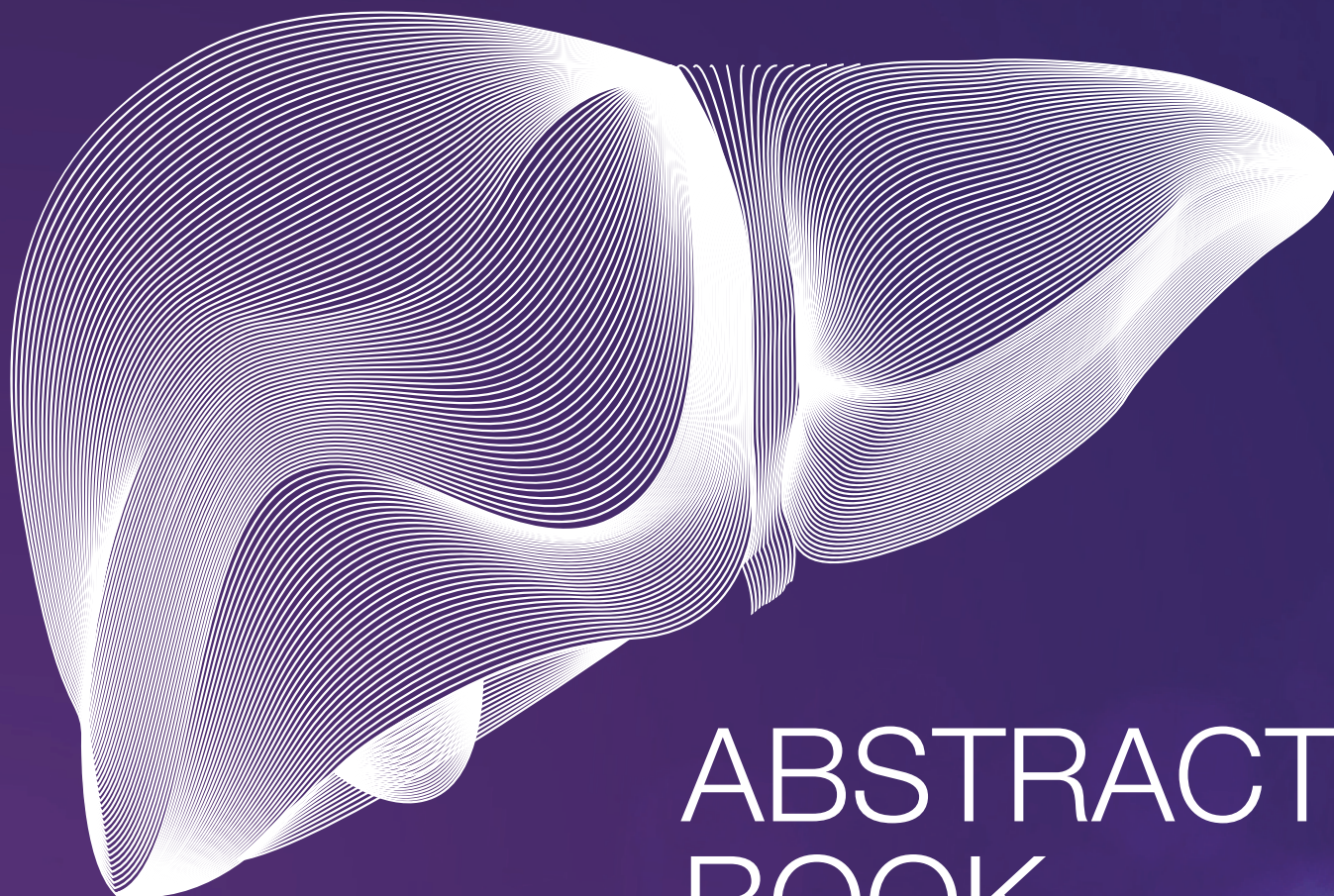


JOURNAL OF HEPATOLOGY

The Home of Liver Research



ABSTRACT BOOK

JOURNAL OF HEPATOLOGY

The Home of Liver Research

EDITOR IN CHIEF

Paolo Angeli, Italy

DEPUTY EDITOR

Patrizia Burra, Italy

CO-EDITORS

Vlad Ratziu, France | Bruno Sangro, Spain |
Frank Tacke, Germany | Stefan Zeuzem, Germany

ASSOCIATE EDITORS

Alcohol and Drug-Related Liver Diseases

Einar S. Björnsson, Iceland
Alexandre Louvet, France

Cholestasis and Autoimmune Diseases

Tom H. Karlsen, Norway
Verena Keitel, Germany
Ulrich Beuers, Netherlands

Complications of Cirrhosis and Liver Failure

Paolo Caraceni, Italy
Javier Fernández, Spain
Constantine Karvellas, Canada
Wim Laleman, Belgium

Disease Burden and Public Health

Gregory Dore, Australia

Genetics

Carmen Berasain, Spain

Gut-Liver Axis

Bernd Schnabl, USA
Jonel Trebicka, Germany

Hepatic and Biliary Cancer

Jesper Andersen, Denmark
John Bridgewater, UK
Stephen L. Chan, Hong Kong
Tim Greden, USA

Tom Lüdde, Germany
Jean-Charles Nault, France
Maria Reig, Spain
Lorenza Rimassa, Italy

Imaging and Non-Invasive Tests

Annalisa Berzigotti, Switzerland
Maxime Ronot, France

Immunology

Barbara Rehermann, USA

Liver Fibrosis

Massimo Pinzani, UK

Liver Surgery and Transplantation

Pierre-Alain Clavien, Switzerland
Julie K. Heimbach, USA
Francesco P. Russo, Italy

MASLD

Quentin Anstee, UK
Elisabetta Bugianesi, Italy
George Ioannou, USA
Wajahat Mehal, USA

Pathology

Christine Sempoux, Switzerland

Pediatrics

Lorenzo D'Antiga, Italy

Statistics, A.I. and Modelling Outcomes

Fabrice Carrat, France
Sylvie Chevret, France
Julian Varguese, Germany
Terry CF Yip, Hong Kong

Viral Hepatitis

Thomas Baumert, France
Maria Buti, Spain
Markus Cornberg, Germany
Edward J. Gane, New Zealand
Man-Fung Yuen, Hong Kong

Consultants

Julius Chapiro, USA
Peter Jepsen, Denmark

SPECIAL SECTION EDITORS

Reviews

Michael Trauner, Austria

Snapshot

Sara Montagnese, Italy
Alexander Ploss, USA

Website/Social Media

Jesus Bañales, Spain

What is your diagnosis?

Xavier Forns, Spain

EDITORIAL BOARD

Alcohol and Drug-Related Liver Diseases

Raul Andrade, Spain
Michael R. Lucey, USA
Philippe Mathurin, France
Laura E. Nagy, USA
Georges-Philippe Pageaux, France
Mark R. Thursz, UK

Basic Science

Javier Cubero, Spain
José Fernandez-Checa, Spain
Chandrashekar Gandhi, USA
Mathias Heikenwälder, Germany
Irene Ng, China
Cecilia Rodrigues, Portugal
Detlef Schuppan, Germany

Cholestatic and Autoimmune Diseases

Martti Färkkilä, Finland
Michael Heneghan, UK
Gideon Hirschfield, Canada
Pietro Invernizzi, Italy
Ansgar Lohse, Germany
Xiong Ma, China
Aldo J. Montano-Loza, Canada
Atsushi Tanaka, Japan

Complications of Cirrhosis and Liver Failure

Juan G. Abraldes, Canada
Banwari Agarwal, UK
Jasmohan S. Bajaj, USA
William Bernal, UK
Andrés Cárdenas, Spain
Claire Francoz, France
Guadalupe García-Tsao, USA
Pere Ginés, Spain
Thierry Gustot, Belgium
Matthias Mandorfer, Austria
Sebastian Marciano, Argentina
Manuel Morales-Ruiz, Spain
Salvatore Piano, Italy

Shiv K. Sarin, India
Puneeta Tandon, Canada
Reiner Wiest, Switzerland

Epidemiology/Public Health

Jeffrey Lazarus, Spain
Uwe Siebert, Austria

Genetics

Frank Lammert, Germany
Stefano Romeo, Sweden

Gut-Liver Axis

Sofia Forslund, Germany
Aleksander Krag, Denmark

Hepatic and Biliary Cancer

Ann-Lii Cheng, Taiwan
Laura Dawson, Canada
Peter R. Galle, Germany
Chiun Hsu, Taiwan
Katie Kelley, USA
Josep M. Llovet, USA
Tim Meyer, UK
Pierre Nahon, France
Hayato Nakagawa, Japan
Jinsil Seong, Republic of Korea
Beicheng Sun, China
Juan Valle, UK

Immunology

Mala Maini, UK
Elsa Solà, Spain

Liver Fibrosis

Scott Friedman, USA
Tatiana Kisseleva, USA
Isabelle Leclercq, Belgium
Robert E. Schwartz, USA
Thierry Tordjmann, France
Holger Willenbring, USA

Liver Surgery and Transplantation

Martina Gambato, Italy
Giacomo Germani, Italy

Vincenzo Mazzaferro, Italy
Rajender K. Reddy, USA
Alberto Sánchez-Fueyo, UK
Gonzalo Sapisochin, Canada
Christian Toso, Switzerland

MASLD

Leon Adams, Australia
Guruprasad Aithal, UK
Helena Cortez-Pinto, Portugal
Henning Gronbaek, Denmark
Rohit Loomba, USA
Giulio Marchesini, Italy
Philip N. Newsome, UK
Elizabeth E. Powell, Australia
Manuel Romero-Gómez, Spain
Arun Sanyal, USA
Jörn Schattenberg, Germany
Giovanni Targher, Italy
Luca Valenti, Italy
Grace Wong, Hong Kong
Vincent Wong, Hong Kong
Shira Zelber-Sagi, Israel

Non-invasive Diagnoses and Imaging

Jérôme Boursier, France
Laurent Castera, France
Thierry de Baere, France
Richard (Dick) L. Ehman, USA
Salvatore Petta, Italy
Jordi Rimola, Spain
Riad Salem, USA

Pathology

Karoline Lackner, Austria
Valerie Paradis, France
Peter Schirmacher, Germany
Dina Tiniakos, UK
Achim Weber, Switzerland

Pediatrics

Emmanuel Jacquemin, France
Pietro Vajro, Italy

Statistics, A.I. and Modeling Outcomes

Calogero Camma, Italy

Jeremie Guedj, France

Vascular Liver Diseases

Yasuko Iwakiri, USA
Vincenzo La Mura, Italy
Pierre-Emmanuel Rautou, France

Viral Hepatitis

Alessio Aghemo, Italy
Sandra Ciesek, Germany
James Fung, Hong Kong
Jason Grebely, Australia
Ira Jacobson, USA
Patrick Kennedy, UK
Pietro Lampertico, Italy
Darius Moradpour, Switzerland
Jean-Michel Pawlotsky, France
Thomas Pietschmann, Germany
Charles Rice, USA
Jian Sun, China
Robert Thimme, Germany
Stephan Urban, Germany
Heiner Wedemeyer, Germany
Fabien Zoulim, France

EDITORS EMERITUS

Dame Sheila Sherlock†, Founding
Editor, UK (1985-1989)
Jean-Pierre Benhamou†, France (1990-1994)
Gustav Paumgartner†, Germany (1995-1999)
Juan Rodés†, Spain (2000-2004)
Massimo Colombo, Italy (2005-2009)
Didier Samuel, France (2010-2014)
Rajiv Jalan, UK (2015-2019)

EDITORIAL OFFICE

Manager

Joël Walicki

Coordinators

Kristina Jajcevic
Duncan Anderson

Assistant

Sarita Bhattacharya
Graphic Arts Project Manager
Pablo Echeverria

EASL GOVERNING BOARD

SECRETARY GENERAL

Aleksander Krag, Denmark

VICE SECRETARY

Debbie Shawcross, UK

TREASURER

Francesco Negro, Switzerland
Massimo Pinzani, UK (elect)

SCIENTIFIC COMMITTEE

Tobias Böttler, Germany
Rui Castro, Portugal
Sarwa Darwish Murad, Netherlands
Virginia Hernández-Gea, Spain
Ana Lleo, Italy
Jean-Charles Nault, France
Bogdan Procopet, Romania
Eric Trepo, Belgium

EDUCATIONAL COUNCILLORS

Sven Francque, Belgium

EU POLICY COUNCILLOR

Maria Buti, Spain

Shira Zelber-Sagi, Israel (elect)

EXTERNAL AFFAIRS COUNCILLOR

Francesco Paolo Russo, Italy

INTERNAL AFFAIRS COUNCILLOR

Ahmed Elsharkawy, UK

EASL Office

Journal of Hepatology Editorial Office
7 rue Daubin
1203 Geneva, Switzerland
Tel.: +41 (0) 22 807 0363
E-mail: jhepatology@easloffice.eu

Application for EASL Membership can be done at <https://easl.eu/community/join-the-community/>

© 2024 European Association for the Study of the Liver. Published by Elsevier B.V. All rights reserved.

This journal and the individual contributions contained in it are protected under copyright, and the following terms and conditions apply to their use in addition to the terms of any Creative Commons or other user license that has been applied by the publisher and the European Association for the Study of the Liver to an individual article:

Photocopying: Single photocopies of single articles may be made for personal use as allowed by national copyright laws. Permission is not required for photocopying of articles published under the CC BY license nor for photocopying for non-commercial purposes in accordance with any other user license applied by the publisher and the European Association for the Study of the Liver. Permission of the publisher and the European Association for the Study of the Liver and payment of a fee is required for all other photocopying, including multiple or systematic copying, copying for advertising or promotional purposes, resale, and all forms of document delivery. Special rates are available for educational institutions that wish to make photocopies for non-profit educational classroom use.

Derivative Works: Users may reproduce tables of contents or prepare lists of articles including abstracts for internal circulation within their institutions or companies. Other than for articles published under the CC BY license, permission of the publisher and the European Association for the Study of the Liver is required for resale or distribution outside the subscribing institution or company. For any subscribed articles or articles published under a CC BY-NC-ND license, permission of the publisher and the European Association for the Study of the Liver is required for all other derivative works, including compilations and translations.

Storage or Usage: Except as outlined above or as set out in the relevant user license, no part of this publication may be reproduced, stored in a retrieval system or transmitted in any form or by any means, electronic, mechanical, photocopying, recording or otherwise, without prior written permission of the publisher and the European Association for the Study of the Liver.

Permissions: For information on how to seek permission visit www.elsevier.com/permissions.

Author rights: Author(s) may have additional rights in their articles as set out in their agreement with the publisher and the European Association for the Study of the Liver (more information at <http://www.elsevier.com/authorsrights>).

Notice: Practitioners and researchers must always rely on their own experience and knowledge in evaluating and using any information, methods, compounds or experiments described herein. Because of rapid advances in the medical sciences, in particular, independent verification of diagnoses and drug dosages should be made. To the fullest extent of the law, no responsibility is assumed by the publisher or the European Association for the Study of the Liver for any injury and/or damage to persons or property as a matter of products liability, negligence or otherwise, or from any use or operation of any methods, products, instructions or ideas contained in the material herein.

Although all advertising material is expected to conform to ethical (medical) standards, inclusion in this publication does not constitute a guarantee or endorsement of the quality or value of such product or of the claims made of it by its manufacturer.

Publication information: *Journal of Hepatology* (ISSN 0168-8278). For 2023, volumes 78 and 79 are scheduled for publication. Subscription prices are available upon request from the Publisher or from the Elsevier Customer Service Department nearest you or from this journal's website (<http://www.elsevier.com/locate/jhep>). Further information is available on this journal and other Elsevier products through Elsevier's website: (<http://www.elsevier.com>). Subscriptions are accepted on a prepaid basis only and are entered on a calendar year basis. Issues are sent by standard mail (surface within Europe, air delivery outside Europe). Priority rates are available upon request. Claims for missing issues should be made within six months of the date of dispatch.

Orders, claims, and journal enquiries: Please visit our Support Hub page <https://service.elsevier.com> for assistance.

Advertising information: Advertising orders and enquiries can be sent to: **USA, Canada and South America:** Elsevier Inc., 360 Park Avenue, Suite 800, New York, NY 10169-0901, USA; phone: (+1) (212) 989 5800. **Europe and ROW:** Robert Bayliss, Pharma Solutions, Elsevier Ltd., 125 London Wall, London EC2Y 5AS, UK; phone: (+44) 207 424 4454; e-mail: r.bayliss@elsevier.com.

Author enquiries: Visit the Elsevier Support Center (<https://service.elsevier.com/app/home/supporthub/publishing>) to find the answers you need. Here you will find everything from Frequently Asked Questions to ways to get in touch.

You can also check the status of your submitted article via https://service.elsevier.com/app/answers/detail/a_id/29155/ or find out when your accepted article will be published via https://service.elsevier.com/app/answers/detail/a_id/5981/.

Funding body agreements and policies: Elsevier has established agreements and developed policies to allow authors whose articles appear in journals published by Elsevier, to comply with potential manuscript archiving requirements as specified as conditions of their grant awards. To learn more about existing agreements and policies please visit <http://www.elsevier.com/fundingbodies>.

Special regulations for authors: Upon acceptance of an article by the journal, the author(s) will be asked to transfer copyright of the article to EASL. Transfer will ensure the widest possible dissemination of information.

USA mailing notice: *Journal of Hepatology* (ISSN 0168-8278, USPS 11087) is published monthly by Elsevier B.V. Radarweg 29, 1043 NX Amsterdam, the Netherlands. Airfreight and mailing in the USA by agent named World Container Inc, 150-15, 183rd Street, Jamaica, NY 11413, USA. Periodicals postage paid at Brooklyn, NY 11256.

POSTMASTER: Send address changes to *Journal of Hepatology*, Air Business Ltd, c/o World Container INC 150-15, 183rd St, Jamaica, NY 11413, USA.

Subscription records are maintained at Elsevier B.V. Radarweg 29, 1043 NX Amsterdam, the Netherlands.

Air Business Ltd is acting as our mailing agent.

© The paper used in this publication meets the requirements of ANSI/NISO Z39.48-1992 (Permanence of Paper).

Printed by Henry Ling Ltd., Dorchester, UK



EASLTM
The Home of Hepatology



Let's unite
Hepatology

*Discover your
membership benefits!*



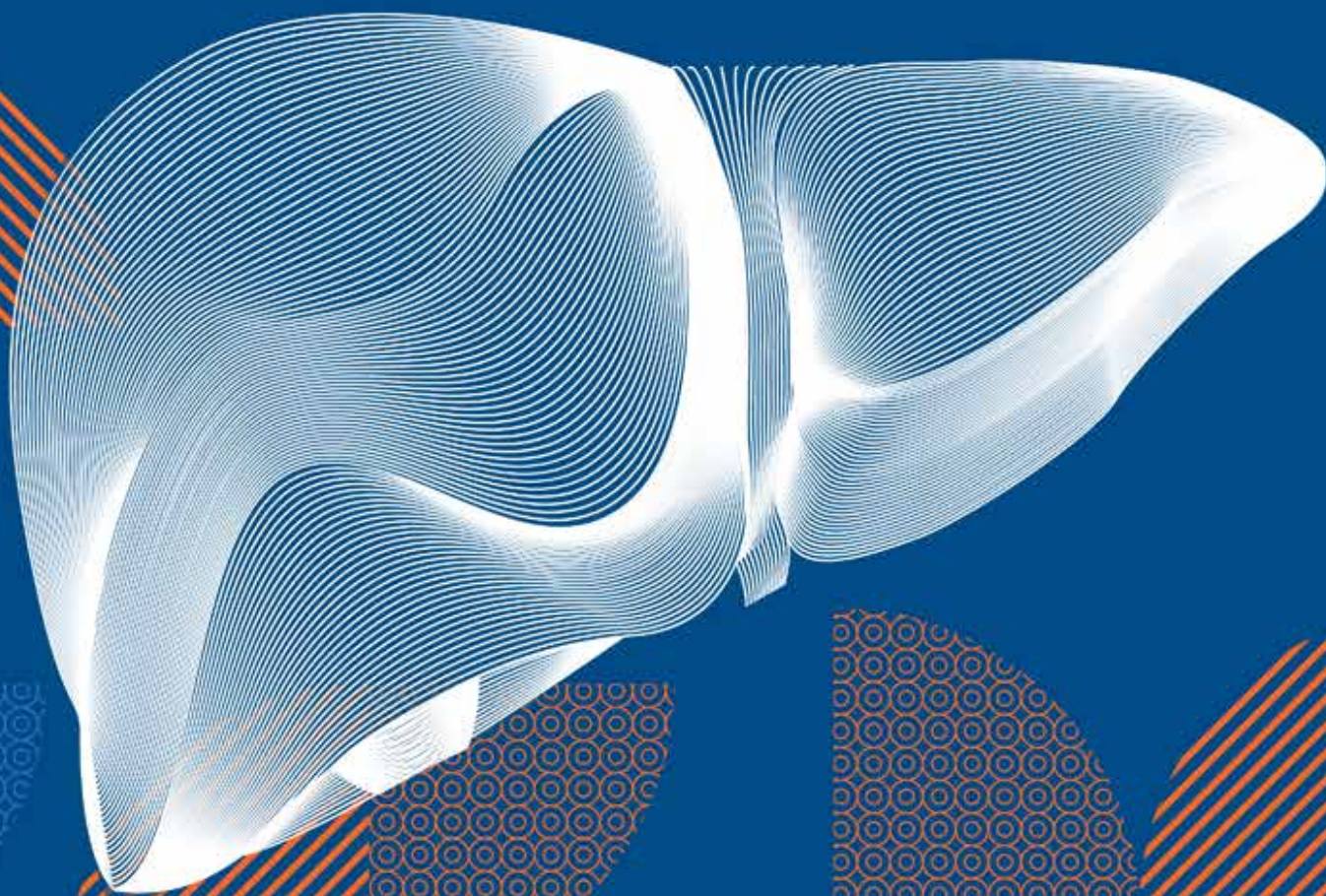
Become a member today



EASL CONGRESS

7-10 May 2025

Amsterdam, the Netherlands



#EASLCongress

easlcongress.eu



HEALTHY LIVERS HEALTHY LIVES

A global coalition for action across the clinical, public health and policy level

Our Vision

A world free of
liver diseases

Our Mission

To mobilise action for
liver diseases

Our Goal

Reducing the prevalence
of liver diseases
worldwide

READ
MORE



The Healthy Livers, Healthy Lives Coalition's activities are supported by MSD and Boehringer Ingelheim. MSD and Boehringer Ingelheim have had no input into the content of the Healthy Livers, Healthy Lives Coalition's activities.

JOURNAL OF HEPATOLOGY

VOLUME **80**, SUPPLEMENT **1**, PAGES **S1–S940**

Abstract Book of EASL Congress 2024
5–8 June 2024, Milan, Italy

Publication of this Abstract supplement was supported by the European Association for the Study of the Liver (EASL)

ELSEVIER

JOURNAL OF HEPATOLOGY

VOLUME 80, SUPPLEMENT 1, PAGES S1–S940

CONTENTS

Oral Presentations	S1
General Session I	S1
General Session II	S4
Late-breaker Orals	S7
Nurses & AHPs	S11
Alcohol-related liver disease	S13
Cirrhosis and its complications: Experimental	S15
Immune-mediated and cholestatic liver diseases – Clinical	S18
Liver transplantation and hepatobiliary surgery	S21
Liver tumours: Experimental and Pathophysiology	S23
Viral hepatitis B/D: New treatments	S26
Cirrhosis and its complications: Clinical	S28
Immune Experimental and rare diseases – Basic	S31
Liver immunology	S34
MASLD: Clinical aspects	S36
Public Health	S39
Viral hepatitis C	S41
Acute liver failure and drug-induced liver injury	S44
Gut microbiota and liver disease	S46
Liver tumours: Clinical aspects except therapy	S49
Rare liver diseases	S52
SLD: Experimental	S55
Viral Hepatitis: Experimental and pathophysiology	S58
Cirrhosis and its complications: Portal hypertension	S60
Hepatocyte and Fibrosis Biology	S63
Liver development and regeneration	S66
Liver tumours: Therapy	S68
SLD: Therapy	S70

Viral hepatitis B/D: Therapy	S73
New CPG and late breaker evidences	S76
Poster Presentations	S78
Late-breaker Posters	S78
Acute liver failure and drug induced liver injury – Basic	S103
Acute liver failure and drug induced liver injury – Clinical	S114
Alcohol-related liver disease and MetALD – Basic	S124
Alcohol-related liver disease and MetALD – Clinical	S136
Cirrhosis and its complications – ACLF and Critical illness	S156
Cirrhosis and its complications – Experimental and pathophysiology	S173
Cirrhosis and its complications – Other clinical complications except ACLF and critical illness	S199
Cirrhosis and its complications – Portal Hypertension	S237
Fibrosis – Stellate cell biology	S261
Gut microbiota and liver disease – Liver-organ crosstalk	S271
Hepatocyte biology	S286
Immune-mediated and cholestatic – Experimental and pathophysiology	S290
Immune-mediated and cholestatic disease Clinical aspects	S305
Liver development and regeneration	S345
Liver immunology	S349
Liver transplantation and hepatobiliary surgery – Basic	S360
Liver transplantation and hepatobiliary surgery – Clinical	S365
Liver tumours – Clinical aspects except therapy	S390
Liver tumours – Experimental and pathophysiology	S411
Liver tumours – Therapy	S436
MASLD – Clinical aspects except therapy	S459
MASLD – Diagnostics and non-invasive assessment	S503
MASLD – Experimental and pathophysiology	S561
MASLD – Therapy	S601
Non-invasive assesment of liver disease except MASLD	S620
Nurses and Allied Health Professionals	S629
Public Health – Except viral hepatitis	S637
Public Health – Viral hepatitis	S656
Rare liver diseases (including paediatric and genetic) – Basic	S692
Rare liver diseases (including paediatric and genetic) – Clinical	S702
Viral Hepatitis – Experimental and pathophysiology	S726
Viral hepatitis AE – Clinical aspects	S757

Viral hepatitis B and D – Clinical aspects	S758
Viral Hepatitis B and D – Current therapies	S792
Viral Hepatitis B and D – New therapies, unapproved therapies or strategies	S806
Viral Hepatitis C – Clinical aspects including follow up after SVR	S817
Viral hepatitis C – Therapy and resistance	S831
Author Index	S837
Disclosures: no commercial relationships	S932
Disclosures: commercial relationships	S936
Reviewers list	S940

Registration of Clinical Trials

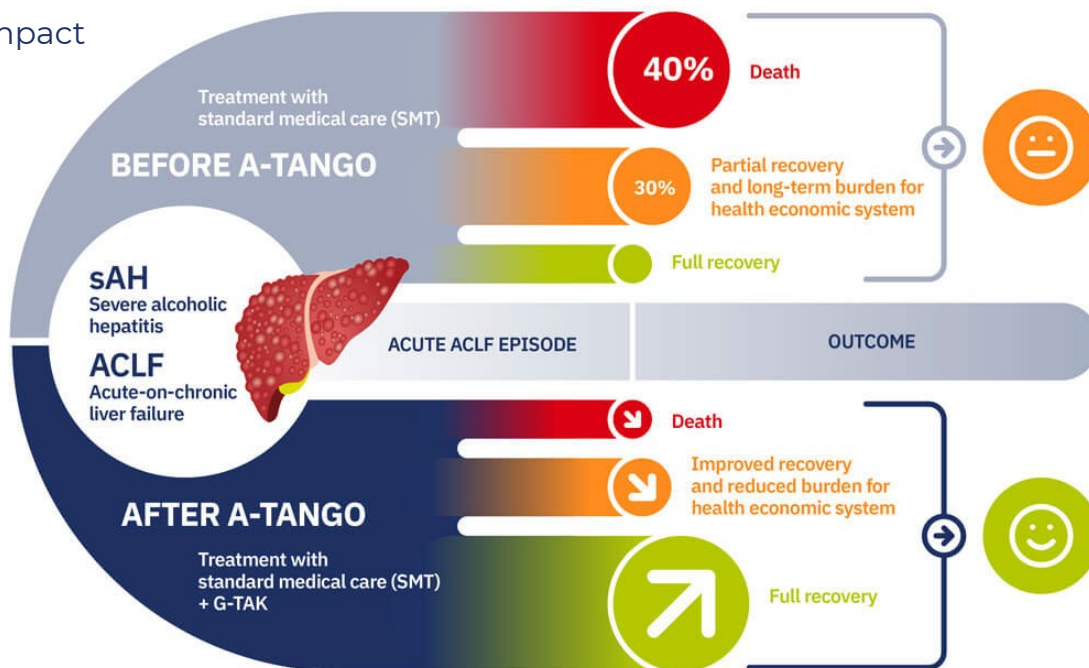
The *Journal of Hepatology* endorses the policy of the WHO and the International Committee of Medical Journal Editors (ICMJE) on the registration of clinical trials. Therefore, any trial that starts recruiting on or after July 1, 2005 should be registered in a publicly owned, publicly accessible registry and should satisfy a minimal standard dataset. Trials that started recruiting before that date will be considered for publication if registered before September 13, 2005.

More detailed information regarding clinical trials and registration can be found in *New Engl J Med* 2004; 351:1250–1251 and *New Engl J Med* 2005; 352:2437–2438.

Available online at www.sciencedirect.com

 **ScienceDirect**
for online access via your library

Expected Impact



- More than **10 million people** suffer from **decompensated cirrhosis** worldwide.
- Effective treatment of ACLF is an urgent and unmet need.
- A-TANGO performs **Phase II clinical studies of G-TAK**, a novel and innovative therapeutic strategy that aims to **reduce inflammation** and **improve hepatocyte proliferation**.
- A-TANGO also strives to identify **reliable biomarkers** for better patient stratification and increased survival.

13 partners, one goal:
Helping cirrhosis patients in Europe and beyond

kick-off

1st March 2021

project duration

5.0 years



www.a-tango.eu
info@atango.eu



grant amount

6.0 million €



DEcompensated CirrhoSis: identification of new cOmBiNatorial therapies based on systems approaches

Key facts

- Project start: 1st April 2020
- Duration: 5.5 years
- Members: 21 institutions from 10 European countries
- EC funding: € 6 million

Follow us on social media:



AIM 1

Understanding at systems level

- Using **high-throughput technologies** to understand decompensated cirrhosis at systems level
- Re-analyzing standardized biobank samples from **2,200 patients** with decompensated cirrhosis by characterizing
 - epigenomics
 - transcriptomics
 - metabolomics
 - microRNA
 - extracellular vesicles
- Publication of results from all molecular characterizations forthcoming

AIM 2

New combinatorial therapy

- COMBAT-Trial**: proof-of-concept, phase II randomized controlled clinical study
- Goal**: Evaluate safety and efficacy of a novel combinatorial therapy (human albumin and enoxaparin) in patients with decompensated cirrhosis discharged from the hospital
- Comparison to standard medical treatment
- Study commencement planned for H1 2024

AIM 3

Preclinical models

- Existing rat models for acute decompensation of cirrhosis leading to ACLF lack full replication of human disease heterogeneity
 - We therefore aim to refine existing animal models
- Two papers will be published in soon:
 - Development and characterization of **novel rodent ACLF models**
 - Acceleration of an advanced **NASH model** by acute and toxic effects of Phenobarbital

AIM 4

Prognostic and response tests

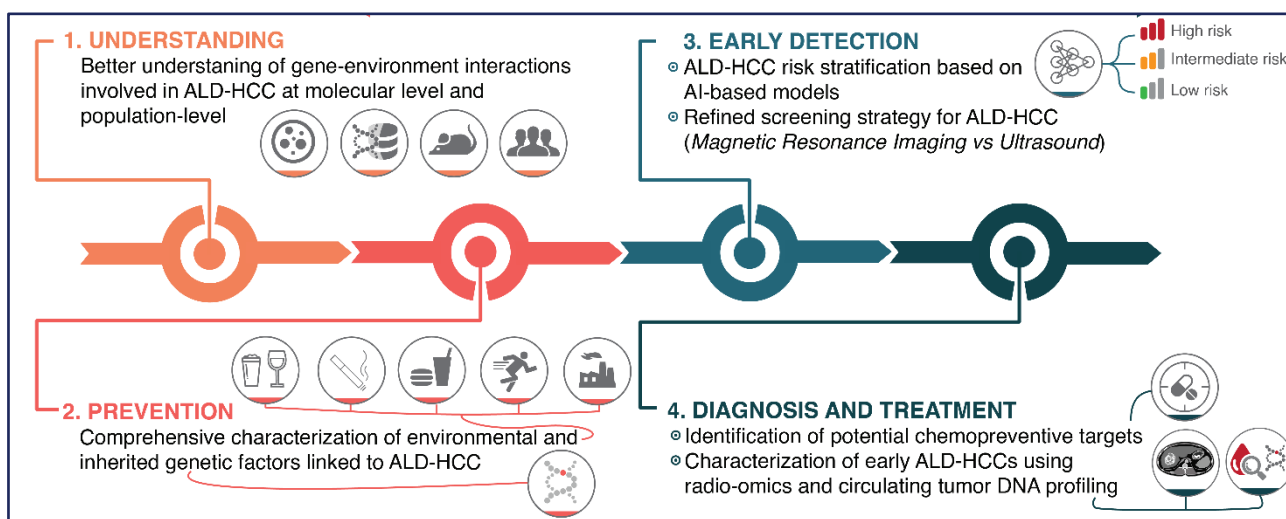
- Novel and robust stratification method identifies three clusters of patients with acute decompensation of cirrhosis (AD)
- Method offers insights that could guide future clinical trial design
- Potential tool for healthcare providers to implement closer monitoring or preventative measures using existing data from electronic health records
- Results will be published soon.

The DECISION consortium





GENIAL is a pioneering initiative targeting **alcohol-related liver cancer (ALD-HCC)**. Our primary goal is to identify **genetic** and **environmental** factors contributing to ALD-HCC risk and unravel how their **interactions** drive alcohol-related liver carcinogenesis. By pinpointing individuals at risk, GENIAL will pave the way for innovative **prevention strategies** and potential **chemopreventive targets** to tackle this devastating disease. Moreover, GENIAL is dedicated to **educating** and empowering the entire EU community with vital knowledge for effective disease prevention and **early detection**.



FONDAZIONE IRCCS CA' GRANDA
OSPEDALE MAGGIORE POLICLINICO



The GENIAL Project is funded by the European Union within the Horizon Europe programme under grant agreement No 101096312.



A biomarker-based platform for early diagnosis of chronic liver disease to enable personalized therapy

Academia and industries are joining forces to undertake the largest project ever in the field of liver diseases

AIM:

To design and validate an AI-powered screening platform using biomarkers for the early diagnosis of liver diseases in the population, and to establish links to care through personalized interventions



This project is supported by the Innovative Health Initiative Joint Undertaking (IHI JU) under grant agreement No 101132901. The JU receives support from the European Union's Horizon Europe research and innovation programme and EFPIA, COCIR, MedTech Europe, Vaccines Europe and EuropaBio. Funded by the European Union, the private members, and those contributing partners of the IHI JU. Views and opinions expressed are however those of the author(s) only and do not necessarily reflect those of the aforementioned parties. Neither of the aforementioned parties can be held responsible for them.



LIVER SCREEN



Screening for liver fibrosis population-based study across European Countries

A project that will change the paradigm
of diagnosis of chronic liver diseases

AIM:

To assess the prevalence of liver fibrosis in the general
population using Transient Elastography, with the
objective of establishing criteria for screening for liver
fibrosis in the population.



This project has received funding from the European Union's Horizon 2020 research and innovation programme under grant agreement No 847989

**MICROBiome-based biomarkers
to PREDICT decompensation of
liver cirrhosis and treatment response**



Project duration
6 1/4 years

Start
01 January 2019

Follow-us on X and LinkedIn:



Grant amount
15 million €

10 Countries
22 Partners

www.microb-predict.eu



the human microbiome to identify predictors and mechanisms associated with the development of decompensation of cirrhosis and progression to **acute-on-chronic liver failure (ACLF)**.

- New microbiome-based tests for better stratification of cirrhosis patients
- Personalized prediction and prevention of decompensation and ACLF
- Clinical trial to predict response to treatment
- Modern, effective nanobiosensors as clinical tools with improved specificity
- More personalized treatment
- Increased survival times
- Decreased costs for the health systems



EF CLIF
EUROPEAN FOUNDATION
FOR THE STUDY OF
CHRONIC LIVER FAILURE



Universität
Münster



UiO : University of Oslo



UNIVERSITY OF
COPENHAGEN



This project has received funding from the European Union's Horizon 2020 research and innovation programme under grant agreement No 825694.



THRIVE

TUMOUR-HOST INTERACTIONS IN LIVER CANCER
OF CHILDHOOD AND ADULTS

THRIVE is a pioneering EU initiative that aims to **enhance** the **outcome of paediatric & adult liver cancer patients** by:

advancing the
understanding
of HCC

identifying
biomarkers for
current therapies

developing novel
treatments to
overcome resistance

THRIVE Consortium

Josep M Llovet - FRCB-IDIBAPS, Spain
Helen Reeves - UNEW, UK
Quentin Anstee - NUTH, UK
Jessica Zucman-Rossi - UPCITE, France
Manel Esteller - IJC-CERCA, Spain
Georg Zeller - LUMC, The Netherlands
Eran Elinav - WEIZMAN, Israel
Carolina Armengol - IGPT-CERCA, Spain

Mathias Heikenwälder - EKUT, Germany
Sven Nahnsen - EKUT, Germany
Manfred Claassen - EKUT, Germany
Jens Puschhof - DKFZ, Germany
Inn-Acta, Italy
ELPA, Belgium
EASL, Switzerland



Funded by
the European Union

Funded by the European Union under Grant Agreement Nr. 101136622. Views and opinions expressed are however those of the author(s) only and do not necessarily reflect those of the European Union or the European Health and Digital Executive Agency (HADEA). Neither the European Union nor the granting authority can be held responsible for them.

THURSDAY 06 JUNE

GENERAL SESSION I

GS-001

Thematic trial: phase 2 dose-ranging randomized clinical trial of capsular or enema fecal microbiota transplant to prevent hepatic encephalopathy in cirrhosis already on Rifaximin and Lactulose

Jasmohan Bajaj¹, Andrew Fagan¹, Edith Gavis¹, Richard Sterling¹, Hannah Lee¹, Brian Davis¹, Puneet Puri¹, Michael Fuchs¹, Amon Asgharpour¹, Travis Mousel¹, Joel Wedd², Scott Matherly², Vaishali Patel², Mohammad Siddiqui², Velimir Luketic¹, Mary Leslie Gallagher¹, Alexander Khoruts³. ¹Virginia Commonwealth University and Richmond VA Medical Center, Richmond, United States; ²Virginia Commonwealth University, Richmond, United States; ³University of Minnesota, Minneapolis, United States
Email: jasmohan.bajaj@vcuhealth.org

Background and aims: Patients with cirrhosis and hepatic encephalopathy (HE) already on lactulose and rifaximin have few options to prevent further HE. Fecal microbiota transplant (FMT) was helpful in small studies, but route/dosage remains unclear. Aim: to compare 2 FMT routes (oral capsule and enema) with dose-ranging in HE prevention.

Method: A double-blind, placebo controlled RCT with 2 modes of FMT administration in cirrhosis pts on lactulose and rifaximin was completed under FDA IND. 4 groups (Gp1: both oral+enema active, Gp2:oral active+placebo enema, Gp3:oral placebo+active enema, Gp4: both oral+enema placebo) received oral+enema FMT at baseline and a 3rd oral dose at day30. 2 donors were used for FMT products. Pts with recent infections, other antibiotics, MELD>22, transplant and immunosuppression were excluded. We needed 60 total (15/gp) for >90% power across gps at 6 mths on ITT analysis. The primary outcome was safety, especially HE recurrence defined as \geq Grade2 on West-Haven criteria. Secondary outcomes were other adverse events, changes in infections/cirrhosis severity/cognition (PHES/Stroop) and patient-reported outcomes (Sickness Impact Profile (SIP), total/physical/psych; high = worse). Regression for HE-recurrence was performed.

Results: 60 pts (15 per group) with similar MELD (13, 12, 12, 12, p = 0.5) and age (65, 63, 61, 63, p = 0.6) on lactulose+rifaximin were included. Last prior HE episode duration was similar (8–13 mths prior, p = 0.51). Baseline cognition, SIP, and cirrhosis severity were similar between gps. Course: All were followed till death or 6 mths in-person/remotely. 6 pts dropped out (2 Gp1 patients died after falls in rehab), 1 Gp2 died after a seizure, 1 Gp2 and 2 Gp 4 did not return for visits), but ITT analysis was performed. 2 pts in Gp 2 and 1 in Gp 1 did not receive the day30 active dose. 5 pts missed some visits due to COVID-19, but were seen remotely. 4 pts developed infections (SBP, cholecystitis and 2 cellulitis), all unrelated to FMT. Primary outcome: HE recurrence was highest in Gp 4 (both placebo: 40%) vs other (Gp 1:13%, Gp 2:13%, Gp3:0%, p = 0.03). Both Gp 1pts who died had HE

prior to death. Secondary outcomes: liver-related hospitalizations tended higher in Gp 4 vs rest (47% vs Gps1–3: 7–20%, p = 0.12). MELD/PHES/Stroop did not change, but SIP total/physical and psych improved with FMT (p = 0.003) on RMANOVA. Regression in all pts: HE recurrence was related to dose number (OR 0.27, 95% CI 0.10–0.79, p = 0.02), male sex (OR 0.16, 0.03–0.89, p = 0.04) and Physical SIP (OR 1.05, 1.01–1.10, p = 0.05). Dose/route/donor: Within FMT recipients neither dose, route, nor FMT donor affected HE recurrence.

Conclusion: HE recurrence was significantly lower in FMT (enema or oral capsule) recipients versus placebo in a phase 2 placebo-controlled, double-blind, dose-ranging RCT in pts with cirrhosis and HE on lactulose and rifaximin. The FMT route, donor, and dose range did not affect HE recurrence.

GS-002

48-week off-therapy efficacy and safety of bulevirtide in combination with pegylated interferon alfa-2a in patients with chronic hepatitis delta: final results from the phase 2b, open-label, randomised, multicentre study MYR204

Tarik Asselah¹, Vladimir Chulanov², Pietro Lampertico^{3,4}, Heiner Wedemeyer⁵, Adrian Streinu-Cercel^{6,7}, Victor Pantea⁸, Stefan Lazar⁹, George Sebastian Gherlan^{7,9}, Pavel Bogomolov¹⁰, Tatyana Stepanova¹¹, Viacheslav Morozov¹², Vladimir Syutkin¹³, Olga Sagalova¹⁴, Dmitry Manuilov¹⁵, Renee-Claude Mercier¹⁵, Lei Ye¹⁵, Grace M. Chee¹⁵, Ben L. Da¹⁵, Audrey H. Lau¹⁵, Anu Osinusi¹⁵, Marc Bourliere¹⁶, Vlad Ratzu¹⁷, Stanislas Pol¹⁸, Marie-Noëlle Hilleret¹⁹, Fabien Zoulim²⁰. ¹Hôpital Beaujon APHP, Université de Paris-Cité, INSERM UMR1149, Clichy, France; ²Sechenov University, Moscow, Russian Federation; ³Division of Gastroenterology and Hepatology, Foundation IRCCS Ca' Granda Ospedale Maggiore Policlinico, Milan, Italy; ⁴Department of Pathophysiology and Transplantation, CRC "A. M. and A. Migliavacca" Center for Liver Disease, University of Milan, Milan, Italy; ⁵Medizinische Hochschule Hannover, Klinik für Gastroenterologie, Hepatologie und Endokrinologie, Hannover, Germany; ⁶Matei Bals National Institute of Infectious Diseases, Bucharest, Romania; ⁷"Carol Davila" University of Medicine and Pharmacy, Bucharest, Romania; ⁸Infectious Clinical Hospital "T. Ciorba", Chisinau, Moldova; ⁹Dr. Victor Babes Foundation, Bucharest, Romania; ¹⁰M.F. Vladimirovsky Moscow Regional Research and Clinical Institute, Moscow, Russian Federation; ¹¹LLC Clinic of Modern Medicine, Moscow, Russian Federation; ¹²LLC Medical Company "Hepatolog", Samara, Russian Federation; ¹³Institute of Emergency Medicine n.a. NV Sklifosovsky, Moscow, Russian Federation; ¹⁴South Ural State Medical University, Chelyabinsk, Russian Federation; ¹⁵Gilead Sciences, Inc., Foster City, United States; ¹⁶Hôpital Saint Joseph, Marseille, France; ¹⁷CH Pitié-Salpêtrière, Paris, France; ¹⁸Hôpital Cochin, Paris, France; ¹⁹Centre Hospitalier Universitaire Grenoble Alpes, Grenoble, France; ²⁰Hospital Croix Rousse, Lyon, France
Email: renee-claude.mercier@gilead.com

Background and aims: Bulevirtide (BLV) is a first-in-class entry inhibitor approved in the European Union for the treatment of chronic hepatitis delta (CHD). This Phase 2b study (MYR204; NCT03852433) evaluated the safety and efficacy of BLV (2 mg and 10 mg) with or without pegylated interferon alfa-2a (PegIFN) in patients with compensated CHD. Here we present the final results at 48 weeks (W) post-end of treatment (EOT).



ORAL PRESENTATIONS

Method: One hundred seventy-four patients with CHD were randomized (1:2:2:2) and stratified based on the absence or presence of compensated cirrhosis to receive: (A) PegIFN for 48W, (B) BLV 2 mg + PegIFN, (C) BLV 10 mg + PegIFN for 48W followed by 48W of monotherapy with BLV 2 mg or 10 mg, respectively; or (D) BLV 10 mg for 96W. All patients were followed for up to 48W after EOT (FU-48). The primary end point was the proportion who achieved undetectable HDV RNA (<lower limit of quantification (LLOQ), target not detected, LLOQ 50 IU/ml, limit of detection 6 IU/ml) at week 24 post-EOT (FU-24) with predefined comparison between arms C and D. The composite response was defined as undetectable HDV RNA and alanine aminotransferase (ALT) normalisation; other end points included ALT normalisation, change in liver stiffness (LS) by transient elastography and hepatitis B surface antigen (HBsAg) loss.

Results: Baseline characteristics were similar between arms and included: mean (SD) age of 41 (8.7) years, 71% male, and 87% White. Overall, 34% had compensated cirrhosis with mean (SD) LS of 13.1 (7.7) kPa, HDV RNA of 5.3 (1.2) log₁₀ IU/ml, and ALT of 114 (94.8) U/L, 48% were on nucleos(t)ide analogue therapy and 48% were interferon experienced.

At FU-48, undetectable HDV RNA was achieved in 25% (6/24) of arm A, 26% (13/50) of arm B, 46% (23/50) of arm C, and 12% (6/50) of arm D (arm C vs D, $p=0.0003$) compared with FU-24 where undetectable HDV RNA was achieved in 17% (4/24) of arm A, 32% (16/50) of arm B, 46% (23/50) of arm C, and 12% (6/50) of arm D (arm C vs D, $p=0.0003$; arms C vs A, $p=0.0197$; arms B vs D, $p=0.0283$). At FU-48, ALT normalisation and composite end point were 42% and 25% in arm A; 38%, 22% in arm B; 46%, 40% in arm C; and 22%, 8% in arm D (arm C vs D, $p<0.05$), respectively. In BLV treated arms, at FU-48, LS (least-square mean) was improved compared with baseline (arm A -0.3, arm B -2.4, arm C -2.5, arm D -0.8). HBsAg loss at FU-48 was only observed in BLV treatment arms (arm A 0%, arm B 10% [5/50], arm C 4% [2/50], arm D 2% [1/50]). Overall, BLV was well-tolerated, one participant discontinued BLV due to an adverse event related to BLV and three participants experienced BLV related serious adverse events in the post-treatment period.

Conclusion: Combination therapy of BLV 10 mg with PegIFN resulted in the highest rates of undetectable HDV RNA at EOT and FU-24 which was sustained through FU-48, providing a viable finite treatment option for patients with compensated CHD.

GS-003-1Y

The role of endothelial cells in the ductular reaction-driven regeneration

Rita Manco¹, Gauthier Neirynck¹, Camilla Moliterni^{1,2}, Isabelle Leclercq¹. ¹UCLouvain, Brussels, Belgium; ²University of Rome La Sapienza, Rome, Italy
Email: rita.manco@uclouvain.be

Background and aims: In chronic liver diseases (CLD), when native hepatocytes enter replicative senescence, new hepatocytes are produced via differentiation of reactive cholangiocytes, also known as ductular reaction-DR-cells. Our previous research demonstrated that during the development of chronic disease, there is a discrete but transient DR expansion and that the disappearance of those DR coincides with the appearance of new DR-derived hepatocytes. The newly formed DR-derived hepatocytes, clonally expand to contribute to the regeneration of the liver tissue. In the injured liver, the two populations of hepatocytes, native and DR-derived, experience similar stress and DNA damage. However, the new DR-derived hepatocytes are better equipped to handle these challenges and are less likely to transform into preneoplastic nodules or HCC. Despite such back-up mechanism exists, it is not enough to fully regenerate and to avoid liver transplantation in patients. Thus, there is a need to better understand the mechanism with the prospective of discovering new targets for the implementation of new therapies to enhance in vivo DR-driven regeneration. We propose that signals driving DR differentiation into hepatocytes might reside in the local niche, such

as ECM composition (i.e. Laminin) and neighbor cells (i.e. Liver sinusoidal endothelial cells-LSEC).

Method: We used the Opn-iCreERT2; Rosa 26RYFP transgenic mouse model to be able to follow the fate of DR. For studying the origin of LSECs we worked with Cdh5-iCreERT2; Rosa 26RmT/mG transgenic mouse model. CLD was simulated by injecting CCl₄ 3x/week for 6 weeks. Liver tissues were analyzed using immunohistochemistry, flow cytometry and RT-qPCR techniques and RESOLVE molecular cartography for spatial transcriptomic. Finally, single-cell sequencing was used to characterize LSECs.

Results: We have identified two populations of DR cells in the liver parenchyma: surrounded or not by laminin. Using the Molecular Cartography RESOLVE, we found that DR with no laminin around have a lower expression of cholangiocytes genes and an increased expression of Hnf4a, suggesting a transition toward a hepatocyte-like state. Conversely, DR surrounded by laminin remain locked in biliary phenotype. Endothelial cells are located in close proximity to DR cells. However, the ones closer to DR with laminin around are characterized by the expression of CD34 and a higher expression of Pecam1 and Cdh5 genes, markers of capillarization. Also, during CLD, the CD34⁺ cells have a more profibrogenic phenotype, with higher expression of the CXCR4 receptor and Timp3 genes. Finally, preventing LSEC capillarization impacts the DR differentiation.

Conclusion: Thus, CD34⁺ capillarized endothelial cells contribute to the maintenance of the biliary phenotype in DR, by preventing the degradation of the laminin that surrounds DR and their differentiation into hepatocytes.

GS-004

Prognostic significance of a change in liver stiffness measurement by vibration-controlled transient elastography-a multicenter cohort study of 10, 920 patients with metabolic dysfunction-associated steatotic liver disease (MASLD)

Terry Cheuk-Fung Yip¹, Hye Won Lee², Huapeng Lin¹, Emmanuel Tsochatzis³, Salvatore Petta⁴, Elisabetta Bugianesi⁵, Masato Yoneda⁶, Ming-Hua Zheng⁷, Hannes Hagström⁸, Jerome Boursier⁹, José Luis Calleja Panero¹⁰, George Boon Bee Goh¹¹, Wah-Kheong Chan¹², Rocio Gallego-Durán¹³, Arun J Sanyal¹⁴, Victor de Lédinghen¹⁵, Philip N. Newsome¹⁶, Jiangao Fan¹⁷, Laurent Castera¹⁸, Michelle Lai¹⁹, Stephen A. Harrison²⁰, Céline Fournier-Pozat²¹, Grace Lai-Hung Wong¹, Grazia Pennisi²², Angelo Armandi²³, Atsushi Nakajima⁶, Wen-Yue Liu⁷, Ying Shang²⁴, Marc de Saint-Loup²⁵, Elba Llop Herrera²⁶, Kevin Kim Jun Teh¹¹, Carmen Lara-Romero²⁷, Amon Asgharpour¹⁴, Sara Mahgoub²⁸, Chan Mandy²⁹, Clémence M Canivet²⁵, Manuel Romero-Gómez³⁰, Seung U Kim³¹, Vincent Wai-Sun Wong¹. ¹The Chinese University of Hong Kong, Hong Kong, China; ²Yonsei University College of Medicine, Seoul, Korea, Rep. of South; ³University College London Institute for Liver and Digestive Health, London, United Kingdom; ⁴University of Palermo, Palermo, Italy; ⁵University of Torino, Torino, Italy; ⁶Yokohama City University Graduate School of Medicine, Yokohama, Japan; ⁷The First Affiliated Hospital of Wenzhou Medical University, Wenzhou, China; ⁸Karolinska Institutet, Stockholm, Sweden; ⁹Centre Hospitalier Universitaire, Angers, France; ¹⁰Hospital Universitario Puerta de Hierro Majadahonda, Madrid, Spain; ¹¹Singapore General Hospital, Singapore, Singapore; ¹²University of Malaya, Kuala Lumpur, Malaysia; ¹³Virgen Del Rocío University Hospital, Seville, Spain; ¹⁴Virginia Commonwealth University, Richmond, United States; ¹⁵University of Bordeaux, Bordeaux, France; ¹⁶University of Birmingham, Birmingham, United Kingdom; ¹⁷Shanghai Jiaotong University School of Medicine, Shanghai, China; ¹⁸Université Paris Cité, Clichy, France; ¹⁹Harvard University, Boston, United States; ²⁰Pinnacle Clinical Research, San Antonio, United States; ²¹Echosens, Paris, France; ²²University of Palermo, Acireale, Italy; ²³University of Turin, Torino, Italy; ²⁴Karolinska Institutet, Solna, Sweden; ²⁵Angers University Hospital, Angers, France; ²⁶Hospital Puerta del Hierro, Madrid, Spain; ²⁷Virgen del Rocío University Hospital, Seville, Spain; ²⁸Queen Elizabeth Hospital, Birmingham, United Kingdom; ²⁹Echosens, Newcastle, United Kingdom; ³⁰University of Seville, Seville,

Spain; ³¹Yonsei University School of Medicine, Seoul, Korea, Rep. of South
Email: wongv@cuhk.edu.hk

Background and aims: To qualify as a surrogate end point for MASLD drug trials, a biomarker should demonstrate not only diagnostic accuracy to assess liver fibrosis but also the ability to predict prognosis, monitor disease progression and assess treatment response. Liver stiffness measurement (LSM) by vibration-controlled transient elastography (VCTE) is a well-established tool to diagnose fibrosis and cirrhosis, but data on the prognostic implication of a change in LSM remain scarce.

Method: This study included data of patients with MASLD who had undergone serial VCTE examinations at 16 centres in Europe, the USA and Asia (prospective at 14 centres). The primary outcome was liver-related events (LREs), defined as hepatocellular carcinoma (HCC) or hepatic decompensation (ascites, variceal haemorrhage or hepatic encephalopathy).

Results: 10,920 patients with MASLD had at least 2 VCTE examinations at a median (IQR) interval of 15 (11, 28) months (mean age 52.3, 57.6% male, body mass index 27.0 kg/m², 36.1% diabetes). Using the Baveno VII cutoffs of 10 and 15 kPa, 9,009 (82.5%), 1,120 (10.3%) and 791 (7.2%) patients were classified as low, intermediate and high risk at baseline, respectively. At the second examination, 9,377 (85.9%) patients had stable risk category, 577 (5.3%) had progressed, and 966 (8.8%) had improved LSM. At a median follow-up of 34.0 months from the second examination, 124 (1.1%) patients developed LREs (55 HCC and 81 decompensation). In the low-risk group, the incidence rate of LREs was 0.9 per 1,000 person-years (PY) in patients who remained at low risk, compared with 4.1 and 8.5 per 1,000 PY in those who progressed to intermediate and high risk. In the high-risk group, the incidence rate of LREs was 38.7 per 1,000 PY in patients who remained at high risk, compared with 7.8 and 19.4 per 1,000 PY in those who regressed to low and intermediate risk. The relative change in LSM correlated with the risk of LREs. In the high-risk group, the incidence of LREs was 16.1, 33.3, and 55.9 per 1,000 PY in patients with >30% relative decrease, stable, and >30% relative increase in LSM.

Conclusion: Changes in LSM over time are predictive of LREs. Serial LSM by VCTE can be used to monitor disease progression and regression in patients with MASLD. (This study is supported in part by the General Research Fund of the Hong Kong SAR Government [14106923]).

GS-005

mRECIST outcomes in EMERALD-1: a phase 3, randomized, placebo-controlled study of transarterial chemoembolization plus durvalumab with/without bevacizumab in participants with embolization-eligible hepatocellular carcinoma

Bruno Sangro¹, Masatoshi Kudo², Joseph Erinjeri³, Shukui Qin⁴, Zhonggang Ren⁵, Stephen Chan⁶, Yasuaki Arai⁷, Jeong Heo⁸, Ahn Mai⁹, Jose Escobar¹⁰, Yamil Alonso Lopez Chuken¹¹, Jung-Hwan Yoon¹², Won Young Tak¹³, Tanita Suttichaimongkol¹⁴, Mohamed Bouattour¹⁵, Shi-Ming Lin¹⁶, Magdalena Zotkiewicz¹⁷, Sajid Ali¹⁸, Gordon Cohen¹⁹, Riccardo Lencioni²⁰. ¹Liver Unit and HPB Oncology Area, Clínica Universidad de Navarra and CIBEREHD, Pamplona, Spain; ²Department of Gastroenterology and Hepatology, Kindai University Faculty of Medicine, Osaka, Japan; ³Interventional Radiology Service, Memorial Sloan Kettering Cancer Center, New York, United States; ⁴Cancer Center of Nanjing, Jinling Hospital, Nanjing, China; ⁵Department of Hepatic Oncology, Liver Cancer Institute, Zhongshan Hospital, Fudan University, Shanghai, China; ⁶State Key Laboratory of Translational Oncology, Department of Clinical Oncology, Sir Yue-Kong Pao Center for Cancer, The Chinese University of Hong Kong, Hong Kong SAR, China; ⁷Department of Diagnostic Radiology, National Cancer Center, Chuo-ku, Tokyo, Japan; ⁸Department of Internal Medicine, College of Medicine, Pusan National University and Biomedical Research Institute, Pusan National University Hospital, Busan, Korea, Rep. of South; ⁹General Surgery Department, Nhan Dan Gia Dinh Hospital, Ho Chi Minh City,

Viet Nam; ¹⁰Hospital San Lucas Cardiológica del Sureste, Chiapas, Mexico; ¹¹I Can Oncology Center, New León, Mexico; ¹²Department of Internal Medicine and Liver Research Institute, Seoul National University College of Medicine, Seoul, Korea, Rep. of South; ¹³Department of Internal Medicine, School of Medicine, Kyungpook National University, Daegu, Korea, Rep. of South; ¹⁴Division of Gastroenterology and Hepatology, Department of Medicine, Faculty of Medicine, Khon Kaen University, Khon Kaen, Thailand; ¹⁵Medical Oncology, AP-HP Hôpital Beaujon, Paris, France; ¹⁶Department of Internal Medicine, Chang Gung Memorial Hospital, Linkou Medical Center, Taoyuan, Taiwan; ¹⁷Oncology Biometrics, Late Oncology Statistics, AstraZeneca, Warsaw, Poland; ¹⁸Late Development Oncology, AstraZeneca, Cambridge, United Kingdom; ¹⁹Global Medicines Development, AstraZeneca, Gaithersburg, United States; ²⁰Department of Diagnostic and Interventional Radiology, University of Pisa School of Medicine, Pisa, Italy
Email: bsangro@unav.es

Background and aims: For over 20 years, transarterial chemoembolization (TACE) has been a standard of care for embolization-eligible unresectable hepatocellular carcinoma (uHCC); however, most people with uHCC treated with TACE progress within 1 year. The primary end point of EMERALD 1 (NCT03778957) was met, with a statistically significant improvement in progression-free survival (PFS) assessed by blinded independent central review (BICR) per Response Evaluation Criteria in Solid Tumors (RECIST) v1.1 with durvalumab (D) + bevacizumab (B) + TACE vs TACE (median [m]PFS (95% confidence interval [CI]), 15.0 (11.1–18.9) vs 8.2 (6.9–11.1) months [mo]; hazard ratio [HR], 0.77; 95% CI, 0.61–0.98; p = 0.032). Safety was consistent with the profiles of D, B, and TACE in uHCC. In addition to RECIST v1.1, efficacy of the regimens was assessed using modified RECIST (mRECIST).

Method: Participants (pts) with embolization-eligible uHCC, Child-Pugh A to B7 liver function, Eastern Cooperative Oncology Group performance status 0–1, and no evidence of extrahepatic disease were randomized 1:1:1 to the D+B+TACE, D+TACE, or TACE arms. TACE was cTACE or DEB-TACE (investigator choice). Pts received D (1500 mg) or placebo for D every 4 weeks (Q4W) plus TACE. After completion of last TACE, pts received D (1120 mg) plus placebo for B, D (1120 mg) plus B (15 mg/kg), or placebos for D and B (Q3W). PFS was assessed by BICR and the investigator per mRECIST as a secondary end point.

Results: Overall, 616 pts were randomised to D+B+TACE (N = 204), D+TACE (N = 207) or TACE (N = 205). PFS improved with D+B+TACE vs TACE as assessed by both BICR per mRECIST (mPFS (95% CI), 14.2 (11.1–17.4) vs 8.2 (6.9–9.5) mo; HR (95% CI), 0.75 (0.60–0.95)) and investigator per mRECIST (mPFS (95% CI), 13.2 (9.4–16.4) vs 7.5 (7.0–9.1) mo; HR (95% CI), 0.69 (0.55–0.86)). The estimation of effect was consistent with that of the primary end point, which showed a statistically significant improvement in mPFS with D+B+TACE vs TACE (p = 0.032, significance threshold 0.0435). D+TACE vs TACE showed similar PFS results as assessed by BICR per mRECIST (mPFS (95% CI), 9.0 (7.0–10.9) vs 8.2 (6.9–9.5) mo; HR (95% CI), 0.99 (0.79–1.25)), by investigator per mRECIST (mPFS (95% CI), 7.0 (6.7–9.0) vs 7.5 (7.0–9.1) mo; HR (95% CI), 1.03 (0.84–1.28)) and BICR RECIST v1.1 (mPFS (95% CI), 10.0 (9.0–12.7) vs 8.2 (6.9–11.1) mo; HR (95% CI), 0.94 (0.75–1.19), p = 0.638).

Conclusion: D+B+TACE is the first immune checkpoint inhibitor-based regimen in a global Phase 3 trial to show statistically significant improvement in PFS vs TACE in pts with embolization-eligible uHCC, as assessed by BICR per RECIST v1.1, with consistent PFS results, as assessed per mRECIST. These results further support the potential for D+B+TACE to set a new standard of care in uHCC.

GS-011

Denifanstat, a fatty acid synthase (FASN) inhibitor, shows significant fibrosis improvement and MASH resolution in FASCINATE-2, a Ph2b 52 week international, randomized, double blind, placebo-controlled trial in patients with F2 or F3 fibrosis

Rohit Loomba¹, Eduardo Martins², Katharine Grimmer², Wen-Wei Tsai², Marie O' Farrell², William McCulloch², George Kemble², Pierre Bedossa³, Jose Cobiella⁴, Eric Lawitz⁵, Madhavi Rudraraju⁶, Stephen A. Harrison⁶. ¹MASLD Research Center, Division of Gastroenterology and Hepatology, Department of Medicine, University of California San Diego, La Jolla, United States; ²Sagimet Biosciences Inc., San Mateo, United States; ³Liverpat, Paris, France; ⁴Global Research Associates, Homestead, Florida, United States; ⁵American Research Corporation, Texas Liver Institute, San Antonio, United States; ⁶Pinnacle Clinical Research, San Antonio, United States
Email: roloomba@health.ucsd.edu

Background and aims: New therapies are needed for MASH in particular drugs that improve fibrosis, the main predictor of poor clinical outcomes. Denifanstat, an oral FASN inhibitor, directly blocks endogenous FASN in stellate cells, immune cells and hepatocytes, thereby directly inhibiting fibrosis, inflammation and steatosis. Denifanstat directly blocks collagen production in human primary stellate cells ex-vivo. Evidence of denifanstat's mechanism was demonstrated in previous studies including Ph2a FASCINATE-1 where denifanstat decreased de novo lipogenesis, liver fat and biomarkers of inflammation and fibrosis. A Ph2b study FASCINATE-2 was conducted to determine safety and efficacy of denifanstat on liver histology in F2/F3 MASH patients after 52 weeks of treatment.

Method: FASCINATE-2 was a phase 2b, multicenter, double-blind, randomized, placebo-controlled international trial. 168 patients (ITT) with biopsy-confirmed F2/F3 MASH were randomized 2:1 to once daily oral denifanstat 50 mg, or placebo. 126 had both pre- and post-treatment biopsies (mITT). Primary end points were liver histology improvement ≥ 2 points in NAS (≥ 1 point in ballooning or inflammation) and no worsening of fibrosis, or MASH resolution and ≥ 2 points improvement in NAS and no worsening of fibrosis, at week 52. Secondary end points included fibrosis improvement, MASH resolution, collagen/fibrosis by AI-assisted digital pathology and liver fat response by MRI-PDFF. Exploratory objectives included FibroScan-AST (FAST) score, biomarkers of liver injury, lipidomics and fibrosis.

Results: Denifanstat successfully met primary and secondary histology end points with statistical significance in both mITT and ITT populations, as follows for mITT: • ≥ 2 -point improvement of NAS without worsening of fibrosis: 51.9% denifanstat vs 20.0% placebo ($p = 0.0003$). • MASH resolution and ≥ 2 -point improvement of NAS with no worsening of fibrosis: 35.8% denifanstat vs 13.3% placebo ($p = 0.0044$). • Improvement of fibrosis by ≥ 1 stage without worsening of steatohepatitis: 40.7% denifanstat vs 17.8% placebo ($p = 0.01$). • Improvement of fibrosis by ≥ 2 stages without worsening of steatohepatitis: 19.8% denifanstat vs 2.2% placebo ($p = 0.0065$). Furthermore, both MASH resolution and fibrosis improvement were achieved in 23% denifanstat-treated patients compared to 7% placebo. Biomarkers of liver fat, inflammation and fibrosis also decreased. Denifanstat was generally well tolerated. Skin and subcutaneous adverse events, all of which were Grade 1 or 2, were more common in denifanstat-treated patients than placebo.

Conclusion: Denifanstat demonstrated a clinically meaningful and statistically significant improvement in both fibrosis regression and MASH resolution end points, consistent with mechanism. These results support progression of denifanstat to Phase 3 clinical trials in MASH.

FRIDAY 07 JUNE

GENERAL SESSION II

GS-006

Glucagon and GLP-1 receptor dual agonist survodutide improved liver histology in people with MASH and fibrosis: Results from a randomized, double-blind, placebo-controlled phase 2 trial

Arun J Sanyal¹, Pierre Bedossa², Mandy Fraessdorf³, Guy Neff⁴, Eric Lawitz⁵, Elisabetta Bugianesi⁶, Quentin M. Anstee⁷, Samina Ajaz Hussain³, Philip N. Newsome^{8,9}, Vlad Ratziu¹⁰, Azadeh Hosseini-Tabatabaei¹¹, Jörn M Schattenberg¹², Mazen Nouredin¹³, Naim Alkhouri¹⁴, Rami Younes³. ¹Virginia Commonwealth University, School of Medicine, Richmond, United States;

²Liverpat and University of Paris, Paris, France; ³Boehringer Ingelheim, Ingelheim, Germany; ⁴Covenant Metabolic Specialists, LLC, Sarasota and Ft Myers, United States; ⁵Texas Liver Institute, San Antonio, United States; ⁶University of Turin, Turin, Italy; ⁷Newcastle University, Newcastle, United Kingdom; ⁸University Hospitals Birmingham NHS Foundation Trust, Birmingham, United Kingdom; ⁹King's College London and King's College Hospital, London, United Kingdom; ¹⁰Sorbonne Université, Paris, France; ¹¹Boehringer Ingelheim Pharmaceuticals Inc, Ridgefield, United States; ¹²Saarland University Medical Center, Homburg, Germany; ¹³Houston Methodist Hospital and Houston Research Institute, Houston, United States; ¹⁴Arizona Liver Health, Chandler, United States
Email: arun.sanyal@vcuhealth.org

Abstract GS-006 is under embargo until Friday 7 June 2024,

10:30. CET, after which this abstract will be made publicly available on the congress website and will be released for publication in the supplement issue of the *Journal of Hepatology*.

Industry must not issue press releases – even under embargo – covering the data contained in abstracts selected to be highlighted during official EASL Press Office activities or in official EASL Press Office materials until the individual embargo for each data set lifts. Media must not issue coverage of the data contained in abstracts selected to be highlighted during official EASL Press Office activities or in official EASL Press Office materials until the individual embargo for each data set lifts.

Journalists, industry, investigators and/or study sponsors must abide by the embargo times set by EASL. Violation of the embargo will be taken seriously. Individuals and/or sponsors who violate EASL's embargo policy may face sanctions relating to current and future abstract submissions, presentations and visibility at EASL Congresses. The EASL Governing Board is at liberty to ban attendance and/or retract data.

Copyright for abstracts (both oral and poster) on the website and as made available during The EASL Congress 2024 resides with the respective authors. No reproduction, re-use or transcription for any commercial purpose or use of the content is permitted without the written permission of the authors. Permission for re-use must be obtained directly from the authors.

GS-007

Prospective validation of the prognostic value of liver stiffness assessed by Fibroscan in primary sclerosing cholangitis: final results of the FICUS study

Olivier Chazouillères^{1,2}, Christoph Schramm^{3,4}, Palak J. Trivedi⁵, Jonathan Bellet⁶, Aymeric Monegier du Sorbier⁷, Douglas Thorburn⁸, Martti Färkkilä^{9,10}, Annarosa Floreani¹¹, Albert Pares^{12,13}, Cynthia Levy¹⁴, Ulrich Beuers^{15,16}, Henriette Ytting^{17,18}, Ehud Zigmond¹⁹, Bertus Eksteen²⁰, Pietro Invernizzi^{21,22}, Sara Lemoine^{2,23}, Ansgar W. Lohse²⁴, Gideon M. Hirschfield²⁵, Nora Cazzagon^{26,27}, Laura Llovet¹², Cyriel Ponsioen²⁸, Marco Carbone^{22,29}, Füssel Katja³⁰, Francesco Pezzato²⁶, Isha Patel¹⁴, Jeltje Helder³¹, Sheeba Khan³², Karima Ben Belkacem³³, Gaouar Farid³⁴, Chantal Housset³⁵, Fabrice Carrat³⁶, Christophe Corpechot³⁷. ¹Reference Center for Inflammatory Biliary Diseases and Autoimmune Hepatitis, Saint-Antoine Hospital, Assistance Publique-Hôpitaux De Paris, Inserm Umr_S938, Sorbonne University, Paris, France; ²ERN RARE LIVER, Paris, France; ³1st Department of Medicine, Martin Zeitz Center for Rare Diseases, Martin Zeitz Center for Rare Diseases, Hamburg, Germany; ⁴ERN RARE LIVER, Hamburg, Germany; ⁵National Institute for Health Research (NIHR) Birmingham Biomedical Research Centre (BRC), University of Birmingham, Birmingham, United Kingdom; ⁶Inserm, Institut Pierre-Louis Epidémiologie Et Santé Publique, Sorbonne Université, AP-HP, Paris, Paris, France; ⁷Sorbonne Université, Inserm, Institut Pierre-Louis Epidémiologie Et Santé Publique, AP-HP, Paris, Paris, France; ⁸Sheila Sherlock liver centre, Royal Free hospital, London, United Kingdom; ⁹Clinic of Gastroenterology, Helsinki University, Helsinki, Finland; ¹⁰ERN RARE LIVER, Helsinki, Finland; ¹¹University of Padova, Padova, Italy; ¹²Liver Unit, Hospital Clinic, University of Barcelona, Barcelona, Spain; ¹³ERN RARE LIVER, Barcelona, Spain; ¹⁴University of Miami, Miller School of Medicine, Miami, United States; ¹⁵Department of Gastroenterology and Hepatology, Tytgat Institute for Liver and Intestinal Research, Amsterdam University Medical Centres, Amsterdam, Netherlands; ¹⁶ERN RARE LIVER, Amsterdam, Netherlands; ¹⁷Gastro Unit, Medical Section, Hvidovre University Hospital Copenhagen, Department of Clinical Medicine, Faculty of Health and Medical Sciences, Copenhagen University, Department of Intestinal Failure and Liver Diseases, Rigshospitalet, Copenhagen University Hospital, Copenhagen, Denmark; ¹⁸ERN RARE LIVER, Copenhagen, Denmark; ¹⁹Tel-Aviv Sourasky Medical Center, Tel-Aviv University, Tel Aviv, Israel; ²⁰University of Calgary, Hepatology department, Calgary, Canada; ²¹Liver Unit, ASST Grande Ospedale Metropolitano Niguarda, Center of autoimmune liver disease, Department of Medicine and Surgery, university of Milano-Bicocca and ERN RARE LIVER, Milano, Italy; ²²ERN RARE LIVER, Milano, Italy; ²³Reference Center for Inflammatory Biliary Diseases and Autoimmune Hepatitis, Saint-Antoine Hospital, Assistance Publique-Hôpitaux De Paris, Department of Hepatology, Paris, France; ²⁴University Medical Center Hamburg-Eppendorf, ERN RARE LIVER, Hamburg, Germany; ²⁵National Institute for Health Research (NIHR) Birmingham Biomedical Research Centre (BRC), Birmingham; ²⁶Department of Surgery, Oncology, and Gastroenterology, University of Padova and ERN RARE LIVER, Padova, Italy; ²⁷ERN RARE LIVER, Padova, Italy; ²⁸Department of Gastroenterology and Hepatology, Tytgat Institute for Liver and Intestinal Research, Amsterdam University Medical Centres and ERN RARE LIVER, Amsterdam, Netherlands; ²⁹Liver Unit, ASST Grande Ospedale Metropolitano Niguarda, Center of autoimmune liver

disease, Department of Medicine and Surgery, university of Milano-Bicocca and ERN RARE LIVER, Milano, Italy; ³⁰Department of Medicine, University Medical Center Hamburg-Eppendorf, ERN RARE LIVER, Hamburg, Germany; ³¹Department of Gastroenterology and Hepatology, Tytgat Institute for Liver and Intestinal Research, Amsterdam University Medical Centres and ERN RARE LIVER, Amsterdam, Netherlands; ³²University Hospitals Birmingham, Birmingham, United Kingdom; ³³Saint-Antoine Hospital, Assistance Publique-hôpitaux de Paris, Reference Center for Inflammatory Biliary Diseases and Autoimmune Hepatitis, Paris, France; ³⁴Saint-Antoine Hospital, Assistance Publique-Hôpitaux De Paris, Reference Center for Inflammatory Biliary Diseases and Autoimmune Hepatitis, Paris, France; ³⁵Reference Center for Inflammatory Biliary Diseases and Autoimmune Hepatitis, Saint-Antoine Hospital, Assistance Publique-Hôpitaux De Paris and centre de Recherche Saint-Antoine, Paris, France; ³⁶INSERM _ UMR-S 1136 Institut Pierre Louis d'Epidémiologie et Sante Publique, Saint-Antoine Hospital, Assistance Publique-Hôpitaux De Paris and centre de Recherche Saint-Antoine, Paris, France; ³⁷Saint-Antoine Hospital, Assistance Publique-Hôpitaux de Paris, Sorbonne University, Reference Center for Inflammatory Biliary Diseases and Autoimmune Hepatitis, ERN RARE LIVER, Paris, France
Email: olivier.chazouilleres@aphp.fr

Background and aims: Predicting the risk and pace of progression of primary sclerosing cholangitis (PSC) by reliable and simple tools is an unmet need. Baseline liver stiffness (LS) and LS changes over time have been associated with adverse clinical outcome in retrospective studies (1). However, prospective validation is lacking.

Method: Clinical, biological and elastographic (LS measurement (LSM) by Fibroscan) data of adult patients with uncomplicated PSC from 13 institutions, members of the International PSC Study Group, were prospectively recorded at baseline and then annually for 5 years. The primary end point was transplant-free survival. Survival free of transplant and liver complications (ascites, variceal bleeding, encephalopathy, hepatocellular carcinoma, biliary cancer, serum bilirubin above 100 micromol/L for at least 3 months, listing for LT) was the main secondary end point. Cox proportional hazard models were used to estimate multivariable adjusted hazard ratios (aHRs). LS was assessed either continuously or according to pre-established fibrosis cut-offs (1). The time-dependent predictive performance of LS was assessed. We present here the final results at 5 years.

Results: 617 patients were included. Follow-up data (median: 60.8 months, Q1-Q3 (48.6-66.0)) were available in 538. Baseline characteristics were: 67% males, age: 43 ± 14 yrs, associated inflammatory bowel disease: 71%, small-duct PSC: 9%, AIH-PSC overlap: 7%, taking UDCA: 76%, bilirubin: 20 ± 24 micromol/L, ALP: 1.9 ± 1.6 ULN, LS: 11.9 ± 12.4 kPa. During follow-up, 19 patients died and 74 were transplanted. Baseline LS was strongly and independently (adjusted for age, gender, bilirubin, and ALP) linked to the risk of death or transplantation: aHR 1.05 (per kPa increase), 95%CI (1.04-1.06), P < 0.001. This association was independent of those observed with the Mayo and Amsterdam-Oxford prognostic scores. Observed transplant-free survival (Kaplan-Meier) at 5 yrs by LS strata was 93.8% CI95% (90.2-96.1), 79.0% CI95% (67.4-86.8) and 48.1% CI95% (36.7-58.5), respectively for [2.5-9.5]kPa group, [9.6-14.3]kPa group and ≥14.4 kPa group with corresponding aHR (vs 2.5-9.5) (95% CI) of 2.7 (1.4-5.4) for [9.6-14.3] kPa group and 7.8 (4.4-13.9) for ≥14.4 kPa group. The predictive performance assessed by the time-dependent area under the ROC curve was 0.85 CI95% (0.78-0.92). Results for the main secondary end point were consistent with those for the primary end point.

Conclusion: This large international prospective study validates the prognostic value of liver stiffness assessed by Fibroscan in PSC. These results support the major role of liver stiffness measurement in clinical trials as a risk stratifying tool and potential surrogate end point.

Reference

1. Corpechot et al. *Gastroenterology* 2014.

GS-008

The combination of therapeutic vaccination with siRNA-mediated silencing of HBV and PD-L1 effectively breaks HBV-specific immunotolerance in high-titer HBV carrier mice

Anna D. Kosinska^{1,2}, Edanur Ates-Öz¹, Till Bunse¹, Merve Gültan³, Swati Singh¹, Ulrike Protzer¹. ¹Institute of Virology, Technical University of Munich/Helmholtz Munich, Munich; ²German Center for Infection Research (DZIF), Munich Partner Site, Munich; ³Institute of Virology, Technical University of Munich/Helmholtz Munich, Munich, Germany
Email: anna.kosinska@tum.de

Background and aims: High levels of hepatic HBV antigens prevent a successful therapeutic vaccination. Reducing HBV levels before vaccination by HBV-specific siRNAs (siHBV) enhanced the immunogenicity and antiviral efficacy of our clinical candidate protein-prime/MVA-boost therapeutic vaccine, TherVacB, in higher-titer HBV-carrier mice. Non-responsiveness to vaccination was associated with high PD-1 expression on vaccine-elicited hepatic CD8 T-cells. Consequently, silencing PD-1 ligand-1 by liver-targeted siRNA (siPD-L1) also improved the TherVacB-mediated therapeutic effects. We hypothesized that combining siHBV with siPD-L1 could further broaden the applicability of TherVacB in high-titer, persistent HBV infection settings.

Method: We established high-titer persistent HBV infection in C57BL/6J mice using AAV-HBV, resulting in over 80% of HBV-positive hepatocytes, HBsAg of 5500 IU/ml and HBeAg of 330 PEI U/ml. We pretreated five mice per group for eight weeks with siHBV before TherVacB and applied siPD-L1 during the two protein priming immunizations. We followed up with the mice for 7.5 months after the MVA boost.

Results: Groups of mice receiving TherVacB and TherVacB+siPD-L1 demonstrated only a minor decrease in serum HBsAg and HBeAg levels shortly after treatment. Without vaccination, siHBV+siPD-L1 reduced HBsAg and HBeAg, as expected, but the antigen load eventually returned baseline values, and no induction of HBV-specific immunity was observed. Combining siHBV+TherVacB reduced HBsAg to undetectable levels for eight weeks, but a partial relapse finally resulted in only a 1-log10 decrease compared to the initial values. By contrast, mice receiving siHBV+TherVacB+siPD-L1 cleared HBsAg for 24 weeks. 3/5 mice remained negative for 7.5 months. Overall, the siHBV+TherVacB+siPD-L1 treatment resulted in a ≥ 3 -log10 reduction in serum HBsAg, a 70% reduction in HBeAg, and, on average, a 90% reduction in intrahepatic HBV-DNA. A strong vaccine-elicited immunity accompanied this impressive antiviral effect.

Conclusion: Our data demonstrate that complementary siRNA-mediated silencing of HBV and the immune checkpoint PD-L1 helps to further enhance the efficacy of therapeutic vaccination in high-titer HBV carriers.

GS-009

Efficacy and safety of carvedilol in cirrhosis patients with uncomplicated ascites without high-risk esophageal varices-a randomized controlled trial [NCT05057572]

Rahul Khajuria¹, Ankur Jindal¹, Shiv Kumar Sarin¹. ¹Institute of Liver and Biliary Sciences, New Delhi, India
Email: dr.rahulkhajuria@gmail.com

Background and aims: Carvedilol is effective in preventing bleeding in patients with cirrhosis and high-risk varices. Although it reduces drivers of clinical decompensation (portal pressure, systemic inflammation and bacterial translocation), the data on carvedilol use for prevention of ascites related complications (SBP, HRS-AKI, refractory ascites or severe hyponatremia) are limited.

Method: Consecutive patients presenting with uncomplicated new-onset ascites and low risk esophageal varices were randomized to receive carvedilol (at the starting dose of 3.125 mg BD) (Group A) or

placebo (Group B) in addition to ST (diuretics with or without albumin). The composite primary outcome was incidence of complicated ascites (any of refractory ascites, HRS AKI, SBP, severe hyponatremia) at 1 year. The secondary outcomes include need for paracentesis, change in HVPG, CTP and MELD score and mortality at 1 year.

Results: Of 302 consecutive patients screened, 104 patients were randomized into two groups. Baseline characteristics were comparable between two groups. In both groups, MAFLD was the most common etiology (overall 41.3%) followed by ethanol (21.2%) with comparable comorbidities. Patients in Group A had lower incidence of complicated ascites at 1 year (39.4% vs. 66.7% $p=0.026$), mainly related to reduction of incident HRS AKI (33.3% vs 63.6% $p=0.014$). Patients in Group A also had less frequent need for large volume paracentesis as compared to Group B at 1 year (27.3% vs 57.6% $p=0.013$). Better resolution of ascites (66.6 vs 39.4% $p=0.06$). Despite comparable at baseline, MELD (18.9 ± 1.3 vs. 15.34 ± 1.38 ; $p=0.06$) and CTP score (9.36 ± 1.43 vs. 8.15 ± 1.7 vs $p=0.003$) were higher in Group B as compared to Group A at the end of one year. Overall, the change in HVPG at one year among responders showed significant reduction from 14.89 to 11.86 mmHg ($p=0.042$). Use of carvedilol was associated with lesser mortality at one year (9.1% vs 24.2% $p=0.05$). None had treatment related severe adverse effects requiring discontinuation of therapy.

Conclusion: Carvedilol use in patients with cirrhosis with uncomplicated ascites and low risk varices is safe and prevented further complications, less frequent need for large volume paracentesis and improved survival.

GS-010

Early liver transplantation for severe alcohol-related hepatitis: long-term data of the french-belgian controlled study (QuickTrans)

Alexandre Louvet¹, Laurie Favier², Julien Labreuche¹, Christophe Moreno³, Claire Vanlemmens⁴, Romain Moirand⁵, Line Carolle Ntandja Wandji¹, Cyrille Feray⁶, Jérôme Dumortier⁷, Georges-Philippe Pageaux⁸, Christophe Bureau⁹, Faiza Chermak¹⁰, Christophe Duvoux¹¹, Dominique Thabut¹², Marie-Noëlle Hilleret¹³, Nicolas Carbonell¹⁴, Ephrem Salame¹⁵, Rodolphe Anty¹⁶, Jérôme Gournay¹⁷, Jean Delwaide¹⁸, Christine Silvain¹⁹, Guillaume Lassailly¹, Sébastien Dharancy¹, Eric Nguyen Khac²⁰, Didier Samuel⁶, Alain Duhamel²¹, Philippe Mathurin¹. ¹CHU de Lille, Lille, France; ²Centre Hospitalier de Valenciennes, Valenciennes, France; ³Erasme Hospital, Brussels, Belgium; ⁴CHU de Besançon, Besançon, France; ⁵CHU de Rennes, Rennes, France; ⁶Hôpital Paul-Brousse, Villejuif, France; ⁷Hospices Civils de Lyon, Lyon, France; ⁸CHU de Montpellier, Montpellier, France; ⁹CHU de Toulouse, Toulouse, France; ¹⁰CHU de Bordeaux, Bordeaux, France; ¹¹Hôpital Henri-Mondor, Créteil, France; ¹²Hôpital de la Pitié-Salpêtrière, Paris, France; ¹³CHU de Grenoble, Grenoble, France; ¹⁴Hôpital saint-Antoine, Paris, France; ¹⁵CHU de Tours, Tours, France; ¹⁶CHU de Nice, Nice, France; ¹⁷CHU de Nantes, Nantes, France; ¹⁸CHU de Liège, Liège, Belgium; ¹⁹CHU de Poitiers, Poitiers, France; ²⁰CHU d'Amiens, Amiens, France; ²¹Université de Lille, Lille, France
Email: alexandre.louvet@chru-lille.fr

Background and aims: The QuickTrans study showed similar survival at 2 years in patients transplanted for alcohol-related hepatitis (AH) compared to alcohol-related cirrhosis but failed to demonstrate non-inferiority of alcohol relapse between the two groups. Long-term data are needed for early liver transplantation (LT) for AH.

Method: Patients were followed-up according to each center local practice after the 2-year end point of the QuickTrans study and our primary end point was alcohol relapse 5 years thereafter (i.e. at 84 months). Secondary end points were survival at 84 months and analysis of alcohol consumption pattern. End points were analyzed

according to 2 time frames: first 24 months and between M24 months and M84. A total of 240 patients were included in 3 groups: A: patients transplanted for AH (n = 68); B: patients transplanted for alcohol-related cirrhosis and 6 months of abstinence (n = 93); C: patients with AH, not transplanted (n = 47).

Results: The rate of any alcohol relapse, whatever the amount consumed, was not different between groups A and B, either during the first 24 months (HR 1.56, 95%CI: 0.87–2.76, p = 0.13) or between M24 and M84 (HR 1.23, 95%CI: 0.48–3.13, p = 0.66). The rate of heavy alcohol relapse (defined by ≥ 30 g/d in women and ≥ 40 g/d in men) was higher in group A than in group B at M24 (23.5 vs. 5.4%, HR 4.86, 95%CI: 1.78–13.2, p = 0.002) but was not different between M24 and M84 (34.3 vs. 16.7%, HR 1.17, 95%CI: 0.44–3.07, p = 0.76). There was a trend toward better survival at M84 in patients transplanted for AH (group A) vs. group B: 83.2 (A) vs. 70% (B), HR = 0, 34, 95%CI: 0.11–1.02, p = 0.054). Rejection rates after LT were not different between the two groups (2.9 vs. 3.2%, p = 0.9) but incidence of de novo alcohol-related cirrhosis was higher in group A (11.8 vs. 3.2%, p = 0.03) while incidence of cancers was more important in group B (22.6 vs. 8.8%, p = 0.02). Among all patients with AH, patients selected for LT (group A) had a better survival at 84 months than non-selected patients (group C): 64 vs. 13%, HR = 4, 2.5–6.67, p < 0.001).

Conclusion: Rates of alcohol relapse between M24 and M84 are similar between patients transplanted for AH and those with alcohol-related cirrhosis selected with the 6-month rule. Heavy alcohol relapse mostly occurs during the first 2 years in AH without significant differences between the two groups thereafter. Early alcohol management should be proposed after LT for AH. Patients transplanted for alcohol-related cirrhosis tend to have a lower long-term survival.

GS-012

Novel DGAT2 antisense inhibitor demonstrates significant MASH resolution in biopsy-proven F2/F3 MASH: results from a 51-week multicenter randomized double-blind placebo-controlled phase 2 trial

Rohit Loomba¹, Erin Morgan², Keyvan Yousefi², Dan Li², Richard Geary², Sanjay Bhanot². ¹UCSD, San Diego, United States; ²Ionis Pharmaceuticals, Carlsbad, United States
Email: roloomba@health.ucsd.edu

Background and aims: ION224 is an investigational ligand-conjugated antisense medicine designed to reduce the production of diacylglycerol acyltransferase 2 (DGAT2), an enzyme that catalyzes the final step in hepatic triglyceride synthesis. ION224-CS2 was an adaptive Phase 2 trial to study the safety and efficacy of monthly subcutaneous injections of ION224 in biopsy-proven MASH patients with MASLD activity score (NAS) ≥ 4 and baseline MRI-PDFF $\geq 10\%$. The primary end point was improvement in steatohepatitis at Week 51 as measured by ≥ 2 -point reduction in NAS with ≥ 1 -point improvement in hepatocellular ballooning or lobular inflammation, and without worsening of fibrosis. An analysis of the primary end point along with key secondary end points was conducted.

Method: The study enrolled 160 patients to receive monthly doses of ION224 or placebo during a 49-week treatment period. In Part 1, 93 patients were randomized to three dose cohorts to receive either 60, 90, or 120 mg of ION224 or placebo (3:1). Based on a pre-specified interim analysis at 3 months, 2 of the 3 dose cohorts were selected by DSMB for expanded enrollment, based on safety and hepatic MRI-PDFF analysis. In Part 2, an additional 67 patients were randomized 1:1 into each of the two expanded dose cohorts (90 and 120 mg) and then in a 2:1 ratio to receive either ION224 or placebo within each cohort.

Results: Baseline characteristics included age 53 (12) (mean (SD)), BMI 37.8 (7.1), type 2 diabetes 50.6%, MRI-PDFF (%) 22.4 (7.4), baseline fibrosis stage: F2–49.6%, F3–39.1%. The primary end point of ≥ 2 -point reduction in NAS was met in both expanded cohorts in 58.8% and 46.2% of patients treated with ION224 120 mg or 90 mg, respectively,

compared to 18.8% for placebo (n = 34, p < 0.001 and n = 39, p = 0.015, respectively, placebo n = 32). Subgroup analysis indicated that significant improvements in the primary end point were observed in patients with both F2 and F3 fibrosis. Additionally, 35.6% of patients treated with 120 mg or 90 mg achieved MASH resolution without worsening of fibrosis versus 15.6% for placebo (p = 0.039). Further, 32.4% of patients treated with 120 mg achieved ≥ 1 stage improvement in fibrosis without worsening steatohepatitis versus 12.5% for placebo. Forty-four (44) % of patients treated with 120 mg achieved $\geq 50\%$ relative reduction in liver steatosis by MRI-PDFF vs 3% of placebo (p < 0.001). ION224 was safe and well-tolerated. There were no treatment-related SAEs, no GI side effects or worsening of hepatic or renal function or plasma lipids (including no hypertriglyceridemia) after ION224 treatment.

Conclusion: This study provides the first clinical evidence that reduction of hepatic fat after DGAT2 inhibition leads to MASH resolution. ION224 was safe and well-tolerated in this study with once-monthly subcutaneous dosing. These data support the potential for ION224 treatment to provide benefit to patients with MASH and liver fibrosis.

Late-breaker Orals

LBO-001

Tirzepatide for the treatment of metabolic dysfunction-associated steatohepatitis with liver fibrosis: results of the SYNERGY-NASH phase 2 trial

Rohit Loomba¹, Mark Hartman², Eric Lawitz³, Raj Vuppalanchi⁴, Jerome Boursier⁵, Elisabetta Bugianesi⁶, Masato Yoneda⁷, Cynthia Behling⁸, Oscar Cummings⁴, Yuanyuan Tang², Bram Brouwers², Deborah Robins², Amir Nikooie², Mathijs Bunck², Axel Haupt², Arun J. Sanyal⁹. ¹MASLD Research Center, Division of Gastroenterology and Hepatology, University of California San Diego, San Diego, United States; ²Eli Lilly and Company, Indianapolis, United States; ³Texas Liver Institute, University of Texas Health, San Antonio, United States; ⁴Indiana University School of Medicine, Indianapolis, United States; ⁵Angers University Hospital, Angers, France; ⁶University of Torino, Torino, Italy; ⁷Yokohama City University, Yokohama, Japan; ⁸Pacific Rim Pathology, San Diego, United States; ⁹Virginia Commonwealth University School of Medicine, Richmond, United States
Email: roloomba@health.ucsd.edu

Background and aims: Metabolic dysfunction-associated steatohepatitis (MASH) is a progressive liver disease associated with liver-related morbidity and mortality. This study evaluated the efficacy and safety of tirzepatide, a dual agonist of the glucose-dependent insulinotropic polypeptide and glucagon-like-peptide-1 receptors, in the treatment of non-cirrhotic MASH with significant liver fibrosis. **Method:** SYNERGY-NASH (NCT04166773) was a multicenter, double-blind, randomized, placebo (PBO)-controlled Phase 2 dose-finding trial in patients with biopsy-confirmed MASH, stage 2 or 3 fibrosis and a non-alcoholic fatty liver disease activity score (NAS) ≥ 4 . Participants (n = 190) were randomly assigned 1:1:1:1 to receive once-weekly s.c. tirzepatide (5 mg, 10 mg or 15 mg) or PBO for 52 weeks. The primary end point was MASH resolution without worsening of fibrosis at 52 weeks. Secondary end points included fibrosis improvement by ≥ 1 stage without worsening of MASH and a reduction in NAS by ≥ 2 points with ≥ 1 point reduction in at least 2 NAS components. Efficacy results were analyzed with the intent to treat population using multiple imputation for missing data.

Results: End-of-treatment liver biopsies were available for 157 participants. The proportion of participants who achieved MASH resolution without worsening of fibrosis was 9.8% for PBO, 43.6% for tirzepatide 5 mg, 55.5% for tirzepatide 10 mg and 62.4% for

tirzepatide 15 mg (differences vs. PBO 33.8–52.6%; $p < 0.001$ for all doses). Among 155 participants who completed the study on treatment with evaluable biopsies, the primary end point was achieved by 51.8%, 62.8%, and 73.3% for tirzepatide 5 mg, 10 mg and 15 mg, respectively, compared with 13.2% for PBO ($p < 0.001$ for all doses). The proportion who achieved ≥ 1 -stage fibrosis improvement without worsening of MASH was 29.7% for PBO, 54.9% for tirzepatide 5 mg, 51.3% for tirzepatide 10 mg and 51.0% for tirzepatide 15 mg (differences vs. PBO 21.3–25.2%; $p < 0.05$ for all doses). A reduction in NAS by ≥ 2 points was achieved by 71.7% to 78.3% of participants across the three tirzepatide dose groups and by 36.7% with PBO ($p < 0.001$ for all doses). Body weight was reduced by up to 17.3% with tirzepatide. Liver enzymes and liver fat decreased, and serum as well as imaging biomarkers of liver inflammation and fibrosis significantly ($p < 0.01$) improved in the tirzepatide groups vs. PBO. Adverse events with tirzepatide were mostly gastrointestinal, and mild to moderate in severity.

Conclusion: In this Phase 2 study of patients with MASH and significant fibrosis, tirzepatide treatment for 52 weeks was more effective than placebo in achieving MASH resolution without worsening of fibrosis. Fibrosis also improved with tirzepatide treatment but without an apparent dose-response effect. Larger and longer trials are needed to further assess the efficacy and safety of tirzepatide for treatment of non-cirrhotic MASH.

LBO-002

Efruxifermin significantly reduced liver fibrosis in MASH patients with F2-F3 fibrosis, with sustained improvement in liver injury and resolution of steatohepatitis over 96 weeks (HARMONY phase 2b study)

Stephen A. Harrison¹, Juan P Frias², Guy Neff³, Gary Abrams⁴, Kathryn Jean Lucas⁵, William Sanchez⁶, Sudhanshu Gogia⁷, Muhammad Y Sheikh⁸, Cynthia Behling⁹, Pierre Bedossa¹⁰, Lan Shao¹¹, Doreen Chan¹², Erica Fong¹², Brittany de Temple¹², Matthew Minerva¹², Kimberly Barrett¹³, Reshma Shringarpure¹², Erik Tillman¹², Tim Rolph¹², Andrew Cheng¹², Vlad Ratziu¹⁴, Kitty Yale¹². ¹Department of Hepatology, University of Oxford, Oxford, United Kingdom; ²Pinnacle Clinical Research, San Antonio, TX, United States; ³Covenant Metabolic Specialists, Sarasota, FL; ⁴Prisma Health, Greenville SC, United States; ⁵Lucas Research, Morehead NC, United States; ⁶Floridian Clinical Research, Miami Lakes, FL, United States; ⁷Texas Digestive Disease Institute, Webster TX, United States; ⁸Fresno Clinical Research Center, Fresno, CA, United States; ⁹Department of Pathology, Sharp Memorial Hospital, San Diego, CA, United States; ¹⁰Liverpat, Paris, France; ¹¹Fortrea Inc, Durham, NC, United States; ¹²Akero Therapeutics Inc, South San Francisco, United States; ¹³Akero Therapeutics Inc, San Francisco, United States; ¹⁴Sorbonne University, Paris, France
Email: reshma@akerotx.com

Background and aims: The HARMONY study met its primary end point of ≥ 1 stage improvement in fibrosis with no worsening of MASH in patients with stage 2 or 3 fibrosis (F2-F3) receiving once weekly (QW) efruxifermin (EFX) 50 mg (41%) or 28 mg (39%) vs placebo (20%; $p < 0.05$) after 24 weeks. The study continued to Week 96 to evaluate longer-term safety, tolerability, and durability of histologic improvements.

Method: 128 patients with MASH (F2-F3) were randomized to placebo or EFX (28 or 50 mg), QW for 96 weeks. Liver biopsies were collected at baseline, Week 24, and Week 96. End-of-study analyses included safety and tolerability, liver histopathology, and non-invasive markers of liver injury and fibrosis, including fibrogenesis.

Results: Among patients with baseline and Week 96 biopsies, 75% ($p < 0.001$) receiving EFX 50 mg and 46% ($p = 0.07$) receiving 28 mg had improvement in fibrosis without worsening of MASH, vs 24% for placebo. Furthermore, 36% ($p < 0.001$) of patients for EFX 50 mg and 31% ($p < 0.01$) for 28 mg had a 2-stage improvement in fibrosis without worsening of MASH, vs 3% for placebo. MASH resolved without fibrosis worsening in 57% ($p < 0.01$) of patients for EFX 50 mg

and 62% ($p < 0.01$) for 28 mg vs 24% for placebo. MASH resolution AND fibrosis improvement of ≥ 1 stage were observed in 54% ($p < 0.001$) of the EFX 50 mg and 42% ($p < 0.01$) of the 28 mg group, vs 9% for placebo. Significant improvements in markers of liver injury and fibrosis were sustained through Week 96, corroborating EFX's durable effects. The most frequent drug-related adverse events over 96 weeks were diarrhea (16%, 40%, and 37%) and nausea (12%, 30%, and 33% for placebo, EFX 28 mg and 50 mg groups, respectively). Discontinuations due to study drug-related AEs by Week 24 were 0, 2, and 2 in the placebo, EFX 28 mg, and EFX 50 mg groups, respectively; another 0, 2, 1, patients discontinued by Week 96 due to drug-related AEs.

Conclusion: In a randomized trial with sequential liver biopsies, EFX demonstrated a significant and durable anti-fibrotic response in MASH patients with fibrosis (F2-F3). From Weeks 24 to 96, the response to EFX broadened (fibrosis improved by ≥ 1 -stage in a more significant proportion of patients) and deepened (a greater proportion of patients experienced a 2-stage improvement in fibrosis). EFX has a promising therapeutic profile for treating MASH with moderate to advanced fibrosis.

LBO-003

Results of a phase 2b multicenter randomized trial of larsucosterol for the treatment of severe alcohol-associated hepatitis (AHFIRM trial)

Mitchell Shiffman¹, Ben Da², Lance Stein³, Christophe Moreno⁴, Ashwini Mehta⁵, Alexandre Louvet⁶, Amanda Nicoll⁷, Aparna Goel⁸, Allison Kwong⁹, Steven Flamm¹⁰, Sanjaya Satapathy¹¹, Alexander Kuo¹², Nikolaos T. Pyrsopoulos¹³, Daniel Ganger¹⁴, Costica Aloman¹⁵, Simone Strasser¹⁶, Edmund Tse¹⁷, Mark Russo¹⁸, Don Rockey¹⁹, Meagan Gray²⁰, Mack Mitchell²¹, Mark R. Thursz²², William Krebs²³, Deborah Scott²³, Christina Blevins²³, James Brown²³, WeiQi Lin²³, Norman Sussman²³. ¹Bon Secours Liver Institute, Richmond, United States; ²Northwell Health, Manhasset, United States; ³Piedmont Healthcare, Transplant Institute, Atlanta, United States; ⁴Université libre de Bruxelles (ULB), Hôpital Erasme, Brussels, Belgium; ⁵Methodist Dallas Medical Center, Liver Institute, Dallas, United States; ⁶CHU de Lille, Services des Maladies de l'appareil digestif, Lille; ⁷Eastern Health, Box Hill Hospital, Box Hill, Australia; ⁸Stanford University Medical Center, Palo Alto, United States; ⁹Stanford University, Palo Alto, United States; ¹⁰Rush University Medical Center, Chicago, United States; ¹¹Zucker School of Medicine at Hofstra/Northwell, Northshore University Hospital, Northwell Health, Manhasset, United States; ¹²Cedars Sinai Medical Center, Los Angeles, United States; ¹³Rutgers-New Jersey Medical School, Newark, United States; ¹⁴Northwestern University, Feinberg Medical School, Chicago, United States; ¹⁵Westchester Medical Center, Valhalla, United States; ¹⁶Royal Prince Alfred Hospital, Sydney, Australia; ¹⁷Royal Adelaide Hospital, Adelaide, Australia; ¹⁸Atrium Health Wake Forest, Charlotte, United States; ¹⁹University of South Carolina, Charleston, United States; ²⁰University of Alabama at Birmingham, Birmingham, United States; ²¹UT Southwestern Medical Center, Dallas, United States; ²²Imperial College, London, United Kingdom; ²³Durect, Cupertino, United States
Email: norman.sussman@icloud.com

Background and aims: Alcohol-associated hepatitis (AH) is a severe form of alcohol-associated liver disease with approximately 30% mortality at 90 days without approved therapy so far. Larsucosterol is an endogenous sulfated oxysterol that inhibits DNA methyltransferases and has been shown to reduce inflammation, lipotoxicity, oxidative stress, and cell death, and promote liver regeneration. In a phase 2a study in subjects with moderate or severe AH, larsucosterol improved liver function markers with 100% 28-day survival. Here we report findings in the Phase 2b AHFIRM trial of larsucosterol in hospitalized patients with severe AH.

Method: AHFIRM was a phase 2b randomized, double-blind, placebo-controlled, international, multicenter study that evaluated the safety and efficacy of larsucosterol in 307 subjects with severe AH (MDF ≥ 32 and MELD 21–30). Subjects were randomized 1:1:1 to

receive 1 or 2 intravenous infusions (72 hours apart) of larsucosterol 30 mg, larsucosterol 90 mg, or Placebo. All subjects received local standard of care at the investigators' discretion. If prescribed, subjects in the Placebo arm would receive 32 mg methylprednisolone daily while those in the larsucosterol arms received matching placebo capsules. The primary end point was death or liver transplant at 90 days measured by win-ratio. The key secondary end point was death at 90 days.

Results: The study did not meet the primary end point. There were more deaths but fewer liver transplants in the Placebo arm than in either larsucosterol arm with win probability differences of 0.078 ($p = 0.196$) in the 30 mg and 0.039 ($p = 0.533$) in the 90 mg larsucosterol arm against Placebo. Mortality at 90 days was reduced by 41% in the larsucosterol 30 mg arm ($p = 0.068$) and 35% in the larsucosterol 90 mg arm ($p = 0.124$). A significant regional difference was observed; US subjects ($n = 232$), which comprised 76% of the study population, showed a 57% and 58% reduction in 90-day mortality ($p = 0.014$ and $p = 0.008$, respectively) following larsucosterol treatment. Both doses of larsucosterol were well tolerated with fewer overall treatment emergent adverse events in the active arms than in the Placebo arm.

Conclusion: AHFIRM showed a compelling signal of mortality reduction with both doses of larsucosterol. A statistically significant reduction in 90-day mortality was observed in the US population. Significant regional differences in clinical practice, sample size, and randomization were seen—these should be addressed when designing future multinational AH trials. Larsucosterol was well-tolerated; both dose groups had numerically fewer adverse events than in Placebo arm.

LBO-004

Excess waitlist mortality and survival benefit of liver transplantation for patients with severe acute-on-chronic liver failure: Interim results of the CHANCE study

Thierry Gustot¹, William Bernal², Javier Fernández^{3,4}, Juan Manuel Díaz³, Carlos de la Peña-Ramírez³, Alberto Farias⁵, Patricia Momoyo Zitelli⁶, Alexander Kuo⁷, Nicholas Nissen⁸, Sebastián Marciano⁹, Adrian Gadano⁹, Rachel Westbrook¹⁰, Rebecca Bateman¹¹, Ashwin Rammohan¹², Dinesh Jothamani¹³, Sudhindran S¹⁴, Arun Valsan¹⁴, Pablo Ruiz¹⁵, Giulia Pagano¹⁶, Luis Bagulho¹⁷, Hugo Pinto Marques¹⁷, Luca Saverio Belli¹⁸, Giovanni Perricone¹⁸, Nazia Selzner¹⁹, Cynthia Tsien²⁰, Juan F. Gallegos-Orozco²¹, Nyingi Kemmer²², Kiran Dhanireddy²³, Manuel Mendizabal²⁴, Josefina Pages²⁴, Christina Lindenmeyer²⁵, Bijan Eghtesad²⁶, Antonella Putignano²⁷, Laure Elkrief²⁸, Joanna Raszeja-Wyszomirska²⁹, Margarita Anders³⁰, Silvio Nadalin³¹, Antonio Siniscalchi³², Giulia Tosetti³³, Carmen Vinaixa³⁴, Michael Kriss^{35,36}, Prasun Jalal³⁷, Baptiste Michard³⁸, Paolo Angeli^{39,40}, Graciela Castro-Narro⁴¹, Karim Boudjema⁴², Kirti Shetty⁴³, Caroline den Hoed⁴⁴, Livia Carone⁴⁵, Sezai Yilmaz⁴⁶, Maria Lúcia Zanotelli⁴⁷, Rosa Martin-Mateos^{48,49,50}, Maximilian Joseph Brol⁵¹, Tomoharu Yoshizumi⁵², Francois Durand⁵³, Sylvie Radenne⁵⁴, Helen Te⁵⁵, Isabel Campos-Varela⁵⁶, Wim Laleman^{57,58}, Masahiro Ohira⁵⁹, Susumu Eguchi⁶⁰, Cornelius Engelmann⁶¹, Constantine Karvellas⁶², Felix Braun⁶³, Marie Sinclair⁶⁴, José Ursic Bedoya⁶⁵, Carmelo Loinaz⁶⁶, Tamara Perera⁶⁷, Arvinder Singh Soin⁶⁸, Ken Liu⁶⁹, Sarah Raevens⁷⁰, Rebecca Bishop⁷¹, Kenneth J. Simpson⁷², Nobuhisa Akamatsu⁷³, Yong Chee Chien⁷⁴, Gabriela Berlakovich⁷⁵, Juan Ignacio Marin Zuluaga⁷⁶, Lance Stein⁷⁷, Ruben Hernaez⁷⁸, Christophe Duvoux⁷⁹, Faouzi Saliba⁸⁰, Constantino Fondevila⁸¹, Geoff McCaughan⁸², Yaman Tokat⁸³, Elizabeth Pomfret⁸⁴, Mohamed Rela¹³, Vinay Sundaram⁷, Joan Claria^{39,85,86,87}, Vicente Arroyo³, Foix Valles^{3,88}, Jorge Carlos Martínez^{3,89}, Pedro Izquierdo-Bueno³, Didier Samuel⁸⁰, Marina Berenguer³⁴, Anna Bosch³, Cristina Sanchez³, Wojciech Polak⁹⁰, Jonel Trebicka^{3,91}, Richard Moreau^{3,92,93}, Rajiv Jalan^{39,94}. ¹Liver Transplant Unit, HUB Hôpital Erasme, Université Libre de Bruxelles, Bruxelles, Belgium; ²King's College Hospital, London, United Kingdom; ³European Foundation for

the Study of Chronic Liver Failure (EF CLIF), Barcelona, Spain; ⁴Hospital Clínic Instituto de Investigaciones Biomédicas August Pi i Sunyer, Universitat de Barcelona, Barcelona, Spain; ⁵The Department of Gastroenterology, Hospital das Clínicas, University of São Paulo School of Medicine, Sao Paulo, Brazil; ⁶Hospital das Clínicas da Faculdade de Medicina da Universidade de São Paulo, Sao Paulo, Brazil; ⁷Cedars-Sinai Medical Center, Karsh Division of Gastroenterology and Hepatology, Comprehensive Transplant Center, Los Angeles, United States; ⁸Cedars-Sinai Medical Center, Department of Surgery, Comprehensive Transplant Center, Los Angeles, United States; ⁹Liver Unit and Department of Research, Hospital Italiano de Buenos Aires, Buenos Aires, Argentina; ¹⁰Royal Free Hospital, London, Spain; ¹¹Royal Free Hospital, London, United Kingdom; ¹²Dr. Rela Institute & Medical Centre, Chennai, India; ¹³Dr. Rela Institute and Medical Center, Chennai, India; ¹⁴Amrita Institute Medical Sciences, Kochi, India; ¹⁵Liver Unit, Hospital Clinic, IDIBAPS, Univ. Barcelona, Barcelona, Spain; ¹⁶Hospital Clinic Barcelona, Barcelona, Spain; ¹⁷Hepato-Biliary-Pancreatic and Transplantation Centre, Curry Cabral Hospital, Local Health Unit of São José. NOVA Medical School, Lisbon, Portugal; ¹⁸Department of Gastroenterology and Hepatology, Liver Transplant Center GOM Niguarda, Milan, Italy; ¹⁹Department of Gastroenterology and Hepatology, Liver Transplant Center GOM Niguarda, Toronto, Canada; ²⁰University of Toronto, Toronto, Canada; ²¹Division of Gastroenterology and Hepatology, Spencer Fox Eccles School of Medicine, University of Utah, Salt Lake City, United States; ²²Medical Director, Liver Transplant Program, TGH. Director, Hepatology Program, TGMG. Professor of Medicine, USF Tampa, Tampa, United States; ²³Tampa General Hospital, Tampa, United States; ²⁴Hepatology and Liver Transplant Unit, Hospital Universitario Austral, Buenos Aires, Argentina; ²⁵Department of Gastroenterology, Hepatology and Nutrition, Cleveland Clinic, Cleveland, United States; ²⁶Department of General Surgery, Cleveland Clinic, Cleveland, United States; ²⁷Liver Transplant Unit, HUB Hôpital Erasme, Université Libre de Bruxelles, Brussels, Belgium; ²⁸CHRU Tours-Hôpital Trousseau, Hepatogastroenterology Department, Tours, France; ²⁹Dept. of General, Transplant & Liver Surgery and the chief of the Dept. of Hepatology and Internal Medicine, Medical University of Warsaw, Warsaw, Poland; ³⁰Hospital Aleman, Buenos Aires, Argentina; ³¹University Hospital Tübingen. Dpt of General, Visceral and Transplant Surgery, Tübingen, Germany; ³²Alma Mater Studiorum University of Bologna, Bologna, Italy; ³³Foundation IRCCS Ca' Granda Ospedale Maggiore Policlinico - Division of Gastroenterology and Hepatology, Milan, Italy; ³⁴Hospital Universitari i Politècnic La Fe, Valencia, Spain; ³⁵Division of Gastroenterology & Hepatology, Department of Medicine, University of Colorado School of Medicine, Aurora, Colorado, United States; ³⁶Colorado Center for Transplantation Care, Research and Education, University of Colorado School of Medicine, Aurora, Colorado, United States; ³⁷Baylor College of Medicine, Houston, United States; ³⁸Liver transplant unit, Strasbourg university hospital, Strasbourg, France; ³⁹European Foundation for the Study of Chronic Liver Failure, Barcelona, Spain; ⁴⁰Unit of Internal Medicine and Hepatology, Department of Medicine, University of Padova, Padova, Italy; ⁴¹National Institute of Medical Sciences and Nutrition "Salvador Zubirán" Mexico City, Mexico City, Mexico; ⁴²CHU Rennes, Hôpital De Pontchaillou, Rennes, France; ⁴³University of Maryland Medical Center, Baltimore, United States; ⁴⁴Department of Gastroenterology and Hepatology, Erasmus MC Transplant Institute, University Medical Center Rotterdam, Rotterdam, Netherlands; ⁴⁵Liver Transplant Unit of Federal University of Ceará, Fortaleza, Brazil; ⁴⁶Inonu University Liver Transplantation Institute, Inonu, Turkey; ⁴⁷Liver Transplant Group, Irmandade Santa Casa de Misericórdia de Porto Alegre, Porto Alegre, Brazil; ⁴⁸Gastroenterology Department, Hospital Universitario Ramón y Cajal, Madrid, Madrid, Spain; ⁴⁹Universidad de Alcalá. Instituto Ramón y Cajal de investigación sanitaria (IRYCIS), Madrid, Spain; ⁵⁰Centro de Investigación Científica en Red de Enfermedades Hepáticas y Digestivas (CIBEREHD), Madrid, Spain; ⁵¹University of Münster, Münster, Germany; ⁵²Kyushu University Hospital, Kyushu, Japan; ⁵³Hôpital Beaujon AP-HP, Clichy, France; ⁵⁴APHP Hôpitaux Universitaires Pitié Salpêtrière, Lyon, France; ⁵⁵Center for Liver Diseases, University of Chicago Medicine, Chicago, United

ORAL PRESENTATIONS

States; ⁵⁶Hospital Universitari Vall d'Hebron, Barcelona, Spain; ⁵⁷Department of Gastroenterology and Hepatology, Section of Liver & Biliopancreatic disorders and Liver transplantation, University Hospitals Leuven, Leuven, Belgium; ⁵⁸Medizinische Klinik B, Universitätsklinikum Münster, Münster University, Munster, Germany; ⁵⁹Hiroshima University Hospital, Hiroshima, Japan; ⁶⁰Department of surgery, Nagasaki University Graduate School of Biomedical Sciences, Nagasaki, Japan; ⁶¹Charité-Universitätsmedizin Berlin, Department of Hepatology and Gastroenterology, Berlin, Germany; ⁶²Department of Critical Care Medicine and Division of Gastroenterology (Liver Unit), University of Alberta, Alberta, Canada; ⁶³University Medical Center Hamburg-Eppendorf, Hamburg, Germany; ⁶⁴Victorian Liver Transplant Unit, Austin Health, Melbourne, Australia; ⁶⁵Hepatogastroenterology Unit, CHU Saint Eloi, Montpellier University, Montpellier, France; ⁶⁶HBP-Transplantation Surgery, 12 de Octubre University Hospital/ Complutense University of Madrid, Madrid, Spain; ⁶⁷Queen Elizabeth Hospital Birmingham, Birmingham, United Kingdom; ⁶⁸Medanta Medcity, New Delhi, India; ⁶⁹AW Morrow Gastroenterology and Liver Centre, Royal Prince Alfred Hospital, Sydney, NSW, Australia; Faculty of Medicine and Health, University of Sydney, Sydney, Australia; ⁷⁰Dept of Gastroenterology and Hepatology, Ghent Liver Research Center, Ghent University Hospital, Ghent, Belgium; ⁷¹Leeds Teaching Hospital, Leeds, United Kingdom; ⁷²Scottish Liver Transplant Unit, Royal Infirmary, Edinburgh UK, Edinburgh, United Kingdom; ⁷³Artificial Organ and Transplantation Surgery Division, Department of Surgery, Graduate School of Medicine, University of Tokyo, Tokyo, Japan; ⁷⁴Kaohsiung Chang Gung Memorial Hospital, Kaohsiung, Taiwan; ⁷⁵Division of Transplantation, Medical University of Vienna, Vienna, Austria; ⁷⁶Hospital Pablo Tobón Uribe, Medellín, Colombia; ⁷⁷Piedmont Transplant Institute, Piedmont Atlanta Hospital, Atlanta, United States; ⁷⁸Michael E. DeBakey VA Medical Center and Baylor College of Medicine, Houston, United States; ⁷⁹Medical Liver Transplant Unit, Department of Hepatology, Henri Mondor Hospital APHP- Paris Est University, Créteil, France; ⁸⁰AP-HP Hôpital Paul Brousse, Centre hépato-Biliaire, Villejuif, France; ⁸¹Department of general and digestive surgery, Hospital Universitario La Paz (IdiPaz), Madrid, Spain; ⁸²Royal Prince Alfred Hospital, Sydney, Australia; ⁸³International Liver Center and Acibadem Healthcare Hospitals, Istanbul, Turkey; ⁸⁴University of Colorado, Denver, United States; ⁸⁵Biochemistry and Molecular Genetics Service, Hospital Clínic-IDIBAPS, Barcelona, Spain; ⁸⁶CIBERehd, Barcelona, Spain; ⁸⁷Department of Biomedical Sciences, University of Barcelona, Barcelona, Spain; ⁸⁸Liver ICU, Hospital Clinic Barcelona, Barcelona, Spain; ⁸⁹Hepatology and Liver Transplantation, Hospital Italiano de Buenos Aires, Buenos Aires, Argentina; ⁹⁰Department of Gastroenterology and Hepatology, Erasmus MC Transplant Institute, University Medical Center Rotterdam, Rotterdam, The Netherlands, Rotterdam, Netherlands; ⁹¹Medizinische Klinik B (Gastroenterologie, Hepatologie, Endokrinologie, Klinische Infektiologie), Münster, Germany; ⁹²Institut National de la Santé et de la Recherche Médicale, Université Paris Cité, Centre de Recherche sur l'Inflammation, Paris, France; ⁹³Assistance Publique-Hôpitaux de Paris, and Hôpital Beaujon, Service d'Hépatologie, Clichy, France; ⁹⁴Liver Failure Group, Institute for Liver Disease Health, University College London, Royal Free Hospital, London, United Kingdom
Email: thierry.gustot@erasme.ulb.ac.be

Background and aims: Mortality of patients with acute-on-chronic liver failure grades 2 and 3 (ACLF 2,3) exceeds 60% within 28-days. Therefore, liver transplantation (LT) is a potential therapeutic option. The current organ allocation systems based on MELD scores could underestimate mortality risk for ACLF 2,3 patients on the waiting list (WL). Moreover, the risk versus benefit of LT for ACLF 2,3 is still debated. The aim of the global CHANCE study was to assess, in the current allocation systems, the outcomes of ACLF 2,3 patients on the WL and for those who underwent LT.

Method: Data from 823 patients (~80% of the overall study cohort) is reported here: 376 patients with ACLF 2,3 (Group 1) and 313 patients with ACLF 0,1 and MELD>20 (Group 2), all listed for LT; and 134

patients with ACLF 2,3 referred but not listed (Group 3). Patients were recruited from 62 LT centers from Asia, Europe, Latin America and North America between July 2021 and October 2023. The rate of death/delisting is presented according to ACLF grade and MELD-Na score at study inclusion and by geographical distribution. Mortality within 3-months after LT is also described.

Results: Death/delisting on the WL occurred in 28% Group 1 patients compared with 16% Group 2 patients ($p<0.001$), while 85% Group 3 patients died. 68% and 79% for Groups 1 and 2 received LT ($p<0.001$). Significant differences in death/delisting on the WL were observed across continents (Asia: 13%; Europe: 18%; Latin America: 40%; North America: 20%; $p<0.001$). The higher rate of death/delisting for ACLF 2,3 patients was observed across all MELD-Na ranges [<25 (50%), 25-29 (35%), 30-34 (22%), >35 (29%)] compared to patients without ACLF 2,3 [MELD-Na <25 (12%), 25-29 (19%), 30-34 (15%), >35 (17%); $p<0.001$]. At the time of LT, 236 patients were ACLF 2,3 and 265 were ACLF 0,1. No differences in 3-month post-LT mortality were observed according to the number of organ failures ($p=0.08$) and ACLF grades ($p=0.07$). Significant differences were observed in 3-month post-LT mortality across continents (Asia: 12%, Europe: 7%, Latin America: 16%; North America: 3%; $p=0.006$).

Conclusion: The interim results of this first global prospective CHANCE study provide clear evidence of transplant benefits for patients with ACLF 2,3 and suggest that the current allocation systems are inadequate for patients with ACLF 2,3, leading to an excess of WL mortality, arguing strongly for a change in the organ allocation systems for these patients.

LBO-005

Intervention with oral LPCN 1148 improves sarcopenia and hepatic encephalopathy (HE) in patients with cirrhosis: a 52-week phase 2 randomized clinical trial

Benjamin Bruno¹, Josh Weavil¹, Jonathan Ogle¹, Nachaippan Chidambaram¹, Elizabeth Carey², Christopher Danford³, Zachary Fricker⁴, Joseph Galati⁵, William M. Lee⁶, Parvez Mantry⁷, Kirti Shetty⁸, Anthony DelConte⁹, Mahesh Patel¹, Arun J. Sanyal¹⁰, Jennifer Lai¹¹. ¹Lipocine Inc, Salt Lake City, United States; ²Mayo Clinic Arizona, Divisions of Hepatology and Gastroenterology, Phoenix, United States; ³Transplant Services, Intermountain Medical Center, Murray, United States; ⁴Department of Gastroenterology, Hepatology, and Nutrition, Beth Israel Deaconess Medical Center, Boston, United States; ⁵Liver Specialists of Texas, Houston, United States; ⁶Division of Digestive and Liver Diseases, University of Texas Southwestern Medical Center, Dallas, United States; ⁷Research and Hepatobiliary Tumor Program, The Liver Institute at Methodist Dallas Medical Center, Dallas, United States; ⁸Division of Gastroenterology and Hepatology, University of Maryland School of Medicine, Baltimore, United States; ⁹Department of Food, Pharma, and Healthcare, Saint Joseph's University, Philadelphia, United States; ¹⁰Stravitz-Sanyal Institute for Liver Disease and Metabolic Health, Virginia Commonwealth University, Richmond, United States; ¹¹Division of Gastroenterology and Hepatology, University of California San Francisco, San Francisco, United States
Email: bjb@lipocine.com

Background and aims: Sarcopenia, a condition of progressive and generalized muscle loss, is prevalent in patients with cirrhosis and is associated with adverse clinical outcomes including HE. Androgens are multimodal hormones which can address these conditions, however their safety and efficacy in patients with cirrhosis have not been well studied.

Method: In this 8-center, phase 2 trial, men with cirrhosis and sarcopenia awaiting liver transplant were randomized 1:1 to receive either oral LPCN 1148, an oral prodrug of testosterone (T), or placebo for 24 weeks (NCT04874350). After week 24, all participants received LPCN 1148 during the study stage 2 open-label extension (OLE). Basal T level was not considered for study eligibility and participants were not asked to change diet, exercise, or background therapies including rifaximin or lactulose during the study. CT scans were performed at 12, 24, 36, and 52 weeks. The primary end point was the change in

skeletal muscle index (SMI) measured by computed tomography (CT) scan at 3rd lumbar spine level (L3-SMI) from baseline to 24 weeks. Secondary end points included overt HE (OHE), defined as HE events with CTCAE severity ≥ 2 .

Results: 29 participants (mean age = 59 ± 8 years, BMI = 29 ± 7 kg/m²) were randomized and received ≥ 1 dose of LPCN 1148 (n = 15) or placebo (n = 14). Baseline characteristics were similar; mean MELD 17 and 76% of participants had a history of HE. At week 24, L3-SMI increased in patients taking LPCN 1148 vs. placebo ($\Delta 4.1 \pm 0.9$ vs $\Delta -0.6 \pm 1.2$ cm²/m²; p = 0.006), representing a placebo-adjusted 9.9% increase in L3-SMI with LPCN 1148. This increase from baseline was maintained with LPCN 1148 through Week 52 ($\Delta 4.1 \pm 1.1$ cm²/m²). All six participants in the placebo arm that converted to LPCN 1148 at Week 24 and had CT scans during stage 2 experienced an increase in SMI at Week 52 ($\Delta 8.1 \pm 1.7$ cm²/m², +16.7%). During stage 1, OHE rates were lower in those on LPCN 1148 vs placebo (2 vs 6 events, p < 0.05), and average time to first OHE recurrence was longer (114 vs 35 days). Two additional OHE events occurred during the OLE; one event from participants from each arm of the prior stage. LPCN-treated participants (vs. placebo) experienced improvements in anemia, patient-reported outcomes, muscle quality, 6-min walk test, and digital Stroop test. The number and severity of treatment-emergent adverse events were similar across both arms with no incident cases of drug-induced liver injury or thrombosis. There were two deaths in placebo-treated, and one in LPCN 1148-treated, participants.

Conclusion: LPCN 1148 is the first therapeutic intervention to both improve sarcopenia and reduce overt HE episodes in men with cirrhosis awaiting liver transplant. Furthermore, LPCN 1148 was well-tolerated with up to 52 weeks of therapy. These results provide support for further study of LPCN 1148 for the treatment of sarcopenia and prevention of HE recurrence in advanced cirrhosis.

LBO-006

A prospective, blinded, multicenter U.S. evaluation of a multi-analyte blood-based test for the detection of hepatocellular carcinoma (HCC) in patients with cirrhosis

David Taggart¹, Shivani Mahajan¹, Maxime Gallant¹, Itai Pinkoviezky¹, Jianfeng Xu², Allison Sorg¹, Curt Roberts¹, Dmitri Slinkov¹, Emmanuel Gorospe³, Abdullah Mubarak⁴, Bal Raj Bhandari⁵, Bradley Freilich⁶, Nadege Gunn⁷, Ju Dong Yang⁸, John Smith⁹, Ziad H. Younes¹⁰, Roniel Cabrera¹¹, Humberto Aguilar¹², Wei Li¹³, Richard Van Etten¹⁴, Mindie Nguyen¹⁵. ¹Helio Genomics, Irvine, United States; ²The Laboratory for Advanced Medicine, Beijing, China; ³Texas Gastro Research, El Paso, United States; ⁴Liver Center of Texas, Dallas, United States; ⁵Delta Research Partners, Bastrop, United States; ⁶Kansas City Research Institute, Kansas City, United States; ⁷Velocity Clinical Research, Wako, United States; ⁸Cedars-Sinai Medical Center, Los Angeles, United States; ⁹Digestive and Liver Disease Specialists, Norfolk, United States; ¹⁰Gastro One, Germantown, United States; ¹¹University of Florida, Gainesville, United States; ¹²Louisiana Research Center, Shreveport, United States; ¹³University of California, Irvine, Irvine, United States; ¹⁴Chao Family Comprehensive Cancer Center, University of California, Irvine, Irvine, United States; ¹⁵Stanford University Medical Center, Palo Alto, United States
Email: davidt@heliogenomics.com

Background and aims: Hepatocellular carcinoma (HCC) surveillance with semi-annual abdominal ultrasound is recommended for patients with cirrhosis, but ultrasound suffers from low adherence and poor early stage sensitivity. To overcome these challenges, the HelioLiver Dx test has been developed to aid in the detection of HCC in cirrhotic patients. This multi-analyte blood test employs a proprietary algorithm utilizing a wide array of biomarkers from cell-free DNA (cfDNA) methylation and serum proteins to accurately detect HCC.

Method: In a prospective, blinded, multicenter study, we enrolled 1,968 adult cirrhosis patients across the U.S. to compare the performance of the HelioLiver Dx test to ultrasound for HCC

detection. Of these, 1,556 participants made up the validation cohort. Multiphasic MRI was the gold standard for HCC diagnosis. The coprimary outcomes were for HelioLiver Dx to possess a superior sensitivity (>5%) and non-inferior specificity (>-10%) compared to ultrasound. The secondary outcome was superior sensitivity of HelioLiver Dx relative to ultrasound for HCC lesions less than or equal to 4 cm in diameter.

Results: 1,268 patients in the validation cohort were evaluable and analyzed (49.4% male, 59.6 in mean age, 33.5% Hispanic, 85.1% white). A total of 46 participants (3.6%) had HCC, with most having HCC lesions of 4 cm or smaller (80%), or 2 cm or smaller (46%). HelioLiver Dx had a sensitivity of 47.8% (95%CI 32.9 to 63.1) for all HCC lesions and 37.8% (95%CI 22.5 to 55.2) for HCC lesions 4 cm or smaller. In contrast, ultrasound demonstrated lower sensitivities of 28.3% (95%CI 16.0 to 43.5) for all HCC lesions and 13.5% (95%CI 4.5 to 28.8) for HCC lesions 4 cm or smaller. Furthermore, HelioLiver Dx detected 28.6% (95%CI 11.3 to 52.2) of HCC lesions 2 cm or smaller, whereas ultrasound failed to detect any (0.0%; 95%CI 0.0 to 16.1). For T1 lesions by the TNM staging system (59%), HelioLiver Dx had a sensitivity of 44.4% (95%CI 25.5 to 64.7) compared to 11.1% (95%CI 2.4 to 29.2) for ultrasound. In subgroup analysis based upon participant sex, ethnicity, race and cirrhosis etiology, HelioLiver Dx consistently demonstrated sensitivities 12.5% to 33.3% higher and specificities 2.9% to 12.2% lower than ultrasound. The overall specificity of HelioLiver Dx and ultrasound were 87.6% (95%CI 85.6 to 89.4) and 94.1% (95%CI 92.6 to 95.4), respectively. The HelioLiver Dx test met both the coprimary and secondary study end points.

Conclusion: Compared to ultrasound, HelioLiver Dx detected more HCC lesions overall, as well as more small HCC lesions in a cohort of diverse patients with cirrhosis. HelioLiver Dx is an accurate and convenient blood-based test that has the potential to reduce HCC morbidity and mortality through improved early detection.

WEDNESDAY 21 JUNE

Nurses & AHPs

OS-001

The second stage of the mobile health application developed for patients with liver cirrhosis: results of the randomized controlled trial

Ferya Celik¹, Hicran Bektas¹. ¹Akdeniz University, Antalya, Turkey
Email: feryacelik@gmail.com

Background and aims: We developed a web-based mobile health application (ReLiver-N App [Rehabilitation of Liver by Nurse Application]) for patients with liver cirrhosis. The aim of this study was to determine the effect of the ReLiver-N App on patient activation, self-efficacy, and quality of life.

Method: The study was carried out between October 2022 and May 2023 with 52 patients with liver cirrhosis by using the Patient Activation Measure, Self-efficacy for Managing Chronic Disease 6-item Scale, and Chronic Liver Disease Questionnaire. Patients in the intervention (ReLiver-N App) group received comprehensive health education and patient activation practices via the ReLiver-N App and were followed up by text messages once a week. Patients in the active control group received patient activation practices via the ReLiver-N App. All of patients reached routine care up in the hospital. Patients in the ReLiver-N App and active control groups completed the measurements for patient activation practice for 12 weeks. The data were evaluated using descriptive statistics, t-tests, Student's t-tests, variance, and regression analyses.

Results: A statistically significant difference was found between the post-test mean scores of the ReLiver-N App and active control groups in terms of patient activation, self-efficacy, and quality of life ($p < 0.01$). The ReLiver-N App group participated in patient activation practices at a rate of 70.8% and the active control group at a rate of 36.0%. At the end of this study 65.4% of the patients in the ReLiver-N App group and 15.4% of the patients in the active control group had an patient activity level of "3."

Conclusion: Mobile educational content and patient activation practices aimed at increasing participation in self-care increased the level of activation, self-efficacy, and quality of life of patients with liver cirrhosis. It is recommended that the use of comprehensive educational content and patient activation practices in the care process of patients be generalized. Keywords: liver cirrhosis, nursing care, patient activation, self-efficacy, quality of life.

OS-002

Patients' experiences of liver cirrhosis health care

Maria Hjorth¹, Ann Karin Svanberg², Daniel Sjöberg³, Fredrik Rorsman⁴, Elenor Kaminsky⁴. ¹Department of Medical Sciences, Centre for Clinical Research in Dalarna, Uppsala, Sweden; ²Department of Medical Sciences, Uppsala, Sweden; ³Centre for Clinical Research in Dalarna, Falun, Sweden; ⁴Department of Public Health and Care Science, Uppsala, Sweden
Email: maria.hjorth@regiondalarna.se

Background and aims: When patients are diagnosed with liver cirrhosis, around 50% already present life-threatening symptoms. Perceived stigma and a hierarchy in the patient-healthcare professional relation may hinder patients' participation in their own care. Further, patients' knowledge regarding their disease, self-care, and medical treatment, may influence both treatment effects and patients' needs of inpatient care. Knowledge about patient experiences of liver cirrhosis health care is scarce. Hence, the aim of this study was to capture patients' descriptions of health care experiences in relation to cirrhosis illness.

Method: Qualitative data from semi-structured interviews ($n = 18$) and open-ended responses in patient surveys ($n = 86$), was collected at six Swedish hospitals, from 2016–2022. Data was analyzed with thematic analysis.

Results: Patients' experiences were reflected in two themes: In the first theme, 'struggle to be in a dialogue', patients expressed troubles in getting understandable information, being involved and being perceived as a person. In the second theme, 'being helped or harmed', most patients described to be satisfied with the received care. Despite this, they 'endured care', 'felt lost' in the healthcare organization and 'not taken care of'. Instead, they described as though they were falling through the cracks.

Conclusion: Patients need assistance to become certain regarding where to turn for cirrhosis health care. They should always be invited to tell their narrative and be provided with information based on their previous knowledge about their disease. Person-centered care where patients are being perceived as a unique person, is vital for patients' sense of a safe and trustful relationship. This may be realized by registered nurse involvement in the hepatology outpatient team, which may prevent patients from falling through the cracks.

OS-003

Longitudinal symptom burden in caregivers for patients with end-stage liver disease

Lissi Hansen¹, Shirin Hiatt¹, Susan Rosenkranz¹, Michael Chang², Nathan Dieckmann¹, Christopher Lee³. ¹Oregon Health and Science University, Portland, United States; ²VA Portland Health Care System, Portland, United States; ³Boston College, Chestnut Hill, United States
Email: hansenli@ohsu.edu

Background and aims: Globally, chronic liver disease (CLD) and cirrhosis is a serious public health problem and accounts for two million deaths annually. The care of patients with end-stage liver disease (ESLD), the final stage of CLD, is most often provided by the

help from informal caregivers. Although, the burden of this care on caregivers has been found to be significant with experience of physical and psychological symptoms, longitudinal research on caregiver symptoms are few. Thus, the aim of this study was to identify trajectories of symptoms to broaden our understanding of caregiver symptom experiences to aid in design of interventions to improve outcomes for caregivers.

Method: Informal caregivers for patients with ESLD were recruited from liver clinics within two healthcare institutions in the Northwestern United States. Inclusion criteria: age ≥ 18 years and identified as the patient's primary caregiver. Exclusion criteria: major uncorrected hearing impairment and uncontrolled psychiatric illness. Survey data were collected at baseline and again at 3, 6, 9, and 12 months. Caregivers completed the Multidimensional Caregiver Strain Index, Patient Health Questionnaire, Uncertainty in Illness Scale for Family Members, Pittsburgh Sleep Quality Index, Short Form Health Survey, and Mutuality Scale (relationship quality with patient). Descriptive statistics and latent growth mixture modelling were used to analyse the data.

Results: The sample ($N = 186$, age 56.7 ± 13.2 years) was predominantly female (75.3%), white (89.2%), and cohabitating with patients (76.9%). Over time caregivers experienced statistically significant improvement in caregiver strain ($p = 0.001$) and uncertainty ($p = 0.001$) but not in sleep quality and depressive symptoms. Patient Charlson comorbidity index was associated with caregiver worsening mental quality of life over time ($p = 0.038$). In contrast to non-spousal caregivers, spousal caregivers had significantly worse mental quality of life at study enrolment ($p = 0.006$) but their mental quality of life improved over time. Relationship quality and female gender were significant predictors of change in caregiver physical quality of life, both were associated with worsening physical quality over time ($p = 0.011$ and $p = 0.012$, respectively).

Conclusion: It is essential for healthcare professionals to address caregiver burden and symptoms experiences by spouse and non-spouse caregivers to improve their overall health and ability to continue to provide care. Future researchers should include longitudinal and dyadic studies to examine how patients' disease progression may affect spouse and non-spouse caregivers differently with the goal of developing effective interventions.

OS-004

Testing for hepatitis C virus infection in prisons in England: room for improvement

Kathryn Jack¹, Brian Thomson¹, William Irving². ¹Nottingham University Hospitals NHS Trust, Nottingham, United Kingdom; ²Nottingham University Hospitals NHS Trust, The University of Nottingham, Nottingham, United Kingdom
Email: katejack2000@hotmail.com

Background and aims: Testing of all new entrants into prisons in England for hepatitis C virus (HCV) infection is a critical policy in the National Health Service England (NHSE) strategy to achieve the World Health Organisation (WHO) hepatitis C elimination goals. This study addresses the extent to which current testing targets are being met in remand prisons, possible reasons for failure, and ways in which testing rates might be improved.

Method: This mixed methods study comprised 4 distinct datasets: (i) HCV testing data was collected from 3 category B prisons (remand or short sentences) in the East Midlands for a period of one year (2022–23), together with location prior to prison arrival and length of stay. Failure to be tested was defined as no test recorded within 4 weeks of arrival. (ii) A questionnaire listing possible reasons for failure to be tested was administered to 166 people in prison (PIP) who were not tested. (iii) A survey, using the tool Expert Recommendations for Implementing Change (ERIC), and containing 76 implementation strategies in 8 clusters, was sent to heads of healthcare at 30 prison establishments in England, with a follow-up telephone call to encourage return. (iv) Face-to-face interviews were semi-structured

according to the five domains of the Consolidated Framework for Implementation Research (CFIR) containing 39 constructs, were held with 13 key healthcare professional staff at the study prisons. All 4 datasets were triangulated to facilitate the development of a novel model of sustainable blood-borne virus testing.

Results: Anti-HCV test uptake rates for the 52-week timeframe for Prisons 1, 2, and 3 were 17.2% (594/3456), 28.3% (590/2081), and 42.5% (558/1307). Testing was more likely if PIP were admitted from the community (39%) as opposed to via prison transfer (31%) and if length of stay was >21 days (39% versus 27%). Two-thirds of 166 PIP not tested gave the reason "I am not interested." Within the ERIC framework, staff education, stakeholder interrelationships, and prisoner engagement were the top three groups with the most interventions implemented, and the financial interventions group was the least implemented. Interviews with healthcare staff revealed 21 barriers and 9 facilitators to HCV testing within the 39 available CFIR constructs. Key barriers include a lack of time and space during the PIP arrival process, competing healthcare and prison regime priorities, and the interpretation that an opt-out approach involves a choice to accept or decline a test. Successful facilitators include incentivising PIP, external support, and adapting opportunities for healthcare delivery.

Conclusion: HCV testing rates within the 3 prisons in this study were far below the intended national target (75%). This study has identified a number of ways that testing rates might be improved, through removal of barriers and adoption of facilitators to testing.

THURSDAY 06 JUNE

Alcohol-related liver disease

OS-005-YI

Single-cell RNA sequencing analysis in alcohol-related liver disease identifies specific cell subpopulations characterized by an inflammatory profile in alcohol-associated hepatitis

Jordi Gratacós-Ginès¹, Alex Guillaumon-Thiery², Aina Rill³, Alicia Martínez², Silvia Ariño², Ana Belén Rubio², Martina Perez-Guasch¹, Celia Martinez-Sanchez², Emma Avitabile², Anna Soria¹, Adrià Juanola¹, Isabel Graupera¹, Mar Coll², Ramon Bataller¹, Elisabetta Mereu³, Pere Ginès¹, Elisa Pose¹. ¹Liver Unit, Hospital Clínic de Barcelona-IDIBAPS, Barcelona, Spain; ²Institut d'Investigacions Biomèdiques August Pi i Sunyer (IDIBAPS), Barcelona, Spain; ³Josep Carreras Leukemia Research Institute (IJC), Badalona, Spain
Email: jgrata@recerca.clinic.cat

Background and aims: Alcohol-related liver disease (ALD) alters the normal architecture of the liver impairing liver function and eventually leading to its severe form, alcohol-associated hepatitis (AH). The phenotypic alterations of the different cell types through ALD progression are largely unknown. The aim of this work was to dissect the transcriptomic identity of cellular populations across ALD stages by using single-cell RNA sequencing (SCRNAseq) of liver biopsies at different stages of the disease.

Method: Liver biopsies were obtained from patients with ALD with different disease stages (patients with compensated liver disease, n = 3 and patients with AH, n = 6) and from healthy donors (n = 3). Samples were processed by mechanical and chemical digestion and SCRNAseq was performed using the 10X Genomics platform. Data were analyzed with Seurat in R and Reactome, KEGG and Gene Ontology databases were used to describe biological function of cellular subtypes.

Results: A total of 30, 092 cells were clustered based on their expression pattern and 60 cell subpopulations with a unique transcriptomic identity were defined. Among these, 12 were found significantly enriched in AH and defined as the specific AH subpopulations. We analyzed the biological processes of every AH subpopulation: 1) 2 subpopulations of hepatocytes that expressed genes of cytokine signaling (IL32⁺), neutrophil degranulation (ORM1⁺) and cellular stress (PRDX1⁺); 2) 2 subpopulations of cholangiocytes that expressed hepatic progenitor cell genes (EPCAM⁺) and epithelial-to-mesenchymal cell transition genes (FGFR1⁺); 3) 2 subpopulations of endothelial cells that expressed genes associated with cytokine production (IRF1⁺) and extracellular matrix interaction (ITGA6⁺); 4) 3 subpopulations of hepatic stellate cells with activated phenotype, expressing genes associated with inflammation and fibrogenesis (COL1A1⁺); 5) 1 lymphocyte subpopulation that expressed genes related to cell stress and heat shock proteins (HSPA1A⁺); and finally 6) 2 macrophages subpopulations characterized by an inflammatory profile expressing cytokines (CCL4⁺) and complement related genes (VTN⁺).

Conclusion: This study unveils for the first time the transcriptomic identity of the liver cell populations during in the progression of ALD at a single cell level. Moreover, the functional analysis of the specific subpopulations associated to AH reveals inflammation and matrix remodeling as common key biological features among cellular compartments.

OS-006

Incretin-based therapies reduce alcohol intake in lean and obese hamster models of chronic alcohol consumption

Francois Briand¹, Estelle Grasset¹, Natalia Breyner¹, Thierry Sulpice¹. ¹Physiogenex, Escalquens, France
Email: f.briand@physiogenex.com

Background and aims: Rodent studies suggested that GLP-1 receptor agonists reduce alcohol intake in mouse and rat, but these species are not truly alcohol dependent. Golden Syrian hamsters spontaneously show a high preference for alcohol and may represent a better animal model. Here we setup two hamster models of chronic alcohol consumption to evaluate incretin-based therapies.

Method: In the first model, normal hamsters were fed a 4-week chow diet with free access to normal water or 15% alcohol-enriched water. Hamsters were then kept on the same diet and treated for 3 weeks with vehicle, semaglutide 0.04 mg/kg or tirzepatide 0.05 mg/kg subcutaneously every 3 days. The second model used hamsters with obesity and metabolic dysfunction-associated steatohepatitis (MASH), induced with a 20-week free choice diet which presents hamsters with a choice between control chow or high fat/cholesterol diet, and normal water or 10% fructose-enriched water. Hamsters were then maintained on the same diet with the 10% fructose water supplemented with 15% alcohol and treated with vehicle or semaglutide 0.06 mg/kg subcutaneously QD for 5 weeks.

Results: In the first model, hamsters reduced their normal water intake by >50% and gradually increased their 15% alcohol-enriched water intake by 275% during the 4-week induction period. Compared with vehicle, semaglutide and tirzepatide significantly prevented weight gain and reduced food intake only during the first week of treatment. Both drugs markedly increased normal water intake and significantly lowered 15% alcohol-enriched water intake during the 3-week treatment. This effect was associated with lower plasma free fatty acids levels and, for tirzepatide only, a significant reduction in hepatic triglycerides content. In the second model, obese hamsters treated with semaglutide showed a 17% body weight loss (p < 0.01 vs. vehicle) with a transient food intake lowering. While vehicle treated hamsters showed a progressive 52% increase in fructose/alcohol-enriched water intake, semaglutide strongly reduced it and significantly raised normal water intake. However, semaglutide did not alter MASH and liver fibrosis.

ORAL PRESENTATIONS

Conclusion: Incretin-based therapies reduce alcohol intake in lean and obese hamsters having free access to alcohol. These preclinical models will be helpful to evaluate the benefits of novel therapies on chronic alcohol consumption.

OS-007-YI

Intelligent liver function test 5 years on-the evolution of an intelligent platform

Damien Leith^{1,2}, Jennifer Nobes^{1,2}, Sava Handjiev^{1,2}, Iain Macpherson¹, Ellie Dow², John F Dillon^{1,2}. ¹University of Dundee, Dundee, United Kingdom; ²Ninewells Hospital, Dundee, United Kingdom
Email: damienleith86@gmail.com

Background and aims: Intelligent Liver Function Testing (iLFT) was introduced in NHS Tayside primary care in August 2018, in response to increasing mortality from chronic liver disease (CLD) and frequent liver function test (LFT) abnormalities without appropriate further investigation. Here we describe the utilisation and evolution of iLFT during the first five years of routine use in a primary care setting serving a population of approximately 400,000 people.

Method: This laboratory platform utilises an automated algorithm which combines clinician-entered clinical information with basic LFT results to reflex fibrosis scoring, relevant aetiological testing and recommended management outcomes. Earlier work demonstrated iLFT to be cost-effective and acceptable to primary care colleagues.

Results: Between August 2018 and August 2023 26,459 iLFT tests were performed. 16,112 (60.9%) cascaded to a full aetiology screen, 1,967 (7.4%) to a partial aetiology screen and 8,380 (31.7%) required no further testing. Over the last 12 months demand has stabilised-averaging 860 requests per month, with 48% cascading further tests. Of the 20,895 outcomes generated from cascaded iLFT, isolated abnormal ALT without fibrosis ($n = 4,962$, 23.7% of all outcomes) was most frequent-the majority of which were likely metabolic dysfunction-associated steatotic liver disease (MASLD) on review. For iLFT with aetiology-specific outcomes, the majority were probable alcohol related liver disease ($n = 3,134$; 15.0%) and MASLD ($n = 2,477$; 11.9%). Additionally, iLFT identified 657 MetALD, 529 alpha-1 antitrypsin phenotypes associated with CLD, 470 possible haemochromatosis, 230 possible autoimmune conditions, 87 active hepatitis C infections and 19 active hepatitis B infections. Biochemical evidence of significant fibrosis was seen in 20.0% of all requests. 69.9% of outcomes recommended that patients could be safely managed in primary care. iLFT has proven rapidly adaptable to evolving clinical need. In response to increasing secondary care hepatology clinic waiting times, reflexive Enhanced Liver Fibrosis (ELF) testing for individuals with indeterminate FIB-4 or NAFLD Fibrosis Scores was introduced in July 2020, reducing referral by around one-third. In addition, new iLFT outcomes were developed in response to new evidence-such as highlighting risk of malignancy in patients with elevated alkaline phosphatase and thrombocytosis-and existing outcomes have adapted in line with new guidance e.g. incorporating new Steatotic Liver Disease nomenclature.

Conclusion: Five years on iLFT is an integral part of the investigation of liver disease in our region, with its high usage demonstrating wide acceptance by primary care. It has proven robust yet adaptable to the Covid pandemic, emerging evidence and nomenclature change. Ongoing work focuses on refining the algorithm and supporting national roll-out.

OS-008-YI

Cellular senescence is reduced following alcohol cessation in severe alcohol-associated hepatitis

Daniel Rodrigo-Torres¹, Alastair M Kilpatrick¹, Stephen R Atkinson², Sofia Ferreira-Gonzalez^{1,3}, Luke D Tyson², Nikhil Vergis², Mark R Thursz², Laura Martinez-Gili², Stuart J Forbes¹. ¹Centre for Regenerative Medicine, Institute for Regeneration and Repair, The University of Edinburgh, Edinburgh, United Kingdom; ²Division of Digestive Diseases, Department of Metabolism, Digestion and

Reproduction, Imperial College London, London, United Kingdom;

³Centre for Inflammation Research, Institute for Regeneration and Repair, The University of Edinburgh, Edinburgh, United Kingdom
Email: drodrigo@ed.ac.uk

Background and aims: Cellular senescence, a state of irreversible cell cycle arrest, has been associated with progression and poor outcomes in chronic liver diseases such as metabolic dysfunction-associated steatohepatitis (MASH). However, the role of senescence in alcohol-related liver disease and alcohol-associated hepatitis (AH) remains unclear. Here, we investigated temporal changes in the transcriptomic expression of senescence markers in a cohort of severe AH (sAH) patients following alcohol cessation.

Method: Liver tissue biopsies were obtained at day 0 (baseline) and day 28 (d28) from participants with sAH enrolled in the ISAIAH clinical trial of canakinumab (CAN), an anti-IL-1 β antibody ($n = 32$; 27 paired samples). RNA was extracted, and bulk RNA sequencing performed. Gene level differential expression analysis was computed with respect to time as categorical variable, and with respect to CAN as an interaction with time, using a linear mixed effects model, adjusting for age and sex as fixed effects and with patient as random intercept. Gene set enrichment analysis (GSEA) was computed with fgsea; cell type specific markers were annotated using the Liver Cell Atlas. False discovery rate <0.05 was considered significant.

Results: CAN treatment revealed no significant transcriptomic differences at d28 compared to the placebo group. However, Model for End-Stage Liver Disease (MELD) score improved at d28 in 93% of patients with paired samples (CAN: 13/14; placebo: 12/13), with 2,921 genes significantly dysregulated with respect to baseline. Expression of senescence markers including Cyclin Dependent Kinase Inhibitors 1A, 2A and 2B (CDKN1A; CDKN2A; CDKN2B) was significantly downregulated at d28. Genes linked to the senescence-associated secretory phenotype (SASP), including chemokine (C-X-C motif) ligand 1 (CXCL1) and transforming growth factor beta 2 (TGFB2) were also significantly downregulated. P53 pathway and apoptosis gene sets were significantly enriched, driven by widespread downregulation of gene set members. Markers of acute inflammation, including C-reactive protein (CRP), were significantly downregulated at d28. Genes associated with fatty acid and bile acid metabolism were upregulated at d28, suggestive of a restoration of liver metabolic function following alcohol cessation. Hepatocyte genes (e.g. albumin [ALB] and hepatocyte nuclear factor 4 alpha [HNF4A]) were also upregulated at d28, while markers of biliary cells (e.g. keratin 7 [KRT7], prominin-1 [PROM1]) and other cell types were downregulated.

Conclusion: Improvement in sAH patients following alcohol cessation is characterized transcriptomically by reduced expression of senescence, SASP and apoptosis-related factors. Concomitant downregulation of inflammatory factors and upregulation of hepatic and metabolic factors further suggest a partial restoration of hepatic gene expression.

OS-009-YI

Phosphatidylethanol complements urinary and scalp hair ethyl glucuronide for the detection of different levels of alcohol use in patients with alcohol-related cirrhosis: establishing a 3-days-3 weeks-3 months alcohol use profile

Benedict Vanlerberghe¹, Catalina Dumitrascu², Nele Van den Eede¹, Schalk van der Merwe¹, Frederik Nevens¹, Alexander van Nuijs², Jef Verbeek¹. ¹University Hospitals Leuven, Leuven, Belgium; ²University of Antwerp, Antwerp, Belgium
Email: b.vanlerberghe@maastrichtuniversity.nl

Background and aims: Phosphatidylethanol (PEth) is a mid-term biomarker (weeks) that could bridge the detection windows of urinary ethyl glucuronide (uEtG) (days) and scalp hair (h)EtG (months), but is barely validated in patients with alcohol-related liver disease (ALD). In addition, the reported detection windows per biomarker are highly variable (1 to 7 days for uEtG and 2 to 4 weeks

for PEth). While the assessment of any alcohol use is important in the follow-up of ALD patients, categorizing patients based on different levels of alcohol use could aid in assessing the contributive effect of alcohol in other liver diseases, such as metabolic dysfunction-associated steatotic liver disease. We assessed the diagnostic accuracy and optimal detection windows of PEth, uEtG, hEtG, and the novel biomarker fingernail (n)EtG, for different levels of alcohol use in patients with ALD cirrhosis.

Method: Alcohol use in the prior 3 months was questioned using the Alcohol Timeline Followback Method in patients with ALD cirrhosis. 1 to 7-day detection windows were assessed for uEtG and 1 to 5 weeks for PEth. hEtG (3 cm proximal hair strand) and nEtG were used to assess alcohol use in the prior 3 months. Increased alcohol use was defined as ≥ 2 U/d for females and ≥ 3 U/d for males, and excessive use as ≥ 5 U/d for females and ≥ 6 U for males. Possible confounding factors were assessed by uni- and multivariate linear regression.

Results: 110 patients (mean age 60.7 yrs (SD 10.7); male 74.5%, CP A 59.1%) were included. For any use, uEtG (n = 98) yielded the highest diagnostic accuracy over a 3-day detection window (sensitivity (SE) 100%, specificity (SP) 93.4%, positive predictive value (PPV) 81.5%, negative predictive value (NPV) 100%), and PEth (n = 105) over a 3-week window (SE 95.2%, SP 98.4%, PPV 97.6%, NPV 96.9%). For any use in the prior 3 months, hEtG (n = 97) had a SE of 89.7%, SP of 86.2%, PPV of 81.4%, and NPV of 92.6%, and nEtG (n = 77) a SE of 78.9%, SP of 97.4%, PPV of 96.8%, and NPV of 82.6%.

PEth and hEtG had high NPV for increased (PEth: SE 76.9%, SP 89.9%, PPV 71.4%, NPV 92.2%; hEtG SE 89.3%, SP 89.9%, PPV 78.1%, NPV 95.4%) and excessive use (PEth: SE 83.3%, SP 80.6%, PPV 35.7%, NPV 97.4%; hEtG: SE 100%, SP 79.3%, PPV 46.9%, NPV 100%).

Absolute values of uEtG (B: 0.860 (SD 0.042); $p < .001$), PEth (B: 1.594 (SD 0.191); $p < .001$), and hEtG (B: 0.931 (SD 0.097); $p < .001$) only correlated with alcohol use and not with renal dysfunction, CP score, or sex in multivariate analysis, nor diuretics use for uEtG and hemoglobin for PEth.

Conclusion: In patients with ALD cirrhosis, uEtG, PEth, and hEtG have excellent and complementary diagnostic accuracies to detect any alcohol use in the prior 3 days, 3 weeks, and 3 months, respectively. PEth and hEtG have high accuracies in excluding increased and excessive alcohol use. Nail EtG can provide an alternative when scalp hair is unavailable but needs further validation.

Cirrhosis and its complications: Experimental

OS-010

Endothelial-to-mesenchymal transition: a targetable mechanism involved in portal vein thrombosis in cirrhosis

Aina Anton^{1,2,3}, Genís Campreciós^{1,2,3}, Sarah Shalaby^{3,4}, María Luisa Botero³, Annabel Blasi^{1,2,5}, Yilliam Fundora⁶, Sergio Barace⁷, Rosa Montañés^{2,3}, Héctor García-Calderó^{1,2,3}, Lara Orts^{1,3}, Carla Montironi⁸, Pol Olivas^{1,2,3}, Gonzalo Crespo^{1,2,3,9}, Cynthia Bazán³, Rommel Zambrano-Huaila³, Olga Tura-Ceida^{2,10,11,12}, Josep Maria Argemi^{1,7,13}, Juan Carlos García-Pagán^{1,2,3,9}, Virginia Hernández-Gea^{1,2,3,9}. ¹Centro de investigación biomédica red de enfermedades hepáticas y digestivas (CIBEREHD), Madrid, Spain; ²Fundació de recerca clínic Barcelona-Institut d'investigacions biomèdiques August Pi i Sunyer (FRCB-IDIBAPS), Barcelona, Spain; ³Liver unit, Hospital clínic, Health care provider of the european reference network on rare liver disorders (ERN-Liver), Barcelona, Spain; ⁴Department of surgery, oncology, and gastroenterology, Padua university hospital, Health care provider of the european reference network on rare liver disorders (ERN-Liver), Padua, Italy; ⁵Anesthesiology department, Hospital clínic, Barcelona, Spain; ⁶Department of surgery, division of hepatobiliary and general surgery, Institut de malalties digestives i metabòliques (IMDiM), Hospital clínic,

Barcelona, Spain; ⁷Center for Applied Medical Research (CIMA), Universidad de Navarra, Gene Therapy Program, Pamplona, Spain; ⁸Pathology department and molecular biology core, Centre de diagnòstic biomèdic (CDB), Hospital clínic, Hospital clínic, Barcelona, Spain; ⁹Medicine department, faculty of medicine, Universitat de Barcelona, Barcelona, Spain; ¹⁰Biomedical research networking centre on respiratory diseases (CIBERES), Madrid, Spain; ¹¹Department of pulmonary medicine, Dr. Josep Trueta university hospital de Girona, Santa Caterina hospital de Salt and the Girona biomedical research institute (IDIBGI), Girona, Spain; ¹²Department of pulmonary medicine, Hospital clínic, University of Barcelona, Department of pulmonary medicine, Barcelona, Spain; ¹³Liver unit. Clinica universidad de Navarra, Pamplona, Spain
Email: anton@recerca.clinic.cat

Background and aims: Portal vein thrombosis (PVT), a common thrombotic complication in cirrhosis (CH), lacks clear pathophysiology. Unlike thrombosis in other areas, in PVT anticoagulation rarely achieve complete recanalization and alternative treatments are scarce. Our study seeks to unravel the molecular-level pathophysiology of PVT in CH patients and to identify new therapeutic targets.

Method: 1) Histological analysis of portal vein segments from explanted livers of patients with cirrhosis with (CH-PVT, n = 15) and without (CH, n = 33) PVT, compared to a control group (CT, n = 28) without portal hypertension; 2) RNA sequencing of primary portal vein endothelial cells (PVECs) obtained during liver transplantation from CH-PVT (n = 5), CH (n = 12), and controls (n = 3); 3) Drug repurposing study using the DrugGene Interactions database; 4) In vitro treatment of previously isolated primary PVECs from CH (n = 7) and CH-PVT (n = 6) patients. Cells were treated with selected drugs for 24 h and analyzed using qPCR and Western blotting.

Results: Tunica Intima (TI) of PVs from CH was mildly increased vs. CT (TI thickness: 0.6 ± 0.5 vs. 0.4 ± 0.3 mm, $p = 0.23$). This increase was much more pronounced when PVT was present (TI thickness: CH-PVT 1.3 ± 0.7 mm; $p = 0.05$ vs CH). Increased thickness was primarily due to endothelial layer proliferation and notable changes in the subendothelial layer composition, which exhibited a secretory phenotype marked by heightened mucin and extracellular matrix (ECM) deposition and reorganization. Transcriptomic analysis of isolated PVECs revealed dysregulation of pathways related to cytoskeletal reorganization, ECM remodeling and TGF β /SMAD signaling with endothelial-to-mesenchymal transition (EndMT) emerging as the predominant mechanism behind CH-PVT. Remarkably no markers of coagulation exhibited deregulation. In silico drug repurposing analysis identified statins as potential agents targeting these changes. In vitro simvastatin treatment of primary human PVECs ameliorated EndMT-related hallmarks, increasing endothelial markers (NOS3) and reducing mesenchymal markers (FSP1), adhesion molecules (VCAM), Snail1 transcription factor and pSMAD2/SMAD2 ratio levels, suggesting a preventive role in EndMT initiation/progression.

Conclusion: Portal vein undergoes significant changes at the endothelial level in cirrhosis, which are particularly pronounced in those patients developing PVT. EndMT has been identified as the underlying process driving these changes in portal endothelium, which appears to unfold gradually, commencing from CH and reaching its peak with the onset of PVT. Simvastatin's potential to modulate EndMT in PVEC makes it a promising option for PVT treatment and prevention.

OS-011

The linoleic acid-derived leukotoxin 9, 10-DiHOME drives immunosuppression in patients with acute-on-chronic liver failure

Bryan J. Contreras^{1,2}, Cristina López-Vicario^{1,2}, Mireia Casulleras^{1,2}, Marta Duran-Güell^{1,2}, Berta Romero-Grimaldo^{1,2}, Jonel Trebicka^{2,3}, Vicente Arroyo², Joan Clària^{1,2,4}, on behalf of the MICROB-PREDICT study group². ¹Biochemistry and Molecular Genetics Service, Hospital Clínic-IDIBAPS, CIBERehd, Barcelona, Spain; ²European Foundation for the Study of Chronic Liver Failure (EF CLIF), Barcelona, Spain; ³Department of Internal Medicine B, University of Münster, Münster, Germany; ⁴Department of Biomedical Sciences, University of Barcelona, Barcelona, Spain
Email: bjcontreras@recerca.clinic.cat

Background and aims: Acute decompensation (AD) of liver cirrhosis is characterized by smoldering systemic inflammation that favors the development of organ failure, a condition known as acute-on-chronic liver failure (ACLF) associated with high short-term mortality. In this context, inflammation-related immunosuppression is a crucial factor contributing to secondary infections and multiple organ dysfunction. In this study we explored the profile of immunomodulatory lipid mediators in patients with AD cirrhosis with and without ACLF and investigated their effects on leukocyte function.

Method: The profile of 101 lipid mediators was determined by targeted lipidomics using liquid chromatography coupled to tandem mass spectrometry in plasma from 84 patients with AD cirrhosis without ACLF (stratified in stable decompensated cirrhosis (n = 53), unstable decompensated cirrhosis (n = 10) and patients with high-risk of developing ACLF (pre-ACLF) (n = 21)), and 9 patients with AD cirrhosis and ACLF. For comparison, 31 healthy donors were included. Bioassays determining degranulation, respiratory burst capacity and phagocytosis were performed to assess changes in polymorphonuclear leukocyte function. Cytokine secretion, autophagy responses and mitochondrial dynamics in mononuclear leukocytes were determined by high-throughput multiplex MILLIPLEX assays and Western blot analysis.

Results: The exploratory analysis of the baseline lipid mediator profile showed higher plasma levels of linoleic acid (LA)-derived lipid mediators in patients with AD cirrhosis as compared to healthy controls. Multiple testing identified the LA-derived 9, 10-dihydroxy-12-octadecenoic acid (9, 10-DiHOME) as the only lipid mediator with discriminating power between AD patients with established ACLF from those without. Plasma levels of 9, 10-DiHOME followed the severity course of the disease, were significantly higher at the time AD patients manifested an active infection and peaked at ACLF presentation. Moreover, expression of soluble epoxide hydrolase (sEH), the enzyme responsible for the biosynthesis of 9, 10-DiHOME, was markedly upregulated in mononuclear leukocytes from AD patients. In the polymorphonuclear leukocyte bioassays, 9, 10-DiHOME impaired degranulation, phagocytosis, and respiratory burst capacity. In the mononuclear leukocyte bioassays, 9, 10-DiHOME significantly impaired cytokine secretion and altered autophagic responses and mitochondrial dynamics.

Conclusion: Leukotoxin 9, 10-DiHOME weakens immune-cell response and therefore the higher circulating levels of this lipid mediator in patients with AD cirrhosis might enhance susceptibility to bacterial infection and precipitate ACLF. These data also position sEH as potential candidate for drug treatment in this condition.

OS-012-YI

Investigating the role of specialized intestinal macrophages in preserving gut-vascular barrier integrity during experimental cirrhosis

Lena Smets¹, Maria Viola^{2,3}, Lukas Van Melkebeke¹, Niels Vandamme⁴, Markus Boesch^{1,5,6}, Marie Wallays¹, Colinda Scheele⁷, Frederik Nevens⁸, Hannelie Korf¹, Guy Boeckxstaens³, Schalk van der Merwe^{1,8}. ¹Laboratory of Hepatology, CHROMETA, KU Leuven, Leuven, Belgium; ²University of Bonn, LINES, Bonn, Germany; ³Laboratory for Intestinal Neuroimmune Interactions, TARGID, KU Leuven, Leuven, Belgium; ⁴VIB Single Cell Core Facility, Leuven, Belgium; ⁵KU Leuven Institute for Single Cell Omics (LISCO), KU Leuven, Leuven, Belgium; ⁶Department of Human Genetics, KU Leuven, Leuven, Belgium; ⁷Laboratory of Intravital Microscopy and Dynamics of Tumor Progression, Center for Cancer Biology, VIB-KU Leuven, Leuven, Belgium; ⁸University Hospitals KU Leuven, Department of Gastroenterology and Hepatology, Leuven, Belgium
Email: lena.smets@kuleuven.be

Background and aims: Cirrhosis is characterised by a progressive decline in liver function coupled with a simultaneous breakdown of both the epithelial and gut-vascular barrier (GVB). This disrupted integrity allows for the translocation of pathogenic bacteria from the gut to the liver, intensifying systemic inflammation and exacerbating hepatic injury. In this study, we elucidate the critical role played by specialized intestinal macrophages in preserving vascular barrier integrity.

Method: Cirrhosis was induced in genetically modified mice by subcutaneous injection of CCl₄ for 20 weeks. We performed single-cell transcriptomics of the small intestinal lamina propria macrophage population from cirrhotic and control animals.

Results: The induction of cirrhosis in Cx3cr1^{CreERT2}.Rosa26-LSL-YFP mice, resulted in a decrease of YFP⁺ cells lining the vasculature, as disease progresses. The loss of long-lived GVB-associated macrophages coincided with increased bacterial translocation to the liver. To investigate the transcriptional changes within lamina propria macrophages that may account for the elevated pathological bacterial translocation, we performed single-cell RNA sequencing on viable, CD45⁺, CD11b⁺ cells. We mapped the transcriptomes of the long-lived GVB-associated macrophages (YFP⁺) along with all other lamina propria myeloid cells in experimentally induced cirrhosis versus control animals. Unbiased hierarchical clustering revealed distinct clusters of cells comprising distinct populations of myeloid cells, dendritic cells and lymphocytes. Further subclustering of myeloid cells revealed a monocyte cluster expressing *S100a4*, *Ly6c2* and *Ccr2* and four macrophage clusters expressing *Adgre1* (*F4/80*), *Cx3cr1* and *Csf1r*. Preliminary findings already suggest an increase in inflammatory monocytes in the experimental cirrhosis group (20% of the total myeloid population in control animals versus 33% in cirrhosis). Additionally, we identified one cluster upregulating core macrophage genes (*C1qa*, *Mrc1*, *Selenop*) (Resident Macs). Another cluster was marked by the upregulation of interferon response genes (*Ifit2*, *Isg15*) (IFN-responding Macs). We further identified an Adamdec1⁺ Macs cluster co-expressing *Hes1* and *Acp5*. Of interest, in this cluster, *Hmox1* and *Vcam1* are downregulated in cirrhosis animals. Finally, we detected a Lyve1⁺ Macs cluster that featured elevated expression of genes associated with phagocytosis (e.g. *Cd163*). Currently, further in-depth analysis on disease differences between control and cirrhosis myeloid cells is ongoing.

Conclusion: Our data provide novel insights into the role of specialized intestinal lamina propria macrophages in GVB barrier failure and bacterial translocation in an experimental model of cirrhosis.

OS-013

Targeting the histamine receptor 2 for HCC chemoprevention

Emilie Crouchet¹, Courtney Katz², Naoto Fujiwara², Frank Jühling¹, Marine Oudot¹, Sarah Durand¹, Antonio Saviano³, Romain Martin¹, Fabio Giannone³, Patrick Pessaux³, Raymond Chung⁴, Catherine Schuster¹, Laurent Mailly¹, Yujin Hoshida², Thomas Baumert⁵. ¹University of Strasbourg, Inserm, Institute of Translational Medicine and Liver Disease (ITM), UMR_S1110, Strasbourg, France; ²Liver Tumor Translational Research Program, Simmons Comprehensive Cancer Center, Division of Digestive and Liver Diseases, Department of Internal Medicine, University of Texas Southwestern Medical Center, Dallas, United States; ³University of Strasbourg, Inserm, Institute of Translational Medicine and Liver Disease (ITM), UMR_S1110, Institut Hospitalo-Universitaire, Pôle Hépato-digestif, Nouvel Hôpital Civil, Strasbourg, France; ⁴Liver Center and GI Division Massachusetts General Hospital Harvard Medical, Boston, United States; ⁵University of Strasbourg, Inserm, Institute of Translational Medicine and Liver Disease (ITM), UMR_S1110, Pôle Hépato-digestif, Strasbourg University Hospitals, Strasbourg, France
Email: ecrouchet@unistra.fr

Background and aims: Advanced liver fibrosis is the key risk factor for hepatocellular carcinoma. Given the absent approved treatment options for treatment of fibrosis, there is a key unmet medical need for HCC chemoprevention to improve patient outcome. The liver tissue-based prognostic liver signature (PLS) and the blood-based prognostic liver secretome (PLSsec) have been shown to robustly predict progression of liver disease, HCC risk and survival in a large number of independent cohorts with chronic liver disease (Fujiwara et al. Sci Transl Med 2022). Using a cell-based assay modeling the clinical PLS, we previously identified the FDA approved histamine 2 receptor (HRH2) antagonist Nizatidine as a candidate compound for HCC chemoprevention (Crouchet et al. Nat Commun 2021). The aim of this study was to evaluate HRH2 as a target for chemoprevention to foster its clinical translation.

Method: HRH2 was evaluated as a driver for MASH-induced hepatocarcinogenesis in a loss-of-function study using a *Hrh2* KO mouse model subjected to CD-HFD. In parallel, HRH2 antagonist Nizatidine was investigated as candidate compound for chemoprevention in patient-derived human liver chimeric mice and patient-derived liver spheroids. Liver fibrosis, progression to HCC and the liquid biomarker PLSsec were used as clinical candidate readouts.

Results: The genetic loss-of-function study in a CD-HFD mouse model for MASH/HCC revealed a robust and significant effect of *Hrh2* KO on liver tumor burden, validating the functional role of HRH2 in hepatocarcinogenesis of MASH and therapeutic target. HRH2 blocker Nizatidine inhibited liver fibrosis progression in a human liver chimeric MASH mouse model without any detectable adverse effects as shown by Sirius red staining and a decreased expression of fibrosis markers. Moreover, macroscopic examination of humanized livers revealed reduced liver nodules in Nizatidine treated animals. Improvement of liver disease was associated with a PLSsec reversal associated with HCC risk in the serum of treated mice. The findings were validated in patient-derived liver spheroids showing a robust PLS reversal after Nizatidine treatment.

Conclusion: HRH2 is a driver of hepatocarcinogenesis in MASH. HRH2 antagonist Nizatidine is a candidate compound for HCC chemoprevention. The reversal of PLSsec offers a simple non-invasive biomarker as a readout. Our results using genetic validation, efficacy and safety studies in patient-derived models pave the way for clinical development of HRH2 inhibitors for HCC chemoprevention using the non-invasive biomarker PLSsec as a clinical readout.

OS-014-YI

Long-term albumin infusion reduces the mortality of cirrhosis and ACLF animal models by modulating the gut-liver axis and hepatic TLR4 signalling

Alexandra Phillips¹, Qianwen Zhao¹, Abeba Habtesion¹, Fausto Andreola¹, Nathan Davies¹, Lindsey Edwards^{2,3}, Jane Macnaughtan¹, Sabine Klein⁴, Jonel Trebicka⁴, Rajiv Jalan¹. ¹Institute of Liver and Digestive Health, University College London, London, United Kingdom; ²Centre for Host Microbiome Interactions, King's College London, Faculty of Dentistry, Oral and Craniofacial Sciences, London, United Kingdom; ³Institute of Liver Studies, King's College London, Department of Inflammation Biology, School of Immunology and Microbial Sciences, Faculty of Life Sciences and Medicine, London, United Kingdom; ⁴Department of Internal Medicine, University of Munster, Munster, Germany
Email: alexandra.phillips5@nhs.net

Background and aims: Long-term albumin infusion has been shown to reduce mortality in cirrhosis, but the mechanism of its beneficial effect remains unknown. The aims of this study were to understand the role of albumin in modulating the gut-liver-axis by studying rat and mouse models of cirrhosis and ACLF, treated with long-term albumin injections.

Method: Models: Rats: 34 Analbuminaemic (NAR) and 36 wild-type (WT); 4-week bile duct ligation (BDL ± LPS (ACLF) (0.025 mg/kg ip) ± Human albumin 20% (1.5 g/kg ip; 2-week). Mice: 39 C57Bl mice 12-week carbon tetrachloride (CCL4) (orally ± 2 mg/kg LPS) (ACLF) ± albumin injections (1.5 g/kg ip; 2-week). Plasma biochemistry and hepatic TUNEL staining. Liver qPCR and RT² PCR profiler for TLR4 genes. Plasma cytokines analysed with Luminex, TLR4 reporter cells assay and plasma cell death ELISA. Gut permeability assessed with plasma D-lactate. Western blot and RT² PCR Profiler of tight junction proteins.

Results: Survival: Coma-free survival was reduced in both WT and NAR ACLF animals of both species, which was significantly increased in the ACLF treated with albumin ($p = 0.027$). Liver injury: Liver injury (assessed by plasma ALT and hepatic TUNEL staining) improved following albumin injection, with significant reduction seen in WT ACLF animals [$p = 0.01$; $p < 0.001$ respectively]. Gut permeability: In both cirrhosis and ACLF models, increased gut permeability (measured using plasma D-lactate) and reduced abundance of tight junction proteins, ZO-1, claudin-4 and occludin was observed, which were restored by albumin infusions (NAR ACLF $p = 0.011$). Cytokines, PAMPs and DAMPs: Albumin infusions decreased circulating cytokines (IL-1beta [WT ACLF 659.2-→522.8 pg/ml, NAR ACLF 123.5-→8.8 pg/ml], IL-10 [NAR ACLF 110.1-→12 pg/ml], IL-6 [WT ACLF 13696.7-→10310.0 pg/ml, NAR ACLF 4915.8-→237.1 pg/ml] and TNFalpha [NAR ACLF 2519.4-→97.7]), pathogen and damage associated molecular patterns (measured by plasma TLR4 activation and plasma markers of cell death respectively) in cirrhosis models and ACLF models significantly (TLR4 reporter NAR ACLF [$p < 0.001$], Cell death WT ACLF [$p < 0.001$], NAR ACLF [$p = 0.012$]). Gene expression: The absence of endogenous albumin was associated with greater hepatic TLR4 expression and related genes (TLR4, TNFalpha, and IL-1beta), with a significant reduction of expression in all disease groups with the addition of albumin injections ($p < 0.05$).

Conclusion: Long-term albumin infusions significantly reduce the mortality of ACLF animals by impacting on hepatic TLR4 related pathways that significantly reduce endotoxin sensitivity. This is manifested by significant reduction in the severity of inflammation, hepatocyte cell death and further endotoxemia. The data show for the first time that these beneficial effects are likely due to the effect of albumin on the integrity of the gut tight junctions and permeability.

Immune-mediated and cholestatic liver diseases – Clinical

OS-015

Time to complete biochemical response and disease progression in autoimmune hepatitis

Martine A.M.C. Baven-Pronk^{1,2}, Charlotte Slooter³, Ana Lleo^{4,5}, Francesca Colapietro^{4,6}, Marco Lenzi^{7,8}, Paolo Muratori^{7,9}, Nanda Kerkar¹⁰, George Dalekos¹¹, Kalliopi Zachou¹¹, Maria Isabel Lucena¹², Mercedes Robles-Díaz¹², Daniel E. Di Zeo-Sánchez¹², Raul J. Andrade¹², Aldo J. Montano-Loza¹³, Ellina Lytvyak¹³, Birgitte Lissenberg-Witte¹⁴, Patrick Maisonneuve¹⁵, Gerd Bouma¹⁶, Guilherme Macedo¹⁷, Rodrigo Liberal¹⁷, Maarten Tushuizen¹, Joost PH Drenth¹⁶, Ynto de Boer¹⁶, Bart van Hoek¹. ¹Departement of Gastroenterology and Hepatology, Leiden University Medical Center, Leiden, Netherlands; ²Groene Hart Hospital, Gouda, Netherlands; ³Department of Gastroenterology and Hepatology Amsterdam University Medical Center, AGEM Institute, Vrije Universiteit Amsterdam, Amsterdam, Netherlands; ⁴Department of Biomedical Sciences, Humanitas University, Pieve Emanuele, Milan, Italy; ⁵Division of Internal Medicine and Hepatology, Department of Gastroenterology, IRCCS Humanitas Research Hospital, Rozzano, Milan, Italy; ⁶Division of Internal Medicine and Hepatology, Department of Gastroenterology, IRCCS Humanitas Research Hospital, Rozzano, Milan; ⁷Department of Clinical Medicine, University of Bologna, Bologna, Italy; ⁸Department of Sciences for the Quality of Life, University of Bologna, Bologna; ⁹Department of Sciences for the Quality of Life, University of Bologna, Bologna, Italy; ¹⁰Department of Gastroenterology, Hepatology and Nutrition, Golisano Children's Hospital, University of Rochester Medical Center, Rochester, United States; ¹¹Department of Medicine and Research Laboratory of Internal Medicine, Expertise Center of Greece in Autoimmune Liver Diseases, European Reference Network on Hepatological Diseases (ERN-RARE LIVER), General University Hospital of Larissa, Larissa, Greece; ¹²Liver Unit, Gastroenterology Service and Department of Medicine, Virgen de Victoria University Hospital, University of Málaga, Málaga, Spain; ¹³Department of Gastroenterology and Hepatology, University of Alberta Hospital, Edmonton, Canada; ¹⁴Department of Epidemiology and Biostatistics, Amsterdam UMC, Vrije Universiteit Amsterdam, Amsterdam, Netherlands; ¹⁵Division of Epidemiology and Biostatistics, IEO European Institute of Oncology IRCCS, Milan, Italy; ¹⁶Department of Gastroenterology and Hepatology Amsterdam University Medical Center, AGEM Institute, Vrije Universiteit Amsterdam, Amsterdam, Netherlands; ¹⁷Department of Gastroenterology and Hepatology, Centro Hospitalar São João, Porto, Portugal
Email: martine.pronk@ghz.nl

Background and aims: The primary goal of treatment in autoimmune hepatitis (AIH) is to achieve complete biochemical response (CBR) and prevent progression of disease, which may result in liver transplantation and death. Not achieving CBR within 6 or 12 months is associated with liver-related adverse outcomes. However, many patients reach CBR after 6–12 months. This may still be prognostically favorable compared to not achieving CBR at all. Also, some patients who achieve CBR may still have progression to cirrhosis or decompensation. This study aimed to investigate to what extent the time to CBR affects the risk of disease progression and adverse outcomes.

Method: This retrospective, observational, multicenter analysis included all patients from the updated international AIH group retrospective registry with data on CBR and follow-up data. Kaplan Meier and Cox regression were used to evaluate timing of CBR in relation to development of cirrhosis development and on liver transplant-free survival.

Results: This analysis included 1105 patients across 7 countries. CBR was achieved in 385 (35%), 115 (10%) and 210 (19%) patients at <6, 6–12 and >12 months respectively. 395 (36%) of the patients never achieved CBR. During a median follow-up of 6 (range 0–43) years, 113 deaths occurred, of which 55 were liver-related, and 43 patients underwent liver transplantation. Of the 814 patients without cirrhosis at diagnosis, 113 (14%) progressed to cirrhosis. Patients who never achieved CBR had a higher risk of progression to cirrhosis (HR 5.2 95% CI 3.4–7.7 p<0.001) and liver-related death or liver transplantation (HR 9.8 95% CI 5.9–16.4 p<0.001) compared to patients who did achieve CBR. Progression to cirrhosis was lower if CBR <6 months (HR 0.3 95% CI 0.1–0.6 p<0.001), but not when CBR 6–12 months (HR 0.6 95% CI 0.2–1.3 p=0.195), compared to CBR >12 months. Survival was not higher in patients with CBR at <6 months (HR 0.6 95% CI 0.2–1 p=0.81) or 6–12 months (HR 0.9 95% CI 0.2–2 p=0.676) compared to patients with CBR at >12 months.

Conclusion: Patients not achieving CBR face markedly higher risks of progression to cirrhosis and liver-related mortality or transplantation. While early CBR (<6 months) was associated with less progression to cirrhosis, there was no association between timing of CBR and liver transplant-free survival. Achieving CBR is crucial for prognosis, with delayed CBR still offering benefits compared to never reaching CBR at all.

OS-016

Elafibranor efficacy in primary biliary cholangitis according to biochemical response criteria in the phase III ELATIVE® trial

Mark Sonderup¹, C Wendy Spearman¹, Vincenza Calvaruso², Nuno Antunes³, Jianfen Shu³, Claudia O. Zein³, Kris V. Kowdley⁴. ¹Division of Hepatology, Department of Medicine, Faculty of Health Sciences, University of Cape Town and Groote Schuur Hospital, Cape Town, South Africa; ²Gastroenterology and Hepatology Unit, Department of Health Promotion Sciences Maternal and Infantile Care, Internal Medicine and Medical Specialties, University of Palermo, Palermo, Italy; ³Ipsen, Cambridge, MA, United States; ⁴Liver Institute Northwest, Seattle, WA, United States
Email: mark.sonderup@uct.ac.za

Background and aims: Elafibranor, a dual peroxisome proliferator-activated receptor- α/δ agonist, is being investigated in primary biliary cholangitis (PBC). In the phase III ELATIVE® trial (NCT04526665), elafibranor efficacy was assessed in patients with PBC with inadequate response or intolerance to ursodeoxycholic acid. PBC is characterised by elevated alkaline phosphatase (ALP) levels. As the disease progresses, total bilirubin (TB) levels increase. ALP and TB have prognostic value and form the basis of several clinical biochemical response criteria.

The primary end point (POISE trial end point criteria: ALP <1.67×upper limit of normal [ULN], ALP reduction \geq 15% from baseline [BL] and TB at or below ULN) was met by a significantly greater proportion of patients receiving elafibranor vs placebo (treatment benefit: 47.2%) at Week 52. Results from other binary biochemical response criteria, secondary outcomes in ELATIVE®, are presented here.

Method: In the global, double-blind, placebo-controlled ELATIVE® trial, patients were randomised 2:1 to once-daily elafibranor 80 mg or placebo. Biochemical response rates at Week 52 were analysed using POISE and: Paris I (ALP <3×ULN, aspartate aminotransferase [AST] <2×ULN and TB \leq 1 mg/dL); Paris II (ALP \leq 1.5×ULN, AST \leq 1.5×ULN and normal TB); Barcelona (ALP normalisation or reduction >40% from BL); Momah/Lindor (ALP \leq 1.67×ULN and TB \leq 1 mg/dL); and complete biochemical response (normal ALP, TB, AST, alanine aminotransferase, albumin and international normalised ratio) criteria. Rotterdam criteria (normalisation of TB and/or albumin) were used but are not reported as few patients had abnormal BLTB or albumin (n=6). Exact Cochran-Mantel-Haenszel tests stratified by the randomisation factors were performed to examine the treatment benefit of elafibranor vs placebo.

Results: 161 patients received elafibranor (n = 108) or placebo (n = 53). Mean age was 57 (standard deviation: 9) years, and 96% of patients were female. BL ALP and TB levels were similar in each group. Responder rates consistently favoured elafibranor over placebo across Paris I (treatment benefit: 22.0%; odds ratio [OR]: 2.85; 95% confidence interval [CI]: 1.34–7.18; p = 0.0061); Paris II (treatment benefit: 37.5%; OR: 16.65; 95% CI: 4.59–91.76; p < 0.0001); Barcelona (treatment benefit: 54.7%; OR: infinity; 95% CI: 20.22–infinity; p < 0.0001); and Momah/Lindor (treatment benefit: 42.8%; OR: 15.42; 95% CI: 4.60–50.00; p < 0.0001) criteria. A complete biochemical response was observed in 10 patients (9.3%) receiving elafibranor; none receiving placebo (OR: infinity; 95% CI: 1.51–infinity; p = 0.0305).

Conclusion: Elafibranor provided a consistent and significantly greater biochemical response in patients with PBC compared with placebo after one year of treatment using several prognostic scoring systems. Study sponsor: GENFIT; publication sponsor: Ipsen.

OS-017

Deep learning discriminates autoimmune hepatitis and primary biliary cholangitis

Alessio Gerussi^{1,2}, Oliver Saldanha^{3,4}, Giorgio Cazzaniga⁵, Damiano Verda⁶, Zunamys Carrero³, Bastian Engel⁷, Richard Taubert⁷, Francesca Bolis⁸, Laura Cristofori^{9,10}, Federica Malinverno⁹, Francesca Colapietro^{11,12}, Reha Akpınar^{13,14}, Luca Di Tommaso^{11,14}, Luigi Terracciano^{11,14}, Ana Lleo^{11,15}, Mauro Viganò^{16,17}, Cristina Rigamonti¹⁸, Daniela Cabibi¹⁹, Vincenza Calvaruso²⁰, Fabio Gibilisco²¹, Nicolò Caldonazzi²², Alessandro Valentino²³, Stefano Ceola⁵, Valentina Canini⁵, Eugenia Nofit⁹, Marco Muselli⁶, Julien Calderaro²⁴, Dina Tiniakos²⁵, Vincenzo L'Imperio⁵, Fabio Pagni⁵, Nicola Zucchini⁵, Pietro Invernizzi^{9,10}, Marco Carbone^{10,26}, Jakob Nikolas Kather^{3,27}. ¹Division of Gastroenterology, European Reference Network on Hepatological Diseases (ERN RARE-LIVER), Fondazione IRCCS San Gerardo dei Tintori, Monza, Italy; ²Center for Autoimmune Liver Diseases, Department of Medicine and Surgery, University of Milano-Bicocca, Monza, Italy; ³Else Kroener Fresenius Center for Digital Health, Medical Faculty Carl Gustav Carus, Technical University Dresden, Dresden, Germany; ⁴Department of Diagnostic and Interventional Radiology, University Hospital RWTH Aachen, Aachen, Germany; ⁵Department of Medicine and Surgery, Pathology, Fondazione IRCCS San Gerardo dei Tintori, Università di Milano-Bicocca, Monza, Italy; ⁶Rulex Innovation Labs, Rulex Inc, Genoa, Italy; ⁷Department of Gastroenterology, Hepatology, Infectious Diseases and Endocrinology, Hannover Medical School, Hannover, Germany; ⁸Division of Gastroenterology, Center for Autoimmune Liver Diseases, European Reference Network on Hepatological Diseases (ERN RARE-LIVER), Fondazione IRCCS San Gerardo dei Tintori, Monza, Italy; ⁹Division of Gastroenterology, Center for Autoimmune Liver Diseases, European Reference Network on Hepatological Diseases (ERN RARE-LIVER), Fondazione IRCCS San Gerardo dei Tintori, Monza, Italy; ¹⁰Department of Medicine and Surgery, University of Milano-Bicocca, Monza, Italy; ¹¹Department of Biomedical Sciences, Humanitas University, Pieve Emanuele, Italy; ¹²Division of Internal Medicine and Hepatology, Department of Gastroenterology, IRCCS Humanitas Research Hospital, Rozzano, Italy; ¹³Humanitas University, Department of Biomedical Sciences, Milan, Italy; ¹⁴Department of Pathology, IRCCS Humanitas Research Hospital, Rozzano, Italy; ¹⁵Division of Internal Medicine and Hepatology, Department of Gastroenterology, IRCCS Humanitas Research Hospital, Rozzano, Italy; ¹⁶Division of Hepatology, San Giuseppe Hospital, Milan, Italy; ¹⁷Gastroenterology Hepatology and Transplantation Unit, ASST Papa Giovanni XXIII, Bergamo, Italy; ¹⁸Department of Translational Medicine, Università del Piemonte Orientale, Novara, Italy; and Division of Internal Medicine, AOU Maggiore della Carità, Novara, Italy; ¹⁹Pathology Institute, PROMISE, University of Palermo, Palermo, Italy; ²⁰Gastrointestinal and Liver Unit, Department of Health Promotion Sciences Maternal and Infantile Care, Internal Medicine and Medical Specialties, University of Palermo, Palermo, Italy; ²¹Department of Medical and Surgical Sciences and

Advanced Technologies, "G. F. Ingrassia", University of Catania, Catania, Italy; ²²Department of Diagnostics and Public Health, Section of Pathology, University of Verona, Verona, Italy; ²³Pathological Unit, Niguarda Hospital, Milan, Italy; ²⁴Assistance Publique-Hôpitaux de Paris, Henri Mondor-Albert Chenevier University Hospital, Department of Pathology, Creteil, France; ²⁵Department of Pathology, Aretaieion Hospital, Medical School, National and Kapodistrian University of Athens, Athens, Greece; ²⁶Liver Unit, ASST Grande Ospedale Metropolitano Niguarda, Milan, Italy; ²⁷Department of Medicine 1, University Hospital and Faculty of Medicine Carl Gustav Carus, Technische Universität Dresden, Dresden, Germany
Email: alessio.gerussi@unimib.it

Background and aims: Differentiating Autoimmune Hepatitis (AIH) from Primary Biliary Cholangitis (PBC) histologically can be difficult. Florid PBC may show interface hepatitis in up to 25% of cases and errors may lead to overestimation of AIH and overtreatment with immunosuppressors. This study applies a deep learning (DL)-based pipeline for the diagnosis of AIH and PBC.

Method: We conducted a multicenter study across six European referral centers, and built a library of digitized liver biopsy slides dating from 1997 to 2023. A training set of 354 cases (266 AIH and 102 PBC) and an external validation set of 92 cases (62 AIH and 30 PBC) were available for analysis. A novel artificial intelligence (AI) model, the Autoimmune Liver Neural Estimator (ALNE), was trained on whole-slide images (WSIs) with haematoxylin and eosin staining. The ALNE model was evaluated against clinico-pathological diagnoses and tested for interobserver variability among general pathologists. Attention heatmaps and explainable machine learning (ML) were used for further characterization of the output.

Results: ALNE demonstrated high accuracy in differentiating AIH from PBC, achieving an AUROC of 0.81 in external validation. Attention heatmaps showed that ALNE tends to focus more on areas with increased inflammation, associating such patterns predominantly with AIH. Inconsistency among general pathologists was noticed when evaluating a random sample of the same cases. A multivariate explainable ML model including clinical variables revealed that misclassified PBC cases were more often characterized by abnormal AST levels. When applied to cases with overlapping features, ALNE was able to recognize the most prevalent disease.

Conclusion: The ALNE model is the first system generating a quantitative and accurate differential diagnosis among AIH, PBC and PBC-AIH cases, using digital pathology slides without preliminary expert annotation. The ALNE model has the potential to support differential diagnosis of autoimmune liver disease.

OS-018

Liver stiffness measurement by vibration-controlled transient elastography predicts adverse clinical outcomes in autoimmune hepatitis: results from a large multicenter longitudinal study

Ellina Lytyvak¹, Narmeen Umar¹, Gideon M. Hirschfield², Christina Plagiannakos³, Hin Hin Ko⁴, Mark G Swain⁵, Julian Hercun⁶, Lawrence Worobetz⁷, Catherine Vincent⁸, Jennifer Flemming⁹, Karim Qumosani¹⁰, Tianyan Chen¹¹, Dusanka Grbic¹², Angela Cheung¹³, Devika Shreekrumar¹, Iffat Iqbal¹, Madeline Cameron¹⁴, Aliya Gulamhusein¹⁵, Andrew L. Mason¹, Bettina Hansen¹⁴, Aldo J Montano-Loza¹, on behalf of the Canadian Network for Autoimmune Liver Diseases (CaNAL)¹⁶. ¹University of Alberta, Edmonton, Canada; ²Toronto Centre for Liver Disease, University of Toronto, Toronto, Canada; ³University Health Network, University of Toronto, Toronto, Canada; ⁴University of British Columbia, Pacific Gastroenterology Associates, Vancouver, Canada; ⁵University of Calgary, Snyder Institute for Chronic Diseases, Calgary, Canada; ⁶Centre hospitalier de l'Université de Montréal (CHUM), Montréal, Canada; ⁷University of Saskatchewan, Saskatoon, Canada; ⁸Centre Hospitalier de l'Université de Montréal (CHUM), University of Montreal, Montreal, Canada; ⁹Queen's University, Kingston Health Sciences Centre, Kingston, Canada; ¹⁰Western University, London, Canada; ¹¹McGill University

ORAL PRESENTATIONS

Health Centre, Montreal, Canada; ¹²University of Sherbrooke, Sherbrooke, Canada; ¹³University of Ottawa, Ottawa, Canada; ¹⁴University Health Network, Toronto, Canada; ¹⁵Toronto Centre for Liver Disease, Toronto, Canada; ¹⁶Canadian Network for Autoimmune Liver Diseases (CaNAL), Edmonton, Canada
Email: lytvayak@ualberta.ca

Background and aims: Non-invasive techniques may have a promising potential in predicting disease outcomes and evaluating the effectiveness of therapies in people living with autoimmune hepatitis (AIH). In this study, we aimed to investigate the usefulness of liver stiffness measurement (LSM) by vibration-controlled transient elastography (VCTE) in predicting clinical outcomes in a large cohort of people living with AIH across Canada.

Method: We conducted a nationwide, multicenter, retro- and prospective cohort study of people with AIH from the Canadian Network for Autoimmune Liver Diseases (CaNAL). Inclusion criteria were a simplified AIH score ≥ 6 and at least one reliable LSM by VCTE (LSM/IQR < 0.30) performed before the occurrence of any adverse events. The primary composite end point was the occurrence of any adverse liver outcomes (development of decompensation, hepatocellular carcinoma (HCC), liver transplantation (LT) or death). Treatment response was defined as the normalization of ALT at 6 months after treatment initiation.

Results: We evaluated 853 people with AIH (73.8% females, 74.5% Caucasians, the median age at diagnosis of 45.9 y.o. [IQR 28.5–58.1]) with 8394 person-years follow-up. The first VCTE was performed at a median of 41.2 months [IQR 4.6–112.0] after the AIH diagnosis, and the median LSM value was 8.7 kPa [IQR 5.7–15.8]. The LSM was strongly associated with the development of adverse outcomes (HR 1.04; 95%CI 1.03–1.05; $p < 0.001$). In a time-dependent multivariable Cox regression analysis, after adjustment for male sex, age at diagnosis, cirrhosis at diagnosis and lack of biochemical treatment response, LSM was independently associated with adverse outcomes (HR 1.03; 95%CI 1.01–1.05; $p = 0.004$). Based on the LSM value, people were stratified into low (< 8.0 kPa), medium (8.0–13.9 kPa) and high-risk (≥ 14.0 kPa) groups. In comparison to the low-risk (reference) group, the medium-risk group had over four-fold (HR 4.64; 95% CI 2.03–10.59; $p < 0.001$) and high-risk-over ten-fold risk (HR 10.12; 95% CI 4.81–21.29; $p < 0.001$) of developing adverse outcomes. The median event-free survival times were comparable (43.6, 40.4 and 43.8 months for low-, medium- and high-risk groups, respectively; $p = 0.477$). After adjustment for the above-mentioned risk factors, only the high-risk group exhibited a significantly higher risk of adverse outcomes (HR 5.53; 95% CI 1.20–25.45; $p = 0.028$).

Conclusion: In people living with AIH, LSM by VCTE is a strong independent predictor for adverse liver outcomes when considering other risk factors and biochemical treatment response. LSM values by VCTE might help to establish risk stratification to identify people with AIH who may benefit from closer screening for liver decompensation, HCC, and timely LT referral. Future studies are warranted to explore the utility of LSM as a non-invasive surrogate end point in clinical trials.

OS-019

Efficacy and safety of seladelpar in patients with primary biliary cholangitis and compensated liver cirrhosis in the open-label, long-term ASSURE safety study: interim results

Stuart C Gordon¹, Ira Jacobson², Ziad H. Younes³, Marina Silveira⁴, Joost P.H. Drenth⁵, Ulrike Morgera⁶, George Dalekos⁷, Jeong Heo⁸, Ke Yang⁹, Carrie Heusner⁹, Daria B. Crittenden¹⁰, Charles A. McWherter¹⁰. ¹Henry Ford Health, Detroit, United States;

²NYU Langone Health, New York, United States; ³Gastro One, Germantown, United States; ⁴Yale School of Medicine, New Haven, United States; ⁵Radboud Universiteit, Nijmegen, Netherlands; ⁶Charité-Universitätsmedizin Berlin, Berlin, Germany; ⁷Larissa General University Hospital, Larissa, Greece; ⁸Pusan National University, Busan, Korea, Rep. of South; ⁹CymaBay Therapeutics, Inc, Fremont, United States; ¹⁰CymaBay Therapeutics, Fremont, United States
Email: cmcwherter@cymabay.com

Background and aims: Seladelpar, a potent and selective PPAR-delta agonist (ie, a delpar), has anti-cholestatic and anti-pruritic activity in patients with primary biliary cholangitis (PBC). The ongoing, international, phase 3 ASSURE study (NCT03301506) is an open-label, long-term study of seladelpar in patients with PBC who participated in a prior seladelpar study. Here we report interim efficacy and safety results on a subset of patients with compensated liver cirrhosis.

Method: Patients with PBC and cirrhosis were eligible for ASSURE if they had an inadequate response or intolerance to ursodeoxycholic acid (UDCA), previously participated in a seladelpar study, and had no history of hepatic decompensation. All patients received open-label seladelpar 10 mg oral daily. As of the data cutoff (29 June 2023), 174 patients from previous seladelpar studies (CB8025–21629, NCT02955602; CB8025–31731, NCT03301506; ENHANCE, NCT03602560; CB8025–21838, NCT04950764) had enrolled, of whom 33 had compensated liver cirrhosis at study entry. Biochemical efficacy end points included the composite response of alkaline phosphatase (ALP) $< 1.67 \times$ upper limit of normal (ULN), ALP decrease $\geq 15\%$, and total bilirubin \leq ULN; ALP normalization; and change from baseline in ALP, total bilirubin, gamma-glutamyl transferase (GGT), alanine aminotransferase (ALT), and aspartate aminotransferase (AST) all at Month 12.

Results: Of the 33 patients with cirrhosis, most were female (91%) with a mean age of 60.4 years. Eight patients (24.2%) had portal hypertension, 93.9% were Child-Pugh (CP) class A, and 6.1% were CP-B. Mean baseline liver stiffness by FibroScan was 19.3 kPa. At baseline, mean ALP was 241.9 U/L, and total bilirubin was 0.92 mg/dL (27.3% $>$ ULN). As of the data cutoff date, 23 patients with compensated cirrhosis had completed 12 months of treatment. Twelve out of 23 (52.2%) patients met the composite biochemical end point at Month 12. ALP normalization occurred in 39.1% (9/23 patients) at Month 12, and the mean percent change from baseline in ALP was -38.1% (absolute change: -99.5 U/L). Reductions were also observed in GGT and ALT (percent changes from baseline: -35.1% and -19.6% , respectively) at Month 12; no change was observed in AST or total bilirubin. There were no serious adverse events that were liver-related or related to study drug and no discontinuations due to adverse events.

Conclusion: In this interim analysis of the ongoing ASSURE study, PBC patients with compensated cirrhosis treated with seladelpar 10 mg for 12 months achieved clinically meaningful improvements in markers of cholestasis and liver injury. Seladelpar appeared overall safe and well tolerated. These findings suggest that seladelpar has the potential to offer a safe and effective therapy for PBC patients with compensated cirrhosis.

Liver transplantation and hepatobiliary surgery

OS-020

MRI-serum based score accurately identifies liver transplant patients without rejection avoiding need for liver biopsy: a multisite european study

Jelte Schaapman¹, Elizabeth Shumbayawonda², Miguel Castelo-Branco³, Filipe Caseiro Alves³, Tania Costa³, Emer Fitzpatrick⁴, Katie Tupper⁴, Anil Dhawan⁴, Maesha Deheragoda⁴, Eva Sticova⁴, Marika French², Cayden Beyer⁵, Soubera Rymell², Dimitar Tonev⁶, Hein W Verspaget¹, Stefan Neubauer⁷, Rajarshi Banerjee², Hildo Lamb¹, Minneke Coenraad¹. ¹Leiden University Medical Center, Leiden, Netherlands; ²Perspectum Ltd., Oxford, United Kingdom; ³Instituto de Ciências Nucleares Aplicadas à Saúde, Universidade de Coimbra, Coimbra, Portugal; ⁴King's College Hospital NHS Foundation Trust, London, United Kingdom; ⁵Perspectum Ltd., London, United Kingdom; ⁶Calliditas, London, United Kingdom; ⁷University of Oxford, Oxford, United Kingdom
Email: j.j.schaapman@lumc.nl

Background and aims: Liver function and histological assessment for fibrosis, inflammation and T-cell mediated rejection are essential elements of post-liver transplant monitoring. However, liver biopsy carries a risk of complications which are preferably avoided in low-risk patients. Multiparametric MRI (mpMRI) is a reliable non-invasive diagnostic method which quantifies liver disease activity (including fibroinflammation (cT1), liver fat content (PDFF) and liver iron) and has shown prognostic utility in chronic liver disease management. Our aim was to determine whether using mpMRI in combination with standard serum biochemistry (serum) tests could non-invasively identify low-risk post-liver transplant patients who are eligible to avoid invasive liver biopsies.

Method: RADICAL2, a multicentre prospective study, included 131 adult and paediatric (children and adolescent) patients with previous liver transplant from the Netherlands, Portugal and UK. Biopsies were centrally read by two expert pathologists. T-cell mediated rejection (rejection) was assessed using BANFF global assessment (BANFF-GA). Diagnostic accuracy to discriminate no rejection vs. indeterminate or T-cell mediated liver transplant rejection was performed using area under the receiver operating characteristic curve (AUC).

Results: In the RADICAL2 cohort, 38% of patients had no rejection, while 62% had either indeterminate (21%) or T-cell mediated rejection (41%). There was a wide range of inter-observer variability ($0 \leq \text{Cohen's Kappa} < 0.85$) across all histology scores with moderate agreement between pathologists ($\text{Kappa} < 0.58$) for BANFF-GA. A combination of mpMRI cT1 and liver fat with standard serum tests had AUC 0.7 (NPV: 0.8) to identify those without rejection (either indeterminate or T-cell mediated rejection). In the 18% of RADICAL2 participants where therapy changed, cT1 (841 ms vs. 789 ms; $p = 0.006$), and GGT (284 vs. 125; $p = 0.013$) were significantly higher compared to those who did not get a change in therapy.

Conclusion: A combination of mpMRI cT1 and liver fat with standard serum tests accurately identified patients without indeterminate or T-cell mediated rejection who could avoid liver biopsy. mpMRI used alongside serum markers has utility to support non-invasive patient management in both adult and paediatric post-transplant populations.

OS-021-YI

Molecular phenotype of chronic antibody-mediated rejection in liver transplant biopsies

Bastian Engel¹, Ahmed Alaswad², Alejandro Campos-Murguía¹, Martijn Zoodma^{3,4}, Anne Höffer¹, Kinan Chihab¹, Emily Bosselmann¹, Sophia Heinrich¹, Björn Hartleben¹, Danny Jonigk¹, Michael Hallensleben¹, Verboom Murielle¹, Robert Geffers⁵, Heiner Wedemeyer¹, Chengjian Xu⁶, Angelina Mensah¹, Theresa Kirchner¹, Elmar Jaeckel^{1,7}, Yang Li⁶, Richard Taubert¹. ¹Hannover Medical School, Hannover, Germany; ²Centre for Individualised Infection Medicine (CiIM), Hannover, Germany; ³Department of Computational Biology for Individualised Medicine, Centre for Individualised Infection Medicine (CiIM), Hannover, Germany; ⁴TWINCORE, joint ventures between the Helmholtz-Centre for Infection Research (HZI) and the Hannover Medical School (MHH), Hannover, Germany; ⁵Research Group Genome Analytics, Helmholtz Centre for Infection Research, Braunschweig, Germany; ⁶Centre for Individualised Infection Medicine (CiIM), Hannover, Germany; ⁷Ajmera Transplant Center, Toronto General Hospital, Toronto, Canada
Email: taubert.richard@mh-hannover.de

Background and aims: The relevance of chronic antibody mediated rejection (cABMR) after liver transplantation (LT) is controversial. Tissue gene expression has been used to better characterize T cell mediated rejection (TCMR) after LT, but a transcriptional signature of cABMR has not been reported. A transcriptional signature could improve the characterization of cABMR and help to establish molecular diagnostic tools in clinical practice. The aim of this retrospective single-center study was to identify a unique transcriptional signature of cABMR after LT.

Method: Graft tissue bulk RNAseq was performed in two independent cohorts of adult LT recipients with well-characterized histological phenotypes retrieved from our prospective institutional biobank including a surveillance biopsy program with more than 1400 liver biopsies. Diagnostic criteria were based on the 2016 Banff criteria. Differentially expressed genes (DEGs) were considered significant with a log2fold change > 1 , and an adjusted p value < 0.05 .

Results: The discovery cohort (2008–2016), included 71 patients with non-histologic rejection (NHR) ($n = 18$), cABMR ($n = 11$), clinical TCMR (clinTCMR) ($n = 26$), and subclinical TCMR (subTCMR) ($n = 26$) matched by age, sex, and time after LT. The validation cohort (2018–2022) included all patients ($n = 58$) within this period with cABMR ($n = 6$) and clinTCMR ($n = 12$), matched by age, sex, and time after LT, with patients with subTCMR ($n = 20$) and NHR ($n = 20$) as controls. cABMR had a prevalence of less than 2%, with normal or mild liver enzyme elevations in 81% of cases. Biologically, cABMR was associated with TNF signaling via NF- κ B, fibrogenesis and complement activation compared to NHR. A unique transcriptional cABMR signature was identified in the discovery cohort, with 946 upregulated and 166 downregulated unique DEGs. Unique DEGs of cABMR were associated with biological fibrogenesis, cell adhesion and NF- κ B signaling. Comparing cABMR and clinTCMR, DEGs relevant to basement membrane remodeling and collagen formation, both processes relevant to liver fibrogenesis, were overexpressed in cABMR. Common features of cABMR and clinTCMR related to chemokine signaling and cytokine responses. The transcriptome of subTCMR was barely distinguishable from biopsies with NHR. There was high concordance between cohorts, with 87% of cABMR DEGs and 93% of clinTCMR DEGs shared between them.

Conclusion: The cABMR transcriptional signature in LT is biologically similar to other solid organ transplants and simultaneously distinct from clinTCMR, strengthening cABMR as a distinct phenotype of graft rejection after LT with a unique transcriptional profile. We highlight a potential application of transcriptomics on liver biopsies to facilitate the diagnosis of cABMR after LT.

OS-022

Kinetics of immune dysfunction in liver transplanted patients and impact on clinical outcome

Marie Charlotte Delignette¹, Arnaud Riff², Céline Guichon³, Kayvan Mohkam⁴, Alice Blet⁵, Solène Pantel⁶, Jérôme Dumortier⁷, Tanguy Soustre⁸, Francois Villeret⁹, Fabien Zoulim¹⁰, Fabienne Venet¹¹, Jean-Yves Mabrut¹², Teresa Antonini¹³, Guillaume Monneret¹⁴, Fanny Lebossé¹⁵. ¹Lyon Liver Institute, Anesthesiology and Critical Care department, Hospices Civils of Lyon, EA7426 "Pathophysiology of Injury Induced Immunosuppression" Hospices Civils of Lyon-bioMérieux-Lyon 1 University, Lyon, France; ²Lyon Liver Institute, Hepatology Department, Hospices Civils of Lyon, EA7426 "Pathophysiology of Injury Induced Immunosuppression" Hospices Civils of Lyon-bioMérieux-Lyon 1 University, Lyon, France; ³Lyon Liver Institute, Anesthesiology and Critical Care department, Hospices Civils of Lyon, Lyon, France; ⁴Lyon Liver Institute, Surgery and Liver transplantation department, Hospices Civils of Lyon, Cancer Research Center of Lyon (CRCL), INSERM U 1052, Lyon, France; ⁵Lyon Liver Institute, Anesthesiology and Critical Care department, Hospices Civils of Lyon*, Cancer Research Center of Lyon (CRCL), INSERM U 1052, Lyon, France; ⁶Lyon Liver Institute, Clinical Research Center, Hospices Civils of Lyon, Lyon, France; ⁷Lyon Liver Institute, Hepatogastroenterology Unit, Hospices Civils of Lyon, Lyon, France; ⁸Lyon Liver Institute, Anesthesiology and Critical Care Department, Hospices Civils of Lyon, Lyon, France; ⁹Lyon Liver Institute, Hepatology Department, Hospices Civils of Lyon, Lyon, France; ¹⁰Lyon Liver Institute, Hepatology Department, Hospices Civils of Lyon, Cancer Research Center of Lyon, INSERM U1052, Lyon, France; ¹¹EA7426 "Pathophysiology of Injury Induced Immunosuppression" Hospices Civils of Lyon-bioMérieux-Lyon 1 University, Immunology laboratory, Hospices Civils of Lyon, Lyon, France; ¹²Lyon Liver Institute, Surgery and Liver transplantation department, Hospices Civils of Lyon, Cancer Research Center of Lyon, INSERM U 1052, Lyon, France; ¹³Lyon Liver Institute, Hepatology department, Hospices Civils of Lyon, Cancer Research Center of Lyon, INSERM U 1052, Lyon, France; ¹⁴EA7426 "Pathophysiology of Injury Induced Immunosuppression" Hospices Civils of Lyon-bioMérieux-Lyon 1 University, Immunology laboratory, Hospices Civils of Lyon, Lyon, France; ¹⁵Cancer Research Center of Lyon (CRCL), INSERM U 1052, Lyon Liver Institute, Hepatology department, Hospices Civils of Lyon, Lyon, France
Email: fanny.lebosse@inserm.fr

Background and aims: Immune dysfunction is an important outcome determinant of end stage liver diseases. There is limited knowledge regarding the kinetic of this immune dysfunction following liver transplantation (LT) and its impact on LT outcomes. Our aim was to describe the post LT evolution of immune dysfunction and its association with clinical outcomes.

Method: Patients with cirrhosis or acute liver failure (ALF) were prospectively enrolled before LT in a monocentric study. The following immune response features were assessed both pre LT and twice a week for a duration of 1 month post LT: HLA-DR monocyte expression (mHLA-DR), neutrophil-to-lymphocyte ratio (NLR), T cell count and function (Interferon-gamma (IFN γ) release assay). If an immune-related event occurred within 1 month post LT (infections or liver graft rejection), immunological data for the affected patients were censored at the time of the event.

Results: 99 patients were included: 20 exhibited compensated cirrhosis (CC), 44 presented with acute decompensation (AD), 30 with acute on chronic liver failure (ACLF) and 5 with ALF. Median MELD score was 20 [15–29]. Pre-LT mHLA-DR level decreased significantly with disease severity (median 26740 antibodies per cell (AB/C) [18740–33220] for AD/CC vs median 16740 AB/C [8250–25050] for ACLF/ALF patients ($p < 0.001$)) and the number of organ failure. T cell count and IFN- γ release were significantly reduced in ACLF patients compared to CC whereas NLR increased with disease severity ($p < 0.001$). Following LT, immune markers kinetic analysis suggested a marked immune dysfunction at day (D) 1

and 3. At D10 post LT, a more profound immune dysfunction was found in patients who died within 1 year post LT ($n = 8$) compared to survivors: respectively median mHLA-DR level 4900 AB/C [4200–8800] vs 15300 AB/C [10000–23000], $p = 0.002$; median NLR 31.7 [11.7–45.6] vs 6.9 [4.9–11.5], $p = 0.005$, median T cell count 260 cells/ μ L [190–340] vs 530 cells/ μ L [350–690], no difference of IFN γ release. Only post LT low mHLA-DR level (since D5, $p < 0.05$), and to a lesser extent high NLR were significantly associated with the occurrence of post LT high-risk infection (intra-abdominal infections, pneumonia, bacteremia). None of the immune markers were associated with liver graft rejection and no difference was found according to immune suppressive treatment.

Conclusion: This longitudinal study showed the early onset of a profound immune dysfunction post LT which is more severe for patients with poor outcomes. mHLA-DR level, NLR and T cell count at D10 differed significantly between 1-year survivors and patients with fatal outcome. The clinical relevance of mHLA-DR to monitor the risk of early post LT high risk infection and to adjust immune suppressive treatment will be assessed in further studies.

OS-023-YI

Liver transplantation due to biliary tract dysplasia in primary sclerosing cholangitis

Sigurd Breder^{1,2}, Christina Villard^{3,4}, Emma Eide¹, Benny Wang³, Lise Engesæter^{1,2,5,6}, Henrik Mikael Reims⁷, Johannes R. Hov^{1,2,5,6}, Espen Melum^{1,2,5,6,8}, Lars Aabakken^{1,9}, Pål Dag Line^{1,9}, Kristine Wiencke⁹, Annika Bergquist^{4,10}, Trine Følseraas^{1,2,6}. ¹Institute of Clinical Medicine, Faculty of Medicine, University of Oslo, Oslo, Norway; ²Norwegian PSC Research Center, Department of Transplantation Medicine, Oslo University Hospital Rikshospitalet, Oslo, Norway; ³Department of Transplantation Surgery, Karolinska University Hospital, Stockholm, Sweden; ⁴Department of Medicine Huddinge, Karolinska Institutet, Stockholm, Sweden; ⁵Research Institute of Internal Medicine, Oslo University Hospital, Oslo, Norway; ⁶Section of Gastroenterology, Department of Transplantation Medicine, Oslo University Hospital, Oslo, Norway; ⁷Department of Pathology, Oslo University Hospital, Rikshospitalet, Oslo, Norway; ⁸Hybrid Technology Hub Centre of Excellence, Institute of Basic Medical Sciences, Faculty of Medicine, University of Oslo, Oslo, Norway; ⁹Department of Transplantation Medicine, Division of Surgery, Inflammatory Medicine and Transplantation, Oslo University Hospital Rikshospitalet, Oslo, Norway; ¹⁰Department of Upper Abdominal Diseases, Karolinska University Hospital, Stockholm, Sweden
Email: sigurd.breder@medisin.uio.no

Background and aims: Primary sclerosing cholangitis (PSC) is a leading indication for liver transplantation (LTX) in the Nordic countries. Pre-emptive LTX in patients with biliary dysplasia to prevent development of cholangiocarcinoma (CCA) has been implemented but remains controversial. We aimed to perform a retrospective study of liver transplanted PSC patients in Oslo or Stockholm with a focus on the subgroup of patients with biliary dysplasia as main indication.

Method: PSC patients were identified using The Nordic Liver Transplant Registry (NLTR), the national PSC registries and data collected from medical records in Norway and Sweden. Patients who received their first LTX between January 1st 2000 and December 31st 2021 at an age ≥ 18 years at time of LTX were included. Clinical and biochemical status at time of listing, results of brush cytology and bile duct biopsies before listing and results of histopathological analyses of the explanted livers were registered. Brush cytology results were classified as reactive changes, low-grade dysplasia (LGD) or high-grade dysplasia (HGD).

Results: In total 512 PSC patients (76% male) were studied. Median age at PSC diagnosis was 33 years (IQR 25–44 years), and median age at first LTX was 45 years (IQR 36–65 years). Main indications for LTX were: LGD $n = 29$ (6%), HGD $n = 58$ (11%), suspicion of CCA $n = 42$ (8%), HCC $n = 25$ (5%), end-stage liver disease $n = 271$ (53%), recurrent

cholangitis/cholestasis symptoms $n = 64$ (13%) and combined indications $n = 23$ (4%). Before listing, $n = 54$ (11%) of the patients had at least one brush cytology sample with LGD and $n = 74$ (14%) with HGD. In patients with LGD as main transplant indication, biliary dysplasia was found in the explant in $n = 15$ (52%), out of which only 1 was HGD. Among those with HGD as main indication, dysplasia was found in the explant of $n = 36$ (62%), 19 of which classified as HGD. Cancer was found in $n = 2$ (7%) and $n = 9$ (16%) in the LGD and HGD groups, respectively. In 12 (41%) and 13 (22%) of the patients in the LGD and HGD groups, there were no signs of biliary neoplasia. CCA was found in 4 (2%) of the patients transplanted for end-stage PSC.

Conclusion: A large proportion (17%) of PSC patients were listed for LTx with biliary dysplasia as the main indication. Dysplasia or cancer were found in the majority of the liver explants with this indication. However, a substantial proportion of patients with LGD in brush cytology had no signs of neoplasia in the explanted liver, suggesting that the criteria for selecting candidates for LTx in the setting of dysplasia may be improved.

OS-024

The gender-equity model for liver allocation built on artificial intelligence (GEMA-AI) improves outcome predictions among liver transplant candidates

Manuel Rodríguez-Perálvarez¹, Antonio M. Gómez-Orellana², David Guijo-Rubio^{2,3}, Pedro Gutierrez², Avik Majumdar⁴, Geoff McCaughan⁵, Rhiannon Taylor⁶, César Hervás², Emmanuel Tsochatzis⁷. ¹Hospital Universitario Reina Sofía, University of Córdoba, Córdoba, Spain; ²Department of Computer Science and Numerical Analysis, University of Córdoba, Córdoba, Spain; ³Department of Signal Processing and Communications, University of Alcalá de Henares, Madrid, Spain; ⁴Victorian Liver Transplant Unit, Austin Health, Melbourne, Australia; ⁵Royal Prince Alfred Hospital, Sydney, Australia; ⁶NHS Blood and Transplant, Bristol, United Kingdom; ⁷Sheila Sherlock Liver Unit and UCL Institute for Liver and Digestive Health, Royal Free Hospital, London, United Kingdom
Email: ropeml@hotmail.com

Background and aims: Current prioritization models for liver transplantation (LT) are hampered by their linear nature, which does not fully capture the severity of patients with extreme analytical values. We aimed to develop and externally validate the Gender-Equity Model for Liver Allocation built on Artificial Intelligence (GEMA-AI) to predict waiting list outcomes in candidates for LT.

Method: Cohort study including adult patients who qualified for elective LT in the United Kingdom (2010–2020, model training and internal validation) and in two Australian institutions (1998–2020, external validation). The Gender-Equity Model for Liver Allocation corrected by serum sodium (GEMA-Na) was compared with GEMA-AI, which was built on a shallow artificial neural network optimized by neuroevolution and hybridization using the same input variables. The primary outcome was mortality or delisting for sickness within the first 90 days. Discrimination was assessed by Harrell's c-statistic (Hc). This study was funded by the Instituto de Salud Carlos III (Project no. PI22/00312) and co-funded by the European Union.

Results: The study population comprised 9,320 patients: training cohort $n = 5,762$, internal validation cohort $n = 1,920$, and external validation cohort $n = 1,638$. The prevalence of 90-days mortality or delisting for sickness ranged from 5.3% to 6% in the different cohorts. The transition from a linear to a non-linear score (from GEMA-Na to GEMA-AI) resulted in improved discrimination in the internal and external validation cohorts (Hc = 0.766 vs Hc = 0.781; $p = 0.035$ and Hc = 0.774 vs Hc = 0.793; $p = 0.003$, respectively), being these differences more pronounced in women (Hc = 0.802 vs Hc = 0.826; $p = 0.048$ and Hc = 0.796 vs Hc = 0.836; $p = 0.014$, respectively). Among 1,403 patients (39.4% of the merged validation cohorts) who showed at least one extreme analytical value, GEMA-AI had Hc = 0.823 compared to Hc = 0.797 ($p = 0.036$). In this subpopulation, GEMA-AI showed a good calibration (chi-square = 5.04; $p = 0.66$) whereas

GEMA-Na did not (chi-square = 18.94; $p = 0.015$). A meaningful change ≥ 2 score prioritization points occurred in 27.8% of patients (11.4% upgraded, 16.4% downgraded). Differential prioritization would occur in 6.4% of the available organs within the first 90 days and would save one in 59 deaths overall, and one in 13 deaths among women.

Conclusion: The use of non-linear explainable machine learning models may improve predictions of waiting list outcomes, particularly in the sickest patients showing extreme analytical values. Their use should be preferred over Cox's regression-based models.

Liver tumours: Experimental and Pathophysiology

OS-025-YI

Spatial single-cell profiling and network analysis reveal the immune architecture of hepatocellular carcinoma associated with immune checkpoint inhibitor therapy outcome

Henrike Salié¹, Lara Wischer¹, Ira Godbole¹, Patricia Otto-Mora¹, Juergen Beck¹, Antonio D'Alessio², Olaf Neumann³, Albrecht Stenzinger³, Andreas Blaumeiser⁴, Melanie Boerries⁴, Maike Hofmann¹, Robert Thimme¹, David J. Pinato², Thomas Longerich³, Bertram Bengsch^{1,5,6}. ¹University Medical Center Freiburg-Clinic for Internal Medicine II, Freiburg, Germany; ²Imperial College London, Department of Surgery and Cancer, London, United Kingdom; ³Heidelberg University Hospital, Institute of Pathology, Heidelberg, Germany; ⁴University Medical Center Freiburg, Institute of Medical Informatics and Systems Medicine, Freiburg, Germany; ⁵German Cancer Consortium (DKTK), Partner Site Freiburg, Germany; ⁶Signalling Research Centres BIOS and CIBSS, Freiburg, Germany
Email: bertram.bensch@uniklinik-freiburg.de

Background and aims: Hepatocellular carcinoma (HCC) is a heterogeneous entity with distinct subtypes treated with immune checkpoint inhibitor (ICI) therapy at an advanced stage. We hypothesized that the immune architecture in the tumor microenvironment (TME) determines response and survival of HCC patients under ICI therapy. We thus aimed to describe the immunotypes of the HCC TME on a spatially resolved, high-dimensional single-cell level to develop a classification that correlates with immunotherapy outcome.

Method: We applied highly multiplexed imaging mass cytometry (IMC) to a discovery cohort of tumors from $n = 54$ HCC patients. Tumor, interface and adjacent liver regions were analyzed in detail using an AI-aided bioinformatic pipeline for cell segmentation, high-dimensional single-cell clustering and neighborhood analysis with microanatomic region mapping to identify spatial immunotypes. The workflow was validated in an independent cohort of HCC patients that received ICI therapy ($n = 42$). Outcome analysis was performed based on spatial immunotype.

Results: Our approach identified several immune, stroma and tumor/hepatocyte clusters that reflect major cell types of the HCC and liver microenvironment. Unsupervised neighborhood detection based on spatial interaction of immune cells identified immune neighborhoods with distinct cellular networks: (1) CD8 T cell dominant, (2) myeloid cell dominant and (3) B/CD4 T cell dominant neighborhoods. The variation of the neighborhood architecture revealed three major spatial subtypes that could be classified based on T cell infiltration and tumor compartments. Their features conceptually resemble immune-deplete, immune-excluded and immune-rich TMEs. We identified the differential contribution of distinct immune subsets and immune checkpoints to spatial immune types. Analysis of the corresponding tumor interface regions showed clear differences between the intratumor stroma and the capsule and between spatial

ORAL PRESENTATIONS

immune types. These findings were validated in an independent cohort. Progression-free survival under ICI therapy differed significantly between the spatial immune types.

Conclusion: The spatial immunotypes identified describe the immune heterogeneity of the HCC tumor immune microenvironment on a spatially resolved level and represent potential pre-therapy biomarkers for ICI based therapies, with implications for the rational choice of treatment regimen.

OS-026-YI

Functional role of CD44⁺ cancer stem cells in intrahepatic cholangiocarcinoma

Paula Cantallops Vilà¹, Laura Sererols Viñas¹, Gemma Garcia Vicién¹, Sílvia Ariño¹, Carmen Cárcamo Giráldez¹, Laura Zanatto¹, Raquel A Martínez-García de la Torre¹, Li Chen², Giancarlo Castellano³, Miguel Torres Martín⁴, Robert F. Schwabe⁵, Daniela Sia⁶, Pau Sancho-Bru⁷, Silvia Affo¹. ¹Institut d'investigacions biomèdiques August Pi i Sunyer (IDIBAPS), Barcelona, Spain; ²PharmaNest, Inc, Princeton, NJ, United States; ³Institut d'Investigacions Biomèdiques August Pi i Sunyer (IDIBAPS), Barcelona, Spain; ⁴Clinical Genomics Research Group, Germans Trias i Pujol Research Institute (IGTP), Genetics Department, Germans Trias i Pujol University Hospital (HUGTIP), Barcelona, Spain; ⁵Department of Medicine, Columbia University, New York, NY, United States; ⁶Division of Liver Diseases, Department of Medicine, Tisch Cancer Institute, Icahn School of Medicine at Mount Sinai, New York, NY, United States; ⁷Institut d'investigacions Biomèdiques August Pi i Sunyer (IDIBAPS), Barcelona, Spain
Email: saffo@recerca.clinic.cat

Background and aims: Intrahepatic cholangiocarcinoma (iCCA) is the second most common primary liver tumor. With increasing incidence and poor survival, there is an urgent need to improve the treatment options for this deadly tumor. Cancer stem cell (CSC) markers are highly expressed in iCCA, however, the role of CSC and their crosstalk with the tumor microenvironment (TME) remain elusive. Here, we aim at investigating the functional role of CD44⁺CSC in iCCA.

Method: GSE154170 was used for scRNA-seq analysis. CD44 floxed mice were injected with AAV8-TBG-Cre (n = 5) or control AAV8-TBG-Null (n = 5) to induce CD44 deletion in tumor cells after iCCA induction by HDTVI of pCaggs-KRAS^{G12D}, CRISPR/Cas9 sg-p19 and SB13 plasmids (KRAS/p19). Samples were submitted to bulk RNA sequencing, followed by Gene Set Enrichment Analysis. FibroNestTM platform was used for single fiber analysis. Statistical Analysis was performed using GraphPad Prism 10.

Results: scRNA-seq and CellphoneDB analysis revealed the presence of CD44⁺CSC strongly interacting with the TME, in human and mouse iCCA. Quantifying CK19⁺CD44v6⁺ cells, we found that CD44⁺CSC constitute the 30% (33.84 ± 8.007) of the tumor cells in human iCCA (n = 3) and the 40% (43.32 ± 2.459) in the KRAS/p19 model (n = 5). After deleting CD44 in tumor cells *in vivo*, we confirmed the depletion by qPCR (p < 0.0001) and by CK19⁺CD44v6⁺ double staining (p = 0.0079). Despite not observing changes in the overall CK19⁺ tumor area (p = 0.8), we found a significant increase in tumor cells proliferation in the CD44-tumor cell deleted vs -non deleted mice, as assessed by double CK19⁺Ki67⁺ staining and quantification (p = 0.0015). In CD44-tumor cell deleted mice, we found increased stroma- (p = 0.024), myCAF- (p = 0.001) and epithelial-mesenchymal transition (EMT)- (p = 0.002) enrichment scores, when compared to the control group. We confirmed increased *Col1a1*- (p = 0.0017) gene expression and collagen deposition by PicroSirius Red (p = 0.048) in the tumors of CD44-tumor cell deleted mice. Moreover, using the AI-based platform FibroNestTM, we found changes in fiber morphometric composite score (p = 0.02) and complexity architecture score (p = 0.01), accompanied by enriched matrisome- (p = 0.001) and core collagen matrisome- (p = 0.024) scores in the CD44-tumor cell deleted vs -non deleted mice. Finally, we found increased immune-

(p = 0.002) and inflammatory stroma STIM class- (p = 0.001) enrichment scores, suggesting T cell exhaustion in the CD44-tumor cell deleted vs non deleted mice.

Conclusion: CD44⁺CSC are dispensable for iCCA initiation in the KRAS/p19 experimental model. Deletion of CD44⁺CSC increases tumor cell proliferation and induces drastic changes in the TME of iCCA. Our study defines a new functional role for CD44⁺CSC as regulator of tumor cell proliferation and as a mediator of collagens and EMT processes in iCCA, opening to new therapeutic opportunities.

OS-027-YI

Immune checkpoint profiles on circulating extracellular vesicles predict response to immunotherapy in hepatocellular carcinoma

Ramsha Masood¹, Gustav Buescher¹, Joao Gorgulho¹, Franziska Giehren¹, Francesca Pagani¹, Lorenz Kocheise¹, Vincent Jörg¹, Constantin Schmidt¹, Lorenz Adlung¹, Moritz Waldmann¹, Thomas Renne¹, Jenny Krause¹, Guido Sauter¹, Franz Ricklefs¹, Cecile Maire¹, Mohsin Shafiq¹, Ansgar W. Lohse¹, Samuel Huber¹, Henning Wege¹, Carolin Zimpel², Jens U. Marquardt², Bernhard Scheiner³, Lorenz Balcar³, Matthias Pinter³, Enrico de Toni⁴, Ignazio Piseddu⁵, Najib Ben Khaled⁴, Kornelius Schulze¹, Johann von Felden¹. ¹University Medical Center Hamburg-Eppendorf, Hamburg, Germany; ²University Hospital Schleswig-Holstein-Lübeck, Lübeck, Germany; ³Medical University of Vienna, Vienna, Austria; ⁴University Hospital, LMU Munich, Germany, Munich, Germany; ⁵University Hospital, LMU Munich, Germany, Munich, Germany
Email: r.masood@uke.de

Background and aims: Atezolizumab and bevacizumab (AB) is the new standard of care for advanced hepatocellular carcinoma (HCC). However, with only 30% objective response, predictive biomarkers are urgently needed. Tissue expression of PD-L1 is associated with better response (Zhu Nat Med 2023), but with limited access to tissue specimens, blood-based biomarkers would be preferable. The aim was to correlate immune checkpoint (IC) expression of tumor-derived circulating extracellular vesicles (EV) with response to AB.

Method: This multicenter study included 4 independent cohorts with 158 HCC patients with 414 sequential blood samples and 50 tissue specimens (2 more cohorts collected: analysis of another 104 patients and 284 samples pending). Tissue specimens were stained for PD-L1 and PD-1 (CTLA-4 pending). EV were extracted from serum using differential ultracentrifugation and quality control of isolates was performed using nanoparticle tracking analysis and electron microscopy. IC were quantified using bead-based multiplex immunoassays, normalized to total protein input, and presented as pg/μl.

Results: Membrane-bound IC were enriched in EV isolates compared to whole serum or EV-depleted serum, e.g. PD-L1: 20.17 vs. 1.3 vs. 1.79, PD-1: 9.27 vs. 1.82 vs. 1.31, CTLA-4: 1.79 vs. 0.06 vs. 0.075, all p < 0.01, (Cohort 1: n = 40 HCC across all stages). Secondly, we found a strong correlation of IC levels between tumor tissue and paired serum EVs (PD-L1: r = 0.80, PD-1: r = 0.82, both p < 0.001; Cohort 2, N = 50 HCC). In HCC patients receiving AB (Cohort 3, N = 49 HCC with 254 sequential samples), baseline EV-IC levels were higher in non-responders (NR) vs. responders (R) (PD-L1 20.57 vs. 18.01, p = 0.053, PD-1 21.85 vs. 18.14, CTLA-4 18.87 vs. 13.35 (both p < 0.01), while clinical parameters, such as age, sex, etiology, or BCLC stage did not differ. Sequential testing at week 6 and 12 revealed significantly different EV-IC dynamics with increase in NR (PD-L1: 52.35 and 59.32, PD-1: 32.48 and 42.63, CTLA-4: 26.22 and 32.01, all p < 0.001) and decrease in R (PD-L1: 6.64 and 1.66, PD-1: 6.06 and 1.94, CTLA-4: 7.82 and 2.90, all p < 0.001). Of note, absolute EV concentrations were not significantly different between timepoints. These findings were validated in an independent cohort of patients treated with AB (Cohort 4, N = 19 HCC with 70 sequential samples). In fact, defining optimal cutoffs for PD-L1, PD-1, and CTLA-4 at baseline in the training cohort 3 was able to predict responders with 63.2%, 89.5%, and 100% accuracy in the validation cohort 4.

Conclusion: Immune checkpoint levels on circulating extracellular vesicles from blood samples are able to predict response to atezolizumab and bevacizumab in two independent cohorts, both before initiation of therapy and based on early dynamics after initiation. Our results hold promise for the development of liquid biopsy-based biomarkers for treatment prediction in HCC.

OS-028

Tumour, immune and parenchymal cell neighbourhoods correlate with survival after cholangiocarcinoma resection

Johannes Eschrich^{1,2}, Zuzanna Kobus¹, Hilmar Berger¹, Yeni Ait Ahmed¹, Natalja Amiridze¹, Marlene Kohlhepp¹, Christian Müller³, Maria Reich³, Niklas Heucke³, Verena Keitel-Anselmino³, Frank Tacke¹, Adrien Guillot¹. ¹Charité University Medicine Berlin, Berlin, Germany; ²Berlin Institute of Health at Charité-Universitätsmedizin Berlin, Berlin, Germany; ³Otto-von-Guericke University Hospital Magdeburg, Magdeburg, Germany
Email: johannes.eschrich@charite.de

Background and aims: Intrahepatic cholangiocellular carcinoma (iCCA) is a malignancy that originates from the bile ducts and accounts for 10–15% of primary liver cancers, with an overall 5-year survival of less than 20%. The poor survival is explained by a late diagnosis, limited treatment options and poor understanding of the disease-relevant pathological mechanisms involved. This project aims at better defining the cellular landscape in iCCA and identifying prognosis-related histological features that could help in patient stratification, improving patient management and identifying relevant therapeutic targets.

Method: We assembled a cohort of >130 patients from multiple centres who underwent iCCA resection. Formalin-fixed paraffin embedded (FFPE) tissues were subjected to a tailored, multiplex (>15 markers) immunostaining protocol. Machine-learning based algorithms were used for digital image (>15 mm² tissue) segmentation and clinical data integration. Spatial clustering was performed using imcRtools-based algorithms to define cellular neighbourhoods (CN).

Results: In-depth characterisation of the individual immune, parenchymal and tumour cells, e.g., distribution, cellular shape or phenotypic marker staining intensities, was performed. In this context, we observed a strong accumulation of immune cells at the tumour border with macrophages particularly densely located adjacent to the tumour in normal tissue. CD45+ leucocytes and in particular CD20+ B cells were almost absent in the tumour area and their numbers increased towards normal liver tissue. Despite these solid observations, a poor correlation was found between single cell-resolved analyses and clinical data. Combined analyses of multiple cell populations identified cellular neighbourhoods (CN). The CN-based image segmentation successfully distinguished between tumour, parenchymal, tumour border, and portal areas, thus supporting the relevance of a multicellular-based digital image analysis. We comprehensively characterised cells and cell interactions on many levels and found several significant correlations between given CN and clinical data. In particular, a CN that encompasses a scattered CK7+ cell distribution and altered lymphoid and myeloid cell accumulation within 300 micrometres from the tumour border was associated with a poor prognosis.

Conclusion: Multiplexed immunohistochemistry together with advanced bioinformatics profoundly expand our horizon for disease-driving mechanism investigations. Within resected iCCA, the cellular landscape varies considerably between tumour, border and non-tumour regions, with a remarkable heterogeneity between patients. The exact cellular composition is associated with prognosis, suggesting that multiplex immunostaining may be suitable to guide personalized treatment decisions after surgery.

OS-029

Claudin-1 is a driver for cholangiocarcinoma by modulating cancer cell plasticity and fate

Zeina Nehme¹, Marion Muller^{1,2}, Emilie Crouchet¹, Frank Jühling¹, Julien Moehlin¹, Romain Desert¹, Fabio Del Zompo¹, Jade Brochon-Toiser¹, Natascha Roehlen¹, Christine Thumann¹, Patrick Pessaux^{1,3}, Emanuele Felli^{1,3}, Aina Venkatasamy⁴, Mihaela Onea^{5,6}, Roberto Iacone⁷, Markus Meyer⁷, Alberto Toso⁷, Nabeel Bardeesy⁸, Lipika Goyal⁹, Vikas Ranvir¹⁰, Mirian Fernández-Vaquero¹⁰, Mathias Heikenwälder^{10,11}, Tessa Ostyn¹², Tania Roskams¹², Patrice Laquerriere², Catherine Schuster¹, Laurent Maily¹, Thomas Baumert^{1,3,13,14}. ¹University of Strasbourg, Inserm, UMR_S1110, Institute of Translational Medicine and Liver Disease (ITM), Strasbourg, France; ²CNRS, Institut Pluridisciplinaire Hubert Curien UMR 7178, Strasbourg, France; ³Pôle Hépato-digestif, Strasbourg University Hospitals, Strasbourg, France; ⁴IHU Strasbourg, Institute of Image-Guided Surgery, Strasbourg, France; ⁵Department of Pathology, Strasbourg University Hospital, Strasbourg, France; ⁶Biological Resource Centre, Strasbourg University Hospitals, Strasbourg, France; ⁷Alentis Therapeutics, Allschwil, Switzerland; ⁸Center for Cancer Research, Massachusetts General Hospital, Harvard Medical School, Boston, MA, United States; ⁹Division of Oncology, Stanford School of Medicine, Palo Alto, CA, United States; ¹⁰Division of Chronic Inflammation and Cancer, German Cancer Research Center, Heidelberg, Germany; ¹¹M3 Research Institute, University of Tuebingen, Tuebingen, Germany; ¹²Department of Imaging and Pathology, University of Leuven, Leuven, Belgium; ¹³Gastroenterology and Liver Service, Strasbourg University Hospitals, Strasbourg, France; ¹⁴Institut Universitaire de France, Paris, France
Email: thomas.baumert@unistra.fr

Background and aims: Cholangiocarcinoma (CCA) is a hepatobiliary adenocarcinoma with dismal prognosis and unsatisfactory treatment options. Claudin-1 (CLDN1) is a transmembrane protein expressed in tight junctions, but also exposed at the cell surface on cancer epithelial cells. The functional role of CLDN1 in the pathogenesis of CCA is unknown. Here, we aimed to investigate the mechanisms by which CLDN1 drives cholangiocarcinogenesis and responds to treatment with target-specific monoclonal antibodies (mAbs).

Method: CLDN1 expression was studied in several cohorts of CCA patient tissues using scRNASeq and spatial transcriptomics. Gain-of-function studies in hydrodynamic tail vein injection (HTVi) mouse models were used to evaluate the role of CLDN1 as an oncogenic driver *in vivo*. Proof-of-concept (POC) studies using humanized CLDN1 mAbs in CDX and PDX mouse models as well as organoids were applied to understand the mechanism of action of antibody-mediated therapeutic intervention.

Results: Comprehensive analysis across several patient cohorts revealed robust CLDN1 upregulation at the transcriptional and protein level of CLDN1 exposed at the cancer cell surface. Spatial transcriptomics of patient CCA tissues revealed a robust association of CLDN1 expression with stemness, EMT and Wnt/beta-catenin, TNFalpha/NF-kB and YAP/Taz signaling. Gain-of-function studies in KRAS/p19 and AKT/YAP orthotopic HTVi models revealed a decrease in survival and enhanced tumor growth, unraveling a functional role of CLDN1 as an oncogenic driver. Mechanistic studies identified TNFalpha/NF-kB and Wnt/beta-catenin signaling as key signaling pathways mediating CLDN1 upregulation in intra- and extra-hepatic CCAs. Targeting exposed CLDN1 using CLDN1 mAbs in PDX and CDX models resulted in robust inhibition of proliferation, stemness and EMT by inhibiting Notch1, SRC-FAK, and Hippo-YAP signaling. Co-immunoprecipitation studies revealed an association of CLDN1 with drivers of cell plasticity and fate. Antibody-mediated inhibition of tumor growth was dependent on CLDN1 expression, observed also in CCA with low CLDN1 expression and a CCA model for lung metastasis. Treatment of patient-derived CCA organoids using mAbs decreased cellular viability and altered cancer cell plasticity and fate by similar pathways as in *in vivo* models.

Conclusion: Integrative spatial transcriptomic and mechanistic studies using CCA patient tissues and patient-derived models uncover CLDN1 as a previously undiscovered driver of cancer cell proliferation, plasticity, stemness and EMT. Robust target expression combined with completed in vivo proof-of-concept studies pave the way for the clinical development of CLDN1-specific mAbs for CCA treatment.

Viral hepatitis B/D: New treatments

OS-030

Efficacy and safety of xalnesiran with and without an immunomodulator in virologically suppressed participants with chronic hepatitis B: end of study results from the phase 2, randomized, controlled, adaptive, open-label platform study (PIRANGA)

Jinlin Hou¹, Qing Xie², Wenhong Zhang³, Rui Hua⁴, Hong Tang⁵, Edward J. Gane⁶, Luis Enrique Morano Amado⁷, Sheng-Shun Yang⁸, Cheng-Yuan Peng⁹, Man-Fung Yuen¹⁰, Xieer Liang¹, Cynthia Wat¹¹, Cong Cheng¹², Katerina Glavini¹³, Sudip Das¹⁴, Yan Huang¹², Farouk Chughlay¹³, Nelson Guerreiro¹³, Ethan Chen¹⁵, Priyanka Kakrana¹³, Avinash Patil¹⁶, Ruchi Upmanyu¹⁴, Maria Teresa Catanese¹³, Rémi Kazma¹³, Tarik Asselah¹⁷. ¹Nanfang Hospital, Southern Medical University, Guangzhou, China; ²Ruijin Hospital, Shanghai Jiaotong University School Of Medicine, Shanghai, China; ³Huashan Hospital, Fudan University, Shanghai, China; ⁴The First Hospital Of Jilin University, Jilin, China; ⁵West China Hospital, Sichuan University, Chengdu, China; ⁶Auckland Clinical Studies Limited, Auckland, New Zealand; ⁷Alvaro Cunqueiro University Hospital, Health Research Institute South Galicia, Vigo, Spain; ⁸Taichung Veterans General Hospital, Taichung, Taiwan; ⁹China Medical University Hospital, Taichung, Taiwan; ¹⁰Queen Mary Hospital, Hong Kong, China; ¹¹Former employee of Roche Products Ltd, Welwyn Garden City, United Kingdom; ¹²China Innovation Center of Roche, Shanghai, China; ¹³Roche Innovation Centre Basel, Basel, Switzerland; ¹⁴Roche Products Ltd, Welwyn Garden City, United Kingdom; ¹⁵Roche (China) Holding Ltd, Shanghai, China; ¹⁶Parexel International (External Business Partner with Roche Innovation Centre Basel), Hyderabad, India; ¹⁷Université de Paris-Cité, Hôpital Beaujon, INSERM UMR1149, Paris, France
Email: tarik.asselah@aphp.fr

Background and aims: PIRANGA (NCT04225715) is a phase 2 platform study designed to evaluate the efficacy and safety of new finite duration therapies in virologically suppressed chronic hepatitis B (CHB) participants (pts) treated with nucleos (t)ide analogues (NUC) aimed at achieving higher functional cure rates than NUC therapy alone. Here, we report end of study results, including seroconversion and durability of HBsAg loss, of xalnesiran (RO7445482), an N-acetylgalactosamine (GalNAc)-conjugated small interfering ribonucleic acid (siRNA) targeting HBsAg transcripts with or without an immunomodulator: ruzotolimod (toll-like receptor 7 agonist, RO7020531) or pegylated interferon alfa-2a (Peg-IFN- α).

Method: Virologically suppressed CHB pts on established NUC therapy for at least 12 months were randomized into one of 5 arms comprising: 1) xalnesiran 100 mg, 2) xalnesiran 200 mg, 3) xalnesiran 200 mg with ruzotolimod, 4) xalnesiran 200 mg with Peg-IFN- α , or 5) NUC control. Xalnesiran was administered subcutaneously (SC) every 4 weeks (wks) for 48 wks. Ruzotolimod 150 mg was administered orally every other day during 2 cycles of 12 wks each (wks 13 to 24 and 37 to 48). Peg-IFN- α 180 mcg was administered SC weekly for 48 wks. The established daily oral administration of NUC therapy was continued in pts from all arms for at least 48 wks and until NUC stopping criteria were met during the 48 wks of post-treatment follow-up. Stratified randomization aimed at recruiting at

least 12 pts per arm with screening HBsAg <1000 IU/ml. HBsAg loss (<0.05 IU/ml) and seroconversion (HBsAg loss and anti-HBsAb \geq 10 IU/L) rates were measured throughout the study.

Results: A total of 160 pts were enrolled. The majority were male (83%) and Asian (94%), with a mean (range) age of 42 (24–65) years. At baseline, 70% were HBeAg negative, 98% had normal ALT levels with a mean (SD) serum HBsAg level of 2.8 (0.9) log₁₀ IU/ml. At 48 wks post-EOT, HBsAg loss was observed in 3/30 (10.0%), 0/30 (0.0%), 4/34 (11.8%), 5/30 (16.7%), and 1/35 (2.9%) pts from arms 1 to 5, respectively. Of these 13 pts, 7 were off NUC therapy at 48 wks post-EOT and 9 had HBsAg seroconversion: 1, 0, 2, 5, and 1 pts from arms 1 to 5, respectively. The change in HBsAg loss between EOT and 48 wks post-EOT was +1 (+3.3%), –1 (–3.3%), –2 (–5.9%), –4 (–13.3%), and +1 (+2.9%) pts in arms 1 to 5, respectively. All pts who achieved HBsAg loss had a baseline HBsAg level <1000 IU/ml. No serious adverse events related to xalnesiran or ruzotolimod and no new safety findings were observed during the study.

Conclusion: The highest HBsAg loss and seroconversion rates were observed when xalnesiran was combined with an immunomodulator. The continued change in HBsAg loss rate between EOT and 48 wks post-EOT warrants adequate follow-up to confirm sustained functional cure. All treatments were generally safe and well tolerated.

OS-031

Imdusiran (AB-729) administered every 8 weeks for 24 weeks followed by the immunotherapeutic VTP-300 maintains lower HBV surface antigen levels in NA-suppressed CHB subjects than 24 weeks of imdusiran alone

Kosh Agarwal¹, Man-Fung Yuen², Stuart Roberts³, Gin-Ho Lo⁴, Chao-Wei Hsu⁵, Wan-Long Chuang⁶, Chi-Yi Chen⁷, Pei-Yuan Su⁸, Sam Galhenage⁹, Sheng-Shun Yang¹⁰, Emily P. Thi¹¹, Katie Anderson¹², Deana Antonello¹³, Elina Medvedeva¹³, Timothy Eley¹³, Tilly Varughese¹³, Louise Bussey¹², Charlotte Davis¹², Antonella Vardeu¹², Christine L. Espiritu¹¹, Sharie C Ganchua¹¹, Christina Iott¹¹, Elizabeth Eill¹¹, Tom Evans¹², Karen D Sims¹³. ¹King's College Hospital, London, United Kingdom; ²The University of Hong Kong, Queen Mary Hospital, Hong Kong, China; ³Alfred Health, Monash University, Melbourne, Australia; ⁴E-Da Hospital, Kaohsiung City, Taiwan; ⁵Chang Gung Memorial Hospital-Lin Kou, Chang Gung University College of Medicine, Taoyuan, Taiwan; ⁶Kaohsiung Medical University Hospital, Kaohsiung Medical University, Kaohsiung, Taiwan; ⁷Chia-Yi Christian Hospital, Ditmanson Medical Foundation, Chiayi City, Taiwan; ⁸Changhua Christian Hospital, Changhua, Taiwan; ⁹Fiona Stanley Hospital, Murdoch, Australia; ¹⁰Taichung Veterans General Hospital, Taichung, Taiwan; ¹¹Arbutus Biopharma, Research, Warminster, PA, United States; ¹²Barinthus Biotherapeutics, Harwell, United Kingdom; ¹³Arbutus Biopharma, Clinical Development, Warminster, PA, United States
Email: ksims@arbutusbio.com

Background and aims: Functional cure of CHB requires suppression of viral replication, reduction of HBsAg and stimulation of host HBV-specific immunity. Imdusiran (AB-729) is a GalNAc-conjugated single trigger siRNA that targets all HBV RNA transcripts and suppresses viral replication and all viral antigens. VTP-300 is an HBV-specific immunotherapeutic consisting of a chimpanzee adenoviral vector (ChAdOx1-HBV) dose and a Modified Vaccinia Ankara (MVA-HBV) dose both encoding the inactivated polymerase, core, and the entire S region from a consensus genotype C HBV virus. Study AB-729–202 is an ongoing, randomized, double-blinded Phase 2a study assessing the safety, pharmacodynamics and immunogenicity of repeat doses of imdusiran followed by VTP-300 \pm low dose nivolumab or placebo in nucleos (t)ide analogue (NA) suppressed, non-cirrhotic CHB subjects.

Method: Sixty-two CHB subjects on stable NA therapy with HBsAg \geq 100 but <5000 IU/ml were enrolled to receive imdusiran 60 mg every 8 weeks for 4 doses. The first 40 subjects were randomized 1:1 at Week (Wk) 24 to receive VTP-300 (Group A) or placebo (Group B) at

Wks 26 and 30. The remaining subjects (Group C) will receive VTP-300 plus 0.3 mg/kg nivolumab at Wk 30 only. Subjects were eligible for NA discontinuation (d/c) based on Wk 48/end of treatment (EOT) data (ALT <2× ULN, HBeAg negative, HBV DNA <lower limit of quantitation [LLOQ] and HBsAg <100 IU/ml). Safety data, HBV parameters and immunology samples were collected at multiple timepoints.

Results: Demographics and baseline characteristics were presented previously. To date 36/40 subjects have completed the VTP-300 or placebo regimen (Wk 30), and 25/40 have reached Wk 48/EOT. At EOT, 92% and 42% of Group A subjects (N = 13) have maintained HBsAg levels <100 IU/ml or <10 IU/ml respectively, vs 73% and 33% of Group B subjects (N = 12). At follow-up Wk 60 (N = 7/group), 100% and 57% of Group A subjects and 29% and 0% of Group B subjects have maintained these levels, respectively. Sixteen of 25 subjects met protocol eligibility criteria at Wk 48/EOT and stopped NA therapy: 11/13 (85%) in Group A vs 5/12 (42%) in Group B. One Group A subject has maintained HBV DNA <LLOQ for 6 months off NA therapy, 1 Group B subject restarted NA therapy after 3 months, the other 14 subjects remain off therapy at various durations of follow-up with no ALT flares. There have been no Serious Adverse Events (AEs), Grade 3 or 4 AEs or treatment d/c during the imdusiran/VTP-300 treatment periods.

Conclusion: Repeat dosing of imdusiran for 24 weeks followed by VTP-300 was well-tolerated and contributes to the maintenance of lower HBsAg levels compared to placebo in subjects who have reached EOT and follow-up Wk 60. More subjects who received VTP-300 have qualified to stop NA therapy at EOT and all remain off therapy. Additional on-treatment, follow-up and NA discontinuation data including HBV parameters and immunology data will be presented.

OS-032

Long-term hepatitis B surface antigen response after finite treatment with siRNAs ARC-520 or JNJ-3989

Lung Yi Loey Mak¹, Christine Wooddell², Oliver Lenz³, Thomas Schlupe², James Hamilton², Heather Davis³, Xianhua Mao¹, Wai-Kay Seto¹, Michael Biermer³, Man-Fung Yuen¹. ¹The University of Hong Kong, Hong Kong, Hong Kong; ²Arrowhead Pharmaceuticals, Madison, United States; ³Janssen Pharmaceutica NV, Beerse, Belgium
Email: loeymak@gmail.com

Background and aims: RNA interference has been extensively explored in patients with chronic hepatitis B (CHB) infection. We aimed to characterize the long-term efficacy of small interfering RNA (siRNA) on hepatitis B surface antigen (HBsAg) suppression.

Method: We prospectively followed up subjects with CHB who received short term siRNA treatment, either ARC-520 (4 injections in study HeparC-2002 [NCT02604199] and HeparC-2003 [NCT02604212]) or JNJ-3989 (3 injections in study AROHBV1001 [NCT NCT03365947]), in combination with nucleoside analogue (NUC) in our centre. Subjects enrolled included 15 receiving ARC-520, 38 receiving JNJ-3989 and 5 receiving placebo in previous clinical trials. Serial blood sampling was performed according to the original protocols and upon completion every 24 weeks until last follow-up (LFU; mean duration 52.5 ± 14.4 months). An integer scoring system was used to construct the model score for achieving qHBsAg <100 IU/ml at LFU according to the results of multivariate regression analysis.

Results: Among the 53 NUC+siRNA-treated subjects (mean age 46.8, baseline HBsAg 3.08 log₁₀ IU/ml, 5.7% <100 IU/ml, 83% previously on NUC, 34% HBeAg+), the proportion of patients achieving HBsAg seroclearance or <100 IU/ml at LFU was 1.9% and 31.2%, respectively, compared to 0% for both end points for placebo. The mean log₁₀ reductions of HBsAg at LFU in siRNA treated and non-treated subjects were 0.85 and 0.52 respectively (p = 0.123). When the two siRNAs were analysed separately, qHBsAg levels were numerically lower at LFU compared to placebo without reaching statistical significance (ARC-520 vs placebo at 72 months: 2.15 vs 2.52 log IU/ml, p = 0.503;

JNJ-3989 vs placebo at 60 months: 1.86 vs 2.63 log IU/ml, p = 0.368). Age was negatively correlated with log reduction of HBsAg at nadir (r = -0.406, p = 0.003) and LFU (r = -0.427, p = 0.001). Compared to placebo, siRNA led to faster annual decline rate of HBsAg (0.08 vs 0.21 log, respectively, p = 0.003). Baseline qHBsAg (OR 0.016, 95% CI 0.001–0.171) and log reduction in HBsAg at nadir (OR 16.979, 95% CI 3.131–92.083) were independently associated with HBsAg <100 IU/ml at LFU. Subjects with siRNA-100 score (derived from these two variables) of 0, 1, 2, 3 and ≥4 had 100%, 80%, 66.7%, 38.5%, and 0% probability of achieving HBsAg <100 IU/ml at LFU.

Conclusion: siRNA treatment suppressed HBsAg expression with a prolonged effect for up to 6 years. The siRNA-100 score consisting of baseline qHBsAg and log reduction at nadir may be indicative of HBsAg level <100 IU/ml at LFU.

OS-033

A phase 2 open-label study to evaluate safety, tolerability, efficacy, and pharmacodynamics of JNJ-73763989, nucleos(t)ide analogs, and a low-dose PD-1 inhibitor in patients with chronic hepatitis B-Interim results of the OCTOPUS-1 study

Tarik Asselah¹, Scott K. Fung², Sila Akhan³, Wan-Long Chuang⁴, Maria Buti⁵, Maurizia Brunetto⁶, Kosh Agarwal⁷, Camellia Diba⁸, John Jerzowski⁹, Thomas Kakuda¹⁰, Catherine Nalpas¹¹, Carine Guinard-Azadian¹¹, Thierry Verbinen⁸, Erkki Lathouwers⁸, An De Creus⁸, Oliver Lenz⁸, Michael Biermer⁸. ¹Université de Paris-Cité, INSERM UMR1149, Department of Hepatology, AP-HP Hôpital Beaujon, Clichy, France; ²Toronto General Hospital, Toronto Center for Liver Disease, Toronto, Canada; ³Department of Infectious Diseases and Clinical Microbiology, Kocaeli University Faculty of Medicine, Kocaeli, Turkey; ⁴Hepatobiliary Division, Department of Internal Medicine, Kaohsiung Medical University Hospital, Kaohsiung City, Taiwan; ⁵Hospital General Universitari Vall d'Hebron, Barcelona, Spain; ⁶Dept of Clinical and Experimental Medicine and Hepatology Unit, University of Pisa, Pisa, Italy; ⁷Institute of Liver Studies, King's College Hospital, London, United Kingdom; ⁸Janssen Research and Development, Beerse, Belgium; ⁹Janssen Research and Development, Trenton, United States; ¹⁰Janssen Research and Development, South San Francisco, United States; ¹¹Janssen Research and Development, Issy-les-Moulineaux, France
Email: tarik.asselah@aphp.fr

Background and aims: Treatment of chronic hepatitis B (CHB) with the small-interfering RNA (siRNA) JNJ-73763989 (JNJ-3989) and nucleos(t)ide analogs (NA) has shown reductions in hepatitis B viral markers. This study aims to assess the efficacy and safety of adding low-dose PD-1 inhibitor nivolumab to JNJ-3989 and NA once HBsAg levels are reduced.

Method: OCTOPUS-1 is a phase 2, randomized, open-label, parallel-group, multicenter study to evaluate safety, efficacy, and pharmacokinetics of JNJ-3989, nivolumab, and NA in hepatitis B e-antigen (HBeAg) negative, virologically suppressed (VS) CHB patients. Patients received daily NA, JNJ-3989 200 mg once a week for the first 4 weeks (loading dose), then once every 4 weeks until W24; nivolumab (0.3 mg/kg) was administered IV at W16 for Arm 1 (A1), and at W16, 20, and 24 for Arm 2 (A2) and follow-up with NA treatment is for 48 weeks. Primary end point is proportion of patients with HBsAg seroclearance (<0.05 IU/ml) at FU W24. Changes in viral markers (HBsAg, HBcrAg, and HBV DNA) and safety were assessed.

Results: At this W24 data snapshot, all patients have reached the end of treatment. Thirty-seven patients were enrolled, 18 in A1, 19 in A2, and received all doses of JNJ-3989. The protocol was amended and dosing of nivolumab was discontinued prior to the 3rd administration of the last two patients. The mean age (standard deviation: SD) was 44.38 years (7.38), 18.9% were female, 37.8% Asian. Mean (SD) baseline HBsAg levels were 3.25 (0.47) and 3.13 (0.54) in A1 and A2, respectively. Receptor occupancy 2 hrs post nivolumab administration at W16 was >90% in 29/35 (83%) of patients. At W24, mean HBsAg levels decreased by 2.0 (0.40) and 2.1 (0.58) log₁₀ IU/ml from

BL in A1 and A2 with HBsAg reduction $\geq 2 \log_{10}$ IU/ml in 58.8% and 55.6%, respectively. 88.2% and 35.3% in A1, 94.4% and 50.0% in A2 achieved HBsAg levels <100 and <10 IU/ml At W24 no patient achieved HBsAg seroclearance. No SAEs or grade 3 or 4 AEs were observed, and no patient discontinued the study prematurely. 48.6% of patients had TEAE, 13.3% were considered related to JNJ-3989 and 5.4% related to Nivolumab. JNJ-3989 loading dose led to mild increases of mean ALT from 23 U/L at BL to 35 U/L at W8 with no further increase until EOT, no patient met flare criteria. 2 cases of TSH suppression 8 weeks post nivolumab in A1 triggered the discontinuation of further nivolumab dosing, both cases resolved rapidly. No other immune-related events or cases of virologic breakthrough were observed.

Conclusion: After 24 weeks of treatment with JNJ-3989 + NA + nivolumab the mean decline of HBsAg from baseline was $2 \log_{10}$ IU/ml in both arms. Cross-study analysis of JNJ-3989 with VS, HBeAg-patients in REEF-1 did not show an apparent benefit of JNJ-3989 loading dose or nivolumab. Treatment was generally safe and well tolerated but administration of low-dose nivolumab in the study was terminated due to observed TSH suppression.

OS-034

Safety and efficacy of REP 2139-Mg in hepatitis D patients with advanced liver disease: an international compassionate use program

Christiane Stern¹, Marc Bourliere², Veronique Loustaud-Ratti³, Edouard Bardou-Jacquet⁴, Laurent Alric⁵, Lea Colombain⁶, Magdalena Meszaros⁷, Sophie Metivier⁸, Philippe Mathurin⁹, Cihan Yurdaydin¹⁰, Mathias Jachs¹¹, Thomas Reiberger¹¹, Giuseppina Brancaccio¹², David Yardeni¹³, Ohad Etzion¹³, Christoph Neumann-Haefelin¹⁴, Mark Douglas¹⁵, Sebastien Poulin¹⁶, Souad Benali², José Ursic Bedoya⁷, Olga Metin¹⁷, Michel Bazinet¹⁸, Michael Schwarz¹¹, Giovanni Battista Gaeta¹⁹, Alessandro Vitale²⁰, Valentina Svicher²¹, Umberto Cillo²², Segolene Brichler²³, Emmanuel Gordien²³, Stéphane Chevaliez²⁴, Andrew Vaillant¹⁸.

¹Centre Hospitalier de Versailles, Le Chesnay-Rocquencourt, France;

²Service Hépatogastro-Entérologie, Hôpital Saint-Joseph, Marseille, France;

³Service d'Hépatogastro-Entérologie, CHU de Limoges, Limoges, France;

⁴Service des Maladies du Foie, CHU de Rennes, Rennes, France;

⁵Service de médecine interne-maladies digestives, CHU Rangueil, Université Toulouse 3, Toulouse, France;

⁶Centre Hospitalier de Perpignan, Perpignan, France;

⁷CHU Montpellier, Montpellier, France;

⁸Service d'hépatologie, CHU Rangueil, Université Toulouse 3, Toulouse;

⁹Service des Maladies de l'appareil digestif et nutrition-Hépatologie, CHRU de Lille, Lille, France;

¹⁰Koç University Medical School, Department of Gastroenterology and Hepatology, Istanbul, Turkey;

¹¹Division of Gastroenterology and Hepatology, Department of Internal Medicine III, Medical University of Vienna, Vienna, Austria;

¹²Department of Molecular Medicine, Infectious Diseases Unit, University of Padua, Padua, Italy;

¹³Soroka Medical Center, Be'er Sheva, Israel;

¹⁴Faculty of Medicine, University of Freiburg, Freiburg, Germany;

¹⁵Westmead Hospital, Westmead, Australia;

¹⁶Clinique L' Agora, Montreal, Canada;

¹⁷Prof. Cemil Taşcıoğlu City Hospital, Department of Gastroenterology, Istanbul, Turkey;

¹⁸Replicor Inc., Montreal, Canada;

¹⁹Infectious Diseases, University L. Vanvitelli, Naples, Italy;

²⁰Department of Surgery, Oncology and Gastroenterology, University of Padua, Padua, Italy;

²¹Department of Biology, University of Rome Tor Vergata, Rome, Italy;

²²Department of Surgical and Gastroenterological Sciences, University of Padua, Padua, Italy;

²³Centre national de référence des hépatites B, C et Delta-Laboratoire associé, Hôpital Avicenne, Bobigny, France;

²⁴Service de Virologie, Hôpital Henri Mondor, Créteil, Créteil, France

Email: avallant@replicor.com

Background and aims: REP 2139 blocks HDV replication and HBV SVP assembly. This study evaluated the real-life safety and efficacy of REP 2139 in HDV patients with advanced liver disease in a compassionate use program (NCT05683548).

Method: Of 33 patients (21–69 y.o.), 24 failed previous pegIFN, 20 failed previous bulevirtide ± pegIFN (11 with viral rebound during therapy) and 1 failed lonarfarnib. NUC therapy continued in all patients during REP 2139-Mg (250 mg qW SC) scheduled for 48 weeks. PegIFN 45–180ug qW SC was added in 17 patients. Safety and liver function were monitored weekly and antiviral response every 4 weeks with standard assays for quantitative HBsAg and anti-HBs, HBV DNA, HDV RNA and HIV RNA (in 2 HIV co-infected patients).

Results: Among 33 patients, 21 had compensated and 6 decompensated cirrhosis. Currently, 29 and 6 patients received ≥ 24 and ≥ 48 weeks of therapy, respectively. No REP 2139-related SAE and no REP 2139 discontinuations occurred. REP 2139 was well tolerated with transient grade 1 injection site reaction in the majority of patients. ALT elevations occurred in 20 patients: 14 with pegIFN (1 requiring pegIFN dose reduction, 1 pegIFN discontinuation) and 6 without pegIFN. Non-response to REP 2139 250 mg SC was rescued with 250 mg IV infusion or 500 mg (SC or IV) in 8/33 patients.

Biochemical response was achieved in 10/33 (30%). HDV RNA decline $>2 \log$ occurred in 24/33 (73%) with HDV RNA negativity in 20/33 (61%). HBsAg decline $>2 \log$ occurred in 17/33 (52%) with HBsAg loss in 7/33 (21%). Anti-HBs >10 mIU/ml occurred in 9/33 (25%). Baseline HDV RNA ($p=0.42$) and HBsAg ($p=0.59$), and HDV RNA decline ($p=0.82$) and HDV RNA loss ($p=0.87$) during REP 2139-Mg were not different between +pegIFN and -pegIFN groups. A trend towards significantly higher HBsAg decline ($p=0.06$) was present in the +pegIFN group ($3.08 \pm 2.19 \log$ IU/ml) than in the -pegIFN group ($1.68 \pm 1.89 \log$ IU/ml). Four patients completed ≥ 48 weeks of REP 2139-Mg with follow-up available. Two patients (compensated cirrhosis, +pegIFN) maintained HDV RNA + HBsAg loss with seroconversion and normal ALT 36 weeks during TDF monotherapy. One achieved HDV cure and functional cure of HBV 14 months after cessation of therapy. One patient (decompensated cirrhosis, -pegIFN) recompensated during therapy and maintained undetectable HDV RNA and HBsAg and anti-HBs seroconversion with normal ALT 24 weeks after cessation of REP 2139-Mg and no longer requires liver transplant. REP 2139-Mg + pegIFN extension therapy in 1 patient (advanced fibrosis) was mistakenly halted at 67 weeks (HDV RNA $<LLOQ$ and HBsAg 4.07 IU/ml). After 12 weeks of TDF, HBsAg is 355 IU/ml, HDV RNA is 426 IU/ml with ALT 40 U/L.

Conclusion: REP 2139-Mg was safe and well tolerated in HDV patients with advanced liver disease and can lead to HDV cure and HBV functional cure. REP 2139-Mg treatment can lead to HDV cure independently of pegIFN, while HBV functional cure may be pegIFN dependent.

FRIDAY 07 JUNE

Cirrhosis and its complications: Clinical

OS-035-YI

Validating and expanding Baveno VII criteria of recompensation in patients with decompensated cirrhosis

Marta Tonon¹, Roberta Gagliardi¹, Gianluca Zilio¹, Simone Incicco¹, Valeria Calvino¹, Antonio Accetta¹, Nicola Zeni¹, Carmine Gambino¹, Anna Barone¹, Paolo Angeli¹, Salvatore Piano¹. ¹Unit of Internal Medicine and Hepatology, Department of Medicine, University of Padua, Padua, Italy

Email: salvatore.piano@unipd.it

Background and aims: Baveno-VII consensus defines recompensation in cirrhotic patients achieving: 1) removal/suppression of cirrhosis's etiology; 2) resolution of ascites (off diuretics), hepatic encephalopathy (off lactulose/rifaximin) and bleeding for >12

months; c) stable improvement of liver function. This study aims to evaluate the incidence and prognostic impact of recompensation in patients with decompensated cirrhosis.

Method: Outpatients with cirrhosis and curable etiologies (alcohol, HCV, HBV) were consecutively included and followed up (median time = 35 months). Demographic, clinical, laboratory and endoscopic data were collected at enrolment and follow-up visits. Recompensation, defined by Baveno VII criteria, was assessed. Since the withdrawal of decompensation treatment is subjective, we evaluated expanded recompensation criteria for patients meeting all criteria, but still on decompensation treatment (low dose diuretics/lactulose/rifaximin). Recompensation was used as a time-varying covariate in survival analysis. In 160 patients (62 compensated, 60 decompensated, 38 recompensated), plasma samples were analyzed for inflammatory cytokines (IL-6, IL-10, IL1beta).

Results: 691 patients were enrolled (mean age = 57 ± 11 years, men = 72.5%; alcohol = 55%). Among decompensated patients (n = 525), 298 achieved an effective etiological treatment and 22 (4.2%) achieved recompensation (Baveno-VII criteria), while 115 patients achieved expanded recompensation criteria (22.3%). MELD score was the only independent predictor of recompensation (aHR = 0.90; p = 0.002). In multivariable analysis (adjusted for age, sex, MELD, albumin, varices and further decompensation), mortality risk was not significantly different between patients achieving recompensation and compensated patients (aHR = 2.53; p = 0.107), while decompensated patients had the highest risk (aHR = 4.74; p < 0.001). Mortality risk was not significantly different between patients meeting expanded recompensation criteria and Baveno-VII criteria (HR = 1.02; p = 0.961). IL-6 and IL-10 were significantly higher in decompensated patients than in compensated ones. Following recompensation, inflammatory cytokines significantly decreased and no difference was found vs compensated patients.

Conclusion: Baveno-VII recompensation criteria identify cirrhotic patients with a good prognosis, comparable to that of compensated patients, but less than 5% of decompensated patients achieve recompensation. Expanding the recompensation criteria to include patients on medical treatment for decompensation identifies patients with a similarly low risk of mortality.

OS-036-YI

Diagnostic potential of speech artificial intelligence analysis in minimal hepatic encephalopathy

Jakub Gazda¹, Peter Drotar², Mate Hires², Sylvia Drazilova¹, Martin Janicko¹, Peter Jarčuška¹. ¹Pavol Jozef Safarik University, I. Pasteur University Hospital, Kosice, Slovakia; ²Technical University in Kosice, Kosice, Slovakia
Email: jkgazda@gmail.com

Background and aims: Hepatic encephalopathy (HE) is defined as cognitive impairment resulting from liver failure and can vary from clinically covert (minimal HE and West Haven I HE), through various degrees of clinically overt HE including hepatic coma. The treatment of HE involves removal of the precipitating factor, an osmotic laxative-lactulose-and a nonabsorbable antibiotic-rifaximin. The diagnosis of minimal HE requires the use of specific psychological tests, but these tests are time-consuming and are characterized by relatively low sensitivity and specificity, leading to underestimation of minimal HE in real world. The aim of this study was to identify the existence of any difference in the speech of patients with liver cirrhosis (with minimal HE and West Haven I HE) compared to a healthy control population, which could be used to diagnose minimal HE.

Method: Patients with known liver cirrhosis and varying degrees of HE (minimal HE diagnosed by STROOP test, West-Haven stage I HE) were included in this prospective study, with the main exclusion criteria being concomitant neurological disease, and an age- and sex-matched healthy control population. Patients' speech was then manually segmented, and concordant passages were compared

using neural networks and tree classifiers, with 10-fold cross-validation.

Results: A total of 62 patients were included in the study, 31 patients with liver cirrhosis (50%) and 31 healthy controls (50%), 36 patients were male (58%) 26 patients were female (42%). The mean age at the time of examination was 56.13 years (± 11.47). Ten patients with liver cirrhosis were diagnosed as West-Haven stage I HE (32%) and the remaining 21 patients as minimal HE (68%). Of the tree classifiers, the XGBoost classifier achieved the best AUROC values, with AUROC ranging from 66.88% (95% CI 58.75–72.4) to 78.6% (95% CI 72.4–82.7), depending on the vowel and its intensity. Of the neural networks, EfficientNet achieved the best AUROC values, with AUROC ranging from 80.65% (95% CI 72.34–88.92) to 88.64% (95% CI 83.28–93.70) depending on the vowel and its intensity.

Conclusion: Artificial intelligence (machine learning in general, and deep learning specifically) detected a difference in the speech of patients with liver cirrhosis (minimal HE and West Haven I HE) compared to a healthy control population, and there is hope that we can use it in the future to diagnose minimal HE.

OS-037

Comparison in epidemiology and outcomes of bacterial infections in patients with cirrhosis between university hospitals with and without liver transplant

Clàudia Torras¹, Juan Bañares², Aina Martí², Victor Acin³, Laura Pagès⁴, Laura Gutiérrez⁵, Antonio Casabell⁶, José Alberto Ferrusquía⁷, Jordi Sánchez⁷, Martina Pérez⁸, Diana Fuertes⁸, Marta García⁴, German Soriano⁹, Helena Masnou⁵, Alberto Amador⁴, Berta Cuyas³, Juan Manuel Pericàs¹⁰, Oriol Gasch¹¹, Cristina Solé⁷. ¹Gastroenterology and hepatology department. Parc Taulí university hospital. Institut d'investigació i innovació Parc Taulí (I3PT-CERCA). Universitat autònoma de Barcelona (UAB), Sabadell, Spain; ²Liver unit. Internal medicine department. Vall d'Hebron university hospital. Vall d'Hebron institut de recerca (VHIR). Vall d'Hebron Barcelona campus hospitalari, Barcelona, Spain; ³Gastroenterology and hepatology department. Hospital de la Santa Creu i Sant Pau. Institut de recerca. Universitat autònoma de Barcelona (UAB), Barcelona, Spain; ⁴Hepatology unit. Gastroenterology and hepatology department. Bellvitge university hospital. Universitat de Barcelona-IDIBELL, Hospitalet de Llobregat, Spain; ⁵Gastroenterology and hepatology department. Germans Trias i Pujol university hospital, Badalona, Spain; ⁶Microbiology department. Parc Taulí university hospital. Institut d'investigació i innovació Parc Taulí (I3PT-CERCA). Universitat autònoma de Barcelona (UAB), Sabadell, Spain; ⁷Gastroenterology and hepatology department. Parc Taulí university hospital. Institut d'investigació i innovació Parc Taulí (I3PT-CERCA). Universitat autònoma de Barcelona (UAB). CIBERehd, Sabadell, Spain; ⁸Research support unit. Parc Taulí university hospital. Institut d'investigació i innovació Parc Taulí (I3PT-CERCA). Universitat autònoma de Barcelona, Sabadell, Spain; ⁹Gastroenterology and hepatology department. Hospital de la Santa Creu i Sant Pau. Institut de recerca. Universitat autònoma de Barcelona (UAB). CIBERehd, Barcelona, Spain; ¹⁰Liver unit. Internal medicine department. Vall d'Hebron university hospital. Vall d'Hebron Institut de Recerca (VHIR). Vall d'Hebron Barcelona campus hospitalari. Universitat autònoma de Barcelona. CIBERehd, Barcelona, Spain; ¹¹Infectious diseases department. Parc Taulí university hospital. Institut d'investigació i innovació Parc Taulí (I3PT-CERCA). Universitat autònoma de Barcelona (UAB), Sabadell, Spain
Email: claudiatorrasv@gmail.com

Background and aims: The prevalence of infections caused by multidrug resistant (MDR) bacteria in patients with cirrhosis is increasing and varies across different regions and hospitals. We aimed to assess and compare the epidemiology, prevalence of MDR infections, and outcomes of bacterial infections in patients with decompensated cirrhosis admitted at five university hospitals, two with liver transplant (LT centers) and three without it (non-LT centers).

Method: We conducted a multicenter retrospective study including all patients with decompensated cirrhosis and bacterial infection that were discharged from the Hepatology Department from January 2021 to 2022. Clinical, laboratory, and microbiological data were collected. Patients were followed for 3 months, until death, or liver transplantation.

Results: A total of 576 infections were reported in 352 patients. LT centers had more nosocomial and healthcare-associated infections, as well as septic shock compared to non-LT centers, while there were no significant differences in cirrhosis severity, ACLF, or comorbidities. Both LT and non-LT centers had similar frequencies of the most common isolated microorganisms, *Escherichia coli* (15% vs. 17%) and *Klebsiella pneumoniae* (10% vs. 7%), and similar rates of negative cultures (42% vs. 37%). However, LT centers had significantly higher rates of extended-spectrum betalactamases (ESBL) (12% vs. 6%), carbapenemases (3% vs. 0%), and resistance to piperacillin-tazobactam (14% vs. 7%) compared to non-LT centers ($p < 0.02$). The most common infections were urinary tract infections (20% vs. 27%) and spontaneous bacterial peritonitis (13% vs. 22%) in both LT centers vs. non-LT centers, respectively ($p < 0.01$). The proportion of MDR infections tend to be higher in LT centers compared to non-LT centers (22% vs. 16%; $p = 0.10$). The proportion of MDR varied among different centers (from 10% to 25%; $p < 0.05$), in addition to resistance mechanisms and types of infections. In-hospital mortality was higher in LT centers compared to non-LT centers (20% vs. 11%; $p = 0.03$). Independent predictors of in-hospital mortality were age (OR of 1.1 [1.01–1.1]; $p = 0.02$), leukocytes (OR 1.1 [1.04–1.2]; $p < 0.01$), healthcare-associated infections (OR 3.4 [1.1–12]; $p = 0.04$), and ACLF (OR 5.8 [1.9–19]; $p = 0.01$).

Conclusion: Our study demonstrates significant differences in the epidemiology and prevalence of MDR infections among university hospitals, particularly between centers with and without liver transplant. Therefore, understanding the epidemiology of infections in each center is crucial for tailoring antibiotic treatment for these patients.

OS-038-1Y

Real-world practice patterns on the use of terlipressin in patients with cirrhosis and acute kidney injury-results from the ICA-GLOBAL AKI study

Ann Thu Ma¹, Adrià Juanola², Kavish Patidar^{3,4}, Anna Barone⁵, Simone Incicco⁵, Anand Kulkarni⁶, José Luis Pérez-Hernández⁷, Brian Wentworth⁸, Sumeet Asrani⁹, Carlo Alessandria¹⁰, Nadia Abdelaaty Abdelkader¹¹, Yu Jun Wong^{12,13}, Qing Xie¹⁴, Nikolaos T. Pyrsopoulos¹⁵, Sung-Eun Kim¹⁶, Yasser Fouad¹⁷, Aldo Torre¹⁸, Eira Cerdá Reyes¹⁹, Javier Díaz-Ferrer²⁰, Rakhi Maiwall²¹, Douglas Simonetto²², Maria Papp²³, Eric Orman²⁴, Giovanni Perricone²⁵, Cristina Solé²⁶, Christian M. Lange²⁷, Alberto Farias²⁸, Gustavo Pereira²⁹, Adrian Gadano³⁰, Paolo Caraceni^{31,32}, Thierry Thévenot³³, Nipun Verma³⁴, Jeong Han Kim³⁵, Julio D. Vorobioff³⁶, Jacqueline Cordova-Gallardo³⁷, Vladimir Ivashkin³⁸, Juan Pablo Roblero³⁹, Rael Maan⁴⁰, Claudio Toledo⁴¹, Oliviero Riggio⁴², Eduardo Fassio⁴³, Mónica Marino⁴⁴, Puria Nabilou⁴⁵, Victor Vargas⁴⁶, Manuela Merli⁴⁷, Luciana Lofego Gonçalves⁴⁸, Liane Rabinowich^{49,50}, Aleksander Krag^{51,52}, Lorenz Balcar⁵³, Pedro Montes⁵⁴, Angelo Z. Mattos⁵⁵, Tony Bruns⁵⁶, Abdulsemed Mohammed Nur⁵⁷, Wim Lecomte⁵⁸, Enrique Carrera Estupiñán⁵⁹, Maria Cecilia Cabrera⁶⁰, Marcos Giralá⁶¹, Hrishikesh Samant⁶², Sarah Raevens⁶³, Joao Madaleno⁶⁴, W. Ray Kim⁶⁵, Juan Pablo Arab⁶⁶, José Presa⁶⁷, Carlos Noronha Ferreira⁶⁸, Antonio Galante⁶⁹, Olivier Roux⁷⁰, Andrew S. Allegretti⁷¹, R. Bart Takkenberg⁷², Murat Harputluoglu⁷³, Sebastián Marciano⁷⁴, Shiv Kumar Sarin²¹, Pere Ginès², Paolo Angeli⁵, Elsa Solà⁶⁵, Salvatore Piano⁵. ¹University Health Network, Toronto, Canada; ²Hospital Clinic de Barcelona, Barcelona, Spain; ³Baylor College of Medicine, Houston, United States; ⁴Michael E. DeBakey Veterans Affairs Medical Center, Houston, United States; ⁵University of Padova, Padova, Italy; ⁶Asian institute of

gastroenterology hospital, Hyderabad, India; ⁷Hospital General de México "Dr. Eduardo Liceaga", Ciudad de Mexico, Mexico; ⁸University of Virginia, Charlottesville, United States; ⁹Baylor University Medical Center, Dallas, United States; ¹⁰A.O.U. Città della Salute e della Scienza di Torino, University of Turin, Turin, Italy; ¹¹Ain Shams University, Cairo, Egypt; ¹²Changi General Hospital, Singapore, Singapore; ¹³Duke-NUS Medical School, Singapore, Singapore; ¹⁴Ruijin Hospital, Shanghai, China; ¹⁵Rutgers-New Jersey Medical School, Newark, United States; ¹⁶Hallym University Sacred Heart Hospital, Hallym University College of Medicine, Anyang, Korea, Rep. of South; ¹⁷Minia University, Minia, Egypt; ¹⁸Medical Center ABC, Mexico City, Mexico; ¹⁹Military Hospital, Ciudad de Mexico, Mexico; ²⁰Hospital Edgardo Rebagliati-Clinica Internacional, Lima, Peru; ²¹Institute of Liver and Biliary Sciences, New Delhi, India; ²²Mayo Clinic, Rochester, United States; ²³University of Debrecen, Debrecen, Hungary; ²⁴Indiana University School of Medicine, Indianapolis, United States; ²⁵ASST Grande Ospedale Metropolitano Niguarda, Milan, Italy; ²⁶Parc Tauli Hospital Universitari, Barcelona, Spain; ²⁷LMU University Hospital Munich, Munich, Germany; ²⁸University of Sao Paulo, São Paulo, Brazil; ²⁹Bonsucesso Federal Hospital, Rio de Janeiro, Brazil; ³⁰Hospital Italiano de Buenos Aires, Buenos Aires, Argentina; ³¹University of Bologna, Bologna, Italy; ³²IRCSS Azienda Ospedaliero-Universitaria di Bologna, Bologna, Italy; ³³CHRU de Besançon, Besançon, France; ³⁴Postgraduate Institute of Medical Education and Research, Chandigarh, India; ³⁵Konkuk University School of Medicine, Seoul, Korea, Rep. of South; ³⁶University of Rosario Medical School, Rosario, Argentina; ³⁷Hospital General Dr Manuel Gea Gonzalez, Tlalpan, Mexico; ³⁸Sechenov First Moscow State Medical University, Moscow, Russian Federation; ³⁹Hospital Clínico Universidad de Chile, Santiago, Chile; ⁴⁰Erasmus University Medical Center, Rotterdam, Netherlands; ⁴¹Universidad Austral de Chile, Valdivia, Chile; ⁴²La Sapienza, University of Rome, Rome, Italy; ⁴³Hospital Nacional Prof. Alejandro Posadas, El Palomar, Buenos Aires, Argentina; ⁴⁴Carlos Bonorino Udaondo Hospital, Buenos Aires, Argentina; ⁴⁵Copenhagen University Hospital Hvidovre, Hvidovre, Denmark; ⁴⁶Hospital Vall d'Hebron, Barcelona, Spain; ⁴⁷Universita' degli Studi di Roma Sapienza, Roma, Italy; ⁴⁸University Hospital-Federal University of Espirito Santo, Vitória, Brazil; ⁴⁹Tel Aviv Sourasky Medical Center, Tel Aviv, Israel; ⁵⁰Tel Aviv University, Tel Aviv, Israel; ⁵¹Odense University Hospital, Odense, Denmark; ⁵²University of Southern Denmark, Odense, Denmark; ⁵³Medical University of Vienna, Vienna, Austria; ⁵⁴Hospital Nacional Daniel A. Carrion, Bellavista, Peru; ⁵⁵Federal University of Health Sciences of Porto Alegre, Porto Alegre, Brazil; ⁵⁶University Hospital RWTH Aachen, Aachen, Germany; ⁵⁷Addis Ababa University, Addis Ababa, Ethiopia; ⁵⁸University Hospitals Leuven, Leuven, Belgium; ⁵⁹Hospital Eugenio Espejo, Quito, Ecuador; ⁶⁰Guillermo Almenara Hospital, Lima, Peru; ⁶¹Universidad Nacional de Asunción, Asunción, Paraguay; ⁶²Ochsner Transplant Center, New Orleans, United States; ⁶³Ghent University Hospital, Ghent, Belgium; ⁶⁴Centro Hospitalar e Universitário de Coimbra, Coimbra, Portugal; ⁶⁵Stanford University School of Medicine, Stanford, United States; ⁶⁶Pontificia Universidad Católica de Chile, Santiago de Chile, Chile; ⁶⁷Trás-os-Montes e Alto Douro Hospital Centre, Vila Real, Portugal; ⁶⁸Hospital de Santa Maria-Centro Hospitalar Universitário Lisboa Norte, Lisboa, Portugal; ⁶⁹Ente Ospedaliero Cantonale and Università della Svizzera Italiana, Lugano, Switzerland; ⁷⁰Beaujon Hospital, Clichy, France; ⁷¹Massachusetts General Hospital, Boston, United States; ⁷²Amsterdam University Medical Centers, Amsterdam, Netherlands; ⁷³Inönü University School of Medicine, Elazığ, Turkey; ⁷⁴Hospital Italiano de Buenos Aires, Buenos Aires, Argentina Email: salvatore.piano@unipd.it

Background and aims: Terlipressin is indicated for the treatment of hepatorenal syndrome (HRS)-acute kidney injury (AKI). However, real-world practice patterns on the use of terlipressin in AKI in general has not previously been reported, and outcomes in non HRS-AKI settings are largely unknown.

Method: International prospective study including patients admitted to the hospital for decompensated cirrhosis at 67 centres in 5 continents from July 2022 to May 2023. This was a subgroup analysis

of patients with AKI who received terlipressin for the treatment of AKI, excluding those who received it for portal hypertension-related bleeding. Primary outcome was absence of AKI resolution, defined as return of serum creatinine to a value within 0.3 mg/dl of the baseline value. Secondary outcomes were respiratory failure, as defined by CLIF-C ACLF, and 28-day mortality. The incidence of respiratory failure was compared with that of patients treated with norepinephrine.

Results: Of 1,456 patients with cirrhosis and AKI, 243 (17%) received terlipressin for treatment of AKI. Most were from Europe (47%), Asia (27%) and Latin America (15%). Terlipressin was predominantly administered in continuous infusion form (75%), with a median maximum daily dose of 3 mg [IQR 2–4] and median duration of 5 days [IQR 3–8]. The AKI phenotype was HRS-AKI in 50%, acute tubular necrosis (ATN) in 17%, hypovolemia-induced in 25%, and others in 8%. Overall, complete AKI resolution occurred in 49% of patients. Lack of AKI resolution was highest in ATN (71%), followed by HRS-AKI (49%) and hypovolemia-induced (37%). On multivariable analysis (adjusted for age, sex, AKI stage, phenotype and acute on chronic liver failure grade [ACLF]), ATN was independently associated with a lack of AKI resolution (OR 2.77; $p = 0.016$), compared to HRS-AKI. AKI stage 3 and ACLF stages 2–3 were also associated to lack of AKI resolution. *De novo* respiratory failure occurred in 20% of patients of patients treated with terlipressin, a rate not higher than that observed in patients treated with norepinephrine (40%). There were no significant differences in amount of albumin or dose of terlipressin received in those who did and did not develop respiratory failure. On multivariable analysis, pneumonia (OR = 8.29; $p < 0.001$) or lack of volume loss/hypovolemia before AKI (OR = 2.70; $p = 0.029$) were independent predictors of respiratory failure. Mortality rate at 28-days was 36%. On multivariable analysis, age, ATN phenotype, ACLF grade and hospital-acquired AKI were independent predictors of 28-day mortality.

Conclusion: Terlipressin is often used for treatment of AKI outside its primary indication of HRS-AKI. AKI response is very poor in ATN. Therefore, terlipressin should be avoided in this setting as the risks associated with the treatment may outweigh its benefits. Respiratory failure is common, but does not seem to be driven by the amount of albumin received.

OS-039

A placebo controlled, randomized, double blinded trial to evaluate the use of Tolvaptan for correction of hyponatremia in liver cirrhosis patients

Zubair Mohamed¹, Arun Valsan², George Malayil³, Anna Paul², S Sudhindran⁴, Nipun Verma⁵, G Unnikrishnan⁶, Anoop Koshy¹, Dinesh Balakrishnan¹, Lakshmi Kumar¹, SaiBala Madathil⁷. ¹Amrita Institute of Medical Sciences, Kochi, Kochi, India; ²Amrita Institute of Medical Sciences, Kochi, Kochi, India; ³Rajagiri Hospital, Kochi, India; ⁴Amrita Institute of Medical Sciences, Kochi, Kochi, India; ⁵Post graduate Institute of Medical Education and research, Chandigarh, Chandigarh, India; ⁶Amrita Institute of Medical Sciences, Kochi, Kochi, India; ⁷Amrita Institute of Medical Sciences, Kochi, Kochi, India
Email: zubairumer@gmail.com

Background and aims: Patients with advanced cirrhosis develop dilutional hyponatremia (<130meq/dL) due to non-osmotic hypersecretion of arginine vasopressin (AVP). Hyponatremia is an independent risk factor for mortality. We undertook this study to ascertain the efficacy of tolvaptan in increasing serum sodium in cirrhosis with hyponatremia.

Method: In this single-centre placebo-controlled randomized double-blind study, all adult patients with established cirrhosis (imaging and/or biopsy) admitted to the hospital between August 2019 and June 2023 were screened. Exclusion criteria included age <18 years, pregnancy, serum creatinine >1.5 mg/dL 48 hours after admission, significant nervous system diseases. Consenting patients were enrolled into either Tolvaptan arm (15 mg orally once daily for 7 days) or the control arm (matched placebo) based on pre-prepared computer-generated randomization sequence. The medical

management of cirrhosis was left to clinicians' discretion. At any point, if there was absolute increase of $S Na^+ \geq 140$ mEq/L or daily increment ≥ 8 mEq/L, the drug was withheld temporarily. All adverse events were evaluated using the common terminology criteria for adverse events (CTCAE) version 5.0. (3) Descriptive statistics, Chi-square and student t-test were used to summarize and analyse categorical and continuous clinical variables respectively. We recruited 50 patients per group based on previous studies. The study received institutional ethics committee approval (IEC-AIMS-2019-ANES-082) and was registered in CTRI (CTRI/2019/10/021479). **Results:** Out of 2441 patients screened, 237 patients were eligible, of which 100 were recruited. No patient withdrew consent or was lost to follow-up. One patient in the tolvaptan group received only 1 dose of the medication and was removed from the final analysis. The results are presented in the following order: tolvaptan (T) and placebo (P). The mean age was $(57.3 \pm 8.5$ (T) and 55.3 ± 7.7 (P), $p < 0.05$) with a male: female ratio was 43:6 and 48:2, $p < 0.05$ respectively. The $S Na^+$ (mmol/L) at enrolment was 120.0 ± 4.2 (T) and 121.91 ± 2.4 (P), $p < 0.05$. The body weight, fluid intake, AST, bilirubin, total protein, urea, creatinine and MELD score were comparable between the groups at enrolment and at day 7. On day 7, $S Na^+$ (mmol/L) was 130.77 ± 5.4 (T) and 125.9 ± 4.8 (P) ($p = 0.004$). $S Na^+$ increased to at least 130meq/dL in 26/49 (T) (53%) versus 5/50 (P) (10%) patients. In the T group, the median time for $S Na^+$ to increase to 130 mg/dL was 4 days (range 2–8 days). The mortality was similar in both groups (22%, $p = 1$) (22%) ($p = 1$). $S Na^+$ increased ≥ 8 mmol/24 hours in 6/49 (12%) patients in the T group and 1/50 (2%) patient in the P group. None of the patients had serious adverse events.

Conclusion: Tolvaptan improved hyponatremia in 53% of cirrhotics and was safe. The optimal dose and duration of tolvaptan needs to be ascertained in larger randomized controlled trials.

Immune Experimental and rare diseases – Basic

OS-040-YI

Claudin-1 is a mediator and therapeutic target of biliary fibrosis by modulating liver progenitor cell fate and signaling

Fabio Del Zompo^{1,2}, Emilie Crouchet^{1,2}, Tessa Ostyn³, Frank Jühling^{1,2}, Julien Moehlin^{1,2}, Natascha Roehlen^{1,2}, Tallulah Andrews^{4,5}, Diana Nakib^{4,5}, Catia Perciani^{4,5}, Sai Chung^{4,5}, Gary L. Bader⁶, Ian McGilvray⁵, Sonya MacParland^{4,5}, Roberto Iacone⁷, Geoffrey Teixeira⁷, Mathias Heikenwälder^{8,9}, Olivier Govaere³, Tania Roskams³, Catherine Schuster^{1,2}, Laurent Maily^{1,2}, Thomas Baumert^{1,2,10,11}. ¹Inserm U1110, Institute of Translational Medicine and Liver Disease (ITM), Strasbourg, France; ²University of Strasbourg, Strasbourg, France; ³Department of Imaging and Pathology, KU Leuven and University Hospitals Leuven, Leuven, Belgium; ⁴Department of Immunology, University of Toronto, Toronto, Canada; ⁵Ajmera Transplant Center, University Health Network, Toronto, Canada; ⁶Donnelly Centre for Cellular and Biomolecular Research, Toronto, Canada; ⁷Alentis Therapeutics, Allschwil, Switzerland; ⁸Division of Chronic Inflammation and Cancer, German Cancer Research Center Heidelberg, Heidelberg, Germany; ⁹M3 Research Institute, Medical Faculty Tuebingen (MFT), Tuebingen, Germany; ¹⁰Institut Universitaire de France, Paris, France; ¹¹Center of Digestive and Liver Diseases, Strasbourg University Hospitals, Strasbourg, France
Email: thomas.baumert@unistra.fr

Background and aims: A key challenge in the clinical course of cholangiopathies is biliary fibrosis with subsequent complications of decompensated liver disease and cancer. We have previously unraveled Claudin-1 (CLDN1) exposed at the basolateral membrane of liver hepatocytes as a mediator and therapeutic target for metabolic dysfunction-associated steatohepatitis (MASH) fibrosis

ORAL PRESENTATIONS

(Roehlen et al. Science Transl. Med. 2022). Here, we aimed to investigate the mechanistic role of CLDN1 as a mediator and therapeutic target for biliary fibrosis using primary sclerosing cholangitis (PSC) as a model disease.

Method: CLDN1 expression in liver tissues of patients with primary sclerosing cholangitis progressing to fibrosis was analyzed using bulk and single cell RNAseq, multicolor immunofluorescence and spatial transcriptomics. Proof-of-concept studies using humanized CLDN1 monoclonal antibodies (mAbs) in mouse models for cholangiopathies and biliary fibrosis, the HepaRG progenitor cell model and primary human cholangiocytes were performed to understand the mechanism of action of antibody-mediated therapeutic intervention.

Results: Analyses of CLDN1 expression in PSC patient tissues identified diseased cholangiocytes, ductular reactive cells, and cholestatic peri-portal hepatocytes as cell-types with the highest CLDN1 expression. Spatial transcriptomics revealed that CLDN1 expression in PSC co-localized with PSC disease drivers at the periphery of scar lesions, including senescence marker p21 and the NFkB pathway. In bile duct ligation, 3, 5-diethoxycarbonyl-1, 4-dihydrocollidine (DDC) and multidrug resistance protein 2-knockout (*Mdr2*^{-/-}) mouse models, human CLDN1-specific mAbs robustly improved liver function by potentially reducing hepatobiliary fibrosis and cholestasis. Mechanistic studies in mouse and cell-based models revealed that mAb treatment resulted in inhibition of pro-inflammatory, pro-fibrotic and pro-carcinogenic signaling perturbed in liver tissues of PSC patients. Gene expression analyses in cell-based models unraveled antibody-mediated maturation of liver progenitor cells into hepatocyte-like cells.

Conclusion: Our results uncover a robust functional role of CLDN1 in the pathogenesis of PSC and biliary fibrosis. Completed in vivo proof-of-concept studies combined with expression analyses in PSC patients pave the way for the clinical development of CLDN1-specific mAb to treat PSC.

OS-041-YI

A spatiotemporal map of the hepatocyte proteome in alpha-1 antitrypsin deficiency by single-cell and visual proteomics

Florian Rosenberger¹, Katrine Thorhaug^{2,3}, Sophia Mädler¹, Malin Fromme⁴, Caroline Weiss¹, Marc Oeller¹, Sophia Steigerwald¹, Marvin Thielert¹, Thierry Nordmann¹, Sönke Detlefsen^{3,5}, Peter Boor⁶, Ondřej Fabián^{7,8}, Soňa Fraňková⁹, Aleksander Krag^{3,10,11}, Pavel Strnad¹², Matthias Mann^{1,13}. ¹Max Planck Institute of Biochemistry, Martinsried, Germany; ²Centre for Liver Research, Department of Gastroenterology and Hepatology, Odense, Denmark; ³Department of Clinical Research, Faculty of Health Sciences, University of Southern Denmark, Odense, Denmark; ⁴Department of Internal Medicine III and IZKF, Gastroenterology, Metabolic Diseases and Intensive Care, University Hospital Aachen, Aachen, Germany; ⁵Department of Pathology, Odense University Hospital, Odense, Denmark; ⁶Institute of Pathology, University Hospital Aachen, RWTH Aachen University, Aachen, Germany; ⁷Clinical and Transplant Pathology Centre, Institute for Clinical and Experimental Medicine, Prague, Czech Republic; ⁸Department of Pathology and Molecular Medicine, 3rd Faculty of Medicine, Charles University and Thomayer Hospital, Prague, Czech Republic; ⁹Department of Hepatogastroenterology, Institute for Clinical and Experimental Medicine, Prague, Czech Republic; ¹⁰Centre for Liver Research, Department of Gastroenterology and Hepatology, Odense University Hospital, Odense, Denmark; ¹¹Danish Institute of Advanced Study (DIAS), University of Southern Denmark, Odense, Denmark; ¹²Department of Internal Medicine III and IZKF, Gastroenterology, Metabolic Diseases and Intensive Care, University Hospital Aachen, Aachen, Germany; ¹³Novo Nordisk Foundation Center for Protein Research, Copenhagen, Denmark
Email: schober@biochem.mpg.de

Background and aims: Alpha-1 antitrypsin deficiency (AATD) is a genetic disorder affecting the structure of the alpha-1 antitrypsin (AAT) protein. Misfolded AAT accumulates in liver cells, causing

variable clinical outcomes, from no/mild liver fibrosis to cirrhosis requiring transplantation. The reasons for this heterogeneity are unclear, and understanding them could enhance risk-stratification and therapeutic interventions. Herein, we (1) identify proteomic signatures of hepatocytes accumulating AAT at various fibrosis stages, (2) map the spatial metabolic niches that drive hepatocyte stress response and (3) aim to define the toxicity of aggregates in relation to their morphology by neural network classifiers.

Method: We performed spatially resolved proteomics on formalin-fixed and paraffin-embedded (FFPE) liver tissues from Pi*ZZ individuals representing the full disease spectrum (F1–4; n = 33). Our Deep Visual Proteomics (DVP) method combined high-content imaging of three-micrometer-thick tissue sections, AI-based cell segmentation and classification, laser microdissection, and the latest generation of mass spectrometry using the Thermo Orbitrap Astral. We introduced a pseudo-time axis by separately measuring up to ten hepatocyte classes with neural network-defined AAT aggregate morphologies. In addition, we performed single-cell DVP in regions with aggregate-stressed and resilient hepatocytes in direct proximity.

Results: We quantified more than 5,000 proteins per sample (n = 134), each of which contained the protein mass of 10 to 15 complete hepatocytes. Fibrosis was the main driver of data separation followed by AAT load. Of all quantifiable proteins, 955 (16.2%) were significantly changed across hepatocytes with high loads to no loads of AAT within the same patient (paired *t* test after multiple testing correction, FDR <5%). We observed most changes among proteins that were produced in the ER and targeted for secretion. This included the structurally similar SERPINS A3 to A7, coagulation factors and albumin, as well as known AATD biomarkers LMAN1 and P4HB. Importantly, our data highlights a robust and late-stage unfolded protein response (UPR) involving all canonical UPR pathways, as well as the calnexin/calreticulin glycosylation rescue pathway. These changes triggered a strong ROS defense response unique to aggregate-positive hepatocytes, followed by a reduction in mitochondrial complex I activity.

Conclusion: We present the first detailed spatially resolved proteomic profile of hepatocytes in Pi*ZZ-homozygous AATD patients, identifying new proteins linked to disease progression and confirming known markers. Our single-cell proteomics approach reveals unique UPR and ROS defense responses in affected cells. This data allows precise tracking of hepatocyte changes during AAT accumulation, suggesting new therapeutic targets in AATD.

OS-042-YI

Metabolic reprogramming induced by pravastatin prevents polycystic liver disease progression improving mitochondrial bioenergetics in cystic cholangiocytes

Enara Markaide¹, Laura Izquierdo-Sánchez^{1,2,3}, Mikel Ruiz de Gauna⁴, Xabier Buque⁴, Pedro M Rodrigues^{1,2,5}, Rui E. Castro³, Matxus Perugorria^{1,2,6}, Luis Bujanda^{1,2,6}, Patricia Aspichueta^{2,4,7}, Jesus M Banales^{1,2,5,8}. ¹Department of Liver and Gastrointestinal Diseases, Biogipuzkoa Health Research Institute-Donostia University Hospital -, University of the Basque Country (UPV/EHU), San Sebastián, Spain; ²National Institute for the Study of Liver and Gastrointestinal Diseases (CIBERehd, "Instituto de Salud Carlos III"), Madrid, Spain; ³Research Institute for Medicines (iMed.Ulissboa), Faculty of Pharmacy, Universidade de Lisboa, Lisbon, Portugal; ⁴Department of Physiology, Faculty of Medicine and Nursing, University of the Basque Country (UPV/EHU), Leioa, Spain; ⁵IKERBASQUE, Basque Foundation for Science, Bilbao, Spain; ⁶Department of Medicine, Faculty of Medicine and Nursing, University of the Basque Country UPV/EHU, San Sebastián, Spain; ⁷Biobizkaia Health Research Institute, Barakaldo, Spain; ⁸Department of Biochemistry and Genetics, School of Sciences, University of Navarra, Pamplona, Spain
Email: enara.markaide@biodonostia.org

Background and aims: Polycystic liver diseases (PLDs) are hereditary genetic disorders marked by progressive development of intrahepatic

fluid-filled biliary cysts, representing a primary source of morbidity. The current pharmacological treatment for advanced disease involves the chronic administration of somatostatin analogs, aimed at reducing the elevated intracellular cAMP levels in cystic cholangiocytes. Nevertheless, this approach demonstrates limited effectiveness. Cystic cholangiocytes exhibit abnormal proteostasis and endoplasmic reticulum (ER) stress, promoting cystogenesis. Considering the interplay between ER and mitochondria, we investigated mitochondrial dynamics, bioenergetics, and metabolism within cystic cholangiocytes, further exploring their potential therapeutic regulatory value *in vitro* and *in vivo*.

Method: Human cystic cholangiocytes (ADPKD^{GANAB-/-} or ADPLD^{PRKCSH-/-}) and normal human cholangiocytes (NHC) as controls were studied. Mitochondrial ultrastructure and its interaction with the ER were analyzed by transmission electron microscopy. Mitochondrial mass, dynamics, and functionality were evaluated using flow cytometry and qPCR. Mitochondrial bioenergetic activity was assessed by Seahorse Analyzer, and protein levels of electron transport chain (ETC) complexes through immunoblotting. Metabolic fluxes including *de novo* synthesis and oxidation of palmitate, glucose, and glutamine were analyzed in radioassays. The effect of pravastatin was investigated in male PCK rats (Pkh1^{-/-}).

Results: Cystic cholangiocytes exhibited higher mitochondria-ER distance and increased mitochondrial mass. The expression of mitochondrial dynamics (*i.e.*, fusion, fission, and mitophagy) and biogenesis-related genes was found upregulated in cystic tissue and cells from PLD patients, compared to gallbladder tissue and NHCs, respectively. Cystic cells displayed higher mitochondrial membrane potential and abnormal bioenergetic capacities compared to NHCs. Consequently, ATP and mitochondrial reactive oxygen species levels were elevated in cystic cells, correlating with upregulation of ETC complexes. Both ADPKD and ADPLD cholangiocytes exhibited enhanced rates of glutamine and palmitate oxidation compared to NHCs, respectively, along with an increased capacity for the *de novo* synthesis of cholesterol. The chronic administration of pravastatin reduced liver volume and weight in PCK rats compared to controls. *In vitro*, pravastatin mitigated mitochondrial metabolic hyperactivity and decreased the proliferation of cystic cholangiocytes.

Conclusion: Cystic cholangiocytes exhibit altered mitochondrial dynamics, bioenergetics, and metabolism, with lipids playing a crucial role as energy substrate. Rewiring lipid metabolism with pravastatin halts hepatic cystogenesis, arising as a novel therapeutic opportunity.

OS-043

Site-specific maturation dynamics of type 2 conventional dendritic cells connect with gamma delta T17 effector differentiation in cholestatic liver disease

Stefan Thomann¹, Ankit Agrawal¹, Helene Hemmer¹, Sagar Sagar², Paul Kießling³, Emilia Scheidereit³, Tanja Poth⁴, Marcell Tóth⁵, Katja Breitkopf-Heinlein⁶, Nuh Rahbari⁷, Christoph Kuppe³, Dominic Grün¹. ¹University of Würzburg, Institute of Systems Immunology, Würzburg, Germany; ²University Hospital Freiburg, Department of Gastroenterology, Hepatology, Endocrinology and Infectious Diseases, Freiburg, Germany; ³University Hospital Aachen, Department of Nephrology and Clinical Immunology, Aachen, Germany; ⁴University Hospital Heidelberg, Center for Model System and Comparative Pathology, Heidelberg, Germany; ⁵University Hospital Heidelberg, Institute of Pathology, Heidelberg, Germany; ⁶Medical Faculty Mannheim, Department of Surgery, Mannheim, Germany; ⁷University Hospital Ulm, Department of Surgery, Ulm, Germany
Email: stefan.thomann@uni-wuerzburg.de

Background and aims: Immunoepithelial crosstalk, immunologic surveillance and niche composition at the biliary niche in cholestatic liver disease involves a complex interplay of diverse immune cell populations residing within portal fields. In this project, dynamical changes of type 2 conventional dendritic cells (cDC2) are linked with

the site-specific initiation of multicellular communication hubs that regulate the inflammatory response in liver cholestasis and in draining lymph nodes (LNs).

Method: Spatial transcriptomics and multicolour immunofluorescence (IF) were used to visualize the biliary niche in steady state. A liver and lymph-node 3, 5-diethoxycarbonyl-1, 4-dihydrocollidine (DDC) diet single-cell RNA-sequencing (scRNA-seq) atlas containing 5 disease timepoints was generated and data compared with publicly available scRNA-seq datasets of other disease modalities. Transcription factor regulon activity was predicted using SCENIC and genomic accessibility was investigated with combined snRNA-seq/snATAC-seq (10x Multiome). Different DC subtypes in hepatic LN were distinguished with the help of CITE-seq. Temporal cell type frequency dynamics were confirmed by FACS analysis and functional validation was performed using an inducible mouse model of cDC2 depletion as well as Tcrd and Il17a/f knockout mice.

Results: Visualization of the biliary niche revealed a spatial co-localization of biliary epithelial cells (BECs), cDC2 and T cells, which was conserved in mouse and human. Our DDC diet scRNA-seq atlas identified a disease-initiating Nfkb2-regulated, Sox9+ BEC cluster, which expressed a common gene expression programme that included Macrophage colony-stimulating factor 1 (Csf1), CC-chemokine ligand 2 (Ccl2) and Il23a. VarID2 predicted a cDC2 cell fate trajectory at disease onset connecting clusters of cDC2 maturation, homing and expression of Il17- inducing genes, while prolonged cholestasis resulted in a perturbed cDC2 differentiation and a cellular shift towards preDCs that were characterized by functional epigenetic restriction. Disease onset led to a gamma delta T cell (gdT cell) -specific Il17a-response, which was attenuated in an inducible model of cDC2-depletion. In draining LNs, gdT cell composition differed compared to the liver, yet T17 polarization could be equally observed.

Conclusion: Inflammatory onset in cholestatic liver disease initiates a multicellular crosstalk between BECs, cDC2, and gdT cells within the biliary niche. cDC2 rapidly mature and home to draining LNs thereby initiating site-specific T17 differentiation in tissue-specific gdT cell subsets.

OS-044-YI

Single-cell profiling of intrahepatic T cells uncovers expanded Th17/MAIT cells with overlapping gene expression in primary sclerosing cholangitis

Lisa R. V. Brynjulfsen^{1,2,3}, Markus S. Jördens^{1,2,3,4}, Jonas Øgaard^{1,2}, Grace Wootton^{5,6,7}, Tom Hemming Karlsen^{1,2,3,8}, Ye Htun Oo^{5,6,7}, Espen Melum^{1,2,3,8,9}, Brian K. Chung^{1,2,3}. ¹Norwegian PSC Research Center, Division of Surgery, Inflammatory Diseases and Transplantation, Oslo University Hospital, Rikshospitalet, Oslo, Norway; ²Research Institute of Internal Medicine, Division of Surgery, Inflammatory Diseases and Transplantation, Oslo University Hospital, Rikshospitalet, Oslo, Norway; ³Institute of Clinical Medicine, Faculty of Medicine, University of Oslo, Oslo, Norway; ⁴Department for Gastroenterology, Hepatology and Infectious Diseases, University Hospital Düsseldorf, Faculty of Medicine, Heinrich-Heine University Düsseldorf, Düsseldorf, Germany; ⁵University Hospitals Birmingham National Health Service Foundation Trust, Birmingham, United Kingdom; ⁶Center for Liver and Gastro Research, Institute of Immunology and Immunotherapy, University of Birmingham, Birmingham, United Kingdom; ⁷National Institute for Health Research Birmingham Biomedical Research Center, European Reference Network Rare-Liver Center, University Hospitals Birmingham National Health Service Foundation Trust and University of Birmingham, Birmingham, United Kingdom; ⁸Section of Gastroenterology, Department of Transplantation Medicine, Division of Surgery, Inflammatory Diseases and Transplantation, Oslo University Hospital, Rikshospitalet, Oslo, Norway; ⁹Hybrid Technology Hub-Centre of Excellence, Institute of Basic Medical Sciences, Faculty of Medicine, University of Oslo, Oslo, Norway
Email: l.r.v.brynjulfsen@medisin.uio.no

Background and aims: Robust HLA associations and lymphocytic infiltration in the liver are consistently reported in both primary sclerosing cholangitis (PSC) and primary biliary cholangitis (PBC) indicating a role for T cells in the pathogenesis of both diseases. To determine if PSC and PBC livers harbour unique T cells, we used single-cell RNA sequencing (scRNA-seq) to compare relative abundances and differential gene expression (DEG) of intrahepatic T cells from PSC, PBC and alcohol-related liver disease (ALD) controls.

Method: Intrahepatic T cells were enriched from 12 PSC, 9 PBC and 3 ALD explants by negative bead selection, sorted for viability and analyzed by 5' scRNA-seq (10X Genomics). Alignment and annotation of sequencing reads was performed using Cell Ranger. Cluster and DEG analysis were computed in Seurat 5 using DESeq2/Pseudobulk. Relative abundances of each cluster per disease were calculated from the median proportion of cells per cluster relative to total T cells per sample. Statistical significance for cluster abundances were determined using the Dunn's multiple comparison test; the Wald test corrected for multiple testing (Benjamini-Hochberg) was used for DEGs.

Results: ScRNA-seq of 42 575 intrahepatic T cells from PSC, PBC and ALD revealed 14 distinct clusters broadly defined by *CD4* (6 clusters), *CD8* (4 clusters) or lack of *CD4* and *CD8* (4 clusters). PSC livers showed a significant increase (PSC: 9.2%, PBC: 5.7%, ALD: 4.4%) in a unique cluster featuring high expression of T helper 17 (Th17) cell markers (*IL17A* and *RORC*) and mucosal-associated invariant T cell (MAIT) markers (*TRAV1-2* and *KLRB1*) compared to PBC ($p=0.016$) and ALD ($p=0.006$). By contrast, PBC livers did not show a significantly greater abundance of any T cell cluster in comparison to all diseases; *CD4*+ effector memory T cells were significantly increased compared to PSC ($p=0.029$) but similar in proportion to ALD (PBC: 12.2%, PSC: 8.7%, ALD: 9.6%). Increased numbers of *FOXP3*+ regulatory T cells were also observed in PSC ($p=0.038$) and PBC livers ($p=0.057$) versus ALD (PSC: 4.6%, PBC: 4.1%, ALD: 1.0%). As expected, DEG analysis showed that gene profiles of T cells in the same cluster were largely similar between diseases except for a 52-fold higher expression of *IL17A* in *CD4*+*TNF*+ effector T cells and 3.2-fold higher levels of *RORC* in *CD4*+ effector memory T cells in PSC livers compared to PBC ($p<0.05$).

Conclusion: We found that gene profiles of intrahepatic Th17 cells more closely resemble liver MAIT cells than other T cell types and a combined Th17/MAIT cell cluster was significantly enriched in PSC livers compared to PBC and ALD controls. This suggests that Th17 and MAIT cells phenotypes may elicit similar molecular pathways in diseased liver.

Liver immunology

OS-045

The combination of TCR-redirected CD4+ and CD8+ T cells in T cell therapy of HBV infection enhances virus control in vivo by increasing IFN- γ and TNF- α secretion

Sophia Schreiber¹, Sven Schreiner¹, Eva Loffredo-Verde¹, Anna D. Kosinska^{1,2}, Ulrike Protzer^{1,2}. ¹Institute of Virology, Technical University of Munich/Helmholtz Munich, Munich, Germany; ²German Center for Infection Research DZIF, Munich, Germany
Email: sophia.schreiber@tum.de

Background and aims: T cell therapy represents a promising therapeutic approach to treating chronic HBV infection and HBV-associated hepatocellular carcinoma. To date, most T cell therapies have focused on CD8+ cells as primary effector cells. Here, we investigate whether redirected HBV-specific CD4+ T cells support CD8+ T cells.

Method: We engrafted human and mouse CD8+ and CD4+ T cells with MHC I- or MHC II-restricted HBV-specific T cell receptors through

retroviral transduction. Human CD8+ and CD4+ T cells were co-cultured with antigen-presenting cells and HBV-positive target cells *in vitro*. In a humanized mouse model of chronic HBV infection expressing human MHC class I and class II, we explored the therapeutic potential of MHC I-restricted HBV surface-specific CD8+ T cells alone or in combination with MHC II-restricted HBV core-specific CD4+ T cells.

Results: Human HBV-specific MHC II-restricted CD4+ T cells enhanced CD8+-mediated cytokine secretion, proliferation, and killing in co-culture with antigen-presenting cells and HBV-positive target cells. Murine CD4+ T cells were successfully engrafted with HBV-specific MHC II-restricted TCRs and secreted IFN- γ and TNF- α upon encountering the target antigen. In a humanized mouse model that was chronically infected with AAV-HBV, both the transfer of CD8+ T cells alone or in combination with CD4+ T cells caused a significant decline of the virological markers HBeAg and HBsAg. In addition, in the combination group, virological markers declined more pronounced by 2 to 3 logs. Upon restimulation of CD8+ T cells isolated from the liver and spleen, cells derived from the combination group secreted higher amounts of IFN- γ and TNF- α . Liver damage was limited, with ALT levels peaking between days 15 and 22 and normalizing again afterward.

Conclusion: We hypothesize a positive helper effect of HBV-specific CD4+ T cells on HBV-specific CD8+ cells for adoptive T cell therapy of chronic HBV infection. This translates into enhanced cytokine secretion, proliferation and killing *in vitro* as well as a stronger antiviral effect *in vivo*.

OS-046

Features of regulatory T cells in primary biliary cholangitis

Naomi Richardson¹, Grace Wootton¹, Ye Htun Oo¹. ¹University of Birmingham, Birmingham, United Kingdom
Email: n.richardson@bham.ac.uk

Background and aims: Regulatory T cells (Treg) are critical components of a homeostatic immune system. In autoimmune diseases, these regulators are overpowered and are insufficient to maintain peripheral tolerance. In primary biliary cholangitis (PBC), inflammatory effector lymphocyte cells damage the intrahepatic bile ducts and cause ongoing biliary damage, eventually leading to liver fibrosis and cirrhosis. We set out to determine whether patients with PBC have defective regulatory T cells in blood and liver and whether Treg functionality has relevance to their disease progression.

Method: We used lymphocytes isolated from peripheral blood and explanted human liver tissue for flow cytometry, scRNAseq and spatial transcriptomic approaches and assessed localization of isolated cell subsets in the liver machine perfusion model system.

Results: We identified that patients with PBC disease have normal frequencies of regulatory T cells in the blood, and an elevated frequency of Treg in the diseased explant liver compared to non-autoimmune chronic liver disease controls (steatotic liver disease). PBC patient Treg also have normal expression of key functional markers CTLA-4, FoxP3 and CD39 which are key to their immunosuppressive capacity. PBC Treg can be readily expanded *in vitro* and used in suppression assays, displaying a similar suppressive capacity to Treg from healthy controls. Interestingly, we found 2 distinct subsets of patients-those with CD39high Treg and those with CD39low Treg. Liver Treg when infused into explant livers migrate and localize around biliary epithelium and our phenotyping data shows that these cells are enriched for biliary homing CCR6 and CXCR3. We identified that PBC liver is highly enriched for innate inflammatory cytokines IL-6 and IL-8 whilst also having low levels of IL-2 or IL-10. IL-6 promotes the generation of Th17 CD4+ T cells and Treg can be polarised to either Th1 or Th17 cells *in vitro*, indicating the propensity of patient cells to become inflammatory when faced with inflammatory milieu.

Conclusion: PBC patient Treg are not numerically deficient in peripheral blood or inflamed liver. PBC Treg also appear to be

functionally comparable to non-autoimmune liver disease patient and healthy controls in peripheral blood. This suggests that PBC Treg are not inherently defective. Their inability to control cholangitis is more likely due to a hostile microenvironment enriched with inflammatory mediators including IL-6. We believe there is a case for further investigation as to whether blocking IL-6 signalling could have therapeutic benefit in PBC.

OS-048

CD4⁺T cells license Kupffer cells to revert the CD8⁺T cell dysfunction induced by hepatocellular priming

Valentina Venzin¹, Cristian Beccaria¹, Valeria Fumagalli¹, Federica Moalli¹, Chiara Laura¹, Pietro Delfino¹, Leonardo Giustini², Elisa Bono², Chiara Perucchini², Marta Grillo¹, Keigo Kawashima¹, Pietro Di Lucia², Anna Celant¹, Sara De Palma², Giorgia De Simone¹, Elena Rodriguez Bovolenta¹, Luca Guidotti^{1,2}, Matteo Iannaccone^{1,2}.
¹Vita-Salute San Raffaele University, Milan, Italy; ²San Raffaele Scientific Institute, Milan, Italy
Email: venzin.valentina@hsr.it

Background and aims: Efficient priming of CD8⁺ T cell responses against non-cytolytic pathogens like HBV is believed to rely on CD4⁺ T cell help within secondary lymphoid organs, as the immunological dogma would dictate. This hypothesis is supported by an observation in experimentally infected chimpanzees, where CD4⁺ T cell depletion prior infection prevents CD8⁺ T cell priming and leads to persistent infection. However, where when and how this issue occurs has never been described or mechanistically elucidated.

Method: We took advantage of unique HBV transgenic mouse models, in which we have demonstrated that adoptive transferred HBV-specific CD8⁺ T cells that recognize hepatocellular viral antigens undergo activation and proliferation but fail to differentiate into antiviral effector cells. To understand the extent to which antigen-specific CD4⁺ T cells help intrahepatic CD8⁺ T cell differentiation, we generated HBV-specific CD4⁺ TCR transgenic mice (Env126), where all CD4⁺ T cells recognize an I-Ab-restricted T cell epitope of the HBV envelope protein.

Results: Here, we show that the adoptive transfer of Th1-like Env126 effector CD4⁺ T cells in HBV-transgenic mice counteracts the CD8⁺ T cell dysfunction induced by hepatocellular priming, boost their proliferation and stimulate their production of IFN γ , TNF α , and GranzymeB. This enhances CD8⁺ T cell-mediated liver immunopathology and suppresses HBV replication. Surprisingly, we found that dendritic cells are dispensable for the observed effect while on the contrary, Kupffer cells' (KCs) cross-presenting capacity is enhanced after adoptive transfer of Env126 effector CD4⁺ T cells. With multiphoton intravital microscopy we indeed revealed that HBV-specific CD4⁺ and CD8⁺ T cells simultaneously interact with individual KCs within the liver, and as such, the restorative process of Env126T effector CD4⁺ T cells help is impeded upon KCs depletion. Preliminary data show that the CD40-CD40L signaling pathway engagement could be key for Env126T cells-mediated KCs licensing.

Conclusion: Our findings underscore the crucial role of antigen-specific CD4⁺ T cells in mitigating the CD8⁺ T cell dysfunction induced by intrahepatic priming through the extra-lymphoid licensing of KCs, revealing a hitherto unexplored dynamic. Deciphering the molecular mechanism behind this effect could lead to the development of innovative immunotherapeutic strategies to eradicate chronic hepatic infections and their life-threatening complications.

OS-049-YI

The anti-tumour effector function of mucosal-associated invariant T cells against hepatocellular carcinoma is impaired by fatty acids and aberrant lipid metabolism

Sebastian Deschler¹, Junika Pohl¹, Lukas Ramsauer², Philippa Meiser², Robin P. Schenk¹, H. Carlo Maurer¹, Juliane Kager¹, Sophia Erlacher¹, Joseph Zink¹, Karyna Pistrenko¹, Enric Redondo Monte¹, Julius Weber¹, Fabian Geisler¹, Douglas Thorburn³, Gabriela M. Wiedemann¹, Karin Kleigrewe⁴, Carolin Mogler⁵, Jan P. Böttcher², Percy A. Knolle², Roland M. Schmid¹, Katrin Böttcher¹.
¹TUM School of Medicine and Health, University Medical Centre, Technical University of Munich, Munich, Germany; ²Institute of Molecular Immunology, School of Medicine and Health, Technical University of Munich, Munich, Germany; ³The Sheila Sherlock Liver Centre, Royal Free London NHS Foundation Trust, London, United Kingdom; ⁴Bavarian Centre for Biomolecular Mass Spectrometry, Technical University of Munich, Munich, Germany; ⁵Institute of Pathology, Technical University of Munich, Munich, Germany
Email: katrin.boettcher@mri.tum.de

Background and aims: Mucosal-associated invariant T (MAIT) cells, the most abundant innate-like T cell population in the liver, harbour anti-cancer potential. However, their effector function is impaired in hepatocellular carcinoma (HCC), a frequent cause of cancer-related deaths worldwide, for reasons that are incompletely understood. Here, we aim to decipher the mechanism by which MAIT cell effector function is impaired in the liver microenvironment. Therefore, we analysed how metabolic changes in metabolic dysfunction-associated steatotic liver disease (MASLD), a common precondition for HCC development, affect the phenotype and effector function of MAIT cells.

Method: MAIT cells from peripheral blood of MASLD patients or healthy controls were stimulated *ex vivo*, and MAIT cells from healthy controls were challenged with fatty acids during stimulation. MAIT cell phenotype and function was analysed by multi-colour flow cytometry, metabolism was investigated by metabolic flux analysis and gene expression by RNA sequencing.

Results: We show that MASLD MAIT cells express significantly higher levels of activation markers and effector cytokines *ex vivo*, suggesting MAIT cell activation in MASLD *in vivo*. However, upon *ex vivo* restimulation, these activated MAIT cells were dysfunctional and failed to produce effector cytokines, such as IFN γ , Granzyme B and TNF α . We further uncover a novel HCC tumour cell killing capacity of MAIT cells. Notably, culture with distinct fatty acid species characteristic of the MASLD microenvironment and accumulating in our MASLD patient cohort, impaired expression of effector cytokines by MAIT cells and abrogated their HCC cell killing capacity. Mechanistically, these effects were mediated by corrupted mitochondrial function, oxidative stress and aberrant lipid metabolism and could be rescued by treatment with redox regulators.

Conclusion: Taken together, we show that impairment of MAIT cell anti-tumour effector function against HCC is mediated by metabolic signals in the hepatic microenvironment in MASLD patients that induce oxidative stress and corrupt MAIT cell mitochondrial function. Our data provide novel mechanistic insight that could be harnessed to develop innovative strategies for MAIT cell-mediated anti-cancer immunity.

OS-050

Therapeutic vaccine (BR11-179) induced immune response associated with HBsAg reduction in a subset of chronic hepatitis B participants

Yun Ji¹, Nina Le Bert², Ariel Lee³, Chong Zhu⁴, Ying Tan⁴, Weihong Liu⁴, Jianxiang Lv⁴, Dong Li⁴, Haiyan Ma³, Xiaofei Chen⁴, Antonio Bertoletti², Qing Zhu¹. ¹Brii Biosciences Inc., Durham, United States; ²Programme in Emerging Infectious Diseases, Duke-NUS Medical School, Singapore, Singapore; ³Hyris/TCO limited, Singapore, Singapore; ⁴Brii Biosciences Co. Ltd., Beijing, China
Email: qing.zhu@briibio.com

Background and aims: BR11-179, a therapeutic vaccine consisting of 3 HBV surface antigens (PreS1, PreS2, and S), is safe and immunogenic when administered alone or in combination with an HBV-targeted small interfering RNA, BR11-835 (VIR-2218). In the study BR11-179-835-001, chronic hepatitis B (CHB) participants on nucleoside reverse transcriptase inhibitor (NRTI) therapy received 9 monthly doses of BR11-835 either alone or in combination with 9 monthly doses of BR11-179 with or without IFN α co-adjuvant. While there was no notable difference of HBsAg reduction at group levels, a heterogeneity of immunological response was detected in CHB participants achieving different HBsAg reduction. In selected participants from the BR11-179-835-001 study we evaluated whether different virological outcomes were associated with specific profiles of treatment-induced anti-HBs and T cell immune responses.

Method: Peripheral blood mononuclear cells (PBMCs) were collected from 49 participants at 6 time points, with an additional 2 time points collected for one participant during NRTI discontinuation. HBV-specific T cell response was analyzed both directly *ex vivo* (cytokine assay upon HBV-specific peptides stimulation of whole blood) or after *in vitro* expansion of PBMCs (ELISpot assays, T cell epitope mapping, intracellular cytokine staining) in selected participants with different levels of HBsAg reduction.

Results: Both anti-HBs and the HBsAg-specific T cell responses were significantly enhanced in the BR11-179 and BR11-835 combination groups compared to the BR11-835 alone group. In addition, HBsAg-specific T cell epitopes were only mappable in participants receiving BR11-179. A unique epitope region adjacent to the NTCP binding site was identified in those participants with high HBsAg reduction (approximately greater than 2log). In contrast, discrete or non-identifiable epitope regions were mapped in those with lower HBsAg reduction relative to the mean HBsAg reduction induced by siRNA. A Th1 cytokine secretion profile upon HBV-specific peptides stimulation was also detected in participants with high HBsAg reduction. These features, as well as the long-term persistence of HBV-specific T cells, were pronounced in the participant who reached HBsAg loss and met NrtI discontinuation criteria.

Conclusion: Therapeutic vaccine BR11-179, in combination with siRNA BR11-835, induced substantial HBV-specific B and T responses in certain CHB participants. The unique immune response pattern observed in these participants receiving combination therapy, and their correlation with the reduction of HBsAg levels among these evaluable participants, suggests that T cells induced by BR11-179 may play a role in reducing HBsAg and controlling HBV. Assessing the neutralizing efficacy of anti-HBs in selected serum against different HBV genotype viruses is currently ongoing.

MASLD: Clinical aspects

OS-047-YI

Prediction of the risk of liver related events with non-invasive models is better than liver biopsy in MASLD cACLD patients

Laia Aceituno^{1,2,3}, Juan Banares¹, Grazia Pennisi⁴, Adele Tulo⁴, Monica Pons^{1,2,5}, Juan Manuel Pericàs^{1,2,5}, Salvatore Petta⁴, Juan G Abraldes⁶, Joan Genesca^{1,2,5}. ¹Liver Unit, Digestive Diseases Division, Vall d'Hebron University Hospital, Barcelona, Spain; ²Vall d'Hebron Institute of Research (VHIR), Vall d'Hebron Barcelona Hospital Campus, Universitat Autònoma de Barcelona, Barcelona, Spain; ³Multi-Organ Transplant, Ajmera Transplant Centre, University Health Network, Toronto, Canada; ⁴Section of Gastroenterology, PROMISE, University of Palermo, Palermo, Italy; ⁵Centro de Investigación Biomédica en Red de Enfermedades Hepáticas y Digestivas (CIBERehd), Instituto de Salud Carlos III, Madrid, Spain; ⁶Liver Unit, Division of Gastroenterology, University of Alberta, Edmonton, Canada
Email: laiaaceituno@gmail.com

Background and aims: Metabolic dysfunction-associated steatotic liver disease (MASLD) is a leading cause of chronic liver disease. Liver biopsy is considered the gold standard for risk stratification. Non-invasive models have been validated to predict clinically significant portal hypertension (CSPH), a major determinant of decompensation. The ANTICIPATE-NASH model uses liver stiffness measurement (LSM), BMI and platelet count to predict the presence of CSPH in MASLD. We recently showed that this model can be used for individualized risk prediction of liver-related events (LRE) in MASLD. This study aimed at evaluating if liver biopsy data improves the prediction of LREs compared to the ANTICIPATE-NASH model alone in MASLD patients with compensated advanced chronic liver disease (cACLD).

Method: European retrospective multicenter cohort study of patients with biopsy-proven F3-F4 MASLD with baseline data and follow-up incidence of LRE (composite event of decompensation, HCC, transplantation, or liver-related death). We estimated the CSPH/LRE risk distribution based on the ANTICIPATE-NASH model. We tested the added value of histology to the risk prediction provided by the ANTICIPATE-NASH model with Cox regression.

Results: 699 patients were included, 52% were male, median age was 60 years (54.3–65.6), and median BMI was 31 kg/m² (27.8–34.5). 324 (46.4%) patients had F3 and 375 (53.6%) F4. Median follow-up was 42.8 months (18.9–66.6). During follow-up, 56 (8.0%) patients developed LRE. F4 patients had significantly higher median LSM (22.6 vs. 15.8 kPa), LRE rates (13.6% vs 1.5%), and CSPH probability estimated by the ANTICIPATE-NASH model (26.9% vs. 18.3%) than F3 patients (all p values <0.001). The ANTICIPATE-NASH model had a higher discrimination (c-statistic 0.93) for LRE compared to histology (0.67). Calibration was excellent. Adding histology to the model did not improve prediction accuracy. Using an ANTICIPATE-NASH model cutoff of 0.25 (which is associated with a pointwise 1.6% estimated 3-year risk of LREs), a substantial difference was observed in LRE rates: 0.98% in <0.25 vs. 18.5% in ≥ 0.25 (p < 0.001); 61% and 39% of the patients were below and above the 0.25 risk threshold of CSPH. This dichotomization provided better separation of the risk of LRE than the F3/F4 classification. Indeed, all LRE occurring in F3 patients (5/68) occurred in patients with an ANTICIPATE-NASH threshold ≥ 0.25 . Similarly, 30% of F4 patients presented a CSPH risk <12% (median value for F3 patients) with no LREs.

Conclusion: The non-invasive ANTICIPATE-NASH model, based on LSM, BMI and platelet count, has better accuracy than histology for LRE prediction in MASLD. Histology does not refine the risk prediction provided by the model.

OS-051

Association between advanced fibrosis and NASH-CRN activity score (NAS) components: combined data from multiple therapeutic trials including more than 10, 000 patients

Stephen A. Harrison¹, Julie Dubourg², Mazen Nouredin³, Naim Alkhouri⁴, Jörn M Schattenberg⁵, Sophie Jeannin⁶, Vlad Ratziu⁷, Michael Charlton⁸. ¹Radcliffe Department of Medicine, University of Oxford, Oxford, United Kingdom; ²Summit Clinical Research, San Antonio, United States; ³Houston Research Institute, Houston, United States; ⁴Arizona Liver Health, Phoenix, United States; ⁵Saarland University Medical Center, Homburg, Germany; ⁶Summit Clinical Research, San Antonio, United States; ⁷Sorbonne Université, Institute for Cardiometabolism and Nutrition, Hospital Pitié-Salpêtrière, INSERM UMRs 1138 CRC, Paris, France; ⁸University of Chicago, Chicago, United States
Email: jdubourg@summitclinicalresearch.com

Background and aims: The association of advanced fibrosis and severity of metabolic dysfunction-associated steatohepatitis (MASH) have been previously described. We aimed to assess the association between NAS, NAS components and advanced fibrosis.

Method: We combined screening data from 10 industry-funded MASH phase 2 trials. We performed univariate and multivariate logistic regression analyses to assess the association between NAS, NAS components and advanced fibrosis, as defined as fibrosis stages 3 or 4. We developed a modified version of the NAS, namely "lean NAS" (=inflammation grade + ballooning grade, excluding steatosis) to predict the presence of advanced fibrosis.

Results: 4, 117 patients with centrally assessed liver biopsy were included. The prevalence of advanced fibrosis in this population was 36%. In univariate analysis, higher NAS, hepatocyte ballooning and lobular inflammation were associated with advanced fibrosis. Advanced fibrosis was observed in 27%, 19%, 19%, 25%, 34%, 47%, 55%, 66%, and 57% of patients with NAS 0 to 8, respectively. The odds of advanced fibrosis was significantly increased in patients with a NAS of 5 or more ($p < 0.0001$). Advanced fibrosis was observed in 15%, 29%, 51% and 71% in patients with inflammation grade 0 to 3, respectively. The odds of advanced fibrosis was 3.4 (95% CI: 2.8–4.0) in the presence of inflammation ($p < 0.0001$). Advanced fibrosis was observed in 15%, 37% and 66% in patients with ballooning grade 0 to 2, respectively. The odds of advanced fibrosis was 5.9 (95% CI: 5.0–6.9) in the presence of ballooning ($p < 0.0001$). Advanced fibrosis was observed in 39%, 39%, 36% and 32% in patients with steatosis grade 0 to 3, respectively. The odds of advanced fibrosis was lower in patients with steatosis grade 3 ($p = 0.048$). In a model including the "lean NAS" and steatosis grade, the presence of high degree of inflammation (grade 3) and ballooning (grade 2) was associated with a 32x greater odds (95% CI: 16.8–62.1) for the presence of advanced fibrosis. Inversely, the presence of steatosis grades 1, 2 or 3 were associated with lower probability of advanced fibrosis: odds ratio of 0.45 (95% CI: 0.31 – 0.66), 0.28 (95% CI: 0.19–0.40), and 0.20 (95% CI: 0.13–0.29), respectively.

Conclusion: Advanced fibrosis is strongly associated with the presence and severity of hepatocyte ballooning and to a lesser extent with the presence and severity of inflammation, independently of the NAS. A modified NAS, namely "lean NAS" can predict the presence of advanced fibrosis, and the severity of steatosis is inversely correlated with the severity of fibrosis.

OS-052

Characteristics and risk of major adverse liver outcomes and major cardiovascular events among swedish patients with diagnosed and high risk of metabolic dysfunction-associated steatohepatitis-a REVEAL-MASH study

Emilie Toresson Grip^{1,2}, Nikolas Scheffer Apecechea³, Ron Basuroy³, Pierre Johansen³, Kamal Kant Mangla³, Helena Skräder², Hannes Hagström⁴. ¹Karolinska Institutet, Stockholm, Sweden; ²Quantify Research, Stockholm, Sweden; ³Novo Nordisk A/S, Denmark,

Copenhagen, Denmark; ⁴Karolinska Institutet, Stockholm, Sweden
Email: emilie.toresson-grip@quantifyresearch.com

Background and aims: Metabolic dysfunction-associated steatohepatitis (MASH) is significantly under-diagnosed and requires liver biopsy. The Fibrotic NASH Index (FNI) is a validated risk score to classify patients at risk of MASH with fibrosis stage ≥ 2 . We used the FNI to characterize patients at risk and to compare the incidence of major adverse liver outcomes (MALO) and major adverse cardiovascular events (MACE) between risk groups.

Method: This cohort study is based on Swedish registry data from 1998–2022, including lab data for patients with ≥ 1 liver-related test in routine clinical care in Stockholm 2001–2020. Patients were classified as high risk if they had $\text{FNI} \geq 0.33$ and a cardiometabolic risk factor (overweight/obesity, type 2 diabetes (T2D), hypertension or dyslipidemia), or low-risk ($\text{FNI} < 0.1 \pm$ cardiometabolic risk factors). Diagnosed patients had a recorded ICD-10 code for MASH (K75.8) in specialist care. Patients with other liver diseases were excluded. All patients were followed from first diagnosis or FNI score.

Results: The FNI score was calculated for 154, 179 patients, of which 47, 154 were considered at high risk of MASH (31%) and 57, 609 at low risk of MASH (37%). Diagnosed patients ($n = 485$ in the register) were younger (median 63 years), included more females (52%) and less commonly had T2D (48%), than patients at high risk (median 66 years, 28% females and 59% with T2D, p for all comparisons < 0.001). Patients at low risk were about the same age as diagnosed (median 62 years, $p > 0.05$) but included more females (65%) and less commonly had T2D (7%; p for all comparisons < 0.01) than both diagnosed and high-risk patients. Diagnosed patients also more commonly had a history of MALO (42%) than patients at high (0.4%) and low risk (0.2%; p for all < 0.001), but less commonly had a history of MACE (Diagnosed: 4.3%, High-risk: 9.5%, Low risk: 4.8%; p for all < 0.01). Among patients with no history of MALO and MACE, respectively, the incidence rate (IR; per 1000 person-years (PY)) for MALO (mean follow-up: 6 years) was higher among diagnosed (IR = 19, 95% CI = 13–27) and high-risk patients (IR = 2.4, 95% CI = 2.2–2.6) vs low-risk patients (IR = 0.5, 95% CI = 0.4–0.6), and also for MACE (Diagnosed: IR = 19, 95% CI = 14–27; High-risk: IR = 31, 95% CI = 30–32; Low-risk: IR = 12, 95% CI = 11.6–12.3). In an adjusted Cox regression model (considering age, sex and T2D), the rate of MALO was higher in patients at high risk vs low risk (aHR = 3.8, 95% CI = 3.2–4.6), but lower for high risk vs diagnosed patients (aHR = 0.08, 95% CI = 0.05–0.12). The rate of MACE was also higher in patients at high vs low risk (MACE: aHR = 1.9, 95% CI = 1.8–2.0) but not significantly in high risk vs diagnosed patients (aHR = 1.3, 95% CI = 0.9–1.8).

Conclusion: The results indicate a large burden of undiagnosed fibrotic MASH in patients from the general population with risk factors for MASH and highlights FNI as a possible risk stratification tool.

OS-053

Screening candidates for therapeutic trials in MASH: choose the right non-invasive test for the diagnostic target considered

Jerome Boursier^{1,2}, Luisa Vonghia³, Charlotte Costentin⁴, Jeanne Fichet², Clemence Moreau¹, Marine Roux¹, Clémence M Canivet^{1,2}, Victor de Lédinghen⁵, Sven Francque³, Ming-Hua Zheng⁶. ¹Angers University, Angers, France; ²Angers University Hospital, Angers, France; ³Antwerp University Hospital, Antwerp, Belgium; ⁴Grenoble University Hospital, Grenoble, France; ⁵Bordeaux University Hospital, Pessac, France; ⁶Wenzhou university Hospital, Wenzhou, China
Email: jeboursier@chu-angers.fr

Background and aims: The screen failure rate in therapeutic trials evaluating MASH treatments is very high, around 70–80%. One of the main reasons is the absence of fibrotic MASH on liver histology, underscoring the need for better selection of candidates for these studies. Our aim was to evaluate the performance of 8 non-invasive tests, specific or not, for the diagnosis of fibrotic MASH.

Method: 1,005 patients with histologically proven MASLD were included in 5 centers across Europe and Asia. Fibrotic MASH was defined as the presence of MASH with a NAS score ≥ 4 and a fibrosis stage ≥ 2 according to the NASH CRN classification. Advanced fibrosis was defined as fibrosis stage ≥ 3 . Three non-invasive tests specifically developed for fibrotic MASH were evaluated (the simple blood test Fibrotic NASH Index [FNI], the specialized blood test MACK-3, and the elastography-based test FAST), as well as 5 non-invasive tests developed for advanced fibrosis (the simple blood test FIB4, the specialized blood tests Fibrotest and ELF, and the elastography tests Fibroscan and Agile3+). The simple blood tests (FNI, FIB4) were available for all the 1005 patients included, the specialized blood tests (MACK-3, Fibrotest, ELF) for 545 patients, and the elastography tests (FAST, Fibroscan, Agile3+) for 817 patients.

Results: Median age was 56.7 years, 62.7% of the patients were male, and 49% had type 2 diabetes. The prevalence of fibrotic MASH and advanced fibrosis were, respectively, 41.8% and 31.9%. For the diagnosis of fibrotic MASH in the 1005 patients included, the simple blood test for fibrotic MASH FNI had a significantly higher AUROC than the simple blood test for advanced fibrosis FIB4 (0.709 [0.677–0.741] vs. 0.662 [0.628–0.695], $p = 0.019$). In the 545 patients with all specialized blood tests available, MACK-3 had a significantly higher AUROC for the diagnosis of fibrotic MASH (0.772 [0.734–0.811]) than Fibrotest (0.615 [0.568–0.663], $p < 0.001$) and ELF (0.700 [0.656–0.744], $p = 0.003$). In the 817 patients with all elastography tests available, FAST had a significantly higher AUROC for the diagnosis of fibrotic MASH (0.774 [0.743–0.806]) than Fibroscan (0.728 [0.694–0.763], $p = 0.001$) and Agile3+ (0.708 [0.672–0.744], $p < 0.001$). The dedicated specialized tests (MACK-3 and FAST) were significantly more accurate than the simple blood tests (FNI and FIB4) for the diagnosis of fibrotic MASH. The thresholds of tests for advanced fibrosis were recalculated for the diagnosis of fibrotic MASH. Despite these optimized thresholds, the specialized non-invasive tests specifically dedicated for fibrotic MASH remained more accurate than the specialized non-invasive tests for advanced fibrosis.

Conclusion: Specialized non-invasive tests specifically dedicated to fibrotic MASH should be preferred to non-invasive tests for advanced fibrosis to improve the screening of candidates for therapeutic trials in MASH.

OS-054

Validation of the Baveno VII 'rule of 5' in a real-life multicentre cohort of patients with metabolic dysfunction associated steatotic liver disease

Elba Llop Herrera¹, Huapeng Lin², Hye Won Lee³, Terry Cheuk-Fung Yip^{4,5}, Emmanuel Tsochatzis⁶, Salvatore Petta⁷, Elisabetta Bugianesi⁸, Masato Yoneda⁹, Ming-Hua Zheng¹⁰, Hannes Hagström^{11,12}, Jérôme Boursier^{13,14}, George Boon Bee Goh¹⁵, Chan Wah Kheong¹⁶, Rocio Gallego-Durán¹⁷, Arun J Sanyal¹⁸, Victor de Lédinghen¹⁹, Philip N. Newsome²⁰, Jiangao Fan²¹, Laurent Castera²², Michelle Lai²³, Stephen A. Harrison^{24,25}, Céline Fournier-Poizat²⁶, Grace Lai-Hung Wong^{4,5}, Grazia Pennisi²⁷, Angelo Armandi⁸, Atsushi Nakajima⁹, Wen-Yue Liu¹⁰, Ying Shang¹¹, Marc de Saint-Loup¹³, Kevin Kim Jun Teh¹⁵, Carmen Lara-Romero²⁸, Amon Asgharpour¹⁸, Sara Mahgoub²⁰, Chan Mandy²⁶, Clémence M Canivet^{13,14}, Manuel Romero-Gómez²⁹, Seung Up Kim³, Vincent Wai-Sun Wong⁴, José Luis Calleja Panero³⁰. ¹Liver Unit, Hospital Universitario Puerta de Hierro Majadahonda, IDIPHISA, Ciberhd., Majadahonda, Spain; ²Medical Data Analytics Centre, Department of Medicine and Therapeutics, The Chinese University of Hong Kong, Hong Kong, China, State Key Laboratory of Digestive Disease, Institute of Digestive Disease, The Chinese University of Hong Kong, Hong Kong, China, Hong Kong, China; ³Department of Internal Medicine, Institute of Gastroenterology, Yonsei University College of Medicine, Seoul, Republic of Korea, Seoul, Korea, Rep. of South; ⁴Medical Data Analytics Centre, Department of Medicine and Therapeutics, The Chinese University of Hong Kong, Hong Kong, China, Hong Kong, China; ⁵State Key Laboratory of Digestive Disease, Institute of Digestive Disease, The

Chinese University of Hong Kong, Hong Kong, China, Hong Kong, China; ⁶University College London Institute for Liver and Digestive Health, Royal Free Hospital and UCL, London, United Kingdom, London, Spain; ⁷Sezione di Gastroenterologia, Di.Bi.M.I.S., University of Palermo, Italy, Palermo; ⁸Department of Medical Sciences, Division of Gastroenterology and Hepatology, A.O. Città della Salute e della Scienza di Torino, University of Turin, Turin, Italy, Torino, Italy; ⁹Department of Gastroenterology and Hepatology, Yokohama City University Graduate School of Medicine, Yokohama, Japan, Yokohama, Japan; ¹⁰MAFLD Research Center, Department of Hepatology, First Affiliated Hospital of Wenzhou Medical University, Wenzhou, China, Wenzhou, China; ¹¹Department of Medicine, Huddinge, Karolinska Institutet, Sweden, Huddinge, Sweden; ¹²Division of Hepatology, Department of Upper GI Diseases, Karolinska University Hospital, Huddinge, Stockholm, Sweden, Stockholm, Sweden; ¹³Hepato-Gastroenterology and Digestive Oncology Department, Angers University Hospital, Angers, France, Angers, France; ¹⁴HIFIH Laboratory, SFR ICAT 4208, Angers University, Angers, France, Angers, France; ¹⁵Department of Gastroenterology and Hepatology, Singapore General Hospital, Singapore, Singapore, Singapore; ¹⁶Gastroenterology and Hepatology Unit, Department of Medicine, Faculty of Medicine, University of Malaya, Malaysia, Malaya, Malaysia; ¹⁷Digestive Diseases Unit and CIBERhd, Virgen Del Rocío University Hospital, Seville, Spain, Sevilla; ¹⁸Division of Gastroenterology, Hepatology and Nutrition, Department of Internal Medicine, Virginia Commonwealth University School of Medicine, Richmond, VA, USA, Richmond, United States; ¹⁹Centre d'Investigation de la Fibrose Hépatique, Haut-Lévêque Hospital, University Hospital of Bordeaux, Pessac, France, Pessac, France; ²⁰National Institute for Health Research, Biomedical Research Centre at University Hospitals Birmingham NHS Foundation Trust and the University of Birmingham, Birmingham, United Kingdom, Birmingham, United Kingdom; ²¹Department of Gastroenterology, Xinhua Hospital Affiliated to Shanghai Jiaotong University School of Medicine, Shanghai Key Lab of Pediatric Gastroenterology and Nutrition, Shanghai, China, Shanghai, China; ²²Université Paris Cité, UMR1149 (CRI), INSERM, Paris, France; Service d'Hépatologie, Hôpital Beaujon, Assistance Publique-Hôpitaux de Paris (AP-HP), Clichy, France, Clichy, France; ²³Division of Gastroenterology and Hepatology, Beth Israel Deaconess Medical Center, Harvard Medical School, Boston, MA, USA, Boston, United States; ²⁴Radcliffe Department of Medicine, University of Oxford Oxford, UK, Oxford, United Kingdom; ²⁵Pinnacle Clinical Research, San Antonio, Texas, USA, San Antonio, United Kingdom; ²⁶Echosens, Paris, France, Paris, France; ²⁷Sezione di Gastroenterologia, Di.Bi.M.I.S., University of Palermo, Italy, Palermo, Italy; ²⁸Digestive Diseases Unit and CIBERhd, Virgen Del Rocío University Hospital, Seville, Spain, Sevilla, Spain; ²⁹Digestive Diseases Unit and CIBERhd, Virgen Del Rocío University Hospital, Seville, Spain, Sevilla, Spain; ³⁰Department of Gastroenterology and Hepatology, Hospital Universitario Puerta de Hierro Majadahonda, IDIPHISA, Ciberhd Madrid, Spain, Majadahonda, Spain
Email: elballop@gmail.com

Background and aims: The Baveno VII 'rule of 5' based on vibration-controlled transient elastography (VCTE) determines the risk of hepatic decompensation and mortality. The aim of our study was to validate the 'rule of 5' in a real-life cohort of obese and non-obese patients with metabolic dysfunction-associated steatotic liver disease (MASLD).

Method: This is a retrospective study in which patients with MASLD undergoing baseline and repeated measurements of VCTE in 16 centers in USA, Europe and Asia were included. The ability of the 'rule of 5' to predict hepatic decompensation (HD) (ascites, variceal hemorrhage, hepatic encephalopathy or hepatorenal syndrome) and liver related death (LRD) was evaluated.

Results: From February 2004 to January 2023 data from 17949 subjects were collected, with 12664 finally included. Mean age was 51.9 years, 58% male, 28% were obese (BMI ≥ 30). 166 (1.3%) had HD and 38 (0.3%) LRD after a median follow-up of 48.0 months (IQR 24.1–72.4 months). The competing risk analysis showed increased risk of

HD for each VCTE 'rule of 5' category in obese and non-obese patients ($p < 0.001$). The cumulative probability of HD at 1, 3 and 5 years of follow-up was: Obese: <10 kPa: 0.2%, 0.3%, 0.9%; 10–15 kPa: 0.2%, 0.9%, 2.9%; 15–20 kPa 1.0%, 3.3%, 6.1%; 20–25 kPa 0%, 4.0%, 8.7%; 25–30 kPa 1.5%, 4.9%, 11.5%; >30 kPa 1.6%, 14%, 23.6% $p < 0.001$; Non-obese: <10 kPa 0.1%, 0.4%, 0.9%; 10–15 kPa 0.9%, 1.6%, 3.0%; 15–20 kPa 1.7%, 5.8%, 12.5%; 20–25 kPa 2.1%, 4.5%, 4.5%; 25–30 kPa 2.8%, 5.8%, 20.5%; kPa; >30 kPa 4.2%, 11.6%, 19.5%; $p < 0.001$. This suggested that the predictive performance of VCTE is lower in patients with obesity. Time-dependent area under receiver operating characteristic (AUROC) curves for the 'rule of 5' to predict HD at 1 and 3 years were 0.71 and 0.86 as well as 0.87 and 0.82 in obese and non-obese, respectively, showing better performance of the 'rule of 5' in non-obese patients for HD. A model including 'the rule of 5' and obesity showed AUROC at 1 and 3 years 0.83 and 0.84 in the whole cohort. Competing risk analysis showed significantly lower risk of LRD for obese and non-obese patients in each category ($p < 0.001$). Incidence of LRD was higher as 'rule of 5' category increased for obese and non-obese patients (Obese: <10 kPa: 0%, 10–15 kPa 0.7%, 15–20 kPa 1.4%, 20–25 kPa 1.6%, 25–30 kPa 2.8%, >30 kPa 6.6% $p < 0.001$; non-obese: <10 kPa: 0.03%, 10–15 kPa 1%, 15–20 kPa 1%, 20–25 kPa 1%, 25–30 kPa 4.1%, >30 kPa 2.9% $p < 0.001$). Again, this suggested that the predictive performance of VCTE is lower in patients with obesity. AUROC for the 'rule of 5' to predict LRD at 3 and 5 years was: Obese: 0.9 and 0.88, non-obese: 0.9, 0.79. A model including 'the rule of 5' and obesity showed AUROC at 3 and 5 years 0.91 and 0.86 in the whole cohort.

Conclusion: The 'rule of 5' predicts HD and LRD in MASLD patients. However, obesity must be taken into account when using it given that the discriminative capacity of VCTE is lower in the presence of obesity.

Public Health

OS-055

Defining the thresholds for alcohol intake on the risk of liver-related mortality in people with metabolic risk factors

Hyunseok Kim¹, Polly Kirsch¹, Yee Hui Yeo¹, Walid S Ayoub¹, Alexander Kuo¹, Vijay Pandeyarajan¹, Hirsch Trivedi¹, Aarshi Vipani¹, Yun Wang¹, Ekihiro Seki¹, Stephen Pandol¹, Debiao Li¹, Shelly C. Lu¹, Ju Dong Yang¹. ¹ Cedars Sinai Medical Center, Los Angeles, United States
Email: hyunseok.kim@cshs.org

Background and aims: The impacts of alcohol consumption in people with metabolic risk factors on the risk of liver-related outcomes are not fully studied. In this study, we investigated the effects of alcohol consumption amount on liver-related mortality in participants with metabolic risk factors in the United Kingdom Biobank study (UKB) study, a prospective cohort.

Method: We included participants without a prior diagnosis of cirrhosis at the time of enrollment. Metabolic traits (hypertension, type 2 diabetes mellitus, dyslipidemia, and obesity) were defined based on self-reported history, medication use, previous hospital diagnosis, or laboratory/anthropometric values. We obtained the alcohol consumption amount from a self-reported alcohol use questionnaire. We categorized the alcohol consumption into <10 g, 10–20 g, 20–30 g, 30–40 g, 40–50 g, 50–60 g, and >60 g per day to identify at which dose people start to have significantly higher risk for liver-related mortality. We performed Cox proportional hazards models to evaluate the effects of alcohol intake amount on time to liver-related mortality. In addition, we investigated whether the effect of alcohol intake can be altered by the *PNPLA3* genotype.

Results: In 263, 052 participants with at least one metabolic trait (mean age 57.39 years, male 51.7%),

92, 481 (35%), 73, 758 (28%), 43, 606 (17%), 22, 499 (8.5%), 13, 358 (5.1%), 6, 832 (2.6%), 10, 518 (3.9%) participants consumed <10 g, 10–20, 20–30, 30–40, 40–50, 50–60, >60 g per day, respectively. During a median follow-up of 12 years, 654 participants developed liver-related mortality. We observed a statistically significantly higher risk of liver-related mortality from those who drank between 20 and 30 g per day (aHR 1.45 [95% CI: 1.10–1.92]) compared to those who drank <10 g per day, after adjusting for age, sex, race/ethnicity, BMI, diabetes, hypertension, hyperlipidemia, and household income. Furthermore, we observed synergistic interaction in those who drank >60 g per day and *PNPLA3* homozygote carriers (p -interaction <0.01, aHR 5.3 [95% CI: 3.7–7.6] in alcohol intake >60 g per day with normal *PNPLA3* trait, aHR 1.6 [95% CI: 0.8–3.4] in *PNPLA3* homozygous carriers who drank <60 g per day, and aHR 25.6 [95% CI: 3.6–182] in both alcohol intake >60 g per day and *PNPLA3* homozygous carriers). While the absolute risks of liver-related mortality were lower in women, we could not find a significant interaction between sex and alcohol consumption.

Conclusion: In the UK Biobank, there was an incremental risk of liver-related mortality by the amount of alcohol consumption. The increased liver-related mortality was observed from those with >20 g/day of alcohol use. The *PNPLA3* genotype status also plays a synergistic interplay in those who drink excessively. We need to counsel the risk of alcohol consumption on the progression to liver-related outcomes in people with metabolic risk factors.

OS-056-YI

Poor referral of migrants with hepatitis B virus infection from primary care: a substantial missed opportunity for successful linkage to specialist care in Catalonia

Camila Picchio^{1,2}, Helena Martí Soler¹, Aina Nicolàs Olivé¹, Sabela Lens^{3,4}, Xavier Fornés^{3,4}, Elisa Martró^{5,6}, Maria Buti^{3,7}, Jeffrey V Lazarus^{1,8}, Ana Requena¹. ¹ Barcelona Institute for Global Health (ISGlobal), Hospital Clínic, University of Barcelona, Barcelona, Spain; ² Department of Community Health and Prevention, Dornsife School of Public Health, Drexel University, Philadelphia, United States; ³ CIBER Hepatic and Digestive Diseases (CIBERehd), Instituto Carlos III, Madrid, Spain; ⁴ Liver Unit, Hospital Clínic, IDIBAPS, University of Barcelona, Barcelona, Spain; ⁵ Microbiology Department, Laboratori Clínic Metropolitana Nord (LCMN), Hospital Universitari Germans Trias i Pujol, Institut d'Investigació Germans Trias i Pujol (IGTP), Badalona, Spain; ⁶ CIBER in Epidemiology and Public Health (CIBERESP), Instituto Carlos III, Madrid, Spain; ⁷ Hospital Campus, Liver Unit, Hospital Universitari Vall d'Hebron, Barcelona, Spain; ⁸ CUNY Graduate School of Public Health and Health Policy (CUNY SPH), New York, United States
Email: camila.picchio@isglobal.org

Background and aims: The impact of chronic hepatitis B virus (HBV) infection is particularly pronounced among vulnerable populations, such as migrants, who face unique challenges related to healthcare access, cultural differences, and social determinants in their host countries. Primary health care is one of the most frequent contact points with the health system migrants have, however, HBV infections in Spain are managed at the tertiary level and therefore referrals from primary care are needed to properly diagnose, manage, and treat chronic HBV infections. We aimed to categorize the referrals of HBV from all of the primary care centers in Catalonia in 2017 and 2018 to specialist care.

Method: We examined all first recorded patient visits in primary care across the autonomous community of Catalonia, Spain in 2017 and 2018 with data the central database primary health care database in Catalonia [Information System for Research in Primary Care (SIDIAP)]. The proportion of people born outside of Spain (classified as migrants) who were HBsAg+ and therefore eligible for a referral to specialist care (e.g. gastroenterology and hepatology or infectious diseases units) was categorized. Region of origin were classified as: North Africa, Central and Southern Africa, Northern Europe, Southern Europe, Central and Eastern Europe, Ibero-America and the

ORAL PRESENTATIONS

Caribbean, Anglo-Saxon America, Asia (Middle East), Eastern Asia, and Oceania. Basic standard descriptive statistics were used to analyze data using R software (R Core Team 2023).

Results: A total of 1,688 and 1,995 migrants had recorded first visits in primary care centers across Catalonia in 2017 and 2018, respectively. Most were female migrants (1553, 56%) and from Northern Africa (892, 24%). Overall, the prevalence of HBsAg+ was 6.5% (n = 239, 108 in 2017 and 131 in 2018). Migrants from Central and Southern Africa region accounted for 55% of all HBsAg+ cases (130/239). While all HBsAg+ patients were eligible for referrals, 73% (175/239) of these migrants did not receive an order for referral to specialist care. Although there is some heterogeneity between regions, no statistically significant differences were observed ($p > 0.05$). Overall, more than half of the HBsAg+ migrants were not referred from their primary care doctor to specialist care in 2017 and 2018, and 77% of migrants from Central and Southern Africa were not referred.

Conclusion: Almost three quarters of migrants who were eligible for and required a referral to specialist care across Catalonia were not provided one from primary care in 2017 and 2018. This presents a substantial missed opportunity to link migrants to indispensable liver care. Training of healthcare workers in primary care should be reinforced and additional strategies, such as community-based care, to diagnose and ensure linkage to specialist care for migrants are needed so that new HBV diagnoses are not missed or lost to follow-up.

OS-057-YI

CORE: a new risk score measuring GGT, AST, and ALT outperforms FIB-4 when predicting the risk of cirrhosis in a primary care setting

Rickard Strandberg¹, Mats Talbäck², Niklas Hammar², Hannes Hagström^{1,3}. ¹Department of Medicine Huddinge, Karolinska Institutet, Stockholm, Sweden; ²Institute of Environmental Medicine, Karolinska Institutet, Stockholm, Sweden; ³Karolinska University Hospital, Stockholm, Sweden
Email: rickard.strandberg@ki.se

Background and aims: Metabolic associated steatotic liver disease (MASLD) has a high prevalence in the general population, and the incidence of MASLD-associated cirrhosis is increasing. The Fibrosis-4 score (FIB-4) is a diagnostic model used in patients with MASLD to estimate the present degree of fibrosis, but the FIB-4 score is inadequate for predicting future cases of severe liver disease. The aim of this study is to develop a risk score—the Cirrhosis Outcome Risk Estimator (CORE)—allowing physicians to identify individuals at a high risk of developing cirrhosis. Correct identification would allow for early intervention and preventive measures.

Method: We used a large Swedish population-based cohort, free of known liver diseases other than possibly MASLD, with available laboratory data—including biomarkers associated with liver disease—and national registry data. Using flexible parametric survival models, a 10-year risk model of cirrhosis or associated complications was created, with non-liver death as a competing event. The new comprehensive risk score initially included age, sex, body mass index (BMI), aspartate aminotransferase (AST), alanine aminotransferase (ALT), gamma-glutamyl transferase (GGT), cholesterol, platelet count, albumin, bilirubin, glucose, and triglycerides. From this, a simplified but clinically feasible model was extracted which includes only age, sex, GGT, AST, and ALT. The performance was assessed in terms of discrimination (time-dependent area-under-curve (AUC)), calibration (calibration curves), and clinical utility (decision curve analysis). The model was compared to the FIB-4 score.

Results: We used data of 504,359 individuals that were followed over an average follow-up time of 25 years. During follow-up, 7604 liver-related outcomes were observed. The cumulative risk of liver cirrhosis at ten years was 0.22%. The new risk score CORE achieved a 10-year AUC of 81% (95%CI: 80–84) compared to the FIB-4 AUC of 73% (95%CI:

71–75). The calibration was considerably better in CORE than FIB, and according to the decision curve analysis CORE has a higher net benefit than FIB-4 for all risk thresholds.

Conclusion: The new risk score, the Cirrhosis Outcome Risk Estimator (CORE), based on a flexible modelling approach and using biomarkers easily accessible in primary care, outperforms FIB-4 when predicting liver-related outcomes in the general population. The model awaits external validation in the FINRISK cohort and the UK biobank.

OS-058

Disparities in hepatocellular carcinoma survival among people with hepatitis B or hepatitis C virus infection in Canada

Naveed Janjua^{1,2}, Stanley Wong¹, Dahn Jeong², Jean Damascene Makuza², Richard Morrow², Sofia Bartlett¹, Héctor Alexander Velásquez García¹, Prince Adu¹, Victor Lei¹, Amanda Yu¹, Maria Alvarez¹, Alnoor Ramji³, Eric Yoshida³, Mel Krajden¹. ¹British Columbia Centre for Disease Control, Vancouver, Canada; ²School of Population and Public Health, University of British Columbia, Vancouver, Canada; ³Division of Gastroenterology, University of British Columbia, Vancouver, Canada
Email: naveed.janjua@bccdc.ca

Background and aims: Liver cancer has one of the fastest increasing incidence and mortality rates among all cancers in Canada. Liver cancer affects populations from diverse background. However, there are limited data on disparities in survival following hepatocellular carcinoma (HCC) diagnosis. We assessed disparities in survival following HCC diagnosis to identify gaps in care in British Columbia, Canada.

Method: We used data from the BC Hepatitis Testers Cohort. This cohort includes data on individuals tested for hepatitis C virus (HCV), hepatitis B virus (HBV), and HIV, integrated with data on cancers, mortality, and healthcare administrative data. The study included individuals diagnosed with HCC among people with HCV or HBV infection between January 2010 and March 2021. Individuals were followed from HCC diagnosis to death or the end of the study (December 31, 2021). We computed the crude mortality rates and constructed survival curves for overall population and by age, sex, ethnicity, and socioeconomic status. We used the Cox proportional hazards models to investigate factors associated with survival duration after HCC diagnosis.

Results: Among 117,524 people with chronic HBV (n = 42,259) or HCV (n = 69,117) or HCV/HBV (n = 6,148) infection, 2,783 (HCV:1,779; HBV:777; HCV/HBV:227) patients were diagnosed with HCC. The median age at HCC diagnosis was 61[57–66] years. Among patients with HCV related HCC, the crude mortality rate (overall: 35.6 per 1000-person years (PY), 95% CI: 33.7–37.5) showed a graded increase with material deprivation (most privileged: 31.2/1000 PY, 95% CI: 27.1–35.74; most deprived: 41.9/1000 PY, 95% CI: 38.0–46.0). Among those with HBV related HCC, the overall crude mortality rate was lower (rate: 13.4, 95%CI: 12.1–14.7) and, there was not a gradient across material deprivation.

In the multivariable model for HCV related HCC, people in the 4th [Adjusted Hazard Ratio (AHR): 1.31, 95% CI: 1.08–1.58] and 5th (AHR:1.29, 95% CI: 1.08–1.55) material deprivation quintiles compared with the most privileged (1st quintile), and people who inject drugs (PWID; AHR: 1.32, 95% CI: 1.16–1.51) had higher mortality rates after adjusting for age, sex, diagnosis stage, and ethnicity. In the multivariable model for HBV related HCC, people from “other” ethnicities (including White and other population groups with anglicized names) compared with people of East Asian ancestry (1.30, 95% CI: 1.04–1.61), and PWID (AHR: 1.89, 95% CI: 1.44–2.46) had higher mortality, although there was no gradient by material deprivation.

Conclusion: This study identified disparities in HCC-related survival by material deprivation and in PWID among those with HCV infection, and by ethnicity and in PWID among those with HBV

infection. As we strive toward hepatitis elimination goals, addressing disparities in HCC diagnosis and care needs to be part of the continuum to improve overall health and survival.

OS-059

Unveiling Socioeconomic Disparities on Liver Disease: A Comparative Study of ALD, MASLD, and MetALD Patients

Helle Lindholm Schnefeld¹, Johanne Kragh Hansen^{1,2}, Katrine Tholstrup Bech¹, Anita Arslanow^{3,4}, Isabel Graupera^{3,4,5,6}, Katrine Prier Lindvig^{1,2}, Maria Kjærgaard¹, Camilla Dalby Hansen^{1,2}, Mads Israelsen¹, Stine Johansen^{1,2}, Peter Andersen¹, Katrine Thorhauge^{1,2}, Nikolaj Torp^{1,2}, Sönke Detlefsen^{2,7}, Núria Fabrellas^{4,6}, Pere Ginès^{3,4,5,6}, Aleksander Krag^{1,2}, Maja Thiele^{1,2}.

¹Centre for Liver Research, Department of Gastroenterology and Hepatology, Odense University Hospital, Odense, Denmark;

²Department of Clinical Research, University of Southern Denmark, Odense, Denmark; ³Liver Unit Hospital Clínic, University of Barcelona, Barcelona, Spain; ⁴Institut D'Investigacions Biomèdiques August Pi I Sunyer (IDIBAPS), Barcelona, Spain; ⁵Centro de Investigación En Red de Enfermedades Hepáticas Y Digestivas (Ciberehd), Barcelona, Spain;

⁶Faculty of Medicine and Health Sciences, University of Barcelona, Barcelona, Spain; ⁷Department of Pathology, Odense University Hospital, Odense, Denmark

Email: helle.lindholm.hansen@rsyd.dk

Background and aims: Steatotic Liver Disease (SLD) poses a major public health concern, requiring focused healthcare approaches. Socioeconomic factors affect disease outcomes, potentially accounting for the variations in progression to significant and advanced liver fibrosis across the SLD spectrum. We aimed to describe socioeconomic disparities across Metabolic Dysfunction-Associated Steatotic Liver Disease (MASLD), MASLD with concurrent moderate-high alcohol consumption (MetALD), and Alcohol-related Liver Disease (ALD). Finally, we sought to explore the impact of socioeconomic elements on liver fibrosis within these SLD subgroups.

Method: We screened individuals from the general population and individuals with SLD using controlled attenuation parameter (CAP) with a CAP-cut-off ≥ 248 dB/m and transient elastography (TE), with significant fibrosis indicated by TE ≥ 8 kPa and advanced fibrosis by TE > 12 kPa. We classified participants according to the nomenclature with either metabolic factors or alcohol intake as predominant factors. We assessed socioeconomic status by self-reported income, education, employment, and marital status, and compared MASLD, MetALD, and ALD, using non-SLD as a comparator. We performed chi-square tests and logistic regression, to explore associations between socioeconomic factors and the distinct subgroups.

Results: We screened 6444 individuals with a median age of 57 (IQR 52–63), 52% female. The distribution of non-SLD/MASLD/MetALD/ALD was 2451 (38%)/2967 (46.0%)/663 (10.3%)/363 (5.6%). More than half of the ALD group earned below 40,000 € (55%), which was significantly more than non-SLD (34%), MASLD (38%), and MetALD (34%), ($p < 0.005$). Within the ALD subgroup, 56% were unemployed, long-term ill, or retired due to disability or age, an overrepresentation compared to MASLD (35%), MetALD (44%), and the non-SLD group (32%) ($p < 0.005$). Nineteen percent of the MetALD group had a longer education, which was more than in the other groups ALD (14%) MASLD (10%) SLD (15%). A third (34%) of the ALD group lived alone, which was significantly more than in MASLD (22%), MetALD (21%), or 23% within the non-SLD group ($p < 0.005$). After adjusting for known risk factors for liver fibrosis, the likelihood of TE ≥ 8 was greater for men (OR 2.3; 95% CI 1.8–3.0), individuals with an income below 40,000€ (OR 2.0; 95% CI 1.3–3.1), and those living alone (OR 1.3; 95% CI 1.1–1.8). These odds escalated for TE ≥ 12 , signifying that being female, earning a higher income, and cohabiting independently decreased the risk of severe liver fibrosis.

Conclusion: Our study reveals that individuals with ALD are more likely to have a lower income, be unemployed, and live alone, while those with MetALD often possess higher educational levels. Being

female, earning a high income, and living with a partner emerge as protective factors against liver fibrosis in these populations.

Viral hepatitis C

OS-060

Hepatocellular carcinoma development despite histological regression of liver fibrosis following HCV cure (ANRS CirVir, Hepather, LICAVIR)

Pierre Nahon¹, Clovis Iusivka-Nzinga², Philippe Merle³, Fabien Zoulim⁴, Thomas Decaens⁵, Nathalie Ganne-Carrié⁶, Georges-Philippe Pageaux⁷, Vincent Leroy⁸, Laurent Alric⁹, Jean-Pierre Bronowicki¹⁰, Marc Bourliere¹¹, Jérôme Gournay¹², Albert Tran¹³, Stanislas Pol¹⁴, Philippe Mathurin¹⁵, Veronique Loustaud-Ratti¹⁶, Sophie Metivier⁹, Victor de Lédinghen¹⁷, Armand Aberger¹⁸, Dominique Thabut¹⁹, Louis Dalteroche²⁰, Mohamed Bouattour²¹, Tarik Asselah²², Denis Ouzan²³, Paul Cales²⁴, Olivier Chazouillères²⁵, Moana Gelu-Simeon²⁶, Dominique Roulot⁶, Jerome Boursier²⁴, Cagnot Carole²⁷, Sonia Tamazirt²⁸, Alina Pascale²⁸, Samuel Nilusmas²⁹, Maite Lewin²⁸, Marianne Ziolf⁶, Fabrice Carrat³⁰, Jean-Charles Duclos-Vallée³¹. ¹APHP Avicenne, Bobigny, France; ²Inserm, Paris, France; ³CHU Lyon, Lyon, France; ⁴CHU Lyon, Lyon, France; ⁵CHU Grenoble, Grenoble, France; ⁶APHP AVICENNE, Bobigny, France; ⁷CHU Montpellier, Montpellier, France; ⁸APHP Mondor, Créteil, France; ⁹CHU Toulouse, Toulouse, France; ¹⁰CHU Nancy, Nancy, France; ¹¹CH Marseille, Marseille, France; ¹²CHU Nantes, Nantes, France; ¹³CHU Nice, Nice, France; ¹⁴APHP Cochin, Paris, France; ¹⁵CHU Lille, Lille, France; ¹⁶CHU Limoges, Limoges, France; ¹⁷CHU Bordeaux, Bordeaux, France; ¹⁸CHU Clermont, Clermont ferrand, France; ¹⁹APHP PITIE, Paris, France; ²⁰CHU TOURS, Tours, France; ²¹APHP BEAUJON, Clichy, France; ²²APHP BEAUJON, Clichy, France; ²³CH St Laurent du Var, St Laurent du Var, France; ²⁴CHU Angers, Angers, France; ²⁵APHP ST Antoine, Paris, France; ²⁶CHU GUADELOUPE, GUADELOUPE, France; ²⁷ANRS, Paris, France; ²⁸APHP PAUL BROUSSE, Villejuif, France; ²⁹INSERM, Paris; ³⁰INSERM, Paris, France; ³¹APHP Paul Brousse, Villejuif, France

Email: pierre.nahon@aphp.fr

Background and aims: The risk of HCC development following HCV cure as a function of liver fibrosis regression is unknown. The aim of this study was to describe and analyze the dynamics of liver fibrosis assessed by both liver histology and non-invasive tests (NIT) at baseline and at the time of HCC occurrence several years after sustained virological response (SVR).

Method: Data were obtained in two prospective French multicenter cohorts of patients with HCV infection recruited since 2006 (ANRS CO22 Hepather and CO12 CirVir). Patients were regularly followed-up and when indicated included in HCC surveillance programs. The dynamics of NIT (Fib4, APRI and LSM) were evaluated in relation to HCC development and histological liver fibrosis in HCC patients was assessed.

Results: 8808 SVR patients (3500 with cirrhosis) were analyzed, among whom 298 (3.6%) HCC occurred during a 62-months follow-up. In the 3500 patients with cirrhosis, all baseline NIT tests (Fib4, APRI, LSM) were higher in patients who ultimately developed HCC. Except for Fib4 in patients who developed HCC, all NIT decreased significantly over time irrespective of subsequent HCC development with a maximum downward slope following antivirals implementation (all $p < 0.005$). This temporal dynamic was similar for all tests irrespective of HCC development ($p = 0.91$, $p = 0.29$ and $p = 0.37$, respectively). Joint modelling of association between the change in NIT and HCC showed that a unit decrease in APRI or Fib-4 scores at any time of follow-up were associated with a decreased HCC risk (HR = 0.62 [0.57–0.69] and HR = 0.91 [0.90–0.93], both $p < 0.0001$). Thirty-eight non-tumour liver biopsies specimen were analyzed at

time of HCC diagnosis, 37/38 (98%) patients having F3 or F4 fibrosis scores before SVR. At time of HCC diagnosis, this proportion was 33/38 (86%) The analysis of fibrosis evolution showed that 7/38 (18%) HCC patients were considered as having liver fibrosis regression (F0: 1 patient, F1: 2 patients, F2: 2 patients, F3: 2 patients). More precisely, 4 patients had a one-point regression and 3 had more than one point of fibrosis regression. Overall, values of NIT tests in these patients suggested the presence of advanced liver fibrosis at the time of HCC. **Conclusion:** HCC occurs despite histological fibrosis regression following HCV cure. The dynamics of NIT may not accurately reflect histological fibrosis changes and may not be sufficient to refine HCC surveillance strategy.

OS-061

Chronic hepatitis C virus infection induces HCC risk by perturbing the human liver circadian transcriptome and epigenome through deregulation of the deacetylase SIRT1

Atish Mukherji¹, Frank Jühling², Yogy Simanjuntak¹, Michio Imamura³, Emilie Crouchet², Fabio Del Zompo¹, Yuji Teraoka⁴, Alexandre Haller⁵, Philippe Baltzinger⁵, Soumith Paritala⁶, Fahmdia Rasha⁶, Naoto Fujiwara⁶, Cléo Gadenne¹, Nevena Slovic¹, Marine Oudot⁷, Sarah Durand¹, Clara Ponsolles¹, Catherine Schuster⁷, Xiaodong Zhuang⁸, Jacinta Holmes⁹, Ming-Lun Yeh¹⁰, Hiromi Abe-Chayama¹¹, Mathias Heikenwälder¹², Angelo Sangiovanni¹³, Massimo Iavarone¹⁴, Massimo Colombo¹⁵, Jane McKeating⁸, Irwin Davidson⁸, Ming-Lung Yu¹⁶, Raymond Chung¹⁷, Yujin Hoshida¹⁸, Kazuaki Chayama¹⁹, Joachim Lupberger⁷, Thomas Baumert¹. ¹University of Strasbourg, Inserm, UMR_S1110, Strasbourg, France; ²University of Strasbourg, Inserm, Institut of Translational Medicine and Liver Disease (ITM), UMR_S1110, Strasbourg, France; ³Yamasaki Hospital, Hiroshima, Japan; ⁴Department of Gastroenterology, National Hospital Organization Kure Medical Center, Hiroshima, Japan; ⁵Department of Functional Genomics and Cancer, Institut de Génétique et de Biologie Moléculaire et Cellulaire, Illkirch, France; ⁶Department of Internal Medicine, University of Texas Southwestern Medical Center, Dallas, United States; ⁷University of Strasbourg, Inserm, UMR_S1110, Strasbourg, France; ⁸Nuffield Department of Medicine, University of Oxford, Oxford, United Kingdom; ⁹St Vincent's Hospital Melbourne, Melbourne, Australia; ¹⁰Hepatobiliary Division, Department of Internal Medicine, Kaohsiung Medical University Hospital, Kaohsiung, Taiwan; ¹¹Center for Medical Specialist Graduate Education and Research, Hiroshima, Japan; ¹²Division of Chronic Inflammation and Cancer, German Cancer Research Center (DKFZ), Heidelberg, Germany; ¹³Foundation IRCCS Ca' Granda Ospedale Maggiore Policlinico, Milan, Italy; ¹⁴Foundation IRCCS Ca' Granda Ospedale Maggiore Policlinico, Milan, Italy; ¹⁵EASL, Geneva, Switzerland; ¹⁶Hepatobiliary Division, Department of Internal Medicine, School of Medicine and Hepatitis Research Center, College of Medicine, and Center for Liquid Biopsy and Cohort Research, Kaohsiung Medical University Hospital, Kaohsiung, Taiwan; ¹⁷Gastrointestinal Division, Hepatology and Liver Center, Massachusetts General Hospital, Boston, United States; ¹⁸Department of Internal Medicine, University of Texas Southwestern Medical Center, Dallas, United States; ¹⁹Department of Collaborative Research Laboratory of Medical Innovation, Graduate School of Biomedical and Health Sciences, Hiroshima, Japan
Email: thomas.baumert@unistra.fr

Background and aims: Chronic liver disease (CLD) progressing to hepatocellular carcinoma (HCC) is a global health challenge. The role of the circadian clock (CC) as a regulator of liver physiology and disease is well established in rodents. However, in the human liver, the status of the CC-oscillator as well as the identity and the epigenetic landscape of circadian gene networks in CLD remain largely unknown. Despite a major research effort, the pathogenesis of hepatitis C virus (HCV)-induced liver disease and HCC is still only partially understood. Here, we aimed to investigate how HCV perturbs the liver CC to cause CLD and HCC.

Method: By performing circadian RNA- and ChIP-sequencing of livers from control and HCV-infected humanized liver chimeric mice (HM mice) combined with their analyses through *dryR* and JASPAR enabled us to identify genes in human liver displaying a circadian expression pattern and their epigenetic landscape under control condition and their perturbation upon HCV-infection. Through molecular analyses we validated key circadian genes and pathways which were perturbed by HCV in human hepatocytes and associated with risk to progress to HCC. Employing cellular models for HCV infection and perturbation studies, we identified the mechanism of HCV-induced CC perturbation. The clinical impact of these findings was validated with investigations in four independent cohorts of patients with chronic hepatitis C progressing to HCC.

Results: We identified numerous genes and biochemical pathways which are rhythmically expressed in the human hepatocytes under control conditions. Amongst rhythmic genes in human hepatocytes we identified master transcription factors, chromatin modifiers and key enzymes regulating different biochemical pathways. We show that HCV infection deregulates the human liver CC, circadian transcriptome, and epigenome, leading to an activation of key pathways mediating metabolic alterations, fibrosis, and cancer. Using cellular models for HCV infection, we identified the non-structural viral encoded proteins NS4 and NS5A to reduce the expression of deacetylase SIRT1. This reduction in SIRT1 levels leads to a decreased expression of key CC component BMAL1 and a concomitant virus-induced perturbation of the hepatocellular clock. HCV-disrupted circadian pathways remain deregulated in patients following HCV cure and advanced liver disease suggesting that the virus-induced perturbation of the liver CC plays a key role in HCC pathogenesis.

Conclusion: We have identified circadian genes and gene regulatory networks in human liver cells under control conditions and upon HCV infection, a major cause of CLD and HCC. We show that virus-induced alteration of the liver clock drives the perturbation of key genes and pathways implicated in HCC development. These results provide opportunities for HCC prevention and discovery of biomarkers to predict HCC risk.

OS-062

Long-term liver morbidity and mortality after HCV elimination by direct-acting antivirals in patients with chronic hepatitis C: results from a large-scale, multicenter cohort study

Eiichi Ogawa¹, Akira Kawano², Motoyuki Kohjima³, Toshimasa Koyanagi⁴, Kazufumi Dohmen⁵, Aritsune Ooho⁶, Takeaki Satoh⁷, Kazuhiro Takahashi⁸, Norihiro Furusyo⁹, Eiji Kajiwar¹⁰, Koichi Azuma¹¹, Yasunori Ichiki¹², Rie Sugimoto¹³, Hiromasa Amagase¹⁴, Takeshi Senju¹⁵, Chie Morita¹⁶, Masatake Tanaka¹⁷, Makoto Nakamuta³, Hideyuki Nomura¹⁸, Jun Hayashi¹⁸. ¹Kyushu University Hospital, Fukuoka, Japan; ²Kitakyushu Municipal Medical Center, Kitakyushu, Japan; ³National Hospital Organization Kyushu Medical Center, Fukuoka, Japan; ⁴Fukuoka City Hospital, Fukuoka, Japan; ⁵Chihaya Hospital, Fukuoka, Japan; ⁶Steel Memorial Yawata Hospital, Kitakyushu, Japan; ⁷National Hospital Organization Kokura Medical Center, Kitakyushu, Japan; ⁸Hamanomachi Hospital, Fukuoka, Japan; ⁹Taihaku Avenue Clinic, Fukuoka, Japan; ¹⁰Kajiwar Clinic, Kitakyushu, Japan; ¹¹Kyushu Central Hospital, Fukuoka, Japan; ¹²JCHO Kyushu Hospital, Kitakyushu, Japan; ¹³Kyushu Cancer Center, Fukuoka, Japan; ¹⁴Amagase Clinic, Kitakyushu, Japan; ¹⁵Kyushu Rosai Hospital, Kitakyushu, Japan; ¹⁶Kyushu Railway Memorial Hospital, Kitakyushu, Japan; ¹⁷Graduate School of Medical Sciences, Kyushu University, Fukuoka, Japan; ¹⁸Haradai Hospital, Fukuoka, Japan
Email: e.ogawa.a65@m.kyushu-u.ac.jp

Background and aims: Treatment of hepatitis C with direct-acting antivirals (DAAs) results in permanent viral clearance (SVR) in the vast majority of patients with chronic hepatitis C (CHC). Many reports have shown that SVR is associated with a significant reduction of liver

morbidity and mortality for up to approximately five years. The aim of this study was to assess long-term liver-related outcomes and mortality after SVR by DAA treatment.

Method: This multicenter, retrospective cohort study consisted of 3, 128 consecutive adult CHC patients without decompensated cirrhosis who were treated with all-oral DAAs. After excluding patients who did not achieve SVR, 3, 024 were included in this study (2, 691 non-HCC experienced, 333 HCC experienced). The index date was the end of DAA treatment. Primary end points were the occurrence or recurrence of hepatocellular carcinoma (HCC), mortality, and the cause of death.

Results: The median follow-up durations were 6.6 (range 0.3–8.9) and 6.3 (range 0.3–8.9) years for the non-HCC and HCC experienced groups, respectively. Although the cumulative de novo HCC incidence rates were longitudinally increased (3-year, 4.0%; 5-year, 5.6%; 8-year, 7.0%), those of the recurrence rates reached a plateau in 3–5 years (3-year, 50.4%; 5-year, 59.1%; 8-year, 62.0%). None of the patients aged under 50 ($n = 377$) developed de novo HCC. In contrast, for patients with cirrhosis aged 50 and over ($n = 536$), the cumulative de novo HCC incidence rates were high (3-year, 11.2%; 5-year, 15.6%; 8-year, 18.9%). Even in patients without cirrhosis, the 8-year cumulative de novo HCC incidence increased with age (age 50–59, 1.8%; age ≥ 60 , 5.5%; age ≥ 75 , 8.7%) (log-rank test: $P < 0.001$). The 3-year, 5-year, and 8-year survival rates for patients with HCC were 85.2%, 74.6%, and 67.4%, respectively. 74% of the deaths were caused by liver-related complications, mainly HCC recurrence. For patients in the non-HCC group, 72% of the deaths were caused by non-liver-related complications (43% non-liver cancer, 20% cerebral/cardiovascular disease).

Conclusion: DAA treatment improves liver-related morbidity and survival irrespective of HCC experience. Non-cirrhotic patients aged over 60 should be considered for long-term HCC surveillance.

OS-063

What happens to HCV incidence after WHO elimination goal is met? Agent-based modeling predicts sustained availability of direct-acting antivirals among people who inject drugs is required to prevent returning to pre-elimination levels

Eric Tatar^{1,2}, Louis Shekhtman^{3,4}, Nicholson Collier^{1,2}, Marian Major⁵, Jonathan Ozik^{1,2}, Basmattee Boodram⁶, Harel Dahari³.

¹Consortium for Advanced Science and Engineering, University of Chicago, Chicago, IL, United States; ²Decision and Infrastructure Sciences, Argonne National Laboratory, Argonne, IL, United States;

³Program for Experimental and Theoretical Modeling, Division of Hepatology, Department of Medicine, Loyola University Chicago, Maywood, IL, United States; ⁴Department of Information Science, Bar-Ilan University, Ramat Gan, Israel; ⁵Division of Viral Products, Center for Biologics Evaluation and Research, Food and Drug Administration, Silver Spring, MD, United States; ⁶Division of Community Health Sciences, School of Public Health, University of Illinois at Chicago, Chicago, IL, United States

Email: harel.dahari@gmail.com

Background and aims: Persons who inject drugs (PWID) are at high risk for acquiring and transmitting hepatitis C virus (HCV). Direct-acting antiviral (DAA) therapy leads to high cure rates. However, high rates of reinfection after cure in PWID and the lack of protective immunity require access to multiple DAA treatments per person to reach the World Health Organization (WHO) goal of HCV elimination, defined as 90% HCV incidence reduction by 2030. A major public health concern is that treatment will be stopped or significantly reduced once the WHO elimination goal is met due to reduced funds or complacency. We use an agent-based model (ABM) to study the effects of varying levels of enrollment in DAA treatment among HCV infected PWID from Chicago, IL and surrounding suburbs and the effects of stopping access to DAAs after 2030.

Method: We extended our Hepatitis C Elimination in PWID (HepCEP) ABM [PMID: 32624641] to identify and optimize DAA therapy scale-up and treatment strategies. HepCEP uses a mathematical model to

determine transmission probabilities relative to the HCV RNA titers of needle/syringe-sharing donors [PMID: 29997251]. Individual temporal viral load profiles are sampled from unique distributions for acute, chronic and reinfected individuals, and for individuals undergoing DAA treatment. DAA treatment enrollment is modelled as (unbiased) random sampling of chronically infected PWID and the annual target enrollment rate, defined as the total annual treatment enrollment as a fraction of the total PWID population, is a model parameter with a range of 2.5–10%. Access to DAAs is started in 2020 and provided through 2030, after which DAA treatment is stopped. We compared the rates of new chronic infections for different combinations of DAA enrollment and frequency of DAA treatment courses, from 2020–2030 when DAAs are available and after 2030 when DAA treatment is stopped.

Results: The model predicts that elimination can be achieved in the PWID population by 2030 for DAA enrollment rates $\geq 7.5\%$ (75 per 1000 PWID). When DAA treatment is stopped in 2030, the rate of new chronic HCV infections rapidly increases and exceeds the WHO 2030 goal within 12 months, regardless of the enrollment rate prior to 2030.

Conclusion: Modeling results indicate that DAA scale-up of $>7.5\%$ is projected to achieve the WHO target of 90% HCV incidence reduction by 2030. HepCEP model simulations underscore the importance of DAA scale-up without any re-treatment prohibition to achieve significant reductions in HCV incidence when the rates of reinfection among PWID networks are high. Unrestricted re-treatment with enrollment rates of $\geq 7.5\%$ should remain beyond 2030 to maintain the WHO elimination goal and prevent resurgence of HCV incidence to current levels. Our data also underscore the importance of other intervention strategies to maintain the elimination goal, such as syringe exchange programs and vaccines.

OS-064

Outcomes following liver transplantation from HCV-seropositive donors to HCV-seronegative recipients

Margaret C. Liu¹, Josiah McCain², Isabella Reitz³, Alyssa K. McGary⁴, Bashar Aqel¹, Surakit Pungpapong², Rolland Dickson¹. ¹Mayo Clinic Arizona, Phoenix, United States; ²Mayo Clinic Florida, Jacksonville, United States; ³Mayo Clinic Alix School of Medicine, Scottsdale, United States; ⁴Mayo Clinic Arizona, Scottsdale, United States
Email: liu.margaret@mayo.edu

Background and aims: The introduction of Direct-Acting Antiviral Agents (DAA) has provided an opportunity to transplant organs from hepatitis C virus (HCV) seropositive donors into HCV RNA negative recipients to help address the donor organ shortage. In 2020, our institution reported outcomes from 34 HCV-seronegative liver transplant (LT) recipients who received HCV-seropositive donors. Our current study expands this group with longer-term follow-up to further assess the outcomes of HCV-seropositive donors for LT.

Method: We conducted a retrospective observational study of HCV RNA negative recipients who received LT grafts from HCV-seropositive donors. Continuous variables were summarized using median and range, and categorical variables were summarized using the frequency and percentage. Comparisons between the groups were performed using Wilcoxon rank sum test for continuous variables and Fisher's exact test for categorical variables. The overall survival and graft survival between the groups were evaluated using Kaplan-Meier curves and compared using the log-rank test. All analysis was performed using R 4.0.3. All tests were 2-sided, and a p value < 0.05 was considered statistically significant.

Results: There were 103 HCV RNA negative recipients who received HCV-seropositive grafts (51 HCV-viremic, 52 non-viremic). The median MELD at listing was 18 for both viremic and non-viremic groups. Primary etiologies of liver disease were metabolic dysfunction-associated liver disease (31%) and alcohol (28%). Other etiologies included HCV s/p DAA therapy with sustained virologic response (SVR) at the time of listing (5%) and previous allograft failure (3%).

ORAL PRESENTATIONS

Twenty-two recipients (21%) underwent simultaneous liver-kidney transplant. Fifty-one patients (50%) developed post LT HCV viremia, 1/51 (2%) from non-viremic donors and 50/51 (98%) from viremic donors. DAA treatment was started at a median of 18 days (range 5–103 days) after LT. Median pre-treatment viral load was 1980000 IU/ml (range 529–100000000). SVR was defined as undetectable HCV RNA 12 or more weeks post-DAA treatment completion and this was achieved in 48/48 with adequate data; three patients did not have an RNA checked after 12 weeks (1 death, 2 lost to follow-up). There was no statistically significant difference in graft ($p=0.3$) or patient survival ($p=0.6$) between the viremic and non-viremic groups. Overall graft and patient survival were 99% and 99% at 1 year, 99% and 95.9% at 2 years, and 99% and 95.9% at 3 years, respectively. No graft loss was related to recurrent HCV.

Conclusion: Our study demonstrates that liver transplantation with HCV-seropositive donors (both viremic and non-viremic) has excellent outcomes in both short and longer-term follow-up, including up to 3 years post-transplantation. Future studies should aim to evaluate a larger sample size and longer-term outcomes.

Acute liver failure and drug-induced liver injury

OS-065

Cerebral oedema at autopsy in acute liver failure: relationship to clinical features and changes over time

William Bernal¹, Mark J W McPhail², Pervez Ali Khan¹, Stacey Calvert¹, Robert Loveridge¹, Christopher Willars¹, Tasneem Pirani¹, Sameer Patel¹, Georg Auzinger¹, Julia Wendon¹. ¹Liver Intensive Therapy Unit, Kings College Hospital, London, United Kingdom; ²Institute of Liver Studies, Kings College Hospital, London, United Kingdom
Email: william.bernal@kcl.ac.uk

Background and aims: Cerebral Oedema (CO) in acute liver failure (ALF) may cause intracranial hypertension (ICH) and fatal cerebral herniation (CH). Reports assessing clinical signs of ICH suggest a falling prevalence over time. In a large series of ALF patients we assessed autopsy findings of CO and CH and their relation to clinical signs and changes over time.

Method: all autopsies of adult patients with ALF at a single specialist centre 2000–22 were studied. CO was classified with brain autopsy signs of external/cut surface swelling, flattened gyri, narrowed sulci or ventricles. Severe CO was present with additional signs of CH. Presentation of ALF was classified as Hyper-acute (HA), Acute (A) or sub-acute (SA) and clinical signs of ICH included pupillary and reflex abnormalities, and administered treatment.

Results: During the study period 1570 patients with ALF were admitted of whom 311 died at median 5 (1–15) days after admission. Mortality fell from 23% in 2000–09 to 18% in 2010–2022. 137 (44%) of those who died underwent autopsy examination. Median age was 44 (IQR 35–56) yrs, 57% female, 58% paracetamol overdose related. Peak hepatic encephalopathy (HE) grade was 3 (3–4) and 21% had clinical signs of ICH and died 1 (0–5) day later.

Overall, at autopsy 28% had findings of CO, in 7% with CH. CO was present in 33% with HA, 16% A and 8% SA presentations. CH was present only in HA cases. 51% of those with autopsy findings of CO did not have clinical signs of ICH, and 38% of those with apparent clinical signs did not have autopsy findings of CO-however 75% with autopsy findings of CH had pre-mortem clinical signs of ICH.

Evaluating only HA cases, autopsy CO closely related to patient age: present in 59% of age 16–30 yrs, 35% 30–50 yrs and 14% >50 yrs ($p < 0.01$), with CH in 29% 16–30 yrs, 7% 30–50 yrs and none >50 yrs ($p < 0.005$). Admission arterial ammonia was highest in those with CH: no

CO 83 (43–117) vs. 144 (111–269) CH ($p < 0.01$). There was no difference in prevalence of CO comparing cases 2000–2009 with 2010–22, (28% in both eras) and no effect of era on adjusted multivariate analysis.

Conclusion: Autopsy findings confirm that CO occurs in only a minority of the most severely ill patients with ALF and severe HE and is associated with young age, HA presentations and high arterial ammonia concentration, features which identify those who may benefit from enhanced monitoring for ICH. CH is very rarely present. Clinical signs were unreliable predictors of CO except when severe. The prevalence of CO at autopsy has not changed significantly over time despite improvements in spontaneous survival in ALF.

OS-066-YI

Polyreactive immunoglobulin G is elevated in autoimmune hepatitis and drug-induced autoimmune-like hepatitis compared to self-limiting drug-induced liver injury

Theresa Kirchner¹, Alejandro Campos-Murguía¹, George Dalekos², Kalliopi Zachou², Mercedes Robles-Díaz³, Raul J. Andrade⁴, Marcial Sebode⁵, Ansgar W. Lohse⁶, Maciej Janik⁷, Piotr Milkiewicz⁸, Mirjam Kolev⁹, Nasser Semmo⁹, Tony Bruns¹⁰, Tom J.G. Gevers¹¹, Benedetta Terziroli¹², Heiner Wedemeyer¹³, Elmar Jaekel¹⁴, Richard Taubert¹, Bastian Engel¹. ¹Hannover Medical School, Hannover, Germany; ²General University Hospital of Larissa, Larissa, Greece; ³University Hospital Virgen de la Victoria, Malaga, Spain; ⁴Serv Aparato Digestivo, Malaga, Spain; ⁵University Medical Center Hamburg-Eppendorf, Hamburg, Germany; ⁶University Medical Center Hamburg-Eppendorf, Hannover, Germany; ⁷Medical University of Warsaw, Warsaw, Poland; ⁸Pomeranian Medical University, Warsaw, Poland; ⁹Department of Visceral Surgery and Medicine, Inselspital, Bern University Hospital, University of Bern, Bern, Switzerland; ¹⁰Department of Medicine III, University Hospital RWTH Aachen, Aachen, Germany; ¹¹Department of Gastroenterology and Hepatology, Maastricht University Medical Centre, Maastricht, Netherlands; ¹²Epatocentro Ticino, Lugano, Switzerland; ¹³Medizinische Hochschule Hannover, Hannover, Germany; ¹⁴University of Toronto, Toronto, Canada
Email: Engel.Bastian@mh-hannover.de

Background and aims: Drug-induced liver injury (DILI), drug-induced autoimmune-like hepatitis (DI-ALH) and autoimmune hepatitis (AIH) are difficult to differentiate from each other as they often share various clinical characteristics. Recently, polyreactive immunoglobulin G (pIgG) was identified as a novel marker for the diagnosis of AIH in a multicenter study. However, the study included only few DILI cases. This retrospective multicenter study aims to evaluate the diagnostic capacity of pIgG to predict AIH in comparison to DI-ALH, DILI, vaccinia-induced liver injury (VILI) and non-AIH-non-DILI-liver disease (non-AIH-non-DILI-LD).

Method: Samples from 125 patients (AIH $n=82$, DI-ALH $n=9$, DILI $n=23$, VILI $n=11$) were recruited from existing biorepositories from 9 centers across Europe. Quantification of pIgG was done using an in-house ELISA with reactivity against human huntingtin-interacting protein 1-related protein in bovine serum albumin blocked ELISA (HIP1R/BSA) as published.

Results: There was no significant difference in median age ($p=.95$) and sex distribution ($p=.14$). Median ALT was highest in patients with DI-ALH (38.4 times upper limit of normal (xULN)) while it was lower in AIH (16.1 xULN) and DILI (8.7 xULN). Median alkaline phosphatase was lowest in AIH (1.11 xULN; DI-ALH: 1.9 xULN; DILI: 2.0 xULN; VILI: 1.9 xULN; $p=0.001$). Positive serology (any positivity for ANA/SMA/SLA/LKM $\geq 1/40$) was significantly more frequent in AIH (97%), DI-ALH (100%) and VILI (91%) compared to DILI (79%, $p=.002$). Median IgG elevation was significantly lower in the DILI-group ($0.8 \times \text{ULN}$; AIH: $1.1 \times \text{ULN}$; DI-ALH: $0.9 \times \text{ULN}$; VILI $1.0 \times \text{ULN}$; $p=.001$). No patient in the DILI-group received immunosuppressive treatment (98% in AIH-, 100% in DI-ALH- and 82% in VILI-group; $p=.000$) while 99% in the AIH-group had immunosuppressive treatment six months after diagnosis (0% in DI-ALH-group, $p=.000$). Median pIgG levels

were significantly higher in the AIH- (1.9 nAU; $p < 0.001$) and DI-ALH-group (1.6 nAU; $p = .04$) compared to the DILI-group (1.1 nAU). No significant difference in plgG levels was seen in AIH vs. DI-ALH and AIH vs. VILI. When comparing AIH to DILI, sensitivity and overall accuracy of plgG (78%/74%), ANA (77%/70%) and SMA (76%/74%) were comparable. Specificity for LKM (100%) and SLA (91%) was higher compared to plgG (61%), ANA (46%) and SMA (67%). In a second step the cohort was compared to a non-AIH-non-DILI-LD group ($n = 596$) that was published before. plgG levels were significantly higher in the AIH- ($p < 0.002$), DI-ALH- ($p = .003$) and VILI-groups ($p = .01$) while they were comparable between DILI and non-AIH-non-DILI-LD.

Conclusion: Immune-mediated liver diseases (AIH, DI-ALH) were characterized by significantly higher plgG levels compared to DILI. Therefore, plgG determination might help to identify patients with self-limiting DILI avoiding unnecessary immunosuppressive treatment.

OS-067

Specific metabolomic and bile acid profiles and their relationship with gut microbiota composition in patients with drug-induced liver injury

Sara Román-Sagüillo¹, Raisa Quiñones Castro², Alba González-Robles¹, María Juárez-Fernández^{1,3}, Susana Martínez-Flórez¹, Javier González-Gállego^{1,3}, Francisco Jorquera^{1,2,3}, María-Victoria García-Mediavilla^{1,3}, Camilla Stephens^{3,4}, Mercedes Robles-Díaz^{3,4}, Esther Nistal^{1,3}, Ramiro Jover^{3,5}, Sonia Sánchez-Campos^{1,3}. ¹Instituto Universitario de Biomedicina (IBIOMED), Universidad de León, León, Spain; ²Complejo Asistencial Universitario de León, Servicio de Aparato Digestivo, León, León, Spain; ³Centro de Investigación Biomédica en Red de Enfermedades Hepáticas y Digestivas (CIBERehd), Instituto de Salud Carlos III, Madrid, Spain; ⁴Unidad de Gestión Clínica de Aparato Digestivo y Servicio de Farmacología Clínica, Instituto de Investigación Biomédica de Málaga-IBIMA, Hospital Universitario Virgen de la Victoria, Facultad de Medicina, Universidad de Málaga, Málaga, Spain; ⁵Hepatología Experimental, IIS Hospital La Fe and Dep. Bioquímica y Biología Molecular, Universidad de Valencia, Valencia, Spain
Email: sroms@unileon.es

Background and aims: Drug-induced liver disease (iDILI) is a multifactorial hepatic disease considered as the fifth cause of liver-related death worldwide and one of the main causes of acute liver failure in the Western world. Bile acids (BAs) are signaling molecules closely related to iDILI progression and development. In this sense, gut microbiota plays a key role not only in the progression of several hepatic diseases but also in BA metabolism and homeostasis. Thus, our aim is to elucidate the existence of BA and metabolomic profiles associated to iDILI patients, as well as a particular gut microbiota composition pattern linked to this metabolic signature.

Method: 46 patients were divided in 3 groups: healthy controls (C), patients with non-acute hepatitis as a liver damage control group (H) and iDILI patients (iDILI). Blood and stool samples were obtained to perform biochemical analysis, determination of serum and fecal bile acids (BAs) as well as metagenomic and metabolomic examination. Moreover, correlation analyses were carried out.

Results: Significant differences were observed between C, H and iDILI. ALT, AST, ALP, GGT and total bilirubin levels were significantly increased in iDILI and H groups compared to C, whereas albumin concentration were markedly decreased, confirming the hepatic injury and dysfunction. Total and conjugated BAs in serum showed a significant increase in iDILI and H groups in comparison with C while unconjugated BAs were significantly reduced. Regarding fecal BAs, a significant reduction in the main secondary BAs was observed in iDILI compared to C. Moreover, a reduction in fecal metabolites such as n-acetylglutamic acid, dodecanedioic acid and pyridoxamine was observed in iDILI compared to the other groups. Concerning metagenomic analysis, a particular microbiota profile linked to iDILI was identified highlighting a reduction in Barnesiellaceae family and

Barnesiella, Clostridia UCG014 and Eubacterium genus as well as an increase in Alloprevotella genera in comparison with the other groups. Additionally, correlation analyses showed significative associations between concrete taxa, the BA profile and the fecal metabolome, highlighting the genus Barnesiella and Eubacterium and their positive correlation with fecal secondary BAs.

Conclusion: iDILI patients showed a particular BA profile and a defined metabolome which could be related to specific modifications in gut microbiota composition. However, more studies are needed. Funding: PID2020-120363RB-I00, LE017-P20. CIBERehd funded by ISCIII.

OS-068

Urinary amatoxin concentration as an early predictor for liver toxicity in patients with amanita spp poisoning

Ona Escoda¹, Valle Molina², Àngels Gispert³, Cándido Díaz-Lagares⁴, Xavier Ichart⁵, Cristina Solé⁶, Lúcia Martínez⁷, Emilio Salgado¹, Jordi To-Figueras¹, Santiago Nogués⁸, Enric Reverter¹. ¹Hospital Clínic, Barcelona, Spain; ²Clínica Universitaria de Navarra, Navarra, Spain; ³Hospital Universitari Dr. Josep Trueta, Girona, Spain; ⁴Hospital Vall d'Hebron, Barcelona, Spain; ⁵Hospital Arnau de Vilanova, Lleida, Spain; ⁶Hospital Universitari Parc Taulí, Sabadell, Spain; ⁷Hospital Sant Joan de Déu, Esplugues de Llobregat, Spain; ⁸Hospital Clínic, Barcelona, Spain
Email: ereverte@clinic.cat

Background and aims: Mushroom poisoning with *Amanita phalloides* can lead to severe liver injury and associates a mortality around 15%. Early prognostic factors for liver injury development are lacking though a pilot study proposed urinary amatoxin concentration as a prognostic biomarker. In this multicenter study we aimed at validating and refining the prognostic role of urinary amatoxin quantification in patients with *Amanitin* spp. intoxication.

Method: 115 patients from 7 centres with a clinical diagnosis of *Amanita* spp. intoxication and in whom urinary amatoxins were determined (2002–22, ELISA technique) were retrospectively collected. We assessed the association of urinary amatoxin and other baseline variables with liver outcome variables: peak ALT, minimum prothrombin (%), severe hepatotoxicity (ALT>1000 U/L), severe acute liver injury (sALI, INR>1.5), acute liver failure (ALF, encephalopathy), transplantation and death.

Results: 115 patients (57% male, mean age 49.8 years) were included, 56 of whom had positive urinary amatoxins (mean concentration 32.9 ng/ml). Ninety-nine of 115 determinations were done within the first 48 hours after intake. Forty-three patients presented an increase in ALT/ALT levels and 25 had ALT>1000 U/L (20/56 among positive amatoxin patients and 5/59 among negative amatoxin patients). The five patients with negative urinary amatoxins developing hepatotoxicity had a late quantification (>48 h after intake). Among 25 patients with severe hepatotoxicity, 24 also developed sALI and 6 of them ALF (1 transplantation and 4 deaths). Urinary amatoxin concentration and prothrombin, along with other baseline variables, were the strongest predictors of all liver-related end points: peak ALT (with creatinine and haemoglobin), minimum INR and ALT>1000 U/L (with leucocyte and intake-quantification interval) and severe ALI (with intake-quantification interval). Predictions of ALT>1000 U/L and severe ALI were highly accurate with the resulting models with AUC/Nagelkerke R² of 0.918/0.624 and 0.908/0.549, respectively. Amatoxin concentrations >55 ng/ml were highly predictive of hepatotoxicity and severe ALI (10/11 patients) while a negative value within 48 h of intake ruled out the development of severe hepatotoxicity.

Sub-analysis in patients admitted within 48 h of intake ($n = 99$), in those with normal ALT at admission ($n = 89$) and only in positive amatoxin patients ($n = 56$), yielded similar results as in overall cohort. **Conclusion:** In patients with *Amanitin* spp. poisoning, urinary amatoxin concentration and baseline prothrombin were the strongest predictors of hepatotoxicity and severe ALI. Urinary amatoxins >55 ng/ml identified patients at extremely high-risk, while negative

ORAL PRESENTATIONS

values within 48 h of intake ruled out the development of hepatotoxicity.

OS-069

3D bioengineered liver for the study of acute and chronic hepatic damage

Ainhoa Ferret Miñana¹, Estefania Alcaraz², Raquel Horrillo², Javier Ramon Azcon^{1,3}, Francesco De Chiara¹. ¹*Institute for Bioengineering of Catalonia, Barcelona, Spain;* ²*Grifols, Barcelona, Spain;* ³*ICREA-Institució Catalana de Recerca i Estudis Avançats, Barcelona, Spain*
Email: aferret@ibecbarcelona.eu

Background and aims: The liver faces acute and chronic insults that disrupt its normal function. Acute damage, caused by toxins or infections, triggers inflammation and necrosis. Chronic insults, such as alcohol abuse or viral hepatitis, lead to fibrosis, cirrhosis, and hepatocellular carcinoma, posing significant clinical challenges. Fibrosis is a hallmark of liver damage driven by the activation of hepatic stellate cells (HSCs). Understanding the mechanisms underlying acute and chronic liver damage is crucial for developing effective treatments. Traditional liver models face several limitations. 2D cultures cannot maintain liver phenotype and functions for extended periods, making it difficult to model chronic exposure. Additionally, replicating fibrosis in 2D cultures is challenging due to HSC activation on plastic or glass surfaces. As a result, 3D models have emerged as a more physiologically relevant cellular microenvironment for investigating disease progression, identifying potential therapeutic targets, and developing new drugs.

Method: We developed a 3D liver using human hepatocytes, HSCs, and monocytes. The cells were encapsulated in a mixture of gelatin methacryloyl and carboxymethyl cellulose methacrylate, and LAP as a photo-initiator. The 3D livers were kept in culture for up to 30 days in serum-free medium. They were challenged with acetaminophen and LPS (APAP-LPS), known hepatotoxic compounds, to recreate the pathophysiological phenotype of liver damage in vitro. Dexamethasone was used as an anti-inflammatory drug to test the ability of 3D livers to predict drug efficacy.

Results: Extensive liver damage characterized by hepatic stellate cell (HSC) activation and proliferation was observed upon challenge with APAP-LPS. These cells exhibited the myofibroblast phenotype typical of activated HSCs. Additionally, impaired gene expression of hepatocyte functionality markers was observed. The transition from monocytes to proinflammatory cytokine-releasing macrophages measured the inflammation level. Dexamethasone demonstrated potent beneficial effects, reducing hepatocyte damage, inhibiting HSC activation, and decreasing collagen production. These results were observed in both acute and chronic models.

Conclusion: The 3D model presented here demonstrates its value as a versatile platform for drug screening in both acute and chronic liver damage scenarios. Its ability to reproduce critical features of liver pathophysiology, including hepatocyte functionality impairment, HSC activation, and inflammation, makes it a valuable tool for studying liver diseases and evaluating potential therapeutic interventions. Furthermore, the adaptability of this model for high-throughput screening provides an opportunity to accelerate the drug discovery process and improve patient outcomes in liver damage-related conditions.

Gut microbiota and liver disease

OS-070

Faecal microbiota transplantation in patients with cirrhosis, reduces antimicrobial resistance and enteric pathogen carriage, and enhances intestinal barrier function, associated with bacteriophage remodelling

Lindsey Edwards^{1,2}, Benjamin Auch³, Theo Portlock¹, Benjamin H. Mullish⁴, Blair Merrick⁵, Charlotte Woodhouse^{2,6}, Thomas Tranah², Jesus Miguens Blanco⁴, Lilianeleny Meoli², Anna Clavé Llavall², Victoria Kronsten², Ane Zamalloa⁶, Vishal C. Patel^{2,6,7}, Julian R. Marchesi⁴, Saeed Shoaie¹, Ivan Liachko³, Simon Goldenberg⁸, Debbie L. Shawcross^{2,6}. ¹*Centre for Host Microbiome Interactions, King's College London, Faculty of Dentistry, Oral and Craniofacial Sciences, London, United Kingdom;* ²*Institute of Liver Studies, King's College London, Department of Inflammation Biology, School of Immunology and Microbial Sciences, Faculty of Life Sciences and Medicine, London, United Kingdom;* ³*Phase Genomics Inc., Seattle, United States;* ⁴*Imperial College London, Faculty of Medicine, Department of Metabolism, Digestion and Reproduction, London, United Kingdom;* ⁵*Centre for Clinical Infection and Diagnostics Research, Department of Infectious Diseases, Guy's and St Thomas' NHS Foundation Trust, London, United Kingdom;* ⁶*Institute of Liver Studies, King's College Hospital NHS Foundation Trust, London, United Kingdom;* ⁷*The Roger Williams Institute of Hepatology, The Foundation for Liver Research, London, United Kingdom;* ⁸*Centre for Clinical Infection and Diagnostics Research, Department of Infectious Diseases, Guy's and St Thomas' NHS Foundation Trust, London, United Kingdom*
Email: lindsey.edwards@kcl.ac.uk

Background and aims: The World Health Organization States Antimicrobial Resistance (AMR) is “the biggest threat to global health.” Patients with cirrhosis are at high risk for AMR because of frequent antimicrobials, regular invasive procedures such as large-volume paracentesis, and recurrent hospitalisations. Gastrointestinal tract (GIT) carriage of Antibiotic Resistance Genes (ARGs) increases with advancing cirrhosis and is associated with increased hospitalisation and mortality. Microbiota perturbations, intestinal inflammation, and barrier damage boost ARG carriage and susceptibility to infection. Translocation of bacteria and their products across the gut-epithelial-barrier induces cirrhosis-associated immune dysfunction. We hypothesised that faecal microbiota transplant (FMT) may reduce GIT ARG carriage and enhance intestinal barrier function and mucosal immunity.

Method: 32-patient prospective, randomised, single-blinded, placebo-controlled trial evaluating jejunally-transplanted FMT [50 g] against placebo [PROFIT Trial: NCT02862249] in patients with advanced stable cirrhosis (MELD 10–16). We assessed the impact of FMT/placebo 7, 30 and 90-days post-intervention on enteric pathogen and ARG carriage. Plasma and faecal cytokines, gut barrier integrity markers (electrochemiluminescence/ELISA), metabolomics (¹H-NMR), and faecal proteomics were performed. Phase-Genomics-ProxiMeta™-Metagenome-Deconvolution was undertaken to capture co-located-DNA enabling strain-level assignment of phages/ARGs within microbes, not previously possible.

Results: FMT reduced intestinal barrier damage and modified mucosal and systemic inflammation. 20% of participants were colonised with Multi-Drug-Resistant-Organisms including vancomycin-resistant *Enterococci*. FMT virtually eradicated carriage of *Enterococcus faecalis*, Enteropathogenic *Escherichia coli* (EPEC) and ARG [e.g., vanD contributing to vancomycin resistance in *E. faecalis*]. A healthy phagosome, via bacterial lysis, drives microbial diversity and stabilizes microbial populations. We observed bacteriophage network remodelling post-FMT such as the presence of beneficial phages from the family *Oscillospiraceae* which includes

Faecalibacterium prausnitzii. This contrasted with loss of phages from *E. faecalis*, EPEC and *Klebsiella*. Faecal proteomics quantified 301 proteins modified post-FMT, including enzymes involved in host/microbial immuno-metabolism alongside reduced proteins involved in bacterial virulence and AMR.

Conclusion: FMT increased gut microbial richness, reduced carriage of enteric pathogens, and reduced vancomycin-associated ARGs. This was associated with favourable phage network remodelling. FMT reduced intestinal barrier damage and systemic inflammation. Findings support continued evaluation of FMT as a treatment to reduce AMR in cirrhosis.

OS-071-YI

Variation of the human microbiome across multiple body sites and temporal dynamics in different stages of decompensated cirrhosis

Wenyi Gu¹, Annelotte Broekhoven², Sebastian Van Blerk³, Marisa Isabell Keller⁴, Michael Kuhn⁴, Jean-Louis-Marie Insonere³, Alain Roulet³, Robert Schierwagen¹, Camila Alvarez-Silva⁵, Rajna Hercog⁴, Anja Telzerow⁴, Quinten Ducarmon^{4,6}, Romy Zwittink⁶, Ed J Kuijper⁶, Frank Erhard Uschner¹, Rajiv Jalan⁷, Wim Laleman⁸, Debbie L. Shawcross⁹, Joan Clària¹⁰, Manimozhiyan Arumugam¹¹, Peer Bork⁴, Maria Papp¹², Florence Servant³, Minneke Coenraad², Benjamin Lelouvier³, Jonel Trebicka¹. ¹Department of Internal Medicine B, University Hospital Muenster, Muenster, Germany; ²Department of Gastroenterology and Hepatology, Leiden University Medical Center, Leiden, Netherlands; ³Vaiomer, Labège, France; ⁴Structural and Computational Biology Unit, European Molecular Biology Laboratory, Heidelberg, Germany; ⁵Novo Nordisk Foundation Center for Basic Metabolic Research, Faculty of Health and Medical Sciences, University of Copenhagen, Copenhagen, Denmark; ⁶Department of Medical Microbiology, Leiden University Medical Center, Leiden, Netherlands; ⁷UCL Medical School, Royal Free Hospital, London, United Kingdom; ⁸Department of Gastroenterology and Hepatology, University Hospitals Leuven, KU Leuven, Leuven, Belgium; ⁹Institute of Liver Studies, School of Immunology and Microbial Sciences, Faculty of Life Sciences and Medicine, King's College London, London, United Kingdom; ¹⁰Biochemistry and Molecular Genetics Service, Hospital Clínic de Barcelona, Catalonia, Spain, Institut d'Investigacions Biomèdiques August Pi i Sunyer (IDIBAPS), Barcelona, Spain; ¹¹Novo Nordisk Foundation Center for Basic Metabolic Research, Faculty of Health and Medical Sciences, University of Copenhagen, Copenhagen, Denmark; ¹²Division of Gastroenterology, Department of Internal Medicine, Faculty of Medicine, University of Debrecen, Debrecen, Hungary
Email: wenyi.gu@ukmuenster.de

Background and aims: Bacterial infections and/or translocation are major precipitants for acute decompensation (AD) in cirrhosis and for the development of acute-on-chronic liver failure (ACLF). This study explores high and low biomass microbiomes across different body compartments and their correlations with development of ACLF in cirrhosis.

Method: The study included 93 patients with decompensated cirrhosis from the PREDICT study, categorized into four groups based on their disease course: stable decompensated cirrhosis (SDC), unstable decompensated cirrhosis (UDC), pre-ACLF, and ACLF at admission.

We analyzed microbiome variations, using 16S metabarcoding optimized for low biomass and complex microbiomes. We longitudinally (up to 308 visits per compartment) analyzed microbiome variations across 11 anatomical locations, including buffy coat, saliva, upper gastrointestinal (GI) tract mucosa biopsies, lower GI tract mucosa biopsies, and feces. The analysis of microbiome correlations with clinical parameters and disease outcomes was conducted using workframes and tools like PLS-DA, ANCOM II, and SECOM.

Results: The analysis revealed that alpha and beta diversity of microbiome communities depends on the sample sites. Notably,

microbiome load in buffy coat increased with cirrhosis severity in non-ACLF patients (SDC, UDC and pre-ACLF) ($p = 0.023$). Additionally, increased dissimilarity in longitudinal samples from different sites from patients who developed ACLF were observed, probably due to bacterial translocation.

Significant correlations were observed between different taxa across various GI tract compartments, suggesting potential bacterial migration from one compartment to another.

In saliva and upper GI, a positive correlation was found between relative abundance of *Lactobacillales* and ACLF severity. Increased *Pseudomonas* levels are significantly linked to the bacterial infections as precipitant of AD in the upper GI. In the lower GI, *Enterobacterales* abundance correlated with model of end-stage liver disease-sodium (MELD-Na) and CLIF-C AD score. *Enterobacterales* was highly increased in small bowel biopsies (duodenum) in ACLF compared to pre-ACLF patients. This association was still relevant after controlling for confounders (e.g. drugs).

Conclusion: This study reveals that dissimilarity of distinct microbiome profiles from different body compartments increased the progression towards ACLF. Further, different taxa are linked to relevant clinical events. Especially in small bowel and buffy coat, the microbiota and bacterial translocation seem to influence ACLF development.

OS-072-YI

Identifying patterns of steatotic liver disease severity: a multi-omic analysis of 834 distinct omics features from healthy to end-stage liver disease in 854 individuals

Johanne Kragh Hansen^{1,2}, Suguru Nishijima³, Robert Schierwagen⁴, Louise Aas Holm^{5,6}, Karolina Sulek⁷, Tommi Suviataival⁷, Julie Steen Pedersen^{8,9}, Mads Israelsen^{1,2}, Nikolaj Torp^{1,2}, Stine Johansen^{1,2}, Cilius Fonvig⁵, Marta Guindo Martínez⁶, Sara Stinson⁶, Yun Huang⁶, Rasmus Tanderup Jensen⁶, Evelina Stankevici⁶, Michael Kuhn³, Marisa Isabell Keller³, Lore Van Espen¹⁰, Camila Alvarez-Silva⁶, Ida Falk Villesen², Katrine Thorhauge^{1,2}, Peter Andersen², Katrine Lindvig², Andressa de Zawadzki¹¹, Maximilian Joseph Brol⁴, Trine Nielsen⁶, Charlotte Brøns⁷, Helene Baek Juel⁶, Lili Niu^{12,13}, Jens-Christian Holm^{5,6,9}, Flemming Bendtsen^{7,8}, Morten Karsdal¹¹, Matthias Mann^{12,13}, Jelle Matthijssens¹⁰, Cristina Legido-Quigly^{7,14}, Jonel Trebicka⁴, Manimozhiyan Arumugam⁶, Maja Thiele^{1,2}, Lars Juhl Jensen¹², Peer Bork³, Torben Hansen⁶, Aleksander Krag^{1,2}. ¹Department of Clinical Research, Faculty of Health Sciences, University of Southern Denmark, Odense, Denmark; ²Centre for Liver Research, Department of Gastroenterology and Hepatology, Odense University Hospital, Odense, Denmark; ³European Molecular Biology Laboratory, EMBL, Heidelberg, Germany; ⁴Department of Internal Medicine B, University of Münster, Münster, Germany; ⁵The Children's Obesity Clinic, accredited European Centre for Obesity Management, Department of Pediatrics, Copenhagen University Hospital Holbæk, Holbæk, Denmark; ⁶Novo Nordisk Foundation Center for Basic Metabolic Research, Faculty of Health and Medical Sciences, University of Copenhagen, Copenhagen, Denmark; ⁷Steno Diabetes Center Copenhagen, Herlev, Denmark; ⁸Gastro Unit, Medical Division, Hvidovre Hospital, Hvidovre, Denmark; ⁹Faculty of Health Sciences, University of Copenhagen, Copenhagen, Denmark; ¹⁰KU Leuven, Department of Microbiology, Immunology and Transplantation, Rega Institute, Division Clinical and Epidemiological Virology, Laboratory of Viral Metagenomics, Leuven, Belgium; ¹¹Nordic Bioscience A/S, Herlev, Denmark; ¹²Novo Nordisk Foundation Center for Protein Research, Faculty of Health and Medical Sciences, University of Copenhagen, Copenhagen, Denmark; ¹³Department of Proteomics and Signal Transduction, Max Planck Institute of Biochemistry, Martinsried, Germany; ¹⁴Institute of Pharmaceutical Science, King's College London, London, United Kingdom
Email: johanne.kragh.hansen@rsyd.dk

Background and aims: Steatotic Liver Disease (SLD) ranges from simple steatosis to end-stage liver disease. Although specific aspects

of SLD development have been investigated in detail, we still lack a complete understanding of the mechanisms driving the disease. To uncover the potential drivers, we conducted a multi-omics analysis across seven cohorts including both metabolic and alcohol-related aetiologies, exploring the complexity of omics profiles across disease severity ranging from healthy to end-stage liver disease.

Method: Combining seven clinical cohorts, from Denmark and Germany, participants were categorized into six disease severity groups: A) healthy without metabolic or alcohol-related risk factors, B) F0-F1 with at least one risk factor, C) F2, D) F3-F4 incl. MELD-Na <10, E) MELD-Na 10–15, and F) MELD-Na >15. Using linear regression, we did multi-omics analyses of faecal metagenomics, targeted faecal metabolomics, targeted plasma inflammation markers, targeted and untargeted plasma metabolomics, and plasma lipidomics. We clustered omics data to reveal dynamic patterns across the spectrum of disease, identifying features with linear changes and those changing early while turning stable in advanced stages.

Results: We included 854 individuals stratified into disease severity groups: A/B/C/D/E/F 149/348/137/82/103/35. Of 834 omics features measured, 485 were significantly associated with higher levels of disease severity (false discovery rate <0.05). Of 92 circulating inflammation markers, 74 were associated with SLD severity mainly clustered into the linear increasing pattern. The strongest associations were hepatocyte growth factor (effect size = 4.5e-01, $p = 1.2e-60$) and interleukin 8 (effect size = 6.3e-01, $p = 2e-57$). Faecal metagenomics (438 microbial species) revealed 272 significant associations. The majority of features ($n = 195$) tended to decrease in abundance with SLD severity, while 47 features showed a significant increase. The strongest association was increasing *Ruminococcus gnavus* (effect size = 2.8e-01, $p = 2.3e-15$). Targeted and untargeted metabolomics showed a similar trend with mainly significant increasing features. Plasma lipidomics (243 lipids) identified 117 features significantly associated with SLD severity, the majority of which showed a decrease. We could not identify a strong influence of genetic risk factors on the severity of SLD in our data sets.

Conclusion: Our extensive multi-omic analysis of SLD identified 485 key omic features significantly associated with disease severity, providing insights to the complex mechanisms of SLD development. These results highlight unique dynamics in inflammation markers, faecal metagenomics, and plasma metabolomics, set the stage for targeted strategies, and enhance our understanding of pathways from no disease to end-stage liver disease.

OS-073

Linking gut microbiome enterotypes and dysbiosis to liver disease severity and prognosis

Marisa Isabell Keller¹, Suguru Nishijima¹, Daniel Podlesny¹, Chan Yeong Kim¹, Shahriyar Mahdi Robbani¹, Christian Schudoma¹, Anthony Fullam¹, Wasiiu Akanni¹, Askarbek Orakov¹, Thomas Sebastian Schmidt¹, Federico Marotta¹, Ivica Letunic², Jonel Trebicka^{3,4}, Maria Papp⁴, Wim Laleman⁵, Frank Erhard Uschner³, Debbie L. Shawcross⁶, Minneke J. Coenraad⁷, Rajiv Jalan^{8,9}, Joan Clària^{9,10,11,12}, on behalf of the MICROB-PREDICT study group⁹, Michael Kuhn¹, Thea Van Rossum¹, Peer Bork^{1,13,14,15}.

¹European Molecular Biology Laboratory, Structural and Computational Biology Unit, Heidelberg, Germany; ²biobyte solutions GmbH, Bothestr 142, Heidelberg, Germany; ³Department of Internal Medicine B, University Hospital Münster, Münster, Germany; ⁴Division of Gastroenterology, Department of Internal Medicine, Faculty of Medicine, University of Debrecen, Debrecen, Hungary; ⁵Department of Gastroenterology and Hepatology, University Hospitals Leuven, KU

Leuven, Leuven, Belgium; ⁶Institute of Liver Studies, King's College London School of Medicine, King's College Hospital, London, United Kingdom; ⁷Department of Gastroenterology and Hepatology, Leiden University Medical Center, Leiden, Netherlands; ⁸Institute for Liver and Digestive Health, University College, London, United Kingdom; ⁹European Foundation for the Study of Chronic Liver Failure, Barcelona, Spain; ¹⁰Liver Unit, Hospital Clínic, Institut de Investigacions Biomèdiques August Pi i Sunyer (IDIBAPS), University of Barcelona, Barcelona, Spain; ¹¹Centro de Investigación Biomédica en Red de Enfermedades Hepáticas y Digestivas, Barcelona, Spain; ¹²Department of Biomedical Sciences, University of Barcelona, Barcelona, Spain; ¹³Max Delbrück Center for Molecular Medicine, Berlin, Germany; ¹⁴Yonsei Frontier Lab (YFL), Yonsei University, Seoul, Korea, Rep. of South; ¹⁵Department of Bioinformatics, Biocenter, University of Würzburg, Würzburg, Germany
Email: marisa.keller@embl.de

Background and aims: The human gut microbiome is recognized as a critical factor in human health. It can be clustered into enterotypes, which are distinct dominant ecological states of the human fecal microbiome that have also been associated with various health and disease states. In many diseases there are both specific alterations of the gut microbiome and a general state of microbial imbalance known as dysbiosis. Although the definition, causes and consequences of this dysbiosis are poorly understood, it is characterized by increased beta-diversity between patient, also in patients with liver disease. This study aims to integrate the concepts of enterotypes and dysbiosis to improve our understanding of the role of the microbiome in liver disease, particularly in patients with decompensated cirrhosis.

Method: The growth of publicly available metagenomic studies allows us to revisit the enterotype concept through an integrated meta-study of 16, 772 fecal metagenomes drawn from 129 studies, including healthy subjects and individuals with pathologies, covering 32 different diseases. We applied fuzzy k-means clustering to the genus-level taxonomic profiles of the samples to define enterotypes. By quantifying the classification strength of each sample for a given enterotype, we introduced an Enterotype Dysbiotic Score (EDS). A lower classification strength, reflecting inconsistency in enterotype assignment across multiple clustering iterations, indicates a higher level of dysbiosis.

Results: Samples from individuals with liver cirrhosis from the MICROB-PREDICT cohorts, as well as from individuals with other pathologies, had a higher EDS than to those from healthy individuals. Among patients with decompensated cirrhosis, those with acute-on-chronic liver failure and those who died within 90 days had more pronounced dysbiotic states compared to the other patients of the cohort. In addition, EDS is associated with the Model for End-Stage Liver Disease (MELD) score, which, when combined, improved prognostic accuracy for survival. To make enterotypes and EDS accessible, we have developed an online 'Enterotyper' tool (<https://enterotype.embl.de>) that requires no bioinformatic expertise to use. It predicts the enterotypes and the EDS for external cohorts using our reference dataset.

Conclusion: We established a dysbiosis marker that accounts for the underlying microbial ecological states, the enterotypes, and validate the dysbiosis measured by EDS as a key factor in liver disease severity. EDS is associated with disease states and health outcomes, suggesting a biomarker potential and its ability to guide clinical decisions in patients with liver diseases.

OS-074

N-acetyl-phenylalanine, a new metabolite derived from the intestinal microbiota participating in hepatic steatosis by altering ER-mitochondria communication

Cyrielle Caussy¹, Rémy Lefebvre², Nadia Bendridi², Chanon Stéphanie¹, Humbert Alexandre², Arquier Delphine³, Aycirix Sophie³, Bertocchini Nicolas¹, Margaux Nawrot¹, Vielle-Marchiset Aurélie¹, Pillot Bruno¹, Pinteaur Claudie², Rohit Loomba⁴, Jennifer Rieusset². ¹CarMeN Laboratory, UMR INSERM U1060/INRA U1393, Pierre-Bénite, France; ²CarMeN Laboratory, UMR INSERM U1060/INRA U1393, Pierre-Bénite, France; ³Institut des Sciences Analytiques, Univ Lyon, CNRS, Université Claude Bernard Lyon 1, Villeurbanne, France; ⁴NAFLD Research Center, Division of Gastroenterology, La Jolla, United States
Email: cyrielle.caussy@gmail.com

Background and aims: The gut-liver axis is a key component in the development of metabolic dysfunction-associated steatotic liver disease (MASLD), potentially mediated by microbial aromatic amino acids (AAA) derived from phenylalanine and tyrosine. However, the causal role of AAA in MASLD and their mechanisms of action are unknown. On the other hand, disrupted calcium coupling between the endoplasmic reticulum (ER) and mitochondria, at contact points called mitochondria-associated ER membranes (MAMs), contributes to the development of hepatic insulin resistance and steatosis. Therefore, some microbial AAAs could induce hepatic steatosis by disrupting MAMs and mitochondrial oxidative capacities.

Method: We analyzed the metabolomic profile of serum AAA in a derivation cohort of 156 subjects with and without MASLD assessed by magnetic resonance imaging proton density fat fraction (MRI-PDFF) and in a validation cohorts of 156 subjects with biopsy-proven MASLD, prospectively recruited at NAFLD Research Center, UCSD, USA. The per se pro-steatogenic role of MASLD-associated AAA were assessed using BODIPY, their actions on MAMs were assessed using *in situ* proximity ligation assay and mitochondria function was assessed by measuring oxygen consumption in the presence of palmitate, *in vitro*, in Huh7 cells and primary mouse hepatocytes (PMH, 500 µM, 16 h). Effect of AAA were confirmed *in vivo* in mice fed with candidate AAA (gavage of 20 mg/day) for 4 weeks.

Results: N-acetyl-phenylalanine (NAPA) had a strong correlation with MRI-PDFF hepatic fat content ($r: 0.51$ $p < 0.001$), in the derivation cohort and was significantly correlated with the grade of steatosis ($r = 0.21$, $p < 0.01$) in the validation cohort. Serum level of NAPA was significantly correlated with bacterial species from human gut-microbiota using the GUTSY Atlas. *In vitro*, NAPA induces lipid accumulation in both Huh7 (+18.5%, $p < 0.0001$) and PMH (+11.4%, $p < 0.001$). It also alters the structure and function of MAMs including a reduction of MAMs in Huh7 (−37.1%, $p < 0.0001$) and PMH (−33.1%, $p < 0.001$). The reinforcement of MAMs using a linker prevented the effect of NAPA in Huh7. Likewise, diazoxide treatment, which inhibits membrane depolarization prevented the effect of NAPA. *In vivo*, chronic NAPA treatment in mice induced a significant increase in NAPA level in the portal vein and NAPA effects on MAMs alteration and hepatic steatosis development were confirmed.

Conclusion: NAPA is a metabolite potentially derived from the microbiota, strongly association with hepatic steatosis in human. NAPA has a causal effect in the development of hepatic steatosis during MASLD, by disrupting ER-mitochondria communication and mitochondrial oxidative capacities mediated by an electrogenic effect.

Liver tumours: Clinical aspects except therapy

OS-075-YI

GALAD score is effective for HCC surveillance among high-risk patients

Grishma Hirode^{1,2,3}, Hooman Farhang Zangneh¹, Orlando Cerocchi¹, Lima Awad El-Karim⁴, Korosh Khalili⁴, Harry L.A. Janssen^{1,5}, Bettina E. Hansen^{1,6,7}, Jordan J. Feld^{1,2,3}. ¹Toronto Centre for Liver Disease, Toronto General Hospital, University Health Network, Toronto, Canada; ²The Viral Hepatitis Care Network Canada (VIRCAN), Toronto, Canada; ³Institute of Medical Science, University of Toronto, Toronto, Canada; ⁴Joint Department of Medical Imaging, University Health Network, Toronto, Canada; ⁵Department of Gastroenterology and Hepatology, Erasmus MC University Medical Center, Rotterdam, Netherlands; ⁶Department of Epidemiology and Biostatistics, Erasmus MC University Medical Center, Rotterdam, Netherlands; ⁷Institute of Health Policy, Management and Evaluation, University of Toronto, Toronto, Canada
Email: grishma.hirode@gmail.com

Background and aims: Although guidelines recommend regular, biannual hepatocellular carcinoma (HCC) surveillance among patients at higher risk, several patients continue to be diagnosed at an advanced stage. Improvements in early-stage HCC diagnoses require a better understanding of current methods, and the exploration of novel strategies. The GALAD score uses a combination of demographics and biomarkers (BMs) to assess HCC risk. We aim to analyze the utility of various surveillance methods for the detection of early-stage HCC.

Method: This is a secondary analysis of a prospective study of patients with cirrhosis or high-risk hepatitis B virus (HBV) infection (REACH-B score ≥ 9) randomized to HCC surveillance with ultrasound (US) alone (Group A) or US and BM (Group B) measuring alpha-fetoprotein (AFP), lectin-reactive fraction of AFP (AFP-L3), and des-gamma-carboxy prothrombin (DCP). For all analyses using Group B data, any BM levels above the specified thresholds (AFP > 100 ng/ml, AFP-L3 $> 10\%$, DCP > 2 ng/ml) or a positive US result triggered further imaging for HCC confirmation. We compared the effectiveness of the GALAD score to US alone, each BM alone, and all three BMs combined using the area under the receiver operating characteristic (AUROC) curve after logistic regression while accounting for patient-level variance.

Results: Among 1,208 patients in this study (baseline age 58 ± 9.8 years, 72% male, 64% HBV, 64% cirrhosis), 35/603 (6%) patients were diagnosed with HCC (30 early-stage, 5 advanced) in Group A and 27/605 (5%) patients were diagnosed with HCC (22 early-stage, 5 advanced) in Group B. AUROCs for both groups were 0.81. In the absence of US in Group B, AUROC for any elevated BM was 0.71 which was higher than elevated AFP alone (0.55, $p = 0.01$), elevated AFP-L3 alone (0.64, $p = 0.11$), and elevated DCP alone (0.59, $p = 0.03$). The AUROC was 0.89 using a longitudinal GALAD score in Group B, which performed better than all three BMs combined at the prespecified thresholds ($p = 0.001$). The optimal cut-point for the GALAD score in Group B was -1.8 which would yield a sensitivity of 0.89, specificity of 0.81, and an AUROC of 0.85. Using a GALAD score threshold of -0.63 in this cohort, as suggested by previous studies, yielded a lower AUROC of 0.77 ($p = 0.17$).

Conclusion: In this large study, use of the GALAD score showed more promise compared to any of the BMs alone. There was no difference in the effectiveness of US alone compared to US plus any elevated BMs using the specified thresholds. However, each elevated BM alone was less effective compared to the use of US alone, US plus BMs, or the GALAD score. Establishing and validating optimal thresholds for the BMs and the GALAD score is crucial to improve surveillance methods for the detection of early-stage HCC.

OS-076-YI

Bile extracellular vesicles hold protein biomarkers for the early diagnosis of cholangiocarcinoma in individuals with primary sclerosing cholangitis

Ainhoa Lapitz^{1,2}, Marit Grimsrud^{3,4,5}, Pedro Miguel Rodrigues^{1,2,6}, Johannes R. Hov^{4,5,7}, Mette Vesterhus^{7,8,9}, Mikel Azkargorta^{2,10}, Krzysztof Grzyb¹¹, Henrik Mikael Reims¹¹, Felix Elortza^{2,10}, Laura Izquierdo-Sánchez^{1,2}, María Jesús Perugorria^{1,2,12}, Luis Bujanda^{1,2,12}, Lars Aabakken⁴, Vemund Paulsen⁴, Tom Hemming Karlsen^{3,4,5}, Jesus Maria Banales^{1,2,6,13}, Trine Følseraas^{5,7,14}, ¹Biogipuzkoa Health Research Institute, San Sebastian, Spain; ²National Institute for the Study of Liver and Gastrointestinal Diseases (CIBERehd), ISCIII, Madrid, Spain; ³Norwegian PSC Research Center, Oslo, Norway; ⁴University of Oslo, Oslo, Norway; ⁵Oslo University Hospital Rikshospitalet, Oslo, Norway; ⁶Ikerbasque, Basque Foundation for Science, Bilbao, Spain; ⁷Norwegian PSC Research Center, Oslo, Spain; ⁸University of Bergen, Bergen, Norway; ⁹University of Bergen, Bergen, Spain; ¹⁰Proteomics Platform, CIC bioGUNE, Derio, Spain; ¹¹Oslo University Hospital, Oslo, Norway; ¹²Faculty of Medicine and Nursing, University of the Basque Country, Leioa, Spain; ¹³University of Navarra, Pamplona, Spain; ¹⁴University of Oslo, Oslo, Spain
Email: ainhoa.lapitz@biodonostia.org

Background and aims: Cholangiocarcinoma (CCA) presents a significant threat to individuals with primary sclerosing cholangitis (PSC), with a 20-year cumulative incidence of approximately 15%. Early diagnosis is challenging due to overlapping symptoms, and recommended MRI/MRCP surveillance every 6–12 months often proves suboptimal in detecting early-stage cancer. PSC-CCA patients face a grim prognosis, with a median overall survival of 5–12 months in unresectable cases, making CCA the primary cause of PSC-associated mortality. There is a critical need for more accurate early detection methods, allowing access to potentially curative options like tumor resection or liver transplantation. In this regard, investigating extracellular vesicles (EVs) in bile, which come into direct contact with CCA tumors, offers a promising avenue for identifying diagnostic CCA biomarkers in PSC, and these were evaluated in this study.

Method: Bile EVs were collected from patients with isolated PSC (PSC, n = 52), PSC with CCA (PSC-CCA, n = 14), or PSC at time of sampling but who later developed CCA (PSC to CCA, n = 8), at Oslo University Hospital Rikshospitalet (Norway). The EV-protein content was characterized using mass spectrometry. Diagnostic biomarkers for PSC-CCA, as well as early-diagnostic/predictive biomarkers for the PSC to CCA group were identified and combined using binary logistic regression multivariable models.

Results: High-throughput proteomics of bile EVs identified 21 diagnostic biomarkers for PSC-CCA, regardless of sex, age, the presence of inflammatory bowel disease, or cirrhosis at the time of sampling. Among these, 14 biomarkers were observed to be more abundant, and 7 exhibited lower levels in patients with PSC-CCA compared to patients with isolated PSC. Machine learning algorithms revealed COPA/ATP5H/VTNC/IQGA1/PRDX2 (AUC = 0.996) and COPA/ATP5H/VTNC/IQGA1/CALX/PRDX2 (AUC = 1.000) as highly effective in diagnosing PSC-CCA versus isolated PSC, surpassing the performance of serum CA19-9 alone (AUC = 0.846). Notably, the logistic model combining TM9S4/RS18/LPPRC/NHRF1 demonstrated predictive capacity for CCA development in PSC before any clinical evidence of malignancy with 100% sensitivity and specificity (AUC = 1.000), whereas serum CA19-9 exhibited no significant predictive capacity for CCA development (AUC = 0.596).

Conclusion: Bile EVs harbor valuable protein biomarkers for predicting the development of CCA and enabling early diagnosis in individuals with PSC. Given the ease of bile collection during stenting for dominant strictures in individuals with PSC, this innovative liquid biopsy tool may be of significant value for monitoring disease progression and aiding access of potentially curative treatment options.

OS-077

Added value of a combination of positron emission tomography with 18F-FDG and 18 F-Fluorocholine for staging optimization and treatment modification in patients with hepatocellular carcinoma: the prospective multicentric PET HCC01 study

Jean Charles Nault¹, Marouane Boubaya², Myriam Wartski³, Anthony Dohan⁴, Stanislas Pol⁵, Gabriel Pop⁶, Michael Soussan⁷, Olivier Serot⁸, Charlotte Costentin⁹, Julie Roux¹⁰, Christian Sengel¹¹, Marie Lequoy¹², Françoise Montravers¹³, Yves Menu¹⁴, Georges-Philippe Pageaux¹⁵, Denis Mariano Goulart¹⁶, Boris Guiu¹⁷, Alain Luciani¹⁸, Marco Dioguardi Burgio¹⁹, Mathilde Wagner²⁰, Philippe Maksud²¹, Sébastien Mulé²², Manon Allaire²³, Sabrina Sidali²⁴, Audrey Coilly²⁵, Florent Besson²⁶, Maïte Lewin²⁷, Hélène Regnault²⁸, Clemence Hollande²⁴, Giuliana Amadio²⁸, Maxime Ronot²⁹, Nathalie Ganne-Carrié^{30,31,32}, Vincent Lévy³³, Lebtahi Rachida³⁴, Julia Chalaye³⁵, Mohamed Bouattour²⁴. ¹Service d'hépatologie, hôpital Avicenne, Bobigny, France; ²URC-CRC GHPSS, Hôpital Avicenne, AP-HP, Bobigny, France; ³Service Médecine nucléaire, Hôpital Cochin, APHP, Paris, France; ⁴Service Radiologie, Hôpital Cochin, APHP, Paris, France; ⁵Service d'hépatologie, hôpital Cochin, APHP, Paris, France; ⁶Service de médecine nucléaire, hôpital Avicenne, APHP, Bobigny, France; ⁷Service de médecine nucléaire, hôpital Avicenne, APHP, Bobigny, France; ⁸Service de radiologie interventionnel, hôpital Avicenne, Bobigny, France; ⁹Hépatogastroentérologie, centre Hospitalier Universitaire Grenoble Alpes, Grenoble, France; ¹⁰Service Médecine nucléaire, centre Hospitalier Universitaire Grenoble Alpes, Grenoble, France; ¹¹Radiologie Grenoble, centre Hospitalier Universitaire Grenoble Alpes, Grenoble, France; ¹²Service d'hépatologie, Hôpital Saint-Antoine, APHP, Paris, France; ¹³Service Médecine nucléaire, Hôpital Tenon, APHP, Paris, France; ¹⁴Service Radiologie, Hôpital Saint-Antoine, APHP, Paris, France; ¹⁵Service d'hépatologie CHU Montpellier-Hôpital Saint Eloi, Montpellier, France; ¹⁶Service Médecine nucléaire, CHU Montpellier, Montpellier, France; ¹⁷Service Radiologie, CHU Montpellier-Hôpital Saint Eloi, Montpellier, France; ¹⁸Service Radiologie, Hôpital Henri Mondor, APHP, Paris, France; ¹⁹Service Radiologie, Hôpital Beaujon, APHP, Clichy, France; ²⁰Service Radiologie, hôpitaux Universitaires Pitié Salpêtrière, APHP, Paris, France; ²¹Service médecine nucléaire, hôpitaux Universitaires Pitié Salpêtrière, APHP, Paris, France; ²²Service Radiologie, Hôpital Henri Mondor, APHP, Créteil, France; ²³Service d'hépatogastroentérologie, hôpital Pitié Salpêtrière, APHP, Paris, France; ²⁴Service d'hépatologie, hôpital Beaujon, APHP, Clichy, France; ²⁵Service d'hépatologie, Hôpital Paul Brousse, APHP, Villejuif, France; ²⁶Service Médecine nucléaire, CHU Bicêtre, AP-HP, Bicêtre, France; ²⁷Service Radiologie, Hôpital Paul Brousse, APHP, Villejuif, France; ²⁸Service d'hépatologie, hôpital Henri Mondor, APHP, Créteil, France; ²⁹Service de radiologie, hôpital Beaujon, APHP, Clichy, France; ³⁰Service d'hépatologie, hôpital Avicenne, APHP, Bobigny, France; ³¹APHP, Hôpital Avicenne and Sorbonne Paris Nord Université, Liver unit, BOBOGNY, France; ³²APHP, Hôpital Avicenne and Sorbonne Paris Nord Université, Liver unit, BOBOGNY, France; ³³URC-CRC GHPSS, Hôpital Avicenne, AP-HP Bobigny, Bobigny, France; ³⁴Service médecine nucléaire, Hôpital Beaujon, APHP, Clichy, France; ³⁵Service Médecine nucléaire, Hôpital Henri Mondor, APHP, Créteil, France
Email: naultjc@gmail.com

Background and aims: The role of positron emission tomography (PET) with 18F-FDG and 18F-Fluorocholine in staging of hepatocellular carcinoma (HCC) and its impact on treatment decisions has never been prospectively assessed.

Method: We conducted a multicentric prospective study in nine centers in France, including patients with a first diagnosis of HCC classified as BCLC A to C (excluding extrahepatic metastasis) and without contraindications to contrast-enhanced CT and MRI (Clinical trial NCT04391348). Patients underwent 18F-FDG-PET-CT and 18F-fluorocholine-PET-CT, liver MRI, and chest and hepatic CT within 4 weeks. A first tumor staging and treatment decision were performed in the multidisciplinary tumor board using morphological imaging, blind to the results of the PET-CTs. The results of the PET-CTs were

then revealed, and a second tumor staging and treatment decision were recorded by the same team. New lesions detected by PET-CT were confirmed as HCC if they increase in size during follow-up or by histology. The primary end point was the proportion of patients whose treatment planned by the multidisciplinary meeting was modified (from curative intent to palliative or from locoregional palliative to systemic treatment) by the combined use of 18F-FDG and 18F-Fluorocholine PET-CTs. The minimal clinically significant difference in the proportion of patients who would have a change in their treatment plan due to the PET-CTs was set at 15% (CI95%: 10–20%), and we planned to include 230 patients.

Results: A total of 230 patients were included, with 215 analyzable for the primary end point. Among these 215 patients, the median age was 65.7, 89.8% were male, and 72% were cirrhotic. Using morphological imaging, HCC was classified as BCLC stage A (n = 140, 65.1%), -stage B (n = 49, 22.8%), and stage C (n = 26, 12.1%, mainly without metastasis). Overall, 202 patients (94%) underwent 18F-FDG and 18F-fluorocholine-PET-CTs; eight patients underwent 18F-fluorocholine only, and four 18F-FDG only. New lesions were identified in 20 patients (9.3%), by PET-CTs (16 new extrahepatic lesions and five new intrahepatic lesions, including eight identified by both tracers, six by 18F-FDG, and seven by 18F-fluorocholine). The PET-CTs modified the BCLC stage in 10 patients (4.7%): from BCLC A to B (n = 2), from BCLC A to C (n = 2), from BCLC B to C (n = 2), and from BCLC C without metastasis to BCLC C with metastasis (n = 4). The primary end point (modification of the initial treatment) was met in four patients (2.9%): SIRT + atezolizumab/bevacizumab to atezolizumab/bevacizumab only (n = 1), partial resection to atezolizumab/bevacizumab (n = 1) or to SIRT (n = 1), and TACE to atezolizumab/bevacizumab (n = 1).

Conclusion: 18F-FDG and 18F-Fluorocholine-PET-CTs should not be systematically performed for staging in patients with a first diagnosis of HCC, as they modified treatment decisions in a minority of patients.

OS-078-Y1

Hepatic decompensation as an aetiology-dependent determinant of mortality in patients with hepatocellular carcinoma treated with atezolizumab plus bevacizumab

Ciro Celsa^{1,2}, Giuseppe Cabibbo¹, Claudia Fulgenzi³, Bernhard Scheiner⁴, Salvatore Battaglia¹, Antonio D'Alessio³, Giulia Manfredi⁵, Bernardo Stefanini³, Naoshi Nishida⁶, Peter R. Galle⁷, Kornelius Schulze⁸, Henning Wege⁸, Roberta Ciccia¹, Wei-Fan Hsu⁹, Caterina Vivaldi¹⁰, Brooke Wietharn¹¹, Po-Ting Lin¹², Angelo Pirozzi¹³, Tiziana Pressiani¹⁴, Andrea Dalbeni¹⁵, Leonardo Antonio Natola^{15,16}, Alessandra Auriemma¹⁷, Cristina Rigamonti¹⁸, Michela Emma Burlone¹⁹, Alessandro Parisi²⁰, Yi-Hsiang Huang²¹, Pei-Chang Lee²¹, Celina Ang²², Thomas Marron²³, Matthias Pinter²⁴, Jaekyung Cheon²⁵, Hong Jae Chon²⁶, Samuel Phen²⁷, Amit Singal²⁸, Anuhya Gampa²⁹, Anjana Pillai²⁹, Robert Thimme³⁰, Arndt Vogel^{31,32}, Noha Soror³³, Susanna V. Ulahannan³⁴, Rohini Sharma³⁵, David Sacerdoti³⁶, Mario Pirisi³⁷, Lorenza Rimassa³⁸, Chun-yen Lin³⁹, Anwaar Saeed⁴⁰, Natascha Röhlen⁴¹, Gianluca Masi⁴², Martin Schoenlein⁸, Johann von Felden⁸, Masatoshi Kudo⁴³, Alessio Cortellini⁴⁴, Calogero Camma⁴⁵, David J. Pinato⁴⁶. ¹University of Palermo, Palermo, Italy; ²Imperial College, London, United Kingdom; ³Department of Surgery and Cancer, Imperial College, London, United Kingdom; ⁴Department of Internal Medicine III, Div. of Gastroenterology and Hepatology, University of Wien, Wien, Austria; ⁵Department of Surgery and Cancer, London, United Kingdom; ⁶Kindai University, Osaka, Japan; ⁷Department of Medicine, University Medical Center of the Johannes Gutenberg-University, Mainz, Germany; ⁸University Medical Center Hamburg-Eppendorf, Hamburg, Germany; ⁹China Medical University Hospital, Taichung, Taiwan; ¹⁰Unit of Medical Oncology 2, Azienda Ospedaliero-, Universitaria Pisana, Pisa, Italy; ¹¹Department of Medicine, Division of Medical Oncology, Kansas University Cancer Center, Kansas City, Kansas, USA, Kansas City, United States; ¹²Department of Gastroenterology and Hepatology, Chang Gung Memorial Hospital, Linkou branch, Taoyuan, Taiwan; ¹³Department of

Biomedical Sciences, Humanitas University, Milan, Italy; ¹⁴Humanitas Research Hospital-IRCCS, Rozzano (MI), Italy; ¹⁵University of Verona and University and Hospital Trust (AOUI) of Verona, Verona, Italy; ¹⁶University of Verona, Division of General Medicine C and Liver Unit, Department of Medicine, Verona, Italy; ¹⁷Section of Innovation Biomedicine-Oncology Area, Department of Engineering for Innovation Medicine (DIMI), University of Verona and University and Hospital Trust (AOUI) of Verona, Verona, Italy; ¹⁸Department of Translational Medicine, Università del Piemonte Orientale, Novara, Italy; and Division of Internal Medicine, AOU Maggiore della Carità, Novara, Italy; ¹⁹Università del Piemonte Orientale, Novara, Italy; ²⁰University della Marche Ancona, Ancona, Italy; ²¹Taipei Veterans General Hospital, Taipei, Taiwan; ²²Mount Sinai Hospital, New York, United States; ²³Mount Sinai Hospital, New York, United States; ²⁴Medical University of Vienna, Wien, Austria; ²⁵Department of Internal Medicine, CHA Bundang Medical Center, CHA University, Seongnam, Korea, Rep. of South; ²⁶CHA Bundang Medical Center, CHA University, Seongnam, Korea, Rep. of South; ²⁷University of Texas Southwestern Medical Center, Dallas, Texas, United States; ²⁸UT Southwestern Medical Center, Dallas, United States; ²⁹University of Chicago, Chicago, United States; ³⁰University Medical Center Freiburg, Freiburg, Germany; ³¹Hannover University, Hannover, Germany; ³²Division of Gastroenterology and Hepatology, Toronto General Hospital, Medical Oncology, Toronto, Canada; ³³Medical Oncology/TSET Phase 1 Program, Stephenson Cancer Center, University of Oklahoma, Oklahoma City, United States; ³⁴Medical Oncology/TSET Phase 1 Program, Stephenson Cancer Center, University of Oklahoma, Oklahoma City, United States; ³⁵Department of Surgery and Cancer, Hammersmith Hospital, London, United Kingdom; ³⁶University of Verona, Verona, Italy; ³⁷Università del Piemonte Orientale, DiMeT, Novara, Italy; ³⁸Humanitas University, Rozzano (MI), Italy; ³⁹Chang-Gung Memorial Hospital, Linkou Medical Center, Taiwan, TaoYuan, Taiwan; ⁴⁰University of Pittsburgh, Pittsburgh, Italy; ⁴¹Department of Medicine II, Medical Center, University of Freiburg, Freiburg, Germany; ⁴²Department of Translational Research and New Technologies in Medicine and Surgery, University of Pisa, Pisa, Italy; ⁴³Kindai University Faculty of Medicine, Osaka, Japan; ⁴⁴Fondazione Policlinico Universitario Campus Bio-Medico, Rome, Italy; ⁴⁵Section of Gastroenterology and Hepatology, University of Palermo, Palermo, Italy; ⁴⁶Department of Surgery and Cancer, Hammersmith Hospital, Imperial College, London, United Kingdom
Email: celsaciro@gmail.com

Background and aims: Unlike other malignancies, hepatic functional reserve competes with tumour progression in determining the risk of mortality from hepatocellular carcinoma (HCC), making overall survival (OS) a uniquely composite end point. Combination immunotherapy is the most effective modality to prolong OS through improved control of tumour progression in advanced HCC. However, the relative contribution of hepatic decompensation over tumour progression in influencing OS has not been assessed in immunotherapy recipients.

Method: From the AB-real observational study (n = 898), we accrued 346 patients with advanced/unresectable HCC, Child-Pugh A class treated with frontline atezolizumab plus bevacizumab. Hepatic decompensation and tumour progression during follow-up were studied in relationship to patients' OS using time-dependent Cox models. Baseline characteristics were evaluated as predictors of hepatic decompensation in competing risks analysis.

Results: During a median follow-up of 9.3 months (95%CI 8.0–10.3), 154 patients (44.5%) developed tumour progression without decompensation and 58 patients (16.8%) developed decompensation. Median OS was 14.9 months (95%CI 12.6–19.7) in patients with HCC progression in absence of hepatic decompensation and 7.1 months (95%CI 5.2–10.5) in patients with hepatic decompensation (p < 0.001). In multivariable time-dependent analysis, hepatic decompensation (hazard ratio[HR] 23.43, 95%CI 8.40–65.31), HCC progression (14.78, 95%CI 5.99–36.45), albumin-bilirubin (ALBI) grade 2/3 (HR 2.12, 95%CI 1.45–3.10) and successful aetiological

ORAL PRESENTATIONS

treatment for underlying chronic liver disease (HR 0.58, 95%CI 0.40–0.83) emerged as covariates independently associated with OS. Pre-treatment platelet count <140*10⁹/L (HR 1.77, 95%CI 1.01–3.12) and ALBI grade 2/3 (HR 2.89, 95%CI 1.50–5.56) were independently associated with hepatic decompensation, whereas successful aetiological treatment was protective (HR 0.53, 95%CI 0.30–0.93). The probability of decompensation at 12 months was higher in patients with metabolic aetiology compared to others (31.4%vs17.5%, $p=0.030$).

Conclusion: Hepatic decompensation identifies patients with the worst prognosis following atezolizumab plus bevacizumab and is more common in thrombocytopenic patients with baseline ALBI>1. Effective management of underlying liver disease may protect from decompensation, highlighting the prognostic disadvantage of patients with metabolic aetiology and the importance of multi-disciplinary management to maximise OS.

OS-079-YI

Development and validation of the CABLE score to estimate individual prognosis of patients with hepatocellular carcinoma treated with 1L atezolizumab and bevacizumab

Simon Johannes Gairing¹, Philipp Mildenberger², Jennifer Gile³, Fabian Artusa⁴, Bernhard Scheiner⁵, Catherine Leyh⁶, Sabine Lieb⁷, Friedrich Sinner⁸, Vincent Jörg⁹, Thorben Fruendt⁹, Vera Himmelsbach¹⁰, Nada Abedin¹⁰, Cennet Sahin¹¹, Katrin Boettcher¹², Jasmin Schuhbaur¹³, Simon Labuhn¹⁴, James Korolewicz¹⁵, Claudia Fulgenzi¹⁵, Antonio D'Alessio^{15,16}, Valentina Zanuso^{17,18}, Florian Hucke¹⁹, Natascha Röhlen²⁰, Najib Ben Khaled²¹, Eleonora Ramadori²², Lukas Müller¹, Arndt Weinmann¹, Roman Kloeckner²³, Peter R. Galle¹, Nguyen H. Tran²⁴, Sudhakar Venkatesh²⁴, Andreas Teufel^{25,26}, Enrico de Toni²¹, Dirk-Thomas Waldschmidt²², Jens U. Marquardt²³, Dominik Bettinger²⁰, Markus Peck-Radosavljevic¹⁹, Andreas Geier²⁷, Florian P Reiter²⁷, Lorenza Rimassa^{17,18}, David J. Pinato^{15,16}, Christoph Roderburg¹⁴, Thomas Ettrich¹³, Michael Bitzer²⁸, Veit Scheble²⁸, Ursula Ehmer¹², Marie-Luise Berres¹¹, Fabian Finkelmeier¹⁰, Maria Angeles Gonzalez-Carmona²⁹, Johann von Felden⁹, Kornelius Schulze⁹, Marino Venerito⁸, Florian van Bömmel⁷, Leonie Jochheim⁶, Matthias Pinter⁵, Raphael Mohr⁴, Sumera I. Ilyas²⁴, Irene Schmidtmann², Friedrich Foerster¹. ¹University Medical Center of the Johannes Gutenberg University Mainz, Mainz, Germany; ²Institute of Medical Biometry, Epidemiology and Informatics of the Johannes Gutenberg-University Mainz, Mainz, Germany; ³Mayo Clinic, Minnesota, USA, Rochester, United States; ⁴Charité-Universitätsmedizin Berlin, Berlin, Germany; ⁵Medical University of Vienna, Vienna, Austria; ⁶Essen University Hospital, Essen, Germany; ⁷University of Leipzig Medical Center, Leipzig, Germany; ⁸Otto von Guericke University Hospital, Magdeburg, Germany; ⁹University Medical Center Hamburg-Eppendorf, Hamburg, Germany; ¹⁰University Hospital Frankfurt, Frankfurt, Germany; ¹¹University Hospital RWTH Aachen, Aachen, Germany; ¹²TUM School of Medicine and Health, University Medical Center, Technical University of Munich, München, Germany; ¹³University of Ulm, Ulm, Germany; ¹⁴University Hospital Düsseldorf, Düsseldorf, Germany; ¹⁵Imperial College London, Hammersmith Hospital, London, United Kingdom; ¹⁶University of Piemonte Orientale, Novara, Italy; ¹⁷Humanitas University, Milan, Italy; ¹⁸Humanitas Cancer Center, IRCCS Humanitas Research Hospital, Milan, Italy; ¹⁹Klinikum Klagenfurt am Wörthersee, Klagenfurt, Austria; ²⁰Medical Center University of Freiburg, Freiburg, Germany; ²¹University Hospital, Ludwig Maximilian University Munich, München, Germany; ²²University of Cologne, Köln, Germany; ²³University Hospital Schleswig-Holstein, Lübeck, Germany; ²⁴Mayo Clinic, Rochester, United States; ²⁵Department of Medicine II, Medical Faculty Mannheim, Heidelberg University, Mannheim, Germany;

²⁶Clinical Cooperation Unit Healthy Metabolism Medical Faculty Mannheim, Heidelberg University, Mannheim, Germany; ²⁷University Hospital Würzburg, Würzburg, Germany; ²⁸University Hospital of Tübingen, Tübingen, Germany; ²⁹University Hospital of Bonn, Bonn, Germany
Email: sgairing@uni-mainz.de

Background and aims: Immunotherapy with atezolizumab plus bevacizumab (a+b) has significantly prolonged survival of patients with unresectable hepatocellular carcinoma (uHCC). However, prognosis is not only dependent on tumor-associated characteristics, but on several other factors such as hepatic function or inflammation. The aim of this study was i) to develop and validate a prediction model allowing to estimate individual prognosis of patients treated with a+b and ii) to compare it with currently used models.

Method: In this retrospective, multinational study, patients with uHCC treated with first-line (1L) a+b from 24 centers across Europe and the US were included. TRIPOD guidelines were used for reporting and analysis. Overall survival (OS) was the primary objective.

Results: A total of 683 patients were analyzed (training set: $n=526$, validation set: $n=157$). In the training set, median age was 67 years (range 25–90), 81% were male and most had preserved liver function (Child A/B: 73%/27%). Median OS was 13.7 months (95% CI: 12.1, 15.8). In total, 235 outcome events occurred during follow-up in the training set. The objective response rate was 32%, the disease control rate 72%. After a stepwise model building procedure, C-reactive protein, albumin, bilirubin, lymphocytes, ECOG performance status, and extrahepatic spread (CABLE score) remained significantly associated with OS. In the training set, the CABLE score had a higher discriminatory performance compared to ALBI, EZ-ALBI, mALBI, CRAFTY, PNI, NLR, PLR, and GPS (time-dependent AUC 0.79, C-index 0.75 (95% CI 0.71–0.78) at 12 months). In the external validation set, the discriminatory accuracy of the CABLE score was comparable to ALBI, EZ-ALBI, and mALBI, but on average higher than PNI, CRAFTY, NLR, PLR, and GPS. To allow the estimation of individual prognosis, we built a web-based calculator for the CABLE score (http://shiny.imbei.uni-mainz.de:3838/CABLE_Score/).

Conclusion: The CABLE score yields good discriminatory accuracy and allows to estimate the individual prognosis of patients with uHCC undergoing 1L immunotherapy with a+b.

Rare liver diseases

OS-080

Performance of spleen stiffness measurement by vibration-controlled transient elastography to rule out high-risk varices in patients with chronic extrahepatic portal vein obstruction without cirrhosis

Lucile Moga¹, Audrey Payancé¹, Luis Téllez², Lucia Giuli³, Asunción Ojeda⁴, Dario Saltini⁵, Elton Dajti⁶, Ekaterina Lusina⁷, Dominik Bettinger⁸, Francisco Capinha⁹, Teresa Monllor-Nunell¹⁰, Joel Silva¹¹, Magdalena Meszaros¹², Markus Peck-Radosavljevic¹³, Sara Noemi Reinartz Groba¹⁴, Christiane Stern¹⁵, Laurent Castera¹⁵, Michael Praktijn¹⁴, Boris Guiu¹², José Alberto Ferrusquía¹⁰, Carlos Noronha Ferreira⁹, Maria Nadinskaya⁷, Federico Ravaioli⁶, Filippo Schepis⁵, Fanny Turon⁴, Francesco Santopaolo³, Agustín Albillos², Pierre-Emmanuel Rautou¹, Aurélie Plessier¹. ¹Service d'Hépatologie, AP-HP, Hôpital Beaujon, DMU DIGEST, Centre de Référence des Maladies Vasculaires du Foie, FILFOIE, ERN RARE-LIVER, Université Paris-Cité, Inserm, Centre de recherche sur l'inflammation, UMR 1149, Clichy, France; ²Department of Gastroenterology and Hepatology, Hospital Universitario Ramón y Cajal, Instituto Ramón y Cajal de Investigación Sanitaria (IRYCIS), Centro de Investigación Biomédica en Red (CIBERehd), Universidad de Alcalá, Madrid, Spain;

³Hepatology Unit, CEMAD Centro Malattie Dell'Apparato Digerente, Medicina Interna e Gastroenterologia, Fondazione Policlinico Universitario Gemelli IRCCS, Roma, Italy; ⁴Liver Unit, Hospital Clinic, Centro de Investigación Biomédica en Red (CIBERehd), IDIBAPS, Barcelona, Spain; ⁵Gastroenterology Unit, CHIMOMO Department, University Hospital of Modena, University of Modena and Reggio Emilia, Modena, Italy; ⁶Department of Medical and Surgical Sciences (DIMEC), University of Bologna, Bologna, Italy; ⁷Gastroenterology Department, Chaika Clinics, National Medical Research Center for Therapy and Preventive Medicine, Moscow, Russian Federation; ⁸University Medical Center Freiburg, Freiburg, Germany; ⁹Serviço de Gastrenterologia e Hepatologia, Hospital de Santa Maria, Centro Hospitalar Universitário Lisboa Norte, Lisboa, Portugal; ¹⁰Liver Unit, Hospital Universitari Parc Taulí, Institut d'Investigació i Innovació Parc Taulí (I3PT), Sabadell, Spain; ¹¹Centro Hospitalar Universitário de São João, Faculdade de Medicina da Universidade do Porto, Porto, Portugal; ¹²CHU Montpellier Saint Eloi, Montpellier, France; ¹³Clinic Klagenfurt am Wörthersee, Klagenfurt, Austria; ¹⁴Department of Internal Medicine B, University Hospital Münster, Münster, Germany; ¹⁵Service d'Hépatologie, AP-HP, Hôpital Beaujon, DMU DIGEST, Clichy, France
Email: lucile.moga@gmail.com

Background and aims: Spleen stiffness is associated with the severity of portal hypertension in patients with cirrhosis. Baveno VII consensus suggests that screening endoscopy can be safely spared in patients with compensated cirrhosis, when spleen stiffness measurement (SSM) by vibration-controlled transient elastography (VCTE) is ≤ 40 kPa, as they have a low probability of high-risk varices (HRV). Conversely, in patients with extrahepatic portal vein obstruction in the absence of cirrhosis (EHPVO), endoscopic screening for varices is recommended in all patients, within 6 months of the acute episode. In the absence of varices, endoscopy should be repeated at 12 months, and 2 years later, for all patients in whom thrombosis have not been recanalized. Whether SSM could spare endoscopies in patients with EHPVO is currently unknown. This study aimed to evaluate the performance of SSM by VCTE to rule out HRV (i.e., large varices, small varices with red spot signs, or previous variceal band ligation for primary prophylaxis) in patients with chronic EHPVO.

Method: All the patients with chronic EHPVO, who underwent SSM by VCTE using FibroScan® performed at our center within 2 years before or after an upper endoscopy, were included. Non-inclusion criteria were a history of variceal bleeding, isolated thrombosis of the splenic or mesenteric vein or of one of the portal vein branch, prior TIPS, portal vein recanalization, or portosystemic surgical shunt, and tense ascites at the time of SSM-VCTE. Performance of SSM by VCTE was externally validated in a cohort of patients with chronic EHPVO from 13 VALDIG centers, according to the same inclusion and non-inclusion criteria.

Results: 141 patients were included in the derivation cohort: 63% men, median age 49; 84% with ≥ 1 risk factor for thrombosis. Median serum bilirubin was 0.76 mg/dL (IQR 0.52–1.12); median serum creatinine 74 μ mol/L (IQR 63–86); and median SSM 45 kPa (IQR 27–74). HRV were present in 38% of the patients. In the validation cohort, including 178 patients with similar characteristics, HRV were present in 31% of them. By univariable analysis, serum bilirubin, spleen size, portosystemic collaterals, liver stiffness measurement and SSM by VCTE were associated with HRV status in both cohorts. By multivariable binary logistic regression analysis, only SSM by VCTE ($p < 0.0001$) remained associated with HRV in both cohorts. In the derivation cohort, SSM by VCTE ≤ 40 kPa had a sensitivity of 96% to rule out HRV, and could spare 43% of screening endoscopies, with 4% of HRV missed, and a negative predictive value (NPV) of 97%. In the validation cohort, SSM by VCTE ≤ 40 kPa could spare 46% of screening endoscopies, with 5% of HRV missed, and a NPV of 96%.

Conclusion: This study gathering a total of 319 patients with chronic EHPVO showed that SSM by VCTE ≤ 40 kPa identifies patients with probability of high-risk varices $\leq 5\%$, in whom screening endoscopy can be spared.

OS-081

Portal vein recanalization in non-cirrhotic patients with portal vein occlusion: first results of a VALDIG study

Pierre Deltenre^{1,2}, Killian Troch¹, Laure Elkrief³, Anna Baiges⁴, Fanny Turon⁴, Aurélie Plessier⁵, Michael Praktiknjo⁶, Astrid Marot⁷, Florent Artru⁸, Veronika Fraitzi⁹, Juan Carlos García-Pagán⁴, Pol Olivas⁴, Marco Dioguardi Burgio⁵, Marta Barrufet¹⁰, Marta Burell¹⁰, Maria Ángeles García-Criado¹⁰, Alexandre Soler¹⁰, Louis Dalteroché³, Carsten Meyer¹¹, Alban Denys⁸. ¹Clinique Saint-Luc, Bouge, Belgium; ²CUB Hopital Erasme, Brussels, Belgium; ³Hôpital Trousseau, Tours, France; ⁴Barcelona Hepatic Hemodynamic Lab, Barcelona, Spain; ⁵Hôpital Beaujon, Paris, France; ⁶Universitätsklinikum, Münster, Germany; ⁷CHU UCL Namur, Yvoir, Belgium; ⁸Centre Hospitalier Universitaire Vaudois, Lausanne, Switzerland; ⁹Universitätsklinikum, Münster, Germany; ¹⁰Clinic Barcelona Hospital, Barcelona, Spain; ¹¹University Hospital, Bonn, Germany
Email: pierre.deltenre01@gmail.com

Background and aims: In non-cirrhotic patients, portal vein recanalization (PVR) is a technique able to treat or prevent complications related to portal hypertension by addressing PVO itself. The aim was to identify factors associated with PVR failure and evaluate long-term stent patency and outcome in a large series of patients with non-cirrhotic PVO.

Method: Retrospective study collecting health-related data of patients with chronic PVO in which placement of a stent has been attempted in 6 VALDIG centers. Extension of occlusion was assessed by portography before PVR. Central review of imaging was performed by a single radiologist expert. A TIPS was inserted at the discretion of each center when blood flow was judged non-sufficient after PVR.

Results: 85 patients were included (55 men [65%], median age 49 years [95% CI: 45–54]). Indications for PVR were gastrointestinal bleeding ($n = 45$, 53%), portal biliopathy ($n = 11$, 13%), the need for reducing portal pressure before surgery ($n = 9$, 11%), abdominal pain ($n = 11$, 13%) and other reasons ($n = 9$, 11%). A procoagulate state was identified in 34 patients (40%) and a local prothrombotic factor in 47 patients (55%). Occlusion involved the mesenteric vein in 55 patients (65%) and/or the splenic vein in 41 patients (50%). Regarding the intra-hepatic extension of PVO, patients were classified according to Marot classification: “type 1” with occlusion limited to the main portal vein ($n = 38$, 45%), “type 2” with involvement of portal bifurcation and extension to segmental branches ($n = 29$, 34%), and “type 3” with extension to distal branches ($n = 18$, 21%). Failure of PVR occurred in 18 patients: 1 in type 1 (3%), 9 in type 2 (31%) and 7 in type 3 PVO (39%) ($p < 0.001$). 18 patients underwent TIPS insertion in addition to PVR (21%), 4 in type 1, 7 in type 2 and 7 in type 3 PVO ($p = 0.048$). The median follow-up was 542 days (95% CI: 374–902). In an intention-to-treat analysis, 2-year PV patency was 58% (95% CI: 47–69): 76% (95% CI: 61–91) in type 1, 51% (95% CI: 33–70) in type 2 and 29% (95% CI: 5–54) in type 3 PVO ($p = 0.005$). In Cox regression analysis, 2-year PV non-patency was independently associated with PVO type 2 (RR: 4.0, 95% CI: 1.5–10.9, $p = 0.006$) and type 3 (RR: 5.6, 95% CI: 2.0–15.8, $p = 0.001$), and with abdominal pain (RR: 3.5, 95% CI: 1.5–8.5, $p = 0.005$). In a per-protocol analysis, 2-year PV patency was 72% (95% CI: 60–83). 2-year cumulative incidence of recurrent symptoms of portal hypertension was 33% (95% CI: 23–46), 33% (95% CI: 20–55) in type 1, 27% (95% CI: 14–51) in type 2, 42% (95% CI: 23–77) in type 3 PVO ($p = 0.6$). 12 patients died (14%). 2-year probability of survival was 88% (95% CI: 80–97).

Conclusion: PVR is feasible in most patients with PVO if there is no extension to distal branches. 2-year PV patency following PVR is 58% and 72% in intention-to-treat and per-protocol analyses. PVO types 2 and 3 and abdominal pain as an indication for PVR are independently associated with 2-year PV non-patency.

ORAL PRESENTATIONS

OS-082

Sustained improvement of alanine aminotransferase levels in patients with lysosomal acid lipase deficiency treated with sebelipase alfa enzyme replacement therapy: longitudinal data from the international lysosomal acid lipase deficiency registry

William Balistreri¹, Jennifer Evans², Florian Abel², Lorenzo D'Antiga³.
¹University of Cincinnati Department of Pediatrics, Cincinnati Children's Hospital Medical Center, Cincinnati, United States; ²Alexion, AstraZeneca Rare Disease, Boston, United States; ³Pediatric Hepatology, Gastroenterology and Transplantation, Hospital Papa Giovanni XXIII, Bergamo, Italy
Email: Idantiga@asst-pg23.it

Background and aims: Data from the International Lysosomal Acid Lipase Deficiency (LAL-D) Registry documented more severe liver disease in patients with LAL-D diagnosed at a younger age (Balwani, et al. Liver Int. 2023;43:1537–47). Alanine aminotransferase (ALT) values <1.5 times the upper limit of normal (\times ULN) have been used to indicate less severe liver damage. This analysis evaluated ALT and aspartate aminotransferase (AST) elevations at baseline and changes reported during treatment with Kanuma® (sebelipase alfa enzyme replacement therapy [ERT]).

Method: This retrospective, observational study focused on children and adults treated with ERT ("treated patients"), excluding infants <6 months of age, identified from the International LAL-D Registry (NCT01633489). All had confirmed LAL-D with baseline results and >1 follow-up in 5 years through Oct 2, 2023. Baseline results were assessed prior to ERT in treated patients and at enrollment for non-treated patients. ALT and AST values for all patients were stratified from normal limits to $>3 \times$ ULN. A subset of treated patients with ALT values at baseline and 3 consecutive annual results was identified. The proportion of patients at each stratified ALT category was calculated. Linear regression analysis was performed to evaluate ALT trends among treated patients with elevated baseline ALT ($>1.5 \times$ ULN).

Results: Of 186 patients (92 [49%] males, median age at diagnosis 10.3 years), 162 (104 [64%] treated) had baseline results for ALT. Prevalence of baseline ALT readings $<1.5 \times$ ULN for ages 0 to <6 ($n = 20$), 6 to <12 ($n = 54$), 12 to <18 ($n = 28$), and >18 ($n = 60$) years were 35%, 22%, 25%, and 50%, respectively. Treated patients showed improvement from baseline at subsequent time points. A subset of 75 patients (53 [71%] treated) had 3 consecutive annual results. Baseline ALT values were $>1.5 \times$ ULN in 41 (77%) vs 11 (50%) of treated and non-treated patients. Of the 41 treated patients with baseline ALT $>1.5 \times$ ULN, 31 (76%) had ALT values $<1.5 \times$ ULN at 1 year of ERT. These trends were maintained throughout the 3-year study period and were similar for AST (to be presented). Results from linear regression indicated improvement in ALT levels (decrease) over time with a slope of -0.40 (95% CI: $-0.57, -0.24$; $P < 0.0001$). No deaths occurred during follow-up. Adverse events (AEs) were mild to moderate in severity. There were 21 serious AEs, 1 of which (non-severe anaphylaxis in an adult male, resolved the same day) was deemed treatment-related.

Conclusion: Findings from this first longitudinal analysis of International LAL-D Registry data reflect a favorable treatment response to ERT. ALT values were elevated in most patients at baseline. Following ERT treatment, most patients experienced improvements in ALT levels. Sustained favorable trends, consistent with findings from clinical trials, were observed during ERT.

OS-083

Highly multiplexed spatial analysis of acute pediatric hepatitis of unknown origin indicates a characteristic immune infiltrate as a possible post-acute sequel of COVID-19

Felix Röttele¹, Andreas Zollner², Muhammed Yuksek³, Cigdem Arkan⁴, Carolin Mogler⁵, Judith Aberle⁶, Stephan Aberle⁷, Lena Wölflle⁸, Felix Maier⁸, Eberhart Lurz⁹, Peter Hasselblatt¹, Maike Hofmann¹, Robert Thimme¹, Thomas Müller¹⁰, Georg-Friedrich Vogel¹¹, Bertram Bengsch¹. ¹Freiburg University Medical Center, Clinic for Internal Medicine II, Freiburg im Breisgau, Germany; ²Medizinische Universität Innsbruck, Innsbruck, Austria; ³King's College Hospital, London, United Kingdom; ⁴Memorial Atasehir Hospital Liver Transplantation Center, Istanbul, Turkey; ⁵Institute of Pathology and Unit of Comparative Experimental Pathology, Department of Pathology, Klinikum rechts der Isar, Technical University of Munich, Munich, Germany, Munich, Germany; ⁶Medical University of Vienna, Vienna, Austria; ⁷Med. Universität Wien, Virology, Vienna, Austria; ⁸University Medical Center Ulm, Department of Pediatric and Adolescent Medicine, Ulm, Germany; ⁹University Hospital Munich, Department of Pediatric Gastroenterology, München, Germany; ¹⁰Univ.-Klinik für Pädiatrie I, Innsbruck, Germany; ¹¹Medical University of Innsbruck, Innsbruck, Germany
Email: felix.roettele@uniklinik-freiburg.de

Background and aims: A rise in cases of acute hepatitis of unknown origin (AHUO) in children was observed in 2022 in several countries, some requiring liver transplantation. Evidence of a link to adeno-associated virus 2 (AAV2) infection and CD4 T cell mediated disease was reported in the UK cohort, but not in other countries and a possible contribution of SARS-CoV2 infection during the pandemic remains unclear.

Method: To understand the underlying pathophysiology in a central European patient cohort, we performed highly-multiplexed spatial and single-cell analysis of ($n = 12$) liver biopsies from children with AHUO manifestation during the pandemic and control patients.

Results: Clinical tests indicated no evidence of AAV2 infection but evidence of a history of SARS-CoV2 infection. We observed significant immune infiltration in patient livers with an enrichment of CD8 T cells. Patients with highest CD8 infiltration had the most severe courses of acute hepatitis and concomitant peripheral immune activation. CD8 T cell infiltration was connected to significant tissue pathology involving tissue necrosis and endothelial damage involving multiple immune cell subsets. Neighborhood analysis indicated disease-associated microanatomic interactions between endothelial cells, CD8 T cells and myeloid cell populations. Of note, we observed evidence for intrahepatic SARS-CoV2 antigens corresponding with ACE2 expression in endothelial cells and myeloid cells in the diseased areas in 11/12 samples using several detection methods. 11/12 patients were treated with corticosteroid therapy and no liver transplantation was required.

Conclusion: In children with AHUO, a possible manifestation of a post-acute sequel to Covid-19 associated with a characteristic immune infiltrate needs to be considered.

OS-084-YI

Hepatopulmonary syndrome in patients with porto-sinusoidal vascular disease: prevalence, characteristics, risk factors and outcome

Ylang Spaes^{1,2}, Sabrina Sidali¹, Kinan El Hussein³, Odile Gorla⁴, Vincent Mallet⁵, Armelle Poujol-Robert⁶, Anne Gervais⁷, Adrien Lannes⁸, Dominique Thabut⁹, Jean-Baptiste Noursbaum¹⁰, Isabelle Ollivier-Hourmand¹¹, Charlotte Costentin¹², Alexandra Heurgue-berlot¹³, Pauline Houssel-Debry¹⁴, Sophie Hillaire¹⁵, Nathalie Ganne-Carrié¹⁶, Nicolas Drillon¹, Shantha Valainathan¹, Aurélie Plessier¹, Francois Durand¹, Sarah Raevens¹⁷, Agnes Cachier¹⁸, Laure Elkrief¹⁹, Pierre-Emmanuel Rautou¹. ¹AP-HP, Hôpital Beaujon, Service d'Hépatologie, DMU DIGEST, Centre de Référence des Maladies

Vasculaires du Foie, FILFOIE, ERN RARE-LIVER, Clichy, France; ²CHU Charles Nicolle, Rouen, France; ³Bichat Hospital, Paris, France; ⁴Gastroenterology and Hepatology department, Charles Nicolle University Hospital Of Rouen, Rouen, France; ⁵AP-HP, Centre, Groupe Hospitalier Cochin Port Royal, DMU Cancérologie et spécialités médico-chirurgicales, Service d'Hépatologie, Paris, France; ⁶Saint-Antoine Hospital, Paris, France; ⁷Hôpital Bichat, AP-HP, Hépatogastroentérologie, Paris, France; ⁸Centre Hospitalier Universitaire Angers, Hépatologie, Angers, France; ⁹Hôpital Pitié Salpêtrière, Paris, France; ¹⁰Centre Hospitalier Régional Universitaire Morvan, Hépatologie, Brest, France; ¹¹Centre Hospitalier Universitaire de Caen Normandie, Hépatologie, Caen, France; ¹²Centre Hospitalier Universitaire Grenoble-Alpes, Hépatologie, Grenoble, France; ¹³Centre Hospitalier Universitaire de Reims, Hépatologie, Reims, Reims, France; ¹⁴Department of Gastroenterology and Hepatology, University Hospital Pontchaillou, Rennes 1 University, Rennes, France; ¹⁵Hôpital Foch, Hépatologie, Suresnes, France; ¹⁶Liver unit, Hôpital Avicenne, Hôpitaux Universitaires Paris-Seine-Saint-Denis, Assistance-Publique Hôpitaux de Paris, Bobigny, France; ¹⁷Department of Gastroenterology and Hepatology, Ghent University, Ghent University Hospital, Ghent, Belgium; ¹⁸Université Paris-Cité, Department of Cardiology, Bichat/Beaujon Hospital (APHP Nord), ENETS Centre of Excellence, Paris/Clichy, France; ¹⁹Centre Hospitalier Régional Universitaire, Hôpital Trousseau, Hépatogastroentérologie, Tours, France
Email: sidali.sabrina@gmail.com

Background and aims: Porto-sinusoidal vascular disease (PSVD) is a rare cause of portal hypertension. Data on hepatopulmonary syndrome (HPS) in PSVD are limited. This study aimed to determine the prevalence, associated factors, and evolution of HPS in patients with PSVD.

Method: Retrospective multicenter observational study of patients with PSVD, according to VALDIG's criteria, with signs of portal hypertension who underwent contrast-enhanced transthoracic echocardiography.

Results: 196 patients were included in 17 centers of the French network for Vascular Liver Diseases. Contrast-enhanced transthoracic echocardiography was performed as part of the investigations carried out at inclusion in the phase III "APIS" clinical trial (NCT04007289) in 80 patients, as part of the initial work-up performed when patients were referred for PSVD in 95 patients and because of dyspnea in 21 patients. Out of the 196 patients included, 14 (7%) had a confirmed diagnosis of HPS. Hypoxemia (PaO₂ <80 mmHg) was found in 9 patients with HPS while 5 patients had elevated AaPO₂ without hypoxemia. Four (2%) additional patients had intrapulmonary shunts at contrast-enhanced echocardiography, but normal arterial oxygenation, precluding diagnosis of HPS. Patients with HPS had more frequently genetic disorder associated with PSVD (43% vs. 6%, p = 0.002). In particular, telomere biology disorders were found in 6 (43%) out of the 14 patients with HPS vs. 6 (3%) out of the 182 patients without HPS (p < 0.001). Liver function was less preserved in patients with HPS, since they had lower prothrombin time (63% vs. 86%, p = 0.04), higher serum total bilirubin (37 µmol/L vs. 14 µmol/L, p < 0.001), and lower serum albumin concentration (32 g/L vs. 38 g/L, p < 0.001). No significant difference was observed concerning signs of portal hypertension, liver and spleen stiffness, nor complications of PSVD. Out of the 14 patients with HPS, 5 underwent liver transplantation after a median follow-up of 34 months, because of HPS requiring long-term oxygen therapy for 4 and because of liver failure for one patient. HPS being an indication for LT in itself, we performed competing risk analyses considering LT for HPS as a competing risk. In this setting, overall cumulative incidence of death and of liver related events was similar between patients with and without HPS.

Conclusion: The prevalence of HPS in patients with PSVD was 7%. HPS in patients with PSVD is associated with genetic disorders, and especially telomere biology disorders. When applying liver transplantation MELD standard exception policy, overall survival of patients with HPS and PSVD is similar to that of patients with PSVD without HPS.

SLD: Experimental

OS-085

Sex and age disparities in MASH and the beneficial effects of estradiol for MASH in old female mice

Madhulika Tripathi¹, Suganya Sakthivel^{2,3}, Priyanka Gupta⁴, Ayako Suzuki⁵, Brijesh Kumar Singh⁶, Paul Yen⁶. ¹Duke-NUS Medical School, Singapore, Singapore; ²Duke-NUS Medical School, Singapore, Singapore; ³Duke-NUS Medical School, Singapore, Singapore; ⁴Duke-NUS Medical School, Singapore, Singapore; ⁵Duke-NUS Medical School, Singapore, Singapore; ⁶Duke-NUS Medical School, Singapore, Singapore
Email: madhulika.tripathi@duke-nus.edu.sg

Background and aims: The prevalence of metabolic dysfunction-associated steatohepatitis (MASH) is higher in males than reproductive age females whereas the prevalence significantly rises in post-menopausal females and eventually equals those in males. The mechanism (s) for these observations is not known so we investigated sex and age differences and the therapeutic potential of estradiol in MASH *in vivo*.

Method: Young/reproductive age (12-week) and old/post-reproductive age (48~50-week) male and female C57BL/6J mice were subjected to control chow, high-fat methionine/choline-deficient (HFMCD) diet for six weeks or WDF (Western diet +fructose) diet for 16~20 weeks to induce MASH. These mice received 17β-estradiol at physiological (200nM) dose for therapeutic groups. Serum and hepatic MASH parameters, ER stress, and lysosome-autophagy defects were analyzed.

Results: Young female mice fed HFMCD or WDF developed milder MASH and lower inflammation (IL-6, IL-1β), inflammasome (Nlrp3, and Asc-1), and fibrosis (Tgf-β1, Col1a1 and α-SMA) gene expression, and decreased hepatic collagen content than age-matched males fed the same diet. Interestingly, Young females fed NASH-inducing diets had no significant changes in glucose sensitivity/insulin tolerance, and less impairment of hepatic autophagy and lysosomal activity than age-matched males fed the same diets. In contrast, post-reproductive age females significantly increased hepatic inflammation, fibrosis, and ER stress gene expression; glucose/insulin impairment; autophagic inhibition; and lysosomal defects to resemble age-matched males. Remarkably, physiological doses of estradiol reduced NASH by decreasing inflammation and fibrosis gene expression and improving lysosomal-autophagic defects in old females.

Conclusion: We found significant sex differences in MASH as males had more severe NASH than age-matched females that further progressed with age. However, old females had a sharp rise in NASH severity and progression and caught up with similar age males. Estradiol markedly decreased inflammation, fibrosis, and other features of NASH in old female mice. Our data suggest that estrogen supplementation may be warranted for post-menopausal patients with NASH who do not have cardiovascular and cancer risk factors.

OS-086-YI

Protein tyrosine phosphatase non-receptor type 2 controls hepatic function of cytotoxic T cells in metabolic dysfunction-associated steatohepatitis

Madita Determann¹, Luise Linzmeier¹, Marlene Schwarzfischer¹, Anna Niechcial¹, Marianne Rebecca Spalinger¹, Yasser Morsy¹, Doris Pöhlmann¹, Marijn Wilmsink¹, Maria Walker¹, Federica Sella², Mitchell Levesque², Viktor Hendrik Koelzer³, Anja Laura Frei⁴, Stephan Buch⁵, Jochen Hampe⁵, Christian Datz⁶, Clemens Schafmayer⁷, Mathias Heikenwälder⁸, Michael Scharl¹, Sena Blümel¹. ¹University of Zurich, University Hospital Zurich, Department of Gastroenterology and Hepatology, Zurich, Switzerland; ²University of Zurich, University Hospital Zurich, Department of Dermatology, Zurich, Switzerland; ³University of Basel, University Hospital Basel, Institute of Medical Genetics and Pathology, Basel, Switzerland; ⁴University of Zurich, University Hospital Zurich, Department of Pathology and Molecular Pathology, Zurich, Switzerland; ⁵University of Technology Dresden, University Hospital Dresden, Medical Department I, Dresden, Germany; ⁶General Hospital Oberndorf, Teaching Hospital of the Paracelsus Medical University Salzburg, Department of Internal Medicine, Salzburg, Austria; ⁷University Hospital Rostock, Department of General Surgery, Rostock, Germany; ⁸German Cancer Research Center, Department Chronic Inflammation and Cancer, Heidelberg, Germany
Email: maditaelena.determann@usz.ch

Background and aims: Obesity and its complications, including metabolic dysfunction-associated steatohepatitis (MASH), cirrhosis, and hepatocellular carcinoma are a growing global epidemic. MASH development involves the hepatic recruitment of cytotoxic CD8⁺ T cells causing liver damage and fibrosis. Protein tyrosine phosphatase non-receptor type 2 (PTPN2) attenuates CD8⁺ T cell responses to self-antigens, tumors and inflammation. Thus, PTPN2 may have a crucial role in MASH pathogenesis by modulating CD8⁺ T cell functionality. Here, we studied the impact of T cell-specific PTPN2 on MASH development and disease progression.

Method: The impact of human hepatic PTPN2 expression on MASH development was analyzed from (1) mRNA data from the sequence read archive (SRA) database (n = 106); (2) protein expression in liver biopsies using multicolor immunofluorescence staining (n = 8–12); (3) the presence of the single nucleotide polymorphism (SNP) rs2542151, which results in PTPN2 non-function, in an Austrian and German Metabolic Dysfunction-associated Steatotic Liver Disease (MASLD) cohort (n = 742–997).

To understand how T cell PTPN2 is connected to MASH development, mice with conditional PTPN2-knock-out in T cells (KO, PTPN2^{fl/fl} × CD4^{Cre}) and their wild-type (WT, PTPN2^{fl/fl}) littermates (n = 4–19 mice per group) were fed 28 weeks with western-style fast food diet (FFD). The mice were investigated regarding their MASH characteristics.

Results: PTPN2 mRNA-expression was increased in livers from MASLD and MASH patients compared to healthy controls, and in MASH compared to MASLD (p < 0.05). PTPN2 expression in patients with non-alcoholic fatty liver disease (NAFLD) activity score (NAS) 5 and NAS 6 was higher compared to patients with NAS 0 (p < 0.05). Immunofluorescence analysis revealed increased numbers of PTPN2⁺, CD3⁺ PTPN2⁺ and CD8⁺ PTPN2⁺ cells in MASH patients compared to controls (p < 0.05).

Of note, the frequency of severe liver fibrosis in MASH patients harboring the SNP rs2542151 was reduced (minor allele frequency (MAF) for F3/4 fibrosis and cirrhosis = 0.108–0.139 vs. fibrosis F0/1-MAF = 0.156).

The FFD-fed KO mice were lighter and their liver-body weight ratio was lower than their WT littermates (p < 0.05) with no differences in water or food consumption. In contrast to their WT littermates, the FFD-fed KO mice were protected from MASH and fibrosis (mean WT-NAS 6 vs. KO-NAS 4 and mean WT-fibrosis F2 vs. KO-fibrosis F0). In flow cytometry, livers of FFD-fed KO mice had higher amounts of

exhausted and central memory CD8⁺ T cells (p < 0.05), while all other immune cell groups were not different between genotypes.

Conclusion: While we observed increased PTPN2 mRNA and protein expression in human MASH livers, SNP analyzes and in vivo data suggested a protective effect of PTPN2 deficiency against MASH likely mediated by impacting on intrahepatic CD8⁺ T cell functionality.

OS-087

Stain-free digital pathology imaging provides microarchitecturally-resolved insights into scar evolution allowing direct clinical outcome prediction in metabolic dysfunction-associated steatotic liver disease

Timothy Kendall¹, Stephen A. Harrison², Dean Tai³, Elaine Chng³, Yayun Ren³, Jonathan Fallowfield¹. ¹University of Edinburgh, Edinburgh, United Kingdom; ²Pinnacle Clinical Research, San Antonio, United States; ³HistoIndex Pte. Ltd, Singapore, Singapore
Email: tim.kendall@ed.ac.uk

Background and aims: Fibrosis stage in metabolic dysfunction-associated steatotic liver disease (MASLD) is associated with increased mortality and liver-related events. Direct prediction of outcomes from tissue has not been possible due to the lack of a suitable event-rich cohort. Using an unstained section from biopsies of the SteatoSITE cohort has allowed quantification of extracellular matrix features that are predictive of clinical outcome but unapparent to human observers.

Method: Sections from 452 SteatoSITE biopsies were randomized into train (300) or test (152) sets and imaged using second harmonic generation/two-photon excitation fluorescence microscopy (SHG/TPEF). Using sequential feature selection, 5 of 184 fibrosis parameters were chosen and linear regression used to construct individual indices for risk of all-cause mortality and hepatic decompensation. Using the test set, Kaplan-Meier analysis, with death a competing risk for decompensation, and Cox proportional hazards modelling was performed. The predictive power of the risk indices was compared with assigned NASH-CRN fibrosis stage (F0/1/2 v F3/4) and stain-free imaging derived qFibrosis stage (qF0/1/2 v qF3/4). Previous indices were established using a training set of 294 biopsies with leave-one-out cross-validation.

Results: Previously established all-cause mortality and hepatic decompensation indices had greater predictive power than either NASH-CRN or qFibrosis stage. New indices generated with these train and test sets from an extended MASLD cohort also outperformed existing predictive metrics. The new all-cause mortality index had greater predictive power (>0.14 vs. ≤ 0.14, hazard ratio (HR) 4.49, 95% confidence intervals (CI) 1.5–13.38) than qFibrosis-derived stage (HR 3.07, CI 1.3–7.26) or NASH-CRN fibrosis score (HR 3.41, CI 1.43–8.15). The new hepatic decompensation index had greater predictive power (>0.31 vs. ≤ 0.31, HR 5.96, CI 2.92–12.14) than qFibrosis-derived stage (HR 3.59, CI 1.79–7.2) or NASH-CRN fibrosis score (HR 3.65, CI 1.81–7.35). Parameters used in separate indices were related to extracellular matrix features in portal tract, periportal, and zone 2 regions.

Conclusion: We show that individual indices composed of micro-architectural features quantified by stain-free imaging have greater predictive value for all-cause mortality and liver-related events than ordinal fibrosis scores. These new indices may be used for more nuanced participant stratification or more meaningful end points in trials. To establish a definitive link between microarchitectural features at baseline, their modification following drug treatment, and associated clinical outcomes, it is essential to incorporate validation within a prospective study.

OS-088-YI

Selective ablation of Caspase 8 in hepatocytes ameliorates development of metabolic dysfunction-associated steatohepatitis following hepatocyte-specific JNK deletion

Ines Volkert¹, Julia Grube¹, Karolina Edlund², Julia Duda³, Adrien Guillot⁴, Hilmar Berger⁴, Jörg Rahnenführer⁵, Frank Tacke⁴, Jan G. Hengstler⁵, Christian Trautwein¹. ¹RWTH University Hospital Aachen, Aachen, Germany; ²University Dortmund, Aachen, Germany; ³TU Dortmund University, Dortmund, Germany; ⁴Charité University, Berlin, Germany; ⁵TU Dortmund University, Dortmund, Germany
Email: ivolkert@ukaachen.de

Background and aims: Metabolic dysfunction-associated steatotic liver disease (MASLD), encompasses a range of liver diseases, spanning from steatosis to cirrhosis and hepatocellular carcinoma (HCC). Despite the global rise in MASLD prevalence, the precise mechanisms driving disease development remains elusive. The c-Jun N-terminal kinases (JNKs) play a pivotal role in liver physiology and disease pathogenesis. This study aims to investigate the mechanisms of liver damage following hepatocyte-specific deletion of Jnk1 and Jnk2 during the development of metabolic dysfunction-associated steatohepatitis (MASH).

Method: Mice with a hepatocyte-specific deletion of Jnk1 and Jnk2 (JNK1/2^{Δhepa}) and corresponding controls underwent an 8-week Western-Style Diet (WSD) to evaluate its impact on MASH progression. Subsequent to gene set pathway analysis, Caspase8/JNK1/2^{Δhepa} animals were generated and subjected to a WSD. Following this, JNK1/2^{Δhepa} and control animals were treated with a WSD for 8 weeks with weekly intravenous (i.v.) injections of hepatocyte-specific Caspase 8 (Casp 8) siRNA, initiated after four weeks of WSD.

Results: WSD led to significantly elevated transaminases, enhanced fibrogenesis and markedly increased inflammation in JNK1/2^{Δhepa} mice compared to control mice. Gene set pathway analysis identified highly upregulated distinct pathways in JNK1/2^{Δhepa} livers, including inflammatory signals and fibrogenesis. Notably, apoptotic pathways exhibited a substantial increase, confirmed by Cleaved Caspase 3 staining. Thus, Casp8/JNK1/2^{Δhepa} mice were generated and subjected to WSD. Triple KO mice displayed a complete reversal of the severe phenotype, with liver transaminases, inflammation, fibrogenesis and cell death fully rescued and significantly reduced. Multiplex staining revealed a significant increase of infiltrating immune cells such as monocyte-derived macrophages in JNK1/2^{Δhepa} mice, which were further reduced in Casp8/JNK1/2^{Δhepa} mice. This was also confirmed by deconvolution of RNA bulk data, based on unpublished liver single-cell datasets. A therapeutic approach employing hepatocyte-specific liposomes containing Casp8 siRNA, administered four weeks after initiating WSD, resulted in significantly reduced liver transaminases, fibrogenesis, inflammatory signals and cell death.

Conclusion: Our results demonstrate that hepatocyte-specific Jnk1 and Jnk2 deletion induces a robust oxidative stress response, leading to increased MASH progression and heightened apoptotic cell death. This phenotype was fully rescued by genetic deletion of Casp8 in hepatocytes. Additionally, therapeutic treatment with Casp8 siRNA significantly mitigated MASH progression, suggesting that Casp8-directed therapy in hepatocytes might be a promising treatment for patients with an increased oxidative stress response and MASH.

OS-089-YI

Transgenerational maternal obesity induces mitochondrial dysfunction and aggravates MASLD, which can be reversed by metabolic drug candidates

Anneleen Heldens^{1,2}, Milton Antwi^{1,2,3}, Louis Onghena^{1,2,4}, Lindsey Devisscher^{2,3}, Xavier Verhelst^{1,2}, Sarah Raevens^{1,2}, Hans Van Vlierberghe^{1,2}, Ruth de Bruyne⁵, Anja Geerts^{1,2}, Sander Lefere^{1,2}. ¹Department of Internal Medicine and Pediatrics, Hepatology Research Unit, Ghent University, Ghent, Belgium; ²Liver Research Center Ghent, Ghent University, Ghent University Hospital, Ghent, Belgium; ³Gut-Liver Immunopharmacology Unit, Department for

Basic and Applied Medical Sciences, Ghent University, Ghent, Belgium; ⁴Department for Human Structure and Repair, Department of Gastrointestinal Surgery, Ghent University Hospital, Ghent, Belgium; ⁵Department of Internal Medicine and Pediatrics, Pediatric Gastroenterology, Hepatology and Nutrition, Ghent University Hospital, Ghent, Belgium
Email: anneleen.heldens@ugent.be

Background and aims: Metabolic dysfunction-associated steatotic liver disease (MASLD) is the most common pediatric chronic liver disease. Although maternal obesity is an independent risk factor, the pathogenesis remains unclear. We aimed to evaluate the effect and mechanisms of transgenerational maternal obesity on MASLD severity, and test drug candidates in a preclinical model.

Method: Maternal obesity was induced by feeding C57BL/6J mice a western diet (WD) from 8 weeks before breeding initiation, with a normal chow (NC)-fed male, throughout pregnancy and lactation. Female offspring were used to produce the next generation. Male offspring were weaned onto NC or WD and MASLD development was assessed at the age of 24 days and 16 weeks. MASLD severity and metabolic alterations were evaluated by histology, serum markers, bulk liver RNA sequencing, flow cytometric analysis of hepatic macrophages, and quantification of hepatic mitochondrial oxidative phosphorylation (OXPHOS) complex content. To evaluate the translational potential of our findings, the publicly available GSE220102 RNAseq dataset on maternal WD in non-human primates (NHP) was analyzed. Finally, we assessed the therapeutic efficacy of wildtype (WT) FGF-21, semaglutide, and an amylin analogue (provided by Novo Nordisk), from 8 to 16 weeks of age.

Results: 16-week-old male offspring exposed to maternal WD, especially multigenerational maternal WD, exhibited higher body, liver and gonadal adipose tissue weight, HOMA-IR, serum ALT levels, and infiltration of monocytes and monocyte-derived macrophages, whereas Kupffer cells were depleted. Maternal WD feeding aggravated steatosis and inflammation, and thus the NAFLD activity score. Fibrosis (F1-F3) was only observed in the offspring exposed to maternal WD. RNA sequencing analysis clustered samples based on maternal and postnatal diet, and presence of fibrosis. Among the top 10 GO-biological processes of significantly altered genes, 4 were related to oxidative phosphorylation. Furthermore, maternal WD exposure was associated with a lower hepatic OXPHOS complex content. Notably, transcriptomic analysis of WD-fed NHP offspring confirmed our findings, as 'oxidative phosphorylation' was one of only two KEGG pathways significantly affected by maternal WD feeding. To isolate the effect of maternal diet, offspring were evaluated at weaning age. Maternal diet alone was sufficient to induce liver steatosis and inflammation at this young age. In our model, treatment with WT FGF-21, semaglutide and the amylin analogue significantly improved steatohepatitis, with WT FGF-21 and the amylin analogue ameliorating fibrosis as well.

Conclusion: Transgenerational obesity aggravates MASLD in male offspring starting from weaning age. While mitochondrial dysfunction contributes to disease progression, WT FGF-21, semaglutide and the amylin analogue are effective treatments.

Viral Hepatitis: Experimental and pathophysiology

OS-090

Novel epigenetic editing technology targets hepatitis B virus in vivo to deeply and durably repress viral markers

Yesseinia Anglero-Rodriguez¹, Sahar Abubucker¹, John Xiong¹, Jhon Medina¹, Caroline Mugambwa¹, Rayman Choo-wing¹, Carrietta Jacques¹, Glen Acosta¹, Scott Clarkson¹, Kendra Bayne¹, Mary Morrison¹, Ari Friedland¹, Narayan Wong¹, Zohan Hoque¹, Amber DiPiazza¹, Parthu Koppa¹, Kuo-Chan Hung¹, Sameer Abraham¹, Adam Zhai¹, Pietro Spinelli¹, Vic Myer¹, Aron Jaffe¹.
¹Chroma Medicine, Boston, MA, United States
 Email: yesse.anglero@chromamedicine.com

Background and aims: Current treatments for chronic hepatitis B virus (HBV) result in a low incidence of functional cure, which is thought to result from the persistence of covalently closed circular DNA (cccDNA) and the deregulation of the immune system resulting from HBsAg expression. Epigenetic editing is a powerful approach that leverages the endogenous cellular mechanism for gene regulation to durably silence or activate genes without introducing unintended genomic consequences associated with traditional gene editing. Our epigenetic editors (EE) consist of a DNA-targeting component fused to a transcriptional repressor domain and a DNA methyltransferase domain. Transient exposure of our HBV-EE results in binding to HBV cccDNA and integrated HBV DNA (intDNA) in a sequence-specific manner and localized DNA methylation of CpG dinucleotides in the viral genome, leading to a deep, durable reduction of multiple HBV viral markers including HBV DNA and HBsAg without cutting or nicking the DNA.

Method: A library of HBV-EEs were screened in vitro and hit confirmation was performed in HepG2.2.15 cells, an immortalized cell line that contains HBV intDNA, and in HBV infected primary human hepatocytes (PHH), which contains both intDNA and cccDNA. Multiple confirmed hits were tested for dose-dependent reduction of HBsAg levels in HepG2.2.15. Hybrid-capture methyl-seq was used to verify that our HBV-EE induced on-target methylation of HBV DNA. RNA-seq and whole genome methylation sequencing to analyze host gene expression and host genome methylation, respectively, were used to evaluate EE specificity in PHHs. In vivo activity was evaluated via IV administration of lipid nanoparticles (LNPs) delivering mRNA encoding our HBV-EE construct into two models: 1) AAV-HBV, a model of episomal DNA and 2) a transgenic (Tg)-HBV mouse, a model of intDNA.

Results: Our HBV-EEs durably and deeply reduced HBsAg and HBeAg in both cccDNA and intDNA in vitro models, demonstrating >80% silencing of each viral antigen. Targeted methylation of HBV DNA correlated with reduction of HBsAg and HBeAg, with no off-target changes seen in host gene expression or methylation in PHHs. In vivo, single administration of our EEs resulted in durable, dose-dependent reduction of HBsAg, achieving a 3.3 log reduction at 84 days in the AAV-HBV model, and 2.1 log reduction at 112 days in Tg-HBV mice.

Conclusion: Our results demonstrate in vivo proof-of-concept with deep, specific, and durable silencing of HBV using our HBV-EE. We believe our novel epigenetic editing approach represents a new therapeutic modality with the potential to achieve higher rates of functional cure in patients with chronic HBV.

OS-091

Precision-cut liver slices as a pre-clinical model for the evaluation of host-targeting agents against hepatitis B virus and hepatitis delta virus infection

Maud Michelet^{1,2,3}, Armando Andres Roca Suarez^{1,2,3}, Anaëlle Dubois^{1,2,3}, Sarah Heintz^{1,2,3}, Marie-Laure Plissonnier^{1,2,3}, Maria Saez-Palma^{1,2,3}, Simon Fletcher⁴, Michel Rivoire⁵, Sandra Phillips^{6,7}, Elena Palma^{6,7}, Shilpa Chokshi^{6,7}, Barbara Testoni^{1,2,3}, Fabien Zoulim^{1,2,3}.
¹INSERM U1052, CNRS UMR-5286, Cancer Research Center of Lyon (CRCL), Lyon, France; ²University of Lyon, Université Claude-Bernard (UCBL), Lyon, France; ³Hepatology Institute of Lyon, Lyon, France; ⁴Gilead Sciences Inc., 324 Lakeside Dr., Foster City, CA, 94404, United States; ⁵INSERM U1032, Centre Léon Bérard (CLB), Lyon, France; ⁶The Roger Williams Institute of Hepatology, Foundation for Liver Research, 111, Coldharbour Lane, London SE5 9NT, United Kingdom; ⁷Faculty of Life Sciences and Medicine, King's College London, London WC2R 2LS, United Kingdom
 Email: fabien.zoulim@inserm.fr

Background and aims: The development of new treatment strategies against hepatitis B virus (HBV) and hepatitis delta virus (HDV) is of high priority to achieve a cure of these infections. In this context, the pre-clinical evaluation of host-targeting agents (HTAs) with the currently available in vitro and in vivo study models remains challenging. The use of precision-cut liver slices (PCLS) represents a promising model that preserves the complex multi-cellular architecture and cellular communication of the hepatic environment, while offering the practical aspects of an in vitro system based on human cells. Therefore, we aimed to assess the potential application of PCLS as an HBV/HDV co-infection model for the evaluation of HTAs.

Method: We employed human PCLS derived from resected liver tissue samples from patients without history of chronic liver disease. Slices were mono- or co-infected ex vivo with HBV and HDV for a five-day period. Tissue architecture and viability were evaluated by immunohistochemistry, detection of ATP and total RNA content. Viral infection was assessed by the presence of HBV RNA, covalently closed circular (ccc)DNA and HDV RNA by RT-qPCR and hepatitis delta antigen (HDAG) by Western blot. The impact of HTAs targeting hepatocytes (i.e. Bulevirtide-1 µM), non-parenchymal immune cells (i.e. Selgantolimod-1 µM) or multiple populations (i.e. Lonafernib-2 µM) was evaluated by the quantification of viral parameters and the production of inflammatory cytokines.

Results: Our ex vivo PCLS infection protocol allowed the detection of HBV RNA, cccDNA, HDV RNA and HDAG at the end of the five-day observation period. Treatment of PCLS with Bulevirtide prior to inoculation (24 h) led to a marked decrease in viral parameters for both HBV and HDV. Lonafernib treatment post-infection (48 h) was associated with the intracellular accumulation of HDAG. In the same context, Selgantolimod induced a significant decrease of HBV RNA levels. The immunomodulatory action of Selgantolimod was confirmed by the production of inflammatory cytokines (e.g. IL-6) in the culture supernatant. PCLS architecture and viability were comparable between the different treatment conditions.

Conclusion: Our results represent the first characterization of PCLS as a relevant ex vivo study model of HBV/HDV co-infection. Moreover, the evaluation of HTAs directed against parenchymal and non-parenchymal hepatic cell populations highlights the potential relevance of this system for the pre-clinical study of novel molecules aimed to achieve HBV/HDV cure.

OS-092

Targeting cellular cathepsins inhibits hepatitis E virus infection

Mara Klöhn¹, Thomas Burkard¹, Juliana Janzen¹, Jil Alexandra Schrader¹, André Gömer¹, Richard Brown¹, Rebecca Fu², Viet Loan Dao Thi^{2,3}, Volker Kinast⁴, Yannick Brüggemann¹, Daniel Todt^{1,5}, Eike Steinmann^{1,6}.
¹Molecular and Medical Virology, Bochum, Germany; ²University Hospital Heidelberg, Heidelberg, Germany; ³German Centre for Infection Research (DZIF), Heidelberg,

Germany; ⁴Carl von Ossietzky University Oldenburg, Oldenburg, Germany; ⁵European Virus Bioinformatics Center (EVBC), Jena, Germany; ⁶German Centre for Infection Research (DZIF), External Partner Site, Bochum, Germany
Email: mara.kloehn@rub.de

Background and aims: HEV is estimated to be responsible for 44,000 deaths annually, yet its therapy is still limited to the off-label use of Ribavirin and pegIFNalpha, despite unsatisfactory cure rates and severe side effects, emphasizing the need for new and improved therapy options. In the pursuit of effective antiviral therapies, targeting viral entry holds promise, as it disrupts the initial stage of viral replication and has been proven effective for other hepatotropic viruses. Cellular proteases have emerged as a class of host factors required for viral surface protein activation and productive cell entry by many viruses. Hence, we aimed to investigate the functional requirement and therapeutic potentials of targeting cellular proteases during HEV infection to identify potential antiviral drugs specifically related to viral entry.

Method: We tested several protease and cathepsin inhibitors in our recently established HEV cell culture model for their ability to interfere with infections of HEV in human hepatoma cells, HepaRGs and primary human hepatocytes (PHHs) by immunofluorescence staining for the HEV capsid protein and microscopic analysis. The cytotoxicity of the compounds was evaluated using MTT and LDH release assay, while the potential impact on viral replication was assessed by employing HEV subgenomic replicon systems. To identify the specific stage of the HEV life cycle targeted by the compounds, we performed time-of-drug-addition experiments. Cathepsin L (CTSL) knockout cells and siRNA transcript knockdown was employed to evaluate CTSL as a potential host and drug target.

Results: We found that blocking lysosomal cathepsins with small molecule inhibitors, impedes HEV infection without affecting RNA replication. Remarkably, the cathepsin inhibitor K11777 exhibited potent suppression of HEV infections with an EC₅₀ of approximately 0.01 nM and no significant toxicity until micromolar concentrations in hepatoma cells. Notably, the inhibitory effects of K11777 were consistently observed in HepaRGs and primary human hepatocytes. Furthermore, we confirmed that HEV entry is potently blocked by inhibition of cathepsins and that CTSL knockout and knockdown reduced permissiveness to HEV.

Conclusion: In summary, our study highlights the pivotal role of cathepsins, especially CTSL, in the HEV entry process. The profound anti-HEV efficacy of the pan-cathepsin inhibitor, K11777, especially with its notable safety profile in primary cells, further underscores its potential as a promising therapeutic candidate.

OS-093

Efficient and heritable elimination of HBV viral antigens in vivo by epigenome editing

Wenbo Peng¹, Junzheng Zhao¹, Dai-tze Wu¹, Shaoshuai Mao¹, Leilei Wu¹, Jing Sun¹, Ruimin Lv¹, Di Sun¹, Bob Zhang¹, YiDi Sun^{1,2}, Changyang Zhou^{1,2}. ¹Epigenic Therapeutics, Shanghai, China; ²Institute of Neuroscience, Chinese Academy of Sciences Center for Excellence in Brain Science and Intelligence Technology, Chinese Academy of Sciences, Shanghai, China
Email: changyang.zhou@epigenictx.com

Background and aims: Chronic hepatitis B virus (HBV) infection is a major global health problem, causing significant morbidity and mortality. However, current therapies do not provide effective functional cure. We have developed EPIREG, a CRISPR-derived epigenetic modulation technology comprising inactivated Cas9 (dCas9) fused with DNA methyltransferase and histone modification effectors, which enables efficient, specific, and durable silencing of targeted genes. Here we evaluated the anti-HBV activity of EPI-003, discovered by the EPIREG technology, in eliminating HBV viral antigens by inhibiting the transcription of cccDNA and integrated DNA.

Method: The anti-HBV efficacy of EPI-003 was evaluated using HBV-infected primary human hepatocytes (PHHs). The *in vivo* efficacy of EPI-003 was assessed by administration of lipid nanoparticles (LNPs) encapsulating EPIREG and single guide RNA (sgRNA) targeting the promoter of the HBV genome in both transgenic (genotype A) and AAV-HBV (genotype D) mouse models. The sgRNA was designed and optimized to target 91–100% of HBV genotypes from A-H. HBV DNA and viral antigen levels were monitored weekly.

Results: In PHHs, EPI-003, following one time treatment at 2.5 µg/ml post HBV infection, potently suppressed over 90% of HBsAg, HBeAg and HBV DNA levels at 14 days post the treatment. In HBV transgenic mouse model, single dose of EPI-003 resulted in a dose-dependent reduction of serum HBsAg by up to 2.0 logs following 2 wks of administration; this reduction was well maintained thereafter in all the animals up to greater than 16 wks (the study is ongoing). Furthermore, among animals treated with safe and efficacious doses, 5 of out of 10 animals further lowered HBsAg from wk 8 by additional 1 to 2 logs, even to the levels close or under the LLOQ (1.5 IU/ml) in 3 animals by wk16. More strikingly, HBsAb was induced in these 2 animals following single dose administration of EPI-003 without need of additional immune stimulation. Mechanistically, methylation of HBV cccDNA was induced and correlated well with the elimination of viral antigens and HBV DNA. Similar anti-HBV results were obtained in AAV-HBV animal model even with the high titer of HBV infection (i.e. HBsAg levels were greater than 10,000 IU/ml). Animals were tolerated well throughout the treatment with normal physical activity and body weight maintenance. No off-target effects were detected by EPI-003 *in vivo* in animal models by host transcriptional and whole genome methylation analyses.

Conclusion: EPI-003 demonstrated superior pharmacological efficacy in eliminating HBV viral antigens and inhibiting HBV DNA with HBsAb recovery and no viral rebound in preclinical studies as compared with other anti-HBV therapies in the same preclinical models. Epigenetic modifications of HBV cccDNA and integrated DNA may provide a potential therapeutic solution to achieve functional cure in chronic hepatitis B patients.

OS-094

Chronic HDV infection is sustained by an intense HBsAg production from integrated HBV-DNA in the setting of a limited or even absent HBV reservoir

Romina Salpini¹, Stefano D'Anna², Lorenzo Piermatteo³, Giuseppina Brancaccio⁴, Elisabetta Teti⁵, Andrea Di Lorenzo⁶, Ilaria Grossi⁷, Giulia Torre⁸, Vincenzo Malagnino⁹, Marco Iannetta⁶, Francesca Ceccherini Silberstein⁷, Caterina Pasquazzi¹⁰, Umberto Cillo¹¹, Alessandro Vitale¹¹, Enrico Gringeri¹¹, Maria Magrofuoco¹¹, Monia Pacenti¹², Leonardo Baiocchi¹³, Simona Francioso¹⁴, Ilaria Lenci¹⁴, Apostolos Koffas¹⁵, Anna Maria Geretti¹⁶, Maria Lorena Abate¹⁷, Antonella Olivero¹⁷, Giovanni Battista Gaeta¹⁸, Loredana Sarmati¹⁶, Mario Rizzetto¹⁷, Upkar Gill¹⁵, Patrick Kennedy¹⁵, Gian Paolo Cavaglia¹⁷, Valentina Svicher¹⁹. ¹Department of Biology Tor Vergata University, Rome, Italy; ²Department of Experimental Medicine, University of Rome Tor Vergata, Rome, Italy, Rome, Italy; ³Department of Biology, University of Rome Tor Vergata, Rome, Italy; ⁴Department of Molecular Medicine, Infectious Diseases, University of Padua, padua, Italy; ⁵Infectious Diseases Unit, University Hospital of Rome Tor Vergata, Rome, Italy; ⁶Department of Systems Medicine, Infectious Disease, University of Rome Tor Vergata, Rome, Italy, Rome, Italy; ⁷Department of Experimental Medicine, University of Rome Tor Vergata, Rome, Italy; ⁸Department of Biology, University of Rome Tor Vergata, Rome, Italy, Rome, Italy; ⁹Department of Systems Medicine, Infectious Diseases, University of Rome Tor Vergata, Rome, Italy, Rome, Italy; ¹⁰Sant'Andrea Hospital, Rome, Italy; ¹¹Hepatobiliary Surgery and Liver Transplantation Unit, Department of Surgery, Oncology and Gastroenterology, University of Padova, Padua, Italy; ¹²Microbiology and Virology Unit, Padova University Hospital, Padua, Italy; ¹³Hepatology Unit, Policlinico Tor Vergata, Rome; ¹⁴Hepatology Unit, Policlinico Tor Vergata, Rome, Italy;

¹⁵Blizard Institute, Barts and The London School of Medicine and Dentistry, Queen Mary University of London, London, United Kingdom; ¹⁶Department of Systems Medicine, Infectious Disease Clinic, University of Rome Tor Vergata, Rome, Italy; ¹⁷Department of Medical Sciences, University of Turin, Turin, Italy; ¹⁸Infectious Disease Unit, University L. Vanvitelli, Naples, Naples, Italy; ¹⁹Department of Biology, University of Rome Tor Vergata, Rome, Italy
Email: rsalpini@yahoo.it

Background and aims: HDV exploits HBV surface glycoproteins (HBsAg) for viral morphogenesis and infectivity. Here, we investigate HBV and HDV replicative activity and their interplay by analysing liver biopsies from patients with chronic HBV/HDV co-infection (CHD) and HBV mono-infection (CHB).

Method: Liver tissues are analysed from 57 HBeAg-negative patients (71% NUC treated): 32 with CHD and 25 with CHB (median [IQR] age: 49 [39–59] and 44 [38–61] years). Intrahepatic levels of covalently-closed circular DNA (cccDNA), pregenomic HBV-RNA (pgRNA) and HDV-RNA were assessed by droplet digital PCR (ddPCR). ddPCR assays were set-up to quantify total HBs transcripts and to distinguish those deriving from cccDNA and integrated HBV-DNA (Grudda, 2022).

Results: Patients with CHD have significantly higher ALT and HBsAg levels than those with CHB (median [IQR]: 68 [45–89] vs 27 [20–46] U/L, $P < 0.001$ and 12,575 [6,322–20,222] vs 5,079 [2,035–9,287] IU/ml, $P = 0.01$) and lower HBV-DNA (median [IQR]: 20 [12–50] vs 1,094 [137–4,170] IU/ml, $P < 0.001$). Median (IQR) serum HDV RNA is 6.0 (3.8–6.7) log IU/ml, positively correlated with intrahepatic HDV-RNA ($Rho = 0.62$, $P = 0.006$; 787 [18–2,782] copies/1000cells). CHD is characterized by a more restricted HBV reservoir in term of cccDNA and pgRNA (median [IQR]: 1 (0.02–16) vs 10 (2–18) copies/1000cells, $P = 0.02$ and 10 [1–173] vs 72 [38–380] copies/1000cells, $P = 0.08$, respectively). Nevertheless, both CHD and CHB are characterized by an abundant production of HBs transcripts (median [IQR]: 6,267 [345–31,387] and 8,081 [314–15,189]), with 99% of them derived from integrated HBV-DNA in both groups. By stratifying CHD patients according to cccDNA reservoir, lower levels of HBV intrahepatic markers are observed in those with less cccDNA (median [IQR] pgRNA and cccDNA-derived transcripts: 1.4 [0.4–77.5] vs 108 [4.5–411], $P = 0.01$ and 0.3 [0.2–1.5] vs 48 [9.6–186] copies/1000cells, $P = 0.002$ in cccDNA<1 vs cccDNA>1 copy/1000cells). Conversely, no differences are observed for intrahepatic HDV-RNA levels (median [IQR]: 782 [0.7–5,559] vs 844 [1–6,371] copies/1000cells in cccDNA<1 vs >1 copy/1000cells, $P = 0.6$). Moreover, a relevant amount of intrahepatic and serum HDV-RNA is also detected in the 8 CHD patients with completely undetectable levels of cccDNA and serum HBV-DNA (median [IQR]: 5,495 [976–15,107] copies/1000cells and 6 [5.9–7.3] log IU/ml, respectively), consistent with HDV replication persisting independently of the HBV reservoir.

Conclusion: CHD is characterized by a restricted HBV reservoir and an intense HBsAg production from integrated HBV-DNA, that can sustain HDV persistence independently of the intrahepatic HBV reservoir. In light of this finding, the silencing/elimination of cccDNA may not necessarily imply the achievement of HDV cure and pharmacological strategies should also target HBsAg production from integrated HBV-DNA.

SATURDAY 08 JUNE

Cirrhosis and its complications: Portal hypertension

OS-095

A machine learning algorithm generated using routine parameters could avoid unnecessary taps to exclude SBP in a national VA cohort with internal and external validation

Scott Silvey¹, Mahum Nadeem², Asiya Tafader², Galvin Dhaliwal², Jinze Liu², Nilang Patel², Jasmohan Bajaj¹. ¹Virginia Commonwealth University, Richmond VA Medical Center, Richmond, United States; ²Virginia Commonwealth University, Richmond, United States
Email: jasmohan.bajaj@vcuhealth.org

Background and aims: Despite the poor prognosis of missed/delayed diagnosis of spontaneous bacterial peritonitis (SBP), there are logistical challenges in providing timely taps. These are related to expertise, training, and time needed in busy emergency settings. Therefore, measures to exclude SBP that obviate taps are needed. Aim: Use machine learning (ML) to create and validate models to exclude SBP without a tap using easily observed and collected parameters.

Method: Training cohort: Using the Veterans Affairs (VA) Corporate Data Warehouse (CDW), records of pts with cirrhosis and ascites who underwent first tap within a day of admission between 2009–2019 were included nationally. SBP was defined as PMN >250/ml, positive culture or validated SBP billing code. Demographics, admission laboratories, medications, vital signs and comorbidities were recorded. XGBoost analysis was performed using variables significant on regression that were collected before the tap to determine probability of excluding SBP based on variables that did not include ascites fluid details. The generated XGBoost model was then tested in 2 validation cohorts: (a) CDW: 2nd para during 2009–2019 and (2) Prospective NACSELD cohort from VCU/Richmond VA admitted non-electively. Negative predictive values (NPV) at 5, 10 and 15% probability were tested.

Results: Training cohort: 9,643 patients (63.14 ± 8.69 years age, 95.5% men, 50.7% alcohol-related) got their first early tap, with 1,448 (15.0%) having SBP after tap. We initially collected 147 predictor variables, which reduced to 20 variables with test set (crude comparisons $p < 0.001$). The variables were BMI, vitals (temp, systolic/diastolic BP) and labs (liver function tests (albumin, ALT/AST/alk phos, bilirubin, INR), basic panel (eGFR, BUN K, CO2) and blood count (Hgb, WBC, Neutrophils and eosinophils)] at/before the tap. Of these only eosinophils and BP were ↓ in SBP; rest were ↑. NPV at 5–15% probability were (92–97%) for SBP. Validation cohort #1: 2844 pts (63.14 ± 8.37 years age, 97.4% men, 54.0% alcohol-related) had repeat tap; 10% had SBP. Using the 20-variable ML model, NPV to exclude SBP at 5–15% probability ranged from 95–99%. Validation cohort #2: 333 pts from NACSELD (57.08 ± 7.74 years age, 65.1% men, 50.1% alcohol-related) were admitted non-electively of whom 9% had SBP. Using the 20-variable ML model, NPV to exclude SBP at 5–15% probability ranged from 97–100%.

Conclusion: A machine learning model to exclude SBP without needing a tap using 20 variables easily available on demographics, labs and vitals showed excellent NPV in a national Veterans cohort. The high NPV for SBP were validated in internal and external cohorts and could be utilized in emergency settings to reliably identify which patient with cirrhosis and ascites can avoid a tap to exclude SBP.

OS-096-YI

Spleen stiffness measurement by transient elastography at 100 Hz refines the non-invasive diagnosis of clinically significant portal hypertension in compensated advanced chronic liver disease-final results of a european multicenter study

Mathias Jachs^{1,2}, Lucile Moga^{3,4}, Wilhelmus J Kwanten^{5,6}, Petra Fischer⁷, Aitor Odriozola⁸, Fanny Turon^{9,10}, Dario Saltini¹¹, Luis Téllez^{12,13}, Angelo Armandi^{14,15}, Yuly Mendoza¹⁶, Elba Llop Herrera¹⁷, Maria Grasso¹⁸, Elton Dajti¹⁹, Emma Vanderschueren²⁰, Lisa Sandmann²¹, Julia Thalhammer^{1,2}, Carlos Pardo^{9,10}, Lotte Schoenmakers⁵, Thomas Vanwolleghem^{5,6}, Luisa Vonghia^{5,6}, Christian Labenz¹⁴, Georg Semmler^{1,2}, Lukas Hartl^{1,2}, Benjamin Maasoumy²¹, Wim Laleman²⁰, Federico Ravaoli¹⁹, José Presa²², Vincenza Calvaruso¹⁸, José Luis Calleja Panero¹⁷, Annalisa Berzigotti¹⁶, Jörn M Schattenberg¹⁴, Agustín Albillos^{12,13}, Antonio Colecchia¹¹, Filippo Schepis¹¹, Juan Carlos García-Pagán^{9,10}, Angela Puente⁸, Jose Ignacio Fortea⁸, Bogdan Procopet⁷, Sven Francke^{6,6}, Pierre-Emmanuel Rautou^{3,4}, Thomas Reiberger¹, Mattias Mandorfer^{1,2}. ¹Division of Gastroenterology and Hepatology, Department of Medicine III, Medical University of Vienna, Vienna, Austria; ²Hepatic Hemodynamic Lab, Department of Medicine III, Medical University of Vienna, Vienna, Austria; ³Université Paris-Cité, Inserm, Centre de recherche sur l'inflammation, UMR 1149, Paris, France; ⁴Service d'Hépatologie, AP-HP, Hôpital Beaujon, DMU DIGEST, Centre de Référence des Maladies Vasculaires du Foie, FILFOIE, Health Care Provider of the European Reference Network on Rare Liver Disorders (ERN RARE-LIVER), Clichy, France; ⁵Department of Gastroenterology and Hepatology, Antwerp University Hospital, Antwerp, Belgium; ⁶Laboratory of Experimental Medicine and Pediatrics (LEMP)-Gastroenterology and Hepatology, University of Antwerp, Antwerp, Belgium; ⁷Third Medical Clinic, Department of Internal Medicine, Iuliu Hatieganu University of Medicine and Pharmacy, Cluj-Napoca, Romania; ⁸Gastroenterology and Hepatology Department, Clinical and Translational Research in Digestive Diseases, Valdecilla Research Institute (IDIVAL), Marqués de Valdecilla University Hospital, Santander, Spain; ⁹Barcelona Hepatic Hemodynamic Laboratory, Liver Unit, Hospital Clínic, Institut de Investigacions Biomèdiques August Pi i Sunyer (IDIBAPS), University of Barcelona, Barcelona, Spain; ¹⁰CIBEREHD (Centro de Investigación Biomédica en Red Enfermedades Hepáticas y Digestivas), Health Care Provider of the European Reference Network on Rare Liver Disorders (ERN-RARE-LIVER), University of Barcelona, Barcelona, Spain; ¹¹Department of Medical Specialties, Gastroenterology Unit, University of Modena and Reggio Emilia and Azienda Ospedaliero-Universitaria di Modena, Modena, Italy; ¹²Gastroenterology and Hepatology Department, Hospital Universitario Ramón y Cajal, Madrid, Spain; ¹³Instituto Ramón y Cajal de Investigación Sanitaria (IRYCIS), CIBEREHD (Centro de Investigación Biomédica en Red Enfermedades Hepáticas y Digestivas), University of Alcalá, Madrid, Spain; ¹⁴Metabolic Liver Disease Research Program, I. Department of Medicine, University Medical Center, Mainz, Germany; ¹⁵Division of Gastroenterology and Hepatology, Department of Medical Sciences, University of Turin, Turin, Italy; ¹⁶Department of Visceral Surgery and Medicine, Inselspital, Bern University Hospital, University of Bern, Bern, Switzerland; ¹⁷Department of Gastroenterology and Hepatology, Puerta de Hierro University Hospital, Puerta de Hierro Health Research Institute (IDIPHIM), CIBEREHD, Universidad Autónoma de Madrid, Majadahonda, Spain; ¹⁸Gastroenterology and Hepatology Unit, Department of Health Promotion Sciences Maternal and Infantile Care, Internal Medicine and Medical Specialties, PROMISE, University of Palermo, Palermo, Italy; ¹⁹Gastroenterology Unit, IRCCS Azienda Ospedaliero-Universitaria di Bologna, European Reference Network on Hepatological Diseases, Bologna, Italy; Department of Medical and Surgical Sciences, University of Bologna, Bologna, Italy; ²⁰Department of Gastroenterology and Hepatology, University Hospitals Leuven, KU Leuven, Leuven, Belgium; ²¹Department of Gastroenterology, Hepatology and Endocrinology, Hannover Medical School, Hannover, Germany; ²²Liver Unit-CHTMD,

Vila Real, Portugal

Email: mattias.mandorfer@meduniwien.ac.at

Background and aims: The ANTICIPATE, and subsequently, the ANTICIPATE-NASH study demonstrated that in compensated advanced chronic liver disease (cACLD), the probability of clinically significant portal hypertension (CSPH) can be non-invasively estimated based on liver stiffness measurement (LSM), platelet count (PLT), and, in obese metabolic dysfunction-associated steatotic liver disease (MASLD), body mass index (BMI).

Spleen stiffness measurement (SSM) is an emerging non-invasive test (NIT) for CSPH which became broadly applicable owing to a recently introduced 100 Hz vibration-controlled transient elastography probe. This study aimed at investigating the diagnostic utility of SSM-100 Hz as a standalone NIT in contemporary cACLD aetiologies and at refining the non-invasive diagnosis of CSPH by adding SSM to the components of the ANTICIPATE models.

Method: This study included Child-Pugh stage A cACLD (LSM ≥ 10 kPa and/or F3/4) patients from 16 specialized European centers who underwent paired assessment of the hepatic venous pressure gradient (HVPG), SSM-100 Hz, and LSM from 2020–2023. The cohort was split into a derivation (2020–2022) and a temporal validation (2023) dataset.

Results: 407 cACLD patients (derivation: n = 202, validation: n = 205) were included (MASLD: 40.3%, ALD: 32.7%, viral: 18.4%, other aetiologies: 8.6%). The median BMI was 28.1 (25th–75th percentile: 24.6–33.1) kg/m², and 39.6% were obese (BMI ≥ 30). The median HVPG was 11 (7–14) mmHg and 59.2% had CSPH (≥ 10 mmHg); median LSM, SSM-100 Hz, and PLT were 21.4 (14.1–31.6) kPa, 45.0 (32.1–65.4) kPa, and 131 (90–181) G/L, respectively. Patients included in the validation cohort showed significantly lower BMI and PLT, while LSM, SSM-100 Hz and CSPH prevalence did not differ significantly. In the derivation cohort, SSM-100 Hz, LSM, PLT, and BMI were independently associated with CSPH in logistic regression analysis. SSM-100 Hz and LSM yielded comparable C-statistics for CSPH (SSM-100Hz: 0.779 vs. LSM: 0.781, DeLong-test: P = 0.973). Notably, a model comprising SSM-100 Hz, PLT, and BMI performed similarly to the ANTICIPATE \pm NASH model (derivation: 0.849 vs. 0.849; P = 0.999, validation: 0.873 vs. 0.863; P = 0.750). Finally, the combined model (SSM-100 Hz, LSM, BMI, and PLT) was superior to the ANTICIPATE \pm NASH model (derivation: 0.889 vs. 0.849, P = 0.022, validation: 0.906 vs. 0.863, P = 0.012). Importantly, the combined model showed excellent calibration in the validation cohort. A nomogram was developed to facilitate point-of-care risk stratification.

Conclusion: The addition of SSM-100 Hz to LSM, BMI, and PLT outperformed the ANTICIPATE \pm NASH model in CSPH risk stratification in our European multicenter study comprising cACLD patients with predominantly steatotic liver disease. Consideration of SSM-100 Hz improves CSPH risk assessment, supporting its implementation into clinical practice.

OS-097

Effect of rifaximin in severe cirrhotic patients with ascites: a double-blind randomized placebo-controlled phase 3 trial

Thierry Thévenot¹, Laure Elkrief², Christophe Bureau³, Edouard Bardou-Jacquet⁴, Isabelle Rosa⁵, Eric Nguyen Khac⁶, Frédéric Oberti⁷, Anais Pitta⁸, Maxime Mallet⁹, Fanny Lebosse¹⁰, Alexandre Louvet¹¹, Lucy Meunier¹², Pierre Nahon¹³, Isabelle Ollivier-Hourmand¹⁴, Rodolphe Anty¹⁵, Claire Francoz¹⁶, Ghassan Riachi¹⁷, Alexandre Meunier¹⁸, Gregory Tio¹⁹, Allison Muller²⁰, Audace Curé-Martin²¹, Didier Hocquet¹⁸, Vincent Di Martino¹, Delphine Weil-Verhoeven¹, Maxime Desmarts¹⁹. ¹Department of Hepatology, CHU Besançon, Besançon, France; ²Department of Hepatogastroenterology, CHU Tours, Tours, France; ³Department of Hepatology, CHU Toulouse, Toulouse, France; ⁴Department of Liver Diseases, CHU Rennes, Rennes, France; ⁵Department of Hepatogastroenterology, CHI Créteil, Créteil, France;

ORAL PRESENTATIONS

⁶Department of Hepatogastroenterology, CHU Amiens, Amiens, France;
⁷Department of Hepatogastroenterology, CHU Angers, Angers, France;
⁸Department of Hepatogastroenterology, CHU Reims, Reims, France;
⁹Department of Hepatogastroenterology, CHU Pitié-Salpêtrière, Paris, France; ¹⁰Department of Hepatology, Hôpital Croix-Rousse, Hospices Civils de Lyon, Lyon, France; ¹¹Service des Maladies de l'Appareil Digestif, Hôpital Huriez, Lille, France; ¹²Department of Hepatogastroenterology and Liver Transplantation, CHU Montpellier, Montpellier, France; ¹³Liver Unit, Hôpitaux Universitaires Paris Seine Saint-Denis, Bobigny, France; ¹⁴Department of Hepatogastroenterology, CHU Caen, Caen, France; ¹⁵Department of Hepatology, CHU Nice, Nice, France; ¹⁶Liver Intensive Care and Liver Transplantation Unit, Hôpital Beaujon, Clichy, France; ¹⁷Department of Hepatogastroenterology, hôpital Charles Nicolle, Rouen, France; ¹⁸Centre de Ressources Biologiques-Filière microbiologique, CHU Besançon, Besançon, France; ¹⁹uMETH, Centre d'investigation Clinique 1431, CHU Besançon, Besançon, France; ²⁰Vigilance Unit, Department of Clinical Research and Innovation, CHU Besançon, Besançon, France; ²¹Centre d'Investigation Clinique-Inserm CIC 1431, Besançon, France
Email: tthevenot@chu-besancon.fr

Background and aims: The strongest evidence supporting the long-term use of antibiotic prophylaxis in cirrhosis concerns patients who recover from a first spontaneous bacterial peritonitis (SBP) and acute gastrointestinal bleeding. Evidence for primary prophylaxis of SBP is weak and the selection of quinolone-resistant bacteria is a concern. Here we present preliminary results from the ProPILA-Rifax study, a phase 3 trial to evaluate whether rifaximin (RIF) has a beneficial effect on 12-month survival in severe cirrhotic patients with ascites (NCT03069131). Data were not fully consolidated at the time of analysis.

Method: In this randomized, double-blind, placebo-controlled trial conducted at 17 French centers, severe cirrhotic patients [1] with grade 2 or 3 ascites and protein level in ascites <15 g/L were randomized 1:1 to receive RIF 550 mg BID or placebo (PBO) for 12 months, as primary prophylaxis of SBP. The primary end point was the 12-month transplant-free survival (TFS). Secondary end points were hospital mortality, 3- and 6-month TFS, incidence of complications of cirrhosis, and safety of rifaximin.

Results: Between March 2018 and June 2022, 1798 cirrhotic patients with ascites were screened and 159 were randomized to the PBO (n = 84) or the RIF (n = 75) arms. Baseline characteristics of patients in RIF/PBO were well balanced: mean (SD) age 59.2 (9.9)/59.6 (9.8) years, male 69.3%/78.6%, alcohol 70.7%/72.6%, mean (SD) MELD score 16.8 (8.9)/13.5 (5). During the study period, 31/30 patients died, but deaths were not related to the study drug, and 7/7 were transplanted. The 12-month TFS rates were comparable between groups (RIF/PBO: 58/64.9%). The 3- and 6-month TFS rates in the RIF/PBO groups were 82.2%/74.7% and 75%/68.4%, respectively. Incidence of infections, hepatorenal syndrome, hepatic encephalopathy and variceal bleeding were not significantly different (all p = NS). The number of patients with adverse events (AEs) (RIF/PBO: 68 [90.7%]/79 [94.1%]) and serious AEs (RIF/PBO: 56 [74.7%]/67 [79.8%]) was similar between groups. The percentage of AEs leading to drug discontinuation, RIF vs PBO, was 44.6% vs 41.8%.

Conclusion: In this phase 3 trial, RIF was well tolerated but had no beneficial role on the 12-month TFS and incidence of complications of liver cirrhosis in severe cirrhotic patients with moderate to large ascites. [1] Fernández J, et al. *Gastroenterology* 2007;133:818–24.

OS-098-YI

Addition of simvastatin to carvedilol improves survival in patients with decompensated cirrhosis after variceal bleed. A randomised controlled trial

Randeep Rana¹, Tabish Mohammad¹, Samagra Agarwal¹, Rajkumar Bayye¹, Syed Ahmed¹, Deepak Gunjan¹, Sanchit Sharma¹, Anoop Saraya¹. ¹All India Institute of Medical Sciences, New Delhi, India
Email: sanchitsharma2188@gmail.com

Background and aims: While linked to improve portal hypertension and prevent complications, data on efficacy and safety of adding simvastatin to standard of care (SOC) in patients with decompensated cirrhosis is limited. We assessed whether addition of simvastatin to carvedilol could reduce mortality in patients with cirrhosis after variceal bleeding.

Method: In this single-centre open-label randomised controlled trial with superiority design, eligible patients with cirrhosis (Child-Turcot-Pugh[CTP] score 5–12) with recent (<5 days) variceal bleed without hepatocellular carcinoma (HCC) or portal-vein thrombosis were randomised to either simvastatin[20 mg once-daily] (n = 130) or no drug (n = 138) in addition to SOC (carvedilol with serial band ligation). Primary outcome was all-cause mortality over 24-month follow-up. Secondary outcomes included rates of individual decompensations with transplant/death before decompensation as competing event. Intention-to-treat analysis included all patients, while per-protocol analysis excluded 17 (12.3%) patients not compliant to simvastatin.

Results: Baseline characteristics (mean age: 45.0 ± 11.5 years, aetiology: alcohol related/NASH/HBV/HCV: 48.1%/15.3%/13.1%/6.7%), severity of liver disease[CTP class- A/B/C:39%/44%/17% in simvastatin vs 30%/56%/14% in no drug arm;p = 0.14]; MELD (median 14[IQR 11–19] vs 14[11–19];p = 0.57)] and follow-up (median 18[14–24] vs 18[12–22] months; p = 0.55) were comparable in both arms. On intention-to-treat analysis, patients on simvastatin had lower mortality (hazard-ratio:0.48[95%confidence-interval:0.29–0.81; Cox-proportional-hazards p = 0.006]. Incidence of ascites was lower (sub distributional hazards-ratio (sHR):0.60[0.39–0.92]; competing risks regression, p = 0.02), All-cause decompensation (sHR:0.74 [0.521.05];p = 0.09), rebleeding (sHR:0.87[0.571.34];p = 0.53), hepatic encephalopathy (HE) (sHR:0.71[0.42–1.19;p = 0.19) and acute-on-chronic liver-failure (ACLF) (0.65[0.39–1.10];p = 0.11) were comparable. On per-protocol analysis (n = 251), rates of mortality (HR:0.48 [0.28–0.84];p = 0.01), all-cause decompensation (sHR:0.65[0.45–0.95];p = 0.025), ascites (sHR:0.54[0.340.86];p = 0.01), HE (sHR:0.51 [0.280.92];p = 0.027) and ACLF (sHR:0.54[0.31–0.95];p = 0.033) were lower in patients on simvastatin. On sub-group analysis, there was no heterogeneity of treatment-effect across CTP-class (p = 0.105) or etiology (p = 0.39). Adverse events on simvastatin included body-aches (n = 19; 14.6%) and transient creatinine-kinase elevation (n = 5; 2.9%) but no patients developed rhabdomyolysis.

Conclusion: Addition of Simvastatin to carvedilol improves transplant-free survival in patients with decompensated cirrhosis with recent acute variceal bleed by reducing the incidence of non-bleed related decompensation. [CTRI/2022/07/044263].

OS-099-YI

Assessment of sarcopenia improves the prediction of post-TIPS mortality in older adult patients with cirrhosis

Dario Saltini¹, Silvia Nardelli², Francesco Vizzutti³, Roberto Miraglia⁴, Daniele Bellafante², Federico Banchelli⁵, Cristian Caporali⁶, Luigi Maruzzelli⁴, Gianmarco Falcone⁷, Marcello Bianchini¹, Biagio Cuffari¹, Tomas Guasconi⁸, Angelica Ingravalle⁹, Federico Casari⁶, Federica Indulti⁸, Prampolini Francesco⁶, Antonio Colecchia⁸, Fabio Marra⁹, Calogero Camma¹⁰, Marco Senzolo¹¹, Oliviero Riggio², Filippo Schepis¹. ¹Division of Gastroenterology, Portal Hypertension Unit (MEC), Azienda Ospedaliero-Universitaria Policlinico di Modena, Surgical, Medical and Dental Department of Morphological Sciences related to Transplant,

Oncology and Regenerative Medicine, CHIMOMO, University of Modena and Reggio Emilia, Modena, Italy; ²Department of Translational and Precision Medicine, Sapienza University of Rome, Rome, Italy; ³Department of Experimental and Clinical Medicine, University of Florence, Italy, Florence, Italy; ⁴Radiology Service, IRCCS ISMETT (Mediterranean Institute for Transplantation and Advanced Specialized Therapies), Palermo, Italy; ⁵Statistics Unit, Department of Clinical, Diagnostic and Public Health Medicine, University of Modena and Reggio Emilia, Modena, Italy; ⁶Division of Radiology, Interventional Radiology Unit, Azienda Ospedaliero-Universitaria di Modena, Modena, Italy; ⁷Interventional Radiology Unit, Azienda Ospedaliero-Universitaria Careggi, Florence, Italy; ⁸Gastroenterology Unit, Department of Specialistic Medicines, University of Modena and Reggio Emilia, University Hospital of Modena and Reggio Emilia, Modena, Italy; ⁹Department of Experimental and Clinical Medicine, University of Florence, Florence, Italy; ¹⁰Section of Gastroenterology and Hepatology, Department of Health Promotion, Mother and Childcare, Internal Medicine and Medical Specialties, PROMISE, University of Palermo, Palermo, Italy; ¹¹Multivisceral Transplant Unit-Gastroenterology, Department of Surgery, Oncology, and Gastroenterology, Padua University Hospital, Padua, Italy
Email: fschepis@unimore.it

Background and aims: Transjugular intrahepatic portosystemic shunt (TIPS) has been demonstrated to be feasible in older adult patients (age ≥ 70 years), but the selection criteria are still suboptimal. Sarcopenia, highly prevalent in the elderly population, may be significantly associated with post-TIPS outcomes. This study aimed at evaluating the impact of baseline sarcopenia on post-TIPS survival in older adults with cirrhosis.

Method: A retrospective analysis of the prospective Italian TIPS Registry (RI-TIPS) was conducted to identify patients ≥ 70 years who received TIPS from June 2015 to March 2023. Availability of a baseline abdominal CT scan was a mandatory inclusion criterion. Skeletal muscle index (SMI) and muscle attenuation (MA) in Hounsfield units (HU) were evaluated at the L3-L4 intervertebral disc level. Sarcopenia was defined as SMI $< 50 \text{ cm}^2/\text{m}^2$ for men and $< 39 \text{ cm}^2/\text{m}^2$ for women; myosteatosis as MA < 41 HU in patients with a BMI < 25 and < 33 HU in those with a BMI ≥ 25 , respectively. Probability of liver-related death was evaluated by competing risks survival analysis. A prediction model for liver-related mortality was created.

Results: One-hundred and fifteen patients were included: median age 74.2 years (IQR 5.0), 61.7% male, median BMI 24.5 (IQR 5.3), 60% prevalence of sarcopenia [median SMI 42.5 (IQR 10.3)] and 80% prevalence of myosteatosis [median muscle attenuation 29.8 HU (IQR 12.2)]. The main etiologies were viral (41.7%), alcohol-associated cirrhosis (30.0%), and metabolic dysfunction-associated steatohepatitis (27.8%). Refractory ascites (54.7%) and secondary prophylaxis of variceal bleeding (33%) were the main indications for TIPS. During a median follow-up of 1-year (IQR 1.9), 40 (34.8%) patients died for liver-related causes and 16 (13.9%) for extrahepatic causes. All-cause mortality was higher in sarcopenic patients than in those without sarcopenia (6-months: 32.0% vs. 8.7%; 1-year: 47.0% vs. 11.0%, respectively; p value 0.005). The impact of sarcopenia was even more significant when considering liver-related mortality (6-months: 25.0% vs. 2.2%; 1-year: 43.0% vs. 4.8%, respectively; p value < 0.001). Interestingly, no significant differences were found in all-cause and liver-related mortality between patients with and without myosteatosis (p values 0.6 and 0.8, respectively). A predictive model that includes INR, creatinine, and sarcopenia was developed to estimate liver-related mortality. The model achieved good predictive performances with AUCs of 0.826, 0.788, and 0.712 at 6-month, 1-year, and 2-years, respectively.

Conclusion: Due to its significant impact on survival, the evaluation of sarcopenia improves the selection of older adults with cirrhosis candidate to TIPS. The new predictive model for post-TIPS liver-related mortality deserves validation.

Hepatocyte and Fibrosis Biology

OS-100

Elevated expressions of NTCP on NK cells from liver fibrosis of metabolic dysfunction-associated steatohepatitis patients are associated with increased bile acid uptake that impaired their function via STAT signaling pathway

Ahmad Salhab¹, Johnny Amer¹, Rifaat Safadi¹. ¹Liver Institute, Hadassah Hebrew University Hospital, Jerusalem, Israel
Email: johnnyamer@hotmail.com

Background and aims: Dysfunctional bile acid (BA) metabolism may influence immune cell activation, thereby exacerbating liver damage. However, the influence of BA on natural killer (NK) cells remains elusive. Our study aimed to assess the impact of the BA signaling pathway on NK cell functions and their immune and molecular features in humans with Metabolic dysfunction-associated steatohepatitis (MASH) and a mouse model of MASH.

Method: Human peripheral NK cells from patients (age ≥ 18 years) of histologically documented MASH with different Metavir scores of liver fibrosis were obtained. NK molecular aspects of BA signaling through NTCP expressions, STAT signaling pathway, RNA single seq, activatory markers [NKp46, NKp30, CD107a], and exhaustion markers [PD-1, TIGIT, LAG-3] were assessed. BA modulatory pathways and trNK phenotypic alterations were assessed in mice models of MASH and adoptive transfer models of immune alterations through NK cells transplantation following sorting cells according to NTCP expressions.

Results: Peripheral blood NK cells obtained from patients with MASH and severe liver fibrosis (METAVIR scores of F3/F4) exhibited 2.5-fold upregulation in sodium+/taurocholate cotransporting polypeptide (NTCP) expression compared with healthy donors, indicating that NTCP may be involved in liver fibrosis. Liver biopsy tissue-resident NK (trNK) cells were sorted based on NTCP expression and higher taurocholic acid (TCA) uptake, and increased exhaustion was observed in trNK^{NTCP+} cells relative to trNK^{NTCP-} cells from the same patients, patients with F1/2 scores, and healthy donors. Moreover, RNA single seq from 5200 genes detected, STAT3, PDCD1, LAG3, TGF β , and TGF β receptor mRNA expression was upregulated in trNK^{NTCP+} cells in the F3/F4 scored patients as compared to their trNK^{NTCP-} from the same patients. The trNK^{NTCP+} cells also exhibited increased levels of STAT3 phosphorylation and decreased STAT1 and STAT5 phosphorylation. trNK^{NTCP+} cells in which STAT3 was inhibited had significantly reduced NTCP expression, reduced NK cell exhaustion, and increased NK cell activity. In MASH mice with epigallocatechin gallate (EGCG)-mediated inhibition of NTCP expression, TCA uptake was reduced, and liver fibrosis was attenuated. Additionally, transplantation of trNK^{NTCP-} cells into immunodeficient MASH model mice alleviated liver fibrosis, along with reducing the levels of proinflammatory and profibrotic cytokines and ameliorating lipid homeostasis.

Conclusion: Taken together, these results indicate that enhancing immune responses would be clinically beneficial though strengthening NK cells activity via treating with NTCP antagonists and therefore a potential strategy for preventing liver fibrosis in MASH patients.

OS-101-YI

Remodelling of hepatocyte cholesterol metabolism mediates colorectal liver metastasis

Ane Nieva-Zuluaga¹, Beatriz Arteta², Mikel Ruiz de Gauna¹, Maider Apodaka-Biguri¹, Idoia Fernández-Puertas¹, Francisco González-Romero¹, Paul Gomez-Jauregui¹, Natalia Sainz-Ramírez¹, Kendall Alfaro-Jiménez¹, Beatriz Gómez Santos¹, Igotz Delgado¹, Andres Valdivieso³, Javier Bustamante³, Luis Bujanda⁴, Jesus Maria Banales⁴, Anastasios Giannou⁵, Samuel Huber⁵, Igor Aurrekoetxea⁶, Xabier Buque¹, Patricia Aspichueta⁷. ¹Department of Physiology University of the Basque Country UPV/EHU, Faculty of Medicine and Nursing, Leioa, Spain, Leioa, Spain; ²Department of Cellular Biology and Histology, University of the Basque Country UPV/EHU, Faculty of Medicine and Nursing, Leioa, Spain, Leioa, Spain; ³Department of HPB Surgery and Liver Transplantation Unit, Hospital Universitario Cruces, Bilbao, Spain, Biocruces Bizkaia Health Research Institute, Cruces University Hospital, Barakaldo, Spain, Cruces, Spain; ⁴Department of Liver and Gastrointestinal Diseases, Biogipuzkoa Health Research Institute, Donostia University Hospital, University of the Basque Country UPV-EHU, Ikerbasque, Donostia-San Sebastian, National Institute for the Study of Liver and Gastrointestinal Diseases (CIBERehd, Carlos III Health Institute), Madrid, Spain, San Sebastian, Spain; ⁵Section of Molecular Immunology und Gastroenterology, I. Department of Medicine, University Medical Center Hamburg-Eppendorf, 20246 Hamburg, Germany, Hamburg Center for Translational Immunology (HCTI), University Medical Center Hamburg-Eppendorf, 20246 Hamburg, Germany, Hamburg, Germany; ⁶Department of Physiology University of the Basque Country UPV/EHU, Faculty of Medicine and Nursing, Leioa, Spain, Biocruces Bizkaia Health Research Institute, Cruces University Hospital, Barakaldo, Spain, Leioa, Spain; ⁷Department of Physiology University of the Basque Country UPV/EHU, Faculty of Medicine and Nursing, Leioa, Spain, National Institute for the Study of Liver and Gastrointestinal Diseases (CIBERehd, Carlos III Health Institute), Madrid, Spain, Leioa, Spain
Email: patricia.aspichueta@ehu.eus

Background and aims: Colorectal liver metastasis (CRLM) stands as the second leading cause of cancer-related mortality, as more than 50% of colorectal cancer (CRC) patients develop CRLM. Comorbidities such as dyslipidaemia are risk factors for the development of CRC. The hepatocyte, being the predominant liver cell, controls lipid and lipoprotein metabolism. However, it remains unclear whether the remodelling of cholesterol (CL) metabolism in hepatocytes is involved in the development of CRLM. Here, we aim to: 1) investigate the reprogramming of CL metabolism in CRLM; and 2) assess whether the modulation of CL metabolism in hepatocytes, achieved through PCSK9 overexpression, influences CRLM progression.

Method: The E-GEOD-14297 human transcriptome array, including healthy liver (HL), CRC and CRLM was analysed. The CRLM model involved intrasplenic injection of MC38 tumor cells in mice fed chow diet (CD), high fat diet (HFD) or Western diet. *In vivo* Pcsk9 overexpression in hepatocytes was induced using adeno-associated virus 8. Metabolic fluxes, lipid content, protein and gene expression were analysed in control and metastatic surrounding (ST) and tumor (T) tissues. An *in vivo* extravasation assay was performed by intrasplenic injection of RFP-labelled MC38 cells. *In vitro* proliferation assays of MC38 cells were performed with conditioned media obtained from isolated hepatocytes.

Results: The analysis of the CRLM transcriptome revealed that one of the most altered pathways in CRLM was "lipid and lipoprotein metabolism". Mice fed HFD or CD exhibited similar tumor numbers, liver fibrosis and reprogramming of CL metabolism in CRLM. CL levels increased in the ST and T of CRLM, with no concurrent increases observed in metabolic fluxes regulating *de novo* synthesis or protein levels of the rate-limiting enzyme HMGCR. However, a decrease in serum CL and an increase in hepatic levels of LDLR in ST and T were observed compared to healthy livers. During CRLM, hepatocyte Pcsk9

overexpression in mice prevented LDL uptake, as indicated by elevated serum CL levels, and induced a marked reduction in tumor number and associated fibrosis compared to their control counterparts. Pcsk9 overexpression induced an increase in the *de novo* synthesis and accumulation of cholesteryl ester in the ST, predominantly in hepatocytes. While the extravasation of CRC cells during CRLM remained unchanged when Pcsk9 was overexpressed in hepatocytes. Conditioned media from hepatocytes overexpressing Pcsk9 decreased the proliferation of CRC cells. Treating hepatocytes with inhibitors of different enzymes of CL synthesis induced changes in the secretome as the proliferation of CRC cells showed.

Conclusion: Targeted remodelling of CL metabolism in hepatocytes reduces CRLM progression without affecting CRC cell extravasation. The results suggest the potential involvement of the hepatocyte secretome in this process.

OS-102

A rule-based multiscale model of hepatic stellate cell plasticity: critical role of the inactivation loop in fibrosis progression

Matthieu Bougueon¹, Vincent Legagneux², Octave Hazard³, Jérémy Bomo², Anne Siegel⁴, Jérôme Féret⁵, Nathalie Theret². ¹Centre national de la recherche scientifique, Paris, France; ²Université de Rennes, Institut national de la santé et de la recherche médicale, Rennes, France; ³École Normale Supérieure Lyon, Lyon, France; ⁴Université de Rennes, Centre national de la recherche scientifique, Rennes, France; ⁵Institut national de recherche en informatique et en automatique, Paris, France
Email: mbougueon@di.ens.fr

Background and aims: Hepatic stellate cells (HSCs) are the source of extracellular matrix (ECM) whose accumulation leads to fibrosis, a condition that impair liver functions in chronic liver disease. Understanding the dynamics of HSCs will provide insight to develop new therapeutic approaches. Few computational models have been proposed for hepatic fibrosis and none include the heterogeneity of HSCs phenotypes recently highlighted by single-cell RNA sequencing analyses. The aim of the study is to develop a rule-based model to study HSCs dynamics during fibrosis and reversion.

Method: Kappa, a graph rewriting language, is used to build models that are calibrated with data from literature. Simulations are performed using the KaSim tool based on the Gillespie stochastic simulation algorithm. We generate biological data from a mouse model of CCL4-induced liver fibrosis to validate the final model and we use RNA sequencing data from patients with fibrosis to verify the predictions.

Results: We develop the first rule-based multi-scale model of HSCs integrating seven HSCs states and their interaction with TGFB1 molecules that regulate HSCs activation and secretion of type I collagen, the main component of the ECM. Simulation studies highlight the critical role of the HSCs inactivation process during fibrosis progression and reversion. While inactivation allows elimination of activated HSCs during reversion steps, reactivation loops of inactivated HSCs (iHSCs) is required to sustain fibrosis. We further have demonstrated the model's sensitivity to TGFB1 parameters, suggesting its adaptability to a variety of pathophysiological conditions in which TGFB1 release associated with the inflammatory response differs. Our model further predicts the accumulation of iHSCs during chronic liver disease and we confirmed this accumulation by using RNA sequencing data from patients with liver fibrosis.

Conclusion: Overall, our study provides the first model of HSCs dynamics during fibrosis and liver reversion that can be used to explore the regulatory role of HSCs in liver homeostasis. Thus, our model provides predictions showing the critical role of the inactivation loop in the development of hepatic fibrosis and identifying iHSCs as potential new markers of fibrosis progression.

OS-103

Antibiotic-mediated microbiota depletion limits IgA-related fibrogenesis in metabolic dysfunction-associated steatohepatitis

Svenja Schuehle^{1,2}, Eleni Kotsiliti^{1,3}, Yotam Cohen⁴, Sisi Deng^{5,6}, Hélène Omer⁷, Feng Han¹, Mengjie Qiu⁸, Aysan Poursadegh Zonouzi⁹, Sabine Schmidt¹, Jose Efrén Barragan Avila^{1,2}, Mirian Fernández Vaquero^{1,2}, Enrico Focaccia^{1,2}, Sandra Prokosch¹, Ulrike Rothermel¹, Florian Müller¹, Jenny Hetzer¹, Danijela Heide¹, Lukas Mager^{5,10}, Daniele Bucci^{5,6}, Ari Waisman⁹, Christoph Trautwein^{5,6}, Dirk Haller⁷, Eran Elinav^{1,11}, Mathias Heikenwälder^{1,5,12,13}, ¹German Cancer Research Center (DKFZ), Heidelberg, Germany; ²University of Heidelberg, Heidelberg, Germany; ³Technische Universität München, München, Germany; ⁴Weizmann Institute of Science, Rehovot, Israel; ⁵The M3 Research Center, Medical Faculty, University Tübingen, Tübingen, Germany; ⁶Werner Siemens Imaging Center, University Hospital Tübingen, Tübingen, Germany; ⁷Technical University of Munich, Munich, Germany; ⁸University Hospital Heidelberg, Heidelberg, Germany; ⁹University medical center of Johannes Gutenberg Mainz, Mainz, Germany; ¹⁰Universitätsklinikum Tübingen, Tübingen, Germany; ¹¹Weizmann Institute of Science, Rehovot, Germany; ¹²Molecular Virology, Heidelberg University, Heidelberg, Germany; ¹³Cluster of Excellence iFIT (EXC 2180) "Image-Guided and Functionally Instructed Tumor Therapies", University of Tübingen, Tübingen, Germany
Email: svenja.schuehle@gmail.com

Background and aims: Metabolic dysfunction-associated steatohepatitis (MASH) is the fastest-growing cause of primary liver cancer, specifically hepatocellular carcinoma (HCC). MASH-to-HCC progression is marked by necroinflammation, metabolic reprogramming and fibrosis. Due to the direct connection between the gut and the liver, the intestinal microbiota is suspected to be involved in inflammatory and metabolic processes during MASH development. Therefore, in this study we aimed to investigate the role of the gut microbiota and gastrointestinal B cells in a mouse model of MASH-to-HCC transition.

Method: C57Bl/6 mice were fed a choline-deficient high fat diet (CD-HFD) for 6 or 12 months to induce MASH and MASH-to-HCC progression. B cells were therapeutically depleted with anti-CD20 and the microbiota was depleted using broad-spectrum antibiotics (ABx) administered through the drinking water. Normal diet (ND) and CD-HFD mice without treatment served as control mice. Microbiota composition and liver pathogenesis were analyzed by shotgun metagenomic sequencing, serology, immunohistochemistry, RNA sequencing and metabolomics.

Results: We showed that B-cell depletion significantly reduced hepatic steatosis and fibrosis and that IgA from gastrointestinal B cells was sufficient to induce fibrosis. This axis was mediated by IgA-dependent activation of hepatic FCGR1⁺ cells which directly correlated with fibrosis development. Fibrosis still developed in AID^{G235} mice with reduced somatic hypermutation indicating that antigen specificity of IgA was not required for fibrosis induction. Furthermore, we found that the role of B cells in MASH was independent of the gut microbiota since germ-free mice were not protected from MASH development. However, therapeutic microbiota depletion using ABx treatment in combination with CD-HFD significantly reduced fibrosis development during MASH progression despite similar obesity and steatosis development compared to non-treated CD-HFD mice. While MASH-associated T-cell infiltration was not affected by ABx treatment, activation of resident and infiltrating myeloid cells was reduced. ABx treatment also significantly decreased intestinal and systemic IgA and consequently the activation of hepatic FCGR1⁺ cells. Moreover, ABx treatment was associated with significant transcriptional and metabolic changes compared to non-treated CD-HFD mice.

Conclusion: Our results demonstrate that the intestinal microbiota promotes MASH progression through IgA-mediated fibrogenesis. Furthermore, our data suggest that certain immunological features of MASH occur independent of the microbiota while metabolic and transcriptional processes regulated by the microbiota might be involved in the pathogenesis.

OS-104

Oxidative stress and metabolic reprogramming of hepatocytes forming liver cell rosettes in patients with primary sclerosing cholangitis

Carlotta Mayer¹, Silvia Radrezza¹, Ignacy Rzagalinski¹, Brian K. Chung², Tom Hemming Karlsen³, Andrej Shevchenko¹, Marino Zerial⁴, ¹Max Planck Institute of Molecular Cell Biology and Genetics, Dresden, Germany; ²Research Institute of Internal Medicine, NoPSC Center, Oslo, Norway; ³Oslo University Hospital, Oslo, Norway; ⁴Max Planck Institute of Molecular Cell Biology and Genetics, Dresden, Germany
Email: zerial@mpi-cbg.de

Background and aims: Patients with impaired bile flow frequently exhibit structural tissue changes described in histological sections as liver cell rosettes. Liver cell rosettes are clusters of >2 hepatocytes arranged around a dilated bile canaliculus lumen, creating segments of epithelial tubes. The hepatocytes in liver cell rosettes have a single apico-basal axis, reflecting a change to the usual hepatocyte polarity. As a shift in polarity requires fundamental intracellular reorganization, we tested the hypothesis that hepatocytes forming liver cell rosettes may lose metabolic functionality, thus contributing to disease progression.

Method: We performed laser capture microdissection on liver tissue of patients with primary sclerosing cholangitis (PSC) (n=7). We collected paired samples of parenchyma with normal hepatocytes and parenchyma of hepatocytes forming liver cell rosettes. From these samples we performed mass spectrometry and compared the proteome. We confirmed our findings using immunofluorescence microscopy and assays for liver metabolic functions.

Results: Principal component analysis revealed broad protein changes between usual parenchyma and liver cell rosette parenchyma. We identified 34 proteins enriched and 59 proteins reduced in liver cell rosette parenchyma (FDR=0.05). Interestingly, the majority of proteins reduced in liver cell rosette parenchyma are enzymes of key metabolic pathways of hepatocytes e.g. glutathione detoxification pathway. Based on this, we quantified the glutathione (GSH) content in the PSC patients. While oxidized glutathione (GSSG) usually remains below 5% of total GSH, we detected an increase of ~45.7% in GSSG. The absolute levels of GSSG positively correlate with the patient's liver cell rosette affection (linear regression analysis, R² = 0.488) and the only known canalicular exporter of GSSG, MRP2, is specifically depleted in liver cell rosettes. Liver cell rosette parenchyma was enriched in lysosomal proteins and proteins involved in ATP production. In line with a decrease of glycolytic enzymes and the glucose transporter GLUT2 this suggests, a reduction of glucose-based energy production and mobilizing alternative energy sources from lysosomal breakdown processes.

Conclusion: Our analysis shows that in PSC patients hepatocytes forming liver cell rosettes are not only structurally (altered cell polarity) but also functionally different from normal hepatocytes. The rosette hepatocytes have a reprogrammed metabolism and accumulate oxidized glutathione, probably as a result of increased oxidative stress and decreased biliary excretion. In summary our results suggest that the changes in liver cell rosettes may have important consequences for hepatocytes to maintain their functionality and, thus, for disease progression.

Liver development and regeneration

OS-105-YI

Collagen-integrin signaling re-establishes bile duct morphogenesis and promotes adult ductular regeneration

Alexander Walker¹, Scott Waddell¹, Anabel Martinez Lyons¹, Paula Olaizola¹, Luke Boulter². ¹MRC Human Genetics Unit, University of Edinburgh, Edinburgh, United Kingdom; ²MRC Human Genetics Unit, University of Edinburgh, Edinburgh, United Kingdom
Email: alex.walker@ed.ac.uk

Background and aims: Bile duct reaction (BDR) is a common feature of many cholangiopathies, characterized by the proliferation and migration of bile ducts between portal triads. How new ducts form with the correct anatomical location and dimensions during regeneration remains unresolved. Integrins are a key cell-surface receptor enabling cells to interact with the extra-cellular matrix (ECM) and move through their extracellular environment. Our group has recently shown that integrin signaling is necessary for morphogenic restructuring of the bile duct. We aimed to address whether ECM-integrin interactions are essential for the formation of complex elongating bile duct networks in adult BDR following damage.

Method: By combining human, pathological tissue and the 3, 5-diethoxycarbonyl-1, 4-dihydrocollidine (DDC) mouse model of biliary inflammation and fibrosis, dynamic changes in biliary integrin expression and peri-portal ECM composition were assessed by quantitative imaging and gene expression analysis. Flow cytometry was used to isolate integrin $\alpha 2$ -high versus low populations which were analysed by bulk RNA sequencing. A transgenic *Krt19:Cre/loxP* mouse model allowed for the conditional knockout of *Itga2* and *Itgb1* in cholangiocytes; this as well as *in vitro* assays were used to assess the role of integrin signaling in biliary regeneration and morphogenesis. Finally reverse phase protein arrays were used to interrogate the downstream mechanisms of integrin signaling in cholangiocytes.

Results: Collagen-binding integrins (particularly $\alpha 2/\beta 1$) are elevated in bile ducts in mouse models of BDR and in human primary sclerosing cholangitis, mirroring an increase in structural collagens I and III in the peri-portal ECM during BDR. Integrin $\alpha 2$ -high bile ducts are formed of predominantly immature cholangiocytes and localize to branching tips throughout the biliary network, partially overlapping with a proliferative cholangiocyte population. Bulk RNA-seq of integrin $\alpha 2$ -high cholangiocytes shows the increased expression of genes involved in migration (*Inhba*, *Aif1l*), mitosis (*Smc2*) and mechano-transduction (*Piezo2*). *In vitro* inhibition of integrin $\alpha 2$ using both siRNA and chemical inhibition (TC-I 15) reduced the proliferation and migration in cholangiocytes, in part attributable to a reduced phosphorylation of FAK and Akt. *In vivo* studies showed that integrin knockout cholangiocytes have reduced regenerative capacity and fail to contribute to extensive regeneration of the biliary tree.

Conclusion: Collagen-binding Integrins are expressed at the leading tip of bile duct growth in biliary inflammation, mirroring increased expression in its cognate ligands between portal triads. Integrin $\alpha 2$ knockout reduces migration and morphogenesis in cholangiocytes, suggesting modulation of the ECM-Integrin axis is important in understanding how ductular systems regenerate.

OS-106-YI

TGR5 deficiency reduces angiocrine factor expression in liver sinusoidal endothelial cells and hepatocyte proliferation after partial hepatectomy

Impreet Kaur¹, Rajnish Tiwari¹, Pinky Juneja², Ashwini Vasudevan³, Akash Kumar Mourya⁴, Michael Trauner⁵, Veronika Mlitz⁶, Dinesh Mani Tripathi⁷, Saneet Kaur⁸. ¹Institute of liver and biliary sciences, Delhi, India; ²Institute of liver and biliary sciences, Delhi; ³Institute of liver and biliary sciences, Delhi, India; ⁴Institute of liver and

biliary sciences, National Institute of Pharmaceutical Education and Research, Delhi, India; ⁵Medical University of Vienna, Vienna, Austria; ⁶Medical University of Vienna, Internal Medicine III, Vienna; ⁷Institute of liver and biliary sciences, Delhi; ⁸Institute of liver and biliary sciences, Delhi, India

Email: savykaur@gmail.com

Background and aims: Bile acid (BA) receptors like FXR and TGR5 have been implicated in liver regeneration. Although FXR-mediated liver regeneration is well known, mechanisms underlying TGR5-mediated liver regeneration remain largely unknown. Here, we investigated role of TGR5 during liver regeneration in rat models of 70% partial hepatectomy (PHx).

Method: PHx rat models were developed and studied at day 2 and day 5 post-PHx. Primary hepatocytes, liver sinusoidal endothelial cells (LSECs) and hepatic stellate cells (HSCs) were isolated by collagenase perfusion. Gene expression of both FXR and TGR5 in liver tissues and liver cells was studied. *In vitro*, effects of silencing and enhancing TGR5 expression was studied in LSECs by RT-PCRs and ELISA. *In vivo* effects of TGR5 deficiency on LSECs was evaluated in TGR5 KO mice. Co-culture of LSECs and hepatocyte organoids were investigated. BA profiling of peripheral serum in PHx rat models and human liver donors (n = 5) undergoing hepatectomy for LDLT was performed using LC-MS.

Results: In liver tissues, TGR5 gene expression was increased by 4 fold ($p < 0.0001$) at day 2 post-PHx, compared to sham while its expression was similar to that of sham at day 5. Among liver cells, TGR5 expression was negligible in hepatocytes at day 2 and day 5 post-PHx, but significantly increased in both LSECs and HSCs compared to sham (3 fold and 2.5 fold at day 2; 5.7 fold and 6 fold at day 5, $p < 0.0001$, each). An inhibition of TGR5 receptor by siRNA in LSECs substantially reduced gene expression of Id1 (2 fold), HGF (2.5 fold), WNT2 (3 fold) ($p < 0.001$ each) and also reduced angiocrine factor release in cell soups (HGF: 2.5 fold, Wnt2: 3 fold, $p < 0.001$ each) compared to controls. This reduction of gene expression and angiocrine factor secretion by LSECs was partially restored by addition of TGR5 agonist, lithocholic acid, LCA in culture for 24 h. Also, compared to cell soups obtained from TGR5-siRNA treated LSECs, cell soups obtained from LCA treated LSECs significantly enhanced proliferation of hepatocyte organoids (3 fold; $p < 0.05$ each). In TGR5 KO, LSECs showed reduced gene expression of Id1 (2 fold), HGF (2.5 fold), Wnt2 (2 fold); $p < 0.001$ each compared to wild-type mice.

BA profiling clearly demonstrated that secondary BAs that activate TGR5, Lithocholic acid (LCA), Deoxycholic acid (DCA) were significantly increased in PHx compared to sham at day 2 post-PHx. Human donors undergoing hepatectomy with remnant liver volume to total liver volume between 35–40% showed increased ratio of serum secondary to primary BAs with specific increase of LCA and DCA levels at day 2 post-hepatectomy.

Conclusion: There is an increase in serum levels of secondary BAs and hepatic TGR5 expression at day 2 post-PHx. Deficiency of TGR5 in LSECs reduces angiocrine gene expression such as Id1, Wnt2 and HGF and hence hepatocyte proliferation during early phases of PHx.

OS-107-YI

Expression and regulation of HNF4 α isoforms in liver development and disease

Paulina Zydowicz-Machtel¹, Lenka Belicova¹, Ting Huang¹, Joanna Sajkowska-Kozielewicz², David Kosek¹, Katja Petzold^{1,2}, Emma Andersson¹. ¹Karolinska Institutet, Solna, Sweden; ²Uppsala University, Uppsala, Sweden
Email: paulina.zydowiczmachtel@ki.se

Background and aims: Hepatocyte nuclear factor 4 alpha (HNF4 α) is a crucial hepatocyte transcription factor controlling liver development and hepatocyte identity in mature livers. However, in mouse and human cells multiple HNF4 α isoforms were found and can be further categorized into two classes: P1- and P2-HNF4 α , based on the

transcription promoter usage. It is increasingly clear that the isoforms have different roles in the liver, while their expression depends on liver developmental stage, and is dysregulated in hepatocellular carcinoma (HCC). Their expression and function during embryonic development and cancer is not well understood, we therefore need detailed understanding of expression patterns and regulation of individual HNF4 α isoforms, as well as comprehensive comparison between mouse and human models. Here, we aim to elucidate the role (s) of P1- and P2-HNF4 α isoforms in hepatoblasts, cholangiocytes, and hepatocytes from healthy and diseased liver using mouse *in vivo* and *in vitro* liver models, human cell lines and gene silencing approaches.

Method: To determine the expression pattern of P1- and P2-HNF4 α isoforms during liver development and maturation, we performed an immunohistochemistry (IHC) staining analysis on wild-type embryonic (embryonic day E17.5, E18.5) and postnatal (postnatal day P1, P7, P15, adult) mouse liver tissues, including livers of aged mice with spontaneous tumor development. For functional characterization of the isoforms, we used both mouse and human *in vitro* systems modeling liver development or liver disease e.g. mouse primary hepatoblasts and cell lines in which the expression of specific isoforms was manipulated using RNAi (RNA interference): *miRNA-34a* (*microRNA-34a*) and siRNAs (small interfering RNA). HNF4 α isoform repression *in vitro* was verified by quantitative PCR (qPCR) and Western blot. Hepatoblasts development into hepatocytes or cholangiocytes after isoform downregulation was characterized by immunofluorescence staining.

Results: Interestingly, P2-HNF4 α was found to be expressed in cholangiocytes at early stages of developing liver (P7 and P15) and in liver tumor tissue, while P1-HNF4 α expression was almost exclusively restricted to hepatocytes. Preliminary experiments in cell lines indicate that *miRNA-34a*, a potential endogenous regulator of HNF4 α , may repress both P1-HNF4 α and P2-HNF4 α . Repression of HNF4 α isoforms in primary hepatoblasts affected the morphology and differentiation of hepatoblasts.

Conclusion: Our data suggests that P1-HNF4 α and P2-HNF4 α isoforms differentially control cell identity of liver epithelial cells in development and may become activated/disactivated in liver cancer. Further studies towards individual manipulation of HNF4 α isoforms in the liver can be a promising tool for more controlled and precise treatment in liver disease.

OS-108-YI

Liver lymphatic endothelial cells regulate hepatic progenitor cells via lymphangiocrine factors in pathological liver regeneration

Aarti Sharma¹, Pinky Juneja², Ashwini Vasudevan², Deepika Jakhar², Jayesh Kumar Sevak², Impreet Kaur², Shiv Kumar Sarin², Dinesh Mani Tripathi², Savneet Kaur². ¹*Institute of Liver and Biliary Sciences, New Delhi, India;* ²*Institute of Liver and Biliary Sciences, New Delhi, India*
Email: savykaur@gmail.com

Background and aims: Liver sinusoidal endothelial cells (LSECs) are known to facilitate hepatocyte proliferation and liver regeneration. However, contribution of liver lymphatics and lymphatic endothelial cells (LyECs) to liver regeneration remains completely unexplored. Here, we comprehensively characterized LyECs vis a vis LSECs and studied their functions in physiological and pathophysiological liver regeneration.

Method: For physiological regeneration, 70% partial hepatectomy (PHx) rat models were used and for pathophysiological, we prepared impaired hepatocyte regeneration models, by 2-Acetyaminofluorene followed by 70% PHx (AAF-PHx). Sham-PHx and AAF-Sham were used as controls for PHx and AAF-PHx. Experiments were performed at day 2 post-PHx and day 8 in post AAF-PHx. Primary LSECs and LyECs were identified by imaging techniques and sorted with specific markers as LyVE1, CD31 and Podoplanin, CD31 respectively. Hepatic lymphatic drainage was assessed via FITC-dextran transport in portal

lymph nodes. Proteomic analysis was performed on sorted LSECs and LyECs and some of secretory proteins were analyzed by ELISAs. Effect of LSEC and LyEC conditioned media (CM) on hepatocytes and OV6+ hepatic progenitor cell (HPC) organoids was studied in co-culture assays.

Results: Histologically, proliferating hepatocytes were seen day 2 post-PHx and in AAF-PHx 8day, we observed damaged hepatocytes, increased inflammation with fibrosis (grade I/II). OV6+ HPCs were increased in AAF-PHx compared to PHx (23 ± 0.5 vs $5.2 \pm 1\%$, $p = 0.003$) near peri-portal region, confirmed with IHC. Dual positive staining and imaging revealed that LyECs were mostly located adjacent to HPCs near portal areas in PHx and AAF-PHx. Increased percentage of LSECs ($17.66 \pm 2\%$) and LyECs ($1.68 \pm 1.2\%$) were observed in PHx verified with confocal imaging, IHC and FACS analysis. Compared to PHx, there was decreased LSECs ($10.4 \pm 0.01\%$; $p = 0.007$) and increased LyECs ($2.59 \pm 0.05\%$; $p = 0.04$) in AAF-PHx. Hepatic lymphatic drainage also increased by about 80% in AAF-PHx compared to PHx ($p = 0.001$). Proteome analysis in LSEC and LyECs identified more than 1000 proteins each and about 400 were differentially expressed among different study groups. Among differentially expressed secretory proteins, secretome of PHx-LSECs showed increased expression of Wnt-2 (4 fold, $p = 0.01$) and secretome of AAF-PHx LyECs showed increased expression of Wnt-2 (2 fold, $p = 0.01$) and R-spondin 3 (2.5 fold, $p = 0.05$) compared to sham. In co-cultures, there was a considerable increase in number of HPCs organoids in AAF-PHx LyECs-CM (9 ± 2 vs 16.6 ± 1.5 , $p = 0.006$). **Conclusion:** The number and drainage function of hepatic lymphatics increase significantly during pathological liver regeneration. Our study provides valuable insights into the novel role of specific lymphangiocrine factors secreted by LyECs in governing proliferation of HPCs during liver injury.

OS-109

Developmental gene regulatory networks driving human liver disease cell states identified by single cell multi-modal data integration

Nigel Hammond¹, Elliot Jokl¹, Syed Murtuza-Baker¹, Sokratia Georgaka¹, Varinder Athwal¹, Neil Hanley¹, Karen Piper Hanley¹. ¹*University of Manchester, Manchester, United Kingdom*
Email: karen.piperhanley@manchester.ac.uk

Background and aims: Chronic liver disease is increasing and a major cause of death worldwide. Iterative injury prolongs an impaired wound-healing response, resulting in fibrosis. This unique microenvironment, involving complex interactions between multiple cell-types, drives progressive disease. We have previously shown similarities at the scar interface in cirrhosis with the ductal plate during liver development. However, it is clear this attempted regenerative response in on-going injury is impaired. To advance understanding of the heterogeneity underlying progressive liver disease we have integrated multi-modal single cell and spatially resolved datasets to uncover developmental gene regulatory networks (GRNs) driving cell state transitions in human liver disease.

Method: Single nuclei RNA and Assay for Transposase-Accessible Chromatin (ATAC) sequencing and spatial transcriptomics (ST) were generated from human cirrhotic tissue. Computational modelling integrated multiple-datasets to provide molecular spatial maps, directional trajectory and infer GRN associated with disease cell states. Molecular mechanisms were validated *in vitro* and *in vivo*.

Results: Data integration from RNA, ATAC and ST sequencing uncovered the cellular patho-architecture and spatial molecular signatures of diseased liver. Our results highlighted a spatial pattern of gene modules specifically localised at the scar interface. Unbiased computational analysis identified these subpopulations containing genes characteristic of both hepatocytes and cholangiocytes (HC1/CC1). Through pseudo temporal analysis of our single nuclei data, we uncovered a directional trajectory and transitional state from

hepatocytes to cholangiocytes. We showed transition of hepatocytes to a disease-associated state (HC1) correlated with the down-regulation of *HNF4A*, a master regulator of hepatocyte identity. Mechanistically, our gene expression and transcriptional motif analysis pointed toward signalling in cirrhosis involving crosstalk between the core developmental pathways Hippo, Notch and Wnt. Using our single cell RNA and ATAC data, we inferred GRNs and identified SOX9/ONECUT1 co-regulation of transitional genes, consistent with their roles in ductal plate development. Through an integrative analysis, we identified a novel transitional axis, marked by *ESRP1* (involved in gene splicing) and *ARHGEF38* (involved in cell migration) expression, driven by ONECUT1 and SOX9 co-accessibility regulating transitional states in cirrhosis.

Conclusion: These data serve as a spatial atlas of gene regulation and altered cell state in human cirrhosis. They highlight developmental regulatory networks as molecular drivers of disease and provide a valuable resource to explore biomarkers and potential therapeutic targets in progressive liver disease.

Liver tumours: Therapy

OS-110

ARMCENVIN: multipolar radiofrequency ablation of HCC using intratumourous versus extratumourous “no-touch” techniques.

French multicentric randomized controlled trial (NCT 01008657)

Olivier Seror^{1,2,3}, Gisele N’Kontchou⁴, Agnès Rode⁵, Philippe Merle⁶, Christophe Aubé⁷, Frédéric Oberti⁸, Valerie Vilgrain⁹, Mohamed Bouattour¹⁰, Hervé Trillaud¹¹, Jean-Frédéric Blanc¹², Boris Guiu¹³, Georges-Philippe Pageaux¹⁴, Patrick Chevallier¹⁵, Albert Tran¹⁶, Jean-Jacques Portal¹⁷, Jean Charles Nault¹⁸, Olivier Sutter¹⁹, Nathalie Ganne-Carrié¹⁸, Pierre Nahon¹⁸, Eric Vicaux²⁰. ¹Interventional radiology unit, Bobigny, France; ²Avicenne Hospital, Bobigny, France; ³Hôpital Avicenne, Bobigny, France; ⁴Liver unit, Avicenne Hospital, Bobigny, France; ⁵Radiology, La Croix Rousse Hospital, Lyon, France; ⁶Liver unit, La Croix Rousse Hospital, Lyon, France; ⁷Radiology, CHU Angers, Angers, France; ⁸Liver Unit, CHU Angers, Angers, France; ⁹Radiology, Beaujon Hospital, Clichy, France; ¹⁰Liver Unit, Beaujon Hospital, Clichy, France; ¹¹Radiology, CHU Bordeaux, Bordeaux, France; ¹²Liver Unit, CHU Bordeaux, Bordeaux, France; ¹³Radiology, CHU Montpellier, Montpellier, France; ¹⁴Hepato-gastroenterology, CHU Montpellier, Montpellier, France; ¹⁵Radiology, CHU Nice, Nice, France; ¹⁶Hepato-gastroenterology, CHU Nice, Nice, France; ¹⁷Clinical Research Unit, Lariboisière Hospital, Paris, France; ¹⁸Liver Unit, Avicenne Hospital, Bobigny, France; ¹⁹Interventional Radiology, Avicenne Hospital, Bobigny, France; ²⁰Clinical Research Unit, Lariboisière, Paris, France
Email: olivier.seror@aphp.fr

Background and aims: Multipolar radiofrequency ablation (mbpRFA) based on “no touch” (NT) concept consists of inserting an arrangement of several electrodes just outside the tumour in order to ablate centripetally first a cancer-free margin then the nodule. The ARMCENVIN randomized trial was aimed to assess if sharing mbpRFA technology, NT concept outperforms IT approach for the treatment of early HCC.

Method: In 52 months, in 6 participating centers 216 naïve patients bearing up to 3 HCC up to 4 cm accepted to be submitted to stratified randomization according to number of nodules >1 and size >3 cm to receive either IT or NT mbpRFA. In the IT arm, conversely to the NT arm, arrangement of electrodes was deliberately inserted just inside the borders of the tumours. To comply with NT requirements for tumours ranging from 1 and 2 cm and from 3 to 4 cm, a supplemental electrode was used in the NT arm as compared to the IT arm. The 2-years recurrence free survival (2y-RFS) was the main end point of the

study. Secondary end points were number of sessions to achieve complete response (up to 3), treatment failure rate, ablation ratio index (ARI) defined as the difference of maximum size of the nodule with the minimum size of ablation zone, the local (LRFS) and distant (DRFS), RFS, overall survival (OS) and complication rates.

Results: In the IT and NT arms 110 and 106 patients were randomized (mean age 65 y, 81% male, 89% Child-Pugh A, 29.15 ± 0.2 BMI, bearing 245 nodules, mean size 19.2 ± 7.7 mm, 84% single), respectively. The 2y-RFS were 56.6% and 50% (median 24.5 and 21.3 months; HR = 0.88 [0.59–1.39], p = 0.4), respectively. More than one procedure were performed in 11 (10.0%) and 12 (11.3%) and failure occurred in 1 (0.9%) and 5 (4.7%) (p = 0.06) patients, respectively. ARI were 10.35 ± 10.02 and 18.12 ± 9.93 in IT and NT arms, respectively (p < 0.0001). The 2y LRFS, DRFS and OS were 88.0% and 84.8% (HR 0.71 [0.34–1.5], p = 0.37), 63.3% and 62.6% (HR 0.93 [0.6–1.46], p = 0.77) and 87.2% and 83.8% (HR 0.7 [0.34–1.42], p = 0.32), respectively. The rates of complications (Dindo Clavien >grade 1) were 43.1% and 24.5%, respectively (p = 0.0042). Subgroup analyses suggested a potential advantage of NT mbpRFA in case of tumours >3 cm and performance in an experienced centre (more than 30 mbpRFA/year).

Conclusion: Using mbpRF technology for the ablation of HCC up to 4 cm diameter, RFS is not improved by extratumourous insertion of electrodes conforming with strict applying of “no touch” concept. Peripheral positioning of applicators within the borders of the tumors provides safely comparable intrahepatic sustained cancer progression free survival and may provide a clinical benefit for ablation of tumours >3 cm by skilled operators.

OS-111

Predictive genomic biomarkers for Atezolizumab plus Bevacizumab combination immunotherapy response in liver cancer: insights from the IMbrave150 trial

Sun Young Yim¹, Seung-Woo Baek², Sung-Hwan Lee³, BoHwa Sohn⁴, Yun Seong Jeong⁵, Sang-Hee Kang⁶, Kena Park⁷, Hyewon Park⁴, Sunyoung Lee⁴, Ahmed Kaseb⁴, Ji Hoon Kim⁶, In-Sun Chu⁸, Ju-Seog Lee⁴. ¹Anam Korea University Hospital, Seoul, Korea, Rep. of South; ²Korea Research Institute of Bioscience and Biotechnology, Daejeon, Korea, Rep. of South; ³CHA Bundang Medical Center, Seongnam, Korea, Rep. of South; ⁴UT MD Anderson Cancer Center, Houston, United States; ⁵UT MD Anderson Cancer Center, Houston, Korea, Rep. of South; ⁶Korea University Guro Hospital, Seoul, Korea, Rep. of South; ⁷Kyung Hee University Hospital at Gangdong, Seoul, Korea, Rep. of South; ⁸Bioneer Corporation, Daejeon, United States
Email: jlee@mdanderson.org

Background and aims: Combination immunotherapy, exemplified by atezolizumab plus bevacizumab, have become the established standard of care for individuals with inoperable hepatocellular carcinoma (HCC). Despite this advancement, the absence of clear predictive biomarkers and an understanding of the mechanisms governing response and resistance to these combined therapies pose challenges. Our aim is to evaluate whether previously defined immune signature scores (ISS) can identify HCC patients likely to derive enhanced benefit from the combination immunotherapy.

Method: We utilized the previously developed ISS predictor from analysis of TCGA pan-cancer data and applied it to gene expression data from the IMbrave150 trial. This phase 3 study compared atezolizumab plus bevacizumab versus sorafenib for treatment-naïve advanced HCC. Using an ISS cutoff of 0.5, patients were stratified into potential immunotherapy responders (high ISS) and non-responders (low ISS). The significance of this ISS-based stratification for predicting clinical outcomes was evaluated through Kaplan-Meier plots, log-rank tests, Chi-square tests, and Cox regression analyses. Multiple statistical approaches assessed the association between ISS groups and progression-free survival in both the immunotherapy combination arm as well as the sorafenib arm.

Results: In the IMbrave150 trial cohort, data on gene expression and outcomes were accessible for 247 patients who received

atezolizumab plus bevacizumab, and 48 patients who received sorafenib. The high ISS demonstrated a significant association with enhanced PFS in the atezolizumab plus bevacizumab group ($p = 0.003$), while no such association was observed in the sorafenib group ($p = 0.6$). Similarly, in the high ISS subgroup, the combination therapy exhibited superior OS ($p.0.001$) and PFS ($p = 0.02$) compared to sorafenib, but no discernible benefit was noted in the low ISS subgroup (both $p > 0.7$). The OS hazard ratio for the combination versus sorafenib was 0.26 (95% CI 0.14–0.51, $p < 0.001$) among high ISS patients, while it was not statistically significant in low ISS (HR 0.88, $p = 0.68$). Interaction testing confirmed a notable interaction between ISS subtype and treatment benefit, particularly for OS ($p = 0.01$). In the combination arm, the objective response rate was 45.6% in the high ISS group versus 22.8% in the low ISS group.

Conclusion: Our study suggests that ISS may serve as a promising predictive biomarker for enhanced therapeutic outcomes in patients undergoing combination immunotherapy for HCC. The identification of such markers is crucial for refining patient stratification and personalized treatment approaches, thereby advancing the effectiveness of current standard-of-care regimens. Further validation studies are warranted to solidify the clinical utility of ISS and its integration into the decision-making process for HCC immunotherapy.

OS-112-YI

Outcome and management of patients with hepatocellular carcinoma who achieved complete response to immunotherapy-based systemic therapy

Bernhard Scheiner¹, Beodeul Kang², Lorenz Balcar³, Pompilia Radu⁴, Florian P Reiter⁵, Gordan Adžić⁶, Jiang Guo⁷, Xu Gao⁸, Xiao Yuan⁹, Long Cheng¹⁰, Joao Gorgulho¹¹, Michael Schultheiß¹², Najib Ben Khaled¹³, Friedrich Sinner¹⁴, Antonio D'Alessio¹⁵, Katharina Pomej³, Anna Saborowski¹⁶, Birgit Schwacha-Eipper¹⁷, Valentina Zarka¹⁷, Katharina Lampichler³, Naoshi Nishida¹⁸, Pei-Chang Lee¹⁹, Anja Krall²⁰, Anwaa Saeed²¹, Vera Himmelsbach²², Giulia Tesini²³, Brooke Wietharn²⁴, Yi-Hsiang Huang¹⁹, Caterina Vivaldi²⁵, Gianluca Masi²⁵, Arndt Vogel^{26,27,28}, Kornelius Schulze¹¹, Michael Trauner³, Rudolf E. Stauber²⁰, Masatoshi Kudo¹⁸, Jeroen Dekervel²⁹, Neehar Parikh³⁰, Jean-François Dufour³¹, Juraj Prejac³², Andreas Geier³³, Bertram Bengsch¹², Johann von Felden¹¹, Marino Venerito¹⁴, Alexander Philipp¹³, Fabian Finkelmeier²², Fanpu Ji⁹, Hung-Wei Wang³⁴, Lorenza Rimassa²³, David J. Pinato¹⁵, Mohamed Bouattour³⁵, Hong Jae Chon², Matthias Pinter³. ¹Medical University of Vienna, Department of Medicine III, Division of Gastroenterology and Hepatology, Vienna, Austria; ²CHA Bundang Medical Centre, CHA University, Seongnam, Korea, Rep. of South; ³Medical University of Vienna, Vienna, Austria; ⁴Inselspital, Bern University Hospital, Bern, Switzerland; ⁵University Hospital Würzburg, Division of Hepatology, Department of Medicine II, Würzburg, Germany; ⁶University Hospital Centre Zagreb, Department of Oncology, Zagreb, Croatia; ⁷Beijing Ditan Hospital, Capital Medical University, Department of Oncology Interventional Radiology, Beijing, China; ⁸Second Affiliated Hospital of Xi'an Jiaotong University, Xi'an, China; ⁹Second Affiliated Hospital of Xi'an Jiaotong University, Xi'an, China; ¹⁰Beijing Ditan Hospital, Capital Medical University, Beijing, China; ¹¹University Medical Center Hamburg-Eppendorf, Hamburg, Germany; ¹²Medical Center-University of Freiburg, Freiburg, Germany; ¹³University Hospital, LMU Munich, Munich, Germany; ¹⁴Otto-Von Guericke University Hospital, Magdeburg, Germany; ¹⁵Imperial College London, London, United Kingdom; ¹⁶Medizinische Hochschule Hannover, Hannover, Germany; ¹⁷Inselspital, Bern University Hospital, University of Bern, Bern, Switzerland; ¹⁸Kindai University, Faculty of Medicine, Osaka, Japan; ¹⁹Taipei Veterans General Hospital, Taipei, Taiwan; ²⁰Medical University of Graz, Graz, Austria; ²¹University of Pittsburgh (UPMC), Pittsburgh, United States; ²²University Hospital Frankfurt, Frankfurt/Main, Germany; ²³Humanitas Cancer Center, IRCCS Humanitas Research Hospital, Rozzano (Milan), Italy; ²⁴University of Kansas Cancer Center,

Kansas, United States; ²⁵University Hospital of Pisa, Pisa, Italy; ²⁶Toronto General Hospital, Toronto, Canada; ²⁷Princess Margaret Cancer Centre, Toronto, Canada; ²⁸Hannover Medical School, Hannover, Germany; ²⁹University Hospitals Leuven, Leuven, Belgium; ³⁰University of Michigan, Ann Arbor, Michigan, United States; ³¹Centre for Digestive Diseases, Lausanne, Switzerland; ³²University of Zagreb, Zagreb, Croatia; ³³University Hospital Würzburg, Würzburg, Germany; ³⁴China Medical University Hospital, Taichung, Taiwan; ³⁵APH Nord, Hôpital Beaujon, Beaujon, France
Email: bernhard.scheiner@meduniwien.ac.at

Background and aims: The management and natural history of patients with hepatocellular carcinoma (HCC) who achieve complete response (CR) to immune checkpoint inhibitor (ICI)-based systemic therapies is not well described.

Method: We conducted a retrospective study of adult patients with HCC who had CR (according to mRECIST) to systemic ICI-based therapies from 18 centers in Europe and Asia. Patients who received immunotherapy as (neo-)adjuvant therapy before/after resection or ablation or in combination with loco-regional therapies were excluded.

Results: Of 2502 patients with HCC treated with ICI-based palliative systemic therapies, 123 patients (4.9%) achieved CR according to mRECIST (CR-mRECIST) and 72 patients (2.9%) had CR according to RECISTv1.1 (CR-RECISTv1.1) as well. The mean age of the total cohort ($n = 123$) was 65.2 ± 9.9 years, 103 were male (84%), and the majority had BCLC stage C ($n = 87$; 71%) and Child-Pugh class A ($n = 112$; 91%). Median follow-up was 32.1 (95%CI, 30.5–33.6) months. The majority ($n = 106$, 86%) received ICI-based combination therapies (atezolizumab/bevacizumab: $n = 80$, 65%). Time from immunotherapy initiation to first CR was 7.4 (95%CI, 5.3–9.5) months. Median alpha-fetoprotein declined from 19 (IQR, 4–1090) ng/ml at baseline to 2 (IQR, 1–3) ng/ml at nadir. Median duration of CR (mRECIST) was 35.5 (95%CI, not estimable) months. Overall, 41 patients (33%) experienced recurrence a median of 11.4 months (95%CI, 8.9–14.0) after mRECIST CR. Recurrence rate was similar in patients with CR-mRECIST only (26%) and CR-RECISTv1.1 (39%; $p = 0.120$), as were recurrence-free survival rates at one and two years (77% and 61% for CR-mRECIST only vs. 74% and 58% for CR-RECISTv1.1; log-rank $p = 0.310$). A total of 93 patients (75.6%) discontinued ICI during follow-up due to adverse events ($n = 11$, 11.8%), recurrence ($n = 15$, 16.1%), durable CR ($n = 41$, 44.1%), or other reasons ($n = 26$, 28.0%). Among those who discontinued treatment for reasons other than recurrence ($n = 76$), recurrence rate was 23.7% ($n = 18$); patients who received systemic treatment for >6 months after complete response had a numerically lower recurrence rate (15.8%, $n = 6/38$) compared to those who discontinued treatment earlier (31.6%, $n = 12/38$; $p = 0.105$). Eleven patients underwent curative conversion therapy after CR (ablation, $n = 4$; transplantation, $n = 4$; resection, $n = 3$); two of them (18%) experienced recurrence. One-/3-/5-year overall survival (OS) rates of the whole cohort were 98%/88%/77%.

Conclusion: Only a small proportion of patients with advanced HCC achieves CR to palliative immunotherapy, but these patients have an excellent overall survival. The recurrence rate was similar between CR-mRECIST only and CR-RECISTv1.1, affecting approximately one in three patients. When considering ICI discontinuation, treatment for >6 months beyond CR may be associated with a lower recurrence rate.

OS-113

Adoptive natural killer cell immunotherapy can increase the recurrence-free survival following transarterial-chemoembolization in patients with intermediate stage hepatocellular carcinoma

Jooho Lee¹, Sooyeon Oh², Min-Ji Ahn³, Su-Kyung Chun³, Seung-Min Lee⁴, Kyumok Lee⁵. ¹Division of Gastroenterology and Hepatology, Department of Internal Medicine, CHA Bundang Medical Center, CHA University, Seoul, Korea, Rep. of South; ²Chaum Life Center, CHA University School of Medicine, Seoul, Korea, Rep. of South; ³Chaum

ORAL PRESENTATIONS

Life Center, CHA University School of Medicine, Seoul, Korea, Rep. of South; ⁴Center for Research and Development, CHA Advanced Research Institute, Seongnam, Korea, Rep. of South; ⁵Department of Internal Medicine, CHA Bundang Medical Center, CHA University, Seongnam, Korea, Rep. of South
Email: piolee2000@naver.com

Background and aims: Transarterial-chemoembolization (TACE) represent a first-line therapy for intermediate stage hepatocellular carcinoma (HCC). Adoptive immunotherapy is one of the important cancer immunotherapies including cytotoxic T lymphocytes and natural killer (NK) cells. Some adoptive cellular immunotherapy treatment exhibited survival benefit in HCC patients. The current study reports the results of a prospective, open label trial investigating the safety and efficacy of the combination of autologous NK cells and TACE in patients with intermediate stage HCC. In this study, we assessed whether post-TACE adjuvant NK cell immunotherapy could lower the frequency of recurrence following conventional TACE.

Method: This prospective pilot study enrolled 10 consecutive patients with HCC of intermediate stage from CHA Bundang medical center in Korea from January 2023 to November 2023. Patients were assigned consecutively to receive adjuvant NK cell immunotherapy (immunotherapy group) or no adjuvant therapy (controls) after TACE. The patients who assigned to immunotherapy group underwent conventional TACE followed by activated autologous NK cell therapy ($2\sim6 \times 10^9$ cells/100 ml, intravenous infusion once a week, 1 weeks after TACE, up to 3 cycles). Tumor response was assessed according to the modified RECIST criteria. We also analyzed the progression-free survival (PFS) and objective tumor response rate (ORR), defined as the percentage of patients with either a complete response or a partial response, in terms of best response experienced.

Results: Mean age was 62 years, with male and hepatitis B predominance (90% and 60%, respectively). The 6-month ORR was significantly higher in the NK cell immunotherapy group compared with the controls (100% vs 60%, $p < 0.05$). Also, NK immunotherapy group showed significantly longer PFS (9.3 vs 3.2 months, $p < 0.05$) than the control group. A significantly higher proportion of patients in immunotherapy group had adverse events, but the proportion of patients with serious adverse events did not differ significantly between groups. The proportion of the patients with worsening liver function, whose ALBI scores increased 3 months after treatment, was not different between groups. However, the proportion of patients with improving liver stiffness (fibrosis), whose liver elastography scores decreased more than 1 kPa, 3 months after TACE, was higher in the immunotherapy group (80% vs 40%; $p = 0.18$).

Conclusion: In patients with intermediate stage HCC who underwent TACE, combination immunotherapy with activated NK cells increased the ORR and PFS. Adoptive immunotherapy with autologous NK cells is a safe, feasible treatment that can lower recurrence and improve recurrence-free outcomes after conventional TACE for HCC.

OS-114

Liver transplantation following hepatocellular carcinoma downstaging with atezolizumab/bevacizumab: preliminary results of the prospective ImmunoXXL study

Sherrie Bhoori¹, Marianna Maspero¹, Michele Droz Dit Busset¹, Marco Bongini¹, Matteo Virdis¹, Davide Citterio¹, Carlo Sposito¹, Valentina Bellia¹, Carlo Battiston¹, Jorgelina Coppa¹, Maria Flores¹, Vincenzo Mazzaferro¹. ¹Fondazione IRCCS Istituto Nazionale dei Tumori, Milan, Italy
Email: sherrie.bhoori@istitutotumori.mi.it

Background and aims: Tumor downstaging (DS) is a viable strategy to increase the access to liver transplantation (LT) in patients with hepatocellular carcinoma (HCC) beyond conventional criteria. Given the exciting results of immune checkpoint inhibitor (ICI)-based combinations in intermediate/advanced stages of HCC, their use within DS protocols is now being investigated. We report the preliminary results of the ImmunoXXL study on LT after DS with

atezolizumab/bevacizumab (A+B) in patients with unresectable intermediate-advanced HCC.

Method: ImmunoXXL (NCT 05879328) is an observational prospective single-arm study that includes patients with HCCs waitlisted for LT after achieving a sustained radiological partial or complete response with A+B. The primary outcome of the trial is recurrence free survival. Secondary outcomes are tumor response, complication rates, overall survival and immunomonitoring.

Results: Out of 66 patients treated with A+B at our center, 16 achieved sufficient response for transplant eligibility, 8 excluded because of non-oncological reasons. Up to now, 7 patients have been enrolled and transplanted (6/7 males, median age 62) into the ImmunoXXL study. Underlying liver disease was HBV (n.2), MetALD (n.2), MASLD (n.1), and HCV-ALD (n.1). All but one patients had received prior loco-regional treatments and all were treated with A+B because of beyond Up-to-7 tumor burden. Median AFP at treatment inception was 135 ng/ml, while at listing within normal limits for all but one (median AFP 2, 5 ng/ml). Mean duration of treatment was 120 days (median of 6 cycles) and the interval between the last A+B dose and LT was 58 days. All patients underwent LT from a cadaveric graft supported with hypothermic oxygenated machine perfusion. Explant pathology revealed 5 HCC within MC (3 complete responses). Post-LT immunosuppression was intensified with a triple regimen with one patient experiencing mild acute cellular rejection responding to steroid pulses. Median post-LT length of hospital stay was 16 days. Three patients (44%) experienced major complications (hepatic artery thrombosis requiring re-LT, biliary fistula requiring endoscopy and post-surgical Budd-Chiari requiring balloon dilation); 4 had high CMV viremia requiring treatment. After a median of 8 months, all patients are alive with no evidence of disease.

Conclusion: Our preliminary results demonstrate that sequential treatment with A+B followed by LT is safe; the higher than expected post-LT morbidity may be related to the intensified immunosuppressive regimen. A+B seems to be effective despite the short follow-up; at this time point, no HCC recurrence has occurred.

SLD: Therapy

OS-115

Results from a phase 2a randomized trial with the transglutaminase 2 inhibitor ZED1227 in patients with MASLD

Jörn M Schattenberg¹, Piotr Rozpondek², Krystyna Opawska³, Sophie Metivier⁴, Veronique Loustaud-Ratti⁵, Luis Ibañez-Samaniego⁶, Pere Ginès⁷, Tobias Böttler⁸, Elzbieta Blach⁹, Diana Leeming¹⁰, Morten Karsdal¹⁰, Markus Proels¹¹, Judith Czarnecki¹¹, Michael Stiess¹¹, Ralph Müller¹¹, Manuel Romero-Gómez¹². ¹Department of Internal Medicine II, Saarland University Medical Center, Homburg, Germany; ²FutureMeds Clinic Krakow, Krakow, Poland; ³ETG Network Lodz, Lodz, Poland; ⁴CHU Toulouse, Hôpital de Rangueil, Toulouse, France; ⁵CHU DUPUYTREN LIMOGES, Hôpital Universitaire Dupuytren, Limoges, France; ⁶Hepatology Department. Hospital Gregorio Marañón. IISGM. CIBEREHD., Madrid, Spain; ⁷Hospital Clínic. Institut d'Investigacions Biomèdiques August Pi i Sunyer (IDIBPAS). Centro de Investigación en Red de Enfermedades Hepáticas y Digestivas (CIBEREHD)., Liver Unit, Hospital Clínic, Faculty of Medicine, University of Barcelona., Barcelona, Spain; ⁸Uniklinik Freiburg. Klinik für Innere Medizin II, Department of Medicine II, Freiburg, Germany; ⁹Centrum Medyczne Katowice-PRATIA-PPDS, Katowice, Poland; ¹⁰Nordic Bioscience A/S, Herlev, Denmark; ¹¹Dr. Falk Pharma GmbH, Freiburg im Breisgau, Germany; ¹²Institute of Biomedicine of Seville (HUVR/CSIC/US), Hospital Universitario Virgen del Rocío-PPDS, University of Seville, Sevilla, Spain
Email: joern.schattenberg@uks.eu

Background and aims: ZED1227 is an inhibitor of transglutaminase (TG) 2, which plays a critical role in the development of liver fibrosis. The CEC-11/NAS trial aimed to show efficacy and safety of ZED1227 in patients (pts) with phenotypic MASLD (Metabolic Dysfunction-Associated Steatotic Liver Disease) and significant fibrosis.

Method: This was a double-blind, randomized, multi-center, placebo-controlled, comparative, exploratory phase II dose-finding trial. Pts were treated orally for 12 weeks with 20, 50 or 100 mg/day ZED1227 or placebo (1:1:1:1). The trial enrolled pts with MASLD and significant fibrosis determined by non-invasive tests or liver biopsy. The primary efficacy end point was the relative change of serum levels of the fibrogenesis marker PRO-C3 (N-terminal propeptide of type III collagen).

Results: 334 pts were screened, 186 were randomized, and 174 received at least one dose of study drug or placebo and were included in the full analysis set (FAS). 168 pts completed the study. Baseline data were comparable between treatment groups (mean age 59.9 years, 55.2% males, mean BMI 33.8 kg/m², mean serum level of PRO-C3 44.12 ng/ml, T2DM 56.3%). Median treatment duration was 84 days and 97.7% of pts had a treatment compliance $\geq 80\%$. The primary efficacy analysis in FAS showed a numerical reduction of PRO-C3 in the low and high dose arms after 12 weeks of treatment (least squares (LS)-mean difference (SE) 20 mg vs placebo (%): -6.5 (4.90) (95% CI [-16.12; 3.10]; $p = 0.0921$ [one-sided]) and 100 mg -8.1 (4.84) (95% CI [-17.57; 1.43]; $p = 0.0479$ [one-sided]; that did not reach statistical significance ($\alpha = 0.025$). No effect was seen in the 50 mg group. In a subgroup analysis in pts with PRO-C3 \geq median at baseline showed a dose-dependent reduction of PRO-C3 levels (LS mean difference (SE) vs placebo (%), 20 mg: -3.5 (6.71), 50 mg: -5.8 (6.78), 100 mg: -14.8 (6.59)). In this subgroup, a dose dependent decrease of PRO-C6, a marker of cardiovascular disease outcome was observed (median reduction after 12 weeks (ng/ml), 20mg: 0.0, 50 mg: -2.46, 100 mg: -6.77, Placebo: 2.69). In a responder analysis, pts responding to ZED1227 had higher baseline PRO-C3 values (mean 54.12 vs 40.55 ng/ml) and showed a trend to higher baseline AST and ALT levels compared to non-responder (AST mean 54.8 vs 41.4 U/L, ALT mean 74.4 vs 59.2 U/L). Treatment with ZED1227 was well tolerated and most of the adverse events (AEs) were of mild or moderate intensity. In three pts AEs led to a discontinuation of IP, two in the 20 mg and one in the placebo group. Nine serious AEs (SAEs) were reported. None of the SAEs were considered related to the study treatment.

Conclusion: ZED1227 was well tolerated and showed a positive trend for reducing profibrogenic PRO-C3 in phenotypic MASLD that however, did not reach statistical significance. In the subgroup of pts with higher PRO-C3 at baseline, the ZED1227 effect was more pronounced and dose dependent.

OS-116

Structured exercise plus mediterranean diet intervention in patients with metabolic-dysfunction associated steatotic liver disease (MASLD): a randomized controlled trial. The EHmet-DIA study

Carmen Lara-Romero¹, Rocío Aller², Miguel Angel Fernández³, Franz Martin-Bermudo⁴, Rocío Munoz-Hernández⁵, Javier García-Rioja², Rebeca Sigüenza², Blanca Escudero-López⁶, Víctor Arroyo-López², Carmen Carnicero², Genoveva Berná⁷, Lucía López-Bermudo⁶, Jesús Funuyet-Salas⁸, Raquel Millán¹, Isabel Fernández-Lizaranzu⁹, Javier Castell¹⁰, Manuel Romero-Gómez¹. ¹Liver and Digestive Diseases Unit. Virgen del Rocío University Hospital; ²SeLiver Group, Biomedicine Institute of Seville (HUVR/CSIC/US), Medicine Department, University of Sevilla; ³CIBEREHD, Sevilla, Spain; ⁴Gastroenterology Department, Centro de Investigación de Endocrinología y Nutrición, Centro de Investigación Biomédica en Red de Enfermedades Infecciosas (CIBERINF), Facultad de Medicina, University of Valladolid, Hospital Clínico de Valladolid, Valladolid, Spain; ⁵Sports Medicine Unit. University of Sevilla., Sevilla, Spain; ⁶Andalusian Center of Molecular Biology and Regenerative

Medicine, Sevilla, Spain, Sevilla, Spain; ⁷SeLiver Group, Biomedicine Institute of Seville (HUVR/CSIC/US), Medicine Department, University of Sevilla; ⁸CIBEREHD, Sevilla, Spain; ⁹Andalusian Center of Molecular Biology and Regenerative Medicine, Sevilla, Spain; ¹⁰Pablo de Olavide University, Sevilla, Spain; ¹¹Faculty of Psychology, Department of Personality, Assessment, and Psychological Treatments, University of Sevilla, Sevilla, Spain; ¹²Interdisciplinary Physics Group. SeLiver Group, Biomedicine Institute of Seville (HUVR/CSIC/US), Medicine Department, University of Sevilla, CIBEREHD, Sevilla, Spain; ¹³Department of Radiology. University Hospital Virgen del Rocío, Sevilla, Spain
Email: carmenlararomero@gmail.com

Background and aims: Exercise independent of weight loss is associated with improved liver steatosis and fibrosis in MASLD patients. Our objective was to study the effect of planned exercise and Mediterranean diet (MD) in patients with MASLD.

Method: Ninety-eight biopsy-proven MASLD patients [54/98 (55%) females, 46/98 T2DM (47%) and AHT (63/98 (64.3%)] were randomized to: Arm A) Hypocaloric MD and intensive structured physical exercise for 12 weeks. Arm B) Hypocaloric MD and standard recommendations for physical activity for 12 weeks. All patients were followed-up for another 12 weeks. Liver assessment included baseline VCTE (kPa and CAP), MR (PDFF (%), MRE (kPa)) and at end-of-treatment at 12 weeks and at the end-of-follow-up at week 24. Bioimpedance and liver biochemistry were also performed. Adherence to exercise was evaluated as adherents (Ad) if ≥ 5 sessions per week or non-adherents (NAd) if ≤ 4 sessions considering frequency, intensity, time, and type. Adherence to the MD and QoL were also evaluated baseline, 12 and 24 weeks.

Results: Patients in Arm A showed a significant improvement in MRE (Baseline MRE: 2.46 ± 0.67 kPa, MRE 12 weeks: 2.31 ± 0.65 kPa; $p = 0.027$) and PDFF-MRI (baseline: $12.4 \pm 6.9\%$, PDFF 12 weeks: $9.5 \pm 6.2\%$; $p = 0.005$), but not in arm B (Baseline MRE: 2.74 ± 0.95 , MRE 12 weeks: 2.70 ± 0.98 ; $p = 0.28$) or steatosis (Baseline PDFF $14.27 \pm 7.27\%$, PDFF 12 weeks: $12.67 \pm 8.01\%$, PDF; $p = 0.26$). Weight loss at 12 weeks follow-up was significantly higher in Arm B (baseline 91.9 ± 19.6 ; 12 weeks 89.6 ± 20.5 Kg; $p = 0.001$) vs Arm A (baseline 91.8 ± 20.4 Kg; 12 weeks 90.8 ± 22.1 Kg; $p = 0.5$). There were also differences in muscle mass in Arm A vs Arm B: $7.6 \pm 12\%$ vs $2.1 \pm 14\%$ ($p = 0.09$). In Ad patients PDFF improved by $-37.16 \pm 28.11\%$, while in NAd there was a worsening in $3.85 \pm 41.8\%$; $p < 0.01$, Hedge's correction 0.15-1.86). Fibrosis improvement was $3.32 \pm 19.1\%$ in NAd patients vs $-12.98 \pm 9.8\%$ in NAd patients; $p < 0.007$; Hedge's correction 0.04-1.84. During 12weeks follow-up no differences were seen between arms and between physical activity adherence groups.

Conclusion: A 12-week life-style intervention allowed stratifying patients in responders and non-responders. The implementation of a physical exercise program with 5 or more sessions per week with moderate/high intensity in patients receiving hypocaloric MD promoted fat removal and liver fibrosis improvement independently of weight loss rate.

OS-117

Assessment of resmetirom efficacy (80 mg vs. 100 mg) stratified by baseline body mass index and weight in patients from the MAESTRO-NASH trial

Jörn M Schattenberg^{1,2}, Rohit Loomba³, Rebecca Taub^{4,5}, Dominic Labriola^{4,6}, Stephen A. Harrison⁷, Mazen Nouredin⁸. ¹Department of Internal Medicine II, Saarland University Medical Center, Homburg, Germany; ²Metabolic Liver Research Program, I. Department of Medicine, University Medical Center of Johannes Gutenberg University Mainz, Mainz, Germany; ³MASLD Research Center, the Division of Gastroenterology and Hepatology, University of California, San Diego, La Jolla, United States; ⁴Madrigal Pharmaceuticals, Inc., West Conshohocken, PA, United States; ⁵Houston Methodist Hospital, Houston Research Institute, Houston, TX, United States; ⁶Houston Methodist Hospital, Houston Research Institute, Houston, TX, United States; ⁷Pinnacle Clinical Research, San Antonio, TX, United States;

ORAL PRESENTATIONS

⁸Houston Methodist Hospital, Houston Research Institute, Houston, TX, United States
Email: joern.schattenberg@uks.eu

Background and aims: MAESTRO-NASH (NCT03900429) is an ongoing 54-month, randomized, double-blind, placebo-controlled Phase 3 trial evaluating the efficacy of resmetirom in patients with biopsy-confirmed non-alcoholic steatohepatitis (NASH) and fibrosis. 966 patients with biopsy-confirmed NASH were randomized 1:1:1 to resmetirom 80 mg, resmetirom 100 mg, or placebo administered once daily. Histologic end points were assessed after 52 weeks. Dual primary end points at Week 52 were achieved with both resmetirom 80 mg and 100 mg: NASH resolution with no worsening of fibrosis (NR) or ≥ 1 -stage reduction in fibrosis with no worsening of NAS (FI). Body weight is the major factor influencing exposure to resmetirom in patients with NASH/MASH. This post-hoc analysis was performed to provide additional evidence of a relationship between resmetirom dose, baseline body weight and body mass index (BMI).

Method: To assess the impact of baseline body weight and BMI on resmetirom response, we stratified resmetirom efficacy data on the dual end points based on baseline patient body weight (≤ 100 and >100 kg) and BMI (≥ 35 and <35 kg/m²).

Results: For patients treated with resmetirom 80 mg who weighed ≤ 100 kg, the 30% PDFF response was 66.9%; and in patients with a Week 52 biopsy, 35.4% showed fibrosis improvement (FI) compared with 32% who showed no worsening of fibrosis (NR). In patients >100 kg, the 30% PDFF response was 56.7%; FI = 22.5%; and NR = 27%. For patients who received resmetirom 100 mg who were ≤ 100 kg, the 30% PDFF response was 71.7%; FI was 33.6% and NR was 35.8%; for patients >100 kg, PDFF = 72.5%; FI = 32.5%; NR = 35.8%. Increases in FI were noted relative to placebo for patients who received resmetirom 80 mg (mITT population) who had BMI <35 : 13.0% (5.2, 20.8); NR = 33.4% (14.2, 30.6); and in patients with BMI ≥ 35 : FI = 7.0% (-0.7, 14.7); NR = 9.8% (3.1, 16.6). Increases were also noted relative to placebo for patients who received 100 mg of resmetirom (mITT population) who had a BMI <35 : FI = 11.8% (4.2, 19.4) NR = 21.0% (13.4, 28.7); for patients with BMI ≥ 35 : FI = 11.1% (3.4, 18.9); NR = 20.0% (12.3, 27.7).

Conclusion: As shown in these stratified data, resmetirom 100 mg was consistently more effective than 80 mg in achievement of the dual primary end points in the sample of patients who had higher baseline body weight and BMI. In patients with a lower BMI, there was no observed difference in efficacy between the 80 and 100 mg resmetirom doses.

OS-118

Week 48 results from the phase 2b ENLIVEN extension study investigating pegozafermin for the treatment of metabolic dysfunction-associated steatohepatitis with fibrosis

Rohit Loomba¹, Manal F. Abdelmalek², Kris V. Kowdley³, Naim Alkhouri⁴, Stephen A. Harrison⁵, Jörn M Schattenberg⁶, Mildred D. Gottwald⁷, Shibao Feng⁷, Germaine D. Agollah⁷, Cynthia L. Hartsfield⁷, Hank Mansbach⁷, Maya Margalit⁸, Arun J Sanyal⁹. ¹Division of Gastroenterology and Hepatology, University of California at San Diego, NAFLD Research Center, La Jolla, United States; ²Mayo Clinic, Division of Gastroenterology and Hepatology, Rochester, United States; ³Liver Institute Northwest, Seattle, United States; ⁴Arizona Liver Health, Chandler, United States; ⁵Pinnacle Clinical Research, San Antonio, United States; ⁶Saarland University Medical Center, Homburg, Germany; ⁷89bio, San Francisco, United States; ⁸89bio, Rehovot, Israel; ⁹Virginia Commonwealth University, Stravitz-Sanyal Institute for Liver Disease and Metabolic Health, Richmond, United States
Email: cindy.hartsfield@89bio.com

Background and aims: FGF21 analogs such as pegozafermin (PGZ) have demonstrated promising direct effects on liver fibrosis as well as additional hepatic and extrahepatic benefits in patients with MASH. The Phase 2b ENLIVEN trial evaluated the efficacy/safety of PGZ given weekly (QW) or every two-weeks (Q2W) versus placebo in MASH patients; the primary end point was assessed at Week 24. Both PGZ

30 mg QW and 44 mg Q2W led to significant improvements in fibrosis without worsening of MASH, MASH resolution without worsening of fibrosis, and markers for liver fibrosis and injury compared to placebo. After the main study, patients began a 24-week blinded extension phase for a total of 48 weeks of treatment.

Method: In the placebo-controlled, blinded, 24-week extension phase patients continued in their assigned treatment arm except for a subset of patients from the placebo arm who were re-randomized to receive PGZ 30 mg QW during the extension phase. The full analysis set includes patients who were F2-F3 and NAS ≥ 4 at baseline (n = 192 of which 163 continued into the extension phase). There were 14 patients, reclassified as F4 fibrosis at baseline per 3-panel read, of which 12 entered the extension study. Efficacy end points include non-invasive tests (NITs) to assess liver fat, markers of fibrosis, inflammation, and extrahepatic metabolic markers. Per protocol, patients did not undergo repeat liver biopsy at Week 48.

Results: PGZ benefit for the 30 mg QW and 44 mg Q2W doses was sustained from Week 24 to Week 48 across a wide range of end points including liver fat (MRI-PDFF), markers of liver fibrosis (VCTE, ELF, Pro-C3), inflammation and injury (ALT, AST), and metabolic markers. At the 30 mg QW dose in the total study population 90% of patients identified previously as ALT responders (defined as ≥ 17 U/L reduction) and 84% of patients classified as MRI-PDFF super-responders (defining as $\geq 50\%$ reduction of liver fat) at Week 24 retained that benefit at Week 48. At Week 48, pegozafermin also had continued benefit on metabolic end points such as lipids and HbA1c. The placebo cohort re-randomized to 30 mg QW recapitulated the robust and rapid treatment effects of PGZ that were observed in the main study, with significant improvements in NITs of liver fat, inflammation, and fibrosis over the extension period. Patients with F4 fibrosis at baseline also showed sustained benefit for markers of fibrosis and liver inflammation at Week 48. Safety and tolerability remained consistent with previously reported data. No new patients on PGZ during the main phase developed treatment-related nausea or diarrhea during the extension phase of the study.

Conclusion: These robust results substantiate the sustained efficacy of PGZ treatment up to 48 weeks on NITs and metabolic markers in MASH patients with advanced fibrosis. PGZ continues to demonstrate a favorable safety and tolerability profile. Confirmatory phase 3 studies are planned for 2024.

OS-119

Survodutide (BI 456906), a glucagon receptor/glucagon-like peptide-1 receptor (GCGR/GLP-1R) dual agonist, in people with compensated and decompensated cirrhosis: a multinational, open-label, phase 1 trial

Eric Lawitz¹, Mandy Fraessdorf², Guy Neff³, Jörn M Schattenberg⁴, Mazen Nouredin⁵, Naim Alkhouri⁶, Bernhard Schmid⁷, Charles P. Andrews⁸, István Takács⁹, Samina Ajaz Hussain², Wiebke K. Fenske¹⁰, Edward J. Gane¹¹, Azadeh Hosseini-Tabatabaei¹², Arun J Sanyal¹³, Daniel Mazo², Ramy Younes². ¹Texas Liver Institute, San Antonio, United States; ²Boehringer Ingelheim, Ingelheim, Germany; ³Covenant Metabolic Specialists, Sarasota and Ft Myers, United States; ⁴University Medical Center Homburg, Homburg, Germany; ⁵Houston Methodist Hospital and Houston Research Institute, Houston, United States; ⁶Arizona Liver Health, Phoenix, United States; ⁷Boehringer Ingelheim, Biberach, Germany; ⁸IMA Research San Antonio, San Antonio, United States; ⁹Semmelweis University, Budapest, Hungary; ¹⁰University Hospital Bonn, Bonn, Germany; ¹¹Auckland City Hospital and University of Auckland, Auckland, New Zealand; ¹²Boehringer Ingelheim, Ridgefield, United States; ¹³Virginia Commonwealth University, Richmond, United States
Email: lawitz@txliver.com

Abstract OS-119 is under embargo until Saturday 8 June 2024, 11:45 CET, after which this abstract will be made publicly available on the congress website and will be released for publication in the supplement issue of the *Journal of Hepatology*.

Industry must not issue press releases – even under embargo – covering the data contained in abstracts selected to be highlighted during official EASL Press Office activities or in official EASL Press Office materials until the individual embargo for each data set lifts. Media must not issue coverage of the data contained in abstracts selected to be highlighted during official EASL Press Office activities or in official EASL Press Office materials until the individual embargo for each data set lifts.

Journalists, industry, investigators and/or study sponsors must abide by the embargo times set by EASL. Violation of the embargo will be taken seriously. Individuals and/or sponsors who violate EASL's embargo policy may face sanctions relating to current and future abstract submissions, presentations and visibility at EASL Congresses. The EASL Governing Board is at liberty to ban attendance and/or retract data.

Copyright for abstracts (both oral and poster) on the website and as made available during The EASL Congress 2024 resides with the respective authors. No reproduction, re-use or transcription for any commercial purpose or use of the content is permitted without the written permission of the authors. Permission for re-use must be obtained directly from the authors.

Foundation IRCCS Ca' Granda Ospedale Maggiore Policlinico, Milan, Italy; ²Clinical Epidemiology and Biometry Unit, Fondazione IRCCS Policlinico San Matteo, Pavia, Italy; ³Hepatology Department, Haut-Lévêque Hospital, Bordeaux, France; ⁴Hepatology Unit, CHU Rangueil, Toulouse, France; ⁵Division of Gastroenterology and Hepatology, Department of Internal Medicine III, Medical University of Vienna, Vienna, Austria; ⁶Division of Infectious Diseases-Hepatology, Department of Transplantation and General Surgery, Istituto Nazionale per le Malattie Infettive "L. Spallanzani" IRCCS, Rome, Italy; ⁷Department of Gastroenterology, Hepatology Infectious Diseases and Endocrinology at Hannover Medical School, Hannover, Germany; ⁸Department of Gastroenterology, General Hospital of Athens "Laiko", Medical School of National and Kapodistrian University of Athens, Athens, Greece; ⁹Department of Clinical and Experimental Medicine, University of Pisa and Hepatology Unit, University Hospital of Pisa, Pisa, Italy; ¹⁰Department of Medical and Surgical Sciences, Unit of Infectious Diseases, "Alma Mater Studiorum" University of Bologna, S. Orsola-Malpighi Hospital, Bologna, Italy; ¹¹Department of Medical Sciences, University of Turin, Gastroenterology Division of Città della Salute e della Scienza of Turin, University Hospital, Turin, Italy; ¹²Hepatology Department, Université Claude Bernard Lyon 1, Hospices Civils de Lyon, INSERM Unit 1052-CRCL, Lyon, France; ¹³Liver Unit, Fondazione IRCCS "Casa Sollievo della Sofferenza", San Giovanni Rotondo, Italy; ¹⁴Service d'hépatogastro-entérologie, CHU Grenoble-Alpes, Grenoble, France; ¹⁵Department of Medical and Surgical Sciences, Infectious Diseases Unit, University of Foggia, Foggia, Italy; ¹⁶Department of Mental Health and Public Medicine-Infectious Diseases Unit, University of Campania Luigi Vanvitelli, Naples, Italy; ¹⁷Liver Unit, San Camillo Hospital, Department of Transplantation and General Surgery, Rome, Italy; ¹⁸Hepato-Biliary Center, AP-HP Hôpital Universitaire Paul Brousse, Paris-Saclay University, Research INSERM-Paris Saclay Unit 1193, Villejuif, France; ¹⁹Hôpital de la Source Orleans, Orleans, France; ²⁰Service d'Hépatogastro-entérologie CHU de Tours, Tours, France; ²¹Department of Digestive Diseases, Hospices Civils de Lyon, Edouard Herriot hospital, France, Claude Bernard Lyon 1 University, Lyon, France; ²²AP-HP, Avicenne Hospital, Hepatology Department, F-93000, Bobigny, France; ²³Centre Hospitalier Annecy Genevois, Annecy, France; ²⁴Department of Hepatogastroenterology, CHU de Caen Normandie, Caen, France; ²⁵Gastroenterology, Hepatology and Transplantation Division, ASST Papa Giovanni XXIII, Bergamo, Italy; ²⁶Division of Hepatogastroenterology, Department of Precision Medicine, Università della Campania "Luigi Vanvitelli", Naples, Italy; ²⁷Division of Internal Medicine and Center for Hemochromatosis, University of Modena and Reggio Emilia, Modena, Italy; ²⁸Institute of Infectious Diseases and Public Health, Università Politecnica delle Marche, Ancona, Italy; ²⁹Division of Internal Medicine, Hepatobiliary and Immunoallergic Diseases, IRCCS Azienda Ospedaliero-Universitaria di Bologna, Bologna, Italy; ³⁰Department of Gastroenterology, CH d'Avignon, Avignon, Italy; ³¹Department of Gastroenterology, Toulouse University Hospital, Toulouse, France; ³²Université de Nantes, INSERM UIC 1413, Department of Infectious Diseases, CHU Hôtel Dieu, Nantes, France; ³³Université Paris Cité, Assistance Publique des Hôpitaux de Paris, Hôpital Cochin, Hepatology/Addictology department, Paris, France; ³⁴Assistance Publique des Hôpitaux de Paris, Hôpital Bichat Claude Bernard, Service des Maladies Infectieuses et Tropicales, Paris, France; ³⁵CHU Dijon, Service d'Hépatogastro-entérologie et oncologie digestive, Inserm EPICAD LNC-UMR1231, Université de Bourgogne-Franche Comté, Dijon, France; ³⁶Service d'hépatogastro-entérologie, Centre Hospitalier Intercommunal, Créteil, France; ³⁷School of Medicine and Surgery University of Milano Bicocca, Milan, Italy; ³⁸CRC "A. M. and A. Migliavacca" Center for Liver Disease, Department of Pathophysiology and Transplantation, University of Milan, Milan, Italy
Email: pietro.lampertico@unimi.it

Background and aims: Bulevirtide (BLV) monotherapy yields high rates of virological and biochemical response in hepatitis Delta (HDV) cirrhotic patients, however clinical benefits on hard outcomes remain unknown.

Viral hepatitis B/D: Therapy

OS-120

Bulevirtide monotherapy prevents liver decompensation and reduces mortality in patients with HDV-related cirrhosis: a case control study with propensity score weighted analysis

Elisabetta Degasper¹, Annalisa De Silvestri², Maria Paola Anolli¹, Dana Sambarino¹, Marta Borghi¹, Riccardo Perbellini¹, Floriana Facchetti¹, Roberta Soffredini¹, Sara Monico¹, Victor de Lédighen³, Sophie Metivier⁴, Mathias Jachs⁵, Thomas Reiberger⁵, Giampiero D'Offizi⁶, Christopher Dietz-Fricke⁷, George Papatheodoridis⁸, Maurizia Brunetto⁹, Gabriella Verucchi¹⁰, Alessia Ciancio¹¹, Fabien Zoulim¹², Alessandra Mangia¹³, Marie-Noëlle Hilleret¹⁴, Teresa Santantonio¹⁵, Nicola Coppola¹⁶, Adriano Pellicelli¹⁷, Bruno Roche¹⁸, Xavier Causse¹⁹, Louis Dalteroche²⁰, Jérôme Dumortier²¹, Nathalie Ganne-Carrié²², Frederic Heluwaert²³, Isabelle Ollivier-Hourmand²⁴, Alessandro Loglio²⁵, Alessandro Federico²⁶, Francesca Pileri²⁷, Monia Maracci²⁸, Matteo Tonnini²⁹, Jean-Pierre Arpurt³⁰, Karl Barange³¹, Eric Billaud³², Stanislas Pol³³, Anne Gervais³⁴, Anne Minello Franza³⁵, Isabelle Rosa³⁶, Massimo Puoti³⁷, Pietro Lampertico^{1,38}. ¹Division of Gastroenterology and Hepatology,

Method: Patients with HDV-related cirrhosis treated with BLV monotherapy in a retrospective multicenter European study (SAVE-D) were compared with untreated HDV cirrhotic patients enrolled in a previous cohort study (Romeo, Gastroenterology 2009). Liver-related events (LRE: HCC, decompensation) and overall mortality were compared by inverse probability treatment weighting (IPTW) analysis.

Results: The BLV-treated cohort included 176 patients (median follow-up: 15 [2–46] months): at BLV start, median age was 50 (19–82) years, 59% men, ALT 77 (23–1,074) U/L, albumin 3.9 (2.8–4.9) g/dL, 100% CPT score A, 55% with varices. The untreated cohort included 140 patients (median follow-up: 91 [3–359] months): at study entry, median age was 40 (18–66) years, 78% men, ALT 102 (11–3,054) U/L, albumin 4.0 (2.0–5.2) g/dL, 94% CPT score A, 46% with varices. Overall, the 2-year cumulative probabilities of LRE were 6.9% (95% CI 3–11%) in the BLV-treated cohort vs. 15.7% (95% CI 9–22%) in untreated patients ($p=0.02$): 4.9% vs. 6.7% for de-novo HCC ($p=0.45$) and 2.0% vs. 9.1% for decompensation ($p=0.01$), respectively. The 2-year probability of overall mortality was 1.2% (95% CI 0.3–3%) vs. 3% (95% CI 0.5–6%) in BLV-treated vs. untreated patients ($p=0.13$). By IPTW analysis adjusted for confounding baseline factors and competing mortality risks, the BLV-treated cohort had a significantly decreased risk of all-type liver-related events (HR 0.38; 95% CI 0.24–0.60, $p<0.0001$), decompensation (HR 0.15; 95% CI 0.06–0.36, $p<0.0001$) and mortality (HR 0.27; 95% CI 0.08–0.93, $p=0.04$) compared to untreated patients. Conversely, the HCC risk was similar (HR 0.76; 95% CI 0.42–1.40, $p=0.38$).

Conclusion: Compared to an untreated matched control group, a 2-year course of BLV monotherapy significantly reduced the risk of decompensation and mortality but not of HCC in HDV patients with compensated cirrhosis.

OS-121

Multinational randomized trial to investigate the efficacy of tenofovir alafenamide in reducing adverse clinical events in chronic hepatitis B patients who are beyond treatment indications by current guidelines (ATTENTION trial): first interim analysis

Young-Suk Lim¹, Jonggi Choi¹, Won-Mook Choi¹, Wonseok Kang², Gi-Ae Kim³, Hyung Joon Kim⁴, Jeong-Hoon Lee⁵, Yun Bin Lee⁵, Neung Hwa Park⁶, So Young Kwon⁷, Eun Sun Jang⁸, Soo Young Park⁹, Ji Hoon Kim¹⁰, Ming-Lung Yu¹¹, Chien-Hung Chen¹², Yao-Chun (Holden) Hsu¹³, Ming-Jong Bair¹⁴, Pin-Nan Cheng¹⁵, Hung-Da Tung¹⁶, Te-Sheng Chang¹⁷, Chi-Yi Chen¹⁸, Chingchu Lo¹⁹, Kuo-Chih Tseng²⁰, Sheng-Shun Yang²¹, Cheng-Yuan Peng²². ¹Asan Medical Center, Seoul, Korea, Rep. of South; ²Samsung Medical Center, Seoul, Korea, Rep. of South; ³Kyung Hee University Hospital, Seoul, Korea, Rep. of South; ⁴Chung-Ang University Hospital, Seoul, Korea, Rep. of South; ⁵Seoul National University Hospital, Seoul, Korea, Rep. of South; ⁶Ulsan University Hospital, Ulsan, Korea, Rep. of South; ⁷Konkuk University Medical Center, Seoul, Korea, Rep. of South; ⁸Seoul National University Bundang Hospital, Seongnam, Korea, Rep. of South; ⁹Kyungpook National University Hospital, Daegu, Korea, Rep. of South; ¹⁰Korea University Guro Hospital, Seoul, Korea, Rep. of South; ¹¹National Sun Yat-sen University, Kaohsiung, Taiwan; ¹²Kaohsiung Chang Gung Memorial Hospital, Kaohsiung, Taiwan; ¹³Fu-Jen Catholic University, Kaohsiung, Taiwan; ¹⁴Mackay Memorial Hospital, Taichung, Taiwan; ¹⁵National Cheng Kung University Hospital, Tainan, Taiwan; ¹⁶Chi Mei Hospital, Tainan, Taiwan; ¹⁷Chiayi Chang Gung Memorial Hospital, Puzy city, Taiwan; ¹⁸Chia-Yi Christian Hospital, Chia-Yi, Taiwan; ¹⁹St Martin Hospital, Chia-Yi, Taiwan; ²⁰Dalin Tzu Chi Hospital, Chia-Yi, Taiwan; ²¹Taichung Veterans General Hospital, Taichung, Taiwan; ²²China Medical University Hospital, Taichung, Taiwan
Email: limys@amc.seoul.kr

Background and aims: There is lack of robust evidence regarding the efficacy of early antiviral therapy in reducing adverse clinical events among non-cirrhotic chronic hepatitis B (CHB) patients with

significant viremia but without notable alanine aminotransferase (ALT) level elevation.

Method: The ATTENTION trial, an ongoing randomized, open-label, multicenter, phase 4 study (NCT03753074), is actively enrolling 780 participants across 22 sites in Korea and Taiwan. Key inclusion criteria are: age between 40 and 80 years, serum HBV DNA levels between 4–8 log₁₀ IU/ml, serum ALT levels <70 U/L for males and <50 U/L for females, and absence of cirrhosis. Participants are randomly assigned at a 1:1 ratio to receive either 25 mg/day of tenofovir alafenamide (TAF) or no antiviral treatment (observation). The primary end point was a composite of hepatocellular carcinoma (HCC), death, liver transplantation, or hepatic decompensation, with the first interim analysis planned at year 4.

Results: From 2019 to 2023, 734 patients were randomized to either TAF group (n = 369) or observation group (n = 365). As of October 2023, the median follow-up duration was 1.5 years. Participants in the first interim analysis set had an average age of 53.4 years, with 46.5% male, and 82.7% HBeAg-negative. The median ALT level was 31 U/L. No significant differences were observed in baseline characteristics between the two groups. A total of 11 primary clinical events occurred: 2 in the TAF group (both HCC) and 9 in the observation group (7 HCC, 1 death, 1 hepatic decompensation), corresponding to incidence rates of 0.33 and 1.57 per 100 person-years, respectively. The hazard ratio for TAF was 0.21 (99.997% CI: 0.01–5.45). The log-rank test yielded $Z=2.22$ ($p=0.027$), which did not exceed the pre-defined upper stopping boundary ($Z=4.17$; $p=0.00003$) in this first interim analysis.

Conclusion: Preliminary findings from the ATTENTION trial suggest that early initiation of TAF treatment may significantly reduce the risk of liver-related adverse clinical events in non-cirrhotic CHB patients with significant viremia, but without elevated ALT levels. These results highlight the potential benefit of proactive antiviral therapy in these patients.

OS-122

Bulevirtide in combination with pegylated interferon alfa-2a shows a sustained off-treatment response in the liver

Lena Allweiss^{1,2}, Annika Volmari¹, Dmitry Manuilov³, Stephan Urban^{4,5}, Heiner Wedemeyer^{6,7}, Wildaliz Nieves³, Jeffrey Wallin³, Renee-Claude Mercier³, Audrey H. Lau³, Maura Dandri^{1,2}. ¹University Medical Center Hamburg-Eppendorf, Hamburg, Germany; ²German Center for Infection Research, Hamburg-Lübeck-Borstel-Riems, Germany; ³Gilead Sciences, Inc., Foster City, United States; ⁴University Hospital Heidelberg, Heidelberg, Germany; ⁵German Center for Infection Research, Heidelberg, Germany; ⁶Hannover Medical School, Hannover, Germany; ⁷German Center for Infection Research, Hannover, Germany
Email: l.allweiss@uke.de

Background and aims: Bulevirtide (BLV) is a first-in-class entry inhibitor approved in the EU for the treatment of chronic hepatitis D (CHD). In a multicentre, open-label, randomized phase 2b study (MYR204; NCT03852433), safety and efficacy of BLV (2 and 10 mg/day) with or without pegylated interferon alfa-2a (PegIFN α) were evaluated in patients with CHD and compensated liver disease. This sub-study aimed to evaluate intrahepatic virologic changes 24 weeks after end of treatment (EOT) compared to baseline. To further understand the effect of treatment, the relationship between intrahepatic outcomes and peripheral parameters, including intrahepatic innate and inflammatory gene expression profiles, was evaluated.

Method: 174 CHD patients were randomized (1:2:2:2) to receive (A) PegIFN α for 48 weeks (48w); (B) BLV 2 mg + PegIFN α or (C) BLV 10 mg + PegIFN α for 48w, both followed by 48w of monotherapy with BLV 2 mg or 10 mg, respectively; or (D) BLV 10 mg for 96w. Paired liver biopsies were available at baseline and 24w after EOT in a subset of patients (n = 42 for molecular and 44 for histological analysis). HDV

parameters and infection-related host genes were assessed by qPCR and HDAG immunohistochemistry.

Results: At follow-up (FU), 24w after EOT, median intrahepatic HDV RNA declines from baseline were 1.9Log10 in arm A (n = 5), 2.0Log10 in arm B (n = 14), 3.2Log10 in arm C (n = 11), and 0.8Log10 in arm D (n = 12). Intrahepatic HDV RNA levels strongly correlated with the number of HDAG positive cells ($r = 0.85$; $p < 0.0001$), which declined by 1.9Log10 in arm A (n = 6), 1.0Log10 in arm B (n = 14), 1.9Log10 in arm C (n = 11), and 0.8Log10 in arm D (n = 13). In the two combination arms B and C, 8/14 (57%) and 8/11 (73%) patients, respectively, were negative for HDV RNA at FU, while in monotherapy arms A and D, 3/5 (60%) and 1/12 (8%) patients had undetectable intrahepatic HDV RNA levels, respectively. Intrahepatic changes of HDV RNA mirrored HDV RNA changes determined in the serum ($r = 0.82$; $p < 0.0001$) while intrahepatic HBV parameters did not change significantly apart from a modest median reduction of total HBV RNA in both combination arms. Transcriptional levels of inflammatory chemokines and infection-related genes were decreased at FU in combination treatment arms. Notably, decreases from BL to FU in chemokines, such as CXCL10, strongly correlated with the reduction of intrahepatic HDV RNA ($r = 0.67$; $p < 0.0001$) and with changes of peripheral ALT levels ($r = 0.75$; $p < 0.0001$), suggesting an amelioration of liver inflammation.

Conclusion: Intrahepatic analysis in paired BL and post-treatment biopsies demonstrated a strong correlation between intrahepatic and serum HDV RNA reductions. Concomitant with the decrease of HDV parameters, expression levels of innate immune genes declined. The highest rate of the off-treatment virologic response in the liver was observed in the arm that received combination of BLV 10 mg + PegIFN α .

OS-123

Progression and risk factors after treatment with tenofovir or entecavir for chronic hepatitis B based on a multistate modeling approach

Wan-Jung Wu¹, Wen-Jie Liu¹, Chih-Lin Lin², Chun-Jen Liu³, Yi-Wen Huang⁴, Jui-Ting Hu⁵, Ming-Whei Yu¹. ¹Institute of Epidemiology and Preventive Medicine, College of Public Health, National Taiwan University, Taipei, Taiwan; ²Department of Gastroenterology, Ren-Ai Branch, Taipei City Hospital, Taipei, Taiwan; ³Division of Gastroenterology, Department of Internal Medicine, National Taiwan University Hospital and Graduate Institute of Clinical Medicine, National Taiwan University College of Medicine, Taipei, Taiwan; ⁴Graduate Institute of Clinical Medicine, College of Medicine, Taipei Medical University, Taipei, Taiwan; ⁵Liver Center, Cathay General Hospital Medical Center, School of Medicine, Fu-Jen Catholic University College of Medicine, Taipei, Taiwan
Email: wendy1234599@gmail.com

Background and aims: Conflicting evidence exists on hepatocellular carcinoma (HCC) risk in patients with chronic hepatitis B (CHB) receiving tenofovir (TDF)- vs. entecavir (ETV)-based regimens, and data are lacking on whether there is a difference between the two agents in preventing hepatic decompensation. We aimed to compare clinical profile and long-term prognosis between the two drugs and examine the effects of age, sex, alcohol use, diabetes, and cirrhosis on transition rates using a multistate modeling approach.

Method: We conducted a retrospective nationwide cohort study using data from Taiwan's National Health Insurance Research Database, including 47478 treatment-naïve patients with CHB aged 30–75 years receiving TDF/TAF (n = 14353) or ETV (n = 33125) for at least 3 months between November 2009 and December 2019, and followed until December 2021. Multistate analysis modeled CHB progression by describing transitions between distinct disease states, including CHB with or without cirrhosis, hepatic decompensation, HCC, death (liver-related and unrelated death) and a switching treatment state. Propensity score matching (PSM) and inverse probability of treatment weighting (IPTW) methods were used for sensitivity analyses.

Results: During follow-up (median [interquartile range]: 4.7 [3.2–6.8] in TDF/TAF and 5.8 [3.8–8.7] in ETV group), 1228 patients developed hepatic decompensation and 2671 developed HCC. Comparing TDF/TAF-treated and ETV-treated patients, the risks of progression to hepatic decompensation (adjusted hazard ratio [aHR] 0.81, 95% CI 0.70–0.93) and HCC (aHR 0.76, 95% CI 0.68–0.84) were significantly lower in TDF/TAF-treated patients after adjusting for age, sex, excess alcohol use/alcohol-related disorder, diabetes, and cirrhosis. PSM (aHR 0.82 [$p = 0.0080$] and 0.75 [$p < 0.0001$] for decompensation and HCC, respectively) and IPTW (aHR 0.81 [$p = 0.0032$] and 0.75 [$p < 0.0001$] for decompensation and HCC, respectively) analyses yielded similar patterns of results. The 5-year absolute risks of HCC were 3.3% and 4.9% for TDF/TAF and ETV group, respectively; after hepatic decompensation, the 5-year risks of HCC were 12.2% and 27.3% for TDF/TAF and ETV group. Transition rates significantly increased with age, male sex, diabetes, excess alcohol use/alcohol-related disorder, and cirrhosis.

Conclusion: Using data from a large real-world cohort over a median follow-up time of 5 years, we provided detailed absolute risks and indicated a significantly reduced risk for both hepatic decompensation and HCC among TDF/TAF-treated patients compared with ETV treatment.

OS-127

Efficacy and safety of tobevibart (VIR-3434) alone or in combination with elebsiran (VIR-2218) in participants with chronic hepatitis delta virus infection: preliminary results from the phase 2 SOLSTICE trial in non-cirrhotic and compensated cirrhotic participants

Tarik Asselah¹, Anca Streinu-Cercel², Alina Jucov³, Edward J. Gane⁴, Heiner Wedemeyer⁵, Pietro Lampertico^{6,7}, Michael A. Chattergoon⁸, Pan Wu⁸, Sonia Maciejewski⁸, Cara Pilowa⁸, Afshar Hassani⁸, Todd Correll⁸, Carey Hwang⁸, Kosh Agarwal⁹. ¹Université de Paris Cité, Hôpital Beaujon, Paris, France; ²National Institute for Infectious Diseases Matei Bals, Carol Davila University of Pharmacy and Medicine, Bucharest, Romania; ³Arensia Exploratory Medicine GmbH, Düsseldorf, Germany and Nicolae Testemitanu State University of Medicine and Pharmacy, Chişinău, Moldova; ⁴Auckland Clinical Studies, Auckland, New Zealand; ⁵Department of Gastroenterology, Hepatology, and Endocrinology, Hannover Medical School, Hannover, Germany; ⁶Division of Gastroenterology and Hepatology, Fondazione IRCCS Ca' Granda Ospedale Maggiore Policlinico, Milan, Italy; ⁷CRC "A. M. and A. Migliavacca" Center for Liver Disease, Department of Pathophysiology and Transplantation, University of Milan, Milan, Italy; ⁸Vir Biotechnology, Inc., San Francisco, United States; ⁹King's College Hospital, London, United Kingdom
Email: tarik.asselah@aphp.fr

Background and aims: Hepatitis D virus (HDV) infection is the most severe form of viral hepatitis with limited treatment options. The phase 2 SOLSTICE study is investigating the antiviral activity and safety of the monoclonal antibody tobevibart (VIR-3434) alone and in combination with the silencing RNA elebsiran (VIR-2218) in chronic HDV infection (NCT05461170).

Method: Participants with chronic HDV infection, with or without compensated cirrhosis (CPT-A) on NRTI therapy, were randomized 1:1 to receive either tobevibart 300 mg plus elebsiran 200 mg subcutaneously (SC) every 4 weeks (Combo Q4W) or tobevibart 300 mg SC every 2 weeks (tobevibart Q2W) for 96 weeks. The primary end point is a combined response (CR) defined as a virologic response plus normalization of ALT at week 24. A virologic response was defined as HDV RNA less than limit of detection (LOD, 14 IU/ml) or a decrease of $\geq 2 \log_{10}$ IU from baseline. Lower limit of quantification (LLOQ) for HDV RNA was 63 IU/ml.

Results: Preliminary results from all participants completing 12 weeks of Combo Q4W (n = 18, 50% CPT-A) and tobevibart Q2W (n = 15, 27% CPT-A) are presented. Five participants who received tobevibart or elebsiran monotherapy for 12 weeks and failed to

achieve virologic response ($n=3$) or normalize ALT ($n=2$) transitioned to Combo Q4W. Week 40 results on combination treatment for these participants are reported. After 12 weeks of Combo Q4W treatment, 100% (18/18) of participants achieved a virologic response with 50% (9/18) <LOD, mean ALT decreased from 87 ± 53 IU/ml at baseline to 48 ± 30 U/L, 39% (7/18) achieved ALT normalization, 39% (7/18) achieved the CR and 28% (5/18) achieved HDV RNA <LOQ + ALT normalization. Among tobevibart Q2W participants, 80% (12/15) achieved a virologic response with 13% (2/15) <LOD, mean ALT decreased from 56 ± 22 U/L at baseline to 36 ± 12 U/L, 60% (9/15) achieved ALT normalization, 40% (6/15) achieved the CR and 13% (2/18) achieved HDV RNA <LOQ + ALT normalization after 12 weeks. ALT and HDV RNA declines, and CR were comparable among non-cirrhotic and compensated cirrhotic participants in both cohorts and no ALT flares were observed. All Combo roll-over Q4W participants (5/5) who have completed 40 weeks of combination therapy had HDV RNA <LOD. Both regimens were well tolerated with no reported serious adverse events, Grades 3 and 4 treatment-emergent adverse events (TEAEs) or TEAEs leading to discontinuations.

Conclusion: After 12 weeks of treatment, high rates of virologic response were observed in tobevibart and elebsiran combination therapy and tobevibart monotherapy cohorts. Reductions in ALT values occurred over time with no ALT flares. Similar results were observed in participants with non-cirrhotic and cirrhotic chronic HDV infection. Additional 12- and 24-week data will be presented. These results support continued development of tobevibart alone or in combination with elebsiran.

New CPG and late breaker evidences

OS-124

Identification and validation of pre-identified morphological baseline features for prediction of fibrosis progression in MAESTRO-NASH

Stephen A. Harrison¹, Rebecca Taub², Dominic Labriola², Hang Zhang², Elaine Chng³, Yayun Ren³, Dean Tai³, Jörn M Schattenberg⁴. ¹Pinnacle Research, San Antonio, Texas, United States; ²Madrigal Pharmaceuticals, Pennsylvania, United States; ³Histoindex Pte. Ltd., Singapore, Singapore ⁴Saarland University Medical Center, Homburg, Germany
Email: Dean.Tai@histoindex.com

Background and aims: Fibrosis staging remains the pinnacle predictor of clinical outcomes in metabolic-associated steatohepatitis (MASH) clinical trials, with liver biopsies as the gold standard. However, the ability to reflect dynamic fibrotic changes using ordinal scores in interventional trials remains contentious. Various non-invasive tests (NITs) have been developed but without success in replacing biopsies thus far. qFibrosis, an AI-driven fibrosis assessment methodology, has identified specific fibrotic features potentially more predictive of clinical outcomes than ordinal stages and the aim is to validate whether these pre-identified fibrotic features can distinguish fibrosis progressors in MAESTRO-NASH. MAESTRO-NASH is an ongoing 54-month phase 3 study which achieved NASH resolution and fibrosis reduction end points.

Method: Based on sample availability at baseline, 845 patients had qFibrosis assessment and corresponding selected NITs (VCTE, MRE, ProC3, AST, GGT and platelets), except for MRE where there were only 495 patients. 30 fibrosis features previously identified from SteatoSITE are used in this analysis and Spearman correlation against pathologist scores. Using univariate analyses and random

forest model with baseline fibrosis stage as the outcome, 6 fibrosis features (5 from periportal region, 1 from zone 2) were chosen for exploration with clinical data and subsequent validation.

Results: Correlations of NITs with pathologist scores were modest, with MRE exhibiting the highest correlation (0.489), followed by VCTE (0.309). Against the NITs, these 6 fibrosis features showed varying degrees of correlation, albeit generally mediocre (0.05~0.46). Notably, the feature from zone 2 (number of short strings) exhibited a negative correlation ($-0.07 \sim -0.324$), while the rest showed positive correlation. MRE and VCTE correlations with these 6 features aligned closely with pathologist scores, ranging from 0.393 to 0.464 with MRE and 0.233 to 0.342 with VCTE, suggesting nuanced fibrosis progression markers. Note that the correlation of zone 2 fibrosis feature to MRE and VCTE are -0.324 and -0.255 , respectively.

Conclusion: Using pre-identified fibrosis features from SteatoSITE, which is an event-rich resource containing clinical and pathological data from MAFLD 940 cases, we validated them with MAESTRO-NASH for predicting fibrosis progression. The identification of negatively correlating features underscores the complexity of fibrosis progression markers. The findings argue against the sufficiency of NITs for predicting fibrosis progression based solely on fibrosis stages or specific fibrosis features. This highlights the necessity for a composite NIT approach, incorporating both positively and negatively correlating fibrosis features. Confirmation of clinical significance is necessary with month 54 biopsies and eventual clinical outcomes.

OS-125

15-year liver outcomes after metabolic surgery in patients with compensated cirrhosis due to metabolic dysfunction-associated steatohepatitis (MASH)

Ali Aminian¹, Abdullah Aljabri¹, Sarah Wang¹, James Bena¹, Daniela Allende¹, Hana Rosen¹, Rickesha Wilson¹, Alex Milinovich¹, Rohit Loomba², Arun J Sanyal³, Naim Alkhouri⁴, Jamile Wakim-Fleming¹, Srinivasan Dasarathy¹, Arthur McCullough¹, Steven Nissen¹. ¹Cleveland Clinic, Cleveland, United States; ²University of California San Diego, La Jolla, United States; ³Virginia Commonwealth University, Richmond, United States; ⁴Arizona Liver Health, Phoenix, United States
Email: aminiaa@ccf.org

Background and aims: No therapy has been shown to reduce the risk of serious adverse outcomes in patients with compensated cirrhosis due to metabolic dysfunction-associated steatohepatitis (MASH).

Method: Among 36,912 liver biopsies performed at the Cleveland Clinic Health System in the U.S. between 1995 and 2020, adult patients with obesity and compensated histologically-proven MASH-related cirrhosis (Child-Pugh class A with MELD-Na ≤ 10) were selected in the Surgical Procedures Eliminate Compensated Cirrhosis In Advancing Long-term (SPECCIAL) observational study. A doubly robust estimation combining the overlap weighting and multi-variable-adjusted Cox regression analysis was utilized to compare time-to-incident major adverse liver outcomes (MALO), defined as first occurrence of ascites, variceal hemorrhage, hepatic encephalopathy, hepatocellular carcinoma, liver transplantation, or all-cause mortality, between patients who received metabolic bariatric surgery versus patients who received usual care. The secondary composite end point was the progression to decompensation, defined as the first occurrence of ascites, variceal hemorrhage, or hepatic encephalopathy. Follow-up ended in February 2024.

Results: The study analyzed 168 patients (69.6% female) including 62 metabolic surgery and 106 nonsurgical control patients with compensated MASH-related cirrhosis. Follow-up was over a 25-year period with a mean follow-up of 10.0 ± 4.5 years. Distribution of key baseline characteristics was precisely balanced after overlap weighting including the mean age of 54.4 years, BMI of 42.7 kg/m^2 , fibrosis-

4 score of 2.1, albumin of 4.1 g/dL, bilirubin of 0.6 g/dL, platelet count of 208.8 k/uL, and Elixhauser comorbidity index of 9.0 in both groups (standardized difference = 0 for all). In each group, 84.5% had type 2 diabetes and 79.1% had Ishak stage 6. The cumulative incidence of MALO at 15-years was 20.9% (95% CI, 2.5-35.9) in the surgical group and 46.4% (95% CI, 25.6-61.3) in the nonsurgical group, an adjusted absolute risk difference of 22.1% (95% CI, 4.6-37.2), with an adjusted HR of 0.28 (95% CI, 0.12-0.64), $P = 0.003$. The cumulative incidence of progression to decompensated stage at 15-years was 15.6% (95% CI, 0-31.3) in the surgical group and 30.7% (95% CI, 12.9-44.8) in the nonsurgical group, an adjusted absolute risk difference of 20.6% (95% CI, 3.7-35.2), with an adjusted HR of 0.20 (95% CI, 0.06-0.68), $P = 0.01$. The mean total weight loss at 15 years in the surgical and nonsurgical groups was 26.6% (95% CI, 24.5-28.7) and 9.8% (95% CI, 7.8-11.8), respectively (mean difference: 16.8% [95% CI, 13.9-19.7], $P < 0.001$). Ten (16.1%) patients developed postoperative adverse events.

Conclusion: Metabolic surgery, compared with nonsurgical management, was associated with a significantly lower risk of incident MALO among patients with compensated MASH-related cirrhosis and obesity.

OS-126

Steatotic liver disease classification is highly dynamic impacting eligibility for clinical trials and subclass-specific interventions

Katrine Thorhauge^{1,2}, Mads Israelsen^{1,2}, Peter Andersen¹, Nikolaj Torp^{1,2}, Stine Johansen¹, Ellen Lyngbeck Jensen¹, Helle Schnefeld¹, Johanne Kragh Hansen^{1,2}, Katrine Tholstrup Bech¹, Ida Falk Villesen¹, Katrine Lindvig¹, Camilla Dalby Hansen¹, Maja Thiele^{1,2}, Aleksander Krag^{1,2}. ¹Odense University Hospital, Odense, Denmark; ²University of Southern Denmark, Odense, Denmark
Email: mads.eigerod.israelsen@rsyd.dk

Background and aims: Steatotic liver disease (SLD) includes several subclasses including metabolic-dysfunction associated steatotic liver disease (MASLD), metabolic and alcohol-related liver disease MetALD and alcohol-related liver disease (ALD). The classification is based on the presences of hepatic steatosis, cardiometabolic risk factors

(CMRF) and current alcohol use. However, these criteria may be sensitive to spontaneous changes in lifestyle making the SLD diagnoses dynamic. Our aim was to investigate the dynamics of SLD diagnoses over time.

Method: We performed a prospective cohort study among individuals from the general population and individuals at risk of SLD (obesity, type 2 diabetes or a history of excessive alcohol use). We defined presence of steatosis as CAP >275 dB/m and presence of advanced fibrosis as TE >12 kPa. Subclassification of SLD was based on the presence of at least one CMRF and self-reported current alcohol use (MASLD <20/30 (female/male) gram/day; MetALD 20-50/30-60 (female/male) gram/day; ALD >50/60 (female/male) gram/day). The SLD classification was assessed at baseline and after 2 years follow-up.

Results: We included 994 participants, mean age was 57 (± 10) years, 633 were male (64%) and 361 (36%) female and 54 (5%) had advanced fibrosis. At baseline, 551 (55%) had SLD (CAP >275 dB/m and/or TE >12 kPa) while 443 (45%) did not have SLD. Among the patients with SLD, 337 (61%) met the criteria for MASLD, 133 (24%) for MetALD and 79 (14%) for ALD, and 2 (0.4%) were classified as cryptogenic SLD. Median time between baseline and follow-up visit was 25 months (IQR 25-31). At follow-up, 382 (38%) of the 994 participants were reclassified. Among the 443 participants that did not have SLD at baseline, 113 (26%) met the criteria for SLD at follow-up. Among the 551 participants classified as having SLD at baseline, 269 (49%) were reclassified of which 186 (69%) did not meet the criteria for SLD at follow-up and 83 (31%) changed SLD subclass. For the 382 participants reclassified, 299 (78%) were due to changes in steatosis, 83 (22%) due to changes in alcohol use, and 0 due to changes in presences of CMRFs.

Conclusion: SLD and the subclassification hereof is highly dynamic, especially driven by changes in alcohol use and steatosis. This affects eligibility for clinical trials and imply that patients with SLD should be reassessed regularly to ensure correct subclass diagnosis and management.

Late-breaker Posters

LBP-001

Rapid reductions of HDV RNA and ALT with the monoclonal antibody, BJT-778: results from a phase 2 study

Kosh Agarwal¹, Marta Dobryanska², Alina Jucov³, Patrick Kennedy⁴, Edward J. Gane⁵, Man-Fung Yuen⁶, Grace Lai-Hung Wong⁷, Simone Strasser⁸, Jacinta Holmes⁹, Stuart Roberts¹⁰, Hassan Javanbakht¹¹, Nancy Shulman¹¹. ¹Kings College Hospital, London, United Kingdom; ²ARENSIA Exploratory Medicine, Kyiv, Ukraine; ³ARENSIA Exploratory Medicine, Chisinau; ⁴Queen Mary University Hospital, London, United Kingdom; ⁵New Zealand Clinical Research, University of Auckland, Auckland, New Zealand; ⁶Queen Mary University Hospital, Hong Kong, Hong Kong; ⁷Prince of Wales Hospital, Hong Kong, Hong Kong; ⁸Royal Prince Alfred Hospital, Sydney, Australia; ⁹St. Vincent's Hospital, Melbourne, Australia; ¹⁰The Alfred Hospital, Melbourne; ¹¹Bluejay Therapeutics, Inc., San Mateo, United States
Email: nshulman@bluejaytx.com

Background and aims: BJT-778 is a fully human anti-HBsAg monoclonal antibody that exhibits potent antiviral activity against HBV and HDV in vitro. BJT-778 is currently being evaluated in a Phase 1/2 study, BJT-778-001, for the treatment of chronic hepatitis B and chronic hepatitis D (CHD). We report the preliminary safety and efficacy results from the phase 2 portion of the study, where BJT-778 administered subcutaneously (SC) for a duration of up to 48 weeks in subjects with CHD.

Method: Approximately 10 subjects per arm were to be enrolled into: Arm 1: BJT-778 300 mg SC once weekly (QW); Arm 2: BJT-778 600 mg SC QW for 12 weeks followed by Q2W; and Arm 3: BJT-778 900 mg SC Q2W for 4 weeks followed by Q4W. Primary end points are safety and tolerability. Efficacy end points include absolute reductions and changes from baseline in HDV RNA and ALT levels, and the proportion of subjects achieving (i) virologic response defined as ≥ 2 log₁₀ HDV RNA IU/ml reduction from baseline or below the limit of detection (BLD), (ii) ALT normalization (defined as \leq ULN in subjects with $>$ ULN at baseline), and (iii) composite response (defined as virologic response and ALT normalization). Eligible patients have quantifiable HDV RNA, HBsAg levels of ≥ 10 IU/ml and HBV DNA < 100 IU/ml on nucleos (t)ides. Arm 1 limited enrolment to non-cirrhotic patients, whereas Arms 2 and 3 included patients with compensated cirrhosis. Here, we provide results from Arm 1, with up-to-date results from all three arms to be presented.

Results: 10 subjects were enrolled into Arm 1 and 11 subjects into Arm 2. Recruitment for Arm 3 is ongoing. All subjects in Arm 1 have completed 16 weeks of treatment, with the data presented here. Baseline characteristics: Median (range) age of 41 years (31 to 47), ALT of 54 U/L (19 to 117), HDV RNA of 5.3 (2.9 to 7.1) log₁₀ IU/ml, and HBsAg of 4.2 (3.8 to 4.9) log₁₀ IU/ml. Six were men and all were Caucasian. In Arm 1, 90% of the subjects (9 out of 10) achieved a virologic response, with 40% (4 out of 10) falling below the limit of quantification (BLQ) and 30% (3 out of 10) BLD. Additionally, 67% (6/9) achieved ALT level normalization and composite response. One subject had a normal ALT at baseline, which remains normal. The

mean reduction in HDV RNA at Week 16 was 3.0 logs. Across all treatment arms, BJT-778 at doses up to 900 mg have been well tolerated, with no reported serious or Grade 3/4 adverse events, and no treatment discontinuations in any of the arms. Available data from all arms will be presented.

Conclusion: Monotherapy with BJT-778 was safe and well-tolerated and achieved rapid virologic responses with ALT normalization in most subjects with CHD. Comprehensive data from all study arms will be presented, offering further insights into the therapeutic potential of BJT-778.

LBP-002

GM-60106 (a peripheral 5HT2A antagonist) as a clinical candidate for metabolic dysfunction-associated steatohepatitis (MASH)

Jin Hee Ahn^{1,2}, Hail Kim³, Sungmin Song⁴, Peter Goughnour⁴, Myung Ae Bae⁵. ¹JD Bioscience INC, Gwangju, Korea, Rep. of South; ²Gwangju Institute of Science and Tehcnology, Gwnagju, Korea, Rep. of South; ³Korea Advanced Institute of Science and Technology, Daejeon, Korea, Rep. of South; ⁴JD Bioscience INC, #1414 B complex, Tera Tower, 167, Songpa-daero, Seoul, Korea, Rep. of South; ⁵Korea research institute of chemical technology, Daejeon, Korea, Rep. of South
Email: hailkim@kaist.edu

Background and aims: Metabolic Dysfunction-Associated Steatotic Liver Disease (MASLD) is a leading cause of chronic liver disease globally. Metabolic Dysfunction-Associated Steatohepatitis (MASH) represents an advanced stage of MASLD, capable of progressing to liver fibrosis, cirrhosis, and hepatocellular carcinoma. This study aimed to assess the safety profile and tolerability of GM-60106, a peripheral 5HT2A antagonist, in healthy adults and otherwise healthy adults with markers of metabolic dysfunction-associated fatty liver disease (MAFLD) in a Phase 1 trial (NCT05517564).

Method: The Phase 1 clinical trial is a randomized, double-blind, placebo-controlled study involving single and multiple ascending doses to evaluate the safety, tolerability, pharmacokinetics (PK), and pharmacodynamics (PD) of GM-60106 in healthy adult male and female participants, as well as otherwise healthy adults with elevated markers of MAFLD. The study was structured into three parts: Part A (Single Ascending Dose) included 64 healthy participants divided into 8 cohorts, assessing the safety, tolerability, PK, PD profiles, and food effects of GM-60106. Part B (Multiple Ascending Dose, 14 days once daily) involved 24 healthy participants divided into 3 cohorts, evaluating the safety, tolerability, PK, and PD profiles of GM-60106. Part C (Multiple Ascending Dose, 28 days once daily) included 8 otherwise healthy participants with elevated biomarkers for NAFLD, examining the safety, tolerability, PK, and PD profiles of GM-60106.

Results: The part A study has been completed, revealing that adverse events (AE) were mostly mild to moderate in severity following a single dose of GM-60106 and demonstrated minimal effect on a high-fat meal. Notably, at the maximum tolerated dose (160 mg), grade 2 AEs such as posture dizziness were documented. Pharmacokinetic (PK) data shows that the absorption of GM-60106 increased in a dose-proportional manner from 2.5 mg to 160 mg dosing.

Conclusion: In the first-in-human clinical trial, GM-60106, a novel HTR2A antagonist, has been determined to be safe and well-tolerated, displaying PK profiles optimal for oral administration. A multiple ascending dose study is currently ongoing to assess the



safety, PK, and PD of the compound, paving the way for further long-term toxicity assessments and human proof-of-concept studies to establish the potential of GM-60106 as a promising treatment for MASH.

LBP-003

Semaglutide achieves resolution of metabolic dysfunction-associated steatohepatitis via modulation of multiple pathogenic pathways: insights from human and animal studies

Maximilian Kurt Jara¹, Jenny Egcioglu Norlin², Mette Kjaer¹, Kasper Almhol², Kristian Bendtsen², Elisabetta Bugianesi³, Kenneth Cusi⁴, Elisabeth Galsgaard², Milan Geybels⁵, Lise Lotte Gluud⁶, Lea Mørch Harder², Rohit Loomba⁷, Gianluca Mazzoni², Philip N. Newsome^{8,9}, Louise Maymann Nitze¹, Mads Sundby Palle⁵, Vlad Ratziu¹⁰, Anne-Sophie Sejl¹, Vincent Wai-Sun Wong¹¹, Quentin M. Anstee^{12,13}, Lotte Bjerre Knudsen². ¹Novo Nordisk, Clinical Development, Søborg, Denmark; ²Novo Nordisk, Research and Early Development, Måløv, Denmark; ³Division of Gastroenterology, Department of Medical Sciences, University of Torino, Torino, Italy; ⁴Division of Endocrinology, Diabetes, and Metabolism, University of Florida, Gainesville, FL, United States; ⁵Novo Nordisk, Data Science, Søborg, Denmark; ⁶Gastro Unit, Copenhagen University Hospital Hvidovre, Hvidovre, Denmark and Department of Medicine, University of Copenhagen, Hvidovre, Denmark; ⁷Radcliffe Department of Medicine, Oxford University, Oxford, United Kingdom; ⁸National Institute for Health Research Birmingham Biomedical Research Centre and Liver Unit at University Hospitals Birmingham NHS Foundation Trust, and Centre for Liver and Gastrointestinal Research, Institute of Immunology and Immunotherapy, University of Birmingham, Birmingham, United Kingdom; ⁹Institute of Hepatology, Faculty of Life Sciences and Medicine, King's College London and King's College Hospital, London, United Kingdom; ¹⁰Sorbonne University, ICAN-Institute for Cardiometabolism and Nutrition, Hôpital Pitié Salpêtrière, Paris, France; ¹¹Department of Medicine and Therapeutics, The Chinese University of Hong Kong, Hong Kong, China; ¹²Translational and Clinical Research Institute, Faculty of Medical Sciences, Newcastle University, Newcastle upon Tyne, United Kingdom; ¹³Newcastle NIHR Biomedical Research Centre, Newcastle upon Tyne Hospitals NHS Trust, Newcastle upon Tyne, United Kingdom
Email: quentin.anstee@newcastle.ac.uk

Background and aims: Metabolic dysfunction-associated steatohepatitis (MASH) increases the risk of cardiovascular (CV) events and liver fibrosis. Semaglutide, a glucagon-like peptide-1 (GLP-1) receptor agonist, reduces CV risk associated with overweight and obesity in the absence of diabetes and has a profound effect on weight reduction and MASH resolution. Management of MASH may benefit from an understanding of the mechanistic basis of semaglutide-induced MASH resolution; thus, it is of interest to explore its effect on the hepatic microenvironment and fibrosis development.

Method: GLP-1 receptor expression was assessed using RNA *in situ* hybridization and immunohistochemistry in human liver tissue and immunohistochemistry in liver tissue from DIO-NASH and CDA-HFD mice. The effect of semaglutide treatment on liver fibrosis was assessed using liver transcriptome analysis in both mouse models of MASH. Proteomic analyses of 4979 proteins using the SomaScan Platform were conducted on serum samples from 293 patients with MASH who received semaglutide or placebo in a phase 2b study (NCT02970942), and an independent cohort of 141 patients with MASH and 89 healthy volunteers.

Results: GLP-1 receptor mRNA or protein expression were not detected in human or mouse liver tissue. However, semaglutide improved histological markers of fibrosis and expression of genes involved in collagen turnover in two distinct mouse models of MASH; one that phenocopies the metabolic-associated features of human disease and another that exhibits non-abdominal obesity-induced advanced steatohepatitis and rapid fibrosis. In semaglutide-treated patients with MASH, proteomics identified 72 proteins significantly

associated with MASH resolution after 72 weeks of treatment. These 72 proteins were also identified as differentially expressed in patients with MASH who were not treated for MASH, relative to healthy individuals. In semaglutide-treated patients with MASH, the abundance of the 72 proteins was similarly altered; however, semaglutide reverted the altered disease profile to that seen in non-pharmacologically treated healthy individuals. In contrast, changes in the levels of the 72 proteins in patients who received placebo were negligible. Notably, changes in the abundance of 26 of the 72 proteins were significant even after correction for weight loss. Although most of these 26 proteins are associated with metabolic functions, several are implicated in fibrosis-related pathways and CV disease (e.g. ADAMTSL2 and ACY1), and hepatocellular carcinoma (e.g. SERPINC1). **Conclusion:** Based on circulating proteomic profiling, semaglutide-induced MASH resolution is associated with changes in multiple pathogenic pathways even after correction for weight loss. Semaglutide appears to re-balance the expression levels of disease-associated proteins in MASH to levels found in healthy individuals.

LBP-005

Efficacy, safety, tolerability, and immunogenicity of JNJ-0535 following a reduction of viral antigen levels through administration of siRNA JNJ-3989 in patients with chronic HBsAg negative hepatitis B-interim data of the OSPREY study

Stefan Bourgeois¹, Maria Buti², Edward J. Gane³, Kosh Agarwal⁴, Ewa Janczewska⁵, Yao-Chun (Holden) Hsu⁶, Maurizia Brunetto⁷, Pietro Lampertico⁸, Joaquin Cabezas⁹, Gloria Kim¹⁰, Leen Slaets¹¹, Adam Bakala¹¹, Joris Vandenbossche¹¹, Simon Verheijden¹¹, Bart Fevery¹¹, An De Creus¹¹, Michael Biermer¹², Dessislava Dimitrova¹³. ¹ZNA, Cadix, Antwerp, Belgium; ²Hospital General Universitari Vall Hebron, CIBER-EHD del Instituto Carlos III, Barcelona, Spain; ³New Zealand Liver Transplant Unit, University of Auckland, Auckland, New Zealand; ⁴Institute of Liver Studies, King's College Hospital, London, United Kingdom; ⁵Faculty of Health Sciences, Medical University of Silesia, Katowice, Poland; ⁶Department of Medical Research, Center for Liver Diseases and Center for Clinical Trials, E-Da Hospital, I-Shou University, Kaohsiung, Taiwan; ⁷Hepatology Unit and Laboratory of Molecular Genetics and Pathology, University Hospital of Pisa, Pisa, Italy; ⁸Division of Gastroenterology and Hepatology, Foundation IRCCS Ca' Granda Ospedale Maggiore Policlinico, Division of Gastroenterology and Hepatology, CRC "A. M. and A. Migliavacca" Center for Liver Disease, Department of Pathophysiology and Transplantation, University of Milan, Milan, Italy; ⁹Servicio de Aparato Digestivo, Hospital Universitario Marqués de Valdecilla, Clinical and Translational Research in Digestive Diseases, Valdecilla Research Institute (IDIVAL), Santander, Spain; ¹⁰IQVIA, Durham, United States; ¹¹Janssen Pharmaceutica, Beerse, Belgium; ¹²Janssen Pharmaceutica NV, Beerse, Belgium; ¹³Janssen Research and Development, LLC, Titusville, United States
Email: stefan.bourgeois@zna.be

Background and aims: JNJ-64300535 (JNJ-0535), a DNA vaccine with two plasmids encoding HBV core and polymerase (pol) proteins, delivered through electroporation-mediated intramuscular injection, has previously shown to induce strong to modest T-cell responses in healthy adults and weak responses in patients with chronic hepatitis B (CHB). The OSPREY study (NCT05123599) was designed to assess whether a reduction of viral antigens by siRNA JNJ-73763989 (JNJ-3989) prior to JNJ-0535 vaccination, can enhance HBV-specific T cell responses and improve HBsAg kinetics in CHB patients.

Method: OSPREY is a phase 1b, open-label, single-arm, multicenter study in virologically suppressed patients with HBeAg-negative CHB receiving daily doses of nucleos(t)ide analogs (NA) for 36 weeks (W), 7 JNJ-3989 injections (Q4W) until W24, and 4 doses of JNJ-0535 (Q4W) from W14 to W28. NA stopping criteria (HBsAg <10 IU/ml, DNA <LLOQ and ALT <ULN) are assessed based on W36 results and patients are followed up (FU) with or without NA treatment for 48W, accordingly. Changes in virologic markers are assessed in serum and peripheral blood mononuclear cells (PBMCs) are evaluated for T cell

POSTER PRESENTATIONS

responses against core, pol, and surface using ex vivo intracellular cytokine staining (ICS). Intrahepatic changes in immunology markers are assessed from fine needle aspirates (FNA) at baseline (BL) (n = 22), W14 (n = 19) and W28 (n = 14) by single-cell RNA-sequencing. We report interim data with all patients at FUW24.

Results: Of the 23 patients who completed dosing, 11 achieved the primary end point of $\geq 2 \log_{10}$ IU/ml reduction in HBsAg from baseline (BL) at W36. NA treatment was stopped in 7 patients based on W36 results and was restarted in 2 following an HBV DNA flare. Mean change in HBsAg in \log_{10} IU/ml (SE) from W28 to FUW24 was 0.41 (0.148; n = 22) with -0.29 (0.248) in 7 patients who stopped NA (NA completers) versus 0.73 (0.113) in 15 NA non-completers. Among the 7 NA completers, polypositive CD4 T cells (PP CD4) to 32 HBV antigens was enhanced at W28 in 4, detected at pre-vaccination and W28 in 1 and not in the 2 NA completers who re-started NA during FU. Among the 14 non-completers with available data, 3 had enhanced PP CD4 at W28 and 1 had PP CD4 at pre-vaccination and W28 with no further enhancement. NA completers had higher proportions of intrahepatic mucosal-associated invariant T cells (MAIT), at all timepoints with FNAs available. Except 1 grade 3 injection site reaction, no grade 3 or 4 adverse events (AE) or serious AEs were reported until FUW24.

Conclusion: Treatment with JNJ-3989, JNJ-0535 and NA, continued or stopped was generally safe and well tolerated. HBsAg lowering, followed by vaccination in OSPREY, showed more favourable HBsAg kinetics during FU in patients that were able to stop NA treatment versus patients who continued NA treatment. A potential role of HBV specific polypositive CD4 T cells needs further elucidation.

LBP-006

Efficacy of elafibranor in primary biliary cholangitis: results from the variable double-blind period of ELATIVE®, a randomised, placebo-controlled phase III trial

Christopher L. Bowlus¹, Kris V. Kowdley², Cynthia Levy³, Ulus Akarca⁴, Mario Alvares-da-Silva⁵, Pietro Andreone⁶, Marco Arrese⁷, Christophe Corpechot⁸, Sven Francque^{9,10}, Michael Heneghan¹¹, Pietro Invernizzi^{13,13}, David Jones¹⁴, Frederik Kruger^{15,16}, Eric Lawitz¹⁷, Marlyn J. Mayo¹⁸, Mitchell Shiffman¹⁹, Mark G. Swain²⁰, José Miguel Valera²¹, Victor Vargas Blasco²², John M. Vierling²³, Alejandra Villamil²⁴, Julie Dietrich²⁵, Jianfen Shu²⁶, Nuno Antunes²⁶, Marwan Sleiman²⁷, Nathan Touati²⁷, Jörn M. Schattenberg²⁸. ¹Division of Gastroenterology and Hepatology, UC Davis School of Medicine, Sacramento, CA, United States; ²Liver Institute Northwest, Seattle, WA, United States; ³Schiff Center for Liver Diseases, University of Miami, Miami, FL, United States; ⁴Department of Gastroenterology, Ege University Faculty of Medicine, İzmir, Turkey; ⁵Gastroenterology and Hepatology Division, Hospital de Clinicas de Porto Alegre, Universidade Federal do Rio Grande do Sul, Porto Alegre, Brazil; ⁶Medicina Interna Metabolica, Baggiovara Hospital, Azienda Ospedaliero-Universitaria di Modena and Università di Modena e Reggio Emilia, Modena, Italy; ⁷Departamento de Gastroenterología, Escuela de Medicina, Pontificia Universidad Católica de Chile, Santiago, Chile; ⁸Reference Center for Inflammatory Biliary disease and Autoimmune Hepatitis, European Reference Network RARE-LIVER, Saint-Antoine Hospital and Research Center, APHP, Sorbonne University, Paris, France; ⁹InflaMed Centre of Excellence, Laboratory of Experimental Medicine and Paediatrics, Faculty of Medicine and Health Sciences, Antwerp University, Antwerp, Belgium; ¹⁰Department of Gastroenterology and Hepatology, Antwerp University Hospital, Antwerp, Belgium; ¹¹Institute of Liver Studies, King's College Hospital NHS Foundation Trust, London, United Kingdom; ¹²Division of Gastroenterology, Center for Autoimmune Liver Diseases, Department of Medicine and Surgery, University of Milano-Bicocca, Monza, Italy; ¹³European Reference Network on Hepatological Diseases (ERN RARE-LIVER), Fondazione IRCCS San Gerardo dei Tintori, Monza, Italy; ¹⁴Institute of Cellular Medicine and NIHR Newcastle Biomedical Research Center, Newcastle University, Newcastle Upon Tyne, United Kingdom; ¹⁵Department of Gastroenterology and Hepatology, Mediclinic Durbanville, Cape Town, South Africa; ¹⁶Tiervlei Trial Centre, Cape Town, South Africa; ¹⁷The Texas Liver Institute, University of Texas Health, San

Antonio, TX, United States; ¹⁸Division of Digestive and Liver Diseases, University of Texas Southwestern Medical Center, Dallas, TX, United States; ¹⁹Liver Institute of Virginia, Bon Secours Mercy Health, Richmond, VA, United States; ²⁰Liver Unit, Department of Medicine, Cumming School of Medicine, University of Calgary, Calgary, AB, Canada; ²¹Sección de Gastroenterología, Hospital San Juan de la Serena, Coquimbo, Chile; ²²Liver Unit, European Reference Network RARE-LIVER, Hospital Universitari Vall d'Hebron, Universitat Autònoma de Barcelona, CiberEhd, Barcelona, Spain; ²³Departments of Medicine and Surgery, Baylor College of Medicine, Houston, TX, United States; ²⁴Hepatic Autoimmunity Unit, Hospital Italiano de Buenos Aires, Buenos Aires, Argentina; ²⁵GENFIT Corp, Cambridge, MA, United States; ²⁶Ipsen, Cambridge, MA, United States; ²⁷Ipsen, Boulogne-Billancourt, France; ²⁸Department of Internal Medicine II, Saarland University Medical Center, Homburg, Germany
Email: clbowlus@ucdavis.edu

Background and aims: Primary biliary cholangitis (PBC) is a rare autoimmune cholestatic liver disease characterised by the destruction of interlobular bile ducts, resulting in cholestasis and liver fibrosis. Elafibranor, a dual peroxisome proliferator-activated receptor (PPAR)-alpha/delta agonist, significantly improved prognostic biomarkers of cholestasis at Week 52 in patients with PBC in the phase III ELATIVE® trial.¹ Here, efficacy data from ELATIVE® beyond Week 52 are reported.

Method: In ELATIVE® (NCT04526665), patients with PBC and an inadequate response or intolerance to ursodeoxycholic acid, with alkaline phosphatase (ALP) $\geq 1.67 \times$ upper limit of normal (ULN) and total bilirubin (TB) $\leq 2 \times$ ULN, were randomised 2:1 to elafibranor 80 mg or placebo once daily for at least 52 weeks. Patients continued their assigned regimen after Week 52 until all patients had completed the Week 52 visit or for a maximum of 104 weeks, whichever came first. We report efficacy outcomes beyond Week 52, in the variable double-blind period, with a focus on Week 78. Biochemical response, the primary end point at Week 52, was defined as ALP $< 1.67 \times$ ULN, with $\geq 15\%$ reduction from baseline, and TB \leq ULN. Week 78 data presented are descriptive; some patients had missing data at Week 78.

Results: Of 161 randomised patients, 96/108 (89%) receiving elafibranor and 47/53 (89%) receiving placebo completed treatment to Week 52; 30/108 (28%) patients receiving elafibranor and 13/53 (25%) receiving placebo attended a Week 78 visit. Efficacy data to Week 52 have been reported previously.¹ At Week 78, 19/27 (70%) patients receiving elafibranor achieved a biochemical response compared with 0/13 (0%) patients receiving placebo. ALP normalisation occurred in 5/27 (19%) patients receiving elafibranor compared with 0/13 (0%) patients receiving placebo. Mean change from baseline to Week 78 in ALP was -135.3 U/L in patients receiving elafibranor (n = 26) versus 31.0 U/L in patients receiving placebo (n = 12). Mean change from baseline to Week 78 in TB was -1.2 μ mol/L in patients receiving elafibranor (n = 25), while patients receiving placebo had a worsening of mean TB levels with an increase of 3.1 μ mol/L (n = 12). Mean change from baseline to Week 78 in gamma glutamyl transferase (GGT) was -56.3 U/L in patients receiving elafibranor (n = 26) versus -10.3 U/L in patients receiving placebo (n = 12).

Conclusion: Following previously reported efficacy outcomes to Week 52,¹ the results presented here indicate that treatment of patients with PBC with elafibranor results in improvements in prognostic biomarkers of cholestasis longer-term, through 78 weeks.

Reference

1. Kowdley KV. *N Engl J Med.* 2024;390 (9):795–805. Study sponsor: GENFIT; secondary analysis and publication sponsor: Ipsen.

LBP-007

Beneficial effects of autologous macrophage therapy on clinical outcomes in patients with compensated cirrhosis: extended follow-up data from a randomized controlled phase 2 trial

Paul Brennan¹, Iain Macpherson², Debbie Troland², Alastair M. Kilpatrick³, Thomas Manship⁴, Neil McGowan⁵, John Campbell⁵, Alasdair Fraser⁶, Chloe Pass⁶, Francesca Moroni⁷, David Morris³, Alison Glover⁵, Scott Semple³, Mark MacMillan³, Cat Graham³, Marc Turner⁵, John F. Dillon¹, Neil Lachlan², Jonathan Fallowfield⁸, Stuart J. Forbes³. ¹University of Dundee, University of Edinburgh, Dundee, United Kingdom; ²NHS Greater Glasgow and Clyde, Glasgow, United Kingdom; ³University of Edinburgh, Edinburgh, United Kingdom; ⁴Northumbria Healthcare NHS Foundation Trust, Newcastle-Upon-Tyne, United Kingdom; ⁵Scottish National Blood Transfusion Service (SNBTS), Edinburgh, United Kingdom; ⁶Scottish National Blood Transfusion Service (SNBTS), Edinburgh; ⁷NHS Grampian, Aberdeen, United Kingdom; ⁸University of Edinburgh, Institute of Regeneration and Repair, Edinburgh, United Kingdom Email: p.z.brennan@dundee.ac.uk

Background and aims: Preclinical models and early human studies using macrophage cell therapy for liver cirrhosis have produced promising results. We recently performed a multicentre, open-label, Phase 2, randomized controlled trial of autologous monocyte-derived macrophage therapy for cirrhosis (MATCH01; ISRCTN10368050). The long-term effects of advanced cellular therapies are vital to understanding the efficacy, duration of response, and adverse safety signals, but are poorly described. Here, we present an interim analysis of extended follow-up of participants from the MATCH01 study.

Method: In MATCH01, autologous monocyte-derived macrophage therapy was compared with standard medical care in adults (18 to 75 years inclusive) with compensated cirrhosis (minimum 3 months since decompensation episode) and MELD score ≥ 10 and ≤ 17 . The trial was designed to administer three infusions in the treatment arm, but was later amended to a single infusion protocol. Treatment comprised leukapheresis, cell isolation and maturation with reinfusion of macrophages up to a maximum dose of 1×10^9 cells. In total participants were randomized to triple infusion ($n=3$), single infusion ($n=23$) or standard medical care ($n=24$). Participants were followed-up for 12 months as part of the original trial which was reported (Brennan PN et al., *Hepatology* 2023;78 (S1):S168–169). Here, time-to-event analysis over 30 months post-randomization was estimated for each group using the Kaplan-Meier method and compared statistically using the log-rank test.

Results: After 18 months of additional follow-up (i.e., 30 months post-randomization)- there were 7 deaths, 2 liver transplants, 1 patient listed for transplant, and 3 malignancies (no HCC) in the control group; compared to 2 deaths, no liver transplants, no patients listed for transplant, and 1 malignancy (HCC) in the macrophage infusion group. The macrophage treated groups had significantly improved overall survival (Chi-square = 4.35; $p=0.037$) and transplant-free survival (Chi-square = 7.07; $p=0.0078$).

Conclusion: This study demonstrates proof-of-concept for the beneficial effect of macrophage therapy on clinical outcomes in patients with compensated cirrhosis and reinforces their longer-term safety profile. Further development of macrophage therapy for cirrhosis/end-stage liver disease is warranted.

LBP-008

AAV8 gene therapy for mitochondrial neurogastrointestinal encephalomyopathy

Teresa Brevini¹, Lisa Swift², Helen Reynolds³, Richard Stopforth⁴, Yogeshkumar Malam³, John Ong³, Harry Spiers², Emilija Jovanovic³, Miki Scaravaglio³, Vitushan Vakeeswarasarma³, James Heslop³, Sarah Hosgood², Claudia Fuchs⁵, Michael Trauner⁵, Adam Duckworth², Anna Paterson², Arthur Kaser⁴, Jelle van Den Ameel⁴, Vassillis Kosmoliaptis², Gwilym Webb², Christopher Watson², Andrew Butler², Fotios Sampaziotis^{2,3}. ¹Jeffrey

Cheah Biomedical Centre, Cambridge Biomedical Campus, Puddicombe Way, Cambridge, United Kingdom; ²Cambridge University Hospital, Cambridge, United Kingdom; ³Cambridge Stem Cell Institute, Cambridge, United Kingdom; ⁴University of Cambridge, Cambridge, United Kingdom; ⁵Medical University of Vienna, Vienna, Austria Email: fs347@cam.ac.uk

Background and aims: Mitochondrial neurogastrointestinal encephalomyopathy (MNGIE) is a rare genetic disorder caused by mutations in the thymidine phosphorylase (TYMP) gene. This results in nucleoside accumulation, mitochondrial damage, and progressive gastrointestinal and neurological dysfunction leading to cachexia and death before 40 years. There is no established treatment for MNGIE. Liver transplantation restores nucleoside levels, but it is not indicated in all patients (e.g. severely malnourished patients) and it is associated with complications. Adeno-associated-virus (AAV) gene therapy could provide an attractive therapeutic alternative, as it is already clinically approved for other genetic diseases and has been successful in MNGIE animal models. Nevertheless, it has not been tested in human and due to the rarity of MNGIE (<200 cases described) obtaining sufficient numbers for robust AAV trials is challenging. *Ex situ* machine perfusion (ESMP) of human organs has emerged as a new avenue to trial novel therapies in the liver and could address this limitation. Our aim was to test AAV gene therapy for MNGIE in the explanted liver of a patient transplanted for this disease, which was maintained on ESMP.

Method: A 34-year-old patient with MNGIE was listed for liver transplantation as enzyme replacement therapy. The explanted liver was divided into anatomical right and left lobe and perfused *ex situ* using 2 XVIVO Liver Assist devices for 9 days. Nucleoside levels in the perfusate were measured with mass spectrometry. An AAV type 8 encoding for the human TYMP gene was used at a dose of 10^{11} viral genomes/kg of liver. Perfusion parameters (flow, pressure), biochemistry (ALT, pH, glucose) and histology were used to assess treatment toxicity.

Results: Within 24 hours of perfusion nucleosides accumulated in the perfusate recapitulating key features of MNGIE. Subsequently, one lobe received AAV8-TYMP, while the other received carrier injection. The viral vector was uptaken by hepatocytes and TYMP expression was restored in the treated lobe within 3 days. Importantly, AAV8-TYMP treatment resulted in clearance of nucleoside from the perfusate which recapitulated nucleoside clearance from the patient's blood following liver transplant. Furthermore, long-term ESMP of the 2 liver lobes revealed no evidence of hepatotoxicity following AAV8 gene therapy, including normal ALT.

Conclusion: Our report provides the first demonstration of the safety and efficacy of AAV gene therapy for MNGIE in a human liver, paving the road for clinical trials. Our results shift the paradigm of using ESMP exclusively for donor livers and establishes perfusion of patient explanted pathological livers as a novel platform for drug testing. Finally, our study provides proof-of-principle for the efficacy of AAV gene therapy for treating diseased livers on ESMP which could be applied to various other liver diseases.

LBP-009

Liver-infiltrating activated HBV-specific tissue-resident memory T cells and atypical memory B cells were correlated with acute-on-chronic liver failure

Yang Cheng¹, Nina Le Bert², Nicole Tan², Loghman Salimzadeh², Bavani Gunasegaran³, Seng Gee Lim⁴, Evan Newell⁵, Antonio Bertoletti². ¹Institute of Biomedical Science, Academia Sinica, Taipei, Taiwan; ²Duke-NUS Medical School, Singapore, Singapore; ³Singapore Immunology Network, A*STAR, Singapore, Singapore; ⁴National University Health System, Singapore, Singapore, Singapore; ⁵Fred Hutchinson Cancer Center, Seattle, United States Email: ycheng@ibms.sinica.edu.tw

Background and aims: Chronic HBV infection can lead to liver fibrosis and cirrhosis, and in some cases, patients develop into

POSTER PRESENTATIONS

chronic liver failure (CLF), a progressive loss of liver function for more than 6 months. On the contrary, patients who characterized as acute-on-chronic liver failure (ACLF) have dramatic clinical conditions and high short-term mortality due to the sudden loss of substantial amount of hepatocytes, with 80% of the cases lead to death or liver transplantation. However, how the adaptive immunity targeting HBV in the liver contribute to the development of two clinically distinct liver diseases is largely unknown. Studies of adaptive immunity in human liver has been often limited to total T or B cell population without the understanding of antigen-specificity, which prevents the accurate interpretation of disease-specific immune responses and restrain the therapeutic implications of findings.

Method: Here, we combined the utility of highly multiplexed combinatorial peptide-MHC tetramer staining and mass cytometry to probe >100 HBV epitopes on intrahepatic CD8⁺ T cells isolated from HBV-associated ACLF and CLF patients in conjunction with deep-profiling of T cell phenotype. In parallel, intrahepatic B cells were sorted and examined by HBcAg- and HBsAg-probe with a panel focusing on memory B cell responses.

Results: We identified a subset of HBV-specific tissue-resident memory T (T_{RM}) cells expressing tissue homing and activation molecules, including CXCR6 and CD38, were significantly enriched in the liver of ACLF patients compared with CLF patients. Importantly, this subset was not observed in paired blood isolated from the same patients. Similarly, we found that intrahepatic HBcAg-specific B cells, but not HBsAg-specific B cells, were substantially elevated in ACLF patients compared with CLF patients. Of note, these cells obtained an atypical memory B cell phenotype in the liver.

Conclusion: Thus, by comprehensively probing intrahepatic HBV-specific T and B cells, we provide novel insights of adaptive immune responses occurs during the development of HBV-associated liver failure in great details. Our data implies that these cells might have therapeutic potential such as tolerogenic vaccine.

LBP-010

Azemiglitazone in combination with GLP1 agonists increases benefit and could preserve lean body mass

Jerry Colca¹, Kelly Pyles², Kyle McCommis². ¹Cirius Therapeutics, Kalamazoo; ²St. Louis University School of Medicine, St. Louis
Email: jcolca@ciriusx.com

Background and aims: Azemiglitazone (0602K) is a second-generation insulin sensitizer designed based on the activity of metabolites of the first-generation insulin sensitizer pioglitazone to specifically bind to the recently identified target of the TZDs, the mitochondrial pyruvate carrier. Accumulating data suggests that this agent may preserve lean mass in the face of programs designed to cause weight loss.

Method: Here we provide data from a new post-hoc analysis of the Phase 2b EMMINENCE trial (Harrison et al, J Hepatol. 2020 Apr;72(4):613–626) and examined the body composition in db/db mice treated with the combination of 0602K and liraglutide under conditions where there are synergistic improvements in liver histology including ballooning with the 0602K/lira combination (Kamm et al, J Biol Chem 2021: 296:100807).

Results: Analysis of the 23 subjects with NASH (MASH) and type 2 diabetes who had been enrolled in the trial while on a stable dose of a GLP1 receptor agonist (GLP1-RA; 11 liraglutide, 8 dulaglutide, and 4 exenatide) demonstrated that any dose of 0602K was able to further lower fasting glucose, insulin and liver enzymes. HbA1c decreased by more than 2% in some subjects (average 0.5%). No subjects on a GLP1-RA without 0602K had a reduction in fibrosis score, while 5 of the 19 subjects who had been on both 0602K and a GLP1-RA had a reduction in the liver fibrosis scores (52-week liver biopsies). Some subjects who had been on a GLP1-RA continued to lose weight while others did not,

often with a reduction in waist circumference. Given the major effects of this pharmacology to improve insulin sensitivity in skeletal muscle, maintenance of lean mass could be a component of the overall pharmacology. To this end, we performed additional analysis of a preclinical study in db/db mice that examined the combination of 0602K and liraglutide. Here we report that the addition to 0602K to lira maintains lean body mass without significantly affecting overall adipose mass. Statistically significant increases in adipose mass occurred only in subcutaneous and brown adipose tissue.

Conclusion: Together these results suggest that clinical evaluation of azemiglitazone should include GLP1 incretins to take advantage of the combined efficacy of these mechanisms of action and to produce more favorable effects on body composition.

LBP-011

Streamlined serodiagnosis of hepatitis delta: a novel lateral flow assay kit for on-site rapid diagnostics

Arghun Dashdorj¹, Nomin Ariungerel², Sunguck Han³, Gichan Choi³, Su Ah Kim³, Tae-Hoon Kim³, Kyongman An³, Minsup Chung³, Odgerel Oidosambuu², Byambasuren Ochirsum⁴, Purevjargal Bat-Ulzii⁴, Enkhnomiin Ochirbat⁴, Sanjaasuren Enkhtaivan⁴, Saruul Enkhjargal², Naranbaatar Dashdorj¹, Naranjargal Dashdorj⁴, Nam Joon Choi³. ¹Onom Foundation, The Liver Center, Ulaanbaatar, Mongolia; ²Laboratory of Genetic Engineering, NUM, The Liver Center, Ulaanbaatar, Mongolia; ³LUCA AICell, Inc., Anyang-si, Korea, Rep. of South; ⁴The Liver Center, Onom Foundation, Ulaanbaatar, Mongolia

Email: a.dashdorj@onomfoundation.org

Background and aims: Hepatitis Delta Virus (HDV), the most severe form of viral hepatitis in humans, exacerbates the liver disease caused by Hepatitis B Virus (HBV). Despite an estimated global prevalence of 15–20 million, HDV infections often go underdiagnosed due to insufficient training, testing, and funding. To address this challenge, we have developed and validated an anti-HDV Antibody Rapid Diagnostic Test (RDT), leveraging the lateral flow assay (LFA) technique to detect antibodies against Hepatitis Delta antigen (anti-HDV) in serum and plasma. The LFA, integral to our RDT, operates in a streamlined mechanism. When a sample, such as serum or plasma, is applied it migrates via capillary action, encountering reagents including antibodies labeled with colored particles. These particles bind to any present anti-HDV, producing a test line indicating a positive result. A control line further validates this procedure. Aim: Develop and validate LUCA AICell anti-HDV Antibody Rapid Diagnostic Test (RDT), leveraging the lateral flow assay (LFA) technique to detect antibodies against Hepatitis Delta antigen (anti-HDV) in serum and plasma.

Method: 10 µl of serum was collected using a micropipette. Held the micropipette at a 90° angle to the testing device and added the collected specimen into the specimen well. Held the buffer bottle at a 90° angle to the testing device without touching the specimen well to avoid buffer contamination. Added 3 drops of the buffer into the specimen well. Checked the results after 15 minutes. Then compared the results to conventional anti-HCV and HBsAg ELISA tests, as well as HDV-RNA quantification PCR kits.

Results: Our evaluation involved 200 samples, encompassing 122 HDV-RNA positive, 49 HDV-RNA negative but HBsAg and HBV-DNA positive, and 29 healthy individuals. The RDT showcased 100% sensitivity and specificity compared to conventional anti-HCV and HBsAg ELISA tests, as well as HDV-RNA quantification PCR kits.

Conclusion: The anti-HDV Antibody RDT emerges as an accessible, reliable tool for HDV diagnosis. Its simplicity, rapidity, and accuracy make it particularly valuable in both hospital and remote settings, paving the way for improved HDV screening and management worldwide.

LBP-012

Epidemiological trends and clinical impact of multidrug-resistant bacterial infections in patients with cirrhosis across Latin America: results from the ACLARA study

Juan Manuel Diaz^{1,2}, Alberto Farias³, Eva Usón², Patricia Momoyo Zitelli⁴, Gustavo Pereira⁵, Luciana Lofego Goncalves⁶, Aldo Torre⁷, Adrian Gadano⁸, Angelo Z. Mattos⁹, Mario Álvares-da-Silva¹⁰, Liliana Sampaio Costa Mendes¹¹, Paulo Bittencourt¹², Carlos Benitez¹³, Cláudia Alves Couto¹⁴, Manuel Mendizabal¹⁵, Claudio Toledo¹⁶, Daniel Mazo¹⁷, Mauricio Castillo¹⁸, Padilla Machaca Martín¹⁹, André Castro Lyra⁴, Adelina Lozano²⁰, René Malé Velazquez²¹, Milagros Davalos²², José Luis Pérez-Hernández²³, Oliveira Ximenes Rafael²⁴, Faria Silva Giovanni²⁵, Oscar Beltran²⁶, Maria Sarai González-Huezo²⁷, Fernando Bessone²⁸, dos Santos da Rocha Tarciso Daniel²⁹, Eduardo Fassio³⁰, Terra Carlos³¹, Juan Ignacio Marín Zuluaga³², Patricia Sierra², Carlos de la Peña-Ramirez², Ferran Aguilar², Fernandes Souza Fernanda³³, Zago Gomes Maria da Penha⁶, Sebastián Marciano⁸, Mendez Osvely⁷, Liana Codes¹², Marco Arrese¹³, Camila Marques de Alcanatara Barreto⁵, Cristina Sanchez², Jonel Trebicka², Thierry Gustot², Joan Claria², Rajiv Jalan², Paolo Angeli², Vicente Arroyo², Flair Jose Carrilho³, Richard Moreau², Javier Fernández². ¹Liver Unit and Department of Research, Hospital Italiano de Buenos Aires, Buenos Aires, Argentina, Buenos Aires, Argentina; ²European Foundation for the Study of Chronic Liver Failure, Barcelona, Spain; ³H. das Clínicas da Universidade São Paulo, São Paulo, Brazil; ⁴The Department of Gastroenterology, Hospital das Clínicas, University of São Paulo School of Medicine, São Paulo, Brazil, São Paulo, Brazil; ⁵H. Federal de Bonsucesso, Rio de Janeiro, Brazil; ⁶H. Universitário Cassiano Antonio Moraes, Vitória, Brazil; ⁷Inst. Nac. Ciencias Médicas y Nutrición Salvador Zubirán, Ciudad de México, Mexico; ⁸H. Italiano de Buenos Aires, Buenos Aires, Argentina; ⁹Irmandade Sta. Casa de Misericórdia de Porto Alegre, Porto Alegre, Brazil; ¹⁰H. de Clinicas de Porto Alegre, Porto Alegre, Brazil; ¹¹H. de Base do Distrito Federal, Brasília, Brazil; ¹²H. Português de Salvador Bahia, Salvador de Bahia, Brazil; ¹³Pontificia Univ. Católica de Chile, Santiago de Chile, Chile; ¹⁴H. das Clinicas da Universidade Federal de Minas Gerais., Belo Horizonte, Brazil; ¹⁵H. Universitario Austral, Buenos Aires, Argentina; ¹⁶Univ. Austral de Chile. Hospital Valdivia, Valdivia, Chile; ¹⁷Universidade Estadual de Campinas, Campinas, Brazil; ¹⁸Hospital de Especialidades Centro Médico Nacional La Raza, Ciudad de México, Mexico; ¹⁹H. Nac. Guillermo Almenara, Lima, Peru; ²⁰Unidad de Hígado, Hospital Nacional Arzobispo Loayza, Lima, Perú, Lima, Peru; ²¹Instituto de Salud Digestiva y Hepática, Guadalajara, Mexico; ²²H. Nac. Edgardo Rebagliati Martins, Lima, Peru; ²³H. Gral. de México Dr Eduardo Liceaga, Ciudad de México, Mexico; ²⁴H. das Clínicas da Universidade Federal de Goiás, Goiânia, Brazil; ²⁵Faculdade de Medicina de Botucatu, Botucatu, Brazil; ²⁶Fundación Cardio Infantil, Bogotá, Colombia; ²⁷Centro Médico INSSEMYN, Metepec, Mexico; ²⁸H. Provincial del Centenario. Univ. Nac. de Rosario, Rosario, Argentina; ²⁹H. Universitario Walter Cantídio, Fortaleza, Brazil; ³⁰H. Nacional Profesor Alejandro Posadas, Buenos Aires, Argentina; ³¹H. Universitario Pedro Ernesto, Rio de Janeiro, Brazil; ³²Hospital Pablo Tobón Uribe, Medellín, Colombia; ³³H. das Clinicas da Faculdade Medicina Ribeirão Preto, Ribeirão Preto, Brazil
Email: juanmanuel.diaz@efclif.com

Background and aims: Decompensated cirrhosis represents a significant public health challenge in Latin America, with bacterial infections likely exacerbating morbidity and mortality. Multidrug-resistant (MDR) bacteria further complicate infection management and prognosis. We aimed to investigate the current epidemiology and prognostic impact of MDR bacterial infections in patients with cirrhosis across Latin America.

Method: Multicenter prospective study involving 1274 non-elective hospitalized patients with acutely decompensated cirrhosis across 44 centers in 7 Latin American countries (Brazil, Argentina, Chile, Mexico, Peru, Colombia, and Paraguay) from 2018 to 2020.

Results: Among the 1274 patients, 524 (41.1%) developed a total of 619 bacterial infections, of which 41.7% were culture-positive. Acute-on-Chronic Liver Failure (ACLF) developed in 47.1% of cases, while septic shock occurred in 26.9%, with higher rates observed in Mexico (ACLF: 62.5%, septic shock: 45.7%) and Peru (ACLF: 53.3%, septic shock: 37.8%), with p values of 0.042 and <0.001, respectively. Gram-negative bacteria (67.8%; *Escherichia coli*: 34.8%) were the most frequently isolated strains. MDR bacteria were isolated in 29.4% of the culture-positive infections, with higher rates observed in Mexico (41.7%), Argentina (35.1%), and Peru (33.3%). ESBL-producing *Escherichia coli* was the most prevalent MDR bacteria (27.6%). Relevant differences in the types of MDR bacteria were observed among countries. ESBL- and Amp-C producing *Enterobacteriaceae* were the most prevalent in Mexico (36.1%), followed by Colombia and Paraguay (25% each), Peru (22.2%), Chile (18.2%), Argentina (16.2%), and Brazil (12.1%). Methicillin-resistant *Staphylococcus aureus* (MRSA) and Vancomycin-resistant *enterococci* (VRE) were predominant in Argentina (5.4% and 2.7%, respectively). Carbapenem-resistant *Klebsiella pneumoniae* was prevalent in Argentina (5.4%) and Carbapenem-resistant *Pseudomonas* was prevalent in Brazil (2%). MDR infections were more frequently associated with septic shock (40%) and ACLF (57.4%). The 28-day mortality rate among infected patients was 29.4%, with a higher proportion in Mexico (47.1%, p < 0.001), whereas it increased to 47.8% in MDR-infected patients, with no difference between countries.

Conclusion: MDR bacterial infections are prevalent and associated with poor prognosis in patients with decompensated cirrhosis in Latin America. Predominant resistant strain varies markedly among countries.

LBP-013

Deciphering the role of mechanical forces in liver regeneration by a biomimetic liver regeneration chip

Xinyu Shu^{1,2}, Ning Li^{1,2}, Yu Du^{1,2}, Mian Long^{1,2}. ¹Institute of Mechanics, Chinese Academy of Sciences, Beijing, China; ²University of Chinese Academy of Sciences, Beijing, China
Email: duydu@imech.ac.cn

Background and aims: Mechanically regulated angiocrine signals induced by the increased blood flow have a key role in liver growth and regeneration. Although mechanical stretching has been proven to contribute to the regeneration in vivo, if shear stress which also changes in the blood perfusion contribute to the regeneration and how shear stress affect liver regeneration with mechanical stretch synergistically remains unclear. Part of the reason is the lack of in vitro models that allow manipulating mechanical stretch and shear stress independently and synergistically. To address this issue, we developed a biomimetic liver regeneration chip (LRC) consisting of a tubular blood vessel and neighbouring hepatocytes monolayer, which integrates stretch and shear stress to elucidate the underlying mechanisms that how two types of forces synergistically regulate liver regeneration.

Method: PDMS microfluidic devices were replicated from a high-resolution 3D printed resin mold. The LRC was fabricated by filling collagen gel into the PDMS microfluidic device with an inserted needle and two open ports nearby to create a tubular channel and two neighbouring defined hollow space for cell seeding. Primary murine liver sinusoidal endothelial cells (LSECs) and hepatocytes were isolated by collagenase perfusion and MACS sorting. LSECs were seeded through the tubular channel while hepatocytes were seeding into a plate form by side. Mechanical forces were applied by a pressure driven pump system. Various mode of applying mechanical forces to the vascular channel were achieved by restricting flow and adjusting the stiffness of surrounding matrix. By exerting shear stress and stretch separately and synergistically, we have then investigated how mechanical forces regulate the angiocrine signals and hepatocyte proliferation.

POSTER PRESENTATIONS

Results: In the LRC, LSECs were able to form a tubular monolayer with intact cell junctions and barrier function. Hepatocytes grew into a confluent monolayer with canaliculi formed between cells. The separated and synergistic mechanical loading of shear stress and stretch was validated by time lapse imaging and particle tracking visualization. Compared with static control, the LSECs in LRC under flow expressed higher genes of secretory factors such as HBEGF to promote hepatocytes proliferation. We are currently using the LRC as a model to study the role of shear stress and stretch in regulating the angiocrine signals and related mechanical sensing pathways to elucidate a mechanism for mechanical forces-initiated liver regeneration.

Conclusion: Overall, these results demonstrated that the LRC not only recapitulate liver sinusoid structurally and functionally, but also allow manipulation of shear stress and stretch separately and together. The LRC represents a novel tool for investigation of mechanical stimuli regulating the angiocrine signals to promote liver regeneration.

LBP-014

Enhancing prediction of moderate fibrosis in MASLD patients for Resmetirom treatment via machine learning

Winston Dunn¹, Naim Alkhour², Terry Cheuk-Fung Yip³, Laurent Castera⁴, Marina Takawy⁵, Leon Adams⁶, Nipun Verma⁷, Juan Pablo Arab⁸, Syed-Mohammed Jafri⁹, Bihui Zhong¹⁰, Julie Dubourg¹¹, Vincent Chen¹², Ashwani K. Singal¹³, Luis Antonio Diaz¹⁴, Nicholas Dunn¹, Rida Nadeem¹⁵, Vincent Wai-Sun Wong³, Manal F. Abdelmalek⁵, Zhengyi Wang¹⁰, Ajay Kumar Duseja⁷, Yousef Almahanna¹⁶, Amani Bajunayd¹⁶, Haya A. Omeish⁹, Junzhao Ye¹⁷, Stephen A. Harrison¹⁸, Grace Lai-Hung Wong¹⁹, Marco Arrese¹⁴, Sage Robert¹, Congxiang Shao¹⁰. ¹University of Kansas, Kansas City, United States; ²Arizona Liver Health, Fairview, United States; ³CUHK, Hong Kong, China; ⁴Hospital Beaujon, AP-HP, Clichy, France; ⁵Mayo Clinic, Rochester, MN, United States; ⁶The University of Western Australia, Nedlands, Australia; ⁷Postgraduate Institute of Medical Education and Research, Chandigarh, India; ⁸Western University, London; ⁹Henry Ford Health, Detroit, United States; ¹⁰First Affiliated Hospital, Sun Yat-sen University, Guangzhou, China; ¹¹Summit Clinical Research, San Antonio, United States; ¹²Summit Clinical Research, Ann Arbor, United States; ¹³University of Louisville, Louisville, Louisville, United States; ¹⁴Pontificia Universidad Católica de Chile, Santiago, Chile; ¹⁵Arizona Liver Health, Phoenix, United States; ¹⁶London Health Sciences Centre, London, Canada; ¹⁷The First Affiliated Hospital, Sun Yat Sen University, Guangzhou, China; ¹⁸University of Oxford, London, United Kingdom; ¹⁹CUHK, Kansas City, United States
Email: winstondunnmd@gmail.com

Background and aims: Metabolic Dysfunction-Associated Steatotic Liver Disease (MASLD) affects approximately 30% of the global adult population and poses significant risks of disease progression, particularly in patients with moderate to advanced fibrosis (stages 2–3). Following the FDA's approval of Resmetirom for treating Metabolic Dysfunction-Associated Steatohepatitis (MASH) in these stages, there is a need for a surrogate marker to refine the selection of patients for liver biopsy. The ALADDIN study introduces a novel machine learning-based web calculator to estimate the probability of stage ≥ 2 fibrosis in MASLD using routine laboratory parameters, with and without Vibration Controlled Transient Elastography (VCTE).

Method: A total of 3708 patients with biopsy-confirmed MASLD from six centers worldwide were divided into Derivation and Internal Validation cohorts on a 1:1 basis, supplemented by 1289 patients from nine centers for External Validation. ALADDIN models, employing Random Forest, Gradient Boosting Machines, and XGBoost enhanced by Bayesian updates, were developed to evaluate moderate fibrosis (stage ≥ 2).

Results: The VCTE model achieved an Area Under the Curve (AUC) of 0.800 (95% CI 0.773–0.827) in external validation, significantly outperforming the FAST (AUC: 0.707, 95% CI 0.674–0.739, $p <$

0.0001) and Agile-3 (AUC: 0.764, 95% CI 0.735–0.793, $p = 0.001$) models. The model using routine laboratory parameters without VCTE reached an AUC of 0.757 (95% CI 0.730–0.783), comparable to FAST and Agile-3. The VCTE model also demonstrated superior decision curve analysis, calibration, and classification accuracy, using a dual cut-off approach, and outperformed existing models in predicting moderate fibrosis.

Conclusion: The ALADDIN study, via an international consortium, has successfully developed and externally validated machine learning models that predict moderate fibrosis with notable accuracy. Our VCTE model, available at <https://aihepatology.shinyapps.io/ALADDIN1/>, and our routine laboratory parameter model without VCTE, available at <https://aihepatology.shinyapps.io/ALADDIN2/>, demonstrate statistical superiority and comparable performance, respectively, against traditional models including Agile-3 and FAST. These algorithms will facilitate targeted liver biopsy in line with the new FDA approval for Resmetirom treatment.

LBP-015

The effect of precursors on extracellular nicotinamide adenine dinucleotide in plasma

Sue Easaw¹, Can Kamali¹, Al-Hussein Saqr¹, Naomi Chioma Okpala¹, Eriselda Keshi¹, Simon Moosburner¹, Karl Hillebrandt¹, Philipp Brunnbauer¹, Felix Krenzien¹. ¹Charité-Universitätsmedizin Berlin, Berlin, Germany
Email: ellen-sue.easaw@charite.de

Background and aims: The presence of extracellular Nicotinamide adenine dinucleotide (eNAD⁺) and its effects have been investigated recently, it remains questionable whether it can be synthesized in the extracellular space. This study aims to investigate the effect of three different NAD⁺ precursors on eNAD⁺ content of plasma, to test the presence of enzymatic activity capable of converting these precursors into eNAD⁺.

Method: Initially, the individual impact of nicotinamide riboside (NR), L-Tryptophan (L-Trp), and nicotinic acid (NA) on plasma eNAD⁺ levels was evaluated. After incubating at 37°C for various time periods (0 min, 30 min, 60 min), the sample eNAD⁺ levels were measured using an enzymatic assay based on the principle of reactant cycling, employing alcohol dehydrogenase as the converting enzyme. Ultimately, a revised-simulated body fluid adjusted with albumin (r-SBFA) served as a NAD⁺-free negative control. All plasma samples were obtained from healthy volunteers ($n = 2$).

Results: Plasma samples without any added precursors showed a noticeable decreasing trend in eNAD⁺ concentration after both 30 and 60 minutes (-3.20% and -11.66% , respectively $p < 0.05$). Furthermore, the effect was more pronounced when plasma samples were spiked with NAD⁺ (-90% , $p < 0.05$). In contrast, samples spiked with all precursors added (NR + L-Trp + NA) and NA-only-samples presented a stable eNAD⁺ within the first 30 min (with a percentage change in plasma with all precursors added: -0.02% and plasma with NA-only: $+0.09\%$, respectively $p > 0.05$). The plasma samples with added L-Trp were the only ones that demonstrated a slight increase in eNAD⁺ after 30 minutes of incubation (3.82% , $p > 0.05$). However, after 60 minutes, the eNAD⁺ levels dropped within all observed precursor conditions for NR, L-Trp and NA (-3.51% , -13.3% , -8.49% , and -8.52% , respectively, $p < 0.05$). In contrast, there were no eNAD⁺ changes observed in r-SBFA.

Conclusion: This study demonstrates the effects of NAD⁺ precursors on plasma samples. The results indicate that the presence of NAD⁺ precursors in blood plasma, such as NR, L-Trp, and NA, can induce temporary eNAD⁺ homeostasis as seen within the first 30 minutes of incubation post spiking. These findings suggest the presence of enzymatic activity within plasma, which might play a role in NAD⁺ metabolism, whereby the addition of NAD⁺ precursors seem to affect the synthesis of eNAD⁺ or stabilize the extracellular consumption of NAD⁺.

LBP-016

Carvedilol versus propranolol in the prevention of decompensation and mortality in patients with compensated and decompensated cirrhosis

Jose Fortea¹, Edilmar Alvarado-Tapias², Benedikt Simbrunner³, Irazu Ezcurra¹, Virginia Hernández-Gea⁴, Carlos Ferre Aracil⁵, Elba Llop Herrera⁶, Angela Puente¹, Cristina Roig², Thomas Reiberger³, Juan Carlos García-Pagán⁴, José Luis Calleja Panero⁶, Mattias Mandorfer³, Cándid Villanueva², Javier Crespo¹. ¹Gastroenterology and Hepatology Department, Clinical and Translational Research in Digestive Diseases, Valdecilla Research Institute (IDIVAL), Marqués de Valdecilla University Hospital, Santander, Spain; ²Hospital de la Santa Creu i Sant Pau, Biomedical Research Institute Sant Pau (IIB Sant Pau), Universitat Autònoma de Barcelona, Centro de Investigación Biomédica en Red de Enfermedades Hepáticas y Digestivas (CIBERehd), Barcelona, Spain; ³Division of Gastroenterology and Hepatology, Department of Medicine III, Medical University of Vienna, Hepatic Hemodynamic Lab, Department of Medicine III, Medical University of Vienna, Vienna, Austria; ⁴Barcelona Hepatic Hemodynamic Laboratory, Liver Unit, Hospital Clínic, Health Care Provider of the European Reference Network on Rare Liver Disorders (ERN-Liver), Institut d'Investigacions Biomèdiques August Pi i Sunyer (IDIBAPS), Barcelona, Catalonia, Spain; ⁵Digestive Diseases Unit, Hospital Arnau de Vilanova, Lleida, Spain; ⁶Department of Gastroenterology and Hepatology, Puerta de Hierro University Hospital, Puerta de Hierro Health Research Institute (IDIPHIM), CIBEREHD, Universidad Autónoma de Madrid, Majadahonda, Spain
Email: jifortea@gmail.com

Background and aims: Data on the effectiveness of classic non-cardioselective beta-blockers (cNSBBs, i.e., propranolol and nadolol) versus carvedilol in patients with cirrhosis are scarce. We aimed to compare their potential to prevent decompensation and mortality in patients with compensated and decompensated cirrhosis.

Method: Multicenter retrospective study, including patients with cirrhosis and clinically significant portal hypertension undergoing measurement of hepatic venous pressure gradient (HVPG) to assess the acute hemodynamic response to intravenous propranolol prior to the initiation of primary prophylaxis for variceal bleeding. A competitive risk analysis was performed after adjusting for baseline covariates using Inverse Probability of Treatment Weighting (IPTW). The main objectives were (i) the prevention of decompensation in compensated patients and (ii) death or further decompensation in decompensated patients, considering death, liver transplantation, and viral clearance as competitive events.

Results: A total of 540 patients with cirrhosis were included, 256 compensated (cNSBBs n = 111; carvedilol n = 145) and 284 decompensated (cNSBBs n = 134; carvedilol n = 150). In patients with compensated cirrhosis, the median age was 61.5 years (IQR 53.4–69.4), viral disease was the predominant etiology (39.5%) and the median MELD score was 9 (IQR: 8–11). Decompensated patients were younger (59.0 years; IQR: 51.9–65.7), with alcohol-related liver disease as the primary etiology (66%) and a higher MELD score (12 points; IQR: 10–15). In both cohorts, cNSBB were more frequently used in earlier years (i.e., 2008–2014) and among acute hemodynamic responders. Median follow-up were 43.8 months (compensated) and 32.5 months (decompensated). After covariate balancing with IPTW, Carvedilol, compared to cNSBBs, significantly reduced the risk of first decompensation in compensated patients (SHR 0.57; 95% CI 0.36–0.90; p = 0.014) and the combined end point of further decompensation/death in decompensated patients (SHR 0.68, 95% CI 0.49–0.96; p = 0.026). A second HVPG was conducted in 176 (68.8%, compensated cohort) and 177 patients (62.3%, decompensated cohort). Among non-responders, both compensated (11.1% vs. 29.4%; p = 0.422) and decompensated patients (16.0% vs. 43.6%; p =

0.0247) showed a threefold increase in likelihood of response with Carvedilol. Discontinuation rates for cNSBB and Carvedilol were comparable in compensated patients (6.3% vs. 9.0%; p = 0.488), but cNSBB discontinuation was higher in decompensated patients (11.3% vs 4.7%; p = 0.046), predominantly due to non-safety-related factors. **Conclusion:** Our data endorse the current recommendation favoring the use of carvedilol in the prevention of the first decompensation of cirrhosis and extend its preferential use in patients with decompensated cirrhosis without refractory ascites.

LBP-017

Liver-kidney crosstalk: the influence of hepatic oxalate release on kidney gluconeogenesis

Philipp Gabrys¹, Katharina Grgas¹, Jörg Reinders¹, Eduardo Salido², Jan G. Hengstler¹, Cristina Cadenas¹. ¹Leibniz Research Centre for Working Environment and Human Factors, Dortmund, Germany; ²Hospital Universitario de Canarias, Universidad La Laguna, San Cristobal de La Laguna (Canary Islands), Spain
Email: philipp.gabrys21@gmail.com

Background and aims: Primary hyperoxaluria type 1 is a metabolic disease that affects the kidney by the formation of oxalate precipitates. The elevated oxalate levels originate in the liver due to a dysfunction of the enzyme, alanine-glyoxylate aminotransferase (Agxt). Our previous studies identified a downregulation and promoter hypermethylation of Agxt in steatotic liver disease. Evidence exists that Agxt is implicated in amino acid-driven gluconeogenesis, and oxalate is reported to inhibit key enzymes in gluconeogenesis, such as pyruvate carboxylase and phosphoenolpyruvate carboxykinase. Consequently, the oxalate effect on global glucose homeostasis and how organs driving gluconeogenesis are affected, is still elusive. Thus, the aim of the study is to understand the contribution of Agxt/oxalate to gluconeogenesis in gluconeogenic organs, such as the liver and the kidney, which together maintain glucose homeostasis under fasting.

Method: The effect of oxalate on gluconeogenesis driven by gluconeogenic substrates like pyruvate/lactate, alanine and glycerol was studied in vitro in primary mouse hepatocytes (PMHs) isolated from Agxt knockout (KO) and wild type mice using a hepatic glucose production assay. Hormonal and substrate-dependent regulation of Agxt was studied *in vivo* and *in vitro* with common biomolecular techniques. Additionally, abnormalities in glucose homeostasis were investigated in AgxtKO mice analyzing gene expression changes in the liver and kidney using qPCR and immunoblots and plasma biochemistry and metabolites after fasting.

Results: In primary mouse hepatocytes (PMHs), exposure to oxalate or precursors, e.g. hydroxyproline, significantly decreased the *de novo* production of glucose from pyruvate/lactate and amino acids, but not from glycerol. Although fasting glucose levels did not significantly differ between wt and AgxtKO mice (which represent oxalemia and hyperoxaluria), gene expression alterations in gluconeogenic genes in response to fasting were more pronounced in the kidney of AgxtKO mice, indicating a compensatory shift towards glycerol-driven gluconeogenesis. Moreover, Agxt was upregulated by glucagon administration *in vivo* and *in vitro*, and by the gluconeogenic substrates pyruvate/lactate, amino acids, but not by glycerol.

Conclusion: The results suggest a role for Agxt in glucose homeostasis via regulation of oxalate generation in hepatocytes. High hepatic oxalate release resulting from Agxt downregulation appears to influence gluconeogenesis in the kidney where oxalate levels massively increase. When oxalate rises to levels high enough to inhibit pyruvate carboxylase, gluconeogenesis from pyruvate/lactate is expected to be impaired, and compensatory gluconeogenesis from glycerol will be predominant. The consequences of the switch to global glucose homeostasis are currently under investigation.

LBP-018

Promising first-in-human, first-in-class, Phase 1B immunogenicity data of VRON-0200, a novel checkpoint modifier containing immunotherapy, for HBV functional cure

Edward J. Gane¹, Sue Currie², Andrew Lubert², Hildegund Ertl³, Marie Bonhomme⁴, Grace Lai-Hung Wong⁵. ¹New Zealand Liver Transplant Unit, Auckland City Hospital, University of Auckland, Auckland, New Zealand; ²Virion Therapeutics, Philadelphia, United States; ³The Wistar Institute, Philadelphia, United States; ⁴PPD, Part of Thermo Fisher Scientific, Richmond, United States; ⁵The Chinese University of Hong Kong, Hong Kong, Hong Kong
Email: edgane@adhb.govt.nz

Background and aims: VRON-0200 is a therapeutic vaccine for functional cure of chronic hepatitis B virus (HBV) infection that expresses a genetically encoded checkpoint modifier (herpes simplex virus type 1 (HSV-1) glycoprotein D), fused with HBV core and polymerase antigens, designed to enhance, broaden, and prolong CD8⁺ T cell responses. Here we report the first-ever immunogenicity data, and ongoing safety data, in VRON-0200 vaccinated patients.

Method: Chronic HBV-infected, virally suppressed adults, with HBsAg levels ≤ 500 IU/ml, are randomized to receive VRON-0200 1×10^{10} vp via one of 2 different chimpanzee adenoviral vectors intramuscularly. Cohort 1a receives a prime, followed by a heterologous boost, on day 91; Cohort 1b receives prime only. A higher dose Cohort 2 (5×10^{10} vp) may begin once 12 Cohort 1 patients reach Day 28. Study assessments include safety, virologic, and immunologic parameters. T cell frequencies are assessed pre-vaccination (two timepoints) and at multiple post-vaccination timepoints, via ELISpot (IFN- γ ; LLOD <30 SFU/1e6) from PBMCs isolated from whole blood and incubated overnight using 3 separate peptide pools (core and pol representing the vaccine peptides, and peptides representing S antigen).

Results: As of March 15, 2024, 10 Cohort 1 pts received one dose of VRON-0200 (n = 5 each viral vector), and are included in the safety analysis; 6 pts have IFN- γ ELISpot results for 4 timepoints through Day 28 (2 pre-treatment (-28 to -7 , Day 1) and Days 14 and 28). For the 10 pts, 100% are male, 80% Asian, mean age, 44.5 yrs (range 41–54), median baseline HBsAg, 244 IU/ml (range: 16–623). After 641 pt safety days, there were no SAEs reported, and no study discontinuations; 1 pt reported 2 discrete AEs (1 considered TEAE; both resolved without treatment). In the 6 pts with ELISpot results, all are male, 5 Asian, with mean age of 44 yrs (range: 41–49); 5 are HBeAg-. As of Day 28, after VRON-0200 vaccination: 50% (3 of the 6 pts) showed increases in T cell frequencies to core; 2 of these 3 pts showed increases to both core and pol, despite having frequencies below LOD at baseline to both antigens. Three pts showed no consistent changes in T cell frequencies, after vaccination; one of those 3 had frequencies below LOD, at all timepoints evaluated. No sustained changes in frequencies to S antigen were observed in any pts through Day 28.

Conclusion: As of March 15, 2024, a single, intramuscular low dose of VRON-0200 was safe, well tolerated, and, in 50% of pts, increased or induced T cell responses, to one or both peptides, even in pts without immune responses at baseline, prior to vaccination. These data support VRON-0200's continued evaluation as a potential simple, easy-to administer, interferon-sparing immunotherapy for HBV functional cure. Further immunologic and safety analyses are ongoing and will be presented.

LBP-019

Safety and antiviral activity of AHB-137, a novel antisense oligonucleotide, in healthy volunteers and subjects with chronic hepatitis B

Edward J. Gane¹, Man-Fung Yuen², Wen Wang³, Chi-Yi Chen⁴, Yao-Chun (Holden) Hsu⁵, Eric Lawitz⁶, Joel Chua⁷, Jinlin Hou⁸, Hong Ren⁹, Xian Yu⁹, Chongyuan Xu⁸, Paul Yien Kwo¹⁰, Shyamasundaran Kottlilil⁷, Ira Jacobson¹¹, Wan-Long Chuang¹², Lung-Yi Mak², Wai-Kay Seto², Christian Schwabe¹³, Mingyue Chen¹⁴,

Di Zhao¹⁴, Chen Yang¹⁴, Miao Wang¹⁴, Cheng Yong Yang^{14,15}, Guofeng Cheng^{14,15}, Junqi Niu¹⁶, Yanhua Ding³. ¹University of Auckland, Auckland, New Zealand; ²Queen Mary Hospital, The University of Hong Kong, Hong Kong, China; ³Phase I Clinical Trial Center, The First Hospital of Jilin University, Changchun, China; ⁴Division of Gastroenterology and Hepatology, Department of Medicine, Ditmanson Medical Foundation Chiayi Christian Hospital, Chiayi, Taiwan; ⁵Center for Liver Diseases, E-DA Hospital, Kaohsiung, Taiwan; ⁶Texas Liver Institute, University of Texas Health San Antonio, San Antonio, United States; ⁷Division of Clinical Care and Research, Institute of Human Virology, University of Maryland School of Medicine, Baltimore, United States; ⁸Nanfeng Hospital, Southern Medical University, Guangzhou, China; ⁹The Second Affiliated Hospital, Chongqing Medical University, Chongqing, China; ¹⁰Division of Gastroenterology and Hepatology, Stanford University School of Medicine, Stanford, United States; ¹¹NYU Grossman School of Medicine, New York, United States; ¹²Kaohsiung Medical University Chung-Ho Memorial Hospital, Kaohsiung, Taiwan; ¹³New Zealand Clinical Research, Auckland, New Zealand; ¹⁴Asuper Biopharma, Hangzhou, China; ¹⁵AsuperBio Therapeutics, San Mateo, United States; ¹⁶The First Hospital of Jilin University, Changchun, China
Email: edgane@adhb.govt.nz

Background and aims: AHB-137 is a novel naked antisense oligonucleotide (ASO) that targets a highly conserved sequence close to the 3' end of hepatitis B virus (HBV) mRNA. AHB-137 has demonstrated a favorable pharmacokinetic (PK) and safety profile and potent antiviral activity in preclinical studies. Here, we report the safety and preliminary efficacy results from two phase I clinical studies of AHB-137 in healthy volunteers (HVs) and chronic hepatitis B (CHB) subjects.

Method: 40 HVs received either a single dose of AHB-137 up to 450 mg or multiple doses of 300 mg on Day 1, 4, 8, 15, and 22. A total of 52 hepatitis B e antigen (HBeAg) negative CHB subjects under stable nucleos(t)ide analogue (NA) treatment were enrolled and were dosed with up to 6 doses of 150 mg or 300 mg of AHB-137 within 4 weeks. All doses were administered subcutaneously. The baseline hepatitis B surface antigen (HBsAg) level was $<1,000$ IU/ml in 35 CHB subjects and was between 1,000 and 10,000 IU/ml in 17 CHB subjects (HighS subjects).

Results: All HVs successfully completed the study. There were no grade 4 adverse events (AEs), no study drug discontinuations due to AEs and no study drug related serious AEs (SAE). Overall, 30 HVs (75%) experienced treatment-related adverse events (TRAEs). All TRAEs were Grade 1 or 2, except for one Grade 3 injection site erythema. The most common TRAEs (incidence >1 subject) were injection site reactions, headache, nausea, pyrexia, and myalgia. CHB subjects enrolled were aged 26–63, mostly male (81%) and Asian (92%). To date, a total of 37 CHB subjects completed at least Day 29 visit. Among them, AHB-137 was dosed at 150 mg and 300 mg in 8 and 18 CHB subjects with HBsAg $<1,000$ IU/ml respectively and was dosed at 300 mg in 11 HighS subjects. HBsAg reduction $>1 \log_{10}$ IU/ml was achieved in 37.5% (3/8) subjects at 150 mg, in 55.6% (10/18) subjects at 300 mg, and in 45.4% (5/11) in HighS subjects at 300 mg. HBsAg reduction $>2 \log_{10}$ IU/ml was achieved in 12.5% (1/8) subjects at 150 mg, in 33.3% (6/18) subjects at 300 mg, and in 36.4% (4/11) in HighS subjects at 300 mg. To date, 5 subjects have achieved sustained HBsAg loss (HBsAg below lower limit of quantitation), including 2 with seroconversion (detectable hepatitis B surface antibody (HBsAb)) with a 4-week AHB-137 treatment. Maximum HBsAg reduction was reached between Day 29 and Day 50.

Conclusion: Single doses of AHB-137 up to 450 mg and multiple doses up to 300 mg for 4 weeks were safe and well tolerated in HVs and CHB subjects. Over $2 \log_{10}$ IU/ml HBsAg reduction was achieved in $>30\%$ CHB subjects with baseline HBsAg $<10,000$ IU/ml and could lead to sustained HBsAg loss with a 4-week AHB-137 treatment at 300 mg. AHB-137 monotherapy with background NA treatment demonstrated promising potential for achieving a functional cure of CHB.

LBP-020

A phase 1, double-blinded, randomized, placebo-controlled, multicenter global study evaluating the safety, tolerability, and antiviral activity of DF-006 in chronic hepatitis B, virologically-suppressed patients

Edward J. Gane¹, Eshwari Kovoov², Alina Jucov³, Igor Anastasiy⁴, Marta Dobryanska⁵, Susan Parker², Carl Cook², Cong Xu⁶, Tian Xu⁷, Henri Lichenstein², Jeysen Yogaratnam². ¹New Zealand Clinical Research, Auckland, New Zealand; ²Drug Farm, Inc., Guilford, United States; ³PMSI Republican Clinical Hospital "T. Mosneaga," Arensia Exploratory Medicine Phase I Unit, Nicolae Testemitanu State University of Medicine and Pharmacy, Chisinau, Moldova; ⁴Medical Center of LLC "Arensia Exploratory Medicine" Department of Clinical Trials, Kyiv, Ukraine; ⁵Municipal Non-Profit Enterprise "Kyiv City Clinical Hospital #12" Department of Emergency Medical Care, Kyiv, Ukraine; ⁶Drug Farm, Inc., Zhejiang Yao Yuan Biotechnology Ltd, Jiashan, China; ⁷Zhejiang Yao Yuan Biotechnology Ltd; Shanghai Yao Yuan Biotechnology Ltd, Shanghai, China
Email: edgane@adhb.govt.nz

Background and aims: DF-006, an oral (PO), small molecule prodrug, activates alpha-protein kinase 1 and stimulates host immune response in the liver. The ongoing Phase 1 study DF-006-1001 evaluates safety, pharmacokinetics, and pharmacodynamics (PD) of DF-006 or placebo (PBO) in healthy volunteers and the safety, antiviral activity, and PD of DF-006 in virologically-suppressed (VS) hepatitis B e antigen (HBeAg)-negative chronic hepatitis B (CHB) patients. Preliminary blinded safety and antiviral results from 2 completed CHB cohorts are presented below.

Method: The study consists of 3 CHB cohorts. The first (0.4 mcg DF-006/PBO) and second (0.7 mcg DF-006/PBO) cohorts have completed the study; the last cohort (1 mcg DF-006/PBO) is ongoing. DF-006 or PBO (6:2) was administered PO once weekly (QW) for 4 weeks (Days 1, 8, 15, and 22) with a previously prescribed nucleotide reverse transcriptase inhibitor (NRTI). After the last dose, subjects were followed up on Days 29, 36, 43, and 50. Of the 16 subjects randomized in the completed cohorts, 2 subjects from the 0.4 mcg DF-006/PBO cohort were excluded from efficacy analysis due to a protocol deviation pre-dosing.

Results: There were no serious adverse events, study discontinuations, adverse events of special interest, Grade 3–4 treatment emergent adverse events (TEAEs) or clinically significant vital signs, ECG, or urinalysis abnormalities. One subject (0.7 mcg DF-006/PBO) had mild alanine aminotransferase elevation 1 week after the last dose of the investigational product (IP); it was not related to the IP. There were 2 subjects with 3 TEAEs reported as possibly related to the IP (dysgeusia, asthenia, and fatigue); all were Grade 1 (mild) and resolved in 1–3 days without medical interventions. In subjects with baseline hepatitis B surface antigen (HBsAg) >2000 IU/ml (0.4 mcg DF-006, N=3; 0.7 mcg DF-006, N=4; PBO, N=1), at Day 36, reduction in HBsAg was seen in 33% and 75% for doses of 0.4 mcg and 0.7 mcg DF-006, respectively. At Day 50, reduction in HBsAg was seen in 67% and 50% subjects dosed with 0.4 mcg and 0.7 mcg DF-006, respectively. The PBO subject missed sample collection on Days 36 and 50, though no HBsAg reductions were seen on Days 22 and 29. Days 36 and 50 HBsAg reductions in DF-006 subjects ranged from approximately 0.02 log₁₀ IU/ml to 0.40 log₁₀ IU/ml. Throughout the study, hepatitis B virus (HBV) DNA and HBV RNA remained below the lower limit of quantification for all subjects.

Conclusion: DF-006 is safe and well tolerated in VS HBeAg-negative CHB subjects after 4 weeks of PO QW dosing up to 1 mcg. Most VS CHB subjects with baseline HBsAg >2000 IU/ml achieved off-treatment HBsAg reductions. These data support further evaluation of DF-006 in a Phase 2 study.

LBP-021

BRIL-179 induced functional immune response, demonstrating potential to improve chronic hepatitis B functional cure

Zhiliang Gao¹, Libo Yan², Jianping Li³, Rong Hu⁴, Peng Hu⁵, Wei Yue⁶, Fangfang Lv⁷, Yiwen Liu⁸, Chunming Li⁹, Yue Wu⁹, Weihong Liu⁹, Xiaofei Chen⁸, Qing Zhu⁹. ¹The Third Affiliated Hospital Sun YAT SEN University, Guangzhou, China; ²West China Hospital of Sichuan University, Chengdu, China; ³Guangzhou Eighth People's Hospital, Guangzhou, China; ⁴Public Health Clinical Center of Chengdu, Chengdu, China; ⁵The Second Affiliated Hospital of Chongqing Medical University, Chongqing, China; ⁶The First People's Hospital of Yunnan Province, Kunming, China; ⁷Sir Run Run Shaw Hospital, Hangzhou, China; ⁸Brii Biosciences, Shanghai, China; ⁹Brii Biosciences, Beijing, China
Email: yiwen.Liu@briibio.com

Background and aims: BRIL-179, a novel therapeutic vaccine comprised of PreS1, PreS2 and S hepatitis B virus (HBV) surface antigens that can induce functional HBV specific B-cell and T-cell immune responses is currently under evaluation in a randomized, double-blind, placebo-controlled phase 2a study in China. In the previous interim analyses, BRIL-179 as an add-on therapy in patients with chronic hepatitis B (CHB) receiving Peginterferon alfa (PEG) and nucleos (t)ide reverse transcriptase inhibitors (NRTI) therapy improved HBsAg loss at end-of-treatment (EOT) (Primary end point, 26.3% vs. 19.3% in full analysis set [FAS]) and the numerical difference maintained through 24-week post EOT. Besides, HBsAb ≥10 IU/L was strongly associated with sustained HBsAg loss at 12 weeks and 24 weeks post EOT.

Method: 114 HBeAg and HBsAb negative virally suppressed CHB patients who have been treated with 24–28 doses of PEG and HBsAg levels reduced to ≥0.05 and <100 IU/ml were randomized 1:1 to BRIL-179 or placebo every 3 weeks for 7 doses with PEG continued in both groups for another 24 weeks. Eligible patients with HBsAg <0.05 IU/ml for 2 consecutive visits at 12–24 weeks post EOT (Week 36 to 48) would be eligible to discontinue NRTI and be monitored for another 48 weeks. Safety and efficacy data as of the data cut-off date when all patients remain in study who discontinued NRTI and completed 24 weeks off-NRTI follow-up (36–48 weeks post EOT) were analysed and reported here.

Results: BRIL-179 + PEG combination was generally safe and tolerated with adverse events (AEs) similar to those observed with PEG or BRIL-179 as previously reported. The majority of AEs were Grade 1 or 2 in severity and the frequency of Grade 3 and above AEs were comparable between BRIL-179 group and PEG alone group. BRIL-179 + PEG group had higher percentage of patients discontinued NRTI by 24-week post EOT (FAS: 15/57, 26.3% vs. 9/57, 15.8%) and earlier NRTI discontinuation. No participant who discontinued NRTI required NRTI retreatment, 11 patients in BRIL-179 + PEG group and 7 patients in placebo + PEG group remain HBsAg loss and were still in follow-up. Within the NRTI discontinuation group, a higher percentage of patients on BRIL-179 had maximum post-baseline HBsAb ≥10 IU/L, ≥100 IU/L and ≥1000 IU/L. All but one patient experienced HBsAg rebound in the study had HBsAb <10 IU/L at EOT suggesting that strong treatment induced antibody responses are necessary to sustain the HBsAg loss.

Conclusion: The investigational BRIL-179 and PEG combination treatment was generally safe and tolerated. The BRIL-179 add-on induced functional immune responses, which improved HBsAg loss and NRTI discontinuation, demonstrating potential to improve CHB functional cure.

LBP-022

Preclinical safety data for PBGENE-HBV gene editing program supports advancement to clinical trials as a potentially curative treatment for chronic hepatitis B

Emily Harrison¹, Keely Dulmage¹, Katie Evans¹, Haley Grimason¹, Nicole Heard¹, Adepeju Aseyiga¹, Whitney Lewis¹, Ben Morris¹, Arpan Mukherjee¹, Traci Reddick¹, Andrew Van Cott¹, Dan Nazarenko¹, Ying Tam², Sean Semple², Neil Leatherbury¹, Janel Lape¹, Jeff Smith¹, Cassandra Gorsuch¹. ¹Precision BioSciences Inc., Durham, United States; ²Acuitas Therapeutics, Vancouver, Canada
Email: emily.harrison@precisionbiosciences.com

Background and aims: ARCUS nucleases are single-component gene editors that can be engineered for optimal safety leveraging the unique 3' DNA overhangs generated by ARCUS cuts. Systemically-administered ARCUS nucleases recently received approvals to initiate clinical trials for Ornithine Transcarbamylase (OTC) deficiency in neonatal patients. PBGENE-HBV is composed of an mRNA that encodes an ARCUS nuclease formulated in a clinically-utilized lipid nanoparticle (LNP) formulation. Preclinical efficacy models have shown that ARCUS nucleases have potential as a finite curative regimen for chronic hepatitis B due to their ability to eliminate covalently closed circular DNA and inactivate integrated HBV DNA resulting in durable reductions of HBV DNA and HBsAg. Given the potential for functional cure with this mechanism of action, preclinical safety of PBGENE-HBV was evaluated through a comprehensive specificity assessment and preclinical program to support advancement to clinical trials.

Method: The potential for PBGENE-HBV to create double strand breaks at unintended off-target sites in the human genome was assessed through a tiered approach. Potential off-target sites were identified orthogonally using genome-wide *in silico*, cellular, and biochemical assays and quantified using deep sequencing in HBV-infected primary human hepatocytes (PHH). Potential genomic rearrangements in untreated and ARCUS-treated PHH infected with HBV were evaluated using hybrid capture followed by long-read sequencing. The tolerability and pharmacokinetics of LNP-delivered ARCUS nucleases were tested at multiple dose-levels and after multiple administrations in non-human primates (NHPs).

Results: No off-target editing or editing-associated translocations were observed in HBV-infected PHH after treatment with PBGENE-HBV at therapeutically relevant doses. LNP-delivered ARCUS nucleases were well tolerated by NHPs and produced minor and transient elevations in liver transaminases typically associated with LNPs. Transaminase elevations normalized within 2 weeks after each dose administration and did not increase in magnitude after subsequent administrations. Components of the drug product, novel lipids and ARCUS mRNA, showed rapid clearance after administration without evidence of altered pharmacokinetics after multiple administrations.

Conclusion: ARCUS is a single-component gene editor that has been engineered to specifically cut HBV DNA leading to elimination of cccDNA and inactivation of integrated HBV DNA without impacting any sites in the human genome. LNP delivery of ARCUS mRNA was well tolerated in nonhuman primates over multiple administrations. Robust preclinical safety data supports the advancement of PBGENE-HBV to clinical trials as a potential curative, finite treatment for HBV.

LBP-023

Targeting RuvBL1 hampers NASH-HCC progression by tipping the scale from mTOR-driven lipogenesis to AMPK-induced lipolysis

Alice Guida¹, Irene Simeone¹, Dimitri Papini¹, Alice Giovannini¹, Simone Polvani¹, Gabriele Dragoni¹, Lucia Picariello¹, Andrea Galli¹, Tommaso Mello¹. ¹Department of Clinical and Experimental Biomedical Sciences "Mario Serio," University of Florence, Florence, Italy
Email: tommaso.mello@unifi.it

Background and aims: RuvBL1 belongs to the highly conserved AAA + ATPases. It is deregulated in various human cancers and its

expression correlates with a worse prognosis in HCC patients. We previously found that RuvBL1 haploinsufficiency impairs the PI3 K/ Akt/mTOR pathway in liver.

Given the relevance of mTOR pathway hyperactivation in HCC, we hypothesized that RuvBL1 genetic targeting could reduce mTOR-driven hepatocarcinogenesis.

Method: Pten^{hep-/-} and Ruvbl1^{hep±} mice were crossed to generate Pten^{hep-/-}Ruvbl1^{hep±} mice. NASH was assessed by histology at 12 weeks of age. Metabolic and inflammatory markers were evaluated by qPCR and IHC. mTOR pathway was analysed by WB of liver lysates. RuvBL1 interactome was evaluated by MS proteomics of RuvBL1-IP. HCC development was assessed by macroscopic tumour count and by histology. AML-12 PTEN KO cells were generated by CRISPR-Cas9 genome editing. TFEB nuclear translocation was evaluated by immunofluorescence. PPARalpha activity was evaluated by luciferase reporter assay. The publicly available dataset LIHC_TCGA was explored to investigate *in vivo* and *in vitro* pre-clinical models for human HCC.

Results: Pten^{hep-/-}Ruvbl1^{hep±} developed significantly less steatosis, fibrosis, and inflammation compared to Pten^{hep-/-} mice at 12 weeks of age. Pten^{hep-/-}Ruvbl1^{hep±} mice aged to 15 months showed better survival than Pten^{hep-/-} which developed significantly more HCC and of higher grade. The mTOR-driven lipogenic targets were similarly expressed in the two mice models. However, Ppara and its target CPT1 was increased in Pten^{hep-/-}Ruvbl1^{hep±}. The spontaneous and insulin-induced accumulation of lipid droplets in PTEN KO AML-12 cells was completely abrogated by RuvBL1 inhibition with CB-6644. Analysis of RuvBL1-IP in AML-12 revealed that RuvBL1 interacts with members of the lysosomal AMPK complex. Furthermore, p-AMPK and p-RAPTOR were increased in Pten^{hep-/-}Ruvbl1^{hep±} compared to Pten^{hep-/-} mice. Inhibition of RuvBL1 activity by CB-6644 increased TFEB nuclear translocation and PPARalpha transcriptional activity in AML-12 WT and PTEN KO. TCGA pathway analysis highlights a significant correlation between RUVBL1 expression and hyperactivation of the PI3K-mTOR pathway, clearly portrayed by the inverse correlation between RUVBL1 and PTEN. Accordingly, RUVBL1 positively correlates with PPARG and negatively correlates with PPARα, PGC1α, their direct targets CPT1A and several Acyl-CoA-dehydrogenases. Intriguingly, RUVBL1 shows either strong positive or negative correlation with different subunits of the AMPK complex.

Conclusion: RuvBL1 targeting reduces mTOR hyperactivation hampering NASH-HCC progression in Pten^{hep-/-} mice, likely promoting the switch from mTOR-driven lipogenesis to AMPK-induced fatty acid catabolism.

LBP-024

Performance of AASLD, AGA, AACE guidelines to identify patients for resmetirom treatment: pooled dataset including more than 4, 000 patients with liver biopsy

Stephen A. Harrison¹, Julie Dubourg², Sophie Jeannin Megnien², Larissa Goli³, Mazen Nouredin⁴, Naim Alkhouri⁵, Jörn M. Schattenberg⁶, Vlad Ratziu⁷. ¹Radcliffe Department of Medicine, University of Oxford, Oxford, United Kingdom; ²Summit Clinical Research, San Antonio, United States; ³Summit Clinical Research, San Antonio, United States; ⁴Houston Medical Research, Houston, United States; ⁵Arizona Liver Health, Chandler, United States; ⁶Saarland University Medical Center, Homburg, Germany; ⁷CH Pitié-Salpêtrière, Paris, France
Email: jdubourg@summitclinicalresearch.com

Background and aims: Resmetirom, a THR-β agonist, is the first and only treatment approved for metabolic dysfunction-associated steatohepatitis (MASH) as of March 2024. Resmetirom label indicates to treat patients with MASH and moderate to advanced fibrosis consistent with F2/F3. There is no requirement for liver biopsy. We aimed to describe the accuracy of AASLD, AGA and AACE guidelines and of non-invasive biomarkers to identify patients for resmetirom treatment.

Method: We combined screening data from 10 industry-funded MASH phase 2 trials. The target population for resmetirom treatment was defined as patients with MASH (at least 1 point in each component) and moderate (F2) to advanced (F3) fibrosis. We described the proportion of patients meeting those criteria according to existing guideline thresholds. We also explored additional biomarkers to further identify patients for resmetirom treatment.

Results: 4,025 patients with centrally assessed liver biopsy were included in this analysis. Among them, 1,490 (37%) met the criteria for resmetirom treatment, 441 (11%) had cirrhosis, 1,787 (44%) had F0-F1, and 307 (8%) had F2-F3 without MASH. Among the patients considered as low risk who would not have an indication for resmetirom treatment according to existing guidelines, 31% met the criteria for resmetirom treatment, 4% had cirrhosis, 58% had F0-F1, and 7% had F2-F3 without MASH. Among the patients considered as intermediate or high risk who would have an indication for resmetirom treatment according to guidelines, 46% met the criteria for resmetirom treatment, 20% had cirrhosis, 27% had F0-F1, and 7% had F2-F3 without MASH. Among the group of patients with AST ≥ 40 (if HbA1c $< 6.5\%$) or AST ≥ 30 (if HbA1c $\geq 6.5\%$), 53% met the criteria for resmetirom treatment, 13% had cirrhosis, 28% had F0-F1, and 6% had F2-F3 without MASH. In the patients who do not meet these AST/HbA1c thresholds, 25% met the criteria for resmetirom treatment, 9% had cirrhosis, 58% had F0-F1, and 8% had F2-F3 without MASH. Among the group of patients with FAST ≥ 0.67 (if HbA1c $< 6.5\%$) or FAST ≥ 0.50 (if HbA1c $\geq 6.5\%$), 60% met the criteria for resmetirom treatment, 19% had cirrhosis, 17% had F0-F1, and 4% had F2-F3 without MASH.

Conclusion: The current guidelines support the appropriate selection of patients for resmetirom treatment. However, there is a significant proportion of patients requiring treatment that will not be identified and a non-negligible proportion of patients who do not require treatment that will be treated. Alternative simple biomarkers increase accurate selection of patients. This highlights the need for a refined approach to identify patients for resmetirom treatment using combinations of NITs and their correlation to outcomes.

LBP-025

Shortened telomeres impact liver regeneration in mice

Michael Hu¹, Mark Tiguer¹, Melissa Rowe¹, Yehuda Tzfati², Klaus Kaestner¹. ¹University of Pennsylvania, Philadelphia, United States; ²The Hebrew University of Jerusalem, Jerusalem, Israel
Email: kaestner@pennmedicine.upenn.edu

Background and aims: Telomeres, or the ends of linear chromosomes, consist of a short repeat sequence (TTAGGG in humans and mice) which is complexed with shelterin proteins that protect chromosome ends and are thus critical for maintaining genomic integrity. The *Mus musculus* strain C57BL/6 is the most widely used inbred strain of laboratory mouse to model human disease. The C57BL/6 mouse has telomeres about 5 times longer than those present in humans. We recently engineered the C57BL/6 "telomouse" with human-length telomeres by introducing into *Mus musculus* a single amino acid variation in the helicase 'Regulator of telomere elongation 1' (*Rtel1*), enabling the study of human length telomeres in proliferation during short-term liver regeneration. In a partial hepatectomy (PHx) experiment, where two-thirds of the liver is surgically resected, strikingly, the remaining lobes of the liver grow to compensate for the excised liver mass within one-week post-surgery. Here, we employed our unique telomouse model to study the effects of shortened telomeres on short-term liver regeneration.

Method: 70% PHx surgical procedures were performed on telomice and age-matched wild-type C57BL/6 control mice. At 36 hours post-PHx, mice were intraperitoneally injected with 5-chloro-2'-deoxyuridine (CldU) with a dose of 100 mg/kg of weight. At 46 hours post-PHx, mice were intraperitoneally injected with 5-iodo-2'-deoxyuridine (IdU) with a dose of 100 mg/kg of weight. CldU and IdU are both thymidine analogs that incorporate into nuclear DNA during cells'

S-phase. Staggering CldU and IdU injections allowed us to observe the different timings of proliferation for particular cell types. At the 48-hour end point the remaining liver was perfused and processed for histology. Immunofluorescence staining visualized CldU, IdU, and DAPI (nuclear stain). Other markers such as CK19 (cholangiocyte marker) and HNF4alpha (hepatocyte marker) were used to differentiate cholangiocytes and hepatocytes.

Results: By using CK19/CldU labeling, we found that *Rtel1* mutant mice display decreased cholangiocyte proliferation at the 36 hours time point compared to the wild type control. By using CK19/IdU labeling, we found that the cholangiocyte proliferation rate of *Rtel1* mutant mice further decreased at the 46 hours time point. In contrast, wild type control mice display increased proliferation at the 46 hours time point compared to the 36 hours time point. We did not observe significant hepatocyte proliferation in either *Rtel1* or control mice at the 36 hours time point. However, at the 46 hours time point, analysis of the HNF4alpha/IdU staining results showed that *Rtel1* mutant mice also exhibit reduced proliferative capacity compared to the wildtype control.

Conclusion: Our results suggest that human-length telomeres limit the proliferative capacity of cholangiocytes and hepatocytes in short-term liver regeneration in mice.

LBP-026

The global prospective observational study to evaluate the role of 'liver transplantation in patients with cirrhosis and severe acute-on-chronic liver failure (CHANCE)': study design, demographics and overall outcome

Thierry Gustot¹, William Bernal², Javier Fernández^{3,4}, Juan Manuel Diaz³, Carlos de la Peña-Ramírez³, Alberto Farias⁵, Patricia Momoyo Zitelli⁶, Alexander Kuo⁷, Nicholas Nissen⁸, Sebastián Marciano⁹, Adrian Gadano¹⁰, Rachel Westbrook¹¹, Rebecca Bateman¹¹, Ashwin Rammohan¹², Dinesh Jothamani¹³, Surendran Sudhindran¹⁴, Arun Valsan¹⁴, Pablo Ruiz^{15,16}, Giulia Pagano¹⁷, Luis Bagulho^{18,19}, Hugo Pinto Marques^{20,21}, Luca Saverio Belli²², Giovanni Perricone²³, Nazia Selznér²⁴, Cynthia Tsien²⁴, Juan F. Gallegos-Orozco²⁵, Nyingi Kemmer^{26,27}, Kiran Dhanireddy²⁸, Manuel Mendizabal²⁹, Josefina Pages²⁹, Christina Lindenmeyer³⁰, Bijan Eghtesad³⁰, Valerio Lucidi³¹, Laure Elkrief³², Joanna Raszeja-Wyszomirska³³, Margarita Anders³⁴, Silvio Nadalin³⁵, Antonio Siniscalchi³⁶, Giulia Tosetti³⁷, Carmen Vinaixa³⁸, Michael Kriss³⁹, Prasun Jalal⁴⁰, Baptiste Michard⁴¹, Paolo Angel^{3,42}, Graciela Castro-Narro⁴³, Karim Boudjema⁴⁴, Kirti Shetty⁴⁵, Caroline den Hoed⁴⁶, Livia Carone⁴⁷, Sezai Yilmaz⁴⁸, Angelo Z. Mattos⁴⁹, Rosa Martin-Mateos^{50,51}, Maximilian Joseph Brol⁵², Tomoharu Yoshizumi⁵³, Francois Durand⁵⁴, Sylvie Radenne⁵⁵, Helen Te⁵⁶, Isabel Campos-Varela⁵⁷, Wim Laleman^{58,59}, Masahiro Ohira⁶⁰, Susumu Eguchi⁶¹, Cornelius Engelmann⁶², Felix Braun⁶³, Marie Sinclair⁶⁴, José Ursic Bedoya⁶⁵, Carmelo Loinaz^{66,67}, Thamara Perera⁶⁸, Arvinder Singh Sooin⁶⁹, Ken Liu⁷⁰, Sarah Raevens⁷¹, Rebecca Bishop⁷², Kenneth J. Simpson⁷³, Nobuhisa Akamatsu⁷⁴, Yong Chee Chien⁷⁵, Gabriela Berlakovich⁷⁶, Juan Ignacio Marin Zuluaga⁷⁷, Lance Stein⁷⁸, Yaman Tokat⁷⁹, Ruben Hernaez⁸⁰, Christophe Duvoux⁸¹, Faouzi Saliba⁸², Geoff McCaughan⁸³, Constantino Fondevila⁸⁴, Elizabeth Pomfret⁸⁵, Mohamed Rela¹³, Vinay Sundaram⁷, Joan Claria^{3,86,87,88}, Vicente Arroyo³, Foix Valles^{3,89}, Jorge Carlos Martínez^{3,90}, Pedro Izquierdo-Bueno³, Didier Samuel⁹¹, Marina Berenguer³⁸, Anna Bosch³, Cristina Sanchez³, Wojciech Polak⁴⁶, Constantine Karvellas⁹², Jonel Trebicka^{3,93}, Richard Moreau^{3,94}, Rajiv Jalan^{95,96}. ¹Liver Transplant Unit, HUB Hôpital Erasme, Université Libre de Bruxelles, Bruxelles, Belgium; ²King's College Hospital, London, United Kingdom; ³European Foundation for the Study of Chronic Liver Failure (EF CLIF), Barcelona, Spain; ⁴Liver unit Hospital Clínic Barcelona, Barcelona, Spain; ⁵Department of Gastroenterology, Hospital das Clínicas, University of São Paulo School of Medicine, Sao Paulo, Brazil; ⁶Hospital das Clínicas da Faculdade de Medicina da Universidade de São Paulo, Sao Paulo, Brazil; ⁷Cedars-Sinai

POSTER PRESENTATIONS

Medical Center, Karsh Division of Gastroenterology and Hepatology, Comprehensive Transplant Center, Los Angeles, United States; ⁸Cedars-Sinai Medical Center, Department of Surgery, Comprehensive Transplant Center, Los Angeles, United States; ⁹Liver Unit and Department of Research, Hospital Italiano de Buenos Aires, Buenos Aires, Argentina; ¹⁰Liver Unit and Department of Research, Hospital Italiano de Buenos Aires, Buenos Aires, Argentina; ¹¹Royal Free Hospital, London, United Kingdom; ¹²Rela Institute of Liver Disease and Transplantation, Chennai, India; ¹³Dr.Rela Institute & Medical Centre, Chennai, India; ¹⁴Amrita Institute of Medical Sciences, Kochi, India; ¹⁵Liver unit Hospital Clinic, Barcelona; ¹⁶IDIBAPS, Universitat de Barcelona, Barcelona, Spain; ¹⁷Liver Unit, Hospital Clinic, IDIBAPS, Univ. Barcelona, Barcelona, Spain; ¹⁸Hepato-Biliary-Pancreatic and Transplantation Centre, Curry Cabral Hospital, Local Health Unit of São José, Lisbon, Portugal; ¹⁹NOVA Medical School, Lisbon, Portugal; ²⁰Hepato-Biliary-Pancreatic and Transplantation Centre, Curry Cabral Hospital, Local Health Unit of São José, Lisbon, Portugal; ²¹NOVA Medical School, Lisbon; ²²Department of Gastroenterology and Hepatology, Liver Transplant Center GOM Niguarda, Milan, Italy; ²³Department of Gastroenterology and Hepatology, Liver Transplant Center GOM Niguarda, Milan; ²⁴Ajmera Transplant Center, University of Toronto, Toronto, Canada; ²⁵Division of Gastroenterology and Hepatology, Spencer Fox Eccles School of Medicine, University of Utah, Utah, United States; ²⁶Liver Transplant Program, TGH, Director, Hepatology Program, TGMG, Tampa, United States; ²⁷USF Tampa, Tampa, United States; ²⁸Tampa General Hospital, Tampa, United States; ²⁹Hepatology and Liver Transplant Unit, Hospital Universitario Austral, Pilar, Argentina; ³⁰Department of Gastroenterology, Hepatology and Nutrition, Cleveland Clinic, Cleveland, United States; ³¹Liver Transplant Unit, HUB Hôpital Erasme, Université Libre de Bruxelles, Bruxelles, Belgium; ³²CHRU Tours-Hôpital Trousseau, Tours; ³³Medical University of Warsaw, Warsaw, Poland; ³⁴Hospital Aleman, Buenos Aires, Argentina; ³⁵University Hospital Tübingen, Dpt of General, Visceral and Transplant Surgery, Tübingen, Germany; ³⁶Alma Mater Studiorum University of Bologna, Bologna, Italy; ³⁷Foundation IRCCS Ca' Granda Ospedale Maggiore Policlinico - Division of Gastroenterology and Hepatology, Milan, Italy; ³⁸Hospital Universitari i Politècnic La Fe, Valencia, Spain; ³⁹Division of Gastroenterology & Hepatology, Department of Medicine, University of Colorado School of Medicine and Colorado Center for Transplantation Care, Research and Education, University of Colorado School of Medicine, Denver, United States; ⁴⁰Baylor St. Luke's Medical Centre, Houston, United States; ⁴¹Liver transplant unit, Strasbourg university hospital, Strasbourg, France; ⁴²Unit of Internal Medicine and Hepatology, Department of Medicine, University of Padova, Padova, Italy; ⁴³National Institute of Medical Sciences and Nutrition "Salvador Zubirán" Mexico City, Mexico City, Mexico; ⁴⁴CHU Rennes, Hôpital De Pontchaillou, Rennes, France; ⁴⁵University of Maryland Medical Center, Baltimore, United States; ⁴⁶Department of Gastroenterology and Hepatology, Erasmus MC Transplant Institute, University Medical Center Rotterdam, Rotterdam, Netherlands; ⁴⁷Liver Transplant Unit of Federal University of Ceará, Fortaleza, Brazil; ⁴⁸Inonu University Liver Transplantation Institute, Malatya, Turkey; ⁴⁹Federal University of Health Sciences of Porto Alegre, and Gastroenterology and Hepatology Unit, Irmandade Santa Casa de Misericórdia de Porto Alegre, Porto Alegre, Brazil; ⁵⁰Gastroenterology Department, Hospital Universitario Ramón y Cajal, Madrid. Universidad de Alcalá. Instituto Ramón y Cajal de investigación sanitaria (IRYCIS), Madrid, Spain; ⁵¹Centro de Investigación Científica en Red de Enfermedades Hepáticas y Digestivas (CIBEREHD), Madrid; ⁵²University of Münster, Münster, Germany; ⁵³Kyushu University Hospital, Kyushu, Japan; ⁵⁴Hopital Beaujon AP-HP, Paris, France; ⁵⁵APHP Hôpitaux Universitaires Pitié Salpêtrière, Paris, France; ⁵⁶Center for Liver Diseases, University of Chicago Medicine, Chicago, United States; ⁵⁷Hospital Universitari Vall d'Hebron, Barcelona, Spain; ⁵⁸Department of Gastroenterology and Hepatology, Section of Liver & Biliopancreatic disorders and Liver transplantation, University Hospitals Leuven, Leuven, Belgium; ⁵⁹Medizinische Klinik B, Leuven, Belgium; ⁶⁰Hiroshima University Hospital, Hiroshima, Japan; ⁶¹Department of surgery, Nagasaki University Graduate School of Biomedical Sciences, Nagasaki,

Japan; ⁶²Charité-Universitätsmedizin Berlin, Department of Hepatology and Gastroenterology, Berlin, Germany; ⁶³University Medical Center Hamburg-Eppendorf, Hamburg; ⁶⁴Victorian Liver Transplant Unit, Austin Health, Austin, Australia; ⁶⁵Hepatogastroenterology Unit, CHU Saint Eloi, Montpellier University, Montpellier, France; ⁶⁶HBP-Transplantation Surgery. 12 de Octubre University Hospital, Madrid, Spain; ⁶⁷Complutense University of Madrid, Madrid, Spain; ⁶⁸Queen Elizabeth Hospital Birmingham, Birmingham, United Kingdom; ⁶⁹Medanta Medcity, Medanta, India; ⁷⁰AW Morrow Gastroenterology and Liver Centre, Royal Prince Alfred Hospital, Sydney, NSW, Australia; Faculty of Medicine and Health, University of Sydney, Sydney, Australia; ⁷¹Dept of Gastroenterology and Hepatology, Ghent Liver Research Center, Ghent University Hospital, Ghent, Belgium; ⁷²Leeds Teaching Hospital, Leeds, United Kingdom; ⁷³Scottish Liver Transplant Unit, Royal Infirmary, Edinburgh, United Kingdom; ⁷⁴Artificial Organ and Transplantation Surgery Division, Department of Surgery, Graduate School of Medicine, University of Tokyo, Tokyo; ⁷⁵Kaohsiung Chang Gung Memorial Hospital, Kaohsiung, Taiwan; ⁷⁶Division of Transplantation, Medical University of Vienna, Vienna, Austria; ⁷⁷Hospital Pablo Tobón Uribe, Medellín, Colombia; ⁷⁸Piedmont Transplant Institute, Piedmont Atlanta Hospital, Atlanta, United States; ⁷⁹International Liver Center and Acibadem Healthcare Hospitals, Acibadem, Turkey; ⁸⁰Michael E. DeBakey VA Medical Center and Baylor College of Medicine, Houston, United States; ⁸¹Medical Liver Transplant Unit, Department of Hepatology, Henri Mondor Hospital APHP- Paris Est University, Paris, France; ⁸²AP-HP Hopital Paul Brousse, Centre hépatobiliaire, Paris, France; ⁸³Royal Prince Alfred Hospital, Sydney, Australia; ⁸⁴Hospital La Paz, Madrid, Spain; ⁸⁵University of Colorado, Denver, United States; ⁸⁶Biochemistry and Molecular Genetics Service, Hospital Clínic-IDIBAPS, Barcelona, Spain; ⁸⁷CIBERehd, Barcelona, Spain; ⁸⁸Department of Biomedical Sciences, University of Barcelona, Barcelona, Spain; ⁸⁹Liver unit Hospital Clínic, Barcelona, Spain; ⁹⁰Hospital italiano de Buenos Aires, Buenos Aires, Argentina; ⁹¹Centre Hepatobiliaire, Hopital Paul Brousse, Université Paris-Saclay, Inserm Unit 1193, Paris, France; ⁹²Department of Critical Care Medicine and Division of Gastroenterology (Liver Unit), University of Alberta, Alberta, Canada; ⁹³Medizinische Klinik B, Münster, Germany; ⁹⁴Institut National de la Santé et de la Recherche Médicale, Université Paris Cité, Centre de Recherche sur l'Inflammation, Paris, France; ⁹⁵European Foundation for the Study of Chronic Liver Failure, Barcelona; ⁹⁶Liver Failure Group, Institute for Liver Disease Health, University College London, Royal Free Hospital, London, United Kingdom
Email: rajiv.jalan@efclif.com

Background and aims: Acute-on-chronic liver failure (ACLF) is characterized by increasing risk of short-term mortality with number of organ failures. Liver transplantation (LT) improves the survival of these patients. However, the current worldwide organ allocation systems are principally based on the model for end-stage liver disease (MELD) scores or its variations, which underestimate death of ACLF patients. The aim of the global CHANCE study sponsored by EF CLIF and supported by ILTS and ELITA was to characterize, in the current allocation systems, the clinical outcomes of patients with ACLF 2,3 undergoing LT. This interim study describes the study design, demographics and overall outcomes.

Method: 66 LT centers from 21 countries recruited patients to this prospective observational study, (12 Asia [AS], 35 Europe [EU], 8 Latin America [LA], 11 North America [NA]). 549 investigators were involved and managed by 16 regional coordinators. Patients were recruited from July 2021 to October 2023. ACLF was defined by the EASL-CLIF-C criteria. The intention-to-treat survival of patients from the Group 1 (patients with ACLF 2,3 listed for LT), the Group 2 (patients with ACLF 0,1 listed for LT) and the Group 3 (patients with ACLF 2,3 referred to the waitlist evaluation but not listed) were assessed.

Results: Data from 823 patients (80% of the overall study cohort) is reported here: 92 patients were recruited from AS, 354 from EU, 188 from LA and 189 from NA; 376 patients were in Group 1, 313 in Group

2, and 134 in Group 3. LA patients were older than patients from other regions [57 (46, 64)] and higher proportion of male was observed in AS (83%). The main etiology of cirrhosis was related to alcohol in all continents but less frequently in LA (50–67% vs. 33%, $p < 0.001$). Centers from NA included patients with higher MELD [34 (30–40)] compared to those from other regions. Centers from EU and NA recruited more ACLF 3 patients compared to those from AS and LA (33% and 39% vs. 16% and 26% respectively, $p < 0.001$). In an intention-to-transplant analysis, less patients of the Group 1 were alive the 3-month post-LT time point compared to those of the Group 2 (66% vs. 78%, $p < 0.001$). Only 15% of Group 3 patients survived.

Conclusion: The interim results of the CHANCE study reveal significant differences in the characteristics of ACLF patients listed for LT. In those that were not transplanted, mortality exceeded 85%. Patients with ACLF 2,3 have a lower probability of accessing LT and being alive at 3-months than patients with ACLF 0,1, providing the rationale for expedited LT for these patients.

LBP-027

Combined effect of obeticholic acid and bezafibrate in patients with primary biliary cholangitis and inadequate response or intolerance to ursodeoxycholic acid: 6-month results from a phase 2 trial

David E. Jones¹, Alexandre Louvet², Christophe Corpechot³, Vaclav Hejda⁴, Heng Zou⁵, Antonio Civitarese⁵, Alejandra Villamil⁶, Frederik Nevens⁷. ¹Newcastle University, Newcastle upon Tyne, United Kingdom; ²University Hospital of Lille, Lille, France; ³Reference Center for Inflammatory Biliary Diseases and Autoimmune Hepatitis, European Reference Network on Hepatological Diseases (ERN Rare-Liver), Sorbonne University, Paris, France; ⁴University Hospital in Pilsen, Pilsen, Czech Republic; ⁵Intercept Pharmaceuticals, Inc., Morristown, United States; ⁶Hospital Italiano de Buenos Aires, Buenos Aires, Argentina; ⁷University Hospital KU Leuven, Leuven, Belgium
Email: david.jones@newcastle.ac.uk

Background and aims: Obeticholic acid (OCA) and bezafibrate (BZF) have each improved serum biomarkers of primary biliary cholangitis (PBC)-related liver damage. We assessed the effects of combination OCA + BZF vs placebo + BZF on serum biomarker levels and safety/tolerability. A range of doses and formulations was explored in patients (pts) with PBC who had inadequate response or intolerance to ursodeoxycholic acid.

Method: This randomized, double-blind (DB), active-controlled, phase 2 trial randomized pts 1:1:1:1 to once-daily oral BZF 200 mg (B200) immediate release (IR), BZF 400 mg (B400) sustained release (SR), OCA 5 mg titrated to 10 mg at week 4 + BZF 200 mg IR (OCA/B200 IR), or OCA 5 mg titrated to 10 mg at week 4 + BZF 400 mg SR (OCA/B400 SR) during a 12-week DB treatment period. After a DB follow-up period, pts then received once daily OCA/B400 SR in a 96-week open-label long-term safety extension (LTSE). Here, we present data from month 6 (12-week DB treatment period + 12 weeks of LTSE). Percentage change from baseline and normalization rate of alkaline phosphatase (ALP; \leq upper limit of normal [ULN]) and total bilirubin (TB; $\leq 0.6 \times$ ULN) were assessed. Biochemical remission was defined as normalization (\leq ULN) or $\geq 40\%$ reduction in ALP; gamma-glutamyl transferase, alanine aminotransferase, and aspartate aminotransferase \leq ULN; and TB $\leq 0.6 \times$ ULN. GLOBE and UK-PBC scores estimated the risk of death and liver transplantation and were compared at baseline and month 6. Safety was assessed by treatment-emergent adverse events (TEAEs). Metabolic safety outcomes, including percentage change in total and low-density lipoprotein (LDL) cholesterol, were also assessed.

Results: The DB treatment period included 75 pts; 66 pts continued to the LTSE. At month 6, OCA/B400 SR demonstrated a 65.3% reduction in ALP and 27.6% reduction in TB; 61.1% of pts in this cohort achieved ALP \leq ULN and 83.3% achieved TB $\leq 0.6 \times$ ULN. OCA/B400 SR induced biochemical remission in 66.7% of pts, and 77.8% of pts experienced $\geq 40\%$ reduction in ALP from baseline. Compared with

the other cohorts, OCA/B400 SR induced the greatest change in GLOBE (−0.7) and UK-PBC (−1.1) scores. TEAEs were generally balanced across cohorts. In the OCA/B400 SR cohort, 1 pt discontinued due to a serious TEAE of pruritus. The rate of new events of pruritus with OCA/B400 SR was low (11.1%) at month 6. OCA/B400 SR also demonstrated the greatest percentage reductions in total cholesterol (19.6%) and LDL cholesterol (18.7%).

Conclusion: These results suggest that OCA + BZF is generally well tolerated and has therapeutic potential to normalize multiple serum biomarkers associated with improved transplant-free and decompensation-free survival. Low rates of pruritus were observed with OCA/B400 SR, which were substantially lower than those with OCA in the phase 3 POISE study (56%–68%). The data support phase 3 development of the SR formulation of BZF with low doses of OCA.

LBP-028

Effect of elafibranor on pruritus in primary biliary cholangitis: symptom severity and quality of life measurements from the phase III ELATIVE® trial

Andreas E. Kremer¹, Kris V. Kowdley², Cynthia Levy³, Marlyn J. Mayo⁴, Jörn M. Schattenberg⁵, Nuno Antunes⁶, Elaine Böing⁶, Dimitar Tonev⁷, Nathan Touati⁷, David Jones⁸. ¹Department of Gastroenterology and Hepatology, University Hospital Zurich, University of Zurich, Zurich, Switzerland; ²Liver Institute Northwest, Seattle, WA, United States; ³Schiff Center for Liver Diseases, University of Miami, Miami, FL, United States; ⁴Division of Digestive and Liver Diseases, University of Texas Southwestern Medical Center, Dallas, TX, United States; ⁵Department of Internal Medicine II, Saarland University Medical Center, Homburg, Germany; ⁶Ipsen, Cambridge, MA, United States; ⁷Ipsen, Boulogne-Billancourt, France; ⁸Institute of Cellular Medicine and NIHR Newcastle Biomedical Research Center, Newcastle University, Newcastle Upon Tyne, United Kingdom
Email: andreas.kremer@usz.ch

Background and aims: Primary biliary cholangitis (PBC) is a rare autoimmune cholestatic liver disease, in which pruritus is a commonly reported symptom that negatively impacts quality of life (QoL). In the phase III ELATIVE® trial, elafibranor, a dual peroxisome proliferator-activated receptor (PPAR)-alpha/delta agonist, significantly improved prognostic biomarkers of cholestasis in PBC. Here, the effect of elafibranor on the patient (pt)-reported pruritus measures 5-D Itch and PBC-40 Itch is reported.

Method: The 5-D Itch and PBC-40 questionnaires were recorded at each study visit in ELATIVE® (NCT04526665), in which pts with PBC were randomised to elafibranor 80 mg or placebo. 5-D Itch has 5 domains, with scores for each ranging from 1 to 5, for a total of 5 (no pruritus) to 25 (most severe). PBC-40 has 6 domains, including a PBC-40 Itch domain consisting of 3 questions for a maximum score of 15 (most severe). Change from baseline (BL) to Week (Wk) 52 in 5-D Itch and PBC-40 Itch in pts with moderate-to-severe pruritus (BL PBC Worst Itch Numeric Rating Scale [PBC WI-NRS] $\geq 4/10$) is reported. Analyses of total scores used a mixed model for repeated measures with treatment, visits until Wk 52 and treatment by visit interaction as fixed factors, and adjusted for BL scores and stratification factors; p values are nominal. Shifts in responses from BL to Wk 52 to specific individual 5-D Itch domains/questions and PBC-40 Itch questions were analysed post hoc and are descriptively presented.

Results: Of 161 randomised pts, 66 (41%) had moderate-to-severe pruritus at BL (elafibranor: 44; placebo: 22). Pts receiving elafibranor had greater reductions at Wk 52 in 5-D Itch total score vs placebo (LS mean difference [95% CI]: −3.0 [−5.5, −0.5]; $p = 0.0199$). For the Duration domain, 14/24 (58%) pts receiving elafibranor had itching duration reduced from ≥ 6 hours/day to < 6 hours/day from BL to Wk 52 vs 3/11 (27%) pts receiving placebo. In response to the sleep question of the Disability domain, 20/25 (80%) pts receiving elafibranor with at least frequently delayed sleep (score ≥ 3) improved to occasionally delayed sleep or no disturbance (score < 3) from BL to Wk 52 vs 3/10 (30%) pts receiving placebo.

POSTER PRESENTATIONS

Pts receiving elafibranor had greater, clinically meaningful, ^{1, 2} reductions at Wk 52 in PBC-40 Itch total score vs placebo (LS mean difference [95% CI]: -2.3 [-4.0, -0.7]; p = 0.0070). Similar reductions to those observed in 5-D Itch domains from BL to Wk 52 were seen in mean scores for the individual PBC-40 Itch questions with elafibranor vs placebo.

Conclusion: In pts with PBC, elafibranor resulted in improvements in 5-D Itch and PBC-40 Itch, emphasising its potential to reduce both the severity of pruritus and impact on QoL, and address an important unmet need.

References

1. Jones D. *Hepatol Commun.* 2023;7(3):e0057.
2. Jopson L. *BMJ Open.* 2015;5(8):e007985. Study sponsor: GENFIT; secondary analysis and publication sponsor: Ipsen.

LBP-029

Efficacy and safety of 144 weeks of bulevirtide 2 mg or 10 mg monotherapy from the ongoing phase 3 study, MYR301

Pietro Lampertico^{1,2}, Soo Aleman³, Maurizia Brunetto^{4,5}, Antje Blank⁶, Pietro Andreone⁷, Pavel Bogomolov⁸, Vladimir Chulanov⁹, Nina Mamonova⁹, Natalia Geyvandova¹⁰, Viacheslav Morozov¹¹, Olga Sagalova¹², Tatyana Stepanova¹³, Grace M. Chee¹⁴, Dmitry Manuilov¹⁴, Mingyang Li¹⁴, Steve Tseng¹⁴, Audrey Lau¹⁴, Anu Osinusi¹⁴, Julian Schulze zur Wiesch¹⁵, Markus Cornberg¹⁶, Stefan Zeuzem¹⁷, Heiner Wedemeyer¹⁶. ¹Division of Gastroenterology and Hepatology, Foundation IRCCS Ca' Granda Ospedale Maggiore Policlinico, Milan, Italy; ²CRC "A. M. and A. Migliavacca" Center for Liver Disease, Department of Pathophysiology and Transplantation, University of Milan, Milan, Italy; ³Karolinska University Hospital/Karolinska Institutet, Department of Infectious Diseases, Stockholm, Sweden; ⁴University Hospital of Pisa, Hepatology Unit, Reference Center of the Tuscany Region for Chronic Liver Disease and Cancer, Pisa, Italy; ⁵University of Pisa, Department of Clinical and Experimental Medicine, Pisa, Italy; ⁶Heidelberg University Hospital, Medical Faculty Heidelberg/Heidelberg University Hospital, Department of Clinical Pharmacology and Pharmacoevidemiology, Heidelberg, Germany; ⁷University of Modena and Reggio Emilia, Internal Medicine, Baggiovara Hospital, Modena, Italy; ⁸State Budgetary Institution of Health Care of Moscow Region "Moscow Regional Research Clinical Institute Named After M.F. Vladimirov", Moscow, Russian Federation; ⁹FSBI National Research Medical Center for Phthysiolpulmonology and Infectious Diseases of the Ministry of Health of the Russian Federation, Moscow, Russian Federation; ¹⁰Stavropol Regional Hospital, Stavropol, Russian Federation; ¹¹LLC Medical Company "Hepatolog", Samara, Russian Federation; ¹²Federal State-Funded Institution of Higher Education "South Ural State Medical University of Ministry of Health of the Russian Federation", Chelyabinsk, Russian Federation; ¹³Limited Liability Company "Clinic of Modern Medicine," Moscow, Russian Federation; ¹⁴Gilead Sciences, Inc., Foster City, United States; ¹⁵Universitätsklinikum Hamburg-Eppendorf, Medizinische Klinik Studienambulanz Hepatologie, Hannover, Germany; ¹⁶Medizinische Hochschule Hannover, Klinik für Gastroenterologie, Hepatologie und Endokrinologie, Hannover, Germany; ¹⁷Department of Medicine, University Hospital Frankfurt, Frankfurt, Germany
Email: pietro.lampertico@unimi.it

Background and aims: Bulevirtide (BLV) is a first-in-class entry inhibitor approved in Europe for chronic hepatitis delta (CHD). In a Phase 3 study over 96 weeks (wk), BLV 2 mg or 10 mg monotherapy was effective and safe. Here, we present week (W) 144 results.

Method: 150 patients (pts) with CHD were randomised: Arm A (delayed treatment): observed for 48 wk followed by BLV 10 mg/d for 96 wk (n = 51); Arm B: BLV 2 mg/d for 144 wk (n = 49); Arm C: BLV 10 mg/d for 144 wk (n = 50). All pts will be followed for 96 wk posttreatment. W144 efficacy end points included virologic response (VR; undetectable HDV RNA or ≥ 2 log decline from baseline [BL]), alanine aminotransferase (ALT) normalisation, combined response (CR; VR and ALT normalisation), and undetectable HDV RNA (target

not detected). Univariate logistic regression was used to discern if any BL characteristics predicted undetectable HDV RNA at W144 for pts in Arms B/C who completed W144 and had BL HDV RNA ≥ 250 IU/ml. Predictors with p value <.05 were considered significant.

Results: BL characteristics were previously published. At W144, 96% (49/51), 91.8% (45/49), and 88% (44/50) in Arms A, B, and C remained in study. Arms B and C had similar rates of CR, VR, and ALT normalisation; rates increased through W96 and were maintained through W144. At W144, 57%, 73%, 59% (Arm B) and 54%, 76%, 60% (Arm C) of pts achieved CR, VR, and ALT normalization. Undetectable HDV RNA rates continually increased with BLV treatment and were 29% in Arm B and 50% in Arm C at W144. Time to first reaching undetectable HDV RNA (mean wk [SD]) was faster in Arm C (69.3 [41.2]) vs Arm B (77.3 [44.5]). BL predictors of W144 undetectable HDV RNA were lower HDV RNA log₁₀ IU/ml (BLV 2 mg: OR 2.9, p = .0145; BLV 10 mg: OR 2.1, p = .0258) and lower hepatitis B surface antigen (HBsAg) log₁₀ IU/ml (BLV 2 mg: OR 5.1, p = .0319; BLV 10 mg: OR 6.0, p = .0390). W144 HBsAg (mean change from BL log₁₀ IU/ml [SD]) was -0.36 (0.596) and -0.19 (0.39) with BLV 2 mg and BLV 10 mg. At W144 in Arm A (96 wk of BLV), rates of CR, VR, ALT normalisation, and undetectable HDV RNA were 56%, 92%, 58%, and 52%. There was no progression to liver-related outcomes over 144 wk except for 1 case of mild ascites in Arm A (pt with BL cirrhosis). Platelet count and liver chemistries remained stable/improved including in pts with cirrhosis. Through 144 wks of BLV therapy, there were no drug discontinuations, serious adverse events, or deaths attributed to BLV; the safety profile was similar for BLV 2 mg and 10 mg doses. Dose-dependent increases in bile acids remained asymptomatic.

Conclusion: Long-term therapy with BLV therapy over W144 remains safe and effective. Improvements in biochemical, fibrosis and virologic markers including increased rates of undetectable HDV RNA, as well as low occurrence of liver-related events are supportive of the potential clinical benefits of long-term BLV therapy.

LBP-030

Use of tocilizumab for the treatment of steroid and mycophenolate-refractory hepatitis and cholangiohepatitis induced by immune checkpoint inhibitor immunotherapy

Sophia Ling¹, Bishma Jayatilaka¹, Chee Hui¹, Jonathan Segal¹, Andrew Trinh¹. ¹Peter MacCallum Cancer Centre, Parkville, Australia
Email: liying@gmail.com

Background and aims: The use of immune checkpoint inhibitor (ICI) therapies to engage the immune system against a growing number of tumour types has seen a rise in unwanted immune-mediated hepatitis (IMH) and cholangiohepatitis (IMCH). The optimal strategy for complete resolution without need for ongoing immunosuppression is still being refined. Tocilizumab, an IL-6 receptor antagonist, is emerging as a safe and effective agent beyond steroids and mycophenolate. We aim to describe our experience with patients who received tocilizumab as third-line treatment for IMH/IMCH, and discuss its use in both acute and protracted episodes.

Method: Patients with IMH/IMCH who were given at least one dose of tocilizumab 8 mg/kg i.v. after an unsatisfactory response to steroids and mycophenolate were assessed. Clinical trajectory, imaging results, liver biopsies when available, outcomes and liver enzymes across each episode were analysed.

Results: Eight patients (6 IMH, 2 IMCH) received ICIs for advanced cancer (melanoma, mucosal melanoma, non-small cell lung, cervical adenoma and prostate). All patients reached at least grade 3 IMH/IMCH during their clinical course (ALT>). Four patients (including one with acute IMCH) had normalization of liver enzymes by mean 85.5 days of a single tocilizumab dose. Two patients improved after a single dose, but died before normalization of liver enzymes: one (who also had third line tacrolimus before tocilizumab) with progression of cervical adenocarcinoma 76 days after tocilizumab; another of neutropaenic sepsis secondary to peptide receptor radionuclide therapy for prostate cancer, 26 days after tocilizumab. The seventh patient with protracted IMCH proceeded to a

second dose of tocilizumab 8 mg/kg at 12 weeks after a liver biopsy confirmed persisting mild IMCH. The final patient with protracted IMH for 1088 days demonstrated only marginal improvement after four doses of tocilizumab, which was ceased. There were no cases of tocilizumab toxicity.

Conclusion: Tocilizumab can be a safe and effective third-line agent in a group of patients in whom prompt resolution of adverse events improves quality of life and allows for ongoing cancer treatment. Current guidelines lack a clear alternative for IMH when steroids and mycophenolate are inadequate, nor treatment strategies upfront for IMCH, where response to steroids and mycophenolate is known to be poor. This study highlights an important need for high-quality data addressing the safety and efficacy of tocilizumab in such patients.

LBP-031

AZD2693, a potent PNPLA3 antisense oligonucleotide, decreases hepatic PNPLA3 mRNA and liver fat content in participants with presumed MASH and homozygous for the PNPLA3 148M risk allele

Javier Armisen¹, Mitra Rauschecker², Janeli Sarv³, Mathias Liljeblad⁴, Mohammad Niazi⁵, Oskar Clewe⁵, Olof Eklund⁶, Thérèse Sandell⁶, Daniel Linden⁷, Stefan Hallen⁷, Linda Wernevik⁸, Sofia Köster⁸, Erika Morizzo⁹, Jeanna Sundelin⁸, Björn Carlsson⁴, Lars Hansen², Jane Knöcher⁵, Sanjay Bhanot¹⁰, Shuling Guo¹⁰, Ola Fjellstrom⁴, Jenny Blau², Rohit Loomba¹¹. ¹Research and Early Development, Cardiovascular, Renal and Metabolism, BioPharmaceuticals, RandD, AstraZeneca, Cambridge, United Kingdom; ²Research and Early Development, Cardiovascular, Renal and Metabolism, BioPharmaceuticals, RandD, AstraZeneca, Gaithersburg, MD, United States; ³Late Stage Development, Cardiovascular, Renal and Metabolism, BioPharmaceuticals, RandD, AstraZeneca, Gothenburg, Sweden; ⁴Research and Early Development, Cardiovascular, Renal and Metabolism, BioPharmaceuticals, RandD, AstraZeneca, Gothenburg, Sweden; ⁵Clinical Pharmacology and Quantitative Pharmacology, Clinical Pharmacology and Safety Sciences, RandD, AstraZeneca, Gothenburg, Sweden; ⁶Global Patient Safety, Cardiovascular, Renal and Metabolism, BioPharmaceuticals, RandD, AstraZeneca, Gothenburg, Sweden; ⁷Bioscience Metabolism, Research and Early Development Cardiovascular, Renal and Metabolism (CVRM) BioPharmaceuticals, RandD, AstraZeneca, Gothenburg, Sweden; ⁸Clinical Operations, Cardiovascular, Renal and Metabolism, BioPharmaceuticals, RandD, AstraZeneca, Gothenburg, Sweden; ⁹Clinical Operations, Cardiovascular, Renal and Metabolism, BioPharmaceuticals, RandD, AstraZeneca, Cambridge, United Kingdom; ¹⁰Ionis Pharmaceuticals, Inc., Carlsbad, CA, United States; ¹¹MASLD Research Center, Division of Gastroenterology and Hepatology, University of California at San Diego, La Jolla, CA, United States

Email: javier.armisengarrido@astrazeneca.com

Background and aims: A common genetic variant (rs738409) encoding isoleucine (I) to methionine (M) at position 148 in the PNPLA3 protein is a key genetic determinant of hepatic steatosis, inflammation, fibrosis, cirrhosis and liver-related mortality. AZD2693 is a potent GalNAc-conjugated PNPLA3-targeted, antisense oligonucleotide (ASO) designed to specifically silence liver PNPLA3 mRNA and subsequent protein expression. This phase 1 program evaluated the safety, tolerability, pharmacokinetic and pharmacodynamic effects of AZD2693.

Method: The single ascending dose (SAD) study was a single-blind, placebo-controlled study to evaluate 5–110 mg in obese but otherwise healthy volunteers. The multiple ascending doses (MAD) study was a double-blind, placebo-controlled study to evaluate three monthly doses of 25 mg, 50 mg, and 80 mg in participants with MRI-PDFF >8%. The MAD study included MRI-PDFF assessment of liver fat content (LFC) at baseline and after 8 and 12 weeks. The 80 mg MAD cohort included liver biopsy at baseline and one week after third dose for target engagement of PNPLA3 mRNA knock-down.

Results: A total of 73 participants were randomized in the SAD study and 74 in the MAD study. There were no deaths or AEs leading to discontinuation in either study. AZD2693 displayed a typical ASO PK

profile with rapid absorption and distribution followed by a slower terminal phase and a half-life ranging from 14 to 22 days across investigated doses. Baseline MRI-PDFF mean values were 16.5%, 15.5%, 18.6% for 25 mg (n = 15), 50 mg (n = 16), and placebo (n = 12) groups, respectively. Week 12 reduction in LFC of 11% and 15% (placebo-corrected LS means) was observed for the 25 mg and 50 mg MAD study cohorts, respectively. The mean knockdown of liver PNPLA3 mRNA after 80 mg treatment was 87% (n = 4, p < 0.0001). There was a dose-dependent increase of polyunsaturated fatty acids (PUFA) in serum triglycerides (50 mg, p < 0.01), as well as a numerical reduction in hs-CRP levels.

Conclusion: AZD2693 treatment induced a potent reduction of liver PNPLA3 mRNA with a safety, tolerability and PK profile consistent with that of other ASOs. Therapeutic knock-down of PNPLA3 is impacting proposed mechanistic drivers in homozygous PNPLA3 148MM risk allele patients. These data support the continued development of AZD2693 in the FORTUNA Ph2b study.

LBP-032

Semaglutide improves cardiovascular outcomes in patients with high risk for metabolic dysfunction-associated steatohepatitis-a subgroup analysis from the SELECT trial

Sebastian Meyhoefer^{1,2}, Bertrand Cariou³, Cintia Cercato⁴, Helen Colhoun⁵, Anne Duun-Henriksen⁶, Iris Kliers⁶, A. Michael Lincoff⁷, Ildiko Lingvay⁸, Michelle Long^{6,9}, Philip N. Newsome¹⁰, Stephen Nicholls¹¹, Maria De Los Angeles Quiroga Pelaez⁶, Ferruccio Santini¹², Arun J. Sanyal¹³, Steven Kahn¹⁴. ¹Department of Internal Medicine 1-Endocrinology and Diabetes, University Medical Centre Lübeck, Lübeck, Germany; ²Clinical, Medical and Regulatory, Novo Nordisk Pharma GmbH, Mainz, Germany; ³Nantes Université, CHU Nantes, CNRS, INSERM, l'institut du thorax, Nantes, France; ⁴Obesity Unit, Department of Endocrinology, Hospital das Clínicas, University of São Paulo, São Paulo, Brazil; ⁵Institute of Genetics and Cancer, The University of Edinburgh, Edinburgh, United Kingdom; ⁶Novo Nordisk A/S, Søborg, Denmark; ⁷Department of Cardiovascular Medicine, Cleveland Clinic and Cleveland Clinic Lerner College of Medicine of Case Western Reserve University, Cleveland, OH, United States; ⁸Department of Internal Medicine/Endocrinology and Peter O'Donnell Jr. School of Public Health, University of Texas Southwestern Medical Center, Dallas, TX, United States; ⁹Department of Medicine, Section of Gastroenterology, Boston University Chobanian and Avedisian School of Medicine, Boston, MA, United States; ¹⁰Institute of Hepatology, King's College London and King's College Hospital, London, United Kingdom; ¹¹Victorian Heart Institute, Monash University, Melbourne, Victoria, Australia; ¹²Obesity and Lipodystrophy Centre, University Hospital of Pisa, Pisa, Italy; ¹³Division of Gastroenterology, Hepatology and Nutrition, Virginia Commonwealth University School of Medicine, Richmond, VA, United States; ¹⁴Department of Medicine, VA Puget Sound Health Care System and University of Washington, Seattle, WA, United States

Email: sebastian.meyhoefer@uni-luebeck.de

Background and aims: Cardiovascular (CV) risk is increased in people living with metabolic dysfunction-associated steatohepatitis (MASH). Although liver biopsy remains the gold standard to diagnose MASH, it is not practical to implement on a large scale. However, non-invasive tests, such as the Fibrosis-4 score (FIB-4), are useful for staging patients with fibrotic MASH and predict overall, CV- and liver-related mortality. In the SELECT CV outcome trial, which included patients with a body mass index ≥ 27.0 kg/m² and established CV disease but without diabetes, those treated with the glucagon-like peptide-1 receptor agonist semaglutide had a 20% CV risk reduction compared with those receiving placebo. We examined the CV benefits of semaglutide in a subgroup of participants at high risk of MASH as defined by FIB-4.

Method: SELECT was a multicentre, randomised, double-blind, placebo-controlled, event-driven trial that enrolled 17,604 patients aged ≥ 45 years. Patients were randomly assigned in a 1:1 ratio to receive once-weekly subcutaneous semaglutide 2.4 mg or placebo in

POSTER PRESENTATIONS

addition to standard of care recommendations for CV disease prevention. This subgroup analysis for the primary composite end point of 3-point major adverse cardiovascular event (MACE; non-fatal myocardial infarction, non-fatal stroke, CV death) was performed for patients with increased MASH risk as indicated by FIB-4 ≥ 1.3 for patients aged <65 years and FIB-4 ≥ 2.0 for patients aged ≥ 65 years, and for a second subgroup of patients of any age with FIB-4 >2.67 , respectively. As identified by review of medical history and co-medication, patients with a cause of liver disease other than MASH were not included in this analysis.

Results: From the SELECT cohort, 3,665 patients (20.8% of all) aged <65 years with FIB-4 ≥ 1.3 and aged ≥ 65 years with FIB-4 ≥ 2.0 were included in this analysis. The primary CV end point occurred in 140 of the 1,834 patients (7.6%) in the semaglutide group and in 176 of the 1,831 patients (9.6%) in the placebo group (hazard ratio [HR] 0.79; 95% confidence interval [CI] 0.63, 0.98; $p < 0.03$). In the subgroup of 475 patients with suspected MASH and advanced fibrosis (FIB-4 >2.67 irrespective of age), there were 22 CV events in 235 patients treated with semaglutide 2.4 mg compared with 35 events in 240 placebo-treated patients, yielding an HR of 0.64 (95% CI 0.37, 1.08; $p = 0.10$).

Conclusion: In line with the primary analysis of the SELECT trial, use of semaglutide 2.4 mg in a subgroup of patients at high risk of fibrotic MASH as defined by FIB-4 produced a 21% reduction in MACE outcomes.

LBP-033

Metabolic flux analysis using a ^{14}C microtracer approach combined with accelerator mass spectrometry analysis-a proof of concept study on de novo lipogenesis

Martine C. Morrison¹, Lianne Stevens¹, Robert Kleemann¹, Elwin Verheij¹, Wouter Vaes¹. ¹The Netherlands Organisation for Applied Scientific Research (TNO), Department of Metabolic Health Research, Leiden, Netherlands
Email: martine.morrison@tno.nl

Background and aims: Metabolic flux measurements play an important role in advancing our understanding of (patho)physiology, disease mechanisms and the development of new therapeutics. By incorporating stable or radioactive isotopes into specific molecules (tracers), the distribution and fate of the isotope can be followed—thereby providing insight into the movement and metabolic transformation of biomolecules. An isotope that is frequently used for such analyses is ^{13}C , which is analysed by isotope ratio mass spectrometry. The high natural abundance of ^{13}C ($\sim 1\%$) requires the use of large amounts of labelled substrates, especially in clinical studies. An alternative isotope is ^{14}C , which has an extremely low natural abundance (1 in 10^{12}). In combination with analysis by extremely sensitive accelerator mass spectrometry (AMS), this enables the detection of very small amounts of ^{14}C -labelled product/biomarker formed at very low (microtrace) amounts of labelled substrate administration. Here we provide proof of concept for this ^{14}C microtracer approach to assess activity of the de novo lipogenesis (DNL) pathway, an important metabolic pathway that is deregulated in various disease states, including metabolic dysfunction-associated steatotic liver disease (MASLD).

Method: De novo lipogenesis activity was assessed in Ldlr^{-/-}-Leiden MASLD mice fed a standard chow or a MASH-inducing high-fat diet (HFD) with/without the DNL inhibitor firsocostat (ACCi), as well as in an ex vivo porcine liver perfusion model. Incorporation of ^{14}C from ^{14}C -acetate into total lipid extracts (from plasma and liver samples), bile, fatty acids and cholesterol was assessed by LC/MS and AMS.

Results: Using this method, we show that DNL activity is significantly higher in HFD-fed Ldlr^{-/-}-Leiden MASH mice than in chow-fed controls. This is demonstrated by increased incorporation of ^{14}C into total lipid extracts, which we confirmed to be DNL by demonstrating incorporation into fatty acids profiled by LC/MS. Treatment with the DNL inhibitor firsocostat significantly reduced DNL activity as expected. In the ex vivo liver perfusion model we similarly

demonstrate that ^{14}C from acetate is incorporated into total lipids and fatty acids. In addition, we show in this model that this method can also be used for assessment of de novo synthesised cholesterol using the same labelling protocol.

Conclusion: We show here that this ^{14}C microtracer approach combined with AMS analysis can be used for assessment of metabolic fluxes in various experimental models at much lower amounts of tracer used than in conventional tracer methodologies. This allows study of metabolic pathways without disrupting the pathway of interest by adding large quantities of precursor and opens up opportunities to study the activity of other (metabolic) pathways in which only very small amounts of product are produced.

LBP-034

Evaluation of the PIKfyve kinase inhibitor Apilimod against hepatitis E virus infections

Julian Ring¹, Sarah Schlienkamp², Jil Haase², Xin Zhang³, Johan Neyts³, Suzanne J.F. Kaptein³, Mara Klöhn², Daniel Todt^{2,4}, Yannick Brüggemann², Eike Steinmann^{2,5}. ¹Department of Molecular and Medical Virology, Ruhr University Bochum, Bochum, Germany, Bochum, Germany; ²Department of Molecular and Medical Virology, Ruhr University Bochum, Bochum, Germany; ³KU Leuven Department of Microbiology, Immunology and Transplantation, Rega Institute for Medical Research, Laboratory of Virology and Chemotherapy, Leuven, Belgium; ⁴European Virus Bioinformatics Center (EVBC), Jena, Germany; ⁵German Center for Infection Research (DZIF), External Partner Site, Bochum, Germany
Email: Julian.Ring@ruhr-uni-bochum.de

Background and aims: Hepatitis E Virus (HEV) is the most common cause of viral hepatitis with over 20 million cases and up to 70,000 deaths annually. Despite its high risks especially among immunosuppressed patients and pregnant women, the treatment of HEV is limited to the off-label use of nucleoside-analogue ribavirin (RBV) and PEGylated interferon- α . Since both cause significant side effects and are contraindicated in selected patients, there is an urgent need to develop novel antiviral strategies against HEV. The phosphoinositide kinase PIKfyve plays a crucial role during various endocytotic processes by modulating endosome morphology, function and biogenesis. Inhibition of PIKfyve kinase activity has been shown to prevent the entry of different viruses, including Ebola virus and SARS-CoV-2. However, the role of PIKfyve during HEV infections still remains unclear. Here we investigated the antiviral potential of different PIKfyve inhibitors against HEV infections *in vitro* and *in vivo*.

Method: Using a robust HEV cell culture model, we investigated the dose-dependent effect of three PIKfyve kinase inhibitors. To identify which step of HEV life cycle is affected by PIKfyve inhibition, we performed time-of-addition as well as subgenomic replicon assays. The requirement of PIKfyve during the HEV live cycle was further validated via siRNA-mediated knockdown. In addition, we evaluated the antiviral effect of the PIKfyve kinase inhibitors in primary human hepatocytes (PHH) and in a chronic rat HEV infection model.

Results: All three tested PIKfyve kinase inhibitors, Apilimod, YM201636 and APY0201 lowered HEV infectivity at nanomolar efficacy in hepatoma cells. Consistent with this, siRNA-mediated knockdown of PIKfyve lowered the infectivity of HEV. Time-of-addition experiments showed that the PIKfyve inhibitors exert its antiviral effect during virus entry, without affecting viral replication, as observed in the replicon assay. In PHH, Apilimod exhibited a potent effect in reducing the HEV infectivity. Moreover, treatment with Apilimod (75 mg/kg/day, once-daily for 12 consecutive days) resulted in decreased viral RNA replication kinetics in the feces as compared to vehicle-treated rats. In addition, rats treated with Apilimod showed strong reductions in viral loads in the liver, spleen and intestine.

Conclusion: Overall, our data suggests that PIKfyve plays a crucial role during the viral entry of HEV. Considering the proven safety profile of Apilimod in previous human clinical trials (unrelated to viral conditions), the pharmacological targeting of PIKfyve kinase activity might guide novel antiviral strategies against HEV infections.

LBP-035

Luji-1 reduces fibrosis by blocking Neuroligin-4 and β -neurexin and overexpressing thyroid hormone receptor- β , suggesting Rezdiffra sensitization and synergism in combination

Johnny Amer¹, Ahmad Salhab¹, Baker Saffouri¹, Ashraf Imam¹, Abed Khalaileh¹, Rifaat Safadi¹. ¹Liver Institute- Hadassah Medical Hospital, Jerusalem, Israel
Email: johnnyamer@hotmail.com

Background and aims: The anti-fibrotic effect of Natural Killer (NK) cells against active hepatic stellate cells (HSCs) is impaired in advanced fibrosis. Following uncover of a novel immune inhibitory checkpoint, Luji-1 designed as dual antagonist peptide to HSCs ligand β -neurexin (β NRXN) and NK Neuroligin-4 receptor (NLGN4). Rezdiffra, a thyroid hormone receptor- β (THR- β) agonist, added 11% fibrosis improve in metabolic dysfunction-associated steatohepatitis (MASH). Here-in, THR- β modulation by Luji-1 assessed on addition to its anti-fibrotic effects.

Method: Luji-1, scrambled-peptide (both 8 μ g/ml), L-Thyroxin (T4, 10 nM) and combinations were *in vitro* incubated 6 hours with LX2 [HSCs cell line] monocultures in 1% FCS [quiescent] and 10% [activated]. Similar incubations assessed in peripheral-blood NK cells from F1/F2 and F3/F4 MASH donors monocultured in 10% FCS. Luji-1 vs scrambled-peptide treated NK cells were then cocultured 6 hours with LX2. For the *in vivo* study, biweekly i.p CCl₄ (0.5 μ l/g body weight) fibrosis model induced in C57/Bl mice for 6 weeks; and biweekly Luji-1 (8 μ g/mice) treatment provided along last 2 weeks.

Results: Using flow cytometry, active LX2 monocultured cells significantly overexpressed α Smooth Muscle Actin (α SMA) and β NRXN (suggesting pro-fibrotic features), but reduced THR- β expressions by 8.3-folds compared to quiescent state. Treated LX2 cells with Luji-1, T4 and combination significantly reduced α SMA expressions (61%, 31% and 85%, respectively). As Luji-1 induced 3.2-folds THR- β overexpression, the achieved synergism by combination was significant. Monocultured F3/F4 NK cells with scrambled-peptide were impaired (low CD107a); associated with 3.2-folds NLGN4 overexpress and 2.4-folds THR- β down express as compared to active F1/2 counterparts and quiescent healthy donors ($p < 0.05$). Luji-1 or T4 promoted F3/F4 NK cytotoxicity against activate HSCs and enhanced THR- β expressions. Both Luji-1 and T4 achieved a significant synergistic increase of NK cytotoxic effect. In the *in vivo* CCl₄ model, Luji-1 significantly activated NK cells (increased CD107a and F-actin expressions) and improved all markers of liver inflammation and fibrosis (serum liver enzymes, histology HandE and serious red stains, liver extracts for α SMA and Collagen). Luji-1 downregulated NLGN4 and β NRXN expressions while increased THR- β expressions in liver extracts.

Conclusion: Luji-1 improved liver injury via: (1) direct β NRXN inhibition in myofibroblasts and decreased their activation, (2) NK cells stimulation against myofibroblasts directly via NLGN4 inhibition in NK cells and indirectly by blocking the myofibroblast β NRXN that serves as NK inhibitor and (3) THR- β over expressions that sensitizes Rezdiffra in combination.

LBP-036

Final results from the phase 3 REGENERATE trial evaluating the effects of obeticholic acid in patients with pre-cirrhotic fibrosis due to metabolic dysfunction-associated steatohepatitis

Arun J. Sanyal¹, Rohit Loomba², Quentin M. Anstee³, Vlad Ratziu⁴, Kris V. Kowdley⁵, Eric Lawitz⁶, Christopher White⁷, Sangeeta Sawhney⁷, Thomas Capozza⁷, Rina Leyva⁷, Zobair Younossi⁸, Mary E. Rinella⁹, Manal F. Abdelmalek¹⁰. ¹Division of Gastroenterology, Hepatology and Nutrition, Virginia Commonwealth University, Richmond, VA, United States; ²University of California, San Diego, La Jolla, CA, United States; ³Translational and Clinical Research Institute, Faculty of Medical Sciences, Newcastle University, Framlington Place, Newcastle upon Tyne, United Kingdom; ⁴Sorbonne Université, Assistance Publique-Hôpitaux de Paris, Hôpital Pitié-Salpêtrière, Institute for

Cardiometabolism and Nutrition, Paris, France; ⁵Liver Institute Northwest, Seattle, WA, United States; ⁶Texas Liver Institute, University of Texas Health San Antonio, San Antonio, TX, United States; ⁷Intercept Pharmaceuticals, Inc., Morristown, NJ, United States; ⁸Beatty Liver and Obesity Research Program, Center for Liver Diseases, Inova Medicine, Falls Church, VA, United States; ⁹University of Chicago, Pritzker School of Medicine, Chicago, IL, United States; ¹⁰Division of Gastroenterology and Hepatology, Mayo Clinic, Rochester, MN, United States
Email: arun.sanyal@vcuhealth.org

Background and aims: Fibrosis is the strongest predictor of clinical outcomes in metabolic dysfunction-associated steatohepatitis (MASH). The phase 3 REGENERATE study of the farnesoid X receptor agonist obeticholic acid (OCA) evaluated progression to clinical outcomes over 48 months, with an interim analysis of histologic improvement at month 18 (M18). At M18, OCA demonstrated a statistically significant antifibrotic benefit. REGENERATE was discontinued in September 2023 for failure to achieve marketing approval after a consensus re-analysis of the M18 data. Final end-of-study results are presented.

Method: In this multicenter, randomized, double-blind, placebo (PBO)-controlled study, patients (pts) with biopsy-confirmed fibrosis (F2-F3) were randomized 1:1:1 to PBO, OCA 10 mg, or OCA 25 mg. The primary end point was time to first occurrence of prespecified clinical outcomes, including progression to cirrhosis. Secondary end points included measures of histologic improvement and biochemical markers of liver function. Efficacy was assessed in the intent-to-treat population ($n = 2187$); safety was assessed in 2477 pts with a median of >4 years of exposure. An independent expert committee adjudicated all outcomes.

Results: Baseline demographics and clinical characteristics were balanced across treatment groups. Clinical outcomes occurred in 18.8%, 15.8%, and 14.7% of pts treated with PBO, OCA 10 mg, and OCA 25 mg, respectively. Compared to PBO, the hazard ratio was 0.814 for OCA 10 mg and 0.772 for OCA 25 mg, driven by fewer pts receiving OCA progressing to cirrhosis. More pts receiving OCA had fibrosis improvement ≥ 1 stage with no worsening of MASH compared to PBO ($p < 0.001$ for both dose groups). Improvement in fibrosis by ≥ 1 stage was achieved in 27.0%, 37.1%, and 39.3% of pts treated with PBO, OCA 10 mg, and OCA 25 mg, respectively; worsening of fibrosis by ≥ 1 stage occurred in 23.5%, 19.3%, and 18.5%, respectively. OCA treatment produced dose-dependent reductions in mean serum alanine aminotransferase, aspartate aminotransferase, and gamma glutamyl transferase levels to a greater extent than PBO. Treatment-emergent adverse events (TEAEs), serious TEAEs, and deaths were similar across groups. Consistent with the M18 analysis, pruritus and gallbladder- and gallstone-related TEAEs occurred more frequently with OCA 25 mg than with PBO or OCA 10 mg.

Conclusion: Our end-of-study analysis demonstrated a trend for benefit in clinical outcomes, and histological progression to cirrhosis was reduced in patients receiving OCA 25 mg. Fibrosis improvement ≥ 1 stage and reductions in biochemical markers of liver injury and oxidative stress were observed for OCA 10 mg, which may be relevant in the treatment of primary biliary cholangitis. The safety results add to the largest safety database in MASH, with a median OCA exposure of 52 months and no new safety concerns with >2 years of additional exposure.

LBP-037

Role of early on-treatment serum hepatitis B virus RNA declines in the prediction of hepatocellular carcinoma risk in patients with chronic hepatitis B

Shi Liu¹, Grace Lai-Hung Wong², Rong Fan¹, Junqi Niu³, Hong Ma⁴, Wanying Liang¹, Xingyu Lu¹, Jianping Xie⁵, Jia Shang⁶, Dong-Ying Xie⁷, Yali Liu⁸, Bin Zhou¹, Qing Xie⁹, Jie Peng¹, Hongbo Gao¹⁰, Huiying Rao¹¹, Jinjun Chen¹, Jifang Sheng¹², Sheng Shen¹, Song Yang¹³, Xiaoguang Dou¹⁴, Zhengang Zhang¹⁵, Vincent Wai-Sun Wong², Jinlin Hou¹, Jian Sun¹. ¹Nanfang Hospital, Southern Medical University,

POSTER PRESENTATIONS

Guangzhou, China; ²State Key Laboratory of Digestive Disease, Institute of Digestive Disease, The Chinese University of Hong Kong, Hong Kong, China; ³No. 1 Hospital affiliated to Jilin University, Changchun, China; ⁴Beijing Friendship Hospital, Capital Medical University, Beijing, China; ⁵Department of Infectious Diseases, Xiangya Hospital, Central South University, Changsha, China; ⁶Henan Province People's Hospital, Zhengzhou, China; ⁷Sun Yat-Sen University 3rd Affiliated Hospital, Zhengzhou, China; ⁸Beijing Youan Hospital, Capital Medical University, Beijing, China; ⁹Ruijin Hospital, Shanghai Jiao Tong University School of Medicine, Shanghai, China; ¹⁰Guangzhou 8th People's Hospital, Guangzhou Medical University, Guangzhou, China; ¹¹Peking University People's Hospital, Beijing, China; ¹²The First Affiliated Hospital, Zhejiang University of School Medicine, Hangzhou, China; ¹³Beijing Ditan Hospital, Capital Medical University, Beijing, China; ¹⁴Shengjing Hospital of China Medical University, Shenyang, China; ¹⁵Tongji Hospital, Tongji Medical College, Huazhong University of Science and Technology, Wuhan, China

Email: doctorsunjian@qq.com

Background and aims: Hepatocellular carcinoma (HCC) risk prediction models established in patients with chronic hepatitis B (CHB) under nucleoside analogue (NA) treatment rarely included viral factors because of mediocre predictability of traditional viral markers. Here, we investigate the role of serum hepatitis B virus (HBV) RNA, a novel biomarker, in predicting HCC risk in NA-treated patients.

Method: A total of 1374 patients treated with entecavir or tenofovir disoproxil fumarate were enrolled from two prospective CHB cohorts. Serum HBV RNA levels were detected at baseline and year 1, 2 and 3 of treatment by a commercial automated quantitative serum HBV RNA assay (Rendu Biotechnology, Shanghai, China), with lower limit of detection of 50 copies/ml. Restricted cubic spline analyses and Cox proportional hazard models were used to investigate the association of serum HBV RNA kinetics and HCC risk.

Results: After a median follow-up of 5.4 years, 76 patients developed HCC. Restricted cubic spline analyses showed significant non-linear parabolic associations of serum HBV RNA levels at baseline and year 1 with HCC risk (all p for non-linear trend <0.050). Similar trend was observed between serum HBV RNA levels at year 2 and HCC risk with marginal statistical significance (p for non-linear trend = 0.114). Interestingly, early on-treatment serum HBV RNA declines (at year 1 and 2) showed independent linear associations with HCC risk (all p for linear trend <0.05). Patients with lower HBV RNA decline at year 1 ($= <0.4 \log_{10}$ copies/ml) or 2 ($= <0.6 \log_{10}$ copies/ml) had 2.22- and 2.09-folds higher HCC risk, respectively, than those with higher declines. When incorporating these early on-treatment HBV RNA declines into existing HCC risk scores, including PAGE B, mPAGE B and aMAP score, they could enhance their predictive performance [i.e. C-index of models based on baseline parameters, 0.814 vs. 0.788, Model (PAGE B + HBV RNA decline at year 1) vs. PAGE B score; 0.825 vs. 0.804, Model (mPAGE B + HBV RNA decline at year 1) vs. mPAGE B score; 0.825 vs. 0.811, Model (aMAP + HBV RNA decline at year 1) vs. aMAP score], which were internally validated by repeated K-fold cross-validation.

Conclusion: Serum HBV RNA declines at year 1 and 2 were significantly associated with on-treatment HCC risk. Incorporating early on-treatment HBV RNA declines into HCC risk prediction models can be useful tools to guide appropriate surveillance strategies in NA-treated patients.

LBP-038

Expanding knowledge regarding real-world treatment of patients with primary biliary cholangitis with obeticholic acid from the Italian RECAPITULATE cohort

Francesca Terracciani¹, Antonio De Vincentis², Daphne D'Amato³, Miki Scaravaglio³, Pietro Invernizzi³, Ester Vanni⁴, Daniela Campion⁴, Annarosa Floreani⁵, Nora Cazzagon⁵, Domenico Alvaro⁶, Rosanna Venere⁶, Edoardo Giannini⁷, Sara Labanca⁷, Ana Lleo⁸, Francesca Colapietro⁸, Elisabetta Degasperis⁹, Mauro Viganò¹⁰,

Eugenia Vittoria Pesatori¹⁰, Stefano Fagioli¹⁰, Marco Marzoni¹¹, Valerio Buzzanca¹¹, Raffaella Viganò¹², Federico D'Amico¹², Andrea Galli¹³, Armando Curto¹³, Fabio Marra¹³, Paola Begini¹⁴, Leonardo Baiocchi¹⁵, Paola Carni¹⁵, Luigi Muratori¹⁶, Barbara Coco¹⁷, Maurizio Brunetto¹⁷, Fabrizio Pizzolante¹⁸, Nicoletta De Matthaeis¹⁸, Elisabetta Falbo¹⁹, Lorenzo Surace¹⁹, Alberto Mattalia²⁰, Donatella Ieluzzi²¹, Federico Salomone²², Guido Delle Monache²³, Riccardo Tatonetti²³, Ilaria Cavalli²⁴, Valentina Cossiga²⁵, Filomena Morisco²⁵, Vincenzo Valiani²⁶, Pietro Gatti²⁶, Vincenzo Boccaccio²⁶, Debora Angrisani²⁷, Giovanni Vettori²⁸, Biagio Cuffari²⁹, Alessandra Moretti³⁰, Gerardo Nardone³¹, Alba Rocco³¹, Paolo Scivetti³², Martina Costanzo³², Valentina Boano³³, Giulia Francesca Manfredi³⁴, Loredana Simone³⁵, Valeria Pace Palitti³⁶, Maurizio Rusello³⁷, Maria Rita Cannavò³⁷, Evelise Frazzetto³⁸, Gaetano Bertino³⁸, Marco Distefano³⁹, Antonio Izzi⁴⁰, Federica Cerini⁴¹, Luchino Chessa⁴², Michela Miglianti⁴², Valentina Feletti⁴³, Alessandro Mussetto⁴³, Raffaele Cozzolongo⁴⁴, Francesco Losito⁴⁴, Grazia Anna Niro⁴⁵, Rosa Cotugno⁴⁵, Rodolfo Sacco⁴⁶, Chiara Ricci⁴⁷, Paolo Poisa⁴⁷, Luca Cadamuro⁴⁸, Antonino Castellaneta⁴⁹, Francesco Squeo⁴⁹, Natalia Terreni⁵⁰, Niccolò Bina⁵⁰, Pietro Pozzoni⁵¹, Silvia Casella⁵², Francesca Zani⁵², Olivia Morelli⁵³, Giuseppe Cuccorese⁵⁴, Carlo Saitta⁵⁵, Teresa Zolfino⁵⁶, Cristina Rigamonti³⁴, Vincenza Calvaruso⁴⁸, Marco Carbone³, Umberto Vespasiani-Gentilucci¹. ¹Internal Medicine and Hepatology, University Campus Bio-Medico of Rome, Rome, Italy; ²Internal medicine unit, Fondazione Policlinico Universitario Campus Bio-Medico, 00128, Italy; ³Division of Gastroenterology, Centre for Autoimmune Liver Diseases, Department of Medicine and Surgery, University of Milano-Bicocca, European Reference Network on Hepatological Diseases (ERN RARE-LIVER), San Gerardo Hospital, Monza, Italy, Monza, Italy; ⁴Gastroenterology Unit, Città della salute e della scienza, Turin, Italy, Turin, Italy; ⁵Gastroenterology Unit, Department of Surgery, Oncology and Gastroenterology, Padua University Hospital, Padua, Italy, Padua, Italy; ⁶Department of Translation and Precision Medicine, Sapienza University of Rome, Rome, Italy, Rome, Italy; ⁷Gastroenterology Unit, Department of Internal Medicine, University of Genoa, IRCCS Ospedale Policlinico San Martino, Genoa, Italy, Genoa, Italy; ⁸Internal Medicine and Hepatology, Humanitas Clinical and Research Center IRCCS, Humanitas University, Milan, Italy, Milan, Italy; ⁹Foundation IRCCS Ca' Granda Ospedale Maggiore Policlinico-Division of Gastroenterology and Hepatology-CRC "A.M. and A. Migliavacca" Center for Liver Disease, Milan, Italy, Milan, Italy; ¹⁰Hepatology and Liver Transplant Unit, Papa Giovanni XXIII Hospital, Bergamo, Italy, Bergamo, Italy; ¹¹Clinic of Gastroenterology and Hepatology, Università Politecnica delle Marche, Ancona, Italy, Ancona, Italy; ¹²Hepatology Unit, Niguarda Hospital, Milan, Italy, Milan, Italy; ¹³Internal Medicine and Hepatology Unit, Department of Experimental and Clinical Medicine, University of Firenze, Firenze, Italy, Firenze, Italy; ¹⁴Digestive and Liver Disease Department, School of Medicine and Psychology University "Sapienza", Azienda Ospedaliera S. Andrea, Rome, Italy, Rome, Italy; ¹⁵Hepatology Unit, University of Rome "Tor Vergata," Rome, Italy, Rome, Italy; ¹⁶DIMEC Università di Bologna, Policlinico di Sant'Orsola, Bologna, Italy, Bologna; ¹⁷Hepatology Unit, University Hospital of Pisa, Italy, Pisa, Italy; ¹⁸UOC of Gastroenterology, Gastroenterological, Endocrine-Metabolic and Nephro-Urological Sciences Department, Fondazione Policlinico Universitario A.Gemelli IRCCS, Università Cattolica del Sacro Cuore, Rome, Italy, Rome, Italy; ¹⁹Azienda Sanitaria Provinciale di Catanzaro, Presidio Ospedaliero "Giovanni Paolo II" Lamezia Terme (CZ), Lamezia Terme, Italy; ²⁰Division of Gastroenterology, Santa Croce e Carle General Hospital, Cuneo, Italy, Cuneo, Italy; ²¹USD Liver Unit, Azienda Ospedaliera Universitaria Integrata di Verona, Verona, Italy; ²²Ospedale di Acireale, Azienda Sanitaria Provinciale di Catania, Catania, Italy, Catania, Italy; ²³Ospedale di Penne, Pescara, Pescara, Italy; ²⁴Division of Internal Medicine, Cremona Hospital, Cremona, Italy; ²⁵Department of Clinical Medicine and Surgery, Gastroenterology Unit, University of Naples "Federico II", Naples, Italy; ²⁶Internal Medicine Unit, Perrino Hospital, Brindisi, Italy, Brindisi, Italy; ²⁷AORN Antonio Cardarelli di

Napoli, Naples, Italy; ²⁸Gastroenterology and Endoscopy Unit, Santa Chiara Hospital, Trento 38014, Italy, Trento, Italy; ²⁹Division of Gastroenterology, Azienda Ospedaliero-Universitaria di Modena and University of Modena and Reggio Emilia, Modena, Italy, Modena, Italy; ³⁰UOC GASTROENTEROLOGIA, Ambulatorio di Epatologia, P.O. San Filippo Neri, Rome, Italy; ³¹Gastroenterology and Hepatology, Department of Clinical Medicine and Surgery, University Federico II, Naples, Italy, Naples, Italy; ³²Internal Medicine Unit, Azienda Sanitaria Locale di Biella, Biella, Italy, Biella, Italy; ³³Department of Gastroenterology and Endoscopy, Cardinal Massaia Hospital, Asti, Italy, Asti, Italy; ³⁴Dipartimento di Medicina Traslazionale, Università del Piemonte Orientale, Novara, Italy and Division of Internal Medicine, AOU Maggiore della Carità, Novara, Italy, Novara, Italy; ³⁵Azienda Ospedaliero-Universitaria Di Ferrara, Ferrara, Italy, Ferrara, Italy; ³⁶Internal Medicine Unit, Santo Spirito Hospital, Pescara, Italy, Pescara, Italy; ³⁷Liver Unit, Arnas Garibaldi, Catania, Italy, Catania, Italy; ³⁸Gastroenterology and Hepatology Unit, University Hospital Policlinico Vittorio Emanuele, Catania, Italy, Catania, Italy; ³⁹Department of Infectious Diseases, Umberto I Hospital, Siracusa, Italy, Siracusa, Italy; ⁴⁰Department of Infectious Diseases, D. Cotugno Hospital, Napoli, Italy, Naples, Italy; ⁴¹Hepatology Unit, San Giuseppe Hospital, Milan, Italy, Milan, Italy; ⁴²Liver Unit, University Hospital of Cagliari, Cagliari, Italy, Cagliari, Italy; ⁴³Gastroenterology Unit, Santa Maria Delle Croci Hospital, Ravenna, Italy, Ravenna, Italy; ⁴⁴Gastroenterology Unit, National Institute of Gastroenterology "S de Bellis" Research Hospital, Castellana Grotte (Bari), Italy, Castellana Grotte (Bari), Italy; ⁴⁵Gastroenterology Unit, Fondazione Casa Sollievo Della Sofferenza IRCCS, San Giovanni Rotondo, Foggia, Italy, Foggia, Italy; ⁴⁶Gastroenterology Unit, Ospedali Riuniti, Foggia, Italy, Foggia, Italy; ⁴⁷Internal Medicine, Spedali Civili, Brescia, Italy, Brescia, Italy; ⁴⁸Gastroenterology and Hepatology Unit, University of Palermo, Palermo, Italy, Palermo, Italy; ⁴⁹Gastroenterology Unit, Policlinico di Bari Hospital, Bari, Italy, Bari, Italy; ⁵⁰Hepatology Unit, Valduce Hospital, Como, Italy, Como, Italy; ⁵¹Hepatology Unit, Alessandro Manzoni Hospital, Lecco, Italy, Lecco, Italy; ⁵²Hepatology Unit, Spedali Civili Gardone Val Trompia, Brescia, Italy, Val Trompia, Italy; ⁵³Clinic of Gastroenterology and Hepatology, Department of Medicine, Università degli Studi di Perugia, Perugia, Italy, Perugia, Italy; ⁵⁴Internal Medicine Ospedale "R.Dimiccoli", Barletta, Italy, Barletta, Italy; ⁵⁵Division of Medicine and Hepatology, University Hospital of Messina "Policlinico G. Martino", Messina, Italy, Messina, Italy; ⁵⁶Department of Gastroenterology, Brotzu Hospital, Cagliari, Italy, Cagliari, Italy Email: f.terraciani@unicampus.it

Background and aims: Obeticholic acid (OCA) is the only conditionally approved second-line treatment in PBC patients non-responder/intolerant to ursodeoxycholic acid. After OCA approval, a number of studies provided confirmations of the drug's effectiveness and safety in a real-world context. The aim of this study is to expand knowledge on long-term treatment with OCA in the largest real-world cohort described to date and with the longest follow-up.

Method: The RECAPITULATE cohort includes all PBC adult patients on OCA therapy from Italian centres belonging to "Italian PBC registry" and "CLEO/AIGO" groups. Efficacy was evaluated according to POISE (ALP < 1.67/upper limit of normal (ULN) with a reduction of 15% from baseline and a normal total bilirubin) or "normal range" (NR) criteria (normal ALP, ALT, bilirubin). Cumulative incidences of OCA response and discontinuation were evaluated through Aalen-Johansen (taking into account the competing risk of discontinuation) and Kaplan-Meier estimators, respectively. Risk factors analysis was carried out using Cox proportional hazard models.

Results: After excluding those with less than 6 months follow-up, 759 individuals (median age 58 years, women 87%, median time on OCA 24 months -IQR 12–42 months-) from 66 Italian centres were analyzed. The cohort includes 221 cirrhotic patients (29%), 104 with PBC/autoimmune hepatitis (AIH) overlap (14%) and 105 on concomitant off-label fibrate therapy (14%). Out of the total number of patients prescribed OCA, the relative percentage of cirrhotics has

halved over time (~40% of those prescribed OCA in 2017–2020 Vs ~20% of those prescribed in 2021–2023). According to POISE criteria, response probabilities were 40.6%/49%/55.6%/54.7% at 12/24/36/48 months. Discontinuation probabilities were 10%/15%/20%/26% at 12/24/36/48 months. Pruritus (49 patients, 35%) and hepatic events (43 patients, 31%) were the main causes of OCA discontinuation. When compared with non-cirrhotics, cirrhotic patients showed significantly lower response ($p=0.02$ for POISE, $p=0.003$ for NR) and higher discontinuation ($p<0.001$) probabilities, while no differences were observed between PBC/AIH overlap and "pure" PBC in terms both of response ($p=0.8$) and discontinuation ($p=0.07$) probabilities. Pre-treatment ALP (HR 0.72, IC 0.64–0.81), total bilirubin (HR 0.23, IC 0.16–0.33), pruritus (HR 0.70, IC 0.55–0.88), and AMA positivity (HR 1.53, IC 1.10–2.14) were independent predictors of POISE response in the multivariate analysis.

Conclusion: These results, derived from a large real-world dataset, confirm that the efficacy and safety profiles of OCA in treating PBC remain consistent in the long term. Although cirrhotics are a challenging population to treat, their proportion is reducing over time, aligning with earlier PBC diagnosis and the decline in more severe cases accumulated prior to the drug's availability.

LBP-039

Oral alpha-v/beta-6 and alpha-v/beta-1 integrin inhibitor bexotegast in primary sclerosing cholangitis: updated 12-week interim safety and efficacy analysis of the INTEGRIS-PSC phase 2a trial

Michael Trauner¹, Kris V. Kowdley^{2,3}, Gideon M. Hirschfield⁴, Eric Lefebvre⁵, Martin Decaris⁵, Johanna Schaub⁵, Annie Clark⁵, Mandy Lin⁵, Mahru An⁵, Aarthi Balasubramanyam⁵, Chris N. Barnes⁵, Richard Pencek⁵, Douglas Thorburn⁶, Aldo J. Montano-Loza⁷, Christopher L. Bowlus⁸, Christoph Schramm⁹, Cynthia Levy¹⁰, Palak J. Trivedi^{11,12}. ¹Division of Gastroenterology and Hepatology, Department of Internal Medicine III, Medical University of Vienna, Vienna, Austria; ²Liver Institute Northwest, Seattle, United States; ³Elson S. Floyd College of Medicine, Washington State University, Seattle, United States; ⁴Toronto Centre for Liver Disease, Toronto General Hospital, University of Toronto, Toronto, Canada; ⁵Pliant Therapeutics, Inc, South San Francisco, United States; ⁶Sheila Sherlock Liver Centre and UCL Institute for Liver and Digestive Health, London, United Kingdom; ⁷University of Alberta, Edmonton, Canada; ⁸University of California, Davis, Sacramento, United States; ⁹University Medical Center Hamburg-Eppendorf, Hamburg, Germany; ¹⁰Schiff Center for Liver Diseases, University of Miami, Miami, United States; ¹¹NIHR Birmingham Biomedical Research Centre, Centre for Liver and Gastrointestinal Research, University of Birmingham, Birmingham, United Kingdom; ¹²Liver Unit, University Hospitals Birmingham, Birmingham, United Kingdom

Email: michael.trauner@meduniwien.ac.at

Background and aims: Primary sclerosing cholangitis (PSC) is characterized by biliary inflammation and progressive fibrosis. Two integrins, alpha-v/beta-6 on cholangiocytes and alpha-v/beta-1 on myofibroblasts, are regulators of transforming growth factor (TGF)-beta signalling, which drives fibrosis. Bexotegast (BEXO), an oral, once-daily, dual-selective inhibitor of these integrins, is in development for the treatment of PSC. We report 12-week safety and efficacy results, focusing on BEXO 320 mg vs placebo (PBO), from the double-blind, dose-ranging, randomized, Phase 2a INTEGRIS-PSC study (NCT04480840).

Method: Participants with PSC were randomized to once-daily BEXO 320, 160, 80 or 40 mg or PBO for 12 weeks. Analyses of 40-, 80- and 160-mg doses were presented previously, and results of the 320 mg dose vs PBO presented herein. Key entry criteria were large-duct PSC, stable inflammatory bowel disease (if present), ursodeoxycholic acid <25 mg/kg/day (if used), alkaline phosphatase (ALP) ≤10x upper limit of normal and suspected liver fibrosis (without cirrhosis) as evidenced by ≥1 of the following: enhanced liver fibrosis (ELF) score ≥7.7,

POSTER PRESENTATIONS

transient elastography ≥ 8 to ≤ 14.4 kPa, magnetic resonance [MR] elastography ≥ 2.4 to ≤ 4.9 kPa or historical biopsy indicating fibrosis. The primary end point was safety and tolerability at Week 12. Secondary and exploratory end points included changes in ELF score, PRO-C3 and gadoxetate contrast-enhanced MR imaging (MRI).

Results: Of 121 participants in the study, 27 were randomized to BEXO 320 mg and 30 to PBO (pooled group). A total of 20 (74.1%) and 20 (66.7%) BEXO 320 mg- and PBO-treated participants, respectively, reported treatment-emergent adverse events (TEAEs); no BEXO 320 mg-related TEAEs or serious TEAEs were reported. TEAEs of pruritus and cholangitis were less frequent with BEXO 320 mg (7.4% and 0%, respectively) than with PBO (20.0% and 13.3%, respectively). At Week 12, mean (SD) [n] change from baseline in ELF score (BEXO 320 mg vs PBO) was 0.2 (0.6) [25] vs 0.4 (0.7) [28], PRO-C3 mean percent change (SD) [n] from baseline was 3.3% (24.6) [25] vs 12.4% (25.5) [28] and mean (SD) [n] change from baseline in time to arrival of gadoxetate in the common bile duct was -22.2 (196.0) [10] vs 86.5 (217.6) [15] seconds. In the subgroup with elevated ALP, mean (SD) [n] change from baseline was 1.5 (50.3) [20] U/L with BEXO 320 mg vs 49.7 (150.4) [21] U/L with PBO.

Conclusion: In this study population with PSC enriched for liver fibrosis, BEXO 320 mg was well tolerated and associated with prevention of worsening of biomarkers of fibrosis and hepatobiliary excretory bile flow (as suggested by MRI) compared with PBO over 12 weeks, consistent with findings with lower doses. This analysis supports proof of mechanism for targeting integrin-mediated TGF-beta activation as a therapeutic approach for PSC.

LBP-040

Long-term efficacy and safety of open-label seladelpar treatment in patients with primary biliary cholangitis (PBC): interim results for 2 years from the ASSURE study

Palak J. Trivedi¹, Cynthia Levy², Kris V. Kowdley³, Stuart C. Gordon⁴, Christopher L. Bowlus⁵, María Carlota Londoño⁶, Gideon M. Hirschfield⁷, Aliya Gulamhusein⁷, Eric Lawitz⁸, Alejandra Villamil⁹, Alma Laura Ladrón de Guevara¹⁰, Marlyn J. Mayo¹¹, Ziad H. Younes¹², Oren Shibolet¹³, Kidist Yimam¹⁴, Daniel Pratt¹⁵, Jeong Heo¹⁶, Ulrike Morgera¹⁷, Pietro Andreone¹⁸, Andreas E. Kremer¹⁹, Christophe Corpechot²⁰, Aparna Goel²¹, Adam Peyton²², Hany Elbeshbeshy²³, Daria B. Crittenden²⁴, Carrie Heusner²⁴, Sarah Proehl²⁴, Shuqiong Zhou²⁴, Charles A. McWherter²⁴. ¹University of Birmingham, Birmingham, United Kingdom; ²University of Miami, Miami, United States; ³Liver Institute Northwest, Seattle, United States; ⁴Henry Ford Health, Detroit, United States; ⁵University of California Davis, Davis, United States; ⁶Hospital Clinic Barcelona, Barcelona, Spain; ⁷University of Toronto, Toronto, Canada; ⁸Texas Liver Institute, San Antonio, United States; ⁹Hospital Italiano de Buenos Aires, Buenos Aires, Argentina; ¹⁰Roma Gastroenterology and Research Center, Mexico City, Mexico; ¹¹UT Southwestern Medical Center, Dallas, United States; ¹²Gastro One, Germantown, United States; ¹³Tel Aviv University, Tel Aviv, Israel; ¹⁴California Pacific Medical Center, San Francisco, United States; ¹⁵Massachusetts General Hospital, Boston, United States; ¹⁶Pusan National University, Busan, Korea, Rep. of South; ¹⁷Universitätsmedizin Berlin, Berlin, Germany; ¹⁸University of Modena and Reggio Emilia, Modena, Italy; ¹⁹University Hospital Zurich, Zurich, Switzerland; ²⁰Saint-Antoine Hospital, Paris, France; ²¹Stanford University, Palo Alto, United States; ²²Eastern Pennsylvania Gastroenterology and Liver Specialists, Allentown, United States; ²³Saint Louis University, Saint Louis, United States; ²⁴CymaBay Therapeutics, Fremont, United States Email: p.j.trivedi@bham.ac.uk

Background and aims: Seladelpar, a potent and selective PPAR-delta agonist, has been shown to reduce biochemical markers of cholestasis and pruritus in PBC patients. ASSURE (NCT03301506) is an ongoing, open label, long-term phase 3 trial of seladelpar in patients rolling over from the phase 3 registrational study RESPONSE (NCT04620733) or with prior participation in legacy studies: phase 3

ENHANCE (NCT03602560) study; CB8025-21629 (NCT02955602); CB8025-31731 (NCT03301506); and CB8025-21838 (NCT04950764). Here, we report interim 2-year efficacy and safety results for 337 enrolled patients.

Method: Patients with insufficient response or intolerance to first line PBC treatment ursodeoxycholic acid and prior participation in a seladelpar clinical trial could enroll in ASSURE. Key end points were the composite biochemical response (alkaline phosphatase (ALP) $<1.67\times$ upper limit of normal (ULN), ALP decrease $\geq 15\%$, and total bilirubin \leq ULN) and ALP normalization. Pruritus was reported using a numerical rating scale (NRS; 0–10). Baseline for participants who entered ASSURE from RESPONSE was entry to RESPONSE, analyzed as continuous seladelpar or crossover from placebo. Legacy patients were analyzed separately with baseline set as the entry to ASSURE.

Results: As of 31 January 2024, 158 patients from RESPONSE and 179 patients from legacy studies had received 10 mg seladelpar, daily, for up to 155 weeks in ASSURE. In RESPONSE, 61.7% (79/128) of seladelpar patients met the composite end point at Month 12 vs 20% (13/65) for placebo. With continued treatment in ASSURE, 61.8% (63/102) at 6 months in ASSURE and 72.4% (21/29) at 12 months in ASSURE met the composite end point. Among placebo patients crossing over to seladelpar, 75% (39/52) at 6 months and 93.8% (15/16) at 12 months met the composite end point. ALP normalized in 25% of seladelpar and 0 placebo patients at Month 12 in RESPONSE. With continued treatment, 33.3% (6 months) and 17.2% (12 months) had ALP normalization. For crossover patients, 26.9% and 50% had ALP normalization at these timepoints. The change in pruritus NRS with seladelpar in ASSURE was similar to RESPONSE: -3.8 and -3.7 change from baseline at 6 months in continuous and crossover patients, respectively, corresponding to the key secondary end point in RESPONSE. Among legacy patients, 73.2% (120/164) and 69.7% (69/99) met the composite end point at Month 12 and Month 24 in ASSURE. Normalization of ALP was achieved by 42.1% at 12 months and 42.4% at 24 months. Reduction in pruritus NRS in this group was -3.8 at Month 12 and -3.1 at Month 24. The safety profile was favorable with no treatment-related serious adverse events.

Conclusion: Continuous treatment with seladelpar for RESPONSE and legacy patients led to sustained effects on biochemical markers and pruritus. Seladelpar appeared safe and well tolerated with long-term use.

LBP-041

Screening and comparison of current clinical candidates in MASH using human 3D liver spheroids

Philip Vonschallen¹, Thomas Hofstetter¹, Radina Kostadinova¹, Jesus Glaus¹, Angelina Freitag¹, Francine Spalinger¹, Joel Zwick¹, Francisco Verdeguer¹. ¹InSphero AG, Schlieren, Switzerland Email: philip.vonschallen@insphero.com

Background and aims: Metabolic dysfunction-associated steatohepatitis (MASH) is a progressive severe disease characterized by hepatic lipid accumulation, inflammation, and fibrosis which lacks any approved drug therapy. Novel approaches to identify therapeutic candidates that predict clinical responses are needed. Human pre-clinical models, including organoids/spheroids, are powerful models for drug testing and discovery. Pre-clinical models combining fast, robust, high-throughput compatible and predictive outputs are still a limiting factor to identify novel clinical therapies. We aimed at performing a comparison of the safety and efficacy of existing clinical candidates for MASH in high-throughput manner using a human-derived 3D liver spheroid model and multiplex readouts.

Method: We used a previously developed a human-derived 3D liver spheroid model in 96-well plates, containing primary human hepatocytes, Kupffer cells, endothelial cells, and stellate cells from healthy donors. Incubation with a MASH-inducing cocktail of the 3D liver model during 10 days lead to the recapitulation of the main hallmarks of MASH including steatosis, inflammation, and fibrosis. We screened simultaneously the safety and efficacy of 20 current

clinical candidates in a concentration-dependent manner. We selected secreted lactate dehydrogenase (LDH), intracellular triglycerides (TGs) and secreted pro-collagen 1 (PC-1) as surrogate markers of cytotoxicity, steatosis and fibrosis. LDH was measured at day 3, 5, 7 and 10, TGs at day 10 and PC-1 at day 7 and 10.

Results: The screen of 20 clinical candidates comprised different modalities including small molecules, antibodies, and antisense oligos (ASOs) targeting different mechanisms of action. The majority of compounds did not show signs of toxicity at lower doses but some lead to high LDH release at higher doses. We generated a matrix of anti-steatotic versus anti-fibrotic effect to plot the comparison of all tested clinical candidates. Examples of successful translational effect are the FASN inhibitor TVB2640 (Sagimet) showing a significant reduction of triglycerides and the α v β 1 integrin inhibitor (PLN-1474) demonstrating a strong reduction of PC-1 secreted levels.

Conclusion: We show for the first time a screening platform that combines safety and MASH efficacy readouts. We show the translational capacity of this human in-vitro 3D platform by recapitulating the clinical effects of several drug candidates.

LBP-042

First-in-human clinical result of a novel HBV-specific TCR T cell therapy (SCG101) in patients with HBV-related hepatocellular carcinoma (HCC)

Xueshuai Wan¹, Wei Wu², Yunpeng Liu³, Shunda Du¹, Wei Li⁴, Dongmei Quan², Ke Zhang⁵, Karin Wisskirchen⁶, Ulrike Protzer⁷, Yuhong Zhou⁴, Xiujuan Qu³. ¹Peking Union Medical College Hospital, Beijing, China; ²The Sixth People's Hospital of Shenyang, Shenyang, China; ³The First Hospital of China Medical University, Shenyang, China; ⁴Zhongshan Hospital, Fudan University, Shanghai, China; ⁵SCG Cell Therapy, Shanghai, China; ⁶SCG Cell Therapy, Munich, Germany; ⁷Institute of Virology, Helmholtz Munich, Munich, Germany
Email: qu_xiujuan@hotmail.com

Background and aims: SCG101, a first-in-class autologous HBV-specific TCR-T cell therapy that utilizes a natural, high-affinity TCR, has been evaluated for its antiviral and antitumor activities in patients with HBV-related HCC in an investigator-initiated phase I trial. Here, we present the summary of the clinical results of the trial.

Method: The trial enrolled 6 HLA-A*02:01 (+), serum HBsAg (+), and HBeAg (-) patients with advanced HBV-related HCC (BCLC B/C) who had received one to three prior systemic therapies. All patients received a single dose of SCG101 at 5×10^7 or 1×10^8 cells/kg intravenously 3 days after lymphodepletion. Safety, pharmacokinetics, pharmacodynamics, and efficacy of SCG101 were evaluated.

Results: After infusion, SCG101 showed dose-dependent proliferation. Serum HBsAg levels dropped in all six patients; four (66.7%) had a reduction $>1 \log_{10}$, with three of them maintaining <10 IU/ml for up to 21 months. Transient ALT elevation, correlating with serum HBsAg reduction, was observed in all patients, indicating on-target activity of SCG101. Tumor control was achieved in all four patients with HBsAg reduction $>1 \log_{10}$, with two exhibiting a partial response (PR) and two stable disease (SD) per mRECIST. The objective response rate (ORR) was 33.3%. Both patients with PR maintained remission for over 6 months. One patient achieved complete remission of the target lesion and remained progression-free for 27 months (data cut-off 9-Mar-2024). The other achieved durable remission with a tumor reduction of 74.6%. Patients with HBsAg reduction $<1 \log_{10}$ experienced disease progression. Median progression-free survival (mPFS) and overall survival (mOS) in patients with HBsAg reduction $>1 \log_{10}$ were longer than those without (mPFS: 5.9 vs 0.7 months, mOS: 19.0 vs 6.3 months as of the data cut-off). Overall, SCG101 treatment was well-tolerated, with no dose-limiting toxicity or neurotoxicity observed. The most common treatment-related adverse events were elevated liver enzymes, cytokine release syndrome, and cytopenia.

Conclusion: SCG101, as a monotherapy for patients with HBV-related HCC, demonstrated antiviral and antitumor activities alongside a

survival benefit and manageable safety profile. The persistence of SCG101, reduction of serum HBsAg, and tumor response collectively underscore its on-target activity. A phase II trial to evaluate the safety and efficacy of SCG101 in HLA-A*02:01 (+) patients with HBV-related HCC will be initiated.

LBP-043

A phase 1, dose-escalation and dose-expansion study evaluating the safety, tolerability, pharmacokinetics and preliminary efficacy of AHB-137 in Chinese healthy volunteers and subjects with chronic hepatitis B

Wen Wang¹, Xieer Liang², Hong Ren³, Xian Yu³, Chongyuan Xu², Jiajia Mai¹, Jinlin Hou², Hong Zhang¹, Fu Kuang³, Junting Wang⁴, Tianwen Lan⁴, Yilei Wen⁴, Haixia Cao⁴, Bingxia Lu⁴, Xiaoli Wu⁴, Tingting Lu⁴, Xiao Qiu⁴, Chen Yang⁴, Lidan Wang⁴, Di Zhao⁴, Miao Wang⁴, Cheng Yong Yang⁴, Guofeng Cheng⁴, Junqi Niu⁵, Yanhua Ding¹. ¹Phase I Clinical Trial Center, The First Hospital of Jilin University, Changchun, China; ²Nanfang Hospital, Southern Medical University, Guangzhou, China; ³The Second Affiliated Hospital, Chongqing Medical University, Chongqing, China; ⁴Ausper Biopharma, Hangzhou, China; ⁵The First Hospital of Jilin University, Changchun, China
Email: dingyanhua2003@126.com

Background and aims: AHB-137, an antisense oligonucleotide (ASO) with a favorable preclinical safety profile and strong antiviral activity, is in early-stage clinical development. Here, we report the safety and pharmacokinetics (PK) data of AHB-137 from an ongoing phase I clinical study in China.

Method: 52 Chinese healthy volunteers (HVs) were enrolled into four placebo-controlled single ascending dose (SAD, 6:2) cohorts of 75 mg, 150 mg, 300 mg, and 450 mg and two multiple ascending dose (MAD, 8:2) cohorts of 150 mg and 300 mg. As of April 2nd, 2024, 20 hepatitis B e antigen (HBeAg) negative chronic hepatitis B (CHB) subjects under stable nucleos (t)ide analogue (NA) treatment with hepatitis B surface antigen (HBsAg) between 100 and 1,000 IU/ml were sequentially enrolled into 150 mg or 300 mg placebo-controlled MAD cohorts (n = 10, 8:2, 6 doses within 4 weeks). 10 CHB subjects with baseline HBsAg up to 3,000 IU/ml were enrolled into a 300 mg expansion cohort (open-label, 6 doses within 4 weeks). All doses were administered subcutaneously.

Results: The 52 HVs, with average age of 40.8 years and equal ratio of gender, had successfully completed the study. The 30 enrolled CHB subjects were mostly male (73.3%) with average age of 44.9 years. There were no serious adverse events (SAEs) and no treatment discontinuations due to adverse events (AEs) in HVs and CHB subjects. Most treatment-related adverse events (TRAEs) were mild or moderate. The most common TRAEs (incidence >1 subject) included injection site reactions, ALT increased, AST increased, and the following AEs that transiently occurred after the first dose: pyrexia, C-reactive protein increased, and lymphocyte count decreased, in both HVs and CHB subjects. Single dose of AHB-137 was well absorbed (T_{max} 3.5–5.0 hours), with rapid distribution to peripheral tissues, and slow elimination ($t_{1/2}$ approximately 85.8–90.5 hours). Plasma exposure increased with dose from 75 mg to 450 mg. No accumulation observed with repeated doses. Doses of 150 mg and 300 mg for 4 weeks resulted in a rapid dose-dependent reduction in HBsAg levels. Significant HBsAg reductions were observed in CHB subjects with HBsAg between 100 and 1,000 IU/ml as well as between 1,000 and 3,000 IU/ml.

Conclusion: AHB-137 administered subcutaneously as SAD up to 450 mg and MAD up to 300 mg was safe and well tolerated in both HVs and CHB subjects. Overall, AHB-137 was well tolerated, had favourable PK profile, and promising efficacy results, supporting the further development of AHB-137 as a candidate for functional cure of CHB.

LBP-044

Robust reduction of HBsAg and HDV RNA levels with low risk for ALT elevations in JNJ-73763989 treated patients with chronic hepatitis D (CHD) and baseline HBsAg levels below 10,000 IU/ml: part 2 of the REEF-D study

Heiner Wedemeyer¹, Pietro Lampertico², Edward J. Gane³, Kosh Agarwal⁴, Fehmi Tabak⁵, Ulus Akarca⁶, Soo Aleman⁷, Maria Buti⁸, Kathrin Sprinzl⁹, Kathleen Donohue¹⁰, John Jerzowski¹¹, Thomas Kakuda¹², Thierry Verbinen¹³, Adam Bakala¹³, Oliver Lenz¹³, Michael Biermer¹³. ¹Department of Gastroenterology, Hepatology and Endocrinology, Hannover Medical School, Excellence Cluster RESIST, and D-SOLVE Consortium, Hannover, German Center for Infection Research (DZIF) Partner Site Hannover-Braunschweig, Hannover, Germany; ²Division of Gastroenterology and Hepatology, Foundation IRCCS Ca' Granda Ospedale Maggiore Policlinico, CRC "A. M. and A. Migliavacca" Center for Liver Disease, Department of Pathophysiology and Transplantation, University of Milan, Milan, Italy; ³New Zealand Liver Transplant Unit, University of Auckland, Auckland, New Zealand; ⁴Institute of Liver Studies, King's College Hospital, London, United Kingdom; ⁵Department of Infectious Diseases, Cerrahpasa Medical Faculty, Istanbul University-Cerrahpasa, Istanbul, Turkey; ⁶Division of Gastroenterology, Department of Internal Medicine, Ege University, School of Medicine, Izmir, Turkey; ⁷Department of Infectious Diseases, Karolinska University Hospital/Karolinska Institutet, Stockholm, Sweden; ⁸Hospital General Universitari Val de Hebron, CIBER-EHD del Instituto Carlos III, Barcelona, Spain; ⁹Goethe University Frankfurt, University Hospital, Medical Clinic 1, Frankfurt a.M., Germany; ¹⁰Cytel Inc., Waltham, MA, United States; ¹¹Janssen Research and Development, LLC, Trenton, NJ, United States; ¹²Janssen Research and Development, LLC, Brisbane, CA, United States; ¹³Janssen Pharmaceutica NV, Beerse, Belgium
Email: wedemeyer.heiner@mh-hannover.de

Background and aims: The siRNA JNJ-73763989 (JNJ-3989) profoundly reduced HBsAg in patients with chronic hepatitis B. In Part-1 of the REEF-D study, this reduction was associated with serum HDV RNA decline in patients with chronic hepatitis D (CHD). Treatment discontinuation due to relevant ALT elevations was primarily seen in patients with high HBsAg and HDV RNA levels at screening. Based on predefined virologic response criteria in Part-1, the confirmatory Part-2 was initiated with modified inclusion and stopping criteria for ALT elevations.

Method: In REEF-D, a phase 2, multicenter, randomized, double-blind, placebo-controlled study, adult participants with CHD were enrolled. After observing ALT elevations in Part-1, Part-2 excluded patients with liver cirrhosis and those with a combination of HBsAg >10,000 IU/ml and HDV RNA >100,000 IU/ml. Patients were randomized 4:1 to receive JNJ-3989 (100 mg sc. Q4W) + NA for 144 weeks (immediate active) or placebo + NA for 52 weeks followed by JNJ-3989 + NA for 96 weeks (deferred active). Changes in serum viral markers and safety were assessed. For Part-2, the primary composite end point reported here is the proportion of patients with HDV RNA decline from baseline (BL) of $\geq 2 \log_{10}$ IU/ml (or undetectable) and normal ALT at treatment week (TW) 48.

Results: Of 30 patients enrolled in Part-2, 24 and 6 were randomized to the immediate and deferred treatment arms and 15 and 6 completed the double-blind phase up until TW48, respectively. The primary end point was met by 7/15 completers (47%) and 7/24 overall (29%) versus 0 in the deferred arm. Among 15 completers in the immediate active arm 10 (67%) reached an HDV RNA decline from BL of $\geq 2 \log_{10}$ IU/ml and 7 (47%) had HDV RNA <LOQ at TW48 and mean (SE) reductions of HBsAg and HDV RNA from BL were 2.44 (0.238)/2.09 (0.294) \log_{10} IU/ml in the immediate arm versus 0.02 (0.026)/0.19 (0.199) \log_{10} IU/ml in the deferred arm. Nine of 24 (37.5%) patients in the immediate arm had treatment-emergent ALT elevations ($\geq 3 \times$ upper limit of normal and $\geq 2 \times$ nadir), which resulted in early discontinuation of JNJ-3989 in 7 patients. Six of those 7 patients had HBsAg levels at screening of >10,000 IU/ml. In contrast, only one

of 16 (6%) patients with HBsAg <10,000 IU/ml at screening had an on-treatment ALT elevation leading to discontinuation. In general, ALT elevations returned to BL values after treatment discontinuation and no cases of liver decompensation occurred. Besides ALT elevations, no other safety issues were observed including four participants from Part-1 who continued treatment with JNJ-3989 for up to 144 weeks. **Conclusion:** Patients with screening HBsAg <10,000 IU/ml had a low risk for ALT flares and showed a profound and sustained on-treatment suppression of HBsAg and HDV RNA. ALT elevations seen in patients with HBsAg $\geq 10,000$ IU/ml were safely managed with strict stopping criteria for JNJ-3989.

LBP-045

Efficacy and safety of HSK31679, a thyroid hormone receptor β agonist, for the treatment of asian non-alcoholic fatty liver disease: a multicenter randomized, double-blind, placebo-controlled, phase 2a trial

Feng Xue¹, Wei Ma², Jixian Gao³, Jinjun Chen⁴, Wei Yue⁵, Peili Bu⁶, Qincong Chen⁷, Hao Chen⁷, Jianlong Sheng⁸, Liang Chen⁹, Fei Liu¹⁰, Chuanwu Zhu¹¹, Bihui Zhong¹², Guang-Ming Li¹³, Jianming Zhang¹⁴, Le Wang¹⁵, Qingxian Cai¹⁶, Zhaohui Pei¹⁷, Ying Chen¹⁸, Lvfang Yao¹⁹, Lingchun Lv²⁰, Yanhang Gao²¹, Bihua Xia²², Xianyou Ji²³, Yang Liu²⁴, Laijing Du²⁵, Genshan Ma²⁶, Kunyan Hao²⁷, Yong Huo², Lai Wei¹. ¹School of Clinical Medicine, Tsinghua University, Hepatopancreatobiliary Center, Beijing Tsinghua Changgung Hospital, Tsinghua University, Beijing, China; ²Department of Cardiology, Peking University First Hospital, Beijing, China; ³Department of Cardiology, Cangzhou People's Hospital, Cangzhou, China; ⁴Department of Infectious Diseases, Nanfang Hospital, Southern Medical University, Guangzhou, China; ⁵Department of Infectious Disease, The First People's Hospital of Yunnan Province, Kunming, China; ⁶Department of Cardiology, Qilu Hospital of Shandong University, Jinan, China; ⁷Department of Cardiology, Shijiazhuang People's Hospital, Shijiazhuang, China; ⁸Department of Cardiology, The Second Hospital of Anhui Medical University, Hefei, China; ⁹Department of Hepatic Diseases, Shanghai Public Health Clinical Center, Shanghai, China; ¹⁰Department of Infectious Diseases, Xiangya Hospital Central South University, Changsha, China; ¹¹Department of Hepatology, The Fifth People's Hospital of Suzhou, Suzhou, China; ¹²Department of Gastroenterology, The First Affiliated Hospital, Sun Yat-sen University, Guangzhou, China; ¹³Department of Hepatology, The Sixth People's Hospital of Zhengzhou, Zhengzhou, China; ¹⁴Department of Cardiology, Chongqing University Three Gorges Hospital, Chongqing, China; ¹⁵Department of Cardiology, The First Hospital of Hebei Medical University, Shijiazhuang, China; ¹⁶Department of Hepatic Diseases, Shenzhen Third People's Hospital, Shenzhen, China; ¹⁷Department of Cardiology, Nanchang People's Hospital, Nanchang, China; ¹⁸Department of Cardiology, The Fourth People's Hospital of Chenzhou, Chenzhou, China; ¹⁹Department of Hepatic Diseases, Mengchao Hepatobiliary Hospital of Fujian Medical University, Fuzhou, China; ²⁰Department of Cardiology, Lishui Central Hospital, Lishui, China; ²¹Department of Hepatology, The First Hospital of Jilin University, Changchun, China; ²²Department of Cardiology, The Second Affiliated Hospital of Guizhou Medical University, Qiandongnan Miao and Dong Autonomous Prefecture, China; ²³Department of Cardiology, Daqing Shi People's Hospital, Daqing, China; ²⁴Department of Endocrinology, Daqing Shi People's Hospital, Daqing, China; ²⁵Department of Cardiology, The First Affiliated Hospital of Henan University of Science and Technology, Luoyang, China; ²⁶Department of Cardiology, Zhongda Hospital Southeast University, Nanjing, China; ²⁷Department of Hepatic Diseases, Chinese People's Liberation Army East Theater General Hospital, Nanjing, China
Email: weelai@163.com

Background and aims: Non-alcoholic fatty liver disease (NAFLD) may progress to non-alcoholic steatohepatitis (NASH), which is associated with high liver-related or all-cause mortality. We

evaluated the efficacy and safety of the thyroid hormone receptor β agonist HSK31679 in Asian patients with NAFLD.

Method: This was a phase 2a, multicenter, randomized, double-blind, placebo-controlled study at 26 centres in China. Liver fat content (LFC) was assessed by magnetic resonance imaging-proton density fat fraction (MRI-PDFF) at screening and Week 12. Subjects with an LFC of $\geq 8\%$ at screening and low-density lipoprotein cholesterol (LDL-C) ≥ 3.44 mmol/L were eligible. Subjects were stratified according to the LFC $\geq 17.5\%$ or $< 17.5\%$ and were randomized 1:1:1:1 to oral HSK31679 doses of 40 mg QD, 80 mg QD, 160 mg QD, placebo, or ezetimibe 10 mg QD. The primary end point was a relative reduction from baseline in LFC (%) after 12 weeks of treatment.

Results: 784 participants were screened and 210 were randomly assigned to the five groups at 26 sites in China. At baseline, 10.0% had 2 diabetes mellitus, 27.8% had hypertension, mean BMI was 29.0 kg/m², mean LFC was 17.0% and mean LDL-C was 4.37 mmol/L. At week 12, the least squares mean relative reduction from baseline in LFC was -4.1% in the placebo group, -14.0% in the 40 mg group (mean difference versus placebo -9.9% [95% CI -21.5% to 1.6%], $p = 0.092$), -22.7% in the 80 mg group (-18.6% [-30.2% to -7.0%], $p = 0.002$), and -29.2% in the 160 mg group (-25.2% [-36.8% to -13.5%], $p < 0.001$). The proportions of participants with $\geq 30\%$ relative reduction of LFC was 23.8% in the 40 mg HSK31679 group, 47.6% in the 80 mg HSK31679 group (difference versus placebo, $p = 0.006$), 50.0% in the 160 mg HSK31679 group (difference versus placebo, $p = 0.002$), 11.9% in the 10 mg ezetimibe group, and 17.1% in the placebo group. At least one treatment-emergent adverse event (TEAE) occurred in 24 (57.1%) of 42 patients in the 40 mg group, 31 (73.8%) of 42 patients in the 80 mg group, 31 (73.8%) of 42 patients in the 160 mg group, 24 (57.1%) of 42 patients in the ezetimibe group, and 17 (40.5%) of 42 patients in the placebo group. The most common TEAE was diarrhoea (11 [26.2%] of patients in the 40 mg group, 13 [31.0%] in the 80 mg group, 16 [38.1%] in the 160 mg group, 4 [9.5%] in the ezetimibe group, and 2 [4.8%] in the placebo group). Non-drug-related serious adverse events or grade 3 events were reported.

Conclusion: In Asian patients with NAFLD, 12 weeks of HSK31679 treatment was safe and well tolerated, with 80 mg and 160 mg treatment significantly reducing LFC.

LBP-046

A phase IIa basket clinical trial of allogeneic CD362-enriched umbilical cord-derived mesenchymal stromal cells (ORBCEL-CTM) in patients with primary sclerosing cholangitis and autoimmune hepatitis

Julian Yeh^{1,2,3}, Sheeba Khan^{1,3}, Sara Mahgoub^{1,2,3}, Nguyet Luu³, Victoria Homer⁴, Janine Fear⁵, Migena Tushe⁵, Pamela Jones⁶, Shahida Begum⁶, Diana Hull⁶, Kathryn Rodden⁷, Helen Coulthard⁸, Emma Burke⁶, Rhian Jones⁴, Anna Rowe⁴, Steven Elliman⁹, Tina McLeod¹⁰, Jacqui Thompson¹⁰, Darshna Patel¹⁰, Jon Smythe¹⁰, Amisha Desai¹¹, Debashis Halder¹, Ashnila Janmohamed¹, Ye Htun Oo^{1,2,3}, Palak J. Trivedi^{1,2,3}, Gideon M. Hirschfield¹², Philip N. Newsome^{1,2,3}. ¹Liver Unit, University Hospitals Birmingham NHS Foundation Trust, Birmingham, United Kingdom; ²National Institute for Health Research, Biomedical Research Centre at University Hospitals Birmingham NHS Foundation Trust and the University of Birmingham, Birmingham, United Kingdom; ³Centre for Liver and Gastrointestinal Research, Institute of Immunology and Immunotherapy, University of Birmingham, Birmingham, United Kingdom; ⁴Cancer Research UK Clinical Trials Unit, University of Birmingham, Birmingham, United Kingdom; ⁵Centre for Liver and Gastrointestinal Research, Institute of Immunology and Immunotherapy, University of Birmingham, Birmingham, United Kingdom; ⁶Liver Research Team, University Hospitals Birmingham NHS Foundation Trust, Birmingham, United Kingdom; ⁷University Hospitals Birmingham, NHS Foundation Trust-Liver Research Team, Birmingham, United Kingdom; ⁸University of Birmingham, Cancer Research UK Clinical Trials Unit, Birmingham, United Kingdom; ⁹Orbsen Therapeutics, Galway, Ireland; ¹⁰NHS Blood and Transplant Birmingham, Birmingham, United Kingdom; ¹¹University

Hospitals Birmingham NHS Foundation Trust, Pharmacy, Birmingham, United Kingdom; ¹²Toronto Centre for Liver Disease, Division of Gastroenterology and Hepatology, University Health Network, Toronto General Hospital, Toronto, Canada
Email: julian.yeh@nhs.net

Background and aims: Mesenchymal stromal cells (MSC) are novel therapeutics for inflammatory diseases. MERLIN is a single-arm, adaptive, basket trial investigating safety and efficacy of a single MSC infusion in patients with primary sclerosing cholangitis (PSC) and autoimmune hepatitis (AIH).

Method: Allogeneic umbilical cord derived, antibody-purified allogeneic CD362⁺ MSC (ORBCEL-CTM) were investigated at three potential doses; 1×10^6 cells/kg (start dose A), 2.5×10^6 cells/kg (dose B) and 0.5×10^6 cells/kg (dose C), using 3 + 3 design with de-escalation if the dose-limiting toxicity (DLT) rate was > 1 per 6 patients. The Highest Safe Dose (HSD) of MSC was determined by observing DLT defined as occurrence of adverse events graded 3–5 per the Common Terminology Criteria for Adverse Events within 14 days of infusion. Primary outcomes were safety/ascertainment of the HSD and a principal mechanistic outcome of change in circulating regulatory T cells (Treg) across both cohorts. Other outcomes included changes in serum ALP for PSC, serum ALT for AIH and circulating immune cell populations.

Results: For AIH ($n = 6$); mean age 48 (28–77) and 2 females. For PSC ($n = 12$); mean age 41 (27–73) and 3 females. 75% had concurrent PSC colitis. In the AIH cohort, 3 patients were recruited to dose levels A and B with no DLTs reported. In the PSC cohort there was one DLT at each dose level and thus 6 patients were treated at each dose. The HSD for both arms was 2.5×10^6 cells/kg. There were 7 reported serious adverse events across 5 patients. Related/possibly related events included fever, cholangitis, viral myocarditis, ALT and AST rises. The DLTs consisted of a rise in ALT/AST > 10 times the upper normal limit at 1×10^6 cells/kg dose, later identified as a flare of AIH in a PSC patient with immune overlap syndrome. The second DLT was an episode of viral myocarditis at the 2.5×10^6 cells/kg dose, possibly related to COVID19. In repeated measures analysis of the primary mechanistic outcome there was an increase in total circulating CD25^{HI} Tregs following MSC infusion from 3.12% of CD4 population to 3.84% at day 14; $p = 0.0085$, with a rise in activated Tregs (FOXP3^{HI}CD45RA⁺) peaking at day 3 from 1.23% to 1.39%; $p = 0.0016$. At the HSD for patients with AIH, there was a significant decrease in ALT by day 28 post MSC; -41.54% (95% CI: -70.7 – 12.4). ALP values in patients with PSC showed no change. Repeated measures analysis of M1:M2 polarisation in the PSC cohort (but not for AIH) demonstrated a reduction in mean M1:M2 ratio from 5.85 to 4.17 by day 14 post MSC $p = 0.043$.

Conclusion: In this population of 18 patients the HSD of MSC was identified as 2.5×10^6 cells/kg. MSC were well tolerated in both AIH and PSC patients albeit with two DLT events in the PSC group. We observed expansion of Treg in response to the administration of MSC in both groups, a reduction in ALT in the AIH group, and a shift in macrophage polarisation toward a more immune-tolerant M2 state in PSC.

LBP-047

Development and validation of CLDQ-MASH: a disease specific health related quality of life instrument for patients with metabolic dysfunction-associated steatohepatitis (MASH)

Zobair Younossi¹, Maria Stepanova¹, Issah Younossi¹, Andrei Racila¹.
¹The Global NASH Council, Washington, United States
Email: zobair.younossi@cldq.org

Background and aims: The new nomenclature for metabolic dysfunction associated steatohepatitis (MASH) requires presence of steatohepatitis in the context of at least one cardiometabolic risk (CMR). MASH is now considered the most common form of chronic liver disease with a global prevalence of 5–7%. MASH not only causes significant clinical burden (cirrhosis, hepatocellular carcinoma and liver mortality) but also leads to impairment of health-related quality

POSTER PRESENTATIONS

of life (HRQL) and other patient reported outcomes (PROs). Given the changes in the definition (requirement for CMR) with the new terminology, a HRQL instrument specifically for patients with MASH is important for clinical research and clinical trials.

Method: From our NASH/MASH Databases, we included patients with established diagnosis of MASH according to the new criteria. Patients had completed CLDQ, CLDQ-NAFLD, and other PRO instruments [Functional Assessment of Chronic Illness Therapy-Fatigue (FACIT-F)] and had available clinico-laboratory data. The CLDQ-MASH was developed following a standard pipeline (Younossi Z et al. Gut 1999) to develop and validate disease-specific HRQL instruments; the instrument was validated in a non-overlapping set of subjects.

Results: There were 8003 metabolic dysfunction-associated steatotic liver Disease (MASLD) patients in our databases who also had PRO scores collected (age: 54 ± 12 years, male: 46%, body mass index (BMI): 33 ± 7 , BMI >25 : 94%, type 2 diabetes: 55%, biopsy-proven MASH: 53%, biopsy-proven advanced fibrosis (F3-F4): 36%). The MASH sample was split 1:2 into training set used for development of the instrument and testing set which was used for validation. After item reduction and exploratory factor analysis with the training set, the CLDQ-MASH was developed to contain 35 items and 7 domains. With the non-overlapping testing set, CLDQ-MASH demonstrated excellent face validity and internal consistency (Cronbach's $\alpha > 0.85$ for 6/7 domains) as well as known-groups validity (based on disease severity and the presence of non-hepatic comorbidities) and high correlations with relevant domains of other instruments ($p < 0.01$). Other psychometric assessments are current ongoing and will be available.

Conclusion: The CLDQ-MASH is a disease-specific HRQL instrument developed and validated using an established methodology and useful for clinical trials of MASH.

LBP-048

Preclinical proof of concept and discovery of siRNA therapeutics targeting CIDEB for metabolic dysfunction-associated steatohepatitis

Jianhua Zhang¹, Xujie Liu², Xudong Mao¹, Xueli Xu¹, Xing Zhang¹, Ke Shang¹, Xian Jin¹, Yuan Xu¹, Guofeng Meng², Ming Yue², Song Yang², Jinyu Huang², Jianwu Fang², Ling Pan², Lei Jiang¹, Stella Shi², Jianyong Shou¹. ¹Shanghai EnnovaBio Pharmaceuticals Co., Ltd., Shanghai, China; ²Shanghai RONA Therapeutics Co., Ltd., Shanghai, China

Email: jianyong.shou@ennovabio.com

Background and aims: CIDEB, a member of the CIDE (cell death-inducing DNA fragmentation factor alpha-like effector) family of

proteins, is a lipid droplet (LD)-associated protein with high expression in the liver. It is involved in the regulation of very-low-density lipoprotein secretion, LD fusion and growth, and lipogenesis. Germline mutations in CIDEB have been found to confer protection against various liver diseases in humans, highlighting its significance as a potential therapeutic target for the treatment of metabolic dysfunction-associated steatohepatitis (MASH) as well as other related liver diseases. However, whether liver specific inhibition of CIDEB will bring potential clinical benefits remains to be determined. Our goals are to establish preclinical proof of concept by liver-targeting *Cideb* siRNAs for MASH and to develop siRNA drug candidates for clinical investigations in humans.

Method: Surrogate siRNAs targeting rodent *Cideb* were designed and tested via *in vitro* and *in vivo* assays for knock-down (KD) efficiency, duration, and cytotoxicity. *In vivo* administration of the surrogate siRNAs was conducted in two animal models: 1) diet-induced obesity (DIO) model and 2) choline-deficient L-amino acid defined high fat diet (CDAA-HFD) model. In each study, plasma and liver lipid levels were measured and liver histopathology features were analyzed. Additionally, RNA-seq analysis of liver tissues was also performed to gain a comprehensive systems biology understanding of *Cideb* target biology. Concurrently, humanized *Cideb* knock-in mice were generated to serve as a research tool for screening and validating human therapeutic siRNAs.

Results: The lead surrogate siRNA potentially reduced *Cideb* mRNA level in primary mouse hepatocytes (IC_{50} 0.012 nM) without obvious cytotoxicity and off-target risks. Dose-dependent *Cideb* target KD effects were confirmed in both efficacy studies. Single administration of the surrogate siRNA (2, 10 mg/kg) resulted in more than 80% target KD up to two weeks. In the DIO model, *Cideb* KD led to significant reductions of plasma total cholesterol (TC) and triglyceride (TG) levels, a significant decrease in hepatic macro-steatosis and notable body weight loss. Furthermore, in the CDAA-HFD model, siRNA treatment resulted in significant reductions of liver weight as well as liver TC and TG levels. Consistently, remarkable reductions of both macro- and micro-steatosis and a significant NAS score reduction were observed. Importantly, histopathology analysis indicated a significant improvement of liver fibrosis. In parallel, candidate-like human *CIDEB* targeting molecules have been discovered through our proprietary siRNA drug discovery platform.

Conclusion: CIDEB exhibits significant potential as a therapeutic target for the treatment of MASH. Liver-targeting siRNA candidates are being developed to test the therapeutic hypothesis in humans.

Acute liver failure and drug induced liver injury – Basic

TOP-349-YI

Plasma lipidomics and fungal peptide-based community analysis identifies signatures of severity and early mortality in acute liver failure

Neha Sharma^{1,2}, Jaswinder Maras¹, Sushmita Pandey¹, Gaurav Tripathi¹, Manisha Yadav¹, Nupur Sharma¹, Babu Mathew¹, Vasundhra Bindal¹, Sadam H Bhat¹, Rakhi Maiwall¹, Shvetank Sharma¹, Shiv Kumar Sarin¹. ¹Institute of Liver and Biliary Sciences, NEW DELHI, India; ²Institute of Liver and Biliary Sciences, Molecular and cellular medicine, Delhi, India
Email: jassi2param@gmail.com

Background and aims: Acute liver failure (ALF) is a rapidly progressive disease with high mortality. Ongoing hepatocellular injury is likely to produce severe metabolic alterations that compromise the immune system and increase vulnerability to bacterial and fungal infections. We performed lipidome- (Lipid Species) landscape and fungal peptide-based community analysis- (mycobiome) to identify integrated metabolic signatures that segregate ALF non-survivors; (ALF-NS) and survivors; (ALF-S).

Method: Baseline plasma samples of 300 subjects (270-ALF, 30-healthy) were enrolled. Lipidomics and mycobiome analysis were performed in training cohort; [40 ALF, 5 controls]. Weighted lipid/ Fungal correlation network analysis- (WL/FCNA) was correlated to disease severity and outcome. The probability of detection for mortality based on lipids and fungal-peptides was validated on test cohort [230 ALF; non-survivor-146, survivor-84] using High-resolution-mass-spectrometry- (HRMS) and machine learning- (ML).

Results: Untargeted lipidomics provided plasma lipid landscape in which total of 2, 013 lipid species and lipid-like metabolites associated with 8 lipid groups were identified from which 5 Lipid Species Phosphatidylcholine; PC (15:0/17:0), PC (20:1/14:1), PC (26:4/10:0), PC (32:0) and TG (4:0/10:0/23:6) significantly segregated ALF-NS (FC > 10, p < 0.05, FDR < 0.01). Fungal peptide-based diversity was significantly higher (Alpha/Beta diversity) linked to 4 phyla and >20 species were found dysregulated in ALF-NS (p < 0.05). Functionally ALF-NS specific fungal peptide was linked with lipid-metabolism, fatty acid elongation in ER and others (p < 0.05). We observed striking correlation between Shannon-lipid and Shannon-fungal diversity profile in ALF-NS ($r^2 > 0.7$, p < 0.05). MMCN analysis showed striking associations between lipid and Fungal-peptides modules, functionality and Clinical parameters specific to ALF-NS (p < 0.05). Increased Basidiomycota; *Trametes pubescens*, *Cryptococcus amyloletus* CBS6039, Ascomycota; *Penicillium oxalicum* 1142, *Cladophialophora bantiana* CBS173.52 and their functionality directly correlated with lipid classes such as Phosphatidylcholine, Triglycerides, others and severity in ALF-NS ($r^2 > 0.85$, p < 0.05). POD-lipid associated with hepatic encephalopathy whereas POD-fungus associated with infection, necrosis and multi-organ-failure (Beta > 1.2, p < 0.05). POD-Lipid (AUC = 0.969) superseded POD-Mycobiome and severity with HR = 1.5 (1.021–1.844) for early mortality. Finally, POD-lipid > 25% predicted early mortality and the lipid panel

showed > 95% accuracy/sensitivity/specificity (ML) for prediction of mortality.

Conclusion: In ALF plasma lipidome and mycobiome are dysregulated. Increased plasma levels of Phosphatidylcholine could stratify ALF predisposed to early mortality or require emergency liver transplantation.

TOP-350-YI

DNA differential methylation as a potential drug-induced liver injury biomarker and genome-wide DNA methylation functional analysis

Romina De los Santos Fernández¹, Marina Villanueva², Ismael Alvarez-Alvarez¹, Hao Niu¹, Camilla Stephens¹, Andrés González Jiménez³, Guillermo Paz López³, Jose Pinazo Bandera⁴, Gonzalo Matilla⁴, Maria Isabel Lucena⁴, Inmaculada Medina-Caliz⁵, Raul J. Andrade⁴. ¹Servicios de Aparato Digestivo y Farmacología Clínica, Hospital Universitario Virgen de la Victoria, Instituto de Investigación Biomédica de Málaga y Plataforma en Nanomedicina-IBIMA Plataforma BIONAND, Universidad de Málaga, Málaga, Spain; ²Servicios de Aparato Digestivo y Farmacología Clínica, Hospital Universitario Virgen de la Victoria, Instituto de Investigación Biomédica de Málaga y Plataforma en Nanomedicina-IBIMA Plataforma BIONAND, Universidad de Málaga, Málaga, Spain; ³Instituto de Investigación Biomédica de Málaga y Plataforma en Nanomedicina-IBIMA Plataforma BIONAND, Málaga, Spain; ⁴Servicios de Aparato Digestivo y Farmacología Clínica, Hospital Universitario Virgen de la Victoria, Instituto de Investigación Biomédica de Málaga y Plataforma en Nanomedicina-IBIMA Plataforma BIONAND, Universidad de Málaga, Málaga, Spain; ⁵Servicios de Aparato Digestivo y Farmacología Clínica, Hospital Universitario Virgen de la Victoria, Instituto de Investigación Biomédica de Málaga y Plataforma en Nanomedicina-IBIMA Plataforma BIONAND, Universidad de Málaga, Málaga, Spain
Email: imcaliz@uma.es

Background and aims: Idiosyncratic drug-induced liver injury (DILI) is a complex pathology involving drug, host and environmental factors. In a previous analysis of our group, an overall tendency towards DNA hypomethylation was observed in the DILI group when compared to healthy subjects. This study aimed to identify the most affected cellular processes during a DILI episode and if DNA methylation in CpG sites is a good DILI biomarker when compared with healthy controls.

Method: Peripheral blood DNA was extracted from 32 DILI patients enrolled in the Spanish DILI Registry and 32 healthy controls. DNA methylation analysis was carried out by microarray assays using Infinium MethylationEPIC BeadChip Kit (Illumina). Whole-genome amplification and hybridization were performed with BeadChip microarray (Illumina). Cytosine methylation state was assessed by single-base extension and analysis with the HiScan SQ module (Illumina). Analysis of differentially methylated CpG sites, gene ontology (GO), and KEGG enrichment and kNN classification were done with R.

Results: The kNN classification analysis for the 347 most significant differentially methylated CpG sites (FDR ≤ 0.05 | Δ beta-value | ≥ 0.125) between groups has shown an AUC = 0.965. The kNN analysis using the minimum p value approach for the top 6 most significant differentially methylated CpG sites between groups resulted in an AUC = 0.932. The GO cellular component enrichment analysis has shown the top cellular functions associated with the most significant differentially methylated genes in DILI were related to cell junction processes and early endocytosis. The GO biological process enrichment analysis revealed the most significant differentially methylated genes in DILI were related to adaptive immune system activation, especially the ones involved in T-cell activation. Regarding the KEGG pathway enrichment analysis, the most relevant were those

POSTER PRESENTATIONS

implicated in endocytosis, platelet activation, MAPK and T-cell receptor signalling pathways.

Conclusion: This preliminary study has shown that differential CpG site methylation during a DILI episode is a potential DILI biomarker when compared with healthy controls. Moreover, during DILI episodes differential CpG site methylation was especially associated with genes involved in diverse processes on the cell membrane (early endocytosis, cell-cell junction and signalling pathways) and adaptive immune system activation. Funding: P119/00883, PEMP-2020-0127, PI21/01248, P18-RT-3364, PI-0310-2018, ISCIII CIBERehd, POSTDOC_21_00780, CD20/00083, CD21/00198. Funded by European Union: HORIZON-HLTH-2022-STAYHLTH-02, grant number 101095679.

TOP-351-YI

A therapeutic strategy to target CD47 using SIRP alpha expressed extracellular vesicles derived from engineered mesenchymal stem cells to promote liver regeneration following severe injury

Seohyun Kim¹, Yoonjeong Choi¹, Gi-Hoon Nam^{1,2}, In-San Kim^{3,4,5}.

¹SHIFTBIO INC., Seoul, Korea, Rep. of South; ²Korea University College of Medicine, Seoul, Korea, Rep. of South; ³SHIFTBIO INC, Seoul, Korea, Rep. of South; ⁴KU-KIST Graduate School of Converging Science and Technology Korea University, Seoul, Korea, Rep. of South; ⁵Korea Institute of Science and Technology, Seoul, Korea, Rep. of South
Email: kkksh03@shiftbio.net

Background and aims: CD47 is known to transmit a 'don't eat me' signal to immune cells and is overexpressed in pathological cells, including inflammatory dying cells. Consequently, uncleared dead cells in liver injury significantly contribute to a high pro-inflammatory process, exacerbating the condition. In this study, we aim to develop and validate the therapeutic efficacy of SIRP alpha over-expressed mesenchymal stem cell-derived extracellular vesicles (SIRP-EVs). SIRP-EVs can effectively block CD47 on dying hepatocytes, thereby facilitating their clearance through macrophages, mediating anti-inflammatory and pro-resolutive effects in acute liver injury.

Method: To explore CD47 as a promising therapeutic target in acute liver injury, we established various severe injury models using acetaminophen (APAP), thioacetamide (TAA), or carbon tetrachloride (CCl₄) and evaluated through histological analysis and spatial transcriptomics. SIRP-EV we developed strongly binds and blocks CD47, the 'don't eat me signal.' Using the IVIS Spectrum in vivo imaging system, we validated the biodistribution of SIRP-EV in normal and liver-injured mice. The therapeutic potential of SIRP-EV was evaluated in diverse mouse models by treating them with SIRP-EV and subsequently assessing liver enzyme levels, histological changes, survival rates, and inflammatory cytokine profiles.

Results: In this study, we observed CD47 overexpression in severely injured liver, predominantly on necroptotic hepatocytes. We found that SIRP-EV preferentially accumulated in the injured liver in a CD47-dependent manner; however, this accumulation was noticeably reduced when CD47 was pre-blocked using an anti-CD47 antibody. Treatment with SIRP-EV in acute liver-injured mice led to a notable improvement in liver histology and reductions in serum ALT and AST levels. Furthermore, SIRP-EV significantly increased survival rates, and the immune profile was transmitted from pro-inflammatory to pro-resolutive. We also demonstrated the therapeutic superiority of SIRP-EV over naïve MSC derived EVs and CD47 antibodies.

Conclusion: CD47 is a potent therapeutic target for acute liver injury. Importantly, SIRP-EV, which targets CD47, offers a promising strategy for treating acute liver injury by mitigating the inflammatory responses and inducing pro-resolutive immune responses.

TOP-352

Serum proteomics can help identify new prognostic biomarkers in adults with acute liver failure

Katharina Remih¹, Franziska Hufnagel¹, Anna Karl¹, Valerie Durkalski-Mauldin², William M. Lee³, Zemin Su², Jody Rule³, Petra Tomanova⁴, Laura Krieg⁵, Isabel Karkossa⁵, Kristin Schubert⁵, Martin von Bergen⁵, Sonja Luckhardt^{6,6}, Nicole Ziegler⁶, Aimo Kannt⁶, Robert Fontana⁷, Pavel Strnad¹. ¹University Hospital RWTH Aachen, Clinic for Gastroenterology, Metabolic Disorders, and Internal Intensive Medicine, Aachen, Germany; ²Medical University of South Carolina, Department of Public Health Sciences, Charleston, SC, United States; ³UT Southwestern Medical Center, Department of Internal Medicine, Division of Digestive and Liver Diseases, Dallas, TX, United States; ⁴Quantitative Consulting, Prague, Czech Republic; ⁵Helmholtz Centre for Environmental Research, Department of Molecular Systems Biology, Leipzig, Germany; ⁶Fraunhofer Institute for Translational Medicine and Pharmacology ITMP, Frankfurt am Main, Germany; ⁷University of Michigan, Department of Internal Medicine, Division of Gastroenterology, Ann Arbor, MI, United States
Email: kremih@ukaachen.de

Background and aims: Acute liver failure (ALF) is defined as rapid onset coagulopathy and encephalopathy in patients without prior history of liver disease. Liver transplantation (LT) represents the only curative treatment, but the decision for/against LT remains challenging. We used untargeted and targeted proteomics to explore novel diagnostic and prognostic proteomic/cytokine profiles in adult ALF patients.

Method: Serum proteomic and cytokine patterns were compared in 200 and 119 (discovery/validation cohort) adult ALF patients, ~50% were acetaminophen (APAP)-related and there were 30 healthy controls without liver disease. The former were randomly selected from admission samples (<48 h) of the multi-center US ALF study group database. Non-survivors had died or required LT within 21 days. Biomarkers were mapped to their presumed cell of origin from single cell RNAseq data and Ingenuity pathway analysis (Qiagen) was used to obtain mechanistic insights. Novel prognostic scores were calculated and compared to MELD and ALFSG Prognostic index scores.

Results: In the discovery cohort, 188 proteins were detected. 82% of these differed between ALF cases and healthy controls. The key altered pathways involved IL-6 signaling, acute phase response and prothrombin activation. 167 proteins differed between 95 APAP and 105 non-APAP cases of which 47% were hepatocyte derived. Among those hepatocyte derived proteins, 3 proteins (ALDOB, CAT and PIGR) were robust discriminators of ALF etiology (AUROCs ~ 0.9 in both cohorts). 37 proteins significantly differed between 21-day survivors and non-survivors (discovery cohort). The majority were secreted hepatocellular proteins that were nearly uniformly decreased in non-survivors. Activated immune and acute-phase responses were the most significantly enriched pathways and the latter associated with a better outcome. Cytokine profiling revealed most cytokines to be elevated in non-survivors, with interleukin 6 being most prominently affected. Alpha1-antitrypsin and leucine-rich alpha-2 glycoprotein constituted the best discriminators of 21-day survival (AUROCs >0.7 in both cohorts). Two mathematically derived 5-feature models including SERPINA1 outperformed MELD and ALFSG PI and were reproduced in the validation cohort (AUROCs of 0.83 and 0.85). Finally, combining SERPINA1 with the ALFSG PI numerically improved patient prognostication (from AUROC of 0.75 to 0.77).

Conclusion: Unbiased proteomics and cytokine profiling identified several new biomarkers associated with APAP vs non-APAP etiology and 21-day transplant free survival. Use of these biomarkers may improve prognostication and guide medical decision making in ALF patients and lead to improved understanding of the etiopathogenesis of ALF.

FRIDAY 07 JUNE

FRI-318-YI

NGFR inhibition by TAT-Pep5 protects mice from acetaminophen-induced liver injury

Laura Kitto¹, John Wilson-Kanamori¹, Neil Henderson¹. ¹Institute for Regeneration and Repair, Edinburgh, United Kingdom
Email: Laura.kitto@ed.ac.uk

Background and aims: Acetaminophen (APAP) poisoning is the commonest cause of acute liver failure (ALF) in the Western world. Therapeutic options for the treatment of APAP-induced liver injury (AILI) are limited. In severe AILI, transplantation remains the only curative option, but donor organ demand outstrips supply. Hepatic stellate cells (HSCs) play a central role during liver injury and regeneration. Traditionally HSCs were considered a functionally homogeneous population. However, single cell RNA sequencing (scRNA-seq) studies have revealed heterogeneity. Identification of an NGFR-expressing HSC subpopulation following AILI prompted us to specifically inhibit NGFR using TAT-Pep5 (TP5), which inhibits activation of Rho signalling through NGFR.

Method: 6–12-week-old male mice were fasted for 12 hours prior to intraperitoneal (IP) injection of APAP (300 mg/kg). eGFP⁺ (PDGFRβ⁺) mesenchymal cells were FACS-sorted from PDGFRβ-bac-eGFP mouse livers for scRNA-seq (10X Chromium). TP5 (1.7 mg/kg, dissolved in 10% DMSO/PBS) or N-acetylcysteine (NAC, 150 mg/kg) were administered by IP injection, 2 hours following APAP. Alanine aminotransferase (ALT) and glutathione (GSH) levels were assessed, along with percentage necrotic area in liver tissue. Flow cytometry and immunofluorescence staining was used to quantify hepatic immune cells.

Results: (1) scRNA-seq analysis of mesenchymal cells from healthy and APAP-injured mouse livers demonstrated an NGFR-expressing peri-portal subpopulation of HSCs, in both human and murine liver. Significant upregulation of NGFR was seen following both human (mean %area NGFR positive using IF, 12.96% uninjured vs. 38.70% AILI, $p=0.0022$) and murine (2.03% vs. 12.01%, $p=0.029$) AILI. (2) TP5 inhibition of NGFR *in vivo* reduced hepatic injury post-APAP, with a significant reduction in necrosis apparent from 12 hours post-injury (control mean necrosis 62.1% vs. TP5 39.2%, $p=0.0087$). (3) TP5 did not interfere with APAP metabolism, with comparable GSH levels in both groups (control mean GSH 2.47 μmol/g liver vs. TP5 2.35 μmol/g, $p=0.93$). (4) TP5 was as effective as NAC in reducing liver injury at 24 hours following AILI (ALT: NAC 1448 u/L, TP5 728 u/L, $p=0.11$, necrosis: 8.24% vs. 9.86%, $p=0.39$). (5) Delayed administration of NAC and TP5 led to loss of benefit (mean necrosis, 24 hours: control 26.6%, TP5 26.6%, NAC 22.8%, $p=0.642$). (6) TP5 treatment was associated with an early increase in infiltrating immune cells located specifically around the portal vein.

Conclusion: TP5 administration resulted in a significant reduction in hepatic injury following murine AILI. We have performed single nuclei RNA-seq of hepatic tissue from TP5 and control treated mice to help understand the mechanisms by which NGFR inhibition protects against AILI. Modulation of HSC NGFR signalling could represent a novel therapeutic strategy for patients with AILI.

FRI-319

SEMA6B triggers macrophage mediated systemic inflammation in acute-on-chronic liver failure

Hui Yang¹, Qun Cai², Jiaxian Chen¹, Xi Liang³, Jiaojiao Xin¹, Dongyan Shi¹, Jing Jiang¹, Jun Li¹. ¹State Key Laboratory for Diagnosis

and Treatment of Infectious Diseases, National Clinical Research Center for Infectious Diseases, National Medical Center for Infectious Diseases, The First Affiliated Hospital, Zhejiang University School of Medicine, Hangzhou, China; ²Department of Infectious Diseases and Liver Diseases, Ningbo Medical Center Lihuli Hospital, Affiliated Lihuli Hospital of Ningbo University, Ningbo, China; ³Precision Medicine Center, Taizhou Central Hospital (Taizhou University Hospital), Taizhou, China

Email: lijun2009@zju.edu.cn

Background and aims: Acute-on-chronic liver failure (ACLF) is a complex syndrome characterized by high short-term mortality. Semaphorin-6B (SEMA6B) crucial role in its pathogenesis is unclear. This study aims to clarify mechanisms of SEMA6B in ACLF.

Method: Fifty ACLF patients underwent mRNA sequencing with peripheral blood mononuclear cells (PBMCs). The mechanisms were validated *in vivo* with SEMA6B knockout mice, and *in vitro* with macrophage and hepatocytes.

Results: Transcriptome analysis of PBMCs showed that the expression of 5 genes (SEMA6B/PPARG/MERTK/ADAMTS2/FAM20A) were significantly higher in patients with ACLF than with liver cirrhosis, chronic hepatitis B and healthy subjects (all, $p<0.05$). Area-under-ROC analysis demonstrated that SEMA6B was the most robust diagnostic performance for ACLF development and prognostic performance for 28-day mortality (AUROCs = 0.9788/0.7692). Significant high-expression of SEMA6B was observed in ACLF-2/3, INR (≥ 2.5) and coagulation failure groups, and was significantly correlated with clinical indicators (INR, ALT) and pathways involved in 28-day ACLF non survivors (inflammatory-related pathways, apoptosis and oxidative phosphorylation). SEMA6B high-expression was observed in macrophage/hepatocytes in liver tissue of ACLF patients. Overexpression of SEMA6B in macrophages activated the immune-response and inflammatory-cytokines secretion (IL-6/IL-1β/IL-10/CCL2; all, $p<0.05$). The knockout of SEMA6B in liver failure mice improved the liver functions (ALT/AST/TBil/TBA; all, $p<0.05$) and downregulated the inflammatory cytokines expression (TNF-α/IL-6/IL-1β/IL-10; all, $p<0.05$), and significantly rescued liver failure mice ($p<0.05$). The downregulation of inflammation related biological processes (T cell proliferation and activation, interleukin-1 beta type II interferon and production, chemokine-/integrin-mediated pathways) and immuno-inflammation related IL-17 signaling pathway, and the low expression of IL-17 pathway receptor (IL17a/IL17f) were observed in the knockout of SEMA6B mice with liver failure.

Conclusion: SEMA6B, as is a potential diagnostic and diagnostic biomarker in the progression of ACLF, aggravates liver failure by macrophage mediated systemic inflammation, providing a novel clinical target for treating ACLF.

FRI-321

Clinical and molecular features of immune-mediated and drug-induced liver injury

Thais Leonel¹, Anna Pocurull¹, Ignasi Olivas¹, Ester García-Pras¹, Sofia Pérez-del-Pulgar¹, María Carlota Londoño¹, Xavier Fornis¹. ¹Liver Unit, Hospital Clínic, IDIBAPS, University of Barcelona, CIBEREHD, Barcelona, Spain
Email: leonel@recerca.clinic.cat

Background and aims: Differential diagnosis of drug-induced liver injury (DILI) from autoimmune hepatitis (AIH) can be difficult due to the common presence of serum autoantibodies and similar histological findings. Likewise, “autoimmune-like hepatitis” (DI-ALH) is a particular phenotype linked to drugs (Andrade R et al., J Hepatol 2023) with laboratory and histological characteristics that closely resemble those of AIH. However, our understanding of DI-ALH pathogenesis is limited due to the lack of well-defined biological markers. Hence, the aim of our study was to evaluate liver transcriptome profiles in patients diagnosed with DILI, HAI and DI-ALH.

POSTER PRESENTATIONS

Method: We included 44 patients (with liver biopsy) that were classified into 3 groups: DILI (n = 16), DI-ALH (n = 13) and AIH (n = 15). FFPE liver samples from healthy controls (n = 7) were provided by the IDIBAPS Biobank. DILI and AIH were diagnosed according to EASL guidelines. DILI-ALH was defined as liver injury with analytical (positive ANA or SMA plus IgG elevation) and histological features of autoimmunity within 3 months of drug exposure. Gene expression analysis was performed by using the nCounter Host Response Panel (770 genes), Nanostring.

Results: Median age of patients diagnosed with AIH was 63 years (IQR 56–72), 46 (IQR 34–57) for DILI and 43 (IQR 43–62) for DI-ALH (p = 0.01). Most patients were women, 93% AIH, 56% DILI and 92% DI-ALH. ALT levels were significantly higher in DILI than AIH patients (2350 IU/L [IQR 632–3451] vs 853 IU/L [IQR 592–1211], p = 0.049). ANA were detected in 100% of patients with AIH, 77% with DI-ALH and 63% with DILI patients (p = 0.03), whereas SMA were detected in 87% AIH, 77% DI-ALH and 56% DILI (p = ns). Both AIH and DI-ALH patients were positive for either ANA or SMA. Median IgG levels were significantly higher in patients with AIH (28.4 g/L) as compared to the other groups (12.5 g/L in DILI and 13.6 g/L in DI-ALH; p = 0.01). Principal component analysis (PCA) showed that healthy controls clustered separately but there was not a clear delineation between DI-ALH, DILI, and AIH patients. Differential expression (DE) analysis showed that 292, 250 and 231 genes were upregulated in DI-ALH, DILI and AIH patients, respectively, compared to healthy controls (Log2 fold-change > 1, p-adj < 0.05. Proinflammatory (IL-17 and chemokine signaling) and immune activation (BCR and TCR signaling) pathways were enriched in the DI-ALH group. In addition, pathways related to liver damage such as apoptosis or oxidative stress were upregulated in DI-ALH patients compared to AIH.

Conclusion: Despite observing slight differences in liver damage and inflammation pathways among AIH, DI-ALH and DILI, our data show significant overlap at the transcriptomic level. This indicates potential common pathophysiological mechanisms, as well as the lack of accuracy of current clinical criteria to distinguish the three groups.

FRI-322

Up-regulation of hyaluronan synthase 2 in hepatocytes contributes to oxaliplatin-induced portal hypertension

Ling Wu^{1,2}, Xiaoquan Huang¹, Feng Li^{1,3}, Siyu Jiang¹, Detlef Schuppan^{2,4}, Shiyao Chen^{1,3}. ¹Zhongshan Hospital, Fudan University, Shanghai, China; ²Institute of Translational Immunology and Research Center for Immunotherapy, University Medical Center, Johannes Gutenberg University, Mainz, Germany; ³Minhang Hospital, Fudan University, Shanghai, China; ⁴Beth Israel Deaconess Medical Center, Harvard Medical School, Boston, United States
Email: wuling01@uni-mainz.de

Background and aims: Oxaliplatin is a first-line drug in chemotherapy regimens, while the incidence of portal hypertension (PH)-related symptoms during follow-up of oxaliplatin (Op)-treated patients without prior liver disease is increasing. However, oxaliplatin-related PH studies are mainly clinical reports, and the specific mechanism is still unclear. We aimed to explore the potential pathological mechanism, discover key molecules, and provide clinical clues for the prevention and treatment of Op-related PH.

Method: Gene expression profiles related to Op treatment were obtained from the GEO database. Key molecules and pathways were identified by screening differentially expressed genes (DEG) between Op-treated and untreated patients. Transcriptome analysis was performed on liver samples from rats with Op-induced PH. Focus was on Op related pathways common to patients and rats. Key molecular pathways were validated in liver samples from rats and oxaliplatin-treated patients. Since main RNA-seq detected signatures in liver are due to abundant hepatocytes, the direct effect of oxaliplatin was studied in human LO2-hepatocytes, and subsequently in co-cultures of human hepatocytes with primary human liver sinusoidal endothelial cells (HHSEC).

Results: Based on the DEG between 19 oxaliplatin-treated patients and 5 untreated patients, hyaluronan synthase 2 (HAS2) and the ERK pathway showed the highest regulation by Op. PH was induced by a 6-week Op treatment in rats, showing a comparable regulation of the ERK pathway. Liver samples from Op-treated patients showed hepatic sinusoidal dilatation, combined with central vein dilatation and fibrosis. Op-treated rats lacked overt sinusoidal obstruction, but showed prominent perivenous monocyte-macrophage infiltration. Moreover, as in humans Op treatment of rats upregulated HAS2, and induced (sinusoidal) endothelial cell activation in vivo. Op could directly upregulate HAS2 in hepatocyte culture and activate the ERK pathway in both LO2 human hepatocytes and HHSEC. The co-culture of HHSEC and Op-treated LO2-hepatocytes showed that mediators released from LO2 cells induced HHSEC damage and activation with increased expression of tissue plasminogen activator, von Willebrand factor and tissue factor, as well as increased cell migration. The migration of HHSEC was also increased after hyaluronic acid treatment, which in co-culture was mainly secreted from hepatocytes after the upregulation of HAS2 with Op treatment.

Conclusion: The MAPK/ERK pathway activation is a key signaling pathway underlying oxaliplatin-induced portal hypertension. It induces the upregulation of HAS2 in hepatocytes, which releases hyaluronic acid, resulting in the activation of hepatic sinusoidal endothelial cells, likely promoting sinusoidal endothelialitis.

FRI-323

The TAK1- β -catenin signaling is essential for inducing chaperone-mediated autophagy and M2 macrophage polarization in acetaminophen-induced liver injury

Xiao Wang¹, Tao Yang¹, Xiaoye Qu¹, Dongwei Xu¹, Xiyun Bian², Christopher King², Jun Li³, Longfeng Jiang³, Bibo Ke². ¹The Dumont-UCLA Transplant Center, Department of Surgery, David Geffen School of Medicine at UCLA, Los Angeles, United States; ²The Dumont-UCLA Transplant Center, Department of Surgery, David Geffen School of Medicine at UCLA, Los Angeles, United States; ³Department of Infectious Diseases, the First Affiliated Hospital, Nanjing Medical University, Nanjing, China
Email: xiawang@mednet.ucla.edu

Background and aims: TAK1 plays a central role in triggering an inflammatory signaling cascade. β -catenin is essential for immune regulation during inflammatory response. However, it is unknown how macrophage TAK1- β -catenin signaling may regulate macrophage autophagy and cell differentiation in acetaminophen (APAP)-induced liver inflammatory injury. This study was designed to dissect the regulatory mechanism of the macrophage TAK1- β -catenin axis on inflammatory and immune responses during APAP-induced liver damage.

Method: A mouse model of APAP-induced liver injury was used in the myeloid-specific TAK1 knockout (TAK1^{M-KO}) and floxed TAK1 (TAK1^{fllox/fllox}) mice (n = 10/group). Mice were intraperitoneally injected with APAP (400 ug/g) or PBS. The animals were sacrificed at the indicated time. For the *in vitro* study, bone marrow-derived macrophages (BMMs) from these conditional knockout mice were transfected with CRISPR/Cas9-mediated β -catenin knockout (KO), Heb1 KO or control vector followed by LPS (100 ng/ml) stimulation.

Results: TAK1^{M-KO} reduced APAP-induced liver damage with decreased serum ALT/AST levels and proinflammatory mediators and increased animal survival compared to the TAK1^{FL/FL} controls. TAK1^{FL/FL} mice treated with APAP increased JNK and β -catenin phosphorylation, leading to increased β -catenin degradation. However, TAK1^{M-KO} reduced JNK and β -catenin phosphorylation, increasing β -catenin nuclear translocation. Interestingly, TAK1^{M-KO} increased autophagic gene ATG5, ATG7, and LC3B but reduced SQSTM1/p62 expression compared to the TAK1^{FL/FL} controls. Moreover, TAK1^{M-KO} increased macrophage Arginase1 and reduced iNOS expression after the APAP challenge. Chromatin immunoprecipitation (ChIP) coupled with massively parallel sequencing (ChIP-

Seq) revealed that macrophage β -catenin activated its target gene *Hebp1*. Activating macrophage *Hebp1* increased cFLIP and Rab10 expression and the cFLIP-Rab10 interaction, which augmented p-ULK1, Hsc70, and LC3B but diminished NLRP3, cleaved caspase-1, and IL-1 β expression. However, disruption of macrophage *Hebp1* or cFLIP with CRISPR/Cas9 KO inhibited p-ULK1, Hsc70, LC3B, NLRP3, Arginase1, and augmented iNOs with reduced IL-10 and TGF- β expression. Furthermore, adoptive transfer of *Hebp1*-expressing macrophages in TAK1^{M-KO} mice ameliorated APAP-induced liver damage.

Conclusion: Macrophage TAK1 deficiency promotes β -catenin activity in APAP-challenged livers. Activating β -catenin targets *Hebp1* and activates cFLIP. The cFLIP-Rab10 interaction is crucial for the modulation of chaperone-mediated autophagy and M2 macrophage polarization in APAP-challenged livers. Our findings underscore a novel role of the macrophage TAK1- β -catenin axis in APAP-induced liver injury, implying the potential therapeutic targets in liver immune and inflammatory diseases.

FRI-324

Advancing in drug-induced liver injury models development: high content screening in cell-based models derived from skin tissues

Antonio Segovia-Zafra^{1,2,3,4}, Marina Villanueva^{1,2,3,4}, Joel Posligua-García⁵, Nieves Montenegro-Navarro^{5,6}, Manuel Bernal Muñoz^{3,5}, Maria Isabel Lucena^{1,3,4,7,8}, Raul J. Andrade^{1,3,4,7,8}. ¹Centro de Investigación Biomédica en Red Enfermedades Hepáticas y Digestivas (CIBERehd), Madrid, Spain; ²Servicios de Aparato Digestivo y Farmacología Clínica, Hospital Universitario Virgen de la Victoria, Málaga, Spain; ³IBIMA-Bionand Platform, Málaga, Spain; ⁴Universidad de Málaga, Málaga, Spain; ⁵Departamento de Biología Molecular y Bioquímica, Facultad de Ciencias, Universidad de Málaga, Málaga, Spain; ⁶IBIMA-Bionand platform, Málaga, Spain; ⁷Servicios de Aparato Digestivo y Farmacología Clínica, Hospital Universitario Virgen de la Victoria, Málaga, Spain; ⁸Plataforma de Investigación Clínica y Ensayos Clínicos UICEC-IBIMA, Plataforma ISCIII de Investigación Clínica, Málaga, Spain
Email: anseza9@gmail.com

Background and aims: Idiosyncratic Drug-Induced Liver Injury (DILI) encompasses unexpected liver damage from both prescribed and over-the-counter medications and herbal and dietary supplements (HDS). Developing human-relevant *in vitro* models is vital for studying DILI and mitigating drug development risks. Recently, keratinocytes, skin-derived cell cultures, showed gene overexpression linked to DILI when exposed to DILI-inducing drugs, providing new alternatives to traditional models. Our study aims to harness this discovery for early-stage DILI prediction, emphasizing the importance of High Content Screening (HCS) methods for speed and automation to enhance these models' accuracy and relevance.

Method: The human immortalized keratinocyte cell line HaCaT was used to perform all the experiments. Cells were seeded onto a 96-well. After 24 hours they were exposed to the drugs of study at eight different concentrations for 24 hours. Cells were stained with different fluorescent markers (membrane, nucleus, mitochondria, and ROS markers) and fixated with formalin. Six different drugs (3 DILI positive and 3 DILI negative) were studied. The HCS imaging was performed using the Operetta CLS system. The image analysis was implemented and automated using the Harmony 4.9 software measuring nine different morphological and functional end points.

Results: 14 different parameters were examined for each of the concentrations, to investigate which could best predict hepatotoxicity. Among all the concentrations studied, the one at which the greatest number of parameters could distinguish between hepatotoxic and non-hepatotoxic drugs was 30 times the base study concentration. Under these conditions, using five distinct parameters (nuclei count, cell area, nucleus area, nuclear marker intensity, and nuclear marker intensity per squared micrometer), all non-

hepatotoxic and two out of three hepatotoxic drugs were correctly classified. This yielded an accuracy value of 83%, sensitivity of 66%, specificity of 100%, a positive predictive value of 1, and a negative predictive value of 0.75.

Conclusion: Although the drug panel need to be expanded, the HaCaT cell line exhibits substantial potential as a predictive model for DILI. This bears considerable preclinical significance, as the need for valid models to study DILI is pressing. Furthermore, it holds crucial clinical value, given that keratinocytes are more accessible than hepatocytes, opening up new avenues for clinical investigations.

FRI-325

DDX3X regulates the functional transition of endoplasmic reticulum stress in the pathogenesis of liver failure

Ling Xu¹, Zihao Fan¹, Yao Gao¹, Yaling Cao¹, Yuan Tian¹, Xiangying Zhang¹, Feng Ren¹. ¹Capital Medical University Beijing Youan Hospital, Beijing, China
Email: renfeng7512@ccmu.edu.cn

Background and aims: The functional transition of endoplasmic reticulum stress (ERS) plays a critical role in the pathogenesis of liver failure (LF), but the underlying molecular mechanisms remain unclear. Here, we explored the role of DDX3X under ERS to regulate cell fate in the progression of LF.

Method: Primary hepatocytes were isolated from C57BL/6J mice and induced ERS with tunicamycin (TM). C57BL/6J mice were induced ERS with TM and liver injury with concanavalin A (ConA), respectively. The expression level of DDX3X in liver tissue and serum were analyzed in healthy, chronic hepatitis B (CHB) patients and HBV-associated LF patients. Quantitative real-time PCR (qRT-PCR) and western blotting (WB) methods were used to detect the expression of related genes and proteins; cell viability, cell death rate and cell apoptosis rate was detected by cell counting kit-8 (CCK-8), lactate dehydrogenase (LDH) assays and flow cytometry, respectively; serum alanine transaminase (ALT) and aspartate aminotransferase (AST) levels and hematoxylin-eosin (HandE) staining of liver sections were used to evaluate liver injury in this study.

Results: We demonstrated that DDX3X increased and translocated into nucleus with prolonged ERS; secondly, DDX3X plays dual roles under different periods of ERS mediated cell fate; in addition, phosphorylation modification of DDX3X is the key mechanism to regulate its subcellular localization. Under short-term ERS, DDX3X was mainly expressed in cytoplasm and interacted with peroxisome proliferators-activated receptor alpha (PPAR α), which translationally up-regulated transcription factor EB (TFEB) to promote the adaptive cell response. Under prolonged ERS, phosphorylated DDX3X increased nuclear translocation to promote cell apoptosis by CCAAT enhance-binding protein homologous protein (CHOP) activation. In addition, we demonstrated that DDX3X was increased in ConA-induced liver injury in mice and its nuclear translocation was increased; secondly, DDX3X plays dual roles during ConA-induced liver injury, which exerts a protective effect in early phase (6 h) and a pro-injury effect in the late phase (24 h). Furthermore, we found that DDX3X levels were significantly increased in serum and liver tissues of HBV-related LF patients; secondly, the fluctuation of DDX3X serum level is correlated with the prognosis of HBV-LF patients, which consistent decline was correlated with the good prognosis.

Conclusion: Our novel findings document the key regulatory function of DDX3X signaling under ERS in the pathophysiology of liver failure, and provide a rationale to target DDX3X as a refined therapeutic strategy to ameliorate liver injury.

FRI-326-YI

Multi-omics uncovers spatial remodelling of the hepatic lipidome in acute liver injury

Aleksandra Gruevska¹, Kylie Matchett², Evangelos Triantafyllou¹, Neil Henderson², Zoe Hall¹. ¹Department of Metabolism, Digestion and

POSTER PRESENTATIONS

Reproduction, Imperial College London, London, United Kingdom;
²Centre for Inflammation Research, Institute for Regeneration and Repair,
University of Edinburgh, Edinburgh, United Kingdom
Email: zoe.hall@imperial.ac.uk

Background and aims: Drug-induced liver injury (DILI), including acetaminophen (APAP) poisoning, is a major cause of acute liver failure (ALF) with limited therapeutic choices. Dysregulated lipid metabolism has been implicated in DILI, however, lipids and lipid metabolism remain underexplored targets for improving drug safety. Further investigation is also needed to understand the complex interplay between the immune system and local metabolic remodelling during the resolution of injury. The aim of this study is to map the spatial hepatic lipid signature following APAP-induced injury and subsequent resolution.

Method: A multimodal approach including mass spectrometry imaging (MSI) for spatial lipidomics, spatial transcriptomics (ST) and single nuclei RNA sequencing (snRNA-seq) was applied to analyse human APAP-ALF liver explant tissue samples and control background liver tissue (n = 3). The same multimodal approach was used to analyse APAP-induced acute liver injury in wild-type mice (male C57BL/6J, i.p. dosage: 300 mg/kg) across multiple timepoints.

Results: Haematoxylin and eosin staining was used to identify necrotic or remnant viable regions (RVR) in APAP-ALF samples and periportal/pericentral zones in control samples. Spatial lipidomics performed on adjacent tissue sections revealed that metabolic lipid zonation was disrupted in APAP-ALF. The necrotic regions of the APAP-ALF liver tissue exhibited a strikingly different lipid profile to the RVR, with increased sphingolipids, ether lipids, saturated and monosaturated fatty acid-containing phospholipids. Further analysis of the MSI data revealed that cardiolipins (CLs; key mitochondrial lipids) and their precursors phosphatidylglycerols (PGs), had characteristic perinecrotic (PNR) spatial distribution. In line with the MSI data, ST analysis of an adjacent cryosection, demonstrated that genes implicated in PG and CL metabolism (*PGS1*, *CDS2*, *TAZ*, *PLSCR3*) had increased expression in necrotic and PNR regions of human APAP-ALF liver tissue, compared to RVR. In APAP-treated mice, PG and CL lipid abundance and *Pgs1* gene expression were increased in the PNR regions, during the resolution of injury phase. Of note, CL is involved in mitochondrial biogenesis and dynamics, mitophagy, as well as in the apoptotic process. We found that genes implicated in mitophagy (*ULK1*, *BECN1*, *BNIP3L*) had increased expression in the same histological regions as increased abundance of CL lipids. Interestingly, analysis of human snRNA-seq data showed that genes involved in CL metabolism and mitophagy were upregulated specifically in endothelial and myeloid cells.

Conclusion: Overall, we have shown that mitochondrial lipids have increased abundance in PNR regions of APAP-induced ALF. Altered PG and CL metabolism in endothelial and myeloid cells may be involved in mitigating APAP poisoning-related injury and promoting liver regeneration.

FRI-327-YI

Plasma multi-omic reveals dysregulated gut arbitrated increase in bacterial peptides and metabolites predictive of poor outcomes in acute liver failure

Sushmita Pandey¹, Neha Sharma¹, Nupur Sharma¹, Gaurav Tripathi¹, Babu Mathew¹, Manisha Yadav¹, Vasundhara Bindal¹, Sadam H Bhat¹, Rakhi Maiwall¹, Shvetank Sharma¹, Shiv Kumar Sarin¹, Jaswinder Maras¹. ¹Institute of Liver and Biliary Sciences, NEW DELHI, India

Email: jassi2param@gmail.com

Background and aims: Acute liver failure (ALF) has high mortality and identification of microbial/metabolic signatures in plasma could stratify ALF patients predisposed to early mortality.

Method: Plasma multi-omics was performed on 40 ALF patients and 5 controls (training-cohort). Multi-omics signatures differentiating ALF Non-survivor (ALF-NS) from ALF Survivor (ALF-S) were validated

in 270 ALF patients (TC-1; plasma and paired one drop blood (n = 160); TC-2; external validation (n = 70)) and Diseases control (TC-3 (n = 70)), using High Resolution Mass Spectrometry (HRMS), Machine-Learning (ML) and correlated with clinical parameters and outcome. **Results:** Multi-omics signature were distinct for ALF, more so for ALF-NS. Non-survivors showed increased metabolites; bile-acids, tryptophan, tyrosine linked to inflammation, cell death, stress and proteins linked to hyper-inflammation (p < 0.01, FDR < 0.01, FC > 1.5). Bacterial-peptide based alpha/beta diversity was higher in ALF-NS corresponding to Proteobacteria, Firmicutes, Actinobacteria functionally associated to energy, amino-acid and xenobiotic metabolism (p < 0.05). ALF-NS specific metaproteomic modules/functionality directly correlated with metabolic modules/functions and clinical parameters (R² > 0.7, p < 0.05). Metabolomic signature directly correlated with clinical parameters and bacterial-peptides e.g., (chenodeoxycholic acid-Firmicutes: alkaliphilus oremlandii and Proteobacteria: phyllobacteriaceae; (R² > 0.75)). Probability of detection (POD) of Non-survival built on top five metabolites, namely, chenodeoxycholic acid, 4-(2-Amino phenyl)-2, 4-dioxobutanoate, L-Tyrosine, carnosine and alanyl-tyrosine showed diagnostic accuracy of 98% (AUC = 0.98 (0.92–1.0)) and distinguish ALF predisposed to early mortality (log-rank < 0.05). Validation using HRMS on TC-1, TC-2 and TC-3 and 5 ML-algorithm on (ALF = 270) the metabolome panel showed > 98% accuracy/sensitivity and specificity for prediction of mortality.

Conclusion: Plasma multi-omics outlines hyper-inflammation and hydrophobic bile acid accumulation as characteristic features for ALF-NS. Baseline plasma metabolite signatures could segregate ALF predisposed to early mortality.

FRI-330

MiRNA/mRNA network topology in acute-on-chronic liver failure identified miR-503-5p as a regulatory hub of lymphocytes activation through antigen-presentation suppression

Heng Yao¹, Xi Liang², Jing Jiang¹, Jiaojiao Xin¹, Dongyan Shi¹, Xin Chen^{3,4}, Jun Li¹. ¹State Key Laboratory for Diagnosis and Treatment of Infectious Diseases, National Clinical Research Center for Infectious Diseases, National Medical Center for Infectious Diseases, The First Affiliated Hospital, Zhejiang University School of Medicine, Hangzhou, China; ²Precision Medicine Center, Taizhou Central Hospital (Taizhou University Hospital), Taizhou, China; ³Institute of Pharmaceutical Biotechnology and the First Affiliated Hospital Department of Radiation Oncology, Zhejiang University School of Medicine, Hangzhou, China; ⁴Joint Institute for Genetics and Genome Medicine between Zhejiang University and University of Toronto, Zhejiang University, Hangzhou, China

Email: lijun2009@zju.edu.cn

Background and aims: The pathology of acute-on-chronic liver failure (ACLF) remains uncharted. This study aimed to uncover the disease mechanisms by identification of regulatory hubs in the disease-related miRNA/mRNA network using topological analysis.

Method: Ninety peripheral blood mononuclear cell samples (ACLF, n = 30, liver cirrhosis (LC), n = 25; chronic hepatitis B (CHB), n = 25; normal controls (NC), n = 15) were collected from a prospective cohort for paired miRNA/mRNA sequencing. Differentially expressed (DE) transcripts were used to construct miRNA/mRNA networks enabling topological analysis and capturing the regulatory hubs through the disease progression of ACLF.

Results: Two miRNA/mRNA networks were constructed based on the DE-miRNA/mRNA of NC/ACLF and Chronic disease group (LC and CHB)/ACLF containing 83 and 100 miRNA/mRNA pairs. MiRNA/mRNA sequence matching and tissue miRNA level screening were performed to confirm these miRNA/mRNA were potentially matched in targeting region and expressed in liver tissue. Topological analysis identified miR-503-5p as the most influencing miRNA nodes shared by two networks, whose co-expressed gene set were closely related to acute inflammatory response, humoral immune response, heterotypic cell-cell adhesion, and lymphocyte mediated immunity in

enrichment analysis, which indicates miR-503-5p's participation in the complex immune disorder through the disease progression. The potential target genes of miR-503-5p were down-regulated through ALCF disease progression and involved in the decrease of lymphocytes activation, which were confirmed in the validation group independently.

Conclusion: Topological analysis of the miRNA/mRNA network in ALCF reveals its regulatory complexity through the disease progression and identified miR-503-5p as a hub involved in the lymphocytes activation by suppressing its potential targets to hamper antigen presentation, which may help to discover novel early-warning markers or therapeutic targets of ALCF.

FRI-331

IL-1B exacerbates acute-on-chronic liver failure by promoting neutrophil extracellular traps formation via IL1R1/MyD88/TBK1 axis

Jia Chen¹, Qiongchi Zhang², Zhipeng Li¹, Qiumin Luo¹, Wenxiong Xu¹, Liang Peng¹. ¹Third Affiliated Hospital of Sun Yat-sen University, Guangzhou, China; ²Xi'an Jiaotong University Health Science Center, Xi'an, China
Email: pliang@mail.sysu.edu.cn

Background and aims: Acute-on-chronic liver failure (ACLF) is characterized by hepatic damage and systemic inflammation, particularly notable for significant neutrophil accumulation within the liver. Our research focuses on understanding the role of neutrophils in ACLF to gain insights into disease mechanisms.

Method: In this study, four ACLF-related datasets retrieved from the Gene Expression Omnibus (GEO) database were conducted comprehensive bioinformatics analyses. Furthermore, We established an ACLF mouse model and utilized IL-1R1 knockout mice to confirm IL1R1's role in vivo. In vitro, we stimulated neutrophils with IL-1B, co-cultured them with hepatocytes, and employed co-immunoprecipitation (CO-IP). Finally, we recruited peripheral blood samples from ACLF patients for experiments and tracked the patients' 28-day prognosis.

Results: Bioinformatics analysis indicated elevated IL-1-related pathways in the peripheral blood of ACLF patients, which were validated by Bulk-RNA sequencing. Simultaneously, ACLF mice exhibited significant GSDME/Caspase3-mediated hepatocyte pyroptosis and notable neutrophil infiltration which were alleviated in IL-1R1 knockout mice. In vitro, IL1R1 deficiency in neutrophils exposed to IL-1B had reduced ROS levels, neutrophil extracellular traps (NETs) formation, and chemotactic factor release. CO-IP results suggested that MyD88, the downstream molecule of IL-1B/IL-1R1, interacts with TBK1 to mediate NETs formation and promote the transcriptional expression of interferon-beta (IFNB). IFNB, upon acting on neutrophils, induces mitochondrial oxidative stress damage. Additionally, a novel MyD88 inhibitor (ST2825) significantly reduced hepatic damage and neutrophil aggregation in ACLF mice. Serum levels of IL-1, soluble IL-1R1, IL-18, CXCL-1, and CXCL-2 significantly increased in ACLF patients, along with increased neutrophil IL-1R1, MyD88, MPO, and CD177 expression. Furthermore, soluble IL-1R1 was identified as a risk factor for 28-day mortality in patients.

Conclusion: In ACLF, hepatocyte pyroptosis-induced IL-1B release triggers NETs formation via the IL1R1/MyD88/TBK1 pathway, worsening hepatic damage and increasing hepatic neutrophil infiltration. IL-1R1 and MyD88 are potential therapeutic targets in ACLF.

FRI-332

Mechanical stress of acute portal hypertension aggravates PA-HSOS by damaging gut-vascular barrier targeting NR4A3/PV1

Han Zhang¹, Si Zhao¹, Rui Fang¹, Xue Wang¹, Suzhen Yang¹, Bing Xu¹, Ming Zhang¹, Yuzheng Zhuge¹, Jiangqiang Xiao¹. ¹Department of

Gastroenterology, Nanjing Drum Tower Hospital, Affiliated Hospital of Medical School, Nanjing University, nanjing, China
Email: jiangqiang86@drumtowerhosp.group

Background and aims: Portal hypertension is considered to play an important role in the progression of many liver disease which is associated with impaired intestinal barrier and increasing gut vascular permeability. However, the specific mechanism is yet to be defined. This study focused on the relationship between portal hypertension, gut vascular permeability and liver injury progression based on pyrrolizidine alkaloids-induced hepatic sinusoidal obstruction syndrome (PA-HSOS), a kind of drug-induced vascular liver disease characterized by acute portal hypertension.

Method: Plasma, hepatic and intestinal tissue from PA-HSOS patients were collected and PA-HSOS mice model was established by MCT intragastric administration. In addition, we also performed partially ligation of the posterior hepatic segment of inferior vena cava (pIVCL) in mice to simulate the portal hypertension of PA-HSOS. Gut vascular permeability was measured in these mice by intravenous injection of FITC -dextran. Propranolol was used to reduce portal pressure to observe the effects of pressure on intestinal vascular barrier and liver damage. The effect of MCT on endothelial cell proliferation and permeability was explored in vitro. HUVECs under mechanical stress with a stretch device were used to perform RNA-sequencing analyses to identify gene expression patterns associated with stretch.

Results: We found increased intestinal permeability in patients with PA-HSOS and gut-vascular barrier (GVB) is disrupted in mice gavaged MCT which is marked by up-regulation of PV1 and impaired structure of endothelial cells. We confirmed that activated MCT damaged endothelial cells in vitro, meanwhile, confocal laser endomicroscopy revealed hyperpermeability of GVB in the both PA-HSOS mice and post-hepatic portal hypertension (pIVCL) mice, a model to simulate the portal hypertension in PA-HSOS. Reducing portal pressure by pharmacological intervention ameliorated the GVB and liver function. RNA-sequencing of HUVECs identified genes that were altered in response to mechanical stretch, including NR4A subfamily. Mechanical stretch of HUVECs increased expression of NR4A3 and NR4A3 repressed wnt signaling pathway to mediate stretch-induced PV1 expression.

Conclusion: We have identified the important role of portal hypertension in PA-HSOS progression. Treatment aimed at reducing portal pressure have protected against intestinal barrier damage and PA-HSOS development. Mechanical stress of portal hypertension is an important component of GVB destruction through the NR4A3/PV1 pathway, which enriches the liver injury mechanism of PA-HSOS and provides new targets for therapeutic strategies.

FRI-333

Sibiriline, an inhibitor of regulated necrosis, protects mice against Acetaminophen-induced liver injury, alone or in combination with N-acetyl-cysteine

Mélanie Simoes Eugenio^{1,2}, Ghiles Imerzoukene², Annaïg Hamon³, Claire Piquet-Pellorce², Alison Rapin², Claire Delehouze¹, Sophie Belal¹, Axelle Autret¹, Jeph Akakpo⁴, Hartmut Jaeschke⁴, Stephane Bach⁵, Michel Samson², Jacques Le Seyec², Marie-Thérèse Dimanche-Boitrel², Morgane Rousselot¹. ¹SeaBeLife Biotech, Roscoff, France; ²Univ Rennes, Inserm, EHESP, Irset (Institut de recherche en santé, environnement et travail)-UMR_S 1085, Rennes, France, Rennes, France; ³Univ Rennes, Inserm, EHESP, Irset (Institut de recherche en santé, environnement et travail)-UMR_S 1085, Rennes, France, Rennes, France; ⁴Department of Pharmacology, Toxicology and Therapeutics, University of Kansas Medical Center, Kansas City, United States; ⁵Kinase Inhibitor Specialized Screening Facility, Station Biologique, UMR 8227 CNRS-UPMC, Roscoff, France
Email: melanie.simoesugenio@seabelife.com

Background and aims: Acetaminophen, also known as APAP (N-acetyl-para-aminophenol) or paracetamol is one of the most commonly used analgesics. Overconsumption of more than 4 g/day

POSTER PRESENTATIONS

of APAP could lead to liver injury. Thus, APAP-induced liver injury (AILI) is the second cause of liver transplantation worldwide and is involved in more than 50% of acute liver failure. For patients diagnosed within 8 hours after APAP ingestion, N-acetyl-cysteine (NAC) is the only approved antidote treatment capable to resolved AILI. For late diagnosis, the mortality is higher since NAC is not effective and liver transplantation remains the only solution. With the aim of discovering a new therapy, SeaBeLife Biotech has developed a new compound, named Sibiriline (SBL01), able to rescue liver after AILI.

Method: After overnight fasting, AILI was induced by intraperitoneal injection of APAP (400 or 450 mg/kg) in C57Bl6J male mice. One hour later, mice were treated with intravenous injection using either vehicle, NAC (200 mg/kg), SBL01 (10 mg/kg) or a combination of NAC and SBL01. Mice survival was followed during 72 hours. Blood and liver tissue samples were collected 8 hours after AILI for further analyses.

Results: 24 hours after APAP intoxication, survival rates increased from 40% to 70% if the vehicle contains SBL01 or NAC. No deaths occurred in mice injected with APAP and treated with a combination of SBL01 and NAC. AILI in mice only treated with the vehicle was associated with an increase of hepatic transaminase levels in plasma (AST and ALT) and the presence of centrilobular necrosis in liver tissue stained with HandE. When AILI mice were treated with SBL01, a decrease of hepatic transaminases and a reduction of hepatic necrosis area were observed showing a protective effect of SBL01. Similar results were also observed in AILI mice treated with NAC. The combination of NAC and SBL01 provided complete and synergistic protection to AILI mice against liver injury. Thus, plasma levels of hepatic transaminases were comparable to those measured in healthy mice and HandE staining of liver sections did not show any centrilobular necrosis. In order to understand the mechanism of SBL01 protection, further analyses were performed. NAPQI-adducts quantification and JNK signalling pathway analyses showed that SBL01 exerted a protective action different from that obtained with NAC.

Conclusion: When AILI mice were treated with SBL01 and NAC, a super-additive effect of SBL01 improve NAC treatment of AILI. SBL01 is a news promising molecule in APAP-induced liver injury.

FRI-334

Adipose-derived mesenchymal stem cells ameliorate APAP-induced liver injury via REDD1-ULK1-FUNDC1 axis-mediated mitophagy

Yelei Cen¹, Guohua Lou¹, Caixia Xia¹, Min Zheng¹, Yanning Liu¹. ¹The State Key Laboratory for Diagnosis and Treatment of Infectious Diseases, The First Affiliated Hospital, College of Medicine, Zhejiang University, National Clinical Research Center for Infectious Diseases, Collaborative Innovation Center for Diagnosis and Treatment of Infectious Diseases, Hang Zhou, China
Email: liuyanning@zju.edu.cn

Background and aims: Acetaminophen (APAP) overdose is the leading cause of drug-induced acute liver failure in the United States and Europe. Mitochondrial dysfunction is a major contributor to APAP-induced liver injury (AILI). Mesenchymal stem cell (MSC) therapy is a potential method to reduce AILI. We found that adipose-derived mesenchymal stem cells (AMSCs) can promote mitochondrial function and significantly upregulate REDD1, a classical inhibitor of mTOR signaling and serves an important role in autophagy. This study aims to explore the role and mechanism of REDD1 in regulating mitochondrial function in AILI by AMSC therapy.

Method: AMSCs were injected into mice with APAP-induced liver injury to assess changes in serology, liver pathology and the function of mitochondria. RNA sequencing was used to identify differentially expressed genes between APAP-intoxicated and AMSC-treated mice. The results were verified in APAP-injured AML12 cells co-cultured with AMSCs using a transwell model. To further reveal the molecular

mechanism, AML12 cells were transfected with a plasmid over-expressing REDD1 and exposed to excess APAP. And hepatocyte-specific REDD1 knockout mice were used to evaluate the role and mechanism of AMSCs-induced REDD1 expression in AILI.

Results: Treated mice with AMSCs showed significant reductions in liver injury and improvements in mitochondrial function compared to APAP-intoxicated mice. RNA sequencing showed a significant increase in REDD1 expression in mouse liver tissue after AMSCs infusion and was verified by western blot and immunohistochemistry. In *in vitro* experiments, we also found that co-culture of AMSCs and AML12 cells could upregulate REDD1 expression and alleviate the mitochondrial dysfunction in the hepatocytes with APAP exposure, whereas the effect of AMSCs on restoring mitochondrial function in APAP-injured hepatocytes was impaired by interfering REDD1 expression in AML12 cells. Furthermore, we found that overexpression of REDD1 in AML12 cells can promote phosphorylation of FUNDC1 by activating ULK1, a kinase substrate in the mTOR pathway, and thereby promote mitophagy. This effect can be inhibited by the ULK1 inhibitor SBI-0206965. In addition, we detected a decrease in the expression of ULK1 and p-FUNDC1 and more severe liver necrosis in hepatocyte-specific REDD1 knockout mice after APAP overdosing. Moreover, AMSCs infusion could increase ULK1 and p-FUNDC1 expression and promote mitophagy in the liver of APAP-intoxicated mice.

Conclusion: These results showed AMSCs therapy mitigating mitochondrial damage in AILI by upregulating REDD1-ULK1-FUNDC1 axis-mediated mitophagy.

FRI-335

An exploration of plasma neurofilament protein as a marker of neuronal damage in acute liver failure

Marilena Stamouli^{1,2}, Christos Konstantinou^{1,2}, Francesca M Trovato^{2,3}, Ane Zamalloa³, Mark J W McPhail^{2,3}, Anna Hadjihambi^{1,2}, Vishal C Patel^{1,2,3}. ¹The Roger Williams Institute of Hepatology, Foundation for Liver Research, London, United Kingdom; ²Faculty of Life Sciences and Medicine, King's College London, London, United Kingdom; ³Institute of Liver Studies and Transplantation, King's College Hospital, London, United Kingdom
Email: m.stamouli@researchinliver.org.uk

Background and aims: Acute liver failure (ALF) is a life-threatening condition marked by an abrupt liver dysfunction, disordered coagulation and high-grade hepatic encephalopathy (HE), in individuals without pre-existing liver disease. HE in ALF has several manifestations with a reduction in consciousness driven by disruptions in neurotransmission. Neurofilaments (NfL), structural proteins indicative of neuronal damage, are potential markers for various neurological conditions. This study aims to elucidate the associations of plasma NfL in ALF as a circulating marker of neuronal damage.

Method: A cohort of 22 ALF patients underwent baseline sampling, compared to 19 healthy controls (HC) and 25 acute-on-chronic liver failure (ACLF) patients with HE, serving as positive chronic liver disease controls. ALF and ACLF patients were longitudinally sampled on days 3, 7, and 10, where feasible and prior to liver transplantation. HE severity was clinically assessed using the West Haven criteria (scale 1–4). Plasma levels of NfL and IL-6 were quantified utilising electrochemiluminescent-based assays (MSD). Clinical outcomes and ammonia data were extracted from the patients' clinical records.

Results: Median plasma NfL levels were significantly elevated in ALF patients compared to HC (66 vs 13 pg/ml, $p < 0.0001$), but did not reach the levels observed in ACLF patients (66 vs 158 pg/ml, not significant). However, there was a greater fold change between baseline and follow-up NfL in ALF patients compared to ACLF patients (6.4 vs 1.3, $p = 0.002$). Longitudinal NfL levels remained elevated in both ALF (61 vs 346 pg/ml, $p < 0.0001$) and ACLF patients (158 vs 390 pg/ml, $p < 0.0001$) compared to baseline levels irrespective of outcomes, such as transplant-free survival and HE resolution. Baseline NfL levels were unable to distinguish ALF spontaneous

survivors from non-survivors (deceased and transplanted patients). Additionally, baseline NFL in both ALF showed no correlation with IL-6 nor ammonia levels.

Conclusion: This study demonstrates that plasma NFL levels are elevated in ALF, indicative of neuronal damage that is associated with HE. Elevated NFL levels persist in the systemic circulation of ALF patients up to 10 days, even after the improvement in HE and liver injury, at significantly higher levels than ACLF. However, baseline NFL did not predict transplant-free survival in ALF. The lack of correlation with conventional systemic inflammation cytokines or ammonia levels emphasises that there may be other contributory mechanisms in the pathophysiology of HE in ALF.

FRI-338

Obeticholic acid promotes the hepatic ductular reaction via hepatocyte-mediated HMGB1 by disrupting autophagosome-lysosome fusion in cholestasis

Jie Wang¹, Qianhui Tang¹, Weishuang Shen¹, Qingyu Chen¹, Qinwei Yu¹, Luyong Zhang^{1,2}, Zhenzhou Jiang^{1,3}. ¹China Pharmaceutical University, New drug screening center, Nanjing, China; ²Guangdong Pharmaceutical University, Center for drug research and development, Guangdong, China; ³China Pharmaceutical University, Jiangsu center for pharmacodynamics research and evaluation, Nanjing, China
Email: jiangcpu@163.com

Background and aims: Obeticholic acid (OCA) is the established second line therapy for primary biliary cholangitis (PBC) patients. However, OCA-induced liver injury in PBC patients puts them at risk for liver failure and increases mortality. OCA exacerbated biliary injury when used during biliary obstruction. The safety studies of OCA will help to guide the clinical medication. High-mobility group box 1 (HMGB1), a extracellular damage/danger associated molecular pattern (DAMP) molecule, is closely involved in various liver diseases. And HMGB1 is a critical regulator of autophagy, which the deficiency also leads to inflammation, ductular reaction (DR) and fibrosis. However, it is not clear how these events are mechanistically linked to OCA-induced liver injury.

Method: Bile duct ligation (BDL) was performed as the complete biliary obstruction model. Ethyl pyruvate (EP) was chosen to pharmacological inhibition of HMGB1 release. The primary mouse hepatocytes were used to investigate the mechanism of HMGB1 and autophagy. ELISA, immunohistochemistry, immunofluorescence, Western blot, Kits and Flow analysis were performed for in vitro and vivo experiments.

Results: The serum concentration of HMGB1 was obviously increased in OCA-treated BDL mice. The images revealed that the positive staining area of HMGB1 in cytoplasm was significantly increased in BDL OCA group. OCA induced the enhancement of cytoplasmic HMGB1 level analyzed by flow in BDL mice. Pharmacological inhibition of HMGB by EP alleviated ductular reaction, necrosis and fibrosis caused by OCA in BDL mice. In vitro, OCA 100 μ M treatment induced the increased release of lactate dehydrogenase (LDH) (about 30–40%) and HMGB1 (about 100 pg/ml) from the supernatant of primary hepatocytes. And the release of LDH was significantly reduced in OCA combination with EP group. As reported, secretory autophagy and multivesicular body formation mediate HMGB1 secretion. So, the expression of markers of autophagy were detected. Significantly augmented expression of LC3-II and p62 proteins were observed in OCA dose-dependent manner. Immunofluorescence analysis revealed increased numbers of LC3- and p62-positive puncta in OCA-treated hepatocytes. Furtherly, the release of LDH was upregulated by OCA in the presence of chloroquine (CQ), indicating the compromised process of autophagosome-lysosome fusion. Consistent with this, OCA-treated hepatocytes showed a reduction in acridine orange (AO)-stained acidic organelles, an enhanced release of the lysosomal enzyme CTSB (cathepsin B) into

the cytosol, increased expression of lysosome-associated membrane protein (LAMP-1) and the reduction of acidification of lysosomes.

Conclusion: OCA triggered cell death of hepatocytes via lysosomal membrane permeabilization and subsequent HMGB1 release, and the increased release of HMGB1 accelerated the process of liver injury in cholestasis.

FRI-339

Obeticholic acid promotes the hepatic ductular reaction via macrophage-mediated Relb-TNFSF14 signaling in cholestasis

Jie Wang¹, Zihang Yuan¹, Haoran Zhang¹, Qianhui Tang¹, Qingyu Chen¹, Weishuang Shen¹, Qinwei Yu¹, Luyong Zhang^{1,2}, Zhenzhou Jiang^{1,3}. ¹China Pharmaceutical University, New drug screening center, Nanjing, China; ²Guangdong Pharmaceutical University, Center for drug research and development, Guangdong, China; ³China Pharmaceutical University, Jiangsu Center for Pharmacodynamics Research and Evaluation, Nanjing, China
Email: jiangcpu@163.com

Background and aims: Obeticholic acid (OCA) is approved as a second-line treatment in Primary Biliary Cholangitis (PBC). However, several side effects were reported in clinical studies. And long-term feeding of 30 mg/kg OCA even slightly induced proliferation of cholangiocytes in normal mice. Recent studies have reported that the non-classical NF-kappaB pathway plays an essential role in the process of ductular reaction (DR). But, the effect of OCA on the non-classical NF-kappaB pathway and the mechanism involved have not been clarified.

Method: The bile duct ligation (BDL) model was chosen for in vivo experiments. And the primary mouse bone marrow derived macrophages (BMDMs), Kupffer cells, THP-1 and human intrahepatic bile epithelium cells (HiBECs) were used for in vitro experiments.

Results: The dose of 40 mg/kg of OCA significantly increased the level of serum alkaline phosphatase (ALP) in BDL mice. The mRNA level of *F4/80*, *Il-1beta* and *Tnf-alpha* were elevated by OCA compared with BDL mice. The protein of CK19 in liver was obviously increased in OCA-treated BDL group. And the serum level of TNFSF14, one of the non-classical NF-kappaB pathway ligands, was significantly induced by OCA in BDL mice. In liver non-parenchymal cells, OCA induced the upregulation of LTbetaR mediated Relb signaling, such as the increased mRNA expression of Ltbr, Relb and Tnfsf14 (one of the ligands combined with LTbetaR), while Ltbr (another ligand combined with LTbetaR) unchanged. To further identify the Relb-positive cells in liver, immunohistochemistry was performed. The images showed that the expression pattern of Relb was located not only in cholangiocytes but also in non-parenchymal cells around the portal area and OCA led to an apparently increased area in BDL mice. So, we isolated the liver primary Kupffer cells. And OCA could induce the increased fluorescence intensity of Relb compared with BDL group, indicating the participation of macrophages. In addition, OCA 20 μ M upregulated the Relb and Tnfsf14 expression in mouse BMDMs and THP-1 cells. The content of TNFSF14 in OCA-treated conditional medium of THP-1 cells was significantly increased. And OCA-treated conditional medium could promote the proliferation of HiBECs. Clodronate liposomes were used to deplete macrophages. The depletion of macrophages alleviated the liver injury caused by OCA in BDL mice. After macrophage depletion, the protein expression of Relb in liver was downregulated compared with BDL OCA group. And the protein of CK19, SOX9, alpha-SMA and Fibronectin 1 were also significantly reduced in BDL OCA group with depletion of macrophages.

Conclusion: The OCA-treated BDL mice displayed aggravated inflammatory infiltration and ductular reaction. OCA induced the upregulation of LTbetaR-Relb signaling in macrophages and subsequent TNFSF14 production to further enhance TNFSF14-mediated proliferation of cholangiocytes.

POSTER PRESENTATIONS

FRI-340

Hepatocyte TAF15 promotes APAP-induced acute liver injury via activating NF- κ B to induce PANoptosis

Si Zhao¹, Bing Xu¹, Jiangqiang Xiao¹, Yuzheng Zhuge¹. ¹Department of Gastroenterology, Nanjing Drum Tower Hospital, Affiliated Hospital of Medical School, Nanjing University, Nanjing, Jiangsu, China, nanjing, China

Email: 2469981887@qq.com

Background and aims: Drug-induced liver injury (DILI) has become the leading reason of acute liver failure (ALF), posing a serious threat to human health worldwide. Acetaminophen (APAP), commonly used as an analgesic and antipyretic drug, is the principal cause of drug-induced ALF after APAP overdose. TATA-binding protein-associated factor 15 (TAF15) is a FET membrane protein participating in the regulation of gene transcription and inflammation signalling pathways in multiple diseases although its role in DILI remains elusive. Here, we examined whether PANoptosis, a novel type of programmed cell death closely associated with inflammation damage, was involved in APAP-induced liver injury, and TAF15-mediated regulation of hepatocyte PANoptosis, if any.

Method: Human DILI liver tissues and control liver samples were collected for detecting TAF15 expression. The APAP models of DILI (350 mg/kg) were established and compared between hepatocyte-specific TAF15 knockout (TAF15^{Δhep}) and wild-type control (TAF15^{fl/fl}) mice. HE, western blotting, PCR, Co-immunoprecipitation (IP), immunofluorescence (IF), primary hepatocyte cells extraction, and immunohistochemistry (IHC) staining were performed to further clarify the mechanism by which TAF15 regulates the occurrence and development of DILI.

Results: epatic expression of TAF15 and PANoptosis was significantly increased in the pathogenesis of DILI compared with controls in human and mice. TAF15 deficiency alleviated APAP-induced liver dysfunction, inflammatory responses, and hepatocyte PANoptosis. Further examination revealed that TAF15 promoted inflammatory responses and the activation of PANoptosome through interaction with NF- κ B factor p65, a key factor in the transcript expression and regulation of programmed cell death. Moreover, NF- κ B activation inhibitor JSH-23 markedly blocked APAP-induced PANoptosis in primary hepatocytes.

Conclusion: Our findings shed light toward a deleterious role of TAF15 in hepatocyte PANoptosis, thus offering therapeutic promises in APAP-induced acute liver injury.

FRI-341

Clusterin deficiency exacerbates cholestatic liver disease through ER stress and NLRP3 inflammasome activation

Hye-Young Seo¹, So-Hee Lee¹, Ji Yeon Park¹, Jae-Seok Hwang¹, Mi-Kyung Kim², Byoung Kuk Jang¹. ¹Keimyung University School of Medicine, Daegu, Korea, Rep. of South; ²Keimyung University School of Medicine, Daegu, Korea, Rep. of South

Email: jangha106@dsme.or.kr

Background and aims: Cholestatic liver disease, characterized by impaired bile flow leading to the accumulation of harmful metabolites and toxins, results in liver damage. Inflammatory cytokines play a crucial role in the progression of this condition. This study investigates the potential anti-inflammatory effects of clusterin, a glycoprotein known for its roles in cell death, lipid transport, and cellular protection, on liver injury induced by a DDC diet.

Method: The study examined the impact of clusterin on liver injury using C57BL/6 mice and Clusterin knockout mice fed a DDC diet for 10 to 20 days. Both primary kupffer cells (KC) and hepatocytes (HC) from these mice were analyzed. Assessments included Sirius red staining, immunohistochemistry, real-time RT-PCR, ELISA, and western blot analysis to determine the effects of clusterin.

Results: In Clusterin knockout mice, elevated levels of ALT, AST, collagen, and α SMA were observed post DDC diet-induced liver injury. These mice also showed increased ER stress markers (CHOP,

ATF6, p-eIF2 α) and inflammasome markers (NLRP3, ASC, caspase1, IL1 β protein expression, and IL1 β and IL18 secretion). Thapsigargin, an ER stress inducer, escalated the NLRP3 inflammasome response in primary KC and HC, which was reduced by overexpressing clusterin.

Conclusion: This study demonstrates that the absence of clusterin exacerbates ER stress and NLRP3 inflammasome activation in mice fed a DDC diet. Conversely, overexpression of clusterin suppresses ER stress and NLRP3 activation. Therefore, clusterin deficiency is linked to an increased inflammatory response in the liver, which is associated with the upregulation of ER stress.

FRI-342

Visualisation of intrahepatic activation of coagulation and its contribution to disease progression in mice with acetaminophen-induced acute liver injury

Fien von Meijenfeldt¹, Agostina Carestia², Laura Godin², James Luyendyk³, Ton Lisman¹, Craig Jenne². ¹University Medical Center Groningen, Groningen, Netherlands; ²University of Calgary, Calgary, Canada; ³Michigan State University, East Lansing, United States

Email: f.a.von.meijenfeldt@umcg.nl

Background and aims: Acute liver failure (ALF) is a life-threatening disease that is most often caused by acetaminophen overdose. ALF is characterized by profound hemostatic changes, and experimental evidence suggests that activation of coagulation contributes to disease progression. Here, we aimed to study and visualize intrahepatic activation of coagulation in a mouse model of acetaminophen-induced acute liver injury.

Method: Acute liver injury was induced by intraperitoneal injection of acetaminophen in mice. To study the contribution of activation of coagulation to progression of disease we treated mice with argatroban, DNase, or saline (n = 6 per group). We imaged formation of thrombin, and influx of platelets and neutrophils in mice livers using intravital microscopy. Liver injury was studied by plasma alanine transferase levels and histology (HandE staining).

Results: Acetaminophen overdose resulted in extensive liver injury, intrahepatic platelet aggregation and neutrophil influx in the injured liver at 6 and 24 hours after overdose. Interestingly, we observed formation of bursts of thrombin in extravascular spaces in the liver, presumably the space of Disse. Mice treated with argatroban prior to acetaminophen overdose showed a remarkable reduction in liver injury and platelet aggregation with levels similar to controls. In these mice we did not observe intrahepatic thrombin formation. DNase treatment had no effect on liver injury or intrahepatic thrombin formation.

Conclusion: Acetaminophen-induced acute liver injury in mice results in formation of thrombin, formation of platelet aggregates, and influx of neutrophils in the injured liver. Intrahepatic thrombin formation likely contributes to liver injury as livers of mice that were pre-treated with argatroban showed minimal injury. We did not find a role for neutrophil extracellular traps or extracellular DNA in acetaminophen-induced liver injury in mice.

FRI-343-YI

APAP induced liver damage is prevented by activation of PPAR-gamma and PPAR-alpha

Paul Gomez-Jauregui¹, Francisco Gonzalez-Romero¹, Beatriz Gómez Santos¹, Maider Apodaka-Biguri¹, Xabier Buque¹, Maria Crespo², Alfonso Mora^{2,3}, Mariana Mesquita^{4,5}, Igor Aurrekoetxea^{1,6}, Igotz Delgado¹, Ane Nieva-Zuluaga¹, Mikel Ruiz de Gauna¹, Idoia Fernández-Puertas¹, Natalia Sainz-Ramírez¹, Kendall Alfaro-Jiménez¹, María Esther Irizar⁷, Ainhoa Iglesias⁸, Francisco Javier Cubero^{5,9,10}, Guadalupe Sabio^{2,3}, Ana Zubiaga⁸, Patricia Aspichueta^{1,6,9}. ¹Department of Physiology

University of the Basque Country UPV/EHU, Faculty of Medicine and Nursing, Leioa, Spain; ²Centro Nacional de Investigaciones Cardiovasculares Carlos III, Madrid, Spain; ³Centro Nacional de Investigaciones Oncológicas Carlos III, Madrid, Spain; ⁴Institute of Biology, Department of Plant Biology, PPG BMM, University of Campinas (UNICAMP), São Paulo, Brazil; ⁵Department of Immunology, Ophthalmology and ENT, Complutense University School of Medicine, Madrid, Spain; ⁶Biocruces Bizkaia Health Research Institute, Cruces University Hospital, Barakaldo, Spain; ⁷IMQ Clínica Zorrotzaurre, Bilbao, Spain; ⁸Department of Genetic, Physical Anthropology and Animal Physiology, Faculty of Science and Technology, University of Basque Country UPV/EHU, Leioa, Spain; ⁹National Institute for the Study of Liver and Gastrointestinal Diseases (CIBEREHD, Carlos III Health Institute), Madrid, Spain; ¹⁰Instituto de Investigación Sanitaria Gregorio Marañón (IISGM), Madrid, Spain
Email: patricia.aspichueta@ehu.eus

Background and aims: Acetaminophen (APAP), a common pain reliever, is the leading cause of hepatotoxicity. Thus, effective antidotes are required. The APAP induced toxicity involves the dysregulation of pathways involved in liver metabolism, immunity and regeneration, processes in which E2F1 and E2F2 might also be involved. The aims were: 1) to investigate if E2F1 and/or E2F2 are involved in APAP-induced liver injury; 2) to identify the mechanism and investigate whether the activation of beneficial processes improve the survival.

Method: *E2f1*^{-/-}, *E2f2*^{-/-} and wild-type (WT) mice were used. CD45.1 WT mice underwent bone marrow (BM) transplant. Hepatotoxicity was induced by IP injection of 750 mg/kg or 360 mg/kg APAP. Mice were sacrificed 6, 24 and 48 h post treatment. Survival and metabolic studies, anatomopathological evaluation of necrosis and immune infiltrate, immunohistochemistry, and protein and lipid levels analysis were performed. Additionally, both a PPAR-gamma protein agonist (Rosiglitazone) and inhibitor (GW9662), a PPAR-alpha/PPAR-gamma agonist (Saroglitazar), and a Pan-PPAR agonist (Lanifibranor) were administered.

Results: E2F1 deficiency exacerbated APAP-induced liver injury, whereas E2F2 deficiency conferred protection. Accordingly, the increased inflammatory component, with neutrophils as the main recruited cells, was found in *E2f1*^{-/-} mice, while was decreased in *E2f2*^{-/-} mice when compared to WT mice. This was reinforced with the determination of CD45⁺, CD11b⁺ and F4/80⁺ cells in the whole liver. BM transplantation showed that the protection of *E2f2*^{-/-} mice or the susceptibility of *E2f1*^{-/-} mice was related to the effect of its deficiency in the liver rather than to changes in myeloid cell activity. The higher survival and protection in *E2f2*^{-/-} mice were linked to increased levels of ATGL, lipase involved in hydrolysis of lipid droplets, and LC3-II levels while decreased p62 levels. This pro-lipophagy profile was associated with higher β -oxidation rate (FAO) and mitochondrial mass. Simultaneously, increased levels of the autophagy and FAO regulators, PPAR-alpha and PPAR-gamma were observed in *E2f2*^{-/-} mice livers. Pharmacological inactivation of PPAR-gamma exacerbated APAP induced hepatotoxicity in *E2f2*^{-/-} mice, while rosiglitazone, saroglitazar or lanifibranor administration protected against APAP-induced hepatotoxicity in *E2f1*^{-/-} mice and WT mice, prolonging survival and reversing transaminases levels. Notably, anatomopathological evaluation revealed no necrotic foci in the livers of agonist-treated mice.

Conclusion: PPAR-gamma activation is involved in the protection of *E2f2*^{-/-} mice against APAP-induced hepatotoxicity. The activation of both PPARs confers protection against APAP-induced liver injury and might be consider as a potential treatment in the future.

FRI-347

HYX1-derived exosomal let-7c-5p protects against acute liver failure by inhibiting SLC11A2-mediated ferroptosis

Huixin Tang¹, Li Bai¹, Yu Chen¹. ¹Capital Medical University, Beijing, China
Email: tender78@126.com

Background and aims: Acute liver failure (ALF) is characterized by rapid progression, high short-term mortality, and poor prognosis. Unfortunately, there is no effective therapy for ALF currently except for liver transplantation, which is limited by critical shortage of donor liver. Therefore, it is imperative to seek for novel therapeutic means for ALF. We previously have documented that the transfer of hepatic stem cell HYX1 confers the hepatoprotection against ALF. In the present work, we aimed to demonstrate the hepatoprotection conferred by HYX1-derived exosomes (Exos) against D-GalN/LPS-induced ALF and to dissect the underlying molecular mechanism.

Method: Normal mice were pre-treated with HYX1-Exos or negative control, followed by D-GalN/LPS insult. HYX1-Exos were subjected to miRNA sequencing and KEGG enrichment analysis. The pivotal role of ferroptosis in ALF was confirmed. The ferroptosis levels were evaluated after HYX1-Exos treatment. The special miRNAs related to ferroptosis were screened out and identified. Let-7c-5p agomir or negative control was injected into normal mice followed by acute insult. And the expression of ferroptosis-related markers was detected. The targeted relationship between let-7c-5p and SLC11A2 was analyzed. The molecular basics underlying the hepatoprotection conferred by let-7c-5p was dissected using stable AML cells with SLC11A2 overexpression (OE) or knockdown.

Results: HYX1-Exos alleviates ALF, as shown by improved hepatic architecture and reduced pathology scores. miRNA sequencing analysis displayed that miRNAs derived from HYX1-Exos could be enriched in ferroptosis signaling pathway. The administration of fer-1 led to significant mitigation in hepatic damage. HYX1-Exos treatment resulted in remarkable decrease in the levels of ferroptosis signaling molecules. Let-7c-5p was screened out as the potential miRNA responsible for the hepatoprotection conferred by HYX1-Exos. The administration of let-7c-5p agomir brought about obvious alleviation in hepatic damage and marked inhibition in ferroptosis signaling. Let-7c-5p targetedly inhibited SLC11A2. The cell viability was decreased but the ferroptosis levels were enhanced in SLC11A2-OE cells compared with control (CT) cells. Especially, the hepatoprotection conferred by HYX1-Exos or let-7c-5p agomir was obviously weakened in SLC11A2-OE cells compared with CT cells. On the other hand, the cell viability was increased but the ferroptosis levels were reduced in SLC11A2-knockdown cells compared with CT cells.

Conclusion: Let-7c-5p carried by HYX1-Exos protects from ALF by inhibiting SLC11A2-mediated ferroptosis. Our finding will shed novel insights into the pathogenesis and treatment of ALF.

FRI-348

Endogenous Annexin A1 has a protective effect on the liver in a diabetic mouse model

Diego Dias dos Santos¹, Rafael André da Silva², Luiz Philipe de Souza Ferreira¹, Cristiane Damas Gil¹. ¹Federal University of São Paulo, Department of Morphology and Genetics, São Paulo, SP, Brazil; ²Institute of Biosciences, Letters and Exact Sciences, Department of Biology, São José do Rio Preto, SP, Brazil
Email: dias.diego@unifesp.br

Background and aims: Diabetes mellitus (DM) is a global public health problem, which leads to systemic dysregulations affecting several tissues, including severe liver complications. Patients with DM2 have increased plasma levels of annexin A1 (AnxA1) and, in an experimental murine model of DM2, the AnxA1 protein plays a fundamental role in attenuating the effects caused by insulin resistance, such as hepatosteatosis. Despite these important findings, its role has been little explored in hepatocytes in DM1. Thus, this study aims to evaluate the role of AnxA1 in hepatocyte biology in a streptozotocin (STZ)-induced DM1 mouse model.

Method: Male C57BL/6 mice (AnxA1^{+/+} and AnxA1^{-/-}) were randomly distributed into two experimental groups (n = 6 animals/

POSTER PRESENTATIONS

group): control (CTR) and DM. DM was induced in mice with intraperitoneal injection of STZ (65 mg/kg \times 5 days) or citrate vehicle. After 12 weeks, livers were collected for different analysis. GSE39752 study, which presents murine liver transcriptome from control ($n = 7$) and STZ-induced DM ($n = 6$) groups, was selected from the Gene Expression Omnibus repository (<http://www.ncbi.nlm.nih.gov/geo/query/acc.cgi?acc=GSE39752>). The datasets were analyzed using the GEO2R tool to detect expressions of AnxA1, Fpr1, Fpr2/3 (formyl peptide receptors) and S100A11 (S100 calcium-binding protein A11). The procedures were approved by the UNIFESP Animal Experimentation Ethics Committee (n° 5520161123).

Results: Morphological evaluation of the AnxA1+/+ CTR livers showed a normal appearance of hepatocytes and sinusoids, contrasting with the AnxA1-/- CTR group where 70% of mice showed hepatocytes with cytoplasmic vacuolation. In the AnxA1+/+ DM group, ~50% presented hepatocytes with vacuolated and damaged cytoplasm and nucleus, exacerbated in AnxA1-/- DM mice (~75%). Both AnxA1+/+ and AnxA1-/- DM livers exhibited a significant reduction in glycogen, fibroblast growth factor 2 and vascular endothelial growth factor A levels compared to the respective CTR groups. AnxA1+/+ DM livers showed higher levels of reactive oxygen species, IL-10 and TNF- α compared to the CTR ones. The lack of AnxA1 in DM livers was associated with raised monocyte chemoattractant protein-1 levels and no alterations were detected in ROS levels. Transcriptome analysis revealed an increase in the transcriptional levels of Fpr1, Fpr2/3 (AnxA1 receptors), and S100A11 (marker of hepatic steatosis and AnxA1 adaptor protein) in the DM livers compared to the controls, with no changes in AnxA1 transcripts.

Conclusion: Our study showed that AnxA1 deficiency exacerbates the pathological aspect of the liver, suggesting its important hepatoprotective role in the context of DM1.

Acute liver failure and drug induced liver injury – Clinical

TOP-344-YI

Personalized prediction of spontaneous recovery in acute liver failure listed for liver transplantation

Xun Zhao¹, Yingji Sun², Hannah Wozniak², Mamatha Bhat³.

¹University of Toronto, Toronto, Canada; ²Toronto General Hospital, Toronto, Canada; ³University Health Network, Toronto, Canada
Email: xun.zhao@mail.mcgill.ca

Background and aims: Acute liver failure (ALF) is a rare clinical presentation characterized by rapid deterioration of hepatic function in people without pre-existing liver disease. Transplant-free survival is low at 50%, and early referral to liver transplantation is crucial. In the United States, ALF can be considered for urgent organ allocation and listed as status 1A if life expectancy is anticipated to be less than 7 days. However, spontaneous recovery is still possible in certain patients, even when listed under status 1A. Currently there is no clinical tool that predicts spontaneous recovery. We have built and validated a machine learning algorithm that accurately predicts spontaneous recovery in patients listed with the highest urgency for liver transplantation.

Method: We used the Scientific Registry of Transplant Recipients to train, test, and validate our model. We identified all patients listed as status 1A for ALF. Patients who died or spontaneously recovered on the waitlist were included. Patient demographic data, comorbidities, and intensive care unit specific variables were collected (37 variables in total). Clinical findings and serum variables up to 72 hours from the time of listing were collected. We built two machine learning models, a logistic regression model, and a random forest model to predict spontaneous recovery or death on the waitlist. Training and testing of

the data was split 70% and 15%, with 15% of data held out for validation.

Results: 2,347 patients were included in our study, with 1,335 dying on the waitlist (mean age 41, MELD 35) and 1,012 recovering spontaneously (mean age 34, MELD 32). 33.2% of the recovery group had ALF to acetaminophen overdose, compared to 17.6% in the deceased group. Mean change in MELD from initial MELD and most recent MELD within 72 h was -0.1 in those who died and -2.6 in those who recovered. Logistic regression had an accuracy of 0.77 ± 0.01 , and an AUC of 0.76 ± 0.01 . Our random forest model had an accuracy of 0.92 ± 0.01 , a F1 score of 0.91 ± 0.01 , and AUC of 0.92 ± 0.01 . This corresponded to a sensitivity of 89.2% and specificity of 94.3%. SHAPLEY analysis showed that bilirubin, mechanical ventilation, MELD score, encephalopathy grade, and age were top features contributing to our model.

Conclusion: We have built a score that accurately predicts spontaneous recovery in listed ALF patients based on variables at time of listing and is personalized to individual patients.

TOP-345

Clinical and HLA associations of fluoroquinolone induced liver injury: results from the drug induced liver injury network (DILIN)

Jawad Ahmad¹, Andrew Dellinger², Paola Nicoletti³, Huiman Barnhart⁴, Marwan Ghabril⁵, Robert Fontana⁶, Victor Navarro⁷, Gina Choi⁸, Paul Hayashi⁹. ¹Recanati-Miller Transplantation Institute, Icahn School of Medicine at Mount Sinai, New York, United States; ²Duke University School of Medicine, Durham, NC, United States; ³Icahn School of Medicine at Mount Sinai, New York, United States; ⁴Duke University School of Medicine, Durham, United States; ⁵Indiana University, Indianapolis, United States; ⁶University of Michigan, Ann Arbor, United States; ⁷Einstein University, Philadelphia, United States; ⁸UCLA, Los Angeles, United States; ⁹FDA, Silver Spring, United States

Email: jawad.ahmad@mountsinai.org

Background and aims: Fluoroquinolones are widely prescribed antimicrobials with a favorable safety profile but a well-described risk of drug-induced liver injury (DILI). The aim of this study was to identify clinical features and HLA genetic variants associated with fluoroquinolone-induced DILI in a large national registry.

Method: Analysis was limited to cases of fluoroquinolone-induced liver injury enrolled in DILIN between 2004 and 2022, adjudicated as definite, highly likely or probable (high confidence). HLA class I and II alleles were sequenced by Illumina MiSeq platform and compared to population controls from publicly available datasets inferred by HIBAG software.

Results: 61 high-confidence cases (13% definite, 49% highly likely, and 38% probable) were included: 32 from ciprofloxacin, 22 from levofloxacin, and 7 from moxifloxacin. Clinical features of liver injury for the 3 drugs were similar. Indication for use were genitourinary (41%), gastrointestinal (13%), respiratory (20%), orthopedic/cutaneous (10%), and other/unknown (16%) infections. The median duration of therapy was 7 (range 2–54) days; median age 53 (range 22–80) years; 67% female; 72% non-Hispanic-white, 10% non-Hispanic-black, 5% Asian, and 13% other. Median latency to onset was 10 (range 1–83) days; 28% had rash, 26% had fever, 64% were hospitalized, 61% were jaundiced; 44% had hepatocellular, 30% mixed, 26% cholestatic pattern of liver injury as determined by the R-value; 31% were ANA and 18% SMA positive; median time to recovery was 65 days, but 13% developed evidence of chronic injury, 15% died (11% due to liver failure). HLA association results were available on 60 cases. Two HLA alleles were associated with an increased risk of liver injury compared to controls: HLA-DQA1*03:01 (carriage frequency (CF) 0.38 in cases vs 0.19 in controls) and HLA-B*57:01 (0.15 vs 0.06). There was a significant difference between the combined CF of the two alleles of 0.48 in cases vs 0.24 controls, OR: 2.8 (1.7–4.8), $p = 0.0001$. For each individual drug the associations were: ciprofloxacin HLA-DQA1*03:01 (CF 0.28 in cases vs 0.19 in controls) and HLA-B*57:01

(0.16 vs 0.06), combined 0.40 vs 0.24, OR: 2.0 (1.0–4.1), $p=0.06$; levofloxacin HLA-DQA1*03:01 (CF 0.53 in cases vs 0.19 in controls) and HLA B*57:01 (0.10 vs 0.06), combined 0.53 vs 0.24, OR: 3.2 (1.2–8.9), $p=0.01$; moxifloxacin HLA-DQA1*03:01 (CF 0.43 in cases vs 0.19 in controls) and HLA B*57:01 (0.29 vs 0.06), combined 0.71 vs 0.24, OR: 9.3 (1.5–97.4), $p=0.006$. No clinical characteristics or outcomes were associated with carriers compared to non-carriers.

Conclusion: Fluoroquinolone-induced liver injury typically presents with a short latency, variable pattern of liver injury, and carries a significant risk of chronicity and mortality. There is a significant association with HLA-DQA1*03:01 and HLA B*57:01.

TOP-346-YI

Therapeutic plasma exchange in Amatoxin associated acute liver failure-results from an interim analysis of the Amanita-PEX study

Klaus Stahl¹, Bahar Naibant¹, Tobias Laue², Filipe Sousa Cardoso³, Joao Madaleno⁴, Petra Stöckert⁵, Daniel Tegtmeyer⁶, Angelo Di Giorgio⁷, Karsten Große⁸, Uta Merle⁹, Nikola Mareljic¹⁰, Dominik van de Loo¹¹, David Toapanta¹², Dominic Lenz¹³, Tanja Fritz¹⁴, Alexandra Linke¹⁵, Peter Nissen Bjerring¹⁶, Oscar M. Fierro-Angulo¹⁷, Ricardo Ulises Macias Rodriguez¹⁸, Anja Geerts¹⁹, Sarah Raevens²⁰, Marcial Sebode²¹, Martina Sterneck²², Ekkehard Sturm²³, Alexander Fichtner⁹, Enric Reverter²⁴, Phil Robin Tepasse²⁵, Christian M. Lange²⁶, Tony Bruns²⁷, Jun Oh²⁸, Stephan Schmid⁹, Martina Müller-Schilling⁹, Catarina Borges²⁹, Hugo Pinto Marques³⁰, Ulrich Baumann², Heiner Wedemeyer¹, Richard Taubert³¹. ¹Hannover Medical School, Hannover, Germany; ²Medizinische Hochschule Hannover, Hannover, Germany; ³Hospital Curry Cabral, Lisbon, Portugal; ⁴Centro Hospitalar e Universitário de Coimbra, Coimbra, Portugal; ⁵University Hospital Regensburg, Regensburg, Germany; ⁶Universitätsklinikum Hamburg, Hamburg, Germany; ⁷Hospital Papa Giovanni XXIII, Bergamo, Italy; ⁸University Hospital Aachen, Aachen, Germany; ⁹Universitätsklinikum Heidelberg, Heidelberg, Germany; ¹⁰University Hospital Munich, Munich, Germany; ¹¹University Hospital Muenster, Muenster, Germany; ¹²Hospital Clínic Barcelona, IDIBAPS and CIBERhd, Barcelona, Spain; ¹³Universitätsklinikum Heidelberg, Heidelberg, Germany; ¹⁴Universitätsklinikum Tübingen, Tübingen, Germany; ¹⁵Universitätsklinikum Hamburg, Hamburg, Germany; ¹⁶University of Copenhagen, Copenhagen, Denmark; ¹⁷Instituto Nacional de Ciencias Médicas y Nutrición Salvador Zubirán, Mexico, Mexico; ¹⁸Instituto Nacional de Ciencias Médicas y Nutrición Salvador Zubirán, Mexico, Mexico; ¹⁹Ghent University Hospital, Ghent, Belgium; ²⁰Ghent University Hospital, Ghent, Belgium; ²¹I. Dept. of Medicine, University Medical Center Hamburg-Eppendorf (UKE), Hamburg, Germany; ²²University Hospital Hamburg Eppendorf, Hamburg, Germany; ²³University Hospital Tuebingen, Tuebingen, Germany; ²⁴Hospital Clinic, Barcelona, Spain; ²⁵Universitätsklinikum Münster, Münster, Germany; ²⁶LMU University Hospital Munich, München, Germany; ²⁷University Hospital RWTH Aachen, Aachen, Germany; ²⁸University Hospital Hamburg, Hamburg, Germany; ²⁹Centro Hospitalar e Universitário de Coimbra, Coimbra; ³⁰Centro Hospitalar Lisboa Central, Lisboa, Portugal; ³¹Medical School, Hannover, Germany
Email: stahl.klaus@mh-hannover.de

Background and aims: Amatoxin related acute liver failure (AT-ALF) is associated with high mortality if no urgent liver transplantation (LTX) is performed. Therapeutic plasma exchange (PEX) has been demonstrated to improve LTX-free survival in patients with ALF of other etiologies. It is however unclear, if PEX may also improve LTX-free survival in AT-ALF and clinical practice in utilizing PEX in AT-ALF varies substantially between different centers. Of note, due to the scarcity of this ALF entity, realization of a randomized controlled trial investigating use of PEX in AT-ALF does not appear to be feasible in the future.

Method: This is an interim analysis of a multicenter, international, retrospective cohort study (Amanita-PEX study, NCT06187220) investigating the effect of additive PEX compared to standard

medical therapy (SMT) alone in AT-ALF. So far, 57 patients diagnosed with AT-ALF over the past 10 years have been successfully recruited into the study from fifteen liver transplant referral centers across seven countries. LTX-free and overall survival within the first 28 days following fulfillment of ALF criteria (encephalopathy and INR >1.5) were recorded and compared between patients receiving PEX and SMT, respectively.

Results: In this interim analysis, 49 adults with AT-ALF were included (of anticipated total $n=60$ patients), of which 18 received PEX in six centers and 31 SMT only (all but one center). Median (Interquartile Range (IQR) patient age, BMI, INR, bilirubin, MELD- and SOFA-Scores in the adult cohort were: 57 (41–65) years, 25.8 (22.7–28) kg/m², 4.0 (2.4–6.4), 75 (44–124) umol/l, 31 (26–38) and 6 (4–10) points, respectively (without significant differences between groups). 96% and 90% of patients received intravenous silibinin and n-acetylcysteine. LTX-free survival up to day 28 was 61.1% (11/18) and 41.9% (13/31) in patients receiving PEX and SMT, respectively (HR 0.544 (95%-Confidence Interval (CI): 0.246–1.205), $p=0.125$ for 28 day survival (Kaplan-Meier test); $p=0.064$ for early survival (Gehan-Breslow test)). In patients with higher grade (>1°) encephalopathy, LTX-free survival was 41.7% (5/12) and 20% (4/20) in the PEX and SMT group, respectively (HR 0.526 (95%-CI: 0.231–1.194, $p=0.094$ for 28 day survival (Kaplan-Meier test); $p=0.049$ for early survival (Gehan-Breslow test)).

Conclusion: In this interim analysis of a multicenter retrospective study, adjunctive PEX was associated with a trend towards improved LTX-free survival in patients with AT-ALF. Data retrieval is ongoing in 10 further centers. The study is still open for new study centers.

SATURDAY 08 JUNE

SAT-306

Time to use the right classification to predict the severity of checkpoint inhibitor-induced liver injury

Lina Hountondji¹, Stéphanie Faure¹, Pascale Palassin¹, Philine Witkowski Durand Viel², Marie Dupuy¹, Dominique Larrey^{1,3}, Anouck Lamoureux¹, Dimitri Pureur¹, Cyril Coustal¹, Candice Lesage¹, Eric Assenat¹, Benjamin Riviere¹, Jean-Luc Faillie¹, Xavier Quantin², Alexandre Maria¹, Georges-Philippe Pageaux¹, Lucy Meunier^{1,4}. ¹Montpellier University Hospital, Montpellier, France; ²Montpellier Cancer Institute, Montpellier, France; ³REFEPS, Montpellier, France; ⁴REFEPS, Montpellier
Email: lina.hountondji@outlook.fr

Background and aims: Immune checkpoint inhibitors (ICIs) targeting CTLA-4 and PD (L)1 have revolutionized the prognosis of many cancers. ICIs may induce several immune-related adverse events, including checkpoint inhibitor-induced liver injury (CHILI). The CTCAE classification grades all multi-system toxicities and considers the elevation of liver enzymes in CHILI. Thus, CTCAE does not include liver function, whereas European guidelines call for liver function assessment to evaluate the severity of drug-induced liver injury. The aim of this study is to evaluate and compare the severity of CHILI according to the CTCAE, DILI-N and DILI IEWG classifications.

Method: CHILI-S is an observational multicenter study of CHILI patients grade CTCAE ≥ 2 presented to the ToxImmun meeting in Montpellier. Clinico-biological data were collected at diagnosis, S2, S4, and then once a month for 6 months. CHILI was classified according to CTCAE, DILI-N and DILI IEWG: non-severe (grade 1–2) and severe (grade 3–4–5). The primary end point was the occurrence of severe liver dysfunction (ALI), defined by hyperbilirubinemia and INR ≥ 1.5 . Secondary end points were critical liver dysfunction (ALF), 3-month survival, overall survival, hospitalization, optimization of steroids, and use of a second-line immunosuppressant. EasyMedstat software was used for statistical testing. Survival curves were calculated using the Kaplan Meyer method and compared with the

POSTER PRESENTATIONS

log-rank test. The prognostic performances of the 3 classifications were compared with ROC curves.

Results: 114 patients were included in the study between December 2018 and September 2023, mostly men ($n = 67$, 58.8%), with a median age of 65.5 years (23–88). The most common cancers were lung adenocarcinoma ($n = 38$, 33.3%) and melanoma ($n = 37$, 32.5%). Anti-PD1 was the most prescribed ICI ($n = 103$, 90.3%), either alone ($n = 72$, 63.2%) or in combination with anti-CTLA4 ($n = 31$, 27.2%). Hepatitis severity according to classifications was predominantly grade 3–4 CTCAE ($n = 102$, 89.5%), and grade 1–2 DILI-N ($n = 99$, 86.8%) and DILI IEWG (107, 93.9%). Hyperbilirubinemia was present in 27 patients (23.7%), and 16 patients were hospitalized (14%). Liver biopsy was significantly more performed for severe CHILI according to CTCAE, DILI-N and DILI IEWG (37.3%, 66.7% and 71.4%). ALI was not significantly associated with any histological lesion, but lobular necrosis with bridge necrosis tended to be more frequent in patients with ALI. The DILI-N and DILI IEWG classifications performed better in predicting liver dysfunction (AUC 0.988 and 0.994), compared with CTCAE (AUC 0.795).

Conclusion: The CTCAE classification, which is recommended in clinical practice to assess the severity of CHILI, does not accurately predict liver dysfunction, in contrast to the DILI-N and DILI IEWG classifications. These results support the need to revise current CHILI management recommendations.

SAT-314

Impact of hepatic steatosis on risk of acute liver injury among people with chronic hepatitis B and SARS-CoV-2 infection

Matthew Shing Hin Chung^{1,2}, Carlos King Ho Wong^{2,3,4}, Xue Li^{1,2,3}, Francisco Tsz Tsun Lai^{2,3}, Eric Yuk Fai Wan^{2,3,4}, Celine Sze Ling Chui^{3,5,6}, Franco Wing Tak Cheng², Esther Wai Yin Chan^{2,3}, Ching Lung Cheung^{2,3}, Xi Xiong², Lanlan Li^{1,2}, Wai-Kay Seto^{1,7}, Man-Fung Yuen^{1,7}, Lung Yi Loey Mak^{1,7}, Ian Chi Kei Wong^{2,3,8,9}, ¹Department of Medicine, School of Clinical Medicine, Li Ka Shing Faculty of Medicine, The University of Hong Kong, Hong Kong, Hong Kong; ²Centre for Safe Medication Practice and Research, Department of Pharmacology and Pharmacy, Li Ka Shing Faculty of Medicine, The University of Hong Kong, Hong Kong, Hong Kong; ³Laboratory of Data Discovery for Health (D24H), Hong Kong, Hong Kong; ⁴Department of Family Medicine and Primary Care, School of Clinical Medicine, Li Ka Shing Faculty of Medicine, The University of Hong Kong, Hong Kong, Hong Kong; ⁵School of Nursing, Li Ka Shing Faculty of Medicine, The University of Hong Kong, Hong Kong, Hong Kong; ⁶School of Public Health, Li Ka Shing Faculty of Medicine, The University of Hong Kong, Hong Kong, Hong Kong; ⁷State Key Laboratory of Liver Research, The University of Hong Kong, Hong Kong, Hong Kong; ⁸Research Department of Practice and Policy, UCL School of Pharmacy, University College London, London, United Kingdom; ⁹Aston School of Pharmacy, Aston University, Birmingham, United Kingdom
Email: loeymak@gmail.com

Background and aims: SARS-CoV-2 infection was known to be associated with higher risk of liver impairment in people with chronic hepatitis B infection (CHB). However, evidence regarding the impact of concomitant hepatic steatosis (HS) on the risk of liver disease among people with CHB and SARS-CoV-2 infection is lacking. We investigated the impact of concomitant HS on people with CHB suffering from SARS-CoV-2 infection.

Method: This retrospective cohort study was performed using an electronic health database for people in Hong Kong with CHB and confirmed SARS-CoV-2 infection between 1st January 2020 and 31st January 2023. People with HS diagnosis (HS+CHB+COVID-19) were identified and matched 1:1 by propensity-score with those without (CHB + COVID-19). Each person was followed up until death, outcome event, or 31st January 2023. Study outcome was incidence of acute liver injury (ALI) within first 28 days since COVID-19 diagnosis. Severity of ALI and comparison of ALI risk stratified by the presence of

CHB infection and HS were also analyzed. Incidence rate ratios (IRRs) were estimated by Poisson regression models.

Results: Of 52, 259 COVID-19 patients with CHB infection in the cohort, 15, 391 people with HS + CHB + COVID-19 and 15, 391 people with CHB + COVID-19 were included after matching. HS + CHB + COVID-19 was associated with increased risk of ALI (IRR: 1.41, 95% CI: 1.05–1.90, $p = 0.023$), compared to CHB + COVID-19. Over 99% ALI cases were mild to moderate severity and there were no differences in the severity of ALI between HS + CHB + COVID-19 and CHB + COVID-19 ($p = 0.127$).

Conclusion: Concomitant HS was associated with increased risk of ALI among people with CHB infection suffering from SARS-CoV-2 infection.

SAT-315

High volume plasma exchange may improve transplant-free survival in patients with severe paracetamol-induced acute liver failure: a case control study

Sébastien L'Hermite¹, Valentin Coirier¹, Pauline Houssel-Debry¹, Baptiste Giguot¹, Florent Artru¹, Claire Francoz², Sophie Pellegrin², Emmanuel Weiss², Federica Dondero², Kieran Pinceaux¹, Francois Durand², Christophe Camus¹, Olivier Roux², ¹Centre Hospitalo-Universitaire de Rennes, Rennes, France; ²Hopital Beaujon-APHP, Clichy, France
Email: sebastienlhermite7@gmail.com

Background and aims: Paracetamol-induced Acute Liver Failure (P-ALF) is a severe condition that may justify emergency liver transplantation (LT). It has been suggested that High Volume Plasma Exchange (HVPE) may improve survival of ALF patients who are not candidate for LT. Yet indication for and timing of HVPE in candidates for LT remain to be defined. The aim of this study was to compare 28-day transplant-free and overall survival in patients admitted for P-ALF, depending on HVPE.

Method: We included all consecutive patients admitted in two high-volume liver transplant centers between 2016 and 2023 with P-ALF. All patients met King's College Hospital (KCH) transplant criteria. Clinical and biological data were collected retrospectively. In one center, HVPE was the first-line option whereas in the second center, LT without HVPE was the first-line option.

Results: Seventy-three patients were included: 31 (42.5%) in HVPE-group and 42 (57.5%) in non-HVPE group. There were 74% of female, with a median age of 41 years. Admission severity scores were similar in the 2 groups (SOFA score: 7 in both groups, IGS-2: 42.5 in HVPE group and 45 in non-HVPE group, ns). The proportion of patients requiring mechanical ventilation, or vasopressors, were similar (51.6% and 45, 2% in the HVPE group and 40.5% and 42, 9% in the non-HVPE group, respectively, $p = ns$). Patients in the HVPE group received a median of two sessions. Thirty-two (76.2%) patients out of 42 in the non-HVPE group had renal replacement therapy. At admission ALAT, INR, bilirubin, were similar in the 2 groups (4825 UI/L, 6.69, 3.7 mg/L in the HVPE group vs 4507 UI/L, 5.81, 3.8 mg/L in the non-HVPE group respectively, $p = ns$), as well as creatinine and lactate levels (1.01 mg/L and 5.4 mmol/L vs 1.51 mg/L and 7.85 mmol/L, $p = ns$). Arterial ammonia was significantly lower in the HVPE group (95.5 vs. 190 $\mu\text{mol/L}$, $p < 0.0001$). One (3.2%) of 31 patients was transplanted in the HVPE group, compared with 17 (40.5%) of 42 patients in the non-HVPE group. Five (16.1%) patients died at day 28 in the HVPE group, versus 18 (42.9%) patients in the non-HVPE group ($p = 0.012$). In the HVPE group, none of the 5 deceased patients received LT, in the non-HVPE group 15 patients died prior to LT and 3 after (at day 1 or 2 post LT). 28-day transplant-free survival was significantly higher in the HVPE group (80, 7% vs 23.8%, $p < 0.0001$), as well as overall survival (83.9% vs 57.1%, $p = 0.002$). Lactate level at admission and the use of HVPE were significantly associated with both transplant-free and overall survival in a multivariate analysis.

Conclusion: This study suggests that in patients with P-ALF meeting the KCH criteria, the use of HVPE may improve transplant-free and

overall survival. Whether HVPE is an alternative to LT or serves as a bridge to LT remains to be evaluated in larger populations.

SAT-316

β-adrenergic drive impairs small intestinal gut-vascular barrier (GVB): mechanism involved in gut-vascular-barrier dysfunction in acute-on-chronic liver failure (ACLF)

Marco Felber^{1,2}, Tim Wolfisberg^{1,2}, Lorena Wyss^{1,2}, Sheida Moghadamrad³, Oriol Juanola³, Andrea De Gottardi³, Reiner Wiest¹. ¹Department of Visceral Surgery and Medicine, Inselspital, Bern University Hospital, University of Bern, Bern, Switzerland; ²Department for BioMedical Research, Visceral Surgery and Medicine, University of Bern, Bern, Switzerland; ³Laboratories for Translational Research, Ente Ospedaliero Cantonale and Faculty of Biomedical Science, Università della Svizzera italiana, Lugano, Switzerland
Email: marco.felber@unibe.ch

Background and aims: Acute on chronic liver failure (ACLF) is often characterized by precipitating events of which pathological bacterial translocation (BT) from the gut and/or bacterial infections have been proposed to be of particular pathophysiological relevance. In ACLF i) excessive adrenergic drive has been shown by markedly increased serum levels of norepinephrine (Jalan et al. (2015) *Liver international*) and ii) non-selective beta-blocker therapy appears to improve short-term mortality (Mookerjee et al. (2016) *Journal of Hepatology*). The gut-vascular-barrier (GVB) is fundamental for limiting access of pathological BT to the gut-liver-axis but has not been addressed as for changes induced by adrenergic drive and/or ACLF. Thus, we aimed to characterize the small intestinal GVB in terms of function, structure and integrity in dependency on beta-adrenergic stimulation, blockade (by propranolol) and/or presence of liver cirrhosis and ACLF.

Method: ACLF was induced in C57Bl/6 cirrhotic mice (bile-duct-ligation) via LPS i.p. and beta-adrenergic hyperactivity was induced by chronic intraperitoneal delivery of isoproterenol (by osmotic mini pump) for 7 days. Duodenal GVB-function was determined in-vivo by confocal laser endomicroscopy assessing extravasation of FITC-albumin. Endothelial intercellular junctions (VE-cadherin, claudin-5) were evaluated in duodenal tissues by immunofluorescence. To evaluate the direct effects of beta-adrenergic hyperstimulation on murine vascular endothelial cells (MIVECs), we performed transwell-permeability-assays for FITC-albumin.

Results: Chronic beta-adrenergic hyperstimulation caused pathological increases in FITC-albumin extravasation into the duodenal lamina propria being even more pronounced in cirrhotic and ACLF mice. Moreover, propranolol-treatment ameliorated FITC-albumin-extravasation in ACLF mice. Changes in GVB-function induced by beta-adrenergic stimulation were associated with significant reductions in VE-cadherin and claudin-5 in duodenal capillaries and disrupted murine vascular endothelial cell monolayer in in-vitro.

Conclusion: Beta-adrenergic hyperstimulation modulates intercellular junctions impairing vascular barrier integrity and function of small intestinal GVB. This GVB-dysfunction may be a leading cause of pathological loss of albumin as well as pathological BT fueling the gut-liver-axis in ACLF.

SAT-317

Assessment of liver fibrosis in patients taking Methotrexate: long-term outcomes and changes in measurements over time

Lucy O'Reilly¹, Robert Greig¹, Stephen Barclay¹, Ewan H. Forrest². ¹Glasgow Royal Infirmary, Glasgow, United Kingdom; ²Glasgow Royal Infirmary, University of Glasgow, Glasgow, United Kingdom
Email: loreilly24@gmail.com

Background and aims: Methotrexate is used to treat a variety of inflammatory diseases, particularly inflammatory arthritis and psoriasis. Despite its effectiveness, there have been concerns about the risk of liver fibrosis, although the relationship has been poorly understood. Recently there has been greater acknowledgement of the

importance of metabolic dysfunction risk factors. In this context we have reviewed our use of FibroScan for Liver Stiffness Measurement (LSM) in patients prescribed Methotrexate over 12 years.

Method: This was a retrospective, single-centre study. Patients on Methotrexate referred to our Liver Service with suspicion of liver injury were identified from FibroScan studies. Data was collated between October 2008 and December 2020. LSM was categorised as <8 kPa, 8–12 kPa and >12 kPa with regards to risk of subsequent liver related events. From the laboratory data, the AST-to-ALT ratio, APRI and FIB-4 index were calculated and P3NP value, if available, recorded. A reliable FibroScan was defined as an IQR percentage of median LSM ≤30%, or >30% if LSM <7.1 kPa as previously described.

Results: 369 LSMs were obtained, of which 325 (88.1%) were reliable. The most common indication for Methotrexate was psoriasis (68.9%). The Medium probe was used in 180 scans (61.8%). Overall, abnormal LSM (>8 kPa) were seen in 25.8% with just 10.8% having high risk scores >12 kPa. On logistic regression analysis diagnosis of diabetes ($p < 0.0001$ (6.21; 2.58, 14.96)), use of the XL probe ($p = 0.006$ (3.76; 1.46, 9.6)) and FIB-4 index ($p = 0.0004$ (2.52; 1.51, 4.21)) were related to a LSM >12 kPa. In total there were 44 deaths (15.9%) after a median follow-up of 2767 (2536, 3011) days from their index assessment. Two of these deaths were liver-related (following decompensation with ascites) and both of these patients had a LSM >12 kPa. The 33 patients with a LSM >12 kPa had a median follow-up of 3509 (2672, 3954) days. Of these patients there were just 3 (9.1%) who experienced liver related events: the 2 deaths as above and 1 patient with bleeding from portal hypertensive gastropathy. Forty eight patients had more than 1 LSM: median time interval between scans was 726 (623, 817) days. The median change in LSM -0.3 ($-0.7, 0.3$) and change in FIB-4 $+0.04$ ($-0.08, 0.08$). Sixteen patients changed LSM category: 7 to a lower and 9 to a higher category. 1 patient progressed to LSM >12 kPa.

Conclusion: Liver-related events are rare in patients taking Methotrexate and occurred only in those with a baseline LSM >12 kPa. FIB-4 index and markers of metabolic dysfunction (diabetes and XL probe use) were related to high LSM values. Clinically significant change in LSM on interval scanning after a median of 2 years was rare.

SAT-318

Evaluating the life-saving potential of liver transplantation for acute-on-chronic liver failure with circulatory failure: an observational cohort study

Jinjin Luo¹, Peng Li^{1,2}, Meiqian Hu¹, Xi Liang³, Jiaojiao Xin¹, Jing Jiang¹, Dongyan Shi¹, Huazhong Chen⁴, Jinjun Chen⁵, Yu Chen⁶, Jun Li¹. ¹State Key Laboratory for Diagnosis and Treatment of Infectious Diseases, National Clinical Research Center for Infectious Diseases, National Medical Center for Infectious Diseases, The First Affiliated Hospital, Zhejiang University School of Medicine, Hangzhou, China; ²Department of Gastroenterology, The First Affiliated Hospital, Zhejiang University School of Medicine, Hangzhou, China; ³Precision Medicine Center, Taizhou Central Hospital (Taizhou University Hospital), Taizhou, China; ⁴Department of Infection Diseases, Taizhou Hospital of Zhejiang Province Affiliated to Wenzhou Medical University, Linhai, China; ⁵Hepatology Unit, Department of Infectious Diseases, Nanfang Hospital, Southern Medical University, Guangzhou, China; ⁶Beijing Municipal Key Laboratory of Liver Failure and Artificial Liver Treatment Research, Fourth Department of Liver Disease, Beijing Youan Hospital, Capital Medical University, Beijing, China
Email: lijun2009@zju.edu.cn

Background and aims: Circulatory failure (CF) is a severe type of extrahepatic organ failure in acute-on-chronic liver failure (ACLF), but its clinical characteristics and outcomes were undefined. This study aimed to clarify the clinical characteristics and survival benefit of liver transplantation (LT) in hepatitis B virus-related ACLF (HBV-ACLF) patients with CF.

POSTER PRESENTATIONS

Method: Data from 2247 hospitalized HBV-ACLF patients, with and without CF, were enrolled from the Chinese Group on the Study of Severe Hepatitis B open cohort to assess the survival benefit of LT by propensity score matching (PSM) analysis and stratification analysis.

Results: Among all patients, 222 individuals were diagnosed with CF, while 2025 did not exhibit CF. Patients with CF were older, had worse laboratory indicators, and had higher proportions of cirrhosis and complications, more frequent multiorgan failures and mortality (28/90/360-day: 93.6%/95.2%/95.7% vs. 26.9%/37.7%/43.1%, $p < 0.001$) than those without CF. Age, white blood cell counts, and international normalized ratio (INR) were identified as independent risk factors for the onset of CF during hospitalization. HBV-ACLF patients with CF who underwent LT exhibited significantly improved survival rates compared to those without transplantation (28-/90-/360-day: 62.9%/54.3%/54.3% vs. 6.4%/4.8%/4.8%, $p < 0.001$), supported by PSM analysis (28-/90-/360-day: 62.9%/54.3%/54.3% vs. 7.1%/7.1%/7.1%, $p < 0.001$). Furthermore, stratification analysis showed that CF patients with an INR < 3.5 had a higher 360-day post-LT survival rate.

Conclusion: HBV-ACLF patients with CF exhibited a poor prognosis, and LT significantly improved their survival. Patients with INR < 3.5 had a higher survival benefit from LT. These findings could provide evidence for the appropriateness and limitations of LT in ACLF patients with CF and help refine candidate selection for LT in clinical practice.

SAT-319

RECAM-J 2023-validation of RECAM and development of the Japanese version for the diagnosis of DILI

Atsushi Tanaka¹, Keiji Tsuji², Yasuyuki Komiyama³, Kota Tsuruya⁴, Keisuke Kakisaka⁵, Akemi Tsutsui⁶, Keiko Ichimoto⁷, Masayuki Ueno⁸, Yuki Okazaki⁹, Hiroteru Kamimura¹⁰, Atsushi Takai¹¹, Noriyo Yamashiki¹², Takanori Ito¹³, Masaaki Watanabe¹⁴, Masanori Abe⁹, Tatehiro Kagawa¹⁵. ¹Department of Medicine, Teikyo University School of Medicine, Tokyo, Japan; ²Department of Gastroenterology, Hiroshima Red Cross Hospital and Atomic-Bomb Survivors Hospital, Hiroshima, Japan; ³Gastroenterology and Hepatology Department of Internal Medicine, Faculty of Medicine, University of Yamanashi, Kofu, Japan; ⁴Division of Gastroenterology and Hepatology, Department of Internal Medicine, Tokai University School of Medicine, Isehara, Japan; ⁵Division of Gastroenterology and Hepatology, Department of Internal Medicine, School of Medicine, Iwate Medical University, Morioka, Japan; ⁶Department of Hepatology, Kagawa Prefectural Central Hospital, Kagawa, Japan; ⁷Department of Metabolism, Chiba Children's Hospital, Chiba, Japan; ⁸Department of Gastroenterology and Hepatology, Kurashiki Central Hospital, Kurashiki, Japan; ⁹Department of Gastroenterology and Metabolism, Ehime University Graduate School of Medicine, Ehime, Japan; ¹⁰Division of Gastroenterology and Hepatology, Graduate School of Medical and Dental Sciences, Niigata, Japan; ¹¹Department of Gastroenterology and Hepatology, Kyoto University Graduate School of Medicine, Kyoto, Japan; ¹²Department of Gastroenterology and Hepatology, Kansai Medical University Medical Center, Osaka, Japan; ¹³Department of Gastroenterology and Hepatology, Nagoya University Graduate School of Medicine, Nagoya, Japan; ¹⁴Department of Gastroenterology, Tosenen Kitamoto Hospital, Saitama, Japan; ¹⁵Division of Gastroenterology and Hepatology, Department of Internal Medicine, Tokai University School of Medicine, Isehara, Japan
Email: a-tanaka@med.teikyo-u.ac.jp

Background and aims: The diagnosis of drug-induced liver injury (DILI) is very challenging, because there is no highly sensitive and specific biomarker or pathological findings for the diagnosis. In Japan, a scoring system based on RUCAM was developed in 2004, but it has not been revised since then. In 2022, a revised electronic version of RUCAM (RECAM) was reported based on the American and Spanish DILI databases. In this study, we validated the RECAM using Japanese DILI database and aimed to develop a Japanese version of the RECAM.

Method: Clinical information on Japanese patients with DILI were retrospectively collected from 5 centers. The diagnosis of DILI was made by expert's causality decision in each center. We collected the clinical information required for validation of RECAM, included suspected drug, time from taking or discontinuing suspected drug to onset of liver injury, liver function test values at onset (AST, ALT, ALP, GGT), dechallenge or washout, and information to exclude alternative diagnosis for liver injury, such as hepatitis virus markers, autoantibodies, imaging results, and alcohol intake. The obtained clinical information was then used to score each case using RECAM to examine the likelihood of DILI for each case. Finally, we investigated the factors contributing to instances where scores were low, leading to a determination of "possible" or "unlikely" with RECAM.

Results: We collected 533 patients with DILI in Japan, and the scoring using RECAM revealed that the median score was 2 [range -16-13] and the categorization into highly probable (≥ 8), probable (4-7), possible (-3-3), and unlikely (≤ -4) yielded 53 (10%), 146 (27%), 254 (48%), and 80 (15%) cases, respectively. The combined percentage of highly probable + probable was only 37%, indicating a low concordance rate with the experts' diagnosis. Upon investigating the reasons for low scores, it was observed that the primary cause of low scores was due to the deduction with missing hepatitis virus markers, such as anti-HBc IgM, which was not measured in cases with negative HBs antigen, or anti-HEV IgM; anti-HEV IgA is used in Japan instead. Deductions related to other domains were minimal. Since it is unlikely that deductions related to missing hepatitis virus markers will be issues in prospective applications of RECAM, we decided to re-score without deductions related to hepatitis virus markers. At this time, the median score increased to 7 [range -13-15]. The categorization into highly probable, probable, possible, and unlikely resulted in 197 (37%), 216 (41%), 106 (20%), and 14 (3%) cases, respectively, with a combined percentage of highly probable + probable reaching 78%.

Conclusion: By modifying the scoring related to viral hepatitis markers, RECAM has demonstrated improved alignment with the DILI diagnosis by Japanese experts. We hereby announce the modified Japanese version as RECAM-J 2023.

SAT-320

Early diagnosis and treatment with Terlipressin for adults with hepatorenal syndrome improves clinical outcomes and reduces healthcare resource utilization

Juan F. Gallegos-Orozco¹, Jacqueline G. O'Leary², Gautham Reddy³, Khurram Jamil⁴, Jas Bindra⁵, Ishveen Chopra⁶, John Niewoehner⁴, Xingyue Huang⁴. ¹University of Utah, Salt Lake City, Utah, United States; ²Dallas Veteran Affairs Medical Center, Dallas, Texas, United States; ³University of Chicago Medicine, Chicago, Illinois, United States; ⁴Mallinckrodt Pharmaceuticals, Bridgewater, New Jersey, United States; ⁵Falcon Research Group, North Potomac, Maryland, United States; ⁶Manticore Consultancy, Bethesda, Maryland, United States
Email: juan.gallegos@hsc.utah.edu

Background and aims: Hepatorenal syndrome (HRS) is a potentially reversible form of acute kidney injury. A recent analysis of 3 North American clinical trials showed that patients with lower serum creatinine (SCr) levels at diagnosis derived greater benefit from terlipressin (TERLIVAZ®), emphasizing the importance of early identification and treatment of HRS. Terlipressin is currently the only Food and Drug Administration-approved medication to treat HRS in adults. This study evaluated the potential impact of a national strategy for earlier HRS diagnosis and terlipressin treatment in the United States (US).

Method: A decision-analytic model was developed to compare various scenarios, assessing the distribution of patients across 3 different SCr groups at the time of HRS diagnosis (Curry et al, 2023). Under the current clinical practice scenario, patients were grouped by SCr level based on the CONFIRM trial data (< 3 mg/dL: 45%; ≥ 3 to < 5 mg/dL: 55%). Under the early diagnosis and treatment scenario,

the distribution of patients was assumed (<3 mg/dL: 85%; ≥3 to <5 mg/dL: 15%) based on the results of an HRS medical chart review study from the United Kingdom. The model only assessed terlipressin on-label treatment, hence patients with SCr ≥5 mg/dL or grade 3 acute-on-chronic liver failure (ACLF) were excluded. Terlipressin HRS reversal rate for the on-label population (SCr <5 mg/dL and ACLF grade 0 to 2), 52.2% and 33.3% for SCr <3 mg/dL and ≥3 to <5 mg/dL, respectively were generated from the CONFIRM trial. The annual HRS incidence of 50, 000 was used to assess the impact of the early diagnosis and treatment strategy. The incremental benefit was calculated based on the difference between the scenarios multiplied by the 40, 000 patients (based on the label).

Results: Earlier HRS diagnosis and treatment with terlipressin yields 3, 040 greater HRS reversals compared with the current clinical practice. Consequently, this early treatment strategy results in 1200 more patients with 90-day survival without transplant and 960 fewer patients with renal replacement therapy rate during hospitalization compared with the current clinical practice. This strategy also leads to fewer intensive care unit (ICU) days and a shorter overall length of hospitalization. Further, a reduction in hospitalization, including ICU stay, results in \$11, 504 savings/cost offset per person and total annual national savings of \$460.2 million in the US (2023 US dollars).

Conclusion: Earlier HRS diagnosis and treatment with terlipressin shows improved clinical outcomes including transplant-free survival and reduced healthcare resource utilization compared to the current clinical practice.

SAT-321

A nationwide, multi-center, prospective study of drug-induced liver injury in mainland China

Yan Wang¹, Mengmeng Zhang¹, Yao Meng¹, Tiantian Guo¹, Zikun Ma¹, Yun Zhu², Zhengsheng Zou², Fangcheng Zhao³, Juan Li⁴, Xiaojie Liu⁵, Liuyi Chang⁶, Rongkuan Li⁷, Xinyan Zhao¹. ¹Liver Research Center, Beijing Friendship Hospital, Key Laboratory on Translational Medicine on Cirrhosis, National Clinical Research Center for Digestive Disease, Capital Medical University, Beijing, China; ²The Fifth Medical Center of PLA General Hospital, Beijing, China; ³The Second Affiliated Hospital of Dalian Medical University, Beijing, China; ⁴Qinghai Provincial People's Hospital, Qinghai, China; ⁵The First People's Hospital of Qinzhou, Qinzhou, China; ⁶Shanxi Yuncheng Central Hospital, Shanxi, China; ⁷The Second Affiliated Hospital of Dalian Medical University, Dalian, China Email: zhao_xinyan@ccmu.edu.cn

Background and aims: A majority of studies have reported the clinical characteristics and outcomes of drug-induced liver injury (DILI), which originated from retrospective DILI cohorts in China. No nationwide prospective study of DILI has been reported yet. Since June 2022, we commenced a nationwide, multi-center, prospective study (NCT05060289) to better understand the nature of DILI in China.

Method: DILI patients hospitalized in the eight clinical centers, located in the north, south, east, and west of mainland China were enrolled. Eligible patients were those meeting the diagnostic criteria of DILI with a RUCAM higher than three points with an acute clinical course (<three months since onset). Competing etiologies of liver injury were all excluded. They were followed up to either normalization of liver biochemical tests or appearance of outcome events (chronicity, acute liver failure, and death/liver transplantation). Demographic, laboratory, disease severity, liver pathology (if any), and prognostic data were collected.

Results: A total of 130 patients were enrolled with 88 (67.7%) females and the median age was 53 (42, 63) years old. 54.6% were attributed to herbal and dietary supplements (HDS) and 22.3% were associated with conventional agents and 22.3% with combination of HDS and conventional agents. The median latency was 20 (7, 40) days. Most of

the cases were hepatocellular injury type 103 (79.2%), the mixed type was 12 (9.2%) and the cholestatic type was 15 (11.5%). The alanine aminotransferase (ALT) and aspartate aminotransferase (AST) were significantly stepwise decrease along with hepatocellular, mixed, and cholestatic group (ALT: 1037.0 (694.0, 1483.6), 345.0 (185.0, 429.0), 111.0 (89.3, 160.7), $p < 0.001$; AST: 709.0 (363.0, 975.4), 204.0 (145.0, 306.0), 93.5 (56.8, 202.0), $p < 0.001$). Mild, moderate and severe liver injury occurred in 49 (37.6%), 77 (59.2%) and 4 patients (3.1%), respectively. Liver biopsy was completed in 25 patients (19.2%) and cholestatic hepatitis [11/25 (44%)] and acute hepatitis [9/25 (36%)] were the top two common pathological patterns. Significantly more patients with hepatocellular injury type had liver chemistries normalization [85/103 (75%) vs. 9/12 (75%) vs. 8/15 (53.3%), $p = 0.171$]. Two patients with hepatocellular injury type died of liver failure.

Conclusion: This is the first nationwide, multi-center, prospective DILI study in mainland China. HDS were the leading cause of DILI, accounting for about half of the cases. Patients with hepatocellular injury type have more proportion of liver normalization.

SAT-322

Longitudinal single-cell transcriptomics analyses reveal distinct peripheral immune characteristics linked to ACLF progression

Xi Liang^{1,2}, Qian Zhou¹, Jinjin Luo¹, Jiaqi Li¹, Jun Li¹. ¹State Key Laboratory for Diagnosis and Treatment of Infectious Diseases, National Clinical Research Center for Infectious Diseases, National Medical Center for Infectious Diseases, The First Affiliated Hospital, Zhejiang University School of Medicine, Hangzhou, China; ²Precision Medicine Center, Taizhou Central Hospital (Taizhou University Hospital), Taizhou, China Email: lijun2009@zju.edu.cn

Background and aims: Acute-on-chronic liver failure (ACLF) is a life-threatening syndrome involving dysfunction in multiple immune cells. This study aims to comprehensively depict the dynamic immune responses along the progression of ACLF.

Method: We conducted single-cell RNA-sequencing (scRNA-seq) of 45 samples from 32 subjects using peripheral blood mononuclear cells (PBMCs). Among the subjects, 17 hospitalized hepatitis B virus-related ACLF and early stage non-ACLF patients were included to exhibit a progressive, stable or recovering course of ACLF. Bulk RNA-Seq, flow cytometry and histological assays were employed for external validation.

Results: The scRNA-seq identified forty-one immune cell clusters, including 4 low-density neutrophil clusters, revealing cell-type-specific changes in ACLF progression. FCGR4B⁺-neutrophil with hyper-inflammatory phenotype and CD163⁺-macrophage emerged as pivotal in progressive ACLF, especially in the end stage. Enhanced CD39 and IL10 signaling have been identified, showing an anti-inflammation effect in the end stage of ACLF. A significant reduction in highly activated cytotoxic T cells, including GZMK⁺CD4⁺- and GZMK⁺-COTL1⁺-CD8⁺- T cells, was correlated with disease severity. Cellular interferon response and antigen presentation process gradually decreased with the progression of ACLF. The patients were stratified into six subtypes with specific features, significantly associated with ACLF outcome. External validation confirmed the specificity of cell cluster signatures in ACLF progression.

Conclusion: Our comprehensive immune profiling reveals dynamic changes in the innate and adaptive immune responses in progressive ACLF, highlights anti-inflammatory role of macrophage and provides diverse immune subtypes for ACLF stratified medicine.

SAT-323

Establishing a predictive nomogram for 21-day transplant-free survival in drug-induced liver failure

POSTER PRESENTATIONS

Mengyu Tao¹, Xiaoping Wu¹, Zhilong Wen², Jiwei Fu¹, Wentao Zhu¹.

¹The First Affiliated Hospital of Nanchang University, National Medical Center for Infectious Diseases, Nanchang, China; ²The First Affiliated Hospital of Gannan Medical University, Ganzhou, China
Email: wuxiaoping2823@aliyun.com

Background and aims: The high prevalence of drug-induced liver failure (DILF) have drawn great attention from clinicians.

Method: 202 DILF patients were enrolled between January 2016–December 2022, and were followed up from DILF diagnosis to death, liver transplantation, or 91 days afterward, whichever came first. The primary end point, though, was 21-day TFS. Clinical data was collected from all patients, and independent risk factors associated with death/liver transplantation was identified using both uni- and multi-variate Cox regression analyses.

Results: Independent risk factors incorporated into the predictive nomogram are neutrophils (HR = 1.148, 95% CI = 1.048–1.257), prothrombin time (HR = 1.048, 95% CI = 1.017–1.080), albumin (HR = 0.880, 95% CI = 0.823–0.941), acute kidney injury (HR = 2.487, 95% CI = 1.134–5.452), and hepatic encephalopathy (HR = 3.378, 95% CI = 1.744–6.543). The resulting nomogram was highly predictive, with an area under the curve of 0.947 for 21-day TFS.

Conclusion: Compared to existing models, such as the Model for End-Stage Liver Disease score, the predictive nomogram is more accurate, only requires easily-measurable clinical and laboratory metrics, as well as being able to directly calculate TFS at various time points.

SAT-324

Efficacy of magnesium isoglycyrrhizinate in patients with immune checkpoint inhibitor-related hepatotoxicity

Yang Zhi¹, Yinuo Dong¹, Yimin Mao¹. ¹Division of Gastroenterology and Hepatology, Renji Hospital, Shanghai Jiaotong University School of Medicine, NHC Key Laboratory of Digestive Diseases, Shanghai, China
Email: maoyim11968@163.com

Background and aims: Liver injury significantly impacts the continuity of antineoplastic therapy, and even leads to drug discontinuation in patients receiving immune checkpoint inhibitors (ICIs). Currently available management for ICI-related hepatotoxicity (IRH) is limited including glucocorticoids (GC) and certain immunosuppressants. In this study, we explore the efficacy of magnesium isoglycyrrhizinate (MgIG), a therapeutic agent previously proven to be safe and effective in acute drug-induced liver injury (DILI), in patients with IRH.

Method: We conducted a 3-year, retrospective, multicenter, electronic medical record-based real-world study to evaluate the efficacy of MgIG compared to GC in patients with IRH. Patients above 18 years old who received only MgIG or GC after IRH episode with liver biochemistry fulfilling the International DILI Expert Working Group criteria for DILI were included. Liver injury due to other competitive etiologies were excluded based on differential diagnosis by investigators. Propensity score matching (PSM) was used to match age, sex, and baseline alanine aminotransferase (ALT) between groups. The primary end point is the change of ALT from baseline 10 days after treatment. Secondary end points include change of aspartate aminotransferase (AST), alkaline phosphatase (ALP), and total bilirubin (Tbil) from baseline at day 10; change of liver biochemistry before discharge; normalization rate and the proportion of patients with >50% reduction of liver biochemistry 10 days after treatment and before discharge.

Results: From December 2019 to December 2022, a total of 504 cases were included, among which 358 received only MgIG and 146 received only GC. After PSM in a 2:1 ratio, these cases were divided into MgIG group (n = 260) and GC group (n = 130). In MgIG group, the change of ALT (–142.56 vs. –131.95 p = 0.047) was more remarkable compared to GC group 10 days after treatment, as well as AST (–255.86 vs. –178.64, p = 0.013). The proportion of patients with >50% reduction in ALT (60% vs. 46.92%, p = 0.014) and AST (55.38% vs.

50%, p = 0.046) were higher compared to GC group 10 days after treatment. Before discharge, a higher proportion of patients with >50% reduction in ALT (65.77% vs. 50.77%, p = 0.004), AST (61.15% vs. 53.08%, p = 0.008), and Tbil (32.69% vs. 20.77%, p = 0.014) were observed in the MgIG group. Moreover, MgIG achieved a greater change in AST (–264.51 vs. –166.91, p = 0.008) and higher normalization rate in ALP (30% vs. 15.38%, p = 0.025) before discharge.

Conclusion: The study provided preliminary evidence that MgIG improves recovery of liver injury in IRH with possibly better efficacy than GC. Further rigorous studies are warranted to support the use of MgIG in IRH.

SAT-325

Incidence and outcomes of drug-induced liver injury in a large primary care urban area

Anna Pocurull¹, Elia Canga¹, Luis González-de Paz^{2,3}, Joaquín Sáez-Peñataro^{4,5}, Naira Rico⁶, Maria Calvo-Orteu⁴, Mireia Sans-Corrales^{2,3}, Carlos Gómez^{2,3}, Antoni Sisó-Almirall^{2,3}, Xavier Forns¹. ¹Liver Unit. Hospital Clínic. IDIBAPS and CIBEREHD. University of Barcelona, Barcelona, Spain; ²Consorci d'Atenció Primària de Salut Barcelona Esquerra (CAPSBE), Barcelona, Spain; ³Primary Healthcare Transversal Research Group. Institut d'Investigacions Biomèdiques August Pi I Sunyer (IDIBAPS), Barcelona, Spain; ⁴Clinical Pharmacology Service. Hospital Clínic., Barcelona, Spain; ⁵Pharmacovigilance Program. Hospital Clínic, Barcelona, University of Barcelona, IDIBAPS, Barcelona, Spain; ⁶Biochemistry and Molecular Genetics Service, CDB, Hospital Clínic, Barcelona, Spain
Email: pocurull@recerca.clinic.cat

Background and aims: Drug-induced liver injury (DILI) represents a diagnostic challenge for both general practitioners (GPs) and hepatologists. Its estimated incidence ranges between 5 and 20 cases per 100,000 persons/year. Since prospective studies assessing DILI in the primary care setting are scarce, our study aimed to assess its incidence, causes and outcomes among patients attending three primary healthcare centers in Barcelona.

Method: This prospective study involved three primary care centres attending a population of 100,600 residents. An automated system was designed to trigger an alert whenever a patient undergoing a blood test (including liver function assessment), met one of diagnostic DILI criteria: 1) ALT >5 ULN (upper limit of normal), 2) ALP >2 ULN, or 3) ALT >3 ULN and total bilirubin (TB) >2 ULN. We excluded other potential causes of abnormal liver function. The study started in August 2022 and is scheduled to conclude in July 2024.

Results: During the initial 18 months, a total of 88 patients met the specified analytical criteria: 37 (42%) ALT >5 ULN, 47 (53%) ALP >2 ULN, and 4 (5%) ALT >3 ULN and TB >2 ULN. Among these patients, half (52%) were male, with a median age of 61 years (IQR 39–82). DILI was confirmed in 10 cases, with an estimated incidence of 7 cases per 100,000 inhabitants/year (95%CI 1.5–11.8). Implicated drugs included metamizole (2), atorvastatin (2), diclofenac (1), ibuprofen (1), oral contraceptives (1), and metamizole plus diclofenac (1). Energetic protein supplements were implicated in the remaining 2 cases. All patients were managed by their GPs and subsequent analyses returned to normal after discontinuation of the respective drug or supplement. Among the 37 patients with ALT >5 ULN, the most prevalent diagnoses were DILI (8; 22%) and infectious mononucleosis (7; 19%). Among patients with ALP >2 ULN the most common diagnoses were cancer involving the liver (12; 26%), heart failure (7; 15%), and primary biliary cholangitis (4; 47%). Notably, only 1 patient (2%) received a diagnosis of DILI in this group. Among those with ALT >3 ULN and TB >2 ULN, one individual (25%) had DILI. Thus, the positive predictive value for diagnosis of DILI was acceptable for patients with hepatocellular or mixed patterns (22% and 25%, respectively) and very low for cholestatic pattern (2%).

Conclusion: The incidence of DILI in primary care is low, but GPs should consider this diagnosis if ALT are significantly elevated (>5 ULN). Pain killers, statins and dietary supplements are among

the most common causes. Outcomes are good and liver test normalization is the rule after drug interruption.

SAT-326

Immune-mediated liver injury induced by PD-1/PD-L1 checkpoint inhibitors is different from idiosyncratic drug-induced liver injury

Yan Wang¹, Yao Meng¹, Mengmeng Zhang¹, Tiantian Guo¹, Wei Chen¹, Liwei Liu², Xinyan Zhao¹. ¹Liver Research Center, Beijing Friendship Hospital, Key Laboratory on Translational Medicine on Cirrhosis, National Clinical Research Center for Digestive Disease, Capital Medical University, Beijing, China; ²Fourth Department of Liver Disease (Difficult and Complicated Liver Diseases and Artificial Liver Center), Beijing You'an Hospital, Capital Medical University, Beijing, China
Email: zhao_xinyan@ccmu.edu.cn

Background and aims: Immune-mediated liver injury induced by immune checkpoint inhibitors (ILICI) has been reported in recent years. However, ILICI differs from idiosyncratic drug-induced liver injury (iDILI) in various aspects. In this study, we aimed to study the differences of clinical characteristics between ILICI induced by PD-1/PD-L1 inhibitors and iDILI.

Method: Data of ILICI and iDILI patients from January 2016 to December 2022 at Beijing Friendship Hospital were retrospectively collected. The clinical and laboratory data were collected and compared between the two groups. Patterns of injury were defined according to the R value.

Results: A total of 66 cases of ILICI and 316 cases of iDILI were included in this study. The ILICI group exhibited a significantly higher age compared to the iDILI group [65 (57, 70) vs. 56 (46, 64) years old, $p < 0.001$] and a lower proportion of females [17 (25.8%) vs. 254 (80.4%), $p < 0.001$]. Among the ILICI group, 18 (27.3%) cases had no available ALP at the time of onset, resulting in the absence of the R value. Among the remaining 48 cases, a higher proportion of patients were classified as cholestatic and mixed [39 (59.1%) vs. 93 (29.4%), $p < 0.001$], while a lower proportion were categorized as hepatocellular [9 (13.6%) vs. 223 (70.6%), $p < 0.001$] than that in the iDILI group. The alanine aminotransferase (ALT) and aspartate aminotransferase (AST) in the ILICI group were significantly lower compared to iDILI group at peak levels [ALT: 125.0 (75.8, 231.0) vs. 635.0 (340.8, 1087.0) U/L, $p < 0.001$; AST: 132.9 (85.1, 296.3) vs. 476.0 (221.5, 820.5) U/L, $p < 0.001$]. The serum immunoglobulin G levels were similar between the ILICI and iDILI group [1220.0 (972.5, 1435.0) vs. 1350.0 (1100.0, 1612.5) mg/dL, $p = 0.078$].

Conclusion: The ILICI demonstrates distinct clinical characteristics that differ from iDILI, with a higher prevalence of older individuals and males in the ILICI group. Additionally, ILICI tends to present as cholestatic and mixed liver injury, in contrast to iDILI. Notably, there was no difference in the levels of serum immunoglobulin G between the two groups.

SAT-327

The combination of s-ademethionine with Bifidobacterium infantis 35624 inhibits oxidative stress as a risk factor for cytostatic-induced liver injury

Igor Skrypnyk¹, Ganna Maslova¹, Roman Skrypnyk¹. ¹Poltava State Medical University, Poltava, Ukraine
Email: inskrypnyk@gmail.com

Background and aims: The conduction of chemotherapy (CT) in patients with chronic lymphoproliferative disorders (CLPD) is associated with oxidative stress which is considered a key pathogenic mechanism of cytostatic-induced liver injury.

The aim is to investigate the effect of s-ademethionine (s-AMe) in combination with Bifidobacterium infantis 35624 on oxidative stress, as a method of prevention of liver injury in patients with CLPD during CT.

Method: 38 patients with CLPD were examined. 20 (53%)-B-cell Chronic lymphocytic leukemia, 18 (47%)-B-cell Non-Hodgkin

lymphoma, 8 (21%) females and 30 (79%) males, age 30–76. Patients received CT according to current guidelines. Patients were divided into groups: I-A (n = 13)-patients with CLPD, who underwent only CT; I-B (n = 12)-patients with CLPD who during CT received s-AMe 1000 mg/day for 30 days, I-C (n = 13)-patients with CLPD who during CT received S-AMe 1000 mg/day and Bifidobacterium infantis 35624 1 capsule/day for 30 days and group II (n = 20) -the control group of practically healthy individuals. Several biochemical markers were determined: the activity of alanine aminotransferase (ALT) and aspartate aminotransferase (AST), alkaline phosphatase (ALP), gamma glutamyl transferase (GGT), level of plasma bilirubin and concentration of substances that form a trimethine complex with 2-thiobarbituric acid (TBA).

Results: Preexisted liver function test abnormalities were determined in 38.5% (5/13) patients in group I-A, in 25% (3/12) patients in group I-B and in 38.5% (5/13) patients in group I-C. At the same time in patients of groups I-A and I-B, the concentration of TBA in plasma was in 1.38 ($p = 0.0479$) and 1.3 times ($p = 0.0122$) accordingly higher compared to controls. After the 3d course of CT liver function test abnormalities were present more frequently in patients of group I-A compared to group I-B χ^2 (1, N = 25) = 9.07 ($p = 0.002$) and group I-C χ^2 (1, N = 26) = 9.90 ($p = 0.001$). At the same time after the conduction of CT the level of several biochemical markers in group I-A were higher compared to I-B and I-C groups: ALT was higher in 2.1 ($p = 0.012$) and 2.5 times ($p = 0.046$) accordingly, AST in 1.74 ($p = 0.009$) and 2.0 times ($p = 0.0037$) accordingly, GGT in 2.13 times ($p = 0.0195$) and in 2.4 times ($p = 0.002$), ALP in 1.5 times ($p = 0.012$) and in 1.3 times ($p = 0.0149$) accordingly, without reliable changes in the level of bilirubin. Important that in groups I-B and I-C after the conduction of CT the level of TBA was in 1.39 ($p = 0.0005$) and 1.46 times ($p = 0.0002$) accordingly lower compared to group I-A.

Conclusion: The infusion of s-AMe and the combination of s-AMe with Bifidobacterium infantis 35624 during CT in patients with CLPD provides inhibition of oxidative stress that can prevent abnormalities in liver function.

SAT-330

Depressed TFAM promotes acetaminophen-induced hepatotoxicity regulated by DDX3X- PGC1 α -NRF2 signaling pathway

Sisi Chen¹, Qin Ouyang¹, Mei Liu², Feng Ren², Jian Huang¹. ¹Beijing Friendship Hospital, Capital Medical University, Beijing, China; ²Beijing Youan Hospital, Capital Medical University, Beijing, China
Email: thoughtfmu@163.com

Background and aims: Acetaminophen-induced acute liver injury (AILI) is the most prevalent cause of acute liver failure in developed countries and mitochondrial dysfunction plays a dominant role in the pathogenesis of AILI. Mitochondrial transcription factor A (TFAM) is an important marker for maintaining mitochondrial functional homeostasis and also helps to maintain the integrity of mitochondrial DNA (mtDNA), while its possible functions in AILI are unclear. This study aimed to investigate the function of TFAM and its regulatory molecular mechanism in the progression of AILI.

Method: TFAM was detected in the liver of AILI patients and mouse models. The role of TFAM and DEAD (Asp-Glu-Ala-Asp) box polypeptide 3 X-linked (DDX3X) in AILI was determined in mouse and cellular models with TFAM overexpression or DDX3X knock-down, respectively.

Results: TFAM expression is suppressed in the liver of AILI patients and mtDNA levels are increased in serum. Overexpression of TFAM alleviates the liver necrosis, activated inflammatory and apoptotic responses, and mitochondrial dysfunction caused by APAP overdose. Treatment of the AILI mouse model with N-acetylcysteine (NAC), a drug used to treat APAP overdose, resulted in significant activation of TFAM. In vivo experiments confirmed that TFAM expression was negatively regulated by DDX3X. Knockdown of TFAM superseded the protective effect of DDX3X knockdown on APAP overdose induced

POSTER PRESENTATIONS

liver injury. Mechanistic studies showed that nuclear respiratory factor 2 (NRF-2), a key regulator of TFAM, was selectively activated after DDX3X knockdown via activated peroxisome proliferator-activated receptor γ coactivator 1 (PGC-1 α), both in vivo and in vitro experiments.

Conclusion: This study demonstrates that depressed hepatic TFAM plays a key role in the pathogenesis of AILI, which is regulated by DDX3X- PGC1 α -NRF2 signaling pathway.

SAT-331

Anticancer drugs are the first cause of drug-induced liver injury in the REFHEPS network

Lucy Meunier¹, Eleonora De Martin², Bénédicte Delire³, Fanny Lebosse⁴, Amel Zahhaf¹, Dominique Larrey⁵, Yves Horsmans⁶.
¹CHU Montpellier, Montpellier, France; ²Centre Hepato Biliaire, Villejuif, France; ³Saint Luc Hospital, Bruxelles, Belgium; ⁴Hopital Croix Rousse, Lyon, France; ⁵CHU Montpellier, Montpellier; ⁶Hopital Saint Luc, Bruxelles, Belgium
Email: lucy-meunier@chu-montpellier.fr

Background and aims: Drug hepatotoxicity is the main cause of drug withdrawals from the market and halted development of new molecules. International hepatotoxicity networks are essential for the emergence of hepatotoxicity data. At the end of 2021, REFHEPS was created to collect hepatotoxicity cases in France and Belgium and provide specialist advice on request. We report data from the first 2 years of the network's existence.

Method: All cases submitted to REFHEPS were analyzed retrospectively by a panel of hepatotoxicity experts. The profile of liver damage (cytolytic, cholestatic or mixed), its severity and the imputability of suspected drugs or other health products were assessed according to recently defined international criteria (RUCAM score and American DILIN method (1–3)).

Results: In 2022 and 2023, 213 cases were submitted to REFHEPS. Four cases were excluded for differential diagnosis, and 36 are currently being adjudicated. A total of 173 cases were analyzed, 116 (67%) with a single implicated drug, 46 (26.6%) with 2 and 11 (6.4%) with 3 or more drugs. The mean age of patients was 55.8 years (95% CI: 53.0–58.5), and the majority were women (n = 106; 63.6%). Drugs causing DILI were antineoplastic (65%), antibiotics (5%), analgesics (7%), herbal and dietary supplement (2%), biotherapy and immunosuppressive drugs (4%), non-steroidal anti-inflammatory drugs (3%) and recreational drugs (1%). In 13% of cases, the drug involved is more unusual. The main category of drugs incriminated were antineoplastic. In this category, the therapeutic classes most frequently found were: immune checkpoint inhibitors (n = 66, 38.2%) and CDK4/6 inhibitors (n = 24, 13.9%).

Conclusion: After 2 years of REFHEPS existence, over 200 cases have been submitted. The majority of cases are related to anticancer drugs. In two-thirds of cases, several drugs are potentially responsible for toxicity. Antineoplastic drugs have become the first cause of DILI in our network, mainly represented by immune checkpoint inhibitors. Some cases are currently being analyzed, and more complete data may be presented at the EASL congress.

References

- 1) Fontana RJ, Seef LB, Andrade RJ, Björnsson E, Day CP, Serrano J, Hoofnagle JH. Standardization of nomenclature and causality assessment in drug-induced liver injury: summary of a clinical research workshop. *Hepatology* 2010;52:730–42.
- 2) Danan G, teschke R. RUCAM in Drug and herb Induced Liver Injury: The Update. *International J Mol Sci* 2016;17:14.
- 3) EASL Clinical practice Guidelines: Drug-induced liver injury. The group of experts included: Andrade Raúl, Aithal Guruprasad, Björnsson Einer, Kaplowitz Neil, Kullak-Ublick Gerd, Larrey Dominique, Karlsen Tom. *J Hepatol* 2019;70:1222–1261.

SAT-332-YI

Frequency and clinical features of tamoxifen-induced liver injury

Masayuki Ueno^{1,2}, Takahisa Kayahara¹, Hiroyuki Takabatake¹, Youichi Morimoto¹, Motowo Mizuno¹, Hirokazu Mouri¹.
¹Department of Gastroenterology and Hepatology, Kurashiki Central Hospital, Kurashiki, Japan; ²Department of Gastroenterology and Hepatology, Graduate School of Medicine, Kyoto University, Kyoto, Japan
Email: masayuki.u.0819@outlook.jp

Background and aims: Tamoxifen (TAM) is the most widely used hormonal treatment for breast cancer, and it is well-known for causing drug-induced steatotic liver disease. However, the clinical manifestation and optimal management of TAM-induced liver injury remain insufficiently understood. Therefore, we aimed to explore the frequency and clinical characteristics of drug-induced liver injury in breast cancer patients receiving TAM treatment.

Method: We retrospectively analyzed 192 breast cancer patients who initiated TAM treatment between January 2008 and December 2017 at our institution. Patients who underwent blood tests and abdominal ultrasonography after receiving TAM for at least one year were included. In this study, liver injury was defined as alanine transaminase (ALT) exceeding twice the upper limit of normal and/or alkaline phosphatase (ALP) exceeding the upper limit.

Results: Among the 192 patients, 191 (99.5%) were female, with a median age of 47 years. The median duration of TAM treatment at the time of the last abdominal ultrasonography was 3.4 years. Pretreatment abdominal ultrasonography was performed in 155 patients, revealing liver steatosis in 83 patients. After TAM treatment, 140 patients (72.9%) exhibited liver steatosis, with ALT elevation in 6 cases, ALP elevation in 3 cases, and both in 3 cases. Two patients (1.0%) showed morphological changes in the liver and splenomegaly, which suggested progression to cirrhosis. Thirteen patients (6.8%) discontinued TAM treatment due to liver injury or severe steatosis. Several years were required to recover from liver steatosis after TAM discontinuation. Among the 72 patients without pre-existing liver steatosis, 32 patients (44.4%) developed liver steatosis after TAM treatment, but no patients showed elevated ALT or ALP.

Conclusion: In patients without pre-existing steatotic liver disease, approximately 40% developed liver steatosis after TAM treatment, but no patients showed significant elevation of ALT or ALP. On the other hand, some patients with pre-existing liver steatosis developed significant liver injury, with two cases progressing to cirrhosis. During TAM treatment, careful monitoring of liver function is needed, especially in patients with pre-existing steatotic liver disease.

SAT-333

Efficacy of magnesium isoglycyrrhizinate as add-on therapy to glucocorticoids in immune checkpoint inhibitor-related hepatotoxicity

Yinuo Dong¹, Yang Zhi¹, Yimin Mao¹.
¹Division of Gastroenterology and Hepatology, Renji Hospital, Shanghai Jiaotong University School of Medicine, NHC Key Laboratory of Digestive Diseases, Shanghai, China
Email: maoyim11968@163.com

Background and aims: Immune checkpoint inhibitor (ICI)-related hepatotoxicity (IRH) impedes antineoplastic therapy and often requires glucocorticoids (GC) as treatment. In this study, we explore the efficacy of magnesium isoglycyrrhizinate (MgIG), a therapeutic agent previously proven to be safe and effective in acute drug-induced liver injury (DILI), as add-on therapy to GC in IRH.

Method: We conducted a 3-year, retrospective, multicenter, electronic medical record-based real-world study to evaluate the efficacy of MgIG as add-on therapy to GC compared to GC monotherapy in patients with IRH. Patients above 18 years old who received GC in combination with MgIG or GC monotherapy after IRH episode with liver biochemistry fulfilling the International DILI Expert Working Group criteria for DILI were included. Liver injury due to other competitive etiologies were excluded based on differential diagnosis by investigators. Propensity score matching (PSM) was used to match age, sex, and baseline alanine aminotransferase (ALT) between groups. The primary end point is the change of ALT from baseline

10 days after treatment. Secondary end points include change of aspartate aminotransferase (AST), alkaline phosphatase (ALP), and total bilirubin (Tbil) from baseline at day 10; change of liver biochemistry before discharge; and normalization rate of liver biochemistry 10 days after treatment and before discharge.

Results: From December 2019 to December 2022, a total of 318 cases were identified, among which 172 received GC in combination with MglG and 146 received only GC. After PSM in a 1:1 ratio, these cases were divided into MglG + GC group (n = 134) and GC group (n = 134). In MglG + GC group, the change of ALT (−187.19 vs. −134.27, p = 0.004) was more remarkable compared to GC group 10 days after treatment, as well as AST (−232.94 vs. −180.16, p = 0.028), and Tbil (−16.56 vs. −9.49, p < 0.001). Before discharge, MglG + GC achieved a higher normalization rate in AST (49.25% vs. 28.36%, p < 0.001), Tbil (49.25% vs. 35.82%, p = 0.026), and ALP (26.12% vs. 16.42%, p = 0.029) compared to GC group. The change in ALT (−196.1 vs. −136.86, p = 0.006) and Tbil (−21.68 vs. −9.39, p < 0.001) were also more significant in MglG + GC group before discharge. There was no statistical difference in the dose of GC or course of treatment after the occurrence of liver injury between two groups.

Conclusion: The study provided preliminary evidence that MglG may aid to improve recovery as add-on therapy to GC in patients with IRH. Further rigorous studies are warranted to explore whether MglG can partially substitute GC in IRH.

SAT-334

Histopathological findings in liver biopsies of patients affected by multiple sclerosis undergoing disease-modifying therapies and pulse methylprednisolone

Joana Sorino^{1,2}, Vittorio Viti^{1,3}, Chiara Zanetta³, Massimo Memoli⁴, Martina Rubin^{5,6}, Lucia Moiola⁷, Maria Assunta Rocca^{1,8,9}, Massimo Filippi^{1,8,9,10,11}, Federica Pedica^{1,2}. ¹Vita-Salute San Raffaele University, Milan, Italy; ²IRCCS San Raffaele Scientific Institute, Pathology Unit, Milan, Italy; ³IRCCS San Raffaele Scientific Institute, Neurology and Neurorehabilitation Units, Milan, Italy; ⁴IRCCS San Raffaele Scientific Institute, Medicina Generale Ind. Specialistico e della Comunità Assistenziale, IRCCS San Raffaele Scientific Institute, Milan, Italy; ⁵Neurorehabilitation, Neurology Unit and Neurophysiology Unit, San Raffaele Scientific Institute, Milan, Italy; ⁶Neuroimaging Research Unit, Institute of Experimental Neurology, Division of Neuroscience, San Raffaele Scientific Institute, Milan, Italy; ⁷IRCCS San Raffaele Scientific Institute, Neurology Unit, Milan, Italy; ⁸Neuroimaging Research Unit, Division of Neuroscience, IRCCS San Raffaele Scientific Institute, Milan, Italy; ⁹Neurology Unit, IRCCS San Raffaele Scientific Institute, Milan, Italy; ¹⁰Neurorehabilitation Unit, IRCCS San Raffaele Scientific Institute, Milan, Italy; ¹¹Neurophysiology Service, IRCCS San Raffaele Scientific Institute, Milan, Italy
Email: pedica.federica@hsr.it

Background and aims: Patients affected by multiple sclerosis (MS) undergoing disease-modifying therapies (DMTs) may develop liver injury, due to their hepatotoxic potential. Even today, the differential diagnosis between drug-induced liver injury and autoimmune hepatitis remains a challenge. In this study, we report a case series of 8 patients, 3 exposed to methylprednisolone (MTP), 2 undergoing fingolimod therapy and 2 treated with natalizumab. One more patient underwent MTP administration during fingolimod long-standing treatment. We document the pattern of liver disease, diagnosis and consequences on therapy.

Method: From 2015 and 2023, 8 patients with MS (pwMS) underwent liver biopsy because of elevation of liver enzymes during or after DMTs administration. Indices of hepatocellular damage, autoimmune antibodies, viral serology were evaluated and liver biopsies were investigated for all patients.

Results: Six patients were females (75%) and 2 males (25%). Mean age at presentation of liver enzyme elevation was 41 years and mean MS duration was 7.10 years. All patients displayed a relapsing remitting phenotype and median Expanded Disability Status Scale at liver enzyme elevation was 1.5 (interquartile range 1.0–2.0). In 5 of the 8 (62, 5%) patients anti-nucleus autoantibodies (ANA, equal or superior to 1:160) and in 1 of them anti-smooth muscle autoantibodies (ASMA, equal to 1:40) were found and possible autoimmune hepatitis was suspected. No hypergammaglobulinemia was detected. No patients had viral infection. There was no evidence of metabolic and storage liver disease. On liver biopsies, none of the patients had histology consistent with autoimmune hepatitis. PwMS treated with MTP and natalizumab developed severe acute hepatitis, with confluent necrosis. Portal tracts were only mildly affected. Patients on treatment with fingolimod exhibited vascular alterations, resembling porto-sinusoidal vascular disease, with minimal lobular inflammation. The patient undergoing MTP during fingolimod treatment had overlapping features with those administered with MTP.

Conclusion: In all cases, the hepatocellular damage indices returned to the normal range when the aforementioned drugs were discontinued. The results emerged from liver biopsies turned out to be decisive, allowing patients to benefit from the switch to new therapies for MS. This highlights liver biopsy contributes, with clinical and laboratory data, to the management of pwMS with liver injury, avoiding an overdiagnosis of autoimmune hepatitis, which can impact negatively on the follow-up and therapy.

SAT-335

Pathological dynamics and clinical implications of hepatitis in cancer patients undergoing immune checkpoint inhibitor

Ryo Izai¹, Sadahisa Ogasawara¹, Teppei Akatsuka¹, Chihiro Miwa¹, Takuya Yonemoto¹, Sae Yumita¹, Miyuki Nakagawa^{1,2}, Ryuta Kojima¹, Hiroaki Kanzaki¹, Keisuke Koroki¹, Masanori Inoue¹, Kazufumi Kobayashi¹, Soichiro Kiyono¹, Masato Nakamura¹, Naoya Kanogawa¹, Takayuki Kondo¹, Shingo Nakamoto¹, Mina Komuta³, Naoya Kato¹. ¹Department of Gastroenterology, Graduate School of Medicine, Chiba University, Chiba, Japan; ²Department of Gastroenterology, Asahi General Hospital, Asahi, Japan; ³Department of Pathology, International University of Health and Welfare, Narita Hospital, Narita, Japan
Email: izai.ryo@chiba-u.jp

Background and aims: With the widespread use of immune checkpoint inhibitors (ICIs) in cancer therapy, cases of suspected hepatitis as an immune-related adverse event have increased. However, detailed investigations of the clinical course and liver biopsy findings at the onset of hepatitis are limited, especially in patients with coexisting chronic liver diseases such as hepatocellular carcinoma (HCC). Our study investigates the clinical course and pathologic liver biopsy findings during ICI-related hepatitis in our institution, focusing on the changes from ICI initiation to hepatitis onset in HCC patients.

Method: We analyzed the clinicopathologic features of patients treated with ICIs who underwent liver biopsy for suspected ICI-related hepatitis.

Results: The study included 23 patients: 13 with HCC, 4 with renal cell carcinoma, 2 with lung cancer, and one each with malignant melanoma, paranasal sinus cancer, esophageal cancer, and breast cancer. The median time from the start of ICI to the development of hepatitis was 52 days. Eighteen patients had grade 3 or higher hepatitis as indicated by elevated aspartate aminotransferase (AST), alanine aminotransferase (ALT), alkaline phosphatase (ALP), or total bilirubin (T-BIL), with 14 requiring steroid treatment. Pathologic

examination revealed 19 cases (82.6 percent) of hepatitis type, 2 of bile duct type, and 2 of mixed type. In hepatitis type, the inflammation was limited to the lobule in 5 cases, to the pericentral vein in 5 cases, and to both in 9 cases. Among 14 patients with periportal inflammation, 12 had elevated AST/ALT of grade 3 or higher. In HCC patients, comparison of liver biopsies taken before ICI and at the onset of hepatitis provided detailed insights into the progression of inflammation.

Conclusion: ICI-related hepatitis predominantly presents as hepatitis type with lobular or central venous perivascular inflammation. Specifically, 11 patients with central venous perivascular inflammation showed significant AST/ALT elevation requiring steroid therapy. Comparison of liver biopsies before and after ICI treatment in HCC patients was critical for accurate diagnosis and treatment planning.

SAT-336

Monocytes/macrophages imbalance in chronic drug-induced liver injury: potential candidates for disease pathogenesis

Xing-Ran Zhai¹, Zhe-Rui Liu¹, Ya-Wen Lu², Shao-Ting Chen³, Yun Zhu³, Ying Sun³, Ang Huang⁴, Jia-Bo Wang², Zhengsheng Zou³. ¹Peking University 302 Clinical Medical School, Beijing, China; ²Capital Medical University, Beijing, China; ³The Fifth Medical Center of PLA General Hospital, Beijing, China; ⁴The Fifth Medical Center of PLA General Hospital, The First Medical Center of PLA General Hospital, Beijing, China Email: zszou302@163.com

Background and aims: Monocytes/macrophages are core immune cells involved in the initiation, development, progression, and/or resolution of drug-induced liver injury (DILI). However, it is unclear whether monocytes/macrophages are involved in the chronicity of DILI. In this study, we aimed to characterize monocytes/macrophages in chronic DILI and provide a basis for understanding the pathogenesis of DILI chronicity.

Method: This study was conducted according to the ethical guidelines of the 1975 Declaration of Helsinki (6th revision, 2008), and approved by the Ethics Committees of Fifth Medical Center of Chinese PLA General Hospital (No. R2015139DC020). Participating patients provided written consent for both liver biopsy and blood collection during the period of hospitalization. Plasma cytokines related to monocytes/macrophages [interleukin (IL)-12p70, IL-6, and IL-10], immunophenotype of peripheral monocytes and hepatic macrophages were evaluated by flow cytometry and immunofluorescence staining in patients with chronic DILI, acute DILI, and healthy volunteers.

Results: In patients with chronic DILI, plasma levels of IL-12p70 and IL-6 (M1-related cytokines) were significantly increased ($p < 0.01$, $p < 0.05$, respectively), whereas the plasma level of IL-10 (M2-related cytokine) was significantly decreased ($p < 0.01$). The secretion of IL-12 (M1-like marker) was increased ($p < 0.05$), while the secretion of IL-10 (M2-like marker) was decreased ($p < 0.05$) by lipopolysaccharide-stimulated peripheral monocytes in patients with chronic DILI. The expression of CD206 (M2-like marker) on peripheral monocytes was significantly decreased ($p < 0.05$). An increase in CD68 + CD80+ macrophages (M1-like macrophages) and a decrease in CD68 + CD206+ macrophages (M2-like macrophages) was also observed in the liver tissue of chronic DILI.

Conclusion: M2-like monocytes/macrophages are significantly decreased and M1-like monocytes/macrophages are significantly increased in chronic DILI, potentially contributing to the disease pathogenesis. These findings would inspire monocyte/macrophage-based targeted therapies for this challenging disease.

Alcohol-related liver disease and MetALD – Basic

TOP-312

Functional characterization of intrahepatic CD8+ T lymphocytes in patients with severe alcohol-associated hepatitis

Luca Maccioni^{1,2}, Yukun Guan¹, Yang Wang¹, Dechun Feng¹, George Kunos³, Bin Gao¹. ¹Laboratory of Liver Diseases, National Institute on Alcohol Abuse and Alcoholism (NIAAA), Bethesda, United States; ²Laboratory of Physiologic Studies, National Institute on Alcohol Abuse and Alcoholism (NIAAA), Bethesda, United States; ³Laboratory of Physiologic Studies, National Institute on Alcohol Abuse and Alcoholism (NIAAA), Bethesda, United States Email: luca.maccioni@nih.gov

Background and aims: Intrahepatic neutrophil and T lymphocyte infiltrations have been associated with severe alcohol-associated hepatitis (SAH). Our previous study identified two SAH phenotypes despite a similar clinical presentation, one with high intrahepatic neutrophils but low numbers of CD8+ T cells (Neu^{hi}CD8^{lo}), and one with low neutrophils but high CD8+ T cells (Neu^{lo}CD8^{hi}) and explored the neutrophil function in SAH. Interestingly we have previously found that patients with alcohol use disorder have markedly reduced T cells in small intestines. However, the functions of T cells in SAH and the effects of intestinal T cells on SAH remain largely unknown. This translational study aims to characterize the role of T cell infiltration in SAH pathogenesis.

Method: Multiplex immunofluorescence, bulk RNA-Seq and single-cell RNA sequencing were performed in livers from SAH patients. Mechanisms were evaluated using the chronic-plus-binge model.

Results: Multiplex immunofluorescence and transcriptomic analyses confirmed two SAH phenotypes. Strikingly, CD8+ T cells in Neu^{lo}CD8^{hi} positively correlated with degree of cirrhosis and fibrotic gene signatures. Furthermore, single-cell RNA sequencing revealed different specific subpopulations of T cells in patients with SAH. To study specifically the mechanisms of CD8+ T cell infiltration and the role of CD8 in the pathogenesis of SAH, wild-type control mice and several strains of genetically modified mice were subjected to the chronic plus-binge alcohol model, and we found that intrahepatic CD8 T cells control neutrophil infiltration and ethanol-induced liver cell apoptosis. We also found that intestinal T cells, but not intrahepatic T cells were markedly reduced in mice with chronic-plus-binge ethanol feeding.

Conclusion: High number of CD8+ T cells infiltrate the liver in SAH patients with underlying cirrhosis. CD8+ T cells control intrahepatic neutrophil infiltration and liver cell death during SAH. Future studies will investigate how the reduced intestinal T cells affects SAH.

TOP-313

Farnesoid X receptor agonist INT-787 protects human liver organoids from alcohol-induced injury

Francesca De Franco¹, Daniela Passeri¹, Sanjay Kansra², Luciano Adorini², Mary Erickson², Roberto Pellicciari¹. ¹TES Pharma S.r.l., Perugia, Italy; ²Intercept Pharmaceuticals, Inc., Morristown, United States Email: fdefranco@tespharma.com

Background and aims: Alcohol-associated liver disease (ALD) represents a spectrum of liver injury ranging from steatosis to cirrhosis, and potentially to hepatocellular carcinoma. Activation of the farnesoid X receptor (FXR) has been shown to decrease liver steatosis, inflammation, and fibrosis in multiple animal models and in patients with primary biliary cholangitis or metabolic dysfunction-associated steatohepatitis. We assessed the therapeutic potential of a semisynthetic bile acid analog and potent FXR agonist, INT-787, to

determine its effect on alcohol-induced liver injury using an in vitro human liver organoid model.

Method: Human liver organoids (3D InSight™) were obtained from InSphero and were produced from primary human hepatocytes in co-culture with non-parenchymal cells, including primary human Kupffer cells and primary liver endothelial cells. Organoids were cultured in human liver lean maintenance medium (InSphero). To determine alcohol-induced liver injury and any mitigating effects by INT-787, liver organoids were exposed to 0.5% ethanol (EtOH) or 0.5% EtOH in presence of 0.3 micromolar INT-787 for 96 hours. Steatosis was evaluated using Nile red staining; bead-based multiplex enzyme-linked immunosorbent assay and adenosine triphosphate (ATP) bioluminescence were used to quantify pro-inflammatory cytokines (interleukin-6 [IL-6], tumor necrosis factor [TNF]-alpha) and cell viability, respectively. Expression of genes implicated in inflammation (COX2), fibrosis (TGFB1), oxidative stress (CYP2E1), disruption of bile canaliculi (MRP2), and apoptosis (BAX) were measured by real-time quantitative reverse transcription polymerase chain reaction. Eight organoids per treatment group were pooled for each assay. Statistical significance was determined using 1-way analysis of variance with Dunnett's multiple comparison test.

Results: EtOH-induced steatosis was significantly reduced in the presence of INT-787 ($p < 0.001$). Treatment with INT-787 also led to decreases in EtOH-dependent IL-6 ($p < 0.001$) and TNF-alpha production ($p < 0.01$). EtOH-induced COX2, TGFB1, and CYP2E1 expression was reduced in the presence of INT-787 ($p < 0.001$). Decreased MRP2 expression with EtOH was inhibited by INT-787 ($p < 0.001$). Treatment with INT-787 significantly mitigated the nearly 50% reduction in cell viability observed with EtOH ($p < 0.01$) and suppressed the EtOH-induced expression of BAX ($p < 0.001$).

Conclusion: Human liver organoids exposed to 0.5% EtOH demonstrated alcohol-induced liver injury, providing a reliable in vitro model to study ALD. INT-787 significantly reduced the effects of alcohol-induced liver injury via multiple protective mechanisms, including inhibition of steatosis, inflammation, fibrosis, oxidative stress, and apoptosis. Thus, INT-787 represents a promising molecule for clinical evaluation of ALD treatment.

TOP-328-YI

Single-nucleus RNA sequencing of the liver identifies predictive markers to corticosteroid treatment in patients with severe alcohol-related hepatitis

Lukas Van Melkebeke^{1,2,3,4}, Markus Boesch^{1,3,4}, Hannelie Korf¹, Tessa Ostyn⁵, Dóra Bihary^{6,7}, Marie Wallays¹, Rita Feio-Azevedo¹, Bram Boeckx^{6,7}, Lena Smets¹, Ann Reekmans⁸, Isabelle Colle⁸, Hannah Van Malenstein², Halit Topal⁹, Joris Jaekens⁹, Eveline Claus¹⁰, Lawrence Bonne¹⁰, Geert Maleux¹⁰, Tania Roskams⁵, Frederik Nevens^{1,2}, Diether Lambrechts^{6,7}, Olivier Govaere⁵, Schalk van der Merwe^{1,2}, Jef Verbeek^{1,2}. ¹Laboratory of Hepatology, CHROMETA Department, KU Leuven, Leuven, Belgium; ²Department of Gastroenterology and Hepatology, University Hospitals Leuven, Leuven, Belgium; ³KU Leuven institute of single cell omics (LISCO), KU Leuven, Leuven, Belgium; ⁴Department of Human Genetics, KU Leuven, Leuven, Belgium; ⁵Department of Imaging and Pathology, Translational Cell and Tissue Research, KU Leuven, Leuven, Belgium; ⁶Laboratory for Translational Genetics, Department of Human Genetics, KU Leuven, Leuven, Belgium; ⁷VIB Center for Cancer Biology, Leuven, Belgium; ⁸Department of Gastroenterology and Hepatology, AZZ Aalst, Aalst, Belgium; ⁹Department of Abdominal Surgery, University Hospitals Leuven, Leuven, Belgium; ¹⁰Department of Interventional Radiology, University Hospitals Leuven, Leuven, Belgium
Email: lukas.vanmelkebeke@kuleuven.be

Background and aims: Severe alcohol-related hepatitis (sAH) has a high 28-day mortality and corticosteroids are the only proven therapy. However, 45% of patients do not respond, resulting in a dismal prognosis and a 70% mortality rate. In this study, we elucidate

the intricacies of therapy response in the liver through an integrated transcriptomics analysis.

Method: We performed single-nucleus RNA sequencing (snRNA-seq, 10X) on liver biopsies from sAH patients ($n = 8$) before initiation of corticosteroids, acutely decompensated alcohol-related liver disease patients (AD) ($n = 5$) and healthy controls ($n = 4$). A definite diagnosis of sAH was established excluding patients with infection or acute-on-chronic liver failure (ACLF) grade 0 or 1. We followed patients for one year or until death. Mean Maddrey score was 18.8 ± 3.4 for the AD group, and 59.1 ± 13.8 for the sAH group. Protein validation of selected targets was done using immunohistochemistry (IHC) in an independent cohort and associated with outcome.

Results: We retrieved 152,283 good quality nuclei after analysis. Comparing sAH to healthy, we observed changes in cell proportions in immune and parenchymal cells. In hepatocytes at the RNA level, 1701 genes were differentially expressed (DEGs, $\log_{2}FC > 0.25$), including a decrease in SULT2A1 ($\log_{2}FC = 0.78$, $p_{adj}\text{-value} < 0.0001$), an enzyme that plays an essential role in bile acid and steroid metabolism. No significant differences were observed in cell proportions in sAH vs. AD. However, multiple differences were found at the RNA level. 478 DEGs were observed in hepatocytes, including a decrease in SULT2A1 ($\log_{2}FC = 0.54$, $p_{adj}\text{-value} < 0.0001$). When stratifying sAH based on therapy response at day 7, a higher proportion of monocytes in responders (R, $n = 4$) vs non-responders (NR, $n = 4$) ($0.67 \pm 0.28\%$ vs 0.28 ± 0.19 , $p_{adj}\text{-value} = 0.02$) was observed. At the RNA level (372 DEGs), SULT2A1 expression was significantly increased in R ($\log_{2}FC = 0.71$, $p_{adj}\text{-value} < 0.0001$) which was confirmed at the protein level using IHC in an independent sAH cohort ($p = 0.02$) including patients with infection and ACLF grade 2–3. In addition, S100A9, as a monocyte marker, was significantly more expressed in R vs NR on IHC ($p = 0.04$).

Conclusion: We have constructed a snRNA-seq liver atlas for sAH, providing a comprehensive resource to unravel its pathophysiology and to identify novel therapeutic targets within the molecular landscape of the liver during sAH. Additionally, we have developed innovative models based on protein markers, enhancing our ability to predict the response to corticosteroid therapy before its initiation. This advancement holds promise for a more precise and personalized approach in determining the most effective treatment strategies for individual patients with sAH.

TOP-329-YI

Integrated plasma multi-omics analysis classifies key microbiome, microbiome and metabolome changes linked to development of poor outcome in severe alcoholic hepatitis

Gaurav Tripathi¹, Vasundhara Bindal², Sushmita Pandey³, Neha Sharma⁴, Manisha Yadav⁵, Nupur Sharma¹, Babu Mathew⁵, Rimsha Saif⁵, Sadam H. Bhat⁵, Rakhi Maiwall⁵, Shiv Kumar Sarin⁵, Jaswinder Maras⁶. ¹Institute of Liver and Biliary Sciences, Delhi, India; ²Institute of Liver and Biliary Sciences, Delhi; ³Institute of Liver and Biliary Sciences, Delhi, India; ⁴Institute of Liver and Biliary Sciences, Delhi, India; ⁵Institute of Liver and Biliary Sciences, Delhi, India; ⁶Institute of Liver and Biliary Sciences, Delhi
Email: jassi2param@gmail.com

Background and aims: Severe Alcoholic Hepatitis (SAH) often encompasses complication such sepsis, shock, fungal growth and has high mortality rates. Plasma indicators linked to predisposition to shock and early mortality, and microbiome and its association in SAH is elusive.

Method: Plasma multi-omics (Metabolomics, Metaproteomics and fungal peptide based microbiome) analysis was performed in derivative cohort (50 healthy (HC), 50 alcoholic cirrhosis (AC) and 100 SAH patients (50 with sepsis and 50 with septic shock) using High Resolution Mass Spectrometry (HRMS). The results were validated using HRMS and Machine Learning (ML) in 300 SAH patients, cross correlated and benchmarked with clinical parameters and severity indices.

POSTER PRESENTATIONS

Results: SAH patients median age (46) and MDF score >32 were enrolled in the study. A total of 482 metabolite were upregulated and 356 metabolite were down regulated in the plasma of SAH as compared to AC or HC (FC >1.5, $p < 0.05$). Alpha and beta diversity of microbiome and mycobiome was significantly higher in SAH as compared to AC or HC ($p < 0.05$). Patients with Septic shock and those attaining early mortality (SAH-NS) were enriched for B-oxidation, TCA Cycle, Fatty acid, and Tryptophan metabolism. Plasma level of Stearaldehyde (FC >4), L-Dihydroorotic acid (FC >6), 2-Hydroxyglutaric acid (FC >4.34), and others significantly stratified patients with Septic shock or those predisposed to early mortality in SAH patients ($p < 0.05$). The microbiome and mycobiome diversity were distinct in SAH patients with sepsis, septic-shock, Vasoplegic shock or those attaining early mortality. Plasma microbiome/metabolome-based Probability for Diagnosis (POD) for sepsis was >90% and of Septic-shock was 89% in SAH patients. Microbiome modules/functionality directly correlated with metabolite modules, clinical parameters, and severity indices in SAH-NS ($R^2 > 0.5$, $p < 0.05$). Increased bacterial and fungal taxa Clostridia species (FC > 2.3), Actinomycetes (FC > 3.75), Chlorobiia (FC > 5.4), Bacteroidia (FC > 81), Gammaproteobacteria (FC > 3.2), and Erysipelotrichia (FC > 2.7) and functionality showed a direct correlation with bile acids, tryptophan metabolites, others, and development of Shock ($r^2 > 0.85$). ML Validation of SAH-NS metabolite panel on 300 SAH patients showed accuracy (>90%) and sensitivity/specificity (>95%) for mortality prediction.

Conclusion: SAH septic patients showed increase in bacterial/fungal taxa which reduces as patients become sicker due to prolonged antibiotic administration. Further, we identified novel clinical indicators and mycobiome for sepsis, shock and early mortality which outperforms the diagnostic capabilities of current markers like SIRS, SOFA and identify outlier patients, which do not fall under current diagnostic criteria's but have similar clinical presentation thus covering a broader range of SAH patients.

THURSDAY 06 JUNE

THU-315

HSD17B13 loss-of-function splice variant delays onset of incident steatotic liver disease and suggests slower progression in established liver disease

Audrey Chu¹, Jonathan Davitte², Damien Croteau-Chonka¹, Jessica Chao², Diogo Ferrinho³, Nikhil Vergis³, Cathy O'Hare⁴. ¹GSK, Cambridge, MA, United States; ²GSK, Collegeville, PA, United States; ³GSK, Brentford, United Kingdom; ⁴GSK, South San Francisco, CA, United States

Email: audrey.y.chu@gsk.com

Background and aims: The genetic variant rs72613567 in hydroxysteroid 17-beta dehydrogenase 13 (*HSD17B13*) leads to enzymatic loss of function (LOF) reducing the risk of developing steatotic liver diseases (SLD) including metabolic dysfunction-associated steatotic liver disease (MASLD), metabolic dysfunction-associated steatohepatitis and alcohol-related liver disease. Most research uses simple case-control comparisons to measure the relationship between LOF and SLD susceptibility, yet linkage of electronic health records and whole-genome sequencing (WGS) in the UK Biobank (UKB) in nearly 500,000 participants enables exploration beyond SLD susceptibility. We leveraged UKB's longitudinal follow-up to measure *HSD17B13* LOF impact on age of SLD onset, progression from MASLD to cirrhosis, and risk for liver-related or all-cause mortality.

Method: We captured *HSD17B13* rs72613567 LOF genotype from WGS data in 416,000 unrelated UKB participants of non-Finnish ancestry and modelled genotype additively. We used primary care, hospital episodes and mortality registry data to identify clinical diagnoses for MASLD and cirrhosis, and Cox-proportional hazards regressions (CPH) to measure hazard ratios (HR) and 95% confidence

intervals (CI) for the association between *HSD17B13* and age-of-onset for MASLD and cirrhosis. CPH were adjusted for standard covariates to evaluate *HSD17B13* impact on progression risk from MASLD to cirrhosis over 10 years post-MASLD diagnosis in 5600 cases, *HSD17B13* impact on 10 year liver-related mortality, and all-cause mortality within each of 374,000 participants without SLD, 7000 MASLD and 2500 cirrhosis cases. We used Kaplan-Meier survival curves (KM) to inspect survival rates between *HSD17B13* LOF allele carriers and non-carriers.

Results: Each *HSD17B13* LOF allele significantly reduced MASLD (HR [95% CI], 0.94 [0.90–0.97]; $p = 0.00046$) and cirrhosis (0.87 [0.83–0.93]; $p = 0.0000039$) risk; KM showed delayed age-of-onset for LOF carriers. For MASLD cases, KM showed separation by *HSD17B13* allele with slower progression from MASLD to cirrhosis for LOF carriers; CPH results were not significant (0.85 [0.69–1.05]; $p = 0.14$). From CPH, the LOF allele was not significantly associated with liver-related or all-cause mortality in the non-SLD ($p > 0.58$), MASLD ($p > 0.57$) or cirrhosis cohorts ($p > 0.20$), with no clear separation by *HSD17B13* LOF allele carriers in the KM. While not statistically different, deaths in *HSD17B13* LOF allele carriers in the cirrhosis cohort were lower than non-carriers (8.8% [96/1092] vs 9.4% [136/1446], respectively).

Conclusion: *HSD17B13* LOF variant rs72613567 was associated with delayed age-of-onset for SLD and trends to delayed progression from MASLD to cirrhosis. There was no significant effect of *HSD17B13* LOF on liver-related or all-cause mortality in this analysis; however, the small number of deaths observed limits inference.

THU-316

Farnesoid X receptor agonist INT-787 exhibits high intestinal localization

Jennifer Burkey¹, Sanjay Kansra¹, Antonio Macchiarulo², Kenneth Brouwer³, Luciano Adorini¹, Mary Erickson¹, Roberto Pellicciari⁴. ¹Intercept Pharmaceuticals, Inc., Morristown, United States; ²Department of Pharmaceutical Sciences, University of Perugia, Perugia, United States; ³ADME-TOX Division, BioIVT, Chapel Hill, United States; ⁴TES Pharma S.r.l., Perugia, Italy
Email: jennifer.burkey@interceptpharma.com

Background and aims: Disruption of the intestinal barrier and dysbiosis-driven inflammation are key factors in the pathogenesis of alcohol-associated liver disease. Farnesoid X receptor (FXR) activation within the intestine reduces inflammation and preserves the integrity of the intestinal epithelial and endothelial barriers. INT-787 is a hydrophilic, semisynthetic bile acid-derived FXR agonist with significant intestinal activity in animal models, protecting intestinal barrier integrity and promoting gut microbial reshaping. Here, we report unique distribution properties of INT-787 that support its potential for treatment of severe alcohol-associated hepatitis (sAH).

Method: In a phase 1, single-center, open-label study, 8 healthy male subjects were administered a single oral dose of 50 mg [¹⁴C]-INT-787. Mass balance recovery of total radioactivity and concentrations of INT-787 and its conjugates (glyco-INT-787 and tauro-INT-787) were measured in urine, fecal, and plasma samples. Additionally, intestinal permeability of parent and conjugated INT-787 were evaluated in a Caco-2 human intestinal epithelial cell model (American Type Culture Collection). Binding affinity for the ileal bile acid-binding protein (IBABP), a regulator of bile acid transport and activity in the small intestine, was assessed by MicroScale Thermophoresis (MST).

Results: Overall mean recovery of [¹⁴C]-INT-787 from feces and urine over the 504-hour study was 94.1%; the primary route of elimination was through the feces, with an arithmetic mean fecal recovery of 86.3%. INT-787 underwent moderate metabolism via glycine and taurine conjugation and oxidation to yield a total of 17 metabolites. The major compounds recovered from feces and urine were INT-787 (72.3%) and glyco-INT-787 (4.85%), respectively. Major plasma components were glyco-INT-787 (40.3%), INT-787 (32.8%), and tauro-INT-787 (8.89%). In vitro intestinal absorption of INT-787 in Caco-2 cells was low compared to FXR agonist obeticholic acid (OCA;

P_{app} (A-to-B): 6.4×10^{-6} cm/s vs 38.3×10^{-6} cm/s, respectively) and even lower for tauro-INT-787 and glyco-INT-787 (P_{app} (A-to-B): 0.7×10^{-6} cm/s and 0.3×10^{-6} cm/s, respectively). INT-787 and its metabolites demonstrated markedly weaker binding affinity to IBABP compared to OCA and its metabolites (MST dissociation constant [K_D] >1000 microM for INT-787, glyco-INT-787, and tauro-INT-787 vs 135 ± 22 microM, 33 ± 6 microM, 43 ± 8 microM for OCA, glyco-OCA, and tauro-OCA, respectively).

Conclusion: Oral INT-787 is a unique FXR agonist with low intestinal absorption resulting in high gut localization, likely due to the inability of INT-787 and its metabolites to bind to IBABP. These findings further support clinical studies evaluating the therapeutic use of INT-787 in alcohol-associated liver disease, including sAH, in which the integrity of the intestinal barrier is critical.

THU-317

Alcohol-related hepatitis is associated with a distinctive pattern of disordered bile acid metabolism and reduced bile acid transporter expression

Luke D. Tyson^{1,2,3}, Stephen R. Atkinson^{1,2,4}, Benjamin H. Mullish^{1,2}, Alexandros Pechlivanis¹, Michael Allison⁵, Andrew Austin⁶, Katie Chappell¹, Stuart J. Forbes⁷, Ewan H. Forrest^{8,9}, Alastair M. Kilpatrick⁷, Laura Martinez-Gili¹, Steven Masson¹⁰, Mark J. W. McPhail¹¹, Paul Richardson¹², Daniel Rodrigo Torres⁷, Stephen D. Ryder^{13,14}, Mark Wright¹⁵, Vishal C. Patel^{11,16,17}, Nikhil Vergis^{1,2,18}, Elaine Holmes¹, Mark R. Thursz^{1,2}. ¹Imperial College London, Department of Metabolism, Digestion and Reproduction, London, United Kingdom; ²Imperial College Healthcare NHS Trust, The Liver Unit, St Mary's Hospital, London, United Kingdom; ³London North West University Healthcare NHS Trust, Department of Hepatology, London, United Kingdom; ⁴GSK, Stevenage, United Kingdom; ⁵Cambridge NIHR Biomedical Research Centre, Liver Unit, Cambridge, United Kingdom; ⁶University Hospitals of Derby and Burton NHS FT, Department of Hepatology, Derby, United Kingdom; ⁷University of Edinburgh, MRC Centre for Regenerative Medicine, Edinburgh, United Kingdom; ⁸Glasgow Royal Infirmary, Department of Hepatology, Glasgow, United Kingdom; ⁹University of Glasgow, Glasgow, United Kingdom; ¹⁰Newcastle Freeman Hospital, Department of Hepatology, Newcastle, United Kingdom; ¹¹Institute of Liver Studies, Kings College Hospital, London, United Kingdom; ¹²Liverpool Foundation NHS Trust, Liverpool, United Kingdom; ¹³Nottingham University Hospitals NHS Trust, NIHR Nottingham Biomedical Research Centre, Nottingham, United Kingdom; ¹⁴University of Nottingham, Nottingham, United Kingdom; ¹⁵University Hospitals Southampton, Department of Hepatology, Southampton, United Kingdom; ¹⁶King's College London, School of Immunology and Microbiology, London, United Kingdom; ¹⁷The Roger Williams Institute of Hepatology, Foundation for Liver Research, London, United Kingdom; ¹⁸GSK, Brentford, United Kingdom Email: luke.tyson@nhs.net

Background and aims: Alcohol-related hepatitis (AH) is characterised by acute cholestasis and liver dysfunction in patients misusing alcohol. We aimed to characterise the bile acid (BA) profile of AH and explore its aetiology.

Method: BA concentrations were measured using UHPLC-MS in serum and stool samples from patients with severe AH, healthy controls, and controls with acute decompensation of alcohol-related cirrhosis; classified as moderately decompensated (MDC, MELD <21) or severely decompensated (SDC, MELD >21). Fibroblast growth factor 19 (FGF19) concentrations were measured by ELISA in fasted, early morning serum. RNA was extracted from liver biopsies (AH patients only). Pairwise comparisons were made by Mann-Whitney U test; correlation assessed by Spearman's Rank.

Results: Serum conjugated primary BAs were notably elevated in AH, even compared to SDC (n = 69 vs 36; glycochenodeoxycholic acid median 82.0 microM vs 48.0, taurochenodeoxycholic acid [TCDCA] 59.8 vs 25.0, glycocholic acid 36.3 vs 9.1, taurocholic acid [TCA] 16.0 vs 3.8; all p < 0.001). However, the serum concentrations of the

unconjugated primary BAs were highest in MDC (n = 135; chenodeoxycholic acid [CDCA] median 0.861 microM; cholic acid [CA] 0.176). In AH, the serum unconjugated primary BA concentrations were comparable to HC (n = 69 vs n = 63; CDCA median 0.201 microM vs 0.179; CA 0.071 vs 0.066; all p > 0.05). Faecal unconjugated primary BA were higher in AH compared to HC (n = 39 vs 51; CDCA median 74.9 microgram/gram dry stool vs 16.6, CA 47.7 vs 13.3; all p < 0.003), yet secondary BA were significantly lower (deoxycholic acid median 9.8 microgram/gram dry stool vs 970.7, ursodeoxycholic acid 4.1 vs 24.5, lithocholic acid 3.8 vs 734.0; all p < 0.001). The faecal concentration of conjugated primary BA in AH was negligible, with many samples below the lower limit of quantification of the assay. FGF19 was markedly elevated in AH compared to SDC and MDC (n = 10 vs 10 vs 8; median 5.84 ng/ml vs 0.61 vs 0.34; all p < 0.005). Hepatocyte BA transporter gene expression, particularly NTCP, inversely correlated with MELD score and serum conjugated BAs such as TCDCA and TCA (n = 25; NTCP vs MELD rho = -0.562; vs TCDCA rho = -0.549; vs TCA rho = -0.581; all p < 0.004).

Conclusion: In AH, conjugated primary BAs accumulate in the serum, even compared to SDC. Unconjugated primary BA do not. FGF19 is elevated implying reduced BA synthesis. Unlike the passive, non-ionic diffusion of unconjugated BA, conjugated BA require transporters to cross hepatocyte cell membranes for excretion into bile. Downregulation of hepatocyte BA transporters appears to explain the accumulation of conjugated BA in serum which distinguishes AH from acute decompensation. BA transporter expression inversely correlates with MELD score.

THU-318

Deep lipidomic analysis of plasma classifies lipid species capable of segregating septic-shock and predictive of early mortality in severe alcoholic hepatitis (SAH)

Gaurav Tripathi¹, Vasundhara Bindal¹, Sushmita Pandey¹, Neha Sharma¹, Manisha Yadav¹, Nupur Sharma¹, Babu Mathew¹, Rosmy Babu¹, Sadam H. Bhat¹, Rimsha Saif¹, Rakhi Maiwall¹, Shiv Kumar Sarin¹, Jaswinder Maras¹. ¹Institute of Liver and Biliary Sciences, Delhi, India Email: jassi2param@gmail.com

Background and aims: SAH encompasses high mortality, primarily due to complications like sepsis and septic shock. Lipids play crucial role in cell signaling, energy metabolism. There is limited understanding of role of lipids in sepsis initiation, shock induction, and early mortality in SAH patients.

Method: Plasma lipidomics was used to explore the roles and diagnostic efficacy of lipids in derivative cohort of (50 healthy (HC), 50 alcoholic cirrhosis (AC) and 100 SAH patients (50 with sepsis; 50 with septic shock) using high resolution mass spectrometry (HRMS). Lipid species and based Probability of detection (PODs) for sepsis, shock, and early mortality were validated by HRMS and Machine Learning (ML) in 300 SAH patients and were cross-correlated and benchmarked with clinical parameters/severity indices (MELD, SOFA, and others).

Results: Lipidomics identified 3388 lipid species (8 major classes; 94 classes; 570 subclasses). Progressive decrease of total lipid pool was seen, with increasing severity in SAH patients. SAH patients showed (>1300 differentially expressed lipid species (DEL)'s vs AC or HC) with significant downregulation of sphingolipids (31%), ceramides (15%), and upregulation of Eicosanoids (15%), Bile acid derivatives (18%), Fatty esters (11%) and others. Lipid Alpha diversity was significantly lower in SAH and POD-SAHS showed AUC>0.959 (p < 0.05). Patients with sepsis, septic shock, and Vasoplegic shock showed distinct lipidomic signatures (>1.5 FC, p < 0.05). Lipid species-based diagnostic accuracy of sepsis (POD-Sepsis = 98%) and shock (POD-Shock = 97%) were found in SAH patients. Lipid Species; 2, 5-dihydro-D-glucuronic acid (157 FC), 2, 5-Diaminopentanoic acid (14 FC), and others significantly segregated non-survivors. POD-Mortality showed >94% accuracy (p < 0.05). All PODs directly correlated with clinical

POSTER PRESENTATIONS

parameters (lactate, NORAD, FIO₂, MELD, AARC and others R²>0.5, $p < 0.05$). POD-shock/mortality showed highest beta-coefficient with AKI/HE grades ($p < 0.05$). POD-mortality had highest AUC>0.99 and hazard ratio (HR = 10, $p < 0.05$) when benchmarked against severity parameters. Finally, POD-mortality>45% predicted early mortality and the mortality lipid panel showed>95% accuracy/sensitivity and specificity in ML for mortality prediction.

Conclusion: SAH patients have hypolipidemia which worsens as the patients become sicker. Restoring lipid pool in patients can reverse the outcome. Also, clearance of classes like Fatty esters, eicosanoids, bile acid- derivatives, and others could change patient's outcome. Further, we identified novel clinical indicators for sepsis, shock and early mortality which outperforms the diagnostic capabilities of current markers like SIRS, SOFA and identify outlier patients, which do not fall under current diagnostic criteria's but have similar clinical presentation thus covering a broader range of SAH patients.

THU-319

Hepatocyte response to metabolic stress in alcoholic fatty liver leads to sublethal cell toxicity through the perturbation of protein translation-elongation machinery

Go Sugahara^{1,2}, Muranaka Hayato³, Yuji Ishida^{1,2}, Jae-Jin Lee⁴, Hyungjin Eoh⁴, Z. Gordon Jiang⁵, Meng Li⁶, Chise Taten², Takeshi Saito⁷. ¹Department of Medicine, Division of Gastrointestinal and Liver Diseases, Keck School of Medicine, University of Southern California, Los Angeles, United States; ²RandD, PhoenixBio Co., Ltd., Higashi Hiroshima, Japan; ³Department of Medicine, Cedars-Sinai Medical Center, Los Angeles, United States; ⁴Department of Molecular Microbiology and Immunology, Keck School of Medicine, University of Southern California, Los Angeles, United States; ⁵Department of Medicine, Division of Gastroenterology, Beth Israel Deaconess Medical Center, Harvard Medical School, Boston, United States; ⁶Bioinformatics Service, University of Southern California, Norris Medical Library, Los Angeles, United States; ⁷Department of Medicine, Molecular Microbiology and Immunology, and Pathology, Keck School of Medicine, University of Southern California, Los Angeles, United States
Email: saiotak@usc.edu

Background and aims: Alcoholic fatty liver (AFL) and metabolic dysfunction-associated fatty liver (MAFL), representing the initial stages of steatotic liver disease, serve as prerequisites for disease progression to advanced stages. ALF and MAFL are distinguished solely by clinical context as these conditions share histological and radiographic features, as well as genetic risk factors. Hence, it remains elusive whether they represent distinctive or shared pathophysiology. This study aims to characterize the hepatocytic response to the metabolic stress of AFL by contrasting it with that of MAFL, with the goal of advancing our understanding of how AFL primes the development of advanced stages of alcoholic liver disease (ALD).

Method: Human hepatocytes (HH), either primary or derived from humanized liver chimeric mice (HLCM), were seeded onto collagen-coated plates and cultured with DMSO-containing medium for 7 days, promoting the reinstatement of genuine characteristics. Subsequently, HH were cultured with either ethanol (EtOH) or a free fatty acid-sugar cocktail for an additional 7 days, during which time DMSO was replaced with DMSO2 due to its potent inhibitory effect on a multitude of hepatic metabolic enzymes. were characterized via mRNA-seq, ribosome profiling, and quantitative proteomics to decipher the impact of metabolic stresses on the transcriptome, translome, and proteome. The results obtained from in vitro studies were validated through in vivo experiments with HLCM.

Results: In vitro cultured HH exhibits the efficient EtOH metabolism to acetate, the final metabolite, at a rate comparable that of the human liver. In parallel, HH treated with EtOH developed macrovesicular steatosis at a comparable level to AFL liver tissue. HH treated with the free fatty acid-sugar cocktail also developed macrovesicular steatosis to an extent indistinguishable from AFL-HH. Despite the identical appearance, mRNA-seq analysis revealed substantial

differences in the number and type of differentially expressed genes, with only a small proportion exhibiting overlap. Furthermore, polysome profiling of AFL-HH but not MAFL-HH revealed substantial dissociation of mRNAs from ribosomes, indicating that metabolic stress in AFL results in potent suppression of translome. Subsequent in vitro and in vivo biochemical and protein studies indicate that the translome perturbation in AFL-HH is largely attributed to an impairment of elongation processes rather than initiation machineries. We also found that the translome deficiency results in the sublethal activation of cell death pathways in AFL-HH but not in MAFL-HH upon exposure to inflammatory cytokines.

Conclusion: Our work revealed a marked translome perturbation at the elongation stage and consequential cell toxicity in HH of AFL, uncovering a previously unrecognized pathophysiology of ALD.

THU-320-YI

The pan-cyclophilin inhibitor rencofilstat exhibits therapeutic anti-fibrotic effects in human relevant models of alcohol-related liver disease via extracellular matrix remodelling

Una Rastovic^{1,2,3}, Sara Campinoti^{1,3,4}, Lai Wei^{2,3}, Bruna Almeida^{2,3}, Sergio Bozzano^{2,3}, Ramin Amir⁵, Nicola Harris^{2,3}, Omolola Ajayi^{2,3}, Tsin Shue Koay^{2,3}, Caoimhe Kerins⁶, Fiona Kenny⁷, Ane Zamalloa⁸, Lissette Adofina⁸, Rosa Miquel⁸, Yoh Zen⁸, Parthi Srinivasan⁸, Krishna Menon⁸, Nigel Heaton⁸, Camilla Luni⁵, Eileen Gentleman⁶, Tanya Shaw², Daren Ure⁹, Shilpa Chokshi^{2,3}, Luca Urbani^{3,4,10}, Elena Palma^{2,3,10}. ¹Equal Contribution, London, United Kingdom; ²Faculty of Life Sciences and Medicine, King's College London, London, United Kingdom; ³The Roger Williams Institute of Hepatology, Foundation for Liver Research, London, United Kingdom; ⁴Faculty of Life Sciences and Medicine, King's College London, London, United Kingdom; ⁵Dept. Civil, Chemical, Environmental and Materials Engineering (DICAM), University of Bologna, Bologna, Italy; ⁶Centre for Craniofacial and Regenerative Biology, King's College London, London, United Kingdom; ⁷Faculty of Life Sciences and Medicine, King's College London, London, United Kingdom; ⁸Institute of Liver Studies, King's College London, London, United Kingdom; ⁹Hepion Pharmaceuticals, Edison, United States; ¹⁰Joint Senior Authorship, London, United Kingdom
Email: u.rastovic@researchinliver.org.uk

Background and aims: Alcohol-induced liver disease (ALD) represents a substantial challenge to global health as the foremost cause of cirrhosis. The severity of hepatic fibrosis is a crucial prognostic factor contributing to liver-related morbidity and mortality. Improved diagnostic methods have enabled the early detection of fibrosis in ALD patients, consequently driving a significant demand for pharmaceutical interventions aimed at halting the progression to end-stage liver disease. Inhibition of cyclophilins, peptidyl-prolyl isomerases that facilitate protein folding and are overexpressed in fibrosis, has been proven beneficial in several diseases, but the impact on ALD and the mechanism of action is still unclear. Here, we investigate the efficacy of a pan-cyclophilin inhibitor (rencofilstat) currently in Phase 2 clinical evaluation for metabolic dysfunction-associated steatohepatitis, on patient-derived models of ALD and liver fibrosis.

Method: Rencofilstat was tested in human Precision Cut Liver Slices (PCLS) exposed to ethanol and other stimuli to mimic key characteristics of ALD, and in primary human hepatic stellate cells (HSCs) activated by TGFβ to model fibrogenesis. Fibrosis and cell activation were assessed by gene (RNAseq, Quantigene) and protein analysis (proteomics, immunofluorescence, ELISA). A comprehensive characterisation of changes in the extracellular matrix (ECM), biochemical composition and fibre patterns/orientation, was performed in PCLS and HSC-derived matrix using immunofluorescence, confocal imaging, proteomics and TWOMBLI pipeline. Stiffness of PCLS upon treatment was assessed by atomic force microscopy.

Results: The expression and secretion of pro-fibrogenic markers was decreased in PCLS by the cyclophilin inhibitor. This was accompanied

by a reduced amount of cell-derived matrix deposited by HSCs treated with the drug in presence of TGFβ. RNAseq and proteomic analysis highlighted a consistent effect of rencofilstat on pathways involved in ECM and collagen fibril organisation in PCLS and HSC-derived matrix *in vitro*. These results were supported by significant changes in fibre alignment, matrix density, and bundle arrangement, suggesting ECM remodelling towards a potentially softer 3D matrix structure, which was confirmed by a reduced stiffness of PCLS exposed to rencofilstat.

Conclusion: Despite promising results in animal models, a substantial “translational gap” persists and there are no approved therapies to target alcohol-related fibrosis. This study demonstrates the therapeutic effects of rencofilstat in relevant patient-derived 3D models of ALD and fibrosis and proves the significant impact of cyclophilin inhibition on ECM remodelling, with direct consequences on tissue stiffness.

THU-321

Protein source differentially alters the outcome of fecal microbiota transplant in mouse model of alcohol-related liver disease

Shvetank Sharma¹, Ashi Mittal², Nishu Choudhary¹, Kavita Yadav¹, Anupama Kumar¹, Jaswinder Maras¹, Shiv Kumar Sarin³. ¹Molecular and Cellular Medicine, Institute of Liver and Biliary Sciences, Delhi, India; ²Molecular and Cellular Medicine, Institute of Liver and Biliary Sciences, D1 Vasant Kunj, Delhi, India; ³Hepatology, Institute of Liver and Biliary Sciences, Delhi, India
Email: shvetanks@gmail.com

Background and aims: Fecal microbiota transplantation (FMT) is an effective therapeutic option in alcohol-related liver disease (ALD). Selection of donor and its microbiota composition defines the FMT success. We evaluated the efficacy of pre-educating the donor microbiota with variable protein sources (plant or animal based) prior to FMT in remission of ALD.

Method: ALD mice were developed in 8wks by using Lieber-DeCarli diets with incremental ethanol (5–25%) and twice a week thioacetamide (150 mg/kg, i.p.). Donors (n = 6) for FMT were fed egg or soya protein isocaloric diet (1000 kcal/L) for 2 weeks. Gut microbiota changes were assessed by 16 s rRNA sequencing post day7 of FMT. PICRUSt analysis was performed to capture the functional pathways. Histopathology, serum biomarkers of liver injury, and gene expression (RT-PCR) of inflammation were assessed.

Results: Egg-FMT (eFMT) reduced the liver injury significantly compared to abstinence [AST (1.5-fold, p = 0.002), ALT (1.4-fold, p = 0.002), bilirubin (1.4-fold, p = 0.02), steatosis (6-fold, p = 0.001), fibrosis (2.8-fold, p = 0.001)], or soya-FMT (sFMT) [AST (1.2-fold, p = 0.002), ALT (1.06-fold, p = 0.1), bilirubin (1.2-fold, p = 0.03), steatosis (1.7-fold, p = 0.01)]. Both the FMTs reduced fibrosis similarly (1.1-fold, p = 0.14). eFMT also reduced the gene expression of hepatic pro-inflammatory markers [TNFα (1.5-fold, p = 0.02), IL6 (1.6-fold, p = 0.02)]. sFMT or eFMT lead to significant variation (79.54%, p = 0.001) in gut microbiota composition when compared to abstinence. eFMT increased the Shannon diversity more than sFMT (1.08-fold, p = 0.06). eFMT significantly increased the abundance of beneficial taxa *Dubosiella* (13.7-fold, p = 3.23E-14) and commensals *Bacillus* (7.8-fold, p = 2.77E-10) and *Vagococcus* (5.7-fold, p = 3.05E-05) compared to sFMT. eFMT reduced opportunistic pathogens *Muribaculum* (10.9-fold, p = 3.23E-14) and *Enterococcus* (3.7-fold, p = 0.0003). Bacterial pathways involved in amino acid, lipid, and carbohydrate metabolism were significantly modulated by eFMT (2-fold increase in hexitol degradation, p = 0.005 and phenylpropanoate degradation, p = 0.013; 1.5-fold increase in toluene degradation, p = 0.04 and glycerol degradation, p = 0.004) in comparison to sFMT.

Conclusion: Protein source in FMT donors is an important controller of post-FMT outcome in ALD. FMT from egg protein donor improves ALD injury better compared to FMT from soya donor. Along with increases in abundance beneficial species there is a concomitant

increase in carbohydrate and amino acid metabolism accompanied by significant reduction in hepatic inflammation and steatosis.

THU-322-YI

Plasma cell-free mtDNA is released in alcohol-associated liver disease and correlates with liver injury

Maram Alenzi¹, Gao Wen¹, Heansika Matta¹, Pinzhu Huang¹, Disha Badlani¹, David Guardamino Ojeda², Gloria Horta¹, Michelle Lai¹, Z. Gordon Jiang¹, Yury Popov¹. ¹Division of Gastroenterology and Hepatology, Beth Israel Deaconess Center, Harvard University, Boston, United States; ²Beth Israel Deaconess Medical Center-Harvard Medical School, Division of Gastroenterology and Hepatology, Boston, United States
Email: malenzi@bidmc.harvard.edu

Background and aims: Mitochondrial DNA (mtDNA) is a pro-inflammatory and pro-fibrogenic damage-associated molecular pattern (DAMP) with a pathogenic role in several inflammatory diseases. Due to common evolutionary origins, mtDNA shares many similarities with immunogenic bacterial DNA. We performed a pilot study to evaluate the potential significance of circulating mtDNA as a functional disease driver and biomarker in patients with alcohol-associated liver disease (ALD).

Methods: We collected EDTA-plasma and serum from 71 ALD patients (40 alcohol-associated hepatitis [AH] and 31 alcohol-associated cirrhosis [AC]) and 27 healthy controls in our tertiary hospital Liver Center (BIDMC) and measured absolute copy number of circulating mtDNA using our novel in-house high sensitivity duplex digital droplet polymerase chain reaction (ddPCR) mtDNA assay. The relationship between multiple clinically relevant AH parameters and mtDNA levels was assessed using linear regression analysis.

Results: Plasma mtDNA levels were significantly increased in both AH (2219 ± 5445 copies/ul of plasma, P = 0.01) and AC (1233 ± 1716 copies/ul of plasma, P = 0.008) compared with healthy controls (387.6 ± 426.5 CI copies/ul of plasma). In active AH, mtDNA levels were significantly higher compared to AC (p = 0.01). Plasma mtDNA level in alcohol-associated hepatitis, but not alcohol-associated cirrhosis, significantly correlated with parameters of liver injury-alanine aminotransferase (ALT, P < 0.001) >alkaline phosphatase (ALK-P, P < 0.001) >white cell count (WBC, P = 0.02), and markers of abnormal lipid metabolism-triglycerides (TG, P = 0.005) >lipoprotein X (LPX, P = 0.01) >lipoprotein Z (LPZ, P = 0.03) but not with aspartate aminotransferase (AST, P = 0.06), and total bilirubin (TBIL, P = 0.38). mtDNA levels in AH serum were about two-fold lower compared to those detected in plasma, and demonstrated similar pattern of significant, but weaker associations with above clinical parameters.

Conclusion: Using our novel ddPCR assay for circulating mtDNA we show for the first time that pro-inflammatory and pro-fibrogenic mtDNA is released during active AH and correlates with parameters of alcohol-related liver injury and dyslipidemia. These results support multi-center disease biomarker validation studies. The potential pathogenic role of mtDNA in AH should also be interrogated in follow-up mechanistic studies.

THU-324

Differential apoptotic and non-apoptotic cell death profiles in alcohol associated liver disease and their prognostic impact on acute-on-chronic liver failure

Pratibha Garg¹, Nipun Verma¹, Parminder Kaur¹, Samonee Ralmilay¹, Aishani Wadhawan¹, Rohit Nadda¹, Jiya Prajapati¹, Sahaj Rath¹, Arka De¹, Madhumita Premkumar¹, Sunil Taneja¹, Ajay Kumar Duseja¹. ¹Postgraduate Institute of Medical Education and Research, Chandigarh, India
Email: nipun29j@gmail.com

Background and aims: Cell death as a driver of disease progression in alcohol-associated liver disease (ALD) remain underexplored. This study aims to compare apoptotic and non-apoptotic forms of cell

POSTER PRESENTATIONS

death across distinct ALD stages and assess their prognostic impact using plasma-based biomarkers.

Method: 301 patients across stages of ALD were enrolled; 125 with acute-on-chronic liver failure (ACLF), 50 with acute decompensation (AD), 95 with non-acute decompensation (non-AD), 17 with compensated cirrhosis (CC), and 14 with alcohol use disorder-fatty liver (AUD-FL). Baseline plasma samples were collected and analysed for various forms of cell death using immunoassays. Expression profiles of these markers were evaluated across ALD spectrum, between ACLF grades, and their potential associations with short-term outcomes within ACLF were investigated. ROC analysis and AUC comparison through DeLong's test were performed.

Results: The cohort comprised mostly males (98%) with mean age of 45.2 years, with relatively older patients in non-AD and CC subgroup. MELD score increased significantly from AUD-FL to ACLF [8.2 (IQR: 6.5–11.5) to 29.3 (IQR: 24.9–35.8), $p < 0.001$]. A progressive, step-wise elevation in the concentrations of apoptotic (M30), total cell death (M65), pyroptosis (Gasdermin D), and necroptosis (RIPK3, MLKL) was seen across the ALD spectrum ($p < 0.001$ each). Overall, non-apoptotic forms of cell death became more prominent with increasing ALD severity, and specifically, MLKL exhibited significantly higher expression in ACLF than AD, serving as an indicator for the progression to ACLF (AUC: 0.761, $p < 0.001$). A consistently increasing trend was noted in all cell death markers between the ACLF grades ($p < 0.001$ each), except for M65 ($p = 0.056$).

All cell death markers, except M65 ($p = 0.061$) were associated with short-term mortality in ACLF patients ($p < 0.05$, each). Notably, Gasdermin D (HR: 2.970) and RIPK3 (HR: 2.213) remained significantly elevated in non-survivors even after adjusting for severity scores (MELD) ($p < 0.05$ each). Gasdermin D emerged as a pivotal prognostic marker in ACLF; strongly associated with mortality [HR: 2.970; adjusted for MELD with AUC of 0.732, $p < 0.001$] which was better than the MELD score (HR: 1.071; AUC: 0.644, $p = 0.008$). Adding Gasdermin D with MELD significantly enhanced the predictive performance of the MELD for 30-day mortality (AUC: 0.741), representing substantial improvement of 10%, (DeLong's test, $p = 0.017$).

Conclusion: Pyroptosis and necroptosis are predominant forms of cell death driving the progression of ALD. Non-apoptotic cell death exhibited a progressive increase with greater ACLF severity and mortality, offering valuable prognostic insights. Dynamic assessments of cell death and their targeted manipulation are promising avenues for disease modification in ALD.

THU-326

Improvement in alcohol-associated hepatitis is characterized by reduction of RNA modification processes

Alastair M. Kilpatrick^{1,2}, Daniel Rodrigo Torres¹, Stephen Atkinson², Luke D. Tyson², Nikhil Vergis², Mark R. Thursz², Laura Martinez-Gili², Stuart J. Forbes¹. ¹Centre for Regenerative Medicine, The University of Edinburgh, Edinburgh, United Kingdom; ²Department of Metabolism, Digestion and Reproduction, Imperial College London, London, United Kingdom

Email: alastair.kilpatrick@ed.ac.uk

Background and aims: Alcohol-associated hepatitis (AH) has a high mortality rate; however, disease mechanisms are still poorly understood. Here, we investigated the hepatic transcriptomic expression of a cohort of severe AH (sAH) patients to determine potential molecular mechanisms associated with disease prognosis.

Method: Paired baseline and day 28 (d28) liver tissue biopsies were obtained from participants with sAH enrolled in the ISAIAH randomised controlled clinical trial of canakinumab (CAN), an IL-1 β blocking antibody ($n = 32$; 27 paired samples). RNA was extracted and sequenced and gene level differential expression (DE) analysis was computed with respect to Model of End-Stage Liver Disease (MELD) score using a linear mixed effects model, adjusting for age, sex and timepoint as fixed effects and with patient as random intercept. Gene

set enrichment analysis (GSEA) was computed with fgsea. A false discovery rate < 0.05 was considered significant.

Results: MELD score improved at d28 similarly in both treated and untreated patients with paired samples (CAN: 13/14; placebo: 12/13). We identified 3,557 genes significantly differentially expressed with respect to MELD. Posttranscriptional regulation of gene expression was significantly enriched. Core enrichment genes included several eukaryotic initiation factors (eIFs) significantly upregulated with decreasing MELD. RNA modification, methylation and splicing processes were also enriched. Common to all these processes were methyltransferases 14 and 16 (METTL14; METTL16), significantly upregulated with decreasing MELD and known factors in m6A modification of RNA. Non-coding RNA (ncRNA) processing is also enriched with MELD; enrichment drivers include terminal uridylyl transferases 1 and 7 (TUT1; TUT7), upregulated with decreasing MELD and responsible for 3' RNA uridylation, a process important in epitranscriptomics. A substantial proportion of genes significantly downregulated with decreasing MELD are small nuclear and small nucleolar RNAs (snRNAs; snoRNAs) (12.6%), while almost all upregulated are protein coding. TUT1 has a known role in modification of snRNAs and may mediate gene expression and cell proliferation. Integrator complex subunits (INTSs) 2, 6, 7 and 12 also contribute to the enrichment of ncRNA-related gene sets; the integrator complex is a multiprotein complex involved in the 3' end processing of snRNAs.

Conclusion: Diverse posttranscriptional RNA modification processes and expression of snRNAs and snoRNAs are depleted with decreasing AH severity following alcohol cessation. Epitranscriptome and epigenome modulation may therefore be promising therapeutic targets in alcohol-related liver disease.

THU-327

Exploring the AhR molecular pathways to improve gut microbiota and liver injury in alcohol-associated liver disease

Wanchao Hu¹, Geraldine Schlecht-louf¹, Nicolas Trainel¹, Françoise Mercier-nome¹, Aurore Desmons², Sophie Viel³, Gabriel Perlemuter⁴, Dragos Ciocan⁴, Anne-Marie Cassard⁵.

¹Université Paris-Saclay, INSERM, Inflammation, Microbiome and Immunosurveillance, 91400 Orsay, France; ²Clinical metabolomic department, Sorbonne Université, INSERM, CRSA, Saint Antoine Hospital, AP-HP, Paris, France; ³INSERM, CNRS, Institut Paris-Saclay d'Innovation Thérapeutique, 91400 Orsay, France; ⁴Université Paris-Saclay, INSERM, Inflammation, Microbiome and Immunosurveillance, AP-HP, Hepato-Gastroenterology and Nutrition, Antoine-Béclère Hospital, 92140 Clamart, France; ⁵Université Paris-Saclay, INSERM, Inflammation, Microbiome and Immunosurveillance, Paris Center for Microbiome Medicine (PaCeMM) FHU, 91400 Orsay, France
Email: wanchao.hu@universite-paris-saclay.fr

Background and aims: Alcohol-associated liver disease (ALD) is the leading cause of cirrhosis worldwide, with few therapeutic options other than alcohol withdrawal. Intestinal microbiota (IM) plays a causal role in the severity of the disease both in mice and humans. Among metabolites produced by IM, bile acids and tryptophan metabolites are mainly modified in ALD. We previously demonstrated that pectin, a soluble fiber, improves liver and gut injuries in ALD through bile acid metabolism and indoles production acting through the aryl hydrocarbon receptor (AhR) signaling. However, the potential of tryptophan metabolites to improve ALD through the AhR and which cells are involved in mechanisms remain unknown. In this study, we aimed to decipher the involvement of AhR, specifically in the liver and the gut.

Method: We established conditional knockout mice models for AhR in hepatocytes, enterocytes, or dendritic cells (DCs) and CD11c expressing macrophages, followed by implementing preventative treatments with tryptophan or pectin in the context of ALD. Based on metagenomic and metabolomic analyses, we focused on changes in IM and microbiota tryptophan metabolites, which are ligands of AhR.

Results: We found that a tryptophan-enriched diet partially reproduced the effect of pectin without major changes in IM but with significant modification in the relative abundance of some bacteria. The tryptophan diet also modifies tryptophan metabolism and AhR ligands. These changes are closely related to IM but differ from the effect of the pectin diet. Serum tryptophan levels increased in the tryptophan group but not in the pectin group, while the serum tryptamine levels exhibited the opposite trend. Through conditional AhR knockout mice, we observed that AhR deficiency in hepatocytes or enterocyte-expressing cells worsened the ALD. However, the protective effect of pectin and tryptophan is not abrogated by AhR deficiency. In these AhR deficient mice, pectin and tryptophan treatments improve the alcohol-induced liver injury, conversely, the improvement of the gut barrier was abrogated.

Conclusion: Our data showed that tryptophan reproduces a part of the effect of pectin on the improvement of liver and gut injuries, which is independent of the AhR expression in hepatocytes and enterocytes. Conversely, the improvement of the gut injury depends at least on part of the AhR expression in the gut but not in the liver, suggesting that gut improvement is not a prerequisite to improve the liver injury.

THU-330

Complement protein signatures in patients with alcohol-associated hepatitis

Laura Nagy¹, Moyinoluwa Taiwo², Emily Huang³, Vai Pathak³, Esperance Schaefer⁴, Jay Luther⁴, Le Day⁵, Jon Jacobs⁵, Russell Goodman⁴, Daniel Rotroff^{6,7}, Gyongyi Szabo⁸, ¹Cleveland Clinic, Cleveland; ²Cleveland, Cleveland, United States; ³Cleveland Clinic, Lerner Research Institute, Cleveland, United States; ⁴Massachusetts General Hospital, Alcohol Liver Center, Boston, United States; ⁵Pacific Northwest National Laboratory, Richland, United States; ⁶Cleveland Clinic, Endocrine and Metabolism Institute, Cleveland, United States; ⁷Cleveland Clinic, Center for Quantitative Metabolic Research, Cleveland, United States; ⁸Beth Israel, Boston, United States
Email: len2@po.cwru.edu

Background and aims: Diagnostic challenges continue to impede development of effective therapies for successful management of alcohol-associated hepatitis (AH), thus creating an unmet need to identify and develop non-invasive biomarkers for AH. In murine models of ethanol-induced liver injury, complement activation contributes to hepatic inflammation and injury. Therefore, we hypothesized that complement proteins could be rational diagnostic/prognostic biomarkers in AH.

Method: We performed a comparative analysis of data derived from the human hepatic and serum proteome to identify and characterize complement protein signatures in severe AH (sAH). The hepatic proteomics data were generated by liquid chromatography-mass spectrometry analysis of de-identified liver samples acquired by University of Louisville and Johns Hopkins University Clinical Resource Center for Alcohol Hepatitis Investigations (R24AA025017). Samples used included healthy controls ($n = 12$; UL-7 and JHU-5) and patients with severe AH ($n = 6$ JHU) with an average Model for End-Stage Liver Disease (MELD) score of 37.2 ± 1.8 . The dataset was generated from the MS resources at PNNL (accession number MSV000089168; <https://massive.ucsd.edu/ProteoSAFe/static/massive.jsp>). The circulating proteomic data were acquired using the aptamer-based, proteomic SomaScan platform by Luther et al. (10.1172/jci.insight.159775). Serum samples from healthy controls (HC) ($n = 6$), patients with alcohol use disorder (AUD) ($n = 20$) and patients with mild ($n = 21$) (MELD < 10), moderate ($n = 15$) (MELD $11-20$), or severe ($n = 18$) (MELD > 20) AH, and patients with alcohol-associated cirrhosis (AC) ($n = 13$) were included in the cohort.

Results: The quantity of multiple complement proteins was perturbed in liver and serum proteome of patients with sAH. Multiple complement proteins differentiated patients with sAH from those with AC, AUD and HCs. Notably, serum collectin 11 and

C1q binding protein were strongly associated with sAH and exhibited good discriminatory performance amongst patients with sAH, AC, AUD, and HCs. Furthermore, lower serum mannose-binding lectin associated serine protease 1 and coagulation factor II were associated with and independently predicted 90-day mortality.

Conclusion: In summary, meta-analysis of proteomic profiles from liver and circulation revealed complement protein signatures of AH, highlighting a complex perturbation of complement and identifying potential diagnostic and prognostic biomarkers for patients with sAH.

THU-331-YI

The humoral profile of immunoglobulins specific for microbiota antigens stratifies the severity of patients affected by alcohol-related liver disease and predicts their 90-d mortality

Antonella Putignano^{1,2,3,4}, Natasha Kelkar⁵, Anaïs Thiriard^{3,6}, Shilpee Sharma^{3,6}, Dalila Lakhouloufi^{3,6}, Anne Botteaux^{3,6}, Samuel Meuree³, Christophe Moreno^{2,3,4}, Yiwei Jiang^{3,6}, Degré Delphine^{2,3,4}, Patrice Filee⁷, Margaret Ackerman^{8,9}, Thierry Gustot^{2,3,4}, Arnaud Marchant^{3,6}, ¹European Plotkin Institute for Vaccinology, Anderlecht, Belgium; ²HUB, Brussels, Belgium; ³Université Libre de Bruxelles, Brussels, Belgium; ⁴Laboratory of Experimental Gastroenterology, Brussels, Belgium; ⁵Geisel School of Medicine at Dartmouth, Dartmouth College, Department of Microbiology and Immunology, Hanover, United States; ⁶European Plotkin Institute for Vaccinology, Brussels, Belgium; ⁷Centre d'Economie Rurale, Liège, Belgium; ⁸Geisel School of Medicine at Dartmouth, Dartmouth College, Department of Microbiology and Immunology, Hanover, United States; ⁹Thayer School of Engineering, Dartmouth College, Hanover, United States
Email: putignano.anto@gmail.com

Background and aims: severe forms of alcohol-related liver disease (ALD) are burdened by high short-term mortality. Translocation of microbiota components might trigger immunoglobulins production (M-Ig) and M-Ig might contribute to ALD progression and prognosis. Systems serology (SS) profiles biophysical and functional features of antigen-specific antibodies and their relationship with clinical outcomes. The aims of this study were to characterize M-Ig using a SS approach and to investigate their role in ALD severity stratification and outcomes prediction.

Method: Single-center retrospective study enrolling ALD patients with steato-fibrosis ($n = 48$), compensated cirrhosis ($n = 54$), decompensated cirrhosis (CP B/C, $n = 59$) and severe alcoholic hepatitis (sAH, $n = 46$). M-Ig specific for 11 classes of microbiota antigens were considered. M-Ig titers, subclasses, Fc receptors (FcR) binding and antibody-dependent complement deposition were determined by Multiplex Immunoassay; antibody-dependent NK cells activation and antibody-dependent neutrophil and monocytes phagocytosis were assessed with *in vitro* cellular models. Unsupervised computational analysis (PCA) was used to determine M-Ig humoral signature of ALD severity groups, dBScan to identify clusters of patients, Chi Square or Fisher Test and Kruskal-Wallis test to compare variables or outcomes, Cox Regression to model predictors of 90-day mortality ($p < 0.05$).

Results: M-Ig titers, subclasses, and FcR binding increased according to ALD severity, however this was not associated to a parallel increment in the respective M-Ig function. PC1, PC2 and PC3 discriminated between ALD severity groups ($p = 0.0009$, < 0.0001 and $= 0.031$ respectively). VIP ranking showed that ALD humoral variability defined by PC1 was related to M-Ig specific for *E. Coli* and to FcR binding, whilst PC2 depended on *S. Aureus* specificities and IgA/IgG titers and PC3 on *C. Albicans* and IgG titer and subclasses. The DBscan analysis performed on CP B/C and sAH identified two clusters of patients ("nested" and "dispersed" cluster), clinically comparable, however septic shock occurrence and 90-day mortality were higher for patients belonging to the "dispersed" cluster (28.1% vs 10.8%, $p = 0.03$ and 36.4% vs 16.7%, $p = 0.029$ respectively). At the multivariate

POSTER PRESENTATIONS

analysis, to belong to the “dispersed” cluster resulted to increase the 90-day mortality risk (HR 4.2, CI 1.7–10.2, $p = 0.002$) independently from the MELD score (HR 1.2, CI 1.1–1.3, $p < 0.0001$).

Conclusion: Despite increased titers in severe ALD groups, M-Ig do not show higher functional potential, suggesting that other Fc biophysical factors might affect M-Ig final function and a reduced M-Ig potential to clear infection. M-Ig humoral signature defined by PCA discriminates between ALD severity groups and identifies a cluster of patients at higher 90-day mortality, independently from the stage and severity of the disease.

THU-332-YI

Growth differentiation factor 15 and adrenergic receptor beta 2 modulate free fatty acid release by inducing foamy macrophage in adipose tissue under chronic alcohol consumption

Min Jeong Kim¹, Kyurae Kim¹, Sung Eun Choi¹, Won-il Jeong^{1,2}. ¹Korea Advanced Institute of Science and Technology (KAIST), Daejeon, Korea, Rep. of South; ²Center for the Hepatic Glutamate and Its Function, KAIST, Daejeon, Korea, Rep. of South
Email: wijeong@kaist.ac.kr

Background and aims: Alcohol-related liver disease (ALD) is a leading cause of liver-related illness and death worldwide. Especially, among various organs influencing ALD, adipose tissue (AT) contributes the acceleration of alcohol-related hepatic steatosis by releasing free fatty acids (FFAs). Particularly, foamy macrophages in AT contribute to lipid metabolism and modulate inflammatory responses by accumulating cytosolic lipid droplets, subsequently participating in the systemic regulation of fat metabolism. Previous studies have reported that hepatic growth differentiation factor 15 (GDF15) increased the expression of adrenergic receptor beta-2 (ADRB2) in Kupffer cells (KCs) and the resultant activation of ADRB2 induced apoptosis of inflammatory KCs in ALD. However, GDF15 production and ADRB2 expression in AT macrophages have not been investigated clearly in ALD. Here we explored the GDF15/ADRB2 axis in AT macrophages and its effect on hepatic steatosis in ALD.

Method: To investigate the roles of GDF15 and ADRB2 on AT macrophage in ALD, wild-type mice were fed Lieber-DeCarli liquid EtOH diet (4.5%) for 8 weeks. Liver, blood, and AT samples were analyzed for biochemical parameters, histopathology, and bulk RNA-sequencing. In vitro experiments, Raw 264.7 cell were treated with recombinant GDF15 and ADRB2 agonist for BODIPY staining, flow cytometry, western blot, and qRT-PCR analyses.

Results: Chronic alcohol consumption induced hepatic steatosis and increased blood levels of catecholamine and FFA. AT decreased in weights and increased the numbers of crown-like structures, followed by elevated expression of GDF15 in adipocytes and ADRB2 in AT macrophages. Interestingly, flow cytometry revealed an increase of foamy macrophages in AT. In vitro, EtOH exposure increased GDF15 expression in adipocytes. Moreover, ADRB2 expression was induced in Raw 264.7 cells by GDF15 treatment. Furthermore, co-treatments of GDF15 and ADRB2 agonist enhanced not only lipid metabolism-related gene expression but also anti-inflammatory gene expression, thereby promoting foamy appearance in Raw 264.7 cells. These findings suggest a peculiar role of GDF15 and ADRB2 in regulating fat storage in AT macrophages.

Conclusion: Our study revealed that alcohol intake produced GDF15 in adipocytes, and increased ADRB2 expression in neighboring AT macrophages, increasing uptake of FFAs and promoting fat storage through triglyceride synthesis. Thus, targeting the GDF15/ADRB2 axis may provide novel therapeutic strategy for ALD by alleviating the blood levels of FFAs and inducing foamy macrophages.

THU-333

Novel mechanism of golgiphagy in hepatocytes and the protective impact of hydroxychloroquine on alcohol-induced liver damage and steatosis

Armen Petrosyan¹, Carol Casey², Amanda Macke², Taylor Divita².

¹University of Nebraska Medical Center, Omaha, United States;

²University of Nebraska Medical Center, Omaha, United States

Email: ccasey@unmc.edu

Background and aims: The progression of alcohol-associated Liver Disease (ALD) involves the disruption of the Golgi apparatus and the accelerated formation of phagophores. Although Golgi membranes may play a role in phagophore development, the connection between ethanol (EtOH)-mediated Golgi alterations and autophagy remains unclear. The research from our laboratory identified the impact of Rab3D GTPase downregulation in the development of EtOH-mediated intracellular alterations, including impaired trafficking of one of the critical hepatic proteins, the asialoglycoprotein receptor (ASGP-R). Herein, we studied the pivotal role of the dimeric Golgi matrix protein, p230, the regulator of trans-Golgi protein transport, in phagophore formation.

Method: VA-13 cells (mouse ADH1-transfected HepG2 cells) and WIF-B cells underwent exposure to 35–50 mM EtOH for a duration of 72–96 hours. In our in vivo studies, primary hepatocytes and liver homogenates from rats and mice were analyzed after being fed a control diet or the EtOH-containing Lieber-DeCarli diet for 5–7 weeks, along with the NIAAA chronic/binge mice model. We used various methodologies, including high-resolution, electron, and atomic force microscopies.

Results: We revealed that the morphology of the trans-Golgi is regulated by the cooperative actions of Rab3D, p230, and the motor protein non-muscle Myosin IIB (NMIIB). In the context of EtOH-induced Golgi scattering, Rab3D undergoes redistribution from trans-Golgi compartments to cis-medial, disrupting its complex with p230 and NMIIB. This redistribution induces conformational changes in the p230 molecule, specifically a shift from its bent configuration to an extended form, leading to the formation of p230-positive phagophores and their incorporation into autolysosomes. Deficiency in Rab3D within the trans-Golgi also results in the segregation of NMIIB from Golgi membranes, while its isoform NMIIA becomes tethered to the Golgi, giving rise to NMIIA-positive phagophores. Inhibition of NMIIA, both in vitro and in vivo, effectively prevents EtOH-induced Golgi dispersal. Additionally, in both chronic and chronic/binge models, we observed that Hydroxychloroquine (HCQ)-mediated autophagy inhibition prevents Golgi disorganization. This rescue of Golgi architecture re-establishes ASGP-R distribution. Significantly, HCQ blocks collagen deposition and steatosis and reduces the expression of upregulated hepatic cytochrome P450 2E1 (CYP2E1), suggesting the protective impact of HCQ on alcohol metabolism in hepatocytes.

Conclusion: Rab3D deficiency at the trans-Golgi and p230 conformational changes emerge as crucial events in NMIIA-driven, EtOH-mediated Golgiphagy. The promising results of HCQ treatment indicate its potential as a novel therapeutic approach for ALD.

THU-334

Supplementation of the amino acid L-arginine attenuates the onset of alcohol-related liver diseases

Anja Baumann¹, Franziska Kromm¹, Victor Sánchez¹, Katja Csarman¹, Raphaela Staltner¹, Annette Brandt¹, Ina Bergheim¹.

¹University of Vienna, Vienna, Austria

Email: ina.bergheim@univie.ac.at

Background and aims: Alcohol-related liver diseases (ALD) are still one of the major chronic liver diseases world-wide. Ethanol intake has been shown to alter intestinal barrier function, leading to an increased translocation of bacterial toxins and activation of toll-like receptor-dependent signaling cascades thereby promoting hepatic inflammation and progression of ALD. Studies suggest that changes of

intestinal nitric oxide (NO) metabolism are critical in the development of intestinal barrier dysfunction and that amino acids like L-citrulline and L-arginine may attenuate these alterations. Here, we assessed the effect of an oral L-arginine supplementation on the development of ALD in mice.

Method: Female C57BL/6J mice (n = 8/group) were pair-fed a control or an ethanol-enriched Lieber deCarli diet (EtOH, 5% ethanol) \pm 2.49 g L-arginine/kg bw/d for 28 days. Parameters of liver damage and intestinal permeability as well as markers of NO homeostasis in small intestine were determined. Moreover, everted small intestinal tissue sacs were challenged with EtOH in the presence of 0–4 nM L-arginine.

Results: The concomitant treatment of EtOH-fed mice with L-arginine significantly attenuated the development of ALD with markers of hepatic steatosis and inflammation such as the number of neutrophils, hepatic interleukin 6 concentration, 4-hydroxynonenal protein adducts and NO levels, all being significantly lower compared to mice fed only EtOH. The protective effect of L-arginine on the development of alcohol-related liver damage was associated with a protection from the significant increase in intestinal permeability in EtOH-fed mice. Moreover, the beneficial effects of supplementing L-arginine in EtOH-fed mice on changes in intestinal barrier function were associated with an alleviation of the significant increase of NO in small intestine. Additionally, in everted gut sacs ex vivo, EtOH-induced intestinal barrier dysfunction was almost abolished by L-arginine being associated with a normalisation of NO levels.

Conclusion: Our data suggest that L-arginine may attenuate the development of ALD in mice and that this is associated with a protection against the development of intestinal barrier dysfunction and alterations in intestinal NO homeostasis.

THU-335

The new nomenclature of steatotic liver disease identifies different risk trajectories for liver-related complications

Bocquillon Adrien¹, Jackie Bitton¹, Lauren-Ange Djia Meyapyal¹, Delphine Degré¹, Antonia Lepida¹, Laura Weichselbaum¹, Nathalie Boon¹, Thierry Gustot¹, Eric Trépo¹, Guillaume Lassailly², Lukas Otero Sanchez¹, Christophe Moreno¹. ¹HUB Erasme, Brussels, Belgium; ²CHU Lille, Lille, France
Email: adrien.bocquillon@ulb.be

Background and aims: A new nomenclature for Steatotic Liver Disease (SLD) was endorsed by EASL and AASLD. It encompasses Metabolic dysfunction Associated Steatotic Liver Disease (MASLD), Metabolic dysfunction and alcohol-related Steatotic Liver Disease (MetALD) and Alcohol-related Liver Disease (ALD). Data regarding liver-related complications according to this new nomenclature in compensated SLD are lacking. The aim of this study was to assess risk factors associated with liver-related events (LRE) in compensated patients with SLD, aiming to identify at-risk individuals regarding the new nomenclature.

Method: In this single-center study we included all patients with compensated biopsy-proven SLD performed at Erasme hospital (Brussels, Belgium) between January 2009 and December 2021. The main inclusion criteria were: \geq 18 years old, biopsy-proven SLD (steatosis $>5\%$); exclusion criteria were: other causes of chronic liver diseases, decompensated liver disease at the time of the biopsy or previous liver decompensation. We defined LRE as the occurrence of at least one of the following complications: ascites, encephalopathy, variceal hemorrhage, or hepatocellular carcinoma (HCC). To assess factors predicting outcomes of interest, univariate and multivariable regression analyses were performed using the Fine and Gray competing risks regression model, with non-liver-related death considered as competitive risk event.

Results: 316 patients were included and were followed for a median of 3.4 years. 233 patients were categorized as MASLD, 36 as MetALD and 47 as ALD. 47% of MASLD patients had advanced fibrosis stage

(F3–F4), compared to 58% and 81% for MetALD and ALD respectively. During follow-up, 8.2% of MASLD patients presented a LRE, compared to 22.3% for MetALD patients and 27.4% for ALD patients. The cumulative incidences of LRE at 2, 4 and 8 years were 4.61% (95% CI \pm 0.032), 6.06% (95% CI \pm 0.037) and 10.58% (95% CI \pm 0.056) for patients with MASLD, compared to 3.13% (95% CI \pm 0.061), 14.04% (95% CI \pm 0.121) and 18.65% (95% CI \pm 0.153) for patients with MetALD and to 9.67% (95% CI \pm 0.091), 18.83% (95% CI \pm 0.130) and 32.23% (95% CI \pm 0.182) for patients with ALD. In the multi-state model, fibrosis stage (HR = 1.62, 95% CI [1.04–2.51], p = 0.031), units of alcohol per day (HR = 1.08, 95% CI [1.01–1.15], p = 0.027), diabetes (HR = 4.36, 95% CI [1.56–12.01], p = 0.005) and bilirubin serum level (HR = 1.64, 95% CI [1.28–2.11], p < 0.001) were associated with LRE.

Conclusion: The new SLD classification identifies distinct at-risk groups for liver-related complications, highlighting liver fibrosis, daily alcohol consumption, and diabetes mellitus as key drivers. These findings underscore the critical necessity of screening for liver fibrosis in more at-risk SLD population for liver-related complications, including individuals with diabetes and those with significant daily alcohol consumption.

THU-338

Portal neutrophils exhibit an activated phenotype in alcohol-related liver disease

Sara Reinartz Groba¹, Mathis Richter², Raphael Chevre², Jonel Trebicka¹, Michaela Praktijn¹, Oliver Soehnlein². ¹Medicine B (Gastroenterology, Hepatology, Endocrinology, Infectious Diseases), University Hospital Münster, Münster, Germany; ²Institute of Experimental Pathology, University of Münster, Münster, Germany
Email: sara.reinartz@uni-muenster.de

Background and aims: Neutrophils are drivers of hepatic injury in alcohol-related liver disease (ALD). However, the neutrophil population is heterogeneous and disease-driving neutrophil subsets were identified in many pathological conditions, also in ALD. The portal venous compartment in ALD-related cirrhosis is distinct from those in other etiologies likely due to changes in gut microbiome and bacterial translocation. Immune cells passing through the splanchnic vascular bed are exposed to high levels of bacterial metabolites. This study aimed to examine the effects of the portal venous milieu on the neutrophil phenotype in ALD and non-ALD related cirrhosis.

Method: During transjugular intrahepatic portosystemic shunt (TIPS) placement blood was collected from the jugular, hepatic and portal vein prior to the establishment of the TIPS stent. Leukocytes were isolated from whole blood by red blood cell lysis, stained with a multicolor antibody panel and subsequently analyzed by spectral flow cytometry. For statistical analysis geometric mean of fluorescent intensities within the neutrophil populations were compared using Wilcoxon matched-pairs signed rank test. Further, inducibility of the portal phenotype was assessed by exposure to portal plasma. Neutrophils isolated from the jugular vein were treated with autologous portal plasma and characterized by spectral flow cytometry as described above.

Results: A total of 22 cirrhotic patients were included in this study (ALD = 12, non-ALD = 10). ALD and non-ALD groups had similar severity of liver disease (MELD, Child-Pugh-Score, portosystemic pressure gradient). Portal neutrophils of patients with ALD showed an increased expression of CD11b, CD10, CD45, and CD177 (all p < 0.01) compared to neutrophils from the jugular vein. Uniform Manifold Approximation and Projection for Dimension Reduction revealed that portal neutrophils clustered apart from neutrophils derived from the hepatic and jugular vein. Upon incubation with portal plasma, neutrophils from the jugular vein adopted the portal phenotype with increased expressions of CD11b, CD10 and CD45 (all p < 0.01) compared to controls. Those differences in phenotype could not be observed in patients with etiologies of cirrhosis not related to ALD.

POSTER PRESENTATIONS

Conclusion: Neutrophils derived from the portal vein of ALD patients exhibit a highly activated phenotype compared to those isolated from the jugular vein. This phenotype is probably induced by plasma factors from the portal vein.

THU-339

Abstinence induces site-specific metabolomic alterations in resolution from alcohol-related liver disease

Nupur Sharma¹, Sadam H. Bhat¹, Babu Mathew¹, Manisha Yadav¹, Sushmita Pandey¹, Gaurav Tripathi¹, Vasundhara Bindal¹, Neha Sharma¹, Shiv Kumar Sarin¹, Jaswinder Maras¹. ¹*Institute of Liver and Biliary Sciences, New Delhi, India*
Email: nupush1995@gmail.com

Background and aims: Alcohol increases gut permeability, allowing endotoxins to enter the blood, activating inflammation, and inducing not only liver injury but also affecting other organs. Continued alcohol drinking and abstinence from alcohol are likely to produce different metabolites, which are likely to be site specific and may influence gut permeability and disease pathophysiology. We investigated site-specific metabolomic changes upon alcohol or abstinence and correlated them to disease pathophysiology to identify potential therapeutic targets.

Method: Male and female LE rats (6–8 weeks old) were randomly assigned to Control (Lieber Di Carli control diet, n = 6), or alcohol-related liver disease (ALD, LDC ethanol diet for 24 weeks, n = 6), and Abstinence groups (24 weeks ALD rats abstained from alcohol for 7 days, n = 6). Liver, plasma, and intestine samples were subjected to metabolomic analysis.

Results: In ALD model, histology showed increased steatosis (28%, p < 0.05) and fibrosis (15%, p < 0.05) while in abstinence group, it resolved by 19% (p < 0.05) and 12%, respectively. The AST, ALT, bilirubin, triglycerides, and cholesterol, were significantly elevated in plasma of ALD rats but decreased in abstinence group (p < 0.05). Metabolomics analysis in liver of abstinence rats showed induction of steroid biosynthesis, terpenoid pathways, and reduction of amino acid metabolism (pathway intensity: >2fold, p < 0.05) associated with ameliorating inflammation. Plasma of rats under 7 days of alcoholic abstinence showed metabolites with phenylalanine metabolism surged while fatty acid metabolism reduced compared to ALD rats (>2fold, p < 0.05).

Intestine of alcoholic abstinence rats exhibited increased malate aspartate shuttle and glutamate metabolism whereas methionine metabolism was decreased (>4fold, p < 0.05). Metabolite integration analysis showed that abstinence resolved metabolites linked to pyrimidine (Deoxyuridine, 5-Thymidylic acid, Deoxycytidine, Thymidine, Uridine) and galactose metabolism (Melibiose, D-Gal alpha 1->6D-Gal alpha 1->6D-Glucose, Stachyose, Galactosylglycerol) in liver, plasma and intestine thereby producing a systemic increase in energy metabolism which corroborates with improvement in the liver injury. In-depth analysis revealed metabolic shift from pyrimidine to arginine synthesis resulting in increased urea formation. Interestingly, urea showed inverse correlation (r² > 0.6) with clinical parameters in abstinence from alcohol.

Conclusion: Our results demonstrate that alcohol abstinence for 7 days induces site specific alterations and a metabolic shift towards arginine synthesis. This promotes functioning of urea cycle, reducing ammonia, and facilitating the recuperation from ALD. Consequently, targeting arginine biosynthesis and urea cycle could be a beneficial approach in ALD treatment.

THU-340-YI

Multimomics landscape of alcohol detoxification and the role of PNPLA3 genotype

Anna Karl¹, Katharina Remih¹, Franziska Hufnagel¹, Francesca Barletta², Mohamed Ali Jarbou³, Johannes Müller⁴, Sebastian Mueller⁴, Zbyněk Zdráhal⁵, David Potěšil⁵, Pavel Hruška⁵, Olivia Plešow⁶, Ulrike Rolle-Kampczyk⁶, Martin von Bergen⁶,

Pavel Strnad¹. ¹*University Hospital RWTH Aachen, Aachen, Germany;* ²*University of Tübingen, Tübingen, Germany;* ³*University of Tübingen, Tübingen, Germany;* ⁴*University of Heidelberg, Heidelberg, Germany;* ⁵*Masaryk University, Brno, Czech Republic;* ⁶*Helmholtz Centre for Environmental Research, Leipzig, Germany*
Email: akarl@ukaachen.de

Background and aims: Alcohol-related liver disease (ALD) is the most predominant type of chronic liver disease and accounts for 50% of all cases of liver-related death. Despite that, the underlying mechanism remains incompletely understood. To change that, we systematically analyzed the proteomic and metabolomic changes in subjects undergoing inpatient alcohol detoxification and studied the relevance of PNPLA3 variant as the major genetic ALD modifier.

Method: Sera from 95 ALD subjects (44 PNPLA3^{WT/WT}, 20 PNPLA3^{I148M/I148M}) were collected prior to and after inpatient detoxification (median duration: 6 days) and were compared to sera of 32 liver-healthy controls. Liver fibrosis was assessed through liver stiffness measurement via transient elastography. All samples were subjected to untargeted mass spectrometry-based proteomic analysis and a subset was studied by depleted proteomics (14 most abundant proteins were removed). For targeted metabolomics, samples were extracted with the AbsoluteIDQ p180 kit and analyzed via high-throughput QTRAP mass spectrometry.

Results: The nondepleted dataset of ALD subjects strongly differed from healthy controls and changes were more pronounced in subjects with advanced vs. low fibrosis. Several inflammation-related proteins (CD14, immunoglobulin chains, PIGR etc.) were increased in alcoholic while protease inhibitors were often diminished (ITIHs, SERPINF2). The changes in immunoglobulin chains and protease inhibitors were even more pronounced at advanced liver disease stages. Detoxification was associated with a decrease in controlled attenuation parameter (CAP) values as surrogate of steatosis as well as diminished levels of several apolipoproteins (APOA1, APOA2, APOC3). Compared to PNPLA3^{WT/WT}, PNPLA3^{I148M/I148M} subjects harbored more pronounced changes in apolipoproteins suggestive of stronger lipidomic alterations. Depleted proteomics provided a better coverage of hepatocellular injury markers that typically decreased after alcohol withdrawal. Metabolomics revealed that detoxification led to a decrease in several acylcarnitines and an elevation in various glycerophospholipids.

Conclusion: Our multiomic-approach provides novel insights into changes occurring in ALD subjects during inpatient alcohol detoxification treatment.

THU-341

Mouse models of MetALD and metabolic dysfunction-associated steatohepatitis elicit similar patterns of liver injury

Naomi Lange^{1,2}, Amani Lee³, George Marek⁴, Luke Doskey⁴, P. Vineeth Daniel⁴, Amy Mauer⁴, Vijay Shah⁴, Harmeet Malhi⁴.

¹*Graduate School for Health Sciences, University of Bern, Bern, Switzerland;* ²*Department of Visceral Surgery and Medicine, Inselspital, Bern University Hospital, University of Bern, Bern, Switzerland;*

³*University of Minnesota, Minneapolis, Minnesota, United States;*

⁴*Division of Gastroenterology and Hepatology, Mayo Clinic, Rochester, Minnesota, United States*

Email: malhi.harmeet@mayo.edu

Background and aims: Both MetALD and metabolic dysfunction-associated steatohepatitis (MASH) are characterized by severe progressive liver injury. To gain further insight into shared and unique patterns of liver injury, we compared mouse models of advanced MetALD and MASH against several control groups.

Method: Liver injury was evaluated in 40 male C57Bl/6 (Jackson) mice at 16 and 24 weeks (n = 4 per group per timepoint). In the control groups (n = 8 per group), mice were fed chow diet with water (CW), sugar water containing glucose and fructose (CS), or 10% ethanol in sugar water (CE). In the condition groups (n = 8 per group), MetALD mice were fed a high-fat, -fructose, and -cholesterol (FFC)

diet with 10% ethanol sugar water (FE), and MASH mice were fed FFC with sugar water (FS). Liver tissue specimen were evaluated using NAFLD activity score (NAS), Sirius Red histological staining for fibrosis, immunohistochemistry for myofibroblasts (aSMA) and BODIPY staining for lipid droplet morphology. Liver injury and inflammation were measured by alanine aminotransferase (ALT) and aspartate aminotransferase (AST) levels, differential gene expression by multiplex nucleic acid hybridization (NanoString nCounter), and quantitative PCR (qPCR). Statistical analysis was performed in R, NanoString nSolver and GraphPad Prism.

Results: At 16 and 24 weeks, absolute body weight and liver mass to body mass index were significantly increased in both MetALD and MASH compared to controls. At 16 weeks, both MetALD and MASH exhibited increased ALT levels whereas AST levels did not differ from controls. Analysis of lipid droplet morphology in BODIPY staining demonstrated higher steatotic area and lipid droplet size in both conditions compared to controls. The number of lipid droplets per nucleus was lower in MetALD compared to MASH. Relative fibrotic area under polarized light (Sirius Red) was increased in MetALD compared to MASH at 16 weeks. Analysis of fibrotic gene expression revealed comparable patterns in both conditions, distinctly differing from controls. At 24 weeks, both NAS histological scoring and Sirius Red polarized light fibrosis assessment showed increased steatosis, inflammation and fibrosis in both conditions compared to controls, but indicated no differences between conditions. Accordingly, qPCR assessment revealed an increased expression of inflammatory (IL1beta and Mac2) and fibrotic (aSMA and Col1a) genes in both conditions. Multiplex hybridization of an immune gene panel revealed comparable patterns of differential gene expression in both MetALD and MASH.

Conclusion: In male C57Bl/6 mice, both MetALD and MASH demonstrate similar patterns of liver injury at 16 and 24 weeks. However, our data suggest a potentially distinct pattern of lipid droplet morphology as well as distinct dynamic of fibrosis progression, characterized by more pronounced early fibrosis in MetALD compared to MASH.

THU-342

Establishment of a mouse model of severe alcoholic hepatitis and study on the material basis of traditional chinese medicine rhubarb in the treatment of severe alcoholic hepatitis

Min Liu¹, Xue-Jin Zhu², Jia-Bo Wang¹. ¹Capital Medical University, Beijing, China; ²Fujian University of Traditional Chinese Medicine, Fuzhou, China
Email: jiabo_wang@ccmu.edu.cn

Background and aims: Severe alcoholic hepatitis is a fatal liver disease with limited therapeutic options, and the lack of accurate animal models impedes research progress. Traditional Chinese medicine has demonstrated potential in the treatment of severe alcoholic hepatitis, and the development of efficient animal models is crucial for drug advancement.

Method: To establish a murine model of severe alcoholic hepatitis (SAH) in C57Bl/6 mice using an enhanced NIAAA model, it is necessary to incorporate the final high-dose alcohol administration and bacterial endotoxin stimulation to mimic acute severe hepatitis induced by excessive alcohol consumption and gut toxins. Subsequently, the effects of rhein and sennoside A should be investigated in vivo.

Results: Observe the presence of abundant lipid vacuoles and neutrophil infiltration in liver tissue of SAH group using HandE staining and immunohistochemical staining. Compared with the control group, the serum ALT and AST in the NIAAA group and the SAH group increased, and there was a significant difference, especially in the SAH group ($p < 0.001$). The survival rate of mice in the SAH group was 66.7%, the survival rate of the positive drug hydrocortisone group was 83.3%, and the survival rate of the control group, the rhein dose group and the sennoside A dose group was

100%. Mitigate hepatic neutrophil infiltration and suppress hepatitis in SAH mice through the administration of varying dose of rhein and sennoside A. The administration of a low dose of rhein (30 mg/kg) and a moderate dose of sennoside A (30 mg/kg) significantly ameliorate hepatic function indicators in mice, including reducing the levels of alanine transaminase (ALT), aspartate transaminase (AST), direct bilirubin (DBIL), lactate dehydrogenase (LDH), and total bile acids (TBA), while increasing the levels of albumin (ALB) and cholinesterase (CHE). The research findings indicate that different doses of sennoside A (low, medium, and high) significantly impact LDH, TBA, ALB, and CHE indicators when compared to the model group. Moreover, varying concentrations of emodin A and rhein also demonstrate regulatory effects on factors such as TNF-alpha, IL-6, IL-1beta, and CCL2.

Conclusion: We established an animal model of SAH. The hepatic inflammation in mice, primarily characterized by neutrophil infiltration, was aberrant. Concurrently, there was significant impairment in liver function, mimicking the pathogenesis of clinical SAH. Rhein and sennoside A exhibited pronounced therapeutic effects on severe alcoholic hepatitis by significantly reducing levels of neutrophil infiltration and inflammatory factors in the liver. Among them, a low dose of rhubarb extract (30 mg/kg) and a moderate dose of sennoside A (30 mg/kg) demonstrated superior therapeutic efficacy compared to hormone drugs as they not only reduced mortality in SAH mice but also preserved their body weight.

THU-343

Dissecting metabolic dysfunction-associated steatotic liver disease with increased alcohol intake (MetALD): clinical and molecular insights and classification

Jun Liu¹, Sile Hu², Sihao Xiao¹, Rui Huang¹, Lingyan Chen², Jeremy Tomlinson^{3,4}, Jeremy Cobbold^{4,5}, Joanna Howson², Cornelia van Duijn¹. ¹Nuffield Department of Population Health, University of Oxford, Oxford, United Kingdom; ²Genetics Centre-of-Excellence, Novo Nordisk Research Centre Oxford, Oxford, United Kingdom; ³Oxford Centre for Diabetes, Endocrinology and Metabolism, University of Oxford, Churchill Hospital, Oxford, United Kingdom; ⁴NIHR Oxford Biomedical Research Centre, Oxford University Hospitals NHS Foundation Trust and the University of Oxford, Oxford, United Kingdom; ⁵Translational Gastroenterology Unit, University of Oxford, Oxford, United Kingdom
Email: jun.liu@ndph.ox.ac.uk

Background and aims: Metabolic dysfunction-associated SLD (MASLD) with increased alcohol intake (MetALD) is a condition that straddles MASLD and alcohol-related liver disease (ALD). This study aims to elucidate the distinct clinical and molecular characteristics of MetALD and to refine its subtypes using metabolomics and proteomics data.

Method: We analyzed 475, 204 European participants from UK Biobank with 33, 877 MetALD patients detected. We compared clinical, metabolomic, and proteomic profiles of MetALD with pure MASLD and ALD. Logistic or Cox regression were used to analyse features and assess risk of serious outcomes over 15 years. Classification models were developed using Elastic Net Regression.

Results: MetALD patients exhibited generally intermediate features between pure MASLD and ALD. Despite a significant overlap in metabolite and protein profiles among the three SLDs, MetALD still shared 10% metabolites and 4% proteins exclusively with either ALD or pure MASLD. The proteome model achieved an Area Under Curve (AUC) of 0.97 to differentiate pure MASLD from ALD in a separate dataset, while the metabolome combined with traditional markers reached an AUC of 0.91. The metabolome model identified a significantly higher risk for hepatocellular carcinoma (247%), cirrhosis (198%), mortality (50%), and heart failure (39%) in patients with ALD-predominated MetALD than MASLD-predominated MetALD. The proteome model identified a higher risk for cirrhosis (222%) and mortality (127%). In contrast, the alcohol model either did not

POSTER PRESENTATIONS

identify significant differences or identified much smaller differences (38% for cirrhosis and 22% for mortality).

Conclusion: This study provides a robust classification framework for MetALD and highlighting the prognostic significance of differentiating between MASLD-predominated and ALD-predominated MetALD. This could help healthcare providers tailor interventions more effectively, potentially improving prognosis and reducing complications.

THU-347-YI

Minibioreactor arrays (MBRAs) to model microbiome response to tryptophan and alcohol in the context of alcohol-associated liver disease (ALD)

Wanchao Hu¹, Nicolas Trainel¹, Vanessa Liévin-Le Moal¹, Gabriel Perlemuter², Benoit Chassaing³, Sabrine Naimi³, Dragos Ciocan², Anne-Marie Cassard⁴. ¹Université Paris-Saclay, INSERM, Inflammation, Microbiome and Immunosurveillance, 91400 Orsay, France; ²Université Paris-Saclay, INSERM, Inflammation, Microbiome and Immunosurveillance, AP-HP, Hepato-Gastroenterology and Nutrition, Antoine-Béclère Hospital, 92140 Clamart, France; ³INSERM U1016, CNRS UMR8104, Institut Cochin, Université Paris Cité, Paris, France; ⁴Université Paris-Saclay, INSERM, Inflammation, Microbiome and Immunosurveillance, Paris Center for Microbiome Medicine (PaCeMM) FHU, 91400 Orsay, France
Email: wanchao.hu@universite-paris-saclay.fr

Background and aims: Intestinal microbiota (IM) plays a causal role in the severity of alcohol-associated liver disease (ALD). Using IM transplantation in mice, we proved that the dysbiosis of alcohol use disorder (AUD) patients with severe alcohol-associated hepatitis (sAH) could be modified, leading to an improvement in alcohol-induced liver injury by increasing tryptophan metabolites to activate aryl hydrocarbon receptor (AhR) signaling pathway. However, the effect of tryptophan on IM in AUD patients, as well as its interactions with alcohol, remain to be elucidated. For this purpose, we used an in vitro approach with Minibioreactor arrays (MBRAs) that allows for the study of IM in a continuous-flow culture with well-controlled factors.

Method: Fecal samples from AUD patients with sAH (n = 2) or with noAH (n = 2) were transferred to MBRAs chambers. After 24 hours of adaptation in the initial medium, treatments with different tryptophan concentrations (low: 8 mg/L, normal: 24 mg/L and high: 72 mg/L) were initiated for 48 hours. Subsequently, alcohol was introduced in the system for 5 days (50 mM ethanol/Day). Finally, alcohol was removed and the cultures were maintained for an additional 5 days. IM analysis was conducted by 16 s sequencing. AhR activity of tryptophan derivatives in supernatants was determined using two reporter lines: intestinal epithelial cells (HT-29) and hepatocytes (HepG2) labelled with Lucia-AhR.

Results: After 24 h of stabilization, MBRA effectively maintains each fecal community. Tryptophan had no effect on the alpha and beta diversity of the IM from sAH and noAH patients. However, normal tryptophan level decreased the relative abundances of *Escherichia-Shigella* and increased *Bacteroides* in noAH IM, decreased *Proteobacteria* and increased *Bacillus* in sAH IM. In the absence of alcohol, tryptophan changed more number of bacteria in noAH IM (43 species) than in sAH IM (8 species). However, with alcohol conditions, tryptophan had minimal effect on the noAH IM. Compared to low tryptophan, normal and high tryptophan levels increased the AhR activity.

Conclusion: Our results suggest that maintaining a normal tryptophan level in patients with noAH could be essential to prevent dysbiosis and high concentrations of tryptophan may have a beneficial effect on the IM of sAH patients. Tryptophan holds potential as a novel therapeutic agent for ALD treatment but these results must be confirmed in vivo.

THU-348

Identification of alcoholic associated hepatitis-related genes and mesenchymal stem cell treatment target genes by meta analysis

Seul Ki Han¹, Taesic Lee², Sang Gyune Kim³, Yeon Seok Seo⁴, Soon Koo Baik¹, Young Uh⁵, Moon Young Kim¹. ¹Department of Internal Medicine, Yonsei University Wonju College of Medicine, Wonju, Korea, Rep. of South; ²Department of Family Medicine, Yonsei University Wonju College of Medicine, Wonju, Korea, Rep. of South; ³Department of Internal Medicine, Soonchunhyang University Bucheon Hospital, Bucheon, Korea, Bucheon, Korea, Rep. of South; ⁴Department of Internal Medicine, Korea University College of Medicine, Seoul, Korea, Rep. of South; ⁵Department of Laboratory Medicine, Yonsei University Wonju College of Medicine, Wonju, Korea, Rep. of South
Email: drkimmy@yonsei.ac.kr

Background and aims: Alcoholic associated hepatitis (AH) is a life-threatening condition and widespread chronic liver condition that places patients at risk of short-term mortality if it is not properly managed. This study aimed to identify transcriptomic biomarkers and cell therapy targets for AH.

Method: We conduct a systematic meta-analysis of published human gene expression studies on liver biopsies and blood derived gene data. First, three liver AH transcriptome datasets and a blood AH dataset were combined to discover a common phenotype. Second, two AH prognosis datasets were compiled, which are including gene phenotype reflecting prognosis. Using inverse weighted variance-based method mounted in METAL software, the candidate genes related to AH in liver and blood tissues and annotated them as the liver-blood AH meta genes. Third, three MSC datasets were curated for gene identification in stem cell response. Meta-analysis was implemented on the individual cohort-specific summary statistics obtained from differential expression methods to identify the AH-related biomarkers. To narrow down the candidate hub genes among stem cell treated data, TF database, protein-protein interaction network, disease-gene association database, and disease- and expression-related SNP database were used to analysis.

Results: With previously identified alcoholic gene-related databases, external verification was performed and 47 upstream AH-related genes were presented. The analysis contains some genes that have not been previously characterized in the context of alcoholic liver disease.

Conclusion: We present key genes involved in the progression of AH and provide a meta-analysis of results in a objective, statistically-based format. And at the same time, we suggest this biomarkers that can predict the prognosis of AH and treatment response. By using these genes, we can confirm the genetic changes caused by stem cell treatment and this can be used to lay the foundation for targeted cell therapy or function-enhanced genetic therapy.

Alcohol-related liver disease and MetALD – Clinical

TOP-311-YI

Subtypes of steatotic liver disease have differing clinical outcomes

Katrina Pekarska¹, Alexander Hinkson¹, Ian Rowe¹, Richard Parker¹.

¹Leeds Teaching Hospitals NHS Trust, St James's University Hospital, Leeds, United Kingdom

Email: katrina.pekarska@gmail.com

Background and aims: Steatotic liver disease (SLD) is a major health problems because of their potential to evolve into cirrhosis. SLD is an umbrella term for diseases typified by accumulation of fat in the liver. SLD includes a spectrum of diseases caused by cardiometabolic risk factors (CMRF) and alcohol including metabolic dysfunction

associated steatotic liver disease (MASLD), metabolic alcohol associated liver disease (MetALD) and alcohol related liver disease (ALD). This spectrum has made it possible to recognize patients having CMRF with increased alcohol consumption. Little data is available on all-cause mortality of the newly suggested SLD subtypes. We aimed to investigate the risk of all cause and liver-related outcomes in MASLD, MetALD and ALD.

Method: Patients who underwent liver biopsy for diagnosis or staging of NAFLD (non-alcoholic fatty liver disease) or ALD in routine practice at a single centre were included. Patient electronic records were reviewed for variable extraction. These two patient cohorts were then reclassified according to the new SLD nomenclature into three cohorts. Cox proportional hazards regression analysis was performed to understand the outcomes in MASLD, MetALD and ALD patients. Statistical analysis was done in R.

Results: In total 712 patients were included with a mean age of 51 (SD = 12.7) years. In old classification terms, 528 (74%) had a diagnosis of NAFLD, and 184 (26%) had ALD. After reclassification 477 (67%) had MASLD, 100 (14%) metALD and 135 (19%) patients had ALD. Patients with MASLD had significantly higher BMI ($p < 0.001$), cholesterol levels ($p < 0.001$), higher prevalence of diabetes mellitus ($p < 0.001$). Patients were followed up after biopsy for a median of 55.5 months (IQR 26–81), during which time 75 (11%) of patients died, including 30 liver-related deaths (40% of all deaths). Mortality was commonest in ALD (49 deaths, 36% of cohort), compared to metALD (13 deaths, 13%) and MASLD (13 deaths, 2.7%). Death due to decompensated liver disease was more frequent in ALD patients ($p = 0.044$), accounting for 16 deaths (66.7% of all deaths in ALD cohort). Multivariate Cox proportional hazards regression adjusting for baseline fibrosis stage showed a hazard ratio for death of patients with ALD of 5.59 (95% confidence interval, 2.74–11.4, $p < 0.001$) compared to MASLD.

Conclusion: ALD carries the highest risk of all-cause and liver-related mortality. To reduce the burden of liver disease alcohol should be a priority for policy makers. It is more important now than never to alert physicians to advise against any amount of alcohol intake as well as to have a good public education regarding alcohol intake and its effect on liver health. We should work with public health campaigns to tackle the ever-growing burden of the disease that leads to cirrhosis and decompensation.

SATURDAY 08 JUNE

SAT-249

Reduced Pannexin-1 and IL-33 in liver tissue are associated with lesser neutrophilic satellitosis and a higher rate of infections in severe alcoholic hepatitis patients

Shraddha Singh¹, S. Muralikrishna Shasthry¹, Archana Rastogi¹, Shiv Kumar Sarin¹, Chhagan Bihari¹. ¹Institute of Liver and Biliary Sciences, Delhi, India
Email: drcbsharma@gmail.com

Background and aims: Pannexin-1 releases nucleotide “find me” signals from apoptotic cells for the recruitment of inflammatory cells in tissue via IL-33 and promotes tissue innate immunity. Genetic predisposition to low Pannexin 1 (PANX1) expression can reduce hepatic recruitment of macrophages and neutrophils with higher chances of infections. In severe alcohol related hepatitis (SAH) patients, lower neutrophilic satellitosis is a poor prognostic indicator. We aimed to assess the status of PANX-1 and IL-33 in SAH patients’ liver biopsies and their association with neutrophilic satellitosis and sepsis/infections within four weeks.

Method: We analyzed the patients who underwent trans-jugular liver biopsies, performed per the standard protocol before treatment administration. Patients who had active infections, sepsis, recent bleeding, renal insufficiency, active tuberculosis, associated viral hepatitis, drug-induced liver injury, and inadequate liver biopsy were excluded. Standard treatment was administered per the institutional

protocol. We followed up patients for 28 days; the development of infection/sepsis was registered as an outcome measure. Liver biopsies were assessed for Pannexin-1 and IL-33 by immunohistochemistry (IHC) and calculated by Image-J software using an IHC analyzer, and the score was calculated as intensity \times cell positivity. We performed a quantitative real-time reverse transcriptase-polymerase chain reaction (RT-PCR) for PANX1, NLRP3, IL-33, and IL1beta.

Results: A total of 287 patients were screened and after applying exclusion criteria, 120 patients [median age 38 (IQR 32–46.2), 95% males, MELD Na 28.8 (25.6–34.5)] were included. Amount of alcohol days was 360 (200–375), median jaundice and ascites days were 30 (15–42.5) and 9 (6–21). Thirty six out of 120 (30%) patients developed infections within 4 weeks. The baseline IHC PANX1 score was significantly lower in those who developed infections [25 (0–50) vs. 150 (100–200), $p < 0.001$]. Likewise, IL-33 was more deficient in these patients [20 (0–50) vs. 120 (100–225), $p < 0.001$]. 80% of patients who developed infection had lower neutrophilic satellitosis of \leq grade 1 vs 13% of those who did not have the infection. PANX1 and IL-33 intensity correlated with the neutrophilic satellitosis grades ($p < 0.001$ and $p = 0.004$, respectively). RT-PCR of liver tissues also showed downregulated PANX1 (–1.8 folds) and IL33 (–3.4 folds) in those who eventually had infection compared to those who did not.

Conclusion: Downregulated PANX1 and IL-33 in liver biopsies were associated with lesser neutrophilic satellitosis and higher chances of infection in SAH patients.

SAT-250

Substituting FIB-4 with LiverPRO as an initial test for detecting advanced fibrosis leads to a 6-fold reduction in false positive results

Katrine Lindvig¹, Katrine Thorhauge^{1,2}, Helle Schnefeld¹, Johanne Kragh Hansen^{1,2}, Camilla Dalby Hansen¹, Stine Johansen^{1,2}, Peter Andersen¹, Ida Falk Villesen¹, Katrine Tholstrup Bech¹, Nikolaj Torp^{1,2}, Mads Israelsen^{1,2}, Aleksander Krag^{1,2}, Maja Thiele^{1,2}. ¹Department of Gastroenterology and Hepatology, Center for Liver Research, Odense University Hospital, Odense C, Denmark; ²Institute of Clinical Research, University of Southern Denmark, Odense M, Denmark
Email: katrine.prier.lindvig@rsyd.dk

Background and aims: EASL recommends starting with the Fibrosis-4 Index (FIB-4) in a fibrosis screening sequence for individuals at risk of Steatotic Liver Disease (SLD), followed by confirmatory Transient Elastography (TE), and the Enhanced Liver Fibrosis (ELF) test if available. Our study evaluates this pathway and compares it to an alternative approach where FIB-4 is replaced by LiverPRO, a CE-marked diagnostic tool, that utilizes a machine learning model to assess the likelihood of liver fibrosis based on routine blood samples. **Method:** We retrospectively applied the EASL pathway to a Danish screening cohort of at-risk individuals, recruited based on either metabolic or alcohol-related risk factors. We evaluated the accuracy of patient classification by FIB-4 and LiverPRO using TE as a reference. We used LiverPRO as the first-tier test in the alternative pathway, LiverPRO is considered positive, when the risk is $>65\%$. SLD groups were defined according to the new nomenclature and based on the past three months alcohol intake. The outcomes of both pathways were validated against liver biopsy data in the subgroup of patients who received a liver biopsy due to elevated TE (≥ 8 kPa).

Results: We included 4,869 patients with risk factors for SLD. Average age was 57 (IQR 52–63), with males comprising 52%. We found that 31% had Metabolic Dysfunction Associated Steatotic Liver Disease (MASLD), 7% had MASLD and associated alcohol intake (MetALD), 3% had Alcohol-related Liver Disease (ALD), and 59% had no SLD according to the new nomenclature. Using the FIB-4 initiated pathway, 35% ($n = 1,724$) had a FIB-4 score ≥ 1.3 , necessitating a subsequent TE measurement. Of these, 218 (13%) had TE ≥ 8 kPa, meaning FIB-4 showed 1501 false positives (87%). If LiverPRO replaced FIB-4, 388 patients (8%) would have been referred for further testing, and of these, 35% were identified as high-risk by TE.

POSTER PRESENTATIONS

LiverPRO had 252 false positives (65%). The effectiveness in patient classification was therefore higher with LiverPRO, with 90% of patients correctly classified (true negatives + true positives), compared to 66% in the FIB-4 pathway. Looking in a biopsied subgroup ($n = 238$), FIB-4 had an AUC of 0.70 (0.62–0.77), and LiverPRO an AUC of 0.79 (0.73–0.84) for predicting advanced fibrosis ($\geq F3$).

Additionally, when analyzing ELF as a third-tier assessment, 62% (88 out of 143) of those with positive FIB-4 and high TE score had a positive ELF (>9.8), compared to 63% (63 out of 100) in the high-risk LiverPRO and high TE group. In cases where TE and ELF disagreed a liver biopsy showed mild to significant liver fibrosis (F1–F2).

Conclusion: Substituting FIB-4 with LiverPRO as the initial test for individuals at risk of SLD, significantly improves the accuracy of participant classification, notably decreasing the incidence of false positives 6-fold.

SAT-251

Semaglutide can reduce alcohol use in patients with metabolic dysfunction-associated steatotic liver disease

Vladislav Fomin¹, Adam Buckholz¹, Yihan Liu¹, Himel Mallick¹, Sonal Kumar^{1,2}. ¹Weill Cornell Medicine, New York, United States; ²New York Presbyterian Hospital-Weill Cornell Medicine, New York, United States

Email: sok9028@med.cornell.edu

Background and aims: In patients with metabolic dysfunction-associated steatosis liver disease (MASLD) moderate alcohol use is associated with less steatosis reduction and less steatohepatitis resolution; heavy use is associated with accelerated liver injury and fibrosis progression. As a result, patients with MASLD are recommended to avoid alcohol. Glucagon-like peptide-1 (GLP-1) receptor agonists such as semaglutide are approved for diabetes and obesity, and associated with steatohepatitis resolution in clinical trials. GLP-1 receptors in brain areas are associated with reward and addiction and in primate studies GLP-1s reduce alcohol intake. We hypothesize semaglutide use decreases self-reported alcohol use through neuro-hormonal mechanisms.

Method: This single-center retrospective cohort study evaluated semaglutide use on weekly alcohol intake in patients with MASLD. The intervention group was started on semaglutide for obesity or overweight with complications in the setting of MASLD. The control group was patients with MASLD not started on semaglutide due to a variety of recorded factors. Both groups received standard counseling to discontinue alcohol. The primary end point was change in self-reported drinks per week (d/w) at 6, 12, and 24 months. Groups were stratified by BMI. A linear mixed effects model was used to compare changes both across and within cohorts. Age, sex, race, diabetes, HLD, metformin use, and use of other weight loss medications were controlled as covariates in the models of each cohort.

Results: 175 patients were included, 60 in the control and 115 in the semaglutide group. Age, liver enzymes, and liver stiffness per transient elastography were similar between groups. The semaglutide group had more women, diabetes, a lower mean BMI (31 vs 35), metformin use, and use of other weight loss medications. Mean initial alcohol use per week was similar (5.2 d/w with semaglutide, 6.6 d/w in control, $p = 0.36$). The semaglutide group decreased alcohol use during the first 6 months of treatment -4.2 d/w (95%CI $-7.3, -1.4$ $p = 0.0108$). The change in alcohol use was -4.5 d/w (95%CI $-9.0, -1.1$, $p = 0.0407$) at 12 months and -7.1 d/w (95%CI $-26.4, 12, 2$, $p = 0.0407$) at 24 months. The control group decreased -1.8 d/w (95%CI $-6.4, 0.2$, $p = 0.4791$). Compared to the control the semaglutide group decreased alcohol use -2.8 d/w (95%CI $-5.2, -0.4$, $p = 0.027$). When stratified for obesity at the combined time points with a BMI >30 , patients trended towards decreased use -3.0 d/w (95%CI $-6, 0$ $p = 0.067$).

Conclusion: In patients with MASLD semaglutide was associated with decreased alcohol use when combined with counselling. Semaglutide is increasingly used in patients with MASLD to treat

comorbid conditions like obesity and diabetes and may be a powerful tool to decrease alcohol use. Further studies in prospective randomized controlled trials can further evaluate the utility of GLP-1s in these patients.

SAT-254

Diet modifies the association between alcohol intake and alcohol-related liver disease: a prospective study of individual patient data from the UK Biobank

Fanny Petermann¹, Ziyi Zhou², John Mathers³, Carlos Celis-Morales², David Raubenheimer⁴, Naveed Sattar², Jill Pell², Ewan H. Forrester⁵, Frederick Ho². ¹Universidad Diego Portales, Santiago, Chile, Santiago, Chile; ²University of Glasgow, Glasgow, United Kingdom; ³Institute of Population Health Sciences, Newcastle University, Newcastle upon Tyne, United Kingdom; ⁴University of Sydney, Sydney, United Kingdom; ⁵Glasgow Royal Infirmary, University of Glasgow, Glasgow, United Kingdom

Email: fanny.petermann@udp.cl

Background and aims: Whilst alcohol-related liver disease (ALD) incidence is proportional to the amount of alcohol consumed, only 10 to 20% of individuals with chronic heavy alcohol use develop advanced ALD. Other factors must influence the effect of alcohol intake and the evolution of ALD. Associations between diet and the development of ALD have previously been seen only in animal models or in ecological studies. This study aimed to investigate if the incidence of ALD is influenced by an individual's diet.

Method: This was a prospective study of UK Biobank participants. At baseline, participants completed a questionnaire to collect the frequency of consumption of 20 food items over the previous year. Alcohol intake in units (u) was estimated using self-reported consumption of alcoholic beverages. ALD was defined as ICD-10 K70. The food items were included in Cox regression models with a 'Least Absolute Shrinkage and Selection Operator' algorithm. A 10-fold cross-validation for Cox Models was used to predict food items to be included in the diet score and determine dietary risk (DR). Joint association of diet and alcohol with ALD were investigated using Cox proportional hazard models. Results are reported as hazard ratios (HR) and their 95% confidence intervals (95%CI). Analyses were adjusted for sociodemographic factors, components of the metabolic syndrome, and lifestyle factors.

Results: Of the 303,269 participants included in the main analyses, 539 (0.2%) were diagnosed with incident ALD over a median follow-up of 10.7 years (IQR 10.0–11.4). Four food items achieved the minimum error and were used in the score: processed meat, beef, cereal, and salt intake (coefficients 0.0098, 0.0061, -0.098 and 0.202 respectively). Those at highest risk (higher DR and ≥ 14 u alcohol/week) were younger, more likely to be men, to smoke previously and to drink alcohol daily: hyperglycaemia, high triglycerides, central obesity and hypertension were also more prevalent. There was a non-linear association between the score and ALD incidence. The highest ALD incidence risk was in those with higher DR and ≥ 14 u alcohol/week (HR: 6.08 [95%CI: 4.30 to 8.59]), followed by those with lower DR and ≥ 14 u alcohol/week (HR: 3.01 [95%CI: 2.04 to 4.44]), and those with higher DR and <14 u alcohol/week (1.52 [95%CI: 1.02 to 2.26]) compared with those who were in the healthiest classification. A higher dietary score accounted for 40.5% (95%CI: 39.1% to 41.9%) of incident cases of ALD, while alcohol accounted for 50.9% (95%CI: 48.6% to 53.4%) assuming causality.

Conclusion: Using the UK Biobank study with individual patient data, we identified that diet amplified the association between alcohol consumption and ALD. Poor diet appears to exacerbate disease progression beyond alcohol intake and metabolic dysfunction. If these findings are corroborated, relevant guidelines should consider diet change to address ALD incidence.

SAT-255

Assessing LSM thresholds to identify clinically relevant SLD in individuals with excessive alcohol intake and absence of steatosis

Mette Lehmann Andersen^{1,2}, Nikolaj Torp^{1,3}, Stine Johansen^{1,3}, Camilla Dalby Hansen¹, Emil Deleuran Hansen^{1,3}, Ellen Lyngbeck Jensen^{1,3}, Katrine Thorhauge^{1,3}, Johanne Kragh Hansen^{1,3}, Ida Falk Villesen¹, Katrine Tholstrup Bech^{1,3}, Charlotte Wernberg^{1,4}, Peter Andersen¹, Katrine Lindvig¹, Maja Thiele^{1,3}, Aleksander Krag^{1,3}, Mads Israelsen^{1,3}.
¹Liver Research Centre, Department of Gastroenterology and Hepatology, Odense University Hospital, Odense C, Denmark; ²Department of Gastroenterology and Hepatology, Herlev Hospital, Herlev, Denmark; ³Institute of Clinical Research, Faculty of Health Sciences, University of Southern Denmark, Odense C, Denmark; ⁴Institute for Regional Health Science, Liver Research Group, Department of Gastroenterology and Hepatology, University Hospital of South Denmark, Esbjerg, Denmark
 Email: mette_98@hotmail.com

Background and aims: According to the new nomenclature for steatotic liver disease (SLD), a diagnosis of alcohol-related liver disease (ALD) or metabolic dysfunction and alcohol-associated steatotic liver disease (MetALD) requires the presence of hepatic steatosis or advanced fibrosis indicated by liver stiffness measurement (LSM) >14 kPa. However, alcohol-induced steatosis typically resolves with abstinence, why many patients with a history of excessive alcohol use do not meet the SLD criteria. We aimed to identify the threshold of LSM that associate with increased risk of decompensation in patients with a history of excessive alcohol use but without steatosis.

Method: This prospective cohort recruited individuals aged 18–75 with a current or previous alcohol overuse (>24 g/day for women, >36 g/day for men) for over a year and no history of decompensation. Participants were categorized based on the absence of steatosis, confirmed through histological assessment per NASH-CRN standards and controlled attenuation parameter (CAP) score <290 dB/m. A valid LSM was also required. Follow-up was done through manual reading of electronic medical records with decompensation events categorized according to the Baveno VII criteria.

Results: Of 441 patients with a history of excessive alcohol intake, 178 (40%) had absence of steatosis according to the histological assessment and CAP. For patients without steatosis 116 (65%) were male, mean age 54 years (SD 11), mean BMI 26 kg/m² (SD 4), and 110 (62%) were reported at least one week of abstinent at baseline. LSM was <8 kPa in 133 patients (75%), 8–14 kPa in 18 patients (10%), and >14 kPa in the remaining 27 patients (15%). Over a mean follow-up of 68 months (IQR 40), 21 (12%) patients developed decompensation (11 ascites, 5 hepatic encephalopathy and 5 variceal bleeding). In the subgroup with LSM <8 kPa, 2 of 133 patients (2%) had a decompensating event. For LSM 8–14 kPa, the rate increased to 17% (3 of 18 patients), whereas in the LSM >14 kPa group, 16 events occurred among 27 patients (59%). The risk of decompensation increased stepwise from LSM <8 kPa to LSM 8–14 kPa (HR = 7.8 95%; CI 1.1–55.8) and LSM >14 kPa (HR = 63.3, 95%; CI 13.1–307.2) independent of age, gender, and current alcohol intake.

Conclusion: In patients with a history of excessive alcohol use, 40% show no signs of hepatic steatosis. Due to the significant risk of developing hepatic decompensation in these patients with LSM >8 kPa, it is necessary to incorporate distinct thresholds for MetALD and ALD when classifying these patients according to the nomenclature for SLD.

SAT-256

Liver-related complications are the fastest growing cause of mortality from alcohol consumption: results from the global burden of disease 2019 study

Benedix Sim¹, Pojsakorn Danpanichkul², Darren Jun Hao Tan³, Cheng Han Ng¹, Wen Hui Lim³, Benjamin Nah¹, Benjamin Koh³, Christen Ong³, Nicholas Syn³, Jia Hong Koh¹, Daniel Tung¹,

Karn Wijarnpreecha⁴, Mark Muthiah¹, Margaret Teng¹, Daniel Huang¹.
¹Division of Gastroenterology and Hepatology, Department of Medicine, National University Hospital, Singapore, Singapore, Singapore, Singapore; ²Immunology Unit, Department of Microbiology, Faculty of Medicine, Chiang Mai University, Thailand, Chiang Mai, Thailand; ³Yong Loo Lin School of Medicine, National University of Singapore, Singapore, Singapore, Singapore; ⁴Division of Gastroenterology and Hepatology, Department of Medicine, University of Arizona College of Medicine, Phoenix, Arizona, USA, Phoenix, United States
 Email: benedix.sim@mohh.com.sg

Background and aims: Alcohol consumption plays a major role in global disability and mortality. Excessive alcohol consumption leads to liver-related complications, alcohol use disorder (AUD), and cardiovascular complications. Furthermore, alcohol significantly contributes to disparities in health outcomes across different socioeconomic groups. We aimed to investigate the global burden of disease attributable to alcohol consumption, in terms of AUD, liver and cardiac-related complications.

Method: Utilizing data from the 2019 Global Burden of Disease (GBD 2019) study, our study focused on assessing the annual age-standardized rates (ASRs) of prevalence, deaths and disability-adjusted life years (DALYs) attributable to AUD, liver-related complications, and cardiovascular complications from alcohol. We also conducted stratified analysis by sex and sociodemographic index (SDI).

Results: In 2019, the greatest contributor of DALYs ASRs was AUD (207.31 per 100,000; 95%CI 163.71 to 261.66 per 100,000), followed by alcohol-associated cirrhosis (133.31 per 100,000; 95%CI 112.68 to 156.17 per 100,000). Prevalence ASRs decreased in AUD (APC [annual percentage change] −0.38%), and alcohol-induced cardiomyopathy (APC −1.85%), but increased in alcohol-associated cirrhosis (APC +0.44%) and liver cancer (APC +0.53%). Death ASRs from alcohol generally decreased, but there was an increase in death ASRs from alcohol-associated liver cancer (APC +0.51%). Between 2010 and 2019, there was a rise in the contribution of alcohol-related complications to the overall burden in countries with low and low-to-middle SDI, relative to the global scale. The contribution of DALYs from these complications among young adults was more pronounced in countries with lower SDI.

Conclusion: There was a significant rise in the global impact of cardiovascular and liver complications due to alcohol over the past decade, particularly in alcohol-associated liver disease. Countries with lower income levels are contributing more to this global burden from alcohol. There is a pressing need for effective strategies in response to the escalating burden.

SAT-257

Hepatorenal syndrome markedly impacts prognosis of patients with alcohol-associated hepatitis. Results from the spanish registry of alcohol-associated liver disease (REHALC)

Jordi Gratacós-Ginès¹, Pilar Ruz-Zafra², Miriam Celada-Sendino³, Aina Martí⁴, Federico Cáceres⁵, Rosa Martín-Mateos⁶, Víctor Echavarría⁷, Luis Frisancho⁸, Sonia García-García⁹, Mónica Barreales Valbuena¹⁰, Javier Tejedor-Tejada¹¹, Sergio Vaquez Rodríguez¹², Nuria Cañete¹³, Carlos Fernández-Carrillo¹⁴, María Valenzuela¹⁵, David Martí-Aguado¹⁶, Diana Horta¹⁷, Marta Quiñones¹⁸, Vanesa Bernal¹⁹, Silvia Acosta-López²⁰, Tomás Artaza²¹, José Pinazo Bandera²², Carmen Villar²³, Ana Clemente²⁴, Esther Badia-Aranda²⁵, Maria Jose Moreta¹, Adrià Juanola¹, Pere Ginès¹, Pau Sancho-Bru²⁶, Joaquín Cabezas⁷, Meritxell Ventura Cots⁴, Conrado Fernández-Rodríguez¹⁸, Victoria Aguilera Sancho⁹, Santiago Tomé²⁷, Ramon Bataller¹, Joan Caballería¹, Elisa Pose¹.
¹Liver Unit, Hospital Clínic de Barcelona-

POSTER PRESENTATIONS

IDIBAPS, Barcelona, Spain; ²Virgen del Rocío University Hospital, Sevilla, Spain; ³Hospital Universitario Central de Asturias, Oviedo, Spain; ⁴Hospital Universitari Vall d'Hebrón, Barcelona, Spain; ⁵Hospital de la Santa Creu i Sant Pau, Barcelona, Spain; ⁶Hospital Universitario Ramón y Cajal, Madrid, Spain; ⁷Hospital Universitario Marqués de Valdecilla, Santander, Spain; ⁸Parc Taulí Hospital Universitari, Sabadell, Spain; ⁹Hospital Universitari i Politècnic La Fe, Valencia, Spain; ¹⁰Hospital Universitario 12 de Octubre, Madrid, Spain; ¹¹Hospital Universitario de Cabueñes, Gijón, Spain; ¹²Xerexia Xestión Integrada de Vigo SERGAS, Vigo, Spain; ¹³Hospital del Mar, Barcelona, Spain; ¹⁴Hospital Universitario Puerta de Hierro, Madrid, Spain; ¹⁵Hospital Universitari Dr. Josep Trueta, Girona, Spain; ¹⁶Hospital Clínico Universitario de Valencia-INCLIVA, Valencia, Spain; ¹⁷Hospital Universitari Mútua Terrassa, Terrassa, Spain; ¹⁸Hospital Universitario Fundación Alcorcón, Alcorcón, Spain; ¹⁹Hospital Universitario Miguel Servet, Zaragoza, Spain; ²⁰Hospital Universitario Nuestra Señora de Candelaria, Santa Cruz de Tenerife, Spain; ²¹Complejo Hospitalario Universitario de Toledo, Toledo, Spain; ²²Hospital Universitario Virgen de la Victoria, Málaga, Spain; ²³Hospital de Salamanca, Salamanca, Spain; ²⁴Hospital Universitario Gregorio Marañón, Madrid, Spain; ²⁵Hospital Universitario de Burgos, Burgos, Spain; ²⁶Institut d'Investigacions Biomèdiques August Pi i Sunyer (IDIBAPS), Barcelona, Spain; ²⁷Hospital Universitario de Santiago, Santiago de Compostela, Spain
Email: jgrata@recerca.clinic.cat

Background and aims: Acute kidney injury (AKI) is common and is associated to high morbimortality in patients with alcohol-associated hepatitis (AH). Hepatorenal syndrome (HRS) is a severe form of AKI arising in patients with advanced cirrhosis. Information regarding prevalence and prognostic implications of HRS-AKI in patients with AH is scarce.

Method: Retrospective analysis of patients with AH admitted to 28 Spanish hospitals from 2014 to 2022. AH was defined based on the NIAAA criteria of "probable" or "definite" AH. Patients were classified into 3 groups based on AKI occurrence and phenotype: AH with HRS-AKI, HA with non-HRS-AKI (including prerenal AKI, acute tubular necrosis and unable to classify), and AH without AKI. We analyzed the prevalence of the different AKI phenotypes, and assessed survival at 28 and 90 days with Kaplan-Meier curves and log-rank test. Patients with AH and HRS-AKI were compared to a prospective cohort of patients with cirrhosis and HRS-AKI (n = 63) from Hospital Clínic of Barcelona.

Results: Out of 1,746 patients with AH, 408 (23%) developed AKI; 77 (19%) were HRS and 331 (81%) were non-HRS-AKI (187 [46%] prerenal AKI, 36 [9%] acute tubular necrosis y 108 [26%] unable to classify). Patients with HRS-AKI had the lowest survival out of the three AH groups, followed by non-HRS-AKI and no-AKI (44%, 77%, 96% at 28 days; 24%, 65%, 91% at 90 days; both p < 0.01). Compared to patients with cirrhosis and HRS-AKI, patients with AH and HRS-AKI were younger, had higher median MELD, greater proportion of ACLF and lower survival (44% vs 75% at 28 days; 24% vs 54% at 90 days; both p < 0.01). Terlipressin was used in 46/77 (60%) patients with AH and HRS-AKI, with a 50% response rate. HRS-AKI recurrence rate among responders was 57%. Six (13%) patients developed severe adverse events related to terlipressin (acute respiratory failure [n = 2]; gastrointestinal hemorrhage [n = 2]; acral ischemia [n = 2]); 5 of them required treatment discontinuation. Predictive factors of response were AKI stage at diagnosis (HR 3.1 [1.1–9.2]) and absence of ACLF (HR 3.3 [1.3–10.0]). Terlipressin responders had higher 28-day survival (71% vs 24% in non-responders; p < 0.01).

Conclusion: HRS has the worst prognosis out of all AKI phenotypes in patients with AH. Terlipressin may be useful in patients with AH and HRS-AKI as a bridge to liver transplant or to recovery.

SAT-260

Metadoxine improves alcohol abstinence and is related to a lower risk of decompensation in cirrhosis at a median five-year follow-up: propensity score matching analysis

Fátima Higuera-de-la-Tijera¹, Alfredo Servin-Caamaño², Juan Miguel Abdo-Francis³, Elia Hernández-Labra⁴, Adriana Tovar-Aguilar⁵, José Luis Pérez-Hernández⁶. ¹Head of Gastroenterology and Hepatology Department, Hospital General de México "Dr. Eduardo Liceaga," Facultad de Medicina, Universidad Nacional Autónoma de México (UNAM), Mexico City, Mexico; ²Internal Medicine Department, Hospital General de México "Dr. Eduardo Liceaga," Facultad Mexicana de Medicina, Universidad La Salle, Mexico City, Mexico; ³Gastroenterology Department, Hospital Angeles Acoxa, Mexico City, Mexico; ⁴Psychology and Psychiatry Department, Hospital General de México "Dr. Eduardo Liceaga," Mexico City, Mexico; ⁵Social work assistant from Gastroenterology and Hepatology Department, Hospital General de México "Dr. Eduardo Liceaga," Mexico City, Mexico; ⁶Liver Clinic, Hospital General de México "Dr. Eduardo Liceaga," Facultad de Medicina, Universidad Nacional Autónoma de México (UNAM), Mexico City, Mexico
Email: fatimahiguera@hotmail.com

Background and aims: Abstinence is the key in alcohol-related cirrhosis (AC). Some studies suggest metadoxine (MTD) reduces alcohol craving (OHc), but its long-term impact on AC has not been evaluated. Aim was to compare long-term MTD vs. non-pharmacological therapy on alcohol abstinence in compensated AC.

Method: Patients with compensated AC were included in a retrospective cohort. Data were collected on attendance at Alcoholics Anonymous (AA) meetings, adherence to psychiatric therapy provided by addiction-trained personnel (PTA), family support (FS), self-reported commitment to stop drinking (CSD), decompensations, and relapse in alcohol intake (RAI) during follow-up. Patients were divided in 2 groups: A) MTD, B) without specific pharmacological therapy. To compare between groups, a propensity score matching (PSM) was conducted. The risk of RAI was assessed using Kaplan-Meier analysis with a log-rank test in the PSM cohort. A p value < 0.05 was significant.

Results: In the pre-matched cohort were 1042 pts, 79.1% men, mean age 52 ± 11 y/o, media follow-up 5.2 ± 1.3 years, 31.9% received long-term MTD to reduce OHc (median dose 1000 [500–2000] mg/d). Despite 67.7% reporting CSD and 68.9% having FS; adherence to AA meetings attendance and PTA was low: 31.2 and 27.3%. RAI occurred in 53.4%, median time to relapse was 22 (4–58) months, median number of relapses was 3 (1–10) times. Four covariables were associated with lower RAI: Age >40 y/o (456/877 [51.9%] vs. 100/165 [60.6%]; p = 0.04), MTD (122/332 [36.7%] vs. 434/710 [61.1%]; p < 0.0001), assistance to AA meetings (156/325 [48%] vs. 400/717 [55.8%]; p < 0.02), PTA (129/284 [45.4%] vs. 427/758 [56.3%]; p = 0.002). FS, CSD and sex were not significant. We conducted PSM to estimate the effect of MTD by pairing cases based on sex, age, AA attendance, PTA, FS and CSD. In the PSM cohort, 662 pts were obtained. MTD remained effective for reducing RAI (122/332 [36.7%] vs. 194/330 [58.7%]; OR: 0.41, 95%CI: 0.30–0.56; p < 0.0001). Even in those who experienced RAI, MTD prolonged the median time to the first RAI event (32 [8–84] vs. 17 [4.72] months; p < 0.0001). The total number of RAI events was lower in those receiving MTD (2 [1–6] vs. 3 [1–10]; p < 0.0001). Long-term MTD was also associated with fewer complications: variceal bleeding (28.3% vs. 37.9%; OR: 0.65, 95%CI: 0.47–0.89; p = 0.009), ascites (27.4% vs. 37.6%; OR: 0.63, 95%CI: 0.45–0.87; p = 0.005), encephalopathy (8.7% vs. 19.4%; OR: 0.39, 95%CI: 0.25–0.64; p < 0.0001), acute kidney injury (0% vs. 8%; OR: 0.97, 95%CI: 0.96–0.99; p = 0.004). MTD did not have an impact on development of spontaneous bacterial peritonitis, progression to Child-Pugh B/C, development of hepatocellular carcinoma, or mortality.

Conclusion: MTD is effective to improve alcohol abstinence. It is not clear whether the reduction of complications in patients with AC is directly driven by MTD or is indirectly related to abstinence itself.

SAT-261

Preliminary results of a phase I study of SZN-043, a novel R-Spondin mimetic, in healthy volunteers and subjects with liver cirrhosis

Edward J. Gane¹, Michael Lauw², Jay Tibbitts², Josh Koons², Jianyong Huang², Trudy Vanhove³, Mark Yen⁴, Chris Stevens², Christian Schwabe⁵, Craig Parker². ¹Faculty of Medicine, University of Auckland, Auckland, New Zealand; ²Surrozen Inc., South San Francisco, United States; ³Longitude Capital, Menlo Park, United States; ⁴Prometheus BioSciences, Los Angeles, United States; ⁵New Zealand Clinical Research Limited, Auckland, New Zealand
Email: jtibbitts@surrozen.com

Background and aims: Severe alcohol-associated hepatitis (SAH) is a huge unmet medical need, associated with high mortality. Corticosteroids have not been associated with improved long-term survival benefit and there has been no improvement in survival in SAH with medical management during the last 60 years. SAH is associated with impaired hepatocyte proliferation. Elevated Wnt signaling and increased hepatocyte proliferation have been linked to greater survival, suggesting that therapies that can enhance hepatocyte proliferation can benefit patients. R-spondins (RSPOs) are known enhancers of Wnt signaling. SZN-043 is a bispecific fusion protein and hepatocyte-specific RSPO mimetic shown to induce hepatocyte-targeted Wnt signaling and hepatocyte proliferation in preclinical studies. SZN-043 was evaluated for safety, pharmacokinetics, and pharmacodynamics in a single center, first-in-human, Phase 1, randomized, double-blind, placebo-controlled, single ascending dose (SAD) and multiple ascending dose (MAD) study in healthy volunteers (HV) and subjects with liver cirrhosis (LC).

Method: Thirty-five (35) subjects were recruited across SAD and MAD cohorts. In Part 1, 12 HVs (6 active/2 placebo per cohort) received a single IV dose of SZN-043 at 1 or 3 mg/kg. In Part 2, 8 LCs (3 active/1 placebo per cohort) received a single IV dose at 0.5 or 1 mg/kg. In Part 3, 18 HVs (6 active/2 placebo per cohort) received 0.5, 1, or 1.5 mg/kg of SZN-043 on Days 0 and 4.

Results: SZN-043 was well tolerated across all populations and dosing regimens. No serious adverse reactions nor infusion reactions were observed. Asymptomatic serum transaminase elevations were observed in 4 HVs in Part 1 and 2 HVs in Part 3. No transaminitis was observed in any LC subject. Severity appeared to be dose dependent, with 5 subjects experiencing no more than a mild (Grade 1) transaminase elevation and a Grade 2 alanine aminotransaminase elevation observed in 1 subject at 3 mg/kg. All resolved without intervention. No clinical sequelae or other related significant indicators of liver dysfunction were observed. In all other subjects, only mild to moderate adverse events judged to be at least possibly related were observed in 4 (other) subjects. Serum SZN-043 exposure was consistent with an IgG-based fusion protein. Pharmacologic activity in the liver was observed, as measured by increased metabolism of methacetin by cytochrome P450 1A2, a Wnt-target gene.

Conclusion: Administration of SZN-043 to HVs and LCs was well tolerated at doses where evidence of pharmacology was observed. Combined with the promise of the underlying biological mechanisms, the results from this study warrant further clinical investigation of SZN-043. A Phase Ib study in subjects with severe alcohol-associated hepatitis is under way.

SAT-262

Assessing efficacy and safety of baclofen in the management of alcohol dependence among patients with alcoholic liver disease

Berta López-Sáez¹, Cristina Solé¹, José Alberto Ferrusquía¹, Mireia Miquel¹, Meritxell Casas¹, Ariadna Altadill¹, Carme Massons², Alicia Capilla², Mireia Agut², Martí Guinovart², Irina Olasz², Lidia Rius², Alfred Reyes², Pilar Guillen², Deyanira Bártulos², Nora Mesa², Albert Cosculluela², Maria Rosa Blanco³, Francisco Verjano³, Vanessa Martín³, Mercedes Vergara¹,

Laia Grau Lopez⁴, Jordi Sánchez¹. ¹Gastroenterology and Hepatology Department, Parc Taulí University Hospital, Institut d'investigació i innovació Parc Taulí (I3PT-CERCA), Universitat Autònoma de Barcelona (UAB), Sabadell, Spain; ²Psychiatry and Psychology Department, Parc Taulí University Hospital, Institut d'investigació i innovació Parc Taulí (I3PT-CERCA), Universitat Autònoma de Barcelona (UAB), Sabadell, Spain; ³Psychiatry and Psychology Department, Parc Taulí University Hospital, Institut d'investigació i innovació Parc Taulí (I3PT-CERCA), Universitat Autònoma de Barcelona (UAB), Sabadell, Spain; ⁴Hosp. Universitario Germans Trias i Pujol, Barcelona, Spain
Email: bertalopezsaez@gmail.com

Background and aims: Alcohol use disorder (AUD) is the main cause of cirrhosis. Abstinence enhances survival, with clinical guidelines favoring baclofen as the first choice for preventing/reducing consumption in alcohol-related liver disease (ALD). Limited evidence exists regarding its real-world use. Our study assesses baclofen's efficacy (abstinence/reduction) and safety in ALD patients.

Method: A retrospective, single-center observational study was conducted, involving patients with ALD and alcohol-related cirrhosis (AC) who initiated baclofen between December 2022 and October 2023. Demographic, clinical and laboratory data were collected at baclofen onset (baseline) and 3 and 6 months thereafter.

Results: A total of 46 patients were included. The mean age was 53.8 (SD \pm 9.3) years, 84.7% were men, and 84.7% had AC (Child A: 38.5%, Child B/C: 61.5%). The median Child-Pugh score and MELD score in patients with AC was 7 [IQR: 5–11] and 11 [IQR: 6–22], respectively. At 3 months, 54.3% were abstinent and 24% had reduced consumption, while 54.3% continued with baclofen, 15.2% reduced the dose and 30.4% discontinued it. Abstainers presented a decline of 1.06 (SD 0.6) points in MELD score, while that of consumers increased by 2.25 (SD 2.9) points compared to baseline (p = 0.001). Among patients followed up at 6 months (n = 33), 54.5% were abstinent and 15.2% had reduced consumption. Of these, 44% continued with baclofen, 23.5% had reduced the dose and 30.3% had discontinued it. The MELD of abstainers decreased by 1.47 (SD 1.3) points, whereas that of consumers increased by 2.87 (SD 2.1), p < 0.001. Concerning safety, there were no instances of renal or hepatic impairment attributable to baclofen. However, 32.6% experienced drowsiness without signs of hepatic encephalopathy. Abstinent patients were compared to those non-abstinent. The univariate analysis showed that the use of psychotropic drugs (68% vs 31%, p = 0.04), Child-Pugh score (7 [5–11] vs 5 [5–11], p = 0.01), MELD score (12 [6–22] vs. 9 [6–22], p = 0.02); baclofen treatment (80% vs 24%, p < 0.01), and baclofen onset during hospital admission (60% vs 14%, p = 0.02) were associated with abstinence at 3 months. Only treatment with baclofen was independently associated with abstinence (OR 13.4, CI 2.4–24.9, p = 0.002). The univariate analysis showed that the baclofen onset during hospital admission (66.7% vs 26.7%, p = 0.03) and baclofen treatment (66.7% vs 26.7%, p = 0.02) were associated with abstinence at 6 months. Only treatment with baclofen was independently associated with abstinence (OR 4.5, CI 1.3–6.8, p = 0.03).

Conclusion: Baclofen demonstrates efficacy in achieving alcohol abstinence in ALD and AC, with rates of 78% and 70% at 3 and 6 months. Drowsiness, the most common side effect, led to dose adjustments or withdrawal in one-third of patients. Baclofen treatment emerged as an independent predictor of abstinence, supporting its use in ALD.

SAT-263

Resmetirom treatment of a subgroup of patients with possible MetALD enrolled in MAESTRO-NASH, a phase 3 NASH/MASH serial liver biopsy study

Stephen A. Harrison¹, Jörn M. Schattenberg^{2,3}, Rebecca Taub⁴, Dominic Labriola⁴, Brandon Hill⁴, Vlad Ratziu⁵. ¹Pinnacle Clinical Research, San Antonio, TX, United States; ²Metabolic Liver Research Program, I. Department of Medicine, University Medical Center of Johannes Gutenberg University Mainz, Mainz, Germany; ³The

POSTER PRESENTATIONS

Department of Internal Medicine II, Saarland University Medical Center, Homburg, Germany; ⁴Madrigal Pharmaceuticals, Inc., West Conshohocken, PA, United States; ⁵Pinnacle Clinical Research, San Antonio, TX, United States
Email: vlad.ratzu@gmail.com

Background and aims: MAESTRO-NASH (NCT03900429) is an ongoing 54-month, randomized, double-blind, placebo-controlled Phase 3 trial evaluating efficacy of resmetirom in patients with biopsy-confirmed non-alcoholic steatohepatitis (NASH/MASH) and fibrosis. 966 patients with biopsy-confirmed NASH were randomized 1:1:1 to resmetirom 80 mg, resmetirom 100 mg, or placebo once daily. Dual primary end points at Week 52 were achieved with both resmetirom 80 mg and 100 mg: NASH resolution with no worsening of fibrosis (NR) or ≥ 1 -stage improvement in fibrosis with no worsening of NAS (FI). The benefit of resmetirom in patients with and without indicators of increased alcohol consumption above protocol-allowed limits for NASH/MASH was assessed on biopsy end points and MRI-PDFF (liver fat reduction).

Method: Carbohydrate Deficient Transferrin (CDT) was collected longitudinally in all patients over 52 weeks. Post-randomization, a PEth test was performed in patients suspected of increased alcohol consumption. Patients with baseline or post-baseline CDT $>2.5\%$ (ULN 2.47) and/or a PEth >20 ng/ml (ULN 20 ng/ml) were assigned to a possible "MetALD" subgroup. Analyses were performed on 782 patients who had both a baseline and Week 52 biopsy.

Results: Of the 782 patients, 75 patients (9.6%) were included in the MetALD subgroup and 707 were not. Baseline characteristics, mean (SD), for the MetALD and non-alcohol subgroups included Age = 57.7 (10.5), 60.1 (10.7); percent male = 59%, 42%; Presence of diabetes = 50.7%, 67.9%; CDT% = 2.2 (1.0), 1.6 (0.3); BMI 33.0 (5.5), 35.8 (6.6); MRI-PDFF = 21.7% (7.4), 17.4 (6.5), Fibroscan VCTE = 13.4 (6.7), 13.2 (6.6); Fibroscan CAP = 348.5 (38.5), 347.0 (38.7); FIB-4 = 1.67 (0.69), 1.37 (0.66); AST = 45.6 (21.8), 40.3 (22.9); ALT = 55.2 (24.8), 55.5 (32.2); GGT = 117.9 (170.8), 75.3 (85.6); Bilirubin = 0.69 (0.31), 0.65 (0.29); MCV = 92.3 (5.8), 90.3 (5.6); Platelets = 200, 229; NAS (median) = 5 (5, 6), 5 (5, 6); and %F3 = 66.7, 62.5. For the group of patients with low or no alcoholic consumption:

Patients treated with 80 mg and 100 mg resmetirom doses ($n = 224$ and 228 , respectively): 29.9% and 36% had NR, 29% and 33.3% had FI, 59.2% and 71.2% showed a $\geq 30\%$ reduction from baseline in MRI-PDFF. For patients treated with placebo ($n = 255$), the corresponding results were 10.3%, 13.7%, and 24.5%. For the possible MetALD group: Patients treated with 80 mg and 100 mg resmetirom doses ($n = 34$ and 20 , respectively): 29% and 35% had NR, 35% and 30% had FI, and 88% and 81% showed a $\geq 30\%$ reduction from baseline in MRI-PDFF. For patients treated with placebo ($n = 21$), the corresponding results were 10%, 19%, and 14%.

Conclusion: A total of 75 (9.6%) of patients had possible MetALD during the first 52 weeks of MAESTRO-NASH. Baseline characteristics showed a higher mean GGT and FIB-4 in the MetALD versus low alcohol group. Response rates to resmetirom in patients with suspected MetALD were similar to those without MetALD.

SAT-266

Fibrosis stage progression in alcohol-related liver disease evaluated by repeated biopsies

Ellen Lyngbeck Jensen^{1,2}, Nikolaj Torp^{1,2}, Stine Johansen^{1,2}, Katrine Thorhauge^{1,2}, Camilla Dalby Hansen¹, Johanne Kragh Hansen^{1,2}, Peter Andersen², Emil Deleuran Hansen^{1,2}, Ida Falk Villesen^{1,2}, Katrine Tholstrup Bech^{1,2}, Charlotte Wernberg¹, Katrine Lindvig¹, Sönke Detlefsen^{2,3}, Aleksander Krag^{1,2}, Maja Thiele^{1,2}, Mads Israelsen^{1,2}. ¹Centre for Liver Research, Department of Gastroenterology and Hepatology, Odense University Hospital, Odense, Denmark; ²Department of Clinical Research, University of Southern Denmark, Odense, Denmark; ³Department of Pathology, Odense University Hospital, Odense, Denmark
Email: ellen.lyngbeck.jensen@rsyd.dk

Background and aims: Alcohol-related liver disease (ALD) is recognised as the most severe form of steatotic liver disease, yet precise progression rates are not well established. Understanding the annual rate of fibrosis progression in ALD patients, along with the impact of current alcohol intake and cardiometabolic risk factors, is crucial for optimizing management and informing clinical trial design. We therefore assessed annual fibrosis progression from patients with ALD in a repeated biopsy design.

Method: We included patients with ALD who had undergone liver biopsies twice in randomised trials and prospective cohorts at Centre for Liver Research in Odense. Biopsies were assessed by a single expert pathologist who was masked to all clinical data. Liver fibrosis was evaluated according to the Kleiner scoring system for fibrosis: F0, F1, F2, F3, and F4. We excluded patients who could not have progression of fibrosis stage (F4 at baseline). We calculated annual fibrosis stage progression rates along with 95% confidence intervals (CI). In multivariable models, we calculated the impact of self-reported current alcohol use and cardiometabolic risk factors (type 2 diabetes, BMI) on fibrosis stage progression, adjusted for age and sex.

Results: We included 80 patients from four studies from 2013 to 2022. The median age at baseline was 60 (IQR: 11) years, 69 (86%) were male and 35 (44%) reported abstinence for at least one week. The median BMI was 29 (IQR: 8) and 18 (23%) had type 2 diabetes at baseline. At baseline, fibrosis stages 0, 1, 2, and 3 were detected in 4 (5%), 23 (29%), 32 (40%), and 21 (26%) of the patients. Over a median follow-up of 2.2 (IQR: 1.5) years, 36 (45%) experienced fibrosis stage progression, 30 (38%) had stable disease, and 14 (18%) regressed. The number of patients who experienced fibrosis stage progression was higher compared to patients with improvement and stable disease ($p = 0.027$). We calculated the mean change in fibrosis stage based on the difference between fibrosis stage in the paired biopsies and found a fibrosis progression rate of 0.22 stages/year (95% CI: 0.053–0.382, $p = 0.010$). This is equivalent to fibrosis progression of one stage over 4.5 years. After adjusting for sex and age in a multivariate analysis, the fibrosis progression rate was 0.24 stages/year (95% CI: 0.084–0.401, $p = 0.003$) and no significant associations were observed with BMI and type 2 diabetes. In the same analysis, current alcohol use at baseline exhibited an impact correlating with a 0.66-stages increase (95% CI: 0.224–1.105, $p = 0.004$) compared to patients reporting abstinence.

Conclusion: In this study we show the disease dynamic of ALD and found that patients with ALD progress one stage per 4.5 years and is accelerated in patients with current alcohol intake. These data should be used for guiding clinical management of patients with ALD and informing clinical trial design.

SAT-267

The interaction between metabolic syndrome and alcohol consumption after an episode of alcohol-associated hepatitis is associated with increased mortality: results from de spanish registry of alcohol-associated liver disease (REHALC)

Jordi Gratacós-Ginès¹, María Del Barrio², Pilar Ruz-Zafra³, Miriam Celada-Sendino⁴, Ares Villagrasa⁵, Federico Cáceres⁶, Rosa Martín-Mateos⁷, Luis Frisancho⁸, Sonia García-García⁹, Mónica Barreales Valbuena¹⁰, Javier Tejedor-Tejada¹¹, Sergio Vaquez Rodríguez¹², Nuria Cañete¹³, Carlos Fernández-Carrillo¹⁴, María Valenzuela¹⁵, David Martí-Aguado¹⁶, Diana Horta¹⁷, Marta Quiñones¹⁸, Vanesa Bernal¹⁹, Silvia Acosta-López²⁰, Tomás Artaza²¹, José Pinazo Bandera²², Carmen Villar²³, Ana Clemente²⁴, Esther Badia-Aranda²⁵, Javier Crespo², Pau Sancho-Bru²⁶, Meritxell Ventura Cots⁵, Conrado Fernández-Rodríguez¹⁸, Victoria Aguilera Sancho⁹, Santiago Tomé²⁷, Ramon Bataller¹, Joan Caballería¹, Joaquín Cabezas², Elisa Pose¹. ¹Liver Unit, Hospital Clínic de Barcelona-IDIBAPS, Barcelona, Spain; ²Hospital Universitario Marqués de Valdecilla, Santander, Spain; ³Hospital Universitario Virgen del Rocío, Sevilla, Spain; ⁴Hospital Universitario Central de Asturias, Oviedo, Spain; ⁵Hospital Universitari Vall d'Hebrón, Barcelona, Spain;

⁶Hospital de la Santa Creu i Sant Pau, Barcelona, Spain; ⁷Hospital Universitario Ramon y Cajal, Madrid, Spain; ⁸Parc Taulí Hospital Universitari, Sabadell, Spain; ⁹Hospital Universitari i Politècnic La Fe, Valencia, Spain; ¹⁰Hospital Universitario 12 de Octubre, Madrid, Spain; ¹¹Hospital Universitario de Cabueñes, Gijón, Spain; ¹²Xerencia Xestión Integrada de Vigo, Sergas, Vigo, Spain; ¹³Hospital del Mar, Barcelona, Spain; ¹⁴Hospital Universitario Puerto de Hierro, Madrid, Spain; ¹⁵Hospital Universitari Dr. Josep Trueta, Barcelona, Spain; ¹⁶Hospital Clínico Universitario de Valencia-INCLIVA, Valencia, Spain; ¹⁷Hospital Universitari Mútua Terrassa, Terrassa, Spain; ¹⁸Hospital Universitario Fundación Alcorcón, Alcorcón, Spain; ¹⁹Hospital Universitario Miguel Servet, Zaragoza, Spain; ²⁰Hospital Universitario Nuestra Señora de la Candelaria, Santa Cruz de Tenerife, Spain; ²¹Complejo Hospitalario Universitario de Toledo, Toledo, Spain; ²²Hospital Universitario Virgen de la Victoria, Málaga, Spain; ²³Hospital de Salamanca, Salamanca, Spain; ²⁴Hospital General Universitario Gregorio Marañón, Madrid, Spain; ²⁵Hospital Universitario de Burgos, Burgos, Spain; ²⁶Institut d'Investigacions Biomèdiques August Pi i Sunyer (IDIBAPS), Barcelona, Spain; ²⁷Hospital Universitario de Santiago, Santiago de Compostela, Spain
Email: jgrata@recerca.clinic.cat

Background and aims: Metabolic risk factors (MRF) and harmful alcohol consumption often coexist in the same patient. The synergistic effect of both risk factors on the risk of liver disease has been previously described; however, information regarding prevalence and prognostic implications of MRF in patients with alcohol-associated (AH) is scarce.

Method: Retrospective analysis of patients admitted to 28 Spanish hospitals for an episode of AH meeting the NIAAA criteria between 2014 and 2022. We assessed the prevalence of both individual MRF and metabolic syndrome (MS), and their impact on mid-term (90 days) and long-term (1 year) survival. MS was defined based on the National Cholesterol Education Program, Adult Treatment Panel III (NCEP-III) criteria. As an exploratory analysis, we also assessed the prevalence of steatotic liver disease associated with MRF and moderate alcohol consumption (MetALD) in this population as defined by a recent consensus (Rinella ME et al, *J Hepatol* 2023). We used Chi-square and Mann-Whitney tests for the descriptive analyses, the Kaplan-Meier curves and log-rank test for the survival analyses and the Cox regression analysis to identify risk factors of mortality. All statistical analyses were performed with SPSS version 27.0.1.0.

Results: Out of 1,746 patients included, 403 (23%) had arterial hypertension, 324 (19%) had obesity (BMI ≥ 30) and 208 (12%) had diabetes. One hundred eighty-seven (11%) patients met criteria for MS. Patients with MS were older (median age of 53 [48–60] vs 51 [45–57] years, $p < 0.01$), less frequently women (14% vs 29%, $p < 0.01$) and had slightly higher baseline serum creatinine (median of 0.8 [0.6–0.9] vs 0.7 [0.6–0.9] mg/dL, $p < 0.01$). Patients with and without MS had both similar alcohol intake (10 [7–14] vs 10 [7–14] units/day, $p = 0.992$) and duration of alcohol consumption prior to AH (24 [14–35] vs 20 [15–30] years, $p = 0.384$). MS was not associated with mortality in the total cohort; however, it was an independent risk factor of mortality (HR 1.7 [1.1–2.9]) in the subgroup of patients who survived an episode of AH and resumed alcohol intake during follow-up. In this latter subgroup, 1-year survival was lower in patients with MS (65.2% vs 82.8, $p < 0.01$). Only 249 (14%) patients met the MetALD consensus criteria; the most frequent reason for failing to meet the criteria was an alcohol consumption > 50 g/day in women and > 60 g/day in men (80%). Survival in patients with and without MetALD was similar (84.2% vs 83.6% at 90 days, $p = 0.873$; 76.2% vs 73.8% at 1 year, $p = 0.352$).

Conclusion: MRF are common in patients with AH. After surviving an episode of AH, the combination of active alcohol consumption and the presence of metabolic risk factors defines a population at high risk of death.

SAT-268

Bariatric surgery is a major independent factor of disease progression in cirrhotic patients with alcohol-related liver disease

Louis Onghena^{1,2,3}, Lindsey Devisscher⁴, Hans Van Vlierberghe⁵, Sarah Raevens⁵, Xavier Verhelst⁵, Yves Van Nieuwenhove⁶, Sander Lefere⁵, Anja Geerts⁵. ¹Liver Research Center Ghent, Ghent University, Ghent University Hospital, Ghent, Belgium; ²Department for Human Repair and Structure, Department of Gastrointestinal Surgery, Ghent University Hospital, Ghent, Belgium; ³Department of Internal Medicine and Paediatrics, Hepatology Research Unit, Ghent University, Ghent, Belgium; ⁴Gut-Liver Immunopharmacology Unit, Ghent, Belgium; ⁵Hepatology Research Unit, Ghent, Belgium; ⁶Department of Gastrointestinal Surgery, Ghent, Belgium
Email: Louis.onghena@ugent.be

Background and aims: Patients with a history of bariatric surgery (BS) are susceptible to developing alcohol use disorder, potentially resulting in end-stage liver disease. There is paucity of data on the evolution of cirrhotic disease. Our aim was to describe the demographics and mortality in hospitalizations over time in patients diagnosed with alcohol-related liver disease, in relation to BS.

Method: We included patients hospitalized at our hospital between 1/1/2010 and 30/09/2023 with ARLD. Data were retrieved retrospectively from the most recent hospitalization. Statistical analysis was performed using Mann-Whitney U and Chi² tests.

Results: 46/275 (16.7%) of cirrhotic patients admitted with ARLD had a history of bariatric surgery. Patients with a history of BS were predominantly female (76.1%), in contrast to the non-BS population (29.7%) ($p < 0.0001$) and were significantly younger at the time of diagnosis (46 vs 58 years, $p < 0.0001$), as well as the first hospitalization (48 vs 61, $p < 0.0001$). Liver disease evolved at a faster pace in BS group with a shorter time to first hospitalization (5 vs 13 months, $p = 0.036$), and a shorter time between first and second (45 vs 114 months, $p = 0.011$) and second and third (31 vs 86, $p = 0.006$) hospitalizations. The population with primary hospitalization due to ACLF was significantly larger in the BS group (60.9% vs 27.6%, $p < 0.0001$) and throughout the following hospitalizations remained more prominent in the BS group; with significantly more patients hospitalized with pre-ACLF as well (8.7% vs 2.6%, $p = 0.045$). Conversely, stable decompensated cirrhosis occupied a substantial share in the group without BS during the first four ($p = 0.004$, $p < 0.0001$, $p < 0.001$, $p = 0.034$) hospitalizations. Modeled transplant-free survival, through Cox proportional regression analysis with age at diagnosis, was lower in the BS group ($p = 0.004$), with the main cause of death was ACLF in 81.3% vs 25.0% in the control group. Within the ACLF hospitalizations, alcoholic steatohepatitis (25.0% vs 12.9%, $p = 0.0014$) and bacterial infection (57.1% vs 43.5%, $p < 0.0001$) were predominant triggers for the BS group, whereas gastro-intestinal bleeding (3.6% vs 21.0%, $p = 0.037$) occurred significantly more often in the non-BS group. The weekly amount of alcohol consumed during drinking periods (41.0 (22.5, 64.5) vs 55.0 (35.0, 80.0) units/week, $p = 0.002$) and duration of use (8.0 (5.0, 15.0) vs 23.0 (15.0, 30.0) years, $p < 0.001$) were significantly lower in the BS group.

Conclusion: Cirrhotic BS patients hospitalized with ARLD develop acute decompensations at a faster pace, with more overall ACLF hospitalizations, with an equally evolving cumulative mortality, despite being 12 years younger on average. There is a need for prospective research to substantiate stricter pre-BS patient selection guidelines, especially regarding alcohol use.

SAT-269

Portal hypertension in alcohol-related hepatitis: natural history and prognostic value

Karim Gebara¹, Lionel Moulis¹, Benjamin Riviere¹, Stéphanie Faure¹, Georges-Philippe Pageaux¹, José Ursic Bedoya². ¹Montpellier University Hospital, Montpellier, France; ²Montpellier University Hospital, Université de Montpellier, Montpellier, France
Email: jose.ursicbedoya@chu-montpellier.fr

Background and aims: Portal hypertension (PH) is a prominent feature in the setting of alcohol-related hepatitis (AH). It is however unclear whether the severity of PH has a prognostic impact in this context. Moreover, the natural history of PH after an episode of AH is not thoroughly understood. The aim of our study was to evaluate the impact of severe PH on 6-months transplant-free survival (TFS) in patients admitted for histologically proven symptomatic AH and describe natural history of PH in this context.

Method: We retrospectively included all patients with a histologically proven AH diagnosis admitted to our tertiary care center, between January 2013 and December 2021. We excluded transplanted patients and patients with uncontrolled infection/gastro-intestinal bleeding or multi-organ failure at admission. Severe PH was defined by endoscopic PH and ascites or portal pressure gradient >22 mmHg. We defined persistence of PH at 6 months: by the persistence of ascites and/or an episode of GI bleeding linked to PH and/or the need for a TIPS placement and/or the persistence of at least grade II oesophageal varices. Primary outcomes were 6-month TFS and the impact of severe PH on 6-month TFS. We also aimed to describe the evolution of PH and investigate if there were factors associated with severe PH at admission and its persistence at 6 months.

Results: 127 patients were included; median follow-up was 20 months. Mean age was 52 (± 9.45) and 83% were male patients. Mean discriminant function (DF) was 59.54 (± 23.40) and mean MELD score was 25.17 (± 6.59). PH was severe in 71.6%. During the follow-up 25% died and 25% underwent liver transplantation, median TFS was 16.8 months (95% CI [7.75; 24.31]). Severe PH was not significantly associated with 6-month TFS ($p = 0.96$). On multivariate analysis, independent factors associated with 6-month TFS were MELD score (OR 1.22 95% CI [1.07; 1.38]) and non-response to corticosteroids (OR 6.39 95% CI [1.63; 25.10]). On multivariate analysis, independent factors associated with severe PH at admission were male gender (OR 3.84 95% CI [1.28; 11.55]), Child-Pugh score (OR 1.35 95% CI [1.00; 1.82]) and CLIF-C ACLF score (OR 1.08 95% CI [1.02; 1.13]). At 6 months 39 patients (30.7%) had persistent PH, among whom 25 (59.5%) were considered abstinent. In the multivariate model among patients with initial PH only the baseline CLIF-C ACLF score (which includes leukocytes count) was identified as a risk factor for the persistence of PH at 6 months (OR = 1.07 95% CI [1.00; 1.15], $p = 0.05$).

Conclusion: Severe PH was not significantly associated with 6-month TFS. Our results underscore a central role of systemic inflammation in the development and persistence of PH over time after an episode of AH, irrespective of alcohol withdrawal. These results are consistent with recent reports highlighting the role of extracellular vesicles persistent over time.

SAT-272

Updated definition of healthy alanine aminotransferase levels in a metabolically and histologically normal population

Jonggi Choi¹, Ji Won Yang¹, Hyeyeon Hong¹, Sung Won Chung¹, Chaeyeon Lim¹, Jina Park¹. ¹Asan Medical Center, Seoul, Korea, Rep. of South

Email: jkchoi0803@gmail.com

Background and aims: This study re-evaluates the upper limit of normal (ULN) for alanine aminotransferase (ALT), traditionally set at 40 U/L, using histological and metabolic parameters in Asian living liver donors.

Method: We conducted a retrospective analysis of 5,455 potential living liver donors from 2005 to 2019. Patients were screened for hepatitis B, C, HIV, and alcohol use. Histologically and metabolically healthy participants was assessed using the modified Prati criteria (body mass index <23 kg/m², triglyceride ≤ 200 mg/dL, fasting glucose ≤ 105 mg/dL, total cholesterol ≤ 220 mg/dL). The new healthy ULN of ALT was determined at the 95th percentile among participants without hepatic steatosis or metabolic dysfunction.

Results: The median age of the cohort was 30 years, with a predominance of males (66.2%). While 3,162 (58.0%) did not have hepatic steatosis, 1,553 (49.1%) met the modified Prati criteria, being metabolically healthy. The new healthy ULN of these participants was 34 U/L for males and 22 U/L for females, significantly lower than the conventional 40 U/L. A 'borderline' ALT category (34–40 U/L for males, 22–40 U/L for females) was also introduced to participants at risk of hepatic steatosis or metabolic dysfunction.

Conclusion: Our study suggests that the traditional ALT ULN is higher than healthy levels for a metabolically and histologically verified Asian population. The proposed ULN values are 34 U/L for males and 22 U/L for females. The introduction of a 'borderline' category aids in better disease risk stratification, highlighting the need for updated ULN of ALT.

SAT-273-YI

Is it worth staining for hepatic glucocorticoid receptors in alcohol related hepatitis?

Mina Ignat^{1,2,3}, Ioana Rusu^{1,2}, Adelina Horhat², Bumbu Andreea Livia^{1,2,3}, Andreea Fodor^{1,2,3}, Petra Fischer^{1,2,3}, Oana Nicoara-Farcu^{1,2,3}, Bogdan Procopet^{1,2,3}, Horia Ștefănescu^{1,2,3}. ¹Regional Institute of Gastroenterology and Hepatology "Prof. Dr.

O. Fodor," Cluj-Napoca, Romania, ²Cluj-Napoca, Romania; ³University of Medicine and Pharmacy "Iuliu Hatieganu," Cluj Napoca, Romania, ³rd Medical Clinic, Cluj-Napoca, Romania; ³Liver Research Club, Cluj-Napoca, Romania

Email: ignat.mina@gmail.com

Background and aims: The precise mechanism of action of corticotherapy for treating severe alcohol related hepatitis (AH) is still unknown. The function of glucocorticosteroids (CS) are mediated by intracellular glucocorticoid receptors (GR). The most known GR isoform is GR alpha, which is the most widely expressed, being responsible for the classic functions of glucocorticoids. Other isoform, such as GR beta, acts as a dominant negative inhibitor of GR alpha. Our aim is to evaluate the role of hepatic GR as a prognostic tool in AH.

Method: All consecutive patients with a history of alcoholism, suggestive liver chemistry data, biopsy proven AH, were included between November 2015–December 2020. Immunohistochemistry (IHC) staining was performed using a fully automated slide preparation system (Leica automatic Bond-Max system). IHC staining was performed with Anti-Glucocorticoid Receptor alpha antibody (Abcam3580) and Beta antibody (ab233165). The staining was scored according to intensity (0-no staining, 1-weak, 2-moderate and 3-strong), in hepatocyte nuclei, cytoplasm and biliary epithelium.

Results: We included 110 patients with severe alcohol related hepatitis, 75.5 were male and the median age was 52. 90.9% were decompensated, 36.5% patients had an infection at admission and 25.5% developed a nosocomial infection. Median Child-Pugh at diagnostic was 11 (6; 14), Meld 23 (6; 51), Maddrey 72.2 (32; 203). Median follow-up was 23 months (0–78) with 1 month survival of 80%. Out of all patients, 85 (83.8%) were treated with corticotherapy and 82.9% responded to the corticotherapy treatment, evaluated with Lille score at day 7. 28.9% had none-low alpha GR, 71.7% had moderate-strong alpha GR. Otherwise, 65.6% had none-low beta GR and 34.4% had moderate-strong GR. In the biliary epithelium, alpha GR 34.1% had no receptors, 45.9% had weak receptors and 20% had moderate receptors. In the group of patients treated with corticotherapy, the patients with low intensity of alpha biliary GR receptors had a worst survival at 1 month ($p = 0.01$). Patients with lower expression of the biliary GR receptors had higher bilirubin level ($p = 0.04$), Maddrey score (0.03) and Meld score ($p = 0.04$). Alpha biliary GR were not associated with infections. Overall expression of alpha GR receptors (hepatocyte nuclei, cytoplasm and biliary epithelium) was associated with higher risk of mortality on short term ($p = 0.06$) and medium term, $p = 0.01$.

Conclusion: Alpha glucocorticoid receptors subclasses show distinct prognoses. Biliary epithelium GR expression could be a marker for short term survival, possibly by mediating the effects of glucocorticoids. The glucocorticoid receptors in the liver may not be the only ones implicated in GS response, others sites such as intestinal epithelium could have an important role.

SAT-274

Serum proteomic analyses reveal elevated HGF and IL-8 in patients with alcohol-related hepatitis compared to decompensated alcohol-related cirrhosis and can differentiate patients with AH at risk of infection from those at risk of acute kidney injury

Luke D. Tyson^{1,2,3}, Stephen R. Atkinson^{1,2,4}, Vishal C. Patel^{5,6,7}, Michael Allison⁸, Andrew Austin⁹, James W. Dear¹⁰, Ewan H. Forrest^{11,12}, Robert W. Hunter¹⁰, Tong Liu¹, Steven Masson¹³, Mark J. W. McPhail¹⁴, Joao Nunes¹⁵, Paul Richardson¹⁶, Stephen D. Ryder^{17,18}, Mark Wright¹⁹, Elaine Holmes¹, Mark R. Thursz^{1,2}, Nikhil Vergis^{1,2,20}. ¹Imperial College London, Department of Metabolism, Digestion and Reproduction, London, United Kingdom; ²Imperial College Healthcare NHS Trust, The Liver Unit, St Mary's Hospital, London, United Kingdom; ³London North West University Healthcare NHS Trust, Department of Hepatology, London, United Kingdom; ⁴GSK, Stevenage, United Kingdom; ⁵The Roger Williams Institute of Hepatology, Foundation for Liver Research, London, United Kingdom; ⁶Institute of Liver Studies, King's College Hospital NHS Foundation Trust, London, United Kingdom; ⁷King's College London, School of Immunology and Microbiology, London, United Kingdom; ⁸Cambridge University Hospitals NHS Foundation Trust, Cambridge NIHR Biomedical Research Centre, Cambridge, United Kingdom; ⁹University Hospitals of Derby and Burton NHS FT, Derby, United Kingdom; ¹⁰University of Edinburgh, Centre for Cardiovascular Science, Edinburgh, United Kingdom; ¹¹Glasgow Royal Infirmary, Department of Hepatology, Glasgow, United Kingdom; ¹²University of Glasgow, Glasgow, United Kingdom; ¹³Newcastle Freeman Hospital, Department of Hepatology, Newcastle, United Kingdom; ¹⁴Institute of Liver Studies, King's College Hospital, London, United Kingdom; ¹⁵Meso Scale Discovery, Rockville, United States; ¹⁶The Royal Liverpool University Hospital, Department of Hepatology, Liverpool; ¹⁷Nottingham University Hospitals NHS Trust, NIHR Nottingham Biomedical Research Centre, Nottingham, United Kingdom; ¹⁸University of Nottingham, Nottingham, United Kingdom; ¹⁹University Hospital Southampton NHS Foundation Trust, Department of Hepatology, Southampton, United Kingdom; ²⁰GSK, Brentford, United Kingdom
Email: luke.tyson@nhs.net

Background and aims: Alcohol-related hepatitis (AH) is the most severe alcohol-related liver disease (ALD). Infection and acute kidney injury (AKI) are associated with mortality. Multiple serum cytokines and growth factors have been associated with AH in comparison to compensated ALD or healthy controls. Our aim was to compare AH to controls with decompensated ALD cirrhosis to identify analytes associated with severe AH and to characterize endophenotypes of severe AH at risk of incident infection and AKI.

Method: Using MSD U-PLEX assays, the serum concentrations of IL-1alpha, IL-1beta, IL-6, IL-8, IL-10, IL-18, IL-22, IL-1 receptor antagonist, TGF-beta1, TGF-beta2, TGF-beta3, TNF-alpha, IFN-gamma, epidermal growth factor, hepatocyte growth factor (HGF), insulin-like growth factor, platelet-derived growth factor subunit A, vascular endothelial growth factor, cluster of differentiation 163, lipopolysaccharide binding protein, programmed cell death protein 1, programmed death-ligand 1, TWEAK, cystatin C, neutrophil gelatinase-associated lipocalin, and beta-2 microglobulin (B2M) were quantified in baseline (day-0) serum from patients recruited to several RCTs and cohort studies with similar inclusion criteria. AH was defined by Steroids or Pentoxifylline for Alcoholic Hepatitis (STOPAH) criteria; controls had decompensated ALD cirrhosis without AH. Incident infection was defined as infection at day-7 without infection at day-0; incident AKI as AKI at day-7 without AKI

at D0, AKI defined by an adapted International Club of Ascites definition. Significance was tested by Mann-Whitney U, adjusted for multiple comparisons by Bonferroni correction.

Results: HGF and IL-8 were notably elevated in AH vs decompensated ALD cirrhosis (n = 856 vs n = 187; 7.90 ng/ml vs 2.61 ng/ml, p < 2.60E-16; 0.39 vs 0.07, p < 2.60E-16, respectively), other analytes less so. Within the AH cohort, IL-6, IL-22, and B2M were elevated at day-0 in those who died at day-90, compared to those alive at day-90 (n = 170 vs n = 556; 0.027 ng/ml vs 0.018 ng/ml, p = 1.95E-8; 0.004 vs 0.002, p = 2.05E-4; 169 vs 96, p = 1.05E-3, respectively). Day-0 IL-6 was elevated in those who developed incident infection compared to those who did not (n = 76 vs n = 656; 0.029 ng/ml vs 0.019 ng/ml, p = 3.09E-3). Day-0 HGF and IL-8 were elevated in those who developed incident AKI compared to those without AKI at day-0 or day-7 (n = 75 vs n = 300; 12.66 ng/ml vs 7.49 ng/ml, p = 1.70E-3; 0.73 vs 0.39, p = 7.25E-3).

Conclusion: In severe AH, HGF and IL-8 are markedly elevated compared to decompensated ALD cirrhosis without AH. Different AH endotypes may suffer different complications, implying differing pathophysiology with implications for putative treatments. Further work exploring the role of IL-6 in patients with AH who develop infection, and IL-8 and HGF in those who develop AKI, may help in the early identification and treatment of these deadly complications.

SAT-275

Role of neutrophil lymphocyte ratio in transition of alcoholic cirrhosis with acute decompensation to unstable decompensated cirrhosis

Feixiang Xiong¹, Tingting Jiang², Lihua Yu³, Yandan Jiang², Qin Zhang², Zhiyun Yang², Xian-bo Wang², Yuyong Jiang². ¹Beijing Ditan Hospital, Capital Medical University, Dongzhimen Hospital, Beijing University of Chinese Medicine, Beijing, China; ²Beijing Ditan Hospital, Capital Medical University, Beijing, China; ³Beijing Ditan Hospital, Capital Medical University, Beijing, China
Email: xiangakb@163.com

Background and aims: According to PREDICT research conducted by EASL, the 90-day mortality rate of unstable decompensated cirrhosis (UDC) can be up to 21%, with the recurrence of infection being the main cause for the worsening of patients with acute decompensation (AD). As a key indicator of inflammation and immunity, neutrophil lymphocyte ratio (NLR) is regarded as an important predictor of liver diseases and inflammatory diseases, such as acute-on-chronic liver failure (ACLF) and sepsis. The aim of this study is to investigate the predictive value of NLR in the progress from AD of alcoholic cirrhosis (AC) to UDC within 90 days.

Method: We enrolled 679 patients of AC with AD in Beijing Ditan Hospital of Capital Medical University and collected all previous data of the patients within 48 hours of admission. With the previous data and the clinical and laboratory data collected within 90 days, we predicted the possibility of UDC. The end point was hospitalization due to liver-related complications (bacterial infection, variceal bleeding, hepatic encephalopathy, or grade 2 or worsening ascites). Multivariable COX regression analysis was conducted to predict the risk factors for UDC and to test NLR's value of prediction in liver-related complications. Kaplan-Meier survival curve, restricted cubic spline, and subgroup analysis were performed to analyze the predictive value of NLR.

Results: 185 (27.2%) cases of AD progressed to UDC in 90 days. In multivariable analysis, NLR was an independent predictor of UDC (HR 1.51; 95% CI 1.06–2.15; p = 0.024). COX regression showed that NLR was an independent risk factor for UDC in 3 patients groups separately with ascites (HR: 1.58, 95%CI:1.07–2.32, p = 0.021), infection (HR:1.6 4, 95%CI:1.03–2.6, p = 0.036) and variceal bleeding (HR:2. 12, 95%CI:1.21–3.71, p = 0.009). Maximally selected rank statistics were utilized to find 2.45 as the optimal cut-off to divide patients into high-risk group and low-risk group and statistical differences existed in the two groups when it came to predict the

POSTER PRESENTATIONS

progress from AD to UDC and the mortality within 90 days ($p < 0.001$ and $p = 0.012$ respectively). Restricted cubic splines showed that the risk of UDC was associated with increasing NLR in both groups regardless of high or low CLIF-C AD scores. NLR remained the key predictor for UDC across all Age, TB, Creatinine, INR subgroups and was correlated with Sodium ≤ 135 mmol/L, Leukocyte ≤ 10 subgroups. **Conclusion:** NLR was a novel indicator predicting the transition of AC with AD to UDC, which can help identify patients with UDC early and prevent deterioration of clinical end points.

SAT-278

FIB-4 score as a predictor of mortality outcomes in individuals with metabolic dysfunction-associated steatotic liver disease with moderate alcohol consumption: a nationwide cohort study

Majd Aboona¹, Pojsakorn Danpanichkul², Vincent Chen³, Pooja Rangan¹, Donghee Kim⁴, Naim Alkhouri⁵, Mazen Nouredin⁶, Juan Pablo Arab^{7,8}, Karn Wijarnpreecha^{1,9,10}. ¹University of Arizona College of Medicine-Phoenix, Phoenix, United States; ²Chiang Mai University, Thailand, Thailand; ³University of Michigan Health System, Ann Arbor, United States; ⁴Stanford University School of Medicine, Stanford, United States; ⁵Arizona Liver Health, Chandler, United States; ⁶Houston Research Institute and Houston Methodist Hospital, Houston, United States; ⁷Pontificia Universidad Catolica de Chile, Santiago, Chile; ⁸Western University and London Health Sciences Centre, London, Canada; ⁹Banner University Medical Center, Phoenix, United States; ¹⁰BIO5 Institute, University of Arizona College of Medicine-Phoenix, Phoenix, United States
Email: aboona@arizona.edu

Background and aims: Steatotic liver disease, more specifically Metabolic dysfunction-associated steatotic liver disease (MASLD) has become a leading cause of chronic liver disease worldwide. MASLD is defined as patients with steatosis meeting 1 of 5 cardiometabolic criteria. The global prevalence of MASLD is thought to be 30% and its prevalence is increasing yearly by 0.7%. A new subcategory termed MetALD has also been described and defined as individuals with MASLD with increased alcohol intake. In males, increased alcohol consumption is defined as 3–6 drinks (210–420 g) per week. In females, increased alcohol consumption is defined 2–5 drinks (140–350 g) per week. We conducted a population-based study with the aim to compare the longitudinal outcomes of individuals with MetALD stratified by FIB-4 scores.

Method: This study was performed within the National Health and Nutrition Examination Survey (NHANES) data from 2017 to 2018. Vibration controlled transient elastography (VCTE, FibroScan) was used to evaluate the presence of steatosis. Steatosis was defined as a Controlled Attenuation Parameter ≥ 288 dB/m. We excluded patients with other causes of liver disease, underweight, baseline decompensated cirrhosis, baseline cancer diagnosis, prior bariatric surgery, or missing data on race, body mass index (BMI), aspartate and alanine aminotransferase, and platelet. Patients who met 1/5 cardiometabolic criteria including BMI >25 (BMI >23 in Asians), hypertension, DM, dyslipidemia, hypertriglyceridemia were included in the study. We used Cox proportional hazard model to assess mortality risk among patients stratified by FIB-4 scores.

Results: The cohort consisted of 2,557 individuals with MetALD. The median age of the cohort was 45 (33–56). Race was classified as 36.72% Non-Hispanic White, 33.32% Hispanic, 22.29% Black, 3.71% Asian. In Multivariable cox analysis adjusted for age, sex, race, smoking status, hypertension, dyslipidemia, insulin resistance, when compared to patients with FIB-4 ≤ 2.67 , patients with FIB-4 >2.67 were at increased risk of all-cause mortality (Hazard Ratio (HR) 2.95; 95% Confidence Interval (CI), 1.46–6.00; p value, <0.01), cardiovascular mortality (HR 2.68; 95% CI, 1.18–6.07; p value, 0.02), and cancer related mortality (HR 5.08; 95% CI, 1.08–23.96; p value, 0.04).

Conclusion: In this cohort of patients with MetALD, individuals with high FIB-4 scores were at higher risk for all-cause mortality, cardiovascular mortality, and cancer-related mortality. It is known

that hepatic fibrosis is considered a prognostic factor in advanced liver disease. This suggests that FIB-4 scores can also be used in metALD, as they have been used in MASLD as a non-invasive score which can help determine advanced fibrosis or higher risk of death.

SAT-279

Transplantation for alcoholic liver disease: impact of on-site substance use disorder treatment on outcome

Shehzad Niazi¹, Aaron Spaulding², Emily Brennan², Terry Schneekloth³, Sheila Jowsey-Gregoire², Adriana Vasquez², Burcin Taner². ¹Mayo Clinic, Jacksonville, United States; ²Mayo Clinic, Jacksonville, United States; ³Mayo Clinic, Rochester, United States
Email: niazi.shehzad@mayo.edu

Background and aims: About 63% of the US transplant centers lack Substance Use Disorder (SUD) treatment programs¹. We compared the outcomes of those who received liver transplant (LT) due to alcoholic liver disease at centers that offered SUD services with those that did not.

Method: Using CMS identification codes, we merged the United Network for Organ Sharing and the American Hospital Association (AHA) 2011–2018 Annual Survey data. Study included subjects aged 18–60 with alcoholic cirrhosis who received LT between 2011 and 2018. The primary end points were graft failure and patient survival. We identified centers offering SUD services from the AHA dataset. Patient-related variables from UNOS, included age and functional status, body mass index (BMI), race/ethnicity, sex, diabetes status, encephalopathy, MELD score, and the center's transplant volume. Patients receiving a transplant from a center offering SUD services vs. those who did not were matched (1:1). Patient age was matched within ten years, the MELD closest to transplant was matched within 5 points, and all other were matched exactly. We used Chi-square and Kruskal-Wallis tests to evaluate differences among unmatched and matched LT recipients. Cox proportional hazard models were used to compare the time till graft failure and death.

Results: Of 5,383 LT recipients, 2,850 (53%) received a LT from a center with SUD services. Recipients from non-SUD service centers had a higher MELD (28.37 vs. 27.07, $p < 0.0001$), likely to be Hispanic (17.8% vs 11.6%, $p < 0.0001$), higher representation in the highest volume centers (37.5% vs 31.9%, $p < 0.0001$), and among the highest BMI category (37.6% vs. 34.5%, $p = 0.009$). LT recipients from centers providing SUD services were more likely to be White (80.8% vs. 75.0%, $p < 0.0001$) and receive care at the lowest volume centers (34.0% vs. 32.6%, $p < 0.0001$). There were no differences in the proportion of deaths or graft failures in unmatched outcomes. After matching, we evaluated 1,624 recipients who received LT at centers providing SUD services vs those that did not. The hazard of graft failure was 0.97 (95% CI: 0.71–1.32) for SUD service facilities, and the hazard of death was 0.96 (95% CI: 0.78–1.18).

Conclusion: We found no differences in LT outcomes between centers offering SUD services and those that did not. While only about 37% of the US transplant centers provide SUD services, a substantial 87% offer mental health services, which may have adequately addressed the SUD evaluation and treatment. However, the increasing number of patients receiving LT due to acute alcoholic hepatitis² may change future trends.

References

1. Niazi SK, et al. Mental health and chemical dependency services at US transplant centers. *AJT*. Apr 2020;20(4):1152–1161.
2. Bittermann T, et al. Trends in Liver Transplantation for Acute Alcohol-Associated Hepatitis During the COVID-19 Pandemic in the US. *JAMA Netw Open*. Jul 1 2021;4(7):e2118713.

SAT-280

Emergence of co-morbidities in alcohol-related hepatitis over time: insights from the WALDO cohort

Douglas Corrigan¹, Keval Naik², Guruprasad Aithal³, Mayur Brahmanian⁴, Ewan H. Forrest⁵, Hannes Hagström⁶, Anne McCune⁷, Steven Masson⁸, Neil Rajoriya⁹, Juan Pablo Arab¹⁰, Richard Parker¹¹, Michael Allison¹². ¹North Middlesex Hospital, London, United Kingdom; ²Mid and South Essex NHS Foundation Trust, Chelmsford, United Kingdom; ³Nottingham Digestive Diseases Centre, School of Medicine, University of Nottingham, UK, Nottingham, United Kingdom; ⁴University of Toronto, Toronto, Canada; ⁵Glasgow Royal Infirmary, Castle Street, Glasgow, United Kingdom; ⁶Karolinska Institutet, Stockholm, Sweden; ⁷University of Bristol, Bristol, United Kingdom; ⁸Liver Unit, Freeman Hospital, The Newcastle Upon Tyne Hospital Trust, Newcastle, United Kingdom; ⁹Liver Unit, University Hospital Birmingham NHS Foundation Trust, Birmingham, Birmingham, United Kingdom; ¹⁰Pontificia Universidad Católica de Chile, Santiago de Chile, Chile; ¹¹Leeds Teaching Hospitals NHS Trust, St. James's University Hospital, Leeds, United Kingdom; ¹²Cambridge Liver Unit, Cambridge, United Kingdom
Email: michael.allison6@nhs.net

Background and aims: Alcohol-related Liver disease (ALD) is a major cause of liver disease. Alcohol-related Hepatitis (AH) is the most florid manifestation of ALD conferring significant morbidity and mortality¹. We aim to examine the natural history of AH.

Method: WALDO is an international multi-centre cohort of 723 patients with biopsy-proven ArLD and associated outcome data. Baseline clinical data and events occurring after index biopsy were collected retrospectively. Patients with a diagnosis² of AH were examined (n=185). The primary outcome was overall survival (OS) and the effects on this of liver-associated clinical events and major adverse medical events both at the time of biopsy and subsequently were examined. Median follow-up was 900 days. Survival analysis was performed using Kaplan-Meier/Log rank analysis. Time-dependent variables and their effect on mortality were assessed using Cox-proportional hazards.

Results: 69% (128/185) had severe AH at baseline (SAH) defined by a discriminant function of >32. 67% (124/185) died in the follow-up period. The presence of SAH significantly decreased survival (HR 1.891, 95% CI 1.332–2.687, p<0.05). Ongoing alcohol use was recorded in 59% (110/185). In those who survived past 5 years, abstinence significantly associated with survival (HR 2.339, 95% CI 1.220–4.485, p<0.05). Subsequent liver-related adverse clinical events occurred in 29% (53/185). 3 developed a new HCC. 21 developed ascites, 25 varices, 18 had a variceal bleed, 27 developed hepatic encephalopathy (HE) and 6 Hepatorenal Syndrome (HRS). Additional mortality risk was conferred by development of HE (HR 2.78 95% CI 1.58–4.88, p<0.001) and new episodes of AH (HR 2.80 95% CI 1.37–5.72, p=0.005). Baseline medical comorbidities were present in 21% (38/185) of patients and their presence did not significantly affect OS. Subsequent major medical comorbidities developed in 16% (30/185). 14 developed a new cancer. 15 developed cardiovascular disease, and 7 developed diabetes. Time dependent analysis reveals that development of diabetes conferred a significantly higher risk of death (HR 3.29 95% CI 1.21–8.92, p=0.020).

Conclusion: Cardiovascular disease and diabetes were the most common medical co-morbidities that developed in this cohort. This may have consequences for long term management and decisions about transplant in these patients.

References

1. Bataller R, Arab JP, Shah VH. Alcohol-Associated Hepatitis. *N Engl J Med*. 2022;387(26):2436–2448. doi:10.1056/NEJMra2207599
2. Crabb DW, Bataller R, Chalasani NP, et al. Standard Definitions and Common Data Elements for Clinical Trials in Patients With Alcoholic Hepatitis: Recommendation From the NIAAA Alcoholic Hepatitis Consortia. *Gastroenterology*. 2016;150(4):785–790. doi:10.1053/j.gastro.2016.02.042

SAT-281

Clinical characteristics, surveillance, treatment allocation and outcomes of alcohol-related hepatocellular carcinoma: meta-analysis of 37 studies and 66, 559 patients

Daniel Tung¹, Rebecca Wenling Zeng², Christen En Ya Ong², Elden Ong², Charlotte Chung Hui Ong², Benedix Sim¹, Jia Hong Koh¹, Wen Hui Lim², Jieliang Xiao², Nicholas Syn³, Alfred Kow⁴, Cheng Han Ng³, Darren Jun Hao Tan², Sung Won Lee⁵, Hirokazu Takahashi⁶, Takumi Kawaguchi⁷, Nobuharu Tamaki⁸, Atsushi Nakajima⁹, Yock-Young Dan¹⁰, Karn Wijarnpreecha¹¹, Mazen Nouredin¹², George Ioannou¹³, Mark Muthiah¹, Margaret Teng¹, Rohit Loomba¹⁴, Daniel Huang¹. ¹Division of Gastroenterology and Hepatology, Department of Medicine, National University Hospital, Singapore, Singapore, Singapore, Singapore; ²Yong Loo Lin School of Medicine, National University of Singapore, Singapore, Singapore, Singapore; ³National University Hospital, Singapore, Singapore, Singapore; ⁴Division of Hepatobiliary and Pancreatic Surgery, Department of Surgery, National University Hospital, Singapore, Singapore, Singapore; ⁵Seoul St. Mary's Hospital, College of Medicine, The Catholic University of Korea, Seoul, Korea, Rep. of South; ⁶Liver Center, Saga University Hospital, Saga, Japan, Saga, Japan; ⁷School of Medicine, Department of Digestive Disease Information and Research, Kurume University, Fukuoka, Japan, Fukuoka, Japan; ⁸Musashino Red Cross Hospital, Tokyo, Japan; ⁹Department of Gastroenterology and Hepatology, Yokohama City University Graduate School of Medicine, Yokohama, Japan, Yokohama, Japan; ¹⁰Division of Gastroenterology and Hepatology, Department of Medicine, National University Hospital, Singapore, Singapore, Singapore; ¹¹Division of Gastroenterology and Hepatology, University of Arizona College of Medicine Phoenix, Phoenix, United States; ¹²Houston Liver Institute, Houston Research Institute, Houston, TX, United States, Houston, United States; ¹³Division of Gastroenterology and Hepatology, University of Washington, Seattle, Washington, USA, Seattle, United States; ¹⁴NAFLD Research Center, Division of Gastroenterology, University of California at San Diego, La Jolla, CA, United States, La Jolla, United States
Email: daniel.tung@mohh.com.sg

Background and aims: The disease burden of alcohol-related hepatocellular carcinoma (HCC) is increasing globally with rising per-capita alcohol consumption. Data regarding clinical characteristics and outcomes of alcohol-related HCC versus other etiologies are limited by geographical location or by etiology of liver disease. We aimed to assess the clinical characteristics, treatment allocation, and survival outcomes of alcohol-related HCC via a systematic review and meta-analytic approach.

Method: Medline and Embase were searched from inception to January 2023 for articles in English that compared clinical features, and outcomes of alcohol-related HCC versus HCC from other causes. Primary outcomes included (1) the proportion of HCC related to alcohol, (2) a comparison of clinical characteristics, and (3) survival outcomes between alcohol-related HCC and HCC from other causes. Proportional data was analysed using a generalized linear mixed model. A pairwise meta-analysis was conducted to obtain the odds ratio (OR) or mean difference comparing alcohol-related HCC and non-alcohol-related HCC. Survival outcomes were evaluated using hazard ratio pooled analysis. p values <0.05 were considered statistically significant. All analyses were conducted in RStudio 2021.09.0.

Results: 37 articles comprising 67, 045 patients with HCC were included in the overall analysis (25, 779 with alcohol-related HCC and 41, 266 patients with HCC of other etiologies). Overall, 27.48% (CI: 18.93% to 38.09%) of HCC were alcohol-related, with the highest proportion in Europe and the lowest in the Americas. Patients with alcohol-related HCC were more likely to be male, and there was no significant difference in age or comorbidities between alcohol-related HCC and HCC from other causes. Patients with alcohol-related HCC were more likely to have cirrhosis (OR: 1.87, CI: 1.46 to 2.38; p<0.001) and BCLC stage C/D cancers (OR: 1.30, CI: 1.05 to 1.61;

POSTER PRESENTATIONS

$p = 0.021$) compared to HCC from other causes. A lower proportion of alcohol-related HCC patients underwent surveillance (17.04%, CI: 7.58% to 33.95% versus 20.08%, CI: 6.99% to 45.65%) and were less likely to receive curative therapy (OR 0.72, CI: 0.53 to 0.97; $p = 0.037$) compared to HCC from other causes. In terms of overall survival, alcohol-related HCC was associated with increased mortality (HR: 1.27, CI: 1.13 to 1.42, $p < 0.001$) compared to non-alcohol-related HCC.

Conclusion: We found that alcohol-related HCC was associated with a lower likelihood of receiving surveillance, more advanced BCLC stage, and higher mortality compared to HCC from other etiologies of liver disease. Further research and collective efforts are required to address these disparities in care.

SAT-284

Diagnostic performance of non-invasive tests in patients with metabolic dysfunction-associated steatotic liver disease (MASLD) with increased alcohol intake (MetALD) in a primary care setting

Eileen Yoon¹, Jihyun An², Ha Il Kim², Joo Hyun Sohn², Huiyul Park³, Sang Bong Ahn⁴, Joo Hyun Oh⁵, Hyunwoo Oh⁶, Hyo Young Lee⁷, Dae Won Jun¹. ¹Department of Internal Medicine, Hanyang University College of Medicine, Seoul, Korea, Rep. of South; ²Department of Internal Medicine, Hanyang University College of Medicine, Guri, Korea, Rep. of South; ³Department of Family Medicine, Myoungji Hospital, Hanyang University College of Medicine, Goyang, Korea, Rep. of South;

⁴Department of Internal Medicine, Nowon Eulji Medical Center, Eulji University, College of Medicine, Seoul; ⁵Department of Internal Medicine, Nowon Eulji Medical Center, Eulji University, College of Medicine, Seoul, Korea, Rep. of South; ⁶Department of Internal Medicine, Kangbuk Samsung Hospital, Sungkyunkwan University School of Medicine, Seoul, Korea, Rep. of South; ⁷Department of Internal Medicine, Sanggye Paik Hospital, Inje University College of Medicine, Seoul, Korea, Rep. of South

Email: noshin@hanyang.ac.kr

Background and aims: Non-invasive tests (NITs) for liver fibrosis have been recognized for its clinical utility in metabolic dysfunction-associated steatotic liver disease (MASLD); however, its diagnostic efficacy is notably diminished in alcohol-related liver disease. It is essential to ascertain the reliability of NITs in MASLD with increased alcohol intake (MetALD) patients.

Methods: In this cross-sectional study, we reviewed data from 7,918 health checkup participants who underwent both magnetic resonance elastography (MRE) and ultrasound with hepatic steatosis diagnosed by ultrasound. Participants were categorized into MASLD and MetALD, and the performance of fibrosis-4 (FIB-4) and NAFLD fibrosis score (NFS) were assessed. Advanced hepatic fibrosis (F3) was defined as MRE ≥ 3.6 kPa.

Results: In this health check-up cohort, the prevalence of MetALD was 5.8%, and 1.5% of these cases exhibited advanced hepatic fibrosis. Both MetALD and MASLD displayed similar metabolic profile and hepatic fibrosis burdens but the alcohol consumption levels were significantly higher in MetALD group (0.85 vs 0.80 in FIB-4). The diagnostic performance of FIB-4 and NFS for significant fibrosis revealed no noticeable differences in the area under the receiver operating characteristic values between the two groups. Moreover, the sensitivity (71.4%), specificity (77.3%), and both positive (4.6%) and negative (99.4%) predictive values of NITs for MetALD closely mirrored those observed in MASLD.

Conclusion: The newly defined MetALD showed high performance of FIB-4 with reasonable sensitivity and negative predictive value for the first screening tier for advanced hepatic fibrosis in MetALD.

SAT-285-YI

Incorporation of cholestasis into prognostic models improves predictive outcome in alcohol-related liver disease: a retrospective multicenter study

Mohsan Subhani^{1,2}, Minjun Chen³, Hannes Hagström^{4,5}, Michael Allison⁶, Mayur Brahmanian⁷, Ewan H. Forrest⁸, Anne McCune⁹, Steven Masson¹⁰, Neil Rajoriya¹¹, Juan Pablo Arab¹², Guruprasad Aithal¹, Richard Parker¹³. ¹Nottingham Digestive Diseases Biomedical Research Centre (NDDC), School of Medicine, University of Nottingham, Nottingham, United Kingdom; ²NIHR Nottingham Biomedical Research Centre, Nottingham University Hospitals NHS Trust and the University of Nottingham, Nottingham, United Kingdom; ³Division of Bioinformatics and Biostatistics, National Center for Toxicological Research, U.S. Food and Drug Administration, Jefferson, Arkansas, United States; ⁴Division of Hepatology, Department of Upper GI, Karolinska University Hospital, Stockholm, Sweden; ⁵Department of Medicine, Huddinge, Karolinska Institute, Stockholm, Sweden; ⁶Cambridge University Hospitals NHS Foundation Trust, Cambridge, United Kingdom; ⁷Calgary Liver Unit, University of Calgary Cumming School of Medicine, Calgary, Canada; ⁸Department of Gastroenterology, Glasgow Royal Infirmary, Glasgow, United Kingdom; ⁹University Hospitals Bristol and Weston NHS Foundation Trust, Bristol, United Kingdom; ¹⁰Liver Unit, Freeman Hospital, The Newcastle Upon Tyne Hospital Trust, Newcastle, United Kingdom; ¹¹Liver Unit, University Hospital Birmingham NHS Foundation Trust, Birmingham, United Kingdom; ¹²Western University, Toronto, Canada; ¹³Leeds Teaching Hospitals NHS Trust, Leeds, United Kingdom
Email: mohsan.subhani@nottingham.ac.uk

Background and aims: Cholestasis has been associated with various liver disorders, but its role in predicting outcomes in alcohol-related liver disease (ARLD) remains unclear. This study aims to investigate the role of cholestasis on liver biopsy and serum alkaline phosphatase (ALP) in predicting survival in patients with ARLD.

Method: This cohort study with historical data included adult patients (≥ 18 years), with biopsy proven ARLD from nine international centres in UK, Sweden, and Canada. Data from the UK centres were used as a training cohort and from non-UK centres as validation cohort. The primary outcome was transplant-free survival (TFS) measured as survival without transplantation from the time of liver biopsy to the end of the study. Concordance of the area under the receiver operating characteristic curve (AUC) was used to quantify the prognostic performance of scoring models and Model for End-stage Liver Disease (MELD) scores. ROC curves were used to compare the predictive ability of cholestasis alone, ALP alone, MELD scores plus cholestasis, and MELD score plus ALP. A reclassification approach was used to compare the added values of selected variables in the MELD score. We used the incidence of the event ($p = 0.45$) values as the cutoff, i.e., 0, $p/2 = 0.23$, $p = 0.45$, and 1 for risk categories used in the reclassification model.

Results: A total of 485 patients were included (training $n = 345$, validation $n = 140$), the mean age was 53 years (IQR 44–61), and 60% ($n = 289$) were male. The median alcohol use at the peak was 63 grams/day (IQR 20, 129), the drinking duration was 10 years (IQR 5, 21), and 27% ($n = 132$) had cholestasis on liver histology. On multi-variable Cox analysis, the histological findings of cholestasis, cirrhosis, Mallory-Denk bodies, and steatohepatitis were significantly associated with reduced TFS. Among the laboratory investigations, increased ALP, Bilirubin, Urea, and decreased Albumin were significantly associated with reduced TFS. MELD plus ALP presents a higher AUC value (0.78) than the MELD score alone (0.74), while MELD plus cholestasis (0.74) also showed a comparable AUC value. Of 232 subjects who experienced TFS events, classification improved in 53 subjects using the model with cholestasis, but for 7 subjects it became worse, with an overall net gain in reclassification proportion of 0.198. On the other hand, the net gain in reclassification proportion for subjects who did not experience a TFS event ($n = 178$) was 0.112; 25 individuals were reclassified down and 5 were reclassified up. The

NRI for MELD plus cholestasis was estimated at 0.086 and was statistically significant (p value = 0.04). Similarly, the NRI for MELD plus ALP was estimated at 0.13 ($p < 0.001$).

Conclusion: The study shows that adding ALP and cholestasis to standard scoring systems (MELD) for ARLD could improve the predictive outcomes in patients with biopsy proven ARLD.

SAT-286-YI

Long-term risk of alcohol-related liver disease after community-based treatment for alcohol use disorder: a nationwide register based cohort study from Denmark

Line Molzen^{1,2}, Matilde Winther-Jensen², Lone Madsen³, Merete Osler², Peter Jepsen⁴, Gro Askgaard^{1,2}. ¹Section of Gastroenterology and Hepatology, Medical Department, Zealand University Hospital, Køge, Denmark; ²Center for Clinical Research and Prevention, Bispebjerg and Frederiksberg Hospital, Copenhagen, Denmark; ³Section of Gastroenterology and Hepatology, Medical Department, Zealand University Hospital, Køge, Denmark; ⁴Department of Hepatology and Gastroenterology, Aarhus University Hospital, Aarhus, Denmark

Email: limol@regionsjaelland.dk

Background and aims: Screening for ALD (Alcohol-related Liver Disease) is suggested in individuals with a high alcohol consumption such as individuals in community-based treatment for Alcohol Use Disorder (AUD). Our primary aim was to examine the risk of developing ALD in individuals attending community-based treatment for AUD according to sex-, age-, and diabetes. Our secondary aim was to estimate their absolute risk of mortality due to alcohol-related causes.

Method: We used nationwide health registries to identify individuals 18 years or older with no prior ALD diagnosis who attended community-based treatment for AUD in Denmark from 2006 to 2019. Individuals were followed for an ICD-10 diagnosis of ALD (K70) until 2021. We estimated the cumulative risk of ALD in a competing risk setting according to age group (18–34, 35–44, 45–54, 55–64 and >64 years), sex (men/women) and diabetes at treatment start. In a secondary analysis, we estimated the 10-year risk of death due to any cause, ALD; other alcohol-specific cause and due to external causes, based on the underlying cause of death. Finally, we estimated the 10-year risk of death due to cancer and cardio- and cerebrovascular disease.

Results: There were 58,408 individuals attending community-based treatment for AUD, their median age was 47 years and men constituted 69.5%. The average number of years with excessive drinking (>15 units/week) was 25.8 at treatment start. During 423,056 person-years of follow-up, 3,933 was diagnosed ALD and 11,590 died. Overall, the 10-year risk of ALD was 5.7% (95%CI 5.5–5.9) and according to age the highest risk was found for 45–54 years (7.3%), the lowest for 18–34 years (2.0%) and no difference was found according to sex. The 10-year cumulative risk was higher in individuals with diabetes. For example at age 45–64 years, it was 11.8% (95%CI 9.0–14.6) for individuals with diabetes vs 6.9% (95%CI 6.5–7.3) for individuals without diabetes. The 10-year risk of death from any cause was 14.3% (95%CI 14.0–14.6), and it was 1.6% (95%CI 1.5–1.7) for ALD, 2.5% (95%CI 2.3–2.6) for other alcohol-specific causes, and 0.6% (95%CI 0.5–0.7) for external causes. The 10-year risk of death from cancer was 2.7 (95%CI 2.6–2.9) and for cardio- and cerebrovascular death it was 1.8 (95%CI 1.7–1.9).

Conclusion: About 6% of individuals attending community-based AUD treatment was diagnosed with ALD within 10 years, although the risk was nearly doubled in those with diabetes. Only a small fraction of deaths during follow-up could be attributed ALD. These findings imply that the potential number of lives saved by screening for ALD in this population is likely limited.

SAT-287

Association between serum homocysteine levels and advanced hepatic fibrosis in alcohol-related liver disease: a cross-sectional study

Hui Yang^{1,2}, Cheng Ma², Xiaoqian Zhang^{1,2}, Wenxin Zhang², Jianzhou Duan², Lubing Gu², Wenhong Zhang³. ¹Department of Infectious Diseases, the First Hospital of Shanxi Medical University, Taiyuan, China; ²First Clinical Medical College, Shanxi Medical University, Taiyuan, China; ³Department of Infectious Diseases, National Medical Centre for Infectious Diseases, Huashan Hospital, Shanghai Medical College, Fudan University, Shanghai, China
Email: sydyhyh@163.com

Background and aims: In Western and industrialized countries, Alcohol-related liver disease (ALD) has replaced viral hepatitis as the main cause of advanced hepatic fibrosis and cirrhosis. The liver is the primary site of methionine metabolism and transsulfuration pathways, and alcohol-induced hepatic parenchymal cell injury will cause impaired homocysteine (HCY) metabolism. This study aimed to investigate the relationship between serum HCY and advanced hepatic fibrosis in ALD patients.

Method: We included 10,033 participants from the 1999–2006 National Health and Nutrition Examination Survey (NHANES). 496 individuals with excessive alcohol consumption, elevated liver enzymes, and no other chronic liver disease were identified as ALD. Fibrosis-4 index (FIB-4), aspartate aminotransferase to platelet ratio index (APRI), and Forns index were used as non-invasive indicators for assessing the extent of liver fibrosis. Weighted multivariate logistic regression was used to analyze the correlation between serum HCY and advanced hepatic fibrosis in ALD participants.

Results: Compared to non-ALD, ALD participants had higher serum HCY levels. In weighted multivariable-adjusted logistic regression models, we observed a positive correlation between serum HCY levels and the risk of advanced hepatic fibrosis in ALD (OR = 1.07, 95% CI, 1.01–1.12), and the highest tertile of HCY was significantly associated with an increased risk of advanced hepatic fibrosis (OR = 3.36, 95% CI, 1.34–8.43). In subgroup analyses, this association remained significant in men (OR = 1.07, 95%CI, 1.01–1.13), vigorously physically active (OR = 1.46, 95%CI, 1.06–2.01), and obese participants (OR = 1.36, 95%CI, 1.10–1.67). In ALD participants, the area under the working characteristic curve (AUROC) of HCY for advanced hepatic fibrosis was 0.686 (95% CI, 0.639–0.733).

Conclusion: Serum HCY levels were independently associated with an increased risk of advanced hepatic fibrosis in ALD. This study supports the predictive value of HCY for advanced hepatic fibrosis and suggests that HCY may become a therapeutic entry point for ALD.

SAT-290-YI

Natural history of varices in patients with severe alcohol-associated hepatitis

Sharath S¹, Sowmya Iyengar², Manasa Alla², Shantan Venishetty³, Rajesh Gupta⁴, Mithun Sharma², Padaki Nagaraj Rao⁵, Nageshwar Reddy², Anand Kulkarni¹. ¹Asian Institute of Gastroenterology, Hyderabad, India; ²AIG Hospitals, Hyderabad, India; ³AIG Hospitals, Hyderabad, India; ⁴Asian Institute of Gastroenterology, Hyderabad, India; ⁵Asian Institute of Gastroenterology, Hyderabad, India
Email: sharath.sitaram@gmail.com

Background and aims: Severe alcoholic hepatitis (SAH) pose a significant threat, often accompanied by complications such as the development of oesophageal varices. Variceal bleeding in patients with severe alcohol-associated hepatitis (SAH) is associated with poor outcomes. Beta blockers are most commonly recommended medications to decrease portal pressures and prevent bleeding from varices. However, there are no studies evaluating the role of beta blockers on the course of variceal/portal hypertensive gastropathy (PHG) progression in patients with SAH, which we aimed to assess.

POSTER PRESENTATIONS

Method: We conducted a prospective analysis of data collected over five years from patients with SAH, focusing on endoscopy reports. The objectives were to assess the variceal and PHG stage at baseline, and the course of variceal/PHG progression, and the impact of non-selective beta blockers (NSBB) and alcohol relapse on variceal progression and PHG.

Results: A total of 133 patients with SAH were identified and 103 with baseline endoscopy reports were included in the study. Of the 103 patients, 29.1% did not have any varices at baseline, 57.2% had small low-risk varices and 13.6% had large high-risk varices. 11 patients underwent prophylactic variceal ligation. Of the 30 patients with no varices at baseline, 13 underwent follow-up endoscopy, 4 developed small low-risk varices, 1 developed fundal varix and 8 had no varices. Of the 59 patients with small low-risk varices, only 13 underwent follow-up endoscopy with 1 having no varices, 7 still having small low-risk varices and 5 developing large high-risk varices, including 1 with fundal varices. A total of 38.4% (10/26) had progression of varices. 6 of the 14 patients with high-risk varices underwent endoscopy and all had large high-risk varices. Of the 24 patients who received NSBB, 12.5% (3/24) had progression of varices compared to 6.42% (7/109) in those who did not receive BB ($p=0.3$). Of the patients who were evaluated endoscopically, only 25% (3/12) had stage migration in the BB group compared to 35% (7/20) in the non-BB group ($p=0.56$). One patient in the non-BB group developed variceal bleeding and required EVL, while none in the BB group developed variceal bleeding. 15% (3/20) in the abstainer group compared to 50% (6/12) in the relapse group had progression of varices ($p=0.03$). Of the total cohort, sixty-nine patients had no evidence of PHG, while 30 patients had mild PHG, and two had both severe PHG and gastric antral vascular ectasia (GAVE). 5% (1/20) in the non-beta-blocker and 25% (3/12) in the beta-blocker group had progression of PHG by one grade ($p=0.1$).

Conclusion: 70% of patients with SAH had varices and an additional 38.4% developed varices during the five-year study period. Alcohol relapse was identified as a significant factor increasing the risk of variceal progression in this population.

SAT-291

Screening for alcohol related liver disease in acute hospital admissions

Jessica Lovatt¹, Kerry Badger¹, Claire Cussons¹, Richard Parker¹. ¹Leeds Teaching Hospitals NHS Trust, Leeds, United Kingdom
Email: jessicalovatt@nhs.net

Background and aims: Heavy alcohol consumption has a major impact on both morbidity and mortality but also on healthcare systems: in the UK alcohol is linked to 5.7% of all hospital admissions. Of those, 74220 admissions were linked to alcohol related liver disease (NHS data). Despite heavy drinkers often having multiple contacts with healthcare, these patients frequently remain undiagnosed and present at a later stage of the disease. To address this NHS England recently offered an incentive to hospitals to screen hazardous drinkers for liver disease. This is a service evaluation of this initiative in a single centre.

Method: A prospective project as part of NHS England 'CQUIN' service development initiative between July 2022 and July 2023; acute admissions to hospital who had evidence of alcohol misuse-defined as AUDIT-C >12 and/or requiring treatment for alcohol withdrawal were offered testing for liver fibrosis. The enhanced liver fibrosis (ELF) test was used, taken at the same time as other routine blood sampling. A cut off of 9.5 was used to differentiate between low risk and high risk requiring further investigation in the form of a transient elastography.

Results: At baseline (pre-screening period) only 7% (10 of 138) of hazardous drinkers were offered a test for liver fibrosis, during the assessment period this rose to 47% of hazardous drinkers being offered testing. During the service evaluation, a total of 1015 patients were identified as suitable for testing, of whom 669 (66%) had an ELF

test done. Of these tests, 164 (24%) were considered low risk (<9.5) and 505 (76%) were high risk (>9.5) requiring further investigation. Of the high-risk tests, 82 patients (16%) had a previous diagnosis of liver disease and a further 34 (7%) patients presented with decompensated disease at the time of ELF testing. This left 389 high risk patients (65% of all tests, 84% of high-risk tests) with no previous history of liver disease. After ELF testing, 59 patients died before further tests could be done (58 cases from non-liver causes, 98%), 145 underwent transient elastography, and 84 patients were discharged from follow-up after review. To date, 49 new cases of compensated advanced chronic liver disease (cACLD) have been confirmed and are in clinical follow-up (5% of total population tested, 7% of patients who had a test). At the time of analysis 114 patients are pending further investigation.

Conclusion: ELF testing can be used to screen acute hospital admissions with high-risk alcohol use for underlying cACLD. The results of the ELF test can allow for non-invasive transient elastography to be used more efficiently in high-risk populations. By identifying cACLD earlier, patients can receive specialist hepatology input, ongoing alcohol cessation support and commence surveillance for hepatocellular carcinoma.

Reference

NHS data/stats: Statistics on Alcohol, England 2021-NHS Digital.

SAT-292

Coinfection with viral hepatitis increases the short-term but not the long-term risks of hepatocellular carcinoma and hepatic events in adults with alcohol-related cirrhosis

Vicki Wing-Ki Hui¹, Terry Cheuk-Fung Yip¹, Zeyuan Yang², Ramsey C. Cheung^{2,3}, Robert Wong^{2,3}, Vincent Wai-Sun Wong⁴, Grace Lai-Hung Wong⁵. ¹Department of Medicine and Therapeutics, Medical Data Analytics Centre (MDAC), and Institute of Digestive Disease, The Chinese University of Hong Kong, Hong Kong, Hong Kong; ²Gastroenterology and Hepatology Section, Veterans Affairs Palo Alto Healthcare System, Palo Alto, CA, Palo Alto, United States; ³Division of Gastroenterology and Hepatology, Stanford University School of Medicine, Palo Alto, CA, Palo Alto, United States; ⁴Department of Medicine and Therapeutics, Medical Data Analytics Centre (MDAC), and Institute of Digestive Disease, The Chinese University of Hong Kong, Hong Kong, Hong Kong, Hong Kong; ⁵Department of Medicine and Therapeutics, Medical Data Analytics Centre (MDAC), and Institute of Digestive Disease, The Chinese University of Hong Kong, Hong Kong, Hong Kong
Email: 1155063467@link.cuhk.edu.hk

Background and aims: Rapid urbanization and economic growth in Hong Kong have led to increased alcohol consumption, resulting in a rise in alcohol-related cirrhosis (AC). Chronic hepatitis B virus (HBV) and hepatitis C virus (HCV) infections are prevalent, with rates of 6.2% for HBV and 0.3% for HCV in the general population. This research focuses on examining the interaction between AC and chronic viral hepatitis in Hong Kong.

Method: Patients with AC from 2000 to 2023 were identified from a territory-wide database in Hong Kong. Exclusions were made for those with other chronic liver diseases namely autoimmune hepatitis, hemochromatosis, only non-alcoholic fatty liver disease (NAFLD)-specific codes, and primary biliary cholangitis. AC was identified using a combination of ICD-9/10 codes, based on previously validated algorithms. Chronic HBV and HCV infections were identified through diagnosis codes and laboratory tests. Liver complications, including hepatocellular carcinoma (HCC) and hepatic events, were identified using diagnosis codes. Baseline events were defined as those occurred with 30 days from baseline, incident events were defined as those happened beyond 30 days.

Results: We identified 10,670 AC patients, with 3,155 (30%) having concurrent chronic HBV (2,612 [83%]) and/or HCV (685 [22%]) infection. The cohort predominantly consisted of males (91%, 9,752

patients), with an average age of 60.8 ± 12.5 years and a body mass index of 22.9 [20.6 , 25.6]. Over 44% were unhealthy drinkers, consuming more than 50 ml/day of alcohol. Patients with HBV/HCV displayed worse liver conditions, showing higher median AST (73 vs. 65) U/L, ALT (40 vs. 33) U/L, total bilirubin levels (30.5 vs. 27.6) $\mu\text{mol/L}$. The follow-up duration for the 5, 526 patients (4, 068 without hepatitis, 1, 458 with hepatitis) with at least 30 days of follow-up was 31.9 [11.1, 75.0] months. Baseline HCC were identified in 84 (3.0%) patients without hepatitis and 47 (3.7%) patients with hepatitis. Baseline hepatic events were observed in 920 (32.7%) patients without hepatitis and 412 (32.5%) patients with hepatitis. A significant number of patients with (517, 40.8%) and without (998, 35.4%) hepatitis died within 30 days. Beyond 30 days, HCC cases were 14 (0.3%) without hepatitis and 9 (0.6%) with hepatitis. Hepatic events were recorded in 903 (22.2%) without hepatitis and 319 (21.9%) with hepatitis, with deaths in 2, 636 (64.8%) without hepatitis and 823 (56.4%) with hepatitis.

Conclusion: Coinfection with HBV or HCV worsens liver conditions in AC patients at the time of diagnosis, whereas the clinical courses of AC patients with or without chronic viral hepatitis are similar afterwards. Our findings emphasize the importance of prompt recognition and interventions for the unhealthy alcohol use as well as chronic viral hepatitis to slow disease progression and reduce the burden of liver-related morbidity and mortality.

SAT-293-YI

Dietary habits and ultra-processed food consumption in steatotic liver diseases: differences among etiologies and impact on liver histology

Salomé Declerck¹, Guillaume Henin^{1,2}, Stéphanie André-Dumont², Alexis Goffaux¹, Pamela Baldin³, Paulina Henry⁴, Audrey Loumaye⁵, Peter Stärkel^{1,2}, Nicolas Lanthier^{1,2}. ¹Laboratory of Hepatogastroenterology, Institut de Recherche Expérimentale et Clinique, UCLouvain, Brussels, Belgium; ²Service d'Hépatogastroentérologie, Cliniques universitaires Saint-Luc, UCLouvain, Brussels, Belgium; ³Service d'Anatomie pathologique, Cliniques universitaires Saint-Luc, UCLouvain, Brussels, Belgium; ⁴Institut de Pathologie et de Génétique, Gosselies, Belgium; ⁵Service d'Endocrinologie, diabétologie et nutrition, Cliniques universitaires Saint-Luc, UCLouvain, Brussels, Belgium
Email: nicolas.lanthier@saintluc.uclouvain.be

Background and aims: The consumption of ultra-processed foods (UPF) has increased in recent years and has been associated with a higher risk of metabolic dysfunction-associated steatotic liver disease (MASLD), obesity, and diabetes. However, the relationship between UPF consumption and liver histology is unknown, as well as its evaluation in alcohol-related liver disease (ALD) patients. Our aim is to assess the nutritional intake and UPF consumption in individuals with histologically evaluated steatotic liver disease (SLD).

Method: Patients with histologically confirmed SLD (MASLD or ALD) are prospectively recruited. Anthropometric and biological data are collected. Dietary intake is assessed through a 24-hour recall, and UPF consumption in grams is quantified using the NOVA classification. Fermented alcoholic beverages fall under the category of processed foods, while both fermented and distilled alcoholic beverages are classified as UPF. Histological evaluation of hepatic phenotype severity is conducted using the Beaujon score (SAF).

Results: We analyze 62 patients with SLD, including 46 with MASLD and 16 with ALD. The average age and body mass index (BMI) for MASLD and ALD patients are 54 and 52 years (ns), and 35 and 22 kg/m² ($p=0.0001$), respectively. Three patients are classified as F0 (4.9%), 12 as F1 (19.7%), 28 as F2 (45.9%), 17 as F3 (27.9%), and 1 as F4 (1.6%). One patient could not be evaluated due to the small size of the biopsy. In terms of nutritional intake, compared to patients with ALD, MASLD patients consume more lipids (73 vs. 53 g/day; $p=0.050$), saturated fatty acids (29 vs. 22 g/day; $p=0.0201$) and fibers (17 vs. 8 g/day; $p=0.0003$) but fewer calories (1806 vs. 2716 kcal/day; $p=$

0.0003). Nevertheless, there are no significant differences in the average consumption of proteins or carbohydrates between patients with MASLD and those with ALD. Patients with ALD consume more processed foods than MASLD patients (2628 vs. 196 g/day; $p=0.0001$). The average consumption of UPF among individuals with moderate or severe steatosis, low or high activity, or absence or presence of fibrosis in MASLD or ALD patients does not demonstrate any difference (ns).

Conclusion: ALD patients exhibit higher caloric consumption compared to MASLD patients, despite their lower BMI. The disparity in energy intake between the two groups is primarily attributed to the caloric contribution from alcohol consumption, which is also associated with a greater consumption of processed foods. In MASLD and ALD patients, UPF consumption evaluated through a 24-hour recall does not impact the severity of the hepatic phenotype.

SAT-294

The prognostic value of the hepatic venous pressure gradient in severe alcohol-related hepatitis

Andreea Livia Bumbu¹, Adelina Horhat², Mina Ignat³, Bogdan Procopet⁴, Horia Ștefănescu⁵. ¹Iuliu Hatieganu University of Medicine and Pharmacy, Cluj Napoca, Romania; ²Iuliu Hatieganu University of Medicine and Pharmacy Cluj-Napoca, Cluj Napoca, Romania; ³Octavian Fodor Institute of Gastroenterology and Hepatology, Iuliu Hatieganu University of Medicine and Pharmacy, Cluj Napoca, Romania; ⁴Octavian Fodor Regional Institute of Gastroenterology and Hepatology, Iuliu Hatieganu University of Medicine and Pharmacy, Cluj Napoca, Romania; ⁵Octavian Fodor Regional Institute of Gastroenterology and Hepatology, Cluj Napoca, Romania
Email: andreea_bumbu@yahoo.com

Background and aims: Severe alcohol-related hepatitis (SAH) has a high mortality rate. In this study we aimed to evaluate the prognostic role of the hepatic venous pressure gradient (HVPG) in alcohol-related hepatitis and to determine which of the cut-off values proposed by previous studies (22 mmHg in the study conducted by Rincon et al in 2007 or 20 mmHg in the one by Dominguez et al in 2009) best correlates with mortality.

Method: We enrolled 246 consecutive patients with a clinical suspicion of SAH (MaddreyDF >32). 233 patients underwent HVPG measurement before the transjugular liver biopsy (TJLB) procedure. Mortality at 1, 3 and 9 months was recorded.

Results: The age of the patients ranged from 23 to 78 (median 51.5), 178 (72.4%) were male and 68 (27.6%) female. Regarding the complications, 85% of patients had ascites, 37.8% had hepatic encephalopathy, out of which 36.6% was covert, 18.7% had variceal bleeding, 33.3% of patients were infected at admission time and 11% developed hepatorenal syndrome. A total of 172 patients (69.9%) were administered 40 mg/day of Prednisone, out of which 66.9% were responders according to the day 7 Lille score. The mean and median survival were 31.8 months (S.E. 2.26; 27.4–36.3; 95%CI) and 22 months (11.3–32.6; 95%CI), respectively. Mortality at 1 month was 23.9%, at 3 months was 29.6% and at 9 months 43.4%. The median HVPG in our cohort was 19 mmHg (range 7–40). HVPG correlated with the overall mortality ($p < 0.01$, HR 1.083; 1.029–1.141; 95%CI) in the binary logistics regression. Both the 22 mmHg and the 20 mmHg threshold correlated with the disease severity scores (MELD, Child-Pugh, MaddreyDF), while only the 20 mmHg cut-off correlated with the hepatic rigidity in kPa, and only the 22 mmHg cut-off correlated with the platelets number ($p < 0.01$) in the Man Whitney U test. The Cox regression model showed that the higher the HVPG, the higher the probability of death (HR 1.050; 1.015–1.086 95%CI; $p < 0.01$). Both values associated very strongly with the overall mortality: Chi-square test for HVPG <20 mmHg ($p < 0.05$) with a Phi coefficient of 0.487, and Chi-square test for HVPG <22 mmHg ($p < 0.05$) with a Phi coefficient of 0.549.

Conclusion: HVPG is a good predictor of short and medium term mortality in SAH, but needs to be validated in bigger cohorts of

POSTER PRESENTATIONS

patients. It is not far-fetched to assume that it could be included in the MELD score. Both the 20 mmHg and the 22 mmHg values correlate with mortality.

SAT-295

Sarcopenia, frailty and growth hormone-insulin like growth factor axis among decompensated and alcohol-associated hepatitis patients

Aishani Wadhawan^{1,2}, Nipun Verma¹, Parminder Kaur¹, Pratibha Garg¹, Samonee Ralmilay¹, Rohit Nadda¹, Naveen Kalra¹, Sahaj Rathi¹, Arka De¹, Madhumita Premkumar¹, Sunil Taneja¹, Ajay Kumar Duseja¹, Virendra Singh¹. ¹Post Graduate Institute of Medical Education and Research, Chandigarh, India; ²Postgraduate Institute of Medical Education and Research, Chandigarh, India
Email: nipun29j@gmail.com

Background and aims: Sarcopenia, frailty and growth hormone insulin like growth factor axis impairment in alcohol-associated hepatitis (AH) and decompensated cirrhosis (ALD-DC) remain elusive. This study investigates sarcopenia, frailty and GH IGF 1 axis between ALD-DC and AH patients.

Method: We enrolled patients with ALD-DC and ALD-AH at single cross-section at a tertiary care institute between 2023–24. Sarcopenia and frailty assessments were done through DEXA or CT-SMI and liver frailty index, respectively and GH IGF 1 levels through immunoassays.

Results: A total of 100 patients were recruited (99% males, median age of 44 years) exhibiting ascites (grade-I: 24%, grade-II: 32%, grade-III: 40%), HE (grade-I: 5%, grade-II: 6%) and CTP of 9 (8–11) [CTPA-7%, CTP B-51%, CTP C-42%]. Median MELD score, MELDNa score, GH and IGF 1 levels were 17.4 (IQR: 13.9–23.3), 19.9 (IQR: 15.5–25.6), 4.23 ng/ml (IQR: 2.1–7.2) and 39.8 ng/ml (IQR: 31.6–52.4). Sarcopenia and frailty were noted in 59.6% and 25.6% patients. Patients with AH had worse CTP, MELD and MELD-Na scores than ALD-DC patients. Although GH levels were similar, patients with AH had lower IGF 1 levels 36.2 (20.1–43.1) than DC patients 43.9 (38.8–54.1). AH patients exhibited more frailty and malnutrition ($p=0.001$) than ALD-DC (41.3% vs 9%, $p=0.001$). Sarcopenia through either DEXA or CT-SMI and osteodystrophy was not statistically different between AH and DC patients ($p>0.05$, each). Patients with sarcopenia had lower IGF1 levels [39.3 (IQR: 34.4–45.8)] compared to patients without sarcopenia [48.8 (IQR: 35.3–59.5)] with a trend significance ($p=0.056$). Within the subset of frail and pre-frail patients, frail individuals exhibited significantly diminished IGF-1 levels [37.5 (IQR: 32–40)] compared to their pre-frail counterparts [42.4 (IQR: 35.8–55)] ($p=0.006$). We observed a stepwise decline in IGF 1 levels with worsening CTP classes [CTP A [54.6 ng/ml (IQR: 48.8–60.3)] to CTP B [41 ng/ml (IQR: 36.7–50.2)] and CTP C [36.5 ng/ml (IQR: 29–53.7)] ($p=0.012$). Linear regression analysis revealed, log IGF1 was negatively associated with MELD (beta = -11, $p<0.001$), MELDNa (beta = -12.7, $p<0.001$) and CTP score (beta = -3, $p<0.001$).

Conclusion: AH patients are sicker and frailer than DC patients, possibly mediated by lower IGF 1 levels. Reduced IGF 1 levels are associated with sarcopenia, frailty and disease severity in alcohol associated cirrhosis patients with DC or AH. Modulation of GH IGF 1 axis is a potentially disease modifying target in cirrhosis.

SAT-296

Prevalence and characteristics of MASLD with greater alcohol consumption (MetALD) in the general population

Eileen Yoon¹, Jihyun An¹, Ha Il Kim², Joo Hyun Sohn¹, Bo-Kyeong Kang³, Eun Chul Jang⁴, Huiyul Park⁵, Hye-Lin Kim⁶, Sang Bong Ahn⁷, Joo Hyun Oh⁸, Hyunwoo Oh⁹, Hyo Young Lee¹⁰, Dae Won Jun¹. ¹Department of Internal Medicine, Hanyang University College of Medicine, Seoul, Korea, Rep. of South; ²Department of Internal Medicine, Hanyang University College of Medicine, Guri, Korea, Rep. of South; ³Department of Radiology, Hanyang University College of Medicine, Seoul, Korea, Rep. of South; ⁴Department of Occupational and

Environmental Medicine, Soonchunhyang University College of Medicine, Chun An, Korea, Rep. of South; ⁵Department of Family Medicine, Myoungji Hospital, Hanyang University College of Medicine, Goyang si, Korea, Rep. of South; ⁶College of Pharmacy, Sahmyook University, Seoul, Korea, Rep. of South; ⁷Department of Internal Medicine, Nowon Eulji Medical Center, Eulji University, College of Medicine, Seoul; ⁸Department of Internal Medicine, Nowon Eulji Medical Center, Eulji University, College of Medicine, Seoul, Korea, Rep. of South; ⁹Department of Internal Medicine, Kangbuk Samsung Hospital, Sungkyunkwan University School of Medicine, Seoul, Korea, Rep. of South; ¹⁰Department of Internal Medicine, Sanggye Paik Hospital, Inje University College of Medicine, Seoul, Korea, Rep. of South
Email: noshin@hanyang.ac.kr

Background and aims: The term MetALD has been introduced to describe individuals who have metabolic dysfunction-associated steatotic liver disease (MASLD) with greater alcohol consumption, according to the new nomenclature for steatotic liver disease (SLD). This study aims to evaluate the prevalence and clinical characteristics of MetALD in the general population.

Method: This study is a retrospective, cross-sectional analysis that utilizes the population-based data from the Fifth Korea National Health and Nutrition Examination Survey (KNHANES) conducted between 2019 and 2021. A total of 16,521 participants aged over 18 years were included in the analysis. The presence of hepatic steatosis was determined based on a hepatic steatosis index of 36 or higher.

Results: The prevalence of MetALD was 2.8% (95% CI, 2.5–3.2). Individuals with MetALD were predominantly men (85.4%) and tended to be younger compared to those with MASLD. They exhibited a higher prevalence of hypertension and had significantly higher levels of aspartate aminotransferase, fasting glucose, triglycerides, HDL cholesterol, and creatinine compared to individuals with MASLD. The average daily total energy intake, with and without energy from alcohol, was higher in the MetALD group (2496 and 4250 kcal) compared to the MASLD group (1821 and 1963 kcal). The amount of fat and sodium intake levels were also higher in the MetALD group than in the MASLD group. In addition, the MetALD group had a higher proportion of clerical support workers and technicians, machine operators, and assemblers with higher income compared to the MASLD group.

Conclusion: MetALD exhibited distinct characteristics from MASLD, which was similar to those of ALD. Therefore, MetALD would be on the spectrum of ALD than MASLD.

SAT-297

Recidivism and post-transplant outcomes in patients with alcohol-associated liver disease

Nilofar Najafian¹, Suaka Kagbo-Kue², Rachana Punukollu¹, Margaret C. Liu¹, Laura Budvytyte³, Xingjie Li¹, Alyssa K. McGary¹, David M. H. Chascsa¹, Caroline Jadlowiec¹, Channa Jayasekera⁴, Michele S. Barnhill⁵, Rolland Dickson¹. ¹Mayo Clinic Arizona, Phoenix, United States; ²Intermountain Medical Center, Salt Lake City, United States; ³Mayo Clinic Alix School of Medicine, Scottsdale, United States; ⁴Mayo Clinic Arizona, Phoenix, United States; ⁵Mayo Clinic Arizona, Phoenix, United States
Email: najafian.nilofar@mayo.edu

Background and aims: Alcohol-associated liver disease (ALD) is the most common indication for liver transplant (LT) in the USA. Alcohol recidivism, a complication of ALD, is associated with decreased graft and patient survival. Identifying risk factors prior to LT, post-LT recidivism, and strategies to improve survival are not well defined. We aim to describe post-LT outcomes and identify predictive risk factors for relapse among patients transplanted for ALD.

Method: Patients with LT for ALD at Mayo Clinic Arizona from 2019 to 2022 were reviewed retrospectively. Patients had at least one screening test for alcohol. We examined medical comorbidities, clinical and psychosocial characteristics, relapse, and 1-year patient and graft survival. Subgroup analysis compared patients with and

without relapse and by alcohol transplant pathways: traditional (6 months of sobriety pre-LT), expedited (cirrhotic patients with less than 6 months sobriety), and alcohol-associated hepatitis (AH).

Results: 157 patients were transplanted for ALD, 17 were excluded given lack of alcohol screening. Most were Caucasian (76%) and male (76%), with mean age of 55.9 years. Ninety-one percent were transplanted through the traditional pathway, 6% expedited, and 3% for AH. Twenty-three patients (16%) resumed alcohol use post-LT. Of the relapsed, 43% had sustained alcohol use and 22% had relapse prevention therapy post-transplant. Relapse was detected by alcohol testing alone in 15/23, by self-report alone in 2/23, and by combination of self-report and alcohol testing in 6/23 patients. Relapsed patients were more likely to have psychiatric disease ($p = 0.004$) or depression ($p = 0.04$) than those without relapse. There was no difference in relapse by transplant pathway, medical comorbidities, substance use history, length of pre-transplant sobriety, prior rehabilitation attempts, alcohol related legal issues, or SIPAT (Stanford Integrated Psychosocial Assessment for Transplantation). Overall survival at 1-year was 99.1% in those without relapse vs 100% in those with relapse ($p = 0.17$). Graft survival at 1-year was 96.5% in those without relapse vs 91.3% in those with relapse ($p = 0.16$). No significant difference was noted in fibrosis or steatosis at 1-year post-LT regardless of transplant pathway or alcohol recidivism.

Conclusion: Traditional, expedited and AH pathways resulted in similar outcomes, arguing against a defined period of sobriety. Early identification with routine alcohol testing and intervention is essential for patients transplanted for ALD given inaccuracy of self-reporting, high rate of relapse (16%), and trend toward worsened graft outcomes in those with relapse.

SAT-298

Annual decompensation and death in patients with intermediate severity of alcohol-related liver fibrosis

Sara Hauskov¹, Mads Israelsen², Katrine Lindvig³, Katrine Thorhauge³, Johanne Kragh Hansen³, Camilla Dalby Hansen³, Stine Johansen³, Ida Ziegler Spedtsberg³, Helle Lindholm Schnefeld³, Peter Andersen¹, Ida Falk Villesen³, Katrine Tholstrup Bech¹, Nikolaj Torp³, Aleksander Krag³, Maja Thiele³. ¹Centre for Liver Research, Fibrosis, Fatty Liver and Steatohepatitis Research Center Odense (FLASH), Odense C, Denmark; ²Centre of Liver Research, Fibrosis, Fatty Liver and Steatohepatitis Research Center Odense (FLASH), Odense C, Denmark; ³Centre of Liver Research, Fibrosis, Fatty Liver and Steatohepatitis Research Center Odense (FLASH), Odense C, Denmark
Email: sara.tonder.hauskov@rsyd.dk

Background and aims: Patients with alcohol-related liver disease (ALD) of intermediate severity of liver fibrosis experience a far higher rate of progression to decompensation than other liver disease aetiologies. We therefore aimed to identify variables contributing to five year decompensation or death in ALD patients with intermediate disease severity.

Method: We defined intermediate severity as either moderate fibrosis (F2), transient elastography (TE) 10–15 kPa, or ELF test 9.8–10.5. We selected patients from a prospective, biopsy-controlled cohort of patients with a history of harmful drinking and followed them for 4–9 years. We used Cox regression analyses to investigate baseline predictors of decompensation-free survival: histological features (fibrosis, lobular inflammation, ballooning and steatosis), metabolic risk factors, alcohol intake, Transient Elastography (TE) and Enhanced Liver fibrosis (ELF) test.

Results: We included 157 patients, 78% male, with a median age of 58 ± 13 years, a TE of 9.5 ± 5.7 kPa, and an ELF score of 9.8 ± 1.2. Concordant ELF and TE results were seen in 62% ($n = 96$): 48 with ELF < 9.8 and TE < 10 kPa, and another 48 with both elevated. Over a median of 6.3 years (IQR 4.6–7.9), 22 patients decompensated and 39 died, with 38% of deaths following decompensation. Decompensation and death rates were 2.2% and 4.1% per year. Univariable analyses identified higher fibrosis stage, severe steatosis,

ballooning and lobular inflammation, ELF and TE as predictors of death or decompensation. Alcohol abstinence and insulin resistance measured by HOMA-IR ≥ 2.5 were protective. Multivariable analysis showed severe steatosis (hazard ratio 5.94, 1.68–21.00), significant fibrosis (HR 4.33, 1.33–14.15), insulin resistance (HR 0.33, 0.14–0.79), ELF ≥ 9.8 (HR 2.27, 1.03–4.99), and TE ≥ 10 kPa (HR 5.36, 2.28–12.62) as independent predictors of decompensation-free survival. While 23% (11/48) with concordance between low ELF < 9.8 and TE < 10 kPa met the end point, only 3 were decompensations. Conversely, 32% (35/109) with high ELF and/or high TE met the end point, with 19 decompensations.

Conclusion: In patients with ALD and intermediate fibrosis most fatalities occur without prior decompensation. However, not to neglect liver-related morbidity as it exceeds 2% annually. Patients with high ELF or TE require management in secondary care due to an increased decompensation risk. Notably, insulin resistance may be associated with improved prognosis, while severe steatosis suggests poorer outcomes.

SAT-299

There is a need to improve retention of people with alcohol-related liver disease in clinical trials: a systematic review and meta-analysis of retention rates in interventional trials

Paula Boeira¹, Kris Bennett², Tamar Avades², Ashwin Dhandu², Jaiveer Arora³, Matthew Cramp². ¹University of Plymouth, Plymouth, United Kingdom; ²University Hospitals Plymouth NHS, Plymouth, United Kingdom; ³University of Bath, Bath, United Kingdom
Email: paula.boeira@plymouth.ac.uk

Background and aims: Alcohol-related liver disease (ARLD) is the leading cause of cirrhosis and liver-related mortality in Europe but few interventional clinical trials have been completed in this patient group. Such patients can experience challenges accessing and engaging with their treatment. High levels of retention in clinical trials enable more efficient trial design and ensure that the outcomes can be fully assessed as intended. However, it is not known how well patients with ARLD and recent or ongoing alcohol use engage with clinical trials. This study aimed to quantify retention rates of ARLD patients recruited to interventional clinical trials at 1, 3, 6 and 12 months after recruitment.

Method: According to our published review protocol (<https://osf.io/5kuge/>), we conducted systematic searches of Medline, Embase, Web of Science, and Scopus. We included interventional clinical trials, published 2008 onwards in people with ARLD (including alcohol-related hepatitis [AH]). We excluded studies where patients had been abstinent from alcohol for more than 6 months. Data were extracted on study design, population and retention rates and a risk of bias assessment was made. Two-step meta-analysis was conducted to generate a random effects model.

Results: 3072 studies were identified, of which 55 were eligible for inclusion, 37 in AH and 18 in alcohol-related cirrhosis. Studies were heterogeneous in design, intervention and outcome. Median study duration was 90 days. The primary outcome was mortality in 25 and 3 of the AH and cirrhosis trials, respectively. Overall retention rates at 1, 3 and 6 months were: 89% (95% CI 85–92%), 67% (61–72%) and 56% (47–66%), respectively. Only 6 trials reported retention at 12 months at 59% (38–79%; $I^2 = 97\%$). In cirrhosis trials ($n = 5$), retention (excluding mortality) at 3 months was 92% (67–100%; $I^2 = 94\%$) versus 97% (94–99%; $I^2 = 91\%$) in AH trials ($n = 24$).

Conclusion: Most ARLD trials have been conducted in AH, with an outcome of mortality with relatively good short-term retention. In contrast, few interventional trials have been reported in people with alcohol-related cirrhosis. ARLD cirrhosis trials have lower short-term retention that may undermine interpretation of outcome data. Estimated retention in cirrhosis trials was 92% at 3 months, substantially lower than in comparable interventional trials in other chronic diseases e.g. tirzepatide for diabetes; retention excluding mortality: 96% at 72 weeks. Methods to improve

POSTER PRESENTATIONS

participant engagement in ARLD cirrhosis trials needs to be tested and applied to improve the quality of future studies.

SAT-302

Long-term trends in the prevalence of alcohol-related cirrhosis among national U.S. veterans affairs data and territory wide Hong Kong data-an east-west perspective

Robert Wong¹, Terry Cheuk-Fung Yip², Zeyuan Yang³, Vicki Wing-Ki Hui², Jimmy Che-To Lai², Vincent Wai-Sun Wong², Ramsey C. Cheung¹, Grace Lai-Hung Wong². ¹Veterans Affairs Palo Alto Health Care System, Stanford University School of Medicine, Palo Alto, United States; ²The Chinese University of Hong Kong, Hong Kong, Hong Kong; ³Veterans Affairs Palo Alto Health Care System, Palo Alto, United States

Email: rwong123@stanford.edu

Background and aims: The increasing prevalence of alcohol-related cirrhosis (AC) has been exacerbated by the COVID-19 pandemic and is rapidly becoming a major cause of end-stage liver disease. However, it is not clear if the prevalence and trends in AC are similar in Asia-Pacific regions (where viral hepatitis is endemic) vs. U.S. populations. We aim to evaluate long-term trends in the prevalence of AC across two large population-based cohorts in the U.S. and Hong Kong (HK).

Method: Trends in the prevalence of AC were analyzed using two separate cohorts representing distinct populations in the U.S. and HK from 2010 to 2023: 1) U.S. National Veterans Affairs data and 2) HK territory-wide data of adults. AC was identified using a combination of ICD-9/10 codes based on previously validated algorithms. Annual prevalence of AC (per 100,000 person-years (py)) were stratified by sex and age groups, and compared between groups using the z-statistic. Patients were censored during follow-up if they died, received a liver transplant, or were lost to follow-up (defined as no healthcare encounters within a 12-month period).

Results: Among 3.0 million U.S. Veterans, 45,670 were identified with AC (96.5% men, mean age 59.6 ± 11.8 years). The prevalence of AC was significantly higher in men vs. women throughout the study period, and in 2023, AC prevalence was 787 per 100,000-py in men vs. 315 per 100,000-py in women, $p < 0.01$. When stratified by age, the highest AC prevalence was observed among Veterans age 50–59 years. However, following onset of the COVID-19 pandemic, the prevalence of AC among young Veterans age 18–29 years rose rapidly, and in 2023, the prevalence was similar to that of Veterans age 50–59 years (1382 vs. 1392 per 100,000-py, $p = 0.87$). Among 6.15 million HK adults, 5,591 patients with AC were identified (93.4% men, mean age 60.7 ± 12.6 years). While AC prevalence was significantly lower than the U.S. cohort, similar gender-specific differences were observed. In 2023, AC prevalence was more than 10 times higher in men vs. women (55.7 vs. 4.3 per 100,000-py, $p < 0.01$). In the HK cohort, AC prevalence rose steadily from 2010 to 2023, and similar to the U.S. cohort, the highest prevalence was observed among adults age 50–59 years.

Conclusion: Among U.S. Veterans, the prevalence of AC was highest among adults age 50–59 years. While the prevalence of AC among most age groups plateaued or declined following the pandemic, there was a rapid rise among young Veterans age 18–29 years, highlighting the need for greater awareness about the dangers of high-risk alcohol use in this group. Among HK adults, while the prevalence of AC was overall lower than the U.S. cohort, prevalence of AC has continued to rise among all age groups, particularly after the pandemic. Similar to the U.S. cohort, adults age 50–59 years had the highest prevalence of AC.

SAT-303

Vitamin D deficiency is associated with advanced liver fibrosis and Type 2 diabetes mellitus in alcohol use disorder

Paola Zuluaga^{1,2}, Julia Casado-Carbajo¹, Daniel Fuster¹, Anna Hernandez-Rubio¹, Marvin Bueno-Vélez¹, Carmen Garcia-Martin³, Xael Pena³, Robert Muga¹. ¹Universitat Autònoma de Barcelona, Barcelona, Spain; ²University Hospital Germans Trias i Pujol, Badalona; ³University Hospital Germans Trias i Pujol, Badalona, Spain

Email: ypzuluaga.germanstrias@gencat.cat

Background and aims: Vitamin D deficiency is a risk factor for liver disease including cirrhosis and HCC. Individuals with Alcohol Use Disorder (AUD) are comorbid, with a heavy burden of liver disease and metabolic complications including Type 2 Diabetes Mellitus (T2DM). We aimed to analyze the prevalence and associations of Vitamin D deficiency in AUD patients enrolled in a detoxification program.

Method: Cross-sectional study in patients consecutively admitted for the treatment of AUD between January 2017 and October 2023. Socio-demographic, substance use characteristics and blood parameters were available at admission. Vitamin D status was assessed through the level of 25-Hydroxyvitamin D (25 (OH)D) using a direct competitive chemiluminescent Immunoassay method. Vitamin D deficiency was defined as serum 25 (OH)D concentration < 20 ng/ml. Impaired Fasting Glycaemia (IFG) was defined by fasting blood glucose > 100 mg/dl and advanced liver fibrosis by a FIB-4 index > 3.25 .

Results: 243 patients (75% M) with mean age of 49 ± 10 years, mean BMI of 26.4 ± 7 , 3 kg/m², mean alcohol consumption of 163 ± 81 gr/day and mean duration of AUD of 18.1 ± 11.2 years, were included. Mean of 25 (OH)D, fasting blood glucose, AST, ALT and platelets were 14.4 ± 10.2 ng/ml, 103.4 ± 40.9 mg/dl, 55.1 ± 75.8 U/L, 44.8 ± 76.6 U/L, and $206.3 \pm 84.8 \times 10^9/L$, respectively. Overall prevalence of Vitamin D deficiency was 80.6% (41.1% of them having serum levels of 25 (OH)D < 10 ng/ml). In addition, 32.3% of patients had IFG and 20.5% a FIB-4 index suggestive of advanced liver fibrosis. Vitamin D deficiency was associated with older age ($p < 0.05$), IFG ($p < 0.05$) and FIB-4 > 3.25 ($p < 0.05$). In multivariate analysis adjusted for renal function, IFG (OR, 2.33; 95% CI 1.00–5.49, $p < 0.05$) and FIB-4 > 3.25 (OR, 4.1; 95% CI 1.18–14.5, $p < 0.05$) were the only factors associated with Vitamin D deficiency.

Conclusion: Type 2 Diabetes Mellitus and Vitamin D deficiency may have a synergistic effect in AUD patients at risk of adverse liver-related outcomes.

SAT-304

Screening of compensated alcohol-related liver disease: efficacy of a holistic approach (hepatology visit, brief intervention and non-invasive test) on alcohol abstinence and relapses

Ares Villagrasa¹, Sonia Carramiñana², Marta Selvi³, Francesc Xavier Belvis Costes⁴, Maria Asuncion Ubeda Pastor⁵, Mireia Valle⁶, Carla Morer⁶, Patricia Alvarez⁷, Mariana Gutierrez-Zamora Navarro⁸, Alba Prió⁹, Aina Martí Carretero¹⁰, Anna Aguilar¹⁰, Natalia Tumas¹⁰, Joan Benach¹¹, Izabela Pera², Juan Manuel Pericàs¹², Meritxell Ventura Cots¹³. ¹Liver Unit, Hospital Universitari Vall d'Hebron, Vall d'Hebron Institut de Recerca (VHIR), Universitat Autònoma de Barcelona, Barcelona, Spain; ²Vall d'Hebron Institut de Recerca (VHIR), Barcelona, Spain; ³Servicio Atención Primaria (SAP) Muntanya, Àmbit d'atenció Primària Barcelona Ciutat, Institut Català de la Salut, Departament de Salut | Generalitat de Catalunya, Barcelona, Spain, CAP Sant Andreu, Equipo Atención Primària (EAP) Sant Andreu, Servicio Atención Primaria (SAP) Muntanya, Àmbit d'Atenció Primària Barcelona Ciutat, Barcelona, Spain, Barcelona, Spain; ⁴Research Group on Health Inequalities, Environment, and Employment Conditions (GREDS-EMCONET), Department of Political and Social Sciences, Universitat Pompeu Fabra, Barcelona, Spain, Johns Hopkins University-Universitat

Pompeu Fabra Public Policy Center, Barcelona, Spain, Barcelona, Spain;
⁵Servicio Atención Primaria (SAP) Muntanya, Àmbit d'atenció Primària Barcelona Ciutat, Institut Català de la Salut, Departament de Salut | Generalitat de Catalunya, Barcelona, Spain, CAP Horta, Equipo Atención Primària (EAP) Horta 7D, Servicio Atención Primaria (SAP) Muntanya, Àmbit d'Atenció Primària Barcelona Ciutat, Barcelona, Spain, Barcelona, Spain;
⁶Servicio Atención Primaria (SAP) Muntanya, Àmbit d'atenció Primària Barcelona Ciutat, Institut Català de la Salut, Departament de Salut | Generalitat de Catalunya, Barcelona, Spain, Centro de Salud (CAP) Rio de Janeiro | Servicio Atención Primaria (SAP) Muntanya, Àmbit d'Atenció Primària Barcelona Ciutat, Barcelona, Spain, Barcelona, Spain;
⁷Unitat de VIH/ITS Drassanes-Hospital Universitari Vall d'Hebron, Barcelona, Spain;
⁸Research Group on Health Inequalities, Environment, and Employment Conditions (GREDS-EMCONET), Department of Political and Social Sciences, Universitat Pompeu Fabra, Barcelona, Spain, Barcelona, Spain;
⁹Emergency department, Hospital Universitari Vall d'Hebron, Barcelona, Spain;
¹⁰Liver Unit, Hospital Universitari Vall d'Hebron, Vall d'Hebron Institut de Recerca (VHIR), Universitat Autònoma de Barcelona, Barcelona, Spain, Barcelona, Spain;
¹¹Research Group on Health Inequalities, Environment, and Employment Conditions (GREDS-EMCONET), Department of Political and Social Sciences, Universitat Pompeu Fabra, Barcelona, Spain, Barcelona, Spain;
¹²Liver Unit, Hospital Universitari Vall d'Hebron, Vall d'Hebron Institut de Recerca (VHIR), Universitat Autònoma de Barcelona, Barcelona, Spain, Centro de Investigación Biomédica en Red de Enfermedades Hepáticas y Digestivas (CIBERehd), Instituto de Salud Carlos III, Madrid, Spain, Barcelona, Spain;
¹³Liver Unit, Hospital Universitari Vall d'Hebron, Vall d'Hebron Institut de Recerca (VHIR), Universitat Autònoma de Barcelona, Barcelona, Spain, Centro de Investigación Biomédica en Red de Enfermedades Hepáticas y Digestivas (CIBERehd), Instituto de Salud Carlos III, Madrid, Spain, Barcelona, Spain
 Email: meritxell.ventura@vallhebron.cat

Background and aims: The asymptomatic forms of alcohol-related liver disease (ArLD) have been ignored worldwide leading to the late diagnosis of the disease. The main factor linked to progression and mortality among ArLD patients is the lack of abstinence. We aim to compare an intervention (i.e. hepatology visit, psychology visit including brief intervention and assessment of the underlying liver disease with non-invasive test) with a historical control group to establish a better strategy to promote abstinence.

Method: Prospective interventional study (currently recruiting) including subjects ≥ 30 years old with a diagnosis of alcohol use disorder or excessive alcohol consumption as well as ALT and AST < 5 times UNL, bilirubin < 3 mg/dL, AST/ALT ratio > 1.5 and GGT > 100 mg/dL gathered from primary care and the emergency department (ER). Patients with known liver disease were excluded. Patients from the historical cohort were gathered from the ER (discharge with the recommendation to cease drinking and control for either primary care and/or addiction center). Patients were followed for 1 year with an initial assessment of the underlying liver disease with Fibroscan® and thereafter visited every three months by the psychologist. Control patients (n = 19) were followed for 1 year.

Results: Up to date 23 patients had been included in the intervention group and 21 completed 3 month follow-up. In summary, most patients were men (81.82% intervention vs 78.95% control, $p = 0.8$) with a mean age of 50.58 vs 49.07 years ($p = 0.6$). There were no differences in the prevalence of diabetes, hypertension, and dyslipidemia. There was a higher use of cannabis in the intervention group 54.55% vs 21.05% $p = 0.02$, with no differences between other drugs. The average of standard drink units was 81.64 [IQR = 33.6–129.6] for the intervention group vs 128.3 [IQR = 67.7–189] in the control ($p = 0.2$). Both groups presented similar Fib-4 score 4.4 vs 3.4, $p = 0.5$, without relevant differences in the analytical parameters. At 3 months follow-up, 8 patients from the intervention group stopped drinking while only 5 of the control did ($p = 0.3$). Of note, 14 patients in the intervention vs 6 in the control cohort achieved a $\geq 50\%$ reduction of baseline consumption ($p = 0.02$). A reduction in total

number of standard drink units/week among the intervention group was also observed 17.2 vs 69.5; $p = 0.02$. While up to 6 patients from the control group required a second ER admission, none of the study group did ($p = 0.009$). Finally, up to 9 patients from the study group presented advanced liver disease assessed by Fibroscan (10.8 kPa).

Conclusion: Asymptomatic forms of advanced ArLD are common and frequently underdiagnosed. A holistic approach including hepatology, psychology and assessment of the underlying liver disease decreases alcohol consumption and promotes abstinence in patients with a suspected underlying ArLD as compared with a historical cohort.

SAT-305

Impact of corticosteroid treatment and clinical risk factors in patients with alcohol-associated hepatitis and clinically significant portal hypertension

Petra Dinjar Kujundžić¹, Marko Milosevic¹, Mislav Barišić-Jaman¹, David Dohoczky¹, Viktoria Skurla¹, Marta Defar², Sara Cepić², Frane Pastrovic³, Ivica Grgurević³. ¹University Hospital Dubrava, Zagreb, Croatia; ²School of Medicine, University of Zagreb, Zagreb, Croatia; ³University Hospital Dubrava, School of Medicine, University of Zagreb, Zagreb, Croatia
 Email: petra.dinjar@gmail.com

Background and aims: There is limited knowledge about the clinical features and prognostic factors of hospitalized patients diagnosed with alcohol-associated hepatitis (AH) and clinically significant portal hypertension (CSPH) who undergo corticosteroid (CS) treatment. This study aims to analyse impacts of CS treatment and identify mortality-associated risk factors within this specific subgroup of patients with AH.

Method: A retrospective analysis was conducted of patients hospitalized for AH at University Hospital Dubrava from January 2012 to December 2023. The primary outcome assessed was 90-day mortality. AH was defined based on the criteria established by the NIAAA AH Consortia, and CSPH was defined clinically based on either endoscopic evidence of esophageal varices, or platelet count $< 150 \times 10^9/L$ plus splenomegaly (> 12 cm).

Results: Our cohort comprised 168 AH patients, with 81% males and a with median age of 54. Half of patients (n = 84) received CS treatment and 58.9% (n = 99) had CSPH. At admission patients with CSPH were more likely to have ascites, experienced more decompensation events and were treated more often with CS ($p < 0.05$ for all, using Chi-squared test). The 90-day mortality rate was slightly higher in CSPH patients (42.4%) than in non-CSPH patients (33.3%), but without statistical significance ($p = 0.23$). Moreover, there wasn't statistically significant difference in CSPH group depending on the use of CS (39.7% vs 47.2%, $p = 0.47$). The same outcome was observed in non-CSPH group depending on CS therapy (31.2% vs 38.1% $p = 0.13$). Higher leukocytes and neutrophil counts, lower lymphocytes and higher AST/ALT ratios and lipid levels at admission were observed in CSPH group ($p < 0.05$ for all, using Kruskal-Wallis test). Although GAHS and MELD scores showed no differences at day 0, variations emerged on the 7th day where CSPH patients had higher scores. Encephalopathy (HR = 2.506, 95% CI: 2.506–2.506, $p < 0.001$) and number of decompensated events at admission (HR = 1.641, 95% CI: 1.641–1.641, $p < 0.001$) were independently associated with 90-day mortality in CSPH group. CS treatment did not significantly impact 90-day survival in the CSPH group (HR = 1.365, 95% CI: 0.838–2.223, $p = 0.21$). However, in the non-CSPH group, CS treatment independently associated with lower 90-day mortality (HR = 0.383, 95% CI: 0.161–0.911, $p = 0.04$).

Conclusion: CSPH had no significant impact on 90-day survival in AH patients. CS treatment didn't significantly affect 90-day survival in CSPH patients but was linked to lower mortality in non-CSPH. A larger cohort should be considered for further evaluation.

Cirrhosis and its complications – ACLF and Critical illness

TOP-097-YI

Dynamics of systemic inflammation after TIPS implantation and their impact on acute-on-chronic liver failure and liver-related death

Andrea Kornfehl¹, Lukas Hartl¹, Theresa Müllner-Bucsics¹, Michael Schwarz¹, Benedikt Hofer², Nina Dominik³, Benedikt Simbrunner³, Mathias Jachs³, Lukas Reider⁴, Maria Schoder⁴, Michael Trauner³, Matthias Mandorfer⁵, Thomas Reiberger³. ¹Division of Gastroenterology and Hepatology, Department of Medicine III, Medical University of Vienna, Vienna, Austria; ²Division of Gastroenterology and Hepatology, Department of Medicine III, Medical University of Vienna, benedikt.s.hofer@meduniwien.ac.at, Austria; ³Division of Gastroenterology and Hepatology, Department of Medicine III, Medical University of Vienna, Vienna, Austria; ⁴Division of Interventional Radiology, Department of Radiology, Medical University of Vienna, Vienna, Austria, Vienna, Austria; ⁵Medical University of Vienna, Vienna, Austria
Email: andrea.kornfehl@meduniwien.ac.at

Background and aims: Transjugular intrahepatic portosystemic shunt (TIPS) placement is an option for treatment of portal hypertension (PH)-related complications. Systemic inflammation is associated with acute-on-chronic liver failure and death in patients with cirrhosis.

Method: Patients undergoing covered TIPS implantation at two Viennese centers with available data on longitudinal levels of C-reactive protein (CRP) were included from a prospective cohort (AUTIPS study, NCT03409263; 01/2017 to 11/2022; n=64) and a retrospective cohort (09/2000 to 09/2019, n=191). Inflammation parameters CRP (available in n=84), interleukin 6 (IL-6; n=80), procalcitonin (PCT; n=84) and lipopolysaccharide-binding protein (LBP; n=75) were measured before (BL) and 3 (M3), 6 (M6), 9 (M9) and 12 (M12) months after TIPS implantation. Competing risk regression (CRR) was performed considering liver transplantation and death as competing events. For the analysis of the association of the difference in CRP and IL-6 with clinical outcomes, only events that occurred at least 3 months after TIPS implantation were considered for CRR.

Results: A total of 255 patients (71% male, median age 57 years) were included and followed for a median of 22 (IQR 47) months. Main indications for TIPS were PH bleeding (n=81, 32%) and refractory ascites (n=174, 68%). At BL, median levels were 0.91 (IQR 1.51) mg/dL for CRP, 25.15 (IQR 27.89) pg/ml for IL-6, 0.13 (IQR 0.15) ng/ml for PCT and 8.37 (IQR 4.69) µg/ml for LBP. Among patients with available CRP at each time point (n=84; BL: 0.96; 1.12 mg/dL), CRP increased 3 months after TIPS implantation (1.29; IQR 1.80 mg/dL) before decreasing significantly at M6 (0.47; IQR 0.94 mg/dL), 9M (0.37; IQR 1.15 mg/dL) and M12 (0.45; IQR 0.98 mg/dL; p<0.001). IL-6 decreased from BL to M3 in 53% (ΔIL-6 median -1.61; IQR 13.94 pg/ml), PCT in 37% (ΔPCT median 0.01; IQR 0.16 ng/ml) and LBP in 84% (ΔLBP median -2.21; IQR 4.13 µg/ml) of patients. In multivariable CRR adjusted for age, albumin and MELD at BL, IL-6 at BL was independently associated with post-TIPS ACLF (aSHR: 1.007; 95%CI: 1.004–1.010; p<0.001) and liver-related death (aSHR: 1.020; 95%CI: 1.008–1.020; p<0.001). Moreover, multivariable CRR adjusted for age, albumin and MELD at 3M revealed that ΔIL-6 after three months was independently associated with subsequent ACLF aSHR: 1.014; 95%CI: 1.006–1.020; p=0.001) and liver-related death; aSHR: 0.018; 95%CI: 1.010–1.030; p<0.001). ΔCRP was not independently associated with ACLF und liver-related death.

Conclusion: In patients with decompensated cirrhosis, several biomarkers of inflammation show a consistent decrease after TIPS

implantation. The decrease in LBP early (M3) after TIPS also suggests an improvement of bacterial translocation. Importantly, a favourable dynamic of IL-6 3 months after TIPS implantation is independently associated with a lower risk of ACLF and liver-related death.

TOP-108

Evaluation of the scoring systems dedicated to liver transplantation in acute-on-chronic liver failure (ACLF) in an international multicenter cohort

Sébastien L'Hermite¹, José Ursic Bedoya², Sébastien Halter³, Philippe Ichai⁴, Line Carolle Ntandja Wandji⁵, Audrey Coilly⁴, Christophe Camus¹, Samir Jaber², Rhiannon Taylor⁶, Sébastien Dharancy⁵, Douglas Thorburn⁷, Filomena Conti³, Georges-Philippe Pageaux², Faouzi Saliba⁴, Constantine Karvellas⁸, Antoine Monseil³, Alexandre Louvet⁵, William Bernal⁹, Florent Artru¹. ¹Rennes University Hospital, Rennes, France; ²Regional University Hospital Center of Montpellier, Montpellier, France; ³Pitié-Salpêtrière University Hospital-APHP, Paris, France; ⁴Centre Hépatobiliaire, Paul Brousse Hospital, Villejuif, France; ⁵Lille University Hospital, Lille, France; ⁶Statistics and Clinical Research, NHS Blood and Transplant, Bristol, United Kingdom; ⁷The Sheila Sherlock Liver Centre, London, France; ⁸University of Alberta Hospital, Edmonton, France; ⁹Institute of Liver Studies, Kings College Hospital, London, United Kingdom
Email: sebastienlhermite7@gmail.com

Background and aims: Liver transplantation (LT) in patients with acute-on-chronic liver failure (ACLF) require a thorough selection process to optimise post-procedural survival. The Transplantation for ACLF-3 model (TAM) and Sundaram ACLF LT models (SALT) have been proposed to aid in the selection process. To date the performance of these models has not been assessed in a large independent cohort.

Method: All patients transplanted in the context of ACLF grade 3 from 6 retrospective cohort (involving 5 French and 1 Canadian centres) and 1 prospective cohort (a multicentric cohort from the United Kingdom) covering the period 2008–2023 were included in this study. The primary end point was 1-year patient survival. All variables included in both scores and their cut-offs were included in logistic regression analyses.

Results: Two hundred thirty-two patients, median age of 55 years (IQR:46–61), were included. Alcohol consumption was the main cause of cirrhosis (51%). Median BMI was 26.4 kg/m² (22.9–30.3), 23% had diabetes. At LT, CLIF-C-ACLF score was 67 (61–73), MELD 40 (34–40), PaO₂/FiO₂ ratio 280 (206–502), leukocytes count 10 G/L (6–15), 67% patients needed vasopressors; TAM and SALT were 1 (1–2) and 14 (10–18). Median follow-up was 858 days (218–2429) with a 1-year survival of 77% (95%CI:71–82) without difference in overall comparison. At 1-year, 53 deaths (23%) occurred in a median timeframe of 77 days (16–156). PaO₂/FiO₂ ratio as continuous (OR 0.98, 95%CI:0.99–0.98, p=0.04) or according to the threshold of TAM and SALT (200 mmHg-OR 3.39, 1.68–6.86, p<0.0006) and lactate level according to TAM threshold (4 mmol/l -OR 2.26, 1.02–5.07, p=0.04) were independently associated with 1-year post transplant mortality. All other components of the TAM and SALT including age, diabetes, BMI, leukocytes counts or vasopressors were not associated with 1-year mortality after transplantation. Discriminant abilities of TAM (AUC 0.63, 0.54–0.70) and SALT (AUC 0.63, 0.53–0.71) were moderate and not different (p=0.86) in the overall cohort. However, AUCs varied widely between groups (from 0.38 to 0.79 and 0.48 to 0.74 respectively) and were best in the three cohorts with the lowest survival rate (1-year survival 70–72%, accounting for 120 patients) with an AUC of 0.69 (0.56–0.76) for TAM and 0.70 (0.56–0.81) for SALT. Both scores showed good performance in calibration testing with a median difference in observed vs. expected 1-year survival after LT of 6% and 5% respectively.

Conclusion: Both TAM and SALT have acceptable discriminative abilities supported by good calibration of 1-year post-LT survival in patients with ACLF-3. These scores could aid the decision-making process to optimise outcome after LT. Thresholds of 200 for PaO₂/FiO₂

ratio and 4 mmol/l for arterial lactate are confirmed to be independently associated with 1-year mortality in this population.

THURSDAY 06 JUNE

THU-049

Supplemental low-dose hydrocortisone in cirrhotic patients with septic shock: a double-blind, randomised, placebo-controlled, multicentre trial; the SCotCH study

Philippe Meersseman¹, María Hernández-Tejero², Juan Manuel Díaz³, Joost Wauters¹, Greet Hermans¹, Fatima Aziz⁴, Helga Ceunen¹, Veronica Enith Prado Gonzalez⁵, Mireya Arteaga⁴, Juan Acevedo Haro⁶, Miriam Valdivieso⁴, Cristina Sanchez³, Vicente Arroyo³, Alexander Wilmer¹, Javier Fernández⁷. ¹University Hospital Leuven, Leuven, Belgium; ²Mayo Clinic, Rochester, Rochester, United States; ³EF-Clif, Barcelona, Spain; ⁴Hospital Clinic Barcelona, Barcelona, Spain; ⁵C.H. Luxembourg, Luxembourg, Luxembourg; ⁶University Hospitals Plymouth NHS Trust, Plymouth, United Kingdom; ⁷Hospital Clinic Barcelona, EF-Clif, Barcelona, Spain
Email: jfdez@clinic.cat

Background and aims: Steroid treatment in septic shock remains controversial, partially due to a heterogenous study population. Ample evidence suggests that cirrhotic patients frequently develop relative adrenal insufficiency in case of sepsis. Therefore, we hypothesized that early administration of low-dose hydrocortisone (HCS) in cirrhotic patients with septic shock, a specific population, might reduce mortality and facilitate shock reversal and organ recovery.

Method: Double-blind, randomised, placebo-controlled multicentre trial, enrolling adult cirrhotic patients with septic shock. Patients were assigned to receive an i.v. bolus of 100 mg HCS prior to a continuous infusion of 200 mg/24hr or placebo, for at least 3 days, followed by a tapering period of 3 to 7 days, depending on the time of hemodynamic recovery. Primary end point was 28-day all-cause mortality.

Results: After enrolment of 83 patients, the trial was stopped early due to slow inclusions. There was no difference in 28-day (14/40 (35%) in HCS and 16/43 (37.2%) in placebo group, $p = 1$) and 90-day mortality (23/40 (57.5%) versus 20/43 (46.5%), $p = 0.43$). Moreover, no difference was seen in shock resolution (34/40 (85%) versus 31/43 (72.1%), $p = 0.25$) or in days to shock resolution (3 days (2.2–4, IQR) versus 4 (2–7.5, IQR), $p = 0.34$). More patients died of refractory shock in the placebo group (2/23 (8.7%) vs 9/20 (45%), $p = 0.01$), whereas ACLF was the main cause of death in the HCS group (15/23 (65.2%)). No difference was seen in new shock episodes or new bacterial, CMV or fungal infections during hospital stay between groups. Severity of ACLF (HR = 3.25, 95% CI: 1.94–5.46) and inadequacy of empirical antibiotic therapy (HR = 6.25, 95% CI: 3.03–12.5) were the only independent predictors of 28-d mortality.

Conclusion: Supplemental hydrocortisone did not improve survival in cirrhotic patients with septic shock. Its role in refractory shock deserves further evaluation.

THU-050

Urinary biomarkers of tubular and glomerular damage predict renal recovery in patients with hepatorenal syndrome-acute kidney injury

Salvatore Piano¹, Stefano Dall'Acqua¹, Carlos de la Peña-Ramirez², Cristina Sanchez¹, Ferran Aguilar², Gianluca Zilio¹, Alessandra Brocca¹, Alberto Farias³, Maria Papp⁴, Gustavo Pereira⁵, Paolo Caraceni^{6,7}, Aldo Torre⁸, Carlo Alessandria⁹, Adrian Gadano¹⁰, Wim Laleman¹¹, Angelo Z. Mattos¹², Frank Erhard Uschner¹³, Agustín Albillos¹⁴, Rafael Bañares¹⁵, Martin Janicko¹⁶, Víctor Manuel Vargas Blasco¹⁷, Rajeshwar Prosad Mookerjee¹⁸, Javier Fernández¹⁹, Thierry Gustot²⁰, Rajiv Jalan²¹, Joan Clària²², Richard Moreau^{2,23}, Vicente Arroyo², Flair Jose Carrilho²⁴,

Jonel Trebicka¹³, Paolo Angeli¹. ¹University of Padova, Padova, Italy; ²European Foundation for the Study of Chronic Liver Failure, Barcelona, Spain; ³University of Sao Paulo, Sao Paulo, Brazil; ⁴University of Debrecen, Debrecen, Hungary; ⁵Bonsucesso Federal Hospital, Rio de Janeiro, Brazil; ⁶University of Bologna, Bologna, Italy; ⁷IRCSS Azienda Ospedaliero-Universitaria di Bologna, Bologna, Italy; ⁸Instituto Nacional de Ciencias Médicas y Nutrición "Salvador Zubirán", Mexico City, Mexico; ⁹University of Turin, Torino, Italy; ¹⁰Hospital Italiano de Buenos Aires, Buenos Aires, Argentina; ¹¹University Hospitals Leuven, Leuven, Belgium; ¹²Federal University of Health Sciences of Porto Alegre, Porto Alegre, Brazil; ¹³Universitätsklinikum Münster (UKM), Münster, Germany; ¹⁴Hospital Universitario Ramon y Cajal, Madrid, Spain; ¹⁵Hospital General Universitario Gregorio Marañón, Madrid, Spain; ¹⁶Pavol Jozef Safarik University in Kosice, Kosice, Slovakia; ¹⁷Hospital Vall d'Hebron, Universitat Autònoma Barcelona, Barcelona, Spain; ¹⁸UCL Inst. of Liver and Digestive Health, London, United Kingdom; ¹⁹University of Barcelona, Barcelona, Spain; ²⁰Hôpital Erasme, Brussels, Belgium; ²¹University College London, London, United Kingdom; ²²Hospital Clinic, Barcelona, Spain; ²³Institut National de la Santé et de la Recherche Médicale, Université Paris Cité, Centre de Recherche sur l'Inflammation, Paris, France; ²⁴Hospital das Clínicas da Faculdade de Medicina da Universidade de São Paulo, Sao Paulo, Brazil
Email: salvatore.piano@unipd.it

Background and aims: Hepatorenal syndrome (HRS-AKI) is the most severe type of acute kidney injury in patients with cirrhosis. Less than 50% of patients with HRS-AKI show renal function recovery with albumin and vasoconstrictors. The lack of renal recovery is still poorly understood and there is a lack of biomarkers able to predict it. We aimed to identify biomarkers of renal recovery and 90-day mortality in patients with HRS-AKI.

Method: We identified patients with a clinical diagnosis of HRS-AKI and serum creatinine >1.5 mg/dl among those enrolled in the PREDICT and ACLARA studies. Demographics, clinical and laboratory characteristics were collected. Urinary biomarkers of tubular damage (neutrophil gelatinase-associated lipocalin [NGAL], Cystatin C, Albumin, Epidermal growth factor, Osteopontin) and cell cycle arrest (insulin growth factor binding protein 7 [IGFBP-7]) were measured by multiplex ELISA. Urinary metabolites of de novo NAD⁺ biosynthetic pathway were measured by HPLC-MS. Serum inflammatory cytokines (IL-1beta, IL-1ra, IL-6, IL-8, TNF-alpha, MCP-1, VEGF-A) were measured by a multiplexed immunoassay. Primary outcome was renal recovery (defined as serum creatinine <1.5 mg/dl) and all the analysis were adjusted for false discovery rate. Predictors of 90-day mortality were explored using renal recovery as a time-varying covariate.

Results: Overall, 171 patients with HRS-AKI were identified. Most frequent etiology was alcohol-related cirrhosis (61%) and 138 patients (81%) had acute on chronic liver failure (ACLF). Renal function recovery was achieved in 69 patients (40%). Patients with renal recovery were younger (57 vs 62 years; $p = 0.021$), had lower serum creatinine (2.1 vs 2.7 mg/dl; $p < 0.001$) and lower prevalence of ACLF (69 vs 88%; $p = 0.033$). Patients with renal recovery had lower levels of urinary NGAL (184 vs 533 ng/ml; $p = 0.007$), urinary albumin (4.3 vs 8.2 mg/dl; $p = 0.025$) and serum MCP-1 (235 vs 329 pg/ml; $p = 0.033$) than those without. Metabolites of de novo NAD⁺ biosynthetic pathway were not significantly different between the two groups. During 90-day follow-up 88 patients died. In multivariable analysis, white blood cell count (subdistribution hazard ratio [sHR] = 1.05; $p = 0.001$), bilirubin (sHR = 1.04; $p < 0.001$) and IGFBP-7 (sHR = 1.27; $p = 0.002$) were identified as independent predictors of 90-day mortality, while renal recovery was associated with a lower risk of 90-day mortality (sHR = 0.31; $p < 0.001$).

Conclusion: Urinary biomarkers of tubular (NGAL) and glomerular damage (albumin) are strong predictors of renal recovery in patients with HRS-AKI. Urinary IGFBP-7, a biomarker of cell cycle arrest, predicts survival independently from renal recovery in patients with HRS-AKI.

THU-051

Extended validation of proteomics and machine learning guided biomarker discovery and pathway perturbations in infection-related acute-on-chronic liver failure

Nipun Verma¹, Pratibha Garg^{2,3}, Arun Valsan⁴, Vivek Sarohi⁵, Trayambak Basak⁶, Parminder Kaur², Shreya Singh⁷, Arka De², Madhumita Premkumar², Sunil Taneja², Ajay Kumar Duseja², Virendra Singh⁸. ¹Department of Hepatology, Postgraduate Institute of Medical Education and Research, Chandigarh, India; ²Post Graduate Institute of Medical Education and Research, Chandigarh, India; ³Postgraduate Institute of Medical Education and Research, Hepatology, Chandigarh, India; ⁴Amrita Institute of Medical Sciences, Kerala, India; ⁵Indian Institute of Technology, Mandi, India; ⁶Indian Institute of Technology, Mandi, Himachal Pradesh, India; ⁷Post graduate Institute of Medical Education and Research, Ambedkar Institute of Medical Sciences, Chandigarh, India; ⁸Post Graduate Institute of Medical Education and Research, Punjab Institute of Liver and Biliary Sciences, Chandigarh, India
Email: nipun29j@gmail.com

Background and aims: Evaluating infections in acute-on-chronic liver failure (ACLF) presents a formidable challenge. This study deciphers protein signatures and pathway perturbations associated with bacterial or fungal infections in ACLF.

Method: We prospectively enrolled 391 patients with ACLF (92% males, median age: 41 years, 63% alcohol-associated hepatitis), with and without bacterial or fungal infections. High-resolution-untargeted proteomics was performed on plasma samples from 84 patients for biomarker discovery utilizing differential expression, discriminant analysis, and machine learning. Selected biomarkers were validated through immunoassays in two cohorts (N = 147 and 160) with predictive modelling for identifying infections. Perturbed pathways between groups were analyzed.

Results: Patients with infection exhibited higher leucocytosis, procalcitonin, organ failures, severity scores, and 30-day mortality ($p < 0.001$; each). Of 516 identified proteins, 27 were upregulated and 38 were downregulated in infected-cases (adjusted $p < 0.05$). A four-protein panel (LGALS3BP, PLTP, CFP, GPX3) yielded an AUC of 0.854 (0.787–0.922) in validation cohort-I, retaining significance after adjusting for severity (MELD or CLIF-C OF) and systemic inflammatory response criteria. We developed a PACIFY model (LGALS3BP + procalcitonin + CLIF-C OF + lactate) with excellent discrimination (AUC: 0.965; 0.933–0.997), sensitivity: 92%, and specificity: 91.7% for diagnosing infections. Its utility for identifying infections was further established in validation cohort-II with an optimal AUC: 0.906; 0.860–0.952, sensitivity: 80.6%, and specificity: 86.5%. PACIFY model's discriminatory ability outperformed procalcitonin, SIRS, WBC, NLR, neutrophil%, and composite models ($p < 0.001$). Pathway analysis unveiled diverse perturbations including impaired pathogen-response, reduced-phagocytosis, neutrophilic extracellular traps, complement functions, hypocoagulation and hypofibrinolysis, dysregulated carbohydrate metabolism, autophagy, heightened cell death and proteolysis.

Conclusion: A PACIFY model emerges as a robust tool for identifying infections in ACLF, surpassing existing markers. Pathway disruptions provide novel therapeutic targets for managing infections in ACLF.

THU-052

Therapeutic plasma-exchange improves short-term survival in patients with ACLF admitted to intensive care unit with organ failures-a multinational AARC data analysis

Rakhi Maiwall¹, Samba Siva Rao Pasupuleti², Ashok Kumar Choudhury¹, Vinod Arora¹, Mohd. Rela³, Dinesh Jothimani³, Mamun Al-Mahtab⁴, Harshad Devarbhavi⁵, CE Eapen⁶, Ashish Goel⁷, Cesar Yaghi⁸, Qin Ning⁹, Tao Chen⁹, Jidong Jia¹⁰, Zhongping Duan¹¹, Saeed Sadiq Hamid¹², Amna Subhan¹², Wasim Jafri¹², Akash Shukla¹³, Soek-Siam Tan¹⁴, Dong Joon Kim¹⁵, Anoop Saraya¹⁶, Jinhua Hu¹⁷, Ajit Sood¹⁸,

Omesh Goyal¹⁸, Vandana Midha¹⁸, Manoj Sahoo¹⁹, Guan-Huei Lee²⁰, Sombat Treeprasertsuk²¹, Kessarin Thanapirom²², Ameet Mandot²³, Samir Shah²³, Laurentius A. Lesmana²⁴, Hasmik Ghazinyan²⁵, Mohan Prasad V G²⁶, A. Kadir Dokmeci²⁷, Jose Sollano²⁸, Zaigham Abbas²⁹, Ananta Shrestha³⁰, George Lau³¹, Diana Payawal³², Gamal Shiha³³, Ajay Kumar Duseja³⁴, Sunil Taneja³⁴, Nipun Verma³⁴, Nagaraja Rao Padaki³⁵, Anand Kulkarni³⁵, Mithun Sharma³⁵, Md. Fazal Karim³⁶, Radha Krishan Dhiman³⁷, Ajay Mishra³⁷, Shahinul Alam³⁸, Osamu Yokosuka³⁹, Debashis Chowdhury⁴⁰, Chandan Kedarisetty⁴¹, Sanjiv Saigal⁴², Anil Arora⁴³, Ashish Kumar⁴⁴, Abraham Koshy⁴⁵, Ajay Kumar⁴⁶, Mohammed Elbasiony⁴⁷, Pravin Rath⁴⁸, Sudhir Maharshi⁴⁹, V.M. Dayal⁵⁰, Ashish Kumar Jha⁵⁰, Kemal Fariz Kalista⁵¹, Rino Gani⁵², Man-Fung Yuen⁵³, Virendra Singh⁵⁴, Ayaskant Singh⁵⁵, Sargyan Violeta⁵⁶, Chien-Hao Huang⁵⁷, Saurabh Mukewar⁵⁸, Shaojie Xin⁵⁹, Ruveena Bhavani⁶⁰, Charles Panackel⁶¹, Sunil Dadhich⁶², Sanjeev Sachdeva⁶³, Ajay Kumar⁶³, Sanatan Behera⁶⁴, Prabir Maji⁶⁴, Lubna Kamani⁶⁵, Hemamala Venugopal Saithanyamurthi⁶⁶, Dr. Joy Varghese⁶⁷, Pathik Parikh^{68,69}, P Javed⁷⁰, Neeraj Saraf⁷¹, Narendra S. Choudhary⁷¹, Akash Roy⁷², Mahesh Goenka⁷², Chetan Kalal⁷³, Krishnadas Devadas⁷⁴, Janaka De Silva H⁷⁵, Shiv Kumar Sarin⁷⁶. ¹Institute of Liver and Biliary Sciences, New Delhi, India; ²Department of Statistics, Mizoram University (A Central University), Pachhunga University College Campus, Aizawl, India; ³Dr. Rela Institute, Chennai, India; ⁴Bangabandhu Sheikh Mujib Medical University, Dhaka, Bangladesh; ⁵St John Medical College, Bangalore, India; ⁶CMC, Vellore, Vellore, India; ⁷CMC, Vellore, British Indian Ocean Territory; ⁸Saint Joseph University, Lebanon, Beirut; ⁹Tongji Hospital, Wuhan, China; ¹⁰Tongji Hospital, Wuhan, China; ¹¹Hepatology Institute Capital Medical University, China; ¹²Aga Khan University Hospital, Karachi, Pakistan; ¹³Lokmanya Tilak Municipal General Hospital and Lokmanya Tilak Municipal Medical College (LTMMC), Mumbai, India; ¹⁴Hospital Selayang, Bata Caves, Selangor, Malaysia; ¹⁵Hallym University Medical Centre, Chuncheon, Republic of Korea; ¹⁶All India Institute of Medical Sciences, New Delhi, India; ¹⁷302, Military Hospital, China; ¹⁸Dayanand Medical College, Ludhiana, India; ¹⁹IMS and SUM Hospital, Bhubaneswar, Odisha, India; ²⁰Department of Medicine, National University Health System, Singapore; ²¹Chulalongkorn University, Bangkok, Thailand; ²²Chulalongkorn University, Bangkok, Thailand; ²³Global Hospitals, Mumbai, India; ²⁴Digestive Disease and GI Oncology Centre, Medistra Hospital, Jakarta, Indonesia; ²⁵Nork Clinical Hospital of Infectious Disease, Yerevan, Armenia; ²⁶VGM Hospital, Coimbatore, India; ²⁷Ankara University School of Medicine, Ankara, Turkey; ²⁸University of Santo Tomas, Manila, Philippines; ²⁹Dr. Ziauddin University Hospital Clifton Karachi Pakistan; ³⁰Department of Hepatology, Alka Hospital, Nepal; ³¹Humanity and Health Medical Group, New Kowloon, Hong Kong; ³²Fatima University Medical Center Manila, Philippines; ³³29. Egyptian Liver Research Institute And Hospital, Egypt; ³⁴Postgraduate Institute of Medical Education and Research, Chandigarh, India; ³⁵Institute of Gastroenterology, Hyderabad, India; ³⁶Sir Salimullah Medical College Hospital, Bangladesh; ³⁷SGPGI, Lucknow, India; ³⁸Crescent Gastroenterology and General Hospital, Bangladesh; ³⁹Chiba University, Japan; ⁴⁰CMOSH Medical College, Bangladesh; ⁴¹Global Hospitals, Hyderabad, India; ⁴²38. Max Super Specialty Hospital, Saket, New Delhi, India; ⁴³Ganga Ram Hospital, New Delhi, India; ⁴⁴Sir Ganga Ram Hospital, New Delhi, India; ⁴⁵Lakeshore Hospital, Kochi, India; ⁴⁶KGMC, Lucknow, India; ⁴⁷Mansoura University, Egypt; ⁴⁸TN Medical College and BYL Nair Hospital, Mumbai, India; ⁴⁹SMS Jaipur, India; ⁵⁰IGIMS, Patna, India; ⁵¹Cipto Mangunkusumo Hospital, Indonesia; ⁵²Cipto Mangunkusumo Hospital, Indonesia; ⁵³Queen Mary Hospital, Hong Kong; ⁵⁴Punjab Institute of Liver and Biliary Sciences, Mohali, India; ⁵⁵SUM Ultimate Medicare, Bhubaneswar, India; ⁵⁶Violeta Medical Centre, Armenia; ⁵⁷Linkou Chang Gung Memorial Hospital, Taiwan; ⁵⁸Midas Multispeciality Hospital Pvt. Ltd.-Nagpur, Nagpur, India; ⁵⁹Medical school of Chinese PLA, China, China; ⁶⁰University of Malaya Medical Centre, Malaysia; ⁶¹Aster Medcity,

Kochi, India; ⁶²SMNC, Jodhpur, India; ⁶³G.B. Pant Hospital, New Delhi, India; ⁶⁴SCB Medical College and Hospital, Cuttack (Odisha), Odisha, India; ⁶⁵Liaquat National Hospital, Pakistan; ⁶⁶MIOT International Hospital, Chennai, India; ⁶⁷Gleneagles Global Health City, Chennai, India; ⁶⁸Zydus Hospital, Ahmedabad, India; ⁶⁹Apollo Hospital International Limited Blood Bank, Hepatology, Ahmedabad, India; ⁷⁰Aster MIMS Hospital, Kannur, India; ⁷¹Medanta, The Medicity Multispeciality Hospital, Gurgaon, Gurgaon, India; ⁷²Apollo Multispeciality Hospital, Kolkata, India; ⁷³Nanavati Max Super speciality Hospital, Mumbai, India; ⁷⁴Government Medical College, Trivandrum, Trivandrum, India; ⁷⁵University of Kelaniya, Ragama, Srilanka; ⁷⁶Institute of Liver and Biliary Sciences, New Delhi, India
Email: rakhi_2011@yahoo.co.in

Background and aims: Therapeutic plasma-exchange (TPE) could ameliorate systemic inflammation and reduces liver-failure related deaths in patients with acute on chronic liver failure (ACLF). We aimed to study the outcomes of TPE in patients admitted to the intensive care unit with organ failures from the multicentric-multinational AARC database.

Method: Prospectively collected data from AARC was analysed. Our primary outcome was to evaluate TPE compared to standard medical treatment (SMT) in improving 15-day transplant-free survival and secondary outcomes included 28-day survival and predictors of mortality in patients treated with TPE. The decision of TPE was taken by the treating physician at each center. In a subset of 50 patients pre and post TPE, an analysis of cytokines (interleukin-6, C-reactive protein), endotoxin, and nitric oxide was performed.

Results: Patients with ACLF (n = 1053) who underwent TPE (n = 117) were significantly older (46.7 ± 11.8 vs. 44.2 ± 11.6 ; $p = 0.03$), majority being males (78% vs. 89%), predominantly alcoholics (89% vs. 92%), and sicker with higher AARC score (9.9 ± 2.4 vs. 8.3 ± 1.9 ; $p < 0.001$) and number of extrahepatic organ failures (EH-OFs) [4 (21% vs. 6%) and 3 (20% vs. 10%) vs. 1 (39% vs. 75%) and 2 (20% vs. 9%); $p < 0.001$] respectively. Majority of patients, 90% underwent low-volume TPE with mean of 2 ± 0.6 sessions per patient. At day 28, 536 (51%) died and 171 (16%) underwent liver transplant. TPE (HR 0.73, 0.56–0.95) independently improved 15-day transplant free survival. Higher AARC (HR 1.21, 1.06–1.38) and SOFA scores (HR 1.05, 1.02–1.08) (Model-1) while number of EH-OFs (HR 1.16, 1.11–1.22) (Model-2) predicted higher 15-day mortality. TPE however, could not improve 30-day survival. On competing-risk survival analysis, considering liver transplant as the competing event, the survival benefit with TPE was not observed. In the subgroup of patients who underwent TPE, higher SOFA (HR 1.11, 1.02–1.22), age (HR 1.04, 1.01–1.06) and AARC score (HR 1.21, 1.06–1.38) (Model-1) and higher arterial lactate (≥ 3 mmol/L) (2.61, 1.49–4.57) and MELD (HR 1.03, 1.01–1.06) (Model-2) predicted 15-day mortality. Survivors (n = 22) post-TPE had significant improvement in markers of systemic inflammation, nitric oxide, endotoxin, oxidative stress and arterial lactate compared to non-survivors (n = 28).

Conclusion: TPE could only improve short-term 15-day transplant-free survival without improving long-term outcomes in patients with ACLF admitted to the intensive care unit with organ failures. Severity of liver failure and number of extrahepatic organ failures determine mortality in these patients. Patients with higher age, AARC score and arterial lactate have higher mortality with TPE.

THU-053

Longitudinal salivary metagenomics in acute-on-chronic liver failure patients

Manolo Laiola¹, Maria Papp², Wenyi Gu³, Nathalie Galleron¹, Benoit Quinquis¹, Mamadou-Gabou Thiam¹, Emmanuelle Le Chatelier¹, Hervé Blottière¹, S. Dusko Ehrlich⁴, Mathieu Almeida¹, Jonel Trebicka^{3,5}. ¹INRAE MetaGenoPolis, Jouy-en-

Josas, France; ²University of Debrecen, Debrecen, Hungary; ³University of Münster, Münster, Germany; ⁴UCL, London, United Kingdom; ⁵EF CLIF, Barcelona, Spain
Email: laiola.manolo@gmail.com

Background and aims: The main clinical events precipitating acutely decompensated cirrhosis (AD) patients are bacterial infections and alcoholic hepatitis, while in 30–40% of the cases no clinical event is identifiable [1]. When not identified, bacterial translocation is thought to be causal for the AD. Recent studies showed evidence for the presence of oral microbes in stool [2], and salivary microbiome could reflect changes in the cirrhotic patients' gut microbiome [3]. Hence, elucidating the role of the salivary microbiome might pave the way for the development of new diagnostic and therapeutic strategies in the etiology of AD cirrhosis and progression to ACLF [4]. The aim of the study is to longitudinally assess the clinical and oral microbial evolution of 91 patients of the MICROB-PREDICT project.

Method: Shotgun metagenomic analysis was performed on saliva samples collected from 91 patients, collected over more than 75 days after baseline. The samples were DNA extracted then sequenced using Ion Proton technology. A human oral microbial gene catalog was used as a reference database [5]. The sequenced DNA was mapped to the reference using Meteor software [6] to generate the microbial taxonomical abundance profile and identify biomarkers of ACLF progression.

Results: At the inclusion, ACLF patients showed significantly lower levels of oral dominant species in saliva compared to AD subjects. Over time, a loss of oral-related taxa was observed for some AD patients independently of rifaximin treatment, along with an accumulation of non-oral species, after adjustment from known confounders. A microbial drift towards a unique compositional state was significantly associated to the accumulation of non-oral taxa like *Enterococcus faecalis* only for pre-ACLF subjects (53.7% mortality rate in 3 months), whereas this pattern was not evident for stable AD individuals (9% of mortality per year).

Conclusion: Our analysis shows the potential of saliva as reservoir of microbiome-based biomarkers for acute decompensated cirrhosis and progression to ACLF. The monitoring of opportunistic pathogens in the salivary microbial composition might support the management of precipitating events, delivering guidance in a personalized medicine approach.

Funding: The MICROB-PREDICT project has received funding from the European Union's Horizon 2020 research and innovation program under grant agreement No 825694. This reflects only the author's view, and the European Commission is not responsible for any use that may be made of the information it contains.

References

1. Trebicka et al., *J Hepatol*, 2021
2. Qin et al., *Nature*, 2014
3. Bajaj et al., *Hepatology* 2015
4. Trebicka et al., *Nat Rev Gastro and Hepatol*, 2021
5. <https://doi.org/10.15454/WQ4UTV>
6. <https://forgemia.inra.fr/metagenopolis/meteor>

THU-055

Differential impact of proton pump inhibitors, statins, and non-selective beta-blockers on survival in different stages of chronic liver disease

Wenqi Gu¹, David Tornai², Josune Cabello Calleja¹, Aleksander Krag³, Katrine Thorhaug³, Richard Moreau^{4,5,6}, Vicente Arroyo⁶, Jasmohan Bajaj⁷, Michael Praktiknjo¹, Robert Schierwagen¹, Pere Ginès⁸, Frank Erhard Uschner¹, Rajiv Jalan⁹, Joan Clària^{10,11}, Manimozhiyan Arumugam¹², Minneke Coenraad¹³, Wim Laleman^{1,14}, Debbie L. Shawcross¹⁵, Maria Papp¹⁶, Jonel Trebicka¹. ¹Department of Internal Medicine B, University Hospital Muenster, Muenster, Germany; ²Division of Gastroenterology, Department of Internal Medicine, Faculty of Medicine, University of Debrecen, Debrecen, Germany; ³Fibrosis Fatty

POSTER PRESENTATIONS

Liver and Steatohepatitis Research Centre, Department of Gastroenterology and Hepatology, Odense University Hospital, Institute of Clinical Research, University of Southern Denmark, Odense, Denmark; ⁴Centre de Recherche sur l'Inflammation, INSERM, Université Paris Cité, Paris, France; ⁵Service d'Hépatologie, Assistance Publique-Hôpitaux de Paris and Hôpital Beaujon, Clichy, France; ⁶European Foundation for Study of Chronic Liver Failure, Barcelona, Spain; ⁷Virginia Commonwealth University and Richmond VA Medical Center, Richmond, Virginia, United States; ⁸Liver Unit Hospital Clínic, Institut d'Investigacions Biomèdiques August Pi i Sunyer (IDIBAPS), Barcelona, Spain; ⁹UCL Medical School, Royal Free Hospital, London, United Kingdom; ¹⁰Biochemistry and Molecular Genetics Service, Hospital Clínic de Barcelona, Catalonia, Spain; Institut d'Investigacions Biomèdiques August Pi i Sunyer (IDIBAPS), Centro de Investigación En Red de Enfermedades Hepáticas y Digestivas (CIBEREHD), Barcelona, Spain; ¹¹European Foundation for the Study of Chronic Liver Failure (EFCLF), Grifols Chair, Barcelona, Spain; ¹²Novo Nordisk Foundation Center for Basic Metabolic Research, Faculty of Health and Medical Sciences, University of Copenhagen, Copenhagen, Denmark; ¹³Department of Gastroenterology and Hepatology, Leiden University Medical Center, Leiden, Netherlands; ¹⁴Department of Gastroenterology and Hepatology, Section of Liver and Biliopancreatic disorders, University Hospitals Leuven, KU Leuven, Leuven, Belgium; ¹⁵Institute of Liver Studies, School of Immunology and Microbial Sciences, Faculty of Life Sciences and Medicine, King's College London, London, United Kingdom; ¹⁶Division of Gastroenterology, Department of Internal Medicine, Faculty of Medicine, University of Debrecen, Debrecen, Hungary
Email: wenyi.gu@ukmuenster.de

Background and aims: Patients with chronic liver disease (CLD) receive frequently proton pump inhibitors (PPIs), statins, and non-selective beta-blockers (NSBB). The role of these drugs on the overall survival of CLD patients at different disease stages are still debated.

Method: This study includes a comprehensive univariable analysis of 2029 patients from six multicentric studies (PREDICT, CANONIC, FCRB, NEPTUNE, VA-US and GALA-ALD), assessing the effects on short- and long-term survival associated with PPIs, statins, and NSBB usage during hospital admission across different stages of liver disease, including CLD without cirrhosis, stable decompensated cirrhosis (SDC), unstable decompensated cirrhosis (UDC), pre-acute-on-chronic liver failure (pre-ACLF), and ACLF.

Results: Notably, PPI was associated with increased long-term mortality, especially in less severe disease (SDC [90-day: 5.8% vs. 2.1%, $p = 0.043$] and CLD without cirrhosis [overall: 16.2% vs. 4.4%, $p < 0.001$]). Patients with statin therapy had improved survival across all patient groups, with a significant effect on 1-year survival (mortality: 21.4% vs. 24.2%, $p = 0.040$). However, in SDC patients, statins were associated with lower long-term survival (overall mortality: 10.2% vs. 20.0%, $p = 0.037$). Finally, NSBB use demonstrated the most consistent benefit on short-term mortality (28-day and 90-day) in all patient categories. Of note, patients with ACLF (28-day mortality: 14.0% vs. 33.5%, $p = 0.009$; 90-day: 21.9% vs. 45.9%, $p < 0.001$) and with pre-ACLF (90-day mortality: 43% vs. 61.6%, $p = 0.024$; 1-year: 58.1% vs. 74.4%, $p = 0.013$) seem to benefit as well from NSBB therapy.

Conclusion: Our comprehensive study of 2029 CLD patients indicates that PPI and statins may not be beneficial in stable decompensated cirrhosis. In contrast, statins were associated with better survival when all disease stages were analyzed. Notably, patients with NSBBs consistently linked to improved survival outcomes, even in advanced stages like pre-ACLF and ACLF. These findings highlight the necessity for personalized treatment approaches to maximize patient outcomes in chronic liver disease.

THU-056

Soluble PD-L1 levels as predictors of ACLF in decompensated cirrhosis: findings from two independent cohorts

Adrià Juanola¹, Gabriel Mezzano², Elisa Pose¹, Maria Jose Moreta³, Jordi Ribera⁴, Joaquín Andrés Castillo³, Natalia Jimenez-Esquivel⁵, Martina Perez-Guasch¹, Ana Belén Rubio⁶, Marta Cervera⁶, Marta Carol⁶, Ruth Nadal⁶, Jordi Gratacós-Ginès¹, Anna Soria¹, Núria Fabrellas⁷, Manuel Morales-Ruiz⁴, Mar Coll⁸, Isabel Graupera⁹, Elsa Solà¹⁰, Pere Ginès¹¹, the Investigators of the Liverhope Consortium¹². ¹Liver Unit, Hospital Clínic de Barcelona. Institut d'Investigacions Biomèdiques August Pi i Sunyer (IDIBAPS). Centro de Investigación Biomedica en Red Enfermedades Hepáticas y Digestivas (CIBEREHD), Barcelona, Spain; ²Gastroenterología-Hepatología, Hospital del Salvador, Universidad de Chile, Santiago de Chile, Chile; ³Liver Unit, Hospital Clínic de Barcelona, Barcelona, Spain; ⁴Biochemistry and Molecular Genetics Department, Hospital Clínic of Barcelona, Institut d'Investigacions Biomèdiques August Pi i Sunyer (IDIBAPS), Centro de Investigación Biomédica en Red de Enfermedades Hepáticas y Digestivas (CIBEREHD), Barcelona, Spain; ⁵Liver Unit, Hospital Clínic de Barcelona, Barcelona, Spain; ⁶Institut d'Investigacions Biomèdiques August Pi i Sunyer (IDIBAPS), Centro de Investigación Biomedica en Red Enfermedades Hepáticas y Digestivas (CIBEREHD), Barcelona, Spain; ⁷Liver Unit, Hospital Clínic de Barcelona, Institut d'Investigacions Biomèdiques August Pi i Sunyer (IDIBAPS), Centro de Investigación Biomedica en Red Enfermedades Hepáticas y Digestivas (CIBEREHD), Faculty of Medicine and Health Sciences, Universitat de Barcelona (UB), Barcelona, Spain; ⁸Institut d'Investigacions Biomèdiques August Pi i Sunyer (IDIBAPS), Centro de Investigación Biomedica en Red de Enfermedades Hepáticas y Digestivas (CIBEREHD), Barcelona, Spain; ⁹Liver Unit, Hospital Clínic de Barcelona, Institut d'Investigacions Biomèdiques August Pi i Sunyer (IDIBAPS), Centro de Investigación Biomedica en Red de Enfermedades Hepáticas y Digestivas (CIBEREHD), Barcelona, Spain; ¹⁰Institute for Immunity, Transplantation and Infection, Stanford University School of Medicine, Stanford, United States; ¹¹Liver Unit, Hospital Clínic de Barcelona, Institut d'Investigacions Biomèdiques August Pi i Sunyer (IDIBAPS), Centro de Investigación Biomedica en Red de Enfermedades Hepáticas y Digestivas (CIBEREHD), Faculty of Medicine and Health Sciences, Universitat de Barcelona (UB), Barcelona, Spain; ¹²Liverhope Consortium, Barcelona, Spain
Email: juanola@clinic.cat

Background and aims: Acute-on-chronic liver failure (ACLF) is the most severe complication in patients with decompensated cirrhosis (DC). In recent years, studies have demonstrated the activation of inflammatory pathways as liver cirrhosis progresses. Notably, increased expression of the PD-L1 pathway has been associated with the risk of bacterial infection due to impaired phagocytic capacity of macrophages in patients with DC. Additionally, its soluble form (sPD-L1) has been linked to the risk of bacterial infections. However, the potential relationship between sPD-L1 levels and ACLF has not been evaluated. This study aims to evaluate the role of sPD-L1 as biomarker in the prediction of ACLF.

Method: This is a sub-analysis of the LiverHope Efficacy trial. Serum samples from patients recruited in the study were collected at baseline. Data on ACLF development in patients enrolled in the study was evaluated. PD-L1 pathway activity was estimated by measuring serum levels of PDL1 (ELISA), which estimates the soluble isoform of PDL1 (sPDL1) expressed in monocytes. Factors associated with ACLF development were identified in a bivariate analysis. Competing risk analysis was performed, being transplant and mortality considered as competing events for ACLF development. A second prospective cohort, previously reported (EASL-ILC 2022), was used to validate the findings.

Results: Baseline samples from the Liverhope cohort were available for analysis in 214 patients (out of 254 patients included in the trial, 84%). The most common etiology was alcohol-related in 82% of cases, followed by MASLD in 7%. At inclusion, the median MELD Na score was 14 (11–17), and the median levels of soluble PD-L1 (sPD-L1) were

97 (74–121) pg/ml. Over the course of a 1-year follow-up, 25 patients (12%) experienced at least one episode of ACLF. Baseline levels of sPD-L1 were higher in patients who developed ACLF versus those of patients who did not develop ACLF: 116 (97–151) vs 93 (74–118) pg/ml, p value = 0.019. A multivariate competing risk analysis revealed that MELD Na, a history of hepatic encephalopathy (HE), and levels of sPD-L1 were independently associated with ACLF development during 1 year of follow-up. To validate these findings, an independent prospective cohort consisting of 305 hospitalized patients with decompensated cirrhosis (DC) was analyzed. In this new cohort, levels of sPD-L1 and MELD-Na were the only two independent factors predicting ACLF at the 3-months of follow-up.

Conclusion: Levels of sPD-L1 are associated with the risk of ACLF in patients with DC. These may reflect the degree of immune dysfunction reported in patients with DC. Soluble PD-L1 is a promising biomarker, providing the potential to predict the risk of ACLF in the context of DC.

THU-057-YI

Distinguishing clinical profiles in acute-on-chronic liver failure: a comparative analysis of alcohol-related hepatitis versus infection precipitated acute-on-chronic liver failure

Julian Pohl¹, Annarein Kerbert², Carlos de la Peña-Ramirez³, Nirbaanot Walia⁴, Cristina Sanchez⁵, Pavitra Kumar⁵, Ingrid Wei Zhang⁵, Lilli Rausch⁵, Richard Sittner⁵, Maria Papp⁶, Paolo Caraceni⁷, Carlo Alessandria⁸, Wim Laleman⁹, Agustín Albillos¹⁰, Martin Janicko¹¹, Víctor Manuel Vargas Blasco¹², Rajeshwar Prosad Mookerjee¹³, Alberto Farias¹⁴, Gustavo Pereira¹⁵, Aldo Torre¹⁶, Sebastián Marciano¹⁷, Angelo Z. Mattos¹⁸, Flair Jose Carrilho¹⁹, Vicente Arroyo³, Jonel Trebicka²⁰, Richard Moreau²¹, Joan Clària²², Paolo Angeli²³, Salvatore Piano²⁴, Thierry Gustot²⁵, Fausto Andreola¹³, Rajiv Jalan¹³, Cornelius Engelmann²⁶. ¹Charité- Universitätsmedizin Berlin, Berlin, Germany; ²Leiden University Medical Center, Leiden, Netherlands; ³EF Clif, Barcelona, Spain; ⁴Charité Universitätsmedizin Berlin, Berlin, Germany; ⁵Charité-Universitätsmedizin Berlin, Berlin, Germany; ⁶University of Debrecen, Debrecen, Hungary; ⁷University of Bologna, Bologna, Italy; ⁸A.O.U. Città della Salute e della Scienza di Torino, University of Turin, Turin, Italy; ⁹University Hospitals Leuven, Leuven, Belgium; ¹⁰Hospital Universitario Ramón y Cajal, Madrid, Spain; ¹¹Pavol Jozef Safarik University in Kosice, Kosice, Slovakia; ¹²Hospital Vall d'Hebron, Universitat Autònoma Barcelona, CIBEREHD, Barcelona, Spain; ¹³University College London, London, United Kingdom; ¹⁴University of São Paulo, São Paulo, Brazil; ¹⁵Bonsucesso Federal Hospital, Rio de Janeiro, Brazil; ¹⁶Medical Center ABC, Mexico City, Mexico; ¹⁷Hospital Italiano de Buenos Aires, Buenos Aires, Argentina; ¹⁸Federal University of Health Sciences of Porto Alegre, Porto Alegre, Brazil; ¹⁹Hospital das Clínicas da Faculdade de Medicina da Universidade de São Paulo, São Paulo, Brazil; ²⁰University Hospital Münster, Münster, Germany; ²¹Inserm and Université de Paris, Paris, France; ²²Hospital Clinic, Barcelona, Spain; ²³University of Padova, Padova, Italy; ²⁴University and Hospital of Padova, Padova, Italy; ²⁵HUB Erasme, Brussels, Belgium; ²⁶Charité—Universitätsmedizin Berlin, Berlin, Germany
Email: julian.pohl@charite.de

Background and aims: Severe alcohol-related hepatitis (sAH) and infection are the most common precipitating factors for the development of acute-on-chronic liver failure (ACLF). The pathophysiological basis and prognostic impact of sAH progressing to ACLF (sAH-ACLF) is still poorly understood. Here, we aimed to characterize the clinical profile and disease course of patients with sAH-ACLF as compared to those with infection-induced ACLF (inf-ACLF).

Method: We studied cirrhotic patients admitted with sAH-induced acute decompensation (sAH-AD, $n = 546$), sAH-ACLF ($n = 239$) and inf-ACLF ($n = 234$), that were included in three prospective observational cohort studies (CANONIC, PREDICT and ACLARA). Organ failures and the presence of ACLF were defined according to the

CLIF-consortium organ failure (CLIF-C OF) score. Clinical and laboratory baseline data were compared between the three groups. A competing-risk regression analysis was performed to evaluate the impact of clinical and laboratory factors on 28-day mortality and ACLF development.

Results: Patients with sAH-ACLF had more often liver or coagulation failure as compared to those with inf-ACLF ($p < 0.001$ and $p = 0.001$, respectively), whereas kidney, circulatory and respiratory failure were more frequently present in inf-ACLF ($p < 0.001$, $p = 0.002$ and $p < 0.001$, respectively). Plasma C-reactive protein (CRP) was higher in inf-ACLF as compared to sAH-ACLF ($p < 0.001$), whereas white blood cell count (WBCC) was higher in sAH-ACLF ($p = 0.001$). Despite their different phenotype, cumulative incidence of 28-day mortality was comparable between sAH-ACLF and inf-ACLF (42.2 vs. 39.3%). When dividing the sAH-ACLF group into patients with and without an infection at admission, patients with an infection showed higher CRP and creatinine levels ($p = 0.01$ and $p < 0.001$, respectively), higher CLIF-C OF scores ($p = 0.036$) and higher mortality rates (53.6 vs. 32.6%) as compared to those without. Multivariate analysis for 28-day mortality revealed INR as the only independent predictor in sAH-ACLF, whereas age, creatinine, CRP, WBCC, INR and bilirubin independently predicted mortality in inf-ACLF. In the sAH-AD group, creatinine and sodium levels were independent predictors of mortality and ACLF development at 28 days.

Conclusion: sAH-ACLF is distinct from inf-ACLF and is characterized by 'liver-centered' OFs, whereas inf-ACLF is characterized by extra-hepatic OFs. Despite the different phenotypes, short-term mortality rates are the same. As opposed to inf-ACLF, markers of systemic inflammation do not predict outcome in sAH-ACLF, nor disease progression in sAH-AD which speaks against the notion that inflammation is a hallmark in alcohol-related severe liver disease. These findings underline the need for a better understanding of the pathophysiological basis of sAH progressing to ACLF and for more accurate risk stratification in these patients.

THU-058

Portal vein thrombosis increases short-term mortality independent of liver disease severity score among hospitalized patients of decompensated cirrhosis-result from CLEARED consortium

Ashok Kumar Choudhury¹, Qing Xie², Mark Topazian³, Aldo Torre⁴, Peter Hayes⁵, Hailemichael Desalegn⁶, Ramazan Idilman⁷, Zhujun Cao⁸, Mario Álvares-da-Silva⁹, Jacob George¹⁰, Wai-Kay Seto¹¹, Florence Wong¹², Patrick S. Kamath¹³, Shiv Kumar Sarin¹⁴, Brian Bush¹⁵, Leroy Thacker¹⁶, Anoop Saraya¹⁷, Haydar Adanir¹⁸, Busra Haktaniryan¹⁹, Anand Kulkarni²⁰, Sezgin Barutcu²¹, Sumeet Asrani²², Hong Tang²³, Maria Sarai González-Huezo²⁴, CE Eapen²⁵, Kessarar Thanapirom²⁶, Jing Liu²⁷, Elizabeth Verna²⁸, Mohd. Rela²⁹, Alper Uysal³⁰, Jacqueline Cordova-Gallardo³¹, Jose Antonio Velarde-Ruiz Velasco³², Matheus Truccolo Michalczuk³³, Gustavo Pereira³⁴, Oscar Morales Gutiérrez³⁵, Abraham Ramos Pineda³⁶, Abha Nagral³⁷, David Nyam P³⁸, Dibya Lochan Praharaj³⁹, Rahmi Aslan⁴⁰, Paul J. Thuluvath⁴¹, Hugo Vargas⁴², Tolga Kosay⁴³, Beiling Li⁴⁴, Jie Li⁴⁵, Suresh Vasan Venkatachalapathy⁴⁶, Sunil Taneja⁴⁷, Stephen Riordan⁴⁸, Jawaid Shaw¹⁶, Diana Yung⁴⁹, Adam Doyle⁵⁰, Yan Yue James Fung⁵¹, Huan Deng⁵², Lei Wang⁵³, Hiang Keat Tan⁵⁴, Al-Tamimi Hala⁵⁵, Amany Zekry⁵⁶, Liane Rabinowich⁵⁷, Man Su⁵⁸, Xiaoping Wu⁵⁹, Xinrui Wang⁶⁰, Yaodi Zhang⁶¹, Caiyan Zhao⁶², Zhiliang Gao⁶³, Feng Guo⁶⁴, Michael Schultheis⁶⁵, Puneeta Tandon⁶⁶, Bilal Bobat⁶⁷, K. Rajender Reddy⁶⁸, Ricardo Cabello Negrillo⁶⁹, Scott Biggins⁷⁰, Nipun Verma⁷¹, Jasmohan Bajaj⁷². ¹Institute of Liver and Biliary Sciences, New Delhi, India; ²Ruijin Hospital, Shanghai Jiaotong University School of Medicine, Shanghai; ³Mayo Clinic, Minnesota, United States; ⁴Instituto Nacional de Ciencias Médicas y Nutrición Salvador Zubirán, Mexico city, Mexico; ⁵The Royal Infirmary of Edinburgh, Edinburgh, United Kingdom; ⁶St Paul's Hospital Millennium Medical College, Ethiopia, Ethiopia; ⁷Ankara University School of

POSTER PRESENTATIONS

Medicine, Ankara, Turkey; ⁸Rui Jin Hospital Affiliated to Shanghai Jiao Tong University School of Medicine, Sanghai, China; ⁹Hospital de Clínicas de Porto Alegre, Porto Alegre, Brazil; ¹⁰Westmead Hosp/Westmead Institute, Westmead, Australia; ¹¹The University of Hong Kong, Hongkong, Hong Kong; ¹²Toronto General Hospital, Toronto, Ontario, Canada; ¹³Mayo Clinic, Rochester, United States; ¹⁴Institute of Liver and Biliary Sciences, Vasant Kunj, India; ¹⁵VCU Richmond, Richmond, United States; ¹⁶VCU, Richmond, United States; ¹⁷All India Institute of Medical Sciences, New Delhi, New Delhi, India; ¹⁸Department of Gastroenterology, Akdeniz University School of Medicine, Antalya, Turkey; ¹⁹University of Ankara, Ankara, Turkey; ²⁰Asian Institute of Gastroenterology, Hyderabad, India; ²¹Gaziantep University Faculty of Medicine, Gaziantep, Turkey; ²²Baylor Dallas (Baylor University Medical Center), Texas, United States; ²³West China Hospital of Sichuan University, Chengdu, China; ²⁴Centro Medico ISSEMyM, Ciudad de México, Mexico; ²⁵CMC Vellore, Vellore, India; ²⁶Division of Gastroenterology, Department of Medicine, Faculty of Medicine, Bangkok, Thailand; ²⁷Department of Infectious Diseases, Union Hospital, Tongji Medical College, Huazhong University of Science and Technology, Wuhan, China; ²⁸Columbia University, New York, United States; ²⁹Dr. Rela Institute and Medical Centre, Chennai, India; ³⁰Ege University, Izmir, Izmir, Turkey; ³¹Hospital General Dr Manuel Gea Gonzalez, Talalpan, Mexico; ³²Hospital Civil de Guadalajara, Guadalajara, Mexico; ³³Hospital de Clínicas de Porto Alegre, Porto Alegre, Brazil; ³⁴Hospital Federal de Bonsucesso, Rio de Janeiro, Brazil; ³⁵Hospital General de Mexico "Dr. Eduardo Liceaga, Mexico, Mexico; ³⁶Instituto Nacional de Ciencias Médicas y Nutrición "Salvador Zubirán", Mexico City, Mexico city, Mexico; ³⁷Apollo Hospitals, Delhi, Delhi, India; ³⁸Jos University Teaching Hospital, Lagos, South Africa; ³⁹KIMS Bhubaneswar, Bhubaneswar, India; ⁴⁰Marmara University, Istanbul, Turkey; ⁴¹Institute of Digestive Health and Liver Disease, Mercy Medical Center and University of Maryland School of Medicine, Baltimore, United States; ⁴²Mayo Clinic in Arizona, Phoenix, AZ, USA, Scottsdale, United States; ⁴³Mersin University, Mersin, Mersin, Turkey; ⁴⁴Nanfeng Hospital, Southern Medical University, Guangzhou, China; ⁴⁵Nanjing Drum Tower Hospital, Affiliated Hospital of Medical School, Nanjing University, Nanjing, China; ⁴⁶NIHR Nottingham Biomedical Research Centre, Nottingham, United Kingdom; ⁴⁷PGIMER, Chandigarh, India; ⁴⁸Prince of Wales Hospital, Sydney, Sydney, Australia; ⁴⁹Royal Infirmary of Edinburgh, Edinburgh, United Kingdom; ⁵⁰Royal Perth Hospital, Perth, Australia; ⁵¹Queen Mary Hospital, Hong Kong, Hong Kong; ⁵²Second Affiliated Hospital of Chongqing Medical University, Chongqing, China; ⁵³The Second Hospital of Shandong University, Jinan, China; ⁵⁴Singapore General Hospital, Singapore, Singapore; ⁵⁵Sir Charles Gairdner Hospital, Nedlands, Australia; ⁵⁶University of New South Wales, Sydney, Australia; ⁵⁷Tel Aviv Sourasky Medical Center, Tel Aviv, Israel; ⁵⁸The First Affiliated Hospital of Guangxi Medical University, Nanning, China; ⁵⁹The First Affiliated Hospital of Nanchang University, Nanchang, China; ⁶⁰The First Hospital of Jilin University, Changchun, China; ⁶¹The First People's Hospital of Lanzhou, Lanzhou, China; ⁶²Third Hospital of Hebei Medical University, Shijiazhuang, China; ⁶³The Third Affiliated Hospital of Sun Yat-sen University, Guangzhou, China; ⁶⁴Traditional Chinese Medical Hospital Affiliated to Xinjiang Medical University, Urumqi, China; ⁶⁵UMC Freiburg (University Medical Center Freiburg), Freiburg im Breisgau, Germany; ⁶⁶University Of Alberta, Edmonton, Canada; ⁶⁷Wits Donald Gordon Medical Centre, Johannesburg, South Africa; ⁶⁸University of Pennsylvania, Philadelphia, United States; ⁶⁹University of Pittsburgh, Pennsylvania, United States; ⁷⁰University of Pittsburgh Medical Center, Pittsburgh, United States; ⁷¹PGIMER, Chandigarh, Chandigarh, India; ⁷²Virginia Commonwealth University, Richmond, United States
Email: doctor.ashokchoudhury@gmail.com

Background and aims: Portal Vein Thrombosis (PVT) in cirrhosis is multifactorial and is associated with poor outcome in the natural history. However, etiology, presentation and implications of PVT in decompensated cirrhosis as well as its distribution across different regions is unclear.

Method: The multi-national CLEARED consortium enrolled prospectively non-electively admitted patients with cirrhosis with 30-days follow-up post-discharge. PVT was diagnosed on USG and/or CT scan and was analysed in relation to demographic, aetiology, clinical presentation, mode of decompensation, complications, course in hospital and survival at 30-days post discharge across all 6 continents.

Results: Total of 4305 patients from 107 centres in 27 countries were included. The predominant aetiology was alcohol (1723, 40%) followed by NASH/Cryptogenic (1104, 25.6%), HBV (903, 17.7%), Autoimmune (495, 11.5%), HCV (420, 9.8%). PVT was seen in 420 (9.8%) patients and is more among NASH/Cryptogenic (32.6%) and lesser with ethanol (27.9%) than other aetiologies. PVT prevalence increased in proportion to WHO income group i.e. with lower, middle- or high-income region as 17.1%, 39.8% and 43.1% respectively, more among diabetics (39% vs 28.5%). More hospital visit (13.6% vs 9.1%) and infection (23% vs 19%) was observed in the preceding 6 months than those without PVT. At admission the CTP and MELD Na score were comparable. Those with PVT get admitted more with infections (25.5% vs 20.2%, $p = 0.03$) or GI bleed (27.6% vs 21.4%, $p = 0.01$), and during hospital course higher ICU transfers (21. % vs 17.2%), AKI (37.4% vs 32.2%, $p = 0.02$) and brain failure (15.5% vs 11.4%, $p < 0.004$) was observed. The in-hospital mortality (14.8% vs 10.8%, $p = 0.02$), 30-day mortality (23% vs 12.4%, $p = 0.004$) were more with PVT. In multivariate (MV) analysis, the in-patient mortality [OR 1.69 (1.23, 2.34), $p < 0.001$], 30-day mortality [OR 1.71 (1.27, 2.31), $p < 0.001$] were increased significantly with presence of PVT.

Conclusion: In a prospective global cohort of hospitalized decompensated cirrhosis, PVT was seen in 10% cases, more often among those with diabetics, or NASH related cirrhosis and is associated a higher in-hospital complications and greater mortality even when the CTP or MELD Na score were comparable. All decompensated cirrhosis needs to be evaluated for the presence of PVT and deserve special focus and monitoring during and after discharge from the hospital worldwide.

THU-059

Therapeutic plasma exchange improves organ function and potentially increases short-term survival in ACLF-3 patients who do not respond to standard medical treatment: a single centre propensity score-matched retrospective study

Jonas Schumacher¹, Rhea Veelken¹, Adam Herber¹, Lorenz Weidhase², Raymund Buhmann³, Reinhard Henschler³, Sirak Petros², Thomas Berg¹. ¹Leipzig University medical center, Division of Hepatology, Leipzig, Germany; ²Leipzig University Medical Center, Medical ICU, Leipzig, Germany; ³Leipzig University Medical Center, Institute of Transfusion Medicine, 04103 Leipzig, Germany
Email: thomas.berg@medizin.uni-leipzig.de

Background and aims: Acute on chronic liver failure (ACLF) is a severe syndrome, with Grade 3 having a 28-day mortality approaching 80%. The prognosis becomes crucial within 3–7 days of full organ support. Beyond transplantation, there is no causative therapy. ACLF is marked by an inflammatory response syndrome, and therapeutic plasma exchange (TPE) holds promise in eliminating circulating pro-inflammatory mediators. Thus, TPE emerges as a potential therapeutic intervention for ACLF patients showing resistance to standard medical treatment (SMT).

Method: This retrospective study focused on ACLF patients receiving SMT with TPE from January 1, 2017, to March 11, 2023, at a tertiary care medical centre in Germany. Patients were monitored for at least 90 days post-ACLF diagnosis. The primary end point measured transplant-free survival at 28, 60, and 90 days. Secondary end points included changes in organ dysfunction, CLIF-C scoring systems, and global inflammatory markers. Data were collected by chart review. A cohort of 23 patients treated with SMT+TPE and 25 patients undergoing SMT alone was identified. Propensity scores, accounting for age, sex, ACLF grade, CLIF-C-ACLF Score, CLIF-C-OF Score, and

white blood cell count, facilitated 1:1 patient matching. 40 patients (N = 20 SMT + TPE; N = 20 SMT) underwent final analysis. Statistical analysis utilized non-parametric methods. Each patient underwent a median of 3 TPE sessions (SD 2.3), initiated a median of 14 days after the ACLF diagnosis (SD 15.27).

Results: The 28-day transplant-free survival rates were 65% (SMT + TPE) compared to 45% (SMT alone). Four patients died on the day of TPE or the following day, all attributed to uncontrolled septic shock. No TPE-related adverse events were observed. At day 60, the survival rates were 30% (SMT + TPE) versus 25% (SMT alone), and at 90 days, the rates were 25% versus 20%, respectively. Evaluation of ACLF grade, and CLIF-C scoring systems 24–48 hours after the last TPE application revealed improvements in ACLF grade (Median grade 3, SD 0.686 vs. grade 1.5, SD 1.125, $p = 0.046$), CLIF-C-ACLF Score (Median 59.5, SD 11.08 vs. 50, SD 23.14, $p = 0.049$), CLIF-C-OF Score (Median 13, SD 2, 53 vs. 10, SD 2.579, $p = 0.079$), Bilirubin levels (Median 282.45 $\mu\text{mol/l}$, SD 196.12 $\mu\text{mol/l}$ vs. Median 184.9 $\mu\text{mol/l}$, SD 170.82 $\mu\text{mol/l}$, $p = 0.07$), and PT levels (Median 32%, SD 16.89% vs. Median 38%, SD 17.72%, $p = 0.009$). Patients who did not show improvement in ACLF with SMT and were subsequently treated with TPE demonstrated a significantly improved 28-day transplant-free survival compared to patients in the SMT alone cohort (50% vs. 21%, $p = 0.012$). This improvement was consistent specifically in patients with ACLF-3 (36.4% vs. 11.1%, $p = 0.026$).

Conclusion: TPE demonstrates efficacy in improving organ dysfunction in ACLF patients. In the subset of severe ACLF patients unresponsive to standard medical treatment, TPE may enhance short-term survival.

THU-060

Lower inpatient mortality and second infections in inpatients with cirrhosis managed between 2021–22 than between 2011–13 in prospective North American cohorts

Jasmohan Bajaj¹, Puneeta Tandon², Paul J. Thuluvath³, Florence Wong⁴, Patrick S. Kamath⁵, Hugo Vargas⁶, Sumeet Asrani⁷, Jacqueline O'Leary⁸, Leroy Thacker⁹, K. Rajender Reddy¹⁰. ¹Virginia Commonwealth University and Richmond VA Medical Center, Richmond, United States; ²University of Alberta, Edmonton, Canada; ³Mercy Medical Center and University of Maryland School of Medicine, Baltimore, United States; ⁴University of Toronto, Toronto, Canada; ⁵Mayo Clinic, Rochester, United States; ⁶Mayo Clinic, Phoenix, United States; ⁷Baylor Scott and White, Dallas, United States; ⁸Dallas VA Medical Center, Dallas, United States; ⁹Virginia Commonwealth University, Richmond, United States; ¹⁰University of Pennsylvania, Philadelphia, United States

Email: jasmohan.bajaj@vcuhealth.org

Background and aims: With changing demographics, etiology and treatments for cirrhosis, a temporal analysis of inpatient outcomes is needed. Aim: Determine inpatient mortality, organ failures and ICU in cirrhosis patients admitted non-electively at the same centers 10 years apart.

Method: The CLEARED Consortium (max 50/site from 2021 to 22) and NACSELD2 (from 2011 to 13) prospectively enrolled pts with cirrhosis admitted non-electively across 9 North American centers using identical eligibility criteria. Both consortia required non-electively admitted cirrhosis patients without HIV, organ transplant, or inability to consent. CLEARED pts were COVID negative. Patients were followed for inpatient course. We matched CLEARED to NACSELD2 pts using age, gender and admission MELD-Na using 1:2 propensity matching. Outcomes included inpatient ICU use, second infections, death and liver transplant.

Results: 450 pts were enrolled from 9 centers in CLEARED while 2067 were enrolled from the same centers in NACSELD2. Cohort details: 441 CLEARED pts were matched 1:2 with 882 NACSELD2 patients on age (57.2 vs 57.3, $p = 0.92$), Male sex (57 vs 58%, $p = 0.67$) and MELD-Na (median 22 each). More pts in CLEARED had alcohol etiology (48 vs 30%, $p < 0.001$), MASH (33 vs 22%, $p < 0.001$) but lower HCV (5 vs

17%, $p < 0.001$) and HCV + alcohol (9 vs 14%, $p = 0.004$). More CLEARED pts were admitted for liver-related conditions (81 vs 73%, $p = 0.002$), especially HE (25 vs 15%), AKI (27 vs 8%) and fluid overload (19 vs 8%, all $p < 0.001$). Admission due to infections (24 vs 27%, $p = 0.2$) or liver-unrelated reasons (13 vs 14%, $p = 0.2$) were similar. Admission WBC (8.7 vs 8.0, $p = 0.08$) and serum albumin (2.9 vs 2.8, $p = 0.06$) trended higher in CLEARED. Admission beta-blocker use was lower in CLEARED (27 vs 38%, $p = 0.001$) and PPI were higher (60 vs 53%, $p = 0.02$). Lactulose, rifaximin and SBP prophylaxis use was similar. Outcomes: A lower % of CLEARED pts (6% vs 9%, $p = 0.04$) died or had second infection (1 vs 8%, $p < 0.0001$) while transplant (5 vs 4%, $p = 0.4$), and ICU transfer (21 vs 20%, $p = 0.8$) were similar. On multivariable analysis, being in CLEARED vs NACSELD2 (OR 0.4, 95% CI 0.24–0.67, $p = 0.006$), age (1.04, 1.02–1.07, $p < 0.001$), admission AKI (2.66, 1.59–4.43, $p = 0.002$), admission albumin (0.64, 0.47–0.88, $p = 0.006$) and MELD-Na (1.12, 1.09–1.16, $p < 0.0001$) were linked with death. Etiology, admission reasons and medications were not contributory.

Conclusion: In two inpatient cirrhosis cohorts using similar eligibility criteria enrolled in the same North American centers 10 years apart and propensity score matched on age, sex and admission MELD-Na, the more recent cohort had a lower risk of inpatient death and second infections (likely related to COVID restrictions). This persisted on multi-variable analysis despite higher alcohol and MASH etiology vs hepatitis C and greater liver-related causes of admission in the later versus the earlier cohort.

THU-067

Predictors of clinical response to empirical antibiotic therapy in patients with cirrhosis and bacterial infections: results from a resource-constrained setting

Chitta Ranjan Khatua¹, Prajna Anirvan², Manas Kumar Panigrahi³, Shivaram Prasad Singh². ¹MKCG Medical College And Hospital, Brahmapur, Brahmapur, India; ²Kalinga Gastroenterology Foundation, Cuttack, India; ³All India Institute Of Medical Sciences, Bhubaneswar, India

Email: gudduchhotu3@gmail.com

Background and aims: Multidrug-resistant (MDR) bacterial infections pose a significant challenge in cirrhosis, hampering the efficacy of empirical antibiotic treatments and thus, adversely affecting patient outcomes. The International Club of Ascites Global Study Group had determined the predictors of lack of response to empirical antibiotic therapy in patients with cirrhosis. In this study, we sought to validate the predictors of clinical response to empirical antibiotic treatment in a South Asian cohort of cirrhosis patients with infections.

Method: From October 2016 to September 2023, all cirrhosis patients with bacterial infections were included and on hospitalization, all parameters were recorded. The outcomes were compared between patients with and without MDR bacterial infections, with a three-month follow-up to discern the short and long-term impacts of MDR infections.

Results: Out of 1203 patients, 44.2% had infections, with MDR infections prevalent in 21.8% ($n = 116$). Urinary tract infection (UTI) was the most common at 73.3%, followed by pneumonia at 30.2%, spontaneous bacterial peritonitis (SBP) at 26.7%, skin and soft tissue infection at 11.2%. Patients with MDR infections had higher Model for End-Stage Liver Disease (MELD) scores, MELD-Na scores, Child-Turcotte-Pugh (CTP) scores, and a higher incidence of acute-on-chronic liver failure (ACLF). MDR infection was also associated with decreased serum albumin levels. Furthermore, patients with MDR infection demonstrated increased multiple site infections (36.2% vs. 8.2%; $p < 0.001$), increased use of vasopressors, prolonged hospital stay, elevated in-hospital mortality (57.8% vs. 8.9%), decreased survival at 28 days (25% vs. 75.2%), and 90 days (11.2% vs. 52.9%). The presence of respiratory infections (OR = 3.813; 95%CI = 1.062–13.690; $p = 0.40$), UTIs (OR = 4.973; 95%CI = 1.125–21.977; $p = 0.34$),

POSTER PRESENTATIONS

and SBP (OR = 0.109; 95%CI = 0.017–0.718; $p = 0.021$) were identified as factors associated with increased in-hospital mortality and lack of clinical response to antibiotic treatment.

Conclusion: Bacterial infections were observed in approximately half of cirrhosis patients, with one-fifth having MDR infection. MDR infection was associated with multiple site infections, hypotension, an increased prevalence of ACLF, and prolonged hospitalization. MDR infection, respiratory infections, UTIs, and SBP were associated with a lack of clinical response to antibiotic treatment and increased short-term mortality.

THU-068

Predicting with the “POAD” score the course of acute kidney injury in acute-on-chronic liver failure: a metabolomics approach

Rakhi Maiwall¹, Neha Chauhan², Ashini Hidam¹, Gaurav Tripathi¹, Jaswinder Maras¹, Shiv Kumar Sarin³. ¹Institute of Liver and Biliary Sciences, Delhi, India; ²Institute of Liver and Biliary Sciences, Delhi, India; ³Institute Liver and Biliary Sciences, Delhi, India
Email: rakhi_2011@yahoo.co.in

Background and aims: Acute kidney injury is an ominous complication in patients with acute on chronic liver failure. The rapidity of AKI progression in ACLF patients is an ongoing clinical challenge. The serum metabolites and pathways associated with AKI progression could be useful for timely identification and institution of therapeutic interventions.

Method: ACLF patients with AKI at enrolment were enrolled and carefully followed. Plasma metabolomic studies using LC-MS/MS were conducted. We utilized area under the receiver operating curve (AUC), random forest analysis, for identification of biomarkers and pathways associated with AKI progression.

Results: A total 242 ACLF patients with AKI, 91% males, aged 43.2 ± 9.8 years, 73% with alcohol as etiology were enrolled. At day 4, AKI progression was seen in 42.6% and 26% required dialysis. AKI progression was an independent predictor of 28-day mortality (HR 1.98, 1.25–3.16). Plasma metabolomic analysis identified 54, 372 LC-MS/MS peaks, leading to the annotation of 778 metabolites. PLSDA and hierarchical clustering analysis demonstrated a distinct separation between AKI progressors and non-progressors with a total of 445 differentially expressed metabolites (241 upregulated, 231 downregulated; $FC > 1.5$; $p < 0.05$). The top 5 biomarkers predicting AKI progression were arachidonic acid ($FC > 35$, p value < 0.05 , $AUC > 0.95$), alpha-linolenic acid ($FC > 5$, $p < 0.05$, $AUC > 0.90$), oleamide ($FC > 3$, $p < 0.05$, $AUC > 0.91$), cysteic acid ($FC > 2.5$, $p < 0.05$, $AUC > 0.87$), and 10-Nitrolinoleate ($FC > 4$, $p < 0.05$, $AUC > 0.88$). This panel of five biomarkers- together POAD score (Probability Of AKI Detection score) reliably predicted AKI progression ($AUC > 0.91$, $p < 0.05$). The score positively correlated with the serum creatinine, and urine NGAL and also surpassed the prediction accuracy of these known biomarkers for AKI progression. The progressors further exhibited upregulated pathways such as arginine and proline metabolism, primary bile acid biosynthesis, taurine and hypotaurine metabolism, alpha-linolenic acid metabolism, among others. Conversely, downregulated pathways included glutathione metabolism, alanine metabolism and sphingolipid metabolism.

Conclusion: We identified and developed the “POAD score” (comprising top 5 metabolites-arachidonic acid, alpha-linolenic acid, oleamide, cysteic acid, and 10-Nitrolinoleate) implicated in cellular toxicity from differentially expressed metabolites for prediction of AKI progression in ACLF patients. AKI progressors exhibited altered metabolic pathways, providing insights into potential mechanisms for developing novel therapeutic interventions for improving AKI outcomes of ACLF patients.

THU-069

Serum bile acids determine AKI progression and terlipressin non-response in patients with acute-on-chronic liver failure with acute kidney injury

Rakhi Maiwall¹, Neha Chauhan¹, Ashini Hidam¹, Gaurav Tripathi², Sherin Sarah Thomas², Jaswinder Maras², Shiv Kumar Sarin².

¹Institute of Liver and Biliary Sciences, Delhi, India; ²Institute of Liver and Biliary Sciences, Delhi

Email: rakhi_2011@yahoo.co.in

Background and aims: Acute-on-chronic liver failure (ACLF) patients frequently have hyperbilirubinemia and limited response to vasoconstrictors. Cholemic nephropathy (CN) is distinctly noted in patients with ACLF; however, the association of the number and type of bile acids with AKI progression, and non-response to terlipressin, has not been studied.

Method: In a prospective cohort of ACLF patients ($n = 242$) with AKI, quantitative serum bile acids, urine neutrophil-gelatinase associated lipocalin (NGAL), and LC-MS/MS-based conventional serum bile acid profiling for 16 bile acids was performed for all patients at enrolment.

Results: ACLF patients, aged 43.2 ± 9.8 years, 91.2% males, 73% with alcohol etiology, 87% with sepsis, AKI stages (1:2:3) (40%:31%:29%), 61% with HRS-AKI were enrolled. The mean total serum bile acids were 154.2 ± 45.8 $\mu\text{mol/L}$, and NGAL was 1881 ± 1714 ng/ml. AKI progression at day 4 was observed in 42.6%, 26% required dialysis, and 48% died at 28 days. The bile acids showed a significant direct but weak correlation with total bilirubin ($p = 0.001$, $r = 0.21$ and with NGAL ($p = 0.04$, $r = 0.13$). On multivariable analysis, serum bile acids (OR 1.008, 1.001–1.016), higher AARC score (OR 1.72, 1.37–2.15), NGAL (OR 1.56, 1.01–2.46) and number of organ failures (OR 1.89, 1.27–2.83) predicted AKI-Prog. AKI progression was an independent predictor of 28-day mortality (HR 1.98, 1.25–3.16). Bile acids > 175 $\mu\text{mol/L}$ predicted non-response in HRS-AKI (3.25, 1.38–7.67) and AKI-Prog (OR 2.52, 1.42–4.45). The bile acid profiling showed a significant increase in the glycochenodeoxycholic ($FC > 10$; $p < 0.05$) acid while taurothiocholic acid ($FC > 12$ folds, $p < 0.05$) and glycodeoxycholic acid ($FC > 3$ folds, $p < 0.05$) were downregulated in the AKI-Prog compared to non-progressors. In the subset of patients with HRS-AKI, 6 bile acids were differentially expressed. Levels of deoxycholic acids ($FC > 9$, $p < 0.05$), taurodeoxycholic acids ($FC > 5$, $p < 0.05$), taurourso-deoxycholic acid ($FC > 3.1$, $p < 0.05$) were found upregulated while glycodeoxycholic acid, chenodeoxycholic acid, glyoursodeoxycholic acid were found downregulated in terlipressin non-responders ($FC > 10$ folds, $p < 0.05$).

Conclusion: Severity of liver failure, number of organ failures, presence of tubular injury, and total serum bile acids independently predict AKI progression and non-response in HRS-AKI in ACLF patients. High levels of glycochenodeoxycholic acid in AKI progressors and deoxycholic acid in terlipressin non-response (PMID: 23685124, 26351365) could be used as markers of mitochondrial destruction by these cell-toxic bile acids which in-turn drive worse outcomes of AKI in ACLF patients.

THU-070

Dynamic assessment of lactate and AARC-Lactar score could determine survival in acute-on-chronic liver failure with septic shock admitted to the intensive care unit: a prospective cohort study [NCT06116305]

Rakhi Maiwall¹, Vishnu Girish¹, Shiv Kumar Sarin¹, Manoj Kumar¹, Ashok Kumar Choudhury¹, Chitranshu Vashistha¹, Harshvardhan Tevethia¹, S. Muralikrishna Shashtry¹, Vinod Arora¹, Vijayraghavan Rajan¹, Ankur Jindal¹, Satender Pal Singh¹, Dr Babu Lal Meena¹. ¹Institute of Liver and Biliary Sciences, Department of Hepatology, Delhi, India

Email: rakhi_2011@yahoo.co.in

Background and aims: Data on acute-on-chronic liver failure (ACLF) and septic shock is few. We aimed to study impact of lactate kinetics

on outcome in ACLF with septic shock and effect of therapeutic interventions on lactate kinetics.

Method: Prospective cohort study; ACLF with septic shock and lactate >3.0 mmol/L were checked for arterial lactate every 6 h until 72 h and outcomes of survivors and non-survivors compared. Primary outcome was impact of lactate kinetics at 6 h on 7-d survival. Delta lactate, defined as difference in lactate at inclusion and at specific time and lactate clearance, percentage decrease in lactate from time of inclusion, were noted.

Results: One hundred five ACLF patients with septic shock, age 43.4 ± 10.4 years, 92.3% males, 49% alcohol-related, model for end stage liver disease (MELD) 33.8 ± 6.2 , sequential organ failure assessment (SOFA) 12.26 ± 2.6 , and Asia Pacific ACLF research consortium (AARC) score 11.35 ± 1.6 , were enrolled. Mean arterial pressure (MAP)- 54 mmHg (Interquartile Range [IQR] 46, 62), norepinephrine equivalent (NEE) was 0.12 ± 0.06 mcg/kg/min and mean lactate was 3.8 ± 1.3 mmol/l at inclusion, at day 7, 66% patients were alive. Of these, 42 received continuous renal replacement therapy (CRRT). Predominant focus was pneumonia (74.8%). Admission lactate (3.53 ± 1.72 vs. 4.46 ± 1.96 , $p = 0.045$), Lactate at 6 h (2.13 ± 0.81 vs. 4.70 ± 1.57 ; $p < 0.001$), delta lactate at 6 h (1.39 ± 0.78 mmol/L vs. -0.326 ± 0.71 , $p < 0.001$), lactate clearance at 6 h ($33.38 \pm 3.3\%$ vs. $-15.75 \pm 4.23\%$, $p < 0.001$) all significantly correlated with 7d survival. Lactate clearance at 6 hours had highest predictive accuracy for determining 7d survival (AUROC of 0.826 (cutoff = 15%, sensitivity = 75%, specificity = 71%). High lactate at 12, 24, 48, and 72 h were significantly associated with high mortality (HRs: 1.513, 1.413, 1.492, 1.493, 1.477) while higher lactate clearance at 12 h (HR 0.993, $p = 0.033$) predicted better survival, but not at 24 and 48 h. Fluid resuscitation correlated positively ($r = 0.21$, $p = 0.031$) and NEE negatively with 6 h lactate clearance ($r = -0.20$, $p = 0.040$). CRRT was associated with lactate clearance after 24 h of start ($r = 0.20$, $p = 0.043$). Multivariable analysis derived two models; Model-1 (based on delta lactate)-need of mechanical ventilation, [HR 6.219, 95% CI 1.467–26.360, $p = 0.013$], higher AARC [HR 1.258, 95% CI 1.03–1.54, $p = 0.026$] and delta lactate at 6 hours [HR 0.637, 95% CI 0.514–0.791, $p < 0.001$]; Model-2- (lactate clearance at 6 hours) [HR 1.236, 95% CI 1.013–1.509, $p = 0.037$], mechanical ventilation [HR 6.205, 95% CI 1.467–26.39, $p = 0.013$], and AARC [HR 1.236, 95% CI 1.013–1.509, $p = 0.037$] predicted 7-d survival.

Conclusion: Predictive models incorporating lactate kinetics and AARC score (AARC-Laclear) are predictors of short-term survival in ACLF with septic shock. Need of mechanical ventilation, high AARC and failure to clear lactate at 6 h predict early death.

THU-071

Impact of underlying portal hypertension and systemic inflammation on acute-on-chronic liver failure (ACLF) severity and outcome

Vlad Taru^{1,2,3}, Georg Kramer^{1,2}, Lorenz Balcar¹, Benedikt Hofer^{1,2}, Michael Schwarz¹, Nina Dominik¹, Lukas Hartl¹, Mathias Jachs¹, Mathias Schneeweiss-Gleixner¹, Bogdan Procopet³, Michael Trauner¹, Bernhard Scheiner¹, Philipp Schwabl^{1,2}, Mattias Mandorfer¹, Thomas Reiberger^{1,2,4}, Benedikt Simbrunner^{1,2}. ¹Division of Gastroenterology and Hepatology, Department of Medicine III, Medical University of Vienna, Vienna, Austria; ²Christian-Doppler Laboratory for Portal Hypertension and Liver Fibrosis, Medical University of Vienna, Vienna, Austria; ³Regional Institute of Gastroenterology and Hepatology "Octavian Fodor," Hepatology Department and "Iuliu Hatieganu" University of Medicine and Pharmacy, 3rd Medical Clinic, Cluj-Napoca, Romania; ⁴Center for Molecular Medicine (CeMM) of the Austrian Academy of Science, Vienna, Austria
Email: vlad.taru@meduniwien.ac.at

Background and aims: In patients with cirrhosis, acute-on-chronic liver failure (ACLF) may develop on top of acute decompensation (AD) and is characterized by profound systemic inflammation (SI) and extra-hepatic organ failure (s). The impact of portal hypertension

(PH) in the context of AD/ACLF remains poorly investigated. We have analyzed the impact of PH on the incidence, the severity and the course/outcome of ACLF.

Method: We have retrospectively identified patients developing ACLF (EASL-CLIF criteria) at the Vienna General Hospital between 11/2003 and 11/2022. Data at several timepoints was collected: Pre-ACLF (30–180 days prior to ACLF), ACLF diagnosis (D0) and 7 days after ACLF (D7). Post-ACLF mortality was recorded at D90, D180 and 1 year (Y1). Pre-ACLF results on hepatic venous pressure gradient (HVPG), liver stiffness measurement (LSM), platelet count (PLT), presence/size of varices Von Willebrand factor levels (VWF) served as surrogates of PH severity. Severity of SI was evaluated by WBC, CRP, and IL-6.

Results: The study included 192 patients with ACLF (Grade G1: 91 [47.4%], G2: 62 [32.3%], G3: 39 [20.3%]). When comparing pre-ACLF surrogates of PH (PLT $p = 0.908$, LSM $p = 0.692$, VWF $p = 0.340$, presence of varices $p = 0.078$) and of systemic inflammation (WBC $p = 0.575$, CRP $p = 0.814$, IL-6 $p = 0.565$), there was no difference across different ACLF grades. Accordingly, HVPG (available in $n = 95$) was non significantly different across ACLF grades (G1: 20.9 ± 6.1 vs. G2: 20.3 ± 6.1 vs. G3: 17.3 ± 5.8 mmHg; $p = 0.148$). Pre-ACLF MELD-Na scores were similar in patients with different grades of ACLF (G1: 18.4 ± 5.9 vs. G2: 19.9 ± 4.6 vs. G3: 19.5 ± 5.3 ; $p = 0.133$). At D0 systemic inflammation increased significantly in parallel to ACLF severity (WBC $p = 0.020$, CRP $p = 0.132$, IL6 $p = 0.032$); while PLT tended to decrease with higher ACLF grades (G1: 91 (93) vs. G2: 81 (93) vs. G3: 72 (86) G/L; $p = 0.094$), and were significantly lower in higher ACLF grades at D7 (G1: 89 (84) vs. G2: 64 (47) vs. G3: 39 (80) G/L; $p < 0.001$). D90 mortality increased with ACLF severity (G1: 41.8%, G2: 58.1%, G3: 79.5%, log-rank $p < 0.001$). The CLIF-C ACLF score at D0 was predictive of D90, D180 and Y1 mortality in univariate Cox regression analyses (all $p < 0.001$). The addition of PLT at D0 to the CLIF-C-ACLF score components improved the model fit (C-indexes, likelihood ratio tests) of D90 (0.72 vs. 0.70, $p = 0.005$), D180 (0.71 vs. 0.69, $p = 0.004$) and Y1 (0.71 vs. 0.69, $p = 0.004$) mortality prediction.

Conclusion: While PH represents an established risk factor for AD, pre-ACLF PH severity does not impact on the severity of subsequent ACLF. Interestingly, pre-ACLF SI levels were not associated with subsequent ACLF grade, however, were linked to ACLF severity at ACLF onset. Our results indicate that PH is not a major driver of ACLF severity, but ACLF severity impacts on PLT and the addition of PLT to the CLIF-C-ACLF scores improves prediction of mortality.

THU-074

Effect of terlipressin on patients with hepatorenal syndrome, alcohol-associated hepatitis, and acute-on-chronic liver failure grade 0–2

Kevin Moore¹, Priya Grewal², Marco Olivera³, Khurram Bari⁴, Khurram Jamil⁵. ¹University College London, London, United Kingdom; ²Mount Sinai Medical Center, New York, NY, United States; ³University of Nebraska Medical Center, Omaha, NE, United States; ⁴University of Cincinnati, Cincinnati, OH, United States; ⁵Mallinckrodt Pharmaceuticals, Bridgewater, NJ, United States
Email: kevin.moore@ucl.ac.uk

Background and aims: Patients with severe alcohol-associated hepatitis (AAH) frequently have underlying liver cirrhosis, which leads to the development of acute kidney injury (AKI) in 10–40% of these patients. Hepatorenal syndrome (HRS) is a potentially reversible form of AKI. Terlipressin is the first and only treatment for adult patients with HRS-AKI approved by the United States Food and Drug Administration and is more likely to clinically benefit those with acute-on-chronic liver failure (ACLF) grade 0–2. In this study, we determined the effect of terlipressin on renal function among patients with AAH and HRS-AKI who had ACLF grades 0–2.

Method: Data from a subpopulation (pooled from the Phase III studies: OT-0401, CONFIRM, and REVERSE) of patients with AAH, HRS-AKI, and ACLF grades 0–2 who received terlipressin or placebo were examined. Change in renal function—measured as least squares

POSTER PRESENTATIONS

(LS) mean changes in serum creatinine (SCr) with and without interaction between treatment and day—from baseline through the end of treatment (EOT) was evaluated within and between treatment arms. Incidence of death and renal replacement therapy (RRT) on Days 30, 60, and 90 were reported.

Results: For the 141 patients evaluated, the LS mean decrease in SCr from baseline to EOT with and without interaction between treatment and day were -0.98 mg/dL and -1.02 mg/dL for terlipressin, and -0.35 mg/dL and -0.26 mg/dL for placebo, respectively. The decrease in SCr from baseline to EOT was significantly larger in the terlipressin vs placebo arms; the difference in LS mean change in SCr between terlipressin and placebo was -0.64 mg/dL without interaction, and -0.76 mg/dL with interaction between treatment and day (both $p < 0.001$). In the terlipressin ($n = 84$) and placebo ($n = 60$) arms, the incidence of HRS reversal (defined as at least 1 SCr value of ≤ 1.5 mg/dL while on treatment by Day 14 or discharge) was 44.0% vs 11.7% ($p < 0.001$ respectively; incidence of death on Days 30, 60, and 90 were 33% vs 48% ($p = 0.070$), 41% vs 58% ($p = 0.034$), and 44% vs 60% ($p = 0.059$), respectively. Incidence of RRT on Days 30, 60, and 90 were similar between the terlipressin and placebo arms: 24% vs 25%, 26% vs 27%, and 26% vs 27% ($p > 0.800$ for all), respectively.

Conclusion: Compared with placebo, terlipressin significantly improved renal function and increased HRS reversal among patients with AAH and HRS-AKI who had ACLF grades 0–2 and was associated with fewer deaths on Day 60. However, the need for RRT was similar between treatment arms in this population.

THU-075-YI

Incidence and prognostic value of zinc and selenium deficiency in cirrhosis

Nina Dominik¹, Lorenz Balcar¹, Georg Semmler¹, Benedikt Simbrunner¹, Michael Schwarz¹, Benedikt Hofer¹, Lukas Hartl¹, Mathias Jachs¹, Bernhard Scheiner¹, Matthias Pinter¹, Michael Trauner¹, Mattias Mandorfer¹, Alexander Pilger², Thomas Reiberger¹. ¹Division of Gastroenterology and Hepatology, Department of Medicine III, Medical University of Vienna, Vienna Hepatic Hemodynamic Lab, Division of Gastroenterology and Hepatology, Department of Medicine III, Medical University of Vienna, Vienna, Austria; ²Department of Laboratory Medicine, Medical University of Vienna, Vienna, Austria
Email: nina.dominik@meduniwien.ac.at

Background and aims: Zinc and selenium are essential trace elements involved in important (patho)physiological processes. The incidence and prognostic implications of zinc and selenium deficiency in patients with cirrhosis remain unknown.

Method: We determined serum zinc and selenium concentrations in 309 patients with cirrhosis undergoing hepatic venous pressure gradient (HVPG) measurement between 2017–2022. We evaluated the prevalence of zinc/selenium deficiency and assessed its association with cirrhosis severity and liver-related events (i.e. hepatic decompensation/liver-related death).

Results: Among 309 cirrhotic patients [median: age: 57 (IQR 50–64) years, MELD: 11 (IQR 9–16) points, HVPG: 17 (IQR 11–20) mmHg], 73% ($n = 227$) and 63% ($n = 195$) were deficient in zinc and selenium, respectively. Decompensated (dACLD) patients showed significantly lower serum zinc [median: 48 (IQR 38–59) vs. compensated, cACLD: 65 (IQR 54–78) $\mu\text{g/dL}$, $p < 0.001$] and selenium levels [median: 4.9 (IQR 4.0–6.2) vs. cACLD: 6.1 (IQR 5.1–7.3) $\mu\text{g/dL}$, $p < 0.001$]. Significant correlations of zinc and selenium levels were found with MELD (zinc: Spearman's $Rho = -0.498$, $p < 0.001$; selenium: Spearman's $Rho = -0.295$, $p < 0.001$), HVPG (zinc: Spearman's $Rho = -0.400$, $p < 0.001$; selenium: Spearman's $Rho = -0.157$, $p = 0.006$), and liver disease-driving mechanisms (IL6, bile-acid homeostasis). Zinc and selenium consistently decreased with progression of liver disease as evaluated by disease severity scores (CTP score: $p < 0.001$ for zinc, $p = 0.001$ for selenium; MELD score: $p < 0.001$ for zinc and selenium) as well as with the severity of portal hypertension ($p < 0.001$ for zinc, $p = 0.003$

for selenium) and across clinical stages of cirrhosis ($p < 0.001$ for zinc and selenium). On multivariable analysis adjusting for clinically important co-factors, only low zinc levels [adjusted HR, aHR: 0.98 (95% CI: 0.96–0.99), $p = 0.014$] and the MELD score [aHR: 1.06 (95% CI: 1.00–1.11), $p = 0.044$] remained independently associated with liver-related events. Selenium was also found to be a prognostic parameter in univariable analysis [HR: 0.78 (95% CI: 0.64–0.95), $p = 0.016$], but did not independently predict liver-related events after multivariable adjustment. We evaluated a data-driven cut-off for zinc at 44.6 $\mu\text{g/dL}$ to stratify patients at distinct risk.

Conclusion: Zinc and selenium deficiencies are highly prevalent in patients with cirrhosis and are associated with key disease-driving mechanisms, most importantly with disease progression/hepatic dysfunction (i.e., MELD) and portal hypertension severity (i.e., HVPG). Patients with low serum zinc levels had a significantly increased risk of hepatic decompensation and liver-related death. Further studies should evaluate the impact of zinc and selenium supplementation on liver-related outcomes in patients with cirrhosis.

THU-076-YI

Machine learning algorithms predict survival in patients with cirrhosis hospitalized due to infections based on routine features obtained within 24 hours of admission

Shoham Dabbah^{1,2}, Yana Davidov^{1,2}, Ehud Zigmond^{1,2}. ¹Tel-Aviv University Faculty of Medicine, Tel-Aviv, Israel; ²Sheba Medical Center, Ramat Gan, Israel
Email: shohamdbh@gmail.com

Background and aims: Infections in cirrhotic patients increase the risk for death by a factor of 4 with mortality rates estimated as 30%, 44% and 63% at 1-, 3-, and 12-month, respectively. Hence, infection is considered a prognostic landmark in cirrhosis. Management entails decisions regarding the spectrum of therapeutic intervention, referral for critical care evaluation and liver transplantation, all rely heavily on the determination of prognosis. We aimed to train machine learning algorithms (MLAs) to predict survival in cirrhotic patients hospitalized due to infections and to provide explanations for the predictions.

Method: In this cross-sectional study 14 readily available features documented within 24 hours of hospitalization due to a diagnosis of an infection were used to train three MLAs. Hyperparameters were tuned to maximize time dependent ROC (tdROC) at 1-, 3-, and 12-month across 3-folds cross-validation of the training sample ($n = 472$). In order to stratify patients into three risk categories, two thresholds were tuned to maximize Youden index at 3- and 12-month for each MLA. The tdROC of MLAs were compared to model of end-stage liver disease (MELD) 3.0 and log-rank test was utilized to compare between survival curves of different risk categories from the validation sample ($n = 118$). Feature importance via permutation and partial dependence for survival probability were used to explain the best-performing MLA.

Results: In the validation sample mortality rates were 25%, 36% and 47% at 1-, 3-, and 12-month, respectively. Mean tdROC for random forest (RF), gradient boosting machine (GBM), penalized cox proportional hazard (COXPH) and MELD 3.0 were 0.8, 0.82, 0.76 and 0.71 respectively. RF and GBM, but not COXPH, outperformed MELD 3 at all time points ($p < 0.05$). The thresholds derived for GBM achieved sensitivity of 93% and 100% with specificity of 45% and 25% for mortality at 3- and 12-month, respectively. Patients from the validation sample were stratified into high, intermediate and low risk categories based on these thresholds. Survival curves differed significantly between these categories ($p < 0.05$). In contrast to COXPH, GBM identified time-dependent feature importance; while serum lactate had stronger influence on the survival probability at 3- compared to 12-month, the opposite was true for serum creatinine. Overall, the most important features considered by GBM were albumin, urea, age, creatinine and alkaline phosphatase.

Conclusion: An explainable GBM algorithm outperformed MELD 3.0 in determining prognosis among cirrhotic patients hospitalized due to infections using easily obtainable features measured within 24 hours of hospital admission. This risk stratification algorithm enables clinicians to understand the relationship of features with the survival probability and to tailor management at an early stage, hopefully translating into improvement in prognosis.

THU-077

Prognostic value of nutritional index in patients with decompensated cirrhosis: a single-center cohort study

Heechul Nam¹, Hee Yeon Kim¹, Chang Wook Kim¹. ¹The Catholic University of Korea, Seoul, Korea, Rep. of South
Email: hcnam128@catholic.ac.kr

Background and aims: Nutritional assessment is critical in patients with decompensated liver cirrhosis to maintain quality of life and improve survival. Nevertheless, the predictive value of nutritional index for the outcome of decompensated cirrhosis remains uncertain. This study aims to determine the potential prognostic value of nutritional index in predicting the liver transplantation (LT)-free survival of decompensated cirrhosis.

Method: This is a single-center, retrospective study that included consecutive patients presenting with first-onset decompensated complications to Uijeongbu St. Mary's Hospital from January 2013 to December 2022. Nutritional assessment in this study utilized the nutritional risk index (NRI), which was calculated based on serum albumin levels, body weight, and height. The primary end point was LT-free survival.

Results: The study included 1273 patients, with a median age of 57 years, of whom 69.5% were male. Alcoholic-related liver disease was the most common cause of liver disease in this cohort (65.2%), followed by chronic hepatitis B (15.9%), non-alcoholic steatohepatitis (11.6%), chronic hepatitis C (3.7%), and autoimmune hepatitis or primary biliary cholangitis (3.5%). The median MELD score of the patients was 16 (IQR, 12–22), and 19.8% of them met the criteria for APASL ACLF. At the time of the first admission, the most common complications observed were ascites (71.2%), followed by variceal bleeding (52.2%), hepatic encephalopathy (26.6%), spontaneous bacterial peritonitis (5.4%), and hepatorenal syndrome (11.8%). The median LT-free survival was 22.2 months (95% CI; 18.7–25.6 months). We conducted analysis based on ACLF; ACLF group (n = 1021) and non-ACLF (n = 252). The median LT-free survival was 29.5 months (95% CI, 26.4–33.1) in the non-ACLF group and 2.6 months (95% CI, 2.1–3.8) in the ACLF group (p < 0.001), respectively. In the non-ACLF group, Age ≥ 55 (HR, 1.53; 95% CI, 1.30–1.80, p < 0.001), MELD ≥ 20 (HR, 1.63; 95% CI, 1.33–2.04, p < 0.001), Child-Pugh class C (HR, 1.94; 95% CI, 1.42–2.65, p < 0.001), and NRI ≤ 83.5 (HR, 1.61; 95% CI, 1.23–2.10, p < 0.001) were identified as independent predictors of LT-free survival. In the ACLF group, NRI ≤ 83.5 (HR, 1.47; 95% CI, 1.10–1.96, p = 0.010) was only independently associated with LT-free survival.

Conclusion: In conclusion, nutritional index is independent predictor of LT-free survival in patients with decompensated cirrhosis irrespective of ACLF. Integrating nutritional index with established prognostic factors may improve prognostic accuracy and guide treatment decisions.

THU-078

Extra-hepatic organ failure in ACLF patients is associated with poor survival and limited curative therapy-results from AARC cohort

Ashok Kumar Choudhury¹, Vinod Arora², Mohd. Rela³, Dinesh Jothimani⁴, Mamun Al-Mahtab⁵, Harshad Devarbhavi⁶, CE Eapen⁷, Ashish Goel⁷, Cesar Yaghi⁸, Qin Ning⁹, Tao Chen¹⁰, Zhongping Duan¹¹, Saeed Sadiq Hamid¹², Wasim Jafri¹³, Akash Shukla¹⁴, Soek-Siam Tan¹⁵, Dong Joon Kim¹⁶, Anoop Saraya¹⁷, Jinhua Hu¹⁸, Ajit Sood¹⁹, Omesh Goyal²⁰, Manoj Sahoo²¹, Guan-Huei Lee²², Sombat Treeprasertsuk²³, Kessarin Thanapirom²⁴,

Ameet Mandot²⁵, Samir Shah²⁶, Laurentius A. Lesmana²⁷, Hasmik Ghazinyan²⁸, Mohan Prasad V C²⁹, A. Kadir Dokmeci³⁰, Jose Sollano³¹, Zaigham Abbas³², Ananta Shrestha³³, George Lau³⁴, Diana Payawal³⁵, Gamal Shiha³⁶, Ajay Kumar Duseja³⁷, Sunil Taneja³⁷, Nagaraja Rao Padaki³⁸, Anand Kulkarni³⁸, Md. Fazal Karim³⁹, Radha Krishan Dhiman⁴⁰, Ajay Mishra⁴⁰, Shahinul Alam⁵, Osamu Yokosuka⁴¹, Dr. Debashis Chowdhury⁴², Chandan Kedarisetty⁴³, Dr Sanjiv Saigal⁴⁴, Anil Arora⁴⁵, Ashish Kumar⁴⁵, Ghulam Nabi Yattoo⁴⁶, Abraham Koshy⁴⁷, Ajay Kumar⁴⁸, Mohammed Elbasiony⁴⁹, Pravin Rath⁵⁰, Sudhir Maharshi⁵¹, V.M. Dayal⁵², Ashish Kumar Jha⁵³, Kemal Fariz Kalista⁵⁴, Rino Gani⁵⁵, Man-Fung Yuen⁵⁶, Virendra Singh⁵⁷, Ayaskant Singh⁵⁸, Sargsyan Violeta⁵⁹, Chien-Hao Huang⁶⁰, Saurabh Mukewar⁶¹, Shaojie Xin⁶², Ruveena Bhavani⁶³, Charles Panackel⁶⁴, Sunil Dadhich⁶⁵, Sanjeev Sachdeva⁶⁶, Ajay Kumar⁶⁷, Sanatan Behera⁶⁸, Prabir Maji⁶⁹, Lubna Kamani⁷⁰, Hemamala Venugopal Saithanyamurthi⁷¹, Dr. Joy Varghese⁷², Pathik Parikh⁷³, P Javed⁷⁴, Neeraj Saraf⁷⁵, Narendra S. Choudhary⁷⁵, Akash Roy⁷⁶, Mahesh Goenka⁷⁷, Chetan Kalal⁷⁸, Krishnadas Devadas⁷⁹, Gupse Adali⁸⁰, Janaka De Silva H⁸¹, Masao Omata⁸², Manoj Sharma⁸³, Shiv Kumar Sarin⁸³. ¹Institute of Liver and Biliary Sciences, Delhi, India; ²Institute of Liver and Biliary sciences, Delhi, India; ³Dr. Rela Institute and Medical Centre, Chennai, India; ⁴Dr. Rela Institute and Medical Centre, Chennai, India; ⁵Bangabandhu Sheikh Mujib Medical University, Dhaka, Bangladesh; ⁶St Johns Medical College, Bangalore, India; ⁷CMC Vellore, Vellore, India; ⁸Hotel Dieu de France University Hospital, Beirut, Lebanon; ⁹Tongji Hospital of Tongji Medical College, Huazhong University of Science and Technology, Wuhan, China; ¹⁰Tongji Hospital, Tongji Medical College, Huazhong University of Science and Technology, Wuhan, China; ¹¹Beijing Youan Hospital, Beijing, China; ¹²Aga Khan University, Karachi, Pakistan; ¹³Aga Khan University Hospital, Karachi, Pakistan; ¹⁴Seth GS Medical College and KEM Hospital, Mumbai, India, Mumbai, India; ¹⁵Hospital Selayang, Bata Caves, Selangor, Malaysia; ¹⁶Hallym University College of Medicine, Chuncheon, Korea, Rep. of South; ¹⁷Institute of Liver and Biliary Sciences, New Delhi, India; ¹⁸302 Military Hospital, Beijing, China; ¹⁹Dayanand Medical College (DMC), Ludhiana, Ludhiana, India; ²⁰Dayanand Medical College and Hospital, Ludhiana, Ludhiana, India; ²¹IMS and SUM Hospital, Bhubaneswar, India; ²²National University Hospital, Singapore, Singapore; ²³Chulalongkorn University, Bangkok, Thailand; ²⁴Chulalongkorn University and King Chulalongkorn Memorial Hospital, Thai Red Cross Society, Bangkok, Thailand; ²⁵Global Hospital, Mumbai, India; ²⁶Global Hospital- Super Speciality and Transplant Center, Mumbai, India; ²⁷RS Medistra, Jakarta, Indonesia; ²⁸Nikommed Medical Center, Yerevan, Armenia; ²⁹VGM Hospital, Tamil Nadu, India; ³⁰Ankara University School of Medicine, Ankara, Turkey; ³¹University of Santo Tomas, Manila, Philippines, Manila, Philippines; ³²Ziauddin University, Karachi, Pakistan; ³³Alka Hospital, Kathmandu, Nepal; ³⁴Humanity and Health Clinical Trial Centre, Hong Kong, Hong Kong; ³⁵Fatima University Medical Center, Valenzuela City Metro Manila, Philippines; ³⁶ELPA-Egypt, Cairo, Egypt; ³⁷PGIMER, Chandigarh, India; ³⁸AIG Hospitals, Hyderabad, India; ³⁹Sir Salimullah Medical College Hospital, Bangladesh, Dhaka, Bangladesh; ⁴⁰SGPGI, Lucknow, India; ⁴¹Department of Gastroenterology and Nephrology, Chiba University, Chiba, Japan; ⁴²CMOSH Medical College, Bangladesh, Agrabad, Chattogram, Bangladesh; ⁴³Gleneagles Global Hospitals, Hyderabad, India; ⁴⁴Max Super Specialty Hospital, Saket New Delhi, India, Delhi, India; ⁴⁵Sir Ganga Ram Hospital, New Delhi, India; ⁴⁶Sher-i-Kashmir Institute of Medical Sciences, Srinagar, Jammu and Kashmir, India; ⁴⁷Lakeshore Hospital, Kochi, India; ⁴⁸King George's Medical University, Lucknow, India; ⁴⁹Egyptian Liver Research Institute and Hospital (ELRIAH), Mansoura, Egypt; ⁵⁰Topiwala National Medical College and BYL Nair Hospital, Mumbai, India; ⁵¹SMS Medical College and Hospital, Jaipur, India; ⁵²IGIMS, Patna, India, Patna, India; ⁵³IGIMS, Patna, Patna, India; ⁵⁴Cipto Mangunkusumo Hospital, Indonesia, Jakarta, Indonesia; ⁵⁵RSCM, Jakarta, Indonesia; ⁵⁶The University of Hong Kong, Hong Kong SAR, China; ⁵⁷Postgraduate Institute of Medical Education and Research, Chandigarh, India; ⁵⁸IMS and SUM

POSTER PRESENTATIONS

Hospital, Bhubaneswar, India; ⁵⁹Violeta Medical Centre, Yerevan, Armenia; ⁶⁰Chang-Gung University, College of Medicine, Tao Yuan, Taiwan; ⁶¹Midas Multispeciality Hospital Pvt. Ltd.-Nagpur, Nagpur, India; ⁶²Beijing 302 Hospital, Beijing, China; ⁶³University of Malaya, Kuala Lumpur, Malaysia; ⁶⁴Aster Medcity, Kochi, India; ⁶⁵SMNC, Jodhpur, India; ⁶⁶G B Pant Hospital, New Delhi, India; ⁶⁷G.B. Pant Hospital, New Delhi, India; ⁶⁸SCB Medical College and Hospital, Cuttack (Odisha), Odisha, India; ⁶⁹SCB Medical College and Hospital, Cuttack (Odisha), Odisha, India; ⁷⁰Liaquat National Hospital, Karachi, Pakistan; ⁷¹MIOT International, Chennai, India; ⁷²Gleneagles Global Health City, Chennai, India; ⁷³Apollo Hospitals, Ahmedabad, India; ⁷⁴Aster MIMS Hospital, Kannur, India; ⁷⁵Medanta The Medcity, Haryana, India; ⁷⁶Postgraduate Institute of Medical Education and Research, Chandigarh, India; ⁷⁷Apollo Multispeciality Hospital, Kolkata, India; ⁷⁸Global Hospitals, Mumbai, India; ⁷⁹Government Medical College, Trivandrum, India; ⁸⁰University of Health Sciences Istanbul Umraniye Training and Research Hospital, Istanbul, Turkey; ⁸¹University of Kelaniya, Ragama, Sri Lanka; ⁸²University of Tokyo, Tokyo, Japan; ⁸³Institute of Liver and Biliary Sciences, New Delhi, India
Email: doctor.ashokchoudhury@gmail.com

Background and aims: ACLF syndrome is liver failure with or without extra-hepatic organ failure (OF) like- renal, circulatory and cardiac. Therapy, liver transplant and survival are confounded by the organ failures often with or without sepsis. We studied the impact of the type, time frame, evolution and impact on therapy as well as survival of the extra-hepatic OF (EHOF) among hospitalized patients of ACLF.

Method: We analysed prospectively collected data of ACLF patients (APASL criteria) from AARC registry. History, clinical course and OF development, sepsis laboratory parameters, treatment received and survival were compared among those with ACLF with or without EHOF. Liver failure is defined as jaundice, coagulopathy or HE whereas extra-hepatic OF is defined as per CLIF-SOFA.

Results: Total of 8, 683 ACLF patients [mean age 44.5 ± 8.9 years, 86.8% male], predominant aetiologies being alcohol (57.1%) and HBV reactivation (12.4%). At presentation majority (6258, 72.1%) of ACLF patients had an additional EHOF i.e. renal (42.1%), circulatory (8.6%) and respiratory (2.2%). Those with EHOF were younger, male, with high WBC, MELD, AARC score, low platelet, low albumin ($p < 0.01$) and often sepsis (39.6% vs. 30.1%, $p < 0.001$). They had greater new onset sepsis (6.9% vs 2.2%), need of RRT (27.4% vs 0.5%) or ventilator (3.6% vs 0.5%) and higher mortality (26.1% vs 18.4%) in first week. In absence of EHOF at baseline and at day 4, a lower 90-day mortality (21.9%) noted, while single EHOF at baseline or day 4 increases it to 50.8% and 85.5% respectively. With organ support and improved EHOF at end of first week-mortality showed a decline. Two or three EHOF were uniformly associated with high mortality (>80%). The 90-day mortality increased proportionately with 1 [HR 1.23 95 CI (1.22–1.29)], 2 [HR 1.49 95 CI (1.46–1.53)] and 3 [HR 2.38 95 CI (2.35–2.41)] EHOF respectively. These patients could be offered LT in limited cases (2.9% vs. 10.7%, $p < 0.001$). Presence of EHOF associated with high 90-days mortality (55.3% vs. 37.1%, $p < 0.01$) and is an independent predictor HR [1.23 95 CI (1.22–1.29), $p < 0.001$] at 90 days.

Conclusion: ACLF is serious condition with only half surviving at the 90 days and two third patients have associated EHOF at presentation to tertiary centres, most common being renal. Presence of EHOF is an independent and dynamic predictor of survival, also precludes liver transplant, whereas optimisation of the organs is associated with improved survival.

THU-079

Pre-transplant work-up for acute-on-chronic liver failure patients in intensive care units, a nationwide french survey

Claire Bellec¹, Romain Moirand², Armand Aberger³, Teresa Antonini⁴, Rodolphe Anty⁵, Isabelle Mabile-Archambeaud⁶, Aurore Baron⁷, Christophe Bureau⁸, Jean-François Cadranet^{9,10}, Nicolas Carbonell¹¹, Paul Carrier¹², Audrey Coilly¹³, Filomena Conti¹⁴,

Charlotte Costentin¹⁵, Victor de Lédinghen¹⁶, Sebastien Dharancy¹⁷, Claire Francoz¹⁸, Armand Garioud¹⁹, René Gerolami²⁰, Elia Gigante²¹, Adrien Lannes²², Marianne Latournerie²³, Jean Charles Nault²⁴, Georges-Philippe Pageaux²⁵, Claire Perignon²⁶, Noemi Reboux²⁷, Valentin Rolle²⁸, Isabelle Rosa²⁹, Delphine Weil-Verhoeven³⁰, Faustine Wartel³¹, Laure Elkrief¹, Florent Artru². ¹CHU Tours, France; ²CHU Rennes, France; ³CHU Clermont Ferrand, France; ⁴CHU Lyon, France; ⁵CHU Nice, France; ⁶CHU Nantes, France; ⁷CH Sud Francilien, Noisy Le Grand, France; ⁸CHU Toulouse, France; ⁹GHPSO, Creil, France; ¹⁰GHPSO, Liver and Digestive Diseases Department, Creil, France; ¹¹CHU Saint Antoine, Paris, France; ¹²CHU Limoges, France; ¹³CHU Paul Brousse, Villejuif, France; ¹⁴CHU Pitié Salpêtrière, Paris, France; ¹⁵CHU Grenoble, France; ¹⁶CHU Bordeaux, France; ¹⁷CHU Lille, France; ¹⁸CHU Beaujon, Paris, France; ¹⁹CH Villeneuve Saint Georges, France; ²⁰CHU Marseille, France; ²¹CHU Reims, France; ²²CHU Angers, France; ²³CHU Dijon, France; ²⁴Sorbonne Université, Paris, France; ²⁵CHU Montpellier, France; ²⁶CHU Caen, France; ²⁷CHU Brest, France; ²⁸CHU Poitiers, France; ²⁹CHIC Créteil, France; ³⁰CHU Besançon, France; ³¹CH Valenciennes, France
Email: claire.blc@gmail.com

Background and aims: The outcome after liver transplantation (LT) for acute-on-chronic liver failure (ACLF) is acceptable with a 1-year survival exceeding 80%. However, access to LT lies on a narrow timeframe as death commonly occurs early after admission. Hence, the period dedicated to the pre-transplant work-up is shortened. Notably, cardiovascular (CV) events emerge as a prominent cause of post-LT mortality in ACLF cases questioning the adequacy of the screening. There is a current lack of consensus regarding the components of the pre-transplant work-up for these patients. We aimed to investigate the status of pre-transplantation work-up practices in patients with ACLF.

Method: A questionnaire was devised with hepatologists and addictologists' involvement and distributed to 39 French centers. It was divided into 3 sections: work-up for ambulatory patients (AP group), work-up for hospitalized patients with decompensated cirrhosis but without ACLF (DC), and work-up for patients with ACLF in intensive care units (ACLF). Each section was divided into 4 parts including CV and respiratory comorbidities, oncological, nutritional and addictology assessment.

Results: 31 (80%) centres answered to the survey. 15 (48%) were LT centres with 67% of them transplanting ≥6 patients with ACLF/year. Of the 16 non-LT centres, 67% estimated to transfer ≥6 patients with ACLF/year to LT centre. Electrocardiogram and transthoracic echocardiography were the only CV work-up performed in 97% of centres in patients with ACLF whilst 58% and 68% centres performed a least another CV exploration in DC and AC respectively ($p < 0.0001$). While chest CT-scan was performed in all groups and centres, respiratory function testing was performed in 19% of the centers in ACLF vs. 68% vs. 87% in DC and AP respectively ($p < 0.0001$). Regarding addictology assessment, there was a non-significant increase of centres considering transplantability without a minimal period of abstinence in patients with ACLF 68% vs. 45% in DC and vs. 42% in AP, $p = 0.08$. Relative requesting to investigate the addictology profile was more frequent in ACLF patients 81% vs. 68% in DC, vs. 52% in AP, $p = 0.05$. An esophagogastrroduodenoscopy combined with a thoraco-abdominopelvic CT-scan and PSA concentration in males was considered sufficient to screen for cancer in most cases of ACLF 55% but not in DC (0%) or AP (0%), $p < 0.0001$. The estimated timeframe to placement on waiting list was 7 days in ACLF vs. 21 days in DC vs. 45 days in AP, $p < 0.0001$. 97% of centres agreed that the pre-LT work-up had to be shortened to optimise access to LT but 26% thought that it increased the risk of not identifying LT contraindication.

Conclusion: The survey results emphasize the distinctive nature of the pre-LT assessment in ACLF patients compared other groups. The definitive impact of the shortened work-up on outcome after LT remain to be prospectively investigated.

THU-080-YI

The predictive role of immunoglobulins indicative of gut barrier dysfunction in a prospective patient cohort with cirrhosis and acute decompensation

David Tornai¹, Boglarka Balogh¹, Aniko Csillag¹, Istvan Tornai¹, Zsuzsanna Vitalis¹, Patricia Kovats¹, Péter Antal-Szalmás², Florian Rosenberger³, Matthias Mann^{3,4}, Wim Laleman⁵, Minneke J. Coenraad⁶, Jonel Trebicka^{7,8}, Maria Papp¹. ¹Division of Gastroenterology, Department of Internal Medicine, Faculty of Medicine, University of Debrecen, Debrecen, Hungary; ²Department of Laboratory Medicine, Faculty of Medicine, University of Debrecen, Debrecen, Hungary; ³Department for Proteomics and Signal Transduction, Max-Planck Institute of Biochemistry, Martinsried, Germany; ⁴NNF Center for Protein Research, Faculty of Health Sciences, University of Copenhagen, Copenhagen, Denmark; ⁵Department of Gastroenterology and Hepatology, University Hospitals Leuven, KU Leuven, Leuven, Belgium; ⁶Department of Gastroenterology and Hepatology, Leiden University Medical Center, Leiden, Netherlands; ⁷Department of Internal Medicine B, University Hospital Muenster, Muenster, Germany; ⁸European Foundation for Study of Chronic Liver Failure, Barcelona, Spain
Email: tornai.david@med.unideb.hu

Background and aims: Cirrhosis is associated with impaired gut mucosal immunity, thereby facilitating bacterial translocation, which activates the proinflammatory cascade, further exacerbating tissue damage and progression of liver disease. However, little is known about the role of antibody-mediated adaptive immunity in this process. Therefore, we measured serum levels of immunoglobulin (Ig) indicators of gut barrier function in a prospective patient cohort with cirrhosis and acute decompensation (AD) to determine their ability to predict outcomes.

Method: Serum samples of 128 patients recruited in the frame of MICROB-PREDICT have been assayed at inclusion and acute-on-chronic liver failure (ACLF) development to determine levels of IgA and IgG antibodies against various targets (F-actin; *Saccharomyces cerevisiae* [ASCA]; glycoprotein 2 [GP2]; gliadin; endotoxin core [EndoCab]), secretory (s)IgA, total IgA, IgG, IgM and free Ig kappa and lambda light chains. Disease severity was assessed by CLIF-C AD, MELD and Child-Pugh scores and presence of ACLF. ACLF development and liver-related death were assessed in a 3-month follow-up period.

Results: The presence of target specific IgA type antibodies increased in parallel to diseases severity as defined by Child-Pugh stages. Higher total IgA level was associated with increased detection of IgA type antibodies and elevated levels of individual antibodies in patients. At inclusion, high CLIF-C AD score (≥ 50) was associated with decreased total IgG levels (median [IQR]: 16 [11.15–19.89] vs. 18.8 [13.45–24.05] mg/ml; $p = 0.042$), while the presence of ACLF was associated with elevated free Ig kappa light chain (29.6 [20.18–40.65] vs. 20.5 [14.23–31.93] $\mu\text{g/ml}$; $p = 0.043$) and decreased total IgG levels (12.4 [8.23–19.3] vs. 17.3 [11.6–22.5] mg/ml; $p = 0.046$). ACLF development during follow-up was associated with increased free Ig kappa light chain level ($p = 0.018$).

Ninety-day mortality in all patients with ACLF (at inclusion and during follow-up) was associated with increased sIgA levels (AUROC: 0.819; at the cut-off of $>20.9 \mu\text{g/ml}$: 15% vs 79% mortality $p < 0.001$).

Conclusion: Mucosal immune activation as indicated by increased total IgA level occurs along the increasing severity of Cirrhosis. The presence of target specific IgA antibodies suggest a link to enhanced BT. Increased sIgA level is a promising marker of 90-day mortality in ACLF patients.

THU-082

A clinical decision support tool to identify predictors of decompensation, acute-on-chronic liver failure and mortality in liver cirrhosis from the multi-center SingHealth chronic liver disease registry (SoLiDaRity-DAM)

Jason Pik Eu Chang¹, Wei-Quan Teo², Amber Chung², Rahul Kumar³, Marianne DeRoza⁴, Hiang Keat Tan¹, Prema Raj². ¹Singapore General Hospital, Singapore, Singapore; ²SingHealth Duke-NUS Transplant Center, Singapore, Singapore; ³Changi General Hospital, Singapore, Singapore; ⁴Sengkang General Hospital, Singapore, Singapore
Email: jason.chang@singhealth.com.sg

Background and aims: Chronic liver disease, particularly cirrhosis, poses a significant health burden resulting in substantial mortality rates. Timely identification of decompensation and acute-on-chronic liver failure (ACLF) in cirrhosis patients is crucial to reduce mortality and improve outcomes. In this study, we address the pressing need for predictive tools by leveraging electronic health records (EHR) and advanced machine learning techniques to develop an automated clinical decision support system using data from the multi-center SingHealth Chronic Liver Disease Registry (SoLiDaRity-DAM). This system aims to predict decompensation events, facilitate timely referral for liver transplantation, and enhance patient care in cirrhosis management.

Method: SoLiDaRity-DAM encompasses a comprehensive approach to convert longitudinal structured and unstructured patient data from diverse EHR sources into predictive algorithms and machine learning models. The development process places a strong emphasis on merging clinical expertise with statistical methods. In this proof-of-concept (POC) study, we generated a Random Forest Classifier model using clinically annotated data from our registry. The model's primary objective was to predict the likelihood of cirrhosis patients developing decompensation based on collected clinical indicators. Furthermore, we applied linear regression to estimate the time to decompensation events in the cirrhotic cohort.

Results: The Random Forest Classifier achieved an impressive accuracy score of $\sim 89\%$, highlighting its potential for identifying patients at risk of decompensation. Feature selection identified the top 10 ranking variables, with biomarkers like Alpha Fetoprotein (AFP) and the presence of ascites and varices highlighted as critical factors in distinguishing patients with decompensated cirrhosis. Among the five regression models we used for the prediction of the time to decompensation, Random Forest is identified as the best model with the lowest loss function value.

Conclusion: SoLiDaRity-DAM demonstrates the feasibility of utilizing AI and machine learning techniques to predict decompensation events in cirrhosis patients with high accuracy. By integrating clinical expertise and EHR data, this AI-powered clinical decision support system holds promise in improving patient outcomes by enabling timely interventions, including the referral for liver transplantation. The development of SoLiDaRity-DAM represents a crucial step towards personalized, data-driven cirrhosis management, with the potential to significantly reduce mortality and healthcare costs in Singapore's population.

THU-083

Acute kidney injury (AKI) severity in critically-ill patients with decompensated liver cirrhosis and acute-on-chronic liver failure (ACLF)

Martin Schulz¹, Lena Wolters¹, Helen Jurr¹, Wenyi Gu¹, Maximilian Joseph Brol¹, Frank Erhard Uschner¹, Michael Tischendorf¹, Konrad Buscher¹, Alexander Zarbock¹, Robert Schierwagen¹, Sabine Klein¹, Stefan Zeuzem², Kai-Henrik Peiffer¹, Jonel Trebicka^{1,3}. ¹University Hospital Münster, Münster, Germany; ²Goethe University, Frankfurt, Germany; ³European Foundation for Study of Chronic Liver Failure, Barcelona, Spain
Email: martinsebastian.schulz@ukmuenster.de

POSTER PRESENTATIONS

Background and aims: Acute kidney injury (AKI) is a frequent complication in patients with acutely decompensated liver cirrhosis (AD) and acute-on-chronic liver failure (ACLF). Although it has been acknowledged that underlying pathomechanisms and clinical courses may differ between AKI in AD and ACLF, differences in clinical trajectories between AKI in AD and ACLF are not well characterized to date.

Method: In this retrospective analysis 498 patients with cirrhosis and IMC/ICU admission were included. To assess differences of AKI severity in the spectrum of AD/ACLF, patients were enrolled into the following subgroups: AD-AKI, ACLF-AKI, ACLF-renal failure (ACLF-AKI-RF) or ACLF-AKI requiring renal replacement therapy at admission (ACLF-AKI-RRT). AKI was defined according to ICA criteria. ACLF was defined according to EASL-CLIF criteria. All patients with history of chronic kidney disease (CKD) were excluded. Clinical data, laboratory and urinary results were retrospectively collected. Urine analysis was performed in spot-urine.

Results: Median age was 60 years, 71.5% were male. At admission, 173/498 (34.7%) of patients presented defined ACLF. While only 19% of ACLF patients (33/173) presented AKI, 43.9% (76/173) presented ACLF-AKI-RF and an additional 12.7% (22/173) required RRT at admission due to AKI. 28-day mortality was strongly associated with AKI and ACLF severity (AD-AKI: 14.3%, ACLF-AKI: 51.1%, ACLF-AKI-RF: 53.6%, ACLF-AKI-RRT: 77.8% $p < 0.001$). Surrogates of SI increased among AD/ACLF progression (leucocytes: AD-AKI: 8.6/nl vs. ACLF-AKI: 9.3/nl vs. ACLF-AKI-RF: 11.6/nl, ACLF-AKI-RRT: 15.0/nl, $p < 0.001$; neutrophil-to-monocyte-ratio 7.9 vs 10.1 vs 13.2 vs 14.23, $p = 0.01$). Upon disease progression among the subgroups, and colinear to SI severity, patients showed increasing proteinuria (AD-AKI: 17 mg/dl, ACLF-AKI: 24 mg/dl, ACLF-AKI-RF: 38 mg/dl, ACLF-AKI-RRT: 87 mg/dl, $p < 0.001$). This was also reflected in protein-to-creatinine ratio, showing a significant association within ACLF severity grades ($p < 0.05$). BUN-to-creatinine-ratio >20 , a hallmark of prerenal AKI, decreased upon AKI progression (AD-AKI: 50.9%, ACLF-AKI: 51.7%, ACLF-RF: 30%, ACLF-RRT: 21.1% $p < 0.05$).

Conclusion: AKI in AD and ACLF is closely linked to patient outcomes. Interestingly, our data show that increasing severity of SI is paralleled by increased proteinuria upon ACLF progression and urinary surrogates of intrarenal kidney injury. While AD-AKI patients present urinary profiles predominantly associated with prerenal injury, our data suggests that the aggravation of AKI upon ACLF progression could be increasingly driven by intrarenal injury mechanisms.

THU-086

Proton pump inhibitors does not impact on the severity and mortality of the acute-on-chronic liver failure: andalusian multicentric prospective study

María Carmen García-Gavilán¹, Marta Guerrero-Misas², Alberto García-García³, Marta Casado-Martin⁴, Laura Castillo-Molina⁵, Yolanda María Sanchez-Torrijos⁶, Carmen Sendra^{7,8}, Jose Miguel Rosales-Zábal¹. ¹Costa del Sol University Hospital, Marbella, Spain; ²Reina Sofia Regional Hospital Complex, Córdoba, Spain; ³Virgen de la Victoria Specialty Hospital Complex, Málaga, Spain; ⁴Torrecañadas Specialty Hospital Complex, Almería, Spain; ⁵Jaén Hospital, Jaén, Spain; ⁶Virgen del Rocío Regional Hospital Complex, Seville, Spain; ⁷Virgen del Rocío University Hospital, Seville, Spain; ⁸Virgen del Rocío University Hospital, Seville, Spain. Email: marigarcagavilan@hotmail.es

Background and aims: The proton pump inhibitors (PPI) are widely consumed worldwide and there is no prospective study that evaluates their influence on acute-on-chronic liver failure (ACLF). The main objective was to assess the possible influence of the chronic PPI consumption and the severity of the ACLF. The secondary objectives were to assess its possible relation with the mortality and different types of decompensation of the ACLF.

Method: Prospective cohort study (7 participants hospitals from Spain) between august 2020 to 2023. We recruited all patient with diagnosis of ACLF and classified them as exposed or not exposed, according to the chronic PPI intake. All patients with hepatocellular carcinoma, immunosuppression, digestive surgery or PPI intake under 3 months were excluded. On admission, chronic PPI intake, norfloxacin, rifaximin, lactulose, statins, antiaggregation and anticoagulation were recorded. The CLIF-C-OF was determined at admission, the CLIF-C-ACLF at admission, 3 and 7 days, the Child-pugh score, MELD-Na score and the type of decompensation were registered too. Analytical variables of liver, kidney and hematological function were collected as well as critical care unit admissions, new hospitalizations for ACLF and the mortality at 28 days, 3 and 6 months were recorded.

Results: 60 patients were enrolled with a median age of 59 years: 26 chronic IBP users (76.9% Omeprazole) and 33 non-users. Among consumers, 69% do not have an established indication for PPI consumption. They regularly take lactulose in the 27.1% of the cases, rifaximin in 10.2%, norfloxacin in 16.9%, simvastatin in 6.8%, chronic antiaggregation in 7.3% and chronic anticoagulation in 10.9%. At admission they had a median CLIF-C-OF of 9, CLIF-C-ACLF of 52, CHILD of 10 and MELD-Na of 29. The most frequent type of decompensation was the hepatic encephalopathy, followed by the hydropic decompensation and infections (66.7%, 56.7% y 48.3% respectively). The urine infection was the most frequent one (20%), followed by spontaneous bacterial peritonitis and respiratory infections (18.3%). 15.8% were admitted to the critical care unit and 45.8% died during the hospitalization. When analyzing, no relation was found between the chronic PPI consumption and the severity of the ACLF ($p = 0.44$ for the CLIF-C-OF score and $p = 0.87$ for the CLIF-C-ACLF score), with the mortality during the admission ($p = 0.63$), at 28 days ($p = 0.70$) and 3 months ($p = 0.98$). Nor was a significant relationship found with each type of decompensation within the ACLF.

Conclusion: This is the first prospective study assessing the influence of the PPI and the ACLF. With our results we can conclude that no relationship is observed between chronic PPI consumption and the severity of the ACLF, the mortality of the ACLF and the different types of acute decompensation within the ACLF.

THU-087

Herpesvirus viremia-cause or consequence of ACLF? Higher prevalence of cytomegalovirus, Epstein-Barr virus and herpes simplex virus viremia in patients with acute-on-chronic liver failure

Jannik Sonnenberg¹, Keerthihan Thiyagarajah², Esra Görgülü³, Mirco Glitscher², Nico Kraus³, Toska Wiedemann³, Marcus Maximilian Muecke³, Michael Praktikno¹, Hans-Peter Erasmus³, Frank Erhard Uschner¹, Wenyi Gu¹, Maximilian Joseph Brol¹, Martin Schulz¹, Michael Tischendorf¹, Robert Schierwagen¹, Sabine Klein¹, Jessica Vasseur³, Stefan Zeuzem³, Holger Storf³, Christoph Welsch³, Jonel Trebicka¹, Sandra Ciesek⁴, Eberhard Hildt², Kai-Henrik Peiffer¹. ¹Medizinische Klinik B, Uniklinikum, Münster, Germany; ²Paul-Ehrlich-Institut, Langen, Germany; ³Goethe University Hospital, Frankfurt, Germany; ⁴Institute for Medical Virology, Frankfurt, Germany. Email: jannik.sonnenberg@ukmuenster.de

Background and aims: Acute-on-chronic liver failure (ACLF) is a life-threatening clinical syndrome characterized by the rapid deterioration of liver and other organ function in individuals with pre-existing chronic liver disease. In 40–60% of patients, the precipitants contributing to ACLF remain unknown. Herpesviruses, including Cytomegalovirus (CMV), Epstein-Barr virus (EBV) and Herpes simplex virus (HSV) are highly prevalent viruses, which may cause isolated self-limiting hepatitis in immune competent patients, but severe infections leading to fulminant hepatic failure in immuno-compromised patients, such as liver cirrhosis.

Method: We analysed blood samples from 212 patients (42 ACLF vs. 170 liver cirrhosis patients) registered in the ACLF-I-study for viremia of the herpesviruses CMV, EBV and HSV. Viral nucleic acids were extracted from 200 µl serum and multiplex-qPCR was performed. Absolute copy numbers were calculated based on standard curves and were correlated with clinical data.

Results: Higher prevalence of overall viremia (47, 6% vs. 26, 4%, $p < 0,001$), CMV (28, 6% vs. 16, 0%, $p = 0,016$), EBV (16, 7% vs. 9, 0%, $p = 0,039$) and HSV1 (7, 1% vs. 2, 4%, $p = 0,025$) were observed in ACLF patients in comparison to non-ACLF patients. Viremia remained clinically undetected and there was no suspicion for viral infections documented. In a third of ACLF patients with experimentally detected viremia the precipitant of ACLF was unknown. Viremia was associated with overall higher bilirubin levels, CLIF score and ACLF grade. CMV and HSV1 were significantly associated with liver failure while EBV correlated with failure of the respiratory system.

Conclusion: The presence of viral infections may tip the balance towards ACLF and impair hepatocellular function in individuals with chronic liver disease. However, the observed high prevalence of herpesviruses in our study may be a cause or a consequence of acute-on-chronic liver failure.

THU-088

Blood and peritoneal metabolomics suggest VS-01 actively captures metabolites associated with acute-on-chronic liver failure

Olaf Tyc¹, Frank Erhard Uschner^{1,2}, Berenice Alard³, Meriam Kabbaj⁴, Jeremy Magnanensi³, Désirée Füglistaller⁴, Marie Bobowski-Gerard³, Dean Hum³, Bart Staels⁵, Katharina Staufer⁴, Jonel Trebicka^{1,2}.

¹Department of Internal Medicine I, Hospital of the Goethe University, Frankfurt, Germany; ²Department of Internal Medicine B, University Hospital, Münster, Germany; ³Genfit S.A., Loos, France; ⁴Versantis AG (Genfit Group), Zurich, Switzerland; ⁵Univ. Lille, INSERM, CHU Lille, Institut Pasteur de Lille, Lille, France
Email: berenice.alard@genfit.com

Background and aims: Acute-on-Chronic Liver Failure (ACLF) is characterized by systemic inflammation, organ failure, and high short-term mortality. ACLF is associated with an accumulation of metabolites in blood, altering major metabolic pathways which may contribute to disease progression. VS-01 is a novel investigational intraperitoneal (*i.p.*), pH-gradient, liposomal suspension that enhances the clearance of ammonia and potentially of other metabolites as suggested by prior metabolomic analysis in blood. Using both peritoneal and blood data from the Phase 1 clinical trial evaluating VS-01 safety in patients with decompensated cirrhosis, ascites and covert hepatic encephalopathy, we aimed to confirm the captures of metabolites previously proposed and to explore further metabolites in the context of ACLF.

Method: Metabolomic analyses were performed in blood and peritoneal fluid samples of 9 patients in whom a single dose of VS-01 (15, 30 or 45 ml/kg body weight, 3 patients each) was administered *i.p.* and left to dwell for 2 h following paracentesis. Blood samples were collected concomitantly with ascites at baseline (T0), and with peritoneal fluid samples at the end of the dwell time (T2) and 24 h after VS-01 infusion start (T24). Metabolomic analyses were first performed on all samples using an untargeted LC/MS approach. Among identified metabolites, we focused on 24 compounds which were already described in the literature as being potentially related to organ failures and ACLF and aimed to analyze the potential capture of these metabolites by VS-01. Statistical analyses, using MetaboAnalyst package in R, were performed on the peak lists containing mass features of identified compounds, computing fold changes and t-tests.

Results: At the end of the 2 h dwell time (T2), we observed a significant capture of 10 metabolites out of the 24 in ascites when compared to T0 ($p < 0.05$). Among the 10 metabolites, 5 were concomitantly associated with a numerical decrease in blood at T2

vs T0, suggesting a potential specific capture of these metabolites by VS-01. Moreover, comparing fold changes, 4 of these metabolites were associated with an increase at T2 vs T0 compared to T24 vs T0 in the peritoneal fluid, whereas a decrease was observed in blood, respectively, confirming a potential removal of those metabolites by VS-01. The identified compounds which appeared to be captured by VS-01 are Trimethylamine N-Oxide (TMAO), Carnitine, N-Acetyl-Alanine and 4-Acetamidobutanoic acid.

Conclusion: VS-01 seems to specifically capture metabolites that may be associated with organ failures and inflammation, which are hallmarks of ACLF. TMAO, reported to be toxic for the kidney and associated with the progression of multiple diseases, could represent an interesting metabolite to clear out in the context of ACLF. Further analyses should be performed to confirm our findings.

THU-089

Bilirubin monoglucuronides play an important role in the pathophysiology of acute-on-chronic liver failure

Stephany Castillo-Castañeda¹, Jacqueline Cordova-Gallardo², Liliana Rivera-Espinosa³, Juan Chavez-Pacheco³, Mariana Ramírez-Mejía¹, Nahum Méndez-Sánchez¹. ¹Medica Sur Clinic and Foundation, National Autonomous University of Mexico, Mexico City, Mexico; ²General Hospital Dr. Manuel Gea González, National Autonomous University of Mexico, Mexico City, Mexico; ³National Pediatric Institute, Mexico City, Mexico
Email: nmendez@medicasur.org.mx

Background and aims: Acute-on-chronic liver failure (ACLF) is a syndrome characterized by acute decompensation of chronic liver disease associated with organ failures and high short-term mortality. ACLF frequently occurs in a closed temporal relationship to a precipitating event, involving systemic inflammation due to infections and acute liver damage. The development of organ failures may be a result of a combination of tissue hypoperfusion, direct immune-mediated damage and mitochondrial dysfunction. The aim of the present study was to evaluate the molecular species of bilirubin in patients with compensated liver cirrhosis (LC) and those with ACLF.

Method: We included patients diagnosed with LC and ACLF, and healthy subjects (HS) as controls. The ACLF patients were diagnosed using the EASL-CLIF definition and ACLF grades. We collected all clinical and biochemical data. Bilirubin molecular species: BMG, BDG and UCB were measured in serum by LC-MS, monitoring their m/z. Results are expressed as median, IQR, frequency and percentages. Statistical analyses were performed by the Mann-Whitney and Kruskal-Wallis tests, with p values < 0.05 as significant.

Results: A total of 58 consecutive patients were included, 29 with ACLF diagnosis, 11 with LC, and 18 HS. The median age of the ACLF patients was 54 years, compared with 46 years for LC and 63 years for HS. The most common etiology was alcohol-associated liver disease, 63.3% in ACLF and 28.6% in LC. Bilirubin molecular species levels (BMG, BDG and UCB) in ACLF patients were 28.57, 1.32 µmol/L and 19.69 µmol/L. In the LC, the median concentrations were 1.49, 0.055 and 11.29 µmol/L, respectively. In the HS, levels were 0.52, 0.028 and 6.42 µmol/L. With a p value of 0.000.

According to ACLF grade, BMG, BDG and UCB were 11.36, 0.62 and 36.08 µmol/L for NO ACLF, 15.87, 1.19 and 21.16 µmol/L for ACLF 1, 28.07, 1.21 and 18.76 µmol/L for ACLF 2 and 239.07, 7.37 and 23.04 µmol/L for ACLF 3. The p values were 0.007 and 0.009 for BMG and BDG.

Conclusion: We found that bilirubin molecular species levels are significantly higher in cirrhosis, especially in those who develop ACLF. We believed that at high concentrations, bilirubin lost its protective antioxidant and anti-inflammatory effects, contributing to the distinctive feature of ACLF development including systemic inflammation. As more bilirubin is released into the system, more toxicity occurs, causing membrane and mitochondrial dysfunction, oxidative stress, apoptosis, inflammation, and even epigenetic modifications in susceptible organs. All these bilirubin-induced toxic mechanisms can

POSTER PRESENTATIONS

exacerbate multiple organ dysfunction. In addition, BMG was the most elevated molecular species in the serum of ACLF patients, suggesting that the conjugation process is not well completed by UGT1A1 enzyme and therefore the normal excretion of diglucuronide into the bile is impaired making it difficult to get into the serum.

THU-090

Safety and efficacy of liver hemodialysis in managing hepatic dysfunction: a systematic review and meta-analysis

Eyad Gadour^{1,2}, Moahammed Kabbalo³, Khalid Shrwani⁴, Zeinab Hassan⁵, Ahmed Koth⁶, Ahmed Aljuraysan⁷, Bogdan Miutescu^{8,9}, Nouf Sherwani¹⁰, Alaa Sherwani¹¹, Waleed Mahallawi¹², Mohammed Raza¹³. ¹King Abdulaziz National Guard Hospital, Department of Gastroenterology and Hepatology, Alahsa, Saudi Arabia; ²Zamzam University College, School of Medicine, Khartoum, Sudan; ³King Abdulaziz National Guard Hospital, Department of Nephrology, Al-Ahsa, Saudi Arabia; ⁴Saudi Center for Disease Prevention and Control, Public Health Authority, Jazan, Saudi Arabia; ⁵Stockport Hospital NHS Foundation Trust, Internal Medicine, Manchester, United Kingdom; ⁶Glan Clwyd Hospital, Department of Vascular Surgery, Rhyl, United Kingdom; ⁷King Abdulaziz National Guard Hospital, Department of Gastroenterology and Hepatology, Al-Ahsa, Saudi Arabia; ⁸"Victor Babes" University of Medicine and Pharmacy Timisoara, Department of Gastroenterology and Hepatology, Timisoara, Romania; ⁹"Victor Babes" University of Medicine and Pharmacy, Advanced Regional Research Center in Gastroenterology and Hepatology, Timisoara, Romania; ¹⁰Mohammed bin Nasser Hospital, Department of Surgery, Jazan, Saudi Arabia; ¹¹Abu-Arish General Hospital, Department of Pediatrics, Jazan, Saudi Arabia; ¹²Taibah University, College of Applied Medical Sciences, Madinah, Saudi Arabia; ¹³Al-Fatima University College, Karachi, Pakistan
Email: eyadgadour@doctors.org.uk

Background and aims: Since not all liver dysfunction patients are suitable for transplantations and there is a shortage of grafts, liver support therapies have gained interest. In this regard, extracorporeal albumin dialysis devices such as Single-Pass Albumin dialysis (SPAD), Prometheus, and Molecular Adsorbent Recycling System (MARS) have been valuable in supplementing standard medical therapy (SMT). However, the efficacy and safety of these devices is often questioned. Therefore, we performed a systematic review to summarize the efficacy and safety of MARS, SPAD, and Prometheus as supportive treatments for liver dysfunction.

Method: PubMed, Medline, Cochrane Library, Web of Science, and Google Scholar electronic databases were extensively searched for all randomized trials published in English. In addition, meta-analytic analyses were performed with the Review Manager software, and Cochrane's risk of bias tool embedded in this software was used for bias assessment.

Results: 12 trials with 653 patients were eligible for inclusion. Subgroup analyses of data from these trials revealed that MARS and Prometheus were associated with significant removal of bilirubin (MD: -5.14 mg/dL; 95% CI: -7.26-3.02; $p < 0.00001$ and MD: -8.11 mg/dL; 95% CI: -12.40-3.82; $p = 0.0002$, respectively) but not bile acids and ammonia when compared to SMT. Furthermore, MARS was as effective as Prometheus and SPAD in the reduction of bilirubin (MD: 2.98 mg/dL; 95% CI: -4.26-10.22; $p = 0.42$ and MD: 0.67 mg/dL; 95% CI: -2.22-3.56; $p = 0.65$), bile acids (MD: -17.06 $\mu\text{mol/L}$; 95% CI: -64.33-30.20; $p = 0.48$) and MD: 16.21 $\mu\text{mol/L}$; 95% CI: -17.26-49.68; $p = 0.34$), and ammonia (MD: 26 $\mu\text{mol/L}$; 95% CI: -12.44-64.44; $p = 0.18$). In addition, MARS had a considerable effect in improving hepatic encephalopathy (HE) (RR: 1.54; 95% CI: 1.15-2.05; $p = 0.004$). However, neither MARS nor Prometheus had a mortality benefit compared to SMTRR: 0.86; 95% CI: 0.71-1.03; $p = 0.11$ and RR: 0.87; 95% CI: 0.66-1.14; $p = 0.31$, respectively).

Conclusion: MARS, SPAD, and Prometheus as liver support therapies are equally effective in reducing albumin-bound and water-soluble substances. Moreover, MARS is associated with HE improvement.

However, none of the therapies was associated with a significant reduction in mortality or adverse events.

THU-091

Predictors of acute-on-chronic liver failure (ACLF) and mortality in ambulatory cirrhotic patients

Maamoun Basheer¹, Prof Nimer Assy². ¹Internal Medicine Department, Galilee Medical Center, Nahariya, Israel, Nahariya, Israel, Israel; ²Internal Medicine Department, Galilee Medical Center, Nahariya, Israel, Nahariya, Israel, Israel
Email: maamon.basheer@mail.huji.ac.il

Background and aims: Acute-on-chronic liver failure (ACLF) is the most life-threatening complication of cirrhosis. ACLF's prevalence and outcomes have been described in hospitalized patients with cirrhosis. However, no data is available on the prevalence and predictors of ACLF in ambulatory cirrhotic patients. Aims: Assessment of the incidence and predictors of ACLF in cirrhotic ambulatory patients.

Method: A retrospective study of 204 ambulatory patients with cirrhosis consecutively evaluated in a tertiary hospital at the Galilee Medical Center from Feb. 2015 to Dec. 2022 and followed for eight years. Data on developing hepatic and extrahepatic organ failures were collected. ACLF was defined and graded according to the European Association for the Study of Liver-Chronic Liver Failure (EASL-CLIF) Consortium definition.

Results: Outpatients with cirrhosis developed ACLF in 40% of cases (82 patients). The mortality rate was significantly high in the ACLF group as compared to the non-ACLF group (38% VS 8.5%, respectively $P < 0.001$). Patients with ACLF were older, had increased CRP, NLR and WBC, increased LFTS and kidney function, and increased MELD, Child-Pugh, CLIF-C and PADUA scores than the non-ACLF group. Univariate regression analysis determined that the MELD score was the most powerful predictor of organ failure. Multivariate analysis showed that MELD and CLIF-C scores were associated with organ failure and developing ACLF (OR 4.5, $P < 0.001$, OR 3.2, $P < 0.001$, respectively). Discriminant analysis showed that BUN, MELD, CLIF-C and PADUA scores predicted mortality in ambulatory outpatients with cirrhosis with 87% accuracy. Inflammatory markers CRP and NLR were not selected as independent predictors of ACLF or of mortality.

Conclusion: Outpatients with cirrhosis developed ACLF in 40% of cases. MELD and CLIF-C scores are the best ACLF development predictors. PADUA, CLIF-C and MELD scores are the best predictors of mortality. Therefore, we should use MELD, PADUA and CLIF-C scores to evaluate and follow-up cirrhotic outpatients in liver units.

THU-092

Enrolling patients in ACLF trials-the need to increase ACLF awareness (DHELIVER trial)

Dominique Thabut¹, Marika Rudler², Ewa Janczewska³, Schalk van der Merwe⁴, Frederik Nevens⁴, Adrien Lannes⁵, Luc Lasser⁶, Thomas Reiberger⁷, Vadim Brjalin⁸, Desislava Pavlova⁹, Svetlana Adamcova Selcanova¹⁰, Krum Katzarov¹¹, Ventseslav Draganov¹², Christine Collienne¹³, Christophe Bureau¹⁴, Antonio Saviano¹⁵, Pierluigi Toniutto¹⁶, Javier Martínez González¹⁷, Jordi Sánchez¹⁸, Julia Borissova¹⁹, Jordan Genov²⁰, Ivaylo Nikolov²¹, Thierry Gustot²², Georges-Philippe Pageaux²³, Teresa Antonini²⁴, Patrick Borentain²⁵, Vincent Leroy²⁶, Giovanni Perricone²⁷, Henning Grønbaek²⁸, Benjamin Maasoumy²⁹, Tony Bruns³⁰, Aldis Pukitis³¹, Juozas Kupcinskas³², Kalina Grivcheva Stardelova³³, Magdalena Genadieva Dimitrova³³, Beti Todorovska³³, Fabienne Eggermont³⁴, Yelena Vainilovich³⁴, Frederic Lin³⁴, Noelia Gordillo³⁴, Griet Goddemaer³⁴, Mustapha Najimi³⁴, Etienne Sokal^{34,35}. ¹Groupement Hospitalier Aphp-Sorbonne Université, Hôpital De La Pitié-Salpêtrière, Unité de Soins Intensifs d'Hépatogastro-Entérologie, Paris, France; ²Groupement Hospitalier Aphp-Sorbonne Université, Hôpital De La Pitié-Salpêtrière, Paris, France; ³ID Clinic, Myslowice, Poland; ⁴UZ Leuven, Leuven, Belgium; ⁵CHU Angers,

Hepatology Department, Angers, France; ⁶CHU Brugmann, Brussels, Belgium; ⁷Medical University Vienna, Internal Medicine III Gastroenterology and Hepatology department, Vienna, Austria; ⁸West Tallinn Central Hospital, Tallinn, Estonia; ⁹UMHAT Dr. Georgi Stranski, Gastroenterology Department, Pleven, Bulgaria; ¹⁰FNSP Roosevelt University Hospital, Hepatology Division, Banská Bystrica, Slovakia; ¹¹MMA-Sofia, Gastroenterology, Sofia, Bulgaria; ¹²UMBAL Medica, Ruse, Bulgaria; ¹³Cliniques Universitaires Saint Luc, Brussels, Belgium; ¹⁴Hôpital Rangueil, Hepatology, Toulouse, France; ¹⁵NHC Strasbourg, Nouvel Hôpital Civil de Strasbourg, Strasbourg, France; ¹⁶A.S.U. Friuli Centrale, Hepatology and Liver Transplant Unit, Udine, Italy; ¹⁷University Hospital Ramón y Cajal, Hepatology, Madrid, Spain; ¹⁸Hospital Parc Taulí Sabadell, Hepatology Department, Barcelona, Spain; ¹⁹North Estonia Medical Centre Foundation, Tallinn, Estonia; ²⁰UMHAT Tzaritza Joanna, Sofia, Bulgaria; ²¹UMHAT Sveta Anna, Gastroenterology, Sofia, Bulgaria; ²²C.U.B. Hôpital Erasme, Gastroenterology and Hepato-Pancreatology, Brussels, Belgium; ²³CHU Montpellier, Pôle Digestif, Montpellier, France; ²⁴Hospices Civils De Lyon, Hôpital de la Croix Rousse, Lyon, France; ²⁵Assistance Publique Hôpitaux de Marseille, Hôpital de la Timone, Marseille, France; ²⁶Henri Mondor University Hospital, Paris, France; ²⁷ASST Grande Ospedale Metropolitano Niguarda, Gastroenterology and Hepatology, Milan, Italy; ²⁸Aarhus University Hospital, Department of Hepatology and Gastroenterology, Aarhus, Denmark; ²⁹Medical University Hannover, Clinic for Gastroenterology, Hepatology and Endocrinology, Hannover, Germany; ³⁰University Hospital Aachen RWTH, Internal Medicine III/Gastroenterology and Hepatology, Aachen, Germany; ³¹Pauls Stradins Clinical University Hospital Pilsone, Riga, Latvia; ³²Lithuanian University of Health Sciences, Kaunas, Lithuania; ³³PHI University Clinic of Gastroenterohepatology, Skopje, Macedonia; ³⁴Cellaion, Mont-Saint-Guibert, Belgium; ³⁵Cliniques Universitaires Saint-Luc (UCLouvain), Woluwe-Saint-Lambert, Belgium
Email: dominique.thabut@aphp.fr

Background and aims: Inclusion of ACLF patients in clinical trials requires awareness of existing clinical trials, prompt recognition of the disease characteristics and thorough pre-screening for inclusion/exclusion criteria. In addition to major investigational hospitals, the HEP102 DHELIVER ACLF phase IIB study enrolled patients referred from other hospitals through local information sessions to support patient recruitment in the study. We reviewed the data of all screened patients to better understand the reasons for delayed diagnosis and screening.

Method: Retrospective analyses of dates of hospitalization (at investigational sites or other hospitals) and ACLF diagnosis were performed in relation to the causes of admission.

Results: Of the 185 patients screened in the DHELIVER study (up to mid-December), 107 were randomized. Complete hospitalization data have been available for 99 patients so far. These patients were hospitalized either in investigational sites (63%) or other hospitals (37%) before being randomized. The average number of days between initial healthcare encounter and ACLF diagnosis was 2.7 days when hospitalized in investigational sites and 7.5 days when hospitalized in other hospitals. Causes of admission to the hospital varied widely. Of the 99 randomized patients for whom hospitalization data are available, only 10% were admitted for diagnosed or suspected ACLF, while 61% were admitted for signs of acute decompensation (AD) including jaundice, ascites, hepatic encephalopathy, gastrointestinal bleeding, and 17% for acute alcoholic hepatitis (AAH). When the causes of admission were not specifically ACLF, the average time to ACLF diagnosis was 3.0 days in investigational sites, vs 7.7 days in other hospitals. Forty-four percent of patients were admitted to intensive care units (ICU) before being randomized. Overall, the average time from initial healthcare encounter to ACLF diagnosis was the same between ICU vs non-ICU patients (4.5 days). However, the average time to ACLF diagnosis in other hospitals compared to investigational sites was 3.3 times longer for non-ICU patients (8.0 vs 2.5 days), and 2.3 times longer for ICU-patients (6.8 vs 3.0 days).

Conclusion: The DHELIVER study has demonstrated those hospitals that are not participating in the study have high potential in recruiting patients in ACLF trials (37%). The DHELIVER data have also highlighted the challenges facing the recruitment of ACLF patients due to late diagnosis of ACLF in hospitalized patients, as only 10% of patients displaying ACLF symptoms are admitted for ACLF itself. Early and regular assessment of ACLF criteria in patients with signs of AD and AAH in ICU and non-ICU wards and better awareness campaign on ACLF diagnosis would allow timely identification of ACLF. This would allow earlier transfer of patients to tertiary hospitals with better access to clinical trials.

Cirrhosis and its complications – Experimental and pathophysiology

TOP-072

Red blood cell distribution width-to-platelet ratio estimates the 3-year risk of decompensation in patients with metabolic dysfunction-associated steatotic liver disease-related cirrhosis

Mario Romeo¹, Marcello Dallio¹, Marina Cipullo¹, Paolo Vaia¹, Simone Mammone¹, Salvatore Auletta¹, Silvio Naviglio², Luigi Sapio², Angela Ragone², Marco Niosi¹, Alessandro Federico¹.

¹Hepatogastroenterology Division, Department of Precision Medicine, University of Campania "Luigi Vanvitelli", Naples, Italy; ²Clinical Biochemistry Division, Department of Precision Medicine, University of Campania "Luigi Vanvitelli", Naples, Italy
Email: mario.romeo@virgilio.it

Background and aims: For compensated advanced chronic liver disease (cACLD) patients, the first decompensation represents a dramatically worsening prognostic event. Based on the first decompensation event (DE), the transition to decompensated advanced chronic liver disease (dACLD) can occur through two modalities referred to as acute decompensation (AD) and non-acute decompensation (NAD), respectively. Clinically Significant Portal Hypertension (CSPH) is considered the strongest predictor of decompensation in these patients. However, CSPH is seldom evaluated in clinical practice due to its invasiveness and costs. Therefore, recognizing non-invasively predicting tools still has more appeal across healthcare systems. The red blood cell distribution width-to-platelet ratio (RPR) has been reported to indicate hepatic fibrosis in Metabolic Dysfunction-Associated Steatotic Liver Disease (MASLD). However, its predictive role in decompensation has never been explored. In this observational study, we investigated the clinical usage of RPR in predicting DEs in MASLD-related cACLD patients.

Method: 40 controls and 150 MASLD-cACLD patients were consecutively enrolled and followed up (FUP) semiannually for 3 years. At baseline, biochemical, clinical, and Liver Stiffness Measurement (LSM), Child-Pugh (CP), Model for End-stage Liver Disease (MELD), AST to Platelet Ratio (APRI), Fibrosis-4 (FIB-4), Albumin-Bilirubin (ALBI), and RPR were collected. During FUP, DEs (timing and modalities) were recorded. CSPH was assessed through methods proposed by the Clinical Practice Guidelines.

Results: Of 150 MASLD-cACLD patients, 43 (28.6%) progressed to dACLD at a median of 28.9 months (29 NAD; 14 AD). Baseline RPR values were significantly higher in cACLD compared to controls, as well as MELD, CP, APRI, FIB-4, ALBI, ALBI-FIB-4, and LSM in dACLD-progressing compared to cACLD individuals [all $p < 0.0001$, except for FIB-4 ($p:0.007$) and ALBI ($p:0.011$)]. ROC analysis revealed RPR ≥ 0.472 and ≥ 0.894 as the best cut-offs [AUC: 0.95; AUC: 0.94] in the prediction respectively of 3-year first DE and relative modality (AD), as well as its superiority for both the outcomes compared to APRI [AUC: 0.88; AUC: 0.88], FIB-4 [AUC: 0.72; AUC: 0.75], ALBI [AUC: 0.90; AUC: 0.77], ALBI-FIB-4 [AUC: 0.93; AUC: 0.79], MELD [AUC: 0.81;

POSTER PRESENTATIONS

AUC: 0.73], CP [AUC: 0.79; AUC: 0.82], and LSM [AUC: 0.88; AUC: 0.85] (all $p < 0.0001$). The RPR [adjusted Hazard Ratio (aHR): 1.91; 95% C.I.: 1.72–1.98; $p: 0.02$] and the presence of baseline-CPSH [aHR: 1.84 95% C.I.: 1.72–1.91; $p: 0.04$] were significantly associated with the DE. Patients presenting baseline-CSPH and RPR ≥ 0.472 showed a higher risk [HR: 3.10; $p: 0.0023$] of decompensation.

Conclusion: RPR is a valid and potentially applicable non-invasive tool in predicting the timing and modalities of decompensation in MASLD-related cACLD patients.

TOP-073

Extensive characterization of new biomarkers associated with infection and outcome of decompensation of cirrhosis using high throughput metabolomics, lipidomics and cytokinomics

Cristina López-Vicario^{1,2,3}, Carlos de la Peña-Ramírez², Marta Duran-Güell^{1,2}, Bryan J. Contreras^{1,2}, Berta Romero-Grimaldo^{1,2}, María Belén Sánchez-Rodríguez^{1,2}, Sara Palomino-Echevarría⁴, Ferran Aguilar², Wim Laleman⁵, David Gómez-Cabrero⁴, Alberto Queiroz Farias⁶, Sebastián Marciano⁷, Francois Fenaille⁸, Florence Castelli⁸, Jonel Trebicka^{2,9}, Richard Moreau^{2,10,11}, Vicente Arroyo², Pierre-Emmanuel Rautou^{10,11}, Joan Clària^{1,2,3,12}. ¹Biochemistry and Molecular Genetics Service, Hospital Clínic-IDIBAPS, Barcelona, Spain; ²European Foundation for the Study of Chronic Liver Failure (EF CLIF), EASL-CLIF Consortium and Grifols Chair, Barcelona, Spain; ³CIBERehd, Barcelona, Spain; ⁴Navarrabiomed, Universidad Pública de Navarra (UPNA), Pamplona, Spain; ⁵University of Leuven, Leuven, Belgium; ⁶Department of Gastroenterology, Hospital das Clínicas, University of São Paulo School of Medicine, São Paulo, Brazil; ⁷Liver Unit and Department of Research, Hospital Italiano de Buenos Aires, Buenos Aires, Argentina; ⁸Université Paris-Saclay, CEA, INRAE, Département Médicaments et Technologies pour la Santé (MTS), MetaboHUB, Gif-sur-Yvette, France; ⁹Department of internal medicine B, University of Münster, Münster, Germany; ¹⁰Université Paris Cité, INSERM, Centre de Recherche sur l'Inflammation (CRI), Paris, France; ¹¹Service d'Hépatologie, Hôpital Beaujon, APHP, Clichy, France; ¹²Department of Biomedical Sciences, University of Barcelona, Barcelona, Spain
Email: clopezv@recerca.clinic.cat

Background and aim: Patients with acutely decompensated (AD) cirrhosis present a systemic hyperinflammatory response causally linked to the development of acute-on-chronic liver failure (ACLF), characterized by multi-organ failure and short-term mortality. In this study, we analyzed the systemic circulation secretome through a combination of omics to identify biomarkers associated with infection, 28-day ACLF development and 90-day mortality in patients with AD cirrhosis.

Method: The study included patients with AD cirrhosis from PREDICT (discovery cohort, $n = 766$) and ACLARA (validation cohort, $n = 580$). Plasma cytokines/chemokines were evaluated using multiplex bead-based immunoassays. Bioactive lipids and low-molecular weight metabolites were assessed by targeted lipidomics and untargeted metabolomics in plasma and serum, respectively. A multifactorial regression network was built to identify significant associations between high-dimensional multi-omics data and infection and outcome of AD cirrhosis.

Results: Among the 292 features included in the integrated network analysis, we identified a strong connection between arachidonic acid (a hydrogenated product of arachidonic acid) and glucuronic acid (a marker of extramitochondrial glucose oxidation) and a high negative association with the anti-inflammatory marker 15-HETE in patients with active infections. Considering ACLF development as outcome, we identified a network that strongly correlated with the arachidonic acid-derivative 20-HETE and the hydroxylated fatty acid hydroxydo-decanoic acid with acylcarnitines (established markers of mitochondrial dysfunction). In addition, arachidonic acid together with interleukin-8 interconnected with glucuronic acid. Importantly, levels of sphingosine-1-phosphate, a signaling molecule that controls

immune cell trafficking, were strongly and negatively associated with this outcome. When we interrogated mortality as outcome, we identified a network of lipids that converged into acylcarnitines, hydroxy-3-methoxyphenylglycol sulfate (MPHG, a major metabolite of norepinephrine) and glucuronic acid. Most features appearing in the above described immunometabolic networks were primarily associated with the ramping neutrophilia existing in these patients, except sphingosine-1-phosphate which was linked to thrombocytopenia. Furthermore, glucuronic acid, interleukin-6 and hydroxydo-decanoic acid were the best predictors of ACLF development (AUC > 0.66) whereas MPHG sulfate (AUC > 0.72) was the best prognostic marker of imminent death, findings that were validated in the ACLARA cohort.

Conclusion: A network-based multi-omics analysis allowed us to uncover new pathophysiological events associated with ACLF development and death and to identify new biomarkers to fuel prognostic tests to improve prediction of outcome in patients with AD cirrhosis.

TOP-084

Galectin 9 predicts clinical outcome and regulates immune dysfunction in acute-on-chronic liver failure

Antonio Riva^{1,2}, Douglas Corrigan^{1,2,3}, Hio Lam Phoebe Tsou^{1,2}, Nicola Harris^{1,2}, Dhruvi Devshi^{1,2}, Sarah Fairclough³, Gavin Wright³, Jonel Trebicka^{4,5}, Carlo Alessandria⁶, Paolo Angeli⁷, Rajiv Jalan⁸, Joan Clària⁹, Richard Moreau¹⁰, Vicente Arroyo⁵, Shilpa Chokshi^{1,2}. ¹Roger Williams Institute of Hepatology, Foundation for Liver Research, London, United Kingdom; ²King's College London, Faculty of Life Sciences and Medicine, London, United Kingdom; ³Basildon and Thurrock University Hospitals NHS Foundation Trust, Basildon, United Kingdom; ⁴Medical Department I, Goethe University Clinic, Frankfurt, Germany; ⁵European Association for the Study of the Liver-Chronic Liver Failure (EASL-CLIF) Consortium and European Foundation for the study of Chronic Liver Failure (EF-CLIF), Barcelona, Spain; ⁶Division of Gastroenterology and Hepatology, San Giovanni Battista Hospital, Torino, Italy; ⁷Unit of Internal Medicine and Hepatology, Dept. of Medicine, DIMED, University of Padova, Padova, Italy; ⁸Institute for Liver Disease Health, University College London, Royal Free Hospital, London, United Kingdom; ⁹Hospital Clínic, IDIBAPS, Barcelona, Spain; ¹⁰Inserm, U1149, Centre de Recherche sur l'Inflammation (CRI), Paris, France
Email: a.riva@researchinliver.org.uk

Background and aims: Acute-on-Chronic Liver Failure (ACLF) is an immunological paradox characterised by a highly activated hyperinflammatory immune system that is simultaneously profoundly suppressed in its antibacterial functionality. We have previously revealed the importance of immune checkpoints (membrane-bound and soluble) in modulating antipathogen and inflammatory responses in alcohol-related liver disease, but their role in the immunopathogenesis and progression of ACLF are unknown.

Method: We quantified 17 soluble (s) immune checkpoints and D-Lactate (DL) as a marker of bacterial translocation by Luminex and ELISA in the serum of 511 patients with decompensated cirrhosis from the CANONIC Cohort (at inclusion: 334 acute decompensation, AD, ACLF 0; 177 ACLF 1/2/3). Predictive multivariable regression models were used to quantitatively weigh contributions to ACLF grade, development, resolution, and day (d)28/90 transplant free survival (TFS). Kaplan-Meier analyses were used to find TFS cutoffs. Peripheral blood mononuclear cells (PBMC) from AD and ACLF patients ($n = 10$) were assessed for antibacterial immune functionality (IFN γ , IL-17, TNF α , IL-10, CD107a, Granzyme B, Perforin on CD4 and CD8 T cells by flow cytometry) upon bacterial challenge with/without Galectin (Gal)9 blockade.

Results: Gal9, Gal1 ($p < 0.002$), sCD40, sBTLA, sCD137, sCD27 ($p < 0.008$), and DL ($p = 0.002$) were all significantly associated with ACLF and ACLF grade. In predictive models, Gal9 and Gal1 were found to be significant positive predictors of ACLF severity ($p < 0.005$; standardised Gal9 odds ratios (OR) > 1.3; 95% CI 1.1–1.6) and transplant/death

(day 28 and day 90) ($p < 0.015$; st. Gal9 hazard ratios > 1.2 ; 95% CI 1.1–1.6). Gal9 was also significantly unfavourable to ACLF resolution ($p < 0.003$; st. Gal9 OR < 0.7 ; 95% CI 0.5–0.8). Immune scoring based on Gal9 was able to discriminate ACLF from AD ($p < 0.001$; AUROC 0.71, 95% CI 0.67–0.76, Sens/Spec $> 65\%$) and addition of Gal9 marginally enhanced the CLIF ACLF score, increasing discriminating accuracy for both AD vs ACLF (78 to 80%) and between ACLF grades (59 to 63%). Significant TFS cutoffs were also found for Gal9 (d28 TFS, $p = 5.6E-9$, < 22611 pg/ml; d90 TFS, $p = 1.8E-10$, < 22402 pg/ml). Post-hoc analyses by sex (as assigned at birth) showed that Gal9 associations with ACLF and ACLF grade were similar in male and female patients, unlike other receptors. In vitro blockade of Gal9 in PBMCs restored antipathogen responses boosting antibacterial cytokines and also anti-inflammatory IL-10 in both AD and ACLF.

Conclusion: Gal9 is a promising biomarker of AD and ACLF progression and represents a promising novel therapeutic target for restoration of anti-pathogen immunity in these patients.

TOP-085

Final results from the Italian real-world experience on lusutrombopag treatment in cirrhotic patients with severe thrombocytopenia: insights from the reality study

Paolo Gallo¹, Antonio De Vincentis¹, Valeria Pace Palitti², Maurizio Russello³, Anthony Vignone⁴, Domenico Alvaro⁵, Raffaella Tortora⁶, Marco Biolato⁷, Maurizio Pompili⁷, Vincenza Calvaruso⁸, Marzia Veneziano⁸, Marco Tizzani⁹, Francesco Frigo⁹, Alessandro Caneglias¹⁰, Gesualdo Marcantonio¹⁰, Alfredo Marzano¹⁰, Valerio Rosato¹¹, Ernesto Claar¹¹, Rosanna Villani¹², Antonio Izzi¹³, Raffaele Cozzolongo¹⁴, Aldo Airoldi¹⁵, Chiara Mazzarelli¹⁵, Marco Distefano¹⁶, Claudia Iegri¹⁷, Stefano Fagioli¹⁷, Vincenzo Messina¹⁸, Enrico Ragone¹⁹, Rodolfo Sacco²⁰, Pierluigi Cacciatore², Flora Masutti²¹, Lory Saveria Croce²¹, Alessandra Moretti²², Francesca Terracciani¹, Andrea Falcomatà¹, Giulia Di Pasquale¹, Valentina Flagiello¹, Antonio Picardi¹, Umberto Vespasiani-Gentilucci¹. ¹Fondazione Policlinico Universitario Campus Biomedico, Rome, Italy; ²ASL Pescara, Pescara, Italy; ³Arnas Garibaldi, Catania, Italy; ⁴Sapienza University of Rome, Rome, Italy; ⁵Sapienza University of Rome, Rome, Italy; ⁶AORN Cardarelli, Naples, Italy; ⁷Fondazione Policlinico Universitario Gemelli, Rome, Italy; ⁸University of Palermo, Palermo, Italy; ⁹Città della salute e della scienza, Torino, Italy; ¹⁰Città della salute e della scienza, Torino, Italy; ¹¹Betania Hospital, Naples, Italy; ¹²University of Foggia, Foggia, Italy; ¹³D. Cotugno Hospital, Naples, Italy; ¹⁴"S de Bellis" Research Hospital, Castellana Grotte, Bari, Italy; ¹⁵ASST GOM Niguarda, Milano, Italy; ¹⁶Umberto I Hospital, Siracusa, Italy; ¹⁷ASST Papà Giovanni XXIII, Bergamo, Italy; ¹⁸S. Anna and S. Sebastiano Hospital, Caserta, Italy; ¹⁹Monaldi Hospital, Naples, Italy; ²⁰University of Foggia, Foggia, Italy; ²¹A.S.U. Giuliano Isontina, University of Trieste, Trieste, Italy; ²²San Filippo Neri Hospital, Rome, Italy
Email: paolo.gallo@policlinicocampus.it

Background and aims: Severe thrombocytopenia (platelet count $< 50,000/\mu\text{L}$) presents management challenges in patients with chronic liver disease (CLD). Recently, thrombopoietin receptor agonists, such as lusutrombopag, have been developed as alternatives to platelet transfusions. However, existing real-world data are limited to sporadic reports or administrative databases. We aimed to assess the first post-marketing real-world European cohort of cirrhotic patients treated with lusutrombopag to verify the efficacy and safety of the drug.

Method: In the REAL-world Lusutrombopag treatment in Italy (REALITY) study, we collected data from consecutive cirrhotic patients who underwent lusutrombopag treatment before invasive procedures between March 2021 and March 2023. The data were collected from 19 Italian hepatologic centers, mostly affiliated with the "Club Epatologi Ospedalieri" (CLEO). Efficacy, defined as the ability of lusutrombopag to raise platelet count to $\geq 50,000/\mu\text{L}$ and

avoid transfusions, as well as treatment-related adverse events, were recorded and analyzed.

Results: A total of 73 patients were enrolled in the study (median age 66 years, female 32%, Child-Pugh A/B/C 63/28/9%). Twelve patients (15%) had a previous medical history of portal vein thrombosis. Chronic viral hepatitis emerged as the leading cause of chronic liver disease (55%), with endoscopic band ligation being the most frequently performed procedure (38% of cases). Lusutrombopag induced a significant increase in platelet count [from 37,000 (33,000–44,000/ μL) to 58,000 (49,000–82,000), $p < 0.001$]. The overall efficacy of lusutrombopag was determined to be 74%. Multivariate logistic regression analysis identified baseline platelet value as the only independent factor associated with the response (OR 1.13, CI95% 1.04–1.26, $p < 0.01$) and with an adequate discriminative ability (AUROC of 0.78). Notably, a baseline platelet count of $\leq 29,000/\mu\text{L}$ was identified as the threshold for identifying patients unlikely to respond to the drug, exhibiting a sensitivity of 91%. Finally, de novo portal vein thrombosis was observed in 4 patients (5%), while no other safety events were recorded.

Conclusion: In this first real-world European series of CLD, lusutrombopag demonstrated efficacy and safety consistent with findings from registrative trials. Finally, according to our results, patients with baseline platelets $\leq 29,000/\mu\text{L}$ are unlikely to respond to the drug.

TOP-096

Glucagon-like peptide-1 receptor agonist, semaglutide attenuates liver cirrhosis-related skeletal muscle atrophy in diabetic mice

Kosuke Kaji¹, Shohei Asada¹, Shinya Sato¹, Tadashi Namisaki¹, Hitoshi Yoshiji¹. ¹Department of Gastroenterology, Nara Medical University, Kashihara, Japan
Email: kajik@naramed-u.ac.jp

Background and aims: Recent studies have demonstrated the molecular role of the glucagon-like peptide-1 receptor agonist (GLP-1RA) in skeletal muscle homeostasis; however, the therapeutic efficacy of semaglutide, a GLP-1RA, on skeletal muscle atrophy in liver cirrhosis. The aim of the present study was to investigate the effect of semaglutide on skeletal muscle wasting and dysfunction in liver cirrhosis-related skeletal muscle atrophy under diabetic conditions.

Method: To induce liver cirrhosis under diabetic condition, male diabetic KK-Ay mice were fed with diethoxycarbonyl-L, 4-dihydrocollidine (DDC) diet for 6 weeks. Semaglutide (3 nmol/kg) was subcutaneously injected every 3 days. We assessed the effect of semaglutide on psoas muscle mass index by using CT image and grip strength as well as hepatic and muscular phenotypes. Moreover, in vitro assay was performed to evaluate direct effect of semaglutide on C2C12 myocytes.

Results: Semaglutide inhibited psoas muscle atrophy and suppressed declines in grip strength in mice. Moreover, semaglutide inhibited ubiquitin-proteasome-mediated skeletal muscle proteolysis and promoted myogenesis in C2C12 myocytes. Mechanistically, this effect of semaglutide on skeletal muscle atrophy was mediated by multiple functional pathways. First, semaglutide protected against hepatic injury in mice accompanied by increased production of insulin-like growth factor 1 and reduced accumulation of reactive oxygen species (ROS). These effects were associated with decreased proinflammatory cytokines and ROS accumulation, leading to suppression of ubiquitin-proteasome degradation in the skeletal muscle tissue. Moreover, semaglutide inhibited the amino acid starvation-related stress signaling which was activated under chronic liver injury, resulting in the recovery of mammalian target of rapamycin activity in the skeletal muscle of mice. Second, semaglutide improved skeletal muscle atrophy by directly stimulating GLP-1R in myocytes. Treatment with semaglutide induced cAMP-mediated activation of PKA and AKT, enhanced mitochondrial biogenesis, and reduced ROS accumulation, thereby resulting in inhibition of NF- κ B/myostatin-mediated ubiquitin-proteasome

POSTER PRESENTATIONS

degradation and the augmentation of heat-shock factor-1-mediated myogenesis.

Conclusion: Semaglutide may have potential as a new therapeutic strategy for liver cirrhosis-related skeletal muscle wasting.

WEDNESDAY 05 JUNE

WED-055

Effect of long-term treatment with Simvastatin and Rifaximin in mitochondrial and proinflammatory pathways in patients with decompensated cirrhosis. A single-cell RNA seq analysis in PBMCs

Adrià Juanola^{1,2,3}, Núria Planell⁴, Elisa Pose^{1,5,6}, Martina Perez-Guasch⁷, Marta Carol⁸, Ana Belén Rubio⁸, Marta Cervera⁸, Ruth Nadal⁸, Sara Palomino-Echevarria⁹, Estefania Huergo Iglesias⁹, Jordi Gratacós-Ginès¹⁰, Anna Soria⁷, Alex Guillamon-Thiery¹¹, Celia Martinez-Sanchez¹², Núria Fabrellas¹³, Isabel Graupera¹⁴, Elsa Solà¹⁵, Mar Coll¹⁶, Pere Ginès¹⁷. ¹Liver Unit, Hospital Clinic de Barcelona, Spain; ²Institut d'Investigacions Biomèdiques August Pi i Sunyer, Barcelona, Spain; ³Centro de Investigación Biomedica en Red Enfermedades Hepáticas y Digestivas, Barcelona, Spain, Madrid, Spain; ⁴Universidad de Navarra, Centro de Investigación Médica Aplicada (CIMA), Computational Biology Program, Instituto de Investigación Sanitaria de Navarra (IdiSNA), Pamplona, Spain; ⁵Institut d'Investigacions Biomèdiques August Pi i Sunyer (IDIBAPS), Barcelona, Spain; ⁶Centro de Investigación Biomedica en Red Enfermedades Hepáticas y Digestivas (CIBEREHD), Barcelona, Spain; ⁷Liver Unit, Hospital Clinic de Barcelona. Centro de Investigación Biomedica en Red Enfermedades Hepáticas y Digestivas Institut d'Investigacions Biomèdiques August Pi i Sunyer, Barcelona, Spain; ⁸Centro de Investigación Biomedica en Red Enfermedades Hepáticas y Digestivas Institut d'Investigacions Biomèdiques August Pi i Sunyer, Barcelona, Spain; ⁹Translational Bioinformatics Unit, Navarrabiomed, Universidad Pública de Navarra (UPNA), Instituto de Investigación Sanitaria de Navarra (IdiSNA), Pamplona, Spain; ¹⁰Liver Unit, Hospital Clinic de Barcelona. Centro de Investigación Biomedica en Red Enfermedades Hepáticas y Digestivas. Institut d'Investigacions Biomèdiques August Pi i Sunyer, Barcelona, Spain; ¹¹Institut d'Investigacions Biomèdiques August Pi i Sunyer Centro de Investigación Biomedica en Red Enfermedades Hepáticas y Digestivas, Barcelona, Spain; ¹²Institut d'Investigacions Biomèdiques August Pi i Sunyer. Centro de Investigación Biomedica en Red Enfermedades Hepáticas y Digestivas, Barcelona, Spain; ¹³Institut d'Investigacions Biomèdiques August Pi i Sunyer. Faculty of Medicine and Health Sciences, University of Barcelona. Centro de Investigación Biomédica en Red Enfermedades Hepáticas y Digestivas, Barcelona, Spain; ¹⁴Liver Unit, Hospital Clinic de Barcelona. Institut d'Investigacions Biomèdiques August Pi i Sunyer. Centro de Investigación Biomédica en Red Enfermedades Hepáticas y Digestivas, Barcelona, Spain; ¹⁵Institute for Immunity, Transplantation and Infection, Stanford University, Stanford, California, USA, Stanford, United States; ¹⁶Institut d'Investigacions Biomèdiques August Pi i Sunyer. Centro de Investigación Biomedica en Red Enfermedades Hepáticas y Digestivas, Barcelona, Spain; ¹⁷Liver Unit, Hospital Clinic de Barcelona. Institut d'Investigacions Biomèdiques August Pi i Sunyer. Centro de Investigación Biomedica en Red Enfermedades Hepáticas y Digestivas. Faculty of Medicine and Health Sciences, University of Barcelona, Barcelona, Spain
Email: juanola@clinic.cat

Background and aims: The progression of cirrhosis is associated with an activation of immune cells in response to liver injury and bacterial translocation. However, immune tolerance mechanisms that follow proinflammatory state, are also increased at latter stages, mainly in the monocyte subsets. Furthermore, metabolic alterations have been also described to play a role in the progression of the disease. The LiverHope Efficacy study has evaluated the treatment combination of simvastatin and rifaximin against placebo in patients with decompensated cirrhosis to prevent the development of acute-

on-chronic liver failure. This study aims to describe the effect that this treatment induces on peripheral blood mononuclear cells (PBMCs).

Method: This is a sub-study of the LiverHope Efficacy trial (NCT03780673). Single-cell RNA-Seq analysis was performed in PBMCs collected in 6 patients with decompensated cirrhosis: 4 from the treatment group and 2 from the placebo group. For each individual, paired samples of PBMCs were obtained before the start of treatment and at month 6 of treatment. Baseline/follow-up differences between the placebo and treatment groups were evaluated.

Results: A total of 17 cell populations were identified from the 44,709 cells analyzed. Compositional analysis showed no changes in the proportion of cell subpopulations according to the treatment group. Differential gene expression analysis revealed classical monocytes as the population with higher transcriptional changes, detecting a total of 1,253 differentially expressed genes (p value <0.05 and fold-change >1.5) in the classical monocyte population treated with simvastatin/rifaximin when compared with patients treated with placebo (944 genes up-regulated and 309 genes down-regulated). Functional enrichment analysis using the gene set enrichment analysis (GSEA) showed a decrease in the expression of molecular pathways involved in the immune response, as well as an increase in the expression of pathways related to mitochondrial metabolism in monocytes from patients treated with the drug combination.

Conclusion: Treatment with simvastatin/rifaximin decreases the expression of proinflammatory genes and promotes changes in mitochondrial metabolism in monocytes of patients with decompensated cirrhosis. These findings reveal beneficial effects at the cellular level of treatment with simvastatin and rifaximin.

WED-056

Activated cytotoxic T-cells in mesenteric lymph nodes limit systemic bacterial dissemination, inflammation, and disease progression in chronic liver injury

Pinky Juneja¹, Aarti Sharma², Deepika Jakhar², Impreet Kaur², Ashwini Vasudevan², Dinesh Mani Tripathi², Savneet Kaur². ¹Institute of Liver and Biliary Science, Delhi, India; ²Institute of Liver and Biliary Sciences, Delhi, India
Email: savykaur@gmail.com

Background and aims: Mesenteric lymph nodes (MLNs) are immune inductive sites that limit pathogens in gut, preventing their systemic spread. We studied the role of MLNs in bacterial spread, systemic inflammation, and progression of fibrosis using MLN resection models (MLNx).

Method: MLNs were resected from healthy rats (C-MLNx) and allowed to reconstitute lymphatic connections for next 3wk, and were compared with healthy rats (control). CCl₄-MLNx model was prepared by administering CCl₄ to 3wk post MLNx rats for next 8wk and compared with 8wk CCl₄ fibrotic model. LPS, 1 mg/Kg, i.p., was administered in all groups. Tissues and blood were collected 24 h post-LPS. Immune cells were quantified in liver, spleen, and blood. Endogenous bacterial load was quantified in these organs along with lung and MLNs. Cytokines and endotoxin levels were examined in plasma and MLNs. Gut permeability was studied by Claudin-1 expression.

Results: In C-MLNx vs. control, inflammatory CD43 monocytes (2.6 fold, p < 0.01), IL-6 (0.8 fold, p < 0.05), and TNF-alpha (0.6 fold, p < 0.05) were increased in blood 24 h post-LPS. Endogenous bacterial load was observed in lungs (540 CFU/g) of C-MLNx, while no bacteria were present in control. Plasma endotoxin levels were increased in C-MLNx compared to control (5.1 vs. 4.4 EU/ml, p > 0.05). No mortality, fibrosis, or cell infiltration was observed in C-MLNx. Endogenous bacterial load in MLNs (2000 CFU/g) and other organs in CCl₄ were higher in comparison to control, where bacteria were contained in MLNs (564 CFU/g) only. Bacterial load was further increased in liver (785 CFU/g), spleen (352 CFU/g), and lung (1084 CFU/g) in CCl₄-MLNx vs. CCl₄. Chronic lung inflammation and splenomegaly were observed in CCl₄-MLNx vs CCl₄ with no change in gut permeability. TNF-alpha

(3.2 fold) and IFN-gamma (2.1 fold) were increased in MLNs of CCl₄ vs control ($p < 0.03$). IL-6 (2.4 fold) and TNF-alpha (2.3 fold), along with endotoxin levels (2.8 fold), were increased in plasma of CCl₄ vs control ($p < 0.03$ each). This was aggravated in CCl₄-MLNx vs CCl₄ (IL-6: 1.4 fold, TNF-alpha: 1.5 fold, endotoxins: 1.4-fold, $p < 0.04$ each). Compared to control, activated CD134+ Tc cells are higher in MLNs (1.28 vs. 10.96%) and blood (1.03 vs. 3.23%) of CCl₄ ($p < 0.04$ each). However, in CCl₄-MLNx vs. CCl₄, activated CD134+Tc cell count was reduced (2.03 vs. 3.23%, $p < 0.05$), and Treg cells were increased (8.7 vs. 3.5%, $p < 0.001$) in blood. In CCl₄-MLNx, we observed increased liver fibrosis (30% F3, 70% F4 grade fibrosis) with 30% mortality rate compared to CCl₄ (90% F3, 10% F4) 24 h post LPS.

Conclusion: In the absence of MLNs, fibrosis progression and mortality are enhanced owing to increased systemic dissemination of bacterial endotoxins, causing systemic inflammation, gut immunosuppression, and endotoxemia. Hence, the preservation of MLNs functionality is crucial for limiting the spread of bacterial infections and disease progression.

WED-057

Exercise alters immune cell senescence and inflammation in cirrhosis patients with sarcopenia

Preeti Negi¹, Nidhi Nautiyal¹, Swati Thangariyal¹, Ashmit Mittal¹, Rakesh Kumar¹, Akhil Deshmukh², Vinod Arora², Shiv Kumar Sarin¹, Sukriti Baweja³. ¹Institute of Liver and Biliary Sciences, Delhi, India; ²Institute of liver and biliary sciences, Delhi, India; ³Institute of Liver and biliary Sciences, Delhi, India
Email: sukritibiochem@gmail.com

Background and aims: Sarcopenia is a gradual and widespread reduction of skeletal muscle mass, commonly associated with physical impairment. In cirrhosis, sarcopenia is linked to immune cells aging and inflammation. The aim of the study was to investigate the association of exercise with immune cells rejuvenation, inflammation and muscle strength in cirrhosis patients.

Method: Cirrhosis patients (n = 70) [78.1% male, age 54 ± 12 yr; MELD 14.5 (IQR 9.7–20.2)] sarcopenic (SP; n = 44) or non-sarcopenic (NSP) as assessed by Appendicular skeletal muscle index [ASMI (<5.5 kg/m² for women, <7.0 kg/m² for men)], dual-energy X-ray absorptiometry (DXA), gait speed, liver frailty index were included. Samples were collected before and immediately post-exercise (exercise by pedaling a half bicycle, sitting on a chair for 20 minutes with maximal effort). High-dimensional immune profiling was done using flow cytometry, plasma cytokines and myokines (TNF α , IL-6, Myostatin and Follistatin by ELISA and senescence associated secretory proteins [SASP; (IL-6, IL-1b, CXCL10, MAPK3, TNF α , p21, p53IL-10, IL-22, IL-17A) mRNA was assessed.

Results: In SP patients gait speed, liver frailty index were significantly low than NSP ($p < 0.001$). At baseline we observed, high absolute counts of neutrophils (77.2 ± 12.9 vs 64.7 ± 13.6; $p = 0.03$), low lymphocytes ($p < 0.001$; 17.5 ± 5.6 vs 26.3 ± 9.4) and neutrophil/lymphocyte ratio (NLR) (4.23 ± 1.1 vs 2.9 ± 0.8; $p = 0.03$) in SP patients. In plasma, inflammatory markers, IL-6 and TNF- α levels were high in SP than NSP ($p < 0.05$), myostatin (MYST) and follistatin levels were comparable between the groups. Interestingly, the number of neutrophils and IL-6 levels were significantly low ($p = 0.05$; $p = 0.015$) post-exercise in SP than NSP patients, but without differences in MYST and Follistatin levels. NLR and IL-6 were found to be independent predictors of sarcopenia (AUROC-0.75, $p = 0.004$ and 0.72, $p = 0.014$) and the levels of MYST were inversely proportional to MELD-Na ($r = -0.289$; $p = 0.002$). The mRNA levels IL-6 ($p = 0.031$) and p21 ($p = 0.008$) were decreased significantly in SP, but no differences in CXCL10 and MAPK3 in both the groups post-exercise. IL-10 ($p = 0.05$; $p < 0.0001$) and IL-22 ($p = 0.04$; $p = 0.02$) were increased significantly in both SP and NSP post-exercise.

Conclusion: Our results clearly document the positive immunological and molecular alterations associated with exercise in sarcopenic cirrhosis patients. Single supervised exercise program,

improve immune senescence, and reduce inflammation and can be of great help in patients with advanced cirrhosis and high MELD.

WED-058-YI

High shear stress induced PIEZO1 activation promotes cytoskeleton remodelling and a nuclear deformation develops pro-thrombotic microenvironment and contributes to portal hypertension

Rajni Yadav¹, Parul Singh², Vaibhav Tiwari¹, Aishwarya Bhatnagar¹, Ashwini Vasudevan¹, Himanshi Himanshi¹, Prem Prakash², Shiv Kumar Sarin¹, Savneet Kaur¹, Dinesh Mani Tripathi¹. ¹Institute of Liver and Biliary Sciences, New Delhi, India; ²Jamia Hamdard University, New Delhi, India
Email: dineshmanitripathi@gmail.com

Background and aims: LSECs sense and respond to both shear stress and hydrostatic pressure via mechanocrine signalling and regulates endothelial homeostasis. Aberrant shear mediates endothelial dysfunction and promote portal hypertension through varied mechanisms is still unexplored. We investigated high shear-induced mechanosensors and involved signalling in the development of portal hypertension.

Method: Experimental high shear rat model was developed by resection of 70% liver (PHx). Intrahepatic shear flow was evaluated by transonic flow system and intra-vital imaging with Rhodamine-6G-fluorophore-stained platelet. Hepatic hemodynamic was monitored at 24 and 48 hrs post PHx. Sham animals were used as controls. Further in liver tissues proteomics, gene expression and histological analysis and electron microscopy was performed.

Results: Hemodynamic studies revealed significant increase in portal blood flow index by +222% and +200% at 24 hrs and 48 hrs respectively post 70% PHx and PP was raised (17.19 ± 3.28 +83.33% and 17.66 ± 2.51 +150%) at 24 h and 48 h respectively in comparison to controls. Intra-vital imaging revealed Intrahepatic shear flow was raised 2-fold at 48 h post PHx. Mechanistically, at mRNA level PIEZO1 pathway was upregulated including NOTCH-1, TRPV4 in PHx at 24 h and 48 h. Hepatic proteome analysis confirmed significant upregulation (L2FC = -1 to +1) of α , β -integrin, cadherins, ICAM1 while FAK and cytoskeleton proteins such as f-actin, ROCK, myosin, Kinesin, dynein, vimentin were downregulated in high shear. Interestingly, downregulated nucleoskeleton proteins- Lamin A/C, Lamin B1, and nuclear matrix protein matrin-3 were evident and promotes nuclear deformation further confirmed with Electron Microscopy. Elevated calcium binding proteins calmodulin, calpain, and SERCA complex, and calcium-calmodulin kinase II confirms elevated intracellular calcium influx in high shear, which is re-validated increase expression of PIEZO1 and TRPV4. Additionally, increased expression of coagulation factors XII, IX and neutrophil elastase and MPO was observed suggest NETosis and pro thrombotic milieu. Mechanosensors like VEGFR2, VEGFR3, VE-cadherin, CD-31 were also upregulated, as well as in the expression of α -SMA, vWF, ET-1 genes by RT-PCR in high shear further established disturb vascular homeostasis.

Conclusion: High shear stress activates coagulation cascade and mechanosensitive PIEZO1 dependent cytoskeleton rearrangement promotes nuclear deformation. Which leads hepatic trans-endothelial migration and vascular adhesion.

WED-059

Effects of albumin treatment on cell death markers in patients with decompensated cirrhosis and in acute-on-chronic liver failure

Estefania Alcaraz¹, Anna Mestre¹, Raquel Horrillo¹, Jordi Vidal¹, Mireia Torres¹, Joan Clària^{2,3,4}, Javier Fernández^{2,4}, Vicente Arroyo⁴, Isabel Bravo¹, Montserrat Costa¹. ¹Scientific Innovation Office, Grifols, Barcelona, Spain; ²Hospital Clínic, IDIBAPS and CIBERehd, Barcelona, Spain; ³Department of Biomedical Sciences, University of Barcelona

POSTER PRESENTATIONS

Medical School, Barcelona, Spain; ⁴EF CLIF, EASL-CLIF Consortium and Grifols Chair, Barcelona, Spain
Email: estefania.alcaraz@grifols.com

Background and aims: Cytokeratin 18 (K-18) and caspase-cleaved keratin 18 (cK-18) are cell death markers which reflect overall cell death and apoptosis, respectively. They are released into the plasma and increased in patients with decompensated cirrhosis and in acute on chronic liver failure (ACLF). For these liver pathologies, albumin-based therapies are under clinical investigation where the potential beneficial effects of albumin administration may be related to its non-oncotic properties (i.e. antioxidant, transport, immunomodulation). This study evaluated whether albumin-based treatments decrease cell death markers in patients with different stages of cirrhosis.

Method: Plasma samples from patients included in Pilot-PRECIOSA and Pilot-APACHE trials were assessed at baseline and during their follow-up. The Pilot-PRECIOSA trial (NCT00968695) analyzed the long-term albumin 20% administration (high dose, 1.5 g/kg weekly or low dose, 1 g/kg every 2 weeks, for 12 weeks, n = 5–6 patients each dose) to treat patients with decompensated cirrhosis and ascites. The Pilot-APACHE trial (NCT01201720) evaluated the effects of plasma exchange with human serum albumin 5% (PE-A5%) in 6 patients with ACLF for 10 days (6 sessions). Additionally, samples from age-matched healthy controls (HC, n = 7) were included. K-18 and cK-18 levels were detected by M65 and M30 ELISA kits, respectively.

Results: At baseline, both cell death markers were elevated in patients with decompensated cirrhosis and ACLF compared with HC. This increase was related to clinical disease severity, being higher in patients with ACLF. In patients with decompensated cirrhosis, necrotic cell death was decreased only in patients receiving high albumin dose (change from baseline, K-18 = −188 IU/L) vs low albumin dose (−20 IU/L). Similarly, high dose albumin treatment, but not low dose, reduced apoptotic cell death (p = 0.0343, between arms after 10 weeks). High dose albumin resulted in a cK-18 change from baseline of −257 IU/L while low albumin dose was 4 IU/L. In patients with ACLF, just after each PE-A5% session a reduction of both cell death markers was observed. After the last (sixth) PE-A5%, K-18 was reduced in 1300 IU/L and cK-18 in 118 IU/L. The effect on necrosis cell death was statistically significant for K-18 (ANOVA, p = 0.0003), and maintained longer (24–48 h after session), while the effect on apoptotic cell death marker was more transient.

Conclusion: Both apoptotic and necrotic cell death markers were increased in patients with decompensated cirrhosis and ACLF, being this increase associated with disease severity. Two different albumin-based treatments proposed for different stages of liver disease decreased circulating cell death markers. Further investigation is warranted to elucidate the beneficial effects of albumin, and its mechanism of action as a therapeutic agent in cirrhosis.

WED-060-YI

Type-I interferon shapes peritoneal immunity in cirrhosis and drives caspase-5-mediated progranulin release during spontaneous bacterial peritonitis

Michael Rooney¹, Shivalee Duduskar², Mohamed Ghait², Johanna Reißing³, Sven Stengel¹, Philipp Reuken¹, Alexander Zipprich¹, Michael Bauer⁴, Ashley Russo⁵, Vijay Rathinam⁵, Andreas Stallmach¹, Ignacio Rubio⁴, Tony Bruns³. ¹Department of internal medicine IV, Jena university hospital, Friedrich schiller university, Jena, Germany; ²Integrated research and treatment center, center for sepsis control and care, Jena university hospital, Jena, Germany; ³Department of internal medicine III, University hospital RWTH Aachen, Aachen, Germany; ⁴Integrated research and treatment center, Center for sepsis control and care, Jena university hospital, Department of anesthesiology and intensive care medicine, Jena university hospital, Friedrich schiller university, Jena, Germany; ⁵Department of immunology, University of connecticut health school of medicine, Farmington, United States
Email: michael.rooneyd@gmail.com

Background and aims: Gut-derived translocation of bacteria and their components contributes to alterations in immune responses and development of infections such as spontaneous bacterial peritonitis (SBP) in cirrhosis. Many bacterial products including bacterial DNA and lipopolysaccharide (LPS) are capable of producing type-I interferon (IFN) thereby influencing numerous important immune responses. We hypothesized peritoneal macrophage (PMs) exposure to bacterial-derived DNA or type-I IFN shapes their subsequent responses, activation of the inflammasome and release of certain damage-associated molecular patterns (DAMPs).

Method: PMs were isolated from the ascitic fluid of patients with decompensated cirrhosis and treated with *E. coli* single-stranded DNA (ssDNA), LPS, and type-I or II IFN or infected with *E. coli*, *S. aureus*, and Group B streptococcus. Inflammasome activation, changes in gene expression and release of cytokines and progranulin utilizing primary PMs, monocytes, and IFN pathway/caspase-deficient THP-1 cells were measured by qPCR, ELISA, western blot, and IFN-alpha/beta reporter cells. The concentration of serum progranulin was analyzed for correlation with transplant-free survival in 77 patients who developed SBP.

Results: *E. coli* ssDNA was a strong activator of type-I IFN in PMs and monocytes from patients and subsequently primed these cells for tumor necrosis factor production in response to LPS stimulation. During live-bacterial infection, PMs released type-I IFN and upregulated the expression of IFN-inducible genes, IFN-regulatory factors (IRF)1/IRF2, guanylate binding proteins (GBP)2/GBP5 and inflammasome components such as caspase-4/5. Exposure of PMs to bacterial ssDNA or type-I IFN also upregulated important inflammasome-associated proteins. PMs release significant amounts of interleukin-1beta and progranulin upon *S. aureus* or *E. coli* infection and utilizing THP-1 macrophages progranulin release through gasdermin-D pores occurs via a type-I IFN and caspase-5 dependent manner. A serum progranulin concentration greater than 93 ng/ml was found to be a marker for poor 90-day transplant-free mortality following SBP.

Conclusion: Type-I IFN influences the immune response in the peritoneal cavity and regulates caspase-5-mediated progranulin release during SBP. Progranulin may be a novel and useful biomarker for disease severity and caspase-5 mediated non-canonical inflammasome activation during SBP.

WED-068-YI

Cell-free DNA dynamics in advanced cirrhosis: unravelling the role of nuclear and mitochondrial DNA in inflammation, coagulation dysfunction and short-term mortality

Marilyna Stamouli^{1,2}, Jelle Adelmeijer³, Dana Huskens⁴, Elena Palma^{1,2}, Neil Youngson^{1,2}, Ane Zamalloa⁵, Shilpa Chokshi^{1,2}, William Bernal^{2,5}, Mark Roest⁴, Ton Lisman³, Vishal C Patel^{1,2,5}. ¹The Roger Williams Institute of Hepatology, Foundation for Liver Research, London, United Kingdom; ²Faculty of Life Sciences and Medicine, King's College London, London, United Kingdom; ³Surgical Research Laboratory and Section of Hepatobiliary Surgery and Liver Transplantation, Department of Surgery, University of Groningen, University Medical Center Groningen, Groningen, Netherlands; ⁴Synapse Research Institute, Cardiovascular Research Institute Maastricht, Maastricht University Medical Center, Maastricht, Netherlands; ⁵Institute of Liver Studies, King's College Hospital, London, United Kingdom
Email: m.stamouli@researchinliver.org.uk

Background and aims: Cirrhosis is characterised by increased cell death, leading to the release of cell-free DNA (cfDNA) into the systemic circulation, previously identified as a predictor of mortality. cfDNA primarily composed of nuclear (nDNA) and mitochondrial (mtDNA), each with distinct genomes, is thought to contribute to systemic inflammation and coagulation dysfunction. However, the patterns of cfDNA abnormalities at varying stages and severities of cirrhosis are poorly understood.

Method: Patients with varying cirrhosis severities [stable cirrhosis (SC, n = 30), decompensated cirrhosis (DC, n = 60) and acute-on-

chronic liver failure (ACLF, n = 40)] were included and compared to healthy controls (HC, n = 40) and to patients with sepsis without cirrhosis (non-liver sepsis/NLS, n = 25) as 'positive disease' control group. Plasma-derived total cfDNA (tDNA), nDNA, and mtDNA were quantified using Nanodrop, quantitative and digital droplet PCR. nDNA and mtDNA levels were related to cirrhosis severity and 30-day mortality. Markers of systemic inflammation and haemostasis including platelet activation proteins, coagulation and fibrinolysis factors were measured using a combination of ELISA, multiplex electrochemiluminescence assays, and on optimised in-house developed assays.

Results: Elevated tDNA and nDNA levels were detected in cirrhosis compared to HC but not as profoundly as in NLS, with a step-wise increase with worsening cirrhosis severity. However, mtDNA levels decreased progressively in cirrhosis compared to both HC and NLS. Notably, nDNA outperformed mtDNA in discriminating between patients with SC and DC (AUROC 0.79 vs 0.62) whereas both were equally effective in differentiating DC and ACLF (AUROC 0.73 vs 0.72). Higher nDNA levels were associated with a 10-fold higher risk of death or transplantation within 30 days. However, higher mtDNA levels were linked to a 6-fold increase of transplant-free survival. nDNA exhibited more robust correlations with inflammatory cytokines (IL-6, $r = 0.70$), and haemostatic markers (vfw, $r = 0.73$ and D-dimer, $r = 0.71$) compared to the overall weaker associations observed in mtDNA.

Conclusion: These findings reveal new insights into cirrhosis-specific cfDNA dynamics, compared to health and sepsis. To the best of our knowledge, we are the first to describe that circulating nDNA levels increase while mtDNA decrease proportionally to the severity of cirrhosis, suggesting differential release mechanisms for the two cfDNA subtypes. Both nDNA and mtDNA levels may serve as valuable biomarkers for predicting short-term mortality in cirrhosis patients, as well as offering insights into differential roles in disease processes. These data are in line with the established role of nDNA release with aberrant immunoregulatory processes, and support a plausible role of nDNA in endothelial dysfunction and haemostasis that requires further study.

WED-069

Bone morphogenic protein 9 (BMP9): a novel therapeutic agent for the prevention of extrahepatic organ failure in acute-on-chronic liver failure (ACLF)

Alexandra Phillips¹, Abeba Habtesion¹, Fausto Andreola¹, Nathan Davies¹, Paul Upton², Nick Morrell², Rajiv Jalan¹. ¹Institute of Liver and Digestive Health, University College London, London, United Kingdom; ²Heart and Lung Research Institute, University of Cambridge, Cambridge, United Kingdom
Email: alexandra.phillips5@nhs.net

Background and aims: Endothelial dysfunction in ACLF is associated with severity of inflammation and extrahepatic organ dysfunction resulting in reduced organ perfusion and lactatemia. Bone morphogenic protein 9 (BMP9), a member of the transforming growth factor beta (TGF β) superfamily, is involved in the regulation of endothelial cell function. BMP9 is reduced in cirrhosis and this correlates with increased liver and renal injury. We hypothesise that BMP9, by virtue of its known effect on the endothelium may be a novel therapeutic agent for prevention and treatment of extrahepatic organ dysfunction in models of cirrhosis and ACLF, reducing organ injury and improving survival.

Method: Rat cirrhosis model induced by 4-week bile duct ligation (BDL) \pm 0.025 mg/kg intraperitoneal (ip) Lipopolysaccharide (LPS) to induce acute-on-chronic liver failure (ACLF) \pm 90 μ g/kg/day BMP9 ip. Mouse fibrosis induced by 12-week oral gavage of 0.5 ml/kg carbon tetrachloride (CCL4) \pm 2 mg/kg LPS (ACLF) \pm 90 μ g/kg/day BMP9 ip in C57Bl mice. Mean arterial pressure assessed by arterial catheterisation under gaseous anaesthesia. Plasma biochemistry analysed by COBAS and Fujifilm DriChem slides. Histological staining with TUNEL

assay, Sirius red and Haematoxylin and Eosin. Survival assessed by absence of coma. Statistical analysis performed using SPSS.

Results: BMP9 administration led to a significant increase in coma-free survival at 3-hours post LPS injection in the rat ACLF models [75% vs 22%, $p = 0.03$]. An increase in body weight change was observed in BDL and BDL+LPS animals treated with BMP9 [1.9% to 4.2% $p = 0.076$, 5.8% to 9.4% $p = 0.037$], and a reduction in liver weight compared to vehicle control was observed in BMP9-treated animals [20.9 g to 17.4 g in BDL animals, 21.2 g to 17.8 g in BDL+LPS animals]. BMP9 increased the mean arterial pressure (MAP) at termination in all models, with a significant increase in the ACLF model [82.1 to 108.5 mmHg, $p = 0.01$]. BMP9 administration modulated renal injury in the ACLF model with a reduction in plasma creatinine [82.3 to 65.4 μ mol/L, $p = 0.056$], in addition to a reduction in plasma lactate [10.4 to 6.6 mmol/L, $p = 0.019$]. No significant changes were observed in the severity of liver injury, portal pressure, portal vein flow, markers of cell death and systemic inflammation. The effects seen in BDL animals were validated in the CCL4 mouse model.

Conclusion: This study provides novel insights that directly targeting the endothelium can prevent circulatory and renal failure improving effective organ perfusion resulting in significant survival benefit in ACLF animal models. BMP9 is therefore, an attractive therapeutic strategy that should be explored in clinical trials.

WED-070

Isolation and immortalization of human endothelial cells from the portal vein

Aina Anton^{1,2,3}, Genís Campreciós^{1,2,3}, Sarah Shalaby^{1,3,4}, Annabel Blasi^{1,2,5}, Yilliam Fundora⁶, Rosa Montañés^{1,3}, Héctor García-Calderó^{1,2,3}, Juan Carlos García-Pagán^{1,2,3,7}, Virginia Hernández-Gea^{1,2,3,7}. ¹Fundació de recerca clínic Barcelona-Institut d'investigacions biomèdiques August Pi i Sunyer (FRCB-IDIBAPS), Barcelona, Spain; ²Centro de investigación biomédica red de enfermedades hepáticas y digestivas (CIBEREHD), Madrid, Spain; ³Liver unit, Hospital Clínic, Health care provider of the european reference network on rare liver disorders (ERN-Liver), Barcelona, Spain; ⁴Department of surgery, oncology, and gastroenterology, Padua University hospital, Health care provider of the european reference network on rare liver disorders (ERN-Liver), Padua, Italy; ⁵Anesthesiology department, Hospital Clínic, Barcelona, Spain; ⁶Department of surgery, division of hepatobiliary and general surgery, Institut de malalties digestives i metabòliques (IMDiM), Hospital Clínic, Barcelona, Spain; ⁷Medicine department, Faculty of medicine, Universitat de Barcelona, Barcelona, Spain
Email: anton@recerca.clinic.cat

Background and aims: Cirrhosis (CH) profoundly affects the portal venous system that frequently develops thrombosis (PVT). The exact mechanisms responsible for PVT development are not well understood and the contribution of endothelial cells (EC) to thrombosis, although well established in other vascular territories, remains unexplored in the portal vein, mainly due to its remote access. To the best of our knowledge portal vein EC (PVEC) have never been isolated and EC from other areas may not fully represent the splanchnic characteristics during CH. Moreover, for the study of PVT we lack suitable preclinical models (i.e., rodents do not develop PVT) challenging splanchnic vascular bed research in CH. The aim of our study is to generate a unique tool that can facilitate a more in-depth exploration of splanchnic vasculature diseases by isolating and immortalizing PVECs.

Method: 1) PVECs were isolated from human portal vein (PV) tissue obtained during hepatic transplantation. PV samples were trypsinized, scratched and cells detached from the inner wall were cultured until confluence. FACS sorting, based on CD31 and CD144 positive markers, was performed to select pure EC. Cells were expanded, characterized through functional assays (tub formation assay) and phenotypically analyzed using flow cytometry and immunofluorescence staining (CD31, CD144, eNOS and Von Willebrand markers). 2)

POSTER PRESENTATIONS

PVECs were immortalized (IM cells) with lentiviral particles expressing the SV40 large T-antigen containing the GFP-puromycin marker, selected and characterized as previously described.

Results: Human primary PVECs were successfully obtained from PV tissues, exhibiting a uniform morphology, forming monolayers that proliferate normally as plaques of small, tightly clustered cells. PVECs showed endothelial features, including positive staining for eNOS and vWF and demonstrated endothelial behavior by forming tubes in a matrigel matrix. PVECs were able to grow and expand until passage 6–9, when they started to gain a senescent phenotype –enlarged and multinucleated- and ceased growth. Compared to primary PVECs, IM cells exhibited a normal growth rate but could grow until passage 25–40. IM cells maintained a normal phenotype, expression of EC markers, and tube-forming capacity across all passages. Importantly, they did not exhibit a tumorigenic phenotype, as evidenced by the absence of colony formation in a soft agar assay.

Conclusion: For the first time, we successfully isolated PVEC utilizing an innovative strategy. Moreover, we have generated IM cell lines for physiopathological investigations and drug screening. This advance may deep our understanding of conditions like PVT, with treatment limited to anticoagulation-often falling to achieve complete recanalization-but also enhance our comprehension of vascular complications in liver diseases, paving the way for precise translational research.

WED-071

The association of hepatocyte large extracellular vesicles with plasma biomarkers levels improve prediction of mortality in patients with cirrhosis

Audrey Payancé¹, Louise Biquard², Sara Thietart³, Gilberto Silva-Junior⁴, Marion Tanguy², Tazime Issoufaly⁵, Cristina Levi⁶, Julien Bissonnette⁷, Dominique Valla⁸, Francois Durand⁹, Juan Carlos García-Pagán¹⁰, Pierre-Emmanuel Rautou¹. ¹Université Paris-Cité, Inserm, Centre de recherche sur l'inflammation, UMR 1149, Paris, France., AP-HP, Hôpital Beaujon, Service d'Hépatologie, DMU DIGEST, Centre de Référence des Maladies Vasculaires du Foie, FILFOIE, ERN RARE-LIVER, Clichy, Paris, France, ²Université Paris-Cité, Inserm, Centre de recherche sur l'inflammation, UMR 1149, Paris, France, ³Sorbonne Université, Assistance Publique-Hôpitaux de Paris (AP-HP), Hôpital Pitié-Salpêtrière, Département de Gériatrie, Paris, France, ⁴Hospital Clinic-Institut d'Investigacions Biomèdiques August Pi i Sunyer, IMDIM, barcelona, Spain, ⁵AP-HP, Hôpital Beaujon, Service d'Hépatologie, DMU DIGEST, Centre de Référence des Maladies Vasculaires du Foie, FILFOIE, ERN RARE-LIVER, Clichy, France, ⁶Centre Hospitalier Sud-Francilien, Service d'hépatogastroentérologie, Corbeil-Essonnes, France, ⁷Department of Hepatology and Liver Transplantation, University of Montreal Hospital, Montreal, Canada, ⁸AP-HP, Hôpital Beaujon, Service d'Hépatologie, DMU DIGEST, Centre de Référence des Maladies Vasculaires du Foie, FILFOIE, ERN RARE-LIVER, Clichy, France, ⁹Université Paris-Cité, Inserm, Centre de recherche sur l'inflammation, UMR 1149, Paris, France, ¹⁰AP-HP, Hôpital Beaujon, Service d'Hépatologie, DMU DIGEST, Centre de Référence des Maladies Vasculaires du Foie, FILFOIE, ERN RARE-LIVER, Clichy, France, ¹⁰Barcelona Hepatic Hemodynamic Laboratory, Liver Unit, Hospital Clínic de Barcelona, IDIBAPS, CIBERehd, European Reference Network for Rare Vascular Liver Diseases, Universitat de Barcelona, Spain
Email: audrey.payance@gmail.com

Background and aims: Biomarkers and scores used to predict mortality in patients with decompensated cirrhosis are still imperfect tools. We identified 8 biomarkers reflecting tissues and processes altered in patients with decompensated cirrhosis. The aims of this study were to 1) evaluate features associated with circulating concentrations of these 8 biomarkers, 2) define a prognostic signature including some of these biomarkers and test its accuracy to predict mortality in patients with stable decompensated cirrhosis.

Method: All patients with cirrhosis undergoing liver catheterization at two centers were prospectively included (derivation cohort, n = 239; validation cohort n = 103). Circulating concentrations of hepatocyte large extracellular vesicles (IEVs) and of 7 biomarkers derived from the kidneys (podocalyxin), gut (Villin), platelets (P-selectin), reflecting systemic inflammation (leukosialin, C-reactive protein and complement C6) and mitochondrial function (GPD2) were measured. Univariate and multivariate analyses were conducted using the Fine and Gray model with liver transplantation considered as a competing event.

Results: In the derivation cohort, 162 (68%) Child-Pugh score B or C cirrhosis. During the 6 months follow-up, 45 (19%) patients underwent liver transplantation and 16 (7%) patients died. Among the 8 biomarkers, circulating concentrations of hepatocyte IEVs, C-reactive protein, and Villin were significantly associated with features reflecting liver disease severity, i.e. Child-Pugh score, MELD and HVP. We then focused on the 162 patients with Child-Pugh B or C cirrhosis to assess the predictive ability of the identified plasma biomarkers. We observed that plasma concentrations of hepatocyte IEVs, of CRP, and of Villin were associated with 6-month mortality by univariate analysis. Cut-off values of plasma biomarkers were identified using the Youden Index for CRP and Villin and a previously identified value for hepatocytes IEVs. Values above those cut-offs are thereafter referred to as “high-risk plasma biomarkers.” Patients with one or more high-risk plasma biomarkers had a 6-month cumulative incidence of death higher than that of patients with no high-risk plasma biomarkers (19% vs. 2.8%, p = 0.007). This association with survival was independent from Child-Pugh score and MELD. When separating patients according to a threshold of MELD of 15, we observed that patients with one or more high-risk plasma biomarkers and MELD >15 were at higher risk for 6-month mortality than the other patients (27% vs. 4.5%; p = 0.004). Similar results were obtained in the validation cohort.

Conclusion: A signature including circulating concentrations of hepatocyte IEVs, C-reactive protein, and Villin combined with MELD, is able to identify a population of patients with cirrhosis at particularly high risk of 6-month mortality.

WED-074

The role of endothelial FoxO1 pathway in decompensated liver cirrhosis and acute-on-chronic liver failure

Fabian Schachteli¹, Yang Zhang^{2,3}, Sabine Klein^{1,4}, Maximilian Joseph Brol^{1,4}, Robert Schierwagen^{1,4}, Pia Lembeck¹, Sara Noemi Reinartz Groba¹, Wenyi Gu^{1,4}, Stefan Zeuzem⁴, Jonel Trebicka^{1,4,5}, Michael Potente^{2,3}, Frank Erhard Uschner^{1,4}. ¹University Hospital Münster, Münster, Germany; ²Max Delbrück Center for Molecular Medicine (MDC), Berlin, Germany; ³Max Plank Institut for Heart and Lung Research, Bad Nauheim, Germany; ⁴Hospital of the Goethe University Frankfurt, Frankfurt am Main, Germany; ⁵European Foundation for the Study of Chronic Liver Failure, Barcelona, Spain
Email: frankerhard.uschner@ukmuenster.de

Background and aims: Endothelial dysfunction, in response to severe systemic inflammation, is majorly involved in the development of acute decompensation (AD) and Acute-on-Chronic Liver Failure (ACLF). The transcription factor Forkhead Box O1 (FoxO1) regulates the activity and growth of healthy endothelium as well as its stress response. The aim of this study was to investigate the role of FoxO1 signaling in human endothelial cells *in vitro* as well as in experimental and human liver cirrhosis and ACLF *in vivo*.

Method: Liver cirrhosis was induced in rats using bile duct ligation (BDL), CCl₄ injections with Western diet (WD rats) or CCl₄ injections with ethanol in drinking water (EtOH rats), and compared to healthy and sham operated animals respectively. Acute alcohol binge, lipopolysaccharide (LPS) i.p. injections, transnasal stool inoculation or cecal pole ligation and puncture were used for ACLF induction. FoxO1 signaling was analyzed in rat liver tissue and patient samples using cRNA microarray, Western Blot and qPCR. Human umbilical

vein endothelial cells (HUVECs) were treated with FoxO1 inhibitor AS1842856 or plasma of healthy patients, patients with AD or with ACLF to reproduce disease conditions *in vitro*. FoxO1 pathway expression and endothelial cell functional assays (apoptosis, senescence, quiescence, proliferation and angiogenesis) were performed after FoxO1 inhibitor or plasma incubation.

Results: Gene expression levels of FoxO1 pathway components, nuclear and cytoplasmic protein expression, as well as mRNA levels of FoxO1 and its downstream target MYC, were markedly reduced after ACLF induction in BDL, WD and EtOH rats. Similarly, FoxO1 signaling was downregulated in liver explants from patients undergoing liver transplantation with alcohol-related liver disease and ACLF. Thus, FoxO1 correlates with severity of experimental and human liver cirrhosis and ACLF *in vivo*. Incubation of HUVECs with AD plasma, mimicking systemic inflammation *in vitro*, decreased FoxO1 and MYC expression. Interestingly, FoxO1 downregulation was even more pronounced after incubation with ACLF plasma, thus reflecting the changes observed *in vivo*. Incubation with ACLF plasma and FoxO1 inhibitor AS1842856, however, not with plasma from AD patients, inhibited angiogenesis and proliferation without inducing apoptosis or autophagy in HUVECs.

Conclusion: Loss of FoxO1 expression and function is associated with experimental and human liver cirrhosis and ACLF. Furthermore, incubation with plasma of ACLF patients or pharmacological inhibition decreased FoxO1 expression *in vitro* and induced endothelial dysfunction. Therefore, the FoxO1 pathway seems to be crucial for the development of endothelial dysfunction in ACLF.

WED-075-YI

Exploring the immunomodulatory potential of TLR7/8 agonism in decompensated cirrhosis

Dimitrios Patseas¹, Rosey Sheth², Wing Yu Lee¹, Georgina Hagger¹, Eoin Mitchell¹, Francesca M Trovato², Cathrin L C Gudd¹, Lucia A Possamai¹, Mark R Thursz¹, Mark J W McPhail², Evangelos Triantafyllou¹. ¹Department of Metabolism, Digestion and Reproduction, Imperial College London, London, United Kingdom; ²Department of Inflammation Biology, King's College London, London, United Kingdom
Email: d.patseas@imperial.ac.uk

Background and aims: Immune dysfunction and bacterial infections are common in patients with acute decompensation (AD) of cirrhosis, contributing to high morbidity and mortality. This is more profound in those with accompanying organ-failure (acute-on-chronic liver failure; ACLF). Toll-like receptors (TLRs) recognize microbial-related factors such as LPS (via TLR4) or single-stranded RNA (via TLR7 and TLR8). TLR7 and 8 are expressed within the myeloid compartment and some of their ligands are currently considered in clinical trials as potential therapeutics. We utilized an ex-vivo whole blood culture setting to study the functional effects of TLR7, TLR8 or dual TLR7/8 agonism on AD/ACLF patient-derived monocytes and T cells.

Method: AD/ACLF patient (n = 13) and healthy control (HC; n = 13) derived whole blood was cultured overnight in the presence (5 µg/ml) of TLR7-L (R837), TLR8-L (ssRNA40/LyoVec), or TLR7/8-L (R848) in comparison to PBS. The effects of TLR agonism on immune function were evaluated by flow cytometry assays; apoptosis (Annexin-V/7-AAD stain) and intracellular cytokine production by monocytes and T cells following 4-hour whole blood stimulation with LPS (100 ng/ml) or PMA/ionomycin were measured. Monocyte phagocytosis of E. coli GFP+ bacteria was also evaluated.

Results: TLR7/8 (R848) dual agonism improved the E. coli uptake of monocytes in AD/ACLF patients (PBS:44.7% vs TLR7/8:65.3%, p = 0.001). Notably, individual TLR7 or TLR8 agonism did not exert a similar effect, whilst HC monocyte phagocytosis was not impacted by TLR treatment. PBS-treated patient monocytes produced less pro-inflammatory cytokines such as TNFα (HC:59.8% vs AD/ACLF:11.6%, p < 0.0001), IL-1β, IL-6, and more of IL-10 and OPN, in comparison to HC. We found that TLR7/8 dual agonism reduced OPN production by

AD/ACLF monocytes (PBS:71.6% vs TLR7/8-L:46.8%, p = 0.0017) while an increased, non-significant, TNFα and IL-1β production by monocytes was observed. In addition, PBS-treated CD4+ T cells from patients produced less IL-4 (HC:69.4% vs AD/ACLF:8.85%, p = 0.0317) and more IL-2, in comparison to HC samples, and CD8+ T cells showed higher production of IL-4 (HC:60.85% vs AD/ACLF:84.6%, p = 0.0635) and TNFα (HC:45.3% vs AD/ACLF:59.2%, p = 0.0635). Overall, TLR7, 8 or 7/8 agonism did not alter T cell cytokine production, in both HC and AD/ACLF samples, nor impacted apoptosis of monocytes or T cells.

Conclusion: We demonstrate that TLR7/8 agonism improves the bacterial phagocytosis of AD/ACLF monocytes, while showing promise in augmenting their pro-inflammatory cytokines. Our findings suggest TLR7/8 agonism (using R848) as an immunomodulatory approach for improving monocytic function that could prove beneficial for AD/ACLF patients. Future ex vivo and in vivo studies will further evaluate this TLR-directed approach for improving antimicrobial responses in cirrhosis.

WED-076

Increased gut urease activity contributes to hyperammonemia and is a potential biomarker of disease severity in cirrhosis

Deepika Jakhar¹, Pinky Juneja², Aarti Sharma², Nishu Choudhary², Ashi Mittal³, Shiv Kumar Sarin², Dinesh Mani Tripathi³, Shvetank Sharma², Savneet Kaur⁴. ¹institute of liver and biliary sciences, vasant kunj, new delhi, India; ²institute of liver and biliary sciences, new delhi, India; ³institute of liver and biliary sciences, new delhi; ⁴Institute of liver and biliary Sciences, Vasant Kunj, Delhi, India
Email: savykaur@gmail.com

Background and aims: Hyperammonemia is an important prognostic factor for liver related complications. Gut is one of the main source of endogenous ammonia and it is generated from urea by urease expressing bacteria. In view of the fact that gut microbiota undergoes profound changes, we hypothesised that higher gut urease bacteria is associated with increased gut ammonia production and hence hyperammonemia in cirrhosis.

Method: For experimental cirrhosis, 10 wk CCl4 rat model was prepared. Ammonia was measured in plasma and stool. Gut ammonia metabolism was studied. 16S rRNA gene sequencing analysis was done in stool samples to see gut microbiota. To ascertain role of gut urease bacteria in ammonia production, we gavaged representative live and attenuated urease producing bacteria, *Klebsiella pneumoniae* (Kp) in bowel cleansed controls and cirrhotic rats for 7 days, and then studied ammonia metabolism and its levels in gut, stool and plasma. In clinical study, stool and plasma of healthy controls (n = 15) and cirrhotic patients (n = 32) were obtained and their normalized plasma ammonia and stool urease activity was studied.

Results: In cirrhotic rats, plasma ammonia (3.6 fold change (fc) p = 0.02), stool ammonia (1.5 fc p = 0.1) and stool urease (2 fc p = 0.05) activity were significantly increased as compared to controls. 16S rRNA analysis of stool samples showed reduced species diversity (p = 0.01) and evenness (p = 0.01) in cirrhotic rats as compared to controls. Taxonomic analysis revealed that abundance of *Lactobacillus acidophilus* (probiotic) was relatively reduced while that of *Kp* and *Prevotella* (pathogenic) was increased in cirrhotic animals as compared to controls. In gut microbiota replenishing studies, in controls, after bowel cleansing, rats given live *Kp* showed higher colon (4.3 fc p = 0.05), stool urease activity (3.8 fc p = 0.05) and increase stool ammonia (6000 ± 50 vs 4500 ± 50 µg/dl p = 0.08) than rats given attenuated bacteria. While, there was no change in plasma ammonia between two groups. In cirrhotic rats, given live urease bacteria, both colon, stool urease activity (4 fc and 4.5 fc p = 0.05 each) and plasma ammonia (2 fc p = 0.02) were increased as compared to those given attenuated *Kp*. In clinical study, normalized plasma ammonia (3 ± 0.5 vs 1 ± 0.2 p = 0.01) and stool urease activity (2.5 fc p = 0.009) was significantly higher in cirrhosis patients than healthy subjects. Both stool urease activity (2 fc p = 0.05) and normalized plasma ammonia levels (3.4 ± 0.5 vs 1.1 ± 0.1 p = 0.04) of CTP class C

POSTER PRESENTATIONS

was significantly higher than class A patients. There was however no significant direct correlation between stool urease activity with plasma ammonia in our patients.

Conclusion: Our experimental findings elucidate the role of gut microbial urease activity as a significant contributor of stool and plasma ammonia. Stool urease activity increases with severity of cirrhosis and indicates higher gut ammonia production.

WED-077

APASL-ACLF without previous decompensation is rare but immunological distinct from ACLF with previous decompensation in a european cohort

Mona-May Langer¹, Sabrina Guckenbiehl², Alina Bauschen¹, Gerald Denk¹, Christian M. Lange¹. ¹Department of Medicine II, University Hospital, LMU Munich, Munich, Germany; ²Department for gastroenterology and hepatology, University hospital Essen, Essen, Germany

Email: monamay.langer@med.uni-muenchen.de

Background and aims: Definitions of acute-on-chronic liver failure (ACLF) are heterogeneous. EASL-CLIF-definition focusses on extra-hepatic organ failures, whereas in APASL-definition the liver is the most important organ failure. More importantly, APASL-ACLF definition excludes patients with previous decompensation. In the present study, we provide an updated analysis of associations between the presence and absence of ACLF without/with previous decompensation and correlate these with inflammatory molecules, immune cell phenotyping, clinical parameters and outcome.

Method: 207 hospitalized patients with liver cirrhosis without or with ACLF were recruited from a prospective cohort study. 76 inflammatory molecules were quantified by proximity extension analysis assay (Olink, Uppsala, Sweden). Associations between inflammatory profiles and types of ACLF were determined. Moreover, surface expression profiles of immune cells were analyzed by flow cytometry.

Results: Of 207 patients, 126 had no ACLF at all, while 81 had any ACLF. Of patients with ACLF, 30 had ACLF exclusively based on the EASL-CLIF-definition. 17 patients had ACLF based on the APASL-definition without/with previous decompensation events. Of these patients, 9 have been decompensated before, while 8 have never been decompensated. Overall, patients who met the EASL-definition of ACLF showed signatures of substantial systemic inflammation. Discrimination of APASL-ACLF regarding previous decompensation event shows striking differences in inflammatory profiles of these patients compared to patients with AD or EASL-CLIF-ACLF. Patients with APASL-ACLF without previous decompensation show, among others, significant lower levels of NT-3, FGF-5 and IL-17. Patients with EASL- or APASL-ACLF-definition show significant decreased frequencies of CD8⁺ T cells in peripheral blood (APASL-ACLF 7%, CLIF-ACLF 16%) compared to healthy donors (36%) and AD (26%). Moreover, the frequency of specific surface markers on T cells are significantly decreased in APASL-ACLF (46%) compared to healthy donors (90%, $p = 0.4$) or AD (92%, $p = 0.2$), leading to presumption of senescent T cell subpopulations in the blood of these patients.

Conclusion: Not only do patients with APASL- versus EASL-CLIF-ACLF show distinct inflammatory profiles, but moreover inflammatory profiles of patients fulfilling APASL-ACLF without vs. with previous decompensation differ significantly. The changes in surface expression of T cells may point towards distinct pathophysiological mechanisms in different types of ACLF.

WED-078

Systemic albumin administration improves the gut microbiome and intestinal permeability in animal models of cirrhosis and ACLF

Alexandra Phillips¹, Yi Jin², Florian Rosenberger³, Qianwen Zhao¹, Abeba Habtesion¹, Fausto Andreola¹, Nathan Davies¹, Frederick Clasen⁴, Lindsey Edwards^{5,6}, Jane Macnaughtan¹,

Sabine Klein⁷, Jonel Trebicka⁷, Saeed Shoaie⁸, Matthias Mann³, Rajiv Jalan¹. ¹Institute of Liver and Digestive Health, University College London, London, United Kingdom; ²Centre for Host-Microbiome Interactions, King's College London, London, United Kingdom; ³Department of Proteomics and Signal Transduction, Max Planck Institute of Biochemistry, Munich, Germany; ⁴Cancer Metabolism Laboratory, The Francis Crick Institute, London, United Kingdom; ⁵Centre for Host Microbiome Interactions, King's College London, Faculty of Dentistry, Oral and Craniofacial Sciences, London, United Kingdom; ⁶Institute of Liver Studies, King's College London, Department of Inflammation Biology, School of Immunology and Microbial Sciences, Faculty of Life Sciences and Medicine, London, United Kingdom; ⁷Department of Internal Medicine, University of Munster, Munster, Germany; ⁸Centre for Host Microbiome Interactions, Kings College London, London, United Kingdom
Email: alexandra.phillips5@nhs.net

Background and aims: Gut dysbiosis impacts negatively on gut permeability, bacterial translocation and endotoxemia, which is a target of therapy in patients with decompensated cirrhosis. Long term albumin administration in cirrhosis patients reduces endotoxemia, modulates inflammatory response and improves survival. This study was designed to test the hypothesis that albumin modulates the composition of the gut microbiome and permeability. We also tested whether the administered albumin could cross into the gut lumen.

Method: Cirrhosis induced in 70 rats by 4-week bile duct ligation (BDL) and acute-on-chronic liver failure (ACLF) model induced by lipopolysaccharide (LPS) 0.025 mg/kg intraperitoneal injection (ip) to BDL model. Human albumin 20% administered (1.5 g/kg ip; 2-week) to cirrhosis and ACLF models in albuminaemic (NAR) and wild-type (WT) rats. Caecal stool 16 s PCR analysis of microbiome and mass spectrometry analysis for gut proteome of ileal, caecal and left colon stool. Plasma biochemistry and cytokines were measured. Plasma D-lactate was used as a measure of gut permeability.

Results: The absence of endogenous albumin in NAR rats was associated with significant differences of 3 operational taxonomic unit (OTUs) in healthy rats. Albumin infusion in NAR rats restored these OTUs to that observed in wild-type (WT) rats. In both WT and NAR cirrhotic rats, 20 and 25 OTUs were different compared with their sham controls. Treatment of both WT and NAR rats with albumin ameliorated the differential abundance seen in cirrhosis. Proteomic analysis of stool detected *human albumin* in the gut of albumin-treated animals, with the highest levels in the left colon. Otherwise, albumin treatment did not change the proteome. The highest number of significant changes in proteins following albumin treatment was seen in ACLF models of WT rats, where proteomic differences were associated with pathways of precursor metabolites, energy generation, and protein digestion and absorption. These microbiome changes in human albumin-replete rats were associated with preserved gut permeability, reduced systemic inflammation, severity of liver injury and survival in the ACLF animals.

Conclusion: The results of this study show for the first time the importance of albumin in maintaining the health of the gut microbiome. The detection of administered human albumin in the rat colonic lumen suggests that this effect of albumin may at least partially be mediated by the action of administered albumin directly in the colonic lumen. These novel data allow development of potential new therapeutic uses of albumin.

WED-080

Hepatic inflammation-senescence-regeneration gene expression during recovery from ACLF and the effect of granulocyte-colony stimulating factor (G-CSF), toll-like receptor-4 (TAK-242) inhibition and their combination (G-TAK)

MohammadMahdi Saeidinejad¹, Daniel Shaw², Cornelius Engelmann^{3,4}, Abeba Habtesion⁴, Fausto Andreola⁴, Rajiv Jalan^{4,5}. ¹Liver failure Group, Institute for Liver and Digestive

Health, Division of Medicine, London, United Kingdom; ²Institute for Liver and Digestive Health, Division of Medicine, London, United Kingdom; ³Medical Department, Division of Hepatology and Gastroenterology, Berlin, Germany; ⁴Liver failure Group, Institute for Liver and Digestive Health, Division of Medicine, London, United Kingdom; ⁵European Foundation for the Study of Chronic Liver Failure, Barcelona, Spain
Email: mohammad.saeidinejad@nhs.net

Background and aims: Failure of hepatic regeneration in acute-on-chronic liver failure (ACLF) is pathophysiologically related to inflammation and hepatocyte senescence but how these evolve during recovery from ACLF is unknown. Toll-like receptor-4 antagonist (TAK242) with or without GCSF (G-TAK), improves survival of animal models. The aims of this study were to explore the inflammation-senescence-regeneration gene expression in animals that survived an episode of ACLF with or without treatment.

Method: Six groups of animals were studied: Control (vehicle), carbon tetrachloride (CCL4 0.5 mg/ml, 0.5 ml/kg twice weekly for 6 weeks) (cirrhosis), CCL4+ Lipopolysaccharide (LPS, 6.25 µg/µl, 4 mg/kg i.p.) (ACLF), CCL4+LPS+GCSF, CCL4+LPS+TAK242, and CCL4+LPS+G-TAK. Of the 86 mice in the study, 24 mice (4/group), surviving 5-days were studied. Liver samples were then assessed at the NanoString nCounter laboratory for expression of genes in the metabolic pathways panel and analysed using NanoString Software.

Results: 5-day survival was 100% except for the mice treated with G-CSF (mortality-66%). Within 24 hours, LPS injection led to significant liver and renal injury (mean ALT >1500 U/L, creatinine >30 µmol/L in CCL4+LPS mice), which was prevented by TAK242 and G-TAK. By day-5, ALT and creatinine normalised and were similar in all groups. TLR signalling: In animals recovering spontaneously, hepatic TLR signalling pathway remained upregulated; in those treated with GCSF alone this was further accentuated but in those treated with TAK-242 or GCSF+TAK-242, this was normalised. Chemokine and cytokine signalling pathways (Ccl5 and 9) were similar. Senescence: G-CSF increased p53 gene expression. Treatment with TAK242, or G-TAK, downregulated p53 pathway compared to ACLF mice recovering spontaneously. Regeneration: Spontaneous recovery and TAK-242, in terms of pro- and anti-regeneration genes was not different to control. G-TAK significantly augmented proliferation and cell survival genes as evidenced by the increase in expression of Cyclin A2, Cyclin D1, Ki67, and STAT3.

Conclusion: The results of this study show for the first-time that despite spontaneous recovery from liver and renal injury in ACLF, pathways involved in inflammation through TLR signalling and senescence remain elevated leaving animals prone to future episodes of decompensation and ACLF. Treatment with TAK242 with or without G-CSF downregulates senescence pathways but only G-TAK improved regeneration. These data indicate that G-TAK may reduce the risk of future decompensation and ACLF.

WED-081

Carvedilol decreases hepatic vascular resistance in cirrhosis by deactivating hepatic stellate cells (HSC) and improving liver sinusoidal endothelial cells (LSEC) dysfunction, resulting in decreased liver fibrosis and improved nitric oxide release

Yeldos Nulan^{1,2,3}, Eric Felli^{2,3}, Cong Wang^{2,3}, Sonia Emilia Selicean^{2,3}, Annalisa Berzigotti^{2,3}, Jordi Gracia-Sancho^{2,3,4}, Jaime Bosch^{2,3}.

¹Graduate School for Cellular and Biomedical Sciences (GCB), University of Bern, Bern, Switzerland; ²Department of Visceral Surgery and Medicine, Inselspital, Bern University Hospital, University of Bern, Bern, Switzerland; ³Department for BioMedical Research, Hepatology, University of Bern, Bern, Switzerland; ⁴Liver Vascular Biology Research Group, CIBEREHD, IDIBAPS Research Institute, Barcelona, Spain
Email: jaime.bosch@unibe.ch

Background and aims: Portal hypertension (PH) in cirrhosis results primarily from increased hepatic vascular resistance, promoted by structural changes (architectural remodeling, parenchymal

extinction, fibrosis and nodular regeneration) and increased hepatic vascular tone (endothelial dysfunction with decreased availability of nitric oxide-NO, and increased production and sensitivity to vasoconstrictors). Later on, PH is aggravated by extrahepatic circulatory abnormalities. Non-selective-beta-blockers (NSBBs) are the mainstream of medical therapy, reduce PH by decreasing the cardiac output and splanchnic blood flow. Carvedilol, a new generation NSBB with anti-alpha1-adrenergic activity, causes a greater fall in portal pressure than traditional NSBBs and is better tolerated. Carvedilol is thought to decrease the hepatic vascular tone, but its effects on the determinants of hepatic vascular resistance in cirrhosis have not been well characterized. In this study we analyze the effects of carvedilol on the HSCs and endothelial cells function in vitro, as well as on liver fibrosis and hepatic hemodynamics after in vivo administration to cirrhotic rats.

Method: *In vitro*: LSECs and HSCs were isolated from cirrhotic rats (ip thioacetamide for 12 weeks) and then cultured with 10 µM Carvedilol/vehicle for 24 hours. Endothelial function was assayed by immunocytochemistry (DAF-FM NO assay) in human umbilical vein endothelial cells (HUVECs) and cirrhotic LSECs. Cell contraction assays were performed in human hepatic stellate cell line (LX2) and cirrhotic HSCs. (n = 3–5 per condition).

In vivo: hepatic hemodynamic studies were performed in thioacetamide cirrhotic rats treated with carvedilol (10 mg/kg/day, p.o.) or vehicle for 2 weeks (n = 14 per group). Hepatic remodeling was assessed in collagen-stained sections by calculating the collagen proportionate area (CPA), and HSC activation by immunofluorescence of alpha-smooth muscle actin (αSMA) in liver sections.

Results: NO release was significantly increased in carvedilol vs vehicle in HUVECs and in cirrhotic LSECs, by 2 and 2.2 fold-change respectively. Carvedilol significantly reduced cell contraction in LX2 and HSCs, by 32% and 48% respectively vs vehicle. Oral administration of carvedilol in cirrhotic rats significantly reduced portal pressure by 27.1% and decreased CPA and αSMA positive area in liver tissue slides, by -29.8% and -32.1% respectively vs vehicle (all p < 0.01).

Conclusion: These results suggest that carvedilol improves portal hypertension in liver cirrhosis not only by its systemic hemodynamic effects, but also by its intrahepatic effects ameliorating HSCs function with ensuing reduction of liver fibrosis, and by counteracting LSECs dysfunction, leading to increased hepatic NO delivery and decreased hepatic vascular tone.

WED-082

Multifactorial modulation of the endothelial transcription factor ERG in chronic liver disease

Sonia Selicean^{1,2,3}, Eric Felli^{2,3}, Cong Wang^{1,2,3}, Yeldos Nulan^{1,2,3}, Horia Ștefănescu⁴, Jaime Bosch^{2,3}, Annalisa Berzigotti^{2,3}, Jordi Gracia-Sancho^{2,3,5}. ¹Graduate School for Cellular and Biomedical Sciences (GCB), University of Bern, Bern, Switzerland; ²Department of Visceral Surgery and Medicine, Inselspital, Bern University Hospital, University of Bern, Bern, Switzerland; ³Department for BioMedical Research, Hepatology, University of Bern, Bern, Switzerland; ⁴Regional Institute of Gastroenterology and Hepatology Octavian Fodor, Cluj-Napoca, Romania; ⁵Liver Vascular Biology Research Group, IDIBAPS Research Institute, CIBEREHD, Barcelona, Spain
Email: jgracia@recerca.clinic.cat

Background and aims: Chronic liver disease (CLD) is characterized by profound dysfunction of liver sinusoidal endothelial cells (LSECs). The escalation of matrix stiffness during fibrosis progression predisposes LSECs to adopt a proinflammatory phenotype. Despite recent significant advances in the mechanobiology of CLD, the impact of stiffness and inflammation on the regulation of transcription factors remains unclear. The ETS-related gene (ERG) is a well-known endothelial-specific transcription factor involved in maintaining endothelial cell quiescence and homeostasis in the post-developmental phase of adult vasculature. Recent findings have implicated ERG in lung and liver disease, demonstrating its role in preventing

POSTER PRESENTATIONS

endothelial-to-mesenchymal transition. However, the effects of stiffness and inflammation on ERG expression in LSECs during CLD is not well understood. This study aims to elucidate the potential role of ERG as mechanosensitive transcription factor in the context of CLD.

Method: ERG knockdown RNA sequencing data were retrieved from the Gene Expression Omnibus database. Functional enrichment was conducted using GSEA and Panther. ERG expression was assessed in human liver tissue slides obtained from two cohorts of patients (n = 11 healthy vs 41 CLD). Cirrhotic rat models were developed in male rats through chronic carbon tetrachloride (CCl₄) inhalation (10 weeks) or i.p. thioacetamide (TAA) (12 weeks). Freshly isolated LSECs from healthy or cirrhotic rats, as well as human umbilical vein endothelial cells (HUVEC), were cultured on polyacrylamide substrates with low (0.5 kPa) and high stiffness (30 kPa). Interleukin 1 β (IL1 β) was employed as an in vitro inflammatory stimulus (n = 3–5 independent experiment per condition).

Results: Gene set enrichment analysis revealed that loss of ERG has a major influence on the upregulation of inflammatory pathways and in integrin signaling. ERG expression was significantly downregulated in liver samples from patients with cirrhosis compared to healthy (–53%, p < 0.01), irrespective of disease stage or aetiology. Endothelial ERG expression, sensitive to substrate stiffness (–69% at 30 kPa vs 0.5 kPa; p < 0.001), faced additional downregulation by inflammation at physiological stiffness (–36% control vs IL1 β at 0.5 kPa; p = 0.03). Interestingly, no synergistic effect between stiffness and inflammation was noted. In cirrhotic rat liver, ERG displayed a –20% downregulation vs healthy (p = 0.02), followed by recovery in the regression phase.

Conclusion: ERG downregulation by stiffness and inflammation, without a synergistic effect, implies their complementary and sequential role in suppressing ERG, aligning with CLD's pathophysiology. Our findings emphasize ERG as a responsive transcription factor to inflammation and mechanical cues, confirming its downregulation in the dysfunctional LSEC phenotype in CLD.

WED-083

Multi-compartment metabolomics for stratifying cirrhotic patients with acute decompensation

Sylvain Dechaumet¹, Sebastian Burz², Wenyi Gu³, Robert Schierwagen³, Florence Castelli¹, Emeline Chu-Van⁴, Francois Fenaille¹, Wim Laleman⁵, Frank Erhard Uschner³, Debbie L. Shawcross⁶, Minneke Coenraad⁷, Rajiv Jalan⁸, Joan Clària⁹, Maria Papp¹⁰, Jonel Trebicka¹¹, Christophe Junot¹², ¹Université Paris-Saclay, CEA, INRAE, Département Médicaments et Technologies pour la Santé (MTS), F-91191 Gif-sur-Yvette, France., MetaboHUB, F-91191 Gif-sur-Yvette, France; ²Université Paris-Saclay, CEA, INRAE, Département Médicaments et Technologies pour la Santé (MTS), F-91191 Gif-sur-Yvette, France., MetaboHUB, F-91191 Gif-sur-Yvette, France;

³Department of Internal Medicine B, University Hospital Muenster, Muenster, Germany; ⁴Université Paris-Saclay, CEA, INRAE, Département Médicaments et Technologies pour la Santé (MTS), F-91191 Gif-sur-Yvette, France, MetaboHUB, F-91191 Gif-sur-Yvette, France;

⁵Department of Gastroenterology and Hepatology, Section of Liver and Biliopancreatic disorders, University Hospitals Leuven, KU LEUVEN, Leuven, Belgium, Belgium; ⁶Institute of Liver Studies, School of Immunology and Microbial Sciences, Faculty of Life Sciences and Medicine, King's College London, London, UK., Institute of Liver Studies, King's College Hospital NHS Foundation Trust, London, United Kingdom;

⁷Department of Gastroenterology and Hepatology, Leiden University Medical Center, Leiden, The Netherlands; ⁸Liver Failure Group, Department of Medicine, Institute for Liver and Digestive Health, University College London, London, United Kingdom. Hepatology Department, Royal Free Hospital, London, United Kingdom., European Foundation for Study of Chronic Liver Failure, Barcelona, Spain., London, United Kingdom; ⁹Hospital Clínic-IDIBAPS, CIBERehd, Universitat de Barcelona, Barcelona, Spain., European Foundation for Study of Chronic Liver Failure, Barcelona, Spain; ¹⁰Division of Gastroenterology,

Department of Internal Medicine, Faculty of Medicine, University of Debrecen, Debrecen, Hungary; ¹¹Department of Internal Medicine B, University Hospital Muenster, Muenster, Germany., European Foundation for Study of Chronic Liver Failure, Barcelona, Spain., Muenster, Germany; ¹²Université Paris-Saclay, CEA, INRAE, Département Médicaments et Technologies pour la Santé (MTS), MetaboHUB, F-91191 Gif-sur-Yvette, France

Email: christophe.junot@cea.fr

Background and aims: Acute decompensation (AD) of cirrhosis and its progression to acute-on-chronic liver failure (ACLF) are associated with intense systemic inflammation, multiple organ dysfunctions, and a major risk of short-term mortality. There is a need to develop tools to stratify patients in order to improve their management and reduce the mortality observed in decompensated patients and ACLF. Metabolomics has already been proved to its relevance to the field with the identification of a 38-metabolite blood fingerprint specific for ACLF whose intensity correlates with systemic inflammation and which revealed mitochondrial dysfunction in peripheral organs (Moreau R et al., J. Hepatol., 2020). Here, the aims are to evaluate (i) the added value of investigating urine and feces compartments for improving the description of the metabolite landscape in cirrhotic patients with decompensations, (ii) the ability of multi-matrix metabolomics to improve the stratification of patients with decompensated cirrhosis.

Method: We performed untargeted metabolomics using liquid chromatography coupled to high-resolution mass spectrometry from serum, urine and stool samples of the MUCOSA-PREDICT cohort, which deals with the longitudinal follow-up of 93 cirrhotic patients with acute decompensation (300 samples for each biological matrix).

Results: A total of 402 metabolites were detected and identified in the three biological matrices. A greater number of metabolites were detected in urine (326 metabolites) and fecal (314 metabolites) samples compared to serum (222 metabolites) samples, whereas 162 metabolites are shared within the 3 biological matrices. Our results show that metabolomic signatures of ACLF can be drawn from serum, fecal and urinary samples of the MUCOSA-PREDICT cohort. Twenty-five metabolites out of the 38-metabolite blood fingerprint specific for ACLF previously established (Moreau R. et al., J Hepatol, 2020) were detected and had similar concentration trends (i.e., 65% of the fingerprint). The greatest number of metabolites whose concentrations are impacted by ACLF is observed in serum samples. Interestingly, some urinary and fecal metabolites not detected in serum also have their concentrations impacted by ACLF. However, ROC curve analyses performed for the metabolomics signatures in individual or combined matrices indicated that the best performance in terms of discrimination between AD and ACLF is obtained with the serum signature.

Conclusion: Blood, but also urine and fecal metabolomic signatures can discriminate between AD patients having or not ACLF. Although the three compartments provide complementary metabolic information, data obtained from the blood compartment enabled the best stratification performances.

WED-086

Nicotinamide riboside supplementation improves bacterial clearance and mitigates fibrosis in animal model of cirrhosis

Nidhi Nautiyal^{1,2}, Deepanshu Maheshwari³, Sandeep Kumar¹, Manisha Bhardwaj⁴, Sunidhi Diwakar¹, Shivi Chauhan⁵, Jaswinder Maras¹, Anupama Kumari¹, Subhrajit Biswas⁶, Chhagan Bihari¹, Shiv Kumar Sarin¹, Anupam Kumar¹. ¹Institute of Liver and Biliary Sciences, Delhi, India; ²Amity Institute of Molecular Medicine and Stem Cell Research, Amity University, NOIDA, Uttar Pradesh, India; ³Institute of Liver and Biliary Sciences, Molecular and Cellular Medicine, New Delhi, India; ⁴Institute of Liver and Biliary Sciences, Delhi, India; ⁵Institute of Liver and Biliary Sciences, Delhi,

India; ⁶Amity Institute of Molecular Medicine and Stem Cell Research, Amity University, NOIDA, India
Email: nidhinautiyal113@gmail.com

Background and aims: Poor liver clearance of invading intestinal/systemic bacteria are one of the major hallmarks of cirrhosis. The underlying cause of bacterial translocation in cirrhosis is not well established. In this study, we examined the kinetic changes in protein landscape and investigated whether Nicotinamide Riboside (NR) supplementation can improve the bacterial clearance in animal models of cirrhosis, explored the underlying mechanism.

Method: C57BL/6 (J) mice were used to develop chronic liver injury through intraperitoneal injections of carbon tetrachloride (0.1–0.5 ml/kg) for 15 weeks (W) and studied at specific time points for quantitative liver proteome using LC-MS. NR supplemented in animals (3 mg/ml) and mice bone marrow derived macrophages (BMDM, 2 mM) for 7 days and studied.

Results: Histopathology of liver showed progressive increase in chronic liver injury (steatosis (W3), fibrosis (W6), compensated cirrhosis (W10) and decompensated cirrhosis (W15)). Proteome analysis of liver tissue showed defect in NAD metabolism and cellular bioenergetics in transition from healthy to W3, followed by increase in bacterial response, inflammation and ECM accumulation from W3 to W10 with further increase in apoptosis and cell-cycle arrest from W10-W15. Further analysis of liver tissue showed significant reduction in NAD level in both cirrhosis animal ($p=0.0065$) and human ($p=0.0084$) liver tissue. Prolonged LPS treatment reduced NAD level ($p=0.0063$), mitochondrial respiration ($p<0.0001$) and phagocytic function of BMDM ($p=0.0079$). This was mitigated with NR supplementation with improved mitochondrial respiration ($p=0.0003$) and phagocytic activity ($p=0.0079$). In-vivo supplementation of NR showed improved OXPHOS and Glycolysis in BMDM. It also increases the phagocytic function of BMDM ($p=0.0084$) as well as Liver macrophages ($p<0.0001$). In comparison to cirrhosis, NR showed improved in-vivo bacterial clearance. Further analysis of liver tissue showed reduction in fibrosis (Massons trichrome, $p=0.0004$). Both in-vivo and in-vitro data suggested that NR improves the health of BMDM by improving their energy metabolism and effective clearance of bacteria by increasing their phagocytic activity.

Conclusion: Early dysfunction of NAD metabolism and cellular bioenergetics in liver cells may contribute to loss of liver macrophages mediated bacterial clearance during chronic liver injury. NR supplementation augments energy metabolism and bacterial clearance of resident macrophages.

WED-087

Exploring the potential of human serum albumin to reprogram B cell function

Berta Romero-Grimaldo^{1,2,3}, Mireia Casulleras^{1,2,3}, Marta Duran-Güell^{1,2,3}, Bryan J. Contreras^{1,2,3}, Javier Fernández^{3,4}, Vicente Arroyo³, Richard Moreau³, Cristina López-Vicario^{1,2,3}, Joan Clària^{1,2,3,5}. ¹Biochemistry and Molecular Genetics Service-Hospital Clínic, Barcelona, Spain; ²Hospital Clínic-IDIBAPS and CIBERehd, Barcelona, Spain; ³European Foundation for the Study of Chronic Liver Failure (EF CLIF) and Grifols Chair, Barcelona, Spain; ⁴Liver Unit-Hospital Clínic, Barcelona, Spain; ⁵Department of Biomedical Sciences of University of Barcelona, Barcelona, Spain
Email: romerog@recerca.clinic.cat

Background and aims: Recent randomized clinical trials have demonstrated that immunocompromised patients with acutely decompensated (AD) cirrhosis receiving albumin infusions have lower incidence of infections than patients receiving standard medical therapy. In the current study, we explored the potential actions of albumin on the production of immunoglobulins by B cells, an essential host defense response to microorganisms.

Method: B cell immunophenotyping was performed by flow cytometry in peripheral blood from patients with AD cirrhosis and healthy subjects. In vitro studies were performed in peripheral blood mononuclear cells (PBMCs) isolated by ficoll and B cells isolated by magnetic-activated cell sorting incubated with human serum albumin (15 mg/ml) or vehicle for increasing periods of time (from 24 to 72 hours). In some experiments, cells were stimulated with T-dependent or T-independent stimuli. Immunoglobulin levels in plasma and cell supernatants were assessed by nephelometry and enzyme-linked immunosorbent assay (ELISA), respectively. mRNA expression was determined by FLUIDIGIM technology and conventional real-time PCR.

Results: The systemic adaptive immune cell landscape of patients with AD cirrhosis was characterized by a profound suppression of the B cell compartment. These patients also showed a notable dysregulation in the circulating levels of IgM, IgG, and IgA, an alteration that was more evident in female patients. PBMCs isolated from patients with AD cirrhosis showed lower capacity to produce immunoglobulins under both unstimulated conditions and following T-dependent and T-independent stimulation than PBMCs from healthy subjects. Incubation of PBMCs with albumin significantly increased IgG production and the IgG/IgM ratio, an observation that was confirmed in isolated B cells and was independent of the gender of the blood donor. The increase in IgG levels was the result of the gain of the IgG2 subtype, which responds to bacterial capsular polysaccharide antigens. Consistent with these findings, albumin induced a significant upregulation of immunoglobulin-related genes. Notably, albumin up-regulated the expression of activation-induced cytidine deaminase (AID), a key enzyme for class switch recombination and somatic hypermutation, which are crucial processes for the humoral responses of adaptive immunity.

Conclusion: These data provide direct evidence of the ability of albumin to reprogram B cell function and to boost the production of immunoglobulins by these adaptive immune cells. This observation might contribute to explain why long-term albumin infusions are associated with lower incidence of infections.

WED-088-YI

Enhancing infection diagnostics and antimicrobial resistance detection in cirrhosis: a clinical metagenomics approach for blood culture assessment

Merianne Mohamad^{1,2}, Veena Ramachandran³, Dhaarica Jeyanesan³, Marilena Stamouli^{1,2}, Jack Wright³, Themoula Charalampous⁴, Kyle Leung^{1,2}, Ane Zamalloa³, Tasneem Pirani^{2,3,5}, Vishal C Patel^{1,2,3}. ¹The Roger Williams Institute of Hepatology, Foundation for Liver Research, London, United Kingdom; ²School of Immunology and Microbial Sciences, Faculty of Life Sciences and Medicine, King's College London, London, United Kingdom; ³Institute of Liver Studies, King's College Hospital NHS Foundation Trust, London, United Kingdom; ⁴Centre for Clinical Infection and Diagnostics Research, Department of Infectious Diseases, School of Immunology and Microbial Sciences, King's College London, London, United Kingdom; ⁵Liver Intensive Therapy Unit, King's College Hospital NHS Foundation Trust, London, United Kingdom
Email: m.mohamad@researchinliver.org.uk

Background and aims: The adverse consequences of increasing rates of antimicrobial resistance (AMR) in cirrhosis patients, coupled with suboptimal and delayed infection detection, persistently impact outcomes and mortality (Fernandez et al., 2019). Harnessing antibiotic efficacy depends on promptly and precisely identifying the causative bacterial and fungal pathogens and their AMR profiles (Patel and Williams, 2020). This study seeks to assess the utility of clinical metagenomics (CMg) for rapidly identifying pathogens and profiling AMR genes in positive blood culture (+BC) samples from

POSTER PRESENTATIONS

hospitalised cirrhosis patients, in comparison to standard microbiological testing (SMT).

Method: +BC samples identified as positive through SMT were obtained from acutely decompensated cirrhosis patients with a strong clinical suspicion of infection. Oxford Nanopore MinION platform and optimised protocols were employed for CMg sequencing. The accuracy and speed of pathogen identification and AMR profiling were evaluated by comparing CMg data with SMT results. The results were not shared with clinicians for decision-making purposes.

Results: 19 +BC samples obtained from 16 cirrhosis patients were subjected to CMg sequencing and SMT. The time required for reporting AMR profiling through CMg ranged from 10–16 hours from BC positivity, contrasting with an average of 72 hours for SMT. In all 19 samples, CMg results demonstrated concordance with both the bacterial and fungal species identified by SMT. Moreover, CMg detected an additional pathogen in two of the samples. CMg AMR profiling matched resistance phenotypes reported by SMT in 52.6% (10/19) of cases, while in the remaining 9 samples, CMg results diverged from SMT. In 6 samples, CMg identified AMR determinants that conferred resistance to clinically prescribed antibiotics, contradicting SMT, which classified these pathogens as fully sensitive. In 3 samples, CMg failed to detect AMR genes or mutations associated with resistance phenotypes reported by SMT, suggesting a distinct phenotypic resistance profile. In 1 case, CMg revealed genes conferring resistance to aminoglycosides, macrolides, and tetracyclines, which were not reported by SMT.

Conclusion: These initial findings indicate that CMg pathogen detection align with SMT and could offer more precise and rapid identification. Implementing CMg as an adjunct to SMT may improve the ability to more rapidly diagnose bloodstream infections in cirrhosis. Nevertheless, additional research is required to explore the disparities in AMR profiles between the approaches given their inherent differences (genotype versus phenotype), evaluate cost implications and feasibility within healthcare settings, and assess the impact on clinical outcomes.

WED-089-YI

Characterising the hemodynamic and pro-inflammatory profile of a CCL4/LPS-induced acute-on-chronic liver failure (ACLF) rat model

Vlad Taru^{1,2,3}, Thomas Sorz-Nechay^{1,2,4}, Benedikt Hofer^{1,2}, Oleksandr Petrenko^{1,2,4}, Philipp Königshofer^{1,2}, Katharina Bonitz^{1,2,4}, Georg Kramer^{1,2}, Henriette Horstmeier^{1,2}, Katharina Regnat^{1,2}, Kerstin Zinöber^{1,2}, Bogdan Procopet³, Michael Trauner¹, Philipp Schwabl^{1,2}, Thomas Reiberger^{1,2,4}, Benedikt Simbrunner^{1,2}

¹Division of Gastroenterology and Hepatology, Department of Medicine III, Medical University of Vienna, Vienna, Austria; ²Christian-Doppler Laboratory for Portal Hypertension and Liver Fibrosis, Medical University of Vienna, Vienna, Austria; ³Regional Institute of Gastroenterology and Hepatology "Octavian Fodor", Hepatology Department and "Iuliu Hatieganu" University of Medicine and Pharmacy, 3rd Medical Clinic, Cluj-Napoca, Romania; ⁴Center for Molecular Medicine (CeMM) of the Austrian Academy of Science, Vienna, Austria
Email: vlad.taru@meduniwien.ac.at

Background and aims: Acute-on-chronic liver failure (ACLF) is defined as hepatic and extrahepatic organ failure (s) and often triggered by infections. A systemic proinflammatory state and high short-term mortality are important hallmarks of ACLF. We aimed to develop and characterize a representative rat model of ACLF.

Method: Cirrhosis was induced in 18 male Sprague-Dawley rats (10 weeks old) by repeated i.p. of carbon tetrachloride (CCL4, 0.3 ml/kg)- or olive-oil (Healthy control, HC) 3x/week for 12 weeks. ACLF was induced by a single i.p. injections of lipopolysaccharide (LPS, E. coli

O111:B4, 1 mg/kg) 3 hours prior to hemodynamic characterization (portal pressure, PP; mean arterial pressure, MAP) and organ/blood harvesting. The following groups were examined: HC (n = 3), HC+LPS (n = 3), CCL4 (n = 6), and CCL4+LPS (n = 6). Collagen proportionate area (CPA) was quantified on picro-sirius red (PSR)-stained full liver lobe scans. Gene expression and plasma protein expression were quantified by RT-qPCR of bulk liver tissue (expressed as log₁₀-fold change) and ELISA. Results are expressed as mean ± SD and significance level was set at p < 0.05.

Results: Body weight was similar across the different animal groups after 12 weeks (p = 0.25). The CCL4 animals showed a trend towards higher PP (9.4 ± 1.7 vs. 7.4 ± 0.3 mmHg, p = 0.184 and higher liver fibrosis (CPA: 3.3 ± 1.2 vs. 1.7 ± 0.8%, p = 0.059) compared to HC. The CCL4+LPS animals had lower MAP (52.9 ± 18.1 vs. 78.4 ± 8.9 mmHg, p = 0.019) and higher HR (410 ± 51.2 vs. 376 ± 18.6 bpm, p = 0.188) compared to the CCL4 group, while PP was not significantly different (10.9 ± 3.9 vs. 9.4 ± 1.7 mmHg, p = 0.462). Blood lactate levels were significantly elevated in CCL4+LPS animals (7.8 ± 2.8 vs. 2.8 ± 1.3 mmol/L, p = 0.005) indicating circulatory failure. Hepatic gene expression analysis revealed significantly increased IL-1β (1.86 ± 0.27), IL-6 (3.5 ± 0.27), TNF-α (2.1 ± 0.30), MCP1 (2.46 ± 0.28) and IL-10 (0.89 ± 0.21) mRNA levels in CCL4+LPS (all p < 0.001 vs. CCL4). The plasma levels of IL-1β (4093 ± 2111 vs. 33 ± 7 pg/ml; p = 0.031), IL-6 (12142 ± 6206 vs. 77 ± 67 pg/ml; p = 0.030), TNF-α (2935 ± 2001 vs. 42 ± 67 pg/ml; p = 0.028), MCP1 (219.2 ± 29.2 vs. 2.5 ± 1.1 ng/ml; p < 0.001) and IL-10 (2391 ± 756 vs. 74 ± 29 pg/ml; p = 0.009) were significantly elevated in the CCL4+LPS as compared to the CCL4 group. Blood biochemistries suggested renal dysfunction (creatinine: 1.41 ± 0.25 vs. 0.92 ± 0.12 mg/dL; p = 0.008) and hepatic injury/liver dysfunction (AST: 1341 ± 491 vs. 635 ± 355 U/L, p = 0.031; ALT: 894 ± 394 vs. 515 ± 513 U/L, p = 0.228; glucose: 59 ± 56 vs. 176 ± 21 mg/dL, p = 0.003) in CCL4+LPS vs. CCL4, respectively.

Conclusion: Our rat model induced by CCL4+LPS resembled key features of the ACLF syndrome with high-grade hepatic and systemic inflammation, circulatory, kidney, and liver dysfunction and failure. These features qualify this rat ACLF model for preclinical drug research.

WED-090

Developing a discovery platform for engineered macrophage cell therapies for end stage liver disease

Niya Aleksieva¹, Kayleigh Thirlwell¹, Philip Starkey Lewis¹, Mark Cant¹, Moony Su¹, Hollie Bartley¹, Alejandro Armesilla Diaz¹, Amol Ketkar¹, Benjamin J Dwyer², John Campbell¹, Stuart J Forbes^{1,3}, Lara Campana¹. ¹Resolution Therapeutics, Edinburgh, United Kingdom; ²Curtis University, Perth, Australia; ³University of Edinburgh, Edinburgh, United Kingdom

Email: lara.campana@resolution-tx.com

Background and aims: Patients with end-stage liver disease (ESLD) have extensive fibrosis and inflammation, which result in loss of organ function leading to decompensation events, and limited life expectancy. Incidence and prevalence of ESLD is projected to increase in western countries, and currently there are no licensed therapies to treat ESLD. Macrophages play a pivotal role in fibrosis remodeling, dampening the inflammatory response, and in coordinating liver regeneration. Autologous non-engineered macrophages have been tested in patients with cirrhosis in the MATCH clinical studies ("MATCH cells"), displaying an excellent safety profile and significant efficacy with a significant reduction of all-cause mortality one-year post-treatment in a population of patients with liver cirrhosis and baseline MELD score 10–16.

Method: Further enhancement of the pro-regenerative profile of the native macrophage therapy is needed to provide a long-term solution for a more severe patient population with ESLD. To achieve this, a

novel, genetically engineered autologous macrophage is under development. To support the development of such a product, three key technological advancements are necessary, namely: (i) an improved differentiation protocol to maximise yields without compromising phenotype (no significant changes in surface expression levels of 25F9, CD206, CD163, CD169 vs MATCH); (ii) a robust engineering method to allow for overexpression of candidate therapeutic genes; (iii) a cryopreservation method which allows administration of multiple doses from a single leukapheresis collection.

Results: Herein, we show results from the optimisation of a culture protocol that delivers increased yields (average increase 10% over previous method); we also report the definition of an engineering method based on transfection delivering high transfection efficiency (>80%) without affecting cell viability (>70%). Finally, we defined a cryopreservation method based on progressive temperature lowering as best to ensure macrophage viability and function post-thawing (viability \geq 70% and maintenance of ability to phagocytose beads coated with bacterial particles).

Conclusion: Resolution Therapeutics has established a reliable discovery platform to differentiate, engineer and cryopreserve macrophages for therapeutic use in patients with ESLD. Further studies will determine what genes are best suited to enhance macrophage efficacy in this clinical setting.

WED-092

Hyperuricemia leads to early cognitive dysfunction and neuronal cell injury in bile-duct ligated rats

Sydnée L'écuyer^{1,2}, Maximilian Steger³, Farzaneh Tamnanloo⁴, Mariana M. Oliveira⁴, Mélanie Tremblay⁴, Emmanuel Charbonney^{5,6}, Christopher F. Rose^{4,6}. ¹Hepato-Neuro Lab, CRCHUM, Montreal, Canada; ²Department of Pharmacology and Physiology, Université de Montréal, Montréal, Canada; ³University of Applied Sciences Weihenstephan-Triesdorf, Munich, Germany; ⁴Hepato-Neuro Lab, CRCHUM, Montréal, Canada; ⁵Intensive Care Unit, CHUM, Montréal, Canada; ⁶Department of Medicine, Université de Montréal, Montréal, Canada
Email: christopher.rose@umontreal.ca

Background and aims: Hyperammonemia plays a major role in the pathogenesis of hepatic encephalopathy (HE). However, other factors may be involved in cognitive dysfunction in patients with chronic liver disease (CLD). Hyperuricemia, an increase in plasmatic uric acid (UA), arises with excessive alcohol and fructose consumption, both factors known to contribute to the onset of CLD. Hyperuricemia has been demonstrated to be associated the progression of liver steatosis and fibrosis as well as negatively impacting cognitive function. We investigated the impact of hyperuricemia on neurological dysfunction and brain integrity in a rat model of CLD with HE.

Method: In Sprague-Dawley rats, CLD was induced following bile-duct ligation (BDL) for 5 weeks, with SHAM-operated rats as controls. To induce hyperuricemia, rats were fed a diet containing 3% UA (HUAD) compared to regular diet (RD). Fifty-six male rats were randomly assigned to 1 of 4 experimental groups: (1) SHAM+RD, (2) SHAM+HUAD, (3) BDL+RD et (4) BDL+HUAD. Behavioural assessment for anxiety (Open-Field and Elevated Plus-Maze) and memory (New-Object Recognition) was performed at day 14 to evaluate for early cognitive impairments. At day 33, animals were sacrificed, to measure plasma UA and liver injury markers. Liver was collected for histological analysis (HandE and Sirius Red staining). The frontal cortex, amygdala and hippocampus were isolated to measure apoptosis (caspase-8, 9 and 3) and neuronal loss (NeuN and SMI311) by Western Blot and immunohistochemistry. All statistical analysis used a one-way ANOVA with Tukey's or Games-Howell post-hoc.

Results: The HUAD diet leads to a significant increase in plasma UA in BDL+HUAD animals at day 33 compared to BDL+RD animals. No significant increase in liver injury evaluated by plasmatic markers and histology was observed in either HUAD-fed groups. For behavioural assessment, we detected an impairment of short-term memory for both SHAM+HUAD and BDL+HUAD animals compared to their RD counterparts. We also observed an increase of anxiety and long-term memory impairments for BDL+HUAD rats compared to all three other groups. Regarding neuronal cell loss in the frontal cortex, both apoptosis pathways (caspase-8, 9 and 3) are increased and neuronal markers are decreased for both HUAD groups compared to their RD counterparts. In the amygdala and hippocampus, the intrinsic pathway of apoptosis (caspase-9 and 3) is activated in BDL-HUAD rats compared to all three other groups which was associated with a decrease in neuronal markers.

Conclusion: In a BDL rat model, the administration of a high UA diet leads to the early-onset of anxiety-like behaviour and memory impairments. The behavioural alterations are associated with increased apoptosis and neuronal cell loss in the frontal cortex, amygdala and hippocampus. These results suggest a potential role for UA in irreversible brain damage in the context of CLD.

WED-094

Food antigen-specific antibodies contribute to hypergammaglobulinemia in patients with decompensated liver cirrhosis

Lara Kelsch¹, Jill Werner¹, Giuseppe Rusignuolo¹, Dominik Bettinger¹, Michael Schultheiß¹, Maike Hofmann¹, Robert Thimme¹, Tobias Böttler¹. ¹Department of Medicine II, Medical Center-University of Freiburg, Freiburg, Germany
Email: lara.kelsch@uniklinik-freiburg.de

Background and aims: Portal hypertension is the major driver in disease progression from the compensated to the decompensated stage of liver cirrhosis. Hypergammaglobulinemia (HGG), characterized by elevated immunoglobulin G (IgG) levels, is a common feature of decompensated liver cirrhosis (dCirr). The mechanisms underlying HGG and the antigen specificity of these IgG antibodies remain incompletely understood. As the healthy liver mediates local and systemic tolerance to self and foreign antigens, including antigens from ingested food, we hypothesize that food antigens can bypass the liver in the presence of portal hypertension, thereby failing to undergo tolerization and subsequently eliciting immune responses contributing to increased IgG levels.

Method: Food-specific IgGs against 90 different food antigens were analyzed in a cohort of 11 healthy controls (HCs), 26 individuals with dCirr and 8 with a transjugular intrahepatic portosystemic shunt (TIPS) via an ELISA assay. As the generation of IgGs is a T cell-dependent process, T cell markers indicative of tolerance induction were analyzed by flow cytometry in bulk peripheral blood mononuclear cell (PBMCs). Additionally, food antigen-specific T cell responses were measured using overlapping peptides (OLPs) targeting previously described immunodominant regions of four different food antigens and evaluated by intracellular cytokine staining.

Results: Individuals with dCirr showed significantly increased food-specific antibodies (mean values: 9.1 µg/ml in dCirr patients, 16.6 µg/ml with TIPS and 1.9 µg/ml in HCs) with percentages of food-specific IgGs relative to the total IgGs of 1.6% in HCs, 3.8% in dCirr and 5.8% in patients with TIPS. While there was no difference in markers indicative of tolerance induction in bulk analysis, food-specific CD4 T-cells responses were enriched in dCirr compared to HCs (mean values: 7.9 responses in dCirr and 5.6 responses in HCs).

Conclusion: Our data demonstrate that food-specific immune responses contribute to HGG in dCirr patients with portal hypertension that might result from portosystemic shunting of gut-derived antigens, circumventing tolerance induction in the liver parenchyma.

WED-095-YI

Pharmacological inhibition of high mobility group box 1 ameliorate sepsis induced hepatic micro vascular dysfunction and portal hypertension in non-cirrhotic and cirrhotic animals

Vaibhav Tiwari¹, Rajni Yadav², Akash Kumar Mourya¹, Aishwarya Bhatnagar¹, Himanshi Himanshi², Parul Singh², Kanchi Sharma², Savneet Kaur¹, Dinesh Mani Tripathi¹. ¹Institute of Liver and Biliary Sciences, New Delhi, India; ²Institute of Liver and Biliary Sciences, New Delhi, India

Email: dineshmanitripathi@gmail.com

Background and aims: Septic shock is shattering multiple cellular injury progress to organ failure, leading to short-term mortality. Sepsis is key event that promotes early hepatic decompensation, disturb vascular homeostasis, hepatic microvascular complications and aggravates portal pressure. High mobility group box1 (HMGB1) initiates immune responses that triggers hepatic injury in response to pathogens. We investigated the role of HMGB1 in sepsis induced hepatic microvascular-dysfunction and portal-hypertension in cirrhosis.

Method: Experimentally, sepsis was induced by intraperitoneal administration of LPS 4 mg/kg in non-cirrhotic and CCl₄-cirrhotic animals. Controls (Ct1). Non cirrhotic Ct+LPS (Ct2), Ct+LPS+Glycyrrhizin (Ct3) were compared with CCl₄ cirrhotic rats (Gr1), CCl₄+LPS (Gr2), CCl₄+LPS+Glycyrrhizin (Gr3). HMGB1 pharmacological inhibition was achieved by glycyrrhizin (GLZ). Hepatic hemodynamic was monitored followed by *in-situ-ex-vivo* Hepatic microvascular functionality analysis. To investigate the changes in HMGB1 *in-vitro*, vascular endothelial cells were stimulated with LPS after giving pretreatment of Glycyrrhizin. Cellular, Molecular and histological analysis was performed in hepatic tissues.

Results: Studies shows a noticeable increased PP (9.2 ± 1 ; +27.7% (Ct2), vs 7.2 ± 1 in Ct1) a marked reduction in CT3 (8.1 ± 0.5 ; -15.2%) vs Ct2 ($p=0.01$) was observed. Ct2 animals also had increased SMABF ($p=0.001$) and PBF ($p=0.05$) in comparison to Ct1 and Ct3. However, in cirrhotic animals we observed significantly raised PP (12.6 ± 1 ; +26% (Gr2), vs 10 ± 1 ; in Gr1) a marked reduction in Gr3 (10.8 ± 0.2 ; -14%) vs Gr2 ($p=0.01$) was observed. Gr2 animals had increased SMABF ($p=0.001$) ($p=0.001$) and PBF ($p=0.05$) ($p=0.001$) in comparison to Gr1 and Gr3. Endothelial dysfunction assay under perfused *ex-vivo* condition showed improvement in endothelial activity showed by percentage change in Portal perfusion pressure ($p=0.005$) in Gr3andCt3 vs Gr2andCt2. Periportal inflammation and inflammatory cells infiltration was evidently reduced in both Ct3 and Gr3 rats vs Ct2andGr2 respectively. Gene expression of TNF- α , IL-6, HMGB1, TLR4 were significantly upregulated in Gr2 andCt2 ($p<0.05$) vs Gr3 and Ct3. Moreover, Endothelial dysfunction genes ICAM1, VCAM1, fold was downregulated ($p<0.05$) in Gr3andCt3 vs Gr2andCt2. Gene expression analysis of endothelial cells showed that upregulation of VCAM-1 ($p=0.001$) and ICAM-1 ($p=0.001$) as well as HMGB1 ($p<0.05$) was effectively abolished by Glycyrrhizin without affecting cell viability.

Conclusion: This study demonstrated that pharmacological inhibition of HMGB1 ameliorates PP and protects vascular function during sepsis in liver cirrhosis.

WED-098-YI

Low-density lipoprotein can predict hospital readmissions and outcomes following acute decompensation of cirrhosis

Kohilan Gananandan¹, Jonel Trebicka^{2,3}, Joan Clària^{3,4}, Wim Laleman⁵, Javier Fernández^{3,6}, Maria Papp⁷, Paolo Caraceni⁸, Salvatore Piano⁹, Frank Erhard Uschner², Thierry Gustot¹⁰, Agustín Albillos¹¹, Rafael Bañares¹², Martin Janicko¹³, Víctor Manuel Vargas Blasco¹⁴, Carlo Alessandria¹⁵, Paolo Angeli^{3,16}, Cristina Sanchez², Ferran Aguilar³, Richard Moreau^{3,17}, Rajiv Jalan^{3,18}, Vicente Arroyo³, Rajeshwar Prosad Mookerjee^{18,19}. ¹University College

London, London, United Kingdom; ²Münster University Hospital, Münster, Germany; ³European Foundation for the Study of Chronic Liver Failure, Barcelona, Spain; ⁴Hospital Clinic, Barcelona, Spain; ⁵University Hospitals Leuven, Leuven, Belgium; ⁶Hospital Clinic, Barcelona, Spain; ⁷University of Debrecen, Debrecen, Hungary; ⁸University of Bologna, Bologna, Italy; ⁹University and Hospital of Padova, Padova, Italy; ¹⁰Université Libre De Bruxelles, Brussels, Belgium; ¹¹Hospital Universitario Ramon y Cajal, Madrid, Spain; ¹²Complutense university school of medicine, Madrid, Spain; ¹³Pavol Jozef Safarik University in Kosice, Kosice, Slovakia; ¹⁴Hospital Vall d'Hebron, Barcelona, Spain; ¹⁵University of Turin, Turin, Italy; ¹⁶University of Padova, Padova, Italy; ¹⁷Université de Paris, Paris, France; ¹⁸University College London, London, United Kingdom; ¹⁹Aarhus University Hospital, Aarhus, Denmark
Email: k.gananandan1@nhs.net

Background and aims: In liver cirrhosis, serum lipid and lipoprotein levels are altered due to pathological changes in synthesis, secretion and catabolism. Whilst most research has focussed on the role of high-density lipoprotein (HDL), relatively little attention has been given to the predictive capacity of low-density lipoprotein (LDL). We aim to explore the role of serial LDL measurements in predicting liver-related events following acute decompensation (AD).

Method: 232 patients from the PREDICT cohort were included in this study. This was a European, multicentre, prospective, observational study recruiting patients admitted non-electively with an episode of AD of cirrhosis. Blood tests including lipids were performed at baseline and day 7. Patients were followed up for 3 months to obtain clinical outcome data.

Results: There was no difference in baseline LDL and HDL levels when comparing patients treated with statins versus those who were not. During the 3-month follow-up period, 32 (14%) patients developed acute-on-chronic liver failure (ACLF), 62 patients (27%) had readmissions and 13 patients (6%) died. HDL measurements and LDL/HDL ratios were not associated with outcomes. In contrast, when comparing patients who were subsequently re-admitted versus those who were not, day 7 LDL results were significantly lower (55.0 vs 78.6 mg/dL, $p=0.003$). Indeed, day 7 LDL remained an independent predictor of subsequent readmissions in both univariable and multivariable analyses (OR 0.984 [95% CI 0.972–0.995], $p=0.01$). With regards to ACLF development, a marked difference was noted in the delta change between baseline and day 7 LDL in those who developed ACLF versus those who did not (-7.7 vs 3.8 mg/dL, $p=0.05$). Finally, with respect to 90-day transplant-free mortality, when comparing those who died versus those who survived, there was a trend towards lower day 7 LDL levels (42.5 vs 75.8 mg/dL, $p=0.06$) as well as decreased LDL between baseline and day 7 (-12.3 vs 3.9 mg/dL, $p=0.08$).

Conclusion: This study demonstrates novel findings that decreased LDL, independent of statin treatment, can predict readmissions and provide a potential signal for other liver-related events, including mortality, though this needs further validation. Given its biological relevance, ease of measurement, and low cost, LDL may be an ideal biomarker for predicting outcomes in patients with decompensated cirrhosis.

WED-099-YI

Hyperammonemia-induced mitochondrial dysfunction is abrogated by targeting toll-like receptor 4

Supachaya Sriphoosanaphan^{1,2}, Annarein Kerbert³, Abeba Habtesion³, Fausto Andreola³, Gautam Mehta³, Jan-Willem Taanman⁴, Rajiv Jalan³. ¹Institute for Liver and Digestive Health, University College London, London, United Kingdom; ²Division of Gastroenterology, Department of Medicine, Faculty of Medicine, Chulalongkorn University and King Chulalongkorn Memorial Hospital, Thai Red Cross Society, Bangkok, Thailand; ³Institute for Liver and Digestive Health, University College London, London, United Kingdom;

⁴Department of Clinical and Movement Neurosciences, Queen Square Institute of Neurology, University College London, London, United Kingdom
Email: r.jalan@ucl.ac.uk

Background and aims: Inhibition of the toll-like receptor 4 (TLR4) protects against hyperammonemia but the underlying mechanism is unknown. We hypothesized that TLR4 inhibition protects against hyperammonemia-induced mitochondrial dysfunction, thereby preserving the urea cycle enzyme (UCE) function. The aims of this study were to investigate the impact of hyperammonemia and TLR4 inhibition on oxidative phosphorylation (OXPHOS), a key mitochondrial function.

Method: Hyperammonemia was induced in wild type (WT) and TLR4 knock-out (TLR4KO) mice by an amino acid (AA) diet for 14 days. WT mice fed with the AA diet (WT-AA) were treated with a vehicle, the TLR4 antagonist TAK-242 (10 mg/kg i.p.), or the ammonia scavenger Ornithine Phenylacetate (OP, 300 mg/kg i.p.) during days 10–14. Plasma ammonia and protein expression of UCes were studied, while isolated mitochondria from the liver were assessed for concentration and activity of OXPHOS complexes I–V by immunoblot and in-gel activity assay, respectively.

Results: A significant increase in ammonia levels was observed in WT-AA compared to controls (333.4 ± 54.5 vs. 47.0 ± 11.9 $\mu\text{mol/L}$, $p < 0.0001$). Treatment with both TAK-242 and OP significantly reduced ammonia levels (121.1 ± 51.5 and 131.6 ± 79.8 $\mu\text{mol/L}$; both $p < 0.0001$). Hepatic protein expression of key mitochondrial UCes, carbamoyl phosphate synthase and ornithine transcarbamylase, was significantly reduced in WT-AA as compared to controls and restored with both TAK-242 and OP. Although the concentration of the OXPHOS complexes were similar, the activity of all of the OXPHOS complexes were increased in hyperammonemic mice compared to controls. TAK-242 treatment significantly reduced enzyme activities of all OXPHOS complexes compared to WT-AA (all $p < 0.05$). OP only led to a significantly reduced activity of complex I. TLR4KO mice fed with the AA diet had significantly lower blood ammonia levels compared to WT-AA (149.9 ± 104.6 $\mu\text{mol/L}$, $p < 0.0001$). No changes were observed in complex I–V concentration and activity between TLR4KO mice with or without the AA diet.

Conclusion: Hyperammonemia increases the activity of OXPHOS complexes, which is associated with the downregulation of mitochondrial UCes. In contrast to treatment with OP, TLR4 inhibition prevented an increase in OXPHOS complex activity. This points towards TLR4 as a mediator of hyperammonemia-induced oxidative stress and mitochondrial dysfunction, providing an explanation why TLR4 inhibition preserves the expression of mitochondrial UCes and ammonia levels.

WED-100-YI

Role of apoptosis in B-cell compartment retraction during decompensation of cirrhosis and acute-on-chronic liver failure

Lorena Paule^{1,2}, Javier Martínez González^{2,3,4}, Elisa Castillo^{2,4}, Alejandro Miranda^{2,4}, Leticia Muñoz^{2,4}, Luis Téllez^{2,4,5}, Jorge Monserrat^{2,4}, Melchor Álvarez-Mon^{2,4,6}, Agustín Albillos^{2,4,5}.
¹Laboratory of Immune System Diseases. Department of Medicine. University of Alcalá., Alcalá de Henares, Spain; ²Center for Biomedical

Research Network on Liver and Digestive Diseases (CIBERehd), Instituto de Salud Carlos III., Madrid, Spain; ³Department of Gastroenterology and Hepatology, Hospital Universitario Ramón y Cajal, IRYCIS., Madrid, Spain; ⁴Laboratory of Immune System Diseases. Department of Medicine. University of Alcalá., Alcalá de Henares, Spain; ⁵Department of Gastroenterology and Hepatology, Hospital Universitario Ramón y Cajal, IRYCIS., Madrid, Spain; ⁶Department of Internal Medicine, Hospital Universitario Príncipe de Asturias, Alcalá de Henares. Madrid., Alcalá de Henares, Spain
Email: lorena.paule@uah.es

Background and aims: Cirrhosis-associated immune dysfunction involves various abnormalities, such as altered activation and reduced effector functions of the innate and adaptive immune systems. The impact of B lymphocyte compartment dysregulation on immune dysfunction in cirrhosis has been minimally explored. Our aims consist of investigate in patients at different cirrhosis stages: i) the differentiation/activation stage of circulating B lymphocytes, ii) the degree of apoptosis within this compartment, and iii) the role of cirrhosis-related metabolic abnormalities in apoptosis.

Method: Analysis by flow cytometry of circulating B lymphocytes' differentiation (CD27/IgD), thymus-dependent/independent (CD5) subpopulations in patients with cirrhosis or with ACLF. Groups: compensated cirrhosis (CC, $n = 10$), decompensated cirrhosis (DC, $n = 12$), ACLF ($n = 9$), healthy controls (HC, $n = 10$). B-lymphocyte apoptosis was studied using Annexin-V and Caspases-3–8–9 at baseline and after 48 h culture of B lymphocytes from HC with serum from HC or patients.

Results: The percentage and absolute values of B lymphocytes in patients were lower ($p < 0.01$) than in HC, with a more pronounced difference observed in DC and ACLF groups (HC: 5.2%, 102200 cells/ml; CC: 4.0%, 59200 cells/ml; DC: 3.2%, 28800 cells/ml; ACLF: 3.0%, 31900 cells/ml). Lymphopenia affected all B lymphocyte subpopulations. In patients with CC and DC, there was a decrease in naive and an increase in memory populations, while ACLF showed a decrease in naive and an increase in effector populations. At baseline all groups of patients exhibit a significant increase in the frequency of apoptosis markers (Annexin-V and Caspases-3, –8, and –9) in B-lymphocytes compared to HC. Notably, apoptosis significantly escalated when B lymphocytes from HC were cultured with serum from patient CC or DC or ACLF, showed increased expression of apoptosis markers: Annexin-V (7.2, 13.7, 16.7%) and Caspases-3 (8.3, 8.7, 14.9%), –8 (7.7, 9.4, 13.0%), and –9 (7.6, 10.1, 11.0%).

Conclusion: Cirrhosis leads to severe abnormalities in the circulating B lymphocyte compartment, correlating with disease severity. Despite the redistribution causing an increase in effector cells, it is inadequate to compensate for the compartmental retraction in decompensated cirrhosis and ACLF. This inadequacy is partly due to increased apoptosis, activated through the caspase pathway by cirrhosis-induced metabolic alterations.

WED-101-YI

Modulation of portal and hepatic venous flow leads to fibrotic liver changes and can be prevented through anticoagulation

Beat Moeckli^{1,2}, Graziano Oldani³, Andrea Peloso⁴, Florence Slits⁵, Quentin Gex⁶, Neil Theise⁷, Stéphanie Lacotte¹, Christian Toso^{1,2}.
¹Université de Genève, Genève, Switzerland; ²Hôpitaux Universitaires de Genève, Genève, Switzerland; ³University of British Columbia, Vancouver BC, Canada; ⁴University of Geneva Hospitals, Departement of Surgery, Genève, Switzerland; ⁵University of Geneva, Hepatology and Transplantation Laboratory; 1206 Geneva, Switzerland; ⁶University of Geneva, Transplantation and Hepatology Laboratory, Geneva, Switzerland; ⁷New York University, Departement of Pathology, New York, United States
Email: beat.moeckli@gmail.com

Background and aims: Cirrhosis is a progressive, irreversible liver disease with a myriad of diverse etiologies. We hypothesize that different etiologies share a common vascular injury pattern that occurs early in the disease course. Hence, two simultaneous insults to the liver vasculature are responsible for the initiation and progression of the fibrotic disease process.

Method: Adult male C57Bl6 mice were subjected to the following procedures: 1) Partial ligation of the inferior vena cava (IVC) to generate an outflow obstruction 2) Injection of microspheres in the portal vein to obstruct distal venules. Animals were sacrificed at 6, 12, and 18 weeks after the interventions (n=6-8/group). Controls received either a sham surgery, partial IVC ligation, or portal embolization. As a preventive intervention, an additional group received a vitamin K antagonist (warfarin) for anticoagulation.

Results: At 12 weeks, two-thirds of animals subjected to combined partial ligation of the IVC and portal embolization developed macronodular liver disease resembling cirrhosis, compared to none in the control groups (62.5 vs. 0%, p=0.002). Combining both procedures resulted in elevated serum bilirubin levels (5.9 vs. 0.3 µmol/L, p=0.001), increased portal pressure (12.5 vs. 5.0 mmHg, p=0.008), and an increased collagen staining in the liver (2.84 vs. 0.13%, p<0.001) compared to controls. Moreover, animals with combined interventions exhibited an overexpression of fibrotic markers such as *Col1a1*, *αSMA*, *TGFβ* and *Timp1*. Continuous anticoagulation improved the rate of macronodular liver disease (37.5 vs 62.5%) and portal pressure (6 vs. 12.5 mmHg, p=0.002). Furthermore, it decreased aspartate transaminase serum levels (95 vs 202 IU/L, p=0.002) and expression of fibrotic markers. Additionally, anticoagulation led to a marked compensatory proliferation characterized by increased Ki67 staining (0.03 vs 0.08% +cells, p<0.001).

Conclusion: The results of our study highlight the importance of vascular mechanisms in the development of cirrhosis. The combination of portal and hepatic venous intervention potentiates the effect on liver fibrosis. Anticoagulation potentially slows the progression of liver disease and, therefore, represents a therapeutic target common to all etiologies of cirrhosis.

WED-102

Transplanted acellular liver scaffold is not affected by the cirrhotic liver remaining a healthy template for cell growth

Marlon Dias¹, Ines Wajsenzon¹, Raysa de Sousa¹, Bruno Paranhos¹, Victoria Monteiro², Cherley de Andrade³, Debora Mello⁴, Regina Goldenberg¹. ¹Precision Medicine Research Center, Carlos Chagas Filho Biophysics Institute, Federal University of Rio de Janeiro, Rio de Janeiro, Brazil; ²Federal University of Rio de Janeiro, Rio de Janeiro, Brazil; ³Department of Histology and Embryology, Rio de Janeiro State University, Rio de Janeiro, Brazil; ⁴National Center for Structural Biology and Bioimaging, CENABIO, Federal University of Rio de Janeiro, Rio de Janeiro, Brazil

Email: marlonlemons@biof.ufrj.br

Background and aims: Acellular Liver Scaffolds (ALS) are a promising tool in tissue engineering that can help overcome the organ shortage problem. While the potential of using ALS has been demonstrated, it remains unclear whether the transplanted scaffold can be affected by the cirrhotic liver that received it, either by becoming cirrhotic or by remaining a healthy template for healthy cell growth. This study aimed to evaluate the influence of the cirrhotic liver on the recellularization of transplanted liver scaffolds in cirrhotic rats.

Method: To address this issue, donor Wistar rats (n = 5) underwent a surgical procedure to promote liver procurement, which was approved by the Animal Care Committee CEUA/CCS-UFRJ 097/20.

The livers were decellularized by being perfused through the portal vein using an infusion pump at 3 ml/min with water for 2 hours, followed by 1% Triton X-100 for 2 hours and SDS 1% for 18 hours. Subsequently, the livers were washed with distilled water for 8 hours and then subjected to DNA quantification and histological analysis (HandE). Cirrhotic recipient rats (n=5), which had previously received 5% ethanol in drinking water and intraperitoneal injections of carbon tetrachloride (1 ml/Kg) every other day for 8 weeks, underwent median lobe hepatectomy (10%) and partial ALS orthotopic transplantation. Various histological analyses (HandE, Sirius red, Gomori's trichrome, Periodic Acid-Schiff), Ki67, CK19 and CK7 immunohistochemistry and non-invasive ultrasound analysis were performed to evaluate the transplanted ALS at different time points post-transplantation.

Results: The decellularization process effectively removed the cells and preserved the 3D vascular structure and extracellular matrix (ECM) components of the ALS, as evidenced by whole liver macroscopy, HandE staining, and DNA quantification. Serum biochemical analysis showed that the transplanted ALS normalized the ALB and ALT serum biochemical parameters after transplantation in cirrhotic rats. Histological findings revealed that liver resident cells migrated to the ALS, promoting full recellularization 30 days post-transplantation. Various cell types were detected including hepatocytes, cholangiocytes, endothelial, and immune cells. Furthermore, the ALS underwent ECM remodeling after transplantation and no signal of fibrotic ECM deposition was observed.

Conclusion: The study concluded that the transplanted ALS was not affected by the cirrhotic livers and remained a template for healthy cell growth. In a translational context, this study demonstrates that ALSs derived from decellularization can be transplanted into patients with liver disease undergoing hepatectomy procedures in the future.

WED-104

Loss of heterogeneity and CD4+ T-cell differentiation in patients with alcohol-related cirrhosis

Paola Zuluaga^{1,2}, Coral Zurera¹, Daniel Fuster¹, Anna Hernandez-Rubio¹, Eva Martínez-Cáceres³, Robert Muga¹. ¹Universitat Autònoma de Barcelona, Barcelona, Spain; ²University Hospital Germans Trias i Pujol, Badalona; ³Universitat Autònoma de Barcelona, Barcelona, Spain

Email: ypzuluaga.germanstrias@gencat.cat

Background and aims: CD4⁺ T-cells have a central role on the immune response through different subsets. Lymphopenia is common in patients with alcohol-related cirrhosis (AC); however, changes in CD4⁺ T-cell subsets are not sufficiently studied. The present pilot study analyzes the changes over time in the CD4⁺ T-cell subsets and the interactions between them in patients with AC.

Method: Patients with Alcohol Used Disorder (AUD) admitted at least twice for treatment and evaluated for alcohol-related liver disease, were included in the study. The presence of AC was evaluated according to clinical and ultrasound criteria. Patients without clinical evidence of alcohol-related liver disease were the control group. The following CD4⁺ T-cell subsets were analyzed through flow cytometry: naïve (CCR7⁺/CD45RA⁺), central memory (CCR7⁺/CD45RA⁻), effector memory (CCR7⁻/CD45RA⁺), terminally differentiated effector memory (TEMRA) (CCR7⁻/CD45RA⁺), Th1 (CXCR3⁺/CCR6⁻), Th2 (CXCR3⁻/CCR6⁻), Th17 (CXCR3⁻/CCR6⁺), early activated cells (CD38⁺/HLA-DR⁺) and late activated cells (CD38⁺/HLA-DR⁻).

Results: 27 patients (46 ± 8 years, 81% male, IMC 25 ± 5.7 kg/m²) with a mean alcohol consumption of 186.5 ± 112 gr/day and a mean AUD duration of 17.4 ± 9.5 years were included. During the follow-up, TEMRA CD4⁺ T-cells were increased (1.24 ± 1.16 vs. 2.14 ± 1.14, p = 0.03) in patients with AC (n = 5) and Th17 cells were decreased (14.16

± 4.31 vs. 12.35 ± 6.40 , $p = 0.03$) in the control group ($n = 22$). Early activated cells were associated with an increase of memory cells in the control group ($r = 0.51$, $p = 0.01$), and late activated cells were associated with a decrease of memory cells in both groups. This association was stronger in patients with AC than in control group ($r = -0.90$, $p = 0.04$; $r = -0.44$, $p = 0.05$, respectively). The proportion of memory cells was associated with an increased proportion of Th1, Th2 and Th17 cells in the control group ($r = 0.70$, $r = 0.68$, $r = 0.63$; $p < 0.01$, respectively), while in patients with AC the proportion of memory cells was associated with a decrease in the Th17 cells ($r = -0.90$, $p = 0.03$).

Conclusion: Patients with alcohol-related cirrhosis experience an increase in the proportion of CD4⁺ TEMRA cells, lymphocyte populations associated with the presence of inflammation and immunosenescence. The loss in heterogeneity and the decreased lymphocyte differentiation in patients with alcohol-related cirrhosis are findings that suggest an inappropriate immune response.

WED-105

Nitazoxanide directly protects from stress-induced cell death to alleviate liver damage in preclinical models of acute-on-chronic liver failure

Marie Bobowski-Gerard¹, Simon Debaecker¹, Nicolas Stankovic Valentin¹, Alexia Tessier², Hana Elkhatib¹, Philippe Delataille¹, Remy Hanf³, Sakina Sayah Jeanne¹, Dean Hum¹, Vanessa Legry¹, Bart Staels^{2,4}. ¹Genfit S.A., Loos, France; ²Univ. Lille, INSERM U1011, Lille, France; ³Pradial consulting, Lille, France; ⁴CHU Lille, Institut Pasteur de Lille, Lille, France
Email: marie.gerard@genfit.com

Background and aims: Acute-on-chronic liver failure (ACLF) is characterized by an acute decompensation of liver function in patients with cirrhosis; associated with multiple organ failures and high short-term mortality rates. We previously showed that the anti-parasitic drug nitazoxanide (NTZ) counteracts LPS-induced inflammatory responses and organ failures in disease models of ACLF (*J Hepatol.* 2022 vol. 77, THU-528 and *J Hepatol.* 2023 vol. 78, THU-342). The aim of this study was to investigate the effect of NTZ on liver damage and cell death, using animal and cellular models of ACLF.

Method: ACLF was triggered through lipopolysaccharide (LPS) injection in rats displaying cirrhosis induced by bile duct ligation (BDL). A single dose of NTZ (100 mg/kg) or vehicle was orally administered concomitant to LPS injection. Liver samples were collected 3 h post-LPS for RNA sequencing and transcriptomic analysis. To assess NTZ's effect on cell death, immortalized human hepatocytes were stimulated with two pathogenic factors contributing to ACLF pathophysiology: H₂O₂ (0.5 mM) and ethanol (0.6 mM). In parallel, necroptotic cell death was induced in HT-29 cells using a combination of the pan-caspase inhibitor zVAD (10 μ M), the Smac mimetic BV6 (2 μ M) and TNF-alpha (20 ng/ml). Cells were treated with Tizoxanide (TZ), NTZ's circulating active metabolite, at the same time or after the stress inducer. Cell death was evaluated through measurement of caspase 3 activation and cleavage, and LDH release.

Results: ACLF induction with LPS injection significantly remodeled the transcriptome of cirrhotic rat liver. Enrichment analysis showed that NTZ reversed the hepatic ACLF-related gene signature, modifying cell death-related pathways such as apoptosis and necroptosis, two modes of cell death reported in patients with ACLF (Adebayo *et al.*, *Liver Int.*, 2015; Kondo *et al.*, *CDD*, 2022). Cellular models were therefore used to investigate direct effect of NTZ on stress-induced cell death. In human hepatocytes, TZ blunted apoptosis induced by H₂O₂ or ethanol treatment in a dose dependent manner as shown by a reduction of caspase 3/7 activity and caspase 3 cleavage (IC₅₀ = 2 to 2.8 μ M). When stressed with necroptotic stimuli, HT-29 cells displayed an activation of the necroptosis effectors MLKL and

RIPK3, accompanied by plasma membrane leakage, as measured by lactate dehydrogenase (LDH) release. Interestingly, TZ inhibited LDH release in this model with a maximum efficacy of 57% at 7.5 μ M. These results highlight a direct protective effect of TZ on stress-induced cell death.

Conclusion: The direct protective effects of TZ on apoptosis and necroptosis suggest that NTZ treatment is a promising approach to protect the liver of patients with ACLF from cell death. Combined with its antibacterial and anti-inflammatory activities, this further supports NTZ development for the potential treatment of ACLF.

WED-106

Liver cirrhosis and epithelial damage-The gut-liver axis in spontaneous bacterial peritonitis and its modulation by p53

Martha Ernst¹, Celina Macek², Carina Steindl¹, Marika Haderer¹, Christoph Brochhausen³, Arne Kandulski¹, Kunst Claudia¹, Karsten Guelow¹, Martina Müller-Schilling¹. ¹University Hospital Regensburg, Regensburg, Germany; ²University Hospital Regensburg, Regensburg, Germany; ³Medical Faculty Mannheim, Mannheim, Germany
Email: martina.mueller-schilling@ukr.de

Background and aims: The gut-liver axis is pivotal in preserving overall health and modulating essential (patho)physiological processes. Patients with liver cirrhosis show reduced mucus thickness, facilitating direct contact of bacteria with epithelial cells and the breakdown of cell junctions (Haderer *et al.*, *Gut* 2022). The translocation of gut bacteria into mesenteric lymph nodes constitutes a pivotal event in spontaneous bacterial peritonitis (SBP). Cellular stress triggered by direct contact with bacteria involves the p53 family of transcription factors, serving as crucial regulators of the cell cycle, repair mechanisms, and cell death. We investigate the effects of ascites-derived bacteria on the expression of p53 isoforms concerning cell death induction in epithelial cells using a novel reporter system.

Method: Three exon-specific intein-luciferases (EXSISERS) were cloned into exons 2, 4, and 7 of the TP53 gene. Split inteins allow for the cleavage of luciferase from the p53 polypeptide, preserving the structural integrity of p53 isoforms (Truong *et al.*, *Nat Cell Biol* 2021). This method precisely quantifies p53 protein isoform ratios at the cellular level. HCT116-EXSISERS cells were co-cultured with patient-derived *Escherichia coli*, and the three main groups of p53 isoforms—cell cycle-arrest-inducing full-length p53, cell death-inducing $\Delta 40p53$, pro-proliferative $\Delta 133p53/\Delta 160p53$ —were measured. Concurrently, bacterial-induced cell death was quantified in HCT116 p53 wild-type and p53 knockout cells. Electron microscopy was used for determination of the type of cell death.

Results: Co-culturing patient-derived bacteria with HCT116-EXSISERS cells initially enhanced the production of the cell death-inducing p53 isoform $\Delta 40p53$ within 15 minutes. This was followed by a decrease in the pro-proliferative p53 isoforms $\Delta 133p53/\Delta 160p53$. Concurrently, the induction of cell death was detected in response to bacterial contact, exhibiting morphological characteristics of paraptosis, including mitochondrial swelling, and cytoplasmic vacuolization. In parallel with the observed morphological changes, damage to the mitochondria and plasma membrane was confirmed through flow cytometry. The known paraptosis inhibitor Acinomycin D efficiently blocked bacteria-induced cell death. In accordance with the measured induction of the $\Delta 40p53$ isoform, the induction of cell death was significantly delayed through a CRISPR/Cas9-mediated p53 knockout.

Conclusion: Bacterial translocation occurs due to an impaired epithelial integrity in patients with liver cirrhosis. Cellular responses to bacterial-induced stress are regulated by specific p53 isoforms. Thus, the p53 status exerts a crucial influence on paraptosis

POSTER PRESENTATIONS

susceptibility. Targeted induction or stabilization of particular p53 isoforms could thus represent a therapeutic option for the management of SBP.

WED-107

Administration of xyloglucan alone or in combination with norfloxacin improves intestinal barrier homeostasis in cirrhotic rats with ascites

Ramon Bartoli^{1,2}, Ignacio Iborra^{1,3}, Helena Masnou^{1,2,3}, Alba Ardevol³, Maria Torner³, Maria Bermudez³, Ana Bargallo⁴, Rosa M Morillas^{1,2,3}.
¹Germans Trias i Pujol Research Institute (IGTP), Badalona, Spain; ²CIBER de Enfermedades Hepáticas y Digestivas, Instituto de Salud Carlos III, Madrid, Spain; ³Hepatology Unit, Gastroenterology Department, Germans Trias i Pujol University Hospital, Badalona, Spain; ⁴EndosMedicina. Gastroenterology Department, HM Nou Delfos Hospital, Barcelona, Spain
Email: rbartoli@igtp.cat

Background and aims: Cirrhosis leads to a multifactorial alteration of the intestinal barrier, resulting in increased intestinal permeability that promotes bacterial translocation (BT) and is associated with infections in these patients. Currently, selective intestinal decontamination with norfloxacin is the only effective strategy to reduce BT. Xyloglucan, a hemicellulose obtained from land plants, has been shown to be effective in improving the integrity of the intestinal mucosa in various pathologies due to its mucoprotective and mucin-like properties. However, there is a lack of data on its role in the intestinal barrier in cirrhosis with ascites. The aim was to evaluate the effect of xyloglucan alone or in combination with norfloxacin on the mucosal and vascular intestinal barrier in cirrhotic rats with ascites.

Method: Cirrhosis and ascites decompensation was induced in 32 rats using carbon tetrachloride. Subsequently, they were orally administered xyloglucan (group 1), norfloxacin (group 2), xyloglucan + norfloxacin (group 3), or water (group 4, control), for one week. The following parameters were determined in colonic mucosa: IFN- γ and IL-23 as markers of inflammatory activity, occludin (a tight junction protein) as a marker of mucosal barrier integrity, PV1/CD34 ratio as a marker of vascular permeability, in addition to endotoxemia and the incidence of BT.

Results: All treatment groups (groups 1, 2 and 3) significantly showed an increase of the parameters of mucosal barrier integrity (occludin) and a significantly decrease in vascular permeability (PV1/CD34 ratio) compared to controls (group 4). Regarding inflammatory activity, there were no differences in IL-23 levels but all treatment groups showed a decrease in IFN- γ , significantly in groups 2 and 3. Similarly, BT was lower in all treatment groups compared to controls but differences were only significant in groups 2 and 3. Furthermore, all treatment groups showed a significant decrease of endotoxemia compared to controls, which values significantly correlated with BT incidence, occludin expression, IFN- γ levels, IL-23 levels, and PV1/CD34 ratio.

Conclusion: Xyloglucan reduces inflammation of the intestinal mucosa and improves both mucosal integrity and vascular permeability, thereby reducing endotoxemia and the incidence of BT; two factors implicated in the pathogenesis of infections in cirrhosis. This would justify evaluating the use of xyloglucan as a new therapeutic strategy to prevent infections associated with cirrhosis.

WED-109

Evaluation of statins as a new therapy to alleviate hepatic encephalopathy in cirrhotic mice

Subas Aroob¹, Qamar Niaz¹, Muhammad Ovais Omer¹, Syed Muhammad Muneeb Anjum², Ghulam Mustafa³, Sania Mehreen⁴, Muhammad Bilal Khan⁵, Muhammad Adil Rasheed¹.
¹Department of Pharmacology and Toxicology, Faculty of Bio-Sciences, University of Veterinary and Animal Sciences (UVAS), Lahore, Punjab-Pakistan; ²Institute of Pharmaceutical Sciences, Faculty of Bio-Sciences,

University of Veterinary and Animal Sciences (UVAS), Lahore, Punjab-Pakistan; ³Department of Pathology, Faculty of Veterinary Sciences, University of Veterinary and Animal Sciences (UVAS), Lahore, Punjab-Pakistan; ⁴Department of Zoology, Faculty of Fisheries and Wildlife, University of Veterinary and Animal Sciences (UVAS), Lahore, Punjab-Pakistan; ⁵Department of Zoology, Faculty of Biological Sciences, Quaid-I-Azam University, Islamabad, Pakistan
Email: qamar.niaz@uvas.edu.pk

Background and aims: Hepatic encephalopathy (HE) is a neurological disorder of liver cirrhosis characterized by elevated plasma ammonia levels, oxidative stress, and neuronal inflammation and death. Current therapies for HE target the ammonia levels to decrease. Statins, antilipidemic drugs, reduce the portal pressure (PP), fibrosis, inflammation, and oxidative stress in liver cirrhosis. Therefore, we evaluated the atorvastatin (Ato) effect on HE in cirrhotic mice.

Method: Total 64 male albino mice were randomly selected and divided into two groups of sham (control) i.e., Sham/Saline, Sham/Ato-15 mg/kg, Sham/Ato-30 mg/kg, and Sham/Lac-1.43 g/kg sub-groups and bile duct ligated (cirrhotic) i.e., BDL/Saline, BDL/Ato-15 mg/kg, BDL/Ato-30 mg/kg, and BDL/Lac-1.43 g/kg sub-groups. BDL surgery was performed to induce liver cirrhosis for 28 days, while sham surgery was used for control groups. Each group was gauged orally the respective drug once daily for 14 days. Following the treatment, the plasma ALT, AST, bilirubin, cholesterol, and ammonia levels were evaluated along with histopathology for the liver (inflammation and fibrosis) and brain (inflammation and vacuolar degeneration). Finally, the anxiety and cognitive functions were assessed through the elevated plus maze test and open field test and Y-maze test, respectively.

Results: The findings revealed that the spleen weight was decreased in the BDL/Ato-30 group in comparison to the BDL/Saline group. The liver inflammation and fibrosis and brain inflammation and vacuolar degeneration were noted as moderate and mild in the BDL/Ato-15 and BDL/Ato-30 groups, respectively than the BDL/Saline group. The plasma ALT, cholesterol, and ammonia levels were decreased equally in the BDL/Ato-15 and BDL/Ato-30 groups, while the plasma AST level was decreased in the BDL/Ato-30 group than BDL/Saline group. The plasma bilirubin level was reduced more in the BDL/Ato-30 group than the BDL/Ato-15 group as compared to the BDL/Saline group. The anxiety (the distance traveled in the open field) was high in the BDL/Saline group and was raised further in the BDL/Ato-15 group than in the BDL/Ato-30 group. The anxiety (time spent in the center of the open field) was high in the BDL/Saline group and was not treated in the BDL/Ato-15 and BDL/Ato-30 groups. The anxiety (number of entries and time spent in closed arms in the elevated plus maze) was absent in the BDL/Saline group and was reduced in the BDL/Ato-30 group. No change in cognitive function (percent spontaneous alteration in Y-maze) in the BDL/Saline group was observed and the BDL/Ato-30 group decreased the cognitive functions.

Conclusion: The atorvastatin at 30 mg/kg body weight alleviates the HE in cirrhotic mice by decreasing the plasma ammonia level and treating the liver inflammation and fibrosis and brain inflammation and vacuolar degeneration without affecting anxiety and cognitive functions.

WED-110

Alterations in plasma neuronal and glial proteins in varying severities of cirrhosis and differing grades of hepatic encephalopathy

Marilena Stamouli^{1,2}, Christos Konstantinou^{1,2}, Jack Wright³, Ane Zamalloa³, Neil Youngson^{1,2}, Mark J W McPhail^{2,3}, Anna Hadjihambi^{1,2}, Vishal C Patel^{1,2,3}.
¹The Roger Williams Institute of Hepatology, Foundation for Liver Research, London, United Kingdom; ²Faculty of Life Sciences and Medicine, King's College London, London, United Kingdom; ³Institute of Liver Studies and Transplantation, King's

College Hospital, London, United Kingdom
Email: m.stamouli@researchinliver.org.uk

Background and aims: Hepatic encephalopathy (HE) is a challenging neuropsychiatric complication that contributes to cognitive and motor symptoms frequently observed in cirrhosis. Central to the pathophysiology of HE are neuronal injury and astrocyte swelling. Neurofilament light chain (NfL), a neuronal cytoplasmic protein reflecting neuroaxonal damage, and glial fibrillary acidic protein (GFAP), the principal intermediate filament found in astrocytes serving as a marker of astrocytic activation, are potential diagnostic tools for HE in cirrhosis. This study aims to investigate the diagnostic potential of these circulating proteins and explore their roles in the complex underlying mechanisms that cause HE.

Method: Cirrhosis patients were stratified based on disease severity into three groups: stable cirrhosis (SC, n = 14), decompensated cirrhosis (DC, n = 13), and acute-on-chronic liver failure (ACLF, n = 20), and compared to healthy controls (HC, n = 8) and non-liver sepsis patients (NLS, n = 14). HE was assessed at the time of blood sampling using the West Haven criteria, ranging from patients with no detectable symptoms (grade 0, n = 32) to mild behavioral and cognitive alterations (grades 1/2, n = 9) and severe symptoms including coma (grades 3/4, n = 6). Plasma levels of NfL and GFAP were quantified using electrochemiluminescent-based assays (MSD R-plex™).

Results: Plasma NfL concentration progressively increased with cirrhosis severity, while GFAP showed an upward trend without reaching statistical significance. NfL effectively discriminated cirrhosis patients with HE from those without (median: 183 vs 51 pg/ml, p = 0.007). Receiver-operating curve analysis discriminated HE grades 1/2 compared to grade 0 based on NfL levels (r = 0.87, p = 0.0009). Circulating NfL and GFAP levels directly related to each other in all cirrhosis patients, regardless of severity of liver disease (r = 0.59, p < 0.0001), with stronger associations observed in patients with ACLF (r = 0.67, p = 0.01) or HE (r = 0.75, p = 0.002). Both markers exhibited an inverse correlation with estimated glomerular filtration rate (eGFR), a marker of renal function (NfL: r = -0.61, p < 0.0001; GFAP: r = -0.30, p = 0.04). Notably, NfL, but not GFAP, positively correlated with IL-6 (r = 0.63, p < 0.0001), while neither of them showed a correlation with ammonia.

Conclusion: Plasma NfL and GFAP exhibit potential as diagnostic tools for HE in cirrhosis, especially at the challenging to diagnose more covert stage. NfL, particularly, demonstrated superior discriminatory capabilities between HE grades and stronger associations with cirrhosis severity. Their correlations with renal function and inflammatory markers further underscore their clinical and mechanistic relevance, respectively. The neuronal and glial-derived proteins may offer valuable insights into the complex pathophysiology of HE that warrant further evaluation.

WED-111

Plasma proteomics uncovers progression markers of acute-on-chronic liver failure

Florian Rosenberger¹, Peter Treit¹, Vincent Albrecht¹, Maximilian Zwiebel¹, Johannes Müller-Reif¹, Robert Schierwagen², Wenyi Gu², David Tornai³, Frank Erhard Uschner⁴, Debbie L. Shawcross⁵, Minneke Coenraad⁶, Rajiv Jalan⁷, Joan Clària⁸, Maria Papp³, Wim Laleman⁹, Jonel Trebicka², Matthias Mann^{1,10}. ¹Max Planck Institute of Biochemistry, Dept. Proteomics and Signal Transduction, Martinsried, Germany; ²Department of Internal Medicine B, University of Münster, Münster, Germany; ³Division of Gastroenterology, Department of Internal Medicine, Faculty of Medicine, University of Debrecen, Debrecen, Hungary; ⁴Department of Internal Medicine B, University of Münster, Münster, Germany; ⁵Institute of Liver Studies, School of Immunology and Microbial Sciences, Faculty of Life Sciences and Medicine, King's College London, London, United Kingdom; ⁶Leiden University Medical Center, Dept. of Gastroenterology-Hepatology, Leiden, Netherlands; ⁷Institute for Liver and Digestive

Health, Royal Free Hospital, UCL Medical School Rowland, London, United Kingdom; ⁸Biochemistry and Molecular Genetics Service, Hospital Clínic de Barcelona, Institut d'Investigacions Biomèdiques August Pi i Sunyer (IDIBAPS), Barcelona, Spain; ⁹Department of Gastroenterology and Hepatology, University Hospitals Leuven, KU Leuven, Leuven, Belgium; ¹⁰NNF Center for Protein Research, Faculty of Health Sciences, University of Copenhagen, Copenhagen, Denmark
Email: schober@biochem.mpg.de

Background and aims: Acute-on-Chronic Liver Failure (ACLF) is a life-threatening condition that includes failure of one or more organs after acute decompensation of cirrhosis. The clinical mode of action depends on accurate predictions of near-future events. Herein, we aim to identify prognostic biomarkers of ACLF events in patient plasma.

Method: We deployed mass spectrometry-based proteomics to quantify the in-depth plasma proteome profile of 93 patients in four disease groups (stable and unstable decompensated cirrhosis, pre-ACLF, at ACLF onset and after ACLF recovery) across multiple timepoints (n = 346). These discovery samples were part of the MICROB-PREDICT study cohort MUCOSA-PREDICT. We used an automated processing protocol for patient plasma and the highly reproducible Evosep system for liquid chromatography, coupled to a Thermo Scientific Orbitrap Exploris 480 mass spectrometer. Validation of the data on additional 550 plasma samples of VALIDATION-PREDICT measured on the latest Thermo Orbitrap Astral mass spectrometer is currently ongoing.

Results: On average, we detected 410 proteins across all discovery samples, and around 1,500 proteins in the validation cohort. The data complied with quality control standards, including low coefficient of variation across 80% of all proteins, and low levels of typical erythrocyte, platelet and coagulation contamination markers. A set of nine differentially abundant proteins (p < 0.05 after multiple testing adjustment) was identified in a paired longitudinal analysis of pre-ACLF patients (n = 15). The levels of all nine potential biomarkers increased drastically upon ACLF onset compared to the admission timepoint, and dropped in the recovery period. This signature correlate strongly with creatinine levels and kidney failure.

Conclusion: We identified nine potential plasma biomarkers for ACLF that are significantly elevated upon disease onset compared to the baseline inclusion timepoint within the same patients. In combination with already established clinical read-outs, these proteins can contribute to predicting ACLF onset and to specifying the clinical mode of action.

WED-112

Plasma extracellular vesicles improve prediction of 90 day mortality in patients with acute decompensation of cirrhosis

Shantha Valainathan¹, Marion Tanguy², Damarys Loew³, Florent Dingli³, Louise Biquard⁴, Sara Thietart⁵, Jonel Trebicka⁶, Paolo Caraceni⁷, David Gomez-Cabrero⁸, Paolo Angeli⁹, Carlo Alessandria¹⁰, Alberto Queiroz Farias¹¹, Sebastián Marciano¹², Vicente Arroyo¹³, Cristina Sanchez¹⁴, Joan Clària¹⁵, Pierre-Emmanuel Rautou¹⁶. ¹Hôpital Beaujon AP-HP, Liver Unit, Hepatology unit, Clichy, France; ²INSERM UMR 1149, Paris, France; ³Institut Curie, Paris, France; ⁴INSERM 1149, Paris, France; ⁵Centre de recherche sur l'inflammation, INSERM, UMR 1149, Paris, France; ⁶Universitätsklinikum Münster (UKM), Münster, Germany; ⁷University of Bologna, Bologna, Italy; ⁸Navarrabiomed-Fundación Miguel Servet, Pamplona, Spain; ⁹University and Hospital of Padova, Padova, Italy; ¹⁰AOU Città della Salute e della Scienza di Torino, Turin, Italy; ¹¹Department of Gastroenterology, Hospital das Clínicas, University of São Paulo School of Medicine, São Paulo, Brazil; ¹²Hospital Italiano de Buenos Aires, Buenos Aires, Argentina; ¹³EF CLIF, Barcelona, Spain; ¹⁴EF Clif, Barcelona, Spain; ¹⁵Hospital Clinic, Barcelona, Spain; ¹⁶Hôpital Beaujon, Clichy, France
Email: shantha.valainathan@gmail.com

Background and aims: Accurate prediction of survival in patients with acute decompensation of cirrhosis (AD) is key to orientate

POSTER PRESENTATIONS

patients with a poor predicted outcome to liver transplantation or to novel therapeutic approaches. The Clif-Consortium Acute Decompensation (Clif-C AD) score, dedicated to predict mortality in patients with AD, has been a step forward in that respect, but its predictive ability needs further improvements. Extracellular vesicles are released by cells undergoing a stress and are attractive biomarkers. The aim of the study was to identify plasma large extracellular vesicles (IEVs) able to improve prediction of death at 90 days in patients with AD.

Method: A pilot proteomic analysis was performed on plasma IEVs from two cohorts: 25 patients with AD, including 7 who died at 90 days, and 14 patients with stable decompensated cirrhosis, including 6 who died at 180 days. The identified IEV proteins were measured in plasma samples from patients with AD without ACLF at inclusion included in two prospective multicenter cohorts: PREDICT (serving as derivation cohort, $n = 763$) and ACLARA (serving as validation cohort, $n = 579$). Fine-Gray models were used to assess the risk of death at 90-days, liver transplantation being considered as a competing event.

Results: Proteomic analysis identified tenascin-C, IgG-Fc binding protein (FCGBP) and olfactomedin-4 on IEVs to be associated with mortality in patients with AD. We thus measured the three IEV proteins in plasma samples from patients of the PREDICT cohort (68% men, median age 59, median MELD 15, 90-day mortality rate 14%). Using multivariate analysis, concentrations of all three IEV were independently associated with 90-day mortality after adjustment on Clif-C AD and MELD scores. Mortality at 90 day gradually increased with the number of IEV above cut-off values identified using Youden index, from 3% to 30% for 0 and 3 high IEV, respectively. When combined with Clif-C AD score, plasma concentration of the 3 IEV improved prediction offered by Clif-C AD, reaching a 93% specificity for 90-day mortality vs. 40% for Clif-C AD score alone. We then measured these 3 IEVs on plasma samples from patients of the ACLARA validation cohort (65% men, median age 59, median MELD 15, 90-day mortality rate at 20%) and confirmed our Results: 90 day mortality increased with the number of high IEVs from 15% to 31% for 0 and 3 high IEV, respectively; the 3 IEV improved prediction offered by Clif-C AD, reaching a 95% specificity for 90-day mortality vs. 50% for Clif-C AD score alone.

Conclusion: We identified a IEV signature, including tenascin-C, FCGBP and olfactomedin-4 on IEVs able to identify a group of AD patients at high risk of short-term mortality. This added prognostic value might be explained by the fact that these IEV are released by organs and tissues (fibroblasts, gut and neutrophils) strongly implicated in the pathophysiology of AD.

WED-113

Histological, molecular, and neuromotor alterations of the liver-brain axis in an aged model of experimental cirrhosis

Oriol Juanola¹, Sebastian Martinez^{1,2}, Marina Serrano-Maciá¹, Enrique Angel^{1,2}, Isabel Gómez-Hurtado^{2,3}, Paula Boix¹, Francisco Navarrete Rueda⁴, Maria Salud García Gutierrez⁴, Esther Caparrós^{1,2}, Rubén Francés^{1,2,3}. ¹Grupo de Inmunobiología Hepática e Intestinal, Dpto. Medicina Clínica e Instituto IDIBE, Universidad Miguel Hernández, San Juan de Alicante, Spain; ²IIS ISABIAL, Hospital General Universitario de Alicante, Alicante, Spain; ³CIBERehd, Instituto de Salud Carlos III, Madrid, Spain; ⁴Grupo de Neuropsicofarmacología Traslacional, Instituto de Neurociencias CSIC-UMH, San Juan de Alicante, Spain
Email: rfrances@umh.es

Background and aims: During chronic liver disease (CLD), dysregulation of hepatic immunosurveillance and intestinal dysbiosis promote systemic inflammation and metabolic alterations, affecting neurocognitive function through the liver-brain axis. As aging may worsen neurological damage and CLD and its complications are more prevalent in the aging population, our aim was to assess differences in hepatic and neurocognitive damage based on age during experimental CLD.

Method: CLD was induced by oral administration of carbon tetrachloride (CCl₄) for 12 weeks (w) in young mice (6 w old) and aged mice (40 w old). Liver damage was assessed through histology and molecular biology. Levels of ammonia in different tissues were examined, and a panel of behavioural assays was conducted to assess neurological impairment.

Results: Hepatic damage was more severe following the induction of CLD in aged mice compared to young ones, exhibiting significantly elevated levels of ALT and AST, as well as, higher levels of red Sirius staining and lymphocyte recruitment (CD3), compared to the latter. Ammonia concentrations were higher in cirrhotic aged mice than in young ones in both serum (2.47 ± 0.74 vs 5.18 ± 2.36 nmol/uL, $p = 0.015$) and the brain (4.65 ± 0.41 vs 5.27 ± 0.86 nmol/uL, $p = 0.114$). Cirrhotic animals showed motor impairment and a tendency towards anxiety compared to healthy controls. Aged cirrhotic animals exhibited a significantly higher severity index in motor function than the young ones ($p = 0.023$). Interestingly, only ammonia levels in the brain correlated with results in the open field test ($r = -0.544$, $p = 0.003$) and motor evaluation test ($r = 0.444$, $p = 0.018$), suggesting a direct relationship between brain ammonia and neurological impairment. The increased anxiety shown by aged cirrhotic animals did not reach significant differences compared to the young ones.

Conclusion: Aged animals exhibit more severe liver damage during the experimental cirrhosis model, with higher levels of ammonia in the brain, and worse neurological function. Neurocognitive damage in young cirrhotic animals is similar to the impairment observed in healthy aged animals, suggesting a contribution of liver damage to neurological impairment during experimental cirrhosis.

WED-114

In vivo experiments and network pharmacology to explore the effect and mechanism of JiGuCao capsule in treating liver cirrhosis

Shihao Zheng¹, Wenying Qi², Size Li², Xu Cao², Xiaoke Li², Xiaobin Zao². ¹Dongzhimen Hospital, Beijing University of Chinese Medicine, Beijing 100700, China, Institute of Liver Diseases, Dongzhimen Hospital, Beijing University of Chinese Medicine, Beijing 100700, China; ²Dongzhimen Hospital, Beijing University of Chinese Medicine, Beijing 100700, China
Email: A3417@bucm.edu.cn

Background and aims: Liver cirrhosis (LC) has been a serious threat to the health of people all over the world which has no effective treatment for now. Traditional Chinese medicine (TCM) has shown a good therapeutic effect for LC. The JiGuCao capsule (JGC) is a commonly used TCM that is already on the market for the treatment of acute and chronic hepatitis. However, the effect and mechanism of JGC in treating LC is not clear.

Method: The LC mice model was established by intraperitoneal injection of 10% CCl₄ of olive oil mixture for 12 weeks. From the seventh week, the treatment group was given JGC granule aqueous solution by gavage. After treatment, the mice's body weight was recorded, and the mice's serum was used to detect biochemical indicators including alanine aminotransferase (ALT) and aspartate aminotransferase (AST). The rats' liver tissues were used to perform pathological examinations including HE staining, Masson staining, and Sirius red staining. The key compounds of JGC were detected by UHPLC-MS/MS analysis, and target genes of JGC in treating LC were obtained from the public databases. Then constructed the protein-protein interaction network and performed further enrichment analyses including the Gene Ontology (GO) and the Kyoto Encyclopedia of Genes and Genomes (KEGG) of the target genes.

Results: Compared to the control group, after modeling, the weight of the model mice was significantly decreased. Compared to the model group, significantly lower levels of serum ALT and AST in the JGC group than in the model were observed. The HE staining, Sirius red staining, and Masson staining showed less inflammatory damage and collagen production after JGC treatment compared to the model.

After UHPLC-MS/MS analysis and database mining, we obtained 337 overlapping genes (OGEs) between JGC targets and LC targets. The GO analysis of OGEs was mainly enriched in protein phosphorylation, cytosol, and enzyme binding. KEGG pathway enrichment analysis of OGEs showed that the key targets were significantly associated with the HIF-1 signaling pathway and PI3K-Akt signaling pathway.

Conclusion: JGC exerted a reversion effect on the progress of earlier LC in mice. Its molecular mechanism may be related to the regulation of the HIF-1 signaling pathway and PI3K-Akt signaling pathway.

WED-116

Primary biliary cholangitis increases the risk of hepatocellular carcinoma: results from Mendelian randomization analysis and bioinformatics analysis

Yikai Wang¹, Muqi Wang¹, Xiaqing Zhou¹, Chenrui Liu¹, Meng Zhang¹, Miao Hao¹, Wenjun Wang¹, Yaping Li¹, Juanjuan Shi¹, Shuangsoo Dang¹. ¹The Second Affiliated Hospital of Xi'an Jiaotong University, xi'an, China
Email: dang212@126.com

Background and aims: Primary biliary cholangitis (PBC) is an inflammatory factor closely associated with hepatocellular carcinoma (HCC); however, the relationship between these two liver diseases has not been well studied.

Method: GWAS data was obtained from the IEU Open GWAS database. Gene expression profiles were retrieved from the GEO and ICGC databases, respectively. A prediction model was constructed using COX regression with TCGA data, and its performance was assessed using ROC curves. Additionally, differentially expressed genes (DEGs) analysis at various stages was conducted using UALCAN, and their prognostic significance was evaluated using Kaplan-Meier (KM) curves. The correlation between DEGs and immune infiltration was assessed using TIMER. Finally, Cytoscape was employed to identify hub genes and perform enrichment analysis.

Results: MR analysis revealed a significant causal relationship between PBC and an elevated risk of HCC (OR >1, p < 0.05). Following prognostic analysis, LGALS3 and PRKCD exhibited associations with patient prognosis. These genes exhibited upregulation in HCC and were correlated with tumor grade and lymphatic metastasis. KM analysis further confirmed their close relationship with HCC prognosis. The prognostic model exhibited lower prognostic outcomes in the high-risk group. Both two genes exhibited positive correlations with tumor immune cell infiltration. Subsequent hub gene identification and enrichment analysis underscored their pivotal role in immune cell recruitment and migration in HCC.

Conclusion: This study establishes that PBC may contribute to an elevated risk of developing HCC, and the overexpression of LGALS3 and PRKCD may facilitate the progression of HCC.

WED-117

Targeted breath biopsy® profiling of induced biomarkers unveils a metabolic adaptation in cirrhosis toward alcohol production

Giuseppe Ferrandino¹, Federico Ricciardi¹, Antonio Murgia¹, Menisha Manhota¹, Daniela Fonseca¹, Louise Nicholson-Scott¹, Chloe Fitzpatrick¹, Olga Gandelman¹, Max Allsworth¹, Billy Boyle¹, Agnieszka Smolinska^{1,2}, Alexandra Ginesta Frings^{3,4}, Jorge Contreras³, Victor Gabrielli³, Claudia Asenjo-Lobos⁵, Francisca Bascuro⁵, Viviana Barrientos⁴, Nataly Clavo⁴, Melissa Jerez⁶, Luis Mendez^{3,4}. ¹Owlstone Medical, Cambridge, United Kingdom; ²Department of Pharmacology and Toxicology, School for Nutrition and Translational Research in Metabolism (NUTRIM), Maastricht University Medical Center, Maastricht, Netherlands; ³Unidad de Gastroenterología y Endoscopia, Clínica Alemana, Facultad de Medicina Clínica Alemana, Universidad de Desarrollo, Santiago, Chile; ⁴Unidad de Endoscopia, Hospital Padre Hurtado, Santiago, Chile; ⁵Centro de Estudios Clínicos, Instituto de Ciencias e Innovación en Medicina (ICIM), Facultad de Medicina Clínica Alemana, Universidad del Desarrollo, Santiago, Chile;

⁶Nursing School, Universidad de Las Américas, Santiago, Chile
Email: giuseppe.ferrandino@owlstone.co.uk

Background and aims: Subjects with chronic liver disease have shown higher circulating ethanol levels after fasting or carbohydrates ingestion. However, clinical functional data about the capability of the injured liver to cope with alcohols remain limited. In this study we used exhaled breath analysis to explore the conversion of an alcohol to the corresponding ketone, and a ketone to the corresponding alcohol, to establish the suitability of potential metabolic alterations and identify subjects with cirrhosis using a non-invasive breath test.

Method: 2-butanol, and 2-pentanone (the substrates) were selected as an alcohol and a ketone based on their safe profile for human consumption, their reported hepatic metabolism, and their presence in breath. Hepatic metabolism was confirmed by simultaneous treatment of human suspension hepatocytes with 10 ng/μl of 2-butanol, and 2-pentanone to measure their conversion to respectively 2-butanone, and 2-pentanol (the bioproducts) by using headspace analysis coupled with gas-chromatography mass-spectrometry (GC-MS). Clinical metabolism of these compounds was evaluated by measurement of the breath profile in 14 subjects with cirrhosis and 14 healthy controls before and at different timepoints (10–120 minutes) after simultaneous ingestion of 2-butanol (100 mg) and 2-pentanone (100 mg) using Breath Biopsy® OMNI.

Results: The bioproducts were present in the head space of primary hepatocytes treated with the substrates and absent in control conditions omitting primary hepatocytes or substrates. After an overnight fasting all the participants showed breath levels of investigated compounds with no differences between healthy and cirrhosis groups (p > 0.05). After ingestion of the substrates, all the subjects showed a >100-fold increase of investigated compounds within 10 minutes. Subjects with cirrhosis showed higher levels of 2-butanol and 2-pentanol (p < 0.05) compared to healthy controls between 20- and 90-minutes post-administration. An exploratory classification model built on these breath-induced biomarkers at 20 minutes showed an area under the ROC curve of 0.92.

Conclusion: 2-butanol and 2-pentanone are metabolized to the corresponding ketone and alcohol in primary hepatocytes, supporting previous findings reporting hepatic metabolism. Subjects with cirrhosis showed higher breath levels of secondary alcohols independently from administration of the alcohol or the corresponding ketone, suggesting that the hepatic function is more balanced toward the alcohol production compared to healthy controls. This metabolic adaptation may contribute to higher circulating ethanol levels observed in subjects with chronic liver disease and be exploited in a breath test for cirrhosis detection.

WED-118

Mitoquinol intervention ameliorates cirrhosis associated hematopoietic imbalance and improves innate immune function

Deepanshu Maheshwari¹, Nidhi Nautiyal^{1,2}, Sandeep Kumar¹, Manisha Bhardwaj³, Sunidhi Diwakar¹, Shivi Chauhan¹, Anupama Kumari¹, Archana Rastogi¹, Chhagan Bihari¹, Shiv Kumar Sarin¹, Anupam Kumar¹. ¹Institute of Liver and Biliary Sciences, New Delhi, India; ²Amity Institute of Molecular Medicine and Stem Cell Research, Amity University, Noida, India; ³Institute of Liver and Biliary Sciences, New Delhi, India
Email: deepanshu.maheshwari@gmail.com

Background and aims: Myeloid-biased hematopoiesis play a key role in promotion and resolution of injuries and infections. In cirrhosis, this process becomes dysregulated, leading to poor resolution of infections and impaired healing. In this study, we aim to elucidate mechanism behind this and evaluate the potential of Mitoquinol (MQ) in improving innate immune function during cirrhosis.

Method: Cirrhosis was induced in C57Bl/6 (n = 35) mice using CCl₄. Mice were culled for studying bone marrow (BM) hematopoietic stem cells (HSC), myeloid progenitors (MyP), multipotent progenitors

POSTER PRESENTATIONS

(MPP), and long-term HSCs (LT-HSC). Myeloid cell populations and functions were studied. In vitro, bone marrow-derived macrophages (BMDM) were treated with MQ (50 nM). In vivo, cirrhotic mice received MQ treatment (50 µM), controls were treated with PBS.

Results: We show progressive increase in myeloid-biased differentiation of HSC during chronic liver injury. During the transition from healthy to steatosis, there was an increase in monocytes and neutrophils in BM, along with elevation in MyP and MPP, without any loss of LT-HSC. From steatosis to fibrosis and cirrhosis, there was increase in MyP and MPP at the expense of LT-HSC. During this transition, while neutrophils increased, there was decline in monocytes and their phagocytosis and efferocytosis. Liver showed increased influx of neutrophils ($p < 0.01$), loss of the monocytes ($p < 0.01$), and impaired function ($p < 0.05$). Both BM-HSCs and monocytes showed progressive increase in cellular and mitochondrial (mt) ROS with loss of mt biomass and potential during cirrhosis. In vitro treatment of BMDM with MQ demonstrated elevated production of naïve macrophages with improved phagocytosis ($p < 0.05$) and efferocytosis ($p < 0.01$). MQ-BMDM showed increased mt potential. In vivo treatment with MQ resulted in reduced neutrophil infiltration and decreased Kupffer cell loss. HSCs from MQ-treated mice showed increased glucose uptake and mt biomass compared to controls. MQ-HSCs displayed lower TLR2 expression compared to controls. MQ mice did not show changes in MyP but showed increased production of functional monocytes ($p < 0.01$) with reduced neutrophils ($p < 0.01$). BMDM from MQ mice showed increased mt respiration and ATP-linked oxygen consumption. MQ mice showed reduced liver injury and fibrosis compared to controls.

Conclusion: Our study shows an increase in myeloid-biased differentiation of HSC during chronic liver injury. Shift from steatosis to fibrosis and cirrhosis show increased myelopoiesis, impacting LT-HSC, along with altered monocyte and neutrophil dynamics. Overall, suggesting potential role of dysregulated hematopoiesis in the loss of liver monocyte/macrophages and their function. In vivo and in vitro MQ treatments demonstrated therapeutic potential by mitigating neutrophil infiltration, enhancing macrophage function, and reducing liver injury.

WED-120

Albumin infusion in decompensated cirrhotic patients with ascites induced decreasing serum active form of vitamin D, 1, 25 dihydroxy vitamin D, an opposite effect on promoting systemic inflammatory cytokines reduction

Thitaporn Roongrawee¹, Sirinporn Suksawatamnuay², Nunthiya Srisoonthorn³, Nipaporn Siripon⁴, Panarat Thaimai⁵, Prooksa Ananchuensook⁶, Supachaya Sriphoosanaphan⁷, Kessarin Thanapirom⁸, Piyawat Komolmit⁹. ¹King Chulalongkorn Memorial Hospital, Bangkok, Thailand; ²Division of Gastroenterology, Department of Medicine, Faculty of Medicine, Chulalongkorn University and King Chulalongkorn Memorial Hospital, Thai Red Cross Society, Bangkok, Thailand; ³Center of Excellence in Liver Diseases, King Chulalongkorn Memorial Hospital, Bangkok, Thailand; ⁴Center of Excellence in Liver Diseases, King Chulalongkorn Memorial Hospital, Thai Red Cross Society, King Chulalongkorn Memorial Hospital, Bangkok, Thailand; ⁵Division of Gastroenterology, Department of Medicine, Faculty of Medicine, Chulalongkorn University and King Chulalongkorn Memorial Hospital, Thai Red Cross Society, Bangkok, Thailand, King Chulalongkorn Memorial Hospital, Bangkok, Thailand; ⁶Division of Gastroenterology, Department of Medicine, Chulalongkorn University, Bangkok, Thailand; ⁷Institute for Liver and Digestive Health, University College London, London, United Kingdom; ⁸Division of Gastroenterology, Department of Medicine, Faculty of Medicine, Bangkok, Thailand; ⁹Chulalongkorn University and King Chulalongkorn Memorial Hospital, Bangkok, Thailand
Email: thitagiftr@gmail.com

Background and aims: Decompensated cirrhosis, characterized by excessive inflammation, contributes to multiorgan dysfunction.

Current comprehension of albumin extends beyond its oncotic properties to encompass anti-inflammatory effects. A prior study, in a small number of cases, exhibited a notable decrease in inflammatory cytokine levels following high-dose albumin infusion in cirrhotic patients, suggesting a potential link between albumin replacement therapy and its anti-inflammatory mechanisms. This study aims to explore the intricate role of albumin infusion by focusing on its immunomodulatory properties. The hypothesis posits that the anti-inflammatory attributes of albumin replacement therapy in cirrhotic patients might be partially linked to alterations in 1, 25 (OH)₂ vitamin D levels, thereby influencing immune regulation.

Method: This prospective open-label study was conducted at the Liver Clinic of King Chulalongkorn Memorial Hospital, and targeted patients diagnosed with decompensated cirrhosis with ascites. Participants meeting inclusion criteria underwent high-dose albumin infusion therapy (80 grams of albumin). Primary objectives centered on evaluating changes in 1, 25 (OH)₂ vitamin D levels, and 25 (OH) vitamin D levels before and after albumin infusion over one week. Secondary outcomes involved assessing alterations in ten inflammatory cytokine levels pre- and post-albumin infusion.

Results: Interim analysis encompassed seventeen cases of decompensated cirrhosis with ascites. Alcohol-associated cirrhosis was the most prevalent cause (N=5), followed by NASH (N=4), chronic hepatitis B infection (N=3), cryptogenic (N=2), and other causes. Ten patients had Child Pugh scores B, while seven had Child-Pugh scores C, averaging a Child-Pugh score of 9 points. The average MELD-Na score was 15.7 ± 5.11 . Post-albumin infusion, 1, 25 (OH)₂ vitamin D levels significantly decreased over a week ($p = 0.011$), while 25 (OH) vitamin D levels slightly decreased ($p = 0.101$). Importantly, IL-1 beta, IL-6, TNF-alpha, and IFN-gamma levels significantly decreased post-intervention ($p = 0.043, 0.037, 0.005$, and 0.02 , respectively). However, no correlation was observed between changes in vitamin D levels and cytokine levels.

Conclusion: This study evidenced a significant reduction in 1, 25 (OH)₂ vitamin D and inflammatory cytokine levels following high-dose albumin infusion in decompensated cirrhosis patients. While the direct relationship remains unclear at this stage, these findings hint at a potential mechanism influencing the complex interplay between albumin therapy, vitamin D alterations, and immune modulation. Further comprehensive investigations are warranted to elucidate this intricate relationship.

WED-121-YI

Increased procoagulant activity of tissue factor-expressing microvesicles in patients with liver cirrhosis

Adonis Protopapas¹, Anna Takardaki², Nefeli Protopapa¹, Ioanna Papagiouvanni³, Andreas Protopapas¹, Lemonia Skoura^{2,2}, Christos Savopoulos¹, Ioannis Goulis³. ¹First Propaedeutic Department of Internal Medicine, Aristotle University of Thessaloniki, AHEPA University Hospital, Thessaloniki, Greece; ²Department of Microbiology, Aristotle University of Thessaloniki, AHEPA University Hospital, Thessaloniki, Greece; ³Fourth Internal Medicine Department, Aristotle University of Thessaloniki, Hippokraton General Hospital, Thessaloniki, Greece
Email: adoprot@hotmail.com

Background and aims: Cirrhosis is characterized by significant perturbations of the coagulation mechanism. Tissue factor (TF) is the main activator molecule of the coagulation cascade. The main mode of TF activation is through its expression by microvesicles, establishing them as an important research focus in multiple prothrombotic syndromes. Therefore, their study may provide valuable insights into the hypercoagulability of cirrhosis and possible mechanisms by which it contributes to disease progression. Our study aimed to assess TF levels and activity of TF-expressing microvesicles in the plasma of cirrhotic patients and correlate them with disease severity.

Method: Sixty-one cirrhotic patients [including 11 with hepatocellular carcinoma (HCC)] and 21 controls were prospectively enrolled in

the study. Exclusion criteria were history of cancer (except HCC), haematological diseases, thrombophilia, history of thrombosis, recent hospitalization, anticoagulant, antiplatelet or contraceptive drugs, ongoing infection or alcohol use and chronic kidney disease. In addition to workup for disease staging and exclusion criteria testing, plasma TF antigen concentration (Quantikine®ELISA) and TF-expressing plasma microvesicle activity (ZYMUPHEN MP-TF) were measured.

Results: 50% of the patients had decompensated cirrhosis (DeCi). The patients' Child-Pugh (CP) stage was A in 56%, B in 26% and C in 18% of cases, respectively. TF antigen concentration (TFa) was 71.2 [56.8–81.9], 59.7 [47.1–66.6] and 43.9 [29.4–47.9] pg/ml in the cirrhosis with HCC (group 1), cirrhosis without HCC (group 2) and control (group 3) groups, respectively. There was a statistically significant difference between groups 1 and 3 ($p < 0.001$) and groups 2 and 3 ($p < 0.001$), while group 1 had higher values than group 2 without statistical significance ($p = 0.133$). The activity of TF-expressing microvesicles (MV-TF) showed values of 4.03 [3.35–4.92], 3.22 [2.44–4.09] and 2.17 [1.49–3.05] pg/ml in groups 1, 2 and 3 respectively. There was a statistically significant difference between groups 1 and 3 ($p < 0.001$) and groups 2 and 3 ($p = 0.003$), while group 1 had higher values than group 2 without statistical significance ($p = 0.088$). There was a significant correlation of MV-TF but not TFa with DeCi ($p = 0.005$ and $p = 0.404$), with DeCi patients having higher MV-TF values. There was also a significant correlation with CP stage ($p = 0.011$ for MV-TF and $p = 0.037$ for TFa), with higher values reported in patients of higher CP stage.

Conclusion: Increased TFa and MV-TF values in cirrhotic patients highlight the prothrombotic dynamics of the disease, which increase with disease severity. The fact that all patients had stable disease indicates that these dynamics are intrinsic to cirrhosis and independent of acute complications. The next step is to investigate the association of these with disease progression and thrombotic complications.

WED-122-YI

The soluble guanylate cyclase pathway is dysregulated in rodent models of cirrhosis and portal hypertension

Thomas Sorz-Nechay^{1,2,3}, Ksenia Brusilovskaya^{1,3}, Philipp Königshofer^{1,3}, Benedikt Hofer^{1,3}, Oleksandr Petrenko^{1,2,3}, Benedikt Simbrunner^{1,2,3}, Vlad Taru^{1,3}, Kerstin Zinöber^{1,3}, Katharina Regnat^{1,3}, Katharina Bonitz^{1,2,3}, Henriette Horstmeier¹, Ines Trübenbach⁴, Peng Sun⁴, Stefan Günther Kauschke⁴, Larissa Pfisterer⁴, Michael Trauner¹, Philipp Schwabl^{1,2,3}, Thomas Reiberger^{1,2,3}. ¹Division of Gastroenterology and Hepatology, Department of Internal Medicine III, Medical University of Vienna, Vienna, Austria; ²Center for Molecular Medicine (CeMM) of the Austrian Academy of Sciences, Vienna, Austria; ³Christian Doppler Lab for Portal Hypertension and Liver Fibrosis, Medical University of Vienna, Vienna, Austria; ⁴Department of CardioMetabolic Diseases Research, Boehringer Ingelheim Pharma GmbH and Co.KG, Biberach an der Riss, Germany
Email: thomas.sorz-nechay@meduniwien.ac.at

Background and aims: Stimulation of the nitric oxide (NO)-soluble guanylate cyclase (sGC) pathway represents a promising approach for the treatment of liver disease. We investigated key molecular nodes of the NO-sGC pathway in different rodent models of liver fibrosis and portal hypertension (PH).

Method: 44 Sprague Dawley rats were used in four models of liver disease: 4 weeks (W) bile duct ligation (BDL, $n = 4$), W12 choline deficient high fat diet (CDHFD, $n = 6$), W12 carbon tetrachloride induced (CCl4, $n = 6$) and W12 thioacetamide induced (TAA, $n = 6$). Controls were: sham-operated (SHAM, $n = 4$), chow fed (CHOW, $n = 6$), olive oil (OO, $n = 6$) and sodium-chloride (NaCl, $n = 6$). Portal pressure (PP) measurement and livers were collected at the end of each timeline. Fibrosis was evaluated by collagen proportionate area (CPA). Gene expression and protein levels were assessed via RT-qPCR and Western-blot.

Results: All models developed liver fibrosis (CPA: BDL: $9.01 \pm 3.09\%$; CDHFD: $8.97 \pm 4.27\%$; CCl4: $4.86 \pm 1.54\%$; TAA: $8.67 \pm 1.84\%$) and PH (PP: BDL: 13.57 ± 2.85 mmHg; CDHFD: 11.30 ± 2.91 mmHg; CCl4: 9.03 ± 0.63 mmHg; TAA: 12.68 ± 2.94 mmHg). The BDL model showed potent upregulation of inducible nitric oxide synthetase (iNOS, 28.10 ± 11.95 -fold; $p = 0.029$) and downregulation of sGC beta2 (0.19 ± 0.07 -fold; $p = 0.029$). In the CDHFD model, the sGC alpha1 (1.75 ± 0.57 -fold, $p = 0.004$) and beta1 (2.04 ± 0.72 -fold, $p = 0.004$) subunits were upregulated; sGC beta1 was also upregulated in the CCl4 model (1.40 ± 0.17 -fold, $p = 0.030$). The TAA model also showed upregulation of sGC beta1 (1.64 ± 0.27 -fold, $p = 0.004$) and a down-regulation of sGC alpha2 (0.66 ± 0.09 -fold; $p = 0.026$) subunits. Protein kinase G1 (PKG1) was upregulated only in CDHFD (1.90 ± 0.62 -fold, $p = 0.002$) and TAA (1.90 ± 0.34 -fold, $p = 0.002$) models. In all models, we observed significant upregulation of phosphodiesterase (PDE) 5 (BDL: 5.72 ± 0.75 -fold; $p < 0.029$; CDHFD: 5.70 ± 2.22 -fold, $p = 0.004$; CCl4: 1.97 ± 0.33 -fold, $p = 0.002$; TAA: 5.56 ± 0.74 -fold, $p < 0.002$). Protein content of all three sGC subunits, PKG1 and PDE5 on Western-blot was concordant to the respective changes on the RNA level.

Conclusion: The NO-sGC pathway was dysregulated, albeit at different molecular nodes in all rat models of PH induced by distinct types of liver injury. These results underline the potential of sGC activators for the treatment of cirrhotic portal hypertension.

WED-123

Female mice with cirrhosis are more prone to acute and chronic effects of psilocybin exposure without tolerance compared to male mice

Jessica Maltman¹, Derrick Zhao¹, Alaina Jaster¹, Yunling Tai¹, Jing Zeng¹, Javier Maeso-Gonzalez¹, Huiping Zhou¹, Jasmohan Bajaj¹.
¹Virginia Commonwealth University, Richmond, United States
Email: jasmohan.bajaj@vcuhealth.org

Background and aims: Use of psychedelics such as psilocybin for treating psychiatric disorders including PTSD and recalcitrant depression is rising. Preclinical findings indicate sex differences in response to psychedelics. Cirrhosis often coexists in subjects using psychoactive substances, but the safety profile is unclear. Aim: Define the impact of sex and of concomitant cirrhosis on response to psilocybin in a mouse model.

Method: MDR2KO and wild type (WT) mice (both male and female, 8–10 mths old) were included; we ensured the MDR2KO mice had developed cirrhosis. The head-twitch response (HTR) is a rapid side-to-side rotational head movement used as a behavioral proxy of human psychedelic potential in rodents. Psilocybin or vehicle was administered i.p. dose of 1 mg/kg (5 µl/g) at days 1, 12 and 21. HTR was tested 60 min post injection at days 1 and 21. 3-way ANOVA (drug x genotype-sex) analyses for genotype, sex, and drug effects were performed along with separate sex-collapsed and genotype-collapsed analyses.

Results: We included 3–4 mice/subgroup (MDR2KO vs WT, males vs females). Day 1: After a single psilocybin dose, the acute HTR showed significant interactions between treatment, sex and genotype (MDR2KO vs WT); while psilocybin increased HTR across all groups, only MDR2KO females showed a significant HTR increase vs all vehicle/psilocybin-Rx groups. 3-way ANOVA revealed a significant effect of psilocybin ($p < 0.0001$), genotype ($p = 0.0237$), sex ($p = 0.0044$). Significant interactions were observed between all variables (psilocybin x Genotype $p = 0.03$, psilocybin x Sex $p = 0.015$, Genotype x Sex $p = 0.0414$, and psilocybin x Genotype x Sex $p = 0.02$). Day 21: After 3 psilocybin doses (days 1, 12 and 21), the HTR showed a significant effect of treatment, and only MDR2KO females displayed a significant effect of psilocybin vs all vehicle groups. On multiple comparisons, a significant difference between psilocybin-treated KO females vs vehicle groups (WT males $p = 0.016$, WT females $p = 0.019$, KO males $p = 0.021$, KO females $p = 0.022$) was seen. Combined day 1 +21 data: HTR showed several significant interactions, again showing

POSTER PRESENTATIONS

that psilocybin's impact is greater in MDR2KO females vs both vehicle- and psilocybin-treated groups. 3-way ANOVA showed significant effect of psilocybin ($p < 0.0001$), genotype ($p = 0.037$), sex ($p = 0.007$), and an interaction between psilocybin x genotype ($p = 0.008$) and psilocybin x genotype x sex ($p = 0.034$).

Conclusion: MDR2KO female mice with cirrhosis have an increased acute response to psilocybin in the head twitch assay, and do not develop a potential tolerance effect developed by other groups with repeated exposure to psilocybin. This suggests that females with cirrhosis may display differences in the establishment of tolerance to psilocybin and increased subjective effects from this psychedelic and should inform upcoming investigations into safe use of this drug in patients.

WED-124

Assessment of plasma VCAM-1 levels in pediatric portal hypertension and its relationship with disease severity

Tengfei Si¹, Huihong Yu², Bethany Tucker³, Fabiola Di Dato¹, Xiaohong Huang¹, Qing Shao¹, Bowen Gao¹, Xuan Luo¹, Eirini Kyrana³, Yun Ma¹, Tassos Grammatikopoulos⁴. ¹Institute of Liver Studies, King's College London, London, United Kingdom; ²Institute Of Liver Studies, King's College London, London, United Kingdom; ³King's College Hospital, King's College London, London, United Kingdom; ⁴King's College Hospital, Paediatric Liver Department, London, United Kingdom
Email: tengfei.si@kcl.ac.uk

Background and aims: Portal hypertension (PHT), often a consequence of chronic liver disease (CLD) or portal vein thrombosis (PVT), lacks specific inflammatory biomarkers for early detection and monitoring. This study explores the potential of plasma VCAM-1 as a biomarker in children with PHT.

Method: We analysed plasma samples from 55 children (33 males) with PHT and oesophageal varices, alongside 15 healthy, age-matched controls. The study involved investigation of various immune markers and collection of clinical data for correlation studies.

Results: In the PHT group, levels of soluble CD163 (sCD163) and vascular cell adhesion molecule-1 (VCAM-1) were significantly higher (633.5 ng/ml vs. 414.8 ng/ml, $p = 0.0028$; 861 ng/ml vs. 397.7 ng/ml, $p < 0.0001$, respectively) compared to controls. A positive correlation was noted between VCAM-1 and both sCD163 ($r = 0.5267$, $p = 0.0002$) and matrix metalloproteinase 7 (MMP7) ($r = 0.3374$, $p = 0.014$). VCAM-1 exhibited a high diagnostic accuracy for PHT (ROC curve area: 0.957), with an optimal cut-off of 549.1 ng/ml yielding a sensitivity of 93.3% and specificity of 91.1%. VCAM-1 levels were stable across different PHT subgroups but were lower in patients with a history of bleeding (816 ng/ml vs. 964 ng/ml, $p = 0.04$). A positive correlation was found between VCAM-1 levels and liver stiffness. Notably, treatment with non-selective beta blockers significantly reduced VCAM-1 levels (869.7 ng/ml to 651.9 ng/ml, $p < 0.0001$).

Conclusion: Plasma VCAM-1 levels are closely linked to the development and progression of PHT in children, offering high diagnostic accuracy. This suggests its potential as a reliable biomarker for the condition.

WED-125

Differential regulation of soluble guanylate cyclase signaling during liver fibrosis regression

Thomas Sorz-Nechay^{1,2,3}, Ksenia Brusilovskaya^{1,3}, Philipp Königshofer^{1,3}, Benedikt Hofer^{1,3}, Oleksandr Petrenko^{1,2,3}, Benedikt Simbrunner^{1,2,3}, Vlad Taru^{1,3}, Kerstin Zinöber^{1,3}, Katharina Regnat^{1,3}, Katharina Bonitz^{1,2,3}, Henriette Horstmeier¹, Ines Truebenbach⁴, Peng Sun⁴, Stefan Günther Kauschke⁴, Larissa Pfisterer⁴, Michael Trauner¹, Philipp Schwabl^{1,2,3}, Thomas Reiberger^{1,2,3}. ¹Division of Gastroenterology and Hepatology, Department of Internal Medicine III, Medical University of Vienna, Vienna, Austria; ²Center for Molecular Medicine (CeMM) of the Austrian Academy of Sciences, Vienna, Austria; ³Christian Doppler Lab for Portal Hypertension and Liver Fibrosis, Medical University of Vienna, Vienna,

Austria; ⁴Department of CardioMetabolic Diseases Research, Boehringer Ingelheim Pharma GmbH and Co.KG, Biberach an der Riss, Germany
Email: thomas.sorz-nechay@meduniwien.ac.at

Background and aims: Pharmacologic agonists of the nitric oxide (NO)-soluble guanylate cyclase (sGC) pathway exert antifibrotic effects when administered during ongoing liver disease. We aimed to investigate key molecular nodes of the hepatic NO-sGC pathway in mouse models of ongoing fibrogenesis and fibrosis regression.

Method: Male C57BL/6 mice were used for two models of liver fibrosis: carbon tetrachloride induced (CCl₄, oral gavage 3x/week for 12 weeks, $n = 8$) and thioacetamide induced (TAA, intraperitoneal injection 3x/week for 12 weeks, $n = 8$). The respective controls received olive oil (OO, $n = 5$) or sodium chloride (NaCl, $n = 8$). Both models included additional groups with 1 or 2 week (s) of regression ($n = 7$ for CCl₄-R1 and R2, $n = 8$ for TAA-R1 and R2), when no toxic agent was administered. Portal pressure (PP) measurement and sample collection occurred at the end of each timeline. Collagen-proportionate area (CPA) was measured via histomorphometry of digitized picrosirius-red stained liver sections. Gene expression was assessed via RT-qPCR and expressed as fold-change to healthy controls. Liver cGMP content was determined by LC/MS.

Results: Both models developed fibrosis and increased PP which decreased during regression: CCl₄: CPA: $16.91 \pm 3.64\%$ vs R1 $10.93 \pm 2.83\%$ vs R2 $5.43 \pm 1.33\%$, $p < 0.001$; PP: 9.98 ± 1.09 mmHg vs R1 8.35 ± 0.73 mmHg vs R2 7.89 ± 1.07 mmHg, $p < 0.001$; TAA: CPA: $3.87 \pm 0.34\%$ vs R1 $3.49 \pm 0.59\%$ vs R2 $2.90 \pm 0.28\%$, $p < 0.001$; PP: 7.71 ± 0.53 mmHg vs R1 7.28 ± 0.44 mmHg vs R2 6.04 ± 0.48 mmHg, $p < 0.001$. In the CCl₄ model, we found transcriptional changes mostly at R2 with increased expression of inducible nitric oxide synthase (4.80 ± 2.28 -fold vs CCl₄ 2.23 ± 1.89 -fold, $p = 0.108$), sGC $\alpha 1$ (3.15 ± 0.74 -fold vs CCl₄ 1.80 ± 1.13 -fold, $p = 0.054$), sGC $\alpha 2$ (1.98 ± 0.18 -fold vs CCl₄ 0.64 ± 0.44 -fold, $p = 0.001$), phosphodiesterase (PDE) 5 (2.50 ± 0.72 -fold vs CCl₄ 1.23 ± 0.78 -fold; $p = 0.020$) and PDE9 (0.82 ± 0.15 -fold vs CCl₄ 0.14 ± 0.08 -fold; $p = 0.001$). In the TAA model transcriptional changes occurred already at R1 with increases in sGC $\alpha 2$ (1.30 ± 0.13 -fold vs TAA 0.65 ± 0.07 -fold, $p < 0.001$), sGC $\beta 1$ (2.04 ± 0.35 -fold vs TAA 1.36 ± 0.12 -fold, $p = 0.018$), and PDE9 (0.72 ± 0.15 -fold vs TAA 0.11 ± 0.02 -fold, $p = 0.007$). Hepatic cGMP levels were decreased in diseased livers vs healthy controls (CCl₄: 3.86 ± 0.63 nM vs. OO 4.13 ± 0.37 nM, $p = 0.985$; TAA 2.96 ± 0.73 vs NaCl 5.23 ± 0.90 nM, $p = 0.001$) and recovered with liver disease regression: CCl₄-R1 (6.28 ± 1.46 nM; $p = 0.030$) and R2 (5.49 ± 2.41 nM; $p = 0.162$); TAA-R1 (5.22 ± 1.26 nM, $p = 0.001$) and R2 (6.68 ± 1.04 nM, $p < 0.001$).

Conclusion: The NO-sGC-cGMP pathway is dysfunctional in CCl₄/TAA mouse models with dysregulated sGC subunits and decreased hepatic cGMP bioavailability. With liver disease regression, hepatic cGMP levels recover spontaneously. Future studies should evaluate if pharmacological sGC activation can promote fibrosis regression.

WED-126

Biglycan as a biomarker in acute-on-chronic liver failure (ACLF)

Martin Schulz^{1,2,3}, Esther Roth³, Jinyang Zeng-Brouwers³, Konrad Buscher¹, Robert Schierwagen¹, Maximilian Joseph Brol¹, Frank Erhard Uschner¹, Sabine Klein¹, Stefan Zeuzem², Kai-Henrik Peiffer¹, Jonel Trebicka^{1,4}, Liliana Schaefer³. ¹University Hospital Münster, Münster, Germany; ²University Hospital Frankfurt, Frankfurt am Main, Germany; ³Institute of Pharmacology and Toxicology, Frankfurt, Germany; ⁴European Foundation for Study of Chronic Liver Failure, Barcelona, Spain
Email: martinsebastian.schulz@ukmuenster.de

Background and aims: Acute-on-chronic liver failure (ACLF) is characterized by systemic inflammation (SI), development of organ failures and a high short-term mortality in patients with liver cirrhosis. Recently, danger-associated molecular pattern (DAMPs) have received an increased focus as endogenous triggers of SI. Biglycan is a proteoglycan of the extracellular matrix (ECM), which is

released into the blood as a response to tissue injury. Soluble biglycan can trigger distinct pro-inflammatory pathways by direct toll-like receptor 2 (TLR2) and TLR4 interaction. However, its role in ACLF remains uncharted.

Method: In this observational study we collected plasma samples from patients with compensated cirrhosis (CC, n=10), acute decompensation (AD, n=10) and ACLF (n=10). ACLF was defined according to EASL-CLIF definition. Samples were centrifuged (2,000 rpm, 10 min), biglycan was extracted, semipurified and analysed by western blot. Pro-inflammatory cytokines were measured by a human-specific ELISA assays.

Results: Median age of CC patients was 66 years (IQR 58–70), while AD and ACLF patients were younger (57 years, n.s.) and predominantly male (70%). Median MELD was 6 (IQR 6–15) in CC patients, 17 (IQR 11–19) in AD and 36 (IQR 30–40) in ACLF. 28-day mortality was 0% in CC patients, 12.5% in AD and 30% in ACLF ($p < 0.001$). In AD patients, plasma levels of soluble biglycan were 2.6-fold higher compared to CC, while ACLF patients showed an even steeper increase by 7.5-fold ($p < 0.001$). Compared to AD, ACLF biglycan levels were also significantly elevated (2.9-fold, $p < 0.01$). Moreover, soluble biglycan was strongly correlated with severity of liver disease (MELD, $r = 0.88$, $p < 0.0001$) and ACLF grade ($r = 0.86$, $p < 0.001$). It also showed significant correlations with markers of systemic inflammation, such as IL-8 ($r = 0.663$, $p < 0.001$) and IL-6 ($r = 0.587$, $p < 0.001$). In ACLF patients, soluble biglycan was the strongest predictor for short-term mortality (AUC 0.91), higher than IL-6 (AUC 0.81) or MELD score (AUC 0.67).

Conclusion: Our data show that soluble biglycan could constitute a novel biomarker in ACLF. As a biomarker, biglycan could synthesize distinctive characteristics of hepatic fibrosis and the inflammatory liver microenvironment, since it can be released from the cirrhotic liver upon tissue injury. Moreover, in its role as a canonical ECM-derived DAMP, increased levels of soluble biglycan could then possibly trigger and perpetuate SI upon ACLF progression. However, further studies are necessary to elucidate the mechanistical role of biglycan in ACLF and its utility as a biomarker.

Cirrhosis and its complications – Other clinical complications except ACLF and critical illness

TOP-062

Global epidemiology of acute kidney injury in hospitalized patients with cirrhosis: the ICA-GLOBAL AKI study

Kavish Patidar^{1,2}, Ann Thu Ma³, Adrià Juanola⁴, Anna Barone⁵, Simone Incicco⁵, Anand Kulkarni⁶, José Luis Pérez-Hernández⁷, Brian Wentworth⁸, Sumeet Asrani⁹, Carlo Alessandria¹⁰, Nadia Abdelaaty Abdelkader¹¹, Yu Jun Wong^{12,13}, Qing Xie¹⁴, Nikolaos T. Pyrsopoulos¹⁵, Sung-Eun Kim¹⁶, Yasser Fouad¹⁷, Aldo Torre¹⁸, Eira Cerda Reyes¹⁹, Javier Diaz-Ferrer²⁰, Rakhi Maiwall²¹, Douglas Simonetto²², Maria Papp²³, Eric Orman²⁴, Giovanni Perricone²⁵, Cristina Solé²⁶, Christian M. Lange²⁷, Alberto Farias²⁸, Gustavo Pereira²⁹, Adrian Gadano³⁰, Paolo Caraceni^{31,32}, Thierry Thévenot³³, Nipun Verma³⁴, Jeong Han Kim³⁵, Julio D. Vorobioff³⁶, Jacqueline Cordova-Gallardo³⁷, Vladimir Ivashkin³⁸, Juan Pablo Roblero³⁹, Rael Maan⁴⁰, Claudio Toledo⁴¹, Oliviero Riggio⁴², Eduardo Fassio⁴³, Mónica Marino⁴⁴, Puria Nabilou⁴⁵, Victor Vargas⁴⁶, Manuela Merli⁴⁷, Luciana Lofego Goncalves⁴⁸, Liane Rabinowich^{49,50}, Aleksander Krag^{51,52}, Lorenz Balcar⁵³, Pedro Montes⁵⁴, Angelo Z. Mattos⁵⁵, Tony Bruns⁵⁶, Abdulsemed Mohammed Nur⁵⁷, Wim Laleman⁵⁸, Enrique Carrera Estupiñan⁵⁹, Maria Cecilia Cabrera⁶⁰, Marcos Giralá⁶¹, Hrishikesh Samant⁶², Sarah Raevens⁶³, Joao Madaleno⁶⁴, W. Ray Kim⁶⁵, Juan Pablo Arab⁶⁶, José Presa⁶⁷, Carlos Noronha Ferreira⁶⁸, Antonio Galante⁶⁹,

Andrew S. Allegretti⁷⁰, R. Bart Takkenberg⁷¹, Murat Harputluoglu⁷², Sebastián Marciano⁷³, Shiv Kumar Sarin²¹, Pere Ginès⁴, François Durand⁷⁴, Paolo Angeli⁵, Elsa Solà⁶⁵, Salvatore Piano⁵. ¹Baylor College of Medicine, Houston, TX, United States; ²Michael E. DeBakey Veterans Affairs Medical Center, Houston, TX, United States; ³Toronto Centre for Liver Disease, University Health Network, Toronto, Canada; ⁴Hospital Clinic de Barcelona, Barcelona, Spain; ⁵University of Padova, Padova, Italy; ⁶Asian institute of gastroenterology hospital, Hyderabad, India; ⁷Hospital General de México "Dr. Eduardo Liceaga", Ciudad de México, Mexico; ⁸University of Virginia, Charlottesville, United States; ⁹Baylor University Medical Center, Dallas, United States; ¹⁰University of Turin, Turin, Italy; ¹¹Ain Shams University, Cairo, Egypt; ¹²Changi General Hospital, Singapore, Singapore; ¹³Duke-NUS Medical School, Singapore, Singapore; ¹⁴Shanghai Jiao Tong University School of Medicine, Shanghai, China; ¹⁵Rutgers New Jersey Medical School, Newark, United States; ¹⁶Hallym University Sacred Heart Hospital, Anyang, Korea, Rep. of South; ¹⁷Minia University, Minia, Egypt; ¹⁸Medical Center Abc, Mexico City, Mexico; ¹⁹Military Hospital, Ciudad de México, Mexico; ²⁰Hospital Edgardo Rebagliati-Clínica Internacional, Lima, Peru; ²¹Institute of Liver and Biliary Sciences, New Delhi, India; ²²Mayo Clinic, Rochester, United States; ²³University of Debrecen, Debrecen, Hungary; ²⁴Indiana University School of Medicine, Indianapolis, United States; ²⁵ASST Grande Ospedale Metropolitano Niguarda, Milan, Italy; ²⁶Parc Tauli Hospital Universitari, Barcelona, Spain; ²⁷LMU University Hospital Munich, Munich, Germany; ²⁸University of Sao Paulo, São Paulo, Brazil; ²⁹Bonsucesso Federal Hospital, Rio de Janeiro, Brazil; ³⁰Hospital Italiano de Buenos Aires, Buenos Aires, Argentina; ³¹University of Bologna, Bologna, Italy; ³²IRCSS Azienda Ospedaliero-Universitaria di Bologna, Bologna, Italy; ³³CHRU de Besançon, Besançon, France; ³⁴Postgraduate Institute of Medical Education and Research, Chandigarh, India; ³⁵Konkuk University School of Medicine, Seoul, Korea, Rep. of South; ³⁶University of Rosario Medical School, Rosario, Argentina; ³⁷Hospital General Dr Manuel Gea Gonzalez, Tlalpan, Mexico; ³⁸Sechenov First Moscow State Medical University, Moscow, Russian Federation; ³⁹Hospital Clínico Universidad de Chile, Santiago, Chile; ⁴⁰Erasmus University Medical Center, Rotterdam, Netherlands; ⁴¹Universidad Austral de Chile, Valdivia, Chile; ⁴²La Sapienza, University of Rome, Rome, Italy; ⁴³Hospital Nacional Prof. Alejandro Posadas, El Palomar, Buenos Aires, Argentina; ⁴⁴Carlos Bonorino Udaondo Hospital, Buenos Aires, Argentina; ⁴⁵Copenhagen University Hospital Hvidovre, Hvidovre, Denmark; ⁴⁶Hospital Vall d'Hebron, Barcelona, Spain; ⁴⁷Università degli Studi di Roma Sapienza, Roma, Italy; ⁴⁸University Hospital-Federal University of Espirito Santo, Vitória, Brazil; ⁴⁹Tel Aviv Sourasky Medical Center, Tel Aviv, Israel; ⁵⁰Tel Aviv University, Tel Aviv, Israel; ⁵¹Institute of Clinical Research, University of Southern Denmark, Odense, Denmark; ⁵²Department of Gastroenterology and Hepatology, Odense University Hospital, Odense, Denmark; ⁵³Medical University of Vienna, Vienna, Austria; ⁵⁴Hospital Nacional Daniel A. Carrion, Bellavista, Peru; ⁵⁵Federal University of Health Sciences of Porto Alegre, Porto Alegre, Brazil; ⁵⁶University Hospital RWTH Aachen, Aachen, Germany; ⁵⁷Addis Ababa University, Addis Ababa, Ethiopia; ⁵⁸University Hospitals Leuven, Leuven, Belgium; ⁵⁹Hospital Eugenio Espejo, Quito, Ecuador; ⁶⁰Guillermo Almenara Hospital, Lima, Peru; ⁶¹Universidad Nacional de Asunción, Asunción, Paraguay; ⁶²Ochsner Transplant Center, New Orleans, United States; ⁶³Ghent University Hospital, Ghent, Belgium; ⁶⁴Centro Hospitalar e Universitário de Coimbra, Coimbra, Portugal; ⁶⁵Stanford University School of Medicine, Stanford, United States; ⁶⁶Pontificia Universidad Católica de Chile, Santiago de Chile, Chile; ⁶⁷Centro Hospitalar de Trás-os-Montes e Alto Douro, Vila Real, Portugal; ⁶⁸Hospital de Santa Maria-Centro Hospitalar Universitário Lisboa Norte, Lisboa, Portugal; ⁶⁹Ente Ospedaliero Cantonale and Università della Svizzera Italiana, Lugano, Switzerland; ⁷⁰Massachusetts General Hospital, Boston, United States; ⁷¹Amsterdam University Medical Centers, Amsterdam, Netherlands; ⁷²Inönü University School of Medicine, Elazığ, Turkey; ⁷³Hospital Italiano de Buenos Aires, Buenos Aires, Argentina; ⁷⁴Beaujon Hospital, Clichy, France

Email: salvatore.piano@unipd.it

POSTER PRESENTATIONS

Background and aims: Acute kidney injury (AKI) is a serious complication of cirrhosis. Little is known about the epidemiology of AKI in different regions in the world. We performed a multicenter prospective intercontinental study to assess the global differences in the characteristics, management and outcomes of AKI in hospitalized patients with cirrhosis.

Method: Patients admitted to the hospital for decompensated cirrhosis were enrolled from July 2022 to May 2023 at 67 centers in 5 continents (Africa, Asia, Europe, North America and South America). We captured demographics, AKI precipitants, stage and phenotypes [hypovolemic, hepatorenal syndrome (HRS-AKI), acute tubular necrosis (ATN), and others] and details on AKI management and clinical course. Data on AKI resolution and 28-day mortality were collected. AKI characteristics, management and outcomes were compared among the five regions, utilizing multivariable models to assess the independent association between regions and outcomes.

Results: Among 3,792 enrolled patients, 1,456 (36%) developed AKI, of which the majority were community-acquired (71%). The most common precipitant for AKI was volume loss (47%), followed by infections (42%). Peak AKI stage was highest in North America and lowest in Europe ($p < 0.001$). Significant differences in the management of AKI (use of albumin, crystalloids, diuretics and vasoconstrictors) were found between regions. Overall, hypovolemic AKI was the most common phenotype (58%). The prevalence of HRS-AKI was similar among regions (ranging from 14% to 20%; $p = 0.275$), while ATN was more frequent in Asia and North America (25% and 17%, respectively; $p < 0.001$ vs other regions). AKI outcomes also differed significantly between regions. Non-resolution rates were highest in North America and lowest in Europe (51% vs 32%; $p < 0.001$). On multivariable analysis (adjusted for age, sex, etiology of cirrhosis, ascites, hepatic encephalopathy, MAP, ACLF grade, AKI stage and phenotype), patients admitted in North America and Asia had higher risk of AKI non-resolution [odds ratio 2.42 ($p < 0.001$) and 2.14 ($p < 0.001$), respectively]. Overall, 23% of patients died at 28 days. On multivariable analysis, patients admitted in Asia and North America had an increased risk for 28-day mortality [subdistribution-hazard ratio 1.85 ($p = 0.002$) and 1.73 ($p < 0.001$), respectively].

Conclusion: This global study found important regional differences in AKI severity, phenotype, management and outcomes. In particular, the differences identified in AKI resolution and mortality rates across regions should be further explored and drive the implementation of strategies to improve kidney- and patient-related outcomes.

TOP-063

The efficacy of Glucagon-like Peptide-1 receptor agonists in patients with compensated cirrhosis and obesity

Wee Han Ng¹, Yee Hui Yeo², Amit Singal³, Neehar D. Parikh⁴, Alexander Kuo², Hyunseok Kim², Yun Wang², Hirsch Trivedi², Nicole Rich⁵, Jamil Samaan², Walid S Ayoub⁶, Kevin Ma⁷, Ju Dong Yang². ¹Bristol Medical School, Bristol, United Kingdom; ²Karsh Division of Gastroenterology and Hepatology, Cedars-Sinai Medical Center, Los Angeles, United States; ³UT Southwestern Medical Center, Dallas, Texas, United States; ⁴University of Michigan Medical School, Ann Arbor, United States; ⁵UT Southwestern Medical Center, Dallas, United States; ⁶Karsh Division of Gastroenterology and Hepatology, Cedars-Sinai Medical Center, Bristol, United States; ⁷Department of Epidemiology, Harvard T. H. Chan School of Public Health, Boston, United States
Email: qx21999@bristol.ac.uk

Background and aims: Glucagon-like Peptide-1 receptor agonists (GLP-1RAs) are effective treatment for type 2 diabetes mellitus (T2DM) and obesity. Herein, we aimed to investigate the association between the use of GLP-1RAs and overall survival, hepatocellular carcinoma (HCC), and hepatic decompensation in patients with compensated cirrhosis and obesity.

Method: We conducted a retrospective cohort study using a multi-center nationwide database (TriNetX). We compared patients with

obesity (body mass index (BMI) ≥ 35 kg/m²) and compensated cirrhosis who started GLP-1RA after the diagnosis of cirrhosis vs. never received any GLP-1RA between 28 April 2005 (date of FDA approval of exenatide) and 31 October 2022 using propensity score matching (based on age, sex, race, diabetes status, BMI, cardiovascular risk factors, chronic kidney disease, AST, ALT, INR, albumin, bilirubin, creatinine, cirrhosis etiology, diabetic, hypertensive, antiviral drugs for hepatitis B and C infections, lipid-lowering agents including statins, and aspirin). The primary end point was overall survival, and secondary end points were HCC and hepatic decompensation events.

Results: Of 27497 obese patients with compensated cirrhosis, 1699 were GLP-1RA users and 25797 non-users. After propensity score matching, 1498 users and 1496 non-users were included. The two arms were well-balanced in all examined demographic and clinical characteristics. GLP-1 RA user non-user groups had a mean (SD) age of 56.1 (12.1) vs 56.2 (13.2); 68.7% vs. 70.7% were White, and 42.0% vs. 40.6% were males, respectively. At 10-year follow-up, GLP-1 RA use was associated with significantly lower all-cause mortality (Hazard ratio (HR) 0.56, 95%CI 0.45–0.68). Compared to short duration GLP-1 RA use (1–3 refills), both medium (3–6 refills) and long (>7 refills) durations were associated with lower all-cause mortality (medium: HR 0.58, 05% CI 0.37–0.93) (long: HR 0.43, 95% CI: 0.25–0.73). GLP-1 RA use was associated with significantly lower risk of decompensated cirrhosis (HR 0.52, 95%CI 0.38–0.72), including a lower risk of hepatic encephalopathy (HR 0.50, 95%CI 0.35–0.72) and ascites (HR 0.57, 95% CI 0.33–0.99). GLP-1 RA use was also associated with a lower risk of developing HCC (HR 0.41, 95%CI 0.19–0.88). As a negative control, GLP-1 RA use was not associated with lower risk of overall cancer (HR 0.71, 95%CI 0.49–1.03) or lung cancer (HR 0.86, 95%CI 0.31–2.4).

Conclusion: GLP-1RA use is associated with a lower risk of overall mortality, HCC development, and hepatic decompensation in patients with obesity and compensated cirrhosis. Future trials investigating the safety and efficacy of GLP-1RA in patients with compensated cirrhosis and obesity are needed.

TOP-064-YI

Impact of bacterial infections on kidney function and survival in patients with decompensated cirrhosis and acute kidney injury worldwide-analysis of the ICA-GLOBAL AKI study

Adrià Juanola¹, Kavish Patidar^{2,3}, Ann Thu Ma⁴, Anna Barone⁵, Simone Incicco⁵, Anand Kulkarni⁶, José Luis Pérez-Hernández⁷, Brian Wentworth⁸, Sumeet Asrani⁹, Carlo Alessandria¹⁰, Nadia Abdelaaty Abdelkader¹¹, Yu Jun Wong^{12,13}, Qing Xie¹⁴, Nikolaos T. Pyrsopoulos¹⁵, Sung-Eun Kim¹⁶, Yasser Fouad¹⁷, Aldo Torre¹⁸, Eira Cerdá Reyes¹⁹, Javier Díaz-Ferrer²⁰, Rakhi Maiwall²¹, Douglas Simonetto²², Maria Papp²³, Eric Orman²⁴, Giovanni Perricone²⁵, Cristina Solé²⁶, Christian M. Lange²⁷, Alberto Farias²⁸, Gustavo Pereira²⁹, Adrian Gadano³⁰, Paolo Caraceni^{31,32}, Delphine Weil-Verhoeven³³, Nipun Verma³⁴, Jeong Han Kim³⁵, Julio D. Vorobioff³⁶, Jacqueline Cordova-Gallardo³⁷, Vladimir Ivashkin³⁸, Juan Pablo Roblero³⁹, Rael Maan⁴⁰, Claudio Toledo⁴¹, Oliviero Riggio⁴², Eduardo Fassio⁴³, Mónica Marino⁴⁴, Puria Nabilou⁴⁵, Victor Vargas⁴⁶, Manuela Merli⁴⁷, Luciana Lofego Gonçalves⁴⁸, Liane Rabinowich^{49,50}, Aleksander Krag^{51,52}, Lorenz Balcar⁵³, Pedro Montes⁵⁴, Angelo Z. Mattos⁵⁵, Tony Bruns⁵⁶, Abdulsemmed Mohammed Nur⁵⁷, Wim Laleman⁵⁸, Enrique Carrera Estupiñán⁵⁹, Maria Cecilia Cabrera⁶⁰, Marcos Giralá⁶¹, Hrishikesh Samant⁶², Sarah Raevens⁶³, Joao Madaleno⁶⁴, W. Ray Kim⁶⁵, Juan Pablo Arab⁶⁶, José Presa⁶⁷, Carlos Noronha Ferreira⁶⁸, Antonio Galante⁶⁹, Claire Francoz⁷⁰, Andrew S. Allegretti⁷¹, R. Bart Takkenberg⁷², Murat Harputluoglu⁷³, Sebastián Marciano⁷⁴, Shiv Kumar Sarin²¹, Pere Ginès¹, Paolo Angeli⁵, Elsa Solà⁶⁵, Salvatore Piano⁵. ¹Hospital Clinic de Barcelona, Barcelona, Spain; ²Baylor College of Medicine, Houston, United States; ³Michael E. DeBakey Veterans Affairs Medical Center, Houston, United States; ⁴University Health Network, Toronto, Canada; ⁵University of Padova, Padova, Italy; ⁶Asian institute of

gastroenterology hospital, Hyderabad, India; ⁷Hospital General de México "Dr. Eduardo Liceaga", Ciudad de México, Mexico; ⁸University of Virginia, Charlottesville, United States; ⁹Baylor University Medical Center, Dallas, United States; ¹⁰A.O.U. Città della Salute e della Scienza di Torino, University of Turin, Turin, Italy; ¹¹Ain Shams University, Cairo, Egypt; ¹²Changi General Hospital, Singapore, Singapore; ¹³Duke-NUS Medical School, Singapore, Singapore; ¹⁴Ruijin Hospital, Shanghai, China; ¹⁵Rutgers-New Jersey Medical School, Newark, United States; ¹⁶Hallym University Sacred Heart Hospital, Hallym University College of Medicine, Anyang, Korea, Rep. of South; ¹⁷Minia University, Minia, Egypt; ¹⁸Medical Center ABC, Mexico City, Mexico; ¹⁹Military Hospital, Ciudad de México, Mexico; ²⁰Hospital Edgardo Rebagliati-Clínica Internacional, Lima, Peru; ²¹Institute of Liver and Biliary Sciences, New Delhi, India; ²²Mayo Clinic, Rochester, United States; ²³University of Debrecen, Debrecen, Hungary; ²⁴Indiana University School of Medicine, Indianapolis, United States; ²⁵ASST Grande Ospedale Metropolitano Niguarda, Milan, Italy; ²⁶Parc Taulí Hospital Universitari, Barcelona, Spain; ²⁷LMU University Hospital Munich, Munich, Germany; ²⁸University of São Paulo, São Paulo, Brazil; ²⁹Bonsucesso Federal Hospital, Rio de Janeiro, Brazil; ³⁰Hospital Italiano de Buenos Aires, Buenos Aires, Argentina; ³¹University of Bologna, Bologna, Italy; ³²IRCSS Azienda Ospedaliero-Universitaria di Bologna, Bologna, Italy; ³³CHRU de Besançon, Besançon, France; ³⁴Postgraduate Institute of Medical Education and Research, Chandigarh, India; ³⁵Konkuk University School of Medicine, Seoul, Korea, Rep. of South; ³⁶University of Rosario Medical School, Rosario, Argentina; ³⁷Hospital General Dr Manuel Gea Gonzalez, Tlalpan, Mexico; ³⁸Sechenov First Moscow State Medical University, Moscow, Russian Federation; ³⁹Hospital Clínico Universidad de Chile, Hospital Clínico Universidad de Chile, Chile; ⁴⁰Erasmus University Medical Center, Rotterdam, Netherlands; ⁴¹Universidad Austral de Chile, Valdivia, Chile; ⁴²La Sapienza, University of Rome, Rome, Italy; ⁴³Hospital Nacional Prof. Alejandro Posadas, El Palomar, Buenos Aires, Argentina; ⁴⁴Carlos Bonorino Udaondo Hospital, Buenos Aires, Argentina; ⁴⁵Copenhagen University Hospital Hvidovre, Hvidovre, Denmark; ⁴⁶Hospital Vall d'Hebron, Barcelona, Spain; ⁴⁷Università degli Studi di Roma Sapienza, Roma, Italy; ⁴⁸University Hospital-Federal University of Espirito Santo, Vitória, Brazil; ⁴⁹Tel Aviv Sourasky Medical Center, Tel Aviv, Israel; ⁵⁰Tel Aviv University, Tel Aviv, Israel; ⁵¹Centre for Liver Research, Odense, Denmark; ⁵²Institute of Clinical Research, University of Southern Denmark, Odense, Denmark; ⁵³Medical University of Vienna, Vienna, Austria; ⁵⁴Hospital Nacional Daniel A. Carrion, Bellavista, Peru; ⁵⁵Federal University of Health Sciences of Porto Alegre, Porto Alegre, Brazil; ⁵⁶University Hospital RWTH Aachen, Aachen, Germany; ⁵⁷Addis Ababa University, Addis Ababa, Ethiopia; ⁵⁸University Hospitals Leuven, Leuven, Belgium; ⁵⁹Hospital Eugenio Espejo, Quito, Ecuador; ⁶⁰Guillermo Almenara Hospital, Lima, Peru; ⁶¹Universidad Nacional de Asunción, Asunción, Paraguay; ⁶²Ochsner Transplant Center, New Orleans, United States; ⁶³Ghent University Hospital, Ghent, Belgium; ⁶⁴Centro Hospitalar e Universitário de Coimbra, Coimbra, Portugal; ⁶⁵Stanford University School of Medicine, Stanford, United States; ⁶⁶Pontificia Universidad Católica de Chile, Santiago de Chile, Chile; ⁶⁷Centro Hospitalar de Trás-os-Montes e Alto Douro, Vila Real, Portugal; ⁶⁸Hospital de Santa Maria-Centro Hospitalar Universitário Lisboa Norte, Lisboa, Portugal; ⁶⁹Ente Ospedaliero Cantonale and Università della Svizzera Italiana, Lugano, Switzerland; ⁷⁰Beaujon Hospital, Clichy, France; ⁷¹Massachusetts General Hospital, Boston, United States; ⁷²Amsterdam University Medical Centers, Amsterdam, Netherlands; ⁷³Inönü University School of Medicine, Elazığ, Turkey; ⁷⁴Hospital Italiano de Buenos Aires, Buenos Aires, Argentina Email: salvatore.piano@unipd.it

Background and aims: Acute kidney injury (AKI) is a common complication in patients with decompensated cirrhosis. Bacterial infection (BI) is a frequent precipitating factor for AKI. However, it is unknown whether BI-related AKI has different characteristics and outcomes than AKI not precipitated by BI.

Method: We performed a multicenter, prospective, intercontinental study to investigate global differences in the characteristics,

management and outcomes of AKI in patients with cirrhosis. Patients admitted to the hospital for decompensated cirrhosis were included at 67 hospitals in 5 continents, between July 2022 and May 2023. Demographical data, AKI precipitants, phenotypes and treatment were collected. Patients were followed until 90 days, death, or liver transplantation. AKI characteristics and outcomes were compared between patients with BI-related AKI and those in whom AKI precipitant was other than BI. In this analysis, competing-risk multivariable models were used to determine the independent association of BI-related AKI with 28-day mortality.

Results: Among 3,792 enrolled patients, 1,456 patients (36%) had AKI and BI was the second most common AKI precipitant after volume loss/hypovolemia. BI was identified as the precipitant of AKI in 598 patients (41%), with urinary tract infection, spontaneous bacterial peritonitis (SBP), and pneumonia as the most common types of infection (28%, 26% and 25%, respectively). Patients with BI-related AKI had worse kidney and liver function at the time of AKI diagnosis, as shown by higher AKI stage (peak AKI stage 2/3 70% vs 55%; $p < 0.001$), higher MELD score (25 vs 22; $p < 0.001$) and higher prevalence of acute-on-chronic liver failure (ACLF, 64 vs 56%; $p = 0.003$). In addition, those with BI-related AKI had increased signs of systemic inflammation, with higher C-reactive protein (6.0 vs 2.4, $p < 0.001$) and white blood cell (WBC) count (10.7 vs 7.5, $p < 0.001$). The prevalence of acute tubular necrosis (ATN) was significantly higher in patients with BI-related AKI than in those with AKI not triggered by BI (22% vs 10%, $p < 0.001$) while no difference was found in the prevalence of hepatorenal syndrome-AKI. Complete AKI resolution was significantly lower in BI-related AKI (55% vs 62%; $p = 0.004$). Mortality rates at 28 days were higher in patients with BI-related AKI than in those with non BI-related AKI (31% vs 17%, $p < 0.001$). In multivariable analysis (adjusted for age, sex, etiology of cirrhosis, ascites, hepatic encephalopathy, MAP, WBC, ACLF grade, and AKI stage) BI-related-AKI was associated with higher risk of 28-day mortality (sHR 1.35; $p = 0.013$). Among infections, pneumonia and SBP were associated with the highest risk of mortality.

Conclusion: Bacterial infection-related AKI is common and associated with worse kidney function, ATN, ACLF and worse survival. Preventive strategies to avoid BI may be helpful in improving AKI outcomes.

TOP-065

Outcomes of thromboelastography guided versus routine empirical or on-demand platelet transfusion in patients with liver cirrhosis and severe thrombocytopenia undergoing high-risk invasive percutaneous and vascular procedures: an open-label, randomized controlled trial

Sagnik Biswas¹, Shekhar Swaroop¹, Arnab Aggarwal¹, Tushar Sehgal², Manas Vaishnav¹, Ayush Agarwal¹, Abhinav Anand¹, Piyush Pathak¹, Shubham Mehta¹, Anshuman Elhence¹, Soumya Jagannath Mahapatra¹, Deepak Gunjan¹, Shivanand Gamangatti¹, Shalimar Shalimar¹. ¹All India Institute of Medical Sciences, New Delhi, New Delhi, India; ²All India Institute of Medical Sciences, New Delhi, India Email: sagnik_biswas@yahoo.co.in

Background and aims: There is a lack of consensus regarding periprocedural platelet transfusions in patients with liver cirrhosis and severe thrombocytopenia (platelet counts less than 50,000/mm³) undergoing high risk invasive procedures. We aimed to compare the utility of thromboelastography (TEG) guided platelet transfusion to routine empirical or on-demand transfusions in this patient group in avoiding unnecessary platelet transfusions and for outcomes in terms of post-procedural bleeding.

Method: Patients with liver cirrhosis and severe thrombocytopenia undergoing high-risk invasive procedures were randomized into three groups- Group 1: Transfusion based on deranged TEG parameters, group 2: routine empirical platelet transfusion, group 3: on-demand transfusions (platelets or packed red cells) based on

POSTER PRESENTATIONS

the procedural complications. All patients underwent thromboelastography pre-procedurally. In group 1, patients with maximum amplitude <32 mm were transfused 3 units of random donor platelets (RDP) pre-procedure, while in group 2, all patients received 3 units of RDP routinely pre-procedure. In group 3, patients did not receive any pre-procedure transfusions and were transfused blood products if they developed post-procedure bleeding. No correction was done for deranged INR. Primary outcome was assessment of periprocedural platelets transfused in each randomized arm.

Results: Eighty-seven patients were randomized (29 in each group). There were no differences in baseline demographics, hemostatic profile, and types of procedures between the three groups. The median platelet count was 33 (26–43) $\times 10^3/\text{mm}^3$. The most commonly performed procedure was percutaneous liver biopsy (46) followed by transjugular intrahepatic portosystemic shunt (13). Median MELD scores in groups 1, 2 and 3 were 13 (9.5–16), 13 (10.5–16) and 12 (10.5–14.5) respectively. Significantly lower numbers of patients in the TEG guided transfusions group received platelets (4 cases, 13.8%; 95% CI: 3.9–31.7) as compared to those receiving routine transfusions (100%; 95% CI: 88.1–100) ($p < 0.001$). Four cases in the on-demand group received RDPs (13.8%; 95% CI: 3.9–31.7). Minor (CTCAE grade 1) post-procedure related bleeding was seen in 3 (10%; 95% CI: 2.2–27.4) patients in the TEG guided transfusion group as compared to 1 (3.4%; 95% CI: 0.1–17.8) each in groups 2 and 3 respectively ($p = 0.43$). The bleeding episodes in the TEG group were from the local site and did not require packed red cell transfusions. There were no bleeding related mortality in any of the 3 groups at the 28-day follow-up period.

Conclusion: Thromboelastography guided transfusion reduces unnecessary platelet transfusions in patients with liver cirrhosis and severe thrombocytopenia undergoing high risk invasive procedures without a significant increase in major bleeding events as compared to those receiving empiric transfusions.

TOP-066-YI

Development and validation of a prognostic model (AMMON-AD) to define risk of overt hepatic encephalopathy in cirrhosis patients with acute decompensation

María Pilar Ballester¹, Juan Antonio Carbonell-Asins², Shalimar Shalimar³, Rajiv Jalan⁴. ¹Clinic University Hospital of Valencia, INCLIVA Biomedical Research Institute, Valencia, Spain; ²INCLIVA Biomedical Research Institute, Valencia, Valencia, Spain; ³All India Institute of Medical Sciences, New Delhi, New Delhi, India; ⁴University College London, London, United Kingdom
Email: mapibafe@gmail.com

Background and aims: Overt hepatic encephalopathy (OHE) is the most common cause of hospitalization in patients with cirrhosis, but which patients with an acute decompensation (AD) will develop OHE is unknown. In addition, the real impact of OHE occurrence during admission on the patient's prognosis is not clear, and therefore, prophylactic therapies are not routinely used. The aims of the study were to determine the impact of OHE development on the risk of death and to develop and validate a prognostic model (AMMON-AD) that defines the group of patients at risk of OHE during hospitalization. Secondary aims were to evaluate the impact of OHE recovery on survival and to assess the utility of the new prognostic model on the probability of recovery from OHE.

Method: This observational, prospective study included 310 consecutive patients with cirrhosis hospitalized for an AD (non-ACLF). Patients were followed up to 90-days. Ammonia was normalized to upper limit of normal (AMM-ULN) of the laboratory. Fast unified random forest was performed to predict future OHE and recovery and Kaplan-Meier curves were used to compare risk of death according to development of OHE during hospitalization. An independent cohort of 50 patients was included for validation.

Results: 76% were male with a mean age of 42 (SD 12) years and an AD-CLIF score of 56 (SD 11). Out of 243/310 patients without OHE at

admission, 102 (42%) developed OHE within 90-days. Development of OHE was associated with an increased risk of death (HR = 4.3; 95%CI = 3.03–5.97; $p < 0.001$), with significant differences in time to death between patients with and without OHE occurrence during hospitalization (Log Rank $p < 0.001$). The best model (AMMON-AD) to predict development of OHE included sodium, albumin, AMM-ULN, white cell count, INR and bilirubin, with an integrated Brier score (IBS) of 0.180 (Child-Pugh 0.187, MELD-Na 0.191, AD-CLIF score 0.194). Out of 67 patients with OHE at admission, 39 (58%) resolved the episode, with a significant impact in time to death compared with patients who did not recover from OHE (Log Rank $p < 0.001$). AMMON-AD also predicted OHE recovery with an IBS of 0.181. Out of 17/50 patients that did not present OHE at admission in the validation cohort, 8 (47%) developed OHE, with an accuracy of the model of 71%.

Conclusion: This study revealed that development of OHE during hospitalization is associated with a high risk of death, highlighting the importance of prophylactic therapies. In addition, we developed and validated the AMMON-AD model to select patients that may benefit from prophylaxis. This new model can also be used to evaluate the probability of recovery from OHE and risk of death.

FRIDAY 07 JUNE

FRI-038-YI

Silver-coating of tunneled peritoneal drainage system is associated with a lower incidence of spontaneous bacterial peritonitis and device explanation

Sarah Lisa Schütte¹, Heiner Wedemeyer^{1,2,3}, Benjamin Maasoumy^{1,2}, Tammo Lambert Tergast¹. ¹Hannover Medical School, Department of Gastroenterology, Hepatology, Infectious Diseases and Endocrinology, Hannover, Germany; ²German Center for Infection Research (DZIF), Hannover-Braunschweig, Germany; ³Excellence Cluster Resist, Hannover Medical School, Hannover, Germany
Email: schuette.sarah@mh-hannover.de

Background and aims: Patients with refractory ascites (RA) have limited treatment options, if contraindications for the implantation of transjugular intrahepatic portosystemic shunt (TIPS) are present or liver transplantation (LTx) is not available. Novel therapeutic devices such as tunneled peritoneal catheter systems (PeCa) have emerged to enable home-based care of RA. However, device infections are a common reason for device explantation or rehospitalization. Recently, silver-coated PeCa (scPeCa) have been introduced. The silver coating has been associated with a lower bacterial burden in in-vitro studies and presumably leads to a lower rate of device infections. However, clinical data to support this are lacking. This study compared conventional PeCa with scPeCa regarding the incidence of device explantations and the incidence of spontaneous bacterial peritonitis (SBP).

Method: All patients that received a PeCa at Hannover Medical School between 2012 and 2023 were considered for this study. Exclusion criteria included presence of malignant diseases, except for HCC within the MILAN criteria or absence of cirrhosis. Overall, 177 patients were included in this study of whom 27 received scPeCa (15%). To adjust for potential group differences, propensity score matching (PPSM) was applied. Matching factors included MELD and history of SBP. After PPSM, we compared 81 patients with PeCa and 27 patients with scPeCa. Competing risk analysis was conducted to analyse longitudinal end points. Analysed end points included SBP incidence, device explantation within one year and LTx-free survival.

Results: At the time of device implantation, history of SBP was less frequent and MELD score was numerically lower in patients with scPeCa (33% vs. 61%, $P = 0.008$; 16 vs. 18, $P = 0.15$). After PPSM, baseline factors like age, MELD score, history of SBP or intake of Norfloxacin after device implantation were comparable between patients with and without scPeCa (Age: 64 ± 13.5 vs 61 ± 10.6 , $p =$

0.29, MELD: 16 ± 5 vs 16 ± 5 , $p = 0.91$; History of SBP: 33% vs 33%, $p = 1.00$; Intake of Norfloxacin: 70% vs 59%, $p = 0.40$, respectively). One year LTx-free survival was comparable between both groups (57% vs 63%, HR 1.66, 95% CI 0.65–4.22, $p = 0.29$). However, presence of scPeCa was associated with a significantly lower SBP incidence within one year after device implantation (69% vs 74%, HR 0.38, 95% CI 0.17–0.86, $p = 0.02$). Moreover, device explantation within one year was significantly less frequent in those with scPeCa (61% vs 87%, HR 0.39, 95% CI 0.016–0.95, $p = 0.038$, median time to explantation: 344 days vs 83 days). Device infections were the most frequent reason for explantation in both groups (scPeCa: 3 (60%) vs. PeCa: 19 (66%)).

Conclusion: Compared to conventional uncovered PeCa, scPeCa were associated with a lower SBP incidence and less device explantations within one year.

FRI-039

Terlipressin therapy is associated with increased risk of colonization with multidrug-resistant bacteria in patients with decompensated cirrhosis

Marcus Mücke¹, Maria Hernandez-Tejero², Wenyi Gu³, Michael Kuhn⁴, Malte Janz¹, Marisa Isabell Keller⁴, Anthony Fullam⁴, Laura Altepeter¹, Victoria Mücke¹, Fabian Finkelmeier¹, Katharina Maria Schwarzkopf¹, Cremonese Carla¹, Peter Hunyady¹, Myriam Heilani¹, Frank Erhard Uschner^{1,3}, Robert Schierwagen^{1,3}, Maximilian Joseph Broil^{1,3}, Sabine Klein^{1,3}, Kai-Henrik Peiffer^{1,3}, Michael Hogardt⁵, Saeed Shoaie⁶, Minneke Coenraad⁷, Jörg Bojunga¹, Vicente Arroyo⁸, Stefan Zeuzem¹, Volkhard A. J. Kempf⁹, Christoph Welsch¹, Wim Laleman⁹, Peer Bork⁴, Javier Fernandez², Jonel Trebicka^{1,3}. ¹Medical Clinic 1, University Hospital, Goethe-University Frankfurt, Frankfurt a.M., Germany; ²Liver ICU, Liver Unit, Hospital Clinic, University of Barcelona, IDIBAPS and CIBERehd, Barcelona, Spain; ³Department of Internal Medicine B, University of Münster, Münster, Germany; ⁴Structural and Computational Biology Unit, European Molecular Biology Laboratory, Heidelberg, Germany; ⁵Institute of Medical Microbiology and Infection Control, Goethe University Frankfurt, Frankfurt a.M., Germany; ⁶Science for Life Laboratory, KTH-Royal Institute of Technology, Stockholm, Sweden; ⁷Department of Gastroenterology and Hepatology, Leiden University Medical Center, Leiden, Netherlands; ⁸European Foundation for the Study of Chronic Liver Failure, Barcelona, Spain; ⁹Department of Gastroenterology and Hepatology, Section of Liver and Biliopancreatic Disorders, University Hospitals Leuven, Leuven, Germany
Email: marcus.m.muecke@gmail.com

Background and aims: Patients with liver cirrhosis are susceptible to develop bacterial infections, the most frequent trigger for acute decompensation (AD) and progression to acute-on-chronic liver failure (ACLF). The CANONIC and the PREDICT study demonstrated that infection with multidrug-resistant organisms (MDROs) are associated with deleterious outcome. MDRO infections are frequent following MDRO colonization. The influence of non-antibiotic medication contributing to MDRO colonization and selection remains unclear.

Method: 324 patients with AD and ACLF admitted to the ICU with MDRO screening and details concerning past medication intake were eligible for inclusion. Regression models were performed to identify drugs associated with MDRO colonization. A second series ($n = 129$ patients with AD and ACLF from Barcelona, Spain) was included to validate results. A third multi-center validation cohort ($n = 203$ decompensated cirrhosis patients) with metagenomic sequencing data was included to detect antibiotic resistance genes.

Results: Upon admission, 97 patients (30%) were defined to have MDRO colonization and 35 of them (11%) developed MDRO infection. Patients with MDRO colonization had a significantly higher risk of MDRO infection than those without ($p = 0.0098$). Apart from antibiotic therapy (OR 2.91, 95%-CI 1.72–4.93, $p < 0.0001$), previous terlipressin therapy over 14 days was the only independent covariate associated with MDRO colonization in both, the overall (OR 12.6, 95%-

CI 4.04–39.0, $p < 0.0001$) and the propensity score matched cohort (OR 6.79, 95%-CI 1.55–29.79, $p = 0.011$). In the second series, prior terlipressin therapy appeared as a risk factor for MDRO colonization (OR 2.49, 95%-CI 0.911–6.823, $p = 0.075$) and was associated with an increased risk of MDRO infection during follow-up ($p = 0.017$). The external validation cohort confirmed these results and demonstrated that antibiotic inactive genes were significantly associated with terlipressin administration ($p = 0.001$).

Conclusion: Our study reports an increased risk of MDRO colonization in patients with AD or ACLF, who recently received terlipressin therapy, while other commonly prescribed non-antibiotic comedication had negligible influence. Further studies are needed to confirm our results and to identify the underlying mechanisms.

FRI-040

Male sex is associated with worse outcomes in primary biliary cholangitis

Nirbaanot Walia¹, Julian Pohl¹, Matthias Reinhardt¹, Frank Tacke¹, Cornelius Engelmann¹. ¹Gastroenterology and Hepatology, Charité-Universitätsmedizin Berlin, Berlin, Germany
Email: nirbaanwalia@gmail.com

Background and aims: Although Primary Biliary Cholangitis (PBC) predominantly affects women, limited evidence suggests men experience worse outcomes. The aims of this study were to assess sex related differences in outcomes in PBC, and to determine whether these differences are more specific to PBC compared to other causes of cirrhosis.

Method: This was a retrospective study conducted at The Charité-Universitätsmedizin Berlin. Inpatient admissions with a documented diagnosis of PBC based off the International Statistical Classification of Diseases and Related Health Problems (ICD-10) codes were extracted from 2011–2022. Further information such as patient age, sex, comorbidities, inpatient complications, procedures, blood test results and in-hospital mortality were obtained. The primary outcome was a composite of in-hospital mortality or liver transplant. Secondary outcomes included in-hospital mortality, liver transplant, decompensated cirrhosis, and length of hospital admission. Univariable and multivariable logistic and linear regression was used to assess the impact of sex on outcomes in PBC. A control group of patients with alternate cirrhosis aetiologies, matched on age and comorbidities on a 1:1 ratio, was compared against, and an interaction term for sex and PBC was included in the modelling.

Results: 940 patient admissions with a diagnosis of PBC were obtained, with 82% being female. Men with PBC had higher rates of most acute and chronic complications of liver disease, and significantly higher ALT, AST, GGT, ALP, Bilirubin and INR levels. Women had a reduced odds of the primary outcome on univariable analysis (OR = 0.23, 95% CI: [0.14, 0.40], $p < 0.001$) and following adjustment for age and comorbidities (OR = 0.27, 95% CI: [0.15, 0.49], $p < 0.001$). This was in contrast to the control group, where female sex was associated with an increased odds of death or transplant on univariable (OR = 1.54, 95% CI: [1.02, 2.30], $p = 0.036$) and multivariable (OR = 1.58, 95% CI: [1.04, 2.39], $p = 0.030$) logistic regression. The interaction analysis across the combined cohort revealed a modification effect of PBC on the risk of the primary outcome by sex (OR for interaction = 0.15, 95% CI: [0.08, 0.30], $p < 0.001$). Similar findings were noted in the assessment of secondary outcomes.

Conclusion: Men with PBC experience worse outcomes across a spectrum of measures. This difference appears to be more specific to PBC compared to other causes of cirrhosis, suggesting the pathological progression of PBC in males may be more severe than in females. Further research is required to consolidate these findings.

FRI-041

Evaluating the influence of human albumin infusions on the MELD and MELD-Na scores in patients hospitalized with an acute decompensation of cirrhosis: an ATTIRE trial analysis

Nikolaj Torp^{1,2}, Nicholas Freemantle³, Aleksander Krag^{1,2}, Alastair O'Brien^{3,4}. ¹Centre for Liver Research, Department of Gastroenterology and Hepatology, Odense University Hospital, Odense, Denmark; ²Department of Clinical Research, University of Southern Denmark, Odense, Denmark; ³Comprehensive Clinical Trial Unit, University College London, London, United Kingdom; ⁴Royal Free Hospital, London, United Kingdom
Email: nikolaj.christian.torp@rsyd.dk

Background and aims: The model for end-stage liver disease (MELD) score is widely used in hospitalized patients with cirrhosis and changes in MELD has been proposed as a surrogate end point for phase II trials. Albumin can affect the levels of creatinine, bilirubin and sodium, but if human albumin infusions represent a confounder for changes in MELD score is unknown. Therefore, we studied the effect of 20% human albumin infusions on the MELD and MELD sodium (MELD-Na) scores in patients hospitalized with cirrhosis.

Method: We used data from ATTIRE trial, which consisted of 777 patients randomized to daily 20% human albumin infusions or standard of care, during a hospitalization due to an acute decompensation of cirrhosis. Dosing of human albumin was based on a target serum albumin >30 g/L and human albumin infusions were allowed in the standard of care group as per clinical practice guidelines. We only included patients discharged during the trial period (within 15 days) in the analysis. We compared changes in MELD models from baseline to discharge according to the human albumin use. We looked at three- and six-month mortality to investigate the prognostic utility of MELD and MELD-Na after albumin infusions.

Results: We included 499 discharged patients during the trial period. Majority were men (71%) with mean age 53 years (SD: +11 years). Median baseline MELD was 18 (IQR: 15–22) and MELD-Na 22 (IQR: 18–26). Of included patients, 335 (68%) received 20% human albumin during their hospitalization, where the median amount of albumin given was 140 grams (IQR: 80–220). On average, one vial of 20% human albumin (20 gram) was associated with a $-0.82 \mu\text{mol/L}$ decrease in creatinine (95% CI: -1.63 ; -0.01 , $p = 0.046$), a $-1.13 \mu\text{mol/L}$ decrease in bilirubin (95% CI: -2.04 ; -0.22 , $p = 0.015$) and a $+0.24 \text{ mEq/L}$ increase in sodium (95% CI: $+0.16$; $+0.32$, $p < 0.001$). Discharge MELD (median 17, IQR: 14–21) and MELD-Na (median 20, IQR: 16–24, $p < 0.001$) were both lower compared to baseline MELD ($p < 0.001$) and MELD-Na ($p < 0.001$). Number of deaths were 69 (14%) and 113 (23%) after three- and six months, respectively. MELD at discharge, predicted death at three months (HR = 1.11, 95% CI: 1.08–1.15, $p < 0.001$) and six months (HR = 1.09, 95% CI: 1.06–1.12, $p < 0.001$). Similarly, discharge MELD-Na predicted death after three months (HR = 1.13, 95% CI: 1.09–1.17, $p < 0.001$) and six months follow-up (HR = 1.10, 95% CI: 1.07–1.13, $p < 0.001$). Divided into MELD and MELD-Na severity groups, a stepwise increase in mortality was observed for both models.

Conclusion: Human albumin infusions were associated with statistically significant but not clinically significant changes in components of the MELD and MELD-Na scores. A MELD and MELD-Na calculated at discharge in patients hospitalized with an acute decompensation of cirrhosis, may therefore serve as a surrogate for survival and prognostication, irrespective of human albumin use.

FRI-042

Comparison of clinical outcomes among patients with refractory ascites and implantation of either Alfapump®, tunneled peritoneal drainage system or transjugular intrahepatic portosystemic shunt

Sarah Lisa Schütte¹, Anja Tiede^{1,2}, Jim Benjamin Mauz¹, Hannah Schneider¹, Nicolas Richter³, Heiner Wedemeyer^{1,4,5},

Benjamin Maasoumy^{1,2}, Tammo Lambert Tergast¹. ¹Hannover Medical School, Department of Gastroenterology, Hepatology, Infectious Diseases and Endocrinology, Hannover, Germany; ²German Center for Infection Research (DZIF), Hannover-Braunschweig, Germany; ³Hannover Medical School, Department of Abdominal and Transplant surgery, Hannover, Germany; ⁴German Center for Infection Research (DZIF), Hannover, Germany; ⁵Excellence Cluster Resist, Hannover Medical School, Hannover, Germany
Email: schuette.sarah@mh-hannover.de

Background and aims: Onset of refractory ascites (RA) is a severe complication in patients with liver cirrhosis. If liver transplantation (LTx) is not available, implantation of a transjugular intrahepatic portosystemic shunt (TIPS) is the current standard of care. If TIPS implantation is not possible due to contraindications, alternative treatment options with devices such as Alfapump® or tunneled peritoneal catheters (PeCa) have been introduced to enable home-based treatment. Currently, data comparing TIPS, Alfapump® and PeCa are limited. This study investigated clinical outcomes between patients that received TIPS, Alfapump® or PeCa due to RA.

Method: All patients with liver cirrhosis and RA who received treatment at Hannover Medical School between 2009 and 2023 were considered. Patients with malignancies were excluded from this study. Study end points comprised one-year incidences of mortality, acute kidney injury (AKI), hyponatremia ($<130 \text{ mmol/L}$) and spontaneous bacterial peritonitis (SBP). Competing risk regression analysis was conducted, treating death and/or LTx as competing events. Due to expected differences in baseline characteristics, propensity score matching (PPSM) was performed. Patients with PeCa (Analysis 1) or TIPS (Analysis 2) were matched in a 2:1 manner with individuals from the Alfapump® group, respectively. Afterwards, patients with PeCa underwent 1:1 matching with TIPS patients (Analysis 3).

Results: Overall, 35 patients with Alfapump®, 126 with PeCa and 138 patients with TIPS were included in this study.

Analysis 1: After PPSM, 60 patients who underwent PeCa implantation were compared with 30 patients with Alfapump®. Mortality (HR 0.74, $p = 0.53$), incidence of AKI (HR 1.46, $p = 0.13$) and hyponatremia (HR 0.92, $p = 0.77$) did not differ. Yet, incidence of SBP (32% vs 81%, HR 0.32, $p = 0.006$) and explantation of the device (41% vs. 86%, HR 0.25, $p = 0.005$) were significantly less frequent in patients with Alfapump®.

Analysis 2: Overall, 70 patients with TIPS were matched with 35 patients with Alfapump®. Mortality and SBP incidence were comparable (HR 0.84, $p = 0.69$ and HR 1.47, $p = 0.44$, respectively). However, incidences of AKI and hyponatremia were significantly higher in patients with Alfapump® (AKI: 84% vs 46%, HR 3.84, $p < 0.001$ and hyponatremia: 78% vs. 27%, HR 4.46, $p < 0.001$).

Analysis 3: Finally, 118 patients with PeCa were matched against 118 patients with TIPS. Mortality did not differ (HR 1.15, $p = 0.58$), while incidences of AKI (81% vs 30%, HR 6.05, $p < 0.001$), hyponatremia (75% vs 37%, HR 3.72, $p < 0.001$) and SBP (81% vs. 35%, HR 2.50, $p < 0.001$) were significantly higher in patients with PeCa.

Conclusion: Overall, TIPS implantation is associated with lower incidences of clinical complications when compared to devices like Alfapump® or PeCa. Furthermore, Alfapump® was linked with a lower SBP incidence and a lower rate of device explantations compared to PeCa.

FRI-043

A multi-center randomized controlled study of primary prevention of esophageal variceal bleeding in cirrhotic patients treated with HVPG-guided therapy or standard heart rate-guided therapy: an interim analysis of the PORTHOS trial

Annelotte Broekhoven¹, Jelte Schaapman¹, Annarein Kerbert¹, Hein W Verspaget¹, Bart van Hoek¹, Suzanne Cannegieter², Arian van Erkel³, Wilbert van den Hout⁴, Bart Mertens⁵, Roeland Veenendaal¹, Ulrich Beuers⁶, R. Bart Takkenberg⁶,

Karin van Nieuwkerk⁷, Johan P.H. Kuyvenhoven⁸, Sunje Abraham⁹, Thomas Vanwolleghem¹⁰, Minneke Coenraad¹. ¹Department of Gastroenterology and Hepatology, Leiden University Medical Center, Leiden, Netherlands; ²Department of Clinical Epidemiology, Leiden University Medical Center, Leiden, Netherlands; ³Department of Radiology, Leiden University Medical Center, Leiden, Netherlands; ⁴Department of Medical decision Analysis, Leiden University Medical Center, Leiden, Netherlands; ⁵Department of Medical Statistics, Leiden University Medical Center, Leiden, Netherlands; ⁶Department of Gastroenterology and Hepatology, Amsterdam University Medical Center, location AMC, Amsterdam, Netherlands; ⁷Department of Gastroenterology and Hepatology, Amsterdam University Medical Center, location VuMC, Amsterdam, Netherlands; ⁸Department of Gastroenterology and Hepatology, Spaarne Gasthuis, Haarlem, Netherlands; ⁹Department of Gastroenterology and Hepatology, Alrijne Hospital, Leiderdorp, Netherlands; ¹⁰Department of Gastroenterology and Hepatology, University Hospital Antwerpen, Antwerpen, Belgium Email: a.g.c.broekhoven@lumc.nl

Background and aims: Nonselective beta-blockers (NSBB) are the standard of care for primary prevention of esophageal variceal bleeding in patients with liver cirrhosis. However, about 50% of these patients do not reach target hemodynamic response. These non-responders have significantly higher rate of first variceal hemorrhage as compared to NSBB responders. In clinical practice, NSBB therapy is evaluated according to heart rate. However, the reduction in heart rate due to NSBB does not correlate with the reduction in portal venous pressure. We aimed to compare the effectiveness of hepatic venous pressure gradient (HVPG)-guided NSBB therapy to standard heart rate-guided NSBB therapy.

Method: Randomized controlled multi-center trial comparing NSBB therapy guided HVPG-measurements before and after start of NSBB therapy, to standard heart rate-guided NSBB therapy in patients with liver cirrhosis and large (≥ 5 mm) esophageal varices without a history of variceal hemorrhage. Follow-up period was 2 years. In patients randomized to the HVPG group, a HVPG-measurement was performed before and 4 weeks after the start of propranolol to determine the hemodynamic response. In hemodynamic responders, NSBB's were continued. In hemodynamic non-responders, NSBB's were continued and additional repeated endoscopic band ligation was performed until complete obliteration of large varices. In the control group propranolol was started, and NSBB's were continued throughout the whole study period, no routine gastroscopy was required. This study constitutes the planned interim analysis according to the protocol.

Results: In total 64 patients were included in this interim analysis: 33 were randomized to the HVPG group, 31 to the control group. The median follow-up time was 9.6 months (IQR 3.38–23.95). Within the HVPG group 20 (60.6%) patients were non-responders to propranolol. Within the HVPG group, 5 (15.2%) patients experienced a variceal hemorrhage versus 5 (16.1%) within the control group (NS). The observed risk reduction was 0.9% (95% CI –0.25–0.26). The cumulative incidence of having a variceal bleeding within 2 years was 19% in the HVPG group and 17.8% in the control group (NS).

Conclusion: In this randomized controlled trial, no clinical benefit from HVPG guided NSBB therapy could be demonstrated. Although around 60% of the patients were hemodynamic non-responders to NSBB treatment and were subsequently treated with endoscopic band ligation on top of NSBB therapy as primary prophylaxis of variceal bleeding, no risk reduction in variceal hemorrhage could be demonstrated.

FRI-044-YI

Impact of underlying etiology of liver cirrhosis on tests for diagnosing minimal hepatic encephalopathy

Julius Egge¹, Alena Friederike Ehrenbauer¹, Maria Magdalena Gabriel¹, Jana Al-Ayoubi¹, Lea Wagner¹, Jennifer Witt¹, Jim Benjamin Mauz¹, Anja Tiede¹, Heiner Wedemeyer¹, Anika Grosshennig¹, Gerrit M. Grosse¹, Benjamin Maasoumy¹, Karin Weissenborn¹. ¹Hannover Medical School, Hannover, Germany Email: Egge.Julius@mh-hannover.de

Background and aims: Diagnosing minimal hepatic encephalopathy (mHE) is a challenge. Many determinants may affect mHE test results. One major issue discussed is the impact of liver cirrhosis etiology. It remains unclear whether different tests for mHE are differentially affected by etiology. This study aims to investigate the effect of cirrhosis etiology on mHE test results.

Method: A total of 215 patients with liver cirrhosis underwent six mHE tests: Portosystemic-Encephalopathy-Syndrome Test (PSE), Continuous Reaction Time Test (CRT), Animal-Naming-Test, Stroop Encephal_App (Stroop), Inhibitory Control Test, and Critical Flicker Frequency. The effect of cirrhosis etiology on test results was analyzed using multivariable linear and binary logistic regression models. A directed acyclic graph model identified the factors sex, age, native language, and diabetes mellitus as minimal sufficient adjustment set for multivariable analyses.

Results: The cause of liver cirrhosis was alcohol-related (AC) in 73, metabolic dysfunction-associated steatohepatitis (MASH) in 32, metabolic dysfunction and alcohol associated steatotic liver disease (MetALD) in 24, autoimmune hepatitis, cholangitis or Hepatitis C in 44 (infectious or autoimmune liver disease (IALD)), and cryptogenic or of other etiology in 42 patients. MetALD patients exhibited the lowest results in PSE (mean –4.25), while the IALD group performed best (mean –2.02). Abnormal PSE was most prevalent in AC patients (39.7%) and least in IALD (20.7%). Stroop test results were comparable. In line with this, in multivariable linear regression analyses IALD was associated with higher PSE score values (adjusted regression coefficient beta = 1.59, 95% confidence interval (CI) 0.24–2.95) in comparison to patients with AC. In multivariable binary logistic regression analyses, the adjusted odds ratio (aOR) for an abnormal PSE result was 0.42 (95% CI 0.17–1.034) in IALD patients compared to AC patients. For other etiologies, similar effects to AC patients were observed. Regarding CRT, patients with cryptogenic or other etiology showed an aOR of 3.02 (95% CI 1.28–7.12) for an abnormal result compared to AC patients. For the other mHE tests, no effect of cirrhosis etiology on test results was observed.

Conclusion: The etiology of cirrhosis appears to impact mHE test results. Patients with cirrhosis due to metabolic syndrome and/or alcohol exhibit similar results, while those with autoimmune hepatitis, cholangitis or Hepatitis C fare better compared to the aforementioned etiologies. This discrepancy is especially notable in the surrogate gold standard for diagnosing mHE, the PSE-Test. As shown in the past, alcoholism per se has no observable effect upon PSE test results. Thus, these data suggest an amplification of the liver cirrhosis associated harm on brain function in patients with nutritive/toxic etiology of cirrhosis compared to IALD.

FRI-045

Superior prognostic accuracy of the LiverPRO score versus FIB-4 in predicting liver-related events in a cohort of 457, 152 individuals

Katrine Lindvig¹, Sören Möller^{2,3}, Katrine Thorhauge^{1,3}, Johanne Kragh Hansen^{1,3}, Camilla Dalby Hansen¹, Stine Johansen^{1,3}, Helle Schnefeld¹, Mads Israelsen^{1,3}, Peter Andersen¹, Ida Falk Villesen¹, Katrine Tholstrup Bech¹, Nikolaj Torp^{1,3}, Aleksander Krag^{1,3}, Maja Thiele^{1,3}. ¹Department of Gastroenterology and Hepatology, Centre for Liver Research, Odense University Hospital, Odense C, Denmark; ²Open Patient data Explorative Network, Odense University Hospital and Research unit OPEN, 5000, Denmark; ³Institute

POSTER PRESENTATIONS

of Clinical Research, University of Southern Denmark, Odense M, Denmark
Email: katrine.prier.lindvig@rsyd.dk

Background and aims: Steatotic liver disease (SLD) poses a growing healthcare burden, often undetected until advanced stages. Improved prognostic tools are urgently needed. LiverPRO is a CE-marked decision tool that utilizes a machine learning model to assess the percentage likelihood of having liver fibrosis based on routine blood samples and has shown strong diagnostic capabilities, surpassing current solutions. However, its prognostic potential remains unexplored. In this study, we compared the prognostic accuracy of LiverPRO to Fibrosis-4 Index (FIB-4) for prediction of liver-related events in the UK Biobank.

Method: We conducted a retrospective study on data from UK Biobank collected between 2006 and 2010 and followed until 2020. Information on ICD-10 codes and mortality is included in the database. The outcome was the risk of liver-related events, analysed using Cox regression and cumulative incidence curves, and the overall prognostic accuracy was presented with Harrell's C statistic and hazard ratios (HR).

We have used the following ICD-10 codes for defining a liver related event: ascites (R18.9), Esophageal and gastric varices, not bleeding (I85.9, I85.2, I86.4), Esophageal and gastric varices, bleeding (I85.0, I85.3, I86.4A), Spontaneous bacterial peritonitis (K65.8), Liver failure (K72.1, K72.0, K72.9), Liver cirrhosis (K74.6), Portal hypertension (K76.6), Hepatorenal syndrome (K76.7), Hepatocellular carcinoma (C22.0).

Results: The analysis encompassed 457,152 participants with a mean age of 58 years (interquartile range, IQR: 51–64), 56% male. In the cohort a total of 1,174 liver related events was observed. LiverPRO predicted liver-related events with a Harrell's C of 0.86 (95% confidence interval, CI: 0.85–0.87), compared to 0.78 (95%CI: 0.76–0.79) for FIB-4. Furthermore, a HR of 64.21 (95%CI: 53.18, 77.54) with $p < 0.001$ was observed for LiverPRO in the high-risk category ($>65\%$) versus the low-risk category ($<25\%$). Similarly, an elevated HR of 41.07 (95%CI: 35.03, 48.16) with $p < 0.001$ was estimated for FIB-4 >2.67 compared to FIB-4 <1.3 . These findings means that patients with elevated FIB-4 (≥ 2.67) have an 311% increased risk compared to patients with a low FIB-4, for developing a liver related event. Similarly, patients with a high risk LiverPRO ($>65\%$) have a 542% increased risk of developing a liver related event.

Conclusion: This extensive study demonstrates the superior prognostic accuracy of LiverPRO over FIB-4 in predicting liver-related events, underscoring its potential as a vital tool in early detection and management of liver disease. The marked difference in hazard ratios highlights the need for integrating advanced non-invasive diagnostic methods like LiverPRO in routine clinical practice, significantly enhancing risk stratification and patient care in SLD.

FRI-046

Alfapump implantation significantly improved quality of life and showed similar safety outcomes compared to a contemporaneously enrolled refractory ascites cohort

Jasmohan Bajaj¹, Patrick S. Kamath², K. Rajender Reddy³, Puneeta Tandon⁴, Jennifer Lai⁵, Jacqueline O'Leary⁶, Gijis Klarenbeek⁷, Jeroen Capel⁸, Scott Biggins⁹, Hugo Vargas¹⁰, Guadalupe Garcia-Tsao¹¹, Leroy Thacker¹², Florence Wong¹³, ¹Virginia Commonwealth University, Richmond, United Arab Emirates; ²Mayo Clinic, Rochester, United States; ³University of Pennsylvania, Philadelphia, United States; ⁴University Of Alberta, Edmonton, Canada; ⁵University of California San Francisco, San Francisco, United States; ⁶Dallas VA Medical Center, Dallas, United States; ⁷Sequana Medical, Ghent, Belgium; ⁸Sequana Medical, Zurich, Switzerland; ⁹University of Pittsburgh Medical Center, Pittsburgh, United States; ¹⁰Mayo Clinic in Arizona, Phoenix, United States; ¹¹VA-CT Healthcare System, West Haven,

United States; ¹²Virginia Commonwealth University, Richmond, United States; ¹³Toronto General Hospital, Toronto, Canada
Email: jasmohan.bajaj@vcuhealth.org

Background and aims: The POSEIDON study evaluated alfapump to relieve refractory ascites (RA) in a multi-center North American cohort but a contemporaneous cohort of RA to compare outcomes is needed. NACSELD3 (North American Consortium for Study of End-Stage Liver Disease), is a prospective outpatient cirrhosis cohort that includes RA patients which is enrolled contemporaneously to POSEIDON and could serve as comparators. Aim: Determine changes in quality of life (QOL), and safety outcomes (death, hospitalization, liver transplant) over 6 months vs baseline in POSEIDON compared to age, gender, Ascites-Q and MELD-Na matched NACSELD3 patients.

Method: NACSELD3 included outpatients with cirrhosis enrolled from 10 North American centers who were followed at 6 monthly intervals. 157 NACSELD3 patients with RA were matched to the 40 POSEIDON patients with propensity score matching calculated using age, sex, MELD-Na, and Ascites-Q score. Patients were matched 1:1, minimizing the difference between logits of the calculated propensity scores for cases and controls with a caliper of 0.2 using greedy nearest neighbor match. Ultimately 37 of 40 POSEIDON patients were matched 1:1 with the NACSELD3 RA subgroup. Ascites-Q and SF-36 are QOL questionnaires validated for ascites and overall health respectively. Outcomes were QOL [Ascites-Q, low = good and SF-36 physical component summary (PCS), high = good], any serious adverse event (SAE) resulting in death or hospitalization, and liver transplant (LT) through 6 months.

Results: Baseline parameters were comparable between POSEIDON and NACSELD3 (mean age 62.5 vs 61.0 years, 65% vs 62% men, MELD-Na 15.5 vs 16.6, Ascites-Q 50.1 vs 52.1). QOL: Ascites-Q improved over 6 months in POSEIDON (Delta -17 ± 16 , $p < 0.001$) but not in NACSELD3 (Delta -4 ± 20 , $p = 0.37$). Similarly, SF-36 PCS improved at 6 months over baseline in POSEIDON (Delta 6 ± 8 , $p = 0.002$) but not NACSELD3 (Delta 0.2 ± 8 , $p = 0.92$). Safety outcomes: Mortality was equal (10.8% each). Hospitalization rate was statistically similar (35.1% vs 46.9%, $p = 0.48$) but trended higher in POSEIDON due to implant-related events for the alfapump. LT occurred in 8.1% of NACSELD3 and 5.4% of POSEIDON patients, which was similar statistically ($p = 1.0$).

Conclusion: The POSEIDON open-label trial of alfapump demonstrated significant improvement in quality of life focused on ascites symptoms and physical function compared to baseline, which is not seen in refractory ascites patients enrolled contemporaneously in the prospective NACSELD3 cohort despite matching for Ascites-Q, age, sex, and enrollment MELD-Na. No statistically significant difference in mortality, hospitalizations, or transplant were observed. Within the limitations of not being a RCT, this matched comparison provides evidence that the alfapump significantly improves QOL over standard paracentesis without significant impact on 6-month safety outcomes.

FRI-047-YI

Predictors of ascites resolution in patients with cirrhosis receiving long-term albumin treatment. Results from a real-world study in Italy (Real-ANSWER)

Enrico Pompili^{1,2}, Giulia Iannone^{1,2}, Salvatore Piano³, Antonino Lombardo⁴, Davide Bitetto⁵, Stefania Gioia⁶, Giacomo Zaccherini^{1,2}, Roberta Gagliardi³, Vincenza Calvaruso⁴, Marta Tonon³, Clara De Venuto¹, Maurizio Baldassarre², Greta Tedesco¹, Silvia Nardelli⁶, Pierluigi Toniutto⁵, Vito Di Marco⁴, Paolo Angeli³, Paolo Caraceni^{1,2}. ¹Department of Medical and Surgical Sciences, University of Bologna, Bologna, Italy; ²Unit of Semeiotics, Liver and Alcohol-related diseases, IRCCS Azienda Ospedaliero-Universitaria di Bologna, Bologna, Italy; ³Unit of Internal Medicine and Hepatology, Department of Medicine-DIMED, University and Hospital of Padova, Padua, Italy; ⁴UOC di Gastroenterologia, Dipartimento di Promozione

della Salute, Materno Infantile, Medicina Interna e Specialistica (PROMISE), University of Palermo, Palermo, Italy; ⁵Hepatology and Liver Transplantation Unit, University Academic Hospital, Udine, Italy; ⁶Department of Translational and Precision Medicine, Sapienza University of Rome, Rome, Italy
Email: paolo.caraceni@uniibo.it

Background and aims: Long-term albumin (LTA) treatment in patients with cirrhosis and ascites has become widespread in Italy, but several issues still deserve clarification. The present study focuses on predictors of ascites resolution in patients receiving LTA in a real-world setting.

Method: We performed a multicenter, retrospective, observational study enrolling patients with cirrhosis and ascites who received LTA for at least one month between January 2016 and February 2022. Ascites resolution was defined as improvement to grade 0–1.

Results: 312 patients were included in the present analysis. The most common etiology was alcohol (60%) followed by MASLD (30%). Median Child-Pugh was 8, MELD 15 and MELD-Na 18. Ascites was grade 2 in 55% of patients, grade 3 in 36% and refractory in 28%, while 47% received paracentesis in the prior 6 months. Median dose of albumin was 40 grams/week (IQR 40–40). Albumin dose was decreased in 24% of patients before discontinuation for ascites resolution or increased in 12% due to the lack of response. At the time of the last observation (at treatment interruption due to any cause or at the end of follow-up in patients still on treatment [February 2023]), ascites was grade 0/1 in 56% of patients, with a median length of treatment of 11 (6–19) months. Notably, of the 123 patients who received a paracentesis prior LTA, 53% had no additional paracentesis between 3 and 6 months of treatment. At multivariable logistic regression analysis, independent predictors of response were age ($p = 0.007$), baseline grade of ascites ($p = 0.007$), no paracentesis in the previous 6 months ($p = 0.001$), etiological treatment in the past 12 months or during LTA ($p = 0.005$), weekly albumin dose ($p = 0.014$) and a serum albumin concentration of 40 g/L after one month of treatment ($p = 0.017$). Ascites resolution often occurred within few months after the start of LTA. Indeed, ascites improved to grade 0/1 in 34% of patients within the first 3 months, in 37% within 6 months and in 46% within 12 months. Factors independently associated with ascites resolution within 3 months were: baseline grade of ascites ($p = 0.038$) and no paracentesis in the previous 6 months ($p = 0.004$), baseline INR ($p = 0.003$), weekly dose of albumin ($p = 0.025$) and a serum albumin level of 40 g/L at one month of treatment ($p = 0.003$).

Conclusion: These data indicate that: 1) LTA on top of diuretic therapy greatly facilitates the management of ascites, leading to a significant reduction in the need for paracentesis and ascites resolution in almost 60% of cases, including in some with a previous diagnosis of refractory ascites; 2) one-third of patients achieved grade 0/1 ascites within 3 months, and 3) clinical and treatment-related factors could help in predicting response to LTA, providing useful information for tailoring treatment at the individual level.

FRI-050-YI

Development of a screening tool for covert hepatic encephalopathy through automated speech signal analysis in patients with chronic liver diseases and/or portosystemic shunts

Apolline Leproux^{1,2,3}, Lyès Kheloufi^{1,2}, Kishanthan Kingston⁴, Philippe Sultanik^{1,2,3}, Sarah Mourj^{1,2,3}, Charlotte Bouzbib^{1,2,3}, Marika Rudler^{1,2,3}, Jean-Luc Zarader⁴, Mohamed Chetouani⁴, Nicolas Weiss^{1,2,5}, Dominique Thabut^{1,2,3}. ¹AP-HP, Brain-Liver Pitié-Salpêtrière Study group (BLIPS), Paris, France; ²INSERM UMR_S 938, Centre de recherche Saint-Antoine, Maladies métaboliques, biliaires et fibro-inflammatoire du foie, Institute of Cardiometabolism and Nutrition (ICAN), Paris, France; ³AP-HP, Sorbonne Université, Liver Intensive Care Unit, Hepatogastroenterology Department, Pitié-Salpêtrière Hospital, Paris, France; ⁴Sorbonne Université, Institut des Systèmes Intelligents et de Robotique (ISIR), Paris, France; ⁵AP-HP, Sorbonne Université,

Neurology Intensive Care Unit, Neurology Department, Pitié-Salpêtrière Hospital, Paris, France
Email: apolline.leproux@aphp.fr

Background and aims: Covert hepatic encephalopathy (CHE) encompasses a range of neurological and neuropsychological symptoms associated with chronic liver diseases (CLD) and/or portosystemic shunts. The current diagnostic approach relies on clinical and paraclinical work-up, which are often not available in routine practice. This lack of sensitive and specific tools leads to underdiagnosis of CHE, despite its impact on patient prognosis and quality of life, and the availability of effective therapies. The aim of this study was to develop a screening tool for CHE through automated speech signal analysis, by developing a machine-learning algorithm dedicated to our CLD patients.

Method: Cross sectional analysis of a cohort of patients with CLD evaluated by the BLIPS (Brain Liver Pitié-Salpêtrière) study group (outpatient's clinics with complete neuropsychological assessment, clinical evaluation by hepatologist and neurologist, blood sample with ammonia, MRI with spectroscopy, electroencephalogram) between March and June 2023. The diagnosis of CHE and the presence of factors of brain injury (FBI : vascular leucopathy, sequelae of alcohol abuse, epilepsy, stroke) was set based on an adjudication committee. This organization led to two classifications : presence or absence of CHE (two-class model) and presence or absence of CHE and/or FBI (four-class model). Patients were recorded during two verbal tasks: a short text reading and the animal naming test in 2 minutes, enabling to extract 63 rhythm, prosody and acoustic features. Three machine learning algorithms were developed (SVM : Support Vector Machine, RF : Random Forest, GB : Gradient Boosting).

Results: The study included 39 patients: 69% were males, median of age was 61 (55–66), 64% had cirrhosis, with a median MELD score of 14 (11–16). The two-class model led to 51% of patients with CHE. The four-class model led to 15% of patients with only CHE, 36% with CHE and FBI, 28% with only FBI and 21% without CHE nor FBI. SVM demonstrated significantly greater results than GB and RF, its prediction based solely on rhythmic features yielded an accuracy of 67.6% and a precision of 65.0% (two-class model). For the four-class model, it yielded an accuracy of 55.9% and a precision of 86.1%. However, by combining the 20 best rhythm, prosody, and acoustic features, it achieved an accuracy and precision of 100% in the two-class model, and an accuracy of 97.1% with a precision of 98.1% for the four-class model.

Conclusion: This automated speech signal analysis could represent a cost-effective and reliable screening tool for CHE and differential diagnosis of neurocognitive impairment in patients with CLD. The best results combined rhythm, prosody, and acoustic features analysis, and yielded to an excellent accuracy and precision. Our results could translate into a rapid CHE screening tool in hospital and at home, if larger validation studies confirm these findings.

FRI-051

Differences between urgent and elective major surgery in patients with advanced chronic liver disease and discriminatory capacity of the VOCAL-Penn

Lidia Canillas^{1,2,3}, Amalia Pelegrina^{2,3,4}, Elena Colominas-González^{3,5}, Aina Salis^{3,6}, Antonia Caro¹, César Enríquez-Rodríguez^{2,3}, Teresa Broquetas^{1,2}, Susana Coll^{1,2}, Nuria Cañete^{1,2}, Marc Puigvehí^{1,2}, Diego Rojo¹, Montserrat García-Retortillo^{1,2}, Xavier Bessa^{1,2,3}, Juan Álvarez⁷, Jose A. Carrión^{1,2,3,6}. ¹Liver Section, Gastroenterology Department, Hospital del Mar, Barcelona, Spain; ²Hospital del Mar Medical Research Institute (IMIM), Barcelona, Spain; ³Department of Medicine and Life Sciences, Universitat Pompeu Fabra, Barcelona, Spain; ⁴General Surgery Department, Hospital del Mar, Barcelona, Spain; ⁵Pharmacy Department, Hospital del Mar, Barcelona, Spain; ⁶Department of Medicine, Universitat Autònoma de Barcelona, Barcelona, Spain; ⁷Anesthesia Department, Hospital del Mar, Barcelona,

POSTER PRESENTATIONS

Spain

Email: lidia.canillas.alaves@gmail.com

Background and aims: In patients with advanced chronic liver disease (ACLD), emergent surgery has been related to higher mortality (up to 4–10 times) in contrast to elective surgery. Studies that reevaluate these results in recent populations are required. Our main aim was to evaluate the predictive capacity of the VOCAL-Penn in urgent surgery compared to elective surgery. As secondary objectives, we wanted to describe the baseline differences and complications of patients with ACLD undergoing urgent and elective surgery.

Method: Retrospective and unicentric study in patients with ACLD operated on major surgeries between 2010–2019. Patients undergoing emergent and elective surgery were compared (test de Fisher, X^2 o U-Mann Whitney), as well as the discriminant capacity of the VOCAL-Penn to predict mortality (ROC curves and agreement statistics) at 30 and 90 days.

Results: We included 512 patients, and 206 (40%) required an emergent surgery. Patients who underwent emergent surgery had more frequently ACLD due to alcohol consumption (56% vs. 47%; $p = 0.04$), higher comorbidity (ASA-IV 39% vs. 14%; $p < 0.01$), worse liver function (Child B/C 46% vs. 19%; $p < 0.01$ and MELD-Na 14 vs. 10; $p < 0.01$) and ascites (27% vs. 8%; $p < 0.01$). Abdominal (cholecystectomy, colectomy, etc.) and abdominal wall (hernia repair) surgeries were performed more frequently urgently (49% and 25%) than electively (39% and 20%) ($p < 0.01$). Fifteen percent of urgent surgeries (30/206) were related to previous known diseases, and 63% of these (19/30) were already on the waiting list for elective surgery. After surgery, the urgently operated patients developed more frequently ascites (29% vs. 11%; $p < 0.01$), AKI (54% vs 38%; $p < 0.01$), and infection (59% vs 26%; $p < 0.01$). The mortality observed at 30 and 90 days after emergent surgery was 10% (21/206) and 16% (32/206) and after elective surgery 4% (12/306) and 6% (18/306) ($p < 0.01$). The cause of mortality after urgent surgery was hepatic (38%) or infection (33%); and after elective surgery it was hepatic (50%) or cardiovascular (17%) ($p = ns$). The median (IQR) 30- and 90-day mortality estimated by VOCAL-Penn in emergent surgeries was 3.4% (1.4–10.5%) and 6.7% (2.7–16.3%) and in elective surgeries 0.5% (0.2–1.8%) and 1.3% (0.5–4.2%) ($p < 0.01$). VOCAL-Penn's c-statistic at 30- and 90-days for urgent surgery (0.83 and 0.82) was lower than for elective surgery (0.87 and 0.90), without reaching statistical significance.

Conclusion: The VOCAL-Penn has a good discriminant capacity in patients with advanced chronic liver disease undergoing emergent surgery. However, the mortality of emergent surgeries was 2–3 times higher than elective surgery. Patients undergoing emergent surgeries had more comorbidity, worse liver function, and more postoperative complications. Thus, improving the waiting list and perioperative management should be enhanced in patients with advanced chronic liver disease.

FRI-052

Anthropometric muscle mass indicators are effective in diagnosing muscle mass loss but are unable to diagnose myosteatosis, thus failing to identify all patients with sarcopenia in liver cirrhosis

Eleni Geladari¹, Theodoros Alexopoulos², Larisa Vasilieva³, Meropi Kontogianni⁴, Roxani Tenta⁴, Vasilios Sevastianos¹, Iliana Mani⁵, Alexandra Alexopoulou⁵. ¹3rd Department of Internal Medicine and Liver Outpatient Clinic, Evangelismos General Hospital, Athens, Greece; ²Gastroenterology Department, National and Kapodistrian University of Athens, Medical School, Laiko General Hospital, Athens, Greece; ³Gastroenterology Department, Alexandra Hospital, Athens, Greece; ⁴Department of Nutrition and Dietetics, School of Health Sciences and Education, Harokopio University, Athens, Greece; ⁵2nd Department of Internal Medicine and Research Laboratory, Medical School, National and Kapodistrian University of Athens, Hippokraton

Hospital, Athens, Greece

Email: elgeladari@gmail.com

Background and aims: In patients with liver cirrhosis (LC), sarcopenia is correlated with more frequent complications such as hepatic encephalopathy and increased mortality. To date, the use of computed tomography (CT) at the level of the third lumbar vertebra (L3) is considered one of the most sensitive approaches to evaluate muscle quantity and quality. However, radiation exposure and the need for experienced staff and expensive software render CT scans a challenging tool in daily clinical practice. In this study we aimed to explore the effectiveness of anthropometric measurements in assessing muscle mass compared to CT.

Method: Muscle mass was assessed by measuring the muscle mass area at L3 by CT scan, using appropriate software (SliceOmatic V4.3, Tomovision, Montreal, PQ). The area was then adjusted to height to calculate the skeletal mass index (SMI) ($\text{cm}^2/\text{height}^2$ (in m^2). Myosteatosis (low muscle quality) was defined as muscle radio-density at L3 < 41 HU for patients with dry BMI < 24.9 kg/m^2 and < 33 HU for those with ≥ 25 kg/m^2 . Handgrip (HG) strength was measured using a calibrated hydraulic hand dynamometer. Sarcopenia diagnosis, according to the latest European Working Group on Sarcopenia in Older People-2 (EWGSOP-2) criteria, consisted of low muscle strength in combination with low muscle quantity and/or quality. Low (below the 5th percentile) mid-arm circumference (MAC), mid-arm muscle circumference (MAMC), and mid-arm muscle area (MAMA) were also assessed.

Results: One hundred ninety-seven consecutive patients with LC [65.7% male, median age 61 years (IQR 52–68.5), MELD 10.5 (7.7–16), 60.9% with decompensated LC] were included. Low MAC, MAMC, MAMA, and low SMI were determined in 20.8%, 53.3%, 52.3%, and 43.4%, respectively. Sarcopenia was diagnosed in 45.2% and was the Method of Reference. HG strength in combination with low SMI (without myosteatosis) showed a sensitivity of 61.8%, specificity 100%, positive predictive value (PPV) 100%, and negative predictive value (NPV) 76%. If SMI is replaced by MAC, then the combination of low MAC with low HG offered a sensitivity of 69.7%, specificity 99%, PPV 98.4%, and NPV 79.8% in diagnosing sarcopenia. If low SMI is replaced by the presence of any one of the following: low MAC or MAMC or MAMA in combination with low HG, then sarcopenia is diagnosed with sensitivity of 61.8%, specificity 89.1%, PPV 83.3%, and NPV 74.5%. If MAC was replaced by low MAMC or low MAMA, the combination with low HG was inferior compared to MAC in diagnosing sarcopenia.

Conclusion: Among anthropometric indices, MAC is as effective as the skeletal mass index in identifying sarcopenia in LC. However, no anthropometric marker assessing muscle mass can diagnose myosteatosis, and therefore about one third of sarcopenic cases could be misdiagnosed as non-sarcopenic, if myosteatosis is not determined by imaging studies.

FRI-053

Wide variations in proton pump inhibitor use in hospitalized patients with cirrhosis in a worldwide cohort shows little impact on clinically significant outcomes

Jasmohan Bajaj¹, Patrick S. Kamath², Qing Xie³, Mark Topazian⁴, Peter Hayes⁵, Aldo Torre⁶, Hailemichael Desalegn⁷, Ramazan Idilman⁸, Zhujun Cao⁹, Mario Álvares-da-Silva¹⁰, Jacob George¹¹, Florence Wong¹², Brian Bush¹³, Wai-Kay Seto¹⁴, Leroy Thacker¹⁵, Shiv Kumar Sarin¹⁶, Alexandra Alexopoulou¹⁷, Samagra Agarwal¹⁸, R. Bart Takkenberg¹⁹, Abha Nagral²⁰, Mithun Sharma²¹, Bin Xu²², Libo Yan²³, Mauricio Castillo²⁴, Marie Jeanne Lohoues²⁵, Tongluk Teerasartipant²⁶, Danielle Ho Wei Ling²⁷, Zheng Xin²⁸, Kara Wegermann²⁹, Zeki Karasu³⁰, Damien Leith³¹, Maria Mercedes Rodriguez Gazari³², Alberto Farias³³, Federico Vilamil³⁴, Livia Victor³⁵, Adrian Gadano³⁶, Lilian Torres Made³⁷, Godolfino Miranda Zazueta³⁸, Alexander Prudence³⁹, Edith Okeke⁴⁰, Scott Davison⁴¹,

Mussagy Tarmamade⁴², Andrew Keaveny⁴³, Haibing Gao⁴⁴, Somya Sheshadri⁴⁵, Belimi Hibat Allah⁴⁶, Jinjun Chen⁴⁷, Dalia Allam⁴⁸, Aloysious Aravinthan⁴⁹, Carlos Benitez⁵⁰, Neil Rajoriya⁵¹, Danielle Adebayo⁵², Cameron Gofton⁵³, Hooi Ling Si⁵⁴, Surendra Kumar⁵⁵, Fuchen Dong⁵⁶, Peng Hu⁵⁷, Chenghai Liu⁵⁸, Liou Wei Lun⁵⁹, Henok Fisseha⁶⁰, Anil Arora⁶¹, Yanhang Gao⁶², Chuanwu Zhu⁶³, Minghua Su⁶⁴, Mingqin Lu⁶⁵, Wei Wang⁶⁶, Feng Peng⁶⁷, Ruveena Bhavani⁶⁸, Jin Guan⁶⁹, Xiaozhong Wang⁷⁰, Suditi Rahematpura⁷¹, Nik Ma Nik Arsyad⁷², Somaya Albhaisi⁷³, Chinmay Bera⁷⁴, Ning-Ping Zhang⁷⁵, Akash Roy⁷⁶, Ashok Kumar Choudhury⁷⁷. ¹Virginia Commonwealth University, Richmond, United States; ²Mayo Clinic, Rochester, United States; ³Ruijin Hospital, Shanghai Jiaotong University School of Medicine, Shanghai, China; ⁴Mayo Clinic, Minnesota, United States; ⁵The Royal Infirmary of Edinburgh, Edinburgh, United Kingdom; ⁶Instituto Nacional de Ciencias Médicas y Nutrición Salvador Zubirán, Mexico, Mexico; ⁷St Paul's Hospital Millennium Medical College, Ethiopia, Ethiopia; ⁸Ankara University School of Medicine, Ankara, Turkey; ⁹Rui Jin Hospital Affiliated to Shanghai Jiao Tong University School of Medicine, Shanghai, China; ¹⁰Hospital de Clínicas de Porto Alegre, Porto Alegre, Brazil; ¹¹Westmead Hosp/Westmead Institute, Westmead, Australia; ¹²Toronto General Hospital, Toronto, Ontario, Canada; ¹³VCU Richmond, Richmond, United States; ¹⁴The University of Hong Kong, Hong Kong, Hong Kong; ¹⁵VCU, Richmond, United States; ¹⁶Institute of Liver and Biliary Sciences, Vasant Kunj, India; ¹⁷National and Kapodistrian University of Athens, Medical School, Athens, Greece; ¹⁸All India Institute of Medical Sciences, New Delhi, New Delhi, India; ¹⁹Amsterdam University Medical Centers, Amsterdam, Netherlands; ²⁰Apollo Hospitals, Delhi, Delhi, India; ²¹AIIG Hospitals, Hyderabad, India; ²²Beijing Youan Hospital, Capital Medical University, Beijing, China; ²³Center of Infectious Disease, West China Hospital of Sichuan University, Chengdu City, China; ²⁴IMSS Hospital de Especialidades Cent, Ciudad de Mexico, Mexico; ²⁵CHU de Cocody, Abidjan, Côte d'Ivoire; ²⁶Division of Gastroenterology, Department of Medicine, Bangkok, Thailand; ²⁷Department of Gastroenterology and Hepatology, Changi General Hospital, Singapore, Simei, Singapore; ²⁸Department of Infectious Disease, Union Hospital, Tongji Medical College, Huazhong University of Science and Technology, Wuhan, China, Wuhan, China; ²⁹Duke University, Durham, United States; ³⁰Ege Üniversitesi Tıp Fakültesi, İzmir, Turkey; ³¹Glasgow Royal Infirmary, Glasgow, United Kingdom; ³²Favaloro, Buenos Aires, Argentina; ³³University of Sao Paulo, São Paulo, Brazil; ³⁴Hospital El Cruce, Buenos Aires, Argentina; ³⁵Hospital Federal de Bonsucesso, Rio de Janeiro, Brazil; ³⁶Hospital Italiano de Buenos Aires, Buenos Aires, Argentina; ³⁷Instituto de la Salud Digestiva, Guadalajara, Mexico; ³⁸Instituto Nacional de Ciencias Médicas y Nutrición "Salvador Zubirán", Mexico, Mexico; ³⁹Hunter New England Health, New Lambton, Australia; ⁴⁰Jos University Teaching Hospital, Jos, Nigeria; ⁴¹Liverpool Hospital, Liverpool, Australia; ⁴²Maputo Central Hospital, Maputo, Mozambique; ⁴³Mayo Clinic Jacksonville, Jacksonville, United States; ⁴⁴Mengchao Hepatobiliary Hospital of Fujian Medical University, Shanghai, China; ⁴⁵Mercy Medical Centre, Baltimore, Baltimore, United States; ⁴⁶Mustapha Bacha University Hospital, Algiers, Algeria; ⁴⁷Southern Hospital of Southern Medical University, Guangzhou, China; ⁴⁸Ibn. Sina Hospital, Khartoum, Sudan, Khartoum, Sudan; ⁴⁹NIHR Nottingham Biomedical Research Centre, Nottingham, United Kingdom; ⁵⁰Universidad Catolica de Chile, Santiago, Chile; ⁵¹Liver Unit, University Hospital Birmingham NHS Foundation Trust, Birmingham, Birmingham, United Kingdom; ⁵²Royal Berkshire Hospital, Reading, United Kingdom; ⁵³Royal North Shore Hospital, Sydney, Australia; ⁵⁴Royal Perth Hospital, Perth, Perth, Australia; ⁵⁵Sir Ganga Ram Hospital, New Delhi, India; ⁵⁶Department of Gastroenterology, School of Medicine, Ren Ji Hospital, Shanghai Jiao Tong University, Shanghai, China; ⁵⁷The Second Affiliated Hospital of Chongqing Medical University, Chongqing, China; ⁵⁸Shuguang Hospital Affiliated to Shanghai University of Traditional Chinese Medicine, Shanghai, China; ⁵⁹Singapore General Hospital, Bukit Merah, Singapore; ⁶⁰St Paul's Hospital Millennium Medical College, Addis Ababa, Ethiopia; ⁶¹Sir Gangaram Hospital New Delhi, Delhi, India; ⁶²The First Hospital of Jilin University, Changchun, China; ⁶³The Affiliated

Infectious Diseases Hospital of Soochow University, Suzhou, China; ⁶⁴Department of Infectious Diseases, the First Affiliated Hospital of Guangxi Medical University, Nanning, China; ⁶⁵The First Affiliated Hospital of Wenzhou Medical University, Wenzhou, China; ⁶⁶The Third Affiliated Hospital of Hebei Medical University, Shijiazhuang, Hebei, China; ⁶⁷The Second XiangYa Hospital of Central South University, Changsha, Hunan, China; ⁶⁸University of Malaya, Kuala Lumpur, Kuala Lumpur, Malaysia; ⁶⁹The Third People's Hospital of Guilin, Guilin, China; ⁷⁰Traditonal Chinese Medical Hospital Affiliated to Xinjiang Medical University, Urumqi, China; ⁷¹Perelman School of Medicine, Philadelphia, United States; ⁷²University of Malaysia, Kuala Lumpur, Malaysia; ⁷³Virginia Commonwealth University, Richmond, Richmond, United States; ⁷⁴University Health Network, Toronto, Canada; ⁷⁵Zhongshan Hospital, Shanghai, China; ⁷⁶SGPGI Lucknow, LUCKNOW, India; ⁷⁷Institute of Liver and Biliary Sciences, New Delhi, India
Email: jasmohan.bajaj@vcuhealth.org

Background and aims: Proton pump inhibitors (PPI) are linked with infections and cirrhosis complications. A worldwide assessment of patterns, indications and effect on outcomes is unclear. Aim: Determine impact of PPI on outcomes in a multi-national cohort of cirrhosis inpatients.

Method: CLEARED Consortium, consisting of >110 centres across 6 continents enrolled patients with cirrhosis admitted prospectively. Patients are followed through their hospitalization to track deaths, ICU and organ dysfunction, or hospice transfer. Cirrhosis details, admission reasons and medications are recorded. Centres are classified based on World Bank into High/upper or lower middle income (HIC/UMIC/LMICs). PPI type, indications (appropriate/not assessed by site PIs based on guidelines), regional variations and impact on outcomes (AKI, infections, death, ICU) were analysed.

Results: 4305 pts (56yrs, 64% men, 40% alcohol, MELD 21) for 26 countries (37% HIC, 45% UMI and 18% LMICs) were enrolled. 21% were admitted with infections. 33% developed AKI, 18% ICU transfer, 2% got transplanted and 13% died during the admission. PPI use: 1831 (42%) were on PPI; only 58% had adequate indications. Most were pantoprazole (52%) then omeprazole (30) and esomeprazole (9%). A higher percent of HIC pts was on PPI on admission vs UMIC/LMICs (48 vs 31 vs 21%, $p < 0.0001$). Lowest PPI use (~30%) was in China, rest of Asia and Africa, while >48% of pts in rest of the world were on PPI. Rates of adequate PPI indications were lowest in Indian sites (40%) and highest in North American (67%) sites. Infections and PPI: PPI use was higher in pts with spontaneous bacteraemia (9 vs 5%, $p = 0.02$) and lower in respiratory infections (14 vs 20%, $p = 0.004$) on admission. Remaining infections were similar. PPI use was not associated with higher nosocomial infections (12% both). Inpatient course and outcomes: PPI users on admission had similar MELD (21 both, $p = 0.2$) but higher use of NSBB, lactulose, diuretics, rifaximin, statins and HBV antivirals (all $p < 0.001$). PPI users had higher respiratory failure (10 vs 8%, $p = 0.03$), renal failure (5 vs 3%, $p = 0.001$), AKI (35 vs 30%, $p = 0.003$) and transplant (3 vs 1%, $p < 0.001$). Circulatory (11% both) and brain failure (12% both), and mortality (13 vs 12, $p = 0.7$) were similar regardless of PPI use. Multivariable analysis: PPI use was not significantly associated with ICU transfer, AKI, in-hospital mortality or in-hospital transplant. Variables predictive of these outcomes were age, MELD-Na, infections on admission and not being in an HIC.

Conclusion: In a multi-national inpatient prospective cirrhosis cohort across 6 continents, PPI use was seen in 42% of patients, which was highest in Indian sites and lowest across Chinese and African sites. Only 58% of PPI use was for approved indications. Although PPI use was associated with certain infections, transplant, AKI, and ICU on crude analysis none of these associations remained significant on multivariable analysis.

FRI-055

Outcomes of minimal ascites in patients with etiologically controlled liver cirrhosis

Haiyu Wang¹. ¹Nanfang Hospital, Southern Medical University, Guangzhou, China
Email: 375612668@qq.com

Background and aims: Insufficient data are available regarding whether a minimal amount of ascites only detected in imaging procedures can be considered as decompensation. Little is known about the effects of minimal ascites on patient outcome. We aimed to evaluate prognostic significance of minimal ascites in aetiology controlled cirrhosis.

Method: We performed a post-hoc analysis of data from 1674 patients with cirrhosis with etiology controlled (1440 compensated, 234 patients with minimal ascites, 297 with decompensated) who participated a prospective cohort study from April 2019 to October 2022. and we also included homogenous patients who screened in the ultrasound room and defined as minimal ascites in our clinical unit (N = 403). Patients were evaluated at least every 6 months. Liver related events including decompensation events (development of clinically significant ascites, bleeding due to portal hypertensive sources, or overt hepatic encephalopathy), HCC development and death were documented.

Results: Among the 1674 patients, the etiologies included HBV (85.7%), HCV (3.6%), and alcoholic liver disease (6.4%), all of which were removal/suppression. Liver stiffness and spleen stiffness measurements were higher in patients with minimal ascites than in those with decompensation ($p < 0.0001$). Additionally, the prevalence of high-risk varices was higher in patients with minimal ascites compared to those with decompensation (16.7% vs. 52.5%, $p < 0.0001$). Over a median follow-up of 29 months (IQR 20–42), 24 patients developed decompensated episodes, and 46 patients developed HCC among the 1440 compensated cirrhosis cases. In the subgroup of 234 patients with minimal ascites, 34 patients experienced decompensated episodes, and 18 patients developed HCC during follow-up. The risk of developing decompensation in the minimal ascites group was significantly higher compared with compensated cirrhosis (HR = 8.505, 95% CI 5.51–13.12, $p < 0.0001$). Furthermore, compared with the compensated group, the minimal ascites group had a significantly increased risk for the development of HCC (HR = 1.75, 95% CI 1.09–2.80, $p < 0.05$). We also validated a higher incidence of decompensation and HCC in the clinical cohort of 406 cirrhosis cases with minimal ascites.

Conclusion: In an analysis of data from a large cohort of cirrhosis with controlled etiology, we discovered that minimal ascites is associated with more complications, a higher incidence of HCC and increased mortality compared with compensated patients. Patients with cirrhosis with minimal ascites should be monitored closely as they show an increased risk of mortality and complications.

FRI-056-YI

Clinical impact of acute kidney disease in patients with decompensated cirrhosis: insights from a prospective observational study on renal dysfunction

Alberto Calleri¹, Marco Tizzani¹, Francesco Frigo¹, Elisa Bertoldi¹, Daniela Campion¹, Gian Paolo Caviglia¹, Antonio Ottobrelli¹, Alfredo Marzano¹, Giorgio Maria Saracco¹, Carlo Alessandria¹.
¹Division of Gastroenterology and Hepatology, A.O.U. Città della Salute e della Scienza di Torino, University of Turin, Turin, Italy
Email: alberto.calleri.md@gmail.com

Background and aims: Renal dysfunction is very common among patients hospitalized for decompensated cirrhosis. In this setting, acute kidney disease (AKD) has been suggested to impact significantly on prognosis, but data are scant. We aimed to assess prevalence and clinical outcomes of AKD compared to patients with no kidney disease (NKD) and acute kidney injury (AKI).

Method: All patients hospitalized in a 18-month period for decompensated cirrhosis were prospectively evaluated. Patients were classified according to their renal function as per International Club of Ascites definitions and then followed-up until death or liver transplant (LT). Patients with eGFR persistently < 60 ml/min for a follow-up period of at least three months were considered to have new-onset chronic kidney disease (CKD).

Results: 295 patients were screened, 204 enrolled. The most frequent etiology of cirrhosis and cause of hospitalization were alcohol (55%) and ascites (64%), respectively. Renal function was categorized as follows: 17% NKD, 35% AKD, 27% AKI, 10% CKD, 11% acute-on-chronic kidney disease (ACKD). Median serum creatinine was: 0.83, 0.98, 1.70, 1.77, 3.13 mg/dL, respectively. Age was not significantly different between the three groups. Similarly, the proportion of patients with worst liver function (Child C) was not significantly different between patients with AKD (47%) and both NKD (29%, $p = 0.1$) and AKI (57%, $p = 0.2$). Median follow-up was 3.9 months (IQR 1.6–9.2). Overall, 53 patients (26%) were transplanted and 46 (23%) died. Out of 79 patients with follow-up ≥ 3 months, 8 (10%) developed new-onset CKD. The incidence was 0/25 for NKD, 5/33 (15%) for AKD and 3/21 (14%) for AKI (AKD vs NKD, $p = 0.06$; AKD vs AKI, $p = 0.9$; NKD vs AKI, $p = 0.09$). Among the patients discharged after the index hospitalization, the rate of hospital readmission was comparable between the three groups (Log-rank $p = 0.9$). The 1 and 6-month LT-free survival was respectively 100% and 96% in NKD, 96% and 89% in AKD, 77% and 65% in AKI. Survival of AKD patients was then similar to those with NKD (Log-rank $p = 0.22$ and $p = 0.19$, respectively) and significantly better if compared with AKI (Log-rank $p = 0.003$ and $p = 0.002$, respectively).

Conclusion: AKD is very common among patients hospitalized for decompensated cirrhosis. Our preliminary results suggest that AKD, unlike the few data currently available in the literature, is not clinically meaningful, being associated with a short- and medium-term LT-free survival similar to that of NKD and significantly better if compared with AKI.

FRI-057

End of life care in advanced chronic liver disease: results from a national audit of practice in the United Kingdom

Daniel Maggs¹, Emma Saunbury². ¹University Hospitals of Bristol and Weston NHS Trust, Bristol, United Kingdom; ²Somerset NHS Foundation Trust, Taunton, United Kingdom
Email: danrmaggs@gmail.com

Background and aims: The last year of life (LYOL) in advanced chronic liver disease (ACLD) is associated with a high symptom burden and healthcare utilisation. End of life care (EOLC, i.e. palliative care given to patients in their LYOL) is historically poorer in ACLD compared to other life-limiting conditions and barriers to high-quality EOLC in ACLD are recognised. Advance care planning (ACP) and palliative interventions improve EOLC, yet opportunities for ACP are frequently missed and utilisation of specialist palliative care services (SPCS) is variable. EVOLVE (End of life care in adVanced chrOnic LiVeR disease) is the first national audit of EOLC provision in ACLD in the United Kingdom (UK). We aimed to evaluate patient and service level factors associated with quality EOLC and measure the impact of deprivation on EOLC provision.

Method: A retrospective, multi-centre audit was undertaken of adults who died of ACLD between 1st January–30th June 2022 and had at least one non-terminal admission in their LYOL. Site recruitment was undertaken via trainee research networks, social media and promotion via endorsing organisations. Patients were identified by ICD-10 (International Classification of Diseases Tenth Revision) coding and review of electronic records. Patient and service level variables were analysed against markers of quality EOLC (assessed via the surrogate outcomes of documented discussions regarding prognosis, ACP and SPCS referral).

Results: Eighty-three sites contributed data for 803 patients. In the LYOL, 49.9% had a documented discussion about prognosis and 36.9% received ACP. Documentation of prognostic scores (39.6%) and transplant suitability (56.2%) was inconsistent. Only 26.2% of patients were discussed at an ACLD multidisciplinary team (MDT) meeting. 46.9% were referred to inpatient SPCS, though 79.1% of these referrals were only during a terminal admission. Documentation of transplant suitability was significantly associated with prognosis being discussed ($p < 0.001$), prognostic discussion at an earlier stage ($p = 0.04$), ACP ($p < 0.001$) and SPCS referral ($p < 0.001$). Discussions about prognosis were more likely ($p < 0.001$) when a prognostic score was documented. ACP was more likely following ACLD MDT ($p = 0.046$) and in patients having outpatient paracentesis ($p < 0.001$). 11% of patients were in the lowest two Index of Multiple Deprivation centiles, but there was no significant variation in any outcomes.

Conclusion: EVOLVE has revealed inadequacies in EOLC for patient with ACLD in the UK. Utilisation of SPCS prior to a terminal admission was poor. Factors associated with improved EOLC have been demonstrated, highlighting a focus for service improvement. Recent guidance statements from North America highlight standards for EOLC in cirrhosis and similar guidance from professional bodies in the UK and Europe could aid in changing practice.

FRI-058

Smoking cessation correlates with rapid decrease of inflammatory markers in patients with decompensated cirrhosis

Letitia Toma¹, Mihai Daniel Dodot¹, Teodora Isac¹, Simona Ioanitescu¹, Laurentiu Micu¹, Adriana Rusie², Laura Iliescu¹. ¹Fundeni Clinical Institute, Carol Davila University of Medicine and Pharmacy, Bucharest, Romania; ²Fundeni Clinical Institute, Carol Davila University of Medicine and Pharmacy, Bucharest, Romania
Email: letitia_toma@yahoo.com

Background and aims: Smoking is a well-known cardiovascular risk factor as well as an important risk factor for metabolic syndrome-associated steatotic liver disease (MASLD), by promoting systemic inflammation. Recent studies have found significant differences in white blood cell count (WBC) and serum c-reactive protein (CRP) in patients with compensated and decompensated liver disease, in relationship with smoker status. We aim to evaluate the impact on smoking cessation in patients with decompensated cirrhosis.

Method: We performed a prospective observational study in active smoker patients with decompensated cirrhosis (Child B and C) admitted to our clinic between January 2023 and June 2023. Patients were classified as light smokers (less than 1 pack/day) or heavy smokers (more than 1 pack/day). Patients were entered into smoking quitting programs and reevaluated at 6 months after smoking cessation. We determined WBC count and serum levels of CRP, ferritin and B12 vitamin.

Results: Out of 132 patients included, only 74 completed the smoking cessation programs (48 Child B and 26 Child C patients, mean age 51.94 ± 28.17 years, 69% female). Etiology of cirrhosis was: 31% alcohol-related, 28.4% viral, 40.6% MASLD. Initial evaluation revealed 58.1% light smokers and 41.9% heavy smokers. We noted a significant decrease in inflammatory markers after smoking cessation, in light smokers as well as heavy smokers. In light smokers, WBC decreased from 6.82 G/L to 6.23 G/L, $p = 0.04$, CRP decreased from 4.47 mg/L to 3.11 mg/L, $p = 0.02$, ferritin decreased from 213 ng/ml to 176 ng/ml, $p = 0.03$, and B12 vitamin decreased from 987 pg/ml to 881 pg/ml, $p = 0.01$. In heavy smokers, WBC decreased from 7.33 G/L to 5.71 G/L, $p = 0.01$, CRP decreased from 7.22 mg/L to 3.98 mg/L, $p = 0.01$, ferritin decreased from 289 ng/ml to 138 ng/ml, $p = 0.02$, and B12 vitamin decreased from 1387 pg/ml to 935 pg/ml, $p < 0.001$. We also found that inflammation was significantly more diminished in Child B versus Child C patients: WBC 1.52 G/L versus 0.6 G/L, $p = 0.01$, CRP 3.31 mg/L versus 2.04, $p < 0.001$, ferritin 114 ng/ml versus 65 ng/ml, $p = 0.02$, B12 vitamin 421 pg/ml versus 132 pg/ml, $p < 0.001$.

Conclusion: Smoking cessation decreases systemic inflammation in Child B and C cirrhosis at 6 months follow-up. As systemic inflammation is a key point in progression of liver disease, smoking cessation is an important contributor to its management, regardless of the severity of liver disease.

FRI-059

Proton pump inhibitors are not associated with an increased risk of hepatic encephalopathy

Simon Johannes Gairing¹, Chiara Mangini², Lisa Zarantonello², Elise Jonasson Nielsen³, Henrike Dobbermann⁴, Philippe Sultanik⁵, Peter R. Galle¹, Joachim Labenz⁶, Dominique Thabut⁷, Jens U. Marquardt⁴, Patricia Bloom⁸, Mette Lauridsen³, Sara Montagnese^{2,9}, Christian Labenz¹. ¹University Medical Center of the Johannes Gutenberg-University, Mainz, Germany; ²University of Padova, Padova, Italy; ³Hospital of South West Jutland, Esbjerg, Denmark; ⁴University Hospital Schleswig-Holstein, Lübeck, Germany; ⁵Sorbonne Université, Paris, France; ⁶Diakonie Hospital Jung-Stilling, Siegen, Germany; ⁷Sorbonne Université, Paris, Germany; ⁸University of Michigan, Ann Arbor, United States; ⁹University of Surrey, Guildford, United Kingdom
Email: sgairing@uni-mainz.de

Background and aims: Several studies suggest an association between proton pump inhibitor (PPI) use and hepatic encephalopathy (HE). However, multicenter studies including a large number of patients are scarce. This study aimed to analyze the association between PPI use, minimal HE (MHE) and overt HE (OHE) in a large multicenter setting.

Method: This retrospective study included patients with cirrhosis from seven centers (Germany, France, Italy, Denmark, Michigan, US). MHE was defined by the Psychometric Hepatic Encephalopathy Score (PHES) at baseline. Scoring was done according to validated country-specific norms. Patients were followed for the development of OHE, liver transplantation or death. In multivariable competing risk regression analysis, transplantation and death were considered as competing events.

Results: Data from 1160 patients were analyzed. Median age was 60 years (range 23–87), and most patients were male (65%). Median MELD was 11, Child-Pugh stages were A 49%, B 39%, C 11%. MHE was diagnosed in 385 patients (33.2%). On the day of study inclusion, 58% of patients used PPIs of whom only 30% had a hard indication for PPI treatment. During follow-up (median 18.1 months), 20% of patients developed an episode of OHE, and 19% died or underwent liver transplantation. In multivariable logistic regression analysis, PPI use was not associated with MHE at study inclusion (odds ratio 1.07, 95% CI 0.80–1.43, $p = 0.7$). In addition, PPI use was not associated with an increased risk of developing OHE in competing risk regression analysis (subdistribution hazard ratio 1.13, 95% CI 0.81–1.59, $p = 0.5$). These findings were confirmed in subgroup analysis including only patients without a history of OHE ($n = 803$) or only patients with Child-Pugh A or B. In addition, PPI use was neither associated with an increased OHE risk in patients with an indication for PPI treatment nor without an indication.

Conclusion: PPI use does not appear to be associated with an increased HE risk in patients with cirrhosis.

FRI-067

Impact of Farnesoid X receptor polymorphisms on prognosis in hepatocellular carcinoma

Talha Ozudogru¹, Elvan Isik², Fulya Günsar², Ilker Turan², Zeki Karasu², Ulus Akarca². ¹Ege University, Faculty of Medicine, Department of Internal Medicine, Izmir, Turkey; ²Ege University, Faculty of Medicine, Department of Gastroenterology, Izmir, Turkey
Email: ulusakarca@gmail.com

Background and aims: Refining staging and treatment for Hepatocellular Carcinoma (HCC) is crucial, particularly considering the biological behavior and genetic characteristics. The Farnesoid X

POSTER PRESENTATIONS

receptor (FXR) has been implicated as a tumor suppressor in HCC, warranting further investigation.

Objective: This study explores the distribution of genotypes for four FXR-linked single nucleotide polymorphisms (SNPs) in cirrhotic patients with and without HCC, and examines the correlation of these genotypes with prognostic parameters and survival.

Method: A cohort of 101 consecutive newly diagnosed HCC patients developed on cirrhosis (2020–2021) was compared with 101 age, sex, and etiology-matched cirrhotic controls without HCC. Genotyping of SNPs rs56163822, rs35724, rs11110385, and rs11110390 in peripheral blood mononuclear cells was conducted. Statistical analysis assessed allelic distributions between groups and the impact of genotypes on clinical severity, alpha-fetoprotein levels, liver function, and patient survival.

Results: Genotypic distributions of the SNPs did not significantly differ between HCC and cirrhosis patients. However, the rs35724 GG genotype in HCC patients was linked to notably lower survival rates in those with poor prognostic features compared to GC/CC (non-GG) genotypes. This trend was consistent across various patient subgroups, with statistical significance in survival differences for those with vascular invasion, higher ALBI grades, elevated Child-Pugh scores, and increased alpha-fetoprotein levels. In vascular invasion, ALBI grades 2–3, ALBI grade 3, Child-Pugh >5, and AFP >400 ng/ml subgroups, median survivals for GG vs non-GG were 3 vs 12 ($p = 0.0332$), 8 vs 24 ($p = 0.0176$), 6 vs 20 ($p = 0.0103$), 7 vs 24 ($p = 0.0100$), and 3 vs 24 months ($p = 0.0551$), respectively.

Conclusion: FXR polymorphisms, particularly the rs35724 GG genotype, do not increase HCC risk in cirrhotic patients but are associated with reduced survival in HCC patients with adverse prognostic factors. This genotype could be a vital consideration in tailoring therapeutic strategies for HCC, as non-GG variants of rs35724 appear to indicate a more favorable prognosis. Our findings underscore the importance of genetic profiling in HCC management, offering potential for personalized treatment approaches.

FR1-068

Predictors of clinical trajectories in patients surviving an acute decompensation of cirrhosis

Carmine Gambino¹, Antonio Accetta¹, Simone Incicco², Roberta Gagliardi³, Nicola Zeni³, Marta Tonon³, Valeria Calvino³, Anna Barone³, Paolo Angeli⁴, Salvatore Piano³. ¹Unit of Internal Medicine and Hepatology (UIMH), Department of Medicine, University of Padova, Padova, Italy; ²Unit of Internal Medicine and Hepatology (UIMH), Department of Medicine, University of Padova, Padova, Italy; ³Unit of Internal Medicine and Hepatology (UIMH), Department of Medicine, University of Padova, Padova, Italy; ⁴Unit of Internal Medicine and Hepatology (UIMH), Department of Medicine, University of Padova, Padova, Italy
Email: salvatorepiano@gmail.com

Background and aims: three different clinical trajectories have been described in patients surviving an acute decompensation (AD) of cirrhosis, namely stable decompensated cirrhosis (SDC), unstable decompensated cirrhosis (UDC) and pre-ACLF (Acute-on-chronic Liver Failure). The identification of these patients could be crucial in their clinical management, however, predicting the clinical course at time of discharge is challenging. The aim of the study was to investigate predictors of clinical course after discharge for AD and 180-day mortality.

Method: clinical, laboratory and pharmacological data at admission, during hospitalization and at discharge were collected from patients surviving an AD of cirrhosis in our Unit. Patients were followed up until transplant, death, or 180 days.

Results: We included 360 patients (age 62 ± 12 ; male 66%; alcoholic aetiology 55%; MELD 16 [12–22]). At 90-day after discharge, 195 (54%) patients were identified as SDC, 115 (32%) as UDC and 50 (14%) as pre-ACLF. Sixteen (22%) patients underwent LT. At discharge, pre-ACLF patients showed, if compared to SDC and UDC patients, higher serum

creatinine (1.29 vs 0.83 vs 0.85 mg/dl; $p < 0.001$), INR (1.59 vs 1.39 vs 1.38; $p = 0.027$), neutrophils (3.82 vs 2.92 vs $2.97 \times 10^9/l$; $p = 0.033$), MELD (19 vs 14 vs 14; $p < 0.001$). We couldn't find any difference between SDC and UDC patients at discharge. At 180-days after discharge, mortality rate was higher in pre-ACLF respect to UDC and SDC (38% vs 16% vs 2%; $p < 0.0001$), and 30 (8.3%) patients underwent LT. In a multivariable model (adjusted for age, gender, aetiology, presence of varices, AKI or HE during hospitalization, serum creatinine, INR, bilirubin, CRP at discharge, and clinical trajectory) higher levels of CRP (HR 1.02; CI 1.00–1.05; $p = 0.021$), UDC (HR 9, 98; CI 1.76–56; $p = 0.009$) and pre-ACLF (HR 31.4; CI 4.71–209; $p < 0.001$) were independent predictors of 180-day mortality.

Conclusion: Our study is one of the first external confirmation of the clinical trajectories after AD of cirrhosis showed in PREDICT cohort. Pre-ACLF patients showed worse liver and kidney function, and higher systemic inflammation at discharge. We were unable to distinguish SDC from UDC at discharge. Future trials and more raffinate biomarkers could be help in answering this question.

FR1-069

Rifaximin monotherapy has significantly reduced the risk of overt hepatic encephalopathy recurrence versus lactulose monotherapy in patients with cirrhosis and a history of previous episode (s): a post hoc analysis of randomized trials

Jasmohan Bajaj¹, Robert Rahimi², Christopher Allen³, Zeev Heimanson³, Robert Israel³, Kris V. Kowdley⁴. ¹Virginia Commonwealth University, Richmond VA Medical Center, Richmond, United States; ²Baylor University Medical Center, Dallas, United States; ³Salix Pharmaceuticals, Bridgewater, United States; ⁴Liver Institute Northwest, Elson Floyd College of Medicine, Spokane, United States
Email: jasmohan.bajaj@vcuhealth.org

Background and aims: Lactulose monotherapy is recommended as secondary prophylaxis after an initial episode of overt hepatic encephalopathy (OHE), with rifaximin as add-on therapy when additional episodes occur. However, lack of patient adherence and/or adverse effects of lactulose may require alternative management strategies. The aim of this analysis was to compare the efficacy and safety of rifaximin monotherapy with lactulose monotherapy for reducing the risk of OHE recurrence in patients with cirrhosis and a history of OHE.

Method: Two randomized trials (1 phase 3 double-blind and 1 phase 4 open-label) of adults who had cirrhosis and a history of OHE occurrence during the previous 6 months and were currently in OHE remission (Conn score ≤ 1) were included in this post hoc analysis. Only data from patients who received rifaximin 550 mg twice daily (ie, no concomitant lactulose [phase 3 or 4]) or lactulose (titrated to 2–3 soft stools/d) plus placebo (ie, lactulose monotherapy [phase 3]) for up to 6 months were analyzed. The primary efficacy end point in both trials was time to first breakthrough OHE episode (Conn score ≥ 2).

Results: A total of 270 patients were treated with rifaximin monotherapy ($n = 125$) or lactulose monotherapy ($n = 145$). The mean (SD) age in the rifaximin and lactulose groups was 58.2 (9.5) vs 56.6 (9.3) y, respectively; 60.0% vs 68.3% were male, 51.2% vs 46.2% were Child-Pugh class B, and the median Model for End-Stage Liver Disease score was 12 for both groups. The majority of patients had a baseline Conn score of 0 (rifaximin, 68.8%; lactulose, 67.6%). Significantly fewer patients treated with rifaximin monotherapy experienced an OHE episode vs lactulose monotherapy (23.2% vs 49.0%, respectively; $p < 0.0001$), with a 60% reduction in the risk of a breakthrough OHE event during 6 months of monotherapy treatment with rifaximin compared with lactulose (hazard ratio, 0.40; 95% CI, 0.26–0.62). Fewer patients treated with rifaximin monotherapy had an HE-related hospitalization compared with lactulose monotherapy, although the difference was not statistically significant (19.2% vs 23.4%, respectively, $p = 0.18$). The most commonly reported AEs (excluding HE) in rifaximin vs lactulose groups were nausea (13.6% vs

14.5%), fatigue (12.8% vs 12.4%), peripheral edema (16.0% vs 9.0%), constipation (14.4% vs 6.9%), diarrhea (4.8% vs 14.5%), headache (7.2% vs 11.7%), insomnia (11.2% vs 7.6%), and ascites (7.2% vs 10.3%). Discontinuation from study participation was higher in the lactulose monotherapy group (62.1%) vs the rifaximin monotherapy group (36.0%), most commonly due to OHE occurrence.

Conclusion: Rifaximin monotherapy was well tolerated and was associated with significantly fewer episodes of OHE recurrence than lactulose monotherapy in patients with cirrhosis and a history of OHE.

FRI-070-YI

Prevalence of dysgeusia in patients with advanced chronic liver disease, relationship with the liver-disease progression status, and impact on malnutrition-sarcopenia-frailty

Marcello Dallio¹, Mario Romeo¹, Marina Cipullo¹, Annachiara Coppola¹, Simone Mammone¹, Giuseppe Zagaria¹, Giorgia Iadanza¹, Carmine Napolitano¹, Simone Olivieri¹, Luigi Maria Vitale¹, Alessandro Federico¹. ¹Hepatogastroenterology Division, Department of Precision Medicine, University of Campania "Luigi Vanvitelli", Naples, Italy
Email: marioromeo@virgilio.it

Background and aims: Dysgeusia is a disorder defined by a distortion of the sense of taste whose prevalence, relationship with the progression of the disease, and direct contribution to malnutrition (and consequently, sarcopenia-frailty) in advanced chronic liver disease (ACLD) have never been systematically explored.

Method: In this observational study, 40 controls, 50 chronic-liver disease-affected individuals staging initial-mild fibrosis (<F3), and 150 ACLD patients of various etiologies were enrolled. Anthropometrical, biochemical, clinical, and nutritional data were collected. The opportunely-modified CITAS (Chemotherapy-induced Taste Alteration Scale) questionnaire was used to assess the dysgeusia. Child-Pugh (CP) and Liver Frailty Index (LFI) calculations, Liver Stiffness Measurement (LSM), and Bioelectrical Impedance Analysis (BIA) were performed. Skeletal Muscle Mass (SMM) index (SMMI) (SMM/height²) <7 kg/m² (male) and <5.7 kg/m² (female) defined sarcopenia. ACLD patients were 2 years followed up semiannually and Liver-related events (LREs) (ascites, hepatic encephalopathy, bleeding, jaundice, and bacterial infection) were collected.

Results: The prevalence of dysgeusia was significantly higher in ACLD (68%) in comparison to <F3 (8%) individuals and controls (5%) and in decompensated ACLD (dACLD) than compensated (cACLD) (54% vs 6%) patients (all $p < 0.0001$). In line, CITAS-dysgeusia severity positively correlated with CP (R:0.81), as well as with the levels of appetite impairment (R:0.93) (both $p < 0.0001$).

Logistic regression analysis, appropriately weighted for factors notoriously impacting food intake in ACLD patients (low-sodium diet, drugs/supplements taken, physical activity frequency, occurrence of encephalopathy and ascites episodes in the previous 2 weeks), revealed the level of impairment of the appetite as a factor significantly associated with dysgeusia [HR: 2.12; $p:0.02$].

Compared to no-dysgeusia-affected dACLD ($p:0.03$), dysgeusia-affected dACLD patients (dys-dACLD) showed a decreased daily protein intake, reduced Free Fat Mass % ($p < 0.0001$), and SMMI ($p < 0.0001$; $p:0.04$), in contrast with increased LFI ($p < 0.0001$). Consistently, dys-dACLD patients showed a higher prevalence (59% vs 39%) of sarcopenia ($p:0.0002$). The Kaplan-Meier Log-Rank Test analysis on LREs'occurrence showed HR:3.53 for dys-dACLD individuals.

Conclusion: The prevalence of dysgeusia, increasing in parallel to the worsening of liver disease, promoted sarcopenia-frailty pictures, negatively influencing ACLD patients' outcomes.

FRI-071

Complications following percutaneous liver biopsy: results of a nationwide database

Markus Graf¹, Christiana Graf², Sebastian Ziegelmayr¹, Joshua Gawlitzka¹, Markus Makowski¹, Philipp Paprottka³, Nele Willemsen³, Jonathan Nadjiri³. ¹Klinikum rechts der Isar, Technical University Munich; Department of Diagnostic Radiology, Munich, Germany; ²LMU University Hospital Munich, Munich, Germany; ³Klinikum rechts der Isar, Technical University Munich; Department of Interventional Radiology, Munich, Germany
Email: markus.m.graf@tum.de

Background and aims: Liver biopsy is the gold standard for evaluating liver diseases, the diagnosis of liver fibrosis and cirrhosis and malignancy. However, it is susceptible to complications, and safety data on liver biopsies remain scarce. The following study examined the complication rates following percutaneous liver biopsies.

Method: We performed a study using data collected by the German interventional radiology society (DeGIR) from 2018 to 2021 of elective percutaneous liver biopsies. Clinical and biochemical parameters, technical features and adverse events were retrospectively examined.

Results: From 2018 to 2021 a total of 12228, liver biopsies were performed in 194 participating centers in Germany. The median age of the study cohort was 66.16 years (range: 18–104 years) and 6120 were male (50.05%). 8127 punctures were performed CT-guided (66.4%), whereas 4101 interventions (33.5%) were performed with ultrasound. Complications occurred in 224 biopsies (1.83%), of which 183 (1.5%) were major adverse events. Minor complications in form of procedural hypotension and pain occurred in 7 and 34 cases (0.06% and 0.28%, respectively). Major complications such as bleeding, organ injury and pneumothorax were observed in 155, 4 and 24 cases (1.27%, 0.03%, 0.20%). Six subjects (0.05%) died as a result of massive intraperitoneal bleeding. Major complications were significantly more frequently observed in patients with thrombocytopenia ($p = 0.01$) as well as in patients undergoing ultrasound-guided procedure compared to a computed tomography (CT-) guided one ($p < 0.001$). In contrast, the type of needle size used ($p = 0.323$), internationalized ratio (INR) ($p = 0.09$), aPTT ($p = 0.98$), gender ($p = 0.83$), age ($p = 0.08$) and the liver segment punctured ($p = 0.97$) did not influence the frequency of major adverse events. By multivariate logistic regression analysis, platelet count and ultrasound-guided modality were identified as the only independent risk factors of post-biopsy bleeding ($p = 0.001$ and $p < 0.001$, respectively).

Conclusion: Percutaneous liver biopsies are safe with rare procedural morbidity. Our data confirm previous data by showing that post-procedural bleeding was not associated with INR and aPTT in patients undergoing invasive procedures. However, measurement of platelet count is indicated especially in patients with liver cirrhosis to identify patients with increased procedural bleeding risk. Moreover, patients with liver cirrhosis as well as patients with complex findings and difficult localizations should undergo CT-guided puncture.

FRI-074-YI

Rifaximin reduces healthcare utilization but not overall costs in patients with cirrhosis and recurrent episodes of hepatic encephalopathy: a retrospective efficacy study

Diederick van Doorn¹, Kirs van Eekhout¹, Koos de Wit¹, L.C. Baak², Michael Klemt-Kropp³, Bart Verwer⁴, Philip W. Friederich⁵, Gijs J. de Bruin⁶, Xander Vos⁷, R. Bart Takkenberg¹. ¹Amsterdam UMC, Amsterdam, Netherlands; ²OLVG, Amsterdam, Netherlands; ³Noordwest Ziekenhuisgroep, Alkmaar, Netherlands; ⁴Spaarne Gasthuis, Hoofddorp, Netherlands; ⁵Meander Medisch Centrum, Amersfoort, Netherlands; ⁶Tergooi MC, Hilversum, Netherlands; ⁷Dijklander Hospital, Hoorn, Netherlands
Email: d.j.vandoorn@amsterdamumc.nl

POSTER PRESENTATIONS

Background and aims: Hepatic encephalopathy (HE) is a frequent complication of cirrhosis. Rifaximin has been approved and included in guidelines for secondary prevention of HE, but there are few real-world data on its efficacy and impact on healthcare utilization. In this study, we aimed to assess the efficacy of rifaximin as secondary prophylaxis for HE in Dutch patients.

Method: We conducted a real-life cohort analysis from March 2010 to May 2023 in patients from 7 hospitals in the province of North Holland and Utrecht (The Netherlands), reflecting approximately 10% of the Dutch population, who received rifaximin as secondary prophylaxis for HE. Data were collected and compared six months before and six months after the prescription of rifaximin. The primary end point was transplant free survival (TFS). Secondary end points were the effect of rifaximin on healthcare utilization, defined as the quantification of each patient contact with the hospital, such as the number and length of admissions and emergency department visits, and the effect of rifaximin on healthcare costs.

Results: We included 126 patients [65% male; median age 68 (IQR: 61.0–75.3)] with a median Model for End-stage Liver Disease (MELD) score of 15 (IQR: 12–20). Most common etiology was alcohol related liver disease (55%). At end of follow-up, 63% of patients were deceased with a median TFS of 23 months (95%CI: 14.6–31.4). The mean number of HE episodes after starting rifaximin was 0.9 (\pm 1.1), which was lower than before starting rifaximin (2.2; \pm 1.3; 95%CI: 1.0–1.6; p < 0.001). In addition, mean healthcare utilization decreased from 6.1 (\pm 3.3) contacts in the six months before rifaximin to 3.3 (\pm 2.6) contacts in the six months after rifaximin (95%CI: 2.1–3.5; p < 0.001). The mean number of hospital admissions decreased from 1.7 (\pm 1.6) admissions per patient before to 1.0 (\pm 1.3) admissions after starting rifaximin (95%CI: 0.4–1.1; p < 0.001). Mean length of admission did not differ. The mean number of outpatient visits decreased from 2.4 (\pm 1.8) visits per patient before starting rifaximin to 1.7 (\pm 1.4) visits after starting rifaximin (95%CI: 0.3–1.0; p = 0.001). The mean number of visits to the emergency department decreased from 0.33 (\pm 0.6) per patient to 0.15 (\pm 0.5; 95%CI: 0.0–0.3; p = 0.024). An estimate of the annual costs was made based on publicly available data in the Netherlands. The annual costs of rifaximin are € 4.555 per patient. The estimated annual costs of healthcare utilization per patient before starting rifaximin were € 13.320. This was similar to the costs after rifaximin was prescribed (€ 13.120).

Conclusion: In this Dutch real-life cohort, rifaximin significantly reduced the number of episodes of HE, the number of hospital admissions and the number of outpatient and emergency department visits, hereby contributing to a reduction in healthcare utilization. Unfortunately, rifaximin did not lead to reduced overall costs.

FRI-075

The lower, the worse? Impact of PHES results on the risk of overt hepatic encephalopathy in patients with minimal hepatic encephalopathy

Simon Johannes Gairing¹, Chiara Mangini², Lisa Zarantonello², Elise Jonasson Nielsen³, Sven Danneberg⁴, Philippe Sultanik⁵, Peter R. Galle¹, Stefania Gioia⁶, Joachim Labenz⁷, Anna Lok⁸, Jens U. Marquardt⁴, Mette Lauridsen³, Patricia Bloom⁸, Dominique Thabut⁹, Silvia Nardelli⁶, Sara Montagnese², Christian Labenz¹. ¹University Medical Center Mainz, Mainz, Germany; ²University of Padova, Padova, Italy; ³Hospital of South West Jutland, Esbjerg, Denmark; ⁴University Hospital Schleswig-Holstein, Lübeck, Germany; ⁵Sorbonne Université, Hôpital Pitié-Salpêtrière Assistance Publique Hôpitaux de Paris, Paris, France; ⁶Sapienza University of Rome, Rome, Italy; ⁷Diakonie Hospital Jung-Stilling, Siegen, Germany; ⁸University of Michigan, Ann Arbor, United States; ⁹Sorbonne Université, Hôpital Pitié-Salpêtrière Assistance Publique Hôpitaux de Paris, Paris, Germany
Email: christian.labenz@unimedizin-mainz.de

Background and aims: Minimal Hepatic Encephalopathy (MHE), defined by the psychometric hepatic encephalopathy score (PHES), is associated with a higher risk of subsequent OHE. However, it remains unclear if there is a stepwise increase in OHE risk with worse PHES results in patients with MHE.

Method: This multicenter study analyzed data of 1462 patients from eight centers (Italy, France, Denmark, USA, Germany), who underwent testing with the PHES and had available follow-up data. For this analysis, we only included patients with PHES-MHE, no history of OHE, and no prescription for lactulose or rifaximin (excluded: 959 without PHES-MHE, 212 with PHES-MHE but with a history of OHE, 84 with a prescription for lactulose or rifaximin). For subsequent analyses and to make results between centers more comparable, we calculated a scoring system adjusted PHES score (adjusted PHES) by dividing the PHES score by the number of subtests (e.g. for German patients: if a patient had a PHES score of –12, this score was divided by the number of subscores of PHES (in Germany 6 subscores) resulting in an adjusted PHES of –2). All patients were followed for the occurrence of OHE and liver transplantation (LTx)-free survival.

Results: In total, 207 patients with PHES-MHE were included. Median adjusted PHES was –1.20 (range –2.67; –0.80), median MELD score 11 (range 6; 33), and median follow-up time was 18.5 months (95% CI 13.9–20.6). In total, 59 (29%) patients developed an OHE episode during follow-up. There was no stepwise increase in OHE risk with worse PHES results. In multivariable competing risk regression analyses, adjusted PHES as a continuous variable (sHR 1.05, 95% CI 0.55–2.01, p = 0.9) or categorized into quartiles (each p \geq 0.2) were not associated with the development of OHE. In addition, no association was observed in multivariable models only including patients with Child-Pugh A or B/C.

Conclusion: MHE defined by PHES is associated with a higher OHE risk. However, we found no stepwise increase in OHE risk with worse PHES results among patients with PHES below the MHE-defining cutoff. Our findings stress that MHE with PHES just below the cutoff of –4 should be treated with the same rigor as patients with PHES of –18.

FRI-076

Physical frailty diagnosed by short physical performance battery test is an independent poor prognostic factor of 360-day mortality in patients with liver cirrhosis

Eleni Geladari¹, Theodoros Alexopoulos², Larisa Vasilieva³, Meropi Kontogianni⁴, Roxani Tenta⁴, Vasilios Sevastianos¹, Iliana Mani⁵, Alexandra Alexopoulou⁵. ¹3rd Department of Internal Medicine and Liver Outpatient Clinic, Evangelismos General Hospital, Athens, Greece; ²Gastroenterology Department, National and Kapodistrian University of Athens, Medical School, Laiko General Hospital, Athens, Greece; ³Gastroenterology Department, Alexandra Hospital, Athens, Greece; ⁴Department of Nutrition and Dietetics, School of Health Sciences and Education, Harokopio University of Athens, Athens, Greece; ⁵2nd Department of Internal Medicine and Research Laboratory, Medical School, National and Kapodistrian University of Athens, Hippokraton Hospital, Athens, Greece
Email: elgeladari@gmail.com

Background and aims: Physical frailty (PF) is defined as a syndrome of decreased physical function and reserves, preventing patients from coping with stressful factors. The Liver Frailty Index (LFI) and Short Physical Performance Battery (SPPB) in patients with liver cirrhosis (LC) can help evaluate the risk of death and complications before or after liver transplantation. The study aimed to explore the characteristics of frail patients by either method and compare the performance of LFI and SPPB as prognostic markers of mortality in LC.

Method: The Liver Frailty Index (LFI) was calculated using the equation $(-0.330 \times \text{gender-adjusted grip strength}) + (-2.529 \times \text{number of chair stands per second}) + (-0.040 \times \text{balance time}) + 6$. SPPB, including gait speed, chair stand, and balance tests, was also performed. Patients with LFI \geq 4.5 or SPPB \leq 8 were considered frail.

All included patients were prospectively followed up for 360 days, and their mortality was recorded.

Results: A total of 197 consecutive patients with LC without acute events were included [65.7% male, median age 60 years, (IQR 52–68), MELD 10.5 (7.7–16), 60.9% with decompensated LC (DC)]. Causes of LC were 43.1% alcohol-related, 23.3% viral, and 33.5% miscellaneous. PF, as assessed by LFI, was present in 40.8% of DC versus 9.1% of compensated cirrhosis (CC) patients ($p < 0.001$), and by SPPB, in 39.2% versus 9.1% ($p < 0.001$), respectively. Forty-three patients were frail by both tests, 13 by LFI only, and 11 by SPPB only. Overall, frail patients (diagnosed by either LFI or SPPB) were older ($p < 0.001$ for both), underweight ($p = 0.018$ and $p = 0.004$, respectively), had anemia ($p < 0.001$ for both), had more severe liver disease [higher MELD and Child-Pugh scores ($p < 0.001$ for both)], lower serum sodium ($p < 0.001$ for both), and more frequently hepatic encephalopathy ($p < 0.001$ for both). The Kaplan-Meier survival curve at 360 days showed higher mortality in frail compared to non-frail ones (log rank $p < 0.001$ for cases diagnosed by either method). PF defined by both LFI and SPPB was associated with a high mortality rate in univariate binary logistic regression analysis [HR 5.442 (95%CI 2.879–10.286), $p < 0.001$ and HR 0.151 (95%CI 0.079–0.288), $p < 0.001$]. In the multivariate binary logistic regression model, PF defined by SPPB (but not by LFI) and adjusted for age, gender, and MELD score (as a continuous variable) emerged as an independent prognostic factor of 360-day mortality [HR 0.358 (95%CI 0.170–0.753), $p = 0.007$].

Conclusion: PF, defined using either LFI or SPPB, was related to older age, underweight, and advanced liver disease in this cohort of patients with LC. Patients characterized as frail by LFI or SPPB were not identical. PF defined by SPPB (but not by LFI) was proven to be an independent poor prognostic factor for long-term mortality after adjustment for covariates. The assessment of PF is crucial in patients with cirrhosis as it may predict mortality.

FRI-077-YI

Cirrhotic liver transplant candidates with portosystemic shunts benefit from low dietary soluble fiber consumption

Simona Parisse¹, Sara Carnevale², Elio Damato³, Flaminia Ferri⁴, Monica Mischitelli⁵, Mario Corona⁶, Pierleone Lucatelli³, Alfredo Cantafora⁷, Domenico Alvaro⁵, Maurizio Muscaritoli⁵, Stefano Ginanni Corradini⁵. ¹Department of Translational and Precision Medicine, Sapienza University of Rome, Rome, Italy; ²Belcolle Hospital, Viterbo, Italy; ³Department of Radiological, Oncological and Anatomopathological Sciences, Sapienza University of Rome, Rome, Italy; ⁴Department of Translational and Precision Medicine, Sapienza University of Rome, Rome, Italy; ⁵Department of Translational and Precision Medicine, Sapienza University of Rome, Rome, Italy; ⁶Department of Radiological, Oncological and Anatomopathological Sciences, Sapienza University of Rome, Rome, Italy; ⁷Department of Translational and Precision Medicine, Sapienza University of Rome, Rome, Italy

Email: simona.parissee@gmail.com

Background and aims: In cirrhotic patients, spontaneous portosystemic shunts (PS) are associated with liver damage and more severe prognosis. Cholestatic liver damage and fibrosis occur in some patients with congenital PS and, always, in C57BL/6 mice with congenital PS on a diet rich in soluble fiber. Therefore, we aimed to investigate whether there is an association between dietary fiber consumption, cholestasis, and changes in MELD score over time in cirrhotic patients according to the presence of PS.

Method: We enrolled 80 consecutive cirrhotic outpatients under evaluation for liver transplantation who had been abstinent from alcohol and non-viremic for at least 6 months. At baseline we extrapolated the dietary intake of soluble and insoluble fiber, using the FiberTAG repertoire of Neyrinck et al to analyze 3-day food records, we measured serum alkaline phosphatase (ALP), calculated the MELD score and verified the presence of any PS, analyzing the portal venous phase of the abdominal CT. After six months the MELD

score was measured again. Separate multivariable binary logistic regression models were constructed using as dependent variables: a) normal vs abnormal ALP values at enrollment; b) improvement after six months of the MELD score vs its stability or worsening.

Results: PS were found in 48 (60%) patients. At enrollment patients with PS compared to those without had higher MELD score [13.1 (IQR 11.5–15.4) vs. 11.3 (IQR 8.3–14.2); $p < 0.05$] and ALP values [167.5 (IQR 110.8–262.0) vs. 131.0 (IQR 90.5–151.8) IU/L, $p < 0.05$], while fiber intake did not differ. At the end of follow-up there was an improvement in the MELD score compared to enrollment in 19/48 (39.6%) in the group with PS and in 10/32 (31.3%) in the group without PS ($p = 0.448$). Total fiber intake, expressed in mg per kg of body weight per day, was independently and negatively associated with improvement in MELD score after 6 months, both in cirrhotic patients with PS [O.R. 0.985, 95% CI: 0.974–0.997, $p = 0.014$] and in those without [O.R. 0.983, 95% CI: 0.968–0.999, $p = 0.043$]. In cirrhotic patients with PS we found the following independent associations of soluble fiber intake: a) negative with the improvement of the MELD score after 6 months [O.R. 0.946, 95% CI: 0.912–0.982, $p = 0.004$]; b) positive with abnormal ALP values [O.R. 1.032, 95% CI: 1.001–1.064, $p = 0.046$].

Conclusion: In cirrhotic patients with PS, consumption of soluble dietary fiber is associated with cholestatic liver damage and failure to improve prognosis over time. The detrimental effect of soluble fiber is likely due to chronic spillover of cholestatic metabolites stimulated by a dysbiotic microbiota.

FRI-078-YI

Long-term albumin administration in outpatients with decompensated cirrhosis and diabetes mellitus: post-hoc analysis of the ANSWER trial database

Giulia Iannone^{1,2}, Giacomo Zaccherini¹, Enrico Pompili^{1,2}, Greta Tedesco², Clara De Venuto², Maurizio Baldassarre¹, Oliviero Riggio³, Paolo Angeli⁴, Carlo Alessandria⁵, Sergio Neri⁶, Francesco Foschi⁷, Fabio Levantesi⁸, Aldo Airolidi⁹, Loredana Simone¹⁰, Gianluca Svegiati-Baroni¹¹, Stefano Fagioli¹², Giacomo Laffi¹³, Raffaele Cozzolongo¹⁴, Vito Di Marco¹⁵, Vincenzo Sangiovanni¹⁶, Filomena Morisco¹⁷, Pierluigi Toniutto¹⁸, Annalisa Tortora¹⁹, Rosanna De Marco²⁰, Silvia Nardelli²¹, Salvatore Piano⁴, Chiara Elia⁵, Paolo Caraceni^{1,2}, Mauro Bernardi². ¹Unit of Semeiotics, Liver and Alcohol-related diseases, IRCCS Azienda Ospedaliero-Universitaria di Bologna, Bologna, Italy; ²Department of Medical and Surgical Sciences, University of Bologna, Bologna, Italy; ³Department of Translational and Precision Medicine, Sapienza University of Rome, Rome, Italy; ⁴Unit of Internal Medicine and Hepatology, Department of Medicine-DIMED, University and Hospital of Padua, Padua, Italy; ⁵Division of Gastroenterology and Hepatology, Città della Salute e della Scienza Hospital, Turin, Italy; ⁶Department of Clinical and Experimental Medicine, University of Catania, Catania, Italy; ⁷Internal Medicine, Hospital of Faenza, Azienda Unità Sanitaria Locale di Romagna, Faenza, Italy; ⁸Internal Medicine, Hospital of Bentivoglio, AUSL of Bologna, Bentivoglio, Italy; ⁹Department of Hepatology and Gastroenterology, Niguarda Hospital, Milan, Italy; ¹⁰Gastroenterology Unit, University Hospital, Ferrara, Italy; ¹¹Department of Gastroenterology, Polytechnic University of Marche, Ancona, Italy; ¹²Gastroenterology and Transplant Hepatology, Papa Giovanni XXIII Hospital, Bergamo, Italy; ¹³Department of Experimental and Clinical Medicine, University of Florence, Florence, Italy; ¹⁴Division of Gastroenterology, National Institute of Gastroenterology S. De Bellis, Castellana Grotte (Bari), Italy; ¹⁵Unit of Gastroenterology and Hepatology, Biomedical Department of Internal and Specialistic Medicine, University of Palermo, Palermo, Italy; ¹⁶Azienda Ospedaliera di Rilievo Nazionale dei Colli, Cotugno Hospital of Naples, Naples, Italy; ¹⁷Gastroenterology Unit, Department of Clinical Medicine and Surgery, Federico II University of Naples, Naples, Italy; ¹⁸Hepatology and Liver Transplantation Unit, University Academic Hospital of Udine, Udine, Italy; ¹⁹Gastroenterology, Gemelli Foundation,

POSTER PRESENTATIONS

Catholic University, Rome, Italy; ²⁰Gastroenterology Unit, Hospital of Cosenza, Cosenza, Italy; ²¹Department of Clinical Medicine, Sapienza University of Rome, Rome, Italy
Email: g.zaccherini@gmail.com

Background and aims: Type 2 diabetes mellitus (DM) is a frequent comorbidity in patients with liver cirrhosis and an independent risk factor for bacterial infections, occurrence of cirrhosis-related complications, and mortality. Apart from DM control, treatment strategies protecting patients from these risks remain an unmet need. The present study aims to determine whether long-term human albumin (HA) administration improves survival and reduces the incidence of complications in outpatients with decompensated cirrhosis and DM. **Method:** The ANSWER trial enrolled 431 patients with cirrhosis and uncomplicated ascites to receive either the standard medical treatment (SMT) or SMT plus HA (40 g twice weekly for 2 weeks, and then 40 g weekly) up to 18 months. We performed a post-hoc analysis of the trial database extrapolating the subgroup of patients with insulin-treated DM. Overall survival rates during a follow-up of 18 months were determined. To assess the incidence of complications, we calculated and compared their incidence rates (IRs) in the two arms of the trial by calculating incidence rate ratios (IRRs). The SMT group served as the reference category.

Results: Eighty-five (19.7%) patients presented insulin-treated DM at baseline (50 in the SMT and 35 in the SMT+HA arm, respectively). At baseline, diabetic patients who received long-term HA did not significantly differ from those randomized to SMT, as regards age, etiology of cirrhosis, body mass index, Child-Pugh class, and MELD score. During the follow-up, 39 patients ended the study prematurely (17 of them for medically uncontrolled ascites requiring at least 3 paracenteses per month, 14 in the SMT and 3 in the SMT+HA arm). Sixteen patients died (12 in the SMT and 4 in the SMT+HA arm), 13 of them from liver-related causes (10 [83%] in the SMT and 3 [75%] in SMT+HA arm). Eighteen month overall survival was significantly higher in patients enrolled in the SMT+HA arm compared to SMT (86% [95%CI: 66–95] vs 57% [95%CI: 35–74], $p=0.016$). Patients treated with SMT+HA also presented a lower IR of paracenteses (0.89 vs 4.31, IRR 0.21, $p<0.001$), overt hepatic encephalopathy (0.39 vs 1.32, IRR 0.30, $p<0.001$), bacterial infections (0.50 vs 0.95, IRR 0.53, $p=0.023$), acute kidney injury (0.42 vs 1.32, IRR 0.32, $p<0.001$), electrolyte disorders (0.60 vs 1.26, IRR 0.47, $p=0.003$). No significant differences were seen in hospital admissions (IR 1.35 vs 1.52, IRR 0.89, $p=0.53$), but the number of days spent in the hospital was lower in the SMT+HA group (IR 10.95 vs 19.23, IRR 0.57, $p<0.001$).

Conclusion: Long-term HA administration appears a beneficial therapeutic intervention improving survival and reducing the incidence of cirrhosis-related complications in insulin-treated diabetic outpatients with decompensated cirrhosis and ascites.

FRI-080

Hypodynamic cardiocirculatory status measured at echocardiography is associated with one-month mortality in patients admitted for acute decompensation of liver cirrhosis

Alexandru Victor Dragan¹, Ancuta Vijan¹, Caterina Delcea¹, Mihaela Birligea¹, Paul Balanescu², Andreea Bengus¹, Theodor Voiosu³, Ioana Daba³, Bogdan Mateescu³, Cristian Baicus³, Andrei Voiosu³. ¹Colentina Clinical Hospital, Bucharest, Romania; ²University of Medicine and Pharmacy "Carol Davila", Bucharest, Romania; ³Colentina Clinical Hospital, University of Medicine and Pharmacy "Carol Davila", Bucharest, Romania
Email: victoradragan@gmail.com

Background and aims: Systemic inflammation is a crucial component in the cardiocirculatory dysfunction observed in liver cirrhosis. The aim of our study is to assess the mortality and hospital readmission at 1 and 3 months in patients with acute decompensation of liver cirrhosis based on their cardiocirculatory status and to explore their inflammatory profile.

Method: This is a prospective, observational study conducted at a tertiary center, involving the follow-up of patients admitted for acute decompensation of liver cirrhosis without known cardiac comorbidities. We monitored them clinically, electrocardiographically, biologically, and echocardiographically at admission, 5–7 days later, and one month later. A follow-up phone call was conducted at three months. The patients cardiocirculatory status was stratified based on the cardiac index measured by echocardiography into hypodynamic (<3.2 L/min/m²), normodynamic (3.2–4.2 L/min/m²), and hyperdynamic (>4.2 L/min/m²).

Results: We included 66 patients with liver cirrhosis (mean age 59 ± 10 years, 69.6% women), primarily due to alcohol-related liver disease (79%). Mean Child Pugh score was 9 (IQR 8–11) and MELD-Na 19 (IQR 15–23). 86.3% were admitted for acute decompensation, while 13.6% fulfilled the criteria for acute-on-chronic liver failure. The cardiocirculatory status of the patients was hypodynamic in 48.5%, normodynamic in 30.3%, and hyperdynamic in 13.6%. 40.9% of the patients were treated with chronic beta-blockers. Mortality was higher in patients with hypodynamic status compared to those with normo and hyperdynamic status at one-month (24% vs 0% vs 0%, $p=0.049$), but not at 3 months (28% vs 26.6% vs 28.5%, $p=0.9$). The hospital readmission rate did not differ at either one month (33.3% vs 21.0% vs 22.2%, $p=0.5$) or three months (57.6% vs 42.1% vs 66.6%, $p=0.4$). No patients with ACLF on admission had hyperdynamic circulation according to the cardiac index. There was no difference between groups in the serum concentrations of inflammatory markers (C-reactive protein, IL-6, TNF-alpha, GAS6).

Conclusion: Patients with acute decompensation of liver cirrhosis and hypodynamic cardiac status have a higher mortality rate in the first month following admission.

FRI-081

Lisinopril is associated with reduced hepatocellular carcinoma and mortality risk in patients with MASLD-related compensated cirrhosis: a multicenter, nationwide propensity score matching analysis

Yee Hui Yeo¹, Wee Han Ng², Manal F. Abdelmalek³, Seema Khan⁴, Cynthia Moylan⁵, Luz Rodriguez⁶, Augusto Villanueva⁷, Kevin Ma⁸, Ju Dong Yang¹. ¹Karsh Division of Gastroenterology and Hepatology, Cedars-Sinai Medical Center, Los Angeles, United States; ²Bristol Medical School, Bristol, United States; ³Division of Gastroenterology and Hepatology, Mayo Clinic, Rochester, United States; ⁴Department of Surgery, Northwestern University Feinberg School of Medicine, Chicago, United States; ⁵Division of Gastroenterology, Duke University, Durham, United States; ⁶National Cancer Institute, Division of Cancer Prevention, Rockville, United States; ⁷Liver Cancer Program, Divisions of Liver Disease, Tisch Cancer Institute, Department of Medicine, Icahn School of Medicine at Mount Sinai, New York, United States; ⁸Department of Epidemiology, Harvard T. H. Chan School of Public Health, Boston, United States
Email: yeehui.yeo@cshs.org

Background and aims: Lisinopril, an angiotensin-converting enzyme inhibitor (ACEi), appears to have a role in preventing fibrosis progression in a preclinical model of steatotic liver disease. Little is known about the antifibrotic effect of lisinopril in patients with MASLD and cirrhosis. Hepatic fibrosis and cirrhosis are associated with an increased risk for hepatocellular carcinoma (HCC). Our objective was to assess the impact of lisinopril use on the occurrence of HCC in comparison to other antihypertensive medications in patients with MASLD-related compensated cirrhosis.

Method: We conducted a retrospective cohort study utilizing TriNetX, a multicenter, nationwide database with detailed clinical information. We included all patients with MASLD-related compensated cirrhosis from 1/12/2011 to 12/31/2023 defined as having one of the five cardiometabolic risk factors in individuals with steatotic liver disease. Laboratory data, medications for metabolic diseases, physical measurements, and ICD codes were used to define the diagnosis.

Lisinopril users (having three or more prescriptions) were matched with users of non-ACEi, non-angiotensin receptor blocker antihypertensives using propensity score matching (PSM) method based on demographic characteristics, BMI, blood pressure, comorbidities, medications, and laboratory data such as platelet count, INR, liver biochemistry, HbA1c, lipid profile, and renal function test. The index date was defined as the start date of lisinopril or other antihypertensives. Cox regression was used to determine the risk of mortality and HCC. Colorectal cancer, which shares similar sources of bias with the targeted outcome but is unrelated to the treatment of interest, was selected as a negative control.

Results: Of the 16897 eligible patients, 5265 were lisinopril users and 11632 were users of other antihypertensive medications. After PSM, 4769 pairs of users and non-users were well-balanced. For both groups, the mean age was 60.3 years, with 43% males and 75.3% whites. Lisinopril was associated with a significantly decreased mortality risk, with a hazard ratio (HR) of 0.72 (95% confidence interval [CI]: 0.66–0.79). Moreover, lisinopril was associated with a significantly reduced risk of developing HCC, with an HR of 0.70 (95% CI: 0.55–0.89). The effect of lisinopril was duration-dependent, with the HR of mortality in patients who had three to five prescriptions of lisinopril as 0.65 (95% CI: 0.46–0.91) while it was 0.58 (95% CI: 0.39–0.86) in those with six to eight prescriptions. When using colorectal cancer as a negative control, the HR for lisinopril use was non-significant (HR 0.80, 95% CI: 0.57–1.13).

Conclusion: In our cohort lisinopril use in patients with MASLD-related compensated cirrhosis was associated with a reduced risk of mortality and HCC development compared to other antihypertensive medications.

FRI-082

Unveiling the role of GH-IGF1 axis in decompensated cirrhosis: implications for sarcopenia, frailty, decompensations, and mortality

Parminder Kaur¹, Nipun Verma², Aishani Wadhawan³, Pratibha Garg⁴, Samonee Ralmilay⁴, Naveen Kalra⁴, Gaurav Sharma⁴, Sahaj Rathi⁴, Arka De⁴, Madhumita Premkumar⁴, Sunil Taneja⁴, Ajay Kumar Duseja⁴, Pinaki Dutta⁴, Virendra Singh⁵. ¹Postgraduate Institute of Medical Education and Research, Chandigarh, India; ²Postgraduate Institute of Medical Education and research, Chandigarh, India; ³Postgraduate Institute of Medical education and Research, Chandigarh, India; ⁴Postgraduate Institute of Medical education and Research, Chandigarh, India; ⁵Punjab Institute of Liver and Biliary sciences, Mohali, India
Email: nipun29j@gmail.com

Background and aims: The impact of the Growth Hormone-Insulin-like Growth Factor (GH-IGF1) axis on sarcopenia, frailty, bone health, and overall prognosis remains underexplored in cirrhosis. This study investigates their interplay in patients with decompensated cirrhosis, unveiling potential therapeutic targets.

Method: We associated plasma GH (ng/ml) and IGF1 levels (ng/ml) with sarcopenia (CT-SMI), frailty (LFI), decompensations, and outcomes up to 180 days among adult decompensated cirrhosis outpatients at a tertiary care institute between 2021 and 2023.

Results: We recruited 172 patients, 95% males with a median age of 46.5 years, MELD-Na of 16.3 (IQR: 12.8–21.6), Child-Pugh status-A (12.8%), -B (62.2%), or -C (25%), and 180-day mortality of 17.4%. GH and IGF1 levels were 3.6 ng/ml (IQR: 2.02–6.45) and 39.3 ng/ml (IQR: 28.7–50) among patients. Sarcopenia, frailty, and osteodystrophy were observed in 59.5%, 24.3%, and 42% of patients, respectively. Patients were categorized by observed range of IGF1 levels: low IGF1 (first quartile: IGF1 <28.7), intermediate IGF1 (second and third quartile: IGF1 28.7–50), and high IGF1 (fourth quartile: IGF1 >50). \log_{10} IGF1 levels were significant predictors of sarcopenia (OR: 0.094, 0.013–0.676; $p = 0.019$), and osteodystrophy (OR: 0.101, 0.014–0.724; $p = 0.022$). \log_{10} IGF1 levels were negatively associated with frailty (beta = -0.419), MELD-Na (beta = -4.55), and CTP scores (beta = -1.48) (p

<0.05, each). Cumulative incidence of overall complications at 90-day were highest among patients with low IGF1 (39.5%) than intermediate (25%), and high IGF1 levels (17.1%); with a corresponding incidence at 180-days of 48.8%, 39.8%, and 22.0%, $p = 0.001$, respectively. Ascites and hepatic encephalopathy were the main drivers of complications among patients with low IGF1 levels. 90-day and 180-day survival were significantly lower in patients with low IGF1 levels than those with intermediate or high IGF1 levels (90-day: 76.7% vs 93.2% vs 95.1% ($p = 0.023$); 180-day: 69.8% vs 85.2% vs 90.2%; $p = 0.001$). Both \log_{10} IGF1 (AUC: 0.709 and 0.648) and MELD (AUC: 0.710 and 0.659) could predict 90 and 180-day mortality ($p < 0.05$, each). Adding \log_{10} IGF1 with MELD could further improve the discriminative-accuracy of MELD for mortality at 90-day (0.756) and 180-day (0.685), $p < 0.05$. Patients with sarcopenia and osteodystrophy showed lower GH levels than counterparts (sarcopenia: 4.32 vs 3.88; osteodystrophy: 3.88 vs 3.99). A trend towards lower GH levels was observed among 90-day non-survivors compared to survivors [3.11 vs. 4.08, $p = 0.070$].

Conclusion: Reduced IGF1 levels reflect sarcopenia, frailty, and osteodystrophy in cirrhosis. Low IGF1 contributes to complications and mortality in cirrhosis outpatients. Our findings suggest that modulating this axis could be a novel approach for improving patient outcomes in decompensated cirrhosis.

FRI-083

The impact of acute kidney injury in cirrhosis: a meta-analysis of 5, 202, 232 patients

Vasileios Lekakis¹, Ioannis Vlachogiannakos¹, George Papatheodoridis¹, Evangelos Cholongitas². ¹Academic Department of Gastroenterology, General Hospital of Athens "Laiko", Athens, Greece; ²1st Department of Internal Medicine, General Hospital of Athens "Laiko", Athens, Greece
Email: lekakis.vas@gmail.com

Background and aims: Acute kidney injury (AKI) is a commonly seen condition in the natural course of cirrhosis. The aim of this study was to evaluate the pooled incidence and mortality of AKI in different clinical settings and to identify high-risk factors for both the incidence and mortality of AKI.

Method: A systematic search of several databases was performed up to May 2023. Meta-analysis was performed using a generalized linear mixed model, while a random effects model was utilized for all calculations. All analyses followed a pre-specified protocol (PROSPERO: CRD42023487736).

Results: In total, 73 studies with 5, 202, 232 patients fulfilled eligibility criteria and were finally enrolled in the meta-analysis. The overall pooled incidence of AKI was 33% (95% confidence interval [CI]: 29–38%), and prerenal was the most common AKI type [59% (95% CI: 50–67%)]. On admission, patients with infection had the highest AKI rate [47% (95% CI: 40–55%)]. Pooled AKI rates were also high in inpatients with hepatic encephalopathy [41% (95% CI: 32–50%)] and significantly lower in those with gastrointestinal bleeding [31% (95% CI: 24–38%)]. Furthermore, the severity of liver disease proved to be a substantial driver for AKI development, as the pooled incidence of AKI was significant greater in patients at Child-Turcotte-Pugh (CTP) C than B than A class [48% vs 29% vs 16%, $p < 0.01$]. Noteworthy, patients at intensive care unit (ICU) had the greatest AKI incidence [61% (95% CI: 53–69%)], whereas the AKI rate was higher in patients with than without acute on chronic liver failure (ACLF) [43% (95% CI: 32–55%) vs 29% (95% CI: 25–33%), $p = 0.02$]. The overall short-term pooled mortality rate was significantly higher among cirrhotic patients with than without AKI [34% (95% CI: 28–41%) vs 9% (95% CI: 6–13%), $p < 0.01$]. Interestingly, AKI patients in the ICU had the greatest mortality rate [76% (95% CI: 73–79%)], while AKI patients with ACLF experienced higher mortality rates than those without [54% (95% CI: 33–73%) vs 28% (95% CI: 23–34%), $p < 0.01$]. Moreover, the 30-day pooled mortality rate was significant higher in patients with hospital-acquired compared to community-acquired AKI [39% (95% CI: 34–

POSTER PRESENTATIONS

45%) vs 28% (95% CI: 22–36%), $p = 0.03$]. The mortality rates were also significantly correlated with AKI stage being significantly higher in cases with stage 3 than stage 2 than stage 1 (62% vs 50% vs 29%, $p < 0.01$).

Conclusion: Approximately one third of cirrhotic patients experience AKI during follow-up. Patients at ICU and those with severe liver disease, infection, sepsis, hepatic encephalopathy or ACLF upon admission are at higher risk for AKI. AKI patients experience significantly higher mortality rates than non-AKI cases, especially those admitted at ICU or diagnosed with ACLF. Significant risk factors for AKI-associated short-term mortality include both hospital-acquired AKI and high AKI stage.

FRI-086

Untargeted serum metabolomic profiles remain stable over time in large multi-center cohort of >700 outpatients with cirrhosis

Jasmohan Bajaj¹, Puneeta Tandon², Jennifer Lai³, Jacqueline O'Leary⁴, Guadalupe Garcia-Tsao⁵, Hugo Vargas⁶, Scott Biggins⁷, Florence Wong⁸, Patrick S. Kamath⁹, Nicolas Lugon⁵, Ana Limon-Miro², Jawaid Shaw¹, Brian Bush¹, K. Rajender Reddy¹⁰.

¹Virginia Commonwealth University, Richmond, United States;

²University of Alberta, Edmonton, Canada; ³UCSF, San Francisco, United States;

⁴Dallas VA Medical Center, Dallas, United States; ⁵Yale University, New Haven, United States;

⁶Mayo Clinic Arizona, Phoenix, United States;

⁷UPMC, Pittsburgh, United States; ⁸University of Toronto, Toronto, Canada;

⁹Mayo Clinic, Rochester, United States; ¹⁰University of Pennsylvania, Philadelphia, United States

Email: jasmohan.bajaj@vcuhealth.org

Background and aims: Untargeted metabolomics could be biomarkers for disease progression in cirrhosis but stability over time is unclear. Aim: define differences in serum metabolomics at baseline and changes over time in multi-center outpatient cirrhosis cohort.

Method: NACSELD-3 (North American Consortium for Study of End-Stage Liver Disease) is a multi-center outpatient cirrhosis cohort of compensated (comp) and decompensated (decomp) pts seen at 6M intervals. Clinical and demographic data and serum for metabolomics (done with LC/MS) are collected at each visit. Metabolomic profile at baseline and 6M were compared between/within comp vs decomp groups using paired and unpaired t-tests as appropriate.

Results: We enrolled 744 subjects (285 comp, 459 decomp) from 10 centers of whom 165 comp and 150 decomp were seen again at 6M. All pts' comp/decomp status was stable over time. Between group comparisons: 892 metabolites were different between comp/decomp, of which 500 were higher and 392 were lower in decomp pts. At 6M, 676 metabolites were different, of which 350 were higher and 326 were lower in decomp pts. These comparisons were consistent at both timepoints apart from 8 metabolites. 8 metabolites changed direction from baseline to 6M between comp/decomp pts: 2-ketocaprylate (0.81 to 1.36-fold), indole propionate (0.98 to 1.05), 2-aminooctanoate (0.9 to 1.47), N-methylhydroxyproline (0.85 to 1.24) and glycodeoxycholate (0.91 to 1.31) were lower in decomp vs comp at baseline but flipped i.e., increased at 6M post. The reverse (higher at baseline and lower at 6M in decomp) was seen with glycurso-deoxycholate (1.2 to 0.71), 5-hydroxyindole sulfate (1.23 to 0.69) and tauroursodeoxycholate sulfate (1.09 to 0.3). Within group analysis: *Compensated:* 130 metabolites differed of which 95 ↑ and 35 ↓ at 6M vs baseline. Those that reduced at 6M were biliverdin, vitamin C/E metabolites, long-chain fatty acids, phosphocholines, sex steroids, and tauro/glycurso-deoxycholate sulfate. Those that ↑ were amino acid derivatives related to urea cycle (arginosuccinate) and protein breakdown, bioenergetics (aconitate, malate, citrate) and hormones (cortisol). *Decompensated:* 66 metabolites changed (37 ↑/29 ↓) at 6M vs baseline. Those that ↓ were biliverdin, long chain FAs, carnitine derivatives, and serotonin. Metabolites that ↑ were again amino acid derivatives and urea cycle intermediates (citrulline, ornithine), GABA derivatives (imidazole acetate), short/medium fatty acids (butyrate,

valerate) and N-acetylated amino acids that are linked with renal disease.

Conclusion: Serum metabolomics are largely stable over time in outpatients with cirrhosis in a multi-center study across North America, which encourages their use as biomarkers. Few metabolites that changed differentially were microbially modified metabolites (bile acids, indoles, short chain fatty acids), long-chain fatty acids, and urea cycle intermediates.

FRI-087

Cerebral diffusion tensor imaging in patients with liver diseases admitted for evaluation of neurological symptoms

Nicolas Weiss¹, Lyès Kheloufi¹, Philippe Sultanik¹, Sarah Mouri¹,

Charlotte Bouzbib², Marika Rudler², Vincent Perlberg³,

Louis Puybasset², Dominique Thabut². ¹Sorbonne Université, Paris, France;

²Sorbonne Université, PARIS, France; ³BrainTale, PARIS, France

Email: nicolas.weiss@aphp.fr

Background and aims: Hepatic encephalopathy (HE), especially overt HE (OHE), is a common complication of liver diseases. Its occurrence is associated with decreased survival, increased risk of further boots of OHE, altered quality of life. Recent animal data suggested that several boots of OHE could be associated with cerebral neurodegeneration. Diffusion tensor imaging (DTI) is a MRI sequence that enables to study cerebral damage and try to dismantle between axonal and myelin damage. Data are scarce in HE with conflicting results. In this study, we take advantage of DTI in a cohort of patients with chronic liver diseases that were referred for neurocognitive symptoms, and underwent a standardized multimodal work-up.

Method: Patients with chronic liver diseases admitted for a one-day exploration of neurocognitive symptoms were included if they had a cerebral MRI with DTI sequences. They were evaluated with a standardized multimodal work-up and underwent a complete neuropsychological testing by a neuropsychologist encompassing PHES (French and Spanish version, critical flicker frequency (CFF) test and animal naming test (ANT). DTI sequences were analyzed by using the BrainQuant software (BrainTale, Paris) providing automatically global fractional anisotropy (FA) and mean diffusivity (MD). $P < 0.05$ were considered significant and analysis were performed using JMP Pro 17 (SAS Institute).

Results: Among 164 patients that were evaluated, 156 (95%) underwent a cerebral MRI and among them 118 (72%) had DTI sequences acquisition. 94 (80%) had cirrhosis and 24 (20%) had vascular liver disease. Patients with cirrhosis were 61 [55–68] years-old, 68 (72%) were men, Child-Pugh of 8 [7–9] and MELD of 13 [10–15]. In cirrhotic patients FA values were lower ($p = 0.0128$) in patients having a history of previous HE, whereas MD was not different ($p = 0.1436$). MD differed between patients with a history of neurological disease compared to those without ($p = 0.0113$), whereas FA did not ($p = 0.0549$). There was no difference in FA ($p = 0.4309$) nor in MD ($p = 0.5669$) between patients with cHE or not. On neuropsychological testing, FA and MD were correlated with MoCA (Montreal Cognitive Assessment) ($p = 0.0136$ and $p = 0.0112$), and ANT ($p = 0.0081$ and $p = 0.0077$). At long-term, FA decrease and MD increase were correlated to the number of boots of OHE ($p = 0.0057$ and $p = 0.0046$).

Conclusion: FA and MD are altered in patients with liver diseases and neurological symptoms. Cirrhotic patients had lower FA and higher MD values. FA was decreased in cirrhotic patients with previous boots of HE and not in patients with previous neurological diseases. FA and MD correlated to neuropsychological testing especially the ANT. At long-term, a decrease in FA and an increase in MD were positively correlated with number of further boots of OHE.

FRI-088

Patterns and predictors of postacute discharge location other than home in a global cohort of 3, 678 patients hospitalized with cirrhosis

Wai-Kay Seto¹, Qing Xie², Ashok Kumar Choudhury³, Patrick S. Kamath⁴, Mark Topazian⁴, Peter Hayes⁵, Aldo Torre⁶, Hailemichael Desalegn⁷, Ramazan Idilman⁸, ZhuJun Cao⁹, Mario Álvares-da-Silva¹⁰, Jacob George¹¹, Florence Wong¹², Brian Bush¹³, Leroy Thacker¹⁴, Shiv Kumar Sarin¹⁵, Iliana Mani¹⁶, Dinc Dincer¹⁷, Diederick van Doorn¹⁸, Amey Sonavane¹⁹, Mohammad Amin Fallahzadeh²⁰, Linlin Wei²¹, Araceli Bravo Cabrera²², Ashish Goel²³, Ponan Ponan Claude Regis Lah²⁴, Shiva Kumar²⁵, Yu Jun Wong²⁶, Dinesh Jothamani²⁷, Matthew Robert Kappus²⁸, Abdullah Emre Yildirim²⁹, Ewan H Forrest³⁰, Francisco Félix Tellez³¹, Patricia Momoyo Zitelli³², Manuel Barbero³³, José Luis Pérez-Hernández³⁴, Sebastián Marciano³⁵, René Malé Velazquez³⁶, Ajay Jhaveri³⁷, Robert Gibson³⁸, Anil Chandra Anand³⁹, Tahrima Kayes⁴⁰, Feyza Gunduz⁴¹, David Bayne⁴², Minghua Lin⁴³, Enver Ucbilek⁴⁴, Nabil Debzi⁴⁵, Jian Wang⁴⁶, Yashwi Hareesh Kumar Patwa⁴⁷, Ajay Kumar Duseja⁴⁸, Marco Arrese⁴⁹, Rosemary Faulkes⁵⁰, James Kennedy⁵¹, Yu Sung Kim⁵², Radha Krishan Dhiman⁵³, Hai Li⁵⁴, Dedong Yin⁵⁵, Yanyun Zhang⁵⁶, Gerry MacQuillan⁵⁷, Ashish Kumar⁵⁸, Helena Katchman⁵⁹, Yingling Wang⁶⁰, Qunfang Rao⁶¹, Yijing Cai⁶², Liyang Wu⁶³, Yongfang Jiang⁶⁴, Zhen Xu⁶⁵, Yongchao Xian⁶⁶, Dominik Bettinger⁶⁷, Monica Dahiya⁶⁸, Nabih Faisal⁶⁹, Duarte Rojo Andres⁷⁰, Natalia Filipek⁷¹, Fiona Tudehope⁷², Wanqin Zhang⁷³, Jasmohan Bajaj⁷⁴. ¹The University of Hong Kong, Hong Kong; ²Ruijin Hospital, Shanghai Jiaotong University School of Medicine, Shanghai, China; ³Institute of Liver and Biliary Sciences, New Delhi, India; ⁴Mayo Clinic, Rochester, United States; ⁵The Royal Infirmary of Edinburgh, Edinburgh, United Kingdom; ⁶Instituto Nacional de Ciencias Médicas y Nutrición Salvador Zubirán, Mexico City, Mexico; ⁷St Paul's Hospital Millennium Medical College, Ethiopia; ⁸Ankara University School of Medicine, Ankara, Turkey; ⁹Shanghai Jiao Tong University School of Medicine, Shanghai, China; ¹⁰Hospital de Clínicas de Porto Alegre, Porto Alegre, Brazil; ¹¹Westmead Hosp/Westmead Institute, Sydney, Australia; ¹²Toronto General Hospital, Toronto, Canada; ¹³VCU Richmond, Richmond, United States; ¹⁴VCU, Richmond, United States; ¹⁵Institute of Liver and Biliary Sciences, Delhi, India; ¹⁶National and Kapodistrian University of Athens, Athens, Greece; ¹⁷Department of Gastroenterology, Akdeniz University School of Medicine, Antalya, Turkey; ¹⁸Amsterdam UMC, University of Amsterdam, Amsterdam, Netherlands; ¹⁹Apollo Hospital MUMBAI, Mumbai, India; ²⁰Baylor University Medical Center, Dallas, United States; ²¹Beijing Youan Hospital, Capital Medical University, Beijing, China; ²²Centro Médico ISSEMYM, Mexico, Mexico; ²³CMC Vellore, Vellore, India; ²⁴CHU de Cocody, Abidjan, Côte d'Ivoire; ²⁵Cleveland Clinic Abu Dhabi, Abu Dhabi, United Arab Emirates; ²⁶Changi General Hospital, Singapore; ²⁷Rela Institute, Chennai, India; ²⁸Duke University, Durham, United States; ²⁹Gaziantep University School of Medicine, Gaziantep, Turkey; ³⁰NHS GGC, Glasgow, United Kingdom; ³¹Hospital Civil de Guadalajara Fray Antonio Alcalde, Guadalajara, Mexico; ³²Hospital das Clínicas da Faculdade de Medicina da Universidade de São Paulo, Sao Paulo, Brazil; ³³Hospital El Cruce, Buenos Aires, Argentina; ³⁴Hospital General de México, CIUDAD DE MEXICO, Mexico; ³⁵Hospital Italiano de Buenos Aires, Buenos Aires, Argentina; ³⁶Instituto de Salud Digestiva y Hepática, Guadalajara, Mexico; ³⁷Jaslok Hospital, Mumbai, India; ³⁸John Hunter Hospital, Newcastle, Australia; ³⁹KIMS, Odisha, India; ⁴⁰Liverpool Hospital, Sydney, Australia; ⁴¹Marmara University, School of Medicine, Istanbul, Turkey; ⁴²Mayo Clinic Scottsdale, Scottsdale, United States; ⁴³Mengchao Hepatobiliary Hospital of Fujian Medical University, Shanghai, China; ⁴⁴Mersin University, Mersin, Turkey; ⁴⁵CHU Mustapha, Algiers, Algeria; ⁴⁶Nanjing Drum Tower Hospital, Nanjing, China; ⁴⁷Ibn. Sina Hospital, Khartoum, Sudan; ⁴⁸PGIMER, Chandigarh, India; ⁴⁹Pontificia Universidad Católica de Chile, Santiago, Chile; ⁵⁰Queen Elizabeth

University Hospitals, Birmingham, United Kingdom; ⁵¹Royal Berkshire Hospital, Reading, United Kingdom; ⁵²Royal North Shore Hospital, Sydney, Australia; ⁵³SGPGI LUCKNOW, Lucknow, India; ⁵⁴Ren Ji Hospital, School of Medicine, Shanghai Jiao Tong University, Shanghai, China; ⁵⁵Second Hospital of Shandong University, Shandong, China; ⁵⁶Shuguang Hospital Affiliated to Shanghai University of Traditional Chinese Medicine, Shanghai, China; ⁵⁷Sir Charles Gairdner Hospital, Perth, Australia; ⁵⁸Sir Ganga Ram Hospital, New Delhi, India; ⁵⁹Tel-Aviv Sourasky Medical Center, Tel Aviv, Israel; ⁶⁰The Fifth People's Hospital of Suzhou, Suzhou, China; ⁶¹The First Affiliated Hospital of Nanchang University, Nanchang, China; ⁶²The First Affiliated Hospital of Wenzhou Medical University, Wenzhou, China; ⁶³The first people's hospital of Lanzhou, Lanzhou, China; ⁶⁴The Second Xiangya Hospital of Central South university, Changsha, China; ⁶⁵The Third Affiliated Hospital of Sun Yat-sen University, Guangzhou, China; ⁶⁶The Third People's Hospital of Guilin, Guilin, China; ⁶⁷University Medical Center Freiburg, Freiburg, Germany; ⁶⁸University of Alberta, Edmonton, Canada; ⁶⁹University of Manitoba, Winnipeg, Canada; ⁷⁰University of Pittsburgh, Pittsburgh, United States; ⁷¹University of Washington, Seattle, United States; ⁷²Westmead Hospital, Sydney, Australia; ⁷³Fudan University, Shanghai, China; ⁷⁴Virginia Commonwealth University, Richmond, United States Email: wkseto@hku.hk

Background and aims: Postacute out-of-hospital care in cirrhosis is associated with major quality-of-life, resource implications and return to a productive life. But patterns and predictors of post-discharge outcomes are unclear. We aimed to describe global determinants of discharge location other than home for patients with cirrhosis after acute hospitalization.

Method: We prospectively recruited pts with cirrhosis hospitalized non-electively via the CLEARED Consortium, involving >110 centers worldwide across 6 continents, and categorized centers based on World Bank income groups: Low/Lower Middle Income (LIC/LMIC), Upper Middle Income (UMIC) and High Income (HIC). Patients with inpatient death and transplantation were excluded. We recorded demographics and inpatient details, medications, laboratory values and outcomes, and analyzed differences in patients discharged to home vs. non-home locations.

Results: 3, 678 patients (63.9% male, mean age 56.3 ± 13.3 years) were recruited from 26 countries (LIC/LMIC 15.9%, UMIC 46.6%, HIC 37.5%). Alcohol was the most common etiology (39.2%), then hepatitis B (22.4%), MASH (17.5%) and hepatitis C (9.9%). 233 patients (6.8%) were discharged to a non-home location [specialized nursing facilities (49.4%) or non-acute hospitals (50.6%)]. Non-home discharges, vs. home discharges, were more likely to occur in HIC centers (69.5% vs. 35.3%, $p < 0.001$), but with a significantly lower proportion of UMIC centers (14.2% vs. 48.8%, $p < 0.001$) while the proportion of LIC/LMIC centers were similar (16.3% vs. 15.8%). Non-home discharges also had a higher admission median MELD-Na score (23 vs. 19, $p < 0.001$) and a greater mean length of hospital stay (17.6 vs 11.4 days, $p < 0.001$). These patients had higher rates of hepatic encephalopathy (28.3% vs. 22.3% $p = 0.032$); similar associations were observed for nosocomial infection (18.0% vs. 8.1%), acute kidney injury (43.8% vs. 24.3%) and need of intensive care (20.6% vs. 10.2%) (all $p < 0.001$). Concerning inpatient medications, non-home discharges had increased use of spontaneous bacterial peritonitis (SBP) prophylaxis (24.5% vs. 11.4%), and increased use of lactulose, rifaximin and proton-pump inhibitors (all $p < 0.001$). Multivariate analysis found increased age (OR 1.01, 95%CI 1.00–1.03), income group (HIC vs. LIC/LMIC: OR 1.61, 95%CI 1.09–2.44) and SBP prophylaxis (OR 2.51, 95%CI 1.77–3.54) to be independently associated with non-home discharge.

Conclusion: Among patients who survived hospitalization without transplant in a worldwide cohort of inpatients with cirrhosis, 7% are discharged to locations other than home. These were more likely to occur in HIC centers in older patients with more advanced cirrhosis. Our study results show variations in non-home discharges that

POSTER PRESENTATIONS

encourage cirrhosis-specific measures of risk stratification, useful for health system metrics and advance care planning.

FRI-089

Infections and outcomes in patients hospitalized with an acute decompensation of cirrhosis: insights from the ATTIRE trial

Nikolaj Torp^{1,2}, Nicholas Freemantle³, Alastair O'Brien^{3,4}. ¹Centre for Liver Research, Department of Gastroenterology and Hepatology, Odense University Hospital, Odense, Denmark; ²Department of Clinical Research, University of Southern Denmark, Odense, Denmark; ³Comprehensive Clinical Trial Unit, University College London, London, United Kingdom; ⁴Royal Free Hospital, London, United Kingdom
Email: nikolaj.christian.torp@rsyd.dk

Background and aims: Infections in patients hospitalized with cirrhosis are common. We studied the natural history of hospitalized patients with cirrhosis and infection from a large randomized clinical trial, to determine whether outcomes were associated with use of prophylactic antibiotics, proton pump inhibitors (PPIs), statins, non-selective beta-blockers (NSBBs), spironolactone or prednisolone at baseline.

Method: We included patients from the ATTIRE trial, which was a neutral trial of daily in-hospital 20% human albumin infusions to patients admitted with an acute decompensation of cirrhosis. We identified infections upon enrollment, as reported by the attending clinicians. Baseline medication use was captured through the concomitant medication log. Daily biochemistry with white blood cell count (WBC) and C-reactive protein (CRP) was available during hospitalization and until discharge or death. Patients were followed at site for up to 180 days post randomization, by manual review of medical records.

Results: Of 777 patients, 211 (27%) were diagnosed with an infection, upon inclusion into the trial. Patients with baseline infections were older ($p = 0.034$), had higher WBC ($p < 0.001$) and CRP ($p < 0.001$), but a similar baseline MELD score as patients without an infection at baseline (median 19 IQR: 16–23 vs. 20 IQR: 15–23, $p = 0.740$). During 180 day follow-up, 84 (40%) of the patients with a baseline infection died. An infection at baseline was associated with increased risk of death (aHR = 1.51, 95% CI: 1.16–1.97, $p = 0.002$) during follow-up, independent of baseline MELD (aHR = 1.07, 95% CI: 1.05–1.09, $p < 0.001$). For patients with a baseline infection, rifaximin use upon enrollment was associated with an increased risk of death (aHR = 1.90, 95% CI: 1.11–3.25, $p = 0.019$), while a similar trend was observed for antibiotic prophylaxis in general (aHR = 3.09, 95% CI: 0.97–9.90, $p = 0.057$) after controlling for disease severity. No clear associations were observed between 180-day mortality and the use of PPIs ($p = 0.569$), statins ($p = 0.391$), NSBBs ($p = 0.367$), spironolactone ($p = 0.167$) nor prednisolone ($p = 0.790$). During the trial treatment period of 14 days, the overall WBC remained unchanged ($p = 0.425$) while CRP decreased ($p < 0.001$) in patients with a baseline infection. When controlling for disease severity, only increasing WBC was associated with the risk of death during the treatment period (aOR = 1.12, 95% CI: 1.05–1.19, $p < 0.001$), while CRP was not (aOR = 1.01, 95% CI: 1.00–1.02, $p = 0.285$).

Conclusion: Up to one in four patients hospitalized with an acute decompensation of cirrhosis had an infection at baseline. The use of antibiotic prophylaxis upon hospitalization was associated with an increased risk of death, independent of disease severity. However, the association may be due to residual confounding, despite controlling for baseline MELD score.

FRI-090

New concept of cirrhosis recompensation in clinical practice: it's key time

Inês Rodrigues¹, Francisco Capinha¹, Sofia Carvalhana¹, Luís Correia², Helena Cortez-Pinto². ¹Serviço de Gastreenterologia e Hepatologia, Centro Hospitalar Universitário Lisboa Norte, Lisbon, Portugal; ²Serviço de Gastreenterologia e Hepatologia, Centro Hospitalar Universitário Lisboa Norte, Clínica Universitária de Gastreenterologia, Faculdade de Medicina de Lisboa, Universidade de Lisboa, Lisbon, Portugal
Email: mines.bcrodrigues@gmail.com

Background and aims: The concept of liver recompensation challenges the classic unidirectional trajectory in cirrhosis. Suppression of underlying aetiology of liver disease is a necessary factor; however other contributors are still undercover. We aim to evaluate the natural history of hepatic disease, focusing recompensation events and factors that predict the potential of recompensation. **Method:** Retrospective study including all consecutive patients admitted with their first decompensation of cirrhosis, in a tertiary center (2016–2022) and followed >1 year. Recompensation was defined according to Baveno VII consensus: removal of etiological factor; resolution of encephalopathy and ascites without diuretics, and absence of variceal bleeding in the last year; sustained improvement of biochemical liver function. Statistical analysis was performed using SPSSv23 and considered pvalue <0.05.

Results: We included 175 cirrhotic patients, 76% ($n = 133$) males, with a median of 60 years-old at time of first decompensation. Regarding etiology, 69% ($n = 120$) had alcohol-related liver disease (10% with concomitant viral etiologies), 22 (13%) viral hepatitis alone, 12 (7%) metabolic dysfunction-associated steatotic liver disease (MASLD) and 23 (11%) other causes. The mean follow-up was 3.8 years (± 2.7 years). Etiological factor was suppressed in 66% ($n = 116$) of patients, within 55% ($n = 58$) before or at the first decompensation. Due to lack of etiological control definition in MASLD, these patients were considered as non-recompensated, although 42% fulfilled all other recompensation criteria. Recompensation was achieved in 20% ($n = 35$) of patients and 30% of those who controlled etiological factor, positively correlating with etiological factor control before or at the time of first decompensation ($p = 0.02$). Median time from diagnosis to decompensation was 0.5 months, with 86 patients (49%) decompensated at diagnosis. Patients' age at first decompensation ($p = 0.05$) also correlated with recompensation outcome. On logistic regression, for each additional year age, recompensation's probability dropped 3.7%. Gender, different etiological factors and manifestation of decompensation did not correlate with recompensation outcome. Nine (5%) patients without recompensation underwent a liver transplant. There was no correlation between an oncologic disease diagnosis during follow-up, and hepatocellular carcinoma in particular, and recompensation events. Death at the end of follow-up ($n = 83$, 48%) strongly correlated with absence of recompensation ($p < 0.01$).

Conclusion: Patient's age and etiological factor control at first decompensation seems a key element for achieving recompensation. In conclusion, since timely diagnosis and identification of etiological factor is so important, there is a pivotal role for early identification and reference to hepatology differentiated care.

FRI-091

Development of global leadership initiative on malnutrition-dictated nomograms to predict long-term mortality among hospitalized cirrhosis with external validation cohort

Chao Sun¹, Qing Liu¹. ¹Department of Gastroenterology and Hepatology, Tianjin Medical University General Hospital, Tianjin, China
Email: liuqing317@tmu.edu.cn

Background and aims: Global Leadership initiative on Malnutrition (GLIM) gradually accounts for the mainstay evaluating nutritional status. Herein we sought to establish GLIM-dictated nomograms with other factors influencing long-term mortality and further validated

their predictive performance in an independent external cohort among inpatients experiencing decompensated cirrhosis.

Method: The derivation cohort comprised 301 patients hospitalized due to acute insults and the validation cohort recruited 101 cirrhotic subjects from another medical center. Two nomograms were established to predict 1-year all-cause mortality based on the GLIM criteria. Study populations were divided into low-, moderate- and high-risk nutritional groups according to the established nomogram.

Results: By incorporating Child-Pugh class (Nomo#1) and Model for End-stage Liver disease-Sodium (Nomo#2), respectively, GLIM criteria was independently associated with 1-year mortality in multivariate Cox regression models (HR for Nomo#1 = 2.934, CI: 1.529–5.629, $p = 0.001$; HR for Nomo#2 = 3.428, CI: 1.744–6.739, $p < 0.001$). The C index and time-ROC concerning Nomo#1 and Nomo#2 performed significantly better than those of GLIM criteria alone. The survival rate of low-risk nutritional group was significantly higher when compared with moderate- and high-risk groups (Nomo#1: high risk (18/27 = 66.67%) > moderate risk (27/79 = 34.18%) > low risk (8/160 = 5%); Nomo#2: high risk (21/28 = 75%) > moderate risk (22/62 = 35.48%) > low risk (10/176 = 5.68%). Furthermore, the proposed nomograms still exhibited modest predictive accuracy (C index = 0.719) and were capable of identifying malnourished patients with cirrhosis and high mortality risk (log-rank test: $p = 0.013$) in another cohort for external validation.

Conclusion: GLIM criteria-defined malnutrition independently impact long-term mortality in the context of decompensated cirrhosis. Our established nomograms can predict survival status with sufficient accuracy on account of sizable samples and solid analyzing modalities.

FRI-092

Thyroid and adrenal dysfunction is associated with negative mid-term prognosis in decompensated cirrhosis

Laura Iliescu¹, Mircea Istrate², Razvan Rababoc², Simu Razvan-Ioan², Ioana Tanasie², Alexandra Alina Mihaela Mihaila², Letitia Toma².

¹Department of Internal Medicine, Fundeni Clinical Institute, Carol Davila University of Medicine and Pharmacy, Bucharest, Romania;

²Fundeni Clinical Institute, Carol Davila University of Medicine and Pharmacy, Bucharest, Romania

Email: laura_ate@yahoo.com

Background and aims: Chronic liver diseases are associated with a variety of endocrine abnormalities, including pituitary, thyroid and adrenal dysfunction, in correlation to the severity of liver disease. Low levels of thyroid-stimulating hormone (TSH), free triiodothyronine (fT3) and serum cortisol have been described in patients with advanced chronic liver disease. We aim to determine the prognostic value of thyroid and adrenal dysfunction in patients with decompensated cirrhosis.

Method: We performed a prospective observational trial in patients with decompensated cirrhosis (Child B, Child C) admitted to our clinic between June 2013 and June 2023. We excluded patients with hepatocellular carcinoma or other malignancies, vascular liver diseases, infections, liver transplantation or intake of thyroid hormones or cortisone therapy. We measured a jeune serum levels of TSH, fT3 and cortisol. Patients were monitored at 6 months.

Results: We included 635 patients (mean age 65.3 ± 34.1 years, 55.6% male) with cirrhosis Child B (217 patients) and C (418 patients). Main etiologies were: 17.0% alcohol related, 67.4% viral, 15.6% MAFLD related cirrhosis. Patients with Child B cirrhosis has significantly higher levels of TSH, fT3 and cortisol compared to Child C patients (TSH 3.14 uIU/ml versus 2.54 uIU/ml, $p = 0.03$; fT3 3.67 pg/ml versus 2.95 pg/ml, $p = 0.04$; cortisol 465 mmol/L versus 218 mmol/L, $p = 0.02$). At 6 months follow-up, 23 patients (10.6%) progressed from Child B to Child C and 32 Child C patients (7.6%) patients presented with cirrhosis complications, with a mortality rate of 0.7%. Progression of liver disease was associated with decreased TSH, fT3 and cortisol levels in patients with Child B (2.87 uIU/ml versus

3.23 uIU/ml, $p = 0.04$, 3.23 pg/ml versus 3.84 pg/ml, $p = 0.01$, 408 mmol/L versus 482 mmol/L, $p = 0.01$ respectively) and Child C cirrhosis (2.18 uIU/ml versus 2.72 uIU/ml, $p = 0.02$, 2.34 pg/ml versus 3.02 pg/ml, $p = 0.01$, 141 mmol/L versus 235 mmol/L, $p < 0.001$).

Conclusion: Decreases in thyroid and adrenal hormones are associated with a poor mid-term prognosis in patients with decompensated cirrhosis. In this scenario, the serum levels of TSH, fT3 and cortisol may be used to predict rapid deterioration in Child B and C cirrhotic patients. Hormonal supplementation may be an option for these patients and needs to be further investigated.

FRI-093

Clot wave analysis parameters are associated with the severity of liver cirrhosis

Kessarin Thanapirom^{1,2,3}, Pisit Tangkijvanich⁴, Sirinporn Suksawatamnuay^{1,2,3}, Panarat Thaimai^{1,2,3}, Prooksa Ananchuensook^{1,2,3}, Pitiphong Kijrattanakul⁵, Sombat Treeprasertsuk¹, Pantep Angchaisuksiri⁶, Piyawat Komolmit^{1,2,3}. ¹Division of Gastroenterology, Department of Medicine, Faculty of Medicine, Chulalongkorn University and King Chulalongkorn Memorial Hospital, Bangkok, Thailand; ²Center of Excellence in Liver Fibrosis and Cirrhosis, Chulalongkorn University, Bangkok, Thailand; ³Excellence Center in Liver Diseases, King Chulalongkorn Memorial Hospital, Thai Red Cross Society, Bangkok, Thailand; ⁴Center of Excellence in Hepatitis and Liver Cancer, Department of Biochemistry, Faculty of Medicine, Chulalongkorn University, Bangkok, Thailand; ⁵Division of Hospital and Ambulatory Medicine, Department of Medicine, Faculty of Medicine, Chulalongkorn University and King Chulalongkorn Memorial Hospital, Thai Red Cross Society, Bangkok, Thailand; ⁶Department of Medicine, Faculty of Medicine Ramathibodi Hospital, Mahidol University, Bangkok, Thailand Email: kessarin.t@chula.ac.th

Background and aims: Clot wave analysis (CWA) provides a global assessment of hemostasis and may be useful for patients with cirrhosis with complex hemostatic abnormalities. This study aims to assess the association between CWA values of prothrombin time (PT) and activated partial thromboplastin time (aPTT) clotting assays and the severity of cirrhosis. In addition, we prospectively evaluate the role of CWA in predicting acute decompensation in compensated cirrhotic patients.

Method: Adult cirrhotic patients were prospectively enrolled at Chulalongkorn University Hospital from June 2021 to October 2023. At the enrollment, patients with active bleeding, bleeding disorders, antiplatelet or anticoagulant use, hemodialysis, and active malignancy were excluded. Acute decompensation (AD) is defined as the acute development of ascites, variceal bleeding, overt hepatic encephalopathy, bacterial infection, jaundice, or any combination of these complications. CWA values were performed on the CS-2500 (Sysmex Corporation).

Results: A total of 466 cirrhotic patients were enrolled, with 144 (30.9%) having decompensated cirrhosis. Of these, 123 (26.4%) and 40 (8.6%) had Child-Pugh B and C, respectively. Maximum velocity (min1), maximum acceleration (min2), and maximum deceleration (max2) of CWA based on PT and aPTT assays were significantly lower ($p \leq 0.05$) in decompensated patients than in those with compensated cirrhosis. Advanced stage of cirrhosis was associated with more hypocoagulable CWA parameters. In addition, patients with Model For End-Stage Liver Disease (MELD) score of ≥ 18 had lower CWA values than those with MELD score of < 18 . The min1, min2, and max2 of PT CWA assays were significantly negatively correlated with Child-Pugh ($r = -0.37$ to -0.46 , $p \leq 0.001$), MELD score ($r = -0.35$ to -0.41 , $p \leq 0.001$), and transient elastography evaluated by Fibroscan ($r = -0.16$ to -0.26 , $p \leq 0.05$). There was no significant difference in CWA values between patients with and without portal vein thrombosis. Among patients with compensated cirrhosis at baseline, 11.8% (38/322) developed acute decompensation within one year of follow-up. Baseline PT-based CWA values were significantly lower in patients

POSTER PRESENTATIONS

who developed decompensating events compared to those without progression.

Conclusion: Hypocoagulable CWA measurements are associated with advanced cirrhotic stage and the progression to decompensated complications. CWA may be a useful objective marker of the severity of cirrhosis.

FRI-094-YI

Differential diagnosis of covert hepatic encephalopathy in a cohort of outpatients with chronic liver disease

Lyès Kheloufi^{1,2}, Philippe Sultanik^{1,2}, Apolline Leproux^{1,2}, Charlotte Bouzbib^{1,2,3}, Sarah Mouri^{1,2,3}, Antoine Santiago¹, Marika Rudler^{1,2,3}, Nicolas Weiss^{1,2,4}, Dominique Thabut^{1,2,3}. ¹AP-HP, Brain-Liver Pitié-Salpêtrière Study group (BLIPS), Paris, France; ²INSERM UMR_S 938, Centre de recherche Saint-Antoine, Maladies métaboliques, biliaires et fibro-inflammatoire du foie, Institute of Cardiometabolism and Nutrition (ICAN), Paris, France; ³AP-HP, Sorbonne Université, Liver Intensive Care Unit, Hepatogastroenterology Department, Pitié-Salpêtrière Hospital, Paris, France; ⁴AP-HP, Sorbonne Université, Neurology Intensive Care Unit, Neurology Department, Pitié-Salpêtrière Hospital, Paris, France
Email: lyes.kheloufi@aphp.fr

Background and aims: Covert hepatic encephalopathy (CHE) is a complex and multifactorial complication of chronic liver diseases (CLD). Other etiologies may cause neurocognitive impairment (NI) independently from the liver condition, making the differential diagnosis difficult using cognitive tests. The aim of this study was to search for cognitive tools enabling to identify patients with CHE, taking into account the presence of other sources of NI.

Method: Retrospective analysis of a prospective cohort of patients with CLD (March 2018–November 2022) referred to our outpatient clinics for suspicion of CHE. Multimodal work-up was performed in our multidisciplinary team: hepatologists, neurologist, neuropsychologist, biomarkers, electroencephalogram (EEG) and brain MRI (MRI) with spectroscopy (MRS). An adjudication committee involving the aforementioned physicians set the diagnosis of CHE and the presence of factors of brain injury (FBI: alcohol abuse sequelae, vascular leukopathy, stroke, epilepsy) based on medical history, clinical examination, complete neuropsychological evaluation (general cognitive efficiency, attention, executive functions, memory, instrumental functions, including tests validated for HE diagnosis: PHES, Psychometric Hepatic Encephalopathy Score, ANT, Animal Naming Test), EEG and MRI-MRS. Descriptive analyses were conducted with Chi squared test for qualitative data proportions association, and Mann-Whitney U test or Kruskal-Wallis test for quantitative data associations.

Results: 164 pts were included: a majority of males (64%), median age was 60 (50–66) years, 77% cirrhosis (alcohol/MASH/virus in 62/54/16%), 23% portosinusoidal vascular liver disease. Overall, 63% patients were diagnosed with CHE. FBI were found in 36% of patients and 25% with mix causes of NI (CHE and FBI). Only 37% of patients had CHE without FBI. Age, prevalence of cirrhosis, and presence of FBI were similar between CHE and non-CHE groups. MoCA ($p = 0.049$), PHES ($p = 0.003$), ANT ($p = 0.001$), executive and attention evaluating tests were significantly worse in CHE patients. When comparing patients with or without FBI, MMSE ($p = 0.008$), MoCA ($p = 0.027$), and tests evaluating attention, executive functions, and episodic memory were significantly worse in patients with FBI. When separating in four groups taking into account the presence of CHE and FBI, the evaluation of episodic memory (FCSRT, recall of Rey's Figure) enabled to separate patients with FBI from patients without, independently from HE diagnosis.

Conclusion: The diagnosis of HE based only on the presence of NI is complicated. Validated tests (PHES, ANT) can be sensitive for HE but for other sources of NI as well, such as the presence of FBI. The evaluation of episodic memory seems to be a promising tool for differential diagnosis between HE and FBI.

FRI-095

Privative verbal fluency test (PVFT): a quick-to-use cognitive tool for the screening of covert hepatic encephalopathy

Lyès Kheloufi^{1,2}, Aliyya Ahamada¹, Apolline Leproux^{1,2}, Philippe Sultanik^{1,2}, Sarah Mouri^{1,2,3}, Charlotte Bouzbib^{1,2,3}, Marika Rudler^{1,2,3}, Nicolas Weiss^{1,2,4}, Dominique Thabut^{1,2,3}. ¹AP-HP, Brain-Liver Pitié-Salpêtrière Study group (BLIPS), Paris, France; ²INSERM UMR_S 938, Centre de recherche Saint-Antoine, Maladies métaboliques, biliaires et fibro-inflammatoire du foie, Institute of Cardiometabolism and Nutrition (ICAN), Paris, France; ³AP-HP, Sorbonne Université, Liver Intensive Care Unit, Hepatogastroenterology Department, Pitié-Salpêtrière Hospital, Paris, France; ⁴AP-HP, Sorbonne Université, Neurology Intensive Care Unit, Neurology Department, Pitié-Salpêtrière Hospital, Paris, France
Email: lyes.kheloufi@aphp.fr

Background and aims: Hepatic encephalopathy (HE) is a severe complication of chronic liver diseases (CLD). It is associated to a lower survival rate and an alteration of quality of life. Therefore, it is crucial to detect HE as soon as possible, at the stage of covert HE (CHE), in order to start effective therapies. Cognitive tests validated for HE (PHES, Psychometric Hepatic Encephalopathy Score, ANT, Animal Naming Test or Stroop test) are focused on psychomotor speed, attention and executive functions. PHES is currently the gold-standard for CHE diagnosis but is time-consuming and not available in routine clinical practice. The aim of this study was to evaluate the sensibility of a quick cognitive test, the privative verbal fluency test (PVFT) for the diagnosis of HE and comorbidities.

Method: Cross sectional analysis of a prospective cohort (February 2022–October 2023) of patients with CLD referred to our outpatient clinics for suspicion of HE. An adjudication committee involving hepatologists, a neurologist and a neuropsychologist set the diagnosis of HE encompassing the results of brain MRI with spectroscopy, blood sample with ammonia, electroencephalogram and cognitive tests including PHES, ANT, CFF, verbal fluency and cognitive inhibition. The PVFT task consists on giving as many words not containing the letter “a,” in one minute, evaluating verbal fluency and cognitive inhibition. Chi squared test was used for qualitative data and Mann-Whitney U test, Kruskal-Wallis test and Spearman's Rho correlation for quantitative data associations.

Results: Sixty-one patients referred to our outpatient clinics went through all the cognitive tests and clinical evaluation. Among them, 71% were men and the median age was 60 (53–65), 69% had liver cirrhosis with a median MELD score of 13 (10–15). Thirty patients (49%) were diagnosed with CHE. Patients with CHE displayed lower scores in the PVFT ($p = 0.013$), PHES ($p < 0.001$) and ANT ($p = 0.049$). Correlation between PVFT and ANT ($r = 0.76$) and PHES ($r = 0.61$) were significantly high ($p < 0.001$). ROC analysis for PVFT, ANT and PHES yielded to areas under the ROC curve of respectively 0.69, 0.64 and 0.79. The best compromise between sensitivity and specificity for the PVFT was the cut-off of 10 production in one minute (Youden index = 0.32; sensitivity = 0.87; specificity = 0.45), whereas, 20 animals in one minute for the ANT yielded a Youden index of 0.19 (sensitivity = 0.82; specificity = 0.38). The PHES, with a cut-off score of -4 yielded a Youden index of 0.29 (sensitivity = 0.37; specificity = 0.92).

Conclusion: PVFT is a quick (1 min) cognitive sensitive test for the screening of CHE in CLD patients. Correlation analysis have shown a significant association between PVFT, ANT and PHES. PVFT displayed greater sensitivity than ANT and PHES. PVFT can represent a very promising and accessible tool for HE screening.

FRI-098

Feasibility of bedside ultrasonography of rectus femoris muscle for sarcopenia diagnosis in liver cirrhosis

Sara De Monte¹, Philipp Altmann¹, Hans Benno Leicht¹, Roswitha Brandl¹, Florian P Reiter¹, Mathias Plauth², Andreas Geier¹, Monika Rau¹. ¹University hospital Würzburg, Würzburg, Germany; ²Dessau community general hospital, Dessau-Rosslau, Germany
Email: sra.demonte@gmail.com

Background and aims: Malnutrition and sarcopenia are highly prevalent in patients with advanced liver cirrhosis (LC), both serving as independent risk factors for increased morbidity and mortality. The diagnostic algorithm for sarcopenia involves measuring muscle mass and/or muscle function. This prospective study aims at assessing the feasibility of bedside ultrasonography of the Rectus femoris muscle (RFM) as an indicator for muscle mass for diagnosing sarcopenia in patients with LC.

Method: 79 patients with LC hospitalized at a tertiary center from 05/22 to 12/23 were prospectively included. Assessment of sarcopenia was performed 24–48 h after admission, using hand grip strength, chair rising test, ultrasound measurement of RFM and bioelectrical impedance analysis (BIA). Physical performance was tested by Timed Up and Go (TUG) and gait speed test. Statistical analysis was performed by SPSS.

Results: 48/79 (61%) patients were male, and 20 had compensated LC (CHILD A), while 59 had decompensated LC (40 = CHILD B, 19 = CHILD C). RFM thickness (MT) and cross-sectional area (CSA) were significantly lower in CHILD C patients compared to CHILD A (MT 7.3 ± 2.8 vs. 9.0 ± 2.5 mm; $p < 0.05$; CSA 172.1 ± 100.9 vs. 213.6 ± 72.2 mm²; $p < 0.05$) with an even more pronounced difference when adjusting for height (m²) or body surface area (BSA). No significant difference in appendicular skeletal mass (ASM) or fat-free mass (FFM) as determined by BIA was observed in decompensated vs. compensated LC, even when analyzing only patients without ascites and/or edema. However, CHILD C patients had a significantly lower BIA-derived phase angle (PA) compared to CHILD A patients ($3.7 \pm 0.9^\circ$ vs. $4.7 \pm 0.5^\circ$; $p < 0.01$). Patients with low muscle function, assessed by hand grip strength had significantly lower MT and CSA of RFM, as well as lower PA, ASM, and FFM by BIA. MT of RFM and PA were significantly negatively correlated to the chair rising test, but no correlation was found to TUG or gait speed test. ROC curve analysis demonstrated the highest accuracy for MT/m² and CSA/m² of RFM in predicting low PA ($< 4.9^\circ$) (MT/m² 0.68; CSA/m² 0.74)).

Conclusion: In patients with cirrhosis, ultrasound of RFM is a feasible and easily applicable bedside method for detecting those at risk for sarcopenia. Both, low RFM thickness and cross-sectional area are associated with lower muscle strength. These findings underscore the potential of ultrasonography as a practical bedside tool for diagnosing sarcopenia in patients with cirrhosis.

FRI-099

Risk of serious infection in patients with chronic liver disease: a nationwide population-based cohort study

Won Sohn¹, Ju-Yeon Cho², Jung Hee Kim³, Jae Yoon Jeong⁴, Yong Kyun Cho¹, Byung Ik Kim¹. ¹Kangbuk Samsung Hospital, Sungkyunkwan University School of Medicine, Seoul, Korea, Rep. of South; ²Chosun University Hospital, Gwang-Ju, Korea, Rep. of South; ³Hallym University Dongtan Sacred Heart Hospital, Dongtan, Korea, Rep. of South; ⁴National Medical Center, Seoul, Korea, Rep. of South
Email: hand0827@naver.com

Background and aims: This study aimed to investigate the risk of serious infection in patients with chronic liver disease.

Method: This cohort study from the Korean National Health Insurance Service included a population-based data collected from 1, 699, 159 patients with chronic liver disease between 2009 and 2021. The definition of serious infection was hospital admissions with ICD-10 codes for acute meningitis, acute osteomyelitis, bacteremia, pneumonia, pyelonephritis, serious gastrointestinal infection, skin

and soft tissue infections, spontaneous bacterial peritonitis, and COVID-19 infection. We compared the development of serious infection, the admission of intensive care unit (ICU), and mortality between chronic liver disease/compensated cirrhosis and decompensated cirrhosis.

Results: The mean age of the patients was 57.4 years, with 55.6% of them being men. The most common cause of chronic liver disease was chronic hepatitis B (59.5%). The study population consisted of 1, 614, 085 patients (95%) with chronic liver disease/compensated cirrhosis and 85, 074 patients (5%) with decompensated cirrhosis. During the follow-up period, 12.5% of patients with chronic liver disease/compensated cirrhosis, and 23.9% of patients with decompensated cirrhosis experienced serious infections ($p < 0.01$). The most common infections were pneumonia, followed by serious gastrointestinal infection, pyelonephritis, bacteremia, skin and soft tissue infections, spontaneous bacterial peritonitis, acute osteomyelitis, acute meningitis, and COVID-19 infection. The risk of serious infections is higher in decompensated cirrhosis than in chronic liver disease/compensated cirrhosis (adjusted hazard ratio [HR] 2.43 with confidence interval [CI]: 2.38–2.47). Patients with decompensated cirrhosis had higher admission rate on ICU for serious infections compared to chronic liver disease/compensated cirrhosis: 16.9% vs. 1.8%, $p < 0.01$. The mortality rates were 4.2, 40.0, and 107.7 per 1, 000 person years in patients with no, 1, and ≥ 2 serious infections. The adjusted HRs for all-cause mortality in patients with 1 and ≥ 2 serious infections, compared to no serious infection were 5.48 (95% CI: 5.41–5.56), and 11.20 (95% CI: 11.00–11.40).

Conclusion: The risk of serious infection is higher in patients with decompensated cirrhosis. The mortality in patients with chronic liver disease is growing as the risk of serious infection increases.

FRI-100

Bleeding risk after endoscopic polypectomy in patients with cirrhosis

Guenseli Bloch¹, Haedge Frederic², Gabriel Allo³, Philipp Kasper³, Benedikt Hild¹, Tony Bruns², Jassin Rashidi-Alavijeh¹, Hartmut Schmidt¹, Christoph Schramm¹. ¹University Hospital Essen, Essen, Germany; ²University Hospital RWTH Aachen, Aachen, Germany; ³University Hospital Cologne, Cologne, Germany
Email: christoph.schramm@uk-essen.de

Background and aims: Endoscopic polypectomy of colorectal polyps is recognised as a safe procedure and a cornerstone in the prevention of colorectal cancer. In patients with cirrhosis, an increased bleeding risk is often assumed since alterations in global coagulation tests and platelet count are frequently present. However, both are of limited value for predicting bleeding complications in several procedures. We aimed to investigate risk factors for post-polypectomy bleeding complications in patients with cirrhosis.

Method: We performed a retrospective multicenter study of patients with cirrhosis who underwent colonoscopy with polypectomy at three academic medical centers in Germany from 01/01/2013 and 31/12/2022. Clinical significant portal hypertension (CSPH) was diagnosed in the case of liver stiffness > 25 kPa, present or history of ascites, or esophageal, gastric or esophageal varices. Severe bleeding was defined as death, drop in hemoglobin ≥ 2 g/dl and/or transfusion of ≥ 2 red blood cell concentrate.

Results: We included 337 patients with a median age of 61 years (interquartile range (IQR) 54–67), of which 69% were male and 31% female. Alcohol-associated liver disease (40%), chronic hepatitis C (17%), and steatotic liver disease (13%) were the most common etiology of chronic liver disease. 48%, 38%, and 14% of patients were Child Pugh class A, B, and C, respectively, the median MELD score was 11 (IQR 7–16). CSPH was present in 84%, of which 44% received treatment with non-selective beta-blocker and/or transjugular intra-hepatic portosystemic shunt. Platelets $< 50,000/\mu\text{l}$ and/or INR > 1.5 was present in 23%, platelets $< 30,000/\mu\text{l}$ and/or INR > 2.5 in 11%. A total of 664 polyps with a median size of 7 mm (IQR 5–10) were

POSTER PRESENTATIONS

removed by endoscopic polypectomy. 40% of patients had polyps ≥ 10 mm and 9% of patients had polyps ≥ 20 mm in size. Intraprocedural bleeding occurred in 11.6% of patients. Sixteen patients (4.7%) experienced post-polypectomy bleeding, of which 7 (2.1%) were severe. Intraprocedural bleeding was significantly increased in polyps ≥ 20 mm in size (26.7% vs. 10.1%, $p = 0.007$). INR > 1.5 (12.1% vs. 3.3%, $p = 0.004$) and > 2.5 (11.8% vs. 4%, $p = 0.045$), and Child-Pugh class (A: 1.9% vs. B: 6.3% vs. C: 10.2%, $p = 0.034$), but not thrombocytopenia or CSPH were significantly associated with post-polypectomy bleeding.

Conclusion: Post-polypectomy bleeding is infrequent in patients with cirrhosis. Elevated INR and higher Child-Pugh class, i.e. parameters for more advanced chronic liver disease, but not platelet count or CSPH including treatment, were significantly associated with the occurrence of bleeding complications. The benefit of correcting altered coagulation parameters prior to polypectomy needs to be demonstrated.

FRI-101-YI

Rectus femoris cross sectional area predicts 90-day readmission in patients hospitalized for an acute decompensation of cirrhosis

Roberta Gagliardi¹, Paola Campadello¹, Silvia Brocco¹, Simone Incicco¹, Valeria Calvino¹, Beaudelaire Sikadi¹, Marta Tonon¹, Alessandra Brocca¹, Carmine Gambino¹, Nicola Zeni¹, Giorgio De Conti², Chiara Giraud², Paolo Angeli³, Salvatore Piano³.
¹Unit of Internal Medicine and Hepatology, Department of Medicine, University and Hospital of Padova, Padova, Italy; ²Radiology Unit, Department of Medicine, University and Hospital of Padova, Padova, Italy; ³Unit of Internal Medicine and Hepatology, Department of Medicine, University and Hospital of Padova, Padova, Italy
Email: salvatore.piano@unipd.it

Background and aims: Sarcopenia is frequent in patients with cirrhosis and is associated with poor clinical outcomes. Ultrasound measurement of rectus femoris cross sectional area (RF-CSA) is an easy bedside tool for assessing sarcopenia in patients with cirrhosis. The aim of this study was to evaluate the ability of RF-CSA in predicting 90-day readmission in patients hospitalized for an acute decompensation (AD) of cirrhosis.

Method: We prospectively enrolled cirrhotic patients surviving a hospitalization for AD between 2019 and 2023. At discharge, clinical, demographic and laboratory data were collected and RF-CSA was measured at two-thirds of the distance from the anterior superior iliac spine to the superior patellar border. Patients were classified in two groups according to the median values of RF-CSA for males (3.38 cm²) and females (2.60 cm²): "high" if the RF-CSA value was above or equal to the median, and "low" if it was below the median. Follow-up continued until death, liver transplant, or 90 days, during which readmissions were documented.

Results: We enrolled 161 patients (mean age 64 ± 11 years, mean MELD 16 ± 5), the majority had alcohol-related cirrhosis (57%) and ascites (75%). During the 90-day follow-up 69 patients were readmitted (43%). Patients readmitted were older (67 vs 62 years; $p = 0.012$), had higher rate of hepatic encephalopathy during the index admission (44 vs 27%; $p = 0.023$) and lower RF-CSA (3.4 vs 2.8 cm²; $p < 0.001$). Patients with "low" RF-CSA had a higher probability of 90-day readmission than those with "high" RF-CSA (67 vs 46%; $p = 0.005$). In multivariable analysis (adjusted for age, sex, MELD and hepatic encephalopathy during index admission) a "low" RF-CSA was an independent predictor of 90-day readmission (aHR = 1.79; $p = 0.026$), along with the development of HE during index admission (aHR = 5.55; $p < 0.001$).

Conclusion: Low muscle mass assessed by RF-CSA independently predicts 90 day-readmission in patients with cirrhosis surviving a hospitalization for AD. These findings suggest that preventing muscle loss and/or promoting increases in muscle mass could be potential targets for strategies aimed at preventing readmissions.

FRI-103-YI

Screening and assessing Sarcopenia in liver cirrhosis: feasibility and implications for clinical outcomes

Philipp Altmann¹, Sara De Monte¹, Roswitha Brandl¹, Florian P Reiter¹, Hans Benno Leicht¹, Andreas Geier¹, Monika Rau¹. ¹Division of Hepatology, Department of Internal Medicine II, University hospital Wuerzburg, Wuerzburg, Germany
Email: altmann_p@ukw.de

Background and aims: The prevalence of sarcopenia, a nutrition-related condition, is high among patients with advanced liver disease, posing an independent risk for increased morbidity and mortality. This prospective study aims to analyze the feasibility of sarcopenia assessment outlined in the European Working Group on Sarcopenia in Older People (EWGSOP 2) criteria in patients with liver cirrhosis.

Method: A total of 81 cirrhotic patients were included in this prospective study from 05/22–12/23. Sarcopenia assessment was performed between 24–48 h after hospital admission at a tertiary university hospital. The assessment encompassed screening with SARC-F, muscle strength measurements, physical performance tests, and bioelectrical impedance analysis (BIA). Nutritional status was evaluated using Subjective Global Assessment (SGA) and Royal Free Nutrition Prioritizing Tool (RFH-NPT) questionnaires.

Results: Baseline characteristics indicated a mean age of 59 years, with 61.7% males and 38.3% females. Of the patients, 22 (27.2%) had compensated cirrhosis CHILD A, while 59 (72.8%) had decompensated cirrhosis (CHILD B or C). The mean MELD score was 15.6 ± 6.6 . Only 17 (21%) patients had a positive screening with SARC-F (≥ 4), which was significantly associated with higher MELD score (SARC-F pos. 19.6 ± 1.7 vs. SARC-F neg. 14.6 ± 0.8 , $p < 0.05$), but not with age. Reduced muscle strength by low HG strength was observed in 33% of cirrhotic patients and in 60.5% with an impaired chair rise test (> 15 s). There was no significant association between low muscle strength tests and CHILD stage or MELD, but a significant association between both muscle strength tests and malnutrition by SGA in this study cohort. A substantial proportion of patients (75.3%) had a low phase angle ($< 4.9^\circ$) by BIA, significantly associated with a higher CHILD stage, MELD score, and malnutrition assessed by SGA. In terms of physical performance, 18.5% of patients had a low Timed Up and Go (TUG) test (≥ 14 s) and 22.2% had a low gait speed (≤ 0.8 s). Both physical performance tests were significantly associated with impaired muscle strength tests (HG and chair rise test). ROC analysis indicated that grip strength, phase angle and gait speed had the highest accuracy in predicting mortality or transplantation among our participants (0.573 vs 0.726 vs 0.729) in the 12-month follow-up, available at the time point of the abstract for only 28.5% of our study cohort.

Conclusion: The current EWGSOP2 algorithm for diagnosing sarcopenia has limited applicability in patients, as screening by SARC-F identifies only a minority of patients with high risk for sarcopenia characterized by reduced muscle strength and/or low phase angle by BIA-both associated with malnutrition and adverse outcome in this patient group. A valid screening instrument for sarcopenia in patients with liver cirrhosis is needed and should be addressed in further studies.

FRI-104

The respiratory assessment of cirrhotic patients: six-minute walk test is an independent predictor of mortality in cirrhosis

Burcu Gurbuz¹, Aytekin Idikut², Ugur Karakulak³, Ebru Damadoglu⁴, Baris Kaya³, Taylan Kav⁵, Erkan Parlak⁵, Onur Keskin⁵. ¹Hacettepe University School of Medicine Department of Internal Medicine, Ankara, Turkey; ²Hacettepe University School of Medicine Department of Pulmonology, Ankara, Turkey; ³Hacettepe University School Of Medicine Department of Cardiology, Ankara, Turkey; ⁴Hacettepe University School

Of Medicine Department of Pulmonology, Ankara, Turkey; ⁵Hacettepe University School Of Medicine Department of Gastroenterology, Ankara, Turkey
Email: drburcuusta@gmail.com

Background and aims: Respiratory status of cirrhosis patients has not been adequately studied in the literature. The effectiveness of tests showing cardiopulmonary dysfunction in predicting survival in patients with cirrhosis has not been elucidated. This study aimed to investigate the type and frequency of respiratory symptoms in cirrhotic patients, to perform spirometric evaluation, and to investigate the effects of the 6-minute walk test on mortality prediction.

Method: Between September 2022 and June 2023, 75 patients followed up with cirrhosis were included in the study. Patients under 18 years of age and those with known moderate to severe cardiac or pulmonary disease were not included. Patients who came for routine gastroenterological examination were directed to the pulmonology department, whether they had complaints or not, all patients were questioned in detail about respiratory symptoms, spirometric measurements were made and a 6-minute walk test was performed. Walking test results were standardized according to gender, age, height and weight, and percentage values were calculated by proportioning the distances walked by the patients to the expected distances. Hospitalizations, decompensation and exitus status of the patients were recorded during the study period.

Results: Fifty-one patients (68%) reported dyspnea on exertion, 70 patients (93.3%) reported dyspnea on exertion at any time, and 22 patients (29.3%) had orthopnea. In the presence of decompensation, dyspnea ($p < 0.001$), exertional dyspnea ($p:0.001$), orthopnea symptoms ($p < 0.001$) were more common and modified Medical Research Council (mMRC) score was significantly higher ($p: < 0.001$). In spirometric examination, FEV1% ($p:0.003$), FVC % ($p < 0.001$) were significantly lower and 6-minute walk distance was 14% shorter than expected in decompensated patients ($p:0.001$). Patients with FVC $< 70\%$ on spirometry were considered restrictive, and the 6-minute walking distance of patients with restrictive results was found to be 173 meters lower on average ($p < 0.001$). Multivariate analysis showed that the failure to complete the 6-minute walk test was an independent predictor of mortality (OR: 16.00 [95% CI: (2.40–106)], $p:0.004$).

Conclusion: In conclusion, most cirrhotic patients have respiratory symptoms and signs and failure to complete the 6-minute walk test is an independent predictor of mortality in cirrhosis.

FRI-105

Tissue factor pathway inhibitor and serum amyloid A-4 protein are promising to predict occurrence of overt hepatic encephalopathy after transjugular intrahepatic portosystemic shunt

Huan Tong¹, Rui Yang¹, Xin Quan¹, Bo Wei¹, Hao Wu¹. ¹West China Hospital, Sichuan University, Chengdu, China
Email: doctortonghuan@163.com

Background and aims: Transjugular intrahepatic portosystemic shunt (TIPS) is increasingly applied to treat portal hypertension subsequent to liver cirrhosis. However, hepatic encephalopathy (HE) is a complication of concern for TIPS creation. There is still in lack of biomarkers to predict post-TIPS overt HE (OHE) currently. Therefore, this study was conducted to seek for feasible biomarkers to predict post-TIPS OHE.

Method: Serum of liver cirrhosis patients in this study came from another study (register No. ChiCTR2000039674), and those blood samples were collected before TIPS creation. Samples were divided into two groups (OHE group and non-OHE group) depending on the occurrence of OHE within 2 years after TIPS creation. Serum of 5 OHE and 5 non-OHE patients were firstly tested by non-labeled quantitative proteomics to screen for differentially expressed proteins. Proteins with $p < 0.03$ and fold change > 1.3 were eligible for further

validation. The chosen biomarkers were thereafter quantified in 40 OHE and 40 non-OHE patients using enzyme-linked immunosorbent assay (ELISA). Logistic regression were used to determine the significance of biomarkers in predicting post-TIPS OHE and receiver operating characteristic curve was also used to display the diagnostic efficacy.

Results: Non-labeled quantitative proteomics identified 15 differentially expressed proteins between OHE and non-OHE patients. These secretory proteins mainly reside in the extracellular space to negatively regulate peptidase/endonuclease activity and protein hydrolysis to function. ELISA confirmed the up-regulation of tissue factor pathway inhibitor (TFPI), keratin type I cytoskeletal 10 (KRT10), metalloproteinase inhibitor 2 (TIMP2), serum amyloid A-4 protein (SAA4), and coagulation factor IX (F9), and down-regulation of fetuin-B (FETUB) in OHE group (OHE vs. non-OHE: TFPI 72.1 ± 21.9 vs. 52.2 ± 22.3 ng/ml, $p < 0.001$; KRT10 188.1 ± 159.2 vs. 126.4 ± 100.4 ng/ml, $p = 0.042$; TIMP2 417.5 ± 222.0 vs. 325.0 ± 104.2 ng/ml, $p = 0.020$; SAA4 4423.1 ± 2699.9 vs. 3207.1 ± 2592.4 ng/ml, $p = 0.021$; F9 1.4 ± 1.6 vs. 0.7 ± 0.5 ug/ml, $p = 0.014$; FETUB 11.1 ± 2.3 vs. 12.3 ± 3.0 ug/ml, $p = 0.036$). Logistic regression suggested that both serum TFPI and SAA4 were the risk factors to develop post-TIPS OHE in model 0 (6 aforementioned proteins), model 1 (age, gender, HE history, and model 0) and model 2 [alcoholic cirrhosis, portal pressure gradient decrement, blood ammonia, model for end-stage liver disease (MELD) score, hydrothorax, and model 1]. ROC curves showed that TFPI bore a better area under curve (AUC), comparing with SAA4 and MELD score (AUC: TFPI 0.716, $p < 0.001$; SAA4 0.654, $p = 0.018$; MELD score 0.509, $p = 0.889$).

Conclusion: Serum levels of TFPI, KRT10, TIMP2, SAA4, F9 and FETUB before TIPS differ between post-TIPS OHE and non-post-TIPS OHE patients, and serum TFPI and SAA4 are promising to predict the occurrence of post-TIPS OHE.

FRI-106-YI

Change in frailty status with nutritional therapy in patients with cirrhosis-a randomized controlled trial

Sudhir Maharshi¹, Saksham Seth¹, Shyam Sunder Sharma¹. ¹SMS Medical College and Hospitals, Jaipur, India
Email: sudhir.maharshi@gmail.com

Background and aims: Frailty is characterized by low physiologic reserve and decreased functional status and is associated with poor prognosis in patients with cirrhosis. There is limited data on nutritional intervention on frailty status in cirrhosis. Aim was to assess the effects of nutritional therapy on changes in frailty status in cirrhotic patients.

Method: A randomized controlled trial conducted in a tertiary care centre on patients with cirrhosis, who were randomized to assigned to nutritional therapy (group A 30–35 kcal/kg/day, 1.0–1.5 g protein/kg/day) and no nutritional therapy (group B: patients continued on their same diet) for 6 months. Frailty status was assessed by liver frailty index (LFI) and gait velocity (GV). Primary end points were improvement or worsening in frailty status. Secondary end points were improvement of other nutritional parameters and liver functions.

Results: Till date 34 patients were randomized to group -A ($n = 18$, age 43.4 SD 9.8 yr, 14 men) and group-B ($n = 16$, age 42.7 SD 10.1 yr, 12 men). Alcohol was most common (64%) etiology. Baseline characteristics including age, body mass index (BMI), haemoglobin, MELD score, mid arm circumference (MAC), hand grip (HG), GV and LFI were comparable in both the groups. Improvement in GV (delta GV 0.99 SD 0.32 vs -0.82 SD 0.28, $p = 0.001$), LFI (delta LFI -0.62 SD 0.24 vs 0.3 SD 0.32, $p = 0.001$) HG strength (delta HG 4.2 SD 1.3 vs -2.9 SD 1.2, $p = 0.001$), MAC (delta MAC 2.69 SD 0.28 vs -2.15 SD 0.26, $p = 0.01$) was observed in group A compared to group B at the end of study. Liver functions assessed by Child Turcotte Pugh and Model for end stage liver disease also significantly improved in group A compared to group B, p less than 0.001.

POSTER PRESENTATIONS

Conclusion: Nutritional therapy is effective in the improving the frailty status, nutritional parameters and liver functions in cirrhotic patients.

FRI-107-Y1

Folic acid prescription is associated with a lower mortality and hospital readmission in patients with decompensated alcohol-related liver cirrhosis

Laura Buttler¹, Anja Tiede^{1,2}, Marie Griemsmann³, Hannah Schneider¹, Jim Benjamin Mauz¹, Heiner Wedemeyer^{1,2,4,5}, Markus Cornberg^{1,2,5,6}, Tammo Lambert Tergast¹, Benjamin Maasoumy^{1,7}, Katharina Luise Hupa-Breier¹. ¹Department of Gastroenterology, Hepatology, Infectious Disease and Endocrinology, Hannover Medical School, Hannover, Germany; ²German Centre for Infection Research (DZIF), partner-site Hannover-Braunschweig, Hannover, Germany; ³Department of Gastroenterology, Hepatology, Infectious Disease and Endocrinology, Hannover Medical School, Hannover; ⁴RESIST Cluster of Excellence, Hannover Medical School, Hannover, Germany; ⁵Centre for Individualised Infection Medicine (CiIM), A Joint Venture Between the Helmholtz Centre for Infection Research (HZI) and Hannover Medical School (MHH), Hannover, Germany; ⁶TWINCORE, A Joint Venture Between the Helmholtz-Centre for Infection Research (HZI) and the Hannover Medical School (MHH), Hannover, Germany; ⁷German Centre for Infection Research (DZIF), partner-site Hannover-Braunschweig, Hannover, Germany, Hannover, Germany Email: Buttler.Laura@mh-hannover.de

Background and aims: Patients with alcohol-related liver cirrhosis (aLC) frequently develop a state of malnutrition and micronutrient deficiencies, that are linked to a poor prognosis and disease progression. Particularly, an inadequacy of thiamine and folate supply is often observed in this group of patients. Consequently, guidelines recommend broad vitamin B prescription, but the impact on the clinical outcome remains questionable. Therefore, we aimed to evaluate the real-world use of thiamine and folic acid and its effect on liver-related complications and transplant-free survival in patients with decompensated aLC.

Method: The investigated cohort included 289 consecutive patients with aLC and ascites who were treated at our center between 2011 and 2023. Discharge medication was screened for thiamine- or folic acid containing supplements. Patients were followed up for hepatic encephalopathy (HE), infections, spontaneous bacterial peritonitis (SBP) and liver transplantation (LTx) free survival up to one year after hospital discharge.

Results: Thiamine containing supplements were prescribed to 139 (48.1%) patients. Most frequent was intake of a fixed vitamin B combination including vitamin B1 (n=73; 52.5%) and single thiamine (n=66; 47.5%). Only 12 patients (8.6%) took multivitamin supplements. Folic acid was prescribed to a minor proportion of 52 (18.0%) patients. Regarding clinical outcome, 22 (7.6%) patients underwent LTx, 69 (23.9%) died, 168 (58.1%) were readmitted due to a complication of cirrhosis and 100 (34.6%) patients were affected by HE within one year. Moreover, SBP occurred in 85 (29.4%) patients and any infection was acquired by half of the cohort (n=145; 50.2%). Of note, after adjusting for MELD, age, sex and hemoglobin in the multivariable model, competing risk analyses indicated a superior 1-year LTx-free survival in the folic acid group (HR=0.48; p=0.04). Furthermore, folic acid prescription was associated with a significant decreased risk of hospital readmission within one year. This remained statistically significant even after adjusting for the potential confounders MELD, age and hemoglobin (HR=0.55; p=0.01). In contrast, no impact was detected on HE or infections. Similarly, thiamine prescription was not associated with an improved LTx-free survival (HR=0.84; p=0.45) and did not ameliorate the risk of hospital readmission (HR=0.93; p=0.65) or other liver-related complications regarding 365 days follow-up. Additionally, neither

folic acid nor thiamine were linked to an improved clinical outcome when considering a shorter 90 days observation period.

Conclusion: Folic acid prescription is associated with an improved outcome in patients with decompensated aLC. However, possible risks of broad vitamin application, especially the potential aggravation of polypharmacy, have to be investigated.

FRI-109

Differences in the clinical phenotype of decompensated liver cirrhosis between MASLD, MetALD and ALD patients

Laura Buttler¹, Anja Tiede^{1,2}, Marie Griemsmann¹, Hannah Schneider¹, Jim Benjamin Mauz¹, Heiner Wedemeyer^{1,2,3,4}, Markus Cornberg^{1,2,4,5}, Tammo Lambert Tergast¹, Benjamin Maasoumy^{1,2}, Katharina Luise Hupa-Breier¹. ¹Department of Gastroenterology, Hepatology, Infectious Disease and Endocrinology, Hannover Medical School, Hannover, Germany; ²German Centre for Infection Research (DZIF), partner-site Hannover-Braunschweig, Hannover, Germany; ³RESIST Cluster of Excellence, Hannover Medical School, Hannover, Germany; ⁴Centre for Individualised Infection Medicine (CiIM), A Joint Venture Between the Helmholtz Centre for Infection Research (HZI) and Hannover Medical School (MHH), Hannover, Germany; ⁵TWINCORE, A Joint Venture Between the Helmholtz-Centre for Infection Research (HZI) and the Hannover Medical School (MHH), Hannover, Germany Email: Buttler.Laura@mh-hannover.de

Background and aims: Recently, a new nomenclature of steatotic liver disease (SLD) has been implemented, which does not only differentiate MASLD (Metabolic Dysfunction-Associated Steatotic LD) from alcohol-related LD (ALD), but also introduces metabolic and alcohol-related liver disease (MetALD) as a new etiology. The impact of the newly defined etiologies on the clinical management among those with advanced liver disease still needs to be determined. We aimed to analyze whether MASLD, ALD and MetALD patients with decompensated liver cirrhosis (dLC) differ in the clinical phenotypes with regard to the most relevant cirrhosis-associated complications. **Method:** A number of 416 consecutive patients with dLC and undergoing at least one paracentesis between 2011 and 2023 were investigated. All patients were diagnosed with NASH- or alcohol-related LC and reclassified into the SLD groups. Liver transplantation (LTx) free survival, development of infections, spontaneous bacterial peritonitis (SBP), hepatic encephalopathy (HE), portal hypertensive bleeding and hospital readmission due to any further decompensation were examined up to one year of follow-up.

Results: 52 patients were formerly diagnosed with NASH- and 338 with alcohol-related cirrhosis, whereas predominance of metabolic or alcohol-related liver damage was undetermined in 26 cases. When using the new definitions, 55 (13.2%) patients fulfilled the criteria for MASLD, MetALD was present in 67 (16.1%) and ALD in 294 (70.7%) patients. The proportion of male patients was 64% in MASLD, 70% in MetALD and 74% in patients with ALD etiology (p=0.29). Median age was 59 years both in patients with MASLD and MetALD and 56 years in the ALD group (p<0.001). Moreover, median baseline MELD was 18 in MASLD and 17 in MetALD and ALD, respectively (p=0.92). There was no difference between MASLD, MetALD and ALD with regard to the incidence of HE, portal hypertensive bleeding and LTx-free survival. In contrast, ALD was found to be associated with a lower risk for infections within 90 days (HR=0.60; p=0.004) and one year (HR=0.55; p<0.001) compared to MASLD etiology. This remained statistically significant after adjusting for MELD, serum-cholinesterase and diabetes in the multivariable model (90 days: HR=0.61; p=0.04; 1 year: HR=0.59; p=0.02). Of note, incidence of infections in the new MetALD group was lower than in MASLD but numerically higher than in patients with ALD. In all three groups, most common infections were SBP and urinary tract infection.

Conclusion: The risk for infections seems to be elevated among SLD patients with underlying metabolic-dysfunction associated liver

damage. Further studies are necessary to address, whether this could lead to etiology-specific prophylactic measures.

FRI-110

Safety and effectiveness of anticoagulation in patients with cirrhosis listed for liver transplantation: a single center observational study

Riccardo Caccia¹, Giulia Tosetti¹, Massimo Primignani¹, Martina Lucà¹, Sonia Stella¹, Pietro Lampertico^{1,2}. ¹Division of Gastroenterology and Hepatology, Foundation IRCCS Ca' Granda Ospedale Maggiore Policlinico, Milan, Italy; ²CRC "A. M. and A. Migliaiavacca" Center for Liver Disease, Department of Pathophysiology and Transplantation, University of Milan, Milan, Italy
Email: pietro.lampertico@unimi.it

Background and aims: Anticoagulation (AC) in patients with cirrhosis is safe, decreases decompensation and increases survival. However, no data on safety and effectiveness of AC in patients listed for liver transplantation (LT) is available. We evaluated decompensation rate, delisting (either for improvement or progression) and liver-related mortality in patients listed for LT treated with anticoagulants mostly because of portal vein thrombosis (PVT), compared with patients not anticoagulated. Secondary aim was PVT outcome.

Method: Retrospective data of consecutive patients followed at our Center (2017–2021), from listing until LT, delisting or death were collected. Univariate and multivariate logistic regression analyses (adjusted for age, Child-Pugh (CP) class and time in list) were performed to evaluate the effect of AC on bleeding, de-novo decompensation in CP A patients, further decompensation in CP BC patients, delisting for improvement or worsening, OLT and death.

Results: 251 patients listed for OLT, 165 CP class B/C, 34 AC (13.5%), mainly for Portal Vein Thrombosis (PVT) (85%). AC patients were more likely CP class B/C (85% vs 63%, $p = 0.002$). AC included LMWH (67%), fondaparinux (18%), VKA (12%) and DOAC (3%). The bleeding rate was similar in AC and non-AC patients, either for total (23.5% vs. 20.7%; $p = 0.711$), severe (8.8% vs. 9.7%; $p = 0.823$) or portal hypertensive bleedings (2.9% vs. 1.8%; $p = 0.686$). Overall, there was no difference in the rate of de-novo decompensation (14.7% vs 9.7%; $p = 0.398$); in CP class B/C patients there was no difference on further decompensation rate (48.3% vs 41.9%; $p = 0.617$). CP B/C AC patients had more delisting for improvement (10.3% vs 2.2%, $p = 0.034$) and less deaths in list (0.0% vs 13.2%; $p = 0.038$). In CP A patients delisting for worsening (85% due to HCC progression) occurred in 20% AC vs 7% non-AC, while delisting for worsening in CP B/C occurred in 2 patients (1 AC and 1 non-AC). Eight patients were delisted for non-liver related events ($n = 3$) or poor compliance ($n = 5$). Twenty-eight (82%) AC patients and 178 (82.4%) non-AC patients were transplanted ($p = 0.963$). PVT regressed in 13 (45%, 10 total and 3 partial regression), was stable in 12 (14%) and worsened in 4 (14%). None was delisted for PVT worsening.

Conclusion: In cirrhotic patients listed for LT requiring AC for PVT, AC was safe and associated with higher delisting for improvement and improved survival in list.

FRI-111

Risk factors for hepatocellular carcinoma in cirrhosis: a comprehensive analysis from a decade-long study

Daqiong Zhou¹, Lili Liu¹, Jiangyu Liu¹, Jing Zhang¹, Zhenhuan Cao¹. ¹The Third Unit, Department of Hepatology, Beijing Youan Hospital, Capital Medical University, Beijing, China
Email: caozhenhuanyu@mail.ccmu.edu.cn

Background and aims: Cirrhosis represents a significant risk factor for the development of hepatocellular carcinoma (HCC). The variability in HCC risk among cirrhotic patients is notable, particularly when considering the diverse etiologies of cirrhosis. This study aimed to identify specific risk factors contributing to the development of HCC in patients with cirrhosis.

Method: This retrospective study analyzed data from patients with cirrhosis admitted to Beijing Youan Hospital, Capital Medical University, from January 1, 2012, to September 30, 2022, with a minimum follow-up duration of six months. Patient demographics, medical history, liver disease etiology, and clinical characteristics at initial admission were examined. Cox regression was employed to analyze correlations with hepatocarcinogenesis, and competing risk regression was utilized to account for death as a competing event, estimating adjusted hazard ratios (aHR) for identified risk factors.

Results: The study included 5,417 patients, with a median age of 54 years; 65.8% were male, and 76.6% presented with decompensated cirrhosis. During the follow-up, 25% ($n = 1352$) developed HCC. The highest incidence of HCC was observed in patients with hepatitis B virus (HBV) (29.5%), followed by hepatitis C virus (HCV) (26.3%), Alcohol-associated cirrhosis (AC) (20.5%), metabolic dysfunction-associated liver disease (MASLD) (17.6%), primary biliary cirrhosis (15.3%), drug-induced cirrhosis (18.2%), and cryptogenic cirrhosis (26.5%). Competing risk analysis revealed significant associations between increased HCC risk and factors such as male gender (aHR: 1.422, 95% CI: 1.259–1.608), advanced age (aHR: 1.025, 95% CI: 1.021–1.030), HBV (aHR: 1.900, 95% CI: 1.690–2.136), HCV (aHR: 1.523, 95% CI: 1.267–1.832), HBV/HCV co-infection (aHR: 2.171, 95% CI: 1.082–4.356), elevated blood ammonia (aHR: 1.002, 95% CI: 1.001–1.003), and reduced albumin (aHR: 0.984, 95% CI: 0.974–0.994) and platelet levels (aHR: 0.999, 95% CI: 0.998–1.000) were associated. Cumulative incidence function (CIF) curves estimated the HCC risk in cirrhotic patients at 3.24% (1 year), 19.2% (3 years), and 35.2% (5 years).

Conclusion: The study underscores that cirrhosis due to HBV has the highest correlation with HCC incidence. Additionally, male gender, older age, viral hepatitis-related cirrhosis, elevated blood ammonia, and lower albumin and platelet levels significantly elevate HCC risk in cirrhotic patients.

FRI-112

Rapid infection diagnostics in liver disease- evaluation of a multiplex PCR platform to improve infection and antimicrobial resistance detection

Veena Ramachandran¹, Dhaarica Jeyanesan¹, Merianne Mohammed², Zoe Elliott¹, Siva Dwarampudi¹, Marilena Stamouli², Jack Wright¹, Tasneem Pirani^{1,3,4}, Vishal C. Patel^{1,5,6}. ¹Institute of Liver Studies, King's College Hospital NHS Foundation Trust, Denmark Hill, London, SE5 9RS, UK, London, United Kingdom; ²The Roger Williams Institute of Hepatology, Foundation for Liver Research, 111 Coldharbour Lane, London, SE5 9NT, UK, London, United Kingdom; ³Liver Intensive Therapy Unit, King's College Hospital NHS Foundation Trust, Denmark Hill, London, United Kingdom; ⁴School of Immunology and Microbial Sciences, Faculty of Life Sciences and Medicine, King's College London, 125 Coldharbour Lane, London, London, United Kingdom; ⁵The Roger Williams Institute of Hepatology, Foundation for Liver Research, 111 Coldharbour Lane, London, SE5 9NT, UK, London, United Kingdom; ⁶Centre for Clinical Infection and Diagnostics Research, Department of Infectious Diseases, School of Immunology and Microbial Sciences, King's College London, Strand WC2R 2LS, London, London, United Kingdom
Email: v.ramachandran@nhs.net

Background and aims: Chronic liver disease is the second leading cause of work years lost in Europe, driving a significant burden in premature mortality [1]. Cirrhosis is associated with an increased susceptibility to infection [2]. Antimicrobial resistance (AMR) presents a significant risk in cirrhosis, further compounding morbidity and mortality [3]. Early pathogen detection, alongside prompt initiation and de-escalation of antibiotics according to AMR profiles, are therefore critical to improving outcomes [4]. The Curetis Unyvero™ platform (CUP) utilises multiplex polymerase chain reactions (PCR) for rapid pathogen and AMR identification, utilising a range of biofluids based on where infection is suspected. The aim of this study was to compare the CUP against SMT (standard microbial testing) in infection diagnostics and AMR detection in.

POSTER PRESENTATIONS

Method: Ascitic fluid, blood cultures (BC) and bronchoalveolar lavage (BAL) samples were obtained from hospitalised liver disease patients, in whom infection was clinically suspected. Ascites and BAL samples were analysed on CUP prior to culture. Blood cultures—once flagged positive via SMT-based incubation—were in parallel run on CUP for comparison. Following a run time of 4.5hrs, CUP provided pathogen identification data and AMR profiles. Treating clinicians remained blinded to results.

Results: 69 samples from 51 patients were tested: ascites (42), BAL (7), BC (20). Time to positive result was reduced with CUP (4.75hrs) compared with SMT in BAL (mean 73.71hrs; SD = 25.99) and ascites (mean 58.57hrs; SD = 16.38). For all ascites and BAL samples, CUP demonstrated 100% sensitivity and 100% negative predictive value (NPV) in pathogen detection. In positive BCs, CUP showed 94.74% sensitivity for pathogen detection vs SMT. In 1 BC sample, CUP detected *E.coli* spp with corresponding AMR profiles (ctx-M, aacA4) that was SMT negative, retrospective analysis identified a BC sample 24hrs prior that also detected via SMT *E.coli* and a similar AMR profile. In 6 ascites samples, CUP identified pathogens where SMT was negative. On retrospective analysis, 4/6 ascitic samples also showed that prior SMT of earlier samples within 5 days of collection had detected pathogens detected by CUP. CUP identified AMR profiles in 50% (4/8) of BAL and ascites samples, and in 42.85% (3/7) of BC samples, vs SMT, respectively.

Conclusion: These preliminary data demonstrate good concordance in pathogen detection accuracy of CUP vs SMT in all body fluids, with a significant reduction in time to result with CUP. AMR detection with CUP was less optimal, potentially due to PCR limitations in AMR targets. CUP may have a role in rapid infection diagnosis and early de-escalation of antimicrobial therapy in liver disease. Future work will focus on evaluating the cost-effectiveness of CUP vs other sequencing-based approaches.

FRI-113

Diagnostic scoring system for diagnosis of covert hepatic encephalopathy in child-pugh class a cirrhosis patients

Masanori Fukushima¹, Yasuhiko Nakao¹, Ryu Sasaki¹, Masafumi Haraguchi¹, Satoshi Miuma¹, Hisamitsu Miyaaki¹, Kazuhiko Nakao¹. ¹Department of Gastroenterology and Hepatology, Nagasaki University Graduate School of Biomedical Sciences, Nagasaki, Japan

Email: ma-fukushima@nagasaki-u.ac.jp

Background and aims: Covert hepatic encephalopathy (CHE) is a cirrhosis-related complication that warrants diagnosis and treatment. In Japan, a neuropsychiatric test (NPT) performed on a touch-screen tablet has been the diagnostic method. This includes the number connection tests (NCT)-A and B, and the Stroop test. However, the test is time-consuming. Therefore, a simple CHE screening model based on biomedical parameters is desirable. It has been previously reported that hypoalbuminemia and hyperammonemia are useful in diagnosis, but most of these cases were in patients with Child-Pugh class B. For earlier diagnosis, detection of Child-Pugh class A is necessary. This study aimed to establish a simple diagnostic method of CHE in patients with Child-Pugh class A.

Method: Sixty-five patients with Child-Pugh class A cirrhosis who underwent NPT at our hospital were included. They were divided into two groups according to the presence or absence of CHE using the NCT-B. Clinical data, including liver function, fibrosis markers, presence of esophageal varices, and liver volume, were compared. Liver volume was measured with computed tomography using SYNAPSE VINCENT software (Fujifilm) and corrected by liver volume/body surface area.

Results: Of the 65 patients, 23 (35%) were diagnosed with CHE by NCT-B. The Child-Pugh score was 5 in 14 patients (61%) from the CHE group, and in 28 patients (67%) from the non-CHE group. The difference in platelet count between the two groups was 96, 000/microliter in the CHE group and 129, 000/microliter in the non-CHE

group ($p = 0.02$). Hyaluronic acid was 213 ng/ml in the CHE group and 177 ng/ml ($p = 0.02$) in the non-CHE group. Liver volume to body surface area ratio was 550 ml/m² in the CHE group and 726 ml/m² in the non-CHE group ($p = 0.001$). The cut-off values for each of these items in the ROC curve analysis showed that the complication rate of CHE was 55% in patients with a liver volume to body surface area ratio of 618 ml/m² or less, which was 2.8 times higher than that in patients with larger liver volume. Referring to the cut-off values for each item, a score from zero to three was created, with platelet count of 120, 000/microliter or less, hyaluronic acid of 200 ng/ml or more, and liver volume/body surface area ratio of 620 ml/m² or less each counting as 1 point, respectively. Ninety-two percent of cases with 0 points had non-CHE, and 80% of cases with 3 points had CHE.

Conclusion: In a group of patients with Child-Pugh class A liver cirrhosis, platelet count, hyaluronic acid, and liver volume/body surface area ratio were associated with CHE. The score created using these three items made it possible to diagnose or exclude CHE in 80% and 92% of cases, respectively. Since CHE complications can be highly-detected based on clinical test values, these parameters are considered useful as a CHE diagnostic scoring system as an alternative to NPT in patients with Child-Pugh class A liver cirrhosis.

FRI-114

Entecavir can significantly improve the prognosis of patients with first decompensated hepatitis B cirrhosis

Rui Ding¹, Wen Xie², Jidong Jia³, Qi Wang². ¹Beijing Ditan Hospital, Capital Medical University, Beijing Friendship Hospital, Beijing, China; ²Center of Liver Diseases, Beijing, China; ³Liver Research Center, Beijing, China

Email: ddingrui1989@126.com

Background and aims: Untreated patients with HBV infection are at high risk of progression to cirrhosis, clinical decompensation, HCC and liver-related death. Even in patients with HBV-related decompensated cirrhosis, the long-term effect of antiviral therapy significantly modifies the natural history of decompensated cirrhosis, resorting to liver function, and increasing survival. However, data compare the clinical outcomes of them with similar patients who were not subject to antiviral treatment are still limited. Here, we assessed the clinical efficacy of entecavir (ETV) antiviral therapy in patients with decompensated hepatitis B cirrhosis by comparing with the similar patients who do not receive any antiviral therapy, and evaluated the effect of treatment on hepatocarcinogenesis and mortality.

Method: This is a multicenter, ambi-directional cohort study. More than 5 thousand of patients with decompensated hepatitis B cirrhosis between February 2001 and December 2018 were screened for study eligibility. The observation started from the time of first episode of decompensation present with ascites. Propensity score matching (PSM) analysis was used to reduce the potential confounding variables at baseline. Factors associated with all-cause mortality or LT were analysed using the Cox proportional hazards model. Inverse probability of treatment weighting (IPTW) analysis was also carried out using the same variables to confirm the results of the PSM analysis on the cumulative risk of HCC and all-cause mortality or LT.

Results: A total of 480 patients with hepatitis B virus-related first-time decompensated cirrhosis were analysed in this study, of whom 301 were treated with ETV therapy (ETV group) and 179 of whom treatment-naïve (non-antiviral group). PSM analysis was used to reduce the potential confounding variables at baseline and generated 172 pairs of cases. At weeks 48, the changes in ALT, total bilirubin, albumin, platelet count and international normalized ratio over the ETV treatment period were improved dramatically (all $p < 0.005$). However, liver function did not show significant changes in non-antiviral group at 48 weeks. It is interesting to note that ETV antiviral therapy cannot effectively rescue the platelet counts when compared to non-antiviral group ($p > 0.005$). Non-antiviral group (HR = 3.08, $p < 0.001$) and high iMELD score (HR = 1.09, $p = 0.01$) were independently associated with mortality. non-antiviral group (HR = 3.75, $p =$

0.002), low PLT counts (HR = 0.98, $p = 0.036$) and high ALP level (HR = 1.01, $p = 0.047$) were independently associated with HCC occurrence. **Conclusion:** ETV treatment can significantly improve the overall prognosis in patients with first-time decompensated hepatitis B cirrhosis. Further studies are needed to validate our results.

FRI-115

Validation of an easy-to-use malnutrition screening in cirrhosis to predict outcome

Stefan Fürst¹, Julia Traub¹, Jakob Schwarzl¹, Lukas Gulden¹, Johannes Woltsche¹, Angela Horvath¹, Vanessa Stadlbauer¹. ¹Medical University of Graz, Graz, Austria
Email: stefan.fuerst@medunigraz.at

Background and aims: Malnutrition in liver cirrhosis is widespread and often underdiagnosed. The RFH-NPT (Royal Free Hospital Nutritional Prioritizing Tool) as gold standard does not correlate well with other, easier available screening tools, such as GMS (Graz Malnutrition Screening), NRS-2002 (Nutritional Risk Screening), and MNA-SF (Mini Nutritional Assessment-Short Form). (1) It is unclear which of these scores can predict outcome. We tested the predictive merit of these scores either as a standalone score or in combination with easily accessible parameters and comorbidities.

Method: Hospitalized patients aged 18 years or above with cirrhosis were included. Exclusion criteria encompassed hepatic encephalopathy ≥ 2 , other cognitive disorders impeding informed consent, or hepatocellular carcinoma at stage BCLC C or D. Univariate Cox-regression and a stepwise multivariate Cox-regression were utilized for analysis.

Results: One hundred eighteen patients were included (median age 63 years (IQR 13); 88 (74.6%) men; etiology alcohol (57.6%), NASH (18.6%), HCV (16.1%), others (7.6%)). During the median follow-up period of 39 month, 60 patients (50.1%) died. The following parameters were predictive for mortality in a univariate Cox-regression: age, body mass index, severe sarcopenia, gait speed, GMS, Charlson Comorbidity Index, the use of statins and opioids, history of gastrointestinal bleeding due to liver cirrhosis, history of acute kidney injury, presence of hepatocellular carcinoma and blood levels of neutrophils, basophils, eosinophils, C-reactive protein (CRP), gamma-glutamyl transferase (GGT), glomerular filtration rate (GFR) and mean platelet volume (MPV). In contrast to GMS, other malnutrition scores were not predictive. In the multivariate model, accounting for age and CRP, GMS was an independent predictor for mortality. (HR 1.24, $p = 0.046$, 95%CI 1.00–1.53). Using the GMS malnutrition cut-off values, 8.8% of patients in the survivor group and 68.8% in the non-survivor group were classified as malnourished. The percentages for malnutrition according to RFH-NPT, NRS-2022, and MNA-SF were 19.3% vs. 20.0%, 5.2% vs. 6.7%, and 6.9% vs. 5.0% for survivors vs. non-survivors, respectively.

Conclusion: GMS independently predicts mortality in patients with liver cirrhosis. Neither other malnutrition scores such as RFH, NRS and MNA, nor markers of sarcopenia were predictive in the multivariate prediction model for mortality in this patient cohort. GMS can be implemented easily into an electronic patient record system and therefore can provide an added value for cirrhotic patient care to identify patients with malnutrition and high risk of death, who may benefit from intensive nutritional therapy.

Reference

1. Traub J, Bergheim I, Horvath A, Stadlbauer V. Validation of Malnutrition Screening Tools in Liver Cirrhosis. *Nutrients*. 2020;12(5):1306.

FRI-116

Prognostic significance of HDL-associated apolipoproteins in patients with decompensated cirrhosis and spontaneous bacterial peritonitis

Mohamad Murad¹, Johanna Reißing¹, Majda El Hassani¹, Mick Frissen¹, Oluwatomi Ibidapo-Obe¹, Karsten Große¹, Theresa Hildegard Wirtz¹, Christian Trautwein¹, Philipp Reuken², Tony Bruns¹. ¹University Hospital RWTH Aachen, Aachen, Germany; ²University Hospital Jena, Jena, Germany
Email: muradmohamad@outlook.com

Background and aims: Apolipoproteins (Apo) A-I and A-II are the two major components of high-density lipoproteins (HDL) and possess immune-modulating functions, affecting lipopolysaccharide signaling. Recent studies have identified a correlation between low serum apoA-I levels and complications of cirrhosis associated with poor prognosis. This study investigates whether serum and ascitic fluid (AF) concentrations of apoA-II are differentially regulated during spontaneous bacterial peritonitis (SBP) and can be used to predict outcomes.

Method: We performed a case-control study including 118 patients with decompensated cirrhosis and ascites, comprising 59 patients with SBP and 59 without. AF concentrations of apoA-II, apoA-I, and IL-6 were determined using enzyme-linked immunosorbent assay (ELISA). Cumulative 90-day transplant-free survival after SBP was compared using Kaplan-Meier analysis and multivariable Cox regression analysis.

Results: In patients without SBP, lower AF levels of HDL-related biomarkers apoA-I and apoA-II correlated with lower AF protein and albumin levels, higher serum bilirubin, and lower platelet counts, indicating depletion with progression of liver disease. During SBP, apoA-II significantly increased in serum and AF, leading to an increased ratio of apoA-II to apoA-I in AF compared to patients without SBP. Lower levels of serum and/or AF apoA-II correlated with more severe inflammation (white blood cells, AF neutrophils) and organ failure (bilirubin, Model for End-Stage Liver Disease [MELD]). Higher AF levels of apoA-II correlated with higher levels of IL-6, suggesting augmented peritoneal macrophage responses. An AF apoA-II level of 45 $\mu\text{g/ml}$ or higher during an SBP episode indicated an increased risk of death or transplantation within 90 days ($p = 0.01$ in log-rank test). High AF apoA-II levels during SBP remained a predictor of transplant or death after adjustment for age and MELD score (HR 2.59; 95% CI: 1.08–5.91; $p = 0.032$).

Conclusion: The composition of HDL-associated apolipoproteins is altered during SBP, which carries prognostic implications.

FRI-117

Acute kidney injury and infections as the main determinants of outcome in hospitalised patients with liver cirrhosis: a retrospective cohort from a tertiary hospital

Adonis Protopapas¹, Alexandra Tsankof², Vaia Kyritsi¹, Christiana Gogou², Maria Kyziroglou², Erofil Papathanasiou², Charikleia Chatzikosma², Christos Savopoulos², Andreas Protopapas¹. ¹Hepatogastroenterology Unit, First Propaedeutic Department of Internal Medicine, Aristotle University of Thessaloniki, AHEPA University Hospital, Thessaloniki, Greece; ²First Propaedeutic Department of Internal Medicine, Aristotle University of Thessaloniki, AHEPA University Hospital, Thessaloniki, Greece
Email: adoprot@hotmail.com

Background and aims: Complications of portal hypertension, renal dysfunction and infections are the leading causes of hospitalisation of cirrhotic patients, with a significant impact on outcome. Our study aimed to record the specific characteristics of complications and infections in hospitalised cirrhotic patients.

Method: Patients with cirrhosis admitted to our department from 2019 to 2022 were retrospectively analysed. Patients admitted for scheduled investigation or intervention were omitted.

POSTER PRESENTATIONS

Results: A total of 302 hospitalisations from 184 different patients were recorded. Patients had a mean age of 65.4 ± 11.9 years and were predominantly male (74.5%) and with decompensated liver cirrhosis (84.2%). Alcohol-associated liver disease (46.2%) and metabolic dysfunction-associated steatohepatitis (27.7%) were the main causes of cirrhosis. 15.3% of hospitalisations had a fatal outcome (46 patients). Most patients were classified as Child-Pugh stage B (53.3%), followed by patients in stage C (33.8%) and stage A (11.7%), while 36.4% and 15.1% of patients presented with acute kidney injury (AKI) and variceal bleeding, respectively. AKI at presentation had a statistically significant association with prior diuretic use ($p < 0.001$), whereas patients presenting with a combination of AKI and moderate or severe ascites (47 patients, 15.9%) were in a large majority on diuretic treatment (87.2%). 149 (49.3%) patients developed an infection, with almost half being hospital-acquired (48.3%). The leading causes of infection were urinary tract infection (27.9%), spontaneous bacterial peritonitis (21.7%) and respiratory tract infection (19.4%). The majority of the bacterial species were Gram-negative (57.4%) and multi-drug resistant (MDR) (54%). Development of infection was significantly correlated with increased Child-Pugh score, MELD and MELD-Na values ($p < 0.001$). There was no association between PPI use and the presence of infection or the degree of hepatic encephalopathy. In multivariate analysis, patient survival was significantly associated with cirrhosis severity indices (Child-Pugh, MELD, MELD-Na, $p < 0.001$), age ($p = 0.03$), infection ($p < 0.001$) and AKI at presentation ($p = 0.005$). Furthermore, the presence of MDR bacteria was independently associated with survival in patients who developed an infection and the pathogen was successfully isolated ($p = 0.003$).

Conclusion: Inpatients with cirrhosis have significant mortality, which is associated with disease severity and the occurrence of complications such as AKI and infections. In addition, they are often burdened by infections from MDR pathogens, which are an unfavourable outcome indicator. In these patients, proper diuretic management, timely treatment of AKI, safety measures to avoid infections (especially from MDR bacteria) and appropriate antimicrobial therapy are of utmost importance.

FRI-118

Independent association of loss of skeletal muscle mass with long-term liver-related mortality in cirrhotic patients

Jiarui Zheng¹, Shuo Yang², Wenhui Ren³, Bo Feng⁴, Rui Huang¹. ¹Peking University Hepatology Institute, Beijing, China; ²Department of Radiology, Beijing, China; ³Peking University People's Hospital, Beijing, China; ⁴Peking University Hepatology Institute, Beijing, China
Email: strangehead@163.com

Background and aims: Sarcopenia has a detrimental impact on the prognosis of individuals with liver cirrhosis, however, the clinical significance of alterations in muscle mass remains uncertain. This study aimed to investigate the influence of loss of skeletal muscle mass (LSMM) on the prognostic outcomes among patients diagnosed with cirrhosis.

Method: In this retrospective analysis, a total of 158 individuals with cirrhosis who visited our hospital during the period from January 2018 to August 2023 were included. Computed tomography was utilized to measure the cross-sectional area of the skeletal muscles at the level of the third lumbar vertebra, which could enable the determination of the skeletal muscle index for the purpose of diagnosing sarcopenia and all patients underwent a follow-up CT scan performed at least 6 months after the initial scan. The annual relative change in skeletal muscle area ($\Delta\text{SMA}/y$) was calculated for each patient, and LSMM was defined as $\Delta\text{SMA}/y < 0$. To assess the risk factors associated with liver-related mortality, a competing risk model was applied.

Results: Of the 158 cirrhotic patients, 95 (60.1%) patients were identified as LSMM. The median of $\Delta\text{SMA}/y$ was -0.9 (interquartile range [IQR], $-3.8, 1.6$) in all patients. Chronic kidney disease (CKD)

was confirmed as a risk factor of LSMM. During a median follow-up period of 68.1 (IQR, 43.5, 105.0) months, 57 patients (36.1%) died due to the liver-related diseases. The competing risk model found that LSMM was significantly associated with liver-related mortality in cirrhotic patients (hazard ratio [HR], 1.86; 95% CI, 1.01–3.44, $p = 0.047$). Cumulative survival was significantly higher in patients without LSMM than in those with LSMM ($p = 0.004$). Survival rates at 1-, 3-, and 5-years were 96.8%, 81.0%, and 65.1%, respectively, in patients without LSMM, and 97.9%, 80.0%, and 56.8%, respectively, in patients with LSMM.

Conclusion: The utilization of LSMM can be valuable in the prediction of liver-related mortality among individuals diagnosed with liver cirrhosis. Paying attention to the management of skeletal muscle might play a role in enhancing the prognosis of patients with cirrhosis.

FRI-119

Role of HLA DR+ CD4+ T cell %T cell in mediating the effect of Lactobacillus delbrueckii on liver cirrhosis

Xuanchen Liu¹, Ningning Zhang¹, Wei Lu², Yiyan Zhang¹, Kaipeng Liu², Huiru Liu¹. ¹Tianjin Medical University Cancer Institute and Hospital, Tianjin, China; ²Tianjin Medical University Cancer Institute and Hospital, Tianjin, China
Email: 15931873318@163.com

Background and aims: We investigated the causal relationships between the gut microbiota (GM), liver cirrhosis, and potential immunophenotype mediators using Mendelian randomization (MR).

Method: The data on GM, immunophenotype, and liver cirrhosis all come from the GWAS Catalog website (<http://www.ebi.ac.uk/gwas/>). The data of GM were under the study accession numbers GCST90027446–GCST90027857. Immunophenotype from GCST0001391–GCST0002121, and Lactobacillus delbrueckii from GCST90027782. We performed bidirectional MR analyses to explore the causal relationships between the GM and liver cirrhosis, and two mediation analyses, two-step MR to discover potential mediating immunophenotype.

Results: There is a causal relationship between 14 gut microbial taxa and liver cirrhosis, with Lactobacillus delbrueckii showing the most significant association (ivw: $p = 0.0019$, OR:1.2073 (1.0722–1.3595)), and there is no evidence of reverse causation. Performing a bulk MR analysis with Lactobacillus delbrueckii and 731 immunophenotypes revealed causal relationships with 5 immunophenotypes. Subsequently, conducting a bulk MR analysis with these 17 immunophenotypes and liver cirrhosis showed a causal relationship only between the immunophenotype HLA DR+ CD4+ T cell %T cell and liver cirrhosis (ivw: $p = 0.0388$, OR:1.1529 (1.0073–1.3194)).

Conclusion: Through Mendelian randomization, it was revealed that Lactobacillus delbrueckii acts on liver cirrhosis through HLA DR+ CD4+ T cell %T cell as intermediate factors.

FRI-120

Impact of diabetes mellitus on results in the animal naming test in patients with and without liver cirrhosis

Eva Maria Schleicher^{1,2}, Matthias Weber¹, Julia Tuchscher¹, Peter R. Galle^{1,2}, Marcus-Alexander Wörns³, Simon J. Gairing^{1,2}, Christian Labenz^{1,2}. ¹University Medical Center of the Johannes Gutenberg-University, Mainz, Germany; ²Cirrhosis Center Mainz (CCM), Mainz, Germany; ³Department of Gastroenterology, Hematology, Oncology and Endocrinology, Klinikum Dortmund, Dortmund, Germany
Email: eva.schleicher@unimedizin-mainz.de

Background and aims: Diabetes mellitus (DM) is a common comorbidity in patients with cirrhosis and is associated with the development of hepatic encephalopathy (HE) and cognitive dysfunction. The simplified Animal Naming Test (S-ANT1) has been established for detecting minimal HE (MHE). It is currently unknown whether S-ANT1 results are affected by DM in patients with and without cirrhosis.

Method: This study analyzed data from 268 patients with cirrhosis who showed no signs of HE ≥ 1 according to the West-Haven-Criteria. MHE was defined using the psychometric hepatic encephalopathy score (PHES). All patients were also tested with S-ANT1. As controls, 14 patients with severe DM and diabetic foot syndrome but no cirrhosis (DFS), as well as 37 healthy controls, were also tested with S-ANT1.

Results: Diabetes mellitus was present in 79 (29.5%) patients with cirrhosis and MHE according to PHES was detected in 81 (30.2%) patients. Median S-ANT1 in the total cohort was 20 (IQR 16; 24) animals. In the total cohort, results in S-ANT1 did not differ between patients with and without diabetes mellitus (19 vs. 20 animals, $p = 0.108$). Subgroup analyses, stratified by MHE status, showed no difference in S-ANT1 results when comparing patients with and without diabetes mellitus. In multivariable logistic regression analysis, the only variables independently associated with performance in S-ANT1 were PHES-MHE, school education, sodium, and age, while DM was not. Given that patients with DFS were significantly older than patients with cirrhosis and healthy controls, we selected patients with an age >60 years for the following analyses to make the groups comparable. Patients with DFS performed poorer in S-ANT1 compared to healthy controls, while patients with cirrhosis and MHE performed poorer in S-ANT1 compared to patients with diabetic foot syndrome. Performance in S-ANT1 was comparable between patients with cirrhosis without MHE and patients with DFS. Of note, 8 out of 14 patients with diabetic foot syndrome had an S-ANT1 <20 animals (cut-off for MHE according to German norms).

Conclusion: Results in S-ANT1 seem to be affected in patients with severe forms of DM and apparent complications. The S-ANT1 appears to be applicable in patients with liver cirrhosis and compensated DM.

FRI-121

Safety and tolerability of long-term albumin treatment in patients with decompensated cirrhosis

Javier Fernández^{1,2}, Laura Núñez³, Montserrat Costa³, Mireia Torres³, Raquel Horrillo³, Natalia Afonso³, Anna Mestre³, Luis Ruiz Del Arbol⁴, Cándid Villanueva⁵, Antonio Paez³, Vicente Arroyo¹. ¹EF Clif, EASL-CLIF Consortium and Grifols Chair, Barcelona, Spain; ²Hospital Clínic, IDIBAPS and CIBERehd, Barcelona, Spain; ³Scientific Innovation Office, Grifols, Barcelona, Spain; ⁴Department of Gastroenterology, Hospital Ramón y Cajal and CIBERehd, Madrid, Spain; ⁵Department of Gastroenterology, Hospital de Sant Pau and CIBERehd, Barcelona, Spain
Email: jfdez@clinic.cat

Background and aims: Long-term albumin treatment reduces systemic inflammation and cardiocirculatory dysfunction in patients with decompensated cirrhosis and ascites, but safety data are limited. This study was aimed at evaluating the safety and tolerability of long-term human albumin administration in patients with decompensated cirrhosis and ascites.

Method: This was a prospective, open-label clinical trial (Pilot-PRECIOSA study NCT00968695, EudraCT Number: 2008-003920-40), which enrolled decompensated cirrhotic patients with ascites and were treated with a 20% human albumin solution at low doses (1 g/kg every two weeks, LALbD group) or high doses (1.5 g/kg every week, HALbD group) for 12 weeks. Adverse events (AEs), serious adverse events (SAEs), biochemistry and hematology laboratory parameters were assessed during the treatment period in both groups. The effect of long-term albumin therapy on ascites, edema, and hepatic encephalopathy grade was also evaluated. Safety analyses were conducted on intention-to-treat population.

Results: Thirty-one out of 33 screened patients were analyzed ($n = 15$, LALbD; $n = 16$, HALbD). Overall, 140 AEs were reported in 26 patients (83.9%) during the study period and most of them were mild (28.6%) or moderate (25.7%) in severity. There were no differences in the overall incidence of AEs between groups. None of the albumin-treated patients experienced AEs related to pulmonary edema or respiratory failure at any treatment dose. Two AEs (1.4%),

gastrointestinal hemorrhage and pruritus, were related to albumin treatment. Eighty-seven (62.1%) were considered SAEs, being the most frequent: hepatic encephalopathy ($n = 12$, 13.8%), ascites ($n = 6$, 6.9%), gastrointestinal hemorrhage ($n = 6$, 6.9%; including esophageal varices hemorrhage, $n = 3$, 3.4%), anemia ($n = 5$, 5.7%), and dyspnea ($n = 3$, 3.4%). No differences in the main biochemistry and hematology parameters over time and between groups were observed. In the HALbD group, the percentage of patients without ascites at the end of the study period was higher (42.9%) compared with baseline (12.5%). **Conclusion:** Long-term albumin treatment in the patients with decompensated cirrhosis was safe and well-tolerated.

FRI-122

Decompensated cirrhosis is associated with disruption of nuclear positioning in skeletal muscle and selective atrophy of type II myofibers

Aldo J Montano-Loza¹, Maryam Motamedrad², Maryam Ebadi¹, Norberto Sanchez-Fernandez³, Alessandro Parente³, Abha Dunichand-Hoedl², Elora Rider¹, Norman Kneteman³, James Shapiro³, David Bigam³, Khaled Dajani³, Blaire Anderson³, Vickie Baracos⁴, Vera C. Mazurak². ¹Division of Gastroenterology and Liver Unit, University of Alberta Hospital, Edmonton, Canada; ²Division of Human Nutrition, University of Alberta, Edmonton, Canada; ³Division of Transplantation, Department of Surgery, University of Alberta Hospital, Edmonton, Canada; ⁴Department of Oncology, Cross Cancer Institute, Edmonton, Canada
Email: montanol@ualberta.ca

Background and aims: Low skeletal muscle mass is a common complication in cirrhosis and is associated with morbidity and mortality. However, specific muscle pathophysiology in cirrhosis and its decompensated stages is unknown. Muscle fibers type I are oxidative with slow contraction speed adapted for aerobic work, while type II are glycolytic, have fast contraction speed and confer strength. Muscle fibers nuclei are normally situated near the cell membrane. Size and proportions of muscle fiber types and nuclei position may be affected in different pathological conditions. In this study, we aimed to compare muscle morphological features in patients with cirrhosis receiving liver transplantation (LT) and appraise the differences in compensated and decompensated stages.

Method: Biopsies of rectus abdominis muscle were collected from the surgical incision at LT from 57 patients. Fiber type and size was determined immunohistochemically with primary and secondary antibodies for membrane (Laminin and Dystrophin) and myosin heavy chain (MyHC) isoforms [BAD5 (MyHCI) and SC71 (MyHCIIA)]. 4', 6-diamidino-2-phenylindole was used for nuclei staining. Stages of cirrhosis were defined based on the D'Amico classification: 1) no varices, 2) development of varices, 3) variceal bleeding without other decompensation events, 4) first nonbleeding decompensation event, and 5) any second decompensation event. Patients in stages 1 and 2 were classified as compensated cirrhosis, and those in stages 3–5 were classified as decompensated cirrhosis.

Results: Thirty-seven (65%) patients were male, with a mean age of 52 ± 11 years, and BMI of 26.8 ± 4.8 kg/m² at the time of LT. Indication for LT was alcohol-associated cirrhosis in 21 (37%) patients, autoimmune liver diseases in 14 (25%), viral hepatitis in 12 (21%), MASH in 4 (7%), and 6 others (11%). Sixteen patients (28%) had concomitant hepatocellular carcinoma. Thirty-six patients (63%) were in decompensated and 21 (37%) were in compensated stage at the time of LT. Median overall muscle fiber area was smaller in decompensated patients (4407 ± 1882 vs. 3187 ± 1512 μm^2 , $p = 0.01$). Median fiber type I area was similar between compensated and decompensated patients (3727 ± 1670 vs. 3086 ± 1312 μm^2 , $p = 0.068$). However, median size of fiber type IIA was smaller in decompensated patients (5105 ± 2525 vs. 3358 ± 1915 μm^2 , $p = 0.005$). Furthermore, the percentage of centralized nuclei was higher in decompensated patients ($5.1 \pm 2.8\%$ vs. $12.3 \pm 7.4\%$).

POSTER PRESENTATIONS

Conclusion: Patients with decompensated cirrhosis have overall smaller muscle fibers and are more susceptible to fiber type II atrophy and disruption of nuclear positioning. These changes would be likely associated with functional deficits, especially of muscle strength. Further work is warranted to evaluate regimens of muscle rehabilitation for this patient population pre- and post-LT.

FRI-123

Measuring the burden and impact of comorbidity in cirrhosis: insights from clinical database analysis

Dina Ali¹, Jessica Shearer², Lynsey Corless³. ¹Zagazig University, Zagazig, Egypt; ²St James University Teaching Hospital, Leeds, United Kingdom; ³Hull University Teaching Hospitals, Hull, United Kingdom
Email: lynsey.corless@nhs.net

Background and aims: Cirrhosis is a serious long-term condition, with high rates of morbidity and mortality. Effectively managing this long-term condition requires consideration of interlinked factors such as comorbidity, which can influence treatment decisions, the appropriateness of cancer surveillance, and decision making during acute illness. This study was undertaken to determine the burden of comorbidity within our cirrhosis population.

Method: The cirrhosis database in our centre, comprising over 800 individuals, was searched for comorbidities using the widely recognised Charlson comorbidity index (CCI). CCI was calculated from hospital discharge records using an ICD-10 coding algorithm. To mitigate the risk of missing comorbidities not documented at discharge, the CCI was corroborated through a secondary search of Primary Care (PC) records. Only those with both ICD-10 and complete PC data were included.

Results: 331 patients with cirrhosis were included (female 42%; n = 138) with a median age of 61 years (range 30–91). Aetiology was predominantly alcohol-related (ArLD) (42.6%; n = 141) and metabolic dysfunction associated steatotic liver disease (MASLD) (18.1%; n = 60), among other causes. These characteristics were representative of the entire database. Median CCI score was significantly higher by PC record (5) than ICD-10 (2) (difference 2.8; 95% CI 2.56–2.97; p < .05), indicating that ICD-10 under-represents the degree of comorbidity. Consequently, PC records were used for further analysis. The most prevalent comorbidity was diabetes mellitus (n = 119; 36%), followed by COPD (n = 44; 13.3%). MASLD and diabetes were closely linked, with substantial overlap; 39.8% of individuals with diabetes had MASLD, and 78.3% of those with MASLD had diabetes. Almost two thirds of the cohort had five or more comorbidities (CCI ≥ 5; 57.7%), and those with MASLD had the greatest proportion of severe comorbidity (79.3%). 37 patients in the cohort died during follow-up. Whilst there was no significant association between liver aetiology and death (p = 0.124), CCI grade was significantly associated with mortality (p = 0.048).

Conclusion: We found high levels of comorbidity, particularly diabetes, in our cirrhosis population. The greatest burden was observed in those with MASLD. CCI grade was associated with increased mortality, and recording this will inform both individual management plans and development of care pathways. Relying solely on ICD-10 codes underestimates the true burden of comorbidity, and linked databases are recommended for future analysis to provide a more comprehensive understanding of the association between cirrhosis and comorbid disease.

FRI-124

Upper extremity skeletal muscle index to assess sarcopenia in patients with cirrhosis

Anna Ostrovskaya¹, Marina Maevskaya¹. ¹Sechenov First Moscow State Medical University (Sechenov University), Moscow, Russian Federation
Email: mertanen@mail.ru

Background and aims: Sarcopenia is a complication of liver cirrhosis that affects the patient's prognosis. Methods of its objective assessment (including DEXA) are often distorted in lower extremity

edema. The norm for calculating the skeletal muscle index (SMI) of the upper extremities with regard to gender, age has not been clearly developed. Purpose: To develop norm criteria of SMI for patients with decompensated cirrhosis and sarcopenia taking into account sex, age and lower extremity edema.

Method: A prospective cohort study was performed. The main group included patients with.

cirrhosis with lower extremity edema, Child-Pugh class B and C, of various etiologies. There.

was also a group of healthy volunteers to determine the norm criteria for SMI of the upper extremities. All patients were evaluated for muscle mass with DEXA, shoulder volume with a centimeter tape, caliperometry, muscle strength measurement-dynamometry, muscle function-test with lifting from a chair, tests to determine balance.

Results: Fifty-six patients were studied: 39 (main group) with cirrhosis and 17 (control group) healthy volunteers. There were 16 men (41%) and 23 women (59%) with mean age 52.1 ± 11.9 years in main group, and 6 men (35.3%) and 11 women (64.7%) with mean age 60.3 ± 6.7 years in the control group. SMI was evaluated by DEXA method in patients with cirrhosis and had the median of 6.77 (interquartile range: 5.55–7.43), in patients of control group-6.8 (IQR: 6.2–7.3) (p = 0.164). SMI for upper extremity had the median 1.38 (IQR: 1.27–1.68) in patients with liver cirrhosis, and 1.62 (IQR: 1.48–1.98) for the control group (p = 0.007). It indicates statistically significant differences for the upper extremity SMI compared to the standard SMI in the main and control groups. The cutoff value assessed with ROC analysis for SMI for upper extremity was <1.398 (sensitivity 82.35%, specificity 59.0%) compared to the standard SMI cutoff <6.215 (sensitivity 70.59% and specificity 43.6%). Upper extremity SMI is a more accurate marker of sarcopenia than the standard SMI.

Conclusion: Normative values for the upper extremity SMI for patients with decompensated liver cirrhosis and sarcopenia have been developed. It makes it possible to correctly evaluate the index in dynamics against the background of patients' treatment.

FRI-125

Recompensation after TIPS reduces the risk of hepatocellular carcinoma and death in patients with decompensated cirrhosis

Jose Sanchez-Serrano¹, María Pilar Ballester¹, Sheila González-Padilla¹, Paloma Poyatos-García¹, Desamparados Escudero-García², Cristina Montón-Rodríguez¹, Jose Ballester¹, Juan Antonio Carbonell-Asins³, Elisabetta Casula¹, Jorge Guijarro¹, Paloma Lluch-García². ¹Clinic University Hospital of Valencia, Valencia, Spain; ²Clinic University Hospital of Valencia, University of Valencia, Valencia, Spain; ³INCLIVA Biomedical Research Institute, Valencia, Valencia, Spain
Email: josase6195@gmail.com

Background and aims: It has been recently described that some patients with decompensated cirrhosis can recompensate, which results in an improved prognosis. However, recompensation after transjugular intrahepatic portosystemic shunt (TIPS) and its impact on the risk of hepatocellular carcinoma (HCC) and death have not been studied. In addition, whether prognosis of patients who recompensate is similar to those with compensated cirrhosis is not known. The main aim of our study was to evaluate the impact of recompensation at 6 months and 1 year after TIPS placement on the risk of HCC and death.

Method: An observational, single-centre study of consecutive patients with decompensated cirrhosis who underwent TIPS between 2005–2022 was performed. Main outcomes were recompensation after TIPS, development of HCC and death. Recompensation was defined as removal/suppression/cure of the primary aetiology of cirrhosis, resolution of ascites, hepatic encephalopathy (HE) (with or without diuretics/HE prophylaxis) and absence of recurrent variceal haemorrhage and stable improvement

of liver function tests. A prospective cohort of consecutive outpatients with compensated cirrhosis was used for comparison.

Results: 208 patients with cirrhosis were included, 92 compensated and 116 decompensated who underwent TIPS, of whom 28 (24%) were compensated 1 year after TIPS placement.

Liver function at the time of TIPS placement was the only factor associated with recompensation at 1 year, with lower MELD (12 ± 5 vs 15 ± 6 ; p value = 0.049) and Child-Pugh (8; interquartile range [IQR] 7–9 vs 9; IQR 8–10, p value = 0.078) scores in recompensated patients. Median follow-up was 37 months (IQR 12–59). Cumulative incidence of HCC at 1, 3 and 5 years was 4%, 9% and 14% in recompensated patients, 2%, 6% and 16% in the compensated group and 19%, 32% and 38% in non-recompensated patients, respectively. Significant differences were found between non-recompensated patients and the other two groups (log-rank p value <0.001), but not between recompensated and compensated patients (log-rank p value 0.84). Survival was 100%, 88% and 76% at 1, 3 and 5 years follow-up in recompensated, 99%, 95% and 83% in compensated (log-rank p value 0.41 vs recompensated) and 44%, 35% and 24% in decompensated patients, respectively (log-rank p value <0.001 compared with the other groups). Similarly, recompensation at 6 months was associated with a lower incidence of HCC (log-rank p value = 0.004) and longer survival (log-rank p value <0.001).

Conclusion: recompensation at 6 months and 1 year after TIPS has a clear impact on patients with decompensated cirrhosis by reducing incidence of HCC and increasing survival, with a similar prognosis than patients with compensated cirrhosis. Liver function is the only factor associated with recompensation, suggesting the importance of considering early TIPS placement in patients with indication.

FRI-126

Impact of micronutrient deficiencies on the mortality of patients with cirrhosis admitted for acute decompensation

Ariadna Altadill¹, Gemma Llibre-Nieto², Cristina Solé³, José Alberto Ferrusquía³, Mireia Miquel^{3,4}, Meritxell Casas¹, Valentí Puig-Diví¹, Alba Lira¹, Berta López-Sáez¹, Claudia Torras¹, Isabel Laucirica¹, Andrea Peña¹, Carla de Sárraga¹, Judith Cortada¹, Mar Salas¹, Laia Grau⁵, Mercedes Vergara³, Jordi Sánchez³.

¹Gastroenterology and Hepatology Department, Parc Taulí University Hospital. Institut d'Investigació i Innovació Parc Taulí (I3PT-CERCA). Universitat Autònoma de Barcelona (UAB), Sabadell, Spain;

²Gastroenterology and Hepatology Department, Fundació Privada Hospital Assil de Granollers, Granollers, Spain; ³Gastroenterology and Hepatology Department, Parc Taulí University Hospital. Institut d'Investigació i Innovació Parc Taulí (I3PT-CERCA). Universitat Autònoma de Barcelona (UAB), CiberEHD, Sabadell, Spain; ⁴Medicine Department, Universitat de Vic-Universitat Central de Catalunya (UVic-UCC), Vic, Spain; ⁵Statistics. Neurology Department, Hospital Germans Trias i Pujol, Badalona, Spain

Email: a.altadillmauri@gmail.com

Background and aims: Deficiencies in micronutrients, including vitamins and trace elements, are prevalent among patients with decompensated cirrhosis. However, the correlation between these deficiencies and mortality remains unclear. Therefore, we aimed to assess the impact of micronutrient deficiencies on mortality at one, three, six, and twelve months in patients with cirrhosis admitted for acute decompensation.

Method: This is an observational, retrospective, and single centre study that included all cirrhotic patients admitted for acute decompensation from October 2017 to February 2020. During admission, levels of trace elements (iron, ferritin, calcium, phosphorus, magnesium, zinc and copper) and vitamins (A, B1, B6, B9, B12, C, D, E and K) were measured. Different demographic and clinical data, including mortality at one, three, six, and twelve months from admission, were collected. Univariate analysis was used to assess the correlation between micronutrients deficiencies and mortality.

Results: 125 patients were included: 77% male with a mean age of 62 ± 6.3 years. The most common aetiology was alcohol-related cirrhosis (79.2%) and 57.4% had active alcohol consumption. 90% of the patients were Child-Pugh class B or C with a mean MELD score of 16 ± 6 points. At admission, ascites, bacterial infection, hepatic encephalopathy and alcohol-associated hepatitis were present in 80%, 38%, 25% and 14% of the cases. Deficiencies of vitamin D, vitamin A, zinc and vitamin B6 were detected in 95%, 94%, 86% and 61% of the patients, respectively. Mortality at 1, 3, 6, and 12 months was 4.8%, 13.6%, 18.4% and 31.2%, respectively. The univariate analysis showed no association between micronutrient deficiencies or excesses and mortality at any of the assessed time periods. Higher MELD score was associated with lower levels of vitamin A ($p < 0.001$), vitamin E ($p < 0.001$), magnesium ($p = 0.01$) and zinc ($p = 0.001$) and higher levels of ferritin ($p = 0.002$) and vitamin B12 ($p < 0.001$). Factors related to mortality at one, three, six and twelve months were older age and worse liver function measured by Child and MELD points. Admission for alcohol-associated hepatitis was related to mortality in the first month (50% ($n = 3$) vs 12.6% ($n = 15$), $p = 0.03$) and third month (29.4% ($n = 5$) vs 12% ($n = 13$), $p = 0.05$).

Conclusion: In patients with cirrhosis admitted for acute decompensation, neither micronutrient deficiencies nor excesses were associated with mortality at 1, 3, 6, and 12 months. However, diminished levels of zinc, vitamin E and vitamin A, and elevated levels of vitamin B12 and ferritin were associated with a more advanced liver disease according to MELD classification. Further studies are needed to assess the potential influence of correcting micronutrient deficiencies on the severity of liver disease in patients presenting an acute decompensation of cirrhosis.

FRI-127

The relationship between abnormal body composition by computed tomography imaging and long-term mortality in patients with cirrhosis

Jiarui Zheng¹, Wenhui Ren², Shuo Yang³, Rui Huang¹. ¹Peking University Hepatology Institute, Beijing, China; ²Department of Clinical Epidemiology, Beijing, China; ³Department of Radiology, Peking University People's Hospital, Beijing, China

Email: strangehead@163.com

Background and aims: Emerging evidence on cirrhosis suggests a close correlation between abnormality in body composition characteristics and poor prognosis. This study aimed to evaluate the impact of dynamic changes in body composition on the prognostic outcomes in patients with cirrhosis.

Method: This retrospective analysis included patients diagnosed as cirrhosis in our hospital, from January 2018 to August 2023. Skeletal muscle mass index (SMI), visceral adipose tissue index (VATI), subcutaneous adipose tissue index (SATI) and visceral adipose to subcutaneous adipose area ratio (VSR) were evaluated using computed tomography (CT) imaging at the third lumbar vertebra level and all patients underwent a follow-up CT scan performed at least 6 months after the initial scan. Competing risk model was performed in four different body composition status (i.e., normal, only sarcopenia, only myosteatosis, and combined status) for liver-related mortality. We also explored the relationship between the dynamic change in body composition and long-term prognosis by applying Gray's test.

Results: Of the 158 cirrhotic patients (mean [SD] age, 57.1 [12.6] years), sarcopenia was present in 85 (60.1%) patients, while 22 (13.9%) patients had sarcopenic obesity and 68 (43.0%) had myosteatosis. Patients solely diagnosed with sarcopenia exhibited a higher mortality rate compared to those with normal body composition (Gray's test, $P = 0.006$), while patients solely diagnosed with myosteatosis or with a combination of sarcopenia and myosteatosis did not reach statistical significance (Gray's test, $P = 0.076$; $P = 0.140$). Multivariable analysis also revealed that VSR (HR = 1.10 [1.01–1.20]; $P = 0.028$), sarcopenia (HR = 2.73 [1.20–6.22], $P = 0.017$) and

POSTER PRESENTATIONS

myosteatorsis (HR = 2.39 [1.10~5.18], $P = 0.028$) were independent predictors of liver-related deaths. Otherwise, patients exhibiting aggravating body composition during follow-up period were associated with a significantly higher mortality risk compared to those with normal or remission body composition status (HR = 7.63 [1.12~51.14]; $P = 0.036$).

Conclusion: Progressive alterations in body composition status appears to be associated with liver-related mortality in individuals with liver cirrhosis. Focusing on the management of skeletal muscle, along with visceral and subcutaneous adiposity, may contribute to improving the prognosis of cirrhotic patients.

FRI-128

Usefulness of liver volume assessment for simple screening of covert hepatic encephalopathy

Masanori Fukushima¹, Yasuhiko Nakao¹, Ryu Sasaki¹, Masafumi Haraguchi¹, Satoshi Miuma¹, Hisamitsu Miyaaki¹, Kazuhiko Nakao¹. ¹Department of Gastroenterology and Hepatology, Nagasaki University Graduate School of Biomedical Sciences, Nagasaki, Japan

Email: ma-fukushima@nagasaki-u.ac.jp

Background and aims: Covert hepatic encephalopathy (CHE) signifies a precursor to overt hepatic encephalopathy (OHE) and is associated with decreased quality of life. Therefore, it is a clinically significant complication of liver cirrhosis (LC). In Japan, a neuropsychiatric test (NPT) performed on a tablet is used in CHE diagnosis; however, interpretation is challenging because of variations influenced by education levels, cultural backgrounds, cognitive decline in elderly, and physical impairments. Therefore, this study aimed to explore a facile screening method by investigating the characteristics and associated factors of CHE development in patients with LC using various clinical data.

Method: One hundred patients with liver cirrhosis without a history of OHE admitted to our institution from January 2019 to October 2022 were enrolled. CHE diagnosis was conducted using the number connection test B in NPT. Clinical data, including liver function, fibrosis markers, presence of esophageal varices and portal-systemic shunts, and liver volume, were included. Liver volume was measured by CT using SYNAPSE VINCENT software (Fujifilm Medical Co., Tokyo, Japan) and corrected by liver volume/body surface area.

Results: Median age was 68 years, and there were 62 men and 38 women. The causes of LC were alcohol-related in 29 cases, MASLD in 24 cases, HCV in 16 cases, HBV in 15 cases, and others in 16 cases. The distribution of Child-Pugh scores was A (55 cases), B (38 cases), and C (seven cases). Among all cases, 47 (47%) were diagnosed with CHE. The CHE-positive rates in Child-Pugh classes A, B, and C were 30.9% (17/55), 63.2% (24/38), and 85.7% (6/7), respectively. Significant differences between the CHE and non-CHE groups were observed in liver function markers (PT, Alb, T.Bil), fibrosis markers (hyaluronic acid, type 4 collagen 7S, M2BPGi), and liver volume/body surface area ratio. CHE cases (530 vs 691 $p = 0.002$) had significantly lower liver volume/body surface area ratio. ROC curve analysis revealed an AUC of 0.64, with a cutoff value set at 586. In the low liver volume group, 60% had CHE, representing a 1.76-fold increase compared to the high-volume group.

Conclusion: In patients with LC, CHE occurrence is associated with impaired liver reserve function, fibrosis markers, and liver volume. While higher prevalence of CHE in cases with poor liver function is consistent with previous reports, its association with liver volume is a novel finding. The measurement of liver volume can be easily determined within one minute using CT scans. Liver volume calculation may be a simple screening tool independent of blood test to identify high-risk groups for CHE.

FRI-129

Construction and validation of a nomogram prediction model for predicting cirrhosis-related deaths based on severe sarcopenia and clinical serological indicators

Hong Yu¹, Jinhua Jing², Guzainuer Yiliyaer³, Wei Sun¹, Yuyu Li⁴, Feng Guo⁵. ¹The Fourth Clinical Medical College of Xinjiang Medical University, Urumqi, China; ²No.4 Department of Internal Medicine of Traditional Chinese Medicine Hospital of Xinjiang Changji Prefecture, Urumqi, China; ³College of Nursing of Xinjiang Medical University, Urumqi, China; ⁴Fourth Clinical Medical College of Xinjiang Medical University, Urumqi, China; ⁵Department of Hepatology of Traditional Chinese Medicine Affiliated to Xinjiang Medical University, Urumqi, China

Email: gf_sj@163.com

Background and aims: Predicting the risk of liver disease-related death in cirrhotic patients based on severe myasthenia gravis and clinical serological indicators, constructing a nomogram prediction model and validating its predictive power.

Method: We retrospectively analyzed 239 patients with liver cirrhosis in the Department of Hepatology of Traditional Chinese Medicine of Xinjiang Medical University, from January 2019 to December 2020; based on the third lumbar vertebral level Skeletal Muscle Index according to the Malnutrition, Frailty, and Sarcopenia in Patients With Cirrhosis: 2021 Practice Guidance by the American Association for the Study of Liver Diseases, use (L3-SMI) <50 cm²/m² (male) or <39 cm²/m² (female) for the diagnosis of sarcopenia, and a combined 6 m step speed <1.0 m/s for the diagnosis of severe sarcopenia. Using random sampling method, the included patients were randomly assigned to the training cohort (167 cases) and the validation cohort (72 cases) in a ratio of 7:3; using multivariate COX regression and nomogram predicting death at 6, 12, and 24 months in patients with cirrhosis; internal validation was performed on the resulting nomogram through consistency indices (C-index) to check their predictive accuracy, calibration curves to assess their consistency, and clinical decision analyses to assess their clinical benefits; the risk of death in cirrhotic patients was assessed by the Kaplan-Meier curve.

Results: The prevalence of severe sarcopenia in this study was as high as 31.3% (75/239), with a higher prevalence in females than in males (56.0% vs 44.0%), and 81.3% (61/75) of patients with Child-Pugh class B/C. The results of multivariate COX regression analysis based on the training cohort showed that BMI, MELD score, and comorbid severe sarcopenia were risk factors predicting death related to liver disease; severe sarcopenia was independently associated with death in cirrhotic patients, with a multi-factorial-corrected HR of 3.42 (95% CI: 1.19~9.83). These factors were included and evaluated in the construction of a nomogram model, then predicted the risk of liver disease-related deaths at 6, 12, and 24 months with receiver operating characteristic curve, the area under the curve is 0.709 (95% CI: 0.323 ~ 1.096), 0.813 (95% CI: 0.626~1.000), 0.778 (95% CI: 0.558~0.999), and the C-index obtained from internal validation was 0.725 (95% CI: 0.513~0.937) indicating a high predictive value and fair consistency of the validation of the calibration curves for liver disease-related deaths in cirrhotic patients.

Conclusion: Severe sarcopenia increases the risk of death in cirrhotic patients by more than 3-fold and significantly affect the survival prognosis of patients. The nomogram prediction model based on BMI, MELD score, and severe sarcopenia has great clinical predictive value for liver disease-related deaths in cirrhotic patients.

FRI-130

Pre- and post-test diagnostic concordance rates of TJLB for suspected liver and blood diseases

Asako Nogami¹, Naohiro Wada², Tomohiro Otani¹, Michihiro Iwaki¹, Takashi Kobayashi², Satoru Saito¹, Masato Yoneda¹, Atsushi Nakajima¹.

¹Yokohama City University Graduate School of Medicine, Yokohama, Japan; ²Yokohama City University Graduate School of Medicine, Yokohama

Email: nogamia@yokohama-cu.ac.jp

Background and aims: Percutaneous liver biopsy (PLB) is the main method for histological diagnosis of liver disease. However, PLB may be difficult or impossible to perform in cases with signs of liver failure such as ascites effusion or decreased coagulability, or liver damage due to blood disorders. TJLB (transjugular liver biopsy) is an alternative test for PLB. Although there are many reports on the safety of TJLB, there are few reports on the concordance rate between pre- and post-test diagnoses. We investigated the rate of concordance between pre- and post-test diagnoses using TJLB.

Method: We retrospectively examined the concordance rate between pre- and post-test diagnoses in 107 patients who underwent TJLB at our hospital from May 2009 to December 2023.

Results: The median age of patients was 53 years (17–82), 47 males and 60 females. Fifty-seven patients (53.3%) had ascites effusion as a sign of liver failure, 14 patients (14.9%) had platelet counts <50,000/ μ L, and 37 patients (29.8%) had coagulation abnormalities (PT-INR>1.5). HVPG was measured at the time of TJLB in 86 patients. TJLB was successfully performed in 95 patients (88.8%). Seventy-two (75.8%) of the cases in which tissue samples were successfully obtained were for the search for the cause of chronic liver damage, and 23 (24.2%) were for the search for liver damage due to haematological disease. Of the 72 cases in which TJLB was performed to search for the cause of chronic liver disease, the diagnosis before and after the test was consistent in 32 cases (71.6%), the diagnosis of blood disease was reached in 1 case (1.4%), and the diagnosis was not reached in 18 cases (25%). In 4 cases (5.6%), the diagnosis was changed before or after the examination, and symptoms improved with the decision of treatment. Of the 23 patients who underwent TJLB because of suspected hematologic disease, the diagnosis was consistent before and after the examination in 9 cases (39.1%), liver disease was diagnosed in 5 cases (21.7%) based on histological diagnosis, and the diagnosis was not reached in 4 cases (17.4%).

Conclusion: In this retrospective study, the agreement rate of diagnosis before and after TJLB examination was 70% for suspected liver disease and about 40% for suspected haematological disease, suggesting that there is a great possibility that the diagnosis may change after TJLB is performed. On the other hand, the patients who underwent TJLB for suspected liver disease tended to be more difficult to diagnose than those who underwent TJLB for suspected haematological disease. In cases in which PLB is difficult to be performed due to signs of liver failure or hematologic disease, TJLB is a useful method of tissue diagnosis that may influence diagnosis and treatment.

FRI-131

Effect of adipose-related parameters on survival in patients with cirrhosis: a systematic review and meta-analysis

Zhang Wen^{1,2}, Qiu Ju Ran^{1,2}, Shuyue Tuo^{1,2}, Jia Yuan^{1,2}, Yong Li^{1,2}, Chan Li^{1,2}, Shejiao Dai^{1,2}, Jinhai Wang^{1,2}, Xinxing Tantai^{1,2}.

¹Department of Gastroenterology, the Second Affiliated Hospital of Xi'an Jiaotong University, Xi'an, China; ²Clinical Research Center for Gastrointestinal diseases of Shaanxi Province, the Second Affiliated Hospital of Xi'an Jiaotong University, Xi'an, China

Email: xinxingtantai@foxmail.com

Background and aims: Some adipose-related parameters exhibited distinct prognostic value in patients with cirrhosis. However, the association, magnitude, and direction of the association between individual adipose parameter and mortality in patients with cirrhosis

remain to be determined. This study aimed to evaluate the association between individual adipose parameter and mortality in patients with cirrhosis using the meta-analysis method.

Method: PubMed, Embase, Web of Science, and some Chinese databases were searched from inception to November 19, 2023 to identify the eligible studies. The prevalence of dichotomous adipose parameters and their corresponding 95% confidence interval (CI) were pooled using the random-effects model. The impact of each adipose parameter on mortality was assessed by the pooled unadjusted or adjusted hazard ratio (HR) with 95% CIs using the random-effects modeling.

Results: A total of 27 studies involving 7,906 patients were included in our analysis. Initially, 15 adipose parameters were identified and underwent screening, ultimately resulting in the inclusion of 10 parameters: visceral fat area (VFA), visceral adipose tissue index (VATI), subcutaneous fat area (SFA), subcutaneous adipose tissue index (SATI), the visceral to subcutaneous ratio (VSR), myosteatosis, sarcopenic obesity (SO), muscle radiodensity (MR), visceral adipose radiodensity (VAR), and subcutaneous adipose radiodensity (SAR). The pooled prevalence of SO and myosteatosis in patients with cirrhosis was 15.5% and 34.4%, respectively. In unadjusted analyses, associations with mortality were observed for SATI (unadjusted HR 0.99, 95% CI 0.99–0.99), VSR (unadjusted HR 2.46, 95% CI 1.84–3.28), myosteatosis (unadjusted HR 2.52, 95% CI 1.90–3.33), SO (unadjusted HR 2.27, 95% CI 1.63–3.16), MR (unadjusted HR 0.96, 95% CI 0.94–0.98), and SAR (unadjusted HR 1.02, 95% CI 1.01–1.02), while no such associations were found for VFA (unadjusted HR 1.00, 95% CI 0.99–0.101), VATI (unadjusted HR 1.00, 95% CI 1.00–1.00), SFA (unadjusted HR 1.00, 95% CI 0.99–1.00), and VAR (unadjusted HR 1.02, 95% CI 1.00–1.03) in patients with cirrhosis. In adjusted analysis, each unit increase in SATI (adjusted HR 0.99, 95% CI 0.98–1.00) or MR (adjusted HR 0.94, 95% CI 0.90–0.98), and each unit decrease in VSR (adjusted HR 1.92, 95% CI 1.45–2.54), showed an independent association with a decreased risk of mortality. However, concurrent myosteatosis (adjusted HR 1.88, 95% CI 1.48–2.40) or SO (adjusted HR 2.77, 95% CI 1.95–3.93) significantly increased the risk of mortality in patients with cirrhosis.

Conclusion: Different adipose parameters exhibited varying prognostic value: decreased SATI or MR, increased VSR, and concurrent myosteatosis or SO were independently associated with a higher risk of mortality in patients with cirrhosis.

FRI-132

Spontaneous bacterial empyema is a rare yet life-threatening complication in patients with hepatic hydrothorax

Grace Lai-Hung Wong¹, Mandy Sze-Man Lai¹, Jimmy Che-To Lai¹, Terry Cheuk-Fung Yip¹, Lilian Liang¹, Yichong Jiang¹,

Vincent Wai-Sun Wong¹. ¹The Chinese University of Hong Kong, Medical Data Analytics Centre (MDAC), Department of Medicine and Therapeutics, Hong Kong, Hong Kong

Email: wonglaihung@cuhk.edu.hk

Background and aims: Hydrothorax is one of the most debilitating complications in patients with cirrhosis. We aimed to evaluate the detailed pleural fluid analysis and the outcome of spontaneous bacterial empyema in patients with hepatic hydrothorax in a territory-wide cohort over the last two decades in Hong Kong.

Method: This was a territory-wide cohort study of consecutive patients with cirrhosis and hepatic hydrothorax from 2000–2022. We reviewed pleural fluid analysis of patients who underwent diagnostic and/or therapeutic thoracentesis. Spontaneous bacterial empyema was defined as a polymorphonuclear leukocytes (PMN) >500 cells/mm³ with negative pleural fluid culture, or PMN >250 cells/mm³ with positive pleural fluid culture.

Results: Among the 31,542 patients with cirrhosis, 3,251 (10.3%) patients suffered from hydrothorax; their mean age was 58 \pm 14 years; 65.4% were male; cirrhosis was mostly caused by chronic hepatitis B (72.5%). 687/3,251 (21.1%) patients underwent

POSTER PRESENTATIONS

thoracentesis with pleural fluid sent for analysis. Spontaneous bacterial empyema occurred in 43/3, 251 (1.3%) all patients with hydrothorax, and 43/687 (6.3%) of those underwent thoracentesis. Compared with uninfected individuals, patients with spontaneous bacterial empyema had lower median (interquartile range) pleural fluid pH 7.33 (7.21–7.39) vs. 7.46 (7.36–7.51), higher total protein 23.2 (16.7–31.5) vs. 19.5 (12.3–29.2) g/L, higher lactate dehydrogenase (LDH) 107 (79–177) vs. 88 (63–158) IU/L, higher pleural fluid/serum protein ratio 0.52 (0.42–0.83) vs. 0.35 (0.21–0.65). The 30-day and 6-month mortality of patients with spontaneous bacterial empyema was as high as 21.3% and 65.4% respectively, compared to 3.4% and 17.5% respectively in uninfected patients.

Conclusion: Spontaneous bacterial empyema is a rare yet deadly complication in patients with liver cirrhosis and hepatic hydrothorax. A high index of suspicion, timely diagnosis and treatment may improve the clinical outcome.

FRI-133

Decreasing incidence of cirrhosis due to hepatitis C following the treatment as prevention for hepatitis C nationwide elimination campaign

Einar S. Björnsson¹, Halldor A. Haraldsson², Magnús Gottfredsson³, Sigurdur Olafsson³. ¹Landspítali University Hospital, Reykjavik, Iceland; ²University of Iceland, Reykjavik, Iceland; ³Landspítali University Hospital, Reykjavik, Iceland
Email: einarsb@landspitali.is

Background and aims: In the late 20th century the incidence of liver cirrhosis was low in Iceland at 3 cases per 100,000 inhabitants but subsequently increased in the past two decades due to increased alcohol consumption, obesity and hepatitis C virus (HCV) infections to around 10 cases per 100,000 per year in 2015. In 2016 a nationwide elimination program for HCV was initiated, entitled Treatment as Prevention for Hepatitis C (TraP HepC), providing unrestricted access to antiviral treatment. The aims were to describe the changes in risk factors and epidemiology of cirrhosis and to assess the trends in HCV-related cirrhosis following TraP HepC.

Method: The study included all patients newly diagnosed with cirrhosis in Iceland from 2016 to 2022. Diagnosis was based on liver elastography, histology, and/or 2 of 4 criteria: cirrhosis on imaging, ascites, varices, and/or elevated international normalized ratio (INR).

Results: Over the study period, 342 new cirrhosis patients were identified, 223 (65%) males, median age 62 years, MELD 9 (8–14). The crude overall incidence was 13.8 cases per 100,000 inhabitants annually. The most common etiologies were alcohol (40%), metabolic dysfunction associated steatotic liver disease (MASLD) (28%), and HCV with/without alcohol overconsumption (15%). The proportion of cirrhotics with either alcoholic related liver disease or MASLD etiology increased from 53% in a previous prospective study of 2010–2015 to 68% of all cirrhosis etiologies. The number of HCV cirrhosis cases was higher in 2016 (n = 23) due to intensified case-finding in the TraP HepC project but dropped by more than 90% in 2021 and 2022. The overall 5-year survival was 55% (95% CI 48.9–62.3%). The most common causes of death were hepatocellular carcinoma (26%) and liver failure (25%).

Conclusion: During the past two decades the incidence of cirrhosis has increased in Iceland associated with increased alcohol consumption, obesity, and HCV. Alcohol overconsumption *per se* and MASLD now collectively make up two thirds of incident cases in Iceland. Following a nationwide elimination campaign, HCV cirrhosis has dropped by >90% in Iceland.

FRI-134

Six years long-lasting clinical benefits of previous short-term resistance training in cirrhosis-follow-up after a clinical randomized trial

Luise Aamann^{1,2}, Gitte Dam¹, Mette Borre¹, Peter Jepsen¹, Hendrik Vilstrup¹, Niels Kristian Aagaard¹. ¹Aarhus University Hospital, Aarhus, Denmark; ²Copenhagen University Hospital Hvidovre, Copenhagen, Denmark
Email: luise.aamann@gmail.com

Background and aims: In many chronic diseases, training promotes general health and may improve survival. In patients with cirrhosis, our previous randomized clinical trial on supervised resistance training showed reduced risk for the first acute hospital admission and decreased all-cause mortality. The effects were maintained up to three years after randomization. We now extended the follow-up in order to evaluate possible long-lasting effects of resistance training.

Method: 12 weeks of supervised intensive resistance training was the intervention. 39 participants with cirrhosis Child-Pugh stage A/B were randomly assigned to resistance training or continued sedentary living. There was no after-study intervention. After randomization all-cause first acute hospital admissions and deaths were recorded during a 6-year follow-up.

Data were analyzed according to intention-to-treat. We used Fine and Gray regression to analyze time to first admission with death before hospitalization as a competing risk and Cox regression for survival analysis. We adjusted for Child-Pugh, age, gender, and comorbidity (CirCom) at randomization.

Results: Baseline characteristics were similar in both groups. During the 6 years, a total of 15 participants who trained, and 18 who did not were acutely hospitalized. There was a significantly decreased admission risk in the training group (adjusted subdistribution hazard ratio 0.46 (95% CI: 0.24–0.9) p = 0.02).

In total, 17 participants died during the 6 years (7 who trained and 10 who did not) but the reduction was not statistically significant (adjusted hazard ratio 0.37 (95% CI: 0.12–1.09) p = 0.07).

Conclusion: 6 years after an intensive 12-week resistance training program of cirrhosis patients there was still a beneficial effect on their risk of the first acute hospital admission. Also, mortality was lower although not maintaining statistical significance. The mechanisms of this long-lasting positive effect of short-term training are unresolved but are likely related to a reduction in sarcopenia maintained by life-style changes.

The results suggest lasting clinically meaningful benefits of resistance training in cirrhosis and motivate further trials.

FRI-135

Von Willebrand factor is associated with portal vein thrombosis in patients with liver cirrhosis

Wenting Lu¹, Ming Zhang¹, Lei Wang¹, Yuzheng Zhuge¹, Feng Zhang¹. ¹Nanjing Drum Tower Hospital, Affiliated Hospital of Medical School, Nanjing University, Nanjing, China
Email: fzdndx@126.com

Background and aims: von Willebrand factor (vWF) plays a key role in hemostasis and is reported to be related with the outcome of advanced chronic liver disease. The aim of the present study is to investigate the relationship between vWF and portal vein thrombosis (PVT) in patients with cirrhosis.

Method: Consecutive cirrhotic patients with gastroesophageal varices admitted to our hospital between January 2020 and April 2022 were prospectively recruited and divided into PVT and non-PVT groups. We collected clinical, routine blood tests, biochemical tests, coagulation tests, and hemostatic protein profiles data to explore the risk factors of PVT.

Results: A total of 154 patients were enrolled including 83 patients with PVT and 71 patients without PVT. Plasma levels of vWF (OR = 1.013, 95%CI: 1.005~1.021, P = 0.002), D-dimer (OR = 2.263, 95%CI: 1.504~3.877, P = 0.001), and decreased portal blood flow velocity (OR

= 0.827, 95%CI: 0.749~0.897, $P < 0.001$) were the variables independently associated with the existence of PVT. Areas under the curve of ROC (AUROC) analyses for vWF, D-dimer and portal blood flow velocity were 0.773, 0.847, and 0.839, respectively. A nomogram model was established involving the three parameters, and the AUROC was 0.930. In the internal validation using bootstrap, the AUROC was 0.930 (95%CI: 0.887–0.966).

Conclusion: Higher vWF levels were related with PVT in patients with decompensated cirrhosis, indicating that vWF might serve as a risk factor for PVT, and a nomogram containing vWF, D-dimer and portal blood flow velocity could be an important tool of PVT risk prediction in cirrhotic patients. Further external validation is warranted.

FRI-136

Aspirin reduces risk of ascites and encephalopathy in cirrhotic patients without increasing the risk of gastrointestinal bleeding

Roie Tzadok¹, Nir Bar², Ayelet Grupper³, Eugene Feigin⁴, Helena Katchman⁵. ¹Division of Gastroenterology and Hepatology, Tel Aviv Sourasky Medical Center, Faculty of Medicine, Tel Aviv University, Tel Aviv; ²Division of Gastroenterology and Hepatology, Tel Aviv Sourasky Medical Center, Faculty of Medicine, Tel Aviv University, Tel Aviv, Israel; ³Department of Nephrology, Tel Aviv Sourasky Medical Center, Faculty of Medicine, Tel Aviv University, Tel Aviv, Israel; ⁴Department of Endocrinology, Tel Aviv Sourasky Medical Center, Faculty of Medicine, Tel Aviv University, Tel Aviv, Israel; ⁵Division of Gastroenterology and Hepatology, Tel Aviv Sourasky Medical Center, Faculty of Medicine, Tel Aviv University, Tel Aviv, Israel
Email: ROIET@TLVMC.GOV.IL

Background and aims: There is accumulating data regarding the beneficial effects of aspirin on the advancement of liver fibrosis, both in animal models and on laboratory indices of fibrosis. Aspirin was also shown to be associated with reduced HCC risk in cirrhotic patients. This study was aimed to evaluate clinical outcomes in cirrhotic patients treated with aspirin in comparison to non-treated cirrhotic patients.

Method: In a retrospective study at Tel Aviv Sourasky Medical Center, we compared aspirin treated cirrhotic patients for various indications to non-treated patients. Patients were followed-up for composite clinical outcomes, including decompensations, thrombotic and vascular complications (portal vein thrombosis, DVT, TIA, CVA, acute coronary syndrome and myocardial infarction) and HCC. Cox regression multivariate models were used to compare clinical sequelae between the groups.

Results: From 2009–2018, 2413 patients with cirrhosis were treated at our center. One thousand and sixty-nine patients were followed up for a minimum of three months (median 13 months, IQR 33.1–57.67 months). One hundred and thirty-six patients (12.7%) were treated with aspirin for various indications. Baseline clinical and laboratory characteristics of both groups were comparable. Aspirin use was associated with risk reduction for decompensations, including a composite risk of ascites and hepatic encephalopathy, in a multivariate Cox regression analysis ($p = 0.035$). Aspirin use showed a tendency toward encephalopathy risk reduction as a single variable ($p = 0.055$), but not for the development of ascites. Aspirin was not associated with an increased risk of gastrointestinal bleeding in both univariate ($p = 0.281$) and multivariate analyses models adjusted for gender, age, platelet count, MELD score, statin, beta blocker and PPI use ($p = 0.446$).

Conclusion: Aspirin use may confer a protective effect against a composite outcome of hepatic encephalopathy and ascites, and is not associated with increased risk of gastrointestinal bleeding in patients with cirrhosis. Further prospective studies on larger cohorts are necessary to elucidate its mode of action and confirm our findings.

Cirrhosis and its complications – Portal Hypertension

TOP-061-YI

Whole blood thrombin generation improves the understanding of cirrhotic coagulopathy and predicts clinical outcomes in patients with cirrhosis: a prospective cohort study

Alberto Zanetto¹, Elena Campello², Cristiana Bulato², Ruth Willems³, Joke Konings³, Mark Roest³, Sabrina Gavasso², Giorgia Nuozi², Serena Toffanin², Paola Zanaga¹, Patrizia Burra¹, Francesco Paolo Russo¹, Bas de Laet³, Paolo Simioni², Marco Senzolo¹. ¹Gastroenterology and Multivisceral Transplant Unit, Department of Surgery, Oncology and Gastroenterology, Padova University Hospital, Padova, Italy; ²General Internal Medicine Unit, Thrombotic and Hemorrhagic Disease Unit and Hemophilia Center, Department of Medicine, Padova University Hospital, Padova, Italy; ³Department of Functional Coagulation, Synapse Research Institute, Maastricht, Netherlands
Email: alberto.zanetto@yahoo.it

Background and aims: Patients with cirrhosis have an increased thrombin generation (TG) in platelet-poor plasma (PPP). By reflecting the contribution of circulating blood cells, whole blood (WB) TG may allow a more physiological assessment of coagulation, thus improving our understanding of cirrhotic coagulopathy and its clinical implications. We conducted a prospective study to 1) compare WB-TG vs. PPP-TG in cirrhosis; 2) assess whether WB-TG could predict hepatic decompensation, further decompensation/ACLF, bleeding unrelated to portal hypertension and thrombosis.

Method: Assessment of coagulation included routine tests, factor VIII, natural anticoagulants, PPP-TG and WB-TG (with and without thrombomodulin [TM]). Twenty-five healthy subjects were included as controls. All patients were prospectively followed for development of hepatic decompensation and bleeding/thrombosis.

Results: We included 203 patients (Child-Pugh A/B/C 81/55/67). In compensated cirrhosis, both PPP-TG and WB-TG indicated an increased TG capacity, as reflected by an endogenous thrombin potential (ETP) significantly higher than controls; in decompensated cirrhosis, PPP-TG indicated a hyper-coagulable state with increased ETP and higher peak height, whereas WB-TG revealed a progressive impairment of TG kinetics and total capacity, resulting in a profound hypo-coagulable state in Child-Pugh C. Median duration of follow-up was 13 months in compensated and 10 months in decompensated patients. In compensated cirrhosis, patients who experienced 1st decompensation had a significantly higher WB-TG than those who did not, whereas in decompensated cirrhosis WB-TG was comparable in patients with vs. without further decompensation/ACLF during follow-up. In decompensated patients, WB-TG was more severely compromised in patients who experienced bleeding complications, whereas no association was found with thrombosis.

Conclusion: In compensated cirrhosis, a more pronounced hyper-coagulable state, as assessed by WB-TG, indicated a higher risk of decompensation, suggesting that hyper-coagulability may be responsible for cirrhosis progression. In decompensated cirrhosis, contrary to PPP-TG that indicates hypercoagulability, WB-TG reveals a significant hypo-coagulable state, which was associated with bleeding complications.

SATURDAY 08 JUNE

SAT-068

Accuracy of spleen stiffness measurement for the diagnosis of high-risk esophageal varices in patients with advanced chronic liver disease: a systematic review and individual patient data meta-analysis

Elton Dajti¹, Federico Ravaioli¹, Xiaolong Qi², Jinjun Chen³, Horia Ștefănescu⁴, Young Seo Cho⁵, Cristophe Cassinotto⁶, Rui Gaspar⁷, Saveria Lory Croce⁸, Maha Elsabaawy⁹, Mirella Fraquelli¹⁰, Ivica Grgurevic¹¹, Carmen Fierbinteanu Braticević¹², Grace Wong¹³, Renata Bende¹⁴, Maciej Janik¹⁵, Flavia Fernandes¹⁶, Laure Elkrief¹⁷, Pierre-Emmanuel Rautou¹⁸, Atsushi Nakajima¹⁹, Romanas Zyklus²⁰, Matthias Buechter²¹, Giovanni Galati²², Thomas Reiberger²³, Ekaterina Lusina²⁴, Julia Arribas Anta²⁵, Jose Ignacio Fortea²⁶, Jason Pik Eu Chang²⁷, Natalie Lucchina²⁸, Hirooka Masashi²⁹, Giorgio Soardo³⁰, Luigi Colecchia¹, Davide Roccarina³¹, Fabio Piscaglia³², Francesco Azzaroli³³, Giovanni Marasco³⁴, Agostino Colli³⁵, Davide Festi¹, Annalisa Berzigotti³⁶, Antonio Colecchia³⁷. ¹University of Bologna, Bologna, Italy; ²Center of Portal Hypertension, Department of Radiology, Zhongda Hospital, School of Medicine, Southeast University, Nanjing, China; ³Southern Hospital of Southern Medical University, Guangzhou, China; ⁴Regional Institute of Gastroenterology and Hepatology Octavian Fodor, Cluj-Napoca, Romania; ⁵Hanyang University College of Medicine, Hanyang University Guri Hospital, Guri, Korea, Rep. of South; ⁶University Hospital of Montpellier, Montpellier, France; ⁷Centro Hospitalar São João, Porto, Portugal; ⁸Università degli Studi di Trieste, Trieste, Italy; ⁹Menoufia University, Shebeen El-Kom, Egypt; ¹⁰Fondazione IRCCS Ca' Granda-Ospedale Maggiore Policlinico, Milan, Italy; ¹¹Dubrava University Hospital, Zagreb, Italy; ¹²Carol Davila University of Medicine and Pharmacy, University Hospital Bucharest, Bucharest, Romania; ¹³The Chinese University of Hong Kong, Hong Kong, China; ¹⁴Victor Babes University of Medicine, Timisoara, Romania; ¹⁵Department of Hepatology, Transplantology and Department of Hepatology, Transplantology and Internal Medicine, Warsaw, Poland; ¹⁶Bonsucesso Federal Hospital, Rio de Janeiro, Brazil; ¹⁷Tours University Hospitals, Tours, France; ¹⁸Hôpital Beaujon-Assistance Publique-Hôpitaux de Paris, Paris, France; ¹⁹Yokohama City University Graduate School of Medicine, Yokohama, Japan; ²⁰Department of Gastroenterology, Lithuanian University of Health Sciences, Kaunas, Lithuania; ²¹University of Duisburg-Essen, Essen, Germany; ²²University Campus Bio Medico of Rome, Rome, Italy; ²³Medical University of Vienna, Vienna, Austria; ²⁴M. F. Vladimirovskiy Moscow Regional Research Clinical Institute, Moscow, Russian Federation; ²⁵Servicio de Gastroenterología y Hepatología, Hospital Universitario Ramón y Cajal, Universidad de Alcalá, Instituto Ramón y Cajal de Investigación Sanitaria (IRYCIS), Madrid, Spain; ²⁶Marqués de Valdecilla University Hospital, Santander, Spain; ²⁷Singapore General Hospital, Singapore; ²⁸Department of Radiology, University Hospital, Varese, Italy; ²⁹Departments of Gastroenterology and Metabolism, Toon, Ehime, Japan; ³⁰University of Udine, Udine, Italy; ³¹Azienda Ospedaliero-Universitaria Careggi, Firenze, Italy; ³²University of Bologna, Unit of Internal Medicine, Bologna, Italy; ³³IRCCS Azienda Ospedaliero-Universitaria di Bologna Policlinico di Sant'Orsola, Bologna, Italy; ³⁴University of Bologna, Bologna, Italy; ³⁵Fondazione IRCCS Ospedale Maggiore Policlinico, Milano, Milano, Italy; ³⁶Department of Visceral Surgery and Medicine, Inselspital, Bern University Hospital, University of Bern, Bern, Switzerland; ³⁷POLICLINICO DI MODENA, Modena, Italy
Email: e_dajti17@hotmail.com

Background and aims: Diagnosis and management of esophageal varices (EV) is of critical importance in compensated advanced chronic liver disease. We performed an individual patient data (IPD) meta-analysis to investigate the performance of spleen stiffness measurement (SSM)-based algorithms using different elastography

techniques to rule-out high-risk varices (HRV) as compared to the existing standard of care (Baveno-VI criteria).

Method: We systematically researched databases (PubMed, Embase, Scopus, Cochrane) until November 1st, 2023. Studies reporting data on endoscopy and SSM in adult patients were eligible. The main outcome was an acceptable rate (<5%) of missed HRV, defined by a summary sensitivity and negative predictive value (NPV) $\geq 95\%$. The evaluated algorithms for transient elastography (TE) were: i) Baveno-VI Criteria, ruling-out HRV if liver stiffness measurement (LSM) < 20 kPa and platelet count (PLT) > 150 G/L; ii) SSM ≤ 40 kPa; iii) combined Baveno VII-SSM criteria, followed by SSM cut-off ≤ 40 kPa in patients outside Baveno VI criteria. This study is registered with PROSPERO, CRD42019127164.

Results: We assessed 1436 articles for eligibility, of which 37 studies including 4353 patients from 19 countries were included in the analysis. In the TE cohort (18 studies, 1996 patients), the Baveno VI algorithm showed a sensitivity of 100% (95%-CI: 98–100%) and a NPV of 100% (95%-CI: 98–100%); the rate of spared endoscopies was 16% (95%-CI: 12–21%). SSM ≤ 40 kPa alone was accurate to rule-out HRV: sensitivity 98% (95%-CI: 94–99%), NPV 99% (95%-CI: 97–100%), rate of spared endoscopies 30% (95%-CI: 25–35%). The combined Baveno VII-SSM criteria were the best performing for ruling-out HRV: sensitivity 97% (95%-CI: 95–99%), NPV 99% (95%-CI: 97–100%) and rate of spared endoscopies 36% (95%-CI: 30–41%). These results were robust in all sensitivity analyses, including a large subgroup of patients (n = 569) with non-viral etiology. SSM evaluated by other techniques was also accurate to diagnose HRV: the AUROC was 0.69 for two-dimensional shear wave (2D-SWE) (n = 851 patients), 0.74 for VTQ-SWE (n = 1215 patients), and 0.65 for ElastPQ-SWE (n = 291 patients). However, the cut-offs proposed by Baveno VI-VII did not have an acceptable rate of missed HRV in the p-SWE and 2D-SWE cohorts.

Conclusion: This large, multicenter, international study validated SSM-TE as an accurate test for the diagnosis of esophageal varices. The combined Baveno VII-SSM criteria were the best performing algorithm to rule-out HRV.

SAT-069

Effects of zibotentan and dapagliflozin on patients with compensated cirrhosis: a randomized double-blind placebo controlled exploratory pilot study

Juan Carlos García-Pagán¹, Lise Lotte Gluud², Mattias Mandorfer³, Jörn M. Schattenberg⁴, Andrea De Gottardi⁵, Annalisa Berzigotti⁶, Jose Ignacio Fortea⁷, Agustín Albillos⁸, Edilmar Alvarado-Tapias⁹, Marco Berning¹⁰, Pawel Petryszyn¹¹, Min Lin¹², Philip Ambery¹³, Jaime Bosch¹⁴, Jan Oscarsson¹⁵, Don Rockey¹⁵. ¹Hospital Clínic de Barcelona, Barcelona, Spain; ²Copenhagen University Hospital Hvidovre, Hvidovre, Denmark; ³Medical University of Vienna, Vienna, Austria; ⁴Saarland University Medical Center, Homburg, Germany; ⁵Università della Svizzera Italiana, Lugano, Switzerland; ⁶Bern University Hospital, University of Bern, Bern, Switzerland; ⁷Department Hospital Universitario Marqués de Valdecilla, Santander, Spain; ⁸Hospital Universitario Ramon y Cajal, Madrid, Spain; ⁹Autonomus University of Barcelona, Barcelona, Spain; ¹⁰University Hospital Dresden, Dresden, Germany; ¹¹AstraZeneca, Warsaw, Poland; ¹²AstraZeneca, Gaitersburg, United States; ¹³AstraZeneca, Gothenburg, Sweden; ¹⁴Bern University Hospital, Bern, Switzerland; ¹⁵Medical University of South Carolina, Charleston, United States
Email: rockey@muscc.edu

Background and aims: Endothelin-1 is a potent vasoconstrictor that contributes to intrahepatic vasoconstriction and portal hypertension (PH) in patients with cirrhosis. Endothelin receptor antagonists (ERA) may significantly reduce elevated portal pressure gradient but are associated with fluid retention. Sodium-glucose co-transporter 2 inhibitors (SGLT2i) induce osmotic diuresis. In this exploratory pilot study, the effects of the combination of zibotentan, an ERA selective antagonist, and dapagliflozin, a selective SGLT2i, on hepatic venous pressure gradient (HVPG), safety and tolerability, were investigated.

Method: Eligible participants with compensated cirrhosis (MELD <15 and Child-Pugh A) of any etiology, except chronic cholestatic liver diseases, were randomized to placebo (n = 14) or combined 2.5 mg zibotentan/10 mg dapagliflozin (zibo/dapa, n = 14) in a 6 week parallel, double-blind study. The primary objectives were to evaluate change in HVPG, safety and tolerability of the treatment. Secondary objectives included changes in body weight, total body water, extracellular water volume (ECV) and blood pressure (BP). The absolute change in HVPG from baseline to week 6 (primary end point) was analysed in the full analysis set using an ANCOVA model.

Results: Patients had a mean (SD) age of 64.5 (10) years, 71% were males, 36% had type 2 diabetes, and cirrhosis was most commonly caused by ALD (39%) or MASLD (46%). The mean MELD score was 7.4 (range: 6–11); 46% were treated with non-selective beta-blockers. Baseline HVPG ranged from 6.5 to 19 mmHg (median: 10.0), and 16/28 had clinically significant PH (CSPH = HVPG \geq 10 mmHg). One participant in each group did not complete the study. There was no difference in the absolute change in HVPG at week 6 (1.0 mmHg (90% CI: -0.31, 2.35)). In participants with more severe PH treated with zibo/dapa, there was a trend towards a decrease in HVPG (which was not seen in placebo treated participants). Systolic (-20 mmHg (90% CI: -31.8, -8.7)) and diastolic BP (-9.5 mmHg (90% CI: -13.4, -5.7)) decreased significantly with zibo/dapa vs placebo. The estimated difference in body weight and ECV change was -0.8 kg (90% CI: -1.86, 0.34) and -0.9 L (90% CI: -2.1, 0.3), respectively. Adverse events (AEs) were mild or moderate and similar in both groups. Two mild AEs of fluid retention in the zibo/dapa group and one in the placebo group were reported. One AE of orthostatic hypotension and one early withdrawal due to AE (headache) occurred in the placebo group. No serious AEs or DILI were observed.

Conclusion: Six weeks of treatment with zibo/dapa was safe and well tolerated in compensated cirrhosis. Fluid retention events were fewer than described in previous ERA trials. A reduction in HVPG was not observed, possibly reflecting a low number of patients with severe PH. An ongoing phase 2b study investigating patients with CSPH is powered to identify an effect on HVPG.

SAT-070

Argon plasma coagulation or endoscopic band ligation for gastric antral vascular ectasia: a randomized comparative analysis

Ashok Jhaharia^{1,2,3}, Shashank Singh³, Prachis Ashdhir³, Rupesh Pokharna⁴. ¹Sawai Man Singh Medical College and Hospital, Jaipur, India; ²Sawai Man Singh Medical College, Gastroenterology, Jaipur, India; ³Sawai Man Singh Medical College, Jaipur, India; ⁴Sawai Man Singh Medical College, Jaipur, India
Email: drashokjhaharia@gmail.com

Background and aims: Gastric antral vascular ectasia (GAVE) causes iron-deficiency anemia and gastrointestinal bleeding, albeit uncommonly. Some patients need frequent transfusions. While APC effectively treats lesions, new methods like endoscopic band ligation (EBL) in periodic manner are being explored. The study assessed APC versus EBL for GAVE treatment, focusing on lesion obliteration and session frequency.

Method: The Department of Gastroenterology, SMS Medical College and Associated Hospital, Jaipur, conducted a single-centre, prospective, open-label, randomized controlled study. 60 participants with UGI bleeding from GAVE, confirmed by esophagogastroduodenoscopy (EGD), were chosen. Participants without prior GAVE endotherapy were divided into two groups: APC (30) and EBL (30). Sessions were held every 3–4 weeks until GAVE lesions cleared. Afterward, patients followed monthly for 6 months. The study is registered as CTRI Reg. No. CTRI/2023/10/058739.

Results: Outcome analysis compared 27 participants in the EBL group to 29 in the APC group. Both groups had similar baseline parameters. EBL required fewer treatment sessions (2.9 ± 0.6) than APC (3.2 ± 0.7). EBL achieved endoscopic obliteration earlier than APC ($p < 0.01$). At 6 months, both groups showed comparable bleeding control and lesion

obliteration. Initially, both groups had similar hemoglobin levels, prior hospitalizations, and transfusion needs. After 6 months, the EBL group had better hemoglobin levels, fewer transfusions (non-significant), and fewer hospital visits ($p = 0.001$) as compared to APC group. While analysing both groups separately, the pre and post intervention values differ significantly in terms of haemoglobin values, hospitalisation and need for transfusion, with a p value <0.01. **Conclusion:** Both EBL and APC are effective in treating GAVE lesions and relieving associated symptoms. Although outcomes were mostly comparable, EBL exhibited benefits in treatment duration, hospital stays and hemoglobin changes. Nonetheless, more comprehensive, long-term data is needed.

SAT-071

Pre-emptive TIPS should not be contra indicated in high-risk patients with acute variceal bleeding and alcohol hepatitis

Marika Rudler¹, Sarah Mouri¹, Charles Roux¹, Maxime Mallet¹, Manon Allaire¹, Frederic Charlotte¹, Philippe Sultanik¹, Charlotte Bouzbib¹, Dominique Thabut¹. ¹APHP Sorbonne Université Hôpital Pitié-Salpêtrière, Paris, France
Email: marika.rudler@aphp.fr

Background and aims: Patients (pts) with severe alcoholic hepatitis (AH) may have a very bad prognosis, depending on liver function, response to corticosteroids and alcohol withdrawal. pTIPS is improving liver-transplant-free survival in high-risk cirrhotic patients with acute variceal bleeding (AVB). No data have been reported in pts with severe AH requiring a pre-emptive TIPS (pTIPS) placement (i.e. pts with Child-Pugh B and active bleeding or Child-Pugh C10–13 cirrhosis). Clinicians may intuitively think that pTIPS may not be as beneficial in high-risk cirrhotic patients with AVB and severe AH. This study aimed to evaluate the prevalence of severe AH in patients with AVB requiring pTIPS and to compare the clinical outcomes of pts with severe AH and pts with alcohol-related cirrhosis without severe AH.

Method: Monocentric prospective observational study including all consecutive pts with AVB who were treated with pTIPS between January 2018 and December 2022. The pTIPS policy was applied our center since 2011, and all patients with a suspected AH and a Maddrey's discriminant function ≥ 32 had a transjugular liver biopsy. Severe AH was systematically treated with corticosteroids. The primary end point was one-year transplant free survival (TFS) in patients with or without AH. Secondary end points were survival and rebleeding at one year.

Results: 248 pts with variceal bleeding were hospitalized in our ICU during the study period, and 67 were treated with pTIPS in a median delay of 37 hours after admission (male gender 86%, age 53, cause of cirrhosis alcohol in 73%, MetOH in 23%, other in 4%, Child-Pugh score 11, MELD score 21, hemoglobin 8.3 g/dL, HVPG before/after TIPS 15.5/7 mmHg). Overall, 21/67 pts (31.1%) had histologically proven AH. AH pts were significantly younger (49 vs 53 years, $p = 0.04$), had a higher MELD score (21 vs 19, $p = 0.03$) and a higher bilirubin level (130 vs 70 $\mu\text{mol/L}$, $p = 0.03$). Infection rate was similar between the 2 groups (38.1% vs 43.5%, $p = 0.88$). The one-year TFS was similar in AH and in non-AH pts (81% vs 72%, $p = 0.37$), as well as the one-year global survival (81% vs 81%, $p = 0.16$). Rebleeding rate was also similar in the 2 groups. The only factor independently associated with survival was MELD score at admission (OR = 0.92, 95% CI [0.82–0.99], $p = 0.04$).

Conclusion: Severe AH pts with AVB treated by pTIPS presented similar prognosis when compared to pts without severe AH. When suspected, severe AH should be histologically proven and pTIPS should not be contra-indicated in those pts.

SAT-074

Hemodynamic profile of terlipressin and octreotide in patients with cirrhosis and portal hypertension. A randomized, double-blind clinical trial

Valeria Perez-Campuzano^{1,2,3,4,5}, Pol Olivas^{1,2,3,4,5}, Anna Baiges^{1,2,3,4,5}, Lara Orts^{1,2,3,4,5}, Sarah Shalaby^{1,2,3,4,5}, Asunción Ojeda^{1,2,3,4,5}, Fanny Turon^{1,2,3,4,5}, Virginia Hernández-Gea^{1,2,3,4,5}, Andres Cardenas^{1,2,3,4,5}, Juan Carlos García-Pagán^{1,2,3,4,5}. ¹Hospital Clínic Barcelona, Barcelona, Spain; ²Institut de Investigacions Biomèdiques August Pi I Sunyer (IDIBAPS), Barcelona, Spain; ³Departament de Medicina i Ciències de la Salut-University of Barcelona, Barcelona, Spain; ⁴CIBEREHD (Centro de Investigación Biomédica en Red Enfermedades Hepáticas y Digestivas), Barcelona, Spain; ⁵Health Care Provider of the European Reference Network on Rare Liver Disorders (ERN-Liver), Barcelona, Spain
Email: jcgarcia@clinic.cat

Background and aims: In patients with acute variceal bleeding terlipressin is administered by bolus injection every 4–6 hour. Continuous terlipressin infusion administration may achieve a more persistent reduction in portal pressure (PP) with fewer side effects. However, the potential time and profile reduction in PP after continuous terlipressin infusion have yet to be adequately assessed. This study aimed to compare the hepatic and cardiopulmonary hemodynamic effects and safety of terlipressin as a bolus vs. its continuous infusion or octreotide bolus followed by continuous infusion.

Method: This is a single-center, double-blinded, double-dummy, parallel-group, clinical trial in which 38 patients with cirrhosis and portal hypertension (HVPG ≥ 12 mmHg) were randomized to receive (during 2 hours): 1) bolus of octreotide (250 mcg) + continuous infusion (50 mcg/h) (n = 12; group OCTR), 2) bolus of terlipressin (1 mg) followed by continuous infusion of placebo (n = 12; group TERLBOL) or 3) bolus of placebo followed by a continuous infusion of terlipressin (initially 2 mg/day) (n = 14; group TERLINF). Hepatic venous pressure gradient, cardiopulmonary pressures and cardiac output were measured at baseline, and after 30, 60 and 120 minutes. If less than 10% HVPG reduction was observed at 30 min of the infusion, an independent observer, manipulated the infusion rate only doubling the rate of infusion (to 4 mg/day) in the TERLINF group.

Results: 68% of patients were male, with median age 59 years; there were no relevant differences in age, sex, etiology of liver disease, Child-Pugh score, or baseline HVPG in the 3 groups. In OCTR group, there was a non-significant reduction in HVPG (from 20.2 to 19.2 mmHg at 120 min (–4.9%; p:0.08)). PCP significantly decreased at 120 min (from 12.4 to 10.3 mmHg, p:0.0045). No significant changes in other cardiopulmonary parameters were observed. In TERLBOL group, there was a non-significant reduction in HVPG (from 18.4 to 17.5 mmHg at 120 min, –4.9%; p:0.14). However, PAP, PCP, RAP, and mean arterial pressure significantly increased, and cardiac output and heart rate decreased within the 60–120 min of the observation. In TERLINF group, there were no significant changes in cardiopulmonary hemodynamics or HVPG despite doubling the dose after 30 min infusion in all patients. All treatments were well tolerated, and no adverse events were observed.

Conclusion: Octreotide produced a mild reduction in HVPG with no or mild systemic hemodynamic effects. A bolus administration of terlipressin also slightly reduced HVPG but with substantial changes in systemic hemodynamics. However a 2-hour continuous infusion of terlipressin did not induce significant changes in cardiopulmonary or hepatic hemodynamics. Further studies with different doses may help elucidate the optimal dosing of continuous terlipressin infusion in patients with cirrhosis and portal hypertension.

SAT-075-YI

Hemodynamic alterations and survival outcomes in cirrhotic patients with cirrhotic cardiomyopathy undergoing transjugular intrahepatic portosystemic shunt

Yaozu Liu¹, Fangmin Meng², Jingqin Ma¹, Wen Zhang¹, Zhiping Yan¹, Cuizhen Pan², Jianjun Luo¹. ¹Department of Interventional Radiology, Zhongshan Hospital, Fudan University, Shanghai, China, Shanghai, China; ²Department of Echocardiography, Zhongshan Hospital, Fudan University, Shanghai, China, Shanghai, China
Email: luo.jianjun@zs-hospital.sh.cn

Background and aims: Transjugular intrahepatic portosystemic shunt (TIPS) is a commonly used method for managing portal hypertension, effectively reducing the portal pressure gradient (PPG). However, TIPS placement results in a sudden increase in central circulating blood volume, which requires precise regulation of the cardiovascular system. The presence of cirrhotic cardiomyopathy (CCM) indicates myocardial dysfunction which may lead to adverse outcomes in patients treated TIPS. However, evidence is scarce concerning cirrhotic patients with primarily viral etiologies and those undergoing treatment with 8 mm stents. The aim of our study was to explore whether patients with CCM can adapt to acute volume expansion induced by TIPS placement and whether CCM affects patient survival after TIPS in the short term.

Method: A consecutive case series of patients with cirrhosis aged 18–65 years who underwent TIPS were prospectively studied from June 2020 and January 2022. All participants underwent comprehensive transthoracic echocardiography (TTE) prior to (within 24 hours) TIPS and 48 hours postoperatively. Right atrial pressure (RAP), inferior vena cava pressure (IVCP), and portal venous pressure gradient (PPG) were measured before TIPS stent implantation, immediately after implantation, and 48 hours postoperatively. The primary end point of the study was mortality.

Results: From June 2020 to January 2022, 107 patients were included. According to the Cirrhotic Cardiomyopathy Consortium, 38 (35.5%) patients are considered CCM. The results indicate that right atrium pressure (RAP) increased post-TIPS and returned to baseline after 48 hours in CCM patients, while patients without CCM exhibited lower RAP than baseline after 48 hours. The echocardiographic results after 48 hours postoperatively indicated elevated left ventricular filling pressures, and a notable increase in the absolute value of LV-GLS was evident within the CCM cohort. The 1-year probability of all-cause mortality for CCM and no-CCM groups were 13.2% and 4.3% (log-rank test, p = 0.093). E/e' (p = 0.014, HR 1.42, 95%CI [1.073–1.886]), MELD score (p = 0.014, HR = 2.00, 95%CI [1.148–3.497]) and preoperative RAP (p = 0.003, HR = 1.63, 95%CI [1.178–2.266]) were significantly associated with the mortality.

Conclusion: In conclusion, cirrhotic patients with CCM also exhibit an effective regulatory capacity in response to hemodynamic alterations elicited by TIPS, without adversely impacting one-year survival outcomes.

SAT-076

Patients with hepatorenal syndrome and lower baseline mean arterial pressure derive significant survival benefit from treatment with terlipressin

Paul Yien Kwo¹, Nikolaos T. Pyrsopoulos², Paul J. Thuluvath³, Sujit Janardhan⁴, Khurram Jamil⁵. ¹Stanford Health Care, Redwood City, CA, United States; ²Rutgers New Jersey School of Medicine, Newark, NJ, United States; ³Mercy Medical Center, Lutherville, MD, United States; ⁴RUSH University, Chicago, IL, United States; ⁵Mallinckrodt Pharmaceuticals, Bridgewater, NJ, United States
Email: pkwo@stanford.edu

Background and aims: Patients with decompensated liver disease may develop hepatorenal syndrome (HRS), a rapidly progressive form of acute kidney injury. The underlying liver disease can also lead to a hypotensive state. Thus, patients with HRS may present with a mean arterial pressure (MAP) below the optimal target MAP of 65 mm Hg,

used in the management of septic shock. Terlipressin, a vasopressin analogue, is used to treat patients with HRS to improve renal perfusion and kidney function. This post hoc analysis of the largest database of patients treated with terlipressin in prospective Phase III studies aimed to examine the cohort of patients with a MAP <65 mm Hg for their clinical response to terlipressin.

Method: Patient data were collated from 3 Phase III placebo-controlled studies of terlipressin in patients with HRS and rapidly deteriorating kidney function (defined as a serum creatinine ≥ 2.5 mg/dL [OT-0401, REVERSE] or ≥ 2.25 mg/dL [CONFIRM]). Baseline MAP (ie, the pre-study value) <65 mm Hg was assessed for its association with HRS reversal (defined as SCr ≤ 1.5 mg/dL on treatment, up to 24 hours after the last dose of study drug). A multivariate logistic regression analysis was used to determine the association of baseline MAP with overall survival (OS). Patients with low baseline MAP (<65 mm Hg) were assessed for HRS reversal and OS at Day 90. The proportion of patients requiring renal replacement therapy (RRT) at Days 30, 60, and 90, were also assessed.

Results: In the pooled intent-to-treat patient dataset (N = 608), patients with a baseline MAP <65 mm Hg who received terlipressin had a higher likelihood of achieving HRS reversal versus placebo (odds ratio: 4.632, 95% confidence interval [CI]: 0.956–22.448). Further, among patients with a low MAP of <65 mm Hg at baseline (terlipressin, n = 49; placebo, n = 34), significantly more patients achieved HRS reversal with terlipressin than placebo (22.4% [11/49] vs 5.9% [2/34], p = 0.041). Baseline MAP was associated with OS in the terlipressin group (odds ratio: 0.966, 95% CI: 0.947–0.986, p < 0.001). Notably, patients with low MAP (<65 mm Hg) had significant improvements in OS estimates up to 90 days in the terlipressin group (p = 0.002), with 59.2% of patients alive at Day 90 (vs 26.5% in the placebo group). The proportion of patients with low baseline MAP who received RRT was numerically higher in the placebo group, at Days 30, 60, and 90 (terlipressin vs placebo: Day 30, 28.6% [14/49] vs 47.1% [16/34], p = 0.085; Day 60, 30.6% [15/49] vs 47.1% [16/34], p = 0.128; Day 90, 34.7% [17/49] vs 47.1% [16/34], p = 0.258).

Conclusion: Patients with HRS who presented with low MAP (<65 mm Hg) at baseline derived significant benefits from terlipressin treatment, including improved renal function (eg, HRS reversal) and improvements in OS, with over half of these patients surviving at Day 90.

SAT-077

Prevention of hepatic encephalopathy after transjugular intrahepatic portosystemic shunt by live combined Bifidobacterium and Lactobacillus tablets: a randomized controlled trial

Ying Li¹, Xin Quan¹, Xiuling Ye¹, Bo Wei¹, Huan Tong¹, Zhidong Wang¹, Yang Tai¹, Linhao Zhang¹, Can Gan¹, Shuaijie Qian¹, Xu Guo¹, Hao Wu¹.

¹Department of Gastroenterology and Hepatology, West China Hospital, Sichuan University, Chengdu, China

Email: hxxhwh@163.com

Background and aims: Hepatic encephalopathy (HE) is a major complication in cirrhosis after transjugular intrahepatic portosystemic shunt (TIPS) and is closely related to gut microbiota. Efficacy of probiotics in the improvement of minimal HE (MHE) is well studied, but its effectiveness in preventing the first episode of overt HE (OHE) in patients after TIPS has not been established. We aimed to determine whether Live Combined Bifidobacterium and Lactobacillus Tablets, a commonly used probiotic preparation in China, reduce the risk of post-TIPS HE.

Method: We conducted a randomized controlled trial of 142 patients with cirrhosis receiving TIPS (ChiCTR2200062996). Patients were randomly assigned to receive probiotics (2 g three times daily) or not, lasting for 12 weeks after TIPS. The primary outcome was incidence of OHE within 24 weeks after TIPS. The secondary outcomes were the improvement of MHE [defined by number connection test-A (NCT-A)

and digit symbol test (DST)] and incidence of other cirrhosis-related complications at 24 weeks.

Results: The incidence of post-TIPS OHE was 50% in the control group (n = 70), which was significantly reduced in the probiotics group (n = 72, 34%, p = 0.044). DST was significantly worsen at 24 week compared with baseline in the control group (30.95 \pm 8.55 vs 29.34 \pm 9.31, p = 0.017). By contrast, both DST (30.46 \pm 9.95 vs 32.34 \pm 11.16, p < 0.001) and NCT-A (66.28 \pm 33.48 vs 60.63 \pm 30.89, p = 0.001) were significantly improved at 24 week in the probiotics group. There was no significant difference in other cirrhosis-related complications and survival between the two groups.

Conclusion: Live Combined Bifidobacterium and Lactobacillus Tablets reduced the risk for OHE and improved cognitive function in cirrhosis patients receiving TIPS, with good tolerance. Multicenter study should be performed to provide further evidence.

SAT-078-YI

Prospective 5-year follow-up study of spleen stiffness measurement with a spleen-dedicated module (SSM@100 Hz) for predicting hepatic decompensation in cACLD: competitive risk analysis

Luigi Colecchia¹, Federico Ravaoli¹, Elton Dajti¹, Amanda Vestito¹, Arianna Gobbato¹, Francesca Lami², Matteo Renzulli¹, Matteo Serenari¹, Francesco Azzaroli¹, Davide Festi¹, Antonio Colecchia², Giovanni Marasco¹.

¹Department of Medical and Surgical Sciences (DIMEC), University of Bologna, Bologna, Italy;

²Gastroenterology Unit, Department of Specialistic Medicines, University of Modena and Reggio Emilia, University Hospital of Modena and Reggio Emilia, Modena, Italy

Email: luigi.colecchia@studio.unibo.it

Background and aims: Liver and spleen stiffness measurements using FibroScan® (SSM@50 Hz) have been endorsed by the Baveno VII consensus to assess clinically significant portal hypertension (CSPH), which is the main driver of hepatic decompensation (HD) in patients with compensated advanced chronic liver disease (cACLD). A new, dedicated 100 Hz module for spleen stiffness measurement (SSM@100 Hz) seems to increase the clinical applicability of this technique, but there is currently no data available about its diagnostic performance for CSPH and its complications. The aim of our 5-years prospective study was to evaluate the role of the SSM@100 Hz module compared to HVPG in predicting HD in a group of patients with cACLD.

Method: In this prospective study, we included patients with cACLD who underwent paired laboratory tests, liver stiffness measurement (LSM), hepatic venous pressure gradient measurement (HVPG), and SSM@100 Hz. We used univariate and multivariate competing-risks regression analyses to evaluate the outcome, taking liver transplantation or death into account as competitive events.

Results: In this study, 69 patients were enrolled and followed until either HD or a competitive event occurred. During a median follow-up of 69 [31–105] months, 34 patients developed HD. Among the HD events, 17/69 (24.6%), 13/69 (18.8%), and 28/69 (40.6%) patients developed variceal bleeding, hepatic encephalopathy, and ascites, respectively. The results of univariate analysis revealed that SSM median value (SSM@100 Hz), male sex, metabolic etiology, presence of esophageal varices, bilirubin levels, and combined Baveno VII single cut-off rule-in criteria (by SSM@100 Hz) were independent predictors of HD. Further multivariate analysis was conducted, and two models were developed. The first model revealed that age (Hazard Ratio (HR): 0.955, 95% confidence interval: (0.918–0.994), BMI (HR: 0.794 (0.663–0.951)), a higher SSM@100 Hz value (HR: 1.05 (1.029–1.073)), higher bilirubin values (HR: 1.233 (1.108–1.371)), and MASLD (HR: 18.997 (4.486–80.449)) were independent predictive factors of HD. The second model revealed that age (HR: 0.954 (0.918–0.991)), lower BMI (HR: 0.75 (0.604–0.931)), male sex (HR: 7.178 (1.359–37.91)), MASLD (HR: 20.911 (5.639–77.547)), and a higher HVPG value (HR: 1.14 (1.018–1.288)) were predictors of HD. The two

POSTER PRESENTATIONS

models showed comparable accuracy (AUROC 0.869 and 0.868) and competitive risk regression analysis demonstrated that both models could effectively predict the risk of HD over time ($p < 0.001$ for both models).

Conclusion: The SSM@100 Hz dedicated module is an accurate predictor of hepatic decompensation and can be useful to rule out the risk of complications at 5 years in patients with compensated cirrhosis.

SAT-080-YI

Residual minimal ascites 3 months after TIPS implantation indicates risk of further decompensation and death

Lukas Hartl^{1,2}, Jim Benjamin Mauz³, Andrea Kornfehl¹, Sarah Lisa Schütte³, Paul Hemetsberger¹, Theresa Müllner-Bucsics^{1,2}, Mathias Jachs^{1,2}, Anja Tiede^{3,4}, Hannah Schneider³, Michael Schwarz^{1,2}, Bernhard Meyer⁵, Lukas Reider⁶, Maria Schoder⁶, Michael Trauner¹, Matthias Mandorfer¹, Benjamin Maasoumy^{3,4}, Tammo Lambert Tergast³, Thomas Reiberger^{1,2,7}. ¹Division of Gastroenterology and Hepatology, Department of Medicine III, Medical University of Vienna, Vienna, Austria; ²Vienna Hepatic Hemodynamic Lab, Division of Gastroenterology and Hepatology, Department of Medicine III, Medical University of Vienna, Vienna, Austria; ³Department of Gastroenterology, Hepatology, Infectious Diseases and Endocrinology, Hannover Medical School, Hannover, Germany; ⁴German Center for Infection Research (DZIF), Hannover/Braunschweig, Germany; ⁵Department of Diagnostic and Interventional Radiology, Hannover Medical School, Hannover, Germany; ⁶Division of Interventional Radiology, Department of Radiology, Medical University of Vienna, Vienna, Austria; ⁷Christian Doppler Lab for Portal Hypertension and Liver Fibrosis, Medical University of Vienna, Vienna, Austria
Email: lukas.a.hartl@meduniwien.ac.at

Background and aims: Placement of a transjugular intrahepatic portosystemic shunt (TIPS) improves control of recurrent/refractory ascites and increases survival. However, ascites may not fully resolve in all patients after the procedure and especially the impact of residual minimal ascites remains unknown. We investigated the impact of different grades of residual ascites at 3 months after TIPS placement on further clinical outcome of patients.

Method: We included patients with cirrhosis undergoing implantation of covered TIPS due to recurrent/refractory ascites in Vienna (between 2000–2022) and in Hannover (between 2013–2021). Exclusion criteria were hepatocellular carcinoma, vascular liver disease, and previous liver transplantation. Only patients with available abdominal imaging 3 months (M3) after TIPS were included and followed-up for further decompensation (paracentesis or other ascites-related complication, hepatic encephalopathy or variceal bleeding) and death starting at this time point (M3). Competing risk regression was performed considering liver transplantation and death as competing events.

Results: In total, 297 patients (71.7% male, median age 57.5 years, median MELD at M3 14) were included. Alcohol-related liver disease (71.7%) was the main etiology of cirrhosis. With TIPS implantation the median portal pressure gradient (PPG) was reduced from 18 to 7 mmHg. At M3 after TIPS implantation, $n = 106$ (35.7%) patients did not show any ascites on imaging, while $n = 84$ (28.3%) had minimal and $n = 107$ (36.0%) had moderate/severe ascites. PPG after TIPS implantation was similar in all 3 groups (median 6–7 mmHg; $p = 0.284$). Comparing the outcomes of patients with no vs. minimal ascites 3 months after TIPS, competing risk regression adjusted for age, MELD, sodium and albumin at M3 showed that minimal ascites was an independent predictor of further decompensation (adjusted subdistribution hazard ratio [aSHR]: 1.66; 95% confidence interval [95%CI]: 1.03–2.67; $p = 0.038$) and death (aSHR: 1.60; 95%CI: 1.01–2.55; $p = 0.047$). Of note, among patients with moderate/severe ascites, the 1-year-cumulative incidence of further decompensation after M3 tended to be higher than in the no or minimal ascites cohort (34.9% vs. 27.0%; $p = 0.101$) and more patients with moderate/severe

ascites at M3 underwent liver transplantation (9.4% vs. 2.7%; $p = 0.013$). Importantly, patients with moderate/severe ascites at M3 after TIPS had a significantly higher 1-year-cumulative incidence of death (26.0% vs. 9.4%; $p < 0.001$).

Conclusion: Patients with cirrhosis who still exhibit ascites 3 months after TIPS implantation have a worse clinical outcome. While moderate/severe ascites is particularly detrimental without liver transplantation, even minimal residual ascites at M3 represents an independent risk factor for further decompensation and death.

SAT-081

Association between alleviation of portal vein thrombosis and mortality rate in cirrhotic patients: a prospective cohort study

Xiaoquan Huang¹, Yingjie Ai¹, Ling Wu¹, Shiyao Chen¹. ¹Zhongshan Hospital, Fudan University, Shanghai, China
Email: huang.xiaoquan@zs-hospital.sh.cn

Background and aims: Portal vein thrombosis (PVT) is common in patients with cirrhotic patients with a history of variceal bleeding. In the present study, we aimed to investigate the influence of PVT on the endoscopic treatment for prevention of variceal re-bleeding.

Method: This study includes 625 consecutive cirrhotic patients with a history of gastroesophageal variceal bleeding and received endoscopic treatment. They were divided into the PVT group ($n = 166$) and the non-PVT ($n = 459$) group according to computer tomography angiography. Patients were follow-up to 3 years or death, and re-bleeding and mortality rates were compared between the groups.

Results: PVT group had a significantly increased 3-year all-cause mortality rate (18.8% vs. 7.6%, $p = 0.0001$) 3-year rebleeding rate (36.5% vs. 29.3%, RR 1.4, 95% CI 1.0–1.9, $p = 0.0468$) when compared to the non-PVT group. After adjusting covariates including age, Child-Pugh score, type of gastroesophageal varices, the usages of NSBBs, the increased mortality (aHR 2.5, 95% CI 1.5–4.2; $p = 0.001$) and re-bleeding rate (aHR 1.4, 95%CI 1.0–1.9; $p = 0.046$) in the PVT group persists. In patients with PVT, the alleviation of PVT was associated with a significantly lower mortality rate in 3 years (aHR 0.2, 95% CI 0.05–0.095, $p = 0.043$). And anticoagulation treatment did not increase the rebleeding rate.

Conclusion: Cirrhotic patients with PVT had a worse prognosis after endoscopic management for secondary variceal bleeding prophylaxis than patients without PVT. Anticoagulation therapy exhibited predisposition to ameliorate the prognosis without increasing the re-bleeding rate.

SAT-082

A phase 2 study of OCE-205, a novel, selective vasopressin receptor mixed agonist-antagonist: positive proof-of-concept established in subjects with cirrhosis and hepatorenal syndrome/acute kidney injury (HRS-AKI)

Andrew S. Allegretti^{1,2}, Jasmohan Bajaj³, Khurram Bari⁴, Robert S. Brown, Jr.⁵, Giuseppe Cullaro⁶, Daniel Ganger⁷, Tarek Hassanein⁸, Nyingi Kemmer⁹, Saro Khemichian¹⁰, Paul Yien Kwo¹¹, Nicholas Lim¹², Hasan Naqvi¹³, Kavish Patidar¹⁴, Nikolaos T. Pyrsopoulos¹⁵, Robert S. Rahimi¹⁶, Don Rockey¹⁷, Arun J. Sanyal^{18,19}, Kirti Shetty²⁰, Douglas Simonetto²¹, Lance Stein²², Hugo Vargas²³, Philippe Zamor²⁴, David Bernstein²⁵, Lise Kjems²⁵, Jason Lam²⁵, Susan Reid²⁵, Florence Wong^{26,27}. ¹Division of Nephrology, Department of Medicine, Massachusetts General Hospital, Boston, MA, United States; ²Harvard Medical School, Boston, United States; ³Hunter Holmes McGuire VA Medical Center, Richmond, VA, United States; ⁴UC Health-University of Cincinnati Medical Center, Cincinnati, OH, United States; ⁵Center for Liver Disease, Weill Cornell Medical Center, New York, NY, United States; ⁶University of California San Francisco, San Francisco, CA, United States; ⁷Gastroenterology and Hepatology, Northwestern University, Chicago, IL, United States; ⁸Southern California Research Center, Coronado, CA, United States;

⁹Liver Transplant Program, Tampa General Hospital, Tampa, FL, United States; ¹⁰Division of GI and Liver Diseases, Keck Hospital of University of Southern California (USC), Los Angeles, CA, United States; ¹¹Department of Hepatology, Stanford University, Stanford, CA, United States; ¹²Division of Gastroenterology, Hepatology and Nutrition, University of Minnesota, Minnesota, MN, United States; ¹³Department of Medicine, University of Missouri School of Medicine, Columbia, MO, United States; ¹⁴Section of Gastroenterology and Hepatology, Baylor College of Medicine, Houston, TX, United States; ¹⁵Department of Medicine, Rutgers New Jersey Medical School, Newark, NJ, United States; ¹⁶Transplant Hepatology, Baylor University Medical Center, Dallas, TX, United States; ¹⁷Division of Gastroenterology and Hepatology, Medical University South Carolina, Charleston, SC, United States; ¹⁸Virginia Commonwealth University (VCU) School of Medicine, Richmond, VA, United States; ¹⁹Stravitz-Sanyal Institute for Liver Disease and Metabolic Health, Richmond, VA, United States; ²⁰University of Maryland School of Medicine, Baltimore, MD, United States; ²¹Division of Gastroenterology and Hepatology, Mayo Clinic College of Medicine, Rochester, MN, United States; ²²Piedmont Transplant Institute, Atlanta, GA, United States; ²³Transplant Center, Mayo Clinic, Phoenix, AZ, United States; ²⁴Atrium Health-Carolinas Medical Center (CMC), Charlotte, NC, United States; ²⁵Ocelot Bio, Inc., Redwood City, CA, United States; ²⁶Division of Gastroenterology and Hepatology, Department of Medicine, Toronto General Hospital, Toronto, Ontario, Canada; ²⁷Faculty of Medicine, University of Toronto, Toronto, Ontario, Canada
Email: aallegretti@mg.harvard.edu

Background and aims: OCE-205 is a mixed agonist-antagonist selective for the vasopressin 1a (V1a) receptor with no vasopressin 2 (V2) receptor activity across a wide therapeutic range. It is being developed for treatment of HRS-AKI, a serious renal complication in subjects with cirrhosis, portal hypertension and ascites. The safety, pharmacokinetics (PK) and efficacy of OCE-205 were evaluated in subjects with HRS-AKI.

Method: A randomized, double-blind, placebo-controlled, dose-ranging study (ClinicalTrials.gov: NCT05309200) was conducted at 23 North American centers in subjects aged 18–75 years diagnosed with decompensated cirrhosis, ascites and HRS-AKI. Subjects received a continuous IV infusion of OCE-205 8, 15, 30 or 50 mcg/h or placebo. The primary end point was time to confirmed clinical improvement for 2 consecutive days defined as serum creatinine (SCr) <1.5 mg/dL; or if SCr was 1.5 to 1.8 mg/dL at screening, a reduction of 0.3 mg/dL.

Results: Subjects were randomized to OCE-205 (n = 37) or placebo (n = 10). Baseline characteristics were balanced across OCE-205 and placebo cohorts; mean SCr 2.6 vs 2.3 mg/dL, mean MELD score 27.9 vs 25.8, and mean total bilirubin 6.09 vs 4.35 mg/dL. The etiology of cirrhosis for OCE-205 vs placebo cohorts was MASH (29.7% vs 30.0%), alcohol (51.4% vs 60.0%), and other (18.9% vs 10.0%). PK of OCE-205 were dose proportional: clearance, half-life, and volume of distribution were 12.6 L/h, 2.6 h and 30 L, respectively. The primary end point was met in 48.6% of subjects with OCE-205 and 30.0% with placebo (p = NS). Complete response was observed in 54.5%, 54.5%, 28.6% and 50% in 8, 15, 30 and 50 mcg/h cohorts vs 30% in placebo, respectively. Partial response ($\geq 30\%$ reduction in SCr) was observed in 18.2%, 18.2%, 14.3% and 0% at OCE-205 doses of 8, 15, 30 and 50 ug/h respectively vs 10% with placebo. Mean change in MELD score was –2.3 with OCE-205 and –3.4 with placebo. In OCE-205 responders, mean arterial pressure increased (≥ 5 mm Hg) at 2 and 4 h post infusion, then decreased after stopping the infusion. Drug-related AEs occurred in 7 (18.9%) subjects with OCE-205. Drug-related bradycardia (HR <60 bpm) occurred in 6 (16.2%) subjects with OCE-205; most events were asymptomatic, requiring no intervention. No new/unexpected safety findings, no events of ischemia, and no related events of pulmonary edema, fluid overload or cardiac failure occurred.

Conclusion: OCE-205 was well tolerated, with no evidence of excessive vasoconstriction and no ischemic AEs, and no related

events of pulmonary edema or serious infections, at any dose level. OCE-205 had a predictable, capped maximal efficacy that was effective in reversing HRS-AKI in more patients than placebo. OCE-205 carries great promise to become a novel HRS therapy with a favorable risk/benefit profile.

SAT-083-YI

Changes in mean arterial pressure are inadequate to guide treatment with terlipressin and albumin in patients with hepatorenal syndrome-acute kidney injury

Valeria Calvino¹, Anna Barone¹, Marta Tonon¹, Carmine Gambino¹, Simone Incicco¹, Roberta Gagliardi¹, Nicola Zeni¹, Paolo Angeli¹, Salvatore Piano¹. ¹Unit of Internal Medicine and Hepatology, Department of Medicine, University and Hospital of Padova, Padova, Italy

Email: salvatore.piano@unipd.it

Background and aims: Terlipressin and albumin are the first-line treatment of hepatorenal syndrome (HRS-AKI). Terlipressin is titrated according to changes in serum creatinine (SCr) on Day-3. An increase in mean arterial pressure (MAP) was associated with resolution of HRS-AKI, leading some experts to suggest titration of terlipressin according to MAP changes. However, the optimal MAP targets remain unclear. The aim of this study was to evaluate the association between MAP changes on Day-3 and response to treatment with terlipressin and albumin in patients with HRS-AKI.

Method: Patients with cirrhosis and HRS-AKI treated with terlipressin and albumin as continuous infusion were identified. Clinical and biochemical data, including MAP, were collected on Day-0 and Day-3. Patients were followed up until death, liver transplantation or up to 90 days. The primary end point was response to treatment (i.e. SCr <1.5 mg/dL). Death and transplant were considered competing risks for response to treatment. Secondary end points were early response (i.e. reduction of SCr > 25% vs Day-0 on Day-3) and 90-day mortality. **Results:** We enrolled 108 patients (mean age = 59 ± 9 years; male = 70%; MELD = 29 ± 7; alcohol related cirrhosis = 58%). On Day-3 most of patients had an increase in MAP (delta MAP = 5.6 ± 11.5 mmHg; p < 0.001). Response to treatment was found in 56 patients (52%). Delta MAP on Day-3 was not significantly different between responders and non-responders (7.8 vs 4.4 mmHg; p = 0.218). Delta MAP on day-3 was not significantly different between early responders and non-responders (5.3 vs 6.0 mmHg; p = 0.751). Responders had lower baseline SCr (2.91 vs 2.51 mg/dL; p = 0.016) and higher rate of precipitating factors of HRS-AKI (61 vs 38%; p = 0.007). In multivariable analysis (adjusted for age, precipitating factors, baseline SCr and ACLF grade) delta MAP on Day-3 was not significantly associated with response to treatment (sHR = 1.00; p = 0.870). Lower baseline SCr (sHR = 0.75; p = 0.012) and precipitating factors of HRS-AKI (sHR = 1.89; p = 0.014) were independent predictors of response. Delta MAP on Day-3 was not associated with 90-day mortality (sHR = 0.99; p = 0.530). The risk of 90-day mortality was significantly lower in responders than in non-responders (sHR = 0.45; p = 0.004).

Conclusion: Delta MAP on Day-3 was not associated with response to treatment with terlipressin and albumin. These findings do not support the use of MAP changes on Day 3 for titrating the dose of terlipressin in patients with HRS-AKI.

SAT-086-YI

Assessment of portal hypertension risk by liver and spleen stiffness using real-time 2D-shear wave elastography-the prospective AiXplore study

David Bauer^{1,2,3}, Mathias Jachs^{1,2,4}, Lukas Hartl^{1,2,4}, Michael Schwarz^{1,2}, Lorenz Balcar^{1,2,4}, Benedikt Hofer^{1,2,4,5}, Nina Dominik^{1,2,4}, Bernhard Scheiner^{1,2,4}, Albert Friedrich Stättermayer^{1,2}, Benedikt Simbrunner^{1,2,4,5}, Rafael Paternostro^{1,2}, Till Schöchtner¹, Friedrich Haimberger¹, Nicolas Balutsch¹, Michael Trauner¹, Mattias Mandorfer^{1,2,4}, Thomas Reiberger^{1,2,4,5}. ¹Division of Gastroenterology and Hepatology,

POSTER PRESENTATIONS

Department of Medicine III, Medical University of Vienna, Vienna, Austria; ²Vienna Hepatic Hemodynamic Lab, Division of Gastroenterology and Hepatology, Department of Medicine III, Medical University of Vienna, Vienna, Austria; ³IV. Department of Internal Medicine for Gastroenterology and Hepatology, Klinik Ottakring, Vienna, Austria; ⁴LBG clinical research group MOTION, Medical University of Vienna, Vienna, Austria; ⁵Christian-Doppler Laboratory for Portal Hypertension and Liver Fibrosis, Medical University of Vienna, Vienna, Austria

Email: david.bauer@meduniwien.ac.at

Background and aims: Liver (LSM) and spleen (SSM) stiffness measurement using real-time 2D-shear wave elastography (2D-SWE) present as promising non-invasive tests (NITs) for estimating the risk of clinically significant portal hypertension (CSPH), defined as a hepatic venous pressure gradient (HVPG) of ≥ 10 mmHg.

Method: In the prospective AiXplore study, patients with chronic liver disease underwent concurrent measurements of HVPG and real-time 2D-shear wave elastography (2D-SWE) on the Aixplorer Ultimate device. We applied reliability criteria of IQR/Med ≤ 0.30 for 2D-SWE-LSM and median SD of single measurements < 15 kPa for 2D-SWE-SSM. The Pearson correlation of LSM and SSM with HVPG was calculated, and their diagnostic accuracies for CSPH were assessed using receiver operator characteristics analysis (AUC).

Results: Of 366 patients with combined LSM, SSM, and HVPG measurements (66.4% men, median age: 56.5 [IQR: 48.0–64.0] years, median HVPG: 15.0 [10.0–19.0] mmHg) 77.9% and 46.4%, respectively, showed CSPH or HVPG ≥ 16 mmHg. Median 2D-SWE LSM was 38.5 [19.9–60.9] kPa and 269 patients (68.0%) had LSM ≥ 25 kPa. Median SSM was 55.3 [38.3–72.3] kPa and 212 (57.9%) had SSM ≥ 50 kPa. 278 LSM (77.0%) and 256 (69.9%) SSM met the reliability criteria. The Pearson R for HVPG and LSM was 0.53 overall, increasing to 0.59 for reliable LSM; for HVPG, and SSM, it was 0.43, rising to 0.52 in reliable SSM (all $p < 0.001$). The AUC for CSPH was 0.83 (CI95%: 0.77–0.89) for LSM and 0.77 (0.71–0.83) for SSM, increasing to 0.88 (0.82–0.94) and 0.82 (0.75–0.89) for reliable LSM and SSM, respectively. The 90%-specific rule-in and 90%-sensitive rule-out cutoffs for CSPH were ≥ 27.0 kPa and < 18.0 kPa for LSM, and ≥ 52.0 kPa and < 30.0 kPa for SSM, respectively. In patients with both LSM ≥ 25 kPa and SSM ≥ 50 kPa the observed prevalence of CSPH was 98.1% (101/103), while in patients with both LSM < 18 kPa and SSM < 30 kPa, the observed CSPH prevalence was 11.5% (3/26). This algorithm left a grey zone of 37.4% (77/206) of patients.

Conclusion: For 2D-SWE-SSM median SD < 15 kPa seems useful as a reliability criterion. 90% -specific/sensitive 2D-SWE LSM/SSM cut-offs for CSPH assessment were calculated. A clinical algorithm based on 2D-SWE LSM > 25 and SSM > 50 kPa can rule-in and 2D-SWE LSM < 18.0 and SSM < 30.0 kPa can rule-out CSPH.

SAT-087-1Y

The presence of NOD2 risk variants is associated to a higher incidence of first decompensation in patients with cirrhosis and varices

Henrik Karbannek¹, Matthias Reichert², Robin Greinert³, Alexander Zipprich¹, Frank Lammert⁴, Cristina Ripoll¹. ¹Department of Internal Medicine IV, Jena University Hospital, Jena, Germany; ²Department of Internal Medicine II Saarland University Hospital, Homburg, Germany; ³Department of Internal Medicine I, Martin Luther University Halle-Wittenberg, Halle, Germany; ⁴Hannover Medical School (MHH), Hannover, Germany
Email: henrik.karbannek@icloud.com

Background and aims: NOD2 mutations are associated with an impaired gut mucosal barrier function. Prevalence of NOD2 risk variants is higher in patients with cirrhosis than in the general population. According to the systemic inflammation hypothesis, bacterial translocation plays a major role in the development of decompensation. Previous studies indicated that the presence of NOD2 variants modulates the development of infection in

compensated rather than decompensated cirrhosis (PMID 30702490). The aim was to evaluate whether the presence of NOD2 variants is associated with the development of first decompensation in compensated cirrhosis.

Method: Secondary analysis of a prospectively collected database (n = 1000) of consecutive patients with cirrhosis, who were screened for the randomized controlled INCA trial (EudraCT 2013-001626-26) at two academic medical centers between 2014 and 2019. Only patients with previously compensated disease were included in this analysis. Patients were followed up until the first decompensation, as defined by the development of ascites, variceal bleeding, or hepatic encephalopathy. Patients with and without NOD2 variants were compared. Stratified analysis according to the presence or absence of varices was performed. Univariate and multivariate Cox regression analysis was performed.

Results: Overall, 360 patients [239 (66%) men, median age 61 (53–69) years, 70 (19%) with NOD2 variants, 90 (25%) with varices] were followed for a median of 9 (4–16) months. No differences were observed in baseline characteristics between groups according to NOD2 status, except for the use of beta-blockers (45% vs. 32% among NOD2 variant carriers and non-carriers, respectively). During follow-up, 34 patients (12%) developed their first decompensation. There were no differences in the incidence of first decompensation during follow-up according to NOD2 status [HR 1.75 (95%CI 0.84–3.67)]. On multivariate analysis with beta-blockers, MELD, NOD2 variants and varices, only MELD remained an independent predictor. Stratified analysis was performed given the association between varices and decompensation. Among the 90 patients with varices, 18 (24.4%) carried a NOD2 variant. These patients had greater incidence of first decompensation [HR 3.00 (95%CI 1.08–8.32)], determined mainly by a higher incidence of ascites [HR 3.32 (1.07–10.32)] during follow-up as compared to patients with varices without a NOD2 variant. On multivariate analysis in the subgroup with varices, MELD [1.18 (95%CI 1.06–1.32)] and NOD2 variants [2.91 (95%CI 0.95–8.89)] variants were independent predictors of decompensation.

Conclusion: The presence of NOD2 risk variants leads to a greater incidence of first decompensation in compensated patients with varices. This observation could guide individualized strategies for the prevention of complications in cirrhosis.

SAT-088

Safety and Efficacy of the Natriuretic Peptide Ularitide in Refractory Cirrhotic Ascites: Interim Analysis of a Randomized Controlled Trial

Rasmus Gantzel^{1,2,3}, Emilie Møller¹, Niels Kristian Aagaard¹, Hugh Watson⁴, Peter Jepsen^{1,2}, Henning Grønbaek^{2,5}. ¹Department of Hepatology and Gastroenterology, Aarhus University Hospital, Aarhus N, Denmark; ²Department of Clinical Medicine, Aarhus University, Aarhus, Denmark; ³Department of Medicine, Regional Hospital Gødstrup, Herning, Denmark; ⁴Evotec ID, Medical Development and Translational Sciences, Lyon, France; ⁵Department of Hepatology and Gastroenterology, Aarhus University Hospital, Aarhus N, Denmark
Email: ragant@rm.dk

Background and aims: Refractory ascites denotes the most severe ascites status in patients with cirrhosis and portal hypertension. The condition develops as dietary and medical treatments are ineffective or induce intolerable side effects. Therefore, new treatments are warranted for refractory ascites, and we here investigate the efficacy and safety of the natriuretic peptide ularitide in patients with refractory cirrhotic ascites.

Method: We conducted a randomized, placebo-controlled clinical trial using a continuous intravenous infusion of ularitide to manage refractory ascites. We randomized 17 participants in a 2:1 ratio between ularitide (n = 11) and placebo (n = 6). While hospitalized and closely monitored, the participants received the treatment for up to 48 hours as an add-on to any habitual diuretic treatment. The dose regimen allowed individualization of the therapy according to renal

responsiveness and safety. The primary efficacy end point was change in renal water excretion and the main secondary end points were changes in renal sodium excretion rate and body weight. Initially, all participants started with a 30 ng/kg/min dose. However, the starting dose was reduced to 20 ng/kg/min halfway through the trial period because of safety concerns.

Results: The background characteristics were similar for participants randomized to ularitide and placebo. The urine volume decreased after 24 hours of ularitide treatment compared with the baseline level ($p=0.04$) and decreased more in patients randomized to ularitide than placebo ($p=0.06$). There was no effect of ularitide on renal sodium excretion rate or body weight change compared with placebo ($p=0.20$ and $p=0.65$). The participants treated with ularitide developed significant reductions in systolic blood pressure and the incidence rate ratio of adverse reactions in ularitide vs. placebo was 8.5 (95% CI: 2.0–35, $p=0.003$).

Conclusion: Ularitide in doses of 30 and 20 ng/kg/min did not show clinically meaningful effects on urine volume and renal sodium excretion rate after 24 hours of continuous intravenous infusion. The participants randomized to ularitide developed significant reductions in blood pressure and had more adverse reactions compared with placebo. Further studies are needed to clarify the optimal dose and treatment regimen of ularitide in patients with refractory ascites.

SAT-089

Evaluating the correlation between portal pressure, collagen proportional area, and α -smooth muscle actin in patients with portal hypertension due to MASH cirrhosis

Pol Boudes^{1,1}, Michael Inkmann¹, Seth Zuckerman¹. ¹*Galectin Therapeutics, Norcross, United States*
Email: pfbcmo@gmail.com

Background and aims: In liver cirrhosis, the evaluation of the amount of collagen on histology is of interest as it is related to the pathophysiology of the disease. The Kleiner/Brunt and Ishak staging of fibrosis are frequently used in liver diseases but in cirrhotic patients they lack granularity to evaluate disease prognosis or response to treatment. The collagen proportional area (CPA), the amount of tissue that is occupied by collagen could address this shortfall. Similarly, α -smooth muscle actin (α -SMA), an indicator of stellate cells activation, and its proportional area could provide further pathophysiologic information. We studied patients with compensated cirrhosis due to Metabolic-dysfunction Associated SteatoHepatitis (MASH) and portal hypertension (PH) to evaluate the correlation between CPA, α -SMA, and portal pressure estimated by the hepatic venous pressure gradient (HVPG).

Method: The population consisted of patients with MASH cirrhosis (NCT02462967). Cirrhosis was confirmed by liver histology (Ishak 5 or 6, Brunt F4). Patients had no current or recent history of alcohol consumption and no cirrhotic decompensation (varix bleeding, ascites, encephalopathy). Data were collected at time of eligibility. PH was evaluated hemodynamically and HVPG was required to be >6 mm Hg. The collagen proportional area was evaluated with trichrome staining and represented the surface of biopsy tissue occupied by collagen divided by the total amount of tissue, expressed as a %. α -SMA was evaluated with a specific immuno-staining and expressed the same way. Descriptive statistics, mean, standard deviation (SD), and ranges are provided as well as correlation between CPA, α -SMA, and HVPG.

Results: The population consisted of 162 patients. The mean age was 58.2 (8.4), 70% were females. All patients were Brunt F4, and most (70.4%) Ishak 6. The mean (SD) CPA was 10.6 (6.1), range 1 to 29%. The mean (SD) α -SMA was 14.2 (10.8), range 1 to 58%. The mean (SD) HVPG was 12.2 (4.2), range 6 to 27.5 mm Hg. CPA was moderately correlated with α -SMA (R^2 0.427). Neither CPA nor α -SMA were correlated with HVPG, R^2 0.023 and 0.020, respectively.

Conclusion: In this well-defined cohort of patients with PH and compensated MASH cirrhosis while the collagen proportional area

and the α -smooth muscle actin were somewhat correlated, neither of these parameters were correlated with portal pressure (HVPG), a major indicator of disease prognosis.

SAT-090-YI

Improvement of liver frailty, hand grip strength and mid-upper arm circumference in cirrhotic patients after TIPS insertion

Martin Kabelitz¹, Anja Tiede^{1,2}, Hannah Schneider¹, Jim Benjamin Mauz¹, Alena Friederike Ehrenbauer¹, Liv Grete Ahl¹, Lea Wagner¹, Heiner Wedemeyer^{1,2,3}, Benjamin Maasoumy^{1,2}, Lisa Sandmann^{1,3}. ¹*Department of Gastroenterology, Hepatology, Infectious Diseases and Endocrinology, Hannover Medical School, Hannover, Germany;* ²*German Center for Infection Research (DZIF), Hannover/Braunschweig, Germany;* ³*Excellence Cluster RESIST, Excellence Initiative Hannover Medical School, Hannover, Germany*
Email: Kabelitz.Martin@mh-hannover.de

Background and aims: Frailty and sarcopenia are highly prevalent in patients with liver cirrhosis and clinically significant portal hypertension. Moreover, they are associated with an increased risk of hepatic decompensation and reduced quality of life. So far, data on frailty following transjugular intrahepatic portosystemic shunt (TIPS) placement is lacking. Our study aims to investigate the effects of TIPS insertion on frailty and sarcopenia.

Method: From 2019 to 2023, we prospectively enrolled 190 patients who underwent TIPS insertion at Hannover Medical School. A structured follow-up (FU) with outpatient visits at one, three, six, and 12 months after TIPS insertion was conducted. Frailty was assessed using the "Liver Frailty Index" (LFI) categorizing patients into "frail," "pre-frail," and "robust" groups. Hand grip strength (HGS) and mid-upper arm circumference (MUAC) were measured using anthropometric instruments. FU time points were combined into early follow-up (EFU, combining FUs at one and three months) and late follow-up (LFU, combining FUs at six and 12 months). Statistical analyses were performed using paired t-tests and McNemar's test, with p values adjusted using the Bonferroni-Holm method.

Results: A total of 130 patients qualified for the final analysis after excluding cases with Budd-Chiari syndrome, absence of cirrhosis, HCC outside the Milan criteria, or insufficient baseline data on HGS, MUAC or LFI. Patients were predominantly male (65%) with a median MELD score of 11 (IQR 9–14). The main indication for TIPS placement was refractory ascites (70%). At baseline (BL), mean HGS and MUAC were 24.3 ± 9.7 kg and 25.8 ± 5 cm, with 43% and 70% of patients showing abnormal parameters, respectively. After TIPS insertion, HGS improved significantly from BL to LFU (25.4 ± 10.4 kg vs. 28.4 ± 11 kg, $p=0.005$). Similarly, MUAC increased significantly from BL to EFU (25.7 ± 4.8 cm vs. 26.5 ± 4.4 cm, $p=0.002$) and from BL to LFU (26.1 ± 4.4 cm vs. 28.7 ± 4.9 cm, $p<0.001$). At BL, 44%, 50% and 6% of patients were classified as "frail," "pre-frail," and "robust" by LFI, respectively. After TIPS insertion, overall mean numerical LFI did not change from BL to EFU or LFU. However, numerical LFI of "frail" patients improved from BL to EFU (5.31 ± 0.69 vs. 4.79 ± 0.85 , $p=0.005$) and from BL to LFU (5.08 ± 0.55 vs. 4.38 ± 0.65 , $p=0.03$). Overall, the proportion of "frail" patients significantly decreased from BL to EFU (47% to 36%, $p=0.04$) and LFU (48% to 19%, $p=0.03$). No significant differences were found between "frail" patients at BL who did or did not show improvement of frailty during follow-up, while frailty at BL was the only identified risk factor for frailty at EFU.

Conclusion: TIPS insertion has the potential to improve frailty, HGS and MUAC. Furthermore, our results suggest that individuals with a high degree of frailty benefit most. This should be considered for patient selection.

POSTER PRESENTATIONS

SAT-092-YI

The Toulouse algorithm identifies patients with an increased risk of cardiac decompensation only in patients with TIPS for refractory ascites

Emma Vanderschueren^{1,2}, Youri Bekhuis³, Jan Clerick¹, Philippe Meersseman⁴, Alexander Wilmer⁴, Eveline Claus⁵, Lawrence Bonne⁵, Guido Claessen⁶, Chris Verslype¹, Geert Maleux⁵, Wim Laleman^{1,2}. ¹Department of Gastroenterology and Hepatology, University Hospital Leuven, Leuven, Belgium; ²Department of Chronic Diseases, Metabolism and Aging (CHROMETA), Catholic University of Leuven, Leuven, Belgium; ³Department of Cardiology, University Hospital Leuven, Leuven, Belgium; ⁴Department of General Internal Medicine, Medical Intensive Care Unit, University Hospital Leuven, Leuven, Belgium; ⁵Department of Radiology, Interventional Radiology, University Hospital Leuven, Leuven, Belgium; ⁶Department of Cardiology, Jessa Hospital Campus Virga Jesse, Hasselt, Belgium
Email: emma.vanderschueren@student.kuleuven.be

Background and aims: Transjugular intrahepatic portosystemic shunt (TIPS) placement is an effective, possibly life-saving, treatment for complications of portal hypertension. The pressure shift induced by the stent can lead to the development of cardiac decompensation (CD) in some cases. We investigated the incidence of CD, possible variables associated with CD and the validity of the Toulouse algorithm for risk prediction of CD post-TIPS.

Method: All patients receiving TIPS for variceal bleeding (VB) or refractory ascites (RA) between 2011 and 2021 were retrospectively reviewed. A total of 106 patients (41.5% VB, 58.5% RA) had echocardiography and NT-proBNP results available and were included. Development of CD between time of TIPS placement and occurrence of liver transplantation, death or loss-to-follow-up was recorded. Competing risk regression analysis was performed to assess which baseline variables predicted occurrence of CD post-TIPS.

Results: A total of 12 patients (11.3%) developed CD after a median of 11.5 days (IQR 4 to 56.5) post-TIPS. Patients who developed CD were significantly older than patients who did not (66.8 vs 59.8 years old, $p = 0.045$). Other baseline parameters were not significantly different, specifically active alcohol abuse, MELD score, Child-Pugh score, pressure gradients before and after TIPS, NT-proBNP and echocardiographic parameters were similar. Multivariate regression showed age (HR 1.06, CI 1.01–1.11, $p = 0.019$), albumin (HR 1.10, CI 1.03–1.18, $p = 0.009$) and NT-proBNP (for every 100 ng/L increase HR 1.04, CI 1.00–1.07, $p = 0.023$) predicted CD in the RA group. No clear predictors were found in those receiving TIPS for VB. Correspondingly, the Toulouse algorithm successfully identified patients at risk for CD, however only in the RA population (zero risk 0% vs. low risk 12.5% vs. high risk 35.3% with CD; $p = 0.003$). CD post-TIPS was well managed with diuretics in most cases and did not lead to increased mortality in our series (1-year mortality 44.7% without CD vs. 33.3% with CD, $p = 0.455$).

Conclusion: CD is not an infrequent complication post-TIPS occurring in 1/10 patients and mostly in the first month post-TIPS. The Toulouse algorithm can identify patients at risk of CD, though only in patients receiving TIPS for RA. Allocation to the high-risk category warrants close monitoring but should not preclude TIPS placement.

SAT-093-YI

Sustainable endoscopy in hepatology: quantifying the effect of applying BAVENO VII guidelines on the endoscopic carbon footprint; a multi-centred regional assessment

Dylan Angel¹, Sanjayan Anandanadarajah², Mohannad Alqedhr³, Saad Butt², Ayman Elkholi³, Noam Pinchas Gessler Roth⁴, Emily Kooner⁵. ¹East and North Hertfordshire Trust, Stevenage, United Kingdom; ²Queen Elizabeth Hospital Kings Lynn, Kings Lynn, United Kingdom; ³Norfolk and Norwich University Hospital, Norwich, United Kingdom; ⁴Mid and South Essex NHS Foundation Trust, London, United Kingdom; ⁵East and North Hertfordshire NHS Trust, Stevenage, United Kingdom
Email: dylan.angel@nhs.net

Background and aims: With the global move towards net zero, the UK NHS has committed to reduce its carbon footprint by 80% between 2028–2033 and achieve net zero by 2040 [1]. Endoscopy is the third greatest contributing department per daily bed occupied [2], therefore re-evaluation of endoscopic indications is an important factor in achieving net zero. The Baveno VII guidelines recommend that patients with compensated cirrhosis and Fibroscan scores of less than 20 kPa and platelet counts greater than $150 \times 10^9/L$ are unlikely to have clinically significant varices [3], thereby negating the need for endoscopic surveillance. By applying these guidelines in conjunction with estimated energy costs from previously published data [4], we aimed to retrospectively calculate the regional endoscopic carbon footprint generated by potentially avoidable gastroscopies across four NHS trusts with access to Fibroscan.

Method: In this retrospective study, data was analysed from four hospitals in the East of England. Patients undergoing primary variceal surveillance between January 2021 and October 2023 were identified and their pre-endoscopy Fibroscan results and platelet counts were assessed against the criteria listed in Baveno VII. Exclusion criteria comprised features of decompensation, previous variceal haemorrhage or portal- or splenic vein thrombosis. We defined Baveno VII non-compliance as having both Fibroscan and platelet data available but not meeting the required cut offs, or only having a platelet count available above $150 \times 10^9/L$. Patients with no Fibroscan data and a platelet count less than $150 \times 10^9/L$ were deemed indeterminate. Use of water, mass and energy costs per procedure were estimated using previously published data.

Results: 730 patient records meeting eligibility criteria were analysed. 45% ($n = 330$) of procedures were Baveno non-compliant. Of these 330 patients, 38% ($n = 126$) had pre endoscopy Fibroscan and platelet data available but did not fulfil Baveno criteria whilst 62% ($n = 204$) patients underwent endoscopy without Fibroscan and with platelet count above $150 \times 10^9/L$. During the study dates, these 330 procedures generated approximately 37620 L of water and 78 kg of plastic waste. This totalled a carbon cost of 1657 KgCO_{2e}.

Conclusion: The exact carbon cost of a single gastroscopy has yet to be determined, however, our data which is likely to represent a significant underestimate, demonstrates that if used correctly and extrapolated on a larger scale, Baveno VII could rationalise and reduce the significant burden generated by endoscopy.

SAT-094-YI

Mild overt hepatic encephalopathy (HE)-more than meets the eye

Davide Erminelli¹, Chiara Mangini¹, Lisa Zarantonello², Paolo Angeli¹, Sara Montagnese^{1,3}. ¹Department of Medicine, University of Padova, Padova, Italy; ²Department of Medicine, University of Padova, Padova, Italy; ³Chronobiology Section, Faculty of Health and Medical Sciences-University of Surrey, Guildford, United Kingdom
Email: sara.montagnese@unipd.it

Background and aims: The diagnosis of covert/mild overt HE remains a matter of debate. While practices are becoming more homogeneous, the semi-quantitative assessment of overt HE is not necessarily performed, and the interpretation of results when different neuropsychiatric tests are utilized remains poorly defined. The aim of the present study was to assess the impact of a qualitative approach to clinical HE diagnosis, and to describe the features of patients being diagnosed with covert HE on abnormalities in either the Psychometric Hepatic Encephalopathy Score (PHES) or the electroencephalogram (EEG).

Method: 411 patients evaluated in our dedicated HE clinic between April 2009 and June 2023 [292 males (71%), 60 ± 10 years, MELD = 14.4 ± 5.9 , MELD-Na 18.6 ± 16.1] were included. Patients were qualified as: 1) unimpaired, when they were clinically normal and both the PHES and the EEG were normal; 2) having covert HE when they were clinically normal but the PHES and/or the EEG were abnormal, or 3) having overt HE based on the semi-quantitative modification of Conn's criteria (Vilstrup et al., J Hep 2014). Patients

were also classified as having/not having overt HE based on a qualitative impression of the clinician, prior to any formal assessment.

Results: 137 (33%) patients were unimpaired, 174 (42%) had covert HE and 100 (25%) overt HE; 122 (30%) were qualified as having overt HE on qualitative assessment. Of the 100 patients with overt HE, 30% were missed on qualitative assessment. In addition, 17% unimpaired/covert HE patients were erroneously qualified as having overt HE on qualitative assessment. Across the HE spectrum, patients with an abnormal EEG were older (61.5 ± 9.1 vs 58.1 ± 10.3 , $p < 0.001$), had higher MELD (15.8 ± 6.1 vs 12.8 ± 5.2 , $p < 0.001$), higher MELD-Na (21.2 ± 18.9 vs 16.1 ± 13.7 , $p < 0.01$) and higher ammonia levels (76.2 ± 43.6 vs 54.9 ± 41.6 $\mu\text{mol/l}$, $p < 0.001$) compared with their counterparts with normal EEG. Patients with an abnormal PHES were older (60.8 ± 9.3 vs 58.9 ± 10.0 , $p < 0.05$), had lower educational attainment (9.0 ± 3.3 vs 10.6 ± 4.1 years, $p < 0.0001$), higher MELD (15.7 ± 6.4 vs 13.4 ± 5.3 , $p < 0.001$), higher MELD-Na (22.0 ± 20.0 vs 16.3 ± 12.5 , $p < 0.01$) and higher ammonia levels (70.9 ± 48.1 vs 59.7 ± 38.9 $\mu\text{mol/l}$, $p < 0.05$) compared with their counterparts with normal PHES. Amongst patients with covert HE diagnosed on one abnormal test only, those with abnormal PHES had lower educational attainment compared to those with abnormal EEG (8.2 ± 3.1 vs 10.2 ± 4.1 years, $p < 0.002$).

Conclusion: Qualitative clinical evaluation of mild HE is unreliable, with significant proportions of false negatives and, unexpectedly, also false positives. The EEG and PHES work well in this context, with both being affected by age, and PHES also by educational attainment, despite adjustment based on local norms.

SAT-095

Trial of the establishment of shear wave elastography measurement methods for improvement of versatility

Hidemi Unozawa¹, Takayuki Kondo¹, Kentaro Fujimoto¹, Sae Yumita¹, Kisako Fujiwara¹, Keisuke Koroki¹, Masanori Inoue¹, Kazufumi Kobayashi¹, Soichiro Kiyono¹, Naoya Kanogawa¹, Masato Nakamura¹, Sadahisa Ogasawara¹, Shingo Nakamoto¹, Naoya Kato¹. ¹Graduate School of Medicine, Chiba University, Chiba, Japan
Email: unozawa.hidemi@chiba-u.jp

Background and aims: Liver stiffness measurement using ultrasound is widely used to understand the pathophysiology of liver diseases due to its low invasiveness and simplicity. Although various devices have been used to measure liver stiffness, and the results of shear wave elastography (SWE) may depend on how the region of interests (ROIs) at placed, and there are no clear standards on how to place ROIs. In this study, we investigated the correlation between FibroScan and clinical and the intraclass correlation coefficient (ICC) between FibroScan and SWE to establish a measurement method of SWE.

Method: This retrospective study included 215 patients from our institutual database, who underwent abdominal ultrasonography for liver disease and had FibroScan and SWE at the same site on the same day. Correlation between liver reserve function and FibroScan was analyzed. In addition, the correlation between the waveform of the right hepatic vein. The ICC between FibroScan and SWE was analyzed in patients with or without cirrhosis, ascites, and fatty liver. The definition of fatty liver was based on the Controlled Attenuation Parameter value, and fatty liver was defined as 240 dB/m . To determine the optimal area of treatment in SWE, ROIs of 1 cm^2 were placed at 1 cm, 2 cm, and 3 cm from the liver surface, and the units of measurement were nified as kPa.

Results: Correlation between FibroScan and clinical findings. The FibroScan reading increased significantly with decreased hepatic function ($r = 0.555$, $p < 0.001$). The correlation coefficient between the right hepatic vein and FibroScan was -0.267 ($p < 0.001$). As the values of Fibroscan increased, the waveform of the right hepatic vein changed from 3-phase wave to 2-phase wave to 1-phase wave.

Conformity between FibroScan and SWE. The ICCs between FibroScan and SWE were -0.050 ($p = 0.638$), 0.845 ($p < 0.001$), and 0.762 ($p < 0.001$) for 1 cm, 2 cm, and 3 cm, and especially the values of shear wave at 2 cm was significantly consistent with FibroScan. Stratifying into various groups the ICCs were -0.231 ($p = 0.892$)/ -0.382 ($p = 0.932$) for 1 cm, 0.808 ($p < 0.001$)/ 0.897 ($p < 0.001$) for 2 cm, and 0.709 ($p < 0.001$)/ 0.835 ($p < 0.001$) for 3 cm in patients with cirrhosis/without, $(0.216 [p = 0.190]/-0.249 [p = 0.919])$ for 1 cm, $0.847 [p < 0.001]/0.816 [p < 0.001]$ for 2 cm, $0.718 [p < 0.001]/0.741 [p < 0.001]$ for 3 cm in patients with ascites/without, $0.146 [p = 0.252]/-0.274 [p = 0.913]$ for 1 cm, $0.872 [p < 0.001]/0.831 [p < 0.001]$ for 2 cm, $0.813 [p < 0.001]/0.718 [p < 0.001]$ for 3 cm in patients with fatty liver/without), with the measurement at 2 cm from liver surface showing the most consistency.

Conclusion: SWE at 2 cm from the liver surface showed the highest conformity with FibroScan, which may help in the establishment of future measurement methods in SWE.

SAT-098

Prognostic factor which can predict esophageal varices aggravation after plug-assisted retrograde transvenous obliteration (PARTO)

Chan Jin Yang¹, Jeong-Ju Yoo¹, Sang Gyune Kim¹, Young Seok Kim¹, Hong Soo Kim², Gab Jin Cheon³, Jong Joon Shim⁴, Jae Myeong Lee⁴. ¹Division of Gastroenterology and Hepatology, Department of Internal Medicine, Soonchunhyang University Bucheon Hospital, Bucheon, Korea, Rep. of South; ²Soonchunhyang University College of Medicine Cheonan Hospital, Cheonan, Korea, Rep. of South; ³Department of Internal Medicine, Gangneung Asan Hospital, University of Ulsan College of Medicine, Gangneung, Korea, Gangneung, Korea, Rep. of South; ⁴Department of Radiology, Soonchunhyang University Bucheon Hospital, Bucheon, Korea, Bucheon, Korea, Rep. of South
Email: liverkys@schmc.ac.kr

Background and aims: Plug-assisted retrograde transvenous obliteration (PARTO) is known to be an effective treatment for gastric varices. However, it is also known that it worsens esophageal varices after PARTO. The aim of this study is to identify prognostic factors which can predict the worsening of esophageal varices after PARTO in patients with gastric varices.

Method: Ninety-nine patients who underwent PARTO between Jun 2015 and Jan 2023 were enrolled in this study. Esophageal varices and their exacerbation were evaluated by esophagogastroduodenoscopy (EGD).

Results: Of the 99 patients, 74 patients who could confirm the change in esophageal varix with EGD performed after PARTO were analyzed. The mean age of patients were 57.9 ± 9.9 years and 64.9% were male. Most common etiology of liver cirrhosis was alcoholic liver disease (40.5%) followed by hepatitis B virus (28.4%). The cumulative worsening rate of esophageal varices at 1, 2, and 3 years were 32.4%, 48.6% and 50.0%. In the univariate logistic regression analysis, total bilirubin, aspartate aminotransferase, albumin, prothrombin time international normalized ratio, previous hepatic vein pressure gradient (HVPG) which measure before PARTO, post HVPG which measure after PARTO, MELD score, Child-Pugh class were associated with worsening of esophageal varices after PARTO. Additionally, from the perspective of vascular anatomy, left gastric vein (LGV) dilatation which LGV diameter more than 3.55 mm and type 2 gastric varix according to the Saad-Caldwell classification were also associated with worsening of esophageal varices after PARTO. In multivariate logistic regression analysis, previous HVPG (OR 1.172; 95% CI 1.011–1.358; $p = 0.035$) was independent risk factor of worsening of esophageal varices.

Conclusion: HVPG is associated with esophageal varices aggravation after PARTO. The left gastric vein diameter tended to predict EV exacerbation after PARTO.

SAT-099-YI

Splenic stiffness using spleen-dedicated 100 Hz transient elastography compared with the Baveno criteria to predict high risk esophageal varices in cirrhosis

Harsh Jain¹, Prajna Anirvan², Mohd. Imran Chouhan³, Biswajit Sahoo¹, Hemanta Nayak¹, Subash Samal¹, Manas Kumar Panigrahi⁴. ¹All India Institute of Medical Sciences, Bhubaneswar, India; ²Kalinga Gastroenterology Foundation, Cuttack, India; ³Government Medical College, Rajouri, Jammu and Kashmir, Jammu, India; ⁴All India Institute of Medical Sciences, Bhubaneswar, India
Email: imharshjain@gmail.com

Background and aims: Spleen-dedicated Transient Elastography (TE) utilizes 100 Hz shear waves to estimate Splenic Stiffness Measurement (SSM). Recent Baveno consensus suggests the use of SSM to rule out High Risk Esophageal Varices (HREV) in patients not fulfilling the Baveno VI criteria. The evidence supporting the role of SSM is limited. This study was designed to establish the diagnostic accuracy of SSM in predicting HREV using spleen-dedicated 100 Hz TE, and compare it with the existing Baveno criteria.

Method: Single centre cross-sectional study including patients with cirrhosis. Endoscopy was done to grade esophageal varices, LSM was estimated using standard 50 Hz TE and SSM was estimated using spleen-dedicated 100 Hz TE. Area under Receiver Operating Characteristic (AUROC) curves were obtained for LSM, SSM individually as well as for the combination of parameters used in the Baveno VI and VII criteria. SSM cut-off value was derived from the study cohort. The diagnostic performance of SSM was compared with the existing cut-offs proposed by the Baveno VI and VII criteria by determining the endoscopy spare rate and HREV miss rate.

Results: Out of 156 patients with cirrhosis included in the study, 34% (n = 53) had HREV. SSM could not be obtained in 3 patients (1.9%). The AUROC of SSM alone, LSM alone, combined LSM and platelet count (PC), and, combined LSM, PC and SSM was 0.805, 0.643, 0.735 and 0.801, respectively. An SSM cut-off value of 35 kPa was selected, having a corresponding sensitivity of 96.2%. At this cut-off, SSM alone spared more endoscopies as compared to the Baveno VI criteria (37.2% vs 16.6%) and had a lower HREV miss rate as compared to the Baveno VII criteria (3.8% vs 11.3%). All the non-invasive parameters performed better in the compensated cirrhosis subgroup (n = 97) as compared to those having prior history of decompensating event (n = 59). SSM alone had an AUROC of 0.705 in the decompensated cirrhosis subgroup, possibly avoiding 23.7% endoscopies in this subgroup.

Conclusion: SSM can accurately rule out HREV in cirrhosis and save a significant number of endoscopies in these patients. The SSM cut-off to rule out HREV may vary in different populations and may depend on the etiology of cirrhosis. The combination of LSM, platelet count and SSM was not superior to SSM alone in predicting HREV. SSM may have a role in stratifying the risk of HREV in patients with decompensated cirrhosis.

SAT-100

Heart failure outcomes following transjugular intrahepatic portosystemic shunts

Jemima Finkel¹, Silke Francois², Amine Benmassaoud³, Louise China⁴, David Patch⁵, Emmanouil Tsochatzis⁶. ¹Institute of Liver and Digestive Health, London, United Kingdom; ²Royal Free Hospital, London, United Kingdom; ³McGill University, Montreal, Canada; ⁴Institute of Liver and Digestive health, Royal Free Hospital, London, United Kingdom; ⁵Institute of Liver and Digestive Health, London, United Kingdom; ⁶Institute for Liver and Digestive Health, Royal Free London, London, United Kingdom
Email: jfinkel@doctors.org.uk

Background and aims: Transjugular intrahepatic portosystemic shunts (TIPSS) are increasingly used for the management of variceal bleeding and diuretic refractory ascites. Complications include

cardiac failure in up to 20%. TIPSS outcomes over a 12-year period were reviewed for predictors of the occurrence of heart failure.

Method: Data was collated retrospectively for TIPSS performed at a tertiary referral centre between 2010 and 2022. The primary outcome was the occurrence of heart failure. Referring hospitals were contacted and information requested for data missing up to 12 month follow-up. Statistical analysis included Mann-Whitney and t-tests for comparison of continuous variables between groups and binary logistic regression to determine predictive factors for the occurrence of heart failure.

Results: 472 patients underwent TIPSS, including 279 for ascites (A) and 193 patients for variceal bleeding (B). Overall, 65% of patients were male and the mean age was 55 years. The most common aetiology was alcohol at 64%, 13% were due to metabolic dysfunction-associated steatotic liver disease and 8% were secondary to hepatitis C infection. In 57.5% (46/80) heart failure was detected in the outpatient setting, most commonly due to new onset peripheral oedema, and was successfully managed with outpatient diuretic therapy. 10% (8/80) required re-admission to hospital for fluid overload (3% of the overall cohort). Five patients had multi-system involvement driving their symptoms as opposed to solely the TIPSS. Two patients required haemodialysis for fluid removal before subsequently undergoing TIPSS reductions as definitive management. Heart failure was documented in 80/472 (16.9%). Similar proportions of patients developed heart failure between the two cohorts, 40/279 (14.3%) in ascites and 32/193 (16.5%) in bleeding. Univariate analysis showed that age and cryptogenic cirrhosis were predictive factors for heart failure, with both remaining significant at multivariate analysis (Age: aOR 1.024, 95% C.I 1.001–1.049, cryptogenic cirrhosis: aOR 2.979, 95% C.I 1.118–7.937).

93 patients had a pro-BNP within 6 months of the TIPSS, with no significant baseline increase in those who developed heart failure.

Conclusion: The majority of heart failure following TIPSS procedures is manageable in an outpatient setting and does not require re-admission to hospital or intervention beyond diuretic therapy. Cardiovascular risk factors did not predict the risk of heart failure in this cohort.

SAT-101

Morphological changes in esophageal varices in patients with HCV related cirrhosis who achieved sustained virological response by direct-acting antivirals

Chikako Nagao¹, Masanori Atsukawa¹, Tadamichi Kawano¹, Taeng Arai¹, Akihito Tsubota², Chisa Kondo¹, Tomomi Okubo³, Hidenori Toyoda⁴, Koichi Takaguchi⁵, Makoto Nakamura⁶, Tsunamasa Watanabe⁷, Asahiro Morishita⁸, Hironao Okubo⁹, Atsushi Hiraoka¹⁰, Akito Nozaki¹¹, Kazuhito Kawata¹², Haruki Uojima¹³, Chikara Ogawa¹⁴, Toru Ishikawa¹⁵, Hiroki Nishikawa¹⁶, Motoh Iwasa¹⁷, Yasuhito Tanaka¹⁸, Katsuhiko Iwakiri¹. ¹Division of Gastroenterology and Hepatology, Nippon Medical School, Tokyo, Japan; ²Project Research Units (PRU) Research Center for Medical Science, The Jikei University School of Medicine, Tokyo, Japan; ³Department of Gastroenterology, Nippon Medical School Chiba Hokusoh Hospital, Chiba, Japan; ⁴Department of Gastroenterology, Ogaki Municipal Hospital, Gifu, Japan; ⁵Department of Hepatology, Kagawa Prefectural Central Hospital, Kagawa, Japan; ⁶National Hospital Organization Kyushu Medical Center, Fukuoka, Japan; ⁷Department of Internal Medicine, St. Marianna University School of Medicine, Kanagawa, Japan; ⁸Department of Gastroenterology, Kagawa University Graduate School of Medicine, Kagawa, Japan; ⁹Department of Gastroenterology, Juntendo Nerima University Hospital, Tokyo, Japan; ¹⁰Gastroenterology Center, Ehime Prefectural Central Hospital, Ehime, Japan; ¹¹Gastroenterological Center, Yokohama City University Medical Center, Kanagawa, Japan; ¹²Hepatology Division,

Department of Internal Medicine II, Hamamatsu University School of Medicine, Hamamatsu, Japan; ¹³Department of Gastroenterology, Kitasato University School of Medicine, Kanagawa, Japan; ¹⁴Department of Gastroenterology and Hepatology, Takamatsu Red Cross Hospital, Takamatsu, Japan; ¹⁵Department of Hepatology, Saiseikai Niigata Hospital, Niigata, Japan; ¹⁶Second Department of Internal Medicine, Osaka Medical and Pharmaceutical University, Osaka, Japan; ¹⁷Department of Gastroenterology and Hepatology, Mie University School of Medicine, Mie, Japan; ¹⁸Department of Gastroenterology and Hepatology, Faculty of Life Sciences, Kumamoto University, Kumamoto, Japan
Email: gachi@nms.ac.jp

Background and aims: Portal hypertension is the main pathophysiology of liver cirrhosis that forms collateral vessels such as esophageal varices. DAAs have markedly improved treatment outcomes and have been approved for patients with HCV related cirrhosis including decompensated cirrhosis, which is frequently complicated by esophageal varices. Although some studies reported that achievement of SVR with DAAs decreased portal pressure to some extent, post-SVR portal pressure decreased only slightly or not at all in patients with high baseline portal pressure or poor hepatic functional reserve. Recent studies reported post-SVR changes in the morphology of esophagogastric varices in patients with compensated cirrhosis. However, post-SVR esophageal variceal changes in patients with decompensated cirrhosis remain unclear. Therefore, this multicenter retrospective study aimed to clarify the morphological changes in esophageal varices and factors associated with esophageal varix aggravation after achieving SVR with DAAs in patients with cirrhosis, including decompensated cirrhosis.

Method: A total of 1,768 patients with chronic HCV infection achieved SVR with DAAs at 26 participating institutions in Japan. Among them, 243 patients underwent esophagogastroduodenoscopy before DAAs treatment and after achieving SVR, and the morphological changes in esophageal varices were examined.

Results: This study included 125 males and 118 females with compensated or decompensated cirrhosis with a median age of 68 (range, 44–91) years. Esophageal varices before DAAs treatment were classified into no varix in 155, F1 in 59, F2 in 25 and F3 in 4 patients. The improvement, unchanged, and aggravation rates of esophageal varices after SVR were 11.9%, 73.3%, and 14.8%, respectively. Low platelet count was extracted as an independent factor associated with esophageal varices aggravation. Of the 155 patients without esophageal varices before DAAs treatment, 17 developed de novo post-SVR esophageal varices. High ALBI score was extracted as an independent factor associated with de novo post-SVR esophageal varices. The cumulative incidences of de novo esophageal varices were 0%, 6.7%, and 17.7% at 1, 3, and 5 years, respectively.

Conclusion: In conclusions, patients with cirrhosis can experience esophageal varices aggravation despite achieving SVR. In particular, patients with low platelet count and high ALBI score such as decompensated cirrhosis had a high likelihood of developing esophageal varices aggravation and de novo esophageal varices, respectively, even after achieving SVR, and should periodically undergo esophagogastroduodenoscopy in patients with such factors.

SAT-102

The safety and technical success of endoscopic ultrasound-guided portal pressure gradient measurement: a systematic review and meta-analysis

Yousaf Zafar¹, Hamid Ullah², Faisal Bukeir², Brett Fortune³.

¹University of Mississippi Medical Center, Madison, United States;

²University of Mississippi Medical Center, Jackson, United States;

³Montefiore Medical Center- The University Hospital for Albert Einstein College of Medicine, Bronx, United States

Email: yousuf.zafar.iqbal@gmail.com

Background and aims: Portal hypertension (PH) is a serious complication that is linked to significant morbidity and mortality in

patients with cirrhosis. Unlike the indirect measurement of the hepatic venous pressure gradient, the portal pressure gradient (PPG) directly reflects the degree of PH including presinusoidal causes of PH. As endoscopic sonography techniques expand, the use of endoscopic ultrasound-guided porto-systemic pressure gradient (EUS-PPG) provides a novel procedure that is minimally invasive and can obtain direct portal pressure measurements, thus providing potentially clinically meaningful information. Our aim of using this systematic review is to assess the technical success and safety of this procedure in liver patients.

Methods: A comprehensive literature search was conducted in PubMed, EMBASE, Web of Science and Google Scholar to query for studies that assessed the safety and technical success of EUS-PPG. All articles published from inception to January 2024 were included. The primary outcomes were the overall technical success rate, and incidence of adverse events. The risk of bias was assessed by Egger's test. Results were synthesized using I² to test heterogeneity.

Results: Six published studies including 212 patients met inclusion criteria. In 4 of the studies with mean age 59.6 years, 59% male while two had no mention of demographics. The pooled technical success rate of EUS-PPG measurements was 97.1% with (95% CI 92.9%–98.8%, I² = 0%). A 25-gauge needle was used in 84.3% (135/160) of patients. The mean PPG was 12.99 (range 5.63–20.35) mmHg. Ninety-five patients underwent simultaneous EUS-LB using 19G needle with wet suction technique. The technical success rate of EUS-LB was 100% and specimen was adequate in 99% (94/95) patients to establish histological diagnosis. There were no major life-threatening complications of the EUS-PPG procedure. The pooled incidence of adverse events for EUS-PPG was 6.8% (95% CI 3.8–11.8%; I² = 0%). Low heterogeneity was noted in the analysis.

Conclusion: EUS-PPG measurement carries a high technical success rate with excellent safety with or without EUS-LB when performed for the assessment of portal pressure in patients with chronic liver disease. Future studies are needed to evaluate whether there is strong correlation between EUS-PPG measurements and histologic fibrosis stage by liver biopsy as well as linkage to meaningful clinical outcomes.

SAT-104-YI

Impact of albumin dosing on the need for terlipressin therapy and prognosis in patients with liver cirrhosis

Eva Maria Schleicher^{1,2}, Christian Reinhardt¹, Julia Weinmann-Menke¹, Peter R. Galle^{1,2}, Simon J. Gairing^{1,2}, Christian Labenz^{1,2}. ¹University Medical Center of the Johannes Gutenberg-University, Mainz, Germany; ²Cirrhosis Center Mainz (CCM), Mainz, Germany
Email: eva.schleicher@unimedizin-mainz.de

Background and aims: If acute kidney injury (AKI) is detected in patients with cirrhosis, current guidelines recommend volume expansion with albumin at the dosage of 1 g/kg body weight per day for 48 h. The dosage and its prognostic relevance for albumin therapy have not been supported by conclusive evidence so far but are based on expert consensus. Therefore, this study aimed to investigate the influence of different doses of albumin in the context of volume expansion therapy on the need for therapy with terlipressin and prognosis in patients with liver cirrhosis and AKI.

Method: Data from 124 patients with cirrhosis and AKI were recruited at the Cirrhosis Center Mainz (Germany). Albumin doses within the first 48 h were recorded. To make the doses of albumin comparable between patients, normalization for body weight (BW) (albumin dose in g/kgBW per day) was performed. Patients were followed up for the need for therapy with terlipressin in hepatorenal syndrome (HRS) and liver transplant-free (LTx-free) survival.

Results: Patients received a median of 80 g (IQR 80; 120) albumin within the first 48 h. The median albumin dose normalized to body weight (Alb/kg) was 0.58 (IQR 0.42; 0.83). During the AKI episode, 46 (37%) patients required therapy with terlipressin. In a multivariable

POSTER PRESENTATIONS

logistic regression model, lower Alb/kgBW (OR 0.048, $p = 0.001$) was shown to be significantly associated with the need for therapy with terlipressin. The same result was found in a model with the inclusion of Alb/kgBW dichotomized by median (OR 0.320, $p = 0.010$). A total of 24 (19%) patients died or required LTx within 30 days of diagnosis of AKI. In a multivariable logistic regression model, only a higher MELD (OR 1.082, $p = 0.006$) was found to be associated with a worse prognosis, while Alb/kgBW was not ($p = 0.915$). These results were confirmed in a further analysis after 1:1 matching of patients with Alb/kgBW above and below the median ($n = 33$ per group).

Conclusion: Guideline-recommended administration of intravenous albumin in patients with cirrhosis and AKI is associated with a reduced need for therapy with terlipressin. However, patients' prognosis appears to be independent of albumin dosage.

SAT-105

Neutrophil extracellular traps are not linked to the development of decompensation, ACLF, or death in clinically stable patients with advanced chronic liver disease

Lorenz Balcar¹, Bernhard Scheiner¹, Benedikt Simbrunner¹, Mathias Jachs¹, Lukas Hartl¹, Georg Semmler¹, Benedikt Hofer¹, Nina Dominik¹, Michael Schwarz¹, Albert Friedrich Stättermayer¹, Matthias Pinter¹, Michael Trauner¹, Thomas Reiberger¹, Ton Lisman², Mattias Mandorfer¹. ¹Medical University of Vienna, Vienna, Austria; ²University of Groningen, Groningen, Netherlands

Email: lorenz.balcar@meduniwien.ac.at

Background and aims: Neutrophil extracellular traps (NETs) are part of the body's innate immune response. In animal models, they aggravated liver injury and promoted disease progression/portal hypertension by the formation of (micro)thrombi leading to parenchymal extinction. This study aimed to investigate NETosis in patients with clinically stable advanced chronic liver disease (ACLD).

Method: We investigated stable ACLD patients undergoing hepatic venous pressure gradient (HVPG) measurement in whom an extensive panel of laboratory tests related to coagulation and NET biomarkers were assessed. First/further hepatic decompensation (HD; according to disease stage)/liver-related death (LRD; in a multistate model) as well as development of ACLF/LRD and non-tumoural portal vein thrombosis (PVT) were the outcomes of interest.

Results: Overall, 194 patients (70 compensated ACLD [cACLD], 124 dACLD; mean Child-Turcotte-Pugh score (CTP): 7 ± 2 points; mean HVPG: 17 ± 6 mmHg) were included. Compared to healthy controls ($n = 29$), levels of cell free-DNA (cf-DNA) levels were higher (0.88 [IQR 0.84–0.93] vs. 0.94 [IQR 0.88–1.03] $\mu\text{g/ml}$; $p = 0.001$) in ACLD patients, whereas myeloperoxidase-DNA (MPO-DNA) values were similar (0.32 [IQR 0.17–0.54] vs. 0.39 [IQR 0.18–0.76] mAU/ml ; $p = 0.400$). Compared to cACLD, syndecan-1, platelet factor 4 (PF4), and plasmin antiplasmin complex were significantly higher in dACLD, while activated factor XIII was lower. However, after correcting for platelet count, the differences in PF4 disappeared. While these differences were also observed when stratifying according to disease severity indices (i.e., CTP score), there were no differences throughout HVPG strata. Activated factor XIII, soluble platelet (P)-selectin, and cf-DNA but not MPO-DNA were associated with HD/LRD in univariable analysis. However, no coagulation test predicted HD/LRD death after adjusting for established prognostic indicators. Similarly, soluble P-selectin and cf-DNA were also associated with ACLF/LRD univariably, but associations vanished after appropriate adjustment. Finally, while thrombin antithrombin complex was predictive of non-tumoural PVT development in univariable analysis, after adjusting for CTP score, the association was lost.

Conclusion: Patients with clinically stable ACLD showed increased cf-DNA levels (i.e., NETosis, but also apoptosis/necrosis). However, the more specific marker of NETosis, MPO-DNA, was comparable to healthy controls. NETosis does not appear to drive disease progression in humans with clinically stable ACLD, as it was not linked to

clinical end points. Thus, findings obtained in animal models may not be translatable to humans.

SAT-106

Gadoxetic acid-enhanced MRI-derived functional liver imaging score (FLIS) predicts acute-on-chronic liver failure in patients with acute decompensation

Lorenz Balcar¹, Sarah Poetter-Lang¹, Ahmed Ba-Ssalamah¹, Nina Bastati¹, Raphael Ambros¹, Antonia Kristic¹, Julia Krawanja¹, Katharina Pomej¹, Benedikt Simbrunner¹, Georg Semmler¹, Viktor Schmidbauer¹, Svitlana Pocheptnia¹, Daniel Sobotka¹, Jacqueline Hodge¹, Michael Trauner¹, Thomas Reiberger¹, Lucian Beer¹, Mattias Mandorfer¹. ¹Medical University of Vienna, Vienna, Austria

Email: lorenz.balcar@meduniwien.ac.at

Background and aims: The Functional Liver Imaging Score (FLIS), derived from gadoxetic acid-enhanced MRI (GA-MRI), can identify patients with advanced chronic liver disease (ACLD) who are at increased risk of hepatic decompensation and liver-related death. In decompensated ACLD (dACLD) patients (i.e., combining clinically stable/unstable), a FLIS of 0–3 was independently associated with an increased risk of acute-on-chronic liver failure (ACLF). However, it is unclear whether the semiquantitative FLIS or its individual complex quantitative (GA-MRI) imaging components (i.e., relative liver enhancement [RLE], relative enhancement ratio of the biliary system [REB], and liver-to-portal vein contrast ratio [LPC]), are capable of predicting ACLF in acutely decompensated (AD) patients; the main at-risk population for ACLF development.

Method: ACLD patients with GA-MRI derived semiquantitative FLIS, in whom the RLE, REB and LPC were additionally computed by two independent, experienced radiologists, were included. According to disease stage, patients were stratified into stable ACLD (cACLD and stable, non-hospitalised dACLD) and AD patients (GA-MRI in non-elective liver-related hospitalisation). The predictive values of semiquantitative FLIS and quantitative (GA-MRI) imaging parameters for ACLF development were investigated by Cox regression analyses.

Results: We included 322 patients of whom 253 (69%) were stable ACLD ($n = 187$, 58% cACLD, $n = 66$, 21% stable dACLD), and 69 (21%) AD patients. The inter-observer variability was good to excellent for all evaluated GA-MRI parameters. The FLIS was associated with ACLF development/liver-related death in AD patients in univariable and multivariable analyses (adjusted hazard ratio [aHR]: 2.49 [95%CI 1.15–5.37]; $p = 0.030$), even after adjusting for known predictive factors such as the CLIF-C ACLF-D score. In stable ACLD patients, the FLIS was only associated the end point of interest in univariable analysis; after correction for well-established prognostic indicators, the association did not attain statistical significance (aHR: 2.01 [95%CI 0.96–4.23]; $p = 0.070$).

Notably, RLE, REB, and LPC did not predict ACLF/liver-related death, neither in AD, nor stable ACLD patients.

Conclusion: The FLIS is a simple imaging biomarker for prognostication of ACLF in AD patients in whom ACLF risk stratification is clinically valuable to identify patients who may benefit from intensified monitoring or timely liver transplant evaluation and potentially enrich study populations of clinical trials investigating preventive measures with high-risk patients.

SAT-107-YI

Assessment of the diagnostic accuracy of cell count on spontaneous bacterial peritonitis

Prebhashan Moodley¹, Mohamed Waddah¹, Oliver Bendall¹, Kris Bennett¹, Nigel Keelty¹, Sally Chan¹, Joanne Hosking², Wayne Thomas³, Robert Tilley⁴, Juan Acevedo Haro⁵. ¹South West Liver Unit, University Hospitals Plymouth NHS Trust, Plymouth, United Kingdom; ²Medical Statistics Group Peninsula Clinical Trials Unit, University of Plymouth, Plymouth, United Kingdom; ³Haematology Service, University Hospitals Plymouth NHS Trust, Plymouth, United

Kingdom; ⁴Microbiology Service, University Hospitals Plymouth NHS Trust, Plymouth, United Kingdom; ⁵South West Liver Unit, University Hospitals Plymouth NHS Trust, Peninsula Medical School, University of Plymouth, Plymouth, United Kingdom
Email: jacevedo@nhs.net

Background and aims: The current definition of SBP, cell count ≥ 250 PMN/mm³ on ascitic fluid (AF), is based on small studies performed in the 70's–80's using the manual cell count method. Only a few published studies showed the automated cell count method has good agreement with the manual method. However, the automated counters assessed are no longer available or have been superseded by new models and no independent comparison was made against the gold standard (GS). The accuracy to diagnose SBP is key to avoid delays in its diagnosis and treatment. Therefore, it is important to employ the most accurate diagnostic method. Our aim is to compare both methods independently against the GS diagnosis of SBP.

Method: This is a 5-year long retrospective study including all cases admitted to University Hospitals Plymouth NHS Trust from Dec. 2017 to Nov. 2022, fulfilling the GS positive-SBP criteria: pathogenic bacteria isolated on AF and at least one sign/symptom of peritonitis. And including all day cases having elective paracentesis between Dec. 2021 and Nov. 2022, fulfilling the GS negative-SBP criteria: no admission to hospital within 4 weeks, asymptomatic, AF culture negative and no antibiotics received. The automated method was performed by the Abbott Alinity HQ high-throughput blood count analyser. Only 1 case per patient per admission was included.

Results: 89 cases in 46 patients were identified, 37 with SBP and 52 without SBP according to GS criteria. GS positive-SBP cases had worse liver function: higher levels of bilirubin (161 ± 159 vs 42 ± 27 μ mol/L, $p < 0.001$), more prolonged INR (2.1 ± 1.8 vs 1.3 ± 0.2 , $p = 0.001$) and higher Child-Pugh score (11.5 ± 2.0 vs 9.3 ± 1.3 points, $p < 0.001$); worse renal function: higher creatinine levels (142 ± 110 vs 69 ± 18 μ mol/L, $p < 0.001$) and MELD score (23.0 ± 10.6 vs 12.2 ± 4.0 points, $p < 0.001$); and were more critically ill: higher prevalence of ACLF grade 2–3 (30% vs 0%, $p < 0.001$), septic shock (22% vs 0%, $p < 0.001$), admission to ITU (27% vs 0%, $p < 0.001$), and in-hospital mortality (42% vs 0%, $p < 0.001$) compared to GS negative-SBP cases. GS positive-SBP cases showed higher degree of inflammation: higher CRP levels (58 ± 46 vs 22 ± 17 mg/L, $p < 0.001$), serum leukocyte count (11.3 ± 5.2 vs 7.3 ± 2.1 , $p < 0.001$) and higher prevalence of Systemic Inflammatory Response Syndrome (SIRS) (52% vs 13%, $p < 0.001$) than GS negative-SBP cases. In order to compare the sensitivity and specificity of the manual and automated cell count methods, only those cases having both methods performed (76/89) were selected and compared with the GS cases. The sensitivity of the automated method was superior to the manual method, 79% vs. 59%, $p = 0.02$. Both methods showed Specificity of 100%.

Conclusion: The sensitivity of the modern automated method is superior to the classic manual cell count. It is also cheaper and readily available out of hours. The diagnosis of SBP should be made using a modern automated cell counter.

SAT-111

Lower levels of Insulin-like growth factor 1 are independently associated with unfavorable prognosis in patients with advanced chronic liver disease

Lukas Hartl¹, Michael Schwarz¹, Benedikt Simbrunner¹, Mathias Jachs¹, Peter Wolf², David Bauer¹, Bernhard Scheiner¹, Lorenz Balcar¹, Georg Semmler¹, Benedikt Hofer¹, Nina Dominik¹, Rodrig Marculescu³, Michael Trauner¹, Mattias Mandorfer¹, Thomas Reiberger¹. ¹Division of Gastroenterology and Hepatology, Department of Medicine III, Medical University of Vienna, Vienna, Austria; ²Division of Endocrinology, Department of Medicine III, Medical University of Vienna, Vienna, Austria; ³Department of Laboratory Medicine, Medical University of Vienna, Vienna, Austria
Email: thomas.reiberger@meduniwien.ac.at

Background and aims: Insulin-like growth factor 1 (IGF-1) acts as the primary mediator of growth hormone's (GH) anabolic effects. Secretion of liver-derived circulating IGF-1 is affected by GH, insulin, and nutritional status. In advanced chronic liver disease (ACLD), low IGF-1 levels are linked to insulin resistance, disturbances in lipid and carbohydrate metabolism, malnutrition, hypogonadism, and osteopenia.

Method: We assessed consecutive patients with suspected ACLD (i.e., liver stiffness measurement [LSM] ≥ 10 kPa), who underwent hepatic venous pressure gradient (HVPG) measurement between 05/2018 and 01/2022 within the prospective VICIS (NCT03267615) study. Exclusion criteria were hepatocellular carcinoma out of Milan criteria, vascular liver disease, occlusive portal vein thrombosis, and a history of liver transplantation/TIPS. Patients were stratified into seven clinical stages of ACLD: pACLD: probable ACLD with LSM ≥ 10 kPa, but HVPG < 6 mmHg; S0: non-significant portal hypertension (PH), i.e. HVPG 6–9 mmHg; S1: clinically significant portal hypertension (CSPH), i.e. HVPG ≥ 10 mmHg, without esophageal varices; S2: CSPH with esophageal varices; S3: CSPH with previous variceal bleeding; S4: CSPH with previous non-bleeding decompensation event; S5: further decompensation. Competing risk regression considering liver transplantation and death as competing events was performed.

Results: Overall, we included 283 patients (pACLD: 7.1%; S0: 11.0%, S1: 7.8%, S2: 13.8%, S3: 3.9%, S4: 33.9%, S5: 22.6%) and alcohol-related liver disease (45.2%) was the main liver disease etiology. Median GH levels significantly increased with progressive clinical stages (from pACLD: 1.7 ng/ml [IQR 0.3–4.2] to S5: 2.2 ng/ml [IQR 1.1–5.7]; $p = 0.006$), while median levels of IGF-1 decreased (from pACLD: 83.5 ng/ml [IQR 60.5–108.0] to S5: 51.0 ng/ml [37.0–69.9], $p < 0.001$). IGF-1 showed a moderate inverse correlation with MELD ($\rho = -0.433$), HVPG ($\rho = -0.307$), and interleukin 6 ($\rho = -0.445$, all $p < 0.01$), but did not correlate with GH ($\rho = -0.063$, $p = 0.288$). In multivariate competing risks analyses adjusted for age, sex, body mass index, MELD, albumin, sodium, HVPG, and C-reactive protein, lower IGF-1 was independently associated with (further) decompensation (adjusted subdistribution hazard ratio [aSHR] 0.99, 95% confidence interval [95%CI] 0.98–1.00), acute kidney injury (aSHR 0.98, 95%CI 0.97–0.99), acute-on-chronic liver failure (ACLF, aSHR 0.98, 95%CI 0.97–0.99), and liver-related death during follow-up (aSHR 0.98, 95%CI 0.96–0.99) (all $p < 0.05$).

Conclusion: With progression of ACLD severity IGF-1 decreases, while GH increases, suggesting increasing GH resistance. IGF-1 levels correlated with liver disease severity and systemic inflammation. Lower levels of IGF-1 were independently linked to hepatic decompensation and liver-related death during follow-up.

SAT-112

Spleen-dedicated stiffness measurement higher than 50 kPa is sufficient to diagnose clinically significant portal hypertension in cACLD individuals

Xiaofeng Zhang¹. ¹Hepatology Unit, Department of Infectious Diseases, Nanfang Hospital, Southern Medical University, Guangzhou, China
Email: 1282614092@qq.com

Background and aims: The Baveno VII consensus recommends transient elastography derived non-invasive tools including spleen stiffness measurement (SSM) for clinically significant portal hypertension (CSPH) differentiation in compensated advanced chronic liver disease (cACLD) patients. We aimed to prospectively evaluate the performances of these algorithms with spleen-dedicated probe in cACLD individuals.

Method: Consecutive cACLD individuals who underwent hepatic venous pressure gradient (HVPG) measurement, liver stiffness measurement (LSM) and SSM measured with 100 Hz probe were prospectively enrolled.

Results: From July 2021 to December 2023, 303 patients were screened and 160 were enrolled for analysis, and 77 patients were

POSTER PRESENTATIONS

with CSPH. For ruling in CSPH, the SSM >50 kPa had positive predictive value (PPV) at 97.4% and specificity at 98.8%. The Baveno VII-SSM dual cutoff (50 kPa) model had PPV at 89.1% and specificity at 92.8%, which correctly identified comparable CSPH cases (49/77, 63.6%) with the SSM >50 kPa (37/77, 48.1%, $p = 0.051$). For ruling out CSPH, 30 individuals met LSM <15 kPa plus platelet count >150,000/ μ L, with negative predictive value at 96.7% and sensitivity at 98.7%.

Conclusion: We validated that SSM >50 kPa using 100 Hz shear wave frequency was sufficiently accurate to rule in CSPH in cACLD individuals and initiate non-selective β -blockers. The Baveno VII-SSM dual cutoff (21–50 kPa) algorithm for identifying CSPH still need further studies.

SAT-113

Long-term therapy with intravenous human albumin increase survival in patients with decompensated cirrhosis and refractory ascites

Antonino Lombardo¹, Luigi Capodicasa², Domenico Alaimo³, Francesco Mercurio³, Angelo Zimbaro³, Fabio Simone³, Nicola Alessi³, Ciro Celsa³, Grazia Pennisi³, Giuseppe Cabibbo³, Salvatore Petta³, Calogero Camma³, Vincenza Calvaruso³, Vito Di Marco³. ¹Section of Gastroenterology and Hepatology, University of Palermo, Palermo, Italy; ²Section of Gastroenterology and Hepatology, Dipartimento Promozione Della Salute, Materno Infantile, Medicina Interna e Specialistica Di Eccellenza, Palermo, Italy; ³Section of Gastroenterology and Hepatology, Dipartimento Promozione Della Salute, Materno Infantile, Medicina Interna e Specialistica Di Eccellenza, University of Palermo, Palermo, Italy
Email: lombanino@gmail.com

Background and aims: Refractory ascites in cirrhosis is associated with 50% survival at six months. International guidelines recommend the use of human albumin in cirrhotics with acute decompensation. Recently, the benefit of long-term human albumin therapy (HAT) was proven by ANSWER study in decompensated cirrhosis and have become best practice in Italian Liver Units, but there is no evidence in patients with refractory ascites.

Method: We reported data of an observational study including 143 patients with cirrhosis and refractory ascites undergoing large-volume paracenteses (LVP) in the Day Hospital of our Liver Unit. The group 1 included 90 patients, observed from January 2019 and April 2022, who received HAT only during LVP. The group 2 of 53 patients, observed from May 2022 and January 2024, received HAT during LVP and long-term (40 grams/week). Chi-square test was used to analyze differences between two groups.

Results: The mean age of patients was 68 years, 70% were male and the mean of MELD score was 14. The mean value of serum albumin was 32 g/L, sodium 135 mmol/L, bilirubin 2 mg/dL and INR 1.35. The etiology was MASH in 46 patients, alcohol abuse in 37, HCV in 30, HBV 11, autoimmune in 2, while 7 patients had a cryptogenic cirrhosis and 10 had a mixed etiology. Thirty-three patients (23%) had HCC and 19 (13%) had portal thrombosis. There were no significant clinical differences between 2 groups at baseline. In group 1, 8 patients (8%) received liver transplant and in 9 patients (10%) was placed a TIPS, only 1 had a post-TIPS complication. In group 2, 4 patients (7%) received liver transplant, 2 patients (4%) were on the waiting list, 31 patients (58%) had a contraindication to transplantation; in 5 patients (9%) was placed a TIPS, 1 patient had a post-TIPS complication, 31 patients (58%) had a contraindication for TIPS. Seventy-four patients (82%) of group 1 and 23 patients (43%) of group 2 needed at least one hospitalization for complications ($p < 0.0001$). In group 1 all patients (100%) undergoing LVP during follow-up, while in group 2, 24 patients (45%) no longer performed LVP ($p < 0.0001$). Finally, during the first year of follow-up 71 patients (78%) of group 1 and 9 patients (16%) of group 2 died during the follow-up ($p < 0.0001$), with a mean survival of 5 months in patients in the group 1, of 7 months in patients in the group 2.

Conclusion: Long-term human albumin therapy treatment can significantly improve prognosis and reduce mortality in patients with refractory ascites. It is a well-tolerated treatment with no complications or contraindications.

SAT-114

Heartbeats and Platelets: unveiling the symphony of heart failure and congestive hepatopathy

Anas Zaher¹, Jude Elsaygh¹, Harsh Patel², Navim Mobin², Gres Karim^{3,4}, Kumudha Ramasubbu⁵, Ilan Weisberg². ¹New York Presbyterian Brooklyn Methodist Hospital-Department of Internal Medicine, Brooklyn, United States; ²New York Presbyterian Brooklyn Methodist Hospital-Department of Gastroenterology, Brooklyn, United States; ³New York Presbyterian Brooklyn Methodist Hospital, New York, United States; ⁴New York Presbyterian Brooklyn Methodist Hospital, Brooklyn, United States; ⁵New York Presbyterian Brooklyn Methodist Hospital-Department of Cardiology, Brooklyn, United States
Email: qks9002@nyp.org

Background and aims: Heart failure (HF) resulting in elevated central venous pressure is frequently associated with poor cardiac output and decreased hepatic perfusion. This subsequently leads to liver injury due to congestive hepatopathy (CH). Platelets, a surrogate for portal hypertension, have a prognostic value since worsening thrombocytopenia in HF is associated with higher all-cause mortality. This study explores the effect of diuresis on hepatic parameters and platelets during an acute HF (AHF) exacerbation to understand their effect on mortality.

Method: Patients who were >18 years with an ejection fraction (EF) of $\leq 40\%$ admitted for an AHF exacerbation between 1/2020 to 5/2023 were identified through the electronic medical record at a high-volume New York City hospital. All patients underwent diuresis until they became euvoletic. CH was defined as aspartate transferase (AST) and alanine transaminase (ALT) levels exceeding two times the upper normal limit (35 U/L). Patients were categorized into three groups based on platelet values ($\times 10^9/L$): moderate-severe (≤ 99), mild (100–149), and normal (≥ 150). Continuous variables were represented using means, while categorical variables were expressed as percentages.

Results: Among 614 patients, 51 (10.3%) were found to have CH and the majority (56%) were black. On average, those with CH had a lower EF (20% vs 25%), higher mean AST levels on admission (152 vs 35)/ALT levels on admission (126 vs 30), and elevated mean natriuretic peptide (15,011 vs 14,140 pg/ml) compared to non-CH patients. Among patients with CH, 6% had moderate-severe thrombocytopenia, 18% had mild thrombocytopenia, and 76% had normal platelets count. Patients with moderate-severe thrombocytopenia had higher in-hospital mortality (19%) when compared to patients with mild thrombocytopenia (7%) and a normal platelet count (3%). Additionally, the mean days of diuresis were longer with moderate-severe thrombocytopenia (6.5 days) compared to mild thrombocytopenia and normal platelets (5.6 and 5 days, respectively). Finally, platelet counts on admission when compared to discharge were significantly different between the two groups (193 and 246 CH vs. 229 and 233 non-CH, $p = 0.004$). There was an observed 30% improvement in platelet count in the CH group compared to 2% in the non-CH group.

Conclusion: This study highlights the significance of platelets in predicting mortality and assessing HF severity during exacerbations. Patients with CH were noted to have a substantial improvement in platelet count post-diuresis, emphasizing its potential as a therapeutic target in the future. A greater severity of thrombocytopenia on admission was associated with higher mortality, a longer length of stay, and a longer duration of diuresis. Recognizing platelet count as a dual marker for mortality risk and therapeutic response underscores its importance in managing HF patients with CH.

SAT-116

Association between pre-operative TIPS and post-operative mortality in a veterans affairs cohort

Nadim Mahmud¹, David Kaplan¹. ¹Hospital of the University of Pennsylvania, Philadelphia, United States
Email: nadim.mahmud@gmail.com

Background and aims: Patients with cirrhosis have an increased risk of post-operative mortality, a component of which may be attributable to portal hypertension in some patients. Performance of pre-operative TIPS, therefore, may plausibly reduce operative risk. Recent literature suggests benefit with pre-operative TIPS, however these studies are limited by residual confounding and lack of exploration of longitudinal liver function data. To address these limitations we used granular longitudinal data from the Veterans Health Administration (VHA).

Method: This was a retrospective cohort study of well-characterized patients with cirrhosis in the VHA who underwent major surgery between 2008 and 2022. A six-month window prior to surgery was utilized to identify patients who underwent pre-operative TIPS. Detailed data regarding demographics, comorbidities, surgery type, ASA class, and longitudinal laboratory data were collected and incorporated into a propensity score using 3:1 caliper matching for receipt of TIPS. Cox regression was then used to evaluate the impact of TIPS on post-operative mortality through 12 months. This process was iterated an additional 500 times using a random number generator to identify variability around the hazard ratio point estimate. Liver function parameters were descriptively compared between TIPS and no TIPS groups 6 months prior to surgery and immediately prior to surgery.

Results: After comprehensive propensity matching including by surgery type, 47 patients underwent pre-operative TIPS and 134 did not. Cohort data included median age 63 years, 94.5% male, and 58.6% ALD-related cirrhosis. In Cox regression, pre-operative TIPS was associated with increased risk of post-operative mortality (HR 1.94, 95% CI 1.02–3.69, $p = 0.04$). In random 500 resampling events, the samples demonstrated an HR >1 and the median HR was 1.91. In evaluating longitudinal lab data, TIPS and no TIPS patients had similar albumin, bilirubin, INR, and platelet count 6 months prior to surgery (each $p > 0.05$), however immediately prior to surgery patients with TIPS patients had lower albumin ($p = 0.004$) and platelet counts ($p = 0.02$), and higher bilirubin ($p = 0.03$) and INR ($p = 0.02$).

Conclusion: In this propensity matched analysis, pre-operative TIPS was associated with increased post-operative mortality in patients with cirrhosis undergoing major surgery. Patients with TIPS had worsened liver synthetic function in the immediate pre-operative period, suggesting that theoretical operative benefits of portal pressure reduction are likely offset by worsened liver synthetic function that may drive increased risk.

SAT-117

Evaluation of Baveno VII criteria and other non-invasive tests for clinically significant portal hypertension in chronic hepatitis D

Mathias Jachs^{1,2}, Lisa Sandmann^{3,4,5}, Lukas Hartl^{1,2}, Tammo Lambert Tergast³, Michael Schwarz^{1,2}, David Bauer^{2,6}, Lorenz Balcar^{1,2}, Alena Friederike Ehrenbauer³, Benedikt Hofer^{1,2}, Markus Cornberg^{3,4,5,7,8}, Henrike Lenzen³, Katja Deterding³, Michael Trauner¹, Matthias Mandorfer^{1,2}, Heiner Wedemeyer^{3,4,5,7}, Thomas Reiberger¹, Benjamin Maasoumy^{3,7}. ¹Division of Gastroenterology and Hepatology, Department of Medicine III, Medical University of Vienna, Vienna, Austria; ²Vienna Hepatic Hemodynamic Lab, Division of Gastroenterology and Hepatology, Department of Medicine III, Medical University of Vienna, Vienna, Austria; ³Department of Gastroenterology, Hepatology, Infectious Diseases and Endocrinology, Hannover Medical School, Hannover, Germany; ⁴D-SOLVE consortium, an EU Horizon Europe funded project (No 101057917), Hannover, Germany; ⁵Excellence Cluster RESIST, Excellence Initiative Hannover Medical School, Hannover, Germany; ⁶Department of Medicine IV, Klinik

Ottakring, Vienna, Austria; ⁷German Center for Infection Research (DZIF), Braunschweig/Hannover, Germany; ⁸Centre for Individualised Infection Medicine, Helmholtz Centre for Infection Research/Hannover Medical School, Hannover, Germany
Email: mathias.jachs@meduniwien.ac.at

Background and aims: Non-invasive tests (NIT) have been endorsed by international guidelines for the diagnosis of clinically significant portal hypertension (CSPH) in compensated advanced chronic liver disease (cACLD) patients, but limited data exists on their utility in chronic hepatitis delta (CHD).

Method: This study included CHD-cACLD (LSM ≥ 10 kPa or F3/4) patients from two specialized European centers who underwent paired assessment of the hepatic venous pressure gradient (HVPG) and NIT from 2013 to 2023. Liver stiffness measurement (LSM), platelet count (PLT), von Willebrand factor to PLT ratio (VITRO), and spleen stiffness measurement (SSM) were assessed, and the utility of previously proposed models/algorithms for CSPH risk estimation (ANTICIPATE, 3P/5P) or diagnostic algorithms (Baveno-VII criteria, Baveno-VII-VITRO, and Baveno-VII-SSM) was evaluated.

Results: Fifty-one CHD-cACLD patients (HDV-RNA detectable: 90.2%, median HDV-RNA: 3.8 [25th–75th percentile: 3.2–5.0] log₁₀ IU/ml) with a CSPH prevalence (HVPG ≥ 10 mmHg) of 62.7% were included. CSPH patients showed higher LSM (25.8 [17.2–31.0] vs. 14.0 [10.5–19.8] kPa; $p < 0.001$), VITRO ($n = 31$, 3.5 [2.7–4.5] vs. 1.3 [0.6–2.0] %/[G/L]; $p < 0.001$), and SSM ($n = 20$, 53.8 [41.7–75.5] vs. 24.0 [17.0–33.9] kPa; $p < 0.001$), as compared to patients without CSPH. The ANTICIPATE (0.885), 3P (0.903) and 5P (0.912) models yielded excellent AUC for CSPH. When applying the Baveno-VII criteria, CSPH could be ruled out (LSM <15 kPa and PLT >150 G/L) in 15.7% of patients with 100% sensitivity and ruled in (LSM ≥ 25 kPa) in 43.2% of patients with 84.2% specificity. The diagnostic 'grey zone' of Baveno-VII criteria (41.1%) could be significantly reduced whilst maintaining diagnostic accuracy when applying the previously proposed Baveno-VII-VITRO (final 'grey zone': 19.4%) and Baveno-VII-SSM (final 'grey zone': 15.0%) sequence, respectively.

Conclusion: NIT for CSPH show a high diagnostic accuracy in CHD-cACLD, thereby facilitating individualized surveillance for portal hypertension, prognostication and prioritization for novel antiviral treatment options against CHD.

SAT-118

Ongoing alcohol use after TIPS implantation is associated with increased rates of ACLF and liver related death among individuals with alcohol related ACLD

Caroline Schwarz^{1,2}, Andrea Kornfehl¹, Reema Abid¹, Theresa Müllner-Bucsics¹, Michael Schwarz¹, Benedikt Hofer¹, Nina Dominik¹, Benedikt Simbrunner¹, Mathias Jachs¹, Lukas Reider¹, Maria Schoder¹, Matthias Mandorfer¹, Michael Trauner¹, Thomas Reiberger¹, Lukas Hartl¹. ¹Medical University of Vienna, Vienna, Austria; ²Klinik Ottakring, Vienna, Austria
Email: thomas.reiberger@meduniwien.ac.at

Background and aims: Transjugular intrahepatic portosystemic shunt (TIPS) placement is the recommended treatment for severe complications of portal hypertension (PH). Alcohol-related liver disease (ALD) represents the most common cause of cirrhosis and PH, yet data on the effect of alcohol use (AU) after TIPS implantation remain scarce.

Method: Individuals with ALD cirrhosis undergoing TIPS implantation at two Viennese tertiary care centers were included with a pooled prospective cohort (AUTIPS study, NCT03409263: 01/2017 to 11/2022; $n = 41$) and retrospective cohort (09/2000 to 09/2019, $n = 235$). Demographic, laboratory, and clinical parameters (decompensation events; acute-on-chronic liver failure = ACLF; bacterial infections, mortality) were recorded. AU after TIPS implantation was determined by documentation of the treating physician and patients' reporting.

POSTER PRESENTATIONS

Results: A total of 276 patients with ALD cirrhosis receiving a TIPS were included in the study and followed for a median of 29 (IQR 54) months. Main indications for TIPS were bleeding in 80 (29.0%) of the patients and refractory ascites in 196 (71.0%). Two-hundred and fifteen (77.9%) were male, the median age was 56 (IQR 13) years, and 24 (8.7%) had coexisting viral hepatitis. At TIPS implantation (baseline, BL) the median MELD was 11 (IQR 9) and 38 (13.8%) were classified as Child-C. Overall, 85 (30.8%) of the study population reported AU after TIPS implantation. Baseline characteristics were similar between individuals with and without ongoing AU, including prevalence of ascites ($p = 0.51$), variceal bleeding ($p = 0.87$), encephalopathy ($p = 0.87$), and hepatocellular carcinoma ($p = 0.54$). Bacterial infections occurred more frequently in patients with post TIPS AU (log-rank $p = 0.002$). Importantly, patients with ongoing AU had a higher incidence of ACLF (log-rank $p < 0.001$) and had higher overall mortality (log-rank $p = 0.005$; including liver-related death [log-rank $p < 0.001$]). The cumulative incidence of ACLF ($p = 0.014$) and liver-related death ($p = 0.004$) was significantly higher in patients with ongoing AU. In multivariable competing risk analysis, adjusted for age, MELD and PPG after TIPS implantation, ongoing AU was independently associated with ACLF (aHR: 1.66; 95%CI: 1.13–2.44; $p = 0.010$) and liver-related death (aHR: 2.09; 95%CI: 1.32–3.33; $p = 0.002$).

Conclusion: Our data reveal an alarming deterioration in outcomes associated with ongoing AU after TIPS implantation as an independent risk factor. These findings underline the paramount role of harm reduction measures and linkage to psychiatric care to treat AU and promote abstinence in addition to optimized hepatologic treatment after TIPS implantation.

SAT-119

Frequency of chronic liver disease after chemotherapy for gastrointestinal tumors

Fernanda Sales¹, Liana Codes², Gabriel Nogueira³, Beatriz Cunha³, Vivianne Mello⁴, Anelisa Coutinho⁴, Paulo Bittencourt⁵. ¹Bahiana School of Medicine and Public Health, AMO Oncology Clinic, Salvador, Brazil; ²Bahiana School of Medicine and Public Health, AMO Oncology Clinic, Salvador, Brazil; ³Bahiana School of Medicine and Public Health, Salvador, Brazil; ⁴AMO Oncology Clinic, Salvador, Brazil; ⁵Bahiana School of Medicine and Public Health, Unit of Gastroenterology and Hepatology, Portuguese Hospital, Salvador, Bahia, Salvador, Brazil
Email: nandaspmelo@gmail.com

Background and aims: Chronic liver disease (CLD) either due to steatosis, steatohepatitis or sinusoidal obstructive syndrome (SOS) has been increasingly reported in long-term survivors of gastrointestinal (GI) tumors treated with 5-fluorouracil (5-FU), irinotecan and/or oxaliplatin based chemotherapy. Cumulative prevalence of CLD in those patients, its major risk factors and liver-related outcomes remain largely unknown. The aim of this study is to investigate the frequency and risk factors for CLD in long-term survivors of GI tumors treated with chemotherapy as well as to assess their liver-related outcomes. Method: All patients with GI tumors older than 18 years admitted to AMO oncology clinic between January 2017 and January 2022 were retrospectively reviewed. Evaluation of CLD was carried out in all patients without prior evidence of CLD who survived more than 12 months after chemotherapy. The diagnosis of CLD was assumed in the presence of radiologic features of cirrhosis or portal hypertension by imaging, advanced fibrosis, or cirrhosis by histology or esophagogastroduodenoscopy. In addition, vibration-controlled transient elastography (VCTE) was offered to all patients irrespective of CLD diagnosis.

Results: 328 patients (165 males, mean age: 64 ± 13 years) were studied. Most had colorectal cancer (58%) and grade III or IV (69, 6%) tumors by TNM staging system. They were treated with 15, 5 (8–28) cycles mainly with oxaliplatin (86%), 5-FU (76%), irinotecan (49%), capecitabine (43%). After a mean follow-up of 30, 5 (21–49) months, CLD was observed in 47 (14, 3%) subjects. 2% of patients developed

decompensated cirrhosis due to ascites ($n = 5$) and hepatic encephalopathy ($n = 1$), but only one patient died due to end-stage liver disease. No difference in survival was observed in patients without CLD when compared to their counterparts with CLD (85, 7 [69–102] vs. 77, 0 [51–102] months in those with CLD, $p = 0.385$). Number of chemotherapeutic agents (4 [2–4] vs. 3 [3–4], $p = 0.002$) and number of chemotherapy cycles (21 [12–37] vs. 13 [8–27]) of those patients without CLD, $p = 0.005$ employed, exposure to 5-FU (89% vs. 73% of those patients without CLD, $p = 0.02$) and irinotecan (66% vs. 46% of those patients without CLD, $p = 0.01$) were significantly correlated to development of CLD, but only number of chemotherapy cycles was independently associated with CLD on multivariate analysis.

Conclusion: Evidence of CLD was observed in a considerable number of patients treated with chemotherapy due to GI tumors. Few developed either decompensation or liver-related mortality. Number of chemotherapy cycles was independently associated with CLD. Screening for CLD should be recommended for long-term survivors of GI tumors, particularly those previously exposed to several cycles of chemotherapy.

SAT-121

Point-of-care ultrasound of the inferior vena cava for intravascular volume assessment in patients with cirrhosis during intravenous albumin infusion

Daniel Segna¹, Pompilia Radu¹, Gerard Angeles Fite¹, Jaime Bosch^{1,2}, Annalisa Berzigotti^{1,2}. ¹Department of Visceral Surgery and Medicine, Hepatology, Inselspital, Bern University Hospital, Bern, Switzerland; ²Department for BioMedical Research, Visceral Surgery and Medicine, University of Bern, Bern, Switzerland
Email: daniel.segna@insel.ch

Background and aims: In patients with decompensated cirrhosis, current guidelines recommend intravenous (i.v.) albumin for different indications (i.e. large volume paracentesis; hepatorenal syndrome; spontaneous bacterial peritonitis). However, an increasing number of studies reported on iatrogenic volume overload related to albumin i.v. in this population. Point-of-care ultrasound (POCUS) of the inferior vena cava (IVC) is a non-invasive tool for monitoring intravascular volume status, but data in cirrhosis is scarce. Our aim is to explore the use of POCUS of the IVC for assessing changes in diameters and collapsibility reflecting intravascular volume status during passive leg raise (PLR) and its potential prediction of volume response after albumin i.v.

Method: In this prospective proof-of-concept study including 55 patients with decompensated cirrhosis and absent right heart failure requiring albumin i.v. for clinical indications, we assessed changes in minimal and maximal IVC diameters (IVC min, IVC max) and collapsibility (IVCCI) during an entire respiratory cycle during PLR and after albumin i.v. using POCUS (Venue Fit, GE Healthcare). We defined intravascular volume overload as IVC max > 2.1 cm and IVCCI $< 20\%$.

Results: In our study population (78% male, median age 61 years, 53% alcohol-related cirrhosis, 57% Child-Pugh stage B, median model for end-stage liver disease score 16), 94% received albumin i.v. (median 40 g) following paracentesis (median 5.2 l ascites). We found a significant increase in IVC min and IVC max both during PLR (mean IVC min 9.5 to 11.2 cm, mean IVC max 14.1 to 16.1 cm, all $p < 0.01$) and after albumin i.v. (mean IVC min 9.8 to 14.9 cm, mean IVC max 14.0 to 20.4 cm, all $p < 0.01$). Moreover, we observed a significant decrease in IVCCI during PLR (mean IVCCI 33% to 31.3%, $p < 0.01$) and after albumin i.v. (mean IVCCI 31.2% to 27.1%, $p < 0.01$). After albumin i.v., changes in IVC min, IVC max, but not IVCCI, were significantly higher than during PLR. In multivariate regression models adjusting for age, sex and body mass index, only an increase in IVC min ($p = 0.03$), but not IVC max and IVCCI during PLR, was significantly associated with an increase in IVC min after albumin i.v. Intravascular volume overload significantly increased after albumin i.v. (3 patients at baseline vs. 11 patients after albumin i.v., $p = 0.02$).

Conclusion: Patients with decompensated cirrhosis showed significant increases in IVC diameters and decreases in IVCCI after albumin i. v., thereof 13% with intravascular volume overload. Changes in IVC max and IVCCI during PLR did not accurately predict the same parameters after albumin i.v., potentially related to variable extents of intra-abdominal pressure. However, increases in IVC min during PLR were found to correlate with corresponding increases after albumin i. v. The clinical use of POCUS of the IVC individualizing albumin i.v. should be further investigated.

SAT-122

Biomarkers of extracellular matrix remodelling are linked to portal hypertension and disease progression in patients with stable advanced chronic liver disease

Benedikt Simbrunner¹, Ida Falk Villesen², Lorenz Balcar¹, Georg Semmler¹, Lukas Hartl¹, Benedikt Hofer¹, Mathias Jachs³, Michael Schwarz¹, Nina Dominik¹, Bernhard Scheiner¹, Rodrig Marculescu⁴, Michael Trauner¹, Morten Karsdal⁵, Thomas Reiberger¹, Diana Leeming⁶, Mattias Mandorfer¹. ¹Division of Gastroenterology and Hepatology, Department of Medicine III, Medical University of Vienna, Vienna, Austria; ²Department of Gastroenterology and Hepatology, Center for Liver Research, Odense University Hospital, Odense, Odense, Denmark; ³Division of Gastroenterology and Hepatology, Department of Medicine III, Medical University of Vienna, Vienna, Austria; ⁴Department of Laboratory Medicine, Medical University of Vienna, Austria, Vienna, Austria; ⁵Nordic Bioscience, Hepatic and Pulmonary Research, Herlev, Denmark, Herlev, Denmark; ⁶Nordic Bioscience, Hepatic and Pulmonary Research, Herlev, Denmark, Herlev, Denmark
Email: benedikt.simbrunner@meduniwien.ac.at

Background and aims: Advanced liver fibrosis in advanced chronic liver disease (ACLD) results from excessive remodeling of the extracellular matrix (ECM) characterized by collagen deposition in the interstitial matrix (ISM) and basement membrane (BM). Accumulating liver fibrosis induces portal hypertension (PH), and promotes clinical complications. This study assessed collagen remodeling biomarkers and their relationship with PH and clinical outcome.

Method: Patients with stable ACLD (n = 232) undergoing hepatic venous pressure gradient (HVPG) measurement were included. Blood biomarkers reflecting collagen formation and degradation of the interstitial matrix (collagen III: PRO-C3, C3M; VI: PRO-C6, C6M) and basement membrane (collagen IV: PRO-C4, C4M; XVIII: PRO-C18L), as well as tissue inhibitor of metalloproteinases-1 (TIMP-1) were measured. Using Cox regression models the predictive value was assessed for the composite end point of first/further decompensation, acute-on-chronic liver failure, or liver-related death.

Results: The study cohort comprised 131 (57%) patients with decompensated ACLD (dACLD), median HVPG and MELD were 18 (13–21) mmHg (HVPG 6–9: n = 28, 10–19: n = 124, ≥20: n = 80) and 11 (9–14) points, respectively. Biomarkers of ISM and BM formation (PRO-C3 and PRO-C6: p < 0.001; PRO-C4: p = 0.033) significantly increased across HVPG strata, except for PRO-C18L (p = 0.231). Collagen degradation markers C3M and C4M also increased with HVPG (p < 0.01), while no difference was observed for C6M (p = 0.542). A relative increase of collagen III and VI formation (PRO-C3/C3M and PRO-C6/C6M ratios; i.e. ISM) but not collagen IV ratio (p = 0.729; i.e. BM) was associated with PH severity: 0.90 (0.58–1.14) vs. 1.34 (0.89–1.92) vs. 1.12 (0.73–2.04, p < 0.001) and 33.9 (22.5–39.8) vs. 45.3 (33.3–61.4) vs. 48.6 (32.6–64.0, p < 0.001) across HVPG groups. Notably, the ECM degradation inhibitor TIMP-1 was significantly linked to PRO-C3/C3M and PRO-C6/C6M ratios in linear regression models adjusted for HVPG and MELD (all p < 0.001), but not to PRO-C4/C4M (p = 0.671). Multivariate Cox regression models assessing the prognostic value of ECM biomarkers (median follow-up 28.9 months, IQR 12.0–43.6) for the composite end point were adjusted for established prognostic indicators. Next to HVPG and dACLD at baseline, PRO-C4 (aHR per 100 ng/ml: 1.12, 1.02–1.23, p =

0.019) and TIMP1 (aHR per 100 ng/ml: 1.20, 1.05–1.36, p = 0.006) remained independently linked to disease progression.

Conclusion: ECM remodeling biomarkers are closely linked to PH in patients with stable ACLD. While a net increase of ISM formation primarily corresponds with PH severity, BM formation markers were prognostic for disease progression independently from PH severity. These data indicate that distinct compartments of ECM remodeling and their individual pathophysiological and prognostic impact should be explored further.

SAT-123

Evaluation of portal hemodynamics after etiological factor removal and persistence of varices in patients with an HVPG <10 mmHg and NITs within the grey zone

Pol Olivas Alberch¹, Alexandre Soler², Luis Téllez³, Jose A. Carrión⁴, Edilmar Alvarado-Tapias⁵, José Alberto Ferrusquía⁶, Sabela Lens^{7,8}, Antonio Guerrero⁹, M. Àngels Falgà¹⁰, Pamela Vizcarra¹¹, Lara Orts⁷, Valeria Perez¹², Sarah Shalaby¹³, Anna Baiges¹³, Fanny Turon⁷, Juan Carlos García-Pagán^{8,14}, Maria Àngeles García-Criado¹⁵, Virginia Hernández-Gea^{16,17}. ¹Liver Unit, Hospital Clínic, Health Care Provider of the European Reference Network on Rare Liver Disorders (ERN-Liver), Barcelona, Fundació de Recerca Clínic de Barcelona-Institut d'Investigacions Biomèdiques August Pi Sunyer (FRCB-IDIBAPS), Barcelona, Barcelona, Spain; ²Radiology Department. CDI. Hospital Clínic Barcelona. Barcelona. Spain., Barcelona, Spain; ³Hospital Universitario Ramón y Cajal. Universidad de Alcalá. Servicio de Gastroenterología y Hepatología, Madrid, Spain; ⁴Liver Section, Gastroenterology Department, Hospital del Mar, Barcelona, Institut Hospital del mar d'investigacions Mèdiques, PSMAR, Universitat Pompeu Fabra, Facultat de ciències de la Salut i de la Vida, Barcelona, Spain; ⁵Gastroenterology Department Hospital de la Santa Creu i Sant Pau, Institut d'Investigacions Biomèdiques Sant Pau, Barcelona, Spain, Centro de Investigación Biomédica Red de Enfermedades Hepáticas y Digestivas (CIBEREH), Madrid, Barcelona, Spain; ⁶Unitat Hepatologia, Servei d'Aparell digestiu. Parc Taulí Hospital Universitari. Institut d'Investigació i Innovació Parc Taulí (I3PT-CERCA). Universitat Autònoma de Barcelona, Sabadell, Spain; ⁷Liver Unit, Hospital Clínic, Health Care Provider of the European Reference Network on Rare Liver Disorders (ERN-Liver), Fundació de Recerca Clínic Barcelona-Institut d'Investigacions Biomèdiques August Pi i Sunyer (FRCB-IDIBAPS), Centro de Investigación Biomédica Red de Enfermedades Hepáticas y Digestivas (CIBEREHD), Barcelona, Spain; ⁸Medicine Department, Faculty of Medicine, Universitat de Barcelona, Barcelona, Spain; ⁹Hospital Universitario Ramón y Cajal. Universidad de Alcalá. Servicio de Gastroenterología y Hepatología, Madrid, Spain; ¹⁰Hospital Clínic Barcelona, Barcelona, Spain; ¹¹Hospital Clínic Barcelona, Barcelona, Spain; ¹²Liver Unit, Hospital Clínic, Health Care Provider of the European Reference Network on Rare Liver Disorders (ERN-Liver), Fundació de Recerca Clínic Barcelona-Institut d'Investigacions Biomèdiques August Pi i Sunyer (FRCB-IDIBAPS), Centro de Investigación Biomédica Red de Enfermedades Hepáticas y Digestivas (CIBEREHD), Barcelona, Spain; ¹³Liver Unit, Hospital Clínic, Health Care Provider of the European Reference Network on Rare Liver Disorders (ERN-Liver), Fundació de Recerca Clínic Barcelona-Institut d'Investigacions Biomèdiques August Pi i Sunyer (FRCB-IDIBAPS), Centro de Investigación Biomédica Red de Enfermedades Hepáticas y Digestivas (CIBEREHD), Barcelona, Spain; ¹⁴Liver Unit, Hospital Clínic, Health Care Provider of the European Reference Network on Rare Liver Disorders (ERN-Liver), Fundació de Recerca Clínic Barcelona-Institut d'Investigacions Biomèdiques August Pi i Sunyer (FRCB-IDIBAPS), Centro de Investigación Biomédica Red de Enfermedades Hepáticas y Digestivas (CIBEREHD), Barcelona, Spain;

POSTER PRESENTATIONS

¹⁵Radiology Department, CDI, Hospital Clínic de Barcelona, Universitat de Barcelona, Barcelona, Spain, Barcelona, Spain; ¹⁶Liver Unit, Hospital Clínic, Health Care Provider of the European Reference Network on Rare Liver Disorders (ERN-Liver). Fundació de Recerca Clínic Barcelona-Institut d'Investigacions Biomèdiques August Pi i Sunyer (FRCB-IDIBAPS), Barcelona, Spain, Medicine Department, Faculty of Medicine, Universitat de Barcelona, Barcelona, Catalonia, Spain, Barcelona, Spain; ¹⁷Centro de Investigación Biomédica Red de Enfermedades Hepáticas y Digestivas (CIBEREHD), Madrid, Spain, Barcelona
Email: olivas.alberch@gmail.com

Background and aims: Etiological factor removal (ER) drives recompensation and improves portal hypertension (PH) in cirrhosis. Non-invasive tests (NITs) effectively identify patients at both low and high risk of clinically significant PH after viral elimination. However, a substantial grey zone persists. Interestingly, varices and portosystemic shunts (PPS) have been found in patients despite hepatic vein pressure gradient (HVPG) dropping below 10 mmHg after ER, questioning its accuracy in reflecting true portal pressure. The role of persistent presinusoidal vascular changes, resistant to regression, in potentially contributing to a pre-sinusoidal component of PH not captured by HVPG remains unclear. Our aim is to evaluate the correlation of HVPG with direct portal pressure in patients with persistence of varices after ER despite having an HVPG below 10 mmHg, and NITs in the grey zone and provide insights into the management of PH in cirrhosis regression.

Method: Bicentric "proof of concept" study in patients with HCV or alcohol-related cirrhosis with persistent varices, liver stiffness measurement (LSM) <25 kPa but >12 kPa and HVPG <10 mmHg after at least 5 years of ER. Evaluation of PH. Gastroscopy, LSM, spleen stiffness measurement (SSM), abdominal image, and simultaneous US-guided direct portal vein pressure and HVPG.

Results: 7 patients with HCV and 3 with alcohol-related cirrhosis were included. Median years of SVR and abstinence were 6 (5–7) and 14 (5–17) respectively. Before ER, all patients have varices and 3 were decompensated. At time of evaluation, all patients had a patent portal vein and were compensated. Median platelet counts were 129.5 (95–145) 10^9 /ml, median SSM 35.1 (29.3–43.6) kPa, and median LSM 16.5 (14.4–22.3) kPa. In 7 patients, varices remained the same size despite ER (4 large and 3 small), and 3 downsized to small. Median HVPG was 7 (6–9) mmHg and median portal pressure gradient (PPG) 6 (5–8) mmHg. The correlation between wedge hepatic vein pressure and portal pressure was excellent ($R\ 0.926\ p < 0.0001$). All patients had both PPG and HVPG below 10 mmHg.

Conclusion: In the context of ER and cirrhosis regression, varices may persist despite HVPG <10 mmHg. Due to its excellent correlation with direct portal pressure, HVPG is useful in identifying patients without PH despite the presence of varices. Whether these patients would require prophylaxis is unknown. Future studies with clinical end points are needed to validate our findings.

SAT-124

Lower post-transjugular intrahepatic portosystemic shunt overt hepatic encephalopathy and mortality in patients with hepatic venous communication

Li Ma¹, Jingqin Ma¹, Yaozu Liu¹, Wen Zhang¹, Zhiping Yan¹, Jianjun Luo¹. ¹Department of Interventional Radiology, Zhongshan Hospital, Fudan University, Shanghai, China, Shanghai, China
Email: luo.jianjun@zs-hospital.sh.cn

Background and aims: Intrahepatic venovenous shunt (IHVS) can result in underestimation of wedged hepatic venous pressure (WHVP), but its prognostic value remains unknown.

Method: The single-center data (2020–2022) of patients with sinusoidal portal hypertension (PHT) undergoing concurrent balloon-occluded hepatic venography and transjugular intrahepatic portosystemic shunt (TIPS) were retrospectively analyzed. The study hypothesized that patients with IHVS have less preexisting intrahepatic portal shunting.

Results: 131 patients (male/female: 94/37, mean age: 56.3 years) were eligible and classified by the presence ($n = 49, 37.4\%$) or absence ($n = 82, 62.6\%$) of IHVS. Model of end-stage liver disease score and blood ammonia were lower in IHVS group ($p < 0.001$). Agreement between WHVP and portal venous pressure (PVP) was poor in IHVS group (intraclass correlation coefficients [ICC]: 0.133, difference: 13.4 mmHg, $p < 0.001$), but almost perfect in non-IHVS group (ICC: 0.827, difference: 1 mmHg, $p = 0.005$). The WHVP/PVP ratio in non-IHVS group, reflecting total/functional portal perfusion, was negatively correlated with hepatic function and post-TIPS pressure reduction ($p < 0.05$). Within 1-year post-TIPS, IHVS group had a lower incidence of overt hepatic encephalopathy (HE) (12.4% vs. 32.0%, $p = 0.015$, HR: 0.35, 95% CI: 0.14–0.85) and an improved liver transplantation-free survival (98.0% vs. 87.8%, log-rank/Cox: $p = 0.046/0.081$, HR: 0.16, 95% CI: 0.02–1.25). The 1-year incidences of clinical relapse ($p = 0.767$), shunt dysfunction ($p = 0.916$), and survival ($p = 0.095$) were not significantly different between groups. **Conclusion:** For patients with sinusoidal PHT treated with TIPS, IHVS was associated with a reduced risk of overt HE and a potential survival benefit. Abnormal hepatic venous communication should be well-identified to evaluate prognosis.

SAT-125

Comparison of endoscopic variceal ligation and endoscopic cyanoacrylate injection for the treatment of acute variceal bleeding from the cardia to the lesser curvature of the stomach

Yu-Fu Chen^{1,2}, Tsung-Chieh Yang^{3,4,5}, Ping-Han Hsieh^{1,5}, Yu-Jen Chen^{6,7}, Jiing-Chyuan Luo⁵, Ming-Chih Hou^{1,7,9}. ¹Therapeutic and Research Center of Liver Cirrhosis and Portal Hypertension, Taipei Veterans General Hospital, Taipei, Taiwan; ²Division of Gastroenterology and Hepatology, Department of Medicine, Taipei Veterans General Hospital, Taipei, Taiwan; ³Therapeutic and Research Center of Liver Cirrhosis and Portal Hypertension, Taipei Veterans General Hospital, Taipei, Taiwan; ⁴School of Medicine, College of Medicine, National Yang Ming Chiao Tung University, Taipei, Taiwan; ⁵Division of Gastroenterology and Hepatology, Department of Medicine, Taipei Veterans General Hospital, Taipei, Taiwan; ⁶Therapeutic and Research Center of Liver Cirrhosis and Portal Hypertension, Taipei Veterans General Hospital, Taipei, Taiwan; ⁷School of Medicine, College of Medicine, National Yang Ming Chiao Tung University, Taipei, Taiwan; ⁸Division of Gastroenterology and Hepatology, Department of Medicine, Taipei Veterans General Hospital, Taipei, Taiwan
Email: tcyang@vghtpe.gov.tw

Background and aims: Practice guidelines endorse endoscopic variceal ligation (EVL) for the treatment of esophageal variceal bleeding and endoscopic cyanoacrylate injection (ECI) for the treatment of fundal variceal bleeding. However, the optimal treatment for acute variceal bleeding (AVB) from the cardia to the lesser curvature of the stomach is undefined. This study aims to compare the efficacy of EVL and ECI for the treatment of AVB from the cardia to the lesser curvature of the stomach. Varices extending for 0 to 2 cm below the gastroesophageal (GE) junction are defined as cardiac varices (CVs), and varices extending for 2 to 5 cm below the GE junction along the lesser curvature of the stomach are defined as type 1 gastroesophageal varices (GOV1 s).

Method: Patients with bleeding from CVs or GOV1 s who were treated by EVL or ECI at Taipei Veterans General Hospital were retrospectively evaluated. Clinical indicators, such as the presence of active spurting, active oozing, blood clots, or white nipple sign over CVs or GOV1 s were documented carefully during endoscopy. Outcomes including the cumulative incidences of six-week rebleeding and probability of six-week survival were compared between the EVL group and the ECI group by Kaplan-Meier method and log-rank test. Cox proportional hazards regression analysis was used to determine the indicators of six-week rebleeding and mortality. Subgroup analyses based on the bleeding location were performed.

Results: Between February 2006 and August 2023, a total of 97 patients (mean age 59 years, 71.1% male) were evaluated. Fifty-two and 45 patients were treated with EVL and ECI, respectively. Baseline characteristic were similar between the two groups. Both groups achieved high hemostasis rates with no significant differences regarding to five-day treatment failure rates ($p = 0.246$). No significant differences were noted between the two groups in terms of the cumulative incidences of six-week rebleeding ($p = 0.874$) and probability of six-week survival ($p = 0.715$). In multivariate analyses, ALT >40 U/L was the only independent predictor of six-week rebleeding (HR 5.281, 95% CI 1.066–26.172, $p = 0.042$), and Child-Pugh class C (HR 4.235, 95% CI 1.578–11.361, $p = 0.004$) as well as creatinine >1.3 mg/dL (HR 3.684, 95% CI 1.448–9.376, $p = 0.006$) were the independent predictors of six-week mortality. In subgroup analyses, the cumulative incidences of six-week rebleeding were lower in the EVL group than in the ECI group for bleeding from CVs ($p = 0.031$), but not for bleeding from GOV1s ($p = 0.840$).

Conclusion: EVL and ECI offer similar efficacy for the treatment of AVB from the cardia to the lesser curvature of the stomach. Notably, EVL displays a lower six-week rebleeding rate than ECI for bleeding from CVs, but not for bleeding from GOV1s.

SAT-126

Clinical Value of 4D Flow MRI in Assessing Varices Needing Treatment in Cirrhotic Patients with Portal Hypertension: A Prospective Study

Qian Zhang¹, Mingfeng Wu², Xinhua Luo¹, Hong Peng¹. ¹Guizhou Provincial People's Hospital, Guiyang, China; ²Guizhou Provincial People's Hospital, Guiyang, China
Email: 331610287@qq.com

Background and aims: Esophageal and gastric variceal (EGV) bleeding poses a critical threat in liver cirrhosis. Early identification of varices prone to hemorrhage is crucial for primary prevention, significantly reducing mortality rates. Non-invasive models for assessing portal hypertension are still evolving. 4D flow MRI, an advanced imaging technique, offers a comprehensive view of blood flow patterns and precise hemodynamic parameter quantification. Our study aims to fill this research gap, prospectively assessing the efficacy of 4D flow MRI in cirrhotic portal hypertension, validating its role as a non-invasive tool for risk stratification in this susceptible population.

Method: This study constitutes a cross-sectional analysis derived from our ongoing prospective cohort at Guizhou Provincial People's Hospital (Clinical Trial.gov: ChiCTR2300076380). We enrolled 85 participants, comprising 12 with compensated cirrhosis, 44 with decompensated cirrhosis, and 29 healthy volunteers. The study focuses on profiling portal circulation utilizing hemodynamic parameters obtained through 4D flow MRI.

Results: Comparing baseline characteristics between compensated and decompensated cirrhotic patients, we observed significant differences in sex, laboratory indicators, non-invasive markers, and endoscopic findings. 4D flow MRI enabled direct anatomic visualization of varices in 14 of 56 (25.0%) cirrhotic patients, with 13 (92.9%) of them having varices needing treatment (VNT). We conducted a quantitative analysis using 4D flow MRI and observed significant differences in portal vein fractional flow change (FFC), maximum pressure gradient, cross-sectional area, and wall shear stress for the portal vein, splenic vein, and superior mesenteric vein among the three groups ($p < 0.05$). In multivariable logistic regression models, portal vein's maximal pressure gradient, cross-sectional area, and FFC were independent predictors of VNT ($p < 0.05$). We constructed a 4D flow model model using the three mentioned indicators. The model had a sensitivity of 96.4%, negative predictive value of 95.7%, and negative likelihood ratio of 0.045, which avoided esophagogastroduodenoscopy (EGDs) comparable to the Baveno VII criteria (76.2% vs. 71.4%), while the missed VNT rate of the 4D flow model was lower than the Baveno VII criteria (3.6% vs. 14.3%).

Conclusion: Our initial findings suggest that FFC, portal vein maximum pressure gradient, and portal vein cross-sectional area measured through 4D flow MRI serve as valuable markers for stratifying esophagogastric varices in liver cirrhosis patients. The model built on these indicators demonstrates superior performance in identifying varices requiring treatment while minimizing unnecessary endoscopic examinations. Compared to the latest Baveno VII algorithm, our model shows improved efficacy and broader applicability.

SAT-128

Circulating fibronectin levels are linked to endothelial dysfunction, fibrogenesis, and portal hypertension in advanced chronic liver disease

Benedikt Simbrunner¹, Lorenz Balcar¹, Fabian Hammer¹, Benedikt Hofer¹, Georg Semmler¹, Mathias Jachs¹, Lukas Hartl¹, Nina Dominik¹, Philipp Schwabl¹, Rodrig Marculescu², Peter Quehenberger³, Bernhard Scheiner¹, Michael Trauner¹, Mattias Mandorfer¹, Thomas Reiberger¹. ¹Division of Gastroenterology and Hepatology, Department of Medicine III, Medical University of Vienna, Vienna, Austria; ²Department of Laboratory Medicine, Medical University of Vienna, Austria, Vienna, Austria; ³Department of Laboratory Medicine, Medical University of Vienna, Austria, Vienna
Email: benedikt.simbrunner@meduniwien.ac.at

Background and aims: Fibronectin (FN) is considered an important mediator of extracellular matrix remodelling and angiogenesis in the context of liver fibrosis. FN also interacts with von Willebrand factor (VWF) and may thereby impact on the haemostatic equilibrium. We investigated the relationship between FN and portal hypertension (PH), hepatic dysfunction, and biomarkers reflecting liver fibrogenesis and endothelial dysfunction in patients with advanced chronic liver disease (ACLD).

Method: Patients with stable ACLD ($n = 236$) undergoing measurement of hepatic venous pressure gradient (HVPG) without active malignancies, intake of platelet inhibitors or antithrombotic medication were included. FN levels and biomarkers of extracellular matrix (ECM) remodelling (ELF score, including single components P3NP, TIMP1, HA), endothelial activation/dysfunction (VWF, factor VIII [FVIII]) were measured.

Results: The study cohort displayed a median HVPG of 17 (12–21) mmHg (HVPG 6–9: $n = 37$, 10–19: $n = 118$, ≥ 20 : $n = 81$), median MELD was 11 (9–16), and 138 (58%) had decompensated ACLD. FN levels decreased across HVPG strata (median [IQR]: 38.5 [31–45.6] vs. 32.5 [25.2–41.8] vs. 29.5 [24.1–36.6] mg/dL; $p < 0.001$) and exhibited a significant negative correlation with MELD ($r = -0.521$, $p < 0.001$), VWF ($r = -0.232$; $p < 0.001$), ELF ($r = -0.207$; $p = 0.001$); particularly HA: $r = -0.322$; $p < 0.001$), but not with FVIII ($p = 0.082$). Multivariable linear regression models suggested an independent link between FN and biomarkers of endothelial dysfunction and ECM remodeling, since FN exhibited a positive coefficient to ELF ($\beta = 0.022$, $p < 0.001$) and to VWF ($\beta = 0.810$, $p = 0.067$) after adjusting for MELD and HVPG.

Conclusion: FN decreases in ACLD patients with severe PH and more pronounced hepatic dysfunction. Mechanistically, FN seems to be involved in ECM remodelling and endothelial dysfunction-as we observed a positive association after accounting for hepatic dysfunction and PH severity. Future studies should investigate the pathophysiological role of FN in liver fibrogenesis and sinusoidal dysfunction in ACLD.

POSTER PRESENTATIONS

SAT-129

Role of serum Mac-2 binding protein glycosylation isomer in identifying patients with chronic liver diseases at risk for portal hypertension-related complications

Kessarin Thanapirom^{1,2,3}, Pisit Tangkijvanich⁴, Sirinporn Suksawatamnuay^{1,2,3}, Panarat Thaimai^{1,2,3}, Sakunkan Marnmana¹, Sombat Treeprasertsuk¹, Piyawat Komolmit^{2,3,5}. ¹Division of Gastroenterology, Department of Medicine, Faculty of Medicine, Chulalongkorn University and King Chulalongkorn Memorial Hospital, Bangkok, Thailand; ²Center of Excellence in Liver Fibrosis and Cirrhosis, Chulalongkorn University, Bangkok, Thailand; ³Excellence Center in Liver Diseases, King Chulalongkorn Memorial Hospital, Thai Red Cross Society, Bangkok, Thailand; ⁴Center of Excellence in Hepatitis and Liver Cancer, Department of Biochemistry, Faculty of Medicine, Bangkok, Thailand; ⁵Division of Gastroenterology, Department of Medicine, Faculty of Medicine, Chulalongkorn University and King Chulalongkorn Memorial Hospital, Bangkok, Thailand
Email: kessarin.t@chula.ac.th

Background and aims: BAVENO VII consensus classifies portal hypertension (PHT) as compensated advanced chronic liver disease (cACLD) and clinically significant portal hypertension (CSPH) based on liver stiffness measurement (LSM) using transient elastography (TE). However, the availability of TE is still limited. The Mac-2 binding protein glycosylation isomer (M2BPGi) has emerged as a novel serum biomarker for liver fibrosis. This study aims to assess the association between serum M2BPGi, cACLD, and CSPH, as well as the role of M2BPGi in predicting liver decompensation (LD) during one-year follow-up.

Method: We prospectively enrolled patients with chronic liver diseases at Chulalongkorn University Hospital in Bangkok, Thailand, from June 2021 to October 2023. cACLD and CSPH are identified by LSM ≥ 10 kPa and ≥ 25 kPa, respectively. LD is characterized by the acute development of ascites, variceal bleeding, overt hepatic encephalopathy, or any combination of these complications.

Results: Overall, 376 patients were included, with 98 (26.1%) and 142 (37.8%) having cACLD and CSPH, respectively. At enrollment, 57 (15.2%) patients met the criteria of LD. Chronic liver diseases were caused by HBV ($n = 114$, 30.3%) and HCV ($n = 77$, 20.5%). M2BPGi levels were associated with the severity of PHT stages with a median of 0.79 (IQR: 0.41–1.34), 1.75 (IQR: 0.97–4.36), and 5.38 (IQR: 3.11–9.71) cutoff index (COI) in those with no cACLD, cACLD, and CSPH, respectively. The optimal M2BPGi cutoff for identifying cACLD was 1.71 COI (AUROC = 0.80, sensitivity 86%, specificity 74%) and 2.07 COI (AUROC 0.79, sensitivity 74.6%, specificity 83.6%) for CSPH. Patients with LD had higher M2BPGi than those without [6.95 (IQR: 4.17–11.56) vs 1.51 (IQR: 0.73–4.16) COI, $p < 0.001$]. At baseline, serum M2BPGi (OR = 1.13, 95%CI: 1.00–1.27, $p = 0.04$) and albumin (OR = 0.27, 95%CI: 0.13–0.56, $p < 0.001$) were independent factors associated with LD. During one-year follow-up, 21/319 (6.6%) patients without LD at baseline developed LD. Baseline serum M2BPGi (OR = 1.19, 95%CI: 1.07–1.32, $p < 0.001$) was associated with an increased risk of developing LD.

Conclusion: Serum M2BPGi is associated with stages of PHT and may be a potential serum biomarker for identifying risk for PHT-related complications in patients with chronic liver diseases.

SAT-130

Three-dimensional transjugular intrahepatic portosystemic shunt geometry predicts shunt dysfunction in decompensated liver cirrhosis

Markus Kimmann¹, Carsten Meyer², Sebastian Nowak², Alba Maria Paar Pérez³, Jörn Arne Meier¹, Sara Noemi Reinartz Groba¹, Juliana Goediker¹, Torid Jacob¹, Feras Sanoubara¹, Karsten Wolter², Chang Johannes³, Jonel Trebicka¹, Alois Martin Sprinkart², Michael Praktijn¹. ¹University Hospital Münster, Department of

Internal Medicine B, Münster, Germany; ²University Hospital Bonn, Department of Radiology, Bonn, Germany; ³University Hospital Bonn, Department of Internal Medicine I, Bonn, Germany
Email: markus.kimmann@googlemail.com

Background and aims: Patients with decompensated liver cirrhosis are at risk for complications of portal hypertension, especially refractory ascites or variceal bleeding. Transjugular intrahepatic portosystemic shunt (TIPS) is the most effective mean to reduce portal hypertension and treat these complications. However, development of TIPS dysfunction may lead to recurrence of these complications. This study investigated the prognostic value of three-dimensional (3D) TIPS geometry to predict TIPS dysfunction.

Method: We screened 330 patients undergoing TIPS insertion between 2014 and 2019 for this retrospective monocentric study. Overall, 108 patients could be included for the final analysis. Multiplanar reconstructions of computer tomography (CT) scans, which were performed after TIPS insertion, were used to investigate 3D TIPS geometry. Exclusion criteria were non-availability or insufficient quality of CT after TIPS insertion. Parameters of 3D TIPS geometry were calculated using a semi-automated algorithm. Additionally, angiograms were reviewed to determine two-dimensional (2D) geometric characteristics of the TIPS. Primary outcome was the development of TIPS dysfunction, which was defined by need for invasive TIPS revision. Uni- and multivariate Cox regression analysis with TIPS dysfunction as end point was performed to identify predictors for the development of TIPS dysfunction.

Results: Overall, 32 patients developed TIPS dysfunction and were compared to 76 patients without TIPS dysfunction. Both groups were comparable in regard of general characteristics (e.g., age, MELD and Child-Pugh Score). The median time from TIPS insertion to TIPS dysfunction was 539 days. In terms of 3D TIPS geometry parameters, a longer distance of the cranial stent end to the inferior vena cava ($p < 0.001$, hazard ratio 1.069, 95% confidence interval 1.039–1.101) and a more pronounced stent curvature ($p = 0.001$, hazard ratio 1.023, 95% confidence interval 1.009–1.037) were significantly associated with the development of TIPS dysfunction in a multivariate Cox regression analysis. Of note, none of the 2D TIPS geometry parameters was significantly associated with TIPS dysfunction in the univariate Cox regression analysis, while a distance of the cranial stent end to the inferior vena cava of more than one centimeter closely failed to reach statistical significance ($p = 0.053$, hazard ratio 2.333, 95% confidence interval 0.989–5.501).

Conclusion: This monocentric study demonstrates the prognostic value of 3D TIPS geometry using an algorithmic approach for the first time. Overall, a longer distance of the cranial stent end to the inferior vena cava as well as a more pronounced stent curvature could be identified as independent predictors of TIPS dysfunction.

SAT-131

End-procedural complete hemodynamic response may not be essential for the clinical success of tips in patients with cirrhosis

Davide Roccarina¹, Valentina Adotti¹, Martina Rosi¹, Dario Saltini², Marco Senzolo³, Silvia Nardelli⁴, Tomas Guasconi⁵, Silvia Aspite¹, Stefano Gitto¹, Umberto Arena¹, Lara Biribin⁶, Stefania Gioia⁴, Federica Indultti⁵, Claudia Campani¹, Patrizia Burra⁶, Oliviero Riggio⁴, Fabio Marra⁷, Filippo Schepis⁵, Francesco Vizzutti¹. ¹Department of Experimental and Clinical Medicine, University of Florence, Florence, Italy; ²Unit of Gastroenterology, Hepatic Hemodynamic Laboratory, Azienda Ospedaliero-Universitaria Policlinico di Modena and University of Modena and Reggio Emilia, Modena, Italy; ³Gastroenterology, Multivisceral Transplant Unit, Department of Surgical and Gastroenterological Sciences, University of Padua, Padua; ⁴Department of Translational and Precision Medicine, Sapienza University of Rome, Rome, Italy; ⁵Division of Gastroenterology, Modena Hospital, University of Modena and Reggio Emilia, Modena, Italy; ⁶Gastroenterology,

Multivisceral Transplant Unit, Department of Surgical and Gastroenterological Sciences, University of Padua, Padua, Italy;
⁷Department of Experimental and Clinical Medicine, University of Florence, Center for Research, High Education and Transfer DENOTe, University of Florence, Florence, Italy
 Email: davideroccarina@gmail.com

Background and aims: Transjugular intrahepatic portosystemic shunt (TIPS) is a well-established treatment for variceal bleeding (VB) and refractory ascites (RA) in liver cirrhosis. Immediate post-TIPS complete haemodynamic response (CHR), defined as a post-TIPS porto-caval gradient (PCG) <12 mmHg in VB and RA, or 50% PCG reduction in VB, is used to define a treatment success. TIPS underdilation reduces post-derivative complications, although with this strategy CHR is not always achieved, raising concerns on control of PH complications and survival.

We compared ascites control, bleeding recurrence and mortality rate among patients achieving CHR or partial (PHR) haemodynamic response after TIPS.

Method: From the prospective Italian TIPS Registry (RI-TIPS), we retrospectively analysed a series of cirrhotic patients who consecutively received TIPS for RA or secondary prophylaxis of VB at four referral Italian Centers from 2007 to 2021.

Results: 415 patients with liver cirrhosis, median age 61 (15), 28% females were enrolled. TIPS was indicated in 51% for VB and in 49% for RA. Fifty-percent received underdiluted TIPS (<8 mm). Overall, a CHR was achieved in 65%, with a median post-TIPS PCG of 8 (4) mmHg and a median percentage of PCG reduction of 60 (19)%. In PHR, post-TIPS PCG was 15 (4) mmHg while percentage of PCG reduction was 36 (14)%. Non-significant differences were observed in rebleeding rate (5% vs 4%, $p=0.73$, in CHR vs PHR, respectively). On binary logistic regression, stent dysfunction was the only predictor of rebleeding. The grade of ascites or the need for large volume paracentesis at 3, 6, 12 months did not significantly differ ($p=0.76, 0.77, 0.86$, respectively) between CHR and PHR. The median overall survival was 24 (34) months. Regardless of TIPS indication, survival as well as cumulative incidence of mortality were not significant different between CHR and PHR accounting for liver transplantation as a competing risk event. Advanced age and disease severity before TIPS turned out to be predictors of mortality.

Conclusion: CHR immediately after TIPS may not be essential to define the clinical success, with a substantial reduction in PCG exerting a pivotal role. Further studies are needed to identify a minimal threshold for PCG reduction.

SAT-134

Paired assessment of the hepatic venous pressure gradient with the push-wedge versus balloon-occlusion technique: impact of intrahepatic collaterals

Naomi Gestels¹, Wilhelmus Kwanten^{1,2}, Jolien Derdeyn¹, Toon Steinhäuser¹, Luisa Vonghia^{1,2}, Sven Francque^{1,2}, Thomas Vanwolleghem^{1,2}. ¹Antwerp University Hospital, Edegem, Belgium; ²Laboratory of Experimental Medicine and Paediatrics (LEMP), Antwerp, Belgium
 Email: naomi.gestels@uza.be

Background and aims: Two methods exist for hepatic venous pressure gradient (HVPG) assessment: the balloon-occlusion and push-wedge technique, but little information exists on comparability and influencing factors of both methods to assess portal hypertension (PHT).

We performed a pairwise comparison of the push wedge versus occlusion balloon technique and examined influencing factors of discordance.

Method: Clinical, biochemical, histological data and haemodynamic measurements were analysed for consecutive transjugular HVPG measurements between January 2018 and October 2023. Included variables were: 1) liver histology, on simultaneous transjugular biopsies; 2) MELD and Child-Pugh score; and 3) presence of

intrahepatic or extrahepatic collaterals on imaging. HVPG with both occlusion balloon and end-hole catheter were compared. A pressure difference of ≥ 2 mmHg ("disagreement") between the methods was considered clinically relevant. A separate analysis stratified patients as having PHT (HVPG >5 mm Hg) or clinically significant PHT (CSPH, HVPG ≥ 10 mm Hg), according to the technique.

Results: From 725 cases, 274 had a paired measurement and a complete dataset for analyses; 159 (57.6%) were male, mean age was 56.1 ± 12.9 years (SD); and 182 (66.4%) had advanced fibrosis (F3-F4). Most common aetiologies were alcohol-related liver disease (34.3%) and metabolic dysfunction-associated steatotic liver disease (29.9%). Intra- and extrahepatic collaterals were observed in 13.5% and 30.3% of cases respectively. Mean HVPG was $11.01 \text{ mmHg} \pm 6.63$ and $11.13 \text{ mmHg} \pm 6.67$ for the occlusion-balloon and push wedge technique respectively (ns). Disagreement was observed in 80 cases (29.2%) independent of the liver disease aetiology (Chi-Square 0.37), but significantly more in case of intrahepatic collaterals (Kruskal-Wallis $p=0.019$). Intrahepatic collaterals were observed in 37 cases; HVPG disagreement was found in 16/37 (43.2%). In case of HVPG disagreement in presence of collaterals a clear pattern was noted: in 11/16 the push wedge technique yielded the highest HVPG value whilst in 5/16 it was the opposite (Kruskal Wallis $p<0.01$). Discordance was not related to the severity of liver disease (Child-Pugh) or MELD in the subgroup of patients with advanced fibrosis. The PHT classification changed according to the applied technique in 32/274 (11.7%) of cases: 15/274 (5.5%) were discordantly classified concerning presence or absence of PHT, whereas 17/274 (6.2%) were differently classified regarding CSPH. When restricted to those with a disagreement between techniques, 19/80 cases (23.8%) were differently classified.

Conclusion: Occlusion balloon and push wedge technique yield comparable HVPG measurements in most patients (70.1%). In case of intrahepatic collaterals discordance occurred more frequently. We suggest using the push wedge technique when intrahepatic collaterals are found.

SAT-135

Soluble urokinase plasminogen activator receptor (suPAR) levels predict survival in patients with portal hypertension undergoing TIPS

Sven H. Loosen¹, Fabian Benz², Raphael Mohr², Philipp Reuken³, Theresa Hildegard Wirtz⁴, Wenyi Gu⁵, Lioba Junker⁴, Christian Jansen⁶, Carsten Meyer⁷, Michael Praktijn⁵, Alexander Wree², Johanna Reissing⁴, Münevver Demir², Mihael Vucur⁸, Robert Schierwagen⁵, Andreas Stallmach³, Anselm Kunstein⁸, Johannes Bode⁸, Christian Trautwein⁴, Frank Tacke², Tom Luedde⁸, Tony Bruns⁴, Jonel Trebicka⁵, Christoph Roderburg⁸. ¹Department of Gastroenterology, Hepatology and Infectious Diseases, University Hospital Düsseldorf, Medical Faculty of Heinrich Heine University Düsseldorf, Düsseldorf, Germany; ²Department of Gastroenterology and Hepatology, Campus Virchow Klinikum and Campus Charité Mitte, Charité Universitätsmedizin Berlin, 13353 Berlin, Germany, Berlin, Germany; ³Department of Internal Medicine IV, Jena University Hospital, Am Klinikum 1, 07747 Jena, Germany, Jena, Germany; ⁴Department of Medicine III, University Hospital RWTH Aachen, Pauwelsstrasse 30, 52074 Aachen, Germany, Aachen, Germany; ⁵Department of Internal Medicine B, University of Münster, Münster, Germany, Münster, Germany; ⁶Department of Internal Medicine I, University Clinic Bonn, Bonn, Germany, Bonn, Germany; ⁷Department of Radiology, University Clinic Bonn, Bonn, Germany, Bonn, Germany; ⁸Department of Gastroenterology, Hepatology and Infectious Diseases, University Hospital Düsseldorf, Medical Faculty of Heinrich Heine University Düsseldorf, 40225 Düsseldorf, Germany, Düsseldorf, Germany
 Email: Sven.Loosen@med.uni-duesseldorf.de

Background and aims: Transjugular intrahepatic portosystemic shunt (TIPS) is the most effective therapy for complications of

POSTER PRESENTATIONS

portal hypertension. However, clinical outcomes following TIPS placement vary widely between patients and identifying ideal candidates remains a challenge. Soluble urokinase plasminogen activator receptor (suPAR) is a circulating marker of immune activation that has previously been associated with liver inflammation, but its prognostic value in patients receiving TIPS is unknown. In the present study, we evaluated the potential clinical relevance of suPAR levels in patients undergoing TIPS insertion.

Method: suPAR concentrations were measured by enzyme-linked immunosorbent assay (ELISA) in hepatic vein (HV) and portal vein (PV) blood samples from 99 patients (training cohort), as well as peripheral venous blood samples from additional 150 patients (validation cohort) undergoing TIPS placement. The association between suPAR levels and patients' outcome was assessed using Kaplan-Meier methods and Cox-regression analyses.

Results: suPAR concentrations were significantly higher in HV samples compared to PV samples and correlated with the presence of ascites, renal injury, and consequently with the Child-Pugh and MELD scores. Patients with higher suPAR levels had a significantly worse short- and long-term survival after TIPS insertion, which remained robust after adjustment for confounders in multivariate Cox-regression analyses. Sensitivity analysis showed an improvement in risk prediction in patients stratified by Child-Pugh or MELD score. In an independent validation cohort, higher levels of suPAR predicted poor transplant-free and overall survival after TIPS, particularly in patients with Child-Pugh A/B cirrhosis.

Conclusion: suPAR seems to largely derive from the injured liver and its levels may predict of outcome in patients undergoing TIPS. suPAR, as a surrogate of hepatic inflammation, may be used to stratify care in patients undergoing TIPS insertion.

SAT-136

The modified child-turcotte-pugh score based on plasma ammonia to predict survival in patients with cirrhosis after transjugular intrahepatic portosystemic shunt: a multicenter validation

Binlin Da¹, Wei Wu², Wuhua Guo³, Kai Xiong⁴, Chao Cheng⁵, Qiao Ke³, Moran Zhang⁴, Taishun Li¹, Jiangqiang Xiao¹, Lei Wang¹, Ming Zhang¹, Feng Zhang¹, Yuzheng Zhu¹. ¹Nanjing Drum Tower Hospital Clinical College of Nanjing Medical University, Nanjing, China; ²The First Affiliated Hospital of Wenzhou Medical University, Wenzhou, China; ³Mengchao Hepatobiliary Hospital of Fujian Medical University, Fuzhou, China; ⁴The Second Affiliated Hospital of Nanchang University, Nanchang, China; ⁵The First Affiliated Hospital of Wenzhou Medical University, Wenzhou, China
Email: yuzheng9111963@aliyun.com

Background and aims: The modified Child-Turcotte-Pugh score based on plasma ammonia (aCTP) score was created to predict survival for patients with decompensated cirrhosis. Aims: The aim of this study was to perform the first external validation of the aCTP score and compare it with other risk scoring systems to predict survival in patients with cirrhosis after transjugular intrahepatic portosystemic shunt (TIPS) placement.

Method: We retrospectively reviewed 473 patients from three cohorts between January 2016 and June 2022 and compared the aCTP score with the Child-Turcotte-Pugh (CTP) score, albumin-bilirubin (ALBI), model for end-stage liver disease (MELD) and sodium MELD (MELD-Na) in predicting transplant-free survival by the concordance index (C-index), area under the receiver operating characteristic curve (AUROC), calibration plot, and decision curve analysis (DCA).

Results: The median follow-up time of the cohort was 29 months, during which a total of 62 (20.74%) patients died or underwent liver transplantation (LT). The survival curves for the three aCTP grades

differed significantly. Patients with aCTP grade C had a shorter expected lifespan than patients with aCTP grades A and B ($p < 0.0001$). The aCTP score showed the best discriminative performance using the C-index compared with other scores at each time point during follow-up, it also showed better calibration in the calibration plot and the lowest Brier scores, and it also showed a higher net benefit than the other scores in the DCA curve.

Conclusion: The aCTP score outperformed the other risk scores in predicting survival after TIPS placement in patients with cirrhosis and may be useful for risk stratification and survival prediction.

SAT-137

Multivariable models for prediction of decompensation in compensated advanced chronic liver disease often lack external validation and measures of calibration

Vincent Haghnejad^{1,2}, Laura Burke³, Richard Parker⁴, Ian Rowe². ¹Department of hepatology and gastroenterology, University Hospital of Nancy, University of Lorraine, INSERM UMR_S 1256, Nutrition, Genetics, and Environmental Risk Exposure (NGERE), Faculty of Medicine of Nancy, Nancy, France; ²Leeds Institute for Medical Research, University of Leeds, Leeds, United Kingdom; ³Leeds Liver Unit, Leeds Teaching Hospitals NHS Trust, Leeds Institute for Medical Research, University of Leeds, Leeds, United Kingdom; ⁴Leeds Teaching Hospitals NHS Trust, St. James's University Hospital, Leeds, United Kingdom
Email: v.haghnejad@chru-nancy.fr

Background and aims: Prediction of decompensation in persons with compensated advanced chronic liver disease (cACLD) provides opportunities to personalise therapy. Prediction of decompensation is however challenging and multiple predictive models have been developed. The aim of this study was to systematically identify, collate, and critically appraise the performance of published multivariable models for the prediction of decompensation in patients with cACLD or compensated cirrhosis.

Method: From inception to November 2023, MEDLINE and EMBASE databases were searched for studies deriving and/or validating prediction models for the development of decompensation. The study was registered on PROSPERO (CRD42023488395) done according to the Checklist for critical Appraisal and data extraction for systematic Reviews of prediction Modelling Studies (CHARMS).

Results: We included 17 retrospective and 3 prospective studies. 9 studies were focused on a single aetiology, most commonly MASLD and HCV. There was no study describing a model specifically predicting outcomes in persons with alcohol-related liver disease. Outcome definition was heterogeneous across studies with 6 models predicting hepatocellular carcinoma together with decompensation. In total, 29 predictors of decompensation were included in the models assessed. The most frequent predictors were albumin, platelets, age, liver stiffness, bilirubin, MELD score, the presence of esophageal varices, and international normalized ratio. 7 predictors were non-standard analytes. Only 2 studies included an a priori power calculation to guide predictor selection. All studies reported discrimination measures, such as area under the curve (AUC), yet only 11/20 had any evaluation of calibration. External validation was done in 10/20 studies.

Conclusion: For clinical utility a predictive model must accurately describe future risks. Models developed for the prediction of decompensation in persons with cACLD are often poorly described and lack external validation. The inclusion of non-standard analytes and parameters limits opportunities for independent external validation and clinical applicability. Future model development should focus on the context in which models will be used, incorporation of routinely measured parameters, and ensuring that model performance is appropriately reported.

Fibrosis – Stellate cell biology

TOP-564

Dual alpha-v/beta-6 and alpha-v/beta-1 integrin inhibitor bexotegast targets TGF-beta inhibition to specific cell types in human liver explant tissue with biliary fibrosis

Johanna Schaub¹, Richard Ahn¹, Chris Her¹, Steve Ho¹, Vikram Rao¹, Jessie Lau¹, Mahru An¹, Jennifer Yuzon¹, Scott Turner¹, Martin Decaris¹. ¹Pliant Therapeutics, South San Francisco, United States
Email: jschaub@pliantrx.com

Background and aims: TGF-beta is a master regulator of fibrotic disease, however systemic inhibition of TGF-beta signaling has limited therapeutic utility due to the pleiotropic nature of TGF-beta in regulating homeostatic cellular pathways. Bexotegast (PLN-74809) is a dual inhibitor of the TGF-beta-activating integrins alpha-v/beta-6 (expressed by injured cholangiocytes) and alpha-v/beta-1 (expressed by myofibroblasts) currently in clinical development for the treatment of primary sclerosing cholangitis (PSC). The aim of this study was to combine 10× single nuclei RNA sequencing with the precision-cut liver slice (PCLivS) platform to test the hypothesis that bexotegast targets reduction of TGF-beta signaling to specific liver cell types in biliary fibrosis.

Method: Liver explants were collected from patients with PSC (n = 3) and primary biliary cholangitis (n = 1) at the time of transplant. PCLivS were generated and cultured for 2 days with bexotegast, TGF-beta receptor I kinase inhibitor (ALK5i, R-268712), or vehicle. Nuclei were isolated and processed for single nuclear barcoding using 10× Chromium Next GEM 3' HT kits. Resulting libraries were sequenced, processed using Cell Ranger, and analyzed using Seurat. Custom annotation of cell types was performed using gene markers from published data sets. Differentially expressed genes (DEGs) were determined using a non-parametric Wilcoxon rank sum test and defined as genes with absolute log2 fold-change ≥ 0.5 and an FDR ≤ 0.05.

Results: Differential gene expression analysis of PCLivS from explants with biliary fibrosis revealed a strong overlap in the pharmacodynamic effects of bexotegast and ALK5i in key pathologic cell types. A similar number of DEGs and similar pathways (e.g. extracellular matrix organization) were downregulated in myofibroblasts (124 vs 153 DEGs), cholangiocytes (71 vs 56 DEGs), and scar-associated endothelial cells (183 vs 227 DEGs) following treatment with bexotegast or ALK5i, respectively. In contrast, bexotegast treatment induced fewer gene expression changes in immune cell types than ALK5i. Notably, effects of bexotegast differed from ALK5i in B cells (27 vs 317 total DEGs) and Kupffer cells (149 vs 415 total DEGs). Pathway enrichment analysis identified interferon signaling (B cells) and immune system (B cells and Kupffer cells) as pathways altered by ALK5i, consistent with the immunomodulatory role of TGF-beta.

Conclusion: Dual alpha-v/beta-6 and alpha-v/beta-1 integrin inhibition with bexotegast showed clear differences from ALK5 inhibition in PCLivS from human liver explants with biliary fibrosis, targeting reduction of TGF-beta signaling pathways to fibrogenic cell populations. These findings provide valuable insight into the mechanism of action of bexotegast and demonstrate the utility of this approach for distinguishing the cell-specific effects of anti-fibrotic therapies.

THURSDAY 06 JUNE

THU-522

Proteomics analysis of liver fibrosis reveals Fibulin-3 as a new regulator of hepatic stellate cells

Célia Thomas¹, Dominique Bonnier², Vincent Legagneux², Nathalie Thérêt². ¹Univ Rennes, Inserm, EHESP, Irset (Institut de recherche en santé, environnement et travail)-UMR_S1085, Rennes, France; ²Univ Rennes, Inserm, EHESP, Irset (Institut de recherche en santé, environnement et travail)-UMR_S 1085, Rennes, France
Email: celia.thomas@univ-rennes.fr

Background and aims: Chronic liver diseases (CLD) are associated with the development of liver fibrosis, characterized by excessive accumulation of extracellular matrix (ECM). This fibrotic microenvironment affects tissue homeostasis and favors initiation and progression of hepatocellular carcinoma (HCC). During liver injury, hepatic stellate cells (HSCs) are activated and differentiate into myofibroblasts that secrete ECM components, therefore contributing to fibrosis. The present study aimed to identify and investigate new proteins involved in the remodeling of the hepatic microenvironment in order to decipher the mechanisms of CLD progression.

Method: A proteomics screening was conducted using ECM-enriched samples from adjacent non-tumor tissues from 20 patients with HCC and data were compared to the matrisome signature (Naba et al., 2015). Analyses of Fibulins mRNA expression were performed in cultured human hepatocytes (HHs) and HSCs using RT-qPCR. The expression of Fibulin-2 and -3 was silenced using RNA interference in the human HSC-derived cell line, LX-2. Protein extracts were analyzed using Western Blot. Phenotypic changes were assessed by immunofluorescence studies using Phalloidin for actin fibers and Paxillin antibody for focal adhesions. Cell migration and spreading were evaluated using transwell assay and xCELLigence real-time cell analysis, respectively. Integrative analyses of protein-protein interaction (PPI) networks were performed using PSICQUIC web service from EMBL-EBI database (Aranda et al., 2011).

Results: Proteomics analyses of human fibrotic liver tissues identified three members of the Fibulin family, Fibulin-2, -3 and -5, associated with fibrosis progression. mRNA analyses from cultured hepatic cells revealed that these Fibulins are highly expressed in cultured HSCs compared to HHs. We showed that LX-2 cell line express Fibulin-2 and -3 while Fibulin-5 is only detected after TGF-β stimulation. Upon silencing, we observed smaller, less spread-out cells with shorter cell body extensions in Fibulin-3 but not Fibulin-2 depleted cells. These cells displayed a disorganized cytoskeleton network and smaller nuclei indicating that less tensions are exerted through the stress fibers. Silencing Fibulin-3 also affects cell spreading and migration. Consistently, both focal adhesions and the activity of the focal adhesion-associated protein kinase, FAK, are impaired in Fibulin-3 depleted cells. In line with the differential effects of Fibulin-2 and -3 silencing, PPI networks demonstrated that Fibulin-2, -3 and -5 have different binding partners, suggesting involvement in different biological processes.

Conclusion: While Fibulin-2, -3 and -5 are all upregulated in liver fibrosis, our study suggest that Fibulin-3 plays an important role in regulating contact of HSC with the microenvironment.

THU-523

Single cell resolution of hepatic heterogeneity in liver fibrosis progression and regression

Le Thi Thanh Thuy¹, Pham Minh Duc², Hoang Hai², Nguyen Thi Ha², Norifumi Kawada². ¹Department of Global Education and Medical Sciences, Graduate School of Medicine, Osaka Metropolitan University, Department of Hepatology, Graduate School of Medicine, Osaka Metropolitan University, Osaka, Japan; ²Department of Hepatology, Graduate School of Medicine, Osaka Metropolitan University, Osaka, Japan
Email: kawadanori@omu.ac.jp

POSTER PRESENTATIONS

Background and aims: Single Cell Fixed RNA Profiling (FRP) is a novel technology that measures RNA expression in single cells from frozen tissues fixed with formaldehyde, using probes targeting the whole transcriptomes. Here we applied this novel technology in the murine model of advanced liver fibrosis progression and regression to discover novel targets for anti-fibrosis therapy.

Method: scRNA-seq was performed on primary cells isolated from frozen mouse liver tissues of the age-matched control, 10 weeks TAA-induced liver fibrosis group, and 2 weeks recovery after TAA injection group (n=3, each group) using the 10X Genomics Chromium platform. Computational analysis was performed in R.

Results: Integration and annotation of liver cells from control, fibrosis, and recovery revealed 10 cell types. Reclustering of Hepatocytes identified 20 subpopulations. Two main phenotypes in liver fibrosis were pericentral apoptotic and periportal proliferation hepatocytes. The fibrosis recovery generated a specific hepatocytes subcluster associated with antioxidant pathways by gene set enrichment analysis and exposed marked increased genes such as Cat, Gpx1, Sod1, Adh1, Gsta3. Reclustering of hepatic stellate cells (HSCs) identified 13 subpopulations. The fibrotic livers had 3 distinct subclusters, including one representing fibrogenic myofibroblast, and two intermediate-activated subclusters. Recovery of liver fibrosis revealed two specific HSCs subclusters, both reduced expression of fibrogenic markers, and restored expression of quiescence markers, whereas upregulated unique markers including Agtr1a, Ehd3, Cadm3, Gpx3, Emp1, and Fmo2. Receptor-ligand interaction analysis between Hepatocytes and HSCs by CellChat revealed significantly upregulated interaction pairs including Vitronectin Vtn- (Itga8+Itgb1), Fn1- (Itga8+Itgb1), Gdf15-Tgfb2, Igf1- (Itga6+Itgb4), and Agt-Agr1a.

Conclusion: Hepatocytes and HSCs in liver fibrosis progression and regression exposed cellular heterogeneity and their interaction play important role in both liver fibrosis progression and regression. Regulating receptor-ligands interactions could be potential targets for anti-fibrosis therapy.

THU-524-Y1

Single-cell atlas reveals conserved HSC activation process and therapeutic opportunities

Vincent Merens¹, Vincent De Smet¹, Stefaan Verhulst¹, Leo van Grunsven¹, ¹Vrije Universiteit Brussel, Brussels, Belgium
Email: vincent.merens@gmail.com

Background and aims: Chronic liver diseases are a major cause of death globally. Hepatic stellate cells (HSC) will produce most of the excessive scar-tissue that disrupts the liver function. Although HSCs have been extensively investigated in the past decades, we do not know if their activation process from quiescent HSC to a scar-tissue producing cell is similar in different liver disease settings. In this project, we pool recently generated single-cell RNA-sequencing (scRNA-Seq) datasets containing HSCs in different injury settings to investigate what ligands and transcription factors drive HSC activation in different injury settings.

Method: 10 different mouse scRNA-Seq datasets, representing 7 different liver injuries, were integrated to create the mouse HSC activation atlas. Similarly, 3 different human scRNA-Seq datasets were integrated consisting of varying chronic liver diseases. Comparison of ligands and transcription factors inducing HSC activation was done using the Seurat, pySCENIC, Slingshot and NicheNet packages in R and Python. Plasma levels of COLEC10 were assessed with ELISA. Parathyroid hormone induced HSC activation was assessed in primary mouse HSC-hepatocyte cultures with qPCR for fibrosis related genes and sirius red stainings for scar tissue formation.

Results: We found that in all investigated liver injuries, HSCs can be divided into 3 subtypes: quiescent HSCs, initiatory HSCs and myofibroblasts. The genesets and transcription factors defining these subtypes are conserved between liver injuries in mice and men: *Rxra*, *Nr1h4* and *Foxf1* for quiescent HSCs, *Fosl1*, *Egr3* and *Nfkb2* drive the initiatory phenotype while *Wt1*, *Prrx1* and *Mef2c* drive the

myofibroblast phenotype. The ligands inducing this activation process are conserved as well, with TGFβ1, SPP1 and EGF being the top predicted ligands inducing activation in almost all liver injuries. Additionally, we identified parathyroid hormone as a novel HSC activating ligand and validated its profibrotic effect in primary mouse HSCs-hepatocyte spheroid cultures. Finally, we identified COLEC10 as a gene that is almost exclusively expressed by quiescent HSCs in mice and humans. Strikingly, plasma levels of COLEC10 are correlated with the fibrosis stage of chronic liver disease patients and outperforms FIB-4 and APRI to predict the fibrosis stage.

Conclusion: We generated a mouse and human single cell HSC activation atlas and show that HSC activation is a very conserved process between different species and liver injuries, and is driven by a limited set of ligands and transcription factors across 3 conserved HSC stages. Additionally, we validate the use of COLEC10 as a biomarker for fibrosis as well as the profibrotic effect of a novel ligand, parathyroid hormone. Finally, we provide a user-friendly explorable versions of both the human and mouse HSC atlas through <https://livr.research.vub.be/rnaseq-projects>.

THU-525-Y1

Temporal and spatial development of cholestasis induced liver injury

Jonas Øgaard^{1,2}, Kathrine Sivertsen Nordhus^{1,2,3}, Markus S. Jørdens^{1,2,3,4}, Brian K. Chung^{1,2,3}, Espen Melum^{1,2,3,5,6},
¹Norwegian PSC Research Center, Oslo University Hospital and Institute of Clinical Medicine, University of Oslo, Oslo, Norway; ²Research Institute of Internal Medicine, Oslo University Hospital, Rikshospitalet, Oslo, Norway; ³Institute of Clinical Medicine, University of Oslo, Oslo, Norway; ⁴Department of Gastroenterology, Hepatology and Infectious Diseases, Medical Faculty, Heinrich Heine University Düsseldorf, University Hospital Düsseldorf, Düsseldorf, Germany; ⁵Section for Gastroenterology, Department of Transplantation Medicine, Division of Surgery, Inflammatory Diseases and Transplantation, Oslo University Hospital, Rikshospitalet, Oslo, Norway; ⁶Hybrid Technology Hub-Centre of Excellence, Institute of Basic Medical Sciences, Faculty of Medicine, University of Oslo, Oslo, Norway
Email: jonas.ogaard@medisin.uio.no

Background and aims: Cholestasis is a hallmark of liver diseases, resulting from a functional impairment of bile formation or mechanical obstruction of bile-flow through the bile ducts. Several animal models of this phenotype using either chemical or surgical interventions exist. Here we used the well described bile-duct ligation (BDL) model as this allows us isolate the biophysical consequences of bile duct obstruction which is commonly seen in primary sclerosing cholangitis, cholangiocarcinoma, and primary biliary cholangitis without being biased by the disease process itself. To assess the transcriptomic and cellular feature to an unprecedented temporal and spatial granularity we used high dimensional transcriptomic data along with spatial barcoding to track changes in different morphological compartments.

Method: C56Bl/6 mice underwent BDL or sham surgery and were sacrificed at 6 timepoints to capture transcriptomic events during the acute phase (4 h, 8 h, 24 h), as well as the recovery phase (3 d, 5 d, 7 d). Liver samples were snap frozen and processed for spatial transcriptomics using 10X Visium technology. The sequencing data was adjusted, normalized and finally spatially and cellularly deconvoluted using CARD, to generate a spatiotemporal map of cellular identities.

Results: Based on the transcriptomic data we clearly observed liver zonation and differential disease characteristics in periportal vs perivenous zones in a temporal manner. The CARD deconvolution predicted presence of hepatocytes matching the observed morphology and reduced abundance of hepatocytes was seen periportal. Known markers for liver disease activity were altered both spatially and temporally with *Alb* ($P_{\text{adj}} = 4.3 \times 10^{-9}$) and *Acta2* ($P_{\text{adj}} = 0.02$) exhibiting a zonated pattern, whereas *Ptprc* ($P_{\text{adj}} = 0.034$), *Timp1* (P_{adj}

= 0.04), *Acta2* ($P_{\text{adj}} = 0.015$) and *Mki67* ($P_{\text{adj}} = 0.011$) showed chronological modulations. Notably, *Ptprc* expression was dampened during the acute phase (fold-change (FC) = 0.51 to sham), while increased during the recovery phase (FC = 1.23), while *Timp1*, *Acta2* displayed an increasing, monotonic development over time.

Conclusion: Herein we have developed a spatiotemporal map of cellular and molecular development of cholestatic fibrosis during the extended acute phase. By integrating the spatial and temporal dimensions of this model condition, we have identified changes in key factors to a granularity no achievable using traditional technologies that can be of key relevance for developing novel treatment approaches targeting these pathways. Specifically, we demonstrate that molecular disease development in the BDL-model aligns with morphological and chronological expectations. The current results demonstrate the potential of dissecting cholestatic damage in 4 dimensions, giving promise to further investigate cholestasis despite challenges posed by morphological heterogeneity.

THU-526

The hepatoprotective role of ECM1: inhibition of mediators of latent TGF- β 1 activation and implications for anti-fibrotic treatment strategies in chronic liver disease

Frederik Link¹, Yujia Li¹, Jieliang Zhao^{2,3}, Stefan Munker^{4,5}, Weiguo Fan⁶, Zeribe Nwosu⁷, Ye Yao⁸, Seddik Hammad⁸, Peter ten Dijke⁹, Matthias Ebert^{1,10,11}, Roman Liebe¹², Honglei Weng⁸, Dirk Drasdo^{2,3}, Steven Dooley⁸, Sai Wang⁸. ¹University Medical Center Mannheim, Medical Faculty Mannheim, Heidelberg University, Department of Medicine II, Mannheim, Germany; ²INRIA, Paris, France; ³IfADO, Dortmund, Germany; ⁴Department of Medicine II, University Hospital, LMU, Munich, Germany; ⁵Liver Center Munich, University Hospital, LMU, Munich; ⁶School of Medicine, Stanford University, Palo Alto, United States; ⁷Department of Molecular Biology and Genetics, Cornell University, Ithaca, NY, United States; ⁸Department of Medicine II, University Medical Center Mannheim, Medical Faculty Mannheim, Heidelberg University, Mannheim, Germany; ⁹Oncode Institute and Department of Cell and Chemical Biology, Leiden, Netherlands; ¹⁰DKFZ-Hector Cancer Institute at the University Medical Center Mannheim, Mannheim, Germany; ¹¹Molecular Medicine Partnership Unit, European Molecular Biology Laboratory, Heidelberg, Germany; ¹²Clinic of Gastroenterology, Hepatology and Infectious Diseases, Otto-von-Guericke-University, Magdeburg, Magdeburg, Germany
Email: Frederik.Link@umm.de

Background and aims: Extracellular Matrix Protein 1 (ECM1) serves as a gatekeeper of hepatic fibrosis by maintaining liver tissue homeostasis, whereas its knockout causes lethal hepatic fibrosis resulting from an excessive activation of latent transforming growth factor- β 1 (TGF- β 1). In patients suffering from chronic liver disease (CLD) and HCC, the expression of ECM1 is decreased. We sought to investigate the mechanisms underlying the regulation of TGF- β 1 bioavailability by ECM1 and its impact on CLD progression.

Method: RNAseq was performed to analyze hepatic gene expression in *Ecm1*-knockout (*Ecm1*-KO) mice. Functional assays were performed using matrix metalloproteinases (MMP)-2/9 and thrombospondin 1 (TSP-1) or ADAMTS1 as extracellular matrix-resident mediators of latent TGF- β 1 activation in primary and immortalized hepatic stellate cells (HSCs) and TSP-1/ADAMTS1-derived peptides in WT or *Ecm1*-KO mice, and patient liver tissue. Computer modeling was employed to demonstrate consistency of experimental findings.

Results: *Ecm1*-KO mice sequencing data indicated the presence of severe liver fibrosis, in addition to an upregulation of mediators of latent TGF- β 1 activation including TSPs, ADAMTS proteases and MMPs. ECM1 overexpression or the addition of the recombinant protein abrogated TSP-1, ADAMTS1, MMP-2/9-mediated latent TGF- β 1 activation in HSCs. Interaction studies pinpointed ECM1's inhibitory effect to an interaction with intrinsic latent TGF- β 1-activating amino acid sequences of TSP-1 and ADAMTS1, KRFK and KTRF, respectively, while also reducing MMP-2/9 proteolytic activity.

In mice, ECM1 overexpression prevented KRFK-induced liver injury and fibrosis, whereas KTRF mimicked ECM1 and reverted *Ecm1*-KO-induced liver injury and fibrosis. In patients suffering from alcohol- or virus-related liver disease, ECM1 was inversely correlated with increasing expression of TSP-1, ADAMTS1 and MMP-2/9 and TGF- β 1 activation. Lastly, we integrated our findings into a computational model for validation.

Conclusion: Our findings underscore the hepatoprotective effect of ECM1 that inhibits mediators of latent TGF- β 1 activation. Strategies for maintaining or restoring ECM1 expression or functions in diseased livers could inform novel and safe anti-fibrotic therapies for CLD.

THU-527

Aging-associated liver sinusoidal endothelial cell dysfunction is involved in the progression of diet-induced liver steatosis and fibrosis

Qingqing Dai¹, Quratul Ain¹, Michael Rooney¹, Alexander Zipprich¹. ¹Jena University Hospital, Jena, Germany
Email: alexander.zipprich@med.uni-jena.de

Background and aims: Aging increases the susceptibility to fatty liver and accelerates liver fibrosis progression, but the underlying mechanisms are still not fully understood. Liver sinusoidal endothelial cells (LSECs) possess distinctive location and function in the liver microenvironment. Therefore, the aim of this study was to investigate the effect of aging-associated LSECs dysfunction on the hepatic microcirculation and the progression of diet-induced liver steatosis and fibrosis.

Method: Young (8 weeks) and aged (78 weeks) rats were subjected to methionine-choline deficient (MCD) diet-induced liver steatosis and fibrosis. Afterwards the liver tissue and blood samples were collected for histology staining and biochemistry tests. Moreover, bivascular liver perfusion (portal vein and hepatic artery) including measurement of sinusoidal resistance was performed in the presence of vasodilator Acetylcholine and nitric oxide donor S-Nitroso-N-acetyl-DL-penicillamine (SNAP) or vasoconstrictor methoxamine (MTX) with and without NOS inhibitor NG-Methyl-L-arginine acetate salt (L-NMMA) to evaluate hepatic hemodynamics and liver endothelial microcirculatory function.

Results: MCD-rats showed higher levels of serum alanine aminotransferase, hepatic triglyceride, and hepatic alpha-smooth muscle actin protein ($p < 0.05$ for all parameters, $N = 6$), which exacerbates with aging ($p < 0.05$ for all parameters, $N = 6$). Aged MCD-rats also showed higher basal portal venous vascular resistances (PVR; 0.32 VS 0.29 mmHg*ml⁻¹*min⁻¹, $p < 0.05$, $N = 9-12$) and sinusoidal vascular resistances (SVR; 0.20 VS 0.16 mmHg*ml⁻¹*min⁻¹, $p < 0.05$) than young-MCD rats. Hepatic arterial vascular resistance (HAR) was significantly lower in aged-MCD rats (3.01 VS 5.54 mmHg*ml⁻¹*min⁻¹, $p < 0.05$). The hepatic p-eNOS protein level was significantly reduced in MCD-fed rats ($p < 0.05$ for both young and aged groups, $N = 6$) and more noticeable in aged MCD-rats ($p < 0.05$). Endothelial impairment and microcirculatory dysfunction were also considerably more pronounced in aged MCD-rats as evidenced by decreased sensitivity to Acetylcholine-induced vasodilation in PVR and SVR and increased sensitivity to MTX-induced vasoconstriction in HAR ($p < 0.05$, $N = 9-12$). In contrast, no significant difference in SNAP-induced vasodilation was observed between young and aged MCD-rats in PVR and SVR ($p > 0.05$, $N = 9-12$). L-NMMA supplementation abolished the difference in MTX-induced vasoconstriction in HAR between the two groups ($p > 0.05$, $N = 9-12$).

Conclusion: Aging aggravates MCD diet-induced liver injury, steatosis, and fibrosis. Moreover, LSECs dysfunction was also more severe in aged rats, putatively contributing to hepatic stellate cells activation and fibrosis. Therefore, aging-related LSECs dysfunction may serve as a potential therapeutic target to treat the progression of liver steatosis and fibrosis.

THU-530

Roles of intrahepatic IgA on the fibroblast activation in livers with steatotic liver diseases

Jae-Sung Yoo¹, Jong Geun Park², Sung Woo Cho², Jeong Won Jang¹, Jong Young Choi¹, Pil Soo Sung¹. ¹Department of Gastroenterology and Hepatology, Seoul St Mary's Hospital, The Catholic University of Korea, Seoul, Korea, Rep. of South; ²The Catholic University Liver Research Center, College of Medicine, Department of Biomedicine and Health Sciences, The Catholic University of Korea, Seoul, Korea, Rep. of South
Email: pssung@catholic.ac.kr

Background and aims: Immunoglobulin A (IgA) is known to facilitate inflammation and dismantle anti-tumor immunity in the inflamed liver. In this study, we aimed to elucidate the role of intrahepatic IgA complex on the fibroblast activation in the inflamed livers with steatotic liver diseases (SLDs).

Method: Serum levels of IgA were measured in various chronic liver diseases with diverse fibrosis stages. Fibroblasts isolated from SLD livers were characterized using flow cytometry. In vitro IgA treatment on cultured patient-derived fibroblasts was done. A choline-deficient, L-amino acid-defined, high-fat diet (CDAHFD) as a dietary NASH model with rapidly progressing fibrosis was used.

Results: Patients with SLD showed increased levels of serum IgA levels than other chronic liver diseases ($p < 0.01$) and SLD patients with advanced fibrosis stages (F3, 4) showed higher serum IgA levels than those with F1 or F2 fibrosis ($p < 0.01$). Flow cytometry using ex vivo fibroblasts in livers with SLD showed higher levels IgA binding and PD-L1/FAP expression in patients with advanced fibrosis ($p < 0.01$). Moreover, SLD transplant explants with very high serum IgA levels (> 800 mg/dL) showed the highest number of IgA+FAP+PD-L1+ fibroblasts. In vitro treatment of IgA complex to cultured, SLD patient-derived fibroblasts provoked STAT3 phosphorylation and PD-L1/FAP/CXCL12 upregulation, suggesting the inflammatory and pro-tumorigenic fibroblasts. In vivo experiments using CDAHFD mouse model demonstrated that increased levels of IgA+FAP+PD-L1+ fibroblasts were found in the 3rd week livers. Treatment of nintedanib, an approved drug for idiopathic pulmonary fibrosis, to these activated fibroblasts selectively induced killing of these cells at a very low concentration, suggesting that nintedanib may be used to treat fibrotic SLD with activated fibroblasts.

Conclusion: Our data demonstrate that intrahepatic IgA activates fibroblasts in SLD liver, leading to pro-tumorigenic phenotype changes in these cells.

THU-531

DA-1241, a GPR119 agonist, combined with Semaglutide synergistically improved liver fibrosis in mice with CCl₄-induced liver fibrosis

Il Hoon Jung¹, Tae Hyoung Kim¹, Sujin Lee¹, Yuna Chae¹, Hyung Heon Kim², Mi-Kyung Kim³. ¹Dong-A ST Co., Ltd., Yongin-Si, Korea, Rep. of South; ²NeuroBo Pharmaceuticals Inc., Cambridge, United States; ³Dong-A ST Co., Ltd, Yongin-Si, Korea, Rep. of South
Email: kmk@donga.co.kr

Background and aims: DA-1241 is a novel chemical drug candidate that selectively and efficiently activates GPR119 and is currently in Phase 2a clinical development for the treatment of metabolic dysfunction-associated steatohepatitis (MASH). Previously, we confirmed that anti-MASH effect of DA-1241 combined with a dipeptidyl peptidase 4 (DPP4) inhibitor was synergistically enhanced through increasing plasma active GLP1 levels compared to each treatment alone. In connection with this, we attempted to determine the combination effects of DA-1241 and a GLP-1 analogue *per se* on liver fibrosis in this study.

Method: Liver fibrosis mice were generated by feeding a western diet in adjunctive with CCl₄ injections. After administering CCl₄ twice weekly for 3 weeks, mice with elevated plasma ALT levels were allocated to receive DA-1241 (oral) or semaglutide (subcutaneous) alone and in combination for 4 weeks.

Results: At the end of treatment, semaglutide reduced body weight by approximately 17% ($p < 0.05$ vs. vehicle control), while DA-1241 (−2.8%) showed little effect. There was no additional weight loss in the combination group (−19%, $p < 0.05$) compared to semaglutide alone. After four-week-treatment, three drug-treated groups had significantly lower plasma ALT levels than the vehicle control group, suggesting alleviation of liver damage. Collagen fiber deposition was prominent in mice treated with vehicle compared to the normal control group. However, DA-1241 or semaglutide alone lowered collagen-positive area compared to the vehicle-treated group (17.8%, 17.1% vs. 25.8%, $p < 0.05$), and their combination therapy elicited a further reduction to 6.05% ($p < 0.05$) compared with each treatment alone, which was recapitulated in changes of fibrosis score. Hepatic hydroxyproline contents and gene expression of various collagen subtypes (*Col1a1*, *Col3a1*, *Col5a1*, *Col6a1*) were also altered correspondingly, supporting the beneficial combination effects against the liver fibrogenesis. Notably, gene expression of Hedgehog-interacting protein (*Hhip*), a suppressor of hepatic stellate cell activation, was lower in mice with liver fibrosis than in normal mice, and were increased by DA-1241 or semaglutide alone. Intriguingly, their combination therapy fully restored the gene expression of *Hhip*. Additionally, the expression of inflammatory cytokines (*Tnfa*, *Il1b*, *Ccl2*, *Cxcl10*) was significantly reduced by each monotherapy, and combination treatment reduced gene expression of *Tnfa* and *Cxcl10* more than monotherapy. These data indicate that liver inflammation status has improved as well.

Conclusion: For the first time, we suggest a beneficial combination effect of DA-1241 and semaglutide in the treatment of liver fibrosis, which may be attributed to augmented inhibition of fibrogenesis and inflammation in the liver.

THU-532

New insight of liver fibrosis: altered chromatin accessibility in hepatic stellate cells

Tingting Jia¹, Yi Shen¹. ¹Department of Gastroenterology and Hepatology and Sichuan University-University of Oxford Huaxi Joint Centre for Gastrointestinal Cancer, West China Hospital of Sichuan University, Chengdu, Sichuan, China, Chengdu, China
Email: 2018151621145@stu.scu.edu.cn

Background and aims: The treatments for liver fibrosis are still in need so far. As the crucial initiators, activated hepatic stellate cells (aHSCs) undergo a series of epigenetic changes. The study intends to explore transcription factors (TFs) that facilitate HSCs activation and provide novel therapeutic targets for liver fibrosis.

Method: Three distinct HSCs activation models were established in present study. Firstly, *in vitro* activation involved isolating primary HSCs from normal Sprague-Dawley rats and culturing them for two days ($n = 5$) and seven days ($n = 5$), namely natural activation model. Secondly, *in vivo* activation entailed isolating primary HSCs from bile duct ligated rats ($n = 4$) and normal controls ($n = 4$), followed by culturing until the next day. Lastly, transforming growth factor- β (TGF- β , 2.5 ng/ml) ($n = 10$) or control buffer ($n = 10$) were added to the human HSCs cell line LX2 and cultured for 24 hours. Subsequently, Assay for transposase-accessible chromatin using sequencing (ATAC-seq) was conducted on the abovementioned cells, along with motif prediction. RNA sequencing (RNA-seq) was employed to analyze gene expression profiles of primary HSCs in the natural activation model ($n = 4$). The integration of ATAC-seq and RNA-seq further identified potential key TFs. Finally, RT-qPCR and differential expression analysis was utilized to confirm the dysregulation of TFs.

Results: For ATAC-seq, primary HSCs exhibited higher chromatin accessibility after activation compared with the controls. In the motif enrichment analysis, 150 aHSCs related TFs and 54 quiescent HSCs (qHSCs) related TFs were identified in the *in vitro* activation model. The three models shared 12 aHSCs related TFs, namely *Runx-a*, *Runx1*, *Runx2*, *Runx*, *Ets:Runx*, *Atf2*, *Atf4*, *Atf7*, *c-Jun-Cre*, *Creb5*, *Smad3* and *CAR*; and 19 qHSCs related TFs, including *Foxf1*, *Foxo3*, *Foxk1*,

Foxp1, Hoxa1, Hoxa2, Stat3, Hnf4a, Hnf6, Elk1, Elk4, Cux1, Crx, Duxbl, Vdr, Tr4, Ebf2, Gata2, Gata6. Integration of ATAC-seq and RNA-seq showed that gene expression was significantly correlated with chromatin accessibility, among which *Runx2, Creb5, and Smad3* were significantly upregulated in aHSCs at transcription level. Finally, the dysregulation of *Runx2* and *Smad3* in different HSCs activation models was verified.

Conclusion: We generated chromatin accessibility profiles of different HSCs activation models, highlighting the significance of *Runx2* and *Smad3* as key TFs mediating HSCs activation. These findings proposed these TFs as promising targets for future liver fibrosis treatment.

THU-533

MCPIP1 RNase inhibits liver fibrosis by targeting TGF- β 1 mRNA

Natalia Pydyn¹, Anna Ferenc¹, Katarzyna Trzos¹, Mateusz Wilamowski¹, Pedro Miguel Rodrigues², Jesus Maria Banales², José María Herranz³, Matías A. Avila⁴, Jolanta Jura¹, Jerzy Kotlinowski¹. ¹Jagiellonian University, Krakow, Poland; ²Biodonostia Health Research Institute, San Sebastian, Spain; ³Center of Applied Medical Research (CIMA), Pamplona, Spain; ⁴CIMA, CCUN, University of Navarra, Pamplona, Spain
Email: j.kotlinowski@uj.edu.pl

Background and aims: Monocyte-chemoattractant protein-induced protein 1 (MCPIP1) is an RNase that degrades a wide variety of transcripts, for example, those coding for proinflammatory cytokines such as IL-1 β , IL-6 or IL-2. Hepatic fibrosis is characterized by enhanced deposition of extracellular matrix (ECM), which results from the wound-healing response of the liver to a chronic and repeated injury. Liver fibrosis is commonly associated with non-alcoholic steatohepatitis, HCV infection, alcoholic liver disease, cholestatic disorders or autoimmune hepatitis. In the present study, we analyzed the role of MCPIP1 in liver fibrosis and its levels in fibrotic liver samples collected from patients. Next, we evaluated the impact of MCPIP1 on the activation status of hepatic stellate cells (HSCs).

Method: Effect of Mcpip1 on HSCs activation was studied by coculture of Mcpip1 KO or WT primary hepatocytes with HSCs and by modulating ZC3H12A expression in LX-2 cell line. Next, We analyzed MCPIP1 level in patients' fibrotic livers and hepatic cells isolated from fibrotic murine livers. We used both CCl₄ treated mice and livers from Mcpip1 knock-out animals (Mcpip1fl/flAlbCre).

Results: MCPIP1 levels are induced in patients' fibrotic livers compared to their nonfibrotic counterparts. Similarly, in murine models of fibrosis Mcpip1 level is increased in HSCs and hepatocytes. Overexpression of MCPIP1 in LX-2 cells led to decreased mRNA expression of HSCs activation markers e.g. ACTA2, TGF β 1, COL1A1 and α -SMA protein level. Protein-RNA IP experiments demonstrated binding of TGF β 1 mRNA by MCPIP1 RNase indicating its involvement in degradation of TGF β 1 transcript. Contrary, MCPIP1 silencing in LX-2 cells resulted in their increased activation status. Moreover, hepatocytes with Mcpip1 deletion trigger HSCs activation in a paracrine manner via the release of connective tissue growth factor (CTGF).

Conclusion: MCPIP1 inhibits activation of HSCs in autocrine manner by targeting TGF β 1 mRNA and in paracrine manner via regulating CTGF expression. This study was supported by National Science Centre, grant number K/PBM/000672 and 2017/27/B/NZ5/01440.

THU-534-YI

Circulating matricellular fibrosis markers TSP2, IGFBP7, TSP4 and M2-macrophage marker CD163 as predictors of fibrosis and outcome in people with primary sclerosing cholangitis

Ludwig J. Horst¹, Rambabu Surabattula², Füssel Katja¹, Marcial Sebede¹, Ansgar W. Lohse¹, Detlef Schuppan^{2,3}, Christoph Schramm^{1,4}. ¹I. Department of Medicine, University Medical Centre Hamburg-Eppendorf, Hamburg, Germany; ²Institute of Translational Immunology and Research Center for Immunotherapy, University Medical Center, Johannes Gutenberg University, Mainz, Germany; ³Division of Gastroenterology, Beth Israel Deaconess Medical Center, Harvard Medical School, Boston, United States; ⁴Martin-Zeititz Center for Rare Diseases, University Medical-Center Hamburg-Eppendorf, Hamburg, Germany
Email: l.horst@uke.de

Background and aims: Primary sclerosing cholangitis (PSC) remains one of the most complex, least understood liver diseases. There is a lack of biomarkers for the assessment of fibrosis stage and disease progression. This poses a continuous challenge for clinical trials and drug development. The four serum markers Thrombospondin-2 and -4 (TSP2/-4), Insulin-like growth factor-binding protein 7 (IGFBP7) and Cluster of Differentiation 163 (CD163) reflect key pathogenic mechanisms in general liver and biliary fibrosis. We therefore hypothesised that these markers may serve as predictors of fibrosis and outcome in PSC.

Method: 142 people with PSC were selected from the biobank of the University Medical Center Hamburg-Eppendorf. All patients had their serum marker levels determined by validated in-house sandwich ELISAs. Liver stiffness was measured by transient elastography (TE). In addition, parameters of disease activity and patient outcome were assessed.

Results: In multivariable regression analyses adjusted for ALT, ALP and creatinine, TSP2, IGFBP7, CD163 and TSP4 were independently and positively associated with liver stiffness assessed by TE ($p < 0.001$, $p < 0.001$, $p = 0.014$, $p < 0.001$). The association between fibrosis stage and elevated serum markers was verified in a sub-cohort of people with PSC ($n = 26$) and histologically confirmed fibrosis status. ROC curve analyses showed that all markers were able to distinguish patients with and without cirrhosis. TSP2 in particular showed excellent discrimination with an area under the receiver characteristic curve (AUC) of 0.898 (95% CI: 0.841–0.955, $p < 0.0001$). A newly developed fibrosis score, encompassing TSP2 and IGFBP7 was able to further improve the discriminatory value for cirrhosis with an AUC of 0.932 (95% CI: 0.890–0.975, $p < 0.0001$). Patients with baseline serum levels of TSP2, IGFBP7 and CD163 indicating advanced fibrosis ($\geq F3$) had significantly reduced transplant-free survival (Log Rank $p < 0.001$). An external validation of the present results on persons with PSC is currently in preparation.

Conclusion: Circulating TSP2, IGFBP7, CD163 and TSP4 levels were highly associated with the presence of advanced fibrosis and cirrhosis in people with PSC. TSP2, IGFBP7 and CD163 serum levels were associated with transplant-free survival in PSC, indicating their potential as prognostic biomarkers in cholestatic liver disease.

THU-535-YI

SOX9 is influential in type 2 immune mediated liver fibrosis

Kim Su^{1,2}, Alice Costain³, Elliot Jokl⁴, Kara Simpson⁴, Andrew MacDonald⁵, Karen Piper Hanley⁶. ¹University of Manchester, Manchester; ²Stepping Hill Hospital, Manchester, United Kingdom; ³Lydia Becker Institute of Immunology and Inflammation, University of Manchester, Manchester, United Kingdom; ⁴University of Manchester, Manchester, United Kingdom; ⁵Lydia Becker Institute of Immunology and Inflammation, University of Manchester, Manchester, United Kingdom; ⁶Wellcome Trust Centre for Cell-Matrix Research, University of Manchester, Manchester, United Kingdom
Email: kim.su@nhs.net

POSTER PRESENTATIONS

Background and aims: *Schistosomiasis mansoni* is a neglected tropical disease affecting over 200 million people worldwide. *S. mansoni* egg deposition in affected organs elicit an intense type 2 (Th2) immune reaction, triggering granuloma formation around the schistosome egg. Progressive granuloma fibrosis in the liver leads to development of complications of portal hypertension and hepatic synthetic dysfunction. Despite the high burden of disease related to schistosomiasis, there is a paucity of anti-fibrotic targets in Th2 mediated liver fibrosis. Previous work in our group has shown that SRY-Box Transcription Factor 9 (SOX9) expression in hepatic stellate cells (HSCs) and disease-associated hepatocytes is influential in regulating Th1/17 liver fibrosis. In this study, we investigated whether *in vivo* SOX9 depletion could diminish Th2 immune mediated fibrosis in the murine *S. mansoni* model of liver fibrosis.

Method: Control and SOX9 knockout (KO) mice infected with *S. mansoni* were utilised. Immunohistochemistry (IHC), immunofluorescence staining (IF), and immunoblotting were undertaken to assess SOX9 expression, granuloma size and markers of fibrosis. Hepatic cytokine subsets, myeloid and T-cell populations were determined using flow cytometry. Statistical analyses utilised Graphpad Prism v8.

Results: SOX9 expression was significantly increased in *S. mansoni* infected livers, in contrast to uninfected controls ($p < 0.05$). SOX9 levels correlated with hepatic fibrosis ($R^2 = 0.77$) and localised to areas of granuloma fibrosis and HSC activation, reflected in picrosirius red (PSR) and alpha-smooth muscle actin (ASMA) staining. Dual IF revealed SOX9 co-localises with ASMA, indicative of expression by activated granuloma HSCs. SOX9 was also detected in hepatocytes, where it co-localises with Hepatocyte Nuclear Factor 4-alpha (HNF4a). Significantly, *in vivo* SOX9 depletion was associated with reduced granuloma size ($p < 0.01$), reduced granuloma fibrosis and reduction in hepatic collagen I protein levels ($p < 0.01$). SOX9 KO animals displayed marked alterations in hepatic immune profile, with increased hepatic IL4 and IL5, reduced proinflammatory Ly6C^{hi} monocytes ($p < 0.01$) and upregulation of CD4⁺ T cell subsets expressing ST2 ($p < 0.001$) and CD25 ($p < 0.001$).

Conclusion: SOX9 is relevant in the pathogenesis of Th2 mediated liver fibrosis. Excitingly we provide novel evidence that SOX9 depletion reduces hepatic granuloma fibrosis in the setting of chronic *S. mansoni* infection, rendering it a potential anti-fibrotic target in Th2 mediated liver fibrosis. Our data also reveals marked immune alterations are associated with fibrosis abrogation. Deciphering the interplay between fibrosis biology and the hepatic immune niche is of crucial importance and could pave the way towards developing combination anti-fibrotic and immunology-based treatments in chronic liver disease.

THU-538

Delivery of anti-miR-155 using lipid nanoparticles ameliorate liver fibrosis by alleviating macrophage-driven liver inflammation

Vishal Tuli^{1,2}, Miranda Turkal^{1,2}, Cheng Lin², Eline Geervliet¹, Matthias Bartneck², Ruchi Bansal¹. ¹University of Twente, Enschede, Netherlands; ²Uniklinik RWTH Aachen, Aachen, Germany
Email: v.tuli@utwente.nl

Background and aims: Upon liver injury, (resident) macrophages get activated and contribute to liver inflammation. MicroRNAs (miRs) are implicated in liver inflammation and disease progression. miR-155 is considered as a master regulator of inflammation and has shown to promote liver inflammation and fibrosis. The aim of this project is to deliver anti-miR-155 to macrophages to attenuate liver inflammation. Lipid nanoparticles (LNPs) are one of the most advanced non-viral delivery platforms for negatively charged nucleic acids. We evaluated different LNPs with various helper lipids for their biodistribution, more specifically for liver uptake, *in vivo*, and used DSPC-based LNPs to deliver anti-miR-155 *in vitro* and *in vivo*.

Method: DSPC/DOPC/DOPE-LNPs were prepared using a microfluidic device by injecting volumes of lipid mix (12.5 mM) containing ionizable MC3 lipid/helper lipids (DSPC or DOPC or DOPE)/

cholesterol/structural lipid DSPE-PEG at respective mol% ratios of 50/10/38.5/1.5 in ethanol with aqueous phase containing negative control (NC)-antimiR or anti-miR-155 (amine-to-phosphate ratio of 4). Following the successful synthesis of the LNPs, their organ specific uptake as well as cellular uptake was performed using DiR- and DiD-LNPs respectively. Therapeutic efficacy of anti-miR-155-LNPs (DSPC) was evaluated *in vitro* in LPS/IFN γ -stimulated RAW264.7 macrophages and *in vivo* in a chronic CCl₄-induced liver injury mouse model.

Results: Average size of empty LNPs, DiD-LNPs, anti-miR-155-LNPs were 110 nm, 126 nm, 142 nm respectively. The size of DiR-LNPs with DSPC, DOPC and DOPE helper lipids were 81.8 nm, 119 nm and 114 nm respectively. Among other LNPs, DSPC-LNPs showed highest liver accumulation *in vivo* and higher uptake in macrophages *in vitro*. LPS/IFN γ -stimulated mouse macrophages showed higher miR-155 expression levels, compared to non-stimulated or IL4/IL13 stimulated macrophages, that correlated with higher TNF α and IL6 expression. Anti-miR-155-LNP treatment significantly reduced miRNA-155 levels and mRNA and protein levels of IL6 and TNF α , without affecting cell viability. Anti-miR-155-LNP treatment in CCl₄-induced chronic liver injury mouse model attenuated liver inflammation and fibrosis as assessed by immunostainings and by decrease in the mRNA levels of major inflammation and fibrotic markers.

Conclusion: We have developed a LNP platform to deliver anti-miR-155 to ameliorate macrophage-driven liver inflammation and liver fibrosis.

THU-539

Exploring novel targets in hepatic stellate cell activation: interference with the mitochondrial function as part of the antifibrogenic effect of Rilpivirine

Ana Benedicto^{1,2}, Federico Lucantoni³, Isabel Fuster-Martínez^{1,2}, Cristina Benavides^{1,2}, Pedro Díaz², Dimitri Dorcaratto⁴, Elena Muñoz⁴, Victor M. Víctor², Ángeles Álvarez^{1,2}, Juan V. Esplugues^{1,2,5}, Ana Blas-García^{2,5,6}, Nadezda Apostolova^{1,2,5}. ¹Departamento de Farmacología, Facultad de Medicina, Universidad de Valencia, Valencia, Spain; ²FISABIO-Hospital Universitario Dr. Peset, Valencia, Spain; ³Centro Investigación Príncipe Felipe, Valencia, Spain; ⁴Departamento de Cirugía, Unidad de Hígado, Biliar y Páncreas, Instituto de Investigación Biomédica, INCLIVA, Hospital Clínico, Universidad de Valencia, Valencia, Spain; ⁵Centro de Investigación Biomédica en Red de Enfermedades Hepáticas y Digestivas (CIBERehd), Valencia, Spain; ⁶Departamento de Fisiología, Facultad de Medicina, Universidad de Valencia, Valencia, Spain

Email: a.benedictoelena@gmail.com

Background and aims: Activation and subsequent trans-differentiation of hepatic stellate cells (HSC) from quiescent to myofibroblast-like (activated, aHSC) are pivotal in the liver's response to injury and development of liver fibrosis. This energy-intensive transformation involves major reprogramming of the mitochondrial function. Our group demonstrated the hepatoprotective effects of the anti-HIV drug Rilpivirine (RPV) interfering with aHSC, *in vivo* and *in vitro*. The current study investigates whether changes in mitochondrial function contribute to RPV's antifibrogenic action in aHSC.

Method: HSC (the human cell line LX-2 or primary HSC isolated from healthy human liver samples (hHSC) were activated with the profibrotic cytokine TGF- β (2.5 ng/ml) and co-exposed to clinically relevant concentrations of RPV (1–8 μ M) or vehicle (DMSO) for 48 h. A set of parameters indicative of mitochondrial function and morphology were analyzed through Western blot, qRT-PCR, live-cell fluorescence microscopy (Leica) and the Seahorse Cell Mito Stress kit (Agilent). RNA sequencing analysis was performed through a single read of 75 cycles (1 \times 75 bp) (Agilent).

Results: LX-2 cells activated with TGF- β (48 h) displayed altered mitochondrial function (increased oxygen consumption and diminished mitochondrial membrane potential), morphology (diminished branching) and dynamics (increased fission). They were much bigger

(hypertrophied) and displayed enhanced mitochondrial signal (NAO). Co-treatment with RPV fully or partially rescued virtually all these TGF- β -induced effects. mRNA sequencing analysis of hHSC resulted in the generation of expression data for 13156 protein-coding sequences. Mitochondria-related genes were identified among the differentially expressed genes (DEG) using the MitoCarta 3.0 database. Altered expression patterns of genes encoding mitochondrial proteins (mitoDEG) were detected when cells were exposed to TGF- β , with 139 up- and 199 down-regulated genes. Co-treatment with RPV led to substantial changes in mRNA levels of 90 mitoDEG (4 μ M RPV) and 110 mitoDEG (8 μ M RPV). Notably, a portion (31 in 4 μ M and 80 in 8 μ M) of these genes displayed reversed expression compared to TGF- β , some of them shared between both concentrations. Further investigation into the mitoDEG common for both RPV concentrations (compared to TGF- β alone) and their involvement in mitochondrial pathways revealed essential processes such as the “Mitochondrial central dogma,” “Metabolism,” and “OXPHOS” for up-regulated mito-DEG, and “Protein import, sorting and homeostasis,” “Signaling,” and “Mitochondrial dynamics and surveillance” for down-regulated mitoDEG.

Conclusion: RPV interferes with mitochondrial function in TGF- β aHSC. This underscores the potential of targeting mitochondria in the pursuit of novel therapies for liver fibrosis.

THU-540

Characterization of in vivo mouse models of regressive fibrosis and resolving portal hypertension

Katharina Bonitz^{1,2,3}, Philipp Königshofer^{1,3,4}, Benedikt Hofer^{1,3}, Oleksander Petrenko^{1,2,3}, Thomas Sorz^{1,2,3}, Vlad Taru^{1,3}, Benedikt Simbrunner¹, Henriette Horstmeier¹, Kerstin Zinöber¹, Katharina Regnat¹, Hubert Scharnagl⁵, Michael Trauner¹, Stefan Günther Kauschke⁶, Larissa Pfisterer⁶, Peng Sun⁶, Ines Truebenbach⁶, Philipp Schwabl¹, Thomas Reiberger^{1,2,3}. ¹Division of Gastroenterology and Hepatology, Department of Internal Medicine III, Medical University of Vienna, Vienna, Austria; ²Center for Molecular Medicine (CeMM) of the Austrian Academy of Sciences, Vienna, Austria; ³Christian Doppler Lab for Portal Hypertension and Liver Fibrosis, Medical University of Vienna, Vienna, Austria; ⁴Core Facility Laboratory Animal Breeding and Husbandry, Medical University of Vienna, Vienna, Austria; ⁵Clinical Institute of Medical and Chemical Laboratory Diagnostics, University Hospital Graz, Graz, Austria; ⁶Department of CardioMetabolic Diseases Research, Boehringer Ingelheim Pharma GmbH and Co.KG, Biberach an der Riss, Germany
Email: katharina.bonitz@meduniwien.ac.at

Background and aims: Liver fibrosis regression and improvement of portal hypertension (PH) has been observed both in patients and in experimental models after cure of the primary liver disease and cessation of liver injury. However, the dynamics of liver disease regression and the underlying molecular mechanisms remain poorly understood. We characterized two murine liver disease models at different stages of regression in regards to fibrosis and PH severity.

Method: Liver fibrosis was induced in male wildtype C57BL/6 mice by either oral gavage of carbon tetrachloride (CCl₄, 2 ml/kg, 3 \times per week) for 8 or 12 weeks or repeated intraperitoneal injections of thioacetamide (TAA, 150 mg/kg, 3 \times per week) for 8 or 12 weeks, while healthy controls received olive oil gavage or NaCl injections. Animals were sacrificed at peak injury (W8 or W12) or 1 (R1) or 2 (R2) weeks after last CCl₄/TAA dose. We measured portal pressure (PP) and spleen/bodyweight ratio for PH, collagen proportionate area (CPA) for fibrosis, and AST/ALT for liver injury severity, respectively.

Results: Increasing fibrosis severity was confirmed for CCl₄ (CPA in OO-W8: 1.55 \pm 0.88% vs. CCl₄-W8: 8.53 \pm 5.04%, OO-W12: 0.83 \pm 0.16% vs CCl₄-W12: 16.9 \pm 3.90%) and for TAA (CPA in NaCl-W8: 0.89 \pm 0.14% vs. TAA-W8: 3.03 \pm 0.18%, NaCl-W12: 0.87 \pm 0.20% vs. TAA-W12: 3.87 \pm 0.36%) induction. The CCl₄ model animals developed more pronounced PH (PP: OO-W8: 4.92 \pm 0.78 mmHg vs CCl₄-W8: 8.45 \pm 1.28 mmHg, OO-W12: 5.19 \pm 0.20 mmHg CCl₄-W12: 9.99 \pm

1.17 mmHg) than the TAA model (PP: NaCl-W8: 5.30 \pm 0.29 mmHg vs TAA-W8: 6.80 \pm 0.35 mmHg, NaCl-W12: 5.51 \pm 0.42 mmHg vs TAA-W12: 7.71 \pm 0.57 mmHg). Serum AST/ALT levels regressed to levels non-significantly different to healthy control animals already at R1 across all models. During regression, fibrosis decreased in both the CCl₄ (CPA: W8 + R1: 8.47 \pm 3.69%, p = ns; W8 + R2: 5.40 \pm 2.20%, p = ns; W12 + R1: 10.90 \pm 3.05%, p = 0.01; W12 + R2: 5.43 \pm 1.44% p < 0.001) and the TAA (CPA: W8 + R1: 2.60 \pm 0.28%, p = 0.01; W8 + R2: 2.34 \pm 0.21% p < 0.001; W12 + R1: 3.49 \pm 0.63%, p = ns; W12 + R2: 2.90 \pm 0.30%, p < 0.001) models. PP decreased in both the CCl₄ (W8 + R1: 5.84 \pm 0.24 mmHg, p = 0.004; W8 + R2: 6.02 \pm 0.92 mmHg, p = 0.004; W12 + R1: 8.35 \pm 0.79 mmHg, p = 0.01; W12 + R2: 7.89 \pm 1.16 mmHg, p = 0.008) and the TAA (W8 + R1: 6.74 \pm 0.40 mmHg, p = ns; W8 + R2: 6.01 \pm 0.22 mmHg, p < 0.001; W12 + R1: 7.28 \pm 0.47 mmHg, p = ns; W12 + R2: 6.04 \pm 0.52 mmHg, p < 0.001) models.

Conclusion: Peak fibrosis and PP were more severe in the CCl₄ than the TAA models. Normalized AST/ALT levels at all R1 timepoints suggested rapid cessation of liver injury. Fibrosis regressed significantly after 2 weeks except for the 8-week CCl₄ model. PP decreased significantly in all regression models. Both severity and the therapeutic window were most prominent in the 12-week CCl₄ model, qualifying this animal model for pre-clinical testing of therapeutics aiming at promoting fibrosis resolution and improving PH after etiologic cure.

THU-541

Cell communication network in diseased livers reveals lymphotoxin beta as a potential inducer of hepatic stellate cell activation

Stefaan Verhulst¹, Vincent Merens¹, Ayla Smout¹, Leo van Grunsven¹. ¹Vrije Universiteit Brussel, Brussels, Belgium
Email: stefaan.verhulst@vub.be

Background and aims: Liver pathologies cause approximately 2 million deaths per year worldwide, including 1 million due to complications of liver cirrhosis. Common causes include hepatitis infection, excessive alcohol intake or unhealthy diets. Cirrhosis is an advanced stage of fibrosis characterized by an excessive accumulation of extracellular matrix proteins. Key players in this fibrotic process are hepatic stellate cells (HSCs). During any type of liver injury, HSCs start to activate into a myofibroblast phenotype which produce large amounts of ECM that results in an increased stiffness of the liver. There are currently no approved anti-fibrotic therapies available in the clinic that can cure patients with liver fibrosis. In this study we aimed to create an interactive network that incorporates available scRNA seq data of healthy and diseased human and mouse livers. With this network, we want to further unravel the signalling pathways that drive HSC activation.

Method: To establish an intercellular communication network between diverse liver cell types, we used publicly available single-cell RNA sequencing (scRNAseq) datasets from human cirrhotic livers (GSE48452) and different diseased mouse livers, including fatty livers (GSE192742, GSE129516) and fibrotic livers (GSE171904, GSE145086). We extracted potential ligands capable of activating HSCs using an in-house developed cell communication algorithm (LiNiCom) and validated these through in vitro experiments, using 2D monolayer cultures of primary mouse HSCs and primary multicellular mouse liver spheroids containing HSCs, liver sinusoidal endothelial cells, Kupffer cells, and hepatocytes.

Results: To create a comprehensive cell communication network in diseased livers, we developed a novel cell communication tool that combined LIANA and NicheNet. Using this integrative cellular communication network tool, we identified ligands capable of promoting HSC activation; 39 ligands in cirrhotic human livers and 49 in diseased mouse livers, with an overlap of 12 ligands in both species. Overlapping ligands include the well-known activators such as TGF β , TNF α , and LGALS3, alongside less known ligands, including lymphotoxin beta (LTB), calreticulin, and lumican. None of these

POSTER PRESENTATIONS

newer ligands were able activate mHSCs in 2D cultures, however, LTB activated HSCs in primary liver spheroid cultures by increasing the gene expression of HSC activation markers Acta2, Lox, Col1a1 and Col3a1.

Conclusion: Using LiNiCom we successfully generated a cell communication network between all cell types in diseased and revealed potential ligands that promote HSC activation, including LTB, that can effectively activate HSCs in primary liver spheroid cultures. While in vivo validation is required to further establish the role of LTB in chronic liver disease, we believe that LTB can be a new target for the development of anti-fibrotic therapies.

THU-542

Inhibition of hyaluronic acid synthase by hyaluronan synthase 2 targeting siRNA downregulates expression of chemokine (C-X-C motif) ligand 16 and suppresses liver fibrosis in mice

Noreen Halimani¹, Mikhail Nesterchuk¹, Alexandra Tsitrina², Marat Sabirov³, Irina Andreichenko⁴, Nataliya Dashenkova³, Alexey Kulikov³, Timofei Zatspein⁵, Roman Romanov⁶, Arsen Mikaelyan³, Yuri Kotelevtsev¹. ¹Skolkovo Institute of Science and Technology, Moscow, Russian Federation; ²IKI-Ilse Katz Institute for Nanoscale Science and Technology, Ben Gurion University of the Negev, Beersheba, Israel; ³Koltzov Institute of Developmental Biology of Russian Academy of Sciences, Moscow, Russian Federation; ⁴AO Reproduction Head Centre of Agricultural Animals, Moscow, Russian Federation; ⁵Lomonosov Moscow State University, Moscow, Russian Federation; ⁶Center for Brain Research, Medical University of Vienna, Vienna, Austria
Email: Noreen.Halimani@skoltech.ru

Background and aims: Hepatic fibrosis remains a major clinical challenge characterised by excessive deposition of extracellular matrix components (ECM). Recent studies have shown that Hyaluronic acid synthase 2 (HAS2) is critical in driving hepatic stellate cell (HSC) activation and liver fibrosis, making it an important pharmacological target for therapeutic intervention. Our study aimed to investigate the suppression of liver fibrosis by knocking down HAS2 using small interfering RNA (siRNA). Additionally, we aimed to elucidate the molecular mechanisms underlying the antifibrotic effects of this approach through total liver transcriptome analysis.

Method: Female BALB/c mice were exposed to repeated intraperitoneal administration of CCl₄ twice a week for two weeks to induce liver fibrosis. Nanoparticle-encapsulated HAS2 targeting siRNA (siHAS2) was administered twice a week intravenously, and to the control mice, luciferase targeting siRNA was administered.

Results: Iterative CCl₄ administration induced excessive HA deposition in the periportal zone of the liver, inferring elevated HAS2 activity. Furthermore, HA serum levels were also elevated post-repeated CCl₄ injections. Knockdown of HAS2 decreased the deposition of both collagen and HA. Transcriptome analysis showed that downregulated genes were enriched in cell chemotaxis, ECM organisation and collagen biosynthesis. In contrast, upregulated genes were enriched in meiotic chromosome segregation and epigenetic regulation of gene expression. Interestingly, transcriptomics identified the CXCR6-CXCL16 as a potential therapeutic target network due to its role in lymphocyte trafficking. Our analysis revealed that CXCL16 expression was significantly downregulated, which was confirmed with real-time PCR.

Conclusion: Our analysis of the hepatic transcriptome has shed light on the antifibrotic effect of knocking down HAS2. This effect is primarily achieved by reducing cell chemotaxis, extracellular organisation, and response to growth factor stimuli. These processes play a crucial role in the initiation and progression of hepatic fibrosis. Additionally, we demonstrate that RNA interference therapy using siHAS2 is a feasible and practical approach to ameliorating fibrosis. Our findings highlight the potential of siHAS2 as a promising agent for combating hepatic fibrosis and targeting its critical pathways.

THU-546

The improvement of Bortezomib on cirrhosis and its potential mechanism

Ling Wu^{1,2}, Feng Li^{1,3}, Xiaoquan Huang¹, Chenyi Rao¹, Detlef Schuppan^{4,5}, Shiyao Chen^{1,3}. ¹Zhongshan Hospital, Fudan University, Shanghai, China; ²Institute of Translational Immunology and Research Center for Immunotherapy, University Medical Center, Johannes Gutenberg University, Mainz, Germany; ³Minhang Hospital, Fudan University, Shanghai, China; ⁴Institute of Translational Immunology and Research Center for Immunotherapy, University Medical Center, Mainz, Germany; ⁵Beth Israel Deaconess Medical Center, Harvard Medical School, Boston, United States
Email: wuling01@uni-mainz.de

Background and aims: Bortezomib (B), a proteasome inhibitor, has been shown to attenuate fibrosis of skin, lung and kidney. We therefore aimed to evaluate the efficacy of B to improve advanced parenchymal and biliary liver fibrosis in rats and potential underlying mechanisms.

Method: Advanced liver fibrosis was induced in 8-week-old rats by intraperitoneal injection of thioacetamide (TAA) for 12 weeks or bile duct ligation (BDL) for 3 weeks. Rats with advanced fibrosis were divided into 2 groups: intravenous injection of B at 0.1 mg/kg in PBS (B) or injection of PBS alone three times a week for 3 weeks (fibrotic controls, FC). Age matched rats with no intervention served as normal controls (NC). Portal vein pressure was measured after anesthesia before sacrifice. Liver and renal function parameters were determined to evaluate liver inflammation and potential toxicity of B. HE and Masson staining were used to evaluate liver inflammation and fibrosis. Liver collagen was quantified via hydroxyproline content. Fibrosis-related gene and protein expression were determined by RT-qPCR and Western blot. Liver samples were subjected to NGS analysis. LX-2 human hepatic stellate cells and LO2 human hepatocytes were cultured with different concentrations of B for 24 h. Cell apoptosis was quantified via flow cytometry.

Results: Portal vein pressure (mmHg) showed a decrease after B treatment, though the p values did not yet reach statistical significance in the two fibrosis models (B vs FC: TAA, 6.86 ± 0.76 vs 11.42 ± 2.37 ; BDL, 9.49 ± 2.92 vs 18.57 ± 16.83). ALT and AST decreased with B treatment in both fibrosis models, and serum creatinine and bilirubin levels remained unchanged, indicating a beneficial effect of B on liver function with no apparent liver or renal toxicity. Morphometry and biochemical quantification showed a significant amelioration of fibrosis, as evidenced by a 50% decrease of liver hydroxyproline content (B vs FC: TAA, 0.21 vs 0.41, $p = 0.001$; BDL, 0.13 vs 0.20, $p = 0.016$) and a 70% reduction of Masson-positive area in both fibrosis models. Fibrosis related protein and transcript levels showed significant downregulation of α SMA, Col1a1, and fibronectin 1. Gene set enrichment analysis indicated the upregulation of pro-inflammation-related Ugt2b7 and anti-proliferation-related gene Marvled1, and downregulation of Cdc 20, which is a key regulator in ubiquitin-mediated proteolysis and cell cycle pathways upon treatment with B. B-treated hepatic stellate cells but not hepatocytes showed prominent apoptosis.

Conclusion: Bortezomib induces activated hepatic stellate cell apoptosis and has a prominent antifibrotic potential in parenchymal and biliary fibrosis.

THU-547

Ex-vivo translational assay of hepatic stellate cells using patient-derived serum characterizes the anti-fibrotic activity of CM-101

Johnny Amer¹, Ahmad Salhab¹, Raanan Greenman², Tom Snir², Avi Katav², Revital Aricha², Matthew Frankel², John Lawler², Francesca Saffioti³, Douglas Thorburn⁴, Massimo Pinzani⁴, Ilan Vaknin², Adi Mor², Rifaat Safadi¹. ¹Hadassah Hebrew University Medical Center, Jerusalem, Israel; ²Chemomab, Tel Aviv, Israel; ³UCL Institute for Liver and Digestive Health, University College of London, Oxford University Hospitals NHS Foundation Trust, London, United

Kingdom; ⁴UCL Institute for Liver and Digestive Health, University College of London, Sheila Sherlock Liver Centre, Royal Free London NHS Foundation Trust, London, United Kingdom
Email: raanan@chemomab.com

Background and aims: CCL24, a chemokine that regulates inflammatory and fibrotic activities, was found to be highly expressed in livers of patients with liver fibrosis including those with primary sclerosing cholangitis (PSC) and metabolic dysfunction-associated steatohepatitis (MASH). Treatment with CM-101, a first-in-class humanized antibody targeting CCL24, has impacted consequential biomarkers of liver fibrosis in patients with MASH (NCT05824156) and in multiple PSC preclinical models. This study aimed to further characterize CM-101's anti-fibrotic activity in patients using an ex-vivo hepatic stellate cells (HSC) activation model.

Method: Activation of HSC was evaluated using the human LX2 cell line by quantification of the fibrotic marker alpha-SMA (smooth muscle actin). Cell activation was assessed following a 24-hour incubation period with either CCL24, CCL24 in the presence of CM-101, or with sera from MASH patients before or after 16 weeks of exposure to either placebo (vehicle) or CM-101 (5 mg/kg subcutaneous every 3 weeks). Placebo MASH participants without clinical response vs. CM-101 which showed improved liver fibrosis biomarkers were included. The secretome of CCL24-stimulated LX2 was examined by RayBio L-507 protein array. To compare the LX2 secretome to serum proteins of PSC patients, sera from PSC patients and healthy controls were analyzed using Olink proximity extension assay.

Results: CCL24 activated HSC, as manifested by increased alpha-SMA expression, while pre-incubation of CCL24 with CM-101 restored alpha-SMA expression to baseline levels. Notably, the expression of alpha-SMA in HSC was significantly lower after incubation with sera from CM-101-treated MASH patients, compared to placebo-treated patients. Moreover, it was found that proteins secreted by CCL24-activated HSC were upregulated in sera from PSC patients with extensive fibrosis (as defined by an enhanced liver fibrosis (ELF) score >9.8). Five of the CCL24-dependent secreted proteins demonstrated a high predictive area under the receiver operator characteristic (AUROC) curve for both PSC and fibrosis severity (by ELF score), while their combination achieved AUROC of more than 0.95.

Conclusion: A serum-based ex-vivo assay derived from MASH patients treated with CM-101 restored HSC activation. Additionally, a protein signature generated from CCL24-activated HSC predicted PSC disease and its severity, underscoring the relevance of this translational assay to PSC. These findings support CM-101's mode of action in liver fibrosis and may serve as a translational tool in the ongoing clinical trial in PSC.

THU-548-YI

Activation of the GABAA receptor counteracts hepatic steatosis and fibrosis: a novel first-in-class approach for MASH therapy
Elisabeth Rohbeck^{1,2}, Leonie Koester¹, Juergen Eckel¹. ¹CMR CureDiab Metabolic Research GmbH, Düsseldorf, Germany; ²CMR CureDiab Metabolic Research GmbH, Düsseldorf, Germany
Email: juergen.eckel@curediab.de

Background and aims: Liver fibrosis represents a pathological wound-healing response to chronic liver injury, characterized by the excessive accumulation of extracellular matrix proteins. The degree of liver fibrosis predicts the long-term prognosis of metabolic-dysfunction associated steatohepatitis (MASH). However, no specific pharmacological therapy has been approved for the treatment of liver fibrosis. Therefore, the proposed study aimed to investigate if the hepatoprotective thioacrylamide compound, HK3, could also ameliorate fibrosis in a human 3D spheroid MASH model.

Method: Cryopreserved primary human hepatocytes and non-parenchymal cells from patients with clinically confirmed MASH were seeded in ultra-low attachment plates and further analyzed at HepaPredict, Sweden. After forming spheroids, the media were

supplemented with 10 ng/ml insulin (control group) or 10 µg/ml insulin and 240 µM albumin-conjugated palmitic acid (PA) and 240 µM oleic acid (OA) (MASH group). The CellTiter-Glo Luminescent Cell Viability Assay kit was used to assess viability in an upfront toxicity test for up to two weeks with repeated exposure to HK3. Subsequently, the effects of HK3 (1, 3, and 10 µM) for 1 week on intracellular lipid content were quantified using the AdipoRed Assay. The secreted cytokines IL-6 and IL-8 or pro-Collagen alpha 1-type I (COL1A1) were measured in the culture supernatants using a customized Magnetic Luminex Assay or ELISA.

Results: Acute exposure to HK3 did not result in hepatotoxicity at any concentration tested. A moderately strong time-dependent reduction in viability was apparent upon concentrations of 30 µM. The PA/OA-induced hepatic lipid content of spheroids exposed to HK3 was reduced by 51–54% (all $p < 0.001$). A concentration of 3 µM HK3 led to a reduction in IL-6 levels to 55% ($p < 0.01$), while IL-8 levels decreased to 80% ($p < 0.05$), compared to MASH group. In line, HK3 resulted in a significant reduction in pro-COL1A1 levels. Exposure was dose-dependent and reached levels of 82%, 73% ($p < 0.05$), and 64% ($p < 0.01$), respectively.

Conclusion: Our thioacrylamide compound promotes the regression of hepatic fibrosis mediated by anti-steatotic and anti-inflammatory properties. Consequently, this compound might represent an innovative pharmacological approach to treat or prevent fibrosis as a first-in-class drug.

THU-549

Pioglitazone ameliorates fibrotic niche of HBV transgenic mice by restoring NK cell function and inhibiting macrophage activation
HuanYu Xiang¹, Taiyu He¹, Jing Xiao¹, Yong Sun¹, Ming-Li Peng¹.

¹Department of Infectious Diseases, Key Laboratory of Molecular Biology for Infectious Diseases (Ministry of Education), Institute for Viral Hepatitis, The Second Affiliated Hospital, Chongqing Medical University, Chongqing, China, Chongqing, China
Email: peng_mingli@hospital.cqmu.edu.cn

Background and aims: The restoration of NK cell function and inhibition of macrophage activation are novel strategies to improve HBV-related liver fibrosis. Recent Studies have shown PPAR γ agonists can effectively promote IFN γ secretion in NK cells and inhibit macrophage activation. Therefore, the study is aimed to investigate the efficacy of pioglitazone, a clinically used PPAR γ agonist, in HBV-related liver fibrosis.

Method: Histopathological characteristics and serum markers were used to evaluate the efficacy of pioglitazone in CCl₄-induced fibrotic HBV transgenic mice. Flow cytometry was used to explore the effects of pioglitazone on macrophages and NK cells in the liver and peripheral blood.

Results: Pioglitazone effectively reduced serum ALT, AST and liver extracellular matrix deposition, and significantly improved liver inflammation and fibrosis. Interestingly, in vivo, we found pioglitazone significantly reduced serum HBV DNA levels in HBV-Tg mice, but no significant inhibition of HBV DNA by pioglitazone was observed in vitro. The above results suggested the reduction in serum HBV DNA levels caused by pioglitazone treatment may act through non-hepatic parenchymal cells rather than hepatocytes. The flow cytometry results showed pioglitazone increased the proportion of NKG2D⁺ NK, NKG2A⁺ NK cells and promoted IFN- γ secretion in hepatic NK cells. Meanwhile, pioglitazone reduced the proportion of hepatic pro-inflammatory Ly6c^{high} macrophages and peripheral blood Ly6c^{high} monocytes and inhibited TNF- α secretion in both cells.

Conclusion: Pioglitazone inhibits HBV replication by promoting IFN γ secretion in NK cells, and inhibits macrophage activation to attenuate hepatic inflammation and fibrosis. Therefore, pioglitazone deserves further study in treating HBV-related liver fibrosis.

THU-550

Magnetic levitation culture: a step towards quiescent hepatic stellate cell in vitro models

Nataliya Rohr-Udilova¹, Martha Seif¹, Matthias Pinter², Michael Trauner¹. ¹Medical University of Vienna, Division of Gastroenterology and Hepatology, Internal Medicine III, Vienna, Austria; ²Medical University of Vienna, Division of Gastroenterology and Hepatology, Internal Medicine III, Vienna, Austria
Email: nataliya.rohr-udilova@meduniwien.ac.at

Background and aims: Hepatic Stellate Cells (HSCs) play a pivotal role in the development of hepatic fibrosis. There is a substantial need for experimental models that facilitate the study of HSC activation. Traditional 2D in vitro cell culturing leads to the activation of HSCs upon adherence to plastic surfaces used in labware, which results in a switch to an activated HSC phenotype. Magnetic levitation is a technique that involves the nonspecific binding of nanomagnetic beads to the cell surface, followed by the application of a magnetic field above the cell culture flask. This method enables cells to form 3D spheroids that levitate in the medium, thereby avoiding contact with labware plastic. This study aimed to establish a 3D spheroid culture of HSCs using magnetic levitation to revert them to their quiescent state and to assess its effectiveness as an in vitro model for studying HSC activation.

Method: The human LX-2 stellate cell line was used as a model for HSCs and cultured in DMEM under standard tissue culture conditions. Nanoshuttle-PL beads combined with a Bioassembler magnet were utilized to induce magnetic levitation. Cell viability was evaluated using the ATP-Glow assay, and the expression levels of alphaSMA and Col1A1 were quantified via real-time RT-PCR.

Results: We have developed an optimized protocol for LX-2 cell treatment with magnetic beads which resulted in stable 3D spheroid formation without impairing cell viability. After eight days of culture, magnetic levitation led to a significant reduction in Col1A1 mRNA levels by $20.1 \pm 3.1\%$ and alphaSMA mRNA levels by $74.2 \pm 4.1\%$ ($p < 0.01$, $n=3$), compared to traditional 2D adherent controls. Additionally, levitated 3D LX-2 spheroids retained responsiveness to TGF-beta, a known inducer of HSC activation.

Conclusion: Magnetic levitation effectively reduces the in vitro activation of HSCs by preventing direct contact with labware plastic, favoring a more quiescent HSC state that is conducive to studying their activation. This technique offers a promising approach for the in vitro study of hepatic stellate cell biology, especially in the context of fibrotic disease research.

THU-554

Evaluation of liver fibrosis: reproducibility of transient elastography

Cyrine Ben Mehrez¹, Meriam Sabbah¹, Jlassi Houssaina², Sabrine Soua³, Norsaf Bibani⁴, Dalila Gargouri³. ¹Habib Thameur Hospital, Department of Gastroenterology, Tunis, Tunisia; ²Habib Thameur Hospital, Department of Gastroenterology, Tunis, Tunisia; ³Habib Thameur Hospital Department of Gastroenterology, Tunis, Tunisia; ⁴Habib Thameur Hospital, Department of Gastroenterology, Tunis, Tunisia
Email: cyrine.benmehrez@etudiant-fmt.utm.tn

Background and aims: Transient elastography is considered a reliable surrogate marker for assessing the severity of liver fibrosis. The aim of our study was to evaluate the reproducibility of this examination and the factors associated with discordance between experienced and novice operators.

Method: This was a prospective cross-sectional study over a period of eight months, including patients for whom a transient elastography was indicated in the diagnostic or monitoring of liver disease. An experienced operator is defined as an operator who has previously performed more than 100 examinations. Discordance was defined by a difference of at least one fibrosis stage between the results of the operators. Cohen's Kappa coefficient was calculated to study the

agreement between fibrosis stages. The overall agreement rate between two qualitative variables was estimated based on the value of the Kappa coefficient (K): Excellent if $K > 0.81$, good if K between 0.61 and 0.8, moderate if K between 0.21 and 0.6, poor if K between 0 and 0.2, and very poor if $K < 0$. The agreement was assessed using the intra class correlation coefficient (Ric) for quantitative variables: Excellent if $Ric > 0.9$, good if Ric between 0.75 and 0.9, moderate if Ric between 0.5 and 0.75, and poor if $Ric < 0.5$. We defined the variables crude and relative differences to identify factors associated with a significant difference between the two operators.

Results: One hundred and thirty-two patients, with a mean age of 51.5 years and a male-to-female ratio of 0.9, were included.

The results showed excellent inter-observer agreement with an intra class correlation coefficient of 0.99 ($p < 0.001$). Inter-observer agreement was good for elasticity values ≤ 6.5 kPa ($Ric = 0.736$) and excellent when elasticity > 6.5 kPa ($Ric = 0.99$; $p < 0.001$). The agreement between the two operators was excellent with ($K = 0.834$; $p < 0.001$). However, the discordance rate for METAVIR fibrosis stages was high in F2 (25%) and F3 (50%), and low in F1 (9%) but absent in F4. Multivariate analysis revealed that male gender, waist circumference, Alanine Aminotransferase, and Hemoglobin A1C were independently associated with discordant results. The crude difference was significantly associated with high body mass index, waist circumference, and elevated Alanine Aminotransferase level, fasting glucose, and Hemoglobin A1C. It decreased with increasing elasticity ($p = 0.01$). The relative difference was significantly associated with elevated levels of Aspartate and Alanine Aminotransferase, Gamma-Glutamyl Transferase, and hyperbilirubinemia. It was inversely proportional to the degree of fibrosis ($p = 0.005$).

Conclusion: In conclusion, although the Fibroscan[®] is a reproducible technique, this study emphasizes the importance of operator training and result confirmation by an experienced operator in the presence of discordance risk factors.

THU-555

The effect of the novel selective and orally bioavailable CXCR7 modulator in carbon tetrachloride (CCl₄)-induced liver fibrosis using mouse model

Yunhee Kim¹, Yoon Suk Lee¹, Eun Hee Chae¹. ¹IleadBMS Ltd., Hwaseong-si, Korea, Rep. of South
Email: lisa.kim@ileadbms.com

Background and aims: Liver fibrosis is the process underlying chronic liver diseases, characterized by the repeated destruction and regeneration of liver cells. This leads to an abnormal deposition and distribution of extracellular matrix components like collagen, glycoproteins, and proteoglycans in the liver. Emerging research suggests that CXCR7 plays a role in both liver regeneration and fibrosis. In this study, we investigate whether our novel compound, CXCR7 modulator has a therapeutic impact in CCl₄-induced hepatic fibrosis in mice.

Method: Male C57BL/6N mice were injected intraperitoneally with carbon tetrachloride (CCl₄) twice a week for a period of 6 weeks. The treatment (vehicle, IL1512 and Elafibranor) commenced right before the administration of CCl₄ on day 0 and was sustained for a duration of 6 weeks, concurrently with the administration of CCl₄. After the termination of dosing, liver injury was evaluated through liver weight, serum AST, ALT, liver hydroxyproline, Ishak fibrosis score, and % collagen proportion area (% CPA).

Results: In the disease control group, levels of liver hydroxyproline and liver enzymes ALT and AST were significantly higher than those in the normal control group. However, treatment with Elafibranor (30 mg/kg, po) and IL1512 (10, 30, and 60 mg/kg, po) demonstrated a significant reduction in hydroxyproline and ALT levels compared to the disease control group. Moreover, the administration of Elafibranor and IL1512 resulted in a notable, dose-dependent decrease in liver fibrosis when compared to the disease control group.

Conclusion: Prophylactic treatment with IL1512 in a CCL₄-induced liver fibrosis model demonstrated a potent efficacy equal to or greater than Elafibranor. This study identified IL1512 as the first CXCR7 modulator showing notable efficacy in an animal model of liver fibrosis.

THU-556

Liver fibrosis in NLRP3^{tm1Hhf/J} knockout mice suffering from apical periodontitis

Cristiane Cantiga¹, Mariana Justo¹, Flávio Faria¹, Pedro Oliveira¹, Laís Barroti¹, Almir Rodrigues¹, Nathália Machado¹, Juliana Goto¹, Edilson Ervolino¹, Tiago Pinheiro², Luciano Cintra¹. ¹School of Dentistry, São Paulo State University (Unesp), Araçatuba, São Paulo, Brazil; ²School of Health Sciences, Amazonas State University (UEA), Manaus, Amazonas, Brazil
Email: cristiane.cantiga@unesp.br

Background and aims: Aimed to evaluate the effect of NLRP3 silencing on the immunological response of liver fibrosis (LF) alone or combined with apical periodontitis (AP).

Method: Forty C57BL/6J wild type (wt) mice were used, divided into 4 groups (n = 10): Cwt-control; APwt-with AP; LFwt-with LF; APLFwt-with AP and LF. Another forty Nlrp3^{tm1Hhf/J} knockout (ko) mice were divided into 4 groups (n = 10): Cko-control; APko-with AP; LFko-with LF; APLFko-with AP and LF. The animals were induced to liver fibrosis by injecting intraperitoneally 0.2 µl/g of carbon tetrachloride (CCl₄) twice a week for 60 days. On day 30, dental pulp exposure of the 1st and 2nd right upper molars was performed to induce AP. On day 60 the animals were euthanized. Histological analysis of AP was performed by HandE staining. Livers were analyzed by HandE, PSR staining and immunohistochemistry. Statistical tests were applied (p < 0.05).

Results: Periapical inflammation was more severe in the wt mice. These animals presented larger periapical bone resorption. In the livers, hepatic inflammation was more severe in wt animals compared to ko and between LFwt and APLFwt (p < 0.05). There was no difference between the LFko and APLFko groups (p > 0.05). The stage of liver fibrosis was higher in the wt animals compared to ko (p < 0.05). There was no difference between the LFwt and APLFwt, LFko and APLFko groups (p > 0.05). Immunostaining revealed greater activity of IL-1β, IL-17, IL-18 and CD20 in the wt mice compared to ko (p < 0.05). NLRP3 and IL-17 had a significant difference between the LFwt and APLFwt groups (p < 0.05). There was no difference in immunostaining between the LFko and APLFko groups (p > 0.05).

Conclusion: NLRP3 inflammasome silencing plays an important role in modulating LF, reducing inflammatory mediators. Furthermore, the presence of AP influences the increase in NLRP3 and IL-17, aggravating liver fibrosis in wt mice.

Gut microbiota and liver disease – Liver-organ crosstalk

TOP-561

Butyrate induces epigenetic and metabolic reprogramming in myeloid-derived suppressor cells to alleviate primary biliary cholangitis

Rui Wang¹, Bo Li¹, Zhengrui You¹, Xiong Ma¹, Ruqi Tang¹. ¹Shanghai Jiao Tong University School of Medicine Affiliated Renji Hospital, Shanghai Institute of Digestive Disease, Shanghai, China
Email: azureocean0107@gmail.com

Background and aims: Gut dysbiosis and myeloid-derived suppressor cells (MDSCs) are implicated in primary biliary cholangitis (PBC) pathogenesis. However, it remains unknown whether gut microbiota

or their metabolites can modulate MDSCs homeostasis to rectify immune dysregulation in PBC.

Method: We measured fecal short-chain fatty acids (SCFAs) levels by targeted GC/MS and analyzed circulating MDSCs by flow cytometry in two independent PBC cohorts. Human and murine MDSCs were differentiated *in vitro* in the presence of butyrate, followed by transcriptomic, epigenetic (CUTandTag-seq and ChIP-qPCR) and metabolic (untargeted LC/MS, mitochondrial stress test, and isotope tracing) analyses. The *in vivo* role of butyrate-MDSCs was evaluated in 2-octynoic acid-BSA-induced cholangitis murine model.

Results: Decreased butyrate levels and defective MDSCs function were found in patients with incomplete response to ursodeoxycholic acid (UDCA), compared to those with adequate response. Butyrate induced expansion and suppressive activity of MDSCs in a manner dependent on PPARD-driven fatty acid β-oxidation (FAO). Pharmaceutical inhibition or genetic knockdown of the FAO rate-limiting gene CPT1A abolished the effect of butyrate. Furthermore, butyrate inhibited HDAC3 function, leading to enhanced H3K27ac modifications at promoter regions of PPARD and FAO genes in MDSCs. Therapeutically, administration of butyrate or adoptive transfer of butyrate-MDSCs alleviated immune-mediated cholangitis in mice. Importantly, reduced expression of FAO genes and impaired mitochondrial physiology were detected in MDSCs from UDCA non-responders, and their impaired suppressive function was restored by butyrate.

Conclusion: We identify a critical role for butyrate in modulation of MDSCs homeostasis by orchestrating epigenetic and metabolic crosstalk, proposing a novel therapeutic strategy for treating PBC.

TOP-562

KYNA induced by short-term fasting through gut microbiota remodelling ameliorates hepatic ischemia/reperfusion injury via activating AhR-YAP signalling in mice

Xiaolong Chen¹, Xiaowen Wang², Genshu Wang³, Wenfeng Zhu⁴, Xuejiao Li⁵, Haoqi Chen⁴, Zhilong Liu¹, Zhiwei Chen¹. ¹Department of Hepatobiliary Surgery, The First Affiliated Hospital of Jinan University, Guangzhou, China; ²The Third Affiliated Hospital of Sun Yat-sen University, Guangzhou, China; ³Department of Hepatic Surgery, Liver Transplantation, Guangdong Provincial Hospital of Chinese Medicine, Guangzhou, China; ⁴Department of Hepatic Surgery, Liver Transplantation, The Third Affiliated Hospital of Sun Yat-sen University, Guangzhou, China; ⁵The Third Affiliated Hospital of Sun Yat-sen University, Guangzhou, China
Email: 519781497@qq.com

Background and aims: Hepatic ischemia-reperfusion (IR) injury often occurs during liver transplantation (LT), partial liver resection and shock, and is an important factor affecting the prognosis of corresponding patients. Fasting is thought to improve a variety of inflammatory diseases, but its role in IR injury remains controversial. Our study aimed to determine the role of fasting in liver IR injury and to identify its underlying mechanisms.

Method: A mice model of hepatic IR injury with pretreatment of a 24-hour fasting was established first. Gut microbiota and metabolites were obtained for analysis by 16S rRNA sequencing and targeted/non-targeted metabolomics approaches. The effects of fasting on the changes of RNA in liver were further examined by RNA sequencing. Finally, clinical liver samples after LT were collected for further study.

Results: Short-term fasting remarkably attenuated liver IR injury, which relied on gut microbiota remodeling. The metabolite Kyna induced by *A.muciniphila* is necessary for the protection effect of fasting, and the administration of Kyna significantly reduce hepatocytes apoptosis and promote their proliferation during IR. Mechanistically, liver RNA sequencing results suggested that the AhR-YAP signaling axis plays an important role in the Kyna-dependent hepatocyte protection, which was confirmed by inhibiting AhR and knocking down YAP. Further, the correlation between

POSTER PRESENTATIONS

AhR-YAP signal and hepatic IR injury in post reperfusion liver grafts after transplantation was validated.

Conclusion: Our results demonstrated that metabolite Kyna induced by short-term fasting through gut microbiota remodelling ameliorates hepatic ischemia/reperfusion injury via activating AhR-YAP signalling in mice.

TOP-563

Phages targeting *Enterococcus B* bacteria associated with increased short-term mortality and proven bacterial infection in patients with decompensated liver cirrhosis and ACLF

Lore Van Espen¹, Lila Close², Robert Schierwagen³, Wenyi Gu³, Marisa Isabell Keller⁴, Anthony Fullam⁴, Michael Kuhn⁴, Wim Laleman⁵, Peer Bork⁴, Maria Papp⁶, Jonel Trebicka³, Jelle Matthijnsens². ¹KU Leuven, Rega Institute, Leuven, Belgium; ²KU Leuven, Leuven, Belgium; ³Universitätsklinikum Münster (UKM), Münster, Germany; ⁴EMBL, Heidelberg, Germany; ⁵University Hospitals Leuven, Leuven, Belgium; ⁶University of Debrecen, Debrecen, Hungary
Email: lore.vanespen@kuleuven.be

Background and aims: Bacterial infections and translocation are not only key precipitants, but also complications of ACLF. Especially the gut microbial ecosystem seems to play hereby an important role. Gut phages play a key role in the human gut microbial ecosystem, mainly through their influence on the interaction of the gut bacteria with the human host. This study will explore the relevance of the human gut virome in the context of decompensated liver cirrhosis and acute-on-chronic liver failure (ACLF).

Method: The fecal virome was longitudinally assessed in 93 patients with decompensated liver cirrhosis or ACLF from the PREDICT study. Phages were grouped according to their predicted bacterial host and lifestyle to associate them with clinical parameters.

Results: Phage alpha-diversity was higher in ACLF patients and increased with ACLF severity (CLIF-C ACLF score, Pearson's correlation coefficient = 0.41). In the absence of ACLF, the phageome was dominated by virulent phages, whereas the emergence of ACLF diminished this dominance of virulent phages at the expense of more temperate phages. This shift suggests ACLF causes induction of prophages, potentially as a consequence of inflammation. Inflammation status (white blood cell count, $R^2 < 1\%$), as well as markers of liver damage ($R^2 < 1\%$), timepoint ($R^2 < 1\%$), and most importantly patient-identifier ($R^2 = 32\%$) were contributing to the between-sample phage diversity. Furthermore, *Lactococcus A* phages were identified as potential predictors for ACLF development and were associated with increased short-term (90-day) mortality. While their phages were implicated, *Lactococcus A* bacteria themselves were not associated with disease progression. An elevated relative abundance and prevalence of *Enterococcus B* phages and *Enterococcus B* bacteria were observed in case of systemic bacterial infection and their presence was linked to worsened 90-day survival rates. Due to the novelty of this dataset, only the association between *Enterococcus B* phages and bacterial infection could be validated in an external cohort.

Conclusion: This study provides a first evidence that gut virome alterations are implicated in patients with decompensated liver cirrhosis and ACLF. Specifically, *Lactococcus A* phages may predict ACLF development, and especially *Enterococcus B* phages, in parallel to *Enterococcus B* bacteria, are associated with bacterial infection and mortality. This insight may be instrumental for development of strategies to prevent ACLF and improve outcome.

WEDNESDAY 05 JUNE

WED-517

Oatmeal a day does not keep the doctor away: the impact of the combination of inulin and exercise on MASLD amelioration and gut-liver crosstalk

Artemiy Kovynev^{1,2}, Mikolaj Charchuta^{1,2}, Quinten Ducarmon^{3,4,5}, Patrick CN Rensen^{1,2}, Milena Schönte^{1,2}. ¹Division of Endocrinology, Department of Internal Medicine, Leiden University Medical Center, Leiden, Netherlands; ²Eindhoven Laboratory for Experimental Vascular Medicine, Leiden University Medical Center, Leiden, Netherlands; ³Structural and Computational Biology Unit, European Molecular Biology Laboratory, Heidelberg, Germany; ⁴Experimental Bacteriology, Department of Medical Microbiology, Leiden University Medical Center, Leiden, Netherlands; ⁵Center for Microbiome Analyses and Therapeutics, Leiden University Medical Center, Leiden, Netherlands
Email: a.kovynev@lumc.nl

Background and aims: Lifestyle interventions such as diet and exercise are currently the only available therapies against metabolic dysfunction-associated steatotic liver disease (MASLD). We have earlier shown that late active period exercise training was associated with fat loss and the enrichment of fiber-digesting gut microbiota, so here we studied the impact of the combination of exercise training and a fiber-rich diet on the amelioration of MASLD via the gut-liver axis.

Method: Male APOE*3-Leiden.CETP mice, a model susceptible to MASLD, were fed a high fat-high-cholesterol diet with or without the addition of 10% inulin and exercise trained on a treadmill for 5 days a week for 1 hour at ZT22, or remained sedentary.

Results: Exercise training alone or in combination with fiber reduced the gain of fat mass throughout the study and lowered plasma glucose levels. Only the combination of fiber and exercise training, however, also decreased plasma triglyceride levels compared to sedentary control mice. Exercise training both with (3.3 ± 1.35) and without the addition of fiber (4.06 ± 1.78) had a similar ameliorating effect on the MASLD score compared to sedentary controls (5.675 ± 1.32), while fiber alone did not result in any improvement (5.57 ± 1.86). Interestingly, only exercise without fiber significantly decreased the expression of inflammatory markers in the liver. Both interventions remodeled the gut microbial composition. Exercise and fiber in combination enriched the fat-lowering and fiber-digesting bacterium *Anaerostipes hadrus*, while exercise training alone or in combination with fiber decreased the abundance of the genus *Alistipes* that has been linked to MASLD in mice and rats. Finally, exercise training increased the levels of health-promoting short-chain fatty acids (SCFA) in the portal vein blood, with the combination of exercise and fiber leading to the highest levels, which also correlated with the lowest levels of plasma triglycerides.

Conclusion: The combination of exercise training and dietary fiber decreases fat mass and restores insulin sensitivity, but does not have an additional positive effect on liver health compared to exercise training alone, despite the shift of the gut microbiota towards a healthier, SCFA-producing profile.

WED-518-YI

Protein-modulated microbiota for fecal transplantation improves metabolic functions in alcohol-related liver disease model

Nishu Choudhary¹, Ashi Mittal², Kavita Yadav³, Jaswinder Maras², Anupama Parasar³, Shiv Kumar Sarin³, Shvetank Sharma³. ¹Institute of Liver and Biliary Science, New Delhi, India; ²Institute of Liver and Biliary Sciences, New Delhi, India; ³Institute of Liver and Biliary Sciences, New Delhi, India
Email: shvetanks@gmail.com

Background and aims: Fecal microbiota transplantation (FMT) is a promising treatment for alcohol-related liver disease (ALD). To understand FMT-induced metabolic alterations post-FMT, we

investigated the outcome of protein-modulated FMT (pFMT) vs standard FMT in murine ALD model.

Method: Male C57BL/6N mice (n=8 each group) were pair-fed control or ethanol (22%) Lieber-DeCarli diet with thioacetamide (TAA, 150 mg/kg body weight, i.p.) for 8 weeks to induce ALD. FMT from standard diet and high protein (isocaloric, 20% from soya protein) fed donors was performed in ALD animals. Tissue, blood, and stool were collected at baseline and post-FMT day 7. Liver injury and inflammatory markers were assessed. Fecal 16S rRNA sequencing was performed to capture microbiota variations. Fecal and plasma metabolome was assessed by high-resolution mass spectrometry.

Results: There was a decrease in opportunistic taxa *Staphylococcus*, *Jeitgalicoccus*, and *Sporosarcina* (8 fold, $p < 0.001$), and *Desulfovibrio* (2.3 fold, $p < 0.001$) post pFMT, which was increased in ALD. Liver histopathology showed pericellular lesion in ALD and post pFMT showed significant overall improvement: steatosis (15 fold reduction, $p = 0.002$), fibrosis (6 fold reduction, $p = 0.005$), AST (3 fold reduction, $p = 0.016$), ALT (3 fold reduction, $p = 0.04$), serum bilirubin (2 fold reduction, $p = 0.04$). Significant reduction in hepatic pro-inflammatory markers IL6 (3 fold, $p = 0.03$) and TNF α (2.5 fold, $p = 0.06$) was observed after pFMT. Metabolomics identified a total of 503 plasma and 647 fecal metabolites across all groups. pFMT significantly ($p < 0.05$) altered 212 fecal and 124 plasma metabolites. 33 plasma metabolites were significantly ($p < 0.05$) upregulated, involved in: bile acid metabolism [taurocholic acid (9.7 ± 1.2 vs 6.2 ± 0.9 $p = 0.04$), chenodeoxycholic acid (9 ± 1.7 vs 7.0 ± 1.15 $p = 0.09$), deoxycholic acid (15.4 ± 1.9 vs 12.0 ± 1.2 $p = 0.08$)] and oxidative stress reducers glutamate, glutathione, and methionine metabolism [involving glutathione (10.9 ± 0.3 vs 8.9 ± 0.3 $p = 0.006$), s-adenosylmethionine (14.5 ± 0.2 vs 12.6 ± 0.4 $p = 0.001$) and 5-Phosphoribosylamine ($7.9 \pm 6.1 \pm 0.07$ $p = 0.001$) metabolites]. There was also an increase in mitochondrial beta-oxidation [3-oxododecanoic acid (12.7 ± 0.2 vs 11.5 ± 0.5 $p = 0.001$), octanoylcarnitine (12.3 ± 0.4 vs 11.3 ± 0.5 $p = 0.008$)], and amino acid metabolism, indicating the enhanced energy production, and concurrent increase in purine and histidine metabolism (deoxyuridine, 11.1 ± 0.6 vs 10 ± 0.2 $p = 0.02$) related to cell proliferation. 59 plasma metabolites were significantly down-regulated, including arachidonic acid (2 fold, $p = 0.009$) and linoleic acid (2.4 fold, $p = 0.001$) metabolism.

Conclusion: In alcohol-related liver disease, pFMT reduces the load of opportunistic taxa and expression of inflammatory pathways concomitantly increasing bile acid and energy metabolism, resulting in hepatic recovery.

WED-519-YI

Criss-cross fecal microbiota transplant identifies hepatic steroid biosynthesis and linoleic acid metabolism linked with liver injury and dysbiosis in rat

Manisha Yadav¹, Jaswinder Maras², Neha Sharma², Nupur Sharma², Gaurav Tripathi², Sadam H. Bhat³, Sushmita Pandey², Vasundhara Bindal², Babu Mathew², Anupama Kumari², Shiv Kumar Sarin². ¹Institute of Liver and Biliary Sciences, New Delhi, India; ²Institute of Liver and Biliary Sciences, New Delhi, India; ³Institute of Liver and Biliary Sciences, New Delhi, India
Email: jassi2param@gmail.com

Background and aims: Chronic and excessive alcohol consumption induces significant inflammation oxidative stress and produce hepatic lesions, including steatosis, hepatitis, and fibrosis/cirrhosis. Fecal microbiota transplant (FMT) has shown promise in ameliorating liver disease by modulating the gut microbiota. However, systemic change in the metabolome profile post FMT from healthy to ALD model or vice versa (criss-cross) are obscure and identification of such metabolic pathways may have therapeutic importance.

Method: We used human associated rats, Criss-cross FMT (intestinal microbiota of healthy donors given to ALD rats and intestinal microbiota from ALD patients given to healthy rats) was performed to look onto the pathways regulated by alcohol associated bacteria.

Metabolomics evaluation was performed in the liver, plasma, intestine and stool to understand pathways and metabolites which specifically got altered post FMT at different sites i.e., in liver, intestine, plasma and stool.

Results: Six-month chronic ethanol consumption in Long Evans rats led to significant liver injury, and perturbed butanoate, amino acid, bile acids, arachidonic acid, linoleic acid, microbial metabolism, tryptophan, steroid biosynthesis, and others in liver, intestine, stool, and plasma ($p < 0.05$) as seen in SAH patients and led to high Streptococcus and low Bifidobacterium prevalence. The chronic ethanol exposure reduced energy metabolism in liver ($p < 0.05$). FMT from healthy to ALD rats, significantly reduced inflammation, fibrosis ($p < 0.05$) and pathways such as arachidonic acid, tryptophan, linoleic acid, bile acid synthesis (liver, plasma and intestine) compared to control groups ($p < 0.05$). Conversely, FMT from ALD patients to healthy rats majorly impacted liver metabolism and specifically upregulated linoleic acid (4.5 folds), steroid biosynthesis, NAD and tryptophan metabolism ($p < 0.05$). The stool showed higher prevalence Streptococcus, Salmonella, Bacillus, Helicobacter, Haemophilus. Also, hepatic gene expression showed increase in cyp1a1 (50 fold), nox1 and mcp1 (5 fold) in the rat model treated with ALD microbiota ($p < 0.05$). A higher expression of cyp1a1 is associated with increased linoleic, steroid and arachidonic metabolism. Together hepatic gene expression and metabolome analysis of healthy rat treated with ALD microbiota outlines that alcohol associated microbiota induces cyp1a1 mediated increase in steroid biosynthesis (11 fold), linoleic acid (4 fold) and arachidonic acid metabolism (3 fold) which corroborated with ROS/inflammation as seen in SAH.

Conclusion: Our findings suggest that alcohol associated microbiome change in the intestine impact liver metabolism with significant effect on steroid biosynthesis and linoleic acid metabolism. Thus, targeting hepatic steroid biosynthesis and linoleic acid metabolism may have therapeutic importance in ALD.

WED-521-YI

Tissue-specific roles of Farnesoid X Receptor in gut-liver axis and influence on progressive cholestatic liver injury

Lina Ludwigs¹, Ines Volkert¹, Mona Peltzer¹, Antonio Molinaro², Marcus Henricsson³, Hanns-Ulrich Marschall⁴, Karolina Edlund⁵, Kai Markus Schneider⁶, Thomas Longerich⁷, Peter Boor⁸, Jan G. Hengstler⁹, Christian Trautwein⁶, Lena Susanna Candels¹.
¹University Hospital RWTH Aachen, Aachen, Germany; ²The Sahlgrenska Academy, Gothenburg, Sweden; ³University of Gothenburg, Gothenburg, Sweden; ⁴Department of Molecular and Clinical Medicine, Gothenburg, Sweden; ⁵University Dortmund, Dortmund, Germany; ⁶Uniklinik RWTH Aachen, Aachen, Germany; ⁷Universitätsklinikum Heidelberg, Heidelberg, Germany; ⁸Rheinisch-Westfälische Technische Hochschule Aachen, Aachen, Germany; ⁹IfADO, Aachen, Germany
Email: lludwigs@ukaachen.de

Background and aims: The Farnesoid X Receptor (FXR) is a broadly expressed receptor with diverse functions. Extensive research has been conducted on FXR and FXR agonist have been tested for the treatment of chronic liver diseases e.g., primary biliary cholangitis (PBC). However, a deeper understanding of the distinct functions of FXR within the gut-liver axis is still lacking. The aim of this study was to explore the tissue-specific roles of FXR in the gut and liver.

Method: We developed a novel mouse model using tissue-specific FXR knockouts for hepatocytes (FXR^{Δhepa}), intestinal epithelial cells (FXR^{ΔIEC}), and a combination of both—the FXR^{ΔhepaΔIEC} animals. We analysed liver tissue, ileal tissue, blood, and caecum stool samples after eight and 52 weeks.

Results: FXR^{ΔIEC} mice only showed a mild cholestatic phenotype with liver function tests within the normal range, while FXR^{Δhepa} mice exhibited a more severe phenotype with elevated transaminases, moderate cholestasis, and hepatic inflammation. In contrast, 8-week-old combined FXR^{ΔhepaΔIEC} animals demonstrated exacerbated liver damage with elevated transaminases, increased hepatic infiltration of

inflammatory cells, and strongly upregulated fibrosis markers. Gene pathway analysis of hepatic tissue confirmed these results, showing minor changes in gene regulation in FXR^{ΔIEC} mice, slightly more in FXR^{Δhepa} mice, but a severe dysregulation in FXR^{ΔhepaΔIEC} animals. While in FXR^{ΔIEC} mice and FXR^{Δhepa} mice bile acid synthesis was only mildly upregulated, it was severely increased in the FXR^{ΔhepaΔIEC} mice. Furthermore, we found changes in bile acid transporter expression, which, in combination with the increased bile acid synthesis, led to cholestatic liver disease in the FXR^{ΔhepaΔIEC} mice. Age progression led to an aggravation of this cholestatic phenotype after 52 weeks in FXR^{ΔhepaΔIEC} mice. Severe fibrosis and dysplastic nodules were evident.

Conclusion: Our data show that the loss of either the intestinal or the hepatic FXR, respectively, leads to minor dysregulations of gut-liver axis related pathways without any strong impact on the phenotype of these mice. The combined FXR loss however, leads to severe cholestatic liver injury associated with increased liver fibrogenesis and malignant growth. It appears that the interaction of both receptors is needed to maintain a balanced bile acid homeostasis. FXR^{ΔhepaΔIEC} animals are a novel model of progressive cholestatic liver injury and can contribute to a better understanding of the tissue-specific roles of FXR within the gut-liver axis.

WED-522-YI

Effect of various edible exosomes in restoring gut homeostasis and hepatic metabolic axis: a comparative study

P. Debishree Subudhi¹, Jitendra Kumar², Anupama Kumari¹, Shivani Gautam¹, Shruti Sureshan¹, Dinesh Mani Tripathi¹, Chhagan Bihari¹, Shiv Kumar Sarin¹, Sukriti Baweja¹. ¹Institute of Liver and Biliary Sciences, New Delhi, India; ²Department of Immunology, Mayo Clinic, College of Medicine and Science, Rochester, United States
Email: sukritibiochem@gmail.com

Background and aims: Edible Exosomes known to restore gut commensals and integrity, hence could configure gastro-hepatic alignment, attribute of hyperammonemia. We investigated the effects of Edible Exosomes on gut-microbiome and hepatic injury.

Method: Edible Exosomes isolated from carrot (CarEx), ginger (GinEx), garlic (GarEx), turmeric (TurEx) and lemon (LemEx) by differential ultracentrifugation, characterized by TEM and NTA. Cargoes evaluated by proteomics. Stability assessed by *in vitro* stomach/intestine-like digestion. Prophylactic oral administration of exosomes assessed in Thioacetamide (TAA) induced hyperammonemia model, compared to vehicle and lactulose. Biochemical markers of hepatic injury, ammonia, histology and behaviour were assessed. Microbiomics assessed by stool metagenomics and untargeted LC-MS metabolomics and by *in vitro* coculture of exosomes with probiotic *Lactobacillus rhamnassus* GG (LGG).

Results: Size and concentration of exosomes ranges 52 nm–200 nm and $2.65 \times 10^9 \pm 0.65$ particles/ml with zeta potential -7 to -16.0 ± 2.4 mV. Cargoes found enriched with anti-oxidants and proteins associated to metabolism, gingipain, allinase, and defensin. After *in-vitro*-digestion, particle size was reduced ($p = 0.02$) with intact zeta potential. Edible Exosomes administration in TAA rats reduced plasma ammonia [Vehicle- 97.9 ± 22.9 ; lactulose- 157.9 ± 46.6 umol/L ($p = 0.42$); CarEx- 92.2 ± 13.6 umol/L ($p = 0.002$); GinEx- 124.2 ± 11.9 umol/L ($p = 0.004$); GarEx- 179.9 ± 66.5 umol/L; LemEx- 159.6 ± 36.7 umol/L], ALT and bilirubin ($p < 0.004$; $p < 0.008$) but only CarEx improved albumin ($p = 0.03$). Edible Exosomes improved motor activity ($p < 0.0001$), cognitive caper ($p = 0.004$), hepatic cholestasis, necrosis and inflammation. Edible Exosomes altered the gut flora in TAA rats (β -diversity; $p = 0.001$) but CarEx ($p = 0.02$)/TurEx ($p = 0.01$) decreases growth of urease positive *Escherichia-Shigella* responsible for elevated ammonia levels. CarEx improved colonisation of Firmicutes [Lachnospiraceae ($p = 0.03$), Ruminococcaceae ($p =$

0.017), Lactobacillaceae ($p = 0.028$)] that maintains gut homeostasis and upon coculture with probiotic microbe LGG *in-vitro* showed enhanced growth ($p = 0.004$). Stool metabolome of CarEx found enriched metabolites guanidosuccinic acid, $p = 0.030$, D-proline, $p = 0.05$, 8amino7oxonononate, $p = 0.017$ associated with ammonia excretion, converting through urea/L-arginine/biotin metabolism pathways and improves gut integrity (glutathione, retinol metabolism). Meanwhile D-glutamine associates with ammonia scavenging, N-acetyl-DL-serine improves cognition, malic acid/arctigenin having anti-inflammatory/microbial effects found upregulated in serum of CarEx administered rodents.

Conclusion: CarEx potentiates ammonia excretion helps alleviating hyperammonemia, configures gut and improves cognition, considered 'Ammonia scavengers'.

WED-523

Sulphated progesterone metabolites undergo apical sodium bile acid transporter-mediated enterohepatic recycling and stimulate glucagon-like peptide 1 and peptide YY release

Alice Mitchell^{1,2}, Iain Tough¹, Caroline Ovadia¹, Anita Lövgren-Sandblom³, Jenny Chambers², Anastasia Tsakmaki¹, Patricia Pedro¹, Gavin Bewick¹, Helen Cox¹, Catherine Williamson^{1,2}. ¹King's College London, London, United Kingdom; ²Imperial College London, London, United Kingdom; ³Karolinska Institute, Sweden, United Kingdom
Email: am13309@ic.ac.uk

Background and aims: Sulphated progesterone metabolites (PMxS) increase during gestation and are elevated further in intrahepatic cholestasis of pregnancy (ICP), characterised by elevated serum bile acids (BA). Both PMxS and BA are derived from cholesterol and have a steroid backbone, and PMxS have previously been shown to activate BA receptors. We investigated whether PMxS could undergo enterohepatic recycling and stimulate intestinal Takeda G-protein coupled receptor 5 (TGR5)-mediated release of gut hormones glucagon-like peptide-1 (GLP-1) and peptide YY (PYY).

Method: Ussing chambers were used to evaluate colonic ion secretion changes (ΔI_{sc}) in wildtype, TGR5^{-/-}, and PYY^{-/-} mice by two PMxS metabolites, PM3S and PM5S, and in wildtype mice with or without apical sodium bile acid transporter (ASBT) inhibition ($n = 6$ /condition). PM3S/PM5S and taurodeoxycholic acid (TDCA) stimulation of GLP-1 release from wildtype and TGR5^{-/-} murine crypts and human colonoids was measured by ELISA ($n = 3$). PMxS were quantified in faeces ($n = 18$) and pre-/postprandial serum samples ($n = 20$) by ultra-performance liquid chromatography-tandem mass spectrometry in prospectively recruited third trimester of pregnancy outpatients with uncomplicated pregnancy or ICP.

Results: Apical and basolateral PM3S and PM5S stimulated PYY-mediated $-\Delta I_{sc}$ in wildtype ($p < 0.01$) but not TGR5^{-/-} or PYY^{-/-} colons. PM3S and PM5S stimulated GLP-1 secretion in murine crypts and human colonoids ($p < 0.001$) to levels comparable to a canonical agonist, TDCA. PMxS are present in faeces; ASBT inhibition blunted $-\Delta I_{sc}$ by 68% after apical PM3S and PM5S addition ($p < 0.001$). Serum PMxS increase postprandially in women with ICP but are unaltered in uncomplicated pregnancies.

Conclusion: ASBT can transport steroid-based progesterone metabolites alongside the canonical conjugated bile acids and may be involved in the postprandial rise in serum PMxS levels in cholestatic pregnancies. PMxS were able to stimulate GLP-1 and PYY release via activation of TGR5 to a similar extent as TDCA, suggesting they may play a role in modulating gut hormone response during pregnancy. This work demonstrates a novel substrate for ASBT beyond bile acids and suggests a role for hormone metabolites elevated in pregnancy undergoing enterohepatic recycling to modify metabolic responses in the gut.

WED-524-YI

Multi-omics study of chronic liver diseases with rifaximin treatment

Yingjie Ai¹, Sitao Ye¹, Xiaoquan Huang¹, Shiyao Chen¹. ¹Zhongshan Hospital, Fudan University, Shanghai, China
Email: 23111210016@m.fudan.edu.cn

Background and aims: Chronic liver diseases including cirrhosis and non-alcoholic fatty liver disease (NAFLD) are worldwide health concerns and are closely interrelated. Multiple clinical and experimental studies have found that rifaximin, an oral non-absorbable antibiotic, can be used in the treatment of cirrhosis and NAFLD and their complications but the common mechanisms and targets of rifaximin for the treatment of both chronic liver diseases still need to be clarified. The aim of this study was to investigate the biomolecular characteristics and targets of rifaximin for the treatment of two chronic liver diseases by multi-omics.

Method: Rat and mouse models of cirrhosis and NAFLD were constructed and followed by rifaximin gavage intervention for 2 weeks. The therapeutic effects of rifaximin on dual chronic liver diseases were verified by pathological and hematological tests. Common hepatic genetic targets regulated by rifaximin were discovered by liver transcriptome sequencing of rats and validated with experiments in mouse, biochemical indices of clinical patients and public transcript data. Fecal 16S rDNA sequencing was performed to explore the regulatory effect of rifaximin on intestinal flora and explore the common microbial targets.

Results: Staining and other assays demonstrated that rifaximin could improve liver fibrosis in cirrhotic model and hepatic steatosis in NAFLD model. Hepatic transcriptome analysis of rats suggested that rifaximin could regulate metabolism-related pathways in both models, and metabolism-related genes such as Ephx1 and Cbr1 were significantly dysregulated. Identical rifaximin-induced transcriptional changes were observed in mouse by RT-PCR. Meanwhile, lipid levels in cirrhotic patients showed a decrease in cholesterol, LDL, and non-HDL after rifaximin intervention, corresponding with the transcriptional changes. Analysis of public datasets showed that hepatic EPHX1 and CBR1 in patients with NAFLD showed corresponding pathological dysregulation. Rifaximin could affect the structure and function of gut microbiome in rats with cirrhosis and NAFLD as alpha diversity and beta diversity of the microbiota were altered. Plentiful intestinal taxa showed reversible alterations after rifaximin intervention, including *Candidatus Saccharibacteria*, *Actinobacteria*, *Firmicutes*, and *Bacteroidetes*, which are reported to undergo dysregulation during the pathological process and predicted to have metabolic function. Shared differential-abundant taxa were mostly related with carbohydrate metabolism and amino acid metabolism.

Conclusion: The multi-omics study of chronic liver disease with rifaximin treatment uncovered common hepatic genetic and gut microbial targets of rifaximin for treating both cirrhosis and NAFLD, providing novel ideas to advance and understand the clinical application of rifaximin.

WED-525

Hepatocellular carcinoma risk associated with circulating metabolites of gut microbiome origin assessed by targeted mining of high-resolution untargeted metabolomics data

Anastasia Chrysosvalantou Chatziioannou¹, Nikolaos Papadimitriou¹, David Hughes², Mazda Jenab^{1,3}, Pekka Keski-Rahkonen¹.

¹International Agency for Research on Cancer (IARC-WHO), Lyon, France; ²University College Dublin, Dublin, Ireland; ³International Agency for Research on Cancer, Nutrition and Metabolism Branch, Lyon, France

Email: chatziioannouc@iarc.who.int

Background and aims: Alterations in the composition and metabolic activity of the human gut microbiome, favoring the growth of pathogenic or unhealthy species, have been implicated in the

development of hepatocellular carcinoma (HCC). Some gut-derived microbial metabolites may be pro-inflammatory and growth-promoting, while others may be cancer protective. Much of the current knowledge about metabolic alterations occurring in HCC is derived from case-control studies, while information from prospective, observational cohort studies remains limited. We explored associations between circulating metabolites related to gut microbial metabolism and HCC risk in a case-control study nested within the European Prospective Investigation into Cancer and Nutrition (EPIC) cohort.

Method: A detailed literature search of peer-reviewed articles and on-line metabolite databases was conducted to compile a diverse target list of microbial metabolism-related metabolites to be examined in association with HCC development. We employed untargeted, high-resolution liquid chromatography-mass spectrometry (LC-MS), using reversed phase and hydrophilic interaction chromatography both in positive and negative polarities, to detect thousands of metabolic features in pre-diagnostically collected serum samples from n = 110 first incident HCC cases matched 1:1 with healthy control participants from the EPIC cohort. In EPIC detailed lifestyle data and biospecimens were collected at baseline from >520,000 apparently healthy participants from 10 European countries who were then followed up over time for cancer diagnoses. Gut microbiome-related metabolites were annotated from LC-MS features detected in the serum samples. Multivariable adjusted conditional logistic regression models were applied to assess the relationship between each matched metabolite and HCC risk.

Results: The detailed literature search identified 473 microbiome-related metabolites. A large number of LC-MS features were successfully matched to these metabolites based on chemical formula and isotopic pattern. After Benjamini-Hochberg correction for multiple testing, HCC risk associations were observed for 14 annotated metabolites from diverse chemical classes. In general, bile acids, amino acids and their metabolites, tocopherols, amines and choline were associated with risk of HCC, suggesting a role for microbiome alterations in the development of this cancer.

Conclusion: These novel findings contribute to the evidence base on microbial metabolism-related compounds and HCC risk, providing preliminary insight into metabolic perturbations linked to gut microbiome composition and metabolic activity and their potential involvement in HCC development. They also highlight a unique approach of targeted analysis of specific metabolites from within high-resolution untargeted metabolomic features.

WED-526

Hepatic steatosis in young adults is associated with altered intestinal microbiology

Yasmina Tashkent^{1,2,3}, Jocelyn Choo^{1,3}, Alyson Richard³, Zhengyi Wang⁴, Luis Bertot⁴, Trevor Mori⁴, Lawrence Beilin⁴, Oyekoya Ayonrinde⁴, John Olynyk⁵, Therese O'Sullivan⁶, Kerry Ivey⁷, Alan Wigg^{1,2}, Kate Muller^{1,2}, Geraint Rogers^{1,3}, Leon Adams^{4,8}.

¹Flinders University, Adelaide, Australia; ²Flinders Medical Centre, Adelaide, Australia; ³South Australian Health and Medical Research Institute (SAHMRI), Adelaide, Australia; ⁴The University of Western Australia, Perth, Australia; ⁵Curtin University, Perth, Australia; ⁶Edith Cowan University, Perth, Australia; ⁷Harvard University, Boston, United States; ⁸Sir Charles Gairdner Hospital, Perth, Australia
Email: yasmina.tashkent@gmail.com

Background and aims: Steatotic liver disease (SLD) is a leading cause of chronic liver disease worldwide. The gut microbiome and the metabolites that are produced by intestinal microbes (e.g. short-chain fatty acids [SCFA]), are increasingly linked to SLD risk, with specific bacterial taxa associated with steatosis in children, adolescents and older adults. We aimed to characterise changes to the gut microbiome in young adults with steatosis, previously undescribed in this age group.

POSTER PRESENTATIONS

Method: 1082 participants of the longitudinal population-based Raine Study underwent cross-sectional assessment at the age of 27 years, including magnetic resonance imaging (MRI) of the liver and fasting serum biochemistry. Clinical metadata and stool samples were also collected. Hepatic steatosis was quantified using a validated MRI volumetric liver fat fraction (VLFF) equation (HepaFat) and a previously established cut-off of greater than 3.55% was used to indicate the presence of steatosis. Participants were divided into three groups for analysis (no steatosis [NS]: VLFF \leq 3.55%, mild-moderate [MM] steatosis: VLFF 3.56–13.55% and severe steatosis [SS]: VLFF $>$ 13.55%). Gut microbiome profiling was performed using 16S rRNA V4 amplicon sequencing to assess microbial alpha diversity (Shannon entropy, Pielou evenness and observed features) and microbiota composition similarity (based on weighted UniFrac distance).

Results: Of 588 participants (305 [51.9%] female) who had complete data, 488 (83%) had NS, 76 (12.9%) had MM steatosis and 24 (4.1%) had SS. Compared to NS, individuals with SS exhibited significantly lower microbiota alpha diversity. Faecal microbiota composition also differed significantly between NS and both MM ($p=0.0064$) and SS groups ($p=0.0015$). Compared to NS, the SS group exhibited significantly lower relative abundance of a number of SCFA-producing bacterial taxa, including Christensenellaceae R.7 group, Lachnospiraceae ND3007 group, Lachnospiraceae NK4A136 group, *Eubacterium xylanophilum* group, *Eubacterium eligens* group, *Alistipes*, *Coprococcus*, *Odoribacter* and *Clostridia vadin* BB60 group (False-Discovery Rate [FDR] corrected $p < 0.05$). UCG-001 (family XIII), UCG-002 (family Oscillospiraceae) and UCG-005 (Oscillospiraceae) were also significantly lower in SS compared to the NS group. In contrast, members of the SS group displayed significantly increased levels of *Lachnoclostridium* and *Ruminococcus gnavus* group (FDR corrected $p < 0.05$), bacterial taxa that have been implicated in cardiovascular disease and SLD pathogenesis.

Conclusion: Hepatic steatosis in young adults is associated with reduced intestinal microbial diversity compared to those without hepatic steatosis, including lower relative levels of bacteria that are capable of SCFA biosynthesis and higher relative levels of bacterial clades associated with cardiovascular disease.

WED-527-YI

Protein-educated fecal cell-free transplant enhances remission better than protein-educated fecal microbiota transfer in alcohol-related liver disease

Ashi Mittal¹, Nishu Choudhary¹, Kavita Yadav¹, Anupama Kumari¹, Jaswinder Maras¹, Shiv Kumar Sarin¹, Shvetank Sharma¹. ¹*Institute of Liver and Biliary Sciences, New Delhi, India*
Email: shvetanks@gmail.com

Background and aims: Fecal microbiota transfer (FMT) is an effective treatment for alcohol related liver disease (ALD). During FMT, cell free component consisting of metabolites, proteins and other molecules from host and gut bacteria is also transferred. Cell free transfer (CFT) is known to be as beneficial as FMT. We compared the efficacy of protein pre-educated (PE)-FMT and CFT.

Method: Male C57BL/6N mice were fed ethanol Lieber-DeCarli diets along with thioacetamide (150 mg/kg bw, i.p., twice weekly) for 8 weeks to induce ALD. Donors were fed soya protein diet (1000 kcal/L, 50% protein, 36% fat, 14% carbohydrate) for 2 weeks. Fecal slurry was prepared for FMT and CFT (slurry was sterile filtered using 0.22 micron filter). Standard (Std) FMT/CFT and abstinence served as controls. Microbiota was assessed using 16 s rRNA sequencing post-day7 of transplant. PICRUSt analysis was used to assess microbial functional pathways. Hepatic recovery was assessed by histopathology, serum biomarkers and gene expression of inflammatory markers.

Results: PE-CFT showed significant reduction in AST (1.4 fold change (FC) $p=0.008$; 1.3 FC $p=0.02$), ALT (1.4 FC $p=0.05$), steatosis (1.5 FC $p=0.04$; 1.4 FC $p=0.05$) and fibrosis (1.2 FC $p=0.06$; 1.3 FC $p=0.05$) as

compared to Std CFT and Std FMT respectively. Comparison of PE-CFT with PE-FMT showed reduction in serum biomarkers [ALT (1.2 FC $p=0.05$), AST (1.2 FC $p=0.02$), steatosis (2 FC $p=0.04$) and fibrosis (1.1 FC $p=0.07$). PE-CFT also resulted in a reduced gene expression of hepatic pro-inflammatory markers IL1 beta (1.7 FC $p=0.01$), TNF alpha (1.4 FC $p=0.01$) and TLR4 (1.7 FC $p=0.07$) along with an increased expression of anti-inflammatory marker IL10 (1.7 FC $p=0.0005$) when compared to PE-FMT, suggests enhanced efficacy of PE-CFT over PE-FMT in remission of liver injury. PE-FMT and PE-CFT led to significant variation (76% $p=0.001$) in gut microbiota composition. PE-CFT increased the relative abundance of probiotic taxa *Akkermansia muciniphila* and *Parabacteroides goldsteinii* over PE-FMT. Though PE-CFT increased the abundance of pathogenic taxa significantly (*Citrobacter freundii*, 5.7 FC $p=5.2E-05$; *Enterococcus faecalis*, 3.5 FC $p=0.007$; *Helicobacter typhlonius*, 3.7 FC $p=0.02$), they did not exert any adverse effect on outcome. Bacterial pathways involved in energy, amino acid, lipid, and carbohydrate metabolism were significantly modulated by PE-CFT (NAD salvage pathway II: 4.7 FC, $p=2.1E-04$; polyamine biosynthesis: 3.4 FC $p=3.0E-07$; fatty acid and beta-oxidation: 2 FC $p=0.02$; TCA cycle: 2 FC $p=0.03$; glycolysis (-1.3 FC $p=0.03$).

Conclusion: Protein pre-educated CFT alleviates the ALD injury better than protein pre-educated FMT. It improves the energy and amino acid metabolism accompanied with significant reduction in hepatic inflammation and steatosis. Thus, donors gut milieu may be pre-educated with high protein diet prior to cell-free transfer in ALD subjects.

WED-528-YI

Isolation and characterization of extracellular vesicles in faecal matter: implications for future biomarker discovery

Hector Leal-Lassalle¹, Olga Estévez-Vázquez¹, Raquel Benedé-Ubieto¹, Raquel Castillo-González^{1,2}, Lucía Sancho-Temiño¹, Aranzazu Cruz-Adalia^{1,2}, Rafael Bañares^{1,3,4,5}, Javier Vaquero^{3,4,5}, Francisco Javier Cubero^{1,3,4}, Yulia Nevzorova^{1,3,4}. ¹*Complutense University School of Medicine, Madrid, Spain*; ²*Instituto de investigación sanitaria Hospital 12 de octubre, Madrid, Spain*; ³*Centro de investigación biomédica en red de enfermedades hepáticas y digestivas, Madrid, Spain*; ⁴*Instituto de investigación sanitaria Gregorio Marañón, Madrid, Spain*; ⁵*Servicio de aparato digestivo, Hospital general universitario Gregorio Marañón, Madrid, Spain*
Email: hecleal@ucm.es

Background and aims: Extracellular vesicles (EVs) are microscopic particles (with size ranging from 30 nanometers to 10 micrometers) abundantly released into body fluids by all types of cells. EVs are of growing interest due to their potential diagnostic, disease surveillance, and therapeutic applications. While several studies have evaluated EV isolation methods in various biofluids, there are only few data on these techniques when applied to stool. However, the feces are an ideal biospecimen for studying intestinal inflammation and damage. In this study, we aimed to assess EVs from murine feces (fEVs) for reproducibility, purity, and protein expression in stool supernatant as well as to evaluate their effects *in vivo* and *in vitro*.

Method: We used stool from 33 weeks old C57BL/6J male mice. fEVs were isolated by ultracentrifugation, and fully characterized by flow cytometry, Nanoparticle Tracking Analysis (NTA), western blotting and Transmission Electron Microscopy (TEM). HepG2 cells were cocultured with different amounts of isolated fEVs marked with a fluorescent probe, assessing their survival and proliferation at different timepoints. The morphology of the cells was analyzed by fluorescent staining and observation under a Leica TCS SP5 confocal microscope.

Results: NTA of the isolated fEVs confirmed size homogeneity in the nanoparticle population at the range of 50–100 nanometers, together with high fEV concentration and high protein yield in the isolated samples. TEM visualization confirmed crucial EV characteristics, i.e. shape and size as well as purity of the preparation. Vesicle-associated

markers CD63, CD81 and Alix were present in fEV fractions. Importantly we showed, the fEVs are released by two main domains-eukaryotes and bacteria. The presence of fEVs from gram-negative and gram-positive bacteria was detected by western blot using anti-lipid A and anti-lipoteichoic acid antibodies, whereas western blot using anti-beta-actin antibody was employed to detect host-derived EVs. Furthermore, bacteria-free fEVs were administered into healthy C57BL/6J mice by intraperitoneal injection and did not cause any peritoneal inflammation as it has been confirmed by flow cytometry analysis of intraperitoneal liquid. Consistently, fluorescently labeled fEVs applied to HepG2 human hepatoma culture did not affect cellular morphology and have been localized either in the cytoplasm or the nuclei of treated cells.

Conclusion: These findings serve as the groundwork for future studies in order to investigate the potential of fEVs as a source for novel biomarkers for diagnosis of intestinal homeostasis.

WED-529

Transplantation of fecal microbiota derived from idiosyncratic drug-induced liver injured patients caused by amoxicillin-clavulanate determines a specific bile acid profile in germ-free mice

Sara Román-Sagüillo¹, María Juárez-Fernández^{1,2}, Alba González-Robles¹, Raísa Quiñones Castro³, Susana Martínez-Flórez¹, Javier González-Gállego^{1,2}, Francisco Jorquera^{1,2,3}, María-Victoria García-Mediavilla^{1,2}, Esther Nistal^{1,2}, Sonia Sánchez-Campos^{1,2}. ¹Instituto Universitario de Biomedicina (IBIOMED), Universidad de León, León, Spain; ²Centro de Investigación Biomédica en Red de Enfermedades Hepáticas y Digestivas, Instituto de Salud Carlos III, Madrid, Spain; ³Servicio de Aparato Digestivo, Complejo Asistencial Universitario de León, León, Spain
Email: sroms@unileon.es

Background and aims: Drug-induced liver injury is a multifactorial hepatic disease and amoxicillin-clavulanate (AC) is one of the main causing agents of its idiosyncratic (iDILI) and cholestatic form. Bile acids are important signaling molecules related to the progression and development of cholestatic iDILI. In this sense, gut microbiota composition is linked not only to the onset and progression of various hepatic diseases, but also to the enterohepatic circulation of bile acids. Thus, our aim is to evaluate the effect of fecal microbiota transplantation (FMT) from patients with iDILI caused by AC (iDILI-AC) on bile acid metabolism in germ-free mice (GFm).

Method: Two patients with iDILI-AC (diDILI-AC+), two patients treated with AC who did not develop iDILI (diDILI-AC-) and a healthy subject (dC) were selected as FMT donors based on iDILI-related biochemical parameters and gut microbiota characterization. Stool samples from these donors were processed for FMT to GFm. Then, GFm were divided in 3 groups per donor being treated with amoxicillin (A), AC or its vehicle. After 7 days of treatment, serum, liver and fecal samples were obtained to evaluate biochemical parameters, hepatic gene expression, fecal bile acid quantification and gut microbiota composition. Moreover, correlation analysis between fecal bile acids and gut microbiota composition were performed.

Results: Serum biochemical analysis showed an increase in bilirubin levels referred to diDILI-AC+ in comparison with the other groups. Moreover, an altered expression of hepatic genes related to bile acid synthesis and transport (*Cyp8b1* and *Abcg5*) was observed not only associated with the treatment, but also with the donor. In this sense, the quantification of fecal bile acids showed a modification in primary (cholic and ursodeoxycholic acid) and secondary (deoxycholic, lithocholic and 12-Ketolithocholic acid) bile acid concentration in feces. These alterations in bile acid concentration levels were affected by both donor and treatment, highlighting a significant reduction of secondary bile acids in dC/A and dC/AC compared to dC/H₂O, a trend that was not observed in diDILI-AC+ and diDILI-AC-. Furthermore, secondary fecal bile acids were positively correlated with specific gut

microbial genera, remarking *Barnesiella*, *Desulfovibrio* and *Howardella*. The relative abundance of these genera was affected by the donor type, while *Barnesiella* also showed a higher abundance after AC treatment regardless of the donor.

Conclusion: Transfer of a particular gut microbiota profile associated with iDILI-AC could affect the enterohepatic circulation of GFm bile acids and the response to treatment. However, further studies are needed. Funding: PID2020-120363RB-I00, LE017-P20. CIBERehd funded by ISCIII.

WED-530-YI

Comparative analysis of the gut-liver axis in preclinical models of decompensated cirrhosis

Elisa Castillo^{1,2}, Leticia Muñoz^{1,2}, Lorena Paule^{1,2}, Manuel Ponce-Alonso^{3,4}, Olaya de Dios^{5,6}, Alejandro Miranda González^{1,2}, Rosa del Campo^{3,4}, Miguel A. Ortega^{1,2}, Agustín Albillos^{1,2,4}. ¹University of Alcalá, Faculty of Medicine and Health Sciences, Alcalá de Henares, Spain; ²CIBERehd Biomedical Research Networking Center in Hepatic and Digestive Diseases, Madrid, Spain; ³CIBERinfec - Center for Biomedical Research Network of Infectious Diseases, Madrid, Spain; ⁴Hospital Universitario Ramón y Cajal IRYCIS, Madrid, Spain; ⁵Hospital 12 de Octubre Health Research Institute (i+12), Madrid, Spain; ⁶Carlos III Health Institute, Majadahonda, Spain
Email: elisa.castillo@uah.es

Background and aims: Liver-gut axis comprehension is crucial in cirrhosis research, yet the specific alterations in animal models of cirrhosis with this domain remain under-characterized. Addressing this gap, our study conducts an in-depth comparative structural and functional analysis of the gut analysis of the two most used preclinical models of cirrhosis: bile duct ligation (BDL) and carbon tetrachloride (CCl₄). Our aim was to elucidate differences in the structure and function of the gut barrier and microbiota in these models.

Method: Cirrhosis with ascites was induced in Wistar rats by CCl₄ oral gavage or bile duct ligation (BDL). Once animals developed ascites, we evaluated different aspects of the structure and function of the gut at the terminal ileum: muco-epithelial barrier (PAS), structure (by endothelial co-expression PV1/CD34) and function (4kD dextran-FITC visualized in liver after intestinal loop assay) of the gut vascular barrier, microbiota adhered to the mucosa and feces (by 16S metagenomic, NGS) and bacterial translocation (BT) to the mesenteric lymph nodes (by MALDI-TOF).

Results: Compared to the BDL model, the muco-epithelial barrier of the ileum in the CCl₄ model showed lower mucus thickness (27.0 [20.2–29.1] vs. 32.7 [27.9–38.5] μm, p < 0.05) and fewer goblet cells (0.17 [0.13–0.19] vs. 0.32 [0.30–0.35]/μm villus, p < 0.05). Impairment of the gut vascular barrier was also more severe in CCl₄ cirrhosis, indicated by higher PV1 expression (0.80 ± 0.08 vs. 0.57 ± 0.14, p < 0.05) and increased passage of dextran-FITC particles from the intestine to the liver (10.7 ± 2.3 vs. 6.7 ± 1.5 particles/field, p < 0.05) compared to the BDL model. In terms of microbiota composition, the CCl₄ model showed significantly greater relative abundance of Firmicutes and Bacteroidetes, while Proteobacteria were similar to the BDL model. Small intestinal bacterial overgrowth was more frequent in BDL (12.1 ± 1.1 vs. 6.9 ± 0.4 CFU/g, p < 0.05). Conversely, BT was more common in CCl₄ (86% vs. 60%, p < 0.05). Transcriptomic analysis revealed distinct expression patterns with upregulation of immune genes in BDL and of cholesterol homeostasis genes in the CCl₄.

Conclusion: The abnormalities of the intestinal barrier and microbiota of the CCl₄ and the BDL models of cirrhosis exhibit distinctive differences. These disparities underscore the importance of analysing the results in both models when studying abnormalities in the gut-liver axis in cirrhosis and identifying potential therapeutic targets.

WED-531

The double-edged sword of bariatric surgery: extending the excluded limb can trigger bacterial translocation, liver inflammation and death

Louis Onghena¹, Anneleen Heldens², Milton Antwi², Lindsey Devisscher³, Hans Van Vlierberghe², Sarah Raevens², Xavier Verhelst², Anne Hoorens⁴, Yves Van Nieuwenhove⁵, Anja Geerts², Sander Lefere². ¹Liver Research Center Ghent, Ghent University, Ghent University Hospital, Ghent, Belgium; ²Hepatology Research Unit, Ghent, Belgium; ³Liver Research Center, Ghent, Belgium; ⁴Department of Diagnostic Sciences, Ghent, Belgium; ⁵Department of Gastrointestinal Surgery, Ghent, Belgium
Email: Louis.onghena@ugent.be

Background and aims: Bariatric surgery (BS) is an effective treatment for obesity and associated comorbidities, including metabolic dysfunction-associated steatotic liver disease (MASLD). We applied several novel BS procedures in mice to examine the effects of surgery selection and biliary limb length on metabolic health, bacterial translocation, and survival.

Method: Mice were fed a Western diet (WD) for 12 weeks, followed by surgery with continued WD feeding and sacrifice at weeks 13 and 20. Six different types of BS (vertical sleeve gastrectomy and plication, Roux-en-Y gastric bypass (RYGB), and one-anastomosis gastric bypass (OAGB) with three different biliary limb lengths (25% = Ω_1 , 50% = Ω_2 , 75% = Ω_3) were performed and compared with sham surgery procedure. Gut decontamination with an oral antibiotic cocktail (amoxicillin, vancomycin, neomycin, and metronidazole) was performed in a subset of Ω_3 mice, starting one week before surgery until the end of the experiment. Statistical differences between groups were assessed by one-way ANOVA with Tukey post-hoc tests.

Results: Relative weight loss differed significantly amongst the groups at week 20. In RYGB, $\Omega_{1\text{and}2}$, significantly lowered relative visceral adipose tissue weight ($p < 0.0001$) and ALT ($p < 0.01$) compared to sham surgery. Histologically, sham-operated mice had developed severe liver steatosis, moderate inflammation, and mild fibrosis after 20 weeks of WD feeding, which was attenuated by RYGB and $\Omega_{1\text{and}2}$. Bacterial translocation to the liver was observed in RYGB, $\Omega_{1\text{and}2}$ ($p < 0.001$).

Unexpectedly, the Ω_3 surgery resulted in 100% mortality after 20 days. To further dissect the cause of this event, we sacrificed mice with the varying Ω loop limb lengths one week after surgery. The number of bacterial colonies in the spleen and biliary limb were significantly higher after Ω_3 ($p < 0.05$), combined with higher levels of hepatic inflammation and bacterial content ($p < 0.05$), compared to sham. Liver histology in Ω_3 mice was characterized by a mediovesicular steatosis, which we compared to histopathology features in humans. This entity closely resembled the typical histological picture observed in patients with end-stage liver disease after BS. Critically, oral gut decontamination significantly increased one-week-survival of Ω_3 mice from 31.3% to 80.0%. Antibiotic treatment not only prevented bacterial overgrowth in biliary fluid ($p < 0.05$) and spleen ($p < 0.01$), but also significantly decreased serum ALT and AST levels ($p < 0.01$) in these mice.

Conclusion: BS procedures in mice, especially RYGB, $\Omega_{1\text{and}2}$ improve MASLD. Our studies show that mortality in longer biliary limb surgery is caused by bacterial overgrowth and inflammation of the gut-liver axis, which can be treated with oral gut decontamination. Our novel procedures open the field of research into the mechanisms of action of BS on hepatic and intestinal physiopathology.

WED-533

The narcolepsy drug sodium oxybate improves metabolism in developing and existing obesity

Cong Liu^{1,2}, Sen Zhang^{1,2}, Mik Zwaan^{1,2}, Aswin Verhoeven³, Mink Schinkelshoek^{2,4}, Yanan Wang^{2,4,5}, Martin Giera³, Mariëtte Boon^{2,4}, Patrick CN Rensen^{2,4,5}, Milena Schöнке^{2,4}. ¹Department of Medicine, Division of Endocrinology, Leiden University Medical Center, Leiden, Netherlands; ²Eindhoven Laboratory for Experimental Vascular Medicine, Leiden University Medical Center, Leiden, Netherlands; ³Center for Proteomics and Metabolomics, Leiden University Medical Center, Leiden, Netherlands; ⁴Department of Medicine, Division of Endocrinology, Leiden University Medical Center, Leiden, Netherlands; ⁵Med-X institute, Center for Immunological and Metabolic Diseases, and Department of Endocrinology, First Affiliated Hospital of Xi'an Jiaotong University, Xian, China
Email: c.liu@lumc.nl

Background and aims: Clinical studies have reported that sodium oxybate (SXB), the sodium salt of gamma-hydroxybutyric acid (GHB) used for the treatment of narcolepsy, exerts weight loss-promoting effects. These metabolic effects of SXB are believed to be mediated by peripheral organs, particularly the liver. In addition, GHB is a short-chain fatty acid (SCFA) and other structurally closely related SCFAs have been shown to alleviate obesity-associated metabolic diseases at least partially through the beneficial modulation of the gut microbiota.

Method: The anti-obesity effect of SXB was investigated in both existing and developing obesity in mice. In existing obesity, male C57BL/6J mice were first fed a high fat diet (HFD) for 8 weeks to induce obesity, and then treated with either SXB or water by daily oral gavage for 8 weeks. In developing obesity, mice were subjected to HFD feeding and concurrently received either daily SXB treatment or water for 8 weeks. In a follow-up experiment to study the contribution of the gut microbiota to the SXB treatment effect, we performed a fecal microbiota transplantation (FMT) from SXB-treated mice (SXB donor) to untreated mice (SXB recipient) for 6 weeks following an antibiotics-induced microbiota depletion. For this, fresh feces from donor mice were collected and fecal bacteria were transferred to recipient mice by oral gavage three times per week.

Results: SXB treatment reduced body weight gain and plasma glucose levels only in existing but not in developing obesity. In both conditions, SXB treatment, however, reduced liver steatosis and alleviated liver damage. This was likely associated with improved hepatic mitochondrial function, as suggested by the upregulated expression of hepatic genes encoding mitochondrial respiratory complexes. 16S rRNA sequencing furthermore indicated that SXB beneficially modulated the gut microbiota composition both in existing and developing obesity. FMT from SXB-treated to untreated mice attenuated HFD-induced body weight gain accompanied by decreased plasma glucose levels in the untreated recipient mice. In line, FMT alleviated hepatic steatosis in the recipient mice as evidenced by decreased liver triglyceride levels and lipid droplets.

Conclusion: SXB treatment counteracts obesity and the associated metabolic dysfunction of the liver, at least in part, through the improvement of gut microbiota dysbiosis.

WED-534

Mir122 expression regulates liver immune tolerance and microenvironment

Maytal Gefen¹, Shanny Layani¹, Emma Klahr¹, Reut Tzig¹, Nofar Rosenberg¹, Aurelia Markezana¹, Dyana Yaish¹, Zohar Shemuelian¹, Adi Sheena Yehzekel¹, Nathalie Abudi¹, Inbal Mishalian¹, Michal Abraham¹, Ophir Hay¹, Lucy Ghantous¹, Jacob Rachmilewitz¹, Daniel Goldenberg¹, Amnon Peled¹, Samuel Huber², Nicola Gagliani², Christoph Schramm², Lorenz Adlung², Christoph Kilian², Johannes Herkel², Thomas Jacobs³, Johannes Brandi³, Rifaat Safadi⁴, Stefan Rose-John⁵, Dirk Schmitt-Arras⁶, Mathias Heikenwälder⁷, Eithan Galun¹,

Hilla Giladi¹. ¹Gene Therapy Institute, Hadassah Hebrew University Hospital, Jerusalem, Israel; ²University Medical Center Hamburg-Eppendorf, Hamburg, Germany; ³Bernhard-Nocht-Institut für Tropenmedizin, Bernhard-Nocht-Hamburg, Hamburg, Germany; ⁴Liver Institute, Hadassah Hebrew University Hospital, Jerusalem, Israel; ⁵Christian-Albrechts-Universität zu Kiel, Kiel, Germany; ⁶University of Salzburg, Salzburg, Austria; ⁷German Cancer Research Center (DKFZ), Heidelberg, Germany
Email: eithang@hadassah.org.il

Background and aims: MiR-122 is downregulated in many liver pathologies all associated with chronic liver inflammation e.g. NASH, AIH and others and may have a role in regulating the immune tolerance of the liver. We generated miR-122 KO mice and found that they develop spontaneous liver inflammation.

Method: This model enables to study the the immune response developing in the absence of miR-122.

Results: The liver of the miR-122 KO is inflamed and fibrotic from 3 weeks of age. In the inflamed livers of these mice, there is an increase in Kupffer and T cells as well as an increase in liver damage markers-including fibrosis, ductular proliferation and apoptosis. Gene expression analysis demonstrates overexpression of TLR genes in miR-122 KO mice and enrichment of genes that are associated with TNF α and NF κ B signaling. In microbiome depleted miR-122 KO mice, the liver damage was mildly decreased. Specific subsets of T cells were analyzed and we found that in effector CD8 cells, immune checkpoints are downregulated. In a preliminary Comparing RNAseq data of these mice with humans with AIH showed a significant overlap. In AIH patients an anti-correlation between levels of miR-122 in the liver and inflammation activity index was observed. Specifically, TLR signaling, NF κ B signaling and Th17 signaling pathways are all significantly differentially expressed in AIH patients with high inflammation activity index as in the miR-122 KO mice.

Conclusion: We hypothesize that the immune response exhibited in the miR-122 KO mice is a result of a dysregulated response to the natural microbiome in the absence of miR-122. Overexpression of TLRs could lead to excessive NF κ B activation and TNF α signaling. Further analysis is required in order to determine the pathways and specific cellular responses involved in regulation of the liver immune tolerance by miR-122.

WED-535-YI

Association of HLA alleles with Oral Microbiome in Liver Cirrhosis patients

Rosmy Babu¹, Shruti Sureshan², Satender Singh², Chhagan Bihari².
¹Institute of Liver and Biliary Sciences, Delhi, India; ²Institute of Liver and Biliary Sciences, Delhi, India
Email: rosmy.1995@gmail.com

Background and aims: The composition of gut microbiome can be influenced by host immunity, which is partly regulated by HLA. HLA classes play an important role in inducing tolerance, through its immunosuppressive effects on all types of immune cells. Immune tolerance is a key issue in the liver, both in liver homeostasis and in the response to liver injury. It would therefore appear likely that association between HLA motifs and gut microbiome plays an important role in liver diseases. We profiled the salivary microbiome and tested the association between each microbial taxa with HLA motifs.

Method: Saliva and blood samples of cirrhosis patients (n=52) between the age group 18–65 years were collected. V3–V4 Amplicon sequencing and HLA typing (HLA-A, -B, -C, -DRB1, -DQB1 and -DPB1) were performed to see any plausible relation between HLA and oral microbiome in cirrhosis patients. We used Generalized linear models to test the association between HLA motifs and microbial taxa.

Results: Upon sequencing of HLA-A, B, C, DQB1, DPB1 and DRB1 to see any plausible relation between HLA and oral microbiome, the generated data identified 68 distinct HLA alleles, and these alleles

were used to determine their association with the oral microbiome. Presence of HLA-DRB1*07 had positive effect on the relative abundance of Lactobacillaceae (p=0.019) in cirrhosis patients. Lactobacillaceae activate hepatic Nrf2 to protect against oxidative liver injury and acute ethanol toxicity. Similar positive co relation were observed between pairs HLA-DQB1*06-Flavobacteriaceae (p=0.046), Bifidobacteriaceae (p=0.001) HLA-DRB1*07-Lactobacillaceae (p=0.019) and HLA-B*15-Prevotellaceae (p=0.025). These bacterial classes produce SCFAs from dietary fibre, have anti-inflammatory and modulating effects on the intestinal mucosa, maintaining gut health. When HLA-A*11 was present in the patient samples, we observed a decline in the relative abundance of family Veillonellaceae (p=0.042). Higher abundance of Veillonellaceae, affects the clinical benefit response associated with energy metabolism which may modulate the clinical response to immunotherapy in liver cirrhosis.

Conclusion: We see plausible relation between HLA and oral microbiome in cirrhosis patients based on the positive effect of presence of different HLA alleles on abundance of certain bacterial taxa.

WED-538-YI

Toll-like receptor 2 signaling cascades are a trigger of aging-associated liver decline in mice

Annette Brandt¹, Patricia Olivera Prada¹, Anja Baumann¹, Julia Jelleschitz², Annika Höhn², Ina Bergheim¹. ¹University of Vienna, Vienna, Austria; ²German Institute of Human Nutrition Potsdam-Rehbrücke, Nuthetal, Germany
Email: ina.bergheim@univie.ac.at

Background and aims: Old age has been identified as an independent risk factor in the development of various liver diseases. Indeed, across species, even healthy aging is associated with the development of hepatic inflammation and fibrosis. Studies further suggest that intestinal microbiota composition, an impairment of intestinal barrier function and an induction of toll-like receptors (TLRs) in liver tissue and dependent signaling cascades are critical herein. Here, employing different mouse models, we assessed the role of TLR2 in the development of aging-related liver degeneration.

Method: In the first experiment, markers of liver damage, senescence and inflammation were assessed in 4 and 20 months old male C57BL/6 and TLR2 Knockout (TLR2 KO, B6.129-Tlr2tm1Kir/J) mice. In a second experiment, old male C57BL/6 mice (17 months) showing signs of impaired intestinal barrier function and senescence were treated either with the TLR2 inhibitor ortho-vanillin (60 mg/kg BW in drinking water) or plain water for 4 months and markers as determined for the first experiment were assessed.

Results: As expected, 20 months old wild-type mice developed clear signs of aging including an increase in markers of senescence such as p16, and liver inflammation as well as liver fibrosis. In contrast, 20 months old TLR2 KO mice were significantly protected from these alterations showing significantly lower levels of markers of senescence but also less hepatic inflammation (e.g. significant lower number of neutrophil granulocytes, significant lower expression of interleukin 1beta mRNA) and significantly less fibrotic alterations in the liver such as lower expression of alpha smooth muscle actin mRNA. In line with these findings, treatment of old mice, showing beginning signs of senescence and intestinal barrier dysfunction, with the TLR2 inhibitor significantly attenuated the development of inflammatory and fibrotic alterations in liver tissue. Also, markers of senescence like p16 in blood were significantly lower than in untreated mice.

Conclusion: Taken together, our data so far suggest that an alteration of TLR2 and associated signaling cascades may be critical in aging-associated liver degeneration in mice. (funded by FWF and DFG).

POSTER PRESENTATIONS

WED-539

Gut dysbiosis-induced humoral dysregulation in metabolic dysfunction-associated steatotic liver disease

Hong Sheng Cheng¹, Yolanda Wei Ling Koo¹, Esha Bharathwaj Vijay¹, Damien Chua¹, Sunny Hei Wong¹, Nguan Soon Tan¹. ¹Nanyang Technological University Singapore, Singapore, Singapore
Email: hscheng@ntu.edu.sg

Background and aims: Metabolic associated steatotic liver disease (MASLD), a silent and chronic liver disease, poses a growing threat with limited treatment options. The gut microbiome is increasingly known to interact with the adaptive immunity during the progression of MASLD but the underpinning mechanism remains largely elusive. Hence, this study aims to explore deeper understanding of the gut-immune-liver crosstalk by investigating the dynamic changes of humoral response in gut dysbiosis-exacerbated MASLD.

Method: We humanized the gut microbiome of male C57BL/6 mice via fecal microbiota transplantation (FMT) and performed MASLD induction using a specialized Liver Disease Progression Aggravation Diet (LIDPAD) and thermoneutral housing. Fecal microbiome was obtained from the humanized mice that developed metabolic dysfunction-associated steatotic liver (MASL) and metabolic dysfunction-associated steatohepatitis (MASH) and subsequently transplanted into naïve mice to study the impact of MASL- and MASH-associated microbiome on the humoral response and liver histology.

Results: Mice with humanized gut microbiome developed gut dysbiosis upon MASLD induction, characterized by the emergence of *Romboutsia-Marvinbryantia* cluster and loss of *Akkermansia-Bifidobacterium* cluster. Gut dysbiosis in MASLD were associated with the onset of auto-immunogenicity against liver antigens which are positively correlated with disease severity scores. We identified an increased abundance of CD19⁺CD45R⁺CD93⁺IgM^{hi}IgD^{lo} B-cells in the livers, blood circulation and large intestine of MASLD mice. FMT of MASL- and MASH-associated microbiome markedly accelerated MASLD progression and the onset of IgG- and IgM-mediated auto-immunogenicity, suggesting a causative role of gut dysbiosis in dysregulated humoral response and MASLD deterioration.

Conclusion: Our results highlight a potential role of gut-immune-liver axis in the exacerbation of MASLD.

WED-540-YI

Gender-dependent HCC development in X/MYC mouse model

Vincenzo Alfano¹, Alexia Paturel¹, Valerio Iebba², Giulia Canarutto³, Massimiliano Cocca¹, Alice Lombard¹, Francesca De Nicola⁴, Jamila Faivre⁵, Silvano Piazza³, Massimo Levrero¹, Claude Caron de Fromental¹, Francesca Guerrieri¹. ¹Cancer Research Center of Lyon (CRCL), INSERM U1052, Lyon, France; ²Università di Trieste, Trieste, Italy; ³ICGEB, Trieste, Italy; ⁴IRCCS Regina Elena National Cancer Institute, Rome, Italy; ⁵INSERM U785, Paris, France
Email: vincenzo.alfano@inserm.fr

Background and aims: Hepatocellular carcinoma (HCC), the most frequent primary malignancy of the liver, is among the leading causes of cancer-related death worldwide. The vast majority of HCCs is associated with chronic liver disease due to a known underlying aetiology, including chronic viral hepatitis (B and C), alcohol intake and non-alcoholic steatohepatitis (NASH). It has been reported that epigenetics plays an important role in liver oncogenesis and gut microbiome changes in HCC patients, but the relationship between them over the course of carcinogenesis is not clear. Finally, epidemiological reports indicate that the incidence of HBV-related HCC is higher in males and postmenopausal females than other females, but the cause underlie this notion is largely unknown. The aim is to understand the interplay between the transcriptomic profiles and the microbiome in the hepatocarcinogenesis of X/MYC mice model.

Method: WT and X/Myc double transgenic mice, expressing in the liver both HBV HBx under control of viral regulatory elements and c-myc, were characterized by liver tumor (T) and peri-tumor (PT) RNA-

seq (75×2 Novaseq Illumina). 16 s rRNA of mice stools was sequenced by Miseq Illumina platform at 10 and over 20 months, during liver carcinogenesis and at the development of HCC respectively.

Results: Integrative transcriptome analysis of T and PT indicated that X/MYC mice correlated with human subclass S2 HCC, characterized by proliferation as well as stemness. RNA species of WT, PT and T tissues showed a different transcriptomic profile depending on the gender. This difference could explain the low penetrance of HCC in females' mice. In particular we found a different pattern of mitochondrial metabolism according to sex. The distinctive sex molecular etiologies were confirmed by rRNAs 16 s results both during the carcinogenesis and at HCC development. The ecological parameters of males and females X/MYC mice are different and females' mice, while presenting a dysbiosis, they would seem to have a less harmful microbial community than males. The X/MYC females' distinctive species have been previously reported have a role in clinical response to anti-PD-1 immunotherapy. Finally, we defined a specific network of relevant RNA and bacterial species that characterized females and male hepatocarcinogenesis.

Conclusion: We found that X/MYC females and males mice developed a different liver tumor (time and transcriptomic profile) and that they exhibited a specific microbiota profile depending on the gender.

WED-541

Gut Akkermansia improves liver injury in D-penicillamine treated copper exposure model

Xi Huang¹, Yanqi Jin², Tianyuan Wang³, Danting Fu⁴, Yu Chen⁴, Ren Yan³, Yimin Zhang⁵. ¹The First Affiliated Hospital, College of Medicine, Zhejiang University, Hangzhou, China; ²The First Affiliated Hospital, School of Medicine, Zhejiang University, Hangzhou First People's Hospital, Hangzhou, China; ³The First Affiliated Hospital, School of Medicine, Zhejiang University, Hangzhou, China; ⁴Zhejiang Academy of Traditional Chinese Medicine, Hangzhou, China; ⁵The First Affiliated Hospital, School of Medicine, Zhejiang University, Hang, China
Email: 1307020@zju.edu.cn

Background and aims: Accumulation of copper is toxic to organs such as liver. Metal-chelators such as D-penicillamine (DPA) are commonly used in the treatment of copper overload. Proper manipulation of gut microbial composition can improve drug efficacy and safety. The objective of this study is to examine how targeted intervention of gut microbiota affects the effectiveness of copper removal in a copper exposure model while undergoing DPA treatment.

Method: First, after a 4-week treatment of DPA, the liver copper concentration and gut microbial composition in the copper exposure mice were evaluated to identify potential candidates for specific regulation of gut microbiota. Second, after 8 weeks of manipulating the gut microbiota during DPA treatment, the blood liver function indicators, tissue copper load, hepatic histopathological features and gut microbiota in copper exposure mice were investigated.

Results: The result showed that *Akkermansia* can enhance the effectiveness of DPA in treating copper exposure mice, whereas *Butyrivibrio* has a counteractive impact. Supplementing with *Akkermansia muciniphila* (Akk) improved the effectiveness of DPA in eliminating copper from tissues, leading to a greater improvement in liver injury, liver dysfunction and gut dysbiosis in copper exposure mice. Gene function prediction analysis results indicated that the altered gut microbial function by DPA and Akk is primarily linked to the energy generation/utilization, amino acid, fatty acid, lipid and nucleic acid metabolism.

Conclusion: Our findings offered an experimental basis for the possible uses of targeted regulation of gut microbiota in the supplementary therapy of copper dysregulation disease.

WED-542-YI

Unravelling bacterial metabolites using high-resolution magic angle spinning nuclear magnetic resonance spectroscopy in intact hepatocellular carcinoma liver tissue

Wendy Fernandes^{1,2}, Nicola Harris^{1,2}, Lissette Adofina³, Ane Zamalloa³, Nigel Heaton³, Krishna Menon³, Parthi Srinivasan³, Rosa Miquel⁴, Yoh Zen⁴, Geoff Kelly⁵, James Jarvis⁶, Alain Oregioni⁵, Shilpa Chokshi^{1,2}, Antonio Riva^{2,7}, I. Jane Cox^{1,2}. ¹The Roger Williams Institute of Hepatology, Foundation for Liver Research, London, United Kingdom; ²King's College London, Faculty of Life Sciences and Medicine, London, United Kingdom; ³Institute of Liver Studies, King's College Hospital and King's College London, London, United Kingdom; ⁴Liver Histopathology Laboratory, Institute of Liver Studies, King's College Hospital, London, United Kingdom; ⁵MRC Biomedical NMR Centre, The Francis Crick Institute, London, United Kingdom; ⁶Randall Centre for Cell and Molecular Biophysics and Centre for Biomolecular Spectroscopy, King's College London, London, United Kingdom; ⁷The Roger Williams Institute of Hepatology, Foundation for Liver Research, London, United Kingdom
Email: wendy.fernandes@kcl.ac.uk

Background and aims: Hepatocellular carcinoma (HCC) ranks among the top 5 global causes of cancer mortality, with 5-year survival rates of only 18%. Immune checkpoint inhibitors (ICIs) show promise in treating advanced HCC, achieving objective response rates (ORR) of 15%–20%. However, ICI resistance is still high, limiting efficacy, and has recently been linked to the gut microbiota, a pivotal factor in the development of anti-tumour immunity. Notably, increased intestinal permeability, bacterial translocation and high immune checkpoint expression in cirrhosis, a precursor to HCC, suggest possible links between gut microbiota, HCC, and ICI treatment response. This study used High-Resolution Magic-Angle-Spinning Nuclear Magnetic Resonance spectroscopy (HRMAS-NMR) to detect bacterial signatures in intact HCC tumour (TUM) and adjacent non-tumour (ADJ) tissue.

Method: Paired TUM/ADJ HCC tissue samples [n = 10 patients, M/F = 5/5, median (IQR) age 70 (65–79) years underwent HRMAS-NMR analysis [16.7 (16.0–18.0) mg] at stable 5000 Hz spinning rate and temperature (4°C) on a 600 MHz magnet, within 30 minutes of preparation. The human metabolome database and gutSMASH were used to curate a preliminary list of bacterial metabolites of interest. Untargeted analysis of HRMAS-NMR spectra was performed using KnowItAll and Metaboanalyst, in correlation with clinical/histological assessments.

Results: HRMAS-NMR identified dominant lipids with histopathological assessments indicating steatotic liver disease (SLD) and glucose in correlation with type-2 diabetes mellitus (T2DM) diagnoses. Distinctive HRMAS-NMR bacterial metabolite peaks, specifically formate and TMAO, were also identified in 7 patients, with variations in matched TUM/ADJ tissue. Ethanol detection was consistent in tumour tissue only from alcohol-consuming patients. No distinct clustering based on tissue, patient, or sex was observed even when considering non-bacterial metabolites.

Conclusion: HRMAS-NMR reveals bacterial metabolites in intact HCC liver tissue, reinforcing the gut microbiota-HCC connection. Tissue metabolic profiles dynamically characterise diverse histological patterns, offering crucial patient-specific information for improved data interpretation. This understanding can potentially shape subject-centric approaches for innovative HCC treatment strategies.

WED-543

Crosstalk between liver spheroids and pancreatic islets in the anterior chamber of the eye promotes growth and vascularization

Noah Moruzzi¹, Francesca Lazzeri-Barcelo¹, Nuria Vilarnau¹, Barbara Leibiger¹, Ingo Leibiger¹, Per-Olof Berggren¹. ¹Karolinska Institutet, Stockholm, Sweden
Email: noah.moruzzi@ki.se

Background and aims: Metabolic disorders such as type 2 diabetes mellitus (T2DM) and metabolic associated fatty liver disease (MASLD) are comorbid and characterized by dysfunctional lipid and glucose homeostasis controlled by the endocrine pancreas and the liver. Therefore, monitoring of functional changes in these organs, currently hindered by their anatomical localization, and their crosstalk during disease development is pivotal to identify early disease mechanisms. The anterior chamber of the eye (ACE) has been proven to be a suitable transplantation site to monitor pancreatic islets non-invasively and longitudinally at cellular resolution. Recently, we showed that liver spheroids transplanted into the ACE engraft, become vascularized, innervated, and preserve the liver-like features and functions. The aim of this study is to implement our in vivo platform to study crosstalk between endocrine pancreas and liver in health and disease and identify responsible factors.

Method: Mouse liver spheroids generated in vitro and isolated pancreatic islets are transplanted singularly or together into the ACE of recipient mice and imaged by confocal microscopy. Human liver spheroids and islets are co-transplanted into immunodeficient mice. Light backscatter is used to longitudinally measure the size of the spheroids. Fluorescent probes are administered intravenously during in vivo imaging to identify vascularization. Islets and spheroids from Fucci reporter mice are used to identify cell cycle/proliferation. Aqueous humor extracted from the ACE is subjected to mass-spectrometry to identify secreted factors. Mice transplanted with islets/spheroids are fed a high-fat-high-sucrose/fructose diet to identify changes in crosstalk factors during MASLD/T2DM development.

Results: Preliminary results show that liver spheroids and islets from mouse transplanted to mouse recipients engraft on the iris and become vascularized. Co-transplantation in the same eye results in growth of the liver spheroids compared to the spheroids transplanted without islets in the contralateral eye. Human liver spheroids solely made by purified hepatocytes fail to engraft on their own while co-transplantation with human islets results in fast and full vascularization.

Conclusion: We established a co-transplantation platform for non-invasive imaging of liver spheroids and islets in vivo, which enables identification of key factors involved in crosstalk between these two tissues. Our preliminary data suggest that crosstalk between islets and liver-like tissue from humans allows rapid vascularization while increased proliferation/hypertrophy occurs when tissues are derived from mouse. This ongoing study will help understanding the communication between the endocrine pancreas and the liver in physiology and during MASLD/T2DM development.

WED-544

Aging promotes liver injury: studies on C57Bl/6 mice

Karuna Rasineni^{1,2}, Sathish Kumar Perumal^{1,2}, Natalia Osna^{1,2}, Kusum Kharbanda^{1,2}. ¹VA Medical Center, Omaha, United States; ²University Nebraska Medical Center, Omaha, United States
Email: kharbanda@unmc.edu

Background and aims: Many extrahepatic factors determine the liver disease phenotype and outcome. Among these, aging is a predominant risk factor for the development of advanced chronic liver diseases of various etiologies. Emerging evidence indicates that advanced age alters liver anatomy and physiology and causes dysfunction in many other organs including the gut that can increase the pro-inflammatory environment of the liver. Since the global population is aging and is predicted to double by 2050, this study was undertaken to establish a baseline of liver injury parameters in the young and old mice.

Method: Young (8–10 weeks old) and aged (20–22 months old) C57Bl/6 mice were purchased from the Charles River Laboratories (Wilmington, MA, USA). These chow-fed mice were housed in an AAALAC-accredited Animal Research Facility at the Omaha VA Medical Center. Metabolic phenotyping was conducted using the Sable Systems International Promethion system. The animals were

POSTER PRESENTATIONS

euthanized, and the serum and tissues (liver and gut) removed for subsequent analyses.

Results: Aged mice exhibited higher body weight and fat mass compared to their younger counterparts despite aged females exhibiting lower food and water consumption, and higher energy expenditure. Aged mice of both sexes showed higher hepatic triglycerides, elevated lipid peroxidation products and lower lysosomal acid lipase activity compared to their younger counterparts. However, only aged females displayed reduced hepatic S-adenosyl-methionine levels, methylation potential, trypsin-like proteasome and lysosomal cathepsin B and cathepsin L activities compared to young female mice. Further, the increased hepatic expression of chemokine (C-C motif) ligand 2 and chemokine (C-X-C motif) ligand 2 in aged female mice was associated with a lower ileal methylation potential and increased intestinal permeability. Aging had no effect on serum AST and ALT levels, hepatic activities of alcohol metabolizing enzymes or the liver's ability to utilize betaine.

Conclusion: To conclude, chow-fed aged mice of both sexes exhibited some parameters of liver injury compared to their younger counterparts. However, more severe liver injury was seen in aged female mice. The data from this study will be used as a baseline to determine the effect of alcohol on gut-liver axis in aged versus younger mice.

WED-545-YI

Restoration of mucosa-associated invariant T (MAIT) cell function and metabolism in cirrhosis with rifaximin- α

Thomas Tranah^{1,2}, Juan Carlos Lopez Rodriguez², Lindsey Edwards^{1,3}, Patricia Barral², Debbie L. Shawcross¹. ¹King's College London, Institute of Liver Studies, Department of Inflammation Biology, School of Immunology and Microbial Sciences, Faculty of Life Sciences and Medicine, London, United Kingdom; ²King's College London, Centre for Inflammation Biology and Cancer Immunology, School of Immunology and Microbial Sciences, Faculty of Life Sciences and Medicine, London, United Kingdom; ³King's College London, Centre for Host Microbiome Interactions, Faculty of Dentistry, Oral and Craniofacial Sciences, London, United Kingdom
Email: t.tranah@nhs.net

Background and aims: Reduced gut microbial diversity with increased pathobionts is a hallmark of cirrhosis and is associated with liver disease progression and susceptibility to infection. Mucosa-associated invariant T (MAIT) cells are an innate-like population of T cells that represent a sentinel system for homeostatic sensing of the intestinal microbiota and mucosal antimicrobial defence as they respond to riboflavin metabolites produced by bacteria. We aimed to characterise circulating MAIT cell function in cirrhosis before and following manipulation of the intestinal microbiota with rifaximin- α .

Method: Peripheral blood mononuclear cells were isolated from healthy donor controls and from cirrhotic patients at baseline and 7, 30 and 90 days after administration of the non-absorbable antibiotic, rifaximin- α 550 mg, twice daily. We utilised a combination of bulk RNA sequencing, flow-cytometry and *in vitro* experiments to characterise MAIT cell function, metabolic requirements and response to inflammatory stimulus.

Results: Circulating MAIT cells are present at reduced frequency in cirrhotic patients and display an activated phenotype with distinct gene expression profiles indicating enrichment of cytotoxic effector clusters with cytotoxic transcriptional programmes [normalised enrichment score (NES) 1.893; $p < 0.0001$]. This corresponded with upregulation of canonical markers of early and late T cell activation CD69 (31.5 vs 10.9%, $p < 0.0001$), HLA-DR (53.2 vs 12.1%, $p < 0.0001$) and the cytolytic agent granzyme B (43.5 vs 6.5%, $p < 0.0001$). MAIT cells from cirrhotic patients demonstrate enrichment of oxidative phosphorylation gene signatures (NES 2.758; $p < 0.0001$) with enhanced mitochondrial mass ($p < 0.001$) and membrane potential ($p < 0.001$). Hyperammonaemic conditions *in vitro* enhanced healthy control MAIT cell mitochondrial energy metabolism ($p < 0.001$) and

cytotoxic effector responses to stimulation ($p < 0.001$). Rifaximin- α treatment led to a reduction in circulating ammonia levels ($p = 0.007$) in cirrhotic patients and was associated with reduced MAIT cell metabolic requirements and an improvement in the cytotoxic effector phenotype.

Conclusion: MAIT cells display enrichment of cytotoxic effector clusters in cirrhotic patients underpinned by distinct cellular metabolic requirements with enhanced mitochondrial oxidative phosphorylation observed in the context of circulating hyperammonaemia that is improved with rifaximin- α treatment.

WED-546

Evidence of gut microbiome differences in post-menopausal females with metabolic dysfunction-associated liver disease compared to pre-menopausal females and males

Laura Martinez-Gili^{1,2}, Roberta Forlano^{2,3}, Jesus Miguens Blanco², Panteleimon Takis¹, Mark R. Thursz^{2,3}, Julian R. Marchesi², Benjamin H. Mullish², Pinelopi Manousou^{2,3}. ¹Division of Systems Medicine, Department of Metabolism, Digestion and Reproduction, Imperial College London, London, United Kingdom; ²Division of Digestive Diseases, Department of Metabolism, Digestion and Reproduction, Imperial College London, London, United Kingdom; ³Department of Hepatology, St Mary's Hospital, Imperial College Healthcare NHS Trust, London, United Kingdom
Email: laura.martinez@imperial.ac.uk

Background and aims: Prevalence and severity of metabolic dysfunction-associated liver disease (MASLD) is increased in females after menopause compared to age-matched males. The gut microbiome could be an important contributor to sex-specific phenotypes by modulating reproductive hormones. We investigated clinical, metabolic and gut bacterial differences between pre- and post-menopausal females and males in a prospective cohort of patients with type-2 diabetes mellitus (T2DM) screened for liver disease.

Method: Gut bacterial composition was determined by 16S rRNA gene sequencing, metabolomic profiling done with ultra-high performance liquid chromatography mass spectrometry and proton nuclear magnetic resonance spectroscopy and cytokines assessed by ELISA. Microbiome and metabolic signatures were analysed in post-versus pre-menopausal females, and post-menopausal females versus age-matched males diagnosed with MASLD. We used Mann-Whitney U test for continuous and Fisher test for categorical variables. ANCOMBC was used to assess bacterial composition. Linear mixed models (LMM) were fitted to metabolic and cytokine features and p values obtained with likelihood ratio test. All models were adjusted for age, alcohol, PPI, metformin, insulin use and index of multiple deprivation (random intercept in the LMM).

Results: Overall, 285 patients were enrolled. MASLD prevalence, based on US and CAP score, was 74% (210/285), while the prevalence of advanced fibrosis was 13% (36/285) and newly diagnosed cirrhosis secondary to MASLD was 3% (8/285). 128 were females; 87 post-menopausal. Post-menopausal females had a lower controlled attenuation parameter score than pre-menopausal ones ($p = 0.04$) and no difference in stiffness. Gut bacterial alpha diversity evenness was higher, and *Bacteroidota* phylum lower in post-menopausal than pre-menopausal females. Microbial-derived bile acids in stool, including taurodeoxycholic acid-3 sulfate and tauroolithocholic acid, were lower in post-menopausal compared to pre-menopausal females, as well as tricarboxylic acid cycle metabolite fumaric acid. Serum interleukin-6 (IL-6) was higher, while stool IL-2, IL-13, tumour necrosis factor-alpha and interferon-gamma lower in post-menopausal with respect to pre-menopausal females. Compared to males, post-menopausal females had higher BMI, serum cholesterol, HDL and alkaline phosphatase, but lower alanine aminotransferase levels ($p = 0.002$). *Oscillospiraceae* NK4A214 genus was lower in post-menopausal females, as well as serum metabolites glutamic acid, citric acid and leucine.

Conclusion: We identified changes in systemic and gut inflammation and a lower abundance of bacterial-derived bile acids that were specific to post-menopausal females. The gut microbiome may be important in developing a personalised and sex-tailored therapeutic approach in females.

WED-547

Amelioration of metabolic dysfunction-associated steatohepatitis by *Lactobacillus delbrueckii* subsp. *lactis* CKDB001 restoring gut microbiota

Hyunchae Joung¹, Yoojin Kwon¹, Yukyung Choi¹, Kyunghwan Kim¹.

¹CKDBiO, Seoul, Korea, Rep. of South

Email: hcjoung@ckdbio.com

Background and aims: Many studies have reported on the prevention or treatment of various diseases, including inflammatory and metabolic diseases, cancer, and even mental disorders, by promoting a balanced gut microbiome, known as eubiosis. The gut microbiome can be influenced using probiotics, prebiotics, synbiotics, and postbiotics. In particularly, live biotherapeutic products (LBPs) have been suggested as innovative therapeutic substances. We isolated numerous bacteria from different sources and conducted *in vitro* screening to assess their safety and probiotic effects. Following screening, *Lactobacillus delbrueckii* subsp. *lactis* (*L. lactis*) CKDB001 was selected, and this *in vivo* study was carried out to evaluate the therapeutic efficacy of *L. lactis* CKDB001 against metabolic dysfunction-associated steatohepatitis (MASH).

Method: The genome of *L. lactis* CKDB001 was sequenced using PacBio RS II and assembled by Canu. Antimicrobial resistance (AMR) genes were identified based on the public databases. *L. lactis* CKDB001 was prepared for this animal study, and the viable cell concentration was measured. To evaluate the therapeutic effect against MASH, 5-week-old C57BL/6J male mice were fed a Gubra amylin NASH (GAN) diet for 16 weeks to induce the disease. Following disease induction, *L. lactis* CKDB001 was orally administered for 8 weeks at varying doses: 1.0×10^8 , 1.0×10^9 , or 1.0×10^{10} CFU/day. At the end of the administration, body and tissue weights were measured. Liver samples were fixed in 10% formalin and stained with HandE. RNA-sequencing analysis was performed on liver tissues, and metagenomic analysis was conducted using cecum samples.

Results: The genome of strain CKDB001 was fully sequenced, revealing a single circular chromosome of 2,052,085 base pairs without any plasmids. Bioinformatic analysis confirmed *L. lactis* CKDB001's safety as a probiotic, showing no harmful genes like AMR genes. Treatment with *L. lactis* CKDB001 led to a reduction in liver weight and fat mass in mice, coupled with improvements in liver enzyme concentrations and lipid profiles in the serum. The decrease in hepatic triglycerides and cholesterol showed a dose-dependent response in *L. lactis* CKDB001-treated groups. No side effects were observed in any of study groups over its duration. Moreover, the *L. lactis* CKDB001-treated groups showed enhanced alpha- and beta-diversity in the gut microbiota, accompanied by a decrease in the *Firmicutes/Bacteroidetes* (F/B) ratio. Additionally, RNA expression levels associated with inflammation significantly decreased in *L. lactis* CKDB001-treated mice.

Conclusion: The findings from our study suggest that *L. lactis* CKDB001 exhibits therapeutic potential for MASH by restoring the gut microbiome and reducing inflammation and lipid accumulation in the liver.

WED-548

Rifaximin-alpha acts through increased abundance of *Lactobacillus* spp. in murine models of chronic liver disease

Maximilian Joseph Brol¹, Camila Alvarez-Silva², Robert Schierwagen¹, Frank Erhard Uschner¹, Sabine Klein¹, Jonel Trebicka^{1,3}, Manimozhiyan Arumugam². ¹Department of Internal Medicine B, University Hospital Münster, Münster, Germany; ²Novo Nordisk Foundation Center for Basic Metabolic Research, University of

Copenhagen, Copenhagen, Denmark; ³European Foundation for the Study of Chronic Liver Failure-EFCLF, Barcelona, Spain
Email: maximilian.brol@ukmuenster.de

Background and aims: Rifaximin-alpha is a poorly absorbable broad spectrum antibiotic used for the prevention of recurrent hepatic encephalopathy. Despite its well-proven clinical benefit, the mechanism of action is not understood. In this study, we aim to investigate the effects of rifaximin-alpha on the microbiome in murine models of alcohol-related liver disease (ArLD) and metabolic dysfunction-associated steatotic liver disease (MASLD) without the use of lactulose.

Method: 12-week-old, C57BL/6 mice were treated for 7 weeks with either a Methionine-Choline deficient diet (MCD), Western diet (WD), carbon tetrachloride (CCl₄) inhalations or a standard chow with or without ethanol treatment. Mice were further divided whether to receive rifaximin-alpha (30 µg/mouse/day) or not (n=5 per group, total 16 groups). 16S sequencing was performed on fecal samples collected before and after injury induction. The experiment was repeated with a resolution phase of 7 weeks afterwards (control chow ± rifaximin-alpha). Liver phenotype was analyzed with regard to fibrosis (Sirius red, *col1a1* expression), steatosis (Oil Red O stains, *fasn* expression) and inflammation (*ccl2*, *ccr2*, *emr1* expression).

Results: MCD-treated mice showed the strongest decrease in alpha-diversity, though not significant, followed by WD and CCl₄, irrespective of ethanol intake. Permutational multivariate analysis of variance (PERMANOVA) revealed that changes in beta-diversity are mostly driven by diet (p value = 0.001, R² = 47.6%), with MCD showing the strongest effect compared to WD and control chow. Differential abundance analysis, adjusted for diet and ethanol intake, revealed a statistically significant difference only in the abundance of *Lactobacillus* spp. between the treated and untreated rifaximin groups (adj. p value = 0.0013). Interestingly, after further 7 weeks of resolution, *Lactobacillus* and *Bifidobacterium* are more abundant in non-rifaximin-alpha treated mice. Despite limited changes in hepatic cytokine expression, liver phenotypes were not significantly altered by rifaximin-alpha treatment.

Conclusion: Rifaximin-alpha treatment lead to an increase of *Lactobacillus* in different murine models of steatotic liver disease, possibly explaining fair effects in patients treated with lactulose.

WED-549

Urobilinogen promotes leaky gut by impacting intestinal integrity in a three-dimension intestinal organoid model system

Manisha Yadav¹, Jaswinder Maras², Abhishak Gupta³, Babu Mathew⁴, Nishu Dalal⁵, Neha Sharma², Gaurav Tripathi⁶, Vasundhara Bindal⁶, Nupur Sharma⁷, Sushmita Pandey⁸, Rita Singh⁹, Ashima Bhaskar¹⁰, Ved Dwivedi¹¹, Anil Kumar¹², Niraj Kumar¹³, Shvetank Sharma¹⁴, Shiv Kumar Sarin¹⁵. ¹Institute of Liver and Biliary Sciences, New Delhi, India; ²Institute of Liver and Biliary Sciences, New Delhi, India; ³Artimis Hospital, Gurgaon, India; ⁴Institute of Liver and Biliary Sciences, New Delhi, India; ⁵National Institute of Immunology, New Delhi, India; ⁶Institute of Liver and Biliary Sciences, New Delhi, India; ⁷Institute of Liver and Biliary Sciences, New Delhi, India; ⁸Institute of Liver and Biliary Science, New Delhi, India; ⁹Translational Health Science and Technology Institute, Faridabad, India; ¹⁰International Centre for Genetic Engineering and Biotechnology, New Delhi, India; ¹¹National Institute of Immunology, New Delhi, India; ¹²National Institute of Immunology, New Delhi, India; ¹³Translational Health Science and Technology Institute, New Delhi, India; ¹⁴Institute of Liver and Biliary Sciences, New Delhi; ¹⁵Institute of Liver and Biliary Sciences, New Delhi, India
Email: jassi2param@gmail.com

Background and aims: Severe alcohol related hepatitis (SAH) is accompanied by compromised liver functions with high levels of bilirubin and its derivatives production, with metabolic conversions occurring primarily in the intestine. Previously, we reported in 223 SAH patients, increased urobilinogen (bilirubin metabolic byproduct) levels resulting in inflammation and glucocorticoid receptor

POSTER PRESENTATIONS

suppression (<https://doi.org/10.1101/2023.03.06.23286831>). We investigated the effects of high urobilinogen on intestinal integrity and inflammation contributing to progression of SAH.

Method: We used a 3-D intestinal organoid model system as they provide more accurate representation of the in vivo microenvironment compared to traditional two-dimensional cell cultures, which was developed using HCT116 cell line was used to develop the organoid. This was exposed to different doses of urobilinogen (40 uM, 120 uM, and 120 uM). Various assessments were conducted to gauge the integrity of intestinal cells, including Transwell and TEER assays to measure permeability and resistance changes as compared to ethanol. The treatment dose of urobilinogen was comparable to that seen in SAH. Confocal microscopy for intestinal junction proteins along with genomic and proteomic evaluation were performed to elucidate effect of urobilinogen on the organoids as compared to ethanol.

Results: Progressive increase in urobilinogen concentration enhanced FITC-labelled dextran permeabilization through HCT116 monolayer by 6 folds similar to ethanol treatment ($p < 0.05$). We observed significant decrease in the transepithelial electrical resistance from 150 to 63.5 ohm cm⁻², indicating leakage in the monolayer post urobilinogen and ethanol treatment compared to control ($p < 0.05$). Exposure of intestinal organoids with 40 uM, 120 uM, and 120 uM urobilinogen (conc. observed in SAH) significantly reduced the expression of critical proteins like TJP1 (4 folds) and claudin 1 (5.5 folds) (>1.5 FC, $P < 0.05$). Notably, genes responsible for maintaining cell integrity, such as desmoplakin, plakoglobin, desmoglein, and occludin, were downregulated both at the gene and protein level urobilinogen treatment ($p < 0.05$). Urobilinogen exposure stimulated proteins linked to inflammatory pathways, including interleukins, mTOR, and TNF-alpha, while simultaneously suppressed pathways associated with maintaining cell integrity (30% genes), such as focal adhesion and integrin ($p < 0.05$) suggesting inflammatory and intestinal compromising nature of urobilinogen.

Conclusion: Our findings demonstrate that urobilinogen, at concentrations comparable to those observed in SAH patient's blood, can detrimentally impact intestinal epithelial permeability, and promote leaky gut akin to the effects of ethanol. Clearance of urobilinogen may lead to therapeutic benefits in ALD patients.

WED-550

Unveiling the myth and truth of “Yellow Soup” in managing acute liver injury

Sen-Yung Hsieh¹, ¹Chang Gung Memorial Hospital, Taoyuan, Taiwan
Email: siming.shia@gmail.com

Background and aims: The historical use of feces for treating acute ailments traces back to China's 4th Century, notably termed as “yellow soup” in Li Shizhen's *Compendium of Materia Medica* (Bencao Gangmu) during the 16th Century. However, the application in treating human diseases had not been widely recognized. Recently, fecal microbiota transplantation (FMT), specifically via colonic administration, has shown promise in treating certain diseases. Although oral fecal administration is more acceptable and accessible to patients, the microbe selection in the upper gastrointestinal tract (UGIT) through oral administration remains unclear. This study aimed to explore the effects of gut microbes and their metabolites post oral-route administration in addressing acetaminophen-induced liver injury (AILI) in mice.

Method: Acetaminophen was intraperitoneally administered to conventionally housed or germ-free C57BL/6 mice. Oral gavage of fresh or pasteurized fecal samples collected from healthy mouse donors was performed. Assessment of fecal microbiota and metabolites pre- and post-gavage was conducted. Mechanistic investigations were carried out in cultured hepatocytes and verified in AILI mice.

Results: Despite varying effects of commensal microbes on AILI in antibiotic-treated mice, short-term oral fecal gavage (OFG) consistently mitigated AILI severity and mortality. Oral gavage with

pasteurized feces (OPG) produced comparable AILI alleviation to OFG. Microbiota profiling revealed time-dependent shifts in gut microbiome composition, particularly the enrichment of Lachnospiraceae post three-dose OFG within one week. Crucially, short-term OFG enriched butanoate biosynthesis pathways and short-chain fatty acids (SCFAs) in feces, among which butyrate significantly alleviated AILI in mice. Mechanistically, butyrate inhibited acetaminophen-induced ferroptosis by activating the AMPK-ULK1-p62 pathways, stimulating Nrf2 antioxidant responses, and promoting mitophagy. A combination of N-acetylcysteine and butyrate synergistically improved survival rates in AILI mice.

Conclusion: Oral administration of fecal microbiota exhibits a time-dependent shifts in gut microbiota composition. Our findings underscore the UGIT's role in reshaping administered fecal microbiota and its importance in healthcare management. Further, this study provides a new paradigm by employing oral FMT and microbial metabolites to treat acute liver injury.

WED-551

Nitrogen recycling by the gut microbiome in sarcopenia

Rosa Haller^{1,2}, Olha Hazia^{1,2}, Julia Traub³, Angela Horvath^{1,2}, Vanessa Stadlbauer^{1,2}, ¹Department of Gastroenterology and Hepatology, Medical University of Graz, Graz, Austria; ²Center of Biomarker research in Medicine (CBmed) GmbH, Graz, Austria; ³Department of Clinical Medical Nutrition, University Hospital Graz, Graz, Austria
Email: rosa.haller@medunigraz.at

Background and aims: Sarcopenia is the loss of skeletal muscle mass and strength, and affects up to 70% of patients with cirrhosis. As many animals survive hibernation without extensive muscle loss, they are often studied in the context of sarcopenia. It was recently shown that the abundance of urease-producing bacteria is increased in hibernating squirrels and that the resulting nitrogen is incorporated into muscle protein. In the light of that finding, we aimed to gain a better understanding of nitrogen recycling potential in sarcopenia with a specific focus on sex differences since cirrhosis and sarcopenia have a male predominance.

Method: Stool samples of 152 patients (96 cirrhotics, 56 non-cirrhotics) with and without sarcopenia were obtained. We predicted the functional profiles of microbial communities based on 16S rRNA sequencing data (Tax4Fun2) and extracted the predicted abundance of urease subunits (alpha, beta and gamma). In addition, we conducted a systematic literature search to identify urease-producing taxa, extract their abundance from 16S rRNA sequencing data to compare them between patients with and without sarcopenia.

Results: Sarcopenia, but not cirrhosis nor sex was associated with lower urease gene abundance ($p < 0.05$). In women irrespective of cirrhosis ($n = 49$; 28 sarcopenic) and in patients with cirrhosis irrespective of sex ($n = 64$; $p < 0.05$) urease gene abundance was lower in sarcopenia. The systematic literature search yielded 120 taxa, of which 35 were present in sequencing data. Overall abundance of potentially urease-producing taxa was comparable between the groups with only slight and divergent differences in abundance of *Bacteroides fragilis*, *Micrococcaceae* and *Clostridiaceae* 1.

Conclusion: We found lower levels of predicted urease gene abundance in patients with sarcopenia. This gives first indications for the potential role of the gut microbiome and its nitrogen recycling potential in sarcopenia. More pronounced differences in women and patients with cirrhosis, two groups who are disproportionately affected by sarcopenia, point towards a potential precision medicine target.

WED-554

Lean and non-lean non-alcoholic fatty liver disease patients differ significantly with regard to gut microbiota expression: results of an observational study

Prajna Anirvan¹, Zaiba Khan², Pallavi Bhuyan³, Giriprasad Venugopal², Manas Kumar Panigrahi², Balamurugan Ramadass², Shivaram Prasad Singh¹. ¹Kalinga Gastroenterology Foundation, Cuttack, India; ²All India Institute of Medical Sciences, Bhubaneswar, India; ³Dharanidhar Medical College and Hospital, Keonjhar, India
Email: prajnaeatchiranjeet@gmail.com

Background and aims: Lean non-alcoholic fatty liver disease (NAFLD) has been described as a distinct pathophysiological entity. Gut microbiota dysbiosis has been linked to the pathophysiology of NAFLD. But studies comparing the expression of gut microbiota between lean and non-lean NAFLD patients are few. We aimed to compare the gut microbiota profile between lean and non-lean NAFLD patients.

Method: Fecal microbiome analysis was carried out on 71 (33 lean and 38 non-lean) NAFLD patients and an equal number of matched controls. Duration of study was two years—from January 2020 to December 2021. A total number of 1048727 sequence reads were obtained through 16 s rRNA gene sequencing and clustered into 685 OTUs, at the 3% dissimilarity threshold. 28 phyla, 133 genus and 259 species were identified. At species level, 259 OTUs were obtained. Data filtering was performed to improve downstream statistical analysis. By removing counts less than 4 and 20% prevalence and 10% low variance from inter quartile range, 44 OTUs were obtained.

Results: Firmicutes, Bacteroidetes, Actinobacteria and Proteobacteria comprised the 44 OTUs.

Proteobacteria were more prevalent in the NAFLD group as compared to the controls. Non-lean NAFLD patients had less Bacteroidetes and more Firmicutes whereas the opposite trend was observed for Lean NAFLD group. Although, there was no difference in alpha diversity between lean and non-lean NAFLD patients, beta diversity was found to be significantly different across all groups ($p < 0.05$). Higher abundance of *Coprococcus eutactus* in the lean group and *Streptococcus luteciae* in the non-lean group was observed. *Streptococcus anginosus* and *Rothia mucilaginosa* were found to be indicators of Lean NAFLD whereas *Veilonella dispar* was found to be an indicator of non-lean NAFLD group. Regression analysis revealed strong positive and negative association of microbes with various clinical parameters. *Bifidobacterium adolescentis* was positively associated with fibrosis in lean NAFLD patients while *Coprococcus catus* was negatively associated with fibrosis in the obese NAFLD group. Species network analysis too showed significant association of microbes with clinical parameters.

Conclusion: Although there was significant difference in beta diversity among lean NAFLD, non-lean NAFLD, lean control and non-lean control groups, lean and non-lean NAFLD patients did not differ with regard to alpha diversity. We hypothesise a shift in the gut microbiome profile of lean patients towards that of the non-lean phenotype to account for this finding. Longitudinal studies are required to prove this. There is also strong correlation of gut microbiota with clinical parameters in NAFLD patients.

WED-555

Metabolic dysfunction-associated steatotic liver disease and gut microbiota

Vitalii Petryna¹. ¹Ivano-Frankivsk National Medical University, Ivano-Frankivsk, Ukraine
Email: petryna.vitaliy@gmail.com

Background and aims: Metabolic syndrome, cardiovascular disease, type 2 diabetes, obesity, and their complications lead to increased mortality and reduce quality of patient's life. Metabolic dysfunction-associated steatotic liver disease (MASLD) is currently recognized as one of the most common causes of chronic liver disease worldwide.

Current scientific evidence suggests that there is a close relationship between the gut microbiota and chronic pathologies.

Method: To evaluate the frequency of development of bacterial overgrowth syndrome in the small intestine in MASLD and to determine the relationship between the presence of this syndrome, cytolytic activity, and the degree of liver fibrosis.

Results: Analysis of the frequency of bacterial overgrowth syndrome showed that changes in microbiota of the small intestine were observed in 75.0% of patients with MASLD. In 37.5% of patients, the level of liver transaminases at the time of the study did not exceed the reference values, in 42.7% moderate biochemical activity was noted (within 2–5 norms), in 20.8% of cases the level of transaminases was 5–10 norms, which indicated the pronounced activity of the process. Moderate fibrosis predominated in 70.8% of patients, while a significantly smaller number of patients (29.2%) had severe fibrosis. As a result of the correlation analysis of the data, no connection between the bacterial overgrowth syndrome and the degree of cytolytic activity in patients with MASLD was found (the value of the χ^2 criterion was 0.879; the critical value of χ^2 at the significance level of $p < 0.05$ is 5.662; the relationship between factorial and outcome features statistically insignificant, probability level $p > 0.05$ ($p = 0.547$). There was also no relationship between bacterial overgrowth syndrome and the degree of fibrosis in the liver tissue (criterion $\chi^2 = 0.211$; the critical value of χ^2 at the significance level $p < 0.05$ is 3.752, the relationship between factor and outcome features is statistically insignificant, the probability level is $p > 0.05$ ($p = 0.580$).

Conclusion: The results of studies have established the existence of cause and effect relations between impaired microbiota of the intestine, imbalance of the immune system, as well as in one of the key pathogenetic roles in the development and progression of MASLD, reducing the protective properties of mucosa, enhancing translocation of microorganisms into the systemic circulation. Disturbance of small intestinal microbiota observed in three quarters of MASLD patients. However, the relationship between the presence of this syndrome and severity of cytolytic activity, as well as the degree of fibrotic changes in the liver were not detected.

WED-556

Gut microbiota promotes macrophage M1 polarization in hepatic sinusoidal obstruction syndrome via regulating intestinal barrier function mediated by butyrate

Si Zhao¹, Jiangqiang Xiao², Bing Xu², Yuzheng Zhuge². ¹Department of Gastroenterology, Nanjing Drum Tower Hospital, Affiliated Hospital of Medical School, Nanjing University, Nanjing, Jiangsu, China, Nanjing, China; ²Department of Gastroenterology, Nanjing Drum Tower Hospital, Affiliated Hospital of Medical School, Nanjing University, Nanjing, Jiangsu, China, Nanjing, China
Email: 2469981887@qq.com

Background and aims: Hepatic sinusoidal obstruction syndrome (HSOS) is a rare disease targeting hepatic sinusoids, sublobular veins and central veins of the hepatic lobules, which results in destructive damage of hepatic sinusoidal endothelial cells, congestion of hepatic sinusoids, and intrahepatic portal hypertension. The intestinal-liver axis is associated with various liver diseases. Here, we verified the role of the gut microbiota and macrophage activation in the progression of pyrrolizidine alkaloids-induced hepatic sinusoidal obstruction syndrome (PA-HSOS), and explored the possible mechanisms and new treatment options.

Method: The HSOS murine model was induced by gavage of monocrotaline (MCT). An analysis of 16S ribosomal DNA (16S rDNA) of the feces was conducted to determine the composition of the fecal microbiota. Macrophage clearance, fecal microbiota transplantation (FMT), and butyrate supplementation experiments were used to assess the role of intestinal flora, gut barrier, and macrophage activation and to explore the relationships among these three variables.

POSTER PRESENTATIONS

Results: Activated macrophages and low microflora diversity were observed in HSOS patients and murine models. Depletion of macrophages attenuated inflammatory reactions and apoptosis in the mouse liver. Moreover, compared with control-FMT mice, the exacerbation of severe liver injury was detected in HSOS-FMT mice. Specifically, butyrate fecal concentrations were significantly reduced in HSOS mice, and administration of butyrate could partially alleviated liver damage and improved the intestinal barrier in vitro and in vivo. Furthermore, elevated lipopolysaccharides in the portal vein and high proportions of M1 macrophages in the liver were also detected in HSOS-FMT mice and mice without butyrate treatment, which resulted in severe inflammatory responses and further accelerated HSOS progression.

Conclusion: These results suggested that the gut microbiota exacerbated HSOS progression by regulating macrophage M1 polarization via altered intestinal barrier function mediated by butyrate. Our study has identified new strategies for the clinical treatment of HSOS.

WED-557

Investigating gut microbial biomarkers for early detection of sarcopenia in individuals at various stages of alcohol-related liver disease

Haripriya Gupta¹, Seol Hee Song², Jeong Ha Park², Jeong Su Kim², Min Ju Kim², Sang Jun Yoon², Young Lim Ham³, Ki Tae Suk². ¹Hallym University College of Medicine, Chuncheon; ²Hallym University College of Medicine, Chuncheon, Korea, Rep. of South; ³Daewon University, Jaechon, Korea, Rep. of South
Email: ktsuk@hallym.ac.kr

Background and aims: Sarcopenia and alcohol-related liver disease (ALD) are closely connected, affecting the liver and muscles. Excessive alcohol exacerbates protein breakdown during stress, influencing muscle function. Gut dysbiosis is explored in ALD, but its link to sarcopenia is underexplored. Our objective is to examine gut microbiota at early stage and correlate sarcopenia indices in ALD patients.

Method: Total 142 subjects were enrolled and categorized under non-sarcopenia (HC=13, alcoholic hepatitis (AH)=25, alcoholic cirrhosis (AC)=27, alcoholic hepatocellular carcinoma (HCC)=16) and sarcopenia (SC=11, S-AH=18, S-AC=20, S-HCC=12) having ALD for the study. Sarcopenia was assessed by Skeletal muscle area (SMA) divided by height (meter) squared index. Liver function test and stool microbiome analysis by 16S rRNA-based sequencing were examined.

Results: Sarcopenia indices ($p < 0.01$) were significantly decreased in sarcopenia vs non-sarcopenia ALD. Microbiome analysis showed significant shifts in sarcopenia vs non-sarcopenia ALD. In stagewise comparison, species *Parabacteroides goldsteinii*, *Phocaeicola dorei*, *Parasutterella excrementihominis* and *Prevotella copri* were significantly low ($p < 0.05$, LDA > 2.5, AUC of > 0.69) in S-AH vs AH. Differentiating S-AC vs AC, species *Phocaeicola dorei*, *Bacteroides ovatus*, *Bifidobacterium catenulatum* were significantly low ($p < 0.05$, LDA > 2.5, AUC of > 0.67). S-HCC vs HCC, *Bacteroides faecis*, *Megamonas rupellensis* were significantly low ($p < 0.05$, LDA > 2.1, AUC > 0.74). Correlating those bacteria, increased and decreased bacteria in sarcopenia at different ALD stages were inversely and directly significantly correlated with sarcopenia indices ($p < 0.05$).

Conclusion: These findings suggest that early-stage ALD patients with sarcopenia, displaying a depleted *Bacteroides* species profile, may benefit from modifying gut microbiota. This could enhance clinical outcomes and improve the quality of life in ALD with sarcopenia individuals.

WED-558

Inhibition of miR-21 improves muscle activity in experimental metabolic dysfunction-associated steatotic liver disease

Diogo Fernandes¹, Mariana Moura Henrique¹, José Rodrigues¹, Ana Brígido¹, Carolina Palma¹, Laura Izquierdo-Sanchez^{2,3,4}, Jesus Maria Banales^{3,4,5}, Pedro Miguel Rodrigues^{3,4,5}, Rui E. Castro¹, André Simão¹. ¹Research Institute for Medicines (iMed.Ulisboa), Faculty of Pharmacy, Universidade de Lisboa, Lisbon, Portugal; ²Research Institute for Medicines (iMed.Ulisboa), Faculty of Pharmacy, Universidade de Lisboa, Lisbon, Portugal; ³Biogipuzkoa Health Research Institute, Liver and Gastrointestinal Diseases Area, San Sebastian, Spain; ⁴Carlos III National Institute of Health, Centre for the Study of Liver and Gastrointestinal Diseases (CIBERehd), Madrid, Spain; ⁵IKERBASQUE, Basque Foundation for Science, Bilbao, Spain
Email: diogofernandes@gmail.com

Background and aims: Metabolic dysfunction-associated steatotic liver disease (MASLD) presents as a complex multifactorial disease, in which dysregulation of metabolic homeostasis in the liver, as well as in distant organs, plays a substantial role. Recent evidence places skeletal muscle and the muscle-liver axis at the center of the MASLD pathogenic cascade. In fact, low muscle mass and muscle fat infiltration associates with increased risk of advanced MASLD, namely metabolic-associated steatohepatitis (MASH). In parallel, we showed that microRNA-21 (miR-21) is increased in the liver and skeletal muscle of MASH patients, with its abrogation ameliorating disease progression in vivo. Here, we investigated the effects of miR-21 on muscle function in the context of experimental MASLD.

Method: miR-21 knockout (KO) and wild-type (WT) mice were fed ad libitum with a high-fat/calorie diet (HFD) with high fructose/glucose corn syrup in drinking water for 20 weeks, or with a standard diet (SD), to recapitulate key, complementary metabolic features of human MASLD. Muscle phenotype and function were evaluated through grip strength and wheel running assays one week before sacrifice. In parallel, glucose tolerance test was also performed.

Results: Comparing to WT mice, HFD-fed miR-21 KO mice displayed lower weight increments and increased voluntary wheel-running distance, similarly to SD-fed WT mice. In parallel, miR-21 KO mice exhibited higher grip strength levels and presented with a glucose area under the curve lower than those of HFD-fed WT mice.

Conclusion: Our results suggest that miR-21 abrogation may ameliorate MASLD by acting upon the skeletal muscle, improving tissue function. These findings highlight the relevance of the muscle-liver axis in MASLD pathogenesis and, possibly, therapeutic targeting (PTDC/MED-PAT/31882/2017, 2022.08837.PTDC, FCT).

Hepatocyte biology

TOP-560

Establishing a Liver-on-Chip using tissue-resident progenitor cells from adult human liver

Defu Kong¹, Hans Blokzijl², Vincent de Meijer³, Klaas Nico Faber⁴. ¹Renji Hospital, Shanghai Jiao Tong University, School of Medicine, Shanghai, China; ²Department of Gastroenterology and Hepatology, University of Groningen, University Medical Center Groningen, Groningen, Netherlands; ³Department of Surgery, Division of Hepato-Pancreato-Biliary Surgery and Liver Transplantation, University Medical Center Groningen, Groningen, Netherlands; ⁴Department of Gastroenterology and Hepatology, University of Groningen, University Medical Center Groningen, Groningen, Netherlands
Email: dfkong@163.com

Background and aims: Organoids derived from tissue-resident liver progenitor cells (LPC) are increasingly recognized as valuable *in-vitro* models to study hepatic function and pathophysiological

mechanisms underlying liver disease. Also, Organ-on-Chip (OoC) microfluidic systems have become available that aim to reconstruct organ functions of selected or a combination of specific cell types. So far, LPC-derived organoids have not been applied in an OoC to build a Liver-on-Chip (LoC). Here, we aimed to culture LPC-derived cells in an OoC to study hepatocyte specific features.

Method: LPC-derived organoids were established from healthy human liver, digested into single cells, and then seeded in the MIMETAS Organoplate® 3-lane 40. After generating 3D tubular structures, cells were differentiated to mature hepatocytes. Hepatocyte markers (HNF4A, albumin, MRP2, BSEP) were visualized by immunofluorescence, and MRP2 functionality was analyzed by fluorescent bile acids. LoCs were incubated with troglitazone or free fat acids to analyze drug-induced toxicity and mimic the process of MASH.

Results: Human LPC-derived cells expanded and formed cellular tubules in the Organoplate OoC. After differentiation, the cells expressed albumin, MRP2 and BSEP of which both transporter proteins accumulated in the plasma membrane. The fluorescent bile acid CDFDA accumulated in an intercellular network, resembling canaliculi, in hepatocyte-differentiation conditions, while this was not observed in undifferentiated cellular tubules. Troglitazone disturbed the subcellular location of MRP2 and BSEP and impaired CDFDA transport to the intercellular network. In addition, Free fat acids led to an increasing ROS accumulation and lipid storage, without injuring cell viability in Organoplate OoC.

Conclusion: We developed a liver-on-chip system based on human tissue-resident hepatic progenitor cells, which can be used to study hepatocyte functions in health and diseases and allows mechanistic analysis of therapeutic drugs.

FRIDAY 07 JUNE

FRI-538

Novel regulatory mechanisms of the transforming growth factor β signaling pathway by the histone Methyltransferase G9a

Borja Castello¹, Amaya Lopez-Pascual², Jose Maria Herranz³, Jasmin Elurbide-Tardio⁴, Elena Adan-Villaescusa⁵, Ainara Irigaray-Miramon⁵, Maria U. Latasa⁵, Iker Uriarte³, Maria Arechederra⁶, Isabel Fabregat⁷, Bruno Sangro⁸, Carmen Berasain³, Maite G. Fernandez-Barrena³, Matías A. Avila³.
¹CIMA, CCUN, University of Navarra, Pamplona; ²Hepatology Unit, CCUN, Navarra University Clinic, Instituto de Investigaciones Sanitarias de Navarra IdiSNA, Pamplona, Spain; ³Hepatology Laboratory, Solid Tumors Program, CIMA, CCUN, University of Navarra, CIBERhd, Instituto de Salud Carlos III, Pamplona, Spain; ⁴Hepatology Laboratory, Solid Tumors Program, CIMA, CCUN, University of Navarra, CIBERhd, Instituto de Salud Carlos III, Madrid, Spain, Pamplona, Spain; ⁵Hepatology Laboratory, Solid Tumors Program, CIMA, CCUN, University of Navarra, Pamplona, Spain; ⁶Hepatology Laboratory, Solid Tumors Program, CIMA, CCUN, University of Navarra, Instituto de Investigaciones Sanitarias de Navarra IdiSNA, Pamplona, Spain; ⁷TGF- β and Cancer Group, Oncobell Program, Bellvitge Biomedical Research Institute (IDIBELL), CIBERhd, Instituto de Salud Carlos III, Barcelona, Spain; ⁸Hepatology Unit, CCUN, Navarra University Clinic, CIBERhd, Instituto de Salud Carlos III, Pamplona, Spain
 Email: maavila@unav.es

Background and aims: Transforming growth factor β (TGF β) is a pluripotent cytokine that participates in all stages of liver disease. TGF β has antiproliferative effects in hepatocytes and controls liver regeneration. High levels of TGF β results in the activation of stellate cells to myofibroblasts. During liver tumorigenesis, TGF β behaves as a suppressor factor at early stages; however, there is strong evidence that overactivation of TGF β signaling might contribute to later tumor progression, once cells escape from its cytostatic effects. Recent findings indicate that the histone lysine-methyltransferase G9a is

involved in the cellular responses to TGF β but its contribution and the underlying mechanisms of action are still unclear. This work aims at elucidating the role of G9a in TGF β signaling and to explore its potential as a mechanistic target in different aspects of liver disease.

Method: G9a overexpression and inhibition was performed in human and murine HCC cells. G9a chemical inhibitors (CM272 and UNC0642) were used. The effects of G9a gene expression manipulation and enzymatic inhibition on TGF β 1 actions were evaluated by RNAseq. Mechanistic studies were carried out by gene and protein expression analyses, promoter-luciferase reporter and ChIP assays. The role of G9a in TGF β 1 pathway was assessed in primary hepatocytes from mice with hepatocyte-specific G9a deletion (G9^{Δhep}) and in a model of acute liver damage induced by CCl₄ administration in wild type and G9^{Δhep} mice.

Results: Inhibition of G9a in HCC cell lines resulted in an impaired transcriptional response to TGF β 1 stimulation. These results were supported by the use of specific G9a inhibitors and observations in primary hepatocytes from G9^{Δhep} mice. Transcriptomic analyses in Huh7 human HCC cells revealed significant alterations in TGF β -mediated gene expression regulation when G9a was knocked down. G9a inhibition led to a profound decrease in TGFBR1 mRNA and protein levels. Luciferase assays confirmed that G9a inhibition or overexpression negatively or positively modulated TGFBR1 promoter activity, respectively. Analysis of regulatory elements controlling TGFBR1 promoter activity identified SMAD3 as a likely candidate. G9a inhibition resulted in a downregulation of SMAD3 expression. ChIP analyses showed binding of G9a to a specific site in the SMAD3 gene promoter, suggesting a potential role for G9a as a coactivator of this central effector in the TGF β pathway. In an acute liver injury mouse model induced by CCl₄, the upregulation of genes involved in fibrogenic and reparative processes mediated by TGF β 1 was significantly attenuated in G9^{Δhep} mice compared to WT.

Conclusion: G9a acts as a potent regulator of the TGF β pathway, directly modulating the expression of its central effector SMAD3. These findings provide a novel regulatory mechanism for a signaling pathway highly relevant in liver pathophysiology.

FRI-539

EGF/STAT1 signals to maintain ECM1 expression in hepatic homeostasis are disrupted by IFN γ /NRF2 in chronic liver disease

Yujia Li¹, Frederik Link², Weiguo Fan³, Rilü Feng⁴, Seddik Hammad⁴, Honglei Weng⁴, Matthias Ebert⁴, Steven Dooley⁵, Sai Wang⁴. ¹Medical Faculty Mannheim, Heidelberg University, Mannheim, Germany; ²Medical Faculty Mannheim, Heidelberg University, Mannheim, Germany; ³Stanford University, Stanford, United States; ⁴Heidelberg University, Mannheim, Germany; ⁵Heidelberg University, Mannheim University, Germany
 Email: yujia.li@medma.uni-heidelberg.de

Background and aims: In healthy livers, latent TGF- β (LTGF- β) is stored in the extracellular matrix and kept quiescent by extracellular matrix protein 1 (ECM1). Upon damage, ECM1 is downregulated in hepatocytes, facilitating LTGF- β activation and hepatic fibrosis. This study investigates the regulatory mechanism of ECM1 expression in the liver under pathophysiological conditions.

Method: *In silico* promoter analysis was used to predict pathways for ECM1 transcription regulation. Functional assays were performed in AML12 cells, mouse and human primary hepatocytes (MPHs, HPHs), and in liver tissue of mice and patients.

Results: In healthy liver, EGF/EGFR signaling maintains ECM1 expression through phosphorylation of STAT1 at S727, which promotes its binding to the *Ecm1* gene promoter to enhance gene transcription. During inflammatory liver injury, accumulated IFN γ interferes with EGF signaling by downregulating EGFR expression and by disrupting EGF/EGFR/STAT1-mediated *Ecm1* promoter binding. Mechanistically, IFN γ induces STAT1 phosphorylation at position Y701, which is competing with the ability of p-STAT1 S727 to bind to the *Ecm1* gene promoter. Additionally, IFN γ induces NRF2

POSTER PRESENTATIONS

nuclear translocation and repressive binding to the *Ecm1* gene promoter, thus further reducing ECM1 expression. As a result, decreased levels of ECM1 facilitate LTGF- β activation, TGF- β signaling and fibrogenesis. Importantly, patients suffering from liver cirrhosis lacking nuclear expression of NRF2 consistently maintain higher levels of ECM1, inferring a better prognosis.

Conclusion: ECM1 expression in healthy livers is controlled by EGF/EGFR/STAT1 signaling. Upon liver injury, ECM1 expression is repressed by accumulating IFN γ /NRF2, which results in the activation of LTGF- β and the onset of hepatic fibrosis.

FRI-540

Role of hepatocyte-intrinsic humoral factors in establishing bioscaffold that regulates the fate determination of primary hepatocytes

Yuji Ishida^{1,2}, Go Sugahara^{1,2}, Chihiro Yamasaki², Sho Morioka², Mikaru Yamao², Jae-Jin Lee³, Yasuhito Tanaka⁴, Meng Li⁵, Hyungjin Eoh³, Chise Tateno², Takeshi Saito⁶. ¹Department of Medicine, Division of Gastrointestinal and Liver Diseases, Keck School of Medicine, University of Southern California, Los Angeles, United States; ²RandD, PhoenixBio Co., Ltd., Higashi Hiroshima, Japan; ³Department of Molecular Microbiology and Immunology, Keck School of Medicine, University of Southern California, Los Angeles, United States; ⁴Faculty of Life Sciences, Kumamoto University, Kumamoto, Japan; ⁵USC Libraries Bioinformatics Service, University of Southern California, Los Angeles, United States; ⁶Department of Medicine, Molecular Microbiology and Immunology, and Pathology, Division of Gastrointestinal and Liver Diseases, Keck School of Medicine, University of Southern California, Los Angeles, United States
Email: saiotak@usc.edu

Background and aims: In vitro culture of human hepatocytes (HH) results in rapid quality deterioration, attributed to both the injury inflicted during cell procurement processes and the absence of a tissue-specific microenvironment. Our refined 2D culture approach, however, demonstrates that freshly isolated single-cell suspension HH undergo dynamic processes of in vitro wound healing, resulting in the reinstatement of genuine characteristics. These processes include the restoration of tight junctions, proper cellular polarity, morphological architecture, and the expression of hepatocyte marker genes at levels comparable to those observed in liver tissue. Our work also shows that the degree of fate restoration and maintenance is inversely correlated with the frequency of culture medium replacement, indicating the involvement of hepatocyte-derived humoral factors in this process. This study aims to decipher the autocrine role of hepatocyte-intrinsic humoral factors in determining the cell fate of HH.

Method: HH, either primary or derived from humanized liver chimeric mice (HLCM), were seeded onto collagen-coated plates and cultured for 14 days in medium containing hepatocyte-specific supplements. Subsequently, the culture medium was pooled as the conditioned medium (CM), and its impact on the fate restoration and maintenance of freshly isolated HH was compared with that of fresh medium (FM) via transcriptome analysis to identify responsible pathways, and loss of function approaches were employed for validation. Immunofluorescent and electron microscopic analyses were also conducted to characterize the impact of the conditioned medium (CM) on cellular and extracellular architectures. Lastly, HH cultured with the CM or FM were transplanted into uPA/SCID mice to determine their fate status by assessing the capacity to establish HLCM.

Results: The transcriptome of HH cultured with the CM exhibits a pattern highly resembling that of freshly isolated HH, normal human liver tissue, as well as the liver of HLCM. In contrast, HH cultured with FM show a significant upregulation of the TGF β -YAP/TAZ pathway, as well as signature genes indicative of dedifferentiation or trans-differentiation to cholangiocytes. Microscopic analyses reveal that CM treatment promotes the accumulation of extracellular matrix

(ECM) composed of fibrin, fibronectin, laminin, and vitronectin, preventing HH from developing morphological deformities. Studies employing a loss-of-function approach indicate that ECM formation is the key fate-protective effect of the CM. Lastly, the transplantation of HH cultured with the CM, but not with FM into HLCM host mouse showed efficient engraftment.

Conclusion: This study demonstrates the critical role of hepatocyte-derived humoral factors in shaping the fate of in vitro cultured HH by establishing ECM that mimics the liver tissue microenvironment.

FRI-541-YI

Taurine supplementation plays hepato-protective role against steatosis in mouse hepatocytes

Pavitra Kumar¹, Frank Tacke¹, Cornelius Engelmann^{1,2}. ¹Charité—Universitätsmedizin Berlin, Department of Hepatology and Gastroenterology, Berlin, Germany; ²University College London, Institute for Liver and Digestive Health, Berlin, Germany
Email: cornelius.engelmann@charite.de

Background and aims: Taurine, a semi essential micronutrient is taken up by cells through taurine transporter (SLC6A6). It has anti-aging potential shown in multiple organisms including humans. In liver, aging is associated with hepatic steatosis, fibrosis, dysregulated metabolism, and immune cells infiltration leading to metabolic dysfunction-associated steatotic liver disease (MASLD). A few anti-aging studies have shown 'what' taurine does to the liver however there is no study exploring 'how' taurine improves liver health. Therefore, the present study explores 'how' taurine supplementation affects the steatosis and steatosis-associated metabolism in hepatocytes.

Method: Primary mouse hepatocytes (PMH) were cultured overnight, were supplemented with optimized dose of 1 mM taurine for 24 hours, followed by 0.3 mM free fatty acids (FFA) (1:1 palmitic acid and oleic acid) for 24 hours. Neutrophils were isolated by negative selection-based microbeads and bone marrow-derived microphages (BMDM) were isolated by anti-F4/80 microbeads from mice bone marrow. Cellular bioenergetics and fuel dependency were assessed using XFe Seahorse analyser.

Results: FFA treatment increased SLC6A6 expression. Taurine-supplemented PMH showed 2-fold reduced lipid accumulation ($p < 0.001$) compared to FFA-treated cells. Taurine suppressed fatty acid uptake and lipogenesis, maintaining this even during FFA treatment. Taurine did not increase fatty acid oxidation, indicating reduced lipid accumulation resulted from decreased FFA uptake and lipogenesis. The metabolic landscape saw distinctive shifts in fuel preferences for ATP generation. Steatotic hepatocytes prioritized fatty acids, glucose, and glutamine, in that order. In contrast, taurine-supplemented steatotic PMH had a preference for glucose as their primary fuel source for ATP generation, followed by fatty acids and glutamine. Notably, taurine alone led to a reduction in glucose-dependent oxidative phosphorylation 2-fold ($p < 0.001$). Taurine's influence extended beyond fatty acid metabolism reaching into the inflammatory milieu. FFA treatment triggered an upregulation of pro-inflammatory cytokines and chemokines (IL6, TNF α , CCL2, and CXCL2), with taurine effectively suppressing all except CXCL2. Furthermore, the pro-inflammatory response translated into increased migration of neutrophils 1.5-fold ($p < 0.001$) and BMDM 2-fold ($p < 0.001$) in a trans well migration assay. Taurine alone, however, demonstrated a remarkable reduction in the migration of both neutrophils and BMDM, underscoring its potential anti-inflammatory impact.

Conclusion: Taurine supplementation robustly impacted hepatocyte metabolism and inflammation by suppressing fatty acid uptake and de novo lipogenesis. This effect persisted post-FFA treatment, highlighting taurine's hepato-protective role against free fatty acids-induced steatosis.

FRI-542

Induced pluripotent stem cell-derived hepatocytes revisited: improved liver functionality compared to liver cancer cell lines and a better model for pre-clinical large-scale therapeutic screening and drug safety

Magdalena Lukasiak¹, Gemma Gatti¹, George Kiloh¹, Samuel Chung¹, Ka Cheung¹, Chloe Robinson¹, Bhavik Chouhan², Dominic Williams³, Lia Panman¹, Carlos Gil¹, Nikolaos Nikolaou¹. ¹DefiniGEN Ltd., Cambridge, United Kingdom; ²AstraZeneca, Gothenburg, Sweden; ³AstraZeneca, Cambridge, United Kingdom
Email: nikolaos.nikolaou@definigen.com

Background and aims: Liver disease is a rising cause of mortality worldwide. Despite careful approaches taken during drug development, most therapeutics fail to reach clinical trials due to the lack of translatability between pre-clinical models and the clinic. Primary human hepatocytes (PHH) and hepatocellular cancer cells (e.g., HepG2) are currently used, however, they come with limitations, including short life-span, rapid loss of function, and malignant origin. We have hypothesized that induced pluripotent stem cell (iPSC)-derived hepatocytes can overcome these limitations, offering a sustainable *in vitro* platform in pre-clinical liver research.

Method: Healthy iPSCs were differentiated to hepatocytes (Opti-HEP) for six weeks. Characterisation of Opti-HEP, HepG2, and PHH functionality was assessed, including liver maturity marker expression and secretion by qPCR and ELISA, *de novo* gluconeogenesis by qPCR and glucose assays, urea synthesis by western blotting and urea assays, and cytochrome P450 expression and activity by qPCR and luciferase assays. Suitability of Opti-HEP to predict drug-induced liver injury (DILI) was evaluated by cell viability assays following 48 h treatment with 27 drugs of known DILI liability.

Results: HepG2, Opti-HEP, and PHH expressed similar levels of *ALB*, *A1AT*, and *HNF4A*, however, albumin secretion was higher in Opti-HEP and HepG2 cells compared to PHH (HepG2: 23.0 ± 2.6 vs. Opti-HEP: 25.0 ± 4.5 vs. PHH: 1.4 ± 0.9 µg/day/10⁶ cells, n = 3–4). Urea-synthesizing enzyme expression (*OTC*, *ASS1*, *ASL*, *CPS1*, *ARG*) were higher in Opti-HEP compared to HepG2 cells, consistent with higher urea secretion (HepG2: 4.3 ± 0.3 vs. Opti-HEP: 18.5 ± 0.5 µg/day/10⁶ cells, n = 3–4). *De novo* gluconeogenesis in Opti-HEP was investigated revealing increased *G6PC* and *PEPCK* mRNA levels following 0.1 mM dbcAMP treatment, consistent with enhanced glucose secretion upon pyruvate (PYR) challenge (0 mM PYR: 1.6 ± 0.01 vs. 1 mM PYR: 2.5 ± 0.02 vs. 2 mM PYR: 3.2 ± 0.03, fold change, n = 3). *CYP3A4*, *2B6*, *2C9*, *2C19*, *2A6*, and *ABCB11* mRNA levels were higher in Opti-HEP compared to HepG2 cells, in line with higher basal *CYP3A4* activity (HepG2: 12.3 ± 2.2 vs. Opti-HEP: 338.7 ± 104.5 nmol Luciferin/µmol ATP). Crucially, Opti-HEP treatment with 1α, 25-hydroxy-vitamin D3 (*CYP3A4* inducer; 100 nM) resulted in a >2.5-fold change increase in *CYP3A4* activity, confirming successful *CYP3A4* induction. Cell viability assessment following treatment with 27 drugs of known DILI liability showed similar levels of accuracy in predicting DILI between Opti-HEP and HepG2 cells.

Conclusion: Opti-HEP is a superior hepatocyte model compared to HepG2 cells, with liver functionality comparable to PHH. This data alongside the expansion capacity and amenability of Opti-HEP showcase the spectrum of opportunities this model can offer in the fields of disease modelling, large-scale therapeutic screening, and drug safety.

FRI-543

Relevance of hepatic estrogen receptor alpha in liver metabolic adaptation during pregnancy

Arianna Dolce¹, Clara Meda², Sara Della Torre¹. ¹Università degli Studi di Milano, Department of Pharmaceutical Sciences, Milan, Italy; ²Università degli Studi di Milano, Department of Health Sciences, Milan, Italy
Email: sara.dellatorre@unimi.it

Background and aims: Males and females show different susceptibility, progression and outcome of several acute and chronic liver diseases. Among the factors that may account for these differences are estrogens, acting mainly through estrogen receptor alpha (ERα) at the hepatic level. We previously demonstrated that, in the liver of females, hepatic ERα acts as a sensor of food availability and regulates the hepatic metabolism according to the needs of the several stages of reproduction, thus linking metabolism and reproduction to each other. In particular, hepatic ERα activation by nutrients such as amino acids (AA) is necessary for the proper progression of the estrous cycle. The role of hepatic ERα in the regulation of liver metabolism and reproduction could be even more complex and relevant during pregnancy; however, it still needs to be investigated. Deregulations of hepatic estrogen signaling could also be implicated in pathological liver conditions related to pregnancy, such as intrahepatic cholestasis and acute fatty liver of pregnancy. In this view, a better understanding of the role of hepatic ERα during physiological progression of pregnancy could be crucial for the development of strategies to prevent or limit the progression of these conditions. Therefore, the aim of this study was to assess the specific relevance of hepatic ERα in the physiological adaptation of liver metabolism in different stages of pregnancy.

Method: To assess the specific relevance of hepatic ERα in the metabolic adaptation during pregnancy, we compared female control (CTRL) and liver-specific ERα-knockout (LERKO) pregnant mice at different timepoints (gestational day 6.5, 14.5 and 17.5). Virgin females at proestrus (the phase of the estrous cycle in which circulating 17β-estradiol levels are highest) were used as the reference group.

Results: Results show that in the livers of female pregnant mice most of the genes analyzed, that are involved in lipid metabolism, glucose homeostasis and amino acid metabolism, display different expression patterns according to the progression of pregnancy. Moreover, hepatic ERα concurs to regulate the expression of some of the genes analyzed, especially those involved in AA metabolism. These findings are in line with our previous data and further demonstrate the tight connection between ERα and AA metabolism in the female liver.

Conclusion: Altogether, our results suggest that liver adapts its metabolism according to the different stages of pregnancy, to sustain the energetic needs of the developing embryo. Moreover, a contribution of hepatic ERα can be observed in the regulation of some of the analyzed pathways, hinting to this receptor as a possible key player in the orchestration of the metabolic adaptation during pregnancy.

FRI-544

KLB depletion fosters stem-like properties and epithelial-mesenchymal transition plasticity in HepG2 cells

Nadia Panera¹, Marica Meroni², Nicolò Cicolani¹, Francesca Tiano¹, Anna Ludovica Fracanzani², Paola Dongiovanni², Anna Alisi¹. ¹Bambino Gesù Children's Hospital, IRCCS, Rome, Italy; ²Fondazione IRCCS Cà Granda Ospedale Maggiore Policlinico, Milan, Italy
Email: anna.alisi@opbg.net

Background and aims: Beta-Klotho (KLB), the co-receptor of fibroblast growth factor receptor 4, was found reduced at circulating and hepatic levels in both pediatric and adult patients with non-alcoholic fatty liver disease (NAFLD). This reduction was associated with inflammation, ballooning, and fibrosis. The genetic ablation of KLB in hepatocytes resulted in enhanced oxidative stress and inflammation, supporting its role in liver homeostasis but also suggesting a potential involvement of KLB in the hepatocyte transformation toward a neoplastic phenotype.

Here, we evaluated the impact of KLB depletion on the acquisition of stem-like properties and epithelial-mesenchymal transition (EMT) plasticity in the HepG2 *in vitro* model.

Method: We generated a complete full knock-out model of the KLB gene (KLB-KO) in HepG2 hepatoma cells by using CRISPR/Cas9. Subsequently, we performed functional assays to investigate cell

proliferation, self-renewal, and pluripotency. Critical EMT effectors were explored through gene and protein expression analysis.

Results: KLB mRNA and protein levels were reduced in KLB-KO cells ($p < 0.01$). Functional assays revealed the increase of cell proliferation ($p < 0.001$) and cell cycle S-phase ($p < 0.01$) in KLB-KO cells, if compared to Cas9 controls. The self-renewal ability of KLB-KO cells was assessed by analyzing the formation of free-floating cell aggregates in a 3D multicellular Tumor Spheroid model (TS) over 96 hours. Thus, KLB-KO cells reported the enlargement of the TS area and diameter at the last timepoints (72 hours, $p < 0.01$; 96 hours, $p < 0.0001$). Furthermore, the expression of 609 stem and pluripotency-related genes was analyzed by TaqMan OpenArray Human Stem Cell Panel, resulting in the upregulation of a total of 114 genes and the downregulation of a total of 49 genes. Among the enriched genes we found several mediators of the EMT process, such as the transforming growth factor beta 2 ($p < 0.01$), the matrix metalloproteinase-14, ($p < 0.01$), WNT3a ($p < 0.05$) which is involved in the modulation of beta-catenin and c-Myc ($p < 0.01$). Moreover, several effectors involved in lipid metabolism and storage and the alpha-fetoprotein (AFP) ($p < 0.0001$) were found downregulated in KLB-KO cells, suggesting the loss of the hepato-specific proprieties. Interestingly, the epithelial markers E-cadherin ($p < 0.001$), N-cadherin ($p < 0.01$), and cytokeratin 18 ($p < 0.001$) were found downregulated at gene and protein levels in KLB-/- cells, while the mesenchymal effectors Vimentin ($p < 0.0001$) and phosphorylated-FAK ($p < 0.01$) were increased in our model.

Conclusion: We demonstrated that KLB-KO confers in vitro stemness and pluripotency features and may mediate the downregulation of epithelial markers prompting the EMT. Thus, we hypothesize that KLB depletion may have a central role in the switching towards a phenotype that could have acquired pro-oncogenic features.

FRI-545

Dickkopf-1 inhibitor treated with sorafenib inhibited Wnt/PI3 K/Akt pathway in hepatocellular carcinoma

Seung Up Kim¹, Sang Hyun Seo¹, Hye Won Lee¹, Beom Kyung Kim¹, Jun Yong Park¹, Do Young Kim¹, Sang Hoon Ahn¹. ¹Yonsei University College of Medicine, Seoul, Korea, Rep. of South
Email: ksukorea@yuhs.ac

Background and aims: Sorafenib prolongs overall survival of patients with advanced hepatocellular carcinoma (HCC). Overexpression of Dickkopf-1 (DKK1) was detected in HCC patients. Therefore, we studied combination effects and signaling pathways of sorafenib treated with DKK1 inhibitor in HCC models.

Method: Human HCC cells (Huh7 and Hep3B) were used to identify the IC₅₀ values of sorafenib and DKK1 inhibitor. Hep3B cells and hydrodynamic tail vein injection were used to conduct HCC xenograft mouse and transgenic mouse. Mouse models were orally treated with sorafenib (32 mg/kg) and/or DKK1 inhibitor (16 mg/kg) for 10 days. Signaling pathways of sorafenib treated with DKK1 inhibitor were confirmed by immunoblot assays (western blot, IHC, IF staining) and qRT-PCR.

Results: Combination treatment of sorafenib and DKK1 inhibitor reduced the expression levels of Wnt/PI3 K/Akt related molecules [p110 α , p-Akt (all $P < 0.05$), β -catenin (all $P < 0.05$), p-GSK3 β -Ser9], but the expression level of p-GSK3-Tyr216 was augmented, compared to a single treatment in HCC models. The expression levels of PI3 K/Akt pathway inhibitory genes were augmented and the expression levels of canonical Wnt pathway target genes were reduced by combination treatment of sorafenib and DKK1 inhibitor (all $P < 0.05$), compared to a single treatment. Moreover, co-expression of Hras, miR53 and PI3 K significantly augmented the expression levels of Wnt/PI3 K/Akt pathway molecules, compared to injected with Hras and miR53 in transgenic mouse model.

Conclusion: Combination treatment of sorafenib and DKK1 inhibitor significantly inhibited Wnt/PI3 K/Akt pathway through regulation of GSK3 β in HCC. Accordingly, inhibition of DKK1 may be a novel strategy in HCC. inhibition of DKK1 may be a novel strategy in HCC.

Immune-mediated and cholestatic – Experimental and pathophysiology

TOP-147

Long-term, real-world outcomes under obeticholic acid treatment in primary biliary cholangitis: a nationwide multicentre study

Nadir Abbas¹, Amal Almahroos², Rachel Smith³, Emma Culver⁴, Douglas Thorburn⁵, Neil Halliday⁶, Jessica Dyson⁷, George F. Mells⁸, David E. Jones⁹, Palak J. Trivedi¹⁰. ¹NIHR Birmingham Biomedical Research Centre, Centre for Liver and Gastroenterology Research, University of Birmingham, UK, Liver Unit, University Hospitals Birmingham Queen Elizabeth. Birmingham UK, Birmingham, United Kingdom; ²The Liver Unit, Queen Elizabeth Hospital, Birmingham, United Kingdom; ³Academic Department of Medical Genetics, University of Cambridge, Cambridge, United Kingdom; ⁴John Radcliffe Hospital, University of Oxford, Oxford, United Kingdom; ⁵The Sheila Sherlock Liver Centre, Royal Free, London, United Kingdom; ⁶Institute of Liver and Digestive Health, University College London, London, United Kingdom; ⁷Newcastle upon Tyne Hospitals NHS Foundation Trust, Newcastle, United Kingdom; ⁸Academic Department of Medical Genetics, University of Cambridge, Cambridge, United Kingdom; ⁹Newcastle University Medical School, Newcastle, United Kingdom; ¹⁰NIHR Birmingham Biomedical Research Centre, Centre for Liver and Gastrointestinal Research, University of Birmingham, Birmingham, United Kingdom
Email: nadir.abbas@uhb.nhs.uk

Background and aims: Obeticholic acid (OCA) is the only licensed second-line therapy for primary biliary cholangitis (PBC). However, real-world evidence is limited to data captured over 1–2 years following treatment initiation. The aim of this study was to evaluate long-term safety, tolerability and efficacy amongst the index series of patients (pts) treated with OCA following initial market approval in the United Kingdom (UK).

Method: Our cohort consisted of PBC pts who initiated OCA between 2017–19, with follow-up continuing to 2023. Pts were censored at the date of last clinic visit free of a clinical event, or at the point of switching from OCA to non-licensed therapy in fibric acid derivatives (fibrates), or on starting fibrates in combination with OCA.

Results: In all, we accrued data from 240 pts who initiated OCA (216 women; 218 also treated with ursodeoxycholic acid). Median transient elastography at baseline was 9.5 kPa IQR 7–14 kPa with 20% of pts having cirrhosis. Median ALT, ALP and bilirubin values at baseline (ratio to upper limit of normal) were 1.35 (1.02–2.04), 2.81 (2.02–3.96) and 0.55 (0.35–0.95). Over 48 months, 106 pts (44%) discontinued OCA because of side effects, most often pruritus (26%). Moreover, 45/106 pts switched from OCA to fibrates due to persistent biochemical non-response, with an additional 74 starting fibrates alongside OCA as combination therapy. In the group of pts who continued OCA (without switching/starting fibrates), the median reduction in serum ALP from baseline to 12-, 24-, 36- and 48 months was 27% (21–31%), 40% (35–51%), 43% (32–49%) and 54% (40–60%) ($p < 0.001$ for all). In turn, median reductions in serum ALT at 12-, 24-, 36- and 48 months were 25% (17–34%), 40% (32–56%), 42% (39–52%) and 43% (35–54%) ($p < 0.001$ for all). Biochemical response rates according to POISE and normal range criteria (normalisation in bilirubin, ALT and ALP) were 30% and 2%, 46% and 9%, 62% and 10% and 64% and 17% at 12-, 24-, 36- and 48 months, respectively ($p < 0.01$ for all). Forty pts experienced at least one clinical event; including hepatocellular carcinoma ($n = 4$); decompensation ($n = 29$); referral for transplantation ($n = 27$); or death from any cause ($n = 13$). Cirrhosis (hazard ratio [HR] 3.93; 95% CI: 2.09–7.38), not being treated with UDCA (HR: 1.96; 1.67–5.70), high bilirubin (HR: 1.08; 1.04–1.12), low albumin (HR: 0.91; 0.93–0.97), low platelets (HR: 0.98; 0.97–0.99) and being a non-responder according to POISE

criteria at 12 months of OCA therapy (HR: 5.49; 2.29–13.72) were risk factors for developing clinical events ($p < 0.01$ for all).

Conclusion: Biochemical response rates increase over time among pts under long-term OCA treatment. We also show, for the very first time, that the POISE criteria can be used to stratify risk of developing clinical events in an OCA-treated PBC cohort. However, drug discontinuation rates remain high, underscoring need for new treatment paradigms in PBC.

TOP-148

Interleukin-2 mediated regulatory T cell expansion is associated with dual outcomes of ductular reaction and liver fibrosis

Man Chun Wong¹, Gareth Hardisty¹, Nuruhiro Kimura², Wei-Yu Lu¹.

¹Institute for Regeneration and Repair, University of Edinburgh, Edinburgh, United Kingdom; ²Division of Gastroenterology and Hepatology, Niigata University, Niigata, Japan
Email: s2425254@ed.ac.uk

Background and aims: Regulatory T cells (Tregs) exert immune-modulatory functions through suppressing immune responses. Expanding Tregs number has become an attractive option for controlling excessive inflammation during liver disease. Methods to manipulate Tregs as therapeutics have been performed in mouse models and clinically, including the use of IL-2 aiming to control the development and proliferation of CD4⁺ T cells. However, mixed results have been reported from these studies. To investigate the underlying mechanisms of the discrepancy using Tregs to contain disease progression, we explore the possibility of using IL2-antibody complex to expand Tregs in biliary and hepatocellular injury models to make IL2-mediated Tregs expansion more efficient.

Method: Tamoxifen was given to the Foxp3CreERTAi14 Tregs fate-mapping mice, inducing the expression of red fluorescence (RFP) in Tregs. A low dose of IL-2 complexes (IL-2 protein and anti-IL2 antibody) or PBS control was injected into the mice. All mice were then given the 3, 5-Diethoxycarbonyl-1, 4-Dihydrocollidine (DDC) diet to induce biliary injury. Immunostaining and PSR staining examined the degree of liver damage, ductular reaction and liver fibrosis. Immune cells, intrahepatic Tregs and their subsequent populations were analysed by flow cytometry. Similar experiments were also conducted in the context of hepatocellular injury using the Mdm2^{fl/fl} mice receiving hepatotropic AAV-8 Cre.

Results: We found that Tregs expansion decreases the magnitude of ductular reaction, indicating less liver inflammation during the start of biliary injury. Interestingly, the decrease in the ductular reaction was not linked to a decrease in fibrosis as the fibrosis level was increased three-fold in the IL2 complex injected group. Flow cytometry analysis indicated that the IL-2 complex preferentially doubled the Foxp3⁺ Tregs population; however, a three-fold increase in the Foxp3⁺ Tregs population was also observed. Using the fate mapping mice, we concluded that the expanded Foxp3⁺ Tregs are “ExTreg,” which originally belonged to the Foxp3⁺ population but acquired a pro-inflammatory phenotype.

Conclusion: IL-2 complex successfully expanded intrahepatic Treg during biliary injury. Tregs expansion does not decrease liver fibrosis during injury but causes a reduction in ductular reaction. The magnitude of the ductular reaction does not positively correlate to liver fibrosis, suggesting cholangiocytes are not the main driver of fibrogenesis. Further investigation is required on the dose and timing of Tregs expansion and the effects of expanded ExTreg. This study highlights the plasticity of Tregs in the liver and precautions for Tregs' stability if we aim to use Tregs expansion as a therapeutic approach.

TOP-149-YI

Plasmatic expression of miR122-5p and miR21-5p predicts relapse of autoimmune hepatitis after treatment withdrawal

Pinelopi Arvaniti^{1,2}, Olga Millán^{3,4}, Ignasi Olivas¹, Mar Riveiro Barciela^{3,5}, Montserrat García-Retortillo⁶, Mercé Roget⁷, Thais Leonel^{1,3}, Sergio Rodriguez-Tajes^{1,3}, Judit Julian⁴,

Mercè Brunet^{3,4}, María Carlota Londoño^{1,3}. ¹Liver Unit, Hospital Clinic, Institute of Biomedical Investigation August Pi y Sunyer (IDIBAPS), Barcelona, Spain, Barcelona, Spain; ²Department of Medicine and Research Laboratory of Internal Medicine, Expertise Center of Greece in Autoimmune Liver Diseases, ERN RARE-LIVER, General University Hospital of Larissa, Greece, Larissa, Greece; ³Biomedical Research Center in Hepatic and Digestive Diseases (CIBERehd), Instituto de Salud Carlos III, Madrid, Spain, Barcelona, Spain; ⁴Pharmacology and Toxicology, Biochemistry and Molecular Genetics, Biomedical Diagnostic Center (CDB), IDIBAPS, Hospital Clinic of Barcelona, University of Barcelona, Spain, Barcelona, Spain; ⁵Unit of Hepatology, Department of Internal Medicine, University Hospital Vall de Hebron, Barcelona, Spain, Barcelona, Spain; ⁶Seccion of Hepatology, Department of Gastroenterology, Hospital del Mar, Barcelona, Spain, Barcelona, Spain; ⁷Unit of Hepatology, Department of Gastroenterology, Health Consortium of Terrassa, Spain, Barcelona, Spain
Email: peni.arvaniti@gmail.com

Background and aims: More than 50% of patients with autoimmune hepatitis (AIH) relapse after immunosuppression (IS) withdrawal. Unfortunately, there are no available biomarkers for predicting disease flares after treatment discontinuation. Circulating microRNAs (miRNA) are associated with disease activity and could potentially serve as predictors of relapse in AIH. We aimed to evaluate the capacity of a circulating miRNA panel to predict relapse after treatment discontinuation in patients with AIH.

Method: This was a multicenter prospective study of IS withdrawal in 30 patients with AIH. Treatment was progressively tapered until complete withdrawal according to published guidelines. Circulating plasma expression of miR155-5p, miR122-5p, miR181-5p, miR21-5p, miR221-3p, miR4725-3p, miR6125, miR3196-3p, and miR4634 was assessed by reverse-transcription quantitative PCR using the $2^{-\Delta\Delta Cq}$ formula in samples obtained before IS withdrawal (T0), during follow-up (T1, before relapse with normal transaminases and IgG), and at the time of relapse (T2, or similar in patients with sustained complete biochemical response, CBR).

Results: Sixteen patients (53%) were female, with a median age of 59 years (IQR 49–70) and a median time of complete biochemical response of 44 months (IQR 37–55). At T0, the median levels of the liver tests were AST 19 IU/L (IQR 16–22), ALT 15 IU/L (IQR 11–22), and IgG 10 g/L (IQR 9–11). All patients were in histological remission (mHAI <4) at T0. After a median follow-up of 7 months (T2), 14 (47%) patients presented with disease relapse. Relapsers presented a significantly higher expression of miR122-5p at T0, T1 (median follow-up of 4 months, IQR 2–12) and T2 ($p < 0.05$ for all comparisons). In contrast, miR21-5p levels were significantly lower at T1, compared to non-relapsers (21 vs. 31, $p = 0.02$). No significant differences were detected among the remaining miRNAs analyzed. Using a general linear model with repeated measures, a significant increase in miR122-5p levels over time was observed among relapsers ($F_{(1, 28)} = 8.460$, $p = 0.007$), with a significant interaction effect on the probability of relapse ($F_{(1, 28)} = 8.772$, $p = 0.004$). Plasma levels of miR122-5p at T0 (AUC 0.771, 95%CI 0.592–0.951; $p = 0.013$), as well as the combination of miR122-5p and miR21-5p levels at T1 (AUC 0.901, 95%CI 0.734–0.978; $p = 0.001$), accurately predicted relapse after IS discontinuation.

Conclusion: Progressive elevation of miR122-5p along with a significant decrease in miR21-5p plasma levels was observed before any alteration in liver biochemistry in patients with AIH who relapsed after IS withdrawal. Assessment of miR122-5p expression before and at consecutive time points after discontinuation of IS can serve as a non-invasive predictor of relapse in AIH.

TOP-150-YI

Molecular analysis of checkpoint inhibitor-induced liver injury

Sarp Uzun¹, Carl Zinner¹, Asmita Pant¹, Amke Beenen¹, Hélène Heusler¹, Ilaria Alborelli¹, Anna Stalder¹, Magdalena Filipowicz Sinnreich², Kirsten Mertz³, Jürg Vosbeck¹,

POSTER PRESENTATIONS

Luigi Maria Terracciano⁴, Markus Heim⁵, Heinz Läubli⁶, Christine Bernsmeier⁵, Matthias Matter¹. ¹Institute of Medical Genetics and Pathology, University Hospital Basel, Basel, Switzerland; ²University of Basel, University Hospital Basel, Basel, Switzerland; ³Institute of Pathology, Cantonal Hospital Baselland, Liestal, Switzerland; ⁴Pathology Unit, Head of Anatomic Pathology Unit, Rozzano (MI), Italy; ⁵University Center for Gastrointestinal and Liver Diseases Basel, Basel, Switzerland; ⁶Department of Biomedicine, University of Basel, Division of Oncology, University Hospital Basel, Basel, Switzerland
Email: sarp.uzun@usb.ch

Background and aims: The advent of immune checkpoint inhibitors (ICIs) has led to a major change in the management of different cancer types. However, ICI treatment can trigger treatment-limiting immune-mediated toxicity, so-called immune-related adverse events (irAEs). Checkpoint inhibitor-induced liver injury (ChILI) is a relatively common adverse event of ICI therapy, with a wide range of incidence between 1% to 15%. Although several mechanisms have been proposed, the pathophysiology of ChILI has not been fully understood. In this study, we aimed to perform a molecular comparison of ChILI with autoimmune hepatitis (AIH), a well-characterized immune-mediated liver disease, to enhance our understanding of this disease.

Method: Formalin-fixed and paraffin-embedded (FFPE) liver biopsy samples were collected from ChILI (n = 12), AIH (n = 9), alcoholic steatohepatitis (n = 18), hepatitis C virus hepatitis (n = 13), and normal liver samples (n = 3). Total RNA was isolated from FFPE samples and whole transcriptome sequencing was performed with HTG Transcriptome Panel. To explore the T-cell architecture of ChILI and AIH, FFPE extracted total RNA from AIH, ChILI and matching tumor samples of ChILI samples were sequenced for their T-cell receptor (TCR) by using the OncoPrint TCR Beta-SR assay.

Results: Whole transcriptome analysis indicated that ChILI cohort has a different gene expression profile than AIH and other additional cohorts with liver inflammation. Transcriptome deconvolution revealed significantly lower enrichment of B cells and plasma cells in ChILI compared to AIH. Both ChILI and AIH cohorts presented a polyclonal distribution of T-cell clones with no significant differences in the diversity metrics, CDR3 nucleotide length distribution, and VDJ usage. Interestingly, we observed overlapping high-frequency T-cell clones in ChILI samples and their matched tumor samples obtained from the same patient.

Conclusion: ChILI has a different gene expression profile and immune cell distribution than AIH, supporting the notion that they are two distinct disease entities. However, both diseases share a similar T-cell repertoire architecture in liver biopsies. Interestingly, we detected overlapping T cell clones between ChILI and matched tumor samples, suggesting a role for shared epitopes between liver and tumor samples.

TOP-156

SRT-015: Novel therapeutic for cholestatic liver diseases

Kathleen Elias¹, S. David Brown¹, Neil D. McDonnell¹, Artur Plonowski¹. ¹Seal Rock Therapeutics, Inc, Seattle, United States
Email: kelias@sealrocktx.com

Background and aims: SRT-015, a best-in-class apoptosis signal-regulating kinase 1 (ASK1) inhibitor, has demonstrated preclinical efficacy in a therapeutic, diet-induced obese mouse MASH model with biopsy-confirmed fibrosis and in acute models of liver injury including alcohol-related liver disease and acetaminophen overdose. In vitro studies have demonstrated direct dose-dependent anti-apoptotic, anti-inflammatory and antifibrotic effects of SRT-015. Human safety and PK profile was established in a phase 1 clinical trial. Here we evaluate SRT-015 effects on fibrosis in a rat 14-day Bile Duct Ligation (BDL) model of severe cholestatic disease.

Method: Male Sprague Dawley rats (7–8 weeks,) were randomized to treatment groups (n = 4–10): 1) Sham vehicle 2) BDL + vehicle 3) BDL + 15 mg/kg SRT-015 4) BDL + 50 mg/kg SRT-015. SRT-015 or vehicle

was dosed PO, starting at Day1, 1 h before surgery then daily for 14 days. BDL surgery included ligation of the common bile duct below the junction of the hepatic ducts and above the pancreatic ducts entrance. Sham animals underwent laparotomy without ligation. On terminal Day 14, 2 h after the last dose, whole blood and plasma was collected for blood chemistry (ALT, AST, ALP, TBil and TBA) or SRT-015 levels. Livers were evaluated for SRT-015 concentrations, fibrosis by biochemical hydroxyproline (HP) content, picrosirius red staining (PSR), and stellate cell activation (alpha-smooth muscle actin staining, α -SMA) by histomorphometry (Aperio ImageScope analysis software).

Results: BDL + vehicle group showed increased fibrosis and elevated blood chemistries compared to sham vehicle. The BDL + 50 mg/kg SRT-015 group demonstrated a significant ($p < 0.05$) antifibrotic effect by reducing fibrotic area by –40% (PSR staining) and –33% (HP content), and decreased α -SMA positive area –54% ($p < 0.0001$) vs. BDL + vehicle. BDL + 15 mg/kg SRT-015 group trended to decrease fibrotic area by PSR (–19%) and HP content (–28%) and significantly ($p < 0.01$) decreased α -SMA positive area (–32%) compared to BDL + vehicle. These significant decreases in fibrosis and stellate cell activation with SRT-015 were observed with no significant change in blood chemistries demonstrating the severity of this 14-day model. SRT-015 liver concentrations, in line with previous studies, showed liver-preferred distribution. The observed efficacious exposures of SRT-015 in this BDL model were within the range of observed clinical plasma levels, and predicted hepatic exposure, in the phase 1 clinical trial.

Conclusion: SRT-015 significantly, and dose-dependently, decreased BDL-induced fibrosis shown by multiple end points after 14 days of treatment in this robust model. These antifibrotic data, with previously demonstrated anti-inflammatory activity, suggests that SRT-015 is a promising therapeutic for human cholestatic liver diseases with an established safe clinical dosing regimen.

SATURDAY 08 JUNE

SAT-151-YI

The role of interleukin-8 in primary sclerosing cholangitis-associated immune cell dysregulation

Lander Heyerick^{1,2}, Kevin De Muynck^{1,2}, Zenzi De Vos^{1,2}, Sander Lefere^{2,3}, Jana Roels^{4,5}, Niels Vandamme^{4,5}, Anja Geerts^{2,3}, Sarah Raevens^{2,3}, Xavier Verhelst^{2,3}, Hans Van Vlierberghe^{2,3}, Lindsey Devisscher^{1,2}. ¹Department of Basic and Applied Medical Sciences, Gut-Liver Immunopharmacology Unit, Ghent University, Ghent, Belgium; ²Liver Research Center Ghent, Ghent University, Ghent University Hospital, Ghent, Belgium; ³Department of Internal Medicine and Paediatrics, Hepatology Research Unit, Ghent University, Ghent, Belgium; ⁴VIB Single Cell Core, VIB, Ghent-Leuven, Belgium; ⁵VIB Center for Inflammation Research, Ghent, Belgium
Email: lander.heyerick@ugent.be

Background and aims: Primary sclerosing cholangitis (PSC) is a chronic, progressive, fibroinflammatory liver disease. Dysregulated systemic and hepatic immune cell responses are implicated in the pathogenesis of PSC and could serve as a diagnostic and therapeutic target. However, PSC-associated systemic immune cell profiles remain insufficiently characterised. Therefore, we unravelled peripheral immune cell subsets of PSC patients and healthy controls at the single cell level and further investigated its implications in PSC pathogenesis.

Method: Peripheral blood mononuclear cells (PBMCs) were isolated by density gradient centrifugation from fresh EDTA-anticoagulated peripheral blood from PSC patients and healthy controls (HCs). PBMC cell suspensions were FACS-purified, single cell Gel Bead-in-Emulsions were generated and RNA-Sequencing libraries were created and analysed. IL-8 concentrations were determined in the sera of PSC-patients, without prior liver transplantation, and of

healthy controls. Adult male C57BL6/J mice were subjected to common bile duct ligation (CBDL) surgery and monocyte/macrophage populations were sorted by FACS and processed for bulk sequencing.

Results: Based on single cell analyses of PBMCs, we identified a population of CD14-positive monocytes with enriched IL8-expression in PSC patients (n = 7) compared to HCs (n = 4). Serum protein analyses showed that PSC patients are also characterised by increased IL-8 levels in the systemic circulation (n = 57 for PSC, n = 15 for HCs, age- and sex-matched). In addition, PSC patients with advanced fibrosis (Metavir stage F3/F4) had significantly higher serum concentrations of IL-8 compared to patients without advanced fibrosis (F0/F2, $p < 0.05$). AUROC analysis showed good performance of IL-8 to assess risk of liver-transplant free survival at 3 years of follow-up (AUROC 0.78). Bulk sequencing of isolated mouse liver monocytes and monocyte-derived macrophages in CBDL-induced cholestasis showed significantly upregulated expression of the IL-8 mouse homologs Cxcl1 (in monocyte-derived macrophages) and Cxcl2 (in monocytes and monocyte-derived macrophages) 2 weeks after surgery compared to sham-operated mice.

Conclusion: PSC patients are characterised by a population of CD14-positive monocytes enriched in IL8-expression and by elevated IL-8 concentrations in the systemic circulation. Serum IL-8 concentrations might serve as prognostic marker for liver-transplant free survival, but validation in larger cohorts is necessary. Further research is directed towards the role of IL-8 in monocytes and macrophages in the context of PSC pathogenesis to unravel its potential as therapeutic target.

SAT-152

The deletion of PTP1B protects against liver biliary damage by shutting immune cell recruitment and enhancing oval cell proliferation

Silvia Calero Pérez^{1,2}, Pilar Valdecantos^{1,2},
Angela Martínez Valverde^{1,2}. ¹IIBm Sols-Morreale (CSIC-UAM), Madrid, Spain; ²CIBERdem (ISCIII), Madrid, Spain
Email: scalero@iib.uam.es

Background and aims: Oval cells (OCs) are hepatic progenitor cells implicated in liver regeneration and repair upon injury. However, the impact of the inflammatory environment in oval cell expansion during primary sclerosing cholangitis (PSC) is unclear. Inhibition of protein tyrosine phosphatase 1B (PTP1B encoding by the *Ptpn1* gene) modulates immune cell responses and protects against acute and chronic liver damage. Our aim was to investigate the effect of *Ptpn1* deletion in the inflammatory compartment surrounding the OC niche and to characterize the proliferation/survival of *Ptpn1*^{+/+} and *Ptpn1*^{-/-} OCs in the context of PSC.

Method: *Ptpn1*^{-/-} and *Ptpn1*^{+/+} mice were fed a diet supplemented with 0.1% of 3, 5-Diethoxycarbonyl-1, 4-Dihydrocollidine (DDC) for 2 weeks. For the analysis of the role of PTP1B in the inflammatory compartment of the OC niche *Ptpn1*^{+/+} mice were transplanted with *Ptpn1*^{-/-} or *Ptpn1*^{+/+} bone marrow (BM) and mice were fed a DDC diet for 2 weeks. *Ptpn1*^{+/+} primary hepatocytes were treated with a mixture of glycochenodeoxycholic and taurocholic acid for 8 h after which the conditioned medium (CM1) was used to stimulate *Ptpn1*^{+/+} or *Ptpn1*^{-/-} bone marrow-derived macrophages (BMDM) for 16 h. Then, *Ptpn1*^{+/+} OCs were treated for different time-periods with *Ptpn1*^{-/-} or *Ptpn1*^{+/+} BMDM-CM (CM2).

Results: *Ptpn1*^{-/-} mice presents lower plasma bilirubin and porphyrin aggregates in the liver compared to *Ptpn1*^{+/+} mice. Increased A6/SOX9 positive cells and expression levels of the OC markers *Krt19* and *Epcam* were observed in livers from *Ptpn1*^{-/-} mice. Moreover, elevations in the number of recruited monocytes (Ly6c⁺), macrophages (F4/80⁺) and lymphocytes (CD3⁺) were observed in the OC niche from *Ptpn1*^{-/-} mice. Flow cytometry analysis revealed increased M2-like macrophages as well as CD4⁺, Treg and Th2 lymphocytes in *Ptpn1*^{-/-} mice concurrently with a

decrease in M1-like macrophages, CD8⁺, Th1, Th17 lymphocytes and NKTs. All these parameters were recapitulated in mice transplanted with *Ptpn1*^{-/-} BM. In vitro results demonstrated that stimulation of OCs with *Ptpn1*^{-/-} CM2 enhanced survival signaling cascades (ERK and AKT phosphorylation) and promoted OCs proliferation.

Conclusion: Our results demonstrated that PTP1B deletion protects against biliary damage through the modulation of the inflammatory compartment in the OC niche. Moreover, in vitro studies revealed that the specific deletion of PTP1B in BMDM induced a molecular signature that favors OC proliferation and survival. These results open new therapeutic perspectives in cellular regenerative therapies against PSC.

SAT-153-YI

Single-cell RNA sequencing identifies the fundamental role of intrahepatic CD8⁺ T cells in the pathogenesis of autoimmune hepatitis

Ignasi Olivas^{1,2}, Aina Rill³, Georgios Koutsoudakis², Yasmin Roldan²,
Pinelopi Arvaniti^{1,2,4}, Sergio Rodríguez-Tajes^{1,2,5}, Sabela Lens^{1,2,5},
Elisabetta Mereu³, María Carlota Londoño^{1,2,5}. ¹Liver Unit, Hospital Clínic Barcelona, Barcelona, Spain; ²Institut d'Investigació Biomèdica August Pi y Sunyer (IDIBAPS), Barcelona, Spain; ³Instituto de Investigación contra la Leucemia Josep Carreras (IJC), Badalona, Spain; ⁴Department of Medicine and Research Laboratory of Internal Medicine, Expertise Center of Greece in Autoimmune Liver Diseases, ERN RARE-LIVER, University Hospital of Larissa, Larissa, Greece; ⁵Centro de Investigación Biomédica en Red de Enfermedades Hepáticas y Digestivas (CIBERehd), Instituto de Salud Carlos III, Madrid, Spain
Email: ignasiolivasalberch@gmail.com

Background and aims: The treatment of autoimmune hepatitis (AIH) has remained unchanged since the 70 s. This is partially due to a lack of knowledge regarding the mechanisms involved in the pathogenesis of the disease. Detailed analysis of lymphocyte populations in liver tissue using single-cell RNA sequencing (scRNAseq), single-cell T-cell receptor sequencing (scTCRseq), and flow cytometry (FC) would allow the design of targeted therapeutic strategies that are more effective and have fewer adverse effects. The aims of the study were to: 1) analyze the clonality and characteristics of lymphocytes in liver tissue at diagnosis and during follow-up, and 2) study the differences between patients with or without response to treatment.

Method: Ten patients diagnosed with AIH were prospectively included in this study. Mononuclear cells isolated from liver tissue (using fine needle aspiration) obtained at diagnosis (M0) and at 6 months of treatment (M6) were analyzed by scRNAseq/scTCRseq (Chromium 5' protocol) and FC. Inflammation in baseline biopsy was evaluated using the modified activity index (mHAI). Complete biochemical response (CBR) was defined as normalization of ALT and IgG at M6.

Results: Most patients were women (n = 8, 80%), with a median age of 59 years. At M0 median ALT was 302 IU/L, IgG 17 g/L, and mHAI 7. Six patients reached M6, 3 of them in CBR. scRNAseq in liver tissue resulted in 35,509 single cells showing a great diversity of CD4⁺, CD8⁺, and myeloid lineage. By integrating scRNAseq and scTCRseq into liver cells, we observed an expansion of activated CD8⁺, tissue-resident memory CD8⁺ (TRM-CD8⁺), CD8⁺-NKT "like," and NK cells. Using FC, we confirmed a high frequency of TRM-CD8⁺, which significantly correlated with mHAI ($r_s = 0.72$; $p = 0.02$). In addition, central memory, and terminal effector memory CD8⁺ cells correlated with ALT levels ($r_s = 0.68$; $p = 0.04$; $r_s = -0.95$; $p < 0.01$, respectively). Patients who achieved CBR had a significantly lower frequency of NK cells and a higher frequency of macrophages than those without CBR ($p < 0.05$). At M6, we observed an expansion of CD4⁺ T cells, mainly regulatory T cells. In addition, there was a significant decrease in the frequency of TRM-CD8⁺ and naïve/transitional B cells and a significant increase in class-switched B cells by CF ($p < 0.05$). By analyzing the TCR repertoire, we observed a pronounced TCR diversity at M0, with a significantly higher proportion of hyper-

POSTER PRESENTATIONS

expanded clonotypes (100 >x ≤500) in CD8+ subpopulations, especially in patients without CBR. This percentage decreased at M6 in both groups.

Conclusion: CD8+ and NK cells seem to play an essential role in the pathogenesis of AIH and the regulation of the immune response. The diversity of TCR in M0 suggests that further expansion of self-reactive clones could hinder response to treatment. The increase in regulatory T cells might indicate partial recovery of immune homeostasis after treatment.

SAT-154-1Y

Studying cholangiocyte properties and functions using a bile duct on a chip

Henry Hoyle^{1,2,3,4}, Anna Katharina Frank^{1,2,3,4,5}, Mathias Busek^{3,6}, Aleksandra Aizenshtadt³, Fotios Sampaziotis^{7,8,9,10}, Tom Hemming Karlsen^{1,2,4,11}, Stefan Krauss^{3,6}, Espen Melum^{1,2,3,4,11}.
¹Norwegian PSC Research Center, Department of Transplantation Medicine, Division of Surgery, Inflammatory Diseases and Transplantation, Oslo University Hospital Rikshospitalet, Oslo, Norway; ²Research Institute of Internal Medicine, Division of Surgery, Inflammatory Diseases and Transplantation, Oslo University Hospital Rikshospitalet, Oslo, Norway; ³Hybrid Technology Hub, Institute of Basic Medical Science, University of Oslo, Oslo, Norway; ⁴Institute of Clinical Medicine, Faculty of Medicine, University of Oslo, Oslo, Norway; ⁵Scientia Fellowship, European Union's Horizon 2020 research and innovation program under the Marie Skłodowska-Curie grant agreement No 801133, Norway; ⁶Department of Immunology and Transfusion Medicine, Oslo University Hospital, Oslo, Norway; ⁷Wellcome Trust-Medical Research Council Cambridge Stem Cell Institute, Jeffrey Cheah Biomedical Centre, University of Cambridge, Cambridge, United Kingdom; ⁸Department of Surgery, University of Cambridge, Cambridge, United Kingdom; ⁹Department of Medicine, University of Cambridge, Cambridge, United Kingdom; ¹⁰Cambridge Liver Unit, Cambridge University Hospitals NHS Foundation Trust, Cambridge, United Kingdom; ¹¹Section of Gastroenterology, Department of Transplantation Medicine, Division of Surgery, Inflammatory Diseases and Transplantation, Oslo University Hospital Rikshospitalet, Oslo, Norway
Email: h.w.hoyle@medisin.uio.no

Background and aims: Studies of bile duct function and diseases are limited by a lack of effective experimental models with relevance to human physiology. Cholangiocyte organoids have become a powerful *in vitro* tool but suffer drawbacks such as lack of a tubular structure similar to the bile ducts and difficulties in accessing their apical interior. To address these shortcomings, we have created an *in vitro* bile duct on a chip model incorporating patient derived primary human cholangiocytes. This provides a platform for studies ranging from basic cholangiocyte biology to modelling aspects of bile duct diseases. We aimed to demonstrate that this model is effective and scalable in studies of biliary processes with direct relevance for human medicine.

Method: A collagen gel containing a hollow channel was formed within a 3D printed bile duct chip. Primary human cholangiocytes were derived from brushings during endoscopic retrograde cholangiopancreatography (ERCP) and propagated as organoids prior to being seeded as a single cell suspension into the channel. Cells were grown in the chip for approximately 7 days before reaching confluency, forming the bile duct epithelium. The properties of the bile duct on a chip system were investigated using confocal microscopy and biochemical assays. Functional properties of the cholangiocytes were also tested using transport assays, with drug treatments to investigate the impacts of transport inhibition.

Results: Human cholangiocytes formed a robust and well differentiated epithelial monolayer around the channel lumen with clear similarities to a human bile duct. A fluorescent-labeled dextran permeability assay demonstrated that the epithelial layer was effective in blocking passive diffusion of molecules of different sizes (3, 10, 40, 70 kDa). Using lipopolysaccharide (LPS) as an external

challenge relevant for inflammation we observed that the barrier was compromised. Staining for proteins such as actin, zonula occludens-1 (ZO-1) and multidrug resistance-associated protein 3 (MRP3) demonstrated a strong apical-basal cellular polarization and active transport of molecules across the epithelium was proven using the rhodamine 123 assay. This transport could be pharmacologically modulated using treatment with verapamil, inhibiting the multidrug resistance protein 1 (MDR1) transporter.

Conclusion: We have established a human and disease relevant bile duct on a chip using cholangiocyte organoids that is robust and scalable, and that can be readily created to study basic biology and disease pathways. When the model is challenged with addition of compounds such as bacterial components and drugs, robust and dynamic changes in the physiological properties were observed. This work paves the way for a completely new generation of future *in vitro* studies of the bile ducts that can probe deeper into disease-specific pathways and drug targets.

SAT-155

Impaired hepatic sympathetic neuronal communication intensifies hepatic inflammation, fibrosis and metabolic dysregulation, exacerbating liver injury

Sadam H. Bhat¹, Nupur Sharma¹, Csaba Adori², Anupama Kumari¹, Savneet Kaur¹, Babu Mathew¹, Ravinder Singh¹, Hami Hemati³, Adil Bhat⁴, Manisha Yadav¹, Gaurav Tripathi¹, Sushmita Pandey¹, Neha Sharma¹, Vasundhara Bindal¹, Abhishak Gupta¹, Roshan Koul¹, Viniyendra Pamecha¹, Nilesh Patil¹, Rakhi Maiwall¹, Tore Bengtsson⁵, Manoj Kumar¹, Jaswinder Maras¹, Shiv Kumar Sarin¹.
¹Institute of liver and biliary sciences, New Delhi, India; ²Karolinska Institute, Stockholm University, Stockholm, Sweden; ³University of Kentucky, Lexington, United States; ⁴University of California, Los Angeles, Los Angeles, United States; ⁵Stockholm University, Stockholm, Sweden
Email: sadam.m11@gmail.com

Background and aims: The predominant innervation within liver is sympathetic. It originates from T7 to T12 segments of the spinal cord and plays crucial role in regulating various liver functions, including metabolism and regeneration. Injury to sympathetic nerves effect these hepatic functions, although their specific roles in disease progression and the associated molecular pathways remained obscure. Our aim is to identify the molecular pathways that altered due to sympathetic neuronal damage and are associated with liver injury.

Method: Liver-specific sympathetic denervation (Sx) models were developed by intraportal injection of 6-OHDA hydrobromide in male Sprague Dawley rats, 8-10 weeks old. Four distinct groups were formed: GR-1 (Veh; n = 21), rats with intact nerves; GR-2 (Sx; n = 24), sympathectomized rats; GR-3 (Veh + BDL; n = 30), rats having intact hepatic sympathetic nerves with BDL; and GR-4 (Sx + BDL; n = 51), sympathectomized rats with BDL. Histological, confocal microscopy, serum AST/ALT, and proteomic analysis were conducted at baseline, Day-7 (D7), D15, and D30 for all groups.

Results: Liver-specific sympathectomy in GR-2 and GR-4 was validated through observable changes including urine coloration, ptosis, and absence of sympathetic nerves marker (tyrosine hydroxylase; TH) in the liver sections. At D7 and D15, GR-2 exhibited mild steatosis and inflammation, but no significant difference in AST and ALT levels compared to GR-1. Histologically, increased fibrosis and inflammation was observed in GR-4 versus GR-3 (p < 0.05). Remarkably, at D15, fibrosis in GR-4 resembled that in GR-3 at D30 (p < 0.05). GR-4 displayed elevated AST and ALT values versus GR-3 (p < 0.05). GR-3 exhibited progressive disorganization of sympathetic nerves correlating with fibrosis severity and inflammation. Hepatic adrenergic receptors and gap junction proteins showed a gradual decrease in gene expression in GR-4 (p < 0.05), suggesting an impaired hepatic neuronal communication. Hepatic proteome revealed a significant difference between groups. In GR2 vs GR-1, 127 were upregulated and 80 were downregulated and in GR-4 vs GR-

3, 462 were upregulated and 235 were downregulated. These differentially expressed proteins were involved in the activation of both fibrogenic (TNFR2, Wnt, FGF) and inflammatory (NLRP3, MAPK, PDGF) pathways ($p < 0.05$). Interestingly, we also observed a significant metabolic dysregulation with the upregulation of TCA cycle ($p < 0.05$) and downregulation of urea cycle ($p < 0.05$) not only in GR-4 vs GR-3 but also in GR-2 vs GR-1, suggesting the role of sympathetic fibers in metabolic regulation in both healthy and diseased liver.

Conclusion: Degeneration of sympathetic innervations may lead to impaired hepatic neuronal communication, which is associated with an increased liver inflammation, fibrosis, and metabolic dysregulation resulting in exacerbation of liver injury.

SAT-158

Machine learning-driven identification of serum protein signature for primary sclerosing cholangitis and enhanced liver fibrosis score

Tom Snir¹, Raanan Greenman¹, Avi Katav¹, Revital Aricha¹, Matthew Frankel¹, John Lawler¹, Francesca Saffioti², Douglas Thorburn³, Massimo Pinzani⁴, Ilan Vaknin¹, Adi Mor¹.
¹Chemomab, Tel Aviv, Israel; ²UCL Institute for Liver and Digestive Health, London, United Kingdom; ³The Sheila Sherlock Liver Centre, London, United Kingdom; ⁴University College London, London, United Kingdom
Email: tom.snir@chemomab.com

Background and aims: Primary sclerosing cholangitis (PSC) is a rare disease, lacking treatment and reliable prognostic biomarkers to assess changes in disease activity. Proximity extension assay (PEA) of sera allows for extensive profiling of patients' proteome, and when combined with machine learning based methods, enables for the discovery of markers of disease presence and severity. CM-101, a monoclonal antibody that neutralizes CCL24, was shown to be safe and active in early clinical trials and is currently tested in a PSC phase 2a clinical study. Here, we present a potential PSC protein signature that may monitor and assess drug activity in clinical trials.

Method: Sera from 30 healthy controls (HC) and 45 patients with PSC were profiled with PEA, quantifying the expression of 2870 proteins (Olink Explore), which are used to train a regularized regression model, accounting for feature abundance. An elastic net model was trained using a 10-fold repeated cross validation, and proteins that contributed most (by importance, averaged across 100 runs) to differentiate between HC or patients with PSC were then tested for their correlation (< 0.05 , FDR) with their underlying enhanced liver fibrosis (ELF) scores. This signature was then used for overrepresentation analysis to obtain biological pathways and functions. Receiver operating characteristic (ROC) curves were generated for each protein.

Results: Elastic net successfully predicted disease (accuracy 0.98, ± 0.2) while handling the relatively large number of variables. When combined with proteins correlated to ELF score, a ranked signature related both to disease presence and severity was apparent. The top-ranked proteins are associated with cell adhesion, immune response, and inflammation—all with area under receiver operator characteristic (AUROC) curves greater than 0.9 for disease presence and greater than 0.85 for ELF level (using a 9.8 threshold). Pathway analysis found that elastic fiber formation, cell adhesion, and extracellular matrix (ECM) organization was over-represented. Heatmaps showed successful unsupervised clustering of HC and patients with PSC with low or high ELF scores, with each individual protein showing a positive correlation to ELF score in patients with PSC.

Conclusion: A data driven, disease-agnostic approach characterizing PSC and its severity highlights potential serum protein biomarkers. The large proteomic data and the use of penalized regression points to a predictive protein signature associated with fibrosis, ECM, cell adhesion and migration. Notably, these functions were shown to be affected by CCL24 neutralization in clinical trials and pre-clinical models. These proteins will be monitored as markers for disease

activity in an ongoing clinical trial in PSC patients treated with CM-101.

SAT-159-YI

Mitochondrial integrity and auto (mito)phagy are disrupted in experimental models of primary biliary cholangitis, contributing to disease pathogenesis

Iruñe Lasa-Elosegi¹, Laura Izquierdo-Sánchez^{1,2}, Paula Olaizola^{1,2}, Ainhoa Lapitz^{1,2}, Luis Bujanda^{1,2,3}, Matxus Perugorria^{1,2,3}, Pedro M. Rodrigues^{1,2,4}, Jesus Maria Banales^{1,2,4,5}. ¹Department of Liver and Gastrointestinal Diseases, Biogipuzka Health Research Institute-Donostia University Hospital - University of the Basque Country (UPV/EHU), San Sebastian, Spain; ²National Institute for the Study of Liver and Gastrointestinal Diseases (CIBERehd, "Instituto de Salud Carlos III"), Madrid, Spain; ³Departments of Medicine, Faculty of Medicine and Nursing, University of the Basque Country UPV/EHU, Donostia-San Sebastian, Spain; ⁴IKERBASQUE, Basque Foundation for Science, Bilbao, Spain; ⁵Department of Biochemistry and Genetics, School of Sciences, University of Navarra, Pamplona, Spain
Email: irune.lasaelosegui@biodonostia.org

Background and aims: Primary biliary cholangitis (PBC) is a chronic cholestatic and immune-mediated liver disease of unknown origin. Our prior research revealed an increased expression of microRNA-506 (miR-506) in PBC cholangiocytes, targeting the Cl⁻/HCO₃⁻ exchanger AE2. This leads to intracellular pH (pHi) disturbances and PBC-like features, including PDC-E2 overexpression and immune activation. Autophagy, and particularly mitophagy, is a crucial cell-intrinsic, quality-control and anti-inflammatory mechanism designed to eliminate dysfunctional organelles, such as mitochondria. Although these processes are critically dependent on pHi, their role in PBC remains unknown. Our aim was to characterize the mitochondrial dynamics and auto (mito)phagy processes in PBC and evaluate their contribution to disease pathogenesis.

Method: Experimental *in vitro* PBC models, including miR-506-overexpressing cholangiocytes (H69 miR-506) and control cells (H69 miR- and H69), were subjected to high-throughput proteomic analysis. Additionally, these cells were assessed for mitochondrial dynamics, integrity, activity, auto (mito)phagy, and cell viability under baseline conditions and in the presence of various anti-cholestatic drugs.

Results: High-throughput proteomics revealed significant alterations in several proteins related to mitochondrial dynamics and autophagy/mitophagy in H69 miR-506 cholangiocytes compared to control cells. Notably, gene-set enrichment analysis (GSEA) indicated a stronger association of processes related to antigen presentation, inflammation, and mitochondrial organization and translation in H69 miR-506 cells. Specifically, genes involved in mitochondrial fusion (linked to increased functionality) were downregulated, while a gene related to mitochondrial biogenesis (associated with *de novo* mitochondrial generation) was upregulated. These changes were accompanied by decreased mitochondrial functionality, as measured by flow cytometry, indicating an accumulation of defective mitochondria and impaired mitophagy. Consistently, the presence of auto (mito)phagy inhibitors potentiated toxic bile acid-induced cell death, particularly in miR-506 cells. Importantly, incubation of H69 miR-506 cholangiocytes with ursodeoxycholic acid (UDCA), obeticholic acid (OCA), or bezafibrate (BZF) improved mitochondrial functionality and energy metabolism, normalizing the overexpression of PDC-E2.

Conclusion: Our findings suggest that cholangiocytes in PBC exhibit disruptions in mitochondrial integrity and auto (mito)phagy, resulting in the accumulation of dysfunctional mitochondria and abnormal presentation of mitochondrial antigens. Current anti-cholestatic and anti-fibrotic drugs used in PBC can modulate these mitochondrial disturbances, emphasizing that the regulation of mitophagy represents a novel target in PBC.

SAT-160

Lysophosphatidic acid (LPA)-receptors, a group of established itch receptors, show elevated agonism during cholestasis and are likely to contribute to cholestasis-associated itch

Frank Wolters¹, Dagmar Tolenaars¹, Michel van Weeghel², Rudi de Waart³, Stan van de Graaf¹, Coen Paulusma¹, Ulrich Beuers¹, Ronald Oude-Elferink¹. ¹Tytgat Institute for Liver and Intestinal Research, Amsterdam Gastroenterology Endocrinology Metabolism (AGEM), Amsterdam UMC, Amsterdam, Netherlands; ²Core Facility Metabolomics, Amsterdam UMC, Amsterdam, Netherlands; ³Tytgat Institute for Liver and Intestinal Research, Amsterdam Gastroenterology Endocrinology Metabolism (AGEM), Amsterdam UMC, Amsterdam, Netherlands
Email: f.wolters@amsterdamumc.nl

Background and aims: The etiology of cholestasis-associated pruritus is poorly understood, resulting in suboptimal treatment. The search for itch factors continues, but is hindered by a lack of molecular understanding of the involved itch receptors in this form of pruritus. Recently, we showed that a panel of established itch receptors (TRPA1, TRPV1, TRPV3, TRPV4 and MRGPRX4) poorly respond to bile salts, bilirubin and patient serum and plasma, questioning their direct involvement in itch (Wolters *et al.*, manuscript in preparation). Based on our previous observations that the activity of the lysophosphatidic acid (LPA)-forming enzyme autotaxin correlates with pruritus intensity in cholestasis (PMID: 20546739), we studied which LPA-receptors as established itch receptors are activated due to elevated patient plasma autotaxin activity.

Method: LPAR-TANGO constructs were obtained from the Presto-TANGO library. LPA-receptor activation by patient plasma was quantified by means of dual-luciferase assays in HEK293-HTLA cells. LPA species and concentrations were identified and quantified by means of HPLC-MS in 45 cholestatic patient samples and in 15 healthy controls.

Results: HEK293-HTLA cells, transfected with LPAR-TANGO constructs, showed significantly higher activation upon incubation with patient plasma compared to healthy controls. This activation could be abrogated by the autotaxin inhibitor HA155. Particularly strong activation was observed with LPAR2. The extent of LPAR receptor activation significantly correlated with pruritus intensity in patients ($p = 0.0004$) and with their plasma autotaxin activity ($p = 0.0026$). HPLC-MS analysis showed elevated levels of LPA in patients. Particularly LPA 20:4 levels showed significant correlation with pruritus intensity ($p = 0.0099$).

Conclusion: Unlike the other investigated receptors, LPA receptors show marked activation by cholestatic patient plasma compared to healthy controls. The significant correlation between autotaxin, levels of its product, LPA, and the extent of in situ LPA receptor activation on the one side and itch severity on the other strongly suggests that LPA is a dominant pruritogen in cholestatic itch with LPA 20:4 as the most potent LPA species. Hence, the LPA-receptors, and particularly LPAR2, are likely to be involved in the generation of cholestasis-associated pruritus. The autotaxin-LPA receptor pathway is a promising target for treatment of cholestasis-associated pruritus.

SAT-161

Inhibition of bile acid conjugation improves DDC-induced cholestatic liver injury in mice with a humanized bile acid pool

Claudia Fuchs^{1,2}, Oleksandr Petrenko^{1,3,4,5}, Veronika Mlitz^{1,2}, Hubert Scharnagl⁶, Tatjana Stojakovic⁷, Thomas Reiberger^{1,3,4,5}, Benjamin Garfinkel⁸, Michael Trauner^{1,2}. ¹Division of Gastroenterology and Hepatology, Department of Internal Medicine III, Medical University of Vienna, Vienna, Austria; ²Hans Popper Laboratory of Molecular Hepatology, Division of Gastroenterology and Hepatology, Department of Internal Medicine III, Medical University of Vienna, Vienna, Austria; ³Vienna Experimental Hepatic Hemodynamic Lab (HEPEX), Division of Gastroenterology and Hepatology, Department of Internal Medicine III, Medical University of Vienna, Vienna, Austria; ⁴Christian Doppler

Laboratory for Portal Hypertension and Liver Fibrosis, Medical University of Vienna, Vienna, Austria; ⁵CeMM Research Center for Molecular Medicine of the Austrian Academy of Sciences, Vienna, Austria; ⁶Clinical Institute of Medical and Chemical Laboratory Diagnostics, Medical University of Graz, Graz, Austria; ⁷Clinical Institute of Medical and Chemical Laboratory Diagnostics, University Hospital Graz, Graz, Austria; ⁸Alnylam Pharmaceutical Inc., Cambridge, MA, United States
Email: claudia.fuchs@meduniwien.ac.at

Background and aims: In cholestasis, intrahepatic accumulation of bile acids (BAs) results in liver and bile duct injury. We hypothesized that inhibition of BA conjugation, subsequently increasing levels of non-amidated BAs in the BA pool and changing BA composition, may induce bile flow, thus improving cholestatic liver and bile duct injury. **Method:** Male FVB/N mice received 3, 5-diethoxycarbonyl-1, 4-dihydrocollidine (DDC) over 4 weeks to induce sclerosing cholangitis-like phenotype/injury and cholestasis with/without siRNA treatment to silence Cyp2c70 (siCyp2c70) to humanize the BA pool. DDC-fed mice with/without siCyp2c70 were treated with siRNA to inhibit BACL (siBACL) and subsequently BA conjugation. Liver injury was assessed biochemically and by (immuno)histology. Bile flow measurements, BA profiling from serum and bile as well as biliary glutathione levels, hepatic hydroxyproline content were also investigated. RNA sequencing from bulk liver tissue as well as mRNA profiling by RT-PCR and immunoblotting were performed.

Results: Silencing BACL in mice challenged with DDC and siCyp2c70 (WT DDC siCyp2c70+siBACL), improved biochemical and histological features of liver and bile duct injury. CK19 and VCAM protein levels-as surrogate markers for reactive cholangiocytes-were significantly reduced by siBACL treatment by 60% and 80%, respectively. Hepatic fibrosis was improved in DDC siCyp2c70+siBACL in comparison to DDC siCyp2c70 controls as reflected by reduction of hydroxyproline levels by 50%. Accordingly, RNA sequencing revealed significant downregulation of fibrosis markers (e.g. Col12e1, Col14a1, Col4a2, Fbn1). Moreover, RNA sequencing showed increased levels of GSTa1, GSTa3, GSTa5, GSTm2 and GSTm3 (all involved in ROS detoxification) among the top upregulated genes in the DDC siCyp2c70+siBACL group. siBACL treatment reduced biliary levels of conjugated BAs (90% in DDC siCyp2c70 vs 50% in DDC siCyp2c70+siBACL mice), with cholic acid being the most prominent unconjugated BA in DDC siCyp2c70 +siBACL animals, that demonstrate a 2-fold and 4-fold increase in bile flow and biliary glutathione output, respectively.

Conclusion: Our data indicate that inhibition of BA conjugation improves liver and bile duct injury, presumably by increasing bile flow and biliary glutathione levels and by reducing oxidative stress.

SAT-163-YI

Spatial characteristics of cell compartments in primary sclerosing cholangitis

Markus S. Jørdens^{1,2,3,4}, Jonas Øgaard^{1,2}, Tom Luedde⁴, Tom Hemming Karlsen^{1,2,3,5}, Brian K. Chung^{1,2,3,6}, Espen Melum^{1,2,3,5,7}. ¹Norwegian PSC Research Center, Oslo University Hospital and Institute of Clinical Medicine, University of Oslo, Oslo, Norway; ²Research Institute of Internal Medicine, Oslo University Hospital, Rikshospitalet, Oslo, Norway; ³Institute of Clinical Medicine, University of Oslo, Oslo, Norway; ⁴Department of Gastroenterology, Hepatology and Infectious Diseases, Medical Faculty, Heinrich Heine University Düsseldorf, University Hospital Düsseldorf, Düsseldorf, Germany; ⁵Section for Gastroenterology, Department of Transplantation Medicine, Division of Surgery, Inflammatory Diseases and Transplantation, Oslo University Hospital, Rikshospitalet, Oslo, Norway; ⁶Research Institute of Internal Medicine, NoPSC Research Center, Oslo, Norway; ⁷Hybrid Technology Hub-Centre of Excellence, Institute of Basic Medical Sciences, Faculty of Medicine, University of Oslo, Oslo, Norway
Email: markus.joerdens@med.uni-duesseldorf.de

Background and aims: Primary sclerosing cholangitis (PSC) is characterized by peribiliary immune infiltration and cholangiocyte destruction. To detect disease driving interactions between immune

cells and cholangiocytes that may represent novel treatment targets, we analyzed explanted early non-fibrotic and late end-stage cirrhotic livers using spatial transcriptomics.

Method: Fresh frozen liver explants (n = 28) were analyzed by spatial transcriptomics (10x Genomics), including 21 PSC patients (4 recurrent cholangitis and no fibrosis, 7 dysplasia and no fibrosis and 10 cirrhosis) and 7 non-PSC controls with advanced cirrhosis. Sequencing data were analyzed by SpaceRanger and unsupervised K-means clustering was performed using Loupe Browser (10x Genomics). Statistical significance for differential gene expression (DEG) analysis was calculated using the exact negative binomial test. All stated DEG have a p value <0.01 (Benjamini-Hochberg corrected). Relative cell abundances were estimated from spatial transcriptomes using a public human liver single cell reference and CIBERSORTx deconvolution analyses.

Results: Clustering analysis identified two parenchymal clusters and two fibrotic clusters closely correlating with tissue morphology visualized by HE staining. Independent of disease, DEG analysis revealed a hepatocyte-dominated profile for the central parenchymal cluster (*ALB*, *APOC1*, *HP*) whereas the parenchymal cluster adjacent to fibrosis showed upregulation of several inflammatory markers (*SAA1*, *SAA2*, *CRP*) compared to the other clusters. Both fibrotic clusters showed a significant increase in inflammatory markers (*S100A6*, *TIMP1*, *CCL19*, *IGHG1*, *CD74*, *HLA-DRA*) relative to parenchymal clusters. Cell type abundances identified mainly hepatocytes and cholangiocytes within the central parenchymal cluster, whereas the parenchymal cluster adjacent to the fibrotic tissue showed immune infiltration dominated by monocytes and pDCs. Fibrotic regions adjacent to the parenchyma contained mesenchymal and endothelial cells, monocytes and ILCs, with the majority of B and T cells localized within the central fibrotic cluster. When comparing PSC and controls, both parenchymal PSC clusters showed higher expression of oxidative stress markers (*MT1H*, *MT1G*) or immune regulation/response (*HLA-DRB5*, *HLA-DRB1*, *FOXP3*, *CCL18*). In fibrotic clusters, PSC samples also showed increased markers of chronic inflammation (*SAA1*, *SAA2*), oxidative stress (*MT1H*, *MT1G*) and immune activation (*THY1*, *CXCL8*, *CCL16*).

Conclusion: Diseased PSC livers have distinct gene expression patterns in both fibrotic and non-fibrotic tissues. Gene expression profiling and cell type deconvolution indicate specific upregulation of inflammatory markers in clusters adjacent to fibrotic areas, highlighting a diverse cellular landscape within different liver tissue compartments.

SAT-164-YI

Mice lacking the NO receptor develop primary sclerosing cholangitis

Muhammad Ashfaq-Khan¹, Cornelius Caesar¹, Andreas Friebe¹.

¹Physiologisches Institut, Würzburg, Germany

Email: m.ashfaq_biotech@yahoo.com

Background and aims: Primary sclerosing cholangitis (PSC) is a form of cholestatic liver disease that finally leads to biliary cirrhosis. Lack of full understanding of mechanistic drivers of chronic liver disease in general and of PSC in particular hamper the development of innovative treatment strategies. In the present study, we have characterized the role of the NO receptor, NO-sensitive guanylyl cyclase (NO-GC).

Method: 8–10-week-old male mice carrying a global deletion of NO-GC and their wildtype siblings (C57BL/6J background) were fed control diet and Western diet (21% fat, 0.2% cholesterol) and 42 g/l fructose in drinking water for 16 weeks. Thereafter, mice were sacrificed, and liver tissues were fixed in paraformaldehyde for histological evaluation to assess the rate of disease progression. Analyses included HE, Sirius red staining, immunofluorescence, and confocal microscopy.

Results: In contrast to wildtype siblings, NO-GC knock mice on control diet had altered ductular architecture of the biliary system

and increased ductular proliferation (between PSC stage 1 and stage 2) which worsened on Western diet (≥stage 2). Compared to the WT mice on control diet, fibrosis stage in NO-GC KO mice had increased significantly (p = 0.0001) which enhanced two-fold upon feeding Western diet. In addition, cytokeratin 19 was upregulated significantly in NO-GC KO mice both on control diet (p = 0.0179) and on Western diet (p = 0.0227) vs WT mice. Moreover, α-SMA expression was increased in NO-GC KO mice compared to mice on control diet. Furthermore, CD3, CD4 and CD8 expression was increased significantly in NO-GC KO mice on control diet which had upregulated in NO-GC KO mice fed on Western diet. MASLD-related events under Western diet were obvious in WT but absent in NO-GC KO mice.

Conclusion: Deletion of the NO receptor in mice led to spontaneous primary sclerosing cholangitis and biliary fibrosis. The PSC phenotype worsened upon feeding Western diet. Thus, we identify a so far unknown role of NO-GC in primary sclerosing cholangitis.

SAT-165-YI

Impaired muscle metabolism during exercise is associated with elevated IL-6 in PBC patients with fatigue: is this a new therapeutic target?

Aaron Wetten^{1,2}, Laura Jopson², Amardeep Khanna^{1,2}, Denise Howel³, Andy Bryant³, Andrew Blamire², Julia Newton², Jennifer Wilkinson⁴, Alison Steel⁵, Jennifer Bainbridge¹, Renae Stefanetti⁶, Sophie Cassidy⁶, David Houghton⁶, Jessica Dyson^{1,2}, David E. Jones^{1,2}. ¹Newcastle upon Tyne Hospitals NHS Foundation Trust, Newcastle, United Kingdom;

²Institute of Cellular Medicine, Newcastle University, Newcastle, United Kingdom;

³Institute of Health and Society, Newcastle University, Newcastle, United Kingdom;

⁴Clinical Trials Unit, Newcastle University, Newcastle, United Kingdom;

⁵Newcastle Clinical Trials Unit, Newcastle University, Newcastle, United Kingdom;

⁶Institute of Neuroscience, Newcastle University, Newcastle, United Kingdom

Email: aaron.wetten@nhs.net

Background and aims: Primary Biliary Cholangitis (PBC) is progressive autoimmune cholestatic liver disease. Significant peripheral fatigue affects over 50% of PBC patients, and has the greatest impact on functional status, leading to social isolation and worsening quality of life. Muscle fatigability and mitochondrial dysfunction have been demonstrated in PBC, but mechanisms are poorly understood and there is no effective treatment. Interleukin-6 (IL-6) has a significant role in muscle metabolism during exercise, whilst chronically elevated IL-6 has been implicated in skeletal muscle fatigability and mitochondrial dysfunction. This study explored the association between serum IL-6 and muscle metabolism in a cohort of PBC patients with significant peripheral fatigue.

Method: Forty-one participants enrolled in the phase 2 Rituximab as a treatment for fatigue in PBC (RITPBC) trial had serum IL-6 levels measured using electrochemiluminescence immunoassays. They completed two 180 s cycles of controlled plantar flexion at 25% and then 35% maximal voluntary contractions, using purpose-built exercise apparatus. Muscle metabolism was recorded by phosphorous spectra via novel magnetic resonance spectroscopy. Anaerobic thresholds (AT), the point at which muscles switch from aerobic to anaerobic metabolism, were measured using integrated cardiopulmonary exercise testing on a stationary ergometer.

Results: A positive correlation was observed between serum IL-6 and total pH fall (increased acidosis) during all exercise and as well as recovery time (return to baseline pH), as assessed by area under the curve (AUC) [0.340, CI 95% 0.031–0.590, p = 0.027]. A greater fall in pH with individual exercise (increased acidosis) was observed in those with higher serum IL-6 levels [0.324, CI 95% 0.01–0.578, p = 0.036]. Overall, the lower the pH during exercise the longer the pH recovery time [–0.522, CI 95% –0.719––2.46, p < 0.01]. A higher baseline pH correlated with a superior AT threshold [0.443, CI 95% 0.148–0.666, p = 0.004], but no correlation between serum IL-6 levels and AT was observed.

POSTER PRESENTATIONS

Conclusion: Impaired muscle metabolism, exhibited by increased muscle acidosis during exercise, was observed in patients with elevated serum IL-6. This translated across all exercise periods, with increased falls in pH (increased muscle acidosis) and extended recovery times to baseline pH (resolving muscle acidosis) after exercise occurring in patients with higher IL-6 levels. This suggests chronic IL-6 elevation may play a pivotal role in PBC peripheral fatigue. IL-6 blockade therapies significantly improve fatigue in other chronic inflammatory conditions and may present a new therapeutic strategy for fatigue in PBC.

SAT-166

Functional relevance of CD44 for hepatocyte proliferation in diet-induced liver injury models

Sophia Bernatik¹, Franziska Ihli¹, Kohnke-Ertel Birgit¹, Fabian Delugre¹, Carolin Mogler², Fabian Geisler¹, Roland M. Schmid¹, Ursula Ehmer¹. ¹Clinical Department for Internal Medicine II, TUM School of Medicine and Health, University Medical Center, Technical University of Munich, Munich, Germany; ²Institute of Pathology and Unit of Comparative Experimental Pathology, Klinikum rechts der Isar, Technische Universität München, Munich, Germany
Email: ge54key@mytum.de

Background and aims: The cellular adhesion molecule CD44 has been linked to liver regeneration and fibrosis development. In animal models of cholestatic liver injury, high expression of CD44 is observed in ductular reactions (DR) around the portal triad, while in acute, diet-induced hepatocyte injury, expression of CD44 is strongly increased in hepatocytes. To date, the functional relevance of CD44 for regeneration in different liver injury models is unknown.

Method: Acute hepatocyte injury was induced by choline-deficient and ethionine-supplemented (CDE), while the 3, 5-diethoxycarbonyl-1, 4-dihydrocollidine (DDC) diet was utilized to specifically cause damage to intrahepatic bile ducts in male *Cd44*^{-/-} (KO) mice and age-matched C57BL/6J control mice. As a model of a chronic liver injury, *Mdr2*^{-/-}; *Cd44*^{-/-} mice and age-matched *Mdr2*^{-/-} control mice were used. Livers were analyzed at different time points by liver immunohistopathology for expression of CD44 and the proliferation marker Ki67.

Results: In acute hepatocyte injury induced by 3 weeks of CDE diet, CD44-deficient mice comprised a significantly lower number of proliferating cells (Ki67+) in the liver (23.11% vs 14.73% *p* = 0.0434) with a dramatic decrease of hepatocyte proliferation (18.56% vs 6.927% *p* = 0.0175). Similarly, hepatocyte proliferation decreased after 2 weeks of DDC diet in CD44-deficient mice (30.51% vs 9.94% *p* = 0.0176). Even though CD44 in acute cholestatic liver injury (DDC diet) was highly expressed in DR, no difference in ductular proliferation was observed in *Cd44*^{-/-} mice in comparison to controls. In contrast, chronic cholestatic injury in *Mdr2*^{-/-} mice was associated with proliferation of DR and almost no proliferation in hepatocytes. Here, a significant difference in proliferation between *Mdr2*^{-/-}; *Cd44*^{-/-} and *Mdr2*^{-/-} was observed after 3 months (39% vs 18.20% *p* = 0.0421) with no difference in hepatocyte proliferation.

Conclusion: Our study utilized two well-established dietary models and a genetic model of chronic cholestasis to assess the functional role of CD44 in acute and chronic liver damage. In acute liver damage, high expression of CD44 correlates with proliferation in hepatocytes but not in DR, while CD44-deficiency in chronic cholestatic injury influences proliferation also in periportal DR. These findings highlight the cell type-specific and possibly injury-dependent role of CD44 in liver regeneration and further research will be needed to identify the differential cellular mechanisms mediating CD44-dependent cell proliferation.

SAT-167-YI

Generation and utilisation of an advanced iPSC-derived hepatocyte model for cholestasis modelling

Elena Garitta¹, Adam Syanda², Cyril Lemerle³, James Boot¹, Jemima Burden³, Chris Stefan³, Richard J. Thompson⁴, Kenneth Linton¹, Tamir Rashid². ¹Queen Mary University of London, London, United Kingdom; ²Imperial College London, London, United Kingdom; ³University College London, London, United Kingdom; ⁴Kings College London, London, United Kingdom
Email: e.garitta@qmul.ac.uk

Background and aims: Cholestasis is a pathology of the liver characterised by impaired bile formation and flow. It can be caused by genetic mutations in canalicular transporters ABCB11 (BSEP), ABCB4 or ATP8B1, or by drugs. Drug-induced cholestasis (DIC) can be life threatening and often results in clinical trial failures or withdrawal of licenced drugs. Our inability to faithfully replicate human cholestasis with current pre-clinical models limits our mechanistic understanding of this disease and accordingly restricts our ability to identify DIC-causing drugs before they reach patients. These gaps are largely due to species specific differences in composition of human and rodent bile acid pools that reduce disease penetrance in murine models and the rapid loss of bile production seen with primary human hepatocyte ex vivo culture. Patient derived iPSC-human hepatocytes (iHEPs) and advanced ex vivo culture techniques offer a potential solution to these problems. Indeed, recent advances with iHEP technology have resulted in an ability to phenocopy key features of metabolic and virally mediated pathology. To date however, there has been less success in generating iHEPs with functional bile canaliculi (BC) and canalicular transporters as is critical for modelling cholestasis. This study accordingly aimed to overcome this roadblock by developing iHEPs which are multipolar, possess functional canalicular transporters and could model DIC.

Method: iPSCs underwent an optimised 25-day hepatocyte differentiation protocol. DIC was induced with bosentan, a BSEP inhibitor, or by feeding excess chenodeoxycholic acid for 6 days. Functional, immunological and gene expression assays, along with confocal and transmission electron microscopy (TEM), were employed to validate iHEP physiology and characterise the induced cholestatic phenotype.

Results: The new differentiation cocktail in combination with an ECM sandwich-culture significantly improved the hepatocyte functionality, polarisation, and ultrastructural phenotype of iHEPs. BC expressed canalicular ABC transporters, were sealed by junctional complexes and developed a brush border, closely resembling normal liver tissue. BC functionality was confirmed by active excretion of a fluorescent MRP2 substrate into the canalicular lumen. DIC caused by BSEP inhibition and bile acid overload demonstrated changes in BC and mitochondrial morphology and ultrastructure, such as canalicular dilatation and curling of mitochondrial cristae, as seen in patient tissue samples, as well as mitochondrial dysfunction, ER stress and the secretion of inflammatory cytokines.

Conclusion: Our new iHEP model provides a more physiologically relevant platform for human cholestasis modelling, offering insights into disease mechanisms and facilitating screening of compounds that cause DIC.

SAT-170

Establishing a cholangioid library for biliary niche-on-a-chip multicellular models for the study of liver disease-associated ductular reaction

Tian Lan^{1,2}, Natalia Martagón Calderón¹, Guo Yin¹, Hanyang Liu¹, Queeny Okechukwu¹, Milad Rezvani¹, Frank Tacke¹, Adrien Guillot¹. ¹Charité Universitätsmedizin Berlin, Berlin, Germany; ²West China Hospital, Sichuan University, Chengdu, China
Email: tian.lan@charite.de

Background and aims: Ductular reaction (DR) that includes ductular cell and macrophage accumulation is a disease progression hallmark

in virtually all chronic liver conditions. Hence, ductular cells are proposed as disease progression drivers. Yet, optimal models for functional studies of ductular cell biology are still lacking. We aim to evaluate the direct influence of ductular cells on liver macrophage activation. For this purpose, we generated a library of mouse intrahepatic cholangioids (mICO) from healthy and DR mouse models, and established a biliary niche-on-a-chip (BoC) as an *in vitro* perfusable multicellular system.

Method: Intrahepatic cholangiocytes were isolated from wild-type and Mdr2-deficient (KO) mice by magnetic-activated cell sorting and expanded to generate 3-dimensional mICO. Quantitative RT-PCR (qPCR) and immunostaining were performed to confirm cell identity and functionality. Dissociated WT and KO mICO were seeded into the BoC together with mouse primary hepatic stellate cells, endothelial cells, and hepatic macrophages. The BoC system was perfused with freshly isolated blood circulating immune cells.

Results: Both WT and KO mICO expressed the biliary markers CK19, CK7, and acetylated tubulin (the marker of primary cilium). KO mICO showed distinct features when compared to WT mICO, notably increased proliferation (PCNA staining) and expression of chemokines (*Cxcl1*, *Ccl2*), bile acid transporters and receptors (*Gpbar1*, *Slc10a2*, *Slc51a*), and bicarbonate secretion-related genes (*Cftr*, *Aqp1*). KO mICO also showed decreased stemness (*Sox9*, *Lgr5*, *Tpm2*), and altered chemo/osmosensing function of the primary cilium (*Trpv4*, *P2ry12*). mICO reversed their polarity and turned to apical-out cholangioid (AOO) when cultured in suspension, as showed by staining of polarity markers such as ZO-1 and beta-catenin. Both WT-AOO and KO-AOO exposed their apical side for potential further treatment and were more proliferative than corresponding mICOs. Mouse primary liver macrophages treated with conditioned medium from WT mICO showed increased expression of *Il1a*, *Il1b*, *Il6*, *Il10*, *Ccl2*, *Inos*. This effect was further enhanced when macrophages were cultured with conditioned medium from KO mICO. Cholangiocytes were successfully seeded into the BoC, and perfused immune cells were effectively recruited to the layer of liver parenchymal cells, mimicking the pathobiological processes observed in DR.

Conclusion: The mICO, AOO, and BoC are promising *in vitro* models for understanding the cell phenotype changes and cellular crosstalk within the biliary niche during DR. Our data shows drastic differences in the steady-state phenotype of WT and KO ductular cells, including their metabolic adaptability and their potential to induce immune cell response. Ongoing efforts aim at further dissecting the molecular pathways involved and to develop comparable human cell-based systems.

SAT-171

Advancements in liver biopsy analysis: convolutional neural networks for portal tract segmentation

Giorgio Cazzaniga¹, Vincenzo L'Imperio¹, Nicola Zucchini¹, Laura Cristofari^{2,3}, Fabio Pagni¹, Pietro Invernizzi^{2,3}, Marco Carbone^{3,4}, Alessio Gerussi^{2,3}. ¹Department of Medicine and Surgery, Pathology, Fondazione IRCCS San Gerardo dei Tintori, University of Milan-Bicocca, Monza, Italy; ²Center for Autoimmune Liver Diseases, Department of Medicine and Surgery, University of Milano-Bicocca, Monza, Italy; ³European Reference Network on Hepatological Diseases (ERN RARE-LIVER), Division of Gastroenterology, Fondazione IRCCS San Gerardo dei Tintori, Monza, Italy; ⁴Hepatology and Gastroenterology Unit, ASST Grande Ospedale Metropolitano Niguarda, Milano, Italy
Email: giorgio9cazzaniga@gmail.com

Background and aims: Detection and evaluation of portal tracts (PT) in liver biopsy play a crucial role in the diagnostic process of liver diseases. Lack of standardized definitions and high inter-observer variability hamper current diagnostic protocols. Artificial intelligence (AI) tools can streamline the histological examination assisting pathologists in time-consuming and highly operator-dependent tasks. In our study, we investigated an AI-driven automatic

identification and segmentation of PT, with the aim of automating and standardizing the process.

Method: Our study utilized a dataset of 94 hematoxylin and eosin stained liver biopsies from the European Reference Network on Hepatological Diseases (ERN RARE-LIVER) center at Fondazione IRCCS San Gerardo dei Tintori, Monza, Italy, including several liver diseases to capture a broad phenotypic landscape of liver pathology. These biopsies, collected during 2021–2022, were annotated by a pathologist using a standardized definition for PT. We trained an Attention UNet, a semantic segmentation model, for automatic identification and segmentation of PT. The training involved analyzing 256px image tiles extracted at 5×, 10×, and 20× magnifications. For the model test, we used a distinct 2023 cohort comprising 12 cases including autoimmune hepatitis (AIH), primary biliary cholangitis (PBC), primary sclerosing cholangitis (PSC), and cases of metabolic dysfunction-associated steatohepatitis (MASH). Performance metrics were recorded to evaluate their ability to binary segment classify the biopsy samples into PT and non-PT regions.

Results: The model trained with image tiles at 20x magnification, which included 1,691 tiles for training, 188 for development, and 838 for testing, demonstrated superior performance and scalability. This was evident from key metrics on the test set, such as Intersection over Union (IoU), dice coefficient, accuracy, precision, recall, and F1 score, which were 0.87, 0.71, 0.94, 0.77, 0.70, and 0.71, respectively. These metrics outperformed those of models trained with 10× and 5× magnification tiles, which had IoUs of 0.84 and 0.56, respectively. Moreover, the ability to piece together these tiles allowed for the reconstruction of the original virtual slide, complete with annotations for all PT at the whole-slide image (WSI) level, ready for diagnostic routine use and morphometric features extraction.

Conclusion: This study demonstrates high performances in distinguishing and segmenting PT, especially when the model is fed with very close detail of liver tissue, offering a preoperative, objective evaluation of sample adequacy, enhancing workflow efficiency, and shortening diagnostic timelines. Additionally, this technique may prove highly beneficial in understanding disease mechanisms, as it efficiently extracts crucial morphometric data from histologic samples.

SAT-173-YI

TAZ and YAP play an interdependent role in biliary development and adaptation to cholestasis

Adelya Gabdulkhakova¹, Yekaterina Krutsenko², Satdarshan Monga^{2,3}, Laura Molina². ¹Heidelberg University Hospital, Heidelberg, Germany; ²University of Pittsburgh School of Medicine, Pittsburgh, United States; ³Pittsburgh Liver Research Center, University of Pittsburgh Medical Center, Pittsburgh, United States
Email: adelya.gabdulkhakova@med.uni-heidelberg.de

Background and aims: Most young patients with bile duct disorders such as progressive familial intrahepatic cholestasis (PFIC), biliary atresia, Alagille syndrome, and others, will require a liver transplant. Understanding the pathogenesis of cholangiopathies and liver adaptation mechanisms to biliary injury is crucial. We previously showed that deletion of yes-associated protein 1 (YAP) in early liver development leads to Alagille syndrome-like phenotype. YAP^{KO} mice were born without intrahepatic biliary tree and exhibited severe cholestasis. A paralog of YAP, TAZ, was significantly overexpressed in YAP^{KO} hepatocytes and interacted with TEAD transcription factors, suggesting possible compensatory activity. In this study we aimed to investigate the relationship between TAZ and YAP and their role in biliary development and cholestasis.

Method: Both Yap1 and Wwtr1 (a gene encoding TAZ) were knocked out in mice during early liver development by employing the Foxa3 promoter to drive Cre expression, resulting in diverse combination of alleles. Littermates were used as wild-type controls. We analysed these mice at stages of embryos (E17.5), new-borns (postnatal days

POSTER PRESENTATIONS

1–2), and adults (at the age of 3 weeks and 3–4 months) by immunohistochemistry, immunoprecipitation, western blotting, serum biochemistry, bile acid profiling, and RNA sequencing.

Results: YAP/TAZ double knockout mice were not viable and embryonic lethal. Their livers appeared grossly normal but had no intrahepatic bile ducts. We observed a 50% decrease in the expected birthrate of YAP^{KO} with TAZ heterozygosity (YAP^{KO}TAZ^{HET}) mice. While male YAP^{KO}TAZ^{HET} mice were also embryonic/perinatally lethal, YAP^{KO}TAZ^{HET} females survived and exhibited pronounced cholestasis. In response, their livers adapted by bile transport reversal and changes in the composition of bile acids to enhance hydrophilicity. Liver transaminases were more elevated in YAP^{KO}TAZ^{HET} mice, compared to YAP^{KO} mice, suggesting worsened hepatocyte injury. TAZ heterozygosity impacted the expression of canonical YAP targets *Ctgf* and *Cyr61*. Alterations in gene expression resulting from partial TAZ loss were found to align with immunohistochemical findings, which included enhanced inflammatory signalling, cell cycling, apoptosis, and increased macrophage infiltration.

Conclusion: Biliary development is aborted without YAP (both in presence and absence of TAZ). Our results point to the unique roles of TAZ in liver injury repair. TAZ is implicated in regulating key YAP targets and in the setting of YAP loss, TAZ contributes to hepatocyte adaptation to chronic cholestasis through promoting cell survival and dampening macrophage recruitment. Together, they play an essential, interdependent role in the development of the intrahepatic biliary system and in the liver's response to cholestatic injury.

SAT-174

Expression of inflammatory markers in cholangiocyte organoids from patients with primary sclerosing cholangitis recapitulate disease severity

Philip Puchas¹, Farzaneh Kashfi¹, Chengcheng Zhang-Hagenlocher¹, Uta Merle¹, Patrick Michl¹, Peter Sauer¹, Michael Dill^{1,2}. ¹Department of Gastroenterology, Infectious Diseases, Intoxications, Heidelberg University Hospital, Heidelberg, Germany; ²German Cancer Research Center (DKFZ) Heidelberg, Research Group Experimental Hepatology, Inflammation and Cancer, Heidelberg, Germany
Email: michael.dill@med.uni-heidelberg.de

Background and aims: Primary sclerosing cholangitis (PSC) is a rare liver disease defined by inflammation and consecutive fibrotic alterations of the bile ducts. Importantly, PSC has a highly variable clinical course and mechanisms driving interindividual progression are incompletely understood. Cholangiocytes can adapt a highly secretive phenotype and therefore facilitate PSC pathogenesis. It is unclear whether susceptibility and reactivity of cholangiocytes influences the course of the disease, but differences in cytokine expression (e.g. Interleukin-8) in bile of PSC patients has been shown. 3D culture allows for culture of primary patient-derived cholangiocytes as organoids (chol-orgs). We aimed to investigate whether chol-orgs could be used as a tool to study potential molecular differences based on interindividual PSC severity.

Method: 31 chol-org lines (controls n = 10, mild PSC = 10, severe PSC = 11) were generated from bile sampled endoscopically. Severe PSC cases were defined having evidence of advanced liver fibrosis and severe cholangiographic findings, while mild cases were selected for minor cholangiographic changes and limited fibrosis of the liver. Controls consisted of cases without evidence of chronic inflammation (i.e. choledocholithiasis, postoperative biliary leakage, papillary stenosis and polycystic liver disease). Chol-orgs were analysed at passage 4–8 for mRNA expression of selected genes and this correlated with clinicopathological parameters. Statistical analysis was performed via T-tests, linear regression and Pearson correlation. Written informed consent was obtained from all patients.

Results: mRNA expression of the genes *CCL20*, *P21*, *TFF1*, *CFTR* and *GGT* was not significantly different between all chol-org groups. However, severe PSC chol-orgs showed >2-fold upregulated mRNA expression of Interleukin-8 (IL8) compared to mild PSC chol-orgs (p =

0.0139). Interestingly, IL8 expression in controls was similar compared to severe PSC chol-orgs. In PSC, IL8 expression positively correlated with disease stage as indicated by liver stiffness (p = 0.0113, r = 0.5539) and worsening of liver function in a 6–12 month follow-up by change in labMELD score (p = 0.031, r = 0.5395). Further, IL8 expression correlated moderately with serum bilirubin and GGT across all groups (p = 0.0032, r = 0.5122 and p = 0.0091, r = 0.4609). CCL20 expression also positively correlated with worsening of liver function in PSC (p = 0.0256, r = 0.5551).

Conclusion: Under regular culturing conditions, IL8 and CCL20 mRNA expression in PSC chol-orgs still correlated with worsening of liver function in PSC, indicating a rationale for more comprehensive molecular and functional analyses of chol-orgs between PSC severity subgroups. The selection of good bile controls has to be carefully considered in this setting.

SAT-175

PPAR-delta activation with seladelpar regulates cholangiocyte inflammation

Xia Wu¹, Yen-Wen Chen², Jiangao Song¹, Edward Cable¹, Jeff Johnson¹, Joanne Elliott², Francisco Caballero-Camino³, Xin Chen¹, Robert Martin¹, Jeffrey Stebbins¹, Jesús M. Banales³, Charles A. McWherter¹. ¹CymaBay Therapeutics, Inc., Fremont, United States; ²Triple Ring Technologies Inc., Newark, United States; ³Biogipuzkoa Health Research Institute, San Sebastian, Spain
Email: xwu@cymabay.com

Background and aims: Cholangiocytes, epithelial cells lining bile ducts, play a crucial role as the primary site of injury in primary biliary cholangitis (PBC). The Phase 3 RESPONSE trial in patients with PBC demonstrated that the selective PPAR-delta agonist seladelpar effectively reduced bile acid pools, improved cholestatic and liver injury markers (ALP, GGT and ALT), and decreased the pruritogenic cytokine IL-31, leading to an accompanying alleviation of patient-reported pruritus. Given the central role of cholangiocytes in PBC pathobiology, we investigated the response to seladelpar treatment of human cholangiocyte cells as a potential translational model to understand its observed clinical profile.

Method: H69 human cholangiocytes were cultured and exposed to varying concentrations and durations of seladelpar treatment. Inflammatory PBC mediators like IL-17 were used in addition to seladelpar. Gene expression changes were analyzed by bulk RNAseq and qPCR assays. Secreted cytokines in culture media were analyzed with Meso Scale Discovery (MSD) assays.

Results: Treatment of cholangiocytes cells with seladelpar (10 µM) resulted in substantial changes in gene expression. Genes pivotal in lipid pathways, particularly those involved in fatty acid beta-oxidation, exhibited significant up-regulation with seladelpar, including *ANGPTL4*, *CPT1A*, *ACADVL*, *HADHA*, *HADHB*, *ACAA2*, *ECH1*. PPAR-delta-activated genes, such as *PKD4* and *ANGPTL4*, showed increases by 4-fold and 8-fold, respectively, even at low seladelpar concentrations (10 nM). Furthermore, IL-17 incubation induced an inflammatory response in cholangiocytes, leading to the up-regulation of *CXCL10*, *CCL5*, *CXCL1*, *CXCL8*, and *IL-6*. MSD assays confirmed the secretion of IL-6, CXCL8, IL-1beta and TNFα cytokines induced by IL-17 in cholangiocytes. Notably, co-incubation of cholangiocytes with IL-17 and seladelpar attenuated the IL-17 induced response. Cholangiocytes co-incubated with IL-17 and seladelpar exhibited reduction in gene expression of interferon genes *IFNB1* and *IFNL1*, interferon stimulated genes (*IFIT1*, *ISG15*, *RSAD2*, *CXCL10*), chemokine genes (*CCL5*, *CXCL1*, *CXCL8*, *CCL20*), and HLA genes (*HLA-F*, *HLA-E*, *HLA-DPB1*) compared with IL-17 alone.

Conclusion: This is the first evidence on the impact of selective PPAR-delta activation in a human cholangiocyte cell line. These findings indicate that seladelpar modulates multiple inflammatory mediators and this warrants further in-depth investigation.

SAT-176

Ilg-Cre/DTA mice develop the autoimmune biliary disease that serologically and pathogenically models human primary biliary cholangitis

Jiaqi Zhang¹, Mayu Ouchi¹, Ryo Nakagawa², Akane Kurosugi¹, Goto Chihiro², Ryuta Kojima¹, Tatsuya Kaneko¹, Yuki Ohta¹, Motoyasu Kan¹, Masato Nakamura¹, Shingo Nakamoto¹, Jun Kato¹, Yoshihiro Hirata³, Naoya Kato¹. ¹Department of Gastroenterology, Graduate School of Medicine, Chiba University, Chiba, Japan; ²Division of Advanced Preventive Medicine, Department of Gastroenterology, Chiba University, Chiba, Japan; ³The Institute of Medical Science, The University of Tokyo, Tokyo, Japan
Email: zhangjiaqi@chiba-u.jp

Background and aims: Primary biliary cholangitis (PBC) is an autoimmune liver disease that has progressive destruction of the intra-hepatic bile ducts that causes the retention of bile and other toxins. The incidence of PBC in European, North American, Asia, and Australian populations is between 0.9 and 5.8 per 100,000 population per year, and the prevalence per 100,000 is 1.9 to 40.2. The disease is female-predominant, and an estimated 1 in 1000 women over 40 live with PBC. Multiple murine models of PBC have been developed in recent years, which aim to provide a new idea to elucidate the pathological mechanism and design for new target drugs. However, each model had different similarities to human PBC, which cannot cover all features. In the Ilg-Cre/DTA (ID) mouse model, dendritic cells (DCs) are genetically depleted, immune tolerance is disrupted, and systemic autoimmune disorders occur spontaneously. It will contribute to unraveling the mechanisms underlying PBC pathogenesis and advancing its treatment options.

Method: In this murine model, hepatobiliary changes were assessed by HE staining, immunohistochemistry (IHC-p), and flow cytometry (FCM). IFN-gamma production capacity of CD4⁺ T lymphocytes was analyzed by intracellular staining. Gene expression of cholangitis-related cytokines was analyzed using quantitative RT-PCR (reverse transcription PCR). Serum anti-mitochondrial antibodies (AMA) and secreted IFN-gamma were evaluated by Enzyme-Linked Immunosorbent Assay (ELISA).

Results: ID mice developed extensive portal inflammation with neutrophils, CD4⁺ T lymphocytes, and CD8⁺ T lymphocytes surrounding bile ducts and portal veins. The severity of cholangitis increased with age in weeks, with intense cholangitis from 10 to 20 weeks, and partial disappearance of bile ducts was observed over 36 weeks. In addition, the ID model mice showed the presence of serum AMA and the inflammatory cytokine IFN-gamma. Moreover, the liver injury indicator ALT was observed to be elevated. Immunohistochemistry of liver tissue revealed inflammation around the bile ducts and portal vein by neutrophils, macrophages, CD4⁺ T lymphocytes, and CD8⁺ T lymphocytes. Furthermore, there was an increase in the CD4/CD8 ratio of T lymphocytes, coupled with elevated IFN-gamma production from CD4⁺ T lymphocytes. Besides that, Th1-dependent cytokines such as IFN-gamma, TNF-alpha, IL-2, IL-6, and IL-12p35 showed an increased expression.

Conclusion: The deficiency of DC leads to immunologic and hepatobiliary changes that resemble human PBC, and this model is characterized by the lack of direct modification of T cells compared to existing PBC models. We expect that new ID model mice will help us elucidate PBC's pathogenesis through T cell regulation and develop new treatments for PBC.

SAT-177

Assessment of PPARdelta target engagement in mouse liver assessed by single nuclei sequencing following a single oral dose of seladelpar

Edward Cable¹, Yun-Jung Choi¹, Xia Wu¹, Jiangao Song¹, Jeff Johnson¹, Charles A. McWherter¹. ¹CymaBay Therapeutics, Newark, United States
Email: ecable@cymabay.com

Background and aims: Seladelpar is a selective PPARdelta agonist that recently completed a Ph 3 trial as a second-line therapy for patients with an inadequate response, or intolerance, to ursodeoxycholic acid. The results of the trial have been previously published and demonstrated significant reductions of alkaline phosphatase and improvements in pruritus. Published data in mice demonstrate seladelpar-mediated reductions of bile acid synthesis, including reduction of *Cyp7a1*, following a single oral dose in mice as well as in PPARalpha knockout mouse hepatocytes. To investigate the molecular mechanisms of seladelpar in the various liver cell types, mice were treated with a single dose of seladelpar and single nuclei harvested and analyzed by sequencing.

Method: Male CD-1 mice, five per group, were treated with vehicle (1% CMC dosed at 5 ml/kg) or seladelpar (10 mg/kg in vehicle) and sacrificed 6 hours after dosing. Sections of liver were removed and snap frozen. Nuclei were isolated using the Parse Evercode kit. 100,000 nuclei were used to make the Evercode library. Sequencing was performed on an Illumina NovaSeq X. Data were demultiplexed with NovaSeq X Plus DRAGEN onboard BCLConvert 4.1.7. Single cell alignment was performed with Split-Pipe 1.1.2. Single cell analysis was performed with Seurat 4.4.0. Data visualization and analyses were completed on CellxGene (1.2.0).

Results: Leiden clustering identified 30 different clusters. Hepatocytes, cholangiocytes, Kupffer cells, endothelial cells, and dendritic cells were identified and were spread over different clusters. Analysis of the expression levels of PPARalpha, gamma, and delta in the vehicle group indicate that PPARalpha is the dominant PPAR isoform expressed in the liver of mice with delta and gamma being expressed at lower levels in all cell types. As expected, the PPAR responsive genes *Pdk4* and *Angptl4* were induced, and *Cyp7a1* was reduced, in hepatocytes following seladelpar treatment. Seladelpar changed gene expression patterns in every identified cell type. Correlation of *Pdk4* and *Angptl4* was variable indicating unexpected differences in expression patterns for two "prototypical" PPAR responsive genes.

Conclusion: Identification of changes in gene expression six hours following a single dose of seladelpar, indicate that there are PPARdelta mediated changes in all identified cell types in the mouse liver. Single-cell analyses, such as this, can provide a framework in which to understand the primary PPARdelta responsive genes following seladelpar treatment and can be used to deconvolute the gene expression patterns leading to the beneficial pharmacodynamic effects reported in either humans or mice.

SAT-178-YI

Galectin-3 and prohibitin 1 are autoantigens in IgG4-related cholangitis without clear-cut protective effects against toxic bile acids

Remco Kersten¹, David Trampert¹, Lowiek Hubers¹, Dagmar Tolenaars¹, Harmjan Vos², Stan van de Graaf¹, Ulrich Beuers¹. ¹Department of Gastroenterology and Hepatology, Tytgat Institute for Liver and Intestinal Research, Amsterdam Gastroenterology Endocrinology Metabolism (AGEM), Amsterdam University Medical Center, Amsterdam, Netherlands; ²Oncode Institute and Molecular Cancer Research, Center for Molecular Medicine, University Medical Center Utrecht, Utrecht, Netherlands
Email: d.c.trampert@amsterdamumc.nl

Background and aims: IgG4-related cholangitis (IRC) is the hepatobiliary manifestation of IgG4-related disease, a systemic fibroinflammatory disorder. Four autoantigens have recently been described in IgG4-RD: annexin A11, galectin-3, laminin 511-E8, and prohibitin 1. We have previously reported a protective role of annexin A11 and laminin 511-E8 in human cholangiocytes against toxic bile acids. Here, we explored the potentially protective role of galectin-3 and prohibitins 1 and 2.

Method: Anti-galectin-3, anti-prohibitin 1 and 2 autoantibody positivity was assessed by ELISA/LC-MS/MS in IRC, primary sclerosing

POSTER PRESENTATIONS

cholangitis (PSC) and healthy control sera. IgG's were isolated from a healthy control and an IRC patient with anti-galectin 3 and anti-prohibitin 1 autoantibodies. Human H69 cholangiocytes were subjected to short hairpin RNA knockdown targeting galectin-3 (*LGALS3*), prohibitin 1 (*PHB1*), and prohibitin 2 (*PHB2*). H69 cholangiocytes were also exposed to recombinant galectin-3, the inhibitor GB1107, recombinant prohibitin 1 and the pan-prohibitin inhibitor rocaglamide. Protection against bile acid toxicity was assessed by intracellular pH (pHi) measurements using BCECF-AM, 22, 23-³H-glycochenodeoxycholic acid (³H-GCDC) influx, and GCDC-induced apoptosis using Caspase-3/7 assays.

Results: Anti-galectin-3 autoantibodies were detected in 13.5% of individuals with IRC but not in PSC. Knockdown of *LGALS3* and galectin-3 inhibition with GB1107 did not affect pHi, whereas recombinant galectin-3 incubation lowered pHi. *LGALS3* knockdown increased GCDC influx but not GCDC-induced apoptosis. GB1107 reduced GCDC influx and GCDC-induced apoptosis. Recombinant galectin-3 tended to decrease GCDC influx and GCDC-induced apoptosis. Anti-prohibitin 1 autoantibodies were detected in 61.5% and 35.7% of individuals with IRC and PSC respectively. *PHB1* knockdown, combined *PHB1/2* knockdown, treatment with rocaglamide, and recombinant prohibitin 1 all lowered pHi. *PHB1*, *PHB2*, or combined *PHB1/2* knockdown did not alter GCDC influx, yet *PHB1* knockdown increased GCDC-induced apoptosis. Conversely, rocaglamide reduced GCDC influx but did not attenuate GCDC-induced apoptosis. Recombinant prohibitin 1 did not affect GCDC influx or GCDC-induced apoptosis. Finally, IRC patient-derived anti-galectin-3 and anti-prohibitin 1 autoantibody pretreatment did not lead to increased GCDC influx into H69 cholangiocytes.

Conclusion: A subset of individuals with IRC have autoantibodies against galectin-3 and prohibitin 1. Gene-specific knockdown, pharmacological inhibition and recombinant protein substitution did not clearly disclose a protective role of these autoantigens in human cholangiocytes against toxic bile acids. The involvement of these autoantibodies in processes surpassing epithelial secretion remains to be elucidated.

SAT-179

A DNA methylation signature associated with inflammation is found in primary sclerosing cholangitis and IgG4-related cholangitis

Alexandre Adams¹, Silvia Cabras¹, Alexandra Noble¹, Rodrigo Motta¹, Belen Moron Flores¹, Jan Nowak², Aleksandra Glapa-Nowak², Alessandra Geremia¹, Jack Satsangi¹, Emma Culver¹. ¹Translational Gastroenterology and Liver Unit, Nuffield Department of Medicine, University of Oxford, Oxford, United Kingdom; ²Department of Pediatric Gastroenterology and Metabolic Diseases, Poznan University of Medical Sciences, Poznan, Poland
Email: rodrigo.vieiramotta@ndm.ox.ac.uk

Background and aims: Primary sclerosing cholangitis (PSC) and IgG4-related cholangitis (IgG4-C) are chronic fibro-inflammatory hepatobiliary conditions, with genetic, environmental, and immunologic risk factors. We sought to study epigenetic alterations that may provide insights into pathophysiology and novel disease biomarkers.

Method: Whole blood DNA methylation profiling and genotyping was performed by MethylationEPIC and Global Screening arrays (Illumina) in a cohort of 214 individuals; 56 patients with IgG4-C, 70 patients with PSC, and 88 healthy controls (HC). Epigenome-wide methylation changes were processed with minfi and limma, genotyping analysed with PLINK and methylation quantitative trait loci (meQTL) with linear models, and Horvath's epigenetic clock was used to assess age acceleration. Genome-wide significance was defined by Holm correction.

Results: Epigenome-wide methylation changes were identified between PSC and IgG4-C cohorts. In IgG4-C, there were 13 individual CpG sites with methylation alterations, including IFNAR1 ($p = 3.19 \times 10^{-10}$) and PYY ($p = 7.8 \times 10^{-10}$). meQTL analyses identified 36

significant loci in IgG4-C, including TESPA1 ($p < 3.18 \times 10^{-13}$), which is associated with B cell function and onset of autoimmune diseases. Gene ontology showed enrichment of T-cell activation, proliferation and endosome membrane recycling pathways ($p < 0.001$). DNA methylation age acceleration was observed in IgG4-SC ($p = 0.0006$). In PSC, there were 31 individual CpG sites with methylation alterations compared with HC, including TXK ($p = 2.89 \times 10^{-9}$), CEP97 ($p = 6.66 \times 10^{-15}$) and MTRNR2L1 (1.47×10^{-10}). meQTL analyses revealed a strong HLA signal in PSC. 19/40 significant findings occurred in 5 clusters (HLA-DRB1, HLA-DPB1, BTNL2, CSNK2B, and SFTA2). PSC and IgG4-C shared 8 individual CpG sites with methylation alterations, including genes associated with inflammation (CEP97) and loci associated with mitochondrial DNA copy number (C5orf36, PYY).

Conclusion: This is the first description of the methylome in IgG4-C as compared to PSC, with alterations centred on inflammatory and immune-related pathways, and age acceleration demonstrated in IgG4-C.

SAT-180

Targeting neutrophil injury-pathways and fibrogenesis in non-parenchymal immune tissue-like liver organoids generated from human induced pluripotent stem cells

Susanna Quach¹, Kyle Lewis², Kentaro Iwasawa², Yuka Milton³, Adrien Guillot⁴, Yeni Ait Ahmed⁴, Takanori Takebe^{2,5,6}, Rose Yinghan Behncke^{7,8}, Milad Rezvani^{1,7}. ¹Charité Universitätsmedizin Berlin, Berlin, Germany; ²Division of Gastroenterology, Hepatology and Nutrition, Cincinnati Children's Hospital Medical Center, Cincinnati, United States; ³Division of Gastroenterology, Hepatology and Nutrition, Cincinnati Children's Hospital Medical Center, Cincinnati, Cincinnati, United States; ⁴Charité Universitätsmedizin Berlin, Department of Hepatology and Gastroenterology, Berlin, Germany; ⁵Institute of Research, Tokyo Medical and Dental University, Tokyo, Japan; ⁶Premium Research Institute for Human Metaverse Medicine (WPI-PRiMe), Osaka University, Osaka, Japan; ⁷Berlin Institute of Health, Center for Regenerative Therapies, Berlin, Germany; ⁸Charité, Institute of Medical Genetics and Human Genetics, Berlin, Germany
Email: susanna.quach@charite.de

Background and aims: Hepatic non-parenchymal cells (NPCs), including hepatic stellate cells (HSCs), biliary epithelial cells (BECs), endothelial cells (ECs), and various myeloid innate leukocytes, play a critical role in liver injuries induced by lipotoxic milieu. Here, we develop human induced pluripotent stem cell (hiPSC)-derived non-parenchymal immune tissue-like liver organoids (NPC-HLOs), inclusive of syngeneic neutrophils, heterogenous monocyte and macrophage subsets, as a platform to investigate injuries involving innate immune-fibrogenic pathways and hepatocyte injury.

Method: NPC-HLOs were developed from hiPSCs by co-inducing endoderm and mesoderm, followed by cluster embedding with BMP4, FGF2, FGF4, and CHIR. From day 10, NPC-HLOs were treated with basal medium for self-organization or hematopoietic cytokines for enhanced myeloid differentiation. Cell populations were identified via anti- or nanobody based immunofluorescence and flow cytometry. For modeling steatohepatitis, NPC-HLOs were treated with a lipid mix (LM) or palmitic acid (PA) and assessed using electrochemiluminescence for cytokine secretion. Intercellular pathways were identified using single-cell RNA sequencing and CellChat, and modulated via CXCR1/2-blockade-using Reparixin for macrophage-to-neutrophil recruitment and Notch-mediated fibrogenesis-using DAPT.

Results: We co-developed FOXA2+/CXCR4+ endoderm and KDR+/CD235a+ mesoderm and observed without adding further growth factors spontaneous in vitro organogenesis, including a reticular CD31+ EC system, CK19+ CK7+ EPCAM+ luminal BECs, PDGFRA+ alphaSMA+ HSCs, AFP+ ALB+ ECAD+ hepatocytes and CD68+ IBA-1+ macrophages with partial polarization (CD45+ CD64low

CD163+ CD206-). Including GM-CSF completed macrophage polarization and yielded CD45+CD14-CD16+CD66b MPO+ segmented, reactive oxygen species (ROS)-releasing neutrophils. Under lipotoxicity, NPC-HLOs exhibited a 5-fold decrease in HNF4alpha expression, a 1.3-fold MPO+ expansion, low-frequency detection of neutrophil extracellular traps (NETs), and a 2-fold increase in IL8 secretion. Reparixin mitigated HNF4alpha loss to 1.8-fold. Organoid-encapsulating fibrogenesis was observed after inflammatory cytokine addition, further intensified by Notch-agonism via DLL1, resembling bridging fibrosis. In contrast, treatment with DAPT prevented fibrogenesis, maintaining a non-fibrotic state. Inferring intercellular pathways via CellChat supported Notch signaling across hepatocytes-to-NPCs, primarily HSCs and ECs, in addition to autocrine NPC-signaling.

Conclusion: NPC-HLOs recapitulate the majority of cell populations of the human liver, enabling studies of parenchymal-NPC crosstalk. Our findings highlight Notch as a key regulator in fibrogenesis involving NPCs and the druggable IL8 pathway, for recruiting tissue-injurious neutrophils.

SAT-181-YI

WTAP deficiency in mice hepatocyte induces cholestatic liver diseases by modulating nuclear receptor FXR

Chuanhui Peng¹, Xueyu Zhou¹, Guomin Ju¹. ¹The First Affiliated Hospital, Zhejiang University School of Medicine, Hangzhou, China
Email: peng_chuanhui@zju.edu.cn

Background and aims: Cholestatic liver diseases are characterized with bile accumulation, hepatocyte damages, liver fibrosis and cirrhosis. Wilms' tumor-1 associated protein (WTAP), a key regulator of N6-methyladenosine (m6A) modification, has been reported to play a crucial role in MASH and liver tumors. However, there is little known about WTAP's role and its underlying mechanism in cholestatic liver diseases.

Method: Hepatocyte conditional knockout of WTAP mice were generated by CRISPR/Cas9, and compared with wild type mice at different time points. Liver zonation, inflammation, fibrosis, metabolic and immune alternation were analyzed by histology, serology, multi-omics and single cell sequencing.

Results: Here, we have identified WT1-associated protein (WTAP) as a key regulator in cholestatic liver injury. Knocking out WTAP with Alb Cre (WTAP LKO) during the perinatal period induces liver injury and cholestasis. Metabolomics and transcriptomic analyses showed that the bile acid metabolism of WTAP LKO mice was significantly affected. Biliary duct ligation (BDL) was used to induce cholestasis in control and WTAP LKO mice. Compared with wild-type mice, WTAP LKO mice showed significantly increased inflammation and liver injury. Single cell sequencing delineated the landscape of liver architecture after WTAP deletion in hepatocyte. Deleting WTAP down-regulated nuclear receptor FXR, a key protein for bile acid transport via decreasing its transcript stability. Clinically, WTAP was associated with cholestatic liver diseases.

Conclusion: WTAP was crucial in maintaining liver homeostasis. Targeting WTAP may be a promising strategy for treating cholestatic diseases.

SAT-182

Immunokinetics of CD4+ T cells in primary sclerosing cholangitis by functional transcriptome analysis

Mayu Ouchi¹, Ryo Nakagawa¹, Jiaqi Zhang¹, Naoya Kato¹. ¹Chiba University, Chiba, Japan
Email: aromarokarisuo@yahoo.co.jp

Background and aims: Primary sclerosing cholangitis (PSC) is a chronic progressive cholangiopathy of unknown cause. Since PSC recurs even after liver transplantation, it is assumed that auto-immune mechanisms play a major role in the pathogenesis of the disease. In recent years, various attempts have been made to understand the immune microenvironment of PSC, and it has been suggested that TNFα and IL-17 responses to intestinal bacteria are

involved in the pathogenesis of the disease. In particular, it has been reported from Japan that intestinal bacteria specific to PSC patients induce IL-17-producing CD4+ T cells in the liver of PSC patients via systemic circulation from mesenteric lymph nodes, and this immune mechanism has attracted attention. Therefore, we analyzed the gene expression profile of its CD4+ T cells to further explore the immune mechanism in PSC patients.

Method: Gene expression in peripheral blood CD4+ T cells from PSC patients and healthy controls was analyzed using RNA sequencing and quantitative RT-PCR. In vitro analysis was performed using CD4+ T cells for functional analysis of genes that showed expression variation.

Results: Expression analysis of CD4+ T cells from PSC patients (n = 3) and healthy controls (n = 3) by RNA sequencing showed 1,035 genes showed variation (up/down: 974/61, p < 0.005). Pathway analysis of expression variation genes extracted 16 pathways (p < 0.001). Based on the similarity of the genes they encompassed, they were classified into two clusters. Among them, we focused on the cluster consisting of NFκB signaling pathway, Cytokine-cytokine receptor interaction, and Chemokine signaling pathway. We analyzed the expression of CXCL2, CXCL3, CXCL8, CCL4L2, and NFKBIA in CD4+ T cells from PSCs (n = 6) and healthy controls (n = 5), and found that CXCL2, CXCL3, CXCL8, CXCL4L2, CXCL4L2, CXCL4L2, CXCL4L2, CXCL4L2, CXCL8, CXCL8, CXCL8, and CXCL2 are common genes in these three pathways, NFKBIA showed significantly higher expression in PSCs (p < 0.05). Therefore, we analyzed the regulation of CXCL8 expression in vitro. First, CXCL8 was induced by TNFα stimulation in CD4+ T cells from healthy subjects (n = 3). Furthermore, when we compared the expression and secretion of CXCL8 in CD4+ T cells from patients with PSC (n = 4) and healthy controls (n = 4) after TNFα stimulation, the PSC group secreted more CXCL8 than the healthy group (p < 0.01).

Conclusion: CD4+ T cells from PSCs showed enhanced secretion of chemokines associated with NFκB signaling activity. Since CXCL8 enhances neutrophil chemotaxis and promotes inflammation, it is possible that CXCL8 produced by CD4+ T cells may contribute to the pathogenesis of PSCs. may contribute to the pathogenesis of PSC. Gene expression analysis of CD4+ T cells in PSCs revealed some of their immune mechanisms.

SAT-183

Moderate overexpression of c-Met in hepatocytes decreases cholestatic liver injury

Carlos González-Corrales^{1,2}, Juan García-Sáez^{1,2}, Cesáreo Roncero^{1,2}, María Figueroa², Adrián Jiménez², Nerea Lazcanoiturburu², Beatriz Pacheco², Almudena Porras^{1,2}, Flavio Maina³, Isabel Fabregat^{4,5}, Blanca Herrera^{1,2,5}, Aránzazu Sánchez^{1,2,5}. ¹Health Research Institute of the "Hospital Clínico San Carlos" (IdiSSC), Madrid, Spain; ²Department of Biochemistry and Molecular Biology, Faculty of Pharmacy, Complutense University of Madrid (UCM), Madrid, Spain; ³Aix Marseille Univ, Inserm, CNRS, Centre de Recherche en Cancérologie de Marseille (CRCM), Institut Paoli-Calmettes, Turing Center for Living Systems, Marseille, France, Marseille, France; ⁴TGF-β and Cancer Group, Oncobell Program, Bellvitge Biomedical Research Institute (IDIBELL), Barcelona, Spain; ⁵Biomedical Research Networking Center in Hepatic and Digestive Diseases (CIBEREHD-ISCIII), Madrid, Spain
Email: carlgo17@ucm.es

Background and aims: The hepatocyte growth factor (HGF) and its receptor mesenchymal-epithelial transition factor (c-Met) signaling axis plays a critical role during liver regeneration upon chronic damage through its mitogenic, survival, and morphogenic activities on hepatocytes and hepatic progenitor cells/oval cells (HPC/OC). However, the molecular mechanisms underneath HGF/c-Met pro-regenerative effects are not fully elucidated. The aim of this study was to analyze the impact of c-Met overexpression on liver regeneration upon cholestatic injury and uncover how it affects hepatocyte and HPC/OC function.

POSTER PRESENTATIONS

Method: Transgenic mice with moderate overexpression of c-Met receptor in the liver (albumin-positive cells) were fed with a diet supplemented with the cholestatic agent 3, 5-diethoxycarbonyl-1, 4-dihydrocollidine (DDC). Serum biomarkers of liver function and liver histological features were analyzed. A biochemical and molecular analysis of oxidative stress and antioxidant pathways was also performed both *in vivo* and *in vitro* in hepatocytes derived from c-Met transgenic mice treated with bile acids and TGF-beta to mimic the cholestatic and fibrotic liver microenvironment.

Results: Overexpression of c-Met led to a diminished liver damage in response to DDC, evidenced by lower serum levels of bilirubin and alkaline phosphatase. Interestingly, decreased damage was associated with a decreased HPC/OC expansion and an enhanced hepatocyte proliferation. In parallel, c-Met transgenic livers displayed an enhanced upregulation of the nuclear factor erythroid 2-related factor 2 (Nrf2), together with an up-regulation of the rate-limiting enzyme of glutathione biosynthetic pathway, increased levels of reduced glutathione and decreased reactive oxygen species levels during DDC treatment, along with a decreased activation of TGF-beta-induced signaling. Consistently, c-Met transgenic hepatocytes were more resistant to the cytotoxicity induced by bile acid and TGF-beta combined treatment and presented an ameliorated oxidative stress response *in vitro*.

Conclusion: Our work evidence that a moderate overexpression of c-Met in hepatocytes is sufficient to promote a strong antioxidant response in the liver that efficiently protects against chronic cholestasis thus allowing an optimal liver regeneration.

SAT-184

Primary biliary cholangitis symptoms are reduced in liver specific Mcp1 knock-out mice after treatment with probiotic *Lactobacillus rhamnosus*

Katarzyna Trzos^{1,2}, Tomasz Hutsch³, Gabriela Machaj⁴, Guillem Ylla⁴, Jolanta Jura², Jerzy Kotlinowski². ¹Doctoral School of Exact and Natural Sciences, Cracow, Poland; ²Jagiellonian University, Faculty of Biochemistry, Biophysics and Biotechnology, Cracow, Poland; ³University of Warsaw, Warsaw, Poland; ⁴Jagiellonian University, Laboratory of Bioinformatics and Genome Biology, Cracow, Poland
Email: kat.trzos@doctoral.uj.edu.pl

Background and aims: Primary biliary cholangitis (PBC) is a chronic autoimmune liver disease that results from slow, progressive destruction of the intrahepatic bile ducts. PBC progression leads to the development of fibrosis, cholestasis, liver cirrhosis. Mcp1fl/flAlbCre mice, with the Zc3h12a gene (encoding Mcp1 protein) deleted in liver epithelial cells, exhibit typical PBC symptoms (increased levels of antimitochondrial and antinuclear antibodies, elevated total bile acids, and intrahepatic bile duct hyperplasia, disruption of bile duct epithelium and fibrosis). The primary objective of this project is to elucidate PBC symptoms in these mice following the administration of first- and second-line therapies commonly employed in PBC patients. Additionally, the study incorporates the use of a probiotic (*Lactobacillus rhamnosus*) due to emerging evidence suggesting that gut microbiota regulates host immunity.

Method: Mcp1fl/fl and Mcp1fl/flAlbCre male mice at 6 weeks of age were randomly divided into five groups for drug treatment. Control group received corn oil, other groups received consecutively Lakcid (*L. rhamnosus*, 10⁹ CFU per day) suspended in water, ursodeoxycholic acid (UDCA, 15 mg/kg body mass per day) diluted in corn oil, UDCA and Lakcid, UDCA and obeticholic acid (OCA, 10 mg/kg body mass per day) both diluted in corn oil. After 6 weeks of treatment, all mice were sacrificed, and the collected material analysed by, amongst other, detailed serum liver tests, ELISA tests for the presence of anti-PDC-E2 autoantibodies, histological stainings (HandE, PSR), qPCRs and next generation sequencing (NGS) of total RNA from livers.

Results: After 6-weeks of treatment significant proliferation of cholangiocytes and fibrosis in livers from Mcp1 knock-out mice

was detected, together with high serum level of total IgM, total bile acids and anti-PDC-E2 autoantibodies. Animals receiving Lakcid had the most significant weakening of the PBC symptoms (reduced amount of total bile acids in the serum, proliferation of cholangiocytes and fibrosis). NGS analysis revealed 1131 up-regulated and 390 down-regulated genes in control knock-out mice compared to control Mcp1fl/fl mice. Processes such as humoral immune response, regulation of lymphocyte activation and T cell activation are significantly enriched in these mice. Comparison of Lakcid-treated and control knock-out mice revealed 178 up-regulated and 308 down-regulated genes. Most importantly, NGS revealed a significant suppression of biological processes related to T cells activation and inflammatory response.

Conclusion: Treatment of Mcp1fl/flAlbCre mice with Lakcid has beneficial effects on PBC symptoms and suggest that the gut-liver axis and intestinal microflora can be a master-regulator of PBC progression and is an interesting therapeutical target in chronic inflammatory liver diseases.

SAT-185

Human leukocyte antigen-DRB1 expression in cholangiocytes of 'early' primary sclerosing cholangitis

Ynto de Boer¹, Frank Sun², Vincent de Meijer², Klaas Nico Faber², Naomi Karmi², Sofie de Jong², Joris Erdmann¹, Eleonora Festen², Cyriel Ponsioen¹. ¹Amsterdam UMC, Amsterdam, Netherlands; ²University Medical Center Groningen, Groningen, Netherlands
Email: y.deboer1@amsterdamumc.nl

Background and aims: Primary sclerosing cholangitis (PSC) is a chronic cholestatic liver disease, for which there is currently no therapy to halt disease progression. PSC is generally regarded as an immune-mediated disease, but disease etiology and pathogenesis is still largely unknown. The aim of the study was to characterize the cellular composition of the tissue in stenoses in the larger bile ducts of 'early' PSC patients, as relevant literature on pathogenesis is mostly based on explant and resection material. This is done by analysis of expression profile of affected bile duct tissue on a single cell RNA sequencing (scRNAseq) level, elucidating antigen presenting properties and senescence signaling of affected cholangiocytes.

Method: PSC patients with dominant or suspected dominant strictures and a clinical reason for biliary drainage who underwent endoscopic retrograde cholangiography (ERC) were included in this study. Strictures were sampled using Spybite max forceps. After dissociation into single cells we performed scRNAseq to characterize the cellular composition of the biopsies. We used cluster specific genetic markers with Cell-ex to obtain cluster specific cell type expression profiles.

Results: 5 PSC patients undergoing ERC were successfully biopsied. Cell dissociation proved challenging due to adherent bile, but was successful in one patient. After Cell-ex associated clustering we performed manual annotation on each cluster based on its expression profile in combination with literature and histopathological evaluation. We identified a subset of activated cholangiocytes that express abundant *HLA-DRB1* in addition to CK7, which suggests a primary role in the early phase of inflammation as antigen presenting cells. The evaluated material showed a paucity of lymphocellular infiltrate, concurrent with the histopathological evaluation of this biopsy.

Conclusion: We have now successfully implemented a sampling protocol to perform scRNAseq to ascertain the variation of the cellular composition of the biliary inflammation in ERC guided biopsies of 'early' PSC patients, hence establishing a reference dataset for bile duct cell type annotation. Furthermore, this preliminary single patient dataset has revealed a potential role of a subset of activated cholangiocytes that express abundant *HLA-DRB1*, a key-factor in lymphocyte activation and a known genetic risk locus for PSC development.

Immune-mediated and cholestatic disease Clinical aspects

TOP-157

Risk of extrahepatic malignancies in patients with autoimmune hepatitis: a nationwide cohort study

Sung Won Chung¹, Won-Mook Choi¹, Ye-Jee Kim², Sehee Kim², Jonggi Choi¹, Danbi Lee¹, Ju Hyun Shim¹, Kang Mo Kim¹, Young-Suk Lim¹, Han Chu Lee¹. ¹Department of Gastroenterology, Liver Center, Asan Medical Center, University of Ulsan College of Medicine, Seoul, Korea, Rep. of South; ²Department of clinical epidemiology and biostatistics, Asan Medical Center, Seoul, Korea, Rep. of South
Email: dr.choi85@gmail.com

Background and aims: Nationwide, population-based data on the risk of extrahepatic malignancy in autoimmune hepatitis (AIH) patients in Asian countries are scarce. This study aimed to examine the risk of developing extrahepatic malignancy in a nationwide cohort of patients with AIH.

Method: Using claims data from the Korean National Health Insurance Service database between 2007 and 2020, patients with AIH (n = 7, 382) were matched in a 1:8 ratio with age- and sex-matched control population (n = 58, 320) to compare the incidence of extrahepatic malignancies. We compared the incidence rates (IRs) and hazard ratios (HRs) of overall and specific extrahepatic malignancies between the two groups, also examining the impact of immunosuppressant use.

Results: During a median follow-up period of 5.4 years, a total of 3, 713 extrahepatic malignancies were developed. The IR of extrahepatic malignancy in AIH patients (990.8 cases per 100, 000 person-years) was comparable to that in the matched controls (937.6 cases per 100, 000 person-years), with an HR of 0.93 (95% CI, 0.81–1.07; p = 0.30). However, a significantly higher risk of hematologic malignancies, particularly lymphoma or myeloma (HR, 2.66; 95% CI, 1.70–4.17; p < 0.001) was observed. The use of glucocorticoids (HR, 1.09; 95% CI, 0.87–1.38; p = 0.44) or azathioprine (HR, 0.92; 95% CI, 0.73–1.17; p = 0.51) had no impact on the risk of lymphoma or myeloma in patients with AIH.

Conclusion: In this Korean nationwide, population-based cohort, AIH was not associated with an increased risk of overall extrahepatic malignancy compared with age- and sex-matched controls. However, AIH itself increased the risk of lymphoma or myeloma, independent of immunosuppressant use.

TOP-168-YI

Urgent call to action: people living with primary sclerosing cholangitis-inflammatory bowel disease (PSC-IBD) lose 10 years of life compared to those with IBD alone

Kristel Leung¹, Wenbin Li², Bettina E. Hansen³, Amanda Ricciuto⁴, Eric Benchimol^{4,5}, Aliya Gulamhusein¹, Jennifer Flemming^{6,7}, Gideon M. Hirschfield⁸. ¹Toronto Centre for Liver Disease, Toronto, Canada; ²Institute for Clinical Evaluative Sciences (ICES), Kingston, Canada; ³Erasmus Medical Center, Rotterdam, Netherlands; ⁴The Hospital for Sick Children (SickKids), Toronto, Canada; ⁵Institute for Clinical Evaluative Sciences, Toronto, Canada; ⁶Queen's University, Kingston, Canada; ⁷Institute of Clinical Evaluative Sciences, Kingston, Canada; ⁸Toronto Centre for Liver Disease, University Health Network, University of Toronto, University Health Network, Toronto, Canada
Email: gideon.hirschfield@uhn.ca

Background and aims: We sought to evaluate current outcomes for people living with primary sclerosing cholangitis and inflammatory bowel disease (PSC-IBD) as compared to IBD.

Method: Using linked health administrative data (population ≥15 million) with previously derived and validated PSC-IBD incidence (by PSC diagnosis) and IBD incidence cohorts in Ontario, Canada from

January 1, 2002, to December 31, 2018, the number of deaths (censored December 31, 2021) and underlying cause of death (up to 2018) were ascertained. To align disease observation periods for direct comparison, a subcohort with PSC-IBD (both diagnoses) and IBD alone diagnosed from 2002 to 2018 was examined to determine liver transplant-free survival from IBD diagnosis, the number of PSC and IBD-related surgeries, and related cancer cases.

Results: Of 1046 incident PSC-IBD cases with PSC diagnosed between 2002 and 2018 (median age 45 y.o., IQR 20–61), there were 325 deaths (31%) (median age 65 y.o., IQR 49–78), of which 254 (78%) had an underlying cause of death reported. Of 55, 067 incident IBD cases with IBD diagnosed between 2002 and 2018 (median age 38 y.o., IQR 24–54), there were 4757 deaths (8.6%) (median age 74 y.o., IQR 63–84), of which 3048 (64%) had cause of death reported. Cause of death was most commonly due to liver disease in 94 (37%) PSC-IBD individuals, while cardiovascular (19%) and pulmonary (19%) disease were the most common causes of death amongst the IBD incidence cohort. Those with PSC-IBD experienced a significant burden of death due to hepatopancreatobiliary malignancy compared to those with IBD (26% vs. 3.1%), while death from gastrointestinal luminal malignancy was similar (5% for both). Amongst the subcohort, those with PSC-IBD had up to a 4.5-fold worse liver transplant-free survival compared those with IBD alone. There were 98 (21%) deaths amongst PSC-IBD (median age 63 y.o. IQR 46–80), compared to 4, 672 (8.5%) deaths amongst those with IBD alone (median age 74 y.o., IQR 63–84). People with PSC-IBD compared to IBD alone underwent significantly more liver transplants (17% vs. 0.2%), cholecystectomies (12% vs. 3.5%), pouch surgery (9.5% vs. 3.4%) and ileostomy creation (16% vs. 3.4%) (p value < 0.001 for all), but a similar number of colectomies (15% vs. 13%, p = 0.13). Those with PSC-IBD had significantly more hepatocellular carcinoma (19% vs. 0.8%), cholangiocarcinoma (4.2% vs. 0.1%), colon cancer (2.7% vs. 0.6%), and pancreatic cancer (1.4% vs. 0.2%) compared to those with IBD alone (p < 0.001 for all).

Conclusion: In contrast to people living with IBD alone, people with PSC-IBD experience significantly worse outcomes with a high burden of disease-related morbidity and earlier mortality. Those with PSC-IBD experience more hepatopancreatobiliary malignancies, colon cancer, and PSC disease-related surgeries compared to those with IBD alone. Colectomy rates are as frequent in PSC-IBD, and pouch surgery is more common.

TOP-169

Sex, ethnicity and clinical outcomes in autoimmune hepatitis: results from a large multicenter longitudinal cohort

Ellina Lytvayak¹, Devika Shreekumar¹, Gideon M. Hirschfield², Christina Plagiannakos³, Hin Hln Ko⁴, Mark G Swain⁵, Julian Hercun⁶, Lawrence Worobetz⁷, Catherine Vincent⁸, Jennifer Flemming⁹, Karim Qumosani¹⁰, Tianyan Chen¹¹, Dusanka Grbic¹², Angela Cheung¹³, Narmeen Umar¹, Iffat Iqbal¹, Madeline Cameron¹⁴, Aliya Gulamhusein¹⁵, Andrew L. Mason¹, Bettina Hansen¹⁴, Aldo J Montano-Loza¹, on behalf of the Canadian Network for Autoimmune Liver Diseases (CaNAL)¹⁶. ¹University of Alberta, Edmonton, Canada; ²University of Toronto, Toronto, Canada; ³University Health Network, University of Toronto, Toronto, Canada; ⁴University of British Columbia, Pacific Gastroenterology Associates, Vancouver, Canada; ⁵University of Calgary, Snyder Institute for Chronic Diseases, Calgary, Canada; ⁶Centre hospitalier de l'Université de Montréal (CHUM), Montréal, Canada; ⁷University of Saskatchewan, Saskatoon, Canada; ⁸Centre Hospitalier de l'Université de Montréal (CHUM), University of Montreal, Montreal, Canada; ⁹Queen's University, Kingston Health Sciences Centre, Kingston, Canada; ¹⁰Western University, London, Canada; ¹¹McGill University Health Centre, Montreal, Canada; ¹²University of Sherbrooke, Sherbrooke, Canada; ¹³University of Ottawa, Ottawa, Canada; ¹⁴University Health Network, Toronto, Canada; ¹⁵Toronto Centre for Liver Disease, Toronto, Canada; ¹⁶Canadian Network for Autoimmune Liver Diseases (CaNAL), Edmonton, Canada
Email: lytvayak@ualberta.ca

POSTER PRESENTATIONS

Background and aims: Sex and ethnicity have been shown to impact prognosis in liver diseases of different aetiologies; however, data on their impact on outcomes in people living with autoimmune hepatitis (AIH) are limited. We aimed to identify and quantify the magnitude of associations between sex, ethnicity, treatment response and clinical outcomes in a large multicentric cohort of people with AIH across Canada.

Method: A multicentre, retro- and prospective cohort study was conducted using data from the Canadian Network for Autoimmune Liver Diseases (CaNAL). Adverse events were defined as the development of decompensation, hepatocellular carcinoma (HCC), liver transplantation (LT), or death. Treatment response was defined as the normalization of ALT at 6 months after treatment initiation.

Results: Data of 1198 people living with AIH with 13443 person-years follow-up and median disease duration of 9.5 years [IQR 4.6–15.4] were analyzed. The cohort had a high female predominance (73.6%), and the vast majority were Caucasians (76.9%). Males were significantly younger at the time of AIH diagnosis compared to females (35.2 [IQR 21.9–55.5] vs. 47.9 years [IQR 31.2–59.0]; $p < 0.001$). No significant difference was observed between males and females in the frequency of cirrhosis at diagnosis (29.4% vs. 26.1%; $p = 0.249$) or during follow-up (39.0% vs. 33.3%; $p = 0.124$), decompensation at diagnosis (9.6% vs. 8.7%; $p = 0.632$) or during follow-up (21.6% vs. 17.3%; $p = 0.112$), and mortality (13.9% vs. 13.2%; $p = 0.729$). However, males had twice the frequency of HCC (4.0% vs. 1.8%; $p = 0.034$) and LT (19.3% vs. 9.1%; $p < 0.001$) compared to females as well as poorer transplant-free survival (71.2% vs. 80.5%; $p = 0.001$). Moreover, males have substantially lower biochemical treatment response compared to females (36.6% vs. 56.7%; $p < 0.001$). Compared to other ethnicities, Indigenous Canadians had the highest frequency of adverse events (44.1% vs. 27.0%; $p = 0.027$), mainly driven by twice the frequencies of development of decompensation over follow-up (34.6% vs. 18.0%; $p = 0.031$), LT (26.5% vs. 11.3%; $p = 0.007$), mortality (26.5% vs. 13.0%; $p = 0.023$) and poorer transplant-free survival (21.5% vs. 38.2%; $p = 0.020$). They also had a substantially shorter event-free survival time (4.3 [IQR 1.5–9.5] vs. 8.2 [IQR 3.8–14.2] years; $p < 0.001$). In a time-dependent Cox regression, Indigenous people have a significantly higher risk of developing adverse outcomes (HR 2.70, 95% CI 1.60–4.54; $p < 0.001$) that remained strong after adjusting for male sex, age and cirrhosis at diagnosis and lack of treatment response (HR 2.80, 95% CI 1.01–7.80; $p = 0.049$).

Conclusion: Males living with AIH have lower rates of treatment response and higher frequency of HCC and need for LT compared to females. From the ethnicity perspective, Indigenous Canadians living with AIH have a higher risk of developing adverse liver outcomes compared to other ethnic groups.

THURSDAY 06 JUNE

THU-093

Biochemical response and liver stiffness variation over time predict liver-related events in patients with primary biliary cholangitis treated with Obeticholic acid

Antonio De Vincentis¹, Francesca Terracciani¹, Daphne D'Amato², Miki Scaravaglio³, Pietro Invernizzi⁴, Ester Vanni⁵, Daniela Campion⁶, Annarosa Floreani⁷, Nora Cazzagon⁷, Domenico Alvaro⁸, Rosanna Venere⁸, Edoardo Giannini⁹, Sara Labanca⁹, Ana Lleo¹⁰, Francesca Colapietro¹⁰, Elisabetta Degasperis¹¹, Mauro Viganò¹², Eugenia Vittoria Pesatori¹², Stefano Fagioli¹², Marco Marzoni¹³, Valerio Buzzanca¹³, Raffaella Viganò¹⁴, Federico D'Amico¹⁴, Andrea Galli¹⁵, Armando Curto¹⁶, Fabio Marra¹⁶, Paola Begini¹⁷, Leonardo Baiocchi¹⁸, Paola Carni¹⁸, Luigi Muratori¹⁹, Barbara Coco²⁰, Maurizia Brunetto²⁰, Fabrizio Pizzolante²¹, Nicoletta De Matthaeis²¹, Elisabetta Falbo²², Lorenzo Surace²², Alberto Mattalia²³, Donatella Ieluzzi²⁴, Federico Salomone²⁵, Guido Delle Monache²⁶, Riccardo Tatonetti²⁶, Ilaria Cavalli²⁷, Valentina Cossiga²⁸,

Filomena Morisco²⁸, Vincenzo Valiani²⁹, Pietro Gatti³⁰, Vincenzo Boccaccio²⁹, Debora Angrisani³¹, Giovanni Vettori³², Biagio Cuffari³³, Alessandra Moretti³⁴, Alba Rocco³⁵, Gerardo Nardone³⁵, Paolo Scivetti³⁶, Martina Costanzo³⁶, Valentina Boano³⁷, Giulia Francesca Manfredi³⁸, Loredana Simone³⁹, Valeria Pace Palitti⁴⁰, Maurizio Russello⁴¹, Maria Rita Cannavò⁴¹, Evelise Frazzetto⁴², Gaetano Bertino⁴², Marco Distefano⁴³, Antonio Izzi⁴⁴, Federica Cerini⁴⁵, Luchino Chessa⁴⁶, Michela Miglianti⁴⁶, Valentina Feletti⁴⁷, Alessandro Mussetto⁴⁷, Raffaele Cozzolongo⁴⁸, Francesco Losito⁴⁸, Grazia Anna Niro⁴⁹, Rosa Cotugno⁴⁹, Rodolfo Sacco⁵⁰, Chiara Ricci⁵¹, Paolo Poisa⁵¹, Luca Cadamuro⁵², Antonino Castellaneta⁵³, Francesco Squeo⁵³, Natalia Terreni⁵⁴, Niccolò Bina⁵⁴, Pietro Pozzoni⁵⁵, Silvia Casella⁵⁶, Francesca Zani⁵⁶, Olivia Morelli⁵⁷, Giuseppe Cuccorese⁵⁸, Carlo Saitta⁵⁹, Teresa Zolfino⁶⁰, Cristina Rigamonti³⁸, Vincenza Calvaruso⁵², Marco Carbone³, Umberto Vespasiani-Gentilucci¹. ¹Internal Medicine and Hepatology, University Campus Bio-Medico of Rome, Rome, Italy, ²Gastroenterology Unit, Città della salute e della scienza, Turin, Italy, ³Division of Gastroenterology, Centre for Autoimmune Liver Diseases, Department of Medicine and Surgery, University of Milano-Bicocca, European Reference Network on Hepatological Diseases (ERN RARE-LIVER), San Gerardo Hospital, Monza, Italy, ⁴Division of Gastroenterology, Centre for Autoimmune Liver Diseases, Department of Medicine and Surgery, University of Milano-Bicocca, European Reference Network on Hepatological Diseases (ERN RARE-LIVER), San Gerardo Hospital, Monza, Italy, ⁵Gastroenterology Unit, Città della salute e della scienza, Turin, Italy, ⁶Gastroenterology Unit, Città della salute e della scienza, Turin, Italy, ⁷Gastroenterology Unit, Department of Surgery, Oncology and Gastroenterology, Padua University Hospital, Padua, Italy, ⁸Department of Translational and Precision Medicine, University La Sapienza, Rome, Italy, ⁹Gastroenterology Unit, Department of Internal Medicine, University of Genoa, IRCCS Ospedale Policlinico San Martino, Genoa, Italy, ¹⁰Internal Medicine and Hepatology, Humanitas Clinical and Research Center IRCCS, Humanitas University, Milan, Italy, ¹¹Foundation IRCCS Ca' Granda Ospedale Maggiore Policlinico-Division of Gastroenterology and Hepatology-CRC "A.M. and A. Migliavacca" Center for Liver Disease, Milan, Italy, ¹²Hepatology and Liver Transplant Unit, Papa Giovanni XXIII Hospital, Bergamo, Italy, ¹³Clinic of Gastroenterology and Hepatology, Università Politecnica delle Marche, Ancona, Italy, ¹⁴Hepatology Unit, Niguarda Hospital, Milan, Italy, ¹⁵Department of Experimental and Clinical Biochemical Sciences, University of Florence, Florence, Italy, ¹⁶Internal Medicine and Hepatology Unit, Department of Experimental and Clinical Medicine, University of Firenze, Firenze, Italy, ¹⁷Azienda Ospedaliera Sant'Andrea, Rome, Italy, ¹⁸Hepatology Unit, University of Rome "Tor Vergata," Rome, Italy, ¹⁹DIMEC Università di Bologna, Policlinico di Sant'Orsola, Via Massarenti 9, 40138 Bologna, Italy, ²⁰University Hospital of Pisa, Pisa, Italy, ²¹Hepatology Unit, Pisa, Italy, ²²UOC of Gastroenterology, Gastroenterological, Endocrine-Metabolic and Nephro-Urological Sciences Department, Fondazione Policlinico Universitario A.Gemelli IRCCS, Università Cattolica del Sacro Cuore, Rome, Italy, ²³Azienda Sanitaria Provinciale di Catanzaro, Presidio Ospedaliero "Giovanni Paolo II" Lamezia Terme (CZ), Lamezia Terme, Italy, ²⁴Division of Gastroenterology, Santa Croce e Carle General Hospital, Cuneo, Italy, ²⁵Liver Unit, Department of Medicine, University and Azienda Ospedaliera Universitaria Integrata di Verona, Verona, Italy, ²⁶Ospedale di Acireale, Azienda Sanitaria Provinciale di Catania, Catania, Italy, ²⁷Ospedale di Penne, Pescara, Penne, Italy, ²⁸Division of Internal Medicine, Cremona Hospital, Cremona, Italy, ²⁹Department of Clinical Medicine and Surgery, Gastroenterology Unit, University of Naples "Federico II", Naples, Italy, ³⁰Unità di medicina interna, Ospedale Perrino di Brindisi, Italy, ³¹Unità di medicina interna, Ospedale Perrino di Brindisi, Brindisi, Italy, ³²AORN Antonio Cardarelli, Naples, Italy, ³³Gastroenterology and Endoscopy Unit, Santa Chiara Hospital, Trento 38014, Italy, ³⁴Division of Gastroenterology, Azienda Ospedaliero-Universitaria di Modena and University of Modena and Reggio Emilia, Modena, Italy, ³⁵UOC GASTROENTEROLOGIA, Ambulatorio

di Epatologia, P.O. San Filippo Neri, Rome, Italy, ³⁵Gastroenterology and Hepatology, Department of Clinical Medicine and Surgery, University Federico II, Naples, Italy, ³⁶Internal Medicine Unit, Azienda Sanitaria Locale di Biella, Biella, Italy, ³⁷Department of Gastroenterology and Endoscopy, Cardinal Massaia Hospital, Asti, Italy, ³⁸Dipartimento di Medicina Traslazionale, Università del Piemonte Orientale, Novara, Italy and Division of Internal Medicine, AOU Maggiore della Carità, Novara, Italy, ³⁹Department of Gastroenterology, University Hospital Sant'Anna, Ferrara, Italy, ⁴⁰Internal Medicine Unit, Santo Spirito Hospital, Pescara, Italy, ⁴¹Liver Unit, Arnas Garibaldi, Catania, Italy, ⁴²Gastroenterology and Hepatology Unit, University Hospital Policlinico Vittorio Emanuele, Catania, Italy, ⁴³Department of Infectious Diseases, Umberto I Hospital, Siracusa, Italy, ⁴⁴Department of Infectious Diseases, D. Cotugno Hospital, Napoli, Italy, ⁴⁵Hepatology Unit, San Giuseppe Hospital, Milan, Italy, ⁴⁶Liver Unit, University Hospital of Cagliari, Cagliari, Italy, ⁴⁷Gastroenterology Unit, Santa Maria Delle Croci Hospital, Ravenna, Italy, ⁴⁸Gastroenterology Unit, National Institute of Gastroenterology "S de Bellis" Research Hospital, Castellana Grotte (Bari), Italy, ⁴⁹Gastroenterology Unit, Fondazione Casa Sollievo Della Sofferenza IRCCS, San Giovanni Rotondo, Foggia, Italy, ⁵⁰Gastroenterology Unit, Ospedali Riuniti, Foggia, Italy, ⁵¹Internal Medicine, Spedali Civili, Brescia, Italy, ⁵²Gastroenterology and Hepatology Unit, University of Palermo, Palermo, Italy, ⁵³Gastroenterology Unit, Policlinico di Bari Hospital, Bari, Italy, ⁵⁴Hepatology Unit, Valduce Hospital, Como, Italy, ⁵⁵Hepatology Unit, Alessandro Manzoni Hospital, Lecco, Italy, ⁵⁶Hepatology Unit, Spedali Civili Gardone Val Trompia, Brescia, Italy, ⁵⁷Clinic of Gastroenterology and Hepatology, Department of Medicine, Università degli Studi di Perugia, Perugia, Italy, ⁵⁸Internal Medicine Ospedale "R.Dimiccoli", Barletta, Italy, ⁵⁹Division of Medicine and Hepatology, University Hospital of Messina "Policlinico G. Martino", Messina, Italy, ⁶⁰Department of Gastroenterology, Brotzu Hospital, Cagliari, Italy
Email: a.devincentis@policlinicocampus.it

Background and aims: In primary biliary cholangitis (PBC), the prognostic significance of alkaline phosphatase, bilirubin and liver stiffness measurements (LSM), and of their variation over time, have been well established. However, the association between their change during treatment with Obeticholic acid (OCA) and the occurrence of liver-related events (LRE) has never been investigated. In a large cohort of OCA-treated PBC patients, we aimed to evaluate whether the biochemical response to OCA is associated with longitudinal changes of LSM and, ultimately, with the risk of LRE.

Method: Data were extracted from the Italian RECAPITULATE cohort, including OCA-treated PBC patients from centers belonging to the Italian PBC Registry and/or the CLEO/AIGO PBC study groups. After excluding subjects with <6 months' observation and cirrhotic patients in Child-Pugh B-C classes, biochemical response was evaluated through POISE criteria. Linear mixed models were used to describe on-treatment variations of liver enzymes and LSM, while Cox-models to assess their impact on LRE. Joint models were applied to estimate the association between changes in LSM and LRE, defined as the occurrence of hepatic decompensation, liver transplantation or liver-related death.

Results: 631 PBC subjects (median age 58, women 89%, cirrhotics 27%) were followed for a median of 30 months (19, 164 patient-months), and 29 LRE were registered. A sub-sample of 243 individuals with at least two LSMs repeated during treatment (total 656 LSMs, median interval 12 months) was also analysed. POISE response rates were 42% and 58% at 1 and 3 years, respectively. LSM progressively increased in POISE non-responders (slope +0.44 KPa/year, 95%CI 0.04, 0.85), while decreased over time in responders (slope -0.45 KPa/year 95%CI -0.75, -0.13; p interaction <0.001). Patients attaining 1-year-POISE response showed a significantly reduced incidence of LRE during follow-up (HR 0.22, 95%CI 0.08, 0.59). Any increase in LSM was associated with an increased risk of

LRE, with an overall HR per 10% increase in LSM/year of 1.39 (95%CI 1.18, 1.67).

Conclusion: In patients with PBC, biochemical response to OCA translates into a reduction of LSM and of LRE during follow-up, while non-response is associated with increased LSM and risk of LRE.

THU-094

Clinical benefits with maralixibat for patients with Alagille syndrome are durable through 7 years of treatment: data from the MERGE study

Binita M. Kamath¹, Emmanuel Gonzalès², Deirdre Kelly³, Douglas B. Mogul⁴, Will Garner⁴, Pamela Vig⁴, Emmanuel Jacquemin². ¹The Hospital for Sick Children and the University of Toronto, Division of Gastroenterology, Hepatology and Nutrition, Toronto, Ontario, Canada; ²Service d'Hépatologie et de Transplantation Hépatique Pédiatriques, Centre de Référence de l'Atrésie des Voies Biliaires et des Cholestases Génétiques (AVB-CG), FSMR FILFOIE, ERN RARE LIVER, Hôpital Bicêtre, AP-HP, Faculté de Médecine Paris-Saclay, Le Kremlin-Bicêtre, and Inserm U1193, Hépatinov, Université Paris-Saclay, Orsay, France; ³Liver Unit, Birmingham Women's and Children's Hospital NHS Trust and University of Birmingham, Birmingham, United Kingdom; ⁴Miram Pharmaceuticals, Inc., Foster City, California, United States
Email: binita.kamath@sickkids.ca

Background and aims: Maralixibat (MRX), an ileal bile acid transport inhibitor (IBATi), is approved for the treatment of cholestatic pruritus in patients with Alagille Syndrome (ALGS) ≥3 months of age in the US and ≥2 months of age in Europe. Improvements in pruritus, serum bile acids (sBA), and height have been demonstrated from prior clinical trials including ICONIC (NCT02160782), which followed participants up to 4 years, as well as IMAGO/IMAGINE (NCT01903460/NCT02047318) and ITCH/IMAGINE-II (NCT02057692/NCT02117713), which reported outcomes to approximately 1.5 years. Participants from ICONIC, IMAGINE, and IMAGINE-II trials were invited to enroll in MERGE for additional long-term follow-up (LTFU) and prior long-term outcomes (e.g., liver transplant, death) for this group have been previously reported. Here we report on efficacy in participants with additional LTFU from MERGE, including some participants that have received treatment for 7 years.

Method: All participants from ICONIC, IMAGINE and IMAGINE-II were included in the analysis. Impact of MRX was assessed for pruritus [ItchRO (Obs) 0–4 scale, with a ≥1-point reduction considered clinically meaningful], sBA, height and weight z-scores, ALT, and total bilirubin (TB). Change from Baseline (CFB) was determined by comparing median (Q1, Q3) values from enrolment in the initial trial (i.e., ICONIC, IMAGO or ITCH) to data from the visit in MERGE that best aligned with an annual visit.

Results: Data were analyzed for 84 participants at Baseline, with follow-up to 1 year for 77 participants, 4 years for 40 participants, and 7 years for 26 participants. Baseline mean (SD) ItchRO (Obs) was 2.65 (0.75) and clinically meaningful reductions over time with CFB of -1.57 (-0.83, -2.14), -2.00 (-1.43, -2.56), and -2.14 (-1.43, -3.00) at 1 year, 4 years and 7 years, respectively. Likewise, Baseline sBA was 254 (207) µmol/L and decreased with CFB of -57 (-8, -150) µmol/L, -62 (-32, -152) µmol/L, and -105 (-41, -266) µmol/L at 1 year, 4 years and 7 years. Improvement was observed in height, with Baseline z-score of -1.7 (1.27) and CFB of 0.1 (-0.1, 0.3), 0.3 (0.0, 1.0), and 0.7 (0.0, 1.2) at 1 year, 4 years and 7 years while weight z-scores were largely unchanged. TB was stable with seven years of follow-up, with Baseline 5.5 (5.82) mg/dL, and CFB of 0.0 (-0.6, 0.5) mg/dL, 0.2 (-2.0, 0.2) mg/dL, and 0.0 (-0.9, 0.4) mg/dL over 1 year, 4 years, and 7 years. Changes in ALT showed modest increases with Baseline 158 (90) U/L and CFB of 23 (-2, 65) U/L, 36 (-4, 98) U/L, and 65 (-3, 87) U/L over 1 year, 4 years, and 7 years. There were no new safety signals.

Conclusion: In this unmatched cohort, the benefit of MRX in ALGS patients, including both improvements in clinical outcomes and sBA, persist through 7 years of treatment. No new safety concerns were identified in the long-term.

THU-095

Novel machine learning algorithm for risk prediction of cholangiocarcinoma in primary sclerosing cholangitis

Ewa Wunsch¹, Marcin Horecki², Małgorzata Milkiewicz¹, Beata Kruk³, Katarzyna Fischer⁴, Agnieszka Winikajtis-Burzyńska⁵, Gary Norman⁶, Dirk Roggenbuck⁷, Piotr Milkiewicz^{1,3}. ¹Pomeranian Medical University in Szczecin, Szczecin, Poland; ²Pomeranian Medical University in Szczecin, Department of Infectious, Tropical Diseases and Acquired Immunodeficiency, Szczecin, Poland; ³Medical University of Warsaw, Warsaw, Poland; ⁴Pomeranian Medical University in Szczecin, Independent Laboratory of Rheumatic Diagnostics, Szczecin, Poland; ⁵University Clinical Hospital 1, Szczecin, Poland; ⁶Werfen, San Diego, United States; ⁷Brandenburg University of Technology Cottbus-Senftenberg, Senftenberg, Germany
Email: ewa.wunsch@gmail.com

Background and aims: Single serum biomarkers are insufficient to predict the risk of primary sclerosing cholangitis-related cholangiocarcinoma (PSC-CCA). Recently novel autoantibodies have been postulated to correlate with the risk of PSC-CCA. We aimed to construct an original PSC-CCA risk prediction model based on a combination of clinical and laboratory variables and an autoantibody profile in a large cohort of patients with PSC. Artificial intelligence (AI) and machine learning techniques were used.

Method: A total of 606 patients with PSC (age range 16–73, 66% male, 23% cirrhotic) from the Polish prospective PSC registry were enrolled between 2010–2022. During the median follow-up period of 41 months, 42 patients (7%) were diagnosed with CCA by tissue samples and radiology. Enzyme-linked immunosorbent or chemiluminescence assays were utilizing to detect anti-gliadin IgA, anti-F-actin IgA, anti-GP2 IgA, and PR3-ANCA IgG antibodies. Input data consisted of 37 variables previously shown to correlate with unfavorable outcome and CCA. The estimation algorithm was developed based on a Python Scilearn package and Pandas using built-in machine learning algorithms. Various types of estimation algorithms were evaluated, including MLP, Random Forest, Decision Tree, Gaussian Naïve Bayes, SVC, and Logistic Regression. Variables were pre-selected using the Recursive Feature Elimination with cross-validation. Eleven variables were selected for the estimation algorithm, including the presence of PR3-ANCA IgG, anti-GP2 IgA, and anti-gliadin IgA antibodies; abnormal laboratory parameters (ALP, GGT, bilirubin, albumin, INR, ALT, AST), and diagnosis of inflammatory bowel disease (IBD). Each algorithm was evaluated using C-Statistics and individual metrics were calculated. All results were cross-validated and the data were divided into 5 folds.

Results: All applied algorithms revealed C-statistics >0.7. Logistic Regression showed the highest recall score and was chosen for the final algorithm. Individual metrics for this model were: C-Statistics 0.85, Accuracy Score 0.86, Recall Score 0.83, Precision Score 0.29, F1 Score 0.42. Finally, the model was placed in a docker container and can be implemented in an easy-to-use mobile app, where users could calculate the CCA risk for individual patients after entering input parameters in an online form.

Conclusion: We identified autoantibodies, IBD, and worse liver biochemistry as CCA risk factors and constructed a novel AI algorithm to estimate the risk of developing CCA in patients with PSC. The algorithm uses easily available data and may therefore be valuable in routine medical practice. Further external validation however is needed before clinical application.

THU-098

Appraising gain of an extended 2-year placebo-controlled trial in primary biliary cholangitis: challenges for evaluating clinical outcomes

Bettina E. Hansen¹, Gideon M. Hirschfield², Carla Fiorella Murillo Perez³, Charles A. McWherter³, Klara Dickinson⁴, Andrew L. Mason⁵, Aldo J. Montano-Loza⁵, Ellina Lytvyak⁵, George Dalekos⁶, Nikolaos Gatselis⁶,

Frederik Nevens⁷, Nora Cazzagon⁸, Cynthia Levy⁹, Nadir Abbas¹⁰, Palak Trivedi¹¹, Douglas Thorburn¹², Alan Bonder¹³, Vilas Patwardhan¹³, María Carlota Londoño¹⁴, Marco Carbone¹⁵, Laura Cristofori¹⁵, Adriaan J. van der Meer¹, Rozanne C. de Veer¹, Atsushi Tanaka¹⁶, Harry L.A. Janssen¹, Ehud Zigmund¹⁷, Eyal Yehezkel¹⁷, Andreas E. Kremer¹⁸, Ansgar Deibel^{18,19}, Tony Bruns²⁰, Karsten Große²¹, Kris V. Kowdley²², Ana Lleo²³, Marlyn J. Mayo²⁴, Xavier Verhelst²⁵, Christophe Corpechot²⁶. ¹Erasmus University Medical Center, Rotterdam, Netherlands; ²Toronto Centre for Liver Disease, University of Toronto, Toronto, Canada; ³Cymabay Therapeutics, Newark, United States; ⁴Cymabay Therapeutics, Newark, United States; ⁵University of Alberta, Edmonton, Canada; ⁶General University Hospital of Larissa, Larissa, Greece; ⁷University Hospitals KU, Leuven, Belgium; ⁸University of Padua, Padua, Italy; ⁹University Of Miami, Miami, United States; ¹⁰University Hospitals Birmingham National Health Service Foundation Trust, Birmingham, United Kingdom; ¹¹University of Birmingham, Birmingham, United Kingdom; ¹²Royal Free Hospital, London, United Kingdom; ¹³Beth Israel Deaconess Medical Center, Boston, United States; ¹⁴Liver Unit Hospital Clinic, Universidad de Barcelona, Barcelona, Spain; ¹⁵University of Milano-Bicocca, Monza, Italy; ¹⁶Teikyo University School of Medicine, Tokyo, Japan; ¹⁷Tel Aviv Sourasky Medical Center, Tel Aviv, Israel; ¹⁸University Hospital Zürich, Zürich, Switzerland; ¹⁹Department of Gastroenterology and Hepatology, University Hospital Zurich, University of Zurich, Zurich, Switzerland; ²⁰University Hospital RWTH Aachen, Aachen, Germany; ²¹University Hospital RWTH Aachen, Aachen, Germany; ²²Liver Institute Northwest, Seattle, United States; ²³Humanitas University, Milan, Italy; ²⁴UT Southwestern, Dallas, United States; ²⁵Ghent University Hospital, Ghent, Belgium; ²⁶Saint-Antoine Hospital, Assistance Publique-Hôpitaux de Paris, Sorbonne University, Paris, France
Email: b.hansen@erasmusmc.nl

Background and aims: Placebo-controlled trials in primary biliary cholangitis (PBC) assess biochemical response at 1 year. Recent European regulatory guidance proposes using trials of two years to assess safety and efficacy on clinical outcomes. The aim of this study was to determine whether it is feasible to detect a meaningful difference in event-free survival by extending a placebo-controlled trial to two years.

Method: A cohort of patients from the Global PBC Study group with similar eligibility criteria as the phase 3 RESPONSE study (EudraCT: 2020-004348-27) were selected; PBC diagnosis after 1990, age between 18 and 75 years, ursodeoxycholic acid (UDCA)-treatment for ≥12 months, or if untreated 12 months follow-up, total bilirubin (TB) <2 × ULN, and ALP > 1.67 × ULN. A random visit out of all eligible visits was selected as the index time. The RESPONSE population was used to estimate propensity scores based on: sex, age at visit, ALP, AST, ALT, TB, UDCA duration and use, and cirrhosis. These were subsequently used to calculate the IPTW-ATT weights. Weighted time-to-event analyses were conducted for transplant-free survival and event-free survival (hepatic decompensation [ascites, variceal bleeding, and hepatic encephalopathy], death, and liver transplantation). The incidence rate of events at two years was used for a power calculation based on a two-sided alpha of 0.05 with Fisher's exact test.

Results: There were 199 patients, 95% were female and 93% were UDCA-treated with a mean age at inclusion of 56 years (SD 10.3). The median year of diagnosis was 2004 (25th–75th percentile 1999–2009). Balance assessment between the RESPONSE cohort and the GLOBAL PBC cohort was successful after weighting. The incidence of death or liver transplantation after weighting in the first year was 1.0% as compared to 2.4% for two years, with a delta of 1.4% between one and two years. The incidence of hepatic decompensation, death, or liver transplantation after weighting in the first year was 3.3% as compared to 5.4% for two years, with a delta of 2.1% between one and two years. With the 5.4% incidence rate of events at two years in the control population and an estimated 2% incidence rate for the treated

group, a calculation with 80% power suggests that a total of 1050 patients would be required to detect a significant difference at 2 years based on Fisher's exact approach.

Conclusion: In a cohort of 199 PBC patients matched to a clinical trial population, the incidence of hepatic decompensation, death, and liver transplantation was 3.3% at one year and 5.4% at two years. Around 1000 patients would need to be included in a clinical trial for a significant difference to be detected between placebo and treatment at 2 years, which is unattainable in a rare disease and with a short inclusion time-frame. These findings emphasize the challenges of conducting placebo-controlled trials in PBC to inform on clinical outcomes.

THU-099-YI

Small duct primary sclerosing cholangitis is not associated with a heightened risk of colorectal cancer compared to inflammatory bowel disease alone

Sarah Al-Shakhshir¹, Nadir Abbas², Nasir Hussain³, Sean Morris¹, Tariq Iqbal⁴, Rachel Cooney⁵, James Ferguson⁶, Palak J. Trivedi³. ¹NIHR Birmingham Biomedical Research Centre, Centre for Liver and Gastrointestinal Research, University of Birmingham, Liver Unit, Queen Elizabeth Hospital Birmingham, University Hospitals Birmingham National Health Service Foundation Trust, Birmingham, United Kingdom; ²Liver Unit, Queen Elizabeth Hospital Birmingham, University Hospitals Birmingham National Health Service Foundation Trust, NIHR Birmingham Biomedical Research Centre, Centre for Liver and Gastrointestinal Research, University of Birmingham, Birmingham, United Kingdom; ³NIHR Birmingham Biomedical Research Centre, Centre for Liver and Gastrointestinal Research, University of Birmingham, Liver Unit, Queen Elizabeth Hospital Birmingham, University Hospitals Birmingham National Health Service Foundation Trust, Birmingham, United Kingdom; ⁴Department of Gastroenterology, Queen Elizabeth Hospital Birmingham, University Hospitals Birmingham National Health Service Foundation Trust, University of Birmingham Microbiome Treatment Centre, University of Birmingham, Birmingham, United Kingdom; ⁵Department of Gastroenterology, Queen Elizabeth Hospital Birmingham, University Hospitals Birmingham National Health Service Foundation Trust, Birmingham, United Kingdom; ⁶Liver Unit, Queen Elizabeth Hospital Birmingham, University Hospitals Birmingham National Health Service Foundation Trust, Birmingham, United Kingdom. Email: sarah.al-shakhshir@nhs.net

Background and aims: Primary sclerosing cholangitis (PSC) confers heightened lifetime risks of colorectal cancer (CRC) in patients (pts) with inflammatory bowel disease (IBD). Small duct PSC (sdPSC) is a phenotypic variant, associated with a lower risk of developing PSC-related liver events. However, it is not known if the risks of colorectal outcomes differ in sdPSC compared to IBD alone, and whether the increased incidence of CRC is restricted to pts with large duct disease (ldPSC).

Method: We conducted an observational cohort study across a high-volume autoimmune liver and IBD programme in the UK. The overarching goal was to determine phenotypic differences in IBD between disease groups (sdPSC and ldPSC vs IBD alone) and quantify the risks of colonic high-grade dysplasia (HGD) and CRC. Pts with sdPSC were censored at the time of developing large duct changes on imaging and moved to the ldPSC group using a clock reset approach.

Results: Data was accrued from n=494 pts diagnosed with PSC between 2000 and 2022, of whom 354 (72%) were diagnosed with colitis at some point in their lifetime (92.4% ldPSC-colitis; 7.6% sdPSC-colitis). The majority were men (66% ldPSC; 60% sdPSC), with a median age at PSC diagnosis of 40y and 41y, respectively. Of 27 sdPSC pts, 52% progressed to ldPSC at a rate of 6.6 per 100 follow-up years. Comparatively, 261 pts with colonic IBD (colitis) only, attended our program over the same timeframe. The median age at colitis diagnosis for pts with ldPSC, sdPSC and colonic IBD was 27 y, 29 y and 34 y ($p < 0.001$). Pancolitis was the predominant colonic disease distribution in the PSC group (50% ldPSC; 67% sdPSC), compared to

left-sided colitis in the IBD group (41%) ($p < 0.001$). The ceiling of IBD treatment differed between groups, with at least 1 biologic agent being commenced in 26% of pts with colitis alone, compared to 22% and 14% of pts with sdPSC and ldPSC, respectively ($p < 0.001$). However, colectomy for refractory colitis was performed more often in pts with PSC (sdPSC 22%, ldPSC 22% vs colonic IBD 18% [$p < 0.001$]). In all, 34 cases of high-grade HGD or CRC were identified: 1 patient with sdPSC (4%), who later progressed to ldPSC; 25 in ldPSC (8%) and 8 in colonic IBD (3%). Kaplan Meier estimates (censored by death or colectomy), with log-rank P values comparing the cumulative incidence of HGD or CRC between groups, showed a higher incidence in the PSC-associated colitis group compared to IBD alone (log rank $p = 0.02$). However, in a sub-analysis based on PSC subtype, this trend only persisted for the ldPSC-associated colitis group (log rank $p = 0.01$). The risks of developing HGD or CRC were significantly greater in the ldPSC vs. IBD group (hazard ratio [HR] 1.52, 95% CI: 1.08–2.13, $p = 0.01$) but not for sdPSC vs. IBD (HR 0.72, 0.30–1.50, $p = 0.4$).

Conclusion: Colitis in sdPSC is of a similar distribution and activity to ldPSC, although the risks of developing colonic dysplasia and cancer are no greater than in IBD alone.

THU-100

Factors associated with the real-world biochemical response to fibrate therapy in primary biliary cholangitis

Maria C. van Hooff¹, Rozanne C. de Veer¹, Ellen Werner¹, Ulrich Beuers², Joost P.H. Drenth³, Frans J.C. Cuperus⁴, Bart van Hoek⁵, Bart J. Veldt⁶, Michael Klemm-Kropp⁷, Suzanne van Meer⁸, Robert C. Verdonk⁹, Hajo J. Flink¹⁰, Jan Maarten Vrolijk¹¹, Tom J.G. Gevers¹², Cyriel Y. Ponsioen², Janne van Rooij¹³, Marjo J. Kerbert-Dreteler¹⁴, Jerome Sint Nicolaas¹⁵, Marleen De Vree¹⁶, Elsemieke S. de Vries¹⁷, Philip W. Friederich¹⁸, Merel M. Tielemans¹⁹, Huseyin Aktas²⁰, Daphne M. Hotho²¹, Ulrike de Wit²², Johan P.H. Kuyvenhoven²³, Sunje Abraham²⁴, Edith M.M. Kuiper²⁵, Stephan Schmittgens²⁶, Yasser A. Alderslieste²⁷, Harry L.A. Janssen^{1,28}, Bettina E. Hansen^{29,30}, Nicole S. Erler²⁹, Adriaan J. van der Meer¹. ¹Erasmus University Medical Center, Rotterdam, Netherlands; ²Amsterdam University Medical Center, Amsterdam, Netherlands; ³Radboud University Medical Center, Nijmegen, Netherlands; ⁴University Medical Center Groningen, Groningen, Netherlands; ⁵Leiden University Medical Center, Leiden, Netherlands; ⁶Reinier de Graaf Gasthuis, Delft, Netherlands; ⁷Noordwest Hospital Group, Alkmaar, Netherlands; ⁸University Medical Center Utrecht, Utrecht, Netherlands; ⁹Antonius Hospital, Nieuwegein, Netherlands; ¹⁰Catharina Hospital, Eindhoven, Netherlands; ¹¹Rijnstate Hospital, Arnhem, Netherlands; ¹²Maastricht University Medical Center, Maastricht, Netherlands; ¹³Tjongerschans Hospital, Heerenveen, Netherlands; ¹⁴Medisch Spectrum Twente, Enschede, Netherlands; ¹⁵Amphia Hospital, Breda, Netherlands; ¹⁶Treant Hospital, Hoogeveen, Netherlands; ¹⁷Isala Hospital, Zwolle, Netherlands; ¹⁸Meander Medical Center, Amersfoort, Netherlands; ¹⁹Bravis Hospital, Roosendaal, Netherlands; ²⁰Hospital Group Twente (ZGT), Hengelo, Netherlands; ²¹St Jansdal Hospital, Harderwijk, Netherlands; ²²Elisabeth-Tweesteden Hospital (ETZ), Tilburg, Netherlands; ²³Spaarnse Gasthuis Hospital, Haarlem, Netherlands; ²⁴Alrijne Hospital, Leiderdorp, Netherlands; ²⁵Maasstad Hospital, Rotterdam, Netherlands; ²⁶Nij Smellinghe Hospital, Drachten, Netherlands; ²⁷Beatrix Hospital, Gorinchem, Netherlands; ²⁸Toronto Centre for Liver Disease, Toronto General Hospital, Toronto, Canada; ²⁹Erasmus University Medical Center, Department of Biostatistics, Rotterdam, Netherlands; ³⁰Erasmus University Medical Center, Department of Epidemiology, Rotterdam, Netherlands. Email: m.vanhooff@erasmusmc.nl

Background and aims: Fibrates are off-label second line treatment options for patients with primary biliary cholangitis (PBC). This study aimed to assess the factors associated with the biochemical response at one year of fibrate therapy in patients with PBC.

POSTER PRESENTATIONS

Method: All patients who initiated fibrates in the Dutch PBC Cohort Study—a nationwide retrospective study including every identifiable patient with PBC from 1990 onwards—were evaluated. Biochemical measurements before start of fibrates and those closest to 12 months (within the 9–18 month window) were used. Biochemical response was assessed continuously in change (Δ) of ALP (in the upper limit of normal [ULN]) and dichotomously according to Paris-2 (ALP and AST $\leq 1.5 \times$ ULN and normal bilirubin) or normal ALP. Patients were stratified into a low, medium, and high baseline ALP group based on the 33rd ($<1.84 \times$ ULN) and 66th ($\geq 2.93 \times$ ULN) percentiles.

Results: In total, 317 initiated fibrates (bezafibrate in 310 [97.8%]). Excluded were 56 (17.6%) patients who discontinued therapy prior to response evaluation and 63 (19.8%) who had not yet reached nine months of treatment. Paired baseline and on-treatment ALP results were available for 153 patients, of which 144 (92.3%) were female. At baseline, median age was 54.4 years (IQR 48.5–63.1), 27 (19.6%) had cirrhosis, and median ALP was 2.27 (IQR 1.53–3.47). After one year of fibrate therapy, the median Δ ALP was -1.02 (IQR -1.60 to -0.52 , $p < 0.001$). The 12-month response rates for Paris-2 and normal ALP were 45.7% (64/140) and 34.6% (53/153), respectively. Age-adjusted multivariable logistic regression showed that cirrhosis (OR 0.28 [95%CI 0.08–0.96] $p = 0.043$), baseline ALP (OR 0.59 [95%CI 0.38–0.92], $p = 0.021$) and AST (OR 0.23 [95%CI 0.10–0.55] $p < 0.001$) were negatively associated with fulfilling Paris-2 response at 12 months of therapy. When stratified into a low, medium and high baseline ALP group, the median Δ ALP were -0.56 (-0.80 to -0.31), -1.09 (-1.35 to -0.65), and -2.15 (-3.73 to -1.09), respectively ($p < 0.001$). In contrast, dichotomous response rates reduced with higher ALP at baseline: 78.7%, 48.8% and 13.5%, respectively, for Paris-2 ($p < 0.001$), and 68.6%, 32.0% and 3.8%, respectively, for normal ALP ($p < 0.001$). At 12 months, patients who did not fulfil Paris-2 had a significantly stronger ALP reduction than patients who did (Δ ALP -1.17 [IQR -2.53 to -0.54] vs. Δ ALP -0.85 [IQR -1.29 to -0.56], $p = 0.032$).

Conclusion: In this real-world study, cirrhotic PBC patients had a reduced biochemical response to fibrate therapy. While patients with higher baseline ALP levels showed strongly reduced dichotomous response rates after one year of fibrate therapy, their absolute ALP reduction was substantially larger. As a result, ALP decline was stronger in incomplete Paris-2 responders, emphasizing the importance to value the anticholestatic treatment based on the absolute reduction of ALP.

THU-101

Non-invasive tests for ruling out high-risk esophageal varices in patients with primary biliary cholangitis based on the cholestasis degree

Vincenza Calvaruso¹, Ciro Celsa¹, Laura Cristofori^{2,3}, Miki Scaravaglio², Eugenia Nofit², Rachel Smith⁴, Senamjit Kaur⁵, Gabriele Di Maria¹, Luigi Capodicasa¹, Luca Cadamuro¹, Alessio Gerussi², Federica Malinverno³, Pietro Lampertico⁶, Nora Cazzagon⁷, Marco Marzoni⁸, Umberto Vespasiani-Gentilucci⁹, Francesca Colapietro¹⁰, Pietro Andreone¹¹, Ana Lleo^{10,12}, Cristina Rigamonti¹³, Mauro Viganò¹⁴, Edoardo Giannini¹⁵, Maurizio Russello¹⁶, Ester Vanni¹⁷, Federica Cerini¹⁸, Alessandra Orlandini¹⁹, Maurizia Brunetto²⁰, Grazia Anna Niro²¹, Giovanni Vettori²², Antonino Castellaneta²³, Vincenzo Cardinale²⁴, Domenico Alvaro²⁴, Andrea Mega²⁵, Valeria Pace Palitti²⁶, Francesco Bellanti²⁷, Vito Di Marco¹, George Mells⁴, Emma Culver²⁸, Pietro Invernizzi^{2,3}, Calogero Camma¹, Marco Carbone^{2,29}.

¹Gastroenterology and Hepatology, Department of Health Promotion, Mother and Child Care, Internal Medicine and Medical Specialties (PROMISE), University of Palermo, Palermo, Italy; ²Center for Autoimmune Liver Disease, Department of Medicine and Surgery, University of Milano-Bicocca, Monza, Italy, Monza, Italy; ³Division of Gastroenterology, Fondazione IRCCS San Gerardo dei Tintori, ERN-RARE LIVER center, Monza, Italy; ⁴Cambridge Liver Unit, Cambridge University Hospitals NHS Foundation Trust, Cambridge, United Kingdom; ⁵Oxford

University Hospitals NHS Trust, Oxford, United Kingdom; ⁶CRC “A. M. and A. Migliavacca” Center for the Study of Liver Disease, Division of Gastroenterology and Hepatology, Fondazione IRCCS Cà Granda Ospedale Maggiore Policlinico, Università degli Studi di Milano, Milan, Italy; ⁷Dept. of Surgery, Oncology and Gastroenterology, University of Padova; ⁸Clinic of Gastroenterology and Hepatology, Università Politecnica delle Marche, Ospedali Riuniti, University Hospital Ancona, Italy; ⁹Dept. of Internal Medicine, Unit of Hepatology, University and Fondazione Policlinico Universitario Campus Bio-Medico of Rome, Rome, Italy; ¹⁰IRCCS Humanitas Research Hospital, Rozzano, Milan, Italy; ¹¹Medicina Interna Metabolica, Baggiovara Hospital, Azienda Ospedaliero-Universitaria di Modena and Università di Modena e Reggio Emilia, Modena, Italy, Modena, Italy; ¹²Department of Biomedical Sciences, Humanitas University, Pieve Emanuele, Milan, Italy; ¹³Department of Translational Medicine, Università del Piemonte Orientale, Novara, Italy and Division of Internal Medicine, AOU Maggiore della Carità, Novara, Italy, Novara, Italy; ¹⁴Gastroenterologia 1 - Epatologia e Trapiantologia, ASST Papa Giovanni XXIII, Piazza OMS, 1-24127 Bergamo, Bergamo, Italy; ¹⁵Gastroenterology Unit, Department of Internal Medicine, University of Genoa, IRCCS Ospedale Policlinico San Martino, Genoa, Italy; ¹⁶Liver Unit, ARNAS GARIBALDI-NESIMA, CATANIA, Catania, Italy; ¹⁷Gastroenterology Unit, Città della Salute e della Scienza University Hospital, Turin, Italy; ¹⁸Hepatology Division San Giuseppe Hospital, MultiMedica IRCCS, Department of Clinical Sciences and Community Health, University of Milano, Milan, Italy, Via San Vittore 12, 20123 Milan, Italy; ¹⁹UO Malattie Infettive ed Epatologia, Azienda Ospedaliero-Universitaria di Parma, Via Gramsci 14, 43126 Parma, Parma, Italy; ²⁰Dept of Clinical and Experimental Medicine, University of Pisa and Hepatology Unit, University Hospital of Pisa, Pisa, Italy; ²¹Division of Gastroenterology and Endoscopy, Fondazione IRCCS ‘Casa Sollievo della Sofferenza’, Viale Cappuccini, 71013 San Giovanni Rotondo, Foggia, Italy, Foggia, Italy; ²²Azienda Provinciale per i Servizi Sanitari, Gastroenterology and Digestive Endoscopy Unit, Santa Chiara Hospital, Trento, Italy; ²³Gastroenterology Unit, Policlinico di Bari Hospital, Bari, Italy, Bari, Italy; ²⁴Department of Translational and Precision Medicine, Sapienza Univ. of Rome, Rome, Italy; ²⁵Gastroenterology Unit, Ospedale Generale Regionale di Bolzano, Bolzano, Italy; ²⁶Hepatology Unit, Santo Spirito Hospital, Pescara, Italy, Pescara, Italy; ²⁷Department of Medical and Surgical Sciences, University of Foggia, Foggia 71122, Italy, Foggia, Italy; ²⁸Oxford University NHS Trust and Nuffield Department Medicine, Oxford, UK, Oxford, United Kingdom; ²⁹S.C. Epatologia e Gastroenterologia, ASST Grande Ospedale Metropolitano Niguarda, Milano, Italy
Email: vincenza.calvaruso@unipa.it

Background and aims: Non-invasive tests (NITs) to identify patients with Primary Biliary Cholangitis (PBC) and compensated Advanced Chronic Liver Disease (cACLD) who can avoid esophagogastroduodenoscopy (EGD) are lacking. Aims of this study were to evaluate the diagnostic performance of NITs to rule out high-risk esophageal varices (HRV) in patients with PBC-related cACLD and to assess the influence of cholestasis on the NITs performance.

Method: Data of patients with cACLD were captured from the “Italian PBC registry” and two UK referral centres (Oxford University Hospitals and University Hospital of Cambridge). This study included all PBC patients who performed an EGD for evaluation of signs of portal hypertension within 6 months from liver stiffness and biochemical evaluation. The cohort was split into a derivation (2010–2020) and a validation (2021–2023) dataset. Outcome was the presence of HRV at index EGD.

RESIST criteria (platelets count $>120 \times 10^9/L$ and serum albumin $>3.6 g/dL$) were compared with elastography-based criteria (Baveno VI-BVI, Expanded Baveno VI-EBVI) in patients with Alkaline Phosphatase (ALP) $< \text{or} \geq 1.5$ times the upper limit of normal (ULN). Decision curve analysis (DCA) of NITs were calculated. Rate of patients fitting Baveno VII (BVII) criteria and prevalence of varices among them were also calculated.

Results: The cohort consisted of 303 patients [derivation (DC): n = 201, validation (VC): n = 102]. In the DC, at EGD, 119 patients (59.2%) had no varices, 60 (29.9%) had low-risk varices and 22 (10.9%) had HRV. In the VC, 51 (50%), 32 (31.4%) and 19 (18.6%) had no varices, low-risk and high-risk varices, respectively.

Proportion of correctly spared endoscopies for HRV was 98.2% (108/110), 92.3% (60/65), 92% (92/100) in DC and 94.1% (48/51), 85.2 (23/27), 85.4 (41/48) in VC for RESIST, BVI and EBVI respectively. RESIST criteria were associated with the lowest rate of missing HRV both in DC (1.8% vs 7.7% for BVI and 8.0% for EBVI) and VC (5.9% vs 14.8% for BVI and 14.6% for EBVI).

In both cohorts, patients with ALP ≥ 1.5 ULN (48.3% in DC and 33.3% in VC) had a high false negative rate to miss HRV for BVI (15.2% in DC and 16.7% in VC) and EBVI criteria (16.7% both in DC and VC). RESIST criteria false negative rate was lower (3.9 in DC and 6.2% in VC). DCA demonstrates the highest net benefit of RESIST criteria compared to elastography-based criteria for ruling out HRV, both in patients with ALP \leq or ≥ 1.5 ULN.

Overall, 9/56 (16.1%) patients who fit Baveno VII criteria (PLT >150 and TE <15 kPa) to rule out Clinically Significant Portal Hypertension (CSPH) had varices at EGD; 4/31 (12.9%) with ALP <1.5 and 5/25 (20%) with ALP ≥ 1.5 ULN.

Conclusion: Cholestasis impacts on NITs ability to rule out HRV and CSPH in patients with PBC and cACLD. Biochemical-based RESIST criteria demonstrates the highest net benefit compared to elastography-based criteria for ruling out HRV.

THU-102-YI

Specific glycomic profiles can identify patients at risk of poor transplant-free survival in primary biliary cholangitis

Nicky Somers¹, Nikolaos Gatselis², Maria C. van Hooff³, Vasiliki Lygoura², Emma Butaye¹, Lorenz Grossar¹, Sarah Raevens¹, Anja Geerts¹, Sander Lefere¹, Lindsey Devisscher⁴, Leander Meuris⁵, Marco Carbone⁶, Palak Trivedi⁷, María Carlota Londoño⁸, Cynthia Levy⁹, Atsushi Tanaka¹⁰, Gideon M. Hirschfield¹¹, Christophe Corpechot¹², Nico Callewaert⁵, Hans Van Vlierberghe¹, Adriaan J. van der Meer¹³, George Dalekos², Bettina E. Hansen¹⁴, Xavier Verhelst¹. ¹Department of Gastroenterology and Hepatology, Liver Research Center Ghent, Ghent University Hospital, Ghent, Belgium; ²Department of Medicine and Research Laboratory of Internal Medicine, Institute of Internal Medicine and Hepatology, General University Hospital of Larissa, Larissa, Greece; ³Department of Gastroenterology and Hepatology, Erasmus University Medical Center, Rotterdam, Netherlands; ⁴Gut-Liver Immunopharmacology Unit, Dpt Basic and Applied Medical Sciences; Liver Research Center Ghent, Ghent University, Ghent, Belgium; ⁵VIB-UGent Center for Biotechnology, Department of Biochemistry and Microbiology, Ghent University, Ghent, Belgium; ⁶Department of Medicine and Surgery, University of Milano-Bicocca, Monza, Italy; ⁷Institute of Biomedical Research, Medical School, University of Birmingham, University Hospitals Birmingham NHS Foundation Trust, Birmingham, United Kingdom; ⁸Liver Unit Hospital Clinic, Universidad de Barcelona, Barcelona, Spain; ⁹Division of Digestive Health and Liver Diseases, University of Miami, Miller School of Medicine, Miami, United States; ¹⁰Teikyo University School of Medicine, Tokyo, Japan; ¹¹Toronto Centre for Liver Disease, University of Toronto, Toronto, Canada; ¹²Reference center for inflammatory biliary diseases and autoimmune hepatitis, Saint-Antoine Hospital, Assistance Publique-Hôpitaux de Paris, Sorbonne University, Paris, France; ¹³Erasmus University Medical Center, Gastroenterology and Hepatology, Rotterdam, Netherlands; ¹⁴Epidemiology, Biostatistics and Gastroenterology and Hepatology, Erasmus University Medical Center, Rotterdam, Netherlands Email: nicky.somers@ugent.be

Background and aims: Primary Biliary Cholangitis (PBC) results in progressive liver fibrosis and eventually cirrhosis. Considering the varying pace of disease progression, accurate prognosis becomes essential for fine-tuning disease monitoring and treatment. We investigated the applicability of serum glycomic profiling for the

identification of PBC patients at risk of poor transplant-free survival (TFS).

Method: We used stored serum samples of 858 PBC patients, collected prospectively by three centers of the GLOBAL PBC Study Group. Whole serum N-glycomic analysis was performed using DNA sequencer Aided-Fluorophore Assisted Carbohydrate Electrophoresis (DSA-FACE). Uni- and multivariate Cox regression analyses were conducted to develop the prognostic GlycoRiskScore, with associated Kaplan Meier survival analysis. The GLOBE score and UK-PBC risk score for prediction of TFS were calculated.

Results: Patients had a mean follow-up of 6.43 years since sample collection, with an overall 5- and 10-year TFS of 91.6% and 83.1%, respectively. Cox regression analysis revealed increased fucosylated glycans (NA2Fb, NA3Fb, NA4Fb) and decreased bi-, and tri-antennary glycans (NA2F, NA3) in patients with poor TFS, from which the GlycoRiskScore was derived with an area under the curve (AUC) of 0.82 (95% CI [0.78–0.86], $p < 0.001$) and a hazard ratio (HR) of 3.36 (95% CI [2.82–4.01], $p < 0.001$). Patients with a score above the cut-off value of -1.9 showed an increased risk of poor 5- and 10-year TFS, compared with patients with low values ($p < 0.001$). Furthermore, patients in the 'high risk' group developed more liver cirrhosis (15.5% vs 6.3%, $p < 0.001$), hepatic decompensation (41.4% vs 15.9%, $p < 0.001$), hepatocellular carcinoma (3.2% vs 0.6%, $p = 0.003$) and had a higher mortality rate (37.4% vs 6.6%, $p < 0.001$), when compared to the 'low risk' group. In addition, the precision for TFS estimation of both the GLOBE and UK-PBC risk scores at time of sample collection showed an AUC of 0.75 (95% CI [0.71–0.80], $p < 0.001$). Other risk factors for poor TFS were high total bilirubin and alkaline phosphatase levels, together with low albumin and platelet count-which are signs of severe liver disease. When the GlycoRiskScore was adjusted for these covariates in a multivariable Cox proportional hazards model, the association with poor TFS was confirmed (HR 2.05, 95% CI [1.66–2.53], $p < 0.001$).

Conclusion: The GlycoRiskScore might be a potential predictive biomarker, complementing the current UK-PBC and GLOBE risk scores for assessing the prognosis of PBC patients. It can be useful in identifying individuals at high risk of poor transplant-free survival who need closer monitoring, irrespective of the disease stage.

THU-103

Results from a phase 2a trial with the CD80 antagonist RhuDex as a second line treatment for primary biliary cholangitis

Gideon Hirschfield¹, Vaclav Hejda², Michael Makara³, Tomas Douda⁴, Víctor Vargas Blasco⁵, Radan Brůha⁶, Ferenc Izbéki⁷, Karel Dvořák⁸, Krisztina Hagymási⁹, Mercedes Vergara¹⁰, Marian Oltman¹¹, Xavier Verhelst¹², Michael Stiess¹³, Markus Proels¹³, Michael Heneghan¹⁴. ¹University of Toronto, Toronto Centre for Liver Disease, Toronto, Canada; ²University Hospital in Pilsen, Plzen, Czech Republic; ³Central Hospital of Southern Pest National Institute of Hematology and Infectious Diseases, Saint Laszlo Hospital Outpatient Clinic, Budapest, Hungary; ⁴University Hospital Hradec Kralove, Hradec Kralove, Czech Republic; ⁵Vall d'Hebron University Hospital, Barcelona, Spain; ⁶General University Hospital Prague, Prague, Czech Republic; ⁷Szent György University Teaching Hospital of Fejér County, Székesfehérvár, Hungary; ⁸Regional Hospital Liberec, Liberec, Czech Republic; ⁹Semmelweis University, Budapest, Hungary; ¹⁰Parc Taulí University Hospital, Sabadell, Spain; ¹¹Center for Gastroenterology and Hepatology Thalion, Bratislava, Slovakia; ¹²Ghent University Hospital, Ghent, Belgium; ¹³Dr. Falk Pharma GmbH, Freiburg, Germany; ¹⁴Kings College Hospital, London, United Kingdom Email: gideonhirschfield@gmail.com

Background and aims: About one third of patients with primary biliary cholangitis (PBC) present with a suboptimal response to ursodeoxycholic acid (UDCA) and require additional second line therapy. The RDG-1/PBC trial aimed to evaluate the impact of adding the small molecule CD80 antagonist RhuDex to patients with PBC and inadequate response to UDCA.

POSTER PRESENTATIONS

Method: This was a double-blind, randomized, multi-center, placebo-controlled, comparative, exploratory phase II dose-finding trial. Patients were treated for 12 weeks with 50, 100 or 200 mg/day RhuDex gastro-resistant granules or placebo. The trial included patients with PBC and an inadequate response to UDCA, defined by serum alkaline phosphatase (ALP) levels between 1.5x and 10x the upper limit of normal (ULN) after at least 6 months of UDCA therapy. The primary efficacy end point was the relative change (%) in ALP from Baseline to the end of treatment. The trial was terminated early after a pre-planned interim analysis due to futility.

Results: 120 patients were screened. 82 patients were randomized, and 79 patients received at least one dose of study drug and were included in the full analysis set (FAS). Baseline data were comparable between treatment groups (mean age 55.5 years, 94% females, mean BMI 27.5, mean ALP 266 U/L, mean ALT 52 U/L, mean disease duration of 5.4 years). 58 patients completed the trial as planned and 21 patients of the FAS discontinued the trial prematurely. Mean treatment duration was 69 days and 79% of patients had a treatment compliance of $\geq 80\%$. The primary end point was not met. The mean relative change (%; [95% CI]) in ALP from Baseline to end of treatment were: Placebo (N = 19): -1.53 [-8.03;4.97]; RhuDex 50 mg/day (N = 20): 3.50 [-1.71;8.70]; RhuDex 100 mg/day (N = 21): 1.75 [-8.35;11.85]; RhuDex 200 mg/day (N = 19): 9.86 [-1.69;21.42]. Additional secondary end points including normalization of ALP, relative change in ALT, AST, GGT, ELF score and transient elastography did not reveal any clinical meaningful differences. Patient reported outcomes such as the PBC-40 questionnaire, Pruritus and Fatigue visual analogue scales showed no effect of RhuDex. No clinically relevant changes were observed for immune-activation related markers including TNF-alpha, IgM and IgG. Adverse events (AEs) occurred more frequently in the RhuDex 50, 100, and 200 mg groups (60.0%, 57.1%, and 84.2%, respectively) compared to placebo (52.6%). 28 AEs in 16 patients treated with RhuDex and 1 AE in 1 patient treated with placebo led to the premature trial discontinuation. 2 serious AEs were reported in 2 patients, both under RhuDex treatment, but considered not related to the study drug.

Conclusion: This trial did not show statistically significant or clinically relevant differences between RhuDex and placebo treatment. Higher AE frequencies were observed in the RhuDex groups. In this trial RhuDex did not contribute to potential second line therapies in PBC.

THU-104

Familial risk of biliary tract cancer and colorectal cancer in patients with primary sclerosing cholangitis

Erik von Seth¹, Aiva Båve², Michael Ingre², Caroline Nordenvall³, Annika Bergquist². ¹Department of Medicine Huddinge, Karolinska Institutet, Sweden, Sweden; ²Department of Medicine Huddinge, Karolinska Institutet, Stockholm, Sweden; ³Department of Molecular Medicine and Surgery, Karolinska Institutet, Stockholm, Sweden
Email: Erik.von.seth@ki.se

Background and aims: Primary sclerosing cholangitis (PSC) is a chronic liver disease associated with a high risk of biliary tract cancer (BTC) and colorectal cancer (CRC). Familial clustering of CRC is well-known in the general population and in individuals with inflammatory bowel disease (IBD). The familial clustering and cancer risk in individuals with PSC remains unclear. This study aimed to assess the familial risk of CRC and BTC in a large population with PSC.

Method: In a cohort of 1,594 patients with PSC and 15,940 age-, sex-, and geographically matched comparators from the general population in Sweden, we utilized national Health Registries to identify first-degree relatives and individuals with CRC and BTC across the entire study cohort. To assess the probability of BTC and CRC in individuals with a family history of CRC or BTC, we used logistic regression to calculate odds ratios (ORs) between PSC and their matched controls. In cases where ORs could not be calculated we used Fisher exact test. We also calculated relative risks (RR) in the group of PSC patients.

Results: The prevalence of a first degree relative with CRC and BTC was similar in PSC and in comparators, 6.1% and 1.9% vs. 6.4% and 1.6%. During a median follow-up time of 13.2 years (IQR 0.1–26.2), 5.0% (N = 79) and 13.6% (N = 191) of individuals with PSC were diagnosed with CRC or BTC. PSC with concomitant IBD had a higher likelihood of CRC than their healthy comparators (OR 5.1 (95% CI 3.6–7.0), but a family history of CRC was not associated with an increased risk of CRC in this group, RR 1.4 (95% CI 0.5–3.9). However, having a first-degree relative with CRC was associated with a higher likelihood of colectomy in individuals with PSC and IBD, RR 1.8 (95% CI 1.3–2.5). The odds of BTC in PSC patients was higher compared to matched controls, OR 80.2 (95% CI 54.4–123.1). The prevalence of familial BTC was low and therefore the risk was not assessed. Familial occurrence of either CRC or BTC was not associated with higher risk of BTC, RR 1.4 (95% CI 0.9–2.1). Having a first-degree relative with CRC was associated with an increased risk BTC in PSC, RR 1.6 (95% CI 1.0–2.5). **Conclusion:** A family history of CRC does not seem to increase the risk of CRC among PSC patients with concomitant IBD but increases the risk of colectomy. The high risk of colectomy may be explained by increased tendency for cancer preventive surgery. Having a first-degree relative with CRC was associated with increased risk of BTC in PSC in addition to the already high risk.

THU-105

Improvement in lipid profiles with elafibranor treatment in primary biliary cholangitis during the phase III Elative® trial

Marlyn J. Mayo¹, Nuno Antunes², Mark Pedersen¹, Dimitar Tonev³, Jianfen Shu², Christopher L. Bowlus⁴, Kris V. Kowdley⁵, Claudia O. Zein², Cynthia Levy⁶. ¹Division of Digestive and Liver Diseases, University of Texas Southwestern Medical Center, Dallas, TX, United States; ²Ipsen, Cambridge, MA, United States; ³Ipsen, Boulogne-Billancourt, France; ⁴Division of Gastroenterology and Hepatology, University of California Davis School of Medicine, Sacramento, CA, United States; ⁵Liver Institute Northwest, Seattle, WA, United States; ⁶Schiff Center for Liver Diseases, University of Miami, Miami, FL, United States
Email: marlyn.mayo@utsouthwestern.edu

Background and aims: Primary biliary cholangitis (PBC) is a rare, cholestatic liver disease, commonly associated with comorbid dyslipidaemia, for which patients may receive lipid-modifying therapies. In the ELATIVE® phase III trial, elafibranor, a dual peroxisome proliferator-activated receptor (PPAR)-alpha/delta agonist, demonstrated significant efficacy in improving biomarkers of cholestasis in PBC. This secondary analysis evaluated the effect of elafibranor on the lipid profiles of patients in ELATIVE®, which were divided into subgroups by concomitant lipid therapy.

Method: In ELATIVE® (NCT04526665), patients with PBC with an inadequate response or intolerance to ursodeoxycholic acid were randomized 2:1 to receive once-daily elafibranor 80 mg or placebo. Changes from baseline to Week 52 in lipids (total cholesterol, low-density lipoprotein cholesterol [LDL-c], high-density lipoprotein cholesterol [HDL-c], very LDL-c [VLDL-c] and triglycerides) were assessed in patients who were receiving or were not receiving lipid-modifying therapy (statins, ezetimibe or evolocumab) for ≥ 30 days at start of study treatment. Analyses were performed using a mixed model for repeated measures, with adjustments for baseline values and study stratification factors.

Results: Of 161 randomised patients, 25 (15.5%) were receiving lipid-modifying therapy (elafibranor: n = 18; placebo: n = 7). In the group not receiving lipid therapy, greater improvements in lipids from baseline to Week 52 were observed in patients receiving elafibranor vs placebo according to least-squares mean difference (95% confidence interval): total cholesterol (-11.30 [-23.95, 1.34] mg/dL; p = 0.079), LDL-c (-6.93 [-17.06, 3.20] mg/dL; p = 0.178), VLDL-c (-4.91 [-6.88, -2.93] mg/dL; p < 0.001), and triglycerides (-23.61 [-33.46, -13.76] mg/dL; p < 0.001). Smaller improvements in lipids were also observed in the group receiving lipid therapy; elafibranor vs placebo

(least-squares mean difference [95% confidence interval]): total cholesterol (−2.99 [−45.54, 39.56] mg/dL; $p = 0.884$), LDL-c (−8.80 [−40.96, 23.36] mg/dL; $p = 0.574$), VLDL-c (−4.45 [−10.68, 1.78] mg/dL; $p = 0.150$), and triglycerides (−22.59 [−53.67, 8.49] mg/dL; $p = 0.144$). HDL-c levels remained stable across both groups.

Conclusion: Elafibranor treatment in patients with PBC was associated with an overall improvement in lipid profiles compared with placebo, particularly among patients not receiving lipid-modifying therapy. These data suggest that elafibranor is not only an effective treatment for PBC (as per the primary ELATIVE® analysis), but also has an added benefit on lipid profiles. Ongoing analyses are evaluating lipid parameters in subgroups stratified according to other patient characteristics.

Study sponsor: GENFIT; secondary analysis and publication sponsor: Ipsen.

THU-106-YI

Prospective european reference network registry (R-LIVER) supports improvement in bone disease care delivery at local level for patients with autoimmune liver diseases and enables detailed description of risk elements

Boglarka Bozso^{1,2}, Sandor Mogyorossy^{2,3}, David Tornai^{1,2}, Patricia Kovats^{1,2}, Boglarka Balogh^{1,2}, Nora Sipeki^{1,2}, Fruzsina Olah^{1,2}, Péter Antal-Szalmás^{2,4}, Zsuzsanna Vitalis^{1,2}, Istvan Tornai^{1,2}, Christoph Schramm^{5,6}, Maria Papp^{1,2}. ¹Division of Gastroenterology, Department of Internal Medicine, Faculty of Medicine, University of Debrecen, Debrecen, Hungary; ²The European Reference Network on Hepatological Diseases (ERN RARE-, LIVER), Debrecen, Hungary; ³Division of Rheumatology, Department of Internal Medicine, Faculty of Medicine, University of Debrecen, Debrecen, Hungary; ⁴Department of Laboratory Medicine, Faculty of Medicine, University of Debrecen, Debrecen, Hungary; ⁵Department of Medicine, University Medical Centre Hamburg-Eppendorf (UKE), Hamburg, Germany; ⁶The European Reference Network on Hepatological Diseases (ERN RARE-, LIVER), Hamburg, Germany
Email: bozso.boglarka@mailbox.unideb.hu

Background and aims: Bone loss is a frequently observed complication in patients with autoimmune liver diseases (AILD). The exact risk of osteopenia and osteoporosis is unclear. Risk factors of bone loss require clarification. DEXA is both the screening method and guide for treatment. According to the EASL CPG currently in force, DEXA should be performed for all AILD patients at presentation and during follow-up (FUP). The outline standard is 80% assessment within 5 years.

We aimed to 1) assess bone loss at the time of diagnosis and during the FUP visits; 2) define risk factors of bone loss at the diagnosis; 3) evaluate the accomplishment of quality objectives for the diagnosis of bone loss and analyze how the R-LIVER Registry supported quality improvement in local level.

Method: In 2019, University of Debrecen (UNIDEB) joined the prospective, multicenter, quality-controlled R-LIVER Registry launched by the European Reference Network for Hepatological Diseases (ERN RARE-LIVER). A total of 209 AILD patients were included from UNIDEB. Clinical, laboratory, imaging, and DEXA data were collected prospectively at the time of diagnosis and during FUP visits yearly. A retrospective AILD patient cohort ($n = 176$, 2010–2016) from pre-accession period was used as a control group for monitoring guideline-adherence and clinical care standards of bone loss assessment.

Results: According to DEXA results, 55.7% of patients had some degree of bone loss and 24.5% had osteoporosis at the time of diagnosis with the highest prevalences in PBC (67.5% and 32.5%, respectively). Older age (OR:1.05), post-menopausal status (OR:4.82), vitamin D deficiency (OR:1.02) and presence of significant liver fibrosis (>9.2 kPa; OR:3.97) were risk factors for osteoporosis at diagnosis of AILD ($p < 0.01$ for all). mHAI value was an additional risk factor in AIH, but degree of cholestasis was not in PSC/PBC.

Significantly more patients had DEXA assessment in line with the EASL CPG after joining ERN RARE-LIVER. DEXA assessment rate at diagnosis improved to 50% in the first year after accession and to 64.4% thereafter (12%, $p < 0.001$). In this subpopulation guideline adherence to FUP DEXA requirement improved to 75% and 81.6% (vs 41.4%, $p < 0.001$), respectively. The outline standard was not achieved in the period prior to accession (29.8% had DEXA in 5 yrs), but thereafter DEXA assessment was already 68% in just 2 yrs FUP (IQR: 0.75–4.1).

Conclusion: Bone loss was a frequent complication in our prospective AILD patient cohort. We identified several risk factors. Validation and evaluation off medical treatment on bone loss progression should be performed in the whole R-LIVER Registry cohort. After joining ERN RARE-LIVER program, gradual and significant improvement was observed in the diagnosis of bone loss in AILD that verifies prospective registries as important tools for implementation of complex care in the clinical practice at local level.

THU-107

Short- and medium-term effects of hypnosis and psychoeducational interventions on fatigue associated with primary biliary cholangitis: a randomized controlled trial

Christophe Corpechot¹, Cécile Goffette², Cécile Flahault², Christel Vioulac², Anne-Claire Viret³, Hélène Pérennès⁴, David Da Rin⁴, Karima Ben Belkacem⁵, Gaouar Farid⁵, Nathalie Bernard⁵, Mehdi Kadhefi⁶, Alexandra Rousseau⁶, Pierre-Antoine Soret⁵, Sara Lemoine⁵, Olivier Chazouillères⁵, Aurélie Untas⁷. ¹Reference Center for Inflammatory Biliary Diseases and Autoimmune Hepatitis, Saint-Antoine Hospital, Assistance Publique-Hôpitaux de Paris, Sorbonne University, Paris, France; ²Laboratory of Psychopathology and Health Processes UR 4057, Institute of Psychology, Paris Cité University, Paris, France; ³Paris, France; ⁴Saint-Antoine Hospital, Assistance Publique-Hôpitaux de Paris, Paris, France; ⁵Reference center for inflammatory biliary diseases and autoimmune hepatitis, Saint-Antoine Hospital, Assistance Publique-Hôpitaux de Paris, Sorbonne University, Paris, France; ⁶Clinical Research Platform of the East of Paris, Saint-Antoine Hospital, Assistance Publique-Hôpitaux de Paris, Paris, France; ⁷Laboratory of Psychopathology and Health Processes UR 4057, Psychology Institute, Paris City University, Boulogne-Billancourt, France
Email: christophe.corpechot@aphp.fr

Background and aims: Fatigue is one of the main symptoms associated with primary biliary cholangitis (PBC). It affects quality of life and can lead to social isolation and depression. Although several disease-modifying therapies for PBC have proved effective, no therapeutic intervention has yet improved fatigue in this disease. The present study aimed to explore the efficacy of hypnosis and psychoeducational programs in improving fatigue in PBC patients.

Method: We conducted a randomized controlled trial in which women with stable, compensated PBC but clinically significant fatigue, defined by a PBC-40 fatigue score ≥ 33 , were equally assigned to hypnosis (HY), psychoeducation (PE) (one weekly session for 4 weeks for both interventions) and standard care (SC) programs. Patients completed questionnaires at baseline, week 5 (W5), month 3 (M3) and month 6 (M6). The first 8 patients in each group took part to an interview at baseline and M3. Statistical analysis was performed on the intent-to-treat population. The primary end point was the difference in the PBC-40 fatigue score between M3 and baseline. Secondary end points were differences between M3 and baseline in fatigue dimensions, quality of life, sleep, anxiety and depression scores (MFI, SF-36, PSQI, ESS, HADS). Leximetric analyses were performed on patients' interviews.

Results: A total of 55 patients (median age: 57 years; median fatigue score: 40) were assigned to HY ($n = 18$), PE ($n = 19$) and SC ($n = 18$) groups. Their characteristics at baseline were comparable. No adverse events occurred during the study. The primary end point did not differ statistically between groups, with median (interquartile range)

POSTER PRESENTATIONS

differences in the PBC-40 fatigue score between M3 and baseline in the SC, HY and PE groups of -3.0 ($-10.0; 1.0$), -6.0 ($-11.5; -4.8$) and -6.0 ($-8.0; -4.0$), respectively ($p = 0.15$ and $p = 0.30$ for comparison of SC with HY and PE, respectively). The results at W5 and M6 and those for the secondary end points were consistent with the results for the primary end point. Lexicometric analyses showed that patients in the HY and PE groups no longer spoke of their fatigue in the same way at M3 compared with the initial state, with a positive evolution in fatigue underlining the appropriation of the intervention followed.

Conclusion: Hypnosis and psychoeducational interventions did not result in a significantly greater short- and medium-term reduction in PBC-associated fatigue than standard care. However, a positive change was observed in the perception of fatigue in both intervention groups, suggesting that maintenance sessions could be beneficial in the long term. (Promoted by Assistance Publique-Hôpitaux de Paris; financially supported by Intercept France and ALBI Patient Association; PBC-HOPE ClinicalTrials.gov number, NCT03630718).

THU-109

Increasing prevalence of primary biliary cholangitis in The Netherlands

Rozanne C. de Veer¹, Maria C. van Hooff¹, Ellen Werner¹, Ulrich Beuers², Joost P.H. Drenth³, Frans J.C. Cuperus⁴, Bart van Hoek⁵, Bart J. Veldt⁶, Michael Kempt-Kropp⁷, Suzanne van Meer⁸, Robert C. Verdonk⁹, Hajo J. Flink¹⁰, Jan Maarten Vrolijk¹¹, Tom J.G. Gevers¹², Cyriel Y. Ponsioen², Martijn J. ter Borg¹³, Khalida Soufidi¹⁴, Femke Boersma¹⁵, Hendrik J.M. de Jonge¹⁶, Frank H.J. Wolfhagen¹⁷, L.C. Baak¹⁸, Susanne L. Onderwater¹⁹, Jeroen D. van Bergeijk²⁰, Paul G. van Putten²¹, Gijs J. de Bruin²², Rob P.R. Adang²³, Nieves Aparicio Pages²⁴, Wink de Boer²⁵, Frank ter Borg²⁶, Hanneke van Soest²⁷, Harry L.A. Janssen^{1,28}, Bettina E. Hansen¹, Nicole S. Erler¹, Adriaan J. van der Meer¹. ¹Erasmus University Medical Center, Rotterdam, Netherlands; ²Amsterdam University Medical Center, Amsterdam, Netherlands; ³Radboud University Medical Center, Nijmegen, Netherlands; ⁴University Medical Center Groningen, Groningen, Netherlands; ⁵Leiden University Medical Center, Leiden, Netherlands; ⁶Reinier de Graaf Gasthuis, Delft, Netherlands; ⁷Noordwest Ziekenhuisgroep, Alkmaar, Netherlands; ⁸University Medical Center Utrecht, Utrecht, Netherlands; ⁹St. Antonius Hospital, Nieuwegein, Netherlands; ¹⁰Catharina Hospital, Eindhoven, Netherlands; ¹¹Rijnstate, Arnhem, Netherlands; ¹²Maastricht University Medical Center, Maastricht, Netherlands; ¹³Maxima Medical Center, Eindhoven, Netherlands; ¹⁴Zuyderland Medical Center, Heerlen, Netherlands; ¹⁵Gelre Hospitals, Apeldoorn-Zutphen, Netherlands; ¹⁶Jeroen Bosch Hospital, Den Bosch, Netherlands; ¹⁷Albert Schweitzer Hospital, Dordrecht, Netherlands; ¹⁸Onze Lieve Vrouwe Gasthuis, Amsterdam, Netherlands; ¹⁹Diakonessenhuis, Utrecht, Netherlands; ²⁰Hospital De Gelderse Vallei, Ede, Netherlands; ²¹Medical Center Leeuwarden, Leeuwarden, Netherlands; ²²Tergooi Hospital, Hilversum-Blaricum, Netherlands; ²³VieCuri, Venlo, Netherlands; ²⁴Canisius Wilhelmina Hospital, Nijmegen, Netherlands; ²⁵Bernhoven, Uden, Netherlands; ²⁶Deventer Hospital, Deventer, Netherlands; ²⁷Medical Center Haaglanden, Den Haag, Netherlands; ²⁸Toronto Centre for Liver Disease, Toronto, Canada
Email: r.deveer@erasmusmc.nl

Background and aims: Accurate prevalence rates of Primary Biliary Cholangitis (PBC) remain challenging to determine due to limited comprehensive population-based registries. We assessed the prevalence of PBC in the Netherlands over time through the nation-wide Dutch PBC Cohort Study (DPCS).

Method: The DPCS is a retrospective study which includes every identifiable patient with PBC in the Netherlands from 1990 onwards in all 71 Dutch hospitals. Case identification was performed through diagnosis and treatment codes, antimitochondrial antibodies test results, and locally available registries, by two medical doctors. Data on yearly adult population size (≥ 20 years) on January 1st and

average life expectancy were extracted from Statistics Netherlands. Assessment of point prevalence of PBC was restricted to the period 2008–2018. Patients were censored at time of liver transplantation, death or when moving abroad. Patients lost to follow-up (LFU) were censored based on their average life expectancy. Prevalence Ratios (PR) were calculated using Poisson regression and analyzed among sex and age groups (20–45, 45–65, and ≥ 65 years) over time. Joinpoint regression was used to analyze time trends in prevalence by calculating annual percent changes (APC) and average annual percent changes (AAPC).

Results: On January 1st 2008, 1458 patients had PBC in the Netherlands. Over the study period, 2187 patients were newly diagnosed with PBC, while 46 were transplanted and 468 died. A total of 271 patients were LFU. Point prevalence of PBC increased from 11.93 per 100,000 persons in 2008 to 21.53 in 2018, with a median yearly prevalence of 17.06 (IQR 14.17–19.47) per 100,000 persons. The AAPC was 5.94% (95% CI 5.77–6.15, $p < 0.05$). The APC was 7.73% (95% CI 7.06–8.66, $p < 0.05$) between 2008–2012 and 4.77% (95% CI 4.42–5.09, $p < 0.05$) from 2012 to 2018. In 2018, prevalence of PBC was 37.6 per 100,000 persons for females and 4.9 for males (adjusted PR of 7.72, 95% CI 7.41–8.05, $p < 0.001$, females vs. males). The AAPC was comparable for men (5.53%, 95% CI 4.50–6.70, $p < 0.05$) and women (5.91%, 95% CI 5.73–6.11, $p < 0.05$). When stratified for age, point prevalence in 2018 ranged from 3.04 per 100,000 persons aged 20–45 years to 45.17 aged ≥ 65 years. Over time, compared to the population 20–45 years, adjusted PRs were 7.31 (95% CI 6.94–7.69, $p < 0.001$) and 11.32 (95% CI 10.76–11.90, $p < 0.001$) for those aged 45–65 years and ≥ 65 years, respectively. During the study period the AAPC was higher in older subgroups: 2.12% (95% CI 1.34–2.95, $p < 0.05$) in those aged 20–45 years up to 5.69% (95% CI 5.32–6.36, $p < 0.05$) in those ≥ 65 years.

Conclusion: This nationwide cohort study shows a continuing increase in prevalence of PBC, which remains a rare liver disease. As the proportion of PBC patients ≥ 65 years is becoming larger, future studies need to focus on the clinical impact of (additional) therapy in the elderly population.

THU-110

Time to initiation of the second-line therapy obeticholic acid in patients with primary biliary cholangitis

Sonal Kumar^{1,2}, Joanna P. MacEwan³, Alina Levine³, Leona Bessonova⁴, Radhika Nair⁴, Darren Wheeler⁴, Jing Li⁴, Robert S. Brown, Jr.¹. ¹Weill Cornell Medical College, New York, United States; ²New York Presbyterian Hospital-Weill Cornell Medicine, New York, United States; ³Genesis Research Group, Hoboken, United States; ⁴Intercept Pharmaceuticals, Inc., Morristown, United States
Email: sok9028@med.cornell.edu

Background and aims: Obeticholic acid (OCA) is the only approved second-line (2L) therapy for patients with primary biliary cholangitis (PBC). The objective of this study was to estimate the time from eligibility for 2L therapy to initiation of OCA treatment in patients with PBC.

Method: Patients with PBC (1 inpatient claim or ≥ 2 outpatient claims) eligible for 2L therapy between June 2016 and February 2022 were identified from the US Komodo Healthcare Map™. Eligibility for 2L therapy was determined based on inadequate response to ursodeoxycholic acid. The index date was defined as the first date of 2L eligibility. Patients were enrolled for ≥ 12 months preindex and were ≥ 18 years old at index. Patients were followed up until the initiation of OCA, end of insurance enrollment, long-term care admission, death, or end of study period (May 5, 2023), whichever came first. The proportion of patients initiating OCA and time to OCA initiation were described.

Results: Of 3880 patients with PBC eligible for 2L therapy, 306 (7.9%) initiated OCA, and 3, 574 (92.1%) did not. Eligible patients had a mean

(SD) age of 61.3 years (11.5), they were predominantly female (90.8%), and approximately half were White (50.5%). The mean (SD) time to OCA initiation from the time the patient was eligible for 2L therapy was 15.1 (15.1) months with a median (interquartile range) of 11.0 (3.0–19.3) months. Patients initiating OCA were slightly younger than those who did not, with a mean (SD) age of 57.4 (10.2) vs 61.7 (11.5) years, respectively. Of the patients initiating OCA, 90.8% were female, 42.2% were White. Based on the 1-year baseline period (12 months before and including index date), a higher proportion of patients initiating OCA had cirrhosis (18.3% vs 13.3% who did not initiate OCA) and were diagnosed with other autoimmune disease in addition to PBC (29.4% vs 26.2%). At the time of OCA initiation, the proportion of patients with cirrhosis almost doubled compared to when patients were first eligible for 2L therapy (18.3% to 32.0%). Patients initiating OCA had higher mean (SD) baseline alkaline phosphatase (ALP) levels (IU/L) than those who did not (256.0 [137.6] vs 184.2 [98.6], respectively). At the time of 2L eligibility 55.6% of patients initiating OCA had baseline ALP levels $\geq 1.67 \times$ upper limit of normal (ULN) vs 25.2% of those that did not initiate OCA; by the time of OCA initiation, 66.3% of the patients had ALP $> 1.67 \times$ ULN.

Conclusion: Among patients eligible for 2L therapy, less than 10% initiated OCA. A considerable delay in initiation was observed, indicating that patients may experience disease progression, including onset of cirrhosis, by the time 2L therapy is initiated. Demonstrated clinical benefit on long-term outcomes with OCA may be further improved with more timely initiation of OCA in appropriate patients.

©2023 Komodo Health, Inc. All rights reserved. Used with permission.

THU-111

Second-line treatment in recurrent primary biliary cholangitis after liver transplantation: an international multicentre study

Nadir Abbas¹, Rebecca Mladenovic², Ellina Lytvyak³, Neil Halliday⁴, Douglas Thorburn⁵, Yooyun Chung⁶, Deepak Joshi⁷, Michael Heneghan⁸, Jessica Dyson⁹, David E. Jones¹⁰, Christophe Corpechot¹¹, Aldo J Montano-Loza¹², Palak J. Trivedi^{13,14}.

¹National Institute for Health and Care Research Birmingham Biomedical Research Centre, University of Birmingham, The Liver unit, University Hospital Birmingham Queen Elizabeth, Birmingham, United Kingdom; ²The Liver unit, University Hospital Birmingham, Birmingham, United Kingdom; ³Division of Gastroenterology and Liver unit, University of Alberta, Edmonton, Canada; ⁴Institute of Liver and Digestive Health, University College London, London, United Kingdom; ⁵The Sheila Sherlock Liver Centre, Royal free, London, United Kingdom; ⁶Institute of Liver Studies, Kings college, London, United Kingdom; ⁷Institute of Liver Studies, King's college Hospital, London, United Kingdom; ⁸Institute of Liver studies, Kings College Hospital, London, United Kingdom; ⁹Newcastle upon Tyne Hospitals NHS Foundation Trust, Newcastle, United Kingdom; ¹⁰Newcastle University Medical School, Newcastle, United Kingdom; ¹¹Saint-Antoine Hospital, Assistance Publique-Hôpitaux de Paris, Sorbonne University, Paris, France; ¹²University of Alberta, Gastroenterology and Liver Unit, Edmonton, Canada; ¹³NIHR Birmingham Biomedical Research Centre, Centre for Liver and Gastrointestinal Research, University of Birmingham, Institute of Immunology and Immunotherapy, University of Birmingham, Birmingham, United Kingdom; ¹⁴Institute of Immunology and Immunotherapy, University of Birmingham, Birmingham, United Kingdom

Email: nadir.abbas@uhb.nhs.uk

Background and aims: One in 3 people who undergo liver transplantation (LT) for primary biliary cholangitis (PBC) develop disease recurrence (rPBC) despite treatment with ursodeoxycholic acid (UDCA). This international, multicentre study aimed to assess the safety and tolerability of available second-line treatments (SLTs) in the context of rPBC.

Method: We collected demographic, clinical and laboratory data from patients (pts) who underwent LT from 1999 to 2023 across 6 centres in Europe and North America. Eligible study pts were those with biopsy proven rPBC in the absence of biochemical dysfunction attributable to biliary strictures, vascular complications or allograft rejection, and who were treated with SLTs (obeticholic acid [OCA] or fibric acid derivatives). Biochemical trends, alongside discontinuation rates and tolerability data, were accrued over a 12-month period from the point of starting SLT.

Results: Over the course of the study, 21 individuals with rPBC were treated with SLT (10 OCA, 11 fibric acid derivatives). Fifteen pts were women, with a median age of PBC diagnosis and at time of LT of 41 (IQR 35–49) years and 46 (39–51) years, respectively. All pts were offered UDCA post-LT; however, 9 were UDCA-intolerant and discontinued prior to starting SLT. The median time from LT to rPBC was 1035 (684–1531) days; the earliest diagnosis was made at 183 days. The median transient elastography score at the time of rPBC was 8.8 (6.3–12.2) kPa, with median ALP, ALT, bilirubin, and albumin at baseline of $2.3 (1.8\text{--}2.8) \times$ the upper limit of normal (ULN), $1.2 (0.7\text{--}1.8) \times$ ULN, $12 (8\text{--}18) \mu\text{mol/L}$ and $41 (37\text{--}42) \text{g/L}$, respectively. At 3-, 6- and 12-months follow-up, 16, 14 and 14 pts completed continued SLT. Five pts discontinued OCA due to disease progression ($n=3$), drug intolerance ($n=1$) or pruritus ($n=1$). Comparatively, 4 discontinued fibric acid derivatives due to renal dysfunction ($n=2$) or concerns over liver disease progression ($n=2$). In total, 3/21 pts were referred for re-transplantation and 5 died (4 liver-related deaths). At 3, 6 and 12 months of OCA treatment, median reductions in serum ALP were 18 (12–25) %, $p=0.38$; 30 (19–39) %, $p=0.22$; and 4 (1–7) %, $p=0.40$, median reductions in serum ALT from baseline were 8 (5–12) %, $p=0.08$; 42 (32–51) %, $p=0.02$; and 30 (21–45) %, $p=0.40$. at 12 months. Median ALP reductions in the fibric acid group at 3, 6 and 12 months were 25 (11–37) %, $p=0.03$; 35 (26–49) %, $p=0.01$; and 35 (28–45) %, $p=0.05$; respectively and median ALT reduction was 8 (4–12) %, $p=0.1$; 16 (8–26) %, $p=0.19$; and 8 (4–17) %, $p=0.65$; respectively.

Conclusion: In this first, real-world study of SLT in rPBC, we find treatment with fibric acid derivatives is associated with significant reductions in serum ALP over time. However, discontinuation rates of OCA and fibric acid derivatives are high, underscoring the need for larger studies exploring novel treatment paradigms in the treatment of rPBC.

THU-112-YI

Quantitative magnetic resonance cholangiopancreatography provides additional prognostic value in prediction of transplant-free survival in primary sclerosing cholangitis

Tim Middelburg¹, Bregje Mol¹, Liam Young², Carlos Ferreira³, Tom Davis², Karin Horsthuis¹, Ynto de Boer⁴, Adriaan J. van der Meer⁵, Annemarie de Vries⁶, Roy Dwarkasing⁶, Johannes Bogaards¹, Aart Nederveen¹, Jaap Stoker¹, Cyriel Ponsioen¹. ¹Amsterdam UMC, Amsterdam, Netherlands; ²Perspectum Ltd, Oxford, United Kingdom; ³Perspectum Ltd, Oxford, United Kingdom; ⁴Amsterdam UMC, Amsterdam Gastroenterology, Endocrinology and Metabolism, Amsterdam, Netherlands; ⁵Erasmus MC, Rotterdam, Netherlands; ⁶Erasmus MC, Rotterdam, Netherlands

Email: t.e.middelburg@amsterdamumc.nl

Background and aims: Magnetic resonance cholangiopancreatography (MRCP) is currently used for diagnostic and monitoring purposes in primary sclerosing cholangitis (PSC) and could also prove useful for prediction of transplant-free survival. Current qualitative assessments are limited by intra- and interobserver variability, whereas quantitative assessment could overcome these limitations. This study aimed to validate the additional prognostic value of quantitative MRCP metrics in PSC.

Method: Retrospective clinical and imaging data were collected from the Dutch EpiPSC2 registry, including data from one tertiary and one transplantation center. First available MRCP data was modelled by artificial-intelligence driven software (MRCP+, Perspectum Ltd.) and

POSTER PRESENTATIONS

quantitative metrics were generated. Data were randomized into a derivation and validation set at a 1:1 ratio. Prognostic factors including sex, type of PSC, inflammatory bowel disease phenotype and age and time-related variables were used as covariates. Cox regression analysis was used to develop and assess the predictive performance of a binary risk classifier for transplant-free survival. Subsequently, the derived risk classifier was applied on the validation set.

Results: In total 207 patients were included. Median transplant-free survival from MRCP onwards was 6.3 (IQR: 3.5–8.8) years and an event occurred in 65 patients. Multivariate analysis identified total number of candidate strictures, time from diagnosis to MRCP, proportion of ducts with 3–5 mm diameter and center of inclusion to be associated with transplant-free survival. The derived risk classifier showed good predictive performance (C-statistic = 0.74) for identifying patients at high risk of an event (HR = 5.4, 95% CI 2.3–12.4, $p < 0.001$) in the derivation set and remained consistent under 5-fold cross validation (C-statistic = 0.71). Applying the derived risk classifier on the validation set showed comparable predictive performance (C-statistic = 0.69) for risk assessment (HR = 3.5, 95% CI 1.7–6.9, $p < 0.001$).

Conclusion: This study confirms the additional prognostic value of MRCP+ metrics on long-term transplant-free survival in PSC and warrants further study on the incorporation of quantitative MRCP metrics into existing prognostic risk models.

THU-113

Optimizing thiopurine therapy in autoimmune hepatitis (AIH): a multi-center study on monitoring metabolite profiles and co-therapy with allopurinol

Jan Philipp Weltzsch^{1,2}, Claudius Bartel¹, Moritz Waldmann³, Stephanie Schulze^{1,2}, Ye Htun Oo^{2,4,5}, Maria Papp^{2,6}, Benedetta Terziroli^{2,7}, Adriana Baserga^{2,7}, Marcial Sebode^{1,2}, Ansgar W. Lohse^{1,2}, Christoph Schramm^{1,2,8}, Johannes Hartl^{1,2}.
¹I. Dept. of Medicine, University Medical Center Hamburg-Eppendorf (UKE), Hamburg, Germany; ²European Reference Network on Hepatological Diseases (ERN RARE-LIVER), Hamburg, Germany; ³Institute of Clinical Chemistry and Laboratory Medicine, University Medical Center Hamburg-Eppendorf (UKE), Hamburg, Germany; ⁴Centre for Liver and Gastro Research, Institute of Immunology and Immunotherapy, University of Birmingham, Birmingham, United Kingdom; ⁵Liver Transplant and Hepato-biliary Unit, Queen Elizabeth Hospital, University Hospital Birmingham NHS Foundation Trust, Birmingham, United Kingdom; ⁶Division of Gastroenterology, Department of Internal Medicine, Faculty of Medicine, University of Debrecen, Debrecen, Hungary; ⁷Fondazione Epatocentro Ticino, Lugano, Switzerland; ⁸Martin Zeitz Center for Rare Diseases, University Medical Center Hamburg-Eppendorf (UKE), Hamburg, Germany
Email: j.weltzsch@uke.de

Background and aims: We aimed to assess whether (i) a target range of thiopurine metabolites can be defined in autoimmune hepatitis (AIH), (ii) how modifying thiopurine dose and (iii) the addition of allopurinol to low-dose thiopurines impact metabolite levels and treatment response in AIH.

Method: Metabolite concentrations were tested in 331 individuals from four European centers (Hamburg, Lugano, Debrecen, Birmingham). A subgroup analysis was performed in patients with multiple metabolite measurements over time (N = 146). Thiopurine metabolite levels and treatment response were assessed after thiopurine dose increase in 50 patients and after combination with allopurinol in 36 patients.

Results: Thiopurine doses correlated with 6MMP, but not with 6TGN levels. In a cross-sectional analysis, 6TGN levels were similar in those with complete biochemical remission (CBR) and those without ("CBR": 196 pmol/0.2 ml, IQR 120–312 vs. "No CBR": 204 pmol/0.2 ml, IQR 142–350). However, higher 6TGN levels were observed in those with documented CBR at multiple time points (250 pmol/

0.2 ml, IQR 228–344), compared to those failing to maintain CBR (181 pmol/0.2 ml, IQR 143–231, $p = 0.0014$) or those who never achieved CBR (153 pmol/0.2 ml, IQR 107–218, $p < 0.0001$), with a determined optimal cutoff of 223 pmol/0.2 ml (sensitivity: 76%, specificity: 78%). Increasing azathioprine doses by 36% led to preferential 6MMP formation (6MMP: +127% vs. 6TGN: +34%; $p < 0.0001$). In a difficult-to-treat cohort, adding 100 mg allopurinol to low-dose thiopurines raised 6TGN from 168 to 320 pmol/0.2 ml ($p < 0.0001$) and lowered 6MMP from 2309 to 183 pmol/0.2 ml ($p < 0.0001$), accompanied by improved serum ALT levels (70 to 32 U/L; $p < 0.0001$) in all patients and long-term CBR in 76%.

Conclusion: Maintaining CBR in AIH was associated with 6TGN concentrations above 223 pmol/0.2 ml upon multiple testing. This can be challenging to achieve due to preferential 6MMP formation. Co-administering allopurinol efficiently and safely improved metabolite profiles which was associated with sustained long-term CBR in a difficult to treat cohort.

THU-114

Alkaline phosphatase levels at 6 months as a predictor of response to ursodeoxycholic acid at 1 year in patients with primary biliary cholangitis

Carmen Sendra¹, María del Pilar Silva-Ruiz², Carlota Jimeno Mate³, Patricia Cordero Ruiz⁴, Domingo Pérez-Palacios², Gema Romero⁵, Isabela Angulo-Mcgrath³, Pablo Quiros-Rivero⁶, Jose Miguel Rosales-Zábal⁷, Jose Manuel Sousa-Martin¹.
¹Virgen del Rocio University Hospital, Seville, Spain; ²Infanta Elena Hospital, Seville, Spain; ³Virgen de Valme University Hospital, Seville, Spain; ⁴Virgen Macarena University Hospital, Seville, Spain; ⁵Juan Ramón Jiménez University Hospital, Huelva, Spain; ⁶Juan Ramón Jiménez University Hospital, Seville, Spain; ⁷Costa del Sol University Hospital, Málaga, Spain
Email: csendra.fernandez@gmail.com

Background and aims: Recently, Murillo Pérez et al. on behalf of the Global Primary Biliary Cholangitis (PBC) Study Group identified patients with PBC for second-line therapy at six-months after ursodeoxycholic acid (UDCA) initiation using an alkaline phosphatase (ALP) threshold of $1.9 \times$ upper limit of normal (ULN). The negative predictive value (NPV) of that threshold was 90% (proportion of patients that did not achieve POISE criteria after one year of UDCA). Our aims were:

To assess the reproducibility of these results in our cohort.

To identify the threshold for ALP levels at 6 months that in our cohort achieves a negative predictive value (NPV) nearest to 90% response at 1 year.

Method: This multicenter, retrospective study included 393 patients with CBP from 6 hospitals in southern Spain (Sevilla, Huelva, Málaga) from 1998 to 2022. Two hundred patients were excluded due to incomplete data: lack of knowledge of UDCA initiation date or unavailability of ALP level at the beginning, at 6 months and/or at one year of treatment. Biochemical response at one year was assessed according to POISE criteria. The NPV of the threshold of $ALP > 1.9 \times$ UNL at 6 months was calculated in our cohort, additionally evaluating its predictive capacity for response. Subsequently, the ALP cut-off point at 6 months that achieves an approximate NPV response of 90% at 1 year was identified.

Results: Data from 193 patients were analyzed, 89, 6% women, mean age of 65 years. ALP at six months was the best predictor of insufficient biochemical response at 1 year (AUROC was 0.87 for ALP, 0.72 for bilirubin, 0.83 for GGT, 0.74 for AST and 0.67 for ALT). The median ALP of those who met POISE criteria compared to those who did not was $1.14 \times$ ULN (0, 72–1, 56) vs $2.81 \times$ ULN (0, 91–3, 72) at six months; $p < 0, 001$. Of the 34 patients with serum $ALP > 1.9 \times$ ULN at six months, 76.4% (NPV) did not achieve POISE criteria after one year of UDCA. The ALP threshold at six months with a NPV of response nearest to 90% (89.5%) was $2.5 \times$ ULN. Therefore, out of the 19 patients in our cohort who had $ALP > 2.5 \times$ UNL at 6 months, 89.5% did not achieve biochemical response according to POISE at 1 year of UDCA.

Of those with insufficient response at 1 year according to POISE ($n = 43$, 22.3%), 17 (39.5%) had ALP $>2.5 \times \text{ULN}$ at 6 months and thus could have been identified earlier. 63 out of 174 patients (36.2%) with ALP $<2.5 \times \text{ULN}$ at 6 months achieved normal ALP at 1 year compared to none of the 19 (0%) patients with ALP $>1.9 \times \text{ULN}$ at 6 months.

Conclusion: In our cohort, the ALP threshold $>2.5 \times \text{ULN}$ at 6 months allows us to identify 90% of patients who will not respond after one year of treatment with UDCA.

THU-115-YI

Ursodeoxycholic acid treatment for primary sclerosing cholangitis

Bregje Mol¹, Kim van Munster¹, Rinse Weersma², Akin Anderson³, Kirsten Boonstra⁴, Joost PH Drenth¹, Suzanne van Meer⁵, Elsemieke S. de Vries⁶, B.W. Marcel Spanier⁷, Ton Vrij⁸, Tess Verlaan⁹, Femke van Duijn¹, Willemijn Ponsioen¹, Ulrich Beuers¹, Marcel Dijkgraaf¹, Cyriel Ponsioen¹. ¹Amsterdam University Medical Center, Amsterdam, Netherlands; ²University of Groningen and University Medical Center Groningen, Groningen, Netherlands; ³Leiden University Medical Center, Leiden, Netherlands; ⁴Radboud University Medical Center, Nijmegen, Netherlands; ⁵University Medical Center Utrecht, Utrecht, Netherlands; ⁶Isala Clinics, Zwolle, Netherlands; ⁷Rijnstate Hospital, Arnhem, Netherlands; ⁸Zorggroep Twente, Almelo, Netherlands; ⁹Gelderse Vallei Hospital, Ede, Netherlands
Email: b.mol@amsterdamumc.nl

Background and aims: Ursodeoxycholic acid (UDCA) is often prescribed for primary sclerosing cholangitis (PSC), although evidence to confirm a beneficial long-term effect of UDCA on solid clinical end points is insufficient. The aim of our study is to evaluate the efficacy of UDCA in terms of transplant-free survival in a longitudinal population-based cohort.

Method: Between January 2008 and August 2020, we conducted a retrospective and prospective study based on the Dutch population-based EpiPSC2 cohort. Data regarding medication use were collected by medical chart review, periodic questionnaires, and were retrieved from the national pharmacy prescription database. Survival analyses were performed for the following end points; 1) LT or all-cause mortality, 2) LT, PSC-related death or occurrence of hepatobiliary (HB) malignancies, 3) LT (excluding indication of HB malignancy) or death due to liver failure, and 4) occurrence of HB malignancy. The effect of UDCA use was estimated by using a Fine and Gray proportional hazards model to account for competing risks. Sex, age at diagnosis, PSC type, IBD status, transplant centre inclusion, NSAID use, thiopurine use, and biological use were considered as predictor variables. Events before or in the first three months after PSC diagnosis were censored.

Results: Of the 879 patients included, medication data was available for 739 patients. Patients with uncertain use of UDCA were excluded, resulting in a study population of 567. 64 patients were classified as never users, 67 used UDCA less than half of their disease duration and 415 used UDCA more than half of their disease duration. There were no significant differences in age, alkaline phosphatase levels or PSC type at baseline. UDCA use was significantly associated with a decreased hazard ratio (HR) for LT or all-cause mortality, with the most pronounced effect in the $<50\%$ use group ($<50\%$ HR 0.29 (0.15–0.54) and $>50\%$ HR 0.54 (0.34–0.87)). For the combined end point LT, PSC-related death, or occurrence of HB malignancy, the HR for $<50\%$ UDCA use was 0.33 (0.12–0.91), and 0.71 (0.38–1.34) for $>50\%$ use. No discernible effect of UDCA on LT or death due to liver failure was observed. The HR for HB malignancy occurrence was 0.25 (0.07–0.97) for $<50\%$ UDCA use and 0.60 (0.28–1.28) for $>50\%$. NSAID use less than half of the disease duration was significantly associated with a decreased HR for all end points except LT or death due to liver failure.

Conclusion: UDCA treatment was associated with improved transplant-free survival, in particular when used $<50\%$ of the disease duration. This correlation seems predominantly driven by a reduced

occurrence of hepatobiliary cancer, and supports the use of modest amounts of UDCA in the management of PSC.

THU-116-YI

The skin microbiome diversity differs in regard to age and gender but not presence of pruritus in patients with hepatobiliary diseases

Miriam M. Düll^{1,2}, Rebecca Weiß^{1,2}, Markus F. Neurath^{1,2}, Stefan Wirtz^{1,2}, Andreas E. Kremer^{1,3}. ¹Department of Medicine 1, Friedrich-Alexander-University Erlangen-Nürnberg, Erlangen, Germany; ²Deutsches Zentrum Immuntherapie, DZI, Erlangen, Germany; ³Department of Gastroenterology and Hepatology, University Hospital Zürich, University of Zürich, Zürich, Switzerland
Email: miriam.duell@uk-erlangen.de

Background and aims: Recent data underline microbial components as potential contributors in the pathophysiology of chronic pruritus in different skin conditions. Still, there is very limited data on the influence of the skin microbiome on itch as a symptom in liver diseases. This study therefore investigated the composition of the skin microbiome in a large patient cohort with hepatobiliary disorders with and without pruritus.

Method: We conducted this study at a large tertiary hepatology department, collecting skin microbiome samples at one forearm using the cyanoacrylate glue method. Samples were flash frozen at -80°C immediately after collection, and stored until DNA extraction. Illumina-based next generation sequencing of the 16S V4 ribosomal RNA gene (16S rRNA) regions sequencing was employed, followed by bioinformatic processing using the QIIME2 pipeline and the R programming language. Patients' diagnoses were categorized as "immune-mediated and cholestatic liver diseases" (ICLD), "steatotic liver disease" (SLD, including MASLD, MetALD, ALD), "viral liver diseases" (VLD), "liver transplant recipients" (LTR), and "other liver diseases" (OLD). We assessed clinical and laboratory data, and a questionnaire containing demographic information, quality of life measures and detailed characteristics of pruritus.

Results: A total of 127 patient microbiome specimens were collected (with pruritus $n = 60$; without pruritus $n = 67$). Both patient groups were comparable in regard to age, sex, disease categories and stage of liver disease, with a two-third majority of ICLD patients in both groups. Overall, we observed a very diverse interindividual range of microbiome signatures in this patient cohort. There was no significant difference between the pruritic and non-pruritic patient group in beta diversity, while age and gender had a significant influence here ($p < 0.05$, Bray-Curtis dissimilarity). Similarly, we found no significant difference for beta diversity between disease categories or the presence of cirrhosis. The most prevalent phyla were *Firmicutes* and *Actinobacteriota*, which are common components of the human skin microbiome; but we also observed an overall high relative abundance of gram-negative alpha- and gamma Proteobacteria (28%) with *Enhydrobacter* and *Acinetobacter* as the most frequent genera. Interestingly, we observed the highest amount of alpha- and gamma Proteobacteria in either higher stage fibrotic/cirrhotic patients (38%), patients with ICLD or LTR receiving immunosuppressants (46%) or under UDCA therapy (58%).

Conclusion: The skin microbiome presented as very individually diverse in a large patient cohort with hepatobiliary diseases, with differences in regard to age and gender but not presence of pruritus. Still, relative abundance of certain taxa might present in disease subgroups or with specific medication such as immunosuppressants and UDCA.

THU-117-YI

The course of radiological features and liver stiffness measurement during long-term treatment with fibrates and UDCA in patients with Primary Sclerosing Cholangitis

Elisa Catanzaro^{1,2}, Matteo Peviani^{1,2}, Francesco Pezzato^{1,2}, Emanuela Bonaiuto², Paolo Rollo^{1,2}, Nicola Perin³, Martina Gambato^{2,4}, Annarosa Floreani^{5,6}, Raffaella Motta^{7,8}, Nora Cazzagon^{1,2}. ¹Gastroenterology Unit, Azienda Ospedale—Università Padova, Padova, Italy; ²Department of Surgery, Oncology and Gastroenterology, University of Padova, Padova, Italy; ³Department of Medicine, University of Padova, Padova, Italy; ⁴Multivisceral Transplant Unit, Azienda Ospedale—Università Padova, Padova, Italy; ⁵University of Padova, Padova, Italy; ⁶IRCCS Sacro Cuore Don Calabria, Negrar (Verona), Italy; ⁷Department of Cardiac, Thoracic, Vascular Sciences and Public Health, University of Padova, Padova, Italy; ⁸Radiology Unit, Azienda Ospedale—Università Padova, Padova, Italy
Email: elisa.catanzaro95@gmail.com

Background and aims: Patients with Primary Sclerosing Cholangitis (PSC) lack an effective medical treatment to delay disease progression. According to EASL CPG 2022, ursodeoxycholic acid (UDCA) can be used in PSC since it improves liver function tests (LFTs) and bezafibrate is the 1st-line recommended treatment for pruritus in PSC. Moreover, bezafibrate is under investigation in a phase 3 clinical trial (NCT04309773) due to its beneficial effects in improving LFTs. We here aim at assessing the course of radiological findings and liver stiffness measurement (LSM) by VCTE during long-term treatment with fibrates in PSC.

Method: We conducted a retrospective analysis of PSC patients treated with fibrates (fenofibrate 200 mg/day or bezafibrate 400 mg/day) and UDCA for a minimum of 6 months. Notably, we analyzed the course of magnetic resonance imaging (MRI) prognostic scores, i.e. ANALI score with and without gadolinium (Gd) and DiStrict score from baseline to the end of follow-up alongside LSM, LFTs and pruritus.

Results: Among 27 consecutive PSC patients initiating fibrates between 2017 and 2020, the median age at diagnosis was 31 (21–35) years. Over a median treatment of 33.3 (20.8–51.2) months, fibrates led to a significant reduction of LFTs (ALP 2.6 vs. 1.7 × ULN, $p = 0.002$; ALT 2.0 vs. 1.4 × ULN, $p = 0.038$; GGT 4.3 vs. 3.4 × ULN, $p = 0.012$), Amsterdam-Oxford model (1.75 vs. 1.35 $p = 0.03$) and pruritus (56% vs. 20%, $p = 0.031$) but no improvement in LSM (6.6 vs. 7.1 KPa, $p = ns$) was observed. Regarding radiological scores, the percentage of patients with a high DiStrict score (value = 5–8) remain stable during follow-up (64% vs. 73%, $p = 0.52$) while there was a notable increase in the number of patients high ANALI scores with Gd (value = 2) and without Gd (value = 3–5) (39% vs. 70% and 61% vs. 87%, $p = 0.04$ for both). A more detailed analysis of individual items within the ANALI scores was conducted, revealing a trend toward a worsening of liver parenchymal dysmorphism (43% vs. 87%, $p = 0.08$) compared to other features over time. In particular, the number of patients with moderate to severe intrahepatic bile duct dilatations remained stable over time (69% vs. 78%, $p = 0.35$).

Conclusion: As the first experience of assessing radiological findings during treatment with fibrates in PSC, interesting results emerged from the observation of their course, suggesting the potential role of fibrates in stabilizing biliary alterations but without slowing the progression of parenchymal damage.

THU-118

Prophylaxis for tuberculosis and pneumocystis jirovecii does not seem necessary in patients with autoimmune hepatitis treated with corticosteroid therapy: spanish multicentre study

Alvaro Diaz-Gonzalez¹, Elena Ferreiro², Elena Gómez-Domínguez², Arantxa Caballero³, Magdalena Salcedo³, Alvaro Santos-Laso¹, María Del Barrio Azaceta⁴, Andrea González-Pascual¹, Jose Manuel Sousa-Martin⁵, Judith Gómez-Camarero⁶, Indhira Perez Medrano⁷, Conrado Fernández-Rodríguez⁸,

Beatriz Mateos Muñoz⁹, Ana Arencibia Almeida¹⁰, Mar Riveiro Barciela¹¹, Paula Esteban¹¹, Ignacio VazRomero¹¹, Diana Horta¹², Isabel Conde¹³, Ismael El Hajra Martínez¹⁴, Manuel L. Rodríguez-Perálvarez¹⁵, Marina Orti Cuerva¹⁵, Margarita Sala Llinás¹⁶, Montserrat García-Retortillo¹⁷, Tania Hernaez Alsina¹⁸, Mireia Miquel¹⁹, Jesús M. Gonzalez Santiago²⁰, María Carlota Londoño²¹, Javier Crespo¹. ¹Gastroenterology and Hepatology Department, Clinical and Translational Research in Digestive Diseases Group, Marqués de Valdecilla University Hospital, Santander, Spain, Research Institute Marqués de Valdecilla (IDIVAL), Clinical and Translational Research in Digestive Pathology Group, Santander, Spain, Santander, Spain; ²Hospital Universitario Doce de Octubre, Av. Cordoba, s/n, 28041 Madrid, Madrid, Spain; ³Hospital General Universitario Gregorio Marañón, Madrid, Spain; ⁴Gastroenterology and Hepatology Department, Marqués de Valdecilla University Hospital, Clinical and Translational Digestive Research Group, IDIVAL, Santander, Spain., Research Institute Marqués de Valdecilla (IDIVAL), Clinical and Translational Research in Digestive Pathology Group, Santander, Spain, Santander, Spain; ⁵Hospital Universitario Virgen del Rocío, Sevilla. Instituto de Biomedicina de Sevilla. Universidad de Sevilla. CIBERehd., Sevilla, Spain; ⁶Hospital Universitario de Burgos, Burgos, Spain; ⁷Complejo Hospitalario Universitario de Pontevedra. Instituto de Investigación Sanitaria Galicia Sur (IISGS), Pontevedra, Spain; ⁸Alcorcón Foundation University Hospital, Department of Public Health and Medical Specialties. Rey Juan Carlos University, Alcorcón. Madrid, Spain; ⁹Hospital Universitario Ramón y Cajal, CIBERehd, IRYCIS, Madrid, Madrid, Spain; ¹⁰HOSPITAL UNIVERSITARIO NUESTRA SEÑORA DE LA CADELARIA, Santa Cruz de Tenerife, Spain; ¹¹Liver Unit, Internal Medicine Department, Hospital Universitari Vall d'Hebron, Vall d'Hebron Barcelona Hospital Campus, Barcelona, Spain, CIBERehd, Barcelona, Spain; ¹²Hospital Universitario Mútua de Terrassa, Barcelona, Spain; ¹³Hospital Universitario y Politécnico La Fe, Valencia; Instituto de Investigación Sanitaria La Fe, Valencia, CIBERehd, Valencia, Spain; ¹⁴Hospital Universitario Puerta de Hierro, Madrid, Spain; ¹⁵Unidad de Hepatología y Trasplante Hepático. Hospital Universitario Reina Sofía, IMIBIC, Universidad de Córdoba, CIBERehd, Córdoba, Spain; ¹⁶Hospital Universitari Doctor Josep Trueta. Institut d' Investigació Biomèdica de Girona (IDIBGI), CIBERehd, Girona, Spain; ¹⁷Sección de Hepatología, Servicio de Ap. Digestivo, Hospital del Mar. Institut de Recerca Hospital del Mar, Barcelona, Spain; ¹⁸Hospital Universitario San Pedro, Logroño, Spain; ¹⁹Parc Taulí Hospital Universitari. Institut d' Investigació i Innovació Parc Taulí I3PT, Universitat Autònoma de Barcelona, Sabadell, CIBERehd, Sabadell, Spain; ²⁰Servicio de Aparato Digestivo. Complejo Asistencial Universitario de Salamanca., Laboratorio de Hepatología Experimental y Vectorización de Fármacos (HEVEPHARM). CIBERehd. IBSAL. Salamanca., Salamanca, Spain; ²¹Liver Unit. Hospital Clínic de Barcelona. Health Care Provider of the European Reference Network on Rare Liver Disorders (ERN-Liver). Institut D'Investigacions Biomèdiques August Pi i Sunyer (IDIBAPS), CIBERehd, Barcelona, Spain
Email: diazg.alvaro@gmail.com

Background and aims: Corticosteroid therapy (CS) at doses >15 mg/day for >4 weeks, therapeutic cornerstone of autoimmune hepatitis (AIH) management, increases the risk of active Tuberculosis (TBCa) by 7.7 times in some autoimmune diseases (AID). Guidelines for other AID recommend screening for latent Tuberculosis infection (LTBI) and prophylaxis if appropriate. Furthermore, immunosuppression can also increase the risk of Pneumocystis jirovecii (PJ), with prophylaxis indicated in some situations. However, there are no recommendations for AIH, probably because there are no published data on the incidence of LTBI, TBCa, nor PJ. Our aim was to evaluate the prevalence of LTBI and the incidence of TBCa and PJ.

Method: Retrospective study conducted in 20 Spanish centres, evaluating the diagnosis (dx) of LTBI, TBCa, and PJ between the years 2000 and 2023.

Results: 2893 patients with AIH and treated with CS were evaluated. In 5 centres (25%), routine pre-treatment LTBI screening was

performed. In these, 37 cases (4.9%) of LTBI were identified in 747 studied patients. 7 (19%) patients had previously received prophylaxis, 15 (40.5%) received it at the time of AIH dx –75% received isoniazid-, and 15 (40.5%) did not receive prophylaxis. 3 (20%) of the 15 patients treated presented DILI secondary to prophylaxis. Out of the 2893 patients, only 6 (0.2%) developed TBca during follow-up (3 pulmonary/3 extrapulmonary). 83% were women with a median age of 52.3 years. 50% lived in a rural environment and had another AID. None of the patients had previously received immunosuppression. The time from the start of CS to TBca was 13.3 years (IQR 9.6–22.3). No differences were identified between those who developed TBca and the patients with LTBI in gender ($p=0.6$), AIH presentation (acute/chronic/acute severe; $p=0.7$), respiratory diseases ($p=0.8$), diabetes mellitus ($p=0.6$), BMI ($p=0.4$), presence of other AID ($p=0.5$), AIH treatment ($p=0.7$), nor any other clinical or analytical characteristic. At the time of TBca dx, 5 (83.3%) were treated with CS, 3 (50%) with AZA, and 1 (16.7%) with mycophenolate mofetil. On the other hand, no patient with a dx of LTBI who did not receive prophylaxis developed TBC during follow-up. Regarding *Pneumocystis jirovecii*, 2 (10%) centres routinely perform prophylaxis. During follow-up, no patients were diagnosed with PJ infection (0/2893).

Conclusion: Screening for LTBI, TBca prophylaxis, and PJ prophylaxis do not seem necessary in patients with AIH treated with standard regimens. The incidence of TBca is low, much lower than reported in other AID, and the time from the start of CS and the development of TBca is very long, so its development is probably not related to AIH treatment. Finally, isoniazid was associated with a significant rate of discontinuation due to DILI.

THU-119

Seladelpar treatment increases fatty acid beta-oxidation and serum carnitine levels in patients with primary biliary cholangitis consistent with increased expression of the carnitine transporter OCTN2 and the mitochondrial carnitine shuttle

Yun-Jung Choi¹, Jeff Johnson¹, Charles A. McWherter¹. ¹CymaBay Therapeutics, Inc., Fremont, United States
Email: ychoi@cymabay.com

Background and aims: In a global serum metabolomic study of patients with primary biliary cholangitis treated with seladelpar, a selective PPAR- δ agonist, we found that an increase in carnitine was one of the most biochemically important changes. Carnitine plays an essential role in carrying out beta-oxidation of long-chain fatty acids for energy production. Carnitine is a major substrate of the plasma membrane transporter OCTN2, which is ubiquitously expressed and is involved in carnitine absorption from diet, carnitine reabsorption in the kidney and facilitates cellular uptake of carnitine. Our aim is to further examine seladelpar's effects on serum carnitine as well as expression of OCTN2 and the mitochondrial carnitine shuttle genes.

Method: Serum samples from 160 PBC patients were collected on Day 1 and after 3 months of treatment with placebo ($n=55$), seladelpar 5 mg ($n=52$) or 10 mg ($n=53$) in a randomized phase 3 study (NCT03602560). The abundance of carnitine was examined using UHPLC-MS/MS (Metabolon, Inc). We also measured the effect of seladelpar on expression of OCTN2 and the carnitine shuttle genes in mouse tissues and human primary hepatocytes.

Results: Seladelpar treatment resulted in a significant dose-dependent increases from Day 1 in serum carnitine ($p<0.0001$): placebo (1.02-fold), seladelpar 5 mg (1.18-fold) and 10 mg (1.24-fold). A substantial proportion of patients treated with seladelpar 5 mg (88%) and 10 mg (94%) increased serum carnitine levels compared to the placebo group (58%). RNASeq analysis of tissues from mice treated with seladelpar 10 mg/kg/day for 12 weeks revealed significant increases in *Ocn2* compared to vehicle: intestine (1.9-fold), liver (2-fold) and kidney (1.7-fold). The components of the mitochondrial carnitine shuttle were also induced by seladelpar treatment: *Cpt1a* (intestine, 1.7-fold; kidney, 1.3-fold; skeletal muscle, 1.7-fold); *Cpt2*

(intestine, 1.5-fold; liver, 1.4-fold; kidney, 2.1-fold); *Crat* (intestine, 1.4-fold; liver, 2.7-fold; kidney, 1.9-fold); and *Cact* (intestine, 1.8-fold; liver, 1.7-fold; kidney, 2.7-fold). Similar results were obtained in primary human hepatocytes treated with 10 μ M seladelpar for 24 hours (OCTN2, 1.7-fold; CPT1A, 4-fold; CPT2, 1.7-fold; CACT, 1.6-fold). The rate-limiting carnitine biosynthesis enzyme BBOX1 was not significantly changed by seladelpar.

Conclusion: Seladelpar's upregulation of carnitine transporter in liver, intestine, and kidney may have contributed to the observed increase in serum carnitine levels. Increased gene expression of OCTN2 by seladelpar could result in increased intracellular levels of carnitine and fatty acid beta-oxidation. The effects of seladelpar via the carnitine transporter and carnitine shuttle are proposed to lead to enhanced fatty acid beta-oxidation and further study is needed regarding seladelpar's impact on this aspect of PBC disease pathology.

THU-120-YI

The impact of ursodeoxycholic acid on biochemistry of patients with primary biliary cholangitis in a nationwide cohort

Ellen Werner¹, Maria C. van Hooff¹, Gerjan J. van der Maas¹, Rozanne C. de Veer¹, Ulrich Beuers², Joost P.H. Drenth³, Frans J.C. Cuperus⁴, Bart van Hoek⁵, Bart J. Veldt⁶, Michael Klemt-Kropp⁷, Suzanne van Meer⁸, Robert C. Verdonk⁹, Hajo J. Flink¹⁰, Jan Maarten Vrolijk¹¹, Tom J.G. Gevers¹², Cyriel Y. Ponsioen², Sander de Kort¹³, Paul G. van Putten¹⁴, Djuna L. Cahen¹⁵, Lauren A. van der Waaij¹⁶, Hans H.K. Thio¹⁷, Tim C.M.A. Schreuder¹⁸, Lisette J.H. van Dam¹⁹, Ludger S.M. Epping²⁰, Matthias C. Jurgens²¹, Marcel Cazemier²², J. van Kemenade²³, Edith M.M. Kuiper²⁴, Menno Beukema²⁵, Martijn J. ter Borg²⁶, Khalida Soufidi²⁷, Harry L.A. Janssen^{1,28}, Bettina E. Hansen¹, Nicole S. Erler¹, Adriaan J. van der Meer¹. ¹Erasmus University Medical Center, Rotterdam, Netherlands; ²Amsterdam University Medical Center, Amsterdam, Netherlands; ³Radboud University Medical Center, Nijmegen, Netherlands; ⁴University Medical Center Groningen, Groningen, Netherlands; ⁵Leiden University Medical Center, Leiden, Netherlands; ⁶Reinier de Graaf Gasthuis, Delft, Netherlands; ⁷Noordwest Ziekenhuisgroep, Alkmaar, Netherlands; ⁸University Medical Center Utrecht, Utrecht, Netherlands; ⁹St. Antonius Hospital, Nieuwegein, Netherlands; ¹⁰Catharina Hospital, Eindhoven, Netherlands; ¹¹Rijnstate, Arnhem, Netherlands; ¹²Maastricht University Medical Center, Maastricht, Netherlands; ¹³St. Anna Hospital, Geldrop, Netherlands; ¹⁴Antonius Zorggroep, Sneek, Netherlands; ¹⁵Hospital Amstelland, Amstelveen, Netherlands; ¹⁶Martini Hospital, Groningen, Netherlands; ¹⁷Saxenbergh Medical Center, Hardenberg, Netherlands; ¹⁸Wilhelmina Hospital Assen, Assen, Netherlands; ¹⁹Ommelandse Hospital, Scheemda, Netherlands; ²⁰Maasziekenhuis Pantein, Boxmeer, Netherlands; ²¹St. Jans Gasthuis Weert, Weert, Netherlands; ²²BovenIJ Hospital, Amsterdam, Netherlands; ²³Van Weel-Bethesda Hospital, Dirksland, Netherlands; ²⁴Spijkens Medical Center, Spijkens, Netherlands; ²⁵Streekziekenhuis Koningin Beatrix, Winterswijk, Netherlands; ²⁶Streekziekenhuis Koningin Beatrix, Gorinchem, Netherlands; ²⁷Maxima Medical Center, Eindhoven, Netherlands; ²⁸Toronto Centre for Liver Disease, University of Toronto, Toronto, Canada
Email: e.werner@erasmusmc.nl

Background and aims: Ursodeoxycholic acid (UDCA) is the standard therapy for patients with Primary Biliary Cholangitis (PBC). Biochemical response to UDCA is mainly described in cohorts derived from academic centers. We assessed the biochemical response of UDCA at one year in the nationwide Dutch PBC Cohort Study (DPCS).

Method: The DPCS is a retrospective study which includes every identifiable patient with PBC in the Netherlands from 1990 onwards in all 71 Dutch hospitals. For the assessment of the biochemical response to UDCA monotherapy, available laboratory values (reported in upper limits of normal [ULN]) up to one year prior to start of UDCA and laboratory values closest to the 12 month timepoint, within the 9–18 month window, were included. Patients

POSTER PRESENTATIONS

were censored in case of liver transplantation, immunosuppression therapy and/or second line therapy prior to timepoint of UDCA response evaluation. Complete case analyses were performed per biochemical end point.

Results: In total, 4351 patients were included in the DPCS; 3835 (88.1%) were female, median age was 56.8 (48.5–66.5) years, 198 (4.6%) had cirrhosis at baseline, and 3619 (83.2%) were diagnosed at a secondary center. Of patients with UDCA ($n = 4256$, 97.8%), median ALP at baseline was 1.92 (IQR 1.30–3.25), median AST was 1.53 (IQR 1.06–2.31), median bilirubin was 0.53 (IQR 0.38–0.82), and 714/3025 (23.6%) patients already met PARIS 2 criteria (ALP and AST ≤ 1.5 ULN and normal bilirubin). After one year of UDCA, median Δ ALP was -0.69 (IQR -1.61 – -0.23), median Δ AST was -0.55 (IQR -1.13 – -0.20) and median Δ bilirubin was -0.05 (-0.18 – -0.06) ($p < 0.001$ for all). After one year of UDCA, 1443/2412 (59.8%) patients had a complete response according to PARIS 2, 1009/2576 (39.2%) patients had normal ALP, and 1651/2463 (67.0%) patients had a bilirubin $\leq 0.6 \times$ ULN. These response rates on PARIS 2, normal ALP and bilirubin $\leq 0.6 \times$ ULN were 433 (89.3%), 340 (64.2%) and 382 (76.7%) versus 821 (51.6%), 499 (30.2%) and 1041 (64.2%) among patients who did and who did not fulfill the PARIS 2 criteria at baseline ($p < 0.001$ for all). The median Δ ALP was -0.61 (IQR -1.24 – -0.24) vs -0.95 (IQR -2.42 – -0.18 , $p < 0.001$) and the median Δ bilirubin was -0.05 (IQR -0.15 – -0.06) vs -0.06 (IQR -0.24 – -0.10 , $p = 0.043$) among patients who did and who did not meet the PARIS 2 criteria at one year of UDCA.

Conclusion: This nationwide study shows that 60% of patients have a complete response after one year of UDCA according to the PARIS 2 criteria. The decline of the cholestatic surrogate parameters was higher in patients with an incomplete response versus those with a complete response. Still, considering the discussion on the need of biochemical normalization, one year of UDCA leaves $>60\%$ of all PBC patients in the Netherlands with an elevated ALP.

THU-121

Harnessing synergy of 'triple' anti-cholestatic therapy in patients with primary biliary cholangitis

Guilherme Cançado¹, Bo Chen¹, Madeline Cameron¹, Inbal Hour¹, Kristel Leung¹, Aliya Gulamhusein¹, Bettina E. Hansen^{1,2}, Gideon M. Hirschfield¹. ¹Toronto Centre for Liver Disease, Division of Gastroenterology and Hepatology, Toronto General Hospital, University Health Network, Toronto, Canada; ²Department of Gastroenterology and Hepatology, Erasmus University Medical Center, Rotterdam, Netherlands
Email: gideon.hirschfield@uhn.ca

Background and aims: Treatment goals in primary biliary cholangitis (PBC) increasingly aim for normal serum liver tests. Currently add-on therapy to Ursodeoxycholic acid (UDCA) is with the approved Farnesoid X receptor (FXR) agonist Obeticholic acid (OCA), alongside off-label use of fibrates (PPARs). We report our experience of synergistic FXR-PPAR-UDCA combination therapy in PBC.

Method: Chart review of prevalent patients with PBC seen between July 2022 and July 2023 at the Toronto Centre for Liver Disease was performed.

Results: 470 patients with PBC were seen of which 71% were treated with UDCA only, 7% UDCA-OCA, 11.3% UDCA-fibrates and 10.6% UDCA-OCA-fibrates. Among 50 patients on triple therapy [86% female, median age at diagnosis 43.5 (IQR 14.6) years, median age at triple therapy 53.6 years (13.0), 96% AMA positive, 36% cirrhotic], 82% had OCA as the first add-on therapy. Most patients on fibrates (92%) received bezafibrate, while 8% had fenofibrate. 48 patients were included in final analysis. Median follow-up time after triple therapy was 17.4 months (16.8). Median alkaline phosphatase (ALP) was 396.5 U/L (282.5) before triple therapy and 147.5 U/L (75) at the last available, while bilirubin was 12 (9) $\mu\text{mol/L}$ and 9 (4) $\mu\text{mol/L}$, respectively. Patients on triple therapy demonstrated median ALP reductions after 6 months of 31.1% (95%CI 25.4%–37.0%) and 37.8% (95%CI 31.6%–44.0%) at last follow-up. Patients with cirrhosis showed similar Results: 25.2% (95%CI 17.6%–32.8%) ALP reduction at 6 months

and 31.2% (95%CI 20.6%–42.0%) at last follow-up. Bilirubin values were stable throughout the follow-up. Out of 34 patients with self-reported pruritus before triple therapy, 64.7% reported improvement, 11.8% worsened and 23.5% had no change in itching intensity. Liver stiffness as measured by Fibroscan remained stable after triple therapy initiation [median 7.6 kPa (4.6 kPa) pre; 8.0 kPa (7.6 kPa) at last follow-up].

Conclusion: In people living with at-risk PBC, we confirm FXR-PPAR-UDCA triple therapy significantly improves liver biochemistry.

THU-122

Patient-reported insights on current care practices for primary biliary cholangitis, quality of life and self-management: results of the german PBC online survey

Diane Langenbacher¹, Achim Kautz¹, Christian Trautwein², Carsten Schwenke³, Yuri Sankawa⁴, Andreas E. Kremer⁵. ¹Kautz5 gUG, Köln, Germany; ²RWTH University Hospital, Aachen, Germany; ³SCO: SSiS, Minden, Germany; ⁴Dr. Sankawa GmbH, Stuttgart, Germany; ⁵University Hospital Zürich, Department of Gastroenterology and Hepatology, Zürich, Switzerland
Email: langenbacher@kautzhoch5.de

Background and aims: Primary biliary cholangitis (PBC) is a chronic immune-mediated cholestatic liver disease requiring lifelong stratified treatment and management. Building on an earlier patient survey conducted in Germany in 2017, a comprehensive online survey was carried out in 2021 to obtain representative data on the current care situation, symptom burden and management, quality of life and outcome-relevant influencing factors in PBC.

Method: After a pre-test phase between May and November 2020, the PBC online survey went online in January 2021 for one year. The survey was announced online at leberhilfe.org, pbcnews.info and in digital newsletters. The data was analyzed descriptively.

Results: A total of 1032 patients participated, with 92.6% being female. At the time of diagnosis, 652 patients had no liver fibrosis. Most patients ($n = 697$) were seen by a physician every 3 or 6 months. 56.5% of patients reported on elevated ALP, 23.4% on increased bilirubin levels, however only 14, 8% of patients were put on second line medication. Increased values were more commonly associated with female gender and presence of comorbidities. Female patients were more likely to suffer from comorbidities. QoL was lower in these patients. Factors associated with application of second-line therapies were young age (<30 years), a more recent diagnosis (50% were diagnosed between 2013 and 2022), higher education, and knowledge of lab values. Patients on second-line therapies had a better QoL. Presence of fibrosis was not associated with clinical factors (ALP level, bilirubin level, comorbidities, age, sex, time since diagnosis), but with socio-economic factors (school/professional qualifications, employment/pension status). Fatigue (58.5%), pruritus (37.8%), sicca syndrome (36.3%), and joint complaints (51.9%) were identified as the four most common and severely affecting symptoms. Patients affected by these symptoms had a poorer QoL, including dimensions such as professional/social life, and relationships/sexuality.

Conclusion: Compared to previous survey, no significant improvements were observed in biochemical markers of treatment response such as bilirubin and ALP. Nevertheless, only a minority of patients received additional second-line therapies. This seems to be in line with findings from the German PBC registry. Although fatigue, arthralgia and pruritus remain among the most distressing symptoms, medical and non-medical symptom management and general quality of life appear to have improved. Especially in empowered patients with adequate knowledge of their disease and of strategies to manage symptom burden and improve their overall well-being.

THU-123-YI

External validation of the international autoimmune hepatitis group response criteria in a multicentric real-world cohort

Lorenz Grossar¹, Sarah Raevens², Christophe Van Steenkiste³, Isabelle Colle⁴, Charlotte De Vloo⁵, Hans Orlent⁶, Jeoffrey Schouten⁷, Marie Gallant⁸, Annelien Van Driessche⁹, Sander Lefere¹⁰, Lindsey Devisscher¹¹, Anja Geerts², Hans Van Vlierberghe², Xavier Verhelst². ¹Department of internal medicine and paediatrics, hepatology research unit, Ghent University, Liver research centre Ghent, Ghent, Belgium; ²Ghent University hospital, Hepatology, Ghent, Belgium; ³AZ Maria Middelaers, University hospital Antwerp, Ghent, Belgium; ⁴Algemeen stedelijk ziekenhuis Aalst, Aalst, Belgium; ⁵AZ Delta, Roeselare, Belgium; ⁶AZ Sint-Jan, Brugge, Belgium; ⁷AZ Nikolaas, Sint-Niklaas, Belgium; ⁸Jan Yperman ziekenhuis, Leper, Belgium; ⁹AZ Glorieux, Ronse, Belgium; ¹⁰Department of internal medicine and paediatrics, hepatology research unit, Ghent University, Liver research centre Ghent, Ghent, Belgium; ¹¹Department of internal medicine and paediatrics, hepatology research unit, Ghent University, Department of basic and applied medical sciences, gut-liver immunopharmacology unit, Ghent University, Ghent, Belgium
Email: lorenz.grossar@ugent.be

Background and aims: The goal of treatment in autoimmune hepatitis (AIH) is induction of remission to prevent the development of liver fibrosis, cirrhosis, and its related complications. Considering the need for consistency in definitions of treatment response, the International Autoimmune Hepatitis Group (IAIHG) recently defined consensus criteria for treatment response. Validation of these criteria is necessary for correlation with hard end points to facilitate comparison between studies.

We aimed to validate the IAIHG response criteria in our cohort and establish correlations with survival end points. The primary end point was liver-related survival. Secondary end points were overall mortality and transplant-free survival.

Method: We performed a retrospective, multicentric cohort study in one tertiary and seven secondary care centres in Belgium. Included patients were at least 18 years of age at time of data collection and diagnosed with AIH by a simplified IAIHG score of at least 6. Patients with features of both AIH and primary sclerosing cholangitis (PSC) or primary biliary cholangiopathy (PBC), as defined by the Paris criteria, were excluded from the analysis. Complete biochemical response (CBR) was defined according to the IAIHG consensus criteria as normalisation of transaminases and serum immunoglobulin G (IgG) within the first six months of treatment. Time to development of mortality (all-cause and liver-specific) and liver transplantation was calculated and included in time-to-event analysis. Liver-related survival was defined as freedom from liver-related death or liver transplantation. Outcome was compared between subjects attaining CBR and those with insufficient response.

Results: Biochemical response status could be determined in 200 AIH patients. Median age at diagnosis and median follow-up were 47 years (interquartile range: 29–59) and 7.8 years (interquartile range: 4.1–13.0), respectively. There was a female predominance of 74.2% and 150 individuals (70.4%) were followed up in a tertiary centre. CBR was achieved in 128 (64.0%) individuals. Gender, acute symptoms, and IgG elevation at diagnosis did not associate with CBR status. Patients not achieving CBR presented more frequently with cirrhosis on initial histology (22.2% versus 10.9%, $p=0.035$). Liver-related mortality or liver transplantation combined as a primary end point, occurred in 26 subjects (13.0%). Patients achieving CBR exhibited superior liver-related (HR: 0.118; 95% CI: 0.052–0.267, $p<0.0001$) and overall survival (HR: 0.253; 95% CI: 0.111–0.572, $p=0.0003$).

Conclusion: We externally validated the IAIHG consensus criteria for complete biochemical response and correlate them with survival end points in a multicentric, real-world cohort. AIH patients achieving CBR as an intermediate end point have significantly superior liver-related and overall survival.

THU-124

Population pharmacokinetics of elafibranor in healthy participants and patients with liver diseases: A pooled analysis of 17 clinical studies

Marion Dehez¹, Karl Brendel¹, Dimitar Tonev², Stijn van Beek³, Qing Xi Ooi³, Carol Addy⁴. ¹Ipsen, Les Ulis, France; ²Ipsen, Boulogne-Billancourt, France; ³Pharmetheus, Uppsala, Sweden; ⁴GENFIT Corp., Cambridge, MA, United States
Email: marion.dehez@ipsen.com

Background and aims: Elafibranor is a dual peroxisome proliferator-activated receptor- α/δ agonist in development for the treatment of primary biliary cholangitis (PBC) and primary sclerosing cholangitis. Here, we characterise the pharmacokinetics (PK) of elafibranor and its main active metabolite, GFT1007, in healthy participants and patients with liver diseases, and assess population characteristics that could influence PK parameters.

Method: PK data consisting of 12, 205 elafibranor and 10, 592 GFT1007 samples were pooled from 17 clinical (13 phase I, 2 phase II, 2 phase III) studies in 894 participants receiving elafibranor. The population included 450 healthy participants and 444 patients with PBC, metabolic dysfunction-associated steatohepatitis, or renal or hepatic impairment. Doses ranged from 5 to 360 mg. Regimens included single dosing and daily dosing. Multiple dosing duration ranged from 14 days to >1 year.

Separate population PK models were developed for elafibranor and GFT1007 using nonlinear mixed effects modelling in NONMEM. Elimination half-life, area under the plasma concentration-time curve during a dosing interval at steady state ($AUC_{t,ss}$) and maximum/minimum plasma drug concentration at steady state ($C_{max,ss}/C_{min,ss}$) were derived. Effects of covariates (dose, drug formulation, age, sex, body mass index, Black/African American race, food intake prior to drug administration, bioanalytical method of measuring samples, estimated glomerular filtration rate, National Cancer Institute hepatic impairment score, PBC, levels of hepatic transaminases, albumin and bilirubin) on PK parameters were explored. Clinical significance of covariates on $AUC_{t,ss}$, $C_{max,ss}$ and $C_{min,ss}$ was assessed using Forest plots.

Results: A more than proportional decrease in elafibranor exposure with lower doses was observed, while elafibranor PK was linear between 50 and 360 mg/day. Following daily intake of elafibranor 80 mg in patients with PBC, predicted median elimination half-life (90% confidence interval) of elafibranor was longer versus GFT1007 (59.7 [52.1, 67.3] vs 10.7 [9.84, 11.9] hours). Predicted time to steady state for elafibranor and GFT1007 was 12.4 and 2.22 days, respectively. At this dose, GFT1007 exposure was higher versus elafibranor in patients with PBC: $AUC_{t,ss}$, $C_{max,ss}$ and $C_{min,ss}$ were approximately 5-, 8- and 1.5-fold higher, respectively.

Conclusion: Elafibranor and GFT1007 PK were found to be dose-proportional across a 50–360 mg dose range. As GFT1007 exposure at steady state was 5-fold higher than elafibranor, the pharmacodynamic effect is likely driven more by GFT1007 than by elafibranor under the assumption of equipotency.

THU-125

Key questions that patients with primary biliary cholangitis should ask their physician -Delphi method-

Ellen Werner¹, Maria C. van Hooft¹, Nadir Abbas², Alessio Gerussi³, José A. Willems⁴, Robert Mitchell-Thain⁵, Angela Leburgue⁶, Gideon M. Hirschfield⁷, Christophe Corpechot⁸, Christoph Schramm⁹, Cynthia Levy¹⁰, Frederik Nevens¹¹, Jef Verbeek¹¹, Andrew L. Mason¹², George Dalekos¹³, Nora Cazzagon¹⁴, George F. Mells¹⁵, Kris V. Kowdley¹⁶, Marco Carbone³, David E. Jones¹⁷, Bettina E. Hansen¹, Palak J. Trivedi², Adriaan J. van der Meer¹. ¹Erasmus University Medical Center, Health Care Provider of the European Reference Network on Rare Liver Disorders (ERN RARE LIVER), Rotterdam, Netherlands; ²National Institute for Health and Care Research Birmingham Biomedical Research Centre, University of

POSTER PRESENTATIONS

Birmingham, Health Care Provider of the European Reference Network on Rare Liver Disorders (ERN RARE LIVER), Birmingham, United Kingdom; ³Division of Gastroenterology and Center for Autoimmune Liver Diseases, University of Milano-Bicocca, Health Care Provider of the European Reference Network on Rare Liver Disorders (ERN RARE LIVER), Monza, Italy; ⁴Dutch Liver Patient Association, Hoogland, Netherlands; ⁵PBC Foundation, Edinburgh, United Kingdom; ⁶ALBI Patient Association, Versailles, France; ⁷Toronto Centre for Liver Disease, University of Toronto, Toronto, Canada; ⁸Saint-Antoine Hospital, Assistance Publique-Hôpitaux de Paris, Saint-Antoine Research Center, Sorbonne University, Health Care Provider of the European Reference Network on Rare Liver Disorders (ERN RARE LIVER), Paris, France; ⁹University Medical Center Hamburg-Eppendorf, Health Care Provider of the European Reference Network on Rare Liver Disorders (ERN RARE LIVER), Hamburg, Germany; ¹⁰University of Miami, School of Medicine, Miami, United States; ¹¹University Hospitals KU, Health Care Provider of the European Reference Network on Rare Liver Disorders (ERN RARE LIVER), Leuven, Belgium; ¹²University of Alberta, Edmonton, Canada; ¹³National Expertise Center of Greece in Autoimmune Liver Diseases, General University Hospital of Larissa, Health Care Provider of the European Reference Network on Rare Liver Disorders (ERN RARE LIVER), Larissa, Greece; ¹⁴University of Padua, Health Care Provider of the European Reference Network on Rare Liver Disorders (ERN RARE LIVER), Padua, Italy; ¹⁵University of Cambridge, Cambridge, United Kingdom; ¹⁶Liver Institute Northwest, Seattle, United States; ¹⁷Newcastle University Medical School, Newcastle Upon Tyne, United Kingdom
Email: e.werner@erasmusmc.nl

Background and aims: The goal of this study was to create a question prompt list (QPL) for individuals living with primary biliary cholangitis (PBC), covering key topics to be asked during out-patient consultations which are most likely to improve PBC management.

Method: International PBC experts were invited to rate 43 questions related to 9 aspects of PBC care on a 7-point Likert scale (ranging from 1 = Very Unimportant to 7 = Very Important) in a digital survey. Participants had to consider a) the probability that the specific aspect of care is not optimally managed, and b) their confidence that optimizing that specific aspect of care will benefit patient outcomes. In addition, the top 3 questions within each aspect of care were ranked in order of importance. Questions rated by >70% of the respondents to be moderate/very important were considered best candidate questions (BCQs) for the QPL. Results of the survey were discussed during two in-person meetings, based on which the questions and/or QPL were amended. Hereafter, the study team ratified the final QPL in a consensus meeting.

Results: In total, 108 respondents completed the survey; 61 (56.5%) had >10 years of PBC experience, 71 (65.7%) worked in a tertiary center, and 5 (4.6%) were patient representatives. Eleven questions were rated as BCQs in 6 out of the 9 aspects of care: Symptoms, 2nd line therapy, Disease severity, Monitoring, Extra hepatic disease (s) and Other. During the in-person meetings (64 attendees), experts suggested combining the BCQs regarding symptoms addressing pruritus (rated as moderate/very important by 86.1% of the respondents) and fatigue (75.0%). With respect to treatment, although questions within the category of 1st line therapy failed to achieve the predefined rating for a BCQ (68.5%), attendees agreed there is a strong scientific basis to include the top-ranked question on the correct dosage of ursodeoxycholic acid in the QPL. Also, to avoid overlap, only 1 out of 3 BCQs related to the indication for 2nd line therapy was included in the QPL. With respect to disease severity, attendees approved the inclusion of BCQs related to risks of disease progression (74.1%) and presence of cirrhosis (76.9%), while being aware on a predefined disclaimer that the current QPL is not intended to target specific aspects of cirrhosis care. Attendees suggested rephrasing the BCQ on liver stiffness measurement (71.3%) to focus on the frequency of the measurement and agreed to include the BCQs related to bone health (73.1%) and availability of patient information

and support (70.4%). The final QPL based on the survey results and discussion meetings contained 8 questions and was unanimously approved during the consensus meeting.

Conclusion: Through a Delphi method international expert consensus was reached on a QPL containing 8 key questions patients can ask their physician, which are felt to most likely impact their PBC care.

THU-126

Metabolomic signature in autoimmune hepatitis discriminates disease activity and predicts response to treatment

Kalliopi Zachou^{1,2}, Aikaterini Dimou³, Christina Kostara³, Kalliopi Azariadis^{1,2}, George Giannoulis^{1,2}, Angeliki Lyberopoulou^{1,2}, Eleni Bairaktari³, George Dalekos^{1,2}, ¹Department of Medicine and Research Laboratory of Internal Medicine, National Expertise Center of Greece in Autoimmune Liver Diseases, General University Hospital of Larissa, Larissa, Greece; ²European Reference Network on Hepatological Diseases (ERN RARE-LIVER), General University Hospital of Larissa, Larissa, Greece; ³Laboratory of Clinical Chemistry, Faculty of Medicine, School of Health Sciences, University of Ioannina, Larissa, Greece
Email: zachoukalliopi@gmail.com

Background and aims: Metabolomics were shown to be a useful tool for predicting treatment response or defining disease severity-related phenotypes in diverse autoimmune diseases. Autoimmune hepatitis (AIH) is characterized by altered metabolomic signature but the use of metabolomics in profiling patients according to response to treatment remains unexplored. Therefore, we investigated the ability of metabolites to discriminate disease activity state and predict response to treatment.

Method: Metabolites in plasma samples from 50 AIH patients at diagnosis and 78 AIH patients at complete response (CR) [normal alanine aminotransferase (ALT) and immunoglobuline G (IgG) levels] were determined by ¹H-NMR spectroscopy. For 28 patients matched samples were available. Fifty-two metabolites were quantified. Response to treatment was defined according to the recently reported response criteria by the International AIH Group.

Results: The metabolomic profile of AIH at diagnosis could be sufficiently discriminated from AIH on CR ($p < 0.001$). Eighteen metabolites differentiated AIH at diagnosis from AIH on CR with the top 6 (VIP scores >1.7) being acetoacetate, succinate, 2-aminobutyrate, myoinositol, tyrosine and malonate. Forty-three out of 50 AIH patients received treatment. At week 4 of treatment 36 patients were responders, while at month 6 and end of follow-up 33 and 40 patients, respectively, achieved CR. Treatment could be stopped in 28/43 patients, 16 of whom remained at remission for 59 (3–120) months. Lower carnitine levels at diagnosis could predict response at week 4 of treatment ($p < 0.05$; AOC 0.73), while higher 3-hydroxyisovalerate and choline at diagnosis could predict CR at month six ($p < 0.05$; AUC 0.68 and 0.7, respectively). Interestingly, lower formate and higher lactate levels at diagnosis could predict the possibility to withdraw treatment ($p < 0.05$; AUC 0.69 and 0.72, respectively), while higher formate and lower taurine levels could predict maintenance of remission after treatment withdrawal ($p < 0.05$; AUC 0.76 and 0.72, respectively).

Conclusion: Altered metabolomic profile characterizes active AIH at diagnosis and AIH on CR after treatment initiation. Most importantly, NMR-based metabolomic signature can be used for the prediction of response to treatment in AIH patients.

THU-127-YI

Effects of HLA-G in primary biliary cholangitis: a study on a genetic isolate population

Michela Miglianti¹, Stefano Mocci², Roberto Littera³, Cinzia Balestrieri⁴, Maria Conti⁴, Michela Lorrain², Alessia Mascia², Caterina Mereu², Francesco Pes⁴, Celeste Sanna², Giancarlo Serra⁴, Marina Serra⁵, Teresa Zolfino⁶, Andrea Perra⁵, Luchino Chessa¹, ¹Department of Medical Sciences and Public Health, University of Cagliari, Cagliari, Italy; ²Medical Genetics, Department of Medical

Sciences and Public Health, University of Cagliari, Cagliari, Italy;
³Medical Genetics, R. Binaghi Hospital, Cagliari, Italy; ⁴Liver Unit, Hospital of University of Cagliari, Cagliari, Italy; ⁵Section of Pathology, Oncology and Molecular Pathology Unit, Department of Biochemical Sciences, University of Cagliari, Cagliari, Italy; ⁶Department of Gastroenterology, ARNAS Brotzu, Cagliari, Italy
 Email: m.miglianti420@gmail.com

Background and aims: Primary biliary cholangitis (PBC) is a rare autoimmune cholestatic liver disease. Due to the mosaic etiology of PBC, environmental variables most likely combine with immunogenetic and epigenetic risk to contribute to the disease's development. In this work, we investigated the role of soluble HLA-G (sHLA-G), HLA-G alleles and 3'UTR haplotypes and their potential impact on the onset and therapy response in Sardinian PBC patients. Sardinia, an Italian region, provides an excellent opportunity for research due to its genetic profile; it is considered a "genetic isolate" because of its homogenous genetic traits. With limited variables, a small sample of patients is sufficient to obtain significant results, particularly crucial for rare diseases like PBC.

Method: A cohort of 166 Sardinian PBC patients was compared to two groups, 180 healthy individuals and 205 AIH-1 patients. The HLA-G alleles and 3'UTR haplotypes of the patients and the healthy controls were analyzed. Plasma sHLA-G levels were measured, and the results were categorized based on HLA-G 3'UTR haplotypes linked to affecting HLA-G expression.

Results: Our data showed how the HLA-G UTR-1 haplotype was significantly more frequent in PBC patients, comparing them to the control population [160/332 (48.2%) vs 123/360 (34.3%) respectively; OR = 1.79 (95% CI 1.32–2.44); $p < 0.0001$; $pc = 0.0008$]. Furthermore, this study demonstrated a close correlation between sHLA-G levels and the response to therapy and disease severity (first line therapy response and ALP levels, gamma-GT levels, liver fibrosis score at the last follow-up). Indeed, sHLA-G levels in patients with an inadequate response were significantly lower than patients with a good response to therapy [25.58 (0.0–60.9) U/ml vs 15.53 (6.29–24.77) respectively; $p = 0.010$].

Conclusion: Our study suggests that in PBC, HLA-G extended haplotypes (HLA-G alleles and HLA-G 3'UTR control region) could play a role in disease onset, therapy response and disease progression through advanced fibrosis. This could be related to reduced levels of sHLA-G observed in PBC patients.

THU-128

A randomized phase II proof-of-concept study of beta-lapachone in patients with primary sclerosing cholangitis

Woo Hyun Paik¹, Joo Kyung Park², Moon Jae Chung³, Gunn Huh⁴, Heon Se Jeong⁵, Hee Jin Kim⁵, Do Hyun Park⁴. ¹Seoul National University Hospital, Seoul, Korea, Rep. of South; ²Samsung Medical Center, Seoul, Korea, Rep. of South; ³Yonsei University College of Medicine, Seoul, Korea, Rep. of South; ⁴Asan Medical Center, Seoul, Korea, Rep. of South; ⁵Curome Biosciences, Seoul, Korea, Rep. of South
 Email: dhpark@amc.seoul.kr

Background and aims: Primary sclerosing cholangitis (PSC) is a rare, chronic and cholestatic liver disease caused by inflammation and fibrosis of the bile duct. This condition leads to biliary cirrhosis, liver failure and associated cancer. However, there is still no drug available that can alter the progression or prognosis of the disease. Beta-lapachone (HK-660S) induces an increase in intracellular NAD⁺, thereby improving mitochondrial function and activating the Sirtuins/AMPK pathway, resulting in anti-fibrotic and anti-inflammatory effects. Therefore, we aimed to evaluate the clinical feasibility of HK-660S in patients with PSC.

Method: A randomized, double-blind, placebo-controlled, parallel group phase 2 clinical study was conducted in four tertiary institutions in South Korea. The subjects were randomly assigned to either the active or placebo groups (2:1 ratio) and administered 100 mg of HK-660S or placebo twice a day for 12 weeks and followed

up until 16 weeks. The primary outcomes were the reduction of serum alkaline phosphatase (ALP) after 12-week treatment and percentage of subjects who show improvement of severity PSC as assessed by magnetic resonance cholangiopancreatography (MRCP) with improvement defined as a decrease of –1 or more in the MRCP score (anali score). Secondary outcomes included liver stiffness on fibroscan, and any adverse events after 12-week treatment.

Results: Full analysis set (FAS) comprised 21 patients randomized to experimental (n = 15) and placebo (n = 6) group. After 12 weeks of treatment, among 18 patients who had initial ALP twice higher than upper normal limit, six patients (50.0%) in the experimental group (n = 12) showed a reduction in serum ALP of more than 20%, while none in the control group (n = 6) demonstrated statistically significant results ($p = 0.054$ by Fisher's exact test, significant at two-tailed $\alpha = 0.1$). Among the entire study population, two patients (13.3%) in the experimental group showed an improvement of biliary strictures on MRCP whereas none in the control group. Four patients (26.7%) in the experimental group showed improvement in stiffness measured by ELF score, while no patient in the control group did. There was only one severe adverse event (SAE) in the experimental group, which was bacteraemia not likely associated with HK-660S. No SAEs were reported in the control group.

Conclusion: This 12-week proof-of-concept clinical trial demonstrated that HK-660S was well-tolerated in PSC patients and had the potential to decrease serum ALP levels. Further phase 3 randomized trials with long-term follow-up are warranted to validate these promising results.

(ClinicalTrials.gov NCT05866809).

THU-129

Maralixibat improves growth in patients with progressive familial intrahepatic cholestasis: data from the MARCH/MARCH-ON trials

Regino P. Gonzalez-Peralta¹, Alexander Miethke², Amal A. Aquil³, Douglas B. Mogul⁴, Tiago Nunes⁴, Will Garner⁴, Pamela Vig⁴, Richard J. Thompson⁵. ¹Pediatric Gastroenterology, Hepatology, and Liver Transplant, AdventHealth for Children and AdventHealth Transplant Institute, Orlando, Florida, United States; ²Cincinnati Children's Hospital Medical Center, Cincinnati, Ohio, United States; ³University of Texas Southwestern Medical Center, Dallas, Texas, United States; ⁴Mirum Pharmaceuticals, Inc., Foster City, California, United States; ⁵Institute of Liver Studies, King's College London, London, United Kingdom
 Email: regino.gonzalez-peralta.md@adventhealth.com

Background and aims: Progressive familial intrahepatic cholestasis (PFIC) is a group of disorders resulting in disrupted bile composition and cholestasis leading to debilitating pruritus, growth deficits, vitamin deficiency, and progressive liver damage. A Phase 2 open-label study (INDIGO) of maralixibat (MRX), an ileal bile acid transporter (IBAT) inhibitor, in patients with BSEP deficiency (PFIC2) demonstrated that patients who were serum bile acid (sBA) responders had significant improvements in growth with >5 years of MRX treatment compared to non-responders. MARCH was a 26-week, randomized, placebo-controlled (PBO), Phase 3 trial of MRX that achieved its primary and key secondary end points of pruritus and sBA reduction for individuals across the broadest range of PFIC types studied to date, using a higher dose than INDIGO. Long-term maintenance of effect for up to two years was observed in MARCH-ON, an open-label extension. We report on the long-term impact of MRX on improvements in growth across a variety of PFIC types from the MARCH/MARCH-ON trials.

Method: MARCH/MARCH-ON has been previously described. We analyzed height and weight z-scores based on a participant's sex and age at each scheduled trial visit.

Results: We analyzed 64 participants from the All-PFIC cohort (13 FIC1, 31 nt-BSEP, 9 MDR3, 7 TJP2, and 4 MYO5B). Mean baseline age, sBA, pruritus, and liver biochemistries were well balanced between MRX and PBO groups. Growth (mean [SE]) for the overall PFIC study

population was stunted at Baseline (weight z-score: -1.53 [0.16]; height z-score: -2.07 [0.17]). In MARCH, there was a significant increase in weight z-score in the MRX group vs. PBO with a mean [SE] change from Baseline (CFB) of $+0.23$ [0.11] ($p = 0.039$). There was an increase in height z-score in the MRX group ($+0.08$ [0.09]) and a decrease in the PBO group (-0.13 [0.09]), but relative change between these groups was not statistically significant ($+0.21$ [0.12]; $p = 0.09$). In MARCH-ON, the observed increases in weight z-scores ($+0.52$ [0.18]; $p = 0.011$) were maintained for >2 years of continued treatment with MRX and improvements in height z-scores further increased, resulting in significant improvements starting at Week 30 and maintained for >2 years ($+0.4$ [0.18]; $p = 0.046$). In those participants who were initially on PBO and then subsequently received MRX for up to 1 year, comparable significant improvements were observed in both weight ($+0.32$ [0.13]; $p = 0.03$) and height ($+0.37$ [0.37]; $p = 0.012$) z-scores.

Conclusion: These consistent trends in growth for MRX-treated PFIC patients of various types represents the first report of sustained improvements in weight, as well as improvements in height, with the use of an IBAT inhibitor indicating a potential disease-modifying effect of MRX treatment in PFIC.

THU-130

The role of transient elastography and enhanced liver fibrosis score in IgG4-hepato-pancreato-biliary related disease

Senamjit Kaur¹, Rodrigo Motta², Carolyn Mercer¹, Emma Culver³.
¹Oxford University Hospitals NHS Foundation Trust, Oxford, United Kingdom; ²Translational Gastroenterology Unit, Nuffield Department of Medicine, Oxford, United Kingdom; ³Oxford University Hospitals NHS Foundation Trust, Translational Gastroenterology Unit, Nuffield Department of Medicine, Oxford, United Kingdom
 Email: senamkaur@gmail.com

Background and aims: IgG4-related disease of the liver, pancreas, and bile ducts (IgG4-HPB) can lead to fibrosis and organ damage. Liver stiffness measurement (LSM) by vibration-controlled transient elastography (VCTE) and Enhanced liver fibrosis (ELF) score is a validated, non-invasive method for measuring liver fibrosis in other chronic liver diseases, but little is known in regard to their utility in IgG4-HPB. We aimed to assess LSM using Fibroscan® and ELF in a cohort of patients with IgG4-HPB.

Method: A retrospective observational cohort of patients with IgG4-HPB meeting the ACR/EULAR classification criteria for IgG4-Related Disease at Oxford University Hospitals. Clinical data collected included demographics, organ involvement, clinical flares, serum biomarkers and organ damage. LSM was recorded in 55 IgG4-HPB patients, and sequential LSM was recorded in 32 patients. Serum ELF was measured in 23 patients. Wilcoxon rank, Mann-Whitney U, and Fisher's exact tests were performed.

Results: Ninety-seven patients with IgG4-HPB disease were included; median age 68 years \pm 19, 79% male. Established organ dysfunction and/or damage was seen in 67/97 (69%) of IgG4-HPB patients; (41/57) 72% of those with liver and biliary disease (IgG4-HB); and (26/40) 65% of those with pancreatic disease only (IgG4-AIP).

LSM was recorded in 55 patients: IgG4-HB ($n = 38$) had a higher mean LSM compared with IgG4-AIP ($n = 17$) ($p = 0.04$). IgG4-HB were risk-stratified by LSM: 25/38 (66%) had LSM <8 kPa, 8/38 (21%) had LSM ≥ 8 but <12 kPa, and 5/38 (13%) had LSM ≥ 12 kPa. There was a higher prevalence of metabolic associated steatotic liver disease (MASLD) and its risk factors (diabetes, hypertension, hypercholesterolemia, and ischaemic heart disease) in those with more advanced liver fibrosis (LSM ≥ 12 kPa). There was a higher prevalence of organ damage in those with LSM ≥ 8 kPa and ≥ 12 kPa.

In longitudinal analysis, 32 patients with IgG4-HPB had serial LSM. Of those with IgG4-HB ($n = 22$), 23% showed an increase in LSM over a median of two years (IQR 1–4). The proportion of patients meeting criteria for MASLD increased from 20% to 25% over a median of two

years. In those with paired readings during active disease and remission ($n = 8$), there was no discernible variation in LSM.

Patients with IgG4-HPB ($n = 23$) were stratified by ELF: 13/23 (56%) <9.8 and 10/23 (43%) ≥ 9.8 . ELF accurately identified patients with more significant liver fibrosis; no patient with LSM ≥ 8 kPa was seen in the <9.8 group ($p = 0.0021$). There was no association of ELF with disease activity or serum biomarkers.

Conclusion: This is the first study assessing the role of LSM by Fibroscan® and ELF score in patients with IgG4-HPB. An increased LSM over time was associated with the accumulation of cardiometabolic risk factors, evidence of MASLD, and end-organ damage, while ELF score ruled out advanced fibrosis in this cohort concurrently.

THU-131

Rifaximin helps reduce cholestasis in patients with primary biliary cholangitis and increased fecal calprotectin

Laura Iliescu¹, Andreea Simu², Razvan Rababoc², Mircea Istrate², Ioana Tanasie², Alexandra Alina Mihaela Mihaila², Adriana Rusie³, Letitia Toma².
¹Fundeni Clinical Institute, Carol Davila University of Medicine and Pharmacy, Bucharest, Romania; ²Fundeni Clinical Institute, Carol Davila University of Medicine and Pharmacy, Bucharest, Romania; ³Fundeni Clinical Institute, Carol Davila University of Medicine and Pharmacy, Bucharest
 Email: laura_ate@yahoo.com

Background and aims: Rifaximin is a nonsystemic oral antibiotic used in the prevention of hepatic encephalopathy. Its properties of modulating the gut microbiota suggest its potential use in autoimmune disorders associated with intestinal dysbiosis. We aim to determine the effect of rifaximin in patients with primary biliary cholangitis (PBC) and persistent cholestasis despite optimal treatment with ursodeoxycholic acid (UDCA).

Method: We performed a prospective trial including patients with known PBC and persistent cholestasis admitted to our clinic between January 2022 and June 2023. Diagnosis of PBC was established by presence of serum antibodies or liver biopsy in antibody-negative patients. All patients had a minimum of 6 months of optimal UDCA therapy. Patients with decompensated cirrhosis, history of malignancy or intestinal disease (including signs and symptoms of inflammatory bowel disease) were excluded from the trial. All patients continued UDCA and were given rifaximin 200 mg twice daily, 10 days per month, for a duration of 3 months. Serum transaminases (ALT, AST), gamma-glutamyl transpeptidase (GGT), direct bilirubin (dBili), alkaline phosphatase (AlkP) and fecal calprotectin (fCal) were determined before rifaximin initiation and after the last dose administration.

Results: We included 53 PBC patients (mean age 47.23 ± 12.43 years, 92.4% female). Increased transaminases was observed in 7 patients (median ALT 66 U/L, median AST 57 U/L). All patients had increased GGT (mean 115 ± 28 U/L), 60% had increased AlkP (164 ± 35 U/L) and 18.8% had increased dBili (0.9 ± 0.4 mg/dL). Increased fCal was noted in 37 patients (69.8%) with mean values 87 ± 28 ug/g. After rifaximin therapy we noted a significant decrease in GGT, AlkP, dBili and fCal in patients with initially increased fCal (GGT: 34 U/L versus 86 U/L, $p < 0.001$, AlkP: 103 U/L versus 152 U/L $p = 0.02$, dBil: 0.2 versus 0.9 mg/dL, $p = 0.04$, fCal: 32 ug/g versus 91 ug/g, $p < 0.001$). In patients with normal fCal before therapy, we noted a decrease in serum markers but not reaching statistical significance (GGT 113 U/L versus 121 U/L, AlkP 124 U/L versus 154 U/L, dBil 0.5 mg/dL versus 0.8 mg/dL).

Conclusion: Rifaximin alleviates cholestasis in PBC patients with insufficient response to ursodeoxycholic acid therapy and increased fecal calprotectin, probably by modulating gut microbiota and diminishing systemic inflammation. Therefore, it can become an important therapeutic means in patients with incomplete UDCA response. More information is necessary regarding the use of rifaximin in PBC patients with normal fecal calprotectin.

THU-132

Obeticholic acid normalizes inflammatory biomarkers in patients with primary biliary cholangitis

David E. Jones¹, Christopher L. Bowlus², Arash Thranian³, Mary Erickson³, Jing Li³, Christopher Gasink³, Robert G. Gish⁴.

¹Translational and Clinical Research Institute, Newcastle University, Newcastle-upon-Tyne, United Kingdom; ²University of California Davis, Sacramento, United States; ³Intercept Pharmaceuticals, Inc., Morristown, United States; ⁴Robert G. Gish Consultants, San Diego, United States
Email: david.jones@newcastle.ac.uk

Background and aims: Primary biliary cholangitis (PBC) is an autoimmune cholestatic liver disease characterized by chronic inflammation and progressive destruction of bile ducts. Obeticholic acid (OCA) is a selective, potent farnesoid X receptor agonist that received accelerated approval based on results from POISE, a randomized, double-blind, placebo (PBO)-controlled phase 3 study. Our goal was to evaluate the impact of OCA on normalization of inflammatory and immune biomarkers in patients (pts) from POISE.

Method: Pts with PBC who could not tolerate or had an incomplete response to ursodeoxycholic acid were randomized 1:1:1 to receive PBO, OCA titration (OCA 5 mg daily for 6 months with the option to titrate to 10 mg daily after 6 months), or OCA 10 mg daily for 12 months. Biomarker levels (tumor necrosis factor alpha [TNF-alpha], high-sensitivity C-reactive protein [hsCRP], and immunoglobulin M [IgM]) were measured at baseline (BL) and Month 12. Normalization was defined as reduction to levels ≤ 8.1 pg/ml for TNF-alpha, ≤ 3 mg/L for hsCRP, and ≤ 2.3 g/L for IgM (with abnormal defined as greater than these values). The association between treatment and normalization was assessed using Cochran-Mantel-Haenszel test and the median difference was compared using the Wilcoxon rank-sum test.

Results: In the full intent-to-treat population, median BL levels of TNF-alpha were 11.7, 10.1, and 10.8 pg/ml for PBO, OCA titration, and OCA 10 mg, respectively, and median change from BL at Month 12 was 1.2, 0.8, and -0.2 pg/ml ($p < 0.01$ for OCA 10 mg vs PBO). Among the 79% of pts with TNF-alpha > 8.1 pg/ml at BL, 3% (2/63) on PBO, 23% (10/52) on OCA titration, and 14% (7/56) on OCA 10 mg normalized at Month 12 ($p < 0.05$ for both vs PBO). Median BL hsCRP levels were 3.3, 3.3, and 3.1 mg/L for PBO, OCA titration, and OCA 10 mg, respectively, with median change from BL at Month 12 of 0.4, -0.5, and -0.6 mg/L ($p < 0.001$ for both vs PBO). Among the 53% of pts with elevated hsCRP at BL, 6% (2/38) on PBO, 19% (6/38) on OCA titration, and 39% (13/39) on OCA 10 mg attained ≤ 3 mg/L at Month 12 ($p = 0.1$ and $p < 0.001$ vs PBO, respectively). Median BL levels of IgM were 4.5, 3.7, and 3.5 g/L for PBO, OCA titration, and OCA 10 mg, respectively, with median change from BL at Month 12 of -0.3, -0.7, and -1.0 g/L ($p < 0.001$ for both vs PBO). Of the 77% of pts with high IgM at BL, 0% (0/60) on PBO, 15% (6/51) on OCA titration, and 27% (13/55) on OCA 10 mg normalized IgM at Month 12 ($p < 0.01$ for both vs PBO).

Conclusion: OCA significantly increased the proportion of pts with PBC who achieved normalization of the inflammatory biomarkers TNF-alpha, hsCRP, and IgM, the latter of which is associated with better clinical outcomes. These findings further support improvement of the autoimmune aspects of PBC in pts treated with OCA.

THU-133-YI

Radiomics for prognostication in primary sclerosing cholangitis: a proof-of-concept using GLRLM run entropy

Laura Cristofori¹, Cesare Maino², Davide Bernasconi³, Alberto Savino^{1,4}, Ilaria Ripamonti^{1,4}, Miki Scaravaglio^{1,4}, Eugenia Vittoria Pesatori⁵, Daphne D'Amato⁶, Alessio Gerussi^{1,4}, Chiara Alberzoni², Maria Grazie Valsecchi³, Rocco Corso², Davide Ippolito^{2,4}, Pietro Invernizzi^{1,4}, Elisabetta De Bernardi⁴, Marco Carbone^{4,7}. ¹Fondazione IRCCS San Gerardo dei Tintori-Department of Gastroenterology and Hepatology, European Reference Network on Hepatological Diseases (ERN RARE-LIVER), Monza, Italy; ²Fondazione IRCCS San Gerardo dei Tintori, Department of Radiology, Monza, Italy; ³Bicocca Bioinformatics Biostatistics and Bioimaging

Centre-B4, School of Medicine and Surgery, University of Milan-Bicocca, Monza, Italy; ⁴University of Milano Bicocca, Monza, Italy; ⁵Hepatology and Liver Transplant Unit, Papa Giovanni XXIII Hospital, Bergamo, Italy; ⁶Division of Gastroenterology and Hepatology, Department of Medical Science, University of Turin, Torino, Italy; ⁷ASST Grande Ospedale Metropolitano Niguarda, Hepatology and Gastroenterology Unit, Milan, Italy

Email: l.cristofori@campus.unimib.it

Background and aims: Magnetic resonance imaging (MRI) in primary sclerosing cholangitis (PSC) risk assessment generally relies on qualitative or semi-quantitative analysis, leading to interpretation variability. Radiomics emerges as a promising field for developing quantitative radiological biomarkers for PSC monitoring and risk stratification. This study aims to identify and validate radiomic features from MRI images to identify patients at higher risk of developing poor outcome.

Method: This is a prospective, single-centre, observational study (Jan 2019–Dec-2022) recruiting 102 PSC patients undergoing routine gadoxetate disodium-enhanced MRI with standardized protocol. From PyRadiomics implemented in Python both morphological and radiomics features were extracted by five selected MRI sequences (3D T1 FS GRE (ax) during the arterial phase, 3D T1 FS GRE (THRIVE) (ax) during hepatobiliary phase (20 min), ADC map (mm²/s), In-phase/Out-of-phase (IP/OP) T1 WI (ax), Fat Saturation T2 WI-MultiVane (T2spir) (ax). Patients were categorized into high-risk groups based on the Mayo risk score (MRS) > 0 and the liver stiffness measurement (LSM) > 9.6 kPa. Predictive features from a training cohort of 58 patients were validated in 41 additional PSC patients, followed by survival analysis in the combined 99-patient cohort.

Results: Among 102 patients, 99 were analysed; 2 were excluded due to poor image quality resulting from respiratory artifacts. Of the 58 patients of the training cohort 15 (25.0%) and 17 (30.0%) were defined at high-risk by MRS and LSM. One-hundred and seven radiomic features were extracted from each of the 5 MRI sequences selected. GLRLM-Run Entropy in T2spir significantly correlates with estimates of clinical outcomes with an OR of 4.04 (CI 3.63–4.71, $p = 0.0002$) for MRS and 2.93 (CI 1.71–3.43, $p = 0.009$) for LSM. Its prognostic potential was confirmed on observed clinical events by univariate Cox analysis (HR per 0.1 of increase 1.478 95% CI 1.175;1.860) showing an excellent predicting performance (C-index = 0.85).

Conclusion: This study highlights the potential of a unique, quantitative radiomic feature for monitoring and risk-stratify PSC patients. GLRLM-Run Entropy measures the randomness or complexity of image voxel grey level intensity. Higher values might be indicative of inflammation, edema, and fibrosis. Its quantitative nature, and extraction using free, globally available software makes it a promising candidate in radiological biomarkers' field in PSC. Additional research with wider cohorts and longer follow-up is required to confirm these findings.

THU-134

Metabolomic signature by 1H-NMR spectroscopy discriminates autoimmune hepatitis from other liver diseases

Kalliopi Zachou^{1,2}, Aikaterini Dimou³, Christina Kostara³, Kalliopi Azariadis^{1,2}, George Giannoulis^{1,2}, Angeliki Lyberopoulou^{1,2}, Eleni Bairaktari³, George Dalekos^{1,2}. ¹Department of Medicine and Research Laboratory of Internal Medicine, National Expertise Center of Greece in Autoimmune Liver Diseases, General University Hospital of Larissa, Larissa, Greece; ²European Reference Network on Hepatological Diseases (ERN RARE-LIVER), General University Hospital of Larissa, Larissa, Greece; ³Laboratory of Clinical Chemistry, Faculty of Medicine, School of Health Sciences, University of Ioannina, Ioannina, Greece
Email: zachoukalliopi@gmail.com

Background and aims: Altered metabolomic signature has already been reported in several diseases including autoimmune conditions. However, the metabolomic profile in autoimmune hepatitis (AIH), has not been investigated in depth. We investigated the metabolomic

POSTER PRESENTATIONS

signature of AIH and its ability to discriminate AIH from other liver diseases as well as to study its pathogenesis.

Method: Plasma samples from 50 AIH patients at diagnosis, 43 healthy controls (HC), 72 patients with primary biliary cholangitis (PBC), 26 patients with metabolic dysfunction-associated steatohepatitis (MASH) and 101 patients with chronic viral hepatitis (CVH) were investigated by ¹H-NMR spectroscopy. Fifty-two metabolites were quantified, and metabolic pathway analysis was performed.

Results: AIH could be differentiated from HC and each of the disease controls (multivariate analysis; $p < 0.001$). AIH differentiated also from disease controls as a total (PBC + CVH + MASH) (15 metabolites with 95% sensitivity and 92% specificity). Glutamine and arginine seem the main metabolites separating AIH from HC, while 2-aminobutyrate and kynurenine are the most important metabolites discriminating AIH from other liver diseases including MASH. The pathway of phenylalanine/tyrosine/tryptophan biosynthesis had the greatest impact on separating AIH from HC and other liver diseases. Ten metabolic pathways were altered in AIH compared to disease controls: the metabolic pathway of cysteine/methionine metabolism, butanoate metabolism, tyrosine metabolism, tryptophan metabolism, ketone bodies synthesis and degradation, arginine biosynthesis, arginine/proline metabolism, citrate cycle, phenylalanine/tyrosine/tryptophan biosynthesis, and phenylalanine metabolism ($p < 0.001$). Comparison for the altered metabolic pathways between the two autoimmune liver diseases (AIH and PBC) revealed that the metabolic pathway of branched-chain amino acids (BCAAs) (lower valine, leucine and isoleucine levels and their catabolic intermediates in PBC), methionine (lower methionine, 2-aminobutyrate and 2-hydroxybutyrate levels in PBC), alanine-aspartate-glutamate (lower metabolites in PBC) and that of metabolites associated with gut microbiota (lower choline, betaine and dimethylamine levels in PBC) were significantly different between AIH and PBC ($p < 0.01$).

Conclusion: The metabolomic profile of AIH is distinct and could be used to differentiate AIH from HC but most importantly from patients with other liver diseases including MASH as the panel of 15 metabolites that we detected by ¹H-NMR spectroscopy showed high sensitivity and specificity for AIH diagnosis. Therefore, ¹H-NMR could be used as an additional specific tool for AIH diagnosis and study pathogenesis, given that NMR technology does not need much sample handling, is highly reproducible and with low cost.

THU-135

Real-world study of reasons for non-utilization of second-line treatment in patients with primary biliary cholangitis

Seema T. Meloni¹, Claudia O. Zein¹, Allison R. Smither², Anushree Iyengar², Ediz S. Calay², Tyler E. Wagner², Rohit K. Yenukoti³, Christelle Pommie⁴, Olivier Gattolliat⁴, Vitalii Doban¹, Brian D. Juran⁵, Konstantinos N. Lazaridis⁵. ¹Ipsen, Cambridge, MA, United States; ²Inference, Cambridge, MA, United States; ³Inference Labs, Karnataka, India; ⁴Ipsen, Boulogne-Billancourt, France; ⁵Division of Gastroenterology and Hepatology, Department of Internal Medicine, Mayo Clinic, Rochester, MN, United States
Email: seema.meloni@ipsen.com

Background and aims: Primary biliary cholangitis (PBC) is a rare cholestatic liver disease characterized by autoimmune destruction of intrahepatic bile ducts. Left untreated, PBC can progress to hepatic fibrosis, cirrhosis, decompensation, and death. Ursodeoxycholic acid (UDCA) is the first line treatment for patients with PBC. Patients with inadequate response to UDCA treatment are considered for second line (2L) therapy. Despite availability of 2L treatment options, such as obeticholic acid and fenofibrate in the United States, low numbers of eligible patients have been prescribed these 2L treatments according to Mayo Clinic data. This study utilized natural language processing (NLP) algorithms to identify reasons why patients that met eligibility criteria for initiation of 2L treatment were not receiving it.

Method: This study utilized real-world data from a cohort of patients with PBC who were treated at Mayo Clinic in the United States.

Patients with a PBC diagnosis and evidence of at least one year of UDCA treatment were identified using a combination of structured data (diagnosis codes, lab, and medication orders) and unstructured clinical notes processed using proprietary NLP algorithms. Patients were excluded if they did not have an order of UDCA between February 2016 and February 2023, or if they were part of any interventional clinical trial. 2L treatment eligibility was defined as having alkaline phosphatase (ALP) levels ≥ 1.67 upper limit of normal (ULN) after at least one year of UDCA treatment for PBC, or if there was explicit mention of receiving 2L treatment in clinical notes. Reasons for not initiating obeticholic acid were explored in the unstructured notes using NLP. Results are reported descriptively.

Results: In total, 2,650 patients received UDCA after February 2016. Within that cohort, 753 patients met study criteria for eligibility for 2L treatment; of those, 202 patients (27%) initiated obeticholic acid and 152 (20%) initiated fenofibrate. Of the patients that did not receive a 2L treatment, the majority (72%) had no documentation of discussion of a 2L treatment. For patients with a mention of obeticholic acid in their clinical notes, primary reasons for not initiating obeticholic acid were: concerns were about side effects (48%), decision to wait until disease worsens (28%), and cost/issues with insurance reimbursement (17%).

Conclusion: This study revealed that only about one-quarter of patients who met eligibility criteria for initiating a 2L treatment received an approved 2L treatment. The findings of this study underscore that there remains unmet need in the 2L treatment space and that current 2L treatment options may not fully address patients' and healthcare providers' needs.

THU-136

The epidemiological and prognostic burden of autoimmune liver disease: results of a nationwide population-based study over the past decade

Christophe Corpechot¹, Pierre Hornus², Mallory Calls², Pierre Rinder², Théo Marcille², Amina Malek³, Karima Ben Belkacem⁴, Gaouar Farid⁴, Pierre Corret⁵, Paola Squarzon³, Pierre-Antoine Soret^{6,7}, Sara Lemoine⁸, Olivier Chazouillères⁸, Angela Lebourg⁵. ¹Saint-Antoine Hospital, Assistance Publique-Hôpitaux de Paris, Sorbonne University, INSERM UMR_S938, Saint-Antoine Research Center, Sorbonne University, Paris; ²Semeia@, Paris, France; ³French Network for Rare Liver Disease in Children and Adults FILFOIE, Saint-Antoine Hospital, Assistance Publique-Hôpitaux de Paris, Paris, France; ⁴Reference Center for Inflammatory Biliary Diseases and Autoimmune Hepatitis, Saint-Antoine Hospital, Assistance Publique-Hôpitaux de Paris, Paris, France; ⁵ALBI Patient Association, Versailles, France; ⁶Reference Center for Inflammatory Biliary Diseases and Autoimmune Hepatitis, Saint-Antoine Hospital, Assistance Publique-Hôpitaux de Paris, Sorbonne University, Paris, France; ⁷Sorbonne University, Reference Center for Inflammatory Biliary Diseases and Autoimmune Hepatitis, European Reference Network on Hepatological Diseases (ERN Rare-Liver), Saint-Antoine Hospital, Assistance Publique-Hôpitaux de Paris, Sorbonne University, INSERM, Saint-Antoine Research Center (CRSA), Paris, France, Paris, France; ⁸Reference Center for Inflammatory Biliary Diseases and Autoimmune hepatitis, Saint-Antoine Hospital, Assistance Publique-Hôpitaux de Paris, Sorbonne University, Paris, France
Email: christophe.corpechot@aphp.fr

Background and aims: Autoimmune hepatitis (AIH), primary biliary cholangitis (PBC) and primary sclerosing cholangitis (PSC) are the main autoimmune liver diseases (AILDs). Their incidence and prognosis vary from study to study, with results that may be biased by data coming mainly from tertiary centers and from different time periods. The aim of our study was to assess the epidemiological and prognostic significance of AILDs on a national scale over the last decade.

Method: We conducted a retrospective observational study based on the French National Health Data System (SNDS) from 2009 to 2019.

Diagnoses of AILDs were based on International Classification of Diseases, 10th Revision (ICD-10) codes from health insurance and hospitalization records. In the absence of a specific diagnostic code for PSC, PSC patients were identified using the following composite criterion: 1) ICD-10 code for cholangitis, 2) ICD-10 codes for chronic inflammatory bowel diseases (Crohn disease, ulcerative colitis) and/or iterative hepatobiliary imaging, 3) ursodeoxycholic acid delivery. Patients detected before or after the study period and those who had undergone liver transplantation (LT) prior to this period were excluded. Prevalence, incidence, spatial clustering (Moran's index, MI) and standardized mortality ratio (SMR) with confidence interval (CI) were estimated for each AILD.

Results: The prevalence per 100,000 inhabitants of AIH, PBC and PSC was 18.2 (adults 93%, children 7%; mean age 54 ± 21 years; sex ratio 0.37), 21.7 (adults 98%, children 2%; mean age 62 ± 18 years; sex ratio 0.34), and 5.2 (adults 89%, children 11%; mean age 44 ± 21 years; sex ratio 1.01), respectively. The quarterly incidence of AIH increased significantly (adults $r = 0.030$; $p < 0.01$; children $r = 0.025$; $p < 0.01$) over the study period, while that of PBC ($r = -0.024$; $p < 0.05$) and PSC ($r = -0.020$; $p < 0.01$) decreased in parallel. Prevalence varied from region to region, with strong spatial autocorrelation for patients with AIH (MI: 0.28; $p < 0.001$), PBC (0.30; $p < 0.001$), and to a lesser extent for those with PSC (0.11; $p = 0.06$). The 10-year SMRs for adults with AIH, PBC and PSC were 1.80 (95%CI: 1.68–1.94), 1.74 (1.66–1.83) and 2.59 (2.30–2.91) respectively.

Conclusion: Over the last decade, this study shows: 1) a comparable prevalence for AIH and PBC, and a prevalence 4 times lower for PSC, 2) an increasing incidence of AIH contrasting with a decreasing incidence of PBC and PSC, 3) a non-random territorial distribution of AIH and PBC, and to a lesser extent PSC, 4) the persistence of excess mortality for the 3 AILDs despite the therapeutic and management advances of recent decades.

THU-137

Ulcerative colitis-associated anti-integrin α V β 6 antibodies are highly prevalent in primary sclerosing cholangitis

Dominik Roth¹, Miriam M. Düll¹, Aylin Lindemann¹, Peter Dietrich¹, Ludwig J. Horst², Markus F. Neurath¹, Juergen Siebler¹, Christoph Schramm², Andreas E. Kremer³, Moritz Leppkes¹.

¹Universitätsklinikum Erlangen, Erlangen, Germany;

²Universitätsklinikum Hamburg-Eppendorf, Hamburg, Germany;

³Universitätsspital Zürich, Zürich, Switzerland

Email: moritz.leppkes@uk-erlangen.de

Background and aims: Autoantibodies that target biliary epithelial cells have been identified in a large fraction of patients suffering from primary sclerosing cholangitis (PSC) yet the defining antigens remained elusive for decades. Recently, autoantibodies directed against the epithelial adhesion protein integrin α V β 6 have been identified that strongly associate with ulcerative colitis (UC). To date, it remains unknown whether anti-integrin α V β 6 is also present in PSC and other immune-mediated cholestatic liver diseases.

Method: Anti-integrin α V β 6-directed autoantibodies were detected by an enzyme-linked immunosorbent assay in patient sera, including healthy controls (N = 46), ulcerative colitis (N = 35), Crohn's disease (CD, N = 65), PSC with concomitant IBD (84 samples from N = 42 patients), PSC without clinically manifest IBD (40 samples from N = 18 patients), primary biliary cholangitis (PBC, N = 24), autoimmune hepatitis (AIH, N = 21), metabolic dysfunction associated fatty liver disease (MASLD, N = 24). Furthermore, immunofluorescent analyses of the target antigen were performed in liver and colon tissue samples of PSC patients.

Results: In a cohort derived from a single academic care center anti-integrin α V β 6 antibodies occurred in 91% of UC, 17% of CD, 74% of PSC with IBD, 39% of PSC without manifest IBD, 4% of PBC, 14% of AIH, 55% of AIH with overlap cholangitis and 0% of MASLD patients.

ITGB6 was expressed by PSC cholangiocytes in intrahepatic fibrotic portal fields and periductular glands of the large bile ducts.

Conclusion: UC-associated anti-integrin α V β 6 autoantibodies are highly prevalent in immune-mediated cholestatic liver diseases, especially in primary sclerosing cholangitis with concomitant inflammatory bowel disease. Integrin α V β 6 may represent a major long-sought target of anti-biliary epithelial cell antibodies in primary sclerosing cholangitis. Anti-integrin α V β 6 antibodies distinguish healthy controls and MASLD from primary sclerosing cholangitis, but do not differentiate UC from PSC-IBD.

THU-138

The male-to-female ratio among patients with primary biliary cholangitis depends on age

Ellen Werner¹, Rozanne C. de Veer¹, Maria C. van Hooff¹, Ulrich Beuers², Joost P.H. Drenth³, Frans J.C. Cuperus⁴, Bart van Hoek⁵, Bart J. Veldt⁶, Michael Kempt-Kropp⁷, Suzanne van Meer⁸, Robert C. Verdonk⁹, Hajo J. Flink¹⁰, Jan Maarten Vrolijk¹¹, Tom J.G. Gevers¹², Cyriel Y. Ponsioen², Martijn J. ter Borg¹³, Khalida Soufidi¹⁴, Femke Boersma¹⁵, Hendrik J.M. de Jonge¹⁶, Frank H.J. Wolfhagen¹⁷, L.C. Baak¹⁸, Susanne L. Onderwater¹⁹, Jeroen D. van Bergeijk²⁰, Paul G. van Putten²¹, Gijs J. de Bruin²², Rob P.R. Adang²³, Nieves Aparicio Pages²⁴, Wink de Boer²⁵, Frank ter Borg²⁶, Hanneke van Soest²⁷, Harry L.A. Janssen^{1,28}, Bettina E. Hansen¹, Nicole S. Erler¹, Adriaan J. van der Meer¹. ¹Erasmus University Medical Center, Rotterdam, Netherlands; ²Amsterdam University Medical Center, Amsterdam, Netherlands; ³Radboud University Medical Center, Nijmegen, Netherlands; ⁴University Medical Center Groningen, Groningen, Netherlands; ⁵Leiden University Medical Center, Leiden, Netherlands; ⁶Reinier de Graaf Gasthuis, Delft, Netherlands; ⁷Noordwest Ziekenhuisgroep, Alkmaar, Netherlands; ⁸University Medical Center Utrecht, Utrecht, Netherlands; ⁹St. Antonius Hospital, Nieuwegein, Netherlands; ¹⁰Catharina Hospital, Eindhoven, Netherlands; ¹¹Rijnstate, Arnhem, Netherlands; ¹²Maastricht University Medical Center, Maastricht, Netherlands; ¹³Maxima Medical Center, Eindhoven, Netherlands; ¹⁴Zuyderland Medical Center, Heerlen, Netherlands; ¹⁵Gelre Hospital, Apeldoorn, Zutphen, Netherlands; ¹⁶Jeroen Bosch Hospital, Den Bosch, Netherlands; ¹⁷Albert Schweitzer Hospital, Dordrecht, Netherlands; ¹⁸Onze Lieve Vrouwe Gasthuis, Amsterdam, Netherlands; ¹⁹Diakonessenhuis, Utrecht, Netherlands; ²⁰Hospital De Gelderse Vallei, Ede, Netherlands; ²¹Medical Center Leeuwarden, Leeuwarden, Netherlands; ²²Tergooi Hospital, Hilversum-Blaricum, Netherlands; ²³VieCuri, Venlo, Netherlands; ²⁴Canisius Wilhelmina Hospital, Nijmegen, Netherlands; ²⁵Bernhoven, Uden, Netherlands; ²⁶Deventer Hospital, Deventer, Netherlands; ²⁷Medical Center Haaglanden, Den Haag, Netherlands; ²⁸Toronto Centre for Liver Disease, University of Toronto, Toronto, Canada
Email: e.werner@erasmusmc.nl

Background and aims: Primary Biliary Cholangitis (PBC) predominantly affects the female population. However, the sex distribution differs among epidemiological studies. We assessed differences in sex distribution according to age categories in patients with PBC over time within the nationwide Dutch PBC Cohort Study (DPCS).

Method: The DPCS is a retrospective study which includes every identifiable patient with PBC in the Netherlands from 1990 onwards in all 71 Dutch hospitals. Case identification was performed through diagnosis and treatment codes, antimitochondrial antibodies test results, and locally available registries, by two medical doctors. Data on yearly population size (ages ≥ 20) at January 1st and average life expectancy were extracted from Statistics Netherlands. The assessment of the incidence and point prevalence of PBC was restricted to the period between 2008–2018. With respect to the assessment of point prevalence, patients were censored at time of death, liver transplantation or when moving abroad. Patients lost to follow-up were censored based on their average life expectancy. Incidence Rate Ratios (IRR) were calculated using a Poisson regression to analyze

POSTER PRESENTATIONS

rates among sex and age groups (20–45, 45–65, and ≥65 years) over time.

Results: In total, 2187 patients were diagnosed with PBC between 2008–2018, of which 1927 (88.1%) were female. The mean age at PBC diagnosis was 57.1 (SD 12.7) years. The median yearly incidence rate of PBC in the Netherlands during the study period was 2.6 per 100,000 inhabitants in females and 0.3 in males (age- and calendar year-adjusted IRR was 6.98, 95% CI 6.14–7.95, $p < 0.001$, for females vs. males). The male-to-female ratio was 1: 7.4 among newly diagnosed PBC patients during the study period, which differed based on age category. The ratio was 1: 14.4 in those <45 years, 1: 9.9 in patients aged 45–65 years, and 1: 4.4 in those ≥65 years. In line, the adjusted IRR for females vs males range ranged from 14.51 (95% CI 9.22–22.83, $p < 0.001$) in the population aged 20–45 years to 3.56 (95% CI 2.95–4.30 $p < 0.001$) in those ≥65 years. The age-dependent risk of PBC differed according to sex; as compared to those aged 20–45 years, the adjusted IRRs were 4.21 (95% CI 3.76–4.71, $p < 0.001$) and 6.30 (95% CI 4.18–9.51, $p < 0.001$) among those 45–65 years and 3.50 (95% CI 3.10–3.95, $p < 0.001$) and 14.41 (95% CI 9.62–21.60, $p < 0.001$) among those ≥65 years for females and males, respectively. In 2018, the PBC point prevalence was 37.6 per 100,000 females and 4.9 per 100,000 males. The male-to-female ratio in the DPCS was 1: 7.9, and ranged from 1: 22.0 in those <45 years to 1: 6.1 in those ≥65 years.

Conclusion: Based on this nationwide cohort study, the male-to-female ratio among patients with PBC is lower in the older aged population. The age-dependent risk pattern of PBC differs according to sex; middle-aged females and elderly males are at highest risk of being diagnosed with PBC.

THU-151

A prospective study on the causes of notable elevation of alanine aminotransferase (ALT) as well as elevation of both ALT and alkaline phosphatase (ALP) with special emphasis on drug-induced liver injury (DILI)

Sigurdur S. Sigurdarson¹, Helgi K Björnsson², Einar S. Björnsson³.

¹University of Iceland, Reykjavik, Iceland; ²Sahlgrenska Academy, Reykjavik, Iceland; ³Landspítali University Hospital, Reykjavik, Iceland
Email: einarsb@landspitali.is

Background and aims: In a recent prospective study the most common causes of more than tenfold elevation of ALT were choledocholithiasis, ischemic hepatitis, viral hepatitis and drug induced liver injury (DILI). Very few prospective studies have investigated the most common causes of concomitant elevation of ALT and ALP. The aims of the study were to investigate the etiologies of patients with notably elevated ALT and/or ALT together with ALP elevation and to study the proportion of patients with DILI.

Method: This was a prospective study, in patients with (a) ALT>500 (normal <50 U/L) and (b) ALT>250 U/L and ALP > 210 U/L (normal <105) during an 18-month period from June 2022 to end of 2023. Appropriate diagnostic work-up was undertaken based on clinical features, with relevant imaging, viral and immunological investigations. DILI was identified in patients with exposure to drugs including over-the-counter drugs, herbals and dietary supplements (HDS) prior to the onset of liver injury with exclusion of competing etiologies. DILI cases were diagnosed by expert opinion and with the RUCAM causality assessment method.

Results: A total of 694 patients were identified with either ALT>500 U/L or ALT>250 and ALP > 210. A total of 6 patients were excluded due to lack of information and two cases from a non-liver source, leaving 680 patients for the analysis: 377 females (55%), median age 59 (IQR 40–72), 417 in group A and 263 in group B. The most common causes were choledocholithiasis 43% ($n = 291$), ischemic hepatitis 17% ($n = 113$), hepatobiliary cancer 8% ($n = 56$), DILI 8% ($n = 53$), viral hepatitis 6% ($n = 43$), other etiologies 10% ($n = 68$) and unknown etiology in 8% ($n = 56$). Among patients with DILI, amoxicillin-clavulanate ($n = 11$), HDS ($n = 8$), check point inhibitors ($n = 6$) and acetaminophen ($n = 5$) were the dominating agents. Liver related death was only observed in

patients with ischemic hepatitis and cancer. One DILI patient needed an emergency liver transplantation due to acute liver failure associated with the HDS.

Conclusion: The most common causes of notably elevated ALT as well ALT together with ALP were choledocholithiasis and ischemic hepatitis. DILI was together with hepatobiliary cancer the third most common etiology, with amoxicillin-clavulanate, HDS and check point inhibitors as the most frequent causes.

THU-152-YI

Liver fibrosis in adolescents and young adults with autoimmune hepatitis: magnetic resonance elastography, transient elastography and liver fibrosis changes during transition of care

Maciej Janik¹, Kamil Janowski², Paulina Chodnicka³, Wiesława Grajkowska⁴, Maciej Pronicki⁴, Wojciech Janczyk², Joanna Łącz¹, Sylwia Chełstowska⁵, Elżbieta Jurkiewicz⁵, Piotr Milkiewicz⁶, Piotr Socha². ¹Department of Hepatology, Transplantology and Internal Medicine, Medical University of Warsaw, Warsaw, Poland; ²Department of Gastroenterology, Hepatology, Nutritional Disorder's and Pediatrics, Children's Memorial Health Institute, Warsaw, Poland; ³Department of Radiology, Children's Memorial Health Institute, Warsaw, Poland, Warsaw, Poland; ⁴Department of Pathology, Children's Memorial Health Institute, Warsaw, Poland; ⁵Department of Radiology, Children's Memorial Health Institute, Warsaw, Poland; ⁶Department of Hepatology, Transplantology and Internal Medicine, Medical University of Warsaw, Translational Medicine Group, Pomeranian Medical University, Szczecin, Poland; Warsaw, Poland

Email: mjanik24@gmail.com

Background and aims: Autoimmune hepatitis (AIH) requires an accurate assessment of its progression, particularly in adolescents and young adult (AYA) patients in the transition period from paediatric to adult care. Here, we evaluated liver fibrosis in AYA patients by magnetic resonance elastography (MRE) concerning liver biopsy (LB) and transient elastography (TE) and assessed liver fibrosis changes at the time of transition of care.

Method: Two independent groups of patients with AIH were included: (i) 34 adolescents (mean age 16 ± 2 years, 56% female) to calculate cutoffs of MRE (Avanto 1.5 T) in reference to LB (Ishak); (ii) 64 young adults (mean age 22 ± 4 years, 55% female) were recruited to validate MRE with TE (Fibroscan) and evaluated the liver fibrosis changes by TE in the mean follow-up of 9.4 ± 5.5 years.

Results: MRE cutoffs were calculated in the 34 patients (ALT 165 ± 302 IU/L, IgG 1603 ± 808 mg/dL, 79% on treatment and 59% of them with complete biochemical response (CBR)) in which 35% and 29% had stage ≥4 and ≥5 Ishak Score, respectively. The MRE cutoffs for severe fibrosis and cirrhosis were >2.77 kPa (AUROC 0.87, $p < 0.001$, SP: 68%, SE: 100%) and >3.65 kPa (AUROC 0.89, $p < 0.001$, SP:88%, SE:80%), respectively. Further, 64 patients treated for AIH >6 months (ALT 64 ± 90 IU/L, IgG 1468 ± 506 mg/dL, 9% LKM-positive and 60% CBR) were diagnosed with TE in 24% and 11% as severe fibrosis and cirrhosis, respectively. Regarding TE, the MRE revealed excellent accuracy for excluding severe fibrosis (0.84, PPV 73%, NPV 94%) and cirrhosis (0.87, PPV 53%, NPV 98%). Moreover, MRE classified more patients as severe fibrosis and cirrhosis than TE (both $p < 0.001$), but these patients had smaller spleen, lower FIB-4 and higher platelet count (all $p < 0.05$). During 9.4 ± 5.5 years of the follow-up, 15 patients (23%) had progression of liver fibrosis (i.e. increased liver fibrosis stage according to TE and compared to LB at diagnosis). Patients with liver fibrosis progression did not differ in age, type of AIH and stage of the disease in LB at the diagnosis. At the time of transfer to adult care (the first visit), the progression was linked to increased ALT ($p = 0.03$) but not with serum IgG or TE. Moreover, patients with CBR at the time of transfer to adult service had a lower risk of fibrosis progression (OR 0.17, 95% CI 0.04–0.69, $p = 0.01$). Of note, patients with liver fibrosis progression during transition had elevated ALT, AST, ALP (all $p < 0.05$),

and more advanced liver disease according to MRE and TE (both $p < 0.01$) during follow-up in the adult service.

Conclusion: The MRE revealed excellent accuracy in excluding severe fibrosis and cirrhosis in AYA patients with AIH. MRE identified a significantly higher proportion of patients with severe fibrosis or cirrhosis than TE, but no other clinical signs confirmed the correctness of these identifications. Liver fibrosis progression occurs in a quarter of AYA patients with AIH and is linked to a lack of CBR.

THU-153

Spleen stiffness measurement improves non-invasive prediction of clinically significant portal hypertension in primary biliary cholangitis

Giulia Francesca Manfredi^{1,2}, Ilkay Ergenc^{3,4}, Micol Cittone¹, Elisabetta Degasperis^{5,6}, Maria Cristina Neglia⁷, Rubina Bertetto¹, Carla De Benedittis¹, Hasan Basri Yapici⁸, Mario Pirisi¹, Vincenza Calvaruso⁷, Pietro Lampertico^{5,6}, Yusuf Yilmaz^{3,9}, Cristina Rigamonti¹⁰. ¹Department of Translational Medicine, Università del Piemonte Orientale and Division of Internal Medicine, AOU Maggiore della Carità, Novara, Italy; ²Department of Surgery and Cancer, Imperial College London, Hammersmith Hospital, London, United Kingdom; ³Department of Gastroenterology, School of Medicine, Marmara University, Istanbul, Turkey; ⁴Institute of Liver Studies, King's College Hospital, London, United Kingdom; ⁵Division of Gastroenterology and Hepatology, Foundation IRCCS Ca' Granda Ospedale Maggiore Policlinico, Milan, Italy; ⁶CRC "A. M. and A. Migliavacca" Center for Liver Disease, Department of Pathophysiology and Transplantation, University of Milan, Milan, Italy; ⁷Gastroenterology and Hepatology Unit, Department of Health Promotion, Mother and Child Care, Internal Medicine and Medical Specialties, University of Palermo, Palermo, Italy; ⁸Department of Internal Medicine, School of Medicine, Marmara University, Istanbul, Turkey; ⁹Department of Gastroenterology, School of Medicine, Recep Tayyip Erdoğan University, Rize, Turkey; ¹⁰Department of Translational Medicine, Università del Piemonte Orientale and Division of Internal Medicine, AOU Maggiore della Carità, Novara, Italy
Email: cristina.rigamonti@uniupo.it

Background and aims: Primary biliary cholangitis (PBC) is a slowly progressive cholestatic disease that can lead to portal hypertension (PH). Recently, non-invasive assessment of clinically significant PH (CSPH) in compensated advanced chronic liver disease (cACLD) has been refined by adding spleen stiffness measurement (SSM). In PBC the combination of liver stiffness measurement (LSM) and SSM can significantly improve risk stratification by predicting liver decompensation.

Method: Multicentric and international study of 257 patients from 4 tertiary centres for liver diseases (Novara, Istanbul, Milan and Palermo). From this cohort, 66 patients with cACLD, defined as LSM ≥ 10 kPa were selected. All the patients underwent LSM and SSM by vibration-controlled transient elastography on the same day. Esophagogastroduodenoscopy (EGDS) was performed according to Baveno VI guidelines and in all patients with SSM >40 kPa. The Baveno VII criteria (BVII) for assessing CSPH using LSM alone [LSM ≤ 15 kPa + platelets (PLTs) $\geq 150000/\text{mmc}$ to rule out CSPH; LSM >25 kPa to rule in CSPH] were compared with the BVII for CSPH incorporating both LSM and SSM (at least 2 out of 3 between LS ≤ 15 kPa, PLTs $\geq 150000/\text{mmc}$, SSM ≤ 40 kPa to rule out CSPH; at least 2 out of 3 between LS >25 kPa, PLT $<150000/\text{mmc}$, SSM >40 kPa to rule in CSPH) to evaluate their ability to identify patients with CSPH.

Results: Among the 66 PBC patients with cACLD (LSM ≥ 10 kPa), the vast majority were women (89%), on ursodesoxycholic acid monotherapy (71%), median age was 63.0 years (IQR 53.0–74.1), median disease duration 40.9 (9.9–94.9) months, median LSM 14.1 kPa (IQR 11.8–22.4), median SSM 48.8 kPa (IQR 32.1–66.9). Twenty-nine out of 57 (51%) patients with available EGDS had endoscopic signs of CSPH. Considering the BVII assessing only LSM, 25 patients (38%) belonged

to rule out zone for CSPH, 15 (23%) belonged to rule in zone, 26 (39%) were in the grey zone. According to the BVII incorporating both LSM and SSM, 33 patients (51%) belonged to rule out zone for CSPH, 28 patients to rule in (42%), while 5 patients (7%) belonged to the grey zone. The latter all had endoscopic signs of CSPH and interestingly all had SSM >40 kPa. After excluding 9/66 patients without available EGDS, diagnostic performance of BVII with LSM alone was: sensitivity 83% (LR- 0.34) for ruling out CSPH and specificity 86% (LR 2.66) for ruling in CSPH. Diagnostic performance of BVII for CSPH incorporating both LSM and SSM was sensitivity 79% (LR- 0.34) for ruling out CSPH and specificity 79% (LR 3.22) for ruling in CSPH. SSM ≤ 40 kPa alone best identified patients without CSPH (sensitivity 89%, LR- 0.17).

Conclusion: In patients with PBC, the combined use of SSM with LSM helped in reducing the proportion of patients in the grey zone for ruling in and ruling out CSPH. Moreover, SSM ≤ 40 kPa confirmed its potential role in excluding CSPH in PBC patients.

THU-154-YI

Diabetes mellitus (DM) is associated with worse outcomes in patients with primary biliary cholangitis (PBC) regardless of the presence of liver steatosis: results from the ColHai registry

María Del Barrio Azaceta¹, Margarita Sala Llinás², Diana Horta³, Sílvia Goñi Esarte⁴, Judith Gómez- Camarero⁵, Manuel Hernández Guerra⁶, Lucía Majano⁷, Javier Martínez González⁷, Jesús M. González⁸, Javier Ampuero Herrojo⁹, Magdalena Salcedo¹⁰, Mercedes Vergara¹¹, Javier Salmerón¹², Raquel Ríos León¹³, Montserrat García-Retortillo¹⁴, Sergio Rodríguez-Tajes¹⁵, Rosa M Morillas¹⁵, Margarita Fernández-de la Varga¹⁶, Inmaculada Castello¹⁷, Sara Lorente¹⁸, Indhira Perez Medrano¹⁹, Francisca Cuenca Alarcon²⁰, María Dolores Antón Conejero²¹, Ana Arencibia Almeida²², Mar Riveiro Barciela²³, Elena Gómez-Domínguez²⁴, Sonia Blanco²⁵, Javier Tejedor-Tejada²⁶, Merce Roget Alemany²⁷, Pedro Linares²⁸, Angela Martínez Herreros²⁹, Raul J. Andrade³⁰, Ana Álvarez Cancelo³¹, Javier Crespo³¹, María Carlota Londoño³², Álvaro Díaz-González³¹. ¹Departamento de Gastroenterología y Hepatología. Hospital Universitario Marqués de Valdecilla. Grupo de Investigación Clínica y Traslacional en Enfermedades Digestivas. Instituto de Investigación Valdecilla (IDIVAL), Santander, Spain; ²Servicio Digestivo. Institut d'Investigació Biomèdica de Girona (IDIBGI). Hospital Universitari Dr. Josep Trueta. Ciberehd, Girona, Spain; ³Servicio de Aparato Digestivo. Hospital Universitari Mutua de Terrassa., Terrassa, Spain; ⁴Servicio de Aparato Digestivo. Hospital Universitario de Navarra, Pamplona, Spain; ⁵Servicio de Aparato Digestivo. Hospital Universitario de Burgos., Burgos, Spain; ⁶Servicio de Aparato Digestivo. Hospital Universitario de Canarias., La Laguna, Spain; ⁷Servicio de Aparato Digestivo. Hospital Universitario Ramón y Cajal, CIBERehd, IRYCIS, Madrid., Madrid, Spain; ⁸Servicio de Aparato Digestivo. Complejo Asistencial Universitario de Salamanca. Laboratorio de Hepatología Experimental y Vectorización de Fármacos (HEVEPHARM). CIBERehd. IBSAL., Salamanca, Spain; ⁹Hospital Universitario Virgen del Rocío, Sevilla. Instituto de Biomedicina de Sevilla. Universidad de Sevilla. CIBERehd., Sevilla, Spain; ¹⁰Servicio de Aparato Digestivo. Hospital General Universitario Gregorio Marañón., Madrid, Spain; ¹¹Unitat d'Hepatologia. Servei d'Aparell Digestiu. Hospital Universitari Parc Taulí, Institut d'Investigació i Innovació I3PT. Universitat Autònoma de Barcelona. Departament de Medicina. Uvic-UCC. CIBERehd, Barcelona, Spain; ¹²Servicio de Aparato Digestivo. Hospital Universitario San Cecilio, Granada, Spain; ¹³Servicio de Aparato Digestivo. Hospital Universitario General de Villalba, Madrid, Spain; ¹⁴Sección de Hepatología, Servicio de Ap. Digestivo, Hospital del Mar. Institut de Recerca Hospital del Mar, Barcelona, Spain; ¹⁵Unidad de Hepatología, Hospital Germans Trias i Pujol. Instituto de Investigación Germans Trias i Pujol (IGTP), Badalona, España. Centro de Investigación Biomédica en Red de Enfermedades Hepáticas y Digestivas (CIBERehd), Badalona, Spain; ¹⁶Servicio de Aparato Digestivo. Hospital Álvarez Buylla, Asturias, Spain; ¹⁷Servicio de Aparato Digestivo. Hospital General

POSTER PRESENTATIONS

Universitari de Valencia, Valencia, Spain; ¹⁸Servicio de Aparato Digestivo. Hospital Universitario Lozano Blesa, Zaragoza, Spain; ¹⁹Complejo Hospitalario Universitario de Pontevedra. Instituto de Investigación Sanitaria Galicia Sur (IISGS), Pontevedra, Spain; ²⁰Unidad de Hígado. Servicio de Aparato Digestivo Hospital Clínico San Carlos, Madrid, Spain; ²¹Servicio de Aparato Digestivo. Hospital Universitario Doctor Peset, Valencia, Spain; ²²Servicio de Aparato Digestivo. Hospital Universitario Nuestra Señora de la Candelaria, Santa Cruz de Tenerife, Spain; ²³Liver Unit, Internal Medicine Department, Hospital Universitari Vall d'Hebron, Vall d'Hebron Barcelona Hospital Campus, Barcelona, Spain and CIBERehd, Barcelona, Spain; ²⁴Servicio de Aparato Digestivo. Hospital Universitario 12 de Octubre, Madrid, Spain; ²⁵Servicio de Aparato Digestivo. Hospital Universitario Basurto, OSI Bilbao Basurto, Bilbao, Spain; ²⁶Servicio de Aparato Digestivo. Hospital Universitario de Cabueñes, Gijón, Spain; ²⁷Unidad de Hepatología. Servicio de Aparato Digestivo. Consorci Sanitari de Terrassa, Terrassa, Spain; ²⁸Servicio de Aparato Digestivo. Hospital de León, León, Spain; ²⁹Servicio de Aparato Digestivo. Hospital San Pedro de Logroño, Logroño, Spain; ³⁰Servicio de Aparato Digestivo. Hospital Universitario Virgen de la Victoria, Málaga, Spain; ³¹Departamento de Gastroenterología y Hepatología. Hospital Universitario Marqués de Valdecilla. Grupo de Investigación Clínica y Traslacional en Enfermedades Digestivas. Instituto de Investigación Valdecilla (IDIVAL), Santander, Spain; ³²Liver Unit. Hospital Clínic de Barcelona. Health Care Provider of the European Reference Network on Rare Liver Disorders (ERN-Liver). Institut D'Investigacions Biomèdiques August Pi i Sunyer (IDIBAPS), CIBERehd, University of Barcelona, Barcelona, Spain
Email: maria.del94@gmail.com

Background and aims: The prevalence of metabolic disease is on the rise, and there is a lack of information regarding its impact on PBC. To assess the impact of liver steatosis and metabolic comorbidities on the response, prognosis, and progression of patients with PBC treated with ursodeoxycholic acid (UDCA).

Method: Patients with PBC included in the ColHai registry (Spanish registry for cholestatic and autoimmune liver diseases) were evaluated. Metabolic comorbidities, steatosis, response to treatment and development of cirrhosis were analysed.

Results: A total of 436 patients were included. 89% were female, with a median age of 55 years and a BMI of 25.8. At baseline, 148 (33.9%) presented with hypertension (AHT), 129 (29.6%) with dyslipidaemia, and 94 (21.6%) with DM. Steatosis (radiological and/or elastographic) was present in 126 patients (31%). 95 patients met the MASLD criteria, showing higher baseline liver stiffness (8.1 vs 6.5 kPa, $p=0.03$) than those without MASLD. The latter group had higher ALP levels (173 vs 157 IU/L, $p=0.04$), with no other relevant differences found. All patients received UDCA. After one year of treatment, 34% showed no response according to Paris II criteria and 24.9% presented GLOBE >0.3. Differences in liver stiffness had disappeared among patients with or without MASLD (7.6 vs 6.6, $p=0.18$). In the univariate analysis, we identified that baseline ALP >3 × ULN (OR 6.45 [3.28–12.67]), alcohol consumption (OR: 1.65 [1.04–2.92]) and <50 years of age at diagnosis (OR 13.19 [5.18–33.59]) were associated with worse prognosis. After one year on UDCA, patients with DM and AHT had a lower probability of response according to Paris II (DM: OR 1.79 [1.12–2.86]; AHT: OR 1.58 [1.04–2.39]), had worse prognosis by GLOBE (DM: OR 2.48 [1.34–4.61]; AHT: OR 3.67 [2.21–6.08]) and a higher probability of having a FIB-4 >3.25 (DM: OR 2.30 [1.28–4.14]; AHT: 2.27 [1.43–3.61]).

Data on the development of cirrhosis during the follow-up were available for 281 patients, of which 35 (12.5%) developed it during the follow-up. The presence of DM (OR 3.08 [1.09–8.76]) and alcohol consumption (OR 2.57 [1.01–6.55]) were independently associated in multivariate analysis with an increased risk of cirrhosis during the follow-up, regardless of the presence of steatosis.

Conclusion: DM and AHT, but not steatosis or other metabolic factors, were associated with a lower probability of response and poorer

prognosis. Furthermore, in addition to alcohol, DM independently increases the risk of progression to cirrhosis.

THU-155

Incidence of fungal and other opportunistic infections in patients with autoimmune hepatitis: a spanish multicentre study

Alvaro Diaz-Gonzalez¹, Elena Ferreiro², Elena Gómez-Domínguez², Arantxa Caballero³, Magdalena Salcedo³, Alvaro Santos-Laso¹, María Del Barrio Azaceta⁴, Jose Manuel Sousa-Martin⁵, Judith Gómez-Camarero⁶, Indhira Perez Medrano⁷, Conrado Fernández-Rodríguez⁸, Beatriz Mateos Muñoz⁹, Ana Arencibia Almeida¹⁰, Mar Riveiro Barciela¹¹, Paula Esteban¹², Ignacio VazRomero¹², Diana Horta¹³, Isabel Conde¹⁴, El Hajra Ismael Martínez¹⁵, Manuel L. Rodríguez-Perálvarez¹⁶, Marina Orti Cuerva¹⁷, Margarita Sala Llinás¹⁸, Montserrat García-Retortillo¹⁹, Tania Hernaez Alsina²⁰, Mireia Miquel²¹, Jesús M. González²², María Carlota Londoño²³, Javier Crespo¹. ¹Gastroenterology and Hepatology Department, Clinical and Translational Research in Digestive Diseases Group, Marqués de Valdecilla University Hospital, Santander, Spain, Research Institute Marques de Valdecilla (IDIVAL), Clinical and Translational Research in Digestive Pathology Group, Santander, Spain, Santander, Spain; ²Hospital Universitario Doce de Octubre, Av. Cordoba, s/n, 28041 Madrid, Madrid, Spain; ³Hospital General Universitario Gregorio Marañón, Madrid, Spain; ⁴Gastroenterology and Hepatology Department, Marqués de Valdecilla University Hospital, Clinical and Translational Digestive Research Group, IDIVAL, Santander, Spain., Research Institute Marques de Valdecilla (IDIVAL), Clinical and Translational Research in Digestive Pathology Group, Santander, Spain, Santander, Spain; ⁵Hospital Universitario Virgen del Rocío, Sevilla. Instituto de Biomedicina de Sevilla. Universidad de Sevilla., CIBERehd, Sevilla, Spain; ⁶Hospital Universitario de Burgos, Burgos, Spain; ⁷Complejo Hospitalario Universitario de Pontevedra. Instituto de Investigación Sanitaria Galicia Sur (IISGS), Pontevedra, Spain; ⁸Alcorcón Foundation University Hospital, Department of Public Health and Medical Specialties. Rey Juan Carlos University., Alcorcón. Madrid, Spain; ⁹Hospital Universitario Ramón y Cajal, CIBERehd, IRYCIS, Madrid, Madrid, Spain; ¹⁰HOSPITAL UNIVERSITARIO NUESTRA SEÑORA DE LA CANDELARIA, Santa Cruz de Tenerife, Spain; ¹¹Liver Unit, Internal Medicine Department, Hospital Universitari Vall d'Hebron, Vall d'Hebron Barcelona Hospital Campus, Barcelona, CIBERehd, Barcelona, Spain; ¹²Liver Unit, Internal Medicine Department, Hospital Universitari Vall d'Hebron, Vall d'Hebron Barcelona Hospital Campus, Barcelona, Spain, CIBERehd, Barcelona, Spain; ¹³Hospital Universitario Mútua de Terrassa, Barcelona, Spain; ¹⁴Hospital Universitario y Politécnico La Fe, Valencia; Instituto de Investigación Sanitaria La Fe, Valencia, Valencia, Spain; ¹⁵Hospital Universitario Puerta de Hierro, Madrid, Spain; ¹⁶Unidad de Hepatología y Trasplante Hepático. Hospital Universitario Reina Sofía, IMIBIC, Universidad de Córdoba, Córdoba, Spain; ¹⁷Unidad de Hepatología y Trasplante Hepático. Hospital Universitario Reina Sofía, IMIBIC, Universidad de Córdoba, CIBERehd, Córdoba, Spain; ¹⁸Hospital Universitari Doctor Josep Trueta. Institut d' Investigació Biomèdica de Girona (IDIBGI), CIBERehd, Girona, Spain; ¹⁹Hospital del Mar, Barcelona, Spain; ²⁰Hospital Universitario San Pedro, Logroño, Spain; ²¹Parc Taulí Hospital Universitari. Institut d' Investigació i Innovació Parc Taulí I3PT, Universitat Autònoma de Barcelona, Sabadell, Departament de Medicina. Universitat de Vic-Universitat Central de Catalunya (UVic-UCC). Vic. CIBERehd, Sabadell, Spain; ²²Servicio de Aparato Digestivo. Complejo Asistencial Universitario de Salamanca. Laboratorio de Hepatología Experimental y Vectorización de Fármacos (HEVEPHARM). IBSAL. Salamanca, CIBERehd, Salamanca, Spain; ²³Liver Unit. Hospital Clínic de Barcelona. Health Care Provider of the European Reference Network on Rare Liver Disorders (ERN-Liver). Institut D'Investigacions Biomèdiques August Pi i Sunyer (IDIBAPS), CIBERehd, Barcelona, Spain
Email: diazg.alvaro@gmail.com

Background and aims: Immunosuppression in autoimmune hepatitis (AIH) may predispose patients to the development of fungal and

other opportunistic infections. However, there is no information on their incidence in AIH. We aimed to evaluate the incidence of these infections in patients with AIH.

Method: Retrospective analysis conducted in 20 Spanish institutions to assess the incidence of Aspergillus infection, invasive candidiasis and other opportunistic infections spanning the years 2000–2023.

Results: A total of 2893 patients with diagnosis of AIH and treated with corticosteroids (CS) were included. Aspergillus infection was diagnosed in 16 patients (0.55%). Of these, 11 (68.7%) presented with invasive pulmonary aspergillosis, 3 (20%) had central nervous system infection and 2 (13.3%) were diagnosed with aspergilloma. 62.5% were women with a median age of 58 years. Risk factors (RF): 5 patients (31.2%) had received antibiotics and 3 (18.7%) had been admitted to the ICU. AIH was severe in 12/16 (75%): 8/12 acute-severe and 4/12 with acute liver failure. The time from AIH dx to infection was 1.5 months (IQR 0.8–25.2). At the time of Aspergillus dx, 15 (93.7%) were treated with prednisone (PDN), 8 (50%) with azathioprine (AZA), 2 (12.5%) with tacrolimus (TAC), 2 (12.5%) with mycophenolate and 1 (6.2%) with mercaptopurine (MP). All were treated with amphotericin B (37.5%), voriconazole (25%) or both (37.5%). 10 patients died during follow-up, 8 (80%) due to the infection.

On the other hand, 14 cases (0.48%) of invasive candidiasis were diagnosed: 10 (71.4%) presented as esophagitis, 2 (14.3%) involved lungs, 1 (7.1%) candidaemia, and 1 (7.1%) was nephro-urinary. 57% were women with a median age of 70 years. 9 patients (64.3%) had metabolic comorbidities, 3 (21.4%) were previously diagnosed with cancer and 2 (14.3%) HIV (CD4 >200). Other RF: 2 patients were previously treated with antibiotic, 1 parenteral nutrition, 1 neutropenia (<500) and 1 was admitted to the ICU. No patient presented with AS-AIH at onset (10 chronic, 4 acute). The time from AIH dx to infection was 20.3 months (IQR 1.5–85.8). At the time of dx, 10 (71.4%) patients were treated with CS, 9 (64.3%) with AZA and the rest with MMF, TAC, or MP. 9 patients (64.3%) received fluconazole, 1 (7.1%) isavuconazole and the rest were not treated. 5 patients died during follow-up, none related to fungal infection. Finally, other opportunistic infections included 5 cases of meningitis (2 *Cryptococcus*, 2 herpes simplex virus, and 1 *Listeria*), 2 of herpes zoster, 3 patients with CMV infection (2 pneumonia, 1 severe colitis) and 1 patient with *Nocardia* pleuritis.

Conclusion: Fungal infections are infrequent in patients with AIH. While *Candida* infection appeared late and was not associated with higher mortality, *Aspergillus* infection was diagnosed earlier and was more frequent in patients with severe onset of the disease, carrying an unfavourable prognosis.

THU-158

Improvements in serum bile acid levels are associated with improvements in key markers of liver health after maralixibat treatment in children with progressive familial intrahepatic cholestasis: data from the MARCH/MARCH-ON trials

Lorenzo D'Antiga¹, Alexander Miethke², Simon P. Horslen³, Douglas B. Mogul⁴, Tiago Nunes⁴, Will Garner⁴, Pamela Vig⁴, Richard J. Thompson⁵. ¹Paediatric Hepatology, Gastroenterology and Transplantation, Hospital Papa Giovanni XXIII, Bergamo, Italy; ²Cincinnati Children's Hospital Medical Center, Cincinnati, Ohio, United States; ³UPMC Children's Hospital of Pittsburgh, Pittsburgh, Pennsylvania, United States; ⁴Mirum Pharmaceuticals, Inc., Foster City, California, United States; ⁵Institute of Liver Studies, King's College London, London, United Kingdom
Email: ldantiga@asst-pg23.it

Background and aims: Progressive Familial Intrahepatic Cholestasis (PFIC) refers to inherited disorders of abnormal bile secretion and/or formation causing pruritus, increased serum bile acid (sBA) levels, and chronic liver disease. Most PFIC patients develop ESLD before adulthood and become candidates for liver transplantation, highlighting the importance of liver health in this population. Reductions in bile acids and bilirubin after surgical biliary diversion (SBD) are the

only predictors of longer native liver survival (NLS) in PFIC patients. MARCH was a 26-week, randomized, placebo-controlled (PBO), Phase 3 trial of maralixibat (MRX), an IBAT inhibitor, that achieved its primary and key secondary end points of pruritus and sBA reduction for individuals across a broad range of PFIC types. Long-term maintenance of effect for up to 2 years was observed in MARCH-ON, an open-label extension. We evaluated the impact of MRX on improvements in liver health through a sub-analysis on the correlation of sBA improvements and key liver parameters, including bilirubin, from the MARCH/MARCH-ON trials.

Method: MARCH/MARCH-ON study designs have been summarized. Spearman's (r) coefficients were determined to evaluate the relationship between sBA and key liver health parameters (AST, ALT, total bilirubin [TB], and direct bilirubin [DB]).

Results: This analysis included 64 patients from the All-PFIC cohort (13 FIC1, 31 nt-BSEP, 9 MDR3, 7 TJP2, and 4 MYO5B). Mean baseline age, sBA, pruritus, and liver biochemistries were well balanced between MRX and PBO groups. In MARCH, among MRX-treated participants, there was a positive correlation between average percent reductions in sBA and in AST (r 0.515, p=0.004), TB (r 0.620, p=0.0003), and DB (r 0.686, p<0.0001); correlation between reductions in sBA and in ALT were weaker (r 0.339) and not significant (NS). In PBO participants, there was no correlation between changes in sBA and ALT (r 0.094), AST (r 0.25), TB (r 0.129), and DB (r 0.11). In MARCH-ON, for participants initially on PBO that subsequently received MRX for 26 weeks, a comparable positive correlation was observed between average percent reduction in sBA and in ALT (r 0.578, p=0.002), AST (r 0.696, p<0.0001), and DB (r 0.456, p=0.02); correlation between sBA and TB was weaker (r 0.355) and NS. When analyzed for all participants receiving 26 weeks of MRX, correlations were stronger and statistically significant between reductions in sBA and in ALT (r 0.441, p=0.0007), AST (r 0.616, p<0.0001), DB (r 0.641, p<0.0001) and TB (r 0.557, p<0.0001).

Conclusion: Reductions in sBA following use of MRX, as anticipated by the drug's mechanism of action, are correlated with reductions in important biomarkers of liver disease like bilirubin, which has been shown to be associated with long-term clinical outcomes. These results demonstrate the potential for MRX to have disease-modifying effects in the treatment of PFIC.

THU-159-YI

Assessing the safety, tolerability and efficacy of rituximab in patients with difficult-to-treat autoimmune hepatitis: results from a tertiary UK liver unit

Abhishek Gairola¹, Jessica Dyson^{1,2}. ¹Newcastle upon Tyne Hospitals NHS Foundation Trust, Liver Unit, Newcastle upon Tyne, United Kingdom; ²Translational and Clinical Research Institute, Newcastle University, Newcastle upon Tyne, United Kingdom
Email: a.gairola@nhs.net

Background and aims: Autoimmune hepatitis (AIH) can result in chronic liver disease and liver transplant if biochemical remission is not achieved. Some patients have disease that is refractory to standard therapies or experience toxicity that precludes their use. Recent data suggest that rituximab (RTX), an anti-CD20 monoclonal antibody, may be a safe and effective steroid-sparing agent to maintain biochemical remission. We present our experience of using RTX in difficult-to-treat AIH.

Method: We conducted a retrospective electronic review of all AIH patients in our unit who received RTX between 2013–2023. Data collected included demographics, indication for RTX, baseline bloods (–4 to 0 months prior to 1st dose, median –0.5 months) up to 36 months after treatment started, and prednisolone dose changes. 6 patients also had longer follow-up data (38–96 months). Biochemical remission was defined as normal ALT and IgG. 1 patient was included in safety data but excluded from further analysis due to an adverse event during the 1st infusion.

POSTER PRESENTATIONS

Results: 19 patients were included: 10 (52.6%) female, median age at diagnosis 38.6 years (11–76), median interval to RTX from diagnosis 4.59 years. 12 (63.2%) had 2 or more autoimmune diagnoses. The indication for RTX was refractory disease in 11 (57.9%), treatment of another condition in 7 (36.8%) and intolerance to all other therapies in 1 (5.3%). 17 patients were receiving prednisolone at baseline. At 1 year post-RTX, 12 achieved a mean 63.3% dose reduction, with 1 stopping completely. 12 patients (63.2%) had no adverse effects with RTX. 6 had infectious complications (3 minor, 2 requiring hospitalisation [at 9 and 38 months]), and 1 death from COVID pneumonitis [4 months after last RTX]). All 6 were on 2 or more immunosuppressants. 1 patient had an anaphylactoid reaction to the 1st dose and was not rechallenged. 1 death, 58 months post-RTX, was likely unrelated (decompensated cirrhosis following fracture). Median follow-up for the 18 patients assessed for response was 27 months (5–36). At baseline, 83.3% of patients had active disease, compared with 38.9% at last follow-up within 36 months. 5/7 patients with ongoing disease activity had a mean 65.3% ALT reduction from baseline. For 6 patients with additional data (median follow-up 51 months [38–96]), 3 (50%) remained in remission.

Conclusion: Some AIH patients are at risk of disease progression due to 1st and 2nd line therapies being ineffective or poorly tolerated. Current data for RTX is limited but promising. Using it in very bespoke circumstances, we have found RTX to be effective and well tolerated. It enables reduced prednisolone dosing; a key patient priority. A multicentre trial should be a priority for the community to establish where RTX should sit within our treatment algorithm.

THU-160

Long-term variability of pruritus in primary sclerosing cholangitis and implications for future clinical trial design

Nasir Hussain¹, James Ferguson¹, Nadir Abbas¹, Usha Gungabissoon², Khushpreet Bhandal¹, Emma Burke¹, Diana Hull¹, Penelope Rogers¹, Linda Casillas³, Sumanta Mukherjee³, Andrea Ribeiro⁴, Megan McLaughlin³, Martine Walmsley⁵, Paula Hanford⁵, Palak J. Trivedi¹. ¹University of Birmingham, Birmingham, United Kingdom; ²GSK, London, United Kingdom; ³GSK, Collegeville, PA, United States; ⁴GSK, Madrid, Spain; ⁵PSC Support, Oxford, United Kingdom
Email: nxh100@student.bham.ac.uk

Background and aims: Pruritus is a recognised symptom of primary sclerosing cholangitis (PSC). We conducted a prospective observational clinical trial (ISRCTN:15518794) to capture the burden of pruritus in PSC, including how the temporal variability in symptoms may be used to inform design of future interventional trials.

Method: Adults with PSC (age >16 y; non-transplant) were invited to complete health-related quality of life (QoL) assessments (CLDQ and EQ-5D-5L) alongside pruritus questionnaires (the 5D itch score with 2-week symptom recall, and the itch numerical rating scale (NRS) with 24-hour recall). Baseline factors associated with persistent pruritus were identified, and the inherent variability in symptom intensity quantified over time.

Results: Between Jul 21 and Feb 23, 200 PSC pts were recruited (median age 39y, 115 men, median MELD score 7), of whom 100 (50%) reported pruritus of any degree (median 5D itch score was 8.0, IQR 5.0–12.0), consisting of 25 taking anti-pruritic therapy. Baseline 5D itch scores negatively correlated with age ($r = -0.204$, $p = 0.004$), with low-moderate positive correlations against serum ALT ($r = 0.197$, $p = 0.005$), ALP ($r = 0.319$, $p < 0.001$), bilirubin ($r = 0.251$, $p < 0.001$) and bile acid values ($r = 0.354$, $p < 0.001$). Median baseline 5D-itch scores were greater in pts with cirrhosis vs. no cirrhosis (10.5 vs. 6.0), those with transient elastography scores >8.0 kPa vs. <8.0 kPa (9.0 vs. 5.0) or a history of recurrent acute cholangitis (11.0 vs. 6.0) (all comparisons: $p < 0.001$). Of 31 pts who reported moderate-severe pruritus at baseline (NRS ≥ 4), the majority (61%) reported persistent moderate-severe pruritus at 36–48 weeks. Reciprocally 39% reported improvement to no/mild pruritus (NRS ≤ 3). Amongst pts with an NRS ≤ 3 at baseline ($n = 118$), 11% reported new onset or worsening pruritus to

NRS ≥ 4 . Cirrhosis was a risk factor for pts developing *de novo* or worsening pruritus over time (OR 3.75, 95% CI 1.17–12.05). Anti-pruritic therapy did not significantly impact pruritus score from w0 to w36–48. Applying our data to inform the design of a future long-term placebo-controlled trial, using NRS ≥ 4 as an inclusion criterion, and a primary end point of NRS ≤ 3 at 48 weeks (1:1 randomisation, two-sided alpha, 80% power); treatment response rates of 60%, 70% and 80%, would require 316, 126 and 64 participants per treatment arm, respectively. Comparatively, a primary end point NRS score reduction of ≤ 2 would require 238, 86 and 42 patients per arm, respectively.

Conclusion: Pruritus is common in pts with PSC, is persistent over time in the era of current anti-itch treatment and reported as more intense among pts with advanced disease. Long-term treatment trials will require large pt numbers if powered using conventional, statistical study designs, which is not tenable given the rare disease nature of PSC.

THU-161

Hepatic sarcoidosis diagnosis and management: an italian multicenter study

Cristina Della Corte¹, Daphne D'Amato^{2,3}, Adele Rocchetti⁴, Mauro Viganò⁵, Andrea Martini⁶, Maria Cristina Morelli⁷, Francesca Terracciani⁸, Michele Campigotto⁹, Nicola Pugliese¹⁰, Edoardo Giannini¹¹, Loredana Simone¹², Federica Malinverno¹³, Raffaella Reati¹⁴, Elisabetta Degasperi¹⁵, Alessandro Federico¹⁶, Emanuele Durante Mangoni¹⁷, Gabriele Missale¹⁸, Gianluca Svegliati-Baroni¹⁹, Ester Morana²⁰, Rachele Rapetti²¹, Surace Lorenzo²², Ilaria Arena²³, Annalisa Cespiati²⁴, Paolo Del Poggio²⁵, Giacomo Germani²⁶, Renato Marin²⁷, Mirici Federica²⁸, Piras Maria Rosaria²⁹, Giovanni Perricone³⁰, Salvatore Sciarrone³¹, Maria Grazia Rendina³², Silvia Strona³³, Luca Giampaolo³⁴, Sara Montagnese³⁵, Simone Saibeni²³, Giampiero Manes²³, Marco Carbone¹³. ¹Gastroenterology Unit, ASST Rhodense, Rho (MI), Rho, MI, Italy; ²Division of Gastroenterology and Center for Autoimmune Liver Diseases, Department of Medicine and Surgery, University of Milano-Bicocca, European Reference Network of Hepatological Diseases (ERN RARE-LIVER) San Gerardo Hospital, Monza, Italy, Monza, MB, Italy; ³Gastroenterology Unit, Città della Salute e della Scienza, Turin, Italy, Torino, Italy; ⁴National Center for Rare Diseases, National Institute of Health, Roma, Italy; ⁵Hepatology and Liver Transplant Unit, Papa Giovanni XXIII Hospital, Bergamo, Italy; ⁶Università degli Studi di Padova, Padova, Italy; ⁷IRCCS Azienda Ospedaliero-Universitaria di Bologna, Bologna, Italy; ⁸Internal Medicine and Hepatology, University Campus Bio-Medico of Rome, Rome, Italy, Roma, Italy; ⁹Gastroenterology Unit, Trieste University, Trieste, Italy; ¹⁰Internal Medicine and Hepatology, Humanitas Clinical and Research Center IRCCS, Humanitas University, Rozzano (MI), Italy; ¹¹University of Genoa, IRCCS Ospedale Policlinico San Martino, Genova, Italy; ¹²Gastroenterology and Endoscopy Unit, Ferrara University Hospital, Ferrara, Italy; ¹³Division of Gastroenterology and Center for Autoimmune Liver Diseases, Department of Medicine and Surgery, University of Milano-Bicocca, European Reference Network of Hepatological Diseases (ERN RARE-LIVER) San Gerardo Hospital, Monza, Italy; ¹⁴Gastroenterology Unit, ASST Rhodense, Rho (MI) Italy, Rho, Italy; ¹⁵Foundation Irccs Ca' Granda Ospedale Maggiore Policlinico, Division of Gastroenterology and Hepatology, Milano, Italy; ¹⁶Hepatogastroenterology Unit, Luigi Vanvitelli Hospital, University of Campania, Napoli, Italy; ¹⁷Unit of Infectious and Transplant Medicine, University of Naples, Napoli, Italy; ¹⁸Infectious Diseases and Hepatology University Hospital of Parma, Parma, Italy; ¹⁹Polytechnic University of

Marche, Ancona, Italy;²⁰Gastroenterology and Endoscopy Unit, Umberto Parini Hospital, Aosta, Italy; ²¹Department of Internal Medicine, Università Del Piemonte Orientale, Novara, Italy; ²²Traveler and Migration Medicine Center Provincial Health Authority of Catanzaro, Catanzaro, Italy; ²³Gastroenterology Unit, ASST Rhodense, Rho, MI, Italy; ²⁴Unit of Internal Medicine and Metabolic Disease, Granda IRCCS Foundation, University of Milan, Milano, Italy; ²⁵Gastroenterology and Endoscopy Unit, Policlinico San Marco, Zingonia (BG), Italy; ²⁶Padova Hospital-Multivisceral Transplant Unit, Padova, Italy; ²⁷U.O. Gastroenterology and Digestive Endoscopy Dolo Hospital, Venezia, Italy; ²⁸Transplant Reference Center, Sant'Orsola Polyclinic, Bologna; ²⁹Liver Transplant Coordination Unit, Brotzu Hospital, Cagliari, Italy; ³⁰Hepatology and Gastroenterology Unit, ASST Grande Ospedale Metropolitano Niguarda, Milano, Italy; ³¹U.O. Gastroenterology and Digestive Endoscopy San Bonifacio Hospital, Verona; ³²Gastroenterology Unit, Policlinico University, Bari, Italy; ³³Gastroenterology Department and Daytime Activities in Gastroenterology, ASL Torino, Torino, Italy; ³⁴Gastroenterology Unit, Cervesi Hospital, Cattolica, Italy; ³⁵Department of Medicine, University of Padua, Padova, Italy
Email: cristinadellacorte19@gmail.com

Background and aims: Sarcoidosis is a rare systemic granulomatous disease involving the liver in up to 20% of cases. The RNMNR (National Registry of Rare Disease) reported 3311 sarcoidosis Italian patients (certification period 2017–2018), however data on hepatic sarcoidosis (HS) prevalence and management are lacking. The aim of this study is to enroll all consecutive patients with sarcoidosis followed in hepatologic centers, to describe the real-world experience in disease diagnosis and management.

Method: This cross-sectional study was conducted in 33 AISF (Associazione Italiana per lo Studio del Fegato) affiliated centers across Italy, since April 2022 until October 2023. Each center was firstly asked to answer an online survey (5 domains : localization-8 items, radiology-6 items, histology-3 items, therapy-7 items, liver transplant-2 items) and subsequently each center was prospectively interviewed regarding patient's management.

Results: Through the online survey a total of 78 HS patients were reported; of which 55 [median age 52 (range: 45–57) years, 33 (60%) female, 82% Caucasian] had complete data during a median follow-up of 21 (range 6–51) months. At diagnosis systemic symptoms were reported in 46% of cases, whereas 29% of patients were asymptomatic. Pulmonary and lymphatic involvement was present in 43% and 36%, respectively, while isolated HS was present in 11% of patients. HS diagnosis was histologically proven by liver biopsy in 39 (71%) patients. At diagnosis median ALP/ γ GT and GPT/GOT values were 190/168 and 41/36 \times UI/ml. Males had a significantly higher level of γ GT ($p=0.02$) and bilirubin ($p<0.01$) at presentation. Abdominal lymphadenopathy, hepatosplenomegaly and liver focal lesions were described in 21, 21 and 13 patients, respectively. Bile duct alterations, portal vein ectasia and ascites were reported in 7, 6 and 5 cases, respectively. Clinically-significant-portal-hypertension (CSPH), according to LSM ≥ 25 kPa or esophageal varices was detected in 15% of patients. Liver biopsy showed granulomas in all the specimens, F3/F4 Metavir scores were reported in 7 (32%) patients. Treatment choices included steroids in 26 (48%), steroid+ursodeoxycholic-acid (UDCA) in 11 (20%), UDCA in 6 (11%), combination of different agents (anti-metabolites, hydroxycloquine) in 12 (21%). Median ALP decrease was 56% in 12 months, independently from the medical treatment used ($p=ns$). Seventeen (31%) patients received treatment adjustment with a second-line agent. No liver transplantations or hepatocellular carcinomas were reported. One patient died due to liver-related complications.

Conclusion: This multicentric study provides a first snapshot on the burden and experience of HS in Italy. HS has an intrinsic risk of CSPH, not always related to the presence of cirrhosis. Drug choice does not have an impact on ALP decrease, but UDCA are associated to a better GPT reduction.

THU-162-YI

Lack of association between persistently raised serum transaminase levels and hepatic steatosis/steatohepatitis in autoimmune hepatitis (AIH)

Sarah Flatley¹, Asha Dube¹, Barbara Hoeroldt¹, Laura Harrison¹, Elaine Wadland¹, Dermot Gleeson¹. ¹Sheffield Teaching Hospitals, Sheffield, United Kingdom
Email: s.flatley@nhs.net

Background and aims: The aim of AIH treatment is to achieve complete biochemical and histological remission. We have reported (Flatley, JHep 2023;78:S382) that hepatic steatosis is present in 25% of patients at AIH diagnosis and worsens during steroid treatment in 34%. This can cause confusion as to whether persistent serum transaminase elevation reflects persisting AIH or metabolic dysfunction-associated steatotic liver disease (MASLD). We aimed to assess the associations between serum transaminases and steatosis/steatohepatitis in patients with AIH.

Method: Retrospective/prospective single-centre audit of patients with AIH (1999 IAIHG criteria) presenting 1981–2022. All received corticosteroids and underwent follow-up biopsy after 26 (1–258) months: usually to confirm histological remission, but sometimes for diagnosis in patients with persisting elevated serum transaminases. Necroinflammatory (NI) score (Ishak) and steatosis grade (% hepatocytes containing fat 0: <5%, 1: 5–33%, 2: 34–66%, 3: >67%) were assessed by a single histopathologist (AKD). Steatohepatitis was based on zone 3 hepatocyte ballooning and graded using Brunt criteria. Laboratory values were measured within 2 weeks of the biopsy.

Results: 209 patients (80% women, age (median (range) 53 (3–76) years). 122 patients (47%) had steatosis (Grade 1, 2 and 3: 92, 22 and 8 respectively) and 10 (4%) had steatohepatitis. In 119 (47%) AIH was in histological remission. Serum ALT was normal (cut off 41 IU/L in men and 33 IU/L in women) in 198 patients (76%). Percentage with steatosis (49% vs 39%, $p=0.138$) or steatohepatitis (7% vs 5%, $p=0.613$) did not differ between patients with normal and elevated ALT. Serum ALT did not differ between patients with and without steatosis (median 22.5 vs 24.0, $p=0.463$), or those with and without steatohepatitis (22.0 vs 23.0, $p=0.690$). On regression analysis, there was no association between steatosis and serum ALT ($p=0.492$), AST ($p=0.343$), IgG ($p=0.336$) or NI score ($p=0.318$). There was also no association between steatohepatitis and serum ALT ($p=0.793$), AST ($p=0.600$), IgG ($p=0.247$) or NI score ($p=0.888$). In contrast, serum ALT ($p<0.001$), AST ($p<0.001$) and IgG ($p<0.001$) showed significant associations with NI score.

Conclusion: In patients with AIH, serum transaminases are not associated with steatosis or steatohepatitis, and elevated values are more likely to reflect failure to achieve biochemical remission.

THU-163

Single-cell RNA sequencing of autoimmune hepatitis identifies pathogenic marker MIF and reveals distinctions between CD8-Tc-PDCC1 cells in autoimmunity and cancer

Chao Cai¹, Chenyi Liu¹, Shu Li¹, Chen Chen¹, Yijing Cai¹, Lu Chen¹, Huifang Zhang¹, Bangguo Zhou², Mingqin Lu¹. ¹The First Affiliated Hospital of Wenzhou Medical University, Wenzhou, China; ²Shanghai Tenth People's Hospital, Ultrasound Research and Education Institute, Tongji University School of Medicine, Shanghai, China
Email: lmq0906@163.com

Background and aims: Autoimmune hepatitis (AIH) is characterized by autoimmune-mediated inflammatory liver damage, with mechanism not fully revealed. The low clinical incidence led to a scarcity of single-cell genomics studies related to AIH, leaving a gap in the exploration of new therapeutic targets. Our study aimed to characterize the distinctive immunological microenvironment at the single-cell resolution and identified potential pathogenic markers of AIH.

POSTER PRESENTATIONS

Method: We isolate single cells from liver biopsy tissue of 4 AIH patients and 2 controls. Expression data of 45806 cells was collected through 10× Genomics single-cell RNA sequencing analysis. Downstream analysis was performed using R packages (Seurat, CellChat, Monocle). Multi-colour IHC staining was performed to identify PDCD1, CD68, CD163, CD86, CD8, RORC, CD69, CD103. Serum MIF was tested with MIF Elisa tool kit.

Results: Finally, 45806 cells were captured and analyzed through 10× scRNA sequencing. Initially 19 clusters were identified into six cell types based on expression features: myeloid cells, T and NK cells, Hepatocytes, B cells, Endothelial cells, Plasma cells. To further explore the immune-pathogenesis of AIH, subtyping was performed. Seven myeloid subtypes were identified: Mac_C1QA, Mono_S100A12, Mac_CD86, Mac_CD163, DC_FLT3, Mono_CD16, Neutro_CXCR2. Pseudotime and Cellchat analysis revealed the potential upstream inflammatory factor MIF, highly correlated with AIH, validated by ELISA in serum. T cell identification disclosed distinctions in CD8-Tc-PDCD1 cells between autoimmunity and cancer. The elevated percentage in AIH, however, does not necessarily signify immune exhaustion. Cellchat analysis indicated increased interaction between CD8-Tc-PDCD1 cells and other T cells, as well as myeloid cells, in the AIH group. Additionally, we uncovered a subset of CD8-Tc17-RORc cells, with feature genes enriched in “Nod-like-receptor-signaling-pathway” and “Rig-i-like-receptor-signaling-pathway”, suggesting its potential role in regulating inflammasomes, innate immunity, and inflammation pathway activation. These findings hint at the potential significance of CD8-Tc17-RORc cells in the pathogenesis of AIH. Preliminary validation through multi-color IHC staining supported our scRNA sequencing results.

Conclusion: These findings reveal that MIF, produced by monocytes/macrophages, may serve as a crucial inflammatory factor in AIH. It is likely to modulate immune cells in liver, such as CD8-Tc-PDCD1 and CD8-Tc17-RORc, through paracrine or autocrine mechanisms, reshaping the immune microenvironment and promoting disease progression. Moreover, this study provides a single-cell transcriptomic atlas of AIH, with the potential to enhance our understanding of the complexity of the AIH immune microenvironment and offer insights for the development of new therapies.

THU-164-YI

Evaluation of four chatbots in autoimmune liver disease: a comparative analysis

Jimmy Daza¹, Lucas Bezerra¹, Heike Bantel², Marcos Giralá³, Matthias Ebert⁴, Florian van Bömmel⁵, Andreas Geier⁶, Andres Gomez Aldana⁷, Mario Álvares-da-Silva⁸, Markus Peck-Radosavljevic⁹, Ezequiel Ridruejo¹⁰, Arndt Weinmann¹¹, Andreas Teufel¹. ¹Department of Medicine II, Division of Hepatology, Division of Clinical Bioinformatics, Medical Faculty Mannheim of Heidelberg University, Mannheim, Germany; ²Department of Gastroenterology, Hepatology, Infectious Diseases and Endocrinology, Hannover Medical School, Hannover, Germany; ³Department of Gastroenterology, Hospital de Clínicas, Universidad Nacional de Asunción, Asunción, Paraguay; ⁴Department of Medicine II, Medical Faculty Mannheim of Heidelberg University, Mannheim, Germany; ⁵Department of Medicine II, Clinic of Gastroenterology, Hepatology, Infectious Diseases and Pneumology, Leipzig University Medical Center, Leipzig, Germany; ⁶Department of Internal Medicine II, Division of Hepatology, University Hospital Würzburg, Würzburg, Germany; ⁷Texas Liver Institute, University of Texas Health Science Center, San Antonio, United States; ⁸Department of Gastroenterology, Hospital de Clínicas de Porto Alegre, Universidade Federal do Rio Grande do Sul, Porto Alegre, Brazil; ⁹Internal Medicine and Gastroenterology (IMuG), Clinic Klagenfurt am Woerthersee, Klagenfurt, Austria; ¹⁰Department of Medicine, Section of Hepatology, Centro de Educación Médica e Investigaciones Clínicas Norberto Quirno “CEMIC,” Buenos Aires, Argentina; ¹¹Department of Internal Medicine I, University Medical Center of the Johannes Gutenberg-University Mainz, Mainz, Germany Email: jimmy.daza@medma.uni-heidelberg.de

Background and aims: Autoimmune liver diseases (AILDs) constitute a cluster of rare liver conditions requiring precise evaluation and management, often unfamiliar to many medical providers. With the emergence of chatbots, there is potential for innovative solutions to assist healthcare professionals in order to improve their clinical management. Our study aims to systematically assess the performance of four chatbots in addressing a comprehensive questionnaire as evaluated by global liver specialists, evaluating their utility as potential clinical decision support tools in the field of AILDs.

Method: We developed a questionnaire with 56 questions focusing on AILD evaluation, diagnosis, and management. Three diseases were included: Autoimmune hepatitis (AIH, 20 questions), Primary Biliary Cholangitis (PBC, 18 questions), and Primary Sclerosing Cholangitis (PSC, 18 questions). The list was introduced to four chatbots in December 2023, namely ChatGPT 3.5, Claude, Bing Chat, and Google Bard, in their free and open access subscription tiers. Responses were critically evaluated by ten liver specialists in Europe and the Americas using a standardized 1 to 10 rating scale. The comparative analysis included assessing the mean score and the number of highest rated replies of each chatbot, and identification of common shortcomings in chatbot performance.

Results: Among the evaluated chatbots, the mean rating scores from specialists were: Claude with 7.4 out of 10, ChatGPT with 7.27, Bing Chat with 6.85, and Google Bard with 6.65. Claude also demonstrated superiority with 26 best rated replies, followed by ChatGPT with 20, while Bing Chat and Google Bard lagged significantly with only 10 each. Common deficiencies were observed across all chatbots, including a tendency to list details over providing specific advice, limited practical dosing options, inaccurate information for pregnant patients, a lack of recent data, over-recommendation of CT and MRI, and insufficient discussion on off-label use and fibrates in PBC treatment. Of note, internet access of both Bing Chat and Google Bard did not show a positive impact in chatbot precision when compared to the pretrained models.

Conclusion: While chatbots show promise in AILD support, our findings highlight crucial areas for improvement. Refinement is needed in providing specific advice, accuracy, and focused and up-to-date information. Addressing these shortcomings is essential for enhancing the clinical utility of chatbots in autoimmune liver disease management, guiding their future development, and ensuring their effectiveness as clinical decision support tools.

THU-165

Risk of primary sclerosing cholangitis is increased among patients with gastritis-a nationwide cohort study

Lina Lindström¹, Isabella Ekheden², Marcus Thuresson³, Jonas F Ludvigsson⁴. ¹Department of medicine Huddinge Karolinska Institutet, Stockholm, Sweden; ²Department of Laboratory Medicine, Division of Clinical Pharmacology, Karolinska Institutet, Stockholm, Sweden; ³Statisticon AB, Uppsala, Sweden; ⁴Department of Medical Epidemiology and Biostatistics, Karolinska Institutet, Stockholm, Sweden Email: lina.lindstrom@ki.se

Background and aims: The pathogenesis of Primary Sclerosing Cholangitis (PSC) remains largely unknown. Infection with *Helicobacter pylori* (*H. pylori*) and subsequent gastritis could hypothetically act as a triggering event of PSC in predisposed individuals, as *H. pylori* has been shown to be more prevalent in chronic liver disease. However, the risk of PSC among patients with gastritis and its precursor, *H. pylori* infection, is undetermined. Therefore, our aim was to investigate the risk of PSC in patients with gastritis or *H. pylori* infection.

Method: This is a nationwide cohort study including all Swedish patients undergoing gastroscopy with biopsy showing gastritis or *H. pylori* during 1990–2017 (n = 318 478). For each individual with gastritis/*H. pylori* we matched up to 5 controls by sex and age from the Swedish general population. Patients were followed from the index biopsy until death, emigration, end of follow-up or date of PSC

diagnosis. We calculated the hazard ratio (HR) of PSC development, adjusting for age, sex, calendar year, county, and comorbidities.

Results: Patients with a histological diagnosis of gastritis or *H. pylori* were more likely to be diagnosed with PSC during follow-up. The adjusted HR for PSC among patients with gastritis/*H. pylori* was 3.35 (95% CI 2.67–4.20) compared to the general Swedish population. The incidence rate per 100 000 person-years for PSC in patients with gastritis/*H. pylori* was 3.7 (95% CI 3.1–4.3) and for general population controls 1.2 (95% CI 1.0–1.3).

Conclusion: Patients with a gastroscopy biopsy showing gastritis or *H. pylori* have a moderately increased risk for PSC later in life.

THU-166

Portal hypertension and its prognostic implications in patients with autoimmune hepatitis

Lukas Burghart¹, Sonja Treiber², David Bauer³, Emina Halilbasic⁴, Benedikt Hofer⁵, Mattias Mandorfer⁶, Michael Gschwandler³, Caroline Schwarz⁷, Michael Trauner⁶, Thomas Reiberger⁶, Albert Friedrich Stättermayer⁶. ¹Klinik Ottakring, Vienna, Austria; ²Medical University of Vienna, Department for Medicine III, Division for Gastroenterology and Hepatology, Vienna, Austria; ³Klinik Ottakring, Vienna; ⁴Division of Gastroenterology and Hepatology, Department of Internal Medicine III, Medical University of Vienna, Vienna, Austria; ⁵Division of Gastroenterology and Hepatology, Department of Internal Medicine III, Medical University of Vienna, Vienna, Austria; ⁶Division of Gastroenterology and Hepatology, Department of Internal Medicine III, Medical University of Vienna, Vienna, Austria; ⁷Klinik, Ottakring, Vienna, Austria
Email: burghartlukas@gmail.com

Background and aims: Autoimmune hepatitis (AIH) is a rare autoimmune mediated liver disease that may ultimately progress to advanced chronic liver disease, and clinically significant portal hypertension (CSPH). CSPH is associated with typical features in compensated (splenomegaly, collaterals and varices) and decompensated (ascites, hepatic encephalopathy and variceal bleeding) liver disease and is considered a major driver for hepatic decompensation.

Method: Patients presenting with AIH between Q1/2005 and Q4/2023 at the Medical University of Vienna (N = 282) were identified through a retrospective database query. Patients with a confirmed diagnosis of AIH, based on liver histology and an IAIHG Score of ≥ 6 were included in this study. Relevant clinical information was extracted from individual medical records. Patients with acute liver failure were excluded from further analysis (N = 11).

Results: A total of 271 AIH patients (mean age: 42.5 years (SD:19.1 years), 76.4% female, median follow-up: 7.7 (IQR 2.9–12.7) years) were retrospectively assessed. Overall, 104 (38.4%) showed features of CSPH: 37 (13.7%) developed varices, 40 (14.8%) collaterals, 76 (28.0%) splenomegaly (LDM >13 cm), 50 (18.5%) ascites, 11 (4.1%) hepatic encephalopathy and 9 (3.3%) experienced acute variceal bleeding. Overall, 16 (5.9%) patients died with 7 deaths being caused by CSPH-related complications.

In a cox proportional hazards ratio, esophageal varices (HR 6.3 CI: 2.1–19.3), portosystemic collaterals (HR 5.4 CI: 1.7–17.3) and splenomegaly (HR 6.6 CI: 2.7–15.8) were associated with a significantly increased risk of decompensation.

Overall, patients with features of CSPH showed a significantly increased risk (HR 34.4 CI: 4.6–255.1) to require liver transplantation or to progress to death during the further course of disease. Importantly, the combination of liver stiffness <15 kPa and platelets ≥ 150 G/L indicated excellent prognosis (10 Y decompensation rate: 2.6%, 10Y-TFS of 93.1%), while patients with either liver stiffness ≥ 15 kPa or platelets <150 G/L showed an increased 10 Y decompensation rate of 12.8% (log-rank $p = 0.019$) and a small decrease in 10Y-transplant-free-survival (TFS) of 86.9% (log-rank $p = 0.16$).

Conclusion: In patients with AIH, presence of CSPH associated features as well as liver stiffness ≥ 15 kPa or platelets <150 G/L are

important predictors for future hepatic decompensation and impaired TFS. AIH patients with decompensated liver disease show a dismal prognosis without liver transplantation. Hence, regular CSPH screening by liver stiffness and platelet count seems warranted in order to implement PH-targeted treatment in AIH patients on time.

THU-167

Diagnostic and therapeutic trends in primary biliary cholangitis: insights from the european reference network registry (R-LIVER)

Alessio Gerussi^{1,2,3}, Davide Bernasconi⁴, Claudia Kroll⁵, Finja Groß⁵, Ida Schregel⁵, Alberto Marini², Laura Cristofori^{1,2,3}, Maria Papp^{1,6}, George Dalekos^{1,7}, Eirini Rigopoulou^{1,7}, Nikolaos Gatselis^{1,7}, Maciej Janik^{1,8}, Piotr Milkiewicz^{1,8}, Beata Kruk⁹, Alejandra Villamil¹⁰, Henriette Ytting^{1,11}, Claudia Di Bartolomeo¹², Benedetta Terziroli^{1,12}, Milan Jirsa^{1,13}, Ehud Zigmond¹⁴, Marcial Sebode^{1,5}, Ansgar W. Lohse^{1,5}, Bettina E. Hansen¹⁵, Marco Carbone^{2,16}, Christoph Schramm^{1,5}, Pietro Invernizzi^{1,2,3}. ¹European Reference Network on Hepatological Diseases (ERN RARE-LIVER), Hamburg, Germany; ²Centre for Autoimmune Liver Diseases, Department of Medicine and Surgery, University of Milano-Bicocca, Monza, Italy; ³Division of Gastroenterology, Fondazione IRCCS San Gerardo dei Tintori, Monza, Italy; ⁴Bicocca Bioinformatics Biostatistics and Bioimaging Centre-B4, School of Medicine and Surgery, University of Milan-Bicocca, Monza, Italy; ⁵Department of Medicine, University Medical Centre Hamburg-Eppendorf (UKE), Hamburg, Germany; ⁶Division of Gastroenterology, Department of Internal Medicine, Faculty of Medicine, University of Debrecen, Debrecen, Hungary; ⁷Department of Medicine and Research Laboratory of Internal Medicine, National Expertise Center of Greece in Autoimmune Liver Diseases, General University Hospital of Larissa, Larissa, Greece; ⁸Department of Hepatology, Transplantology and Internal Medicine, Medical University of Warsaw, Warsaw, Poland; ⁹Laboratory of Metabolic Liver Diseases, Department of General, Transplant and Liver Surgery, Medical University of Warsaw, Warsaw, Poland; ¹⁰HIBA, Buenos Aires, Argentina; ¹¹Gastro Unit, Copenhagen University Hospital-Amager and Hvidovre Hospital, Hvidovre, Denmark; ¹²Epatocentro Ticino, Lugano, Switzerland; ¹³Experimental Hepatology Laboratory, Clinical and Experimental Medicine Institute, Prag, Czech Republic; ¹⁴The Research Center for Digestive Tract and Liver Diseases, Tel Aviv Sourasky Medical Center, Tel Aviv, Israel; ¹⁵Department of Epidemiology and Biostatistics, Erasmus MC, University Medical Center, Rotterdam, Netherlands; ¹⁶S.C. Epatologia e Gastroenterologia, ASST Grande Ospedale Metropolitano Niguarda, Milan, Italy
Email: alessio.gerussi@unimib.it

Background and aims: The European Reference Network on Hepatological Diseases (ERN RARE-LIVER) is a Europe-wide network for centers of excellence in the management of rare liver diseases. The aim of this study was to leverage the registry of ERN RARE-LIVER to explore the current diagnostic and therapeutic trends of incident PBC cases.

Method: We analyzed data from PBC diagnosed in the period Jan 2017–Sep 2023 from R-LIVER, a prospective registry of incident cases from the ERN RARE-LIVER network. Patients with available follow-up at 24 months were included. Centers including more than five patients were included.

Results: 313 patients from 10 centers were included in the analysis. Median age at diagnosis was 56 years, 91% were female. Transient elastography was performed in 221 patients (71%) at diagnosis (median liver stiffness (LS) 4.8 [IQR 6.3, 8.5], whereas 64 (20%) individuals had liver biopsy. Cirrhosis was present in 25 (8%) at diagnosis, with median liver stiffness 19.35 (IQR 12.0, 27.6). Two patients died (one of sepsis, one of liver failure), and one underwent transplantation for end-stage liver disease. Three patients suffered from variceal bleeding during follow-up. At diagnosis, median values of ALP were $1.43 \times \text{ULN}$, GGT $4.28 \times \text{ULN}$, ALT $1.39 \times \text{ULN}$, bilirubin $0.5 \times \text{ULN}$. 286 patients (91%) started treatment with Ursodeoxycholic Acid (UDCA) at diagnosis. After 12 months of UDCA, 228 (80%) achieved ALP values $<1.67 \times \text{ULN}$; ALP values $<1.5 \times \text{ULN}$ were

POSTER PRESENTATIONS

achieved in 212 (74%), while ALP normalization occurred in 131 cases (46%). Among 58 patients with incomplete response, 7 (12%) started Obeticholic Acid, 14 (24%) Bezafibrate and one (2%) Fenofibrate.

Conclusion: Our data from the prospective R-LIVER registry highlight diagnostic delay and limited access to second-line therapies in patients with PBC. These should assist healthcare policymakers to improve integrated care pathways in PBC.

THU-170-YI

Paris II criteria are better than Poise to predict liver-related complications after second line therapy in patients with primary biliary cholangitis

Helena Hernández-Èvole^{1,2,3}, Ignasi Olivas^{1,2,3}, Alvaro Giménez Manzorro⁴, Margarita Sala Llinàs⁵, Ares Villagrasa⁶, Montserrat García-Retortillo⁷, Natalia Sobenko⁸, Beatriz Mateos Muñoz⁹, Diana Horta¹⁰, Gabriel Mezzano¹¹, Inmaculada Castello¹², Alejandra Villamil⁸, Magdalena Salcedo⁴, María Carlota Londoño^{1,2,3}, Sergio Rodríguez-Tajes^{1,2,3}. ¹Liver Unit, Hospital Clínic de Barcelona, Barcelona, Spain; ²Centro de Investigación Biomédica en Red Enfermedades Hepáticas y Digestivas, Barcelona, Spain; ³Institut d'Investigacions Biomèdiques August Pi i Sunyer, Barcelona, Spain; ⁴Sección Hepatología y Trasplante Hepático. H.G.U. Gregorio Marañón, Madrid, Spain; ⁵Liver unit, Hospital Universitario Josep Trueta, Girona, Spain; ⁶Liver Unit, Internal Medicine Department, Vall d'Hebron University Hospital. Vall d'Hebron Institute for Research (VHIR), Barcelona, Spain; ⁷Liver Unit, Hospital del Mar, Parc Mar Salut., Barcelona, Spain; ⁸Sección de Hepatología y Trasplante Hepático. Hospital Italiano de Buenos Aires, Buenos Aires, Argentina; ⁹Liver Unit, Hospital Ramón y Cajal, Madrid, Spain; ¹⁰Servicio Digestivo, Hospital Mútua Terrassa, Terrassa, Spain; ¹¹Gastroenterología-Hepatología, Hospital del Salvador-Universidad de Chile, Santiago de Chile, Chile; ¹²Servicio Digestivo, Consorcio Hospital General Universitario Valencia, Valencia, Spain
Email: hernandez.ievole@gmail.com

Background and aims: Diverse criteria exist for assessing the response to UDCA in primary biliary cholangitis (PBC); however, their utility in evaluating the response to second-line therapy has not yet been demonstrated. The aim of our study was to investigate the ability of these criteria in predicting survival and liver-related event-free survival after second-line treatment.

Method: This was a retrospective analysis of 215 PBC patients receiving second line therapy at 10 referral centers. We excluded patients with <1 year of follow-up (FU) and those who received both fibrates and OCA. We assessed the efficacy of response criteria (Paris-II, POISE, and alkaline phosphatase [ALP] normalization) in predicting 1) a combined end point of mortality and liver transplantation (LT), and 2) any liver-related event (LRE, including LT, death, decompensation or hepatocellular carcinoma [HCC]).

Results: Ninety percent were women, with a median age of 57 (IQR: 50–64) years, 195 were treated with fibrates and 20 with OCA. The median FU time after second line treatment initiation was 4.7 (IQR: 2.1–10.6) years. During the FU, 16 patients developed cirrhosis, 6 died from liver-related complications, 7 underwent LT, 18 had decompensation, and 4 HCC. Response criteria were analyzed in 170 patients (79%). According to Paris II, 103 (61%) patients responded. Being a non-responder increased the risk of mortality/LT (HR 5.6; CI95% 1.2–25.9) and LRE (HR 3.5; CI95% 1.1–10.9). On using Poise criteria, 113 (65%) responded, but they were not significantly associated with mortality/LT (HR 2.2; CI95% 0.6–7.5) or LRE (HR 1.9; CI95% 0.7–5.5). Paris II had a ROC curve for predicting mortality of 0.74 (CI95% 0.66–0.8; sensitivity [Se] 0.83, specificity [Sp] 0.64), and 0.71 (CI95% 0.63–0.77, Se 0.76, Sp 0.65) for predicting LRE. On the contrary, ROC curves for Poise were the less accurate, with values of 0.67 (CI95% 0.6–0.74) and 0.63 (CI95% 0.56–0.7) for mortality and LRE, respectively. According to Youden index, the best ALP cut-off for predicting mortality or LRE was $1.56 \times \text{UNL}$. ALP normalization did not result in improved survival compared to ALP between 1 and $1.5 \times \text{UNL}$. Other

factors associated with both, mortality and LRE were AST normalization after 1 year of treatment (HR 0.11; CI95% 0.03–0.43), FU time before second-line treatment (HR 1.1; CI95% 1.02–1.19), albumin (HR 0.8, CI95% 0.71–0.9) and, bilirubin <0.6 mg/dl (0.6–1.2: HR 7.8; CI95% 1.1–63.4 and >1.2: HR 26; CI95% 2.7–262).

Conclusion: Paris II criteria showed better performance than Poise in predicting survival and liver-related events. Normalization of ALP did not improved survival, but bilirubin (<0.6 mg/dl) and AST normalization were excellent predictors. More studies are needed to develop response criteria for second-line treatment able to better predict LT-free survival.

THU-171

Recurrence of primary sclerosing cholangitis after living donor liver transplantation: experience from turkish registry

Gupse Adali¹, Murat Harputluoglu², Meral Akdogan Kayhan³, Dilara Turan Gökçe³, Mesut Akarsu⁴, Nilay Daniş⁵, Dinc Dincer⁶, Haydar Adanir⁶, Ilker Turan⁷, Elvan Isik⁷, Hale Gokcan⁸, Volkan Yilmaz⁹, Zülal İstemihan¹⁰, Sabahattin Kaymakoglu¹¹, Ramazan Idilman¹², Zeki Karasu⁷. ¹University of Health Sciences Istanbul Umraniye Training and Research Hospital, Department of Gastroenterology, Istanbul, Turkey; ²Inönü University School of Medicine, Department of Gastroenterology, Malatya, Turkey; ³University of Health Sciences Ankara Bilkent City Hospital, Department of Gastroenterology, Ankara, Turkey; ⁴Dokuz Eylül University School of Medicine, Department of Gastroenterology, İzmir, Turkey; ⁵Dokuz Eylül University Medical Faculty, Department of Gastroenterology, İzmir, Turkey; ⁶Akdeniz University School of Medicine, Department of Gastroenterology, Antalya, Turkey; ⁷Ege University, Faculty of Medicine, Department of Gastroenterology, İzmir, Turkey; ⁸Ankara University School Medicine, Department of Gastroenterology, Ankara, Turkey; ⁹Ankara University School of Medicine, Department of Gastroenterology, Ankara, Turkey; ¹⁰Istanbul University, Istanbul Faculty of Medicine, Department of Gastroenterology, Istanbul; ¹¹Istanbul University, Faculty of Medicine, Department of Gastroenterology, Istanbul, Turkey; ¹²Ankara University School of Medicine, Department of Gastroenterology, Ankara, Turkey
Email: gupseadali@gmail.com

Background and aims: Liver transplantation (LT) is the only therapeutic option for end-stage liver disease in primary sclerosing cholangitis (PSC). Unfortunately, approximately 10–25% of patients had experienced PSC recurrence after LT. Knowledge of recurrence rates and associated factors in living-donor liver transplantation (LDLT) for PSC is not well established. We aimed to investigate the prevalence and factors associated with PSC recurrence after LT in a predominantly LDLT multicentre cohort from Türkiye.

Method: In this national multicentre (8 centres) cohort study, adult patients with PSC who underwent LDLT between 2000 and 2022 were evaluated. Multivariate logistic regression analyses were used to identify factors associated with PSC recurrence.

Results: A total of 82 patients who underwent LT for PSC were analysed, among them, 63 (77%) had LDLT. The mean age of the patients at diagnosis was 35 ± 11 years, 62.2% were male, the median age at LT was 42 (18–65) years. The mean MELD score was 18 ± 7 . Thirty-seven patients (45%) had inflammatory bowel disease (IBD). PSC recurrence was observed in 16 (20%) patients following LT. The median time of PSC recurrence after LT was 37 months (range: 9–252 months). PSC recurrence was slightly more prevalent in LDLT than in deceased donor LT (DDLTL); (26.3% vs. 6.3%, $p=0.168$). Thirteen recipients (16%) had IBD activation, and five (6%) developed de novo IBD. In the multivariate analysis, LDLT HR 14.8 (95% CI: 1.4–160.8, $p=0.027$), younger age HR 0.85 (95% CI: 0.8–1.0, $p=0.007$), and age at LT HR 1.2 (95% CI: 1.0–1.3; $p=0.012$) were associated with the risk of PSC recurrence.

Conclusion: Based on the results of this preliminary report, LDLT may increase the risk of primary disease recurrence in patients with PSC who underwent LT.

THU-172

Investigating ACOX2 deficiency as an underlying cause of recurrent hypertransaminasemia in the Spanish population: an epidemiological study

Marta Alonso-Peña¹, Maria Menendez², Susana Iraola-Guzman³, David Sordo¹, Sara Arias-Sánchez¹, Ana Álvarez-Cancelo¹, María Del Barrio¹, Álvaro Díaz-González¹, Rafael de Cid³, Javier Crespo¹. ¹Valdecilla Research Institute (IDIVAL), Marqués de Valdecilla University Hospital, Santander, Spain; ²University of Cantabria, Santander, Spain; ³Germans Trias i Pujol Research Institute (IGTP), Badalona, Spain
Email: martaalonsop@gmail.com

Background and aims: Elevated transaminase levels are frequently encountered. ACOX2 deficiency-associated hypertransaminasemia (ADAH) arises from an inherited disruption in bile acid synthesis, leading to recurrent hypertransaminasemia. The frequency of the ADAH-causing variant (rs150832314, c.673C>T) is globally low (0.014–0.089%), suggesting ADAH's rarity, with only five affected families documented in Spain. Our aim is to ascertain the prevalence of recurrent or persistent hypertransaminasemia in the general population and scrutinize the variant's frequency across diverse subpopulations. This exploration aims to distinguish whether ADAH qualifies as a rare disease or possibly goes undiagnosed.

Method: To assess the prevalence of recurrent or persistent hypertransaminasemia (defined as more than two determinations with ALT, AST, or GGT values exceeding normal levels, spaced at least 3 months apart), we conducted a retrospective analysis of clinical records (2018–2022) within the Cantabria Cohort. This cohort recruited individuals aged 40–70 years (n=24852) from the general population. Employing Taqman probes (Ref. C_169947759_10), we genotyped the ACOX2 gene in 97 subjects exhibiting recurrent hypertransaminasemia (DNA supplied by Valdecilla Biobank). Minor Allele Frequency (MAF) information for the c.673C>T variant, as identified in sequencing studies (TopMed, ExAC, 1000Genomes, GO Exome Sequencing Project, Allele Frequency Aggregator, gnomAD, The PAGE Study, Medical Genome Project healthy controls from the Spanish population), was acquired from the dbSNP and Ensembl databases. Additionally, the MAF of the c.673C>T variant was scrutinized within the GCAT cohort, comprising individuals residing in Catalonia, with both genomic sequencing (n = 785) and genotyping data (n = 4988, TopMed panel).

Results: Within the Cantabria Cohort, 13% of participants exhibited recurrent or persistent hypertransaminasemia. Databases indicates that the Spanish population report the highest MAF of the c.673C>T variant (0.70%), with subsequent frequencies observed in the Dominican, Cuban, Central American, and Mexican populations. In the GCAT cohort, sequencing studies revealed a MAF = 0.51%, slightly diminishing in genotyping and imputation analyses (MAF = 0.46%). Regarding the hypertransaminasemia population in Cantabria, three heterozygous carriers of the c.673C>T variant were identified, resulting in a MAF of 1.57%.

Conclusion: According to allele frequency, an estimated prevalence of ADAH ranging from 21 to 49 cases per 10, 000 inhabitants in Spain in 2023 suggests that this condition may not be rare in our country. However, the actual prevalence is anticipated to be lower, considering the unknown penetrance and expressivity of this entity. A multi-center study is currently in progress to elucidate the precise prevalence and clinical spectrum of ADAH.

THU-173

Predicting post-partum flare in Autoimmune Hepatitis- who is at risk?

Charlotte Sewell¹, James Hodson¹, Kathryn Olsen¹, Leena Nagpal², Neil Rajoriya¹, Ellen Knox², Hsu Chong², James Ferguson¹, Fiona Thompson¹, Ye Htun Oo¹. ¹University Hospitals Birmingham NHS Foundation Trust, Birmingham, United Kingdom; ²Birmingham Women's Hospital, Birmingham, United Kingdom
Email: charlottesewell@nhs.net

Background and aims: Autoimmune hepatitis (AIH) is an immune-mediated liver disease with female predominance and a young age of onset. Disease remission is often seen during pregnancy due to immune tolerance, however immune escape after delivery leads to post-partum flare. Identifying which patients are at higher risk of post-partum flare could enable closer monitoring, earlier identification and treatment of flare and therefore may improve outcomes.

Method: In this retrospective single centre study, pregnant patients with AIH were identified from archived Liver Obstetric multidisciplinary team (MDT) discussion notes (births from June 2010–April 2023). Hospital electronic records were then used to collect relevant patient demographics, information regarding the pregnancy outcome, and blood results to identify cases of post-partum flare.

Results: There was a total of 43 pregnancies in 30 patients. The majority of pregnancies were in patients of white ethnicity (61%) and with Type 1 AIH (79%), with a mean age at delivery of 31 years. Post-partum flares developed in 37% of pregnancies, with patients developing post-partum flares found to be significantly younger, with a mean age at delivery of 28 vs. 32 years (p = 0.014). In addition, post-partum flares were significantly more common in pregnancies where there were concerns about treatment compliance (73% vs. 25%, p = 0.010). Other factors that were found to have a higher rate of post-partum flare were Type 2 AIH (56% vs. 33% in type 1 AIH, p = 0.265), disease not controlled at conception (55% vs. 31%, p = 0.278), previous post-partum AIH flare (55% vs. 20%, p = 0.183) and Non-White ethnicity (50% vs 32%, p = 0.314). There was no increased risk of post- partum flare in patients with cirrhosis or in patients with SLA/LC1 antibodies.

Conclusion: Closer monitoring in patients with identified risk factors for post-partum flare may enable earlier detection and treatment. Discussion around medication compliance is important in pregnant patients with AIH, especially in younger patients. Reassurance of drug safety in pregnancy and post-partum could potentially encourage medication adherence, and reduce the risk of post-partum flare.

THU-174

Assessment of the pharmacokinetic drug-drug interaction potential of elafibranor with atorvastatin in healthy adult male participants: an open-label phase I trial

Anna Pedret-Dunn¹, Sarah Mazain², Richard Allan³, Remy Hanf⁴, Carol Addy⁵. ¹Ipsen, Milton Park, United Kingdom; ²Ipsen, Boulogne-Billancourt, France; ³Ipsen, Slough, United Kingdom; ⁴GENFIT S.A., Loos, France; ⁵GENFIT Corp., Cambridge, MA, United States
Email: anna.pedret-dunn@ipsen.com

Background and aims: Elafibranor, a dual peroxisome proliferator-activated receptor-alpha/delta agonist, is under investigation as a treatment for primary biliary cholangitis (PBC). In vitro studies demonstrated that elafibranor and its major active metabolite, GFT1007, inhibit organic anion transporter polypeptide (OATP) 1B3. A phase I trial was conducted to evaluate the drug-drug interaction (DDI) potential of elafibranor as a perpetrator with atorvastatin, an OATP1B3, OATP1B1 and cytochrome P4503A (CYP3A) clinical substrate.

Method: In this phase I, randomised, open-label trial (EudraCT: 2015-000723-88), healthy participants received single doses of atorvastatin 40 mg (Days 1 and 17) and once-daily doses of elafibranor 180 mg (Days 4–19) under fasting conditions. Pharmacokinetic (PK) parameters derived for each treatment included observed maximum

POSTER PRESENTATIONS

plasma concentration (C_{\max}), area under the plasma concentration curve from administration up to the last quantifiable concentration at 72 hours (AUC_{0-72h}), and time to reach C_{\max} (t_{\max}). All adverse events (AEs) were recorded.

Results: Of 25 white male participants, 24 completed the trial; median (range) age was 32.0 (19–45) years. There was no increase in the overall exposure of atorvastatin. Compared with atorvastatin administration alone, C_{\max} was 28% lower following co-administration with elafibranor, with a geometric mean ratio (GMR) of 72 (90% confidence interval [CI]: 60.1–87.2); mean (standard deviation [SD]): 19.7 (11.0) ng/ml vs 14.8 (11.4) ng/ml. Median (range) t_{\max} increased from 0.67 (0.50–3.00) hours (h) to 1.00 (0.67–4.50) h. There was a small decrease of mean (SD) AUC_{0-72h} (12%) following co-administration, and the 90% CIs indicated similarity between the regimens: 81.3 (42.1) ng/ml*h vs 75.0 (51.5) ng/ml*h; GMR: 88 (90% CI: 82.2–93.3). Observed differences between the two regimens were not deemed clinically significant. A total of 16 non-serious and mild to moderate treatment-emergent AEs were reported by 11 participants; all were resolved without treatment discontinuation.

Conclusion: Co-administration of atorvastatin and elafibranor 180 mg had minimal impact on the overall exposure of atorvastatin. Therefore, co-administration of elafibranor 80 mg (clinical dose) with OATP1B1, OATP1B3 and CYP3A substrates, such as other statins, is unlikely to cause clinically significant PK DDIs. Furthermore, co-administration of atorvastatin and elafibranor was well tolerated.

THU-175-YI

Clinical outcome in patients with autoimmune hepatitis and its variant with primary sclerosing cholangitis

Karolina Wronka¹, Maciej Janik¹, Joanna Łącz¹, Joanna Raszeja-Wyszomirska¹, Piotr Milkiewicz^{1,2}. ¹Department of Hepatology, Transplantology and Internal Medicine, Medical University of Warsaw, Warsaw, Poland; ²Translational Medicine Group, Pomeranian Medical University, Szczecin, Poland
Email: karolina.m.wronka@gmail.com

Background and aims: People with autoimmune hepatitis (AIH), primarily a liver parenchyma disease, might present with cholestatic features, which needs to be evaluated in magnetic resonance cholangiopancreatography (MRCP). However, AIH-primary sclerosing cholangitis (PSC) variant syndrome (AIH-PSC) remains a controversial issue. Here, we evaluated the outcome in patients with the pure AIH and AIH-PSC variants.

Method: A total group of 412 adults fulfilling the criteria for diagnosing both conditions were included in the analysis. These included 306 (74%) patients with biopsy-proven AIH and 106 (26%) patients with AIH-PSC, diagnosed in all individuals with liver biopsy and magnetic resonance cholangiopancreatography (MRCP), according to EASL 2015 Guidelines. The complete biochemical response (CBR) was defined as normalization of serum transaminases and IgG. The end point was defined as liver transplantation (LT) or liver-related death. Data were presented as median (IQR) or per cent when appropriated.

Results: Patients with AIH-PSC, compared to pure AIH, were younger at the time of diagnosis (median age of 20 (12) vs 30 (32) years, $p < 0.001$), more frequently diagnosed at the paediatric age (46% vs 29%, $p = 0.013$). Female patients were more common in the pure AIH group (77% vs 36%, $p < 0.001$). In a median follow-up of 8 (10) years, the CBR was observed more frequently in AIH than in AIH-PSC (54% vs 24%, $p = 0.005$). During the 8-year follow-up, 124 patients reached the clinical end point (122 LT (30%) and two deaths (5%)). Patients with AIH-PSC required LT or had liver-related death more frequently than those with pure AIH (51% vs. 23%, $p < 0.001$). Diagnosis of AIH-PSC was an independent risk factor for LT or liver-related death HR 1.98 (95% CI 1.38–2.82, $p < 0.001$), irrespective of sex or age. Of note, hepatocellular carcinoma was diagnosed in 12 patients (3%), including nine (3%) with pure AIH and three (4%) with the AIH-PSC variant.

Conclusion: The diagnosis of AIH-PSC carries a significantly worse prognosis as compared to pure AIH population.

THU-176

Chronic pruritus presents with similar clinical features in metabolic and cholestatic liver diseases

Miriam M. Düll^{1,2}, Vanessa Karlen^{1,2}, Marcel Vetter^{1,2}, Peter Dietrich^{1,2,3}, Jörg Kupfer⁴, Markus F. Neurath^{1,2}, Andreas E. Kremer^{1,5}. ¹Department of Medicine 1, Friedrich-Alexander-University Erlangen-Nürnberg, Erlangen, Germany; ²Deutsches Zentrum Immuntherapie, DZI, Erlangen, Germany; ³Institute of Biochemistry, Emil-Fischer-Zentrum, Friedrich-Alexander-University Erlangen-Nürnberg, Erlangen, Germany; ⁴Institute of Medical Psychology, Justus-Liebig-University Giessen, Giessen, Germany; ⁵Department of Gastroenterology and Hepatology, University Hospital Zürich, University of Zürich, Zürich, Switzerland
Email: miriam.duell@uk-erlangen.de

Background and aims: Real-world experience underlines that pruritus is a common and sometimes difficult-to-treat symptom in various hepatobiliary diseases beyond cholestasis. This analysis aims at further characterizing clinical features of pruritus in patients with cholestatic and non-cholestatic liver diseases in a large cohort of patients.

Method: We performed a cross-sectional questionnaire-based study in a tertiary hepatological center assessing demographics, clinical data, and detailed characteristics of pruritus including quality of life (QoL) measures such as SF-12, 5-D Itch, and ItchQoL. Patients were categorized in “immune-mediated and cholestatic liver diseases” (ICLD), “steatotic liver disease” (SLD, comprising MASLD, MetALD, ALD), “viral liver diseases” (VLD) and “other liver diseases” (OLD). Statistical analyses were performed using Mann-Whitney-U-test and Spearman’s rank correlation. Data are given as mean \pm SEM.

Results: Of a total of 653 patients, 26.2% reported on pruritus, of whom the majority (63.7%) was female. Laboratory values of patients with and without pruritus were comparable in regard to transaminases, cholestasis parameters and liver and kidney function tests. Pruritus was present in 33.7%, 26.9%, 18.4%, and 17.1% in ICLD, SLD, VLD and OLD, respectively. Interestingly, we observed a high itch frequency of 21.4% in liver transplant recipients. Mean and worst NRS itch intensities during the last week were rated comparably high in the ICLD and SLD group at 4.1 ± 0.3 vs 3.9 ± 0.4 and 4.6 ± 0.3 vs 4.7 ± 0.5 on a NRS, respectively, but distinctly lower in patients with VLD with a mean NRS of $3.2 \pm 0.6/3.0 \pm 0.6$ and worst NRS of $3.7 \pm 0.7/3.4 \pm 0.7$. While 44.3% and 48.7% of patients with ICLD and SLD had at least a moderate itch intensity (NRS > 3), only one third received topical (15.3%; 18.9%) and/or systemic treatment (18.9%; 13.5%). Over 80% of all pruritic patients reported on chronic itch with a duration > 6 weeks. 73.9% described a stable or increasing itch level since onset of pruritus, with a majority stating a day-time dependency of worsening in the evening and night. About one third of patients with an NRS > 3 reported difficulty falling asleep or sleeping through the night due to itching. The pruritus-related QoL in both ICLD and SLD correlated with mean and worst NRS itch intensity. Median SF-12 values were significantly lower for physical ($p < 0.01$) and mental scores ($p < 0.05$) in pruritic patients in both ICLD and SLD.

Conclusion: Pruritus is a frequent symptom in patients with non-cholestatic, in particular metabolic liver diseases. In these patients, pruritus exerts comparable clinical features and has similar negative impacts on QoL compared to patients with cholestatic disorders.

THU-177-YI

Patient-reported outcomes in primary sclerosing cholangitis: an australian multicentre cohort perspective

Natassia Tan¹, Christopher Zampogna², Rohit Sawhney², Stephen Bloom², Kate Lynch³, Nicholas Hannah⁴, Siddharth Sood⁴, Kate Collins⁵, Avik Majumdar⁵, Andrew Coulshed⁶, Ken Liu⁶, John Lubel⁷, William Kemp⁷, Stuart Roberts⁷, Ammar Majeed⁷

Amanda Nicoli². ¹Alfred Health, Monash University, Melbourne, Australia; ²Eastern Health, Melbourne, Australia; ³Royal Adelaide Hospital, Melbourne, Australia; ⁴Royal Melbourne Hospital, Melbourne, Australia; ⁵Austin Health, Melbourne, Australia; ⁶Royal Prince Alfred Hospital, Melbourne, Australia; ⁷Alfred Health, Melbourne, Australia
Email: natassiapinintan@gmail.com

Background and aims: Primary sclerosing cholangitis (PSC) is a rare, progressive cholestatic liver condition that has a significant association with inflammatory bowel disease (IBD) and certain malignancies. PSC patients often suffer from impaired health-related quality of life (HRQOL) due to symptoms such as pruritus, pain, and fatigue. We aimed to characterise and compare validated PSC and IBD patient-reported outcomes (PRO) in an Australian prospective cohort and determine if PROs correlated with severity of liver disease.

Method: We conducted a multicentre prospective cohort study enrolling all adult PSC patients with or without IBD. Patients completed a validated PSC PRO questionnaire (Younossi, 2018) and a short IBD questionnaire (SIBDQ, Irvine, 1994) at time of enrolment. Additional baseline demographic and clinical data collected as part of routine clinical care was obtained. Differences in each HRQOL domain was compared using Mann-Whitney's U test. Linear regression was used to determine association between each HRQOL domain and severity of liver disease using Mayo PSC risk score. Spearman's correlation was used to determine if there was a correlation between PSC and IBD PROs within patients.

Results: A total of 55 PSC patients were included. The majority of patients were male (58%) with a median age of 42 years (IQR 33–56), large duct phenotype (82%), and median 7.5 (IQR 3.5–10.9) years of follow-up from PSC diagnosis. Eight patients (15%) were cirrhotic and none of the patients had received a liver transplant. Forty-six (84%) patients had IBD, with the majority having Crohn's disease (61%). There was no significant difference in patient demographics, clinical characteristics, liver disease severity and PSC PRO domains between patients with and without IBD. There was a significant increase in the PSC PRO domains of chronic symptoms (17 vs 7, $p = 0.03$), impairment in activities of daily living (7.5 vs 4, $p = 0.02$) and role function (6 vs 4, $p = 0.003$) in patients with cirrhosis compared to those without, however no difference was seen with the SIBDQ domains. All domain scores except chronic symptoms were significantly associated with disease severity (Mayo risk score). Patients who experienced a higher burden of emotional impairment and symptoms related to PSC also experienced an increased burden of IBD symptoms and related emotional impact ($p < 0.001$).

Conclusion: This is the first Australian study describing PSC and IBD PROs in a well characterised prospective cohort. We have demonstrated that PSC PROs are significantly associated with liver disease severity. PSC and IBD symptoms have a significantly positive correlation which suggests that luminal and biliary disease run a similar course within patients. Further large-scale prospective studies with a more heterogenous cohort are required to further interrogate these findings.

THU-178

Understanding the experience of people living with primary biliary cholangitis (PBC): further development of an experience map

Alexander Artyomenko¹, Abi Bowden², Mo Christie³, Robert Mitchell-Thain², Maria Morais⁴, Carol Roberts⁵, Marwan Sleiman⁶, Sindee Weinbaum⁷. ¹Ipsen, Slough, United Kingdom; ²Health Unlimited, London, United Kingdom; ³PBC Foundation, Edinburgh, United Kingdom; ⁴Canadian PBC Society, Toronto, United Kingdom; ⁵PBCers, Rochester, NY, United States; ⁶Ipsen, Boulogne-Billancourt, France; ⁷ELPA, Brussels, Belgium
Email: alex.artyomenko@ipsen.com

Background and aims: PBC is a rare autoimmune disease of the liver.¹ The experience of living with PBC is highly variable, and current data are limited. A range of non-specific symptoms of varying

severity are reported, which can impact quality of life. The degree of symptoms does not always correlate with liver biochemistry measures or disease progression.¹ This incongruence affects most of the PBC population, with 50% developing symptoms after five years and 95% by 20 years post-diagnosis.² To further understand the patient experience, people living with PBC were consulted to capture their thoughts, feelings, symptoms, and impact on quality of life.

Method: Reviews of publicly available literature, medical and patient organization websites, and patient stories were conducted to identify key themes. These themes guided an international steering committee meeting of patient advocates and 1:1 interviews with patients. Insights were used to co-create an experience survey to validate prior findings and ensure an accurate representation of the PBC population. An experience map was created to represent and visualize findings.

Results: The survey was distributed via a patient app for five weeks in October–November 2023 and was completed by 113 respondents. The demographics reflected the PBC population (96% female, 86% >46 years of age). People living with PBC reported fatigue as the symptom with the biggest impact on quality of life, followed by joint pain, brain fog, and pruritus. Other reported symptoms included abdominal pain, restless legs, and heartburn. Although some patients reported no symptoms (14–15%), 48% were using treatments specifically to alleviate symptoms. When rating their mental health on a scale of 1–10 (1 = worst, 10 = best) before and after their diagnosis of PBC, 25% consistently assigned a rating of 1–3. The proportion of people reporting the highest ratings of 7–10 reduced from 48% before diagnosis to 37% after diagnosis. Emotional responses were variable, with a general trend from anxiety and fear at diagnosis towards more positive emotions at the initiation of treatment. Participants reported receiving support from numerous sources, but support resources were insufficient for patients' needs.

Conclusion: A unique patient experience map for PBC has been developed and validated using insights from a range of people living with this progressive disease. Ultimately, this tool will help to align and inform healthcare approaches and treatment to address the substantial unmet needs of people living with this challenging condition.

Disclosures (funding): Conducted under a collaboration agreement between the PBC Foundation and Ipsen. Financial support was provided to Health Unlimited for project coordination and writing support by Ipsen.

References

- Hirschfield GM *et al.* *Gut* 2018;67:1568–1594
- Prince MI *et al.* *Gut* 2004;53:865–870.

THU-179

Pruritus in primary biliary cholangitis: exploring the itch phenomenon and its progression

Beata Kruk¹, Piotr Milkiewicz^{1,2}, Marcin Krawczyk^{1,3}. ¹Medical University of Warsaw, Warsaw, Poland; ²Pomeranian Medical University in Szczecin, Szczecin, Poland; ³Saarland University Medical Center, Homburg, Germany
Email: marcin.krawczyk@uks.eu

Background and aims: Primary biliary cholangitis (PBC) is a chronic autoimmune liver disease characterized by the progressive destruction of small bile ducts within the liver. Pruritus is one of the hallmark symptoms of PBC. An observation on a decrease of pruritus in patients who progressed to cirrhosis (Sheila Sherlock NEJM 1973) has never been challenged. However, our clinical experience has seemed not to concur with this notion. Thus, here we analyze the relationship between the worsening of liver function and pruritus in a large cohort of patients with PBC.

Method: The study group comprised 616 (554 females, 269 with cirrhosis, age range 22–87 years, MELD range 6.4–38.6) adult Polish Caucasian patients with PBC. All patients were prospectively recruited between 2006 and 2023. Health-related quality of life (HRQoL), including pruritus, was assessed in all patients using PBC-

40 questionnaire at two time points: at inclusion to the cohort and retrospectively at diagnosis of PBC. Associations between markers of liver injury and itch were tested using, Mann-Whitney U, Pearson correlations or paired Student's t tests, as appropriate.

Results: According to the PBC-40 questionnaire, PBC patients with cirrhosis experienced a significantly elevated degree of pruritus ($p = 0.002$) at inclusion compared to those without cirrhosis. The median itch for patients with cirrhosis was 5.0 (range 3.0–15.0), while for patients without cirrhosis it was 3.0 (range 3.0–15.0). Notably, there was a statistically significant positive correlation between the severity of pruritus and MELD score ($R^2 = 0.59$, $p < 0.001$). Examining two distinct time points in patients who progressed to cirrhosis during our observation period ($n = 61$), we noted a consistent correlation ($p = 0.032$) between the progression of liver disease and an increase of pruritus: 6.5 (range 3.0–15.0) in non-cirrhotic PBC vs. 8.0 (range 3.0–15.0) in the same patients once the cirrhosis develops.

Conclusion: Our study shows a notable association between cirrhosis and increased pruritus in subjects with PBC and may suggest a potential, positive relationship between liver function and itching intensity. This reinforces the notion that pruritus may serve as an indicator or symptom associated with the progression of liver condition in PBC.

THU-180

Presence of cholestasis and its impact on survival in patients with COVID-19 associated acute respiratory distress syndrome

Mathias Schneeweiss-Gleixner¹, Katharina Krenn², Mathias Petter¹, Patrick Haselwanter¹, Felix Kraft², Lukas Adam², Georg Semmler¹, Lukas Hartl¹, Emina Halilbasic¹, Nina Buchtele³, Christoph Krall⁴, Thomas Staudinger³, Christian Zauner¹, Michael Trauner¹, Albert Friedrich Stättermayer¹. ¹Department of Medicine III, Division of Gastroenterology and Hepatology, Medical University of Vienna, Vienna, Austria; ²Department of Anesthesia, General Intensive Care and Pain Medicine, Medical University of Vienna, Vienna, Austria; ³Department of Medicine I, Intensive Care Unit 13i2, Medical University of Vienna, Vienna, Austria; ⁴Department of Medical Statistics, Medical University of Vienna, Vienna, Austria

Email: mathias.schneeweiss-gleixner@meduniwien.ac.at

Background and aims: Data on the presence and clinical outcome of liver injury—particularly cholestasis and biliary injury—in patients with COVID-19 are scarce. Development of cholestasis has been associated with disease severity and worse clinical outcomes. The primary aim of this study was to evaluate the prevalence of cholestasis and factors associated with its development and outcome in critically ill patients with COVID-19 associated acute respiratory distress syndrome (ARDS).

Method: In this retrospective exploratory study, all COVID-19 patients with ARDS admitted to the intensive care unit (ICU) at the Medical University of Vienna were evaluated for the development of cholestasis, which was defined as an alkaline phosphatase level of 1.67x upper limit of normal for at least three consecutive days. Simple and multiple logistic regression analysis was used to evaluate parameters associated with development of cholestasis and survival.

Results: 225 critically ill COVID-19 patients (mean age 56.2 ± 12.1 ; male 68%) were included. In total, 119 patients (53%) developed cholestasis during ICU stay. Patients with cholestasis had significantly ($p < 0.001$) higher peak levels of alkaline phosphatase, gamma-glutamyl transferase, bilirubin and inflammation parameters (procalcitonin, interleukin-6) compared to patients without cholestasis. Patients with cholestasis had longer ICU length of stay (40 vs. 18 days; $p < 0.001$), lower PaO₂/FiO₂ ratio nadir (57 vs. 64; $p = 0.001$) and more often required invasive mechanical ventilation (IMV; 99% vs. 87%; $p < 0.001$) and extracorporeal membrane oxygenation (ECMO) support (78% vs. 35%; $p < 0.001$). Further, cholestatic patients more often received norepinephrine (98% vs. 87%; $p = 0.002$), ketamine (93% vs. 69%; $p < 0.001$), continuous neuromuscular blockade (73% vs.

54%; $p = 0.004$) and parenteral nutrition (76% vs. 56%; $p = 0.003$). Factors independently associated with cholestasis were invasive mechanical ventilation (OR: 1.049; CI: 1.022–1.081; $p = 0.001$), ECMO support (OR: 3.315; CI: 1.455–7.733; $p = 0.005$), ketamine use (OR: 1.106; CI: 1.046–1.174; $p = 0.001$), and disease severity as reflected by sequential organ failure assessment score on admission (OR: 1.241; CI: 1.063–1.465; $p = 0.008$). ICU and 6-month survival was 63% and 59%, respectively. Absence of cholestasis was independently associated with better ICU (OR: 0.347; CI: 0.151–0.769; $p = 0.010$) and 6-month survival (OR: 0.389; CI: 0.179–0.822; $p = 0.015$). Treatment with ursodeoxycholic acid in 73% of patients with cholestasis had no effect on ICU survival.

Conclusion: Development of cholestasis is a common complication in critically ill COVID-19 patients and represents a negative prognostic marker for survival. It is primarily associated with disease severity and specific treatment modalities of intensive care, especially ECMO and sedation with ketamine.

THU-181

Sleep disturbance due to pruritus is associated with anxiety, depression, and worse quality of life: evidence for management of pruritus and sleep in chronic liver disease

Alan Bonder¹, Amandeep Kaur², Digant Gupta², Anna Halliday³, Gil Yosipovitch⁴. ¹Division of Gastroenterology and Hepatology, Beth Israel Deaconess Medical Center, Boston, MA, United States; ²Bridge Medical, London, United Kingdom; ³GSK, London, United Kingdom; ⁴Miami Itch Centre, Miller School of Medicine, University of Miami, Miami, FL, United States

Email: anna.c.halliday@gsk.com

Background and aims: Cholestatic pruritus (itch) is common in chronic liver diseases and is even more common in cholestatic liver disease such as primary biliary cholangitis (PBC). Pruritus in PBC, especially severe pruritus, has been associated with depression, and together they have been shown to lead to poorer quality of life (QoL) in PBC. Pruritus has also been associated with sleep disturbance; severe sleep interference is common in patients with PBC and severe pruritus, and impacts QoL. In the GLIMMER study in patients with PBC, change in pruritus severity was strongly correlated (post hoc) with change in sleep interference. Here we present results from a systematic literature review and meta-analysis performed to understand the impact of pruritus-related sleep disturbance on patients' health and QoL.

Method: A systematic literature review was conducted using MEDLINE and Embase databases. Eligible literature was published in the 10 years prior to 13 December 2022 and provided data on medical conditions where pruritus was reported in adults as a specific symptom secondary to any medical condition. Screening was conducted by two independent reviewers. Random effects meta-analyses assessed correlation between sleep quality and depression, anxiety, or health-related QoL (HRQoL). Bias was assessed using a funnel plot, Egger's linear regression test, and Duval and Tweedie's trim-and-fill method.

Results: We identified 51 publications reporting pruritus data secondary to multiple underlying medical conditions including atopic dermatitis, renal impairment with dialysis-dependence and PBC, amongst others. Measures used to assess sleep disturbance/depression/anxiety/QoL were heterogeneous between publications. Lower sleep quality was moderately correlated with depression across multiple studies, with a mean correlation (95% confidence interval [CI]) of 0.392 (0.292 to 0.483; $n = 7$; $p < 0.001$). Similarly, moderate correlations between lower sleep quality and anxiety were identified, with a mean correlation (95% CI) of 0.332 (0.247 to 0.411; $n = 4$; $p < 0.001$). Lower sleep quality was associated with worse disease-specific QoL, with a mean correlation (95% CI) between sleep quality and disease-specific QoL of 0.371 (0.259 to 0.473; $n = 8$; $p < 0.001$). The risk of bias across meta-analyses was generally low.

Conclusion: Poorer sleep quality due to pruritus secondary to any medical condition is correlated with depression, anxiety and worse disease-specific QoL. Given this widespread impact of sleep disturbance on mental health and daily life, healthcare professionals should aim to explore the impact of pruritus on their patient's sleep and identify how best to manage sleep disturbance to improve depression/anxiety and QoL. Optimal management of pruritus, especially when sleep is disrupted, is important for patients with liver diseases such as PBC.

Funding: GSK (219764).

THU-182

Acute liver injury with autoimmune features following SARS-CoV-2 vaccination in an ERN/IAIHG cohort: autoimmune hepatitis versus drug-induced autoimmune-like hepatitis

Donald Malino¹, Greta Codoni², Theresa Kirchner³, Bastian Engel⁴, Alejandra Villamil⁵, Cumali Efe⁶, Elpek Gülsüm Özlem⁷, Soylu Neşe Karadağ⁸, Albert Friedrich Stättermayer⁹, Jan Philipp Weltzsch¹⁰, Marcial Sebode¹¹, Christine Bernsmeier¹², Ana Lleo¹³, Tom J.G. Gevers¹⁴, Limas Kupcinskas¹⁵, Agustin Castiella¹⁶, Jose Pinazo Bandera¹⁷, Eleonora De Martin¹⁸, Ingrid Bobis¹⁹, Thomas Damgaard Sandahl²⁰, Federica Pedica²¹, Federica Invernizzi²², Paolo Del Poggio²³, Tony Bruns²⁴, Mirjam Kolev²⁵, Nasser Semmo²⁶, Fernando Bessone²⁷, Baptiste Giguët²⁸, Guido Poggi²⁹, Masayuki Ueno³⁰, Helena Jang³¹, Andreas Cerny¹, Maria Isabel Lucena¹⁷, Raul J. Andrade¹⁷, Yoh Zen³², Richard Taubert³, Giorgia Mieli-Vergani³³, Diego Vergani³⁴, Benedetta Terzioli Beretta-Piccoli³⁵. ¹Epatocentro Ticino, Lugano, Switzerland; ²Università della Svizzera italiana, Facoltà di Scienze Biomediche, Lugano, Switzerland; ³Hannover Medical School, European Reference Network on Hepatological Diseases (ERN RARE-LIVER), Hannover, Germany; ⁴Hannover Medical School, European Reference Network on Hepatological Diseases (ERN RARE-LIVER), Hannover, Germany; ⁵Hospital Italiano de Buenos Aires, Buenos Aires, Argentina; ⁶Harran University, Şanlıurfa, Turkey; ⁷Department of pathology, Akdeniz University Faculty of Medicine, Antalya, Turkey; ⁸Department of Pathology, Inonu University Faculty of Medicine, Malatya, Turkey; ⁹Medical University of Vienna, Wien, Austria; ¹⁰I. Department of Medicine, University Medical Center Hamburg-Eppendorf, European Reference Network on Hepatological Diseases (ERN RARE-LIVER), Hamburg, Germany; ¹¹I. Dept. of Medicine, University Medical Center Hamburg-Eppendorf (UKE), European Reference Network on Hepatological Diseases (ERN RARE-LIVER), Hamburg, Germany; ¹²University Centre for Gastrointestinal and Liver Diseases, Basel, Switzerland; ¹³Humanitas University, Humanitas Research Hospital IRCCS, Rozzano (Milan), Italy; ¹⁴Maastricht University Medical Center, Maastricht, Netherlands; ¹⁵Lithuanian University of Health Sciences, Kaunas, Lithuania; ¹⁶Donostia University Hospital, Donostia, Spain; ¹⁷Servicios de Ap Digestivo y Farmacología Clínica, Hospital Universitario Virgen de la Victoria, IBIMA, Universidad de Málaga, Málaga, Spain; ¹⁸Hépatologie et Transplantation Hépatique, Hôpital Paul Brousse, Villejuif, France; ¹⁹Städtisches Krankenhaus Kiel, Kiel, Germany; ²⁰Aarhus University Hospital, Aarhus, Denmark; ²¹IRCCS San Raffaele Scientific Institute, Milan, Italy; ²²IRCCS Ospedale San Raffaele, Milan, Italy; ²³Policlinico San Marco, Zingonia, Italy; ²⁴University Hospital RWTH Aachen, European Reference Network on Hepatological Diseases (ERN RARE-LIVER), Aachen, Germany; ²⁵University Hospital of Bern, Inselspital, Bern, Switzerland; ²⁶Inselspital Bern, Bern, Switzerland; ²⁷University of Rosario School of Medicine, Rosario, Argentina; ²⁸Centre Hospitalier Universitaire de Rennes, Rennes, France; ²⁹Istituto Clinico Pavia-Vigevano UO Epatologia Oncologica, Vigevano, Italy; ³⁰Department of Gastroenterology and Hepatology, Kurashiki Central Hospital, Kurashiki, Japan; ³¹Department of Clinical Immunology and Allergy, Royal North Shore Hospital, St Leonards, Australia; ³²King's College Hospital, Institute of liver studies, London, United Kingdom; ³³King's College London School of Medicine at King's College Hospital,

London, United Kingdom; ³⁴Institute of Liver Studies, MowatLabs, King's College Hospital, London, United Kingdom; ³⁵Epatocentro Ticino, Università della Svizzera italiana, Lugano, Switzerland
Email: donald.malino@gmail.com

Background and aims: It is unclear whether the reported rare cases of acute liver injury with autoimmune features after COVID-19 vaccination represent autoimmune hepatitis (AIH) triggered by the vaccines, requiring long-term immunosuppression, or if the liver injury is self-limiting, as observed in drug-induced autoimmune-like hepatitis (DI-AIH). We report follow-up data of our international cohort of well characterized patients aiming at understanding if the disease course is self-limiting or immunosuppression dependent.

Method: Members of the International AIH Group and of the European Reference Network on Hepatological Diseases who had contributed cases to our original cohort were asked to provide follow-up data of all their patients at 6 and 12 months after the hepatitis diagnosis and at last follow-up.

Results: 62 patients were included, median age was 56 years, 35 (56%) female. Median follow-up was 17 months. Fifty-eight patients (94%) were treated with steroids, with or without azathioprine or mycophenolate mofetil. Four patients (6%) died of non-liver related causes. Transaminase levels normalization was achieved by 74%, 85% and 88% of patients at 6 months, 12 months and at last follow-up (median 17 months). Twenty-two patients (35%) had a phenotype and clinical course similar to DI-AIH, characterized by ALT normalization with (n=18) or without (n=4) a short (<9 months) immunosuppressive treatment, and no relapse after treatment discontinuation; 18 patients (30%) had a course similar to AIH, characterized by relapse after immunosuppression discontinuation (n=10), still abnormal ALT levels after 6 months (n=5) or 12 months (n=3) of treatment duration; for 22 patients (35%) it was not possible, based on the available data, to assign them to one of the previous groups. Risk factors for a classical AIH course were: positive anti-smooth muscle antibodies at diagnosis (p=0.04), advanced liver fibrosis (p=0.03), and more severe interface hepatitis (p=0.02).

Conclusion: Most patients with acute liver injury and autoimmune features after COVID-19 vaccination appear to have DI-AIH, but a sizable subgroup with a more severe phenotype requires long-term immunosuppression, akin to classical AIH.

THU-183-YI

Immunosuppressive treatment facilitates hepatic recompensation in patients with decompensated cirrhosis due to autoimmune hepatitis-a pilot study

Benedikt Hofer^{1,2,3,4}, Lukas Burghart⁵, Sonja Treiber¹, Emina Halilbasic^{1,4}, Mattias Mandorfer^{1,2}, Michael Trauner^{1,4}, Thomas Reiberger^{1,2,3,4}, Albert Friedrich Stättermayer^{1,4}. ¹Division of Gastroenterology and Hepatology, Department of Internal Medicine III, Medical University of Vienna, Vienna, Austria; ²Vienna Hepatic Hemodynamic Laboratory, Division of Gastroenterology and Hepatology, Department of Internal Medicine III, Medical University of Vienna, Vienna, Austria; ³Christian Doppler Lab for Portal Hypertension and Liver Fibrosis, Medical University of Vienna, Vienna, Austria; ⁴Rare Liver Diseases (RALID) center of the ERN RARE-LIVER at the Vienna General Hospital, Vienna, Austria; ⁵Klinik Ottakring, Wiener Gesundheitsverbund, Vienna, Austria
Email: benedikt.s.hofer@meduniwien.ac.at

Background and aims: Patients with autoimmune hepatitis (AIH) are at risk of progressing to cirrhosis and hepatic decompensation, and up to 30% are already cirrhotic at time of diagnosis. While a successful treatment of the underlying aetiology may enable hepatic recompensation, e.g. with viral eradication or alcohol abstinence, recompensation has not been assessed in AIH cirrhosis.

Method: We investigated the incidence and implications of recompensation in cirrhosis due to AIH (F3/F4 histology; simplified AIH score ≥6). Patients were included at index decompensation (ascites, variceal bleeding, hepatic encephalopathy [HE]). Acute liver failure

POSTER PRESENTATIONS

patients were excluded due to the high urgency transplantation indication. Recompensation was defined as (i) resolution of ascites/HE despite cessation of diuretic/HE therapy, (ii) absence of variceal bleeding and (iii) improvement in liver function (bilirubin, albumin, INR) to Child-Pugh A values (Baveno VII criteria). Successful aetiological control was defined as a complete biochemical response under immunosuppressive (IS) treatment (transaminase and immunoglobulin G normalisation).

Results: Twenty-one cirrhotic AIH patients (90.5% female, age: 54.6 [39.8–61.6] years, MELD at decompensation: 15 [11–18]) were included at index decompensation (85.7% ascites, 14.3% variceal bleeding) and followed for a median of 80.4 (14.6–133.0) months. Clinically, decompensation occurred in two distinct settings resulting in two subgroups: In the first ($n = 10$; 47.6%), the diagnosis of AIH had already been established prior to baseline and decompensation occurred despite ongoing (median: 128 [70–164] months) IS therapy, primarily due to an insufficient response. No patient within this subgroup recompensated. In the second subgroup ($n = 11$; 52.4%), AIH was first diagnosed at index decompensation. Within this subgroup, in 5 patients (45.5%), IS treatment was initiated >1 month after decompensation, primarily due to delayed diagnosis; none of them recompensated. In contrast, in 6 patients (54.5%), diagnosis and IS treatment were established within 1 month of decompensation and 4 patients recompensated. All recompensated patients achieved a 50% transaminase decrease after 4 weeks of treatment. With regard to prognosis, all recompensated patients survived without liver transplantation for 62.6, 101.3, 106.3 and 202.3 months, respectively. In contrast, of the 17 patients who remained decompensated, 6 (35.3%) died (all liver-related, after median 32.8 [15.1–58.5] months) and 4 (23.5%) required transplantation (after median 37.5 [15.9–57.1] months).

Conclusion: Decompensation in AIH despite ongoing IS treatment is linked to worse outcomes. In patients with decompensated cirrhosis at initial presentation, a prompt diagnosis with early treatment initiation is associated with a higher likelihood of recompensation and better survival.

THU-184

Fatigue is not influenced by chronotype and is reported to be mainly muscular in patients with primary biliary cholangitis

Erica Nicola Lynch^{1,2}, Pietro Rossi¹, Giulia Mengozzi¹, Tommaso Innocenti^{1,2}, Gabriele Dragoni¹, Maria Rosa Biagini¹, Paolo Forte³, Andrea Galli¹. ¹Gastroenterology Research Unit, Department of Experimental and Clinical Biomedical Sciences “Mario Serio,” University of Florence, Florence, Italy; ²Department of Medical Biotechnologies, University of Siena, Siena, Italy; ³Division of Clinical Gastroenterology, University Hospital “Careggi,” Florence, Italy
Email: ericanicola.lynch@unifi.it

Background and aims: Fatigue is considered one of the most frequent and debilitating symptoms in primary biliary cholangitis (PBC), affecting over 50% of PBC patients. The pathophysiology of fatigue and the role of contributing factors are still largely unknown. The aim of the study was to assess whether patient chronotype was associated with fatigue in PBC. In addition, we evaluated the impact on fatigue of environmental and liver disease characteristics, and whether fatigue was perceived by patients as mainly muscular or mental.

Method: All noncirrhotic PBC patients attending our tertiary referral centre were asked to complete the main questionnaires on fatigue, sleepiness, and chronotype (PBC-40, Fatigue Impact Scale [FIS], Epworth Sleepiness Scale [ESS], Morningness-Eveningness Questionnaire [MEQ]) between January 2023 and June 2023. Patients were also questioned on environmental factors (employment, sleep quality, nighttime light exposure) and as to whether fatigue was perceived as mainly muscular or mental. Clinical data of patients who responded was obtained from clinical records.

Results: Of a total of 125 patients, 61 agreed to participate in the study. Most patients reported mainly muscular rather than mental fatigue (69% vs 31%). Chronotype and fatigue did not appear to be related (PBC-40 Fatigue $p = 0.26$; FIS $p = 0.64$). Patients with an intermediate chronotype had slightly less daytime sleepiness vs early and late chronotypes. Nighttime light exposure significantly affected fatigue (PBC-40 $p = 0.01$; FIS $p = 0.004$). Fatigue weakly correlated with alanine-aminotransferase (FIS: $r = 0.28$, $p = 0.03$; PBC-40 Fatigue: $r = 0.34$, $p = 0.007$) and pruritus (FIS: $r = 0.37$, $p = 0.004$; PBC-40 Fatigue: $r = 0.30$, $p = 0.02$). Women were more likely to report fatigue than men (PBC-40 Fatigue: $p = 0.02$; FIS: $p = 0.01$). No other environmental factor or disease characteristic, including treatment, was found to be associated with fatigue or sleepiness.

Conclusion: Chronotype does not appear to have an impact on fatigue in patients with PBC, although nighttime light exposure significantly worsens fatigue, and therefore should be avoided. Treatment with fibrates or obeticholic acid does not affect fatigue. PBC patients report mainly muscular rather than mental fatigue.

THU-185

Second line therapy in patients with primary biliary cholangitis and inadequate response to UDCA: are we choosing the right target population for clinical trials?

Alejandra Villamil¹, Daniela de la Viña¹, Eduardo Mullen¹, Ignacio Lucero¹, Natalia Sobenko¹, Juan Carlos Bandi¹. ¹Hospital Italiano de Buenos Aires, CABA, Argentina
Email: alejandra.villamil@hospitalitaliano.org.ar

Background and aims: Identification of primary biliary cholangitis (PBC) patients who could benefit from second line therapy is uncertain. Most trials rely on 12 month UDCA response status assessed by POISE criteria. Our objective is to evaluate eligible patients and identify epidemiological, clinical and histological findings of high-risk disease that may adversely influence response.

Method: Among 614 patients with established diagnosis of PBC (Jan/16 and Dec/23) 279 were unable to normalize alkaline phosphatase (ALP) and BT after 12 months of therapeutic doses of UDCA. 107/279 (38.3%) fulfilled eligibility criteria for second line trials (ALP >1.67 ULN, bilirubin <2 ULN and non significant portal hypertension) and were analyzed. Fibrosis, bile duct loss, cholangitic and hepatitis activity were obtained in 92/107 patients (Scheuer and Nakanuma scores). All samples were stained with CK 7. Elastography was done in all patients. Statistical analysis using Fisher's exact test and 1-way ANOVA was performed.

Results: Inadequate responders to UDCA fulfilling eligibility criteria had mean age 55.9 ± 11.8 and 87% female ($n = 93$). 22.4% ($n = 24$) <45 years. Mean ALP 366.7 ± 192.5 UI/L, GGT 366.6 ± 326.2 UI/L, ALT 64.7 ± 43.6 UI/L and BT 1.7 ± 4.6 mg/dL. Only GGT differed between women and men (326.3 vs 634.9, $p < 0.05$). Mean MELD score was 7.4 ± 1.8 and 17 patients were cirrhotic (16%). Mean MELD was higher in cirrhotics (9.0 vs 7.1, $p < 0.001$) and correlated with liver events (9.6 vs 7.0 $p < 0.001$), occurring in 14 patients during follow-up and resulting in 4 liver related deaths and 3 transplants. 43/92 patients had moderate to severe ductopenia in histological samples, and it was significantly more frequent in <45 years (66% vs 32%, $p = 0.008$). Moderate to severe portal inflammation with interface hepatitis and lobular spilling was observed in 52/92 samples (56.5%) irrespective of age and associated with progression. No LFT predicted cirrhosis or portal inflammation. ALP was significantly higher in patients with ductopenia (437.9 ± 207.8 UI/L vs 319.2 ± 162.0 UI/L, $p = 0.01$). Elastography correlated with cirrhosis and liver events (10.4 kPa vs 22.9 kPa, $p < 0.001$) but not with inflammation or ductopenia.

Conclusion: A significant proportion of our patients unresponsive to UDCA were not eligible for second line trials. Poise criteria eligibility was associated with the presence of ductopenia and advanced fibrosis, particularly in young patients. The presence of moderate to severe portal inflammation is suggestive of ongoing disease activity. Yet, LFT do not reflect its presence and severity. Higher ALP is linked

to the presence of ductopenia. Elastography and MELD score correlate with cirrhosis and development of liver events. Our data suggest that we are selecting for second line trials a significant proportion of patients with adverse clinical and histological prognostic factors that might impact response.

THU-186

Long term risk assessment of patients with primary sclerosing cholangitis using clinical prognosis models

Matei Manda^{1,2}, Speranta Iacob^{1,2}, Mihaela Ghioca^{1,2}, Razvan Iacob^{1,2}, Cristian Gheorghe^{1,2}, Irinel Popescu¹, Liana Gheorghe^{1,2}. ¹Fundeni Clinical Institute, Bucharest, Romania; ²University of Medicine and Pharmacy "Carol Davila", Bucharest, Romania
Email: matei.manda@drd.umfcd.ro

Background and aims: Primary sclerosing cholangitis (PSC) is a chronic progressive cholestatic disease with poor prognosis, high likelihood of dying without liver transplantation (LT) and high risk of developing cholangiocarcinoma. The assessment of prognosis is important for stratifying the high risk patients. The aim of our study was to evaluate clinical prediction models Revised Mayo Risk Score (rMRS), Amsterdam-Oxford Model (AOM), Model for End-stage Liver Disease (MELD/MELD-Na) and Primary Sclerosing Cholangitis Risk Estimate Tool (PRESto).

Method: Our study is an observational retrospective single center study, that included 107 patients evaluated in our clinic between 2011 and 2023.

Results: From 107 patients included, 54% were female. The average age at diagnosis was 41, 11 years (16–78 years). 24/107 (22, 4%) patients had an IBD associated, 54% (10) of them suffered from Ulcerative Colitis and 46% (11) of Crohn's disease. 92/107 (85.9%) patients had a PSC that affected large bile ducts, 15/107 (14.1%) had a small-duct PSC, 10, 2% (11) had an overlap syndrome with Autoimmune hepatitis and 3.7% (4) had an overlap syndrome with Primary Biliary Cholangitis. The diagnosis was made using either MRCP or liver biopsy and after excluding other causes of cholangitis. 17.3% of the patients had high rMRS, and 42.3% high AOM score. The average PRESto was 6.4% at 1 year and 24.5% at 5 years. There was a significantly higher PRESto score calculated at 1 year in patients that underwent LT compared to those that did not (9.8 ± 2.7 vs 6.3 ± 1.6 , $p = 0.01$), higher MELD score ($p = 0.001$) and higher MELD-Na score ($p = 0.02$). Higher AOM ($p = 0.06$) and rMRS ($p = 0.07$) reached only marginal significance. Patients with PSC that underwent LT had significant more episodes of recurrent cholangitis ($p = 0.04$) as well as antecedents of variceal hemorrhage ($p = 0.02$).

Conclusion: Management of suspected cases should be standardized and a close follow-up could prove useful since most of the patients are asymptomatic, to identify the appearance of complications such as neoplasia, liver decompensation and the optimal moment to include the patients for OLT. In Romanian patients with PSC that underwent LT the following scores can be accurately used in order to evaluate prognosis: PRESto score in addition to MELD/MELD-Na as well as complications like recurrent cholangitis or upper digestive hemorrhage.

THU-187

Landscape of gall bladder cancers in India: a 25 years experience at a tertiary care cancer centre

Rupal Tripathi¹, Anurag Mehta¹, Dinesh Dova¹, K Rana¹. ¹Rajiv Gandhi cancer institute and research centre, DELHI, India
Email: sinharupal@gmail.com

Background and aims: Gall bladder cancer has heterogenous etiology with the incidence rates increasing alarmingly in India and specially in the North Indian population. This has been chiefly attributable to the cumulative effects of genetic, epigenetic and non-genetic modifiable factors. The present study aimed to assess the

landscape of gall bladder cancers at a tertiary cancer care centre in India over a period of 25 years.

Method: All patients who enrolled in the Institute during the period 1996–2021 and diagnosed with gall bladder cancers were included in the study. Details of each patient related to their demographic profile, tumor characteristics and treatment information were recorded from the electronic medical records in the Institute.

Results: During the period 1996–2021, a total of 293262 patients were registered in the Institute. Of these, a total of 8625 patients were diagnosed with gall bladder cancer as the primary site of cancer. Among these, 5883 patients (68.2%) were females. Majority of the patients (2764) were in the age group of 50–59 years. The most common mode of diagnosis of disease was histology in 4271 patients. Chemotherapy or surgery alone was given in 1363 and 345 patients, respectively. Symptomatic treatment only was given in 931 cases whereas 5440 patients did not receive any kind of treatment and presented to the hospital for second opinion only.

Conclusion: The high incidence of gall bladder cancers in India and particularly in the North Indian population and mostly in the females again points to the pressing need for having cost-effective and affordable primary diagnostic tests to ease the diagnosis and management of gall bladder cancers in the rural and urban settings. Further, large scale molecular genomic studies would be required to understand the increasing incidence of this cancer, specially in the females and further explore more cost effective treatment strategies.

THU-188

Hydroxychloroquine as an adjuvant drug to immunosuppressive treatment to achieve histological remission in autoimmune hepatitis

Andreia Evangelista¹, Debora Raquel Terrabuo¹, Ana Luiza Vilar Guedes², Amanda Moreto³, Eduardo Cancado². ¹Hospital das Clinicas da Faculdade de Medicina da Universidade de Sao Paulo, Sao Paulo, Brazil; ²Hospital das Clinicas da Faculdade de Medicina da USP, Sao Paulo, Brazil; ³Hospital das Clinicas da Faculdade de Medicina da USP, Sao Paulo
Email: andreia1179@yahoo.com.br

Background and aims: the standard treatment (ST) of AIH is the association of corticosteroids and azathioprine, however sustained remission rates occur only in 19–40%. Additionally, nearly 10% of patients experience side effects, with discontinuation of medications. These challenges highlight the need for new therapeutic options. To minimize the side effects of higher doses of immunosuppression (IS), we aimed to evaluate the role of adding hydroxychloroquine (HCQ) to the ST in AIH patients with biochemical remission and liver biopsy (LB) with persistent mild inflammatory activity.

Method: patients with AIH with normal levels of IgG, AST, ALT and liver biopsy with persistent discrete inflammatory activity. Patients were selected to add HCQ 400 mg to the ST and were non-randomly compared to historic controls in whom the IS was increased. These patients were reassessed for histological response 18–24 months after implementing this strategy.

Results: 24 patients were selected for the use of HCQ and were compared with 45 controls with standard treatment (Augmentation of IS, AIS). The rates of response were 62.5% and 64.4% ($p = 0.873$) in the HCQ and AIS group, respectively. The levels of IgG were lower in the HCQ group (1144×1335 , $p = 0.029$). Four patients in the HCQ group and six patients in the IS group experienced side effects related to the use of HCQ and increased immunosuppression, respectively.

Conclusion: the addition of Hydroxychloroquine to ST, in patients with partially treated AIH, might be an effective and safety alternative to the increase of the IS.

THU-189

Optimization of treatment in patients with primary biliary cholangitis: Gamma-glutamyl transferase levels as an early prognostic marker for ursodeoxycholic acid response. Results from the ColHai registry

Flor M Fernandez-Gordón Sánchez¹, Sergio Rodriguez-Tajes², María Carlota Londoño³, Álvaro Díaz-González⁴, Margarita Sala Llinás⁵, Manuel Romero-Gómez⁶, Javier Martínez González⁷, Judith Gómez-Camarero⁸, Manuel Hernández Guerra⁹, Mercedes Vergara¹⁰, Tom Stephane Fournot¹¹, Raul J. Andrade¹², Silvia Goñi Esarte¹³, Juan Turnes Vázquez¹⁴, Montserrat García-Retortillo¹⁵, Marina Berenguer¹⁶, Elena Gómez-Domínguez¹. ¹12 de Octubre University Hospital, Madrid, Spain; ²Clinic Hospital of Barcelona, Barcelona, Spain; ³Clinic Hospital of Barcelona, Barcelona, Spain; ⁴Marqués de Valdecilla University Hospital, Santander, Spain; ⁵Dr. Josep Trueta Hospital, Girona, Spain; ⁶Virgen del Rocío University Hospital, Sevilla, Spain; ⁷Ramón y Cajal University Hospital, Madrid, Spain; ⁸University Hospital of Burgos, Burgos, Spain; ⁹University Hospital of the Canaries, La Laguna, Spain; ¹⁰Parc Tauli University Hospital, Sabadell, Spain; ¹¹Hospital de la Santa Creu i Sant Pau, Barcelona, Spain; ¹²Virgen de la Victoria University Hospital, Málaga, Spain; ¹³University Hospital of Navarra, Pamplona, Spain; ¹⁴Pontevedra University Hospital Complex, Pontevedra, Spain; ¹⁵Hospital del Mar, Barcelona, Spain; ¹⁶La Fe University and Polytechnic Hospital, Valencia, Spain
Email: florfgs@hotmail.com

Background and aims: The early identification of non-responding patients with Primary Biliary Cholangitis (PBC) to ursodeoxycholic acid (UDCA) is crucial for prognosis. Elevated levels of gamma-glutamyl transferase (GGT) are associated with a poorer response to UDCA. Further evidence is needed to understand its predictive capacity and the impact of alcohol consumption. To analyze the predictive value of baseline, 6-month, and 1-year GGT elevation for UDCA response. Evaluate the impact of alcohol consumption on GGT levels and its predictive capacity. Establish GGT cutoff points to identify candidates for second-line therapies.

Method: A multicenter retrospective study from the ColHAI Registry with two cohorts of PBC patients treated with UDCA, classified as responders or non-responders (Paris II criteria). Baseline, 6-month, and 1-year variables were compared. Subgroup analysis based on alcohol consumption. U-Mann-Whitney test and Youden Index for optimal cutoff points in ROC curve analysis.

Results: 617 patients included, average age 61 years. 59 responders to UDCA at 6 months and 364 at 1 year. Non-responders at both time points had significantly higher baseline GGT levels compared to responders (465 U/l vs. 53 U/l, 402 U/l vs. 136 U/l, $p < 0.01$). They also had higher GGT at 1 year (229 U/l vs. 108 U/l, $p < 0.01$), with no difference at 6 months.

In non-alcohol consumers (67.6%) who were non-responders, baseline (444 U/l vs. 132 U/l, $p < 0.01$) and follow-up GGT levels (243 U/l vs. 105.2 U/l, $p < 0.01$) were higher.

The cutoff point of baseline GGT at 124 U/l coincides in patients with follow-up at 6 months and annually (Sensitivity 71%, Specificity 43%, AUC 0.57 vs. Sensitivity 55%, Specificity 31%, AUC 0.43).

Cutoff points for GGT non-alcohol consumers (237.5 U/l baseline [Sensitivity 55%, Specificity 75%, AUC 0.65] and 58.5 U/l [Sensitivity 69%, Specificity 50%, AUC 0.60] at 6 months) and alcohol consumers (53.5 U/l [Sensitivity 100%, Specificity 33%, AUC 0.67] baseline and 40.5 U/l [Sensitivity 100%, Specificity 50%, AUC 0.75] at 6 months) to predict treatment response. No differences in predictive capacity between both groups.

Conclusion: GGT levels, regardless of alcohol consumption, are associated with a poorer response to UDCA in PBC patients. Useful baseline GGT cutoff points have been established in the early identification of non-responding patients to antiviral treatment for chronic liver diseases.

THU-190

Quantitative assessment of anti-mitochondrial antibodies in primary biliary cholangitis: a cross-sectional analysis

Lorenzo Canova¹, Elisabetta Degasperis¹, Maria Paola Anolli¹, Marta Borghi¹, Riccardo Perbellini¹, Sonia Stella¹, Pietro Lampertico^{1,2}. ¹Division of Gastroenterology and Hepatology, Foundation IRCCS Ca' Granda Ospedale Maggiore Policlinico, Milan, Italy; ²CRC "A. M. and A. Migliavacca" Center for Liver Disease, Department of Pathophysiology and Transplantation, University of Milan, Milan, Italy
Email: pietro.lampertico@unimi.it

Background and aims: Quantitative assessment of anti-mitochondrial antibodies (AMA)-M2 is available in primary biliary cholangitis (PBC), however its clinical meaning is still unknown. Aim of the study was to analyse quantitative AMA-M2 in PBC patients and its correlation with clinical features.

Method: PBC patients from a single Italian centre with available quantitative AMA-M2 values were included in a cross-sectional analysis. PBC was diagnosed according to international recommendations. Clinical and biochemical features were collected ± 3 months from AMA assessment. AMA was tested by chemiluminescence immunoassay (CLIA) (range 0–3000 AU/ml).

Results: Overall, 92 PBC patients (87% females) were included. At AMA assessment, median age was 67 (39–93) years, ALT 30 (8–258) U/L, ALP 0.7 (0.2–4.4) ULN, 38% patients with ALP > 1.5 ULN, gGT 1.44 (0.2–14.3) ULN, IgM 237 (39–1,037) mg/dl, liver stiffness measurement (LSM) 5.9 (3.9–38.6) kPa, 23% with advanced fibrosis (Stage III–IV Ludwig). Median PBC duration was 89 (1–433) months, 91% UDCA-treated, 19% UDCA non-responder. Overall, in the 49 (53%) patients with quantifiable AMA, median value was 319 (20–2500) AU/ml, AMA-M2 tested >3000 AU/ml in 43 (47%) patients. No statistically significant differences were observed between patients with AMA titers above vs. below 3000 concerning: age ($p = 0.18$), sex ($p = 0.31$), BMI ($p = 0.34$), advanced fibrosis stage ($p = 0.55$), LSM values ($p = 0.73$), disease duration ($p = 0.78$), UDCA response ($p = 0.45$), ALT ($p = 0.97$), ALP values ($p = 0.78$) and ALP ULN categories (<1.5 ULN vs. 1.5–2.0 ULN vs. >2 ULN, $p = 0.84$), gGT ($p = 0.49$) and IgM ($p = 0.84$) values. The same was true when AMA values were analyzed according to multiple thresholds (AMA <300 vs. 300–1000 vs. 1000–3000 vs. >3000). Conversely, in patients with AMA <3000, male sex was associated with lower AMA-M2 values (56 vs. 426, $p = 0.02$).

Conclusion: In UDCA-treated PBC patients, lower AMA-M2 levels were associated with male gender, while they did not correlate with other clinical or disease features.

THU-191

Impact of ursodeoxycholic acid therapy in autoimmune liver disease patients with COVID-19 and its clinical prognosis

Minghui Li¹, Weihua Cao², Tingting Jiang², Wen Deng², Shiyu Wang², Shuling Wu², Lu Zhang², Yao Lu², Min Chang², Ruyu Liu², Xiaoyan Ding², Ge Shen², Yuanjiao Gao², Hongxiao Hao², Xiaoxue Chen², Leiping Hu², Mengjiao Xu², Yuyong Jiang², Wei Yi², Yao Xie², Rui Song². ¹Beijing Ditan Hospital, Capital Medical University, Peking University Ditan Teaching Hospital, Beijing, China; ²Beijing Ditan Hospital, Capital Medical University, Beijing, China
Email: songruii@hotmail.com

Background and aims: To explore impact of ursodeoxycholic acid (UDCA) on COVID-19 infection and clinical outcomes in patients with autoimmune liver disease (AILD).

Method: Patients diagnosed with of AILD were enrolled and divided into UDCA group and non-UDCA group based on whether they received UDCA treatment. Relevant data regarding AILD diagnosis, treatment, biochemical indicators, imaging examination were collected. Incidence and prognosis were observed in COVID-19 infected patients.

Results: 1138 patients completed follow-up. Usage rate of hormone ($p = 0.003$) and immunosuppressant ($p = 0.001$) used for treating AILD in non-UDCA group was markedly lower than that in UDCA group. UDCA usage rate was markedly lower in COVID-19 infected

patients than uninfected ones ($p=0.003$). The rate of COVID-19 infection in non-UDCA group was significantly higher than that in UDCA group ($p=0.018$). Logistic regression analysis showed that UDCA use ($p=0.003$) was correlated to a lower incidence of COVID-19, while immunosuppressant use ($p=0.017$) increased the incidence. Recovery time from COVID-19 infection was markedly longer for those receiving UDCA treatment than those in the non-UDCA group ($p=0.018$).

Conclusion: Using UDCA is associated with low COVID-19 incidence in AILD patients, while using immunosuppressant increases its incidence instead. Patients receiving UDCA treatment have a longer recovery time after being infected.

THU-192

Liver steatosis assessed by controlled attenuation parameter in patients with primary biliary cholangitis

Francesca Bueti¹, Maria Stella Franzè¹, Concetta Pitrone¹, Gaia Caccamo², Irene Cacciola¹, Roberto Filomia², Sergio Maimone², Giovanni Raimondo¹, Carlo Saitta¹. ¹Division of Medicine and Hepatology, Department of Clinical and Experimental Medicine, University Hospital of Messina, Messina, Italy; ²Division of Medicine and Hepatology, University Hospital of Messina, Messina, Italy
Email: csaitta@unime.it

Background and aims: Primary biliary cholangitis (PBC) is a chronic inflammatory autoimmune cholestatic liver disease frequently associated with hyperlipidemia. However, the impact of steatosis on the liver disease in PBC patients has not been studied so far. Aim of the study was to investigate liver steatosis [assessed by controlled attenuation parameter (CAP)] and its relationship with liver stiffness (LS) [evaluated by transient elastography (TE)] in patients with PBC.

Method: All patients with PBC admitted to the Unit of Medicine and Hepatology of the University Hospital of Messina in 2023 underwent contemporaneous LS and CAP measurements. Demographic, anthropometric, biochemical, ultrasonographic data, and treatment information were collected from all patients. The Spearman's rank test was used for analyzing the correlation between CAP values and all the recorded variables. Uni- and stepwise multivariate analyses were performed for identifying factors independently associated with higher liver stiffness values.

Results: Seventy-four patients (68 females, 6 males; mean age 61.3 ± 11.3 years) under ursodeoxycholic acid treatment for at least twelve (range 12–233) months were included in the analysis, and 14 of them (18.9%) had cirrhosis. Mean liver stiffness was 9.1 ± 6.9 kPa, mean CAP values were 228.5 ± 55.7 dB/m. Ultrasonographic signs of steatosis were present in 70/74 (94.6%) patients, mean BMI was 25.7 ± 4.2 Kg/m². The Spearman's rank test showed significant correlation between CAP values and BMI ($p < 0.05$), IgM levels ($p < 0.05$), and liver stiffness ($p = 0.01$). Multivariate analysis showed that higher gamma-globulin levels ($p = 0.002$, OR 4.73), larger spleen diameter ($p = 0.004$, OR 1.02), and higher CAP values ($p = 0.02$, OR 3.11) were independently associated with higher liver stiffness values.

Conclusion: Liver steatosis is highly prevalent in patients with PBC and appears to impact on liver stiffness.

Liver development and regeneration

TOP-559

Metabolic needs dictate the regenerative capacity of the liver

Sara Guerra¹, Dominique L. Birrer¹, Udo Ungethüm¹, Pierre A. Clavien², Humar Bostjan¹. ¹Visceral and Transplantation Surgery Laboratory, University Hospital Zurich, Zurich, Switzerland; ²Privatklinik Bethanien, Zurich, Switzerland
Email: Saralsabel.DaSilvaGuerra@usz.ch

Background and aims: The liver's regenerative capacity is exceptional, but not unlimited. The metabolic duties may be one key factor impeding the proliferative abilities of hepatocytes after tissue loss. To substantiate this view, we exploited a model of accelerated regeneration induced by ALPPS surgery (associating portal vein ligation with transection), a procedure that retains portally ligated lobes (LLs) *in situ*. We sought to explore whether LLs function as auxiliary livers, thereby enabling the future liver remnant to fully focus on regeneration.

Method: Mice were separated into groups undergoing either sham or ALPPS surgery. Sham liver, the future liver remnant (FLR), and the adjacent ligated right median lobe (RML) were individually subjected to omics analysis, including metabolomics, lipidomics, and transcriptomics. A functional surgery approach to test the role of LLs was devised by creating ALPPS variants with loss or gain of ligated volume. Immunohistochemistry was applied to validate omics data and functional surgery outcomes.

Results: Untargeted PCA metabolomics analysis at 4 h and 8 h post-surgery highlighted increased metabolic activities after ALPPS, with a clear distinction between the FLR and the RML specifically during the growth phase. The FLR and RML exhibited heightened energy demands fueled by active lipid oxidation. However, activities related to cell cycle and proliferation were upregulated explicitly in the FLR, whereas the RML was enriched with typical metabolic liver functions such as gluconeogenesis, glycogen synthesis, bile acid metabolism, bilirubin clearance, xenobiotic detoxification, and synthetic function. Functional surgery demonstrated a full dependence of the FLR's regenerative speed on the presence of ligated lobes.

Conclusion: Metabolic pressure during liver regeneration is managed differently by the ligated RML and the FLR. We find that the LLs act as an auxiliary liver in the ALPPS regeneration process. Taking over key metabolic functions, the LLs are needed to unleash the full regenerative capacity of the FLR, as is reflected in accelerated regeneration. This transient macroscopic division of tasks roots on plastic behavior of the different lobes during ALPPS regeneration and reveals how metabolic needs dictate the liver's regenerative capacity.

FRIDAY 07 JUNE

FRI-546

Trained immunity contributes to immunomodulatory plasticity of human bone marrow mesenchymal stem cells

Bingqi Li¹, Xi Liang², Jing Jiang¹, Jiaojiao Xin¹, Dongyan Shi¹, Shiwen Ma¹, Hui Yang¹, Xingping Zhou¹, Jiaxian Chen¹, Jun Li¹. ¹State Key Laboratory for Diagnosis and Treatment of Infectious Diseases, National Clinical Research Center for Infectious Diseases, National Medical Center for Infectious Diseases, The First Affiliated Hospital, Zhejiang University School of Medicine, Hangzhou, China; ²Precision Medicine Center, Taizhou Central Hospital (Taizhou University Hospital), Taizhou, China
Email: lijun2009@zju.edu.cn

Background and aims: The immunoregulatory role of human bone marrow mesenchymal stem cells (hBMSCs) is crucial for addressing cytokine storms associated with severe liver diseases. However, the intricate immune microenvironment *in vivo* poses challenges to the survival and functions of hBMSCs. Trained immunity has been proved to improve the adaptability of immune cells and therapeutic effect. This study aims to enhance the immunoregulation of hBMSCs by trained immunity to optimize stem cell therapy strategies.

Method: Trained immunity was induced in hBMSCs (T-hBMSCs) by exposing them to pro-inflammatory cytokines IFN- γ and TNF- α as "trainers" for 24 hours, while untrained-hBMSCs (UT-hBMSCs) were treated with medium as control. Subsequently, the cells were assessed using the same "trainers" or patient serum derived from acute-on-chronic liver failure (ACLF) after 48 hours of cleaning. Flow

POSTER PRESENTATIONS

cytometry, qRT-PCR, and transcriptome analysis were conducted using cell samples.

Results: The surface markers of T-hBMSCs detected by flowcytometry were positive for CD73, CD166 and CD90, but negative for CD45, CD34 and CD79a, which was consistent with UT-hBMSCs. Trilineage differentiation of hBMSCs after training remained unaffected. Pro-inflammatory genes (IL-1 β , IL-6 and IL-8, all $p < 0.0001$) and immunosuppressive genes (PDL-1 and IDO, both $p < 0.0001$) expressed in T-hBMSCs were higher than UT-hBMSCs. After 48 hours cleaning, the expression of immunomodulatory genes especially IDO remained significantly higher, while the expression levels of inflammatory genes especially IL-1 β gradually returned to baseline in T-hBMSCs. The results revealed a significant increase in IDO expression in T-hBMSCs compared to UT-hBMSCs upon restimulation with the same dosage of “trainers” or ACLF patient-derived serum (5-fold vs. 4606-fold, both $p < 0.0001$). Transcriptome analysis detected a total of 1041 genes with significantly up-regulated expression and 827 genes with significantly down-regulated expression in T-hBMSCs compared to UT-hBMSCs. Gene set enrichment analysis revealed that trained immunity activated NF- κ B signaling pathway, which is associated with innate immune responses, and subsequently induced JAK-STAT pathway in T-hBMSCs causing an increase in IDO expression. The higher expression level of IDO inhibited the proliferation and activation of T lymphocytes, thereby enhancing the immunoregulatory function of T-hBMSCs.

Conclusion: Trained immunity enhances the immunoregulation function of hBMSCs and contributes to optimize stem cell therapy strategies, indicating the potential clinical applications of T-hBMSCs in the future.

FRI-547-YI

Regenerative matrix-based hydrogels repair hepatocellular damage and promote cellular proliferation in pre-clinical models of acute liver injury

Ashwini Vasudevan^{1,2}, Arka Sanyal³, Akash Kumar Mourya^{4,5}, Aarti Sharma⁶, Archana Rastogi⁴, Sourabh Ghosh⁷, Pooja Vijayaraghavan⁸, Shiv Kumar Sarin⁹, Savneet Kaur¹⁰, Dinesh Mani Tripathi⁶. ¹Institute of Liver and Biliary Sciences, Amity Institute of Biotechnology, Vasant Kunj, India; ²Amity Institute of Biotechnology, Noida, India; ³Indian Institute of Technology New Delhi, New Delhi, India; ⁴Institute of Liver and Biliary Sciences, New Delhi, India; ⁵National Institute of Pharmaceutical Education and Research NIPER, SAS Nagar, Mohali, India; ⁶Institute of Liver and Biliary Sciences, New Delhi, India; ⁷IIT-Delhi, New Delhi, India; ⁸Amity Institute of Bioethnology, Noida, India; ⁹Institute of Liver and Biliary Sciences, New Delhi, India; ¹⁰Institute of Liver and Biliary Sciences, New Delhi, India Email: dineshmanitripathi@gmail.com

Background and aims: Acute liver injury is detrimental due to massive hepatocyte damage accompanied by impaired liver functions. In this study, we investigate the potential of regenerative liver extracellular matrix (LEM-PHx) to alleviate acute liver injury in experimental animal models.

Method: 70% partial hepatectomy rat models were developed and decellularized post 96hrs to obtain LEM-PHx. ECM based hydrogels were prepared by blending the matrix proteins with 3% alginate in 1:1 ratio and were characterized by FTIR. Rheological assessment, swelling properties of the hydrogels in vitro were studied. Primary hepatocytes were cultured in the hydrogels for up to 21 days. Fabricated hydrogels were transplanted into subcapsular region of liver 24 hrs post single injection of CCL₄ (Alg-LEM = control liver ECM; Alg-LEM-PHx = PHx liver ECM; Alg = Alginate only, vehicle). The efficacy of the transplanted hydrogels was assessed in serum and by histopathological staining and molecular analysis was performed.

Results: HandE staining, DAPI staining, and DNA quantification confirmed acellularity of the decell tissues. All fabricated alginate-based hydrogels showed gelation at 37°C within 10 mins in the presence of 100 mM CaCl₂. FTIR analysis showed specific peaks for

collagen and proteoglycans only in Alg-LEM and Alg-LEM-PHx. Rheological assessment showed shear thinning behavior of Alg-LEM and Alg-LEM-PHx upon increasing stress, which is ideal for injectable hydrogels. Primary hepatic organoids in Alg-LEM-PHx showed increase in organoid diameter size ($p < 0.05$) with increased albumin secretion ($p < 0.05$) up to 21 days compared with the organoids in Alg-LEM group. Immunocompatibility of the hydrogels was assessed by blood profiling of control vs implantation group in FACS, $\Sigma 67\%$ vs $\Sigma 62.83\%$ T-cells; $\Sigma 13.7\%$ vs $\Sigma 11.8\%$ monocytes; $\Sigma 1.28\%$ vs $\Sigma 1.25\%$ dendritic cells. Transplanted liver lobes showed reduction in injury and oxidative damage to the hepatocytes at the centrilobular region. Liver function improved significantly post LEM-PHx transplant (AST $\Sigma 150$ IU/L; ALT $\Sigma 95$ IU/L; $p < 0.05$) when compared to vehicle group (AST $\Sigma 300$ IU/L; ALT $\Sigma 145$ IU/L). Cell cycle genes Cyclins A, E (+2fold, +4fold; $p < 0.005$) and PCNA (+3fold; $p < 0.05$) and growth factors like HGF (+1.5fold; $p < 0.05$) were significantly upregulated vs vehicle. PCNA-positive proliferating hepatocytes were increased in LEM-PHx group (35 ± 8 cells/field; $p < 0.5$ vs Veh). Proinflammatory genes Tlr4 and IL6 (−6.5fold, −2.5fold; $p < 0.05$ vs Veh) were downregulated, whereas anti-inflammatory genes IL10, SOD (+1.5fold, +2fold; $p < 0.05$ vs Veh) were upregulated in Alg-LEM-PHx.

Conclusion: Regenerative extracellular matrix incorporated alginate hydrogel developed in this study demonstrates reduction in injury and hepatocyte damage and promotes hepatocyte proliferation during acute liver injury serving as a potential adjuvant for regenerative therapy.

FRI-548

Lysosomal protease contributes to hepatocyte proliferation during liver regeneration after partial hepatectomy

Julia Cacho-Pujol^{1,2}, Paloma Ruiz-Blazquez^{1,2,3,4}, Maria Fernandez-Fernandez^{1,2,3,4}, Alejandro del Castillo-Cruz⁵, Anna Moles^{1,3,4}. ¹Institute of Biomedical Research of Barcelona (IIBB-CSIC), Barcelona, Spain; ²University of Barcelona, Barcelona, Spain; ³Institut d'Investigacions Biomèdiques August Pi i Sunyer (IDIBAPS), Barcelona, Spain; ⁴Centro de Investigación Biomédica en Red de Enfermedades Hepáticas y Digestivas (CIBERehd), Barcelona, Spain; ⁵Institut d'Investigacions Biomèdiques August Pi i Sunyer (IDIBAPS), Barcelona Email: anna.moles.fernandez@gmail.com

Background and aims: Liver regeneration is a biological process essential for the restoration of liver mass, homeostasis and function after an injury. During liver regeneration, proteolytic activity is timely regulated in infiltrating and liver resident cells. Protease expression depends on the cellular demands and participates in apoptosis, proliferation and activation and repression of growth factors, amongst others. Despite our growing understanding of the roles played by lysosomal proteases during liver disease, our knowledge of their role in liver regeneration remains still very limited. Thus, the aim of this study was to analyse cathepsin D (CtsD) cell-specific role in hepatocytes during liver regeneration.

Method: We generated and validated a novel knock-out mouse strain by breeding Albumin-Cre (hepatocytes) mice with CtsD floxed mice. Partial hepatectomy (PhX) was performed for 72 hours in CtsD^{F/F} and CtsD ^{Δ Hep} mice. CtsD deletion was assessed by IF and RTqPCR. Liver damage was determined by serum ALT. CtsD activity was determined by an enzymatic assay. Mitotic bodies and BrdU positive cells were analysed and quantified in liver tissue sections using Fiji software. Expression of apoptotic and cell cycle markers was determined by RT-qPCR and/or WB in total liver in CtsD^{F/F} and CtsD ^{Δ Hep} mice at T = 0 and T = 72 h after PhX.

Results: CtsD cell-specific deletion in hepatocytes was confirmed by WB in primary isolated hepatocytes and IF in liver tissue sections from CtsD ^{Δ Hep} mice. Of note, CtsD expression remained unaffected in liver non-parenchymal cells in CtsD ^{Δ Hep} mice. Next, PhX was performed for 72 h in CtsD^{F/F} and CtsD ^{Δ Hep} mice and CtsD deletion

was confirmed by gene expression and IF in liver. Despite CtsD deletion in hepatocytes did not affect liver damaged (ALT), liver BrdU incorporation was significantly increased in CtsD^{ΔHep} mice after PhX indicating an increase in cell proliferation. However, neither the hepatic regeneration rate nor the number of mitotic bodies was affected. Gene expression and WB analysis of PhX livers revealed a significant increase of genes involved in proliferation and cell cycle, such as FoxMB1, Cyclin B1 and NEK2, without changes in apoptotic genes (BCL2, NOXA, BAK1 and FADD) in PhX-CtsD^{ΔHep} mice versus PhX-CtsD^{F/F} ones.

Conclusion: CtsD contributes to the control of hepatocyte proliferation and cell cycle during liver regeneration after partial hepatectomy.

FRI-549-YI

Hepatic loss of the endosomal sorting complex Retromer delays postnatal liver maturation and increases hepatocellular proliferation

Markus Gregorio Barbosa¹, Dyonne Vos¹, Andries Heida¹, Mirjam Koster¹, Vincent Bloks¹, Niels Kloosterhuis¹, Marieke Smit¹, Laura Bongiovanni², Dicky Struik¹, Johan Jonker¹, Jan Albert Kuivenhoven¹, Bart van de Sluis¹. ¹University Medical Center Groningen, Groningen, Netherlands; ²Utrecht University, Utrecht, Netherlands
Email: m.g.barbosa@umcg.nl

Background and aims: Liver cancer, and more specifically hepatocellular carcinoma (HCC), are respectively the third and sixth most common cause of cancer death worldwide. The increasing incidence of HCC in Western countries can be attributed to the growing prevalence of metabolic dysfunction-associated steatotic liver disease (MASLD). Patients with HCC have a poor prognosis due to late diagnosis and lack of effective medical treatments. Efforts to mitigate the rising prevalence of MASLD and enhance early detection strategies are critical in addressing the burden of HCC and improving patient outcomes. Recent studies have identified VPS35 as a novel oncogene. VPS35, a component of an endosomal protein sorting complex, plays a central role in the endosomal recycling of receptors and hereby it can modulate numerous signalling pathways.

Method: To study the role of VPS35 in the development of hepatocellular carcinoma (HCC), we generated a liver-specific *Vps35* knock-out mouse model using the Cre-LoxP system (*Vps35*^{HKO}). We characterized these mice at different ages. Using immunohistochemical staining we studied the level of hepatocellular proliferation. Gene expression, kinome, and western blot analyses were performed to elucidate the pathways underlying the effect of VPS35 deficiency on hepatocellular proliferation.

Results: Using the proliferating markers BrdU and Ki67 we showed that the level of hepatocellular proliferation is increased in hepatocyte VPS35-deficient mice compared to control mice. The increased expression of several proliferating markers, such as *Spp1*, *Hnf4a-p2*, *Sox9*, and cell cycle genes, support the increase in hepatocellular proliferation upon VPS35 ablation. Interestingly, the expression of *Albumin (Alb)* and *Hnf4a-p1* isoform, both markers for differentiated hepatocytes, were markedly decreased. TUNEL assay showed that the level of apoptosis is not changed between control and liver-specific VPS35-deficient mice. Kinome analysis indicated that activity of various tyrosine kinases (TK), including, EGFR and SRC, were increased in *Vps35*^{HKO} mice compared to control mice. This increase in TK activity was accompanied by higher activation of the STAT3 signalling pathway. Remarkably, at the age of 26 weeks, hepatic VPS35 ablation did not affect the level of hepatocellular proliferation.

Conclusion: In contrast to previous studies, we here show that VPS35 inhibits hepatocellular proliferation and mediates the maturation of the postnatal liver. Our data suggest that the loss of VPS35 results in hyperactivation of several TKs, including TKs that are activated in HCC. We are currently studying the effect of VPS35 ablation on carcinogen-induced HCC development in mice.

FRI-550

Regulatory role of host cell factor 1 in metabolic control and epigenomic integrity

Debashruti Bhattacharya¹, Shruti Kaushal², Saran Kumar¹, Viviane Praz³, Maykel Lopes⁴, Winship Herr⁴, Jaspreet Dhanjal⁵, Shilpi Minocha¹. ¹Kusuma School of Biological Sciences, Indian Institute of Technology Delhi, New Delhi, India; ²Indraprastha Institute of Information Technology Delhi, New Delhi, India; ³Centre for Integrative Genomics (CIG), G  nopode, University of Lausanne, Lausanne, Switzerland; ⁴Centre for Integrative Genomics (CIG), G  nopode, University of Lausanne, Lausanne, Switzerland; ⁵Indraprastha Institute of Information Technology Delhi, New Delhi, India
Email: sminocha@bioschool.iitd.ac.in

Background and aims: Effective liver homeostasis and regeneration require dynamic regulation of gene expression, often compromised in metabolic dysfunction-associated liver disease (MASLD). Host Cell Factor 1 (HCF-1), a conserved transcriptional co-regulator encoded by the X-chromosome linked *Hcfc1* gene, plays a crucial role in liver function. Despite its implication in various cellular processes, its impact on the epigenome remains underexplored. Our prior research demonstrated that hepatocyte-specific loss of HCF-1 induces non-alcoholic fatty liver disease (NAFLD) progression to non-alcoholic steatohepatitis (NASH) (Minocha, S. *et al. Mol. Cell. Biol.* 39, (2019).). This study aims to unravel the epigenetic changes in murine liver upon induced hepatocyte-specific loss of HCF-1, elucidating its role in hepatic metabolism and epigenetic integrity.

Method: Tamoxifen-induced hepatocyte-specific HCF-1 knockout (*Hcfc1*^{hepKO}) was validated in mice, followed by 70% partial hepatectomy (PH) to induce liver regeneration. Liver tissue collected at specific time points underwent immunostaining and immunoblotting. Chromatin immunoprecipitation and high throughput sequencing (ChIP-Seq) analysed chromatin from tamoxifen-treated mice, identifying enrichment regions with MACS2. Differential peaks were determined using HOMER and BEDTools. Gene ontology and pathway analysis interpreted ChIP-Seq results.

Results: HCF-1 levels increased post-PH in *Hcfc1*^{lox/y} mice, emphasizing its role in hepatocyte re-entry into the cell cycle for regeneration. HCF-1-negative hepatocytes lacked proliferation capacity, while HCF-1-positive cells exhibited robust regeneration. ChIP-Seq showed altered gene expression patterns, indicating disturbances in the hepatic epigenetic landscape. Dysregulated genes involved in diverse cellular processes highlighted HCF-1's impact on overall hepatic gene expression.

Conclusion: This study unveils HCF-1's role in NAFLD pathogenesis, showcasing its impact on liver damage, epigenetic modifications, and transcriptional regulation. By understanding HCF-1's role in NAFLD pathogenesis, hepatic regeneration, and epigenomic regulation, this research contributes new insights to liver health and disease mechanisms.

FRI-551

  -arrestin2 promotes cytoskeleton polymerization through RhoA-Diaph2 signaling to activate YAP to mediate liver regeneration after hepatectomy in mice

Genshu Wang¹, Wenfeng Zhu², Xiaolong Chen³, Xiaowen Wang², Xuejiao Li⁴, Haoqi Chen², Zhilong Liu³, Zhiwei Chen³. ¹Department of Hepatic Surgery, Liver Transplantation, Guangdong Provincial Hospital of Chinese Medicine, Guangzhou, China; ²Department of Hepatic Surgery, Liver Transplantation, The Third Affiliated Hospital of Sun Yat-sen University, Guangzhou, China; ³Department of Hepatobiliary Surgery, The First Affiliated Hospital of Jinan University, Guangzhou, China; ⁴Department of Hepatology Lab, The Third Affiliated Hospital of Sun Yat-sen University, Guangzhou, China
Email: 15779729700@163.com

Background and aims: As the only regenerative parenchymal organ, the secret of liver regeneration is interesting and far from being revealed.   -arrestin2 (ARRB2) is a ligand of G protein-coupled

POSTER PRESENTATIONS

receptor, which is thought to be involved in a variety of physiological and pathological biological processes. In this study, we aimed to clarify the role of ARRB2 in liver regeneration after hepatectomy and investigate the underlying mechanisms.

Method: Liver samples from patients undergone associating liver partition and portal vein ligation for staged hepatectomy (ALPPS) were obtained to evaluate the correlation between ARRB2 and liver regeneration. ARRB2 knockout (*Arrb2*^{-/-}) mice and wild type littermates were used to establish 70% partial hepatectomy model to determine the exact role of ARRB2 during liver regeneration. In addition, the underlying mechanisms and clinical translation value were further explored.

Results: ARRB2 was found positively correlates with proliferative level of hepatocytes in patients undergone ALPPS. The kinetics of changes in ARRB2 during liver regeneration after hepatectomy in mice was consistent with the trend of hepatocyte proliferation, and knockout of ARRB2 significantly inhibited but not only delayed liver regeneration. In addition, ARRB2 promoted hepatic regeneration in a YAP-dependent way. The regulation of YAP by ARRB2 is not dependent on canonical Hippo signaling, but on the remodeling of cytoskeletal F-actin. Mechanistically, ARRB2 upregulated *Diaph2* by coupling RhoA to promote actin polymerization, thereby promoting YAP translocate into nucleus and initiating the transcription of involved proliferation genes. Moreover, β -receptor blocker carvedilol that up-regulates ARRB2 remarkably promoted liver regeneration after hepatectomy in mice.

Conclusion: Our results demonstrated that ARRB2 plays a key role in liver regeneration after hepatectomy, which activates YAP by regulating actin cytoskeleton polymerization to promote hepatocyte proliferation.

FRI-554

Development of in vitro human organoid models for metabolic dysfunction-associated liver disease (MASLD)

Simran Sharma¹, Ashwini Vasudevan¹, Pooja Bhadoria², Ajeet Bhadoria², Savneet Kaur¹. ¹Institute of Liver and Biliary Sciences, Vasant Kunj, Delhi, India; ²All India Institute of Medical Sciences, Rishikesh, India
Email: savykaur@gmail.com

Background and aims: Organoid systems recapitulate in-vivo organ architecture and help to model complex pathologies. The present research work aims at developing in-vitro organoid model for metabolic dysfunction associated liver disease (MASLD) using human fetal liver cells.

Method: Primary hepatocytes were isolated from aborted human fetal liver samples (n = 5). Viable primary hepatocytes were mixed with Matrigel (Corning), in a 30 μ L dome (seeding density 30,000–50,000 cells/well). The organoid media contained a growth factor cocktail with Acetylcysteine, Gastrin, Nicotinamide and Forskolin. After 7 days of cell seeding and culture, the hepatic organoids were given free fatty acid (FFA) (4 mM palmitic acid) and sugar (25 mM sucrose) insult for 72 hrs. The study groups were designated as Gr1-PBS; Gr2- FFA only; Gr3- Sugar only; Gr4- FFA + Sugar. The developed MASLD organoids were assessed for viability with Calcein and Sytox staining and functional characteristics post insult with BODIPY-lipid staining, RT-PCRs and ELISAs.

Results: The human fetal hepatocyte organoids showed significant increase in organoid diameter (from $35.4 \pm 2 \mu$ m to $112.8 \pm 2 \mu$ m; $p < 0.0001$) from day 0 to day 7. After day 7, the organoids were given different types of insult and studied at 72hrs post insult. There was no significant difference in the diameter of organoids between Gr1 and Gr3. However, as compared to Gr1, in Gr4, the diameter of the organoids was significantly decreased ($120.2 \pm 4 \mu$ m vs $\pm 2 \mu$ m $90.8 \pm 10 \mu$ m, $p < 0.0001$) at day 3 post insult. The viability of the organoids decreased in all the groups vs Gr1 ($p < 0.05$ each). Accumulation of lipid-rich bodies were clearly observed in brightfield imaging in Gr2 and 4, Gr3 did not show much lipid accumulation. We also validated

this observation with BODIPY staining, (34 ± 5 positive organoids/field in Gr4 vs 18 ± 3 positive cells/field in Gr3; $p < 0.05$). RT-PCR analysis of the organoids post insult of Gr4 vs Gr1 organoids, showed increased expression of inflammatory markers such as IL-6 (+2.5 fold, $p < 0.05$) and Serum Amyloid A4 (SAA4) (+1 fold, $p = \text{NS}$). Hepatic functional markers, such as Albumin (–1.5 fold, $p < 0.05$) and CYP3A4 (–0.5 fold, $p = \text{NS}$) reduced in Gr4 vs Gr1. This observation was also confirmed with human rat albumin specific ELISA (albumin levels from organoid conditioned media $5 \pm 2 \mu$ g/ml Gr4 vs $72 \pm 3 \mu$ g/ml Gr1, $p < 0.001$).

Conclusion: The study showed that a combined insult of both sugar and fat to human fetal hepatocyte organoids results in a robust model of MASLD with attributes similar to human disease including steatosis and increase in pro-inflammatory cytokine gene expression. The developed human MASLD organoids may serve as excellent models for drug screening and testing applications.

FRI-555

New insights into the regulation of bile acids synthesis during the early stages of liver regeneration: a human and experimental study

Iker Uriarte^{1,2}, Eva Santamaria^{1,2}, Amaya Lopez-Pascual^{2,3}, Josep Maria Argemi^{1,4,5}, Maria U. Latasa^{2,6}, Elena Adan-Villaescusa², Ainara Irigaray-Miramon², Jose Maria Herranz^{2,7}, Maria Arechederra^{2,3,7}, Jorge Basualdo^{4,8}, Felipe Lucena⁹, Fernando J. Corrales¹⁰, Fernando Rotellar¹¹, Fernando Pardo¹¹, Grégory Merlen¹², Bruno Sangro^{1,4,13}, Thierry Tordjmann¹², Carmen Berasain^{1,2}, Maria J. Monte^{1,14}, Jose J. G. Marin^{1,14}, Maite G. Fernandez-Barrena^{1,2,15}, Jose Ignacio Herrero^{1,4,16}, Matías A. Avila^{1,2,13}. ¹Ciberehd, Instituto de salud Carlos III, Madrid, Spain; ²Hepatology Laboratory, Solid Tumors Program, CIMA, CCUN, University of Navarra, Pamplona, Spain; ³Instituto de investigaciones sanitarias de Navarra Idisna, Pamplona, Spain; ⁴Hepatology Unit, CCUN, Navarra University Clinic, Pamplona, Spain; ⁵RNA Biology and Therapies Program, CIMA, CCUN, University of Navarra, Pamplona, Spain; ⁶Instituto de investigaciones sanitarias de Navarra Idisna, Pamplona, Spain; ⁷Ciberehd, Instituto de salud Carlos III, Madrid, Spain; ⁸Internal medicine department, ICOT hospital ciudad de Telde, Las Palmas, Spain; ⁹Internal Medicine Department, Navarra University Clinic, Pamplona, Spain; ¹⁰Centro nacional de biotecnología (CSIC), Madrid, Spain; ¹¹General Surgery Department, Navarra University Clinic, Pamplona, Spain; ¹²Université Paris-Saclay, Inserm U1193, Orsay, France; ¹³Instituto de investigaciones sanitarias de Navarra Idisna, Pamplona, Spain; ¹⁴Experimental Hepatology and Drug Targeting (Hevefarm), University of Salamanca, IBSAL, Salamanca, Spain; ¹⁵Instituto de Investigaciones Sanitarias de Navarra, Idisna, Pamplona, Spain; ¹⁶Instituto de investigaciones sanitarias de Navarra Idisna, Pamplona, Spain
Email: maavila@unav.es

Background and aims: Liver regeneration is essential for the preservation of homeostasis and survival. Bile acids (BAs)-mediated signaling is necessary for liver regeneration, but BAs levels need to be carefully controlled to avoid hepatotoxicity. We studied the early response of the BAs-fibroblast growth factor 19 (FGF19) axis in healthy patients undergoing hepatectomy for living donor liver transplant. We also evaluated BAs synthesis in mice upon partial hepatectomy (PH) and acute inflammation, focusing on the regulation of cytochrome-7A1 (CYP7A1), the rate-limiting enzyme in BAs synthesis from cholesterol.

Method: Serum was obtained from twelve human liver donors. Mice underwent 2/3 PH or sham-operation. Acute inflammation was induced with bacterial lipopolysaccharide (LPS) in mice fed control or antioxidant-supplemented diets. BAs and 7 α -hydroxy-4-cholesten-3-one (C4) levels were measured by HPLC-MS/MS; serum FGF19 by ELISA. Gene expression and protein levels were analyzed by RT-qPCR and western-blot.

Results: After PH, serum BAs markedly increased. In patients with higher serum BAs levels FGF19 concentrations transiently rose, while

C4 levels (a readout of liver CYP7A1 activity) dropped 2 h post-resection in all cases. Serum BAs and C4 followed the same pattern in mice 1 h after PH, but surprisingly C4 levels also dropped in sham-operated and LPS-treated animals, without marked changes in CYP7A1 protein levels. LPS-induced serum C4 decline was attenuated in mice fed antioxidant-supplemented diet.

Conclusion: In human liver regeneration, FGF19 upregulation may constitute a protective response from BAs excess. Our findings suggest the existence of post-translational mechanisms regulating CYP7A1 activity, and therefore BAs synthesis, independent from *Cyp7a1* gene transcription.

FRI-556

Small nucleolar RNA expression and their prognostic values in non-viral hepatocellular carcinoma

Venkata Ramana Mallela¹, Phanindra Babu Kasi¹, Andriy Trailin¹, Dattatrya Shetti¹, Lenka Cervenková², Richard Pálek³, Václav Liška⁴, Kari Hemminki⁵, Filip Ambrozkiwicz¹. ¹Laboratory of Translational Cancer Genomics, Biomedical Center, Faculty of Medicine in Pilsen, Charles University, Plzeň 1, Czech Republic; ²Laboratory of Cancer Treatment and Tissue Regeneration, Plzeň 1, Czech Republic; ³Laboratory of Cancer Treatment and Tissue Regeneration, Department of Surgery, Plzeň 1, Czech Republic; ⁴Laboratory of Cancer Treatment and Tissue Regeneration, Biomedical Center, Faculty of Medicine in Pilsen, Charles University, Department of Surgery, University Hospital in Pilsen and Faculty of Medicine in Pilsen, Charles University, Plzeň 1, Czech Republic; ⁵Laboratory of Translational Cancer Genomics, Biomedical Center, Faculty of Medicine in Pilsen, Charles University, Department of Cancer Epidemiology, German Cancer Research Center, Im Neuenheimer Feld 280, 69120 Heidelberg, Germany, Plzeň 1, Czech Republic
Email: Mallela.Venkata@lfp.cuni.cz

Background and aims: The absence of accurate prognostic indicators contributes to the ongoing challenge of hepatocellular carcinoma (HCC), resulting in high mortality rates and poor prediction of the recurrence and survival. There has been limited researches exploring the relationship between small nucleolar RNAs (snoRNAs) and HCC. Studies have previously demonstrated that the expression of both SNORA47 and SNORD126 has been altered or dysregulated in liver cancer tissue. In HCC, siRNA transfection suppresses SNORA47, decrease cell invasion, proliferation, and metastasis by modifying an epithelial-mesenchymal transition. Conversely, increased SNORD126 levels have been associated with HCC, contributing to increased cell division. Our aim of study is to provide a better understanding of how snoRNA expression affects patient's outcome in non-viral HCC.

Method: We analyzed HCC and non-tumor adjacent tissue from 35 patients who had undergone resection in Pilsen University hospital between 1997 and 2019. Using q-PCR, we assessed the expression levels of specific snoRNAs namely SNORA47 and SNORD126. Patients were categorized into low and high expression groups based on the median expression of SNORA47 and SNORD126. We then conducted Kaplan-Meier analysis to assess the association of SNORA47 and SNORD126 expression levels with patient outcomes: time to recurrence (TTR), disease-free survival (DFS) and overall survival (OS).

Results: SNORA47 expression was higher in tumor tissue than in non-tumor adjacent tissue. In contrary SNORD126 expression was lower in tumor tissues compared to non-tumor adjacent tissue. Low expression of SNORA47 was associated with longer TTR ($p = 0.03$) and DFS ($p = 0.04$). Whereas low expression of SNORD126 was associated with longer TTR ($p = 0.05$) but not DFS. The combination of SNORA47-SNORD126 low expression was linked to longer TTR and DFS ($p = 0.01$ and 0.02 respectively). Furthermore, there was no association seen between expression and OS. No Correlations with clinical data was observed.

Conclusion: The findings suggest that SNORA47 and SNORD126 show potential as a promising prognostic marker in non-viral HCC.

The analysis revealed that the combination analysis provides better prediction than alone for assessing the prognosis of non-viral HCC patients.

Liver immunology

TOP-552

Oncogenic beta-catenin is using CD155 as a molecular actor to corrupt immunosurveillance of cold HCC

Joana Gonçalves Araujo¹, Céline Pophillat¹, Angélique Gougelet¹, Stefano Caruso², Mathilde Cadoux³, Jing Fang¹, Isabelle Galy-Fauroux⁴, Julien Calderaro⁵, Akira Shibuya⁶, Severine Morizur¹, Manon Allaire⁷, Jessica Zucman-Rossi¹, Chantal Desdouets¹, Jean-Pierre Couty¹. ¹Centre de Recherche des Cordeliers, INSERM U1138, Paris, France; ²INSERM U955, Créteil, France; ³Cherry Biotech, Montreuil, France; ⁴Centre de Recherche des Cordeliers, INSERM U1138, Paris; ⁵Henri Mondor University Hospital, Créteil, France; ⁶University of Tsukuba, Tsukuba, Japan; ⁷Groupe Hospitalier Pitié-Salpêtrière, Paris, France
Email: joana.araujo@inserm.fr

Background and aims: Hepatocellular carcinoma (HCC) belongs to the poor prognosis cancers and is the 3rd most common cause of cancer-related death. Therapies are very limited but immunotherapy (anti-PDL1 + anti-VEGF) is now the first-line treatment for HCC, with only 20% of responders. HCC tumors harboring CTNNB1 activating mutations (30% of all HCCs), constitute a specific entity of cold tumors that fail to respond to immunotherapy. Our team evidenced that oncogenic beta-catenin signaling in hepatocytes subverts the immune system. We found that invariant NKT (iNKT) cells, have a strong anti-tumor potential that diminishes during tumorigenesis. Our recent data also demonstrated that beta-catenin signaling corrupts immune recognition of tumor hepatocytes through the extinction of NKG2D ligand expression. We extended the analysis to other receptor-stress ligand pairs, notably the CD226/CD155 couple. CD226 expression on the surface of CD8+ and NKT cells has recently been shown to reflect the cytotoxic potential of these cells and is a prerequisite for immunotherapy in other cancers. Its ligand CD155 is expressed by tumor cells subjected to various stresses and its expression is associated with a poor patients' prognosis. However, its involvement during Ctnnb1-induced tumorigenesis is still elusive. **Method:** Cohort of HCC patients (N = 500), beta-catenin-HCC mouse models: 1) preneoplastic Apc^{Delta-Hep} (activation of Wnt/beta-catenin pathway in all hepatocytes) 2) spontaneous CTNNB1-mutated, Lpk-c-myc tumors. These mice were crossed with CD226-KO mice. Technologies used: RNA-Seq, FACS, IHC, RTqPCR, Western Blot, ChIP-Seq/ATAC-Seq.

Results: Our study provides molecular evidence that CD226 is an important player in HCC immunosurveillance as we show: 1) in all human HCC subgroups that transcriptional expression of CD155 is increased as its cognate receptor CD226 is downregulated, 2) CD226 expression holds per se a prognostic value for 5-year overall survival, 3) using a model of CTNNB1-mutated HCC an upregulation of CD155 ligand expression in tumors associated with a loss of CD226 expression in iNKT cells, reducing their cytotoxic potential, 4) an exacerbation of tumorigenesis in a CD226-KO mouse model with the emergence of metastasis, 5) that in a forced beta-catenin activation model, a decrease in CD226 expression on iNKTs both dependently and independently of the interaction with its ligand CD155, provoking a reduction of their cytotoxic potential, 6) through ChIP-seq/ATAC-seq analyses that CD155 is a positive target of beta-catenin signaling.

Conclusion: Altogether, our study reveals that beta-catenin drives CD155 expression to subvert CD226-mediated immunosurveillance

in iNKT through the sustained interaction of the CD155 with CD226 receptor.

TOP-553

Deciphering the immunological dynamics of flares following nucleos (t)ide analogue (NA) cessation in HBeAg negative chronic hepatitis B in a large, longitudinal, phase II multi-centred clinical trial (NUC-B study)

Sandra Phillips^{1,2}, Sameer Mistry^{1,2}, Nicola Harris^{1,2}, Dimple Zope^{1,2}, Celia Moore³, Gareth Hahn³, Michelle Rosario³, Camilla Carr-Smith⁴, Maria Cortes Carrillo⁴, Lavanya Elangovan⁵, Kosh Agarwal⁴, James Hand⁵, Chris Sivell⁵, Patrick Kennedy⁵, Susan Congreave⁶, Mathew Barnes⁶, Stephen D. Ryder⁶, Mariam Habib³, Mark R. Thursz³, Shilpa Chokshi^{1,2}. ¹The Roger Williams Institute of Hepatology, Foundation for Liver Research, London, United Kingdom; ²School of Immunology and Microbial Sciences King's College, London, United Kingdom; ³St Mary Hospital Faculty of Life Sciences and Medicine Digestive Diseases Division Imperial College, London, United Kingdom; ⁴Kings college hospital NHS foundation trust, London, United Kingdom; ⁵Barts Health NHS trust Royal London hospital, London, United Kingdom; ⁶Nottingham University Hospitals NHS trust, London, United Kingdom
Email: s.phillips@researchinliver.org.uk

Background and aims: Nucleos (t)ide Analogues (NA) withdrawal in CHB often lead to hepatitis flares which can be beneficial or harmful. Understanding the immunological dynamics underlying these dichotomous outcomes is critical for managing finite NA strategies.

Method: Immune-surveillance was performed during the multi-centred, randomised NUC-B study that included HBeAg-negative patients who had NA-withdrawal (Stop-NA) or NA-cessation followed by a 16-week course of PEG-IFN-alpha (IFN). Flares were defined as mild ($ALT > 2 \times ULN$) or exaggerated ($> 20 \times ULN$), the latter receiving NA retreatment (NA-ReTx). Peripheral blood mononuclear cells (PBMCs) (n = 459) were collected from 23 Stop-NA and 18 IFN patients during the 3-year follow-up with additional sampling during flares. PBMCs were stimulated with 15-mer overlapping genotype-specific peptide pools and recombinant HBcAg/HBsAg. Ex-vivo frequency of HBV-specific IFN-gamma (IFN-g)-producing T-cells was assessed by GCLP-standardised ELISpot assays.

Results: A two-year cumulative incidence of 34.8% for mild and 26.1% for exaggerated flares were found in Stop-NA versus 58.8% and 5.9% in IFN groups. Over 70% of flares occurred within 17 weeks post-NA-withdrawal. Immunological analysis highlighted an elevated frequency of IFN-g-producing-HBV-specific T cells in response to HBcAg-peptides during mild flares in Stop-NA. This is in stark contrast with loss of T-cell response during exaggerated flares in NA-ReTx group (p = 0.010) and mild flares in IFN (p = 0.02). While T-cell response recovered post-flare in IFN, this was not observed in the NA-ReTx group. Wide and broad HBcAg-T-cell responses were only observed in 17% of patients experiencing exaggerated flares in NA-ReTx group (none in the IFN mild flares group) compared to 38% in Stop-NA group experiencing mild flares (p < 0.0001). Notably, epitope recognition significantly contracted during exaggerated flares (p = 0.019) and IFN groups (p = 0.0005). Interestingly, at baseline, a specific region of HBcAg, induced a T-cell response that was significantly associated with RTx and IFN-related flare (p = 0.028).

Conclusion: Immunological analysis revealed distinct T-cell response patterns during mild and exaggerated flares after NA withdrawal and loss of T-cell responses during IFN treatment, that do not recover during NA retreatment. Significant differences in the breadth and specificity of HBcAg-T-cell responses highlight a potential biomarker at baseline associated with deleterious flares post-NA cessation in HBeAg-negative CHB.

SATURDAY 08 JUNE

SAT-531-YI

Testosterone modulates T cells in healthy individuals and women with autoimmune liver disease

Nico Will¹, Lara Henze², Christian Casar², Victor Haas², Jasper Meyer², Dakyung Lee², Stephanie Stein², Tobias Poch², Jenny Krause², Johannes Fuß², Alexandra E. Kulle^{3,3}, Paul-Martin Holterhus⁴, Samuel Huber², Ansgar W. Lohse², Dorothee Schwinge², Christoph Schramm². ¹University Medical Center Hamburg, Hamburg, Germany; ²University Medical Center Hamburg-Eppendorf, Hamburg, Germany; ³University Medical Center Schleswig-Holstein, Kiel, Germany; ⁴University Medical Center Schleswig-Holstein, Kiel, Germany
Email: n.will@uke.de

Background and aims: Female people are more prone to develop the autoimmune liver diseases autoimmune hepatitis (AIH) and primary biliary cholangitis (PBC). The reasons for this high female predominance are still unknown but there is mounting evidence that androgens contribute to the regulation of immune responses. Previous data of our group revealed that testosterone was effective in suppressing liver inflammation in an inducible mouse model of autoimmune cholangitis, which shows female predominance similar to PBC. Within this study, we now aimed to further unravel the influence of testosterone on T cell differentiation and function in women with autoimmune liver diseases.

Method: We combined quantitative serum hormone measurements, *ex vivo* flow cytometry immunophenotyping, *in vitro* T cell conversion assays and single cell CITE-sequencing on multiple cohorts: i) Females with PBC compared to age and sex matched controls, ii) trans men receiving gender-affirming testosterone treatment and iii) a trans man with an AIH/PSC variant syndrome receiving gender-affirming testosterone treatment.

Results: Females with PBC presented with significantly decreased serum testosterone levels compared to age and sex matched healthy controls. Furthermore, we identified elevated frequencies of pro-inflammatory T_H1 and T_H17 $CD4^+$ T cell subsets and increased *in vitro* T_H1 conversion rates of naïve $CD4^+$ T cells in females with PBC. To investigate *in vivo* effects of testosterone in humans, peripheral blood T cells from transmen receiving gender-affirming testosterone treatment were analysed before and during treatment. We observed a shift towards the regulatory T cell population upon six months of treatment with testosterone. To substantiate these findings in disease context, we analysed samples from a trans man diagnosed with autoimmune hepatitis and sclerosing cholangitis variant syndrome. Using single-cell CITE-sequencing we observed a downregulation of proinflammatory pathways and reduced T cell activation marker expression after six months of high dose testosterone treatment. Importantly, this was paralleled by an improvement of disease activity markers and a reduction of immunosuppressive drug dosage.

Conclusion: In summary, we here report a direct effect of testosterone on human $CD4^+$ T cells, shifting them towards anti-inflammatory phenotypes. This effect may contribute to sex differences observed in autoimmune liver diseases and may provide personalized treatment strategies in the future.

SAT-532-YI

Distinct soluble and cellular immunological signatures in various entities of hepatitis flares

Roni Souleiman^{1,2,3,4,5}, Erich Freyer^{1,2,3,4,5}, Tijana Ristic¹, Christine Falk^{3,6}, Benjamin Maasoumy^{1,3,5}, Heiner Wedemeyer^{1,3,5}, Bernd Heinrich¹, Anke R.M. Kraft^{1,2,3,4,5}, Markus Cornberg^{1,2,3,4,5}. ¹Department of Gastroenterology, Hepatology, Infectious Diseases and Endocrinology, Hannover Medical School, Hannover, Germany; ²TWINCORE Center of Experimental and Clinical Infection Research, Hannover, Germany; ³German Center for Infection Research (DZIF), Hannover, Germany; ⁴Center for Individualized Infection Medicine (CiiM), Hannover, Germany; ⁵Cluster of Excellence Resolving Infection

Susceptibility (RESIST; EXC 2155), Hannover Medical School, Hannover, Germany; ⁶Institute for Transplant Immunology, Hannover Medical School, Hannover, Germany
Email: souleiman.roni@mh-hannover.de

Background and aims: The management of hepatitis flares characterized by significant ALT elevations is a major clinical challenge, with consequences ranging from transient liver damage to liver failure. Understanding the immunological mechanisms and identifying predictive markers can be instrumental for effective management. Recent studies indicate, for example, that “auto-aggressive” or “bystander” CXCR6+ CD8+ T cells play a critical role in the immunopathogenesis of various chronic liver diseases.

Method: A comprehensive immunologic analysis was performed by spectral flow cytometry of PBMCs isolated from blood of 73 patients with various hepatitis flares (acute viral, chronic viral and non-viral hepatitis) defined as ALT >5-fold upper limit of normal. In addition, soluble immune markers (SIM) from a sub-cohort (n = 49) were analyzed using the Luminex platform. Results were correlated with clinical data and the Hepatocyte Injury Index (HIX, MS Shearman et al., medRxiv 2022) where possible.

Results: Our results showed a strong correlation between biochemical markers of liver injury and circulating CXCR6+ PD-1+ cytotoxic lymphocytes (CTL), which exhibited increased expression of activity markers compared to all CD8+ T cells. HLA-DR on CXCR6+ PD-1+ CTLs correlated with the real-time liver injury marker HIX ($r = 0.55$, $p < 0.001$). Moreover, CXCR6+ PD-1+ CTLs show distinct granzyme (GZ) expressions in acute and chronic viral infections, with GZB in acute and GZK in chronic infections. The CXCR6+ PD-1+ CD8 T cell subset also significantly correlated with CXCL10 plasma levels ($r = 0.54$, $p < 0.0001$). Besides CXCL10, other pro-inflammatory SIM, such as IL18 and G-CSF, positively correlated with biochemical markers of liver injury, excluding IL-13, which exhibited a negative correlation with HIX ($r = 0.55$, $p < 0.01$). The G-CSF/IL-13 ratio correlated with liver disease severity.

Conclusion: Our study emphasizes the pivotal role of CXCR6+ PD-1+ CTLs in liver inflammation, suggests HLA-DR (on CXCR6+ PD-1+ CTLs) as an activity marker, and proposes the granzyme B/K ratio on CXCR6+ PD-1+ CTLs as a differentiator of acute and chronic hepatitis. In addition, the data underscores the potential of soluble immune markers for characterizing liver inflammation and predicting progression.

SAT-533

Liver immunity index: predicting immune control of chronic hepatitis B from circulating CD8 T cells

Hannah Wintersteller¹, Sainitin Donakonda², Miriam Bosch¹, Anna D. Kosinska³, Edanur Ates-Öz³, Anna Fürst², Gustavo Almeida⁴, Christine Wurmser⁴, Kathrin Heim⁵, Roni Souleiman⁶, Sofia Pérez-del-Pulgar⁷, Sabela Lens⁷, Markus Cornberg⁶, Robert Thimme⁵, Maike Hofmann⁵, Dietmar Zehn⁴, Ulrike Protzer³, Dirk Wohlleber², Percy A. Knolle¹. ¹Institute of Molecular Immunology, Munich, Germany; ²Institute of Molecular Immunology, Technical University of Munich, Munich, Germany; ³Institute of Virology, Technical University of Munich, Munich, Germany; ⁴Division of Animal Physiology and Immunology, School of Life Sciences Weihenstephan, Technical University of Munich, Freising, Germany; ⁵Third Department of Medicine, University Hospital Freiburg, Freiburg, Germany; ⁶Department of Gastroenterology, Hepatology and Endocrinology, Hannover Medical School, Hannover, Germany; ⁷Liver Unit, University Hospital Clinic Barcelona, IDIBAPS, Barcelona, Spain
Email: hannah.wintersteller@tum.de

Background and aims: Chronic hepatitis B (CHB) is characterized by a scarcity and dysfunction of virus-specific CD8 T-cells in the liver. Immunotherapies, such as therapeutic vaccination, aim to reinvigorate and expand intra-hepatic virus-specific CD8 T-cell immunity to control viral infection. This study sought to identify biomarkers on circulating virus-specific CD8 T-cells that reflect the immune

response in the liver and could be used to predict immune control of CHB.

Method: Using pre-clinical models of HBV as well as CHB patient samples, we studied the dynamics of virus-specific T-cell response by flow cytometry and single-cell RNA sequencing.

Results: Single-cell transcriptomic and protein-level analysis detected the generation of virus-specific CD8 T-cells in the liver of preclinical models of persistent as opposed to resolved infection. These HBV-specific CD8 T cells had a tissue-resident phenotype characterized by several markers. During an acute-resolving infection, these CD8 T cells were potent effector cells, as shown in preclinical models, whilst tissue-resident CD8 T-cells during persistent infection were rendered dysfunctional. Strikingly, the phenotype and functionality of HBV-specific CD8 T-cells circulating in peripheral blood were identical to the intrahepatic HBV-specific CD8 in the liver and predicted immune control of infection. Notably, liver-resident HBV-specific CD8 T-cells developed solely when recognizing their antigen in the liver and not after systemic vaccination in the absence of infection or following non-hepatotropic infection.

Conclusion: Our results identify a total of five distinct markers in HBV-specific CD8 T cells that were equally present on circulating and intrahepatic CD8 T cells and predict immune control of infection. Thus, our proprietary biomarker set allows us to study intrahepatic HBV-specific CD8 T cells by targeted analysis of circulating HBV-specific CD8 T cells and use this information for monitoring of immune therapies in CHB patients.

SAT-534

Macrophage-derived IL-15 imprints peritoneal tissue-resident memory T cells during spontaneous bacterial peritonitis in patients with cirrhosis

Oluwatomi Ibidapo-Obe¹, Sven Stengel², Mick Frissen¹, Johanna Reißing¹, Karsten Große¹, Michael Rooney³, Hector Leal-Lassalle⁴, Raquel Benedé-Ubieto⁴, Yulia Nevzorova⁴, Christian Trautwein⁵, Tony Bruns¹. ¹Department of Internal Medicine III, University Hospital RWTH Aachen, Aachen, Germany; ²Department of Internal Medicine IV, University Hospital Jena, Jena, Germany; ³Department of Internal Medicine IV, University Hospital Jena, Jena, Germany; ⁴Department of Immunology, Ophthalmology and ENT, Complutense University School of Medicine, Madrid, Spain; ⁵Department of Internal Medicine III, University Hospital RWTH Aachen, Aachen, Germany, Aachen, Germany
Email: oibidapo@ukaachen.de

Background and aims: Tissue-resident memory T cells (TRM) are long-lived memory T cells residing in tissues and capable of effective immediate response upon re-infection with a familiar pathogen. We investigated whether human peritoneal CD8 T cells from patients with cirrhosis show phenotypic and functional properties of TRM and can be imprinted by inflammatory peritoneal events, such as spontaneous bacterial peritonitis (SBP).

Method: Using mass cytometry, flow cytometry, RT-qPCR, *in vitro* cultures, single-cell RNA sequencing, and ELISA, we evaluated the phenotype and function of human CD8+ T cell subsets present in ascitic fluid (AF) from patients hospitalized for decompensated cirrhosis in the absence or presence of SBP. Observed peritoneal T cell phenotypes were validated in a preclinical, precirrhotic mouse model and potential sources of TRM-activating cytokines were validated using cell-free clinical human AF samples and isolated human peritoneal macrophages.

Results: Unsupervised mass cytometry analysis and validation by flow cytometry confirmed the presence of CD45+ CD3+ CD8+ CD103+ CD69+ CXCR6+ HLADR+ memory T cells in AF, which were largely absent in blood, consistent with the phenotype of human TRM. The presence of peritoneal CD103+ CD69+ T cells in significant numbers was also confirmed in a precirrhotic mouse model of DUAL steatotic liver disease (MetALD). Human CD103+ CD69+ TRM, particularly the CD49+ cells, were potent producers of IFN- γ after T cell receptor (TCR)

POSTER PRESENTATIONS

ligation, which could be augmented by IL-15. In single-cell RNA sequencing, peritoneal CD8 T cells exposed to IL-15 showed increased markers of tissue residency (*RUNX3*, *PRDM1*) alongside transcriptional features of activation and exhaustion. As shown by transcriptomic analysis in absence or presence of LPS, *in vitro* infection with *E. coli* and the analysis of cell-free AF from patients with SBP, activated peritoneal macrophages were a potent source of IL-15, which was able to upregulate cytotoxic granules (Granzyme B) and co-inhibitory receptors such as PD-1 in TRM in a TCR-independent bystander fashion. Clinical serial samples confirmed the upregulation of co-inhibitory receptors on peritoneal TRM during SBP, which persisted after the resolution of infection. Despite the expression of exhaustion markers, TRM retained their effector profiles, and blocking the PD-1/PDL-1 axis *in vitro* had no impact on their cytotoxic functions.

Conclusion: A subset of peritoneal CD8 T cells in patients with cirrhosis resembles the phenotype of tissue-resident memory T cells, which can be imprinted by macrophage-derived IL-15 during bacterial infection in the longer term. Despite the expression of coinhibitory receptors peritoneal TRM from patients with cirrhosis retain potent cytotoxic and proinflammatory effector functions.

SAT-535-YI

The role of the immune checkpoint TIGIT in CD4+ T cell dysfunction in patients with decompensated cirrhosis

Joseph Delo¹, Dan Forton², Evangelos Triantafyllou³, Arjuna Singanayagam⁴. ¹Institute of Infection and Immunity, St George's University, London, United Kingdom; ²Department of Gastroenterology and Hepatology, St George's University Hospital, London, United Kingdom; ³Department of Metabolism, Digestion and Reproduction, Imperial College, London, United Kingdom; ⁴Institute of Infection and Immunity, St George's University, London, United Kingdom
Email: joseph.delo@gmail.com

Background and aims: Patients with decompensated cirrhosis are highly susceptible to bacterial infections. CD4+ T cells, which normally play a key role in supporting and directing anti-bacterial immune responses, are functionally impaired in cirrhosis, but the mechanisms underlying this are not fully understood. TIGIT is an immune checkpoint expressed on T cells that transmits an inhibitory signal when bound to its ligand, CD155, expressed on antigen-presenting cells. This study aimed to determine if TIGIT blockade could improve the function of CD4+ T cells from patients with decompensated cirrhosis.

Method: Patients with stable decompensated cirrhosis (SD, n=9), acute decompensated cirrhosis (AD, n=17) and acute-on-chronic liver failure (ACLF, n=11) were recruited within 48 hours of admission to hospital, along with healthy controls (HC, n=8). Mononuclear cells were isolated from peripheral blood and the expression of membrane-bound TIGIT and CD155 on immune cell subsets was assessed by flow cytometry. An anti-TIGIT monoclonal antibody (MBSA43 clone, at 10 µg/ml) was used for TIGIT functional blockade *ex vivo*. Its impact on CD4+ T cells, following CD3 stimulation, was determined by measuring T cell expression of exhaustion markers (PD-1, LAG-3, TIM-3), proliferation, and cytokine production (IFN-γ, IL-2, and TNF-α).

Results: CD4+ T cells from patients with AD and ACLF expressed more TIGIT compared to those from HC (HC 15.9%, AD 26.1%, and ACLF 27.3% positive; p=0.005). Notably, the expression of TIGIT on CD8+ T cells or NK cells, and the expression of CD155 on CD14+ monocytes, remained the same between groups. Furthermore, patients who died within 90 days had higher TIGIT expression on their CD4+ cells at baseline than those who survived (31.7 versus 21.2% positive; p=0.002). TIGIT blockade reduced expression of the exhaustion markers LAG-3 and PD-1, and increased IFN-γ production by CD4+ T cells from AD and ACLF, but had no impact on CD4+ T cell proliferation.

Conclusion: This study identifies a possible new mechanism for CD4+ T cell dysfunction in cirrhosis. Expression of the inhibitory immune

checkpoint TIGIT is increased on CD4+ T cells in decompensated cirrhosis, in the face of preserved levels of the ligand, CD155, on monocytes. Blockade of TIGIT *ex vivo* partially reversed CD4+ T cell exhaustion and improved proinflammatory cytokine production. It could therefore serve as a novel immunomodulatory target in decompensated cirrhosis, reducing reliance of anti-microbials in the era of emerging multi-drug resistance organisms.

SAT-536

Uptake and T cell stimulation by anti-HBs monoclonal antibody BJT-778-rHBsAg immune complexes

Loghman Salimzadeh^{1,2}, Stuti Shah^{1,2}, Danie La², Hilario Ramos³, Nancy Shulman³, Hassan Javanbakht³, Adam Gehring^{1,2,4}. ¹Schwartz-Reisman Liver Research Centre, University Health Network, Toronto, Canada; ²Toronto Centre for Liver Disease, University Health Network, Toronto, Canada; ³Bluejay Therapeutics, Inc., San Mateo, United States; ⁴Department of Immunology, University of Toronto, Toronto, Canada
Email: adam.gehring@uhn.ca

Background and aims: In chronic hepatitis B patients, the sustained presence of a high quantity of hepatitis B virus surface antigens (HBsAg) contributes to the exhaustion of HBV-specific T and B cell responses. BJT-778 is a fully human IgG1 monoclonal antibody targeting the antigenic loop of HBsAg currently in Phase 1 clinical development. As clearance of HBsAg via immune complex (IC) formation may be a mechanism by which therapeutic antibodies can reduce immune exhaustion, this research-based study investigated the uptake of BJT-778-HBsAg ICs by professional antigen presenting cells and the impact of IC uptake on HBsAg-specific T cell activation.

Methods: Immune complexes were generated using BJT-778 and DyLight-550-labeled recombinant HBsAg. The kinetics of IC uptake across seven distinct professional phagocytic leukocyte populations in peripheral blood samples from healthy individuals and chronic hepatitis B patients were measured using flow cytometry. Fc receptor-mediated uptake of ICs was confirmed using an FcR blocking reagent. T cell-stimulatory effects were tested by loading CD14+ cells with BJT-HBsAg ICs, or HBsAg alone, and measuring activation of a HBsAg-specific CD4+ T cell clone by assessing IFN-γ production via flow cytometry.

Results: BJT-778 significantly increased the uptake of HBsAg compared to an isotype control antibody or HBsAg alone. Within 2h of incubation, nearly all classical (97.40%) and intermediate (94%) monocytes were positive for HBsAg compared to ~50% with HBsAg alone or isotype control. Non-classical monocytes and myeloid dendritic cells (mDCs) also displayed significant increases in HBsAg with ICs compared to HBsAg alone or isotype. CD141+ DCs, plasmacytoid DCs, or B cells did not show significant enhancement of HBsAg uptake with ICs. Cell types where BJT-778 showed significantly enhanced HBsAg uptake displayed high levels of activating FcγR1 (CD64; classical and intermediate monocytes, mDCs) and FcγRIIIa (CD16; intermediate and non-classical monocytes). Fc-mediated uptake was confirmed by blocking FcRs prior to addition of ICs. Notably, classical monocytes and myeloid dendritic cells from CHB patients exhibited significantly slower uptake of ICs compared to healthy donors. Enhanced uptake of BJT-778-rHBsAg-ICs by CD14+ monocytes resulted in increased HBsAg-specific T cell activation.

Conclusion: These data identify the likely *in vivo* targets of BJT-778-HBsAg ICs and demonstrate that BJT-778 ICs lead to enhanced HBsAg uptake in professional antigen presenting cells. Enhanced uptake of HBsAg resulted in increased HBV-specific CD4+ T cell activation, supporting a dual mechanism of action through removal of circulating HBsAg and stimulation of HBV-specific T cell immunity.

SAT-537

Characterization of immune cell populations in the microenvironment of mice liver during the progression of liver fibrosis to hepatocellular carcinoma

Ananya Ajith¹, Françoise Smets¹, Etienne Sokal¹, Mustapha Najimi¹.

¹Université Catholique de Louvain, Brussels, Belgium

Email: ananya.ajith@uclouvain.be

Background and aims: Around 90% of hepatocellular carcinoma (HCC) cases arise in the background of chronic liver diseases (CLD). Chronic inflammation is the underlying cause of CLD and development of HCC. Thus, dysregulated functions of hepatic immune cell populations are playing important roles in CLD and development. In this study we aim to characterize the different immune cell populations dysregulated during liver fibrosis and HCC development using a combination of Diethylnitrosamine (DEN) and carbon tetrachloride (CCl₄) treated mouse model.

Method: A single injection of DEN at 4 weeks of age, followed by continuous injections of CCl₄ for 6 and 21 weeks were administered respectively, to induce liver fibrosis and HCC in mice. Whole liver was perfused and digested using collagenase, to isolate and characterise single-cell suspensions of the non-parenchymal cell fraction (NPF). The different immune cell populations were then identified and sorted using FACS analysis. In parallel, the tissular hepatic immune cells were identified using specific cell surface and nuclear antibody markers and their spatial localisation evaluated using multiplex immunofluorescence on formalin fixed paraffin embedded (FFPE) liver sections.

Results: Based on the FACS analysis results, it was observed that the overall leukocyte population has drastically increased as the disease progressed from liver fibrosis to HCC in comparison to non-treated livers. Among the leukocytes, myeloid cell populations decreased due to a drastic loss of the Kupffer cell (KC) population during the disease progression, while infiltrating monocyte-derived macrophages, monocytes, and granulocyte populations increased. The lymphocyte population increases which seems to be related to an overall increase of the CD4⁺ T cell population than the one of CD8⁺ T cells. Our multiplex immunofluorescence results suggest that all the immune cell populations were distributed near the central vein, which is the site of inflammation in fibrotic mice liver. In HCC liver, immune cells like CD8T cells and granulocytes were found more within the tumor tissue, the hepatic macrophages were distributed throughout the liver parenchyma while Tregs, were more abundant in the invasive margin of the tumor and in the remaining tissue.

Conclusion: By FACS analysis, we observed that the overall populations of different immune cells had significantly dysregulated. By multiplex fluorescence staining the majority of the immune cells were identified to be distributed at the site of inflammation in fibrosis group. In HCC livers, the different immune cell populations were heterogeneously distributed within the tumor, the invasive margin of the tumor or the remaining parts of the liver tissue based on their specific pro-inflammatory and anti-inflammatory properties.

SAT-538-YI

Differential phenotypes of $\gamma\delta$ T cells in hepatitis E virus infection: implications for disease pathogenesis

Erich Freyer^{1,2,3,4,5}, Roni Souleiman^{1,2,3,4,5}, Severin Wulf^{1,2,3,4,5}, Katja Steppich^{1,2,3,4,5}, Patrick Behrendt^{1,2,3}, Heiner Wedemeyer^{1,3,5}, Anke R.M. Kraft^{1,2,3,4,5}, Markus Cornberg^{1,2,3,4,5}. ¹Hannover Medical School, Department of Gastroenterology, Hepatology, Infectious Diseases and Endocrinology, Hannover, Germany; ²Twincore-Centre for Experimental and Clinical Infection Research, Hannover, Germany; ³German Center for Infection Research (DZIF), Hannover, Germany; ⁴Centre for Individualised Infection Medicine (CiM), Hannover, Germany; ⁵Cluster of Excellence Resolving Infection Susceptibility (RESIST, EXC 2155), Hannover Medical School, Hannover, Germany
Email: freyer.erich@mh-hannover.de

Background and aims: Hepatitis E virus (HEV) is a global health problem with diverse outcomes ranging from acute resolving infections to chronic hepatitis in immunosuppressed individuals, highlighting the role of the immune system in disease pathogenesis. Unconventional T cells such as $\gamma\delta$ T cells, which play a key role bridging innate and adaptive immunity, have been poorly studied in this context but may play a crucial role in the pathogenesis of HEV infection. The aim of this study was to investigate $\gamma\delta$ T cells at different stages of HEV infection, distinguishing between immunocompetent and immunosuppressed patients.

Method: A comprehensive analysis of blood $\gamma\delta$ T cells was performed in 29 patients (11 immunocompetent, 18 immunosuppressed) with acute, chronic, or resolved HEV infection at multiple timepoints and 15 healthy controls using spectral flow cytometry with 41 parameters.

Results: No significant differences in $\gamma\delta$ T cell frequencies were observed between HEV groups, but lower frequencies in acute HEV infection compared to healthy controls ($p < 0.05$). In immunosuppressed compared to immunocompetent HEV patients, the V δ 1/V δ 2 ratio was inverted, which was attributed to an increased number of V δ 1 T cells ($p < 0.005$). During acute HEV infection, $\gamma\delta$ T cell phenotypes differed with lower expression of PD-1, lower CXCR6 and higher NKG2A in immunosuppressed compared to immunocompetent patients ($p < 0.05$). Also, individuals with resolved HEV infection showed distinct $\gamma\delta$ T cell phenotypes, e.g. higher CD69 expression and TEMRA markers ($p < 0.05$) and fewer CD8⁺V δ 2⁺ T cells in immunosuppressed compared to immunocompetent patients ($p < 0.005$). Interestingly, in chronic HEV infection (exclusively immunosuppressed), V δ 1 T cell frequency correlated negatively with ALT ($p < 0.05$, $r = 0.55$), while V δ 1 subsets showed positive correlations with ALT (CD69/V δ 1, $p < 0.05$, $r = 0.54$), liver stiffness (CD69/V δ 1, $p < 0.05$, $r = 0.89$), and HEV RNA levels (CD103/V δ 1, $p < 0.005$, $r = 0.87$).

Conclusion: Pan $\gamma\delta$, V δ 1, and V δ 2 T cell subsets in the blood exhibit distinct phenotypes in immunocompetent and immunosuppressed patients across different stages of HEV infection. Particularly, V δ 1 T cell frequencies during chronic HEV infection, along with subset abundance and distinct phenotypes, correlate with markers of liver inflammation, fibrosis, and viral replication. These findings suggest that alterations in $\gamma\delta$ T cells may contribute to the immunopathogenesis of HEV infection.

SAT-539-YI

Sustained macrophage alterations during injury regression beget increased susceptibility to infections

Moritz Peiseler¹, Tashi Rastogi², Yuting Wang³, Bruna Araujo David², Felix Heymann³, Frank Tacke³, Paul Kubes². ¹Department of Hepatology and Gastroenterology, Charité Universitätsmedizin Berlin, Campus Virchow Klinikum and Campus Charité Mitte, Berlin, Germany, Berlin Institute of Health (BIH), Berlin, Germany, Berlin, Germany; ²Snyder Institute for Chronic Diseases, Cumming School of Medicine, University of Calgary, Calgary, Alberta, Canada, Calgary, Canada; ³Department of Hepatology and Gastroenterology, Charité Universitätsmedizin Berlin, Campus Virchow Klinikum and Campus Charité Mitte, Berlin, Germany, Berlin, Germany
Email: moritz.peiseler@gmx.de

Background and aims: The liver is the body's central microbial filter preventing spread of blood-borne pathogens. Kupffer cells (KCs) are the most abundant population of tissue resident macrophages and filter >90% of disseminated bacteria within minutes from the circulation. During liver fibrosis, sinusoidal KCs dramatically change their phenotype, lose their identity and their function. In response, monocytes invade the liver to form KC-like syncytia that compensate for loss of sinusoidal KC function. Chronic liver diseases in patients are characterised by phases of disease activity and disease regression, currently not adequately addressed in rodent models. Thus, it is unclear how the KC compartment responds to injury regression.

POSTER PRESENTATIONS

Method: Using a mouse model of chronic hepatotoxicity with carbon tetrachloride followed by regression of hepatic injury, monocyte and macrophage lineage tracing tools, intravital microscopy and multiplex flow cytometry, we investigated the liver macrophage compartment during injury regression.

Results: Liver architecture and liver damage completely resolved in regression. Surprisingly, we found sustained alterations of the macrophage compartment that included differences in KC identity molecules such as CRIg and TIM-4. Functionally, bacterial capture and survival was impaired in regression compared to control mice. Flow cytometric profiling revealed the sustained presence of monocyte-derived KCs. Lastly, we found a novel macrophage subset expressing the markers MerTK, CD68, CD86 and PD-L1.

Conclusion: Our results demonstrate sustained alteration of the liver macrophage compartment during injury regression, favouring injury repair over antimicrobial responses thus leaving the host vulnerable to infections.

SAT-540-YI

TIGIT + Tregs maintain tolerance in autoimmune hepatitis via CTLA-4 dependent suppressive mechanism

Amber Bozward¹, Grace Wootton¹, Rémi Fiancette¹, Ye Htun Oo^{1,2,3}.

¹Centre for Liver and Gastrointestinal Research, University of Birmingham, Birmingham, United Kingdom; ²Liver Transplant and Hepatobiliary Unit, University Hospitals Birmingham NHS Foundation Trust, Birmingham, United Kingdom; ³European Reference Network Centre-Centre for Rare Disease, University Hospitals Birmingham NHS Foundation TRUST, Birmingham, United Kingdom
Email: a.g.bozward@bham.ac.uk

Background and aims: Immune checkpoint inhibitor, TIGIT, is expressed on T regulatory cells (Tregs). TIGIT⁺Tregs are reported as a highly suppressive subset of Tregs but the mechanism behind the suppressive abilities is unknown. We explore this mechanistic aspect aiming to apply TIGIT⁺Tregs as a potential therapy in autoimmune hepatitis.

Method: Deep immune-phenotypic characterisation of TIGIT⁺Tregs cells in peripheral blood samples (autoimmune hepatitis [AIH, N = 12], chronic immune mediated liver diseases control [N = 7], and healthy volunteers [N = 10]) was investigated with multi-colour flow cytometry. Suppressive capacity of TIGIT⁺Tregs was assessed with expanded and cell-sorted TIGIT⁺Tregs and TIGIT⁻Tregs co-cultured with matched responder CD4 T cells (N = 3). Abatacept was applied to block CTLA-4 pathway of TIGIT⁺Tregs suppressive mechanism. In addition, we examined the effect of TIGIT agonist on TIGIT⁺Tregs proliferation and functional markers of suppression (N = 3).

Results: TIGIT expression is observed on 41.53% ± 31.88 of Tregs in AIH blood. TIGIT⁺Tregs significantly upregulate liver sinusoidal recruitment chemokine receptor (CXCR3, p = 0.0002), biliary localisation chemokine receptor (CCR6, p < 0.0001), hepatic migration and peribiliary localisation integrin (VLA4, p < 0.0001) and tissue residency (CD69, p < 0.0001) markers compared to TIGIT⁻Tregs. Immunohistochemistry of AIH explant liver shows that the expression of TIGIT is within the hepatic sinusoid and lobular and interphase hepatitis inflammatory infiltrates. TIGIT⁺Tregs express significantly higher CTLA-4 (p = 0.0246) and FoxP3 (p < 0.0001) compared to TIGIT⁻Tregs in autoimmune blood. TIGIT agonist upregulates CTLA-4 and FoxP3, on TIGIT⁺Tregs but does not have an impact on cell proliferation. TIGIT agonist leads to plasticity of TIGIT⁺Tregs by increasing TNFα, however, cells remain suppressive. In addition, we demonstrate that TIGIT⁺Tregs are more suppressive than TIGIT⁻Tregs via a CTLA-4 dependent pathway and the use of Abatacept reduces their suppressive ability.

Conclusion: We have identified CTLA-4 as a mechanism of suppression in TIGIT⁺Tregs. TIGIT agonist enhances expression of CTLA-4 and FoxP3 on TIGIT⁺Tregs suggesting TIGIT agonist as a potential therapeutic option for AIH patients.

SAT-541

High-dimensional spectral flow cytometry defines changes in circulating immune cell composition and responsiveness in patients with cirrhosis-associated immune dysfunction

Malgorzata Grzelka¹, William Cambridge¹, Guiquan Jia², Dario Nicetto², Nandhini Ramamoorthi², Jonathan Fallowfield^{1,3,4}, Prakash Ramachandran¹. ¹Centre for Inflammation Research, The University of Edinburgh, Edinburgh, United Kingdom; ²Genentech, South San Francisco, United States; ³Institute for Regeneration and Repair, University of Edinburgh, Edinburgh, United Kingdom; ⁴Institute for Regeneration and Repair, Centre for Inflammation Research, Edinburgh, United Kingdom

Email: grzelka.m@doctors.org.uk

Background and aims: Cirrhosis-associated immune dysfunction (CAID) represents the paradigm of aberrant immune responses as chronic liver disease (CLD) progresses. Clinically, this manifests in cirrhotic patients being prone to infections, resulting in significant mortality and morbidity. Whilst alterations of individual immune cell populations have been reported in CAID, a comprehensive assessment of changes in the composition and function of all major immune cell compartments is lacking. To address this, we utilised the advances in spectral flow cytometry to perform high-parameter analysis of circulating immune cell groups at differing stages of CLD.

Method: A panel of 23 antibody-fluorophore combinations was created for application on 100 µL of whole blood and analysis on a 3-laser Cytek Aurora spectral flow cytometer. Absolute cell count per millilitre of whole blood was established for each cell type. To assess functional responses, we developed a 27-colour panel, including intracellular cytokine staining for a stimulation assay with 6 different TLR ligands. Four study groups were defined as: healthy controls, non-cirrhotic CLD (fibrosan reading < 10 kPa in the absence of other signs of cirrhosis), compensated advanced CLD (cACLD, fibrosan ≥ 10 kPa without clinical signs of decompensation) and decompensated advanced CLD (dACLD, clinical signs of decompensation regardless of fibrosan).

Results: Samples from 13 controls, 17 non-cirrhotic CLD (9 PBC, 8 MASLD, fibrosan mean ± SEM 6.7 ± 0.3 kPa), 59 cACLD (31 MASLD, 16 ALD, 7 other, 5 PBC, 20.3 ± 1.9 kPa) and 20 dACLD (7 MASLD, 6 ALD, 6 PBC, 1 PSC) patients were analysed. We were able to identify and enumerate all major circulating immune cell populations. Quantitation of absolute cell numbers demonstrated significant reductions in CD8⁺ (cytotoxic), CD4⁺CD45RA⁺ (naïve), NKT and gamma delta T cells in patients with dACLD, independent of sex and aetiology. In contrast, numbers of circulating neutrophils, B cells and monocyte subpopulations were not significantly different by CLD stage. Functionally, dACLD CD14⁺ monocytes (n = 8) were activated at baseline compared to cACLD (n = 5) as evidenced by increased IL-1β expression (p < 0.005), and a trend towards increased expression of IL-6 and TNF-α. Stimulation with TLR2 or TLR7/8 agonists (but not TLR3, TLR4, TLR5 or TLR9) showed attenuated upregulation of IL-1β in dACLD monocytes, indicating impaired responsiveness to certain TLR ligands in CAID.

Conclusion: Our high-dimensional spectral flow cytometry method allows for a comprehensive assessment of circulating immune cell composition and function from small sample volumes. This approach has identified loss of multiple circulating T cell subpopulations and aberrant monocyte responses to TLR ligands as key features of CAID. Future work will focus on understanding how these features evolve longitudinally as CLD progresses.

SAT-542

Macrophage Dvl2-HSF1 axis regulates STING-mediated innate immunity and hepatocyte death in liver ischemia and reperfusion injury

Tao Yang¹, Dongwei Xu¹, Xiaoye Qu¹, Mingwei Sheng¹, Yuanbang Lin¹, Xiao Wang¹, Christopher King¹, Jun Li², Longfeng Jiang², Qiang Xia³, Douglas Farmer¹, Bibo Ke¹. ¹The Dumont-UCLA Transplant Center,

Department of Surgery, David Geffen School of Medicine at UCLA, Los Angeles, United States; ²Department of Infectious Diseases, the First Affiliated Hospital, Nanjing Medical University, Nanjing, China; ³Department of Liver Surgery, Renji Hospital, Shanghai Jiaotong University School of Medicine, Shanghai, China
Email: taoyang@mednet.ucla.edu

Background and aims: Dishevelled 2 (Dvl2) is a member of the Wntless/Wnt signaling pathway that regulates cell proliferation, survival, and migration. However, whether macrophage Dvl2-HSF1 signaling may regulate STING function and cell death in oxidative stress-induced liver inflammatory injury is unknown.

Method: A mouse model of hepatic ischemia/reperfusion injury (IRI), the primary hepatocytes, and bone marrow-derived macrophages were used in the myeloid-specific Dvl2 knockout (Dvl2^{M-KO}) and Dvl2-proficient (Dvl2^{FL/FL}) mice.

Results: Dvl2^{M-KO} exacerbated IR stress-induced liver damage with increased serum ALT/AST levels, macrophage/neutrophil infiltration, and proinflammatory mediators compared to the Dvl2^{FL/FL} controls. Notably, Dvl2^{M-KO} inhibited HSF1 and promoted STING, NLRP3, caspase-1, p65 NF- κ B, RIPK3, and p-MLKL, with increased IL-1 β levels in IR-stressed livers compared to the Dvl2^{FL/FL} controls. Interestingly, IR stress increased macrophage Dvl2 and HSF1 nuclear translocation in ischemic livers. Chromatin immunoprecipitation (ChIP) coupled with massively parallel sequencing (ChIP-Seq) revealed that macrophage Dvl2 colocalized with HSF1 and activated its target gene *eEF2*. Activation of HSF1 augmented *eEF2* and inhibited STING, NLRP3, caspase-1, and NF- κ B function. However, disruption of macrophage *eEF2* enhanced STING, NLRP3, caspase-1, and NF- κ B activity, with increased hepatocyte RIPK3 and p-MLKL expression, ROS production, and LDH release after macrophage/hepatocyte co-culture.

Conclusion: Disruption of macrophage Dvl2 activates STING and induces hepatocyte death in IR-stressed livers. The Dvl2 interacts with HSF1 and regulates HSF1 target gene *eEF2* function, which is crucial for the control of STING and RIPK3-mediated necroptotic cell death. Our findings underscore a novel role of macrophage Dvl2 in oxidative stress-induced liver inflammation and cell death, implying the potential therapeutic targets in liver inflammatory diseases.

SAT-543

The surface antigens of circulating small extracellular vesicles, as non-invasive markers of the immune mechanisms involved in liver diseases according to etiology

Albert Guinart-Cuadra^{1,2}, Anna Brujats³, Manuel de la Torre⁴, Rubén Osuna-Gómez¹, Elisabet Cantó¹, Maria Poca⁵, Eva Roman⁶, Javier Fajardo⁷, Eva Santamaria⁸, German Soriano⁵, Cándid Villanueva⁹, Àngels Escorsell⁵, Cristina Gely⁷, Josep Maria Argemi¹⁰, Delia D'Avola¹⁰, Silvia Vidal¹, Edilmar Alvarado-Tapias^{5,11}. ¹Inflammatory Diseases, Biomedical Research Institute Sant Pau (IIB Sant Pau), Barcelona, Spain; ²Inflammatory Diseases, Institut de Recerca de l'Hospital de la Santa Creu i Sant Pau, Biomedical Research Institute Sant Pau (IIB Sant Pau), Barcelona, Spain; ³Hospital de la Santa Creu i Sant Pau, Sant Pau Research Institute, Autonomous University of Barcelona, Department of Gastroenterology, Barcelona, Spain, Barcelona, Spain; ⁴Unidad de Hepatología, Clínica Universidad de Navarra, Departamento de Medicina Interna, Clínica Universidad de Navarra, Pamplona, Spain; ⁵Department of Gastroenterology, Hospital de la Santa Creu i Sant Pau, Institut de Recerca Hospital de Sant Pau-IIB Sant Pau, Universitat Autònoma de Barcelona, CIBERehd, Barcelona, Spain; ⁶Department of Gastroenterology, Hospital de la Santa Creu i Sant Pau, Institut de Recerca Hospital de Sant Pau-IIB Sant Pau, Universitat Autònoma de Barcelona, CIBERehd, Barcelona, Spain, Barcelona, Spain; ⁷Biomedical Research Networking Center for Hepatic and Digestive Diseases (CIBERehd), Carlos III Health Institute, Madrid, Spain, Barcelona, Spain; ⁸University of Navarra, Center for Applied Medical Research (CIMA), Hepatology Laboratory, Centro de Investigación Biomédica en Red de

Enfermedades Hepáticas y Digestivas (CIBERehd), Pamplona, Spain; ⁹Department of Gastroenterology, Hospital de la Santa Creu i Sant Pau, Institut de Recerca Hospital de Sant Pau-IIB Sant Pau, Universitat Autònoma de Barcelona, CIBERehd, Barcelona, Spain; ¹⁰Liver Unit, Hepatology Program, Clínica Universidad de Navarra, CIMA Universidad de Navarra, Centro de Investigación Biomédica en Red de Enfermedades Hepáticas y Digestivas (CIBERehd), Pamplona, Spain; ¹¹Inflammatory Diseases, Biomedical Research Institute Sant Pau (IIB Sant Pau), 08041 Barcelona, Spain, Barcelona, Spain
Email: ealvaradot@santpau.cat

Background and aims: Circulating small extracellular vesicles (sEVs) represent intercellular communication where the donor cell defines the surface antigen composition. Metabolically dysfunction-associated steatotic liver disease (MASLD) and alcohol-associated liver disease (ALD) currently stand as the leading causes of hepatopathy. Characterizing the surface antigens of sEVs may reflect the primary immune mechanisms involved in the pathogenesis of liver diseases. This study aims to characterize the quantity and the surface antigen profile in two cohorts of liver diseases: MASLD vs Alcoholic Hepatitis (AH).

Method: Consecutively and prospectively, metabolically dysfunction-associated steatotic liver disease (MASLD) (Clínica Universidad de Navarra) and patients with alcoholic hepatitis (AH) (Hospital de la Santa Creu i Sant Pau) were included. Blood samples were collected for the study of small extracellular vesicles (sEVs) in plasma, through quantification by flow cytometry (FC) MQ16 (staining with CFSE, CD81-CD9), NTA (NanoSight) and CryoME. The antigen characterization was performed using conventional flow cytometry with MACSplex kit.

Results: A total of 45 patients with MASLD and 39 patients with AH with cirrhosis were included. Patients MASLD have lower peripheral plasmatic sEVs ($27.5 \pm 18.10 \times 10^9$ particle/ml) with significantly higher expression of endothelial-epithelial-lymphocytic and monocytic origin antigens (CD133, CD19, CD20, CD326, CD14, CD24, CD69) in sEVs, unlike patients with MASLD patients with AH have significantly higher peripheral plasmatic sEVs ($78.63 \pm 33.59 \times 10^{11}$ particle/ml) with higher expression of endothelial-epithelial-monocytic and platelet origin antigens (CD133, CD326, CD14, CD49e, CD41b, CD62p, CD42a, CD31). However, despite being etiologically and clinically different, both groups share endothelial-epithelial and monocytic origin antigens (CD133, CD326, CD14). Differentially, AH has a higher expression of platelet antigens. It is possible that from the early stages of MASLD, there is damage not only to the endothelium but also to increased activation of the immune system, which is even more pronounced in different and more advanced scenarios such as AH, where platelet involvement should be further explored.

Conclusion: Circulating sEVs exhibit a distinct surface antigen pattern based on the etiology of liver disease. The characterization of surface antigens allows the identification of early endothelial and monocytic involvement in patients with MASLD, contrasting with platelet involvement in patients with AH. Characterizing the content of sEVs may elucidate the specific cargo according to etiology and open therapeutic possibilities for immune system regulation.

SAT-544

Study on the role of natural killer cells in chronic hepatitis B patients treated with intermittent interferon therapy

Xiaoyue Bi¹, Tingting Jiang¹, Shiyu Wang¹, Ziyu Zhang¹, Xinlin Li¹, Yao Xie^{1,2}, Minghui Li¹. ¹Department of Hepatology Division 2, Beijing Ditan Hospital, Capital Medical University, Beijing, China; ²Department of Hepatology Division 2, Peking University Ditan Teaching Hospital, Beijing, China
Email: wuhm2000@sina.com

Background and aims: To investigate the changes of phenotype, frequency and related cytokines of Natural killer (NK) cells in Chronic

POSTER PRESENTATIONS

hepatitis B (CHB) patients during intermittent treatment with Interferon (IFN).

Method: CHB patients were enrolled and divided into initial treatment group, HBsAg level decreased in interferon treatment group and oral nucleoside (acid) antiviral therapy group according to different conditions of antiviral therapy. After improving the baseline examination, patients in the initial treatment group were treated with IFN alpha. For patients whose HBsAg reached a plateau after IFN alpha treatment, IFN therapy was stopped and restarted after an interval of 12–24 weeks. The oral medication group continued to use the original treatment plan. For the initial treatment group, before IFN treatment, 4 weeks of treatment and 12–24 weeks of treatment; hepatitis B virus virologic, serological and biochemical data were collected when IFN was stopped, before IFN again after a 12–24 weeks interval and at 12–24 weeks after IFN again.

Results: A total of 207 patients with chronic hepatitis B were included, including 68 in the initial treatment group, 50 in the HBsAg lowering platform group and 89 in the oral administration group. At baseline, compared with patients in the initial treatment group, patients in the HBsAg decline plateau stage had lower frequency of CD56^{dim} subgroup and higher frequency of CD56^{bright} subgroup ($p < 0.001$). During IFN treatment, HBsAg level in the initial treatment group showed a downward trend. After 4 weeks of IFN treatment and 12–24 weeks of IFN treatment, the frequency of CD56^{dim} cells decreased significantly ($p = 0.024$; $p < 0.001$), active molecule NKG2D was significantly decreased at 4 weeks of treatment ($p = 0.021$), active molecule NKG2C was significantly decreased at 12–24 weeks of treatment ($p < 0.001$), and inhibitory molecule NKG2A was significantly increased at 12–24 weeks of treatment ($p < 0.001$). The frequency of CD56^{bright} subgroup was increased, and the inhibitory molecule NKG2A and activating molecule NKG2D in CD56^{bright} subgroup were significantly increased ($p < 0.01$).

Conclusion: In CHB patients who have reached a plateau with IFN treatment, intermittent retreatment mode can achieve significant clinical efficacy, which is of clinical significance. During IFN treatment, the CD56^{dim} subgroup responsible for killing effect of NK cells decreased, while the frequency of CD56^{bright} subgroup responsible for cytokine secretion increased. However, the activity of the two subgroups were inhibited to varying degrees, which may be related to the emergence of the plateau period. In the course of IFN treatment, the immune environment, the antiviral effect of immune cells and the pathogenic effect of HBV have been dynamically changing, and the dynamic balance between the two effects may be the cause of the plateau period.

SAT-545

Th2 cell activation in chronic liver disease is driven by local IL-33 and contributes to IL-13 dependent fibrogenesis

Johanna Reißing¹, Marie-Luise Berres¹, Pavel Strnad¹, Alexander Wree², Christian Trautwein³, Tony Bruns³, Zimmermann Henning Wolfgang³. ¹Department of Internal Medicine III, Aachen, Germany; ²Department of Gastroenterology/Hepatology, Berlin, Germany; ³Department of Internal Medicine III, University Hospital RWTH Aachen, Aachen, Germany
Email: joreissing@ukaachen.de

Background and aims: The role of type 2 immune responses is well known for parasite infections caused liver fibrosis, but their role in other liver diseases remains unclear. This study aims to elucidate mechanisms involving Th2 T cell polarization, activation, and recruitment in human liver fibrosis and cirrhosis.

Method: Human liver tissues, cells and serum were analysed by qRT-PCR, ELISA, FISH, immunostaining, flow cytometry and in vitro functional assays. Investigations focused on cellular interactions and soluble mediators influencing T cell polarisation and recruitment, and their impact on hepatic stellate cell (HSC) activation, proliferation and extracellular matrix synthesis.

Results: Human liver fibrosis exhibited a stage-dependent increase in Th2-related transcription factors, Th2 cytokines, and GATA3-expressing T cells, peaking in cirrhotic livers. The alarmin IL-33 was elevated in cirrhotic livers and sera, acting as a chemotactic agent for Th2 cells and inducing type 2 polarization of CD4⁺ T cells. IL-33 originated from oval cells, liver sinusoidal endothelial cells, intrahepatic macrophages, and migrating monocytes. IL-33-activated T cells, not IL-33 alone, induced HSC activation, evidenced by Ki67 and α -SMA staining, increased COL1A1 mRNA expression, and wound healing assays. The pro-fibrotic effect was contact-independent and countered by monoclonal antibodies against IL-13.

Conclusion: In patients with chronic liver disease, the alarmin IL-33 facilitates the recruitment and activation of CD4⁺ T cells with Th2-like properties, triggering paracrine HSC activation in an IL-13-dependent manner, thereby promoting fibrogenesis.

SAT-546

Elevated IL18R+CD8+T cells in Autoimmune Hepatitis patients are associated with a worse therapy response

Katharina Yankouskaya¹, Ida Allabauer¹, Grace Wootton², Naomi Richardson², Amber Bozward², Peter Dietrich³, Markus F. Neurath³, Joachim Woelfle¹, André Hoerning¹, Ye Htun Oo². ¹Pediatric Gastroenterology and Hepatology, Department of Pediatrics and Adolescent Medicine, University Hospital Erlangen, Friedrich-Alexander-University Erlangen-Nuremberg, Erlangen, Germany; ²Centre for Liver and Gastroenterology Research, Institute of Immunology and Immunotherapy, University of Birmingham, Birmingham, United Kingdom; ³Medicine 1, University Hospital Erlangen, Friedrich-Alexander-University Erlangen-Nuremberg, Erlangen, Germany
Email: kyankouskaya@gmail.com

Background and aims: Autoimmune hepatitis (AIH) patients who do not achieve complete biochemical remission with current first-line and second line therapy face a worse prognosis and outcome. The Interleukin 18 Receptor (IL18R) has mostly been described on T cells and has been linked to different autoimmune diseases, making it an interesting target in autoimmune liver diseases. Our aim is to investigate the pathophysiology behind therapy responders (RS) and non-responders (NRS) in AIH, focusing on the role of IL18R+CD8+ T cells.

Method: Initially, Nanostring mRNA analysis of 8 treatment naïve AIH type I patients (4 RS and 4 NRS), and 4 nonhepatitis controls was performed. Liver derived lymphocytes and peripheral mononuclear blood cells (PBMCs) were freshly isolated from human liver explant samples (with established ethics, University of Birmingham) of 4 patients (Primary Biliary Cholangitis (n=1), Primary Sclerosing Cholangitis (n=1), Alcohol-related Liver Disease (n=2)), and 3 unused donor explants as well as peripheral blood samples of 5 AIH RS and 5 AIH NRS patients undergoing treatment and 5 control blood were analysed with Flow Cytometry (FC). PBMCs were either analysed immediately, stimulated overnight with CD3/CD28, or stimulated with cytokines IL18, IL12 or IL18 and IL12 for 5 days and subsequently analysed.

Results: The Nanostring data suggested increased mRNA levels of IL18R in AIH RS compared to AIH NRS ($p < 0.05$). In the unstimulated FC analysis, there was a tendency of an increased frequency of IL18R on CD8⁺ T cells in AIH NRS compared to AIH RS in blood ($p = 0.051$). However, in the liver this tendency in significance was lower in disease livers compared to unused donor livers ($p = 0.057$). After CD3/CD28 stimulation, the frequency of an inflammatory CD8⁺ T cells subset, with IL18R and Tumor Necrosis Factor alpha (TNF α) double positive cells, was higher in NRS than RS or control patients. Also, following IL12 and combined IL12/IL18 stimulation, the frequency of IL18R on CD8 was increased in NRS rather than in RS ($p < 0.005$) and control. Similarly, the frequency of IL18R expression on CD39+CD8+, CD69+CD8+, Ki-67+CD8+, Cytotoxic T-lymphocyte-associated Protein 4 (CTLA-4) +CD8+, Interferon gamma (IFN γ)+CD8+ and T cell

immunoreceptor with Ig and ITIM domains (TIGIT)+CD8⁺ cells was upregulated in NRS compared to RS and HFE patients (all $p < 0.01$). **Conclusion:** IL18R+CD8⁺ T cells seem to be expanded in AIH NRS in blood and seem to display a more exhausted (CTLA-4, TIGIT, CD39) and activated (CD69) phenotype after cytokine stimulation. However, these T cells still appear to be able to secrete inflammatory cytokines such as IFN γ and express high proliferative capacity (Ki-67), thus possibly being at least in part responsible for therapy nonresponse in these patients. Further research in this area is required to better understand the mechanisms behind these pathways and functions of these cells.

SAT-547

Mendelian randomization strengthens the crosstalk of immune traits with primary biliary cirrhosis and primary sclerosing cholangitis

Jing Xu¹, Jie Hao², Ning Ling¹, Ming-Li Peng¹. ¹Department of Infectious Diseases, Key Laboratory of Molecular Biology for Infectious Diseases (Ministry of Education), Institute for Viral Hepatitis, the Second Affiliated Hospital, Chongqing Medical University, Chongqing, China, Chongqing, China; ²Department of Oncology, Southwest Hospital, Third Military Medical University (Army Medical University), Chongqing, China, Chongqing, China
Email: peng_mingli@hospital.cqmu.edu.cn

Background and aims: Immune cells play a crucial role in the onset and progression of liver diseases. However, it is unclear whether the link is merely correlative or orchestrated by causative mechanistic interactions. This study aims to investigate the causal relationship between immune cells and liver diseases using genetic data and Mendelian randomization (MR).

Method: We performed two-sample bidirectional Mendelian randomization (MR) analyses to explore the causal associations between 731 immunophenotypes and 4 liver diseases. Namely, primary biliary cirrhosis (PBC), primary sclerosing cholangitis (PSC), autoimmune hepatitis (AIH) and alcoholic liver disease (ALD) comprehensively sensitive analyses were followed to validate the robustness of results.

Results: After FDR correction, forward MR indicated the following associations remained significant: CD27 on CD24⁺ CD27⁺ (OR = 1.13, PFDR = 0.017), CD27 on IgD⁺ CD38dim (OR = 1.149, PFDR = 0.007), CD27 on IgD⁺ CD24⁺ (OR = 1.209, PFDR = 0.007), CD27 on sw mem (OR = 1.147, PFDR = 0.010), CD27 on unsw mem (OR = 1.162, PFDR = 0.008) may be associated with a higher risk of PBC. CD28 on resting Treg (OR = 0.724, PFDR = 0.004) and CD20-%B cell (OR = 0.806, PFDR = 0.011) had a protective effect on PSC and ALD, respectively. Five immunophenotypes had suggestive association with AIH. In the reverse MR analysis, five immunophenotypes were genetically predicted to be down-regulated in PBC, whereas six were predicted to be up-regulated in PSC. There was no evidence of reverse causality of AIH and ALD on immunophenotype.

Conclusion: This study provide evidence for a bidirectional causal relationship of immunophenotypes with PBC and PSC, which offers a new direction for the early detection of the two diseases and the possibility of developing treatment strategies.

SAT-548

Variations in dynamic T cell response are associated with the HCC recurrence treated with anti-PD-1 immunotherapy after interventional therapy

Yonghong Zhang¹, Tingting Mei², Kang Li³, Chaoran Zang⁴, Wenying Qiao⁴, Jianjun Li⁴, Wenying Qiao⁴, Ling Qin⁴, Caixia Hu⁴, Yinghua Zhang⁴, Chunwang Yuan⁴, Biyu Liu⁴, Yu Sun⁴. ¹Beijing YouAn Hospital, Capital Medical University, Beijing, China; ²Beijing YouAn Hospital, Capital Medical University, Beijing, China; ³Beijing YouAn Hospital, Capital Medical University, Beijing, China; ⁴Beijing YouAn Hospital, Capital Medical University, Beijing Tsinghua Changgung

Hospital, School of Clinical Medicine, Tsinghua University, Beijing, China
Email: mtt18813078830@163.com

Background and aims: Immune checkpoint inhibitors are essential to prevent the recurrence of primary liver cancer after interventional therapy, which is related to the changes in the immune status of the body. The purpose of this research is to demonstrate the association between the dynamic changes in immune response and recurrence in HCC patients who received anti-programmed cell death 1 (anti-PD-1) therapy.

Method: We selected 15 patients with a high risk of recurrence. All enrolled patients were initially treated with TACE combined with ablation and achieved complete remission, followed by anti-PD1 immunotherapy one month later. Peripheral blood samples were collected before each immunotherapy. Laboratory tests were performed on the patients once every 3W. The patients were followed up and divided into two groups according to the recurrence within one year. Then, Elispot assay was used to explore the difference of tumor-associated specific T cell responses between the two groups. Flow cytometry was used to detect the changes in T cell function.

Results: By flow cytometry and Elispot, we found that after PD1 blockade, the expression of PD1⁺CD8⁺ T lymphocytes in HCC patients was significantly reduced, and the expression of Perforin⁺CD8⁺ T lymphocytes and effector CD8⁺ T lymphocytes was increased greatly. Meanwhile, the magnitude of AFP-specific T cell immune response was decreased, and the frequency and magnitude of SMNMS-specific immune response had an increasing trend. In terms of prognosis, compared with the recurrence group, the non-recurrence group had less PD1⁺ CD8⁺ T lymphocytes, effector CD8⁺ T lymphocytes, and PD1⁺ effector CD8⁺ T lymphocytes, and continued to increase the expression of Perforin⁺CD8⁺ T lymphocytes. In addition, the shift of Th1/Th2 balance to Th2 is also associated with relapse.

Conclusion: This study demonstrates the important role of anti-PD1 immunotherapy in patients at high risk for recurrence of liver cancer and reveals that improvement in immune status is closely related to the prevention of recurrence.

SAT-549

Neutrophil-derived miRNA-223 modulates peritoneal immunity in patients with cirrhosis during spontaneous bacterial peritonitis

Mick Frissen¹, Johanna Reißing¹, Oluwatomi Ibidapo-Obe¹, Christian Trautwein¹, Tony Bruns¹. ¹University Hospital RWTH Aachen, Aachen, Germany
Email: mfrissen@ukaachen.de

Background and aims: MicroRNAs (miRNAs) play a pivotal role in modulating inflammatory responses and cell-cell interactions during bacterial infections. This study investigates the alterations in miRNA composition in patients with spontaneous bacterial peritonitis (SBP), identifies cellular sources, and assesses the functional consequences.

Method: Paired serum and ascitic fluid samples, obtained before and during SBP, were subjected to multiplex microRNA profiling. Regulated miRNAs were further validated using LNA miRNA PCR assays. The source of miRNA was assessed by measuring intracellular and supernatant concentrations using cultured neutrophils and mononuclear cells. Functional consequences of miRNA-223 were evaluated using co-culture assays and transfection of THP-1 cells.

Results: Multiplex microRNA profiling identified five miRNAs that were differentially regulated in ascitic fluid during SBP. qPCR validation confirmed the enrichment of miR-223 during SBP. While TLR4 ligation down-regulated miR-223 in peritoneal macrophages and did not affect the release into the supernatant, neutrophils could be identified as a potent source of extracellular miR-223. Peritoneal macrophages show an increased uptake of miR-223 and an increased inflammatory gene expression when cultured with supernatant from isolated neutrophils of SBP patients compared to healthy controls or patients without SBP. The effect of miR-223 on macrophage gene

POSTER PRESENTATIONS

expression was tested by transfection of differentiated THP-1 cells with miR-223-mimic.

Conclusion: During SBP, miR-223 is released from infiltrating neutrophils and is enriched in ascitic fluid. Peritoneal macrophages can take up neutrophil-derived miRNA, which may affect peritoneal inflammation, limit tissue damage, and shape subsequent immune responses in the peritoneal cavity.

SAT-550

Melatonin attenuates LPS-induced acute liver injury by reducing the formation of macrophage extracellular traps through upregulated sirtuin 4 expression

Jun Zheng¹. ¹*the Third Affiliated Hospital of Sun Yat-sen University, Guangzhou, China*

Email: zhengj67@mail2.sysu.edu.cn

Background and aims: Sepsis is a life-threatening systemic inflammatory response syndrome causing multiple organ system dysfunction including liver, namely sepsis-induced acute liver injury (SALI). Macrophages play a crucial role in the pathogenesis of SALI and the modulation of macrophages response can be used to alleviate SALI. However, no effective therapeutics are currently available for clinical application.

Method: In this study, we used lipopolysaccharides (LPS)-induced SALI mouse model and murine macrophage cell lines to uncover the role of macrophages in SALI and the therapeutic potential of melatonin for this model. Moreover, RNA-Seq, detecting mitochondrial function, and adeno-associated virus vector (serotype 2, AAV2) were utilized to analyze the mechanism of melatonin in regulating macrophage extracellular traps (METs) formation.

Results: We investigated the therapeutic efficacy of melatonin in SALI and attempted to explore its underlying basis. Through *in vivo* and *in vitro* studies, we showed that melatonin attenuated SALI by modulating the inflammatory response of intrahepatic macrophages and the formation of METs. Mechanistically, we identified that melatonin directly promoted Forkhead Box M1 (FOXM1) nuclear translocation and upregulated Sirtuin 4 (Sirt4) expression in macrophages. Sirt4 could bind to mitofusin-2 (MFN2) and control its acetylation level in response to MFN2 availability. This effect triggered mitochondrial fusion for repairing the mitochondrial functions and status followed by suppressing METs formation. Notably, the downregulation of macrophagic Sirt4 expression *in vivo* and *in vitro* weakened the hepatoprotective effect and the effect of modulating MET formation of melatonin on SALI.

Conclusion: These data provide pharmacological evidence indicating that melatonin could reduce intrahepatic METs formation to treat LPS-induced SALI by promoting mitochondrial fusion and restoring mitochondrial quality of macrophages through regulating FOXM1/Sirt4 signaling pathway to affect the acetylation level of MFN2.

SAT-551

F-actin in autoimmune liver diseases: a comprehensive evaluation of diagnostic potential using a newly-developed autoimmune liver line immunoassay

Christos Liaskos¹, Tanja Seifert², Eleni Patrikiou¹, Marco Kai³, Alexandra Tsirogianni⁴, Christina Tsigalou⁵, Dimitrios Bogdanos¹.

¹*University of Thessaly, Faculty of Medicine, Department of Rheumatology and Clinical Immunology, Larissa, Greece;* ²*Institute for Experimental Immunology, affiliated to EUROIMMUN Medizinische Labordiagnostika AG, Lubeck, Germany;* ³*Institute for Experimental Immunology, affiliated to EUROIMMUN Medizinische Labordiagnostika AG, Lubeck, Germany;* ⁴*Evangelismos General Hospital, Athens, Greece, Department of Immunology-Histocompatibility, Athens, Greece;* ⁵*Democritus University of Thrace Medical School Laboratory of Hygiene and Environmental Protection, Medical School, Alexandroupolis, Greece*

Email: bogdanos@uth.gr

Background and aims: Antigen-specific profiling assays simultaneously detecting the whole spectrum of AiLD-related autoantibodies

in autoimmune liver diseases (AILDs) such as autoimmune hepatitis (AIH) and primary biliary cholangitis (PBC) are in urgent need, but those so far developed do not allow the comprehensive and reliable analysis of the most frequent autoantibodies in AIH-1, namely smooth muscle autoantibodies against F-actin. The aim was to develop a new line immunoassay that detects disease-specific F-actin SMA for AIH-1 in addition to (CYP2D6) LKM, (FTCD) LC1 for AIH-2, (SepSecS) SLA for AIH, (M2-3E) AMA, (Sp100/PML) MND, (RLM) gp210 for PBC and overlapping features of AIH and PBC, and disease-related SS-A, Ro-52 and (CEN A/B) ACA and to compare its performance in relation to conventional immunofluorescence.

Method: Sera from a meticulously selected cohort of 396 samples including 170 AIH type I, 17 patients with overlapping features of AIH type I/PBC, 32 AIH type II, along with control groups (71 PBC-, 20 PSC-, 32 hepatitis C patients, 50 healthy controls), were employed for a comprehensive, thorough screening using a F-actin line blot (cut off 6; borderline 6–10; pos>10 AU/ml) and ELISA as well as immunofluorescence tests (Liver Kidney Stomach (LKS)- and VSM47 cells).

Results: F-Actin antibody positivity including borderline sera was present in 82.3% (140/170) of the AIH type I cohort (range 6–136 IU, mean \pm SD: 65.1 \pm 28.1) and remarkably in 100% (17/17) patients with overlap features of AIH-1/PBC (range 6–69 IU, mean \pm SD: 32.5 \pm 22.2) while the stringiest 11 AU/ml cut off for clear positive sera revealed F-actin reactivity in 68.2% AIH type I patients and were statistically more frequent in AIH-1 compared to AIH type II ($p < 0.001$), hepatitis C ($p = 0.003$), PBC ($p < 0.001$), PSC ($p < 0.001$) and HC ($p < 0.001$ with a specificity of 87.2% versus SMA negative healthy controls). Levels of F-actin abs were significant higher in AIH type I compared to all other patient groups and HCs ($p < 0.001$ for all comparisons). ELISA and immunofluorescence results supported the line blot results as concordance analysis, assessed through Cohen's kappa statistics, revealed moderate to substantial agreement between F-actin line blot and ELISA ($K = 0.75$) as well as immunofluorescence tests ($K = 0.57$ for VSM47 and $K = 0.51$ for LKS), highlighting the reliability of F-actin as a diagnostic marker.

Conclusion: The comprehensive evaluation underscores the promising diagnostic potential of F-actin in AILDs, particularly through line blot analysis which allows simultaneous detection of the great majority of AILDs specific and disease-related autoantibodies through the reliable detection of F-actin SMA in AIH-1 and AIH-1/PBC overlaps in isolation or in combination with indirect immunofluorescence.

SAT-554-YI

Cellular immunity changes induced by COVID-19 vaccines in patients with chronic liver disease

Carolina Palma¹, Mariana Moura Henriques¹, André Simão¹, Ana Godinho-Santos¹, Miguel Cardoso¹, Diogo Fernandes¹, Sofia Carvalhãna², Miguel Moura², João Gonçalves¹, Helena Cortez-Pinto^{2,3}, Rui E. Castro¹. ¹*Research Institute for Medicines (iMed.Ulisboa), Faculty of Pharmacy, Universidade de Lisboa, Lisbon, Portugal;* ²*Departamento de Gastroenterologia, Centro Hospitalar Universitário Lisboa Norte, Lisbon, Portugal;* ³*Clínica Universitária de Gastroenterologia, Faculdade de Medicina, Universidade de Lisboa, Lisbon, Portugal*

Email: carolina-palma@campus.ul.pt

Background and aims: Patients with chronic liver disease (CLD), particularly those with cirrhosis, exhibit increased risk of developing severe illness when infected with SARS-CoV-2, primarily due to their underlying immune dysfunction and coexisting conditions. As such, vaccination plays a crucial role in safeguarding this population. Here, to fully assess the efficacy and safety of COVID-19 vaccination in patients with CLD, we thoroughly characterized the cellular immune responses of these patients to COVID-19 vaccines.

Methods: Blood samples were systematically collected from patients with CLD and healthy volunteers at various intervals spanning one year after the initial administration of mRNA-1273, BNT162b2,

ChAdOx1, and Ad26.COV2.S vaccines. Peripheral blood mononuclear cells (PBMCs) were isolated and stained with a panel of 22 surface markers and a viability dye, allowing for the detection of 28 immune cell subsets. Immunophenotyping was determined by flow cytometry with acquisition on a four-laser Cytex Aurora[®] spectral analyzer. **Results:** Prior to vaccination, patients with CLD patients were already displaying fewer T cells and an increased number of B cells, comparing to healthy subjects. Within the T cell subsets, differences were significant for CD4⁺ T cells and the Naïve and Central Memory CD4⁺ subsets. At both 6-months and 1-year after vaccination, variances between groups were no longer observed. Rather, at 1-year post-vaccination, T, CD8⁺ and CD4⁺ cells, as well as monocytes, were found increased in both groups, suggesting that the vaccination is critical for inducing a strong cellular immune response. In patients with CLD, minor variations in the percentages of gated cells across the 3 time-points were found to relate with the underlying liver disease etiology and/or the specific vaccine that was administered. Finally, regarding COVID-19 infection in patients with CLD, variations in the percentage of gated cells before and at 1-year after vaccination were similar in almost all cell sub-types except for CD8⁺ T cells and NK cells, which were decreased prior to vaccination in subjects who became infected.

Conclusion: COVID-19 vaccines demonstrated robust immunogenicity in the CLD cohort, despite the differences observed in some cell populations prior to vaccination. Still, additional studies should ideally be performed to determine optimal vaccine strategies; and ascertain whether disease etiology and other disease-associated factors may influence cellular immunity responses to vaccination and/or COVID-19 vaccine efficacy and safety.

SAT-555

Global and Kupffer cell specific Nlrp3 inflammasome in-/activation greatly affects the inflammatory and metabolic progression of alcohol-related liver disease

Lukas Geisler^{1,2}, Marlene Kohlhepp¹, Jana Knorr-Klocke¹, Theresa Holtmann¹, Cornelius Engelmann¹, Frank Tacke¹, Alexander Wree¹. ¹Charité-Universitätsmedizin Berlin, Department of Hepatology and Gastroenterology, Berlin, Germany, ²Humboldt-Universität zu Berlin, Department of Biology, Berlin, Germany
Email: lukas.geisler@charite.de

Background and aims: The NLR family pyrin domain containing 3 (Nlrp3) inflammasome, an intracellular multi-protein complex forming in the presence of a variety of in or extrinsic danger signals, is central to immune response in disease and homeostasis. While its activation is initially pro-inflammatory, it induces an anti-inflammatory cascade to balance the consecutive response. Nlrp3 deficient animal models to study liver disease have been evaluated extensively, showing that it may cause aggravation as well as improvement of induced condition, hence has a heterogeneous impact warranting further studies. Therefore, we evaluated variants of genetically altered Nlrp3, either global deficiency, as well as Kupffer cell specific over and inactivation of the Nlrp3 inflammasome to compare its global and local function in Alcohol-related liver disease (ALD).

Method: Mice carrying a global Nlrp3 deficiency (Nlrp3^{-/-}), Kupffer cell (KC) specific over activation Clec4^{Nlrp3^{ki}}, and inactivation Clec4^{ASC^{flox}} were fed a combined Western Diet + Alcohol (A + WD) for 10 weeks. Ongoing evaluation of liver immune cell populations was performed using flow cytometry and multiplex protocols for histology, alongside extended serum analysis as well as quantitative evaluation of gene expression (qPCR).

Results: While serum AST and ALT remained unaltered when fed chow between all genotypes, we found elevated AST in Nlrp3^{-/-} and Clec4^{Nlrp3^{ki}} mice under A + WD, the latter showing a distinct lymphocytic immune cell infiltration and marked elevation of inflammatory genes e.g. IL-1 β , IL-6, TNF. Nlrp3^{-/-} additionally had a marked increase of serum triglycerides. When fed A + WD

Clec4^{ASC^{flox}} mice showed an increase in weight gain and liver/bodyweight composition alongside cholesterol and histological prevalent steatosis. Under A + WD conditions Sterol regulatory element-binding transcription factor 1 and Cytochrome P450 2A1 were significantly upregulated in Nlrp3^{-/-} mice, which was not found for the other genotypes. Clec4^{Nlrp3^{ki}} mice showed increased immune cell infiltration with pronounced T-cell receptor beta and lymphocyte antigen 6 family member G (Ly6G) positive cell populations, along with signs of fibrosis in Masson's trichrome staining.

Conclusion: The results of our experiments indicate the multifaceted role of the Nlrp3 inflammasome in experimental alcoholic liver disease. While Nlrp3^{-/-} mice had pronounced pathology including increased serum enzymes and IL-10 gene expression, Clec4^{ASC^{flox}} compared to wild type animals showed increased weight gain but hardly any inflammatory reaction towards A + WD. Hence, the role of Nlrp3 inflammasome in liver disease is not limited to its functionality in mediating Kupffer cell differentiation towards a pro or anti-inflammatory phenotype, but may also affect metabolic functions and the development of fibrosis.

SAT-556-YI

Altered immune responses and PD-L1 levels in children with portal hypertension

Tengfei Si¹, Bethany Tucker², Huihong Yu³, Fabiola Di Dato³, Xiaohong Huang³, Qing Shao³, Eirini Kyraia⁴, Yun Ma³, Tassos Grammatikopoulos⁵. ¹Institute of Liver Studies, King's College London, London, United Kingdom; ²King's College Hospital, Paediatric Department, London, United Kingdom; ³Institute of Liver Studies, King's College London, London, United Kingdom; ⁴King's College Hospital, King's College London, London, United Kingdom; ⁵King's College Hospital, Paediatric Department, London, United Kingdom
Email: tengfei.si@kcl.ac.uk

Background and aims: The role of immune dysregulation in children with portal hypertension (PHT) remains unclear. This study aims to delve into the altered immune responses and the immunomodulatory role of Programmed Death-Ligand 1 (PD-L1). By exploring how PHT influences the immune system in children, we seek to unravel the complexity of immune dysregulation in this condition.

Method: We studied a group of 55 children with PHT, stemming from portal vein thrombosis or chronic liver disease, and 15 healthy controls. Assays for plasma PD-L1, various cytokines, and immune biomarkers were conducted. Flow cytometry was used to assess immune cell phenotypes and functions in 33 PHT patients and 12 controls.

Results: PHT patients exhibited higher levels of plasma IFN- γ (95.62 pg/ml vs 25.28 pg/ml, $p=0.03$), PD-L1 (6281 pg/ml vs 454.2 pg/ml, $p=0.032$) and activation markers of M2 macrophage (CD163, 633.5 ng/ml vs 414.8 ng/ml, $p=0.002$; VCAM, 861 ng/ml vs 397.7 ng/ml, $p<0.0001$) compared to controls. PD-L1 levels positively correlated with pro-inflammatory (TNF- α , $R^2=0.8522$, $p<0.0001$; IFN- γ , $R^2=0.188$, $p=0.018$), anti-inflammatory (IL-4, $R^2=0.810$, $p<0.0001$) cytokines, and liver injury marker (MMP7, $R^2=0.423$, $p<0.0001$). Notably, a decrease in peripheral T cells, especially MAIT cells, and an increase in T cell exhaustion markers were observed. There was a significant reduction of CXCR3^{pos} T cells (32.5% vs 42.8%, $p=0.04$), while non-T cells showed altered PD-1 and CD38 expression. Additionally, PHT patients displayed an increase in immunosuppressive PD-1^{pos}CD39^{pos} cells within CD4^{pos} and CD8^{pos} T cell subsets and diminished IFN- γ and IL-17 production in MAIT cells. A positive correlation was established between the count of peripheral PD-1^{pos} non-T cells ($R^2=0.426$, $p<0.0001$), soluble CD25 levels ($R^2=0.7522$, $p<0.0001$), and PD-L1 plasma values.

Conclusion: This study unveils a distinctive pattern of immune dysregulation in pediatric PHT, characterized by T cell exhaustion and altered cytokine profiles. Elevated PD-L1 levels underscore its role in modulating the complex immune responses in PHT.

POSTER PRESENTATIONS

SAT-557-YI

Loss of fibronectin contribute to poor maturation of monocyte to resolving macrophages in acute and chronic liver injury

Sandeep Kumar¹, Dhananjay Kumar¹, Deepanshu Maheshwari¹, Sunidhi Diwakar², Nidhi Nautiyal³, Manisha Bhardwaj¹, Shiv Kumar Sarin¹, Anupam Kumar¹. ¹Institute of Liver and Biliary Sciences, New Delhi, India; ²Institute of Liver and Biliary Sciences, New Delhi; ³Institute of Liver and Biliary Sciences, New Delhi, India
Email: dr.anupamkumar.ilbs@gmail.com

Background and aims: Loss of liver macrophage number and their function have been shown to be associated with poor liver clearance in both acute and chronic liver injury; however, the underlying mechanism is not well defined. The extracellular matrix is a dynamic structural component of tissue and regulate cell behaviour during tissue repair and regeneration. In the current study, we aim to study the role of the liver matrix in the maturation of bone marrow derived monocytes into macrophages and their phenotypic polarisation as well as function.

Method: Human healthy (n = 4), acute liver failure (ALF; n = 5), and chronic liver disease (CLD; n = 5) decellularized liver Extracellular matrix (ECM) was used for label-free quantitative matrix proteome using LC-MS. The decellularized matrices were lyophilized and solubilized for in vitro culture of macrophages. Gelatin and human plasma fibronectin were dissolved and coated over the tissue culture plates (TCP) for monocyte-macrophage culture. Cellular parameters like maturation, phenotype, cytokine release, and functionality were studied by flow cytometry.

Results: To check whether liver ECM has any role in maturation, polarization, and functionality of macrophages, we cultured human peripheral blood monocytes over healthy, ALF, and CLD human liver ECM solution-coated and uncoated TCPs and found that cells cultured over healthy ECM has significant high expression of maturation marker (25f9; $p < 0.001$), resolving macrophage markers ($p < 0.05$; CD163, CD206), and anti-inflammatory cytokine IL-10 ($p < 0.001$), and lower expression of inflammatory cytokines TNF-alpha ($p < 0.01$) and IL-1beta ($p < 0.01$). To further identify the factors that are regulating macrophages, we did a proteomic analysis of decellularized healthy, ALF and CLD human liver ECMs and found that out of 277 shared proteins, fibronectin was downregulated in the ALF and CLD matrix proteomes. For validating the effect of fibronectin on macrophage regulation, we coated the TCP with fibronectin and cultured monocyte-macrophages over it. In-vitro culture of human macrophages over fibronectin showed significantly higher expression of 25f9 ($p < 0.001$), resolving macrophage markers CD163 ($p < 0.05$), CD206 ($p < 0.01$), and a significant increase in their phagocytosis ($p < 0.01$) and efferocytosis ($p < 0.001$) activity as compared to gelatin coated and TCP. Also, the expression of pro-inflammatory cytokines (TNF-alpha and IL-1beta, $p < 0.01$) was significantly lesser in the fibronectin group, while the expression of anti-inflammatory cytokines (IL-10) was significantly higher ($p < 0.001$) when cultured on fibronectin coated plates.

Conclusion: The loss of fibronectin in ALF and CLD may contribute to the loss of macrophage maturation and function. Providing fibronectin enriched matrix may serve as tool for macrophages polarisation for tissue engineering.

SAT-558

CD8⁺ effector T cells expressing low levels of CD127 upregulate GPR56 expression and reside in the hepatic autoimmune and inflammatory microenvironment

Rémi Fiancette¹, Ayma Asif¹, Ye Htun Oo^{1,2}. ¹Institute of Immunology and Immunotherapy, Centre for Liver and Gastrointestinal research, University of Birmingham, Birmingham, United Kingdom; ²Liver Transplant and Hepatobiliary Unit, University Hospitals Birmingham NHS Foundation Trust, European Reference Network Centre-Centre for Rare Disease, University Hospitals Birmingham NHS Foundation trust,

Birmingham, United Kingdom

Email: r.b.fiancette@bham.ac.uk

Background and aims: In contrast to liver cancer and viral hepatitis, little is known about the pathogenic or dysfunctional effector T cells within the proinflammatory microenvironment in inflammatory and autoimmune liver diseases.

Method: Bulk RNA-sequencing and flow cytometric analyses allowed us to identify a specific subset of CD8⁺ T cells in both blood and liver. Immunohistochemistry analysis was performed to detect cell localisation and ligand identification.

Results: We observed a CD8⁺ T cell subset which displays a low level of CD127 and CD160 expression. This population concomitantly upregulates the immune checkpoint GPR56 (25.76% ± 4.21), an adhesion G-protein-coupled receptor, whose ligand, type 3 collagen, is particularly abundant in fibrotic and cirrhotic livers. We performed multicolour flow cytometry analyses on liver-derived lymphocyte T cell populations isolated from end-stage diseased livers with different aetiologies (ALD, n = 2; MASH, n = 4; AIH, n = 1; PSC, n = 2) as compared to non-cirrhotic donor livers not suitable for transplantation (controls, n = 2). Another hallmark of this CD127^{lo} CD8⁺ T cell population is their low expression of the transcription factor TCF-1, consistent with their acquisition of effector properties, potentially sustaining persistent inflammatory processes. GPR56⁺ CD127^{lo} CD8⁺ T cell recruitment and concentration around the portal tract regions could be facilitated by the expression of CXCR3 and CCR6. Immunohistochemistry analysis suggested that these cells reside around fibrous septa expressing collagen 3 and may create a proinflammatory niche establishing a chronic inflammatory disorder. *Ex vivo* assays with flow cytometry staining will help characterise their proinflammatory cytokine (TNF α , IFN γ) and effector molecule (granzyme, perforin) secretion profile, alongside spatial transcriptomic analysis which will enable a deeper description of this newly discovered T cell subset.

Conclusion: We identified a new subset of CD127^{lo} CD8⁺ T cells with a pro-inflammatory cytokine profile and residency to fibrous stromal framework. These T cells may potentially be involved in the pathogenesis of autoimmune and inflammatory liver diseases.

Liver transplantation and hepatobiliary surgery – Basic

WED-008

Adipose tissue as a predictor of morbidity and mortality in patients listed for liver transplantation

Maxence Lepour¹, Delorme Alicia¹, Hubert Piessevaux¹, Pierre Trefois², Nicolas Lanthier¹, Géraldine Dahlqvist¹. ¹Cliniques Universitaires Saint-Luc, Department of Hepato-Gastro-Enterology, Brussels, Belgium; ²Cliniques Universitaires Saint-Luc, Department of Radiology, Brussels, Belgium
Email: max.lepour@gmail.com

Background and aims: Body composition plays a crucial role in the prognosis of liver diseases. However, recent studies have focused mainly on muscle parameters and less is known about the adipose tissue (AT) (=subcutaneous AT (SAT) and visceral AT (VAT)) in terms of prognosis. The aims of our work are to determine the impact of body composition on the morbidity/mortality of patients listed for liver transplantation (LT) and to assess the evolution of these parameters 6 months post-LT.

Method: This single-center prospective observational study screened adult patients who were assessed for LT from June 2021 to October 2023. Clinical data including nutritional and functional status, radiological assessment of muscular compartment and AT were performed at baseline and 6 months post-LT. Measures were

performed on abdominal CT scan at the third lumbar level (L3) using the Slice-O-Matic software. The composite outcome was defined as death and/or emergency admission to hospital. Uni- and multivariate Cox proportional hazard regressions were computed to identify predictors of morbidity and mortality. T-test investigated the evolution of variables between pre- and 6-months post-LT. Spearman correlations were also performed.

Results: We included 158 patients with a mean MELD score of 16 and a mean age of 54 years. 74% were males. 124 were cirrhotic, with alcohol-related cirrhosis in 49.2 and metabolic-associated cirrhosis in 11.3%. 35.2% were listed for hepatocellular carcinoma. During the study period, 58.2% of the patients were transplanted, 63% of them being assessed at 6-month post-LT. During the follow-up, 9, 5% died while waiting for LT, all being cirrhotic. There was at least one acute admission for 28.5%. In univariate analysis, the following variables were significantly associated with the composite outcome : MELD (HR 1.15; IC 1.1–1.201; $p < 0.005$), liver frailty index (LFI) (HR 2.73; IC 1.688–4.408; $p < 0.005$), density of SAT (HR 1.05; IC 1.028–1.072; $p < 0.05$), density of VAT (VAT; HR 1.04; 1.011–1.072, $p = 0.007$) and muscle density (HR 0.97; 0.956–0.987; $p < 0.005$). In multivariate analysis, only MELD and LFI were associated with outcome (HR: 1.14; IC1.078–1.20; $p < 0.005$ and HR: 2.054; IC 1.176–3.588; $p = 0.01$; respectively). Among body composition characteristics, density of SAT was the strongest predictive factor but didn't reach significance (HR 1.033, $p = 0.091$). There was a strong correlation between density of AT and the MELD score (SAT: $r = 0.598$, 95% CI 0, 4747–0, 6987, $p < 0.0001$; VAS: $r = 0.5615$, 95% CI 0, 4306–0, 6692, $p < 0.0001$). At the 6-month post-LT, density of SAT decreased significantly ($p < 0.005$), while density of muscle increased ($p = 0.019$).

Conclusion: High SAT density, compatible with tissue inflammation, is associated with complications on the LT list and improves after LT. However, the MELD score and LFI remain the most robust independent factors for morbidity/mortality.

WED-009

Cytomegalovirus specific polyfunctional t-cells control CMV reactivation, after liver transplantation

Ângela Carvalho-Gomes^{1,2}, Laura Martínez-Arenas^{1,3,4}, Iván Sahuco¹, Almudena Cubells¹, Marina Berenguer^{1,3,5}, F. Xavier Lopez-Labrador^{6,7}, Victoria Aguilera Sancho^{1,3}. ¹Hepatología y trasplante hepático, IIS La Fe, Hospital U. y P. La Fe, Valencia, Spain, Valencia, Spain; ²Ciber-EHD, Instituto De Salud Carlos III, Madrid, Spain; ³Ciber-EHD, Instituto De Salud Carlos III, Madrid, Spain, Madrid, Spain; ⁴Department of Biotechnology, Universitat Politècnica de València, Valencia, Spain, Valencia; ⁵Dep. Medicine, University of Valencia, Valencia, Valencia, Spain; ⁶Virology Laboratory, Genomics and Health Area, FISABIO-Public Health, Generalitat Valenciana, Valencia, Valencia, Spain; ⁷CiberESP Instituto De Salud Carlos III, Madrid, Spain, Madrid, Spain

Email: angela.carvalho@uv.es

Background and aims: Cytomegalovirus (CMV) viral load after liver transplantation (LT) is controlled by cell mediated immune responses (CMI). Quantification of CMV-specific T-cells may allow identifying patients that achieve spontaneous CMV control. In addition, CMI could be used to measure the state of immune-competence status of the patient, and thus useful as a biomarker to predict the risk of infections/reactivations, rejection and *de novo* tumors.

Method: Prospective post-LT clinical, virologic and immunological monitoring was carried out up to 1 year in a cohort of adult LT recipients (LT-R). CMV-specific responses were characterized using flow-cytometry multiparametric analyses.

Results: We analyzed 518 samples from 104 LT-R (83.65% R+, 16.35% R-). CMV reactivation occurred in 52 patients, 36 of which (69.23%) spontaneously controlled viral replication, while 33 had severe reactivation, 78.79% of which was developed in patients at low risk of CMV reactivation (7 in R- and 26 in R+). In pre-LT samples, 48.1% and 56.7% of the patients had detectable CMV-pp65 CD8+ or CD4+ T-

cell response, respectively (at least one cytokine). In contrast, only 24.0% or 16.3% had detectable CMV-specific CD8+ or CD4+ polyfunctional T-cells, respectively. Patients with CMV-specific CD4+ T-cells higher than 0.05% of total T-cells pre-LT had less CMV reactivation episodes ($p = 0.0018$), and less severe CMV events ($p = 0.0043$). Only patients with undetectable CMV-specific CMI pre-LT developed CMV infection and were diagnosed with severe CMV events. No statistically significant differences were detected between polyfunctional CMI driven by CD4+ and CD8+ T-cells in patients who developed a *de novo* tumor, an acute cellular rejection or other infections and those who did not.

Conclusion: While the quantitation of CMV-specific CMI, especially that driven by CD4+ T-cells, showed good diagnostic performance to predict CMV reactivation, it did not predict the development of other clinical events (other infections, *de novo* tumors and rejection). CMV-specific CMI may be a useful biomarker for spontaneous control of CMV reactivation to tailor antiviral treatment after LT.

WED-010

Functions and molecular mechanisms of metformin in ameliorating ischemia-reperfusion injury of steatosis liver by inhibiting ferroptosis

Rong Li¹. ¹the Third Affiliated Hospital of Sun Yat-Sen University, Guangzhou, China

Email: tsfnlr@163.com

Background and aims: Liver transplantation is the only effective treatment for end-stage liver disease. However, the shortage of donors seriously restricts the development of liver transplantation. In recent years, there has been an increasing proportion of steatosis liver in the donor pool. Compared to normal livers, steatosis livers are more susceptible to ischemia-reperfusion injury (IRI), which greatly affects the outcome of liver transplantation. Nevertheless, the underlying mechanisms and corresponding improvement strategies remain largely unexplored. Previous studies have demonstrated that metformin, a first-line drug for type 2 diabetes management, not only effectively reduces blood sugar levels but also significantly improves stroke, myocardial infarction, and renal IRI. However, limited research has been conducted on metformin's role in liver IRI. Therefore, my study aims to investigate whether metformin can mitigate IRI in steatosis livers and elucidate its associated molecular mechanisms.

Method: We utilized clinical samples collected before and after liver transplantation from donors as well as non-alcoholic fatty liver mouse models with hepatic ischemia-reperfusion injury (HIRI) and cell models of non-alcoholic fatty liver to evaluate the effects of metformin in mitigating IRI via inhibiting ferroptosis. Mass spectrometry analysis was employed alongside Chromatin Immunoprecipitation (ChIP) assays and adeno-associated virus (AAV-8) precipitation techniques to identify and validate the potential regulatory mechanisms.

Results: Steatosis liver is indeed more prone to HIRI and exhibits a higher degree of ferroptosis. Treatment with metformin can significantly alleviate the IRI of steatosis liver. Mass spectrometry showed that metformin can down-regulate the level of transcriptional coactivator P300. Corresponding mechanism studies showed that metformin promoted the degradation of P300 by activating AMPK. Further ChIP-seq results showed that P300 could bind to the promoter region of ACSL4, up-regulate its H3K27ac modification, and promote the expression of ACSL4. Overexpression of P300 or ACSL4 can significantly reverse the improvement of metformin on the steatosis liver IRI.

Conclusion: This study reveals that metformin can effectively alleviate steatosis liver IRI through AMPK/P300/ACSL4 pathway, providing an important theoretical basis for clinical use of metformin to reduce the occurrence of steatosis liver IRI and improve its utilization rate in liver transplantation.

WED-015

Prognosticating hepatocellular carcinoma before and after liver transplantation with HepatoPredict

Silvia Gomes Silva¹, Judith Pérez^{2,3}, Laura Frazão⁴, Carolina Peixoto⁴, Almudena Cubells^{5,6}, Eva Montalvá^{6,7}, Antonio Figueiredo⁸, Daniela Proença⁴, Jose Pereira-Leal⁴, Hugo Pinto Marques^{9,10}, Marina Berenguer^{6,11,12}, Joana Cardoso¹³. ¹Hepato-Biliary-Pancreatic and Transplantation Centre, Lisbon, Portugal; ²Pathology Service, Hospital Universitari I Politècnic La Fe, Valencia, Spain; ³CIBERehd, Instituto de Salud Carlos III, Madrid, Spain; ⁴Ophiomics-Precision Medicine, Lisbon, Portugal; ⁵Hepatology Unit, Hospital Universitari I Politècnic La Fe, Valencia, Spain; ⁶CIBERehd, Instituto de Salud Carlos III, Madrid, Spain; ⁷Liver Transplantation and Surgery Unit, Hospital Universitari I Politècnic La Fe, Valencia, Spain; ⁸Pathology Service, Hospital Curry Cabral, Centro Hospitalar de Lisboa Central, E.P.E., Lisbon, Portugal; ⁹Hospital Curry Cabral, Centro Hospitalar de Lisboa Central, E.P.E., Lisbon, Portugal; ¹⁰Centro de Estudos de Doenças Crônicas (CEDOC), NOVA Medical School, Universidade NOVA de Lisboa (NMS/UNL), Lisbon, Portugal; ¹¹Hepatology Unit, Hospital Universitari I Politècnic La Fe, Valencia, Spain; ¹²Universidad de Valencia, Facultad de Medicina, Valencia, Spain; ¹³Ophiomics- Precision Medicine, Lisbon, Portugal Email: jvaz@ophiomics.com

Background and aims: Liver transplantation (LT) is the best curative treatment for hepatocellular carcinoma (HCC) but is limited by the shortage of organs for transplant and by strict pre-LT criteria. Pre-LT evaluation often underestimates tumour burden which leads to cases of tumour progression while on the waiting list or post-LT. Addressing the issue of pre-LT/post-LT prognosis discrepancy is essential to better stratify patients' post-surgery. We have recently developed a gene expression signature (HepatoPredict) to support the selection of HCC patients for LT. In the current work, we test the prognostic value of HepatoPredict to support post-LT stratification of HCC patients.

Method: A retrospective cohort of patients from two main LT centres (PT and ES) with HCC listed for LT from 1998 to 2016 was collected, containing 222 patients who underwent LT. In total 46 patients relapsed and 176 remained recurrence-free at 5 years. The molecular variables measured in each tumour using the HepatoPredict kit were combined with HCC-specific histopathological variables such as tumour number, size of tumour and tumour volume. Data was split into train and test sets and the machine learning algorithms were optimized for Precision or Recall.

Results: In our cohort, 77% of the patients were within Milan criteria pre-LT. At 5 years, 79.3% of the patients remained recurrence-free, with a 5-year incidence of HCC recurrence of 18.9% (median 23 months). The post-LT HepatoPredict algorithm trained with the molecular variables plus clinical variables and presenting the best performance had 88% precision and 90% recall. Compared to other criteria, our best algorithm was the only one showing similar or superior performance for all metrics (e.g., HepatoPredict precision of 88% versus 75% MORAL very low and low scores) with a clear gain in negative predictive value (NPV) (e.g., 65% versus 44% for Milan criteria). When applied to pre-LT prognosis, using radiology-derived tumour measurements as previously described (Pinto-Marques et al.) this algorithm also presented a good performance for all metrics (82% precision, 90% recall, 61% NPV).

Conclusion: HepatoPredict was initially developed to select HCC patients for LT. We now show that using the same algorithm, the same biomarkers and clinical variables defined by radiology or histopathology can aid in the post-LT setting. HepatoPredict-mediated post-LT stratification can identify high-risk patients and improve the definition of more effective surveillance schemes and/or adjuvant therapies.

WED-016

Continuous hemodiafiltration prevents sinusoidal endothelial failure during extended ex situ normothermic perfusion of porcine livers

Jordi Vengohechea Llorens¹, Javier Muñoz², Marina Vendrell³, Josep Martí Sanahuja³, Joaquim Albiol⁴, Javier Salinas¹, Aida Vaquero-Rey¹, Amelia Judith Hessheimer¹, Constantino Fondevila¹. ¹Department of General and Digestive Surgery, Hospital Universitario La Paz, IdiPAZ, CIBERehd, Madrid, Spain; ²Centro de Investigación Biomédica en Red Enfermedades Hepáticas y Digestivas (CIBERehd), Madrid, Spain; ³Anesthesiology, Reanimation, and Pain Management Service, Hospital Clinic, Barcelona, Spain; ⁴Donation and Transplantation Institute, Barcelona, Spain Email: jordivengo@gmail.com

Background and aims: Ex situ normothermic machine perfusion (NMP) is a promising strategy for liver preservation. There is still no consensus on requirements for optimal preservation of graft integrity. We aim to Evaluate the impact of continuous hemodiafiltration (HDF) applied during extended liver NMP.

Method: Porcine livers (N = 16) were perfused for 24H using a blood-based perfusate. Nutrition, vitamins, and trace elements were added after 4H. Insulin and/or glucose were also given, as needed. In a subset of cases, continuous HDF was initiated after 2H (N = 5). Perfusate was sampled serially during perfusion to analyze markers of injury, inflammation, and hepatocellular and biliary function. Liver parenchymal and biliary tissue samples were also taken at the start and end of perfusion to assess histological injury, hepatic stellate cell (HSC) activation (alpha-SMA), and endothelial cell (EC) response (eNOS, KLF2, CD31).

Results: During 24H NMP, AST and LDH levels progressively increased for the first 12H and were higher in grafts without HDF (679 ± 410 vs. 294 ± 93 u/L p < 0.05 and 1636 ± 529 vs. 1013 ± 26 u/L p < 0.01 respectively). HDF also improved glucose consumption and lactate clearance (233 ± 140 vs. 108 ± 40 mg/dL p < 0.02 and 15.9 ± 4.9 vs. 7.3 ± 3.6 p < 0.02 mmol/L), though bile production and quality and histological biliary injury did not vary.

Levels of pro-inflammatory IL-6 and IL-8 were significantly higher in grafts without HDF at 12 (7451 ± 2060 vs. 4152 ± 569 pg/ml and 41930 ± 8960 vs. 3088 ± 791 pg/ml p < 0.001 respectively) and 24H (7045 ± 2174 vs. 3120 ± 587 and 16890 ± 5220 vs. 677 ± 544 pg/ml p < 0.001 respectively). Increased gene and protein expression of alpha-SMA reflected greater HSC activation (4.7 ± 1.6 vs. 1.9 ± 0.19 p < 0.02 and 2 ± 0.3 vs. 1.5 ± 0.2 p < 0.01 for gene and protein expression respectively), while decreased gene and protein expression of eNOS (1.4 ± 0.2 vs. 4 ± 0.6 p < 0.001 and 1 ± 0.5 vs. 2.3 ± 0.7 p < 0.05 respectively) and KLF2 (0.9 ± 0.4 vs. 2 ± 0.4 and 0.9 ± 0.5 vs. 2.7 ± 0.5 p < 0.001 for both expressions) reflected reduced vasodilatory capacity of EC in grafts undergoing NMP without HDF (p < 0.001 for both genes). Consequentially, increased endothelial congestion and decreased EC area were observed among non-HDF livers (22 ± 4% vs. 29 ± 1% p = 0.006).

Conclusion: During extended ex situ NMP, addition of continuous HDF is associated with a less inflammatory environment and maintenance of cellular mechanisms and responses necessary to maintain the normal microarchitecture and size of the sinusoidal lumen in isolated liver grafts.

WED-017-YI

Myeloid Mas-dependent macrophage efferocytosis maintains immune homeostasis in the ischemia-stressed mouse and human livers

Shuai Chen¹, Changqing Yang¹, Zhi Lu². ¹Tongji Hospital, School of Medicine, Tongji University, Shanghai, China; ²Tsinghua University, Beijing, China Email: shuai_chenrj@163.com

Background and aims: Liver ischemia-reperfusion injury (LIRI) is a local sterile inflammatory response driven by the innate immunity

following liver transplantation. Mas is a master regulator of inflammation and has been implicated in both human and murine inflammatory disease models. We aimed to characterize the roles of macrophage-specific Mas in LIRI.

Method: Hepatic expression of Mas was examined in ischemia-stressed mouse and human livers. Myeloid-specific Mas1-knockout strain was generated to study the function and mechanism of macrophage Mas in a murine LIRI model. Single-cell RNA sequencing (scRNA-seq), spatial transcriptomics (ST), multiplex immunohistochemistry (mIHC), flow cytometry, intravital imaging and Mertk-knockout mice were used to describe the efferocytosis and endogenous cell interactions. RNA-seq, ChIP-qPCR, CUTandTag, luciferase reporter assay, adenovirus and mouse primary cells were used for in vitro analysis.

Results: In human specimens, macrophage Mas expression was significantly decreased in liver tissues after transplantation or hepatectomy. Interestingly, lower Mas expressions correlated with more severe liver injury postoperatively. In a mouse model, myeloid deficiency of Mas showed worse inflammation and delayed resolution than controls. scRNA-seq, ST, and intravital imaging collectively revealed that myeloid deficiency of Mas impairs macrophage efferocytosis by downregulating MerTK, leading to the accumulation of aged neutrophils. In vitro, Mas deficiency promoted innate immune activation in macrophages and downregulated the KLF4/MerTK axis through the PKA/CREB signaling pathway. CUTandTag, luciferase reporter assay and ChIP-qPCR further demonstrated KLF4 bound to the promoter region of MerTK. Importantly, Macrophage-specific overexpression of KLF4 rescued the exacerbated phenotype caused by myeloid Mas deficiency by increasing MerTK expression and macrophage efferocytosis.

Conclusion: In conclusion, macrophage Mas mediates innate pro-inflammatory responses and attenuates LIRI by regulating the KLF4/MerTK axis, which provides a therapeutic target for LIRI. These findings identify the macrophage Mas as a putative checkpoint regulator of homeostasis in response to acute hepatic stress in mouse and human livers.

WED-020

JNK signaling activates autophagy of CD8+T cells to promote acute rejection after liver transplantation in rats via regulating BECN1/BCL-2 interaction

Xiaowen Wang¹, Xiaolong Chen², Genshu Wang³, Haoqi Chen¹, Xuejiao Li⁴, Wenfeng Zhu¹, Zhilong Liu², Zhiwei Chen². ¹Department of Hepatic Surgery, Liver Transplantation, The Third Affiliated Hospital of Sun Yat-sen University, Guangzhou, China; ²Department of Hepatobiliary Surgery, The First Affiliated Hospital of Jinan University, Guangzhou, China; ³Department of Hepatic Surgery, Liver Transplantation, Guangdong Provincial Hospital of Chinese Medicine, Guangzhou, China; ⁴Department of Hepatology lab, The Third Affiliated Hospital of Sun Yat-sen University, Guangzhou, China
Email: chxl1446@126.com

Background and aims: Acute rejection (AR) after liver transplantation (LT) remains an important factor affecting the prognosis of patients. Our previous study and other researchers' work confirmed the important role of autophagy in CD8+ T cells during AR after LT. However, the underlying autophagy regulation mechanisms in CD8+ T cells during AR remain unclear.

Method: Human liver biopsy specimens of acute rejection after orthotopic liver transplantation were collected to assess the relationship between JNK and CD8+ T cells autophagy. The effect of JNK inhibition on CD8+ T cells autophagy and its role in AR were further examined in rats. Besides, the underlying mechanisms by which JNK regulates the autophagy of CD8+ T cells were further explored.

Results: The expression of JNK is positive correlated with the autophagy level of CD8+ T cells in AR patients. And similar findings were obtained in rats after LT. Further, JNK inhibitor remarkably inhibited the autophagy of CD8+ T cells in rat LT recipients. In addition, administration of JNK inhibitor significantly attenuated AR injury by promoting the apoptosis and downregulating the function of CD8+ T cells. Mechanistically, JNK activate the autophagy of CD8+ T cells through upregulating BECN1 by inhibiting the formation of Bcl-2/BECN1 complex. Moreover, the acceleration of allograft rejection in rat recipients transferred with JNK-overexpressed CD8+T cells was abrogated after BECN1 knock down.

Conclusion: JNK signalling promoted CD8+ T cells autophagy to mediate AR after LT, providing a theoretical basis for finding new drug targets for the prevention and treatment of AR after LT.

WED-021

Circulating thrombospondin-2 as a novel, highly predictive serum marker of liver fibrosis progression post liver transplant

Rambabu Surabattula¹, Sudha Rani Myneni¹, Tim Zimmermann², Detlef Schuppan^{1,3}. ¹Institute of Translational Immunology, University Medical Center Mainz, Mainz, Germany; ²Department Internal Medicine and Gastroenterology, Klinikum-Worms, Worms, Germany; ³Division of Gastroenterology, Beth Israel Deaconess Medical Center, Harvard Medical School, Boston, MA, United States
Email: rasuraba@uni-mainz.de

Background and aims: Liver transplantation (LTX) is the only curative treatment option for end stage liver disease. However, up to 30% of patients develop recurrent cirrhosis (RC) post LTX within 5 years. In view of emerging antifibrotic therapies, there is an urgent need of non-invasive serum biomarkers to predict RC after LTX. We established and validated novel liver fibrosis serum markers in LTX patients with no, moderate and severe fibrosis progression followed-up for up to >5 years post-transplant.

Method: A sandwich ELISA assay measuring the matricellular fibrosis marker thrombospondin-2 (TSP2) was established using combinations of recombinantly expressed protein, commercial and proprietary monoclonal/polyclonal antibodies. Sensitivity and specificity for serum or plasma showed intra- and inter assay variations below 10% and 15%, resp. 45 LTX patients were divided into super-rapid (<1 year, RC<1) and, rapid progressors (3–5 years, RC<5) to cirrhosis, and non-progressors after LTX. TSP2 was determined at 3, 6 and 12 months post-LTX in the subset of 10 patients of the RC<1 group and in 18 patients of the RC<5 group and in 17 patients of the non-progressors at 1, 2 and 3 years.

Results: Serum levels of TSP2 were significantly increased in RC<1 (mean 253 ng/ml) at 3, 6 and 12 months after LTX compared to non-progressors (mean 86.9 ng/ml) at 1, 2 and 3 years. Super-rapid progressors (RC<1) were clearly differentiated from non-progressors at 1 year after LTX with an AUROC of 0.9. Furthermore, 3 years after LTX, the level of TSP2 was significantly elevated in rapid progressors vs non-progressors (TSP2: 224 vs 90 pg/ml). The AUROC value to distinguish all progressors from non-progressors was 0.89 for TSP2, which outperformed the ELF score (0.84). The levels of TSP2 were significantly correlated with ELF after 1 -year (non-progressors and RC<1) and 3 years (RC<5) post liver transplant. In addition, levels of TSP2 at <6 years (RC<5) and <3 years (RC<1) were significantly elevated in patients who finally died vs survived.

Conclusion: The matricellular fibrosis marker TSP2 reflects fibrogenesis and predicts rapid fibrosis progression in patients post LTX. Other markers contributed to prediction at later stages post LTX. The novel markers may support early antifibrotic interventions post LTX.

WED-022

De novo malignancies after liver transplantation: a twenty years long-single center experience

Stefano Fonte¹, Lucia Lapenna¹, Giulia Cusi¹, Margherita Spigaroli¹, Marco Mattana¹, Simone Di Cola¹, Gianluca Mennini², Massimo Rossi², Manuela Merli³. ¹Department of Translational and Precision Medicine, Sapienza University of Rome, Rome, Italy; ²General Surgery and Organ Transplantation Unit-Policlinico Umberto I, Rome, Italy; ³Department of Translational and Precision Medicine, Rome, Italy
Email: stefanofonte08@gmail.com

Background and aims: Patients after liver transplantation (LT) require lifelong immunosuppressive therapy, exposing them to a higher risk of recurrence or de novo malignancies. The aim of this study is to describe incidence and types of tumors observed in a cohort of patients who underwent LT and were subsequently followed.

Method: We retrospectively enrolled 358 patients undergoing LT between 2000 and 2022. Patients were excluded when survival was lower than 6 months or when follow-up was incomplete. For the statistical analysis Chi squared test and T test were used.

Results: in our cohort 62 (20.9%) patients experienced the onset of malignancy after LT. Among them 8 were HCC recurrences. Among oncological and non-oncological patients no statistically significant differences were observed between the two groups for age and sex. Patients differed for: the prevalence of pre-LT HCC (15% vs 24% in the oncologic group, p value <0.0001); the kind of immunosuppressive therapy, with significantly less patients under combination therapy with tacrolimus and antimetabolites in the oncological group before diagnosis (6.5% vs 17.2%, p value 0.032); etiology of liver disease, with a higher prevalence of alcohol related liver disease in the oncological cohort (38.7% vs 22.3%, p value 0.006) and higher prevalence of viral etiology in the non-oncological group (52% vs 33.9%, p value 0.009). The most frequent non-HCC de novo solid organ malignancy were non-melanoma skin cancers (including squamous and basal cell skin cancers) with a prevalence of 3.9% of the entire cohort, followed by lung cancer with a prevalence of 2% of the entire cohort. The most frequent hematological disorder was non-Hodgkin's lymphoma (prevalence of 2.5% of the entire population).

Conclusion: patients who have undergone liver transplantation, due to their underlying pathology and prolonged immunosuppressive therapy, require careful and specific screening.

WED-027

Long-term post-transplant emergence of metabolic syndrome is associated with gut microbial metabolites in urinary metabolomics

I. Jane Cox^{1,2}, Adrien Le Guennec³, Andrew Fagan⁴, Mette Lauridsen⁵, Mohammad Siddiqui⁶, Scott Matherly⁵, Amy Bartels⁵, Jasmohan Bajaj⁵. ¹The Roger Williams Institute of Hepatology, Foundation for Liver Research, London, United Kingdom; ²Faculty of Life Sciences and Medicine, Kings College London, London, United Kingdom; ³Centre for Biomolecular Spectroscopy, Randall Centre for Cell and Molecular Biophysics, Kings College London, London, United Kingdom; ⁴Richmond VA Medical Center, Richmond, United States; ⁵VCU Medical Center, Richmond, United States; ⁶VCU Medical Center, Richmond, United States
Email: j.cox@researchinliver.org.uk

Background and aims: Liver transplantation (LT), although life-saving, is associated with development of *de novo* metabolic syndrome (MetS) and adverse cardiovascular events in the long-term post-LT course. Gut microbiota-related products, such as trimethylamine-N-oxide (TMAO) and phenylacetylglutamine (PAG), have been associated with negative cardiovascular outcomes in the general population through promotion of atherogenesis. Prior studies have considered the impact of gut microbial diversity on outcome post-LT but long-term impact of LT on microbial functionality, which could modulate the adverse pro-atherogenic profile needs to be

investigated. Our aims were to determine the effect of LT on ongoing gut microbial functionality in outpatients, following patients up to 9 years post-LT, focusing on urinary metabolomics using nuclear magnetic resonance spectroscopy (NMR).

Method: We enrolled 45 patients at baseline (mean age, 57 years; 36 men) with etiologies of HCV and alcohol (n = 12 each), n = 8 with MASH and n = 13 others, Model for End-Stage Liver Disease score mean (sd) 22.6 (6.2), who received LT 11 ± 6 months after enrolment. A sub-set were re-evaluated at 6 months (n = 38), 1 year (n = 19) and 2–9 years (n = 14) after LT. The remaining either died post-LT, did not return for post-LT visits, or did not provide samples. All post-LT patients were on stable calcineurin inhibitor doses. We only included those post-LT pts who did not require re-LT, were stable clinically and did not have recent rejection episodes or infections. Urinary NMR at all these timepoints were analysed and relative signal levels (to total signal intensity) of TMAO and PAG determined. The presence of metabolic syndrome was assessed at follow-up using validated definitions.

Results: An increase in mean relative urinary TMAO and PAG were detected after LT in most patients (mean (sd) TMAO baseline 0.016 (0.009) vs all timepoints post LTx 0.027 (0.021), p < 0.05; PAG baseline 0.0038 (0.0033) vs post LTx 0.0080 (0.0055), p < 0.05. *De novo* MetS post-LT was definitively present in 10 (22%) patients and absent in 18. Metabolite differences between follow-up and baseline were observed according to presence or absence of the MetS in both TMAO (increase of 0.020 in MetS vs 0.005 in absence of MetS, ≥ 6 mo, p = 0.03; increase of 0.039 in MetS vs 0.005 in absence of MetS, ≥ 1 yr; p = 0.01) and PAG (increase of 0.001 in MetS vs 0.003 in absence of MetS ≥ 6 mo, p = 0.34; increase of 0.005 in MetS vs 0.001 in absence of MetS, ≥ 1 yr; p = 0.02).

Conclusion: There is an increase in urinary TMAO and PAG during the months post-LT, which could indicate restoration of microbial diversity. However, these gut microbiota related metabolites were relatively higher in those who developed *de novo* metabolic syndrome post-LT and indicates the role of microbial modulation as a target to modulate these outcomes.

WED-028

Livers undergoing extended ex situ normothermic machine perfusion develop Glutathione- and Methionine-cycle alterations that reverse following transplantation

Aida Vaquero-Rey¹, Jordi Vengohechea Llorens^{1,2,3}, Javier Muñoz³, Joaquim Albiol⁴, Carlota Largo⁵, Fernando Prieto¹, Javier Salinas¹, Amelia Judith Hessheimer^{1,3}, Constantino Fondevila^{1,3}. ¹General and Digestive Surgery Service, Hospital Universitario La Paz, IdiPAZ, Madrid, Spain; ²Department of Surgery and Surgical Specializations, University of Barcelona, Barcelona, Spain; ³CIBERehd, Madrid, Spain; ⁴Donation and Transplantation Institute, TPM-DTI Foundation, Barcelona, Spain; ⁵Experimental Surgery Service, Hospital Universitario La Paz, IdiPAZ, Madrid, Spain
Email: aidavaquero@gmail.com

Background and aims: While *ex situ* normothermic machine perfusion (NMP) is a promising technique for preservation, evaluation, and treatment of livers, current protocols do not provide physiological conditions, and the metabolic state of the liver may be altered while on the device. We aim to evaluate adequacy of support provided during extended *ex situ* liver NMP by characterizing metabolic profiles pre- and post-NMP and post-transplant.

Method: Porcine livers (N = 8) were subjected to NMP during 24H performed using a blood-based perfusate. After 2H, continuous hemodiafiltration was initiated. Parenteral nutrition, vitamins, and trace elements were added after 4H. Insulin and/or glucose were also given, as needed. After 24H, grafts were transplanted into recipients, which were followed for 5D. Tissue samples were collected in the donor, at the end of NMP, post-transplant, and at the end of follow-up. Targeted metabolomic analysis was performed to evaluate 2 metabolites in the glutathione and 9 in the methionine cycles.

PERMANOVA was used to study dissimilarities among samples and univariate analyses to compare differences among times. Principal component analysis was used to identify metabolites with highest explained variance.

Results: During 24H NMP, hepatic artery and portal vein flows, bile production, and biochemical parameters were stable. Grafts functioned well upon reperfusion in their respective recipients. Metabolic profiling was able to group the samples according to time ($p = 0.001$), showing more similarities between baseline and 5D with respect to the end of NMP and 1H post-transplant. Metabolites with highest explained variance included GSH, GSSG, Spermidine, Choline, SAME, SAH and Methionine.

Conclusion: *Ex situ* NMP performed for 24H with continuous hemodiafiltration and nutritional support maintains liver viability, though reversible metabolic derangements do arise. In the future, improved metabolic support is needed to reproduce physiological conditions and maintain homeostasis during extended liver NMP.

WED-029

Adipose-derived stem cell therapy enhances liver regeneration in echinococcus multilocularis infected mice through activation of the wnt/beta-catenin/nestin signaling axis

Xiaojuan Bi¹, Ning Yang¹, Renyong Lin¹. ¹The First Affiliated Hospital Of Xinjiang Medical University, Urumqi, China
Email: renyonglin@xjmu.edu.cn

Background and aims: Stem cell therapy is a promising strategy for liver regeneration, however, its role in alveolar echinococcosis remains unclear. This study aims to evaluate the effect of Adipose-derived stem cells (ADSCs) transplantation on liver regeneration in *E. multilocularis* infected mice through the Wnt/beta-catenin/Nestin axis.

Method: Adult Nestin-cre/Rosa26-tdTomato transgenic C57BL/6 mice were infected echinococcus multilocularis for 1, 3, 5 months. The relative expression of Nestin mRNA in liver tissue was detected by real-time fluorescence quantitative PCR. Immunofluorescence staining was used to observe the relationship between Nestin expression and ALB. The expression of PCNA in the liver was detected by immunohistochemistry to analyze liver regeneration; ADSCs were injected into Em infected mice through tail vein. The underlying mechanisms of liver regeneration by which nestin affected ADSCs were explored using real time-PCR (RT-PCR), Western blot and immunohistochemistry.

Results: The expression of Nestin gradually declined with age in all organs, except for the liver where it showed little expression. However, as the infection worsens, the expression of Nestin becomes concentrated around the lesion and increases. Nestin was found to colocalize with the hepatocyte marker ALB. Through bioinformatics protein interaction (PPI) analysis, it was revealed that Nestin interacts with characteristic genes of embryonic stem cells, such as Nanog and Sox2. The positive rate of CD90 on the cell surface of Nestin+ cells is 45%, while that of CD105 is 60%. Additionally, Nestin+cells demonstrate migration ability in vitro. Furthermore, PCNA expression significantly increased at 5 months after ADSCs transplantation. The transplantation of ADSCs activates the Wnt/beta-catenin/Nestin signal axis in the livers of mice infected with *E. multilocularis*, thereby promoting the expression of Nestin around the lesion.

Conclusion: The high expression of Nestin around liver lesions in mice infected with alveolaris is correlated with hepatocyte proliferation. Adipose mesenchymal stem cell transplantation alleviates liver injury and promotes regeneration in *E. multilocularis* infected mice through Wnt/beta-catenin/Nestin signaling axis.

Liver transplantation and hepatobiliary surgery – Clinical

TOP-001

Socioeconomic deprivation is associated with worse outcomes after adult liver transplantation

Paolo De Simone¹, Juri Ducci², Daniela Campani¹, Piero Marchetti¹.

¹University of Pisa, Pisa, Italy; ²University of Pisa Medical School Hospital, Pisa, Italy

Email: paolo.desimone@unipi.it

Background and aims: Socioeconomic deprivation is a crucial factor for the best possible outcome of pediatric and adult LT. However, the mechanisms linking social deprivation to inferior outcomes are not entirely elucidated, and powered studies are still lacking.

Method: The present study analyzed retrospectively the association between socioeconomic deprivation and graft and patient survival in a cohort of 2, 568 consecutive adult recipients of a whole-size, primary liver transplant from a donor after brain death between 1996 and 2022. The primary exposure was a nationally validated socioeconomic deprivation index (DI) ranking from 1 to 5, with higher ranks indicating more significant socioeconomic deprivation.

Results: At a median (IQR) follow-up of 144.8 (204) months, more deprived patients (DI = 4–5) had a higher risk of death (RR = 1.5; $p < 0.0001$), hypertension (RR = 1.38; $p < 0.0001$), obesity (RR = 1.42; $p = 0.02$), diabetes mellitus (RR = 1.42; $p = 0.02$), graft rejection (RR = 1.8; $p < 0.0001$), chronic kidney dysfunction (RR = 1.9; $p < 0.0001$), major cardiovascular events (RR = 1.9; $p < 0.0001$) and de novo malignancies (RR = 1.5; $p < 0.0001$) than less deprived recipients (DI = 1–2). The overall patient and graft survival rates were 92% and 90.4% at 1 year, 78.4% and 72.2% at 5 years, and 58% and 56.7% at 10 years. Recipients with a DI above the median (i.e., more deprived) had 1, 5, and 10-year patient and graft survival rates of 91% and 89.5%, 70.4% and 68.4%, 48% and 46.7%, respectively, versus 92% and 90.4%, 78.4% and 72.2%, and 58% and 56.7% for less deprived patients (log-rank $p < 0.001$).

Conclusion: Based on our results, socioeconomic deprivation is associated with lower graft and patient survival and a higher risk of graft rejection and cardiovascular, metabolic, and neoplastic complications. Pre-transplant socioeconomic risk profiling is warranted to better tailor post-transplant care to patient's needs and expectations.

TOP-002

Validation of the gender-equity model for liver allocation (GEMA) in a nationwide cohort of liver transplant candidates in Spain

Manuel Rodríguez-Perálvarez^{1,2}, Gloria de la Rosa³, Antonio M. Gómez-Orellana⁴, Victoria Aguilera Sancho⁵, Teresa Pascual-Vicente⁶, Sheila Pereira⁷, María Luisa Ortiz⁸, Giulia Pagano⁹, Francisco Suárez¹⁰, Rocío González-Grande¹¹, Alba Cachero¹², Santiago Tomé¹³, Mónica Barreales Valbuena¹⁴, Rosa Martín-Mateos¹⁵, Sonia Pascual¹⁶, Mario Romero Cristóbal¹⁷, Itxarone Bilbao¹⁸, Carmen Alonso Martín¹⁹, Elena Oton²⁰, María Luisa Gonzalez Dieguez²¹, María Dolores Espinosa Aguilar²², Ana Arias²³, Gerardo Blanco²⁴, Sara Lorente Perez²⁵, Antonio Cuadrado²⁶, Amaya Redín García²⁷, Clara Sánchez Cano²⁸, Carmen Cepeda Franco²⁹, Jose Antonio Pons²⁹, Jordi Colmenero³⁰, Alejandra Otero Ferreiro¹⁰, Nerea Hernández Aretxabaleta¹², Sarai Romero Moreno³¹, María Rodríguez Soler³², César Hervás⁴, Mikel Gastaca³³. ¹Hospital Universitario Reina Sofía, IMIBIC, Córdoba, Spain; ²University of Cordoba, Córdoba, Spain; ³Organización Nacional de Trasplantes (ONT), Madrid, Spain; ⁴University of Córdoba, Córdoba, Spain; ⁵Instituto de Investigación Sanitaria La Fe, Valencia, Spain; ⁶Hospital Universitario de Cruces, Bilbao, Spain; ⁷Hospital Virgen del Rocío, Seville, Spain; ⁸Hospital Universitario Virgen Arrixaca, Murcia, Spain; ⁹Hospital Clinic, Barcelona, Spain; ¹⁰Centro Hospitalario

POSTER PRESENTATIONS

Universitario de A Coruña, A Coruña, Spain; ¹¹Hospital Universitario Regional de Málaga, Málaga, Spain; ¹²Hospital Universitario de Bellvitge, Barcelona, Spain; ¹³Centro Hospitalario Universitario de Santiago, Santiago, Spain; ¹⁴Hospital Universitario 12 Octubre, Madrid, Spain; ¹⁵Hospital Universitario Ramón y Cajal, Madrid, Madrid, Spain, ¹⁶Hospital General Universitario de Alicante, Alicante, Spain; ¹⁷Hospital Gregorio Marañón, Madrid, Spain, ¹⁸Hospital Universitario Vall d'Hebron, Barcelona, Spain; ¹⁹Hospital Rio Hortega, Valladolid, Spain; ²⁰Complejo Hospitalario Universitario de Canarias, Tenerife, Spain; ²¹Hospital Universitario Central de Asturias, Oviedo, Spain; ²²Hospital Universitario Virgen de las Nieves, Granada, Spain; ²³Hospital Universitario Puerta de Hierro, Madrid, Spain; ²⁴Centro Hospitalario Universitario de Badajoz, Badajoz, Spain; ²⁵Hospital Clínico Universitario Lozano Blesa, Zaragoza, Spain; ²⁶University Hospital Marqués de Valdecilla, Santander, Spain; ²⁷Clínica Universidad de Navarra, Navarra, Spain; ²⁸Hospital La Fe e Instituto de Investigación sanitaria La Fe, Valencia, Spain; ²⁹Hospital Universitario Virgen de la Arrixaca, Murcia, Spain; ³⁰Hospital Clínic, Barcelona, Barcelona, Spain; ³¹Hospital Universitari La Fe, Valencia, Spain; ³²Hospital General Universitario Dr. Balmis de Alicante, Alicante, Spain; ³³Hospital Universitario Cruces, Bilbao, Spain
Email: ropeml@hotmail.com

Background and aims: The Gender-Equity Model for liver Allocation corrected by sodium (GEMA-Na) may save a meaningful number of lives while palliating gender disparities among liver transplant (LT) candidates (PMID 36528041). We aimed to validate its performance in Spain, where waiting time for LT is reduced.

Method: Nationwide cohort study including adult candidates for elective LT from 25 centers in Spain (2014–2021). The primary outcome was mortality or delisting for sickness with right-censoring at 90 days. The GEMA-Na score was calculated according to the published formula available at: <http://gema-transplant.com/>. The discrimination of GEMA-Na was assessed by the Harrel's c-statistic (Hc) and compared with MELD-Na, and MELD 3.0. This study was funded by the Instituto de Salud Carlos III (Project no. PI22/00312) and co-funded by the European Union.

Results: Among 6, 206 eligible patients (22.4% women, aged 57.8 ± 8.6 years), 5, 460 patients had sufficient data to calculate the scores and entered the study. The most frequent indications for LT were hepatocellular carcinoma (HCC) (39.4%), hepatic insufficiency (29.4%), and refractory ascites (13%). The primary outcome occurred in 254 patients (5.2% women vs. 4.5% men; $p = 0.24$). Median time in the waiting list was 71 days, without gender disparities ($p = 0.44$). In patients without HCC, women had to wait longer (67 vs. 56 days; $p = 0.025$). GEMA-Na obtained the highest discrimination (Hc = 0.717), followed by MELD-Na (Hc = 0.704; $p = 0.039$), and MELD 3.0 (Hc = 0.701; $p = 0.012$). Differences were more pronounced in patients without HCC: GEMA-Na Hc = 0.776, MELD-Na Hc = 0.756 ($p = 0.004$ vs. GEMA-Na), and MELD 3.0 Hc = 0.752 ($p = 0.005$ vs. GEMA-Na). GEMA-Na obtained the highest discrimination also in patients with ascites: GEMA-Na Hc = 0.745, MELD-Na Hc = 0.724 ($p = 0.002$ vs. GEMA-Na), and MELD 3.0 Hc = 0.724 ($p = 0.011$ vs. GEMA-Na). Differential prioritization between GEMA-Na and MELD-Na occurred in 8.7% of patients, with one-in-20 deaths avoided within the first 90 days ($p = 0.008$). Differential prioritization between GEMA-Na and MELD 3.0 occurred in 9.7% of patients, with one-in-22 deaths avoided within the first 90 days ($p < 0.001$).

Conclusion: GEMA-Na was successfully validated in Spain and confirmed its advantage over the MELD family scores to predict waiting list mortality or delisting for sickness in a context of waiting list shortening.

TOP-003-YI

Model for end-stage liver disease score-based liver allocation is associated with reduced survival in low donation countries-a comparative analysis between Germany and the USA

Leke Wiering^{1,2}, Annette Aigner³, Marieke van Rosmalen⁴, Brigitta Globke^{2,5}, Nathanael Raschzok^{2,5}, Wenzel Schöning⁵, Georg Lurje⁵, Münevver Demir¹, Frank Tacke¹, Johann Pratschke⁵, Robert Öllinger⁶, Paul Ritschl^{2,5}. ¹Charité-Universitätsmedizin Berlin, Department of Hepatology and Gastroenterology, Berlin, Germany; ²Berlin Institute of Health at Charité-Universitätsmedizin Berlin, BIH Biomedical Innovation Academy, Berlin, Germany; ³Charité-Universitätsmedizin Berlin, Institute of Biometry and Clinical Epidemiology, Berlin, Germany; ⁴Eurotransplant International Foundation, Leiden, Netherlands; ⁵Charité-Universitätsmedizin Berlin, Department of Surgery, Berlin, Germany; ⁶Charité-Universitätsmedizin Berlin, Berlin, Germany
Email: leke.wiering@charite.de

Background and aims: The allocation of donor livers based on the Model for End-Stage Liver Disease (MELD) score is the predominant practice in most countries worldwide. Favorable outcomes in waiting list mortality and survival have been described for the USA following its implementation. However, the impact of this policy in countries with low organ donation rates, such as Germany, remains uncertain and is the aim of this investigation.

Method: Waiting list survival and survival after liver transplantation Germany (2003–2016, MELD implementation 12/2006) and the USA (1999–2016, MELD implementation 02/2002) was analyzed using data from the Germany Transplant registry and UNOS registry. A comprehensive cohort of 196, 039 waiting list registrations and 108, 199 liver transplantation was used for this retrospective analysis.

Results: Waiting list mortality did not improve after the introduction of MELD-based allocation in Germany (OR 0.97, 95% CI: 0.91–1.03). Moreover, survival after transplantation deteriorated in Germany (three-year patient survival preMELD 69.3% vs. MELD 65.3%, $p < 0.001$; HR: 1.16, 95% CI: 1.08–1.25). Contrarily to this, an improvement in both waiting list mortality (OR: 0.73, 95% CI: 0.71–0.75) and survival after transplantation (preMELD 75.3% vs. MELD 80.5%, $p < 0.001$; HR 0.75, 95% CI: 0.72–0.77) was found after the implementation of MELD-based policies in the USA. Notably, the disparities between the two countries could be attributed to the significantly higher organ donor numbers in the USA as there was no significant improvement of waiting list mortality in the USA after adjustment for donor number (OR: 1.01, 95% CI: 0.97–1.06). Similarly, survival after transplantation did not show significant improvement after adjustment for donation rates in the USA (HR: 0.96, 95% CI: 0.90–1.01). In addition, a combined multivariable cox-proportional hazards regression model of the two countries showed a markedly reduced difference in patient survival after adjustment for donor number (unadjusted HR for survival in Germany compared to the USA: 2.12, 95% CI: 2.04–2.20; adjusted HR: 1.44 (95%CI: 1.30–1.59).

Conclusion: MELD-based liver allocation demonstrates improved waiting list outcomes and post-transplant survival only in countries characterized by high organ donation rates, exemplified by the USA. Consequently, there is a need for a critical re-evaluation of liver allocation policies in nations with limited organ donation rates like Germany.

TOP-004

Impact of MELD 3.0 on waitlist outcomes of metabolic dysfunction-associated steatohepatitis cirrhosis among liver transplant waitlist registrants

Benedix Sim¹, Wen Hui Lim², Darren Jun Hao Tan², Cheng Han Ng², Nicholas Syn², Benjamin Nah¹, Benjamin Koh², Jieling Xiao², Christen Ong², Jia Hong Koh¹, Daniel Tung¹, Daniel Huang³, Mohammad Shadab Siddiqui⁴, Mark Muthiah¹, Margaret Teng^{5,6}.

¹Division of Gastroenterology and Hepatology, Department of Medicine, National University Hospital, Singapore, Singapore, Singapore,

Singapore; ²Yong Loo Lin School of Medicine, National University of Singapore, Singapore, Singapore, Singapore; ³Yong Loo Lin School of Medicine, National University of Singapore, Singapore, Singapore; ⁴Division of Gastroenterology, Department of Internal Medicine, Hepatology and Nutrition, Virginia Commonwealth University, Virginia, United States; ⁵Division of Gastroenterology and Hepatology, Department of Medicine, Alexandra Hospital, Singapore, Singapore; ⁶Division of Gastroenterology and Hepatology, Department of Medicine, National University Hospital, Singapore, Singapore
Email: margaret.tenglp@gmail.com

Background and aims: Metabolic dysfunction-associated steatohepatitis (MASH) cirrhosis is rapidly growing as an indication for liver transplantation (LT). However, the impact of MELD 3.0 on waitlist outcomes of patients with MASH cirrhosis is not established. The present study aimed to assess the impact of MELD 3.0 on waitlist outcomes of patients with MASH cirrhosis using the Scientific Registry of Transplant Recipient (SRTR) database.

Methods: The study cohort consisted of patients registered on LT waitlist between 1/1/2016 to 12/31/2022. The primary outcomes included probability of LT and waitlist mortality comparing MASH (n = 12, 794) vs. non-MASH (n = 31, 254) cirrhosis.

Results: Patients with MASH cirrhosis were listed with lower Model for End-stage Liver Disease (MELD) 3.0 score despite bearing greater burden of portal hypertension (vs non-MASH). Comparing reclassification between MELDNa and MELD 3.0, more waitlist registrants with MASH cirrhosis were down-categorized (n = 1, 658, 13.0%) than up-categorized (n = 632, 4.94%). Out of 1, 410 female MASH cirrhosis decedents, a net of 14 (0.99%) patients would be correctly reclassified. However, in terms of female LT recipients, there would be a net incorrect down-categorization of 121 (3.56%) patients. The overall transplant probability in LT waitlist registrants with MASH [vs. non-MASH] cirrhosis was significantly lower at 3-months (HR 0.837, p < 0.001) and 12-months (HR 0.836, p < 0.001). Furthermore, both 3-month (HR 1.16, p < 0.001) and 12-month (1.25, p < 0.001) waitlist mortality was significantly higher in patients with MASH cirrhosis compared to non-MASH cirrhosis. Female MASH cirrhosis patients had significantly lower 90-day (HR: 0.878, p < 0.001) and 1-year transplantation probability (HR: 0.863, p < 0.001) compared to male MASH cirrhosis patients. The key contributor to MELD score was serum creatinine among LT waitlist registrants.

Conclusion: LT waitlist registrants with MASH cirrhosis are less likely to receive transplant and more likely to die on waitlist compared to patients with non-MASH cirrhosis. Serum creatinine has the largest contribution to likelihood of LT.

TOP-005

Immune checkpoint inhibitors after liver transplantation: the key role of immunosuppression management

Eleonora De Martin¹, Teresa Antonini², Massih Ningarhari³, Marie-Noëlle Hilleret⁴, Manon Allaire⁵, Arnaud Del Bello⁶, Giuliana Amaddeo⁷, Camille Besch⁸, Martine Neau Cransac⁹, Anais Jaillais¹⁰, Isabelle Ollivier-Hourmand¹¹, Sébastien Dharancy³, Thomas Decaens⁴, Filomena Conti⁵, Faouzi Saliba¹, Olivier Rosmorduc¹, Jérôme Dumortier¹², Audrey Coilly¹. ¹APHP, Hôpital Paul Brousse, Centre Hépatobiliaire, Unité Inserm 1193, Université Paris-Saclay, Villejuif, France; ²Service d'hépatologie et gastroentérologie, Hospices Civils de Lyon, Hôpital de la Croix-Rousse, Lyon, France; ³Services des maladies de l'appareil digestif, Centre Hospitalier Universitaire de Lille, Lille, France; ⁴Service d'hépatogastroentérologie, CHU Grenoble-Alpes, Grenoble, France; ⁵APHP, Groupe Hospitalier Pitié-Salpêtrière, Service d'hépatogastroentérologie, Sorbonne Université, Paris, France; ⁶Département de néphrologie et transplantation d'organes, Hôpital Rangueil, CHU Toulouse, Toulouse, France; ⁷APHP, Hôpital Henri Mondor, Service d'Hépatogastroentérologie, Créteil, France; ⁸Service de chirurgie hépatobilio-

pancréatique et transplantation hépatique, Hôpital Hautepierre, CHRU Strasbourg, Strasbourg, France; ⁹Unité de Soins continus Uro-Vasculaires et greffes rénales, Immunologie Clinique, Biovigilance, Hôpital Pellegrin, CHU de Bordeaux, Bordeaux, France; ¹⁰Hépatogastroentérologie-CHU de Tours, Tours, France; ¹¹Service d'Hépatogastro-Entérologie et Nutrition; CHU de Caen, Caen, France; ¹²Fédération des spécialités digestives, Hôpital Edouard-Herriot, Hospices Civils de Lyon et Université Claude Bernard Lyon, Lyon, France
Email: eleonora.demartin@aphp.fr

Background and aims: The use of immune checkpoint inhibitors (ICI) after liver transplantation (LT) is still controversial considering the potential risk of rejection, that can be fatal, reported in about 40% of treated patients. However, this data come from clinical case or small heterogeneous series and risk factors for rejection haven't been clearly identified yet. The aim of the present study was to characterize patients treated with ICI after LT and clarify risk factors for rejection.

Method: This is a retrospective, multicenter study which included adult patients who received an ICI (anti-PD1, anti-PDL1 or anti-CTLA4) after LT for hepatocellular carcinoma (HCC) recurrence or a *de novo* tumor. Tumor therapy and immunosuppression (IS) management was at physician discretion. Quantitative variables were expressed as median and interquartile (IQR 1st et 3rd quartile), while qualitative variables were expressed as number and %. Utilized tests were Mann-Whitney and Fischer.

Results: Thirty-five patients were included, 27 (77%) males, median age 60.4 (51.5;64.3) years. Fourteen (40%) patients were transplanted for alcohol related cirrhosis and 8 (23%) for HCV related cirrhosis, 28 (80%) had an HCC before LT. The median interval time between LT and cancer diagnosis was 3.27 (1.28; 6.94) years. HCC recurrence was diagnosed in 20 (57%) patients. ICI used were: anti-PD1 in 13 (37%) and anti-PDL1 in 22 (63%) patients. The median interval time between LT and ICI introduction was 4.67 (2.97; 9.66) years. IS was increased a priori in 20 (57%) patients before ICI. Six (17%) patients developed acute rejection. These patients compared to the ones without rejection were less frequently on tacrolimus (33% vs 83%, p = 0.027) and with a trend of being on a single IS drug (67% vs 14%, p = 0.065). Moreover, in patients who developed a rejection, ICI treatment duration was significantly shorter (p = 0.026), and the number of injection lower (p = 0.021) (Table 1). Twenty-four (69%) patients died and among them 4 had a fatal rejection. Survival after ICI initiation was similar in patients with or without rejection (5.10 vs 2.81 months, p = 0.12).

Conclusion: In patients who were treated with ICI after LT, survival is low due to oncological disease progression. In this series, rejection rate is lower compared to the literature (17%), however it was fatal in the majority of the cases. Acute rejection seems to develop rapidly after ICI introduction and in particular in patients on immunosuppression monotherapy and in the absence of tacrolimus. These circumstances should be avoided.

SATURDAY 08 JUNE

SAT-007-YI

Assessing sex differences in access to liver transplantation in Italy: a real-world nationwide study

Chiara Becchetti¹, Silvia Trapani², Lucia Masiero², Francesca Puoti², Francesca D'Arcangelo³, Lucia Lapenna⁴, Manuela Merli⁴, Filomena Morisco⁵, Valentina Cossiga⁵, Maria Guarino⁵, Marta Cilla⁶, Federica Invernizzi⁶, Elisabetta Cerutti⁷, Pierluigi Toniutto⁸, Massimo Cardillo², Patrizia Burra³. ¹Hepatology and Gastroenterology Unit, ASST Grande Ospedale Metropolitano Niguarda, Milan, Italy; ²Italian National Transplant Center, National Institute of Health, Rome, Italy; ³Gastroenterology, Multivisceral Transplant Unit, Department of Surgery, Oncology and Gastroenterology, Padua University Hospital, Padua, Italy; ⁴Department of Translational and Precision Medicine,

POSTER PRESENTATIONS

Sapienza University of Rome, Rome, Italy; ⁵Department of Clinical Medicine and Surgery, Diseases of the Liver and Biliary System Unit, University of Naples "Federico II," Naples, Italy; ⁶Center for Liver Disease, Division of Internal Medicine and Hepatology, IRCCS Ospedale San Raffaele, Milan, Italy; ⁷Department of Anesthesia, Transplant and Surgical Intensive Care, Azienda Ospedaliera Universitaria Delle Marche, Ancona, Italy; ⁸Hepatology and Liver Transplantation Unit, Department of Medical Area, University of Udine, Udine, Italy
Email: burra@unipd.it

Background and aims: sex-based disparities in liver transplantation (LT) have been recognized since several years. This disadvantage is evident to all stages of the LT cascade. Although such disparities are well established in studies from United States, less data are available from European countries. As these differences are affected by the national context, having local data is critical to define the dimensions of the problem.

Method: we performed an observational, retrospective, nationwide study promoted by the Special Interest Group of Gender in Hepatology of The Italian Association for the Study of The Liver in collaboration with the Italian National Transplant Center on LT patients waitlisted in Italy from January 1st, 2017 to December 31st, 2021, using the data entered the Italian Transplant Information System. Demographics and clinical characteristics, as well as time on the waiting-list (WL), access to LT, and reasons for removal were assessed. The probabilities of LT and mortality on WL were analyzed using the competing risk analysis and FineandGray sub-Hazard Ratio (sHR) for sex.

Results: overall, 7609 patients were considered for the analysis, 2004 (26.3%) females. Compared to the latter, males were older (58 vs 56 years, $p < 0.05$) with higher body mass index (BMI) (25.9 vs 24.1 kg/m², $p < 0.05$) at listing. The indication to LT was more often liver cirrhosis (LC) for females (48.2%) and hepatocellular carcinoma (HCC) for males (47%, $p < 0.001$). Among LC etiologies, alcohol-associated disease and hepatitis C virus prevalence were higher in males (42.2 vs 24%, and 22.2 vs 13.8%, respectively, both $p < 0.001$), whereas hepatitis B virus and autoimmune diseases were more prevalent in the female sex (21.8 vs 14.3%, and 25.6 vs 8.2%, respectively, both $p < 0.001$). No significant differences were observed in the HCC etiologies. Females resulted more often listed as urgent LT (5.3 vs 2.4%, $p < 0.001$). LT occurred more frequently in males than females (79.3 vs 74.2%, $p < 0.001$), who experienced more frequently delisting for death (8.7% vs 7%, $p = 0.016$). One-year competing risk analysis for LT and mortality on the WL showed that males had higher probability to receive a LT (Cumulative Incidence Function [CIF] 69.2% [95%CI 68.0–70.4] vs 61.7% [95%CI 68.0–70.4], sHR = 1.17 [95%CI 1.1–1.2], $p < 0.0001$) and lower probability of dying compared to females (CIF 8.3% [95%CI 7.6–9.0] vs 8.9% [95%CI 7.7–10.2]; sHR = 0.89 [95%CI 0.77–1.02], $p = 0.09$). This latter difference resulted significant at 30-days from listing, but not any longer.

Conclusion: in this large Italian cohort, we found that females were less likely undergoing LT and presented with higher rates of death compared with their counterparts. This could be partially explained by a more severe clinical presentation in female at the time of listing. Future studies are needed to better identify causes and ensure equity in providing LT access to the female population.

SAT-008

Significance of routinely measured direct alcohol markers in long-term care after liver transplantation

Julia M. Grottenthaler¹, Johannes Wagner¹, Michael Boettcher², Jannis Altekoester¹, Hannah Kraemer¹, Franziska Trauner¹, Verena Wagner¹, Silke Templin³, Nisar P. Malek¹, Anil Batra⁴, Silvio Nadalin³, Christoph P. Berg¹. ¹Department of Gastroenterology, Gastrointestinal Oncology, Hepatology, Infectiology, and Geriatrics, University Hospital Tuebingen, Tuebingen, Germany; ²MVZ Medizinische Labore Dessau Kassel GmbH, Department of Toxicology, Dessau, Germany; ³Department of General- Visceral- and Transplant Surgery,

University Hospital Tuebingen, Tuebingen, Germany; ⁴Department of Psychiatry and Psychotherapy, Section Addiction Medicine and Addiction Research, Tuebingen, Germany
Email: julia.grottenthaler@med.uni-tuebingen.de

Background and aims: Alcohol misuse after liver transplantation (LTx) can seriously impact graft and patient survival. However, to date, there is no defined standard procedure to identify patients after LTx who are at risk for alcohol-related complications. The aim of this prospective study was to analyze screening methods for alcohol (mis) use after LTx with special focus on the diagnostic value of routinely measured ethanol metabolites: blood phosphatidylethanol (PEth) and urinary ethylglucuronide (uEtG).

Method: In this prospective study, adult patients in post LTx care were consecutively included at their visit in the outpatient clinic of the Tuebingen Transplant Center from August 2022 until September 2023. In order to screen for signs of alcohol consumption, the standardized questionnaire AUDIT-C (alcohol use disorders identification test-concise) was used in combination with measurement of PEth (cutoff <20 ng/ml) and uEtG (cutoff <500 ng/ml).

Results: 351 patients were included in the study (median age 60 years [min-max 20–81 years], 59% male). 22% ($n = 77$) had alcohol-related liver disease (ALD) as underlying liver disease leading to LTx, 19% ($n = 65$) suffered from chronic viral hepatitis, 18% ($n = 63$) had cholestatic liver diseases, in 10% ($n = 35$) acute liver failure led to LTx, 5% ($n = 19$) had cryptogenic liver cirrhosis, in 4% ($n = 14$) MASLD (metabolic dysfunction-associated steatotic liver disease) was present, and 22% ($n = 78$) had other reasons for LTx. Median time since LTx was 8.3 years (min 6 months, max 36 years). 34% ($n = 118$) of the patients had at least one positive sign for alcohol use. In the AUDIT-C, 26% ($n = 93$) of the patients reported at least occasional alcohol use, while 5 patients met the criteria for hazardous drinking. PEth was positive in 14% ($n = 48$), uEtG in 10% ($n = 34$) of the patients. Questionnaire results and positive alcohol metabolites were significantly correlated ($p < 0.001$). However, 25 patients (7%) reported complete alcohol abstinence but presented with at least one positive alcohol metabolite; in 11 of these patients only the longer detectable PEth was positive. There was no significant correlation between ALD as underlying disease and the detection of alcohol use post LTx ($p = 0.40$). In contrast, a longer time since liver transplantation correlated significantly with the detection of alcohol consumption ($p < 0.001$).

Conclusion: Given the high percentage of patients who do not consistently abstain from alcohol after LTx, screening for alcohol use disorders is crucial in order to prevent adverse outcomes. Direct alcohol markers can play a substantial role in detecting patients at risk and closing the gap of patient interviews. In this context, the longer detectable PEth is of special interest. Importantly, with regard to the results of this present study, screening should not be limited to the group of patients transplanted for ALD, nor only to the first few years after LTx.

SAT-009

Increased prevalence of metabolic-alcohol liver disease in Europe and of metabolic dysfunction-associated steatotic liver disease in the Americas. Results of the global IMPROVEMENT study

Alfonso Avolio¹, Luca Miele¹, Patrizia Silvestri², Marco Maria Pascale², Patrizia Burra³, Silvia Martini⁴, Stefano Fagioli⁵, Maurizio Pompili¹, Paulo Martins⁶, Sherrie Bhoori⁷, Mohamed Rela⁸, Ian Leinritz⁹, Marcos Perini¹⁰, Luca Saverio Belli¹¹, Gonzalo Sapisochin¹², Maria Francesca Donato¹³, Ashwin Rammohan⁸, Valerio Giannelli¹⁴, Louise Barbier¹⁵, Ilaria Lenci¹⁶, Felix Braun¹⁷, Maria Rendina¹⁸, Martin De Santibanes¹⁹, Paola Violi²⁰, Deng Feiwen²¹, Lucio Caccamo¹³, Olga Ciccirelli²², Amedeo Carraro²⁰, Mickael Lesurtel²³, Matteo Cescon²⁴, Silvio Nadalin²⁵, Luciano De Carlis²⁶, Wojciech Polak²⁷, Paolo De Simone²⁸, Takashi Ito²⁹, Riccardo De Carlis²⁶, Gupta Subash³⁰, Quirino Lai³¹, Fernandez Hoylan³², Giuseppe Maria Ettore³³, Mikel Gastaca³⁴, Salvatore Gruttadauria³⁵, Patel Madhukar³⁶, Vincenzo Mazzaferro⁷,

Gabriel Oniscu³⁷, Renato Romagnoli³⁸, Cristiano Quintini³⁹, Fabrizio Di Benedetto⁴⁰, Thamara Perera⁴¹, Daniele Dondossola¹³, Taner Timucin⁴², Giuseppe Tisone⁴³, Maíra Godoy⁴⁴, Giovanni Vennarecci⁴⁵, Maria García Guix⁴⁶, Marco Vivarelli⁴⁷, Michele Finotti³⁶, Daniele Ferraro⁴⁸, Jacopo Lanari⁴⁹, Jan Paul Gundlach¹⁷, Emilia Kruk⁵⁰, Salvatore Agnes², Francesco Frongillo⁵¹, Fabio Melandro²⁸, C. Murcia⁵², Duilio Pagano³⁵, Roberta Angelico⁴³, Giammauro Berardi³³, Marco Bongini⁷, Yang Bo⁵³, Eliano Bonaccorsi²², Stefania Camagni⁵, Jessica Bronzoni²⁸, Christopher Chandler⁵⁴, Marco Clasen⁵⁵, Brian Nguyen⁵⁶, Rosaria Calia², Elvan Onur Kırımci⁵⁷, Debora Puzzi⁵⁸, Tommaso Partipilo⁴³, Mathias Vidgren⁵⁹, Lorenzo Cocchi²³, Angus Hann⁶⁰, Femke De Goeij⁶¹, Andrea Della Penna²⁵, Stefano Di Sandro⁴⁰, Songming Li⁶², Isabel Miglior⁶³, Burcin Ekser⁶⁴, Emanuele Felli⁶⁵, Arkaitz Perfecto⁶⁶, Jagadeesh Krishnamurthy⁶⁷, Deniz Balci⁶⁸, Krzysztof Zieniewicz⁵⁰, Matteo Ravaioli⁶⁹, Zhiong Guo⁶², Francesco Tandoi⁷⁰, Tina Pasciuto⁷¹, Umberto Cillo⁷², Vatche Agopian⁵⁴. ¹Fondazione Policlinico Universitario Agostino Gemelli, IRCCS, Catholic University, Rome, Italy; ²Fondazione Policlinico Universitario Agostino Gemelli, IRCCS, Rome, Italy; ³Azienda Ospedaliera Universitaria, University of Padua, Padua, Italy; ⁴Citta' della Salute e della Scienza, Turin; ⁵LTX Center, Bergamo, Italy; ⁶Liver Transplant Center, University of Massachusetts, Worcester, United States; ⁷LTX Center, National Cancer Institute, Milan, Italy; ⁸Rela Transplant Institute, Chennai, India; ⁹LTX Center, Auckland, New Zealand; ¹⁰Austin Liver Transplant Center, Melbourne, Australia; ¹¹Ospedale Niguarda, Milan; ¹²Liver Transplant Center, Toronto General Hospital, Toronto, Canada; ¹³LTX Center-Fondazione IRCCS Ca' Granda Ospedale Maggiore Policlinico, Milan, Italy; ¹⁴San Camillo Hospital, Rome; ¹⁵LTX Center, Auckland, New Zealand; ¹⁶Fondazione Policlinico Tor Vergata, Rome, Italy; ¹⁷LTX Center, Kiel, Germany; ¹⁸LTX Center, Bari, Italy; ¹⁹LTX Center, Buenos Aires, Argentina; ²⁰LTX Center, Verona, Italy; ²¹LTX Center, Foshan, China; ²²LTX Center, Brussels, Belgium; ²³LTX CENTER-Hopital Beaujon, Paris, France; ²⁴LTX CENTER, Bologna, Italy; ²⁵LTX Center, Tubingen, Germany; ²⁶Ospedale Niguarda, Milan, Italy; ²⁷LTX Center, Rotterdam, Netherlands; ²⁸LTX Center, Pisa, Italy; ²⁹Liver Transplant Center, Kyoto; ³⁰LTX Center, New Delhi, India; ³¹LTX Center, Rome, Italy; ³²LTX Center, Dallas, United States; ³³LTX Center-POIT, Rome, Italy; ³⁴LTX Center, Bilbao, Spain; ³⁵LTX Center, Palermo, Italy; ³⁶LTX Center, Dallas, United States; ³⁷LTX Center, Huddinge, Sweden; ³⁸Citta' della Salute e della Scienza, Turin, Italy; ³⁹LTX Center, Cleveland, United States; ⁴⁰LTX Center, Modena, Italy; ⁴¹Queen Elizabeth Hospital, Birmingham, United Kingdom; ⁴²LTX Center, Rochester, United States; ⁴³LTX Center, Rome, Italy; ⁴⁴LTX Center, Blumenau, Brazil; ⁴⁵LTX Center, Napoli, Italy; ⁴⁶LTX Center, Barcelona, Spain; ⁴⁷LTX Center, Ancona, Italy; ⁴⁸LTX Center, Napoli, Italy; ⁴⁹LTX Center, Padua, Italy; ⁵⁰LTX Center, Warsaw, Poland; ⁵¹Fondazione Policlinico Universitario Agostino Gemelli, IRCCS, Rome, Italy; ⁵²LTX Center, Bogota, Colombia; ⁵³LTX Center, Wuhan, China; ⁵⁴David Geffen School of Medicine at UCLA, Los Angeles, United States; ⁵⁵LTX Center, Toronto, Canada; ⁵⁶Liver Transplant Center, Georgetown, United States; ⁵⁷Ankara University School of Medicine, Ankara, Turkey; ⁵⁸Liver Transplant Center, Campinas, Brazil; ⁵⁹Liver Transplant Center, Karolinska Institute, Stockholm, Sweden; ⁶⁰Liver Transplant Center, Birmingham, United Kingdom; ⁶¹Liver Transplant Center, Rotterdam, Netherlands; ⁶²The First Affiliated Hospital, Guangzhou, China; ⁶³Liver Transplant Centre, Newcastle, United Kingdom; ⁶⁴Liver Transplant Center, Indianapolis, Indianapolis, United States; ⁶⁵LTX Center, Tours, France; ⁶⁶Hospital Universitario Cruces-Bilbao, Liver Transplant Centre, Bilbao, Spain; ⁶⁷Liver Transplant Centre, New Delhi, India; ⁶⁸Ankara University School of Medicine, Ankara, Turkey; ⁶⁹Liver Transplant Centre, Bologna, Bologna, Italy; ⁷⁰Liver Transplant Centre, Bari, Italy; ⁷¹GStEP Data Collection-Fondazione Policlinico Universitario "Agostino Gemelli" IRCCS, Rome, Italy; ⁷²LTX Centre, Azienda Ospedaliera Universitaria, Padua, Italy

Email: alfonso.avolio@unicatt.it

Background and aims: There is a widespread occurrence of obesity in the world and an increased indication for liver transplants due to

metabolic dysfunction-associated steatotic liver disease (MASLD). A large global, balanced study investigating the global pattern of etiology and indication for liver transplant (LT) has not been done. The etiology of ESLD-LTs has been reviewed according to 2 time-frames (2018–19 and 2022–23) to show changes in pattern/prevalence.

Method: The IMPROVEMENT project (ClinicalTrials.gov NCT05289609) has been designed to investigate the risk factors that predict outcomes after LT. An international steering committee identified the Centers to be invited. Attention was paid to having an equal number of high-volume Centers (>65 LTs per year) and intermediate-volume Centers (=65 LTs per year) representative of transplant activity in Italy, Europe, Asia, Oceania, and the Americas. An equal number of consecutive cases was requested for each Center. The implementation of the novel multi-society terminology with stratification in metabolic dysfunction-associated steatohepatitis (MASLD), metabolic autoimmune liver disease (Met-AILD), metabolic alcohol liver disease (Met-ALD), alcohol, viral, cryptogenic and others was adopted.

Results: After excluding acute liver failure and retransplant cases, 3599 LTs were stratified in hepatocellular carcinoma (HCC, 1574) and non-HCC (2025) cases. The analysis of HCCs during 2018–19 revealed that Met-ALD was the predominant etiology in Europe, accounting for 37.3% of cases. In contrast, viral etiology was identified as the leading cause in the Asia, Americas, and Oceania. Notably, in the subsequent period of 2022–23, MASLD emerged as the primary etiology in the Americas, comprising 42.9% of cases, while Met-ALD continued to be the most prevalent etiology in Europe, increasing to 48.7%. Viral etiology remained the most frequent cause in Asia and Oceania.

Regarding non-HCC indications, during 2018–19 Met-ALD resulted the most common indication in Europe (28.2%) and the Americas (30.9%), with viral etiology being the most prevalent in Asia, and Met-AILD being the most common in Oceania (28.8). In the 2022–23 period, Met-ALD remained the leading indication in Europe (32.5%) and the Americas (33.7%), while Met-AILD became the most prevalent cause in Asia (22.2%).

Conclusion: The increase in metabolic-related liver diseases in the Americas and Europe highlights the need for integrated healthcare interventions targeting obesity, diabetes, and alcohol consumption. The consistency of viral etiologies in Asia and Oceania emphasises the continued need for effective viral hepatitis control measures, including vaccination and antiviral therapies. LT programs must adapt to the shifting etiological patterns, which may have profound implications for organ allocation policies, patient education, and long-term management.

SAT-010

Elaboration of a one-year mortality score for first elective liver transplantation recipients over 60 years based on the results of the french national cohort between 2007 and 2017

Marie Labruyere¹, Amadou-Khalilou Sow¹, Corinne Antoine², Sebastien Dharancy^{3,4}, Jérôme Dumortier⁵, Celia Turco⁶, Vincent Di Martino⁷, Delphine Weil-Verhoeven⁸, Pauline Housset-Debry⁹, Filomena Conti¹⁰, Claire Francoz¹¹, Georges-Philippe Pageaux¹², Jean-Yves Mabrut¹³, Ephrem Salamé¹⁴, François Faitot¹⁵, Audrey Coilly¹⁶, Jean Hardwigsen¹⁷, Thomas Decaens¹⁸, Faiza Chermak¹⁹, Fabrice Muscarello²⁰, Rodolphe Anty²¹, Christophe Duvoux²², Armand Abergel²³, Anne Minello Franza²⁴, Christine Binquet²⁵, Marianne Latournerie²⁴. ¹CHU Dijon Bourgogne, INSERM, Université de Bourgogne, CIC 1432, Module Épidémiologie Clinique, Dijon, France, Dijon, France; ²Agence de Biomédecine, Direction Prélèvement Greffe Organes-Tissus, Saint-Denis La Plaine, France; ³Service des maladies de l'appareil digestif, CHRU de Lille, France, Lille, France; ⁴Université Lille 2 and Inserm U795, Lille, France; ⁵Service d'Hépatogastroentérologie, Hôpital Édouard Herriot, Hospices Civils de Lyon, Lyon, France; ⁶Service de Chirurgie Hépatobiliaire, Hôpital de la Pitié-Salpêtrière, Paris, France; ⁷Service de Soins Intensifs, Hôpital de la Pitié-Salpêtrière, Paris, France; ⁸Service de Soins Intensifs, Hôpital de la Pitié-Salpêtrière, Paris, France; ⁹Service de Soins Intensifs, Hôpital de la Pitié-Salpêtrière, Paris, France; ¹⁰Service de Soins Intensifs, Hôpital de la Pitié-Salpêtrière, Paris, France; ¹¹Service de Soins Intensifs, Hôpital de la Pitié-Salpêtrière, Paris, France; ¹²Service de Soins Intensifs, Hôpital de la Pitié-Salpêtrière, Paris, France; ¹³Service de Soins Intensifs, Hôpital de la Pitié-Salpêtrière, Paris, France; ¹⁴Service de Soins Intensifs, Hôpital de la Pitié-Salpêtrière, Paris, France; ¹⁵Service de Soins Intensifs, Hôpital de la Pitié-Salpêtrière, Paris, France; ¹⁶Service de Soins Intensifs, Hôpital de la Pitié-Salpêtrière, Paris, France; ¹⁷Service de Soins Intensifs, Hôpital de la Pitié-Salpêtrière, Paris, France; ¹⁸Service de Soins Intensifs, Hôpital de la Pitié-Salpêtrière, Paris, France; ¹⁹Service de Soins Intensifs, Hôpital de la Pitié-Salpêtrière, Paris, France; ²⁰Service de Soins Intensifs, Hôpital de la Pitié-Salpêtrière, Paris, France; ²¹Service de Soins Intensifs, Hôpital de la Pitié-Salpêtrière, Paris, France; ²²Service de Soins Intensifs, Hôpital de la Pitié-Salpêtrière, Paris, France; ²³Service de Soins Intensifs, Hôpital de la Pitié-Salpêtrière, Paris, France; ²⁴Service de Soins Intensifs, Hôpital de la Pitié-Salpêtrière, Paris, France; ²⁵Service de Soins Intensifs, Hôpital de la Pitié-Salpêtrière, Paris, France

POSTER PRESENTATIONS

biliaire; Hôpital Jean Minjoz, Besançon, France; ⁷Service d'Hépatologie; Hôpital Jean Minjoz, Besançon, France; ⁸Service d'Hépatologie; Hôpital Jean Minjoz, Besançon, France; ⁹Service des Maladies du Foie, CHU Rennes, Rennes, France; ¹⁰Service d'Hépatologie, Hôpital Pitié-Salpêtrière, Assistance Publique des Hôpitaux de Paris, Paris, France; ¹¹Service d'hépatologie, Hôpital Beaujon, Assistance Publique des Hôpitaux de Paris, Clichy, France; ¹²Service d'Hépatologie, CHU Montpellier, Montpellier, France; ¹³Service de chirurgie digestive et transplantation, Hôpital La Croix Rousse, Hospices Civils de Lyon, Lyon, France; ¹⁴Service de chirurgie digestive et transplantation hépatique, CHU Tours, Tours, France; ¹⁵Service de chirurgie; CHU Strasbourg, Strasbourg, France; ¹⁶Service d'Hépatologie, Hôpital Paul Brousse, Assistance Publique des Hôpitaux de Paris, Villejuif, France; ¹⁷Service de chirurgie digestive et transplantation hépatique, CHU Marseille, Marseille, France; ¹⁸Service d'Hépatogastroentérologie, CHU Grenoble, LA TRONCHE, France; ¹⁹Service d'Hépatogastroentérologie, CHU Bordeaux, Pessac, France; ²⁰Service Chirurgie Hépatobilio-Pancréatique et Transplantation, CHU Toulouse, Toulouse, France; ²¹Service d'Hépatologie, CHU Nice, Nice, France; ²²Service d'hépatologie, CHU Henri Mondor, Créteil, France; ²³Service d'Hépatologie, CHU de Clermont Ferrand, Clermont Ferrand, France; ²⁴Service d'Hépatogastroentérologie, CHU Dijon-Bourgogne, Dijon, France; ²⁵CHU Dijon Bourgogne, INSERM, Université de Bourgogne, CIC 1432, Module Épidémiologie Clinique, Dijon, France
Email: marianne.latournerie@chu-dijon.fr

Background and aims: Indications for liver transplantation (LT) are changing, with older recipients, with more comorbidities. To help in the selection of recipients who will benefit most from LT in the context of graft shortage, we aimed to develop and validate a score to predict the one-year post-LT risk of death in recipients aged 60 years and over.

Method: This cross-sectional study used data from the national transplantation database managed by French national Biomedicine Agency. Logistic regressions were used to develop the score. The population was split into a training set (70%) and a test set (30%). The predictive ability of the score was assessed using Harrell's C-statistic.

Results: 3158 patients aged 60 years and over who received their first elective LT between 2007 and 2017 were included: 38.4% aged over 65 years and 4.2% over 70 years. 90% had cirrhosis (64% alcoholic), with a median Meld score at 14, and hepatocellular carcinoma (HCC) in 56% of cases. Older patients appeared to more often have cirrhosis unrelated to alcohol consumption ($p < 0.001$). They more often have comorbidities as diabetes ($p = 0.037$) and renal insufficiency ($p = 0.023$). Their cirrhosis was less severe at transplant ($p < 0.001$) and was more often complicated by HCC (68% in patients over 70 years vs 58% in patients between 60 and 65 years, $p < 0.001$). Time on the waiting list increased with age (352 days vs 145 days, $p < 0.001$), as did donor age (62 years vs 58 years; $p = 0.024$).

One-year mortality after LT was 13.7%. Male sex, history of portal vein thrombosis, lower glomerular filtration rate, endotracheal intubation at LT and longer cold graft ischemia were associated with a higher risk of death at one-year post LT, whereas HCC was associated with a lower risk. According to the weight of each of these 6 variables, we constructed a score to predict the risk of death at 1 year post LT and illustrated it with a nomogram. The discriminant ability of the score on the test set was of 0.61 (95%-Confidence Interval = 0.57–0.68).

Conclusion: In this real-life study, we found that careful selection of the oldest patients ensures good results after LT. However, comorbidities and organ failure have a great impact on one-year mortality in this population. This is the first one-year mortality score that can help with the decision to list potential LT recipients aged 60 years and over.

SAT-011

Everolimus and de novo malignancies after liver transplantation in a nationwide french cohort study: an emulated target trial

Ilias Kounis^{1,2,3,4,4}, Long Nguyen⁵, Christophe Desterke², Nathalie Goutte¹, Didier Samuel^{1,2,3,4}, Daniel Azoulay^{1,2,3}, Eric Vibert^{1,2,3,4}, Audrey Coilly^{1,2,3,4}, Paul Landais², Cyrille Feray^{1,2,3,4}.
¹AP-HP Hôpital Paul-Brousse, Centre Hépatobiliaire, Villejuif, France; ²Inserm, Université Paris-Saclay, UMR-S 1193, Villejuif, France; ³Université Paris-Saclay, Inserm, Physiopathogénèse et traitement des maladies du Foie, Villejuif, France; ⁴France FHU Hepatinov, Villejuif, France; ⁵Department of Public Health, Copenhagen, Denmark
Email: ilias.kounis@aphp.fr

Background and aims: De novo malignancies (DNM) following liver transplantation (LT) is as a major cause of post-transplant mortality. Everolimus is an mTor inhibitor with both antitumoral and antirejection properties. We aimed to evaluate the DNM burden after LT at a nationwide level and assess, in emulated target trials, the influence of everolimus in their occurrence.

Method: The French national health data system (SNDS), linked with the national hospital database (PMSI), contains information on 99% of the French population, including ICD-10 codes, medical procedures (MP), prescribed drugs, and vital status. We identified a total of 7,964 patients discharged after LT from 01/01/2009 to 01/01/2020. Different emulated target trials (cloning-censoring-weighting approach) comparing everolimus ($n = 2,036$ (25.5%)) and control were performed with grace periods of 6 months to 4-years after LT, and outcomes being overall survival (OS) and DNM free survival, 2 to 10 years after LT.

Results: The cumulative incidence of de novo malignancies was 15.1% at 5 years and 25.7% at 10 years post-LT. Head and neck cancers and skin cancers were the most common, each accounting for 5.0% of cases. The 10-year overall survival rates varied by cancer type, with gynecological cancer having the highest rate (72.4%) and head and neck cancer the lowest (24.4%). Among the entire cohort, 2,036 (25.5%) received everolimus. In emulated trials, for grace periods <2 years the treated group showed higher DNM free survival rates with a 10-year overall survival difference up to 10%. However, for each grace period, 10y-OS was less for everolimus (up to 10%). Competitive risk (with death) analysis confirmed the favorable effect of everolimus on DNM: 28% less at 10-y.

Conclusion: We confirmed the frequency and severity of DNM after LT previously reported. Systematic screening is clearly insufficient, particularly for ORL and lung. More importantly, emulating randomized trials showed that everolimus lowered DNM free survival when prescribed within the first 2 years following LT.

SAT-013

Sequential normothermic regional and end-ischemic ex-situ machine perfusion allows the safe use of very old DCD donors in liver transplantation (DCDNet trial)

Caterina Martinelli¹, Davide Ghinolfi¹, Daniele Pezzati¹, Jessica Bronzoni¹, Arianna Trizzino¹, Emanuele Balzano², Paola Carrai¹, Gabriele Catalano¹, Stefania Petruccielli³, Giovanni Tincani¹, Simona Palladino¹, Davide Ghinolfi¹. ¹University of Pisa hospital, Division of Hepatic Surgery and Liver Transplantation, Pisa, Italy; ²University of Pisa Hospital, Pisa, Italy; ³University of Pisa hospital, Division of Hepatic Surgery and Liver Transplantation, Pisa, Italy
Email: piero93.vacca@gmail.com

Background and aims: In Italy, 20 minutes of continuous, flat-line electrocardiogram are required for death declaration. Despite prolonged warm ischemia time, Italian centers reported good outcomes in controlled DCD (cDCD) liver transplantation by combining normothermic regional and end-ischemic machine perfusion. This study aimed to evaluate the safety and feasibility of the use of septuagenarian and octogenarian cDCD donors with this approach.

Method: All cDCD older than 70 years were evaluated during normothermic regional perfusion (NRP) and then randomly assigned to dual hypothermic (D-HOPE) or normothermic machine perfusion (NMP).

Results: In the period from April 2021 to December 2023, 25 cDCD older than 70 years were considered. In 9 cases (36%) the graft was not considered suitable for liver transplantation: 3 on NRP parameters, 2 on histology, 1 due to hepatic artery thrombosis at procurement, 2 on NMP parameters, and 1 due to machine perfusion technical failure. Sixteen (64%) liver grafts were eventually transplanted. The median donor age was 82 years (IQR: 79–84), being 9 (56%) older than 80. The mean functional warm ischemia was 39 ± 15 minutes. Grafts were randomly assigned to D-HOPE (9 grafts) and NMP (7 grafts). There were no cases of primary non-function, one of the patients (D-HOPE LT) experienced delayed non-function, treated with retransplantation. Four cases of post-reperfusion syndrome (25%, 50% D-HOPE vs 50% NMP group) and 2 cases (12%) of early allograft dysfunction were observed. At a median follow-up of 12 months, no vascular complications were reported. Three patients experienced biliary complications: 2 anastomotic stenosis and 1 biliary fistula. No patients experienced ischemic cholangiopathy. No major differences were found in terms of post-operative hospitalization or complications based on the type of machine perfusion.

Conclusion: The implementation of sequential normothermic regional and end-ischemic machine perfusion allows the safe use of very old DCD donor grafts in liver transplantation.

SAT-014-YI

Bariatric surgery post-liver transplantation: a Belgian nationwide study

Louis Onghena¹, Anja Geerts², Frederik Berrevoet³, Jacques Pirenne⁴, Jef Verbeek⁵, Eliano Bonaccorsi⁶, Géraldine Dahlqvist⁷, Luisa Vonghia⁸, Olivier Detry⁹, Jean Delwaide¹⁰, Sander Lefere¹¹, Yves Van Nieuwenhove¹². ¹Liver Research Center Ghent, Ghent University, Ghent University Hospital, Ghent, Belgium; ²Hepatology Research Unit, Gent, Belgium; ³Department of General and Hepatobiliary Surgery and Liver Transplantation, Ghent, Belgium; ⁴Department for Abdominal Transplant Surgery and Coordination, Leuven, Belgium; ⁵Department of Gastroenterology and Hepatology, Leuven, Belgium; ⁶Abdominal Transplant Unit, Cliniques Universitaires Saint-Luc, Louvain, Belgium; ⁷Department of Hepatogastroenterology and Liver Transplantation, Brussels, Belgium; ⁸Division of Gastroenterology and Hepatology, Antwerp, Belgium; ⁹Department of Abdominal Surgery and Transplantation, Liege, Belgium; ¹⁰Department of Hepatogastroenterology, Liege, Belgium; ¹¹Hepatology Research Unit, Ghent, Belgium; ¹²Department of Gastrointestinal Surgery, Ghent, Belgium

Email: Louis.onghena@ugent.be

Background and aims: Weight gain and metabolic dysfunction-associated steatotic liver disease (MASLD) pose a rising graft concern post-liver transplantation (LT). Bariatric surgery (BS) can be considered for post-LT weight gain, although the literature is limited and the long-term outcome still uncertain. We previously reviewed the literature and concluded that timing is crucial when considering BS in a population with liver disease or transplantation. Our current aim was to describe the demographics, mortality, and effect of BS in a post-LT population.

Method: We conducted a national retrospective analysis in 5 Belgian transplant centres and included 25 patients with a liver transplantation between 1/1/2000 and 31/12/2018 followed by a bariatric procedure between 1/1/2005 and 31/12/2020. 187 LT patients without BS were included for comparison. Clinical, biochemical and outcome data were retrospectively retrieved. Statistical analysis was performed using the t-test, Mann-Whitney U, and Chi2 tests.

Results: In our nation-wide sample, 25 patients had undergone BS post-LT, at a median 3.5 (2.1, 5.6) years after LT. Twenty-one (84.0%) patients received a sleeve gastrectomy (SG), 3 (12.0%) a Roux-en-Y

gastric bypass (RYGB) and 1 (4.0%) a one-anastomosis gastric bypass. All but one procedure (96.0%) were performed laparoscopically. Patients were predominantly male (72.0%), with a lower age at time of transplantation compared to non-BS population (54.5 vs 60.6, $p < 0.0001$). Transient acute kidney failure (20.0%) was the only short-term complication occurring in more than one patient, all after SG. Weight loss was significant and sustained, with a decrease in BMI from 41.0 ± 4.5 pre-BS to 32.6 ± 5.8 ($p < 0.0001$) 1 to 3 years post-BS and 31.1 ± 5.8 ($p < 0.0001$) 3 to 5 years post-BS. Post-LT pre-BS three (12.0%) patients presented with recurrent and one (4.0%) de novo MASLD, with 100% resolution post-BS ($p = 0.016$). Notable reductions were observed in ALT levels (40.5 ± 28.5 U/L to 27.1 ± 25.1 U/L post-BS, $p = 0.051$) and HbA1c levels (6.9 ± 1.6 to 6.0 ± 1.4 post-BS, $p < 0.0001$). Daily mycophenolic acid intake rose from 1000.0 ± 288.7 mg/day to 1392.8 ± 1619.3 mg/day ($p < 0.0001$), while the dose of ciclosporin decreased from 258.3 ± 91.7 mg/day to 146.0 ± 107.4 mg/day ($p = 0.137$). Three patients were re-transplanted, and eight patients died, of which five (20.0%) due to a non-hepatic malignancy and one (4.0%) due to liver failure. Given the small sample size and relatively high mortality due to competing risks, a statistical analysis of patient or transplant-free survival was not feasible.

Conclusion: SG is the favored BS post-LT and has proven to be safe and feasible in a post-LT setting. SG post-LT is a valid treatment for de novo and recurrent MASLD post-LT. Although we report on the largest cohort to date, there is still a need for larger cohorts to examine the effect of BS on graft survival.

SAT-015-YI

Screening for asymptomatic coronary artery disease in liver transplant recipients: is it time to replace stress echocardiography with coronary CT angiography in selected patients?

Chiara Manuli¹, Margherita Saracco¹, Roberta Lasco¹, Gian Paolo Caviglia¹, Bruna Lavezzo², Donatella Cocchis³, Mauro Giorgi⁴, Riccardo Faletti⁵, Carla Guarnaccia⁵, Angelo Panio², Antonio Ottobrelli¹, Renato Romagnoli³, Silvia Martini¹.

¹Gastrohepatology Unit, AOU Città della Salute e della Scienza di Torino, Turin, Italy; ²Anesthesia and Intensive Care Unit 2, AOU Città della Salute e della Scienza di Torino, Turin, Italy; ³General Surgery 2U, Liver Transplantation Center, AOU Città della Salute e della Scienza di Torino, Turin, Italy; ⁴Cardiology Unit, AOU Città della Salute e della Scienza di Torino, Turin, Italy; ⁵Department of Imaging Diagnostics and Radiotherapy, AOU Città della Salute e della Scienza di Torino, Turin, Italy
Email: chiara.manuli@gmail.com

Background and aims: Asymptomatic coronary artery disease (CAD) has been reported in up to 25% of liver transplant (LT) candidates. Pre-LT cardiovascular (CV) work-up is not yet standardized, but in 2022 coronary-CT angiography (c-CT) was proposed by the American Heart Association in pre-LT selected patients (pts). We aimed to compare two CV screening protocols at our large-volume transplant Centre.

Method: We enrolled all adult cirrhotic pts who underwent first-LT between 01/2019–12/2022 in our Center. In the first period (2019–2021) echostress (EchoS) was performed in the presence of 3 minor (age 60–64 years, arterial hypertension, non-insulin treated diabetes, BMI >29 Kg/m², CAD family history, active smoking) or 1 major CV risk factors (insulin-treated diabetes, age >64 years, peripheral vascular disease, MASLD). From 1/2022 c-CT was performed with 1 major CV risk factor, and EchoS with 3 minor CV risk factors. Coronary angiography (CATH) was performed in pts with CAD history/symptoms, positive/doubtful non-invasive test or cardiology indication. Follow-up was closed on 31/12/2023.

Results: 477 pts were included: 374 (78%) in first period and 103 (22%) in second one. First vs second period: CV risk factors prevalence was similar: age >64 years 26% vs 25% ($p = 0.9$), previous CAD 2% vs 2% ($p = 1$), male sex 74% vs 80% ($p = 0.2$), previous stroke/TIA 2% vs 2% ($p = 1$), diabetes 26% vs 32% ($p = 0.2$), MASLD 10% vs 9% ($p = 0.8$), BMI >29 Kg/m² 12% vs 14% ($p = 0.6$), peripheral vascular disease 1% vs 4% ($p = 0.07$), except for CAD family history which was higher in the first

POSTER PRESENTATIONS

period (15% vs 8%, $p=0.05$). Non-invasive CAD screening was performed in 196 (52%) of the pts of the first period and 55 (53%) of the second one ($p=0.9$). In the second period, the use of EchoS decreased from 52% ($n=196$) to 42% ($n=43$) ($p=0.055$) and the use of c-CT increased from 3% (13 c-CT available outside the Centre protocol) to 23% ($n=24$, $p<0.001$). Positive screening tests increased from 2% ($n=8$) to 8% ($n=8$) ($p=0.01$) and the use of CATH was 6% ($n=23$) in the first period and 11% ($n=11$) in the second ($p=0.1$). 14/477 patients (3%) underwent revascularization, 9 (2%) in the first and 5 (5%) in the second period ($p=0.2$). When considering patients who underwent both CATH and non-invasive screening tests (18 EchoS + CATH and 11 c-CT + CATH), positive predictive value was 62% for EchoS and 67% for c-CT, while negative predictive value (NPV) was 60% for EchoS and 100% for c-CT. The 2-year cumulative incidence of post-LT ischemic CV events was 2.3% and it was similar in the two periods ($p=0.8$). Among 10 pts with post-LT heart ischemic events within 2 years, 7/10 (70%) tested negative at pre-LT EchoS.

Conclusion: In our cohort of 477 LT candidates, 7/10 (70%) pts with 2-year post-LT heart ischemic event tested negative at pre-LT EchoS. The implementation of c-CT in the cardiac work-up decreased the risk of underdiagnosing asymptomatic CAD in LT candidates (NPV: 60% EchoS and 100% c-CT).

SAT-016

Assessment of the role of liver transplantation with or without combined kidney transplantation in polycystic liver or liver and kidney disease

Gwladys Lubuela¹, Dominique Joly², Federica Dondero³, Dany Anglicheau⁴, Corinne Antoine⁵, Christophe Legendre⁶, Olivier Roux¹, Emmanuel Weiss⁷, Carmen Lefaucheur⁸, Arnaud Mejean⁹, Alexandre Hertig¹⁰, Safi Dokmak³, Mickael Lesurtel³, Francois Durand¹, Claire Francoz¹. ¹Hepatology Hopital Beaujon, Clichy, France; ²Hopital Necker, Paris, France; ³Hepatobiliary Surgery and Liver Transplantation Hopital Beaujon, Clichy, France; ⁴Kidney Transplantation Hopital Necker, Paris, France; ⁵Nephrology, Hopital Saint Louis, Paris, France; ⁶Kidney Transplantation Hopital Necker, Paris, France; ⁷Anesthesiology and LICU, Hopital Beaujon, Clichy, France; ⁸Nephrology and Kidney Transplantation Hopital Saint Louis, Paris, France; ⁹Urology, Hopital Pitié-Salpêtrière, Paris, France; ¹⁰Nephrology and Kidney Transplantation, Hopital Foch, Suresnes, France
Email: claire.francoz@gmail.com

Background and aims: Management of severe polycystic liver, or liver and kidney disease, is not standardized. Liver transplantation (LT) could be the best curative option in patients with major disabling related to hepatomegaly or cysts with recurrent episodes of infections difficult to manage with conservative treatments. In Patients with associated end-stage kidney disease, combined liver and kidney transplantation (CLKT) could be proposed. We report here a large monocentric study evaluating the results of LT or CLKT.

Method: From 1995 to 2022, 134 patients were transplanted for polycystic liver, or liver and kidney disease, in a single transplant center, after a median waiting time of 9 months. Among them, 101 received CLKT and 33 LT alone.

Results: There were 84% females, and the median age was 52 years. Indication for LT was large hepatomegaly in 90% of patients and cysts recurrent infections in 10%. Manifestations related to hepatomegaly were abdominal pain and early satiety in most of patients, while as high as 48% had dyspnea. As expected, all had normal liver function. Only 25% of patients had previous radiological or surgical treatment (sclerotherapy = 10%, cyst fenestration = 7% and liver resection = 10%) and 12% had received somatostatin analogues. In patients who underwent CLKT, the mean glomerular filtration rate (GFR) at listing was 14 ml/min and 40% were on dialysis. Among patients who received CLKT, 14% had previous kidney transplantation, while they were 12% in those receiving LT alone. At 10 years, patients' survival was excellent, 85% in CLKT and 83% in LT alone. In CLKT, kidney graft

survival was also excellent: 98% at 10 years while no patients required re LT. Whatever patients received CLKT or LT alone, a marked improvement in quality of life was always observed. However, 7 patients with polycystic liver and kidney disease (21%) who underwent LT alone, all with GFR >60 at transplantation, developed end-stage kidney disease and sequential kidney transplantation with a median interval between LT and KT of 95 months, possibly related to the combination of progression of polycystic kidney disease and calcineurine inhibitors.

Conclusion: This large series shows that a major improvement in quality of life can be achieved in patients with major hepatomegaly and that long term survival is excellent. In patients with CLKT, long-term kidney graft survival exceeds 95% at 10 years, much higher than in patients receiving kidney transplantation alone. These results argue against reluctance to perform liver transplantation in this population.

SAT-017

QuantIFERON monitor as an immune function assay predictive of clinical events in liver transplant recipients: a validation study

Tess McClure^{1,2}, Boris Wong², Fan Zhang², Alexander Dobrovic², Vijayaragavan Muralidharan^{1,2}, Adam Testro^{1,2}. ¹Austin Health, Heidelberg, Australia; ²The University of Melbourne, Parkville, Australia
Email: tess.e.mcclure@gmail.com

Background and aims: Despite the judicious use of immunosuppression, most liver transplantation (LT) recipients experience complications such as rejection and infection. There is a clear need for innovative tools to quantify recipient immune function. QuantIFERON Monitor (QFM) is an immune function assay that involves stimulating whole blood with innate and adaptive immune ligands to induce release of interferon- γ (IFN γ). Between 2012 and 2013, Austin Health pioneered the study of QFM in 75 adult LT recipients, and found that week 1 results correlated with early clinical events. A high IFN γ (>4.45 IU/ml) was associated with a risk of rejection (area under the receiver operating characteristic curve [AUROC], 0.77; $p=0.002$), and a low IFN γ (<1.30 IU/ml) with a risk of infection (AUROC, 0.74; $p=0.008$) within the first month post-LT. The following validation study aimed to re-examine the utility of QFM in a larger cohort of adult LT recipients.

Method: 100 adults were recruited pre-LT from 2019 to 2022 and followed up for 12 months. Additional blood for QFM testing was taken pre- and post-LT (day 1, 3, 5; week 1, 2; month 1, 2, 4, 6, 12). The primary end points were the accuracy of QFM in predicting rejection, defined as treated biopsy-proven acute rejection (tBPAR) and infection, classified as 'probable' or 'definite' as per an international sepsis forum consensus conference.

Results: In these 100 LT recipients, the median age was 55 years and 66% were males. 94% had cirrhosis and 37% had a hepatoma. The most common disease etiologies were alcohol (42%) and hepatitis C (19%). The median pre-LT Model for End Stage Liver Disease-Sodium was 21. The median donor age was 43 years. 89% of donations were after brainstem death, 19% received OrganOx support and 6% proceeded to a split LT. Post-LT, recipients routinely received weaning steroids, a calcineurin inhibitor and an antimetabolite. 75% of patients received basiliximab. 54 recipients experienced 32 episodes of tBPAR and 84 infections. The first event was tBPAR in 14% and infection in 40%. The most common time for tBPAR (10/32) and infections (14/84) was week 1 to month 1 post-LT. At the time of submission, QFM results were available for 98 patients. The median pre-LT QFM was 20.20 IU/ml. The median week 1 QFM varied significantly between patients who were well or had a clinical event ($p=0.0007$) within the first month post-LT. A high IFN γ was associated with the risk of rejection (AUROC, 0.84; $p=0.0049$), and low IFN γ with a risk of infection (AUROC, 0.76; $p=0.0131$), as seen in the original study. Further analysis is ongoing to determine optimal clinical thresholds.

Conclusion: QFM has been shown to be predictive of early rejection and infection post-LT. In this subsequent study, our preliminary

results validate these findings in a larger cohort of adult LT recipients. Further research, in the form a multi-centre randomised trial, is required for clinical translation.

SAT-018-YI

Liver transplantation in cystic fibrosis: the evolving landscape in the United Kingdom

Georgeina L. Jarman¹, Maria Jacobs², Rhiannon Taylor², William J. H. Griffiths¹. ¹Cambridge Liver Unit, Addenbrooke's Hospital, Cambridge University Hospitals NHS Foundation Trust, Cambridge, United Kingdom; ²Statistics and Clinical Research, NHS Blood and Transplant, Bristol, United Kingdom
Email: george.jarman@nhs.net

Background and aims: Cystic fibrosis-related liver disease (CFLD) is a common extra-pulmonary manifestation of cystic fibrosis (CF) with a range of phenotypes, from asymptomatic steatosis to end-stage cirrhosis with portal hypertension. With no specific medical therapies, and exclusion from Cystic Fibrosis Transmembrane conductance Regulator (CFTR) modulator trials, patients with advanced CFLD have historically progressed towards transplantation, often encumbered by multi-morbidity. Here we aimed to review the evolving landscape of liver transplantation in CF in the United Kingdom.

Method: National data through NHS Blood and Transplant identified patients with CF who had been registered for liver transplantation (including multi-organ) between 1989 and 2023. Super-urgent registrations were excluded. Data was collected on registration and transplant numbers, outcomes, donor type and patient and graft survival.

Results: 136 of the 188 patients registered for liver transplant (including multi-organ) between 1990 and 2023 were transplanted (72.3%). Across this period, within 12 months of listing for transplantation, 19 patients died and 10 were removed from the waiting list, including 1 in 2020–2023 due to condition improvement. Most livers came following donation after brainstem death (DBD), with only 3 transplants from donation after cardiac death (DCD), all since 2010. 2 patients received split livers from living-related donors. Historically, multi-organ transplantation was more common, with 3 patients undergoing combined liver-pancreas and 2 liver-kidney transplants. 10 heart-lung-liver transplants were performed between 1991 and 2001 and 6 liver-lung transplants have been completed, though combined liver-cardiothoracic transplants had generally poor survival outcomes (5-year survival 42.9% (95% CI 17.7–66), 1989–2018). No CF patients have been registered multi-organ transplantation since 2019. 5-year survival following isolated liver transplantation remained static at 66.7% (95% CI 19.5–90.4) in 1989–1994 and 2015–2018, respectively ($p = 0.9$).

Conclusion: Liver transplantation has provided a vital therapy to those with end-stage CFLD for almost 35 years in the UK. Trends in solid-organ transplantation have evolved; with a focus on single-organ transplantation, likely in light of combined liver-cardiothoracic outcomes. We may see further shifts in the field, with advancements in machine perfusion of DCD organs helping to close the gap between transplant demand and availability. CFTR modulators may help optimise respiratory health of patients requiring liver transplantation, reducing their burden of co-morbidity, and potentially improving outcomes. With time, optimised medical therapy with CFTR modulators in childhood may help to prevent advanced CFLD and render liver transplantation in CF obsolete.

SAT-019

Recipient donor sex constellation differences in outcome after liver transplantation for hepatocellular carcinoma-an ELTR study

Christian Magyar¹, Noah Arteaga¹, Giacomo Germani², Vincent Karam³, René Adam⁴, Lucienne Christen¹, Federico Storni¹, Corina Kim-Fuchs¹, Anja Lachenmayer¹, Guido Beldi¹, Daniel Candinas¹, Pompilia Radu¹, Birgit Schwacha-Eipper¹,

Annalisa Berzigotti¹, Vanessa Banz¹, for the European Liver and Intestine Transplant Association (ELITA)³. ¹Department of Visceral Surgery and Medicine, Inselspital, Bern University Hospital, University of Bern, Bern, Switzerland; ²Multivisceral Transplant Unit, Department of Surgery, Oncology and Gastroenterology, Padua University Hospital, Padua, Italy; ³The European Society for Organ Transplantation, Amsterdam, Netherlands; ⁴Department of Surgery, Centre Hepatobiliary, Hopital Paul Brousse, Paris, France
Email: vanessa.banz@insel.ch

Background and aims: Hepatocellular carcinoma (HCC) is the third leading cause of cancer-related deaths worldwide. Liver transplantation (LT) is the mainstay of curative treatment, as approximately 90% of HCC develop in chronic liver disease. Donor and recipient sex appears to have an impact on HCC recurrence and death after LT. We describe recipient donor sex constellation (RDSC) specific oncological outcome differences in patients receiving LT.

Method: We performed a European Liver Transplant Registry (ELTR) analysis including patients from 1988 to December 2022. Patients with incomplete tumor variables on histopathology, as well as retransplantation events, were removed. According to the RDSC the following four groups are compiled: female donor female recipient (FDFR), female donor male recipient (FDMR), male donor female recipient (MDFR) and male donor male recipient (MDMR). Survival analysis was performed using Kaplan Meier and Cox regression proportional hazard models. To adjust, factors for an a priori multivariable model were selected (histopathology, number of nodules, largest lesion size and vascular invasion status). Due to design of the registry, no adjustment for comorbidities was feasible. Data was collected in accordance with the General Data Protection Regulation, the European Union legislation and the ELTR privacy policy. The data used in the study was anonymous.

Results: Of the 7601 LT for HCC, 7428 recipients (98%) had concomitant cirrhosis. The median number of HCC lesions on histopathology was 2.0 (IQR 1.0, 3.0), median lesion size 2.8 cm (2.0, 4.0), macrovascular invasion in 275 (4.4%) and in 2822 (42%) the tumor burden was classified as beyond 'Milan criteria'. In 4784 (63%) an HCC pre-transplant specific treatment was registered. Overall median follow-up was 22.6 months (5.8, 60.7) with death registered in 1905 (25%) and, as primary cause of death, HCC tumor recurrence was seen in 496 (26%) of patients. The cohort was split into the four RDSC groups: 743 FDFR, 2325 FDMR, 548 MDFR and 3985 MDMR. There was no statistically significant difference on crude survival estimates (log-rank $p = 0.66$) with 10-year overall survival (OS) of 54% in FDFR, 55% in FDMR, 59% in MDFR and 57% in MDMR. In the a priori multivariable analysis, a trend of the effect of RDSC on OS was seen (FDFR as reference): FDMR (HR 0.91, $p = 0.332$), MDFR (HR 0.78, $p = 0.058$) and MDMR (HR 0.85, $p = 0.086$). Female recipients had a significant higher risk of death with dysfunctioning graft (FDFR 39% MDFR 43%) compared to male recipients (FDMR 29%, MDMR 32%) ($p = 0.035$). Regarding overall registered causes of death, differences between RDSC groups were found in rejection ($p = 0.017$) and cardiovascular ($p = 0.046$) associated deaths.

Conclusion: Female recipients show a trend towards worse long-term oncological outcome, if they receive a sex-mismatched organ.

SAT-020

Evaluation of 18FDG-PET/CT for prediction of waitlist dropout and post transplantation recurrence in patients listed for hepatocellular carcinoma

Catherine Lamarque¹, Anna Sessa¹, Edouard Reizine¹, Sébastien Mulé¹, Julia Chalaye¹, Norbert Ngongang¹, Nadia Oubaya¹, Vincent Leroy¹, Christophe Duvoux¹. ¹University Hospital Henri Mondor, Créteil, France
Email: catherine.lamarque@yahoo.fr

Background and aims: Efficacy of liver transplantation (LT) for HCC is limited by the increasing number of HCC indications and by organ shortage. This results in a 15–20% dropout rate before LT, and in a 10–

POSTER PRESENTATIONS

15% risk of HCC recurrence after LT. To optimize intent-to-treat efficacy, prediction of dropout should be improved. ¹⁸FDG- PET/CT recently showed encouraging results in predicting post-LT recurrence. Yet, whether ¹⁸FDG-PET/CT may also predict waitlist dropout remains unknown. Our objectives were to investigate the value of ¹⁸FDG-PET/CT in the prediction of wait-list dropout in HCC candidates, and to further analyse its role in the prediction of post-LT recurrence.

Method: Retrospective exploratory monocentric study in a cohort of patients listed for HCC between 01/2013 and 11/2018. All patients had been investigated with ¹⁸FDG-PET/CT at work-up. ¹⁸FDG-PET/CT was considered positive when tumor to liver SUV ratio was ≥ 1.15 . The primary end point was the preLT risk of dropout for tumor progression or death; secondary endpoint was 5-year-postLT recurrence free survival.

Results: 105 patients were enrolled: median age 59 yo [55;64], MELD 8 [6;14], number of tumor 2 [1;2], tumor size 1.8 cm [1.2;1.5], Milan criteria in 82.9%, AFP score 0/1/2 in respectively 62%/21.9%/11.4%. Pre-LT 15-month dropout-free survival rate was 77.4%. The 15-month risk of wait-list drop-out tended to be significantly higher in patients with positive ¹⁸FDG-PET/CT compared to patients with a negative one with 28.6% (95% CI: 14.00;52.8) vs 12.3% (95% CI: 6.8;21.7), respectively ($p = 0.08$). By multivariate analysis, ¹⁸FDG-PET/CT tumor to liver SUV ratio, and number of tumors were independent prognostic factors of waitlist dropout for tumor progression or death (OR of 2.56 (95%CI 1.28; 5.15) and 1.7 (95% CI 1.16; 2.5), respectively). Among 72 patients eventually transplanted, 5-year HCC recurrence free survival was significantly higher in patients with negative ¹⁸FDG-PET/CT compared to patients with a positive one: 90.5% (95% CI: 78.6; 95.9) vs 50% (95%CI: 20.8; 73.6), respectively ($p = 0.002$).

Conclusion: This study a- confirms the predictive value of ¹⁸FDG-PET/CT for post-LT recurrence, b- for the 1st time, suggests that ¹⁸FDG-PET/CT has the potential to predict dropout from the waitlist. Subject to retrospective design and population size, this study emphasizes the crucial role that ¹⁸FDG-PET/CT may play in pre-LT work up of HCC patients, to refine selection of HCC candidates and to improve prioritization of these patients. It eagerly calls for a larger multicenter prospective assessment of FDG PET/CT in HCC candidates.

SAT-021

Recurrence of autoimmune hepatitis cholestatic variant syndromes after liver transplantation affects graft and patient survival in an international multicentre cohort

Vincenzo Ronca^{1,2,3,4,5}, Alessandro Parente^{6,7,8}, Ellina Lytyvak⁹, Bettina Hansen¹⁰, Gideon M. Hirschfield¹⁰, Alan Bonder¹¹, Maryam Ebad¹², Saleh Elwir¹³, Mohamad Alsaed¹³, Piotr Milkiewicz¹⁴, Maciej Janik¹⁵, Hanns-Ulrich Marschall¹⁶, Maria Antonella Burza¹⁶, Cumali Efe¹⁷, Ali Riza Caliskan¹⁸, Murat Harputluoglu¹⁹, Gökhan Kabaçam²⁰, Debora Raquel Terrabuio²¹, Fernanda Onofrio²², Nazia Selzner²², Albert Pares²³, Laura Patricia Llovet²³, Murat Akyildiz²⁴, Cigdem Arkan²⁵, Michael P. Manns²⁶, Richard Taubert²⁶, Anna-Lena Weber²⁶, Thomas Schiano²⁷, Brandy Haydel²⁸, Piotr Czubkowski²⁹, Piotr Socha³⁰, Natalia Oldak³⁰, Nobuhisa Akamatsu³¹, Atsushi Tanaka³², Cynthia Levy³³, Eric F. Martin³⁴, Aparna Goel³⁵, Mai Sedki³⁵, Irena Jankowska³⁶, Toru Ikegami³⁷, Maria Rodriguez³⁸, Martina Sterneck³⁸, Christina Weiler-Normann³⁸, Christoph Schramm³⁸, Maria Francesca Donato³⁹, Ansgar W. Lohse⁴⁰, Raul J. Andrade⁴¹, Vilas Patwardhan⁴², Bart van Hoek⁴³, Maaike Biewenga⁴⁴, Andreas Kremer⁴⁵, Yoshihide Ueda⁴⁶, Mark Deneau⁴⁷, Mark Pedersen⁴⁸, Marlyn J. Mayo⁴⁸, Annarosa Floreani⁴⁹, Patrizia Burra⁵⁰, Maria Francesca Secchi⁵¹, Benedetta Terziroli⁵², Marco Sciveres⁵³, Giuseppe Maggiore⁵⁴, Syed-Mohammed Jafri⁵⁵, Dominique Debray⁵⁶, Muriel Girard⁵⁷, Florence Lacaille⁵⁸, Michael Heneghan⁵⁹, Andrew L. Mason¹², Ye Htun Oo^{6,7,60}, Aldo J. Montano-Loza¹². ¹Centre for Liver and Gastro Research,

Birmingham NIHR Inflammation Biomedical Research Centre, Birmingham, United Kingdom; ²Liver Unit, Queen Elizabeth University Hospital, Birmingham, Birmingham, United Kingdom; ³Department of Biomedical Sciences, Humanitas University, Pieve Emanuele, Italy; ⁴IRCCS Humanitas Research Hospital, Rozzano, Italy; ⁵Institute of Immunology and Immunotherapy, University of Birmingham, Birmingham, United Kingdom; ⁶Centre for Liver and Gastro Research, Birmingham, United Kingdom; ⁷NIHR Inflammation Biomedical Research Centre, Birmingham, United Kingdom; ⁸Liver Unit, Queen Elizabeth University Hospital, Birmingham, United Kingdom; ⁹Department of Medicine, University of Alberta, Edmonton, Canada; ¹⁰Toronto Center for Liver Disease, University Health Network, University of Toronto, Toronto, Canada; ¹¹Beth Israel Deaconess Medical Center, Harvard Medical School, Boston, United States; ¹²Division of Gastroenterology and Liver Unit, University of Alberta, Edmonton, Canada; ¹³Baylor University Medical Center, Dallas, United States; ¹⁴Liver and Internal Medicine Unit, Medical University of Warsaw, Warsaw, Poland; ¹⁵Liver and Internal Medicine Unit, Medical University of Warsaw, Warsaw, Poland; ¹⁶Sahlgrenska University Hospital, Gothenburg, Sweden; ¹⁷Department of Gastroenterology, Harran University Hospital, Şanlıurfa, Turkey; ¹⁸Department of Gastroenterology, İnönü University School of Medicine, Malatya, Turkey; ¹⁹Department of Gastroenterology, İnönü University School of Medicine, Malatya, Turkey; ²⁰Clinic of Gastroenterology and Liver Transplantation, Güven Hospital, Ankara, Turkey; ²¹Department of Gastroenterology-University of São Paulo School of Medicine, São Paulo, Brazil; ²²Toronto Center for Liver Disease, UHN, Toronto, Canada; ²³Liver Unit, Hospital Clínic, University of Barcelona, IDIBAPS, CIBERehd, Barcelona, Spain; ²⁴Koç University School of Medicine, Department of Gastroenterology and Liver Transplantation Center, Istanbul, Turkey; ²⁵Koc University School of Medicine Pediatric Gastroenterology and Hepatology, Organ Transplantation Center, Koc University Research Center for Translational Medicine (KUTTAM), Istanbul, Turkey; ²⁶Dept. Gastroenterology, Hepatology and Endocrinology, Hannover Medical School, Hannover, Germany, European Reference Network on Hepatological Diseases, Hannover, Germany; ²⁷Recanati/Miller Transplantation Institute/ Division of Liver Diseases, Mount Sinai Medical Center, New York, United States; ²⁸Adult Liver Transplantation, Mount Sinai Medical Center, New York, United States; ²⁹Department of Gastroenterology, Hepatology, Nutritional Disorders and Pediatrics, The Children's Memorial Health Institute, Warsaw, Poland; ³⁰Department of Gastroenterology, Hepatology, Nutritional Disorders and Pediatrics, The Children's Memorial Health Institute, Warsaw, Poland; ³¹University of Tokyo, Tokyo, Japan; ³²Department of Medicine, Teikyo University School of Medicine, Tokyo, Japan; ³³University of Miami Miller School of Medicine, Miami, United States; ³⁴Miami Transplant Institute, University of Miami Miller School of Medicine, Miami, United States; ³⁵Stanford University, Stanford, United States; ³⁶Children's Memorial Health Institute, Warsaw, Poland; ³⁷Department of Surgery and Science, Graduate School of Medical Sciences, Kyushu University, Fukuoka, Japan; ³⁸UKE Hamburg, Hamburg, Germany; ³⁹Foundation IRCCS Ca' Granda Ospedale Maggiore Policlinico, Liver Transplant Hepatology Unit, Milan, Italy; ⁴⁰University Medical Center, Hamburg, Hamburg, Germany; ⁴¹Gastroenterology Service -IBIMA. University Hospital and CIBERehd. University of Málaga, Malaga, Spain; ⁴²Beth Israel Deaconess Medical Center, Harvard Medical School, Boston, United States; ⁴³Leiden University Medical Center, Leiden, Netherlands; ⁴⁴Leiden University Medical Center, Leiden, Netherlands; ⁴⁵Department of Gastroenterology and Hepatology, University Hospital Zürich, University of Zürich, Zürich, Switzerland; ⁴⁶Department of Gastroenterology and Hepatology, Graduate School of Medicine, Kyoto, Japan; ⁴⁷University of Utah, Salt Lake City, United States; ⁴⁸The University of Texas Southwestern Medical Center, Dallas, United States; ⁴⁹Department of Surgery, Oncology and Gastroenterology, University of Padova, Padova, Italy; ⁵⁰Department of Surgery, Oncology and Gastroenterology, Padova University Hospital, Padova, Italy; ⁵¹University of Padova, Padova, Italy; ⁵²Epatocentro Ticino and Università della Svizzera Italiana, Lugano, Switzerland; ⁵³UPMC Pediatric Liver Center, Palermo, Italy; ⁵⁴Hepatogastroenterology,

Nutrition and Liver Transplant IRCCS Bambino Gesù Pediatric Hospital, Rome, Italy; ⁵⁵*Henry Ford Health System, United States;* ⁵⁶*Pediatric Liver Unit, Paris Descartes University and French National Reference Center for rare diseases BA and Genetic Cholestasis, Paris, France;* ⁵⁷*Université de Paris, Liver hepatology unit Necker Hospital, and French National Reference Center for Rare Diseases BA and Genetic Cholestasis, Paris, France;* ⁵⁸*Hôpital NECKER, Paris, France;* ⁵⁹*King's College Hospital NHS Foundation Trust, London, United Kingdom;* ⁶⁰*Liver Unit, Queen Elizabeth University Hospital, Birmingham, United Kingdom*
Email: Vincenzo.ronca@hunimed.eu

Background and aims: A significant proportion of patients with variant syndromes (VS), namely AIH/PBC or AIH/PSC require liver transplantation (LT), despite treatment. The frequency of disease recurrence and the effect on graft survival is yet to be clarified. The aim of this international, multicentric, retrospective study is to evaluate risk factors associated with recurrence and the impact of the disease recurrence after LT on graft and patient survival.

Method: We evaluated 172 patients undergoing LT for VS in 33 centres in North America, South America, Europe and Asia. Clinical data before and after LT, biochemical data within the first 12 months after LT, and immunosuppression after LT were analysed to identify patients with a higher risk of recurrence of autoimmune disease based on histological and radiological diagnosis. Cumulative probabilities of graft and overall survival after LT were calculated using semi-Markov model.

Results: VS recurred after LT in 23% and 33% of patients after 5 and 10 years, respectively. An increased ALP and ALT at 12 months after LT (HR, 1.60; 95% CI, 1.13–2.25; $p < 0.01$, HR, 1.25; 95% CI, 1.01–1.53; $p = 0.03$) and acute rejection (HR 3.58; 95% CI, 1.60–7.73; $p < 0.01$) were found associated with a higher risk of VS syndrome recurrence, whilst the use of prednisone (lo)ne was associated with a reduced risk (HR 0.30, 95% CI 0.14–0.64, $p < 0.01$). After adjusting for ALT and ALP at 12-months, the use of prednisone (lo)ne was found to be independently and negatively associated with recurrent disease. The recurrence of VS was found significantly associated with graft loss and patients' survival at the multivariate Cox regression analysis with time-dependent covariate. The 5-, 10- year probability of graft survival was 68% and 41% in patients with recurrent VS compared to 83% and 60% in patients without recurrent disease (p value, $p = 0.01$). The overall survival was significantly reduced in patients with recurrent disease ($p = 0.01$), with event probability at 5- and 10- years of 75% and 49% vs 84% and 60% in patients without recurrence.

Conclusion: VS recurrence after LT is frequent and is associated with elevation of liver enzymes within the first year after LT and rejection episodes. VS recurrence negatively impacts graft and patient survival. Strategies are warrant to prevent VS recurrence or mitigate its negative effects.

SAT-022

Post-recurrence survival after liver transplantation for hepatocellular carcinoma: outcomes of an "orphan" disease

Marianna Maspero¹, Carlo Sposito¹, Marco Bongini¹, Sherrie Bhoori¹, Valentina Bellia¹, Andrea Schlegel², Vincenzo Mazzaferro¹.

¹Fondazione IRCCS Istituto Nazionale dei Tumori, Milan, Italy;

²Cleveland Clinic, Cleveland, United States

Email: marianna.maspero@istitutotumori.mi.it

Background and aims: During the last decades, liver transplantation (LT) for hepatocellular carcinoma (HCC) has undergone profound changes regarding patient selection, transplant criteria, downstaging and bridging therapies, allocation policies and immunotherapeutic regimens. Despite this, the main driver of post-transplant mortality in these patients remains HCC recurrence. The aim of this study was to determine whether post-transplant survival has improved during the last two decades.

Method: Using the Scientific Registry of Transplant Recipients (SRTR), we included all patients who underwent LT for HCC between 2003 and 2020 in the United States and experienced HCC recurrence. We

divided them into four eras (2003–2007, 2008–2012, 2013–2016, 2017–2020) according to their year of transplant and analyzed their post-recurrence survival.

Results: 26309 patients underwent LT for HCC (era 1: 4810, 18%; era 2: 7617, 29%; era 3: 7179, 27%; era 4: 6703, 25%). Unadjusted post-transplant 5-year survival was different between the eras (1: 69%, 2: 73%; 3: 80%; 4: 75%; $p < 0.001$) with better survival in more recent eras despite an increase in Milan-OUT patients (1: 3%; 2: 4%; 3: 12%; 4: 13%). Patients who experienced recurrence were 2960 (11%): 689 in era 1, 988 in era 2, 739 in era 3 and 544 in era 4. In later eras, patients with recurrence were older (median age 1: 56; 2: 58; 3: 61; 4: 63), with more MASLD (1: 14%; 2: 28%; 3: 25%; 4: 32%), were more likely to have received bridge therapies (1: 60%; 2: 76%; 3: 90%; 4: 95%) and be outside Milan (1: 4%; 2: 5; 3: 25%; 4: 21%), however had lower AFP scores (AFP score >2 1: 17%; 2: 10.5%; 3: 6%; 4: 2%). Despite these differences, median post-recurrence survival was similar: 10 (IQR 3–27) months for era 1; 12 (IQR 3–31) months for era 2; 12 (IQR 4–31) months for era 3; and 13 (IQR 4–26) for era 4 (log rank p value = 0.178). After adjusting for bridge therapy before transplant, AFP score >2 at transplant and age, post-recurrence survival remained similar.

Conclusion: Post-recurrence survival after LT for HCC has not improved during the last two decades. Research efforts for this "orphan" disease should be made to implement post-recurrence survival, particularly in light of the new available therapeutic options.

SAT-023

Development of a model to preoperatively predict the risk of microvascular invasion for hepatocellular carcinoma patients undergoing liver transplantation

Quirino Lai¹, Suela Ajdini¹, Jean Emond², Arvinder Singh Soin³, Tomoharu Yoshizumi⁴, André Viveiros⁵, Maria Hoppe Lotichius⁶, Takashi Ito⁷, Massimo Rossi¹, Albert CY Chan⁸, Chao-Long Chen⁹, Umberto Cillo¹⁰, Timothy Pawlik¹¹, Jan Lerut¹². ¹Sapienza University of Rome, Rome, Italy; ²Columbia University, New York, United States; ³Medanta-The Medicity, New Delhi, India; ⁴Kyushu University, Fukuoka, Japan; ⁵Medical University of Innsbruck, Innsbruck, Austria; ⁶Universitätsmedizin Mainz, Mainz, Germany; ⁷Graduate School of Medicine, Kyoto, Japan; ⁸The University of Hong Kong, Hong Kong, Hong Kong; ⁹Kaohsiung Chang Gung Memorial Hospital, Kaohsiung, Taiwan; ¹⁰Padua University, Padua, Italy; ¹¹The Ohio State University Wexner Medical Center, Columbus, United States; ¹²Universite Catholique Louvain, Brussels, Belgium
Email: lai.quirino@libero.it

Background and aims: Microvascular invasion (MVI) represents a relevant prognostic factor in the setting of hepatocellular carcinoma (HCC). A recent study by Endo et al. proposed a model in the setting of liver resection. A refined model to predict MVI based on preoperative variables in the setting of liver transplantation (LT) is proposed in the present study.

Method: Patients undergoing LT for HCC between 2000 and 2018 were identified using a multi-institutional database. A total of 2,170 patients were split in a Training (70%) and a Validation Set (30%). Therefore, a preoperative predictive model for MVI was built and externally validated.

Results: Among the entire cohort, MVI was observed in 586 patients (27.0%). On multivariable logistic regression analysis in the Training Set, three preoperative parameters associated with MVI were identified: α -fetoprotein (lnAFP; odds ratio [OR] = 1.19; 95% confidence interval [CI] = 1.13–1.27), imaging tumor burden score (lnTBS; OR = 1.66; 95%CI = 1.39–1.99) and living donor LT (LDLT; OR = 1.99; 95%CI = 1.56–2.53). The c-index of the Validation Set was 0.74 vs. 0.69 observed for the score by Endo (Brier Skill Score +13%). The new score presented a relevant net reclassification index (NRI), with 34.4% of correct reclassification rate for the events and 26.6% for non-events (overall NRI = 0.61). Stratifying the Validation Set in three risk strata (0–50th, 51st–75th, >75th centile of the score), a very good stratification was observed in terms of disease-free (5-year: 89.3,

POSTER PRESENTATIONS

75.5, and 50.7%, respectively) and overall survival rates (5-year: 79.5, 72.6, and 53.7%, respectively).

Conclusion: Preoperative assessment of MVI using the present model showed very good accuracy to predict MVI after LT.

SAT-024-YI

Impact of ISO score on oncological outcomes and survival in HCC patients candidate for liver transplantation

Elisa Pinto¹, Martina Gambato¹, Filippo Pelizzaro¹, Francesco Paolo Russo¹, Victor Echavarria², Patrizia Burra¹, Enrico Gringeri¹, Alessandro Vitale¹, Umberto Cillo¹. ¹University of Padua, Padua, Italy; ²Hospital Universitario Marqués de Valdecilla, Santander, Santander, Spain
Email: pintoelisa93@gmail.com

Background and aims: Liver transplantation (LT) is the most efficacious curative treatment for hepatocellular carcinoma (HCC). Waiting list (WL) prioritization criteria determine patient outcomes. Since 2015, the Italian Score for Organ Allocation (ISO) has been used in Italy to prioritize patients on the WL, introducing a specific policy for HCC. In this study, we aimed to assess the impact of ISO-score on WL dropout, HCC recurrence, and patient survival in LT candidates with HCC.

Method: This retrospective study included all patients with HCC listed for LT (n = 378) at our institute between January 2013 and December 2020. We considered 2 groups: patients prioritized before (group A, 2013–2015) and after (group B, 2016–2020) ISO score implementation. We used cumulative incidence functions within a competing risk time-to-event analysis to assess and compare, between the 2 groups, the probabilities of LT, WL death and dropout. Uni- and multivariable logistic regression models were also used to identify potential risk factors associated with WL mortality.

Results: Group B patients were older than group A patients ($p = 0.01$), presenting more grading 3 HCC in the explanted liver (group A: 8.3%, group B: 16.8%; $p = 0.04$). After the implementation of ISO score, a higher rate of HCC metabolic dysfunction associated steatotic liver disease (MASLD)-related (group A: 7%, group B: 11.7%; $p = 0.03$) have been registered.

During a median follow-up of 49 months, 289 HCC patients underwent LT, 4 patients (13%) died before LT, and 71 patients (18%) were removed from WL for HCC progression. According to the competing risk multivariate analysis, WL dropout rate was similar in the two groups ($p = 0.07$). Downstaging treatments ($p = 0.0001$) and alpha-fetoprotein (AFP) levels ($p = 0.0001$) were identified as risk factors for WL dropout. HCC recurrence after LT rate was significantly lower in group B patients than group A ($p = 0.03$), also confirmed at multivariate analysis ($p = 0.04$). Group B patients showed higher overall survival (OS) than group A patients ($p = 0.04$), without difference in no-HCC related deaths between the two groups ($p = 0.049$).

Conclusion: After the introduction of ISO score, a lower HCC recurrence after LT has been observed as well as an improved overall survival after LT. These findings strongly suggest that the implementation of the ISO score has enhanced the allocation process for HCC patients, resulting in a substantial increased transplant benefit.

SAT-025

“Early” vs “standard” liver transplantation in patients with severe alcoholic hepatitis

Raffaella Viganò¹, Giovanni Perricone¹, Chiara Mazzarelli², Adelaide Panariello³, Chiara Becchetti², Marcello Vangelì⁴, Monica Cucco², Lucia Cesarini², Francesca Aprile², Martina Luca⁵, Giulia Dispenzieri⁶, Elena Roselli⁷, Luciano De Carlis⁸, Aldo Airolidi⁹, Luca Saverio Belli⁹. ¹Hepatology and Gastroenterology Unit, ASST GOM

Niguarda, Milan, Italy; ²ASST GOM Niguarda, Hepatology and Gastroenterology Unit, Milan, Italy; ³ASST GOM Niguarda, Department of Mental Health and Addiction Services, Milan; ⁴ASST GOM Niguarda, Hepatology and Gastroenterology Unit, Milan; ⁵Fondazione IRCCS Ca' Granda Ospedale Maggiore Policlinico, Liver Transplant Hepatology Unit, Milan, Italy; ⁶University of Milano-Bicocca, Division of Gastroenterology and Center for Autoimmune Liver Diseases, San Gerardo Hospital and Department of Medicine and Surgery, Monza, Italy; ⁷ASST GOM Niguarda, Department of Anesthesiology, Milan, Italy; ⁸ASST GOM Niguarda, Department of General Surgery and Transplantation, University of Milano-Bicocca, School of Medicine and Surgery, Milan, Italy; ⁹ASST GOM Niguarda, Hepatology and Gastroenterology Unit, Milan, Italy, Milan, Italy
Email: raffaella.vigano@ospedaleniguarda.it

Background and aims: Liver transplantation (LT) is an established therapeutic option for a subgroup of highly selected patients with alcoholic-hepatitis non[1]responder to medical treatment (MT). While some patients have a rapidly progressive disease leading to an early-LT, others initially improve with MT but need to be evaluated for a standard-LT in the following months for persisting decompensation.

Aim of the study is to describe the features of early-LT versus standard-LT for severe alcoholic hepatitis.

Method: One hundred consecutive patients with severe-AH referred to our center since April 2016 were considered, with those non-responder to medical treatment being evaluated for LT.

Results: Fifty-three patients were non-responder to MT and 17 underwent early-LT within 27 days from admission. Of the 47 responder patients, 14 were subsequently listed with 13 being transplanted after a median of 166 days for persisting decompensation despite initial clinical improvement, Fig.1. Patients receiving standard-LT had lower MELD-Na scores at presentation compared to early-LT (27 vs 34; $p = 0.008$) and a lower prevalence of ACLF-grade 2–3 (23% vs 82.4%; $p = 0.002$). After multivariate analysis patients with MELD-Na ≥ 30 at index hospitalization were 5.88 (95%CI:2.31–16.41) times more likely to be non-responders to MT than those with a MELD-Na < 30 , while those with ACLF grade 2–3 were 12.56 (95% CI:4.95–35.04) times more likely to be non responders as compared to those with ACLF grade 0–1 (Fig). Overall, 15 LT recipients (50%) suffered from depression and 10 (33%) received antidepressants post-LT. Three patients in all (10%) relapsed into any alcohol consumption. Twenty-nine (97%) are currently alive after a median follow-up of 32.2 months from LT.

Conclusion: Patients with SAH have different patterns of progression. Of those transplanted, 57% received an early-LT and 43% a standard LT. Overall, the transplant benefit was huge and relapse into alcohol consumption acceptable, 10%. Treatment of psychiatric comorbidities proved valuable to mitigate the risk of relapse.

SAT-026

Liver stiffness is associated with the results of long-term protocol biopsies in liver transplant patients recipients

Pauline Bozon-Rivière¹, Stéphanie Faure¹, José Ursic Bedoya¹, Magdalena Meszaros¹, Astrid Herrero¹, Benjamin Riviere¹, Georges-Philippe Pageaux¹, Lucy Meunier¹. ¹Regional University Hospital Center of Montpellier, Montpellier, France
Email: pauline.riviere@hotmail.fr

Background and aims: Survival after liver transplantation (LT) is 74% at 5 years and 63% at 10 years. Liver biopsy (LB) is the gold standard for diagnosing post-LT complications (1). However, the use of LB as a monitoring tool is limited by its invasiveness, cost and risk of sampling error. In many indications, Vibration Controlled Transient Elastography (VCTE) has replaced biopsy for assessing liver stiffness. Some preliminary studies have demonstrated the feasibility and diagnostic performance of VCTE for the detection of fibrosis and steatosis following LT (2, 3). However, no data exists concerning the value of VCTE for long-term follow-up after LT compared with a

protocol LB in asymptomatic patients. Our study aimed to compare VCTE with protocol LB in LT patients.

Method: Patients 5 to 10 years post-LT with both protocol LB and VCTE were included. VCTE was used to measure liver stiffness measurement (LSM) and steatosis via Controlled Attenuation Parameter. The primary end point was the performance of the VCTE in predicting an abnormal LB.

Results: Among the 278 patients who underwent LT between 2012 and 2017 in our center, 138 had both LB and VCTE assessment. 80 patients could be analysed. Most of this patients were men (n = 55, 69%), with a mean age of 61 ± 10.2 years. The main indications for LT were alcohol (n = 37; 46.3%) and hepatitis B or C virus (n = 17; 21.3%). The median time between LT and LB was 6 years (IQR 5–8) and between LB and VCTE was 42.5 days (IQR 22–79). Of the 80 LB performed, 40 (50%) were normal and 14 (16%) showed steatosis with no other abnormalities. 26 (32.5%) were abnormal: acute cellular rejection (n = 9), fibrosis (n = 11), recurrence of initial disease (n = 6). Mean LSM was 8.2 ± 8 kPa (range 3.1–74.5) with a mean CAP of 242 ± 55 dB/m. Patients with abnormal LB had higher elastography (12.69 (±14.64) vs 6.02 (±1.95); p < 0.001). Liver tests were more frequently abnormal in patients with high elastography: ASAT (27.62 (±14.22) vs 21.15 (±10.93); p = 0.023), ALT (24.85 (±16.32) vs 18.91 (±13.73); p = 0.046), bilirubin (12.9 (±8.23) vs 8.8 (±4.36); p = 0.011). Elastography (AUC: 0.79 (95% CI: [0.68–0.899])) had the best statistical performance in predicting an abnormal LB compared with ALT (AUC: 0.638 (95% CI: [0.503–0.773])) and bilirubin (AUC: 0.679 (95% CI: [0.555–0.803])). For elastography, the threshold with the highest Youden index was 6.6 kPa. Elastography <5.4 kPa ruled out an abnormal LB (Se 92.3%, Sp 44.4%, VPN 92.3%, VPP 44.4%) and a value above 8.5 kPa predicted an abnormal LB (Se 42.3%, Sp 94.4%, VPN 77.3%, VPP 78.6%). **Conclusion:** For patients in the 5 to 10-year post-LT period, elastography becomes a valuable tool in discerning those who may benefit from a protocol biopsy (>8.5 kPa) or find it unnecessary (<5.4 kPa), particularly in the absence of biological abnormalities. These results underscore the appropriateness of employing VCTE in long-term LT recipients to determine the need for a LB.

SAT-027

Women are also disadvantaged in accessing transplant outside the United States: analysis of the spanish liver transplantation registry

Marta Tejedor¹, Fernando Neria², Gloria de la Rosa³, Carolina Almohalla Alvarez⁴, María Padilla⁵, Andrea Bosca⁶, Yilliam Fundora⁷, Francisco Sánchez-Bueno⁸, Miguel Ángel Gómez Bravo⁹, Marina Berenguer¹⁰. ¹Hospital Universitario Infanta Elena, Madrid, Spain; ²Universidad Francisco de Vitoria, Madrid, Spain; ³Organización Nacional de Trasplante (ONT), Madrid, Spain; ⁴Hospital Universitario Río Hortega, Valladolid, Spain; ⁵Organización Nacional de Trasplantes (ONT), Madrid, Spain; ⁶Hospital Universitari i Politècnic La Fe, Valencia, Spain; ⁷Hospital Clínic de Barcelona, Barcelona, Spain; ⁸Hospital Clínico Universitario Virgen de la Arrixaca, Murcia, Spain; ⁹Hospital Universitario Virgen del Rocío, Sevilla, Spain; ¹⁰La Fe University and Polytechnic Hospital, Valencia, Spain
Email: marta_tejedor@hotmail.com

Background and aims: Sex inequities in liver transplantation (LT) have been documented in several mostly US-based studies. Our aim was to describe the recipient profile over time in Spain, particularly regarding potential sex-related differences in access to LT.

Method: All adult patients registered in the RETH-Spanish Liver Transplant Registry from 2000 to 2022 for LT were included. Baseline demographics, presence of hepatocellular carcinoma (HCC), cause and severity of liver disease, time on the waiting list (WL), access to transplantation, and reasons for removal from the WL were assessed.

Results: 14,385 patients were analysed (77% men, 56.2 ± 8.7 years). Model for end-stage liver disease (MELD) score was reported for 5475 patients (38%), with a mean value of 16.6 ± 5.7. Overall, fewer women received a LT (79% vs 82%, p < 0.001) and a greater proportion were

excluded (10% vs 8%, p = 0.004) from the WL compared to men. Women were less likely to receive a transplant than men (OR 0.78, 95%CI 0.63, 0.97) and more likely to be excluded for deterioration (HR 1.17, 95%CI 0.99, 1.38), despite similar liver disease severity (MELD score for women 16.6 ± 5.7 vs men 16.6 ± 5.7, N.S.). Women waited longer on the WL (198.6 ± 338.9 vs 173.3 ± 285.5 days for men, p < 0.001). In recent years, women's risk of dropout of the WL due to deterioration or death has reduced (2000–2010: HR 1.49 [95%CI 0.99, 2.25]; 2011–2016: HR 0.93 [95%CI 0.64, 1.36]; 2017–2022: HR 0.93 [95%CI 0.57, 1.51]), concomitantly with reduced WL times (mean waiting time for women and men respectively was 473.6 ± 693.7 vs 408.4 ± 593.1 days [p = 0.078] between 2000–2010; 207.0 ± 251.0 vs 186.5 ± 223.1 days [p = 0.005] between 2011–2016; and 104.2 ± 148.2 vs 88.7 ± 118.2 days [p < 0.001] between 2017–2022). The probability of being transplanted was lower for women before 2011 (OR 0.68, 95% CI 0.49, 0.96; p = 0.026). However, recently no significant differences in access to LT were found by sex (2011–2016: OR 0.82 [95%CI 0.60, 1.13]; 2017–2022: OR 0.77 [95%CI 0.57, 1.05]). Time on the WL did not seem to influence the risk of women undergoing transplant (HR 0.95 [95%CI 0.90, 1.01]).

Conclusion: Even in countries with short waiting times, women wait longer and have a higher risk of exclusion from the WL. Policies directed at optimizing the whole LT network should be encouraged to guarantee a fair and equal access of all patients to this life saving resource.

SAT-028

The relationship between spleen stiffness and portal hypertension liver transplant patients

Kanan Nuriyev¹, Zülal İstemihan¹, Pelin Telli¹, Asim Qurbanov¹, Mehmet Akif Yağlı¹, Gizem Dağcı¹, Aynure Rüstemzade¹, Sezen Genç Uluççen¹, Bilger Çavuş¹, Aslı Çıfıbaşı Örmeci¹, Filiz Akyuz¹, Kadir Demir¹, Fatih Beşışık¹, Sabahattin Kaymakoglu¹. ¹Istanbul University, Istanbul Faculty of Medicine, Department of Internal Medicine, Division of Gastroenterohepatology, İstanbul, Turkey
Email: dr_bilgercavus@yahoo.com

Background and aims: In our study, we aimed to reveal the relationship between spleen stiffness and the presence of portal hypertension after post transplant patients who are non cirrhotic.

Method: Spleen and liver stiffness was measured with Fibroscan® in liver transplant patients followed up at the liver transplant outpatient clinic of a tertiary university hospital. “Independent T-test” and “Chi-square test” were calculated. AUC was calculated within the scope of ROC analysis in order to predict the cut-off value of spleen and liver stiffness in revealing the presence of esophageal varices after liver transplantation (LT).

Results: A total of 50 patients who underwent LT at least 6 months ago (mean transplant time was 117 ± 74 months) were included in the study. Patients who developed liver cirrhosis or portal vein thrombosis after LT were excluded from the study. 70% of the patients were women, the mean age was 52.5 ± 12.9 years. 37% of the patients had cadaveric transplants. 60% of the patients had post-transplant gastroscopy results and were included in the study. Gastroscopy examination, which were performed within 6 months after transplantation, were not included in the study. All patients had liver cirrhosis before LT. HBV and cryptogenic liver cirrhosis were the most common etiologies. All patients had esophageal varices before LT, and esophageal varices were detected in 12% of patients during post-transplant gastroscopy. The mean liver stiffness was determined as 6.4 ± 2.4 kPa and the mean spleen stiffness was 29.5 ± 18.7 kPa. The mean spleen size was 136 ± 33 mm. A significant positive relationship was detected between spleen size and spleen stiffness (p < 0.01). Low platelet values after LT were associated with high liver stiffness (p < 0.05). A longer period of time after LT was associated with decreased spleen stiffness (p < 0.05). Male gender, presence of shunt before LT and history of variceal bleeding were found to be associated with increased spleen stiffness (p < 0.05). ROC analysis was performed to

POSTER PRESENTATIONS

evaluate whether spleen and liver stiffness predicted the presence of esophageal varices after LT. It was observed that liver stiffness did not have a statistically significant difference ($p > 0.05$). It was observed that spleen stiffness had 79.5% discrimination (AUC) with its cut-off value of 27.95 kPa, and had a statistically significant discrimination with its sensitivity (%66, 7) and specificity (%66, 7) values ($p = 0.028$). **Conclusion:** In patients with LT due to cirrhosis, spleen stiffness greater than 27.9 kPa on FibroScan® predicts the presence of esophageal varices. Male gender, the presence of portosystemic shunt before LT, and a history of variceal bleeding were associated with increased spleen stiffness.

SAT-029

Induction therapy using rabbit anti-thymoglobulin and IVIG for hyperimmunized liver transplant recipients

Nada El-domiaty^{1,2}, Audrey Coilly¹, Eleonora De Martin¹, Wafaa Ibrahim³, Philippe Ichai¹, Daniel Azoulay¹, Eric Vibert¹, René Adam¹, Jean Luc Taupin¹, Daniel Cherqui¹, Didier Samuel¹, Faouzi Saliba¹. ¹AP-HP Hôpital Paul Brousse, Hepato-Biliary Centre, Villejuif-France, INSERM UMR 1193 and Université Paris Saclay, Paris, France; ²Endemic Medicine Department, Faculty of Medicine, Helwan University, Cairo, Egypt; ³Statistics Department, Faculty of Economics and Political Science, Cairo University, Cairo, Egypt
Email: nadadomty@hotmail.com

Background and aims: Liver transplantation (LT) for hyperimmunized recipients with positive crossmatch or with preformed DSA pose unique challenges due to increased sensitization and risk of antibody-mediated rejection (AMR). Induction therapy, in HLA sensitized liver transplant recipients, with rabbit anti-thymocyte globulin (rATG) has been used to prevent and to treat AMR.

Method: Consecutive hyperimmunized recipients who underwent LT between 2016 and 2022 were retrospectively reviewed. Characteristics of patients, donor, immunological status, liver biopsies and outcomes were collected.

Results: Of the 44 adult recipients (mean age of 47.1 ± 14.4 years) and mean follow-up of 35.1 ± 26.3 months, 29 patients were females (65.9%) and 15 patients were males (34.1%). 36/44 patients (82.8%) had undergone first LT, and 8 (18.2%) recipients had a previous LT. The main indications for primary LT were hepatocellular carcinoma (22.7%), biliary cirrhosis (18.2%), alcoholic related cirrhosis (11.4%). At time of transplant, the mean MELD score was 21.8 ± 9.4 , sensitized recipients with positive HLA antibodies I and II were 83% and 85.4% respectively. 79.5% of the recipients had positive D/R crossmatch. All the recipients received induction therapy with rATG (3 mg/kg/day at day 0, 1, 2) associated to a triple immunosuppression regimen (Methylprednisolone, MMF and tacrolimus). High dose human immunoglobulins (IVIG, 2 g/Kg) were administered to lower anti-HLA antibodies levels. Among 44 patients, 5 patients developed acute cellular rejection (11.4%), 7 patients (15.9%) developed AMR. The 1, 3-year overall survival rates were 83.3%, and 76.7%. The 1, 3 years overall survival among patients respectively with rejection and without rejection were comparable (87.1%, 87.1% and 81.1, 76.3%). 3/44 had re-transplanted due to primary non function graft (2/3) and AMR (1/3). A total of 10/44 patients (22%) died due to sepsis ($n = 5$), cerebral hemorrhage ($n = 3$), HCC recurrence ($n = 2$). Mean intensive care unit stay was 10.4 ± 9.8 days. No serious adverse events were related to induction.

Conclusion: Induction therapy using rATG and IVIG for 3 days for hyperimmunized liver transplant recipients minimize the incidence and impact of antibody mediated rejection on patient and graft survival.

SAT-030

A visual classification scale of biliary anastomotic strictures with per-oral cholangioscopy predicts outcomes in liver transplant recipients

Alex Bofill¹, Lesly Calixto¹, Octavi Bassegoda¹, Alejandro Fernandez-Simon¹, Oriol Sendino¹, Henry Cordova¹, Andres Cardenas². ¹Hospital Clinic, Barcelona, Spain; ²Hospital Clinic, Barcelona, Barcelona, Spain
Email: acardena@clinic.cat

Background and aims: Biliary anastomotic strictures (BAS) after liver transplantation (LT) are the most common biliary adverse events in LT recipients. They are mostly managed with endoscopic retrograde cholangiopancreatography (ERCP). Prior data from our group showed that per-oral cholangioscopy (POCS) identifies two distinct visual stricture patterns: type A (scarring) and type B (erythema with sloughing and/or ulceration). This study analyzed these two stricture patterns and compared treatment outcomes.

Method: Prospective single-center study at Hospital Clinic of Barcelona of LT recipients with BAS that underwent POCS over a 7-year period (2016–2022).

Results: 45 patients with suspected post-LT biliary strictures underwent POCS. Baseline characteristics (age, sex, etiology, time from LT to POCS and therapy) according to the type of stricture were similar. The main indications for POCS were evaluation of complex biliary strictures including selective guidewire placement across strictures (95.6%) and therapy of common bile duct stones above a BAS (4.4%). POCS successfully visualized the biliary tract in 93.3% of patients (42/45). In 38 LT recipients the BAS was successfully visualized, whereas in four POCS no stenosis was confirmed. Type A strictures were present 63.2% (24/38) and Type B in 36.8% (14/38) of LT recipients with BAS. During follow-up (median follow-up 28 months), stricture resolution was successfully accomplished with endoscopic treatment in 83% of type A strictures and in 50% of type B strictures ($p = 0.029$). Additionally, the need for alternative treatments such as percutaneous interventions or surgery was significantly higher in those with type B strictures (50%) compared to pattern A strictures (12.5%) ($p = 0.011$). The cumulative probability of stricture resolution was significantly higher in type A compared to type B ($p = 0.045$). Adverse events (all mild) occurred in 6/45 patients (13.3%): 3 cholangitis, 2 pancreatitis, 1 controlled bleeding.

Conclusion: A visual classification scale of BAS in LT recipients with POCS demonstrates that type A BAS is associated with a higher resolution compared to type B BAS. The proposed classification Barcelona Anastomotic Stricture Scale (BASS) allows to predict outcomes of therapy in LT recipients with BAS. Further validation studies are needed.

SAT-031-YI

Evolution of pre liver transplant cardiovascular risk factors and cardiac work-up: impact on post-transplant events

Margherita Saracco¹, Chiara Manuli¹, Roberta Lasco¹, Mimma Bonomo¹, Bruna Lavezzo², Gian Paolo Caviglia³, Donatella Cocchis⁴, Mauro Giorgi⁵, Antonio Ottobrelli¹, Renato Romagnoli⁴, Silvia Martini¹. ¹Gastrohepatology Unit, AOU Città della Salute e della Scienza di Torino, Turin, Italy; ²Anesthesia and Intensive Care Unit 2, AOU Città della Salute e della Scienza di Torino, Turin, Italy; ³Department of Medical Sciences, University of Turin, Turin, Italy; ⁴General Surgery 2U, Liver Transplantation Center, AOU Città della Salute e della Scienza di Torino, Turin, Italy; ⁵Cardiology Unit, AOU Città della Salute e della Scienza di Torino, Turin, Italy
Email: margherita.saracco@gmail.com

Background and aims: Liver transplant (LT) demographics are changing. Pre-LT cardiac evaluation is crucial to prevent post-LT events, but there are significant differences between Centers in cardiac protocols. We aimed to evaluate the evolution of cardiovascular risk factors (CVRF) and of screening protocol and their impact on major CV post-LT events (MACE).

Method: We retrospectively included all adult patients (pts) who underwent first LT between 01/2015 and 12/2022 (I-era 2015–2018; II-era 2019–2022) in our Center. Pts with 3 minor CVRF [age 60–64 years (y), arterial hypertension, non-insulin diabetes, BMI ≥ 30 Kg/m², family history of coronary artery disease (CAD), active smoking] underwent stress test. Pts with 1 major CVRF [age ≥ 65 y, insulin-treated diabetes, stroke, MASLD, peripheral arterial disease (PAD)] underwent stress test until 2021 and coronary computed tomography (c-CT) since 2022. Coronary angiography (CATH) was performed in pts with CAD history, positive stress tests or cardiology indication. We collected MACE defined as ischemia, de novo arrhythmia and heart failure within 2 y from LT.

Results: 906 cirrhotic pts were included (I-era: 429, II-era: 477). Overall: median age 58 y (20% ≥ 65 y, 25% 60–64 y), 27% AH, 24% diabetics, 2% previous stroke, 11% BMI ≥ 30 kg/m², 15% with CAD family history. 419/906 (46.2%) underwent echostress, 42/906 (4.6%) myocardial scintigraphy, 39/906 (4.3%) c-CT. 52/906 (5.7%) finally underwent CATH (63% for positive non-invasive test, 37% for CAD history or cardiology indication): 15/52 (28.8%) needed pre-LT revascularization. II-era vs I-era: pts were older (59 vs 58 y, $p < 0.01$), with higher rate of diabetes (27 vs 21%, $p = 0.04$), hypertension (30 vs 24%, $p = 0.04$), alcohol cirrhosis (26 vs 20%, $p = 0.03$) and MASLD (9.4 vs 5.6%, $p = 0.03$); 297/477 (62%) vs 203/429 (47%) underwent a non-invasive cardiac test ($p < 0.01$). Pts who underwent CATH in II-era vs I-era were more often revascularized (44 vs 0%, $p < 0.01$). Within 2 y post-LT: 57 MACE were reported [30 (6.3%) in II-era; 27 (6.3%) in I-era]: 63% arrhythmia, 23% ischemia, 14% heart failure. At univariate analysis, MACE were associated with previous CAD ($p = 0.013$), PAD ($p < 0.001$), age ≥ 65 y ($p = 0.026$), male sex ($p = 0.003$). At multivariate cox-regression analysis, PAD (OR = 5.005, $p < 0.001$); previous CAD (OR = 3.645, $p = 0.03$) and male sex (OR = 3.397, $p = 0.008$) remained significantly associated with MACE. 1- and 2-y patient survival was: era-I: 95% and 92%; era-II 96% and 94%, respectively ($p = 0.08$).

Conclusion: In our cohort of 906 LT candidates enrolled between 2015–2022 (I-era 429, II-era: 477 pts), pre-LT CVRF burden increased over time, such as use of non-invasive cardiac test and of pre-LT coronary revascularization. Nevertheless, post-LT MACE incidence and 2-y survival did not differ between the 2 eras. At multivariate analysis, pre-LT PAD, previous CAD and male sex were significantly associated with post-LT MACE.

SAT-032

Risk stratification of emergent living donor liver transplantation from a nationwide survey of the Republic of Korea

Jongman Kim¹, Sang Jin Kim², Dong-Hwan Jung³. ¹Samsung Medical Center, Seoul, Korea, Rep. of South; ²Korea University College of Medicine, Ansan Hospital, Ansan, Korea, Rep. of South; ³Asan Medical Center, Seoul, Korea, Rep. of South
Email: yjongman21@gmail.com

Background and aims: Emergent living donor liver transplantation (LDLT) is vital for acute liver failure or acute-on-chronic liver failure patients facing life-threatening scenarios. Our study aimed to assess risk factors influencing the emergency of patients awaiting LDLT and outcomes of emergent LDLT using Korean nationwide data.

Method: We included patients who applied for emergency LDLT between 2017 and 2021. Subgroups included: 1) LDLT recipients (e-LDLT), 2) deceased donor liver transplant recipients (DDLT; received while waiting), 3) patients who died before receiving LT (death on waiting, DOW), and 4) patients of who recovered without LT or delayed LT > 14 d after application (emergent LDLT unnecessary group, UNN). We compared e-LDLT characteristics and survival between e-LDLT and non-emergency LDLT controls. DOW and UNN groups were compared to establish risk factors and a scoring system. Baseline characteristics, including changes in model for end-stage liver disease (Δ MELD) scores, were analyzed.

Results: Among a total of 594 applicants for emergent LDLT, the number of e-LDLT, DDLT, DOW, and UNN groups was 419, 71, 43, and 37, respectively. Adult e-LDLT 3-year survival rates were 78.3% (overall) and 90.1% (graft); 3-year survival rates of adult non-emergent LDLT patients were 89.1% (overall) and 93.7% (graft). Chronic kidney disease, ventilator use, Δ MELD scores, and retransplantation were associated with worsened adult e-LDLT survival. Leading reasons for emergency LDLT were hepatic encephalopathy, high MELD (>35), and uncontrolled bleeding. When comparing the adult DOW and adult UNN groups, hepatitis B virus (HBV), albumin, care in intensive care unit, ventilator use, and MELD score influenced patient mortality in univariable analysis.

Conclusion: Emergent LDLT showed reasonable survival with CKD, ventilator use, re-LT, and Δ MELD score as risk factors. High baseline MELD score, Δ MELD score, ventilator use, low albumin levels, and HBV relate to pre-LT mortality, reflecting the emergency of LT.

SAT-033

Three- vs. six-monthly measurement of phosphatidylethanol (PEth) in the detection of alcohol use relapse after liver transplantation (RAULT) for alcohol-associated liver disease (ALD)

Lubomir Skladany¹, Svetlana Adamcova Selcanova¹, Natalia Kubanek¹, Daniela Žilincánová¹, Daniel Jan Havaj¹, Karolina Sulejova¹, Michal Patarak¹, Lubos Chvala¹, Juan Pablo Arab², Tomáš Koller³. ¹Roosevelt University Hospital, Banská Bystrica, Slovakia; ²Department of Medicine, Division of Gastroenterology and Hepatology, University Hospital-London Health Sciences Centre, London, Canada, Ontario, Canada; ³Comenius University Faculty of Medicine, Bratislava, Slovakia
Email: lubomir.skladany@gmail.com

Background and aims: Alcohol-associated liver disease (ALD) is the leading cause of liver transplantation (LT). The prevalence of RAULT ranges from 7 to 95% and is usually diagnosed by the patient's history-based clinician's impression in combination with indirect laboratory markers of alcohol intake. The direct marker-phosphatidylethanol (PEth) has gained popularity for its precision and its ability to retrospectively capture alcohol intake over a period of 3–4 weeks. PEth results have been shown to be able to capture an additional 30% of patients with/wo RAULT misdiagnosed by a standard combination of history and indirect markers. In this study, we aimed to investigate the difference between three- and six-monthly PEth measurements in diagnosing RAULT.

Method: A prospective study of ALD patients after LT between May 2008 and June 2023. To diagnose RAULT, we introduced PEth in July 2020 and patients were enrolled in this study until June 2023. We excluded patients with <1 month post-LT follow-up. Data included demographics, direct and indirect history of alcohol use, clinical and laboratory parameters of liver disease, indirect biomarkers of alcohol intake, and quarterly PEth. Moderate and severe RAULT were diagnosed with PEth >0.05 and >0.3 μ g/l, respectively.

Results: Of 380 LTs (360 patients), 143 were analyzed, 101 (70.6%) males, aged 56 y, with median follow-up of 63.4 months (IQR 23.75–114.3). PEth measured at 3- vs. 6-monthly intervals identified any RAULT in 46 (32.2%) vs. 43 (30.1%) of patients ($p = 0.075$) and heavy relapse in 23 (16.1%) vs. 18 (12.6%) of patients ($p = 0.018$). Time was an independent risk factor for any as well as severe RAULT (OR = 1.17, $P = 0.0002$; OR = 1.14, $P = 0.0093$).

Conclusion: To diagnose RAULT, semi-annual and quarterly PEth measurements were comparable. Whether it is cost-effective to keep quarterly intervals in order not to delay diagnosis of severe RAULT, remains to be elucidated.

SAT-034

Acute-on-chronic liver failure in severe acute alcoholic hepatitis: impact on management, prognostication, and urgency of liver transplantation

Giovanni Perricone¹, Chiara Mazzarelli², Raffaella Viganò³, Paola Prandoni⁴, Marcello Vangeli⁵, Francesca Aprile⁶, Monica Cucco⁷, Chiara Becchetti⁶, Rosa Stigliano⁷, Lucia Cesarini⁶, Milki Scaravaglio⁸, Gianpaola Monti⁹, Andrea Lauterio¹⁰, Aldo Airolidi¹¹, Luca Saverio Belli¹². ¹ASST Grande Ospedale Metropolitano Niguarda, Milan, Italy; ²ASST GOM Niguarda, Hepatology and Gastroenterology Unit, Milan, Italy; ³ASST GOM Niguarda, Hepatology and Gastroenterology Unit, Milan, Italy; ⁴ASST GOM Niguarda, Department of Mental Health and Addiction Services, Milan; ⁵ASST GOM Niguarda, Hepatology and Gastroenterology Unit, Milan; ⁶ASST GOM Niguarda, Hepatology and Gastroenterology Unit, Milan, Italy; ⁷ASST GOM Niguarda, Hepatology and Gastroenterology Unit, Milan; ⁸University of Milano-Bicocca, Division of Gastroenterology and Center for Autoimmune Liver Diseases, Monza; ⁹ASST GOM Niguarda, Department of Anesthesiology, Milan, Italy; ¹⁰ASST GOM Niguarda, Department of General Surgery and Transplantation, University of Milano-Bicocca, School of Medicine and Surgery, Milan, Italy; ¹¹SST GOM Niguarda, Hepatology and Gastroenterology Unit, Milan; ¹²SST GOM Niguarda, Hepatology and Gastroenterology Unit, Milan, Italy
Email: giovanni.perricone@ospedaleniguarda.it

Background and aims: A better identification of factors predicting the course, outcome, and need for urgent liver transplantation in patients with severe acute alcoholic hepatitis (SAAH) is needed. Acute-on-chronic liver failure (ACLF) can occur in SAAH, and its impact on management, prognostication, and need for urgent liver transplantation in SAAH should be clarified. Aim of the study is to describe the impact of ACLF on management, prognostication, and need for urgent liver transplantation in SAAH.

Method: Patients with SAAH referred to our center between April 2016 and May 2023 were considered, with those non-responders to medical treatment (MT) being evaluated for LT.

Results: One hundred patients were included, with a median Maddrey Discriminant Function of 72 and a median MELD-Na score of 28. At presentation, 52 patients had ACLF grade 0–1, and 48 ACLF grade 2–3 (31 grade 2, 17 grade 3) (see Figure 1). In the latter group, circulatory failure was present in 3 (6.25%), and respiratory failure in 4 (8.3%). SAAH was the only precipitant factor in 50 (96%) and 36 (75%) patients with ACLF grade 0–1 and ACLF grade 2–3, respectively, with infection being an associated factor in 1 (2%) and 8 (17%), and GI bleeding in 1 (2%) and 5 (10%), respectively. Non-response to MT was significantly higher in patients with ACLF grade 2–3 (39/48, 81%) than in those with ACLF grade 0–1 (14/52, 27%). ACLF grade 2–3 was associated with a corresponding higher need of early LT (ACLF grade 2–3: 14/48, 29% vs ACLF grade 0–1: 3/52, 5.7%; $p = 0.004$). ACLF status at presentation (ACLF grade 2–3 vs ACLF grade 0–1) resulted a better predictor of outcome (death or LT) than MELD-Na (\geq or).

Conclusion: ACLF is a frequent presentation of SAAH. Severe ACLF predicts non-response to MT, indicating the urgency of liver transplantation.

SAT-035

The yield of routine post-operative doppler ultrasound to detect early post-liver transplantation vascular complications

Iulia Minciuna¹, Caroline den Hoed², Adriaan J. van der Meer², Milan J. Sonneveld², Dave Sprengers², Robert J. de Knecht², Jeroen de Jonge³, Rael Maan⁴, Wojciech Polak⁵, Sarwa Darwish Murad². ¹University of Medicine and Pharmacy Iuliu Hatieganu, Cluj-Napoca, Romania, Erasmus MC Transplant Institute, Department of Gastroenterology and Hepatology, Erasmus MC University Medical Center Rotterdam, Rotterdam, The Netherlands, Rotterdam, Netherlands; ²Erasmus MC Transplant Institute, Department of Gastroenterology and Hepatology, Erasmus MC University Medical Center Rotterdam, Rotterdam, The Netherlands, Rotterdam, Netherlands;

³Erasmus MC Transplant Institute University Medical Center Rotterdam, Department of Surgery, Division of HPB and Transplant Surgery, Rotterdam, The Netherlands, Rotterdam, Netherlands; ⁴Erasmus MC Transplant Institute, Department of Gastroenterology and Hepatology, Erasmus MC University Medical Center Rotterdam, Rotterdam, The Netherlands, Rotterdam, Netherlands; ⁵Erasmus MC Transplant Institute University Medical Center Rotterdam, Department of Surgery, Division of HPB and Transplant Surgery, Rotterdam, The Netherlands, Rotterdam, Netherlands

Email: Iuliabreaban@yahoo.com

Background and aims: Early detection and timely management of post liver transplantation (LT) vascular complications are of paramount importance as these early complications can lead to fulminant graft failure. Our aim was to assess if routine Doppler ultrasound (rDUS) improves the detection of hepatic artery thrombosis (HAT), portal vein thrombosis (PVT) and hepatic venous outflow obstruction (HVOO).

Method: This is a retrospective single-centre study of 708 adult patients who underwent primary LT between 2010–2022 and underwent rDUS on post-operative day (POD) 0, 1 and 7, followed by Computed Tomography (CT) if abnormal. Timing and outcomes of HAT, PVT and HVOO, number needed to diagnose one complication (NND) and positive predictive value (PPV) of rDUS was calculated.

Results: HAT developed in $N = 50$ (7.1%; 68% in first week), PVT in $N = 58$ (8.2%) and HVOO in $N = 22$ (3.1%). Most early complications were diagnosed on POD 0 (26.9%), 1 (17.3%) and 5 (17.3%). Of the 26 vascular events on protocol days (0, 1, 7), 21 (80.7%) were detected by rDUS. PPV of rDUS was 53.8% (21/39), detection rate 1.1% (21/1900 ultrasounds) and NND was 90.5. Median time to diagnosis was 4 days for HAT, 21 days for HVOO and 47 days for PVT. The vascular events detected by rDUS led to surgical re-intervention in 14 patients (66.7%), while 7 (33.3%) were treated by anticoagulant therapy alone. This approach preserved the graft in 57.1% patients while 28.6% proceeded to urgent re-LT and 14.3% underwent late re-LT.

Conclusion: The majority of post-LT vascular complications occur during first week. rDUS detects the majority of events, but with low PPV and a high number of ultrasounds needed. Implementing a rDUS protocol, preferably at POD 0, 1 and 5, leads to timely diagnosis and management. However, a true clinical benefit in terms of graft and patient's survival has yet to be shown.

SAT-036-YI

Impact of distance from liver transplant centre on outcomes following liver transplantation-an australian single centre study

Simone Chin^{1,2}, Charlotte Kench^{1,2}, Rena Cao¹, Christina Lee¹, Susan Virtue¹, Claire West¹, Talal Valliani¹, David Bowen¹, Simone Strasser¹, Geoff McCaughan¹, Ken Liu¹. ¹Royal Prince Alfred Hospital, Sydney, Australia; ²The University of Sydney, Sydney, Australia
Email: schin5234@gmail.com

Background and aims: Access to liver transplantation (LT) is affected by geographic disparities. Higher waitlist mortality is observed in patients residing further away from LT centres but impact of distance on post-LT outcomes is unclear. We aimed to evaluate whether the distance LT recipients reside from their LT centre impacts on graft and patient outcomes.

Method: We retrospectively studied consecutive adults who underwent deceased-donor LT from 2006 to 2021 at Royal Prince Alfred Hospital (RPAH), the only LT centre in the state of New South Wales (NSW), Australia. The state covers an area of 801, 150km². Those residing outside of NSW at time of transplant were excluded. Donor and recipient data were collected from a prospective LT database. Patients' regional area code (0 = least remote, 4 = most remote) and socioeconomic code (1 = relatively greater disadvantage, 5 = relative lack of disadvantage) were obtained from the Australian Bureau of Statistics. Patients were grouped based on their distance from LT centre at time of transplant (≤ 100 km vs. > 100 km). For survival

analyses, patients were censored if they moved to a new residential address during follow-up.

Results: During the study period, 973 patients underwent LT (69.7% male, median age 55.6 years (IQR 49.0–60.6)). The median distance from patient residence to LT centre was 44.9 km (IQR 21.9–168.0). 64.2% of patients lived ≤ 100 km from RPAH. 77.6% of patients were from regional area code 0. The distribution of LT recipients across the five socioeconomic codes was similar (17.9–20.2%). Compared to patients living ≤ 100 km from RPAH, those living > 100 km away were less likely to: be male (64.0% vs. 72.7%, $p = 0.004$); have chronic hepatitis B (3.5% vs. 12.6%, $p = 0.001$) or viral hepatitis (35.7% vs. 42.2%, $p = 0.049$) as their cause of liver disease; or have hepatocellular carcinoma as their primary indication for LT (23.3% vs. 32.1%, $p = 0.004$). Patients living > 100 km away had higher body mass indices (27.1 vs. 26.0 kg/m², $p = 0.01$) compared to those living closer.

At a median follow-up of 47.1 months (IQR 13.5–93.7), there were 190 deaths and 42 retransplants. Living > 100 km from the LT centre was associated with fewer face-to-face clinic visits in the first year after LT (10 vs. 11 visits, $p < 0.001$) and fewer overall readmissions to the LT centre (32.4% vs. 67.6%, $p < 0.001$). Distance from LT centre, regional code, and socioeconomic code did not impact on long-term graft or patient survival based on Kaplan-Meier survival analysis (Log-Rank p all > 0.1). There was a trend towards increased likelihood of biopsy-proven rejection in patients living > 100 km away ($p = 0.069$).

Conclusion: In this single centre Australian study, patients living further away from their LT centre had different demographics and fewer face-to-face visits during follow-up. Despite this, distance from the LT centre was not associated with long-term inferior graft or patient survival post-LT.

SAT-037

Impact of recipient sex on long-term survival after liver transplantation in patients with high MELD

Laia Aceituno^{1,2}, Christian Magyar^{1,3,4}, Zhihao Li^{1,3}, Marco Claassen^{3,5}, Tommy Ivanics^{3,6,7}, Erin Winter¹, Roxana Bucur³, Nadia Rukavina³, Woo Jin Choi^{1,3}, Nazia Selzner¹, Mamatha Bhat¹, Leslie Lilly¹, Cynthia Tsien¹, Keyur Patel¹, Markus Selzner^{1,3}, Ian McGilvray^{1,3}, Trevor Reichman^{1,3}, Chaya Shwaartz^{1,3}, Anand Ghanekar^{1,3}, Mark S. Cattral^{1,3}, Blayne Sayed^{1,3}, Elmar Jaeckel¹, Gonzalo Sapichin^{1,3}. ¹Multi-Organ Transplant Program, Ajmera Transplant Centre, University Health Network, Toronto, Canada; ²Liver Unit, Digestive Diseases Division, Vall d'Hebron University Hospital, Barcelona, Spain; ³University Health Network, HPB Surgical Oncology, Toronto, Canada; ⁴Department of Visceral Surgery and Medicine, Inselspital, Bern University Hospital, University of Bern, Bern, Switzerland; ⁵Department of Surgery, Division of HPB and Transplant Surgery, Erasmus MC Transplant Institute, University Medical Center Rotterdam, Rotterdam, Netherlands; ⁶Department of Surgery, Henry Ford Hospital, Detroit, United States; ⁷Department of Surgical Sciences, Akademiska Sjukhuset, Uppsala University, Uppsala, Sweden
Email: laiaaceituno@gmail.com

Background and aims: The MELD score is used to prioritize liver transplant (LT) candidates for deceased donor organs, with a “sickest first” approach. However, it has been shown that MELD score does not accurately reflect disease severity in females. It remains controversial whether recipient sex affects long-term post-transplantation survival. This study aimed to assess the impact of sex in a high MELD cohort on (1) long-term survival post-LT, (2) and its association with underlying diseases, cause of transplant, and comorbidities.

Method: Retrospective cohort study at Toronto General Hospital, including adult LT recipients with a MELD ≥ 25 at transplant between January 2007 and December 2019. Patients were stratified by sex. Survival analysis was performed using a priori multivariable Cox regression and Kaplan-Meier analysis. A post hoc sex-stratified multivariable Cox regression model was performed.

Results: 478 patients with MELD ≥ 25 were included; 196 (40%) were females, with a median BMI of 27.4 kg/m² (IQR 23.7–31.2). The

median follow-up post-LT was 5.7 years (IQR 2.2, 9.2) with a median waitlist of 23.5 days (IQR 0.0, 75.5). The median listing and pre-transplant MELD scores were 28 (IQR 21–34), and 31 (IQR 26–35) respectively. Male recipients had pre-transplant higher rates of ascites (39.8% vs. 53.5%; $p = 0.003$) and hepatic encephalopathy (34.2% vs. 44.3%; $p = 0.026$). Autoimmune hepatitis as underlying disease was more prevalent among females (26.5% vs. 12.4%; $p < 0.005$). Conversely, viral hepatitis (8.7% vs. 24.8%; $p < 0.001$), alcohol-related cirrhosis (ALD) (13.3% vs. 28.7%; $p < 0.001$), and mixed ALD + viral cirrhosis (1.0% vs. 5.0%; $p = 0.018$) were more frequent in males. Females were more frequently transplanted for acute liver failure (16.8% vs. 4.6%; $p < 0.001$) and fewer for cancer (4.6% vs. 11.3%; $p = 0.009$). No statistically significant differences were observed between sex crude overall long-term survival (log-rank $p = 0.681$), or estimated effect (HR 0.92; $p = 0.686$). In the a priori multivariable analysis, sex was not significant (HR 0.94, CI 95% 0.61–1.43; $p = 0.779$). There were no sex differences in early post-transplant mortality (< 90 days) (6.6% females vs. 9.2% males; $p = 0.309$; HR 0.71, $p = 0.329$), mortality in the 1st year (10.7% females vs. 14.5% males; $p = 0.221$), 5th (16.8% females vs. 18.8% males; $p = 0.584$) and 10th year (20.4% females vs. 22.0% males; $p = 0.679$). There was no difference in risk of postoperative complications. On post hoc multivariable analysis stratified by sex, re-transplantation (HR 2.80; CI 95% 1.53–5.14; $p = 0.001$) and ICU stay (HR 1.009; CI 95% 1.005–1.01; $p < 0.001$) were significant risk factors for female mortality.

Conclusion: Our findings show no sex differences in the overall survival in high MELD liver transplant recipients. Female patients with longer ICU admission, or requiring re-transplantation, were at higher risk of all-cause mortality.

SAT-039

Comparing outcomes in patients with portal vein thrombosis undergoing deceased-donor versus living-donor liver transplantation: insights from a major North American center

Zhihao Li¹, Luckshi Rajendran¹, Owen Jones¹, Laia Aceituno¹, Christian Magyar¹, Leah Aspden¹, Elmar Jaeckel¹, Mamatha Bhat¹, Cynthia Tsien¹, Leslie Lilly¹, Nazia Selzner¹, Anand Ghanekar¹, Blayne Sayed¹, Markus Selzner¹, Ian McGilvray¹, Chaya Shwaartz¹, Trevor Reichman¹, Mark S. Cattral¹, Gonzalo Sapichin¹. ¹University Health Network, Toronto, Canada
Email: zhihao.li@uhn.ca

Background and Aims: Portal vein thrombosis (PVT) complicates liver transplantation (LT) due to the need for portal flow restoration. While management strategies have been established, PVT remains a contraindication for living-donor liver transplantation (LDLT) at some centers. This is due to the greater technical complexities in LDLT compared to deceased-donor LT (DDLT).

Method: We retrospectively included adults who underwent LT with main PVT between 2006–2022 and excluded cases with tumor thrombi or re-LT. We employed a 1:1 nearest neighbor propensity score matching to achieve equilibrium in variables age, MELD score, Yerdel classification, cavernous transformation and reconstruction method. Our primary end point was 90-day complication rate; secondary end points were patient and graft survival, assessed via Kaplan-Meier analysis and apriori multivariable cox regression.

Results: Of 122 included patients, 96 were matched (48 in both LDLT and DDLT groups). The median age was 57 (IQR 50–63) years, predominantly male (62%) with a median MELD of 18 (IQR 12–25). Common underlying liver diseases were hepatitis C (26%) and alcohol-related liver disease (20%). 85% had Yerdel grade I/II PVT (DDLT 88%, LDLT 83%, $p = 0.77$) and 15% had grade III/IV (DDLT 13%, LDLT 17%, $p = 0.77$). Cavernous transformation was present in 17% of cases (DDLT 17%, LDLT 17%, $p = 0.99$). Most patients (90%) underwent anatomical portal vein reconstruction (thrombectomy and anastomosis without interposition graft), while 10% received non-anatomical reconstruction using deceased donor iliac vein graft (jump graft to pericholedochal vein $n = 2$, left gastric vein $n = 1$, superior mesenteric vein $n = 7$). There were no significant differences

POSTER PRESENTATIONS

between the DDLT and LDLT group in terms of warm ischemia time (median: 57 vs. 58 min, $p=0.3$), 90-day major complication rate (Clavien-Dindo grade \geq III) (37.5 vs. 39.6%, $p=0.99$) and minor complication rate (47.9 vs. 52.1%, $p=0.84$), portal vein re-thrombosis (12.5 vs. 10.6%, $p=0.99$), posttransplant dialysis requirement (4 vs. 8%, $p=0.65$) and ascites development (25 vs. 30%, $p=0.77$). Over a median follow-up of 2.9 (IQR 1.4–6.8) years, the patient survival rates at 1/3/5 years were similar between the DDLT (90/81/76%) and LDLT group (89/79/79%, log-rank $p=0.8$). Likewise, graft survival rates at these intervals were comparable between DDLT (88/79/74%) and LDLT (85/75/75%, $p=0.9$). Cox regression analysis revealed that neither graft type, Yerdel classification, nor reconstruction method significantly influenced graft survival. However, posttransplant anticoagulation was identified as a protective factor (hazard ratio 0.3, $p=0.02$).

Conclusion: Despite the inherent technical complexities associated with LDLT in the context of PVT, the short-term and long-term outcomes at our center were comparable to those observed in DDLT. Hence, PVT should not be considered a contraindication for LDLT.

SAT-040

Is there a need to screen for ischemic heart disease in liver transplant candidates without coronary calcification on routine chest CT?

Roos Groen¹, Susan Fischer², Fei-lynn Barbero³, Maarten Tushuizen⁴, Jeroen Bax⁵, J. Wouter Jukema^{5,6}, Michiel de Graaf⁵, Minneke Coenraad⁴. ¹Department of Cardiology, Leiden University Medical Center, Leiden, Netherlands; ²Department of Gastroenterology and Hepatology, Leiden University Medical Center, Leiden, Netherlands; ³Leiden University Medical Center, Leiden, Netherlands; ⁴Department of Gastroenterology and Hepatology, Leiden University Medical Center, Leiden, Netherlands; ⁵Department of Cardiology, Leiden University Medical Center, Leiden, Netherlands; ⁶Netherlands Heart Institute, Utrecht, Netherlands
Email: r.a.groen@lumc.nl

Background and aims: Coronary artery disease (CAD) plays an important role in peri- or postoperative mortality in liver transplantation (LT) candidates and recipients. Efficient cardiac pre-operative screening is therefore of utmost importance. Still, the optimal approach for patient-specific cardiac screening is currently debated on. Non-gated computed tomography (CT) of the chest-abdomen are routinely performed, as part of follow-up of patients' liver disease. Patients' coronary artery calcium (CAC) can be readily assessed on these scans, as indicator of patients CAD-burden. This study evaluated the ability of CAC assessment on these earlier acquired scans, to identify a selection of low risk patient, in whom further cardiac imaging is safely withheld.

Method: LT recipients who underwent liver transplantation between 2008–2023 with an available non-gated chest-abdomen CT, were analyzed retrospectively. CAC was scored visually on a semi-quantitative ordinal scale using an established method. This allowed for readily and rapid assessment of atherosclerosis burden. Subsequently, patients were stratified according to CAC severity. Coronary CT angiography (CCTA), stress myocardial perfusion or invasive coronary angiography (ICA) were used as golden standard. The sensitivity and specificity of CAC to exclude or predict obstructive CAD were analyzed. In addition, peri- and postoperative mortality and cardiac events up to 30 days after LT were analyzed.

Results: A total of 149 LT patients of 31–70 years old were included. Most patients (75%) had no or mild CAC. Both no calcifications or mild calcifications could rule out obstructive CAD on CCTA and ICA with 100% certainty. The threshold of mild CAC had a sensitivity of 100% for both CCTA and ICA. The specificity for mild CAC was respectively 91% and 68%. None of the patients with no or mild calcifications experienced peri- or postoperative cardiac events or died of cardiac disease. In terms of dedicated imaging allocation, in patients with severe CAC performance of stress myocardial perfusion or ICA was

most optimal. In patients with no or mild CAC, dedicated cardiac imaging could safely have been withheld.

Conclusion: Visual CAC assessment on available non-gated CT can accurately and safely exclude obstructive CAD in LT recipients. Incorporation of these available data can enhance cardiac risk stratification and dedicated cardiac imaging can efficiently be withheld or allocated in LT recipients. Hereby reducing the test burden for the patient and save health care expenses.

SAT-041

Real-world evidence of magnesium isoglycyrrhizinate for perioperative protection against hepatic injury in patients undergoing hepatectomy

Changzhen Shang¹, Chuanjiang Li², Jinyi Zhong¹, Xuan Luo¹, Jinjing Wei¹, Yajin Chen¹. ¹Department of Hepatobiliary Surgery, Sun Yat-sen Memorial Hospital of Sun Yat-sen University, Guangzhou, 510120, China, Guangzhou, China; ²Division of Hepatobiliopancreatic Surgery, Department of General Surgery, Nanfang Hospital, Southern Medical University, Guangzhou, 510515, China, Guangzhou, China
Email: shchzh2@mail.sysu.edu.cn

Background and aims: Real-world data remain limited on magnesium isoglycyrrhizinate (MgIG) for hepatic injury in patients undergoing hepatectomy. This retrospective, real-world study aims to evaluate the prophylactic and therapeutic effectiveness of MgIG against hepatic injury in patients undergoing hepatectomy.

Method: Clinical data of these patients who underwent hepatectomy between March 2020 and March 2023 were retrospectively collected in two institutes. After propensity score matching (PSM), cohorts were balanced for age, sex, baseline alanine aminotransferase (ALT) levels and extent of resection. The primary outcome was the incidence of moderate and severe liver injury. Key secondary outcomes included changes from baseline in ALT or aspartate aminotransferase (AST), normalization rate and the proportion of patients with a 50% reduction of ALT or AST. No or mild liver injury was defined as ALT or AST $<3\times$ upper limit of normal (ULN) and moderate or severe liver injury as ALT or AST $\geq 3\times$ ULN.

Results: A total of 1711 patients were enrolled in this study. On postoperative day (POD) 1, the incidence of moderate and severe liver injuries was 74.54% among 876 patients who received MgIG prophylaxis versus 79.28% for 835 patients who did not, especially among elderly patients (≥ 65 years) (71.71% vs. 87.75%; $p<0.001$). After PSM, patients receiving prophylaxis ($n=680$) had significantly less increase from baseline in ALT (171.50, IQR 71.75–328.25 vs. 185.5, IQR 93.75–362.75; $p<0.001$) and AST (178.50, IQR 83.00–347.75 vs. 240, IQR 116.50–370.50; $p<0.001$) than those not receiving prophylaxis ($n=680$). Among patients with postoperative abnormal liver function who were treated with MgIG plus other liver protectants, those who received prophylaxis ($n=330$) had a significantly greater reduction in the incidence of moderate and severe liver injuries per ALT (52.12% vs. 65.45%; $p=0.026$) and AST (16.06% vs. 31.82%; $p<0.001$) on POD 3 than those not receiving prophylaxis ($n=110$). In addition, more patients received prophylaxis had an apparently greater reduction in ALT on POD 7 (14.24% vs. 22.73%; $p=0.046$). Among patients who received no prophylaxis and had abnormal postoperative liver function, a significantly greater proportion of patients treated with MgIG plus other liver protectants ($n=110$) experienced a $\geq 50\%$ reduction on POD 7 from baseline in ALT (71.82% vs. 56.67%, $p=0.011$) and AST (79.09% vs. 75.15%, $p=0.029$) than those only treated with other liver protectants ($n=330$). In addition, more patients treated with MgIG had a normal recovery in ALT (21.82% vs. 11.82%, $p=0.015$) and AST (63.64% vs. 52.42%, $p=0.022$).

Conclusion: This study provides real-world evidence that preoperative prophylaxis and postoperative treatment with MgIG is effective in protecting against postoperative liver injury and promoting postoperative liver function recovery.

SAT-042

A HDL-based prognostic model performs better than MELD in chronic liver failure

Rudolf E. Stauber¹, Florian Rainer¹, Vanessa Stadlbauer¹, Alexander Avian², Hubert Scharnagl³, Gunther Marsche⁴. ¹Medical University of Graz, Department of Internal Medicine, Graz, Austria; ²Medical University of Graz, Institute of Medical Informatics, Statistics and Documentation, Graz, Austria; ³Medical University of Graz, Clinical Institute of Medical and Chemical Laboratory Diagnostics, Graz, Austria; ⁴Medical University of Graz, Institute of Pharmacology, Graz, Austria
Email: rudolf.stauber@medunigraz.at

Background and aims: Chronic liver failure is associated with multiple lipidomic alterations including markedly reduced high-density lipoprotein cholesterol (HDL-C) levels. We have previously shown excellent prognostic value of HDL-C comparable to that of MELD (J Hepatol 2020;73:113–120). In the present study we aimed to develop a new prognostic model containing HDL-C and other known prognostic variables in the same cohort of patients with chronic liver failure.

Method: We studied a multinational cohort of patients with chronic liver failure of varying severity, including compensated cirrhosis (CC), AD and ACLF. Prognostic variables including bilirubin, creatinine, INR, HDL-C, WBC, CRP, and albumin were routinely determined in the Clinical Chemistry Laboratory. After checking intercorrelation of variables by variance inflation factors (VIF), multivariable competing risk analysis was performed with death as the event and liver transplantation as a competing risk to identify independent predictors of survival. Cox proportional hazards regression was used to construct a new prognostic model and its performance was compared to that of MELD using ROC analysis (DeLong test) for 3-month and 1-year survival.

Results: We included 508 patients (median age 57 years; 69% male; CC 45%/AD 34%/ACLF 21%; etiology alcohol 56%). Seventy-seven patients (15%) received liver transplantation, 149 (30%) died and 256 (51%) were censored. Multivariable analysis yielded three independent prognostic variables, i.e. HDL-C, INR, and creatinine, hence the new prognostic model was named HIC model. On ROC analysis, the prognostic performance of the HIC model was superior to that of MELD in the prediction of 3-month survival (AUROC 0.88 vs. 0.85, $p = 0.031$ by DeLong test) as well as 1-year survival (AUROC 0.85 vs. 0.82, $p = 0.039$ by DeLong test).

Conclusion: A new prognostic model including HDL-C, INR, and creatinine showed superior accuracy for prediction of 3-month and 1-year survival as compared to MELD. External validation is warranted to confirm our findings.

SAT-043

Liver transplantation for locally advanced, unresectable intrahepatic cholangiocarcinoma following neoadjuvant treatment with chemotherapy and radioembolization

Baptiste Giguët¹, Thomas Uguen¹, Heithem Jeddou¹, Pauline Houssel-Debry¹, Caroline Jezequel¹, Fabien Robin², Alexandre Chebaro³, Karim Boudjema⁴, Etienne Garin⁵, Luc Beuzit³, Turlin Bruno³, Julien Edeline⁵, Edouard Bardou-Jacquet⁶, Florent Artur⁶. ¹university hospital center Pontchaillou, Rennes, France; ²university hospital center Pontchaillou, INSERM U1242, Chemistry Oncogenesis Stress Signaling, Rennes 1 University, Rennes, France, Rennes, France; ³university hospital center Pontchaillou, Rennes, France; ⁴university hospital center Pontchaillou, INSERM U1242, Chemistry Oncogenesis Stress Signaling, Rennes 1 University, Rennes, France, Rennes, France; ⁵centre de lutte contre le cancer Eugène Marquis, Rennes, France; ⁶University Hospital Center Pontchaillou, INSERM CHU Rennes, Institut NUMECAN, CIC 1414, Rennes, France, Rennes, France
Email: baptiste.giguët@chu-rennes.fr

Background and aims: cholangiocarcinoma (CCA) is the second most common primary liver tumor and with three distinct variants (intrahepatic cholangiocarcinomas (iCCA), peri-hilar, and distal).

Liver transplantation (LT) is not a standard indication for iCCA. The largest series of LT for locally advanced unresectable iCCA included 18 patients with heterogeneous neoadjuvant treatment and reported a 5-year survival of 57%. A promising neoadjuvant approach is the combination of selective internal radiotherapy (SIRT) to chemotherapy (CT). The aim of our study was to investigate whether the outcomes of LT in patients with unresectable iCCA treated with SIRT and CT before LT achieve collective utility ($\geq 70\%$ 5-year overall survival after LT).

Method: a single-center retrospective study including all patients who underwent LT for locally advanced unresectable iCCA, treated with SIRT and CT before LT from 2011 until now. The primary and secondary outcomes were 5-year overall and recurrence-free survivals after LT.

Results: five patients were included with a median age of 56.1 years [41.3–61.8]. The cumulative tumor size at diagnosis was 100 mm [64.5–115], and at the time of listing for LT, it was 80 mm [51.5–80]. Advanced chronic liver disease was present in 60% of patients. All 5 patients received neoadjuvant CT (including 4 patients receiving gemcitabine-cisplatin) and SIRT. Lymph node sampling was performed before listing in 4 patients (80%) without evidence of extrahepatic disease. Timeframe between iCCA diagnosis and LT was 516 days [394–866], and LT occurred in a median of 130 days [37–252] after placement on waiting list. Notably, 80% of allocated grafts were from donor with extended criteria. Donor age was 63 years [52.5–89.5], and cold ischemia time was 502 minutes [492–505]. The median follow-up after LT was 77 months [21–103], with 5-year overall and recurrence-free survival rates of 100% and 58.3%, respectively. The post-LT hospitalization length of stay was 12 days [12–16.5]. Long-term immunosuppression included everolimus in 4 patients (80%). 80% of patients exhibited biliary complications of LT with 2 anastomotic strictures, 1 ischemic cholangitis, and 1 biliary fistula. One patient experienced an arterial thrombosis. Oligometastatic tumor recurrence occurred in 2 patients (40%) at 573 and 577 days, both in the pulmonary site. Curative surgery was successfully performed in these patients with no further recurrence.

Conclusion: in our experience, the 5-year outcome of patients undergoing LT for locally advanced, unresectable iCCA treated with a combination of SIRT and CT suggests potential individual therapeutic benefit while maintaining collective utility. However, a higher-than-expected rate of biliary complications was noted. The impact of the neoadjuvant strategy, including SIRT, on these favorable outcomes warrants further investigation in a larger cohort.

SAT-044

Aging with a liver graft: analysis of very long-term survivors after liver transplantation

Paolo DeSimone¹, Jessica Bronzoni², Caterina Martinelli², Juri Ducci², Daniela Campani¹, Piero Marchetti¹. ¹University of Pisa, Pisa, Italy; ²Azienda Ospedaliero Universitaria Pisana, Pisa, Italy
Email: paolo.desimone@unipi.it

Background and aims: Little is known about the health status of very long-term survivors of a liver graft. We aimed to identify predictors of survival and investigate the prevalence of co-morbidities among long-term survivors.

Method: We conducted a hybrid-design study on a historical cohort of 359 adult recipients of a liver graft who received transplants between 1996 and 2002.

Results: The actuarial (95% CI) patient survival of the overall study cohort was 96% (94.6%–98.3%), 69% (64.2%–73.6%), 55% (49.8%–59.9%), 42.8% (37.6%–47.8%), and 34% (29.2%–38.9%) at 1, 5, 10, 15, and 20 years, respectively. The actuarial (95% CI) graft survival was 93.8% (91.6%–97.2%), 67.6% (62.2%–71.5%), 54.3% (49.6%–59.3%), 42.1% (37.3%–47.4%), and 33.8% (29.0%–38.4%) at 1, 5, 10, 15, and 20 years, respectively. The leading cause of death was hepatitis C virus recurrence (24.6%), followed by extrahepatic malignancies (16.9%), infection (14.4%), and hepatocellular carcinoma recurrence (14.4%).

POSTER PRESENTATIONS

The Cox proportional hazards analysis revealed that several independent factors were associated with the survival probability. These factors include younger donor and recipient ages ($p=0.001$ and 0.004 , respectively), female recipient sex ($p<0.001$), absence of HCV ($p<0.01$), absence of HCC ($p=0.001$), and absence of diabetes mellitus at one year ($p<0.01$). At the latest follow-up, the leading comorbidities in the long-term survivors were hypertension (53.6%), obesity (18.7%), diabetes mellitus (17.1%), hyperlipidemia (14.7%), chronic kidney dysfunction (14.7%), and extrahepatic malignancies (13.8%), with 73.9% of patients having more than one complication. The Kaplan-Meier probability (95% CI) of complication-free survival was 65.4% (60.2%–70.3%), 38.4% (33.4%–43.7%), 17.8% (14.1%–22.2%), 7.2% (4.8%–10.5%), and 1.94% (0.85%–4.15%) at 1, 5, 10, 15, and 20 years, respectively.

Conclusion: Aging with a liver graft is associated with an increased risk of complications and requires ongoing care to reduce the long-term attrition rate resulting from chronic immunosuppression.

SAT-045

Outcome of simultaneous heart and liver transplants with HCC: analysis of US national database

Fadi A. Zeineddine¹, Efstathia Polychronopoulou², Prasun Jalal³.

¹Houston Methodist Hospital, Houston, United States; ²University of Texas Medical Branch, Galveston, United States; ³Baylor College of Medicine, Houston, United States

Email: fazeineddine@houstonmethodist.org

Background and aims: Patients with HCC in presence of congestive hepatopathy due to underlying cardiac disease usually undergo combined heart and liver transplant. We aimed to study outcomes of patients with HCC and simultaneous heart and liver transplantation.

Method: We retrospectively analysed United Network for Organ Sharing (UNOS/OPTN) database for patients with simultaneous heart and liver transplants and MELD exception for HCC between April 1, 2012 and June 31, 2023. Tumor characteristics in pre-transplant radiology and explant histology were compared. Patient survival and recurrence were analysed.

Results: A total of 8 patients with MELD exception for HCC underwent simultaneous heart and liver transplant. All had confirmed HCC on explant histopathology. Median age at transplant was 54.5 years (17–67 years). All patients were transplanted due to concomitant cirrhosis with HCC. Three had congenital heart disease, three had dilated cardiomyopathy, and two had pulmonary fibrosis. 62.5% ($n=5$) were HCV positive. Radiologically, five had single lesion with a median diameter of 2 cm. Median AFP level was 46.5 ng/ml (range 3–2960 ng/ml). On explant, median number of lesions was 3 and median maximal tumor size was 2.55 cm (2.5–4.2 cm). Only one patient showed microvascular invasion who also had recurrence after 118 days and expired after 231 days. 87.5% ($n=7$) received locoregional treatment for HCC. Two received chemoembolization, four received thermal ablation and one had radiation microspheres. HCC recurrence occurred in 25% of patients ($n=2$) after 118 and 152 days. 50% of patients ($n=4$) expired after a median follow-up of 245 days (range 74–540 days).

Conclusion: Current radiological parameters used to define HCC may underestimate the size and number of lesions in presence of congestive hepatopathy. Outcome of patients with HCC receiving simultaneous heart and liver transplant remains poor. Appropriate selection process and use of locoregional treatment may improve the outcome.

SAT-046

Detection of conventional adenomas and serrated lesions during repetitive colonoscopies after orthotopic liver transplantation

Sidar Baysal¹, Katharina Willuweit¹, Benedikt Hild¹, Hartmut Schmidt¹, Christoph Schramm¹. ¹University Hospital Essen, Department of Gastroenterology, Hepatology and Transplantational Medicine, Essen, Germany

Email: christoph.schramm@uk-essen.de

Background and aims: Patients with immunosuppression after orthotopic liver transplantation (OLT) are at an increased risk for malignancies. If this applies also to colorectal cancer (CRC) is controversial, especially in the absence of primary sclerosing cholangitis (PSC) and associated inflammatory bowel disease (IBD). Standardized recommendations for CRC screening in this population are not available. We aim to investigate the effect of repetitive colonoscopies on the incidences of colorectal polyps.

Method: We performed a retrospective analysis of patients who underwent screening colonoscopies after OLT at a single liver transplant center in Germany. Exclusion criteria were no post-OLT-colonoscopy, PSC prior to OLT, IBD, hereditary cancer and polyposis syndromes, and CRC prior to OLT. Only the first five post-OLT-colonoscopies per patient were analyzed. Clinically relevant serrated polyps (crSP) were defined as serrated polyps (SP) >5 mm proximal to the splenic flexure, SP ≥ 10 mm, and SP with high grade dysplasia. Insufficient procedure quality was defined as incomplete procedure, i.e. not reaching the cecum, and/or inadequate bowel preparation.

Results: Of 129 patients screened, 59 patients were identified according to inclusion and exclusion criteria. Median age at OLT was 62 years (interquartile range (IQR) 56–65), 2/3 were male and 1/3 were female. Indications for OLT were alcohol-associated liver disease (87%), alpha1-antitrypsin deficiency (5%), autoimmune hepatitis (7%) and Alagille syndrome (2%). A total of 142 post-OLT colonoscopies were performed with a median of 2 colonoscopies per patient (range 1–8). Interval between OLT and first post-OLT colonoscopy, and between consecutive colonoscopies was 33.5 months (IQR 14–47), 33.5 months (IQR 15–42), 23 months (IQR 14–36), 23 months (IQR 8–40), and 30 months (IQR 19–39).

Detection rates for non-advanced conventional adenomas were 18.3%, 20.6%, 19%, 15.4%, and 0% in consecutive colonoscopies. Advanced conventional adenomas were detected in 1.7% and 5.9% of the first two colonoscopies, whereas none were detected hereinafter. Likewise, no crSP was detected on any of the post-OLT colonoscopies. One patient (1.7%) developed CRC, which was detected during the first post-OLT colonoscopy. Colonoscopy prior to OLT was documented in 71%. However, it was not associated with the detection of non-advanced and advanced conventional adenomas during the first post-OLT colonoscopy. Insufficient procedure quality was present in 32%, 27%, 19%, 15%, and 40% of the procedures.

Conclusion: Effectiveness of screening colonoscopies in patients after OLT in terms of detection rates seems to decrease with repetitively performed procedures. Additionally, detection of crSP and procedure quality are suboptimal.

SAT-047

Racial disparities in the receipt of liver transplantation among african american patients with hepatocellular carcinoma in the United States: a systematic review

Nabil El Hage Chehade¹, Isabelle Nguyen¹, Nour El Hage Chehade², Joy-Marie Hermes¹, Adam Deising¹, Paul Pockros¹, Julio Gutierrez¹.

¹Scripps Clinic, La Jolla, United States; ²Cleveland Clinic Foundation, Cleveland, United States

Email: elhagechehade.nabil@scrippshealth.org

Background and aims: Hepatocellular carcinoma (HCC), a leading indication for liver transplantation (LT), is one of the fastest-rising cancers in the United States. Prior studies demonstrate that African American (AA) patients tend to have higher mortality rates as compared with white patients with HCC, despite accounting for

differences in tumor burden, etiology of liver disease, and presence of other comorbidities. Various policies, such as the 2015 MELD exception policy change and the Regional Share 35 policy, were instituted to ensure equitable access to LT for eligible patients. However, it remains unclear whether these efforts have closed the gaps in access to LT or improved post-LT outcomes among different racial groups. Our systematic review aimed to investigate potential racial disparities within LT for patients with HCC.

Method: We performed a review of the literature across major databases including PubMed/MEDLINE, Embase, and Google Scholar in December 2023. Eligible studies included adult patients with HCC who were either waitlisted for or received LT. The primary end point of our study was to assess LT rates in AA patients as compared with white patients with HCC. The secondary end point was to compare post-LT mortality among both racial groups.

Results: 11 retrospective studies involving transplant-eligible patients with HCC were included in our systematic review. 8 studies included data from large LT databases. The years of publication spanned from 2010 to 2023. Pooled results reveal AA patients were significantly less likely to receive LT than white patients with HCC. The odds ratio for AA patients with HCC receiving a LT ranged between 0.03 and 0.60 ($p < 0.05$ across all studies). AA patients had a stronger association with increased post-LT mortality compared to whites. The hazard ratio ranged between 1.03 and 1.53 across all studies ($p < 0.05$ across all but one single center study). AA patients with HCC had higher post-LT mortality rates despite the 2015 MELD exception policy change and the Regional Share 35 policy. In AA patients with HCC due to chronic hepatitis C, post-LT survival rates were mixed despite the introduction of direct acting anti-viral therapy.

Conclusion: Our study highlights a persistent disparity among AA patients with HCC, despite current policies in the United States aimed at achieving equity in liver transplant allocation. Future initiatives should focus on dismantling racial barriers in existing LT policies and providing more support for AA patients to improve access to LT.

SAT-048

Long-term mortality and risk factors associated with mortality after liver transplantation in the modern era

Magdalena Meszaros^{1,1}, Audrey Coilly², Claire Francoz³, Filomena Conti⁴, Christophe Duvoux⁵, Jérôme Dumortier⁶, Teresa Antonini⁷, Sébastien Dharancy⁸, Marie-Noëlle Hilleret⁹, Arnaud Del Bello¹⁰, Rodolphe Anty¹¹, Delphine Weil-Verhoeven¹², Marianne Latournerie¹³, Pauline Houssel-Debry¹⁴, Clara Dassetto¹⁵, Faiza Chermak¹⁶, François Faitot¹⁷, Laure Elkrief¹⁸, Claire Perignon¹⁹, Armand Abergel²⁰, Flora Charpy¹, Nicolas Molinari¹, Georges-Philippe Pageaux¹. ¹CHU Montpellier, Montpellier, France; ²Hopital Paul Brousse, Villejuif, France; ³Hopital Beaujon, Clichy, France; ⁴Hopital Pitie Salpetriere, Paris, France; ⁵Hopital Henri Mondor, Paris, France; ⁶Digestive Diseases Federation, Edouard Herriot Hospital, Hospices Civils de Lyon Université, Lyon, France; ⁷Hepatology Unit, HCL, Hôpital de la Croix-Rousse, Lyon; ⁸CHRU Lille, Hepatology Unit, Claude Huriez Hospital, Lille, France; ⁹Hepato-Gastroenterology Unit, Grenoble, France; ¹⁰Nephrology and Organ Transplantation Unit, CHU Rangueil, Toulouse, France; ¹¹CHU Nice, Nice, France; ¹²Hepatology Unit, CHRU Jean Minjoz Franche Comté University, Besancon, France; ¹³CHU Dijon, Dijon, France; ¹⁴CHU Rennes, Rennes, France; ¹⁵AP HM Hopitaux Marseille, Marseille, France; ¹⁶CHU Bordeaux, Bordeaux, France; ¹⁷CHRU Strasbourg, Strasbourg, France; ¹⁸CHU Tours, Tours, France; ¹⁹CHU Caen, Caen, France; ²⁰CHU Clermont Ferrand, Clermont Ferrand, France
Email: m-meszaros@chu-montpellier.fr

Background and aims: Available robust data on the long-term mortality and associated risk factors in liver transplant (LT) recipients receiving contemporary immunosuppressive agents (Tacrolimus and Mycophenolic acid) are very limited. This study aimed to assess long-term mortality, causes and risk factors of death, in a large cohort of French LT recipients.

Method: A total of 6246 adult LTs were performed between 2008 and 2013 in France. Due to incomplete data in the National Database of the Transplantation Agency, a 20% sample (1249 LTs) was obtained from each LT center to ensure representative characteristics of the total cohort. Clinical and biological data from the pre- and post-LT periods were analyzed, and causes of death were documented in both early (6 months) and late (beyond 5 years) post-transplant periods. Predictive risk factors for death were determined by univariate and multivariate regression analysis.

Results: To date, complete data from 892 LT recipients of the 20% sample (/1249, i.e. 71.4%) were analyzed. Patients' survival in the sample was similar to that of the entire population. Predominant initial liver disease was alcohol-related cirrhosis (37, 6%), with or without hepatocellular carcinoma. The cohort, mainly male (72%), had a mean age of 52.1 ± 11.5 years, and median follow-up after LT was 9.16 years. Survival rates at 5 and 10 years post-LT were 72.6% (95% CI: 69.5–75.4) and 61.7% (95% CI: 58.4–64.8), respectively. During follow-up, 384 (43%) patients died, 26.3% from hepatic causes and 73.7% from non-hepatic causes. Hepatocellular carcinoma recurrence caused liver-related death in 26 (6, 7%) of LT recipients. In the initial 6 months post-LT, 114 patients (29.6%) died, with 32.4% due to hepatic causes and 20.1% to cardiovascular causes. Late mortality (>5 years) was mostly malignancy-related (30.7%): digestive (23%), lung (17.4%) and head and neck (17, 4%). Univariate analysis identified as significant prognostic factors: pre-LT diabetes (HR 1.51 [1.12–2.06]), pre-LT smoking (1.81 [1.34–2.41]), pre-LT stroke (HR 3.18 [1.4–6.4]), pre-LT coronary artery disease (HR = 2.19 [1.51–3.19]), age > 60 years at LT (1.61 [1.31–1.99]), ($p < 0.05$). Multivariate analysis identified as significant prognostic factors: age at LT (HR = 1.02 [1.0–1.03]), pre-LT diabetes (HR = 1.38 [1.05–1.82]), pre-LT coronary artery disease (HR = 1.79 [1.16–2.76]) ($p < 0.05$).

Conclusion: Early post-LT mortality was mainly related to liver or cardiovascular causes, while long-term mortality is predominantly malignancy-related. Risk factors included age at LT, pre-LT diabetes, and pre-LT coronary artery disease. These emphasize the need for cardiovascular risk assessment in LT candidates and implementing cancer screening for long-term care.

SAT-049

Everolimus and hepatocellular carcinoma recurrence post liver transplantation: insights from an emulated target trial

Ilias Kounis^{1,2,3,4}, Christophe Desterke¹, Long Nguyen⁵, Nathalie Goutte², Audrey Coilly^{1,2,3,4}, Didier Samuel^{1,2,3,4}, Daniel Azoulay^{1,2,3,4}, Eric Vibert^{1,2,3,4}, Paul Landais¹, Cyrille Feray^{1,2,3,4}. ¹Inserm, Université Paris-Saclay, UMR-S 1193, Villejuif, France; ²AP-HP Hôpital Paul-Brousse, Centre Hépatobiliaire, Villejuif, France; ³Université Paris-Saclay, Inserm, Physiopathogénèse et traitement des maladies du Foie, Villejuif, France; ⁴France FHU Hepatinov, Villejuif, France; ⁵Department of Public Health, Copenhagen, Denmark
Email: ilias.kounis@aphp.fr

Background and aims: Hepatocellular carcinoma (HCC) is a major indication for liver transplantation (LT). the role of mTOR inhibitors to delay the recurrence is highly debated. No large randomized trials on everolimus and HCC recurrence is available. This study use emulated target trials to assess HCC recurrence.

Method: The French national health data system (SNDS), linked with the national hospital database (PMSI), contains information on 99% of the French population, including ICD-10 codes, medical procedures (MP), prescribed drugs, and vital status. We identified 3, 699 HCC patients from 01/01/2009 to 01/01/2020. Emulated target trials (cloning-censoring-weighting approach) comparing everolimus ($n = 1316$, 35%) and control were performed with grace periods of 6 months to 4 years after LT and outcomes being overall survival (OS) and HCC recurrence-free survival 2 to 10 years after LT.

Results: The 10-y cumulative incidence of HCC recurrence was 16.5% (CI: 12–26). Predictive factors for HCC recurrence were abdominal surgery before LT, gender (male), tobacco and HCV. After recurrence,

POSTER PRESENTATIONS

the 2-y OS was 25%. In emulated trials with grace periods longer than 24 months, the 10-y OS or 10-y recurrence-free survival were not different between groups. For shorter grace period the 10-y recurrence-free survival was up to 25% lower in the everolimus group. Competitive risk analysis did not drop the main conclusions.

Conclusion: Emulated target trial approach recently described controls immortality bias and confounder baseline variables. It is useful when no prospective trials is possible and reflects the “real-life.” The role of everolimus in the prevention of HCC recurrence could not demonstrated through emulated target trials in a large nationwide cohort.

SAT-050

Liver transplantation for biliary tract cancer in primary sclerosing cholangitis

Christina Villard¹, Sigurd Breder², Benny Wang³, Emma Eide², Lise Engesæter⁴, Henrik Mikael Reims⁵, Espen Melum², Pål Dag Line², Kristine Wiencke⁴, Trine Folseraas⁶, Annika Bergquist¹. ¹Department of Medicine Huddinge, Karolinska Institutet, Stockholm, Sweden; ²Institute of Clinical Medicine, Faculty of Medicine, University of Oslo, Oslo, Norway; ³Department of Transplantation Surgery, Karolinska University Hospital, Stockholm, Sweden; ⁴Department of Transplantation Medicine, Division of Surgery, Inflammatory Medicine and Transplantation, Oslo University Hospital Rikshospitalet, Oslo, Norway; ⁵Department of Pathology, Oslo University Hospital, Rikshospitalet, Oslo, Norway; ⁶Institute of Clinical Medicine, Faculty of Medicine, University of Oslo, Oslo
Email: christina.villard@ki.se

Background and aims: Cholangiocarcinoma (CCA) is the most frequent cause of death in patients with primary sclerosing cholangitis (PSC). Liver transplantation (LT) with neoadjuvant chemoradiation could be considered in selected patients with unresectable perihilar CCA and without pre-treatment in patients with bile duct high-grade dysplasia (HGD). Early detection of CCA in patients with PSC is challenging and a number of CCA are incidentally detected in liver explants. This study aimed to evaluate diagnostics and outcome of PSC-CCA treated with LT.

Method: A retrospective cohort study was conducted on patients with PSC undergoing LT due to suspicion of hepatobiliary malignancy, identified by the Nordic Liver Transplant Registry. Patients with PSC, aged ≥ 18 years, receiving their first LT and patients without PSC treated with LT for CCA, from 1st of January 2000 to 31st December 2021 at Oslo University Hospital and Karolinska University Hospital were included. Clinicopathological data including biochemical status at time of listing, results of diagnostics, histopathological analyses of the explants and outcome were analysed by comparative analyses. Survival was assessed by the Kaplan-Meier method and Cox regression.

Results: Out of 133 PSC patients transplanted due to suspicion of malignancy, CCA was confirmed in the explants of 45 patients (33%), HGD was found in 29 patients (22%), and hepatocellular carcinoma in 16 patients (12%). CCA was known prior to LT by brush cytology in 6 patients (13%) and was an unexpected finding in the explant of 5 patients (11%). Recurrence of hepatobiliary malignancy occurred in 26 patients (60%). The cancer-free recurrence was 17 months (9–26 months) and the median overall survival following recurrence was 5 months (2–13 months). The median overall survival in patients with PSC-CCA was 24 months compared with 45 months in PSC patients with HGD. Survival following LT was similar in patients with PSC-CCA and CCA without underlying PSC (9 patients), 24 months, and 20 months, respectively.

Conclusion: The limited survival in patients with PSC-CCA following treatment with LT stresses the importance of early detection of CCA and effective oncological therapy to prevent cancer recurrence.

SAT-051

The clinical relevance of prior bariatric surgery in alcohol-related liver disease in a nationwide belgian liver transplant population

Sander Lefere¹, Roberto Troisi², Vincent Karam³, Constantino Fondevila⁴, Frederik Nevens⁵, Olivier Detry⁶, Nicolas Lanthier^{7,8}, Matteo Serenari⁹, Leke Wiering¹⁰, Thomas Vanwolleghem¹¹, Christophe Moreno¹², Frederik Berrevoet¹³, Anja Geerts¹. ¹Hepatology Research Unit, Dpt. of Internal Medicine and Pediatrics, Ghent University, Ghent, Belgium; ²Dpt. of Clinical Medicine and Surgery, Federico II University of Naples, Naples, Italy; ³Hepatobiliary center, AP-HP Paul Brousse Hospital, University of Paris-Sud, Paris, France; ⁴Department of General and Digestive Surgery, Hospital Universitario La Paz, IdiPAZ, CIBERehd, Madrid, Spain; ⁵Hepatology and Liver Transplantation, University Hospitals KU Leuven, Leuven, Belgium; ⁶Dpt. of Abdominal Surgery and Transplantation, CHU Liege, Liege, Belgium; ⁷Laboratory of Hepato-Gastroenterology, Institut de Recherche Expérimentale et Clinique, Université catholique de Louvain, Brussels, Belgium; ⁸Service d'Hépatogastroentérologie, Cliniques universitaires Saint-Luc, UCLouvain, Brussels, Belgium; ⁹Dpt. of Medical and Surgical Sciences, University of Bologna, Bologna, Italy; ¹⁰Dpt. of Hepatology and Gastroenterology, Charité-Universitätsmedizin Berlin, Berlin, Germany; ¹¹Division of Gastroenterology and Hepatology, University Hospital Antwerp, Antwerp, Belgium; ¹²Dpt. of Gastroenterology, Hepatopancreatology and Digestive Oncology, CUB Hôpital Erasme, Université libre de Bruxelles, Brussels, Belgium; ¹³Dpt. of General and Hepatobiliary Surgery and Liver Transplantation, Ghent University Hospital, Ghent, Belgium
Email: sander.lefere@ugent.be

Background and aims: Patients with a history of bariatric surgery (BS) are susceptible to developing alcohol use disorder, which can lead to alcohol-related liver disease (ALD). Notably, we have previously shown that mortality can be higher compared to non-BS patients. Our aim was to describe the demographics, disease phenotype and mortality of patients transplanted for alcohol-related liver disease, in relation to BS.

Method: In this European Liver Transplant Registry (ELTR)-endorsed study, we included adult patients who underwent a liver transplantation (LT) in Belgium between 1/1/2013 and 31/12/2022 for ALD. We captured all patients with a history of BS prior to developing ALD, and included non-BS control patients from the same cohort. Data were retrieved retrospectively at each centre and collected via REDCap.

Results: We identified 37 patients who underwent BS (83.8% Roux-en-Y gastric bypass) before developing ALD, who received a LT between 2013 and 2022, and included 328 non-BS patients with an LT for ALD as controls. The median time between BS and diagnosis of severe liver disease was 7.2 years. Confirming our previous findings, more BS patients were female, compared to non-BS patients (45.9% vs. 18.9%, $p < 0.001$), and BS patients were 8 years younger at the time of transplantation ($p < 0.001$). MELD score at listing was higher (median 20 vs. 15, $p = 0.003$), and complications including ascites, encephalopathy and bacterial infections were more prevalent in the BS group. These differences disappeared after excluding patients with hepatocellular carcinoma (HCC), which was more prevalent in the non-BS group (8.1% vs. 49.1%, $p < 0.001$). Despite the younger age, survival after a median follow-up time of 5.5 years following LT was similar, and patients with BS trended to have a lower survival after LT in Cox regression analysis (HR 1.86, $p = 0.077$). This risk became statistically significant after exclusion of patients transplanted for HCC ($p = 0.043$). Interestingly, causes of death also differed, with liver disease being listed in 70.0% vs. 14.3% of patients as the main cause of death. Twice as many BS patients experienced a relapse of alcohol use post-transplant (27.0 vs. 14.1%, $p = 0.038$), whereas the occurrence/recurrence of MASLD was similar between both groups.

Conclusion: Following BS, excessive alcohol use can progress to end-stage ALD and need for LT. These patients present at a younger age, with more signs of hepatic decompensation, and can be at a higher risk for post-LT mortality, especially liver-related death. Pre-surgery

screening for risk of excessive alcohol use and continued post-operative follow-up of these patients are warranted.

SAT-052

Artificial intelligence and liver transplantation: post-transplantation chronic kidney disease prediction

Paul Carrier¹, Veronique Loustaud-Ratti¹, Maryline Debette-Gratien¹, Pauline Maurel², Aurélie Prémaud³, Annick Rousseau⁴, Essig Marie⁵, Céline Rigaud², Christine Silvain⁶, Xavier Causse⁷, Pierre Marquet⁸, Ephrem Salamé⁹, Jean-Baptiste Woillard⁵. ¹CHU Limoges, Limoges, France; ²CHU Limoges, Limoges, France; ³UMR 850, Limoges, France; ⁴UMR-850, Limoges, France; ⁵INSERM U-850, Limoges, France; ⁶CHU Poitiers, Poitiers, France; ⁷CHR Orleans, Orleans, France; ⁸Limoges, France; ⁹CHU Tours, Tours, France
Email: pcarrier@hotmail.fr

Background and aims: Renal failure, acute or chronic, is a major issue in the post-organ transplant period, including liver transplantation. It must be prevented and anticipated, eventually through predictive models, obtained thanks to artificial intelligence.

Method: On an available base of 160 patients, we used a Machine Learning approach, based on the xgboost algorithms, generalized linear models and SVM to predict chronic kidney disease post-liver transplantation. Data splitting was carried out to separate the data into a training group (119 patients) and an evaluation group (41 patients). The hyperparameters of the xgboost and SVM algorithms were optimized by cross-validation (10 sets). The choice of the most appropriate algorithm was made by cross-validation on the training base. Finally, the best algorithm was evaluated in the validation base and its performance in terms of AUROC, sensitivity and specificity was studied. Variable importance plots made it possible to evaluate the predictive variables.

Results: The xgboost algorithm provided the best performance in predicting chronic kidney disease post-liver transplantation in crossvalidation in the training database with AUROC = 0.73, sensitivity = 78% and specificity = 69% (vs GLM: AUC ROC = 0.71, sen = 61%, sp = 81%; and SVM: AUROC 0.73, sen = 68%, sp = 67%). The evaluation of Xgboost in the test database shows an AUROC = 0.78, sen = 25%, an sp = 93%. The three algorithms highlighted pre-transplant renal failure as the main risk factor linked to the event.

Conclusion: The predictive performances observed in this study were close to those in the literature studied for post-transplant acute kidney failure (Zhang et al., J. Translationel Med, 2021). We plan to study a larger cohort, with the aim of developing a more efficient predictive tool.

SAT-053

Liver transplantation in patients with autoimmune hepatitis: a large single-center study

Mohssen Nassiri-Toosi¹, Ali Jafarian², Amir Kasraianfard², Ali Mohammad Moradi². ¹Tehran University of Medical Sciences, Tehran, Iran; ²TUMS, Tehran, Iran
Email: mohsen_nasiri@yahoo.com

Background and aims: to find the characteristics and long-term outcomes of the patients who underwent liver transplantation for AIH-related end-stage liver disease at our center.

Method: Adult patients with primary deceased donor liver transplantation from January 2007 to March 2022 at Tehran University of Medical Sciences affiliated hospital, Iran, were enrolled. Exclusion criteria were secondary liver transplantation, patients with diagnosis of acute liver failure, acute on chronic liver failure, and fulminant hepatitis, and patients with age less than 15. AIH was defined by presence of autoantibodies including antinuclear antibodies, anti-smooth muscle antibodies, anti-liver-kidney microsomal type 1 antibody, or high IgG, or plasma cell interface hepatitis in histopathological examination of liver. Patients with overlapping syndromes or concomitant chronic liver disease were excluded. All patients were given triple immunosuppression drugs (Cacinarins,

Cellcept, Prednisolone). Low-dose glucocorticoids (5–7.5 mg/d) were continued lifelong for patients with AIH, unlike the others in whom the glucocorticoids were discontinued within the first year post-transplantation. Recurrent autoimmune hepatitis was defined as presence of portal and periportal lymphoplasmacytic infiltrates in liver tissue in patients with sustained elevations of aminotransferases levels and in the absence of other causes of allograft dysfunction.

Results: During study period, 1107 subjects with a mean age 45.94 ± 12.43 years old (range 16–73, median 48) including 423 (38.2%) females were enrolled. AIH was the underlying cause of cirrhosis in 177 subjects. Other 930 subjects were in the non-AIH group with viral hepatitis in 250 (26.88%), primary sclerosing cholangitis in 153 (16.45%), non-alcoholic steatohepatitis in 119 (12.79%) subjects. All subjects were followed for a mean of 65.14 ± 1.21 months (range 3–187, median 60) post-transplant. Recurrence of AIH was detected in 8 (4.5%) subjects in the AIH group. One out of 8 subjects with a recurrence of AIH died 10 years after liver transplant because of pulmonary sepsis. At the end of the study, 825 subjects were alive, 131 (61.41%) subjects in the AIH group and 694 (74.62%) subjects in the non-AIH group were alive. Survival rates of the subjects at 1 month, 1 year and 3 years after liver transplant were 88%, 81%, and 78%, respectively. In the AIH group survival rate of the subjects at 1 month, 1 year and 3 years were 87%, 81% and 78%. In the non-AIH group survival rate of the subjects at 1 month, 1 year and 3 years were 88%, 81% and 78%. The survival rates were not significantly different between the two groups ($p = 0.445$).

Conclusion: AIH is common etiology of underlying liver disease with safe result and good outcomes after liver transplantation and a low-risk of recurrence of AIH especially the ones who experienced more episodes of acute rejection in our center.

SAT-054

Impact of lymphadenectomy for patients with clinically node-negative intrahepatic cholangiocarcinoma: a retrospective cohort study

Meng Sha¹, Jie Cao¹, Chuan Shen¹, Ying Tong¹, Jianjun Zhang¹, Qiang Xia¹. ¹Renji Hospital, Shanghai Jiao Tong University, School of Medicine, Shanghai, China
Email: simonsha23@163.com

Background and aims: Lymph node status is a prominent prognostic factor for intrahepatic cholangiocarcinoma (ICC). However, the clinical value of performing lymphadenectomy (LND) in patients with clinical node-negative ICC remains controversial. The aim of this study is to determine whether lymphadenectomy improves long-term outcomes in this subgroup of patients.

Method: We retrospectively analyzed patients who underwent radical liver resection for clinically node-negative ICC from three tertiary referral centers. A propensity score matching analysis based on clinicopathological data was conducted between patients with and without lymphadenectomy. Recurrence-free survival and overall survival were compared in the matched cohort.

Results: Among 303 patients who underwent radical liver resection for ICC, a total of 159 clinically node-negative ICC patients were eligible for the study with 102 in the LND group and 57 in the non-LND group. After propensity score matching, two well-balanced group of 51 patients each were analyzed. There was no significant difference of median RFS (12.0 vs. 10.0 months, $p = 0.37$) and median OS (22.0 vs. 26.0 months, $p = 0.47$) between the LND and non-LND group. Also, LND was not identified as one of the independent risks for survivals. On the other hand, postoperative adjuvant therapy was the independent risk factor for both RFS (HR 0.623, 95%CI 0.393–0.987, $p = 0.044$) and OS (HR 0.585, 95%CI 0.359–0.952, $p = 0.031$). Furthermore, postoperative adjuvant therapy was associated with prolonged survivals of non-LND patients ($p = 0.02$ for RFS and $p = 0.03$ for OS).

Conclusion: Based on the data, we found that LND did not significantly improve the prognosis of patients with clinically node-

POSTER PRESENTATIONS

negative ICC. Postoperative adjuvant therapy was associated with prolonged survivals of ICC patients, especially in non-LND individuals.

SAT-055

Post-colectomy liver transplant recipients have higher rates of chronic kidney disease at 1-year

Victoria Kronsten¹, Alison Taylor¹, Varuna Aluvihare¹, Claire Kelly¹.

¹Institute of Liver Studies, King's College Hospital, London, United Kingdom

Email: victoria.kronsten@nhs.net

Background and aims: Ileostomy formation predisposes to volume depletion, acute kidney injury (AKI) and subsequent chronic kidney disease (CKD). This risk persists after ileostomy reversal and formation of an ileal pouch-anal anastomosis (IPAA). CKD is common post liver transplantation (LT), approximate prevalence of 40% at 1-year, and carries significant morbidity and mortality. This study aimed to report post-LT renal function in post-colectomy LT recipients.

Method: A single-centre cohort study was performed. All patients who underwent LT at our institution from 01/09/2012 to 01/09/2022 with a history of colectomy were included. Clinical data was collected retrospectively from electronic patient records. Post-operative CKD was defined based on a sustained estimated glomerular filtration rate (eGFR) <60 ml/min/1.73 m² at 1-year.

Results: 34 patients with a history of colectomy (ileostomy (n = 19) and IPAA (n = 15)) were included. Median age at LT was 47 years (interquartile (IQ) range 38–54). Main indication for colectomy was ulcerative colitis (74%). 59% of patients had primary sclerosing cholangitis. Median MELD at LT was 20 (13–25). Renal sparing induction therapy with an interleukin 2 receptor antibody (IL2Ra) was employed in 26%. Median creatinine at LT was 82 µmol/L (72–100) compared to median creatinine at 1-year of 106 µmol/L (81–130) (p = 0.08). At 1-year, 52% of patients had developed CKD (28% CKD Stage 3a, 24% CKD Stage 3b). Sub-group analysis was performed comparing the ileostomy and IPAA groups. There was no difference in sex, age, creatinine or MELD at LT between the 2 groups. AKI rates were similar in both groups (37% vs 40% and 16% vs 20% at 48 hours and 7-days post-LT, respectively). At 1-year 61% of the ileostomy group were on a calcineurin inhibitor (CNI) sparing regimen with mycophenolate mofetil compared to 23% of the IPAA group (p = 0.03). At 1-year 75% of the ileostomy group had developed CKD (42% CKD Stage 3a, 33% CKD Stage 3b) compared to 31% (15% CKD Stage 3a, 15% CKD Stage 3b) of the IPAA group (p = 0.03).

Conclusion: CKD is more common (>50%) in post-colectomy LT recipients, with the highest rates observed in patients with ileostomies. Fluid replacement peri-transplant, and stoma management where indicated, should be optimised in post-colectomy LT recipients. Consideration should be given to planned renal sparing induction therapy and early use of a CNI sparing regimen in patients with ileostomies undergoing LT independent of pre-LT eGFR.

SAT-056

Long-term survival (≥20 years) after liver transplantation in Italy: a single center retrospective experience

Maria Francesca Donato¹, Clara DiBenedetto¹, Enrico Sguazzini¹, Michele Sagasta¹, Barbara Antonelli², Farina Elisa¹, Federica Invernizzi¹, Lucio Caccamo², Tullia De Feo³, Pietro Lampertico^{1,4}. ¹Division of Gastroenterology and Hepatology, Foundation IRCCS Ca' Granda Ospedale Maggiore Policlinico, Milan, Italy; ²General and Liver Transplant Surgery Unit, Foundation IRCCS Ca' Granda Ospedale Maggiore Policlinico, Milan, Italy; ³North Italy Transplant Program (NITp), UOC Coordinamento Trapianti, Fondazione IRCCS Ca' Granda-Ospedale Maggiore Policlinico, Milan, Italy; ⁴CRC "A. M. and A. Migliavacca" Center for Liver Disease, Department of Pathophysiology and Transplantation, University of Milan, Milan, Italy
Email: francesca.donato@policlinico.mi.it

Background and aims: Nowadays liver transplant (LT) represents the optimal strategy to manage end-stage liver diseases and the post-transplant outcome depends on a complex interaction between donor, recipient and transplant factors. The aim of the study was to retrospectively investigate the prevalence and clinic-epidemiological features of long-term survivors (LTS ≥20 years) LT recipients.

Method: We enrolled consecutive adult patients transplanted in our liver transplant Center from 1983 to 2003 and followed until 2023. The primary end point was assessing factors associated with long term survival (≥20 years).

Results: Overall, 400 patients received 454 liver grafts (re-transplant rate = 12%), 66% were males with a median age of 47 years (range 18–63). Viral etiology was the main etiology of LT (overall 62%: 32% HBV and/or HDV, 30% HCV) followed by PBC/PSC/AIH (16%), alcohol (7%) and mixed etiologies (15%). The most common indication for LT was decompensated cirrhosis (72%) followed by HCC (18%), FHF (5%) and combined liver-kidney transplantation (5%). A CNI-based immunosuppression was used either in monotherapy or combined with steroids, azathioprine or mycophenolate mofetil in all patients. The median follow-up was 16 years (range 0–37). The estimated overall survival at 5–10–20–25 years was 68%, 60%, 43% and 37%, respectively. 171 LT recipients (43%) were classified LTS while 205 (51%) survived less than 20 years (no-LTS); 25 were lost to follow-up (6%). The median follow-up was 25 years (range 20–37) in LTS and 3 years in no-LTS recipients (range 0–19). By univariate analysis, LTS were more often females (40% vs 29%, p = 0.02), younger (44 vs 47 years, p = 0.05) and transplanted with HBV/HDV etiology (42% vs 23%, p = 0.0001) or AIH-PBC-PSC (21% vs 12%, p = 0.01) compared to no-LTS. Conversely, HCV and alcohol-related etiologies were more common in no-LTS compared to LTS (38% vs 20%, p = 0.0001 and 10.5% vs 3%, p = 0.004, respectively). By using liver stiffness (Fibroscan®), LTS recipients showed a good graft function at the last follow-up (median 6 kPa, range 2–58). LTS also showed a lower rate of diabetes and kidney impairment than no-LTS (26% vs 61%, p = 0.05 and 36% vs 54%, p < 0.05, respectively). At the end of study, 76% of LTS and 10% of those without LTS were alive. Deaths due to liver-related or cardio-cerebrovascular causes were more frequently observed in no-LTS recipients compared to LTS group.

Conclusion: This study covers 40 years of our liver transplant program and shows a high overall rate of long-term survivors. HBV and HDV infections together with autoimmune and cholestatic etiologies were more represented in LTS, the former having benefited from the advent, early in the nineties, of anti-HBV prophylaxis and cure by NUCs. The unfavorable outcome of HCV liver transplants observed in our study is justified by the fact that direct anti-HCV drugs became available only in recently.

SAT-057

Poor radiological-histopathological concordance in patients transplanted for hepatocellular carcinoma: a single centre experience

Mzamo Mbelle^{1,2}, Christopher Harlow¹, Charles Gallaher¹, Mercy Karoney¹, Abid Suddle¹, Claire Kelly¹, Rosa Miquel¹, Yoh Zen¹, Varuna Aluvihare¹, Michael Heneghan¹, Sarah Selemani¹, Praveen Peddu¹, Paul Ross¹, Krishna Menon¹, Miriam Cortes Cerisuelo¹, Parthi Srinivasan¹, David Wallace¹, Kosh Agarwal¹, Maria Guerra Veloz¹. ¹King's College Hospital, London, United Kingdom; ²King's College Hospital, Institute of Liver Studies, London, United Kingdom
Email: mzamo.mbelle@nhs.net

Background and aims: Hepatocellular cancer (HCC) is the most common primary liver malignancy and is a leading cause of liver-related mortality. Contrast-enhanced cross-sectional imaging is the cornerstone in the diagnosis, staging and management of HCC, including eligibility for liver transplant (LT). However, it is well known that the radiological and histopathological concordance in liver transplant setting is poor, and this could have a negative impact

in long term outcomes. We audited the radiological-histopathological concordance in our specialised tertiary cancer centre in the United Kingdom.

Method: This retrospective study included all patients who underwent LT for HCC at King's College Hospital and who had been discussed and/or followed-up at a multi-disciplinary tumour board between January 2019 and December 2023. Demographic, clinical data, laboratory parameters and type and date of the scans (dual- or triple-phased computed tomography (CT) scans ± magnetic resonance imaging (MRI)) were collected. Radiological and histological characterisation of the correlation for the number of cancer (s) and the largest lesion size at the time of diagnosis and post liver transplant were analysed using Pearson coefficient.

Results: One hundred eighteen patients were included, 92 (78%) were men, 91 (77%) were Caucasian and the mean age at transplantation was 60.1 (SD 7.5) years. The leading aetiology for liver disease was alcohol-associated cirrhosis (33%) followed by hepatitis C (24%) and metabolic dysfunction-associated steatotic liver disease (19%). The median times between the HCC diagnosis to LT and the wait-list time to LT were 12 (IQR 8–19) months and 4 (IQR 2–7) months respectively. Most of the patients (64%) were diagnosed and staged with dual cross-sectional imaging, and only 45 (38%) had liver contrast-enhanced cross-sectional imaging within 1 month of the LT. Seventy-two patients (65%) were within UK criteria on both imaging and explant. On pre-transplant imaging, the mean of number of cancers was 1.52 (SD 0.7) compared with the 3.4 (SD 2.7) on explant (correlation coefficient of 0.313; $p = 0.001$). The median of the largest cancer size was 28 (20–38.5) mm in the pre-transplant imaging compared 6 (21–35) mm in the explant (correlation coefficient of 0.391; $p = 0.001$).

Conclusion: Despite the poor radiological -histopathological concordance between the number of cancer (s) and the largest lesion size, only one in three patients were outside our national criteria. Staging HCC based on dual cross-sectional imaging did not improve the concordance in our cohort. New AI based imaging techniques may help to improve concordance rate.

SAT-058

The survival benefit of liver transplantation for metabolic dysfunction associated steatotic liver disease: an Italian liver transplant registry study

Alessandro Vitale¹, Silvia Trapani², Francesco Paolo Russo¹, Massimo Cardillo², Umberto Cillo¹. ¹Padua University, Padua, Italy; ²Centro nazionale trapianti, Istituto superiore di sanita', Rome, Italy
Email: alessandro.vitale@unipd.it

Background and aims: A recent international consensus, achieved through the Delphi method, has introduced a new definition of Metabolic Dysfunction-Associated Steatotic Liver Disease (MASLD). Our objective was to analyse past and future epidemiological trends, prognostic features, and transplant survival benefits of MASLD and non-MASLD patients waiting for liver transplantation (LT) in Italy.

Method: Utilizing the Italian Liver Transplant Registry database, we analysed data from adult patients listed for primary liver transplantation due to end-stage chronic liver disease between January 2012 and December 2022. Independent multivariable waiting lists and post-transplant survival models were developed for patients with and without hepatocellular carcinoma (HCC). A Monte Carlo simulation was employed to create 5-year transplant benefit distributions based on the presence of MASLD, HCC, and MELD-sodium values.

Results: A total sample of 16,215 patients was considered, of whom 3,073 were excluded due to positivity for one or more exclusion criteria. A significant increase in the prevalence of MASLD as an indication for liver transplantation was observed from 2012 to 2022, both for HCC and non-HCC cohorts. Projections suggest that, as early as next year, MASLD will overcome HCV as the second most common indication for transplantation after alcoholic liver disease in Italy. According to

univariate and multivariate analyses, MASLD aetiology was not an independent predictive factor for patient survival after transplantation. However, it increased the risk of death for patients on the waiting list without HCC. Consequently, the survival benefit of transplantation in patients with MASLD without HCC was significantly larger than that of other candidates.

Conclusion: The results of this study, if externally validated, could lead to modifications in allocation policies, prioritising MASLD patients over other transplant candidates.

SAT-059

Retrospective population study of liver transplantation in Iceland-An update

Bjarki Leó Snorrason¹, Sigurdur Olafsson², Einar S. Björnsson³. ¹University of Iceland, Reykjavík, Iceland; ²Landspítali University Hospital, Reykjavík, Iceland; ³Landspítali University Hospital, University of Iceland, Reykjavík, Iceland
Email: Bls8@Hi.is

Background and aims: Historically, the incidence of liver cirrhosis in Iceland has been low but has increased in the past two decades due to rising alcohol consumption, obesity and hepatitis C virus (HCV) infections. Since the inception of liver transplantations in Iceland in 1984 up until 2012, the most common underlying liver disease was primary biliary cholangitis (PBC), accounting for 20% of cases. In this study we sought to explore the evolving indications of liver transplantation in Iceland over the last decade.

Method: In this retrospective nationwide study, we systematically collected data pertaining to the indications for adult liver transplantations from 2013 to 2023. A chart review was undertaken, and our findings were compared with data from a previous study to understand the changes in the frequency of liver transplantations.

Results: During the study period a total of 52 liver transplantation (4 re-transplantations) were performed in 48 patients, of whom 30 (63%) were males. The mean age of the cohort was 54 ranging from 24 to 73. The average incidence of liver transplantation in the Icelandic population was 13.1 per million inhabitants per year, representing an increase from the period 2007–2012 (8.9 per million). The most common primary indication for transplantation were cirrhosis (60.4%), cirrhosis with hepatocellular carcinoma (23%). Other indications included acute hepatic failure (4.2%), tumors beyond hepatocellular carcinoma (2.1%) and a combination of various causes (10.4%). The leading etiology for liver transplantation was metabolic-associated steatotic liver disease (MASLD) accounting for 23% of cases with an incidence of 3.03 cases per 1,000,000 person-years annually, compared to an incidence of 0.12 per million inhabitants in the period 1984–2012, a 25-fold increase. The second most common indication was alcohol related cirrhosis (21%). Other indications comprised PBC (8.3%), primary sclerosing cholangitis (8.3%), Hepatitis C (8.3%), drug-induced liver injury (DILI) 4.2%, and a combination of various other causes accounting for 27%.

Conclusion: There has been a significant increase in liver transplantations compared to previously studied periods, particularly driven by MASLD as the leading cause. Notably, alcohol related liver disease surpassed PBC as a leading etiology. These changes underscore the dynamic nature of liver disease etiology, prompting a closer examination of these trends to enhance clinical management and enable the development of targeted public health strategies.

SAT-060

Needle tract seeding of hepatocellular carcinoma after liver transplantation: a single center experience

Chiara Sicuro¹, Gabriella Frassanito¹, Lorenza Di Marco², Alessandra Pivetti¹, Roberta Odorizzi³, Cristiano Guidetti³, Paolo Magistri³, Stefano Di Sandro³, Fabrizio Di Benedetto³, Antonio Colecchia¹, Nicola De Maria¹. ¹Gastroenterology Department-AOU Policlinico di Modena, Modena, Italy; ²Oncology and Hematology Department-AOU Policlinico di Modena, Modena, Italy; ³Onco-Hepato-

POSTER PRESENTATIONS

Biliary-Pancreatic Surgery and Transplantation Unit-AOU Policlinico di Modena, Modena, Italy
Email: chiarasicuro44@gmail.com

Background and aims: Hepatocellular carcinoma (HCC) is one of the leading causes of liver transplantation (LT) worldwide. Most of the patients transplanted for HCC undergo local percutaneous procedures before LT to diagnose/downstage the tumor, to include liver biopsy (LB), thermal ablation (PTA), and ethanol injection (PEI). Needle track seeding (NTS) can occur after such procedures. According to the literature, NTS occurs in 0.01–5% of cases after an LB, 1.4% of cases after a PEI, and 0.95% of cases after a PTA. The incidence of NTS in the setting of LT is poorly investigated, only few studies and case reports about NTS after LT have been published. Aims of our study were: to determine the incidence of NTS following LB or percutaneous treatment in patients with HCC who underwent LT; to assess the impact of NTS on HCC recurrence and patients' survival.

Method: All LTs for HCC performed at our Institution between Jan 2010 and Dec 2022 were considered in this retrospective study. We recorded all percutaneous procedures as well as all HCC treatments performed prior to LT, including liver resection (LR) and trans-arterial chemoembolization (TACE). Radiological imaging of all pts was reviewed.

Results: A total of 347 pts underwent LT for HCC; 137 underwent a percutaneous procedure before LT: 54 underwent LB alone, 19 had an LB followed by a percutaneous treatment, 64 underwent PTA and/or PEI without a previous LB. NTS occurred in 6 pts (4.38%): Pt 1 had LB + TACE (G2 HCC). Peritoneal NTS appeared 13 mo after LT, 23 mo after LB; Pt 2 had LB and no treatment before LT (G3 HCC). NTS in the right rectus abdominis muscle appeared 45 mo after LT, 61 mo after LB; Pt 3 had no LB and underwent TACE + RFA + PEI (G3 HCC). Peritoneal NTS appeared 51 mo after LT, 61 mo after PEI; Pt 4 had LB and then TACE + RFA (G3 HCC). Diaphragmatic NTS appeared 53 mo after LT, 101 mo after LB; Pt 5 had LB and then TACE (G3 HCC). NTS in the right rectus abdominis muscle appeared 22 mo after LT, 34 mo after LB; Pt 6 had LB and then LR + TACE + systemic therapy (G2 HCC). Subcutaneous NTS in the epigastric region appeared 10 mo after LT, 23 mo after LB. The median time of NTS recurrence was 30 mo from PT, 17, 5 mo from LT. Patients 2, 3 and 4 underwent a successful surgical removal of the seeding lesions. No recurrence of HCC has been reported after 27, 14 and 2 mo respectively. Patient 1 is currently awaiting surgical treatment. Patients 5 and 6 underwent surgery with removal of the seeding but had evidence of HCC recurrence respectively 25 mo and 23 mo after LT. They both were Milan out before liver transplantation.

Conclusion: In our experience: 1) NTS is an uncommon but not negligible complication of liver percutaneous procedure for HCC; 2) the occurrence of NTS may not always impact patients' prognosis in terms of HCC recurrence or overall survival. In our small series 3 out of 6 patients had a successful removal of the neoplasm, without recurrence of HCC at least after a short period of follow-up.

Liver tumours – Clinical aspects except therapy

TOP-509-YI

Validation and improvement of the IMbrave050 criteria for high-risk of HCC-recurrence as an indication to adjuvant treatment: results from a 4-year retrospective competitive-risk study

Matteo Serenari¹, Matteo Cescon¹, Chiara Bonatti¹, Bernardo Stefanini¹, Sofia Penazza¹, Edoardo Prosperi¹, Elton Dajti¹, Francesco Tovoli¹, Matteo Ravaioli¹, Fabio Piscaglia¹, Federico Ravaioli¹. ¹Department of Medical and Surgical Sciences, University of Bologna, IRCCS Azienda Ospedaliero-Universitaria di Bologna, Bologna, (IT), Bologna, Italy
Email: f.ravaioli@unibo.it

Background and aims: The IMbrave050 study found that adjuvant treatment with atezolizumab and bevacizumab improved recurrence-free and overall survival in high-risk HCC recurrence (HCC-r) patients after curative-intent liver resection (LR). High-risk criteria for HCC-r are based on the number, dimension, vascular invasion, and HCC differentiation. Authors suggested integrating liver stiffness measurement (LSM) into the risk-stratification algorithm after LR. We aimed to validate the IMbrave050 criteria and improve the criteria for better stratification of patients who would benefit from adjuvant treatment.

Method: We conducted a retrospective analysis on patients with HCC who had undergone curative LR. We followed the patients according to guidelines and assessed the occurrence of HCC-r events. We performed a competing-risks regression analysis to account for liver transplantation or death as competitive events. We stratified the patients as high/low risk for HCC-r events based on the IMbrave050 criteria.

Results: 166 out of 197 HCC patients who underwent LR between 2010–2020 reached oncological radicality (R0) and included in the study. According to IMbrave050 criteria, 105 (63.3%) patients were classified as high-risk for HCC-r, potentially benefitting from adjuvant therapy. During the mean follow-up of 43.5 months, 60.8% of the patients developed HCC-r with an incidence rate of 16.8%/year [95%CI 13.8–20.4] during a follow-up time to HCC-r of 20.7 mo (7.2–43.4). 13.3% of the patients developed competitive events. Kaplan-Meier analysis showed significant stratification of HCC-r risk based on IMbrave050 criteria ($p = 0.0009$). The high-risk group had 71 out of 105 (63.2%) HCC-r, with an incidence rate of 22.5%/y [17.8–28.4]. This was significantly higher ($p = 0.0003$) than in the low-risk group, which had 30 out of 61 (49.1%) HCC-r, with an incidence rate of 10.5%/y [7.3–15]. Based on competitive-risk analysis, $LSM \geq 15$ kPa was significantly ($p = 0.007$) associated with HCC-r with a sub-distribution hazard ratio (SHR) of 1.694 [1.155–2.486]. The incidence rate of HCC-r was significantly different ($p = 0.0019$) between patients with $LSM < 15$ kPa (13%/y [9.9–17]) and $LSM \geq 15$ kPa (24.3%/y [18.4–32.2]). When we applied LSM-based risk stratification in the low-risk HCC-r cohort according to IMbrave050 criteria, we separated the subgroup with $LSM \geq 15$ kPa with a significantly higher incidence of HCC-r (17.5%/y [10.7–28.5]) compared with those with $LSM < 15$ kPa (7.2%/y [4.2–12.1]) ($p = 0.017$).

Conclusion: The study validated the IMbrave050 criteria in radically resected patients to identify high-risk HCC-r patients who need adjuvant therapy. We found that adding $LSM \geq 15$ kPa to the IMbrave050 low HCC-r risk identifies patients at higher risk, which could similarly be considered for adjuvant therapy after radical treatment.

TOP-510

Incomplete thermal ablation plus programmed cell death protein 1 monoclonal antibodies increase the incidence of hyperprogressive disease in hepatocellular carcinoma

Yuzhe Cao^{1,2,3}, Guanglei Zheng¹, Mengxuan Zuo^{1,2,3}, Wang Li^{1,2,3}, Fei Gao^{1,2,3}. ¹Sun Yat-sen University Cancer Center, Guangzhou, China; ²State Key Laboratory of Oncology in South China, Guangzhou, China; ³Guangdong Provincial Clinical Research Center for Cancer, Guangzhou, China

Email: gaof@sysucc.org.cn

Background and aims: Hepatocellular carcinoma (HCC) is the most common type of liver cancer. Programmed cell death protein 1 (PD1) monoclonal antibodies (mabs) are now standard of care for HCC management. However, reports of hyperprogressive disease (HPD) following immunotherapy triggered clinical concern. Though mechanism still not clear, HPD was hypothesized related to interaction between the fragment crystalline (Fc) of PD1 mabs and Fc γ receptors (Fc γ R) on macrophages. Thermal ablation is recommended as the first-line choice for early-stage patients. However, incomplete ablation (IA) is not rare when the tumors are large, multiple or

adjacent to vessels. To deal with metastases or residual lesions, a regimen consisting of ablation and PD1 mabs has raised concern due to synergy between PD1 mabs and tumor-related antigen release caused by ablation. Nonetheless, ablation could induce macrophage infiltration, which may interact with Fc of PD1 mabs and result in HPD. We conducted a retrospective clinical study to explore whether IA plus PD1 mabs increase the incidence of HPD than PD1 mabs in HCC patients. An animal experiment was also performed to validate the clinical findings, study the underlying mechanism of HPD and explore the potential precautions.

Method: This study retrospectively enrolled immunotherapy-naïve HCC patients with Child-Pugh score ≤ 7 who underwent IA plus PD1 mabs (IAP) or PD1 mabs alone (P) from January 2018 to December 2022. Each patient had at least 2 times image data available for baseline tumor growth rate (TGR) assessment before administration of PD1 mabs. The diagnostic criteria of HPD was: 1) Time to progression < 2 months; 2) $\geq 50\%$ increase of sum of target lesions major diameters; 3) Two-fold increase in TGR or at least 10 new lesions after treatment. C57/BL6 mice with subcutaneous tumor were randomly assigned to P (sham ablation + PD1 mab, $n = 4$), IAP (IA + PD1 mab, $n = 3$) and IAMP (IA + modified PD1 mab with D265A mutation on Fc, $n = 3$). Fc with D265A mutation is unrecognized for Fc γ R. The tumor volume is calculated according to the modified ellipsoidal volume formula. And the TGR is the ratio between logarithm of tumor volume and interval time. The difference between pre- and post-treatment TGR was recorded as Δ TGR.

Results: In total, 55 patients met the criteria and were included in the present study (IAP: $n = 12$, P: $n = 43$), the incidence of HPD in the IAP group was significantly higher than that in the P group (58.3% vs. 20.9%, $p = 0.028$). The animal study verified that IAP could accelerate the tumor growth (Δ TGR: IAP vs. P, 0.047 ± 0.0030 vs. -0.0031 ± 0.0080 , $p < 0.001$), and suggested that the blocking the interaction between Fc and Fc γ R receptors could interfere with the phenomenon (Δ TGR: IAMP vs. P, -0.0033 ± 0.0068 vs. -0.0031 ± 0.0080 , $p = 0.96$).

Conclusion: IAP is likely to induce the high incidence of HPD. And the Fc-modified PD1 mabs without the ability to bind to Fc γ R may block the process of HPD.

TOP-511

Trends and evolution of hepatocellular carcinoma due to etiological shift from 2005 to 2020 in Germany: nationwide population-based study

Josune Cabello Calleja¹, Wenyi Gu¹, Robert Schierwagen¹, Maximilian Joseph Brol¹, Frank Erhard Uschner¹, Florian Rennebaum¹, Sara Noemi Reinartz Groba², Michael Praktiknjo², Jonel Trebicka^{1,3,4}. ¹Department of Internal Medicine B, University Hospital Muenster, Muenster, Germany; ²Department of Internal Medicine B, University Hospital Muenster, Muenster, Germany; ³European Foundation for Study of Chronic Liver Failure, Barcelona, Spain; ⁴Department of Gastroenterology and Hepatology, Odense University Hospital, Odense, Denmark
Email: josune.cabello@ukmuenster.de

Background and aims: Hepatocellular carcinoma (HCC) is considered the most frequent primary malignant disease of the liver and it is associated with a high mortality. The main risk of developing HCC consists in the presence of liver cirrhosis. However, its association with other potential drivers, such as comorbidities, still remains unclear. Therefore, we aimed to analyze changing trends of HCC, especially focusing on underlying etiologies and related comorbidities.

Method: This German nationwide study analyzed 393,230 admissions with HCC from 2005 until 2020 based on the diagnosis-related-groups (DRG) system via ICD-10-GM-2023 and OPS-2023 codes. We analyzed the data focusing on the investigation of most probable etiologies related to the development of HCC as well as the all-cause in-hospital mortality rate of these patients. All trend and changes

over the years were compared using linear regression or Mann-Whitney U-test.

Results: The number of recorded admissions of patients with HCC increased significantly during the last 16 years (increase of 21.78%; $p < 0.001$).

The most common underlying etiology was alcohol-related liver disease (ALD) (55.48%), which raised over the time (22.78% of increase; $p = 0.002$), but with a significant decrease of in-hospital mortality rate ($p = 0.010$).

The following most frequent overall etiologies were hepatitis C virus (HCV) (19.79%) and hepatitis B virus (HBV) (9.67%), both showing a decreasing trend in admissions (HCV: -66.99% , $p = 0.001$; HBV: -36.53% , $p < 0.001$), but with a similar in-hospital mortality rate.

In addition, we observed that patients with metabolic dysfunction-associated steatohepatitis/metabolic dysfunction-associated steatotic liver disease (MASH/MASLD) showed a 3.7-fold increase, the strongest among etiologies.

As indicators of metabolic syndrome, comorbidities in patients with HCC (type 2 diabetes mellitus, arterial hypertension (AHT), dyslipidemia and obesity) were significantly more frequent during the observational period (88.89% of increase; $p < 0.001$). In particular, AHT and dyslipidemia seemed to be related to higher risk of HCC development independent of the presence of liver cirrhosis.

Conclusion: This nationwide study shows the increasing prevalence of ALD and MASLD in patients with HCC. Especially metabolic risk factors may be drivers of HCC, even in absence of cirrhosis and should be taken into account in future investigations.

TOP-512-YI

Metformin as a protective factor against hepatocellular carcinoma in chronic hepatitis C patients achieving sustained virologic response: a long-term follow-up study

Henar Calvo^{1,2,3}, Lorena Jara⁴, Irene Villarino¹, Marta Quiñones⁴, Ruben Alvarado⁴, Eva Martinez², Vanessa Díaz⁵, Maria Luisa Gutiérrez⁴, Joaquin Miquel^{1,3}, Eduardo Sanz de Villalobos^{1,3}, Miguel Torralba^{2,3,6}, Sonia Albertos Rubio⁷, Conrado Fernández-Rodríguez^{4,8}, Juan Ramón Larrubia^{1,2,3}. ¹Gastroenterology Section, University Hospital of Guadalajara, Guadalajara, Spain; ²Department of Medicine and Medical Specialties, University of Alcalá, Alcalá de Henares, Madrid, Spain; ³Group of Translational Research in Cellular Immunology (GITIC), IDISCAM, Guadalajara, Spain; ⁴Service of Gastroenterology, Alcorcón Foundation University Hospital, Alcorcón, Madrid, Spain; ⁵Primary Care Health Centre Josep Bertran I Miret, Sant Pere de Ribes, Barcelona, Spain; ⁶Section of Internal Medicine, University Hospital of Guadalajara, Guadalajara, Spain; ⁷Service of Gastroenterology, Hospital Sant Camil-Sitges, Sitges, Spain; ⁸Department of Public Health and Medical Specialties, Rey Juan Carlos University, Alcorcón, Madrid, Spain
Email: hcalvo@sescam.jccm.es

Background and aims: Metformin activates AMPK and the immune system while inhibiting mTORC1 pathway all of which may protect against the development of hepatocellular carcinoma (HCC). The incidence of HCC is reduced in chronic hepatitis C (CHC) after SVR, but the risk factors in advanced fibrosis remain uncertain. The aim of the study was to assess the incidence of HCC according to the grade of fibrosis and the risk factors associated with HCC after SVR, with focus on the potential protective role of metformin.

Method: We conducted an HCC-free survival study assessing incidence rates and proportional risks based on FIB-4 value at the onset of direct anti-viral agents (DAAs) treatment during post-SVR follow-up. Hazard ratio (HR) for model variables were computed, excluding cases emerging within 6 months of treatment initiation. HCC diagnosis relied on radiological and/or histological evidence. The model, developed using the stepwise backward selection with the Wald statistic, was evaluated by calculating the area under the ROC curve for survival.

POSTER PRESENTATIONS

Results: Between August 2012 and December 2022, the prospective data of 1518 patients with SVR after treatment of CHC with DAA (49% women) from three hospitals were retrospectively analysed. Median follow-up of 75 months (IQR 52–90). 53 HCCs were detected. The incidence rates per 100 patient-years according to FIB-4 were: <1.45, 0.03 [95%CI: 0.002–0.15]; 1.45–3.25, 0.35 [95%CI: 0.19–0.59]; >3.25, 1.7 [95%CI: 1.2–2.3], ($p < 0.001$). The multivariate Cox regression model to predict the HR of HCC ($p < 0.001$) included the following variables: FIB-4 at baseline; HR: 1.020 [95%CI: 1.004–1.037; $p = 0.013$], presence of clinically significant portal hypertension (CSPH); HR: 17.544 [95%CI: 9.183–33.516; $p < 0.001$], age in decades; HR: 1.431 [95%CI: 1.104–1.854, $p = 0.007$], smoking; HR: 4.746 [95%CI: 2.284–9.865, $p < 0.001$]; Metformin treatment; HR: 0.35 [95%CI 0.141–0.916; $p = 0.032$], female sex; HR 0.43 [95%CI: 0.232–0.865, $p = 0.017$]; The Cox regression predictive model for HCC yielded an AUC of 0.804 [95%CI: 0.73–0.88, $p < 0.001$]. In F4 with CSPH, HCC incidence rate per 100 patient-years was higher [2.9; 95%CI: 2.1–4] than in F4 without CSPH [0.7; 95%CI: 0.3–1.5], ($p < 0.001$). In F4 with CSPH on metformin, the HCC incidence rate per 100 patient-years was lower [1.3; 95%CI: 0.4–3.3] than without metformin [3.4; 95%CI: 2.3–4.6], ($p = 0.06$).

Conclusion: The incidence rate of HCC in chronic hepatitis C after SVR is very low in patients with FIB4<3.25, which would suggest limiting HCC screening to cases with FIB4>3.25. Within this group, the highest risk is associated with CSPH, followed by tobacco use and age, while metformin treatment and female sex are protective factors.

TOP-520

Machine learning for risk stratification of hepatocellular carcinoma

Jan Clusmann^{1,2}, Paul-Henry Koop¹, Felix van Haag¹, Yazhou Chen¹, Benjamin P.M. Laevens¹, Christian Trautwein¹, Kai Markus Schneider¹, Jakob Nikolas Kather^{2,3,4,5}, Carolin V. Schneider^{3,6}. ¹Medical Clinic III, Gastroenterology, Metabolic Diseases and Intensive Care, University Hospital RWTH Aachen, Aachen, Germany; ²Institute for Clinical Artificial Intelligence, EKfZ for Digital Health, TU Dresden, Dresden, Germany; ³Department of Medicine III, University Hospital RWTH Aachen, Aachen, Germany, Aachen, Germany; ⁴Division of Pathology and Data Analytics, Leeds Institute of Medical Research at St James's, University of Leeds, Leeds, United Kingdom; ⁵Medical Oncology, National Center for Tumor Diseases (NCT), University Hospital Heidelberg, Heidelberg, Germany; ⁶University of Pennsylvania, Philadelphia, United States
Email: janclusmann@ukaachen.de

Background and aims: Hepatocellular carcinoma (HCC) is a highly fatal malignancy. Historically linked to cirrhosis, HCC is increasingly caused by the obesity-related Metabolic Dysfunction-Associated Steatotic Liver Disease (MASLD), expanding the population at risk of HCC along the worldwide epidemic of obesity. While risk constellations for HCC are well characterized and encompass steatotic liver disease (SLD), viral hepatitis, serum indicators, lifestyle and hereditary risk, current screening predominantly targets patients with liver cirrhosis. Stratifying SLD patients in terms of risk of HCC poses a major clinical challenge. This could be addressed through standardized risk stratification methods, augmented by machine learning and big data.

Method: We assessed data from the UK Biobank, a population-based database with electronic health records (EHR), death registers, lifestyle, physical and biological measures as well as genomics (n~500k each) and metabolomics data (n=250k). We trained five-fold cross-validated random forest machine learning (ML) classifiers on multimodal data of all included patients to predict HCC occurrence (n=470). To simulate clinically relevant scenarios, we employed a layered approach in our data analysis, starting with basic physical measurements. We then incrementally integrated more comprehensive data, first adding commonly available blood counts and serum analyses, and subsequently incorporating advanced analyses such as

metabolomics and genomic sequencing, analyzing gain in predictive accuracy for each step. Models were then validated on previously unseen data from UKB centers from Scotland and Wales.

Results: Random-forest classifiers developed using five-fold cross-validation on 18 UKB centers within England achieved high predictive accuracies in the validation dataset. Specifically, models utilizing only EHR and lifestyle data achieved mean AUROC scores exceeding 0.84, which further increased to AUROCs of 0.88 upon integration of serum information. Interestingly, the inclusion of metabolomic or genomic data did not significantly enhance performance. In comparison, the aMAP-score, a widely recognized and utilized score for HCC risk stratification, attained AUROC scores of only 0.74 in our dataset. Secondary analysis revealed feature importance (FI) distributions with high relevance of blood and metabolomic parameters. This was followed by FI of lifestyle and EHR parameters, while genomic factors were assigned relatively lower FI in our models.

Conclusion: Our results underscore the predictive capability of explainable machine learning models in the context of risk stratification approaches developed from real-world data. This establishes machine learning as a potential new benchmark in the realm of HCC risk assessment.

SATURDAY 08 JUNE

SAT-469

Artificial intelligence for classifying liver lesions in contrast-enhanced ultrasound

Adil Oezsoy¹, James Brooks¹, Pompilia Radu², Jakob Nikolas Kather³, Tom Luedde¹, Annalisa Berzigotti², Michael Kallenbach¹, Tobias Paul Seraphin¹. ¹Medical Faculty and University Hospital Düsseldorf, Heinrich Heine University Düsseldorf, Düsseldorf, Germany; ²Bern University Hospital, University of Bern, Bern, Switzerland; ³Else Kroener Fresenius Center for Digital Health, Technical University Dresden, Dresden, Germany
Email: tobiaspaul.seraphin@med.uni-duesseldorf.de

Background and aims: The evaluation of malignancy of focal liver lesions remains an important yet challenging task in routine patient care. Contrast-enhanced ultrasound (CEUS) is a reliable tool but depends on the examiner's expertise. The rise of artificial intelligence has given way to algorithms potentially able to assist clinicians in diagnosing such lesions. In this study, we trained a weakly supervised attention-based multiple instance learning (aMIL) algorithm to classify focal liver lesions as malignant or benign and evaluated its performance.

Method: For this retrospective study we used a cohort of patients from a tertiary care hospital in Germany undergoing routine CEUS for focal liver lesions. Frames were cut from videos recorded during examination and subsequently features extracted using a pretrained convolutional neural network. We randomly removed a class-balanced test set of 20% and used the remaining cohort to train the algorithm. We performed a hyperparameter grid-search, applying a five-fold cross-validation each time.

Of the multiple trained weakly supervised aMIL networks, we evaluated the five best performing models on our held-out test set and chose the final model based on the highest area under the receiver operating curve (AUROC) value. For this model, additional test statistics were calculated and explorative explainability methods deployed.

Results: We included 370 patients with and without cirrhosis, 201 with a benign and 169 with a malignant liver lesion. Our final model was able to diagnose malignant lesions with an AUROC of 0.94 in the cross-validation experiment and of 0.88 in the held-out test set. Accuracy, Sensitivity, and Specificity for the malignant class were 79%, 88%, and 72%, respectively. Our exploratory analysis of the model's decision-making through visual explainability methods

revealed that the model seems to focus on information also highly relevant to expert clinicians in this task.

Conclusion: Weakly supervised deep learning algorithms have shown great potential for the diagnosis of focal liver lesions. Our algorithm can distinguish malignant from benign lesions with a high degree of accuracy. Complex pre-processing (e.g. delineation of regions-of-interest) is not required for this. In the future, such algorithms could support physicians performing CEUS in decision making.

SAT-470

The risk of hepatic decompensation in patients after the treatment for steatotic liver disease-related hepatocellular carcinoma

Tatsuya Minami¹, Tomoharu Yamada¹, Mitsuhiro Fujishiro¹, Ryosuke Tateishi¹. ¹Department of Gastroenterology, Graduate School of Medicine, the University of Tokyo, Tokyo, Japan
Email: minami.tatsu@gmail.com

Background and aims: The effectiveness of surveillance for hepatocellular carcinoma (HCC), especially from a cost-effectiveness perspective, is influenced by the establishment of an effective high-risk group, the proportion of patients diagnosed at an early stage, and the survival prognosis of those found. Assuming that hepatitis will be controlled in many patients with HCC with hepatitis background due to recent advance in anti-viral therapy, it is now expected that the prognosis after treatment will be different for patients with hepatitis background and others, especially those with steatotic liver disease (SLD). This study aims to compare virally controlled and SLD-related HCC in terms of prognosis, recurrence, and risk of decompensation.

Method: Among 1826 patients who underwent curative radiofrequency ablation (RFA) for primary HCC from 1999 to 2020 at our institution, we focused on 255 SLD-related HCC cases and 125 viral controlled HCC (80 hepatitis C with sustained virological response [SVR], 45 hepatitis B on nucleotide analog [NA]) with a maximum tumor diameter of 3 cm or less and three or fewer lesions. Propensity score matching was performed based on age, gender, liver function, and tumor burden in each group, and recurrence rates, decompensation rates, and survival rates were assessed using the Kaplan-Meier method and compared using the log-rank test.

Results: After propensity score matching, 102 cases each of SLD-related HCC and viral controlled HCC were extracted. The 3-year, 5-year, and 10-year recurrence rates were comparable between SLD-related HCC (55.9%, 60.6%, 82.3%) and viral controlled HCC (45.4%, 57.6%, 77.7%) with no significant difference (log-rank test $p=0.2$). However, decompensation rates were significantly higher in SLD-related HCC (11.7%, 18.9%, 38.8%) compared to viral controlled HCC (4.2%, 5.4%, 7.0%) ($p<0.001$), leading to better survival prognosis in viral controlled HCC (92.8%, 87.2%, 63.7%) compared to SLD-related HCC (83.3%, 73.2%, 40.4%) ($p<0.001$).

Conclusion: SLD-related HCC, compared to viral controlled HCC, exhibits similar recurrence rates but higher decompensation rates, suggesting a potential cause for diminished life expectancy. Even with early detection, the high decompensation risk associated with SLD-related HCC underscores the importance of considering this data when planning surveillance strategies for SLD-related HCC.

SAT-472

External validation of hepatocellular carcinoma risk calculators following hepatitis C treatment in a large US cohort

Ellen Green¹, Thad Benefield¹, Rachel Swier¹, Lindsay Lane¹, Louise Henderson¹, Andrew Moon¹. ¹University of North Carolina, Chapel Hill, United States
Email: andrew.moon@unchealth.unc.edu

Background and aims: Many patients with hepatitis C virus (HCV) treated with direct acting antivirals (DAAs) remain at risk of developing hepatocellular carcinoma (HCC). Validated risk stratification models, which utilize commonly available laboratory data, could

guide individualized HCC screening recommendations for patients with cured HCV. Towards this goal, we validated published HCC risk models in a large cohort of patients with chronic HCV who have been treated with DAAs.

Method: Patients with chronic HCV treated with DAAs within a single health system from 1/1/2014 to 12/31/2021 were followed until death, HCC, liver transplant, last follow-up, or 12/31/2022. We excluded those with diagnosis of HCC prior to DAA-treatment. Clinical data was acquired at the time of DAA treatment to validate three published, non-genetic HCC prediction models (age-male sex-ALBI-platelet count score (aMAP), US Veteran Health Affairs (VHA), Toronto HCC risk Index (THRI)). The primary outcome analyzed was the development of HCC, accounting for death and liver transplant as competing risks. Statistical analysis examined the models' discrimination using Uno's Concordance index and calibration using 5-year predicted versus observed HCC incidences. Missing data was imputed using the Markov Chain Monte Carlo (MCMC) method and HCC risk tertiles were computed from the median of the 30 scores.

Results: Our final cohort included 2598 patients with chronic HCV treated with DAAs including 47.5% ($n=1233$) with pre-treatment cirrhosis. The median follow-up interval was 1.4 years (S.D. 1.5 years). After DAA therapy, 0.6% ($n=16$) developed HCC, 0.7% ($n=17$) received liver transplant, and 5.9% ($n=153$) died. Discrimination for aMAP, THRI, and VHA was 0.757, 0.663, and 0.596 respectively, using the multiply imputed datasets. For the aMAP model, the observed 5-year incidences of HCC by tertile were 0.0% (95% CI: [0.0%, 1.0%]), 0.3% (95% CI: [0.0%, 2.3%]), and 3.0% (95% CI: [1.7%, 5.2%]) for low, medium, and high risk, respectively, compared to the predicted values of 0.8%, 4.2%, and 19.9%. The observed incidences for the THRI model were 0.0% (95% CI: [0.0%, 1.0%]), 1.8% (95% CI: [0.9%, 3.5%]), 2.9% (95% CI: [1.2%, 7.1%]) compared to predicted values of 1.5%, 4.9%, and 15.0%. VHA calibration was omitted as only 3-year HCC incidence was reported.

Conclusion: In this cohort of patients with chronic HCV treated with DAAs, the aMAP model had the best discrimination. Observed HCC incidence was much lower for all 3 models, across all tertiles. Validated risk stratification models, which utilize commonly available serum data, are integral to the advancement of HCC health equity through access to earlier, individualized prediction for patients at risk of HCC. However, continued external validation of existing models across diverse patient datasets is needed.

SAT-473

Changes in the landscape of hepatocellular carcinoma-experience of a single tertiary center

Zehnder Jan¹, Jonas Schropp¹, Birgit Schwacha-Eipper², Annalisa Berzigotti^{1,2}, Jean-François Dufour¹, Pompilia Radu². ¹Department for BioMedical Research, Visceral Surgery and Medicine, University of Bern, Bern, Switzerland; ²Department of Visceral Surgery and Medicine, Inselspital, Bern University Hospital, University of Bern, Bern, Switzerland
Email: pia_radu@yahoo.com

Background and aims: In the last decade, the availability of highly effective oral antiviral drugs for chronic hepatitis C and novel immunotherapy agents have modified the landscape of hepatocellular carcinoma (HCC), but detailed data on changes in aetiology and survival are lacking. The aim of the present study was to evaluate how these patterns of HCC changed in the last decade at our academic center.

Method: Data of 505 HCC patients newly diagnosed with HCC included in a prospective HCC cohort of Inselspital, University Hospital of Bern, Switzerland in 2010–2021 was retrospectively reviewed. The analysed timeframe was split in 4 periods (2010–2012, 2013–2015, 2016–2019, 2019–2021) to better reflect the changes and their impact. Chi-squared test/Fisher's exact test for categorical variables. A p value of less than 0.05 was considered statistically significant.

Results: The age of diagnosis has increased over the time from 63 years to 67 years ($p<0.001$). During the analyzed period of time

POSTER PRESENTATIONS

(2010–2021), the viral aetiology (i.e. chronic hepatitis B and chronic hepatitis C) decreased (50% to 23%, $p < 0.001$), while non-viral aetiologies, such as alcohol-related liver disease (ALD) and metabolic dysfunction-associated steatotic liver disease (MASLD)/Metabolic dysfunction-associated steatohepatitis (MASH) increased (48 to 62%, $p < 0.001$ and 25% to 37%, $p = 0.3$, respectively). BMI remained stable over time in newly diagnosed HCC patients, whereas the comorbidities, such as arterial hypertension, hyperlipidemia and diabetes mellitus Type 2 had a significant increase (45% to 60%, $p = 0.027$; 13% vs 40%, $p < 0.001$; 32% vs 44%, $p = 0.006$, respectively). Concerning HCC detection, the proportion of patients diagnosed as BCLC stage 0 increased gradually from 0.9% to 13%, while those diagnosed as BCLC stage C decreased from 23% to 15% ($p = 0.06$). Consequently, the therapy with curative intention increased over the time (39% to 61%, $p < 0.001$).

Conclusion: Our study highlights the important changes in the landscape of HCC that occurred in the last decade. Patients with HCC are currently diagnosed at higher age, have more comorbidities and the landscape of aetiologies changed over time. Alcohol was a major modifiable risk factor for HCC in our population, underlining that prevention in the next years should be a focus to obtain a reduction of new HCC cases. On the other hand, screening programs are likely to result in an increase in proportion of patients diagnosed at earlier stages, which may make them more susceptible to curative treatments.

SAT-474

Lesions hyper- to isointense to the surrounding liver in the hepatobiliary phase of gadoteric acid enhanced MRI

Alicia Furumaya^{1,2}, Francois Willemssen^{3,4}, Razvan Miclea^{5,6}, Martijn Haring^{7,8}, Robbert de Haas^{7,8}, Shirin Feshali^{9,10}, Inge Vanhooymissen^{1,2}, Daniel Bos^{3,4}, Robert A. de Man^{3,4}, Jan Ijzermans^{3,4}, Joris Erdmann^{1,2}, Joanne Verheij^{1,2}, Michail Doukas^{3,4}, Otto van Delden^{1,2}, Maarten Thomeer^{3,4}.
¹Amsterdam UMC, Amsterdam, Netherlands; ²Cancer Center Amsterdam, Amsterdam, Netherlands; ³Erasmus MC, Rotterdam, Netherlands; ⁴Erasmus University Rotterdam, Rotterdam, Netherlands; ⁵Maastricht University Medical Center+, Maastricht, Netherlands; ⁶Maastricht University, Maastricht, Netherlands; ⁷University Medical Center Groningen, Groningen, Netherlands; ⁸University of Groningen, Groningen, Netherlands; ⁹Leiden UMC, Leiden, Netherlands; ¹⁰Leiden University, Leiden, Netherlands
Email: a.furumaya@amsterdamumc.nl

Background and aims: Hyper- or isointensity in the hepatobiliary phase (HBP) of gadoteric acid enhanced MRI has high specificity for focal nodular hyperplasia (FNH). However, hepatocellular adenoma and carcinoma (HCA/HCC) may also be hyper- or isointense in the HBP. The aim of the current study was to identify imaging characteristics to differentiate FNH and HCA/HCC hyper- or isointense on gadoteric acid enhanced MRI.

Method: A multicenter retrospective cohort study was conducted including patients with pathology-proven FNH or HCA/HCC, hyper- or isointense in the HBP of gadoteric acid enhanced MRI between 2010 and 2020. Imaging characteristics were compared between lesions with a pathological diagnosis of FNH and HCA/HCC. Diagnostic performance, univariable analyses, multivariable logistic regression analysis and classification and regression tree analyses were conducted. Sensitivity analyses evaluated imaging characteristics of B-catenin activated HCA.

Results: In total, 124 patients (mean age 40 years, standard deviation 10 years, 108 female) with 128 hyper- or isointense lesions were included. Pathology diagnoses were FNH in 64 lesions (50%) and HCA/HCC in 64 lesions (50%). Imaging characteristics observed only in HCA/HCC and never in FNH were: sinusoidal dilatation on T2-w, raster and atoll fingerprint pattern in the HBP, venous washout, T1-w in-phase hyperintensity or hemosiderin, and nodule-in-nodule participation in the HBP and T2-w. In our selected cohort, 14/48

(29%) of HCA were B-catenin activated, most (13/14) showed extensive hyper- or isointensity.

Conclusion: Aforementioned characteristics should be considered typical for HCA/HCC. If encountered in lesions extensively hyper- or isointense in the HBP, further investigation is warranted.

SAT-476

Development of a preference elicitation tool for treatment choice in unresectable, early/intermediate stage HCC

Andrew Moon¹, Daniel Richardson¹, Donna Evon¹, Hanna Sanoff¹, Jessica Carda-Auten¹, Myra Waheed¹, Gabrielle Ritaccio¹, Jamie Conklin¹, Ethan Basch¹, David Mauro¹, Ted Yanagihara¹, David Gerber², Neil Shah¹, Oren Fix¹, Tammy Triglianios¹, Jonathan Sorah¹, Jingquan Jia¹, Ashwin Somasundaram¹, A. Sidney Barritt, IV¹. ¹University of North Carolina, Chapel Hill, United States; ²University of Cincinnati, Cincinnati, United States
Email: andrew.moon@unchealth.unc.edu

Background and aims: The treatment landscape for early/intermediate stage hepatocellular carcinoma (HCC) is rapidly evolving. Discrete choice experiments (DCE) are preference-elicitation tools that can assess patients' willingness to accept therapeutic risks and inconvenience associated with treatments. We performed a mixed-methods study to identify common and important treatment attributes for inclusion in a DCE for treatment choice in unresectable, early/intermediate stage HCC.

Method: Potential attributes (i.e., treatment characteristics) and attribute levels (i.e., categories of each characteristic) for inclusion in the DCE were identified through (1) patient interviews, (2) clinician interviews, and (3) a scoping review. Interviews of patients and clinicians recruited from a large health system were recorded, transcribed, imported into Dedoose V1.2 and analysed by trained qualitative researchers using code-based thematic analysis. A scoping review was performed of studies that (1) assessed the role of preference elicitation tools for HCC treatment options and (2) included a study population of patients, caregivers and/or clinicians. We searched PubMed, EMBASE, Scopus and Cochrane Library databases for articles published before August 18, 2022 and extracted potential treatment attributes from each included study. Based on these qualitative interviews and scoping reviews, study investigators chose potential attributes and levels that were non-overlapping and relevant to treatment decisions in unresectable, early/intermediate stage HCC.

Results: Qualitative interviews involved 30 patients with HCC (13% BCLC-0, 40% BCLC-A, 33% BCLC-B, 10% BCLC-C, 10% BCLC-D) and 10 clinicians (physicians and nurse practitioners) who cared patients with HCC with representation from medical oncology, hepatology, interventional radiology, radiation oncology and transplant surgery. Based on the qualitative interviews and scoping review, we identified five attributes and levels for inclusion in a DCE: 1) overall survival beyond 3 years (0, 3, 6 months), 2) post-treatment physical function (unchanged, some assistance with daily function, bedbound), 3) short-term treatment-related side effects, such as abdominal pain, nausea and fatigue (mild, moderate requiring medications, severe requiring hospitalization), 4) likelihood of developing worsening liver function over 1 year (10%, 30%, 50%), and 5) duration of treatment (one-time outpatient treatment, few outpatient treatments over 1–2 weeks, ongoing treatments every 3–4 weeks).

Conclusion: This mixed-methods research revealed non-overlapping attributes relevant to treatment decisions in unresectable early/intermediate stage HCC for inclusion in a DCE. Use of this DCE will be used to help better understand tradeoffs between treatment options for HCC and inform patient-centered treatment development.

SAT-477-YI

The impact of etiology on patterns of progression of advanced HCC

Bernardo Stefanini^{1,2}, Fabio Piscaglia^{1,3}, Andrea Dalbeni^{4,5}, Caterina Vivaldi⁶, Piera Federico⁷, Andrea Palloni⁸, Caterina Soldà⁹, Benedetta Stefanini¹⁰, Ingrid Garajova¹¹, Luca Ielasi¹², Stefania De Lorenzo¹³, Gianluca Masi¹⁴, Sara Lonardi¹⁵, Giovanni Brandi¹⁶, Bruno Daniele¹⁷, Franco Trevisani¹, Gianluca Svegliati-Baroni¹⁸, Claudia Campani^{19,20}, Rusi Chen¹, Francesco Tovoli^{1,3}. ¹Department of Medical and Surgical Sciences, University of Bologna, Bologna, Italy; ²Imperial College London, Department of Surgery and Cancer, Hammersmith Hospital, London, United Kingdom; ³Division of Internal Medicine, Hepatobiliary and Immunoallergic Diseases, IRCCS Azienda Ospedaliero-Universitaria di Bologna, Bologna, Italy; ⁴Unit of General Medicine C, Medicine Department, University of Verona and University and Hospital Trust (AOUI) of Verona, Verona, Italy; ⁵Liver Unit, Medicine Department, University of Verona and University and Hospital Trust (AOUI) of Verona, Verona, Italy; ⁶Unit of Medical Oncology 2, Azienda Ospedaliero-Universitaria Pisana, Pisa, Italy; ⁷Medical Oncology Unit, Ospedale del Mare, Napoli, Napoli, Italy; ⁸Oncology Unit, IRCCS Azienda Ospedaliero-Universitaria di Bologna, Bologna, Italy; ⁹Oncology Unit 1, Veneto Institute of Oncology IOV-IRCCS, Padova, Italy; ¹⁰Division of Medical Semeiotics, IRCCS Azienda Ospedaliero-universitaria di Bologna, Bologna, Italy; ¹¹Medical Oncology Unit, University Hospital of Parma, Parma, Italy; ¹²Department of Internal Medicine, Ospedale degli infermi, Faenza, Italy; ¹³Oncology Unit, Azienda USL Bologna, Bologna, Italy; ¹⁴Unit of Medical Oncology 2, Azienda Ospedaliero-Universitaria Pisana, Pisa, Italy; ¹⁵Oncology Unit 3, Veneto Institute of Oncology IOV-IRCCS, Padova, Italy; ¹⁶Oncology Unit, IRCCS Azienda Ospedaliero-Universitaria di Bologna, Bologna, Italy; ¹⁷Medical Oncology Unit, Ospedale del Mare, Napoli, Italy; ¹⁸Liver Injury and Transplant Unit, Polytechnic University of Marche, Ancona, Italy; ¹⁹Department of Experimental and Clinical Medicine, Internal Medicine and Hepatology Unit, University of Firenze, Firenze, Italy; ²⁰Centre de Recherche des Cordeliers, Sorbonne Université, Inserm, Université de Paris Cité, Team «Functional Genomics of Solid Tumors», Paris, France
Email: bernardo.stefanini@gmail.com

Background and aims: Atezolizumab/bevacizumab (A+B) is the recommended first-line treatment for HCC, irrespective of the etiology of the underlying liver disease. Preclinical models showed that only intrahepatic HCC arising in mice with MASLD was less responsive to A+B, while subcutaneous tumor had a decent response, likely related to a higher proportion of exhausted T-cells being recruited in the intrahepatic lesions. Since HCC can progress with different patterns, we aimed to verify whether MASLD etiology had an impact on the pattern of progression to A+B.

Method: Multicenter study including consecutive patients with non-resectable HCC patients from the ARTE database. Patterns of progression were defined as previously proposed by Reig et al: intrahepatic/extrahepatic growth of pre-existing lesions (IHG and EHG, respectively) new intrahepatic/extrahepatic lesions (NIHL, NEHL), new vascular invasion (NVI). A Kaplan-Meier survival analysis was performed to verify whether patients with MASLD were at increased risk of specific patterns of progression.

Results: A total of 202 patients were included. Single-etiology MASLD was the cause of HCC in 46 patients (22.8%). MASLD patients were similar to controls in terms of macrovascular invasion, AFP >400, Child-Pugh Class, ALBI grade, and ECOG. Median OS of MASLD-HCC patients was similar to non-MASLD group (20.6 months vs 14.4, p = 0.084), whereas PFS was longer for non-metabolic HCC (11.6 vs 4.5 months, p = 0.006).

HCC patients with MASLD had a significantly increased risk of progressing both for IHG (HR 2.20 CI 95% 1.32–3.69, p = 0.003). Conversely, the risk of developing progression due to NVI, EHG or NEHL was similar across the etiology groups.

Conclusion: Patients with MASLD-HCC were more likely to develop an intrahepatic progression than non-MASLD patients, confirming

preclinical data and suggesting biologic differences between tumors arising from different etiologies with potential implications in terms of clinical management.

SAT-478

External beam radiotherapy promotes contralateral liver regeneration in primary liver cancer

Ying Zhao¹, Bin Shu², Guangxin Li², Hongxuan Li², Liuqing Yang², Lizhi Xu², Xiaomao Yu², Qiang Li², Gong Li², Shizhong Yang², Jiahong Dong². ¹Beijing Tsinghua Changgung Hospital, School of Clinical Medicine, Tsinghua University, Beijing, China; ²Beijing Tsinghua Changgung Hospital, Beijing, China
Email: zy132829@126.com

Background and aims: Inadequate future liver remnant (FLR) is a contraindication of hepatectomy for primary liver cancer (PLC). Yttrium-90 transarterial radioembolization has been shown to promote FLR hypertrophy, but it is unknown whether external beam radiotherapy has a similar effect. This study aimed to explore whether radiotherapy could promote non-irradiated contralateral liver regeneration and identify the influencing factors of liver regeneration after radiotherapy.

Method: Between June 2018 and December 2022, patients with PLC who had accomplished radiotherapy were eligible for the study. The included patients had an eligibility scan (CT or MRI of the abdomen) <1 month before radiotherapy and <6 months after the end of radiotherapy. FLR was calculated before and again after radiotherapy in patients by the IQQA® –3D Liver System software from enhanced CT images. Independent predictors of contralateral liver regeneration (p value <0.05) were identified by the Logistic proportional hazards regression model.

Results: 179 patients (predominantly Barcelona Clinic Liver Cancer stage C) were enrolled in the final analysis, and 151 patients (84.4%) experienced significant contralateral FLR hypertrophy. Median FLR hypertrophy after radiotherapy was 11.4% (IQR: 3.2%–23.5%). In addition, 61 patients (34.1%) in the high FLR group had an FLR hypertrophy exceeding 20%. By analyzing patient-related factors, tumor-related factors, and treatment-related factors, we found that increasing FLR was more likely to be achieved when the interval to response assessment ≤3 Months. Compared with the patients who received a low dosage of radiotherapy, those receiving a medium to high dosage of radiotherapy (>48 Gy) had more significant FLR hypertrophy. Multivariate logistic regression analysis showed that radiotherapy dosage (OR = 0.089, 95%CI: 0.038–0.211, p < 0.01) and the interval to response assessment (OR = 2.422, 95%CI: 1.127–5.205, p = 0.023) were significantly different between the high FLR group and the low FLR group, which were independent risk factors for contralateral liver regeneration after radiotherapy. Moreover, 22 patients (31.0%) after radiotherapy underwent surgical resection among 71 patients (China liver cancer staging system CNLC stage I-IIIa) with inadequate FLR, median FLR hypertrophy was 17.7% (IQR: 2.1%–43.4%).

Conclusion: This study demonstrates a substantial increase in FLR after radiotherapy and identifies independent predictors. Some PLC patients with inadequate FLR can achieve hepatectomy after radiotherapy. Therefore, external beam radiotherapy deserves further exploration as a non-invasive means of promoting non-irradiated contralateral liver regeneration.

SAT-479-YI

Lower frequency of PNPLA3 in african populations and divergent associations with hepatocellular carcinoma

Perapa Chotiprasidhi¹, Karina Sato Espinoza¹, Jun Ma², Yvonne Nartey³, Yaw Awuku⁴, Adwoa Agyei-Nkansah⁵, Mary Afihene⁶, Amoako Duah⁷, Sally Bampoh⁸, Shadrack Asibey⁹, Joshua Ayawin⁹, Jun Wang¹⁰, Yinan Zheng¹⁰, Lifang Hou^{10,11}, Claudia Hawkins¹¹, Robert Murphy¹², Godwin Imade¹³, Edith Okeke¹³, Alani Akanmu¹⁴, Olufunmilayo Lesi¹⁴, Jose Debes¹⁵,

POSTER PRESENTATIONS

Lewis Roberts¹, Samuel Antwi¹⁶, Kirk Wangenstein¹. ¹Department of Medicine, Division of Gastroenterology, Mayo Clinic, Rochester, United States; ²Department of Quantitative Health Sciences, Division of Computational Biology, Mayo Clinic, Rochester, United States; ³Department of Internal Medicine, Cape Coast Teaching Hospital, Cape Coast, Ghana; ⁴Department of Medicine and Therapeutics, School of Medicine, University of Health and Allied Sciences, Ho, Ghana; ⁵Department of Medicine and Therapeutics, University of Ghana Medical School, Accra, Ghana; ⁶Department of Medicine, Kwame Nkrumah University of Science and Technology, Kumasi, Ghana; ⁷Department of Medicine, University of Ghana Medical Centre, Legon, Ghana; ⁸Department of Internal Medicine, Greater Accra Regional Hospital, Accra, Ghana; ⁹Department of Medicine, Komfo Anokye Teaching Hospital, Kumasi, Ghana; ¹⁰Department of Preventive Medicine, Feinberg School of Medicine, Northwestern University, Chicago, United States; ¹¹Institute for Global Health, Feinberg School of Medicine, Northwestern University, Chicago, United States; ¹²Center for Global Health, Department of Infectious Diseases, Chicago, United States; ¹³College of Health Sciences, University of Jos, Jos, Nigeria; ¹⁴Lagos University Teaching Hospital and College of Medicine, University of Lagos, Lagos, Nigeria; ¹⁵Department of Medicine and Division of Epidemiology and Community Health, School of Medicine, University of Public Health, University of Minnesota, Minneapolis, United States; ¹⁶Department of Quantitative Health Sciences, Division of Epidemiology, Mayo Clinic, Jacksonville, United States
Email: chotiprasidhi.perapa@mayo.edu

Background and aims: Hepatocellular carcinoma (HCC) ranks as the third leading cause of cancer-related deaths globally. A single nucleotide polymorphism (SNP) in patatin-like phospholipase domain-containing protein 3 (*PNPLA3*), rs738409, has been associated with HCC development in European and East Asian populations. However, the relevance of this SNP remains unexplored in African populations. Africa contains the most genetically and phenotypically diverse population and has the highest burden of HCC worldwide. Our study aimed to assess, for the first time, the association of *PNPLA3* with HCC in West Africa in two geographically and ethnically diverse populations, comparing it to European-descent Americans.

Method: We enrolled 363 patients diagnosed with HCC through pathology and/or radiology reports from a predominantly European descent population in the United States ($n = 241$), and from Ghana ($n = 79$), and Nigeria ($n = 43$). Controls comprised 2,817 cancer-free patients from the same sites: United States ($n = 2409$), Ghana ($n = 323$), and Nigeria ($n = 85$). We performed whole-exome sequencing (Exome+, Helix, Inc.) and extracted data on *PNPLA3*-rs738409 for analyses. Prevalence of *PNPLA3*-rs738409 was compared using Chi-square test, odds ratios (OR), and 95% confidence intervals (CI).

Results: In the United States population, there was a significant association between *PNPLA3*-rs738409 (G) and HCC risk, with OR for CG/GG vs. CC of 2.68 (CI: 2.03–3.56, $p < 0.0001$), and with risk allele frequency of 0.46. However, we did not find a significant association between *PNPLA3*-rs738409 and HCC risk in combined West African samples (OR = 1.11, CI: 0.69–1.83, $p = 0.33$), with overall risk allele frequency of 0.12. When the West African samples were examined separately, we found a striking difference in the pattern of association. The Nigerian population demonstrated a strong trend toward an association between *PNPLA3*-rs738409 and HCC risk (OR = 1.87, CI: 0.77–4.35, $p = 0.073$), with risk allele frequency of 0.17, while the Ghanaian sample did not show this trend (OR = 0.82, CI: 0.44–1.52, $p = 0.27$), with a much lower risk allele frequency of 0.09.

Conclusion: Our study indicates a much lower *PNPLA3* minor allele frequency in West Africans from Ghana and Nigeria as compared to European Americans. Furthermore, there were different trends in the association between *PNPLA3* and HCC within Africans, with only the Nigerian population showing the trend toward elevated risk. These findings highlight the genomic heterogeneity of the African continent, emphasizing the importance of population diversity in future

studies and the need for global multi-ethnic genetic association studies to reduce disparities in the clinical application of genetic test results in HCC.

SAT-480-YI

Comparative performance of GAAD and ASAP scores in predicting early-stage hepatocellular carcinoma

Chongkonrat Maneenil¹, Piraya Tantisaranon¹, Pimsiri Sripongpun¹, Naichaya Chamroonkul¹, Maseetoh Samaeng¹, Roongrueng Jarumanokul¹, Lalita Fonghoi¹, Amornkan Numit¹, Teerha Piratvisuth¹, Apichat Kaewdech^{1,1}. ¹Prince of Songkla University, Hatyai, Thailand
Email: apichatka@hotmail.com

Background and Aims: The GAAD score, which includes age, gender, and two tumor markers (alpha-fetoprotein [AFP] and PIVKA-II), has been recently proposed for predicting hepatocellular carcinoma (HCC). It shows comparable performance to the established GALAD score, despite omitting AFP-L3. However, no studies have compared the GAAD score with the ASAP score, which employs similar parameters but utilizes different assays and formulas. Our aim was to assess the performance differences between these two scores.

Methods: We prospectively collected blood samples from treatment-naïve HCC patients and non-HCC chronic liver disease (CLD) patients at a gastroenterology outpatient clinic from April 20, 2023, to December 31, 2023. ASAP and GAAD scores were calculated using AFP and PIVKA-II assays from Abbott and Roche, respectively, with cutoffs set at 0.5256 for ASAP and 2.57 for GAAD. Diagnoses of HCC were confirmed following EASL or AASLD guidelines.

Results: Our cohort of 651 patients had a median age of 63 (interquartile range [IQR] 56–70) years; 58.8% were male, and 69.7% presented with cirrhosis. A total of 174 patients (26.7%) had HCC, with 47.7% in early stages (BCLC stage 0 = 23, A = 60). The leading cause of HCC was hepatitis B virus (HBV) infection (41.4%), followed by metabolic associated steatohepatitis liver disease (MASLD) (20.7%) and hepatitis C virus (HCV) infection (18.4%). The area under the receiver operating characteristic curves (AUROCs) for predicting all stages of HCC were 0.9262 for ASAP and 0.9312 for GAAD ($p = 0.5261$). For early stages, the AUROCs were 0.8985 for ASAP and 0.8718 for GAAD ($p = 0.011$), respectively. ASAP's sensitivity for detecting all-stage HCC was 88.7% with a specificity of 81.7%, while GAAD's sensitivity was 82.5% with a specificity of 89.6%. For early-stage HCC detection, ASAP's sensitivity reached 98.9% with a specificity of 21.7%. Additionally, GAAD's sensitivity for early-stage detection was 96.7% with a specificity of 32.5%.

Conclusion: The GAAD and ASAP scores both demonstrated excellent and comparable abilities in detecting all-stage HCC. However, the ASAP score exhibited superior performance in identifying early-stage HCC.

SAT-481-YI

Improved handling of BCLC 2022 update in the management of hepatocellular carcinoma in clinical practice

Eleonora Alimenti¹, Massimo Iavarone¹, Lorenzo Canova¹, Mariangela Bruccoleri¹, Barbara Antonelli², Anna Maria Ierardi³, Angelo Sangiovanni^{1,4}, Pietro Lampertico^{1,4}. ¹Division of Gastroenterology and Hepatology, Foundation IRCCS Ca' Granda Ospedale Maggiore Policlinico, Milan, Italy; ²General and Liver Transplant Surgery Unit, Foundation IRCCS Ca' Granda Ospedale Maggiore Policlinico, Milan, Italy; ³Radiology Department, Foundation IRCCS Ca' Granda Ospedale Maggiore Policlinico, Milan, Italy; ⁴CRC "A. M. and A. Migliavacca" Center for Liver Disease, Department of Pathophysiology and Transplantation, University of Milan, Milan, Italy
Email: eleonoramenti@gmail.com

Background and aims: In 2022 the BCLC staging and treatment algorithm for hepatocellular carcinoma (HCC) management has been updated, granting for higher flexibility and customized management with a multidisciplinary decision process in the choice of the

therapeutic strategy for HCC patients as compared to the 2018 version. To evaluate the ability to adhere to BCLC 2022 in daily clinical practice as compared to the BCLC 2018 and the impact on patients' overall survival (OS).

Method: We retrospectively evaluated data of 806 prospectively enrolled (year 2006 to 2022) patients with de novo HCC in different stages according to BCLC: 571 0-A, 133 B, 85 C and 17. First line treatment allocations were discussed by a multidisciplinary team (MTD), following updated recommendations and guidelines. All patients were followed until death or end of follow-up.

Results: Overall, the adherence to BCLC increased from 50% for the BCLC 2018 to 68% for the BCLC 2022 ($p < 0.001$) considering all stages of HCC: 48% vs 71% stage 0/A ($p < 0.001$), 50% vs 61% stage B ($p = 0.06$), 59% vs 59% stage C ($p = \text{NS}$), 74% vs 74% for stage D ($p = \text{NS}$). Among BCLC 0/A patients, 131 (32%) were treated with TACE, which is the second choice of treatment according to BCLC 2022, while among BCLC B patients, 5 (6%) underwent LT and 10 (12%) were treated with systemic therapy, which are now considered treatment options for this stage in selected patients. The expected survival rate following the BCLC 2018 recommendations remains unchanged even by adhering to the BCLC 2022 update [74.5% vs 75.2% at year 2 ($p = \text{NS}$) and 41.4% vs 44.6% at year 5 ($p = \text{NS}$), respectively]. Finally, the rate of "upward stage migration" was similar by BCLC 2022 or BCLC 2018 (12% vs 14%, $p = \text{ns}$), while the rate of "downward stage migration" was lower with the new one (19% vs 36%, $p < 0.001$). Overall, the 2-year survival rate of patients treated outside the BCLC 2022 recommendations did not significantly differ from those treated according to the updated algorithm (76% vs 74.5%, $p = \text{NS}$). In BCLC B and BCLC C, an upward stage migration was associated to higher rates of 2-year survival (93.5% vs 60.6%, $p = 0.002$ for BCLC B and 36.9% vs 27.4%, $p = 0.01$ for BCLC C), while there was no difference for stage 0/A between those treated outside and those treated according to the BCLC 2022.

Conclusion: The BCLC 2022 updated version of HCC staging and treatment system allowed a greater adherence to the algorithm in clinical practice, mainly in the early stages, without adversely affecting the survival of patients. In the intermediate and advanced stages, the access to more radical treatment could offer a survival benefit.

SAT-482

A modified Charlson comorbidity index to improve management of patients with hepatocellular carcinoma: a step towards precision medicine

Eleonora Alimenti¹, Massimo Iavarone¹, Lorenzo Canova¹, Elia Fracas¹, Barbara Antonelli², Anna Maria Ierardi³, Silvia Crespi³, Arianna Zefelippo², Angelo Sangiovanni¹, Pietro Lampertico^{1,4}.

¹Division of Gastroenterology and Hepatology, Foundation IRCCS Ca' Granda Ospedale Maggiore Policlinico, Milan, Italy; ²General and Liver Transplant Surgery Unit, Foundation IRCCS Ca' Granda Ospedale Maggiore Policlinico, Milan, Italy; ³Radiology Department, Foundation IRCCS Ca' Granda Ospedale Maggiore Policlinico, Milan, Italy; ⁴CRC "A. M. and A. Migliavacca" Center for Liver Disease, Department of Pathophysiology and Transplantation, University of Milan, Milan, Italy
Email: eleonoramenti@gmail.com

Background and aims: Patients with hepatocellular carcinoma (HCC) frequently have comorbidities that limit access to treatments and might increase mortality. The Charlson comorbidity index (CCI) assigns a numeric score to 17 diseases according to their effect on mortality. In patients with cirrhosis and HCC, these variables might be excluded from the CCI (modified CCI, mCCI). Aim of the study was to evaluate the performance of CCI and mCCI for HCC patients' characterization.

Method: We used data from our retrospective monocentric study of patients with first HCC diagnosis. We evaluated the performance of CCI and mCCI in dissecting our population and predicting overall survival (OS). As secondary end point, the impact of mCCI on

adherence to Barcelona Clinic Liver Cancer (BCLC) staging and treatment allocation was evaluated.

Results: The study included 385 patients (289 males, 68 years median age, 78% Child Pugh (CPT) A, 66% viral etiology) with HCC (271 BCLC 0/A, 64 B, 40 C and 10 D). According to CCI, 94% of our patients were "high-risk" (CCI \geq 5), 5.7% "intermediate-risk" (CCI 3–4) and 0.3% "low-risk" (CCI 0–2). These cutoffs were applied to mCCI: 21% "high-risk," 48% "intermediate-risk," and 31% "low-risk." Patients' mCCI correlated with CCI (Kendall's $\tau = 0.47$; p value < 0.0001). Overall, patients belonging to a "high" or "intermediate-risk" mCCI classes had a shorter OS as compared to "low-risk" patients (median OS 37 vs 49 vs 67 months, p value = 0.007). This was confirmed in BCLC 0/A (p value = 0.002). Moreover, "high-risk" mCCI class, worse CPT class, presence of varices, BCLC stage and AFP > 200 ng/ml were independently associated to mortality [HR1.36 (95% CI 1.09–1.70, p value = 0.006; HR1.62 (95% CI 1.14–2.30), p value = 0.007; HR1.58 (95% CI 1.11–2.24), p value = 0.01; HR1.96 (95% CI 1.66–2.31) p value < 0.001 ; HR1.80 (1.17–2.79) p value = 0.008]. mCCI was also an independent predictor of mortality in BCLC 0/A, with higher tumor burden and worse CPT. No differences were observed in adherence to BCLC2022 algorithm and access to treatment among the mCCI risk classes.

Conclusion: mCCI better stratified patients with HCC as compared to CCI and independently predicted mortality. Implementation of a multiparametric therapeutic approach to treatment allocation including evaluation of comorbidities and frailty is warranted.

SAT-483-YI

The impact of competing risk bias in prognostic models for hepatocellular carcinoma in patients with cirrhosis

Laura Burke^{1,2}, Jessica Shearer¹, Vincent Haghejad^{2,3,4}, Rebecca L. Jones¹, James Ferguson⁵, Richard Parker¹, Ian Rowe^{1,2}.
¹Leeds Liver Unit, Leeds Teaching Hospitals NHS Trust, Leeds, United Kingdom; ²Leeds Institute for Medical Research, University of Leeds, Leeds, United Kingdom; ³Department of Hepatology and Gastroenterology, University Hospital of Nancy, Nancy, France; ⁴Faculty of Medicine of Nancy, University of Lorraine, Nancy, France; ⁵Queen Elizabeth Hospital, University Hospitals Birmingham NHS Foundation Trust, Birmingham, United Kingdom
Email: laura.burke1@nhs.net

Background and aims: Hepatocellular carcinoma (HCC) risk prediction models may provide a more personalised approach to HCC surveillance in patients with cirrhosis. Existing models do not account for competing risk events and may overestimate the probability of HCC. We aimed to demonstrate the impact of considering competing risk when estimating the cumulative incidence of HCC in a contemporary cohort of patients with cirrhosis from the United Kingdom (UK).

Method: Data were collected from consecutive patients undergoing transient elastography (TE) from 2 UK teaching hospitals between 2008 and 2019. Patients with a liver stiffness measurement (LSM) > 10 kPa were included. Electronic health records were analysed to identify clinical events including decompensation, HCC and non-HCC related death. Two HCC prognostic models were developed: (1) a Cox regression model (Cox) ignoring competing risk events and (2) a Fine-Gray regression model (FGR) accounting for non-HCC mortality and decompensation as a competing risk. The same predictors (age, sex, albumin and platelets) were used in both models and were chosen based on well-established outcome associations. The 3-year probability of HCC was calculated for each patient using both models and the predicted risks compared.

Results: A total of 3028 patients (56% metabolic associated steatotic liver disease, 16% viral hepatitis, 15% alcohol related liver disease, 14% other) were included. The total follow-up was 9403 patient years with median per patient follow-up of 3.1 years. 75 patients developed HCC and 411 competing risk events (decompensation and non-HCC deaths) were observed. The mean predicted 3-year probability of HCC

POSTER PRESENTATIONS

for the Cox and FGR model was 1.89% and 1.27% respectively. The majority of patients (58.8%) had a difference in predicted 3-year HCC probability of >0.3% with a mean absolute difference of 0.99%. 13.5% of patients had a large discrepancy (>2%) between model predictions. A Bland-Altman plot indicates substantial disagreement between the model predictions with the disagreement increasing as HCC risk increases. 1517 patients had FIB-4 scores >1.3 and LSM >15 kPa or platelets <150 × 10⁹/L and would typically be considered for HCC surveillance. Applying a 1.5% annual risk threshold for HCC surveillance, the Cox model identified 260 (17.1%) patients meeting the threshold for surveillance. In contrast, the FGR model identified only 99 (6.5%) patients who met the threshold risk level, a reduction in patients requiring surveillance of 62%.

Conclusion: HCC prognostic models that ignore competing risk events overestimate the probability of developing HCC and therefore reduce their clinical utility. Decomensation has been overlooked as a 'competing risk', but its impact on HCC treatment and liver related mortality before HCC develops is substantial and should be accounted for in model development and validation.

SAT-484

Conventional and machine-learning based risk score on survival for patients with hepatocellular carcinoma

Chun-Ting Ho¹, Chien-Wei Su^{2,3,4}, Elise Chia-Hui Tan⁵, Yi-Hsiang Huang^{3,6}, Ming-Chih Hou^{3,6}, Jaw-Ching Wu⁷. ¹Taipei Veterans General Hospital, Taipei, Taiwan; ²Department of General Medicine, Department of Medicine, Taipei Veterans General Hospital, Taipei, Taiwan; ³Division of Gastroenterology and Hepatology, Department of Medicine, Taipei Veterans General Hospital, Taipei, Taiwan; ⁴School of Medicine, College of Medicine, National Yang Ming Chiao Tung University, Taipei, Taiwan; ⁵Department of Health Service Administration, College of Public Health, China Medical University, Taichung, Taiwan; ⁶School of Medicine, College of Medicine, National Yang Ming Chiao Tung University, Taipei, Taiwan; ⁷Institute of Clinical Medicine, School of Medicine, National Yang Ming Chiao Tung University, Taipei, Taiwan
Email: cwsu2@vghtpe.gov.tw

Background and aims: To evaluate the prognostic predictability of non-invasive biomarkers and develop a machine-learning (ML)-based risk score using conventional methods and machine-learning (ML) to categorize HCC patients into distinct prognostic groups.

Method: A total of 4038 HCC patients from BCLC stage 0 to D diagnosed at Taipei Veterans General Hospital from 2012 to 2023 were retrospectively enrolled in the study. The patients were divided into training cohort (n=2827) and validating cohort (n=1211) randomly. The primary end point was overall survival (OS). Non-invasive biomarkers, obtained through blood sample and image at diagnosis, were analyzed by both conventional method (Cox proportional hazards model) and ML-based method (LASSO Cox regression) to determine their prognostic predictability. In the training cohort, factors showing significance in both conventional method and ML-based method were enrolled in the ML-based risk score. The risk score was computed by utilizing coefficients from the Multivariate Cox proportional hazard model and were standardized to a score ranging from 0 to 100. Patients were then categorized into three risk groups (high, medium, and low risk) based on the 33rd and 66th percentiles. The risk score's efficacy was subsequently validated in the validation cohort.

Results: After a median follow-up of 42.0 months (interquartile range IQR 33.6–50.4 months), 1931 patients died, and the 5-year OS rate was 26.0%. Both conventional and ML-based method identified the same 11 factors as significant predictors (Age, curative treatment, extrahepatic metastasis, maximum tumor size, serum albumin, serum creatinine, serum bilirubin, serum aspartate aminotransferase (AST), Lymphocyte-to-monocyte ratio (LMR), albumin bilirubin (ALBI) grade and alpha fetoprotein (AFP) level). The risk score developed accordingly demonstrated excellent predictive ability for

patients' overall survival (AUC=0.800) and showed outstanding predictability for survival within the first five years post-diagnosis (AUC: 0.873 to 0.890). Furthermore, the ML-based risk score can efficiently stratify patients into three different risk groups with significant difference on overall survival ($p < 0.001$).

Conclusion: The ML-based risk score, derived from non-invasive biomarkers through conventional and ML-based methods, can effectively stratify HCC patients into different prognostic groups and aid clinicians in personalized disease management.

SAT-485

Utility of the GAAD algorithm in the screening of hepatocellular carcinoma in a prospective cohort of at-risk patients: preliminary results

Emily Larrea¹, Gemma Serrano¹, Gloria Ruiz-Fernández¹, Eva Marín¹, Joaquín Poza¹, Marta Abadía¹, Clara Amiama¹, Irene González-Díaz¹, Carmen Amor¹, Paula Torrijos¹, Rafael Gayoso¹, José Carlos Erdozaín¹, María Sánchez-Azofra¹, Marta Cuadros¹, Patricia Mayor¹, Yolanda Zarauza¹, Rubén Fernández-Martos¹, Alberto Cerpa¹, Pilar Castillo¹, Miriam Romero¹, Araceli García-Sánchez¹, Francisco Javier García-Samaniego¹, Susana Cano¹, Verónica Ucle¹, Sonia Álvarez¹, Mariana Serrés¹, María Sanz de Pedro¹, Antonio Buño¹, Antonio Oliveira¹. ¹La Paz University Hospital, Madrid, Spain
Email: aolveiram@gmail.com

Background and aims: The current European Association for the Study of the Liver (EASL) Clinical Guideline recommends hepatocellular carcinoma (HCC) screening through semiannual ultrasound in at-risk patients and considers adding biomarkers determination such as alpha-fetoprotein (AFP) suboptimal. There is a need to improve the performance and efficiency of screening programs. The GAAD algorithm (Gender, Age, AFP, and Des-gamma-carboxyprothrombin [DCP]) shows excellent results in HCC diagnosis, with a performance >90%. There are no studies on its utility in screening.

Method: Prospective longitudinal study still in the recruitment phase. Patients were under HCC screening program according to the 2018 EASL risk recommendations. Semiannual ultrasound (Canon Aplio i800) and simultaneous determination (Cobas E 601) of AFP, and DCP (also known as PIVKA-II [prothrombin induced by vitamin K absence-II]) were performed with subsequent calculation of Elecsys GAAD (Roche Dialog. Normal value ≤2.57; range 0–10). Ultrasound (US) findings and exploration quality were categorized according to Liver Imaging Reporting and Data System (LI-RADS) 2018. In short, patient's follow-up was conducted semiannually if US-1 (negative: no suspicious lesions) and GAAD ≤2.57; quarterly if US-2 (subthreshold: suspicious nodule <1 cm) or GAAD >2.57; and they were studied by computed tomography scan and/or magnetic resonance imaging if US-3 (positive: suspicious nodule >1 cm). The diagnosis of HCC was made according to the 2018 EASL Guideline and the disease classified as per Barcelona Clinic Liver Cancer (BCLC). Patients on warfarin or other causes of vitamin K deficiency and those in Child Pugh stage C (except if transplant candidate) were excluded.

Results: Between February and October 2023, 378 patients were included: 63 years old, 70% male, 81.5% cirrhosis, 19.5% non-cirrhotic with chronic hepatitis B ± chronic hepatitis D according to PAGE B screening criteria. The liver disease follow-up time was 8 years (interquartile range 3.9–12), 67.6% with inactive liver disease, platelets 161,000/ml, ALT 28 IU/L. 23.1% of the patients presented US-2 or US-3 categories, and 29.6% had moderate or severe limitations for ultrasound exploration. The GAAD index was >2.57 in 18.7%. 3 patients with HCC have been diagnosed (1 BCLC 0, 2 BCLC A). In these 3 patients, the GAAD index was elevated (5.94, 2.9, 4.75), while AFP values (upper normal limit <8 ng/ml) were 10.27, 2.75, and 2.22, respectively.

Conclusion: Our preliminary results suggest a high sensitivity of the GAAD algorithm in the screening of hepatocellular carcinoma in an at-risk population.

SAT-486

High SAFE scores stratify high risks of hepatocellular carcinoma in patients with chronic liver diseases

Tung-Hung Su¹, Sheng-Shun Yang², Wei-Yu Kao³, Shang-Chin Huang¹, Fen-Fang Chen¹, Francis Poon², Lung-Wen Tsai³, Che Lin⁴, Weichung Wang⁴, W. Ray Kim⁵, Jia-Horng Kao¹. ¹National Taiwan University Hospital, Taipei, Taiwan; ²Taichung Veterans General Hospital, Taichung, Taiwan; ³Taipei Medical University Hospital, Taipei, Taiwan; ⁴National Taiwan University, Taipei, Taiwan; ⁵Stanford University School of Medicine, Stanford, United States
Email: kaojh@ntu.edu.tw

Background and aims: Hepatocellular carcinoma (HCC) surveillance is recommended for high-risk individuals. Indicators of HCC risk to guide surveillance are lacking, especially for chronic liver diseases (CLD) from non-viral etiologies, including non-alcoholic fatty liver disease (NAFLD) and alcohol-related liver disease. The Steatosis-Associated Fibrosis Estimator (SAFE) score was developed to correlate with liver fibrosis in patients with NAFLD. This study explores the role of the SAFE score as a predictor for HCC in CLD.

Method: In this retrospective cohort study, electronic medical records from a tertiary medical center in Taiwan were used to extract data from patients with various CLDs. The SAFE score, consisting of age, BMI, diabetes, and laboratory data, was calculated using the published formula. Statistical analysis assessed the score's performance in predicting HCC risk in the data set and independent external validation sets.

Results: The primary analysis included 12,963 CLD patients with a median follow-up of 4 years, during which 258 developed HCC. The SAFE score correlated with 1, 3, and 5-year HCC risk regardless of liver disease etiologies. High (≥ 100) and intermediate (0–100) SAFE scores increased HCC risk by 11 and 2 folds, respectively, compared to low (< 0) SAFE scores. When lower risk tiers were combined, a high SAFE score (≥ 100) was associated with a 7-fold increased risk of HCC (adjusted hazard ratio [aHR]: 7.28, 95% confidence interval (CI): 5.19–10.21) compared to SAFE < 100 . Data in the external validation sets of 8,103 CLD patients recapitulated the difference (aHR: 7.33, 95% CI: 4.70–11.43).

Conclusion: The SAFE score is a significant predictor of HCC risk in patients with diverse chronic liver diseases and may play a role in selecting candidates for surveillance and early detection of HCC.

SAT-487-YI

Time-trends in cholangiocarcinoma mortality-a danish nationwide cohort study

Morten Daniel Jensen^{1,2}, Joe West^{2,3,4}, Frank Viborg Mortensen^{2,5}, Peter Jepsen^{1,2,6}. ¹Department of Hepatology and Gastroenterology, Aarhus University Hospital, Aarhus, Denmark; ²Department of Clinical Medicine, Aarhus University, Aarhus, Denmark; ³Lifespan and Population Health, School of Medicine, University of Nottingham, NG5 1PB, Nottingham, United Kingdom; ⁴NIHR Nottingham Biomedical Research Centre (BRC), Nottingham University Hospitals NHS Trust and the University of Nottingham, Nottingham, United Kingdom; ⁵Department of Surgical Gastroenterology, Aarhus University Hospital, Aarhus, Denmark; ⁶Department of Clinical Epidemiology, Aarhus University Hospital, Aarhus, Denmark
Email: moje@clin.au.dk

Background and aims: Cholangiocarcinomas (CCA) have a poor prognosis and the incidence of CCA is rising in Denmark. We set out to examine time trends in mortality of CCA in a nationwide Danish cohort.

Method: We included all 3,484 Danish patients with a diagnosis of CCA (ICD-10 codes C22.1, C24.0, C24.8, C24.9) in 1999–2019 recorded in both the Danish Cancer Registry and the National Patient Registry. We computed 1-year mortality and used Cox regression to estimate adjusted mortality hazard ratios (HR) by sex, age, year of diagnosis and type of CCA.

Results: Of the 3,484 CCA patients, 47% were men. The median age of patients diagnosed in 1999 was 73 vs. 71 in 2019. The 1-year mortality decreased between 1999 and 2019 from 76.6% (95% CI 68.9–83.6) in 1999 to 69.5% (63.6–75.2) in 2019, while 1-year mortality for the entire period was 71.7% (70.2–73.2). The 1-year mortality was: for 18–59-year-olds 56.2% (52.4–60.0), for 60–79-year-olds 70.3% (68.4–72.3), for patients over 80 years 88.6% (86.2–90.8), for intrahepatic CCA (iCCA) 71.0% (68.5–73.5), for extrahepatic CCA (eCCA) 66.5% (63.9–69.0), for unspecified CCA 80.5% (77.8–83.0), for females 72.9% (70.8–74.9), and for males 70.4% (68.2–72.6). For year of diagnosis, adjusted mortality HRs decreased with more recent diagnosis year in all age and sex groups and for both iCCA and eCCA. Adjusted HRs of 5-year increase in diagnosis year were: overall 0.90 (0.87–0.92), for 18–59-year-olds 0.87 (0.81–0.93), for 60–79-year-olds 0.90 (0.87–0.94), for patients over 80 years 0.91 (0.85–0.97), for patients with iCCA 0.86 (0.82–0.91), for patients with eCCA 0.89 (0.85–0.93), for females 0.91 (0.87–0.95), and for males 0.89 (0.85–0.93); while for unspecified CCA it was 0.98 (0.92–1.05).

Conclusion: The 1-year mortality of Danish patients diagnosed with CCA in 2019 was 69.5%, but it has decreased since 1999, overall and within subgroups defined by sex, age, or type of CCA.

SAT-490

Competitive risk analysis of spleen stiffness measurement with a spleen-dedicated module (SSM@100 Hz) for predicting de-novo HCC occurrence in cACLD patients: a prospective 5-year follow-up study

Federico Ravaioli¹, Luigi Colecchia¹, Elton Dajti¹, Amanda Vestito¹, Arianna Gobatto¹, Francesca Lami², Matteo Renzulli¹, Matteo Serenari¹, Lorenza Di Marco², Francesco Tovoli¹, Silvia Ferri¹, Alessandra Pivetti², Dante Romagnoli², Francesco Azzaroli¹, Davide Festi¹, Antonio Colecchia², Giovanni Marasco¹. ¹Department of Medical and Surgical Sciences (DIMEC), University of Bologna, Bologna, Italy; ²Gastroenterology Unit, Department of Specialistic Medicines, University of Modena and Reggio Emilia, University Hospital of Modena and Reggio Emilia, Modena, Italy
Email: f.ravaioli@unibo.it

Background and aims: Hepatocellular carcinoma (HCC) impact significantly the survival of patients with liver disease, and it has been shown that portal hypertension (PH) is a major contributor to its development. Notably, clinically significant portal hypertension (CSPH), as identified by HVPG, can predict the occurrence of HCC. To explore the potential of spleen stiffness measurement (SSM) as a predictor of HCC occurrence, particularly with the use of a new spleen-dedicated module (SSM@100 Hz), we conducted a prospective study. Our investigation was aimed to determine whether SSM@100 Hz could identify HCC occurrence in individuals with compensated advanced chronic liver disease (cACLD).

Method: We conducted a prospective study on patients who underwent paired laboratory exams, hepatic venous pressure gradient measurement (HVPG), liver stiffness measurement (LSM), and SSM@100 Hz. Patients were followed as per the current international guidelines for HCC screening, and we assessed the occurrence of HCC or other complications related to liver disease. We used competing-risks regression analysis to account for liver transplantation or death as competitive events.

Results: We enrolled 69 patients with a median follow-up of 68 months until HCC or a competitive event occurrence. Competitive univariate statistical analysis showed how HCC occurrence was predicted by a higher body mass index (BMI), SSM median value (SSM@100 Hz), HVPG, metabolic etiology, and combined Baveno VII single cut-off rule-in criteria (by SSM@100 Hz). Further multivariate analysis was conducted, and two models were developed: one based on SSM@100 Hz and the other based on HVPG. The first one demonstrated that age (hazard ratio (HR): 0.947, 95% confidence interval (CI): (0.906–0.991), metabolic etiology (HR: 20.911 (5.349–77.54)) and higher liver stiffness values (HR: 1.04 (1.013–1.066)) were

POSTER PRESENTATIONS

independent factors for the development of HCC while the second one showed similar results for male sex (HR: 10.296 (1.824–58.1), etiology (HR: 18.35 (4.592–72.97) and HVP (HR: 1.171 (1.021–1.344)). Competitive risk regression analysis demonstrated that both models can effectively predict the risk of HCC occurrence over time ($p < 0.001$ for both models).

Conclusion: SSM@100 hz, mirroring portal hypertension, can predict the de novo HCC occurrence in patients with cACLD with a median follow-up time of 5 years.

SAT-491

Assessing the relationship between human plasma metabolites and hepatocellular carcinoma: a two-sample Mendelian randomization analysis

Xi Wei¹, Ningning Zhang¹, Xuanchen Liu¹. ¹Tianjin Medical University Cancer Institute and Hospital, Tianjin, China

Email: weixi@tmu.edu.cn

Background and aims: Plasma metabolites are small molecules that represent intermediate or final products in metabolic reactions. Their levels are influenced by a variety of factors, including genetics, gut microbiota, and diseases. Plasma metabolites can also affect disease risk. However, the relationship between plasma metabolites and hepatocellular carcinoma (HCC) is unclear. We utilized the Mendelian Randomization (MR) approach to assess the potential causal relationship between plasma metabolites and the risk of hepatocellular carcinoma.

Method: Genetic instrumental variables for serum metabolites were determined through genome-wide association studies (GWAS) of 1,091 metabolites and 309 metabolite ratios in 8,299 individuals from the Canadian Longitudinal Study on Aging (CLSA) cohort. Summary statistics for HCC (hepatocellular carcinoma) were drawn from a GWAS including 1,866 cases and 195,745 controls. We adopted the Inverse Variance Weighted (IVW) method as our primary analysis. We further employed MR Egger, Weighted Mode, and Weighted Median methods.

Results: We identified suggestive associations between 24 plasma metabolites and the risk of HCC (odds ratio (OR): 1.18; $p = 0.015$ for 1-oleoyl-2-arachidonoyl-GPE (18:1/20:4); OR: 1.96; $p = 0.001$ for 1-palmitoleoyl-GPC (16:1); OR: 1.19; $p = 0.001$ for 1-palmitoyl-2-arachidonoyl-GPE (16:0/20:4); OR: 0.74; $p = 0.0046$ for 1-palmitoyl-2-linoleoyl-gpc (16:0/18:2); OR: 1.21; $p = 0.0038$ for 1-stearoyl-2-arachidonoyl-GPE (18:0/20:4); OR: 1.46; $p = 0.035$ for 1-stearoyl-GPE (18:0); OR: 1.51; $p = 0.010$ for 1-stearoyl-GPG (18:0); OR: 1.29; $p = 0.035$ for 5alpha-pregnan-3beta, 20alpha-diol monosulfate (2); OR: 1.41; $p = 0.047$ for 1- (1-enyl-palmitoyl)-2-oleoyl-gpc (p-16:0/18:1); OR: 1.18; $p = 0.028$ for 1- (1-enyl-palmitoyl)-2-palmitoyl-GPC (P-16:0/16:0); OR: 0.76; $p = 0.034$ for 1- (1-enyl-stearoyl)-2-linoleoyl-GPE (p-18:0/18:2); OR: 1.45; $p = 0.048$ for Androstenediol (3alpha, 17alpha) monosulfate (3); OR: 1.33; $p = 0.041$ for Aspartate to mannose ratio; OR: 0.65; $p = 0.0010$ for Campesterol; OR: 1.54; $p = 0.015$ for Carboxyethyl-gaba; OR: 1.16; $p = 0.02$ for Glycocholate sulfate; OR: 1.22; $p = 0.018$ for N-acetyl-isoptreanine; OR: 1.15; $p = 0.039$ for Octadecadienedioate (C18:2-DC); OR: 1.18; $p = 0.038$ for Octadecenedioate (C18:1-DC); OR: 2.41; $p = 0.011$ for Palmitoylcarnitine levels (Metabolon platform); OR: 1.25; $p = 0.041$ for Pregnenediol disulfate (C21H34O8S2); OR: 1.23; $p = 0.028$ for Sphingomyelin (d18:0/20:0, d16:0/22:0); OR: 1.52; $p = 0.039$ for Sphingomyelin (d18:1/22:1, d18:2/22:0, d16:1/24:1); OR: 1.63; $p = 0.012$ for Stearoylcarnitine; OR: 1.27; $p = 0.026$ for X-18922.

Conclusion: Our systematic analyses provide evidence to support a potential causal relationship between several plasma metabolites, and the risk of HCC. More studies are required to show how the plasma metabolites affects the development of HCC.

SAT-492

Different patterns of care and survival outcomes in transplant-centre managed patients with early-stage HCC-real-world data from an Australian multicentre cohort study

Jonathan Abdelmalak^{1,2}, Marie Sinclair³, Simone Strasser⁴, Avik Majumdar³, Natalie Ngu⁴, Claude Dennis⁴, Kate Collins⁵, Anouk Dev⁶, Joshua Abasszade⁶, Zina Valaydon⁷, Susan Byers⁷, Daniel Saitta⁷, Kathryn Gazelakis⁷, Jacinta Holmes⁸, Alexander Thompson⁸, Dhivya Pandiaraja⁸, Steven Bollipo⁹, Suresh Sharma⁹, Merlyn Joseph⁹, Amanda Nicoll¹⁰, Rohit Sawhney¹⁰, Nicholas Batt¹⁰, Myo Tang¹, John Lubel¹, Stephen Riordan¹¹, Siddharth Sood¹², Nicholas Hannah¹², James Haridy¹², Eileen Lam¹³, Elysia Greenhill², John Zalberg², Stuart Roberts^{1,2}. ¹Alfred Hospital, Melbourne, Australia; ²Monash University, Melbourne, Australia; ³Austin Hospital, Heidelberg, Australia; ⁴Royal Prince Alfred Hospital, Camperdown, Australia; ⁵Austin Health, Heidelberg, Australia; ⁶Monash Health, Melbourne, Australia; ⁷Western Health, Melbourne, Australia; ⁸St Vincent's Hospital Melbourne, Melbourne, Australia; ⁹John Hunter Hospital, New Lambton Heights, Australia; ¹⁰Eastern Health, Melbourne, Australia; ¹¹Prince of Wales Hospital, Sydney, Australia; ¹²Royal Melbourne Hospital, Melbourne, Australia; ¹³Monash University, Melbourne, Australia

Email: j.abdelmalak30@gmail.com

Background and aims: Management of very-early and early-stage hepatocellular carcinoma (HCC) is complex with multiple treatment strategies available. There is a paucity of literature regarding variation in patterns of care and outcomes between transplant and non-transplant centres. We performed this real-world multi-centre cohort study in two large liver transplant centres and eight non-transplant tertiary HCC referral centres across Australia to assess for variation in patterns of care and key survival outcomes.

Method: Patients with Barcelona Clinic Liver Cancer (BCLC) 0/A HCC first diagnosed between 01/01/2016 and 31/12/2020 who were managed at a participating site were included in the study. Patients were excluded if they had a history of prior HCC or if they received upfront liver transplantation.

Results: A total of 887 patients were included in the study, with 433 patients managed at liver transplant centres and 454 patients managed at a non-transplant centre. After adjusting for key covariates (age, sex, diabetes, smoking, hepatitis B status, alcohol, Charlson Comorbidity Index, cirrhosis status, portal hypertension status, Child Pugh score, tumour burden category), patients managed at liver transplant centres were significantly more likely to receive transarterial chemoembolization (TACE) as initial treatment compared to non-liver transplant centres ($p = 0.010$) and were significantly more likely to receive liver transplantation during follow-up treatment ($p < 0.001$). After adjusting for the same key covariates using Cox-proportional hazards survival analysis, management at transplant centre was associated with improved overall survival (adjusted OR 0.704, 95%CI 0.508–0.975, $p = 0.035$) and liver-related survival (adjusted OR 0.672, 95%CI 0.461–0.978, $p = 0.038$) but similar transplant-free survival (adjusted OR 1.046, 95%CI 0.786–1.393, $p = 0.758$). Subgroup analyses of those who underwent resection and ablation alone demonstrated no significant difference in overall survival (adjusted OR 1.335, 95%CI 0.350–5.089, $p = 0.672$; and adjusted OR 0.596, 95%CI 0.235–1.509, $p = 0.275$ respectively).

Conclusion: Our study highlights systematic differences in HCC care between large volume transplant centres and other sites, with an associated improvement in overall survival, the key end point in early-stage HCC. Further work is needed to better define the reasons for differences in treatment allocation and to aim to standardise treatment decisions to maximise patient outcomes across Australia.

SAT-493-YI

ASAP score may predict HCC recurrence after complete radiological response to locoregional treatments

Lorenzo Canova¹, Massimo Iavarone¹, Eleonora Alimenti¹, Riccardo Perbellini¹, Sara Uceda Renteria², Roberta D'Ambrosio¹, Elisabetta Degasperi¹, Floriana Facchetti¹, Anna Maria Ierardi³, Angelo Sangiovanni¹, Ferruccio Ceriotti², Pietro Lampertico^{1,4}.
¹Division of Gastroenterology and Hepatology, Foundation IRCCS Ca' Granda Ospedale Maggiore Policlinico, Milan, Italy; ²Clinical Laboratory, Fondazione IRCCS Ca' Granda Ospedale Maggiore Policlinico, Milan, Italy; ³Radiology Department, Foundation IRCCS Ca' Granda Ospedale Maggiore Policlinico, Milan, Italy; ⁴CRC "A. M. and A. Migliavacca" Center for Liver Disease, Department of Pathophysiology and Transplantation, University of Milan, Milan, Italy
 Email: pietro.lampertico@unimi.it

Background and aims: Alpha fetoprotein (AFP) and prothrombin induced by vitamin K absence/antagonist II (PIVKA-II) are biomarkers for hepatocellular carcinoma (HCC), which have been extensively in the diagnosis of HCC, while their use in the prognosis prediction remains poorly assessed. Recently, a new algorithm (ASAP)-including age, gender, AFP and PIVKA-II-has been validated as an alternative to GALAD for prediction of HCC development with a cut-off of 0.52. The identification of predictors of HCC recurrence after curative treatment has always been relevant to patients' management, and now may have further utility with the arrival of adjuvant therapies. The aim of our study was to evaluate the predictive role of AFP and PIVKA-II alone or combined in the ASAP score for HCC recurrence in patients who achieved a complete response (CR) after locoregional treatment.

Method: In this single-center, observational ongoing study, we have enrolled 156 consecutive patients with first diagnosis of HCC treated by ablation (MWTA) or chemoembolization (TACE). CR was evaluated by CT-scan 1 month after treatment, afterwards patients were evaluated every three months by CT-scan, clinical and biochemical features until recurrence, death or last follow-up. PIVKA-II and AFP levels were measured at the day of treatment by Fujirebio assays, Japan.

Results: 81 (52%) patients with HCC who achieved CR after the first treatment were included: median age 66 (40–87); 83% men, 57% HCV-positive, 91% Child-Pugh A, 85% BCLC 0/A, 53% MWTA. The day of treatment, the median AFP was 6.3 ng/ml (1.3–3, 537), median PIVKA-II was 112 (16–5, 090) mAU/ml, median ASAP score was 0.405 (–3.44–6.64; 47% with ASAP value >0.52). During follow-up, HCC recurred in 47 (58%) patients [median time to recurrence was 298 (41–1256) days after achieving CR]. PIVKA-II [HR 2.53 (95%CI 1.47–4.35), $p = 0.001$] and age [HR 1.03 (95%CI 1.00–1.07), $p = 0.013$] were the only independent predictors of overall HCC recurrence by a multivariable model for single variables only, while the ASAP score [HR 1.31 (95%CI 1.12–1.52), $p < 0.001$] was the only independent predictor of recurrence in a multivariable model including only scores and algorithms. PIVKA-II [HR 2.14 (95%CI 1.09–4.18), $p = 0.026$] was the only independent predictor of early recurrence in the first multivariable model, while platelet to lymphocyte ratio [PLR; HR 1.02 (95%CI 1.00–1.04)] and ASAP score [HR 1.30 (95%CI 1.03–1.64)] were independent predictors of early recurrence according to the second model. Adopting the ASAP cut-off of 0.52, the algorithm independently predicted HCC recurrence [HR 3.54 (95%CI 1.86–9.75), $p < 0.001$], but did not predict HCC early recurrence [HR 1.95 (95%CI 0.87–4.34), $p = 0.103$].

Conclusion: The ASAP algorithm may accurately predict HCC recurrence and early recurrence after complete radiological response, deserving further studies to refine the model.

SAT-494

Study on the impact of specific HCC histotypes on patients prognosis

Monica Bernasconi¹, Reha Akpınar^{1,2}, Camilla De Carlo¹, Barbara Durante¹, Angela Palmisano¹, Guido Costa¹, Guido Torzilli¹, Fabio Procopio¹, Luca Di Tommaso¹. ¹IRCCS Humanitas Research Hospital, Rozzano (Milano), Italy; ²Department of Biomedical Sciences, Humanitas University, Pieve Emanuele, Italy
 Email: monica.bernasconi@humanitas.it

Background and aims: The 2021 WHO classification of tumors, 5th edition, describes the existence of eight hepatocellular carcinoma (HCC) subtypes [steatohepatic (SH), clear cell (CC), macrotrabecular massive (MTM), scirrhous, chromophobe, fibrolamellar, neutrophil-rich and lymphocyte-rich (LR)] and suggests that some of these are associated with a better (CC- and LR) or worse (MTM and neutrophil-rich) prognosis. However, large series confirming these clinical features are lacking. The aim of our study is to verify, in a single institution experience, if different HCC histotypes correlate with specific clinico-pathological characteristics, i.e., with different prognoses.

Method: All the histopathological reports of HCC resected at Humanitas from 2005 to 2022 were reviewed. When the report referred to the presence of specific morphological aspects, all the slides of the case were reviewed and cases classified according to the histotypes proposed by WHO. For each case we evaluated for the presence and percentage of features suggestive of special histotypes. When these features exceeded 50% of the lesion, the case was considered as a special histotype. If the percentage did not exceed 50% of the lesion, the case was considered to have special aspects. For each case, morphological (necrosis, satellites, plurifocality, angioinvasion) and clinical data (DFS and OS) were obtained.

Results: The series included 567 HCCs; among them 152 were characterized by specific morphological aspects according to the histopathological report and were reviewed under the microscope. Special features were confirmed in 117 cases (117/567, 20%). In 35 of these cases, the steato-hepatic areas were predominant (SH-HCC, 6%). Clear cell aspects represented the main component in 13 cases (CC-HCC, 2%). Macrotrabecular areas accounted for >50% of the lesion in 8 cases (MTM-HCC, 1.4%). Finally, we observed two cases with a dominant scirrhous component (<1%), one fibrolamellar HCC (<1%) and one lymphocyte-rich HCC (<1%). No cases with chromophobe or granulocyte-rich aspects were present. The co-existence of a specific histotype with other special features was observed in 16% of the series. At clinical level, MTM were most frequently associated with parameters presenting with greater aggressiveness (angioinvasion 81%, necrosis 36%, plurifocality 27%), as opposed to SH histotype lesions (angioinvasion 29%, necrosis 20%, plurifocality 20%).

Conclusion: Our review, based on a large mono-institutional series, confirms that about 20% of HCC cases might present special features; that SH-, CC- and MTM- are the most frequent HCC histotypes; that MTM- HCC is associated with unfavorable morpho-pathological parameters. However, our analysis shows that no histotype correlates with a specific clinical behavior.

SAT-495

Real-World Data of Hepatocellular Carcinoma from 9 Asia-Pacific Countries (The INSIGHT Cohort): Overall Survival associated with choice of first therapy, number of lines of treatment and distance to hospital

Yu Ki Sim¹, Yanan Zhu², Luming Shi², Lequn Li³, Chien-Hung Chen⁴, Masatoshi Kudo⁵, Joon Hyeok Lee⁶, Simone Strasser⁷, Rawisak Chanwat⁸, Pierce Chow^{1,9,10}. ¹Programme in Translational and Clinical Liver Research, National Cancer Centre Singapore, Singapore, Singapore; ²Department of Epidemiology, Singapore Clinical Research Institute, Consortium for Clinical Research and Innovation Singapore, Singapore, Singapore; ³Department of Hepatobiliary Surgery, Guangxi Medical University Cancer Centre, Nanning, China; ⁴Department of

POSTER PRESENTATIONS

Internal Medicine, National Taiwan University Hospital, Taipei City, Taiwan; ⁵Department of Gastroenterology and Hepatology, Kindai University Hospital, Osaka, Japan; ⁶Division of Gastroenterology, Sungkyunkwan University School of Medicine, Samsung Medical Centre, Seoul, Korea, Rep. of South; ⁷AW Morrow Gastroenterology and Liver Centre, Royal Prince Alfred Hospital, Sydney, Australia; ⁸Department of Surgery, National Cancer Institute, Bangkok, Thailand; ⁹Department of Hepatopancreatobiliary and Transplant Surgery, National Cancer Centre Singapore and Singapore General Hospital, Singapore, Singapore; ¹⁰Surgery Academic Clinical Programme, Duke-NUS Medical School, National University of Singapore, Singapore, Singapore
Email: pierce.chow@duke-nus.edu.sg

Background and aims: Hepatocellular carcinoma (HCC) is the 6th most commonly diagnosed cancer and the 3rd leading cause of cancer death worldwide. There is limited real-world data on clinical management practices in HCC, which is essential to guide future public health strategies. Our study aims to evaluate survival outcomes of HCC patients based on clinical and socio-economic factors, stratified by BCLC staging at diagnosis.

Method: The INSIGHT study (NCT03233360) was an investigator-initiated, multi-site longitudinal cohort study that collected information on patient demographics, clinical and socio-economic factors, HCC-directed therapy and outcomes from HCC patients of 9 Asia-Pacific countries [1]. Kaplan-Meier analyses of overall survival (OS) were run, stratified by BCLC staging at diagnosis, with differences between treatment groups assessed by log-rank test. Univariate and multiple Cox proportional hazards regression models with stratification were used to calculate un-adjusted and covariate-adjusted hazard ratios (HRs) and 95% CIs for treatment types and OS. Statistical significance was taken at $p < 0.05$. Data imputations were made for missing data for visits before the start of treatment. Analyses were performed using R (v 4.1.3).

Results: 2,505 patients were analysed after excluding patients with missing death, last contact, last visit dates or wrong dates. Significant biological covariates included BMI, etiology, ALBI score, AFP level and presence of distant metastasis ($p < 0.05$). Education (university or higher) significantly influences OS in early HCC (HR = 0.36, 95% CI 0.14–0.94; BCLC 0 + A; HR = 0.35, 95% CI 0.13–0.94; BCLC B) after adjustment. Interesting, OS differed based on type of first-line treatment received, number of lines of treatment received and distance to hospital ($p < 0.05$) upon stratification. Patients that received liver resection as first line consistently demonstrated good OS across all stages compared to other treatment options like loco-regional and systemic therapies amongst others. Compared to BCLC B and C patients who received a single line of treatment, those who received 2 lines or more had better OS (HR = 0.44, 95% CI 0.26–0.75; BCLC B; HR = 0.45, 95% CI 0.33–0.61; BCLC C) after adjustment. To note, those who lived nearer to hospitals ($< 1/2$ day) fared better than those who lived $1/2$ –1 day away ($p < 0.001$; BCLC 0 + A, $p = 0.01$; BCLC B, $p = 0.03$; BCLC C).

Conclusion: Survival outcomes of HCC depends highly on biological and socio-economic factors. Notably, our findings underscore the need to consider socio-economic factors like distance to hospital and number of lines of treatment in the development of multi-pronged, targeted public health efforts to improve outcomes in HCC.

Reference

1. Sim YK, Chong MC, ..., Chow PKH (2023) Real-World Data on the Diagnosis, Treatment, and Management of Hepatocellular Carcinoma in the Asia-Pacific: The INSIGHT Study, *Liver Cancer*.

SAT-496

Impacts of COVID on HCC care cascade recommendation concordance: maintained surveillance rates and improved linkage to care

Joan Ericka Flores^{1,2}, Alexander Thompson^{1,2}, Stuart Roberts³, Marie Sinclair^{2,4}, Amanda Nicoll⁵, Stephen Bloom⁵, Ammar Majeed³, William Kemp³, Zina Valaydon^{2,6}, Gauri Mishra⁷, Jessica Howell^{1,2}. ¹St

Vincent's Hospital Melbourne, Fitzroy, Australia; ²University of Melbourne, Parkville, Australia; ³Alfred Health, Melbourne, Australia; ⁴Austin Health, Heidelberg, Australia; ⁵Eastern Health, Box Hill, Australia; ⁶Western Health, Footscray, Australia; ⁷Monash Health, Clayton, Australia
Email: ericka@flores.com.au

Background and aims: Optimal Cancer Pathway Recommendations of Hepatocellular Carcinoma (HCC OCP) from the Cancer Council of Australia recommend time intervals for each step in the HCC care cascade. 'Lockdown restrictions' in Victoria affected access to pathology, radiological and outpatient services; leading to a transition to virtual telehealth clinics and MDTs, and community HCC surveillance scans. This study aimed to describe concordance to HCC OCP recommendations and the impact of COVID19 lockdown restrictions.

Method: Incident HCC cases referred to six tertiary hospitals were prospectively identified from 1 January 2018–31 December 2021. 'Pre-lockdown' cases were diagnosed prior to 10 March 2020, and 'during-lockdown' after. Demographic and clinical data were obtained from the hospital electronic medical record and HCC MDT databases. Proportions of concordance were determined against HCC OCP recommendations: 14 days (d) 'time to MDT' review from referral; 28d for 'staging/investigation time' from referral to diagnostic and management consensus; 28d 'time to treatment' receipt from management consensus.

Results: 1015 incident HCC cases were identified: 81% male ($n = 820$), median age 66 years (IQR 59–74 years). Cirrhosis was present in 83% ($n = 842$), of whom 29% had diagnosis made at the time of HCC diagnosis. BCLC 0–A stage HCC occurred in 47% ($n = 482$). 42% ($n = 424$) were diagnosed through surveillance. Where referral information was available ($n = 928$), 70% ($n = 646$) were concordant with time to MDT; 63% ($n = 596$) were concordant with staging/investigation time. Of 957 cases where data were available, 30% ($n = 287$) were concordant with time to treatment, median 19d.

During lockdown, 469 cases (46%) were identified. No difference in the proportion undergoing surveillance pre-lockdown (43%, $n = 225$) vs during lockdown (43%, $n = 199$; $p = 0.984$); however, proportions concordant with time to MDT significantly increased from 64% ($n = 323$) to 76% ($n = 323$) ($p < 0.0001$), and staging/investigation time concordance increased from 58% ($n = 298$) to 69% ($n = 298$) ($p < 0.0001$). There was a significant decrease in the proportion concordant with time to treatment (33%, $n = 171$ vs 27%, $n = 116$ $p = 0.033$). Numerically, there was a decrease in the proportion concordant in non-surgical treatments from 42% ($n = 129$) to 37% ($n = 83$) ($p = 0.117$).

Conclusion: These data highlight effective implementation of telehealth clinics and virtual meetings, leading to an improvement in linking new HCC cases to specialist MDM for follow-up during lockdown. However, timely treatment receipt was significantly impacted by lockdowns, seen particularly in non-surgically treated cases. HCC surveillance uptake remained suboptimal but was maintained during lockdowns through increased use of community radiology services, highlighting the need for increased resource allocation to enable timely receipt of HCC surveillance and management.

SAT-497

A risk prediction model for hepatocellular carcinoma in general population without traditional risk factors for liver disease

Byeong Geun Song¹, Aryoung Kim¹, Dong Hyun Sinn¹. ¹Samsung Medical Center, Seoul, Korea, Rep. of South
Email: sinnndhn@hanmail.net

Background and aims: The available hepatocellular carcinoma (HCC) prediction model for general population without risk factors for chronic liver disease is limited. In this study, we aimed to develop HCC prediction model for individuals without traditional risk factors for HCC.

Method: The total of 138,452 adult participants without chronic viral hepatitis or significant alcohol intake who underwent regular health checkup at a tertiary hospital in South Korea were followed up for the development of HCC. Risk factors for HCC development were analyzed using Cox regression analysis and prediction model was developed using these risk factors.

Results: We developed the HCC prediction model among general population without risk factors for chronic liver disease. The predictors were age, sex, platelet count, aspartate aminotransferase, alkaline phosphatase, total cholesterol, and prothrombin time. The Harrell's C-index and Heagerty's integrated area under the receiver operating characteristics (AUROC) curve of the model were 0.88 (95% confidence interval [CI] 0.84–0.92) and 0.89 (95% CI 0.87–0.91), respectively. The AUROC were 0.89 (95% CI 0.89–0.90) at 5 years and 0.88 (95% CI 0.88–0.89) at 10 years, and the model was well calibrated. In the interval validation, predictive performance was comparable with C-index of 0.88 and 5 years and 10 years AUROC of 0.91.

Conclusion: The new model using clinical parameters is a useful tool for clinicians to stratify HCC risk in general population without risk factors for chronic liver disease.

SAT-498

Patterns and predictors of acute care utilization after liver-directed therapy for hepatocellular carcinoma

Andrew Moon¹, Chidi Iloabachie¹, Sydney Power¹, Gabriel Lupu¹, Joyce Badal¹, Yue Jiang², David Seligson¹, Hanna Sanoff¹, David Mauro¹, David Gerber³, Ted Yanagihara¹, A. Sidney Barritt IV¹.
¹University of North Carolina, Chapel Hill, United States; ²Duke University, Durham, United States; ³University of Cincinnati, Cincinnati, United States

Email: andrew.moon@unchealth.unc.edu

Background and aims: Liver-directed treatments for HCC can cause post-treatment symptoms and decompensation events, resulting in ER visits and hospitalizations. To help prevent these occurrences, it is important to better understand the frequency and predictors of acute care utilization.

Method: We performed a single center retrospective analysis of adult patients with HCC treated with thermal ablation, transarterial therapies (TACE/TAE and Y90) or external beam radiotherapy (EBRT) from 4/2014 to 12/2020. We excluded treatments of metastatic HCC (e.g. external beam radiation to extrahepatic metastases) but did include patients with vascular spread. The primary outcome was any post-treatment acute care utilization defined as an emergency room (ER) visit or inpatient admission (not including post-treatment observation stays) that occurred within 90 days after treatment. We compared baseline characteristics among those with and without health care utilization and created multivariable logistic regression models to identify characteristics associated with post-treatment health care utilization.

Results: This study included 191 unique patients with HCC (10% BCLC-0, 34% BCLC-A, 11% BCLC-B, 34% BCLC-C, 11% BCLC-D) who had 320 separate procedures (40% TAE/TACE, 17% laparoscopic MWA, 17% percutaneous MWA, 11% Y90, 8% EBRT and 8% combination/other). Most patients had CP-A cirrhosis (65%), HCV etiology (39%), and ECOG performance status 0 (56%). ER visits within 90 days occurred for 56 procedures (16%) and unplanned inpatient hospitalizations within 90 days occurred for 34 procedures (11%). Patients who had acute care utilization were older (median 65.5 vs 61.5 years, OR 0.96, 95% CI 0.93–0.99) and more likely to have ER visits (55% vs 24%, OR 4.21, 95% CI 2.38–7.53) and hospitalizations (41% vs 20%, OR 2.68, 95% CI 1.49–4.81) within the prior 12 months. Compared to those with CP-A cirrhosis, post-treatment acute care utilization was more common amongst patients with Child Pugh (CP) B8 (OR 1.53, 95% CI 1.02–5.92), B9 (OR 3.79, 95% CI 1.47–9.46) or C (OR 4.33, 95% CI 1.78–10.30) cirrhosis. Compared to those treated with laparoscopic MWA, patients receiving percutaneous MWA had a significantly lower

likelihood of having post-treatment acute care utilization within 90 days (OR 0.24, 95% CI 0.07–0.68). There were no statistically significant associations with other sociodemographic or clinical factors and no significant associations in multivariable models.

Conclusion: Acute care utilization with 90 days occurred for up to 15% liver-directed therapies, on par with historical cohorts of patients with metastatic non-liver cancer on chemotherapy. CP score and pre-treatment health care utilization are strong predictors of subsequent ER visits and hospitalizations. This study identifies subgroups who may benefit from enhanced nurse navigation or symptom/decompensation monitoring.

SAT-499

The inflammatory state of tumor peripheral liver tissue affects hepatocellular carcinoma progression and prognosis

Zheyu Zhou¹, Jinsong Liu^{2,3}, Shuya Cao⁴, Xiaoliang Xu⁵, Chaobo Chen⁶, Beicheng Sun^{1,5}.
¹Nanjing Drum Tower Hospital, Chinese Academy of Medical Sciences and Peking Union Medical College, Nanjing, China; ²Xinhua Hospital, Shanghai Jiao Tong University School of Medicine, Shanghai, China; ³Shanghai Colorectal Cancer Research Center, Shanghai, China; ⁴The First Affiliated Hospital of Nanjing Medical University, Nanjing, China; ⁵The First Affiliated Hospital of Anhui Medical University, Hefei, China; ⁶Xishan People's Hospital of Wuxi City, Wuxi, China

Email: zhouzheyu_pumc@sina.com

Background and aims: Inflammation has been proven vital in the initiation and progression of hepatocellular carcinoma (HCC), and inflammatory tumor microenvironment was the focus of previous studies. Whether the inflammatory state of HCC peripheral liver tissue also affects tumor progression has not yet been investigated. This study aimed to explore clinical features and underlying gene expression patterns of HCC patients with different G grades (Scheuer's classification).

Method: The medical data of HCC patients at Nanjing Drum Tower Hospital from January 2020 to August 2023 was retrospectively reviewed. Patients were divided into two groups: G 0–1 and G ≥2. Six HCC tissues (three in each group) were collected, and RNA-seq was conducted. Gene Set Enrichment Analysis (GSEA) was conducted to detect differential activation of Hallmarks pathways. Kyoto Encyclopedia of Genes and Genomes (KEGG) and Gene Ontology (GO) analyses were conducted on differentially expressed genes between these two groups to elucidate enriched pathways and biological processes. Integrated machine learning algorithms and multivariate Cox regression analysis were used for prognostic gene screening and model establishment.

Results: 370 HCC patients were included in this study, with 163 patients in the G 0–1 group and 207 patients in the G ≥2 group. More significant liver fibrosis, as well as severe coagulation and hepatic function impairment, were related to the G ≥2 group, characterized by elevated S ≥2 ratio, prothrombin time, international normalized ratio, alanine aminotransferase, and aspartate aminotransferase and lower platelet and albumin. Inflammatory genes (TNFSF9, IL18, and HIF1A), hepatic fibrosis-related genes (COL3A1, COL5A1, and MMP2), and Hallmarks pathways INFLAMMATORY_RESPONSE and TNFA_SIGNALING_VIA_NFKB were significantly upregulated in the G ≥2 group. Conversely, coagulation factors (F2, F7, and F9), complement molecules (C1R, C3, and C5), fibrinolysis-related molecules (SERPINA1, SERPINC1, and SERPIND1), hepatic metabolism-related genes (GOT2, GPT2, and CYP7A1), and Hallmarks pathways COAGULATION and BILE_ACID_METABOLISM were markedly upregulated in the G 0–1 group. KEGG pathways significantly enriched in complement and coagulation cascades, biosynthesis of amino acids, and cholesterol metabolism. Consistently, GO had significant enrichment in blood coagulation, cellular amino acid catabolic processes, and transaminase activity. The established model based on seven inflammatory-related genes performed well in prognostic prediction and risk stratification across multiple datasets.

POSTER PRESENTATIONS

Conclusion: HCC patients with $G \geq 2$ had an inflammatory and fibrotic phenotype with a worse prognosis, while patients with $G 0-1$ retained better coagulation and liver metabolic functions.

SAT-500-YI

Ethnic and racial disparities in the initial presentation of hepatocellular carcinoma: real-world data from a single non-academic hepatology clinic with a large diverse population in Los Angeles County

Isabella Martinez¹, Michel Mendler¹, Edward Mena². ¹California Liver Research Institute, Pasadena, United States; ²California Liver Research Institute, Pasadena Liver Center, Pasadena, United States
Email: isabella.martinez@caliverresearch.org

Background and aims: The increasing incidence of Hepatocellular Carcinoma (HCC) in the U.S. is attributed in part to increasing rates of obesity, diabetes (T2DM), metabolic dysfunction-associated steatotic liver disease (MASLD), and metabolic dysfunction-associated steatohepatitis (MASH). We aim to discern social and clinical characteristics associated with HCC diagnosis in an ethnically diverse population seen at a private Hepatology-focused practice in Los Angeles County, California, USA.

Method: Retrospective study of patients at their initial evaluation for HCC at our hepatology clinic from July 2018 through July 2023. HCC was diagnosed by standard MRI/CT criteria. Underlying causes of liver disease, presence of cirrhosis, pertinent clinical characteristics and socioeconomic factors were stratified according to ethnicity and race and compared by univariate analyses.

Results: 187 patients met inclusion criteria. 45.0% ethnically identified as Hispanic/Latino (HL) and 51.3% non-Hispanic/Latino (NHL). Of HCs, 82.1% racially identified as Non-White and 16.7% as White. Race distribution was 3.2% Black, 28.3% Asian, 20.9% White, 43.3% Other. The median age was 71 (27–88), and 72% were male. No significant differences were observed in gender, median household income by zip code census or satisfying Milan transplant criteria. HCs were found to have a higher prevalence of T2DM (55.3% vs 40.1%, $p = 0.05$) and BMIs [median 28.4 (18.3–46) vs 25.0 (14.3–50), $p = 0.031$] than NHLs. Overall, 88.8% had cirrhosis. When compared to NHLs, HCs had higher prevalence of cirrhosis due to MASLD (53.6% vs 19.8%, $p < 0.001$) and alcohol abuse (17.9% vs 9.4%, $p < 0.001$). Among those with HBV, majority were Asian (93.6%, $p > 0.001$) while for HCV the majority were White (32.1%, $p < 0.001$). Asians had cirrhosis mostly due to HBV and MASLD (56% and 20.8%, $p < 0.001$). Among those without cirrhosis, 61.1% had HBV, and 11.1% had MASLD ($p < 0.001$). Asians (70.7%) and non-white HCs (17.7%) comprised the majority of non-cirrhotic HCC cases ($p = 0.04$). Of those outside of UCSF transplant criteria, majority were non-white HCs (42.3% $p = 0.043$). White-HCs had higher systemic treatment rates than White-NHLs (46.2% vs. 16.0%, $p = 0.007$), with Asians having the lowest rates (5.7%, $p = 0.007$). Additionally, HCs had lower surgical resection rates than NHLs, (3.6% vs 13.5%, $p = 0.044$), while Asians exhibited the highest rates (68.8%, $p = 0.008$).

Conclusion: This real-world data from a diverse population in Los Angeles seen for HCC suggests that HCs exhibit a higher incidence of cirrhosis attributed to MASLD and alcohol-associated liver disease, increased rates of HCC without cirrhosis, higher BMIs and prevalence of diabetes. HCs appear to present with more advanced disease leading to lower rates of surgical resections and a greater need for systemic therapy. Asians had the highest prevalence of HBV-related HCC as well as non-cirrhotic HCC.

SAT-501-YI

The CRAFTY score to predict hepatocellular carcinoma disease control rate at month 12 in patients undergoing transarterial chemoembolization

Rhea Veelken¹, Anne Olbrich¹, Sabine Lieb¹, Aaron Schindler¹, Adam Herber¹, Sebastian Ebel², Timm Denecke², Thomas Berg¹, Florian van Bömmel¹. ¹University Hospital of Leipzig, Division of

Hepatology, Department of Medicine II, Leipzig, Germany; ²University Hospital of Leipzig, Department of Diagnostic and Interventional Radiology, Leipzig, Germany
Email: florian.vanboemmel@medizin.uni-leipzig.de

Background and aims: The CRAFTY score, utilising alpha-fetoprotein (AFP ≥ 100 ng/ml) and C-reactive protein (CRP ≥ 1 mg/dL), classifies patients with hepatocellular carcinomas (HCC) for potential enhanced overall survival (OS) and treatment response to subsequent immunotherapy. This study aimed to assess the predictive utility of the CRAFTY score evaluating disease control rate (DCR) and overall survival within 12 months in patients undergoing transarterial chemoembolization (TACE). Predicting HCC disease control rate after TACE is especially vital in the context of bridging therapy for patients awaiting liver transplantation.

Method: We conducted a retrospective analysis of 1117 HCC patients diagnosed at our center between 2010 and 2020, of which 546 underwent TACE as their initial treatment. Inclusion criteria comprised documented follow-up records >3 months, three-monthly CT or MRI imaging, and availability of baseline CRP and AFP data. The study assessed the association of baseline variables using Cox regression and Kaplan-Meier estimation. The study involved 113 patients, median age 63 [range, 31–85] years, including 15 females (13%). BCLC stages were A ($n = 64$), B ($n = 36$), C ($n = 11$), and D ($n = 2$). Imaging revealed compensated cirrhosis in 101 patients (89%). Twelve months post-TACE, DCR was observed in 27 patients (23.9%), with 14 exhibiting complete response, 9 stable disease, and 4 partial response. Disease progression occurred in 35 (30.9%) patients, with 3 presenting new extrahepatic spread and 32 (28.3%) developing new intrahepatic HCC nodes. Within 12 months, 20 patients (17.7%) underwent liver transplantation.

Results: The assessment of 12-month survival demonstrated the reliability of the CRAFTY score as a predictor of DCR ($p = 0.004$). A CRAFTY score of 2 indicated a threefold higher risk of mortality (HR = 3.4 [95% CI 1.48–7.58]; $p = 0.004$) compared to a score of 0 within 12 months. Additionally, elevated CRAFTY scores, distributed as 0 (59.6%), 1 (33.8%), 2 (6.4%), were significantly associated with the occurrence of new intrahepatic tumor nodes, defining disease progression within 12 months after the first TACE ($p = 0.0114$). Patients with a CRAFTY Score of 2 had a 3.8 times higher risk to develop a new tumor node after 12 months than patients with a CRAFTY Score of 0 (HR = 3.8 [95% CI 1.09–13.24]; $p = 0.036$). AFP at the time of TACE also showed a significant association with treatment response (AUC = 0.679; 95% CI 0.542–0.815; $p = 0.017$), while CRP did not (AUC = 0.568; 95% CI 0.416–0.729; $p = 0.366$).

Conclusion: In addition to its potential for predicting survival, the CRAFTY score could function as a predictive tool for tumor control in HCC patients post-TACE. Further studies are needed to validate these findings, with a particular emphasis on demonstrating its capacity to aid in risk stratification for HCC patients on the liver transplantation waitlist.

SAT-502-YI

Active HCV or HBV infection does not impact on clinical outcomes in patients with hepatocellular carcinoma

Arianna Bertazzoni¹, Francesco Berardi¹, Mariangela Fortunato¹, Matteo Soleri¹, Nicola Pugliese^{1,2}, Francesca Colapietro^{1,2}, Chiara Masetti², Roberto Ceriani², Vittorio Pedicini³, Lorenza Rimassa^{1,4}, Ana Lleo^{1,2}, Alessio Aghemo^{1,2}, Stella De Nicola². ¹Department of Biomedical Sciences, Humanitas University, Pieve Emanuele (Milan), Italy; ²Division of Internal Medicine and Hepatology, Department of Gastroenterology, Humanitas Research Hospital IRCCS, Rozzano (Milan), Italy; ³Department of Interventional Radiology, Humanitas Research Hospital IRCCS, Rozzano (Milan), Italy; ⁴Medical Oncology and Hematology Unit, Humanitas Cancer Center, Humanitas Research Hospital IRCCS, Rozzano (Milan), Italy
Email: arianna.bertazzoni@humanitas.it

Background and aims: Hepatocellular carcinoma (HCC) is the main complication of cirrhosis. Chronic infections with hepatitis B virus (HBV) or hepatitis C virus (HCV) are among the main etiologies for advanced liver disease worldwide. Effective antiviral treatments have changed the course of viral-related liver disease, but access to treatment is not universal and many patients with HCC still present active viral infection. Impact of viral infection on the prognosis of patients with HCC is largely unknown. We analyzed the impact of viral infection on patient outcome after the first diagnosis of HCC in compensated advanced liver disease (cACLD).

Method: We retrospectively analyzed all patients discussed at multidisciplinary meetings, between 2018 and 2022, at our tertiary Hospital. We included all patients with HCC and cACLD without history of previous or active decompensation. The primary outcome was liver decompensation at one year. Secondary outcomes included one-year HCC recurrence, survival and liver transplantation (LT).

Results: 240 cACLD patients were included, of which 75% males. Median age was 71 years (I.Q.63–77). Prevalent etiology was viral cirrhosis (113 cases, 47.09%), specifically 92 patients with HCV (81.42%) and 21 patients with HBV (18.58%). Of viral cirrhoses 52 cases (46%, 52/113) had an active infection, 46 of whom (88%) had HCV infection. The Barcelona Clinic Liver Cancer (BCLC) stages were divided as follows: BCLC-0 (12/52, 23% in active vs 12/61, 19.67% in non-active cases respectively), BCLC-A (24/52, 46.15% vs 32/61, 52.46% respectively), BCLC-B (15/52, 28.85% vs 17/61, 27.87% respectively), BCLC-C (1/52, 1.92% vs 0/61, 0% respectively), BCLC-D (no patients in either case). Active and non-active cases did not differ in number and size of nodules (Milano Criteria in: 30/52, 57.69% in active disease vs 40/61, 65.57% in non-active group respectively, $p = 0.252$) or presence of varices (6/52, 11.54% in active vs 11/61, 10.03% in non-active infection, $p = 0.524$). All active HBV patients started antiviral therapy after HCC diagnosis, while 28/46 (60%) of HCV patients received DAAs. One-year incidence of ascites (2 vs 2 patients, $p = 0.838$), hepatic encephalopathy (1 vs 0 patients, $p = 0.290$) or variceal bleeding (1 vs 0 patients, $p = 0.505$) was similar among active and inactive hepatitis. One-year HCC recurrence (37/52, 71.15% in active vs 32/61, 52.46% in non-active infection, $p = 0.122$), LT (1 vs 3 patients, $p = 0.391$) and one-year liver-related mortality were similar in active vs inactive viral hepatitis.

Conclusion: Active viral infection in Italian patients with HCC and compensated liver disease is common but has limited clinical impact as it does not modify survival, recurrence or liver decompensation. Antiviral treatment is safe and needs to be considered in this setting.

SAT-503

Role of CD27 on IgD+ CD24+ B cell in mediating the effect of Lactobacillaceae on bile duct carcinoma

Xuanchen Liu¹, Ningning Zhang¹, Wei Lu², Yiyang Zhang², Kaipeng Liu¹, Huiru Liu¹. ¹Tianjin Medical University Cancer Institute and Hospital, Tianjin, China; ²Tianjin Medical University Cancer Institute and Hospital, Tianjin, China
Email: 15931873318@163.com

Background and aims: We investigated the causal relationships between the gut microbiota, bile duct carcinoma, and potential immunophenotype mediators using Mendelian randomization.

Method: The data on gut microbiota, immunophenotype, and bile duct carcinoma all come from the GWAS Catalog website (<http://www.ebi.ac.uk/gwas/>). The data of gut microbiota were under the study accession numbers GCST90027446–GCST90027857. Immunophenotype from GCST0001391–GCST0002121, and bile duct carcinoma from GCST90018803. We performed bidirectional MR analyses to explore the causal relationships between the GM and bile duct carcinoma, and two mediation analyses, two-step MR to discover potential mediating immunophenotype.

Results: There is a causal relationship between 12 gut microbial taxa and bile duct carcinoma, with Lactobacillaceae showing the most significant association (ivw: $p = 0.015$, OR:1.224 (1.040–1.441)), and

there is no evidence of reverse causation. Performing a bulk MR analysis with Lactobacillaceae and 731 immunophenotypes revealed causal relationships with 17 immunophenotypes. Subsequently, conducting a bulk MR analysis with these 17 immunophenotypes and bile duct carcinoma showed a causal relationship only between the CD27 on IgD+ CD24+ B cell and bile duct carcinoma (ivw: $p = 0.024$, OR:0.905 (0.829–0.987)).

Conclusion: Through Mendelian randomization, it was revealed that Lactobacillaceae acts on bile duct carcinoma through CD27 on IgD+ CD24+ B cells as intermediate factors.

SAT-513

Hepatocellular carcinoma surveillance in an european tertiary hospital. Where are we failing?

Francisco Capinha¹, Inês Rodrigues¹, Miguel Moura¹, Sofia Carvalhãna¹, Luís Correia², Helena Cortez-Pinto². ¹Serviço de Gastrenterologia e Hepatologia, Hospital de Santa Maria, Centro Hospitalar Universitário Lisboa Norte, Lisboa, Portugal; ²Serviço de Gastrenterologia e Hepatologia, Hospital de Santa Maria, Centro Hospitalar Universitário Lisboa Norte, Clínica Universitária de Gastrenterologia, Faculdade de Medicina de Lisboa, Universidade de Lisboa, Lisboa, Portugal
Email: francisco.capinha96@gmail.com

Background and aims: Surveillance of hepatocellular carcinoma (HCC) is efficient in detecting small tumors, with a positive impact on survival. In clinical practice there are several issues on the application of HCC screening: patients with unknown liver disease, poor patient adherence or problems in the health care system, leading to an underperformance. We aim to evaluate the performance of the HCC surveillance and the reasons of missed/delayed diagnosis in patients with HCC in our center.

Method: Retrospective study which included patients with HCC diagnosis discussed by the multidisciplinary team of liver tumors from 2020 to 2023 in a tertiary hospital. HCC surveillance was defined according to the EASL recommendations (2018). Considering the target population for screening, subgroups were created and compared: (a) diagnosed through screening; (b) missed screening due to poor patient adherence and/or system failure; (c) unknown advanced liver disease (UALD), that would have indication for surveillance if already diagnosed. For patients diagnosed through screening, we considered an error margin of 2 months (8 months) as “complete surveillance” and between 8 and 12 months as “incomplete surveillance.” Statistical analysis has performed using SPSS[®] v23. A p value <0.05 was considered as statistically significant.

Results: We included 174 patients, with a median age 67 years and 90% males. From these, 158 patients had liver disease, among them 136 with cirrhosis (70% CP A; 20% CP B; 10% CP C). The most common etiologic factor for liver disease was alcohol (56%). The proportion of patients diagnosed in surveillance was 26% ($n = 46$). Relatively to the stage at diagnosis, 4% BCLC-0, 37% BCLC-A, 10% BCLC-B, 33% BCLC-C and 15% BCLC-D. Considering the target population (80%, $n = 140$): 33% ($n = 46$) subgroup (a); 24% ($n = 34$) subgroup (b); and 43% ($n = 60$) subgroup (c). The defined subgroups were comparable on sex and age. In subgroup (a) 59% ($n = 27$) have complete surveillance and 41% ($n = 19$) have incomplete surveillance, without any significant difference in terms of outcome. Patients in subgroup (a) had HCC diagnosed at lower stages (BCLC-0 and BCLC-A) compared to subgroups (b) and (c) together ($p = 0.012$), as well as comparing with subgroup (c) ($p = 0.011$). The subgroup (c), comparing to subgroup (a), had higher proportion CP B and C ($p = 0.008$), vascular invasion ($p = 0.01$), extrahepatic involvement ($p = 0.052$) and hepatic dysfunction according to ALBI score ($p < 0.001$) at time of diagnosis.

Conclusion: In our cohort, a minority of HCC cases (26%) were diagnosed through screening. From the patients with indication for screening, only one third achieved diagnostic yield. This study emphasizes not only the need to improve surveillance and early diagnosis of HCC, but also the importance of primary care in early

POSTER PRESENTATIONS

diagnosis of liver disease, since 35% of HCC patients were unaware of the diagnosis of advanced liver disease.

SAT-514

Application of machine learning model-3P to predict portal hypertension in patients with hepatocellular carcinoma

Arianna Bertazzoni¹, Francesco Berardi¹, Mariangela Fortunato¹, Matteo Soleri¹, Roberto Ceriani², Francesca Colapietro^{1,2}, Nicola Pugliese^{1,2}, Chiara Masetti², Guido Torzilli^{1,3}, Vittorio Pedicini⁴, Dario Poretti⁴, Lorenza Rimassa^{1,5}, Tiziana Comito⁶, Ana Lleo^{1,2}, Alessio Aghemo^{1,2}, Stella De Nicola², Emanuela Morengi^{1,7}.

¹Department of Biomedical Sciences, Humanitas University, Pieve Emanuele (Milan), Italy; ²Division of Internal Medicine and Hepatology, Department of Gastroenterology, Humanitas Research Hospital IRCCS, Rozzano (Milan), Italy; ³Division of Hepatobiliary Surgery, Department of General Surgery, Humanitas Research Hospital IRCCS, Rozzano (Milan), Italy; ⁴Department of Interventional Radiology, Humanitas Research Hospital IRCCS, Rozzano (Milan), Italy; ⁵Medical Oncology and Hematology Unit, Humanitas Cancer Center, Humanitas Research Hospital IRCCS, Rozzano (Milan), Italy; ⁶Department of Radiosurgery and Radiotherapy, Humanitas Cancer Center, Humanitas Research Hospital IRCCS, Rozzano (Milan), Italy; ⁷Biostatistics Unit, Humanitas Research Hospital IRCCS, Rozzano (Milan), Italy
Email: arianna.bertazzoni@humanitas.it

Background and aims: The occurrence of decompensation due to portal hypertension (PH) in patients with hepatocellular carcinoma (HCC) could preclude access to treatment. To date, non-invasive methods to predict PH failed their application in HCC patients. Reiniš, J (JHep, 2023) proposed a new non-invasive method developed through machine learning models, called the 3P model, using as reference the invasive measurement of hepatic venous pressure gradient (HVPG). The model considered three laboratory parameters (platelet count, bilirubin, international normalized ratio) and held promising results in predicting the presence of PH in cACLD (compensated advanced chronic liver disease). The aim of our study is to verify reliability of 3P model in a cohort of patients with HCC.

Method: We retrospectively included all consecutive patients discussed in multidisciplinary HCC team (MHT) consultation from 2018 to 2022 with a diagnosis of HCC developed con cACLD. 3P score was calculated using the formula suggested by Reiniš, J., et al. (0.332 for prediction of HVPG >16 mmHg) and was compared to baseline endoscopy. For comparison logistic regression and ROC analysis were performed.

Results: Data from 240 cACLD patients with HCC were collected. 146 patients performed endoscopy at baseline and were included in statistical analysis. Main etiology of cirrhosis was viral infection (64/146, 44%) followed by metabolic disease (44/146, 30%). The HCC stage was classified using the Barcelona clinic liver cancer (BCLC) system: BCLC-0 22 patients (15.7%), BCLC-A 76 (52.5%), BCLC-B 46 (31.51%), BCLC-C 2 (1.37%). A total of 42 patients (28.77%) had varices at endoscopy. Applying the 3P score with a 0.332 cut-off in our cohort, we obtained a sensitivity of 40% and a specificity of 89% (AUC 0.65). Based on our data, another cut-off (0.15) was calculated for prediction of presence of varices at endoscopy, reaching a sensitivity of 80% and specificity of 44%, with a negative predictive value of 83.7%.

Conclusion: 3P model could be a rapid, non-invasive, economic model to predict the absence of severe PH at diagnosis of HCC in cACLD. More data are necessary to validate our proposed cut-off in HCC setting in order to bypass endoscopy and try to limit delays in starting treatment.

SAT-515

Cholangiocarcinoma across England: evidence of regional, socioeconomic, and temporal variations in incidence, survival, routes to diagnosis and treatment

Sophie Jose^{1,2}, Amy Zalin^{1,3}, Daniela Tataru³, Craig Knott^{1,4}, Lizz Paley⁵, Helen Morement⁶, Roger Cherry¹, Kwok Wong³, Mireille Toledano⁷, Shahid Khan⁸. ¹Health Data Insight CIC, Cambridge, United Kingdom; ²National Disease Registration Service, NHS England, Leeds, United Kingdom; ³National Disease Registration Service, NHS England, Leeds, United Kingdom; ⁴National Disease Registration Service, NHS England, Leeds, United Kingdom; ⁵National Disease Registration Service, NHS England, Leeds, United Kingdom; ⁶AMMF-The Cholangiocarcinoma Charity, Essex, United Kingdom; ⁷Imperial College London, MRC Centre for Environment and Health, School of Public Health, London, United Kingdom; ⁸Imperial College London, London, United Kingdom

Email: shahid.khan@imperial.ac.uk

Background and aims: Cholangiocarcinoma (CCA) is increasing in the UK and globally. Whether there are regional, socioeconomic and temporal variations in incidence, mortality, routes to diagnosis (RtD) and treatment within England is unknown. There are no published studies from any country exploring these issues. This work aimed to investigate these issues across England.

Method: Patients diagnosed in England with a CCA between 2001–2018 were extracted from the National Cancer Registration Dataset (NCRD) linked to other data sources: the Hospital Episode Statistics (HES) dataset, the Systemic Anti-Cancer Therapy (SACT) dataset. RtD data were extracted for 2006–2017, and treatment data for 2014–2017, representing the time periods for which respective data were available. Age-standardised incidence (ASRs) and mortality (ASMRs) rates were estimated overall and stratified by gender, area deprivation quintile based on the income domain of the Index of Multiple Deprivation closest to diagnosis, tumour subtype (intra/extrahepatic) and England's 21 regional Cancer Alliances. Net and overall survival estimates were also calculated. Linear probability models were used to quantify geographic variation in RtD and treatment, adjusting for potential confounders. Geographic variation was analysed by Cancer Alliance based on postcode of residence at diagnosis.

Results: ASRs, ASMRs and net survival varied by geography. ASRs and ASMRs were consistently higher in the more socioeconomically deprived groups. The least deprived CCA patients had best overall survival ($p < 0.001$). 3-year net survival rose from 9.2% in 2001–2003 to 12.6% by 2016–2018. The most common RtD was Emergency Presentation (EP), with 49.6% of patients diagnosed thus. The proportion diagnosed via Two Week Wait Urgent GP Referral (TWW) doubled from 9.9% to 19.8%. Statistically significant variation was observed in the proportions of patients diagnosed via a TWW or EP across England's Cancer Alliances. There was also significant variation between Cancer Alliances in the proportions of patients that received potentially curative surgery, systemic therapy without potentially curative surgery, or stent insertion without potentially curative surgery.

Conclusion: Geographic variations in RtD and access to resection and stenting is a novel finding and suggests opportunities for sharing of good practice across NHS organisations to continue to improve on current trends. Local review of treatment pathways and more comprehensive guidelines for the management of CCA could help to reduce potential variation in treatments received across Cancer Alliances. Whilst there were some improvements in overall survival over time, three-year survival rates remained extremely low, highlighting huge unmet need in this population.

SAT-516

In the era of effective antiviral therapy, cured hepatitis C remains a main cause of HCC

Elena Vargas-Accarino¹, Monica Higuera¹, Maria Buti^{1,2,3,4}, Beatriz Minguez^{1,2,3,4}. ¹Liver Diseases Research Group, Vall d'Hebron Institut de Recerca (VHIR), Vall d'Hebron Barcelona Hospital Campus, Barcelona, Spain; ²Department of Medicine, Campus de la UAB, Universitat Autònoma de Barcelona (UAB), Barcelona, Spain; ³Centro de Investigación Biomédica en Red de Enfermedades Hepáticas y Digestivas (CIBERehd), Instituto de Salud Carlos III, Madrid, Spain; ⁴Liver Unit, Hospital Universitario Vall d'Hebron, Vall d'Hebron Barcelona Hospital Campus, Barcelona, Spain
Email: beatriz.minguez@vallhebron.cat

Background and aims: In the last decade, hepatitis B virus infection vaccination, total accessibility to hepatitis B and C antivirals and the global steatotic liver disease epidemic, may impact the underlying liver cancer etiologies. The aim of this study was to analyze the etiological agents of liver disease in patients diagnosed with de novo hepatocellular carcinoma (HCC) in our cohort.

Method: Retrospective study including all new hepatocellular carcinoma diagnosed between January 2019 and December 2022 in an academic center. The demographics, clinical characteristics and risk factors of hepatocellular carcinoma as well as the BCLC stage at diagnosis have been reviewed.

Results: 352 consecutive patients diagnosed with de novo HCC were included. The most frequent underlying etiology was alcoholic-related liver disease in 117 (33.3%) patients, followed by cured hepatitis C in 109 (30.9%), MASLD was detected in 43 (12.2%), active HCV infection in 28 (7.9%) and chronic hepatitis B infection in 21 (6%). The majority were male, mean age of 71 years and 82.7% had liver cirrhosis. BCLC 0 was observed in 28 (8%) of patients at the time of diagnosis, BCLC A in 144 (40.9%) patients, BCLC C in 86 (24.4%), and BCLC B in 58 (16.5%), and BCLC stage D was observed in 36 (10.2%) patients. Significant differences were found between the etiological factor of HCC and patient's sex, median age, BCLC stage at the time of diagnosis and percentage of patients with cirrhosis. Patients with cured HCV were significantly more women than patients with ALD ($p = 0.001$); patients with HBV infection were significantly younger than those with HCV infection ($p = 0.005$) or MASLD ($p = 0.001$); patients with active HCV were significantly more diagnosed at BCLC stage C and less at BCLC stage B than those patients with ALD ($p < 0.05$); and patients with ALD were significantly more cirrhotic than patients with MASLD or HBV infection ($p < 0.05$).

Conclusion: Alcohol liver related disease is the main cause of HCC, followed by solved hepatitis C. The total accessibility to DAA treatment and the high cure rate have not only not eliminated the risk of HCC, but it persists as one of the two predominant causes. The progressive increase in steatosis liver disease is not yet a major cause of HCC development.

SAT-518

Evaluation of the prognostic importance of Gustave Roussy immune score in hepatocellular carcinoma patients

Hatice Gülgün Fırat¹, İlknur Deliktaş Onur¹, Elif Serteser Çamöz¹, Fatih Yıldız¹. ¹Dr. Abdurrahman Yurtaslan Oncology Education and Research Hospital, Ankara, Turkey
Email: drhgtekin@gmail.com

Background and aims: Hepatocellular carcinoma (HCC) is a primary liver tumour that usually develops in the background of chronic liver disease.

Gustave Roussy Immune Score (GRIm score) is a score developed for appropriate patient selection in phase-1 trials using immunosuppressive inhibitors. The HCC-GRIm score was developed by adding the aspartate aminotransferase/alanine aminotransferase ratio and total bilirubin level in hepatocellular cancer patients, in addition to the serum albumin level, serum lactate dehydrogenase level and serum neutrophil/lymphocyte level measured in the GRIm score. In our

study, we aimed to evaluate the prognostic efficacy of GRIm score and HCC-GRIm score in hepatocellular carcinoma patients and to show whether these scores are related to the etiology of HCC.

Method: The study included one hundred thirty two patients aged eighteen years and older with HCC diagnosed between January 2015 and 2023. Age, gender, Ecog performance scores, date of diagnosis, HCC etiology, Barcelona stage at the time of diagnosis, whether local ablative procedure was performed, whether systemic treatment was received, Child Pugg score at the time of diagnosis, Meld score at the time of diagnosis, GRIm score and HCC-GRIm score at the time of diagnosis, final status and dates were recorded. Survival data was last updated in December 2023.

Results: GRIm score was low in seventy-five patients and high in fifty seven patients. Similarly, HCC-GRIm score was low in seventy-six patients and high in fifty six patients. Patients were grouped as low and high according to GRIm score and HCC-GRIm score. As the ECOG performance scores of the patients increased, GRIm score and HCC-GRIm score increased. A significant correlation was found between ECOG performance scores and GRIm scores and HCC-GRIm scores. A significant correlation was also found between BCLC stage and GRIm score and HCC-GRIm score. In the univariate analysis, Ecog, Child score, GRIm, HCC-GRIm score were prognostic for survival. In multivariate analysis, only GRIm and Child were prognostic.

Conclusion: In our study, GRIm score and HCC-GRIm score were found to be prognostic in univariate analysis, whereas only GRIm score was found to be prognostic in multivariate analysis. As these results, we argue that GRIm score alone is prognostic in HCC as in other tumours and there is no need to add additional parameters. In our study, we evaluated the prognostic efficacy of the GRIm score, which was used in Phase-1 studies to identify immune hot tumours suitable for immunotherapy, and its relationship with etiology. In conclusion, we believe that tumour microenvironment studies should be performed to help clinicians in the selection of patients suitable for immunotherapy in HCC. As we solve the microenvironment of the tumour, we can find an answer to the question of which treatment is effective in which patient.

SAT-519

The impact of tumor budding on tumor biology in patients with hepatocellular carcinoma

Osman Fırat Duran¹, Hale Gokcan², Saba Kiremitçi³, Nermin Aras³, Sevinc Tugce Karayel², Volkan Yılmaz², Aslı Çiftçi⁴, Emin Bodakçı⁵, Mesut Gumussoy⁵, Zeynep Melekoğlu Ellik⁶, Abdullah Mübin Özercan⁷, Serkan Duman⁸, Berna Savaş³, Ramazan İdilman². ¹Department of Internal Medicine, Ankara University School of Medicine, Ankara, Turkey; ²Department of Gastroenterology, Ankara University School of Medicine, Ankara, Turkey; ³Department of Pathology, Ankara University School of Medicine, Ankara, Turkey; ⁴Department of Biostatistics, Ankara University School of Medicine, Ankara, Turkey; ⁵Clinic of Gastroenterology, Gaziantep City Hospital, Gaziantep, Turkey; ⁶Clinic of Gastroenterology, Karaman Training and Research Hospital, Karaman, Turkey; ⁷Department of Gastroenterology, Fırat University School of Medicine, Elazığ, Turkey; ⁸Clinic of Gastroenterology, Toros State Hospital, Mersin, Turkey
Email: o.firatuduran@gmail.com

Background and aims: Tumor budding (TB) has recently been evaluated as a histomorphologic indicator of aggressive tumor behavior and is emerging as a valuable prognostic feature in various gastrointestinal carcinomas. However, data regarding tumor budding in hepatocellular carcinoma (HCC) are limited. The aims of the present study were to investigate TB and its effect on tumor biology of HCC.

Method: We conducted a retrospective analysis of 17 years of data from 151 resected or explanted liver tissue samples from HCC patients. TB was counted at 20x magnification, and the "hot-spot" region at the invasive edge of the tumor was selected at 10x magnification. TB has been evaluated according to the International

POSTER PRESENTATIONS

Tumor Budding Consensus Conference (ITBCC) method and classified into Grade 1 (0–4 buds), Grade 2 (5–9 buds), and Grade 3 (≥ 10 buds). **Results:** Among the 151 patients, 107 (70.9%) were male, with a mean age of 69.4 ± 9.5 years. Cirrhosis was present in most patients (58.3%), and hepatitis B virus infection was the main etiology (55.6%). The median AFP level was 8.5 (0.8–123892). In histopathological examination, 23.1% of tumors were well differentiated, 76.9% of tumors were moderately to poorly differentiated. TB was observed in 70% of the patients with HCC. According to TB classification, 43.9% were classified into Grade 1 (0–4 buds), 16.2% Grade 2 (5–9 buds) and 39.9% Grade 3 (≥ 10 buds). No significant difference was found between TB groups and survival ($p = 0.129$). Microvascular invasion was seen in 40.9%, 37.5% 35.6% of patients with 1–4 TB, 5–9 TB, and greater than 10 TB ($p = 0.09$). There was only 16.3% microvascular invasion in the group without tumor budding. Of note, six out of seven poorly differentiated HCC patients exhibited grade 3 tumor budding. The percentage of well-differentiated tumors was higher in patients without TB (33.3%) and 1–4 tumor buds (31.8%) compared to those with 5–9 tumor buds (16.7%) and > 10 tumor buds (16.9%) ($p = 0.07$). **Conclusion:** This preliminary study indicates that tumor budding seems to be correlated with tumor biology.

SAT-521

Impact of centre type on treatment and survival outcomes in hepatocellular carcinoma (HCC)

John Creamer¹, Katy Lillie¹, Molly Bradbury¹, Emma Owen², Gio McGinty³, Gautham Appanna¹, James Orr¹. ¹University Hospitals Bristol and Weston NHS Foundation Trust, Bristol, United Kingdom; ²Somerset NHS Foundation Trust, Taunton, United Kingdom; ³North Bristol NHS Foundation Trust, Bristol, United Kingdom
Email: john.creamer@nhs.net

Background and aims: Centre size and annual hepatocellular carcinoma (HCC) caseload impacted treatment and survival in a French review of HCC patients¹. To our knowledge this has not been investigated in the UK. We aimed to investigate if type of hospital (level 2 liver centre vs district general hospital (DGH)) affected HCC outcomes in the Severn HPB MDT in terms of i) time to MDT discussion and commencing treatment, ii) referral for curative treatment and iii) 12-month survival.

Method: ICD-10 codes (C22.0, C22.9) were used to identify HCC patients discussed at MDT between 1.1.2020–31.12.2022. Data was collected by five reviewers. Differences between groups were assessed using the Chi-squared test for categorical variables and the Mann-Whitney U test for non-parametric data. All analysis was performed on R (ver 4).

Results: 107 patients were included in analysis; 36 presenting at a DGH (3 hospitals) and 71 at a level 2 liver centre (2 hospitals). Median time to MDT discussion from first imaging suggestive of HCC was 25 days and median time from first imaging to treatment was 112 days. Overall 12-month survival was 68% (73/107). Patients diagnosed at a DGH had a trend towards longer time to first MDT discussion (median 28.5 days (IQR 13–57) vs. 21 days (IQR 10.5–37), $p = 0.068$) and longer time from initial imaging to starting treatment (median 137 days (IQR 81.5–203.5) vs. 102 days (IQR 67.3–153.8), $p = 0.117$). A higher proportion of DGH patients also required further tests following first MDT discussion before a treatment decision could be made (33% vs 18%, $p = 0.0135$). There was no significant difference between DGH and level 2 centres for proportion of patients referred for curative treatment (51% vs 48% respectively, $p = 0.94$) or 1 year survival (72% vs 66%, $p = 0.68$).

Conclusion: Although there was a trend towards longer time to MDT discussion and commencing treatment for patients diagnosed at a DGH vs a level 2 liver centre, centre type did not appear to significantly influence treatment or survival outcomes. A small sample size, well-established regional MDT and relatively small distance between hospitals may have contributed to these findings.

Further research may help determine the true influence of centre type on HCC outcomes, addressing known inequalities in HCC outcomes across the UK².

References

1. Goutte N, Sogni P, Bendersky N, Barbare JC, Falissard B, Farges O. Geographical variations in incidence, management and survival of hepatocellular carcinoma in a Western country. *J Hepatol*. 2017;66:537–44.
2. Burton A, Balachandrakumar V, Driver R *et al*. Regional variations in hepatocellular carcinoma incidence, routes to diagnosis, treatment and survival in England. *British Journal of Cancer* 2021; 126:804–814.

SAT-522

Comparison of magnetic resonance imaging (MRI) characteristics of hepatocellular carcinoma (HCC) based underlying liver disease

Hyungjin Rhee¹, Jae Hyon Park², Myeong-Jin Kim¹, Mi Suk Park¹, Jin-Young Choi¹, Yong Eun Chung¹, Young Nyun Park¹. ¹Yonsei University College of Medicine, Seoul, Korea, Rep. of South; ²Armed Forces Daejeon Hospital, Daejeon, Korea, Rep. of South
Email: hjinrhee@yuhs.ac

Background and aims: Although hepatocellular carcinoma (HCC) can occur in the background of various liver diseases, however, the difference of MRI findings according to the underlying liver disease is not well known.

Method: This retrospective study included HCC patients who underwent resection between January 2014 and December 2019. MRI findings and clinic-pathologic findings of HCCs were compared based on the underlying liver disease including hepatitis-B viral (HBV) infection, cirrhosis, and steatohepatitis. Comparison was also performed for HCCs from patients at high risk for HCC according to LI-RADS version 2018.

Results: Out of 465 HCCs in 465 patients, 212 (44%) had cirrhosis, 360 (75%) had hepatitis-B infection, 23 (5%) had hepatitis-C infection and 35 (7%) had steatohepatitis. 399 (83%) patients were at high risk for HCC, wherein 360 (75%) had hepatitis B-infection. Out of 82 (17%) patients not at high risk for HCC, 12 (15%), and 17 (21%) had hepatitis C-infection and steatohepatitis, respectively. The rate of exhibiting major features was not significantly different according to the hepatitis-B infection, cirrhosis, and HCC high-risk. HBV-related HCC and HCC in patients at high risk were commonly associated with smaller size ($p < 0.001$). The non-HBV related HCC and HCC in patients not at high risk were commonly associated with Nodule-in-nodule, mosaic architecture, blood products-in-mass, fat-in-mass, hepatobiliary phase (HBP) hyperintensity, and fatty liver ($P_s < 0.05$). Steatohepatitis was associated with fatty liver, fat sparing in mass, and fat-in-mass ($P_s < 0.05$).

Conclusion: Underlying liver disease is not associated with major features of HCC. In patients not at high risk for HCC, ancillary findings such as nodule-in-nodule, mosaic architecture, HBP hyperintensity, fat-in-mass were more common and these findings may be helpful in image-diagnosis of HCC in patients not at high risk for HCC.

SAT-523

Intrahepatic cholangiocarcinoma: characteristics and outcomes of patients with or without underlying liver disease

Giulia Tesini^{1,2}, Valentina Zanusso^{1,2}, Angelo Pirozzi^{1,2}, Elena Valenzi^{1,2}, Rita Balsano^{1,2}, Tiziana Pressiani¹, Silvia Bozzarelli¹, Lorenza Rimassa^{1,2}. ¹IRCCS Humanitas Research Hospital, Humanitas Cancer Center, Rozzano, Milan, Italy; ²Humanitas University, Department of Biomedical Sciences, Pieve Emanuele, Milan, Italy
Email: giulia.tesini@humanitas.it

Background and aims: Cirrhosis, chronic hepatitis B and C, and metabolic dysfunction-associated steatotic liver disease (MASLD) are risk factors for intrahepatic cholangiocarcinoma (iCCA). We aimed to describe disease characteristics and outcomes of patients (pts) with iCCA with or without underlying liver disease (ULD).

Method: We included consecutive pts from a prospectively maintained dataset diagnosed with iCCA between 2011 and 2023 treated at a single tertiary center. Descriptive statistics were used for pts demographics, tumor and treatment characteristics. Median overall survival (mOS) was calculated from diagnosis with the Kaplan-Meier method. A log-rank test at a two-sided significance level of 0.05 was used to determine the association between ULD and survival.

Results: 248 pts were included, 85 (34%) with ULD; in particular, 17 had liver cirrhosis (LC) and 68 chronic liver disease (CLD). The most common etiology of ULD was MASLD (35 pts, 44%), followed by hepatitis B (17 pts, 22%) and C (12 pts, 15%). 55 pts (65%) with ULD were male vs 76 without (47%, $p = 0.01$). Median age at diagnosis was 65 years (IQR 59–71) and 64 (IQR 56–70, $p = 0.113$) among pts with and without ULD, respectively. 213 pts had molecular testing, 73 (34%) with ULD. Tests were performed either through single-gene analysis (74, 35%) or Next-Generation Sequencing (139, 65%). 42 pts (58%) with ULD had molecular alterations vs 95 pts without (68%, $p = 0.180$). Considering druggable alterations, IDH1 mutation was detected in 10 pts (14%) with ULD vs 23 without (16%, $p = 0.747$), FGFR2 rearrangement in 6 (8%) vs 18 (13%, $p = 0.431$), while FGFR2 mutation in 4 (5%) vs 6 (4%, $p = 0.739$). 48 pts (56%) with ULD had surgery at diagnosis (vs 70, 43%; $p = 0.065$), while more pts without had stage IV disease at diagnosis [104 pts (64%) vs 39 (46%), $p = 0.01$]. 70 pts (82%) with and 135 (83%, $p = 0.97$) without ULD had metastatic disease at some point in their clinical history, but only 47 (67%) and 120 (90%) started first-line systemic therapy (1LT), respectively ($p < 0.001$). Among them, 5 pts (11%) with ULD and 16 pts (13%) without interrupted 1LT due to clinical deterioration ($p = 0.887$). After progression to 1LT, 21 pts (45%) with and 65 (54%) without ULD began second-line therapy ($p = 0.352$). mOS was 25 months (mos) (95% CI, 16–36) vs 24 mos (95% CI, 20–29; $p = 0.85$) among pts with and without ULD, respectively. In the subgroup analysis, pts with LC had a mOS of 18 mos (95% CI 8–NR; HR 1.53; 95% CI, 0.79–2.96, $p = 0.211$), while pts with CLD had a mOS of 26 mos (95% CI, 17–41; HR 1.04; 95% CI, 0.72–1.52, $p = 0.819$).

Conclusion: Pts with iCCA and ULD were primarily male and had stage IV disease at diagnosis less frequently. However, they were less likely to receive 1LT when metastatic disease was found. Although no statistically significant survival differences were observed, there was a trend toward poorer OS among pts with LC. By contrast, pts with CLD had comparable outcomes to those without ULD.

SAT-524

Risk of hepatocellular carcinoma and death among cirrhotics who carry genetic variants of epidermal growth factor, Adiponutrin and 17 β -Hydroxysteroid Dehydrogenase-13: a long-term cohort study

Carla De Benedittis¹, Francesca Caldarone², Maia Lepore², Angelo Strada², Michela Burlone¹, Cristina Rigamonti^{1,2}, Carlo Smirne^{1,2}, Matteo Nazzareno Barbaglia³, Rosalba Minisini², Mario Pirisi^{1,2}. ¹Division of Internal Medicine, AOU Maggiore della Carità, Novara, Italy; ²Department of Translational Medicine, Università del Piemonte Orientale, Novara, Italy; ³Department of Translational Medicine, Università del Piemonte Orientale, 28100, Italy
Email: carla.debenedittis89@gmail.com

Background and aims: Single nucleotide polymorphisms (SNPs) of genes coding for epidermal growth factor (EGF; rs4444903), adiponutrin (PNPLA3; rs738409), and 17 β -hydroxysteroid dehydrogenase-13 (HSD17B13; s72613567) are among the genetic factors thought to be involved in hepatocarcinogenesis. Whether carriage of these SNPs still modulates the risk of developing hepatocellular carcinoma (HCC) and/or survival of patients after they had progressed to cirrhosis is unknown.

Method: A retrospective cohort of 303 adults (183 males, median age 62 years) with any stage of all-cause liver cirrhosis was studied at a single center. All were initially free of HCC and underwent HCC surveillance. Follow-up data were censored at the last follow-up visit.

Each patient was genotyped for rs738409, rs72613567, and rs4444903. The results of genotyping were included as predictor variables in two multivariate models.

Results: Etiologies, not mutually exclusive, were as follows: HCV, 150 (50%); HBV, 25 (8%); alcoholic liver disease, 118 (39%); metabolic dysfunction associated steatotic liver disease, 24 (8%); other, 21 (7%). The distribution for Child-Pugh Class at baseline was as follows: Class A, 228/303 (75%), Class B 64/303 (21%), Class C 11/303 (4%). The median observation time from the diagnosis of cirrhosis was 9.9 years (min 1 year, max 26 years, 2793 person-years). At the end of follow-up, 83/303 patients (27%) had developed HCC (incidence rate 0.032 per year), 160/303 (53%) patients had died and 11/303 (4%) had been transplanted. In a Cox proportional hazards model, with age at diagnosis, history of alcohol use, body mass index, diabetes, Child-Pugh class at baseline, HBV positivity, HCV positivity, as well as rs738409, rs72613567 and rs4444903 genotypes as predictor variables, the factors independently associated with development of HCC were: age (HR 1.04, 95% CI = 1.01–1.06, $p < 0.001$), alcohol (HR 1.74, 95% CI = 1.06–2.84, $p = 0.026$) and HCV (HR 1.95, 95% CI = 1.09–3.05, $p = 0.023$). No statistically significant association was found between the development of HCC and the presence of the allelic variants described above. Instead, in a model having the same predictor variables as above, the factors independently associated with death or transplant were age (HR = 1.07, 95% CI = 1.05–1.09, $p < 0.001$), alcohol (HR = 1.63, 95% CI = 1.15–2.31, $p = 0.006$), Child-Pugh class (HR = 1.95, 95% CI = 1.45–2.60, $p < 0.001$), HBV (HR = 0.48, 95% CI 0.24–0.95, $p = 0.038$) and rs72613567 (HR = 0.76, 95% CI = 0.58–0.98, $p = 0.042$).

Conclusion: Among cirrhotics initially free of HCC followed for nearly 10 years, none of the three SNPs appeared to modulate the risk of developing HCC, suggesting that their postulated hepatocarcinogenic effect is exerted earlier in the natural history of chronic liver disease. Carriage of the rs72613567:TA allelic variant appears to exert a mild protective effect on transplant-free survival of cirrhotics.

SAT-525

Revolutionizing post-surgical outcome predictions: non-invasive tests and AI for hepatocellular carcinoma patients

Iuliana Nenu¹, Ioana Topor², Ioana Cheres³, Mihai Topor⁴, Adrian Groza³, Rares Craciun⁵, Horia Ștefănescu⁵, Gabriela Adriana Filip⁶, Al Hajjar Nadim⁷, Zeno Sparchez⁷, Bogdan Procopet⁷. ¹Regional Institute of Gastroenterology and Hepatology, University of Medicine and Pharmacy “Iuliu Hatieganu,” Cluj-Napoca, Romania; ²University of Medicine and Pharmacy “Iuliu Hatieganu,” Cluj-Napoca, Cluj-Napoca, Romania; ³Artificial Intelligence (Intelligent Systems Group), Department of Computer Science, Technical University of Cluj-Napoca, Cluj-Napoca, Romania; ⁴ULBS, Industrial Business Management, Cluj-Napoca, Romania; ⁵Regional Institute of Gastroenterology and Hepatology “Prof. Dr. O. Fodor,” Cluj-Napoca, Cluj-Napoca, Romania; ⁶“Iuliu Hatieganu” University of Medicine and Pharmacy, Physiology Department, Cluj-Napoca, Romania; ⁷Regional Institute of Gastroenterology and Hepatology “Prof. Dr. O. Fodor,” Cluj-Napoca, “Iuliu Hatieganu” University of Medicine and Pharmacy, Cluj-Napoca, Romania
Email: iuliana.nenu@gmail.com

Background and aims: Hepatic resection is crucial for hepatocellular carcinoma (HCC) treatment, but precise patient selection based on factors like tumor size and portal hypertension is vital for accurate prognosis. This study aimed to assess serum liver tests' effectiveness in identifying clinically significant portal hypertension (CSPH) and predicting post-hepatectomy liver failure (PHLF), comparing them with liver stiffness measurement (LSM). A machine learning approach was also evaluated to develop and validate a mathematical model for PHLF.

Method: A cohort comprising 128 patients with compensated cirrhosis and hepatocellular carcinoma (HCC), who underwent hepatic resection at the Regional Institute of Gastroenterology and

POSTER PRESENTATIONS

Hepatology Cluj-Napoca between 2016 and 2023 was included in the study. Clinically significant portal hypertension (CSPH) was defined as either a hepatic venous pressure gradient (HVPG) of ≥ 10 mmHg or the presence of esophageal varices, splenomegaly, and thrombocytopenia ($<100,000/\text{mm}^3$). Non-invasive serum tests were employed: APRI, FIB-4, NLR, eLIFT, and ALBI. The performance of these non-invasive tests in predicting CSPH and prognosis was evaluated using the area under the receiver operating characteristic (AUROC) curves. Logistic Regression, a machine learning algorithm, established a mathematical model for predicting decompensation.

Results: In the cohort under consideration (mean age: 65 ± 7 years; etiological distribution: 32% alcohol, 43% viral hepatitis C, 20% viral hepatitis B, and 5% other etiologies), 45% exhibited CSPH. Notably, APRI, FIB4, and eLIFT demonstrated commendable predictive capacity for CSPH (AUROC = 0.87, 95% CI: 0.79–0.95; $p < 0.05$; AUROC = 0.88, 95% CI: 0.81–0.96; $p < 0.05$; and AUROC = 0.83, 95% CI: 0.73–0.92; $p < 0.05$, respectively). However, it is noteworthy that liver stiffness measurement (LSM) exhibited superior performance in predicting CSPH (AUROC = 0.913, 95% CI: 0.84–0.98; $p < 0.05$). LSM, APRI, and FIB-4 exhibited a discernible trend in predicting PHLF. Using AI algorithms, we have determined the following equation for probability of PHLF: $\text{probability} = 1 / (1 + e^{(-1 * (-3.4220 + 1.7835 * \text{ACLF_Grade} + 0.0796 * \text{Hospitalisation_days} + -0.5725 * \text{Number_of_Organ_Failures} + -0.3648 * \text{Vent} + 2.6405 * \text{bili}))})$ with an LR accuracy of 0.937.

Conclusion: While liver stiffness measurement (LSM), APRI, FIB-4, and eLIFT demonstrate the capability to identify patients with clinically significant portal hypertension (CSPH) among those with hepatocellular carcinoma (HCC) undergoing hepatic resection, it is noteworthy that they lack the predictive capacity for prognosis in this clinical context. The essence of identifying patients susceptible to postoperative decompensation may be found in the elaboration of mathematical models employing artificial intelligence algorithms.

SAT-526

Predicting non-responsive hepatocellular carcinoma to atezolizumab-bevacizumab therapy: a clinical and imaging-based scoring system

Jaeseung Shin¹, Jae Hyon Park², Hyungjin Rhee³. ¹Sungkyunkwan University School of Medicine, Seoul, Korea, Rep. of South; ²Armed Forces Daejeon Hospital, Daejeon, Korea, Rep. of South; ³Yonsei University College of Medicine, Seoul, Korea, Rep. of South
Email: hjinrhee@yuhs.ac

Background and aims: To develop a model score based on clinical and radiologic markers to predict first response progressive disease (PD) to atezolizumab plus bevacizumab (Atezo-Bev) therapy in advanced hepatocellular carcinoma (HCC) patients.

Method: 140 consecutive HCC patients who received Atezo-Bev therapy between January 2020 and May 2022 at two tertiary care centers were retrospectively enrolled. RECIST version 1.1 was used to assess liver dynamic computed tomography or magnetic resonance imaging, and the first response PD was defined as PD after the 1st cycle of Atezo-Bev therapy. Imaging findings were independently reviewed by two radiologists, and a consensus was reached. Logistic regression analysis was performed to develop a model score for predicting the first response PD.

Results: The first response evaluation of Atezo-Bev therapy was conducted at a median of 56 days (interquartile range, 42–64 days) after treatment initiation. 40% (56/140) of HCC patients showed progression upon the first response evaluation. The model score for predicting first response PD was defined as follows: (age ≥ 60 years; -1 point) + (serum AFP level ≥ 300 ng/ml; 3 points) + (NLR ≥ 2.8 ; 1 point) + (infiltrative appearance; 2 points). At score of 2 or higher, the model score showed sensitivity of 91.1% (95% confidence interval [CI], 83.6–98.5%) and a specificity of 53.6% (95% CI, 42.9–64.2%). At a score of 5 or higher, the model score demonstrated a sensitivity of 55.4% (95% CI, 42.3–68.4%) and a specificity of 91.7% (95% CI, 85.8–97.6%).

Conclusion: A model score combining both clinical and radiologic factors was developed to predict the non-responsiveness to Atezo-Bev therapy in advanced HCC.

SAT-528

Spleen stiffness measurement accurately predicts clinically significant portal hypertension in patients with hepatocellular carcinoma

Razvan Rababoc¹, Simu Razvan-Ioan², Simona Ioanutescu³, Cristian Mugur Grasu⁴, Mircea Istrate¹, Letitia Toma⁵, Laura Iliescu⁶. ¹Fundeni Clinical Institute, Carol Davila University of Medicine and Pharmacy, Bucharest, Romania; ²Fundeni Clinical Institute, "Carol Davila" University of Medicine and Pharmacy, Soseaua Fundeni, Romania; ³Fundeni Clinical Institute, "Carol Davila" University of Medicine and Pharmacy, Bucharest, Romania; ⁴Fundeni Clinical Institute, "Carol Davila" University of Medicine and Pharmacy, Bucharest, Romania; ⁵Fundeni Clinical Institute, Carol Davila University of Medicine and Pharmacy, Bucharest, Romania; ⁶Fundeni Clinical Institute, University of medicine and pharmacy carol davila, Bucharest, Romania
Email: razvan.rababoc@rez.umfcd.ro

Background and aims: Numerous studies have demonstrated the correlation between elevated spleen stiffness values (measured by transient elastography) and the presence of clinically significant portal hypertension (CSPH). Accurate and non-invasive methods for CSPH are essential for timely intervention and improved patient outcome. In hepatocellular carcinoma (HCC) patients, CSPH may translate into decreased access to therapeutic interventions, such as transarterial chemoembolization. Also, liver stiffness measurement in these patients has a low accuracy due to the non-homogenous aspect of the liver. The current study aims to evaluate the diagnostic performance of this novel module for detecting CSPH in a cohort of patients with hepatocellular carcinoma.

Method: We performed an observational clinical trial including patients with hepatocellular carcinoma and compensated liver disease. Spleen stiffness measurement (SSM) was performed during abdominal ultrasonography, using a dedicated software, with a 100 Hz probe. Portal venous pressure was assessed by hepatic venous pressure gradient (HVPG) and a value of over 10 mmHg was considered CSPH.

Results: Our study included 43 patients (58% male; age 54 years [42–67]). Aetiology of HCC was: 46% viral hepatitis B, 17% viral hepatitis C, 37% metabolic syndrome associated steatotic liver disease (MASLD). Mean HVPG in the study lot was 12.5 ± 6.2 mmHg, with 34 patients (79%) with criteria for CSPH. Mean SSM was 32.7 ± 11.3 Kpa. Optimal spleen stiffness cut-off to detect probable CSPH was >25 KPa (likelihood ratio: 5.3, sensitivity: 86%; specificity: 76%, positive predictive value 86.5%, negative predictive value 97.4%). The best performance of SSM was recorded in patient with viral liver disease, compared to patients with MASLD (sensitivity 92% versus 84%, specificity 81% versus 69%, positive predictive value 88.4% versus 81.5%, negative predictive value 98.5% versus 95.2%).

Conclusion: Our findings support the utility of SSM for diagnosing CSPH in patients with HCC. The addition of SSM to the Baveno VII criteria increases accuracy in detecting CSPH and can provide a useful tool in risk stratification for HCC patients.

SAT-529

Comparative performance of GAAD and ASAP scores for predicting hepatocellular carcinoma in MASLD and other etiologies

Chongkonrat Maneenil¹, Pimsiri Sripongpun², Naichaya Chamroonkul², Piraya Tantisaranon², Maseetoh Samaeng², Roongrueng Jarumanokul², Lalita Fonghoi², Amornkan Numit², Suraphon Assawasuwannakit², Teerha Piratvisuth², Apichat Kaewdech². ¹Prince of Songkla University, Hatyai; ²Prince of Songkla University, Hatyai, Thailand
Email: apichatka@hotmail.com

Background and Aims: The increasing incidence of hepatocellular carcinoma (HCC) associated with metabolic associated steatohepatitis liver disease (MASLD) calls for improved surveillance methods. The standard recommendation of ultrasound surveillance faces limitations in this population. Serum biomarkers, incorporating age and gender, including the GAAD and ASAP scores, have recently been proposed for HCC surveillance. However, there is limited data on their comparative performance in detecting HCC within this demographic. Our study aims to assess and compare the effectiveness of these two scores in detecting HCC among patients with MASLD and other etiologies.

Methods: We prospectively collected blood samples from treatment-naïve HCC patients and non-HCC chronic liver disease (CLD) patients at a gastroenterology outpatient clinic from April 20, 2023, to December 31, 2023. The ASAP and GAAD scores were calculated using AFP and PIVKA-II assays from Abbott and Roche, respectively, with cutoffs set at 0.5256 for ASAP and 2.57 for GAAD. Diagnoses of HCC and MASLD were confirmed following EASL or AASLD guidelines.

Results: The study comprised 651 patients, of whom 31 were diagnosed with MASLD-HCC. The area under the receiver operating characteristic curve (AUROC) for predicting HCC was 0.9352 for the ASAP score and 0.9167 for the GAAD score ($p = 0.264$). The AUROC for predicting HCC in patients with other etiologies was 0.923 for ASAP and 0.9315 for GAAD ($p = 0.2254$). Comparing the MASLD-HCC group with those having other causes of HCC, there was no statistically significant difference in the predictive ability of both the GAAD and ASAP scores (p values of 0.6527 and 0.6822, respectively). The GAAD score's sensitivity and specificity for detecting MASLD-HCC were 80.6% and 84.4%, respectively. In contrast, the ASAP score exhibited higher sensitivity at 91.4% but lower specificity at 60%. Conversely, for other causes of HCC, both scores had higher sensitivity and specificity; the GAAD score's sensitivity was 83% with a specificity of 90.1%, while the ASAP score's sensitivity was 88.1% with a specificity of 84.1%.

Conclusion: The GAAD and ASAP scores both display considerable potential for the surveillance of HCC across a range of etiologies. While the ASAP score offers higher sensitivity, its specificity is notably lower, especially in the context of MASLD-associated HCC. Conversely, the GAAD score provides a more balanced sensitivity and specificity profile, suggesting its utility as a surveillance tool in a heterogeneous patient cohort. Future research should aim to refine these biomarkers to improve the early detection of HCC, particularly within the MASLD population where traditional surveillance methods show limitations.

SAT-530

Definite characterization of well-differentiated hepatocellular lesions on biopsy: a 20-year retrospective institutional analysis in the United States of diagnostic challenging cases with long term follow-up

Swachi Jain^{1,1}, Ruihe Lin², Zahra Alipour¹, Kristen Stashek¹, Rashmi Tondon¹. ¹Hospital of the University of Pennsylvania, Philadelphia, United States; ²Hospital of University of Pennsylvania, Philadelphia, United States
Email: jainswachi@gmail.com

Background and aims: Definite characterization of hepatocellular lesions can be challenging, especially in core needle biopsies with atypical or overlapping morphological features. A diagnosis of well-differentiated hepatocellular lesion (WDHCL) is rendered in such cases with a broad differential diagnosis (D/d). However, a definite diagnosis can avoid the need for unnecessary biopsies and appropriate management.

Method: A 20-year retrospective review (1/1/03–6/30/23) of liver biopsies identified 42 patients with atypical/well-differentiated hepatocellular neoplasms/lesions. 19 cases in which one diagnosis was favored were excluded. 23 patients with a broad D/d were included, of which 14 had slides available for review. 3 GI/liver

pathologists independently reviewed and classified lesions in 3 categories: Category 1: morphology alone; Category 2: morphology, reticulin stain and provided clinical history; Category 3: morphology, reticulin stain, additional requested clinical history and IHC. Individual results were compared, and diagnostic consensus was achieved if at least 2/3 pathologists agreed. The medical chart was reviewed for follow-up results.

Results: Of 14 cases, characterization into benign or malignant categories was possible in 3 cases (21.4%) in category 1; additional 2 cases in category 2 (5 cases, 35.7%), and a total of 10 cases (71.4%) could be characterized in category 3. Interestingly, one biopsy did not represent lesional tissue. A consensus diagnosis of WDHCL was rendered in 8 cases (57.1%, category 1), of which a definite diagnosis could be given in 6 cases (Category 3), with a diagnostic yield of 75% using additional history, reticulin and IHC. The final diagnosis was correlated with the patient's long-term follow-up data (3 months to 15 years; Table 1). Two patients with a D/d of hepatic adenoma vs. WD-HCC on final diagnosis were found to have WD-HCC on subsequent resections. Two patients with scant atypical tissue could not be further characterized. IHC was useful in 7 of 11 cases. Beta-catenin, glutamine synthetase and reticulin were the most helpful stains, especially in distinguishing lesional tissue from background liver and FNH.

Conclusion: Overall, a definite characterization of WDHCL was provided in 57.1% of patients (8/14), with likely clinical management implications. Inadequate sample size was a major limiting factor in definite characterization (14.3% in our study). Judicious use of IHC should be considered in diagnostic challenging cases and may prevent the need for a subsequent biopsy.

Liver tumours – Experimental and pathophysiology

TOP-507-YI

Single-cell RNA sequencing-derived gene signatures reveal distinct response mechanisms to atezolizumab + bevacizumab in advanced hepatocellular carcinoma

Sarah Cappuyns¹, Marta Piqué-Gili², Roger Esteban-Fabro³, Gino Philips^{4,5}, Roser Pinyol², Albert Gris-Oliver², Vincent Vandecaveye^{6,7}, Jordi Abril-Fornaguera², Carla Montironi², Laia Bassaganyas⁸, Judit Peix², Marcus Zeithoefler⁹, Agavni Mesropian², Júlia Huguet-Pradell¹⁰, Philipp Haber¹⁰, Raphael Mohr¹¹, Tim Meyer¹², Helen Louise Reeves¹³, Julien Edeline¹⁴, Fabian Finkelmeier¹⁵, Jörg Trojan¹⁶, Peter R. Galle¹⁷, Friedrich Foerster¹⁷, Beatriz Minguez¹⁸, Robert Montal¹⁹, Mathias Heikenwälder²⁰, Chris Verslype^{21,22}, Eric Van Cutsem^{22,23}, Diether Lambrechts^{4,5}, Augusto Villanueva⁹, Jeroen Dekervel^{22,23}, Josep Llovet^{2,9,24}. ¹University Hospitals Leuven, Digestive Oncology, Department of Gastroenterology, Leuven, Belgium; ²Institut d'Investigacions Biomèdiques August Pi i Sunyer (IDIBAPS), Hospital Clínic, Universitat de Barcelona, Liver Cancer Translational Research Laboratory, Barcelona, Spain; ³Institut d'Investigacions Biomèdiques August Pi i Sunyer (IDIBAPS), Hospital Clínic, Universitat de Barcelona, Liver Cancer Translational Research Laboratory, Barcelona, Spain; ⁴KU Leuven, Laboratory for Translational Genetics, Department of Human Genetics, Leuven, Belgium; ⁵VIB Centre for Cancer Biology, Leuven, Belgium; ⁶University Hospitals Leuven, Radiology Department, Leuven, Belgium; ⁷KU Leuven, Laboratory of Translational MRI, Department of Imaging and Pathology, Leuven, Belgium; ⁸Univ. Montpellier, CNRS, INSERM, Institut de Génomique Fonctionnelle, Montpellier, France; ⁹Icahn School of Medicine at Mount Sinai, Mount Sinai Liver Cancer Program (Divisions of Liver Diseases, Department of Hematology/Oncology, Department of Medicine), Tisch Cancer Institute, New York, United States; ¹⁰Charité-Universitätsmedizin Berlin, Department of

POSTER PRESENTATIONS

Surgery, Campus Charité Mitte and Campus Virchow-Klinikum, Berlin, Germany; ¹¹Charité-Universitätsmedizin Berlin, Campus Virchow Klinikum (CVK) and Campus Charité Mitte (CCM), Department of Hepatology and Gastroenterology, Berlin, Germany; ¹²UCL Cancer Institute, University College London, Royal Free Hospital, Research Department of Oncology, London, United Kingdom; ¹³Newcastle upon Tyne NHS Foundation Trust, Freeman Hospital, Newcastle University Translational and Clinical Research Institute and Newcastle University Centre for Cancer; Medical School, Hepatopancreatobiliary Multidisciplinary Team, Newcastle upon Tyne, United Kingdom; ¹⁴Centre Eugène Marquis, Department of Medical Oncology, Rennes, France; ¹⁵University Hospital Frankfurt, Goethe University, Department of Internal Medicine 1 and University Cancer Center, Frankfurt am Main, Germany; ¹⁶University Hospital Frankfurt, Goethe University, Department of Internal Medicine 1 and University Cancer Center, Frankfurt am Main, Germany; ¹⁷University Medical Center of the Johannes-Gutenberg University, Department of Medicine I, Mainz, Germany; ¹⁸Hospital Universitari Vall d'Hebron, Vall d'Hebron Barcelona Hospital Campus, Liver Unit, Barcelona, Spain; ¹⁹Hospital Universitari Arnau de Vilanova, IRBLleida, University of Lleida (UdL), Department of Medical Oncology, Cancer Biomarkers Research Group, Lleida, Spain; ²⁰German Cancer Research Center (DKFZ), Division of Chronic Inflammation and Cancer, Heidelberg, Germany; ²¹University Hospitals Leuven, Digestive Oncology, Department of Gastroenterology, Leuven, Belgium; ²²KU Leuven, Laboratory of Clinical Digestive Oncology, Department of Oncology, Leuven, Belgium; ²³University Hospitals Leuven, Digestive Oncology, Department of Gastroenterology, Leuven, Belgium; ²⁴Institució Catalana de Recerca i Estudis Avançats (ICREA), Barcelona, Spain
Email: sarahcappuyns@hotmail.com

Background and aims: The combination of atezolizumab and bevacizumab (atezo+bev) is the current standard of care for advanced hepatocellular carcinoma (aHCC), providing median overall survival (OS) of 19.2 months. Here, we aimed to leverage the single cell resolution offered by single-cell RNA sequencing (scRNAseq) technologies to uncover the underlying cellular processes driving clinical benefit versus resistance to atezo+bev.

Method: We used scRNAseq data from 31 aHCC tumour biopsies (91,169 single cells) to derive gene signatures recapitulating 21 distinct cell phenotypes. To explore their potential as predictive biomarkers of response to atezo+bev, single-cell derived gene signatures were applied to RNA sequencing datasets comprising $n = 422$ aHCC patients treated with atezo+bev versus atezolizumab ($n = 47$) or sorafenib ($n = 58$) as comparators. Signatures associated with response or resistance to atezo+bev were identified by class prediction and gene set enrichment analysis. Putative biomarkers were then correlated with clinical outcome.

Results: We unveiled two distinct patterns of response to atezo+bev. First, an immune-mediated response characterized by the combined presence of two CD8⁺ T effector cell subtypes and pro-inflammatory CXCL10⁺ macrophages, representing an immune-rich microenvironment. Second, a non-immune, angiogenesis-related response distinguishable by a reduced expression of the vascular endothelial growth factor (VEGF) co-receptor neuropilin-1 (NRP1), a biomarker that specifically predicted improved OS with atezo+bev versus sorafenib ($p = 0.039$). Moreover, we found tumoural enrichment of two immunosuppressive myeloid populations, namely CD14⁺ monocytes and TREM2⁺ macrophages, and Notch pathway activation to be associated with primary resistance to atezo+bev.

Based on these biological insights, we defined "Immune-competent" and "Angiogenesis-driven" molecular subgroups, each associated with a significantly longer OS with atezo+bev versus sorafenib (p of interaction = 0.027), and a "Resistant phenotype" associated with significantly worse OS versus all other subtypes.

Conclusion: Our study unveils two distinct molecular subsets of clinical benefit to atezolizumab plus bevacizumab in advanced HCC: "Immune-competent" and "Angiogenesis-driven" and identifies the

main traits of primary resistance. We provide a molecular framework to stratify patients based on predicted clinical outcome and guide potential strategies to overcome resistance.

FRIDAY 07 JUNE

FRI-454

Prediction of TERT promoter mutations using MALDI imaging and artificial intelligence in small hepatocellular nodules in cirrhosis

Helene Cazier¹, Remy Dubois², Aurélie Beaufrère^{3,4}, Samira Laouirem⁴, Sarah Paisley⁴, Benoit Schmauch², Martin Tabath⁴, Miguel Albuquerque³, Valérie Paradis^{3,4}. ¹Centre de recherche sur l'inflammation INSERM 1149, Université Paris Cité, iMAP platform, Clichy, France; ²Owkin France, Paris, France; ³Hôpital Beaujon APHP Pathology Department, Clichy, France; ⁴Centre de recherche sur l'inflammation, INSERM 1149, Université Paris Cité, Clichy, France
Email: helene.cazier@inserm.fr

Background and aims: Liver carcinogenesis follows a multistep process along hepatocellular carcinoma (HCC) developed from malignant transformation of preneoplastic nodules. The differential diagnosis of small hepatocellular nodules in cirrhosis, ranging from regenerative (LRN), dysplastic nodules [low (LGDN) and high grade (HGDN)] and early HCC, remains challenging, especially on biopsy specimen. The presence of *TERT* promoter (*pTERT*) mutations, the most frequent genetic alterations in HCC, may help to identify the hepatocellular nodules already engaged in the malignant process. We aimed to (1) develop an artificial intelligence-based model to predict *pTERT* mutations, and (2) identify tissue biomarkers associated with *pTERT* mutations using MALDI (Matrix Assisted Laser Desorption Ionization) imaging, an approach providing exhaustive spatial peptidic signatures from fixed and paraffin embedded (FFPE) tissue sections.

Method: We built 7 FFPE tissue microarrays (TMAs) composed of 234 hepatocellular nodules <2 cm from cirrhotic samples, divided respectively in a training set of 164 cases [HCC ($n = 53$), HGDN-HCC ($n = 0$), LGDN ($n = 31$), LGDN ($n = 24$), LRN ($n = 24$) and cirrhotic nodules ($n = 32$)] and a validation set of 70 cases [HCC ($n = 25$), HGDN-HCC ($n = 5$), LGDN ($n = 6$), LRN ($n = 9$) and cirrhotic nodules ($n = 10$)]. *pTERT* mutations were identified by digital droplet PCR in 1 FFPE whole block per nodule. MALDI imaging was applied on all TMAs in order to generate mass-spectrometry library of peptides. A L1 -regularized Logistic Regression model (LASSO) was then trained to predict *pTERT* mutation status from spatially pooled tissue cores spectrum. This model was trained in a leave-one-TMA-out schedule repeated three times with varying algorithm seeds, resulting in 12 trained models in total.

Results: ddPCR revealed *pTERT* mutations in 34% of the 234 nodules including 51 and 28 cases in the training and validation sets, respectively. Our AI model showed good to very good performance in predicting *pTERT* mutations (Area under the curve for all 3 test TMAs [AUC] with 95% confidence interval: 0.73 [0.52–0.95]; 0.80 [0.60–1.0]; 0.82 [0.61–1.0]). The model performed particularly well for predicting *pTERT* mutations in HCC nodules ([AUC]: 0.91 [0.71–1.0]). Finally, we identified 15 peptidic peaks correlated with *pTERT* mutations.

Conclusion: We developed and validated an AI-based model for predicting *pTERT* mutations in small hepatocellular nodules arising in cirrhosis using MALDI imaging data. These analyses led to the identification of a peptidic signature predictive of *pTERT* mutations. The further identification of these peaks will allow the development of a panel of markers that could be performed by immunohistochemistry to identify the malignant hepatocellular nodules on biopsy samples.

FRI-455

Liver cancer in ovo models for preclinical testing

Paul Garcia^{1,2,3}, Yan Wang³, Jean Viallet³, Nour-El-Houda Mehdi^{1,2}, Emilie Montaut^{1,2,4}, Thomas Decaens^{1,2,5}, Anouk Emadali^{1,2,4}, Zuzana Macek Jilkova^{1,2,5}. ¹Université Grenoble Alpes (UGA), Grenoble, France; ²Institute for Advanced Biosciences, Research Center UGA/Inserm U 1209/CNRS 5309, La Tronche, France; ³RandD Department, Inovotion, La Tronche, France; ⁴Pôle Recherche, CHU Grenoble Alpes, La Tronche, France; ⁵Service d'Hépatogastroentérologie, Pôle Digidune, CHU Grenoble Alpes, La Tronche, France
Email: zuzana.mjilkova@gmail.com

Background and aims: Today, more than 70% of patients with advanced liver cancer don't respond to first-line treatments. New combination therapeutic strategies are therefore currently under exploration, drastically increasing the need of models for preclinical testing of immunotherapies. Besides the obvious ethical concerns, classical animal models of HCC lack the capacity to reproduce the tumor-immune system interface that is required to test the new immunotherapy approaches. The *in ovo* (in the egg) model is based on the use of the chorioallantoic membrane (CAM) of the chicken embryo, thus bridging the gap between *in vitro* studies and complex animal models, as an advanced model without the need for ethical approval. The *in ovo* immune status gradually develops over time and can be described as biologically similar to humans. The gradual immune development during embryogenesis in the *in ovo* model allows the cancer cells to be grafted at embryonic development day (EDD) 9 with a low risk of xenograft rejection due to its partial immunodeficiency until it becomes fully competent by EDD18. This dichotomy makes the model interesting for immuno-oncology research, as it allows both tumor xenografting and immune infiltration.

Method: We developed several *in ovo* human liver cancer models, based on the tumor grafting of different liver cancer cell lines (HepG2, Hep3B, HuH7, PLC/PRF/5) on the chicken eggs' CAM, and characterized the collagen accumulation, angiogenesis, as well as the tumor immune microenvironment by immunohistochemistry and RNA sequencing. Treatments with atezolizumab (anti-PD-L1, TECENTRIQ®) and bevacizumab (anti-VEGF, MVASI®) were tested.

Results: Our results show the involvement of chicken immune cells in tumor growth, reproducing a classical non-inflamed "cold" as well as inflamed "hot" tumor status, depending on the *in ovo* liver cancer models. The absence of immune response on gene profile in Hep3B *in ovo* was indicative of a cold tumor profile. On the other hand, a "hot" PLC/PRF/5 *in ovo* tumor was characterized by a high presence of T-cells, and RNA-seq data revealed an increased level of immune activity.

The treatment by atezolizumab and bevacizumab was highly efficient in the "hot" tumor model PLC/PRF/5 *in ovo* with the reduction of tumor size by 76% ($p \leq 0.0001$) compared to control, while the efficacy was limited in "cold" tumor Hep3B *in ovo*. The contribution of anti-PD-L1 blockade to the anti-tumor effect in model PLC/PRF/5 *in ovo* was demonstrated by the efficacy of atezolizumab monotherapy.

Conclusion: This study provides complete information, with detailed characterization and rational arguments that could lead to the partial replacement of conventional laboratory animals with a more ethical model, better suited to the current needs of preclinical research of new immunotherapies for liver cancer.

FRI-456

Characterization of the intratumoral immune microenvironment of hepatocellular carcinoma before selective intrahepatic radiation therapy (SIRT) and study of its prognostic value on response to treatment

Maria Stella Franze^{1,2,3}, Paul Vigneron^{2,4,5}, Stefano Caruso^{1,2,6}, Hélène Regnault^{1,5}, Anna Sessa^{1,2,5}, Pascale Maille^{1,2,6}, Yasmine Bouda^{1,2}, Massimo Iavarone⁷, Lorenzo Canova⁷, Marco Maggioni⁸, Eric Nguyen Khac⁹, Ruxandra Sarba⁹,

Thierry Yzet¹⁰, Alexandra Heurgue-berlot¹¹, Reza Kianmanesh¹², Rami Rhaïem^{1,12}, Jean Charles Nault¹³, Michael Soussan¹⁴, Olivier Sutter¹⁵, Manon Allaire¹⁶, Marie Lequoy¹⁷, Mohamed Bouattour¹⁸, Aurélie Beaufrère¹⁹, Marco Dioguardi Burgio²⁰, Brustia Raffaele^{1,2,21}, Daniele Sommacale^{1,2,21}, Alain Luciani^{1,2,22}, Vania Tacher^{1,2,23}, Jean-Michel Pawlotsky^{1,2,24}, Vincent Leroy^{1,2,5}, Julien Calderaro^{1,2,6}, Giuliana Amaddeo^{1,2,5}. ¹Team "Viruses, Hepatology, Cancer," Institut Mondor de Recherche Biomédicale, INSERM U955, Créteil, France; ²Université Paris-Est Créteil, Créteil, France; ³Department of Clinical and Experimental Medicine, Messina, Italy; ⁴Team "Viruses, Hepatology, Cancer," Institut Mondor de Recherche Biomédicale, INSERM Unit U955, Créteil, France; ⁵Department of Hepatology, Henri Mondor University Hospital, Assistance Publique-Hôpitaux de Paris, Créteil, France; ⁶Department of Pathology, Henri Mondor University Hospital, Assistance Publique-Hôpitaux de Paris, Créteil, France; ⁷Department of Gastroenterology and Hepatology, Fondazione IRCCS Cà Granda-Ospedale Maggiore Policlinico, Milano, Italy; ⁸Department of Pathology, Fondazione IRCCS Ca' Granda Ospedale Maggiore Policlinico, Milano, France; ⁹Hepato-Gastroenterology Department, Centre Hospitalier Universitaire Amiens-Picardie Site Sud, Amiens, France; ¹⁰Radiology Unit, Amiens University Hospital, Amiens, France; ¹¹Department of Hepato-Gastroenterology, Robert-Debré University Hospital, Reims, France; ¹²Department of Hepatobiliary, Pancreatic and Digestive Oncological Surgery, Robert Debré University Hospital, Reims Champagne-Ardenne University, Reims, France; ¹³Liver Unit, Avicenne Hospital, Paris-Seine-Saint-Denis University Hospitals, Assistance Publique-Hôpitaux de Paris, Bobigny, France; ¹⁴Department of Nuclear Medicine, Avicenne Hospital, Paris-Seine-Saint-Denis University Hospitals, Assistance Publique-Hôpitaux de Paris, Bobigny, France; ¹⁵Interventional Radiology Department, Avicenne Hospital, Paris-Seine-Saint-Denis University Hospitals, Assistance Publique-Hôpitaux de Paris, Bobigny, France; ¹⁶Hepato-gastroenterology Department, Pitié-Salpêtrière University Hospital, Assistance Publique-Hôpitaux de Paris, Sorbonne University, Paris, France; ¹⁷Department of Hepatology, Saint Antoine Hospital, Assistance Publique-Hôpitaux de Paris, Paris, France; ¹⁸Liver Cancer Unit, Beaujon University Hospital, Assistance Publique-Hôpitaux de Paris, Clichy, France; ¹⁹Department of Pathology, Beaujon University Hospital, Assistance Publique-Hôpitaux de Paris, Clichy, France; ²⁰Department of Radiology, Beaujon University Hospital, Assistance Publique-Hôpitaux de Paris, Clichy, France; ²¹Department of Digestive and Hepatobiliary Surgery, Henri Mondor University Hospital, Assistance Publique-Hôpitaux de Paris, Créteil, France; ²²Department of Medical Imaging, Assistance Publique-Hôpitaux de Paris, Henri Mondor University Hospital, Créteil, France; ²³Department of Nuclear Medicine, Assistance Publique-Hôpitaux de Paris, Henri Mondor University Hospital, Créteil, France; ²⁴Department of Virology, National Reference Center for Viral Hepatitis B, C, and D, Henri Mondor University Hospital, Créteil, France
Email: mariastellafranze@gmail.com

Background and aims: Internal selective radiation therapy (SIRT) is a validated treatment of hepatocellular carcinoma (HCC). The role of local immune response in achievement of response remains elusive. This study was designed to characterize the HCC immunological status before SIRT and its impact on therapeutic response (primary end point) and survival.

Method: One-hundred patients from 8 University Hospitals (7 French, 1 Italian), affected by histologically proven HCC and treated with SIRT, were enrolled in the study. For each patient, clinical/biological/radiological data were collected at the diagnosis of HCC and during follow-up. Patients were defined as "responders" and "not responders" according to radiological tumor response evaluated 3 and 6 months after SIRT with mRECIST criteria. RNA sequencing was analyzed to study genes expression differences in the intra-tumoral microenvironment.

Results: Twenty-seven patients (81.5% male, median age 63 years, 67% with cirrhosis) were analyzable for primary end point. HCC

distribution across BCLC stage was: 4 A (15%), 10 B (37%), 13 C (48%). Nine patients were responders (1 complete/8 partial response), 17 not responders (3 stable/14 progressive disease). Median overall survival (OS) of patients was 15.9 months. According to RNA sequencing analysis, unsupervised hierarchical clustering identified two clusters (10 C1, 17 C2) of patients (of which most of responders in C2, $p = ns$) with different genes expressions. Clusters were different for cirrhosis ($p = 0.008$), albumin ($p = 0.028$) and AFP levels ($p = 0.015$), histological differentiation ($p = 0.003$) and subtype of HCC ($p = 0.03$), time of OS (C1: 10.6 months; C2: 18.0 months; $p = 0.047$). A supervised analysis for differentially expressed genes showed 480 genes down- and 1121 over-expressed in C1 vs C2. Gene set enrichment analysis with Molecular Signatures Database performed with a hypergeometric test showed that C1 was associated with genes involved in immune responses while C2 with genes involved in proliferation/differentiation liver cells. By Microenvironment Cell Populations counter method, we identified an abundance of immune infiltrates (monocytes, myeloid dendritic cells, cytotoxic lymphocytes, T and B cells) in C1 vs C2. Cox-univariate analysis showed only a higher risk of death for patients not responders at 3 months ($p = 0.004$).

Conclusion: These results suggest that presence of a pro-inflammatory intratumoral immune infiltrate appears predictive of a worse OS with a trend of bad response to SIRT in HCC patients. Our hypothesis is that SIRT, in analogy with external radiotherapy, can trigger the release of pro-inflammatory mediators and increase tumour-infiltrating immune cells. This phenomenon, often described in literature as turning immunologically 'cold' tumours to 'hot', may enhance the efficacy of combined with immunotherapy.

FRI-457

CXCL12 restricts hepatocellular carcinoma progression by shaping the tumor microenvironment in liver fibrosis

Marlene Kohlhepp¹, Julia Onstein², Jana Hundertmark¹, Thomas Ritz³, Alma Diaz Ruiz de Zarate¹, Tobias Puengel¹, Adrien Guillot¹, Frank Tacke¹. ¹Department of Hepatology and Gastroenterology, Charité University Medicine Berlin, Berlin, Germany; ²University Hospital Aachen, Department of Medicine III, Aachen, Germany; ³Institute of Pathology, University Hospital Heidelberg, Heidelberg, Germany
Email: marlene.kohlhepp@charite.de

Background and aims: The chemokine (C-X-C motif) ligand 12 (CXCL12) has been implicated in promoting both progression of fibrosis and primary liver tumour growth, by signaling through its two cognate receptors, C-X-C motif receptor 4 (CXCR4) and atypical chemokine receptor 3 (ACKR3, or CXCR7). In addition, CXCL12 regulates immune cell egress from the bone marrow and their recruitment to the tumour, which is considered to shape a pro-tumourigenic tumour microenvironment. This study aims at exploring the therapeutic potential of CXCL12 inhibition for the prevention and treatment of liver fibrosis and primary liver cancer.

Method: A CXCL12 inhibitor was used in two experimental mouse models of liver fibrosis induced either by repetitive carbon tetrachloride (CCl₄) injections or by feeding a high fat methionine-choline deficient (MCD) diet. To investigate the role of CXCL12 in primary liver cancer in mice, the CXCL12 inhibitor was applied in diethylnitrosamine (DEN)-induced liver cancer combined with either CCl₄ to create a fibrotic environment, or with a high-fat, high-sugar, and high-cholesterol Western diet (WD) to induce metabolic dysfunction-associated steatotic liver disease (MASLD). Immune cells were analyzed by flow cytometry and multiplex immunostaining. Serum chemokines were analyzed with a 12-plex LUNARIS™ biochip.

Results: CXCL12 inhibition had no impact on liver fibrosis (collagen deposition, Sirius Red, hepatic hydroxyproline content) but led to increased tumour burden in both the fibrosis- and MASLD-associated liver cancer model (tumour numbers, liver to body weight ratio). CXCL12 inhibition increased chemokine levels in blood plasma, which was accompanied by an increase of peripheral blood myeloid

cells. In the liver, CXCL12 inhibition provoked changes in hepatic monocyte-derived macrophage (MoMF) populations characterised by a decrease of CD11c⁺MHC-II⁺ MoMF and a relative increase of Ly6C⁺ MoMF. In addition, CXCL12 inhibition specifically reduced eosinophils and B cells in the liver of CCl₄-treated, but not in MASLD livers. Intriguingly, CXCL12 inhibition promoted tumour growth, despite reducing tumour infiltrating MoMF and increasing cytotoxic CD8⁺ T cells in tumour lesions. Moreover, inhibition of CXCL12 activated vascular remodeling in tumour microvessels, evident by an upregulation of CXCR4 on tumour endothelial cells and increased expression of both angiogenic (i.e., Ang2) and anti-angiogenic (Ang1, Thbs1) genes in tumour tissues.

Conclusion: This study demonstrates pro-tumourigenic effects of CXCL12 inhibition in liver cancer and suggests a pivotal role for CXCL12 in tumour control mechanisms. CXCL12 restricts liver cancer progression by a multi-faceted modulation of the tumour microenvironment.

FRI-458

Low-density neutrophils display transcriptome profiles similar to the polymorphonuclear myeloid-derived suppressor cells and predict survival and recurrence in hepatocellular carcinoma patients

Chien-Hao Huang¹, Cheng-Heng Wu², Po-Ting Lin², Tsung-Han Wu², Wei Teng², Yi-Chung Hsieh², Rachel Wen-Juei Jeng^{2,3}, Wei-Ting Chen⁴, Kun-Ming Chan⁵, Shi-Ming Lin², I-Shyan Sheen⁴, Chun-yen Lin⁶. ¹Division of Hepatology, Department of Gastroenterology and Hepatology, Chang-Gung Memorial Hospital, Linkou Medical Center, Taoyuan, Taiwan, College of Medicine, Chang-Gung University, Taoyuan, Taiwan, TaoYuan, Taiwan; ²Chang-Gung Memorial Hospital, Linkou Medical Center, TaoYuan, Taiwan; ³Chang Gung University, College of Medicine, Taoyuan, Taiwan; ⁴Chang-Gung Memorial Hospital, Linkou Medical Center, TaoYuan, Taiwan; ⁵Chang-Gung Memorial Hospital, Linkou Medical Center, TaoYuan, Taiwan; ⁶Division of Hepatology, Department of Gastroenterology and Hepatology, Chang-Gung Memorial Hospital, Linkou Medical Center, Taoyuan, Taiwan, College of Medicine, Chang-Gung University, Taoyuan, Taiwan, TaoYuan, Taiwan
Email: huangchianhou@gmail.com

Background and aims: Hepatocellular carcinoma (HCC) ranks as the sixth most prevalent global cancer, with a sobering third position in cancer-related mortality according to Globocan 2020 data. Current curative treatments are applicable to less than 30% of patients, highlighting the need for novel therapeutic approaches. Immune checkpoint inhibitor (ICI) immunotherapy, despite achieving response rates of 15–30%, has not reached optimal efficacy. Low-density neutrophils (LDNs), a subset implicated in cancer progression and metastasis, present an intriguing avenue for HCC research and novel treatment strategies.

Method: Peripheral blood was collected from both normal controls and HCC patients spanning TNM stages I to IV, with Child-Pugh class A to early B status. Isolation of LDNs from peripheral blood mononuclear cells and tumor tissue was performed using flow cytometric methods. Subsequent analyses involved the examination of clinical data, LDN percentages, and RNA sequencing (RNA-seq) to gain comprehensive insights.

Results: A total of 29 normal controls and 298 HCC patients were included in the study. LDN percentages were observed to be elevated in the peripheral blood mononuclear cells (PBMC) of HCC patients compared to controls, with further accumulation in tumor tissues. LDNs exhibited increased reactive oxygen species (ROS) levels and demonstrated dose-dependent suppression of CD8⁺ and CD4⁺ T cells ex-vivo. Clinically, the LDN percentages in PBMC correlated with advanced TNM staging and served as predictors for 1-year survival, along with neutrophil-to-lymphocyte ratio (NLR) and derived NLR. However, only LDN independently predict 1-year survival by multivariate logistic regression analysis among the three

neutrophil-related scores. Importantly, LDNs were exclusive predictors of HCC recurrence within one year post-curative treatment, in addition to TNM stage. RNA-seq revealed that LDN in patients with HCC shared gene profiles with polymorphonuclear myeloid-derived suppressor cells (PMN-MDSC) and displayed high glycolysis and oxidative phosphorylation potential.

Conclusion: This study highlights LDNs as valuable prognostic predictors for survival and HCC recurrence post-curative treatment in HCC patients. RNA-seq demonstrates their resemblance to PMN-MDSC and high glycolysis and oxidative phosphorylation potential.

FRI-459

Outcome of targeting ATR in high replication stress murine HCC

Jing Fang¹, Qiyuan He², Long Pan², Joana Gonçalves Araujo², Romain Donne³, Céline Pophillat², Christelle Kabore², Amaia Lujambio³, Jessica Zucman-Rossi⁴, Jean-Pierre Couty⁴, Severine Morizur⁴, Chantal Desdouets⁴. ¹Centre de Recherche des Cordeliers, Sorbonne Université, INSERM, Université de Paris, Paris, France; ²INSERM, Université de Paris, Paris, France; ³Icahn School of Medicine at Mount Sinai, New York, United States; ⁴INSERM, Centre de Recherche des Cordeliers, Paris, France
Email: jing.fang@inserm.fr

Background and aims: Hepatocellular carcinoma (HCC) belongs to the five most common malignancies in adult. Much effort is devoted to establishing efficient systemic treatments through many clinical trials. In recent years, targeting DNA Damage Response components has become attractive therapeutics target for cancer therapy. In the present study, we investigate whether targeting DNA Damage Response and more specifically ATR, could offer therapeutic opportunities for High Replication Stress HCC.

Method: Cohort of HCC patients was selected on TCGA dataset (N = 307) and LICA-FR (N = 222) and categorized into two groups related to high and low replication stress (RS) signatures. Pre-clinical HCC murine models were used (Non-germline mosaic GEMMs). Liver-specific deletion of ATR (ATR^{Dhep} or ROSA26^{Δhep} (control)) was carried out by AAV8-CRISPR/Cas9 approach. Cell proliferation, apoptosis were investigated through cellular and molecular analyses. Immune cells were profiled with flow cytometry and immunostaining. Whole transcriptome sequencing (RNA-Seq) was conducted to investigate the impact of targeting ATR in High Replication Stress murine HCC.

Results: Kaplan-Meier analyses of TCGA and LICA-FR databases revealed that HCC patients with a high RS signature had worse overall survival and disease-specific survival compared to HCC patients with a low RS signature. In GEMMs mice models (n = 11), scRNAseq data were used to identify two HCC models: a High Replication Stress (HRS-HCC: MYC, sg-p53) and a Low Replication Stress (LRS-HCC: MYC, sg-Pten). Interestingly, silencing of ATR as no impact on tumoral incidence in LRS-HCC group. By contrast we observed, that in HRS-HCC, deletion of ATR impacts on: (1) tumor incidence 4 weeks after HDI (100%/ROSA26^{Dhep}; 37.5%/ATR^{Dhep}); (2) tumor size (11.71 mm/ROSA26^{Dhep}; 5.57 mm ATR^{Dhep}, p = 0.0105) as well as tumor number/mice (5.12/ROSA26^{Dhep}; 1.42/ATR^{Dhep}); (3) median survival (55 days in ATR^{Dhep} versus 43 days in ROSA26^{Dhep}). We also showed that hepatocyte proliferation was reduced in ATR^{Dhep} compared to ROSA26^{Dhep} in paraneoplastic liver tissues. Furthermore, in ATR^{Dhep} tumoral tissue, apoptosis was more pronounced (cleaved-Caspase-3/cleaved-Caspase-9). To go deeper, bulk RNA-sequencing analysis was performed on tumor tissues. We observed that silencing of ATR enriched specific anti-tumor immune response pathways: "IFN-γ production," "Positive regulation of cell activation," "Response to IFN-γ," "T cell activation." These data were validated by flow cytometry with significantly more CD4⁺ iNKT cells; IFN-γ⁺ iNKT cells and fewer Treg cells in liver tumor tissues in ATR^{Dhep} tumors.

Conclusion: Silencing of ATR in a high RS murine HCC model can delay tumor development via bolstered anti-tumor immune

response. Further works will define whether targeting ATR could be a potentially effective strategy for human HRS-HCC treatment.

FRI-462-YI

Aminoacyl-tRNA synthetases characterization and clinical potential in aggressive hepatocellular carcinoma

Natalia Hermán-Sánchez^{1,2,3,4}, Javier M. Zamora-Olaya^{1,5,6}, Manuel Rodríguez-Perálvarez^{1,5,6}, Raul M Luque^{1,2,3,4}, Juan L. López-Cánovas^{1,2,3,4}, Manuel D. Gahete^{1,2,3,4}. ¹Maimónides Institute of Biomedical Research of Córdoba (IMIBIC), Córdoba, Spain; ²Department of Cell Biology, Physiology and Immunology, University of Córdoba, Córdoba, Spain; ³Reina Sofía University Hospital (HURS), Córdoba, Spain; ⁴CIBER Pathophysiology of Obesity and Nutrition (CIBERObn), Córdoba, Spain; ⁵Department of Hepatology and Liver Transplantation, Reina Sofía University Hospital, Córdoba, Spain; ⁶CIBER Hepatic and Digestive Diseases (CIBERehd), Córdoba, Spain
Email: nataliahermansan@gmail.com

Background and aims: Hepatocellular carcinoma (HCC) genetic and transcriptomic signatures have been widely described. However, its proteomic characterization, which might increase the knowledge of potentially targetable alterations, is scarce. To provide novel insights in this field, we performed non-targeted quantitative proteomics of HCC samples from different aetiologies.

Method: Non-targeted quantitative proteomics were performed on cytosolic and nuclear fractions of hepatic samples (n = 42; HCC vs. non-tumour adjacent tissue). The alteration of the dysregulated proteins was confirmed in 7 *in silico* HCC cohorts. Functional parameters (proliferation, migration, colonies/tumorspheres) were evaluated on HCC-derived cell lines (Hep3B, SNU-387) after silencing/overexpressing VARS1 alone or simultaneously with MAGI1. VARS1-overexpressing Hep3B cells were subcutaneously injected in athymic mice for an Extreme Limiting Dilution Assay (ELDA). Quantitative proteomics were performed on Hep3B and SNU-387 cell lines following VARS1 overexpression.

Results: Non-targeted proteomics revealed the dysregulation of the cytosolic (n = 507 proteins) and nuclear (n = 925 proteins) proteomes in HCC. This proteomic profile discriminated two tumoral subgroups, one of them associated to aggressiveness and to a profound dysregulation of the aminoacyl-tRNA synthetases (ARSs), which catalyse tRNA aminoacylation. Their dysregulation was corroborated in other *in silico* HCC cohorts and associated to clinical features. Indeed, Gene Set Enrichment Analysis (GSEA) confirmed that patients with a general upregulation of the ARSs machinery have genomic (i.e. TP53 mutations) and transcriptomic characteristics of the proliferative HCC. The valine tRNA-aminoacyl synthetase, VARS1, was selected to study the functional and molecular consequences of ARSs dysregulation. VARS1 modulation had a reduced effect on proliferation/migration although it significantly altered the dedifferentiation capacity of the cells and the expression of mesenchymal and stemness-related markers. Untargeted quantitative proteomics on Hep3B and SNU-387 cells overexpressing VARS1 demonstrated a decreased expression of the scaffold protein MAGI-1, a known tumour suppressor in HCC, associated with the overexpression of VARS1. Thus, VARS1 might be exerting its role through the modulation of MAGI-1-mediated cell junctions.

Conclusion: Quantitative proteomics defines two HCC subgroups. The dysregulation of the ARSs machinery is a marker of the most aggressive one, with a potential usefulness as prognostic marker. One of the most dysregulated ARSs, VARS1, promotes aggressiveness, and could therefore be targetable, through the modulation of MAGI1. Fundings: ISCIII (PI20/01301, PI23/00652; co-funded by the European Union), MINECO (FPU20/03957), JdA (PEMP-0036-2020, BIO-0139), FSEEN and CIBERObn/ehd.

FRI-463-YI

Identifying unique cell states in early liver oncogenesis with transcription coupled repair

Elizabeth Carmichael¹, Edward Jarman¹, Luke Boulter¹, Martin Taylor¹.
¹University of Edinburgh, Edinburgh, United Kingdom
 Email: e.carmichael-4@sms.ed.ac.uk

Background and aims: Hepatocellular carcinoma (HCC) is the most common type of primary liver cancer, yet what the early requirements are for a mutant cell to become a cancer remains poorly defined. We utilize the established diethylnitrosamine (DEN) induced mouse model to study HCC formation. Many hepatocytes acquire cancer-driving mutations as a result of DEN treatment, however only a small number of tumors will form per liver. We hypothesize that certain damaged hepatocytes enter cell states that promote them towards tumor formation preferentially over their neighbors. Here we identify the transcriptional states that are permissive to oncogenic transformation.

Method: Transcription coupled repair (TCR) can repair DEN induced DNA damage, and decrease the mutational burden. TCR will only decrease the mutational burden of genes that are transcribed after DEN exposure. As a result, sequenced tumors show low mutation rates in genes active post-DEN treatment, and the inverse for inactive genes. By studying patterns in mutation rates across DEN induced tumors, we can infer gene sets we believe to be up or down regulated after DEN treatment-specifically in damaged hepatocytes that have gone on to form tumors. We also preform single nuclei RNA sequencing (snRNA-seq) of DEN treated liver tissue collected shortly post DEN treatment. Pairing these techniques, we isolate sub populations of hepatocytes we predict to be permissive to HCC formation.

Results: Gene-sets associated with cell adhesion, cell motility, and cell migration appeared to have higher mutational burdens than expected given their levels of transcription in undamaged hepatocytes. These genes also appeared as significantly differentially expressed post DEN treatment compared to the undamaged control (adjusted p value <0, 01). Single nuclear RNA-seq and hierarchical clustering revealed unique expression profiles to the damaged hepatocytes, including differential expression of genes associated with cell motility and adhesion again.

Conclusion: Many gene sets, including those related to cell adhesion, migration, and motility, are been predicted to be down-regulated in response to DEN treatment, due to their high mutational burden in sequenced tumors. RNA sequencing methods identified these genes sets as being unique to post DEN damage hepatocytes, and the down-regulation of these genes sets in response to DEN treatment was directly observed using both single nuclei and bulk RNA sequencing. These findings validate the TCR technique as a robust proxy for identifying gene expression profiles associated with the likely cell type/profile of origin for HCC.

FRI-464

Caspases compromise SLU7 and UPF1 stability and nonsense-mediated RNA decay activity during hepatocarcinogenesis

Carla Rojo¹, María Gárate-Rascón¹, Miriam Recalde¹, Áne Alava¹, María Elizalde¹, María Azkona¹, Elisabet Guruceaga¹, Amaya Lopez-Pascual¹, Maria U. Latasa¹, Bruno Sangro^{2,3,4}, Maite G. Fernandez-Barrena^{1,3,4}, Matías A. Avila^{1,3,4}, María Arechederra^{1,3,4}, Carmen Berasain^{1,3}. ¹CIMA, CCUN, University of Navarra, Pamplona, Spain; ²Clínica Universidad de Navarra, CCUN, Pamplona, Spain; ³CIBERehd, Instituto de Salud Carlos III, Madrid, Spain; ⁴Instituto de Investigación Sanitaria de Navarra (IdiSNA), Pamplona, Spain
 Email: cberasain@unav.es

Background and aims: Cellular transcriptome homeostasis depends on transcription and splicing. Moreover, the fidelity of gene expression, essential to preserve cellular identity and function is secured by different quality control mechanisms including nonsense-

mediated RNA decay (NMD). Our previous findings demonstrated that the expression of the splicing factor SLU7 is reduced in hepatocellular carcinoma (HCC) and the damaged liver, contributing to hepatocellular de-differentiation and genome instability, associated to transcription and splicing changes. Here demonstrate that SLU7 plays a role in NMD which is inhibited in the damaged liver and in HCC. Importantly, we also decipher the mechanism by which SLU7 is downregulated during the progression of liver disease.

Method: We used several human extra-hepatic cancer and HCC cell lines, as well as mouse primary hepatocytes, SLU7 specific siRNAs, apoptosis activators, the antioxidant N-acetylcysteine and the pan-caspase inhibitor zVAD-fmk. Animal models: administration of Fas agonistic antibody Jo2 or acetaminophen (APAP), and Mdr2-/- mice. RNA-seq analysis at the transcript level by Kallisto and SLEUTH, qPCR, Western blot, and immunoprecipitation/mass spectrometry assays. Chemiluminescence-based NMD reporter assay to measure NMD activity. LIHC-TCGA RNA-seq data. Statistical analyses with GraphPad Prism 8.0.1.

Results: TCGA database analysis demonstrate the accumulation in HCC of NMD-target transcripts suggesting the inhibition of NMD activity. RNA-seq analysis in PLC/PRF/5 cells, as well as PCR and qPCR validation in different cancer cell lines revealed that SLU7 depletion induces a significant accumulation of NMD-targets and intron retention isoforms, in parallel to the upregulation of NMD factors, all events associated with NMD inhibition. Moreover, we demonstrate that SLU7 interacts with and stabilizes the NMD core effector UPF1, and that SLU7 is required for a correct NMD activity. Importantly, we found that in two animal models of acute liver injury (Jo2 and APAP) and during the process of hepatocarcinogenesis in Mdr2-/- mice, NMD is inhibited, resulting in the accumulation of different NMD targets, in parallel to the downregulation of UPF1 and SLU7 proteins. Remarkably, we provide in vitro and in vivo evidence showing that caspases activation would be responsible of the cleavage and degradation of SLU7 observed during the process of hepatocarcinogenesis in animal models and patients.

Conclusion: Here we identify the downregulation of UPF1 and the inhibition of NMD as a new molecular pathway contributing to the malignant reshaping of liver transcriptome. Moreover, and importantly, we uncover caspases activation as the mechanism responsible for the downregulation of SLU7 expression during liver disease progression, representing a new link between apoptosis and hepatocarcinogenesis.

FRI-465

The fetal insulin receptor isoform stimulates liver carcinogenesis through non-cell autonomous mechanisms

Fanny Leandre¹, Akila Hamimi², Cécile Godart¹, Isabelle Lagoutte³, Anthony Caldiero², Sandra Pinto², Alexandre Alves², Sabine Colnot², Angélique Gougelet², Christèle Desbois-Mouthon¹. ¹INSERM UMRS1138, Paris, France; ²Centre de Recherche des Cordeliers-INSERM UMRS 1138, Paris, France; ³Institut Cochin-INSERM U1016, Paris, France
 Email: christele.desbois-mouthon@inserm.fr

Background and aims: The insulin receptor (IR) plays a crucial role in the liver by regulating metabolism and proliferation. In the adult liver, these functions are relayed by IRB upon insulin binding. IRA, the fetal isoform, has been reported to be expressed during the progression of hepatocellular carcinoma (HCC). IR isoforms result from the alternative splicing of exon 11 in *Insr* pre-mRNA. Recently, studies detected IRA in murine and human livers with hepatitis or cirrhosis which are risk factors for HCC. These data raise the question of the role of IRA in the pathogenesis of HCC. Therefore, the goal of our study is to investigate the role of IRA on liver homeostasis and carcinogenesis *in vivo*.

Method: An *in vivo* CRISPR strategy using hepatotropic AAV8 expressing saCas9 nuclease and small guide RNAs was developed to delete exon 11 (IRB specific) in *Insr* gene and substitute IRB for IRA in adult mouse hepatocytes. This strategy was conducted in wild-type

mice and in mice with beta-catenin activation in the liver due to hepato-specific APC loss (APC^{ΔHep}) or β-catenin mutation (BCAT^{ΔEx3}). APC^{ΔHep} and BCAT^{ΔEx3} mouse models develop differentiated HCC and undifferentiated hepatoblastoma-like tumors. *Insr* gene editing was evaluated by PCR. Glucose homeostasis was assessed with glucose and insulin tolerance tests. Tumor development was followed by ultrasonography.

Results: Short-term expression of IRA (2 months) in healthy hepatocytes did not induce disturbances in liver homeostasis, but its long-term expression resulted in the appearance of spontaneous tumors (2/8 mice) that were not edited at *Insr*. In APC^{ΔHep} and BCAT^{ΔEx3} models, hepatocyte expression of IRA induced a significant increase in tumor initiation and multiplicity. A higher proportion of differentiated tumors was observed in IRA/APC^{ΔHep} mice compared to APC^{ΔHep} mice (85% vs 44%, *p* < 0.0001). Again, the vast majority of the tumors were not edited at *Insr*, indicating that IRA-expressing hepatocytes were counter-selected during the carcinogenic process. At an early step of carcinogenesis (50 days), livers from Apc^{ΔHep} mice with IRA expression showed increased proliferation of β-catenin-activated hepatocytes together with hallmarks of inflammation (TNFα) and apoptosis. *In vitro*, IRA-expressing hepatocytes displayed increased sensitivity to pro-apoptotic TNFα treatment.

Conclusion: IRA promotes hepatocarcinogenesis through non-cell autonomous mechanisms by modifying liver environment as IRA-expressing hepatocytes do not engage in transformation. Our data suggest a scenario of cell competition in which IRA hepatocytes are eliminated by apoptosis, leaving space for proliferation of preneoplastic APC^{ΔHep}/IRB cells. Therefore, IR-A could be considered as a risk factor for HCC.

FRI-466-YI

Implications and therapeutic potential of neddylation for pediatric liver cancer: hepatoblastoma

Leidy Estefanía Zapata-Pavas¹, Marina Serrano-Maciá¹, Miguel Angel Merlos Rodrigo², Patricia Peña-Sanfelix¹, Claudia Gil-Pitarch¹, Naroa Goikoetxea-Usandizaga^{1,3}, Hana Michalkova², Zbynek Heger², Alvaro del Río-Álvarez⁴, Laura Royo⁴, Claudia M. Rejano-Gordillo¹, Jon Ander Barrenechea-Barrenechea¹, Maria Mercado-Gómez¹, Sofia Lachiondo-Ortega¹, Teresa C. Delgado¹, Dimitris Xirodimas⁵, Jose J. G. Marin^{3,6}, Maite G. Fernandez-Barrena^{3,7}, Matías A. Avila^{3,7}, Carolina Armengol⁴, María Luz Martínez-Chantar^{1,3}. ¹Center for Cooperative Research in Biosciences (CIC bioGUNE), Basque Research and Technology Alliance (BRTA), Liver Disease Lab, Derio, Spain; ²Mendel University in Brno, Department of Chemistry and Biochemistry, Brno, Czech Republic; ³Carlos III National Health Institute, Centro de Investigación Biomédica en Red de Enfermedades Hepáticas y Digestivas (CIBERehd), Madrid, Spain; ⁴Germans Trias i Pujol Research Institute (IGTP), Program for Predictive and Personalized Medicine of Cancer (PMPPC), Childhood Liver Oncology Group, Badalona, Spain; ⁵Univ. Montpellier, CRBM, CNRS, Montpellier, France; ⁶University of Salamanca, IBSAL, Experimental Hepatology and Drug Targeting (HEVEFARM), Salamanca, Spain; ⁷CIMA, University of Navarra, Hepatology Program, Pamplona, Spain
Email: mlmartinez@cicbiogune.es

Background and aims: Hepatoblastoma (HB) is a rare type of primary liver cancer that mainly affects children. Currently, the main treatment options include surgical resection accompanied by chemotherapeutics such as cisplatin or doxorubicin. However, these options are limited or ineffective due to poor prognosis, high recurrence rate and significant side effects. This is a tumor with a low rate of somatic mutations, in which the involvement of other mechanisms modulating its tumorigenic capacity stands out. In this regard, it is crucial to highlight the adaptive advantages conferred to the tumor by post-translational modifications. Neddylation has been extensively studied in this context. Based on this evidence, we have

considered analyzing the impact that neddylation could have on the development of HB.

Method: A cohort of HB patients, preclinical animal model and *in vitro* model in tumor cells were used to characterize NEDDylation pathway in HB. Besides the modulation of NEDP1 levels using an *in vitro* approach was made to study cell proliferation, migration, and metabolic status. *In vivo*, the implications of NEDP1 overexpression as tumor suppressor was evaluated.

Results: Transcriptomic analysis in samples from patients with HB has demonstrated an increase in the neddylation cycle. Likewise, in preclinical models of HB, both *in vivo* and *in vitro*, we have identified an increase in NEDD8 and NAE1 (the NEDD8-activating enzyme E1), which is related to an increase in global neddylation. A significant reduction in the levels and activity of NEDP1 deneddylases has also been observed, which justifies the importance of this process in the development and progression of this pathology. In addition, a positive impact on proliferation driven by neddylation is evidenced. The use of pharmacological inhibitors of neddylation has been shown to decrease such proliferation, while the increase in global neddylation induced by NEDP1 inhibition has resulted in its increase. Moreover, modulation of neddylation through increased levels of NEDP1, *in vitro* and *in vivo* approaches, reveals induction of apoptosis, modulation of migratory and proliferative capacity and metabolic reprogramming, both in HB cell lines (HepT1 and HepG2) and in patient-derived xenografts (PDX) from distal metastasis. *In vivo*, *in Ovo* and *ex Ovo* experiments showed a reduction of tumorigenicity and metastatic phenotype; mice models of HB showed, at the histological level, a reduction of proliferation and tumorigenesis, as well as an increase of necrosis, and a reorganization of the proteome, with an increase of apoptotic processes.

Conclusion: The effect observed with NEDP1 overexpression points to the importance of post translational modifications in pathologies such as HB and highlights the relevance of NEDDylation, not only in the molecular characterization of HB, but also in the development of new specific treatments.

FRI-467

Efficacy of WNTinib, a novel selective therapeutic for CTNNB1 mutant tumors, in preclinical models of hepatoblastoma

Ugne Balaseviciute^{1,2}, Jordi Abril-Fornaguera^{1,2}, Júlia Hugué-Pradell^{1,2}, Alex Rialdi³, Elisa Fernández-Martínez^{1,2}, Albert Gris-Oliver¹, Agavni Mesropian^{1,2}, Gulay Ulukaya^{3,4}, Dan Hasson^{3,4}, Ieva Keraite^{1,2}, Roser Pinyol¹, Swan N. Thung⁵, Ernesto Guccione^{3,4,6}, Josep Llovet^{1,2,7}. ¹Translational Research in Hepatic Oncology, Liver Unit, IDIBAPS, Hospital Clinic, University of Barcelona, Barcelona, Spain; ²Liver Cancer Program, Division of Liver Diseases, Department of Medicine, Tisch Cancer Institute, Icahn School of Medicine at Mount Sinai, New York, United States; ³Department of Oncological Sciences, Icahn School of Medicine at Mount Sinai, New York, United States; ⁴Tisch Cancer Institute Bioinformatics for Next Generation Sequencing (BiNGS) Shared Resource Facility, Icahn School of Medicine at Mount Sinai, New York, United States; ⁵Department of Pathology, Icahn School of Medicine at Mount Sinai, New York, United States; ⁶Center for OncoGenomics and Innovative Therapeutics (COGIT); Center for Therapeutics Discovery, Department of Oncological Sciences and Pharmacological Sciences, Tisch Cancer Institute, Icahn School of Medicine at Mount Sinai, New York, United States; ⁷Institució Catalana de Recerca i Estudis Avançats (ICREA), Barcelona, Spain
Email: ugnebala@gmail.com

Background and aims: Hepatoblastoma (HB), the most frequent pediatric form of liver cancer, is a rare disease with an increasing annual incidence of 1.8 cases per million children and limited therapeutic options (i.e. surgery and chemotherapy). CTNNB1 mutation is the most prevalent alteration and a potential therapeutic target in HB. Here, we aim i) to assess the efficacy of WNTinib -an effective compound blocking Wnt-CTNNB1 activation in

POSTER PRESENTATIONS

hepatocellular carcinoma (HCC)- in HB, and *ii*) to explore mechanisms of resistance to WNTinib in HB.

Method: To assess the efficacy, eight HB patient-derived cell lines were generated and used for testing serial dilutions of WNTinib and cisplatin (Selleckchem, Houston, TX) for IC50 calculations for 3 days. Cell viability was measured using resazurin, with absorbance readings at 560 and 590 nm. Additionally, six subcutaneous patient-derived xenograft (PDX) tumors (n = 5 *CTNNB1* mutant, n = 1 *CTNNB1* wild-type) were implanted in NSG mice and challenged with WNTinib. Animals were treated for 5 days per week with WNTinib (30 mg/kg) until the end of the study and tumor volume was monitored. To investigate WNTinib resistance mechanisms, we performed a kinome-wide CRISPR screen with 3, 052 unique single-guide RNAs targeting 763 human kinase genes using an HB-patient derived cell line and the IC30 dose of WNTinib over the course of 3 weeks.

Results: The calculated WNTinib IC50 values in HB cells were an order of magnitude higher than those in HCC cells (8.99uM vs 0.63uM, respectively). *In vivo*, mean overall survival in the WNTinib arm was longer in 4/5 *CTNNB1* mutant PDX models than in the *CTNNB1* WT model (36.4 vs 14 days, respectively). The CRISPR screen identified as top significantly enriched kinases RPS6KA3, PRKD3 and CAD and as the top significantly depleted DYRK1A, MAPK1, and TESK2, suggesting their potential role in WNTinib's response and resistance mechanisms, respectively. As in HCC, multiple members of the MAPK family were detected as drivers of WNTinib sensitivity. Top significantly depleted kinases such as DYRK1A, PRKCI, and CDK14 are currently being validated as candidate targets for dual treatment options with WNTinib in HB.

Conclusion: We have demonstrated that WNTinib is able to efficiently block tumor progression in HB and identified candidate kinases as potential targets to boost the efficacy of WNTinib activity in HB.

FRI-470

Deciphering the role of FXR in the rewiring of Treg polarization in hepatocellular carcinoma

Yasmeen Attia¹, Rasha Tawfiq¹, Aya Ali², Olfat Hammam³, Mohamed Elmazar¹. ¹Department of Pharmacology, Faculty of Pharmacy, The British University in Egypt, Cairo, Egypt; ²Health Research Center of Excellence, Drug Research and Development Group, Faculty of Pharmacy, The British University in Egypt, Cairo, Egypt; ³Department of Pathology, Theodor Bilharz Research Institute, Giza, Egypt
Email: yasmeen.attia@bue.edu.eg

Background and aims: Once dubbed the immune cell "graveyard", the liver was believed to evade immunosurveillance by promoting T cell dysfunction through T cell disposal/killing. This was later debunked when it became apparent that T cell avidity stems from changes within the tumor microenvironment where regulatory T cells (Tregs) play a pivotal role. Hepatocellular carcinoma (HCC) is often described as immunologically "cold", primarily due to Tregs hijacking the immune response and promoting a tolerogenic milieu with immunosuppressive cytokines such as transforming growth factor (TGF)- β 1 and IL-10. Although the immunomodulatory roles of the farnesoid X receptor (FXR) have been extensively studied in different contexts, its impact on Treg modulation in HCC is not yet addressed. This study, therefore, bridges this gap by exploring how FXR activation, through obeticholic acid (OCA), might affect Treg polarization in an experimental HCC model.

Method: HCC was induced in Swiss albino male mice using diethylnitrosamine (DEN) and carbon tetrachloride (CCl₄). Three-week-old mice received a single i.p. injection of DEN at a dose of 1 mg/kg. After 5 weeks, mice started receiving i.p. injections of 0.2 ml/kg CCl₄ twice per week until the end of the experiment. After 20 weeks from induction, treatment with OCA was initiated at a dose of 10 mg/kg/day, p.o., for 12 weeks. Livers were then harvested for histopathological assessment and alpha-fetoprotein (AFP) immunohistochemical analysis. Other investigations included estimating hepatic levels of the downstream FXR target, cholesterol 7 α -

hydroxylase (CYP7A1) besides TGF- β 1 and IL-10 using ELISA. Additionally, gene expression of forkhead box P3 (Foxp3), a Treg surrogate marker, was measured using qRT-PCR.

Results: OCA demonstrated mitigation in AFP immunoreactivity and HCC histopathological features observed in the DEN+CCl₄ group characterized by enlarged hyperchromatic nuclei and dysplastic alterations. Concurrently, CYP7A1 hepatic levels were decreased in the OCA-treated group, suggesting FXR activation. In the DEN+CCl₄ group, a 5-fold upregulation in hepatic Foxp3 compared to normal mice was observed, hence indicating a potential increase in Treg population. OCA, however, depicted a downregulation in Foxp3 reaching 50% compared to the DEN+CCl₄ group, implying a likely decrease in the Treg pool. In a similar vein, a surge in the levels of the immunosuppressive cytokines, TGF- β 1 and IL-10, paralleled the increase in Foxp3 reaching 10 and 6 folds in the DEN+CCl₄ group compared to normal, whereas OCA treatment reduced their levels by 66% and 90% compared to DEN+CCl₄ group, respectively.

Conclusion: Our findings indicate that FXR activation can likely curb Treg polarization and subsequent immunotolerance in HCC, potentially guiding the development of FXR-targeted therapies to modulate the immune landscape in HCC.

FRI-471

CRISPR metabolic screen identifies UXS1 as a driver of hepatocellular carcinoma progression via regulating hippo signaling pathway

Haoying Ke¹, Zhijie Xu¹, Ruiyang Liu¹, Ji Xiao¹, Fuyuan Xu¹, Fei Xiao¹.
¹The Fifth Affiliated Hospital of Sun Yat-sen University, Zhuhai City, Guangdong Province, China
Email: kehy@mail2.sysu.edu.cn

Background and aims: Metabolic reprogramming is a highlighted hallmark of hepatocellular carcinoma (HCC) and plays an important role in tumorigenesis, progression and drug resistance. However, the mechanisms underlying metabolic reprogramming and how altered metabolism in turn promotes HCC progression remain largely elusive. In this study, we aimed to elucidate the role of UDP-Glucuronate decarboxylase 1 (UXS1) in HCC progression.

Method: A CRISPR knockout screen was used to investigate metabolic genes that contribute to HCC cell proliferation. Colony formation, Incucyte, wound-healing, Transwell migration, and invasion assays, and an animal model were used to examine the role of UXS1 in HCC progression. Immunohistochemical staining was used to evaluate UXS1 expression in HCC tissues and adjacent normal liver tissues. Further, RNA-sequencing (RNA-seq) assays were performed to screen significantly altered metabolic and signaling pathways in HCC cells with UXS1 knockdown.

Results: We identified UXS1, a Golgi enzyme that converts one sugar nucleotide (UDP-glucuronic acid, UDPGA) to another (UDP-xylose), as a key metabolic regulator of HCC cell proliferation using the metabolic CRISPR knockdown screen. UXS1 promotes the proliferation, migration, and invasion of HCC. Clinically, UXS1 is upregulated in HCC and is associated with adverse clinical outcomes in patients with this disease. Mechanistically, UXS1 regulated Hippo signaling pathway and metabolism-related signaling pathways. We found UXS1 knockdown upregulated the phosphorylation levels of Hippo signaling pathway related proteins including LAST1, YAP and TAZ. Conversely, overexpression of UXS1 downregulated their phosphorylation levels. It is indicated that UXS1 up-regulated in HCC promotes tumor progression by inhibiting the Hippo signaling pathway.

Conclusion: Our study suggests that UXS1 has a crucial role in HCC progression by inhibiting the Hippo signaling pathway, providing a potential and therapeutic target for HCC. However, how UXS1 regulates sugar nucleotide metabolism and glycosylation to inhibit Hippo signaling pathway still need further study. We hypothesize that UXS1 has the potential to affect Golgi apparatus function in hepatocellular carcinoma cells, which in turn affects YAP glycosylation levels.

FRI-472-YI

Mitochondrial metabolism is disrupted by ciprofloxacin preventing cholangiocarcinoma cell proliferation

Mikel Ruiz de Gauna¹, Kendall Alfaro-Jiménez¹, Ane Nieva-Zuluaga¹, Maider Apodaka-Biguri¹, Enara Markaide², Laura Izquierdo-Sánchez^{2,3}, Colin Rae⁴, Francisco González-Romero¹, Paul Gomez-Jauregui¹, Natalia Sainz-Ramírez¹, Beatriz Gómez Santos¹, Xabier Buque¹, Igor Aurrekoetxea^{1,5}, Igotz Delgado¹, Idoia Fernández-Puertas¹, Ainhoa Iglesias⁶, Colm O. Rourke⁷, Pedro Miguel Rodrigues^{2,8,9}, Jesper Andersen⁷, Diego Calvisi¹⁰, Jennifer Morton^{4,11}, Chiara Braconi^{4,12,13}, Ana Zubiaga⁶, Jesus Maria Banales^{2,8,9,14}, Patricia Aspichueta^{1,5,8}.

¹University of the Basque Country (UPV/EHU), Faculty of Medicine and Nursing, Department of Physiology, Leioa, Spain; ²Department of Liver and Gastrointestinal Diseases, Biogipuzkoa Health Research Institute, Donostia University Hospital, University of the Basque Country (UPV/EHU), San Sebastián, Spain; ³Carlos III National Institute of Health, Centre for the Study of Liver and Gastrointestinal Diseases (CIBERehd), Madrid, Spain; ⁴School of Cancer Sciences, University of Glasgow, Glasgow, United Kingdom; ⁵Biocruces Health Research Institute, Cruces University Hospital, Barakaldo, Spain; ⁶University of Basque Country (UPV/EHU), Faculty of Science and Technology, Department of Genetic, Physical Anthropology and Animal Physiology, Leioa, Spain; ⁷Department of Health and Medical Sciences, Biotech Research and Innovation Centre (BRIC), University of Copenhagen, Copenhagen, Denmark; ⁸National Institute for the Study of Liver and Gastrointestinal Diseases (CIBERehd, Instituto de Salud Carlos III), Madrid, Spain; ⁹IKERBASQUE, Basque Foundation for Science, Bilbao, Spain; ¹⁰Institute for Pathology, Regensburg University, Regensburg, Germany; ¹¹Cancer Research UK Scotland Institute, Glasgow, United Kingdom; ¹²CRUK Scotland Cancer Centre, Glasgow-Edinburgh, United Kingdom; ¹³Beatson West of Scotland Cancer Centre, Glasgow, United Kingdom; ¹⁴Department of Biochemistry and Genetics, School of Sciences, University of Navarra, Pamplona, Spain
Email: patricia.aspichueta@ehu.es

Background and aims: Metabolic reprogramming is a hallmark of cholangiocarcinoma (CCA), a heterogeneous group of biliary cancers characterized by dismal prognosis. The heightened proliferation of CCA cells has been linked to increased mitochondrial metabolic activity. E2F1 and E2F2, transcription factors regulating cell cycle, also modulate mitochondrial metabolism. Minichromosome maintenance (MCM) proteins, helicases involved in DNA replication and cell cycle, are recognized targets of E2Fs that have been implicated in different cancers. YAP and TAZ, transcriptional coactivators of the Hippo signalling pathway, cooperate with E2Fs to regulate the expression of MCMs. Ciprofloxacin (CPX), a commonly used antibiotic, serves as an inhibitor of MCM helicase activity. Here, we aim to study how targeting the E2F/MCM axis in CCA influences the interplay between cell cycle progression and the associated metabolic adaptation it governs.

Method: CCA was induced in wild type (WT) or *E2f1*^{-/-} mice using the Sleeping Beauty technique, with the overexpression of *Akt1* and *Yap* or *Taz*. Triglyceride (TG) concentration was measured in liver samples from these models, and in cell lines *in vitro*. Cell viability, proliferation, fatty acid oxidation (FAO), and mitochondrial respiration rates were assessed in EGI1 and HUCCT1 human CCA cell lines in the presence or absence of CPX, and an inhibitor of E2F activity (HLM006474). Their impact on the growth of organoids derived from CK19-CreER; KrasG12D^{-/-}; Pten fl/fl CCA mouse model was tested. Data from human CCA tumours from different cohorts (TCGA-CHOL and GSE26566), and levels of these proteins in the proteome of 5 CCA human cell lines and 4 primary cultures of human cholangiocytes were assessed.

Results: Expression of E2F1 and E2F2, as well as MCM2-7, was increased in the two analyzed CCA cohorts. Additionally, a positive correlation was observed between E2Fs and each MCM, which were also upregulated in the proteome of each CCA human cell line and in

the CCA mouse models. Experimental overexpression of *Akt1* and *Yap*, or *Akt1* and *Taz*, in *E2f1*^{-/-} mice resulted in reduced CCA development compared to WT mice. Inhibition of MCM activity with CPX, either alone or in combination with the E2F activity inhibitor HLM006474, induced a dose-dependent decrease in tumour cell and *Kras*/*Pten* CCA mouse organoid viability. CPX also decreased proliferation of human CCA cells *in vitro*. The increased upregulation in FAO previously observed in the most proliferative CCA cells was halted when CCA cells were incubated with CPX and/or HLM006474, significantly decreasing mitochondrial respiration rate and TG accumulation.

Conclusion: Inhibition of MCMs with CPX, either alone or in combination with an E2F inhibitor, reprograms mitochondrial metabolism, leading to a decrease in proliferation and viability of CCA. Combination of MCM and E2F inhibitors arises as a novel potential target in CCA.

FRI-473

The oncogenic m6A demethylase FTO promotes tumorigenesis and immune escape by upregulating GPNMB in hepatocellular carcinoma

Vanilla Xin Zhang^{1,2}, Ao Chen¹, Qingyang Zhang¹, Karen Man-Fong Sze¹, Lu Tian¹, Hongyang Huang¹, Eva Lee¹, Jingyi Lu¹, Xueying Lyu¹, Joyce Man Fong Lee¹, Jack Chun-Ming Wong¹, Daniel Wai-Hung Ho¹, Irene Oi-Lin Ng¹. ¹Department of Pathology and State Key Laboratory of Liver Research, The University of Hong Kong, Hong Kong, Hong Kong; ²The University of Hong Kong, Pathology, Hong Kong, Hong Kong
Email: vanilla6@hku.hk

Background and aims: Hepatocellular carcinoma (HCC) is the 3rd leading cause of cancer-related death worldwide. Immune checkpoint inhibitor (ICI) targeting PD-L1 combined with VEGF is the first-line therapy for advanced HCC. However, the efficiency of Immune checkpoint inhibitor (ICI) is not satisfactory in HCC patients. FTO (Fat mass and obesity-associated protein) is the first identified N6-methyladenosine (m6A) demethylase and has been reported to play an oncogenic or tumor-suppressive role in liver cancer. A better understanding of the functional role and mechanistic basis of FTO in HCC is needed. In this study, we aimed to functionally characterize the roles of m6A demethylase FTO in HCC.

Method: To investigate the tumorigenic functions of FTO, colony formation, proliferation, migration and invasion assays were conducted *in vitro*. Co-culture system of HCC cells and CD8T cells or THP-1 cells was used to examine the activation of effector memory T cells and polarization and recruitment of macrophages upon stable knockdown of FTO (FTO-KD). Multiple xenograft and spontaneous HCC forming mouse models were used to evaluate the effect of FTO on self-renewal, tumor growth, and response to ICI treatment. RNA-sequencing and m6A-sequencing were done to identify the gene targets related to m6A modification by FTO.

Results: FTO expression was up-regulated in patients' HCC tumors, and high FTO expression (2-fold cutoff) was significantly associated with poorer survival rates. Depletion of FTO resulted in reduced pro-oncogenic functions *in vitro*, and suppressed tumor formation, progression, metastasis *in vivo*. Stable FTO-KD significantly increased tumor-infiltrating immune cells and cytotoxic CD8+ T cells in mouse tumor tissues and was accompanied by a significant reduction of PD1 + T cell exhaustion. We also observed a trend of increase in anti-tumoral M1 macrophages in mouse tumors. Consistently, *in vitro* co-culture assays of human HCC cells with T cells isolated from PBMC of healthy human subjects showed that FTO KD increased the proportion of effector memory T cells and enhanced the proliferation of CD8+ T cells. FTO silencing increased the anti-tumoral polarization and migration of M1 macrophages. We identified GPNMB as a novel downstream target of FTO, which reduced the m6A abundance of GPNMB, hence stabilizing it from degradation by YTHDF2. GPNMB was able to inhibit CD8+ T cell activation. Furthermore, targeting FTO by its potential inhibitor CS2 promoted the therapeutic effect of anti-

POSTER PRESENTATIONS

PD1 in a well-established 'cold-tumor' mouse model (Trp53KO/C-MycOE), resulting in significantly smaller tumors and higher tumor-infiltrating CD8T cells in the liver tumor tissues.

Conclusion: We demonstrated that FTO exerts oncogenic function and promotes immune escape in HCC by regulating the m6A demethylation of GPNMB mRNA. Targeting FTO may provide a new therapeutic approach for treating HCC.

FRI-474-YI

Restoring retinoic acid receptor-related orphan receptor alpha reduces intrahepatic cholangiocarcinoma proliferation and modulates cancer-associated fibroblasts

Laura Sererols Viñas¹, Paula Cantalalops Vilà¹, Raquel A. Martínez-García de la Torre¹, Gemma García Vicién¹, Silvia Ariño¹, Carmen Cárcamo Giráldez¹, Joana Ferrer^{2,3}, Alejandro Forner^{3,4}, Loreto Boix^{2,3}, María Reig^{2,3}, Pau Sancho-Bru^{1,3}, Silvia Affo¹. ¹Institut d'investigacions biomèdiques August Pi i Sunyer (IDIBAPS), Barcelona, Spain; ²Barcelona clinic liver cancer (BCLC) group, Liver Unit, Hospital Clínic Barcelona, IDIBAPS, University of Barcelona, Barcelona, Spain; ³Centro de investigación médica en red de Enfermedades hepáticas y digestivas (CIBERehd), Instituto de salud Carlos III, Madrid, Spain; ⁴Barcelona clinic liver cancer (BCLC) group, Liver Unit, Hospital Clínic Barcelona, IDIBAPS, University of Barcelona, Barcelona, Spain
Email: saffo@recerca.clinic.cat

Background and aims: Intrahepatic Cholangiocarcinoma (iCCA) is the second primary liver tumor, with few therapeutic options, late diagnosis, chemotherapy resistance and dismal prognosis. Retinoic acid receptor-related orphan receptor alpha (RORa) is known to be a tumor suppressor in several solid tumors however, its role in iCCA remains unknown. Therefore, with our study we aim at investigating RORa in iCCA, to explore new potential therapies for this deadly tumor.

Method: Human tumoral (n=8) and adjacent non-tumoral (n=8) tissues were obtained after iCCA tumor resection, from the Hospital Clínic, Barcelona. HuCCT1 human iCCA cell line and human primary cancer-associated fibroblasts (CAFs) isolated from iCCA samples (n=3), were treated *in vitro* with RORa agonist SR1078 (5uM). To induce iCCA *in vivo*, 6 weeks old C57BL/6J male mice were injected hydrodynamically through the tail vein with the pCaggs-KRAS^{G12D}, CRISPR/Cas9 sg-p19 and SB13 plasmids (KRAS/p19). 4 weeks after the tumor induction, mice were injected intraperitoneally with vehicle (n=7) or SR1078 (10 mg/kg) (n=9), 3 times per week, for 2 weeks. GraphPad Prism 10 was used for the statistical analysis.

Results: As assessed by qPCR, we detected a reduction in RORa expression in iCCA tumoral (n=8) vs non-tumoral tissue (n=8) (p=0.03) from patients, also confirmed by immunofluorescence (p=0.028). *In vitro*, restoring RORa in cell line using SR1078, reduced tumor cell proliferation and increased apoptotic gene expression. Moreover, when tested on primary human CAFs, RORa agonist reduced the myofibroblastic markers *COL1A1* (p=0.01), *HAS2* (p=0.001) and *ACTA2* (p<0.01), without affecting the inflammatory *STAT3* (p=0.52) and *IL6* (p=0.30), as assessed by qPCR. When testing *in vivo* RORa agonist SR1078 in KRAS/p19 iCCA experimental model, we found a reduction in both tumor number (p=0.03) and tumor size (p<0.001) in the treated mice compared to the vehicle group. After confirming that *Rora* expression was increased in treated mice compared to the vehicle group by qPCR (p=0.01), we found that restoring RORa *in vivo*, reduced tumor cell proliferation (p<0.001) as assessed by double staining and quantification of CK19⁺Ki67⁺ cells. Moreover, we encountered decreased collagen deposition as assessed by PicroSirius Red (p=0.03); and reduction of *Col1a1* (p=0.04) and *Has2* (p=0.03) gene expression in the SR1078 treated-group, compared to the vehicle-group. As promising result, we observed reduction in *Pd-l1* gene expression (p=0.041) in the treated vs control group.

Conclusion: RORa regulates iCCA tumor cells proliferation and affects the tumor microenvironment by modulating the CAF phenotype and reducing the expression of myofibroblastic genes both *in vitro* and *in vivo*. Our data suggest that promoting RORa activity might be a novel therapeutic strategy to target both tumor cells and CAFs in combined therapies in iCCA.

FRI-475-YI

NADPH oxidase 1 inhibition as therapeutic strategy in hepatocellular carcinoma: insights from human-relevant models

Zenzi De Vos^{1,2}, Lander Heyerick^{1,2}, Luís Abreu de Carvalho³, Hasan Eker³, Filip Gryspeerdt³, Frederik Berrevoet³, Sander Lefere^{2,4}, Anja Geerts^{2,4}, Sarah Raevens^{2,4}, Xavier Verhelst^{2,4}, Hans Van Vlierberghe^{2,4}, Lindsey Devisscher^{1,2}. ¹Department of Basic and Applied Medical Sciences, Gut-Liver Immunopharmacology Unit, Ghent University, Ghent, Belgium; ²Liver Research Center Ghent, Ghent University, Ghent University Hospital, Ghent, Belgium; ³Department of General and HPB surgery and Liver transplantation, Ghent University Hospital, Ghent, Belgium; ⁴Department of Internal Medicine and Paediatrics, Hepatology Research Unit, Ghent University, Ghent, Belgium
Email: zenzi.devos@ugent.be

Background and aims: Current preclinical models for hepatocellular carcinoma (HCC) poorly predict human response to therapy as they fail to reliably reflect human pathology and the involvement of human immunity. This is in part responsible for the lack of therapy for patients suffering from advanced HCC. NADPH oxidases (NOX) are reactive oxygen species-producing enzymes of which the isoform NOX1 is present in the tumor microenvironment (TME) of HCC and has been shown to promote HCC development and metastasis. We and others have shown that NOX1 inhibition (NOX1i) alters the TME in classical experimental HCC models and might serve as a therapeutic target. Using human-relevant models, we here aim to provide more evidence for NOX1i, compared to the current standard of care, as potential treatment strategy in HCC with a higher translatability to the clinic.

Method: Hep3B cells were implanted intrahepatically in NSG mice. Ten days post tumor induction, mice were reconstituted with peripheral blood mononuclear cells of human healthy controls and were treated with 25 µM NOX1i ML171, 3 mg/kg anti-programmed death-ligand 1 (anti-PD-L1) antibody + 5 mg/kg anti-vascular endothelial growth factor A (anti-VEGF-A) antibody (standard of care), NOX1i + standard of care or vehicle or IgG control, twice per week for 3 weeks. Immune cell engraftment and phenotype in peripheral blood, liver, tumor and TME was assessed via flow cytometry. Inflammatory markers were evaluated using RT-qPCR. Complementary to the *in vivo* study, *ex vivo* human HCC patient precision cut liver slices (PCLS) of tumor tissue and surrounding non-tumor tissue were treated with 5 µM NOX1i or vehicle for 16 h and analysed for inflammatory markers.

Results: Tumor volume and weight ranged around 4.4 cm³ and 3.9 g, respectively, with no differences between treatments. Human immune cell chimerism reached around 75% in tumors, livers and TME, and around 30% in peripheral blood, with an overall lower engraftment in NOX1i treated mice. Immune cell populations mainly comprised T cells of which CD4⁺ T cells, and in particular the T helper 2 subtype, were present in higher numbers than CD8⁺ T cells in all groups. Within both the CD4⁺ and CD8⁺ T cell populations, effector memory T cells were the most prevalent, next to effector, central memory and naïve T cells. Interestingly, the TME of NOX1i treated mice showed increased CD4⁺ T cells and increased PD-1 expression in CD4⁺ and CD8⁺ T cells, compared to other treatments and control. Tumor tissue of NOX1i treated mice showed reduced expression of inflammatory markers (including tumor necrosis factor-alpha, interleukin (IL)-1 beta, hypoxia-inducible factor-1 alpha and interferon-gamma), which was confirmed in NOX1i-treated *ex vivo* PCLS of patients with advanced HCC.

Conclusion: These findings suggest that NOX1i suppresses immune cell responses in humanized models for HCC.

FRI-478

Histological and molecular characterization of GAN diet-induced obese mouse model of advanced fibrosing MASH with progression to HCC

Monika Lewinska¹, Maja Andersen¹, Susanne Pors¹, Mogens Vyberg², Michael Feigh¹, Henrik B. Hansen¹. ¹Gubra, Hørsholm, Denmark; ²Aalborg University, Center for RNA Medicine, Department of Clinical Medicine, Copenhagen, Denmark
Email: mle@gubra.dk

Background and aims: Metabolic dysfunction-associated steatohepatitis (MASH) is a leading cause of liver cirrhosis and hepatocellular carcinoma (MASH-HCC). However, the molecular alterations leading to onset of MASH-HCC are unclear. The present study aimed to evaluate disease progression in the translational GAN diet-induced obese (DIO) mouse model of advanced fibrosing MASH-HCC (GAN DIO-MASH-HCC mice).

Method: Male C57BL/6J mice were fed the GAN diet high in fat, fructose and cholesterol for 38–78 weeks (n = 15 per group). Mice fed chow for 48–68 weeks (n = 15) served as healthy controls. Terminal end points included AI-assisted histopathological scoring and histomorphometrics, flow cytometry, tumor classification by an expert clinical histopathologist and bulk RNAseq. Single sample gene set enrichment analysis (ssGSEA) and digital cytometry (xCell, EcoTyper) was performed. Transcriptional profiles of murine MASH and MASH-HCC were compared to human hepatic transcriptomes from healthy controls to MASH (n = 57, GSE126848) and MASH-HCC (n = 45, GSE193084).

Results: GAN DIO-MASH-HCC mice demonstrated NASH (NAFLD Activity Score ≥5), progressive fibrosis (all mice demonstrating F3 at ≥60 weeks) and HCC burden consistent with human MASH-HCC. Liver inflammation was characterized by expansions in inflammatory M1 macrophages, Kupffer cells, dendritic cells and CD8+ T-cells. Hepatic neoplasms were detected from 48 weeks with progressive cohort penetrance, resulting in 100% incidence at 72 weeks of GAN diet feeding. 70% of tumors presented histological features of poor prognostic HCC; 30% were classified as hyperplastic nodules. Transcriptional analysis associated murine MASH-HCC tumors with S1 Hoshida signature, activation of immune responses, KRAS, p53 and Wnt/β-catenin signalling pathways. Digital cytometry assigned 50% of murine MASH-HCC tumors carcinoma ecotypes associated with short survival (CE1, CE2), while 30% of tumors presented an ecotype associated with positive response to immune therapy (CE9).

Conclusion: The GAN-DIO-MASH-HCC model spontaneously develops HCC on the background of progressive advanced fibrosis. The HCC molecular signature recapitulates poor prognostic human MASH-HCC and immune microenvironment. The translational GAN DIO-MASH-HCC mouse model is highly applicable for profiling novel drug therapies targeting NASH-HCC, including first-line immune checkpoint inhibitor therapies.

FRI-479-YI

The role of OSM/OSMRβ axis in shaping the immune-microenvironment favouring MASLD-related HCC immune evasion

Beatrice Foglia¹, Jessica Nurcis¹, Alessia Provera², Chiara Rosso³, Gian Paolo Caviglia³, Elisabetta Bugianesi³, Emanuele Albano², Salvatore Sutti², Maurizio Parola¹, Stefania Cannito¹. ¹University of Turin, Dept. Clinical and Biological Sciences, Turin, Italy; ²University Amedeo Avogadro of East Piedmont, Dept. Health Sciences and Interdisciplinary Research Center for Autoimmune Diseases, Novara, Italy; ³University of Turin, Dept. Medical Sciences, Turin, Italy
Email: beatrice.foglia@unito.it

Background and aims: Oncostatin M (OSM), a cytokine from the IL-6 family, is implicated in chronic liver diseases and hepatocellular

carcinoma (HCC) progression. HCC patients with a background of metabolic dysfunction-associated steatotic liver disease (MASLD) showed elevated OSM serum levels correlating with clinical parameters and disease outcome. A murine MASLD-related HCC model showed increasing OSM expression during liver carcinogenesis, correlating with F4/80 gene expression, suggesting OSM's involvement in macrophage recruitment/functions within the tumor microenvironment. This study explores OSM's potential role in modulating the tumor microenvironment, impacting crucial events in HCC progression.

Method: To test this hypothesis, we used: a) OSMRβ^{-/-} mice (where OSMRβ expression into hepatocytes has been abrogated) and wild-type (WT) littermates that underwent the DEN/CDAA protocol of MASLD-related liver carcinogenesis to assessing how disrupting OSM/OSMRβ signaling in hepatocytes influences MASLD-related HCC development and progression of; b) cohort of MASLD patients with/without HCC.

Results: OSMRβ^{-/-} mice exhibited a significant decrease in tumor volumes and weights compared to WT, with unchanged nodule numbers. In terms of inflammation, OSMRβ deletion did not alter the infiltration of F4/80+ cells suggesting OSM's potential role in qualitatively modifying the immune landscape. Analysis of HCC data from the TCGA database, revealed that OSM expression correlates positively with several immunosuppressive markers (CCL2, CCL22, CD25, CXCL12, FOXP3, PD-L1, PTGSE2, TGFβ). Consistently, OSM transcripts levels in WT correlates with these markers and their expression is downregulated in the OSMRβ^{-/-} mice as a consequence of the inhibition of P-STAT3, P-AKT, SMAD4, COX-2 signaling pathways involved in recruiting pro-tumoral Tumor Associated Macrophages (TAMs), T regulatory lymphocytes (T-regs) and Myeloid-derived suppressor cells (MDSC). Multiplex Immunoassay on sera from MASLD cirrhotic and/or HCC patients revealed a significant increase of cytokines characterizing the immunosuppressive tumor microenvironment (IL1β, CCL2, IL8, CXCL13). Transcript levels of these cytokines correlated with OSM expression in MASLD patients. Accordingly, OSMRβ deletion resulted in reduced transcript levels of these genes. Of relevance, CCL15 mRNA levels (a chemokine downregulated in the OSMRβ^{-/-} mice and involved in MDSC recruitment and activation) correlated positively with OSM mRNA levels in MASLD-related HCC patients, assuming a role of independent prognostic factor associated with worse survival.

Conclusion: The experimental data highlight a pro-carcinogenic contribution for OSM in a MASLD background, favoring immunosuppressive tumor microenvironment, suggesting a possible role for the OSM-OSMRβ axes as therapeutic target for MASLD-related HCC.

FRI-480

Multi-dimensional profiling of hepatoblastomas and patient-derived tumor organoids uncovers tumor subpopulations with divergent WNT activation profiles and drug sensitivities

Weng Chuan Peng¹. ¹Princess Maxima Center, Utrecht, Netherlands
Email: wengchuan@gmail.com

Background and aims: Hepatoblastoma, the most prevalent pediatric liver cancer, almost always carries a WNT-activating CTNNB1 mutation, yet exhibits notable molecular heterogeneity. To characterize this heterogeneity and identify novel targeted therapies, we performed comprehensive analysis of hepatoblastomas and tumor-derived organoids using various omic methods and high throughput drug screening.

Method: Single-cell RNA-seq, spatial transcriptomics, single-cell ATAC-seq, patient derived organoid, high throughput drug profiling.

Results: Based on analysis of tumor tissues, we identified two distinct tumor epithelial signatures: hepatic 'fetal-like' and WNT-high 'embryonal-like' signatures, displaying divergent WNT signalling patterns. The liver-specific WNT targets were enriched in the fetal-like group, while the embryonal-like group was enriched in canonical WNT target genes. Gene regulatory network analysis revealed

POSTER PRESENTATIONS

enrichment of regulons related to hepatic function such as bile acid, lipid and xenobiotic metabolism in the fetal-like subgroup but not in the embryonal-like subgroup. In addition, the dichotomous expression pattern of the transcription factors HNF4A and LEF1 allowed for a clear distinction between the fetal- and embryonal-like tumors. Next, we performed high-throughput drug screening using patient-derived tumor organoids and identified sensitivity to multiple inhibitor classes, most notably HDAC inhibitors. Intriguingly, embryonal-like tumor organoids, but not fetal-like tumor organoids, were sensitive to FGFR inhibitor treatments, suggesting a dependency on FGFR signalling. In summary, our data uncover the molecular and drug sensitivity landscapes of hepatoblastoma and pave the way for the development of targeted therapies.

Conclusion: We uncover the molecular and drug sensitivity landscapes of hepatoblastoma, which could pave the way for the development of targeted therapies.

FRI-481

Analysis of HBV DNA integration in patients with intrahepatic cholangiocarcinomas and overt or occult HBV infection

Daniele Lombardo¹, Cristina Musolino², Domenico Giosa³, Valeria Chines⁴, Carlo Saitta⁵, Giuseppina Raffa⁶, Pietro Invernizzi⁷, Domenico Alvaro⁸, Giovanni Raimondo⁹, Teresa Pollicino¹⁰.

¹University Hospital G. Martino Messina, Messina, Italy; ²University Hospital "G. Martino" Messina, Messina, Italy; ³University of Messina, Messina, Italy; ⁴University Hospital "G. Martino" of Messina, Messina, Italy; ⁵University Hospital of Messina, Messina, Italy; ⁶University Hospital "G. Martino" of Messina, Messina, Italy; ⁷University of Milano-Bicocca, Milano, Italy; ⁸Sapienza University of Rome, Rome, Italy; ⁹Division of Medicine and Hepatology, University Hospital of Messina, Messina, Italy; ¹⁰University Hospital "G. Martino" of Messina, Messina, Italy

Email: tpollicino@unime.it

Background and aims: Chronic hepatitis B virus (HBV) infection is associated with an increased risk of developing intrahepatic cholangiocarcinoma (ICC). However, there is no direct evidence of a causal relationship between HBV infection and ICC development. In this study, we sought to investigate the characteristics and mechanisms of HBV integration in HBV-infected ICCs.

Method: We conducted a high-throughput HBV integration sequencing (HBIS) analysis on tumour specimens from 13 HBV positive patients with ICC (3 HBsAg-positive and 10 with occult HBV infection, OBI) and 8 paired non-tumour liver tissues to study HBV integration sites.

Results: A total of 2,753 HBV integration sites were detected in the 13 patients studied, 2,649 in tumours and 104 in non-tumour tissues, with no significant differences between HBsAg- and OBI-positive patients. All patients studied showed HBV integrations, with an average of 221 and 17 integration sites per tumour and non-tumour tissue sample, respectively. HBV integration sites were annotated to analyse their distribution in distinct genomic elements. Integrations were more frequent in intergenic region ($p < 0.001$) in tumours than non-tumour samples, whereas in non-tumours integration sites were more frequent in lncRNA ($p = 0.002$), in SINE ($p < 0.001$), and in the D-Loop region of mitochondrial DNA ($p < 0.001$). Analysis of breakpoints within the HBV genome showed a significant concentration of breakpoints in the HBx gene in tumor samples ($p < 0.0001$). Additionally, there was a notable enrichment of breakpoints in the preS/S gene region in non-tumor tissues ($p < 0.0001$). To elucidate the mechanisms of HBV integration, the presence of microhomology (MH) sequences between cell DNA and HBV DNA integrants at the level of integration sites was investigated. We found that almost all HBV integration sites detected showed the presence of MH sequences (range 3 bp–21 bp).

Conclusion: HBV integration occurs at high frequency in both tumour and adjacent non-tumour tissues of patients with ICC and HBV infection (both in cases with overt and occult HBV infection),

with substantially higher insertion rates in tumours. Furthermore, our data strongly suggest the involvement of an MH-mediated mechanism in HBV integration, which could be triggered by genomic instability/fragility in the proximity of integration sites.

FRI-484

A metastasis-resident B cell subset serves as tumoricidal effectors with checkpoint- expressing in colorectal cancer liver metastasis

Yujie Bao¹, Jiayin Tang², Yupan Bai¹, Jugang Wu¹, Hongsheng Fang², Ming Zhong², Jie Xu¹. ¹Shanghai Jiao Tong University School of Medicine, Shanghai Ninth People's Hospital, Shanghai, China; ²Shanghai Jiao Tong University School of Medicine, Renji Hospital, Shanghai, China
Email: yujie.bao@shsmu.edu.cn

Background and aims: Liver metastasis is the leading cause of mortality in colorectal cancer (CRC), the limited therapeutic efficacy targeting metastatic lesion remains a concern. B cells emerge as a major immune cells within tumor microenvironment (TME), playing multifaceted roles in tumorigenesis. Our study has revealed critical insights into the anti-tumor function of B cells within the liver metastatic TME in CRC.

Method: Three pairs of operational samples were respectively collected from patients with colorectal cancer liver metastasis (CRLM). Each pair concluded the liver metastatic tumor tissue and matched normal liver tissue from one patient. Single-cell RNA sequencing (scRNA-seq) was adopted to map out the transcriptomic atlas of the liver metastasis TME. The main cell types were defined via SingleR and we further integrated all B cells into re-clustering process and nine distinct subclusters were identified based on their Differentially Expressed Genes. Cell-cell communications, Psudotime trajectory and GSEA analysis were performed to study the B cell immune effect on tumor cells. Validation was conducted via immunofluorescent staining, flow cytometry assays and ex vivo functional experiments on another sample cohort. To avoid the sample bias, public database was analyzed to testify our results.

Results: A new B cell subset named as META-CBLs was identified in the liver metastatic TME through scRNA-Seq combined with ex vivo verification and database analysis. These cytotoxic META-CBLs could eliminate tumors through inducing apoptosis via granzyme-perforin pathway. META-CBLs might be activated by tumor associated antigens presented through MHC-I signaling. Nevertheless, CD96 marked META-CBLs could be driven into an immunosuppressive senescent state and restrained the production of GZMB. In addition, PARD3⁺ metastatic tumor cell subset might escape from immunosurveillance of META-CBLs by displaying a poorly immunogenic phenotype and educating META-CBLs by stimulating CD96 checkpoint signaling. Taken together, reinvigorating and harnessing these META-CBLs may hold promise in metastasis tumor immunotherapy.

Conclusion: In summary, our work has improved the common understanding of B cells function in the liver metastatic TME. As CD8⁺T cells and NK cells are the classic icons of tumor killing effector cells, we highlighted the META-CBLs serve as tumoricidal effector cells in the metastatic TME. However, META-CBLs could be driven into immunosuppressive senescent state when expressing CD96. Within the liver metastasis TME, we also discovered a group of PARD3⁺ metastatic tumor cells, which might acquire the capability of immunoescaping from META-CBLs through CD96 checkpoint signaling. Therefore, blocking CD96 might be a promising intervention to reinvigorate META-CBLs against metastatic tumor outgrowth in CRLM.

FRI-485

CHKA, a potential target marker for early-stage metabolic dysfunction associated steatotic liver disease induced hepatocellular carcinoma with low fibrosis level: analysis by metabolomic and transcriptomic

Jihan Sun¹, Fatima Dahboul¹, Estelle Pujos-Guillot², Stephanie Durand², Mélanie Petera², Delphine Centeno²,

Benoit Colsch², Guillaume Zoulm¹, Delphine Weil-Verhoeven³, Vincent Di Martino³, Aicha Demidem¹, Armand Abergel⁴. ¹Team ECREIN, UMR 1019, INRAE, Clermont-Auvergne University, Clermont-Ferrand, France; ²Metabolism exploration platform, MetaboHUB, INRAE Theix, Clermont-Ferrand, France; ³Hepatology and digestive intensive care service, Jean Minjoz hospital, Besançon, France; ⁴Hepato-Gastroenterology unit, university hospital estaing, Clermont-Ferrand, France
Email: jihan.sun@uca.fr

Background and aims: Metabolic dysfunction associated steatotic liver disease (MASLD) can eventually progress to hepatocellular carcinoma (HCC). Thirty to 40% of MASLD-HCC occur in the absence of fibrosis, posing a challenge for early detection. Previously, we reported 2 phenotypes of MASLD-HCC based on the severity of fibrosis (F0F1 vs. F3F4) (Buchard et al., 2021). The objective of this study is to explore lipid metabolism pathways through "omics" and identify biomarkers of MASLD-HCC based on the severity of fibrosis. **Method:** Our cohort included 56 pairs of tumor and non-tumor (NTT) human liver tissues (F0F1 = 28, F3F4 = 28), and 5 healthy liver tissues (HLT) used as control (CRB Foie). A non-targeted metabolomic analysis by liquid chromatography-mass spectrometry (LC-MS) was performed. In addition, a qRT-PCR analysis focused on a panel of 16 genes involved in the main lipid metabolism pathways was conducted (SPTLC1, SPTLC2, SGMS1, SGMS2, SMPD1, SMPD3, CHKA, PCYT1A, CHPT1, PEMT, MBOAT7, DGAT1, DGAT2, ACAT2, AADACL1 and ACOX1). For each group, TT was compared to NTT and to HLT. The study was approved by the Ethic Committee Sud-Est VI Clermont-Ferrand (Agreement number AU887, 04/03/2011).

Results: First, using LC-MS, we identified 130 metabolites and 30 of them exhibited significant difference between TT and NTT. In the MASLD-HCC-F0F1, the levels of ceramide Cer (d18:1/22:0), sphingomyelin SM (41:1) and phosphatidylethanolamine PE (O-16:1_20:4) were decreased. While the levels of SM (35:1), SM (40:2), SM (42:3), phosphatidylcholines PC (16:0_14:0), PC (16:0/16:0), PC (18:0_18:1), PC (40:8) and PE (18:0_18:1) were increased. In contrast, most of metabolites content in MASLD-HCC-F3F4 were reduced compared to NTT, indicating an amplified anabolism. However, the levels of PC (18:0_18:1), PC (18:0_20:3) and phosphatidylinositol PI (16:0_18:1) were increased. Notably, PI (16:0_18:1) is considered as an onco-metabolite (Yang et al., 2018).

Second, transcriptomic data revealed that in MASLD-HCC-F0F1, among the 16 genes studied, the expression of 6 genes coding for CHKA, DGAT1, MBOAT7, SPTLC2, SMPD1 and SGMS1 were up-regulated. However, MASLD-HCC-F3F4 shown no variation in the expression of these genes. Altogether, this data supports the existence of 2 MASLD-HCC phenotypes according to fibrosis severity. Furthermore, the increased expression of CHKA in MASLD-HCC-F0F1 is in line with our previous metabolomic data, reporting a significant accumulation of phosphocholine derivatives in MASLD-HCC-F0F1. This observation suggests that choline may serve as an imaging marker to detect HCC-F0F1.

Conclusion: "Omics" analyses allow: 1) discrimination of MASLD-HCC based on fibrosis severity; 2) propose CHKA as a marker for MASLD-HCC-F0F1, which could lead to a clinical application: labeled choline may be favored as a more effective tracer for PET scanning in HCC patients with minimal fibrosis.

FRI-486

Impact of proliferative and metabolic reprogramming by the lysine-specific demethylase 1 in hepatocellular carcinoma

Jie Wang¹, Lingyu Wang¹, Hardik Makwana¹, Marcel Schmiel¹, Yefeng Shen¹, Anton Ströbel¹, Hannah Eischeid-Scholz¹, Yue Zhao², Evangelos Kondylis³, Mafalda Escobar⁴, Michal Schweiger⁵, Reinhard Büttner¹, Margarete Odenthal⁶. ¹University Hospital of Cologne, Center for Molecular Medicine Cologne, University of Cologne, Cologne, Germany; ²University Hospital of Cologne, Cologne, Germany;

³University Hospital of Düsseldorf, University Hospital of Cologne, Düsseldorf, Germany; ⁴University of Cologne, Cologne, Germany; ⁵University of Cologne, Cologne, Germany; ⁶University Hospital of Cologne, Center for Molecular Medicine Cologne, University of Cologne, Cologne, Germany
Email: m.odenthal@uni-koeln.de

Background and aims: Epigenetic alterations are important features in the process of carcinogenesis. The lysine-specific demethylase 1 (LSD1) mediates chromatin remodeling by demethylation of histone 3 lysine 4 and 9 (H3K4/K9), resulting in gene activation and suppression, respectively. Overexpression of LSD1 in various cancers contributes to cancer progression and malignancy, but its role in hepatocellular carcinoma (HCC) has not yet been addressed. In the present study, we investigated the cell cycle progression as well as metabolic gene expression and function upon LSD1 inhibition in HCC. **Method:** LSD1 was inhibited in different hepatoma cell lines utilizing RNA interferences or the application of specific LSD1 inhibitors. Global transcriptomics was carried out by RNA ultra-deep sequencing. Divergent expression in response to LSD1 inhibition was validated by quantitative PCR. LSD1 influence on promoter interaction and H3K4 methylation was performed by chromatin immunoprecipitation (ChIP) followed by whole genome sequencing (ChIPseq). In addition, a DEN/high-fat diet mouse HCC model was established to investigate the effect of LSD1 in hepatocarcinogenesis based on metabolic liver disease. Characteristics of expression profiles and tumor growth were determined by histology, immunohistology, immunoblot as well as by expression profiling and pathway analysis using RNA sequencing and quantitative PCR.

Results: Pharmacological or siRNA-mediated LSD1 inhibition in hepatoma cells leads to altered H3K4/K9 methylation and cell cycle arrest. Notably, gene expression profiling followed by pathway analysis revealed a prominent dysregulation of genes involved in the cell cycle control and metabolism after LSD1 inhibition in various hepatoma cell types. Subsequent comprehensive ChIPseq analysis provided evidence of alterations in the histone methylation signature and LSD1 binding at the promoter sites of genes, involved in proliferation. Especially, these identified genes are markedly down-regulated after LSD1 inhibition such as the proliferative gene PLK1, indicating that it is a direct target of LSD1 regulation. Furthermore, LSD1 inhibition resulted in a significant reduction in tumor growth and the number of proliferative Ki67-positive cells.

Conclusion: The presented studies show that LSD1 is a crucial mediator in cell cycle control affecting HCC progression not only through cell cycle arrest but also through metabolic dysregulation.

FRI-487

Immunosuppressive CD73 is upregulated on tumour endothelium and may limit effective immune infiltrate in hepatocellular carcinoma

Rosemary Faulkes^{1,2}, Daniel Patten¹, Alex Wilkinson³, Joanne O'Rourke¹, Ayla O'Keeffe¹, James Kennedy¹, Owen Cain², Yuk Ting Ma², Tahir Shah², Chris J. Weston¹, Shishir Shetty^{1,2}.

¹Institute of Immunology and Immunotherapy, University of Birmingham, Birmingham, United Kingdom; ²University Hospitals Birmingham, Birmingham, United Kingdom; ³Mass Therapeutics, Oxford, United Kingdom

Email: rosemary.faulkes@uhb.nhs.uk

Background and aims: Combining vascular and checkpoint inhibitor targets has shown positive results for hepatocellular carcinoma (HCC). We conducted deep RNA sequencing of human liver sinusoidal endothelial cells (LSEC), demonstrating significant differential regulation of immune pathways on tumour LSEC, including upregulation of CD73. The immunosuppressive effect of CD73-generated adenosine is a current target in cancer trials using a monoclonal antibody (Oleclumab). As LSEC are immune gatekeepers, CD73 may contribute to the immune resistant tumour niche. We sought to explore the

POSTER PRESENTATIONS

expression and regulation of CD73 in HCC as a potential future therapeutic target.

Method: Primary human LSEC were isolated and cultured from liver tissue. Regulation of CD73 on primary LSEC exposed to a range of tumour associated factors was explored at gene and protein level using PCR and Western blot respectively. LSEC were incubated with Oleclumab antibody and the interaction was studied using immunocytochemistry. Multiplex imaging with the Lunaphore COMETTM, delineated the relationship between CD73 and immune subsets in HCC tissue. Soluble CD73 (sCD73) was measured in 50 treatment naïve HCC patients using ELISA. Multiple logistic regression compared clinical factors between high and low sCD73 expressing groups.

Results: We found CD73 is highly expressed on peri-tumour vasculature at the border of the immune infiltrate in HCC. In vitro, LSEC significantly upregulate CD73 in response to high shear stress and interferon gamma ($p < 0.05$). LSEC treatment with Oleclumab confirmed that Oleclumab was rapidly internalised by LSEC within 30 minutes. Additionally, two year transplant-free survival for patients with high sCD73 was significantly lower than patients with low sCD73 (43% vs 79% respectively, $p = 0.035$), independent of age, tumour size or number, aetiology of liver disease and AFP.

Conclusion: CD73 is expressed on peri-tumour vasculature at the border of the immune infiltrate. Primary cultured LSEC maintain their expression of CD73 and we confirmed the rapid uptake of the anti-CD73 agent Oleclumab. Our results suggest that CD73 represents a potential barrier to an effective anti-tumour immune response, and peripheral blood measurement provides potential opportunities for personalised medicine in HCC.

FRI-490-YI

Intratumoural microbiome alterations predict postoperative recurrence and mortality in hepatocellular carcinoma after hepatic resection

Saisai Zhang¹, Fung Yu Huang¹, Meng Zhao¹, Tan-To Cheung², Tiffany Wong², Danny Ka-Ho Wong¹, Lung-Yi Mak¹, Man-Fung Yuen¹, Wai-Kay Seto¹. ¹Department of Medicine, School of Clinical Medicine, The University of Hong Kong, Hong Kong, China; ²Department of Surgery, School of Clinical Medicine, The University of Hong Kong, Hong Kong, China

Email: saisaicc@hku.hk

Background and aims: The cancer microbiota, characterized by the colonization of bacteria within tumor tissues, exerts a significant influence on inflammation modulation, tumorigenesis regulation, and the overall cancer microenvironment. While the presence of intratumoral bacteria in hepatocellular carcinoma (HCC) has been documented, their specific functions and associations with HCC outcomes require further elucidation and clarification.

Method: Both tumorous and peri-tumorous tissues were collected from HCC patients who underwent liver resection. DNA was extracted from both tumorous and their corresponding non-tumorous tissues for shotgun metagenomic sequencing. Microbiome analysis was performed on bacterial composition at different taxonomic levels and microbial functions. Early recurrence and survival were monitored after liver resection.

Results: Of the included 12 HCC patients with 2-year outcome data, 11 (91.67%) were male, and the median age was 67.50 (IQR 61.25–77.5) years. The median size of HCC lesions was 7.50 (5.35–12.75) cm for the biggest lesion in each patient. Four (33.33%) patients developed early (≤ 2 years) recurrence; the cumulative 2-year survival rate was 25%. Immunohistochemistry staining showed lipopolysaccharide (LPS)-positive gram-negative bacteria were predominantly identified in both HCC tumorous and peri-tumorous tissues, whereas lipoteichoic acid (LTA)-positive gram-positive bacteria were notably absent. A significant increase in the median abundance of bacterial DNA per 1 μ g DNA was observed in both peri-tumorous and tumorous tissues when compared to negative environmental controls (11.96 [10.25–15.54] ng vs. 0.04 [0.03–0.49]

ng, $p = 0.002$; and 8.22 [4.55–11.11] ng vs. 0.04 [0.03–0.49] ng, $p = 0.015$, respectively), with the dominant phylum being *Proteobacteria*. In HCC tumours, *Peribacillus psychrosaccharolyticus* was significantly enriched in patients with early recurrence when compared to those without recurrence (0.87% [0.20%–1.83%] vs. 0.00% [0.00%–0.00%], $p = 0.0182$); The abundance of *Peribacillus psychrosaccharolyticus* was positively correlated with the presence of satellite tumour nodules in histological specimens ($r = 0.64$, $p < 0.05$). In addition, *Melaminivora* sp. SC2–9 was detected solely in HCC patients with mortality within 2 years, while completely undetectable in patients with a 2-year survival (0.73% [0.21%–0.92%] vs. 0.00% [0.00%–0.00%], $p = 0.0045$). Microbial functional analysis revealed an enrichment of fatty acid metabolism pathway in patients without early recurrence (linear discriminant analysis score 4.02, $p = 0.0296$).

Conclusion: Distinctive profiles of intratumoural microbiota exist in HCC patients and were associated with early recurrence and survival. Our findings encourage more in-depth studies to be conducted to examine the role of tumour microbiome for cancer prognostication.

FRI-491-YI

Targeting inflammasome activation by sorafenib/regorafenib as strategy to enhance efficacy in hepatocellular carcinoma therapy

Anna Tutusaus^{1,2}, Marco Sanduzzi Zamparelli², Loreto Boix², Patricia Rider^{1,2,3}, Silvia Subias¹, Montserrat Mari¹, María Reig², Albert Morales^{1,2}. ¹Institute of Biomedical Research of Barcelona (IIBB-CSIC), IDIBAPS, Barcelona, Spain; ²Barcelona Clinic Liver Cancer (BCLC) Group, Liver Unit, Hospital Clínic de Barcelona, University of Barcelona, CIBEREHD, IDIBAPS, Barcelona, Spain; ³Departament de Biomedicina, Facultat de Medicina, Universitat de Barcelona, Barcelona, Spain
Email: albert.morales@iibb.csic.es

Background and aims: Tyrosine kinase inhibitors (TKIs), such as sorafenib and regorafenib, emerged as standard systemic treatments for advanced hepatocellular carcinoma (HCC) over the last decade before the eruption of immune-based therapies. Although previous research linked sorafenib to inflammasome activation, the beneficial role of inflammasome intervention for sorafenib/regorafenib therapy in liver cancer patients remains mainly unexplored.

Method: Microarray transcriptomic analysis of inflammasome-related genes in a murine HCC model using BCLC9-derived tumors treated with sorafenib and regorafenib. Human databases correlation of transcriptional increases in inflammasome genes with prognosis in HCC patients. Tumor and surrounding tissue from patients diagnosed with HCC (20), untreated (10) or sorafenib/regorafenib treated (10) was analyzed. Experimental tumor growth in BCLC-9 xenografts and immunocompetent Hepa1–6 tumors were evaluated combining sorafenib with inflammasome inhibition (MCC950). ELISA detection of IL1 β released by THP-1 macrophages after sorafenib/MCC950 treatment. Recording of Hep3B tumoroids treated with sorafenib/IL-1 β was taken for 7 days.

Results: Our data confirmed substantial inflammasome activation following treatment with both TKIs, showing a consistent pattern of increased gene expression. Public database analysis associated transcriptional upregulation of inflammasome genes with a poorer prognosis in male liver cancer patients. Our biopsy results from male patients treated with sorafenib/regorafenib demonstrated sustained transcriptional inflammasome activation in both HCC and surrounding tissue. Further supporting the involvement of inflammasome activation in sorafenib action, inhibition of the inflammasome (MCC950) enhanced sorafenib's anticancer activity in experimental HCC models, but not in in vitro treatment of HCC cells. Supporting a pivotal role played by the liver microenvironment, activated THP-1 human macrophages released IL-1 β after sorafenib administration by a inflammasome-dependent mechanism, while 3D Hep3B spheres exhibited increased tumor growth after IL-1 β addition.

Conclusion: This study unveils the inflammasome pathway as a promising and actionable therapeutic target to increase the efficacy of sorafenib/regorafenib therapy for HCC. The identified

inflammasome signature in HCC and surrounding tissue associates with TKI administration, suggesting that targeting inflammasome activation, particularly in male patients, may overcome sorafenib/regorafenib resistance and enhance the overall efficacy of TKI treatments in HCC.

FRI-492-YI

Tumor cell lines and patient derived xenograft models of intrahepatic cholangiocarcinoma maintain histology, transcription profiles and driver mutations of primary tumor but lose human stroma

Denise Schlösser¹, Georgina Schumann¹, Simon Peter¹, Hanna Redeker¹, Tanja Reineke-Plaß¹, Florian Vondran^{1,2}, Nora Nevermann¹, Stephan Bartels¹, Ulrich Lehmann-Mühlhoff¹, Geffers Robert³, Doan Duy Hai Tran¹, Anna Saborowski¹, Arndt Vogel^{1,4}. ¹Hannover Medical School, Hannover, Germany; ²Uniklinik RWTH Aachen, Aachen, Germany; ³Helmholtz Centre for Infection Research, Braunschweig, Germany; ⁴Toronto General Hospital, Toronto, Canada
Email: schloesser.denise@mh-hannover.de

Background and aims: Intrahepatic cholangiocarcinoma (iCCA) is the second common type of primary liver cancer. 5-year-survival remains below 10%, mainly caused by the aggressive biology, late diagnosis and lack of curative therapies. In order to develop more effective therapies, there is an urgent need for a better molecular understanding of CCA as well as for appropriate preclinical models for drug testing. Primary tumor cells enable *in vitro* studies and patient derived xenografts (PDX) serve as valuable tool to mimic original tissue architecture *in vivo*.

Method: Primary material derived from resected tumors was subcutaneously implanted into immunodeficient mice, and monitored for tumor growth. Successfully engrafted tumors were passaged up to four generations; tumor tissue was subjected to histologic evaluation and molecular characterization by DNA and RNA sequencing. In addition, primary and PDX tumors were enzymatically digested in order to generate two-dimensional (2D) cell lines. Stable growing cell lines were subsequently injected into immunodeficient mice; 2D derived tumors were histologically stained. Efficiency of targeted therapy was assessed *in vitro*.

Results: PDX models were successfully established in approximately 50% of cases; tumor penetrance and latency increased upon retransplantation whereas growth kinetics were similar across all generations. Histology of PDX tumors resembled primary iCCA and key characteristics were maintained during four PDX generations, but stroma content was reduced. Additional histologic and transcriptomic analysis revealed that human extracellular matrix components were replaced by murine orthologues. Transcriptome from PDX tumors resembled primary CCA but did not completely overlap. Success rate of 2D tumor cell line generation was approximately 20% and matching PDX models were available. Tumors derived from cell lines displayed comparable histology to their original tumor. Cell lines derived from primary tumor or PDX from the same patient expressed similar features. PDX as well as cell line derived-tumors from ERBB2_{amp} primary tumor overexpressed HER2.

Conclusion: We successfully established and repeatedly passaged seven iCCA PDXs; tumors initially growing as PDX can be passaged for at least four generations with nearly complete penetrance and comparable growth kinetics. PDX tumors retained key morphological and molecular features, but human stroma was lost in PDX tumors. Additionally, we were able to generate iCCA cell lines from three patients. Tumor cell lines derived tumors mimic characteristics from primary iCCA. Driver mutations such as HER2 were stably overexpressed in PDX and cell lines. We expect that thoroughly characterized PDX and tumor cell lines will serve as valuable tool for drug testing and help to understand primary and secondary resistance mechanisms to targeted therapies in iCCA.

FRI-493

CLEC14A regulates neutrophil recruitment across liver endothelial cells and correlates with a neutrophil signature in hepatocellular carcinoma

Joanne O'Rourke¹, Daniel Patten², Dean Kavanagh², Catherine E. Willoughby³, Tahir Shah⁴, Yuk Ting Ma⁵, Owen Cain⁶, Derek A. Mann⁷, Roy Bicknell², Shishir Shetty⁸. ¹Centre for Liver and Gastrointestinal Research, University of Birmingham, Birmingham, United Kingdom; ²University of Birmingham, Birmingham, United Kingdom; ³Translational Research in Hepatic Oncology, Liver Unit, University of Barcelona, Institut d'Investigacions Biomèdiques August Pi i Sunyer (IDIBAPS), Hospital Clínic, Barcelona, Spain; ⁴University Hospitals Birmingham NHS Trust, Birmingham, United Kingdom; ⁵Institute of Immunology and Immunotherapy, University of Birmingham, University Hospitals Birmingham NHS Trust, Birmingham, United Kingdom; ⁶University Hospitals Birmingham NHS trust, Birmingham, United Kingdom; ⁷Newcastle University-Newcastle Fibrosis Research Group, Biosciences Institute, Faculty of Medical Sciences, Newcastle, United Kingdom; ⁸Centre for Liver and Gastrointestinal Research, University of Birmingham, National Institute for Health Research, Birmingham Biomedical Research Centre at University Hospitals Birmingham NHS Foundation Trust, Birmingham, United Kingdom
Email: joanne.orourke@nhs.net

Background and aims: Immune checkpoint inhibition is now standard of care for patients with advanced hepatocellular cancer (HCC) and yet many patients remain resistant to this therapy. The presence of innate immune populations in the tumour microenvironment (TME) have been implicated in regulating the efficacy of these agents. CLEC14A has previously been shown to be upregulated on tumour endothelial cells and we found endothelial upregulation of CLEC14A in a subset of HCC tumours as well as acute liver injuries (alcoholic hepatitis and seronegative hepatitis). This led us to explore the role of CLEC14A in neutrophil recruitment, critical populations in both acute liver injury and cancer.

Method: Immunohistochemical analysis was undertaken of CLEC14A in human liver tissue across a range of liver diseases and HCC. CLEC14A regulation and function was then explored in primary human liver endothelial cells including responses to shear stress and flow based adhesion assays. Acute liver injury models were undertaken in CLEC14A knockout mice followed by intravital microscopy of the liver. Finally, CLEC14A expression was studied in both publicly available HCC data sets and through spatial transcriptomics of HCC tissue.

Results: We found that CLEC14A mediates neutrophil recruitment across liver endothelium in both *in vitro* and *in vivo* models. Specifically, CLEC14A inhibition significantly reduced neutrophil adhesion to liver endothelium in flow based assays and reduced neutrophil sinusoidal recruitment during ischaemia reperfusion injury. This process appeared to be independent of its interaction with its known ligand Multimerin-2. Additionally, we demonstrated a positive correlation of CLEC14A expression in human HCC with a neutrophil transcriptional signature.

Conclusion: This study unveils a new link between a tumour angiogenic receptor and neutrophil infiltration to the liver and highlights the potential of combining current immunotherapy in HCC with agents targeting the CLEC14A pathway.

FRI-494-YI

Cabozantinib induces mtDNA-dependent cytotoxicity through cGAS-STING signaling in experimental hepatocellular carcinoma

Patricia Rider^{1,2,3}, Anna Tutusaus^{1,3}, Carlos Cuño-Gómez^{1,2}, Flavia Savino^{1,2}, Loreto Boix³, Montserrat Marí¹, María Reig³, Albert Morales^{1,3}. ¹Institute of Biomedical Research of Barcelona (IIBB-CSIC), IDIBAPS, Barcelona, Spain; ²Departament de Biomedicina,

POSTER PRESENTATIONS

Facultat de Medicina, Universitat de Barcelona, Barcelona, Spain;
³Barcelona Clinic Liver Cancer (BCLC) Group, Liver Unit, Hospital Clínic of Barcelona, University of Barcelona, CIBEREHD, IDIBAPS, Barcelona, Spain
Email: albert.morales@iibb.csic.es

Background and aims: The tyrosine kinase inhibitor (TKI) cabozantinib is used in clinical practice against hepatocellular carcinoma (HCC). Previous studies demonstrated that TKI inhibitors such as sorafenib and regorafenib induce mitochondrial damage during cancer treatment. However, mitochondrial effects of cabozantinib have not been sufficiently explored in HCC. Cytosolic mitochondrial DNA (mtDNA) from damaged mitochondria emerges as a key driver of innate immunity. mtDNA sensing, contributed by the cyclic GMP-AMP synthase (cGas)-stimulator of interferon genes (STING) pathway is involved in immunomodulation and antitumor response. Here, we describe cabozantinib cytotoxicity as mitochondrial dependent and emphasize its association with the cGas-STING pathway.

Method: Fluorometric assessment of mitochondrial function was conducted by dihydroethidium (DHE) and JC1 staining. Cellular fractionation was performed by digitonin lysis buffer and confirmed by western blot analysis. Immunofluorescence staining and real-time qPCR were performed to detect cytosolic leakage of mtDNA in Hep3B cells. The nucleoside analog 2', 3' dideoxycytidine (ddc) was used for mtDNA depletion. cGas-STING axis activation and interferon stimulated genes (ISGs) downstream signaling was assessed by western blotting and real-time qPCR in hepatoma cells after cabozantinib stimulation.

Results: Cabozantinib caused mitochondrial damage in Hep3B cells increasing ROS production (DHE) and reducing mitochondrial membrane potential (JC1 shifting). We also detected mtDNA leakage into the cytosol in a dose-dependent and time-dependent manner, accompanied by an upregulation of interferon-stimulated genes (ISGs), suggesting that cabozantinib stimulates DNA sensing pathways via the cGas-STING axis. This pathway activation was verified by cabozantinib-mediated TBK-1 and IRF3 phosphorylation. Moreover, short cabozantinib stimulation also induced p65 and IRF3 nuclear translocation. To further verify whether cGas-STING activation and ISGs upregulation is mtDNA dependent, cells lacking mtDNA were generated. After 48 h ddc incubation, mtDNA content was reduced by 80% while ddc-mediated mtDNA depleted cells reduced TBK-1 phosphorylation following cabozantinib stimulation. In parallel, mtDNA depletion blocked mRNA expression of ISGs after cabozantinib treatment. Importantly, while blockage of this pathway (H-151) partially diminished cabozantinib cytotoxicity, vadimezan induction of cGas-STING potentiated the anti-tumor effect in vitro and in a Hepa1-6 3D spheroid model.

Conclusion: Cabozantinib-induced mtDNA leakage to the cytosol induces ISGs signaling by activating the cGas-STING pathway in hepatoma cells. Our results reveal mitochondrial damage and the mtDNA-cGas-STING axis as compelling targets in antitumor efficacy with a potential role in immunological responses.

FRI-495

Regulation of KIF23 by miR-107 controls replicative tumor cell fitness in mouse and human hepatocellular carcinoma

Mirco Castoldi¹, Sanchari Roy², Carolin Lohr¹, Rossella Pellegrino³, Mihael Vucur¹, Michael Singer¹, Veronika Buettner¹, Matthias Dille¹, Lara Heij⁴, Lars Zender⁵, Ulf Neumann⁴, Mathias Heikenwälder⁶, Thomas Longerich³, Christoph Roderburg¹, Tom Luedde¹. ¹Medical Faculty, Heinrich Heine University Düsseldorf, Düsseldorf, Germany; ²Medical Faculty and University Hospital Düsseldorf, Düsseldorf, Germany; ³University Hospital Heidelberg, Heidelberg, Germany; ⁴University Hospital RWTH Aachen, Aachen, Germany; ⁵University Hospital Tübingen, Tübingen, Germany; ⁶Deutsches Krebsforschungszentrum, Heidelberg, Germany
Email: mirco.castoldi@med.uni-duesseldorf.de

Background and aims: In hepatocellular carcinoma (HCC), there is a lack of successful translation of experimental targets identified in

mouse models to human patients. This study utilized a comprehensive transcriptomic approach in mice to identify novel potential targets for therapeutic intervention in humans.

Method: Genome-wide miRNA and mRNA expression data were analyzed in three distinct mouse models of liver cancer. The effects of target genes on hepatoma cell fitness were evaluated through proliferation, survival, and motility assays. The impact of mouse targets on human HCC prognosis was assessed using TCGA and GEO databases, in combination with TMAs. Finally, the functional effects of the identified targets on tumorigenesis were tested in HDTV-based preclinical HCC models in vivo.

Results: We discovered that miR-107, along with other tumor suppressor miRNAs, potentially inhibited the translation of a nexus of genes controlling the assembly and function of the mitotic spindle. Among these potential targets, we identified that Kif23, a protein that controls key stages of cytokinesis, was directly regulated by miR-107 and that the activity of the miR-107/KIF23 signaling module was functionally conserved between mice and humans. In humans, KIF23 expression was found to be a prognostic marker in liver cancer, with high expression associated with poor prognosis. HDTV of vectors carrying either pre-miR-107 or anti-Kif23 shRNA inhibited the development of highly aggressive cMyc-NRas-induced liver cancers in mice.

Conclusion: Disruption of the miR-107/Kif23 axis inhibited hepatoma cell proliferation in vitro and prevented oncogene-induced liver cancer development in vivo, offering a novel potential avenue for the treatment of HCC in humans.

FRI-498-YI

Role of ganglioside GD2 in the stem-like compartment of intrahepatic cholangiocarcinoma

Antonella Mannini¹, Mirella Pastore¹, Margherita Correnti², Elisabetta Rovida³, Cedric Coulouarn⁴, Jesper Andersen⁵, Claudia Campani¹, Fabio Marra¹, Chiara Raggi¹. ¹University of Florence, Florence, Italy; ²University of Milan, Milan, Italy; ³University of Florence, Florence; ⁴University of Rennes, Rennes, France; ⁵University of Copenhagen, Copenhagen, Denmark
Email: chiara.raggi@unifi.it

Background and aims: Among the ganglioside family (sialic acid-containing glycosphingolipids), GD2 has been recently investigated as a potential cancer stem cell (CSC) biomarker in several tumor types. However, the possible role of GD2 and its biosynthetic enzyme, GD3 synthase (GD3S), in intrahepatic cholangiocarcinoma (iCCA) stem subset is currently unknown.

Method: Stem-like subset of iCCA cell lines (HUCCT1, CCLP1) was enriched by sphere culture (SPH) and compared to monolayer parental cells (MON). iCCA ganglioside (GS) profiles were evaluated by chromatographic analytical procedures, after feeding with radioactive sphingosine. Plasma membrane GD2 expression was evaluated by FACS, while GS biosynthesis enzymes were analyzed by RT-qPCR during spherogenesis. The modulation of stem features by GS was investigated *in vitro* and *in vivo* by using iCCA GD3S-transfected cells, and corroborated by global transcriptomic analysis.

Results: In both iCCA lines, SPH showed severe changes in GS composition, including an increased content of GM3 and GD1a, reduction of GM2, and, among complex GS, increase or appearance of GD2. These findings were corroborated by high levels of GM3 synthase as well as GD3- and GM2/GD2 synthase expression. Cancer-stem features related to GD2 availability depend on the GD3S, the synthase that provides the precursor (GD3) to produce GD2. Significant correlations between GD3S expression and lymph node invasion were found in a published iCCA cohort by exploring the possible relevance of GD3S involvement in the clinical setting. After GD3-stable transfection, iCCA cells overexpressing GD3S showed *in vitro* enhanced sphere-forming ability, invasive properties as well as higher drug resistance compared to the transfected control. *In vivo* experiment, CCLP1 cells overexpressing GD3S developed a tumor

mass volume 2–3 fold greater compared to the control. By global transcriptomic analysis, ontology investigations identified 74 processes shared by the iCCA-SPH and GD3S-transfected cells, with enrichment for development and morphogenesis processes, signaling, in particular MAPK pathway and locomotion.

Conclusion: We demonstrate that the iCCA stem-like properties are related to the GS synthetic pathways and patterns. GD3 synthase and GD2 ganglioside could represent potential markers for iCCA stem phenotype.

FRI-499-YI

Counterfactual explanations for histopathology slides of hepatocellular carcinoma and cholangiocarcinoma enhance the understanding of artificial intelligence models

Laura Žigutytė¹, Katherine Hewitt¹, Jakob Nikolas Kather^{1,2,3}. ¹Else Kroener Fresenius Center for Digital Health, Technical University Dresden, Dresden, Germany; ²Department of Internal Medicine I, University Hospital Carl Gustav Carus, Dresden, Germany; ³National Center for Tumor Diseases (NCT), University Hospital Heidelberg, Heidelberg, Germany
Email: laura.zigutyte@tu-dresden.de

Background and aims: Deep learning (DL), a type of artificial intelligence (AI), is increasingly used in biomedical sciences, e.g., for predicting cancer subtypes, or a range of biomarkers from whole slide images. Challenges arise after the training of complex DL models, as it is essential to analyze the underlying reasons for the predictions to avoid biases or confounding factors. Traditional explainability methods, such as saliency maps and feature visualization, are difficult to interpret and may lead to confirmation bias. Therefore, in this work, we explore another type of explainability method-counterfactual explanations that we create using a generative AI model for liver hepatocellular carcinoma (HCC) and cholangiocarcinoma (CCA). These explanations show how an image would look to be classified as a different cancer type, aiding in understanding the reasoning and enhancing trust in the DL model.

Method: We use tiles derived from tumor areas in digitized whole slide images, which are part of The Cancer Genome Atlas Program (TCGA), to train a generative diffusion model. These tiles originate from scanned tissue samples of patients diagnosed with HCC or CCA. Simultaneously with a generative diffusion model, we train a semantic encoder to extract semantic information from each tile. Then, a classifier (HCC vs CCA) is trained, enabling us to determine the direction for the manipulation. By conditioning the generative diffusion model on manipulated semantic information according to the determined direction, we can alter any tile from the dataset to appear like the opposite class. We perform quantitative evaluation of the trained diffusion model, and qualitative analysis of generated counterfactual explanations.

Results: Preliminary results indicate that the trained diffusion model is capable to effectively reconstruct histopathology tiles while maintaining a high level of structural similarity. This model serves as a foundation for generating counterfactual explanations to elucidate the predictions made by the classifier when distinguishing between HCC and CCA. As we gradually modify an image to resemble the opposite class (for example, transforming an HCC image to look like CCA, and vice versa), we are able to observe and pinpoint the specific morphological alterations that transpire during this transformation. By adjusting the degree of manipulation, we create a series of images that depict a gradual transition of the image towards the opposite class, all while retaining a great portion of the original image's distinctive features.

Conclusion: Our work shows the potential of generative AI to aid the analysis of the reasoning behind uninterpretable DL models. The generation of counterfactual explanations offers a promising direction for gaining insights into predictions of other biomedical targets and potentially facilitating a deeper understanding of tissue morphology.

FRI-500-YI

ERAL1 down-regulates NADH: ubiquinone oxidoreductase core subunit V1 through N6-methyladenosine reader Insulin like growth factor 2 mRNA binding protein 2 to inhibit mitochondrial adenosine triphosphate synthesis and metastasis in hepatoma cells

Li Zhou¹, Siqi Liao¹, Siyuan Chen¹, Song He¹, Zhihang Zhou¹.
¹Chongqing medical university, Chongqing, China
Email: zhouzhihang@cqmu.edu.cn

Background and aims: One of the most prevalent malignant tumors is hepatocellular carcinomas (HCC), but its 5-year survival rate is less than 20%. Exploring the genes associated with HCC metastasis and determining the underlying process is a critical and challenging subject. Recent research has demonstrated that alterations in mitochondrial metabolism are directly associated with the development and metastasis of HCC. The primary metabolic activity of mitochondria is oxidative phosphorylation (OXPHOS), and due to mitochondrial dysfunction, this metabolic mode will be reprogrammed in HCC.

Method: We constructed mouse HCC metastasis models using CRISPR/Cas9 genome-wide knockout library to compare HCC primary and metastatic sites. Clinical samples were used to analyze the expression of ERAL1 in HCC and its relationship with prognosis. Then, we constructed cell lines with stable knockdown or over-expression of ERAL1 by lentivirus transfection to verify its effects on tumor development in vivo and in vitro. Metabolomics and transcriptomics were used to search for metabolic pathways and gene information closely related to ERAL1. Lactic acid assay and mitochondrial membrane potential were used to verify cellular glycolysis and oxidative phosphorylation levels. ChIP and MS were used to search for proteins that interact with ERAL1. MeRIP-qPCR, RIP-qPCR and actinomycin D experiments were used to verify whether the mRNA of NDUFV1 binds to IGF2BP2 and affects its stability.

Results: Firstly, we found that the guide RNA of ERAL1 was significantly enriched in the metastasis, suggesting that it was a tumor metastasis suppressor gene. Clinicopathological analysis showed that ERAL1 was low-expressed in HCC and positively correlated with prognosis of patients. Then, we confirmed that ERAL1 could inhibit HCC invasion and metastasis. Mechanically, following ERAL1 knockdown, various metabolites were enriched in the OXPHOS metabolic pathway. ERAL1 inhibited ATP production and metastasis of HCC cells by regulating NDUFV1. Notably, the Warburg effect did not appear in HCC cells after ERAL1 knockdown, and glucose metabolism was still mainly conducted by OXPHOS rather than glycolysis. ERAL1 could bind to and down-regulates the m6A reader protein IGF2BP2, which recognizes NDUFV1 mRNA through the m6A site and enhances its stability. Subsequently, a series of experiments proved that IGF2BP2 regulates NDUFV1 mRNA stability in HCC through m6A modification and facilitates tumor invasion and metastasis.

Conclusion: ERAL1 binds to and down-regulates IGF2BP2, inhibits the m6A modification of NDUFV1 mRNA by IGF2BP2, reduces the stability of NDUFV1 mRNA, and thus inhibits the generation of ATP in mitochondria. This study revealed a new mechanism of regulation of mitochondrial metabolism and metastasis of HCC cells, which is expected to provide a new sight for the treatment of HCC.

FRI-501

Platelet-derived extracellular vesicles (PEVs) as a potential biomarker for hepatocellular carcinoma (HCC)

Ángela Rojas^{1,2}, Rocío Muñoz-Hernández^{1,2}, Antonio Gil-Gómez^{1,2}, Vanessa García-Fernández¹, Sheila Gato-Zambrano^{1,2}, Rocío Montero-Vallejo^{1,2}, Rocío Gallego-Durán^{1,2}, Douglas Maya^{1,2}, Teresa Ferrer³, Javier Ampuero^{1,2,3}, Manuel Romero-Gómez^{1,2,3}.
¹Seliver Group, Instituto De Biomedicina De Sevilla (IBiS), Virgen Del Rocío University Hospital/CSIC/University of Seville., Sevilla, Spain;

POSTER PRESENTATIONS

²Centro De Investigación Biomédica En Red De Enfermedades Hepáticas y Digestivas (CIBEREHD), Madrid, Spain; ³UGC de Enfermedades Digestivas, Hospital Universitario Virgen Del Rocío, Sevilla, Spain
Email: angela_rojas16@hotmail.com

Background and aims: Hepatocellular carcinoma is a primary liver cancer that develops in an environment of chronic inflammation and liver damage where platelets have been proposed as key mediators of carcinogenesis. Platelet activation induces the release of extracellular vesicles (PEVs) which represent around 70–90% of circulating microparticles in the blood. The study aims to determine the use of PEVs as a potential circulating biomarker of HCC.

Method: Eighty-seven patients living with cirrhosis (82% males and average age: 64.5±9.4 years) were followed for 5 years: 35/87 (40%) did not develop HCC during the follow-up and 52/87 (60%) developed HCC. Plasma-heparin samples collected at the entry of the study was used to characterize PEVs by size, (0.2–1 µm Megamix Plus SC protocol, BD) and the expression of CD42b (glycoprotein Ib) and phosphatidylserine (the binding partner of annexin V) cell surface. Levels of PEVs Annexin V CD42b+ were quantified in plasma-heparin samples by flow cytometry.

Results: Alpha-fetoprotein and AST serum level were increased significantly in HCC in comparison with non-HCC cirrhotic patients (AFP: F4: 2.70±0.25 vs HCC: 376.06±147.30 ng/ml; $p < 0.001$ and AST: 35.21±4.99 vs HCC: 49.41±5.31 U/l; $p = 0.024$). In patients with HCC development a significant increase of total EVs (Annexin V+) was found (7816±1310 vs 3147±559 U/µl; $p < 0.001$) and PEVs-CD42b were also increased significantly in HCC (PEVs-CD42b: 1762±266 vs 486±111 U/µl; $p < 0.001$), despite no significant differences in serum total platelets (126.1±43.6 vs 155.4±100.8×10⁹/l; $p = 0.578$). Diagnostic accuracy of PEVs-CD42b was addressed by AUROC: 0.80 (0.70–0.89; $p < 0.001$) with sensitivity 78.8%, specificity 71.4%; PPV 81% and NPV 71.4% for HCC diagnosis (Cut off: 467.47 U/µl). In multivariate analysis age (OR: 1.16 (1.04–1.297; $p = 0.007$), sex (OR: 19.25 (1.23–299.25; $p = 0.035$) AFP serum levels (OR: 1.95 (1.27–2.99; $p = 0.002$) and PEVs-CD42b (OR: 1.001 (1,000–1,002; $p = 0.009$) were independently associated with HCC diagnosis.

Conclusion: Circulating PEVs levels are raised in patients with HCC despite no changes in platelet levels. In clinical settings, PEVs showed a potential as non-invasive biomarker for HCC diagnosis. Further studies are needed to elucidate the role of platelets in cancer.

FRI-502

KDM2A chromatin regulator constrains senescence program and immunoresponse in liver cancer

Elisa Morganti¹, Patrizio Caini², Matteo Lulli³, Rossella Del Frate⁴, Pinuccia Faviana⁵, Laura Gragnani⁶, Krista Rombouts⁷, Vinicio Carloni⁸. ¹Department of Experimental and Clinical Biomedical Sciences, University of Florence, Florence, Italy; ²Department of Experimental and Clinical Medicine, University of Florence, Florence, Italy; ³Department of Experimental and Clinical Biomedical Sciences, General Pathology Unit, University of Florence, Florence, Italy; ⁴Department of Translational Research and New Technologies in Medicine and Surgery, University of Pisa, Pisa, Italy; ⁵Department of Surgical, Medical, Molecular Pathology and Critical Area, University of Pisa, Pisa, Italy; ⁶Department of Translational Research and New Technologies in Medicine and Surgery, University of Pisa, Pisa, Italy; ⁷Institute for Liver and Digestive Health, University College London, London, United Kingdom; ⁸Department of Experimental and Clinical Medicine, University of Florence, Florence, Italy
Email: vinicio.carloni@unifi.it

Background and aims: Maintenance of genomic stability is essential for normal development and to prevent cancer. Genetic information is packaged into chromatin and accumulating evidence suggest that modulation of components of chromatin structure such as histones assumes a relevant significance in genomic integrity. However, how the chromatin remodelers intervene in maintaining genomic integrity and how they affect genetic information remain poorly

understood. KDM2A is a chromatin remodeler and it has been implicated in the regulation of CpG islands and genes transcription. KDM2A specifically removes methyl moieties from lysine 36 of histone H3 (H3K36).

Method: Human HCC cell lines (HepG2, Huh7), mouse HCC cell line (Hepa1-6) and hTert immortalized human hepatocytes (Hus) were employed. To assess the functional role of KDM2A, gain on- and loss-of-function, chromatin immunoprecipitation, RNA-seq, immunofluorescence/live imaging were performed. Mitochondria function, NADPH, lactate and H₂O₂ were evaluated. Hepa 1-6 cells depleted of KDM2A by using CRISPR/Cas9 were further analyzed in vitro and in vivo experiments.

Results: To identify chromatin regulators of genomic stability, knocked down of checkpoint kinase 2 (CHK2) a central effector of DNA repair was performed, hence RNA-seq was performed. RNA-seq analysis revealed that between upregulated genes were several immune response genes. Importantly, Huh7 cells that did not reveal any modifications of immune response genes expressed high levels of KDM2A. To explore the biological function of KDM2A we depleted KDM2A with RNA interfering in Huh7, HepG2 and Hepa1-6 and all cell lines tested showed increased expression of DNA damage marker phospho-histone H2AX. To explain the source of DNA damage we hypothesized an imbalance of redox homeostasis. Indeed, KDM2A depleted cells exhibited a defective antioxidative function represented by reduced NADPH and altered one carbon folate pathway. Furthermore RNA-seq and WB analysis on KDM2A depleted cells showed expression changes of CDKN2A, CDKN1A and LMNB1, markers of senescence. Significantly, we found that depletion of KDM2A coincided with increased H3K36me2 in CpG islands and led to re-expression of adaptive immunity proteins PD-L1 and MHC-I in human cancer cells and H2-D1, H2-T23, Mr1 in Hepa 1-6 cells, activation of AIM2/IFI16-STING signaling, and cell growth inhibition in vitro and in vivo. Consistent with these data, TGCA data analysis showed KDM2A overexpression in liver cancer and inverse correlation between KDM2A expression and CD8⁺ T cell infiltration.

Conclusion: These findings suggest a role for KDM2A as an epigenetic controller of cellular senescence program and its overexpression in liver cancer constrains the program and immune response. Along these lines targeting KDM2A by e.g. siRNA-GalNAc conjugated could represent a novel strategy in liver cancer treatment.

FRI-514

Fatty acids accumulate in intrahepatic cholangiocarcinoma-derived tissue and sera

Stefania Mantovani¹, Michele Dei Cas², Barbara Oliviero¹, Linda Montavoci², Monica Falleni³, Delfina Tosi³, Matteo Donadon⁴, Marcello Maestri⁵, Matteo Barabino⁶, Gaetano Piccolo⁶, Mario Umberto Mondelli^{1,7}, Anna Caretti². ¹Division of Clinical Immunology-Infectious Diseases, Department of Research, Fondazione IRCCS Policlinico San Matteo, Pavia, Italy; ²Department of Health Sciences, University of Milan, Milan, Italy; ³Pathology Division, Health Sciences Department, University of Milan, Milan, Italy; ⁴Department of Surgery, University Maggiore Hospital della Carità, Novara, Italy; ⁵Division of General Surgery 1, Fondazione IRCCS Policlinico San Matteo, Pavia, Italy; ⁶General Surgery Unit, Department of Health Sciences, San Paolo Hospital, University of Milan, Milan, Italy; ⁷Department of Internal Medicine and Therapeutics, University of Pavia, Pavia, Italy
Email: mario.mondelli@unipv.it

Background and aims: Intrahepatic cholangiocarcinoma (iCCA) is the second most common primary hepatic malignancy. Metabolic reprogramming is a hallmark of cancer pathobiology to sustain tumour growth and anabolic pathways. Lipids are crucial for cell survival as components of biological membranes, energy suppliers and bioactive mediators. However, information on the iCCA lipidome profile is still lacking. Fatty acid (FA) synthesis is downregulated in iCCA while active uptake by specific transporters is enhanced, even though conflicting data exist on the mechanism of FA accumulation.

Proliferation of CCA cell lines rely on lipid uptake to fuel FA catabolism and to promote FA storage in lipid droplets (LD) as neutral lipids. Several studies suggested that LDs are associated with cancer cell proliferation, resistance to death, aggressiveness, and support cancer stem cell functionality. In this study we investigated the iCCA lipidome in paired iCCA and non-tumour (NT) liver tissue and serum from iCCA patients, focusing on fatty acid metabolism.

Method: Lipid profile characterization of serum, surgically resected iCCA specimens and NT tissue was analyzed by liquid chromatography-tandem mass spectrometry analysis. In iCCA specimens and NT tissue, gene and protein expression were analysed by qPCR and Western Blot analysis. Immunohistochemistry was performed on iCCA and NT tissues. Healthy subjects' (HC) sera served as control.

Results: The untargeted lipidome profile showed a clear-cut separation between iCCA and NT tissues as well as between iCCA and HC sera. Indeed, FA accumulated both in iCCA tissue and patients' sera. Expression of Acetyl-CoA Carboxylase Alpha ACACA, the rate-limiting enzyme of *de novo* lipogenesis, was higher in iCCA tissue than in NT tissue. FABP5 membrane-associated transporter expression was unchanged; conversely, *FABP4* and *CD36* gene expression was down-regulated in iCCA tissue. Expression of Acyl-CoA Dehydrogenase Medium chain ACADM, which catalyses the initial step of FA β oxidation, was lower in iCCA tissue compared with NT tissue. LD were found in the cytoplasm of hepatocytes and macrophages of non-neoplastic parenchyma. Conversely, only small amounts of LD were found in neoplastic cells, while clusters of small droplets were found in the extracellular matrix and in intratumoral fibrous tissue. Several species of phospholipids and sphingolipids, the main components of plasma membranes, were upregulated in iCCA compared with NT tissues.

Conclusion: These findings suggest that FA accumulation could promote iCCA aggressiveness by supporting membrane biogenesis and generation of bioactive lipids. Differences in lipidome serum profile between iCCA patients and HC suggest a mean to identify individuals with iCCA by liquid biopsy.

FRI-515

TOX3 inhibits the progression of HCC through Jag1/Notch2 pathway

Shaoping She¹, Dongbo Chen¹, Hongsong Chen¹. ¹Peking University People's Hospital, Peking University Hepatology Institute, Beijing Key Laboratory of Hepatitis C and Immunotherapy for Liver Diseases, Beijing, China

Email: sheshaoping@126.com

Background and aims: Hepatocellular carcinoma (HCC) is the most common primary malignancy of the liver and represents a major global health-care challenge. Thymocyte selection-associated high mobility group box factors (TOXs) are members of an evolutionarily conserved DNA-binding protein family, and are expressed in several immune-relevant cell subsets. The transcription factor TOX3 can play different roles in different cancer types as a proto-oncogene or tumor suppressor gene, and can be used to predict the prognosis of certain tumor patients. However, the role and mechanism of TOX3 in HCC have not yet been elucidated.

Method: The expression of TOX3 was detected in different HCC patients cohorts and its correlation with patients' prognosis was analyzed. *In vivo*: In TOX3 knockout (*Tox3*^{-/-}) and wild-type (WT) mice, subcutaneous tumorigenesis models and liver orthotopic tumorigenesis models were established using two mouse HCC cell lines (Hepa1-6, H22); In nude mice, subcutaneous tumorigenesis models were established using two human HCC cell lines (Hep3B, SK-Hep1). The direct effects of TOX3 on HCC cells were studied *in vitro*. In addition, we performed RNA sequencing of HCC cells with TOX3 overexpression or knock out.

Results: Through the detection of clinical HCC patient samples, we found that TOX3 is upregulated in human HCC tissues, and its expression level is positively correlated with the prognosis of HCC

patients. By immunohistochemistry and immunofluorescence staining, we found that TOX3 expression in human HCC tissues was positively correlated with the infiltration level of CD8⁺ tumor-infiltrating lymphocytes (TILs) and negatively correlated with PD-L1 expression. In addition, we found that TOX3 expression in HCC tissues was positively correlated with the infiltration level of M1 macrophages and NK cells based on the TCGA database. *In vivo*, we found that overexpression of TOX3 inhibits the formation of subcutaneous tumors in nude mice. *In vitro*, we observed that overexpression of TOX3 inhibits the proliferation and migration of HCC cells, while knockout of TOX3 promotes the proliferation and migration of HCC cells. Furthermore, analysis of RNA sequencing results showed that TOX3 may inhibit the proliferation and migration of HCC cells through activating the Jag1/Notch2 signaling pathway.

Conclusion: Taken together, TOX3 inhibits the proliferation and migration of HCC cells by activating the Jag1/Notch2 signaling pathway, thereby limiting the progression of HCC and improving the prognosis of patients. The results are expected to clarify the role and mechanism of TOX3 in the liver tumor microenvironment for the first time, and explore the potential value of TOX3 as a prognostic indicator for HCC patients.

FRI-516-YI

Aurora kinase A and programmed death-ligand 1: expression dynamics in hepatocellular carcinoma development and the regulatory role of the kinase in immune checkpoint modulation

Luca Grisetti^{1,2}, Anna Alessia Saponaro^{1,2}, Caecilia Sukowati^{1,3}, Deborah Bonazza⁴, Emiliana Giacomello⁵, Paola Tarchi⁶, Lory Saveria Croce^{1,5,7}, Silvia Palmisano^{5,7}, Beatrice Anfuso⁸, Natalia Rosso¹, Pablo Giraudi¹, Claudio Tiribelli¹, Devis Pascut¹. ¹Fondazione Italiana Fegato ONLUS, Trieste, Italy; ²Department of Life Sciences, University of Trieste, Trieste, Italy; ³Eijkman Research Center for Molecular Biology, National Research, and Innovation Agency of Indonesia (BRIN), Jakarta Pusat, Indonesia; ⁴Surgical pathology, Azienda Sanitaria Universitaria Giuliano Isontina (ASUGI), Trieste, Italy; ⁵Department of Medical, Surgical, and Health Sciences, University of Trieste, Trieste, Italy; ⁶Surgical Clinic, Azienda Sanitaria Universitaria Giuliano Isontina (ASUGI), Trieste, Italy; ⁷Liver Pathology Clinic, Azienda Sanitaria Universitaria Giuliano Isontina (ASUGI), Trieste, Italy; ⁸International Centre for Genetic Engineering and Biotechnology (ICGEB), Trieste, Italy

Email: luca.grisetti@fegato.it

Background and aims: Aurora Kinase A (AURKA) is a pivotal mitotic kinase implicated in tumorigenic processes and overexpressed in most cancer types. Recent evidence suggests a new regulatory role for AURKA in modulating Programmed Death-Ligand 1 (PD-L1) expression in breast cancer. Despite its critical role, limited information exists on AURKA's involvement in hepatocellular carcinoma (HCC), and the regulatory interplay with PD-L1 remains unexplored. This study aims to explore AURKA and PD-L1 expression in HCC and precancerous conditions and the impact of AURKA inhibition and knockdown on the regulation of PD-L1 *in vitro*.

Method: AURKA and PD-L1 (CD274) mRNA and protein expression were assessed using qRT-PCR and Western blot, respectively. Human samples included healthy (n = 14), metabolic dysfunction-associated steatotic liver disease (MASLD) (n = 17), tumor, and paired adjacent non-tumoral (NT) tissues from HCC patients (n = 56). Mouse samples were collected from transgenic (TG) mice with chronic hepatitis B, progressing to HCC by 12 months, and wildtype (WT) mice sacrificed at 3, 6, 9, 12, and 15 months (n = 11 per condition). AURKA was inhibited by alisertib or AK-01 for 72 h, and knockdown was achieved through siRNA for 72 h or 144 h in HCC-derived JHH6 and Huh7 cell lines. The effects were evaluated in terms of cell viability, cell cycle arrest (flow cytometry), and PD-L1 protein expression (Western blot).

Results: AURKA and PD-L1 gradually increased from healthy to MASLD (p < 0.05) and from MASLD to HCC-adjacent NT tissues (p ≤ 0.05). AURKA overexpression was observed in 75% of HCC tissues

POSTER PRESENTATIONS

compared to NT tissues ($p < 0.001$), aligning with the results from the TG mouse model, where the gene was increased in early tumor stages compared to pre-tumoral stages ($p < 0.001$), NT ($p < 0.05$), and WT tissues ($p < 0.001$). *Cd274* exhibited a marked increase during neoplastic progression in mice ($p = 0.01$). *AURKA* positively correlated with *PD-L1* in HCC, NT, and MASLD tissues (all $p < 0.001$). Despite the decrease of *AURKA* protein expression in HCC tissues ($p < 0.001$), the percentage of phosphorylated *AURKA* (Thr288) was increased in HCC, suggesting augmented kinase activity. *AURKA* inhibition or knock-down increased aneuploidy (+19–48%, all $p < 0.01$) and reduced viability ($p < 0.001$) in both cell lines. AK-01 treatment decreased *PD-L1* glycosylated mature forms ($p < 0.01$), while 144-hour knockdown reduced unglycosylated *PD-L1* ($p < 0.05$) in both cell lines.

Conclusion: *AURKA* and *PD-L1* expression positively correlate in liver disease, both increasing with the progression of the disease. *AURKA* exhibits higher kinase activity in tumors than in NT tissues. *In vitro*, *AURKA* inhibition or silencing decreases *PD-L1* expression through two mechanisms, implying multiple roles of *AURKA* in the regulation of *PD-L1*. This suggests a potential use of *AURKA*-targeted therapy in combination with immune checkpoint inhibitors in cancer therapy.

FRI-517

Single-cell sequencing reveals differential efficacy of targeted therapy combined with immunotherapy in patients with hepatocellular carcinoma

Boxiang Zhang¹, Xin Song¹, Xiyao Chen¹, Xingrong Zheng¹, Tao Pan¹, Chan Xie¹, Liang Peng¹. ¹Department of Infectious Diseases, The Third Affiliated Hospital of Sun Yat-sen University, Guangzhou, China
Email: happyxiechan@hotmail.com

Background and aims: In the treatment of hepatocellular carcinoma, targeted therapy combined with immunotherapy is increasingly favored by clinics. However, there are still some patients who do not benefit from it, and the reasons for this are still not clear. In our study, we would like to analyze the tumor microenvironment of patients with different efficacy differences and reveal the reasons for the efficacy differences, so as to improve the efficacy of targeted therapy combined with immunotherapy in patients with hepatocellular carcinoma.

Method: We collected cancer and paracancer tissue samples from three patients with hepatocellular carcinoma who received targeted therapy combined with immunotherapy. Based on the Recist assessment criteria at 6 months after treatment, patients with good efficacy were categorized into the PR group, and those with non-significant efficacy were categorized into the PD group. Cellular heterogeneity and immune cell characteristics of hepatocellular carcinomas with different treatment responses were determined by single-cell nuclear sequencing.

Results: First, we found that the number of tumor cell subpopulations was significantly increased in the PD group. This suggests that the tumor cells of PD patients are significantly heterogeneous. Further functional analysis of up-regulated genes in different subpopulations revealed that tumor cells in the PD group mainly exhibited enhanced fatty acid metabolism, enhanced proliferation ability, and weakened adhesion ability. Next, we found that the tumor microenvironment in the PD group exhibited significant immunosuppression. This was manifested by a significant decrease in the number of T cells and macrophages and a significant increase in the proportion of suppressive immune cells. In the PD group, the proportion of Treg cells was significantly increased. In addition, we performed a pseudotemporal analysis of T cells, which showed that Treg cells were in the middle to late stage of differentiation. This suggests that the tumor-suppressive immune microenvironment is one of the important reasons for the difference in efficacy. At the same time, this immunosuppressive microenvironment promoted the conversion of T cells from tumor-promoting immune CD8⁺ T cells to immunosuppressive Treg cells.

As far as macrophages are concerned, the function of TAM cells in the PD group tended to functionally suppress T cells.

Conclusion: This study provides a comprehensive understanding of the tumor cellular and immune microenvironment in hepatocellular carcinoma and reveals the complex mechanisms underlying tumor response and resistance to anti-targeted therapy combined with immunotherapy. These insights provide potential avenues for improving the efficacy of immunotherapy in cancer patients.

FRI-518

Promoter DNA demethylation restores CYGB expression and attenuates hepatocellular carcinoma progression

Hoang Hai¹, Le Thi Thanh Thuy^{1,2}, Nguyen Thi Ha¹, Pham Minh Duc¹, Shoji Kubo³, Akihiro Tamori¹, Atsushi Hagihara¹, Etsushi Kawamura¹, Sawako Uchida-Kobayashi¹, Masaru Enomoto¹, Norifumi Kawada¹.

¹Department of Hepatology, Osaka Metropolitan University Graduate School of Medicine, Osaka, Japan; ²Department of Global Education and Medical Sciences, Osaka Metropolitan University Graduate School of Medicine, Osaka, Japan; ³Department of Hepato-Biliary-Pancreatic Surgery, Osaka Metropolitan University Graduate School of Medicine, Osaka, Japan
Email: kawadanori@omu.ac.jp

Background and aims: Cytoglobin (CYGB) acts as a tumor suppressor gene and DNA methylation in the CYGB promoter region has been reported in various types of cancers. This study aims to investigate whether CYGB promoter demethylation restoring CYGB expression and attenuating hepatocellular carcinoma (HCC).

Method: Forty-two pairs of tumor and adjacent non-tumor tissues from liver cancer patients with chronic hepatitis C virus infection were evaluated for CYGB promoter methylation using Ion GeneStudio S5. Restoration of CYGB expression was implemented in four HCC cell lines treated with 5-aza-2'-deoxycytidine (DAC). DAC-treated and untreated Huh7 cells were subcutaneously injected into the right and left flanks in 9 nude mice, respectively.

Results: Methylation frequency in tumors is significantly higher than that in non-tumor tissues at all of 33 CpG sites ($p = 1.02E-8$) in promoter region. Reversely, CYGB mRNA expression in tumor is significantly lower than that in non-tumor tissues (-60% , $p < 0.05$). Almost no methylation was found in human HSCs that correspond to positive CYGB expression. In contrast, high methylation frequency and no CYGB expression at RNA and protein levels were found in HCC cells (HepG2, Huh7, SNU-387, HLE) and myofibroblast LX-2 cells. Interestingly, DAC treatment time- and dose-dependently restored CYGB expression at both mRNA and protein levels in SNU-387, HLE and Huh7, and at mRNA level in HepG2 cells while no change in those of LX-2. Notably, after inducing CYGB expression in SNU-387, discontinuation of DAC treatment resulted in regressing of CYGB expression at both mRNA and protein levels. The mean tumor volume in left flanks injected with Huh7 was $3570 \pm 61 \text{ mm}^3$, significantly higher than that of $61 \pm 94 \text{ mm}^3$ in right flanks injected with DAC-treated Huh7.

Conclusion: Down-regulation of CYGB through promoter methylation is associated with HCC progression. Demethylation of CYGB gene promoter may lead to cancer regression.

FRI-519-YI

NKT cells play a protective role against MASH-derived HCC, particularly in female Balb/c mice

Carlos Cuño-Gómez^{1,2}, Anna Tutusaus^{1,3}, Nalika Conesa¹, Patricia Rider^{1,2,3}, Flavia Savino¹, Albert Morales^{1,3}, Montserrat Mari¹.

¹Institute of Biomedical Research of Barcelona (IIBB-CSIC), IDIBAPS, Barcelona, Spain; ²Departament de Biomedicina, Facultat de Medicina, Universitat de Barcelona, Barcelona, Spain; ³Barcelona Clinic Liver Cancer (BCLC) Group, Liver Unit, Hospital Clínic of Barcelona, Barcelona, Spain
Email: monmari@clinic.cat

Background and aims: Metabolic dysfunction-associated steatohepatitis (MASH) is emerging as the new major cause of hepatocellular carcinoma (HCC). Both MASH and HCC are sex-biased diseases, affecting men 3 times more than women due to biological and environmental factors. Intrinsic protection against HCC in females has classically been attributed to estrogen-driven IL-6 inhibition. Previous studies in our lab have demonstrated that natural killer T (NKT) cells, a non-conventional T-cell type mostly found in the liver, play a differential role in males and females in a murine MASH model. NKTs were found to be a protective factor against MASH development in male mice, but not in females. Here, our goal was to determine the role of NKTs in MASH-derived HCC development and to assess the potential differences between sexes.

Method: Male and female, Balb/c (wild-type or WT) or Cd1d^{-/-} (Cd1d-KO, NKT-deficient) mice were injected intraperitoneally with diethylnitrosamine (DEN) at 14 days of age and were fed with a high-fat choline-deficient (HFCD) diet for 20 weeks. Blood samples were taken every 4–5 weeks to quantify alpha-fetoprotein (AFP) and ALT activities. Livers were harvested to determine the presence of tumors, and tissue sections were obtained for hematoxylin-eosin (H&E) staining or immunohistochemistry (IHC). RNA was purified from liver lysates to quantify gene expression by reverse transcription qPCR.

Results: Most mice from all groups (9/10 WT males, 7/8 Cd1d-KO males, 7/9 Cd1d-KO females) developed HCC, except for WT females (0/14). Male Cd1d-KO mice displayed a more aggravated HCC phenotype compared to WT males. An increase in serum AFP concentration was detected at an earlier timepoint in Cd1d-KO males compared to the other groups. AFP was also increased in Cd1d-KO females and WT males at the end of the experiment, but remained unchanged in WT females. The mRNA expression of different tumor associated genes (Afp, Gpc3, Ki67), and ALT activity were significantly increased in Cd1d-KO male mice compared to WT male mice.

Conclusion: From this work the following conclusions were obtained: a) NKT cells in Balb/c mice play a protective role against the development of HCC in a MASH context; b) Female mice are naturally protected against DEN+HFCD-induced HCC, but this protection is eliminated in NKT-deficient individuals.

FRI-521

Mannose receptor (CD206) as a therapeutic target in the liver metastatic microenvironment of colorectal cancer

Ines Alonso¹, Alba Herrero¹, Francesca Mastrotto², Luisa Martinez-Pomares³, Giuseppe Mantovani⁴, Beatriz Arteta¹, Aitor Benedicto¹. ¹Cancer and Translational Medicine, School of Medicine and Nursing, University of Basque Country, Leioa, Spain; ²Department of Pharmaceutical and Pharmacological Sciences, University of Padova, Padova, Italy; ³School of Life Sciences, University of Nottingham, Nottingham, United Kingdom; ⁴School of Pharmacy, University of Nottingham, Nottingham, United Kingdom
Email: aitor.benedicto@ehu.es

Background and aims: Colorectal cancer (CRC) is one of the most prevalent cancers worldwide. Liver metastases of CRC is a very complex scenario that decreases substantially the prognosis of this disease, been the major cause of CRC related deaths. Previous works from this group have shown that in the liver metastatic microenvironment mannose receptor (ManR) expression and activity is modulated by mediating in the regional immune response. While the role of this receptor is well known in antigen presentation and innate immunity, its role as a potential therapeutic target is unknown. Thus, we aim to elucidate the effect of Mannose Receptor blockage in the tumour microenvironment and its role as a prometastatic factor.

Method: *In vitro*, primary liver sinusoidal endothelial cells previously treated with either ManR antibodies or specific sulphated glycopolymers was culture in the presence of either C26 murine colon carcinoma cells or the secretome of basal and sICAM-1 activated C26 cells. Then, endocytosis and processing of ovalbumin was assessed.

Secretome, cell protein and RNA was collected and analysed. Additionally, the motility of LSECs was analysed under such conditions. *In vivo*, experimental metastasis assay was carried out to establish the effect of ManR blockage in the volume of hepatic tissue occupied by the tumour. Also, the recruitment of macrophages, hepatic stellate cells and collagen deposition was analysed.

Results: *In vitro*, the blockage of ManR in LSEC before interaction with C26 cells or the secretome abrogates the stimulation of ManR activity, along with the capacity of motility in treated LSECs. The analysis of the secretome, protein expression and RNA showed decrease of proinflammatory, pro angiogenic and profibrotic markers involved in metastatic development, such as IL-1β, IL-6 and VEGF, while others were slightly, although not significantly, reduced. *In vivo*, a significant reduction in metastatic development was observed under ManR inhibition along with a reduction in myofibroblasts and macrophages recruitment, along with a reduced desmoplastic response.

Conclusion: ManR modulate the prometastatic microenvironment development of colorectal carcinoma. The reduction in prometastatic markers after ManR inhibition *in vivo* and *in vitro* points out ManR as a potential therapeutic target in the treatment of hepatic colorectal metastasis.

FRI-522

Loss of Toll-like receptor 9 protects from hepatocellular carcinoma in murine models of chronic liver disease

Hannes Hatten¹, Leticia Colyn¹, Ines Volkert¹, Twan Lammers², Kai Markus Schneider¹, Christian Trautwein¹. ¹University Hospital RWTH Aachen, Department of Internal Medicine III, Aachen, Germany; ²University Hospital RWTH Aachen, Institute for Experimental Molecular Imaging (ExMI), Aachen, Germany
Email: hhatten@ukaachen.de

Background and aims: Toll-like receptor 9 (Tlr9) is a pathogen recognition receptor, sensing unmethylated DNA derivatives from pathogens and damaged host cells. Hence, it is an important modulator of innate immunity. It has been shown that Tlr9 not only detects CpG motifs but also DNA-containing nucleotide derivatives of other origins, being able to recognize endogenous DNA derived from apoptotic neighboring cells. Given the increase in cell death during chronic liver disease, this further emphasizes the importance of Tlr9 in inflammation-associated cell damage and the progression of inflammatory liver diseases. We aimed to investigate the role of Tlr9 in fibrogenesis and hepatocellular carcinoma (HCC) progression in chronic liver diseases.

Method: We treated mice with constitutive deletion of Tlr9 (Tlr9^{-/-}) with DEN/CCl₄ for 24 weeks. As a second model, we used hepatocyte-specific Nemo knockout (Nemo^{hepa}) mice to induce liver damage and disease progression. We generated double knockout (Nemo^{hepa}Tlr9^{-/-}) animals and sacrificed them without performing any treatment at the age of 52 weeks.

Results: Tlr9 deletion resulted in reduced fibrosis as well as HCC burden. We observed down-regulation of hepatic stellate cell activation and consequently decreased collagen production in both models. Tlr9 deletion was associated with decreased hepatocyte apoptosis and proliferation, modulating the initiation and progression of hepatocarcinogenesis. This observation was accompanied by a decrease in interferon-β (Ifnb1) and an increase in expression of chemokines with anti-tumoral ability. We show that Tlr9 is primarily expressed in Kupffer cells, suggesting a key role of Tlr9 in intercellular communication during liver damage.

Conclusion: Our data define Tlr9 as an important pathway involved in fibrogenesis, but also in the initiation and progression of hepatocellular carcinoma during chronic liver diseases. Here, the downregulation of Ifnb1 seems interesting as it is already known to cause apoptosis leading to compensatory proliferation and disease progression, although potential pleiotropic effects of Tlr9 cannot be excluded.

FRI-523

Enhancing the response of cholangiocarcinoma to chemotherapy by inhibiting MRP3-mediated drug export

Maitane Asensio^{1,2}, Oscar Briz^{1,2}, Elisa Herraiz^{1,2}, Ricardo A. Espinosa-Escudero¹, Laura Perez-Silva¹, Marta Romero^{1,2}, Alvaro Temprano¹, Nazaret Hortelano-Hernandez¹, Kevin Delgado-Calvo¹, Rebeca P. Marijuan¹, Ana Peleteiro Vigil¹, Oliver Poetz^{3,4}, Thomas Efferth⁵, Elisa Lozano^{1,2}, Onat Kadioglu⁶, Jose J. G. Marin^{1,2}, Rocio Macias^{1,2}. ¹University of Salamanca, IBSAL, Salamanca, Spain; ²National Institute for the Study of Liver and Gastrointestinal Diseases (CIBERehd), Carlos III National Health Institute, Madrid, Spain; ³Signatope GmbH, Reutlingen, Germany; ⁴Natural and Medical Sciences Institute at the University of Tübingen (NMI), Reutlingen, Germany; ⁵Institute of Pharmaceutical and Biomedical Sciences, Johannes Gutenberg University, Mainz, Germany; ⁶Institute of Pharmaceutical and Biomedical Sciences, Johannes Gutenberg University, Mainz, Spain
Email: rociorm@usal.es

Background and aims: The activity of ATP-binding cassette (ABC) pumps hinders the response of many cancers to pharmacological treatment. The relevance of MRP3 (gene ABCC3) cholangiocarcinoma (CCA) chemoresistance has been elucidated. Moreover, the effect of inhibiting MRP3 has been evaluated.

Method: MRP3 expression in CCA was investigated in silico using data from the TCGA database (CHOL-TCGA) and determined by RT-QPCR in intrahepatic (iCCA) and extrahepatic (eCCA) CCA and paired adjacent liver tissue (Salamanca cohort). Protein expression and subcellular location were assayed by WB, immunoaffinity LC-MS/MS, and IHC. Several monoclonal cell sublines with overexpression or silencing of MRP3 were developed by transduction with lentiviral vectors. Cell viability was determined by the MTT test. The predicted interaction between MRP3 and ~40,000 natural and semisynthetic compounds (ZINC database) was calculated using a docking approach. Potential inhibitors (EM) were selected based on their interaction score, commercial availability, and price. Tyrosine kinase inhibitors (TKI) were also screened as potential MRP inhibitors. The ability to inhibit MRP3 was validated by flow cytometry and cell viability assays. SynergyFinder online tool was used to calculate the degree of synergistic-additive-antagonistic effects of drug combinations.

Results: MRP3 was the most abundantly expressed ABC pump both in iCCA and eCCA. CCA-derived cells (EGI-1 and TFK-1) showed high mRNA ABCC3 and MRP3 levels at the plasma membrane. Overexpression of ABCC3 in HEK293T cells resulted in a significantly lower cytostatic effect of etoposide (a known MRP3 substrate), platinum-based drugs, SN-38, 5-FU, mitoxantrone, and cabozantinib as compared with Control (Mock) cells. Besides, silencing ABCC3 in EGI-1 cells using shRNAs enhanced the sensitivity to etoposide, cisplatin, SN-38, and mitoxantrone, suggesting a reduction in MRP3-mediated efflux of these drugs. The in silico screening of natural compounds identified 8 potential MRP3 substrates with high ligand binding energy. Flow cytometry-based transport assays of these potential chemosensitizers and 20 TKIs revealed that EM-114, EM-188, and sorafenib reduced the ability of MRP3 to transport carboxyfluorescein (CF), a well-known MRP substrate. However, only sorafenib and MK571 (a pan-MRP inhibitor) could sensitize CCA cell lines to agents presumably transported by MRP3, such as etoposide, SN38, and cisplatin. Thus, the combination of sorafenib with etoposide or cisplatin synergistically reduced the viability of CCA cells.

Conclusion: MRP3, which is highly expressed in CCA, may determine the response of this cancer to several antitumor drugs, such as cisplatin and SN-38. Moreover, pharmacological inhibition of this transporter with sorafenib can be a sound synergistic strategy to enhance the response of CCA to chemotherapy.

FRI-524

Novel genetic loci for hepatocellular carcinoma identified through genome-wide association study meta-analysis from 909,722 individuals

Ifechukwuamaka Chinaka¹, Jake Mann². ¹University of Dublin, Dublin, Ireland; ²University of Birmingham, Birmingham, United Kingdom
Email: jpmann.gsy@gmail.com

Background and aims: Hepatocellular carcinoma (HCC) has high mortality, limited treatment options, and is increasing globally. It is a complication common to all end-stage liver disease. To date, genome-wide association studies (GWAS) for HCC have been aetiology-specific. Here, we conducted trans-ethnic GWAS meta-analysis for all-causes in order to identify genetic drivers independent of aetiology.

Method: Four GWAS were included: FinnGen project (287,590 total, 982 cases), BioBank Japan (197,611 total, 1,866 cases), a European alcohol-associated HCC GWAS conducted by Trepo et al (4,040 total, 1,649 cases) and the Pan-ancestry UK Biobank (420,531 total, 154 cases). Meta-analysis was performed using MR-MEGA (Meta-Regression of Multi-Ancestry Genetic Association).

Results: The complete cohort included 4,651 HCC cases and 905,121 controls, with 4,287,267 variants used in meta-analysis. We established rs72613567:T > A in *HSD17B13* as a protective genome-wide significant locus for all-cause HCC ($p = 4.6e-8$) and replicated well-recognised risk loci in *PNPLA3* (rs738409:C > G, $p = 2.3e-21$) and *TM6SF2* (rs58542926:C > T, $p = 2.0e-12$). In addition, we found five novel loci at suggestive significance, including the tumour suppressor gene *FLI1* (rs1238566:A > G; $p = 9.3e-6$) and *NOTCH4* (rs499691:C > T; $p = 9.3e-7$), which has aberrant expression in HCC. Variants in *MDGA2* (rs2297926:G > A; $p = 1.2e-7$) were also associated with increased risk of HCC; these are also associated with body mass index ($p = 5.6e-24$) and all-cause cirrhosis ($p = 1.1e-4$). Meta-analysis also identified signals in *CCDC63* (rs4766521:T > C, $p = 1.3e-6$), which is associated with alcohol intake, and *IFNL3* (rs12971396:C > G, $p = 3.7e-6$), which influenced hepatitis C viral response.

Conclusion: In the largest genetic study of liver cancer to date, we identified six novel loci that provide insights into aetiology of all-cause HCC.

FRI-525

Phosphoinositide 3-kinase delta promotes plasticity and development of the microenvironment in cholangiocarcinoma

Vanessa Bou Malham^{1,2}, Nassima Benzoubi^{2,3}, Javier Vaquero^{4,5}, Christophe Desterke⁶, Jean Agnetti^{2,3}, PeXuan Song^{2,3}, Ester Gonzalez-Sanchez^{7,8,9,10}, Ander Arbelaiz¹¹, Sophie Jacques¹², Emanuel Di Valentin¹³, Souad Rahmouni¹⁴, Tuan Zea Tan¹⁵, Didier Samuel^{16,17,18}, Jean Paul Thiery¹⁹, Mylène Sebah^{16,17,20}, Laura Fouassier²¹, Ama Gassama-Diagne^{2,3}. ¹University Paris-Saclay, UMR-S 1193, Villejuif, France, villejuif, France; ²INSERM UMRS-1193, Villejuif, France; ³University Paris-Saclay, UMR-S 1193, Villejuif, France, Villejuif, France; ⁴Centro de Investigación del Cáncer, Instituto de Biología Molecular y Celular del Cáncer, CSIC-Universidad de Salamanca, Salamanca, Spain, Salamanca, Spain; ⁵Centre de Recherche Saint-Antoine, CRSA, Sorbonne Université, INSERM, Paris, France, Paris, France; ⁶Université Paris-Saclay, UFR Médecine-INSERM1310, Villejuif, France; ⁷Centre de Recherche Saint-Antoine, CRSA, Sorbonne Université, INSERM, ParisXII; ⁸TGF- β and Cancer Group, Oncobell Program, Bellvitge Biomedical Research Institute (IDIBELL), Barcelona, Spain; ⁹Oncology Program, CIBERehd, National Biomedical Research Institute on Liver and Gastrointestinal Diseases, Instituto de Salud Carlos III, Madrid, Spain; ¹⁰Inovation, PARIS, France; ¹¹Centre de Recherche Saint-Antoine, CRSA, Sorbonne Université, INSERM, Paris, France; ¹²Laboratory of Animal Genomics, GIGA-Medical Genomics, GIGA-Institute, University of Liège, Liège, Belgium; ¹³Plateforme des vecteurs viraux, Université de Liège, GIGA B34, Liège, Belgium; ¹⁴Laboratory of Animal Genomics, GIGA-Medical Genomics, GIGA-Institute, University of Liège, Liège, Belgium 10Plateforme des vecteurs viraux, Université de Liège, GIGA B34, Liège, Belgium; ¹⁵Genomics and Data Analytics Core (GeDaC), Cancer Science

Institute of Singapore, National University of Singapore, Singapore, Singapore; ¹⁶INSERM, Unité 1193, Villejuif, France; ¹⁷Université Paris-Saclay, UMR-S 1193, Villejuif, France; ¹⁸Centre Hepato-Biliaire, AP-HP Hôpital Paul Brousse, Villejuif; ¹⁹Guangzhou Laboratory, International Biological Island Guangzhou, Guangzhou, China; ²⁰Laboratoire d'Anatomopathologie, AP-HP Hôpital Paul-Brousse, Villejuif, France; ²¹Centre de Recherche Saint-Antoine, CRSA, Sorbonne Université, INSERM, Paris
Email: ama.gassama@inserm.fr

Background and aims: The cholangiocarcinoma (CCA) is a highly aggressive liver cancer increasing worldwide. Surgery is the main therapeutic option but few patients are eligible at the time of diagnosis. Unsolved questions on the onset and progression of CCA remain. The high plasticity of liver epithelial cells largely contributes to generate stem cells, promoting resistance to treatment in CCA. We previously reported that PI3Kdelta regulates polarity via extracellular matrix (ECM) assembly and our recent data revealed its critical role in epithelial to mesenchymal transition (EMT)-dependent plasticity. Thus, inducing the reprogramming of liver carcinoma cells into polarized stem-like cells via the transforming growth factor- β (TGF- β) signalling. This study aims to elucidate the involvement of PI3Kdelta in CCA progression and malignancy.

Method: We used different human CCA cell lines including EGI-1 cells, established from the advanced stage of primary bile duct carcinoma (DSMZ, Germany) cultured in 3D. Xenograft tumors were established with PI3K delta -overexpressing EGI-1 cells (EGI-1-PI3Kdelta) injected in immunodeficient mice. Moreover, PI3Kdelta was overexpressed in the mouse liver by Adeno-Associated Virus (AAV) gene transfer plasmids. Protein expression was assessed using immunoblot and immunostaining techniques, and gene expression using RT-qPCR. Besides, ELISA assays were conducted on mouse sera to quantify cytokine secretion. The CCA tumors from patients were obtained from the "Centre de Ressources Biologiques Paris-Sud Villejuif, France".

Results: We showed by immunostaining that PI3Kdelta expression in patient CCA tumors is related to pluripotent stem cell and EMT markers. To evaluate the role of PI3Kdelta in CCA, we analyzed organoids derived from PI3Kdelta-overexpressing CCA cells. The cells exhibited strong expression of mesenchymal markers, stem cell markers and TGF β /Src signaling molecules. The expression of ECM proteins like fibronectin, type IV collagen, and laminin increased, indicating ECM remodeling. The xenografts derived from EGI-1-PI3Kdelta cells showed higher growth rates and volumes compared to controls. Notably, histological staining revealed fibrosis and increased CD31 expression in these xenografts. Analysis of the serum from mice revealed the secretion of pro-angiogenic cytokines. Interestingly, the sinusoids in the AAV-PI3Kdelta liver were wider than in the AAV-control mice liver. The CD31 expression increased by the overexpression of PI3Kdelta, indicating its critical role in angiogenesis. Finally, our recent studies indicated the involvement of PI3Kdelta in lymphangiogenesis and immunity.

Conclusion: This work highlights the crucial role of PI3Kdelta in the development of a dense stroma and tumour progression in CCA by promoting angiogenesis and ECM remodelling through EMT-dependent plasticity signalling.

FRI-526

Role of the splicing factor PCBP2 in cholangiocarcinoma malignancy and chemoresistance

Candela Cives-Losada^{1,2}, Maria Reviejo^{1,2}, Maitane Asensio^{1,2}, Elisa Lozano^{1,2}, Sara Ortiz-Rivero^{1,2}, Maria J. Monte^{1,2}, Maria A. Serrano^{1,2}, Oscar Briz^{1,2}, Rocio Macias^{1,2}, Jose J. G. Marin^{1,3}.
¹Experimental Hepatology and Drug Targeting (HEVEPHARM), University of Salamanca, Institute of Biochemical Research of Salamanca (IBSAL), Salamanca, Spain; ²Spanish Network of Biomedical

Investigation for the Study of Liver and Gastrointestinal Diseases (CIBERehd, Instituto de Salud Carlos III), Madrid, Spain; ³Spanish Network of Biomedical Investigation for the Study of Liver and Gastrointestinal Diseases (CIBERehd, Instituto de Salud Carlos III), Salamanca, Spain
Email: candelacives@usal.es

Background and aims: Poly (rC)-binding protein 2 (PCBP2), a splicing factor member of the hnRNP family of regulatory proteins, was reported to be altered in different types of cancer, affecting tumorigenesis and chemoresistance. However, its relevance in cholangiocarcinoma (CCA) is yet unknown. Thus, this study aimed to elucidate the role of PCBP2 in developing CCA malignant characteristics and drug resistance.

Method: PCBP2 expression was investigated in CCA (n = 36) and adjacent non-tumor (n = 9) tissues in silico using data from The Cancer Genome Atlas (TCGA) and determined by Taqman Low-Density Array (TLDA) and immunohistochemistry in samples from intrahepatic CCA (iCCA; n = 13), extrahepatic CCA (eCCA; n = 10) and adjacent non-tumor tissue (n = 9), obtained at the Salamanca University Hospital. Besides CCA cells (EGI-1), primary human cholangiocytes and hepatocellular carcinoma-derived cells (Huh7) were analyzed as in vitro models. Lentiviral vectors carrying shRNA against PCBP2, and empty vectors (Mock) were generated to transduce liver cancer cells. PCBP2 silencing was confirmed by RT-qPCR and western blot. Transcriptomic analysis of these cells was carried out by RNA-Seq. Migration and proliferation studies were performed by holographic microscopy. Cell cycle characterization was performed by flow cytometry. Induction of apoptosis was assessed by determining the expression of apoptosis-related genes using RT-qPCR. MTT assay was performed to determine the effect on cell viability of anti-tumor drugs (cisplatin, oxaliplatin, gemcitabine, 5-FU, sorafenib, and regorafenib).

Results: In silico analysis showed that PCBP2 is abundantly expressed in CCA, which was confirmed experimentally in tumor samples at mRNA and protein levels. Both iCCA and eCCA presented significantly higher levels of PCBP2 than non-tumor cholangiocytes. Moreover, immunohistochemistry revealed intense nuclear expression of PCBP2 in cancer cells. Compared with Mock cells, silencing of PCBP2 in liver cancer cell lines did not induce changes in the response to the studied anti-tumor drugs. In contrast, a significant decrease in cell proliferation and viability, a lower migration capacity, and enhanced expression of the pro-apoptotic factor BAX, consistent with apoptosis activation, were found. RNA-Seq analyses revealed that PCBP2 silencing affected the expression of several genes known to be associated with the oncogenic process, i.e., downregulation of MEX3A, NRIP1, and NRP2 and alteration of the alternative splicing pattern of MAP4K4.

Conclusion: PCBP2 may act as a relevant factor in regulating cell migration and proliferation in CCA and, therefore, a potential target to be considered in developing novel strategies to treat this cancer.

FRI-527

ACSL4 affects the invasion and metastasis of hepatocellular carcinoma by regulating the activation of arachidonic acid

Yusufkader Maimaitinijati¹, Shizhong Yang¹, Yunfang Wang², Guifang Du², Xiong Chen³, Jiahong Dong¹. ¹Tsinghua University, Beijing, China; ²Tsinghua university, Beijing, China; ³people's hospital of Xinjiang Uyghur Autonomous Region, Beijing, China
Email: 1554504825@qq.com

Background and aims: Hepatocellular carcinoma (HCC) has an insidious onset, easy recurrence and metastasis, and often has a poor prognosis. Tumor invasive front (TIF) is the most active site for tumor cells to invade outwards, and it is also the source of tumor micro-metastasis. Therefore, a comprehensive understanding of the invasive front of HCC and the mining of its key biomarkers may not only deepen the understanding of the mechanisms of HCC invasion and metastasis, but also pave the way for the development of new

therapeutic strategies for HCC. This study was to explore the key biomarkers are closely associated with invasion and metastasis of HCC and its clinical value.

Method: Firstly, we based on the spatial transcriptomic sequencing data of HCC clinical specimens, the biological characteristics of HCC invasive front were deeply analyzed, and an innovative algorithm was used to mine the key biomarker of TIF, which is closely related to HCC invasion and metastasis. Then, the clinical value of biomarker demonstrated through multi-center cohort that recruited 243 HCC patients from 3 clinical centers in China. Finally, the functional mechanism was revealed through in vivo, in vitro and multi-omics joint analysis.

Results: ACSL4 has significant tissue specificity and spatial specificity in HCC, and was strongly positive in the whole process of HCC invasion and metastasis, such as circulating tumor cells, microvascular invasion, intrahepatic metastases and distant metastases lesions. Multicenter study shows that the overall survival rate ($p < 0.05$) and recurrence-free survival rate ($p < 0.05$) of the high ACSL4 expression patients were lower than the low ACSL4 expression patients. Correspondingly, the MVI occurrence rate of patients with high ACSL4 expression was higher than that of patients with low ACSL4 expression ($p < 0.05$). The results of in vivo and in vitro experiments indicate that the ACSL4 gene is closely related to the invasive and metastatic abilities of HCC cells. Transcriptomics and metabolomics joint analysis observed that after knocking down ACSL4, key enzymes (CPT1A, CPT2, ACOX1) and metabolic products (arachidonic acid, Acetyl-CoA) involved in fatty acid beta-oxidation process underwent significant changes ($p < 0.01$).

Conclusion: ACSL4 affects the invasion and metastasis of hepatocellular carcinoma by regulating the activation of arachidonic acid.

FRI-530

Gut microbiome signature is distinct in cirrhosis with HCC compared to cirrhosis without HCC and controls in a southeast asian cohort and is linked with gut permeability and metabolite biomarkers

Thananya Jinato¹, Patrick Gillevet², Masoumeh Sikaroodi², Pisit Tangkijvanich³, Jasmohan Bajaj⁴, Natthaya Chuaypen¹. ¹Center of Excellence in Hepatitis and Liver Cancer, Faculty of Medicine, Chulalongkorn University, Bangkok, Thailand; ²Microbiome Analysis Center, George Mason University, Manassas, United States; ³Center of Excellence in Hepatitis and Liver Cancer, Faculty of Medicine, Chulalongkorn University, Bangkok, Thailand, Bangkok, Thailand; ⁴Virginia Commonwealth University, Richmond VA Medical Center, Richmond, United States
Email: natthaya.ch56@gmail.com

Background and aims: The gut microbiota and bacterial by-products may contribute to the pathogenesis of liver diseases including cirrhosis and hepatocellular carcinoma (HCC). However, most studies are from Western or East Asian countries but not South-East Asia. In this study, we aimed to characterize gut dysbiosis, gut permeability, and butyrate biomarkers in patients with/without HCC from Thailand.

Method: This cross-sectional study included 30 healthy controls, 33 patients with cirrhosis without HCC (16 viral and 17 non-viral), and 44 with HCC (29 viral and 15 non-viral). Fecal samples were sequenced with 16S rRNA and analyzed for alpha/beta diversity and individual taxa comparisons between 3 groups. Circulating biomarkers of gut permeability including intestinal fatty acid-binding protein (I-FABP) and lipopolysaccharide-binding protein (LBP) were measured. The butyrate-associated gene (BCoAT) expression was assessed in fecal samples.

Results: Diversity: alpha-diversity (Chao1 index) was significantly higher in healthy controls (139.0 ± 33.9 , $p < 0.001$) and cirrhosis without HCC (138.0 ± 46.4 , $p = 0.008$) compared to HCC groups (109.0 ± 37.9). Beta-diversity demonstrated distinctions between healthy controls and HCC groups ($p = 0.006$), but not between pts with

cirrhosis with/without HCC. Taxa differences: Multiple pairwise comparisons using ANCOM-BC2 (FDR<0.05) among the top 50 relative abundance at genus level identified significantly increased *Ligilactobacillus*, *Catenibacterium*, and *Alloprevotella* in both cirrhosis (HCC/not) compared to healthy controls. The *[Ruminococcus] gnavus* (*R. gnavus*) group, related to inflammation and metabolic diseases, was significantly increased, while butyrate-producing bacteria including *Coprococcus* and *Subdoligranulum*, were significantly decreased in HCC. However, only *Subdoligranulum* showed a significant decline in HCC compared with no-HCC cirrhosis. For permeability and inflammation, Within the entire cohort, a positive correlation between BCoAT levels and the abundance of *Subdoligranulum* ($r = 0.227$, $p = 0.023$) was observed, while its levels were negatively correlated with the *R. gnavus* group ($r = -0.387$, $p < 0.001$). Additionally, I-FABP and LBP levels exhibited positive correlations with the *R. gnavus* group ($r = 0.401$, $p = 0.001$) and *Alloprevotella* ($r = 0.293$, $p = 0.012$), but were negatively correlated with *Subdoligranulum* ($r = -0.390$, $p = 0.002$).

Conclusion: In a prospective Thai cohort, distinctive gut microbial alterations in cirrhosis, especially related to HCC were found. Increased gut permeability was linked to enriched pathogenic bacteria and lower beneficial bacteria. These data highlight the role of gut dysbiosis and altered bacterial by-products in progressive liver diseases.

FRI-531

Metabolic dysfunction associated steatohepatitis derived HCC model mouse for immune-oncology

Taishi Hashiguchi¹. ¹SMC Laboratories, Inc., Ota-city, Japan
Email: hashiguchi@smclab.co.jp

Background and aims: Metabolic dysfunction-associated steatohepatitis (MASH) is a is linked to type II-diabetes and marked by steatosis, steatohepatitis, fibrosis and eventually HCC. The number of patients with MASH-derived HCC is increasing worldwide. Currently, the first line of cancer treatment drugs are immune checkpoint inhibitors (ICIs). Although ICIs have been approved by the FDA for various cancers, it has been reported that the response rate for HCC is low, and the development of new therapeutic drugs including ICIs for HCC is expected. Therefore, a mouse model for evaluating MASH-derived liver cancer is needed for drug discovery against HCC. In this study, in order to examine whether the STAM mouse, a MASH-HCC model mouse, can be used for the evaluation of ICIs, we conducted an analysis of immunohistochemistry and RNA-seq related to the immuno-oncology (IO) of HCC derived from STAM mice.

Method: MASH was induced in male mice by a single subcutaneous injection of 200 µg streptozotocin solution 2 days after birth and feeding with high fat diet after 4 weeks of age. The mice were sacrificed and livers collected at 6, 8, 10, 12, 16, 20 and 24 weeks of age. For RNA-seq analysis, total RNA from the left lateral lobe was isolated using RNeasy mini kit. Liver specimens were stored at -80°C embedded in Optimal Cutting Temperature compound for immunohistochemistry (IHC). IHC for PD-1, PD-L1, CTLA-4, CD8, FOXP3, a-SMA and FAP was performed.

Results: Expression analysis of IO-related genes was performed. Increased expression was observed in CCL5, CD4, CD8a, CD274, CXCR4, CXCR10 and PDCD1. Additionally, mutations were observed in some genes. As a result of IHC, PD-1, PD-L1, CTLA-4, CD8, a-SMA and FAP -positive signals were detected in the peri-tumor region. Furthermore, CD8-positive signals were also detected in the intra-tumor region.

Conclusion: STAM mouse model, is the model that allows the evaluation of drugs that genetic mutations, immune cells, and tumor microenvironment in addition to molecular targeted drugs.

FRI-532

Metformin boosts the sensitivity of hepatocellular carcinoma to sorafenib via reshaping the tumor microenvironment metabolism

Juan Gao^{1,2}, ¹Karolinska Institutet, Laboratory Medicine/BCM, Stockholm, Sweden; ²The Third Affiliated Hospital of Sun Yat-sen University, Department of Infectious Diseases, Guangzhou, China
Email: gaoj59@mail2.sysu.edu.cn

Background and aims: Metabolic syndrome (MS), such as obesity and type 2 diabetes mellitus (T2DM), is considered an independent risk factor for hepatocellular carcinoma (HCC). Hepatic free fatty acids (FFAs) accumulation, shown as Metabolic-associated fatty liver disease (MAFLD), supports tumor progress by leading the tumor metabolic reprogram. Our previous studies suggested anti-metabolism disorder therapies, such as cold exposure, suppress tumor growth by altering global metabolism (Seki et al., 2022, Nature 608). Sorafenib is the first-line anti-HCC treatment. However, Sorafenib resistance was reported in the MS-HCC combined patients. Metformin, a well-known insulin-sensitizing drug in anti-T2DM treatment and modulator of systematic metabolism. We are interested in how the systematic metabolism reshapes the HCC micro-environment. We also gain insight into the potential mechanisms of combining metabolic stimulators and existing drug therapies.

Method: To establish MS in animal models, adult male C57BL/6N mice were fed with high-fat diet (HFD, 60% fat calories) for more than 3 months to reach obesity. Hepa1-6 cells were implanted in the mice's liver as the orthotopic HCC models. Approximately 1 week after, mice were randomly grouped and orally treated with 10 mg/kg sorafenib (S group), or 10 mg/kg sorafenib with 150 mg/kg metformin (S+M group), or equivalent diluted polyethylene glycol (PEG) (vehicle group) for the next 4 weeks. The Glucose tolerance test (GTT) and insulin tolerance test (ITT) were performed to evaluate the host metabolic condition during the treatment. Terminally, mice were sacrificed, blood, liver with tumor were collected for histological and biochemistry analysis. All data were presented as the mean \pm SEM and analyzed with unpaired Student's t-test or one-way ANOVA analysis.

Results: After 4 weeks of treatment, the body weight and BMI of HCC-HFD mice showed no significant difference between the 3 groups ($p > 0.05$). Surprisingly, compared to the other 2 groups, the liver weight decreased in the S+M group ($p < 0.05$). And the visible tumor volume showed the same difference ($p < 0.05$). Both GTT, ITT (AUC), and metabolite biochemical analysis (blood glucose, triglycerides, total cholesterol) suggested host systematic glucose and lipid metabolic disorders were improved in the S+M group ($p < 0.05$). Histological analysis of the non-tumor liver area showed that the liver steatosis (Oil Red staining) was relieved in the S+M group ($p < 0.05$). Further, histopathology showed the cell proliferation, glucose uptake, and fatty acid uptake of the tumor were decreased in the S+M group, showed by IHC staining of Ki67 and CD36 and Glut1 ($p < 0.05$).

Conclusion: Metformin boosts sorafenib's anti-tumor therapeutic effects and may reshape tumor metabolic programming. The combination of Metformin and Sorafenib may contribute to better outcomes in HCC patients with metabolic syndrome.

FRI-533

Anti-MFAP-5 siRNA loaded polycarbonate nanohydrogels for anti-stromal therapy in hepatocellular carcinoma

Paul Schneider¹, Alexander Fuchs², Lutz Nuhn², Barbara Schroers³, Mustafa Diken³, Twan Lammers⁴, Stephan Grabbe¹, Jörn M. Schattenberg⁵, Leonard Kaps⁶. ¹Department of Dermatology, University Medical Centre of the Johannes Gutenberg University, Mainz, Germany; ²Institute of Functional Materials and Biofabrication, Department of Chemistry and Pharmacy, Julius-Maximilians-Universität Würzburg, Würzburg, Germany; ³TRON-Translational Oncology, Mainz, Germany; ⁴Department of Nanomedicine and Theranostics, Institute for Experimental Molecular Imaging, RWTH Aachen University Clinic, Aachen, Germany; ⁵Department of Medicine II, Saarland University

Medical Center, Saarland University, Homburg, Germany; ⁶Department of Medicine II, Saarland University Medical Center, Saarland University, Homburg, Germany
Email: leonardkaps@googlemail.com

Background and aims: Cancer associated fibroblasts (CAF) are promising target cells for anti-stromal therapy as they support tumor growth and metastasis in the tumor microenvironment (TME) [Kaps, Schuppan, Cells 2020]. CAF derived MFAP-5 promotes tumor angiogenesis in solid tumors [Yeung TL et al., Clinical Cancer Research 2019]. We have designed a novel generation of nanohydrogels with improved biodegradability, consisting of a polycarbonate backbone (NP) for in vivo siRNA delivery [Kaps L et al., J Control Release. 2021]. Anti-MFAP-5 siRNA loaded NP were tested in a murine model of hepatocellular carcinoma for antitumor therapy.

Method and Results: MFAP-5 was highly upregulated in 3T3 fibroblasts and hepatic stellate cells (both precursor cells for CAF in vitro) when co-cultured with the hepatocellular carcinoma (HCC) cells (Dt81Hepa1-6). Transcriptome analysis of HCC cells showed a transcript pattern also found in human HCC as tumor key genes (e.g. AFP, SPATS2) were upregulated, while genes of healthy hepatocytes (e.g. HP, Apoa3/4) were downregulated. For HCC induction, C57BL/6J mice were gavaged with escalating doses of CCl4 for liver fibrosis induction over four weeks. Fibrotic mice received an intrasplenic injection of 500.000 HCC cells to develop macroscopic tumor lesions exclusively in the liver after 28 days. *In vivo* biodistribution of Cy-5.5 siRNA loaded NP was assessed in fibrotic tumor mice. NP accumulated preferentially in the liver (80%), while free Cy-5.5 siRNA was rapidly cleared via the urinary tract. *Ex vivo* FACS analysis of liver single cell suspension revealed preferential colocalization of NP with CAF (α -SMA+) > dendritic cells (CD45+, F4/80+, CD11c+) > macrophages (CD45+, F4/80+). For *in vivo* anti-stromal therapy, fibrotic tumor mice ($n = 5$) received three injections of NP loaded with anti-MFAP-5 (corresponding to 0.5 or 1 mg/kg siRNA) in week four, while controls received equal amounts of scramble siRNA (scsiRNA) loaded NP. Liver weights of mice treated with anti-MFAP-5 siRNA were significantly ($p < 0.05$) lower compared to mice treated with encapsulated scsiRNA, indicating less hepatic tumor burden. Morphometric analysis of liver sections supported ($p < 0.05$) the antitumor effect in siRNA treated mice. *In vivo* knockdown of MFAP-5 was confirmed on RNA and protein level by qPCR and FACS analysis, respectively, while controls had similar MFAP-5 levels like healthy mice. The treatment was well tolerated by the mice and serum parameters for liver- and nephrotoxicity remained in the normal range. Knockdown of MFAP-5 reduced markers for tumor vascularization (e.g. CD34, CD105) in the TME as indicated by histological and qPCR analysis, suggesting an anti-angiogenic effect.

Conclusion: CAF derived MFAP-5 is a promising therapeutic target for anti-stromal therapy in HCC, which can be inhibited by RNA interference with liver targeting NP loaded with anti-MFAP-5 siRNA.

FRI-534

New 3D chimeric model to study hepatic stellate cell activation during primary liver cancer

Alba Herrero^{1,2}, Elisabeth Knetemann², Jens U. Marquardt³, Inge Mannaerts². ¹Basque country university, Leioa, Spain; ²Vrije universiteit Brussels, Jette, Belgium; ³University medical center of the Johannes-Gutenberg university of Mainz, Mainz, Germany
Email: alba.herrero@ehu.eus

Background and aims: Primary liver cancer (PLC) is a frequently occurring cancer worldwide. Around 80% of the PLC cases are from two main types: hepatocellular carcinoma (HCC) and intrahepatic cholangiocarcinoma (iCCA). The etiology of both types is different; however, the development is similar, based on extracellular matrix changes, such as collagen deposition. Moreover, liver non-parenchymal cells, as hepatic stellate cells (HSCs), are activated during PLC helping the development of the cancer. Due to its role during several pro-tumoral processes, these activated HSCs are grouped into cancer-

POSTER PRESENTATIONS

associated fibroblasts (CAFs). However, it is not known if different populations of CAFs are present in HCC or iCCA development. To do so, we have developed a 3D chimera spheroid model to mimic *in vitro* the HSC activation in HCC or iCCA and analyzed the potential of different CAF markers depending on the PLC.

Method: Creation of a 3D chimera spheroid model with mouse primary hepatocytes and HSCs, at a 1:2 ratio with 30 HCC or iCCA human patient-derived cells, labeled with fluorochrome mKate2. Spheroids were seeded in 96-well U-bottom plates and cultured under gentle rotation in an incubator. During the time experiment, spheroids were evaluated with live-dead cell assays, and images at day 7 were taken, to check the viability of the cells into the spheroids. Finally, on day 14 they were collected for further analysis. Moreover, we analyzed public sc-RNAseq databases from mouse and human HCC and iCCA by bioinformatics tools for searching possible specific markers for CAFs based on HCC or iCCA cancer.

Results: 3D chimera spheroids for HCC and iCCA were stable during the time experiment without high cell death and a moderate proliferation of tumor cells into the spheroids. The presence of tumor cells promotes HSC activation based on RNA levels of Acta2, Lox, Col1a1, and Fap. Moreover, the fibrillar collagen deposition was increased in spheroids with both PLC cell lines. After we validated our model, we tested supposedly specific CAFs markers for each PLC, which we found using bioinformatics analysis on public sc-RNAseq databases, on RNA analysis for further investigations.

Conclusion: The 3D chimera spheroid model is a new stable complex *in vitro* model with the capacity to activate HSCs in the presence of HCC or iCCA cells and a valid model for new CAF markers screening.

FRI-535

Effect of the metabotropic glutamate receptor 3 on liver cell survival: a potential biomarker in hepatocarcinoma

Bibiana Elena Juárez-Rivera¹, Andy Hernández-Abrego¹, Ericka de los Ríos-Arellano², Lizeth Vanessa Hernández-Quijano¹, Mauricio Díaz-Muñoz¹, Isabel Méndez¹. ¹Instituto de Neurobiología, UNAM, Querétaro, Mexico; ²Instituto de Neurobiología, UNAM, Querétaro, Mexico
Email: isabelcm@unam.mx

Background and aims: Metabotropic glutamate receptors (mGluRs) are expressed in the liver in physiological and pathological conditions. mGluRs have been characterized into eight types (mGluR1–8) and classified into three groups according to their pharmacology, sequence of amino acid homology, and signal transduction pathways. mGluR2 and mGluR3 belong to group II and are activated by glutamate and selective agonists. Our group has observed mGluR3 expression in normal hepatocytes and its elevated expression in pathological conditions such as cirrhosis and hepatocarcinoma. However, its role in hepatocarcinoma is still being studied. We aim to evaluate the expression of mGluR2 in hepatocarcinoma induced by DEN in rats and the role of mGluR3 on survival using a selective agonist that activates mGluR3 but not mGluR2.

Method: Male Wistar rats received weekly intraperitoneal injections of diethylnitrosamine (DEN- 50 mg/kg body weight) to induce the progressive pathologies fibrosis, cirrhosis, and HCC. Control rats received saline solution. Histopathological analyses confirmed the establishment of each pathology. Expression of mGluR2 and mGluR3 was analyzed in tissue samples by Western-blot and Immunohistochemistry. Both proteins were analyzed in the normal hepatocytes cell line C9 and the hepatocarcinoma cell line HepG2 by Western-blot. Effects of mGluR2 and mGluR3 activation by glutamate or LY354740, a selective group II metabotropic glutamate receptor agonist, were evaluated on live and dead cells. The NF-kappa B activation by glutamate or LY354740 was evaluated using the inhibitor BAY 11-7082. Microarray analysis was performed to further analyze markers of survival in HepG2 cells treated with N-Acetyl-Aspartyl-Glutamate (NAAG), a selective mGluR3 agonist.

Results: Overexpression of mGluR3 was confirmed according to the progression from normal condition to HCC in rats. An opposite expression profile was observed for mGluR2, since it practically disappeared in hepatocarcinoma. These observations were corroborated in HepG2 compared to C9 normal hepatocytes. The activation of mGluR2 and mGluR3 by glutamate and by the selective agonist LY354740 promoted the proliferation in HepG2 and avoided death in C9 cells. These effects were blocked by the NF-kappa B inhibitor. The effect on proliferation by mGluR3 of HepG2 but not in C9 was corroborated by using the selective agonist NAAG.

Conclusion: Our study demonstrates that group II mGluRs contribute to liver cell survival. mGluR2 seems to avoid cell death in normal hepatocytes, while mGluR3 promotes cell proliferation in hepatocarcinoma. Moreover, mGluR2 and mGluR3 have a role in the survival of hepatocytes via NF-kappa B pathway. Also, mGluR3 could be a possible biomarker and therapeutic target in hepatocarcinoma. This research was supported by DGAPA-PAPIIT, UNAM (N222821), and CONAHcyT (CF-2023-I-768).

Liver tumours – Therapy

TOP-488-YI

Fecal microbiota transplant combined with atezolizumab plus bevacizumab in patients with hepatocellular carcinoma who progressed on atezolizumab plus bevacizumab-interim analysis of the FAB-HCC phase II pilot study

Katharina Pomej^{1,2}, Adrian Frick¹, Bernhard Scheiner^{1,2}, Lorenz Balcar^{1,2}, Larissa Pajancic^{1,2}, Anton Klotz¹, Katharina Regnat¹, Kerstin Zinöber¹, Michael Trauner³, Dietmar Tamandl⁴, Christoph Gasche¹, Matthias Pinter^{1,2}. ¹Medical University of Vienna, Division of Gastroenterology and Hepatology, Department of Medicine III, Vienna, Austria; ²Medical University of Vienna, Liver Cancer (HCC) Study Group Vienna, Department of Medicine III, Vienna, Austria; ³Medical University of Vienna, Division of Gastroenterology and Hepatology, Department of Medicine III, Vienna, Austria; ⁴Medical University of Vienna, Department of Biomedical Imaging and Image-guided Therapy, Vienna, Austria
Email: katharina.pomej@meduniwien.ac.at

Background and aims: The gut microbiota is often altered in chronic liver diseases and hepatocellular carcinoma (HCC), and increasing evidence suggests that it may influence response to cancer immunotherapy. Strategies to modulate the gut microbiome (i.e., fecal microbiota transplant (FMT)) may help to improve efficacy of immune checkpoint inhibitors (ICIs) or even overcome resistance to ICIs.

Method: In this single-center phase II pilot study (ClinicalTrials.gov ID: NCT05750030), we plan to include 12 patients with advanced HCC who progressed on atezolizumab/bevacizumab. Patients will receive atezolizumab/bevacizumab every 3 weeks in combination with a single FMT via colonoscopy from donors with HCC who responded to PD-(L)1-based immunotherapy. The primary end point is safety, measured by incidence and severity of treatment-related adverse events (TRAEs). The main secondary end point is best overall response (BOR) according to RECISTv1.1 and mRECIST. Here, we report results of a preplanned interim analysis.

Results: Of 6 patients included so far, 5 were male, 5 had BCLC stage C, and 5 had Child-Pugh class A. All patients underwent successful FMT without any periinterventional complications. TRAEs related to FMT were all low-grade (grade 1–2) and included bloating (n=2), constipation (n=2), and diarrhea (n=1). TRAEs related to atezolizumab included one grade 2 pruritus, and TRAEs related to bevacizumab included arterial hypertension (one grade 3 and two grade 2) and proteinuria (one grade 3 and one grade 1). All patients had at

least one follow-up imaging. Two patients had partial response, 3 patients had stable disease, and 1 patient had progressive disease as BOR according to both RECISTv1.1 and mRECIST, which corresponds to an objective response rate of 33% and a disease control rate of 83%. **Conclusion:** Based on acceptable safety and promising efficacy results, the decision to continue recruitment in this trial was made. An update with longer follow-up will be presented at the meeting, including analyses of the gut microbiome if already available.

TOP-489-YI

Predicting post-hepatectomy liver failure in patient with hepatocellular carcinoma: nomograms based on deep learning-analyzed gadoxetic acid-enhanced hepatobiliary phase images

Boryeong Jeong¹, Seung Soo Lee¹, Subin Heo¹, Seon-Ok Kim².

¹Department of Radiology and Research Institute of Radiology, University of Ulsan College of Medicine, Asan Medical Center, Seoul, Korea, Rep. of South; ²Department of Clinical Epidemiology and Biostatistics, University of Ulsan College of Medicine, Asan Medical Center, Seoul, Korea, Rep. of South
Email: seungssolee@amc.seoul.kr

Background and aims: Post-hepatectomy liver failure (PHLF) remains a serious complication, especially for patients with hepatocellular carcinoma (HCC) due to the coexistence of liver disease. While the potential utility of functional liver volumetry using gadoxetic acid-enhanced MRI has been reported, and it has strength in adequately reflecting regional liver function when liver damage is heterogeneous, a practical model for estimating the risk of PHLF has not yet been established. Therefore, the purpose of our study was to develop nomograms predicting PHLF in patients with HCC, by incorporating clinical and surgical variables, along with functional and volumetric MRI variables derived from the deep learning analysis of the gadoxetic acid-enhanced hepatobiliary phase (HBP) images.

Method: Patients with Barcelona Clinic Liver Cancer stage 0 or A HCC who underwent hepatic resection following preoperative gadoxetic acid-enhanced MRI between January 2017 and December 2020 at Asan Medical Center and between January 2016 and December 2020 at Ajou University Hospital were retrospectively evaluated. The functional and volumetric MRI variables were automatically derived from deep learning-generated whole liver and spleen segmentation. The remnant liver volume was segmented with the expected resection plane drawn by radiologists. The primary outcome was the occurrence of PHLF, assessed and graded according to the International Study Group of Liver Surgery criteria. Two nomograms to predict PHLF grade A-C were developed using multivariable logistic regression analysis: 1) the whole liver nomogram and 2) the remnant liver nomogram.

Results: A total of 1760 patients (1395 male; mean age \pm standard deviation, 60 ± 10 years) were evaluated. The predictors for PHLF in both nomograms included clinical variables such as gamma glutamyl peptidase, platelets, prothrombin time-international normalized ratio, along with liver volume and signal intensity parameters, potentially reflecting hepatic uptake function. Additionally, the extent of liver resection and the spleen volume, reflecting portal hypertension were included for whole liver and remnant liver nomograms, respectively. The whole liver and remnant liver nomograms demonstrated good discrimination performance, with an optimism-corrected AUC of 0.78 (95% confidence interval [CI], 0.74–0.82) and 0.81 (95% CI, 0.77–0.86; $p = 0.001$), respectively, for predicting PHLF grade A-C, and 0.81 (95% CI, 0.77–0.85) and 0.84 (95% CI, 0.80–0.88; $p = 0.02$), respectively, for predicting PHLF grade B-C. The nomograms outperformed most of previously reported models and liver functional indices (apparent AUC range, 0.56–0.79).

Conclusion: The nomograms based on deep learning-analyzed gadoxetic acid-enhanced HBP images accurately stratified the risk of PHLF and may be useful for selecting suitable surgical candidates.

TOP-504

Predicting the efficacy and prognosis of immunotherapy combination therapies for hepatocellular carcinoma based on radiomics and deep learning

Xin Song¹, Xingrong Zheng¹, Xiyao Chen¹, Boxiang Zhang¹, Chan Xie¹.

¹Department of Infectious Diseases, The Third Affiliated Hospital of Sun Yat-sen University, Guangzhou, China
Email: happyxiechan@hotmail.com

Background and aims: With the emergence of immune checkpoint inhibitors, immunotherapy combined with other therapies is increasingly used for the treatment of advanced hepatocellular carcinoma (HCC) and how to identify potential treatment beneficiaries before treatment is particularly important. We aim to develop a predictive model based on patients' clinical characteristics and MRI images to predict efficacy and prognosis for patients receiving immunotherapy combination therapies.

Method: Clinical data and MRI images (including T1 weighted image, T2 weighted image and Liver Acquisition with Volume Acceleration) were retrospectively collected from HCC patients who took immunotherapy with targeted therapy and chemotherapy from January 2019 to June 2022 in our hospital. Patients were divided into response and non-response groups after assessing their response to treatment according to the Modified RESICT criteria. Radiomics and deep learning features were extracted from the MRI sequences, different features were used for modeling and AUC was used to assess the predictive ability of the different models.

Results: 116 patients were included in the final outcome analysis, with 50 patients in the response group and 56 patients in the non-response group. Baseline characteristics (Age, Gender, Barcelona Clinic Liver Cancer, Child-Pugh score, Extrahepatic spread, Macrovascular invasion) were not significantly different between the two groups. The integrated model using Light Gradient Boosting Machine achieved the best prediction performance with AUC of 0.856 (95%CI = 0.698–1.000).

Conclusion: We developed an efficacy prediction model for HCC patients by combining radiomics and deep learning features, which can quickly and accurately predict the efficacy of patients receiving immunotherapy combination therapies. We provided a new approach for non-invasively identifying patients potentially benefiting from therapy before treatment.

TOP-505

Identification of biomarkers for the treatment efficacy of atezolizumab plus bevacizumab in unresectable hepatocellular carcinoma, based on chemokine alterations during treatment

Tomoharu Yamada¹, Tatsuya Minami², Mitsuhiko Fujishiro²,

Ryosuke Tateishi². ¹The University of Tokyo Hospital, Tokyo, Japan;

²Graduate School of Medicine, The University of Tokyo, Tokyo, Japan
Email: tyism123@gmail.com

Background and aims: Atezolizumab plus bevacizumab (atezo + bev) is used as a first-line treatment for unresectable hepatocellular carcinoma (uHCC), however, approximately 20% of patients are non-responders, necessitating the development of biomarkers for predicting therapeutic outcomes and additional combinational agents to enhance the treatment efficacy. We aimed to identify circulating biomarkers predictive for the therapeutic outcomes and to investigate adjunctive drugs that could enhance the treatment efficacy.

Method: We enrolled 54 patients who treated with atezo + bev for uHCC as either first- or later-line systemic therapy in our institution between October 2020 and January 2022. Forty chemokines and cytokines were measured in serum before and after one course of the treatment by multiplex assay. Logistic regression analysis, using the median values of change in each protein before and after the administration, was conducted with progressive disease (PD)/non-PD as the objective variable to identify factors contributing to treatment efficacy. These factors were adjusted with clinical factors (age, gender,

hepatitis B surface antigen, hepatitis C virus antibody, treatment line, total bilirubin, albumin, aspartate aminotransferase (AST), prothrombin time, platelet count, alpha-fetoprotein, Child-Pugh score, Barcelona Clinic Liver Cancer (BCLC) staging) in a multivariate analysis using the Cox proportional hazards model for predicting progression-free survival (PFS).

Results: The median age of the patients was 76 years, with 43 males (80%). Forty-four patients (82%) were Child-Pugh A, and 10 patients (19%) were Child-Pugh B. There were 24 patients (44%) with BCLC stage B and 30 patients (56%) with BCLC stage C. Logistic regression analysis showed that Δ CXCL12 (OR 3.95, $p = 0.0398$), Δ CCL3 (OR 0.25, $p = 0.0398$), and Δ CCL26 (OR 0.25, $p = 0.0398$) as significant predicting factors for PD/non-PD. Multivariate analysis, including significant clinical factors predicting PFS such as treatment line (first vs. later: HR 1.74, $p = 0.0325$) and AST (HR 1.01/1 IU, $p = 0.0884$), revealed that Δ CXCL12 (HR 2.55, $p = 0.0061$) and Δ CCL3 (HR 0.44, $p = 0.0369$) were independent predictors of PFS.

Conclusion: The increase in CXCL12 or decrease in CCL3 contributed to the worsening of PFS for patients treated with atezo + bev. Anti-CXCR4 antibodies that inhibit CXCL12 have already received FDA approval for other diseases, and recently, phase 1–2 trials combining anti-CXCR4 antibodies and immune checkpoint inhibitors in other cancers are in progress. From the results of our study, it is worth considering whether combining anti-CXCR4 antibodies with atezo + bev in uHCC could suppress the increase in CXCL12 and improve PFS.

TOP-506

Atezolizumab/bevacizumab as downstaging in hepatocellular carcinoma: an intention-to-transplant analysis

Marianna Maspero¹, Sherrie Bhoori¹, Veronica Fedele¹, Nicolò Simonotti¹, Valentina Bellia¹, Marco Bongini¹, Carlo Sposito¹, Vincenzo Mazzaferro¹. ¹Fondazione IRCCS Istituto Nazionale dei Tumori, Milan, Italy

Email: marianna.maspero@istitutotumori.mi.it

Background and aims: Atezolizumab-bevacizumab has recently become the standard of care for advanced hepatocellular carcinoma (HCC). Patients who achieve downstaging within transplant criteria after atezolizumab-bevacizumab may undergo liver transplantation within investigational trials.

Method: This was an intention-to-transplant analysis of patients without absolute contraindications to transplant who started atezolizumab/bevacizumab at our center. The primary aim was to determine how many were deemed transplantable into our ImmunoXXL trial (NCT05879328) and were successfully transplanted.

Results: 28 patients without absolute contraindications to transplant started atezolizumab-bevacizumab (86% male, median age 61). Chronic liver disease was due to HBV in 5, HCV in 10, alcohol in 8 and MASLD in 11. Twenty-three (81%) were Child-Pugh score A, 5 (19%) B. Twenty-three (82%) were BCLC B, while 5 (18%) were C due to segmental portal vein thrombosis. At baseline, the median size of the lesions was 60 (IQR 35–81) mm and median number 3 (1–5). Nineteen (68%) had undergone therapies before atezolizumab-bevacizumab (9 chemoembolization, 15 radioembolization, 4 surgery). After a median follow-up of 9 months, five patients died. The mRECIST response to atezolizumab-bevacizumab was complete in 7 (25%) cases, partial in 7 (25%), stable disease in 9 (32%) and progression in 5 (18%). Twenty (74%) patients stopped atezolizumab-bevacizumab after a median of 6 cycles: 8 due to transplant listing, 1 due to curative-intent surgical resection, 2 due to toxicity, 5 due to progression and 4 due to liver decompensation. Of the 8 listed patients, 7 were successfully transplanted while one is still on the waiting list.

Conclusion: Atezolizumab-bevacizumab seems to be a successful downstaging-to-transplant strategy for patients with intermediate-advanced HCC.

THURSDAY 06 JUNE

THU-446

VETC predicts benefit of anti-angiogenic drugs in advanced HCC

Camilla De Carlo^{1,2}, Reha Akpınar^{1,2}, Barbara Durante^{3,4}, Angelo Pirozzi⁵, Salvatore Renne^{1,2}, Tiziana Pressiani⁵, Julien Calderaro⁶, Valentina Zanuso^{2,5}, Irene Oi-Lin Ng⁷, Tanto Cheung⁸, Albino Eccher⁹, Pamela Sighinolfi⁹, Erica Villa¹⁰, Massimo Iavarone¹¹, Marco Maggioni¹², Yu-Yun Shao¹³, Sara Lonardi¹⁴, Mario Domenico Rizzato^{15,16}, Antonio De Rosa^{14,16}, Matteo Fassan^{17,18}, Valentina Angerilli¹⁷, Federica Pedica¹⁹, Margherita Rimini²⁰, Andrea Casadei Giardini²⁰, Armando Santoro²¹, Young Nyun Park²², Massimo Roncalli¹, Luigi Terracciano^{1,23}, Salvatore Piscuoglio^{1,2}, Lorenza Rimassa^{2,5}, Luca Di Tommaso^{1,2}.

¹Pathology Unit, IRCCS Humanitas Research Hospital, Rozzano, Milan, Italy; ²Department of Biomedical Sciences, Humanitas University, Pieve Emanuele, Milan, Italy; ³Pathology Unit, Humanitas Research Hospital, Rozzano, Milan, Italy; ⁴Department of Biomedical Sciences, Humanitas University, Pieve Emanuele, Italy; ⁵Humanitas Cancer Center, IRCCS Humanitas Research Hospital, Rozzano, Milan, Italy; ⁶Hôpitaux Universitaires Henri Mondor-Albert Chenevier, Institut Mondor de Recherche Biomédicale, Créteil, France; ⁷Department of Pathology and State Key Laboratory of Liver Research, The University of Hong Kong, Hong Kong, China; ⁸Department of Surgery and State Key Laboratory of Liver Research, The University of Hong Kong, Hong Kong, China, Hong Kong, China; ⁹Section of Pathology, Department of Medical and Surgical Sciences for Children and Adults, University of Modena and Reggio Emilia, University Hospital of Modena, Modena, Italy; ¹⁰CHIMOMO Department, University of Modena and Reggio Emilia, Modena, Italy; ¹¹Division of Gastroenterology and Hepatology, Fondazione IRCCS Ca' Granda Ospedale Maggiore Policlinico, Milan, Italy; ¹²Division of Pathology, Fondazione IRCCS Ca' Granda Ospedale Maggiore Policlinico, Milan, Italy; ¹³Department of Oncology National Taiwan University Hospital, Graduate Institute of Oncology, National Taiwan University College of Medicine, Taipei, Taiwan; ¹⁴Medical Oncology 1, Veneto Institute of Oncology IOV-IRCCS, Padova, Italy; ¹⁵Medical Oncology 1, Veneto Institute of Oncology IOV-IRCCS, Padova; ¹⁶Department of Surgery, Oncology and Gastroenterology, University of Padua, Padova, Italy; ¹⁷Department of Medicine (DIMED), University of Padua, Padova, Italy; ¹⁸Veneto Institute of Oncology (IOV-IRCCS), Padua, Padova, Italy; ¹⁹Pathology Unit, Vita-Salute San Raffaele University, IRCCS San Raffaele Scientific Institute, Milano, Italy; ²⁰Department of Oncology, Vita-Salute San Raffaele University, IRCCS San Raffaele Scientific Institute Hospital, Milano, Italy; ²¹Humanitas Cancer Center, IRCCS Humanitas Research Hospital, Rozzano, Milano, Italy; ²²Department of Pathology, Graduate School of Medical Science, Yonsei University College of Medicine, Seoul, Korea, Rep. of South; ²³Department of Biomedical Sciences, Humanitas University, Pieve Emanuele, Milan

Email: camilla.decarlo@humanitas.it

Background and aims: VETC (vessel that encapsulate tumor clusters) is a peculiar vascular phenotype associated with a worse prognosis in HCC. It predicts also the response to chemoembolisation and it has been associated with a better response also to sorafenib. The aim of the study is to test the predictive significance of VETC in patients with advanced HCC undergoing systemic treatment.

Method: The predictive significance of VETC was first explored in a retrospective, mono-institutional series of 81 patients with advanced HCC (study cohort) and later validated in an external, retrospective series of 83 patients (validation cohort). The VETC phenotype was determined in the liver biopsy obtained just before systemic treatment.

Results: Both in the study and validation cohorts, VETC+ was associated with a significant better response to anti-angiogenic drugs (TKI and/or bevacizumab). In the whole series of 163 patients, those with VETC+ (43%) treated with TKI and/or bevacizumab had a significant longer OS compared to those treated with Immune

Checkpoint Inhibitors (19.2 months versus 10.2 months, HR 0.4; 95% CI 0.24-0.70; $P = 0.0012$). Similar findings were seen for Sorafenib versus ICI (16.3 months vs 8.7 months; HR 0.4; 95% CI 0.25-0.93; $P = 0.03$). The same benefit from anti-angiogenic drugs was not seen in VETC- cases.

Conclusion: VETC+ is predictive of the response to anti-angiogenic drugs in advanced HCC.

THU-447

Incidence and predictors of complications following percutaneous liver biopsy: a multicenter study

Francesca Colapietro^{1,2}, Mauro Viganò³, Federica Cerini⁴, Riccardo Plebani¹, Alberto Savino³, Maria Pia Calabrese¹, Paolo Marra^{5,6}, Kessy Djonis Martins de Mattos⁷, Agostino Cosenza⁶, Alessandro Loglio³, Carmelo Selvaggio⁶, Tiziana Negri³, Chiara Masellis⁶, Benedetta Mori¹, Nicola Pugliese^{1,8}, Chiara Masetti⁹, Elisa Farina³, Stella De Nicola⁹, Roberto Ceriani⁹, Ana Lleo^{1,9}, Sandro Sironi^{5,6}, Riccardo Muglia^{5,6}, Stefano Fagioli^{3,10}, Alessio Aghemo^{1,9}. ¹Department of Biomedical Sciences, Humanitas University, Pieve Emanuele, Milan, Italy; ²Division of Internal Medicine and Hepatology, Department of Gastroenterology, Humanitas Research Hospital IRCCS, Milan, Italy; ³Gastroenterology, Hepatology and Transplantation Division, ASST Papa Giovanni XXIII, Bergamo, Italy; ⁴Department of Clinical Sciences and Community Health, University of Milan Hepatology Unit, San Giuseppe Hospital, Milan, Italy; ⁵Department of Radiology, ASST Papa Giovanni XXIII Hospital, Bergamo, Italy; ⁶Department of Medicine, University of Milano Bicocca, Milan, Italy; ⁷Department of Radiology, ASST Papa Giovanni XXIII, Bergamo, Italy; ⁸Division of Internal Medicine and Hepatology, Department of Gastroenterology, Humanitas Research Hospital IRCCS, Milan; ⁹Division of Internal Medicine and Hepatology, Department of Gastroenterology, Humanitas Research Hospital IRCCS, Milan, Italy; ¹⁰Department of Clinical Sciences and Community Health, University of Milan Hepatology Unit, San Giuseppe Hospital, Milan, Italy
Email: f.colapietro2@gmail.com

Background and aims: The management of patients undergoing ultrasound (US)-guided percutaneous liver biopsy (PLB) is not standardized. Despite a low risk of major complications (<1%), many scientific societies still recommend repeated blood count and in-hospital stay up to 4 hours. We retrospectively assessed the rates and predictors of complications in a large cohort of patients who underwent US-PLB in three tertiary centers in Lombardia, Italy.

Method: We included all consecutive patients undergoing both parenchymal and lesion targeted PLB from January 2018 to December 2023. We collected clinical, biochemical and procedural features, including needle type, number of insertions, time of observation after the procedure and concomitant antiplatelet/anticoagulant regimens. The safety of US-guided PLB was defined by the incidence of pain and major complications including vaso-vagal reaction, bleeding, pneumothorax, shock; hospitalization; and death.

Results: 1838 patients underwent either parenchymal (1367, 74%) or lesion-targeted (471, 26%) PLB. Mean age was 55.1 years, with 46.1% females and mean BMI of 25.1 Kg/m² (± 4.8); 252 PLB (13.7%) were performed on patients who had undergone previous liver transplantation. Few patients were on anticoagulant/antiplatelet therapy (4.2%/16.2%). Mean platelet count and PT INR value were 209.7 \pm 80.74 x10³/mm³ and 1.04 \pm 0.12, respectively; 17 patients (0.9%) received prophylactic therapy. Needle aspiration was predominant (92.0%), mainly with 18G (59.5%) or 16G (22.1%) needles. After a mean time of observation of 5.4 \pm 2.0 hours, pain occurred in 7.4% of patients (134/1838). Major complications were few (26/1838, 1.4%), with transient hypotension being the most common (14/1838, 0.8%); ten bleeding events were observed (0.5%), with a median time of onset of 1 hour. Hospitalization was rare (12/1838, 0.7%), primarily for bleeding management, though most cases resolved spontaneously. No fatalities were recorded. Pain was the sole significant independent predictor of major complications (18/26, 69.2%, $p < 0.05$), particularly

when referred within one hour following the procedure (15/18, 83.3%, $p = 0.002$). No baseline, procedural or post-procedural variables (including heart rate, mean arterial pressure and hemoglobin values) were associated with major complications.

Conclusion: Complications following PLB are few and associated with pain developing within one hour from the procedure. No other pre-procedure or post-procedure variable was useful in identifying patients with major complications. Our results suggest that in the absence of pain developing within 1 hour following PLB patient monitoring can be safely stopped.

THU-454

Induction of systemic immune activation by liver transplant and effects of previous VEGF/PD-L1 blockade in HCC patients

Sherrie Bhoori¹, Michela Dosi², Valentina Bellia¹, Marco Bongini¹, Maria Flores¹, Luca Lalli², Giovanni Di Maio², Jeanette Salsetta², Marta Zorza², Agata Cova², Martina Stroschia², Licia Rivoltini², Vincenzo Mazzaferro³. ¹Hepato-Pancreatic Biliary Surgery and Liver Transplantation Unit, Fondazione IRCCS Istituto Nazionale dei Tumori, Milan, Italy; ²Translational Immunology Unit, Department of Experimental Oncology, Fondazione IRCCS Istituto Nazionale dei Tumori, Milan, Italy; ³Hepato-Pancreatic Biliary Surgery and Liver Transplantation Unit, Fondazione IRCCS Istituto Nazionale dei Tumori, Department of Oncology, University of Milan, Fondazione IRCCS Istituto Nazionale dei Tumori, Milan, Italy
Email: sherrie.bhoori@istitutotumori.mi.it

Background and aims: HCC patients treated with immune checkpoint inhibitors (ICIs) based combinations can achieve tumor downstaging and become eligible to liver transplantation (LT) for long-term tumor control. However, while ICIs have been described to increase the risk of post-LT graft rejection, post-LT immunosuppression administered at more intensive regimens in this specific setting, may instead exert detrimental effects on ICIs-induced antitumor immunity.

We investigated changes of circulating immune cells on HCC patients undergoing LT with or without ICI pre-treatment, with the purpose of comparing immune kinetics that might jeopardize tumor immunosurveillance.

Method: 7 LT after ICIs (LT-ICI) and 6 LT-alone were enrolled in cirrhotic patients with a downstaged HCC. Lymphoid and myeloid cell subsets were immunomonitoring by high resolution flow cytometry at stringent intervals before and after LT. Post-LT immunosuppressive regimen was intensified in LT-ICI patients.

Results: A significant decrease of most T, B and NK cell subsets was registered, with respect to pre-LT levels, within the first 2 weeks after LT in both groups. At 1 month levels of all circulating immune cell subsets related to anti-tumor surveillance were significantly higher in LT-alone patients as compared to LT-ICI ($p < 0.05$). This refers particularly to CD8+ expressing the early activation markers PD-1 and CD38, NK cells, terminally differentiated effectors (TEMRA), effector memory (TEM), naive CD8+ T cells as well as intermediate and non classical CD14+ monocytes expressing an activated phenotype (HLA-DRbright, PD-L1+ CX3CR1+ and CD36+). No rejection was registered in LT-ICI patients and no cancer recurrence occurred at a median follow-up of 8 months.

Conclusion: Altogether, these data indicate a potent immunostimulating effect of LT on systemic immunity which is suggestive in cancer recipients of a general reprogramming toward antitumor immunosurveillance. The evidence that this effect was instead less pronounced in patients receiving ICIs before LT may be due to the stronger immunosuppressive regimen administered in this specific clinical subset to minimize rejection risk. Longer follow-up is needed to investigate the role of pre-transplant ICIs in reducing peripheral innate immune responsiveness in liver transplant recipients.

THU-455

Efficacy and Safety of Hypofractionated Radiotherapy Combined with Sintilimab and Bevacizumab in Patients with Hepatocellular Carcinoma and Portal Vein Tumor Thrombus: A preliminary single-center prospective study

Xiao Fu¹, Mingfeng He², Yixuan Yang³, Dazhi Zhang³, Hengqiu He⁴, Xuan Jiang⁴. ¹Key Laboratory of Molecular Biology for Infectious Diseases (Ministry of Education), Institute for Viral Hepatitis, the Second Affiliated Hospital, Chongqing Medical University, Chongqing, China; ²The center of Oncology, The Second Affiliated Hospital of Chongqing Medical University, Chongqing, China; ³Department of Infectious Diseases, Key Laboratory of Molecular Biology for Infectious Diseases, Institute for Viral Hepatitis, the Second Affiliated Hospital of Chongqing Medical University, Chongqing, China; ⁴The center of Oncology, The Second Affiliated Hospital of Chongqing Medical University, Chongqing, China
Email: 303722@hospital.cqmu.edu.cn

Background and aims: The efficacy and safety of systemic Sintilimab and bevacizumab (sinti/bev) in the treatment of patients with unresectable hepatocellular carcinoma (HCC) have been demonstrated. However, the efficacy of this treatment in patients with HCC and portal vein tumor thrombus (PVTT) is not satisfactory. Hypofractionated Radiotherapy (HFRT), had be employed as a non-invasive local therapeutic option for HCC. Multiple studies have demonstrated that HFRT can promote tumor antigen release and enhance the efficacy of immunotherapy. Therefore, this study aimed to investigate the efficacy and safety of combining HFRT with systemic sinti/bev treatment in patients with unresectable HCC and PVTT.

Method: This is a single-center, open-label, randomized trial that recruited patients with HCC with type II/III/IV PVTT, who had not previously received systemic therapy. Patients were randomly assigned (2:1) to receive standard treatment Sintilimab (200 mg, every 3 weeks) and bevacizumab (15 mg/kg, every 3 weeks) with or without HFRT [95% planning target volume (PTV), 36Gy/3Gy]. The primary end point was overall survival (OS), and the secondary end points were progression-free survival (PFS), objective response rate (ORR), disease control rate (DCR), and safety.

Results: Ninety patients were enrolled and randomly assigned to two prospective cohorts. The median follow-up was 10.2 months. Median OS were 13.2 months [95% confidence interval (CI), 9.2-not available (NA)] and 8.9 months (95% CI, 5.4-NA), and median PFS were 5.2 months (95% CI, 3.6-8.6) and 3.6 months (95% CI, 2.5-7.0) for the HFRT and non-HFRT cohorts, respectively. The ORR and DCR were 63.5% and 92.5% in the HFRT cohort, and 32.0% and 56.0% in the non-HFRT cohort. The most common TRAEs at all levels were anorexia/nausea 57/90 (63.3%), neutropenia 39/90 (43.8%), and the most common grade 3/4 TRAE was hypertension 14/90 (15.6%). There was no treatment-related deaths.

Conclusion: First-line treatment of HFRT combining with Sintilimab-bevacizumab showed clinical benefits in patients with unresectable HCC and PVTT, with an acceptable safety profile. Thus, these combination regimens may be potential options for such patients.

THU-456

Curative therapy after atezolizumab-bevacizumab and role of liquid biopsy in patient selection

Anand Kulkarni¹, P Kumaraswamy¹, Mithun Sharma¹, Balachandran Menon¹, Anuradha Sekaran¹, Sowmya Iyengar², Manasa Alla¹, Shantanu Venishetty¹, Nagaraja Padaki¹, Nageshwar Reddy¹. ¹AIG Hospitals, Hyderabad, India; ²AIG Hospitals, Hyderabad, India
Email: anandvk90@gmail.com

Background and aims: Locoregional therapy (LRT) is an excellent modality to downstage unresectable hepatocellular carcinoma (uHCC). The role of atezolizumab-bevacizumab (atezo-bev) in downstaging and the outcomes of such patients who undergo curative

surgery, including liver transplantation (LT), is still unknown, which we aimed to assess.

Method: In this single-center retrospective study, we included consecutive patients who received atezo-bev with or without LRT and were subsequently considered for surgical therapy after downstaging (Milan criteria). We describe the course of such patients while assessing the utility of liquid biopsy in this context.

Results: Twelve patients (age-58.4 ± 8.2 years; women-17%; MASH-50%) willing for LT after being downstaged are described here. Fifty-eight percent were in Child-Pugh class A, and the remaining were in Child B, and 41.6% were in BCLC B, while the remaining were in BCLC C at the time of initiation of atezo-bev. The median AFP at the initiation of atezo-bev and at the time of listing was 116.6 (4.1-23,090) ng/ml and 15.9 (2.9-930) ng/ml, respectively. Four patients had undergone LRT prior to listing. Six patients underwent curative therapies: four underwent living donor LT (LDLT) after a median time of 79.5 (54-114) days after the last dose, one underwent deceased donor LT (DDLT) after 38 days of the last dose, and one underwent resection. Three patients (50%) experienced wound healing complications, with one undergoing re-exploration and eventually succumbing to sepsis and graft dysfunction. Except for one, all patients had complete pathologic response with no viable HCC. Of the remaining six patients, three died of infections on the waitlist, and the other three were waiting for LT. Among the patients who underwent curative therapy, there have been no HCC recurrence or rejection episodes after a median follow-up of 8 months. Five patients underwent liquid biopsy using next generation sequencing (NGS) method at the time of listing for LT. Three of the patients who underwent LT had low tumor fraction, no MSI, and <3 mut/mb of blood tumor mutational burden (TMB) and are stable. Of the other two, one had 6 muts/mb of TMB with mutations in CTNNB1 and TP53 and died on waitlist. The other one waiting LT has 3 muts/mb of TMB along with TERT promoter and TP53 mutation.

Conclusion: Curative therapies, including LT, is possible after atezo-bev therapy in well-selected patients after downstaging. Liquid biopsy may be useful in identifying ideal candidates for LT.

THU-457

Outcome of liver transplantation in patients with hepatocellular carcinoma previously treated with immune checkpoint inhibitor-based therapy-first results from an international multicenter registry

Ulrike Bauer¹, Najib Ben Khaled², Julia M. Grottenthaler³, Friedrich Foerster⁴, Sena Blümel⁵, Sophia Heinrich⁶, Friedrich Sinner⁷, Marino Venerito⁷, Richard Taubert⁶, Andreas E. Kremer⁵, Arndt Weinmann⁴, Christoph P. Berg³, Christian M. Lange², Enrico de Toni², Roland M. Schmid¹, Ursula Ehmer¹. ¹TUM School of Medicine and Health, Clinical Department for Internal Medicine II, University Medical Center, Technical University of Munich, Germany, Munich, Germany; ²Department of Medicine II, University Hospital, LMU Munich, Munich, Germany, Munich, Germany; ³Department of Gastroenterology, Gastrointestinal Oncology, Hepatology, Infectiology, and Geriatrics, University Hospital Tuebingen, Tuebingen, Germany, Tuebingen, Germany; ⁴Department of Medicine I, University Medical Center of the Johannes-Gutenberg University Mainz, Germany, Mainz, Germany; ⁵Department of Gastroenterology and Hepatology, University Hospital Zürich, University of Zürich, Zürich, Switzerland, Zuerich, Switzerland; ⁶Department of Gastroenterology, Hepatology, Infectious Diseases and Endocrinology, Hannover Medical School, Hannover, Germany, Hannover, Germany; ⁷Department of Gastroenterology, Hepatology and Infectious Diseases, Otto-von-Guericke University Hospital Magdeburg, Magdeburg, Germany, Magdeburg, Germany
Email: ursula.ehmer@tum.de

Background and aims: Treatment of hepatocellular carcinoma (HCC) with immune checkpoint inhibitor (ICI) combination therapies is the standard of care in advanced stage HCC and in intermediate stage

HCC not amenable to locoregional therapy. Even with successful downstaging of intermediate stage HCC to meet transplant criteria (e.g. Milan or UCSF criteria), liver transplantation (LT) after ICI remains controversial due to the increased risk of acute and potentially fatal organ rejection. As ongoing clinical trials explore the use of ICI in BCLC B patients, the proportion of patients converted to a potentially transplantable stage is going to increase. To evaluate the outcome of LT after ICI and investigate risk factors contributing to rejection, we established a multicenter case registry.

Method: Data from seven liver transplant centers in Germany and Switzerland with one or more patients transplanted after ICI were included. RFS and overall survival (OS) were analyzed by Log-rank test. Patient and tumor characteristics, ICI regimen, duration of ICI, time between ICI and LT, and immunosuppressive therapy after LT were documented.

Results: Nine patients underwent liver transplantation after ICI for HCC (7 male/2 female). The median age at transplant was 63 years, and the majority of patients (7/9) were treated with atezolizumab and bevacizumab. Median follow-up was 531 days (range 155–1062 days). Two rejections were documented in our cohort. One major rejection occurred 21 days after LT with fatal outcome due to subsequent chronic liver failure and infectious complications. One minor rejection (Rejection Activity Index 3–4) was observed five months after LT and was well controlled by increased immunosuppression. HCC recurrence with pulmonary metastasis was histologically confirmed in one patient 229 days after LT. Within this cohort and in line with previously published data, time between ICI and LT was a strong predictor for a major rejection (ICI to LT interval 13 days in the patient with major rejection vs 54–680 days in all other patients).

Conclusion: Despite an overall rejection rate of 22% (2/9), only one major rejection occurred, and this single patient had a short ICI wash-out period of only 13 days. The results of this international registry underscore the critical significance of allowing an adequate time interval between last dose of ICI and liver transplantation (LT), consistent with previously published data. In summary, our study suggests that LT after immunotherapy is generally safe for the majority of patients. However, the optimal and sufficient period for ICI wash-out still needs to be defined.

THU-458

No correlation between MASLD and poor outcome of Atezolizumab-Bevacizumab therapy in patients with advanced HCC

Francisca Copil¹, Claudia Campani², Marie Lequoy³, Philippe Sultanik⁴, Lorraine Blaise⁴, Mathilde Wagner³, Nathalie Ganne-Carrié³, Violaine Ozanne⁴, Jean Charles Nault³, Dominique Thabut⁴, Vlad Ratziu³, Manon Allaire¹. ¹APHP, PARIS, France; ²Centre de recherche des cordeliers, Paris, France; ³APHP, Paris, France; ⁴APHP, Paris, France
Email: allama5@hotmail.fr

Background and aims: Recent concerns have emerged, indicating that non-viral hepatocellular carcinoma (HCC), specifically NASH-HCC, may display limited responsiveness to immunotherapy. We aim to investigate the treatment outcomes of patients facing metabolic-associated steatotic liver disease (MASLD) and associated metabolic risk factors (MRF) when subjected to Atezolizumab-Bevacizumab (AtezoBev) therapy.

Method: Data from all patients treated with AtezoBev in 3 tertiary centers were collected prospectively since August 2020. MRF were defined by the presence of current/past BMI >30 kg/m², type 2 diabetes, arterial hypertension and dyslipidemia. Alcohol intake was less than 30 g daily for men and 20 g in women and no others cause of liver disease was present for MASLD patients. Progression was defined as a composite (progression and/or side effects/hepatic decompensation requiring discontinuation). The influence of

baseline characteristics on events during follow-up was assessed by uni/multivariate analysis using a Cox model.

Results: Data from 295 patients treated with AtezoBev were analyzed (median age 66 years, 16% women, 81% cirrhotic patients). Among the cohort, 27% had 1 MRF, 23% 2 MRF, 15% 3 MRF and 6% 4 MRF. Only 13% had MASLD, 18% MetALD, 17% ALD and 30% viral infection only. At inclusion, 73% of the patients were Child-Pugh A and 49% had esophageal varices. On the day of treatment, 62% of patients were BCLC-C. HCC was multi-nodular in 76% of cases, 41% had infiltrating HCC and 41% vascular invasion. Of the patients, 15% had an ALBI score of 3 and 41% had AFP ≥400 ng/ml. Characteristics of the patients were similar according to the number of MRF.

Median follow-up was 10.3 months and The PFS was 30% at 12 months (median PFS 6.5 months). In univariate analysis, age (HR = 0.99, p = 0.02), MELD score (HR = 1.08, p = 0.002), ALBI grade 3 (HR = 1.86, p < 0.001), AFP level (HR = 1.00, p = 0.02) and the presence of metastasis (HR = 1.61, p = 0.002) were associated with PFS, but not the presence of MASLD (p = 0.49). Only the ALBI grade 3 (HR = 1.60, p = 0.03), AFP level (HR = 1.00, p = 0.01), and the presence of extrahepatic metastasis (HR = 1.77, p < 0.001) were associated with PFS in multivariate analysis.

OS was 59% at 12 months (median OS 15.6 months). Death was related to HCC in 82%, liver failure in 12% and other causes in 6%. In multivariate analysis, only dyslipidemia (HR = 1.69, p = 0.001), the MELD score (HR = 1.07, p = 0.02), AFP ≥400 ng/ml (HR = 1.84, p = 0.001), multinodular HCC (HR = 2.03, p = 0.002), and the presence of infiltrative HCC (HR = 1.44, p = 0.05) were associated with OS.

During the follow-up, 10% of patients presented immune-related adverse events (IRAE). Only age (HR = 1.05, p = 0.004) and female gender (HR = 2.63, p = 0.02) were independently associated with IRAE.

Conclusion: our study suggests that the presence of MASLD or the number of MRF did not lead to worse outcomes in advanced HCC patients treated with AtezoBev.

THU-459-YI

Long-term oncological results of percutaneous radiofrequency ablation for intrahepatic cholangiocarcinoma: a multicentric retrospective study

Clémentine Alitti¹, Agnès Rode², Hervé Trillaud³, Philippe Merle², Jean-Frédéric Blanc⁴, Lorraine Blaise¹, Alix Demory¹, NKontchou Gisèle¹, Véronique Grando Lemaire¹, Marianne Zioli⁵, Pierre Nahon¹, Nathalie Ganne-Carrié¹, Arthur Petit⁶, Olivier Seror⁶, Olivier Sutter⁶, Jean Charles Nault¹. ¹CHU Avicenne, Hepatology, Bobigny, France; ²Croix-Rousse Hospital, Hospices Civils de Lyon, Lyon, France; ³CHU Bordeaux, Bordeaux, France; ⁴Hôpital Haut-Lévêque, Pessac, France; ⁵CHU Avicenne, Anatomopathology, Bobigny, France; ⁶CHU Avicenne, Interventional Radiology, Bobigny, France
Email: alitti.clementine@gmail.com

Background and aims: Percutaneous radiofrequency (RF) is a curative treatment for hepatocellular carcinomas (HCC), but its effectiveness in intrahepatic cholangiocarcinomas (iCCA) remains insufficiently studied.

Method: We conducted a retrospective study in three tertiary liver centers including patients with histologically proven iCCA within Milan criteria treated by percutaneous RFA from December 2020 to December 2022. Primary outcome was overall survival in treatment-naïve patients and secondary outcomes included ablation completeness, adverse events, local and distant recurrence. 494 patients with HCC on cirrhosis treated by RFA were included as a comparison group. Oncological events were analyzed using Kaplan-Meier, log-rank, and univariate/multivariate Cox models.

Results: The main population included 71 patients, mostly cirrhotic (80%) with solitary tumors (66%) with a median size of 24 mm. Underlying liver diseases were attributed to chronic alcohol intake (46%), metabolic syndrome (39%), chronic hepatitis C (20%), and/or chronic hepatitis B (13%). Complete ablation was achieved in 93% of

POSTER PRESENTATIONS

cases. Local recurrence was 45% at 5 years, and was lower in multibipolar versus monopolar RFA (22% vs. 55%, $P=0.007$). In multivariate analysis, both tumor size (HR = 1.09, CI95%: 1.02–1.16, $P=0.13$) and monopolar RFA (HR = 3.48, CI95%: 1.11–10.92, $P=0.03$) were independently associated with a higher local tumor recurrence. In treatment-naïve patients ($n=45$), median overall and recurrence-free survivals were 26 and 11 months, respectively. Tumor size (HR = 1.05, 95%CI 1.009–1.094, $P=0.01$) and Child-Pugh B (HR = 14.9, 95%CI 2.8–79, $P=0.001$) were associated with death. The rate of distant recurrence was 59% at 5 years, and was significantly lower for single tumors of less than 2 ($p=0.002$) or 3 cm ($p=0.02$). The size of the main tumor was the sole factor independently associated with distant tumor recurrence (HR = 1.06, CI95%: 1.02–1.11, $P=0.0007$). Next, we compared the outcomes of 40 patients with iCCA developed in cirrhotic patients naïve of previous treatment with 494 patients with HCC developed in cirrhotic patients naïve of previous treatment. Overall survival was shorter in iCCA than in HCC (26 vs 68 months, $P<0.0001$), with more local recurrences ($p<0.0001$). Among distant recurrences, 50% were extrahepatic metastases in iCCA compared to 12% in HCC ($p<0.001$).

Conclusion: Multibipolar RFA provides better results in term of tumor recurrence than monopolar RFA and could be used to treat small iCCA (<3 cm). Adjuvant chemotherapy should be discussed due to the frequent extra-hepatic metastasis at recurrence.

THU-462

Efficacy and safety of neoadjuvant therapy in narrow-margin hepatocellular carcinoma: a propensity score matching analysis

Hongxuan Li¹, Qiuyang Ren², Pan Qi², Bin Shu³, Xiaojuan Wang³, Xiaoying Zhu², Gong Li³, Yuewei Zhang³, Shizhong Yang¹. ¹Beijing Tsinghua Changgung Hospital, School of Clinical Medicine, Tsinghua University, Beijing, China; ²Qinghai University Affiliated Hospital, Qinghai, China; ³Beijing Tsinghua Changgung Hospital, School of Clinical Medicine, Tsinghua University, Beijing, China
Email: lhxa04369@btch.edu.cn

Background and aims: The clinical role of neoadjuvant therapy (NAT) for narrow-margin hepatocellular carcinoma (HCC) is unclear. The purpose of this study was to investigate the efficacy of NAT combined with surgery versus surgery alone in patients with narrow-margin HCC.

Method: This study retrospectively analyzed the clinical data of 181 patients with narrow-margin HCC who received NAT combined with surgery or surgery alone at two medical centers. NAT is defined as preoperative treatment, which includes local therapy (radiotherapy or interventional therapy) alone, or local therapy plus systemic therapy (PD-1 inhibitor + lenvatinib). Propensity score matching (PSM) was used to balance clinicopathological characteristic differences between the two groups.

Results: A total of 181 patients were included, of which 43 were assigned to the NAT combined with surgery group and 138 to the surgery alone group. Before PSM, the respective 6-, 12-, and 24-month overall survival (OS) rates were 93.0%, 89.6%, and 81.9% in the NAT combined with surgery group and 96.4%, 83.3%, and 56.9% in the surgery alone group ($p=0.062$). The respective 6-, 12-, and 24-month disease-free survival (DFS) rates were 93.0%, 84.6%, and 55.7% in the NAT combined with surgery group and 88.4%, 68.2%, and 40.4% in the surgery alone group ($p=0.047$). After PSM, the 6-, 12-, and 24-month OS rates were 93.9%, 89.7%, and 82.2% in the NAT combined with surgery group and 90.7%, 79.1%, and 49.7% in the surgery alone group ($p=0.033$). The respective 6-, 12-, and 24-month DFS rates were 93.9%, 83.4%, and 54.9% in the NAT combined with surgery group and 81.8%, 54.5%, and 35.3% in the surgery alone group ($p=0.022$). Subgroup analysis of the NAT combined with surgery group demonstrated that patients who received combined local and systemic therapy had significantly better DFS than of those who received local therapy alone ($p=0.028$). According to RECIST, version 1.1, the objective response rate and disease control rate were 51.2%

and 100%, respectively, among 43 evaluable patients in the NAT combined with surgery group. Regarding safety, the incidence of grades 1–3 adverse events (AEs) was 76.7% in patients in the NAT combined with surgery group, with no occurrence of grade 4 or 5 AEs. In addition, postoperative pathological analysis showed that patients in the NAT combined with surgery group had significantly less microvascular invasion ($p=0.0013$) and microvessel density ($p<0.001$) compared with those in the surgery alone group, potentially offering insights into the mechanism of NAT.

Conclusion: Patients with narrow-margin HCC who received NAT combined with surgery had a better prognosis and showed an acceptable safety profile than those who received surgery alone.

THU-463

Pre-treatment serum N-glycans predict poor immunotherapy response and survival in hepatocellular carcinoma

Nicky Somers¹, Theresa Holtmann², Fabian Artusa², Emma Butaye¹, Lorenz Grossar¹, Sarah Raevens¹, Anja Geerts¹, Sander Lefere¹, Lindsey Devisscher³, Leander Meuris⁴, Nico Callewaert⁴, Hans Van Vlierberghe¹, Raphael Mohr², Xavier Verhelst¹. ¹Department of Gastroenterology and Hepatology, Liver Research Center Ghent, Ghent University Hospital, Ghent, Belgium; ²Medizinische Klinik m. S. Hepatologie und Gastroenterologie, Charité-Universitätsmedizin Berlin, Berlin, Germany; ³Gut-Liver Immunopharmacology Unit, Dpt Basic and Applied Medical Sciences, Liver Research Center Ghent, Ghent University, Ghent, Belgium; ⁴VIB-UGent Center for Biotechnology, Department of Biochemistry and Microbiology, Ghent University, Ghent, Belgium
Email: nicky.somers@ugent.be

Background and aims: Patients with hepatocellular carcinoma (HCC) frequently present with advanced disease, for which immunotherapy is the most promising first-line agent despite the fact that only a quarter of patients show a favourable response. Although serum N-glycans (glycomics) are altered in HCC, they have not been assessed as a predictive marker for treatment response. We investigated glycomics as a predictive indicator of poor response to immunotherapy and associated survival in advanced HCC.

Method: A total of 90 immunotherapy-naïve HCC patients were retrospectively recruited with a pre-treatment serum sample. Whole serum N-glycomic analysis was performed using the optimised 96-well on-membrane deglycosylation technique (DSA-FACE). Uni- and multivariate Cox regression analyses were conducted to develop the prognostic GlycanScore and GlycanLabScore, with associated Kaplan Meier survival method (log-rank test). A multivariate Cox proportional hazards model was built to identify independent predictive factors.

Results: This cohort included 90 HCC patients receiving atezolizumab and bevacizumab combination therapy, of which 40 of them had no prior locoregional treatment and were thus completely treatment-naïve. Pre-treatment NA3Fc and NA3Fbc glycans were significantly increased in patients who showed poor response (progressive disease) after a median treatment time of 5.9 months as compared with patients who did not. Other independent risk factors were decreased hemoglobin (Hb) and increased aspartate aminotransferase (AST) pre-treatment levels. For the complete treatment-naïve patients ($n=40$) with a baseline GlycanScore (compositescore of NA3Fc and NA3Fbc) above the cut-off value of 1.75, the HR for poor response was 2.16 (95% CI [1.36–3.42], $p=0.001$). Combination of this GlycanScore with Hb and AST resulted in the GlycanLabScore with an HR of 2.72 (95% CI [1.677–4.401], $p<0.001$) for patients at risk of poor response with low survival ($p<0.001$), exceeding the cut-off value of –0.83. Similar findings could be retained when the total cohort was considered, thus including the 50 patients who did receive prior locoregional treatment before the start of immunotherapy. In these patients, the risk for having progressive disease with low survival ($p=0.0017$, $p=0.028$) was related to a GlycanScore with HR of 1.82 (95% CI [1.40–2.37], $p<0.001$) and a GlycanLabScore with HR of 2.63 (95%

CI [1.91–3.63], $p < 0.001$), based on the same cut-off values. In comparison, the alphafetoprotein (AFP) level was not able to significantly differentiate between treatment response, nor was it retained as an independent predictor in the Cox proportional Hazards model.

Conclusion: Pre-treatment tri-antennary core and branch fucosylated glycans, combined or not with Hb and AST levels, might be predictive of poor immunotherapy response and low survival in advanced HCC.

THU-464

aMAP score predicts progression-free survival in patients receiving atezolizumab plus bevacizumab for hepatocellular carcinoma

Mathew Vithayathil^{1,2}, Antonio D'Alessio^{1,3}, Claudia Fulgenzi^{1,4}, Ciro Celsa¹, Giulia Manfredi¹, Naoshi Nishida⁵, Martin Schoenlein⁶, Johann von Felden⁷, Kornelius Schulze⁷, Henning Wege⁷, Anwaar Saeed⁸, Brooke Wietharn⁸, Hannah Hildebrand⁸, Linda Wu⁹, Celina Ang⁹, Thomas U. Marron⁹, Arndt Weinmann¹⁰, Peter R. Galle¹⁰, Dominik Bettinger¹¹, Chun-yen Lin^{12,13}, Arndt Vogel¹⁴, Bernhard Scheiner¹⁵, Pei-Chang Lee¹⁶, Yi-Hsiang Huang¹⁶, Suneetha Amara¹⁷, Mahvish Muzaffar¹⁷, Abdul Rafah Naqash¹⁷, Valentina Zanuso¹⁸, Tiziana Pressiani¹⁹, Giuseppe Cabibbo²⁰, Andrea Dalbeni²¹, Matthias Pinter¹⁵, Amit Singal²², Hong Jae Chon²³, Alessio Cortellini¹, Masatoshi Kudo⁵, Lorenza Rimassa^{18,24}, David J. Pinato^{25,26}, Rohini Sharma¹. ¹Imperial College London, London, United Kingdom; ²Imperial College London, Surgery and Cancer, London, United Kingdom; ³Humanitas University, Milan, Italy; ⁴Policlinico Universitario Campus Bio-Medico, Rome, Italy; ⁵Department of Gastroenterology and Hepatology, Kindai University Faculty of Medicine, Osaka, Japan; ⁶Department of Oncology, Hematology and Bone Marrow Transplantation with Section of Pneumology, University Medical Center Hamburg-Eppendorf, Hamburg, Germany; ⁷Department of Gastroenterology and Hepatology, University Medical Center Hamburg-Eppendorf, Hamburg, Germany; ⁸Division of Medical Oncology, Department of Medicine, Kansas University Cancer Center, Kansas, United States; ⁹Division of Hematology/Oncology, Department of Medicine, Tisch Cancer Institute, Mount Sinai Hospital, New York, United States; ¹⁰Medical Department, University Medical Center Mainz, Mainz, Germany; ¹¹Department of Medicine II (Gastroenterology, Hepatology, Endocrinology and Infectious Diseases), Faculty of Medicine, Freiburg University Medical Center, University of Freiburg, Freiburg, Germany; ¹²Department of Gastroenterology and Hepatology, Chang Gung Memorial Hospital, Linkou Medical Center, Taoyuan, Taiwan; ¹³College of Medicine, Chang Gung University, Taoyuan, Taiwan; ¹⁴Hannover Medical School, Hannover, Germany; ¹⁵Division of Gastroenterology and Hepatology, Department of Internal Medicine III, Medical University of Vienna, Vienna, Austria; ¹⁶Division of Gastroenterology and Hepatology, Department of Medicine, Taipei Veterans General Hospital, Taipei, Taiwan; ¹⁷Division of Hematology/Oncology, East Carolina University, Greenville, United States; ¹⁸Department of Biomedical Sciences, Humanitas University, Pieve Emanuele, Milan, Italy; ¹⁹Medical Oncology and Hematology Unit, Humanitas Cancer Center, IRCCS Humanitas Research Hospital, Rozzano, Milan, Italy; ²⁰Section of Gastroenterology and Hepatology, Department of Health Promotion, Mother and Child Care, Internal Medicine and Medical Specialties, PROMISE, University of Palermo, Palermo, Italy; ²¹University of Verona, Department of Medicine General Medicine C Unit and Liver Unit, Verona, Italy; ²²Department of Internal Medicine, UT Southwestern Medical Center, Dallas, United States; ²³Medical Oncology, Department of Internal Medicine, CHA Bundang Medical Center, CHA University, Seongnam, Korea, Rep. of South; ²⁴Medical Oncology and Hematology Unit, Humanitas Cancer Center, IRCCS Humanitas Research Hospital, Rozzano, Milan, Italy; ²⁵Imperial College London, London, UK, London, United Kingdom; ²⁶Division of Oncology, Department of Translational Medicine, University of Piemonte Orientale, Novara, Italy
Email: mathew.vithayathil@doctors.org.uk

Background and aims: Atezolizumab plus bevacizumab a first line-treatment for unresectable hepatocellular carcinoma (HCC). The aMAP score comprises of age, sex, bilirubin, albumin and platelets, and has been shown to predict HCC risk in patients with chronic liver disease. aMAP has also been identified as a prognostic tool for patients undergoing resection and ablation, but its role in patients having immunotherapy has not been studied. Our study investigated its prognostic value in a large real-world patient cohort receiving atezolizumab plus bevacizumab.

Method: Patients from twenty-six international centres receiving atezolizumab plus bevacizumab were recorded retrospectively. Overall survival (OS), progression-free survival (PFS), overall response rate (ORR) and disease control rate (DCR) defined by RECIST v1.1 were measured in patients with a low- (<50) and high- (≥50) aMAP score. Kaplan-Meier and Cox regression analysis were measured. For multivariate Cox regression, aMAP group, Barcelona Clinic Liver Cancer Stage (BCLC), Child-Pugh stage, tumour diameter, alpha-fetoprotein and extrahepatic disease were used as co-variables. Treatment-related adverse events (trAEs) were evaluated in each aMAP cohort.

Results: 933 consecutive patients receiving atezolizumab plus bevacizumab were assessed. After exclusion of patients who received previous HCC therapy, 641 patients were studied. Barcelona Clinic Liver Cancer stage and Child-Pugh stage were comparable between low aMAP (n = 67) and high aMAP (n = 574) patients. Patients with a low aMAP score had a significantly shorter median progression-free survival (3.3 months; 95% confidence interval 2.3–4.8) compared to high aMAP patients (6.4 months; 95% CI 5.3–7.6; $p = 0.004$). In Cox regression analysis, high aMAP was associated with a significant reduction in PFS in both univariate (hazard ratio 0.64; 95% CI 0.47–0.87; $p = 0.04$) and multivariate (HR 0.69; 95% CI 0.51–0.94; $p = 0.02$) models. There was no association between aMAP and OS in univariate or multivariate analysis. High aMAP was associated with significantly higher DCR (25.4% vs. 38.0%; $p = 0.04$), with no difference in ORR seen (65.7% vs. 75.8%; $p = 0.07$). The high aMAP group had higher rates of bevacizumab-related toxicity (41.1% vs. 28.4%; $p = 0.04$), with no difference in atezolizumab-related observed (51.9% vs. 40.3%; $p = 0.28$). There was no difference in liver-related toxicity, acute hepatic decompensation or bleeding between aMAP cohorts.

Conclusion: Higher aMAP score is associated with better response to immunotherapy in treatment-naïve HCC patients, independent of BCLC and Child-Pugh stage, with higher rates of bevacizumab-related toxicity. aMAP score has potential use as a theragnostic tool for HCC patients undergoing immunotherapy.

THU-465-YI

Impact of antibiotic exposure and co-medication on the efficacy of immunotherapy for the treatment of advanced hepatocellular carcinoma

Matthias Jeschke¹, Marie Möller², Florian P. Reiter², Sebastian Wiener¹, Hartmut Schmidt¹, Leonie Jochheim¹. ¹University Hospital Essen, Essen, Germany; ²University Hospital Würzburg, Würzburg, Germany
Email: matthias001.jeschke@gmail.com

Background and aims: The advent of immuncheckpoint inhibitors (ICI) has markedly altered the treatment landscape of advanced hepatocellular carcinoma (HCC), and studies are examining its application to the adjuvant and neoadjuvant treatment setting, further extending their utility. However, there is a growing body of evidence that the efficacy of ICI in solid tumors might be impaired by the application of antibiotics, possibly through alterations in the gut microbiome. The aim of this study was to evaluate the association between survival and antibiotic exposure, its timing or co-medication affecting the gut microbiome.

Method: We analysed data from 121 patients, who began treatment with ICI therapy for advanced HCC (BCLC stages B and C) in two tertiary care centers between February 2020 and July 2023. Primary

POSTER PRESENTATIONS

end points included overall survival (OS) and progression-free survival (PFS). Multivariable Cox models evaluated the association between antibiotic exposure or co-medication and OS or PFS.

Results: The mean age in our patient cohort was 68.0 years (SD 11.4 years); 28 patients (23%) were female. In total, 50 patients (41%) received antibiotic treatment during ICI therapy. Among them, early antibiotic treatment (within a time frame of 40 days prior or after initiation of ICI therapy) occurred in 37 patients (30.5%). The most common indications for antibiotic therapy were urinary tract infections (30%), cholangitis (10%) and pneumonia (10%); the most common antibiotic classes included penicillin derivatives (66%) and cephalosporines (20%). Broad-spectrum antibiotic treatment was used in almost half of all cases (48%). Univariate and multivariate analysis did not reveal a significant discrepancy with regards to OS or PFS between patients receiving early antibiotic treatment and those who did not ($p = 0.24$ and $p = 0.38$, respectively). Proton pump inhibitors, Metformin, SGLT2-inhibitors, betablockers or SSRI did not affect Overall survival. The treatment with Rifaximin seemed to negatively affect overall survival ($p = 0.045$) in univariate analysis, although this might be due to a confounding effect.

Conclusion: While some studies report a negative impact of antibiotic exposure on the efficacy of ICI therapy, this could not be shown in our patient cohort. Further studies are needed to improve the management of patients under ICI treatment in clinical practice.

THU-466

Treatment with Atezolizumab-Bevacizumab for hepatocellular carcinoma in the french population outside clinical trials: data from the prospective CHIEF cohort

Manon Allaire¹, Ben Khadhra Hajer², Giuliana Amaddeo³, Mohamed Bouattour⁴, Bleuenn Brusset⁵, Marianne Zioli⁶, Philippe Merle⁷, Jean-Frédéric Blanc⁸, Thomas Uguen⁹, Nathalie Ganne-Carrié¹⁰, Stéphane Cattan¹¹, Ghassan Riachi¹², Veronique Loustaud-Ratti¹³, Thomas Decaens¹⁴, Christine Silvain¹⁵, Jean Marie Peron¹⁶, Aurore Baron¹⁷, Georges-Philippe Pageaux¹⁸, Frédéric Oberti¹⁹, Rodolphe Anty²⁰, Sylvain Manfredi²¹, Marc Bourliere²², Yasmina Ben Merabet²³, Jean-Baptiste Noursbaum²⁴, Alexandra Heurgue-Berlot²⁵, Isabelle Ollivier-Hourmand²⁶, Gerard Ducournau²⁷, Olivier Ganry²⁷, Charlotte Costentin²⁸, Eric Nguyen Khac²⁷. ¹APHP, Paris, France; ²CHU Amiens, Amiens, France; ³Henri Mondor University Hospital, Paris, France; ⁴Beaujon hospital, Clichy, France; ⁵CHU Grenoble, Grenoble, France; ⁶Avicenne, Bobigny, France; ⁷Croix-Rousse Hospital, Hospices Civils de Lyon, Lyon, France; ⁸Hôpital haut-Lévêque, Bordeaux, France; ⁹CHU Pontchaillou, Rennes, France; ¹⁰Hôpital Avicenne, Bobigny, France; ¹¹CHU Lille, Lille, France; ¹²HOPITAL CHARLES NICOLLE, ROUEN, France; ¹³CHU Limoges, Limoges, France; ¹⁴HOPITAL ALBERT MICHALLON, Grenoble, France; ¹⁵CHU La Miletie, Poitiers, France; ¹⁶Toulouse University Hospital, Toulouse, France; ¹⁷Centre Hospitalier Sud Francilien, Creil, France; ¹⁸Regional University Hospital Center of Montpellier, Montpellier, France; ¹⁹CHU Angers, Angers, France; ²⁰CHU de NICE-HOPITAL DE L'ARCHET, Nice, France; ²¹CHU Le-Bocage, Dijon, France; ²²Hôpital Saint Joseph, Marseille, France; ²³Paul Brousse Hospital, APHP, Paris, France; ²⁴CHU BREST, BREST, France; ²⁵CENTRE HOSPITALIER UNIVERSITAIRE DE REIMS, Reims, France; ²⁶CHU de Caen, Caen, France; ²⁷CHU Amiens Picardie, Amiens, France; ²⁸Grenoble Alpes University Hospital, La tronche, France
Email: allama5@hotmail.fr

Background and aims: The results of the Imbrave 150 study have revolutionized the management of advanced HCC with the Atezolizumab-Bevacizumab combination (AtezoBev). In this study, patients were highly selected, with a 30% response rate and a trend to higher response in patients with a viral etiology. Our objective was to evaluate the tolerability and efficacy of AtezoBev in the French HCC population, which is distinctive for its prevalent presence of underlying advanced non-viral chronic liver disease.

Method: Data from all patients treated with AtezoBev as first-line systemic treatment in the multicentric CHIEF cohort (32 centers) were prospectively collected between July 2020 and January 2023. Overall survival (OS) and progression-free survival (PFS) were evaluated using the Kaplan-Meier method. The objective response rate was assessed by the presence of a complete or partial response. The influence of inclusion characteristics on events during follow-up was evaluated using a log-rank analysis.

Results: Prospective data from 552 patients treated with AtezoBev were analyzed (median age 68 [62–75] years, 86% men, 77% cirrhotic patients, Child-Pugh A 81%, 18% Child-Pugh B). Chronic liver disease was of viral origin in 27%, related to excessive alcohol consumption in 58%, to a metabolic cause in 35% of cases. Among these patients, 22% had large esophageal varices (EV) on endoscopy. At the initiation of AtezoBev, 44% of new cases were treatment-naïve for HCC, 28% were classified as BCLC-B, and 67% as BCLC-C. HCC comprised more than 3 lesions in 31% of cases and was infiltrating in 21% of cases, with vascular invasion in 31% of patients and extrahepatic lesions in 27%. Among patients, 4% had an ALBI score of 3, and 32% had an AFP ≥ 400 ng/ml. The median follow-up was 21.2 months, 95% CI [19.8–22.4]. At the first evaluation, 27% of patients showed an objective response (4% complete response and 23% partial response), and 22% of patients progressed. The 12-month overall survival rate was 66%. OS was significantly higher in BCLC-B patients (median OS not reached) versus BCLC-C (17.1 months, $p < 0.001$), as well as in Child-Pugh A patients (median OS not reached) versus Child-Pugh B (12 months, $p < 0.001$). OS was similar across VO stage, etiology of liver disease (viral versus metabolic), and tumor characteristics (AFP ≥ 400 ng/ml, presence of metastases, previous HCC treatment). In the overall cohort, PFS was 15.8% at 12 months (median PFS 4.6 months). PFS was significantly higher in BCLC-B patients (6.8 months) compared to BCLC-C (3.4 months, $p = 0.02$).

Conclusion: These initial real-world data from the prospective multicentric CHIEF cohort show survival and response data similar to those obtained in the phase 3 IMbrave 150 study. These results confirm the effectiveness of the treatment in routine practice, taking into account the clinical and epidemiological characteristics of the French HCC population.

THU-467-YI

Evaluation of overall survival by restricted mean survival time in advanced biliary tract cancer treated with immunotherapy: a systematic review and meta-analysis

Ezequiel Mauro¹, Marco Sanduzzi Zamparelli², Tamara Sauri³, Alexandre Soler⁴, Gemma Iserle¹, Marta Fortuny¹, Alejandro Forner⁵. ¹Barcelona Clinic Liver Cancer (BCLC) Group, IDIBAPS, CIBEREHD, University of Barcelona., Liver Unit, ICDMD. Hospital Clínic de Barcelona, Barcelona, Spain; ²Hospital Clínic de Barcelona. IDIBAPS.CIBEREhd., Liver Unit, ICDMD. Hospital Clínic de Barcelona, Barcelona, Spain; ³Department of Medical Oncology. ICMHO. Hospital Clínic de Barcelona and Translational Genomics and Targeted Therapies in Solid Tumors, IDIBAPS, Barcelona, Spain, Barcelona Clinic Liver Cancer (BCLC) Group, Barcelona, Spain; ⁴Radiology Department. CDI, Hospital Clinic Barcelona, Barcelona, Spain, Barcelona Clinic Liver Cancer (BCLC) group, IDIBAPS, Barcelona, Spain, Barcelona, Spain; ⁵Barcelona Clinic Liver Cancer (BCLC) Group, IDIBAPS, CIBEREHD, University of Barcelona., Liver Unit, ICDMD. Hospital Clínic de Barcelona, Barcelona
Email: mauro@clinic.cat

Background and aims: In biliary tract cancer (BTC), the addition of immunotherapy (durvalumab or pembrolizumab) to gemcitabine and cisplatin (GemCis) has significantly improved overall survival (OS) in phase 3 clinical trials (RCTs). However, the interpretation of the results is challenging because OS and progression-free survival (PFS) Kaplan-Meier curves violate the proportional hazards (PH) assumption. Analysis using the restricted mean survival time (RMST) allows quantification of the absolute benefit in the absence of PH. This systematic review and meta-analysis aim to quantitatively assess

the benefit of immunotherapy-based regimens (IOs) for both OS and PFS at 24 months, using RMST analysis.

Method: Systematic searches were conducted using databases, clinical trial registries, and conference abstracts of studies published until November 8, 2023. Only phase 3 RCTs evaluating the use of anti-PD-1/PD-L1 combined with GemCis and reporting OS and PFS rates were included. KM curves for OS and PFS were digitized using WebPlotDigitizer v.4.6, and the data were reconstructed. A meta-analysis of extracted data for OS and PFS using RMST at 24 months was performed, employing common-effect models to estimate weighted average RMST and mean differences between treatment and control groups. Heterogeneity was assessed using the I^2 statistic.

Results: A total of 1,754 participants from the KEYNOTE-966 and TOPAZ-1 trials were included. In the TOPAZ-1 study, RMST OS at 24 months was 13.52 (7.92) and 12.21 (7.22) months with GemCis plus durvalumab and GemCis, respectively. In the KEYNOTE-966 study, OS at 24 months was 13.60 (7.76) and 12.45 (7.73) months with GemCis plus pembrolizumab and GemCis, respectively. IOs regimens showed a mean OS difference at 24 months by RMST of 1.21 months [(95% CI: 0.49–1.93), $p < 0.001$, $I^2 = 0\%$]. RMST PFS at 24 months in TOPAZ-1 was 8.10 (6.74) and 6.56 (4.82) months with GemCis plus durvalumab and GemCis, respectively. Similarly, in the KEYNOTE-966 study, it was 8.51 (8.54) and 7.49 (7.56) months with GemCis plus pembrolizumab and GemCis, respectively. The meta-analysis of mean PFS difference by RMST was 1.31 [(95% CI: 0.66–1.96), $p < 0.001$, $I^2 = 0\%$] months in patients undergoing IOs.

Conclusion: Combining IOs with GemCis offers a significant benefit for the survival of patients with advanced BTC. With this magnitude of benefit, it is essential to weigh individual patient factors, preferences, and potential risks in therapeutic decision-making. RMST analysis provides valuable information to patients and physicians, facilitating decision-making in a value-based medical environment.

THU-470-YI

Analysis of treatment benefits and prognostic factors for post-transplant hepatocellular carcinoma recurrence in a large Euro-American-Asian cohort

Zhihao Li¹, Itsuko Chih-Yi Chen², Grainne O'Kane³, Arndt Vogel⁴, Luciano De Carli⁵, Leonardo Centonze⁶, Quirino Lai⁷, Neil Mehta⁸, Chao-Long Chen², Gonzalo Sapisochin¹. ¹University Health Network, Toronto, Canada; ²Kaohsiung Chang Gung Memorial Hospital, Kaohsiung, Taiwan; ³Trinity St James's Cancer Institute, Princess Margaret Hospital, Dublin, Ireland; ⁴University Health Network, Hannover Medical School, Toronto, Canada; ⁵Niguarda-Cà Granda Hospital, University of Milano-Bicocca, Milano, Italy; ⁶Niguarda Cà Granda Hospital, University of Modena and Reggio Emilia, Milan, Italy; ⁷Sapienza University of Rome, Rome, Italy; ⁸UCSF, San Francisco, CA, United States

Email: zhihao.li@uhn.ca

Background and Aims: Post-transplant recurrence of hepatocellular carcinoma (HCC) significantly impacts survival, yet its management is challenging due to limited evidence. Improvements in systemic therapies necessitate updated data on managing recurrent disease.

Method: Our retrospective study (2000–2022) across five international centers (Canada, USA, Italy, Belgium, Taiwan) analyzed treatment outcomes and prognostic factors of post-transplant HCC recurrence. We employed Kaplan-Meier analysis to compare survival post-HCC recurrence and utilized multivariable Cox regression to identify prognostic factors.

Results: In our study, 431 of 3630 (12%) transplanted HCC patients developed recurrence with median time from transplant (LT) to recurrence of 18 (IQR 9–33) months. The median age at recurrence was 57 (IQR 51–63), patients were predominantly male (85%), with hepatitis C (41%), hepatitis B (30%) and alcohol-related liver disease (17%) as common underlying liver disease. 25% received deceased-donor LT and 75% living-donor LT. Tumor differentiation varied, with

18% poor, 65% moderate, and 10% well-differentiated; 46% exhibited microvascular invasion. The median RETREAT score was 3 (IQR 2–5). Within the first year post-LT, 35% of patients developed recurrence. Recurrence patterns included 24% intrahepatic-only, 27% both intrahepatic and extrahepatic, and 49% extrahepatic-only. 34% underwent curative-intent treatments (surgery/ablation), 48% received palliative treatments, and 18% were given best-supportive care. Patients undergoing curative-intent treatments had significantly better survival at 1/3/5 years (90%/56%/43%) compared to those receiving non-curative treatments (46%/10%/7%, $p < 0.001$). Patients with recurrence diagnosed in the era 2018–2022 (24%) showed improved 1/3/5-year survival (67%/43%/37%) compared to those diagnosed earlier (59%/22%/16%, $p < 0.001$). No significant survival difference was noted between living-donor and deceased-donor transplants ($p = 0.52$). The median follow-up post-HCC recurrence was 16 (IQR 7–30) months. Multivariable analysis revealed 5 prognostic factors for post-transplant HCC survival: ineligibility for curative-intent treatment (HR 3.7, 95% CI 2.8–4.8, $p < 0.001$), recurrence within 1-year (HR 1.7, 95% CI 1.4–2.2, $p < 0.001$), poor tumor differentiation (HR 1.4, 95% CI 1.1–1.9, $p = 0.02$), higher RETREAT score at transplant (HR 1.1, 95% CI 1.0–1.1, $p = 0.02$) and recurrence diagnosis before 2018 (HR 1.5, 95% CI 1.2–1.9, $p < 0.001$). **Conclusion:** Curative-intent treatments should be advocated for patients with post-transplant HCC recurrence whenever possible. Prognostic factors linked to aggressive tumor biology help to identify high-risk patients for adjuvant therapies and tailored surveillance. Survival outcomes have improved in the past five years reflecting improvements in systemic therapies.

THU-471-YI

From randomised clinical trials to clinical practice: a systematic review and meta-analysis of real-world data on atezolizumab plus bevacizumab for advanced hepatocellular carcinoma

Giulia Francesca Manfredi^{1,2}, Claudia Fulgenzi², Ciro Celsa^{2,3,4}, Bernardo Stefanini^{2,5}, Antonio D'Alessio^{2,6}, Matthias Pinter⁷, Bernhard Scheiner⁷, Nichola Awosika², Yi-Hsiang Huang^{8,9,10}, Chun-yen Lin^{11,12}, Andrea Dalbeni¹³, Arndt Vogel^{14,15}, Peter R. Galle¹⁶, Masatoshi Kudo¹⁷, Lorenza Rimassa^{18,19}, Hong Jae Chon²⁰, Giuseppe Cabibbo³, Fabio Piscaglia^{5,21}, Calogero Camma³, Anjana Pillai²², Mario Pirisi^{1,23}, Amit Singal²⁴, David J. Pinato^{2,6}.

¹Department of Translational Medicine, Università del Piemonte Orientale, Novara, Italy; ²Department of Surgery and Cancer, Imperial College London, Hammersmith Hospital, London, United Kingdom; ³Section of Gastroenterology and Hepatology, Department of Health Promotion, Mother and Child Care, Internal Medicine and Medical Specialties, PROMISE, University of Palermo, Palermo, Italy; ⁴Department of Surgical, Oncological and Oral Sciences (Di.Chir.On.S.), University of Palermo, Palermo, Italy; ⁵Department of Medical and Surgical Sciences, University of Bologna, Bologna, Italy; ⁶Division of Oncology, Department of Translational Medicine, University of Piemonte Orientale, Novara, Italy; ⁷Division of Gastroenterology and Hepatology, Department of Medicine III, Medical University of Vienna, Vienna, Austria; ⁸Healthcare and Service Center, Taipei Veterans General Hospital, Taipei, Taiwan; ⁹Division of Gastroenterology and Hepatology, Taipei Veterans General Hospital, Taipei, Taiwan; ¹⁰Institute of Clinical Medicine, College of Medicine, National Yang Ming Chiao Tung University, Taipei, Taiwan; ¹¹Department of Gastroenterology and Hepatology, Chang Gung Memorial Hospital, Linkou Medical Center, Taoyuan, Taiwan; ¹²College of Medicine, Chang Gung University, Taoyuan, Taiwan; ¹³General Medicine C and Liver Unit, Medicine Department, University of Verona and University and Hospital Trust (AOU) of Verona, Verona, Italy; ¹⁴Toronto General Hospital, UHN and Princess Margaret Cancer Centre, Toronto, Canada; ¹⁵Hannover Medical School, Hannover, Germany; ¹⁶University Medical Center Mainz, I. Dept. of Internal Medicine, Mainz, Germany; ¹⁷Department of Gastroenterology and Hepatology, Kindai University Faculty of Medicine, Osaka-Sayama, Japan; ¹⁸Department of

POSTER PRESENTATIONS

Biomedical Sciences, Humanitas University, Pieve Emanuele, Milan, Italy; ¹⁹Medical Oncology and Hematology Unit, Humanitas Cancer Center, IRCCS Humanitas Research Hospital, Rozzano, Milan, Italy; ²⁰Medical Oncology, Department of Internal Medicine, CHA Bundang Medical Center, CHA University, Seongnam, Korea, Rep. of South; ²¹Division of Internal Medicine, Hepatobiliary and Immunoallergic Disease, IRCCS Azienda Ospedaliero-Universitaria di Bologna, Bologna, Italy; ²²Department of Internal Medicine, Division of Gastroenterology, Hepatology and Nutrition, University of Chicago, Chicago, United States; ²³Division of Internal Medicine, AOU Maggiore della Carità, Novara, Italy; ²⁴Department of Internal Medicine, UT Southwestern Medical Center, Dallas, United States
Email: gf.manfredi01@gmail.com

Background and aims: The treatment landscape of advanced hepatocellular carcinoma (aHCC) has been revolutionised in recent years following demonstration of survival benefit from atezolizumab plus bevacizumab (A+B) in 2019. It is unknown if the efficacy observed from immunotherapy combinations in randomised controlled trials (such as IMbrave150) translates to preserved effectiveness in routine clinical practice.

Method: We conducted a systematic review and meta-analysis of MEDLINE, Embase and Cochrane libraries to compare baseline characteristics and therapy outcomes in patients treated with first-line systemic therapies for aHCC in routine clinical practice. Individual patient-level data were reconstructed from published Kaplan-Meier survival curves. Pooled estimates of overall survival (OS) and progression free survival (PFS) at 6 months and 1 year were calculated using random-effects analysis. Secondary outcomes included pooled overall response rate (ORR), disease control rate (DCR) and adverse events (AEs).

Results: The 12 studies selected for meta-analysis included 2179 patients treated with A+B. Most patients were male (80.5%) median age 66 years (IQR 61.6–73.0). In total, 83.7% were of Child-Pugh (CP) class A, 58.1% classed as albumin-bilirubin grade 1 and the most reported liver disease aetiology was viral (21.4% hepatitis B, 10.9% hepatitis C and 23.8% not further specified). Most patients belonged to Barcelona Clinic Liver Cancer stage C (61.6%). Among the 12 studies, one did not provide published Kaplan-Meier curves for OS but only for PFS, and another study did not present curves for PFS but only for OS. The pooled 6-month and 12-month OS rate were 82% (95% CI: 76–86%; $I^2 = 80\%$) and 68% (95% CI: 63–73%; $I^2 = 66\%$), respectively. No significant difference was found between the median OS of the IMbrave150 cohort (19.2 months, 95% CI 17.0–23.7) and that of real-world patients classified as CP-A (20.9 months, 95% CI 15.7–20.9; $p = 0.58$). The pooled PFS at 6 and 12 months were 57% (95% CI 53–61%; $I^2 = 49\%$) and 35% (95% CI 31–39%, $I^2 = 60\%$), respectively. Median PFS was longer in real world patients (11.8 months, 95% CI 10.45–18.08) compared to IMbrave150 (6.9 months, 95% CI 5.7–8.6, $p < 0.001$). The pooled ORR was 32% (95% CI 29–35%, $I^2 = 50\%$), whereas DCR was 78% (95% CI 73–81%, $I^2 = 63\%$). AEs were reported in 9 studies: pooled all-grade AEs were seen in 75% (7 studies), grade ≥ 3 AEs were 26% (8 studies), and discontinuation due to toxicity was 12% (7 studies).

Conclusion: Combination immunotherapy with A+B confirmed its efficacy and safety for aHCC in routine clinical practice, mirroring estimates published in the registration trial.

THU-472-YI

Sorafenib as a second-line treatment after failure of Atezolizumab/Bevacizumab

Francesco Tovoli¹, Maria Boe², Caterina Vivaldi³, Piera Federico⁴, Andrea Palloni⁵, Andrea Dalbeni⁶, Caterina Soldà⁷, Benedetta Stefanini¹, Ingrid Garajová⁸, Luca Ielasi⁹, Stefania De Lorenzo¹⁰, Alessandro Granito¹, Bernardo Stefanini¹, Gianluca Masi³, Sara Lonardi⁷, Giovanni Brandi¹, Daniele Bruno¹¹, Alessandra Auriemma⁶, Lorenzo Lani¹, Claudia Campani¹², Gianluca Svegliati-Baroni¹³, Fabio Piscaglia¹. ¹Department of Medical

and Surgical Sciences, University of Bologna, Bologna, Italy, Bologna, Italy; ²Department of Medical and Surgical Sciences, University of Bologna, Bologna, Italy, Bologna; ³Department of Translational Research and New Technologies in Medicine and Surgery, University of Pisa, Pisa, Italy; ⁴Medical Oncology Unit, Ospedale del Mare, Napoli, Italy, Naples, Italy; ⁵Oncology Unit, IRCCS Azienda Ospedaliero-Universitaria di Bologna, Bologna, Italy, Bologna, Italy; ⁶University of Verona and University and Hospital Trust (AOUI) of Verona, Verona, Italy; ⁷Medical Oncology 1, Veneto Institute of Oncology Iov-Irccs, Padua, Italy; ⁸Medical Oncology Unit, University Hospital of Parma, Parma, Italy, Parma, Italy; ⁹Ospedale degli Infermi di Faenza, Faenza, Italy; ¹⁰Oncology Unit, Azienda USL Bologna, Bologna, Italy, Bologna, Italy; ¹¹Ospedale del Mare, Napoli, Italy, Naples, Italy; ¹²Department of Experimental and Clinical Medicine, University of Florence, Florence, Italy; ¹³Polytechnic University of Marche, Ancona, Italy
Email: francesco.tovoli@unibo.it

Background and aims: Patients receiving atezolizumab/bevacizumab (AB) for HCC may have a primary resistance to this combination. Another relevant proportion of patients will develop a secondary resistance and, eventually, experience progression disease. Randomized clinical trials (RCTs) trying to identify second-line treatments are undergoing. If such trials are not available or patients are non-eligible, sorafenib is often prescribed, based on European approval and reimbursement policies. However, evidence supporting these policies is lacking, as no RCTs explored sorafenib in this setting. We aimed to assess the efficacy of sorafenib in patients who permanently stopped AB.

Method: The ARTE database collects prospectively enrolled patients treated with AB in a real-life setting (March 2022-ongoing). We analysed the outcome of patients who received sorafenib as second-line treatment. Moreover, we performed a case-control matching with historical controls who had received sorafenib as a frontline treatment before AB had become available in clinical practice. Patients were matched 4:1, based on known predictor of overall survival (OS) in sorafenib-treated patients (Child-Pugh class, AFP > 400 ng/ml, macrovascular invasion, extrahepatic spread, ECOG-PS>0).

Results: Amongst the 157 patients included in the ARTE database as of November 2023, 130 (67.4%) permanently discontinued AB. Of them, 57 received a second-line treatment. Sorafenib was prescribed in 29 patients. The disease control rate (DCR) was 17.2%, with no objective responses. The median PFS and OS were 3.2 and 7.9 months. When compared with historical controls, patients who received sorafenib as a second-line therapy had worse DCR (17.1 vs 47.4%, $p < 0.01$) and PFS. A trend toward a worse OS was also noted.

Conclusion: In the post-AB setting, we found suboptimal efficacy outcome of sorafenib. The very low DCR suggest that resistance to AB might select tumour cells able to escape the therapeutic targets of sorafenib. Enrollment of these patients in RCTs is strongly recommended to identify better therapeutic strategies.

THU-473

Complications of transarterial chemoembolization for hepatocellular carcinoma- 10 years' experience of a tertiary center

Laura Iliescu¹, Simona Ioanitescu², Razvan Rababoc², Andreea Simu², Mihai Toma², Radu Dumitru², Cristian Mugar Grasu². ¹Fundeni Clinical Institute, Carol Davila University of Medicine and Pharmacy, Bucharest; ²Fundeni Clinical Institute, Carol Davila University of Medicine and Pharmacy, Bucharest, Romania
Email: laura_ate@yahoo.com

Background and aims: Transarterial chemoembolization (TACE) is a fundamental therapeutic option in intermediate stage hepatocellular carcinoma (HCC), indicated in patients with preserved liver function, as bridge towards liver transplantation or as means of down-staging. Careful patient selection and increased experience of hospital staff can reduce the incidence of postprocedural complications and mortality (estimated at 2–7% and 1% respectively). This

study aims to determine risk factors for TACE complications in a large cohort in a tertiary care center.

Method: Between January 2013 and November 2023 1673 TACE procedures were performed in our clinic, in 1256 patients. We analyzed incidence and risk factors for developing post TACE complications, by recording demographic, biologic and imagistic data.

Results: Out of 1673 procedures, 22.8% were performed in patients with chronic hepatitis and 77.2% in patients with compensated cirrhosis. Periprocedural complications were: post-embolization syndrome (14.22%), acute liver decompensation (6.45%), infection (2.45%), acute kidney injury (1.01%). Rare complications include acute cholecystitis in 6 patients, acute pancreatitis in 2 patients, hepatic artery dissection in 2 patients, ruptured hepatoma: 4 patients. Overall, TACE related mortality was 0.3% (6 patients). Risk factors for complications included hepatitis B and delta as etiology of liver disease (OR 1.46, CI 1.13–1.89, $p=0.04$), older age (OR 2.17, CI 1.45–2.64, $p=0.02$) and diabetes (OR 3.17, CI 2.89–3.64, $p=0.01$). Tumor size more than 5 cm and the presence of more than 3 nodules were independent risk factors for acute decompensation (OR 2.16, CI 1.98–2.57, $p=0.03$, OR 1.61, CI 1.52–1.83, $p=0.03$ respectively) and post-embolization syndrome (OR 1.42, CI 1.18–1.73, $p=0.02$, OR 1.71, CI 1.55–1.93, $p=0.03$ respectively). Diabetes and older age were independent predictors for development of kidney injury (OR 3.91, CI 3.26–4.18, $p=0.01$ and OR 2.76, CI 2.48–3.12, $p=0.02$). Serologic markers associated with complications were increased transaminases before TACE (OR 2.57, CI 2.11–3.03, $p=0.03$), low total cholesterol (<100 mg/dL, OR 1.82, CI 1.56–2.18, $p=0.02$), low hemoglobin levels (OR 2.12, CI 2.03–2.57, $p=0.01$) and increased C-reactive protein (OR 1.65, CI 1.28–1.93, $p=0.04$).

Conclusion: TACE complications are rare in experienced centers. Risk factors include: diabetes, older age, inflammation and impaired liver synthesis function.

THU-474-YI

Immunotherapy in cholangiocarcinoma: understanding the immune landscape reveals treatment response

Rita Balsano^{1,2}, Tiziana Pressiani², Giulia Milardi³, Silvia Bozzarelli², Valentina Zanuso^{1,2}, Angelo Pirozzi^{1,2}, Giulia Tesini^{1,2}, Ana Lleo^{1,4}, Lorenza Rimassa^{1,2}. ¹Humanitas University, Pieve Emanuele, Milan, Italy; ²IRCCS Humanitas Research Hospital, Medical oncology and hematology unit, Rozzano, Milan, Italy; ³IRCCS Humanitas Research Hospital, Hepatobiliary immunopathology lab, Rozzano, Milan, Italy; ⁴IRCCS Humanitas Research Hospital, Department of gastroenterology, Internal medicine and hepatology, Rozzano, Milan, Italy
Email: rita.balsano@cancercenter.humanitas.it

Background and aims: Cisplatin, gemcitabine and durvalumab has emerged as first-line standard of care for patients (pts) with advanced cholangiocarcinoma (CCA). Despite this result, prognosis remains poor and identification of predictive markers could represent a crucial turning point to select patients who might benefit more from the treatment. Our aim is to dissect pts' immune cell type subgroups to identify markers of treatment response.

Method: This observational study evaluated 26 pts with advanced CCA receiving first-line cisplatin, gemcitabine and durvalumab between April 2022 and December 2023 at a single tertiary center. For 16 pts (61.5%) molecular profiling by Next-Generation Sequencing was available. Peripheral blood cell count was collected at ten different time points. The correlation between immune cell type subgroups and treatment response was analyzed performing a student's t-test. A two-sided $p<0.05$ was considered statistically significant.

Results: Pts were divided into two subgroups based on radiological response within 6 months (range 1–6 months) from treatment start: those with disease control (DC+) (17, 65%) including stable disease (SD) or partial response (PR) and those with progressive disease (PD) as best response (DC-) (9, 35%). Among DC+, 7 pts (41%) had PR and

10 (59%) had SD. We assessed the absolute counts of neutrophils, lymphocytes, eosinophils and the neutrophil-to-lymphocyte ratio (NLR) at baseline and at the last available tumor assessment. We found no difference in lymphocyte count at baseline ($p=0.09$) and at the time of the last tumor assessment ($p=0.07$) between DC+ and DC-. Instead, we observed a significant difference in eosinophil count at baseline (0.84 vs 0.58 M/ml; $p=0.0188$) and at the time of the last tumor assessment (1.18 vs 0.59 M/ml; $p=0.001$) between DC- and DC+. Although there was no difference in neutrophil count at baseline ($p=0.07$), a difference was detected at the time of the last tumor assessment between DC- (7.48 M/ml) and DC+ (3.48 M/ml) ($p=0.005$). This result was confirmed observing the NLR ratio, which showed no difference at baseline but a difference at the time of the last available tumor assessment and it was lower in DC+ (2.30) than DC- (4.79) ($p=0.037$). The molecular profiling showed some differences in the two groups. In the DC+ subgroup, BAP1 mutation was the most common alteration, detected in 3 pts (18.75%) while mutations in AKT1, ARID1A, TP53, KRAS (G12D), and CD22, MDM2 amplification, FGFR2 rearrangement, and BRCA2 truncation were observed in 1 pt each (6.25). In the DC- subgroup, mutations in IDH1 (R132C), ARID1A, NF1, CDKN2A loss and EGFR amplification were observed in 1 pt each (6.25%).

Conclusion: In our study, a lower eosinophil count and NLR ratio were significantly associated with a better disease control. While a more comprehensive analysis is warranted, we observed a higher prevalence of BAP1 mutation in the DC+ subgroup.

THU-475

Tumor burden incorporating AFP improves survival prediction for patients with HCC undergoing TACE: an international multicentre observational study

Dongdong Xia¹, Wei Bai², Qiuhe Wang^{3,4}, Jin Wook Chung⁵, Xavier Adhoute⁶, Roman Kloeckner⁷, Hui Zhang⁸, Yong Zeng⁹, Pimsiri Sripongpun¹⁰, Chunhui Nie¹¹, Seung Up Kim¹², Ming Huang¹³, Wenhao Hu¹⁴, Xiangchun Ding¹⁵, Guowen Yin¹⁶, Hailiang Li¹⁷, Hui Zhao¹⁸, Jing Li¹⁹, Jiaping Li²⁰, Xiaoli Zhu²¹, Jianbing Wu²², Chunqing Zhang²³, Weidong Gong²⁴, Zixiang Li²⁵, Zhengyu Lin²⁶, Tao Xu²⁷, Tao Yin²⁸, Jinlong Song²⁹, Haibin Shi³⁰, Guoliang Shao³¹, Weixin Ren³², Yongjin Zhang³³, Shufa Yang³⁴, Yanbo Zheng³⁵, Jian Xu³⁶, Wenhui Wang³⁷, Xu Zhu³⁸, Dominik Bettinger³⁹, Arndt Vogel⁴⁰, Guohong Han⁴¹. ¹Department of Liver Diseases and Interventional Radiology, National Clinical Research Centre for Digestive Disease and Xijing Hospital of Digestive Diseases, Fourth Military Medical University, Xi'an, China, Xi'an, China; ²Department of Liver Diseases and Interventional Radiology, Digestive Diseases Hospital, Xi'an International Medical Center Hospital, Northwest University, Xi'an, China, Xi'an, China; ³National Clinical Research Centre for Digestive Disease and Xijing Hospital of Digestive Diseases, Fourth Military Medical University, Xi'an, China, Department of Cardiology, Tangdu Hospital, Fourth Military Medical University, Xi'an, China, Xi'an, China; ⁴Department of Cardiology, Tangdu Hospital, Fourth Military Medical University, Xi'an, China, Xi'an, China; ⁵Department of Radiology, Seoul National University Hospital, Seoul, Korea, Seoul, Korea, Rep. of South; ⁶Department of Gastroenterology and Hepatology, Hôpital Saint-Joseph, Marseille, France, Marseille, France; ⁷Department of Diagnostic and Interventional Radiology, University Medical Center of the Johannes Gutenberg University Mainz, Langenbeckstr., Mainz, Germany, Mainz, Germany; ⁸Department of Hepatobiliary Surgery, Southwest Hospital, Third Military Medical University, Chongqing, China, Chongqing, China; ⁹Department of Liver Surgery, West China Hospital, Sichuan University, Chengdu, Sichuan, China, Chengdu, China; ¹⁰Gastroenterology and Hepatology Unit, Division of Internal Medicine, Faculty of Medicine, Prince of Songkla University, Songkhla, Thailand, Songkhla, Thailand; ¹¹Department of Hepatobiliary and Pancreatic Interventional Cancer, The First Affiliated Hospital, School of Medicine, Zhejiang University, Hangzhou, China, Hangzhou, China; ¹²Department of Internal Medicine,

POSTER PRESENTATIONS

Institute of Gastroenterology, Yonsei University College of Medicine, Seoul, Republic of Korea, Seoul, Korea, Rep. of South; ¹³Department of Minimally Invasive International Therapy, The Third Affiliated Hospital of Kunming University, Tumor Hospital of Yunnan Province, Kunming, China, Kunming, China; ¹⁴Department of Interventional Radiology, First Affiliated Hospital of Wenzhou Medical University, Wenzhou, China, Wenzhou, China; ¹⁵Department of Infectious Disease, General Hospital of Ningxia Medical University, Yinchuan, China, Yinchuan, China; ¹⁶Department of Interventional Radiology, Jiangsu Provincial Cancer Hospital, The Affiliated Cancer Hospital of Nanjing Medical University, Nanjing, China, Nanjing, China; ¹⁷Department of Interventional Radiology, The Affiliated Cancer Hospital of Zhengzhou University, Zhengzhou, China, Zhengzhou, China; ¹⁸Department of Interventional Radiology, The Affiliated Hospital of Nantong University, Nantong, China, Nantong, China; ¹⁹Department of Hepatobiliary Surgery, Xinqiao Hospital, Third Military Medical University, Chongqing, China, Chongqing, China; ²⁰Department of Interventional Radiology, The First Affiliated Hospital of Sun Yat-sen University, Guangzhou, China, Guangzhou, China; ²¹Department of Interventional Radiology, The First Affiliated Hospital of Soochow University, Suzhou, China, Suzhou, China; ²²Department of Oncology, The Second Affiliated Hospital of Nanchang University, Nanchang, China, Nanchang, China; ²³Department of Gastroenterology and Hepatology, Shandong Province Hospital Affiliated to Shandong University, Jinan, China, Jinan, China; ²⁴Department of Interventional Radiology, Tangdu Hospital, Fourth Military Medical University, Xi'an, China, Xi'an, China; ²⁵Interventional Medical Centre of the Affiliated Hospital of Qingdao University, Qingdao, China, Qingdao, China; ²⁶Department of Interventional Radiology, First Affiliated Hospital of Fujian Medical University, Fuzhou, China, Fuzhou, China; ²⁷Department of Infectious Diseases, the 910 Hospital of the Chinese People's Liberation Army Joint Logistic Support Force, Quanzhou, China, Quanzhou, China; ²⁸Department of Hepatic and Biliary and Pancreatic Surgery, Hubei Cancer Hospital, Tongji Medical College, Huazhong University of Science and Technology, Wuhan, China, Wuhan, China; ²⁹Department of Interventional Therapy, Shandong Tumor Hospital, Jinan, China, Jinan, China; ³⁰Department of Interventional Radiology, The First Affiliated Hospital of Nanjing Medical University, Nanjing, China, Nanjing, China; ³¹Department of Radiology, Zhejiang Cancer Hospital, Hangzhou, China, Hangzhou, China; ³²Department of Interventional Radiology, The First Affiliated Hospital of Xinjiang Medical University, Urumqi, China, Urumqi, China; ³³Department of Interventional Radiology and Vascular Surgery, Hunan Provincial People's Hospital, Changsha, China, Changsha, China; ³⁴Department of Interventional Radiology, The Affiliated Tumor Hospital of Xinjiang Medical University, Urumqi, China, Urumqi, China; ³⁵Department of Interventional Radiology, Yantai Yuhuangding Hospital, Yantai, China, Yantai, China; ³⁶Department of Medical Imaging, Nanjing General Hospital of the Nanjing Military Command, Nanjing, China, Nanjing, China; ³⁷Department of Interventional Medicine, The First Affiliated Hospital of Lanzhou University, Lanzhou, China, Lanzhou, China; ³⁸Department of Interventional Radiology, Peking University Cancer Hospital, Beijing, China, Beijing, China; ³⁹Department of Medicine II, University Medical Center Freiburg, Freiburg, Germany; ⁴⁰Department of Gastroenterology and Hepatology and Endocrinology, Medizinische Hochschule Hannover, Hannover, Germany; ⁴¹Department of Liver Diseases and Interventional Radiology, Digestive Diseases Hospital, Xi'an International Medical Center Hospital, Northwest University, Xi'an, China, Department of Liver Diseases and Interventional Radiology, National Clinical Research Centre for Digestive Disease and Xijing Hospital of Digestive Diseases, Fourth Military Medical University, Xi'an, China, Xi'an, China
Email: hangh@fmmu.edu.cn

Background and aims: Current prognostic models for patients with HCC undergoing transarterial chemoembolization (TACE) are not extensively validated and widely accepted. The aim of this study was to develop and validate a continuous model incorporating tumour

morphology and biology for individual survival prediction and risk stratification.

Method: 4, 377 treatment-naïve recommended TACE candidates from 37 centres in 5 countries were enrolled and divided into a training dataset, an internal validation dataset and two external validation datasets. The novel model was developed using a Cox multivariable regression analysis, and compared to our original 6-and-12 model (the largest tumour size [ts, centimeters] + tumour number [tn]) and other available models in terms of predictive accuracy.

Results: The proposed model named "6-and-12 model 2.0" was generated as "ts + tn + 1.5 × log10α-fetoprotein [AFP]," showed good discrimination (C-index 0.674) and calibration (Hosmer-Lemeshow test p = 0.147), and outperformed current existing models. An easy-to-use stratification was proposed according to the different AFP levels (≤100, 100–400, 400–2,000, 2,000–10,000, 10,000–40,000, and >40,000 ng/ml) along with the corresponding tumour burden cut-offs (8/14, 7/13, 6/12, 5/11, 4/10, and any tumour burden), ie. if AFP was 400–2,000 ng/ml, the stratification should be low- (≤6)/intermediate- (6–12)/high-risk (>12) strata. Hence, it could divide the patients into three distinct risk categories whose median overall survival 45.0 (95% CI, 40.1–49.9), 30.0 (95% CI, 26.1–33.9), and 15.4 (95% CI, 13.4–17.4) months (p < 0.001) from low-risk to high-risk strata, respectively. These findings were confirmed in validation and subgroup analyses.

Conclusion: 6-and-12 model 2.0 significantly improved individual outcome prediction and better stratified the recommended TACE candidates, which could be used in clinical practice, as well as trial design.

THU-478

RECIST 1.1, mRECIST, and Choi criteria for evaluating treatment response and survival outcomes in hepatocellular carcinoma patients treated with Atezolizumab plus Bevacizumab

Bohyun Kim¹, Dong Hwan Kim¹, Eun Jeong Moon², Joon-Il Choi³, Jong Young Choi⁴. ¹Seoul St. Mary's Hospital, Seoul, Korea, Rep. of South; ²Department of Medical Life Science, College of Medicine, The Catholic University of Korea, Seoul, Korea, Rep. of South; ³Department of Radiology, Seoul St. Mary's Hospital, College of Medicine, The Catholic University of Korea, Seoul, Korea, Rep. of South; ⁴Seoul St. Mary's Hospital, Seoul, Korea, Rep. of South
Email: baboojum@naver.com

Background and aims: The combination of atezolizumab and bevacizumab (atezo-bev) has substantially advanced the systematic therapeutic approach for hepatocellular carcinoma (HCC). However, conventional size-based response assessment criteria may not fully capture treatment effectiveness, particularly in the context of immunotherapy and targeted agents. We compared early responders with advanced HCC receiving atezo-bev. Complete or partial responses were evaluated with Response Evaluation Criteria in Solid Tumors (RECIST) 1.1, modified RECIST (mRECIST), and Choi criteria and correlated with progression-free survival (PFS) and overall survival (OS).

Method: This retrospective study included 65 patients with advanced HCC (56 men, 9 women; mean age, 62.5 ± 12.7 years) treated with ≥3 cycles of atezo-bev. Responses were assessed using RECIST 1.1, mRECIST, and Choi criteria by 2 independent reviewers. Kaplan-Meier curves with log-rank tests and restricted mean survival time (RMST) at 1 year were used to evaluate and compare PFS and OS among responders and non-responders. Cox proportional hazards models identified survival outcome predictors. Kappa statistics assessed inter-reader agreement.

Results: Choi criteria identified the highest proportion of early responders (43.1%–49.2%), followed by mRECIST (33.8%–35.4%) and RECIST 1.1 (24.6%–27.7%), with excellent inter-reader agreement in all criteria (κ, 0.84–0.90). A similar incidence of progressive disease (20–22 patients) was identified consistently across criteria. In responders,

all criteria showed longer PFS (log-rank $p \leq 0.009$), but only Choi criteria demonstrated significantly longer OS (log-rank $p \leq 0.018$). Choi criteria showed cumulative 1-year OS rates of 83.9% for responders and 62.2% for non-responders. RMST analysis at 1 year revealed a significant difference in OS between RECIST 1.1 and mRECIST ($p \leq 0.003$). Univariable Cox analysis identified Choi criteria as a significant OS predictor.

Conclusion: Choi criteria identified more early responders than RECIST 1.1 and mRECIST, and correlated with improved PFS and OS in patients with advanced HCC treated with atezo-bev. Future studies with longer follow-up periods could validate these findings and refine the response assessment.

THU-479

The features of gut microbiota and metabolites in non-viral unresectable hepatocellular carcinoma undergoing immunotherapy

Pei-Chang Lee¹, Ya-Wen Hung², Chi-Jung Wu¹, Chieh-Ju Lee¹, Chen-Ta Chi¹, I-Cheng Lee³, Yu-Lun Kuo⁴, Shih-Hsuan Chou⁴, Jiing-Chyuan Luo¹, Ming-Chih Hou¹, Yi-Hsiang Huang⁵. ¹Taipei Veterans General Hospital, Taipei, Taiwan; ²Taipei Veterans General Hospital, Taoyuan branch, Taoyuan; ³Taipei Veterans General Hospital, Taipei; ⁴Biotech, Co., Ltd, New Taipei City, Taiwan; ⁵Taipei Veterans General Hospital, National Yang Ming Chiao Tung University, Taipei, Taiwan

Email: yhhuang@vghtpe.gov.tw

Background and aims: Growing evidence suggests that non-viral hepatocellular carcinoma (HCC) may derive less benefit from immunotherapy. Gut microbiota and metabolites are considered to be associated with response to immune checkpoint inhibitors (ICIs) in unresectable HCC (uHCC). In this study, we aimed to investigate the features of gut microbiota and metabolites in non-viral uHCC and the association with tumor response to ICI immunotherapy.

Method: From May 2018 to September 2022, patients who received ICI therapy for uHCC in Taipei Veterans General hospital were prospectively enrolled. Pre-treatment fecal and plasma samples from 69 viral uHCC and 25 non-viral uHCC were collected. The differences of fecal microbiota, metabolites and plasma cytokines between non-viral and viral uHCC, and the relationship with tumor response were analyzed.

Results: A significant bacterial dissimilarity was observed between non-viral and viral uHCC before immunotherapy ($p = 0.019$ by Anosim test). *Shigella flexneri* and *Shigella dysenteriae* were predominant and abundant faecal microbiota in non-viral uHCC, whereas *Phocaeicola vulgatus* was predominant in viral uHCC. Significant enriched fecal isocaproic acid and plasma monocyte chemoattractant protein-1 (MCP-1) were also found in non-viral uHCC. In objective responders (16.0%) and durable disease controllers (24.0%) of non-viral uHCC, fecal *Shigella flexneri* and *Shigella dysenteriae* were less abundance, circulatory MCP-1 was less elevated, but significantly enriched anti-inflammatory taurochenodeoxycholic acid, ursodeoxycholic acid and ursocholic acid were noted as compared with non-responders.

Conclusion: Non-viral uHCC are characterized with more inflamed gut microbiota, metabolites and circulatory cytokines. However, responders to ICIs were characterized by more anti-inflammatory bile acids and less pro-inflammatory metabolites in their feces.

THU-480

An artificial intelligence-derived model for classification of tumor morphology based on computed tomography images in patients with hepatocellular carcinoma

I-Cheng Lee^{1,2}, Chia-Hsun Yen³, Yen-Chen Lin³, Chien-An Liu⁴, Shinn-Ying Ho³, Yi-Hsiang Huang⁵. ¹Division of Gastroenterology and Hepatology, Department of Medicine, Taipei Veterans General Hospital, Taipei, Taiwan; ²School of Medicine, College of Medicine, National Yang Ming Chiao Tung University, Taipei, Taiwan; ³Institute of Bioinformatics

and Systems Biology, National Yang Ming Chiao Tung University, Hsinchu, Taiwan; ⁴Department of Radiology, Taipei Veterans General Hospital, Taipei, Taiwan; ⁵Healthcare and Service Center, Taipei Veterans General Hospital, Taipei, Taiwan, Institute of Clinical Medicine, National Yang Ming Chiao Tung University, Taipei, Taiwan
Email: iclee@vghtpe.gov.tw

Background and aims: Tumor morphology pattern had significant impact on the treatment response and survival in patients with hepatocellular carcinoma (HCC). However, the classification of tumor morphology is time-consuming and labor-intensive. The aim of this study is develop an artificial intelligence (AI)-derived model for automatic classification of tumor morphology using dynamic computed tomography (CT) images from HCC patients.

Method: Dynamic CT images before transarterial chemoembolization (TACE) treatment in 515 HCC patients were used for model development ($n = 307$) and validation ($n = 208$). Another cohort of 643 patients receiving surgical resection were used to validate the prognostic value of AI-predicted morphology. Tumor morphology patterns were classified as low-risk (simple nodular type), intermediate-risk (simple nodular type with extranodular growth), and high-risk morphology (confluent multinodular or infiltrative type). A ResNet-based deep-learning model (HCC-MorphoNet model) was developed to classify the tumor morphology of HCC.

Results: The HCC-MorphoNet model achieved the overall accuracy of 86.3% and 86.1% in predicting tumor morphology in the training set and the test set, respectively. The accuracy for predicting low-, intermediate-, and high-risk morphology was 83%, 89.9% and 95.3%, respectively. The AI-classified tumor morphology could significantly discriminate the radiologic response ($p < 0.001$) and overall survival ($p < 0.001$) after TACE, and the predicted outcomes were similar to those from human-classified tumor morphology. The AI-classified tumor morphology also significantly discriminated recurrence-free survival ($p < 0.001$) and overall survival ($p < 0.001$) in HCC patients receiving surgical resection.

Conclusion: We developed an HCC-MorphoNet model based on dynamic CT images for classification of tumor morphology in patients with HCC. The AI-classified morphology significantly discriminated the outcomes of HCC after TACE and surgical resection.

THU-481-YI

Hepatic resection in patients with hepatocellular carcinoma: the message coming from real world data

Lorenzo Lani¹, Laura Bucci¹, Valentina Santi¹, Benedetta Stefanini¹, Franco Trevisani¹. ¹Unit of Semeiotics, Liver and Alcohol-related diseases, IRCCS Azienda Ospedaliero-Universitaria di Bologna. For ITA.LI.CA group, Bologna, Italy
Email: lorenzo.lani@studio.unibo.it

Background and aims: Hepatic resection (HR) is a curative option for hepatocellular carcinoma (HCC). The recently updated Barcelona Clinic Liver Cancer staging system identifies as "ideal candidates" (ICs) for HR patients with single lesion and without clinically significant portal hypertension (CSPH) or hyperbilirubinemia. We aimed to compare the outcome of HR between ICs and non-ICs [bilirubin > 1.1 mg/dL; presence of CSPH; multinodular tumours (mHCC)] in a large population of resected patients for HCC in real-world practice and assess whether their characteristics and outcomes changed over time.

Method: We extracted from the ITA.LI.CA. database 1085 Child-Pugh A patients and without extrahepatic tumour spread undergoing HR for HCC between 2000 and 2022. We analysed 3 periods (T1 = 2000–2008; T2 = 2009–2015; T3 = 2016–2022). CSPH was defined as presence of gastro-oesophageal varices and/or platelet count $< 100,000/\text{mmc}$. Hyperbilirubinemia was accepted up to 2 mg/dL. Overall survival (OS) was measured from the time of HR to death, loss to or end of follow-up (31/12/22). Patients undergoing liver transplantation (LT) were censored at the time of LT. OS was calculated

POSTER PRESENTATIONS

using the Kaplan-Meier method and compared with the log-rank test.

Results: Prevalence of ICs tended to increase over time (32.9%, 42.3% and 42.9% in T1, T2 and T3, respectively; $p=0.083$) but remained lower than that of non-ICs. Among non-ICs, the proportion of those with CSPH alone did not change over time (from 22.4% to 27.6% to 29.5%; $p=0.407$) while mHCC increased (from 33.7% to 48.7% to 49.6%; $p=0.018$). An opposite trend was observed for hyperbilirubinemia alone (from 23.5% to 13.8% to 11.9%; $p=0.018$) and hyperbilirubinemic+CSPH patients (from 20.4% to 10.0% to 9.0%; $p=0.006$). Over a median follow-up of 41.1 months (IQR=56.0), median OS was higher in ICs compared to non-ICs (104.9 months, 95%CI 78.3–131.4 vs 75.0 months, 95%CI 64.0–86.0; $p<0.001$). However, compared to ICs, median OS did not significantly differ in patients with CSPH alone (93.1 months, 95%CI 73.7–112.5, $p=0.417$) or with hyperbilirubinemia alone (86.0 months, 95%CI 58.3–113.8, $p=0.257$), while those with mHCC (63.0 months, 95%CI 45.2–80.8, $p<0.001$) or hyperbilirubinemia+CSPH (60.0 months, 95%CI 42.6–77.4, $p<0.001$) had a worse OS. The 6-month mortality rate (perioperative mortality) of hyperbilirubinemic, CSPH, and mHCC groups did not differ from that of ICs ($p\geq 0.211$), while it was higher in hyperbilirubinemic+CSPH patients ($p<0.001$).

Conclusion: Real-world data show that since 2000 the proportion of ICs remained steady over time and lower than that of non-ICs. HR can be offered to Child-Pugh A patients with CSPH or modest hyperbilirubinemia without compromising its outcome. The presence of two of these features, as well as mHCC, generates a poorer prognosis. In these patients, specific studies assessing if HR is superior to non-surgical therapies are needed.

THU-484

External beam radiation therapy improves the response to Atezolizumab plus Bevacizumab in patients with unresectable hepatocellular carcinoma with portal vein tumor thrombosis

Yunjeong Lee¹, Jin-Wook Kim¹. ¹Seoul National University Bundang Hospital, Seongnam, Korea, Rep. of South
Email: leey217@gmail.com

Background and aims: The combination of atezolizumab plus bevacizumab regimen has been considered the first-line systemic therapy for unresectable hepatocellular carcinoma (HCC). However, the presence of portal vein tumor thrombosis (PVTT) remains a clinical challenge due to more advanced disease burden and poorer response to systemic treatment. The use of external beam radiation therapy may increase tumor control rate in HCC patients with PVTT. However, it is not clear whether the additional radiotherapy improves the tumor response to atezolizumab plus bevacizumab regimen in these patients. In this single-center retrospective cohort study, we assessed the effect of radiotherapy in HCC patients with PVTT who received atezolizumab plus bevacizumab as a first-line therapy.

Method: We reviewed 203 patients who started atezolizumab plus bevacizumab for unresectable HCC at our center between April 2003 and December 2023. The presence of portal vein thrombosis was identified on CT or MRI. The modified response evaluation criteria in solid tumors (mRECIST) was used to assess treatment responses. A multivariate Cox analysis was performed to compare the prognosis of patients who received the combination systemic therapy with or without external beam radiation therapy. A p value of <0.05 was considered significant.

Results: Of the 203 patients, the prevalence of PVTT was 38% ($n=78$). Among the 78 patients, 27 received additional radiotherapy. The radiation dose used ranged from 30 to 60 Gy, with an average of 48 Gy. A multivariate Cox analysis adjusting effects of age and sex showed that the concomitant radiotherapy significantly improved the tumor response to atezolizumab plus bevacizumab therapy and prolonged progression-free survival (hazard ratio=0.50 with 95% confidence interval=0.25–0.99; $p=0.048$).

Conclusion: The addition of external beam radiation therapy improved the tumor response to atezolizumab plus bevacizumab systemic therapy in HCC patients with PVTT. It is notable that this study reached statistical significance in a small patient cohort over a short history of application of the combination regimen. Further experiences with atezolizumab and bevacizumab, as well as the investigation of the nature of HCC with PVTT, would be warranted to validate our finding.

THU-485-YI

Hepatic and peripheral blood neutrophil: lymphocyte ratios offer paradoxical associations with clinical outcome in advanced hepatocellular carcinoma treated with immune checkpoint inhibitors plus transarterial chemoembolization

Paul Armstrong^{1,2}, Aoife Moriarty^{1,2}, Erinn McGrath³, Jennifer Russell¹, Lindsey Clarke³, Stephen Stewart^{1,2}, Austin Duffy², Cliona O'Farrelly⁴. ¹Mater Misericordiae University Hospital, Dublin, Ireland; ²University College Dublin, Dublin, Ireland; ³St. Vincent's University Hospital, Dublin, Ireland; ⁴Trinity College Dublin, Dublin, Ireland

Email: drpaulrichardarmstrong@gmail.com

Background and aims: The complexity of the liver immune environment, which demonstrates significant inter-individual variation, is likely to influence and reflect local tumour growth. Changes in the relative proportions of lymphoid and myeloid populations in the liver may therefore be of useful prognostic value in patients with hepatocellular carcinoma (HCC). Here we aimed to evaluate liver lymphoid and myeloid populations as prognostic biomarkers in patients with advanced HCC treated with immune checkpoint inhibitors (ICI) plus transarterial chemoembolization (TACE).

Method: Patients with HCC (Childs Pugh A/B7; Barcelona Clinic Liver Cancer Stage B/C; ECOG 0/1; sorafenib-naïve or experienced) were enrolled in a clinical trial (UCDRC/19/01 EudraCT no. 2019-002767-98) of tremelimumab plus durvalumab and subtotal TACE performed on week 6. Full blood counts including differential sample assessments were performed at baseline and on treatment (after Cycle 3 Durvalumab). Liver biopsies were taken from the tumour, the tumour margin, portal tracts and uninvolved parenchyma. HandE stained slides were assessed for lymphocyte and granulocyte populations by two experienced independent histopathologists. Neutrophil: lymphocyte ratios (NLR) defined as the hepatic neutrophil count divided by the lymphocyte count in each x40 HPF, were calculated.

Results: Thirteen patients were enrolled in the study. Primary outcome was defined as 6 month progression free survival (PFS) and secondary outcome was overall survival (OS) measured at 1 year. Six patients (46%) exhibited PFS at 6 months, and 9 (69%) achieved one year OS. Lower 'on treatment' peripheral blood NLRs were associated with improved 1 year OS ($p=0.02$, Spearman rho 0.74).

Adequate tissue samples for study were obtained pretreatment from 10 patients. Patients with lower numbers of lymphocytes in their tumour tissue had better rates of 6-month PFS ($p=0.025$, Spearman rho 0.75). Thus, higher NLRs in tumour were associated with improved 6-month PFS ($p=0.011$, Spearman rho 0.85). Cases with a high intratumoural NLR (≥ 0.08) had a median PFS of 7.95 months (6.64–9.41) vs 3.69 (2.78–4.24) for those with low intratumoural NLR (<0.08) ($p=0.048$). In contrast, lower NLRs in the liver portal tracts correlated with improved one year OS ($p=0.036$, Spearman rho 0.734).

Conclusion: Lower NLRs in the peripheral blood and uninvolved liver predict improved survival in advanced HCC treated with ICI plus TACE. Paradoxically, higher NLRs in the tumour correlate with improved clinical response. These findings emphasize the variability of microenvironmental influences on immune populations in primary HCC tumour and surrounding liver tissue. We propose that these interindividual differences have important prognostic value and may also indicate new therapeutic targets.

THU-486-YI

A multi-center comparison of Atezolizumab plus Bevacizumab and Lenvatinib as primary systemic therapy for unresectable hepatocellular carcinoma: focus on thrombotic and hemorrhagic adverse events

Marco Tizzani¹, Chiara Mazzarelli², Michela Emma Burlone³, Patrizia Carucci⁴, Gian Paolo Caviglia⁵, Chiara Lisi¹, Chiara Canalis¹, Lucia Cesarini², Mario Pirisi⁶, Antonio Acquaviva⁷, Emanuela Rolle⁴, Paolo Pochettino⁸, Katia Bencardino⁹, Federica Villa⁹, Martina Angiolillo¹⁰, Eleonora Castellana¹¹, Matilde Scadaferri¹¹, Francesco Cattel¹¹, Mario Airoidi⁸, Giorgio Maria Saracco¹, Silvia Gaia⁴.
¹Division of Gastroenterology and Hepatology-AOU Città della Salute e della Scienza, University of Turin, Turin, Italy; ²Hepatology and gastroenterology ASST GOM Niguarda, Milan, Italy; ³Medicina interna 1, AOU Maggiore della Carità-Novara, Novara, Italy; ⁴Division of Gastroenterology and Hepatology-AOU città della salute e della scienza, Turin, Italy; ⁵Department of Medical Sciences, University of Turin, Turin, Italy; ⁶Università del Piemonte Orientale, dipartimento di Medicina Traslationale, Novara, Italy; ⁷Università del Piemonte Orientale and Division of Internal Medicine, Azienda Ospedaliero-Universitaria Maggiore della Carità, Novara, Italy; ⁸Division of Oncology-AOU città della salute e della scienza, Turin, Italy; ⁹Division of Oncology-ASST GOM Niguarda, Milan, Italy; ¹⁰Division of Hospital Pharmacy, A.O.U. Città della Salute e della Scienza di Torino, University of Turin, Turin, Italy; ¹¹Division of Hospital Pharmacy, A.O.U. Città della Salute e della Scienza, Turin, Italy
 Email: silvia.gaia74@gmail.com

Background and aims: First line therapy for unresectable hepatocellular carcinoma (HCC) are Atezolizumab plus Bevacizumab (AB) and Lenvatinib (Len). The aim is to compare their efficacy and safety, mainly focusing on thrombotic and hemorrhagic adverse events.

Method: A multi-center retrospective study was conducted. All patients treated with Len or AB for HCC in 3 northern Italian centers were consecutively enrolled. Demographic, clinical and radiologic data were collected. All patients were treated following EASL guideline for the HCC systemic therapy.

Results: Overall 173 patients receiving AB (n = 65) or Len (n = 108) were enrolled. At baseline the 2 groups were similar for sex (85% male), median age (69 y), diagnosis of cirrhosis (81%) vs chronic liver disease (19%), Child-Pugh A (100%), HCC staging (75% BCLC-C, 25% BCLC-B), presence of low-risk esophageal varices (39%), median platelet count (150 x10⁹/L), AFP (median 24.5 ng/ml), and anticoagulant therapy (21%). Anti-aggregant therapy was more frequent in Lev group (27.8%) compared to AB (12.3%), p = 0.022. Viral aetiology was higher in AB group (66.7%) vs Len group (48.1%), (p = 0.050). Median follow-up was longer in Lev group (11.3 months, IQR 5.7–21.4) vs AB (6.8 months, 4.1–11.1), p < 0.001. In Len group 6 patients underwent liver transplantation and 1 patient in AB group. Mean overall survival (OS) was 18.7 months (95% CI 15.9–21.5), without difference between Len and AB group (p = 0.682). OS was related to radiological response at 3 months (p < 0.001) in both groups. Baseline AFP value was associated to higher mortality only in Len group (p < 0.001). Disease control rate at 3, 6 and 12 months were similar in Lev group vs AB group: 77% vs 66%, 64% vs 56% and 48% vs 37%, respectively (p = ns). Thrombotic events were uncommon in both groups: 5/108 (4.6%) in Len group [2 acute coronary syndrome, 1 portal vein thrombosis (PVT), 1 Pulmonary embolism, 1 transitory ischemic attack] vs 3/65 (4.6%) in AB group (3 PVT) (p = 0.561). No thrombotic events occurred in patients with anticoagulants. Overall, the use of anti-platelets drug did not reduce the risk of thrombotic events (HR = 1.71, p = 0.472) nor increased the risk of hemorrhagic events (HR = 1.08, p = 0.870). Mild and/or severe hemorrhagic events occurred in 15/108 (13.9%) in Lev group and in 10/65 (15, 3%) in AB group (p = 0.421); the use of anticoagulant drugs showed a trend of association with hemorrhagic events (HR 2.22, p = 0.06). Hospitalization for any reason occurred in 17/108 (15.7%) patients treated with Len and in 22/65 (33.8%) patients treated with AB (p = 0.008); two cases related to hemorrhagic and 2

to thrombotic events in Lev group, whereas 2 related to hemorrhagic events in AB group.

Conclusion: AB or Lev had comparable overall survival and disease control rate. In both group thrombotic events were uncommon: therapy with anticoagulants avoided the risk of thrombotic events but increased the hemorrhagic risks.

THU-487-YI

Upfront multi-bipolar radiofrequency ablation for hepatocarcinoma in transplant-eligible cirrhotic patients with salvage transplantation in case of recurrence

Carina Boros¹, Olivier Sutter¹, Francois Cauchy², Nathalie Ganne-Carrié¹, Pierre Nahon¹, NKontchou Gisèle¹, Marianne Zioli¹, Véronique Grando Lemaire¹, Alix Demory¹, Lorraine Blaise¹, Federica Dondero³, Francois Durand³, Olivier Soubrane⁴, Mickael Lesurtel³, Olivier Seror¹, Jean Charles Nault¹. ¹Avicenne Hospital, Bobigny, France; ²Department of Hepato-biliary and Pancreatic Surgery and Liver Transplantation, Geneva, Switzerland; ³Beaujon Hospital, Paris, France; ⁴Institut Mutualiste Montsouris, Department of Surgery, Paris, France
 Email: carinna.bs@gmail.com

Background and aims: We aim to assess the long-term outcomes of percutaneous multi-bipolar radiofrequency (mbp RFA) as the first treatment for HCC (hepatocarcinoma), in transplant-eligible cirrhotic patients, followed by salvage liver transplantation for an intrahepatic at distance tumor recurrence or for liver failure.

Method: We included transplant-eligible patients with cirrhosis and a first diagnosis of HCC within Milan criteria, treated by upfront mbp RFA. Transplantability was defined by age <70 years, social support, absence of significant comorbidities, no active alcohol use and no recent extrahepatic neoplasia. Baseline variables were correlated with outcomes using Kaplan-Meier and Cox models.

Results: Among 435 patients with HCC, 172 were considered transplantable and had HCCs >2 cm (53%), unimodular tumor (87%) and AFP >100 ng/ml (13%). Median overall survival was 87 months, 75% of patients were alive at 3 years, 61% at 5 years and 43% at 10 years, respectively. Age (p = 0.003) and the MELD score >10 (p = 0.01) were statistically significant associated with the risk of death. Recurrence occurred in 118 patients, among which 81% of cases were within Milan criteria for liver transplantation. At 10 years, local recurrence was observed in 24.5% of patients, while distant recurrence rate was 69%. Furthermore, the 10 year survival rate after a local recurrence was 69%. Patients with local tumor recurrence alone (n = 23) experienced a longer post-recurrence survival rate in compared to patients with distant tumor recurrence (n = 83) or those with concomitant distant and local tumor recurrence (n = 12) (p = 0.0023). At the time of the first tumor recurrence, 75 patients (65%) were considered transplantable. In Cox multivariate analysis, the age (HR = 1.10, 95% CI = 1.04–1.17, p = 0.0008) was the only baseline variable data negatively associated with the transplantability at the time tumor recurrence. Forty-one patients underwent a liver transplantation mainly for distant intrahepatic tumor recurrence. The overall 5-year survival post-transplantation was 72%, with a tumor recurrence rate of 2.4%.

Conclusion: Upfront multi-bipolar RFA as a first treatment of early HCC on cirrhosis followed by salvage liver transplantation has a favorable long-term prognosis, allowing for the preservation of liver grafts.

THU-490

Grip strength complements performance status in assessing general condition in patients with unresectable hepatocellular carcinoma treated with atezolizumab and bevacizumab

Kei Endo¹, Takuya Watanabe¹, Hidekatsu Kuroda¹, Takayuki Matsumoto¹. ¹Iwate medical university school of medicine, Yahaba, Japan
 Email: keiindo@iwate-med.ac.jp

POSTER PRESENTATIONS

Background and aims: Accurate assessment of the general condition of patients with hepatocellular carcinoma (HCC) is essential. We evaluated the impact of grip strength (GS) and Eastern Cooperative Oncology Group performance status (ECOG-PS) on the clinical outcomes of patients with unresectable HCC (u-HCC) who were treated with atezolizumab plus bevacizumab (ATZ+BEV).

Method: This observational cohort study analyzed 89 patients with u-HCC who were treated with ATZ+BEV between October 2020 and October 2023. Low GS was defined as GS <28 kg and GS <18 kg in men and women, respectively. A Cox proportional hazards model and a Kaplan-Meier curve were used to identify the prognostic factors associated with survival outcomes.

Results: There were 33 patients who had low GS, and 16 who had ECOG-PS ≥1. The frequency of low GS was 27.4% (20/73) in patients with ECOG-PS0, 76.9% (10/13) in patients with ECOG-PS1 and 100% (3/3) in patients with ECOG-PS2. The frequency of patients with low GS increased as the ECOG-PS score increased ($p < 0.01$). The overall survival (OS) of the normal GS group was significantly higher than that of the low GS group ($p < 0.01$). There was no significant difference in PFS between the normal GS group and the low GS group ($p = 0.28$). The OS and PFS of the ECOG-PS0 group were significantly higher than those of the ECOG-PS ≥1 group ($p < 0.01$ and < 0.01 , respectively). Among the patients in the ECOG-PS0 groups, the OS in the normal GS group was significantly higher than that in the low GS group ($p < 0.01$). A multivariate analysis revealed that the mALBI 2b (hazard ratio [HR] 2.34; 95% CI, 1.19–4.59), AFP ≥100 ng/ml (HR 2.39; 95% CI, 1.25–4.55) and low GS (HR 3.11; 95% CI, 1.57–6.16) were independently associated with poor OS.

Conclusion: The present study demonstrated that GS is a sensitive marker for detecting a subclinical loss of general condition and a candidate predictor of the outcome of u-HCC patients treated with ATZ+BEV.

THU-491

Prognostic value of the timing of immune checkpoint inhibitors infusion in patients with advanced hepatocellular carcinoma

Alina Pascale¹, Marc Antoine Allard², Amal Benamar¹, Francis Levy², René Adam², Olivier Rosmorduc³. ¹CHU Paul Brousse, APHP, Villejuif, France; ²CHU Paul Brousse, APHP, Paris Saclay University, Villejuif, France; ³CHU Paul Brousse, APHP, Paris Sorbonne University, Villejuif, France

Email: olivier.rosmorduc@aphp.fr

Background and aims: Experimental and clinical data in melanoma and lung cancer suggest that the response to immune checkpoint inhibitors (ICI) may be influenced by circadian rhythms. However, similar findings are lacking in hepatocellular carcinoma (HCC). The aim of this study was to assess the impact of infusion timing of atezolizumab, an ICI, associated or not with bevacizumab, as first line systemic treatment in advanced HCC.

Method: We retrospectively analyzed all consecutive patients, who received, as first line systemic treatment, at least two cycles of atezolizumab ± bevacizumab for advanced HCC in Paul Brousse Hospital, Villejuif, France, between January 2020 and October 2022. We split them in two groups: 1) patients receiving the first two cycles after 1 pm (afternoon group); 2) patients receiving at least one of the two first cycles before 1 pm (morning or mixed group). Cox regression models were used to assess the prognostic value of ICI infusion timing for the overall survival (OS).

Results: A total of 131 patients were analyzed. 119 patients (90.8%) were male, with a median age of 70 years [35; 88]; 40 patients (31%) had performance status (PS) ≥1. 103 patients (79%) had cirrhosis; 61 patients (46.6%) had portal hypertension. 49 patients (37.4%) had metastatic HCC and 52 patients (40.6%) had portal vein thrombosis at diagnosis. The mean initial level of alpha-fetoprotein was 5,212.8 ng/ml (SD: 18,681.8). 36 patients (27.5%) received only atezolizumab. 41 patients were included in the first group and were compared to 90 patients included in the second group. There were no significant

clinical differences between the two groups. The median OS was significantly lower in the afternoon group compared to the morning or mixed group (11.5 months vs 18.7 months, $p = 0.015$). In univariate analysis, PS ≥1 ($p = 0.025$), initial level of alpha-fetoprotein ($p = 0.030$), monotherapy by atezolizumab ($p = 0.004$) and the first two cycles of ICI infusion after 1 pm ($p = 0.018$) were significantly correlated with OS. The first two cycles of ICI infusion after 1 pm remains an independent factor significantly associated with OS in the multivariate Cox model, with HR 2.29, 95% CI: 1.27–4.14, $p = 0.005$.

Conclusion: Our results suggest that the afternoon infusion of the first two cycles of ICI is associated with lower outcomes in patients with advanced HCC, independently of other prognostic factors. There may be confounding factors due to the variability of administration of further perfusions. Larger data are needed to confirm such findings.

THU-492

Prognostic significance of liver decompensation, liver function and portal hypertension in cirrhotic patients with advanced hepatocellular carcinoma treated with Atezolizumab plus Bevacizumab

Maria Pallozzi¹, Leonardo Stella¹, Lucia Cerrito¹, Francesco Santopaolo¹, Maurizio Pompili¹, Antonio Gasbarrini¹, Fabio Marra², Claudia Campani³, Elisa Pellegrini³, Francesco Tovoli⁴, Fabio Piscaglia⁴, Clemence Hollande⁵, Sabrina Sidali⁵, Mohamed Bouattour⁵, Francesca Romana Ponziani¹. ¹Fondazione Policlinico Universitario Agostino Gemelli, IRCCS, Università Cattolica del Sacro Cuore, Roma, Italy; ²AUC Ospedale Universitario Careggi, Università degli studi di Firenze, Firenze, Italy; ³AUC Ospedale Universitario Careggi, Università degli studi di Firenze, Firenze, Italy; ⁴Policlinico Universitario Sant'Orsola-Malpighi, IRCCS, Alma Mater Studiorum-Università di Bologna, Bologna, Italy; ⁵Beaujon University Hospital -Assistance Hopitaux Publique de Paris, Clichy, France
Email: mariapallozzi@yahoo.it

Background and aims: Atezolizumab/Bevacizumab changed the landscape of advanced hepatocellular carcinoma (HCC) treatment but its efficacy and safety in presence of reduced liver function or portal hypertension is still debated. Moreover, it is unknown if liver decompensation may impact on efficacy and safety outcomes. We aimed to evaluate the efficacy and safety of Atezolizumab/Bevacizumab in a real life cohort of patients with unresectable HCC and to evaluate the impact of liver decompensation on survival outcomes and its prognostic significance.

Method: A multicentric cohort of 247 patients with unresectable HCC eligible for Atezolizumab/Bevacizumab treatment was retrospectively enrolled between 2018–2023 and matched in a 1:2 ratio with a cohort of 494 patients treated with tyrosine kinase inhibitors (TKIs). Safety and efficacy outcomes of patients in the Atezolizumab/Bevacizumab cohort were evaluated according to liver function, presence of portal hypertension and development of liver decompensation. We defined time-to-decompensation as the interval from the first treatment administration to the occurrence of any event related to the decline in liver function or the aggravation of portal hypertension. Its impact on the overall survival (OS) was assessed.

Results: Patients in the Atezolizumab/Bevacizumab group showed better median OS (18.3 VS 10.20 months, $p < 0.0001$), time to progression (TTP; 13.6 VS 10.6 months, $p = 0.006$) and progression free survival (PFS; 10.5 VS 6.10 months, $p < 0.0001$) compared with TKIs. Although survival was better in Child Pugh A patients than in Child Pugh B patients (20.2 vs 9.83 months, $p = 0.0008$), no clear difference in TTP ($p = 0.31$) and overall treatment safety was observed. Portal hypertension did not impact on OS and TTP. 63 patients reported liver decompensation (ascites:84.12%, hepatic encephalopathy:38.09% and variceal bleeding:19.04%). Decompensated patients showed a reduced survival (10.50 vs 20.20 months; $p = 0.06$). 26 patients (41.26%) were able to resume Atezolizumab/Bevacizumab after decompensation achieving an OS comparable to that of never decompensated subjects (20.87 vs 20.20

months; $p = 0.77$), and significantly better than patients who had to stop permanently (8.07 months; $p = 0.02$). Treatment interruption following liver decompensation was an independent predictor of survival (HR 3.04, 95%CI 1.97–4.68; $p < 0.0001$), as were Child Pugh B (HR 1.87, 95%CI 1.08–3.25; $p = 0.03$) and portal hypertension (HR 1.86, 95%CI 1.01–3.39; $p = 0.04$) for decompensation.

Conclusion: This real-life multicentric study shows that Atezolizumab/Bevacizumab is equally effective on HCC progression in both Child Pugh A and B patients, who present a higher risk of decompensation.

Because resuming treatment is associated with a survival advantage, integrated hepato-oncology management is critical to maximize Atezolizumab plus Bevacizumab efficacy.

THU-493

Systemic therapy of hepatocellular carcinoma on non-cirrhotic liver: a prospective spanish multicentre study

Marta Romero-Gutiérrez¹, Jorge Barajas¹, Mariano Gómez², Laura Márquez³, Sonia Pascual⁴, Carlos Aracil⁵, Raquel Latorre⁶, Cristina Fernández⁷, Teresa Ferrer⁸, Cristina Alarcón⁹, Vanesa Bernal¹⁰, Mireia Miquel¹¹, Diana Horta¹², Jesús M. González¹³, Belén Piqueras¹⁴, Dalia Morales¹⁵, Maria Luisa Gutiérrez¹⁶, Natalia Arietti¹, Pedro Barrera¹, Olga Ramos¹, Ana Matilla³, Rafael Gómez Rodríguez¹. ¹Complejo Hospitalario Universitario de Toledo, Toledo, Spain; ²Hospital Universitario de Getafe, Madrid, Spain; ³Hospital General Universitario Gregorio Marañón CIBEREHD, Madrid, Spain; ⁴Hospital General Universitario Dr. Balmis de Alicante., Alicante, Spain; ⁵Institute of Biomedical Research, Hospital Universitario Arnau de Vilanova, Lleida, Spain; ⁶Hospital Universitario Son Llàtzer, Palma de Mallorca, Spain; ⁷Hospital Universitario de Burgos, Burgos, Spain; ⁸Hospital Universitario Virgen del Rocío, Sevilla, Spain; ⁹Hospital General de Villalba, Madrid, Spain; ¹⁰Hospital Universitario Miguel Servet, Zaragoza, Spain; ¹¹Hospital Parc Tauli, Barcelona, Spain; ¹²Hospital Universitario Mútua de Terrassa, Barcelona, Spain; ¹³Hospital Universitario de Salamanca, Salamanca, Spain; ¹⁴Hospital Universitario de Fuenlabrada, Madrid, Spain; ¹⁵Hospital Universitario de Canarias, Tenerife, Spain; ¹⁶Hospital Universitario Fundación de Alcorcón, Madrid, Spain

Email: m.romero.gutierrez@gmail.com

Background and aims: Systemic therapy (ST) can be initial (I) or sequential (S) treatment of hepatocellular carcinoma (HCC). However, data are still scarce in patients without liver cirrhosis. We aim to characterize non-cirrhotic patients treated with ST, both in the initial treatment and after progression or recurrence, describing survival benefit and safety profile.

Method: A prospective Spanish multicentre study included 141 non-cirrhotic patients with HCC diagnosed by histology from May 2018 to September 2023. Liver cirrhosis was excluded by histology (89.6%), elastography (4.7%) or Mittal 2 criteria (5.7%). Forty-seven patients (33.3%) treated with ST were evaluated.

Results: ($n = 47$). The median age was 69 years and 85.1% were male. Other cancers 25.5%. DM 38.3%. Non-alcohol 40.4%, non-smoker 21.3%. Seventy-six percent had underlying liver disease, mainly caused by viral infection \pm alcoholic liver disease (ALD) 25.6% (HCV 21.3%, HBV 4.3%), MASLD \pm ALD 25.5%. Liver fibrosis stage: 0–1 in 42.6%, 2–3 in 38.3%, unknown 19.1%. HCC diagnosis was incidental (53.2%), by symptoms (34%) or at follow-up ultrasonography (12.8%). ST was administered at diagnosis in 21 cases (44.7%), and sequentially due to progression or recurrence in 26 (55.3%): 16 after surgery (ST in 11 and TACE-ST in 5), 10 after TACE/IARE. The reason for ST initiation were: 25.5% presentation as BCLC C, 19.1% presentation as BCLC B not candidate for other therapy, 53.2% progression or recurrence, 2.1% others. At the time of ST initiation, 31.9% had macrovascular invasion

and 31.9% had extrahepatic spread. ECOG 0 55.3%. BCLC stage: A 2.1%, B 38.3%, C 59.6%. AFP >200 ng/ml: 25.5%. Drugs at 1st line (1L): sorafenib (SOR) 59.6% (I 17/S 11), lenvatinib (LEN) 14.9% (I 4/S 3), atezolizumab + bevacizumab (AB) 19.1% (I 0/S 9), others 6.4%. Patients received 2 ST lines in 29%, and 3 lines in 8.5%. Adverse events (AE) of any grade: SOR 21/27 (77.8%), LEN 8/10 (80%), AB 5/8 (62.5%). Median treatment time was 15.5 months: 9.5 months (RIQ 3–22) in initial group and 21.1 months (RIQ 12–32) in sequential. Discontinuation 1L was due to symptomatic progression 34%, radiological progression 14.9% or severe AE 12.8%. Median follow-up was 29.1 months. Median overall survival (OS) from ST initiation was 16.3 months (95%CI: 11–22); OS in ST prescribed at diagnosis was 10 months (95% CI 6–14) compared OS sequential ST was 21.4 months (95%CI 12–31) ($p = 0.022$). OS 1L drug: tyrosine kinase inhibitor (SOR/LEN) 13.4 months (95%CI 8–19); AB 26.3 months (95%CI 13–39) ($p = 0.22$). Seventy percent of patients died (87.9% due to HCC).

Conclusion: In our series, patients with HCC on non-cirrhotic liver required more frequently ST due to tumour progression/recurrence after previous treatments than initial therapy for advanced disease. Survival was similar and safety profile was slightly better than clinical trials data, being severe AE uncommon reason for discontinuation.

THU-494

Selective internal radiation therapy for unresectable hepatocellular carcinoma in a tertiary center in France, update and final analysis

Hélène Regnault¹, Julia Chalaye², Athena Galletto², Clara Perrin³, Giuliana Amaddeo², Marie Lequoy⁴, Hicham Kobeiter², Sébastien Mulé², Edouard Reizine², Emmanuel Itti², Christophe Duvoux², Alexis Laurent⁵, Daniele Sommacale², Vincent Leroy², Alain Luciani², Haytham Derbel², Julien Calderaro², Vania Tacher², Brustia Raffaele². ¹Henri Mondor Hospital, Créteil, France; ²Henri Mondor University Hospital, Créteil, France; ³Antoine Bécère, Clamart, France; ⁴Saint Antoine, Paris, France; ⁵Henri Mondor University Hospital, Créteil

Email: helene.regnault@aphp.fr

Background and aims: Selective Internal Radiation Therapy (SIRT) is not yet recommended as first line treatment of unresectable hepatocellular carcinoma (HCC) except in solitary HCC <8 cm. The aim of this study was to report the results of an acquired experience in the real life in a tertiary center.

Method: We conducted a retrospective, observational study using data collected from all consecutive patients undergoing SIRT between October 2013 and June 2020. Downstaging was considered achieved when a curative treatment could be proposed after evaluation 6 months following SIRT.

Results: 127 patients (Male = 90%, 64 ± 11) were included. 112 patients ($n = 88$) had cirrhosis. HCC was mostly advanced according BCLC in 64 patients (50%), with a median diameter of 61 mm, infiltrative pattern in 51 patients (40%) and portal vein invasion in 62 (49%). 50 patients (39%) achieved downstaging 6 months following SIRT, 29 of them (23%) had access to a curative treatment in a median time of 4.3 months: 17 (13%) were transplanted, 11 (85%) had liver resection and one patient had a radiofrequency ablation. Median overall survival (OS) of patients with or without downstaging was 51 months versus 10 months respectively ($p < 0.001$). In patients who achieved downstaging, PFS was higher in patients who underwent surgery (40 vs 13 months). Four variables were independently associated to downstaging: age ($p = 0.02$), baseline AFP ($p = 0.034$), CHC distribution ($p = 0.012$) and ALBI grade ($p = 0.014$).

Conclusion: These results suggest that, in real life, SIRT in HCC patients could be an effective treatment leading to downstaging of about 35% of patients with unresectable HCC, and allowed curative treatment in more than half of them.

THU-495

Baseline neutrophil-to-lymphocyte ratio, liver disease etiology and morphomolecular histological classification could predict clinical outcome in Atezolizumab-Bevacizumab treated cirrhotic patients with advanced hepatocellular carcinoma

Spyridon Pantzios¹, Iakovos Vlachos², Antonia Syricha¹, Orestis Sidiropoulos¹, Emmanouil Nychas¹, Ioanna Maria Grypari², Despoina Myoteri², Dina Tiniakos², Ioannis Elefsiniotis¹. ¹Academic Department of Internal Medicine-Hepatogastroenterology Unit, General Oncology Hospital of Kifissia, National and Kapodistrian University of Athens, Greece, Athens, Greece; ²Dept of Pathology, Aretaieion Hospital, Medical School, National and Kapodistrian University of Athens, Greece, Athens, Greece
Email: spiros_pant@hotmail.com

Background and aims: Non-viral etiology of chronic liver disease has not been related with survival benefit in advanced HCC treated with Atezo-Bev. Moreover, a high neutrophil to lymphocyte ratio (NLR) has been related with worse clinical outcomes whereas data regarding the histological evaluation of these patients are limited. The aim of our study was to evaluate the survival of White European cirrhotic patients with advanced HCC treated with Atezo-Bev according to viral/non-viral etiology as well as baseline NLR and histological HCC status.

Method: Forty-four cirrhotic patients with advanced HCC were included (35 males, mean age = 66.6, median MELD-Na = 8, 39 CPT-A, 18 with MVI, 17 with EHD, 22 with viral etiology). Twenty-three HCCs were classified by morphomolecular analysis as proliferative (PR) and 21 as non-proliferative (N-PR), according to the classification by Nault JC et al, J Hepatol 2018. Baseline NLR was evaluated in all patients and a ratio above 4 was considered as high. Four groups were constructed [A: PR/NLR-H (n = 6), B: PR/NLR-L (n = 17), C: N-PR/NLR-H (n = 6), D: N-PR/NLR-L (n = 15)]. Patients with complete or partial response according to mRECIST were categorized as having objective response (OR).

Results: PR HCC was observed in 13/23 (56.5%) patients of viral and 10/23 (43.5%) of non-viral etiology, whereas N-PR HCC was observed in 9/21 (42.8%) patients of viral and 12/21 (57.2%) of non-viral etiology. Totally, OR was observed in 9/44 (20.45%) patients (1/5/1/2 from group A/B/C/D respectively) and was significantly related with overall survival (OS, p = 0.009).

Baseline characteristics of NLR-L patients (n = 32) were comparable to those of NLR-H (n = 12) but median OS was significantly better in NLR-L (12 m vs 6 m, p = 0.05). Among 22 patients with non-viral etiology, those with PR (n = 10) presented worse survival compared to N-PR (n = 12) HCC (6 m vs 12 m, p = 0.03) in univariate and a significant trend for worse OS (p = 0.07) in multivariate analysis considering age, presence of varices, MELD-Na and MVI. Moreover, patients of non-viral etiology and NLR-L presented the best median OS (26 m) in univariate (p = 0.005) as well as in multivariate analysis (p = 0.01). The 4 groups were comparable for all baseline parameters evaluated. Median OS was 10 m for group A, 12 m for B, 5.5 m for C and 12 m for D. A trend for worse OS was observed in patients with NLR-H and N-PR HCC (p = 0.07) compared to the other groups.

Conclusion: PR and N-PR morphomolecular subgroup HCCs were equally observed among White European cirrhotic patients with advanced HCC of viral or non-viral etiology. Non-viral etiology per se should not be considered as a negative predictor of clinical outcome in patients treated with Atezo-Bev, as the subgroup of them who present low baseline NLR seem to benefit the most from treatment whereas patients with N-PR HCCs and high baseline NLR seem to exhibit a significant trend for worse clinical outcome.

THU-498

Safety and Efficacy of Atezolizumab-Bevacizumab in Non-Viral and Viral Etiologies of Hepatocellular Carcinoma: A Multicenter Retrospective Comparative Study

Anand Kulkarni¹, Karan Kumar², Mithun Sharma¹, Sameer Shaik¹, Sowmya Iyengar¹, Shantanu Venishetty¹, Manasa Alla¹, Vivek Saraswat², Nagaraja Padaki¹, Nageshwar Reddy¹. ¹AIG Hospitals, Hyderabad, India; ²Mahatma Gandhi Medical College, Jaipur, India
Email: anandvk90@gmail.com

Background and aims: Atezolizumab-bevacizumab is the first-line approved drug for unresectable hepatocellular carcinoma (uHCC). There have been conflicting reports suggesting better efficacy of atezo-bev in patients with viral etiology than non-viral etiology due to altered microenvironment in non-viral etiology HCC. We aimed to assess the efficacy and safety of atezo-bev in non-viral and viral etiologies of HCC.

Method: In this multicenter retrospective study, patients who received atezo-bev between November 2020 and December 2023 were included. The primary objective was to compare the overall survival (OS), and the secondary was to compare the progression-free survival (PFS), radiological response rate based on mRECIST criteria, and adverse events among non-viral and viral HCC patients. Propensity-matched analysis (PSM) using multivariate logistic regression analysis was performed using SPSS ver.29.

Results: Eighty-one non-viral etiology (age-61 yrs; females-11.1%; MASH-82.7%) were compared with 52 viral etiology HCC patients (age-57 yrs; females-9.6%; HBV-75%). The proportion of patients with diabetes mellitus (52% vs. 15.4%) and hypertension (40.7% vs. 25%) were higher in the non-viral group. However, the proportion of non-cirrhotics (16% vs. 27%; P = 0.12) and the distribution of CTP class (A/B: 45.5%/54.5% vs. 39.5%/60.5%) was similar in both groups. Most patients were in BCLC C in both groups (86.7% vs. 79%). Twelve percent in non-viral group and 21.2% in viral group had received some form of prior locoregional therapy (LRT) (p = 0.13). On Kaplan Meier analysis, survival was 64.2% (95%CI, 52.7–74.5) in the non-viral group compared to 57.7% (95%CI, 43.2–71.3) in the viral group (p = 0.36). The median overall survival was 12.5 months (95%CI, 9.4–15.6) in non-viral group compared to 9 months (95%CI, 6.8–11.2) in viral group. The median PFS was 9 months (95%CI, 3.9–14.1) in non-viral group compared to 7 (5.2–8.8) months in viral group (p = 0.79). The cumulative overall response rate (32.1% vs. 32.7%; P = 0.94) and disease control rate (49.4% vs. 42.3%; P = 0.42) were similar among both groups. The incidence of adverse events was similar in both groups (64.1% vs. 53.8%; P = 0.24). After PSM, adjusted for age, diabetes, hypertension, non-cirrhosis, prior LRT, absence of portal vein thrombosis, and extrahepatic spread, 52 patients with viral etiology were matched with 39 patients with non-viral etiology HCC. There were no differences in OS, PFS, radiological response rate or adverse event rate even after PSM analysis.

Conclusion: Atezolizumab-bevacizumab is safe and effective in hepatocellular carcinoma, regardless of the etiology.

THU-499

Clinical efficacy of HAIC (FOLFOX) combined with tyrosine kinase inhibitors plus PD-1 inhibitors vs. HAIC combined with bevacizumab plus PD-1 inhibitors in the treatment of advanced hepatocellular carcinoma

Wenwen Zhu¹, Ningning Zhang¹, Wei Lu¹, Yiyan Zhang¹, Kaipeng Liu¹, Huiru Liu¹. ¹Tianjin Medical University Cancer Institute and Hospital, Department of Hepatobiliary Oncology, Liver Cancer Center, National Clinical Research Center for Cancer, Key Laboratory of Cancer Prevention and Therapy, Tianjin's Clinical Research Center for Cancer, Tianjin Medical University, Tianjin, China
Email: zhuwenwenjc@163.com

Background and aims: Unresectable hepatocellular carcinoma (uHCC) still accounts for the majority of newly diagnosed HCC which with poor prognosis. Molecular targeted therapy combined

with immunotherapy significantly and hepatic arterial infusion chemotherapy (HAIC) can improve the prognosis of patients with advanced HCC. This study aimed to evaluate the clinical efficacy of HAIC combined with tyrosine kinase inhibitors (TKIs) and programmed cell death protein-1 (PD-1) inhibitors vs. HAIC combined with bevacizumab and PD-1 inhibitors in the treatment of unresectable hepatocellular carcinoma (HCC).

Method: We retrospectively reviewed data of 133 patients with uHCC treated with HAIC with TKIs and PD-1 inhibitors or HAIC with bevacizumab and PD-1 inhibitors in Tianjin Medical University Cancer Institute and Hospital from 2018 to 2021. The overall survival (OS) and progression-free survival were compared. For sensitivity analysis, inverse probability weighting (IPW) was used to balance the influence of the tested confounding factors between groups to verify the robustness of conversion surgery for survival benefits.

Results: A total of 133 patients were enrolled in this study, including 77 cases in the HAIC+TKIs+PD-1 group and 56 cases in the HAIC+bevacizumab+PD-1 group. The mOS of HAIC+TKIs+PD-1 group and HAIC+bevacizumab+PD-1 group were 24.00 months and NA, respectively ($p = 0.225$). The mPFS of the two groups were 11 and 15 months, respectively ($p = 0.756$). Surgical conversion rate of HAIC+TKIs+PD-1 group and HAIC+bevacizumab+PD-1 group were 37.5% (21/56) and 23.4% (18/77), respectively ($p < 0.05$). IPW-adjusted Kaplan-Meier curves showed that successful conversion surgery was an independent prognostic factor for both PFS and OS.

Conclusion: Compared with HAIC in combination with TKIs and PD-1 inhibitors, HAIC (FOLFOX) in combination with bevacizumab and PD-1 inhibitors can improve tumor response and be more likely to prolong OS, PFS in uHCC patients.

THU-500

Networks in focus: profile of immune-related adverse events in first-line immunotherapy for hepatocellular carcinoma

Marta Fortuny^{1,2,3,4}, Marta García-Calonge⁵, Oscar Arrabal⁶, Marco Sanduzzi Zamparelli^{1,2,7}, Andrés Castano-García⁵, Gemma Iserte², Ana Maria Piedra-Cerezal⁵, Neus Llarch², Ezequiel Mauro^{1,2,4}, Alicia Mesa⁸, Manuel Rodríguez^{5,9}, Belen Saborido^{10,11}, Jordi Rimola^{1,11}, Ferran Torres⁶, Maria Varela^{5,9,12}, María Reig^{2,4,13}. ¹Barcelona Clinic Liver Cancer (BCLC) group. Institut d'Investigacions Biomèdiques August Pi i Sunyer (IDIBAPS), Barcelona, Spain; ²Liver Oncology Unit, Liver Unit, Hospital Clinic de Barcelona, Barcelona, Spain; ³Universitat Autònoma de Barcelona, Barcelona, Spain; ⁴Centro de Investigación Biomédica en Red en Enfermedades Hepáticas y Digestivas (CIBEREHD), Madrid, Spain; ⁵Servicio de Digestivo, Hospital Universitario Central de Asturias, Oviedo, Spain; ⁶Biostatistics Unit, Medical School, Universitat Autònoma de Barcelona, Barcelona, Spain; ⁷Centro de Investigación Biomédica en Red en Enfermedades Hepáticas y Digestivas (CIBEREHD), Barcelona, Spain; ⁸Servicio de Radiodiagnóstico. Hospital Universitario Central de Asturias, Oviedo, Spain; ⁹Universidad de Oviedo, Oviedo, Spain; ¹⁰Barcelona Clinic Liver Cancer (BCLC) group. Institut d'Investigacions Biomèdiques August Pi i Sunyer (IDIBAPS), Barcelona, Spain; ¹¹Liver Oncology Unit, Radiology Department, CDI, Hospital Clinic of Barcelona, Barcelona, Spain; ¹²IUOPA. ISPA. FINBA., Oviedo, Spain; ¹³Barcelona University, Barcelona, Spain

Email: mreig1@clinic.cat

Background and aims: The combination of Atezolizumab +Bevacizumab (AB) and Tremelimumab+Durvalumab (TD) are first-line systemic treatments for hepatocellular carcinoma (HCC). Additionally, Durvalumab (D) and Lenvatinib demonstrated to be non-inferior to sorafenib. The aim of this study is to describe the profile of immune-related adverse events (irAE) that condition temporally treatment interruption (interruption) and/or discontinuation, as well as outcome after AB, TD or D.

Method: Patients (p) treated with first-line immunotherapy from two medical centres in Spain were assessed retrospectively. Demographic characteristics, the number and type of irAEs leading

to treatment interruption or discontinuation, dates of irAEs' appearance, and reasons for interruption/discontinuation of AB, TD, or D, as well as the types of second-line treatments received, were all recorded. The irAE was defined as all those AE \geq grade II in which the relationship with AB, TD or D cannot be excluded.

Results: Of the 109 p included in the study, 83 p were treated with AB, 23 p with TD and 3 p with D. Among them, 52.3% were BCLC-C, 84.4% were Child-Pugh A and the remaining patients did not have cirrhosis. The median follow-up was 8.5 months [range 4.6–16.6], during this period 55 (50%) patients interrupted treatment due to irAE and 32 (29.4%) died, 2p (1.83%) for grade 5 irAE. The median time until the first irAE that led treatment interruption was 64 days [21–192] and 12.8% of patients developed it after the first dose of immunotherapy. The most frequent AEs were proteinuria (7p), diarrhea/colitis (5p), arterial hypertension (4p), myocarditis (4p) and encephalitis (4p). Of the total number of patients, 53.2% discontinued treatment: 22p due to symptomatic progression, 16p radiological progression, 15p AEs (not all irAEs), 1p by patient's decision and 4p for other reasons (3 for a second neoplasia and 1 for an unrelated death). Of those who discontinued treatments such as AB, TD, or D, 29.3% (17p) went on to receive second-line treatment, with 53% (9p) participating in second-line clinical trials.

Conclusion: Although 53.2% of patients discontinued the 1st line immunotherapy schemes, only in 13.8% of them was due to adverse events. The median time to the first adverse event that required treatment interruption was 64 days, and in 12.8% of the patients, this adverse event occurred after the first dose of immunotherapy. This data emphasizes the importance of establishing hospital networks for early detection and management of immune-related adverse events, ensuring timely access to experienced specialists.

THU-501

Safety and efficacy preliminary analysis of first-line systemic therapy with atezolizumab plus bevacizumab in Spanish patients with unresectable hepatocellular carcinoma not previously treated with systemic therapy: phase IIIB ATHECA trial

María Reig¹, Natalia Luque², José Luis Lledó³, Ana Matilla⁴, Jose Luis Montero⁵, Roberto Pazo-Cid⁶, Maria Varela⁷, Mar Borràs⁸, Jose-Manuel Ordóñez⁸, Josep Maria Argemi⁹, Jordi Bruix¹, Carlos Gomez-Martin¹⁰, Raquel Pérez-López¹¹, Jordi Rimola¹², Bruno Sangro¹³, Javier Sastre¹⁴. ¹BCLC Group, Liver Unit, Hospital Clinic y Provincial de Barcelona, IDIBAPS, CIBEREHD, Barcelona, Spain; ²Hospital Universitario de Jaén, Jaén, Spain; ³Gastroenterology and Hepatology Service. Hospital Universitario Ramón y Cajal, IRYCIS, Universidad de Alcalá, CIBEREHD, Madrid, Spain; ⁴Digestive Service, Hospital General Universitario Gregorio Marañón, CIBEREHD, Madrid, Spain; ⁵Liver Unit, Hospital Universitario Reina Sofía, Córdoba, Spain; ⁶Medical Oncology Department, Hospital Universitario Miguel Servet, Zaragoza, Spain; ⁷Department of Gastroenterology. Liver Unit. Hospital Universitario Central de Asturias. IUOPA. ISPA. FINBA. Universidad de Oviedo, Oviedo, Spain; ⁸Medical Department, Roche Farma S.A., Madrid, Spain; ⁹Liver Unit, Clínica Universidad de Navarra, Pamplona, CIBEREHD, Pamplona, Spain; ¹⁰Medical Oncology, University Hospital 12 de Octubre, Madrid, Spain; ¹¹Radiomics Group, Vall d'Hebron Institute of Oncology-Cellex Center, Barcelona, Spain; ¹²BCLC Group, Radiology Dept. Hospital Clinic y Provincial de Barcelona, IDIBAPS, Barcelona, Spain; ¹³Liver Unit, Clínica Universidad de Navarra, CIBEREHD, Pamplona-Madrid, Spain; ¹⁴Medical Oncology, Hospital Clínico Universitario San Carlos, Madrid, Spain

Email: mreig1@clinic.cat

Background and aims: Atezolizumab plus Bevacizumab (ATZ+BEV) was approved as first-line systemic treatment for advanced or unresectable hepatocellular carcinoma (HCC) after showing higher efficacy than sorafenib with manageable safety profile in the pivotal phase III trial IMbrave150. The aim of the ATHECA study was to evaluate the safety and efficacy of ATZ+BEV in Spanish pts with unresectable HCC

POSTER PRESENTATIONS

(uHCC) or unsuitable for locoregional treatments not previously treated with systemic therapy.

Method: Phase IIb, one arm, multicenter, open label study of ATZ + BEV in pts with uHCC or unsuitable for locoregional treatments not previously treated with systemic therapy. This study evaluated 3-week intravenous cycles of ATZ + BEV (1200 mg + 15 mg/kg). Inclusion criteria matched those of the IMbrave150 clinical trial, including prior upper endoscopy. Adverse Events (AEs) were considered for the safety analysis, while overall survival (OS), progression free survival (PFS), time to progression (TTP), duration of response (DOR), and objective response rate (ORR) were considered for the efficacy analysis. Here are presented data from a non-prespecified data cut-off in the study protocol and the study is still ongoing.

Results: 124 pts were screened in 26 Spanish centers and 100 pts were treated (85 males, median age 66 years) with ATZ + BEV. At the cut-off date the median follow-up was 18.5 months (mo), and the median treatments duration were 8.9 mo (ATZ) and 8.1 mo (BEV), 20 pts were still on treatment and 80 discontinued either BEV (80 pts) or ATZ (78 pts) mainly due to disease progression. Treatment Emergent AEs (TEAEs) grade ≥ 3 leading to treatment discontinuation were reported in 16% pts, (gastrointestinal haemorrhage, haemoperitoneum, intestinal perforation, intra-abdominal haemorrhage, oesophageal varices haemorrhage, increased blood bilirubin, increased hepatic enzyme, toxic nephropathy, proteinuria, dyspnoea, pleural effusion, immune-mediated hypothyroidism, hepatitis, abdominal sepsis, fall, and hepatic encephalopathy). Treatment related AE (TRAE) G3–4 occurred in 28% pts. The 7 TEAEs leading to death (1 each) were hepatitis (the only TRAE), abdominal sepsis, aspiration pneumonia, dyspnoea, pleural effusion, hemoperitoneum, jaundice and hepatic encephalopathy (these last two events occurred in the same patient). At this cut-off, 60.6% of pts remained alive, median OS (m OS) was not reached out. Median PFS was 10.9 mo (95% confidence interval (CI) 7.1–12.7), median TTP was 12.4 mo (95% CI 8.4 to 15.2), median DOR was 21.3 mo (95% CI 11.40–NA), and ORR was 26.6% (95% CI 18.7%–36.3%).

Conclusion: At this cut-off data, ATHECA preliminary safety data showed a TEAE profile similar to previous studies and consistent with the underlying disease and known safety profile of each agent, with a higher preliminary efficacy data in terms of OS, PFS, TTP, DOR, and a similar ORR compared to the IMbrave150 trial.

THU-502

Everolimus mitigates the risk of hepatocellular carcinoma recurrence after liver transplantation

Paolo De Simone¹, Arianna Precisi², Quirino Lai³, Juri Ducci², Daniela Campani¹, Piero Marchetti¹, Stefano Gitto⁴. ¹University of Pisa, Pisa, Italy; ²Azienda Ospedaliero Universitaria Pisana, Pisa, Italy;

³Azienda Ospedaliero Universitaria Pisana, Pisa, Italy; ⁴University of Florence, Florence, Italy

Email: paolo.desimone@unipi.it

Background and aims: To obtain long-term data on the use of everolimus in patients who underwent liver transplantation for hepatocellular carcinoma, we conducted a retrospective, single-center analysis of adult recipients transplanted between 2013 and 2021. Patients on everolimus-incorporating immunosuppression were matched with those on tacrolimus using an inverse probability of treatment weighting methodology.

Method: Two propensity-matched groups of patients were thus compared: 233 (45.6%) receiving everolimus versus 278 (54.4%) on tacrolimus.

Results: At a median (interquartile range) follow-up of 4.4 (3.8) years after transplantation, everolimus patients showed a reduced risk of recurrence versus tacrolimus (7.7% versus 16.9%; RR = 0.45; P = 0.002). At multivariable analysis, microvascular infiltration (HR = 1.22; P < 0.04) and a higher tumor grading (HR = 1.27; P < 0.04) were associated with higher recurrence rate while being within Milan criteria at transplant (HR = 0.56; P < 0.001), a successful pre-

transplant downstaging (HR = 0.63; P = 0.01) and use of everolimus (HR = 0.46; P < 0.001) had a positive impact on the risk of post-transplant recurrence. EVR patients with earlier drug introduction (≤ 30 days; P < 0.001), longer treatment duration (p < 0.001), and higher drug exposure (≥ 5.9 ng/ml; P < 0.001) showed lower recurrence rates versus TAC.

Conclusion: Based on our experience, everolimus provides a reduction of the relative risk of hepatocellular carcinoma recurrence, especially for advanced-stage patients and those with earlier drug administration, higher drug exposure, and longer time on treatment. These data advocate for early everolimus introduction after liver transplantation to reduce the attrition rate consequent to chronic immunosuppression.

THU-503

Hepatocellular carcinoma in metabolic dysfunction-associated steatotic liver disease (MASLD): multicenter study comparing patients with or without underlying cirrhosis

Carole Vitellius¹, Elvire Desjonqueres², Marie Lequoy³, Giuliana Amadeo⁴, Isabelle Fouchard¹, NKontchou Gisèle², Clémence M. Canivet¹, Marianne Ziol², Hélène Regnault⁵, Adrien Lannes¹, Frédéric Oberti¹, Jerome Boursier¹, Nathalie Ganne-Carrié². ¹CHU Angers, Angers, France; ²CHU Avicenne, Bobigny, France; ³AP-HP, Saint-Antoine Hospital, Paris, France; ⁴Henri Mondor University Hospital, Créteil, France; ⁵Henri Mondor University Hospital, Créteil, France

Email: carole.vitellius@chu-angers.fr

Background and aims: Despite its growing incidence, hepatocellular carcinoma (HCC) related to metabolic dysfunction-associated steatotic liver disease (MASLD) in non-cirrhotic liver remains poorly characterized. We compared the characteristics, management, survival, and trends of MASLD-related HCC in patients with or without underlying cirrhosis in a large multicenter cohort.

Method: 354 patients with MASLD-related HCC presented at the liver tumor meetings of four French university hospitals between 2007 and 2018 were included in the study. Data were extracted from the meetings' databases and from the French Birth and Death Registry.

Results: 124 HCC (35%) occurred in the absence of cirrhosis. HCC was diagnosed through screening in 60% of patients with cirrhosis, incidentally in 72% of patients without cirrhosis, and as expected more often by histology in non-cirrhotic patients (81% vs. 49% in cirrhotic patients, p < 0.001). Non-cirrhotic patients were older, had greater tumor burden ≥ 5 cm (55% vs. 28%, p < 0.001) but also better liver function than cirrhotic patients. Half the patients had a localized tumor stage (BCLC 0 or A) whether or not they had cirrhosis. In univariate analysis, non-cirrhotic patients showed better overall survival than those with cirrhosis did (p = 0.043). However, cirrhosis was not independently associated with overall survival, for which the independent predictors were age, liver function, tumor burden and BCLC classification. Non-cirrhotic patients underwent surgery more frequently than cirrhotic patients did (41% vs. 11%, p < 0.001), even in cases where the largest tumors were ≥ 5 cm (42% vs. 14%, p = 0.002) or there were four or more lesions (19% vs. 2%, p = 0.024). Among the cirrhotic and non-cirrhotic patients who underwent surgery, survival was not significantly different (p = 0.074). The cirrhosis/no cirrhosis ratio remained stable over the study period.

Conclusion: 35% of MASLD-related HCC occur in a non-cirrhotic liver. While they present poor prognostic factors (higher age and larger tumor), HCC related MASLD in non-cirrhotic liver benefit from more radical management thanks to preservation of liver function, thus probably accounting for the lack of significant difference in overall survival compared with patients with HCC on cirrhosis observed in multivariate analysis.

THU-514

Outcomes of ultrasound-guided artificial ascites induction to facilitate radiofrequency ablation for hepatocellular carcinoma in high-risk positions

Ahmed Hashim¹, Sofia Maria Bakken¹, Fabio Piscaglia¹, Carla Serra¹.
¹IRCCS Azienda Ospedaliero Universitaria di Bologna, Bologna, Italy
 Email: ahmed.hashim@nhs.net

Background and aims: The induction of artificial ascites (or hydrodissection) can potentially be effective in reducing injury to adjacent anatomical structures during radiofrequency ablation (RFA) for hepatocellular carcinoma (HCC) lesions in anatomically high-risk sites. We aimed to evaluate the outcomes of an ultrasound (US)-guided dissection technique to facilitate RFA for such lesions.

Method: Our technique involved the injection of 5% dextrose into the peritoneal space to create a non-target organ gap before undertaking RFA under ultrasound guidance. We retrospectively reviewed the records of all patients who received this technique between December 2013 and March 2021 at the Policlinico St. Orsola Malpighi, Bologna.

Results: A total of 134 procedures were undertaken for 95 patients over the study period. The mean age of the cohort was 68 (SD = 11); 72 (76%) were males. The majority of patients had viral hepatitis (B or C) = 69/95 (73%). Cirrhosis was evident in 87/95 (92%) with 83 (87%) being Barcelona Clinic Liver Cancer (BCLC) stage 0/A. The mean Model For End-Stage Liver Disease (MELD) score was 9.7 (SD = 2.9, n = 92) and the median alpha-fetoprotein was 3.9 ng/ml (IQR = 13.7, n = 78). HCC was diagnosed primarily on imaging criteria alone; only two were confirmed on liver biopsy. At the time of ablation, the majority of HCC lesions treated (n = 134) were new (92), 41 being recurrent and 1 was a completion treatment. Artificial ascites was successfully induced by injecting an average of 232mls (SD = 180) of 5% dextrose and the median duration of RFA treatment was 11 mins (IQR = 6) using a median power of 157W (IQR = 25). Of the 134 procedures, the target lesion was located in segments: 6 (adjacent to the colon, n = 30); 7and8 (adjacent to diaphragm, n = 36); 5 (adjacent to the gallbladder, n = 20); 2and3 (adjacent to the stomach, n = 37), other (n = 11). Procedure-related pain was controlled with simple analgesia in 115/134 cases. Early complications (within 48 hours) occurred in 23/134 (17%) procedures; the vast majority of which were minor with 3 cases recording a hematoma, 1 hepatic insufficiency, and 1 pneumothorax. Fourteen required prolonged hospital stay. On follow-up, progression of the HCC nodule treated was observed in 39/134 (29%) cases at a median duration of 6 (IQR = 9) months post-procedure.

Conclusion: Our work demonstrates that US-guided percutaneous RFA using artificial ascites for treating HCC in difficult anatomical locations is feasible and effective with a good safety profile.

THU-515

Impact of varices on bleeding risks and overall survival in unresectable hepatocellular carcinoma treated with atezolizumab plus bevacizumab

Jeayeon Park¹, Dong Ho Lee², Moon Haeng Hur¹, Yun Bin Lee¹, Eun Ju Cho¹, Jeong-Hoon Lee¹, Yoon Jun Kim¹, Jung-Hwan Yoon¹, Su Jong Yu¹. ¹Department of internal medicine and liver research institute, Seoul National University College of Medicine, Seoul, Korea, Rep. of South; ²Department of Radiology, Seoul National University College of Medicine, Seoul, Korea, Rep. of South
 Email: ydoctor2@snu.ac.kr

Background and aims: The IMbrave150 trial has led first-line systemic therapy for unresectable hepatocellular carcinoma (HCC) to include immunotherapy, remarkably improving life expectancy. However, the use of atezolizumab plus bevacizumab is often challenged due to the increased risk of bleeding. In this study, we aimed to identify factors associated with bleeding events during the treatment with atezolizumab plus bevacizumab, as well as factors that affect overall survival (OS).

Method: We retrospectively included consecutive patients who treated with atezolizumab plus bevacizumab as first-line systemic therapy for unresectable HCC from October 2020 to December 2022 at a tertiary referral center. Primary end point was the incidence of the first bleeding event during treatment. Secondary end point included OS.

Results: A total of 124 patients were included: 82 had varices found on either esophagogastroduodenoscopy (EGD) or computed tomography (CT) (EGD only, n = 3; CT only, n = 46; and both EGD and CT, n = 33; varices group), while 42 showed no varices on both EGD and CT (no varices group). Prior to treatment with atezolizumab plus bevacizumab, no high-risk varices were noted. During the median follow-up duration of 11.1 months (interquartile range, 6.1–14.9), bleeding events occurred in 15 patients. The cumulative incidence of bleeding in the varices group was 12.5%, 21.1%, and 31.0% at 6, 12, and 18 months, respectively, significantly higher than the 0.0% incidence at the corresponding time points in the no varices group (p = 0.003). In addition, the presence of varices was identified as the only significant predictor of bleeding events on multivariate Cox model (adjusted hazard ratio [aHR], 13.56; p = 0.006). However, the median OS was similar between the two groups (11.6 months in the varices group versus 11.8 months in the no varices group), with no significant difference in OS based on the presence of varices (aHR, 0.92; p = 0.74). Baseline PIVKA level ≥ 1000 mAu/ml (aHR 1.98; p = 0.007) and neutrophil to lymphocyte ratio ≥ 3 (aHR 1.77; p = 0.01) were significant predictors of OS.

Conclusion: The presence of varices on baseline imaging study was significantly associated with an increased risk of bleeding events during treatment with atezolizumab plus bevacizumab, although the OS was similar regardless of the presence of varices.

THU-516

Beneficial effect of combined radiation therapy in atezolizumab plus bevacizumab treatment of hepatocellular carcinoma patients with main portal vein tumor thrombosis

Sangyoun Hwang¹, Hyun Young Woo², Jeong Heo², Hyung Jun Kim¹, Young Joo Park², Kiyoun Yi², Yu Rim Lee³, Soo Young Park⁴, Woo Jin Chung⁵, Byoung Kuk Jang⁵, Won Young Tak⁴. ¹Department of Internal Medicine, Dongnam Institute of Radiologic and Medical Sciences, Busan, Korea, Rep. of South; ²Department of Internal Medicine, College of Medicine, Pusan National University and Biomedical Research Institute, Pusan National University Hospital, Busan, Korea, Rep. of South; ³Department of Internal Medicine, School of Medicine, Kyungpook National University, Kyungpook National University Hospital, Daegu, Korea, Rep. of South; ⁴Department of Internal Medicine, School of Medicine, Kyungpook National University, Kyungpook National University Hospital, Daegu, Korea, Rep. of South; ⁵Department of Internal Medicine, Keimyung University School of Medicine, Daegu, Korea, Rep. of South
 Email: jheo@pusan.ac.kr

Background and aims: Atezolizumab (ATE) plus bevacizumab (BEV) was established as the first-line therapy for patients with advanced hepatocellular carcinoma (HCC) through phase 3 clinical trial. However, survival is still poor in HCC patients with main portal vein tumor thrombosis.

Method: This is a multicenter retrospective study. Between January 2020 to June 2022, 215 patients treated for advanced HCC with at ATE +BEV from four tertiary hospital was analyzed. Among them, 70 patients had vp4 portal vein tumor thrombosis. Tumor response was evaluated with the Response Evaluation Criteria in Solid Tumors (version 1.1.).

Results: Among 70 patients with Vp4 portal vein tumor thrombosis, Child-Pugh class was A in 57 (81.5%) and B in 13 (18.5%). 45 (64.3%) received neoadjuvant or concomitant radiation treatment. Baseline characteristics did not differ significantly with or without radiation. In overall, objective response rate was 24.3%. disease control rate was 75.7%. The median progression free survival (PFS) was 7.75 months

POSTER PRESENTATIONS

(95% CI, 5.71–9.79) and median overall survival (OS) was 9.25 months (95% CI, 7.76–10.74). In multivariate analysis, bile duct invasion, preemptive or concomitant radiation therapy and Hb level was significant prognostic factor for survival and progression free survival. Median OS was 10 months (95% CI, 7.85–12.15) in patients with radiation and 7.75 months (95% CI, 3.47–12.03) in patients without radiation. Median PFS was 9.25 months (95% CI, 7.91–10.59) in patients with radiation and 5.00 months (95% CI, 2.23–7.77) in patients without radiation. A total of 58 (82.9%) patients experienced any grade of adverse events (AEs). The most common AEs was proteinuria (14.8%). The rate of grade 3 or higher AE is similar in patients with or without radiation (18.2% vs. 16.7%).

Conclusion: ATE+BEV treatment was tolerable in patients with Vp4 portal vein tumor thrombus. Furthermore, radiation therapy could improve the OS and PFS in these patients.

THU-517

Off-label use of nivolumab beyond first-line in advanced hepatocellular carcinoma: experience from two international centres

Silvia Gaia¹, Francesco Frigo², Najib Ben Khaled³, Gian Paolo Caviglia⁴, Emanuela Rolle¹, Ignazio Piseddu³, Paolo Pochettino⁵, Enrico de Toni³, Matilde Scaldaferri¹, Francesco Cattel¹, Eleonora Castellana¹, Alberto De Giorgi⁶, Giorgio Maria Saracco⁴, Patrizia Carucci¹. ¹AOU Città della salute e della scienza di Torino, Turin, Italy; ²AOU Città della salute e della scienza di Torino, Turin; ³University Hospital, LMU Munich, Munich, Germany; ⁴University of Turin, Turin, Italy; ⁵AOU Città della salute e della Scienza di Torino, Turin, Italy; ⁶University of Turin, Turin
Email: silvia.gaia74@gmail.com

Background and aims: Investigational use of nivolumab as first-line therapy for the treatment of hepatocellular carcinoma (HCC) yielded promising results but failed to demonstrate a statistically significant overall survival (OS) advantage compared to sorafenib. The aims are to evaluate the efficacy and safety of nivolumab as monotherapy beyond first-line in patients with HCC ineligible for other treatments.

Method: we retrospectively analyzed data from 30 HCC patients receiving off-label nivolumab at two referral centers in Italy and Germany between May 2016 and December 2023. Enrolled patients were ineligible for local or surgical therapy, had disease progression or intolerance to prior tyrosine kinase inhibitors therapy, and were not candidates for other systemic therapies. Measured outcomes were overall survival (OS), progression-free survival (PFS), disease control rate (DCR), and biological response (BR), defined as an $\geq 25\%$ decrease in alpha-fetoprotein (AFP) levels after 3 months of therapy. The safety profile of nivolumab was assessed.

Results: 30 patients were enrolled (Italy n=24, Germany n=6). Patient characteristics were as follows: median age 65 (range 30–82) years, Child-Pugh A 80%, BCLC C 87%, viral etiology 83%. One patient received nivolumab as I-line (ineligible for any other therapy), 19 as II-line, 8 as III-line, and 2 as IV-line of systemic treatment. Median OS was 9.1 (95%CI 6.4–14.2) months and median PFS was 3.5 (95%CI 2.8–6.4) months. DCR at 3 months was 27% (8/30) with two patients achieving complete radiologic response after 12 and 21 months of therapy. BR was obtained in 23% (7/30) of patients. Median OS in patients with radiological disease control at 3 months was 27.7 (95% CI 4.7–41.2) months compared to 7.3 (95%CI 4.0–9.1) months in patients with disease progression ($p < 0.001$). Median OS in patients with BR was 38.0 (95%CI 23.5–41.2) months compared to 7.8 (95%CI 3.6–12.1) months in patients without BR ($p < 0.001$). At baseline, better performance status, presence of metastatic lymph nodes, serum AFP ≥ 400 $\mu\text{g/L}$, and lower disease burden were associated with longer OS on univariate analysis (all $p < 0.05$). Ten patients (33%) experienced grade 3–4 adverse events, but only three cases (10%) were deemed treatment-related. Only one patient had to discontinue therapy due to adverse events.

Conclusion: nivolumab could represent a valuable option in patients without other therapeutic alternatives, showing an OS greater than 6 months in 73% of patients and an acceptable safety profile. Radiological response and BR at 3 months predict a significantly longer survival.

THU-518

Analysis of varix bleeding after Atezolizumab plus Bevacizumab for advanced hepatocellular carcinoma patients

Ahlim Lee^{1,2}, Hee Yeon Kim³. ¹Division of Gastroenterology, Department of Internal Medicine, St. Vincent's Hospital, College of Medicine, The Catholic University of Korea, Suwon, Korea, Rep. of South; ²The Catholic University Liver Research Center, College of Medicine, The Catholic University of Korea, Seoul, Korea, Rep. of South; ³Division of Gastroenterology, Department of Internal Medicine, Bucheon St. Mary's Hospital, College of Medicine, The Catholic University of Korea, Bucheon, Korea, Rep. of South
Email: hee82@catholic.ac.kr

Background and aims: After the IMbrave150 trial, atezolizumab plus bevacizumab (AteBeva) became the gold standard for unresectable hepatocellular carcinoma (HCC). However, since this trial included well-selected patients without any history of acute variceal bleeding (AVB) nor high-risk esophageal varices, real-world data from advanced HCC patients with any history of AVB or large varices were unknown under this new combination of treatment. We aimed a study to provide real-life data on the therapeutic effect and the safety of AteBeva and to identify risk factors of AVB during treatment in Korea.

Method: We conducted a prospective study including all patients diagnosed with advanced HCC and received AteBeva from seven centers of Catholic Medical Center between September 2020 to December 2022. We followed up on these patients until December 2023 and analyzed therapeutic efficacy and safety, especially AteBeva-related variceal bleeding. Time-to-events were estimated by Kaplan-Meier with the log-rank test, along with Cox models.

Results: One hundred fifty-four patients treated with AteBeva were included. In baseline characteristics, the median age was 64.0 (56.0–73.0), the male sex was 85.1%, the most common etiology was hepatitis B virus infection (62.2%) and alcohol-related liver disease (26.5%). Child-Pugh class was A or B, and Barcelona Clinic Liver Cancer (BCLC) stage was B or C. The Objective response rate (ORR) of AteBeva was 38.3% and the Disease control rate (DCR) was 70.9%. Median overall survival (OS) 14.000 ± 2.788 (95% CI: 8.536–19.464), median progression-free survival 5.000 ± 0.570 (3.882–6.118), median time-to progression (TTP) was 3.000 ± 0.352 (2.310–3.690). In multivariable analysis, variables associated with OS were the Eastern Cooperative Oncology Group (ECOG) performance scale, liver cirrhosis, Child-Pugh class, largest intrahepatic tumor size, and treatment duration. The patient underwent all grades of gastrointestinal bleeding events after AteBeva was 40 (26.0%), varix bleeding was 23 (14.9%), and 18 (11.7%) received endoscopic band ligation (EBL). In multivariable analysis, variables associated with varix bleeding after AteBeva were Child-Pugh score and ulceration from prophylactic EBL before AteBeva.

Conclusion: In this study, the most common adverse event after AteBeva was all grades of gastrointestinal bleeding events. Risk factors for varix bleeding after AteBeva were Child-Pugh score at baseline and ulceration from prophylactic EBL before AteBeva. Therefore, for patients with prophylactic EBL before AteBeva, ulceration monitoring and management are needed after EBL. Further studies on large scale are needed.

THU-519

Surgical outcomes of laparoscopic versus open liver resection for intrahepatic cholangiocarcinoma: Multicenter study

Jongman Kim¹, Gi Hong Choi², Je Ho Ryu³, Dong-Sik Kim⁴, Hae Won Lee⁵, Ki-Hun Kim⁶. ¹Samsung Medical Center, Seoul, Korea, Rep. of South; ²Yonsei University College of Medicine, Seoul, Korea, Rep. of South; ³Pusan National University College of Medicine, Busan, Korea, Rep. of South; ⁴Korea University College of Medicine, Seoul, Korea, Rep. of South; ⁵Seoul National University Bundang Hospital, Seongnam, Korea, Rep. of South; ⁶Asan Medical Center, Seoul, Korea, Rep. of South
Email: yjongman21@gmail.com

Background and aims: Laparoscopic liver resection (LLR) remains controversial in the treatment of intrahepatic cholangiocarcinoma (IHCCC). The aim of the present study is to investigate the outcomes of LLR for IHCCC compared to open liver resection (OLR).

Method: We retrospectively reviewed patients who underwent hepatectomy for IHCCC from six medical centers between January 2013 and February 2020. During the study period, 616 patients met the inclusion criteria (OLR = 514 patients and LLR = 102 patients).

Results: The median operation time and median blood loss in the LLR group were significantly shorter and less blood loss than in the OLR group. In addition, the incidence of severe postoperative complications in the LLR group was significantly less than in the OLR group. The cumulative disease-free survival and overall survival are comparable between the two groups. Multivariate analyses showed that multiple tumors, R1 resection, intrahepatic metastasis, and metastatic lymph node were predisposing factors for tumor recurrence. Increased age, long operation time, and multiple tumors were closely associated with mortality.

Conclusion: The present study suggests that LLR should be considered in selective IHCCC because of better postoperative short outcomes and comparable disease-free survival and overall survival compared with OLR group.

MASLD – Clinical aspects except therapy

TOP-301

Impact of clonal hematopoiesis of indeterminate potential on hepatocellular carcinoma in steatotic liver disease

Serena Pelusi¹, Alfredo Marchetti², Francesco Malvestiti³, Antony Ricchiuti², Luisa Ronzoni⁴, Marta Lionetti⁵, Vittoria Moretti¹, Elisabetta Bugianesi⁶, Luca Miele⁷, Umberto Vespasiani Gentilucci⁸, Paola Dongiovanni⁹, Alessandro Federico¹⁰, Giorgio Soardo¹¹, Roberta D'Ambrosio¹², Helen Louise Reeves¹³, Vincenzo La Mura¹⁴, Daniele Prati¹⁵, Niccolò Bolli¹⁶, Luca Valenti¹⁷. ¹Transfusion Medicine Unit, Fondazione IRCCS Ca' Granda Ospedale Maggiore Policlinico, Milan, Milan, Italy; ²Hematology Unit, Fondazione IRCCS Ca' Granda Ospedale Maggiore Policlinico, Milan, Milan, Italy; ³Department of Pathophysiology and Transplantation, Università degli Studi di Milano, Milan, Italy; ⁴Transfusion Medicine Unit, Fondazione IRCCS Ca' Granda Ospedale Maggiore Policlinico, Milan, Milan; ⁵Hematology Unit, Fondazione IRCCS Ca' Granda Ospedale Maggiore Policlinico, Milan, Milan; ⁶Department of Medical Sciences, Division of Gastroenterology, University of Turin, Turin, Italy; ⁷Dipartimento Universitario Medicina e Chirurgia Traslazionale, Università Cattolica del Sacro Cuore, Rome, Area Medicina Interna, Gastroenterologia e Oncologia Medica, Fondazione Policlinico A. Gemelli IRCCS, Rome, Rome, Italy; ⁸Clinical Medicine and Hepatology Unit, Department of Medicine and Surgery, Campus Bio-Medico University of Rome, Rome, Italy; ⁹Medicine and Metabolic Diseases, Fondazione IRCCS Ca' Granda Ospedale Maggiore Policlinico, Milan, Milan, Italy; ¹⁰Department of Precision Medicine, University of Campania "Luigi Vanvitelli", Naples, Naples, Italy; ¹¹Clinica Medica,

Department of Medicine, European Excellence Center for Arterial Hypertension, University of Udine, Udine, Italy; ¹²Gastroenterology and Hepatology Unit, Fondazione IRCCS Ca' Granda Ospedale Maggiore Policlinico, Milan, Milan, Italy; ¹³Newcastle University Translational Research Institute, Newcastle University, Newcastle upon Tyne, United Kingdom; ¹⁴Gastroenterology and Hepatology Unit, Fondazione IRCCS Ca' Granda Ospedale Maggiore Policlinico, Milan, Milan; ¹⁵Transfusion Medicine Unit, Fondazione IRCCS Ca' Granda Ospedale Maggiore Policlinico, Milan, Italy; ¹⁶Hematology Unit, Fondazione IRCCS Ca' Granda Ospedale Maggiore Policlinico, Milan, Department of Oncology and Hemato-Oncology, Università degli Studi di Milano, Milan, Italy; ¹⁷Transfusion Medicine Unit, Fondazione IRCCS Ca' Granda Ospedale Maggiore Policlinico, Milan, Department of Pathophysiology and Transplantation, Università degli Studi di Milano, Milan, Italy
Email: alfredo.marchetti@unimi.it

Background and aims: Metabolic dysfunction associated steatotic liver disease (MASLD) is a global epidemic and is the most rapidly rising cause of hepatocellular carcinoma (HCC). Clonal hematopoiesis of indeterminate potential (CHIP) contributes to neoplastic and cardiometabolic disorders and is considered a harbinger of tissue inflammation. CHIP was recently associated with increased risk of liver disease. The aim of this study was to examine whether CHIP is associated with HCC development in patients with SLD.

Method: We considered individuals with MASLD-HCC (n = 208) and controls with (n = 414) and without (n = 259) advanced fibrosis who underwent whole exome sequencing. DNA was extracted from peripheral blood and sequenced by the HiSeq 4000/NextSeq2000 platforms (Illumina). Somatic mutations were identified accepting a minimum variant coverage of 20, a minimum alternative allele count of 3 and a variant allele frequency (VAF) between 0.02 and 0.46. Variants with a population mean allelic frequency higher than 1 in a 1000 were treated as polymorphisms. Variants were then curated to include only variants known to be somatic and associated to either malignancy or CHIP with the use of a semi-automatic pipeline. Age, sex, presence of type 2 diabetes (T2D), advanced liver fibrosis, AST and ALT levels at the time of study enrolment were available in all patients.

Results: CHIP was observed in 116 participants (13.1%), most frequently in DNMT3A (DNA methyltransferase 3 alpha), TET2 (Tet methylcytosine dioxygenase 2), TP53 (tumor protein 53) and ASXL1 (additional sex combs like 1) genes, and correlated with age (p < 0.0001) and advanced liver fibrosis (p = 0.001). Higher AST levels predicted non-DNMT3A-CHIP, in particular with VAF ≥ 10% (OR 1.14, 1.03–1.28 and OR 1.30, 1.12–1.49, respectively, p < 0.05). After adjustment for sex, diabetes and a polygenic risk score of inherited MASLD predisposition CHIP was associated with cirrhosis (2.00, 1.30–3.15, p = 0.02), and with HCC even after further adjustment for cirrhosis (OR 1.81, 1.11–2.00, 1.30–3.15, p = 0.002). Despite the strong collinearity among aging and development of CHIP and HCC, non-DNMT3A-CHIP and TET2 lesions remained associated with HCC after full correction for clinical/genetics covariates and age (OR 2.45, 1.35–4.53; OR 4.8, 1.60–17.0, p = 0.02).

Conclusion: We observed an independent association between CHIP, particularly related to non-DNMT3A and TET2 genetic lesions, and MASLD-HCC.

TOP-307

The interplay between alcohol consumption and cardiometabolic risk factors in patients with MASLD and MetALD

Yee Hui Yeo¹, Fajuan Rui², Yixuan Zhu³, Xiaoming Xu⁴, Xiaoyan Ma³, Wenjing Ni⁵, Xinyu Hu⁶, Chao Wu³, Junping Shi⁷, Jie Li³, Philip N. Newsome⁸. ¹Cedars-Sinai Medical Center, California, United States; ²Nanjing Drum Tower Hospital Clinical College of Traditional Chinese and Western Medicine, Nanjing University of Chinese Medicine, Nanjing, China; ³Nanjing Drum Tower Hospital, Affiliated Hospital of Medical School, Nanjing University, Nanjing, China; ⁴Nanjing Drum

POSTER PRESENTATIONS

Tower Hospital Clinical College of Nanjing University of Chinese Medicine, Nanjing, China; ⁵Nanjing Drum Tower Hospital Clinical College of Traditional Chinese and Western Medicine, Nanjing, China; ⁶Department of Infectious Disease, Shandong Provincial Hospital, Shandong University, Jinan, China; ⁷The Affiliated Hospital of Hangzhou Normal University, Hangzhou, China; ⁸Centre for Liver and GI Research, Birmingham, United Kingdom
Email: p.n.newsone@bham.ac.uk

Background and aims: The synergistic impact of incremental alcohol consumption and cardiometabolic risk factors on the prognosis of patients with metabolic dysfunction-associated steatotic liver disease (MASLD) and metabolic and alcohol-associated liver disease (MetALD) remains unclear. Herein, we aimed to investigate the interplay between varying levels of alcohol consumption and the number of cardiometabolic risk factors (CMRFs) on all-cause mortality in patients with MASLD and MetALD.

Method: Adult participants who underwent ultrasound between 1988 and 1994 were identified from a population-representative cohort, NHANES III. Those with MASLD or MetALD were categorized based on their CMRF count (one, two, or three to five) and alcohol consumption: 0–10/15 g of alcohol/day 0–10/15 g of alcohol/day for females/males (F/M), 10/15–20/30 g/day, and 20/30–50/60 g/day. Multivariate Cox proportional hazards models were conducted to investigate the association between incremental CMRFs and alcohol consumption and mortality, with adjustment for age, sex, race, and poverty income ratio.

Results: During a median follow-up period of 47, 046 person-years, 695 (36.1%) died during this period. The adjusted hazard ratios (aHR) for all-cause mortality showed a stepwise increase with higher levels of alcohol consumption and a greater number of CMRFs. However, statistical significance was only observed in the subgroup with 3–5 CMRFs and alcohol consumption levels greater than 10/15 g/day (F/M). Subgroup analysis by age was performed. For those aged <65 years, the effect of CMRFs and alcohol use was more prominent. Specifically, compared to one CMRF, the aHRs were 1.08 (95%CI: 0.68–1.73) for 2 CMRFs and 2.92 (95%CI: 1.95–4.39) for 3 to 5 CMRFs among participants with 0–10/15 g/day alcohol use. For those who drink 10/15–20/30 g/day, aHRs were 1.05 (95%CI: 0.43–2.57) for one CMRF, 2.06 (95%CI: 1.14–3.73) for two CMRFs, and 3.89 (95%CI: 2.44–6.21) for three to five CMRFs. A synergistic effect between alcohol use and CMRFs was shown, with the aHR peaking at 5.17 (95%CI: 3.20–8.37) for those drinking 20/30–50/60 g/day and with 3–5 CMRFs. Conversely, participants aged ≥65 years displayed no significance in any combination of CMRFs and alcohol use, compared to those with one CMRF and minimal alcohol intake.

Conclusion: We found a significant synergistic effect on mortality risk between CMRFs and alcohol consumption in participants with MASLD and MetALD, particularly in those younger than 65 years. This study has implications for managing modifiable risk factors among those with steatotic liver disease.

TOP-308

Steatotic liver disease subclasses have prognostic relevance for liver-related outcomes in the general population

Ville Männistö^{1,2}, Veikko Salomaa³, Antti Jula³, Annamari Lundqvist³, Satu Männistö³, Markus Perola³, Fredrik Åberg⁴. ¹Kuopio University Hospital, Kuopio, Finland; ²University of Eastern Finland, Kuopio, Finland; ³Finnish Institute for Health and Welfare, Helsinki, Finland; ⁴Helsinki University Hospital, Helsinki, Finland
Email: ville.mannisto@kuh.fi

Background and aims: Steatotic liver disease (SLD) is the most common chronic liver disease. The primary objective of this study was to validate the prognostic relevance of the recently proposed SLD subclasses in a Finnish population-based sample. We also evaluated the relevance of number of metabolic disturbances and the level of alcohol use for liver-related outcomes in SLD subclasses.

Method: A total of 27383 individuals (46% men, mean age 50.8 ± 14.3 years, BMI 27.0 ± 4.8 kg/m²) with registry linkage available were included from Finnish population based FINRISK 2002, 2007, 2012 and Health 2000 studies. SLD was diagnosed as ALT >20 U/l for female and >30 U/l for male. In sensitivity analyses, fatty liver index (FLI) >60 was used. Incident severe liver-related outcomes and non-liver death were identified through linkage with national registries for hospitalization, cancer, or death.

Results: A total of 10380 (43%) individuals in the study cohort had SLD. The overall prevalences of the SLD subclasses were 34.5% for metabolic-dysfunction associated steatotic liver disease (MASLD), 4.2% for co-existent MASLD and alcohol-related liver disease (ALD), i. e. MetALD, and 1.8% for ALD, respectively. During the median follow-up of 13.3 ± 4.7 years, a total of 129 liver-related events were observed (65 in MASLD group, 34 in MetALD group and 30 in ALD group). The absolute cumulative incidences for liver-related outcomes and non-liver death were highest in the ALD group followed by MetALD and MASLD groups. Those with MetALD had 4-fold (HR 3.92, 95% CI 2.56–6.02, p < 0.001) and those with ALD 8-fold (HR 8.08, 95% CI 5.16–12.65, P < 0.001) increase in liver-related outcomes compared to those with MASLD in age- and sex-adjusted Cox regression analysis. Metabolic risk factors were present in 93% and 96% of individuals with SLD or ALD, respectively. The number of metabolic risk factors was significantly associated with liver-related outcomes in MASLD. Furthermore, alcohol use within the limits of MASLD diagnosis increased the risk of liver-related outcomes. The sensitivity analyses using FLI as a marker of SLD provided similar results as our primary analyses.

Conclusion: The prevalence of SLD is considerable high in the general population. Individuals with ALD exhibit the highest risk for both liver-related outcomes and non-liver death when compared to those with MASLD and MetALD, and the prevalence of metabolic disturbances is notably high in individuals with ALD. Alcohol use amplifies the risk of liver-related outcomes in individuals with MASLD.

TOP-309

Identifying patient characteristics associated with the risk of long-term liver and cardiovascular outcomes and high healthcare costs in metabolic dysfunction-associated steatohepatitis: a retrospective cohort analysis using an artificial intelligence model

Kamal Kant Mangla¹, Semiu Gbadamosi², Daniel Semeniuta³, Benjamin Soule², Helene Nordahl¹, Jigar Bandaria³, Joseph Zabinski³, Gary Curhan³, Costas Boussios³. ¹Novo Nordisk A/S, Søborg, Denmark; ²Novo Nordisk Inc., Plainsboro, United States; ³OM1 Inc., Boston, United States
Email: kknm@novonordisk.com

Background and aims: Significant heterogeneity in non-alcoholic steatohepatitis (NASH; also termed metabolic dysfunction-associated steatohepatitis [MASH]) complicates efforts to identify individuals with high unmet need and in need of better management. We used artificial intelligence (AI) phenotyping to identify factors associated with risks of long-term outcomes and high healthcare costs.

Method: Patients diagnosed with NASH between Oct 1, 2015 and Jun 17, 2022 were identified in the OM1 Real-World Data Cloud, a US electronic medical records and claims dataset. The index date was the date of first NASH diagnosis. Core eligibility criteria were a Fibrosis-4 record within 90 days of index, sufficient follow-up data, and no other liver conditions. The AI-based PhenOM™ platform (OM1 Inc., Boston, MA, USA) grouped characteristics from patients' histories (including diagnoses, procedures, and medications) into themes. Using machine learning, these groupings were iteratively refined and evaluated for strength of association with each outcome and clinical plausibility. Cirrhosis and related liver outcomes were assessed in a 'non-cirrhotic' cohort with no evidence of clinical cirrhosis pre-, at, or 6 months post-index. Liver-related outcomes other than cirrhosis were

assessed in a 'cirrhotic' cohort with clinical cirrhosis pre- or at index. Cardiovascular (CV) outcomes were assessed in a 'non-CV' cohort with no evidence of a CV-related outcome pre- or at index. Factors associated with incurring mean annual healthcare costs in the highest decile were also identified.

Results: In total, 37,309 patients met the core eligibility criteria. In the non-cirrhotic cohort (n = 12,555), the strongest factors associated with liver-related outcomes were chronic diseases, kidney issues, and heart issues. In the cirrhotic cohort (n = 807), key factors were medication for coronary heart disease, blood pressure, and type 2 diabetes. In the non-CV cohort (n = 12,566), the strongest factors associated with CV-related outcomes were CV history (other than outcomes of interest), hypertension, atherosclerosis, atrial fibrillation, kidney issues, diabetes, anaemia, osteoarthritis, and metabolic issues. In the healthcare cost analysis (n = 10,133), key factors associated with incurring the highest healthcare costs were myocardial infarction, heart failure, kidney issues, gastrointestinal issues, abdominal imaging, and other chronic comorbidities including diabetes, hypertension, anaemia, and chronic kidney disease.

Conclusion: This study identified factors meaningfully associated with clinical and economic outcomes in NASH, demonstrating the application of AI phenotyping to multidimensional real-world data. The results potentially provide evidence to identify patients in clinical practice, via predictive modelling, who would benefit from closer monitoring and management.

TOP-310

Genetic determinants of disease progression in metabolic dysfunction-associated liver disease patients unresponsive to lifestyle intervention: implications for personalized medicine

Aruhan Yang¹, Xiaoxue Zhu¹, Qiang Yang², Xiao Teng³, Yanhua Ding⁴.
¹Phase One Clinical Research Center, First Hospital of Jilin University, Changchun, China; ²Hangzhou Choutu Technology Co., Ltd., Hangzhou, China; ³HistoIndex Pte Ltd, Singapore, Singapore; ⁴Phase One Clinical Research Center, First Hospital of Jilin University, Changchun, China

Email: arh22@mails.jlu.edu.cn

Background and aims: Lifestyle intervention with 5% weight loss (WL) is the primary approach for managing MASLD. Identifying genetic traits in non-responders may pave the way for personalized pharmacotherapy in this population.

Method: In this study with 724 participants, 146 had liver biopsies. All participants completed questionnaires, blood tests, and MRI-PDFF assessments. Genetic sequencing was performed on collected blood samples, and SHG/TPEF microscopy with computer-assisted analysis was used for pathological specimens. Patients with liver biopsies received lifestyle interventions, while others received health education. MASLD was diagnosed based on new criteria, and disease regression was assessed by comparing two sets of pathological (NAS reduction ≥ 2 points) or MRI findings (Liver Fat Content, LFC reduction $\geq 30\%$).

Results: In this 12-month study, 145 (99%) and 602 (83%) participants were diagnosed with MASLD via liver biopsy and MRI-PDFF, respectively. In individuals achieving MASLD remission (N = 213, 35.3%), significant improvements in liver damage markers (ALT, AST, GGT) and metabolic parameters (Glucose, Insulin, HOMA, LDL, TG) were observed, highlighting enhanced hepatic health and glucose-lipid metabolism. Genetic analysis in the whole cohort revealed significant effects of VPS8 (rs1011147, T > C) and DPP6 (rs144355748, G > A) mutations on disease progression (LFC changes for wild-type vs. mutant: -9.2% vs. 0.3% and -6.5% vs. 0.7%, respectively). After adjusting for lifestyle factors (smoking, alcohol, physical activity, sedentariness), mediation analysis found 25% of the gene's effect on improving MASLD was indirectly mediated through WL > 5%, while the remaining 75% represents the direct influence of the gene independent of WL > 5%. MASLD patients achieving over 5% WL (N = 200) showed an average 34% LFC reduction and 2 points NAS reduction, supported by digital pathology showing significant

decreases in most steatosis markers (Area: -9.7; Area PT: -6.6; ABubblePT: -55.7) and some fibrosis-related markers (Str: -7.7, StrLenthPS: -7093), indicating notable improvements in fat content and select fibrosis-related measures. However, 52 individuals with WL > 5% (26%) didn't achieve remission. 28 SNPs affecting MASLD regression were identified among the WL > 5% group, and GRS scores calculated. Low GRS individuals displayed more improvement in fibrosis (dStrLength: -3.6 vs. 191.5; dSHG: -0.2 vs. 2.8) and steatosis (dArea: -24.5 vs. 5.6; dABubble: -168.2 vs. 58.6; dAreaCV: -14.1 vs. 14.4) compared to high GRS individuals. Functional enrichment analysis revealed a focus on the RISC complex, RNAi effector complex, and Estrogen signaling pathway for these genes.

Conclusion: Our study underscores the role of genetic traits in determining disease progression in MASLD patients resistant to 5% weight loss, pointing towards personalized medicine possibilities.

FRIDAY 07 JUNE

FRI-194-YI

Risk of all-cause mortality and adverse outcomes from steatotic liver disease and its subgroups in the general population

Maurice Michel^{1,2}, Angelo Armandi^{3,4}, Alexander Gieswinkel⁵, Alexander Schuster⁶, Thomas Muenzel^{5,7}, Stavros Konstantinides⁸, Matthias Michal⁹, Beate Straub¹⁰, Irene Schmidtmann¹¹, Oliver Tiescher⁹, Philipp Wild^{5,7,12,13}, Karl Lackner¹⁴, Peter R. Galle¹⁵, Jörn M Schattenberg^{16,17}. ¹I. Department of Medicine, University Medical Centre Mainz, Mainz, Germany; ²Metabolic Liver Research Program, Department of Medicine I, University Medical Center, Mainz, Germany; ³Metabolic Liver Research Program, I. Department of Medicine, University Medical Centre Mainz, Mainz, Germany; ⁴Division of Gastroenterology and Hepatology, Department of Medical Sciences, Turin, Italy; ⁵Preventive Cardiology and Preventive Medicine, Department of Cardiology, University Medical Centre Mainz, Mainz, Germany; ⁶Department of Ophthalmology, University Medical Centre Mainz, Mainz, Germany; ⁷Center for Cardiology-Cardiology I, University Medical Centre Mainz, Mainz, Germany; ⁸Center for Thrombosis and Hemostasis, University Medical Centre Mainz, Mainz, Germany; ⁹Department of Psychiatry and Psychotherapy, University Medical Centre Mainz, Mainz, Germany; ¹⁰Institute of Pathology, University Medical Centre Mainz, Mainz, Germany; ¹¹Institute of Medical Biostatistics, Epidemiology and Informatics, University Medical Centre Mainz, Mainz, Germany; ¹²Institute of Molecular Biology (IMB), Mainz, Germany; ¹³German Center for Cardiovascular Research (DZHK), Partner Site Rhine Main, Mainz, Germany; ¹⁴Institute for Clinical Chemistry and Laboratory Medicine, University Medical Centre Mainz, Mainz, Germany; ¹⁵Department of Medicine I, University Medical Centre Mainz, Mainz, Germany; ¹⁶Metabolic Liver Research Program, Department of Medicine I, University Medical Centre Mainz, Mainz, Germany; ¹⁷Department of Internal Medicine II, Saarland University Medical Centre, Homburg, Germany

Email: maurice.michel@icloud.com

Background and aims: With the implementation of the new nomenclature on steatotic liver disease (SLD), three main subgroups consisting of metabolic dysfunction-associated liver disease (MASLD), MASLD with increased alcohol intake (MetALD), and alcohol-related liver disease (ALD) have been defined. However, the risk of SLD for all-cause mortality and adverse outcomes as well as the different risks between MASLD, MetALD, and ALD needs further clarification.

Method: Data from 13,599 participants without cancer of the population-based Gutenberg Health Study (baseline enrollment between 2007 and 2012) were cross-sectionally and prospectively analysed. The fatty liver index (FLI) with a score of ≥ 60 was used to define SLD. The subgroups of SLD (MASLD, MetALD, and ALD) were defined according to the new nomenclature based on five cardiometabolic criteria and alcohol consumption. The fibrosis-4 score (FIB-4)

POSTER PRESENTATIONS

was calculated to determine patients at risk of fibrosis (≥ 1.3). All-cause mortality (10-year follow-up) and several adverse outcomes (hepatic decompensation, major adverse cardiac events (MACE), extrahepatic cancer) were analysed and compared across the subgroups of SLD. Cox regression models were used to estimate adjusted hazard ratios (aHR) and their 95% confidence intervals (CIs). Adjustments were made for age, sex, socioeconomic status, education, and smoking.

Results: The overall prevalence of SLD was 37.3% ($n = 5,074$), whereas the prevalence of MASLD, MetALD, and ALD were 30.5% ($n = 4,154$), 5.3% ($n = 717$) and 1.5% ($n = 202$), respectively. Almost half of the population were women (48.9%, $n = 6,644$), and the mean age was 54.3 (± 11.0) years. An elevated FIB-4 ≥ 1.3 was present in 20.2% ($n = 1,021$) with SLD compared to 13.9% ($n = 1,184$) without SLD ($p < 0.0001$). The cumulative incidence of all-cause mortality was higher in SLD and all its subgroups MASLD, MetALD, and ALD compared to no SLD ($p < 0.0001$). Stratification by FIB-4 ≥ 1.3 revealed a higher risk of all-cause mortality across all investigated SLD subgroups compared to FIB-4 < 1.3 ($p < 0.0001$). Each subgroup of SLD was associated with a higher risk of all-cause mortality: MASLD (aHR 1.6, 95% CI 1.4–1.9, $p < 0.0001$), MetALD (aHR 1.6, 95% CI 1.3–2.1, $p = 0.00024$) and ALD (aHR 1.6 95% CI 1.0–2.5, $p = 0.033$). The risk of adverse outcomes was increased in MASLD (hepatic decompensation: aHR 1.2, 95% CI 1.0–1.5, $p = 0.0045$; MACE: aHR 1.5, 95% CI 1.2–1.8, $p < 0.0001$; extrahepatic cancer: aHR 1.2, 95% CI 1.1–1.4, $p = 0.0086$), whereas no differences were seen for MetALD and ALD.

Conclusion: The prevalence of SLD and especially MASLD is high in the general population. Patients with SLD and any of its three main subgroups show a higher risk of all-cause mortality, whereas the risk for adverse outcomes is particularly increased in those with MASLD. These results highlight the importance of screening for SLD and related risk factors to improve outcomes.

FRI-195

Genetically determined circulating protein biomarkers and risk of advanced fibrosis

Jun Wang¹, Gabriel Cuellar-Partida¹, Robert W. Read², Karen A. Schlauch², Gai Elhanan³, W. James Metcalf³, Lisa Boyette¹, Timothy R. Watkins⁴, Joseph J. Grzymalski³, Scott D. Patterson¹, Shahed Iqbal¹, Andrew N. Billin¹. ¹Gilead Sciences, Inc., Foster City, United States; ²University of Nevada, Reno, United States; ³University of Nevada, Renown Health, Reno, United States; ⁴Gilead Sciences, Inc., Seattle, United States
Email: jun.wang37@gilead.com

Background and aims: Numerous biomarkers from circulating proteome have been associated with MASH severity. However, it is not known whether any of these biomarkers are also potential drivers of disease. We assessed genetically determined circulating protein biomarkers in relation to risk of advanced fibrosis with the aim of identifying potential drivers for disease progression.

Method: We conducted a case-control study leveraging Renown Health's Healthy Nevada Project (whole exome sequencing and electronic medical records). Participants of European ancestry, including 9078 controls (no MASH and no type 2 diabetes [T2DM]), 1084 MASH at-risk of fibrosis (FIB-4 ≤ 1.3 and with T2DM), and 1200 advanced fibrosis due to MASH (FIB-4 ≥ 2.67 with or without T2DM) were included in this study. Genetically determined circulating protein levels were computed using participants' genotype data and summary statistics of *cis*-protein quantitative trait loci from other proteogenomic studies. Nine previously reported fibrosis-related proteins (ADAMTSL2, ACY1, ASL, ADH4, C7, COLEC11, NFASC, PTGR1, and YKL-40) were evaluated. Multinomial logistic regression models were used to estimate odds ratio (OR) and 95% confidence interval (CI), adjusting for age, sex, genetic ancestry, BMI, and sequencing batch.

Results: More women were included in this study ($N = 7722$, 68%) and the mean age was 52.6, 62.7 and 67.7 years in controls, MASH at-

risk of fibrosis and advanced fibrosis. Genetically predicted circulating proteins were associated with slightly higher risk of MASH without fibrosis, but the risk of advanced fibrosis was significantly elevated for ADAMTSL2, COLEC11, NFASC and PTGR1 in patients with concurrent T2DM. For instance, compared to the lowest tertile, the highest tertile of predicted COLEC11 was linked to 84% higher risk (OR = 1.84, 95%CI = 1.07–3.17) of advanced fibrosis with concurrent T2DM, but no increased risk of advanced fibrosis was noted in those without T2DM (OR = 0.70, 95%CI = 0.46–1.07). Similar results were found for ADAMTSL2, NFASC and PTGR1. Further, associations were different between men and women for ADAMSL2 (interaction $p = 0.01$); for NFASC, associations were notably stronger in men than in women. For the other 5 proteins, significantly increased risk for advanced fibrosis was not observed for higher predicted protein levels. However, genetically predicted ADH4 was inversely associated with advanced fibrosis without T2DM (highest tertile OR = 0.73, 95% CI = 0.84–0.98) but not for advanced fibrosis with T2DM.

Conclusion: Combining genomics and proteomics, we identified several proteins (e.g., ADAMSL2, COLEC11, and NFASC) with their genetically determined circulating levels associated with higher risk of advanced fibrosis in the context of concurrent T2DM. Our integrated analysis provides genetic evidence to support that these protein biomarkers may drive disease progression.

FRI-196

Association between liver histology and long-term clinical outcomes in patients with biopsy-proven metabolic dysfunction-associated steatotic liver disease in Sweden: a real-world cohort study (BRIDGE-MASH)

Ying Shang¹, Johan Vessby², Kamal Kant Mangla³, Elisabeth de Laguiche³, Mattias Ekstedt⁴, Hannes Hagström^{1,5}. ¹Karolinska Institutet, Stockholm, Sweden; ²Uppsala University, Uppsala, Sweden; ³Novo Nordisk A/S, Søborg, Denmark; ⁴Linköping University, Linköping, Sweden; ⁵Karolinska University Hospital, Stockholm, Sweden
Email: ying.shang@ki.se

Background and aims: The link between fibrosis stage and prognosis in metabolic dysfunction-associated steatotic liver disease (MASLD) is well established, however, limited evidence exists for other histologic features of steatohepatitis. We aimed to evaluate the association between these features and the occurrence of major adverse liver outcomes (MALO), cardiovascular (CV) outcomes and mortality in a large cohort of individuals with MASLD.

Method: This cohort study included adults diagnosed with biopsy-proven MASLD between 18 Dec 1974 and 31 Dec 2020 at three Swedish university hospitals. Histologic features were categorized by severity: lobular inflammation (low: grade 0–1; high: grade 2–3), hepatocellular ballooning (low: grade 0–1; high: grade 2), steatosis (low: grade 1–2; high: grade 3) and non-alcoholic fatty liver disease activity score (NAS; low: < 4 ; high: ≥ 4). Outcomes were obtained from medical charts or linkage to national registers. Multivariable hazard ratios (HRs) were calculated using Cox regression models according to fibrosis stage and other histologic parameters, adjusting for age, sex, type 2 diabetes, body mass index, hypertension and hyperlipidemia. An additional analysis assessed event rates stratified by fibrosis stage.

Results: Of 959 eligible patients, median age at diagnosis was 52 years (interquartile range [IQR]: 39–60) and 368 (38.4%) were women. Over a median follow-up of 17 years (IQR: 7–27) there were 99 MALO events. Compared with F4 fibrosis, HRs for MALO and mortality were significantly lower in F0 (MALO: HR 0.10, 95% confidence interval [CI] 0.04–0.24; mortality: 0.44, 0.27–0.73), F1 (MALO: 0.12, 0.05–0.25; mortality: 0.48, 0.30–0.77) and F2 (MALO: 0.28, 0.14–0.56; mortality: 0.50, 0.31–0.80). In addition, compared with corresponding high-grade groups, significantly decreased HRs for MALO were observed in those with low-grade inflammation (HR 0.60, 95% CI 0.38–0.94) and ballooning (0.58, 0.36–0.93). In the stratified analysis, HRs for MALO were numerically higher in more

advanced (F2–3) than earlier (F0–1) fibrosis stages for inflammation, ballooning, steatosis and NAS; for example, HRs (95% CI) for low-versus high-grade ballooning were 0.56 (0.23–1.36) in F0–1 and 0.99 (0.52–1.87) in F2–3. Patients with lower fibrosis stages or inflammation had a reduced incidence of CV outcomes, but no significant reduction was noted after adjusting for covariates.

Conclusion: Lower fibrosis stage is associated with a reduced risk of MALO and overall mortality. The association between inflammation and ballooning and incident MALO appeared to depend on fibrosis stage, indicating that fibrosis is a mediator in the process of cirrhosis. Additional evidence is needed to assess whether reducing inflammation or ballooning would reduce the rate of fibrosis progression and consequently the incidence of MALO.

FRI-197

Implication of recent international consensus criteria for metabolic hyperferritinemia diagnosis and grade in a large cohort of patient with hepatic iron content assessed by magnetic resonance imaging

Sophie Stephant¹, Oumnia Masrouf², Laine Fabrice¹, Jeff Morcet¹, Yves Gandon¹, Edouard Bardou-Jacquet¹. ¹CHU Rennes, Rennes, France; ²CHU Rennes, Rennes, France

Email: edouard.bardou-jacquet@chu-rennes.fr

Background and aims: Metabolic hyperferritinemia (MHF) is the most frequent cause of elevated ferritin. Recently consensus statement has defined diagnosis criteria and grading based on cutoff value for ferritin and hepatic iron concentration (HIC). The impact of this iron overload on metabolic liver disease remains unclear and there is limited data available on the correlation between serum ferritin and liver iron overload in this setting. The aim of our study was to describe in a large cohort of patients with MHF, the relationship between HIC and ferritin, and evaluate the relevance of the proposed cut-off value.

Method: Patients with the following criteria were included: increased ferritin with available HIC as determined by liver MRI, and fulfilling criteria for MHF: fatty liver (as determined by MRI), or type 2 diabetes or BMI>30, or two or more features of altered metabolism associated with insulin resistance (overweight, increased triglycerides, low HDL cholesterol, increased fasting glucose, arterial hypertension). Patient exceeding WHO recommended alcohol consumption were excluded. Multivariate regression analysis were used to identify determinant of HIC and ferritin. ROC curves were used to assess the cut-off suggested.

Results: A total of 534 patients (age: 58.6 ± 10.6; 79.8% male, BMI 29.5 ± 4.6) were included. Diabetes, arterial hypertension, dyslipidemia, were prevalent in 49.6%, 75.8%, 75.5%, and 29.5% of patients respectively. Mean ferritin was 866 ± 655 µg/L, and HIC was 93 ± 65 µmol/g. Strong correlation between ferritin and HIC was observed (rho = 0.70, p < 0.001). Multivariate analysis revealed significant associations of ferritin with HIC, Aspartate amino transferase (ASAT), transferrin saturation (Tsat), triglycerides, and smoking. HIC was associated with ferritin, Tsat, BMI, smoking, ASAT, hemoglobin, age, and alcohol consumption. Grading according to ferritin was 25.3% grade 1, 42.5% grade 2, and 30.9% grade 3. According to HIC grading were 22.3%, 28.3% and 49.4% respectively. The AUC for ferritin diagnosing HIC ≥ 74 µmol/g (Grade 3 MHF) was 0.83, with a 1000 µg/L cutoff showing 51% sensitivity, 90% specificity. For HIC < 36 µmol/g (Grade 1 MHF), the ferritin AUC was 0.91, with a 550 µg/L cutoff providing 83% sensitivity and 81% specificity. Patients with Grade 3 MHF according to HIC, were characterized by older age, male predominance, lower BMI, higher Tsat, lower ASAT, lower ALT, and lower GGT. Fib4 test results were comparable between MHF grade determined by HIC or ferritin.

Conclusion: Our study confirms the strong correlation between ferritin and HIC in MHF. The proposed ferritin and HIC cutoffs effectively stratify MHF severity, patients with higher grade exhibiting distinct clinical features. However, in our population ferritin tends

to underestimate HIC thus emphasizing the importance of integrating both serum ferritin and HIC for comprehensive MHF assessment.

FRI-198

The infamous ballooned hepatocyte-fact or fiction: combined data from multiple therapeutic trials including more than 10, 000 patients

Julie Dubourg¹, Vlad Ratziu², Jörn M. Schattenberg³, Mazen Nouredin⁴, Naim Alkhouri⁵, Michael Charlton⁶, Stephen A. Harrison⁷. ¹Summit Clinical Research, San Antonio, United States; ²Sorbonne Université, Institute for Cardiometabolism and Nutrition, Hospital Pitié-Salpêtrière, INSERM UMRS 1138 CRC, Paris, France; ³Saarland University Medical Center, Homburg, Germany; ⁴Houston Research Institute, Houston, United States; ⁵Arizona Liver Health, Phoenix, United States; ⁶University of Chicago, Chicago, United States; ⁷Radcliffe Department of Medicine, University of Oxford, Oxford, United Kingdom

Email: jdubourg@summitclinicalresearch.com

Background and aims: Due to its high inter- and intra-reader variability, liver histology has been known as a challenge in metabolic dysfunction-associated steatohepatitis (MASH) drug development. One of the most debated histological features is the hepatocyte ballooning. The definition of ballooning is subjective and is highly variable among international recognized liver pathologists. We aimed to compare characteristics between patients with or without ballooning in the setting of similar fibrosis stages; to investigate if the absence of ballooning in a specific population could be reasonably attributed to reading variability.

Method: We combined screening data from 10 industry-funded MASH phase 2 trials. We compared characteristics between patients with or without ballooning in 2 subgroups: 1) fibrosis stage 3 with presence of inflammation and steatosis; 2) fibrosis stage 2 with presence of inflammation and steatosis.

Results: The subgroup of F3 with the presence of inflammation and steatosis, and with or without ballooning, included 1,030 patients. Among them, 103 (10%) did not have hepatocytes ballooning at central reading. Liver enzymes were significantly higher in patients with ballooning (AST: 51 IU/L, SD: 19; ALT 61 IU/L, SD: 36) compared to patients without ballooning (AST: 37 IU/L, SD: 24; ALT 48 IU/L, SD: 28) (p < 0.0001). Glycated hemoglobin (HbA1c), as a reflect of glycemic control, was higher in patients with ballooning (HbA1c: 6.6%, SD: 1.1) compared to patients without ballooning (HbA1c: 6.2%, SD: 1.0) (p < 0.0001). Platelet count was lower in patients with ballooning (227 G/L, SD: 64) versus 245 G/L (SD: 66) in patients without ballooning (p = 0.009). In a multivariate model, the presence of ballooning was associated with age (p = 0.036), AST (p < 0.0001), HbA1c (p = 0.003), and platelets (p = 0.01). The subgroup of F2 with presence of inflammation and steatosis, included 778 patients. Among them, 178 (23%) did not have hepatocyte ballooning at central reading. Liver enzymes were significantly higher in patients with ballooning (AST: 44 IU/L, SD: 27; ALT 61 IU/L, SD: 38) compared to patients without ballooning (AST: 35 IU/L, SD: 15; ALT 51 IU/L, SD: 27) (p < 0.0001). Glycated hemoglobin (HbA1c), as a reflect of glycemic control, was higher in patients with ballooning (HbA1c: 6.5%, SD: 1.1) compared to patients without ballooning (HbA1c: 6.1%, SD: 1.0) (p < 0.0001). In a multivariate model, the presence of ballooning was associated with age (p = 0.017), AST (p < 0.0001), and HbA1c (p = 0.001).

Conclusion: Based on significant differences in clinical parameters between patients with and without hepatocyte ballooning within a similar subset of fibrosis, the presence of ballooning in this patient population seems to be linked to more severe hepatocyte injury/inflammation and glycemic control rather than the variability of histopathological assessment.

POSTER PRESENTATIONS

FRI-199

Insulin resistance as an independent predictor of metabolic dysfunction-associated steatohepatitis (MASH) severity: combined data from multiple therapeutic trials including more than 10,000 patients

Vlad Ratziu¹, Jörn M. Schattenberg², Naim Alkhouri³, Mazen Nouredin⁴, Michael Charlton⁵, Julie Dubourg⁶, Stephen A. Harrison⁷. ¹Sorbonne Université, Institute for Cardiometabolism and Nutrition, Hospital Pitié-Salpêtrière, INSERM UMRS 1138 CRC, Paris, France; ²Saarland University Medical Center, Homburg, Germany; ³Arizona Liver Health, Phoenix, United States; ⁴Houston Research Institute, Houston, United States; ⁵University of Chicago, Chicago, United States; ⁶Summit Clinical Research, San Antonio, United States; ⁷Radcliffe Department of Medicine, University of Oxford, Oxford, United Kingdom
Email: jdubourg@summitclinicalresearch.com

Background and aims: Metabolic dysfunction-associated steatotic liver disease (MASLD) and metabolic dysfunction-associated steatohepatitis (MASH) are closely associated with the metabolic syndrome, with insulin resistance as a key driver of the disease. Advanced fibrosis, defined as fibrosis stages F3 or F4, is the strongest predictor of major liver-related outcomes. We aimed to evaluate whether the level of fasting insulin at baseline, as a reflect of insulin resistance, is associated with the clinical and histological severity of MASH.

Method: Using combined screening data from 10 industry-funded MASH phase 2 trials, we examined patients with biopsy-proven MASLD/MASH and available fasting insulin levels. 1,085 patients with available data were divided into 3 groups according to the fasting insulin tertiles: lower, ≤ 17.19 mIU/L ($n = 362$); middle, 17.20–28.38 mIU/L ($n = 362$); upper ≥ 28.39 mIU/L ($n = 361$). Univariate and multivariate logistic regressions were performed to predict histological severity.

Results: The upper tertile of fasting insulin was associated with a higher histological severity, especially regarding fibrosis and hepatocyte ballooning. While the proportion of F2 patients were unchanged among insulin tertiles, the proportion of F0–F1 was lower with increased insulin levels (42%, 31% and 19% in the lower, middle and upper tertiles, respectively ($p < 0.0001$)) and the proportion of patients with advanced fibrosis (F3–F4) was higher with increased insulin levels (34%, 45%, and 55% in the lower, middle and upper tertiles, respectively ($p < 0.0001$)). The presence of ballooning was highly associated with insulin levels. The proportion of patients with ballooning was 77%, 88%, and 96% in the lower, middle and upper tertiles, respectively ($p < 0.0001$). There was a slight association with steatosis ($p = 0.030$) and no association with inflammation. The upper tertile was also associated more severe clinical characteristics: higher liver enzymes, HbA1c, LDL and triglycerides, uric acid, CK-18, FIB-4, liver stiffness measurement (LSM) by FibroScan, and ELF. In a multivariate model, the upper insulin tertile was associated with fibrosis ($p < 0.0001$) and ballooning ($p < 0.0001$) severity, independent of HbA1c and diabetes level.

Conclusion: Fasting insulin, as a surrogate of insulin resistance, predicts severity of ballooned hepatocytes and hepatic fibrosis, independent of HbA1c level and diabetes status. Insulin resistance is strongly associated with the severity of MASH.

FRI-200

Magnitude of steatotic liver disease before and after liver transplantation and the impact of immunosuppressive medication: a multidimensional study

Ibrahim Ayada¹, Jiajing Li¹, Jiahua Zhou¹, Laurens van Kleef¹, Willem Pieter Brouwer¹, Pengfei Li¹, Yasir J. Abozaid², Maikel P. Peppelenbosch¹, Harry L.A. Janssen^{1,3}, Mohsen Ghanbari², Luc van der Laan^{4,5}, Robert J. de Knegt¹, Caroline den Hoed^{1,5}, Qiuwei Pan^{1,5}. ¹Department of Gastroenterology and Hepatology,

Erasmus MC-University Medical Center, Rotterdam, The Netherlands, Rotterdam, Netherlands; ²Department of Epidemiology, Erasmus MC-University Medical Center, Rotterdam, The Netherlands, Rotterdam, Netherlands; ³Toronto Center for Liver Disease, Toronto General Hospital, University of Toronto, Canada, Toronto, Canada; ⁴Department of Surgery, Erasmus MC-University Medical Center, Rotterdam, The Netherlands, Rotterdam, Netherlands; ⁵Erasmus MC Transplant Institute, Erasmus MC-University Medical Center, Rotterdam, The Netherlands, Rotterdam, Netherlands

Email: i.ayada@erasmusmc.nl

Background and aims: Steatotic liver disease (SLD) is the fastest growing etiology for liver transplantation (LT) in the USA and it remains of concern post-LT as de novo or recurrent steatosis. We aimed to quantify this burden in the pre- and post-LT setting and to identify associated risk factors through a systematic review and meta-analysis. Moreover, we studied the impact of immunosuppressants on steatosis development in a clinical setting and in an experimental model of 3D cultured human liver organoids.

Method: Medline, Embase, Cochrane Central Register of Controlled Trials and Web of Science were searched from inception to March 2023. Data were extracted and cross-checked by two investigators. Analyses were conducted according to the PRISMA guidelines. Included studies reported on the prevalence of LT related to NAFLD/NASH (non-alcoholic steatohepatitis) or recurrent and de novo NAFLD/NASH alongside associated risk factors. Experimentally, the effects of 8 immunosuppressants on the size and number of formed lipid droplet were studied in human liver organoids. Clinically, we attempted to cross-sectionally verify the experimental results by establishing associations between steatosis development and immunosuppressants use in a cohort of LT recipients ($N = 312$).

Results: The meta-analysis included 80 studies and the estimated prevalence of LT related to NAFLD/NASH was 11% (95% CI 9.0%–13.0%). The prevalence of de novo and recurrent NAFLD was 27% (95% CI 19.0%–34.0%) (16 studies) and 42% (95% CI 32.0%–53.0%) (22 studies), respectively. The prevalence of de novo and recurrent NASH was 7% (95% CI 4.0%–10.0%) (11 studies) and 22% (95% CI 14.0%–26.0%) (17 studies), respectively. In organoids, treatment of mTOR inhibitors reduced the size and number of formed lipid droplets. Consistently, the use of mTOR inhibitor containing regimen ($N = 68$, mean age [SD] 51.33 years [11.79]) was inversely associated with steatosis development in the post-LT setting OR (0.51 95% CI 0.28–0.93 $p = 0.03$) in comparison to any other dual immunosuppressive regimen ($N = 244$, mean age [SD] 48.98 years [13.30]).

Conclusion: This study comprehensively estimated the global burden of SLD related LT, revealing that de novo and recurrence of NAFLD/NASH post-LT are highly prevalent which is affected by metabolic dysfunctions. In 3D cultured human liver organoids mTOR inhibitors could ameliorate steatosis which was cross-sectionally validated in our LT cohort. Our findings call for awareness of this post-LT complication and support further investigating the possible protective effects of mTOR inhibitors on steatosis.

FRI-201

Health care resource utilization for patients diagnosed and at high risk of metabolic dysfunction-associated steatohepatitis in Stockholm, Sweden—a REVEAL-MASH study

Emilie Toresson Grip^{1,2}, Nikolas Scheffer Apecechea³, Ron Basuroy³, Pierre Johansen³, Kamal Kant Mangla³, Helena Skróder², Hannes Hagström⁴. ¹Karolinska Institutet, Stockholm, Sweden; ²Quantify Research, Stockholm, Sweden; ³Novo Nordisk A/S, Denmark, Copenhagen, Denmark; ⁴Karolinska Institutet, Stockholm, Sweden
Email: emilie.toresson-grip@quantifyresearch.com

Background and aims: Metabolic dysfunction-associated steatohepatitis (MASH) is underdiagnosed, which can lead to an underestimation of health care resource utilization (HCRU) for this rapidly growing patient group. Here, we aimed to compare HCRU of patients in Swedish routine clinical care with a formal MASH diagnosis with

patients at high- and low risk of MASH based on the validated Fibrotic NASH Index (FNI).

Method: This study is based on registry data from primary- and secondary care (2010–2020) in Stockholm, Sweden. Healthcare-seeking patients with available liver biochemistry were categorized as high- or low-risk for fibrotic MASH based on the first FNI score (low risk: FNI < 0.1, high risk: FNI ≥ 0.33 and cardiometabolic risk factor (s)), or as MASH-diagnosed (ICD-10 K75.8 in specialist care). Patients with liver diseases other than MASH were excluded. Annualized HCRU was measured after index (first diagnosis or FNI score) and was stratified by reason for visit (major adverse liver outcome [MALO] or major adverse cardiovascular event [MACE]).

Results: In total, 101,166 patients with a FNI score (43,557 at high risk and 57,609 at low risk) and 141 diagnosed patients were included and followed for, on average, 4.4 years (range: 0.01–10.8 years). Patients with a diagnosis and high risk had more hospitalizations (total and MALO/MACE-related), longer length of stay, as well as more specialist visits and liver-related lab tests, compared to those at low risk. The mean/median for hospitalization occurrences (total) was 4.1/0.36, 1.6/0.36 and 0.64/0 for diagnosed, high-risk and low-risk patients, respectively (p for all comparisons < 0.001). For MALO- and MACE-related hospitalizations, the corresponding numbers were 2.0/0, 0.0068/0 and 0.00026/0 (MALO; p for all < 0.001) and 0.0070/0, 0.24/0, 0.080/0 (MACE; p for all < 0.033). The mean/median length of stay was 64/18, 19/4.9 and 13/3.3 (p for all < 0.001), the number of visits to a hepatology/gastroenterology clinic was 3.7/0.69, 0.070/0 and 0.037/0 (p for all < 0.001), and the number of AST and ALT tests was 19/3.7, 6.1/1.9 and 3.8/1.6 (p for all < 0.001), respectively. Finally, the number of primary care visits was 6.1/0, 7.2/2.4 and 4.6/2.1 (p for all < 0.001). Out of all diagnosed patients, 38% had cirrhosis at index, compared to only 0.3% and 0.1% of patients at high and low risk, respectively. Sub-group analyses revealed similar differences in HCRU between groups after exclusion of patients with cirrhosis at baseline.

Conclusion: The higher HCRU across all types of visits for diagnosed- and high-risk patients indicate a high future burden on the health care system for this growing patient group, pointing to an urgent need for treatment preventing progression to cirrhosis.

FRI-202

Health-Related Quality of Life (HRQL) assessments in a 52-Week, double-blind, randomized, placebo-controlled phase 3 study of Resmetirom (MGL-3196) in patients with non-alcoholic steatohepatitis (NASH) and fibrosis (MAESTRO-NASH)

Zobair Younossi^{1,2}, Maria Stepanova^{3,4}, Andrei Racila^{4,5}, Linda Henry^{5,6}, Keith Miller⁷, Dominic Labriola⁷, Rebecca Taub⁷, Fatema Nader^{5,8,9}, ¹The Global NASH Council, Washington, United States; ²Beatty Liver and Obesity Research Program, Inova Health System, Falls Church, VA, United States; ³The Global NASH Council, Washington DC, United States; ⁴Beatty Liver and Obesity Research Program, Falls Church, United States; ⁵The Global NASH Council, Washington DC, United States; ⁶Beatty Liver and Obesity Research Program, Falls Church, United States; ⁷Madrigal Pharmaceuticals, West Conshohocken, United States; ⁸Beatty Liver and Obesity Program, Falls Church, United States; ⁹Center for Outcomes Research in Liver Disease, Washington DC, United States

Email: zobair.younossi@cldq.org

Background and aims: NASH, recently renamed as Metabolic Dysfunction-Associated Steatohepatitis (MASH), is highly prevalent liver disease and associated with adverse clinical outcomes and impaired HRQL. Resmetirom is a selective thyroid hormone receptor- β agonist that leads to improvement of fibrosis and resolution of NASH. The aim was to assess HRQL in NASH patients treated with resmetirom.

Method: Non-cirrhotic NASH patients with confirmed or suspected fibrosis were enrolled in a 52-week double-blind randomized placebo-controlled Phase 3 clinical trial with serial biopsy assessments (MAESTRO-NASH, NCT03900429). HRQL was assessed using

Chronic Liver Disease Questionnaire-NASH (CLDQ-NASH; 6 domains and score range 1–7) and Liver Disease Quality of Life (LDQOL; 17 domains and score range 0–100) at baseline, week 24, and week 52. Changes in HRQL scores from subjects' own baseline scores were evaluated in patients receiving resmetirom vs. placebo and compared between subjects with vs. without biopsy response defined as meeting the study histologic end point (improvement of histologic fibrosis without worsening of NASH or resolution of NASH without worsening of fibrosis via in-window baseline/week 52 paired biopsies). Minimally clinically important Difference (MCID) in HRQL scores were defined as previously published.

Results: 966 mITT patients were included (57 ± 11 years, 44% male, 67% type 2 diabetes; 60% baseline fibrosis stage F3, 33% F2, 5% F1b, 84% NAS ≥ 5). Of those, 323 received resmetirom 100 mg, 322 resmetirom 80 mg, and 321 placebo. By weeks 24 and 52, patients receiving both doses of resmetirom experienced improvement of HRQL scores from baseline levels in Worry domain of CLDQ-NASH (mean +0.21 to +0.24, p < 0.05). At week 52, subjects who met the histologic end point after treatment with resmetirom (100 mg and 80 mg pooled) experienced improvement in several HRQL domains: Worry (WO) of CLDQ-NASH +0.46 (41% met MCID), Role Emotional (RE) of LDQOL +3.0 (28% met MCID), Health Distress (HD) of LDQOL +8.1 (38% MCID), Stigma (ST) of LDQOL +3.5 (39% MCID), and total LDQOL +2.2 (35% MCID) (all p < 0.05). Similar improvements in these HRQL domains were observed in biopsy responders from 100 mg and 80 mg resmetirom when groups were studied separately, contrasted by no improvements in both the placebo group and resmetirom biopsy non-responders. In other domains of LDQOL and CLDQ-NASH, MCID was met by 22–41% of resmetirom responders. Biopsy responders with baseline F3 had similar or more pronounced improvements of HRQL (WO +0.57 in F3 vs. +0.32 in F1b/F2, RE +3.6 vs. +1.7, HD +8.8 vs. +7.6, ST +2.9 vs. +5.2, total LDQOL +2.3 vs. +2.5) in comparison to those responders with baseline stage of F2 or F1b.

Conclusion: Patients with NASH who achieve improvement of fibrosis or resolution of NASH with resmetirom experience significant improvements in multiple domains of HRQL by the end of 52-week-long treatment.

FRI-203

Validation of optimal liver biopsy size for reliable quantitation of fibrosis severity in different areas and structures of liver lobule using second harmonic generation microscopy with artificial intelligence analyses

Nikolai V. Naoumov¹, Yayun Ren², Elaine Chng², Kutbuddin Akbary², Dean Tai², Jonathan Fallowfield³, Timothy Kendall³, David E Kleiner⁴, Arun J. Sanyal⁵, ¹Royal College of Physicians, London, United Kingdom; ²HistoIndex Pte Ltd, Singapore, Singapore; ³Institute for Regeneration and Repair, University of Edinburgh, Edinburgh, United Kingdom; ⁴National Cancer Institute, Bethesda, MD, United States; ⁵Division of Gastroenterology, Hepatology and Nutrition, Department of Internal Medicine, Virginia Commonwealth University, Richmond, VA, United States

Email: nikolainauoumov@yahoo.com

Background and aims: Liver fibrosis is a key prognostic determinant for clinical outcomes in patients with metabolic dysfunction-associated steatohepatitis (MASH) and a key end point for clinical trials in MASH. Adequate size of liver specimens is essential for accurate histopathology examination to avoid sampling variability due to heterogeneity of fibrosis, sampling error, or distorted architecture of liver lobules and their anatomical structures. Digital pathology is increasingly used in MASH trials and provides greater sensitivity and precision in determining fibrosis dynamics, however, the influence of sample size on fibrosis quantitation using this technology and the agreement with pathologist's staging is poorly defined. The present study aimed to systematically evaluate the impact of liver specimen size on digital qFibrosis readouts.

POSTER PRESENTATIONS

Method: Wedge biopsies (n = 100) were obtained from liver resections or explants with 20 specimens for each pathologist's determined NASH-CRN fibrosis stage F0 to F4. Unstained sections were examined by Second Harmonic Generation/Two Photon Excitation Fluorescence (SHG/TPEF) microscopy with artificial intelligence (AI) software HistoHepa©. The severity of liver fibrosis was determined by analyzing 184 fibrosis parameters in portal tract (PT), periportal (PP, zone 1), perisinusoidal (PS, zone 2), pericentral (PC, zone 3) and central vein (CV) regions. Virtual needle biopsies were examined from each specimen with a fixed width of 0.9 mm and varying length from 5 to 30 mm. qFibrosis was determined individually for each virtual biopsy specimen and key parameters included the number of PT and CV; % fibrosis area in PT and CV; % fibrosis area in PP, PS and PC (zone 1, 2 and 3) of the liver lobule.

Results: qFibrosis assessment of wedge biopsies showed excellent concordance with NASH-CRN stages ($r = 0.92$; $p < 0.001$). The qFibrosis Coefficient of Variation (CoV) in virtual biopsies was very low for the number of PT-[median (lower quartiles, upper quartiles)]-0.17 (0.12, 0.24), or for % fibrosis in PT area-0.19 (0.13, 0.29), but highest for % fibrosis in CV area 0.50 (0.33, 0.74). Fibrosis assessment in different zones showed the CoV of 0.15 (0.10, 0.20), 0.09 (0.06, 0.14) and 0.35 (0.24, 0.53) for PP (zone 1), PS (zone 2) and PC (zone 3), respectively. Liver specimens with 10 mm length had on average 10 PTs and 5 CVs. The CoV progressively decreased in longer specimens and was consistently < 0.2 for all parameters in biopsies longer than 20 mm.

Conclusion: qFibrosis readouts provide a standardized and highly reproducible assessment of liver fibrosis. The Coefficient of Variation is lower for PT and higher for CV-related parameters, indicating that portal tracts are less prone to sampling variability. qFibrosis assessment reduces errors due to sampling variability by precise and reproducible quantification of features with a higher Coefficient of Variation.

FRI-206-YI

Prevalence and severity of steatotic liver disease in 3, 123 at-risk individuals from the background population

Camilla Dalby Hansen¹, Johanne Kragh Hansen¹, Mads Israelsen¹, Peter Andersen¹, Laura Pikkupera², Katrine Lindvig¹, Maria Kjærgaard¹, Helle Schnefeld¹, Sara Stinson², Julie Tellerup¹, Maria Fogt¹, Nikolaj Torp¹, Katrine Tholstrup Bech¹, Katrine Thorhauge¹, Stine Johansen¹, Ida Ziegler Spedtsberg¹, Emil Deleuran Hansen¹, Ida Falk Villesen¹, Torben Hansen², Aleksander Krag¹, Maja Thiele¹. ¹Department of Gastroenterology and Hepatology, Odense University Hospital, Odense, Denmark; ²Center for Basic Metabolic Research, University of Copenhagen, Copenhagen, Denmark

Email: camilla.dalby.hansen@rsyd.dk

Background and aims: Characterization of the prevalence and severity for the newly defined steatotic liver disease (SLD) categories represent a significant knowledge gap. Our objective was to investigate the prevalence of SLD in the background population with either cardiometabolic or alcohol risk factors. Additionally, we aimed to explore the severity of disease and evaluate the impact of previous alcohol intake on individuals with metabolic dysfunction-associated steatotic liver disease (MASLD).

Method: We conducted a cross-sectional population based study. Participants were recruited based on either 1) cardiometabolic risk defined as BMI ≥ 30 or type 2 diabetes without excessive alcohol consumption, or 2) alcohol as a risk factor defined as a history of excessive alcohol consumption exceeding 24 g/day (W) and 36 g/day (M) for ≥ 5 years. We performed same-day assessments including liver stiffness measurements (LSM), controlled attenuation parameter (CAP) and cardiometabolic risk profiling. We used a validated CAP cut-off of ≥ 248 dB/m as marker of liver steatosis and LSM as a marker of liver disease severity.

Results: We included 3123 at-risk individuals; 1599 with cardiometabolic risk and 1524 with alcohol risk. In the cardiometabolic risk group 1239 (77%) had SLD of whom 1174 (95%) were categorized as MASLD and 56 (5%) as MetALD. In the alcohol risk group 996 (63%) had SLD of whom 431 (45%) were categorised as MASLD, 347 (36%) as MetALD and 188 (19%) as ALD. The prevalence of LSM ≥ 8 kPa were 0.2% in those without SLD (n = 2), 13% in MASLD (n = 211), 12% in MetALD (n = 46) and 24% in ALD (n = 48). The prevalence of LSM ≥ 12 kPa were 0% in those without SLD (n = 0), 5% in MASLD (n = 73), 5% in MetALD (n = 18) and 13% in ALD (n = 25). Compared to individuals without SLD, the odds ratio of LSM ≥ 8 kPa was 68.2 in MASLD (16.9 to 275; $p < 0.0001$), 59.4 in MetALD (14.3 to 245; $p < 0.0001$) and 147.4 in ALD (35.45 to 613; $p < 0.0001$). In individuals with MASLD a previous alcohol intake of ≥ 50 g/d (W)/ ≥ 60 g/d (M) associated with LSM ≥ 12 kPa (OR = 1.82 (1.02 to 3.26; $P = 0.044$)), whereas 20–50 g/d (W)/30–60 g/d (M) did not associate with LSM ≥ 12 kPa (OR = 0.90 (0.40 to 2.01; $P = 0.792$)). Furthermore, a previous excessive alcohol intake of ≥ 20 years associated with LSM ≥ 12 kPa in individuals with MASLD (OR = 2.09 (1.11 to 3.95; $P = 0.023$), whereas a previous excessive alcohol intake from 5 to 20 years did not (OR = 1.00 (0.51 to 1.95); $P = 0.993$)).

Conclusion: Our study reveals a 77% prevalence of SLD in individuals with metabolic risk factors and a 63% prevalence in those with alcohol risk factors. The severity of SLD, as indicated by LSM ≥ 8 kPa, demonstrated rates of 13% in MASLD, 12% in MetALD, and 24% in ALD. Significantly, our findings highlight the impact of long-term and excess alcohol intake on liver disease severity among patients initially classified as MASLD. Our study suggests that the nomenclature for SLD should incorporate historical alcohol intake.

FRI-207-YI

Sarcopenia in metabolic-dysfunction associated steatotic liver disease (MASLD): unraveling its role in cardiovascular damage

Annalisa Cespiati^{1,2}, Rosa Lombardi^{2,3}, Giordano Sigon^{2,4}, Floriana Santomena^{2,3}, Matteo Carlomagno², Margaux Couffon⁴, Beatrice Martino⁴, Jian Huang⁴, Daniel Smith^{2,3}, Giuseppina Pisano³, Giovanna Oberti³, Roberta Forlano⁴, Pinelopi Manousou⁴, Salvatore Petta⁵, Anna Ludovica Fracanzani^{2,3}. ¹SC Medicina ad Indirizzo Metabolico, Fondazione IRCCS Cà Granda Ospedale Maggiore Policlinico, Department of Pathophysiology and Transplantation, University of Milan, Milan, Italy; ²Department of Pathophysiology and Transplantation, University of Milan, Milan, Italy; ³SC Medicina ad Indirizzo Metabolico, Fondazione IRCCS Cà Granda Ospedale Maggiore Policlinico, Milan, Italy; ⁴Liver Unit, Division of Digestive Diseases, Department of Metabolism, Digestion and Reproduction, Faculty of Medicine, Imperial College, London, United Kingdom; ⁵Section of Gastroenterology and Hepatology, PROMISE, University of Palermo, Palermo, Italy

Email: annalisa.cespiati@unimi.it

Background and aims: Patients with MASLD are prone to sarcopenia with the complication rate and severity increasing as fibrosis progresses. MASLD is also associated with subclinical and clinical cardiovascular disease (CVD). However, the impact of sarcopenia on CVD in MASLD patients is undefined. Aims: to assess the impact of sarcopenia and metabolic comorbidities on CVD in a multicentric cohort of MASLD patients.

Method: We included consecutive patients with MASLD followed up in specialised hepatology clinics in Milan, Palermo, and London. Sarcopenia was defined as a skeletal muscle mass/height² $\leq 10.75/ \leq 6.75$ kg/m² (males/females) by bioimpedance. CVD was defined as presence of carotid plaques on Doppler-US. High and very high CV risk was defined by the scores specified for each patient outlined in the ESC 2021 guidelines.

Results: 876 MASLD patients were enrolled, with prevalence of sarcopenia at 34%. Mean BMI was 30 ± 5 kg/m² (44% with BMI ≥ 30 kg/m²), mean age 52 ± 12 years, while 62% were male, 43% had hypertension, 29% type-2 diabetes. Overall, 35% (307) patients had

carotid plaque, 60% (526) had high and 12% (105) very high CV risk. Sarcopenic patients were more frequently male (90 vs 48%, $p < 0.001$), had lower BMI (27.3 vs 31.6 kg/m², $p < 0.001$) and waist circumference (WC) (101 vs 107 cm, $p = 0.003$) compared to non-sarcopenic. There was no difference in terms of prevalence of age (51 vs 52 years, $p = 0.6$), severe steatosis (62% vs 66%, $p = 0.19$), carotid plaques (33% vs 36%, $p = 0.4$), and high/very high CV risk (73% vs 71%, $p = 0.14$). On multivariate analysis (adjusted for age, sex, and factors associated with sarcopenia on univariate analysis) sarcopenia was independently associated with lower BMI (OR 0.6, CI 95% 0.5–0.7, $p < 0.001$), lower waist circumference (OR 0.9, CI 95% 0.8–0.94, $p < 0.001$), male gender (OR 14.2, CI 95% 8.4–24, $p < 0.001$), and age (OR 1.02, CI 95% 1.01–1.04, $p = 0.003$). Analyzing different metabolic subgroups, in diabetic patients, prevalence of carotid plaques was higher in sarcopenic vs non-sarcopenic (56% vs 30%, $p = 0.04$). In hypertensive patients, sarcopenia remained an independent risk factor for carotid plaques (OR 1.9, CI 95% 1.05–3.5, $p = 0.03$) and high/very high CV risk (OR 3.0, CI 95% 1.2–7.2, $p = 0.01$) in multivariate analysis adjusted for age, sex, diabetes, dyslipidemia, smoke and BMI, whereas in non-diabetic subjects for high/very high CV risk (OR 1.44, CI 95% 1.1–2.1, $p = 0.04$).

Conclusion: MASLD patients, particularly non-obese and male, have a high prevalence of sarcopenia. Despite lower BMI, sarcopenic patients exhibit a similar extent of hepatic steatosis and CVD compared to those without sarcopenia. For those with additional metabolic risk factors like diabetes and hypertension, the risk of CVD is aggravated by sarcopenia. A prompt evaluation and treatment of sarcopenia could prevent the onset of CVD, particularly if hypertensive.

FRI-208

qBallooning: AI-based ballooned hepatocyte detection and quantification by second harmonic generation/two photon excitation microscopy

David E. Kleiner¹, Andrew D. Clouston², Zachary Goodman³, Cynthia D. Guy⁴, Elizabeth M. Brunt⁵, Carolin Lackner⁶, Dina G. Tiniakos^{7,8}, Aileen Wee⁹, Matthew Yeh¹⁰, Wei Qiang Leow¹¹, Elaine Chng¹², Yayun Ren¹², George Boon Bee Goh¹³, Elizabeth E. Powell^{14,15}, Mary E. Rinella¹⁶, Arun J Sanyal¹⁷, Brent A. Neuschwander-Tetri¹⁸, Zobair Younossi¹⁹, Michael Charlton²⁰, Vlad Ratziu²¹, Stephen A. Harrison^{22,23}, Dean Tai¹², Quentin M. Anstee^{7,24}. ¹Laboratory of Pathology, Center for Cancer Research, National Cancer Institute, National Institutes of Health, Bethesda, Maryland, United States; ²Molecular and Cellular Pathology, University of Queensland and Envoi Specialist Pathologists, Brisbane, Australia; ³Pathology Department, and Center for Liver Diseases, Inova Fairfax Hospital, Falls Church, Virginia, United States; ⁴Department of Pathology, Duke University Health System, Durham, NC, United States; ⁵Department of Pathology and Immunology, Washington University School of Medicine, Saint Louis, Missouri, United States; ⁶Institute of Pathology, Medical University of Graz, Graz, Austria; ⁷Translational and Clinical Research Institute, Faculty of Medical Sciences, Newcastle University, Newcastle upon Tyne, United Kingdom; ⁸Dept of Pathology, Aretaieion Hospital, National and Kapodistrian University of Athens, Athens, Greece; ⁹Department of Pathology, Yong Loo Lin School of Medicine, National University of Singapore, National University Hospital, Singapore, Singapore; ¹⁰Department of Pathology, University of Washington, Seattle, Washington, United States; ¹¹Department of Anatomical Pathology, Singapore General Hospital, Singapore and Duke-NUS Medical School, Singapore, Singapore; ¹²HistoIndex Pte Ltd, Singapore, Singapore; ¹³Department of Gastroenterology and Hepatology, Singapore General Hospital, Singapore, Singapore; ¹⁴Centre for Liver Disease Research, Faculty of Medicine, University of Queensland, Translational Research Institute, Brisbane, Queensland, Australia; ¹⁵Department of Gastroenterology and Hepatology, Princess Alexandra Hospital, Brisbane, Queensland, Australia; ¹⁶Division of

Gastroenterology and Transplant institute, Pritzker School of Medicine, University of Chicago, Chicago, Illinois, United States; ¹⁷Department of Internal Medicine, School of Medicine, Virginia Commonwealth University, Richmond, Virginia, United States; ¹⁸Division of Gastroenterology and Hepatology, Saint Louis University, Saint Louis, Missouri, United States; ¹⁹Betty and Guy Beatty Center for Integrated Research, Inova Health System, Falls Church, Virginia, United States; ²⁰Center for Liver Diseases, and Transplantation Institute, University of Chicago, Chicago, Illinois, United States; ²¹Department of Hepatology, Sorbonne University and Pitié-Salpêtrière Hospital, Paris, France; ²²Pinnacle Clinical Research, San Antonio, Texas, United States; ²³Hepatology, Radcliffe Department of Medicine, University of Oxford, Oxford, United Kingdom; ²⁴Newcastle NIHR Biomedical Research Centre, Newcastle upon Tyne Hospitals NHS Foundation Trust, Newcastle upon Tyne, United Kingdom
Email: Dean.Tai@histoindex.com

Background and aims: Presence of ballooned hepatocytes (BH) differentiates between metabolic dysfunction-associated steatotic liver (MASL) and metabolic dysfunction-associated steatohepatitis (MASH). The development of qBallooning (qB), an artificial intelligence (AI)-based method for ballooned hepatocytes detection and quantification using Second Harmonic Generation and Two-Photon Excitation images, is useful for pathological diagnosis and feature extraction. This study describes the development and performances of qB algorithm.

Method: A total of 9 expert pathologists conducted three rounds of readings with a total of 95 images ($n = 30, 30, 35$). qB annotated each of the BH in these images and the pathologists reviewed each individual BH afterwards. The pathologists labelled each BH with a yes or no to show if they agreed with qB. qB was further improved during these three rounds, and the new qB was used for the next round of reading throughout the process. The final qB determined BH by overlapping cells detected in both raw and 90°-rotated images. The performance of qB was defined as agreement of at least 5 pathologists, and the definition of the positive diagnostic criteria for MASH was established when ≥ 5 BH were identified in each image.

Results: At the individual cell level, qB exhibited a true positive (TP) of 55% and false positive (FP) of 8%, with BH concurrence from a minimum of 5 pathologists. When we used concurrence from a minimum of 3 pathologists, performance metrics improved TP to 89% but with a higher FP of 42%. On the diagnostic level, a diagnosis of no ballooning (defined as < 5 BH) achieved a 100% TP and 0% FP with agreement from over 5 pathologists.

Conclusion: The study's findings have implications in MASH drug trial context, specifically in the patient inclusion and efficacy evaluation phases. In the patient inclusion phase, employing qB for AI annotation of BH can assist pathologists to achieve a higher consistency on ballooning grade 0 diagnosis. This approach can potentially reduce screening failure rates for clinical trial inclusion. During the efficacy evaluation phase of MASH drug trials, AI annotation on BH can assist pathologists in reviewing and eliminating falsely identified cells. Additionally, utilizing the algorithm's performance metrics (55% TP and 8% FP) with agreement from at least 5 pathologists, the relative change from baseline in the number of BH per unit area can be measured and quantified thus providing an additional tool to assess changes in disease activity.

FRI-209

Differential prevalence and prognostic value of metabolic syndrome components among metabolic-dysfunction associated steatotic liver disease (MASLD) patients

Jesse Pustjens¹, Laurens van Kleef¹, Harry L.A. Janssen^{1,2}, Robert J. de Kneft¹, Willem Pieter Brouwer¹. ¹Department of Gastroenterology and Hepatology, Erasmus MC University Medical Centre, Rotterdam, Netherlands; ²Toronto Centre for Liver Disease, Toronto General Hospital, University Health Network, Toronto, Canada
Email: j.pustjens@erasmusmc.nl

POSTER PRESENTATIONS

Background and aims: Metabolic-dysfunction associated steatotic liver disease (MASLD) is increasingly prevalent in the general population and a growing global health concern. This study aims to describe the cardiometabolic burden of the MASLD population and identify those at highest risk of adverse outcomes and all-cause mortality.

Method: We analysed individuals with MASLD enrolled in the National Health and Nutrition Survey (NHANES) III (N=3, 628) and NHANES 2017–2020 (N=2, 618) studies. MASLD was defined according to the clinical practice guidelines. Hepatic steatosis was assessed by ultrasonography and controlled attenuation parameter (CAP). The primary end points were all-cause mortality and liver stiffness measured by Fibroscan. Significant liver fibrosis was defined as a liver stiffness measurement (LSM) of ≥ 8 KiloPascal (kPa). Cox regression models were adjusted for age, sex, race, marital status, education, and smoking, and results were stratified according to three age groups (20–40, 40–60, 60–80).

Results: Among the total NHANES III MASLD population (median age = 48 [36–62], 44.8% males), 65% had ≥ 3 cardiometabolic disorders. Most frequent were obesity (89.1%), (pre)diabetes (66.6%) and hypo-HDL (54.7%). During a median follow-up of 22.3 [16.9–24.2] years, 1,405 deaths occurred. Hypertension (aHR 1.42, 95% CI 1.26; 1.61), (pre)diabetes (aHR 1.28, 95% CI 1.09; 1.49), and hypertriglyceridemia (aHR 1.19, 95% CI 1.05; 1.34) were the strongest predictors of all-cause mortality. Consistent results were obtained in the NHANES 2017–2020 cohort for the association of cardiometabolic factors and liver fibrosis among the MASLD population. Here, an increased waist circumference (OR 3.45, 95% CI 1.44; 8.25), (pre)diabetes (OR 1.90, 95% CI 1.44; 2.25) and hypertension (aHR 1.84, 95% CI 1.40; 2.43) showed the strongest associations with liver fibrosis.

Conclusion: MASLD patients vary greatly in their cardiometabolic burden and consequently, in their prognosis and risk for significant liver fibrosis. These results highlight MASLD as a disease spectrum rather than a single disease entity, necessitating an individualized treatment approach, also for novel therapeutic regimens assessed in clinical trials.

FRI-210

Increased risk of cancers in metabolic dysfunction-associated steatotic liver disease and MetALD

Yewan Park¹, Jooyi Jung², Gi-Ae Kim¹. ¹Department of Internal Medicine, College of Medicine, Kyung Hee University Hospital, Kyung Hee University, Seoul, Korea, Rep. of South; ²Department of Biostatistics, Korea University, Seoul, Korea, Rep. of South
Email: antiankle@naver.com

Background and aims: Cancer is one of the most common causes of death in non-alcoholic fatty liver disease (NAFLD). With metabolic dysfunction-associated steatotic liver disease (MASLD) now recognized as a replacement of NAFLD and the introduction of a new category of MASLD with increased alcohol intake (MetALD), this study aims to explore the associated cancer risks under this revised nomenclature.

Method: This nationwide cohort study included 3,596,709 participants who underwent a health check-up in 2011 in South Korea. Steatotic liver disease (SLD) was defined as a fatty liver index ≥ 30 . Participants were categorized into four exclusive groups: MASLD, MetALD, other combination etiology, and no SLD. To estimate the cause-specific adjusted hazard ratios (aHRs) for cancer risk, Cox proportional hazards regression was employed.

Results: Over 34 million person-years, 285,845 participants (7.9%) developed cancers. Compared with no SLD, MASLD (aHR, 1.02; 95% CI, 1.01–1.03), MetALD (aHR, 1.06; 95% CI, 1.04–1.08), and other combination etiology (aHR, 1.38; 95% CI, 1.35–1.40) were associated with an increased risk of all cancer. The risk of liver cancer increased in the order of no SLD, MASLD (aHR, 1.17; 95% CI, 1.12–1.22), MetALD (aHR, 1.50; 95% CI, 1.40–1.60), and other combination etiology (aHR, 5.21; 95% CI, 4.97–5.45). Compared with no SLD, MASLD (aHR, 1.13;

95% CI, 1.11–1.15), MetALD (aHR, 1.30; 95% CI, 1.26–1.34), and other combination etiology (aHR, 1.27; 95% CI, 1.23–1.31) had increased risk of gastrointestinal cancer such as the esophagus, stomach, colorectal, pancreas, and biliary cancer. Compared with no SLD, MASLD (aHR, 1.07; 95% CI, 1.04–1.10) and other combination etiology (aHR, 1.13; 95% CI, 1.07–1.20) had a higher risk of lung cancer. Little difference was observed in the risk of hormone-sensitive cancer.

Conclusion: This study showed the newly suggested MASLD and MetALD have an increased risk of all cancers, particularly liver and gastrointestinal cancer. The findings suggest that modifying MASLD and alcohol consumption can serve as a preventative strategy against cancer risk.

FRI-211

The presence of autoimmune characteristics in metabolic associated steatosis liver disease patients increases the risk of liver disease progression. Study from the multicentric spanish register (HEPAMET)

Anna Soria^{1,2,3}, Alba Díaz^{2,4,5}, Paula Iruzubieta⁶, MTeresa Salcedo⁷, Rosa María Martín Mateos^{3,8}, Marlene Padilla^{1,2}, Maria Teresa Arias Loste⁶, Juan Manuel Pericás^{5,9}, Alba Jiménez-Massip¹⁰, Ana Ferrer¹¹, Carolina Jiménez González¹², Cristian Perna¹¹, Sergio Muñoz Martínez¹⁰, Zyanaya Calixto⁷, Clara Sabiote¹⁰, Ignasi Olivas^{1,2}, Helena Hernández Evole¹, Javier Crespo^{3,6}, Agustín Albillos^{3,13}, Pere Ginès^{1,2,3,14}, María Carlota Londoño^{1,2,3,15}, Isabel Graupera^{1,2,3,15}. ¹Liver Unit Hospital Clínic, Universidad de Barcelona, Barcelona, Spain; ²Fundació de Recerca Clínic Barcelona-Institut d'Investigacions Biomèdiques August Pi i Sunyer (FRCB-IDIBAPS), Barcelona, Spain; ³Centro de Investigación Biomédica en Red de Enfermedades Hepáticas y Digestivas (CIBEREHD), Barcelona, Spain; ⁴Servicio de Anatomía Patológica, Centro de diagnóstico biomédico, Hospital Clínic de Barcelona, Barcelona, Spain; ⁵Centro de Investigación Biomédica en Red de Enfermedades Hepáticas y Digestivas, Barcelona, Spain; ⁶Gastroenterology and Hepatology Department, Marqués de Valdecilla University Hospital, Clinical and Translational Digestive Research Group, IDIVAL, Santander, Spain; ⁷Servicio de Anatomía Patológica, Hospital Universitari Vall d'Hebron de Barcelona, Universidad Autónoma de Barcelona, Barcelona, Spain; ⁸Servicio de Digestivo, Hospital Universitario Ramón y Cajal, IRYCIS, Madrid, Spain; ⁹Liver Unit, Digestive Diseases Division, Vall d'Hebron University Hospital, Vall d'Hebron Institute of Research (VHIR), Vall d'Hebron Barcelona Hospital Campus, Universitat Autònoma de Barcelona, Barcelona, Spain; ¹⁰Liver Unit, Vall d'Hebron Hospital Universitari, Vall d'Hebron Institut of Research (VHIR), Vall d'Hebron Barcelona Hospital Campus, Barcelona, Spain; ¹¹Servicio de Anatomía Patológica, Hospital Universitario Ramón y Cajal, Madrid, Spain; ¹²Gastroenterology and Hepatology Department, Marqués de Valdecilla University Hospital, Clinical and Translational Digestive Research Group, IDIVAL, Barcelona, Spain; ¹³Servicio de Digestivo, Hospital Universitario Ramón y Cajal, IRYCIS, Madrid, Spain; ¹⁴School of Medicine and Health Sciences, University of Barcelona, Barcelona, Spain; ¹⁵School of Medicine and Health Sciences, University of Barcelona, Barcelona, Spain
Email: asoriac@clinic.cat

Background and aims: Patients with metabolic associated steatosis liver disease (MASLD) frequently have (15–30%) positive autoantibodies (Ab). Preliminary data suggest that the presence of serologic and histological characteristics of autoimmune hepatitis (AIH) in MASLD patients may increase cirrhosis development and decompensation. The aim of this study was to assess the presence of AIH characteristics in MASLD patients and determine their role in disease prognosis.

Method: Retrospective multicenter cohort study (Spanish HEPAMET register) including patients ≥ 18 years with histologic diagnosis of MASLD and at least 1 year of follow-up. Patients with hepatocarcinoma and other concomitant liver diseases were excluded. The presence of Ab $\geq 1/40$ (ANA, ASMA), gamma globulins (IgG ≥ 12 mg/dl or Gg $\geq 18\%$) and histological features of AIH (interface hepatitis

and/or moderate-severe portal inflammation) were assessed and their relationship with prognosis was analyzed.

Results: Out of the 651 patients in HEPAMET registry, 463 had autoimmune serologies available and 316 had histology assessment of AIH features and therefore were analyzed. Median age of 58 years (IQR 51–64), 48% women, BMI 33.2 kg/m² (IQR 29.7–37.1), liver stiffness 11.4 kPa (IQR 9–16.9) and CAP 330 dB/m (IQR 300–363). After a median follow-up of 10.9 years (IQR 7.5–15, 5), 145 (31%) patients had liver cirrhosis, 49 (11%) hepatic decompensation, 4 (1%) underwent a liver transplantation and 26 (6%) died. Two hundred and sixty-five (36%) had elevated IgG/Gg, 217 (47%) positive Ab (172–37% ANA and 121–26% ASMA) and 93 (20%) had concomitant positive Ab and high Gg/IgG levels. Eighty-two patients (18%) had histological features of AIH. Of those, 54 (12%) had elevated IgG/Gg or positive Ab, and 25 (5.4%) met all three criteria. The presence of any serologic criteria of AIH (in combination or alone) increased the risk of cirrhosis (OR 2.4; CI95%, 1.64–3.68; $p < 0.001$ for positive Ab and OR 2.8; CI95%, 1.7–4.5; $p < 0.001$ for positive Ab with elevated Gg/IgG), decompensation (OR 3.9; CI95%, 2.1–7.3; $p < 0.001$ for positive Ab and OR 5.9; CI95%, 2.8–12.6; $p < 0.001$ for positive Ab with elevated Gg/IgG) and death (OR 2.6; CI95%, 1.1–6.1; $p = 0.016$ for positive Ab with elevated Gg/IgG). Patients with isolated histological features of AIH had higher liver stiffness (13 vs 8.2 kPa; $p = 0.01$) and increased risk of death (OR 5.4; CI95%, 1–9–15.4; $p = 0.004$), but only those with positive serologic tests (Ab + IgG/gg) on top of histological AIH had increased risk of cirrhosis (OR 2.5; CI95%, 1.08–5.7; $p = 0.027$) and decompensation (OR 3.55; CI95%, 1.42–8.86; $p = 0.004$).

Conclusion: The presence of AIH serological markers is frequent in MASLD patients and is associated with an increased risk of cirrhosis development, decompensation and death. Assessing the presence of AIH features in patients with MASLD could help to identify a subgroup of patients with worse prognosis.

FRI-213

Low-to-moderate alcohol consumption is associated with increased fibrosis in subjects with metabolic dysfunction-associated steatotic liver disease

David Marti-Aguado¹, José Luis Calleja Panero², Eduardo Vilar Gomez³, Paula Iruzubietta⁴, Juan Carlos Rodriguez Duque⁵, María Del Barrio⁶, Laura Puchades⁷, Jesús Rivera⁸, Christie Perelló⁹, Angela Puente¹⁰, Concepción Gómez¹¹, Desamparados Escudero-García¹², Miguel Serra¹², Ramon Bataller¹³, Javier Crespo¹⁴, María Teresa Arias Loste¹⁵. ¹Clinic University Hospital of Valencia, INCLIVA Biomedical Research Institute, Valencia, Spain; ²Hospital Puerta de Hierro, Madrid, Spain; ³Indiana University School of Medicine, Indianapolis, United States; ⁴Hospital Marques de Valdecilla, Santander, Spain; ⁵Universitary Hospital Marqués de Valdecilla, Santander, Spain; ⁶Marques de Valdecilla University Hospital, Marqués de Valdecilla Research Institute (IDIVAL), Santander, Spain; ⁷INCLIVA Biomedical Research Institute, Valencia, Spain; ⁸Vall d'Hebron Hospital Universitari, Barcelona, Spain; ⁹Hospital Universitario Puerta de Hierro. Liver Unit. Gastroenterology and Hepatology, Madrid, Spain; ¹⁰Hospital Universitario Marques Valdecilla, Santander, Spain; ¹¹Clinic University Hospital of Valencia, Valencia, Spain; ¹²University of Valencia, Valencia, Spain; ¹³Hospital Clinic, Liver Unit, Barcelona, Spain; ¹⁴Hospital Universitario Marqués de Valdecilla, Marqués de Valdecilla Research Institute (IDIVAL), Santander, Spain; ¹⁵Marqués de Valdecilla University Hospital, Santander, Spain
Email: davidmmaa@gmail.com

Background and aims: Both metabolic dysfunction and alcohol consumption cause steatotic liver disease (SLD). Current definition of metabolic dysfunction-associated SLD (MASLD) allows 140–210 g/week of alcohol intake. We assessed the impact of different levels of alcohol consumption on the prevalence of significant fibrosis in MASLD.

Method: Population-based study with transient elastography (FibroScan®) data from participants in Spain (derivation) and U.S. (validation) cohorts. Controlled attenuation parameter (CAP ≥ 275 dB/m) identified SLD. At least one metabolic comorbidity was required to define MASLD. The FAST score was used to identify significant fibrosis. Low alcohol consumption was defined as an average of 5–9 drinks/week, and moderate consumption as 10–14 and 10–21 drinks/week for female and males respectively.

Results: The derivation cohort included 6,738 adults, of whom 33% had MASLD. Among them, 9% reported low and 14% moderate consumption. Prevalence of significant fibrosis was 14%. In the multivariable analysis, both low (OR = 1.72, 95%CI 1.10–2.69) and moderate (OR = 3.89, 95%CI 2.83–5.35) consumption were independently associated with significant fibrosis. A dose-dependent supra-additive interaction was observed between the number of drinks/week and major metabolic comorbidities (obesity, diabetes, dyslipidemia), with detrimental effect at any level of daily alcohol consumption. The validation cohort included 4,218 participants, 40% MASLD and 13% with significant fibrosis. Among the U.S. population, 39% reported low and 31% moderate consumption. This cohort validated the substantial increase of significant fibrosis in patients with 2/3 major metabolic comorbidities and joint low-to-moderate consumption.

Conclusion: Low-to-moderate alcohol intake is commonly seen in MASLD and increases the risk of advanced disease as compared with minimal consumption.

FRI-214

Risk of non-alcoholic steatohepatitis disease progression to more severe liver disease in medicare patients

Jesse Fishman¹, Yestle Kim¹, Joe Medicis¹, Matthew Davis², Dominic Nunag², Robert G. Gish³. ¹Madrigal Pharmaceuticals, Inc., West Conshohocken, United States; ²Medicus Economics, LLC, Milton, United States; ³Robert G Gish Consultants LLC, La Jolla, United States
Email: jfishman@madrigalpharma.com

Background and aims: Non-alcoholic steatohepatitis (NASH), or metabolic dysfunction-associated steatohepatitis (MASH), is a severe form of metabolic dysfunction-associated liver disease (MASLD). NASH may progress to more advanced liver disease associated with increased mortality, but progression risk and timing have not been well characterized among older adults. This study aimed to estimate risk of NASH disease progression and mortality for Medicare patients.

Method: Patients with NASH (ICD-10: K75.81) in 100% Medicare fee-for-service claims (2015–2021) were required to be ≥ 66 years at index diagnosis, have continuous enrollment for ≥ 12 months prior to and ≥ 6 months following index (unless death), and have no evidence of other causes of liver disease. Diagnoses within 90 days were used to categorize patient-time into five severity states: NASH without advanced liver disease, compensated cirrhosis (CC), decompensated cirrhosis (DCC), hepatocellular carcinoma (HCC), or liver transplant (LT). Survival analyses of disease progression and mortality were conducted for each state overall and by year of progression (Y1–5). Cox proportional hazards models assessed baseline risk factors associated with progression and mortality.

Results: Mean age and follow-up were 72.2 and 2.8 years in 14,806 patients (N = 12,990 NASH; 1,899 CC; 997 DCC; 209 HCC; 140 LT). NASH patients had an annual progression rate of 3%–12% and mortality rates of 2%–12% for Y1–5. CC patients had the highest progression rates (11%–37% for Y1–5) but lower mortality rates (6%–26% for Y1–5) than more severe states. Relative to CC, DCC patients had lower progression rates (3%–18% for Y1–5) but substantially higher mortality rates (41%–76% for Y1–5). HCC patients had low rates of disease progression (2%–4% for Y1–5), but the highest rates of death (41%–85% for Y1–5). LT had mortality rates of 7%–33% in Y1–5. Delayed progression from NASH was associated with lower mortality risk; the 5-year mortality rate of Y2 progressors (32%) was 26% lower than the mortality rate of Y1 progressors (43%). This trend continued

POSTER PRESENTATIONS

for those who progressed in Y3, Y4, Y5, and non-progressors, with 5-year mortality rates of 28%, 18%, 18%, and 12%, respectively. Risk factors varied by state, but older patients and those with previous nursing home use, congestive heart failure, coagulopathy, fluid and electrolyte disorders, or unexplained weight loss faced increased risk of progression or death.

Conclusion: NASH patients have a high risk of disease progression associated with increased mortality rates. The association between unexplained weight loss and progression should be further explored as anti-obesity medications and other strategies are used more broadly. Slower disease progression is associated with lower rates of mortality, suggesting that therapies that can delay or prevent NASH progression may reduce morbidity and mortality.

FRI-215-YI

MASL-B registry: results from a european cohort of patients with chronic hepatitis B and metabolic dysfunction-associated steatotic liver disease

Roberta Forlano¹, Laura Martinez-Gili², Madeleine Lacey², Giordano Sigon², Benjamin H. Mullish², Vincent Mallet³, Lucia Parlati³, Paul Richardson⁴, Niamh Forde⁴, Gaetano Serviddio⁵, Rosanna Villani⁵, Sabela Lens⁶, Maria Buti⁷, Mauro Viganò⁸, Alessandro Loglio⁸, Pietro Lampertico^{9,10}, Roberta D'Ambrosio⁹, Sara Monico⁹, Gabriele Maffi¹¹, Rosa Lombardi¹¹, Anna Ludovica Fracanzani¹¹, Chiara De Luca¹², Patrick Ingiliz¹³, Alessandra Mangia¹⁴, Federica Leserre¹⁴, Valeria Piazzolla¹⁵, Francesco Paolo Russo¹⁶, Giovanni Raimondo¹⁷, George Papatheodoridis¹⁸, Margarita Papatheodoridi¹⁸, Dimitrios N. Samonakis¹⁹, Eleanor Barnes²⁰, Denise O'Donnell²⁰, Jennifer O'Donoghue²⁰, R. Daniel Abeles²¹, Nicola Pugliese²², Alessio Aghemo²², Maud Lemoine², Mark R. Thursz², Ashley Brown², Pinelopi Manousou². ¹Division of Digestive Diseases, Metabolism of Digestion and Reproduction, Imperial college London, London, United Kingdom; ²Division of Digestive Diseases, Department of Metabolism, Digestion and Reproduction, Imperial college London, London, United Kingdom; ³Faculty of Medicine, Université Paris Cité, Cochin Site, 24 rue du Faubourg Saint-Jacques, Paris, France; ⁴Royal Liverpool Hospital Liverpool, Liverpool, United Kingdom; ⁵Liver Unit University of Foggia, Foggia, Italy; ⁶Viral Hepatitis Group, Liver Unit, Hospital Clinic, IDIBAPS, University of Barcelona and CIBERehd, Barcelona, Spain; ⁷Liver Unit, Hospital General Universitari Valle Hebron, Barcelona, Spain; ⁸Gastroenterology Hepatology and Transplantation Unit, ASST Papa Giovanni XXIII, Bergamo, Italy; ⁹Fondazione IRCCS Cà Granda Ospedale Maggiore Policlinico-Gastroenterology and Hepatology Unit, Milan, Italy; ¹⁰CRC "A. M. and A. Migliavacca" Centre for Liver Disease, Department of Pathophysiology and Transplantation, University of Milan, Milan, Italy; ¹¹Fondazione IRCCS Cà Granda Ospedale Maggiore Policlinico-Internal Medicine and Metabolic Disease Unit, Milan, Italy; ¹²Division of Infectious Diseases ASST Fatebenefratelli Sacco, Milan, Italy; ¹³Service Hépatologie, Hôpital Henri-Mondor, Creteil, France; ¹⁴Liver unit, IRCCS Casa Sollievo della Sofferenza, San Giovanni Rotondo, Italy; ¹⁵Liver unit, IRCCS Casa Sollievo della Sofferenza, San Giovanni Rotondo, British Indian Ocean Territory; ¹⁶Gastroenterology and Multivisceral Transplant Unit, Department of Surgery, Oncology and Gastroenterology, University of Padua, Padua, Italy; ¹⁷University of Messina, Messina, Italy; ¹⁸University of Athens, Athens, Greece; ¹⁹University Hospital of Heraklion, Heraklion, Greece; ²⁰Oxford University Hospital, Oxford, United Kingdom; ²¹Chelsea and Westminster Hospital, London, United Kingdom; ²²Department of Biomedical Sciences, Humanitas University, Milan, Italy
Email: r.forlano@imperial.ac.uk

Background and aims: Chronic hepatitis B (CHB) and metabolic-dysfunction associated steatotic liver disease (MASLD) are commonly observed together, with the prevalence and course of disease being debatable. We explored prevalence and risk factors for MASLD with or without fibrosis in patients with CHB in Europe. We also examined the performance of non-invasive markers (NIM).

Method: This multicenter, cross-sectional study included all consecutive CHB patients in 19 liver centers-5 European countries (UK, Italy, Spain, Greece, France). CHB was defined as presence of Hepatitis B surface antigen for at least 6 months. MASLD was defined based on ultrasound, histology or CAP ≥ 275 dB/m, in presence of at least one metabolic factor. Advanced fibrosis was defined as LSM ≥ 8 kPa in those with MASLD or LSM ≥ 9 kPa in those without MASLD. When histology was available, significant fibrosis was F ≥ 2 , advanced fibrosis F ≥ 3 and cirrhosis F ≥ 5 (Ishak). A survey on standard of care for CHB patients with MASLD was circulated.

Results: 1410 CHB patients were included; median age 53 (43–65) years, BMI 25.5 (22–28) kg/m². 62% were White Caucasian, 16% East Asian, 11.2% African or Afro-Caribbean, 5.6% South Asian. Among centers, 70% screened for MASLD all CHB patients, while 30% only those with metabolic syndrome. 50% used imaging, LFTs plus fibroscan, while only 10% serum NIM. Finally, 90% followed same treatment indication as those with CHB only. MASLD prevalence was 32% (465/1410) based on US, 25% (270/1069) on CAP, 49% (151/304) on biopsy. BMI (OR 1.1, 95%CI: 1.14–1.25, p < 0.001), ALT (OR 2.7, 95%CI: 1.02–7.67, p = 0.04), ferritin (OR 1.7, 95%CI: 1.09–2.78, p = 0.02) and history of T2DM (OR 2.1, 95%CI: 1.09–4.47, p = 0.03) predicted MASLD. In those with MASLD, prevalence of advanced fibrosis was 32% (193/598), with age (OR 1.03, 95%CI: 1.01–1.05, p = 0.002), AST (OR 7.8, 95%CI: 1.03–63.55, p = 0.04), PLT (OR 1, 95%CI: 1–1, p = 0.02), insulin treatment (OR 4.2, 95%CI: 1.21–16.8, p = 0.02) and long-term antivirals (OR 4.1, 95%CI: 2.33–7.66, p < 0.001) as predictors for advanced fibrosis. In those without MASLD, advanced fibrosis prevalence was 38%. Overall, 304 (304/1410 = 21%) patients had biopsy. FIB-4 and LSM performed similarly at predicting significant (185/304 = 61%) (AUROC 0.64 vs 0.62, deLong test p = 0.7) and advanced fibrosis (115/304 = 38%) (AUROC 0.64 vs 0.64, deLong test p = 0.9). PPV for FIB-4 and LSM for significant and advanced fibrosis remained modest, while NPV for cirrhosis were 93–95%. The AUROC for CAP predicting steatosis was 0.56 (95%CI: 0.48–0.65, p = 0.01).

Conclusion: In this large European cohort, MASLD and fibrosis were highly prevalent among CHB patients, mirroring host rather than virus-related factors. Biomarkers performed poorly in predicting fibrosis in patients with CHB and MASLD. These results may inform dedicated policies for screening CHB patients for liver disease due to MASLD.

FRI-218

Cost of inaction for metabolic dysfunction-associated steatohepatitis (MASH): the projected economic burden in the United States

Zobair Younossi^{1,2}, Jeffrey V. Lazarus^{1,3,4}, Alina M. Allen^{1,5}, Kenneth Cusi^{1,6}, Frank Tacke^{1,7}, Michael Roden^{1,8,9}, Jörn M. Schattenberg^{1,10}, Henry E. Mark¹, Linda Henry^{1,2,11}, Fatema Nader^{1,12}, James M. Paik^{1,11,13}. ¹The Global NASH Council, Washington DC, United States; ²Beatty Liver and Obesity Research Program, Falls Church, United States; ³Barcelona Institute of Global Health (IS Global), University of Barcelona, Barcelona, Spain; ⁴CUNY Graduate School of Public Health and Health Policy (CUNY SPH), New York City, United States; ⁵Mayo Clinic, Department of Gastroenterology and Hepatology, Rochester, United States; ⁶University of Florida, Division of Endocrinology, Diabetes, and Metabolism, Gainesville, United States; ⁷Universitätsmedizin, Department of Hepatology and Gastroenterology, Berlin, Germany; ⁸Heinrich Heine University, Department of Endocrinology and Diabetology, Medical Faculty and University Hospital Dusseldorf, Dusseldorf, Germany; ⁹Heinrich Heine University, Institute for Clinical Diabetology, German Diabetes Center, Leibniz Center for Diabetes Research, Dusseldorf, Germany; ¹⁰Saarland University Medical Center, Department of Internal Medicine II, Homburg, Germany; ¹¹Center for Outcomes Research in Liver Disease, Washington DC, United States; ¹²Center for Outcomes Research in Liver Disease, Falls Church, United States; ¹³Beatty Liver and Research Program, Falls Church, United States
Email: zobair.younossi@cldq.org

Background and aims: MASH is not only responsible for morbidity and mortality but also significant economic burden. As management strategies are developed, there will be an opportunity to reduce the growing burden of MASH. Our aim was to model the economic burden (direct-medical and societal costs) of MASH in the US.

Method: A Markov Model estimated the burden of MASH in the US. Both MASH prevalent cases in the US (2020) (3.93% or 9.91 million cases) and new (incident) cases (2021: 0.39% or 1.0 million cases to 2040: 0.58% or 1.62 million cases) were considered. Data were sourced from US population projections (2020–2040), National Health and Nutrition Examination (NHANES), National Vital Statistics System (NVSS), global burden of disease (GBD), Scientific Registry of Transplant Recipients (SRTR) data, the Global NASH Registries (GNR) and systematic reviews. Incidence rates were calculated by calibrating against US prevalence rate with the assumption that trends of MASLD in the past decade will continue. Annual all-causes, liver- and cardiovascular-specific mortality were estimated by using NHANES data with 27 years follow-up. The disease states and mortality status were updated over 20-years. Transition probabilities across health states and deaths were updated from our published models, meta-analyses, and calibration. Societal costs were based on the estimated work productivity loss by using WPAI scores from the GNR, US Census Bureau, and the literature. The projections are based on a 3-year moving average trend. Future costs are inflated by +3.5%.

Results: Over the next 2 decades, the model estimates that the cases of NASH, advanced liver disease (F3, compensated cirrhosis, and decompensated cirrhosis) and liver deaths among adults (+18 years) will increase by +81.8% (2021: 4.18% or 10.49 million cases to 2040: 7.61% or 21.04 million cases), +48.4% (2021: 12.28% of MASH or 1.29 million cases to 2040: 13.09% of MASH or 2.75 million cases), and +158% (2021: 6.74 per 100,000 general population or 16,891 cases to 2040: 13.1%, 17.37 per 100,000 or 48,045), respectively. From 2021 to 2040, total annual direct and societal cost of MASH is expected to increase from \$24.26 billion and \$48.33 billion to \$121.44 billion and \$180.69 billion. If the prevalence of MASH is assumed to be lower (1.97%), total annual direct and societal cost for MASH will increase from \$13.95 billion and \$27.36 billion to \$108.85 billion and \$164.20 billion. If the prevalence of MASH is assumed to be higher (5.90%), the expected total annual direct and societal cost will increase from \$32.74 Billion and \$96.17 billion to \$385.38 and \$775.05.

Conclusion: The economic burden of MASH is expected to grow substantially over the next 2 decades. Cost-effective algorithms should be used to identify high-risk MASH patients and the newly developed treatment/management strategies must be adopted to reduce the future economic burden of MASH.

FRI-219-YI

Recompensation and liver function improvement in patients with decompensated cirrhosis due to metabolic-dysfunction associated steatotic liver disease (MASLD): a retrospective cohort study

Alba Jiménez-Masip¹, Teresa Broquetas², Octavi Bassegoda³, Sergio Muñoz Martínez⁴, Isabel Serra⁵, Diego Rojo⁶, Anna Soria³, Cautar El Maimouni³, Jose A. Carrión², Pere Ginès⁷, Joan Genesca⁸, Isabel Graupera⁹, Juan Manuel Pericàs¹⁰. ¹Liver Unit, Digestive Diseases Area, Vall d'Hebron University Hospital, Vall d'Hebron Institute for Research, Universitat Autònoma de Barcelona, Barcelona, Spain; ²Secció d'Hepatologia, Servei de Digestiu, Hospital del Mar, Institut Hospital del Mar d'Investigacions Mèdiques, Universitat Autònoma de Barcelona, Barcelona, Spain; ³Servei d'Hepatologia, Hospital Clínic, Facultat de Medicina i Ciències de la Salut, Universitat de Barcelona, Institut d'Investigacions Biomèdiques August Pi i Sunyer, Barcelona, Spain; ⁴Liver Unit, Digestive Diseases Area, Vall d'Hebron University Hospital, Vall d'Hebron Institute for Research, Universitat de Barcelona, Barcelona, Spain; ⁵Servei de Digestiu Hospital Dr Josep Trueta Girona, Secció d'Hepatologia, Girona, Spain; ⁶Hepatology section,

Gastroenterology Department, Hospital del Mar, Barcelona, Spain; ⁷Servei d'Hepatologia, Hospital Clínic, Facultat de Medicina i Ciències de la Salut, Universitat de Barcelona, Institut d'Investigacions Biomèdiques August Pi i Sunyer, Spanish Centers for Biomedical Research in Liver and Digestive Diseases, Madrid, Spain, Barcelona, Spain; ⁸Liver Unit, Digestive Diseases Division, Vall d'Hebron University Hospital, Vall d'Hebron Institute of Research (VHIR), Vall d'Hebron Barcelona Hospital Campus, Universitat Autònoma de Barcelona, Barcelona, Spain, Centro de Investigación Biomédica en Red de Enfermedades Hepáticas y Digestivas (CIBERehd), Instituto de Salud Carlos III, Madrid, Spain, Barcelona, Spain; ⁹Servei d'Hepatologia, Hospital Clínic, Facultat de Medicina i Ciències de la Salut, Universitat de Barcelona, Institut d'Investigacions Biomèdiques August Pi i Sunyer., Barcelona, Spain; ¹⁰Liver Unit, Digestive Diseases Division, Vall d'Hebron University Hospital, Vall d'Hebron Institute of Research (VHIR), Vall d'Hebron Barcelona Hospital Campus, Universitat Autònoma de Barcelona., Centro de Investigación Biomédica en Red de Enfermedades Hepáticas y Digestivas (CIBERehd), Instituto de Salud Carlos III, Madrid, Spain, Barcelona, Spain
Email: 94jimenezalba@gmail.com

Background and aims: There is lack of a consensus definition and data on frequency of recompensation in MASLD cirrhosis. The aim of this study was to evaluate the incidence and factors associated with recompensation and/or improvement in liver function in decompensated MASLD cirrhosis.

Method: Retrospective study in 4 Catalan university hospitals (Spain). Individuals with MASLD cirrhosis were enrolled at their initial decompensating event (ascites, hepatic encephalopathy, spontaneous bacterial peritonitis and portal hypertension-related bleeding) and followed until death, liver transplantation or last recorded follow-up. Baseline characteristics were collected. The primary end point was a composite of recompensation, defined as sustained absence of clinical decompensation for >1year without specific treatment, and improved and maintained liver function (albumin, bilirubin and INR resulting in Child-Pugh A and/or MELD < 10). Survival analyses were conducted by Kaplan-Meier method. A multivariate analysis of predictors of the primary end point was carried out with variables of the univariate analysis ($p < 0.10$).

Results: 98 patients were included (mean age 64 ± 10 yrs, 57% males). 63% had obesity, 34% overweight, 66% arterial hypertension, 75% type 2 diabetes, and 47% dyslipidemia. Most patients had Child-Pugh B score (68%), 31% Child-Pugh A, and 1 patient Child-Pugh C (1%). Mean (SD) MELD score was 10 ± 3.1 . After a mean follow-up of 32 ± 31 mths, a total of 392 acute decompensation events were recorded (81% ascites, 64% HE, 33% bleeding, and 13% SBP). 65% patients experienced ≥ 2 episodes, 58% patients died and 15% undergone LT. Most deaths were attributed to liver-related events (45% liver failure, 21% hepatocellular carcinoma) while <10% were related to cardiovascular events. During the follow-up period, 15% of patients experienced persistent improvement in liver function, 45% of surviving patients maintained clinical compensation with specific treatment. Only one patient met the fully recompensation criteria. In the univariate analysis, no significant association was found between metabolic risk factors and primary end point, while alcohol consumption and smoking at first decompensation were associated, yet the multivariate analysis did not show significant association with the likelihood of recompensation. At 3-year follow-up, 3 Child-Pugh A patients (10%) and 4 Child-Pugh B patients (6%) exhibited sustained improvement in hepatic function. At 10-year follow-up, 40% and 20% of alive Child-Pugh A and B patients exhibited sustained liver function improvement.

Conclusion: Hepatic recompensation in decompensated MASLD cirrhosis seems very infrequent, possibly due to uncontrolled or unresolved etiology. However, sustained improvement in liver function is achieved in 15% of patients. Further studies are needed to clearly define recompensation criteria in MASLD.

POSTER PRESENTATIONS

FRI-220-YI

The unrecognised burden of pruritus in metabolic dysfunction associated steatotic liver disease

Nasir Hussain^{1,2}, Usha Gungabissoon³, Linda Casillas⁴, Sumanta Mukherjee⁴, Andrea Ribeiro⁵, Megan McLaughlin⁴, Philip N. Newsome^{1,2}, Matthew Armstrong¹, Palak J. Trivedi^{1,2}.

¹National Institute for Health Research, Biomedical Research Centre, Birmingham, United Kingdom; ²University of Birmingham, Birmingham, United Kingdom; ³GSK, London, United Kingdom; ⁴GSK, Collegeville, PA, United States; ⁵GSK, Madrid, United States
Email: nxh100@student.bham.ac.uk

Background and aims: Pruritus is a recognised symptom of cholestasis. However, the prevalence and impact on quality of life (QoL) in metabolic dysfunction associated steatotic liver disease (MASLD) has not been evaluated. We conducted a prospective observational study across a UK tertiary centre to (A) quantify the prevalence of pruritus (B) determine factors associated with pruritus intensity and (C) determine the impact of pruritus on health related QoL in patients (pts) with MASLD.

Method: Adults with MASLD were invited to complete specific itch severity and QoL questionnaires during routine outpatient visits; specifically, 5D-itch, itch numerical rating scale (NRS), chronic liver disease questionnaire (CLDQ) and EuroQoL-5 Dimension 5 level (EQ-5D 5L). QoL assessments were undertaken at baseline and week 48, alongside paired clinical and laboratory data capture. Interim results pertaining to baseline readouts are presented herein. Autoimmune hepatitis, chronic hepatitis B and healthy volunteers served as control groups (each n = 50).

Results: Between Feb 2022 and Aug 2023 we recruited 200 pts with MASLD (115 men; 139 with diabetes mellitus; median age: 60y; median MELD score: 7; and median transient elastography score: 11.0 kPa). Overall, 66 pts were stratified as having no/early fibrosis (elastography <8.0 kPa and/or liver biopsy stage F0-F2), 47 with advanced fibrosis (biopsy F3), 66 with cirrhosis, and 21 as fibrosis unclassified. At baseline, 99 pts (49.5%) reported pruritus to any degree (median 5D-itch: 8.5 vs 5.0 in all control groups, $p < 0.001$), with 62 pts (31%) reporting moderate-severe pruritus (NRS ≥ 4). In the MASLD group, median 5D-itch scores were greater in women (10.0 vs 7.0 in men; $p = 0.04$) and those with more advanced disease (6.0 in no/early fibrosis, 8.0 in advanced fibrosis, and 10.0 in those with cirrhosis; $p = 0.04$). Conversely, individuals taking metformin reported lower itch scores (median 5D-itch: 5.0 vs 10.0 for those not on metformin; $p = 0.03$). 5D-itch scores had moderate positive correlations with body mass index ($r = 0.30$, $p < 0.01$) and serum autotaxin values ($r = 0.33$, $p = 0.02$), weak positive correlations with serum bile acid values ($r = 0.17$, $p = 0.03$), and negatively correlated with serum albumin ($r = -0.24$, $p < 0.01$). No significant correlations were seen for 5D-itch and serum ALT, ALP, gGT or bilirubin. Pruritus severity associated with worse quality of life, with median CLDQ scores in those with no, mild, moderate, and severe itch on NRS of 5.6, 5.1, 4.1 and 3.7, respectively. In turn, median EQ-5D-5L scores for no, mild, moderate, and severe itch were 0.80, 0.77, 0.68 and 0.33, respectively.

Conclusion: One in 3 MASLD pts experience moderate to severe itch, with greater symptom severity in those with advanced fibrosis. Long-term follow-up capturing variability in itch over time, efficacy of anti-cholestatic agents, and factors influencing its persistence are ongoing.

FRI-221

Prevalence and mortality of the spectrum of steatotic liver disease (SLD) in the US populations

Zobair Younossi^{1,2,3}, Pegah Golabi^{1,4}, Leyla Deavila^{1,2}, Ryuuki Hashida^{1,2}, Saleh Alqahtani^{5,6}, Linda Henry^{1,3,7}, James M. Paik^{1,2,3}. ¹The Global NASH Council, Washington DC, United States; ²Beatty Liver and Obesity Research Program, Falls Church, United States; ³Center for Outcomes Research in Liver Disease, Washington DC,

United States; ⁴Beatty Liver and Obesity Research Program, Inova Health System, Falls Church, United States; ⁵Organ Transplant Center of Excellence, King Faisal Specialist Hospital and Research Center, Riyadh, Saudi Arabia; ⁶Division of Gastroenterology and Hepatology, Johns Hopkins University, Baltimore, MD, United States; ⁷Beatty Liver and Research Program, Falls Church, United States
Email: zobair.younossi@cldq.org

Background and aims: The multi-society process to re-name non-alcoholic fatty liver disease led to the creation a new nomenclature. In this context, SLD and its subtypes has provided an opportunity to better assess the interaction of metabolic dysfunction (MetD) with different types of liver diseases. Our aim was to assess the prevalence and mortality of the spectrum of SLD in the U.S.

Method: Data for adults (20–74 years) from the National Health and Nutrition Examination Survey III linked with mortality (follow-up 2019) was utilized. SLD was determined as presence of hepatic steatosis by ultrasound. Definitions of different types of SLD were based on the multi-society consensus. Prevalence and mortality of each subtype of SLD were determined. Multivariable cox regression model with appropriate sample weights was used to investigate factors associated with mortality.

Results: Of 13, 260 adults from NHANES III [mean age 42.9 years; 49.2% male; 76.1% white, 10.7% Black, and 5.4% Mexican American, 7.7% other], 80.8% had at least one cardiometabolic risk (CMR) (65.5% High BMI/WC, 30.7% High Glucose/H1C, 32.1% High Blood pressure, 30.3% High Triglycerides, and 39.1% Low HDL-cholesterol). The following age-adjusted prevalence rates were noted among U.S. adults: SLD (34.3%); metabolic dysfunction-associated steatotic liver disease (MASLD) (25.7%); MetALD (0.62%); ALD with or without MetD (3.03% and 0.20%); viral hepatitis with or without MetD (0.86% and 0.20%); cryptogenic SLD with or without MetD (0.40% and 3.26%); other liver diseases without SLD (9.47%). After a median follow-up of 22.8 years [274, 485 person-years (PY)], the highest mortality rate (per 1, 000 PY) was observed for cryptogenic SLD with MetD (26.73), followed by viral hepatitis with MetD (26.08), ALD with MetD (23.34), MetALD (22.31), MASLD (19.34) and liver diseases without SLD (14.16). Socio-demographic-adjusted model showed that viral hepatitis with MetD had the highest mortality risk (Hazard Ratio [HR] = 3.51 [95% confidence interval, 2.12–5.82]) followed by cryptogenic SLD with MetD (HR = 2.10 [1.36–3.25]), MetALD (HR = 1.76 [1.28–2.42]) and MASLD (HR = 1.19 [1.09–1.29]), while other SLDs without MetD had no significant mortality risk.

Conclusion: Among the spectrum of SLD, MASLD is the most common subtype of SLD while cryptogenic SLD is associated with highest mortality rates. Presence of MetD increases the risk of mortality in different subtypes of SLD (Met-Viral Hepatitis, Met-Cryptogenic SLD, MetALD and MASLD) suggesting the dual impact of both MetD and other liver disease (ALD and Viral Hepatitis) in driving mortality.

FRI-222-YI

A prospective assessment of disease progression impact on patient-reported outcomes in metabolic dysfunction-associated steatotic liver disease

Ian P. O'Connor¹, Brent A. Neuschwander-Tetri², Philip N. Newsome³, Andrea Mospan⁴, Heather Morris⁴, Cheryl Schoen⁴, A. Sidney Barritt Iv⁵, Arun J. Sanyal¹. ¹Stravitz-Sanyal Institute for Liver Disease and Metabolic Health at VCU School of Medicine, Richmond, United States; ²Saint Louis University, St. Louis, United States; ³University of Birmingham, Birmingham, United Kingdom; ⁴Target RWE, Durham, United States; ⁵UNC Liver Center, University of North Carolina, Chapel Hill, United States
Email: ian.oconnor@vcuhealth.org

Background and aims: Metabolic dysfunction associated-steatotic liver disease and steatohepatitis (MASLD and MASH respectively) are major causes of liver-related morbidity and mortality. While several studies have reported clinical event rates in patients with MASLD,

there is a paucity of data on the impact of progression to cirrhosis on patient reported outcomes (PRO) and health related quality of life (HRQOL). The aim of this study was to perform a prospective, cross-sectional analysis of MASLD-specific PRO in patients with MASLD in a real-world setting.

Method: A prospective analysis of the NASH-CHECK PRO in the real-world TARGET-NASH observational longitudinal ongoing cohort in patients enrolled in the United States at academic and community sites was performed from 2021 to 2023. PRO and HRQOL were evaluated in a subset of participants using the NASH-CHECK instrument (version 1.0) that was developed and validated per regulatory guidance. MASLD was defined per the TARGET-NASH definitions using available biopsy, imaging, and clinical criteria as described previously. Three categories of patients were compared using previously published and validated case-definitions: (1) MASL, (2) MASH, (3) MASH cirrhosis. NASH-CHECK has 6 symptom scale scores and three additional HRQOL scores; each has a score of 0–10 with higher scores indicating greater impairment. Scores across classes were compared using ANOVA. A p value < 0.05 was considered significant.

Results: Data from 801 participants with a completed NASH-CHECK PRO and MASLD were obtained (n = 249, 296, 256 for MASL, MASH, and MASH cirrhosis respectively). Median age was 62, 61% female, 81% Non-Hispanic White, 7% Non-Hispanic Black, 7% Hispanic/Latino, 65% obese (BMI ≥ 30), 22% cardiovascular disease, 80% hypertension, 61% type 2 diabetes, 72% dyslipidemia, median follow-up 68 months. Significant differences were noted between MASL, MASH, and MASH cirrhosis: p < 0.001 for itchy skin, activity limitation, emotional impact, social impact; p = 0.011 for fatigue; p = 0.018 for cognitive impact. Scores for those with MASH cirrhosis were significantly higher than MASL and MASH for all domains except abdominal pain, abdominal bloating, and sleep.

Conclusion: In a real-world clinical setting, the recently validated MASLD-specific PRO measure instrument, NASH-CHECK, demonstrated significantly worse scores in patients with MASH cirrhosis vs those with MASL or MASH in 6 out of 9 domains.

FRI-223

Cost-effectiveness of one-time screening for advanced hepatic fibrosis using FIB-4 based two-step algorithm in the general population

Eileen Yoon¹, Jihyun An², Ha Il Kim³, Joo Hyun Sohn³, Bo-Kyeong Kang⁴, Eun Chul Jang⁵, Huiyul Park⁶, Hye-Lin Kim⁷, Sang Bong Ahn⁸, Joo Hyun Oh⁹, Dae Won Jun¹⁰. ¹Department of Internal Medicine, Hanyang University, Seoul, Korea, Rep. of South; ²Department of Internal Medicine, Hanyang University, Guri, Korea, Rep. of South; ³Department of Internal Medicine, Hanyang University College of Medicine, Guri, Korea, Rep. of South; ⁴Department of Radiology, Hanyang University College of Medicine, Seoul, Korea, Rep. of South; ⁵Department of Occupational and Environmental Medicine, Soonchunhyang University College of Medicine, Chun An, Korea, Rep. of South; ⁶Department of Family Medicine, Myoungji Hospital, Hanyang University College of Medicine, Goyangsi, Korea, Rep. of South; ⁷College of Pharmacy, Sahmyook University, Seoul, Korea, Rep. of South; ⁸Department of Internal Medicine, Nowon Eulji Medical Center, Eulji University, College of Medicine, Seoul, Korea, Rep. of South; ⁹Department of Internal Medicine, Nowon Eulji Medical Center, Eulji University, College of Medicine, Seoul, Korea, Rep. of South; ¹⁰Department of Internal Medicine, Hanyang University College of Medicine, Seoul, Korea, Rep. of South
Email: noshin@hanyang.ac.kr

Background and aims: There is currently inadequate evidence supporting one-time screening and intensive lifestyle modification for advanced fibrosis in the general population. Therefore, this study is designed to assess the cost-effectiveness of a screening strategy utilizing the FIB-4 test followed by vibration-controlled transient

elastography (VCTE) for identifying advanced hepatic fibrosis within the general United States population.

Method: We constructed a combined model of the decision tree model and Markov model to compare expected costs and quality-adjusted life-years (QALYs) between 'screening' and 'no screening' groups from healthcare system perspectives. Cardiovascular disease (CVD) conditions, which have the potential combined with advanced hepatic fibrosis, were also incorporated into the model. Patients diagnosed with advanced fibrosis in the screening group were given intensive lifestyle intervention (ILI). The incremental cost-effectiveness ratio (ICER) was calculated for a 30-year horizon.

Results: ICERs of one-time screening for advanced hepatic fibrosis using FIB-4 based two-step algorithm in the general population in their 40 s was \$69, 242 per QALY, respectively, which was under the \$100, 000, regarded as an ICER threshold in the US, indicating that screening is cost-effective. However, those before their 30 s and after 60 s exceeded the threshold. The most influential parameters on cost-effectiveness were the ILI success rate and duration of ILI. If the success rate of ILI drops to less than 28% (as fibrosis regression rate, 14.1%), cost-effectiveness was disappeared.

Conclusion: Screening for detecting advanced hepatic fibrosis using FIB-4 based two-step algorithm followed by ILI was cost-effective in the general population with 40 s.

FRI-224

Intramyocellular lipids are associated with insulin resistance in metabolic dysfunction-associated steatotic liver disease

Guillaume Henin^{1,2}, Maxime Nachit², Harmen Reyngoudt³, Etienne Danse⁴, Pierre Trefois⁴, Frank Peeters⁴, Salomé Declercq², Stéphanie André-Dumont¹, Alexis Goffaux², Benjamin Marty³, Isabelle Leclercq², Audrey Loumaye⁵, Nicolas Lanthier^{1,2}. ¹Service d'Hépatogastroentérologie, Cliniques universitaires Saint-Luc, UCLouvain, Brussels, Belgium; ²Laboratory of Hepatogastroenterology, Institut de Recherche Expérimentale et Clinique, UCLouvain, Brussels, Belgium; ³Institute of Myology, Neuromuscular Investigation Center, NMR laboratory, Paris, France; ⁴Service de Radiologie, Cliniques universitaires Saint-Luc, UCLouvain, Brussels, Belgium; ⁵Service d'Endocrinologie, diabétologie et nutrition, Cliniques universitaires Saint-Luc, UCLouvain, Brussels, Belgium
Email: nicolas.lanthier@saintluc.uclouvain.be

Background and aims: Insulin resistance is considered an indicator of the severity of MASLD. In this context, the role of skeletal muscle fat and its intra- or extra-myocellular localisation on insulin sensitivity remains debated. The aim of this study is to assess muscle lipid content and cellular localisation using proton-magnetic resonance spectroscopy (¹H-MRS) and its relationship with insulin resistance in a cohort of MASLD subjects.

Method: MASLD patients were prospectively recruited based on the co-existence of liver steatosis measured by a controlled attenuation-parameter (CAP) above 251 dB/m and at least one cardiometabolic risk factor. Type 2 diabetes was defined by the intake of hypoglycemic drugs. Insulin resistance was estimated in non-diabetic patients using the homeostatic model assessment of insulin resistance (HOMA-IR). Intra (IMCL) and extramyocellular lipids (EMCL) were measured in vivo using ¹H-MRS. Single voxel ¹H-MRS was performed on a 3-Tesla Signa Premier scanner (GE healthcare) on tibialis anterior (TA) and soleus using a PRESS-sequence (voxel size 10 × 10 × 15 mm³, TE = 27 ms, TR = 1500 ms, 8 averages). JMRUI software, including the AMARES algorithm was used to quantify IMCL and EMCL on non-water suppressed spectra.

Results: 54 MASLD patients were included. 32 patients were male (59%), with a mean age of 54 years (range: 19–75). 27 patients were diabetic (50%). Mean BMI was 35 (range: 24–60). Mean waist circumference was 118 cm (range: 89–160). Mean CAP and liver elasticity were 342 dB/m (range: 242–400) and 14.8 kPa (range: 3.6–35). In the entire cohort, mean TA lipid content was 0.6% for IMCL (range: 0.1–1.5) and 1.8% (0.3–6.8) for EMCL (p < 0.05). Mean soleus

POSTER PRESENTATIONS

lipid content was 0.8% for IMCL (range: 0.2–2.1) and 4.4% for EMCL (range: 0.3–10.9) ($p < 0.05$). In non-diabetic patients, mean fasting glycaemia was 103 mg/dl (range: 76–126) and mean HOMA-IR was 8 (range: 1.7–26). The HOMA-IR index was positively correlated to IMCL content in the TA ($r = 0.63$, $p = 0.017$) but no correlation was found with EMCL content or with soleus fat content (IMCL and EMCL). Diabetic patients had a higher IMCL content in the soleus compared to non-diabetic patients (0.9% versus 0.6%; $p = 0.02$). No difference was highlighted for the EMCL content of soleus (4.1% versus 4.7%; $p > 0.05$) or for IMCL for TA (0.55% versus 0.7%; $p > 0.05$) between diabetic and non-diabetic patients.

Conclusion: The majority of skeletal muscle lipids are extramyocellular. However, IMCL but not EMCL content assessed by ^1H -MRS positively correlates with insulin resistance assessed by the HOMA-IR index in non-diabetic MASLD patients. This observation is reinforced by the IMCL content in diabetic patients being significantly higher compared to non-diabetic patients. This observation highlights a link between IMCL, systemic insulin resistance and type 2 diabetes in MASLD.

FRI-225

Novel digital pathology adequacy score benchmarks the performance of pre-analytical method for digital pathology and AI end-to-end tissue assays

Louis Petitjean¹, Li Chen², Adi Lightstone², Nathan Aist². ¹PharmaNest, Inc, Princeton, United States; ²PharmaNest Inc, Princeton, United States
Email: louis.petitjean@pharmanest.com

Background and aims: The control and monitoring of pre-analytical conditions is key to minimize the noise and variability of Digital Pathology read-outs in the context of Artificial-enabled Digital Pathology tissue assay used for the assessment of liver biopsies. While modern AI algorithms can compensate for most sources of noise (FibroNest, doi: 10.1111/liv.15768), additional opportunities can be addressed for large studies. Inspired by the definition of Adequacy for tissue biopsies, we report the development, validation, and results of a Digital Biopsy Adequacy (DBA) score as a Key Performance Indicator (KPI) to measure liver biopsy pre-analytical quality.

Method: The BDA score is a normalized composite score (1 to 10) to evaluate a digital pathology image along three dimensions and 24 features including (i) Biopsy tissue and glass slide processing (11 features such as area of the biopsy, tissue rupture, folding artifacts) (ii) staining quality (7 features including over or under staining, rinsing artefacts) and (iii) digital scanning (6 features including out-of-focus areas, scanning stripes). The score is based on a point-based method where defects have different penalty weights, such as one single defect can significantly affect the overall score. The method is consistent with the August 2021 FDA Guidance to Industry and Technical Specifications for Submission of Clinical Trials Data Sets for Treatment of NASH, Bio specimen Findings (BS) domain. Digital Pathology images are classified as Non-Adequate (DBA < 5), Minimally Acceptable (5 < DBA < 8) and Acceptable (DBA > 8). We report aggregated DBA results for N = 5227 Digital images processed since 2020 from 13 Phase 2 and 3 MASH studies.

Results: From one operator scoring 385 images and a second independent operator scoring a random subset of 99 images, the Intra-Class Correlation (ICC) is 0.876 ("excellent," Cichetti, 1994) and the Linear Correlation is 0.889 ("good," Koo and Li, 2016). We observe significantly different Not Acceptable ratios (Min 0%, Mean 8%, Median 6% Std 10% Max 41%) and Acceptable Ratios (35%, 71%, 79%, 19%, 97%) across studies. The main root causes for non and minimal adequacy are overstaining, sectioning and folding artefacts, which can be resolved by basic quality control procedures and rework. Best in class performers demonstrate non-acceptable images can be fully avoided.

Conclusion: The use of a KPI for pre-analytical quality in a Digital Pathology end-to-end tissue assay has the potential to significantly improve the Digital Pathology Images used in MASH studies. The

industry benchmark (13 studies, 5227 images) demonstrates that defect rates (not-acceptable biopsies) can be realistically expected to be below 3% and that the rate of fully adequate digital images be above 80%. This KPI should be used to incentivize some pre-analytical laboratories to implement basic Quality Assurance and rework processes.

FRI-226

The impact of light to moderate alcohol consumption on liver and cardiovascular damage in metabolic-dysfunction associated steatotic liver disease

Rosa Lombardi¹, Felice Cinque¹, Andrea Dalbeni², Annalisa Cespiati¹, Floriana Santomenna¹, Jaqueline Currà¹, Daniel Smith¹, Erika Fatta¹, Cristina Bertelli¹, Giuseppina Pisano¹, Edoardo Pulixi¹, Anna Mantovani², Mirko Zoncapè², David Sacerdoti², Anna Ludovica Fracanzani¹. ¹Fondazione IRCCS Ca' Granda Ospedale Maggiore Policlinico of Milan, University of the Study of Milan, Milan, Italy; ²University of Verona and University and Hospital Trust (AOUI) of Verona, Verona, Italy
Email: rosolombardi@hotmail.it

Background and aims: Metabolic-dysfunction associated steatotic liver disease (MASLD) and met-ALD are both characterized by hepatic fat and metabolic alterations without other causes of liver disease but the amount of daily alcohol consumption in their definition differs (0–30/0–20 die vs 30–60/20–50 g/die male/female). MASLD and met-ALD expose patients to progressive liver disease and increased cardiovascular (CV) risk, however the impact of the amount of alcohol in this setting needs to be elucidated. Aim: to evaluate the impact of light alcohol consumption in MASLD on the hepatic and CV damage in a multicentric cohort of steatotic patients with metabolic alterations as compared to total abstinence and met-ALD

Method: 729 patients with ultrasound (US) proven steatosis (mean age 52 ± 12 years, 77% male) without other causes of liver disease were enrolled and classified according to their drinking habits as abstainers (0 g/die) and light consumers in MASLD (<30/20 g/die male/female) or met-ALD (30–60/20–50 g/day male/female). Steatosis was graded by US, hepatic fibrosis diagnosed by LSM > 8.0 kPa at Fibroscan, CVD by carotid US (cIMT > 0.9 mm, plaques) and echocardiography (systolic and diastolic function, epicardial adipose tissue EAT > 7.5/9.5 mm M/F).

Results: 397 (54%) were no alcohol consumers (NAC-MASLD), 290 (40%) light alcohol consumers (LAC-MASLD) and 42 (6%) met-ALD. Considering LAC-MASLD vs NAC-MASLD, there was no difference in the severity of liver disease (severe US steatosis 22% vs 16% $p = 0.06$, LSM > 8 kPa 9% vs 9%, $p = 0.89$). Conversely, LAC had a significantly lower prevalence of cIMT > 0.9 mm compared to NAC (18% vs 28%, $p = 0.005$) and resulted an independent protective factor for increased cIMT (adjusted for age, sex, active smoking, T2DM, hypertension, dyslipidemia, overweight; OR 0.58, CI 95% 0.36–0.93). No difference in other CV parameters was observed. Considering LAC-MASLD vs met-ALD, the latter had significantly higher LSM values (6.4 ± 3.2 vs 5.4 ± 2.2 , $p = 0.02$) despite a not significantly different prevalence of LSM > 8 kPa (19% vs 9%, $p = 0.10$). Met-ALD vs LAC-MASLD had a significantly higher prevalence of carotid plaques (55% vs 30%, $p = 0.003$) and resulted an independent risk factor for carotid plaques (adjusted for sex, active smoking, T2DM, hypertension, dyslipidemia, overweight, statins use; OR 2.01, CI 95% 1.00–4.12). Conversely, there was no difference in the prevalence of severe US steatosis or other CV parameters.

Conclusion: Light alcohol consumption in middle-aged MASLD patients appears to protect against early atherosclerosis without exhibiting more severe liver disease compared to abstiners. However, when alcohol consumption increases up to the level of met-ALD, the cardiovascular protection is hampered and alcohol becomes harmful also for the liver.

FRI-227

Impact of antidiabetic medications on adverse liver outcomes in patients with type 2 diabetes mellitus: independent and interactive effects

Sherlot Juan Song¹, Vincent Wai-Sun Wong¹, Grace Lai-Hung Wong¹, Terry Cheuk-Fung Yip¹. ¹Medical Data Analytics Centre (MDAC), Department of Medicine and Therapeutics, The Chinese University of Hong Kong, Institute of Digestive Disease, Faculty of Medicine, The Chinese University of Hong Kong, HK, Hong Kong
Email: 1155169298@link.cuhk.edu.hk

Background and aims: The impact of antidiabetic medications on liver-related events (LRE) among patients with type 2 diabetes mellitus (T2DM) remains unclear. This study aimed to investigate the independent and interactive effects of antidiabetic medications on the hazards of LRE in patients with T2DM.

Method: This territory-wide retrospective study included adult patients diagnosed with T2DM between January 2007 and December 2021 in Hong Kong. Patients with chronic viral hepatitis, excessive alcohol use, other metabolic and autoimmune liver diseases, malignancies, and pre-existing LRE were excluded. The primary end point was LRE, defined as hepatic decompensation or the development of hepatocellular carcinoma. A cause-specific hazard model was used to calculate hazards ratios (HR) with 95% confidence intervals (CI), with LRE as the event of interest. Time-dependent analysis and interaction analysis were employed to investigate the effects of medications on LRE. LRE-free survival probability was predicted based on combinations of medications with significant interaction.

Results: A total of 575,000 patients with T2DM (mean age 61.9 years; 52.3% males) were included with a median follow-up duration of 6.2 years. 4882 patients developed LRE during the follow-up period. Statin (HR: 0.59, 0.55–0.63), metformin (HR: 0.89, 0.83–0.96), Inhibitors of dipeptidyl peptidase 4 (DPP-4 inhibitors) (HR: 0.85, 0.79–0.93) and sodium-glucose cotransporter-2 inhibitors (HR: 0.70, 0.62–0.78) were all associated with decreased hazards of LRE, while insulin (HR: 1.83, 1.72–1.95) and sulfonylureas (HR: 1.20, 1.13–1.29) increased the risk of LRE. A significant synergistic effect between DPP-4 inhibitors and statin was observed (p value < 0.05). The incidence rate of LRE among patients receiving DPP-4 inhibitors but not statins was 1.341 cases per 1000 person-years, compared with 1.169 cases per 1000 person-years in those receiving both medications.

Conclusion: Antidiabetic medications have varied impact on hazards of LRE. A synergistic interaction was indicated between statin and DPP-4 inhibitors to lower the risk of LRE among patients with T2DM. This study was supported by Health and Medical Research Fund of Health Bureau of HKSAR Government (Reference number: 19202141).

FRI-230-YI

Prevalence and predictors of steatotic liver disease and significant liver fibrosis in an integrated hepatological and non-hepatological healthcare pathway model: preliminary results from a prospective cohort of a tertiary center

Angelo Armandi^{1,2}, Gian Paolo Caviglia¹, Guglielmo Beccuti³, Alessandro Andreis^{4,5}, Federica Barutta³, Matteo Bellettini^{4,5}, Chiara Rosso¹, Arianna Ferro³, Irene Poggolini¹, Giacomo Bonacchi^{4,5}, Gabriele Castelnovo¹, Kamela Gjini¹, Fabrizio Amato¹, Martina Marano¹, Marta Guariglia¹, Eleonora Dileo¹, Nuria Pérez Diaz del Campo¹, Davide Giuseppe Ribaldone¹, Davide Castagno⁵, Giorgio Maria Saracco¹, Gaetano De Ferrari⁵, Gianluca Alunni^{4,5}, Mauro Rinaldi⁴, Gabriella Gruden⁶, Elisabetta Bugianesi¹. ¹Division of Gastroenterology and Hepatology, Department of Medical Sciences, University of Turin, Turin, Italy; ²Metabolic Liver Disease Research Programme, University Medical Center of Mainz, Mainz, Germany; ³Division of Endocrinology, Diabetes

and Metabolism, Department of Medical Sciences, University of Turin, Turin, Italy; ⁴Advanced Cardiovascular Echocardiography Unit, Cardiovascular and Thoracic Department, Città della Salute e della Scienza di Torino University Hospital, Turin, Italy; ⁵Division of Cardiology, Department of Medical Sciences, Città della Salute e della Scienza di Torino University Hospital, Turin, Italy; ⁶Diabetic Nephropathy Laboratory, Department of Medical Sciences, University of Turin, Turin, Italy
Email: angelo.armandi@unito.it

Background and aims: An integrated healthcare pathway model for metabolic-dysfunction associated steatotic liver disease (MASLD) is recommended for a comprehensive evaluation of the metabolic health. In this prospective study we aimed to assess prevalence and predictors of steatotic liver disease (SLD) and significant liver fibrosis (SLF) in consecutive patients first referred for type 2 diabetes mellitus (T2DM) or SLD in two different settings (diabetology and hepatology clinics) of the “AOU Città della Salute e della Scienza di Torino” University Hospital.

Method: All patients underwent vibration-controlled transient elastography for liver stiffness measurement (LSM) and controlled attenuation parameter (CAP), and echocardiography with speckle tracking analysis. SLD was defined by CAP > 247 dB/m. SLF was defined by LSM > 7 kPa. Diastolic dysfunction was defined by mitral E/E' ratio > 9 and systolic dysfunction by left ventricular global longitudinal strain (GLS) > -18.

Results: 544 patients (59% in the liver clinic group [LCG] and 41% in the diabetes clinic group [DCG]) were enrolled. In the LCG all patients fulfilled the criteria for MASLD; prevalence of T2DM and obesity were 21.8% and 42.7%; 4.7% were referred to the DCG for first diagnosed or decompensated T2DM. Median LSM was 5.1 [4.6–6.3] kPa and SLF was detected in 17.8% of cases. In the DCG prevalence of obesity was 52.0% and median LSM was 4.9 [4.1–5.9] kPa. SLD was present in 67.7% of cases, of which 59.6% MASLD, 1.3% ALD (alcohol-related liver disease) and 6.7% metALD. SLF was detected in 13.5% of cases, which were referred to the LCG for hepatological evaluation. A known cardiovascular disease (CVD) was found in 9.7% and 50.2% of patients in the LCG and DCG, respectively. A high Framingham risk score (>20%) was detected in 12.9% in the LCG and 1.3% in the DCG. Prevalence of diastolic and systolic dysfunctions in those without CVD were 27.4% and 18.2% in the LCG and 8.9% and 3.6% in the DCG. In the LCG, Body Mass Index (BMI) and T2DM were the strongest predictors of SLF (aOR 1.13 [95%CI 1.06–1.21], p = 0.0002 and 5.66 [95%CI 2.64–12.07], p < 0.001). In the DCG, only transaminases were independent predictors of SLF (aOR 1.11 [95%CI 1.04–1.19], p = 0.001), while BMI was the only predictor of SLD (aOR 1.09 [95%CI 1.03–1.16], p = 0.001).

Conclusion: Two thirds of SLD in the non-hepatology setting are due to MASLD and associated with BMI. Prevalence of SLF is similar in hepatology and non-hepatology settings, but presence of T2DM results in the strongest association independent of other metabolic risk factors. A higher prevalence of pre-clinical CVD is detected in the hepatology setting by advanced echocardiography, consistent with a higher 10-year risk of CVD-related mortality. This study was funded by the Italian Ministry for Education, University and Research (MIUR) under the programme ‘Dipartimenti di Eccellenza 2018–2022’ Project code D15D18000410001.

FRI-231

Compared to complete abstainers, non-significant alcohol use may be associated with more severe liver disease in patients with metabolic dysfunction-associated steatotic liver disease (MASLD)-The multicentre study of the indian consortium on MASLD

Ajay Kumar Duseja¹, Manu Mehta², Arka De³, Shivaram Prasad Singh⁴, Shrikant Mukewar⁵, Saurabh Mukewar⁵, Shalimar Shalimar⁶, Omesh Goyal⁷, Jayanthi Venkataraman⁸, VK Dixit⁹, Krishnadas Devadas¹⁰, Varun Mehta¹¹, Piyush Ranjan¹², Anil Arora¹³, Abha Nagral¹⁴, Narendra S. Choudhary¹⁵, Sanjib Kar¹⁶,

POSTER PRESENTATIONS

Brij Sharma¹⁷, Sandeep Nijhawan¹⁸, Dibyalochan Praharaj¹⁹, Aakash Shukla²⁰, Nagaraja Rao Padaki²¹, Arun Valsan²², Sanjeev Saigal²³, K Narayanaswamy²⁴, Rajiv Mehta^{25,26}, Pankaj Asati²⁷, Sunil Dadhich^{28,29}, Prasad V G Mohan^{30,31}, Mukul Rastogi³², Abraham Koshy³³, Mallika Bhattacharya^{34,34}, Rohit Gupta^{35,36}, Akash Roy³⁷, Rakhi Maiwall^{38,39}, J Sanyal Arun⁴⁰.

¹Postgraduate Institute of Medical Education and Research, Chandigarh, India; ²Post Graduate Institute of Medical Education and Research (PGIMER), Chandigarh, India; ³PGIMER, Chandigarh, India; ⁴SCB college, Cuttack, India; ⁵MIDAS Hospital, Nagpur, India; ⁶AIIMS, New Delhi, India; ⁷Dayanand Medical College, Ludhiana, India; ⁸Sri Ram Chandran Medical College, Chennai, India; ⁹IMS, BHU, Varanasi, India; ¹⁰Government Medical College, Trivandrum, India; ¹¹Dayanand Medical College and Hospital, Ludhiana; ¹²Sir Gangaram Hospital, New Delhi; ¹³Sir Gangaram Hospital, New Delhi, India; ¹⁴Jaslok Hospital, Mumbai, India; ¹⁵Medanta The Medicity, Gurgaon, India; ¹⁶Gastro Liver Care, Cuttack, India; ¹⁷Indira Gandhi Medical College and Hospital, Shimla, India; ¹⁸SMS Medical College and Hospital, Jaipur, India; ¹⁹Kalinga Institute of Medical Sciences, Bhubaneswar, India; ²⁰Seth GSMC and KEM Hospital, Mumbai, Mumbai, India; ²¹Asian Institute of Gastroenterology, Hyderabad; ²²Amrita Institute, Kerala; ²³Max Hospital, Saket, Gurgaon, India; ²⁴Madras Medical college, Madras, India; ²⁵Surat Institute of Digestive Sciences, Surat; ²⁶SIDS Hospital, Surat, India; ²⁷NSC Bose Medical College and Hospital, Jabalpur; ²⁸MDM hospital, Jodhpur, India; ²⁹SMNC, Jodhpur, India; ³⁰VGM Hospital, Institute of Gastroenterology, Combitor, India; ³¹VGM Hospital, Coimbatore, India; ³²Fortis, Hospital, Noida, India; ³³VPS Lakeshore, Kochi, India; ³⁴Guwahati Medical College and Hospital, Guwahati, India; ³⁵AIIMS, Rishikesh, India; ³⁶All India Institute of Medical Sciences, Rishikesh, India; ³⁷Apollo Multispeciality, Kolkata, India; ³⁸ILBS, New Delhi, India; ³⁹Institute of liver and biliary sciences, New Delhi, India; ⁴⁰Virginia Commonwealth University, Virginia, United States

Email: ajayduseja@yahoo.co.in

Background and aims: Moderate alcohol intake in patients with metabolic dysfunction-associated steatotic liver disease (MASLD) may increase their severity. Met-ALD has been recently defined as metabolic dysfunction associated with moderate alcohol intake of 140/210 g to 350/420 g per week in females and males respectively. There is no data on the effect of alcohol intake less than the moderate amount on the severity of liver disease in patients with MASLD. The aim of the study was to assess the effect of alcohol intake less than the moderate amount on the severity of liver disease in patients with MASLD.

Method: In an on-going real-life Indian Consortium on MASLD study, interim data across 31 centres over 4.5 years (n = 6963) was analysed to compare the severity of non-invasive tests (NITs) namely, aspartate aminotransferase-to-platelet ratio index (APRI), Fibrosis-4 (FIB-4) and FibroScan-AST (FAST) scores among total alcohol abstainers of alcohol Vs those taking <140 g/week alcohol intake within the cohort of MASLD. The study had ethical approval at respective centres and all patients gave an informed consent.

Results: Out of total of 6963 patients [males:61.2%, age:45.8 (32–52)], 5622 (81%) were total abstainers and 1341 (19%) were taking alcohol <140 g/week. Data on the metabolic syndrome, APRI, FIB-4, FAST score and LSM was available in 6097 (87%), 6963 (100%), 2640 (38%), and 2644 (38%) patients. There was no difference in the prevalence of metabolic syndrome amongst the two groups. Total abstainers had significantly lower mean APRI [0.63 ± 0.85 Vs 0.72 ± 0.77, p = 0.03], FAST [0.41 ± 0.24 Vs 0.44 ± 0.22, p = 0.04] and LSM scores (9.43 ± 8.3 Vs 11.7 ± 24.4, p = 0.001) scores than those with alcohol intake with no difference in mean FIB-4 score [1.64 ± 1.87 Vs 1.64 ± 1.87, p = 0.251] among the two groups.

Conclusion: In patients with MASLD, non-significant alcohol use may be associated with severe liver disease in comparison to those with complete abstainers.

FRI-232

In Patients with Metabolic Dysfunction-Associated Steatotic Liver Disease (MASLD), Clinically Significant Pruritus is Associated with High Serum Bile Acid (BA) Level and Advanced Fibrosis (AF)

Zobair Younossi^{1,2}, James M. Estep^{1,3}, Sean Felix¹, Brian Lam^{1,3}, Sumanta Mukherjee⁴, Brandon Swift⁵, Linda Casillas⁴, Andrea Ribeiro⁶, Jake Hunnicutt⁴, Megan McLaughlin⁴, Andrei Racila^{1,3}, Fatema Nader^{1,3,7}, Maria Stepanova^{1,3,7}, ¹Beatty Liver and Obesity Research Program, Inova Health System, Falls Church, VA, United States; ²The Global NASH Council, Washington, United States; ³The Global NASH Council, Washington, DC, United States; ⁴GSK, Collegeville, PA, United States; ⁵GSK, Durham, NC, United States; ⁶GSK, Madrid, Spain; ⁷Center for Outcomes Research in Liver Diseases, Washington, DC, United States
Email: zobair.younossi@cldq.org

Background and aims: Elevated serum BA are associated with pruritus in cholestatic liver diseases. We aimed to assess the associations of serum BA with clinically significant (CS)-pruritus in patients with MASLD.

Method: We used previously collected frozen fasting serum samples and simultaneously collected data (including CLDQ) from patients with MASLD. Patients with viral hepatitis (B, C) and healthy blood donors were used as controls. The diagnosis of non-alcoholic steatohepatitis (NASH), also known as Metabolic Dysfunction-Associated Steatohepatitis (MASH), was based on liver biopsy. Serum was used to measure BA levels using Diazyme Total Bile Acids Assay kit. High BA level was defined as ≥ 5.9 $\mu\text{mol/L}$. Significant fibrosis (SF) was defined as histologic stages 2–4 or liver stiffness by transient elastography > 8 kPa, and advanced fibrosis (AF) was defined as histologic stages 3–4 or liver stiffness > 10 kPa. Pruritus was assessed using the itch item of CLDQ (frequency of itch over the past 2 weeks; score from 1 (all the time) to 7 (none of the time), CS-pruritus defined as ≤ 4 .

Results: This cross-sectional study included 651 subjects: MASLD (N = 497) including MASH/NASH (N = 88), viral hepatitis B and C (VH, N = 98) and healthy controls (N = 56). Across the diagnostic groups, VH patients had the highest BA levels with the lowest levels in healthy controls (p < 0.0001 across groups). There were no differences in the prevalence of CS-pruritus across these groups (p = 0.63). The correlation of higher BA with more itch (lower itch scores) was only seen in MASLD (r = -0.15, p = 0.0006) with stronger correlations according to histologic severity (MASH/NASH: r = -0.23, p = 0.029; SF: r = -0.30, p = 0.0005; AF: r = -0.43, p = 0.0001). Patients with MASH/NASH had higher levels of BA (7.3 ± 11.2 vs. 3.9 ± 5.3 $\mu\text{mol/L}$ in non-MASH MASLD) and 34/88 (39%) vs. 95/409 (23%) met high BA criteria (p < 0.05). Furthermore, MASLD patients with SF and AF had even higher serum BA levels (SF vs no SF: 6.6 ± 10.2 vs. 3.6 ± 4.8 $\mu\text{mol/L}$, high BA 43/130 (33%) vs. 70/334 (21%), p < 0.01; AF vs no AF: 8.1 ± 11.7 vs. 3.7 ± 5.2 $\mu\text{mol/L}$, high BA 27/74 (37%) vs. 86/390 (22%), p < 0.01). MASLD/NAFLD and its subgroups with high BA had more CS-pruritus, and this pattern was more pronounced in patients with greater disease severity (CS-pruritus with high BA vs. those without high BA in all MASLD: 25% vs. 17%; in NASH/MASH 30% vs. 13%; in SF: 33% vs. 12%; in AF: 41% vs. 8%; all p ≤ 0.05). In multivariable logistic regressions adjusted for age, sex, obesity, and type 2 diabetes (T2D), having high BA was an independent predictor of CS-pruritus in MASLD patients with SF [OR = 3.48 (1.37–8.84) (p = 0.009)] and AF [OR = 7.29 (1.95–27.32) (p = 0.003)]. Notably, associations of T2D and obesity with CS-pruritus were not significant (all p > 0.10).

Conclusion: High serum BA level is associated with pruritus in MASLD. High BA is an independent predictor of pruritus in MASLD, especially those with advanced fibrosis.

FRI-233

Cardiovascular disease burden in patients with and without metabolic dysfunction-associated steatohepatitis: data from the unCoVer-MASH longitudinal cohort study

Elisabetta Bugianesi¹, Anurag Mehta², Kamal Kant Mangla³, Abhishek Shankar Chandramouli⁴, Katrine Grau³, Niels Krarup³, Ahsan Shueb Patel³. ¹Department of Medical Sciences, University of Turin, Turin, Italy; ²VCU Health Pauley Heart Center, Richmond, VA, United States; ³Novo Nordisk A/S, Søborg, Denmark; ⁴Novo Nordisk Service Center India Pvt Ltd, Bangalore, India
Email: elisabetta.bugianesi@unito.it

Background and aims: Metabolic dysfunction-associated steatohepatitis (MASH) is linked to increased risk of cardiovascular (CV) disease (CVD), but many aspects of CVD burden in patients with MASH remain unknown. Particularly, data on the clinical burden of CVD and specific CV events in patients with MASH vs those without MASH are limited. This real-world study aimed to assess CVD burden in patients with and without MASH.

Method: Patients with MASH were identified using the International Classification of Diseases code for non-alcoholic steatohepatitis (K75.81) from October 2015–June 2022, using data from a federated network (TriNetX). Index date was defined as the date of first MASH diagnosis. Exclusion criteria were viral hepatitis, alcohol use disorder, chronic liver diseases other than MASH or metabolic dysfunction-associated steatotic liver disease, cirrhosis, decompensated MASH, hepatocellular carcinoma and human immunodeficiency virus. Patients with MASH were matched 1:1 to patients without MASH based on demographics (sex, age, year of start/end of insurance enrolment, and insurance scheme). Outcomes were CVD prevalence (assessed up to 1 year prior to index) and risk of CV events (s) during follow-up (index date to end of enrolment, death or study end) amongst patients with no history of respective CV event (s) at baseline. For CV risk, cumulative incidence was plotted using Aalen-Johansen curves after adjusting for competing risk of non-CV death. Incidence rate (IR) was calculated per 100 person-years (PY) and hazard ratios (HR) were calculated using Cox proportional hazard models (crude and adjusted for CV risk factors [age, sex, type 2 diabetes (T2D), chronic kidney disease (CKD), obesity, hyperlipidaemia and hypertension]).

Results: In total, 9,642 patients (4,821 with MASH; 4,821 without MASH) were included. In both groups, mean (standard deviation) age was 50.8 (13.2) years and 58.5% were women. Compared with those without MASH, more patients with MASH had hypertension (58% vs 31%), hyperlipidaemia (57% vs 30%), obesity (45% vs 17%), T2D (41% vs 14%) and CKD (6% vs 3%) at baseline. Prevalence of any CVD was higher in patients with MASH than without MASH (23% vs 12%), as was risk of any CV event (IR: 11.1 vs 4.5 per 100 PY; crude HR [95% confidence interval]: 2.72 [2.30, 3.22], $p < 0.0001$; adjusted HR: 2.27 [1.95, 2.66], $p < 0.0001$). Similar results were seen for individual CV events, namely ischaemic heart disease (IR: 5.3 vs 2.3), cerebrovascular disease (IR: 4.4 vs 2.1), atherosclerosis (IR: 3.9 vs 1.8), and heart failure (IR: 3.2 vs 1.5).

Conclusion: CVD prevalence at baseline and risk of CV events during follow-up were significantly higher in patients with non-cirrhotic MASH compared with matched controls without MASH in a real-world cohort. These data provide additional evidence of the association between MASH and CVD, and complement a previous analysis of the unCoVer-MASH study.

FRI-234

Association between the duration of comorbidities and steatotic liver disease

Ha Il Kim¹, Hyunji Sang², Jihyun An³, Eileen Yoon³, Dae Won Jun³, Joo Hyun Sohn⁴. ¹Hanyang University Guri Hospital, Guri, Korea, Rep. of South; ²Kyung Hee University Hospital, Seoul, Korea, Rep. of South; ³Hanyang University College of Medicine, Seoul, Korea, Rep. of South; ⁴Hanyang University College of Medicine, Seoul, Korea, Rep. of South
Email: mondosewan@gmail.com

Background and aims: Steatotic liver disease (SLD) is a major cause of chronic liver disease. Previous studies have been reported that SLD interacts with various comorbidities and linked with their outcome. However, there is a paucity of studies on how the duration of the comorbidities is related to SLD development and mortality. We examined the association between comorbidity duration and SLD, focusing on disease-predicting variables and mortality rates.

Method: Data from 12,262 patients aged ≥ 20 years in the 2010 and 2015 Korea National Health and Nutrition Examination Survey were analyzed. Ten comorbidities (hypertension, diabetes mellitus [DM], dyslipidemia, stroke, myocardial infarction [MI], angina pectoris, asthma, chronic obstructive lung disease [COPD], chronic kidney disease [CKD], and depression) were categorized by duration. We investigated the association between presence SLD and the duration of comorbidity by using association rule mining and logistic regression analysis. Survival analysis was conducted using Cox regression analysis.

Results: Among the 2,757 SLD cases and 9,505 non-SLD cases analyzed, shorter durations of DM, MI, CKD, and COPD were associated with a higher proportion in SLD cases, while hypertension, dyslipidemia, stroke, and depression exhibited a lower proportion. Association rule mining highlighted the significance of shorter durations of DM and dyslipidemia, and longer durations of hypertension in predicting SLD. In multivariate logistic regression analysis, DM with a duration ≤ 1 year showed a notably elevated odds ratio (11.53, CI 9.09–14.63). Multivariate Cox regression analysis for survival revealed that longer durations of hypertension and DM were associated with increased hazard ratios beyond 10 years (hazard ratio [HR] 2.222, HR 2.11, respectively). Cardiovascular disease duration ≤ 5 years and lung disease duration > 5 years demonstrated significant hazard ratios (HR 2.486, HR 2.382, respectively). Cardiovascular-related survival showed similar patterns, with longer HTN and shorter cardiovascular disease durations linked to higher risks. The higher FIB-4, longer HTN, and DM durations are independently associated with cancer-related survival.

Conclusion: This suggests that a comprehensive risk stratification should be undertaken, considering the duration of comorbidities, for both the identification of SLD and the assessment of their prognostic significance when they are detected.

FRI-235

Causes of death, mortality rates, and the role of socio-demographic risk factors and biomarkers in metabolic dysfunction-associated steatohepatitis mortality in more than 18,000 real world patients from the United States

Jörn M Schattenberg¹, Claudio Sartin², Ronald Herrera², Mireia Raluy³, Mark Yates⁴, Ramy Younes⁵. ¹Department of Medicine II, Saarland University Medical Center, Homburg, Germany; ²Boehringer Ingelheim International GmbH, Global Epidemiology and Real-World Evidence, Ingelheim, Germany; ³Evidera, Data Analytics, Borlänge, Sweden; ⁴Evidera, Data Analytics, London, United Kingdom; ⁵Boehringer Ingelheim International GmbH, Medicine, Cardio Metabolism and Respiratory, Ingelheim, Germany
Email: joern.schattenberg@uks.eu

Background and aims: To reduce mortality risks in patients with metabolic dysfunction-associated steatohepatitis (MASH) it is critical to have a better disease understanding in real-world populations. Limitations of past studies were small sample size, point in time of

POSTER PRESENTATIONS

data collection, being single center, biopsy based, or broad focus on steatotic liver disease. This study investigates mortality rates, causes of death, and the role of socio-demographic risk factors and biomarkers that could be associated with mortality in a large real-world MASH population.

Method: Retrospective cohort study (2016–2021 years) using Optum Market Clarity (linked claims and electronic health records, EHRs) from the United States. MASH was defined by the first ICD10 diagnosis code (K75.81 Non-alcoholic steatohepatitis) recorded during the study period, presence of AST, ALT and platelets tests carried out 3 months prior/after diagnosis, and absence of diseases prior/at diagnosis, such as alcoholic/chronic liver diseases. Risk factors included age, sex, race, region, comorbidities, FIB-4 fibrosis score and routinely collected biomarkers such as LDL cholesterol, Triglycerides, eGFR, and HbA1c. The associations between risk factors and mortality were estimated using multivariate survival models. To contextualize findings, crude mortality rates were calculated in the subgroup of MASH patients with BMI ≥ 25 and type 2 diabetes (T2D) and in a group of patients in Optum with BMI ≥ 25 who did not report any liver diseases or T2D.

Results: 18,710 MASH patients (mean age 44 years, 54% female, 80% white, 95% with BMI ≥ 25 , 52% with T2D) had been followed-up (FU) for 6.5 years after diagnosis (mean FU = 3 years): 1465 patients died (70% from cardiovascular disease (CVD) and 17% from liver-related causes). The mortality rate was 25 per 1000 persons-year (py). African Americans (vs white) and South residents (vs North-East) had higher all-cause mortality rates [Hazard ratios (HRs) of 1.33 and 1.45 respectively]. A decrease in eGFR of 10 ml/min/1.73 m² and having 3 or more comorbidities (vs none) were also associated with increased mortality (HRs of 1.21 and 1.93 respectively). The mortality rate was 31 per 1000 py in MASH with BMI ≥ 25 and T2D (5 times higher than those with BMI ≥ 25 without liver diseases/diabetes).

Conclusion: CVD risk reduction in patients with MASH will be crucial to improve outcomes. Mortality rates are especially high in MASH patients who are overweight/obese and living with T2D. In addition, racial differences in MASH mortality were observed: African Americans and South residents were at increased risk; this may be due to less access to health care. Also, the eGFR-mortality association signaled that kidney and renal disease prevention is important. This is the largest and most comprehensive study on MASH mortality using claims and EHRs.

FRI-236-YI

Racial disparities in incidence of cirrhosis and extrahepatic manifestations in metabolic dysfunction-associated steatotic liver disease

Majd Aboona¹, Leith Ghani¹, Pooja Rangan¹, Vincent Chen², Cheng Han Ng³, Daniel Huang⁴, Mark Muthiah⁵, Donghee Kim⁶, Moises Nevah Rubin^{7,8}, Ma Ai Thanda Han^{1,9}, Michael Fallon^{1,9}, Karn Wijarnpreecha^{1,9,10}. ¹University of Arizona College of Medicine-Phoenix, Phoenix, United States; ²University of Michigan Health System, Ann Arbor, United States; ³Yong Loo Lin School of Medicine, National University of Singapore, Singapore, Singapore; ⁴National University Hospital, Singapore, Singapore; ⁵National University Health System, Singapore, Singapore; ⁶Stanford University School of Medicine, Stanford, United States; ⁷University of Arizona College of Medicine Phoenix, Phoenix, United States; ⁸Banner University Medical Center, Phoenix, United States; ⁹Banner University Medical Center, Phoenix, United States; ¹⁰BIO5 Institute, University of Arizona College of Medicine-Phoenix, Phoenix, United States
Email: aboona@arizona.edu

Background and aims: Metabolic Dysfunction-associated Steatotic Liver Disease (MASLD) has increased in prevalence in recent years. Data regarding the new cardiometabolic criteria of MASLD, especially in diverse patient population are limited. We conducted a study to estimate the incidence of MASLD and its complications in an ethnically diverse population.

Method: We conducted a multicenter study on MASLD patients seen at the Banner Health System, representing hospitals across Arizona, California, and Colorado, and the University of Michigan Health System from 2012 to June 2023 using ICD codes and natural language processing. We excluded patients with other causes of liver disease, underweight, baseline decompensated cirrhosis, baseline cancer diagnosis, prior bariatric surgery, or missing data on race, BMI, aspartate and alanine aminotransferase, and platelet. Patients who met 1/5 cardiometabolic criteria including BMI > 25 (BMI > 23 in Asians), hypertension, DM, dyslipidemia, or hypertriglyceridemia were included in the study. The primary outcomes are mortality, the incidence of any cardiovascular disease, cirrhosis, liver-related events (ascites, hepatic encephalopathy, variceal bleeding), type 2 diabetes mellitus, any cancer, and major adverse cardiac events (MACE) among racial groups.

Results: We included 51,625 MASLD patients in the cohort. 67.38 % were Non-Hispanic White, 21.57 % Hispanic, 4.93 % African-American, 1.46 % Native American/Alaskan Native (NA), and 1.96 % Asian/Pacific Islanders. Compared to Non-Hispanic White patients, Hispanic patients had a higher mortality (Hazard ratio (HR) 1.19; 95 % Confidence Interval (CI), 1.01–1.40; p value, 0.03) and higher incidence of cirrhosis (HR 1.23; 95 % CI, 1.03–1.45; p value, 0.02). Furthermore, compared to Non-Hispanic White patients, NA patients had a higher mortality (HR 2.18; 95 % CI, 1.39–3.41; p value, < 0.01), higher incidence of liver-related events (HR 1.83; 95 % CI, 1.01–3.32; p value, 0.047), and higher incidence of MACE (HR 1.36; 95 % CI, 1.07–1.74; p value, 0.01).

Conclusion: In this population-based cohort of patients with MASLD, Hispanic patients had higher risk of mortality and cirrhosis despite controlling for other variables. Furthermore, NA had a higher risk mortality, liver related events, and MACE. Attention to racial disparities and cardiac risk stratification is warranted in patients with MASLD, particularly in the NA population.

FRI-237

Natural history of lean and non-lean metabolic dysfunction associated steatotic liver disease

Shun-ichi Wakabayashi¹, Nobuharu Tamaki², Takefumi Kimura¹, Takeji Umemura¹, Masayuki Kurosaki². ¹Shinshu University School of Medicine, Department of Gastroenterology and Hepatology, Matsumoto, Japan; ²Department of Gastroenterology and Hepatology, Musashino Red Cross Hospital, Musashino-shi, Tokyo, Japan
Email: shun_1@me.com

Background and aims: The prognosis of lean metabolic dysfunction-associated steatotic liver disease (MASLD) has not been clear due to some conflicting evidence. This study aimed to clarify the prognosis of lean MASLD by conducting a comprehensive analysis of a vast Asian cohort.

Method: This study used a nationwide, population-based database and analyzed 2.9 million patients. The primary end points were liver-related events (LREs) and cardiovascular events (CVEs) in patients with lean MASLD, non-lean MASLD, and normal liver control groups.

Results: The median observation period was 4.2 years. The 5-year incidence of LREs in the lean MASLD, non-lean MASLD, and normal liver control groups were 0.065%, 0.039%, and 0.006%, respectively. The LRE risk of lean MASLD was significantly higher than that of normal liver control (adjusted hazard ratio [aHR]: 5.94, 95% confidence interval [CI], 3.95–8.92) but comparable to that of non-lean MASLD (aHR: 1.35, 95% CI, 0.87–2.08). By contrast, for CVEs, the non-lean MASLD group exhibited a higher 5-year cumulative incidence rate (0.779%) than the lean MASLD (0.600%) and normal liver control (0.254 %) groups. The lean MASLD group had a reduced risk of CVEs compared with the non-lean MASLD group (aHR, 0.73; 95% CI, 0.64–0.84), and comparable risk of CVEs to the normal liver control group (aHR, 0.99; 95% CI, 0.88–1.12).

Conclusion: Lean MASLD has a similar LRE risk and a lower CVE risk to non-lean MASLD. Therefore, follow-up and treatment strategies should be tailored to the specific MASLD condition.

FRI-238

Histological and clinical disease progression in patients with metabolic dysfunction-associated steatotic liver disease using paired liver biopsy

Merve Ekelik¹, Dilara Turan Gökçe², Mesut Gumussoy³, Saba Kiremitçi¹, Emin Bodakçı⁴, Volkan Yılmaz¹, Sevinc Tugce Karayel¹, Serkan Duman⁵, Zeynep Melekoğlu Ellik⁶, Abdullah Mübin Özercan⁷, Ramazan Erdem Er¹, Fatih Karakaya¹, Hale Gokcan¹, Atilla Elhan¹, Berna Savas¹, Murat Törüner¹, Ramazan Idilman¹. ¹Ankara University Faculty of Medicine, Ankara, Turkey; ²Ankara Bilkent Şehir Hastanesi, Ankara, Turkey; ³Gaziantep Şehitkamil Devlet Hastanesi, Gaziantep, Turkey; ⁴Gaziantep Ersin Arslan Eğitim ve Araştırma Hastanesi, Gaziantep, Turkey; ⁵Mersin Toros Devlet Hastanesi, Mersin, Turkey; ⁶Karaman Eğitim ve Araştırma Hastanesi, Karaman, Turkey; ⁷Fırat University Faculty of Medicine, Elazığ, Turkey
Email: mervekelik@gmail.com

Background and aims: Metabolic dysfunction-associated steatotic liver disease (MASLD) is a dynamic disease. Therefore, the aims of the present study were to assess the histological evolution of patients with MASLD using paired liver biopsies-, to identify the factors associated with fibrosis and clinical disease progression, and to determine the relationship between histological progression and clinical disease outcomes.

Method: This was a single-center study. A total of 114 patients with MASLD who had at least two liver biopsies more than one year apart between January 2001 and December 2021 were included in the analysis.

Results: The median interval between the two biopsies was 46 months (IQR:49.2 months). From the baseline to the follow-up biopsy, 44% of patients showed histological progression. Fibrosis progressed in 28 patients, regressed in 21, and showed no change in 65 patients. The proportion of MASH increased from 83% to 90%, with 95% of the MASH patients remaining MASH and 70% of the MASL patients fulfilling the MASH criteria at the follow-up biopsy. Logistic regression showed no baseline characteristics associated with fibrosis progression. Notably, histological progression was more common in patients with MASL than in patients with MASH ($p = 0.002$). Among the patients with MASL exhibiting histological progression, 87% had lobular inflammation at baseline. During the median follow-up period of 10 years, half of the patients with MASLD showed clinical disease progression, with 73% having MASH at baseline. Ten patients with MASLD developed new-onset cirrhosis. New-onset DM developed in 31% of the 91 patients who did not have DM at baseline, hypertension developed in 25% of the 73 patients without hypertension at baseline, and hyperlipidemia developed in 55% of the 38 patients without hyperlipidemia at baseline. Notably, no metabolic abnormality developed in MASL patients who maintained MASL status at the follow-up biopsy. Multivariable logistic regression showed baseline hypertension (Odds Ratio [OR]: 2.611, $p = 0.024$) and high serum ALT levels (OR: 2.815, $p = 0.049$) were predictors of clinical disease progression in patients with MASLD.

Conclusion: In conclusion, patients with MASLD, both patients with MASL and patients with MASH, exhibit disease progression. Hypertension and abnormal liver injury tests at baseline are predictors of clinical disease progression in patients with MASLD.

FRI-239

An inference model of risk factors for liver-related complications among patients with type 2 diabetes mellitus

Sherlot Juan Song¹, Vincent Wai-Sun Wong¹, Grace Lai-Hung Wong¹, Terry Cheuk-Fung Yip¹. ¹Medical Data Analytics Centre (MDAC), Department of Medicine and Therapeutics, The Chinese University of Hong Kong, Institute of Digestive Disease, Faculty of Medicine, The Chinese University of Hong Kong, HK, Hong Kong
Email: 1155169298@link.cuhk.edu.hk

Background and aims: Data on the prognostic risk factors of liver-related complications among patients with type 2 diabetes mellitus (T2DM) remains limited. This study aims to construct an inference model to explain risk factors associated with adverse liver outcomes. **Method:** This territory-wide retrospective study included 575, 000 adult patients with the diagnosis of T2DM between January 2007 and December 2021 in Hong Kong. Patients with chronic viral hepatitis, excessive alcohol use, other metabolic and autoimmune liver diseases, malignancies, and liver-related events (LRE) before T2DM diagnosis were excluded. The primary end point was LRE, defined as hepatic decompensation or the development of hepatocellular carcinoma. Cause-specific hazard model was fitted in competing risk analysis considering LRE as the event of interest. Restricted cubic spline analysis was used for the non-linear effects of clinical parameters on LRE.

Results: 575, 000 patients with T2DM were included (mean age 61.9 years; 52.3% males). 4887 patients reached the outcome of LRE. 0.05% patients had cirrhosis at baseline, while 0.3% patients presented with compensated cirrhosis over the follow-up. Old age (1.028, 1.025–1.031), male gender (1.19, 1.12–1.26), presence of compensated cirrhosis (3.30, 3.07–3.56) were all associated with an increase in the hazards of LRE, and compensated cirrhosis had the highest estimated hazard ratios among all covariates. Hypertension (1.21, 1.11–1.31) and dyslipidemia (1.14, 1.07–1.21) at diagnosis also heightened the risks of LRE. High albumin (0.977, 0.972–0.982) showed protective effect, while total bilirubin (1.005, 1.004–1.006), international normalized ratio (1.12, 1.08–1.17) and creatinine (1.002, 1.002–1.002) increased hazards of LRE. Both platelet count and hemoglobin A1c (HbA1c) demonstrated a U-shaped relationship with LREs, with the highest risk observed in patients with extreme values of the two parameters.

Conclusion: Compensated cirrhosis had the highest estimated hazard ratios for LRE among patients with T2DM. Bipolar extreme levels of platelet and HbA1c heightened the risk of LRE and warrants extra clinical attention in the management of T2DM.

This study was supported by Health and Medical Research Fund of Health Bureau of HKSAR Government (Reference number:19202141).

FRI-242

Redefining the relationship: the diminished correlation between MASLD and CKD after accounting for diabetes or insulin resistance

Tianyuan Yang¹, JingYa Yin², Yang Bingqing², Qi Wang³. ¹Center of Liver Diseases, Beijing Ditan Hospital, Capital Medical University, Beijing, China; ²Center of Liver Diseases, Beijing Ditan Hospital, Capital Medical University, Beijing, China; ³Center of Liver Diseases, Beijing Ditan Hospital, Capital Medical University, Beijing Key Laboratory of Emerging Infectious Diseases, Institute of infectious diseases, Beijing, China
Email: ty66303@gmail.com

Background and aims: Non-Alcoholic Fatty Liver Disease (NAFLD) is widely regarded as a multisystem condition. Previous studies suggest an independent association between NAFLD and the incidence of CKD. Herein, we explore whether metabolic dysfunction-associated steatotic liver disease (MASLD), as newly defined, is independently associated with CKD after adjusting for five cardiovascular metabolic factors and other covariates.

Method: Analysis included 6567 non-pregnant adult participants from NHANES 2017 to 2020. Fibroscan with controlled attenuation parameter was used to define steatotic liver disease (CAP more than

POSTER PRESENTATIONS

248 dB/m). Stages of CKD were defined according to the KDIGO guidelines. Insulin resistance was defined by HOMA-IR value of more than 2.69. Weighted logistic regression models were utilized to elucidate the correlation between MASLD, covariates, and CKD. Subgroup analyses were performed to evaluate the impact of five cardiovascular metabolic factors, insulin resistance, on the MASLD-CKD association.

Results: Univariate regression analysis revealed that MASLD is significantly linked to a risk of CKD. Further analysis using model 6 (adjustments for age, sex, cardiovascular metabolic factors), the relation was still statistically significant (OR 1.32 95% CI 1.03–1.69 $p = 0.031$). Model 7, expanding on Model 6 by including diabetes among its covariates, indicated that the relationship did not significance. Incorporating insulin resistance as a categorical variable in the Model 8 altered the findings: the association between MASLD and CKD remained non-significant (OR 1.00 95% CI 0.73–1.38 $p = 0.981$), yet insulin resistance itself was significantly linked to CKD. Introduction of an interaction term between insulin resistance and MASLD into the model was statistically significant (OR 2.02 95% CI 1.05–3.89 $p = 0.037$). Faceted bar chart presented the predicted probabilities of CKD across different age and genders, showing that MASLD did not statistically affect CKD risk in the absence of insulin resistance. The presence of insulin resistance significantly increased the likelihood of CKD in those with MASLD compared to those without. Subgroup analyses showed that the associations between MASLD and CKD varied across different subgroups. The analyses identified insulin resistance ($p = 0.02$) as potential modifiers of the MASLD-CKD association. For those without insulin resistance, impact of MASLD on CKD risk is not significant (OR 0.69 95% CI 0.42–1.12 $p = 0.124$), in contrast to its significant effect in those with insulin resistance (OR 1.44 95% CI 1.03–2.23 $p = 0.046$).

Conclusion: Although the prevalence of CKD is higher in patients with MASLD, MASLD does not have an independent association with CKD after adjusting for diabetes or insulin resistance. Therefore, in the community management of comorbid MASLD and CKD, the focus should still be placed on the treatment of diabetes.

FRI-243

Echocardiography-based markers of subclinical cardiac dysfunction in patients with MASLD and preserved ejection fraction: prospective data from the Turin cohort

Kamela Gjini¹, Angelo Armandi¹, Alessandro Andreis^{2,3}, Matteo Bellettini^{2,3}, Irene Poggolini¹, Gabriele Castelnovo¹, Gian Paolo Caviglia¹, Chiara Rosso¹, Nuria Pérez Diaz del Campo¹, Marta Guariglia¹, Davide Giuseppe Ribaldone¹, Giorgio Maria Saracco¹, Davide Castagno^{2,3}, Alberto Milan⁴, Fabrizio Amato¹, Martina Marano¹, Gaetano De Ferrari^{2,3}, Elisabetta Bugianesi¹. ¹Division of Gastroenterology and Hepatology, Department of Medical Sciences, University of Turin, Turin, Italy; ²Division of Cardiology, Department of Medical Sciences, Città della Salute e della Scienza di Torino University Hospital, Turin, Italy; ³Advanced Cardiovascular Echocardiography Unit, Cardiovascular and Thoracic Department, Città della Salute e della Scienza di Torino University Hospital, Turin, Italy; ⁴Hypertension Unit, Department of Medical Sciences, Città della Salute e della Scienza di Torino University Hospital, Turin, Italy
Email: angelo.armandi@unito.it

Background and aims: Individuals with Metabolic dysfunction-Associated Steatotic Liver Disease (MASLD) have abnormal myocardial energy metabolism and reduced coronary functional capacity, even in the absence of risk factors for cardiovascular disease (CVD), potentially associated with cardiac fibrosis and heart failure. We aimed to evaluate diastolic and systolic function in MASLD individuals with preserved ejection fraction.

Method: We prospectively enrolled patients with ultrasound-diagnosed MASLD and without overt CVD undergoing screening echocardiography (Philips, Andover, US) including speckle tracking analysis for myocardial fiber deformation (strain) in all four cardiac

chambers. Significant diastolic dysfunction was defined as mitral E/E' ratio >9, while systolic dysfunction was defined by left ventricular global longitudinal strain (GLS) >–18%. Significant liver fibrosis (SLF) was non-invasively assessed by either FIB-4 score >1.3 or liver stiffness measurement (LSM) >7 kPa by transient elastography. Severe liver steatosis was defined by Controlled Attenuation Parameter (CAP) >300 dB/m.

Results: A total of 94 patients were included (median age 53.0 [44.5–62.5] years, male sex 43.2%). SLF was detected in 20.0% by FIB-4 and in 14.9% by LSM. Severe steatosis was present in 53.8% of cases. FIB-4 values were significantly higher in patients with diastolic ($p = 0.008$) and systolic ($p = 0.006$) dysfunction. In patients with SLF by either FIB-4 or LSM we found lower absolute values of left atrium reservoir strain (indirect marker of reduced compliance) ($p = 0.027$ and $p = 0.021$, respectively), lower values of left atrium conduit strain (indirect marker of impaired passive emptying) ($p = 0.020$ and $p = 0.0003$) and lower values of right atrium reservoir strain ($p = 0.011$ and $p = 0.007$). Patients with severe steatosis had increased epicardial fat tissue deposition ($p = 0.020$). In a multiple stepwise logistic regression model including type 2 diabetes (T2D), obesity, arterial hypertension, dyslipidemia, male sex and SLF by FIB-4, both SLF and T2D were significantly associated with diastolic dysfunction.

Conclusion: MASLD patients with SLF and without overt CVD have impaired pre-clinical markers of cardiac dysfunction. Increased FIB-4 is associated with diastolic dysfunction independently of major CVD risk factors. The research was supported by the Italian Ministry for Education, University and Research (MIUR) under the programme “Dipartimenti di Eccellenza 2018–2022” Project code D15D18000410001.

FRI-244

Barriers and motivators for implementation of lifestyle changes in a large population with MASLD

Sharon Oude Veldhuis^{1,2}, Stans Drossaert², Marjolein den Ouden^{1,3}, Lisette van Gemert-Pijnen², Maureen Guichelaar⁴. ¹Saxion University of Applied Sciences, Enschede, Netherlands; ²University of Twente, Enschede, Netherlands; ³Regional Community College of Twente, Hengelo, Netherlands; ⁴Medisch Spectrum Twente, Enschede, Netherlands
Email: l.s.derksen@saxion.nl

Background and aims: Long-term improvements in lifestyle changes has been shown possible in only a minority of patients with MASLD. This study explored the barriers and motivators in MASLD patients to implement (long-term) lifestyle changes.

Method: A quantitative survey (with some open-ended questions) was distributed via two Dutch patient organizations. The survey included questions about comorbidities, attempts to change lifestyle, motivators and barriers for lifestyle changes, information provision and information needs. The data was analyzed using descriptive statistics.

Results: The survey was completed by 449 MASLD patients (81% female, mean/SD age 56 ± 11 years, BMI 30 ± 5 kg/m²). Patients experienced a high rate of comorbidities, including diabetes mellitus ($n = 98$, 22%), and cardiovascular disease ($n = 83$, 19%). Almost half of the patients ($n = 210$, 47%) experienced joint problems. Sixty-three percent of patients ($n = 283$) self-reported their stage of disease of which 16% reported fibrosis/cirrhosis. The majority of patients attempted lifestyle changes ($n = 365$, 81%), including dietary changes to support weight loss ($n = 320$, 71%). A low percentage of participants succeeded in permanently changing their diet ($n = 174$, 39%), exercise pattern ($n = 159$, 35%) and weight reduction ($n = 90$, 20%). Most frequently mentioned motivators for lifestyle changes were symptoms of MASLD and/or comorbidities ($n = 92$, 20%), desire to live a long and healthy life ($n = 76$, 17%), and discomfort from being overweight ($n = 65$, 14%). Barriers to implement lifestyle changes were lack of knowledge about MASLD-related topics ($n = 122$, 27%), stress ($n = 116$, 26%), and lack of motivation ($n = 97$, 22%). Information

about MASLD was mainly provided by a gastroenterologist (n = 210, 47%) and general practitioner (n = 123, 27%). Less than 20% of participants indicated they had received sufficient information about MASLD-related topics. About 72–90% of patients would like to receive more information on almost all MASLD-related topics including disease specifics and self-management options.

Conclusion: Key reasons to attempt lifestyle changes, in a large population of MASLD patients, included motivation to improve discomfort and comorbidities related to obesity and MASLD. Although the majority of respondents attempted lifestyle changes, only a minority of them were able to sustain long-term improvements (~20% permanent weight loss). Lack of knowledge about MASLD and self-management were key barriers to improve lifestyle in the long-term. Our study supports ongoing efforts to increase patient's knowledge about MASLD and its treatment in order to sustain (long-term) lifestyle changes.

FRI-245

Longitudinal follow-up of Fib-4 in patients at risk of steatotic liver disease (SLD) receiving low-dose Methotrexate treatment (LD-MTX): results from the CIRT randomized placebo-controlled Trial in 4769 patients

Vincent Di Martino¹, Jing Cui², Delphine Weil-Verhoeven³, Daniel Solomon⁴. ¹CHU Besançon, INSERM UMR 1098 Right, Besançon; ²Harvard Medical school, Brigham and Women's Hospital, Boston, United States; ³CHU Besançon, INSERM UMR 1098 Right, Besançon, France; ⁴Harvard Medical School, Brigham and Women's Hospital, Boston, United States
Email: vdimartino@chu-besancon.fr

Background and aims: It seems well established that low-dose methotrexate (LD-MTX), even when administered over the long term, is unable to induce liver fibrosis per se, but the question of whether LD-MTX could worsen SLD and promote fibrosing SLD in at-risk patients remains unanswered so far. The aim of this retrospective study was to report the course of Fib-4 scores in patients included in the CIRT trial, a randomized placebo-controlled trial testing the prevention of cardiovascular events in patients with coronary artery disease by LD-MTX administration (15 to 20 mg/week; Ridker et al, NEJM 2019; NCT 01594333).

Method: Among the 4786 patients included in the CIRT trial, biochemical data enabled calculation of Fib-4 score every 3 months in 4769 patients (2381 in the LD-MTX group; 2388 in the placebo group) for up to 5 years of follow-up. MTX was temporarily discontinued in the event of AST or ALT > 2 ULN, until values were < 1.5 ULN. All patients received folic acid supplementation (1 mg/d). Using a mixed model (type 3 test), we tested whether subjects on LD-MTX had a higher Fib-4 score at study visits, taking into account different MTX dosages, metabolic syndrome, and gender.

Results: Baseline patients characteristics were similar in the two groups (81% males; median age = 65 years, BMI = 32.3 kg/m²; 67% diabetic; 62% alcohol-free; 86% under statins; median Fib-4 = 1.29). On inclusion, 46.5% of patients had a Fib-4 above the alert threshold (>1.3 or >2 depending on age < or > 65 years), and 6.5% had a Fib-4 score > 2.67. Seven patients developed cirrhosis during follow-up (six in the LD-MTX group; one in the placebo group; NS), of whom only two had baseline Fib-4 > 2.67. In multivariate analysis adjusted for gender and the presence of metabolic syndrome, Fib-4 was slightly but significantly higher in the placebo group (+0.042; 95% CI: 0.001–0.075; p = 0.015).

Conclusion: Under the usual conditions of administration and monitoring, LD-MTX is not associated with an increased risk of hepatic fibrosis in patients with coronary artery disease presumed to be at risk of SLD.

FRI-246

Effect of antidiabetics on the risk of hepatocellular carcinoma in patients with diabetes and metabolic dysfunction-associated steatotic liver disease

Han Ah Lee¹, Hwi Young Kim¹, Yeon Seok Seo², Sang Hoon Ahn³, Seung Up Kim³. ¹Ewha Womans University College of Medicine, Seoul, Korea, Rep. of South; ²Korea University College of Medicine, Seoul, Korea, Rep. of South; ³Yonsei University College of Medicine, Seoul, Korea, Rep. of South
Email: amelia86@naver.com

Background and aims: Diabetes is a significant risk factor for the development of hepatocellular carcinoma (HCC). In this retrospective cohort study, we investigated the effects of antidiabetic drugs on the risk of HCC development in patients with diabetes and metabolic dysfunction-associated steatotic liver disease (MASLD).

Method: From 2004 to 2018, patients with diabetes and MASLD were selected from three tertiary academic institutes in South Korea. The patients were followed from the date of MASLD diagnosis until HCC diagnosis, death, or last follow-up. Independent predictors of HCC development were investigated using landmark Cox proportional hazard models.

Results: In total, 4,024 patients with diabetes and MASLD were identified. Their median age was 56.0 years, and 2,184 (54.3%) were male. A total of 3,370 (83.7%) patients received antidiabetics (oral antidiabetic drugs [OADs] in 2,581 and insulin-based therapy in 789), whereas the remaining 16.3% of patients received no antidiabetics. During a median follow-up of 5.1 years, 269 (6.7%) patients developed HCC. The multivariate analysis showed that liver cirrhosis, a fibrosis-4 Index ≥ 1.45, male sex, older age, obesity, hypertension, dyslipidemia, lower albumin level, diabetes complications, longer duration of diabetes, and the type of antidiabetics were significantly associated with an increased risk for HCC (all p < 0.05). No treatment and OAD therapy had comparable risks for HCC, whereas insulin-based therapy was associated with an increased risk for HCC compared to no treatment (hazard ratio [HR] = 1.739, 95% confidence interval [CI] 1.047–2.888) and OAD therapy (HR = 1.717, 95% CI 1.242–2.372) (all p < 0.05). Metformin-based therapy was associated with a reduced risk for HCC in the entire study population (HR = 0.713, 95% CI 0.522–0.973) and in a subgroup of patients receiving OAD therapy (HR = 0.362, 95% CI 0.205–0.640) (all p < 0.05). Metformin-based therapy decreased the risk for HCC in both patients who received OAD monotherapy (HR = 0.148, 95% CI 0.044–0.503) and those who received dual OAD therapy (HR = 0.448, 95% CI 0.200–0.986). However, in patients receiving insulin-based therapy, the combination of metformin treatment did not reduce the risk for HCC compared to insulin monotherapy or combined treatment of insulin and OADs other than metformin.

Conclusion: Metformin use decreased the incidence of HCC in patients with diabetes and MASLD. Careful consideration regarding the choice of antidiabetic drugs is needed for HCC prevention in such patients.

FRI-247

Association of plasma magnesium with MASH and cirrhosis: combined data from multiple therapeutic trials including more than 10,000 patients

Stephen A. Harrison¹, Julie Dubourg², Vlad Ratziu³, Jörn M. Schattenberg⁴, Naim Alkhouri⁵, Mazen Nouredin⁶, Michael Charlton⁷. ¹Radcliffe Department of Medicine, University of Oxford, Oxford, United Kingdom; ²Summit Clinical Research, San Antonio, United States; ³Sorbonne Université, Institute for Cardiometabolism and Nutrition, Hospital Pitié-Salpêtrière, INSERM UMRS 1138 CRC, Paris, France; ⁴Saarland University Medical Center, Homburg, Germany; ⁵Arizona Liver Health, Phoenix, United States; ⁶Houston Research Institute, Houston, United States; ⁷University of Chicago, Chicago, United States
Email: jdubourg@summitclinicalresearch.com

POSTER PRESENTATIONS

Background and aims: Insulin resistance is considered a key driver of metabolic dysfunction-associated steatotic liver disease (MASLD)/metabolic dysfunction-associated steatohepatitis (MASH) pathogenesis. Magnesium has an important role in insulin and glucose homeostasis. We aimed to investigate the association between plasma magnesium and MASLD.

Method: Using combined screening data from 10 industry-funded MASH phase 2 trials, we examined patients with biopsy-proven MASLD/MASH and available magnesium levels. Univariate and multivariate logistic regressions were performed to predict histological severity.

Results: 2,696 patients with available data were included in this analysis. Mean age was 55.0 years (SD: 11.5) and 58% were female. 60% of the patients had MASH, 40% had advanced fibrosis (F3-F4) and 14% had cirrhosis (F4). In univariate analysis, magnesium concentration was associated with advanced fibrosis (Odds Ratio: 0.19, 95% CI: 0.13–0.27), cirrhosis (Odds Ratio: 0.17, 95% CI: 0.10–0.27), hepatocyte ballooning (Odds Ratio: 0.23, 95% CI: 0.15–0.33), and inflammation (Odds Ratio: 0.29, 95% CI: 0.12–0.66). Plasma magnesium concentration was not associated with the presence of steatosis. After adjustment on age, liver enzymes, FIB-4, platelet, HbA1c, magnesium concentration remained independently associated with advanced fibrosis (Odds Ratio: 0.31, 95% CI: 0.20–0.49), cirrhosis (Odds Ratio: 0.28, 95% CI: 0.15–0.59), hepatocyte ballooning (Odds Ratio: 0.40, 95% CI: 0.26–0.63), and inflammation (Odds Ratio: 0.36, 95% CI: 0.14–0.89). Plasma magnesium concentration was significantly lower in patients with cirrhosis (1.96 mg/dL SD 0.23) compared to patients without significant fibrosis (F0-F1) (2.07 mg/dL SD 0.20).

Conclusion: Plasma magnesium was independently and inversely associated with MASH severity. Further studies are warranted to understand this association and mechanistic link.

FRI-248-1Y

The impact of baseline sarcopenia, over time, on liver and cardiovascular damage in patients with metabolic-dysfunction associated steatotic liver disease (MASLD): a prospective study

Floriana Santomena^{1,2}, Annalisa Cespiati^{1,2}, Matteo Carlomagno², Giovanna Oberti¹, Edoardo Pulixi¹, Jaqueline Currà^{1,2}, Daniel Smith^{1,2}, Rosa Lombardi^{1,2}, Erika Fatta¹, Cristina Bertelli¹, Giuseppina Pisano¹, Anna Ludovica Fracanzani^{1,2}. ¹SC Medicina ad Indirizzo Metabolico, Fondazione IRCCS Cà Granda Ospedale Maggiore Policlinico of Milan, Milan, Italy; ²Department of Pathophysiology and Transplantation, University of Milan, Milan, Italy
Email: floriana.santomena@unimi.it

Background and aims: Sarcopenia, defined as the loss of muscle mass, is linked to metabolic comorbidities, connecting to steatotic liver disease and cardiovascular damage (CVD). The impact of sarcopenia on liver and CVD progression over time is not well understood. The aim of this study was to evaluate the impact of baseline sarcopenia on liver and CVD progression after 5 years in non-cirrhotic ultrasound (US) proven metabolic dysfunction-associated liver disease (MASLD) patients.

Method: 180 patients (63% male, mean age 51 ± 10 years) were enrolled. Sarcopenia was defined as skeletal muscle mass/height² ≤ 10.7/7.5 kg/m² in men/women by bioimpedance analysis. CVD was assessed by carotid plaques at US, liver fibrosis and steatosis by liver stiffness measurement (LSM) and controlled attenuation parameter (CAP), respectively. After 5 years, liver disease and CVD severity were reassessed.

Results: At baseline 45% were sarcopenic, 35% obese, 39% hypertensive, 26% dyslipidemic and 13% diabetic. Sarcopenic patients compared to non-sarcopenic had lower BMI (26.6 vs 31.1, $p < 0.001$), lower waist circumference (97 vs 105, $p < 0.001$), lower LSM (4.5 vs 5.1, $p = 0.02$), and lower CAP values ($p = 0.004$), but similar prevalence of carotid plaques ($p = 0.9$). No differences were seen regarding age ($p = 0.99$) and gender ($p = 0.09$). At 5 years of follow-up, despite lifestyle modifications, in sarcopenic patients the mean BMI (26.6 vs

26.5, $p = 0.17$), LSM (4.5 vs 4.8, $p = 0.97$), and CAP (281 vs 285, $p = 0.29$) did not significantly change, while they experienced an increase in carotid plaque (28% vs 53%, $p = 0.002$). Conversely, non-sarcopenic patients showed amelioration in mean BMI (31.1 vs 30.1, $p = 0.02$), and LSM (5.1 vs 4.6, $p = 0.01$), and a decrease in carotid plaques (8% vs 3%, $p = 0.02$) compared with sarcopenic ones. Patients with sarcopenia at baseline, showed less improvement in mean LSM (−0.1 vs −1.1 kPa, $p = 0.04$) than non-sarcopenic patients, with no differences in delta BMI (0.1 vs −0.6 kg/m², $p = 0.18$) and delta CAP (−3 vs −5 dB/m, $p = 0.7$). At multivariate analysis, adjusted for sex, age, and factors associated with sarcopenia at univariate analysis, sarcopenia at baseline remained associated with delta LSM (OR 1.86, $p = 0.04$), irrespective of confounders.

Conclusion: In non-cirrhotic MASLD patients, the presence of sarcopenia at baseline reduces over time, despite lifestyle intervention, the chance of improvement in liver damage and promotes worsening of cardiovascular damage. These findings should prompt us to screen all patients at diagnosis of MASLD for the presence of sarcopenia.

FRI-249

Association between uric acid concentration and MASH: combined data from multiple therapeutic trials including more than 10,000 patients

Stephen A. Harrison¹, Julie Dubourg², Vlad Ratziu³, Jörn M. Schattenberg⁴, Naim Alkhoury⁵, Mazen Nouredin⁶, Michael Charlton⁷. ¹Radcliffe Department of Medicine, University of Oxford, Oxford, United Kingdom; ²Summit Clinical Research, San Antonio, United States; ³Sorbonne Université, Institute for Cardiometabolism and Nutrition, Hospital Pitié-Salpêtrière, INSERM UMRs 1138 CRC, Paris, France; ⁴Saarland University Medical Center, Homburg, Germany; ⁵Arizona Liver Health, Phoenix, United States; ⁶Houston Research Institute, Houston, United States; ⁷University of Chicago, Chicago, United States
Email: jddubourg@summitclinicalresearch.com

Background and aims: Uric acid is considered the ultimate product of purine metabolism and is associated with cardiovascular disease. We aimed to investigate the association between uric acid and metabolic dysfunction-associated steatotic liver disease (MASLD)/metabolic dysfunction-associated steatohepatitis (MASH).

Method: Using combined screening data from 10 industry-funded MASH phase 2 trials, we examined patients with biopsy-proven MASLD/MASH and available uric acid levels. Univariate and multivariate logistic regressions were performed to predict histological severity.

Results: 2,880 patients with available data were included in this analysis. Mean age was 55.1 years (SD: 11.3) and 60% were female. 62% of the patients had MASH, 41% had advanced fibrosis (F3-F4) and 14% had cirrhosis (F4). In univariate analysis, uric acid concentration was inversely associated with advanced fibrosis (Odds Ratio: 0.88, 95% CI: 0.84–0.93), cirrhosis (Odds Ratio: 0.85, 95% CI: 0.79–0.92), hepatocyte ballooning (Odds Ratio: 0.93, 95% CI: 0.89–0.98), and steatosis (Odds Ratio: 1.25, 95% CI: 1.11–1.41). Uric acid concentration was not associated with the presence of inflammation. After adjustment on age, liver enzymes, HbA1c, and triglycerides, uric acid concentration remained independently associated with steatosis (Odds Ratio: 1.22, 95% CI: 1.03–1.44). After adjustment on age, liver enzymes, FIB-4, platelet, HbA1c, uric acid concentration remained independently associated with advanced fibrosis (Odds Ratio: 0.93, 95% CI: 0.87–0.98), cirrhosis (Odds Ratio: 0.91, 95% CI: 0.84–0.99), but was not associated anymore with hepatocyte ballooning. Uric acid concentration was significantly higher in patients with steatosis (5.9 mg/dL SD 1.4) compared to patients without steatosis (5.5 mg/dL SD 1.5).

Conclusion: Uric acid was independently associated with steatosis while it was independently inversely associated with the presence of advanced fibrosis. Further studies are warranted to understand this association and mechanistic link.

FRI-250

An intergenerational study of the prevalence and cardiometabolic significance of steatotic liver disease in adults in the Raine Study
Oyekoya Ayonrinde^{1,2,3}, Leon Adams¹, Trevor Mori¹, Phillip Melton^{1,4}, John Olynyk^{2,3}, Marilyn Zalesko², Andrea Mould⁵, James Fiori², Lawrence Beilin¹, Girish Dwivedi^{1,2}, Frank Sanfilippo¹, Christopher Welman². ¹The University of Western Australia, Perth, Australia; ²Fiona Stanley Hospital, Murdoch, Australia; ³Curtin University, Bentley, Australia; ⁴University of Tasmania, Hobart, Australia; ⁵Fiona Stanley Hospital, Perth, Australia
Email: oyekoya.ayonrinde@uwa.edu.au

Background and aims: Steatotic liver disease (SLD) is the most common chronic liver disease globally. SLD is associated with increased risk of cardiometabolic disorders. We aimed to compare the prevalence and metabolic significance of SLD in two generations of adults participating in the Raine Study, a longitudinal cohort study. **Method:** Middle-aged adults (Gen1) and their adult offspring (Gen2) participating in a cross-sectional follow-up of the Raine Study in Australia, had liver assessments using controlled attenuation parameter (CAP) with transient elastography (TE), anthropometry, and fasting blood tests. SLD was defined by CAP ≥ 275 dB/m, grade 3 steatosis as CAP ≥ 331 dB/m, and significant liver fibrosis as liver stiffness measurement (LSM) ≥ 8.0 kPa. Associations between liver and cardiometabolic characteristics were sought.

Results: The cohort comprised 331 Gen1 adults (63% female) with mean (SD) age 60 (7) and 252 Gen2 adults aged 33 (6) years (46% female). SLD was diagnosed in 26% Gen1s vs. 19% Gen2s ($p=0.05$). Among Gen1s 24% had metabolic dysfunction-associated steatotic liver disease (MASLD), 1% metabolic plus alcohol-related liver disease (MetALD) and 1% alcohol-related liver disease (ALD). Gen2s had 16% MASLD, 0% MetALD and 2% ALD. In both Gen1 and Gen2 mean [SD] body weight (92.6[19.5] kg vs. 76.3[15.3] kg), body mass index (31.3 [6.2] kg/m² vs. 26.2[4.5] kg/m²), waist (104.8[13.5] cm vs. 89.8 [12.7] cm, CAP (315[33] dB/m vs. 213[38] dB/m) were higher in those with SLD compared with those without SLD, $p<0.05$ for all. Mean serum glucose (5.2[1.3] mmol/L vs. 4.7[0.8] mmol/L), alanine aminotransferase (40.9[30.6] IU vs. 28.2[13.9] IU), remnant lipoprotein cholesterol (RLP-C) (0.65[0.30] mmol/L vs. 0.49[0.24] mmol/L), and median[IQR] homeostasis model for insulin resistance (1.9[1.2–2.9] vs. 1.1[0.8–1.6]) were higher in those with SLD, $p<0.05$ for all. Compared with Gen2s, Gen1s had a higher prevalence of central obesity (78% vs. 55%, $p<0.001$), type 2 diabetes mellitus (T2DM) (6.2% vs. 1.3%, $p=0.004$), impaired fasting glucose or T2DM (IFG/T2DM) (16.3% vs. 2.2%, $p<0.001$), and significant hepatic fibrosis (4.7% vs. 1.2%, $p=0.03$), but a similar prevalence of grade 3 hepatic steatosis (6.3% vs. 6.5%, $p=0.94$). Using multivariable logistic regression analyses, grade 3 steatosis (OR 8.14, 95% CI 2.73–24.31), central obesity (OR 4.47, 95% CI 1.27–15.81), and RLP-C (OR 5.27, 95% CI 1.71–16.21) were associated with IFG/T2DM after adjusting for age, sex and LSM in the Gen1s. In the Gen2s, grade 3 steatosis (OR 12.51, 95% CI 1.40–111.72), but not waist, RLP-C, sex, age or LSM, was associated with IFG/T2DM.

Conclusion: The prevalence of SLD and suspected liver fibrosis was higher in middle-aged than in younger adults. Severe hepatic steatosis with or without central adiposity increases the likelihood of a diagnosis of IFG/T2DM. Liver fibrosis was not significantly associated with IFG/T2DM.

FRI-251-YI

Hepatic steatosis contributes to cognitive impairment in patients with metabolic dysfunction-associated steatotic liver disease and/or type 2 diabetes-mellitus

Nuria Pérez Diaz del Campo¹, Arianna Ferro¹, Gabriele Castelnovo¹, Gian Paolo Caviglia¹, Chiara Rosso¹, Marta Guariglia¹, Eleonora Dileo¹, Angelo Armandi^{1,2}, Francesca Saba¹, Giorgio Maria Saracco^{1,3}, Federica Barutta⁴, Guglielmo Beccuti¹, Gabriella Gruden⁴, Elisabetta Bugianesi^{1,3}. ¹University of Turin, Department of Medical

Sciences, Turin, Italy; ²University Medical Center of the Johannes Gutenberg-University, Metabolic Liver Disease Research Program, I. Department of Medicine, Mainz, Germany; ³University Hospital “Città della Salute e della Scienza”, Division of Gastroenterology, Turin, Italy; ⁴Laboratory of Diabetic Nephropathy, Department of Medical Sciences, University of Turin, Turin, Italy
Email: nuria.perezdiazdelcampo@unito.it

Background and aims: Metabolic dysfunction-associated steatotic liver disease (MASLD) coexists with multiple comorbidities such as obesity, type 2 diabetes mellitus (T2DM), and metabolic syndrome, all contributing to impaired vascular function and thus worsening cognitive impairment. However, the biological mechanism underlying the association between MASLD and cognitive dysfunction has not yet been elucidated. In this study, we aimed to assess the impact of hepatic steatosis on cognitive impairment in patients with MASLD and T2DM.

Method: A total of 601 patients diagnosed with MASLD and/or T2DM underwent evaluation of liver stiffness by transient elastography and liver steatosis by controlled attenuation parameter (CAP) (Fibroscan®530, Echosens). According to the established cut-off, a CAP value ≥ 300 dB/m was used to identify severe steatosis (S3). The cognitive function was assessed by the Repeatable battery for assessment of neuropsychological status (RBANS); the questionnaire evaluates the overall cognitive function and five subdomains assessing immediate memory, visuospatial and constructional function, language function, attention and delayed memory. Score values <90 points were indicative of cognitive impairment.

Results: Overall, the median age was 59 years (range 51–65) and 58.6% of patients were male. Impaired overall cognitive function was observed in 288 (47.9 %) patients (median score value 91, 78–107), with the most prevalent deficit in attention ($n=130$; 78.4%), followed by immediate memory ($n=295$; 49.1 %), language function ($n=289$; 48.1%), visuospatial and constructional function ($n=230$; 38.3 %), and delayed memory ($n=225$, 37.4 %). 278 subjects (46.3 %) had severe steatosis and showed increased liver stiffness, AST, ALT, GGT and triglycerides levels compared to those with CAP <300 ($p<0.001$ for all). Moreover, patients with severe steatosis showed a higher prevalence of overall cognitive as compared to patients with CAP <300 dB/m ($p=0.015$). At logistic regression analyses severe steatosis was significantly associated with cognitive impairment (OR = 1.41, 95 % CI 1.0; 1.9; $p=0.048$) along with arterial hypertension ($p=0.023$) and independently from sex, body mass index, diabetes, dyslipidaemia and obstructive sleep apnoea.

Conclusion: Our results suggest that severe hepatic steatosis is associated with cognitive impairment. Other comorbidities such as arterial hypertension may contribute to cognitive deterioration. Further longitudinal and interventional studies with a careful cognitive profile are needed to replicate these results. *This research has been supported by the Italian Ministry for Education, University and Research (MIUR) under the programme “Dipartimenti di Eccellenza 2018–2022” Project code D15D18000410001.*

FRI-254

Global prevalence, clinical characteristics, histology and outcomes of PNPLA3 I148M variant in metabolic dysfunction-associated steatotic liver disease: a systematic review and meta-analysis

Matheus Souza¹, Ivanna Diaz², Lubna Al-Sharif³, Cristiane Villela-Nogueira¹, Alessandro Mantovani⁴. ¹Federal University of Rio de Janeiro, Rio de Janeiro, Brazil; ²Suny Downstate Health Sciences University, New York, United States; ³An-Najah National University, Nablus, Palestine; ⁴University and Azienda Ospedaliera Universitaria Integrata of Verona, Verona, Italy
Email: matheushenrique.gs@hotmail.com

Background and aims: PNPLA3 rs738409 variant is a risk factor for onset and progression of metabolic dysfunction-associated steatotic liver disease (MASLD). We performed a systematic review and meta-

POSTER PRESENTATIONS

analysis to assess the global prevalence, clinical and histological characteristics, and long-term outcomes of the *PNPLA3* variant in MASLD.

Method: We searched PubMed and Embase up to December 2023 for observational studies of *PNPLA3* genotyped adults (≥ 18 years) with MASLD. Proportions were pooled using a generalised linear mixed model. Continuous and dichotomous variables were analysed using random effects modelling. Primary outcome was the minor allele frequency of the G allele [MAF (G)] of the rs738409 at *PNPLA3* in MASLD patients. Secondary outcomes were comparisons of clinical, histological and long-term outcomes of *PNPLA3* variant versus *PNPLA3* CC. We also performed subgroup, meta-regression and sensitivity analyses. Publication bias was assessed using funnel plots, Egger's test and trim-and-fill analysis.

Results: A total of 112 studies (113, 786 MASLD subjects) were included. We found an overall MAF (G) of 0.45 (95%CI 0.43;0.48, $I^2 = 97.9\%$). After adjustment for publication bias, a more conservative MAF (G) estimate of 0.39 (95%CI 0.36;0.42, $I^2 = 98.4\%$) was obtained. This allele frequency varied significantly worldwide, with the highest MAF (G) in the Latin America (0.63 95%CI 0.52;0.72, $I^2 = 96.2\%$) and East Asian (0.50, 95%CI 0.47;0.53, $I^2 = 95.0\%$) regions, and the lowest in Europe (0.38, 95%CI 0.34;0.41, $I^2 = 96.3\%$). Notably, no African countries were identified. Patients with *PNPLA3* variant had lower values of WC (CG: MD -2.18 cm, 95%CI -3.12 ; -1.23 , $I^2 = 0\%$ /GG: MD -2.30 cm, 95%CI -4.36 ; -0.24 , $I^2 = 57.4\%$) and TG (CG: MD -12.04 mg/dL, 95%CI -22.17 ; -1.90 , $I^2 = 50.2\%$ /GG: MD -21.32 mg/dL, 95%CI -39.91 ; -2.73 , $I^2 = 91.4\%$), and higher AST (CG: MD 2.83 U/L, 95%CI 0.99;4.68, $I^2 = 63.2\%$ /GG: MD 5.76 U/L, 95%CI 4.17; 7.35, $I^2 = 66.9\%$) and ALT (CG: MD 5.99 U/L, 95%CI 2.57;9.42, $I^2 = 60.9\%$ /GG: MD 11.40 U/L, 95%CI 7.99; 14.81, $I^2 = 73.2\%$) levels compared to *PNPLA3* CC. Similarly, we observed that *PNPLA3* variant carriers had higher histological severity and odds of advanced stages of MASLD. *PNPLA3* GG carriers had an increased risk of overall mortality, liver-related events and mortality, and cirrhosis. In addition, our univariable meta-regressions showed the influence of adiposity, age and diabetes mellitus on some *PNPLA3* expression parameters.

Conclusion: This study reveals the global pattern of *PNPLA3* prevalence and its clinical, histological and outcomes implications in MASLD. Our findings underscore the importance of *PNPLA3* genotyping in clinical trials and advocate for personalized medicine approaches. Further research is needed on genetic epidemiology for underrepresented populations, challenges of incorporating genotyping into clinical practice, and gene-environment interactions.

FRI-255

Modeling the burden of steatotic liver disease and its subcategories in people living with HIV in Germany

Maurice Michel^{1,2}, Angelo Armandi^{1,3}, Diana Granz^{1,2}, Katharina Bayer^{1,2}, Leonard Kaps^{1,4}, Wolfgang Maximilian Kremer², Christian Labenz^{1,2}, Peter R. Galle^{1,2}, Daniel Grimm², Jörn M. Schattenberg^{1,4}. ¹Metabolic Liver Research Program, I. Department of Medicine, University Medical Centre Mainz, Mainz, Germany; ²I. Department of Medicine, University Medical Centre Mainz, Mainz, Germany; ³Division of Gastroenterology and Hepatology, Department of Medical Sciences, University of Turin, Turin, Italy; ⁴Department of Internal Medicine II, Saarland University Medical Centre, Homburg, Germany
Email: maurice.michel@icloud.com

Background and aims: People living with HIV (PLWH) show a high prevalence of metabolic comorbidities and other partially overlapping liver-related risk factors, including co-infections with hepatitis B (HBV) and hepatitis C (HCV) virus, which increase the risk of steatotic liver disease (SLD) and liver fibrosis, leading to worse outcomes. However, the disease burden of SLD, its different subcategories, and associated risk factors in PLWH under antiretroviral therapy according to the new nomenclature on SLD remain to be determined.

Method: In this prospectively enrolling cohort study, participants with an HIV infection were non-invasively screened using vibration-controlled transient elastography (VCTE) for SLD (controlled attenuation parameter [CAP] ≥ 248 dB/m) and fibrosis (liver stiffness measurement [LSM] ≥ 8 kPa). The subcategories of SLD, including metabolic dysfunction-associated steatotic liver disease (MASLD), MASLD and increased alcohol intake (MetALD), alcohol-associated liver disease (ALD), and associated cardiometabolic criteria were defined according to the recently published new nomenclature on SLD. The Fibroscan-AST (FAST) score was used to identify those with metabolic-dysfunction associated steatohepatitis (MASH) and significant fibrosis, using a cut-off ≥ 0.67 . Uni- and multivariable logistic regression analysis was used to determine predictors of SLD.

Results: In the entire cohort of 325 participants, 71.4% were male and the median age was 51 (41; 58) years. The median HIV disease duration was 12 (5; 20) years and the majority had a CD4 cell count $\geq 500/\mu\text{L}$ (70.2%). A history of HBV and HCV was detected in 19.4% ($n = 63$) and 5.8% ($n = 19$), respectively. Median BMI (kg/m^2) was 25.3 (22.5; 28.5), and 17.5% ($n = 57$) were obese (BMI $\geq 30 \text{ kg}/\text{m}^2$). Insulin resistance was detected in 24.3% ($n = 79$). The overall prevalence of SLD was 50.8% ($n = 165$), with MASLD (42.8%, $n = 139$) showing the highest prevalence as compared to either MetALD (2.5%, $n = 8$) or ALD (0.9%, $n = 3$). Of those with MASLD, 23.7% ($n = 33$) had a history of HBV or HCV coinfection (MASLD-viral). Cryptogenic or other causes (viral, undefined due to missing data) of SLD were identified in 4.3% ($n = 14$). Metabolic comorbidities were overall more prevalent in participants with SLD. Liver fibrosis and MASH were detected in 5.8% ($n = 19$) and 1.8% ($n = 6$), respectively, in those with MASLD. On multivariable analysis, the cardiometabolic criterion with a BMI $\geq 25 \text{ kg}/\text{m}^2$ or a waist circumference $\geq 94/80$ cm (male/female) was associated with the highest risk of SLD (OR 5.2, 95% CI 2.6–10.6, $p < 0.001$). In turn, HIV-related parameters showed no effect on the risk of SLD.

Conclusion: The burden of SLD and especially MASLD is high in PLWH in Germany. Screening for SLD, fibrosis, and associated metabolic comorbidities may reduce the burden of liver disease in PLWH and identify those at higher risk of liver disease progression.

FRI-256-YI

Patients with metabolic-associated steatotic liver disease and portal hypertension have different skeletal muscle and adipose tissue mass than patients with other causes of cirrhosis

Ikram Abow-Mohamed¹, Philip Wong¹, Marc Deschenes¹, Giada Sebastiani¹, Tatiana Cabrera¹, Louis-Martin Boucher¹, David Valenti², Ali Bessissow¹, Amine Benmassaoud¹. ¹McGill University Health Centre (MUHC), Montreal, Canada, ²McGill University Health Centre (MUHC), Montreal, Canada
Email: ikram.abow-mohamed@mail.mcgill.ca

Background and aims: Low muscle mass has been associated with mortality in patients with cirrhosis. The impact of the etiology of liver disease on this association remains unknown especially following the new formal classifications of patients with metabolic-associated steatotic liver disease (MASLD). We aimed to compare the body composition of patients with or without pure MASLD when HVPG ≥ 10 mmHg.

Method: This retrospective cohort study conducted at the McGill University Health Centre included adults with cirrhosis and Hepatic Venous Pressure Gradient (HVPG) between 2012 and 2022. Total skeletal muscle index (SMI), and subcutaneous and visceral adipose tissue indices (SATI, VATI) at the 3rd lumbar vertebrae were measured at the time of HVPG using computed tomography images and CoreSlicer, for body composition analysis. We compared the body composition of patients with or without MASLD. Variables associated with MASLD were assessed using univariate and multivariate logistic regression analyses reporting adjusted odds ratio (aOR) with a 95% confidence interval (CI).

Results: Overall 99 patients were included (mean age: 58.8 years, male gender 61.6%, MASLD 36.4%, clinically significant portal

hypertension: 66.7%, decompensated liver disease: 60.2%, Child-Pugh score A/B/C: 27.8%/45.4%/26.8%, Model for End-stage liver disease [MELD]: 15.6). Patients with MASLD had less decompensated liver disease (42.9% vs 69.8%, $p = 0.01$), and lower MELD score (13.2 vs 16.9, $p = 0.002$), but had similar age, gender, and HVPG than patients without MASLD. Patients with MASLD had higher SMI (51.9 cm²/m² vs 45.0 cm²/m², $p = 0.008$), SATI (94.2 cm²/m² vs 54.2 cm²/m², $p < 0.001$), and VATI (79.5 cm²/m² vs 52.7 cm²/m², $p = 0.001$) compared to patients without MASLD. In univariate logistic regression analysis, when HVPG ≥ 10 mmHg, patients with MASLD were associated with higher SMI (OR1.08, 95% CI 1.02–1.13), SATI (OR1.04, 95% CI 1.01–1.04) and VATI (OR1.02, 95% CI 1.01–1.04) compared to non-MASLD. After adjusting for age, and prior decompensation, when HVPG ≥ 10 mmHg, higher SMI (aOR1.08, 95% CI 1.02–1.15), SATI (aOR1.02, 95% CI 1.01–1.04) and VATI (aOR1.02, 95% CI 1.01–1.04) remained independently associated with patients with MASLD compared to non-MASLD. These associations remained true when adjusted for age and MELD score instead.

Conclusion: In our single-center cohort, after adjusting for confounders, patients with MASLD had different body composition characteristics than patients without MASLD including higher muscle mass.

FRI-257

Metabolic dysfunction associated steatohepatitis (MASH) disease progression phenotyping features based on medical claims

Magda Berberova¹, Petar Nikolov², Deepa Kumar², Liuqiang Lu³.

¹ICON plc, Leopardstown, Dublin 18, Ireland, Dublin, Ireland; ²ICON plc, Dublin 18, Ireland, Ireland; ³ICON plc, Leopardstown, Dublin 18, Ireland, Dublin 18, Ireland, Ireland

Email: magda.berberova@iconplc.com

Background and aims: To define and assess the phenotype of progressing MASH in comparison to the general United States (US) MASH population in regards of the medical claims features and diagnoses reported.

Method: ICON's US medical and prescription longitudinal anonymised records data was leveraged for this analysis of newly diagnosed MASH patients [OCT2018-SEP2020] to collect age, gender and observed conditions information. New diagnoses were confirmed by the absence of MASH and cirrhosis-related conditions records in the two years prior to the MASH diagnosis. For eligible population, disease progression and pace were determined based on the development of cirrhosis-related conditions within three years of MASH diagnosis, categorizing them as Fast Progressors v. Other. Descriptive statistics, significance tests (p value < 0.05) of findings specific parameters/morbidities and speed of progression are performed.

Results: A total of 38 823 individual records have been identified with newly diagnosed MASH followed up for 3 years, based on the above criteria, within them a subpopulation of 5993 cases (15%) meeting the Fast progression definition. More than half of the total population are females, and females gender is significantly higher in the Fast progressors. Mean age is also significantly higher in the Fast progressors (61.3 \pm 13.1) compared to the rest (53.7 \pm 14.2). Between the most frequent co-morbidities significantly more presented in the Fast progressors are the type 2 diabetes mellitus (40% v 28%) and dyslipidaemia (40% v 37%), followed by anaemia (16% v 9%), coronary artery disease (12% v 7%) and heart failure (5% v 1%), all p values < 0.05 . Leading body system affected in the Fast progressors with significant magnitude of difference to the rest of MASH population are assessed as well.

Conclusion: Around 15% of the total MASH population shows disease progression-related medical features diagnosed within a 3 years follow-up period after the initial MASH diagnosis. The Fast progressor phenotype is more frequently female, higher mean age between 55

and 75 years, with a diagnosed cardiovascular or renal co-morbidities, a drug use and dependence records, respiratory morbidities (sleep apnoea), circulatory and endocrinology disease states. Within the most frequent metabolic syndrome related co-morbidities the arterial hypertension and type 2 diabetes are significantly higher in the Fast progressors, similarly like the sleep apnoea, osteoarthritis, depression, anaemia and shortness of breath. We would consider the above features of the MASH phenotype as potential markers of higher medical attention for treatment and prevention within the MASH-related medical care.

FRI-258

Pruritus is frequent, burdensome, and persistent in metabolic dysfunction-associated steatohepatitis (MASH) and primary biliary cholangitis (PBC): a 6-month longitudinal study

Usha Gungabissoon¹, Jake Hunnicutt², Eleanor McDermott³, Andrew Lovley⁴, Monica Frazer⁴, Kaitlin LaGasse⁴, Mark Kosinski⁴, Kristen McCausland⁴, Anna Halliday¹, Ashleigh McGirr⁵, Helen T. Smith¹, Gideon M. Hirschfield⁶, Palak J. Trivedi⁷. ¹GSK, London, United Kingdom; ²GSK, Collegeville, PA, United States; ³GSK, Stevenage, United Kingdom; ⁴QualityMetric Incorporated, LLC, Johnston, RI, United States; ⁵GSK, Mississauga, ON, Canada; ⁶Toronto Centre for Liver Disease, University of Toronto, Toronto, ON, Canada; ⁷University of Birmingham, Birmingham, United Kingdom

Email: usha.2.gungabissoon@gsk.com

Background and aims: Pruritus is a symptom typically associated with cholestasis. However, the burden of pruritus in non-cholestatic liver disorders has not been systematically evaluated. This online, longitudinal, patient (pt)-reported outcome (PRO) study sought to characterise pruritus over 6 months in pts with a range of chronic liver diseases (CLDs). Here, we analyse pruritus in pts with MASH and present these data in the context of PBC-an archetypal chronic cholestatic disease.

Method: Adults with CLDs including MASH or PBC residing in the USA, UK, Canada or Germany were recruited via pt advocacy groups, healthcare provider referral or other methods. Pts were screened online for study eligibility, which included pruritus (reported using worst itch numerical rating scale [WI-NRS] with a 3-month recall) and a confirmed diagnosis of liver disease (via physician note, medical records etc.). Pruritus of extrahepatic origin or prior liver transplant were exclusion criteria. Validated PRO measures including WI-NRS (2-week recall) and 5-D itch, as well as items developed specifically for the study were completed at baseline, 3 and 6 months. In this analysis, pt experience, frequency, impact and persistence of pruritus were examined in pts with MASH or PBC.

Results: Among 97 pts with MASH and 174 with PBC who were screened for this study, 69% and 49% reported any pruritus (WI-NRS score ≥ 1 , 3-month recall), respectively. At baseline, eligible pts in the MASH cohort (N=61) were younger than those with PBC (N=80) (mean [SD] 54.0 [9.9] vs 57.1 [10.6] years) and more often men (44% vs 11%). Overall, 49% of pts with MASH reported moderate-to-severe pruritus (NRS score ≥ 4) on the WI-NRS (2-week recall) compared with 64% in the PBC group. Both cohorts used similar terms to describe their pruritus: 'deep' (64/68%), 'urgent' (59/58%), 'scratching does not help' (46/51%) and 'relentless' (44/45%). Mean (SD) 5-D itch total score indicated moderate pruritus in both cohorts; but was significantly lower in MASH than PBC (12.0 [3.2] vs 13.5 [3.9]; $p < 0.05$). Additionally, mean (SD) disability (2.5 [1.2] vs 3.1 [1.3]) and distribution domain scores (1.9 [0.9] vs 2.3 [1.2]) were lower in MASH vs PBC (both $p < 0.05$). The duration, degree and direction domain scores were similar between cohorts. Longitudinal analyses revealed pruritus, especially moderate-to-severe, recorded on WI-NRS (2-week recall), was largely consistent over 6 months of follow-up; in MASH, 49% of pts had moderate-severe pruritus at baseline, 56% at 6 months, while in PBC, 64% had moderate-severe pruritus at both baseline and 6 months.

POSTER PRESENTATIONS

Conclusion: Our results show that pruritus in MASH is common, burdensome and persists over time.

In both MASH and PBC, moderate-severe pruritus was frequent, pts used similar language to describe pruritus, and itch impact was comparable across many 5-D itch domains.

Funding: GSK (209971).

FRI-259

A real-life multidisciplinary clinic approach for the management of metabolic dysfunction associated steatotic liver disease

Raluca Pais^{1,2}, Thomas Maurel³, Pascal Lebray⁴, Luminita Bonyhay⁴, Charlotte Bouzbib⁴, Stephanie Combet⁵, Marika Rudler⁶, Dominique Thabut⁷, Vlad Ratziu^{2,8}. ¹Sorbonne University, Assistance Publique-Hôpitaux de Paris, Pitié Salpêtrière Hospital, Foundation for Innovation in cardiometabolism and Nutrition (IHU-ICAN), Paris, France; ²Foundation for Innovation in Cardiometabolism and Nutrition (IHU-ICAN), Paris, France; ³Assistance Publique Hôpitaux de Paris, Pitié Salpêtrière Hospital, Paris, France; ⁴Assistance Publique Hôpitaux de Paris, Pitié Salpêtrière Hospital, Paris, France; ⁵Foundation for Innovation in Cardiometabolism and Nutrition (IHU-ICAN), Paris, France; ⁶Sorbonne University, Brain Liver Pitié-Salpêtrière (BLIPS) study group, Assistance Publique-Hôpitaux de Paris, Pitié Salpêtrière Hospital, Paris, France; ⁷Sorbonne University, Brain Liver Pitié-Salpêtrière (BLIPS) study group, Assistance Publique-Hôpitaux de Paris, Pitié Salpêtrière Hospital, Paris, France; ⁸Sorbonne University, Assistance Publique-Hôpitaux de Paris, Pitié Salpêtrière Hospital, Paris, France
Email: raluca.pais@aphp.fr

Background and aims: Metabolic dysfunction associated steatotic liver disease (MASLD) is associated with the metabolic syndrome, type 2 diabetes (T2D), dyslipidemia and cardiovascular (CV) complications. Therefore integrated multidisciplinary clinics (MDCs) for diagnosis and management are preferable to siloed approaches. We aimed to investigate the effectiveness of MDCs for the management of MASLD using surrogate markers of liver injury and CV risk.

Method: Real-life prospectively collected data of patients with known or newly diagnosed MASLD referred to a MDCs with comprehensive hepatological (liver stiffness measurement, LSM), by vibration controlled transient elastography and shear-wave elastography), metabolic and CV risk assessment (coronary calcium score, CAC), dietetic counseling, patients' education program (PEP) and questionnaires to assess disease awareness.

Results: 381 pts were prospectively included between 2019–2023, 288 with previously established and 93 with a newly diagnosed MASLD; 56% males, mean age 59 ± 11 yrs, mean BMI 32.3 ± 5.7 kg/m². 48% T2D, 53% high blood pressure (HBP), 50% dyslipidemia and 12% known coronary artery disease (CAD); 11% had cirrhosis and 25% were F3 by either liver biopsy (LB) or LSM. Following evaluation in the MDCs, 19% of pts were newly diagnosed with T2D or prediabetes, 30% of pts without known CAD had high to moderate CV risk (19% had CAC ≥ 300 and 11% had CAC of 100–300 Agatston UI); 58% had insufficiently controlled LDLc and needed statin dose adjustment) and 14% were initiated on statins. Among patients with newly diagnosed MASLD, 44% had T2D, 54% had HBP, 46% had dyslipidemia, 10% had known CAD; 12% had cirrhosis and 25% F3 fibrosis. Following MDCs, 25% were prescribed LB; 20% were diagnosed with CAD and 26% were seen by a cardiologist for treatment adjustment; 20% were diagnosed T2D or prediabetes; 20% were initiated on statins. Disease awareness was low in 52% of pts: 62% of pts were not aware of the risk factors to develop MASLD; However, 75% of pts believed that MASLD can progress to cirrhosis and 48% expressed anxiety in relation to the MASLD diagnosis. Mean follow-up was 9 ± 5 months. 53% of pts lost weight (mean weight loss, WL = 5 ± 4.7 kg): ≤5% in 65%; 5–10% in 24%; ≥10 in 11%. 14% of patients had stable weight and 33% gained weight (3 ± 2.5 kg). During follow-up there was a significant reduction in ALT ($p < 0.001$), GGT ($p = 0.027$), fasting insulin ($p = 0.05$) and liver fat content assessed by CAP (0.035). 65% of pts entered

a PEP; they had significant WL and reduction in ALT, lipids (total cholesterol and LDLc) and steatosis. There was no significant variation in WL, LFT and lipid parameters in patients without PEP.

Conclusion: MDC models can be effectively implemented in real-life settings with substantial benefit for the diagnosis of hepatic, metabolic and CV comorbidities. Implementation of PEP results in hepatic, metabolic and CV risk improvement.

FRI-260

Diagnosed prevalence of cardio-renal diseases, mental health disorders, sleep apnea, cancer, and mortality rates in more than 18, 000 patients with metabolic dysfunction-associated steatohepatitis with and without cirrhosis from the United States

Jörn M. Schattenberg¹, Claudio Sartini², Ronald Herrera², Mireia Raluy³, Mark Yates⁴, Ramy Younes⁵. ¹Saarland University Medical Center, Homburg, Germany; ²Boehringer Ingelheim International GmbH, Global Epidemiology and Real-World Evidence, Ingelheim, Germany; ³Evidera, Data Analytics, Borlänge, Sweden; ⁴Evidera, Data Analytics, London, United Kingdom; ⁵Boehringer Ingelheim International GmbH, Medicine, Cardio Metabolism and Respiratory, Ingelheim, Germany
Email: joern.schattenberg@uks.eu

Background and aims: The disease burden of metabolic dysfunction-associated steatohepatitis (MASH) extends beyond the liver, impacting especially the cardio-renal system. The prevalence of co-existing diseases in patients with MASH at different disease stages, such as sleep apnea, mental health disorders, and cancer, is not fully understood. This study uses ICD codes to compare the diagnosed prevalence of comorbidities across the disease spectrum including in patients with no evidence of cirrhosis (NC), with compensated cirrhosis (CC), and with decompensated cirrhosis (DC) in the real world setting. We hypothesized that patients with MASH and DC have higher prevalence of comorbidities and that mortality rates were similar in comparison with prior biopsy-based studies.

Method: Retrospective cohort study (2016–2021 years) using Optum Market Clarity (linked claims and electronic health records) from the United States. MASH was defined by the first ICD10 diagnosis code (K75.81 Non-alcoholic steatohepatitis) recorded during the study period, presence of AST, ALT and platelets tests carried out 3 months prior/after diagnosis, and absence of diseases prior/at diagnosis, such as alcoholic, or other chronic liver diseases. Codes for cirrhosis and decompensation were used to classify NC, CC, and DC. Both ICD and National Drug Codes were used to assess comorbidities prevalence at/ or prior to MASH diagnosis. Mortality incidence rates were estimated in each sub-group.

Results: 18, 710 MASH patients were included (mean age 44 years, 95% with BMI ≥ 25 and 52% with diabetes, 73% NC, 9% CC, and 18% DC). In patients with MASH DC vs NC, the prevalence of sleep apnea, heart failure, renal disease, chronic kidney disease, hematological malignancies, and dementia was 38% vs 33%, 32% vs 10%, 31% vs 11%, 28% vs 9%, 16% vs 10%, and 5% vs 1% respectively. Mental health disorders were highly prevalent in all patients (39–43% for anxiety, while 37–41% and 15–19% used at least once anti-depressant and anti-psychotic drugs respectively). In patients with DC, CC, and NC the all-cause mortality incident rate per 1000 person-year was 113, 35, and 8 respectively. 1465 patients died: liver-related causes were responsible for 20%, 14% and 6% of the deaths in MASH DC, CC, and NC.

Conclusion: Patients with MASH live with several comorbidities beyond known metabolic diseases. Patients with DC had higher comorbidities prevalence and remarkably higher all-cause and liver-related mortality rates. Our mortality rates estimations were in line with prior biopsy-based studies: as there is no standard set of ICD codes to define MASH by disease stage, these findings i) contribute to the current debate about consensus of ICD codes that could be the reference standard in the real world studies to classify MASH NC, CC, and DC and ii) inform clinical trials study designs, where inclusion/exclusion criteria for some comorbidities could be applied.

FRI-261-YI

Steatotic liver disease predicts cardiovascular disease and advanced liver fibrosis: a community-dwelling cohort study with 20-year follow-up

Hun Jee Choe¹, Joon Ho Moon², Won Kim³, Bo Kyung Koo³, Nam H. Cho⁴, Young Ho So⁵, Yong Jin Jung⁶. ¹Hallym University Dongtan Sacred Heart Hospital, Hwaseong-si, Gyeonggi-do, Korea, Rep. of South; ²Seoul National University Bundang Hospital, Seongnam, Gyeonggi-do, Korea, Rep. of South; ³Seoul National University College of Medicine, Seoul, Korea, Rep. of South; ⁴Ajou University School of Medicine, Suwon, Gyeonggi-do, Korea, Rep. of South; ⁵Seoul National University College of Medicine, Department of Radiology, SMG-SNU Boramae Medical Center, Seoul, Korea, Rep. of South; ⁶Seoul National University College of Medicine, Department of Internal Medicine, SMG-SNU Boramae Medical Center, Seoul, Korea, Rep. of South
Email: hunjeechoe@snu.ac.kr

Background and aims: Steatotic liver disease (SLD) has emerged as new nomenclature to increase awareness and reflect the pathophysiology of the disease better. We investigated the risk of advanced fibrosis and cardiovascular disease (CVD) in SLD using data derived from a Korean prospective cohort.

Method: We defined SLD using the fatty liver index (FLI) and identified advanced fibrosis with the age-adjusted Fibrosis-4 Index. SLD was further subcategorized into metabolic dysfunction-associated SLD (MASLD), MASLD with increased alcohol intake (MetALD), and alcohol-associated liver disease (ALD).

Results: The Ansung-Ansan cohort of the Korean Genome and Epidemiology study, following 9,497 participants from 2002 to 2020, included 3,642 (38.3%) with MASLD, 424 (4.5%) with MetALD, and 207 (2.1%) with ALD. During the median follow-up of 17.5 years, CVD risk was higher in those with MASLD (hazard ratio [HR], 1.27; 95% confidence interval [CI], 1.12–1.45; $p < 0.001$), MetALD (HR, 1.88; 95% CI, 1.33–2.65; $p < 0.001$), and ALD (HR, 1.95; 95% CI, 1.01–3.77; $p < 0.001$) than in those without SLD, after adjusting for conventional risk factors. Notably, the CVD risk was higher in the MetALD than in the MASLD group ($p = 0.027$). In the MASLD group, the number of cardiometabolic risk factors (CMRFs) correlated positively with CVD risk (HR, 1.34; 95% CI, 1.24–1.45; $p < 0.001$ for trend). Among the CMRFs, hypertension (HR, 1.94; 95% CI, 1.63–2.31; $p < 0.001$) was the predominant contributor to CVD. The MASLD (HR, 1.39; 95% CI, 1.25–1.55; $p < 0.001$), MetALD (HR, 1.75; 95% CI, 1.38–2.23; $p < 0.001$), and ALD (HR, 2.00; 95% CI, 1.30–3.07; $p = 0.002$) groups had a higher risk of advanced fibrosis than did the non-SLD group ($p < 0.001$ for trend).

Conclusion: Our study provides new insight into hepatic and cardiovascular outcomes related to SLD subtypes. A progressive increase in CVD risk was found from MASLD to MetALD. The SLD subcategories, considering CMRFs and alcohol intake, outperformed traditional fatty liver categorizations in predicting CVD risk. The proposed SLD terminology could impact clinical practice, warranting further exploration of the heterogeneity of clinical outcomes among SLD subtypes.

FRI-262

Liver Fibrosis in Metabolic Dysfunction-Associated Steatotic Liver Disease is Independently Associated with Reduced Kidney Function

Gres Karim¹, Carolina Villarroel², Dewan Giri³, Ilan Weisberg¹, Amreen Dinani⁴. ¹New York Presbyterian Brooklyn Methodist Hospital, New York, United States; ²Mount Sinai Beth Israel, New York, United States; ³Mount Sinai Beth Israel, New York, United States; ⁴Duke University Hospital, Durham, United States
Email: karimgres@gmail.com

Background and aims: Metabolic dysfunction-associated steatotic liver disease (MASLD) and chronic kidney disease (CKD) share several phenotypic characteristics, such as type 2 diabetes (T2DM), obesity and hypertension (HTN). Presence of metabolic syndrome, dysbiosis, and unhealthy diets have been postulated as mechanisms linking

MASLD and CKD. The aim of this study is to explore the association and risk factors between MASLD and CKD in a cohort of patients with obesity, a population at high risk for developing both MASLD and CKD.

Method: Patients with obesity (defined as body mass index [BMI] > 30 kg/m²) and MASLD (ICD-10 codes K76.0 and K75.8) were identified using electronic medical record (EMR) at a tertiary care clinic between 06/2019 to 06/2020. Demographics, ethnicity, medical conditions, markers of liver inflammation and synthetic function were recorded. To assess the health of renal function, glomerular filtration rates (GFR) were recorded. Fibrosis Index 4 (FIB4) was calculated to determine the degree of liver fibrosis. Univariate analysis was performed using t-tests for continuous variables and chi-square or Fisher's exact tests for categorical variables. Multivariate analysis and adjustment for confounders was performed using generalized linear models including linear regression.

Results: A total of 546 patients with MASLD were identified from a cohort of patients with obesity. Majority were female (58.6%), mean age 56 years (SD 12.7), and mean BMI 35.7 kg/m² (SD 5.49). Hispanics constituted 24%, 15.2% were black and 37.9% were white. Approximately half (49.6%) had HTN and 34.9% had T2DM. Age ($p < 0.001$), ALT ($p = 0.01$), albumin ($p = 0.011$) and FIB4 ($p = 0.005$) were associated with changes in GFR in univariate analysis. In univariate linear regression, reducing GFR was associated with higher FIB4 (effect size [beta] of one-unit increase in GFR on FIB4 = -0.013 , $p < 0.001$). In multivariate linear regression, T2DM was independently associated with increased liver fibrosis (effect size of T2DM on FIB4 = 0.387925 , $p < 0.02$). After adjustment for T2DM, the relationship between GFR and FIB4 was maintained (beta -0.012 , $p < 0.001$). HTN did not significantly change the relationship between GFR and FIB4 in this model ($p > 0.5$). When compared to white race, only patients of black race had a lower FIB4 (effect size of black race on FIB4 = -0.442 compared to white race, $p < 0.05$). Adjusting for race did not alter the underlying relationship between GFR and FIB4.

Conclusion: MASLD is independently associated with reduced kidney function in obese patients. Black race was associated with lower FIB4. Our analysis revealed an inverse relationship between liver fibrosis and GFR which needs to be further explored.

FRI-263

Severity of hepatic steatosis measured with controlled attenuation parameter as a determinant of carotid atherosclerosis in the Raine Study

Oyekoya Ayonrinde^{1,2,3}, Leon Adams¹, Marilyn Zelesco², Christopher Welman², Trevor Mori¹, Phillip Melton^{1,4}, Andrea Mould², Lawrence Beilin¹, James Fiori², Girish Dwivedi^{1,2}, Frank Sanfilippo¹, John Olynyk^{2,3}. ¹The University of Western Australia, Perth, Australia; ²Fiona Stanley Hospital, Murdoch, Australia; ³Curtin University, Bentley, Australia; ⁴University of Tasmania, Hobart, Australia
Email: oyekoya.ayonrinde@uwa.edu.au

Background and aims: Atherosclerotic cardiovascular disease (ASCVD) is a leading cause of morbidity and mortality in people with steatotic liver disease (SLD). We aimed to examine associations between the severity of SLD and carotid intima media thickness (cIMT) as a measure of carotid atherosclerosis.

Method: Middle-aged adults participating in a cross-sectional follow-up of the longitudinal Raine study in Perth, Australia, had comprehensive liver assessments using controlled attenuation parameter (CAP) with transient elastography (TE), anthropometry, fasting blood tests, blood pressure and carotid artery ultrasound. SLD was defined by CAP ≥ 275 dB/m and grade 3 steatosis as CAP ≥ 331 dB/m. cIMT ≥ 1.0 mm was considered to represent carotid atherosclerosis. The sonographers were blinded to the results of the CAP and TE assessments. We examined the relationship between the severity of hepatic steatosis, cardiometabolic risk factors and cIMT.

Results: Three hundred and thirty-one predominantly Caucasian adults with mean (SD) age 60 (7) years had liver assessments. During

POSTER PRESENTATIONS

the same attendance, 132 also had a B-mode carotid artery ultrasound. Overall, 26% had SLD (38% male and 22% female, $p = 0.45$), 6.3% grade 3 hepatic steatosis (8.5% male and 5.0% female), while 25% had carotid atherosclerosis (39% male and 16% female, $p = 0.006$). Those with carotid atherosclerosis were older (66.1 [5.9] vs. 63.7 [5.2] years), had higher body weight (87.0 [13.7] vs. 76.3 [14.6] kg), waist circumference (102.7 [12.0] vs. 94.2 [13.5] cm), body mass index (29.8 [4.6] vs. 27.7 [4.0] kg/m²), and more severe hepatic steatosis (CAP 261 [56] vs 240 [45] dB/m), $p < 0.05$ for all. Furthermore, a finding of carotid atherosclerosis was associated with higher serum glucose (5.5 [1.7] vs. 5.0 [0.8] mmol/L), lower high density lipoprotein cholesterol (1.4 [0.4] vs. 1.5 [0.4] mmol/L) but similar low density lipoprotein cholesterol (3.1 [1.2] vs. 3.2 [1.0] mmol/L and remnant lipoprotein cholesterol (0.6 [0.3] vs. 0.5 [0.3] mmol/L). Using multi-variable logistic regression analysis, older age (OR 1.11, 95% CI 1.01–1.22, $p = 0.003$), a diagnosis of grade 3 hepatic steatosis (OR 9.14, 95% CI 1.23–67.83, $p = 0.03$) and male sex (OR 3.31, 95% CI 1.25–8.76, $p = 0.02$) were associated with carotid atherosclerosis after adjusting for a diagnosis of type 2 diabetes mellitus (OR 3.99, 95% CI 0.83–19.14, $p = 0.08$), central obesity (OR 2.67, 95% CI 0.74–9.59, $p = 0.13$), remnant lipoprotein cholesterol (OR 3.12, 95% CI 0.63–15.52, $p = 0.16$), and liver stiffness measurement (OR 1.07, 95% CI 0.69–1.66, $p = 0.61$).

Conclusion: Severe hepatic steatosis is associated with increased risk of ASCVD, after adjusting for liver fibrosis and traditional cardiovascular risk factors of obesity, atherogenic dyslipidaemia and type 2 diabetes mellitus. Less severe hepatic steatosis did not appear to increase the risk of ASCVD.

FRI-266-YI

Temporal trends in the profile of non-alcoholic fatty liver disease: a decadal experience

Prajna Anirvan¹, Chitta Ranjan Khatua², Preetam Nath³, Sanjib Kar⁴, Manas Kumar Panigrahi⁵, Shivaram Prasad Singh¹. ¹Kalinga Gastroenterology Foundation, Cuttack, India; ²MKCG Medical College and Hospital, Berhampur, India; ³Kalinga Institute of Medical Sciences, Bhubaneswar, India; ⁴Indian Institute of Gastroenterology and Hepatology, Cuttack, India; ⁵All India Institute of Medical Sciences, Bhubaneswar, India
Email: spsingh.cuttack@gmail.com

Background and aims: The world is seeing an unprecedented burden of non-alcoholic fatty liver disease (NAFLD)—almost one in three people have NAFLD. Of late, there has also been a change in the nomenclature of NAFLD and this has generated a lot of interest among clinicians and patients regarding the pathophysiology, management and other clinical aspects of this entity. India harbours a huge chunk of the world's NAFLD population; however, studies evaluating temporal shifts in the profile of these patients are few. The aim of this study was to compare two separate cohorts of patients—one from 2022 to 2023 and the other from 2013 to 2014.

Method: 1537 NAFLD patients (628 belonging to the 2022–23 cohort and 909 belonging to the 2013–14 cohort) were included in this retrospective study. Anthropometric and biochemical parameters of the two groups were compared. Comparison of liver fibrosis by transient elastography was carried out between the two groups.

Results: The mean age of the subjects in both the cohorts was comparable (43.71 ± 11.01 years in the 2022–23 cohort vs 43.53 ± 11.56 years in the 2013–14 cohort). Males predominated in both the cohorts although the proportion was higher in the 2022–23 cohort (79% vs 70.9%, $p < 0.001$). The mean BMI between the two groups was comparable. However, a greater proportion of patients in the 2013–14 cohort had lean NAFLD (13.31% vs 12.4%, $p < 0.05$). The proportion of patients with diabetes mellitus was greater in the 2013–14 cohort (21.25% vs 14.35%, $p < 0.001$), while the proportion of subjects with hypertension was comparable between the two cohorts. The mean AST and ALT levels were significantly higher in the 2022–23 cohort (ALT, 36.31 ± 23.14 U/L vs 29.98 ± 2.10 U/L, $p < 0.001$; AST, 32.65 ± 17.68 U/L vs 26.40 ± 13.50 U/L, $p < 0.001$) although the proportion of

patients with elevated liver enzymes was higher in the 2013–14 cohort (18.04% vs 14.79%, $p < 0.05$). The proportion of subjects with insulin resistance (HOMA-IR > 2) was slightly higher in the 2013–14 cohort (55.25% vs 54.89%, $p < 0.05$). The proportion of patients with significant fibrosis (≥ F2) was greater in the 2022–23 cohort compared to the earlier cohort (29.9% vs 21.78%, $p < 0.001$).

Conclusion: The results of this study conclusively show that compared to a decade ago, the prevalence of significant fibrosis has markedly increased in NAFLD patients. While there have been some shifts in the anthropological and biochemical parameters, the marked increase in the proportion of patients with significant fibrosis deserves immediate attention.

FRI-267

Regional fibrosis progression analysed by digital pathology with artificial intelligence is associated with renal dysfunction

Dan-Qin Sun^{1,2,3}, Jia-Qi Shen^{1,2,3}, Xiao-Fei Tong⁴, Yangyang Li⁵, Giovanni Targher⁶, Yayun Ren⁷, Haiyang Yuan⁸, Chris D. Byrne⁹, Hong You⁴, Ming-Hua Zheng^{8,10}. ¹Urologic Nephrology Center, Jiangnan University Medical Center, Wuxi, China; ²Affiliated Wuxi Clinical College of Nantong University, Wuxi, China; ³Wuxi No.2 People's Hospital, Wuxi, China; ⁴Liver Research Center, Beijing Friendship Hospital, Beijing Key Laboratory of Translational Medicine on Liver Cirrhosis, National Clinical Research Center of Digestive Diseases, Capital Medical University, Beijing, China; ⁵Key Laboratory of Diagnosis and Treatment for the Development of Chronic Liver Disease in Zhejiang Province, Wenzhou, China; ⁶Section of Endocrinology, Diabetes and Metabolism, Department of Medicine, Azienda Ospedaliera Universitaria Integrata Verona, Verona, Italy; ⁷HistoIndex Pte Ltd, Singapore, Singapore; ⁸MAFLD Research Center, Department of Hepatology, the First Affiliated Hospital of Wenzhou Medical University, Wenzhou, China; ⁹Southampton National Institute for Health and Care Research Biomedical Research Centre, University Hospital Southampton and University of Southampton, Southampton General Hospital, Southampton, United Kingdom; ¹⁰Key Laboratory of Diagnosis and Treatment for The Development of Chronic Liver Disease in Zhejiang Province, Wenzhou, China
Email: sundanqin126@126.com

Background and aims: An association between liver fibrosis and kidney dysfunction in metabolic dysfunction-associated fatty liver disease (MAFLD) patients has recently been demonstrated. However, an analysis of hepatic lobule fibrosis progression and kidney function decline in MAFLD has not been undertaken. The second harmonic generation/two-photon excitation fluorescence (SHG/TPEF) microscopy with artificial intelligence analyses can provide automated quantitative assessment of liver fibrosis (qFibrosis) across the liver lobule. In this study, we aimed to discover the potential relationship between the progression of liver fibrosis and kidney function for MAFLD patients using qFibrosis assessment.

Method: In this longitudinal cohort study, formalin-fixed sections from 58 paired liver biopsies were enrolled with completed a 28-month follow-up. Total 184 fibrosis parameters were quantified in 5 liver regions, including portal tract (PT), peri-portal (PP), zone 2, peri-central (PC) and central vein (CV), and qFibrosis continuous (qFC) values were generated for all samples based on 10 fibrosis parameters using qFibrosis assessment. Liver fibrosis progression (LF+) and regression (LF-) was defined as qFC changes of at least a 20% relative difference, and kidney function decline (or improvement) were defined as eGFR changes of at least a 2% relative difference during the 28-month follow-up period. The two-tailed Wilcoxon rank-sum test and the Spearman nonparametric method were performed to test the independence of associations between liver fibrosis and eGFR.

Results: There was no significant difference in liver fibrosis stage and eGFR at the first and second liver biopsy. However, after 28-month follow-up, eGFR values declined in the LF+ group compared to baseline eGFR. Moreover, eGFR change in LF+ group evaluated by qFibrosis was greater than that in LF- group ($p = 0.043$). In addition,

compared with peri-portal area, zone 2 and portal tract area, kidney function decline was significantly correlated with fibrosis changes in the central vein region and peri-central region. Regional qFibrosis parameters were also able to differentiate kidney injury (%CVDi, AUC:0.737, $P=0.003$; #ThinStrCVDi, AUC:0.791, $P=0.000$; StrLengthCVDi, AUC:0.743, $P=0.003$).

Conclusion: Regional qFibrosis assessment by digital pathology with artificial intelligence can demonstrate specific liver lobular changes that are associated with kidney dysfunction. Further study of specific liver injury in MAFLD and renal dysfunction is required.

FRI-268

MASH not NASH: A contemporary study of the impact of cardiac arrhythmias

Charles Yang¹, Trinava Roy¹, Brian Blair¹, Lucy Joo¹, C. J. Foster¹.

¹Jefferson Health New Jersey, Cherry Hill, United States

Email: cxy206@jefferson.edu

Background and aims: Limited data exists specifically looking at metabolic dysfunction-associated steatohepatitis (MASH), formerly known as non-alcoholic steatohepatitis (NASH), and cardiac arrhythmias. We sought to examine the national inpatient sample database to describe in-hospital outcomes among these patients.

Method: The National Inpatient Sample (NIS) Database was analyzed for the years 2019 and 2020. The NIS was searched for hospitalizations of adult patients greater than 18 years-old with MASH with and without a concomitant diagnosis of atrial fibrillation, atrial flutter, supraventricular tachycardia or ventricular tachycardia. Multivariate logistics were used to adjust for confounders. The primary outcome was inpatient mortality. Secondary outcomes were hospital length of stay (LOS), and total hospital charges (TOTHC).

Results: This study included 237, 215 patients with MASH, of which 40, 275 (16.9%) patients were diagnosed with atrial fibrillation, atrial flutter, supraventricular tachycardia or ventricular tachycardia. Multivariate regression showed that patients with both MASH and selected cardiac arrhythmias had higher inpatient mortality compared to those with MASH alone (OR 1.87, CI 1.67–2.09, $p < 0.0001$). It was also shown that MASH patients with selected cardiac arrhythmias pay significantly more total hospital charges \$16, 108.80 (CI \$13, 048.17–\$19, 167.43, $P < 0.001$) with increased length of stay of 1.58 days (1.39–1.77, $p < 0.0001$).

Conclusion: This nationwide study evaluated the characteristics and outcomes of hospitalized patients with MASH and atrial fibrillation, atrial flutter, supraventricular tachycardia or ventricular tachycardia. Our work highlights longer hospital stays and increased inpatient mortality in this subset of patients. The role of inflammation in the context of cardiac arrhythmias needs elucidation. This relationship may inspire opportunities to screen for arrhythmias that ultimately influence mortality. Further studies are needed on this particular population.

FRI-269

GH agonist use in MASLD: a systematic review and meta-analysis of randomised controlled trials

Islam Mohamed¹, Misha Gautam¹, Hazem Abosheishaa¹, Sophia Hussain¹, Kopal Kumar¹, Anaya Kotak¹, Macy Baugh¹, Raabia Qureshi¹, Rawan Rajab¹, Laura Alba¹. ¹University of Missouri Kansas city, Kansas city, United States
Email: islamh3255@gmail.com

Background and aims: Metabolic Dysfunction Associated Steatotic Liver Disease (MASLD) represents a complex clinical condition characterized by hepatic steatosis and metabolic dysregulation. MASLD poses significant health risks, including the development of insulin resistance, cardiovascular complications, and liver-related morbidity. Growth Hormone (GH) agonists have emerged as potential therapeutic agents, given their role in modulating metabolism, promoting lipolysis, and influencing insulin-like growth factor-1 (IGF-1) levels. However, the comprehensive efficacy outcomes of GH

supplementation in MASLD remain incompletely understood. The primary aim of this study is to systematically evaluate the impact of GH agonist use on a range of clinical and biochemical parameters in MASLD patients.

Method: A systematic literature search across major databases identified randomized controlled trials (RCTs) investigating GH supplementation in MASLD patients. Inclusion criteria encompassed outcomes related to IGF-1 levels, BMI, hepatic fat fraction (relative and absolute), HbA1C, CRP levels, fasting serum glucose, lipid profiles, liver enzymes, and adverse events, with a focus on mean differences (MD), 95% confidence intervals (CI), and p values. Two reviewers independently extracted data, and quality assessment employed the Cochrane Risk of Bias tool. Meta-analyses, utilizing random-effects models and sensitivity analyses, were conducted to synthesize findings. Statistical significance was set at $p < 0.05$.

Results: GH supplementation resulted in a significant reduction in both relative (MD: -46.26 , 95% CI $[-71.52, -21.00]$, $p = 0.0003$) and absolute (MD: -5.15 , 95% CI $[-7.93, -2.37]$, $p = 0.0003$) hepatic fat fraction. No significant changes were observed in HbA1C, CRP levels, fasting serum glucose, BMI, triglycerides, and LDL-C. GH supplementation showed a significant reduction in ALT (MD: -5.97 , 95% CI $[-10.31, -1.62]$, $p = 0.007$) and GGT (MD: -16.18 , 95% CI $[-30.76, -1.59]$, $p = 0.03$) levels compared to placebo. No significant differences were observed in the incidence of arthralgia, myalgia, paresthesia, and injection site reactions between GH and placebo groups.

Conclusion: In summary, our meta-analysis highlights GH supplementation as a promising therapy for MASLD. GH agonists significantly reduced both absolute and relative hepatic fat fraction, indicating potential efficacy in addressing steatosis. Positive effects on liver enzymes, with significant reductions in ALT and GGT levels, were observed. GH agonists showed no significant adverse events compared to placebo, emphasizing their safety. However, further large-scale randomized controlled trials are essential to clarify the long-term effects, safety profile, and potential impact on measures like fibrosis in MASLD patients.

FRI-270-YI

Association of severity of metabolic dysfunction-associated steatotic liver disease with gut dysbiosis and shift in the metabolic function of the gut microbiota in people with HIV

Luz Ramos Ballesteros¹. ¹McGill University Health Centre, Montreal, Canada

Email: luz.ramos@muhc.mcgill.ca

Background and aims: The progression of metabolic dysfunction-associated steatotic liver disease (MASLD) to its severe forms, including metabolic dysfunction-associated steatohepatitis (MASH) and liver fibrosis, might be attributed to a combination of lifestyle and genetic factors. Recently, several studies have emphasized gut microbial dysbiosis as a key driver in this process. However, the role of gut dysbiosis in people with HIV (PWH), a population with a complex MASLD pathogenesis and at risk for severe liver disease, is not known. We aimed to evaluate the association between gut dysbiosis and severe MASLD, that is, MASH and liver fibrosis, in a well-characterized population of PWH.

Method: Consecutive PWH from a prospective Cohort (LIVEr disease in HIV, LIVEHIV) underwent transient elastography with controlled attenuation parameter (CAP) and the measurement of serum cytokeratin-18, a biomarker of hepatocyte apoptosis used to diagnose MASH. All included patients had MASLD, defined as CAP > 238 dB/m. Severe MASLD was defined as presence of MASH (cytokeratin-18 ≥ 130.5 U/L) and/or significant liver fibrosis (liver stiffness measurement ≥ 7.1 kPa). Taxonomic composition of gut microbiota was determined using 16S ribosomal RNA gene sequencing of stool samples. PICRUST-based functional prediction was employed. Bacterial and functional differences were assessed using a

POSTER PRESENTATIONS

generalized linear model, with adjustment for age and sex as confounding factors, using a negative binomial distribution.

Results: 34 patients with MASLD were enrolled (mean age 52 years, 15% females, mean stiffness measurement 6.7 kPa, mean cytochrome-18 184 U/L). Among them, 32% had severe MASLD. After adjusting for age and sex, liver health status (severe MASLD yes vs. no) explained 7% of the overall variation ($r^2 = 0.07$, $p = 0.09$) in bacterial composition. Several genera were found to be significantly different between PWH with severe MASLD. Participants with severe MASLD had increases of genera *Eubacterium*, *Bacteroides*, *Roseburia*, *Ruminococcus*, *Slackia*, *Holdemania*, *Bifidobacterium* and decreases of *Alloprevotella*, *Paraprevotella*, *Prevotella*, *Olsenella*, *Oribacterium*, *Romboutsia*, *Desulfovibrio*, *Dialister*. In severe MASLD, functional analysis revealed increases in fatty acid degradation and flavonoid biosynthesis, and decreases in pyrimidine metabolism, steroid biosynthesis, folate biosynthesis, and alanine, aspartate, glutamate metabolism.

Conclusion: In HIV mono-infection, MASLD severity is associated with gut dysbiosis and a shift in metabolic function of the gut microbiota. Some of these taxa are similar to those associated with MASLD in HIV-negative populations. Thus, gut microbiota analysis adds information to classical predictors of MASLD severity and suggests novel metabolic targets for pre-/probiotics therapies.

FRI-271

Hepatitis C infection increases the risk of new-onset HTN and DM among patients with metabolic dysfunction-associated steatotic liver disease

Ping-Tsung Shih¹, Chin-I Shih², Kuan-Ta Wu³, Meng-Hsuan Hsieh^{3,4,5}, Jeng-Fu Yang³, Yi-Yu Chen³, Wei-Lun Tsai^{6,7}, Wen-Chi Chen^{6,7}, Po-Cheng Liang⁴, Yu-Ju Wei⁴, Pei-Chien Tsai⁴, Po-Yao Hsu⁴, Ming-Yen Hsieh⁴, Yi-Hung Lin⁴, Tyng-Yuan Jang⁴, Chih-Wen Wang^{4,5}, Ming-Lun Yeh^{4,5}, Chung-Feng Huang^{4,5}, Jee-Fu Huang^{4,5}, Chia-Yen Dai^{4,5}, Chi-Kung Ho³, Wan-Long Chuang^{4,5}, Ming-Lung Yu^{4,5,6}. ¹Department of Internal Medicine, Kaohsiung Medical University Hospital, Kaohsiung, Taiwan; ²Department of Medical Education and Department of Internal Medicine, Kaohsiung Veterans General Hospital, Kaohsiung, Taiwan; ³Department of Preventive Medicine, and Health Management Center, Kaohsiung Medical University Hospital, Kaohsiung Medical University, Kaohsiung, Taiwan; ⁴Hepatobiliary Division, Department of Internal Medicine and Hepatitis Center, Kaohsiung Medical University Hospital, Kaohsiung Medical University, Kaohsiung, Taiwan; ⁵School of Medicine and Hepatitis Research Center, College of Medicine, and Center for Liquid Biopsy and Cohort Research, Kaohsiung Medical University, Kaohsiung, Taiwan; ⁶School of Medicine and Doctoral Program of Clinical and Experimental Medicine, College of Medicine and Center of Excellence for Metabolic Associated Fatty Liver Disease, National Sun Yat-Sen University, Kaohsiung, Taiwan; ⁷Division of Gastroenterology, Department of Internal Medicine, Kaohsiung Veterans General Hospital, Kaohsiung, Taiwan
Email: ping289764@gmail.com

Background and aims: Steatotic liver disease (SLD) is associated with higher risks of hypertension (HTN) and diabetes mellitus (DM). A new nomenclature of SLD, metabolic dysfunction-associated steatotic liver disease (MASLD) has emerged recently. Besides, Taiwan is hyperendemic for chronic hepatitis B virus (HBV) and hepatitis C virus (HCV) infections. The interaction between MASLD and viral hepatitis on the risk of HTN and DM remains unclear. We conducted a retrospective cross-sectional and longitudinal cohort design to evaluate the role of viral hepatitis in the risk of co-existing and new-onset HTN and DM among patients with MASLD with and without viral hepatitis.

Method: The cross-sectional cohort consisted of 22,493 adults with SLD who underwent health checkups at a tertiary hospital in Taiwan from 1999 to 2013. Of them, 17,375 subjects with estimated glomerular filtration rate (eGFR) ≥ 30 ml/min/1.73 m², but without

HTN and/or DM at baseline and within 1 year after enrollment were included as a longitudinal cohort (mean, 6.49 years for HTN; 6.85 years for DM). Both cohorts were divided into two groups, MASLD (SLD with at least one cardiometabolic risk factor [CMRF]) as the target group and simple SLD (SLD without CMRF) as the control group. The target group (MASLD) was further divided into three subgroups (NBNC-MASLD, HBV-MASLD, and HCV-MASLD), and the control group (simple SLD) was further divided into simple non-B, non-C (NBNC)-SLD, simple HBV-SLD, and simple HCV-SLD.

Results: In the cross-sectional cohort, HBV-MASLD, but not HCV-MASLD, had significantly lower risk of existing-HTN (adjusted odds ratio [aOR]/95% confidence interval [CI] 0.85/0.77–0.94) compared to those with NBNC-MASLD. The prevalence of existing DM did not differ among HBV-MASLD, HCV-MASLD and NBNC-MASLD. In the longitudinal cohort, 2,084 (13.07%) subjects and 701 (4.40%) subjects developed new-onset HTN and DM, respectively (annual incidence, 20.05 and 6.36 per 1000 person-years; 10-year cumulative incidence, 19.80% and 6.98%, respectively). HCV-MASLD, but not HBV-MASLD, had significantly higher risks of new-onset HTN (adjusted hazard ratio [aHR]/95% CI: 1.46/1.12–1.92) and DM (aHR/95% CI: 1.81/1.22–2.68) than NBNC-MASLD did (annual incidence, 27.89, 20.7, and 19.7, respectively, for HTN and 12.69, 5.85 and 6.33, respectively, for DM per 1000 person-years). The new onset of HTN and DM did not differ among simple NBNC-SLD, simple HBV-SLD, and simple HCV-SLD subjects.

Conclusion: HCV, but not HBV, infection increased the risk of new-onset HTN and DM among patients with MASLD.

FRI-272

Steatotic liver disease with normal liver enzyme: clinical use of ultrasound attenuation method and shear wave elastography

Shunsuke Sato¹, Hidehiko Kawai², Takuya Genda¹. ¹Juntendo University Shizuoka Hospital, Shizuoka, Japan; ²Fuji Town Medical Center, Shizuoka, Japan
Email: syusato@juntendo.ac.jp

Background and aims: Recently, steatotic liver disease (SLD) has emerged as the most common chronic liver disease in Japan. The Nara Declaration, proposed by the Japan Society of Hepatology in 2023, recommends that patients with elevated liver enzyme (ALT level of ≥ 30 IU/L) consult general physicians. However, its disease progression has been known, including patients with normal ALT test. Therefore, we investigated the clinical characteristics and diagnostic significance of SLD with normal ALT test using annual health checkup cohort.

Method: Among the 2,448 patients who underwent a quantitative evaluation of steatosis (attenuation) and fibrosis (shear wave elastography) simultaneously using ARIETTA 850SE (Fujifilm Healthcare, Tokyo, JAPAN) in 2021, 2,397 patients without obvious liver disease were enrolled. Based on previous studies, cut-off values for steatosis were S1 (0.62 dB/cm/MHz), S2 (0.67), and S3 (0.73) and cut-off values for fibrosis were F1 (1.26 KPa), F2 (1.51), and F3 (1.63).

Results: SLD was observed in 850 cases (35.5%). Among them, 599 cases (70.5%) had normal ALT value and 251 cases (29.5%) had elevated ALT value. The degree of steatosis was S1/S2/S3; 51.4/30.1/18.5% vs. 24.3/32.7/43.0% in the patients with normal and elevated ALT test, respectively. Patients with SLD and normal ALT test was less common in obesity (31.2 vs. 66.5%), hypertension (30.6 vs. 47.0%), dyslipidemia (57.8 vs. 77.7%), and diabetes (7.0 vs. 15.1%) ($p < 0.001$). The diagnostic ability of fatty liver index is good in patients with SLD and normal ALT test (AUROC 0.645, $p < 0.001$) and those with elevated ALT test (AUROC 0.708, $p < 0.001$). Conversely, the optimal cut-off value was 45 (sensitivity 66.9/specificity 64.3/PPV 71.8/NPV 80.9%) for patients with SLD and elevated ALT test and 15 (sensitivity 56.4/specificity 64.9/PPV 41.4/NPV) for those with normal ALT test. The degree of fibrosis was F0/F1/F2/F3; 73.6/20.2/4.2/2.2% vs. 53.0/32.7/6.0/8.4% in patients with SLD and normal and elevated ALT test, respectively. The ability of FIB-4 index to diagnose F2 or higher

fibrosis is good only in patients with SLD and elevated ALT test (AUROC; 0.773, $p < 0.001$), while its usefulness did not show in patients with SLD and normal ALT test (AUROC; 0.527, $p = 0.598$).

Conclusion: Approximately 70% of patients with SLD showed normal ALT test. Although mild hepatic steatosis was more common in SLD with normal ALT test, approximately 25% of them showed liver fibrosis. Since it is difficult to identify individuals with SLD and fibrosis; particularly, in normal ALT test, diagnosis using ultrasound measurement was considered important.

FRI-273-YI

Prevalence, characteristics and hepatic fibrosis burden of the different subtypes of steatotic liver disease among a cohort of Egyptian people living with HIV

Rahma Mohamed¹, Heba Omar², Naeema El Garhy¹, Ahmed Cordie¹, Hend Tamim³, Zainab Masoud³, Lamiaa Al Sehem¹, Ammar Hatem¹, Reham Awad Awad¹, Mariam Ismail Abdelraouf¹, Aya M. Al-sharif¹, Mirella Sherif¹, Andrew Saweres¹, Remon Atef¹, Mohamed Nagy¹, Rania Hamza³, Mona Salah Eldin Hamdy³, Engy El Khateeb³, Gamal Esmat². ¹Cairo University Hospitals HIV Clinic, Endemic medicine department, Cairo University Hospitals, Cairo, Egypt; ²Endemic medicine department, Cairo University Hospitals, Cairo, Egypt; ³Department of Clinical and Chemical Pathology, Cairo University Hospitals, Cairo, Egypt Email: ahmedcordie@gmail.com

Background and aims: A consensus was reached to change the nomenclature of non-alcoholic liver disease to steatotic liver disease (SLD), comprising different entities, including metabolic dysfunction-associated steatotic liver disease (MASLD), characterized by the presence of cardiometabolic risk factors (CMRF), met-ALD, which add to MASLD an excessive alcohol consumption, and cryptogenic SLD (cSLD). We aimed to determine the prevalence, clinical characteristics, and frequency of clinically significant fibrosis (CSF) within the SLD subgroups in a cohort of Egyptian people with HIV (PWH).

Method: A cross-sectional study included PWH attending Cairo University Hospital's HIV clinic from July 2022 to September 2023. Patients with viral hepatitis coinfections, alcohol use, or metabolic dysfunction (defined by having ≥ 1 CMRF) were allowed. CSF was defined as liver stiffness measurement > 7.1 KPa, and SLD was defined as controlled attenuation parameter (CAP) ≥ 238 dB/m by transient elastography. Participants were categorized into five subgroups (No-SLD, cSLD, HCV-SLD, HCV+CMRF-SLD, and MASLD). A multivariate analysis was used to identify the predictors of steatosis and CSF.

Results: Of 531 participants, 77.4% were male, mean (SD) age 36 ± 10 years, 90.85% on integrase inhibitors-based antiretroviral therapy (ART), 62.2% were virally suppressed, 13.7% reported occasional alcohol intake, 14.8% cured of HCV and 79.6% had at least one CMRF. The prevalence of SLD was 31.8%, MASLD 23.9%, HCV/CMRF-SLD 4.7%, HCV-SLD 2.8%, cSLD 0.4%, and CSF 7.7%. None of them met the criteria for alcohol-related liver disease or metALD. Within MASLD subgroup, being overweight (OR 4.69, 95%CI, 2.52–8.71, $p < 0.001$) or having hypertension (OR 3, 95%CI, 0.99–9.17, $p = 0.05$) were strongly associated with MASLD, followed by triglycerides > 150 (OR 2.09, 95%CI (1.26–3.44, $p = 0.004$) and age > 35 years (OR 1.81, 95% CI (1.05–3.12, $p = 0.03$). Meanwhile, male gender, intravenous drug use, glycated haemoglobin $> 5.7\%$ and higher CAP reading were significantly associated with CSF (OR, 4.24, 5.37, 2.47, and 1, respectively), but being on ART was protective against having CSF (OR, 0.39, $p = 0.03$). Viral load suppression, CD 4 count and ART type did not affect MASLD risk.

Conclusion: MASLD was the dominant cause of SLD in PWH, with 79.6% of the total cohort having CMRF. Early diagnosis and proactive management of metabolic risk factors are crucial for mitigating the risk of MASLD and subsequent CSF among PWH.

FRI-274

Persistence of fatty liver index (FLI) ≥ 20 as a predictor for hepatocellular carcinoma (HCC) development in non-HBV/non-HCV infected population

Rachel Wen-Juei Jeng^{1,2}, Mei-Hung Pan³, Yi-Chung Hsieh^{1,2}, Hwai-I Yang³. ¹Chang Gung Memorial Hospital, Linkou Medical Center, Department of Gastroenterology and Hepatology, Taoyuan, Taiwan; ²Chang Gung University, College of Medicine, Taoyuan, Taiwan; ³Genomics Research Center, Academia Sinica, Taipei, Taiwan Email: hiyang@gate.sinica.edu.tw

Background and aims: The Fatty Liver Index (FLI) has been employed to exclude hepatic steatosis and is recognized as a factor for incident severe liver disease. However, it has not been thoroughly investigated whether longitudinal changes in FLI can predict hepatocellular carcinoma (HCC) development in the Taiwanese population without viral hepatitis infection.

Method: We enrolled participants from the Taiwan Biobank who tested seronegative for HBsAg and anti-HCV (NBNC). HCC diagnoses were validated through the Taiwan National Cancer Registry, with repeated measurements of body mass index, triglycerides, and liver biochemistry. Subjects were categorized based on their initial and follow-up FLI as follows: persistent lower than 20 (referent), initial < 20 and increased to ≥ 20 (group 1), initial ≥ 20 and reduced to < 20 (group 2), and persistent greater than 20 (group 3). Subjects who experienced an HCC event between the two visits were excluded. Time to the event was calculated from the second visit until the end of the follow-up period (December 31, 2020, as per the National Cancer Registry) or the occurrence of the event. Cox regression analysis was applied to identify the impact of longitudinal changes in FLI on the prediction of HCC.

Results: Among the 116,269 NBNC subjects in the Taiwan Biobank, 28,738 subjects had a second visit with repeated measurements, with a median interval duration of 3.9 (IQR: 3.1–3.8) years. These subjects had a mean age of 51, 35% male, 68% anti-HBcAb positive, 27% with type 2 DM, and 18 developed HCC during a median follow-up of 3.1 (IQR: 1.3–3.9) years. There were 13,284, 2,842, 1,727, and 10,885 subjects in groups 0, 1, 2, and 3, respectively. No HCC developed in group 1 patients. Univariate Cox regression analysis showed that persistent FLI > 20 (group 3) is a factor for HCC development [crude hazard ratio (cHR): 4.0, $P = 0.015$], while group 2 (cHR: 1.8, $P = 0.604$) failed to achieve significance. After adjusting for anti-HBc serostatus, FIB-4, age, gender, and current alcohol consumption, persistent FLI > 20 (group 3) remained the only independent risk factor for HCC development [persistent FLI < 20 as the referent, adjusted HR (aHR): 3.3, $P = 0.042$], while group 2 remained insignificant (aHR: 1.4, $P = 0.752$).

Conclusion: Persistence of FLI greater than 20 is identified as an independent risk factor for HCC development in NBNC subjects. Aggressive reduction of FLI may effectively mitigate their HCC risk.

FRI-275-YI

Liver fibrosis and Lipoprotein (a) levels in individuals with metabolic dysfunction

Sara Margarita¹, Chiara Macchi², Serena Pelusi¹, Cristiana Bianco¹, Giulia Periti¹, Jessica Rondena¹, Francesco Malvestiti³, Daniele Prati¹, Massimiliano Ruscica², Luca Valenti⁴. ¹Transfusion Medicine Unit, Fondazione IRCCS Ca' Granda Ospedale Maggiore Policlinico, Milan, Milan, Italy; ²Department of Pharmacological and Biomolecular Sciences, Università degli Studi di Milano, Milan, Italy; ³Department of Pathophysiology and Transplantation, Università degli Studi di Milano, Milan, Italy; ⁴Transfusion Medicine Unit, Fondazione IRCCS Ca' Granda Ospedale Maggiore Policlinico, Milan, Department of Pathophysiology and Transplantation, Università degli Studi di Milano, Milan, Italy Email: sara.margarita@policlinico.mi.it

Background and aims: Metabolic-dysfunction associated steatotic liver disease (MASLD), characterized by the presence of liver fat and metabolic alterations, has progressively become the most common

POSTER PRESENTATIONS

chronic liver disease, and is associated with accelerated atherosclerosis. Circulating levels of Lipoprotein (a) (Lp (a)) is emerging as an independent cardiovascular (CV) risk factor and a target for novel therapeutic approaches. However, previous studies in small cohorts suggested that Lp (a) may be lower in patients with chronic advanced MASLD, but evidence is not yet conclusive. Aim of the study was to evaluate Lp (a) levels in a cohort of 728 individuals, consecutively enrolled in a primary prevention program for candidate blood donors in Milan, Italy, focused at the early diagnosis of hepatic and extra-hepatic complications of MASLD (the Liver-Bible-2022 Biobank cohort).

Method: The study cohort included apparently healthy subjects, aged 40–65 in the presence of at least three criteria of metabolic dysfunction defining MASLD. Anthropometric data, lipid levels, transaminases and Lp (a) levels were available for all. Hepatic fibrosis and steatosis were non-invasively estimated by measurement of liver stiffness measurement (LSM) and controlled attenuation parameter (CAP) by FibroScan, while Lp (a) was measured by turbidimetric in vitro test and log transformed. Observational associations were performed by fitting data to generalized linear models. Binary outcomes were examined by fitting logistic regression models.

Results: Patients were mainly males (85%), mean age was 53 years, 361 showed CAP ≥ 275 dB/m (49%), 16 (2.2%) had LSM ≥ 8 kPa (>11.9 kPa in two). Of these, 326 subjects (44%) had hypercholesterolemia, only 62 (8%) were on lipid lowering therapy, while 122 (16%) showed increased Lp (a) levels, considering 75 nmol/L as threshold. Increased Lp (a) levels were associated with hypercholesterolemia ($p = 0.02$), while lower Lp (a) concentrations were observed in subjects with LSM above 11.9 kPa ($p = 0.04$), consistent with advanced fibrosis, irrespective of age, sex, use of lipid lowering treatment and overweight. Moreover, participants with lower Lp (a) displayed a trend towards higher ALT levels ($p = 0.08$) and showed an increased NASH score ($p = 0.04$), a non-invasive test taking into account insulin, albumin, AST and PNPLA3 genotype for the estimation of MASH.

Conclusion: We confirm an association between severe liver fibrosis and lower circulating Lp (a) levels. Lp (a) may therefore not be reliable in evaluating CV risk in this subset of patients with increased predisposition to CV events.

FRI-278

The risk of cardiometabolic disease related to increasing amounts of liver fat above the cut-off of 5%

Gabrielle Alblas¹, Jeroen van der Velde¹, Maarten Tushuizen¹, J. Wouter Jukema¹, Hildo Lamb¹, Frits Rosendaal¹, Renée de Mutser¹, Minneke Coenraad². ¹Leiden University Medical Center, Leiden, Netherlands; ²Leiden University Medical Center, Leiden
Email: g.alblas@lumc.nl

Background and aims: Metabolic dysfunction associated steatotic liver disease (MASLD), defined as liver fat content $\geq 5\%$ and the presence of cardiometabolic criteria, is associated with an increased risk of type 2 diabetes and cardiovascular diseases. However, it remains unclear to what extent increasing amounts of liver fat above the cut-off of 5% are associated with more pronounced risks of cardiometabolic disease. We aimed to examine the association between increasing amounts of liver fat content and the risk of cardiometabolic diseases in a middle-aged population during a 10-years follow-up.

Method: In the Netherlands Epidemiology of Obesity study, a prospective cohort study with 10 years of follow-up, liver fat content was assessed using proton magnetic resonance spectroscopy in 1763 participants without pre-existing diabetes or cardiovascular diseases. Incident cardiometabolic diseases were collected via medical records. Cox regression was used to examine associations of MASLD, and of different categories of liver fat content with cardiometabolic diseases, adjusted for age, sex, education, ethnicity, alcohol consumption, physical activity and total body fat.

Results: The overall population had a mean (95% CI) age of 55 (55–56) years, BMI of 29.2 (29.0–29.4) kg/m², liver fat content of 8.1 (7.7–8.5)%. 50% were men, and 751 (43%) had MASLD. During 10 years of follow-up, 140 new cases of cardiometabolic diseases occurred, leading to an adjusted hazard ratio (HR, 95% CI) of 2.2 (1.5–3.3) for those with MASLD as compared with those without MASLD. Compared with those who had a liver fat content between 0 and 2.5%, the adjusted HR for participants with liver fat content between 5 and 10% was 1.8 (1.0–3.2), for 10–15% 1.9 (1.0–3.7), for 15–20% 1.9 (0.9–3.9), for 20–25% 2.4 (1.1–5.2), for 25–30% it was 2.7 (1.2–7.2), and for those with liver fat content of 30% or more the HR was 3.4 (1.7–6.9).

Conclusion: Patients with MASLD have a two-fold increased risk of cardiometabolic disease. Increasing categories of liver fat content above the cut-off of 5% were not associated with strong risk increases. Future studies should reveal to what extent the presence of comorbidities in addition to hepatic steatosis increase the risk of cardiometabolic diseases.

FRI-279-YI

Platelet dynamics in metabolic patients with metabolic dysfunction-associated steatotic liver disease/steatohepatitis and liver cirrhosis

Mirko Zoncapè¹, Marco Castelli², David Sacerdoti¹, Pietro Minuz², Andrea Dalbeni³. ¹Liver Unit, University of Verona and University and Hospital Trust (AOUI) of Verona, Verona, Italy; ²Division of General Medicine C, Department of Medicine, University of Verona and University and Hospital Trust (AOUI) of Verona, Verona, Italy; ³Liver Unit, University of Verona and University and Hospital Trust (AOUI) of Verona, Division of General Medicine C, Department of Medicine, University of Verona and University and Hospital Trust (AOUI) of Verona, Verona, Italy
Email: mirko.zonky@yahoo.it

Background and aims: Metabolic dysfunction-Associated Steatotic Liver Disease (MASLD), affects about 30% globally, potentially leading to cirrhosis. Metabolic dysfunction-Associated Steatohepatitis (MASH) often involves platelets. Platelet roles in MASLD progression remain underexplored. Our aim was to verify the possible platelet contributions to MASLD/MASH genesis and in MASLD-related cirrhosis, compared to healthy subjects, investigating the activation state of platelets *in vitro* and *in vivo*.

Method: Patients with metabolic liver cirrhosis (Child-Pugh classes A/B), MASLD/MASH, and healthy volunteers without metabolic alterations were examined. Patients were diagnosed through abdominal ultrasounds, TC, RM and liver biopsy, Fibroscan and other non-invasive test and scores were also used.

Microfluidic analysis assessed platelet adhesion on collagen, indicating pre-activation states and *in vitro* activation levels. Urinary 11-dehydro-thromboxane-B2 (11-TXB2) measured *in vivo* thromboxane A2 synthesis, indirectly assessing platelet activation *in vivo*. Platelet interaction with coagulation factors, specifically Factor VIII (FVIII) and von Willebrand Factor (vWF) activity, was explored through cross-mixing experiments.

Results: Among 66 participants, platelet count was significantly lower in cirrhotic patients compared to controls ($p < 0.001$). However, no differences were observed in platelet distribution width (PDW), mean platelet volume (MPV), or immature reticulate fraction (IRF) among the three groups. *In vitro* adhesion on collagen was higher in MASLD/MASH and cirrhosis ($p < 0.01$) compared to controls. 11-TXB2 levels were significantly elevated in cirrhotic patients compared to controls ($p < 0.001$). Higher levels of FVIII and vWF were observed in the platelet-poor plasma (PPP) of cirrhotic patients. Cross-mixing experiments indicated that elevated FVIII and vWF levels in cirrhotic patients were associated with these factors in PPP rather than a direct contribution from washed platelets.

Conclusion: MASLD and MASH patients showed normal platelet counts, but increased adhesion, suggesting pro-inflammatory and pro-fibrotic roles. In contrast, cirrhotic patients displayed reduced

platelet count, but increased adhesion function. They also exhibit significantly higher 11-TXB2 levels compared to controls, suggesting higher in-vivo platelet activation.

FRI-280

Dynamic of cardiometabolic components are highly correlated with the risk of hypertension and diabetes among patients with metabolic dysfunction-associated steatotic liver disease

Chin-I Shih¹, Ming-Lun Yeh², Kuan-Ta Wu³, Meng-Hsuan Hsieh³, Jeng-Fu Yang³, Yi-Yu Chen³, Wei-Lun Tsai⁴, Wen-Chi Chen⁵, Po-Cheng Liang², Yu-Ju Wei³, Pei-Chien Tsai³, Ya-Yun Cheng⁶, Po-Yao Hsu³, Ming-Yen Hsieh³, Yi-Hung Lin³, Tyng-Yuan Jang³, Chih-Wen Wang³, Chung-Feng Huang³, Jee-Fu Huang³, Chia-Yen Dai³, Chi-Kung Ho², Wan-Long Chuang³, Wei-Ting Chang⁷, Ming-Lung Yu⁶.

¹Department of Medical Education, Kaohsiung Veterans General Hospital, Kaohsiung, Taiwan; ²Kaohsiung Medical University Hospital, Kaohsiung, Taiwan; ³Kaohsiung Medical University Hospital, Kaohsiung, Taiwan; ⁴Kaohsiung veterans general hospital, Kaohsiung, Taiwan; ⁵Kaohsiung Veterans General Hospital, Kaohsiung, Taiwan; ⁶National Sun Yat-sen University, Kaohsiung, Taiwan; ⁷Chi-Mei Medical Center, Tainan, Taiwan
Email: chini861018@gmail.com

Background and aims: Fatty liver disease (FLD) is associated with higher risks of hypertension (HTN) and diabetes mellitus (DM). A new nomenclature of FLD, metabolic dysfunction-associated steatotic liver disease (MASLD) was proposed recently. We conducted a retrospective cross-sectional and longitudinal study to evaluate the role of cardiometabolic risk factors (CMRF) in MASLD and non-steatotic liver disease (non-SLD) in the risk of new-onset HTN and DM.

Method: The cross-sectional cohort consisted of 32,569 adults without hepatitis or significant alcohol consumption, who underwent health checkups at a tertiary hospital in Taiwan from 1999 to 2013. Of them, 27,109 without HTN and/or DM at baseline and within 1 year after enrollment were included as a longitudinal cohort (mean, 6.28 years for HTN; 6.58 years for DM). Both cohorts were further divided into four groups (MASLD, Simple SLD, CMRF+ Non-SLD, and Healthy control) based on the presence of CMRF and the presence of hepatic steatosis assessed by ultrasound sonography.

Results: In the longitudinal cohort, 12,620 subjects had MASLD, 1,113 subjects had simple SLD, 8,547 subjects had CMRF+ non-SLD, and 4,829 subjects were healthy controls. MASLD subjects had significantly higher risks of new-onset HTN (adjusted hazard ratio [aHR]/CI: 1.89/1.73–2.07) and DM (aHR/CI: 8.24/6.22–10.92) compared to those with non-SLD. The presence of CMRF increased the risk of new-onset HTN in both SLD and non-SLD patients (aHR/CI: 6.45/3.94–10.57 and 10.71/7.78–14.74, respectively) and DM (aHR/CI: 15.38/3.83–61.78 and 9.66/2.35–39.71, respectively). The risk of new-onset HTN and DM significantly increased with the fulfilled number of cardiometabolic components (HTN: aHR/CI from 2.02/1.20–3.41 to 15.53/8.13–29.65 in one-component subjects to five-components subjects; DM: from 2.92/0.68–12.42 to 82.38/18.98–357.58). Resolved cardiometabolic dysfunction (CMD) during follow-up decreased the risk of HTN and/or DM.

Conclusion: Patients with MASLD are at high risk of prevalent and incident HTN and/or DM. The risk increases with the number of CMRF.

FRI-281

Metabolic steatosis in renal transplant recipients does not correlate with CVD, a retrospective cohort study

Pietro Torre¹, Carmine Seconduolo², Letizia Sangiovanni¹, Federica Belladonna¹, Mario Masarone¹, Giancarlo Bilancio², Marcello Persico¹. ¹Internal Medicine and Hepatology Division, Department of Medicine, Surgery and Dentistry, "Scuola Medica Salernitana", Baronissi (Salerno), Italy; ²Nephrology Division, Department of Medicine, Surgery and Dentistry, "Scuola Medica

Salernitana," University of Salerno, Baronissi (Salerno), Italy
Email: pietrotorre90@gmail.com

Background and aims: Metabolic Associated Steatotic Liver Disease (MASLD) is among the main causes of chronic liver disease and is growing. Chronic Kidney Disease (CKD) has a global prevalence of between 8 and 16%, significantly increasing in recent years. This simultaneous increase is not surprising: both recognize common triggering causes, including obesity, diabetes mellitus, hypertension, dyslipidemia and metabolic syndrome. The prevalence of CKD in MASLD patients is between 4 and 40%. The severity of liver disease has been related to the progression of CKD which in turn can aggravate NAFLD by altering the intestinal barrier and microbiota, with the accumulation of uremic toxins and the modification of metabolism of glucocorticoids. To date, there is little data regarding the prevalence of steatosis in renal transplant recipients and how these alterations can modify the outcome of the renal transplant, and particularly the occurrence of CVD. Aims: Investigate the prevalence of steatosis in a population of kidney transplant patients. Evaluate if there is an association between prevalence of CVD and steatosis and its severity in these patients.

Method: 200 patients, followed-up in the Nephrology Unit of Salerno University Hospital, were enrolled after an informed consent. Demographical, clinical and laboratory data have been collected for each patient, as well as abdominal ultrasonography (US). Patients with steatosis underwent liver stiffness measurement and controlled attenuation parameter (CAP). Also, any history of active or inactive CVD was collected (myocardial infarction, angina, stroke). Data were analyzed with parametric and non-parametric tests when indicated, significance was given when a $p < 0.05$ in a two-tailed analysis was reached.

Results: Of the 200 kidney transplant patients, 69% were males, the mean age was 56.8 yrs. The median time of the kidney transplant was 15.88 years (range $\pm 7, 5$). Steatosis was present at the US in 45.5% of the patients, with a median CAP of 219 (208–237.5) and LS of 5.0 (4.3–5.2). Of those with steatosis, 11.1% (8 pts) were at risk of significant fibrosis (> 8 Kpascal). The mean BMI was 26.9 ± 4.8 overall, with 28.5 ± 5.2 vs 25.5 ± 3.9 kg/m² in patients with steatosis vs those without ($p: 0.0001$). Metabolic syndrome was present in 30.8% of patients with steatosis vs 11.0% of those without ($p: 0.001$). The prevalence of CVD among the overall population was of 14.5% with no differences between patients with and without steatosis (14.3 vs 14.7%). At a logistic binary regression CVD was correlated only with age and sex, but not with steatosis, BMI, LS, CAP and MS.

Conclusion: In a cohort of kidney transplant recipients, the prevalence of liver steatosis, as well as overweight and metabolic syndrome was higher than that of the general population. However, previous, or actual CVD did not seem to be correlated with the presence of metabolic steatosis and its causes.

FRI-282

Obese patients with sarcopenic obesity have a more severe metabolic phenotype and hepatic disease and exhibit less metabolic improvement after bariatric surgery

Vittoria Zambon Azevedo¹, Judith Aron-Wisniewsky², Raluca Pais¹, Jean Michel Oppert², Vlad Ratziu². ¹ICAN, Paris, France; ²Sorbonne Université, Paris, France
Email: vlad.ratzu@inserm.fr

Background and aims: Patients (pts) with obesity can have sarcopenia, i.e. reduced muscle mass with increased fat mass, however a precise and consensual definition for sarcopenic obesity (SO) is lacking and different definitions result in widely divergent prevalences. Using an AI-assisted unbiased clustering approach, we identified a body composition-based phenotype that distinguishes SO vs. non-SO patients (Clinical Nutrition ESPEN 2022, PMID 36513443). Here we aimed to externally validate the hepatic and metabolic clinical correlations of the SO phenotype in a population of morbidly obese pts undergoing bariatric surgery (BaS) and to

POSTER PRESENTATIONS

determine if weight loss patterns and metabolic improvement post-surgery differs between SO and non-SO pts.

Method: Pts who underwent BaS, per-operative liver biopsy and body composition assessment by dual-energy X-ray absorptiometry (DEXA) were included (n = 972) and 862 were reassessed 1-year post-surgery. Pts were categorized as having or not SO.

Results: At baseline, 207 (21.3%) pts were diagnosed with SO. They had worse metabolic and cardiovascular profiles than non-SO pts, with a higher prevalence of diabetes (48.8% vs. 37.3%), hypertension (61.8% vs. 44.2%), metabolic syndrome (77.3% vs. 65.4%) and sleep apnea (80.7% vs. 53.7%), all p values ≤ 0.003 , and a higher proportion of android fat-mass ($67.2 \pm 5.0\%$ vs. $62.5 \pm 6.6\%$, $p < 0.001$). SO pts had higher grades of steatosis [$\geq S2$: 64.2% vs. 47.3%], hepatocyte ballooning [≥ 1 : 58.9% vs. 43.9%], portal inflammation [44.4% vs. 32.5%], and fibrosis stage [$\geq F3$: 12.1% vs. 6.0%] than those non-SO ($p < 0.01$). At follow-up, the prevalence of SO was 11.0% and 170 pts no longer had SO. SO pts had a smaller % weight loss than non-SO pts (-31.9 ± 13.3 vs. -35.1 ± 12.2) whereas pts with persistent SO (N = 76) had the lowest % weight loss (23.8 ± 9.7). SO at baseline was associated with lower remission rates of comorbidities (diabetes 46% vs 62.2% in non-SO, $p = 0.031$; hypertension 21.4% vs 41.8% in non-SO, $p = 0.004$; metabolic syndrome 51.3% vs 72.4%, $p < 0.001$). ALT reduction was -12.3 ± 2.4 IU/L vs. -9.6 ± 1.2 in SO vs non-SO pts, $p = 0.037$.

Conclusion: The SO diagnostic index identifies a population of pts with more severe metabolic and hepatic disease, with lower weight loss post-BaS and with lesser metabolic benefit from BaS.

FRI-283

Costs associated with non-alcoholic steatohepatitis disease progression in medicare patients

Jesse Fishman¹, Yestle Kim¹, Joe Medicis¹, Matthew Davis², Dominic Nunag², Robert G. Gish³. ¹Madrigal Pharmaceuticals, Inc., West Conshohocken, United States; ²Medicus Economics, LLC, Milton, United States; ³Robert G Gish Consultants LLC, La Jolla, United States
Email: jfishman@madrigalpharma.com

Background and aims: Non-alcoholic steatohepatitis (NASH), or metabolic dysfunction-associated steatohepatitis (MASH), is a severe form of non-alcoholic fatty liver disease (NAFLD) or metabolic dysfunctional associated steatotic liver disease (MASLD). NASH may progress to more advanced liver disease and is associated with high healthcare resource use (HRU); the risk of progression may be higher in older populations. Costs associated with progression are not well characterized in those ≥ 65 years of age. This study aimed to quantify HRU and costs associated with NASH progression in a Medicare population.

Method: Those diagnosed with NASH (ICD-10: K75.81) in 100% Medicare claims (2015–2021) were required to be ≥ 66 years at index (diagnosis), have continuous enrollment in Parts A, B, and D for ≥ 12 months prior to and ≥ 6 months following index (unless death), and have no evidence of other causes of liver disease. Diagnoses within 90 days were used to categorize patient-time into five baseline severity states: NASH, compensated cirrhosis (CC), decompensated cirrhosis (DCC), hepatocellular carcinoma (HCC), and liver transplant (LT). Annualized HRU and costs were calculated during the baseline and follow-up periods, and for the duration of each severity state. Follow-up period outcomes were stratified by occurrence and timing of progression.

Results: In 14, 806 unique patients, mean age and follow-up were 72.2 and 2.8 years (N = 12, 990 NASH; 1, 899 CC; 997 DCC; 209 HCC; 140 LT). Average annualized costs increased from baseline following diagnosis, generally scaling with severity: \$16, 231 to \$27, 044; \$25, 122 to \$57, 705; \$40, 613 to \$181, 036; \$36, 549 to \$165, 121, and \$35, 626 to \$108, 918 in NASH; CC; DCC; HCC; and LT; respectively. Adjusting for demographics, comorbidities, and baseline HRU, NASH and CC patients with subsequent progression to a more severe disease state (8% of NASH and 20% of CC patients) had significantly

higher follow-up spending (1.6x for NASH and 1.7x for CC) than non-progressors (both $p < 0.001$). NASH and CC progressors were 2.8x and 6.1x more likely to experience inpatient hospitalization and 2.6x and 3.6x more likely to be in the top 20% of spenders, respectively, compared to non-progressors (both $p < 0.001$). Follow-up costs correlated with the time of progression. Within NASH, costs increased for earlier progression; year 1 progressors' costs (\$50, 382) were 1.4x, 1.6x, 1.7x, and 2.2x more than year 2, 3, 4, and 5 progressors' costs, respectively. In CC, year 1 progressors' costs (\$75, 599) were 1.3x, 1.8x, 2.0x, and 2.2x more than year 2, 3, 4, and 5 progressors' costs, respectively.

Conclusion: NASH progression is associated with higher costs that increase in more severe disease states. Slower progression is associated with lower costs, suggesting a potential benefit of interventions to delay or prevent progression for patients with NASH or CC.

FRI-284-YI

A plant-based diet for liver health: the protective role of vegetable fat on MASLD and other liver diseases

Simon Schophaus¹, Paul-Henry Koop², Jan Clusmann¹, Christian Trautwein¹, Kai Markus Schneider¹, Carolin V. Schneider¹.

¹RWTH Aachen University Medizinische Klinik III, Aachen, Germany;

²RWTH Aachen University Medizinische Klinik 3, Aachen, Germany

Email: sschophaus@ukaachen.de

Background and aims: The increasing prevalence of MASLD poses an enormous challenge for Western civilization. Previous research has highlighted the benefits of a vegan diet on MASLD, but the specific impacts of animal versus plant-based fats are not well understood. This study aims to explore their relative effects in relation to total fat consumption.

Method: Utilizing 24-hour dietary data from the UK Biobank (n > 210, 000), excluding individuals with pre-existing liver conditions, we analyzed the impact of higher proportions of animal and plant-based fats in total fat intake on ICD-10-coded liver diseases. Adjustments were made for age, sex, BMI, Townsend index, caloric, alcohol, and carbohydrate intake.

Results: A higher plant-based fat proportion was associated with reduced odds of ICD10-coded MASLD (OR = 0.643 (0.425–0.973), $p = 0.037$), liver diseases in general (OR = 0.740 (0.597–0.917), $p = 0.006$), and liver failure (OR = 0.258 (0.093–0.713), $p = 0.009$). In contrast, increased animal fat intake was associated with higher risks for these conditions (MASLD: OR = 1.555; liver diseases: OR = 1.352; liver failure: OR = 3.876). Cox-proportional hazard models indicated a decreased risk of death from overall (OR = 0.786) and digestive-disease (OR = 0.295) for higher plant-based fat consumption, versus increased risk with more animal fat (OR = 1.273 and OR = 3.393).

Conclusion: Our findings suggest that a higher ratio of plant-based fats in the diet may offer protective benefits against MASLD and related liver conditions, while increased consumption of animal fats appears to raise MASLD risk. These findings open new avenues for dietary interventions in liver disease prevention and underscore the power of plant-based choices for liver health.

FRI-285

Mendelian-randomization study revealed causal relationship between non-alcoholic fatty liver disease and osteoporosis/fractures

Wei Jiang¹, Xiong Pei¹, Qingmin Zeng¹, Yixian You¹, Lang Bai¹, Chang Hai Liu¹, Dongbo Wu¹, Hong Tang¹. ¹Center of Infectious Diseases, West China Hospital of Sichuan University, Chengdu, China
Email: htang6198@hotmail.com

Background and aims: Observational studies have revealed patients with non-alcoholic fatty liver disease (NAFLD) had a higher risk of osteoporosis/fracture. However, due to the existing of reverse causality and confounding factors, whether NAFLD had a causal relationship with osteoporosis/fracture were still unclear. The

purpose of the current study was to examine the potential correlation between NAFLD and the risk of osteoporosis/fractures by using the Mendelian randomization (MR) study design.

Method: Publicly available genome-wide association studies (GWASs) were employed for univariable and multivariable mendelian randomization analyses (MR). GWASs for NAFLD were obtained from the FinnGen consortium. GWASs for bone mineral density (BMD) were derived from a large meta-analysis. To clarify whether the accompanying symptoms of NAFLD contributed to the increased risk of fracture, GWASs for obesity-related traits, liver function metrics, diabetes-related traits, and serum lipids metrics were used for causal inference. GWASs for fractures at different body sites were acquired from FinnGen consortium. Moreover, two additional GWASs of NAFLD were applied to examine the potential correlation between NAFLD and BMD. A range of sensitivity analysis methods were performed to ensure the reliability of the results. The Bonferroni-corrected significance level was applied.

Results: Causal association between NAFLD and reduced BMD using GWASs from FinnGen consortium were not observed. However, in replication GWAS 1, a suggestive relationship between fibrosis and femoral neck BMD (FN-BMD) were observed. In replication GWAS 2, a causal relationship between NAFLD and FN-BMD and a suggestive relationship between NAFLD and osteoporosis were obtained. Moreover, after univariate MR analysis, the genetically proxied body mass index (BMI), high-density lipoprotein (HDL) cholesterol and hip circumference increased the likelihood of lower limb fracture. Waist-to-hip decreased while glycated hemoglobin (HbA1C) and homeostasis model assessment- β (HOMA-B) increased forearm fracture risk. Reduced low-density lipoprotein (LDL) cholesterol and increased HbA1C resulted in a higher femur fracture. Alkaline phosphatase (ALP) predisposed to a rising risk of foot fracture. However, after multivariate MR (adjusting for BMI), all the relationship above became insignificant.

Conclusion: NAFLD caused reduced BMD and genetically predicted HDL, LDL, HbA1C, HOMA-B, ALP, hip circumference, and waist-to-hip causally increased the risk of fracture causally. And the causal relationships were potentially mediated by BMI, but larger GWAS studies were needed to verify.

FRI-286

Muscle function and walking time are associated with better quality of life in MASLD patients

Roberta Forlano¹, Thishana Kirupakaran², Margaux Couffon², Beatrice Martino³, Giordano Sigon³, Jian Huang³, Benjamin H. Mullish³, Michael Yee⁴, Mark R. Thursz³, Pinelopi Manousou³. ¹Division of Digestive Diseases, Department of Metabolism, Digestion and Reproduction, Imperial college London, London, United Kingdom; ²Division of Digestive Diseases, Department of Metabolism, Digestion and Reproduction, Imperial college London, London, United Kingdom; ³Division of Digestive Diseases, Department of Metabolism, Digestion and Reproduction, Imperial College London, London, United Kingdom; ⁴Department of Endocrinology, Imperial college NHS Trust, London, United Kingdom
Email: r.forlano@imperial.ac.uk

Background and aims: Metabolic-dysfunction associated steatotic liver disease (MASLD) is an increasing cause of chronic liver disease worldwide, with lifestyle changes being the mainstay of treatment. Nevertheless, achieving physical activity, weight loss and well-being in this population remains challenging. Here, we aimed to explore the association between exercise and quality of life among MASLD patients.

Method: We included all consecutive MASLD patients, followed up at St Mary's Hospital, London, UK, between October 2022 and June 2023. Patients filled the 36-Item Short Form survey (SF36) for quality of life, which includes 8 domains exploring physical and mental components. They also filled International Physical Activity Questionnaire (IPAQ) for physical activity (PA). Patients were

classified into inactive (total PA<600 MET*min/week), minimally/moderately active (total PA 600–3000 MET*min/week) and health-enhancing physical activity (HEPA, total PA>3000 MET*min/week). Muscle function was evaluated by 5 sit-to stand test (5-STST) and handgrip strength (HST). Multivariate analysis (MVA) was corrected for socio-economic status and psychiatric comorbidity.

Results: In total, 138 patients were enrolled. Median age was 59 (45–67) years, while median BMI was 32.7 (28–36.6) kg/m². HEPA patients were significantly younger (55 vs 60 years, $p=0.025$) and had better muscle mass (56.7 vs 55.6 kg, $p=0.024$) and function (5-STST: 12 vs 13.1 s, $p=0.007$ and HST: 27 vs 26 kg, $p=0.014$). They also scored significantly higher for each of the SF36 domains. 41 (29%) patients showed good social functioning. These patients had better handgrip test (32.3 vs 13.7 kg, $p=0.03$), longer walking (60 vs 45 min/week, $p=0.006$), moderate (40 vs 5 min/week, $p=0.008$) and vigorous exercise time (30 vs 5 min/week, $p=0.001$). On MVA, handgrip strength (OR 1.058, 95%CI: 1.009–1.109, $p=0.02$) and walking time (OR 1.005, 95%CI: 1.001–1.009) predicted better social functioning. 32 patients (32/138 = 23%) reported lower perception of bodily pain. These patients had higher handgrip test (32 vs 26 kg, $p=0.02$), 5STST test (11.6 vs 13.2 s, $p=0.03$) and were more frequently men (78 vs 58%, $p=0.008$). On MVA, 5STST test (OR 0.98, 95%CI: 0.95–0.99, $p=0.05$) predicted lower perception of bodily pain. Finally, 33 patients (32/138 = 24%) had good perception of general health. These were significantly older (63 vs 57 years, $p=0.01$) and reported longer walking (90 vs 30 min/week, $p=0.001$), moderate exercise (42.5 vs 5 min/week, $p=0.038$) and vigorous exercise time (30 vs 0 min/week, $p=0.01$). On MVA, age (OR 1.08, 95%CI: 1.02–1.14, $p=0.004$) and walking time (OR 1.005, 95%CI: 1.001–1.01, $p=0.026$) predicted better perception of general health.

Conclusion: Muscle function and walking time are associated with better quality of life in patients with MASLD. Specific lifestyle interventions should be offered to MASLD patients.

FRI-287

Increased risk of mortality in metabolic dysfunction-associated steatotic liver disease: a nationwide population-based cohort study

Seung Up Kim¹, Jae Seung Lee², Mi Na Kim², Hye Won Lee², Beom Kyung Kim³, Jun Yong Park², Do Young Kim², Sang Hoon Ahn⁴. ¹Yonsei university, Seoul, Korea, Rep. of South; ²Yonsei University, Seoul, Korea, Rep. of South; ³Yonsei University, Seoul, Korea, Rep. of South; ⁴Yonsei University, Seoul, Korea, Rep. of South
Email: skukorea@yuhs.ac

Background and aims: A new fatty liver disease nomenclature, steatotic liver disease (SLD) has been proposed; however, there are no data on clinical outcomes. We investigated the impact of SLD with metabolic dysfunction (MD; SLD-MD) on all-cause mortality.

Method: We evaluated nationally representative participants aged ≥ 19 years using data from the Korea National Health and Nutrition Examination Survey 2007–2015 and their linked death data through 2019. The presence of fatty liver disease was assessed by liver fat score and significant liver fibrosis was evaluated by the Fibrosis-4 Index. SLD-MD was categorized into three groups: metabolic dysfunction-associated steatotic liver disease (MASLD); metabolic alcoholic liver disease (MetALD); and SLD with other combination etiologies.

Results: Among 25,888 individuals (11,087 men and 14,801 women, mean age 48.1 years), 1,624 (6.3%) died during a mean follow-up period of 111.3 ± 33.5 months. Mortality risk was significantly higher in individuals with SLD-MD (hazard ratio [HR] = 1.41) than in those without ($p < 0.001$). Among the three groups, MASLD (HR = 1.38) and SLD with other combination etiologies (HR = 2.47) independently increased mortality risk (all $P < 0.001$). When individuals with SLD-MD had significant liver fibrosis or diabetes, mortality risk increased further (HR = 1.77 and 1.97, respectively; all $P < 0.001$). SLD-MD with both significant liver fibrosis and diabetes showed the highest mortality risk (HR = 2.50, $P < 0.001$).

Conclusion: SLD-MD is associated with a higher mortality risk. When SLD-MD was combined with significant liver fibrosis or diabetes, the mortality risk became much higher. Treatment strategies to reduce fibrotic burden and improve glycemic control in individuals with MASLD are needed.

FRI-290

Evaluation of ChatGPT as a counselling tool for Italian-speaking MASLD patients: assessment of accuracy, completeness and comprehensiveness

Nicola Pugliese¹, Davide Polverini², Rosa Lombardi³, Grazia Pennisi⁴, Federico Ravaioli⁵, Angelo Armandi⁶, Elena Buzzetti⁷, Andrea Dalbeni⁸, Antonio Liguori⁹, Alessandro Mantovani¹⁰, Rosanna Villani¹¹, Cesare Hassan¹², Luca Valenti¹³, Luca Miele¹⁴, Salvatore Petta¹⁵, Giada Sebastiani¹⁶, Alessio Aghemo¹⁷. ¹Division of Internal Medicine and Hepatology, Department of Gastroenterology, IRCCS Humanitas Research Hospital, Rozzano (MI), Italy, Department of Biomedical Sciences, Humanitas University, Pieve Emanuele (MI), Italy, Milano, Italy; ²Department of Biomedical Sciences, Humanitas University, Pieve Emanuele (MI), Italy, Milano, Italy; ³Unit of Internal Medicine and Metabolic Disease, Fondazione IRCCS Ca' Granda Ospedale Maggiore Policlinico of Milan, Italy, Department of Pathophysiology and Transplantation, University of Milan, Italy, Milano, Italy; ⁴Sezione di Gastroenterologia, Dipartimento Biomedico di Medicina Interna e Specialistica, Università di Palermo, Palermo, Italy, Palermo, Italy; ⁵University of Bologna, Bologna, Italy; ⁶University of Turin, Turin, Italy; ⁷University of Modena, Modena, Italy; ⁸University and Azienda Ospedaliera Universitaria Integrata of Verona, Verona, Italy; ⁹Università Cattolica del Sacro Cuore, Roma, Italy; ¹⁰Department of Medicine, University and Azienda Ospedaliera Universitaria Integrata of Verona, Verona, Italy, Verona, Italy; ¹¹Centro C.U.R.E., Dept. of Medical and Surgical Sciences, University of Foggia, Foggia, Italy; ¹²Humanitas University, Milano, MI, Italy; ¹³Fondazione IRCCS Ca' Granda Ospedale Maggiore Policlinico, Università degli Studi di Milano, Milano, Italy; ¹⁴Università Cattolica del S. Cuore, Roma, Italy; ¹⁵Section of Gastroenterology and Hepatology, PROMISE, University of Palermo, Palermo, Italy, Palermo, Italy; ¹⁶Division of Gastroenterology and Hepatology, McGill University Health Centre, Montreal, Canada, Montreal, Canada; ¹⁷Humanitas University, Milano, Italy
Email: nicola.pugliese@live.com

Background and aims: Metabolic dysfunction-associated steatotic liver disease (MASLD) is a significant global public health concern and is expected to become the leading indication for liver transplantation in the coming decades. Chatbots, which utilize artificial intelligence (AI) to simulate conversations with users, could provide counselling and support to English-speaking patients with MASLD. In a recent study, we showed that while ChatGPT 3.5 is complete and comprehensive in answering MASLD-related questions, its accuracy is still suboptimal. Whether language plays a role in modifying these findings is unclear.

Method: We evaluated the accuracy, completeness and comprehensiveness of ChatGPT 3.5 in answering 15 pre-set questions about MASLD in Italian. The questions were grouped into three domains: specialist referral, physical activity, and dietary composition. ChatGPT responses were rated on a 6-point accuracy scale, a 3-point completeness scale, and a 3-point comprehensibility scale by 13 native Italian MASLD experts.

Results: The mean scores for accuracy and completeness were 4.57 ± 0.42 and 2.53 ± 0.51 respectively, with a mean score of 2.91 ± 0.07 for comprehensiveness. The domain of physical activity achieved the most elevated mean score of 4.82 ± 0.22 and 2.35 ± 0.11 for accuracy and completeness respectively, while the domain of specialist referral achieved the lowest mean score of 4.1 ± 0.44 and 1.66 ± 0.29 for accuracy and completeness respectively. The mean Kendall's coefficient of concordance for accuracy, completeness and comprehensiveness across all 15 questions was 0.524, 0.623 and 0.73 respectively. Age and academic role of the evaluators did not affect

the scores. The scores were not significantly different from those reported in our previous study focusing on the English language.

Conclusion: We have shown that language does not affect the ability of ChatGPT to provide complete and understandable counselling for MASLD patients, however its accuracy remains suboptimal in certain domains. To ensure the trustworthiness of medical information provided by AI, the collaboration between healthcare professionals, patient associations and medical literature databases needs to be further improved.

FRI-291

Stigma in steatotic liver disease (SLD): a survey of patients from Saudi Arabia

Saleh Alqahtani¹, Khalid A. Alswat², Mohammad Mawardi³, Faisal Sanai⁴, Faisal Aba Alkhail⁵, Saad Alghamdi⁶, Waleed K. Al-Hamoudi², Fatema Nader⁷, Maria Stepanova⁷, Zobair Younossi⁷. ¹Liver Transplant Center, King Faisal Specialist Hospital and Research Center, Riyadh, Saudi Arabia, Division of Gastroenterology and Hepatology, Johns Hopkins University, Baltimore, MD, United States; ²Liver Disease Research Centre, College of Medicine, King Saud University, Riyadh, Saudi Arabia; ³Department of Internal Medicine, King Faisal Specialist Hospital and Research Center, Riyadh, Saudi Arabia; ⁴Gastroenterology Unit, Department of Medicine, King Abdulaziz Medical City, Jeddah, Saudi Arabia; ⁵Department of Medicine, King Faisal Specialist Hospital and Research Center, Riyadh, Saudi Arabia; ⁶Liver Transplant Center, King Faisal Specialist Hospital and Research Center, Riyadh, Saudi Arabia; ⁷The Global NASH Council, Washington DC, United States, Center for Outcomes Research in Liver Diseases, Washington DC, United States
Email: kalswat@ksu.edu.sa

Background and aims: Non-alcoholic fatty liver disease (NAFLD) and its progressive form non-alcoholic steatohepatitis (NASH) are part of the spectrum of SLD. The terms NAFLD/NASH may be associated with stigma. We aimed to understand stigma among NAFLD/NASH patients enrolled in Saudi Arabia (SA).

Method: Members of the Global NASH Council created a 68-item survey about patients' experience with NAFLD, history of stigma and discrimination due to the disease, various aspects of the disease burden (Liver Disease Burden instrument, 35 items in 7 domains), and perception of various diagnostic terms for NAFLD. We included only patients whose country of residence was SA.

Results: The survey was completed by 804 NAFLD/NASH patients from SA: 63% between 25 and 44 years and 24% ≥ 45 years old, 75% male, 7% obese (BMI > 30), 79% living in urban regions, 76% with a college degree, 84% employed, 9% with type 2 diabetes and 87% with no comorbidities, 1.2% with cirrhosis. Of all patients, 17% ever disclosed having NAFLD/NASH to family/friends; the most used words when discussing the disease were "fatty liver" (96% used it at least sometimes, 79% frequently or always). At the same time, "NAFLD or NASH" and "liver steatosis" were never used by $>94\%$ patients, "liver disease" and "metabolic liver disease" never used by $>75\%$. Interestingly, the term metabolic associated fatty liver or MAFLD was used by 50% at least sometimes, 20% frequently or always. There were 3.7% who reported experiencing stigma or discrimination (at least sometimes) due to obesity/overweight vs. only 2.7% due to NAFLD; female patients reported stigma more frequently than male: 5.9% vs. 3.0% due to obesity ($p = 0.06$), 5.4% vs. 1.8% due to NAFLD ($p = 0.01$). In addition, 43% of patients reported ever missing or avoiding a visit to a primary care provider due to NAFLD (48% male vs. 28% female, $p < 0.0001$). The greatest social-emotional burden among NAFLD patients was being identified as a person with liver disease (10% agree, 4% male vs. 26% female) and feeling like they cannot do anything about their liver disease (6.4% agree, 3% male vs. 16% female). As such, among 7 domains of the Liver Disease Burden instrument, the highest scores (the greatest burden) for both sexes were observed in the Self-Perception domain. Regarding how various diagnostic terms were perceived by patients, there were no

substantial differences between “fatty liver disease,” “NAFLD,” “NASH,” or “MAFLD”: the most popular response was being neither comfortable nor uncomfortable with either term (81%–97%) while only 0.2–1.5% were uncomfortable with any of those terms.

Conclusion: The disease burden, disease-related stigma, and perception of various diagnostic terms as stigmatizing are rarely observed in patients with NAFLD in SA. In comparison to male NAFLD patients from SA, female patients more commonly reported history of stigma and discrimination and a significantly greater disease burden.

FRI-293

Association between liver fibrosis, mental health, and lifestyle behaviors in patients with Metabolic Dysfunction-Associated Steatotic Liver Disease

Tayla Robertson^{1,2}, Nashla Hamdan³, Chinmay Bera², Magdalena Kuczyński², Radin Pakseresh², Bo Chen², Keyur Patel².

¹Princess Alexandra Hospital, Brisbane, Australia; ²University Health Network, Toronto, Canada; ³University Health Network, Toronto, Canada

Email: keyur.patel@uhn.ca

Background and aims: Understanding lifestyle behaviours and psychological factors are necessary to provide personalised interventions for individuals living with Metabolic Dysfunction-Associated Steatotic Liver Disease (MASLD). We hypothesised that advanced fibrosis (F3–4) is associated with poor diet quality, physical inactivity, and impaired mental wellbeing. Our aims were to prospectively examine the relationships between severity of fibrosis, diet quality/behaviour, physical inactivity, and measures of psychological distress.

Method: Patients with MASLD were prospectively recruited from a single tertiary centre between March and October 2023. Four questionnaires were administered to patients during their ambulatory clinic visit: Energy-Restricted Mediterranean Diet Adherence Screener (er-MEDAS), International Physical Activity Questionnaire Short Form (IPAQ-SF), Hospital Anxiety and Depression Scale (HADS), and Binge Eating Scale (BES). Patient demographics, clinical characteristics and laboratory data were collected from their electronic medical records. Fibrosis was assessed by Fibroscan (VCTE) or liver biopsy data, and statistical analysis performed using R (r-project.org).

Results: Our study cohort included 100 MASLD patients with higher proportion of male sex (n = 57), mean age 48.5 years, BMI 33 kg/m², T2DM 31%, and F3–4 27%. Overall, 90% had poor (56%) to moderate adherence to Mediterranean diet, 74% reported low (33%) to moderate physical activity, 22% had anxiety, and moderate-severe binge reported in 21%. In multivariate logistic regression analysis, stage F3–4 was independently associated with weight (OR 1.01, 95% CI: 1.00–1.01; p = 0.04), diabetes mellitus (OR 1.38, 95% CI: 1.16–1.63; p = 0.0003), lower HADS-anxiety score (OR 0.98, 95% CI: 0.97–0.99; p = 0.04) and alcohol intake compliant with er-MEDAS (abstinence or ≤3 glasses red wine/day with meals for men/ ≤2 glasses red wine/day with meals for women, OR 1.17, 95% CI: 1.02–1.35; p = 0.03). In addition, abnormal binge eating (BES) was associated with lower risk of borderline or abnormal anxiety (HADS-A ≥ 8, OR 9.06, 95% CI 1.63–69.3; p = 0.02) and depression (HADS-D ≥ 8, OR 5.92, 95% CI 1.59–23.09; p = 0.008).

Conclusion: In our prospective MASLD cohort, most patients reported poor-moderate diet, reduced activity, and one-fifth reported anxiety and binge-eating behaviour. Advanced fibrosis was not independently associated with poor diet quality, physical inactivity, and impaired mental wellbeing. However, patients with more advanced disease may be modifying their lifestyle behavior in accordance with medical recommendations. Most patients in our cohort had non-advanced disease and further validation is ongoing.

FRI-294

Identification of key predictors of significant weight loss in metabolic dysfunction-associated steatotic liver disease (MASLD) patients: a multicentre study

Ivan Arcari¹, Nicola Pugliese¹, Simone Rocchetto², Rosa Lombardi³, Grazia Pennisi⁴, Michele Sagasta⁵, Matteo Soleri⁶, Federica Cerini⁷, Annalisa Cespiati⁸, Stella De Nicola⁹, Francesca Colapietro¹⁰, Chiara Masetti⁹, Anna Fracanzani¹¹, Salvatore Petta¹², Mauro Viganò¹³, Alessio Aghemo¹. ¹Humanitas University, Rozzano, MI, Italy; ²Università degli Studi di Milano, Milan, Italy; ³Unit of Internal Medicine and Metabolic Disease, Fondazione Ca' Granda IRCCS Ospedale Maggiore Policlinico, Milan, Italy; ⁴Sezione di Gastroenterologia, Dipartimento Biomedico di Medicina Interna e Specialistica, Università di Palermo, Palermo, Italy, Milan, Italy; ⁵Maggiore Hospital and IRCCS Foundation, Milan, Italy; ⁶Humanitas University, Milan, Italy; ⁷Hospital, MultiMedica IRCCS, Università degli Studi di Milano, Milan, Italy; ⁸Fondazione IRCCS Ca' Granda, Ospedale Maggiore Policlinico of Milan, Milan, Italy; ⁹Humanitas Research Hospital IRCCS, Milan, Italy; ¹⁰Humanitas Research Hospital IRCCS, Rozzano, MI, Italy; ¹¹Fondazione IRCCS Ca' Granda Ospedale Maggiore Policlinico, Milan, Italy; ¹²University of Palermo, Palermo, Italy; ¹³MultiMedica IRCCS, Università degli Studi di Milano, Milan, Italy
Email: nicola.pugliese@humanitas.it

Background and aims: Significant weight loss is the only proven therapy for patients with metabolic dysfunction-associated steatotic liver disease (MASLD). This study aimed to identify factors that predict significant weight loss-exceeding 7% of the initial weight-in MASLD outpatients.

Method: We included all MASLD patients referred to four Italian tertiary liver centres between January 2019 and December 2021. They received advice on lifestyle changes according to current guidelines, with reassessment of anthropometric measures after 18 to 24 months.

Results: After evaluating 908 patients meeting the inclusion criteria, the majority were found to be male (518/908, 57%) with a mean age of 61.7 ± 13.31 years and a mean baseline body mass index (BMI) of 30.31 ± 4.49 kg/m². Over a mean follow-up period of 21.88 ± 6 months, only 166 (18.3%) patients achieved significant weight loss. Unadjusted regression analysis revealed significant correlations between dyslipidaemia, baseline BMI ≥ 30 kg/m², and the use of GLP-1 (glucagon-like peptide 1) agonists with significant weight loss (p < 0.05). Multivariate regression analysis identified only BMI ≥ 30 kg/m² (OR = 1.96, 95% CI: 1.37–2.8) and dyslipidaemia (OR = 0.6, 95% CI: 0.44–0.88) as independent predictors of significant weight loss.

Conclusion: A baseline BMI ≥ 30 kg/m² and the absence of dyslipidaemia emerged as significant predictors of achieving substantial weight loss in MASLD patients. These findings highlight the need for personalized interventions to improve the effectiveness of weight management strategies in MASLD.

FRI-295

Risk factors for hepatocellular carcinoma in patients with metabolic dysfunction-associated steatotic liver disease

Ian Yang Liew¹, Hwee Pin Phua², Wei Yen Lim³, Angela Chow³, Xiu Ying Loo¹, Kevin Sim¹, Eng Sing Lee⁴, Kuo Chao Yew³. ¹Ministry of Health (MOH) Holdings Pte Ltd, Singapore, Singapore; ²Tan Tock Seng hospital, Singapore, Singapore; ³Tan Tock Seng Hospital, Singapore, Singapore; ⁴Lee Kong Chian School of Medicine, Nanyang Technological University, Singapore, Singapore
Email: Liewianyang@gmail.com

Background and aims: Metabolic Associated Steatotic Liver Disease (MASLD) is associated with higher risk of Hepatocellular Carcinoma (HCC). For MASLD without advanced fibrosis, the incidence has been estimated to be 0.1 to 1.3 per 1,000 patient-years. In this study, we aim to identify independent risk factors of HCC incidence among individuals with MASLD without advanced fibrosis.

POSTER PRESENTATIONS

Method: We conducted a retrospective cohort study using electronic medical records of MASLD patients with No Advanced Fibrosis (NAF) seen in a multidisciplinary hospital in Singapore. Patients with a diagnosis of MASLD with NAF made between 1st January 2007 and 31st October 2017 were identified using International Classification of Diseases (ICD-10) code, Fibrosis-4 (FIB-4) scoring, imaging, and histology, and followed up till 31st October 2017. The start date of follow-up was defined as the date of MASLD diagnosis. Multivariable Cox regression was performed to identify demographic, clinical, and/or laboratory variables with significant association with increased risk of HCC development. Proportional hazard assumption was tested using Schoenfeld residuals.

Results: Our cohort comprised 2170 patients with a median age of 51 [IQR 41–59] years. Patients were predominantly Chinese (77.1%) and slightly more than half (51.9%) were male. The median length of follow-up was 5.2 years and 19 (0.9%) patients developed HCC at the end of follow-up. There was no statistically significant difference in the proportion of HCC incident cases between patients with more or less than 3 years of follow-up (12/1597 (0.8%) versus 7/573 (1.2%) respectively), $p = 0.300$). Incidence rate of HCC was estimated at 1.6 per 1000 person-year. 431 (19.9%) patients developed advanced fibrosis during follow-up. Older age at diagnosis of MASLD (HR: 1.06, 95% CI: 1.02–1.10), male gender (HR: 5.61, 95% CI: 1.71–18.39), and development of advanced fibrosis over follow-up time (HR: 5.80, 95% CI: 2.14–15.69) were associated with increased risk of HCC incidence. Conversely, the presence of metabolic syndrome at baseline (HR: 1.39, 95% CI: 0.49–3.94) and Charlson Comorbidity Index at baseline (HR: 1.01, 95% CI: 0.73–1.40) were not associated with increased HCC incidence. Due to the retrospective nature of the study, the proportion of patients with missing laboratory data was high. Laboratory variables explored were therefore not included in the analysis.

Conclusion: Our study demonstrated a difference in baseline HCC risk for MASLD. The risk factors could be delineated to identify at-risk subgroups for intensive management or surveillance programme enrolment.

FRI-296

Metabolic dysfunction-associated steatotic liver disease and low handgrip strength are independently associated with a higher risk for cardiovascular disease

Seung Up Kim¹, Jae Seung Lee¹, Hye Won Lee¹, Mi Na Kim¹, Beom Kyung Kim¹, Jun Yong Park¹, Do Young Kim¹, Sang Hoon Ahn¹.
¹Yonsei University, Seoul, Korea, Rep. of South
Email: ksukorea@yuhs.ac

Background and aims: Metabolic dysfunction-associated steatotic liver disease (MASLD) is a term recently proposed to encompass the conventional concept of non-alcoholic fatty liver disease (NAFLD). This study investigated whether muscle function, as indicated by handgrip strength (HGS), is associated with the risk for cardiovascular disease (CVD) in individuals with MASLD.

Method: This study involved the data of 24,682 individuals from the 2014–2019 Korea National Health and Nutrition Examination Survey. Steatotic liver disease was assessed using the Framingham steatosis index and simple NAFLD score, and advanced liver fibrosis was assessed using the Fibrosis-4 index. Low HGS was defined as <26 kg in men and <16 kg in women. The risk for CVD was evaluated using the 10-year atherosclerotic CVD (ASCVD) risk score. High probability ASCVD risk was defined as ASCVD >10%.

Results: The prevalence of MASLD and low HGS were 25.5% ($n = 6,282$) and 6.3% ($n = 1,549$), respectively. Individuals with both MASLD and low HGS were at greater risk for high probability ASCVD (odds ratio = 4.06, $p < 0.001$) than those without MASLD. The impact of low HGS on high probability ASCVD risk was higher when MASLD was

accompanied by advanced liver fibrosis (odds ratio = 8.10, $p < 0.001$). CVD risk was lower in individuals who had low HGS but engaged in regular exercise than in individuals with neither low HGS nor regular exercise. Similar findings were observed when the simple NAFLD score was used to define steatotic liver disease.

Conclusion: Individuals with MASLD and low HGS had a significantly higher risk for CVD than those without MASLD. Concurrent advanced liver fibrosis further enhanced the risk for CVD among individuals with MASLD.

FRI-297

Clinical impact of pre-existing steatotic liver disease on clinical course in acute HEV infection

Kazunari Tanaka¹, Jong-Hon Kang², Takeshi Matsui¹, Hiroaki Okamoto³.
¹Teine Keijinkai Hospital, Sapporo, Japan; ²Teinne Keijinkai Hospital, Sapporo, Japan; ³Jichi Medical University School of Medicine, Shimotuke, Japan
Email: kazunari0511@gmail.com

Background and aims: Steatotic liver disease (SLD) has been recognized as a prevalent underlying condition which could affect clinical course in newly occurred liver diseases including acute hepatitis (AH). Aim of this study was to elucidate the influence of pre-existing SLD on acute infection of hepatitis E virus (HEV).

Method: Among the patients with AHE treated between 2012 and 2017 in Japan, 503 cases collected from 155 medical facilities in Japan, 379 cases well-documented for BMI and alcohol consumption were included. SLD was defined as fatty liver detected by ultrasonography. The patients with chronic liver diseases other than SLD and liver cancer were excluded. They were divided into 2 groups: 27 cases with SLD as a target one and another 352 cases as a control. Acute liver failure (ALF) was defined as PT INR ≥ 1.5 and habitual drinking as ≥ 60 g/day. The impact of background SLD on the clinical course of AHE was retrospectively analyzed.

Results: Among 27 patients with underlying SLD, 23 (85%) were male and median age of years was of 58 (IQR, 50–62). In control patients, showed 292 (83%) were male and median age was of 56 (IQR 45–67). In the current study, SLD consisted of metabolic dysfunction associated steatotic liver disease (MASLD) in 11 patients, Met ALD [MASLD and alcohol-related fatty liver disease (ALD)] in 11, and cryptogenic in 5. In comparison with control, SLD group demonstrated higher BMI (24.8 vs. 23.0, $p = 0.003$), frequently complicated diabetes [$n = 12$ (44%) vs. $n = 57$ (16%), $p = 0.001$], and dyslipidemia [$n = 12$ (44%) vs. $n = 67$ (19%), $p = 0.001$], respectively. On admission, there was no differences in levels of AST, ALT, total bilirubin, and PT-INR between them. Identically, peak value of AST, ALT, total bilirubin, and PT-INR and nadir value of albumin did not differ between two groups. ALF was more frequent in SLD group than in control [$n = 8$ (30%) vs. $n = 36$ (10%), $p = 0.006$]. In univariate analysis, pre-existing SLD (HR 3.81, 95% CI 1.56–9.33), habitual drinking (HR 2.47, 95% CI 1.28–4.79), and diabetes (HR 2.16, 95% CI 1.07–4.39) were associated with progression to ALF, respectively, whereas BMI, ≥ 25 or ≥ 30 , was not. In multivariate analysis, SLD (HR 2.94, 95% CI 1.13–7.62) and habitual drinking (HR 2.34, 95% CI 1.19–4.60) were remained as risk factors related with ALF. The frequency of ALF in MASLD, Met ALD and cryptogenic did not differ. There was no difference in requirement of corticosteroid therapy, hospitalization, or liver disease-related death in each group.

Conclusion: From these results, underlying SLD could affect to deteriorate liver reserve on clinical course of AHE. Clinicians should exercise caution and be cognizant of the potential for severity in the clinical course of AHE in cases with underlying SLD. Additional analyses are warranted to elucidate why SLD affected the course of acute hepatitis E.

FRI-298

Insulin resistance and sarcopenia as comorbid conditions in patients with MASLD

Kateryna Pivtorak¹, Oleksandr Ivanchuk¹, Natalya Pivtorak¹, Iryna Fedzhaga². ¹National Pirogov Memorial Medical University, Vinnytsia, Ukraine; ²National Pirogov Memorial Medical University, Vinnytsia, Ukraine
Email: ekaterina.pivtorak@yahoo.com.ua

Background and aims: Recent studies have shown that sarcopenia often accompanies MASLD. Sarcopenic obesity in combination with the progressive loss of skeletal muscle mass negatively affects the metabolic status of a person, which leads to a decrease in the quality of life and the development of cardiovascular diseases. The aim was to determine the relationship between inflammatory markers, insulin resistance and sarcopenia in patients with MASLD.

Method: The study included 202 normal, overweight, and obese MASLD patients and 106 non-MASLD patients. Anthropometric examination and MRI were performed, AST, ALT, GGT levels, degree of liver fibrosis using elastography (FibroScan), ECG were measured. Cardiovascular risk stratification was assessed using the SCORE version for high-risk countries. The level of inflammatory mediators (TNF- α , IL-1, IL-6), markers (CRP, fibrinogen), myostatin, endothelin-1, the thickness of the intima-media complex, the presence of atherosclerotic plaque and carotid artery stenosis, HOMA-IR insulin resistance index were determined for all patients.

Results: Thus, the body weight of men with MASLD was 1.3 times greater than in the group of healthy men. The body weight of women with MASLD was 1.5 times higher compared to the group of healthy women. There were no significant differences or trends in body length between healthy and MASLD males and MASLD females. The BMI of men with MASLD was 1.4 times higher than that of healthy men. The BMI of women with MASLD was also 1.4 times higher than that of healthy women. The muscle mass of men and women with MASLD was statistically significantly lower ($p < 0.05$) than that of sexually healthy men and women. Moreover, muscle mass in healthy men was statistically significantly higher ($p < 0.05$) than in the corresponding groups of women. Thus, healthy men's muscle mass increased by 20.5% compared to healthy women. Higher levels of inflammation, HOMA index, and decreased adiponectin levels were found in patients with MASLD, and sarcopenia compared to patients with preserved muscle mass. According to the results of the study, the component composition of body weight changes in MASLD. Compared with healthy men with MASLD, body fat mass was 35.2% higher, while muscle mass and bone mass in men were 29.1% and 32.0% lower, respectively. Compared to healthy women with MASLD, body fat mass was 30.2% higher, while muscle mass and bone mass in women were 17.4% and 22.7% lower, respectively. Strong inverse correlations ($r = 0.71$, $p < 0.001$) were found between muscle mass and hs CRP levels in men and women with MASLD.

Conclusion: The mechanisms of pathogenesis of sarcopenia and MASLD are common: insulin resistance, increased inflammation, secretion of myokines by skeletal muscles, myostatin, and decrease in adiponectin level.

FRI-299

Poor diet quality is associated with higher cardiovascular risk in a cohort of non-cirrhotic Italian MASLD (Metabolic dysfunction associated steatotic liver disease) outpatients

Rusi Chen¹, Chiara Abbati¹, Ernestina Santangeli¹, Roberta Capelli¹, Simona Leoni², Federico Ravaioli¹, Fabio Piscaglia¹, Silvia Ferri². ¹University of Bologna, Alma Mater Studiorum, Bologna, Italy; ²IRCCS Azienda Ospedaliero Universitaria di Bologna, Bologna, Italy
Email: silvia.ferri@aosp.bo.it

Background and aims: Poor diet quality accounts for 11 million deaths and approximately 50 % of cardiovascular (CV) disease-related deaths globally. Practical diet screening tools like REAP-S (Rapid Eating Assessment for Participants-Shortened Version) have been

developed to quickly assess the diet quality in clinical settings. The aim of our study was to compare the physical, laboratory and ultrasound features and CV risk of the MASLD patients of our liver clinic, based on their REAP-S score.

Method: We enrolled, from February 2022 to January 2024, 92 consecutive non-cirrhotic subjects (47 % females, median age 61 years) followed in our MASLD outpatient clinic. All patients received a complete anamnestic, physical, laboratory and ultrasound evaluation. Their physical activity and dietary habits were assessed using validated questionnaires, respectively IPAQ (International Physical Activity Questionnaire) score and REAP-S score, the latter ranging from 13 to 39 points (with a higher score indicating a higher diet quality). Skeletal muscle function was evaluated using hand-grip strength. The CV risk was predicted using Italian National Institute of Health calculator "Progetto Cuore." According to a median REAP-S score of 30, we divided our cohort into 2 groups, namely "A" or poor diet quality (with score ≤ 30): 47 subjects and "B" or good diet quality (with score > 30): 45 subjects.

Results: The two groups didn't show statistical differences in demographic and anthropometric data (age, sex, weight, height, BMI, waist circumference), nor in auto-reported physical activity or in hand-grip strength. Similar transaminases, lipid profile, renal function and total protein and albumin levels were found in the two groups. Compared to group A, in group B gamma-GT levels were lower (37 U/L vs. 52 U/L; $p = 0.03$). The two cohorts displayed similar values of non-invasive markers of fibrosis, within the range of normality (NAFLD fibrosis score, FIB-4 and liver stiffness evaluated with two-dimensional shear wave elastography). Regarding CV risks factors, similar prevalence of dyslipidemia and diabetes mellitus were found in the two groups. Compared to group B, more patients in group A were smokers (32% vs 9%, $p = 0.006$) and had been diagnosed and took medications for arterial hypertension (64% vs. 40 %; $p = 0.02$), though the overall probability to experience a major cardiovascular event in the following 10 years was similar in the two groups.

Conclusion: In our cohort of non-cirrhotic MASLD outpatients, a poor diet quality assessed by REAP-S was significantly associated to smoking habit and arterial hypertension. Bad lifestyle habits appear to affect more the cardiovascular system compared to the pathological features of progressive steatotic liver disease, such as liver fibrosis, at least in a context of non-advanced liver disease.

FRI-302

Non-obese non-alcoholic fatty liver disease and the risk of chronic kidney disease: a literature review and meta-analysis

Yixian You¹, Xiong Pei¹, Wei Jiang¹, Qingmin Zeng¹, Chang Hai Liu¹, Lang Bai¹, Dongbo Wu¹, Hong Tang¹. ¹Center of Infectious Diseases, West China Hospital of Sichuan University, Chengdu, China
Email: htang6198@hotmail.com

Background and aims: Data on the risk of incident chronic kidney disease (CKD) in non-obese non-alcoholic fatty liver disease (NAFLD) patients compared to obese NAFLD patients are limited. The purpose of the current study was to examine the risk differences of incident CKD between non-obese and obese NAFLD patients.

Method: We searched PubMed, Embase, and Web of Science databases for studies which reported the incidence of CKD in non-obese and obese patients with NAFLD from inception to 16 July 2023. The primary and secondary outcomes were pooled using random-effects model. Subgroup analyses were used to examine the heterogeneity.

Results: A total of 15 studies were incorporated into the final analysis. The incidence of CKD in non-obese and obese NAFLD were 1450/38720 (3.74%) and 3067/84154 (3.64%), respectively. Patients with non-obese NAFLD had a comparable risk of incident CKD as obese NAFLD patients (random effects odds ratio [OR] 0.92, 95% CI 0.72–1.19, $I^2 = 88\%$). There were also no significant differences in estimated glomerular filtration rate (eGFR) and serum creatinine between non-obese and obese NAFLD. The mean differences (MD) and 95%

POSTER PRESENTATIONS

confidence interval (95%CI) were 0.01 (-0.02–0.04) and 0.50 (-0.90–1.90), respectively. In subgroup analyses, non-obese NAFLD patients were found to have higher eGFR compared to obese NAFLD when diagnosed with ultrasound (MD 1.45, 95%CI 0.11–2.79, $I^2 = 21\%$). In non-Asia populations, non-obese NAFLD patients had higher levels of creatinine (MD 0.06, 95%CI 0.01–0.11, $I^2 = 55\%$). When taking BMI greater than 30 as a criterion for obesity, non-obese NAFLD patients also showed higher levels of creatinine (MD 0.06, 95%CI 0.00–0.12, $I^2 = 76\%$). Non-obese NAFLD patients were also categorized into overweight and normal-weight types, and the occurrence of CKD did not differ among normal-weight, overweight and obese NAFLD patients.

Conclusion: Non-obese NAFLD patients experienced a comparable risk of CKD compared to obese NAFLD patients.

FRI-303

Depression as a determinant of metabolic dysfunction-associated steatotic liver disease (MASLD) risk in the Paracelsus 10, 000 study

Florian Koutny^{1,2}, Elmar Aigner³, Christian Datz⁴, Sophie Gensluckner³, Andreas Maieron², Andrea Mega⁵, Bernhard Iglseder⁶, Patrick Langthaler⁷, Maria Flamm⁸, Vanessa Frey⁹, Bernhard Paulweber¹⁰, Eugen Trinka⁹, Bernhard Wernly⁴.

¹Department of Human Medicine, PhD Medical Science, Paracelsus Medical University, Salzburg, Austria; ²Department of Internal Medicine 2, Gastroenterology and Hepatology and Rheumatology, Karl Landsteiner University of Health Sciences, University Hospital of St. Pölten, St. Pölten, Austria; ³First Department of Medicine, University Clinic Salzburg, Paracelsus Medical University Salzburg, Salzburg, Austria; ⁴Department of Internal Medicine, General Hospital Oberndorf, Teaching Hospital of the Paracelsus Medical University, Oberndorf, Austria; ⁵Gastroenterology Department, Bolzano Regional Hospital, Bolzano, Italy; ⁶Department of Geriatric Medicine, Christian-Doppler-Klinik, Paracelsus Medical University, Salzburg, Austria; ⁷Department of Neurology, Christian Doppler University Hospital, Paracelsus Medical University and Centre for Cognitive Neuroscience, Salzburg, Austria; ⁸Institute of General Practice, Family Medicine and Preventive Medicine, Paracelsus Medical University of Salzburg, Salzburg, Austria; ⁹Department of Neurology, Christian Doppler University Hospital, Paracelsus Medical University and Centre for Cognitive Neuroscience, Salzburg, Austria; ¹⁰First Department of Medicine, University Clinic Salzburg, Paracelsus Medical University, Salzburg, Austria

Email: florian.koutny@stpoelten.lknoe.at

Background and aims: The increasing prevalence of Metabolic Dysfunction-Associated Steatotic Liver Disease (MASLD) comorbid depression is a significant health challenge. Despite the emerging recognition of this health burden, only few studies, particularly those incorporating the new MASLD nomenclature, have explored the interplay between depression and MASLD. Therefore, we aimed here to investigate the association between depression and the risk of MASLD while adjusting for potential confounders. The goal is to better understand how depression affects liver health, and how brain health may interact with metabolic dysfunction contributing new knowledge to this field.

Method: The study included 8,315 participants from the Paracelsus 10,000 study. The fatty liver index (FLI) score ≥ 60 served as a surrogate marker for MASLD. Depression was defined using the Beck Depression Inventory I-II (BDI) score. Initially, we examined the BDI score as a continuous variable. Subsequently, we categorized participants into two groups: those with a BDI score >8 , indicating depression, and those with a BDI score ≤ 8 , serving as the control group. Results were adjusted for covariates such as age, sex, and metabolic syndrome.

Results: The results from the linear regression model indicated that with each additional BDI point, the odds ratio (OR) for MASLD increased by 1% (OR: 1.01, $p < 0.01$, 95% CI: 1.01–1.02). Individuals with depression (BDI score >8) had a significantly higher OR for MASLD compared to those without depression (BDI score ≤ 8), (OR:

1.3, $p < 0.01$, 95% CI: 1.13–1.50). Depression was associated with a 17% increased risk for MASLD after adjusting for confounding factors (Adjusted Relative Risk = 1.17, $p < 0.01$, 95% CI: 1.07–1.28).

Conclusion: Our findings show a significant association between depression and an increased prevalence of MASLD. Early screening for MASLD in high-risk individuals is crucial to enhance health and the overall well-being of patients with depression. Further research is needed to explore the underlying mechanisms and potential interventions.

FRI-304

Assessment of ChatGPT-generated medical arabic responses for patients with metabolic dysfunction-associated steatotic liver disease

Saleh A. Alqahtani¹, Reem S. AlAhmed¹, Waleed S. AlOmair¹, Saad Alghamdi², Waleed K. Al-Hamoudi¹, Khalid I. Bziezi¹, Ali Albenmoussa¹, Alessio Aghemo³, Nicola Pugliese³, Cesare Hassan⁴, Faisal Abaalkhail⁵. ¹King Faisal Specialist Hospital and Research Centre, Riyadh, Saudi Arabia; ²King Faisal Specialist Hospital and Research Centre, Liver and Small Bowel Transplant and Hepatology Surgical Department, Riyadh, Saudi Arabia; ³Humanitas University, Pieve Emanuele (MI), Milan, Italy; ⁴Nuovo Regina Margherita Hospital, Rome, Italy; ⁵King Faisal Specialist Hospital and Research Centre, Department of Medicine, Section of Gastroenterology, Riyadh, Saudi Arabia
Email: drsaleh.a.alqahtani@gmail.com

Background and aims: Metabolic dysfunction-associated steatotic liver disease (MASLD) has become increasingly prevalent in recent years due to the rise in obesity and unhealthy lifestyle choices. Artificial intelligence (AI)-powered chatbots, such as Chat Generative Pretrained Transformer (ChatGPT), have shown promising results in healthcare. These tools can provide guidance and support to individuals with MASLD by offering real-time responses to user queries, ensuring immediate access to relevant information. The present study aimed to explore the potential use of ChatGPT-generated medical Arabic responses for patients with MASLD.

Method: This cross-sectional study firstly involved the Arabic translation of a validated English patient questionnaire on MASLD. Second, the Arabic questions were entered in the ChatGPT 3.5 platform on November 12, 2023. Third, the responses were evaluated for accuracy, completeness, and comprehensiveness by 10 MASLD experts from Saudi Arabia who were native Arabic speakers. Different Likert scales were used to evaluate the three domains: 1) Accuracy: 6-point Likert scale (Correct, Nearly all correct, More correct than incorrect, Approximately equally correct and incorrect, More incorrect than correct, and Completely incorrect), 2) Completeness: 3-point Likert scale: (Incomplete, Adequate, and Comprehensive), and 3) Comprehensiveness: 3-point Likert scale: (Difficult, Partly difficult, and Easy to understand). An additional question was added to the Arabic questionnaire to capture any comments regarding the generated responses.

Results: The mean accuracy score was 4.9 on a 6-point Likert scale corresponding to “Nearly all correct.” Kendall’s coefficient of concordance (KCC) ranged from 0.649 to 0.025, with a mean of 0.28, indicating moderate agreement between all ten experts. The mean completeness score was 2.4 on a 3-point Likert scale corresponding to “Comprehensive” (KCC: 0.553–0.03; mean: 0.22). The average comprehensibility score was 2.74, which indicates that the ChatGPT generated responses were “Easy to understand” (KCC: 0.553–0.03; mean: 0.22).

Conclusion: Arabic-speaking experts in hepatology found that ChatGPT-generated medical Arabic responses for patients with MASLD were accurate, complete, and comprehensive. The results support the increasing trend of leveraging the power of AI chatbots to revolutionize the dissemination of information for patients with MASLD, ultimately improving overall health outcomes.

FRI-305

Lower aspartataminotransferase activity is associated with dynapenia in middle-aged patients with metabolic dysfunction-associated steatotic liver disease

Anna Sheptulina^{1,2}, Elvira Mamutova¹, Ekaterina Lusina¹, Timur Tsoriev¹, Oxana Drapkina¹. ¹National Medical Research Center for Therapy and Preventive Medicine, Moscow, Russian Federation; ²Department of Therapy and Preventive Medicine, A.I. Evdokimov Moscow State University of Medicine and Dentistry, Moscow, Russian Federation
Email: sheptulina.anna@gmail.com

Background and aims: Increasing evidence suggest an important role of skeletal muscles in the pathogenesis of metabolic dysfunction-associated steatotic liver disease (MASLD). Both skeletal muscles and liver express aspartataminotransferase (AST), and non-invasive indices based on the AST activity are widely used for the assessment of liver fibrosis progression, which may depend at least in part on the quality and quantity of skeletal muscles. This study aimed to evaluate the association between the AST activity and grip strength (GS), in middle-aged patients with MASLD.

Method: 83 MASLD patients were included in the study. MASLD was diagnosed based on the ultrasonography findings, the absence of liver disease of other etiology (based on the laboratory data), and the presence of at least one cardiometabolic risk factor. Liver stiffness was measured using two-dimensional shear wave elastography (Affiniti 70, Philips, Amsterdam, Netherlands). Body composition was assessed via dual x-ray absorptiometry (Lunar iDXA, GE HealthCare, USA). Appendicular skeletal muscle mass index (ASMI) was calculated as the sum of the lean muscle mass of the upper and lower extremities adjusted with height. GS was measured using a mechanical hand dynamometer (ZAO "NTMIZ" Russia). Patients were asked to squeeze the dynamometer with as much force as possible three times with their dominant hand. 60 seconds of rest interval was allowed between each trial. The maximum value was registered.

Results: Median age was 59 years (interquartile range (IQR) = 47–65); 74.7 % were female. Median body mass index was 31.2 (28.9–34.8) kg/m². All patients had arterial hypertension and dyslipidemia. Median liver stiffness value was 5.5 (4.1–6.5) kPa. Dynapenia, i.e. decreased GS, was present in 14 (16.9 %) patients. According to the results of correlation analysis, AST activity was associated with liver stiffness ($p < 0.001$), characteristic of liver disease progression, uric acid ($p = 0.05$) and triglyceride ($p = 0.049$) levels, both indicative of disturbed metabolic profile, and the quantity of skeletal muscles (ASMI, $p < 0.001$). Patients with dynapenia had substantially lower AST activity (17 [14–18.5] U/L vs. 20 [17–25] U/L, $p = 0.015$) compared to patients without dynapenia. Results of the logistic regression analysis using ASMI, muscle mass, and AST as covariates showed that AST activity was the only parameter significantly different between the MASLD patients with and without dynapenia ($p = 0.042$).

Conclusion: Our data demonstrate that AST activity which is often used as a marker of liver fibrosis progression (mainly as a component of non-invasive indices), is also associated with the presence of dynapenia in MASLD. Dynapenia is an early symptom of sarcopenia, which may negatively influence the ability of patients to perform physical activity, an established effective treatment strategy in MASLD, and affect disease outcome.

FRI-306

Insulin resistance in metabolic associated steatotic liver disease and its association with liver-related outcomes: a retrospective study and a nationwide, population-based study

Yeo Wool Kang¹, Yang-Hyun Baek², Sang Yi Moon¹, MinKook Son¹. ¹DongA University College of Medicine, Busan, Korea, Rep. of South; ²DongA University College of Medicine, Busan, Korea, Rep. of South
Email: p100100@dau.ac.kr

Background and aims: Insulin resistance (IR) is a well-known factor in the development and progression of in metabolic associated steatotic liver disease (MASLD). Many studies have investigated the development of fatty liver disease and the progression of liver fibrosis in individuals with high insulin resistance (IR); however, limited research exists on IR changes in patients advancing to cirrhosis and hepatocellular carcinoma (HCC). This study investigated the correlation between IR and liver-related outcomes in patients with MASLD.

Method: We retrospectively analyzed data from 361 patients diagnosed with MASLD who underwent liver biopsy at Dong-A University Hospital between January 2015 and November 2023. The study identified changes in insulin surrogate markers, including the triglyceride-glucose (TyG) index, triglyceride to high-density lipoprotein (TG/HDL) ratio, and metabolic score for IR (METS-IR), based on liver fibrosis grade. In a separate analysis, we retrospectively analyzed data from 362, 285 participants who underwent a health screening program in 2009 and 2010 using the Korean National Health Insurance Service (KNHIS) database. The participants were diagnosed and classified using the International Classification of Diseases, 10th Revision. Those with fatty liver were identified using the Fatty Liver Index with a threshold of 30. The study analyzed the relationship between liver-related outcomes such as decompensation or HCC and IR.

Results: 183 patients (50.7%) were in F0, 88 patients (24.4%) were in F1, 31 patients (8.6%) were in F2, and 59 patients (16.3%) were in F3 and F4. The three insulin surrogate markers showed an upward trend from F0 to F2, followed by a downward trend as they progressed to F3, F4. (mean TG/HDL in patients without advanced fibrosis vs with advanced fibrosis = 4.46 ± 2.63 vs 3.05 ± 1.69 , $p < 0.001$). For the analysis of KNHIS data, 67, 908 participants met the MASLD criteria out of a total of 362, 285 participants and were followed for 9.4 years. Throughout this period, 2, 621 cases of decompensation and 2, 056 cases of HCC were documented. Insulin surrogate markers were divided into 4 categories according to their values (Q1, Q2, Q3, and Q4). Lower insulin surrogate markers during the follow-up period were observed to be associated with higher hazard ratios for liver-related outcomes. For example, the Q4 category (highest value) of TyG index had a lower HR for decompensation and HCC at 0.823 and 0.627 compared with Q1 (lowest value).

Conclusion: This study showed the change of IR according to fibrosis grade and revealed a decrease of IR was linked to a rise in fatal liver-related complications, indirectly suggesting nutritional imbalance and decreased liver mediator function during the progression of liver fibrosis. Changes in metabolic parameters in MASLD patients should be reassessed for its association with the liver-related diseases.

FRI-314

Plasminogen activator inhibitor-1 (PAI-1) is associated with hepatic steatosis improvement after lifestyle intervention in overweight/obese subjects with metabolic-dysfunction associated steatotic liver disease

Chiara Rosso¹, Marta Guariglia¹, Angelo Armandi^{1,2}, Gian Paolo Caviglia¹, Eleonora Dileo¹, Francesca Saba¹, Gabriele Castelnovo¹, Marilu' Benedetta Scalici¹, Nuria Pérez Diaz del Campo¹, Kamela Gjini¹, Maria Lorena Abate¹, Antonella Olivero¹, Mirko Parasiliti-Caprino¹, Simona Bo¹, Elisabetta Bugianesi^{1,3}. ¹University of Turin, Department of Medical Science, Turin, Italy; ²University Medical Center of the Johannes Gutenberg University, Department of Internal Medicine I, Mainz, Germany; ³Città della Salute e della Scienza—Molinette Hospita, Gastroenterology Unit, I, Turin, Italy
Email: chiara.rosso@unito.it

Background and aims: Obese/overweight patients with metabolic-dysfunction associated steatotic liver disease (MASLD) are at higher risk of developing cardiovascular (CVD) events over time. Plasminogen activator inhibitor (PAI-1) plays a key regulatory role in fibrinolysis and is predictive of CVD events. Here, we aimed to

POSTER PRESENTATIONS

analyze PAI-1 levels and cardiovascular (CVD) risk in overweight/obese subjects with MASLD, and to assess their association with hepatic steatosis improvement.

Method: We analyzed 73 subjects (mean age 51 ± 12 y; male, $N = 50$) with MASLD who underwent a restricted calories diet for 6 months. At baseline (t0) and after 6-months diet (t6) we collected blood samples, anthropometrical measurements and lifestyle changes through specific questionnaires. PAI-1 was measured by Luminex®. 10 years CVD risk was calculated by Framingham (FRM) score. For all the metabolic parameters, we calculated the variation from t6 to t0 (delta). Hepatic steatosis was determined by CAP (Fibroscan®). 20 % of CAP improvement was considered as clinical end point.

Results: At baseline, PAI-1 levels significantly correlated with fasting insulin ($r = 0.51$, $p < 0.001$), CAP ($r = 0.46$, $p < 0.001$), liver stiffness ($r = 0.29$, $p = 0.013$) and FRM score ($r = 0.24$, $p = 0.037$). The FRM score significantly correlated with waist circumference ($r = 0.27$, $p = 0.023$), fasting glucose ($r = 0.40$, $p < 0.001$), fasting total cholesterol ($r = 0.24$, $p = 0.040$), CAP ($r = 0.33$, $p = 0.005$) and liver stiffness ($r = 0.38$, $p < 0.001$). After 6 months diet, the FRM score decreased by 14 % ($p = 0.002$) independent by the established clinical end point. Conversely, PAI-1 levels improved by 20 % only in patients who ameliorated CAP by 20 % ($p = 0.008$) (Figure 1A-B). At multivariable logistic regression analysis adjusted for age, gender, delta energy intake and delta weight loss, 20 % of CAP decrease after diet was associated with a significant reduction of FRM and PAI-1 (OR = 6.9, 95 % CI = 1.2–39.4, $p = 0.029$ and OR = 3.9, 95 % CI = 1–15, $p = 0.05$).

Conclusion: The decrease in PAI-1 levels and FRM score obtained after a 20 % decrease in hepatic steatosis suggests that this threshold of steatosis improvement is necessary to significantly reduce the cardiovascular risk in MASLD patients. *The research was funded by the University of Turin, g.n. ROSC_RILO_23_01*

FRI-315

Metabolic dysfunction associated steatotic liver disease with development of decompensated cirrhosis as long-term complication after distal gastric bypass surgery

Pamela Meyer-Herbon¹, Irina Bergamin², Patrizia Kuenzler¹, Patrick Folie³, Stefan Aczel³, Sarah Sigrist³, Roman Stillhard¹, Stephan Brand⁴, David Semela⁵. ¹Cantonal Hospital St. Gallen, St. Gallen, Switzerland; ²Cantonal Hospital St. Gallen, St. Gallen, Switzerland; ³Ostschweizer Adipositaszentrum, St. Gallen, Switzerland; ⁴Cantonal Hospital St. Gallen, St. Gallen, Switzerland; ⁵Cantonal Hospital St. Gallen, St. Gallen

Email: pamelameyer@web.de

Background and aims: Bariatric surgeries such as Roux-en-Y gastric bypass and sleeve gastrectomy generally improve metabolic dysfunction, including associated steatotic liver disease (MASLD/MASH). However, some types of bariatric surgeries leading to excessive weight loss and malabsorption can exacerbate these conditions. Notably, distal gastric bypass with a very short common channel can cause iatrogenic short-bowel syndrome with severe malnutrition, dysbiosis and excessive lipolysis potentially promoting progression of MASLD. Our aim was to analyze a series of 12 patients who developed decompensated cirrhosis after distal bypass surgery and recompensated after bypass proximalization.

Method: Retrospective study of patients who underwent distal very long Roux-en-Y gastric bypass (DVLRYGB) between 2005 and 2010 and subsequently progressed to liver cirrhosis with portal hypertension at our tertiary centre with approximately 200 bariatric operations per year

Results: Twelve patients were identified (initial BMI 39.1 to 56.1 kg/m²; 7 females, 5 males) who developed histologically confirmed cirrhosis due to steatohepatitis after DVLRYGB with clinically significant portal hypertension (hepatic venous pressure gradient (HVPG) 10 to 20 mmHg in 11/12 patients) and liver failure. Decompensation occurred on average 10 years (range 6–18) after bypass surgery at the age of 51 years (range 35–68). All except one

patient presented with severe malnutrition, hypoalbuminemia and hepatic encephalopathy (West Haven grade 2–4) necessitating hospitalization. 10/12 (83%) patients presented with ascites, severely limited liver function (Child C, except 2 patients with B 9 points) and elevated MELD scores (mean 22, range 17–30). To date, 6/12 (50%) patients underwent successful proximalization of the gastric bypass. Surgical prolongation of the common channel (mean length 66 cm (range 30–80 cm) before to 274 cm (range 80–425 cm) after conversion) resolved symptoms (malnutrition, hepatic encephalopathy, ascites) and improved liver function (MELD score mean 22 (range 10–30) before to 11 (range 6–19) after conversion). A preoperative TIPS was placed in 4/6 patients with severe portal hypertension (mean HVPG 17 mmHg, range 14–20 mmHg) with a decrease to ≤ 10 mmHg in all patients after TIPS placement. Postoperative follow-up period (range 5–80 months) after conversion showed no new decompensation since proximalization (range 5–80 months). Two patients rejected proximalization surgery, 1 patient died before surgery and 3 patients are currently being prepared for proximalization.

Conclusion: Distal gastric bypass with very short common channel heightens the risk of steatohepatitis with development of long-term hepatic decompensation. Regular surveillance and early conversion to proximal gastric bypass are necessary for DVLRYGB patients to prevent MASLD progression and liver failure.

FRI-316

Influence of reproductive status, synthetic hormone use, and co-medication on serum homocysteine levels and disparities in its contribution to MASLD risk

Ayako Suzuki^{1,2}, Mizuki Suzuki³, George Boon Bee Goh⁴, Brijesh Kumar Singh⁵, Madhulika Tripathi⁵, Xiaoming Xu⁶, Anna Mae Diehl¹, Paul Yen⁵, Manal F. Abdelmalek⁷. ¹Gastroenterology, Duke University, Durham, United States; ²Gastroenterology, Durham VA Medical Center, Durham, United States; ³Brody School of Medicine, East Carolina University, Greenville, United States; ⁴Singapore General Hospital, Singapore, Singapore; ⁵Duke-NUS Medical School, Singapore, Singapore; ⁶Biostatistics, Duke University, Durham, United States; ⁷Division of Gastroenterology and Hepatology, Mayo Clinic, Rochester, United States

Email: ayako.suzuki@duke.edu

Background and aims: Accumulation of hepatic homocysteine (Hcy) has been linked to inflammation and fibrosis, while vitamin B12 and B9 reduce Hcy in the liver and serum, offering protection against steatohepatitis in experimental metabolic dysfunction-associated steatotic liver disease (MASLD). Given the significant influence of sex hormone on Hcy metabolism and the sexual dimorphism in MASLD pathobiology, the contribution of Hcy to MASLD risk may vary based on age, sex, and menopausal status. We aim to assess the association of serum Hcy with the fatty liver index (FLI) and NAFLD fibrosis score (NFS), taking these factors into consideration.

Method: Data from the National Health and Nutrition Examination Survey (NHANES) 1999–2006 were utilized. Excess alcohol use was defined as ≥ 14 servings for males and ≥ 7 servings for females weekly. Pregnancy, synthetic sex hormone use (estrogen or progesterone), menopausal status, and comedication use were defined at evaluation. Fatty Liver Index (FLI) and NAFLD Fibrosis Score (NFS) were computed. After excluding pregnancy, viral hepatitis and excess alcohol use, the cohort was then classified based on FLI (MASLD by FLI of 30 or higher). Serum Hcy comparisons utilized appropriate statistical tests, with multiple linear regression adjusting for confounders.

Results: In 11,249 subjects with available serum Hcy and FLI, serum Hcy was significantly higher in subjects of older age, male, postmenopausal women, and non-Hispanic White ($p < 0.0001$). Lower Hcy correlated with pregnancy and synthetic hormone use among post-menopausal women ($p < 0.0001$). Conversely, higher Hcy correlated with excess alcohol use, active HCV infection, co-

medication with proton pump inhibitors and/or metformin, and synthetic hormone use among premenopausal women ($p < 0.0001$). Following the exclusions, higher FLI was associated with higher Hcy levels (FLI < 30 vs. FLI ≥ 30 , FLI ≥ 60 , $p < 0.0001$), primarily driven by age, sex, menopause, and race/ethnicity. Notably, among postmenopausal women, those with MASLD vs. without tended to have higher Hcy, even after adjusting for age and race/ethnicity ($p = 0.05$). Among MASLD participants, those in a higher NFS group (by median) had elevated Hcy ($p < 0.05$). After adjusting for age and race/ethnicity, MASLD participants in the higher NFS group were associated with higher Hcy specifically among postmenopausal women ($p = 0.015$). **Conclusion:** Serum Hcy is influenced by various patient factors, including age, sex, women's reproductive status, and comedications. While subjects with higher FLI exhibited higher Hcy levels, age, sex, menopause, and race/ethnicity were major contributors to this difference. The association between higher NFS and Hcy was notable among postmenopausal women even after age and race/ethnicity adjustment, suggesting a more prominent contribution of Hcy to MASLD risk in this subgroup.

FRI-317

Clinical outcomes of metabolic liver disease versus non-alcoholic fatty liver disease: a meta-analysis of observational studies

Grazia Pennisi¹, Giuseppe Infantino¹, Ciro Celsa¹, Gabriele Di Maria¹, Marco Enea², Marco Vaccaro², Roberto Cannella³, Carlo Ciccio¹, Claudia La Mantia¹, Alessandro Mantovani⁴, Francesco Mercurio¹, Herbert Tilg⁵, Giovanni Targher⁴, Vito Di Marco¹, Calogero Camma¹, Salvatore Petta¹. ¹Section of Gastroenterology and Hepatology, Dipartimento Di Promozione Della Salute, Materno Infantile, Medicina Interna e Specialistica Di Eccellenza (PROMISE), University of Palermo, Italy, Palermo, Italy; ²Dipartimento di Scienze Economiche, Aziendali e Statistiche, University of Palermo, Italy, Palermo, Italy; ³Department of Biomedicine, Neuroscience and Advanced Diagnostics (BiND), University of Palermo, Italy, Palermo, Italy; ⁴Department of Medicine, Section of Endocrinology, Diabetes, and Metabolism, University of Verona, Verona, Italy, Verona, Italy; ⁵Department of Internal Medicine I, Gastroenterology, Hepatology, Endocrinology and Metabolism, Medical University Innsbruck, Austria, Innsbruck, Austria
Email: grazia.pennisi901@gmail.com

Background and aims: The recent terminology change from non-alcoholic fatty liver disease (NAFLD) to metabolic dysfunction-associated fatty liver disease (MAFLD) and then metabolic dysfunction-associated steatotic liver disease (MASLD) highlights the link between hepatic steatosis and metabolic dysfunction, taking out the stigmata of alcohol. We examined the comparative effects of NAFLD and MAFLD definitions on the risk of overall and cardiovascular (CV) mortality, liver-related events (LRE), nonfatal CV events (CVE), chronic kidney disease (CKD) and extra-hepatic cancers (EHC).

Method: We systematically searched four large electronic databases for cohort studies (published through August 2023) that simultaneously used NAFLD and MAFLD definitions for examining the risk of mortality and adverse cardiovascular, renal, or oncological outcomes associated with both definitions. In total, 21 eligible cohort studies were identified.

Results: Compared with those with NAFLD, MAFLD individuals had significantly higher rates of overall mortality (random-effect OR 1.12, C.I. 1.04–1.21, $p = 0.004$) and cardiovascular mortality (OR 1.15, C.I. 1.04–1.26, $p = 0.004$), and a marginal trend towards higher rates of CKD (OR 1.06, C.I. 1.00–1.12, $p = 0.058$) and EHC events (OR 1.11, C.I. 1.00–1.23, $p = 0.052$). We found no significant differences in LRE and nonfatal CVE between MAFLD and NAFLD. Meta-regression analyses identified male sex and metabolic comorbidities as the strongest risk factors related to the risk of adverse clinical outcomes in MAFLD compared to NAFLD.

Conclusion: Individuals with MAFLD have higher rates of overall and cardiovascular mortality and higher rates of CKD and EHC events than

those with NAFLD, possibly due to the less favorable metabolic risk profile of MAFLD.

MASLD – Diagnostics and non-invasive assessment

TOP-241-YI

Longitudinal changes in liver stiffness measurements in a population-based screening cohort of 5, 517 participants

Katrine Tholstrup Bech^{1,2}, Jesse Pustjens³, Robert J. de Knecht³, Guillem Pera⁴, Laurens van Kleef³, Helle Lindholm Schnefeld^{1,2}, Peter Andersen^{1,2}, Johanne Kragh Hansen^{1,2}, Katrine Lindvig^{1,2}, Ruth Nadal^{5,6}, Marta Carol^{5,6,7,8}, Anna Soria^{5,6,7}, Elisa Pose^{5,6,7}, Adrià Juanola^{5,6,7}, Anita Arslanow^{5,6}, Núria Fabrellas^{6,7,8}, Miquel Serra⁹, Ivica Grgurevic¹⁰, Llorenç Caballeria⁴, Salvatore Piano¹¹, Matthias Reichert¹², Rosa M Morillas¹³, Juan Manuel Pericàs^{7,14,15}, Jörn M Schattenberg^{12,16}, Emmanuel Tsochatzis^{1,17}, Neil Guha¹⁸, Pere Torán⁴, Céline Fournier-Poizat⁹, Anne Llorca¹⁹, Laurent Castera²⁰, Frank Lammert²¹, Isabel Graupera^{5,6,7,8}, Aleksander Krag^{1,2}, Willem Pieter Brouwer³, Pere Ginès^{5,6,7,8}, Maja Thiele^{1,2}. ¹Centre for Liver Research, Department of Gastroenterology and Hepatology, Odense University Hospital, Odense, Denmark; ²Institute of Clinical Research, University of Southern Denmark, Odense, Denmark; ³Erasmus MC, University Medical Center, Rotterdam, Netherlands; ⁴Unitat de Suport a la Recerca Metropolitana Nord, Institut Universitari d'Investigació en Atenció Primària Jordi Gol, Mataró, Barcelona, Spain; ⁵Liver Unit Hospital Clínic, University of Barcelona, Barcelona, Spain; ⁶Institut D'Investigacions Biomèdiques August Pi I Sunyer (IDIBAPS), Barcelona, Spain; ⁷Centro de Investigación en Red de Enfermedades Hepáticas y Digestivas (CIBEREHD), Barcelona, Spain; ⁸Faculty of Medicine and Health Sciences, University of Barcelona, Barcelona, Spain; ⁹Epidemiology, Statistics, and Prevention Institute, University of Zurich, Zurich, Switzerland; ¹⁰Department of Gastroenterology, Hepatology and Clinical Nutrition, University Hospital Dubrava, University of Zagreb School of Medicine and Faculty of Pharmacy and Biochemistry, Zagreb, Croatia; ¹¹Unit of Internal Medicine and Hepatology, Department of Medicine, University of Padova, Padova, Italy; ¹²Department of Medicine II, Saarland University Medical Center, Homburg, Germany; ¹³Liver Unit, Hospital Germans Trias i Pujol, IGTP, Badalona, Spain, Instituto de Investigación Germans Trias i Pujol (IGTP), Badalona, CIBER de Enfermedades Hepáticas y Digestivas, Instituto de Salud Carlos III, Barcelona, Spain; ¹⁴Liver Unit, Department of Internal Medicine, Hospital Universitari Vall d'Hebron, Vall d'Hebron Institut de Recerca, Vall d'Hebron Barcelona Hospital Campus, Barcelona, Spain; ¹⁵Universitat Autònoma de Barcelona, Barcelona, Spain; ¹⁶Metabolic Liver Disease Research Program, I, Department of Internal Medicine, University Medical Center of the Johannes Gutenberg University, Mainz, Germany; ¹⁷UCL Institute for Liver and Digestive Health, Royal Free Hospital, University College of London, London, United Kingdom; ¹⁸NIHR Nottingham Biomedical Research Centre, Nottingham University Hospitals NHS Trust and the University of Nottingham, Nottingham, United Kingdom; ¹⁹Echosens, Paris, France; ²⁰Université Paris Cité, Department of Hepatology, Hospital Beaujon, AP-HP, Clichy, Clichy, France, ²¹Hannover Medical School, Hannover, Germany
Email: katrine.tholstrup.bech@rsyd.dk

Background and aims: The rising prevalence of steatotic liver disease highlights the importance of timely detection of advanced fibrosis and continuous monitoring to detect those who progress. Liver stiffness measurements (LSM) by vibration-controlled transient elastography (VCTE) < 8 kPa effectively rule out advanced fibrosis and therefore often serve as a threshold in fibrosis screening. However, the longitudinal trends in LSM in both general and at-risk

POSTER PRESENTATIONS

populations remain largely unexplored. We therefore aimed to assess the proportion of participants experiencing clinically significant changes in LSM in a longitudinal population-based screening cohort.

Method: This multicenter study, conducted across Spain (ES), The Netherlands (NL) and Denmark (DK), prospectively enrolled participants from the general population (ES and NL), as well as people with current or prior moderate-high alcohol consumption (DK). Participants initially underwent liver fibrosis screening using LSM by VCTE, and were invited to a follow-up investigation after a mean of 3.7 years. We defined a clinically significant LSM change as an alteration (increase or decrease) of $\geq 20\%$, with sub-analyses of examinations crossing the 8 kPa threshold.

Results: We included 5,517 participants for baseline screening, with 3,266 participants (2,530 from the general population and 736 at risk of ALD) undergoing a follow-up investigation. Median ages for the ES, NL, and DK cohorts were 59, 71, and 59 years, respectively. Follow-up participation rate across the cohorts was 73–80% when excluding those lost to follow-up due to various reasons (not found, moved, ill, dead). Among participants with baseline LSM < 8 kPa, 3.0% increased significantly and to a final LSM ≥ 8 kPa, a trend consistent across all cohorts. This group more often comprised male participants with metabolic dysfunction. Within this subset, 63% increased within the 8–9.9 kPa range. Overall, 1.1% participants increased from < 8 kPa at baseline to ≥ 10 kPa at follow-up, most pronounced in the younger, general cohort (ES: 1.4%) and the ALD-risk cohort (DK: 1.2%) compared to the older, general cohort (NL: 0.5%). Of participants with baseline LSM ≥ 8 kPa, 8.8% increased significantly (ES: 6.2%, NL: 10.4%, DK: 10.0%). Conversely, 72% of participants either decreased significantly or decreased to LSM < 8 kPa, with the biggest difference between the two general cohorts (ES: 80% vs. NL 61%).

Conclusion: An 8 kPa liver stiffness threshold provides relevant information for clinical decision making when monitoring steatotic liver disease in the population at intervals spanning 3–4 years. Our findings indicate, that about 1% of individuals screening below this threshold will progress to stages suggestive of advanced fibrosis, whereas up to nearly 10% of patients screening above the threshold will experience a clinically significant increase in liver stiffness.

TOP-252-YI

Longitudinal changes of FIB-4 do not predict outcomes in patients with metabolic dysfunction-associated steatotic liver disease

Hannes Hegmar¹, Terry Therneau², Prowpanga Udompang³, Rachel Canning², Jun Yin², Ross Dierkhising², Joanne Benson², Alina M Allen³. ¹Division of Gastroenterology and Hepatology, Mayo Clinic, Rochester, Minnesota, USA, ²Department of Medicine, Huddinge, Karolinska Institutet, Stockholm, Sweden, Rochester, United States; ²Department of Quantitative Health Sciences, Mayo Clinic, Rochester, Minnesota, USA, Rochester, United States; ³Division of Gastroenterology and Hepatology, Mayo Clinic, Rochester, Minnesota, USA, Rochester, United States

Email: hhegmar@gmail.com

Background and aims: Non-invasive biomarkers may predict the progression to liver-related outcomes in patients with metabolic dysfunction-associated steatotic liver disease (MASLD). The predictive value of longitudinal changes, including the rate of change, is uncertain. We aimed to examine if changes in FIB-4 over time could predict progression to liver and cardiovascular-related outcomes in patients with MASLD.

Method: This is a population-based cohort study of all patients with MASLD from Olmsted County, Minnesota, diagnosed between 1996 and 2016 based on clinical, biochemical, and radiological criteria. Follow-up continued until first outcome, death, or end-of study (2019). Liver-related outcomes included compensated cirrhosis, a decompensation event, liver transplantation, and hepatocellular carcinoma (HCC). Cardiovascular outcomes included myocardial infarction, stroke, heart failure, angina, atrial fibrillation, and cardiac arrest. All outcomes were ascertained and validated

through medical record review. All available FIB-4 scores during follow-up were calculated, and a Cox model treating FIB-4 as a time-dependent covariate was used.

Results: A total of 5,123 patients with MASLD were included. The median age was 52 years (range 18–95 years), 53% were women. Over a median follow-up time of 6.4 (range 1–23 years), 137 patients experienced progression to a liver-related outcome. An elevated FIB-4 at any time point was associated with an increased rate of progression to liver-related outcomes, with a hazard ratio (HR) of 3.29 (95% confidence interval [CI] = 3.17–3.40) per unit increase in FIB-4 until a FIB-4 score of 5, beyond which the rate stabilized. Among the FIB-4 components, the natural logarithms of AST, (HR 9.17, 95% CI = 8.86–9.47), ALT (HR 0.63, 95% CI = 0.32–0.94), and the platelet level (HR 0.09, 95% CI = 0–0.38), respectively, were all individually associated with an increased rate of progression to liver-related outcomes. Additionally, 858 patients experienced a cardiovascular outcome, and an increased FIB-4 was associated with a higher rate of cardiovascular outcomes, HR 1.13 (95% CI = 1.07–1.19) per unit increase of FIB-4. However, longitudinal change in FIB-4 value was not significantly associated with an increased rate of progression to liver ($p = 0.87$) or cardiovascular-related ($p = 0.86$) outcomes.

Conclusion: An increased FIB-4 at any time point, but not the longitudinal trend over time, predicted a higher rate of progression to liver or cardiovascular outcomes in patients with MASLD. This indicates that repeated measurements can provide important prognostic information, but the optimal timing of a repeated measurement remains unknown.

TOP-253

Clinical, biological and imaging predictors of at-risk MASH: combined data from multiple therapeutic trials including more than 10,000 patients

Stephen A. Harrison¹, Julie Dubourg², Naim Alkhouri³, Mazen Nouredin⁴, Jörn M Schattenberg⁵, Sophie Jeannin², Vlad Ratziu⁶, Michael Charlton⁷. ¹Radcliffe Department of Medicine, University of Oxford, Pinnacle Clinical Research, Oxford, United Kingdom; ²Summit Clinical Research, San Antonio, United States; ³Arizona Liver Health, Phoenix, United States; ⁴Houston Research Institute, Houston, United States; ⁵Saarland University Medical Center, Homburg, Germany; ⁶Sorbonne Université, Institute for Cardiometabolism and Nutrition, Hospital Pitié-Salpêtrière, INSERM UMRS 1138 CRC, Paris, France; ⁷University of Chicago, Chicago, United States

Email: jdubourg@summitclinicalresearch.com

Background and aims: The identification of at-risk metabolic dysfunction-associated steatohepatitis (MASH) patients remains a main challenge in both clinical practice and clinical trial settings. Several non-invasive biomarkers have been developed to identify those at-risk MASH patients who would benefit from pharmacological therapy. We aimed to describe the main predictors of at-risk MASH across multiple therapeutic clinical trials.

Method: We combined screening data from 10 industry-funded MASH phase 2 trials. Predictors of at-risk-MASH (MASH + NAS ≥ 4 + F2–3) were examined using logistic regression and excluding patients with cirrhosis.

Results: 3,672 patients with centrally assessed liver biopsy and absence of cirrhosis were included in this analysis. Among them, 1,395 (38%) met the histopathological criteria for at-risk MASH. The proportion of at-risk-MASH patients was 12%, 25%, 41% and 59% in patients with AST < 20 , AST 20–30, AST 30–40, and AST ≥ 40 IU/L, respectively. This rose to 51% in patients with AST ≥ 30 versus 20% in patients with AST < 30 . In patients with FAST < 0.35 , FAST 0.35–0.67, and FAST ≥ 0.67 , 38%, 57%, and 73% were “at-risk MASH,” respectively. This rose to 68% for patients with FAST ≥ 0.5 versus 42% in patients with FAST < 0.5 . When focusing on FIB-4 categories (< 1.3 , 1.3–2.67, ≥ 2.67), the at-risk MASH population represented 27%, 53%, and 65% of the patients, respectively. The proportion of at-risk MASH patients

was 31% in patients with HbA1c <6.5% compared to 50% in patients with HbA1c ≥6.5%. In the population with AST ≥30, 64% of patients with HbA1c ≥6.5% were “at-risk MASH” compared to 43% with HbA1c <6.5%. Similarly, in the subgroup of patients with AST ≥40, 70% of patients with HbA1c ≥6.5% were “at-risk MASH” compared to 51% with HbA1c <6.5%. In the population with FAST ≥0.50, 74% of patients with HbA1c ≥6.5% were “at-risk MASH” compared to 63% with HbA1c <6.5%. Similarly, in the subgroup with FAST ≥0.67, patients with HbA1c ≥6.5% had a higher probability of at-risk MASH (79%) compared to those with HbA1c <6.5% (68%).

Conclusion: Simple non-invasive biomarkers can help stratify at-risk MASH patients. We recommend using the FAST-score or AST as simple tools to target at-risk MASH patients with cut-off points of 0.5 for FAST and/or 30 IU/L for AST in patients with HbA1c ≥6.5% and 0.67 for FAST and/or 40 IU/L for AST in patients with HbA1c <6.5%.

TOP-264

Paired assessment of enhanced liver fibrosis (ELF) and fibrosis-4 (FIB-4) scores is associated with an elevated risk of liver-related clinical events in participants with advanced fibrosis due to metabolic dysfunction-associated steatohepatitis (MASH)

Rohit Loomba¹, Naim Alkhouri², Mazen Noureddin³, Jason H. Melehan⁴, Xiaomin Lu⁴, Xiangyu Liu⁴, Lulu Wang⁴, Catherine Jia⁴, Jun Xu⁴, Andrew N. Billin⁴, Lisa Boyette⁴, Timothy R. Watkins⁴. ¹School of Medicine, University of California San Diego, La Jolla, United States; ²Arizona Liver Health, Chandler, United States; ³Houston Research Institute, Houston Methodist Hospital, Houston, United States; ⁴Gilead Sciences, Inc., Foster City, United States Email: roloomba@health.ucsd.edu

Background and aims: Metabolic dysfunction-associated steatohepatitis (MASH, previously non-alcoholic steatohepatitis [NASH]) is a leading cause of cirrhosis and liver-related mortality. Non-invasive tests (NITs) are commonly used to stratify risk in individuals with MASH. Identifying individuals at risk of liver-related clinical events remains an important unmet need. Our objective was to determine whether a combination of commonly measured NITs was associated with risk of liver-related clinical events in people with advanced MASH.

Method: Data from participants with advanced fibrosis due to MASH enrolled in four placebo-controlled trials evaluating simtuzumab (NCT02466516, NCT01672879) and selonsertib (NCT03053050, NCT03053063) were analyzed. All participants had F3/F4 fibrosis at baseline (centrally read liver biopsy). Baseline Enhanced Liver Fibrosis (ELFTM) and Fibrosis-4 (FIB-4) scores were assessed per trial protocol and categorized into concordant-low, concordant-high or discordant risk groups based on NIT thresholds established in previous studies (ELF ≥11.3 and FIB-4 ≥3.5). Event-free survival for these risk groups was estimated using the Kaplan-Meier method. Hazard ratios (HR) were estimated using a Cox regression model.

Results: Among 2153 participants (F3, n = 1020; F4, n = 1133), the baseline median (Q1, Q3) values of ELF and FIB-4 scores were 10.3 (9.7, 11.0) and 2.1 (1.4, 3.2), respectively. During a median follow-up of 16.5 months, 80 participants experienced liver-related clinical events. The 1-year event rates were 0.5%, 2.5% and 15.0% in the concordant-low, discordant and concordant-high risk groups, respectively. When evaluating ELF and FIB-4, the concordant-high risk group showed the strongest association with liver-related events versus those in the concordant-low risk group (HR 21.4; 95% confidence interval [CI] 11.5–39.5). Discordance between ELF and FIB-4 showed an intermediate association for liver-related events versus the concordant-low risk group (HR 6.5; 95% CI 3.4–12.7).

Conclusion: In this cohort of participants with advanced fibrosis due to MASH, paired evaluation of ELF and FIB-4 demonstrated a significant association with liver-related clinical events. Further research is required to validate this model, which could serve to identify and enrich trials designed to test drugs that could prevent or attenuate MASH disease progression.

TOP-265

Non-invasive predictive markers of resmetirom biopsy response

Rohit Loomba¹, Jörn M Schattenberg², Rebecca Taub³, Dominic Labriola³, Mazen Noureddin⁴, Vlad Ratziu⁵, Stephen A. Harrison⁶. ¹University of California San Diego, La Jolla, United States; ²Metabolic Liver Research Program, I. Department of Medicine, University Medical Center of Johannes Gutenberg University, Department of Internal Medicine II, Saarland University Medical Center, Mainz, Germany; ³Madrigal Pharmaceuticals, West Conshohocken, United States; ⁴Houston Methodist Hospital, Houston Research Institute, Houston, United States; ⁵Sorbonne Université, ICAN Institute for Cardiometabolism and Nutrition, Assistance Publique Hôpitaux de Paris, Paris, France; ⁶Pinnacle Clinical Research, San Antonio, United States Email: roloomba@health.ucsd.edu

Background and aims: MAESTRO-NASH (NCT03900429) is an ongoing 54-month, randomized, double-blind, placebo-controlled Phase 3 trial evaluating the efficacy of resmetirom in patients with biopsy-confirmed non-alcoholic steatohepatitis (NASH) and fibrosis. 966 patients with biopsy-confirmed NASH were randomized 1:1:1 to resmetirom 80 mg, resmetirom 100 mg, or placebo administered once daily. Histologic end points were assessed after 52 weeks. Dual primary end points at Week 52 were achieved with both resmetirom 80 mg and 100 mg: NASH resolution with no worsening of fibrosis (NR) or ≥1-stage reduction in fibrosis with no worsening of NAS (FR). **Method:** Adults with ≥3 metabolic risk factors, liver stiffness ≥8.5 kPa, hepatic fat ≥8%, biopsy-confirmed NASH with F1B-F3 fibrosis, and NAS ≥4 were eligible to participate in MAESTRO-NASH. In this analysis, the relationship of changes in (1) FibroScan CAP, (2) Fibroscan VCTE, and (3) alanine aminotransferase (ALT) to histological response (NR and/or FR) in the resmetirom 80 mg, resmetirom 100 mg, and placebo groups was assessed.

Results: Patients with biopsy-confirmed NASH with fibrosis had high metabolic risk including obesity (mean BMI = 36), type 2 diabetes (70%), hypertension (78%), and 10-year ASCVD risk score >14. Baseline mean (SD) FibroScan VCTE was 13.3 (6.8), 13.6 (7.1), and 12.9 (5.6) kPa for the resmetirom 80 mg, resmetirom 100 mg, and placebo groups. Baseline ELF across all fibrosis groups was 9.8 (0.87). FIB-4 across all dose groups was 1.3. CAP improved with resmetirom treatment. CAP improvement in individual resmetirom patients predicted both NR and FI responses; however, even no change in CAP predicted biopsy responses higher than the mean for placebo. A CAP improvement in placebo patients did not predict an FI on biopsy. VCTE was improved over time (1–3 years) relative to placebo in resmetirom treated patients. Resmetirom treated patients, even those with no VCTE improvement, had higher NASH resolution and fibrosis improvement responses than the mean placebo response rates. VCTE improvement was poorly predictive of a placebo FI or NR response; worsening of VCTE in placebo patients predicted a lower-than-average NASH resolution and fibrosis improvement. Both doses of resmetirom significantly reduced ALT approximately 30% relative to placebo. In resmetirom treated patients, higher % reductions in ALT were associated with higher NR and FI on biopsy. For resmetirom treated patients without a reduction in ALT, the NASH resolution and fibrosis improvement responses were predicted to be higher than the mean placebo biopsy responses.

Conclusion: ALT was reduced and CAP and VCTE improved by resmetirom relative to placebo. However, biopsy responses were not always associated with changes in these markers. Additional analyses, including artificial intelligence (AI)-based assessments of histological response, are ongoing.

POSTER PRESENTATIONS

TOP-276

Time-trends of fibrosis and steatosis in metabolic dysfunction-associated steatotic liver disease (MASLD): a retrospective cohort analysis

Umang Arora¹, Sagnik Biswas¹, Vignesh Dwarkanathan², Sabreena Sheikh¹, Ayush Agarwal¹, Arnav Aggarwal¹, Shubham Mehta¹, Shalimar Shalimar¹. ¹All India Institute of Medical Sciences, New Delhi, India, ²E.S.I.C Medical College and Hospital, Chennai, India

Email: umangarora@gmail.com

Background and aims: The progression of liver stiffness measurement (LSM) and controlled attenuation parameter (CAP) on Transient Elastography (TE), well-accepted surrogates for fibrosis and steatosis, have not been well characterised in patients with metabolic dysfunction-associated fatty liver disease (MASLD). We aimed to identify the rate of progression of LSM and CAP scores and factors associated with this increase.

Method: We performed a retrospective analysis of a large cohort of patients with MASLD (n = 1016). We included all patients for whom at least 2 LSM were available, taken 6 months apart. We excluded LSM observations with baseline LSM >15 kPa (indicating cirrhosis), IQR/LSM value >30 (considered unreliable), and high liver enzymes (ALT >200 IU/ml). Repeated measurements of LSM and weight at each visit were obtained. The last observation (last observation carried forward method) replaced missing values for weight at each visit. The time duration between visits was rounded off to the nearest 6 months. Patient and their visits were assigned as panel data and random effects regression was performed to assess time-variable and time-invariant predictors of an increase in LSM or CAP using 'xtreg' in Stata v14 and coefficients reported with 95% confidence intervals (CI).

Results: A total of 1735 TE measurements were analysed from 421 patients, with a median (IQR) of 3 visits (2–5) and 2.5 years (1–4.5) of follow-up per patient. The mean (SD) age was 41.1 (10.4) years, 289 males (68.8%), 76 (18.1%) with diabetes, 86 (20.4%) with hypertension, and the mean (SD) BMI was 27.31 (3.76) kg/m². The median (IQR) LSM and CAP of the population was 6.1 kPa (4.9–7.9) and 320 dB/m (290–345). Throughout follow-up, the median (IQR) delta change in LSM between the baseline and last follow-up was 0 kPa (–1.20–1.70), and the delta change per year was 0 kPa/year (–0.70–0.57). Unadjusted regression coefficients for time duration (years) for LSM were 0.30 (95% CI 0.20–0.39) and CAP was –2.83 (95% CI –3.92–0.17). After multivariable regression, we found that a rise in LSM was influenced by age (0.03 (0.00–0.07), p = 0.05), presence of diabetes (1.23 (95% CI 0.30–2.16), p = 0.01), BMI (0.10 (0.02–0.18), p = 0.02), and time duration (0.29 (95% CI 0.20–0.39), p ≤ 0.01), indicating a rise during follow-up. Assuming a linear rise in LSM, 1 year of follow-up would lead to an increase in LSM by 0.30 kPa, or a 1 kPa increase would require 3.3 years. The rise in LSM per year was higher among diabetics (0.56 (0.23–0.88) vs 0.24 (0.15–0.33), p < 0.001). On the contrary, only two factors affected change in CAP during follow-up including an increase in BMI (5.03 (4.25–5.81), p < 0.001) while CAP reduced with increased time duration of follow-up (–3.12 (95% CI –4.18––2.07), p < 0.001).

Conclusion: LSM change on follow-up occurs at 0.3 kPa per year and is influenced by older age, higher BMI and presence of diabetes at baseline.

TOP-277

Liver fibrosis assessed via non-invasive tests is associated with incident heart failure in a general population cohort: a UK Biobank study

Theresa Hydes¹, Oliver Kennedy², Kate Glyn-Owen², Ryan M. Buchanan¹, Julie Parkes², Daniel Cuthbertson¹, Paul Roderick², Chris D. Byrne². ¹University of Liverpool, Liverpool, United Kingdom; ²University of Southampton, Southampton, United Kingdom

Email: therasa@doctors.org.uk

Background and aims: Liver fibrosis is associated with cardiovascular events. The association between liver fibrosis and heart failure in a general population cohort is unknown. The relationship between *PNPLA3* rs738409 and *TM6SF2* rs58542926 and heart failure is of interest, given the associations of these polymorphisms with increased risk of liver fibrosis and decreased risk of coronary artery disease. We aimed to determine whether liver fibrosis is associated with heart failure in a general population cohort, and if genetic polymorphisms (*PNPLA3* rs738409; *TM6SF2* rs58542926) linked to increased risk of liver fibrosis and decreased risk of coronary artery disease modify this association.

Method: Using UK Biobank data, we prospectively examined the relationship between non-invasive fibrosis markers (NAFLD fibrosis score (NFS), Fibrosis-4 (FIB-4) and AST to platelet ratio index (APRI)) and incident hospitalization/death from heart failure (n = 413, 860). Cox-regression estimated hazard ratios (HR) for incident heart failure. Effects of *PNPLA3* and *TM6SF2* on the association between liver fibrosis and heart failure were estimated by stratifying for genotype, and testing for an interaction between genotype and liver fibrosis using a likelihood ratio test.

Results: 12, 527 incident cases of heart failure occurred over a median of 10.7 years. Liver fibrosis was associated with an increased risk of hospitalization or death from heart failure (multivariable adjusted high risk NFS score HR 1.59 [1.47–1.76], p < 0.0001; FIB-4 HR 1.69 [1.55–1.84], p < 0.0001; APRI HR 1.85 [1.56–2.19], p < 0.0001; combined fibrosis scores HR 1.90 [1.44–2.49], p < 0.0001). These associations persisted for people with MASLD, Met-ALD or harmful alcohol consumption. *PNPLA3* rs738409 GG and *TM6SF2* rs58542926 TT did not attenuate the positive association between fibrosis markers and heart failure. For *PNPLA3* a statistically significant interaction was found between *PNPLA3* rs738409, FIB-4, APRI score and heart failure.

Conclusion: In the general population, serum markers of liver fibrosis are associated with increased hospitalization/death from heart failure. Genetic polymorphisms associated with liver fibrosis and decreased risk of coronary artery disease were not positively associated with elevated heart failure risk but did not attenuate this risk.

TOP-288

Serum GDF15 level, in combination with the FIB-4 index, is useful for refining the identification of high-risk patients for clinical event occurrence in MASLD patients

Hayato Hikita¹, Shunsuke Kumazaki², Yuki Tahata¹, Ji Hyun Sung¹, Kenji Fukumoto¹, Yuta Myojin¹, Sadatsugu Sakane¹, Kazuhiro Murai¹, Yoichi Sasaki¹, Kumiko Shirai¹, Takahiro Kodama¹, naruyasu kakita³, Hirokazu Takahashi⁴, Hidenori Toyoda⁵, Goki Suda⁶, Eiichi Morii¹, Takashi Kojima¹, Takeshi Ebihara¹, Kentaro Shimizu¹, Yutaka Sasaki⁷, Tomohide Tatsumi¹, Tetsuo Takehara¹. ¹Osaka University, Graduate School of Medicine, Suita, Japan; ²Osaka University, Graduate School of Medicine, Suita, Japan; ³Kaizuka City Hospital, Kaizuka, Japan; ⁴Saga University, Saga, Japan; ⁵Ogaki Municipal Hospital, Ogaki, Japan; ⁶Hokkaido University, Sapporo, Japan; ⁷Osaka Central Hospital, Osaka, Japan

Email: hikita@gh.med.osaka-u.ac.jp

Background and aims: Some MASLD patients develop liver cancer or decompensated liver event emphasizing the need for a biomarker identifying high-risk patients who should be followed up. GDF15 is a cell stress-responsive cytokine related to metabolic syndrome. The aim of the present study was to evaluate the utility of the serum GDF15 level as a novel predictive marker for liver-related events, including liver cancer, decompensated liver event and death, in patients with MASLD.

Method: GDF15 levels were measured in 518 MASLD patients with liver biopsy (biopsy-cohort), and 216 MASLD patients from another institution (validation cohort), and 361 individuals meeting MASLD criteria during health checkups.

Results: In biopsy-cohort, serum GDF15 level was an independent risk factor for liver cancer occurrence along with liver fibrosis stage or Fib-4 index. The AUROC of serum GDF15 level for 3-year and 5-year liver cancer incidence was 0.949 and 0.941, respectively. Using a GDF15 cutoff of 1.75, based on Youden index, GDF15-high patients (n = 153) had significantly higher liver cancer incidence rates with 4.8 and 7.7% at 3 and 5 years, respectively compared to GDF15-low patients (n = 365) with 0.0% within 5 years. Notably, GDF15-high patients exhibited significantly greater liver cancer incidence rates than GDF15-low patients, irrespective of fibrosis status or Fib-4 index levels. While no patients with a Fib-4 index <1.3 (n = 171) or GDF15-low patients with a Fib-4 index >1.3 (n = 209) developed liver cancer within 5 years, GDF15-high patients with a Fib-4 index >1.3 (n = 138) had high liver cancer incidence rates with 5.3% and 8.6% at 3 and 5 years, respectively. GDF15-high patients with a Fib-4 index >1.3 also developed liver decompensated events at higher rate and had poorer prognosis compared to the others. In validation cohort, GDF15-high patients (n = 72) had significantly higher liver cancer incidence rates with 7.2% and 16.8% at 3 and 5 years, respectively compared to GDF15-low patients (n = 144) with 0.8% within 5 years. While patients with a Fib-4 index <1.3 (n = 93) and GDF15-low patients with a Fib-4 index >1.3 (n = 60) rarely developed liver cancer with 1.5% and 1.8%, respectively, at 5 years, GDF15-high patients with a Fib-4 index >1.3 (n = 63) had high liver cancer incidence rates with 6.1% and 16.5% at 3 and 5 years, respectively, and also developed liver decompensated events at high rate and had poor prognosis. Among 364 health checkups with MASLD, 18 individuals (4.9%) had a GDF15 >1.75 ng/ml. Furthermore, 278 individuals (76.4%) had a Fib4 index <1.3, 76 individuals (20.9%) had a Fib4 index >1.3 and a GDF15 <1.75 ng/ml, and only 10 individuals (2.7%) had a Fib4 index >1.3 and a GDF15 >1.75 ng/ml.

Conclusion: Serum GDF15 level is a novel biomarker for liver cancer occurrence with high predictive capability and can be used in combination with the Fib-4 index to identify MASLD patients for close follow-up.

TOP-289

Artificial intelligence-based measurement of non-alcoholic steatohepatitis is an accurate tool for clinical trial enrollment and end point assessment

Hanna Pulaski¹, Hypatia Hou¹, Murray Resnick¹, Stephen A. Harrison², Arun J Sanyal³, Vlad Ratzu⁴, Alastair Burt⁵, Pierre Bedossa⁶, Michael Montalto¹, Katy Wack¹. ¹PathAI, Boston, United States; ²Pinnacle Clinical Research, San Antonio, United States; ³Virginia Commonwealth University, Richmond, United States; ⁴Sorbonne Université, Paris, France; ⁵Newcastle University, Newcastle, United Kingdom; ⁶LIVERPAT, Paris, France
Email: hanna.pulaski@pathai.com

Background and aims: A major obstacle in the development of effective metabolic dysfunction-associated steatohepatitis (MASH) therapies is the lack of a reliable histologic scoring method. The current gold standard is histologic analysis of the liver biopsy, however, the scoring systems have suboptimal inter-reader agreement, even amongst expert pathologists. In this study, Artificial Intelligence-based Measurement of Non-alcoholic Steatohepatitis (AIM-NASH) was evaluated for overall percent agreement (OPA) and for positive and negative percent agreement (PPA and NPA) for main trial inclusion and end point criteria.

Method: In a clinical validation study (Harrison SA, EASL 2023), liver biopsies collected from multiple Phase II and Phase III MASH trials from cirrhotic and non-cirrhotic patients were analyzed. A panel of expert pathologists established GT MASH scores. Cases were also evaluated by at least 3 other experienced pathologists who independently provided MASH scores for the same samples (IMRs). After a minimum 2-week washout period, AI-assisted scores were collected. OPA, NPA and PPA were determined for main trial inclusion and end point criteria (NAS ≥4 with ≥1 in each score category, fibrosis

2 or 3, fibrosis 4 and MASH resolution) for AI-assisted vs GT and individual manual reader (IMR) vs GT.

Results: OPA and PPA for all trial inclusion and enrollment criteria were over 75% (AI-assisted vs GT for NAS ≥4 with ≥1 in each category OPA = 84%, PPA = 87.6%; fibrosis 2 or 3 OPA = 80.5%, PPA = 85.3%; fibrosis 4 OPA = 91.8%, PPA = 79.6% and MASH resolution OPA = 89.0%, PPA = 75.5%) and were higher for all of the categories compared to IMR vs GT, with NAS ≥4, MASH resolution and fibrosis 2 or 3 being superior (NAS ≥4 OPA difference 6.4%, p < 0.001, PPA difference 9.8%, p < 0.001; MASH resolution OPA difference 6.5% p < 0.001, PPA difference 18.3%, p < 0.001, fibrosis 2 or 3 OPA difference 3.3%, p = 0.01, PPA difference 9.3%, p < 0.001). For PPA, fibrosis 2 or 3 was also superior to IMR vs GT (PPA difference 9.3%, p < 0.001). Strikingly, MASH resolution PPA was 18.3% higher for AI-assisted than for unassisted compared to GT. For NPA, AI-assisted vs GT for NAS ≥4 with ≥1 in each NAS category was 76.0%, for fibrosis 2 or 3 71.2%, for fibrosis 4 95.1% and for MASH resolution 90.6%. AI-assisted was superior to IMR vs GT for MASH resolution (difference 4.8%, p < 0.001).

Conclusion: AIM-NASH is an accurate tool for assessment of MASH trial enrollment and end point criteria. AI-assisted pathologists displayed a superior OPA and PPA for trial enrollment criteria of NAS ≥4, MASH resolution and fibrosis 2 or 3, with the PPA of MASH resolution being 18.3% higher for AI-assisted vs IMRs. These data show that AIM-NASH may help to standardize histologic scoring by increasing accuracy for the most relevant clinical trial enrollment and end point criteria, allowing for a more reliable assessment of therapeutics under development.

TOP-300

Clinical, biological and imaging predictors of advanced fibrosis (F3-F4): combined data from multiple therapeutic trials including more than 10, 000 patients

Mazen Nouredin¹, Naim Alkhouri², Vlad Ratzu³, Jörn M Schattenberg⁴, Michael Charlton⁵, Julie Dubourg⁶, Stephen A. Harrison⁷. ¹Houston Research Institute, Houston, United States; ²Arizona Liver Health, Phoenix, United States; ³Sorbonne Université, Institute for Cardiometabolism and Nutrition, Hospital Pitié-Salpêtrière, INSERM UMRS 1138 CRC, Paris, France; ⁴Saarland University Medical Center, Homburg, Germany; ⁵University of Chicago, Chicago, United States; ⁶Summit Clinical Research, San Antonio, United States; ⁷Radcliffe Department of Medicine, University of Oxford, Oxford, United Kingdom
Email: j.dubourg@summitclinicalresearch.com

Background and aims: Advanced fibrosis, defined as fibrosis stages F3 or F4, is the strongest predictor of major liver-related outcomes in metabolic dysfunction-associated steatohepatitis (MASH). We aimed to describe the main predictors of advanced fibrosis across multiple therapeutic clinical trials.

Method: We combined screening data from 10 industry-funded MASH phase 2 trials. Predictors of advanced fibrosis (F3–4) were examined using logistic regression.

Results: 4, 119 patients with centrally assessed liver biopsy were included in this analysis. The prevalence of advanced fibrosis in this population was 37%. The proportion of patients with advanced fibrosis was 22%, 52% and 77% in patients with Fib-4 <1.3, Fib-4 1.3–2.67, and Fib-4 ≥2.67, respectively. The AST:ALT ratio was higher in patients with advanced fibrosis, independently of the baseline liver enzymes. The AST:ALT ratio was 0.90 (SD 0.28) and 0.92 (SD 0.31) in presence of advanced fibrosis versus 0.80 (SD 0.31) and 0.78 (SD 0.29) in absence of advanced fibrosis, in patients with normal liver enzymes, and elevated liver enzymes, respectively. The proportion of patients with advanced fibrosis was 38% and 71% in patients with ELF <9.8, and ELF ≥9.8, respectively. The proportion of patients with advanced fibrosis was 30% and 60% in patients with liver stiffness measurement (LSM) as assessed by FibroScan <9.7 kPa, and LSM ≥9.7, respectively. Glycemic control was a key independent predictor of

POSTER PRESENTATIONS

advanced fibrosis with 48% of the population having a HbA1c $\geq 6.5\%$ compared to 30% in patients with HbA1c $< 6.5\%$. Glycemic control had the biggest impact on the ability of FIB-4 to classify patients with advanced fibrosis. In patients with FIB-4 < 1.3 , FIB-4 1.3–2.67, and FIB-4 ≥ 2.67 , the proportion of patients with advanced fibrosis was 17%, 45% and 72%, respectively in patients with HbA1c $< 6.5\%$ versus 31%, 62%, and 81 %, respectively, in patients with HbA1c $\geq 6.5\%$. ELF and LSM were the best predictors of advanced fibrosis in this population.

Conclusion: Patients with advanced fibrosis can be targeted by using simple non-invasive markers such as FibroScan LSM and ELF. FIB-4 appears to be too influenced by other parameters such as glycemic control and could lead to inadequate follow-up in patients with HbA1c $\geq 6.5\%$.

WEDNESDAY 05 JUNE

WED-194

Diagnostic performance of non-invasive tests and comparison of AGA and EASL algorithm for the screening of MASLD-related advanced fibrosis in diabetes and nutrition clinics

Cyrielle Caussy¹, Bruno Vergès², Leleu Damien², Duvillard Laurence², Abichou-Klich Amna³, Valerie Hervieu⁴, Bérénice Ségrestin⁵, Bin Sylvie⁴, Rouland Alexia⁶, Dominique Delaunay⁵, Hadjadj Samy⁷, Primot Claire⁷, Jean-Michel Petit², Sybil Charrière⁸, Philippe Moulin⁵, Massimo Levvero⁵, Bertrand Cariou⁷, Emmanuel Disse⁹. ¹Hospices Civils de Lyon, Pierre-Bénite, France; ²Dijon University Hospital, Dijon, France; ³Hospices Civils de Lyon, Villeurbanne, France; ⁴Hospices Civils de Lyon, Lyon, France; ⁵Hospices Civils de Lyon, Lyon, France; ⁶Dijon University Hospital, Pierre-Bénite, France; ⁷Nantes Université, CHU Nantes, CNRS, INSERM, l'institut du thorax, Nantes, France; ⁸Hospices Civils de Lyon, Bron, France; ⁹Hospices Civils de Lyon, Pierre-Bénite, France

Email: cyrielle.caussy@gmail.com

Background and aims: The systematic screening for advanced fibrosis (AF) due to metabolic dysfunction-associated steatotic liver disease (MASLD) is recommended in patients with type 2 diabetes (T2D) and obesity. There are very few data of the use of non-invasive tests (NITs) for the detection of AF in this population. We aimed to compare the diagnostic performance of NITs and recommended AGA versus EASL algorithms for the referral in hepatology and the detection of patients with high risk of AF in diabetes and nutrition clinics.

Method: this is an interim analysis of prospective data from a multicenter study performed in 4 French diabetes/nutrition clinics between Oct. 2020 and Oct. 2023 (NCT04435054) enrolling participants with T2D and/or obesity and MASLD, age 40–80 years, BMI < 40 kg/m². All other causes of liver diseases were systematically excluded. All participants had a detailed liver assessment including: NFS, FIB-4, Fibrotest[®], FibroMeter[®], ELF[™] and liver stiffness measurement (LSM) using FibroScan[®]. Low/high risk of AF was defined by a hierarchical composite criterion depending on availability: 1. liver biopsy $< \geq F3$, 2. magnetic resonance elastography $< 2.6 / \geq 3.62$ kPa or overt imaging diagnosis of cirrhosis, or 3. LSM $< 8 / \geq 12$ kPa. Intermediate risk of AF was defined by no biopsy and 1. MRE 2.6–3.63 kPa or 2. TE 8–12 kPa.

Results: 652 patients were included with the following characteristics: T2D: 87%, female: 44%, hypertension: 68%, dyslipidemia 73%, mean 59.8 years and BMI: 32.6 kg/m². Overall, 17% had intermediate/high risk of AF and 9% were classified at high risk of AF, including 22 patients with fibrosis $\geq F3$, 15 with MRE values > 3.6 kPa or overt imaging diagnosis of cirrhosis and 22 with LSM ≥ 12 kPa. The AUROCs of NITs for the detection of high-risk AF were: NFS: 0.72, FIB-4: 0.79, FibroMeter[®]: 0.74, Fibrotest[®]: 0.79, ELF[™]: 0.82. The AGA algorithm using FIB-4/LSM if FIB-4: 1.30–2.66, led to 16% hepatology referral including 47% (47/101) true positive (TP) for high-risk AF, 32% (32/101) with intermediate risk and 22% (22/101) false positive (FP) with low-risk AF. The EASL algorithm using FIB-4/LSM if FIB-4 ≥ 1.30 , led to

14% hepatology referral, including 52% (47/90) TP with high-risk AF, 36% (32/90) with intermediate-risk AF and 12% (11/90) of FP with low-risk AF. Both AGA and EASL algorithm misclassified 4.6% of patients with high/intermediate-risk of AF. Replacement of LSM by ELF[™] $< \geq 9.8$ in the EASL algorithm would increase the referral in hepatology to 18% including 32% TP with high-risk AF (37/114), 14% (16/114) with intermediate-risk AF and 54% FP with low-risk AF (61/114).

Conclusion: The use of AGA or EASL guidelines in patients with T2D or obesity leads to a referral in hepatology of 14 to 18% with good diagnostic performance. The EASL algorithm with LSM should be preferred as it led to lower number of referrals in hepatology, lower FP and higher detection of patients with high-risk of AF.

WED-195

NASH-PI: a randomized trial to compare cost-effectiveness across strategies for screening, referring and management of MASLD patients in clinical practice

Manuel Romero-Gómez^{1,2,3}, Florencia Pollarsky¹, Silvia García Rey¹, Rocío Gallego-Durán^{1,2}, Vanessa García-Fernández¹, Isabel Fernández-Lizaranzu¹, Francisco Javier Atienza Martín⁴, Pablo Remon⁵, Carmen Lara-Romero^{1,3}, María C. Roque-Cuellar¹, Inmaculada Dominguez⁶, Yolanda María Sanchez-Torrijos^{1,3}, Ioanna-Panagiota Kalafati⁷, Sabine Kahl⁸, Michael Roden⁸, Pedro Pablo García-Luna⁹, Jörn Schattenberg¹⁰, George Dedoussis⁷, Davide Fortin¹¹, Abbas Mourad¹¹, Patrizia Carrieri¹¹, Patrizia Marino¹¹, Jeffrey V. Lazarus¹². ¹Seliver Group. Instituto De Biomedicina De Sevilla (IBiS), Hospital Universitario Virgen Del Rocío/Csic/Universidad De Sevilla, Sevilla, Spain; ²Centro De Investigación Biomédica En Red De Enfermedades Hepáticas y Digestivas (CIBEREHD), Sevilla, Spain; ³UCM Digestive Diseases, Hospital Universitario Virgen Del Rocío, Sevilla, Spain; ⁴Centro de Salud El Porvenir, Distrito Sevilla, Sevilla, Spain; ⁵Unidad de Metabolismo y Nutrición, Hospital Universitario virgen del Rocío, Instituto de Biomedicina de Sevilla, Sevilla, Spain; ⁶Departamento de Análisis Clínico, Hospital Universitario Virgen del Rocío, Sevilla, Spain; ⁷Department of Nutrition and Dietetics, School of Health Sciences and Education, Harokopio University of Athens, Athens, Greece; ⁸German Center for Diabetes Research, Neuherberg, Division of Endocrinology and Diabetology, Medical Faculty, Heinrich Heine University, Düsseldorf, Germany; ⁹UCM Endocrinology and Nutrition, Hospital Universitario Virgen del Rocío, Sevilla, Spain; ¹⁰Department of Internal Medicine I, University Medical Center of the Johannes Gutenberg-University, Mainz, Germany; ¹¹Aix Marseille Univ, INSERM, IRD, SESSTIM, Sciences Economiques and Sociales de la Santé and Traitement de l'Information Médicale, ISSPAM, Marseille, France; ¹²Barcelona Institute for Global Health (ISGlobal), Hospital Clínic, University of Barcelona, Barcelona, Spain

Email: mromerogomez@us.es

Background and aims: Cost-effective strategies based on clinical pathways to detect and refer MASLD patients are urgently needed. The NASH-PI study aims to build a stepwise algorithm combining non-invasive freely available methods (FIB-4, NAFLD Fibrosis Score (NFS), Hepamet Fibrosis Score (HFS) alone or in combination) and vibration-controlled transient elastography (VCTE) in diabetic patients from both primary care and endocrinology units.

Method: From January 2021 to May 2023, 506 diabetic patients were prospectively recruited and randomized to one of these three arms: Arm A (n = 159) patients were referred following standard of care; Arm B (n = 168) patients referred due to altered combined fibrosis score (CFS) (FIB4 > 1.3 or NFS > 1.456 or HFS > 0.12); and Arm C (n = 179) patients referred due to HFS > 0.12 or VCTE > 8 kPa. Patients at risk of MASLD-fibrosis (VCTE > 8 kPa or clinical decision) underwent magnetic resonance elastography (MRE) protocols.

Results: Mean age was 58 years old, of them, 56.1% were male and 67.2% obese (BMI > 30 Kg/m²). Average time since diabetes diagnosis was 9.7 years. No significant differences in biochemical, anthropometrical or clinical features were observed among the three arms.

All patients from Arm A were referred, of them, 64/157 (40.7%) showed VCTE >8 kPa or were diagnosed at risk from the hepatologist, 38/64 (59.3%) underwent MRE, 9/38 (23.6%) with liver fibrosis (MRE >3.14 kPa; significant fibrosis). In Arm B, 102/136 (75%) patients were referred, 33/102 (32.3%) showed VCTE >8 kPa, 26/33 (78%) underwent MRE, 6/26 (23%) with significant fibrosis. In Arm C, 77/175 (44%) were referred, 35/77 (45.5%) showed VCTE >8 kPa or were diagnosed at risk from the hepatologist, 17/35 (48%) underwent MRE, 6/17 (35%) with significant fibrosis. The average cost for patient referral for strategy A, B and C was respectively €346, €289 and €275. Estimated cost for MASLD patient referral to the liver unit was approximately €5045, €4577 and €2708 for strategy A, B and C respectively. Strategy B and C dominates strategy A in terms of cost per significant fibrosis case detected. Globally, VCTE >8 kPa was found in 125/453 (27.6%); VCTE >10 kPa in 76/453 (16.6%) and VCTE >15 kPa in 37/453 (8.2%).

Conclusion: The NASH-PI stepwise algorithms for the management of type 2 diabetes patients with HFS and VCTE as well as with combined score between HFS, NFS and FIB-4 were both found to be cost-effective compared with the standard model of care, allowing to save respectively 46% and 9% for each case of significant fibrosis detected.

WED-196

Analyses of fibrosis biomarkers PRO-C3 and ELF in resmetirom treated patients from MAESTRO-NASH, a 52 Week NASH/MASH serial liver biopsy study

Quentin M. Anstee¹, Jörn M Schattenberg^{2,3}, Rebecca Taub⁴, Dominic Labriola⁵, Hang Zhang⁴, Jim Hennan⁴. ¹The Translational and Clinical Research Institute, Faculty of Medical Sciences, Newcastle University, Newcastle-upon-Tyne, United Kingdom; ²Metabolic Liver Research Program, I. Department of Medicine, University Medical Center of Johannes Gutenberg University Mainz, Mainz, Germany; ³Department of Internal Medicine II, Saarland University Medical Center, Homburg, Germany; ⁴Madrigal Pharmaceuticals, Inc., West Conshohocken, PA, United States; ⁵Madrigal Pharmaceuticals, Inc., West Conshohocken, PA, United States

Email: quentin.anstee@newcastle.ac.uk

Background and aims: MAESTRO-NASH (NCT03900429) is an ongoing 54-month, randomized, double-blind, placebo-controlled Phase 3 trial evaluating the efficacy of resmetirom in patients with biopsy-confirmed non-alcoholic steatohepatitis (NASH/MASH) and fibrosis. 966 patients with biopsy-confirmed NASH were randomized 1:1:1 to resmetirom 80 mg, resmetirom 100 mg, or placebo administered once daily. Dual primary end points at Week 52 were achieved with both resmetirom 80 mg and 100 mg: NASH resolution with no worsening of fibrosis (NR) or ≥1-stage improvement in fibrosis with no worsening of NAS (FI). We evaluated the baseline and effect of resmetirom compared with placebo on fibrosis biomarkers PRO-C3 and P3NP/ELF.

Method: Pearson's correlation was used to examine the association between 2 PRO-C3 ELISA assay methods (ELISA GEN1 and ELISA GEN2, NORDIC BIOSCIENCE) using PRO-C3 baseline data (N=919). The rest of the analyses used the ELISA GEN2 assay. Mean SD or SE and median [Q1, Q3] were calculated to summarize PRO-C3 data. ANCOVA was used for comparisons between resmetirom 80 or 100 mg vs. placebo in PRO-C3 change from baseline at week 52 (wk52CHG), while controlling for baseline PRO-C3 level. Mean difference with 95% CI and nominal p values were obtained from the ANCOVA. Scatterplots and Spearman's correlations with 95% CIs were used to assess the associations between P3NP/ELF and PRO-C3 both at baseline and wk52CHG.

Results: The two PRO-C3 assays ELISA GEN1 and ELISA GEN2 data were positively associated with a Pearson's correlation of 0.78 (P value <0.0001). At baseline, PRO-C3 was mean (SD)=137 (71.7) ng/ml. At week 52, PRO-C3 wk52CHG for 100 mg resmetirom = -23.05 (4.76), 80 mg = -17.93 (4.61) and placebo = -0.19, 4.07 with mean difference (95% CI) in PRO-C3 wk52CHG between 80 mg and

placebo = -16.9 (-27.0, -6.76; p=0.0011); 100 mg and placebo = -22.1 (-32.3, -11.84; p<0.0001). Larger reductions in PRO-C3 mean (SD) on the resmetirom arms were observed in F3 patients: 80 mg = -22.42 (6.38) and 100 mg = -27.42 (6.72) compared with placebo = -0.50 (5.46). Baseline P3NP and ELF were correlated with PRO-C3 (0.563 and 0.458, respectively). The wk52CHG in P3NP was positively associated with wk52CHG in PRO-C3 (0.557, 0.548 and 0.524 for 100 mg, 80 mg and placebo; respectively). A weaker positive correlation between wk52CHG for ELF and PRO-C3 (0.483, 0.484 and 0.487 for 100 mg, 80 mg and placebo, respectively) were also observed.

Conclusion: Two Pro-C3 assays (ELISA GEN1 and ELISA GEN2, NORDIC BIOSCIENCE) were correlated at baseline, indicating ELISA GEN2 assay was reasonable for measuring PRO-C3 levels. For PRO-C3 ELISA GEN2, drug effects were statistically significant for both doses of resmetirom vs. placebo. The assay was more sensitive in detecting resmetirom effect in F3 patients. ELF and PRO-C3 was less strongly correlated than P3NP and PRO-C3.

WED-197

How many real world patients diagnosed with metabolic dysfunction-associated steatohepatitis meet clinical trial eligibility criteria? Findings from a large cohort study of more than 18, 000 patients from the United States

Jörn M Schattenberg¹, Claudio Sartin², Ronald Herrera², Mireia Raluy³, Mark Yates⁴, Ramy Younes⁵. ¹Department of Medicine II, Saarland University Medical Center, Homburg, Germany; ²Boehringer Ingelheim International GmbH, Global Epidemiology and Real-World Evidence, Ingelheim, Germany; ³Evidera, Data Analytics, Borlänge, Sweden; ⁴Evidera, Data Analytics, London, United Kingdom; ⁵Boehringer Ingelheim International GmbH, Medicine, Cardio Metabolism and Respiratory, Ingelheim, Germany

Email: joern.schattemberg@uks.eu

Background and aims: The distribution of key eligibility criteria typically used in Phase 2 and 3 metabolic dysfunction-associated steatohepatitis (MASH) trials in real-world data is unknown. Understanding how many real-world MASH patients meet certain criteria (e.g., presence of one metabolic risk factor) will help to refine eligibility requirements in future clinical trials (CTs) and improve representativeness of CT populations. This study estimated the proportion of patients with MASH diagnosed in the real world that could meet eligibility criteria typically used in MASH CTs and described basic socio-demographic patients characteristics, such as age, sex, Body Mass Index (BMI), and FIB-4 fibrosis score.

Method: Retrospective cohort study (2016–2021 years) using Optum Market Clarity (linked claims and electronic health records, EHRs) from the United States (US). MASH was defined by the first ICD10 diagnosis code (K75.81 Non-alcoholic steatohepatitis) recorded during the study period, presence of AST, ALT and platelets tests carried out 3 months prior/after diagnosis, and absence of diseases prior/at diagnosis, such as alcoholic/chronic liver diseases (minimum look-back period of 9 years). We estimated the size and characteristics (age, sex, BMI, and FIB-4) of a CT-like sample of non-cirrhotic patients after the following 6 standard criteria were applied: (1) BMI ≥25 (or weight ≥70 kg), (2) having ≥2 other metabolic risk factors (among obesity, diabetes, hypertension, hyperlipidemia, or hyperglycemia), (3) not having type 1 diabetes, (4) without elevated blood levels for bilirubin (≥1.3 mg/dL), INR (>1.3) ALT and/or AST (>5X ULN ~ 250 U/L), ALP (>2X UNL ~ 250–300 U/L) and MELD score (>12), (5) not using concomitant medications (e.g., vitamin E and pioglitazone among others), and (6) not being cirrhotic.

Results: 18, 710 patients met initial inclusion criteria for MASH. After the six selecting criteria were applied about 2 out of 10 patients with MASH met all criteria (4, 122 corresponding to 22% of the total). In this CT-like sample, the patients were on average 42 years old [standard deviation (SD)=11], 48% female, and with average BMI of 34 (SD=7). The mean FIB-4 score was 1.0 (SD=0.8). In comparison to

POSTER PRESENTATIONS

previous CTs where patients with MASH and without cirrhosis were enrolled, the CT-like sample in Optum showed similar BMI and FIB-4 but younger age; the sex distribution was within the range previously observed (between 30% and 60%).

Conclusion: About 2 out of 10 patients with MASH diagnosed in the real-world setting met standard selecting criteria for enrollment in CTs for MASH without cirrhosis. As recruitment strategies in CTs can vary based on study design and objectives, the real-world evidence from this study brings new insights to inform decisions on inclusion and exclusion criteria.

WED-198

Novel deep learning models utilising domain adaptation outperform conventional statistical models for predicting the risk of liver-related complications in patients with metabolic dysfunction-associated steatotic liver disease

Terry Cheuk-Fung Yip^{1,2,3}, Jingwen Xu⁴, Mandy Sze-Man Lai^{1,2}, Sherlot Juan Song^{1,2}, Yee-Kit Tse^{1,2,3}, Henry L.Y. Chan^{2,5}, Grace Lai-Hung Wong^{1,2,3}, Pong Chi Yuen⁴, Vincent Wai-Sun Wong^{1,2,3}. ¹Department of Medicine and Therapeutics, The Chinese University of Hong Kong, Hong Kong, Hong Kong; ²Medical Data Analytics Centre (MDAC), The Chinese University of Hong Kong, Hong Kong, Hong Kong; ³Institute of Digestive Disease, The Chinese University of Hong Kong, Hong Kong, Hong Kong; ⁴Department of Computer Science, Hong Kong Baptist University, Hong Kong, Hong Kong; ⁵Department of Internal Medicine, Union Hospital, Hong Kong, Hong Kong, Hong Kong
Email: tcfyip@cuhk.edu.hk

Background and aims: We aimed to build novel risk models to predict liver-related events including hepatic decompensation and hepatocellular carcinoma in patients with metabolic dysfunction-associated steatotic liver disease (MASLD).

Method: The training cohort included adult patients with MASLD identified from a territory-wide electronic database in Hong Kong from Jan 2000 to Jul 2021. Five modern domain adaptation (DA) methods were examined. Models were built based on fully connected neural network after different DA methods, assessed by area under the time-dependent receiver operating characteristic curves (AUCs) with death as the competing risk, and compared to FIB-4 index, NAFLD outcomes score (NOS), and a Fine-Gray model. The validation cohort comprised adult patients with type 2 diabetes (T2D) who likely had MASLD detected by NAFLD ridge score we previously developed. Patients with liver-related events before MASLD diagnosis or follow-up <6 months were excluded.

Results: Of 25,166 patients with MASLD in the training cohort (mean age 56.9 ± 13.2 years, 54.3% females, 0.7% cirrhosis), 272 (1.1%) developed liver-related events during 133,816 person-years (PYs) of follow-up. In the validation cohort of 411,395 patients (mean age 61.8 ± 12.4 years, 49.3% females, 0.4% cirrhosis), 5,984 (1.5%) developed liver-related events during 4,386,544 PYs of follow-up. Among the five DA methods, maximum classifier discrepancy (MCD) (AUC [95% CI] 0.822 [0.814–0.829]) and confidence regularised self-training (CRST) (0.825 [0.817–0.832]) performed best in validation cohort; their AUC in training cohort was 0.919 (0.904–0.934) and 0.831 (0.808–0.854) respectively. While the Fine-Gray model had an AUC of 0.804 (0.777–0.831) in the training cohort, the AUC dropped to 0.681 (0.672–0.691) in the validation cohort, showing the benefit of DA in preserving model accuracy in a less definite population at risk of MASLD. The AUC of NOS and FIB-4 was 0.649 (0.640–0.657) and 0.645 (0.635–0.655) in the validation cohort. Among the 19 factors including blood tests (liver and renal tests, lipids, fasting glucose), comorbidities, and demographics incorporated in MCD and CRST, the eight leading factors associated with liver-related events were cirrhosis, diabetes, platelets, aspartate aminotransferase, gamma-glutamyl transferase, international normalised ratio, dyslipidaemia, and albumin. MCD labelled 78.6% of patients with T2D who likely had

MASLD as low risk, with a 99.2% negative predictive value for excluding liver-related events in 15 years.

Conclusion: We developed novel models including common clinical parameters which accurately identify patients who are at low risk for liver-related events among patients with MASLD and patients with T2D who likely had MASLD. This study was supported by Health and Medical Research Fund of Health Bureau of HKSAR Government (Reference number: 19202141).

WED-199

Optimizing MASLD trial recruitment: LiverPRO vs. FIB-4 in reducing false positives and unnecessary biopsies

Katrine Lindvig¹, Naim Alkhoury², Rida Nadeem², Aarya Patel², Manal Chughtai², Sahasraara Hemant², Yasmeen Fallouh², Himanshi Kapoor², Camilla Dalby Hansen¹, Katrine Thorhauge^{1,3}, Johanne Kragh Hansen^{1,3}, Stine Johansen^{1,3}, Helle Schnefeld¹, Peter Andersen¹, Ida Falk Villesen¹, Katrine Tholstrup Bech¹, Nikolaj Torp^{1,3}, Sönke Detlefsen⁴, Mads Israelsen^{1,3}, Maja Thiele^{1,3}, Aleksander Krag^{1,3}. ¹Department of Gastroenterology and Hepatology, Centre for Liver Research, Odense University Hospital, Odense C, Denmark; ²Arizona Liver Health, Chandler, Arizona, United States; ³Institute of Clinical Research, University of Southern Denmark, Odense M, Denmark; ⁴Department of Pathology, Odense University Hospital, Odense C, Denmark
Email: katrine.prier.lindvig@rsyd.dk

Background and aims: Screen failures and high false positive rates present significant challenges in enrolling suitable candidates for clinical trials, yet in high prevalence populations false negatives is a challenge. This study compares the efficacy of two recruitment pathways, employing either Fibrosis-4 (FIB-4) Index or LiverPRO as initial screening tools for clinical trial entry, focusing on Metabolic Dysfunction Associated Steatotic Liver Disease (MASLD). LiverPRO is a CE-marked diagnostic algorithm that utilises a machine learning model to predict the risk of liver fibrosis based on routine blood samples.

Method: We analysed data from a population-based low prevalence cohort study in Denmark (2017–2022), combined with participants from a high prevalence cohort referred for consideration in clinical trials to a tertiary hepatology clinic in the US (2019–2023). The clinical trials included participants with NAFLD activity score ≥4 and fibrosis stage ≥F2, defined as at-risk MASH. Participants underwent non-invasive tests including transient elastography (TE), and those with TE levels ≥8 kPa were referred for confirmatory liver biopsy.

Results: The study included 3,014 participants from Denmark and 705 from the US with risk factors of MASLD. The prevalence of elevated liver stiffness (TE ≥8 kPa) was 6.7% in the Danish cohort and 82% in the US cohort. The Danish and US cohorts were 58% vs. 71% female, with a median age of 57 vs. 58 years (IQR 52–62, IQR 49–65). The US participants exhibited more severe metabolic dysfunction than the Danish participants; BMI was 36 vs. 32 kg/m² (IQR 32–42 vs. IQR 29–35), and 46% vs. 16% had type 2 diabetes. The FIB-4 pathway referred 1,225 participants for TE measurements (cut-off ≥1.3). Of these, 366 of 1,225 (30%) underwent liver biopsy due to a TE ≥8 kPa. Conversely, the LiverPRO pathway referred 684 participants with a high risk LiverPRO score (cut-off >65%) for TE, with 467 of 684 (68%) proceeding to a biopsy. In the Danish cohort, only those with TE ≥8 kPa were referred for biopsy, whereas in the completely biopsied US cohort, at-risk MASH was confirmed in 170 (69%) and 485 (70%) of participants (42 vs. 94 had significant fibrosis, 26 vs. 165 had advanced fibrosis, and 7 vs. 226 had cirrhosis). These results indicate that adopting LiverPRO would result in a 75% reduction (n = 642) in unnecessary TE referrals compared to FIB-4. Finally, the FIB-4 pathway had a false-negative rate for predicting at-risk MASH in liver biopsies of 26% (173 of 673), whereas LiverPRO had a false-negative rate of 14% (99 of 710).

Conclusion: LiverPRO significantly improves MASH trial recruitment precision in both low and high-prevalence populations. In low-

prevalence cases, it reduces screen failures and unnecessary biopsies compared to FIB-4. In high-prevalence scenarios, LiverPRO lowers false negative rates, offering a more efficient participant selection method for clinical trials.

WED-200

Prevalence and tissue characteristics of steatotic liver disease subclassifications in the adult UK population using quantitative MRI clinical thresholds: a UK biobank study

Charlie Diamond¹, John McGonigle¹, Rajarshi Banerjee¹, Helena Thomaides Brears^{1,2}, Andrea Dennis¹, Naim Alkhouri³.

¹Perspectum Ltd., Oxford, United Kingdom; ²Perspectum Ltd., Translational Science, Oxford, United Kingdom; ³Fatty Liver Program, Arizona Liver Health, Chandler, Arizona, United States
Email: charlie.diamond@perspectum.com

Background and aims: Steatotic liver disease (SLD) represents a disease spectrum that results from fat accumulation in the liver. A new consensus nomenclature for the subclassification of SLD aetiologies was developed, including metabolic dysfunction-associated SLD (MASLD), alcohol associated liver disease (ALD), MetALD and cryptogenic SLD. Using data acquired as part of the UK Biobank (UKBB) imaging study, we sought to determine the prevalence of SLD subclassifications in the general UK population of older adults and describe their clinical characteristics using quantitative MRI markers of fat, iron and liver disease activity.

Method: Clinical and imaging data were acquired on 33, 607 volunteers from the UKBB between 2016 and 2020 (application 9914). Liver MRI scans were analysed using LiverMultiScan (for fat (MRI-PDFF), iron concentration (MRI-LIC) and disease activity (iron corrected T1 mapping, cT1). MASLD diagnosis was defined based on MRI criteria of liver fat $\geq 5\%$ and presence of at least one cardiometabolic risk factor. In absence of data describing weekly grams of alcohol consumed, we used daily alcohol consumption as a proxy for ALD. Steatohepatitis (including metabolic-dysfunction associated, MASH) additionally required cT1 ≥ 800 ms. For groupwise statistical comparisons, Wilcoxon rank sum tests were applied for continuous variables and Fishers exact tests for categorical variables.

Results: In our population (mean age 64 (SD 8) years, 47% male, mean BMI 26 (SD 4) kg/m², 17% obese, 4.9% self-reported diabetic), 27% met the criteria for SLD, 20% for MASLD and 3.7% for MASH. ALD was rare (0.6%), whereas MetALD, with concurrent cardiometabolic risk factors, was more prevalent (4.7%). Cryptogenic SLD with no metabolic or alcohol associated risk factors occurred in 2% of the population. People with MASLD had a higher prevalence of abnormally elevated liver disease activity (cT1 ≥ 800 ms) compared to MetALD (19% vs 15%, $p < 0.001$), but similar liver fat distribution (both mean 11% (SD 6)). Advanced liver disease (cT1 ≥ 875 ms, equivalent to significant fibrosis) was also equally prevalent at 3%. Prevalence of clinically elevated iron content (≥ 1.8 mg Fe/g) was significantly higher in ALD (10%) and MetALD (6.4%) groups as compared to cryptogenic SLD (3%, $p < 0.001$) and MASLD (2.6%, $p < 0.001$), respectively.

Conclusion: These data provide the prevalence of SLD and various subgroups in the UK population using state of the art MRI technology. Of interest, the increased liver iron content in the ALD and MetALD groups requires investigation for association with liver outcomes, as seen for hyperferritinaemia.

WED-201

Performance of non-invasive tests to diagnose cirrhosis in MASH trials: combined data from multiple therapeutic trials

Naim Alkhouri¹, Mazen Nouredin², Jörn M Schattenberg³, Vlad Ratziu⁴, Michael Charlton⁵, Julie Dubourg⁶, Stephen A. Harrison⁷.
¹Arizona Liver Health, Phoenix, United States; ²Houston Research Institute, Houston, United States; ³Saarland University Medical Center, Homburg, Germany; ⁴Sorbonne Université, Institute for

Cardiometabolism and Nutrition, Hospital Pitié-Salpêtrière, INSERM UMRs 1138 CRC, Paris, France; ⁵University of Chicago, Chicago, United States; ⁶Summit Clinical Research, San Antonio, United States; ⁷Radcliffe Department of Medicine, University of Oxford, Oxford, United Kingdom
Email: jdubourg@summitclinicalresearch.com

Background and aims: Metabolic dysfunction-associated steatohepatitis (MASH) cirrhosis is a distinct group of patients with a high risk of major adverse liver outcomes. We aimed to assess non-invasive tests (NITs) including ELF, Fibrosis-4 score (FIB-4), vibration-controlled transient elastography (VCTE) and FibroScan-based score Agile 4 to distinguish this group of patients.

Method: We combined screening data from 10 industry-funded MASH phase 2 trials. Liver histology data were assessed centrally, and cirrhosis was defined as a fibrosis stage of 4 with or without MASH. Diabetes status required by the Agile 4 formula was defined using glycated hemoglobin (HbA1c). Areas under the receiver operating characteristic (AUROC) analysis for each NIT were calculated. We calculated the positive likelihood ratio, pre- and post-test probability of cirrhosis to express the clinical utility of each score.

Results: 1, 113 patients with histology results and NITs data were included, with a fibrosis prevalence of: 35 (3%) for F0, 167 (15%) for F1, 269 (24%) for F2, 461 (41%) for F3, and 181 (16%) for F4. AUROC for ELF, FIB-4, VCTE and Agile 4 in this population were 0.76 (95% CI: 0.72–0.79), 0.76 (95% CI: 0.72–0.79), 0.86 (95% CI: 0.83–0.89), and 0.88 (95% CI: 0.86–0.91), respectively. The LR+ of the published ELF rule-in cut-off (≥ 11.3) was 3.97. This reflects a post-test probability of cirrhosis of 43% compared to a pretest probability of 16%. Among the 1, 113 patients included in this analysis, 85 (8%) had ELF ≥ 11.3 with 48 of those having no cirrhosis. The LR+ of the published FIB-4 rule-in cut-off (≥ 3.48) was 7.55. This reflects a post-test probability of cirrhosis of 59% compared to a pretest probability of 16%. Among the 1, 104 patients included in this analysis, 37 (3%) had a FIB-4 ≥ 3.48 , with 15 having no cirrhosis. The LR+ of the published VCTE rule-in cut-off (≥ 20) was 4.52. This reflects a post-test probability of cirrhosis of 46% compared to a pretest probability of 16%. Among the 1, 104 patients included in this analysis, 214 (19%) had a VCTE ≥ 20 , with 114 of those having no cirrhosis but mainly F2 and F3. The LR+ of the published Agile 4 rule-in cut-off (≥ 0.57) was 10.64. This reflects a post-test probability of cirrhosis of 67% compared to a pretest probability of 16%. Among the 1, 113 patients included in this analysis, 138 (12%) had Agile 4 ≥ 0.57 with 45 of those having no cirrhosis.

Conclusion: The FibroScan-based score, Agile 4, has the best diagnostic accuracy for cirrhosis compared to VCTE alone, ELF and FIB-4 in this population.

WED-202

The 2023 AASLD practice guidance for MASLD does not adequately risk stratify MASLD patients in the context of therapeutic trials

Naim Alkhouri¹, Mazen Nouredin², Jörn M Schattenberg³, Vlad Ratziu⁴, Michael Charlton⁵, Julie Dubourg⁶, Stephen A. Harrison⁷.
¹Arizona Liver Health, Phoenix, United States; ²Houston Research Institute, Houston, United States; ³Saarland University Medical Center, Homburg, United States; ⁴Sorbonne Université, Institute for Cardiometabolism and Nutrition, Hospital Pitié-Salpêtrière, INSERM UMRs 1138 CRC, Paris, France; ⁵University of Chicago, Chicago, United States; ⁶Summit Clinical Research, San Antonio, United States; ⁷Radcliffe Department of Medicine, University of Oxford, Oxford, United Kingdom
Email: jdubourg@summitclinicalresearch.com

Background and aims: Metabolic dysfunction-associated steatohepatitis (MASH) is a growing epidemic associated with significant morbidity and mortality. There is an unmet need to identify at-risk MASH patients (NASH + NAS ≥ 4 + F2–F3–F4) because they are the target population for therapeutic trials and future approved therapies. The latest AASLD guidance recommend the use of FIB4 in a first step followed by controlled transient elastography (VCTE) and/or ELF to risk-stratify patients. We aimed to assess the performance of the

POSTER PRESENTATIONS

2023 AASLD guidance in determining the at-risk population in the settings of randomized controlled trials.

Method: We combined screening data from 10 industry-funded MASH phase 2 trials and analyzed the proportion of at-risk MASH patients based on centrally read liver biopsy according to AASLD guidance using FIB-4 data, and VCTE and/or ELF data.

Results: 2,273 patients with histology results and NITs data were included, with a fibrosis prevalence of: 137 (6%) for F0, 484 (21%) for F1, 524 (23%) for F2, 812 (36%) for F3, and 316 (14%) for F4. 1,334 (59%) of patients were considered at-risk MASH. Following the AASLD guidance, FIB-4 classifies 1,087 (48%), 1,016 (45%), and 170 (7%) patients as low- (<1.3), intermediate, and high-risk (>2.67), respectively. Within the low-risk group, 51% were at-risk MASH patients based on liver histology. Within the high-risk group, 67% were at-risk MASH patients based on liver histology. Within the intermediate FIB-4 risk group, 67 (3%), 919 (40%), and 1,287 (57%) of patients were classified in the low-, intermediate, and high-risk groups based on ELF and/or VCTE, respectively. Within these risk groups, 27%, 51%, and 66% of patients were at-risk MASH patients based on liver histology in the low-, intermediate, and high-risk population, respectively. By using the AASLD guidance, 43% of patients with at-risk MASH would have been classified as low-risk.

Conclusion: The use of the current AASLD guidance to risk-stratify MASLD patients would miss a significant number of at-risk MASH patients. Further research, new biomarkers and refinement of guidances are warranted to more accurately risk-stratify patients with MASLD.

WED-203

Evaluation of iATT liver fat quantification for steatosis grading with reference to magnetic resonance imaging-based proton density fat fraction: a multicenter study

Masashi Hirooka¹, Sadanobu Ogawa², Yohei Koizumi³, Yuichi Yoshida⁴, Tatsuya Goto⁵, Satoshi Yasuda⁶, Masahiro Yamahira⁷, Tsutomu Tamai⁸, Ryoko Kuromatsu⁹, Toshihisa Matsuzaki¹⁰, Tomoyuki Suehiro¹¹, Yoshihiro Kamada¹², Yoshio Sumida¹³, Yoichi Hiasa³, Hidenori Toyoda⁶, Takashi Kumada¹⁴. ¹Ehime University Graduate School of Medicine, Department of Gastroenterology and Metabolism, Toon, Japan; ²Department of Imaging Diagnosis, Ogaki Municipal Hospital, Ogaki, Japan; ³Department of Gastroenterology and Metabolism, Ehime University Graduate School of Medicine, Toon, Japan; ⁴Department of Gastroenterology and Hepatology, Suita Municipal Hospital, Suita; ⁵Department of Imaging Diagnosis, Ogaki Municipal Hospital, Ogaki; ⁶Department of Gastroenterology, Ogaki Municipal Hospital, Ogaki, Japan; ⁷Department of Clinical Laboratory Medicine, Suita Municipal Hospital, Suita, Japan; ⁸Department of Gastroenterology, Kagoshima City Hospital, Kagoshima, Japan; ⁹Division of Gastroenterology, Department of Medicine, Kurume University School of Medicine, Kurume, Japan; ¹⁰Department of Gastroenterology, Sasebo City General Hospital, Sasebo, Japan; ¹¹Clinical Research Center, National Hospital Organization Nagasaki Medical Center, Nagasaki, Japan; ¹²Department of Advanced Metabolic Hepatology, Osaka University, Graduate School of Medicine, Osaka, Japan; ¹³Graduate School of Healthcare Management, International University of Healthcare and Welfare, Tokyo, Japan; ¹⁴Department of Nursing, Faculty of Nursing, Gifu Kyoritsu University, Ogaki, Japan
Email: hirooka.masashi.mb@ehime-u.ac.jp

Background and aims: Several preliminary reports have suggested the utility of ultrasound attenuation coefficient measurements based on B-mode ultrasound, such as iATT, for diagnosing steatotic liver disease. Nonetheless, evidence supporting such utility is lacking. This prospective study aimed to investigate whether iATT is highly concordant with magnetic resonance imaging (MRI)-based proton density fat fraction (MRI-PDFF) and could well discriminate between steatosis grades.

Method: A cohort of 846 individuals underwent both iATT and MRI-PDFF assessments. Steatosis grade was defined as grade 0 with MRI-

PDFF <5.2%, grade 1 with 5.2% MRI-PDFF <11.3%, grade 2 with 11.3% MRI-PDFF <17.1%, and grade 3 with MRI-PDFF of 17.1%. The reproducibility of iATT and MRI-PDFF was evaluated using the Bland-Altman analysis and intraclass correlation coefficients, whereas the diagnostic performance of each steatosis grade was examined using receiver operating characteristic analysis.

Results: The Bland-Altman analysis indicated excellent reproducibility with minimal fixed bias between iATT and MRI-PDFF. The area under curve for distinguishing steatosis grades 1, 2, and 3 were 0.887, 0.882, and 0.867, respectively. A skin-to-capsula distance of ≥ 25 mm was identified as the only significant factor causing discrepancy. No interaction between MRI-logPDFF and MRE-LSM on iATT values was observed.

Conclusion: Compared to MRI-PDFF, iATT showed excellent diagnostic accuracy in grading steatosis. iATT could be used as a diagnostic tool instead of MRI in clinical practice and trials.

WED-206

Nash-FibroTest for the diagnosis of significant fibrosis, in severe obesity treated with bariatric surgery and external non-linear trajectories of test' components among obesity classes in a large US population

Thierry Poynard^{1,2}, Olivier Deckmyn¹, Raluca Pais³, Judith Aron-Wisnewsky², Pierre Bedossa⁴, Maharajah Ponnaiah⁵, Jean Michel Oppert², Jean Michel Siksik², Laurent Genser², Frederic Charlotte⁶, Dominique Thabut², Karine Clément², Vlad Ratzu², Valentina Peta¹. ¹BioPredictive, Paris, France; ²Sorbonne University, Paris, France; ³INSERM, Paris, France; ⁴INSERM, Paris; ⁵ICAN, Paris, France; ⁶APHP, Paris, France
Email: thierry@poynard.com

Background and aims: Biopsy (B) is recommended during (B1) and after (B2) bariatric surgery (BS) in severe obesity (sOb). The Nash-FibroTest (NFT), NASHFibroSure in USA, is widely used to predict significant fibrosis (sF = F2toF4), as well as GGT, ALT or AST combos. One study (Netanel 2021) showed that NFT can diagnose sF regression in sOb treated by sleeve gastrectomy (SG). Here, the first objective was to demonstrate, in patients treated with Roux-en-Y (RY) or SG, whether NFTd validated in T2 diabetes (T2D) (Poynard 2023), was similar to B for predicting sF regression. Among BMI classes (BMIC = 27–30 kg/m² as controls, sOb = 30+, 35+, 40+, 45+), the trajectory (Tj) variability between NFT components may induce false positive/negative risks (Mehta 2023) but has never been compared in sOb according to age, sex, and T2D. Therefore, the second aim was to assess the Tj components prescribed consecutively to 60, 366 MASLD sF risk subjects in 2019, 53, 704 US sOb (n = 89%) and 6, 662 controls (11%), according to these factors for each BMIC.

Method: for the first aim, a posthoc analysis of the BARICAN study (Pais 2022) was performed in 55 sOb with 220 paired B and paired NFTd. The main end point was AUC for sF at B1 and B2, then adjusted kappa (K) and F-Test between spline curves for the second aim.

Results: sF prevalence in BS was 53% (29/55) at B1 and 42% (23/55) at B2 6 median years (yrs) later. For the first aim, AUCs were significant at B1 (0.75; 95%CI 0.58–0.86; p = 0.0002) and B2 (0.81; 0.66–0.90 p = 0.0001), with a significant K at B1 (0.75; p = 0.003) and B2 (0.65; p = 0.002). For the second aim in sOb (32, 866/53, 704 = 61% sF by NFT), 4 major differences in Tj were observed (all p < 0.0001): 1) In women (F) with T2D and a BMI of 30–35 (n = 7, 679), ALT and AST reached a plateau between the ages of 40 to 60, not present for other BMIC, nor in men (M), possibly due to menopausal transition. 2) haptoglobin in T2D F has a progressive increase with BMIC, with an age intra-class increase. In T2D M there was no change according to age nor sOb. These results suggest a sex-dependent inflammatory response to sOb and age. 3) A2M in M with BMI 30–45 started and increased with age 10 yrs earlier than in F, with or without T2D. 4) apoA1 levels at age 30 were higher in BMIC <30 regardless of sex and T2D.

Conclusion: NfT predicts sF regression after BS. Tj of sF biomarkers are not linear. Sex, age, T2D and menstrual transition must be taken into account to prevent misinterpretations in sOb novel therapy.

WED-207

Non-invasive biomarkers of liver fibrosis may be used for diagnosing fibrosis and prognostication in patients with metabolic dysfunction-associated steatotic liver disease

Liv Eline Hetland¹, Mikkel Werge¹, Mira Thing¹, Elias Rashu¹, Puria Nabilou¹, Nina Kimer¹, Anders Junker¹, Diana Leeming², Morten Karsdal², Alejandro Mayorga Guiliani², Lise Lotte Gluud^{1,3}.

¹Gastro Unit, Copenhagen University Hospital, Amager and Hvidovre Hospital, Hvidovre, Denmark; ²Nordic Bioscience A/S, Herlev, Denmark; ³Department of Clinical Medicine, Faculty of Health and Medical Sciences, Copenhagen University, Copenhagen, Denmark

Email: livelinehetland@gmail.com

Background and aims: Identification of biomarkers that are both diagnostic and prognostic is essential in metabolic dysfunction-associated steatotic liver disease (MASLD). Fibrosis is the most important predictor of prognosis in MASLD, and we therefore evaluated non-invasive fibrosis biomarkers for diagnosing significant fibrosis (F2-F4) and prognostication in MASLD.

Method: Prospective cohort study including 644 patients MASLD (age 59 years; 47.0% female; 32.3% with type 2 diabetes) and two years of follow-up. The accuracy of biomarkers for diagnosing significant fibrosis and to predict liver-related events was assessed. The analyses included Fibrosis-4 index (FIB-4), FibroScan, Enhanced Liver Fibrosis test (ELF), PRO-C3, and the ADAPT score, which combines age, diabetes, platelet counts and PRO-C3. The area under the Roc-curve (AUROC) was calculated based on prediction values with adjustment for age, gender, and type 2 diabetes.

Results: Significant fibrosis was diagnosed in 148 of 273 who underwent a biopsy (54.2%). Patients with significant fibrosis had increased Fib-4, FibroScan, ELF, Pro-C3, and ADAPT ($p < 0.001$, for all analyses). The diagnostic accuracy of FibroScan was the highest with an adjusted AUROC of 0.88 (95% CI 0.85–0.92, sensitivity 0.89, specificity 0.83). Similar values were found for the remaining biomarkers. Sequential testing with FIB-4 followed by FibroScan increased diagnostic accuracy (adjusted AUROC 0.92 (0.86–0.95, sensitivity 0.91, specificity of 0.84). Sequential testing with FIB-4 followed by remaining biomarkers also accurately predicted significant fibrosis (adjusted AUROC ELF 0.86 (0.81–0.92), Pro-C3 0.83 (0.79–0.87), ADAPT 0.85 (0.80–0.89)). During the follow-up, twenty-three patients developed liver-related events (progression to cirrhosis, development of hepatic decompensation, esophageal varices, liver transplantation, hepatocellular carcinoma, or liver-related death). A FIB-4 cutoff of 1.3 was a significant predictor of liver-related events in unadjusted logistic regression analysis and after adjusting for age, sex, and type 2 diabetes (adjusted odds ratio [OR] 42.92 (95% CI 5.23–5618.90). Increasing the cut-off to 2.67 showed an adjusted OR of 12.87 (4.14–41.70). Remaining biomarkers also predicted liver related events (adjusted OR FibroScan 23.51, ELF 9.79, Pro-C3 4.26, ADAPT 12.10, $p < 0.001$ for all analyses).

Conclusion: Sequential testing with non-invasive fibrosis biomarkers, particularly Fib-4 and FibroScan, is useful for diagnosing significant fibrosis as well as prognostication in MASLD. The results support systematic testing in at-risk patients for identification of patients with an increased risk of liver-related events.

WED-208

Metabolomics-based model for predicting metabolic dysfunction-associated steatotic liver disease and stratifying risk

Takeshi Kimura¹, Masanori Nojima², Yutaka Aoki³, Mai Higashi⁴, Makoto Watanabe⁴, Jyunya Ohtake⁵, Takuya Koshizaka⁶, Takahiro Yagi⁵, Yasuhisa Kumakura⁷, Katsunori Masuda⁷, Taka-Aki Sato⁴. ¹Center for Preventive Medicine, St. Luke's International

Hospital, St. Luke's International University, Chuo-ku, Tokyo, Japan; ²The University of Tokyo, The Institute of Medical Science, Minato-ku, Tokyo, Japan; ³Life Science Research Center, Technology Research Laboratory, Shimadzu Corporation, Nakagyo-ku Kyoto city, Kyoto, Japan; ⁴Life Science Research Center, Technology Research Laboratory, Shimadzu Corporation, Nakagyo-ku Kyoto city, Kyoto, Japan; ⁵St. Luke's International University, Chuo-ku, Tokyo, Japan; ⁶St. Luke's International University, Chuo-ku, Tokyo, Japan; ⁷Center for Preventive Medicine, St. Luke's International Hospital, St. Luke's International University, Chuo-ku, Tokyo, Japan
Email: takekimu@luke.ac.jp

Background and aims: Metabolic dysfunction-associated steatotic liver disease (MASLD; formerly non-alcoholic fatty liver disease [NAFLD]) is a global health concern due to its involvement in the development of a wide variety of non-communicable diseases. Presently, potent MASLD treatments have not been identified; therefore, prevention is essential; a tool able to predict MASLD and stratify disease risk would be practical due to the magnitude of the potentially affected population. We developed a metabolomics-based NAFLD prediction model that stratifies disease risk.

Method: This prospective case-cohort study involved 25,748 participants who underwent annual health checks between 2015 and 2016, followed by three years of follow-up. During these health checks, clinical data, including a lifestyle questionnaire (e.g., alcohol consumption habits), anthropometric measurements, laboratory results, and abdominal ultrasounds, were routinely collected. Gas chromatography-mass spectrometry (GCMS-TQ8040, Shimadzu, Japan), measuring 40 metabolites, was utilized for the metabolomic analysis of residual serum samples collected during the health check-ups. The prediction model for NAFLD development was constructed by the least absolute shrinkage and selection operator (LASSO)-Cox regression algorithm using the "glmnet" package for R (Version 4.2.2). SAS 9.4 was used for time-dependent receiver operating characteristic (ROC) analyses, and incidence rate estimation was performed using the Poisson regression model.

Results: The number of eligible participants in the subcohort was 3141, and the total incident NAFLD cases were 829 (191 were included in the subcohort). A LASSO-based prediction model was developed to forecast NAFLD development, utilizing the measurements of 31 metabolites. This model was initially constructed using the training set and subsequently validated with the test set. Time-dependent ROC analysis in the test set yielded an area under the curve of 0.764 for new-onset NAFLD within three years. Participants were categorized based on hazard ratios (HRs) derived from the log-hazard divided by the median log-hazard in the training set. The yearly incidence rates were determined for different HR groups: 0.4% for HR ≤ 0.5 , 1.1% for $0.5 < \text{HR} \leq 1$, 2.9% for $1 < \text{HR} \leq 2$, 7.6% for $2 < \text{HR} \leq 4$, and 10.0% for HR > 4 . In the highest risk group, the three-year risk of developing NAFLD was 27.1%.

Conclusion: This cutting-edge metabolomics-based model for predicting and stratifying the risk of NAFLD development may contribute to prevention of this disease, globally. Further analysis is needed to ensure that the prediction of MASLD is equally valid.

WED-209

Development of a novel non-invasive biomarker panel for hepatic fibrosis in MASLD

Lars Verschuren¹, Eveline Gart¹, Anne Linde Mak², Arianne van Koppen³, Serdar Özsezen¹, Andre Boonstra⁴, Joanne Verheij⁵, Lise Lotte Gluud⁶, Onno Holleboom², Maarten Tushuizen⁷, Roeland Hanemaaijer¹. ¹TNO, Leiden, Netherlands; ²Amsterdam UMC, Amsterdam, Netherlands; ³TNO, Leiden, Netherlands; ⁴Erasmus Medical Center, Rotterdam, Netherlands; ⁵Amsterdam University Medical Centers, Amsterdam, Netherlands; ⁶Copenhagen University Hospital Hvidovre, University of Copenhagen, Copenhagen, Denmark; ⁷Leiden University Medical Center, Leiden,

POSTER PRESENTATIONS

Netherlands

Email: lars.verschuren@tno.nl

Background and aims: Considering the escalating prevalence of metabolic dysfunction-associated steatotic liver disease (MASLD) and MASLD-related fibrosis, accurate non-invasive biomarkers for diagnosis and staging of fibrosis are urgently needed. This study applied a translational approach with the aim to develop a blood-based biomarker panel for fibrosis detection in MASLD.

Method: A first set of candidate biomarkers was identified using a translational diet-induced MASLD mouse model (LDLr^{-/-}.Leiden), focused on the mechanism of collagen deposition using hepatic gene expression and new extracellular matrix deposition, as detected by dynamic D2O-labeling. To translate these findings to humans, gene expression profiles and biomarkers were analyzed in liver biopsies and serum samples from patients with histologically characterized MASLD and variable degrees of fibrosis and validated in two independent patient cohorts

Results: A panel of blood-based fibrosis biomarkers was identified consisting of IGFBP7, SSC5D and Sema4D. The accuracy of the biomarker panel was validated in a separate cohort of 128 patients with histologically characterized MASLD across different stages of fibrosis. Light Gradient Boosting Machine (LightGBM) modelling demonstrated that fibrosis stage can be predicted in MASLD (F0/F1: AUC = 0.82; F2: AUC = 0.89; F3/F4: AUC = 0.87). Additionally, by validation in an independent second patient cohort (n = 156), we successfully replicated the high-performance predictions for F0/F1 and F3/F4 fibrosis stages with an AUC of 0.84. Although the AUC for predicting F2 fibrosis was modest at 0.62 the overall accuracy of the model outperformed the FIB-4 and Fibroscan predictions.

Conclusion: Using a translational approach to identify novel biomarkers mechanistically related to the dynamics of collagen synthesis, we developed a blood-based biomarker panel with three biomarkers which is able to identify MASH patients with mild (F0/F1) or advanced (F3/F4) hepatic fibrosis with high accuracy.

WED-210

Plasma metabolite profile associates with liver fibrosis and incident liver-related death in men from finnish general population

Ville Männistö^{1,2}, Anniina Oravilahti², Fredrik Åberg³, Markku Laakso². ¹Kuopio University Hospital, Kuopio, Finland; ²University of Eastern Finland, Kuopio, Finland; ³Helsinki University Hospital, Helsinki, Finland
Email: ville.mannisto@kuh.fi

Background and aims: Chronic liver disease is a substantial health challenge and an increasing cause for morbidity and mortality. Metabolic dysfunction associated steatotic liver disease (MASLD) and alcohol-related liver disease (ALD) are the most common causes for the steatotic liver disease in Western countries. These diseases can progress to liver fibrosis and ultimately to cirrhosis. However, it is not completely understood why only some people develop fibrosis and what are the metabolic changes associated with liver fibrosis at population level.

Method: The association between plasma metabolites and liver fibrosis was evaluated using plasma sample metabolomics from Metabolon's Global Discovery Panel and the dynamic Aspartate-to-Alanine Aminotransferase Ratio (dAAR) score for fibrosis in a Finnish population-based METSIM cohort of 10124 male individuals (mean [± standard deviation] age 57.7 ± 7.1 years; body mass index 27.3 ± 4.3 kg/m²). Furthermore, the association between the metabolites and incident liver-related death was evaluated.

Results: A total of 945 metabolites were available from at least 60% of the study individuals, and 498 of these were significantly (p < 5.3 × 10⁻⁵) associated with liver fibrosis in age and BMI adjusted linear

regression analysis. The results were essentially similar with multiple different adjustment models, even when adjusted with fatty liver index and weekly alcohol use. A predictive XGBoost regression model for the dAAR score revealed that the 26 most significant metabolites [selected based on SHapley Additive exPlanations (SHAP) importance values] explained 32% of the variance in dAAR, and the most important metabolites were N-acetylmethionine, alpha-ketoglutarate, aconitate, and xanthine. Among the best predictors were several amino acids, cofactors, products of energy metabolism, lipids (including bile acids), nucleotides, and peptides. The AUROC values for these 26 metabolites, when validated as predictors for liver-related death, varied between 0.82–0.87 depending on the model used (XGBoost, logistic regression or support vector machine).

Conclusion: Liver fibrosis associates with vast amount of plasma metabolites from different metabolic traits in middle-aged men from the general population.

WED-211

Combination of Liverfast (LF) and Liver Stiffness Measurement (LSM) using fibroscan outperforms FIB-4 and LSM, for the identification of MASLD advanced fibrosis (AF) in patients with type 2 diabetes (T2D)

Julie Dupuy¹, Adèle Delamarre², Paul Hermanbessiere³, Ronald Quiambao⁴, Parvez Mantry⁵, Imtiaz Alam⁶, Mona Munteanu⁷, Victor de Lédighen⁸. ¹CHU Bordeaux, Bordeaux, France; ²CHU Bordeaux, Bordeaux, France; ³CHU Bordeaux, Bordeaux, France; ⁴Fibronostics, Florida, United States; ⁵Methodist Dallas Medical Center, The Liver Institute, Dallas, United States; ⁶Austin Hepatitis Center, Texas, United States; ⁷Fibronostics, Medical Affairs, Florida, United States; ⁸CHU Haut Leveque, Bordeaux University, Bordeaux, France
Email: mona_munteanu@hotmail.com

Background and aims: Better identification of T2D patients (pts) with MASH-AF is mandatory as it requires further assessment, specific surveillance or targeted interventions. LF is an AI-based blood test for staging steatosis, activity and fibrosis (LF-Fib) and correlated to the long-term liver outcomes (Alim Pharmacol Ther 2022). We aimed to compare retrospectively two combinations for one-step assessment of AF: LF-Fib and LSM versus FIB-4 and LSM, for the identification of histological AF in T2D pts that undergone liver biopsy (LB).

Method: Data has been collected retrospectively from 583 MASLD pts (NCT01241227). Cut-offs used for AF were: 0.59 for LF-Fib and those recommended by AASLD guidance to rule in/out AF, respectively, 12k/8 kPa for LSM and, 1.3/2.67 for FIB-4, respectively.

Results: 583 MASLD pts had available LF-Fib, LSM, FIB-4 [males 56.4%, age 56 yrs, 51.6%T2DM, BMI 31.5 and LSM 9.6 KPa, 45.2%AF and 17%F4 on LB]. 235 pts had T2D and LB sample ≥ 2 cm and < 6 months apart from biomarkers [males 50%, median age 61 yrs, HbA1c 6.9, LSM 10.4 KPa, 58.3% LB AF]. Among them, the combination LF-Fib and LSM correctly identified AF (F3/F4) as per LB in a higher number of T2D pts, than the combination FIB-4 and LSM [53/56 (94.6%), versus 32/36 (88.9%)]. Using lower LSM cut-off (8 kPa), LF-Fib and LSM correctly identified AF in more pts than FIB-4 and LSM [72/88 (81.8%) versus 37/41 (90%)]. In the overall cohort with LB sample > 2 cm (N = 399), LF-Fib and LSM correctly identified AF in more cases than FIB-4 and LSM [70/74 (94.6%) versus 47/51 (92%)]. Using 8 kPa LSM cutoff LF-Fib and LSM correctly identified 25 pts more [94/117 (80.3%)] than FIB-4 and LSM combination. 74% of AF pts LB had FIB-4 < 2.67; LF-Fib and LSM correctly identified 41% of AF pts having FIB-4 in the indeterminate zone.

Conclusion: The combination LF-Fib and LSM outperformed FIB-4 and LSM for the identification of MASLD-related AF in T2D pts; a lower LSM cutoff could improve AF identification.

WED-212

Pemvidutide treatment is associated with improvement in non-invasive tests indicating greater likelihood of histologic response in subjects with metabolic dysfunction-associated steatotic liver disease: a 24-week, randomized, double-blind, placebo-controlled trial

Naim Alkhouri¹, Shaheen Tomah², John Suschak², Jonathan Kasper², M. Scot Roberts², M. Scott Harris², Sarah Browne², Rohit Loomba³.

¹Arizona Liver Health, Tucson, United States; ²Altimmune, Inc, Gaithersburg, United States; ³University of California, San Diego, United States

Email: naim.alkhouri@gmail.com

Background and aims: Pemvidutide is a long-acting, balanced GLP-1/glucagon dual receptor agonist under development for the treatment of metabolic dysfunction-associated steatohepatitis (MASH) and obesity. We previously reported that pemvidutide led to a greater than 75% reduction in liver fat content (LFC) by MRI-PDFF after 24 weeks of treatment, with up to 50% of subjects achieving normalization of LFC. Herein, we examined the effects of pemvidutide on the likelihood of histologic response.

Method: 64 subjects with metabolic dysfunction-associated steatotic liver disease (MASLD) defined as LFC $\geq 10\%$ by MRI-PDFF, were randomized in a 1:1:1:1 ratio to receive 1.2 mg, 1.8 mg, 2.4 mg pemvidutide, or placebo weekly (QW) for 24 weeks. Subjects with baseline ALT > 75 IU/L or evidence of advanced liver fibrosis, defined by liver stiffness measurement (LSM) by Fibroscan[®] ≥ 10 kPa, were excluded. Outcomes included the proportions of subjects who achieved a Fibroscan-AST (FAST) score < 0.35 and the proportions of subjects with ALT ≥ 30 IU/L at baseline who achieved a simultaneous reduction in MRI-PDFF ($\geq 30\%$) and ALT (≥ 17 IU/L) after 24 weeks of treatment.

Results: Median baseline BMI, LFC, ALT, and LSM, were 36.8 kg/m², 20.6%, 31.0 IU/L, and 6.5 kPa, respectively. Of the subjects, 53% were female and 27% had diabetes. 60%, 67%, and 75% of subjects with intermediate-to-high risk of MASH progression (FAST ≥ 0.35) at baseline achieved low-risk (FAST < 0.35) at Week 24 at pemvidutide 1.2 mg, 1.8 mg, and 2.4 mg, respectively, vs 25% placebo. Simultaneously, 50%, 44%, and 60% of subjects with ALT ≥ 30 IU/L at baseline achieved a combined reduction of MRI-PDFF ($\geq 30\%$) and ALT (≥ 17 IU/L) at Week 24 at pemvidutide 1.2 mg, 1.8 mg, and 2.4 mg, respectively, vs 0% placebo.

Conclusion: Pemvidutide administered QW for 24 weeks was associated with improvement in the FAST score and the combined ALT/MRI-PDFF response rates compared to placebo indicating greater likelihood of histologic response. These findings are expected to result in meaningful histopathological improvement with pemvidutide.

WED-213

Assessment of fibrosis change rates in placebo arm of metabolic dysfunction-associated steatohepatitis drug trials based on pathologist readouts and qFibrosis continuous values

Kutbuddin Akbary¹, Dean Tai¹, Galvin Gan¹, Julie Dubourg², Stephen A. Harrison³. ¹HistoIndex Pte Ltd, Singapore, Singapore;

²Summit Clinical Research, San Antonio, TX, United States; ³Pinnacle Clinical Research, Radcliffe Department of Medicine, University of Oxford, Oxford, UK, San Antonio, TX, United States

Email: akbary.kutbuddin@histoindex.com

Background and aims: Metabolic dysfunction-associated Steatohepatitis (MASH) drug trials face challenges in assessing treatment response due to substantial variability in the placebo group, observed both in pathologist readouts and qFibrosis continuous values (qFc). This significant variability hinders standardizing treatment effect and sample size calculations in MASH clinical trials and challenges the interpretation of the “true” treatment effect. The placebo cohort allows for describing the natural course of the disease. This study aims to describe the placebo response rates in NASH drug

trials, focusing on pathologist readouts (NASH-CRN stage) versus qF continuous values.

Method: Anonymized placebo responses from 5 MASH Phase 2b drug trials are detailed, using NASH-CRN readouts and qFc values. Fibrosis regression, progression, and no-change results are presented. NASH-CRN-based regression/progression was defined as a 1-stage change in fibrosis at end-of-treatment (EOT) compared to baseline (BL). qFc, regression/progression was determined based on the change in qFibrosis continuous values at EOT compared to BL, using the standard error of mean (SEM). No-change in qFc is change of qFc values within SEM at EOT compared to BL, and no-change in NASH-CRN stage in EOT compared to BL, respectively.

Results: Based on qFc values, the average fibrosis regression rate from BL to EOT in the placebo group was 38% (range: 19%–49%), compared to an average regression rate of 21% (range: 7%–30%) based on NASH-CRN staging. Fibrosis progression rates based on NASH-CRN averaged 18% (range: 12%–29%), contrasting with qFc at 45% (range: 33%–76%). The percentage of patients with stable diseases was higher when assessed by the NASH-CRN staging approach (average 62%, range: 46%–81%), compared to qFc (average: 17%, range: 33%–76%).

Conclusion: This study contributes to our understanding of the variance on placebo responses based on both pathologists' staging and qF continuous values. The data underscores considerable variability in placebo response across different studies, reflected in pathologist staging and qFc values. The proportion of patients meeting the definition of progression or regression was higher when assessed by qFc values. As a result, qFc decreased the proportion of patients considering with no change in fibrosis. Both NASH-CRN staging and qFibrosis-based continuous values are essential considerations in understanding placebo responses in MASH drug trials.

WED-214-YI

Ferritin is a predictor of fibrosis, but not liver iron in metabolic hyperferritinaemia

Maria Rosina Troppmair¹, Benedikt Schaefer¹, Michaela Plaikner², Christian Kremser², Benjamin Henninger², Herbert Tilg¹,

Heinz Zoller¹. ¹Department of Medicine I, Medical University of Innsbruck, Innsbruck, Austria; ²Department of Radiology, Medical University of Innsbruck, Innsbruck, Austria

Email: m.troppmair@i-med.ac.at

Background and aims: High serum ferritin is common in patients with metabolic dysfunction-associated steatotic liver disease and a marker of progressive disease. Metabolic hyperferritinaemia (MHF) was recently defined as hyperferritinaemia in patients with metabolic dysfunction. Stage 1-MHF is defined by a normal liver iron content, mild iron overload is MHF Stage 2 and severe iron overload MHF Stage 3. No validated consensus recommendations have been provided when patients should be referred for non-invasive iron quantification by MRI. The aim of the present study was to assess the association of high ferritin with liver iron concentration and fibrosis markers in patients with MHF to evaluate the biologic basis of the proposed staging system for MHF and develop evidence-based thresholds for MRI in MHF.

Method: A cohort of 882 patients with abdominal MRI between 2017 and 2023 was retrospectively evaluated for study inclusion. Of 494 patients with hyperferritinemia (Ferritin ≥ 200 μ g/L in women, ≥ 300 μ g/L in men) without anemia, inflammation or genetic iron overload, 167 patients with MHF could be included. This cohort was also compared with C282Y-homozygous patients (n=71) and patients with MHF characteristics and a hemochromatosis phenotype (TSAT $> 50\%$, n=31).

Results: Staging of MHF by serum ferritin concentration yielded in 44.3% of patients in MHF stage 1, 39.5% in stage 2 MHF and 16.2% of patients in stage 3 MHF. In contrast, disease staging based on liver iron concentration resulted in 70.7% in MHF stage 1, in 27.4% in stage 2 and in 1.8% in stage 3. These results show that ferritin overestimates

POSTER PRESENTATIONS

the degree of iron overload in MHF. Higher levels of ferritin, but not of liver iron concentration were associated with significantly higher FIB-4 values as a surrogate of liver fibrosis. MHF-patients showed higher spleen iron concentrations when compared with C282Y homozygous hemochromatosis patients (45.2 s^{-1} (33.6; 64.4) vs. 32.3 s^{-1} (25.3; 40.6), $p < 0.001$). Further, hepcidin/log (ferritin) ratios in MHF patients were comparable to those in the MHF and TSAT >50% group (12.9 (8.3; 18.9) vs. 11.9 (5.9; 18.8), $p = \text{ns}$), but significantly higher than in hemochromatosis patients (3.4 (1.8; 7.5), $p < 0.0001$). When MHF patients were grouped by HFE genotype, significant differences were observed in liver iron concentrations ($p = 0.02$) but not in spleen iron concentrations ($p = 0.43$). Patients compound heterozygous for p.C282Y and p.H63D in HFE had higher liver iron concentrations than patients with a normal HFE phenotype (72.5 s^{-1} (66.5; 132.6) vs. 56.3 s^{-1} (47.7; 70.2), $p = 0.002$).

Conclusion: The present study shows that the prevalence of significant hepatic iron accumulation as assessed by MRI is low in patients with MHF. HFE genotype is a genetic determinant of liver iron concentration. The strong correlation between ferritin and hepatic fibrosis highlights the prognostic relevance of ferritin in MHF.

WED-215

HeparDx™ (by Metadeq, Inc.) is a reliable biomarker-based non-invasive test for MASH, capable of detecting the presence of inflammation and ballooning

Giulia Angelini¹, Sara Russo¹, Erminia Lembo¹, Ornella Verrastro¹, Caterina Guidone², Antonio Liguori², Stephen A. Harrison³, Aldo Trylesinski⁴, Luca Miele², Geltrude Mingrone^{1,2,5}. ¹Università Cattolica del Sacro Cuore, Rome, Italy; ²Fondazione Policlinico Universitario A. Gemelli IRCCS, Rome, Italy; ³Radcliffe Department of Medicine, University of Oxford, UK, Oxford, United Kingdom; ⁴Metadeq, London, United Kingdom; ⁵King's college, London, United Kingdom
Email: giulia.angelini@unicatt.it

Background and aims: Metabolic dysfunction-associated steatohepatitis (MASH) is the most common liver disease worldwide and the leading cause of liver-related morbidity and mortality. Currently high-risk MASH (NAS ≥ 4 , F ≥ 2) identification is a challenge, as it relies on liver biopsy that is invasive, expensive and fraught with scalability issues. Therefore, there is an urgent need to find non-invasive tests (NITs) for identification of at-risk MASH, to monitor disease progression and future treatment. PLIN2 is a ubiquitously expressed protein that plays an important role in the formation and stability of lipid droplets, contributing to the progression of MASH. Here we aim to evaluate the diagnostic performance of HeparDx™, a test based on the expression of PLIN2 in circulating monocytes, in a cohort of subjects with and without at-risk MASH.

Method: We analyzed data from two trials that included 198 subjects with histologically proven at-risk MASH (BRAVES cohort, $n = 119$) and no MASH (LIBRA cohort, $n = 79$). We used the Area Under the Receiver Operating Characteristic (AUROC) curve to assess the diagnostic performance of HeparDx™ in predicting at-risk MASH and determining the presence of lobular inflammation or ballooning. The Youden criterion was employed to determine the best threshold. To predict the presence/absence of at-risk MASH, inflammation, or ballooning, we used a binomial logistic regression model based on PLIN2 expression.

Results: PLIN2 expression was significantly increased in subjects with at-risk MASH compared with subjects without MASH (5.39 ± 0.31 vs. 2.32 ± 0.10 MFI; $P < 0.0001$). HeparDx™ analysis for the prediction of presence/absence of MASH yielded an AUROC of 91% with a sensitivity and specificity of 93.5% and 90.2% respectively. Positive and negative likelihood ratio were 26 and 0.12 respectively. HeparDx™ was able to detect lobular inflammation and ballooning with a high sensitivity (Lobular inflammation: 82.4%; Ballooning:

71.7%) and specificity (Lobular inflammation: 95.6%; Ballooning: 91.3%). Positive and negative likelihood ratio were 5.42 and 0.05 for lobular inflammation and 3.22 and 0.12 for ballooning. Based on a binomial logistic regression analysis, we estimated that HeparDx™ has the ability to accurately predict the presence of at-risk MASH, inflammation, and ballooning in 94.7%, 87.8%, and 88.1% of the cases, respectively.

Conclusion: NITs that use PLIN2 as a biomarker are reliable for the diagnosis of at-risk MASH subjects. HeparDx™ has the potential to replace invasive liver biopsy-based histology for diagnosis and can help in identifying patients eligible for MASH pharmacotherapy.

WED-218

Circulating mitochondrial bioenergetic profile reflects the hepatic one and represents a non-invasive biomarker of disease severity in MASLD genetically predisposed individuals

Erika Paolini¹, Miriam Longo¹, Marica Meroni¹, Paola Podini², Angelo Quattrini², Anna Ludovica Fracanzani³, Paola Dongiovanni¹. ¹Medicine and Metabolic Diseases, Fondazione IRCCS Ca' Granda Ospedale Maggiore Policlinico, Milan, Italy, Milano, Italy; ²Experimental Neuropathology Unit, Institute of Experimental Neurology (INSPE), Division of Neuroscience, IRCCS San Raffaele Scientific Institute, Milan, Italy, Milano, Italy; ³Medicine and Metabolic Diseases, Fondazione IRCCS Ca' Granda Ospedale Maggiore Policlinico, Milan, Italy, Department of Pathophysiology and Transplantation, Università Degli Studi di Milano, Milan, Italy, milano, Italy
Email: paola.dongiovanni@policlinico.mi.it

Background and aims: Mitochondrial dysfunction is a key player in Metabolic Dysfunction-Associated Steatotic Liver Disease (MASLD) onset and progression. The co-presence of loss-of-function mutations in PNPLA3, TM6SF2 and MBOAT7 genes impacts on mitochondrial morphology and function in vitro models. Conversely, the restore of MBOAT7 and/or TM6SF2 activity in knock-out HepG2 cells decreased the number of misshapen-dysfunctional mitochondria and improved OXPHOS capacity. Therefore, in order to translate our in vitro findings into a clinical perspective and discover novel non-invasive biomarkers, we assessed mitochondrial activity in 41 MASLD patients stratified according to GG-PNPLA3, TT-MBOAT7 and TT-TM6SF2 genotype, of whom frozen liver biopsies and peripheral blood mononuclear cells (PBMCs) were available.

Method: H2O2, ROS, mitochondrial complexes activities were measured by enzymatic assays, the oxygen consumption rate (OCR) by Seahorse.

Results: According to our in vitro results, liver biopsies and PBMCs of GG-PNPLA3, TT-MBOAT7 and TT-TM6SF2 carriers, alone and especially combined (number of risk variants, NRV = 3), showed higher H2O2 and ROS than MASLD patients with no variants. Consistently, the activity of mitochondrial complexes I, III, citrate and ATP synthase was lower in biopsies and PBMCs of GG-PNPLA3, TT-MBOAT7 and TT-TM6SF2 individuals, showing the sharpest effect in their co-presence (* $p < 0.05$, ** $p < 0.001$, *** $p < 0.0001$ vs NRV = 0). Finally, biopsies and PBMCs of NRV = 3 subjects exhibited OCR depletion yielded by complex I/IV and II/IV activities compared to NRV = 0 at Seahorse (*** $p < 0.0001$). At multivariate analysis adjusted for age, gender, BMI, diabetes and MASLD severity, NRV = 3 was associated with reduced OCR in hepatic biopsies ($\beta = -21.24$) and PBMCs ($\beta = -20.08$) ($p < 0.0001$). Finally, at nominal logistic analysis, adjusted for NRV = 3, OCR predicted MASH-fibrosis with AUC of 0.81 and 0.86 in biopsies and PBMCs, respectively.

Conclusion: PBMCs mitochondrial activity is impaired in NRV = 3 carriers and completely reflects the hepatic one. Therefore, PBMCs bioenergetic profile could represent a potential non-invasive biomarker of disease severity in MASLD genetically predisposed individuals.

WED-219

Pemvidutide, a glucagon-like peptide 1/glucagon dual receptor agonist, improves metabolic dysfunction-associated steatohepatitis activity and fibrosis in a clinical quantitative systems pharmacology model

Stephen A. Harrison¹, John Suschak², Matthew McDaniel³, Zackary Kenz³, Shaheen Tomah², Jonathan Kasper², M. Scot Roberts², Scott Siler³, M. Scott Harris², Sarah Browne². ¹*Pinnacle Clinical Research, San Antonio, United States*; ²*Altimmune, Inc, Gaithersburg, United States*; ³*Simulations Plus, Inc, Lancaster, United States*
Email: stephenharrison87@gmail.com

Background and aims: Elevated liver fat content (LFC) is recognized to be the primary pathophysiologic driver of metabolic dysfunction-associated steatohepatitis (MASH). In prior clinical trials, pemvidutide, a balanced (1:1) dual glucagon-like peptide 1 (GLP-1)/glucagon (GCG) receptor agonist, achieved significant reductions in LFC and improvements in two non-invasive markers of MASH inflammation: alanine aminotransferase (ALT) levels and corrected T1 magnetic resonance imaging. In the current study, NAFLDs_{sym}, a mechanistic quantitative systems pharmacology (QSP) model that includes interactive sub-models of steatosis, lipotoxicity, inflammation, and fibrosis, was used to predict the effects of pemvidutide and the relative contributions of GLP-1 receptor agonism and GCG receptor agonism on LFC, non-alcoholic fatty liver disease activity score (NAS), fibrosis, and weight loss in a simulated cohort of MASH subjects.

Method: The QSP modeling of pemvidutide, which included effects on weight loss and hepatocellular adenosine triphosphate (ATP) utilization, was linked to simulated pemvidutide pharmacokinetic profiles via a 1-compartment model. Data from a completed trial of pemvidutide in metabolic dysfunction-associated steatotic liver disease (MASLD) subjects were used to calibrate the quantitative effects of pemvidutide 1.8 mg once weekly dosing over 24 weeks. Simulations were conducted in a MASH cohort with median (Q1, Q3) NAS of 6.0 (4.0, 7.0), a median fibrosis stage of 2.0 (1.0, 3.0), and a median body weight of 106.2 (86.0, 123.8) kilograms.

Results: Excellent correlation was observed between clinically reported and QSP-predicted effects of pemvidutide on LFC at Week 12. The QSP model also predicted pemvidutide 1.8 mg to result in complete resolution of NAS and a 1-point median improvement in MASH fibrosis at 24 weeks of treatment. The addition of GCG receptor agonism to GLP-1 receptor agonism increased the relative reductions in LFC from 21% to 62% and resulted in a 4-point greater decrease in median NAS score. GLP-1 receptor agonism alone was predicted to have no effect on fibrosis within the 24-week timeframe.

Conclusion: The QSP model predicted the additive effects of adding GCG receptor agonism to GLP-1 receptor agonism on LFC, NAS, and fibrosis and suggested that success will be achieved with pemvidutide on these end points in an ongoing 24-week MASH clinical trial.

WED-220

BOS-580, a long-acting FGF-21 analogue, treatment shows beneficial changes in the circulating lipidome and improves MASEF score in patients with phenotypic metabolic dysfunction-associated steatohepatitis in a phase 2a randomized, placebo-controlled, 12-week study

Gerard Bain¹, Alicia Clawson¹, Juan Carlos Lopez-Talavera¹, Tatjana Odrlić¹. ¹*Boston Pharmaceuticals, Cambridge, United States*
Email: gerard.bain@bostonpharmaceuticals.com

Background and aims: BOS-580, a highly engineered fusion of human FGF21 and IgG1 Fc, has a 21-day half-life that enables once-monthly dosing. BOS-580 has shown a statistically significant reduction in liver fat content and markers of liver injury/fibrosis and improved markers of metabolic health in a Phase 2a, double-blind, placebo-controlled, randomized study in phenotypic metabolic dysfunction-associated steatohepatitis (MASH) patients. MASH is driven by dysregulated energy metabolism with extensive changes in the liver and blood lipidome. Here we describe changes in the

circulating lipidome of phenotypic MASH patients treated with BOS-580 and calculate metabolomics advanced steatohepatitis fibrosis (MASEF) scores, a novel composite biomarker to identify at-risk MASH patients (Noureddin M et al., 2024).

Method: Serum samples were collected for lipidomic profiling during a Phase 2a study of phenotypic MASH patients. Multiple dosing regimens were explored, with cohorts of 75 mg every 2 (Q2W) or 4 weeks (Q4W), 150 mg Q2W or Q4W, and 300 mg Q4W, or placebo. Metabolite extraction and analysis was performed according to published methods. Based on 12 lipids, body mass index (BMI), aspartate aminotransferase, and alanine aminotransferase, the MASEF score was calculated to determine at-risk MASH for each patient at baseline and at 12 weeks of BOS-580 treatment or placebo.

Results: A total of 480 lipid metabolic features were detected in the analyzed serum samples. Lipidomic profiles from patients with phenotypic MASH (n = 81) at baseline were enriched in triglycerides (especially those containing short acyl chains), diglycerides, bile acids and diacyl-phospholipids, while levels of non-esterified fatty acids (including mono- and poly-unsaturated and saturated fatty acids) and some lysophosphatidylcholines were reduced compared to a pre-existing obese control group (n = 30). BOS-580 treatment led to extensive changes in the circulating lipidome, including decreased levels of saturated fatty acids and triglycerides. Notably, these samples also had lower levels of lipotoxic molecules such as diglycerides and ceramides. MASEF scores identified 5 subjects in the placebo group with at-risk MASH at baseline, and all of them remained at-risk after 12 weeks, whereas 9 of 10 subjects in the treated group with at-risk MASH at baseline were no longer in the at-risk group after 12 weeks of treatment with BOS-580.

Conclusion: Treatment with once-monthly and bi-weekly BOS-580 improves the MASEF score at 12 weeks. Improvement of the MASEF score suggests reduction of at-risk MASH.

WED-221

A novel point-of-care prediction model for steatotic liver disease: based on bioimpedance analysis

Jaeyeon Park¹, Goh Eun Chung², Yoosoo Chang³, Seungho Ryu³, Yunmi Ko¹, Youngsu Park¹, Hyunjae Shin¹, Moon Haeng Hur¹, Yun Bin Lee¹, Eun Ju Cho¹, Won Sohn⁴, Jeong-Hoon Lee¹, Su Jong Yu¹, Jung-Hwan Yoon¹, Yoon Jun Kim¹. ¹*Department of Internal Medicine and Liver Research Institute, Seoul National University College of Medicine, Seoul, Korea, Rep. of South*; ²*Department of Internal Medicine, Seoul National University Hospital Healthcare System Gangnam Center, Seoul, Korea, Rep. of South*; ³*Center for Cohort Studies, Total Healthcare Center, Kangbuk Samsung Hospital, Sungkyunkwan University School of Medicine, Seoul, Korea, Rep. of South*; ⁴*Division of Gastroenterology, Department of Internal Medicine, Kangbuk Samsung Hospital, Sungkyunkwan University School of Medicine, Seoul, Korea, Rep. of South*
Email: yoonjun@snu.ac.kr

Background and aims: Globally, the incidence of steatotic liver disease (SLD) is increasing across all age groups. The developed non-invasive biomarkers and prediction models for SLD often necessitate laboratory tests or imaging, leading to overlooked early diagnosis in under-screened groups, such as young adults and those with healthcare disparities. To address this challenge, we aimed to develop a machine learning-based point-of-care prediction model for SLD that is readily accessible to the broader population, facilitating early detection, timely intervention, and ultimately reducing the overall disease burden.

Method: We retrospectively analyzed 28,506 adults who had routine health check-ups at Seoul National University Hospital Healthcare Center in South Korea from January 2022 to December 2022. For external validation, 159,351 subjects were included who visited Kangbuk Samsung Hospital Healthcare Center for routine health check-ups during the same period. All participants underwent abdominal ultrasound and bioimpedance analysis, in addition to

POSTER PRESENTATIONS

completing a questionnaire regarding their medical history and alcohol consumption. To analyze the data and make predictions, a logistic regression model was built using machine learning algorithms.

Results: A total of 20,094 subjects were categorized into non-SLD and SLD groups based on the presence of fatty liver on abdominal ultrasound. SLD model 1 was based on age and body mass index (BMI), SLD model 2 was derived from age, BMI, and body fat mass per muscle mass, and SLD model 3 consisted of age, BMI, and visceral fat area per muscle mass. In the derivation cohort, the area under the receiver operating characteristic curve (AUROC) was 0.817 in the SLD model 1, 0.821 in the SLD model 2, and 0.820 in the SLD model 3. In the internal validation cohort, at the optimal upper and lower cutoff values, 86.8%, 86.9%, and 87.1% of subjects were correctly classified in SLD model 1, SLD model 2, and SLD model 3, respectively. In the external validation, all models showed an AUROC of 0.85, and demonstrated predictive values similar to the internal validation at each respective cutoff.

Conclusion: The three derived SLD prediction models, characterized by cost-effectiveness, non-invasiveness, and accessibility in settings outside of hospitals, could serve as novel and validated clinical tools for the mass screening of SLD.

WED-222

Impact of automated FIB-4 reporting on liver-related referral of patients with diabetes

Theodore Feldman^{1,2}, Sarah Altajar³, Emilie Mitten⁴, Nathanael Fillmore^{4,5}, Nhan Do^{3,4,5}, Mary Brophy^{3,4,5}, Gyorgy Baffy^{3,4,6}. ¹Boston Cooperative Studies Program Coordinating Center (CSPCC), VA Boston Healthcare System, Department of Biomedical Informatics, Harvard Medical School, Boston, MA, United States; ²Department of Biomedical Informatics, Harvard Medical School, Boston, MA, United States; ³Department of Medicine, Boston University Chobanian and Avedisian School of Medicine, Boston, MA, United States; ⁴Department of Medicine, Brigham and Women's Hospital, Harvard Medical School, Boston, MA, United States; ⁵Boston Cooperative Studies Program Coordinating Center (CSPCC), VA Boston Healthcare System, Department of Medicine, Brigham and Women's Hospital, Harvard Medical School, Boston, MA, United States; ⁶Department of Medicine, VA Boston Healthcare System, Department of Medicine, Brigham and Women's Hospital, Harvard Medical School, Boston, MA, United States Email: Gbaffy@partners.org

Background and aims: Metabolic dysfunction-associated fatty liver disease (MASLD) is an underrecognized condition in patients with diabetes who are at an increased risk of advanced liver disease. FIB-4 is widely used for primary screening of liver fibrosis in MASLD. In 2020, we began reporting FIB-4 in the electronic health record (EHR) at our hospital and analyzed the impact of this measure on primary care referral practices. Preliminary findings of this work were presented earlier.

Method: Patients diagnosed with diabetes (HgbA1c >6.5% on at least one occasion) and seen in primary care clinics between 2011–2022 were identified. Subgroups of patients with low (<1.3), intermediate (1.3–2.67), and high (>2.67) FIB-4 values were defined based on EHR data. GI consults requested each year were analyzed by individual chart review and data were compared preceding (2011–2019) and following (2020–2022) the start of FIB-4 reporting with a focus on liver-related indications.

Results: A total of 14,280 individual patients with diabetes seen in primary care at our hospital within the study period were identified. The average size of annualized cohorts was 4,403 with the lowest number seen in 2020 (n = 3,016), coinciding with the onset of COVID pandemic. Laboratory parameters allowed FIB-4 calculation in 64.8% of these cases, identifying 37.8%, 51.1%, and 11.1% with low, intermediate, and high FIB-4 scores, respectively, with no significant difference in the annual distribution. The number of outpatient GI consults placed each year ranged from 364 to 712 (10.1% to 15.7%, NS).

Among these, the average rate of liver-related referrals was 11.8% with the highest rate of 14.6% found in 2020, indicating sustained referral rates despite an overall decreased number of GI referrals attributable to the pandemic. Further analysis of the rate of referrals related to abnormal liver tests indicated an average rate of 25.4% prior to FIB-4 index reporting, which increased to 43.4% immediately following its introduction (p = 0.03) and maintained an average of 39.3% (NS). MASLD as a referral indication showed a less robust change (13.1% vs. 19.2%, NS). During the same periods, rates of referrals related to hepatitis C virus infection dwindled from 29.2% to 3.6% (NS), consistent with the fact that most veterans at our center have received antiviral therapy prior to 2020. Finally, the average rate of liver-related referrals among patients with high FIB-4 increased from 4.6% to 8.1% (NS) after FIB-4 reporting.

Conclusion: Automated inclusion of pre-calculated FIB-4 in the EHR may change primary care referral practices and facilitate timely evaluation of patients with diabetes at increased risk of advanced liver disease. Additional steps are needed to bring robust increase in clinician awareness, improve screening rates, and facilitate risk assessment of patients with MASLD who are at increased risk for liver disease.

WED-223

Clinical and biological predictors of liver fat content ≥8% as assessed by MRI-PDFF: combined data from multiple therapeutic trials including more than 10,000 patients

Mazen Nouredin¹, Sophie Jeannin², Naim Alkhouri³, Vlad Ratziu⁴, Jörn M. Schattenberg⁵, Michael Charlton⁶, Julie Dubourg⁷, Stephen A. Harrison⁸. ¹Houston Research Institute, Houston, United States; ²Summit Clinical Research, San Antonio, United States; ³Arizona Liver Health, Phoenix, United States; ⁴Sorbonne Université, Institute for Cardiometabolism and Nutrition, Hospital Pitié-Salpêtrière, INSERM UMRs 1138 CRC, Paris, France; ⁵Saarland University Medical Center, Homburg, Germany; ⁶University of Chicago, Chicago, United States; ⁷Summit Clinical Research, San Antonio, United States; ⁸Radcliffe Department of Medicine, University of Oxford, Oxford, United Kingdom Email: j.dubourg@summitclinicalresearch.com

Background and aims: MRI-PDFF is a common inclusion criterion in metabolic dysfunction-associated steatotic liver disease (MASLD)/metabolic dysfunction-associated steatohepatitis (MASH) and commonly a primary end point in early phase 2 trials, or secondary end points. We aimed to describe the main predictors of liver fat content ≥8% across multiple therapeutic clinical trials.

Method: We combined screening data from 10 industry-funded MASH phase 2 trials. Predictors of liver fat content ≥8% were examined using linear regression.

Results: 2,666 patients with MRI-PDFF data were included in this analysis. Among them, 2,175 (82%) had a liver fat content ≥8%. In a multivariate model, liver fat content was associated with younger age (p = 0.002), and higher CAP-FibroScan (p < 0.0001), ALT (p < 0.0001), triglycerides (<0.0001), and platelet (<0.0001). Body mass index, glycated hemoglobin (HbA1c) and AST were not associated with liver fat content. The proportion of patients with liver fat content ≥8% was 54%, 73%, 84% and 92% in patients with ALT <20, ALT 20–30, ALT 30–40, and ALT ≥40, respectively. This rose to 90% in patients with ALT ≥30 versus 66% in patients with ALT <30. In patients with triglycerides <150 mg/dL, 150–200 mg/dL, and ≥200 mg/dL, 79%, 87%, and 92% had liver fat content ≥8%, respectively. This rose to 90% in patients with triglycerides ≥150 mg/dL versus 79% in patients with triglycerides <150 mg/dL. The proportion of patients with liver fat content ≥8% was 83%, 83%, and 78% in patients with <40 years, 40–60 years, and ≥60 years, respectively.

Conclusion: Simple non-invasive biomarkers can help target patients with liver fat content ≥8%. We recommend using the ALT or triglycerides as simple tools with cutoff points of 30 for ALT and/or 150 for triglycerides.

WED-224

Screening for liver fibrosis in tertiary care using automatic calculation of FIB4 in patients at-risk of diabetes

Clémence M Canivet¹, Celine Rolland¹, Françoise Joubaud¹, Franck Genevieve¹, Stéphane Gervais¹, Frédéric Oberti¹, Delphine Prunier¹, Valérie Moal¹, Sophie Michalak¹, Isabelle Fouchard¹, Adrien Lannes¹, Jerome Boursier¹. ¹CHU of Angers, Angers, France

Email: clemence.canivet@chu-angers.fr

Background and aims: Current recommendations from EASL and AASLD suggest targeted screening for liver fibrosis in patients at risk. For this reason, diabetic and metabolic patients are the first-line patients to be targeted. The aim of this study was to evaluate a targeted screening procedure for advanced liver fibrosis using automatic calculation of FIB-4 in a tertiary centre.

Method: Between March 2021 and February 2023 in a French university hospital, an automatic calculation of the simple FIB-4 blood test was carried out for all blood tests including AST, ALT, platelets and HbA1c to target metabolic or diabetic patients. If the FIB-4 was >2.67, the prescribing physician received an alert message inviting him to request a liver specialized evaluation (SLE) for the patient. If this was not done within 6 weeks, a hepatologist contacted the patient to propose the SLE. The SLE included an assessment of fibrosis using liver elastometry (Fibroscan®) and specialized blood tests (FibroMeter^{V2G} and FibroMeter^{VCTE}). Patients with hepatic elasticity ≥8 kPa were referred to a hepatology consultation. A liver biopsy was then proposed to confirm the diagnosis of advanced fibrosis. In patients without liver biopsy, the diagnosis of advanced hepatic fibrosis was made by an independent adjudication committee of 3 senior hepatologists (procedure in progress which will be available for presentation)

Results: Of the 8796 FIB-4 generated, 835 were >2.67 (9.5%) in 678 patients (7.7%). After excluding patients already followed in hepatology, 364 patients required SLE. 95 patients were deemed to be in too poor a state of health to warrant screening for liver fibrosis, and 62 patients refused or could not be contacted. A total of 207 patients were invited to undergo SLE, half of whom were invited by the prescribing physician (n = 101) and the other half by the hepatologist (n = 106). 185 patients underwent SLE: 52 patients (28.4%) had a liver elastometry ≥8 kPa. Nearly half of these patients came from the diabetology department (24/52), while the cardiology (4/52) and neurology (3/52) departments provided very few patients at risk of advanced fibrosis. Liver biopsy was offered to 34 patients, 5 of whom refused. A total of 29 patients was diagnosed with advanced fibrosis (12 by liver biopsy, 17 by non-invasive tests). The prevalence of advanced liver fibrosis was 7.9% in patients with a FIB-4 >2.67 with no previous liver follow-up and 15.7% in patients who underwent SLE. Patient compliance with the procedure was excellent (87% while compliance by prescribing physicians was 27.7%.

Conclusion: This study shows the value of a targeted automatic screening procedure for advanced liver fibrosis in tertiary centre. Raising awareness among hospital practitioners remains essential to improve compliance with the procedure.

WED-225

An intergenerational population-based cross-sectional study of MASLD in children and their parents

Oyekoya Ayonrinde^{1,2,3}, Shailender Mehta^{1,2}, Stephanie Dowden⁴, Timothy Fairchild⁵, Gina Ambrosini⁶, Desiree Silva^{3,7}, Kemi Wright⁸, Sheeraz Mohd¹, Leela King¹, Seyifunmi Afolabi⁹, Janine Spencer¹.

¹Fiona Stanley Hospital, Murdoch, Australia; ²Curtin University, Bentley, Australia; ³The University of Western Australia, Perth, Australia;

⁴NursePrac Australia, Success, Australia; ⁵Murdoch University, Murdoch, Australia; ⁶Department of Health, Government of Western Australia,

Perth, Australia; ⁷Joondalup Hospital, Joondalup, Australia; ⁸The University of New South Wales, Sydney, Australia; ⁹Oceania University of Medicine, Brisbane, Australia

Email: oyekoya.ayonrinde@uwa.edu.au

Background and aims: Steatotic liver disease (SLD) is the most common chronic liver disorder globally. SLD in childhood reflects prevalent metabolic dysfunction in children and families and poses increased longer-term risk of early-onset cardiometabolic and liver-related complications. We examined the prevalence and significance of SLD in children and their parents.

Method: Population-based children, aged 5–15 years, and their parents participated in a cross-sectional observational study of SLD in Perth, Australia. Assessments included controlled attenuation parameter (CAP) with transient elastography, anthropometry, and blood tests. SLD was defined by CAP ≥249 dB/m in children and ≥275 in parents. Associations between SLD in children and their parents and associations with features of metabolic dysfunction were sought.

Results: One hundred and fifteen children (50% male), with mean [SD] age 9.6[2.7] years, 74 mothers aged 40.7[5.8] years and 24 fathers aged 44.2[5.8] years were examined. Among the children, 73 (64%) were aged 5–10 years. Comparing boys vs. girls, there were no significant differences in modified body mass index (BMI) z-score (-0.17 vs. -0.11), median (IQR) weight (45.6[29.3–59.2] kg vs. 39.5 [27.6–51.0] kg, p = 0.15), waist circumference (WC) (67.0 [53.0–81.0] cm vs. 65.0 [55.5–75.0] cm, p = 0.48), abdominal skinfold thickness (SFT) (23.0 [12.0–32.0] mm vs. 21.0 [11.0–31.0] mm, and CAP (202 [185–244] dB/m vs. 210 [184–251] dB/m (p > 0.05 for all). Mean (SD) WC was 88.3 (13.4) cm in mothers and 91.8 (10.9) cm in fathers. Mean BMI was 27.7 (5.3) kg/m² in mothers and 27.3 (3.0) kg/m² in fathers. SLD was diagnosed in 20.2% children (15.8% male vs. 24.6% female, p = 0.24), 29.9% mothers and 37.5% fathers. SLD was seen in 55% of children with BMI ≥30 kg/m². Children with SLD had higher abdominal SFT, weight, WC, BMI, serum alanine aminotransferase (ALT), high-sensitivity C-reactive protein, and triglycerides, and lower levels of high-density lipoprotein cholesterol, compared with those without SLD (p < 0.05 for all). There was no significant correlation between SLD in children and their parents, however mothers of children with SLD had higher mean BMI than mothers of children without SLD (30.3[5.7] kg/m² vs. 27.1[5.1] kg/m², p = 0.04), and fathers had higher mean liver stiffness measurement (LSM), (7.6[4.6] kPa vs. 4.8[1.2] kPa, p = 0.02. Using multivariable logistic regression analysis, child ALT (OR 1.21, 95% CI 1.01–1.45) and abdominal SFT (OR 1.59, 95% CI 1.03–2.44) were associated with SLD in children, after adjusting for child WC (OR 0.94, 95% CI 0.87–1.04), and maternal BMI (OR 1.22, 95% CI 0.85–1.76).

Conclusion: SLD is common in children, and is associated with increased adiposity, raised ALT, features of metabolic dysfunction, maternal adiposity, and paternal liver stiffness. Our findings suggest possible intergenerational heritability of metabolic and hepatic risk.

WED-226

An algorithm based on serum phospholipid profiles to predict liver fibrosis degree in metabolic dysfunction-associated steatotic liver disease

Mayuko Shimizu¹, Yuko Miyakami¹, Minoru Matsumoto², Kentaro Yoshimura³, Akemi Tsutsui⁴, Yosuke Tsuchiyama¹, Koichi Takaguchi⁴, Sên Takeda^{5,6}, Koichi Tsuneyama¹. ¹Tokushima University, Department of Pathology and Laboratory Medicine, Tokushima, Japan; ²Tokushima University, Department of Molecular Pathology, Tokushima, Japan; ³University of Yamanashi, Division of Molecular Biology, Yamanashi, Japan; ⁴Kagawa Prefectural Central Hospital, Department of Hepatology, Takamatsu, Japan; ⁵Teikyo University School of Medicine, Department of Anatomy, Tokyo, Japan; ⁶University of Yamanashi, Department of Anatomy and Cell Biology, Yamanashi, Japan

Email: ichimura.mayuko@tokushima-u.ac.jp

Background and aims: Metabolic dysfunction-associated steatotic liver disease (MASLD) leads to liver cirrhosis and hepatocellular carcinoma. Although plasma/serum phospholipids are proposed non-invasive biomarkers of MASLD progression, they have not been put into clinical practice, in part because the mechanism underlying their efficacy remains unknown. The aim of this study was to evaluate serum phospholipid profiles in order to develop a novel biomarker for assessing the extent of liver fibrosis in MASLD patients and elucidate the underlying mechanisms.

Method: Liquid chromatography-tandem mass spectrometry was used to comprehensively analyse serum phospholipid profiles in 100 patients with clinically diagnosed MASLD. A total of 550 phospholipid species were analysed, including subclasses of phosphatidylethanolamine (PE), sphingomyelin (SM), phosphatidylcholine (PC), lysophosphatidylethanolamine, and lysophosphatidylcholine. Phospholipid profiles were associated with laboratory data and fibrosis stage in liver biopsy.

Results: MASLD patients with liver fibrosis exhibited distinct changes in serum phospholipids, characterised by reduced SM and PC levels and elevated PE levels. Based on these phospholipid changes, we developed a fibrosis prediction model and evaluated its performance using biopsy data, with samples divided based on classification ($\geq F2$ versus $< F2$). Our phospholipid-based model exhibited both higher area under the curve values (AUC=0.89) and greater specificity in comparison with other fibrosis biomarkers, including FIB-4 index, Mac-2 binding protein glycosylation isomer, and type IV collagen 7s (AUC=0.81, 0.77, and 0.75, respectively). We also elucidated the underlying mechanism of these phospholipid changes in relation to serum lipoproteins of the patients and liver transcriptomics. Specifically, a significant correlation between serum SM and LDL-cholesterol levels was identified ($r = 0.64$, $p < 0.001$ for SM [36:3]; $r = 0.66$, $p < 0.001$ for SM [40:1-d18:1/22:0]). Reduced serum LDL-cholesterol levels could be attributed to fibrotic liver and down-regulated expression of *LIPC*, which encodes the hepatic lipase that catalyzes LDL-cholesterol synthesis.

Conclusion: Serum phospholipid profiles represent an effective biomarker of liver fibrosis and help enhance understanding of the pathology of MASLD.

WED-227

Transient elastography performance for the diagnosis of liver fibrosis in MASLD is independent of steatosis level as determined by MRI proton density fat fraction in a prospective multicenter study

Oumnia Masroui¹, Florent Ehrhard², Maeva Guillaume³, Jérôme Gournay⁵, Karim Aziz⁶, Matthieu Schnee⁷, Ronan Garlantezec¹, Victor de Lédighen⁸, Laine Fabrice⁹, Turlin Bruno¹, Yves Gandon¹, Edouard Bardou-Jacquet⁹. ¹CHU Rennes, Rennes, France; ²CH Lorient, Rennes, France; ³Clinique Pasteur Toulouse, Toulouse, France; ⁴CHU Angers, Angers, France; ⁵CHU Nantes, Nantes, France; ⁶CH Saint Briec, Saint Briec, France; ⁷CH La Roche sur Yon, La Roche sur Yon, France; ⁸CHU Bordeaux, Bordeaux, France; ⁹CHU Rennes, Rennes, France
Email: edouard.bardou-jacquet@chu-rennes.fr

Background and aims: Transient elastography using Fibroscan® (FS) is accurate to screen for severe liver fibrosis in MASLD. Some studies suggest that the severity of steatosis may influence elastography value. Treatment or management modifying liver steatosis might thus impact the relevance of FS in the management of patient. Hepatic steatosis quantification using MRI PDFF is easily accessible and has shown reliability and accuracy. The aim of our study is to evaluate the performance of FS combined with MRI PDFF for severe fibrosis diagnosis.

Method: In this prospective multicenter study, patients with MASLD and indication for biopsy underwent an MRI and FS within a month. Patients with weekly alcohol consumption exceeding 21 UI/14 UI (male/female) were excluded. Biopsies were centrally reviewed using

the SAF score. Hepatic steatosis PDFF was centrally quantified using the MRQuantif software. Elastography quality criteria included an IQR < 0.3 if FS > 7.1 kPa, the M probe was used for patients with BMI < 30 , and the XL probe for BMI > 30 . ROC curves for the diagnosis of fibrosis $\geq F2$ and $\geq F3$ were determined for FS alone and for FS combined with PDFF as a continuous or categorical variable in a logistic regression. ROC curves were compared using the DeLong test.

Results: A total of 270 patients were included. 62 were excluded due to the absence of elastography or MRI, a delay > 30 days, or uninterpretable elastography. The studied population comprised 208 patients. Median age was 57, 63.9% males, median was BMI 32, and 47.6% were diabetic. 56.3% of patients had fibrosis $\geq F2$, and 30.3% had fibrosis F3-F4 on biopsy. 35.7% of patients had MASH according to the SAF score. The mean elastography value was 8.2 kPa. The mean PDFF value was 14.8%. The mean intervals between MRI/biopsy and FS/biopsy were 6.5 and 0.8 days, respectively. The AUC of FS for fibrosis $\geq F3$ was 0.78 (0.72–0.85), with no significant difference compared to AUC considering PDFF as a continuous value = 0.78 (0.72–0.85) or in category = 0.77 (0.70–0.84). The AUC of FS for fibrosis $\geq F2$ was 0.67 (0.60–0.74), with no significant difference compared to AUC considering PDFF as a continuous value = 0.66 (0.59–0.73) or in category = 0.65 (0.58–0.73). Similarly, there was no significant difference in performance within the subgroup of diabetic patients or patients with BMI > 30 .

Conclusion: Quantifying hepatic steatosis using MRI PDFF, allows a comprehensive and accurate assessment of liver steatosis. Fibroscan performance for the diagnosis of liver fibrosis does not seem to be affected by the level of liver steatosis.

WED-230

Association of Quantitative Hepatic Collagen with Non-Invasive Tests (NITs) for Fibrosis in Patients with Metabolic Dysfunction-Associated Steatotic Liver Disease (MASLD)

Zobair Younossi^{1,2}, James M Estep^{1,2}, Sean Felix², Brian Lam^{1,2}, Daisong Tan², Aaron Koenig², Fanny Monge², Andrei Racila^{1,2}, Zachary Goodman², Maria Stepanova^{1,2,3}. ¹The Global NASH Council, Washington, DC, United States; ²Beatty Liver and Obesity Research Program, Inova Health System, Falls Church, VA, United States; ³Center for Outcomes Research in Liver Diseases, Washington, DC, United States
Email: zobair.younossi@cldq.org

Background and aims: Hepatic collagen quantification determined as percent of hepatic collagen (PHC) can provide an accurate assessment of hepatic fibrosis. Although NITs for fibrosis have been shown to correlate with the semi-quantitative assessment of fibrosis by pathologic staging, the association of NITs with PHC in MASLD has not been established. Our aim was to associate PHC with common fibrosis NITs in patients with MASLD.

Method: Biopsy slides of patients with biopsy-proven MASLD and metabolic dysfunction-associated steatohepatitis (MASH) were stained with Sirius red, and PHC was estimated using computer-assisted morphometry (Aperio AT2, Leica Microsystems). The histologic stage of fibrosis was also evaluated using semi-quantitative F0-F4 scoring (NASH CRN system) by the study hepatopathologist (ZG). Serum samples collected at the time of biopsy were used to measure the fibrosis-4 (FIB-4) index and enhanced liver fibrosis (ELF) test, and DNA extracted from buffy coat was used to determine rs738409 (PNPLA3) genotype. Results are reported as % or mean and (SD).

Results: 331 MASLD patients were included [age 45 ± 11 years, 29% male, 97% obese (BMI > 30), 36% type 2 diabetes, 53% hyperlipidemia, 59% hypertension, 44% MASH and 56% non-MASH, 46% with PNPLA3 rs738409 CG or GG genotype, 63% histologic F1, 22% F2, 9% F3, 6% F4; FIB-4 score 1.10 (2.06) with 81% having FIB-4 < 1.30 (low-risk); ELF score 8.97 (1.33) with 77% having ELF < 9.8 (low-risk); PHC was 3.21 (2.79) %]. There was a strong association of PHC with histologic fibrosis stage: F1 patients had PHC 2.38 (1.99) %; F2: 3.45 (2.22) %; F3: 5.31 (3.39) %; F4: 8.19 (4.21) (trend $p < 0.0001$). Pooled together, patients with advanced fibrosis (F3-F4) had significantly higher PHC

than patients with mild or moderate fibrosis: 6.37 (3.93) % vs. 2.65 (2.10) % in F1-F2 ($p < 0.0001$). Among NITs, there were significant correlations of PHC with FIB-4 ($r = +0.23$) and ELF ($r = +0.21$) scores (all $p < 0.05$). Patients with elevated ELF (≥ 9.8) had higher PHC than those with low-risk ELF: 5.66 (4.55) % vs. 3.14 (2.53) %, $p = 0.0095$. Similarly, patients with elevated FIB-4 (≥ 1.30) had higher PHC than those with low-risk FIB-4: 4.83 (3.67) % vs. 2.86 (2.42) %, $p < 0.0001$. Finally, patients with high-risk *PNPLA3* rs738409 genotype (CG/GG) had higher PHC than those with the CC genotype: 3.45 (2.82) % vs. 2.67 (2.46) %, $p = 0.0112$.

Conclusion: In MASLD patients, common NITs are strongly associated with percent of hepatic collagen. These data provide additional validity of NITs as good surrogate of disease severity as determined by PHC and stage of fibrosis.

WED-231

Machine learning-based mortality prediction models for non-alcoholic fatty liver disease in the general United States population

Jiarui Zheng¹, Bo Feng¹. ¹Department of Hepatology, Peking University Hepatology Institute, Beijing, China
Email: fengbo@pkuaph.edu.cn

Background and aims: Nowadays, the global prevalence of non-alcoholic fatty liver disease (NAFLD) has reached about 25%, which is the most common chronic liver disease worldwide, and the mortality risk of NAFLD patients is higher. Our research created five machine learning (ML) models for predicting overall mortality in ultrasound-proven NAFLD patients and compared their performance with conventional non-invasive scoring systems, aiming to find a generalizable and valuable model for early mortality prediction in NAFLD patients.

Method: National Health and Nutrition Examination Survey (NHANES)-III from 1988 to 1994 and NHANES-III related mortality data from 2019 were used. 70% of subjects were separated into the training set ($N = 2262$) for development, while 30% were in the testing set ($N = 971$) for validation. The outcome was all-cause death at the end of follow-up. Twenty-nine related variables were trained as predictor features for five ML-based models: Logistic regression (LR), K-nearest neighbors (KNN), Gradient-boosted decision tree (XGBoost), Random forest (RF) and Decision tree. Five typical evaluation indexes including area under the curve (AUC), F1 score, accuracy, sensitivity and specificity were used to measure the prediction performance.

Results: 3233 patients with NAFLD in total were eligible for the inclusion criteria, with 1231 death during the average 25.3 years follow-up time. AUC of the LR model in predicting the mortality of NAFLD was 0.888 [95% confidence interval (CI) 0.867–0.909], the accuracy was 0.808, the sensitivity was 0.819, the specificity was 0.802, and the F1 score was 0.765, which showed the best performance compared with other models (AUC were: RF, 0.876 [95%CI 0.852–0.897]; XGBoost, 0.875 [95%CI 0.853–0.898]; Decision tree, 0.793 [95%CI 0.766–0.819] and KNN, 0.787 [95%CI 0.759–0.816]) and conventional clinical scores (AUC were: Fibrosis-4 Score (FIB-4), 0.793 [95%CI 0.777–0.809]; NAFLD fibrosis score (NFS), 0.770 [95%CI 0.753–0.787] and aspartate aminotransferase-to-platelet ratio index (APRI), 0.522 [95%CI 0.502–0.543]).

Conclusion: ML-based models, especially LR model, had better discrimination performance in predicting all-cause mortality in patients with NAFLD compared to the conventional non-invasive scores, and an interpretable model like Decision tree, which only used three predictors: age, systolic pressure and glycated hemoglobin, is simple to use in clinical practice.

WED-232-YI

Diagnostic accuracy of two-dimensional shear wave elastography (2D-SWE) for non-invasive assessment of liver fibrosis in biopsy-proven metabolic dysfunction-associated steatotic liver disease (MASLD). Systematic-review and multi-level random effects model meta-analysis

Madalina-Gabriela Taru^{1,2,3,4}, Dan-Corneliu Leucuta³, Silvia Ferri¹, Ahmed Hashim^{1,2}, Olga Orasan³, Bogdan Procopet^{3,4}, Monica Lupsor-Platon^{3,4}, Laura Turco⁵, Horia Ștefănescu⁴, Fabio Piscaglia^{1,2}, Federico Ravaoli^{1,2}. ¹Division of Internal Medicine, Hepatobiliary and Immunoallergic Diseases, IRCCS Azienda Ospedaliero-Universitaria di Bologna, Bologna, Italy; ²Department of Medical and Surgical Sciences, University of Bologna, Bologna, Italy; ³Faculty of Medicine, "Iuliu Hatieganu" University of Medicine and Pharmacy, Cluj-Napoca, Romania; ⁴Regional Institute of Gastroenterology and Hepatology "Octavian Fodor", Cluj-Napoca, Romania; ⁵Internal Medicine Unit for the Treatment of Severe Organ Failure, IRCCS Azienda Ospedaliero-Universitaria di Bologna, Bologna, Italy
Email: madalinagabrielataru@gmail.com

Background and aims: Metabolic dysfunction-associated steatotic liver disease (MASLD) represents a substantial healthcare concern. The early detection of advanced fibrosis (F3) and cirrhosis (F4) in MASLD is essential due to their association with unfavourable long-term outcomes. This systematic review and meta-analysis aimed to provide the best evidence for the diagnostic accuracy by a multiple thresholds model of two-dimensional shear wave elastography (2D-SWE) in detecting different stages of liver fibrosis in adult patients with biopsy-proven MASLD.

Method: We systematically searched PubMed/MEDLINE, EMBASE, Cochrane Library, Scopus, Web of Science, and LILACS electronic databases for full-text articles published in any language from inception to February 2023 and subsequently updated the search to December 2023. We included original studies that reported data on liver fibrosis assessment by 2D-SWE and employed histological diagnosis as the gold standard reference. A linear mixed-effects multiple thresholds model (CICS, Common random intercept and common slope) was endeavoured using the diagmeta R package, and summary estimates for sensitivity (Se), specificity (Sp), and the summary area under the curve (sAUC) were computed for all fibrosis stages. The study protocol was published online at <https://doi.org/10.17605/OSF.IO/9WV8F>.

Results: 23 observational studies (SuperSonic Imagine, GE Healthcare, Canon Medical Systems) were selected for the systematic-review, and 17 fulfilled the inclusion criteria for the subsequent meta-analysis, comprising a total of 1922 participants with biopsy-proven MASLD (mean age 51.4 [SE 2.53] years, mean BMI 28.2 [SE 0.87] kg/m², 51.3% females, prevalence of diabetes 40.3%). The prevalence of any stage of fibrosis (F1), significant fibrosis (F2), advanced fibrosis (F3) and cirrhosis (F4) was 29.2%, 19.6%, 18%, and 11.1%, respectively. The sAUCs [95% CI] in detecting $\geq F1$, $\geq F2$, $\geq F3$, and F4 for Se given Sp were 0.824 [0.129; 0.981], 0.822 [0.741; 0.884], 0.866 [0.756; 0.935], and 0.890 [0.772; 0.955], respectively. The optimal cut-off values were at 6.43 kPa (Se = 0.76, Sp = 0.76) for $\geq F1$, 8.17 kPa (Se = 0.76, Sp = 0.76) for $\geq F2$, 9.61 kPa (Se = 0.80, Sp = 0.80) for $\geq F3$, and 11.55 kPa (Se = 0.82, Sp = 0.82) for F4, respectively.

Conclusion: Our systematic review and meta-analysis suggest that 2D-SWE accurately diagnoses different stages of liver fibrosis in MASLD, underscoring the potential for standardising cut-off thresholds.

POSTER PRESENTATIONS

WED-233-YI

The single nucleotide polymorphism rs780094 C>T in the glucokinase regulator gene (GCKR) is associated with hepatic steatosis improvement after lifestyle intervention in overweight/obese subjects with metabolic dysfunction-associated steatotic liver disease

Eleonora Dileo¹, Chiara Rosso¹, Mariagrazia Tatoli¹, Gabriele Castelnuovo¹, Gian Paolo Caviglia¹, Angelo Armandi^{1,2}, Nuria Pérez Diaz del Campo¹, Marta Guariglia¹, Francesca Saba¹, Maria Lorena Abate¹, Antonella Olivero¹, Fabio Bioletto¹, Mirko Parasiliti-Caprino¹, Simona Bo¹, Elisabetta Bugianesi^{1,3}.

¹University of Turin, Department of Medical Sciences, Turin, Italy;

²University Medical Center of the Johannes Gutenberg University, Department of Internal Medicine I, Mainz, Germany; ³Città della Salute e della Scienza, Molinette Hospital, Gastroenterology Unit, Turin, Italy
Email: eleonora.dileo@unito.it

Background and aims: The rs780094 C >T single nucleotide polymorphism (SNP) in the glucokinase regulator gene (GCKR), involved in the regulation of glucose metabolism, has been associated with obesity and hepatic steatosis in patients with metabolic dysfunction-associated steatotic liver disease (MASLD). Our aim was to assess its impact on metabolic changes after lifestyle intervention in a group of overweight/obese MASLD patients.

Method: We analyzed 95 subjects (mean age 47 ± 52 y; male, N = 67) with MASLD who underwent a 6-month dietary intervention. At baseline (t0) and after 6-months diet (t6) we collected blood samples and anthropometrical measurements. The body composition was assessed by bioelectrical impedance analysis (BIA 101, Anker). GCKR rs780094 C >T genotyping was performed by allelic discrimination assay. Hepatic steatosis was determined by controlled attenuation parameter (CAP, Fibroscan®). A CAP improvement of 15 % was used as clinical end point. For all the metabolic parameters, we calculated the variation from t6 to t0 (delta).

Results: Overall, 57 (60%) patients were obese, 15 (15.8 %) had type 2 diabetes and 32 (33.7 %) had arterial hypertension. The prevalence of the GCKR rs780094 genotypes was 18.9 % (CC), 45.3 % (CT) and 35.8 % (TT). After 6 months of diet, all patients significantly improved body mass index (t0 = 30.8 kg/m² vs. t6 = 29.5 kg/m², p < 0.001), fat mass (FM) (27.9 kg vs. 26.0 kg, p = 0.007) and CAP (306 dB/m vs. 275 dB/m, p < 0.001). Specifically, a 15 % of CAP improvement was observed in 23 patients (24.2 %); among them, 12 carried the TT genotype (52 %), 2 (9 %) carried the CC wild type homozygosity and 9 subjects (39 %) carried the CT heterozygosity (p = 0.042). As expected, we showed that patients carrying the rs780094 TT genotype significantly improved glucose and insulin levels compared to those who carried the CC/CT variants (p = 0.004 and p = 0.001, respectively), while no differences were found concerning lipid profile. At multivariate logistic regression analysis adjusted for age, gender and diabetes, 15 % of CAP decrease after diet was associated with the rs 780094 TT risk homozygosity independent by delta FM (OR = 5.75, p = 0.05).

Conclusion: In overweight/obese subjects with MASLD, the GCKR rs780094 TT genotype predicts CAP improvement after diet. This finding may have implications in clinical practice for risk stratification and personalized medicine. Funded by the University of Turin, g.n. ROSC_RILO_23_01.

WED-234

Identifying the optimal cut off for relative reduction in liver fat content on MRI-PDFF to predict histologic response in MASH clinical trials

Michele Pansini^{1,2}, Cayden Beyer³, Kitty Yale⁴, Tim Rolph⁴, Kenneth Cusi⁵, Andrea Dennis³, Naim Alkhouri⁶. ¹Clinica Di Radiologia EOC, Istituto Di Imaging Della Svizzera Italiana (IIMSI), Lugano, Switzerland; ²John Radcliffe Hospital, Oxford University Hospitals NHS Foundation Trust, Oxford, United Kingdom; ³Perspectum Ltd, Oxford, United Kingdom; ⁴Akero Therapeutics Inc, South San Francisco, United

States; ⁵Division of Endocrinology, Diabetes and Metabolism, University of Florida, Gainesville, United States; ⁶Arizona Liver Health, Chandler, United States

Email: andrea.dennis@perspectum.com

Background and aims: MRI-proton density fat-fraction (PDFF) is a reliable and accurate measure of liver fat content (LFC). Estimates from clinical trials data suggested a threshold of 30% relative reduction in PDFF is indicative of clinically meaningful improvement in liver histopathology, as this had been associated with a 2-point improvement in NAS and with MASH resolution. However, a significant proportion of non-responders on histology achieve a 30% or more relative reduction in PDFF. The aim of this study was to determine the optimal cut off for relative reduction in LFC by PDFF to predict histologic response in patients with MASH.

Method: A retrospective analysis of participants from two interventional clinical trials with histologically confirmed MASH who underwent LiverMultiScan and paired, contemporaneous biopsy at baseline and end of study. The IDEAL post-processing method was used to calculate PDFF as it is the most accurate. Histological responders were defined as (1) a decrease in NAFLD Activity score (NAS) ≥ 2 with no worsening in fibrosis, (2) a decrease in fibrosis ≥ 1 stage with no worsening in NAS, and (3) MASH resolution with no worsening in fibrosis. Optimal thresholds for PDFF were reported using Youden's index.

Results: 132 patients were included in the analysis (age: 57 [IQR: 17.0], BMI: 35 kg/m²; 66% females, 37% diabetic, average baseline PDFF: 19.6%), 18 patients were recorded as in the placebo arms. Median change in PDFF for the 3 histological criteria ranged from 42–64% relative reduction, the median relative difference in PDFF from baseline in those on placebo was 21%. Using AUC, the optimal threshold for identifying histological responders ranged between 57%–63% relative change. For the histological category of MASH resolution, the optimal threshold for relative reduction in PDFF from baseline was –57%, this had an odds ratio of 16.8 (CI 4.7–67.3) and PPV of 65% to predict histological response. This compares to OR of 5.85 (CI 1.82–22.6) and PPV of 36% for a 30% relative reduction from baseline.

Conclusion: Whilst PDFF is a very useful end point in MASH trials, particularly for compounds expected to have a metabolic mechanism of action, the optimal threshold that would indicate a clinically meaningful improvement is much higher than the previous estimates of 30% relative change, which is only marginally more than the mean reduction observed for placebo. These data should be considered when designing clinical trials and setting thresholds for detecting meaningful change in MASH drug development.

WED-235

Prediction of metabolic dysfunction-associated steatohepatitis resolution

Rohit Loomba¹, Maral Amangurbanova¹, Ricki Bettencourt¹, Egbert Madamba¹, Harris Siddiqi¹, Lisa Richards¹, Mildred D. Gottwald², Shibao Feng², Maya Margalit³, Daniel Huang⁴. ¹MASLD Research Center, UC San Diego, La Jolla, United States; ²89 Bio, San Francisco, United States; ³89 Bio, Rehovot, Israel; ⁴Division of Gastroenterology and Hepatology, Department of Medicine, National University Health System, Singapore, Singapore
Email: roloomba@health.ucsd.edu

Background and aims: The resolution of metabolic dysfunction-associated steatohepatitis (MASH) is an accepted regulatory end point for subpart H approval of therapies developed for MASH but requires an invasive liver biopsy for its assessment. The MASH Resolution Index and FibroScan-aspartate aminotransferase (FAST) score have recently been reported to identify MASH resolution. We aimed to compare the diagnostic accuracy of the MASH Resolution Index and the FAST score to detect the histologic resolution of MASH. **Method:** This prospective study included 163 participants (64% female) with biopsy-proven MASH and stage 2 or stage 3 fibrosis from

a randomized, multicenter, placebo-controlled trial of pegozafermin, a fibroblast growth factor 21 analog. Participants received either pegozafermin or placebo and underwent two sets of contemporaneous liver biopsies, magnetic resonance imaging-proton density fat fraction (MRI-PDFF), and FibroScan spaced 24 weeks apart. The *primary outcome* was diagnostic accuracy for MASH resolution. The Delong test was used to compare the area under the receiver operating curves (AUC).

Results: The median (IQR) age and body mass index of participants in the validation cohort were 56.0 (48.0–62.0) years and 36.5 (32.2–40.2) kg/m², respectively. At follow-up biopsy, 29 (21.6%) of participants (pooled placebo and pegozafermin) in the validation cohort had MASH resolution. The AUC of the MASH Resolution Index (0.83, 95% CI 0.76–0.91) for identifying MASH resolution was significantly higher than the FAST score (0.65, 95% CI 0.55–0.75), $p = 0.001$. When the rule-in criteria for the MASH Resolution Index were used, the positive predictive value for MASH resolution was 29%, compared to 23% for change in FAST. When the rule-out criteria for the MASH Resolution Index were used, the negative predictive value was 100% compared to 87% for change in FAST.

Conclusion: The MASH Resolution Index has superior diagnostic accuracy for MASH Resolution, compared to the FAST score.

WED-236-YI

Real world evaluation of a primary care pathway for the assessment of liver fibrosis in metabolic dysfunction-associated steatotic liver disease (MASLD)

Basil Ahmad¹, Oliver Mitchell¹, Sally Pannifex¹, Arjuna Singanayagam¹, Sarah Hughes¹, Sarah Clark¹, Metin Yalcin¹, Nicola Williams², Sarah Davie³, Daniel Forton¹. ¹St George's University Hospitals NHS Foundation Trust, London, United Kingdom; ²South West London Gastroenterology Clinical Network, London, United Kingdom; ³South West London Pathology, London, United Kingdom
Email: daniel.forton@nhs.net

Background and aims: Fibrosis stage is the strongest predictor for disease-specific mortality in MASLD. In 2021 we introduced an initiative in SW London to stratify fibrosis risk in patients in primary care (PC) with MASLD, using non-invasive biomarker (NIB) assessment. FIB-4 was offered as the first test, with nested enhanced liver fibrosis (ELF) for those with indeterminate FIB-4 scores (1.3 >FIB-4 <3.25 if <65 years, 2.0 >FIB-4 <2.67 if >65 years). ELF was only available to PC practitioners and testing was only performed if the FIB-4 was indeterminate. Referrals to Hepatology clinics are only accepted with a qualifying FIB-4 or ELF (>9.5). This two-step (or similar) pathway is recommended by most MASLD guidelines, yet it has not been fully evaluated in real world settings. We assessed utility, and limitations, of PC testing of ELF in patients with MASLD.

Method: Data were obtained for ELF tests performed in the regional laboratory between January 2021 and October 2023. We examined the management of patients who underwent ELF testing in PC and specialty assessment in hospital Hepatology clinics, to determine whether the pathway was effective in enriching the patients referred to hospital with significant fibrosis.

Results: 1371 ELF tests were requested and 1030 were performed for patients in PC with MASLD or MetALD. 588 (57%) patients had ELF >9.5 with a median age of 58 (male 340; female 248). At the time of analysis, 342/588 (58%) patients have been referred and 274 (47%) patients have had a hospital-based Hepatology assessment, including successful Fibroscan in 269. 139 (51%) were discharged to their PC practitioner for follow-up after clinical evaluation revealed a low risk of fibrosis (median liver stiffness measurement (LSM) 5.2 kPa, range 6.1). 126 patients remain under follow-up (median LSM 10.4 kPa, range 72). 106 (39%) patients had F2+ fibrosis (LSM >8.0 kPa), 75 (28%) had F3+ fibrosis (LSM >9.7 kPa). We then considered whether a higher ELF cut-off might improve the performance of the PC pathway. 52/88 patients (59%) with ELF>10.5 had F2+ fibrosis but using this cut-off missed 54 patients with LSM >8 kPa. 41 liver biopsies were

performed in patients with LSM >8 kPa with the following grading of fibrosis: F0–1 (2%); F1–12 (29%, median ELF 10.45, median LSM 10.4 kPa); F2–10 (25%, median ELF 9.7, median LSM 10.9 kPa); F3–11 (27%, median ELF 10.3, median LSM 13.9 kPa); F4–7 (17%, median ELF 11.36, median LSM 18.2 kPa). There was a clear association between LSM and fibrosis stage, which was not seen for ELF.

Conclusion: The ELF cut-off >9.5 successfully enriches hospital referrals with fibrosis, as determined by clinical evaluation and LSM (39% likely F2+). However, >50% of referrals did not have significant fibrosis and there is poor concordance between ELF levels and LSM. For now, ELF has value in a community fibrosis pathway but novel NIBs with a higher positive predictive value are needed for this population.

WED-237

Novel circulating exosomal miRNA-mRNA network is linked to MASL-MASH and offers pathophysiologic insights with potential for biomarkers related to MASLD and hepatocellular carcinoma

Jing Zeng¹, Srinivas Koduru², Derrick Zhao³, Arun J. Sanyal⁴, Jiangao Fan⁵, Huiping Zhou³, Puneet Puri^{3,6}. ¹Virginia Commonwealth University, Richmond Veterans Affairs Medical Center, Richmond, United States; ²Gene Arrays, Omelette Inc., Seaforth, NY, United States; ³Virginia Commonwealth University, Richmond Veterans Affairs Medical Center, Richmond, VA, United States; ⁴Virginia Commonwealth University, Stravitz-Sanyal Liver Institute, Richmond, VA, United States; ⁵Shanghai Jiao Tong University School of Medicine, Shanghai, China; ⁶Virginia Commonwealth University and Richmond VA Medical Center, Richmond, United States
Email: puneet.puri@vcuhealth.org

Background and aims: Metabolic dysfunction-associated steatotic liver disease (MASLD) is the leading cause of end-stage liver disease for liver transplantation. MASLD phenotypes include steatotic liver (MASL) and steatohepatitis (MASH) with MASH conferring a higher risk for disease progression including cirrhosis and hepatocellular cancer (HCC). Exosomes carry a variety of bioactive molecules including miRNAs, lipids, and proteins. The dysregulation of miRNAs is closely related to various pathological aspects of MASLD disease progression. We hypothesized that patients with MASL and MASH will have dysregulated circulating exosomal miRNAs (CE-miRNAs). To test this, we aimed to examine the expression profiles of CE-miRNAs in patients with biopsy proven MASL or MASH compared to healthy controls and identify CE-miRNAs linked with MASL and MASH with potential association with hepatocellular carcinoma.

Method: We extracted serum exosomes and isolated total RNA from exosomes. CE-miRNAs were analyzed using PartekFlow. Potential target genes were identified using TargetScan and mirnet v2.0. Protein-protein interaction (PPI) networks were constructed using STRING database, and Cytoscape software was used to visualize hub genes.

Results: In depth miRNA-seq data analysis of biopsy confirmed MASL (n = 10), MASH (n = 10), and healthy controls (n = 6) revealed 32 differentially expressed CE-miRNAs (DE-CE-miRNAs) in MASL patients compared to healthy controls. Of these, 6 miRNAs were upregulated and 26 were downregulated. In MASH patients, 43 DE-CE-miRNAs were identified, comprising 14 upregulated and 29 downregulated, compared to healthy controls. Interestingly, 5 upregulated DE-CE-miRNAs were common to both MASL and MASH patients, and 8 downregulated DE-CE-miRNAs in MASL were similarly reduced in MASH. Further, GO and KEGG analyses were performed to predict target genes for these 13 overlapping DE-CE-miRNAs. Additionally, a PPI network analysis identified the top 50 hub genes associated with these miRNAs. Specifically, hsa-miR-889-3p and hsa-miR-382 were significantly upregulated in both MASL and MASH. Also, MASL and MASH showed downregulation of hsa-miR-4651 and hsa-miR-940. Previous studies have shown that these miRNAs promote cell invasion, HCC cell growth and progression. Also, downregulated miRNAs which normally facilitate apoptosis via

POSTER PRESENTATIONS

targeting FOXP4 act as an oncogene by dysregulating Wnt/ β -catenin signaling and promote unfavorable prognosis.

Conclusion: Our study has successfully identified DE-miRNAs in the circulating exosomes which may play a significant role in the progression from MASL to MASH and risk of HCC. These findings underscore the potential of exosomal miRNAs as diagnostic and prognostic markers as well as therapeutic targets for MASLD. The identified miRNAs merit further investigation to fully elucidate their clinical utility.

WED-238

High pancreatic fat and reduced volume stratify patients with F4 liver fibrosis

Edward Jackson¹, Alexandre Triay Bagur², Cayden Beyer³, En Ying Tan⁴, Nur Halisah Binte Jumat⁵, Sophie Riddell⁶, Elizabeth Shumbayawonda², Andrea Dennis², Helena Thomaidis Brears², Rajarshi Banerjee², Mark Muthiah⁷, Yock Young Dan⁷. ¹Perspectum Ltd, Oxford, United Kingdom; ²Perspectum Ltd., Oxford, United Kingdom; ³Perspectum Inc, Texas, United States; ⁴Division of Gastroenterology and Hepatology, Department of Medicine, National University Health System, Singapore, Singapore; ⁵Department of Medicine, Yong Loo Lin School of Medicine, National University of Singapore, Singapore, Singapore; ⁶Perspectum Asia Pte Ltd., Singapore, Singapore; ⁷Division of Gastroenterology and Hepatology, Department of Medicine, National University Health System, Yong Loo Lin School of Medicine, National University of Singapore, Singapore, Singapore
Email: edward.jackson@perspectum.com

Background and aims: While there is an emerging body of evidence showing a relationship between the liver and pancreas due to altered metabolism and insulin resistance in diabetes, the relationship between the organs in the advanced stages of liver disease is unclear. Multi-parametric magnetic resonance imaging (mpMRI), with metrics iron-corrected T1 (cT1) and proton density fat-fraction (liver fat), is an established non-invasive alternative to liver biopsy for diagnosis and monitoring of metabolic dysfunction-associated steatotic liver disease (MASLD). Recent development of equivalent metrics in the pancreas, scanner-referenced T1 (srT1), fat and volume allows characteristics of the two organs to be evaluated simultaneously. The aim of this study was to investigate how different stages of liver fibrosis measured by histology relate to mpMRI biomarkers in the liver and pancreas.

Method: 126 individuals across the spectrum of biopsy-proven MASLD, underwent LiverMultiscan as part of the ongoing prospective EMULSION study in Singapore. A semi-assisted pipeline was used to derive additional measures of pancreatic volume, fat and srT1 from 59 mpMRI scans that met adequate quality criteria. Wilcoxon signed-rank test and receiver operating characteristic curve analyses were conducted to compare different liver fibrosis subgroups.

Results: In 59 South-east Asian individuals (19% Malaysian, 61% Chinese, 12% Indian, 46% male, median BMI 29 kg/m², median age 38 years) 44 (75%) showed histological fibrosis (>F0) and MRI confirmed liver steatosis in 47 of 59 (80%). Liver cT1 (median [IQR] 883 ms [114] vs 750 [139], $p < 0.005$), liver fat (15.2% [12.2] vs 5.1 [5.1] $p < 0.001$) and pancreas fat (5.6% [4.3] vs 3.0 [3.1] $p < 0.05$) were elevated in patients with >F0 fibrosis. Pancreatic srT1 (704 ms [78] vs 706 [31]) and volume (74 ml [24] vs 63 [21]) were similar with or without any liver fibrosis. Liver cT1 detected any fibrosis (F1–4) with an area under the curve (AUC) of 0.75. cT1 peaked with F2 fibrosis (888 ms [116]) and remained above reference ranges even at F4 (813 ms [107]). Liver fat was reduced at F4 fibrosis (10% [1]). In contrast, F4 liver fibrosis ($n = 5$) was associated with a combination of increased pancreatic fat (9.5% [2.3] with F4 vs. 5.1% [4.2] all others, $p < 0.05$) and reduced pancreatic volume (59 ml [6.3] vs. 74 [24], $p < 0.05$). Pancreas fat showed very good discrimination of F4 liver fibrosis (AUC = 0.82).

Conclusion: In advanced steatotic liver disease, liver fat begins to decline yet pancreatic fat persists, and this multiorgan pattern of

pathophysiology is highly suggestive of advancing disease. Specifically, increased steatosis and volume atrophy in the pancreas alongside increased liver cT1 is a distinct imaging phenotype to identify F4 fibrosis in the liver.

WED-239

Proteomics identifies a subpopulation of plasma extracellular vesicles able to improve non-invasive diagnosis of MASH in patients with type 2 diabetes: results of the RHU QUID-NASH study

Laure Elkrief¹, Marion Tanguy², Louise Biquard³, Shantha Valainathan², Damarys Loew⁴, Florent Dingli⁴, Alix Cointet⁵, Cedric Laouenan⁶, Philippe Garteiser³, Valérie Paradis⁷, Agnes Lehuen⁸, Laurent Castera⁷, Thierry Poynard⁹, Dominique Valla⁷, Pierre-Emmanuel Rautou¹⁰. ¹Université de Tours, Tours, France; ²Inserm U1149, Université de Paris, Paris; ³Inserm U1149, Université de Paris, Paris, France; ⁴Institut Curie, Paris, France; ⁵Inserm 1149, Université de Paris, Paris, France; ⁶APHP, Hôpital Bichat, Paris, France; ⁷APHP, Hôpital Beaujon, Clichy, France; ⁸Institut Cochin, Paris, France; ⁹Sorbonne Université, Paris, France; ¹⁰APHP Hôpital Beaujon, Inserm UMR1149, Paris, France
Email: laure_elkrief@yahoo.fr

Background and aims: Despite the high prevalence and serious clinical implications of metabolic associated steatohepatitis (MASH) in patients with type 2 diabetes (T2D), MASH is usually overlooked in clinical practice, due to the lack of accurate biomarkers. Aim: to evaluate the ability of plasma large extracellular vesicles (IEVs) to serve as non-invasive biomarkers for the diagnosis of MASH in patients with T2D and investigate the pathophysiological process they reflect

Method: Prior proteomic analysis of IEVs was performed on plasma samples from 23 patients with T2D (8 steatosis, 15 MASH) and 9 healthy individuals. Candidate IEV protein biomarkers were measured in the QUID-NASH patient population (NCT03634098) including consecutive patients with T2D and metabolic dysfunction-associated liver disease (MASLD), separated into a derivation ($n = 278$) and an independent validation cohort ($n = 134$). We then evaluated the relationship between candidate IEV protein biomarkers and the extensive phenotyping performed, including liver histology (centralized reading of liver biopsies), magnetic resonance imaging (MRI) and detailed phenotyping of circulating immune cells.

Results: Prior proteomic analysis identified Transferrin-receptor on IEVs (TFRC-IEVs) as associated with MASH. We thus measured TFRC-IEVs on plasma samples from patients included in the derivation cohort (63% men, median age 59 years, median BMI 32 kg/m², 55% MASH). The proportion of patients with TFRC-IEVs concentration >61 ng/ml (i.e. Youden index threshold) was significantly higher in patients with MASH than in those with steatosis (29% vs. 12%, $p < 0.001$). TFRC-IEVs >61 ng/ml remained associated with MASH after adjustment on either usual laboratory variables (AST, ALT, GGT and triglycerides) (odds ratio (95% CI) 4.15 (2.01–8.57), $p < 0.001$), or on the NASH-Test (odds ratio (95% CI) 4.03 (1.99–6.80), $p < 0.001$) or on the Fibroscan FAST-score (odds ratio (95% CI) 3.01 (1.53–5.92), $p < 0.001$). When combining TFRC-IEVs with available methods (NASH-test >0.50 or FAST score >0.67), the sensitivity for MASH diagnosis were 32% and 29%, versus 22% and 16% for NASH-test or FAST score alone ($p = 0.004$ and $p = 0.0004$, respectively), without decreasing specificity. Similar results were obtained in the validation cohort. TFRC-IEVs >61 ng/ml was associated with hepatocyte ballooning on liver biopsy (32% vs. 15%, $p < 0.001$), but not with liver inflammation nor fibrosis at histology. TFRC-IEVs concentration correlated with serum ferritin concentration ($p < 0.001$), although no association was observed with intra-hepatic iron concentration by MRI nor with circulating immune cells subpopulations.

Conclusion: TFRC-IEVs, an index of hepatocyte ballooning, is an independent biomarker for MASH, able to improve patients' screening to enlarge recruitment of patients with MASH in clinical trials.

WED-242

The use of ELF test, FIB-4 and sequential algorithms to screen the Type 2 Diabetes Mellitus (T2DM) population for advanced fibrosis in Metabolic Dysfunction-Associated Steatotic Liver Disease (MASLD)

Yiying Pei¹, Wei Kwan Sng², Joanne Hui Min Quah², Jin Liu³, Bee Yen Chong², Hwee Khim Lee², Xue Fei Wang², Ngai Chuan Tan², Jason Pik Eu Chang¹, Hong Chang Tan¹, Yong Mong Bee¹, George Boon Bee Goh^{1,3}. ¹Singapore General Hospital, Singapore, Singapore; ²SingHealth Polyclinics, Singapore, Singapore; ³Duke-NUS Medical School, Singapore, Singapore
Email: pei.yiying@singhealth.com.sg

Background and aims: Accurate screening programs for advanced fibrosis in the metabolic dysfunction-associated steatotic liver disease (MASLD) population for at risk subjects such as Type 2 diabetes mellitus (T2DM) are not well established. We compared the performance of serum biomarkers (enhanced liver fibrosis score (ELF) and the fibrosis-4 score (FIB4)) to screen for advanced fibrosis in a population of T2DM, using transient elastography (TE) as the reference standard.

Method: A cross-sectional study was carried out in a primary care and endocrinology clinic in Singapore. Subjects with T2DM were consecutively enrolled and those with chronic liver diseases of other aetiologies were excluded. All participants underwent TE and had their demographics, clinical parameters and biomarkers collected. Validated cut offs for advanced fibrosis (ELF: ≥ 9.8 , FIB4: ≥ 1.3 and TE ≥ 8 kPa) were used.

Results: Analysis was performed on 425 subjects. Both ELF and FIB4 exhibited poor linear correlation with TE (Spearman's rho = 0.29, $p < 0.01$, R squared 0.12 and Spearman's rho = 0.11, $p < 0.02$, R squared 0.06 respectively). However ELF was able to diagnose elevated liver stiffness with moderate accuracy (AUROC 0.74, 95% CI 0.68–0.80) and outperformed FIB4 (AUROC 0.62, 95% CI 0.56–0.69). When using TE ≥ 12 as the reference, diagnostic accuracy improved dramatically, more so for ELF (AUROC of 0.91, 95% CI 0.85–0.97) rather than FIB4 (AUROC 0.70, 95% CI 0.59–0.82). Algorithms using first FIB4 followed by ELF in the cases of indeterminate FIB4 scores (1.3–2.67) resulted in a lower false positive rate of 9.6% (vs 21.2% with ELF and 26.8% with FIB4 alone). False negative rates however were higher than that of ELF alone at 12.5% vs 8%. Out of the 76 patients with TE ≥ 8 , 53 (70%) would have been missed with this referral strategy, though the expense of the ELF test in 69 subjects would have been avoided. BMI and waist circumference impacted performance of FIB4, with mean BMI in the false negative group significantly higher than the true negative group (BMI 28.2 vs 26.4 (kg/m²), $p < 0.001$, 95% CI –2.98 to –0.77). Waist circumference (WC) also was significantly different between the 2 groups for FIB4 ($p < 0.001$, 95% CI –9.71 to –3.53). Similarly, ELF performance was also affected (BMI 27.9 vs 25.7, $p < 0.001$, 95% CI –3.55 to –0.99, WC; $p < 0.001$, 95% CI –12.5 to –4.88). Neither groups showed significant difference in terms of age (FIB4; $p = 0.588$, ELF; $p = 0.554$).

Conclusion: ELF alone as a first line screening tool is more effective than FIB4 in identifying patients with significant fibrosis on transient elastography. The sequential method is also a viable alternative and reduces the false positive rates as compared to ELF test alone, with additional benefit of cost saving.

WED-243-YI

Irisin level as a potential biomarker for hepatic steatosis improvement after a 6-month lifestyle intervention in patients with metabolic dysfunction-associated steatotic liver disease

Gabriele Castelnovo¹, Nuria Pérez Diaz del Campo¹, Chiara Rosso¹, Gian Paolo Caviglia¹, Ilaria Goitre¹, Eleonora Dileo¹, Marta Guariglia¹, Fabio Bioletto¹, Francesca Saba¹, Marilu' Benedetta Scalici¹, Giorgio Maria Saracco^{1,2}, Angelo Armandi^{1,3}, Simona Bo¹, Elisabetta Bugianesi^{1,2}. ¹University of Turin, Department of Medical

Sciences, Turin, Italy; ²University Hospital "Città della Salute e della Scienza," Division of Gastroenterology, Turin, Italy; ³University Medical Center of the Johannes Gutenberg-University, Metabolic Liver Disease Research Program, I. Department of Medicine, Mainz, Germany
Email: gabriele.castelnovo@unito.it

Background and aims: Insulin resistance plays a pivotal role in triggering metabolic dysfunction-associated steatotic liver disease (MASLD) and driving its progression. Irisin, a myokine activated by exercise, is involved in energy homeostasis and the modulation of glucose metabolism. This work aims to explore the conceivable association between irisin levels, anthropometric and biochemical variables in patients with MASLD after a 6-month lifestyle intervention.

Method: A total of 49 patients diagnosed with MASLD underwent a comprehensive lifestyle intervention based on nutritional and physical activity recommendations and were evaluated at baseline and after 6 months. Liver steatosis was assessed with the controlled attenuation parameter (CAP) (Fibroscan®530, Echosens), body composition was determined by bioelectrical impedance analysis (BIA 101, Anker), while leptin, adiponectin and irisin levels were measured by Bioplex (LuminexR).

Results: The median age of participants was 55 years (range 45; 63); 67.3 % of participants were male, 24.4 % had diabetes and the baseline median Body Mass Index (BMI) was 31.4 Kg/m². The lifestyle intervention led to significant reduction in BMI ($p < 0.001$), waist and neck circumference ($p < 0.001$ for both), fat mass ($p < 0.001$), systolic and diastolic blood pressure ($p < 0.001$ and $p = 0.004$, respectively), as well as improvement in biochemical parameters, including ALT ($p = 0.002$), AST ($p = 0.005$), GGT ($p = 0.018$), insulin levels ($p = 0.049$), HOMA-IR ($p = 0.026$) and leptin concentrations ($p = 0.002$). Additionally, handgrip score and adiponectin levels increased significantly ($p < 0.001$ and $p = 0.006$, respectively), while both CAP and liver stiffness values decreased significantly after 6 months (316 dB/m vs. 283 dB/m, $p < 0.001$ and 5.2 vs 4.9, $p = 0.017$, respectively). Notably, negative correlations were observed between the changes in irisin levels and CAP levels ($r = -0.372$, $p = 0.008$) and fat mass ($r = -0.323$, $p = 0.025$). Interestingly, at multiple regression analysis, the decrease in steatosis according to CAP levels was associated with an increase in irisin concentrations (beta = 2.3, 95% CI 0.1; 4.4, $p = 0.035$) and a decrease in HOMA-IR (beta = –9.2, 95% CI –15.7; –2.7, $p = 0.007$), independently from age, sex and the change in fat mass.

Conclusion: A 6-month lifestyle intervention in patients with MASLD is associated with a reduction in hepatic steatosis and HOMA-IR, with a potential restoration of energy and glycid homeostasis reflected by an increase in irisin levels. Along with efforts of non-invasive diagnostic approaches, irisin might be a potential biomarker for the diagnosis and prognosis of this disease. This research has been supported by the University of Torino, grant number ROSC_RILO_21_01.

WED-244

The diminished diagnostic accuracy of existing non-invasive tools for significant fibrosis in MASLD patients concurrent with CHB

Wenjing Ni¹, Fajuan Rui¹, Yee Hui Yeo², Youwen Tan³, Liang Xu⁴, Junping Shi⁵, Jie Li⁶. ¹Nanjing Drum Tower Hospital Clinical College of Nanjing University of Chinese Medicine, Nanjing University of Chinese Medicine, Institute of Viruses and Infectious Diseases, Nanjing University, Nanjing, China; ²Cedars-Sinai Medical Center, Los Angeles, United States; ³The Third Hospital of Zhenjiang Affiliated Jiangsu University, School of Medicine, Jiangsu University, Zhenjiang, China; ⁴Clinical School of the Second People's Hospital, Tianjin Medical University, Tianjin Research Institute of Liver Diseases, Tianjin, China; ⁵The Affiliated Hospital of Hangzhou Normal University, Hangzhou, China; ⁶Nanjing Drum Tower Hospital, Affiliated Hospital of Medical

POSTER PRESENTATIONS

School, Nanjing University, Nanjing Drum Tower Hospital Clinical College of Nanjing University of Chinese Medicine, Nanjing University of Chinese Medicine, Nanjing, China
Email: lijier@nju.edu.cn

Background and aims: The new nomenclature of metabolic dysfunction-associated steatotic liver disease (MASLD) has broadened its definition to encompass populations with viral hepatitis. However, the interplay between chronic hepatitis B (CHB) and MASLD and its implications for non-invasive testings (NITs) accuracy remains under-explored. In this study, we determined the diagnostic accuracy of NITs for significant fibrosis leveraging a large cohort of MASLD patients with CHB.

Method: A total of 1079 adult CHB patients with liver biopsy from eleven medical centers were classified into three groups, (A) with hepatic steatosis (HS) only, (B) with MASLD involving 1–3 cardio-metabolic risk factors (CMRFs), and (C) with MASLD involving 4–5 CMRFs. Significant fibrosis was defined as Scheuer's classification ≥ 2 . The corresponding optimal cutoff values for three non-invasive tests (NITs), namely the fibrosis-4 index (FIB-4), aspartate aminotransferase-to-platelet ratio index (APRI), and non-alcoholic fatty liver disease fibrosis score (NFS), were determined to diagnose significant fibrosis (≥ 2) based on CHB combined with HS population (group A). The performance of these NITs was evaluated for area under the curve (AUC), accuracy, sensitivity, specificity, positive predictive value, and negative predictive value across three groups. The AUCs of these NITs in each group were compared using the DeLong test.

Results: The AUC for diagnosing significant fibrosis (≥ 2) was 0.73 in group A, using an optimal cutoff value of 1.26. However, the AUCs were significantly lower in group B (0.62) and group C (0.57). For APRI, the AUCs in the three groups were 0.75, 0.62, and 0.63, respectively, based on an optimal cutoff value of 0.56. The NFS exhibited more modest performance, with AUCs of 0.67, 0.55, and 0.54 in group A, B, and C, respectively. The diagnostic accuracy of the three NITs was all falling below 0.74, with the lowest accuracy observed for FIB-4 at 0.57 in group C. For APRI, the lowest accuracy was 0.63 in both group B and group C. NFS had the lowest accuracy of 0.52 in group B. The overall diagnostic accuracy showed a downward trend with the increased number of CMRFs.

Conclusion: A notable reduction was observed in diagnostic accuracy of the three NITs for significant fibrosis in patients with concomitant MASLD and CHB. Particularly pronounced in patients with an elevated count of CMRFs, this diagnostic gap underscores an urgent need for the development of more refined NIT methodologies. This is especially critical in regions where CHB prevalence is high, signaling a potential shift in clinical strategies for managing these complex patient profiles.

WED-245

Should specific cutoffs be used for diagnosing fibrotic MASH in patients with type 2 diabetes using FAST, MAST, MEFIB and FNI?

Laurent Castera¹, Philippe Garteiser², Cedric Laouenan³, Tiphaine Vidal-Trecan⁴, Anais Vallet Pichard⁵, Pauline Manchon⁶, Valérie Paradis⁷, Sebastien Czernichow⁸, Dominique Roulot⁹, Etienne Larger¹⁰, Stanislas Pol¹¹, Pierre Bedossa¹², Correas Jean Michel¹³, Dominique Valla¹⁴, Jean-François Gautier¹⁵, Bernard van Beers¹⁶. ¹Université Paris Cité, Department of Hepatology, Hospital Beaujon, AP-HP, Clichy, Clichy, France; ²Université Paris Cité, UMR1149 (CRI), Inserm, Paris, France; ³Université Paris Cité, UMR1137 (IAME), Inserm, Paris, France; ⁴Department of Diabetology, Hospital Lariboisière, AP-HP, Paris, France; ⁵Department of Hepatology, Hospital Cochin, AP-HP, Paris, France; ⁶DEBRC, Hospital Bichat, APHP, Paris, France; ⁷Université Paris-Cité, Department of Pathology, Hospital Beaujon, AP-HP, Clichy, France; ⁸Université Paris-Cité, Department of Nutrition, Hospital European Georges Pompidou, Paris, France; ⁹Université Paris Est, Unit of Hepatology, Hospital Avicenne, AP-HP, Bobigny, France; ¹⁰Université Paris-Cité, Department of Diabetology, Hospital Cochin, Paris, France; ¹¹Université Paris-Cité, Department of

Hepatology, Hospital Cochin, AP-HP, Paris, France; ¹²Liverpat, Paris; ¹³Sorbonne Université, Department of adult imaging, Hospital Necker, AP-HP, Paris, France; ¹⁴Université Paris-Cité, Department of Hepatology, Hospital Beaujon, AP-HP, Clichy, France; ¹⁵Université Paris Cité, Department of Diabetology, Hospital Lariboisière, AP-HP, Paris, France; ¹⁶Université Paris-Cité, Department of Radiology, Hospital Beaujon, AP-HP, Clichy, France
Email: laurent.d.castera@gmail.com

Background and aims: Patients with type 2 diabetes (T2D) with fibrotic metabolic dysfunction associated steatohepatitis (MASH) are at the highest risk of progression to complications of cirrhosis and those who should be treated with forthcoming pharmacologic treatments to be approved. Several non-invasive scores, including FAST (FibroScan-AST), MAST (magnetic resonance imaging [MRI]-aspartate aminotransferase [AST]), MEFIB (magnetic resonance elastography [MRE] plus FIB-4), and FNI (fibrotic NASH index) have been proposed to diagnose fibrotic MASH. However, data in patients with T2D are currently lacking and original published cut-offs may not be suited for this population. The aim of this multicenter prospective study was to compare the performances of these scores, using original and specific cutoffs for the diagnosis of fibrotic MASH in patients with T2D.

Method: 245 T2D outpatients with suspected metabolic dysfunction associated steatotic liver disease (MASLD) (ALT >20 IU/L in female and >30 IU/L in male) seen in secondary/tertiary diabetes clinics from the QUID-NASH study (NCT03634098). All had biopsy-proven MASLD, with FibroScan, MRI-PDFF and MRE data at the time of liver biopsy (LB). The main outcome was fibrotic MASH, defined as NAS ≥ 4 (with at least one point each) and fibrosis stage ≥ 2 (centrally reviewed by a single expert pathologist (PB)). The percentages of correctly classified patients (true positive and true negative) were compared using original rule-in and rule-out cutoffs as well as data driven cutoffs determined to have a sensitivity ≥ 0.90 and a specificity ≥ 0.90 with observed distributions for continuous scores (FAST, MAST, FNI) in our population.

Results: The characteristics of the 245 patients were: median age 59 years; male 65%; BMI 31 kg/m²; HbA1c 7.5%; ALT 48 IU/L; fibrotic MASH 39%. FAST and MAST had similar accuracy (AUROCs 0.81 vs. 0.79, $p = 0.41$) but outperformed FNI (0.74; $p = 0.01$) and MEFIB (0.68; $p < 0.0001$). Using original published cutoffs, MAST (0.165/0.242) outperformed FAST (0.35/0.67), MEFIB and FNI (0.10/0.33) when comparing the percentage of correctly classified patients, in whom LB would be avoided (69% vs. 48%, 46%, 39%, respectively; $p < 0.001$). When using cutoffs specific to our T2D population, FAST (0.38/0.64) outperformed FNI (0.47/0.85) and MAST (0.038/0.199) (56% vs. 40%, and 38%, respectively; $p < 0.001$).

Conclusion: Our findings in this large cohort of well-characterized T2D patients suggest that FAST, MAST and FNI, using specific cutoffs, may be useful tools to identify T2D patients who should be prioritized for forthcoming pharmacologic treatments.

WED-246

A non-invasive index for significant liver fibrosis and stratifying risk of cirrhosis in patients with type 2 diabetes mellitus in primary care

Xiaolong Qi¹, Dongfang You², Jie Shen³, Chuan Liu¹, Yuping Chen⁴, Ming-Hua Zheng⁵, Xiqiao Zhou⁶, Mingxing Huang⁷, Xuan Liang⁸, Tianxurun Deng⁹, Chao Sun¹⁰, Xiao Liang¹¹, Yong-Fen Zhu¹², Fangfang Lv¹², Heng Wan¹³, Fenxiang Li¹⁴, Dengxiang Liu¹⁵, Yan Wang⁸, Tang Dong^{16,17}, Xiaoxiong Hu¹⁸, Baiyun Li¹⁹, Yuting Zhang¹⁸, Rong Zhang¹⁴, Jing Du²⁰, Yanan Han¹⁴, Fang Li¹⁴, Xuanzhe Zhang²¹, Wen-Yue Liu²², Yusen Zhou²³, Xinjie Li²³, Youfang Gao²⁴, Lan Ma²⁴, Wenhua Zhang²⁵, Fengmei Wang²⁵, Jinfen Wei²⁵, Chengyu Liu²⁶, Xing Liu²⁷, Shanghao Liu²⁸, Xiaomei Wang²⁹, Jing Wang³⁰, Xianmei Meng³⁰, Jing Hu²⁰, Jinpeng Hu²⁰, Jiaojian Lv³¹, Chuxiao Shao³¹, Ruiling He^{32,33}, Taolong Zhou³⁴, Yijun Tang³⁵, Xuefeng Li³⁶, Min Li³⁶, Junwei Cai³⁶,

Yuwei Zhang³⁷, Liu Wang³⁷, Qing Shao³⁸, Yuehua Wang³⁹, An Zhou³⁹, Xiaoming Wu³⁹, Wenjing Ni⁴⁰, Jie Li⁴¹, Ling Li⁴², Zhihui Li⁴³, Wannian Liang⁴³, Weimin Jiang⁴⁴, Yang Zhao⁴⁵, Lixin Guo⁴⁶, Vincent Wai-Sun Wong⁴⁷, Gao-Jun Teng⁴⁸. ¹Center of Portal Hypertension, Department of Radiology, Zhongda Hospital, Medical School, Southeast University, Nanjing, China; ²Department of Biostatistics, School of Public Health, Nanjing Medical University, Nanjing, China; ³Department of Endocrinology and Metabolism, Shunde Hospital, Southern Medical University (The First People's Hospital of Shunde), Foshan, China; ⁴Center of Portal Hypertension, Department of Radiology, Zhongda Hospital, Medical School, Southeast University, Nanjing, China; ⁵MAFLD Research Center, Department of Hepatology, The First Affiliated Hospital of Wenzhou Medical University, Wenzhou, China; ⁶Department of Endocrinology, Affiliated Hospital of Nanjing University of Chinese Medicine, Jiangsu Province Hospital of Chinese Medicine, Nanjing, China; ⁷Department of Infectious Diseases, Fifth Affiliated Hospital of Sun Yat-sen University, Zhuhai, China; ⁸The Sixth People's Hospital of Shenyang, Shenyang, China; ⁹Department of Biostatistics, School of Public Health, Nanjing Medical University, Nanjing, China; ¹⁰Department of Gastroenterology and Hepatology, Tianjin Medical University General Hospital, Tianjin, China; ¹¹Key Laboratory of Laparoscopic Technology of Zhejiang Province, Department of General Surgery, Sir Run-Run Shaw Hospital, Zhejiang University School of Medicine, Hangzhou, China; ¹²Department of Hepatology and Infection, Sir Run Run Shaw Hospital, Zhejiang University School of Medicine, Hangzhou, China; ¹³Department of Endocrinology and Metabolism, Shunde Hospital, Southern Medical University (The First People's Hospital of Shunde), Foshan, China; ¹⁴Department of Hepatology, Linfen Third People's Hospital, Linfen, China; ¹⁵Department of Oncology, Affiliated Xingtai People Hospital of Hebei Medical University, Xingtai, China; ¹⁶Inner Mongolia Institute of Digestive Diseases, The Second Affiliated Hospital of Baotou Medical College, Baotou, China; ¹⁷Inner Mongolia University of Science and Technology, Baotou, China; ¹⁸Department of Hepatology, The People's Hospital of Yichun City, Yichun, China; ¹⁹Department of Endocrinology, The People's Hospital of Yichun City, Yichun, China; ²⁰Department of Endocrinology, Ningxia Hui Autonomous Region People's Hospital, Ningxia, China; ²¹Department of General Surgery, Renmin Hospital of Wuhan University, Wuhan, China; ²²Department of Endocrinology, The First Affiliated Hospital of Wenzhou Medical University, Wenzhou, China; ²³Department of Endocrinology, Bozhou People's Hospital, Bozhou, China; ²⁴Department of Infection, Bozhou People's Hospital, Bozhou, China; ²⁵Hepatobiliary Center, Gansu Wuwei Tumor Hospital, Wuwei, China; ²⁶Graduate school of Hebei Medical University, Shijiazhuang, China; ²⁷The Sixth People's Hospital of Shenyang, Shenyang, China; ²⁸The First Clinical Medical College of Lanzhou University, Lanzhou, China; ²⁹Department of Endocrinology, The Sixth People's Hospital of Shenyang, Shenyang, China; ³⁰Inner Mongolia Institute of Digestive Diseases, The Second Affiliated Hospital of Baotou Medical College, Inner Mongolia University of Science and Technology, Baotou, China; ³¹Department of Infectious Diseases, Lishui People's Hospital, Lishui, China; ³²Department of Ultrasound, Donggang Branch the First Hospital of Lanzhou University, Center of Co-management of Diabetes-Liver Diseases, Zhuhai Third People's Hospital, Lanzhou, China; ³³The First Clinical Medical College of Lanzhou University, Lanzhou; ³⁴Center of Co-management of Diabetes-Liver Diseases, Zhuhai Third People's Hospital, Zhuhai, China; ³⁵Taihe Hospital, Hubei University of Medicine, Taihe, China; ³⁶Department of Endocrinology, Taihe Hospital, Hubei University of Medicine, Taihe, China; ³⁷Department of Endocrinology and Metabolism, West China Hospital of Sichuan University, Center for Diabetes and Metabolism Research, West China Hospital of Sichuan University, Sichuan, China; ³⁸Department of Endocrinology and Metabolism, West China Hospital of Sichuan University, Chengdu, Center for Diabetes and Metabolism Research, West China Hospital of Sichuan University, Sichuan, China; ³⁹Jinhua People's Hospital, Jinhua, China; ⁴⁰Department of Infectious Disease, Nanjing Drum Tower Hospital Clinical College of Nanjing University of Chinese Medicine, Nanjing, China; ⁴¹Department of Infectious Disease, Nanjing

Drum Tower Hospital Clinical College of Nanjing University of Chinese Medicine, Department of Infectious Diseases, Nanjing Drum Tower Hospital, Affiliated Hospital of Medical School, Nanjing University, Nanjing, China; ⁴²Department of Endocrinology, Zhongda Hospital, School of Medicine, Southeast University, Institute of Glucose and Lipid Metabolism, Southeast University, Nanjing, China; ⁴³Vanke School of Public Health, Tsinghua University, Institute for Healthy China, Tsinghua University, Beijing, China; ⁴⁴Department of Infectious Diseases, Huashan Hospital, Fudan University, Shanghai, China; ⁴⁵Department of Biostatistics, School of Public Health, Nanjing Medical University, Basic Medicine Research and Innovation Center of Ministry of Education, Zhongda Hospital, Southeast University, Nanjing, China; ⁴⁶Department of Endocrinology, Beijing Hospital, National Center of Gerontology, Institute of Geriatric Medicine, Chinese Academy of Medical Sciences, Beijing, China; ⁴⁷Medical Data Analytics Center, Department of Medicine and Therapeutics, The Chinese University of Hong Kong, State Key Laboratory of Digestive Disease, Institute of Digestive Disease, The Chinese University of Hong Kong, Hongkong, China; ⁴⁸Center of Interventional Radiology and Vascular Surgery, Department of Radiology, Zhongda Hospital, Medical School, Southeast University, Basic Medicine Research and Innovation Center of Ministry of Education, Zhongda Hospital, Southeast University, Nanjing, China
Email: qixiaolong@vip.163.com

Background and aims: To propose a non-invasive index for detecting patients with type 2 diabetes mellitus (T2DM) at risk of significant liver fibrosis and cirrhosis in primary care and indicating these patients to further consult a hepatologist in secondary care.

Method: A total of 38, 160 adults with T2DM were included. Among them, 2, 154 patients (50.0% male), with a mean (standard deviation, SD) age of 52.5 (12.2) years, receiving transient elastography (TE) from the primary care between January 2021 and August 2023 were enrolled to develop and validate a non-invasive index. The accuracy of the proposed index followed by TE in diagnosing significant liver fibrosis was assessed in a liver biopsy-proven cohort of 241 patients (59.3% male), with a mean (SD) age of 46.0 (12.3) years, who were enrolled in the same period. In addition, 35, 765 patients (59.8% male), with a mean (SD) age of 59.8 (7.1) years, from the UK Biobank dataset between 2006 and 2010 were tested for the utility of the index in predicting the development of cirrhosis.

Results: Independent risk factors including Aspartate transaminase and body mass index were identified and fitted to develop a non-invasive index, termed the ADD index (available at: https://chess.nuist.edu.cn/consult/gzconsult/add_index). Using TE as the reference, the ADD index performed better than fibrosis-4 index (FIB-4) and non-alcoholic fatty liver disease fibrosis score (NFS) for significant liver fibrosis, with an area under the curve (AUC) of 0.75 [95% confidence interval (CI): 0.69–0.80], 0.78 [95% CI: 0.70–0.86], and 0.78 [95% CI: 0.74–0.82], in the derivation and two validation cohorts. A cutoff of 0 of the ADD index was selected to stratify patients into low-risk and high-risk group that should receive TE. The AUC of the ADD index followed by TE was significantly higher than that of FIB-4 and NFS followed by TE in predicting significant liver fibrosis proven by liver biopsy, with the AUC of 0.75 [95% CI: 0.68–0.81] vs. 0.59 [95% CI: 0.52–0.65] and 0.59 [95% CI: 0.51–0.67] (all $p < 0.01$), respectively. Notably, using the ADD index combined with TE resulted in 11% cost savings compared to use TE alone to diagnose significant liver fibrosis. Compared with patients in low-risk group, those in high-risk group had a 2.90-fold (95% confidence interval: 1.44–5.82, $p < 0.01$) risk of developing cirrhosis.

Conclusion: The non-invasive ADD index can be applied to screen significant liver fibrosis and cirrhosis in patients with T2DM in primary care, and promoting those in high-risk group to further consult a hepatologist in secondary care.

POSTER PRESENTATIONS

WED-247

Unravelling metabolic dysfunction-associated steatotic liver disease with a Bayesian network approach in the UK biobank

Benjamin P.M. Laevens¹, Yazhou Chen¹, Jan Clusmann¹, Carolin V. Schneider¹. ¹Uniklinik RWTH Aachen, Aachen, Germany
Email: blaevens@ukaachen.de

Background and aims: Data-driven Bayesian methods can be used to augment current understanding of disease development and progression, especially in the context of Metabolic dysfunction-associated steatotic liver disease (MASLD). Using a Bayesian network approach, we characterise (causal) relationships between 30 standard blood biomarkers and steatosis, using 35, 000 participants in the UK Biobank and contrast these with physician drawn networks.

Method: A Random Forest Classifier (RFC), enhanced by grid search hyperparameter tuning and validated through 5-fold cross validation, identifies the eight most important serum parameters that can differentiate between a binary target variable indicating healthy (<5% proton density fat fraction) or steatotic livers (>5%). These blood biomarkers are fed into a Hill Climb Search optimisation algorithm, which searches for the best fitting Bayesian network, scored according to the Akaike Information Criterion, a well known model selection measure. Thus, the favoured network, which best describes the data and the dependencies within them, is selected.

Results: The optimal RFC reveals SHBG, triglycerides, ALT, HDL cholesterol, C-reactive protein, GGT, apolipoprotein A and cystatin C as having the highest predictive value for MASLD (with an ROC AUC of 80% in the training set). The best network structure is characterised by 13 (causal) dependencies. Triglycerides, HDL cholesterol and SHBG point towards MASLD, whereas the remaining biomarkers, such as Cystatin C and ALT, point away from MASLD (i.e. a result of) or are connected more distantly to MASLD (Apolipoprotein A, C-reactive protein and GGT). The Bayesian network displays fewer connections between all the variables, when compared to unbiased physician drawn networks of MASLD, which display 18 strong dependencies. On a global level, the Bayesian and physician drawn networks look similar. Nevertheless, differences on a more detailed level reveal differences in prominence of some biomarkers (e.g. HDL cholesterol) and how they connect to MASLD and other parameters.

Conclusion: The strength of Bayesian Networks is their explainable and intuitive nature. By determining dependencies between serum parameters and disease, insights are obtained that can be used as an additional tool to complement physician-based views of MASLD.

WED-248

A four-country modelling study on doubling MASH diagnostic rates by 2027

Jeffrey V Lazarus¹, Henry E Mark¹, William Alazawi², Alina M Allen³, Paul N Brennan⁴, Chris D Byrne⁵, Laurent Castera⁶, Cyrielle Caussy⁷, Kenneth Cusi⁸, Martin M Grajower⁹, Morten Faarbæk Mikkelsen¹⁰, Michael Roden¹¹, Frank Tacke¹², Mazen Nouredin¹³. ¹Barcelona Institute for Global Health (ISGlobal), Hospital Clínic, University of Barcelona, Barcelona, Spain; ²Barts Liver Centre, Blizard Institute, Queen Mary University of London, London, United Kingdom; ³Division of Gastroenterology and Hepatology, Department of Medicine, Mayo Clinic, Rochester, MN, United States; ⁴Division of Molecular and Clinical Medicine, Ninewells Hospital and Medical School, University of Dundee, Dundee, United Kingdom; ⁵Human Development and Health, Faculty of Medicine, University of Southampton, Southampton, United Kingdom; ⁶Université Paris Cité, Department of Hepatology, Hospital Beaujon, AP-HP, Clichy, Clichy, France; ⁷Endocrinology Diabetes Nutrition Hospices Civils de Lyon, Lyon, France; ⁸Division of Endocrinology, Diabetes and Metabolism, Department of Medicine, University of Florida, Gainesville, United States; ⁹Division of Endocrinology, Department of Medicine, Albert Einstein College of Medicine, New York, United States; ¹⁰Novo Nordisk, Copenhagen, Denmark; ¹¹Department of Endocrinology and Diabetology, Medical Faculty and University Hospital Düsseldorf, Heinrich Heine University, Düsseldorf, Germany; ¹²Department of

Hepatology and Gastroenterology, Charité-Universitätsmedizin Berlin, Berlin, Germany; ¹³Houston Methodist Hospital, Houston Research Institute, Houston, United States
Email: Jeffrey.Lazarus@isglobal.org

Background and aims: With high and increasing prevalence, but low diagnosis rates, identifying people living with MASH who require specialised care remains a significant challenge. Advances in the validation of non-invasive tests (NITs) promise to revolutionise diagnostic pathways. However, little focus has been given to operational considerations for implementing viable, scalable diagnostic pathways for MASH. We developed a model to estimate the testing requirements to double the diagnostic rates of \geq F2 MASH over a 5-year period in 4 countries.

Method: The baseline (2021) prevalence of \geq F2 MASH in the general population and the diagnostic rates, defined as the cumulative proportion of all MASH patients diagnosed with \geq F2 MASH at the end of a given year, were, respectively (%): France 2.9/14.0; Germany 2.6/11.0; UK 2.9/17.0; and USA 4.0/12.5. Using multiple data sources, we constructed diagnostic pathways covering identification (i.e. abnormal LFTs), screening (e.g. FIB-4, NAFLD-Fibrosis Score) and confirmatory diagnosis (e.g. Fibroscan, ELF, biopsy). A weighted average sensitivity and specificity was used for each stage in the pathway depending on the proportion of different NITs used. The model incorporated 5 healthcare settings (primary care, non-liver office (e.g. endocrinologist office), non-liver hospital (e.g. endocrinologist clinic), liver-office, and liver-hospital) and four patient pools (symptom-led presentation, obesity, type 2 diabetes, and cardiovascular disease). We accounted for annual growth in the general population and MASH prevalence. Bottlenecks in provider capacity across healthcare settings were estimated and future testing requirements adjusted accordingly.

Results: A doubling of the diagnostic rates of \geq F2 MASH across the four countries will result in the number of diagnosed patients increasing from 2.6 million (M) to 6.1M between 2022–2027, with the following breakdown by patient pool: 54% type 2 diabetes, 19% obesity, 18% CVD and 9% symptom-led presentations. This will require the number of screening tests to increase from 2.2M to 35.6M, and confirmatory diagnosis tests from 833, 000 to 11.6M between 2022 and 2027. To address capacity bottlenecks, the proportion of confirmatory diagnostic tests completed within liver specific settings must decrease from 95% in 2022 to 29% in 2027, with an increase from 1% to 27% in primary care setting and 4% to 34% in non-liver office and non-liver hospital settings over the same time.

Conclusion: Doubling the diagnosis rate of \geq F2 MASH by 2027 will require enormous expansion of diagnostic pathways. This necessitates a paradigm shift and greater collaboration across disciplines, with much of the testing burden moving from liver specialists to primary care and non-liver specialist settings. Identifying efficient approaches to reduce the operational burden and costs of this expansion will be key for success.

WED-249

Improved risk stratification by combination of FIB-4 with FGF21 serum levels in steatotic liver disease

Martin Franck¹, Katharina John¹, Sherin Al Aoua¹, Monika Rau², Andreas Geier², Jörn Schattenberg³, Heiner Wedemeyer¹, Klaus Schulze-Osthoff⁴, Heike Bantel¹. ¹Department of Gastroenterology, Hepatology, Infectious Diseases and Endocrinology, Hannover Medical School, Hannover, Germany; ²Division of Hepatology, Department of Internal Medicine II, University Hospital Würzburg, Würzburg, Germany; ³Department of Internal Medicine I, University Medical Center Mainz, Mainz, Germany; ⁴Interfaculty Institute of Biochemistry, University of Tübingen, Tübingen, Germany
Email: bantel.heike@mh-hannover.de

Background and aims: Non-alcoholic steatohepatitis (NASH) with significant fibrosis (\geq F2) represents a major prognostic factor in non-alcoholic fatty liver disease (NAFLD). Identification of patients at risk

for NASH with fibrosis $\geq F2$ is therefore important. Although the established fibrosis score FIB-4 is suitable to exclude advanced fibrosis, it does not allow the prediction of significant fibrosis in NAFLD patients. We therefore analysed whether fibroblast growth factor 21 (FGF21), a stress-inducible metabolic regulator, can be used as a non-invasive marker to identify at risk patients in NAFLD.

Method: We analysed FGF21 levels in sera from a retrospective multicenter cohort ($n=225$) of biopsy-proven NAFLD patients with different disease activity and fibrosis stages by enzyme-linked immunosorbent assay. Most of these patients met also the criteria of the new nomenclature metabolic dysfunction-associated steatotic liver disease (MASLD). We evaluated whether the use of FGF21 in patients with low (<1.3) or intermediate ($1.3-2.67$) FIB-4 could improve risk stratification in NAFLD. In addition, we analyzed the diagnostic performance of FIB-4 in combination with FGF21 or transient elastography (TE) for the detection of NASH and fibrosis.

Results: FGF21 levels could significantly discriminate between NASH with fibrosis $\geq F2$ and NAFLD patients without significant fibrosis, even in patients with low or intermediate FIB-4. We calculated a cut-off value for FGF21 which allowed an improved risk stratification of NAFLD patients with low or intermediate FIB-4. NASH could be detected in patients with low FIB-4 and elevated FGF21 levels in 81% of cases, whereas patients with low FIB-4 and increased TE values (≥ 8 kPa) showed NASH in 75% of cases. Moreover, fibrotic NASH was detected in patients with low FIB-4 and elevated FGF21 levels or TE values in 49% and 54%, respectively, half of them had fibrosis stages $\geq F2$. NAFLD patients with intermediate FIB-4 and elevated FGF21 levels or TE values revealed NASH in almost all cases. Fibrotic NASH was detected in patients with intermediate FIB-4 and elevated FGF21 or TE (≥ 8 kPa) values in 71% versus 75% of cases, the majority of them revealed fibrosis stages $\geq F2$. Due to the higher sensitivity of FGF21 compared with TE, less patients were overlooked for fibrotic NASH when FIB-4 was combined with FGF21 instead of TE.

Conclusion: The combination of FIB-4 with serological FGF21 detection might be useful for the identification of patients at risk for progressed NAFLD, especially in primary care when TE is not available.

WED-250-YI

PNPLA3 I148M a useful diagnostic marker for significant fibrosis metabolic dysfunction-associated steatotic liver disease

Elias Rashu¹, Mikkel Werge², Mira Thing², Liv Hetland², Puria Nabilou², Nina Kimer², Anne-Sofie Houlberg Jensen², Anders Junker², Stefan Stender^{3,4}, Lise Lotte Gluud^{2,4}. ¹Gastro Unit, Copenhagen University Hospital Hvidovre, Denmark, Hvidovre, Denmark; ²Gastro Unit, Copenhagen University Hospital Hvidovre, Hvidovre, Denmark; ³Department of Clinical Biochemistry, Rigshospitalet, Copenhagen, Denmark; ⁴Department of Clinical Medicine, Faculty of Health and Medical Sciences, University of Copenhagen, Copenhagen, Denmark
Email: elias.badal.rashu@regionh.dk

Background and aims: Three common genetic variants are known to affect the onset and progression of metabolic dysfunction associated steatotic liver disease (MASLD): *PNPLA3* rs738409, *TM6SF2* rs58542926, and *HSD17B13* rs72613567. We tested if the use of these three variants, alone or combined into a genetic risk score (GRS), can be used in a clinical setting to identify significant fibrosis.

Method: Patients were included in a prospective observational cohort at the Gastro Unit, Hvidovre Hospital, Denmark. In total, 710 patients were evaluated clinically, biochemically, and with Fibroscan. MASLD was defined by the presence of steatosis on Fibroscan (CAP value >250 dB/m), without increased alcohol intake, at least one cardiometabolic risk factor, and exclusion of other liver diseases. A liver biopsy was performed if significant fibrosis was suspected ($\geq F2$) based on the Fibroscan and/or Fibrosis-4 (Fib-4) index. The GRS was calculated as the total number of risk-increasing alleles in the *PNPLA3*, *TM6SF2*, and *HSD17B13* variants (range: from 0 to 6).

Results: Of the 710 patients (50.0 % women, mean age: 54.1 years, mean BMI: 31.2 kg/m²). Significant fibrosis was diagnosed in 149 of 360 who underwent a liver biopsy. The risk of significant fibrosis increased with the number of *PNPLA3* G-alleles; compared to CC homozygotes, CG-heterozygotes had an odds ratio (OR) of 2.38 (95% CI 1.50–3.82, $p=0.0003$) and GG-homozygotes had an OR of 2.51 (95% CI 1.29–4.95 $p=0.007$). The *PNPLA3* G-allele was also associated with the Fib-4 ($p=0.006$) and Fibroscan ($p=0.011$). The variants in *TM6SF2* and *HSD17B13* were not individually associated with fibrosis. None of the individual SNPs predicted cirrhosis. The GRS was associated with an increased risk of significant fibrosis (OR 1.63 (95% CI 1.28–2.04, $p=0.00005$) and cirrhosis (OR 1.42 (95% CI 1.05–1.96, $p=0.03$).

Conclusion: This study found that the *PNPLA3* variant, as well as a 3-variant GRS, were associated with significant fibrosis in MASLD patients. Our findings suggest that these genetic risk factors may hold promise for prediction of significant fibrosis in MASLD patients in a clinical setting.

WED-251

Plasma lipidomic profiling of subjects with overweight or obesity following treatment with the glucagon-like peptide 1/glucagon dual receptor agonist pemvidutide: an investigation of lipid signatures associated with metabolic dysfunction-associated steatohepatitis

John Suschak¹, Bertrand Georges¹, Sarah Browne¹, Cristina Alonso², M. Scot Roberts¹, M. Scott Harris¹. ¹Altimmune, Inc, Gaithersburg, United States; ²OWL Metabolomics, Derio, Spain
Email: jsuschak@altimmune.com

Background and aims: Subjects with metabolic dysfunction-associated steatohepatitis (MASH) frequently have dysregulated serum lipid profiles that can result in increased hepatic and systemic inflammation, exacerbating comorbidities such as cardiovascular disease. Pemvidutide is a long-acting, balanced glucagon-like peptide 1 (GLP-1)/glucagon dual receptor agonist under development for the treatment of MASH and obesity. The balanced 1:1 potency ratio combines the reduced caloric intake effects of GLP-1 receptor agonism with the increased energy expenditure and lipometabolic effects of glucagon receptor agonism. In a 12-week double-blind clinical trial in subjects with overweight/obesity, pemvidutide reduced body weight by up to 10.3% and significantly decreased multiple atherosclerotic lipid mediators such as total cholesterol (-28%), LDL-C (-26%), and triglycerides (-38%). Here we leveraged lipidomics to further investigate the effects of pemvidutide on lipid mediators associated with MASH.

Method: 34 subjects with overweight (BMI 27.0–29.9 kg/m²) or obesity (BMI >30.0 kg/m²) were randomized 1:1:1 to pemvidutide (1.2 mg, 1.8 mg, 2.4 mg) or placebo administered subcutaneously weekly for 12 weeks. Lipidomic profiling covering lipid species across classes of glycoproteins, bile acids, glycerophospholipids, and sphingolipids was performed by ultra-high performance liquid chromatography-mass spectrometry or nuclear magnetic resonance on plasma samples at baseline, Day 43, and Day 84.

Results: Pemvidutide treatment reduced several plasma biomarkers of MASH. Pemvidutide achieved significant reductions from baseline across multiple glycerophospholipid classes associated with MASH, including lysophosphatidylcholines (Lyso-PC) and lysophosphatidylethanolamines (Lyso-PE). Pemvidutide also improved bile acid dysregulation, yielding reductions in taurine and glycine conjugated bile acids. Finally, pemvidutide treatment reduced GlycA and GlycB, composite biomarkers of systemic inflammation correlated with cardiovascular disease.

Conclusion: Pemvidutide administered weekly for 12 weeks induced significant decreases in MASH associated lipid species. These findings support pemvidutide's potential benefit on MASH-associated comorbidities, including atherosclerosis and metabolic syndrome.

WED-254

The true diagnostic performance of magnetic resonance elastography for the detection of advanced fibrosis in metabolic dysfunction-associated steatotic liver disease exceeds the diagnostic performance of liver biopsy

Ian Rowe^{1,2}, Mohsen Farzi¹, Clare McGenity¹, Alyn Cratchley², Alexander Wright², Richard Parker², Darren Treanor^{1,2}. ¹Department of Pathology and Data Analytics, Leeds Institute for Medical Research, University of Leeds, Leeds, United Kingdom; ²Leeds Teaching Hospitals NHS Trust, Leeds, United Kingdom
Email: i.a.c.rowe@leeds.ac.uk

Background and aims: Liver biopsy is recognised as an imperfect reference standard for the assessment of liver fibrosis in metabolic dysfunction-associated steatotic liver disease (MASLD). We aimed to describe the diagnostic accuracy of liver histology for the identification of advanced fibrosis and used this estimate to define the true diagnostic performance of non-invasive biomarkers of fibrosis.

Method: A diagnostic accuracy study of liver biopsy where the reference standard was a liver resection sample was done. Sections were stained with picosirius red for fibrosis area estimation. Sections were divided into 2.5 mm × 1 mm tiles and virtual biopsies between 17.5 and 22.5 mm in length generated. The diagnostic performance of these virtual liver biopsies was then estimated from variation in fibrosis area between known fibrosis stages in silico using individuals drawn from a 100,000 simulated patient cohort. The true performance of non-invasive biomarkers was calculated using apparent biomarker performance (drawn from a recent systematic review and diagnostic test meta-analysis) and the estimated diagnostic accuracy of liver biopsy. All diagnostic performance was assessed where the target condition was advanced fibrosis.

Results: 694 virtual biopsies were assessed. The area under the curve (AUC) for liver biopsy in the identification of advanced fibrosis was 0.93 (range 0.86–0.95), with a mean sensitivity of 0.82 and mean specificity of 0.94. Using this value to estimate true non-invasive test performance led to improvements in performance for imaging biomarkers. For all biomarkers, higher AUC and sensitivity and specificity values for the identification of advanced fibrosis were apparent once the imperfect reference standard was considered. For magnetic resonance elastography the calculated true performance for the detection of advanced fibrosis was as follows: mean AUC 0.97, mean sensitivity 0.97, mean specificity 0.95; all more than the values observed for the performance of liver biopsy. Vibration controlled transient elastography (VCTE, AUC 0.90) and P-shear wave elastography (P-SWE, AUC 0.92) had calculated true performance that was similar to liver biopsy.

Conclusion: Liver biopsy is an imperfect reference standard. Describing its diagnostic accuracy allows the calculation of true non-invasive biomarker performance. MRE has calculated diagnostic performance that is superior to that of liver biopsy while the performance of VCTE and P-SWE is similar to that of liver biopsy. This suggests that imaging biomarkers are sufficiently accurate to replace liver biopsy for the assessment of liver fibrosis in persons with MASLD.

WED-255-YI

Muscle composition as a predictor of advanced fibrosis in chronic liver disease

Wile Balkhed¹, Patrik Nasr¹, Mikael Forsgren^{1,2}, Anna Cederborg^{1,3}, Olof Dahlqvist Leinhard^{2,4}, Simone Ignatova⁵, Peter Lundberg⁶, Nils Dahlström⁷, Christian Simonsson⁸, Stergios Kechagias¹, Mattias Ekstedt¹. ¹Linköping University, Department of Health, Medicine and Caring Sciences, Linköping, Sweden; ²AMRA Medical AB, Linköping, Sweden; ³Sahlgrenska Academy, University of Gothenburg, Department of Medicine, Sahlgrenska University Hospital, Göteborg, Sweden; ⁴Linköping University, Department of Health, Medicine and Caring Sciences, Center for Medical Image Science and Visualization, Linköping, Sweden; ⁵Linköping University, Linköping, Sweden;

⁶Linköping University, Radiation Physics and MR-Physics, Radiology and Center for Medical Imaging and Visualization, Linköping, Sweden;

⁷Linköping University, Department of Radiology in Linköping, Department of Health, Medicine and Caring Sciences, Center for Medical Image Science and Visualization, Linköping, Sweden; ⁸Linköping University, Department of Radiation Physics, Department of Health, Medicine and Caring Sciences, Center for Medical Image Science and Visualization, Department of Biomedical Engineering, Linköping, Sweden

Email: balkhedwile@gmail.com

Background and aims: Sarcopenia and myosteatosis is common in patients with advanced liver disease but associations between muscle degeneration and early-stage liver disease have not been established. We aimed to investigate the relevance of these muscle-related factors at the investigational stage of chronic liver disease.

Method: Patients investigated for liver disease underwent a liver biopsy as well as a neck-to-knee MRI, including liver proton density fat fraction (PDFF) and muscle composition (MC) assessment (thigh muscle fat infiltration [MFI] and fat-free muscle volume z-score [MVZ]) using AMRA[®] Researcher. MC phenotypes were defined as high MFI (myosteatosis), low MVZ (low muscle volume), adverse MC (AMC) i.e., high MFI and low MVZ combined, or normal MC.

Results: Seventy-seven patients were studied. Thirty-one (40 %) were women and mean age and BMI were 58 ± 13 years and 30.9 ± 5.2 kg/m², respectively. Type 2 diabetes was present in 27 (35 %) and the most common etiology was metabolic dysfunction-associated steatotic liver disease (MASLD) in 47 cases (61 %) and MetALD in 8 cases (10 %). Median fibrosis stage was 2 (range, 0–4) and 28 (36 %) patients had advanced fibrosis (≥F3). Forty-seven (61 %) patients had normal MC, 16 (21 %) low MVZ and 24 (31 %) had high MFI. Thus 10 (13 %) had both low MVZ and high MFI (AMC). MVZ had a negative correlation to fibrosis stage ($r = -0.237$, $p = 0.038$) while MFI had a positive correlation ($r = 0.284$, $p = 0.012$). Patients with advanced fibrosis had lower MVZ (-0.26 ± 0.99 vs 0.68 ± 1.33 , $p < 0.001$) and higher MFI (1.72 ± 3.43 vs -0.08 ± 2.12 , $p = 0.012$) compared to patients without advanced fibrosis. Regression analysis of factors predicting advanced fibrosis found low MVZ, irrespective of MFI-status, to be predictive of advanced fibrosis. This was confirmed when adjusting for sex, T2D status and BMI (aOR 5.19, 95 %CI 1.39–19.36; $p = 0.014$). However, adding age to the adjusted model attenuated the predictability of the analysis (aOR 2.57, 95 %CI 0.63–10.52, $p = 0.190$). There were no significant differences in rates of advanced fibrosis comparing patients with or without high MFI or AMC.

Conclusion: Muscle health correlated to fibrosis stage in this cohort of patients under investigation for chronic liver disease. Low MVZ but not high MFI was predictive of advanced fibrosis. However, this relationship did not reach the threshold for significance when adjusting for age. Our findings suggest muscle degeneration could be used as a clinical marker for identifying advanced liver disease.

WED-256

The influence of rifaximin on bile acids composition

Iryna Biriuchenko¹, Olena Barabanchyk². ¹Bogomolet National Medical University, Kyiv, Ukraine; ²Educational and Scientific Center "Institute of Biology and Medicine" of Taras Shevchenko National University of Kyiv, Kyiv, Ukraine
Email: iryna.gastro@gmail.com

Background and aims: Due to some recent publications, intestinal bacteria play a crucial role in the pathogenesis and progression of Metabolic dysfunction-associated hepatitis (MASH) in patients with metabolic dysfunction-associated steatotic liver disease (MASLD), making gut microbiota a potential target for MASH treatment [1]. Rifaximin is a non-systemic selective antibiotic that has almost no absorption into the blood with less adverse reaction, although the full effect of rifaximin on gut flora remains limited. Our hypothesis was whether rifaximin modulation properties on gut flora may have impact on bile acids (BA) composition. Our aim was to assess the

spectrum of bile acids before and after modulation of intestinal flora using rifaximin.

Method: The diagnosis of MASH was established due to the following criteria on the basis of EASL (2016) NAFLD Guidelines. The eligible patients formed the main study group. To compare, we took the results of bile examination of healthy controls, performed during our previous study in 2022 [2]. The bile was obtained after intubation of the duodenum under the ultrasound control. The spectrum of BA was assessed using photocalorimetry. For the modulation of gut flora rifaximin was administered 400 mg 3 times per day for 10 days. The bile composition in the patients of the first group was assessed twice: before and 8 weeks after rifaximin treatment. The data were analysed using parametric and non-parametric methods through StatSoft Statistica program (USA).

Results: 12 adult patients were included into the study. The results of 15 healthy controls formed the second group. The groups were statistically comparable in age and sex. The levels of cholic acid (CA) and deoxycholic acid (DCA) were increased in patients with MASH comparing to healthy controls ($p < 0.05$). Both BA decreased after rifaximin use, especially DCA fast reaching the level of healthy controls ($p < 0.001$). The levels of taurodeoxycholic acid (TDCA) and glycocholic acid (GCA) were not changed significantly comparing to healthy controls either before or after interference with bacteria ($p > 0.05$).

Conclusion: Our study demonstrates the possibility of rifaximin to influence on bile acids composition shortly after application through decreasing the levels of metabolic byproduct DCA and increasing the concentration of CA. We suppose, that because the diet preferences of the patients were not changed/modified after the treatment, the levels of TDCA and GCA were not altered significantly 8 weeks after. This allows to assume that intestinal flora modulation may be a potential target for MASH treatment.

WED-257

FibroScan compared to liver biopsy for accurately detecting recurrent hepatic steatosis and fibrosis after liver transplantation for metabolic dysfunction-associated steatohepatitis

Laura Martínez-Arenas^{1,2,3}, Ângela Carvalho-Gomes^{1,3}, Carmen Vinaixa^{1,3,4}, Isabel Conde^{1,4}, Judith Pérez-Rojas⁴, Eva Montalvá^{1,3,4,5}, Sara Lorente Perez^{6,7,8}, Fernando Diaz Fontela⁹, Marta Guerrero-Misas^{3,10,11}, Jose Ignacio Herrero^{3,12,13}, Marina Berenguer^{1,3,4,5}. ¹IIS La Fe Health Research Institute, Valencia, Spain; ²Universitat Politècnica de València, Valencia, Spain; ³CIBEREHD, Madrid, Spain; ⁴La Fe Hospital, Valencia, Spain; ⁵University of Valencia, Valencia, Spain; ⁶Lozano Blesa Hospital, Zaragoza, Spain; ⁷IIS Aragón, Zaragoza, Spain; ⁸University of Zaragoza, Zaragoza, Spain; ⁹Gregorio Marañón Hospital, Madrid, Spain; ¹⁰Reina Sofia Hospital, Córdoba, Spain; ¹¹Maimonides Institute of Biomedical Research of Cordoba, Córdoba, Spain; ¹²University Clinic of Navarra, Pamplona, Spain; ¹³Navarra Health Research Institute, Pamplona, Spain
Email: laura_munera15@hotmail.com

Background and aims: Metabolic dysfunction-associated steatotic liver disease (MASLD) recurrence after liver transplantation (LT) seems unavoidable and gradual in many patients. We aimed to compare the accurate detection of recurrent hepatic steatosis and fibrosis by vibration-controlled transient elastography (FibroScan) versus liver biopsy during the follow-up of patients transplanted for metabolic dysfunction-associated steatohepatitis (MASH).

Method: This prospective cohort study included adult patients transplanted for MASH between 2010–2022 in 2 LT centers in Spain who underwent both FibroScan and liver biopsy at least one year after LT. Hepatic steatosis and fibrosis were assessed by control attenuation parameter (CAP) and liver stiffness measurement (LSM), respectively. CAP values >275 dB/m were used to diagnose significant steatosis. LSM values <8 kPa and >12 – 15 kPa were used to rule out and rule in advanced fibrosis, respectively. Steatosis and fibrosis evaluation in the graft was performed according to the MASH Clinical Research

Network criteria. MASH diagnosis was defined as a SAF (steatosis, activity and fibrosis) activity score ≥ 2 . Significant and advanced fibrosis were defined as a fibrosis stage $\geq F2$ and $\geq F3$, respectively.

Results: 38 patients transplanted for MASH ($n = 18$ [47.4%] categorized as having MASLD and alcohol-related fatty liver disease) with FibroScan and liver biopsy (89% performed as a protocol biopsy) after LT were included. The median time (interquartile range [IQR]) from LT to liver biopsy and FibroScan was 26 (16–51.5) and 26 (16–46.8) months, respectively. The median time (IQR) between liver biopsy and FibroScan was 2 (0–5) months, with 30 (78.9%) patients having a lag time lower than six months between both techniques. The median CAP and LSM values (IQR) were 273 (245.8–334.3) dB/m and 5.8 (4.4–7.8) kPa, respectively, with significant steatosis diagnosed in half of the patients ($n = 19$, 50%), yet advanced fibrosis in only 1 case (2.6%). On biopsy, about a third of biopsied patients ($n = 11$, 29%) had a MASH diagnosis, 2 (5.3%) with significant fibrosis and 1 (2.6%) with cirrhosis. All patients with LSM values <8 kPa ($n = 30$, 79%) had a fibrosis stage $\leq F1$, whereas of those with LSM values ≥ 8 kPa ($n = 8$, 21%), $n = 2$ (25%) had a fibrosis stage $\geq F2$ ($p = 0.040$).

Conclusion: Although liver biopsy remains the gold standard method for detecting fibrosis, our results suggest that LSM values <8 kPa after LT for MASH are strongly correlated with absence of significant/advanced fibrosis.

WED-258

Head fat correlates with the severity of non-alcoholic fatty liver disease: based on NHANES 2017–2018 data

Jiao Liu¹, Yunhao Xun², Yuecui Li³, Weiyue Hu¹, Chenghang Li¹, Lili Zhang¹. ¹The First People's Hospital of Yongkang, Jinhua, China; ²Xixi Hospital of Hangzhou, Hangzhou, China; ³The First People's Hospital of Yongkang, Jinhua
Email: xyhao1977@126.com

Background and aims: Body fat distribution takes an important part in the pathophysiology of non-alcoholic fatty liver disease (NAFLD), yet the role of head fat remains elusive. The purpose of this study was to explore whether head fat correlates with NAFLD and its severity or not, using the NHANES 2017–2018 dataset.

Method: Body composition values from dual energy X-ray absorptiometry as per the criteria of NHANES 2017–2018, together with medical records of the participants, were retrieved. NAFLD cases were identified on the basis of ultrasonographic steatosis or a controlled attenuation parameters value ≥ 302 dB/m, and without secondary causes of steatosis. Detailed statistical analysis was performed to explore the possible correlation.

Results: A total of 2051 subjects were included, with 22.38% ($n = 459$) of NAFLD. Patients with NAFLD indicated a higher head fat mass and the resulting percentage, and the following known metabolic factors: older, body mass index (BMI), larger waist circumference (WC), higher prevalence of hypertension and diabetes, higher levels of glucose, insulin, HOMA-IR, alanine aminotransferase, aspartate transferase, uric acid, triglyceride (TG), cholesterol and low density lipoprotein cholesterol, and lower level of high density lipoprotein cholesterol, as compared to non-NAFLD subjects. After propensity score matching analysis (1:1 matching, according to gender, age and ethnicity), head fat mass and its percentage in NAFLD patients remained higher than control subjects (1233 vs 1138 [gram]; 24.4 vs 23.9 [%], respectively; $P < 0.05$ for both). Logistic regression analysis showed head fat percentage (OR = 2.162, 95%CI: 1.248–3.746), WC (OR = 1.054, 95%CI: 1.03–1.079), TG (OR = 1.005, 95%CI: 1.002–1.009), and HOMA-IR (OR = 1.151, 95%CI: 1.043–1.271) ($p < 0.05$ for all) were independently associated with NAFLD. In patients with NAFLD, head fat percentage, but not head fat mass and other regional fat deposits, was positively correlated with the liver stiffness measurement, NAFLD fibrosis score and APRI ($r = 0.245$, 0.171, 0.114, respectively; $P < 0.05$ for all). The receiver operating curve by using head fat percentage alone showed an AUC of 0.771 (95%CI: 0.734–0.809) for the diagnosis of NAFLD, with a sensitivity of 55.2% and a specificity of

POSTER PRESENTATIONS

86.6% and an optimal cut-off of 24.35%. No significant correlation between head fat and metabolic syndrome was observed. Mediation effect tests showed that BMI and WC were the mediating variables between head fat percentage and NAFLD, with a mediating ratio of 36.58% and 46.52%, respectively. Head fat percentage was an independent risk factor for NAFLD in overweight people but not in normal weight or obese people.

Conclusion: Head fat is a newer valuable anthropometric parameter for predicting NAFLD and positively correlates with its hepatic severity. The interesting effect of this regional fat is even noteworthy in overweight people.

WED-259

Metabolic dysfunction-associated steatotic liver disease prevalence and predictors in patients with type 2 diabetes in primary care

Wile Balkhed¹, Patrik Nasr¹, Shan Cai¹, Christian Simonsson², Mikael Forsgren¹, Martin Bergman³, Olof Dahlqvist Leinhard^{1,4}, Nils Dahlström⁵, Carl-Johan Carlhäll⁶, Peter Lundberg⁷, Karin Rådholm⁸, Fredrik Iredahl¹, Stergios Kechagias¹, Mattias Ekstedt¹. ¹Linköping University, Department of Health, Medicine and Caring Sciences, Linköping, Sweden; ²Linköping University, Department of Radiation Physics, Department of Health, Medicine and Caring Sciences, Center for Medical Image Science and Visualization, Department of Biomedical Engineering, Linköping, Sweden; ³Linköping University, Division of Prevention, Rehabilitation and Community Medicine, Department of Health, Medicine and Caring Sciences, Linköping, Sweden; ⁴AMRA Medical AB, Linköping, Sweden; ⁵Linköping University, Department of Radiology in Linköping, Department of Health, Medicine and Caring Sciences, Center for Medical Image Science and Visualization, Linköping, Sweden; ⁶Linköping University, Dept. of Clinical Physiology in Linköping, Dept. of Health, Medicine and Caring Sciences, Linköping, Sweden; ⁷Linköping University, Radiation Physics and MR-Physics, Radiology and Center for Medical Imaging and Visualization, Linköping, Sweden; ⁸Linköping University, Department of Health, Medicine and Caring Sciences, Division of Prevention, Rehabilitation and Community Medicine, Linköping, Sweden
Email: balkhedwile@gmail.com

Background and aims: The number of people with metabolic dysfunction-associated steatotic liver disease (MASLD) has increased in parallel with the obesity epidemic. Type 2 diabetes (T2D) is associated with progressive MASLD. Therefore, many guidelines recommend screening for MASLD in T2D patients. Most MASLD studies have been conducted in specialist care, not necessarily representative for primary care. Therefore, we aimed to investigate the prevalence of MASLD and advanced fibrosis in primary care patients with T2D utilizing magnetic resonance imaging (MRI) and transient elastography (TE). In this study, we present results from the EPSONIP study (NCT03864510).

Method: Patients with T2D, without previous liver disease, were prospectively included from primary care. Study participants underwent laboratory investigation, TE with controlled attenuation parameter (CAP) and MRI including liver proton density fat fraction (PDFF).

Results: Two-hundred and seventy-nine participants were included. Out of these, 150 (54%) had a PDFF $\geq 5\%$ and were classified as MASLD. The mean PDFF in participants with MASLD was $12.9 \pm 6.6\%$. There was no difference in sex (37% and 36% were women in the MASLD and non-MASLD groups, respectively), age (63.5 ± 8.5 and 64.2 ± 7.8 years), nor in diabetes- or lipid lowering treatment between groups. However, participants with MASLD had a greater mean BMI (30.6 ± 4.3 vs. 27.3 ± 4.1 kg/m², $p < 0.001$), waist circumference (109 ± 10.4 vs.

99.8 ± 11.7 cm, $p < 0.001$), and HbA1c (52.5 ± 11.2 vs. 49.2 ± 9.2 mmol/mol, $p = 0.018$) compared to those without MASLD. Mean TE was higher in patients with MASLD (6.8 ± 5.3 vs. 5.6 ± 4.8 , $p < 0.001$). In the total cohort, 15% and 4% had a TE > 8 kPa and > 12 kPa, respectively. In patients with MASLD, 23% had a TE > 8 kPa and 4% TE > 12 kPa. CAP was higher in participants with MASLD, with an AUROC of 0.853 for detecting PDFF $\geq 5\%$. Applying a sensitivity of $> 90\%$ for the presence of PDFF $\geq 5\%$, a cut-off for CAP of 248 dB/m had a specificity of 64%. Regression analysis of factors to predict MASLD found BMI, elevated CAP (> 248 dB/m), and elevation of ALT, HbA1c and GT predictive of MASLD, and this relationship was confirmed for all factors except HbA1c when adjusting for age, sex, and BMI. However, in analysis adjusting for all the factors together only elevated CAP was an independent predictor of MASLD (aOR 11.7, 95% CI 5.1–27.2, $p < 0.001$).

Conclusion: In this cohort of highly phenotyped primary care patients with T2D, more than half had MASLD (54%), of whom 23% had suspected advanced fibrosis. Patients with MASLD had greater BMI, waist circumference and HbA1c, but the only independent predictor of MASLD was elevated CAP.

WED-260

Comparative analysis of Agile 3+, NFS, and BARD scores for diagnosing advanced fibrosis in MASLD and MetALD

Donghyeon Lee^{1,2}, Yun Kyu Lee¹, Heejeon Jang¹, Saekyung Joo¹, Won Kim¹, Young Ho So³, Yong Jin Jung⁴. ¹SMG-SNU Boramae Medical Center, Seoul, Korea, Rep. of South; ²Seoul National University, College of Medicine, Seoul, Korea, Rep. of South; ³Department of Radiology, SMG-SNU Boramae Medical Center, Seoul National University College of Medicine, Seoul, Korea, Rep. of South; ⁴Boramae Medical Center, Seoul, Korea, Rep. of South
Email: wonshiri@yahoo.com

Background and aims: Metabolic dysfunction-associated steatotic liver disease (MASLD) and MetALD (MASLD and increased alcohol intake) have emerged as significant public health concerns globally, driven by the rising prevalence of obesity and metabolic syndrome. This study evaluates the performance of commonly used indicators, including Agile 3+, Non-alcoholic Fatty Liver Disease Fibrosis Score (NFS), and BARD score, in diagnosing advanced fibrosis in both MASLD and MetALD.

Method: We conducted a retrospective analysis of 656 patients diagnosed with MASLD and MetALD. Patient data, including clinical, laboratory, and histopathological information, were collected. Agile 3+, NFS, and BARD scores were calculated for each patient. AUROC was employed to assess the discriminatory power of each scoring system, and the DeLong Test was used for pairwise comparisons.

Results: The results indicate no significant differences in the ability to diagnose advanced fibrosis among Agile 3+ (AUROC, 0.931 vs. 0.969; $p = 0.333$), NFS (AUROC, 0.856 vs. 0.792; $p = 0.589$), and BARD scores (AUROC, 0.710 vs. 0.513; $p = 0.287$) in both MASLD and MetALD, respectively. Agile 3+ and NFS demonstrated comparable accuracy and predictive capabilities in identifying advanced fibrosis in both conditions.

Conclusion: These findings suggest the interchangeability of these various scores in diagnosing advanced fibrosis in MASLD and MetALD, emphasizing the importance of selecting the optimal score based on individual patient characteristics and context. Thus, this study provides evidence that Agile 3+ and NFS can be effectively applied for diagnosing advanced fibrosis in MASLD and MetALD, demonstrating no substantial performance differences among these diverse scoring systems.

WED-261-YI

Prognostic significance of ELF test compared to liver biopsy in patients with metabolic dysfunction-associated steatotic liver disease (MASLD)

Antonio Liguori¹, Francesca D'Ambrosio², Nicholas Viceconti³, Fabrizio Termine³, Lucrezia Petrucci³, Riccardo Beschi³, Marco Orienti², Sara Cardinali², Simone Galletti², Laura Riccardi³, Fabrizio Pizzolante³, Nicoletta De Matthaeis³, Maria Elena Ainora³, Maria Assunta Zocco³, Maria Cristina Giustiniani⁴, Giuseppe Marrone³, Marco Biolato³, Fabio Maria Vecchio⁴, Antonio Grieco³, Andrea Urbani², Maurizio Sanguinetti², Antonio Gasbarrini³, Luca Miele³. ¹Department of Translational Medicine and Surgery, Fondazione Policlinico Universitario Agostino Gemelli IRCCS, Rome, Italy; ²Department of Laboratory and Infectious Sciences, Fondazione Policlinico Universitario A. Gemelli IRCCS, Rome, Italy; ³Department of Translational Medicine and Surgery, Fondazione Policlinico Universitario Agostino Gemelli IRCCS, Rome, Italy; ⁴Department of Women, Children and Public Health Sciences, Fondazione Policlinico Universitario A. Gemelli IRCCS, Rome, Italy
Email: lig.antonio91@gmail.com

Background and aims: Liver fibrosis stands out as the main prognostic risk factor in MASLD. The enhanced liver fibrosis (ELF) score is a composite of direct fibrosis biomarkers (tissue inhibitor of metalloproteinases 1, amino-terminal peptide of type 3 procollagen, and hyaluronic acid) that reflect extracellular matrix turnover. While the ELF test exhibits high diagnostic accuracy for advanced liver fibrosis in MASLD patients, its role as a prognostic biomarker remains uncertain. Our aim is to compare the prognostic effectiveness of ELF, FIB4, and liver histology in patients with MASLD.

Method: We retrospectively enrolled 289 patients with MASLD. The ELF score was automatically calculated in accordance with the manufacturer's instruction (Siemens Healthineers) using a serum sample collected at baseline. FIB4 computation and liver biopsy were performed at baseline. Liver fibrosis stage was assessed according to the METAVIR classification. The primary outcome was a composite end point including all-cause mortality, hepatocellular carcinoma, liver transplantation, or complications related to cirrhosis (ascites, variceal bleeding, hepatic encephalopathy, MELD ≥ 15). Subjects were stratified based on existing literature cut-offs for ELF (≤ 9.8 , 9.8–11.3, ≥ 11.3), FIB-4 (< 1.3 , 1.3–2.67, 2.67), and histology (F ≤ 2 , F3, F4) to assess the risk of occurrence of the primary outcome.

Results: We included data of 289 patients (88 [30.4%] were female, median age was 50 years [IQR 39–58], median BMI was 28.7 kg/m² [IQR 25.5–31.8] and 81 [28%] had type 2 diabetes). After a median follow-up of 41 months [IQR 21–68], the composite end point was observed in 34 (11.8%) patients. There was a stepwise increase in the frequency of developing primary outcome according with ELF < 9.8 (0.5%), 9.8 to 11.2 (14.5%), and ≥ 11.3 (69.7%). Survival curves for pairwise comparisons between groups showed significant differences for all index tests according to pre-defined histological and NITs stratification (Log Rank test $p < 0.05$). At multivariate Cox regression analysis, ELF and liver histology were significant predictors of the primary outcome after adjusting for gender, type 2 diabetes, age and BMI. (ELF > 11.2 vs < 9.8 HR 135.4 [95%CI 15.9–1149.0 $p < 0.001$], 9.8–11.2 vs < 9.8 HR 22.5 [95%CI 2.7–183.9 $p < 0.001$]) (Liver fibrosis 4 vs 0–2 HR 216.6 [95%CI 23.5–1999.2 $p < 0.001$], 3 vs 0–2 HR 5.44 [95%CI 1.0–30.9 $p = 0.05$]).

Conclusion: ELF, a simple non-invasive blood test, performed as well as histologically assessed fibrosis in predicting clinical outcomes and should be considered as alternative to liver biopsy for prognostic assessment in patients with MASLD.

WED-262

AI-assisted, quantitative digital pathology-based continuous fibrosis scores perform better than conventional pathology in documenting fibrosis reduction

Vlad Ratziu¹, Louis Petitjean², Raluca Pais³, Judith Aron-Wisniewsky¹, Li Chen⁴, Leila Kara⁵, Frederic Charlotte¹, Pierre Bedossa⁶, Mathieu Petitjean⁷. ¹Sorbonne Université, Paris, France; ²Pharmanest, Inc, Princeton, United States; ³ICAN, Paris; ⁴PharmaNest, Princeton, United States; ⁵ICAN, Paris, France; ⁶LiverPat, Paris, France; ⁷PharmaNest, Princeton, France
Email: vlad.ratziu@inserm.fr

Background and aims: Manual readings of liver biopsies using traditional histological fibrosis semi-quantitative classifications are subject to reader variability and poor sensitivity to change. We studied the performance of AI-assisted, quantitative digital pathology fibrosis scores in detecting fibrosis changes after bariatric surgery (BaS) a procedure with well-documented anti-fibrotic effects.

Method: Pts with morbid obesity who underwent BaS and had liver biopsy performed pre-operatively and at the last clinical follow-up were included. Liver biopsies were stained with Picrosirius red and staged using the NASH-CRN classification by an experienced hepatopathologist. The same slides were digitized (40X) and analyzed using a single-fiber, high-content image analysis platform to extract quantitative traits for collagen content, fiber morphometry and fibrosis architecture, allowing calculation of a continuous, quantitative fibrosis severity score (Ph-FCS, PharmaNest®). Changes in Ph-FCS before and after BaS were studied.

Results: 59 pts were included, 61% females, mean age 51.7 (sd 9.32) yrs. Prevalence of fibrosis stages was: stage 0: 1 (2%); stage 1: 14 (24%); stage 2: 10 (17%); stage 3: 25 (42%) and stage 4: 9 (15%). Gastric bypass (GB) was performed in 47 pts, sleeve gastrectomy (SG) in 11 pts and band ligation in 1 pt. The follow-up biopsy was performed a mean of 5.8 years (s.d. 2.6) post BaS. Overall, BMI was reduced by 11 (sd 3.9) kg/m². Baseline Ph-FCS was 7.07 (sd 1.65) and was reduced to 4.57 (sd 1.65) post-BaS. In the 19 pts with advanced fibrosis (stages 3 or 4) who no longer had advanced fibrosis at follow-up the Ph-FCS dropped by 2.75 (sd 1.89). There was an incremental decrease in Ph-FCS with reduction in histological NASH-CRN fibrosis stage: 1 stage reduction (N = 19): –2.62 (sd 2.26); 2 stage reduction (N = 10): –2.72 (sd 1.44); 3 stage reduction (N = 12): –3.02 (sd 3.13). Among the six patients with a one stage increase in fibrosis post BaS, 4 had an increase in the Ph-FCS (mean 2.34, sd 1.57) while two had a decrease. Importantly, in patients with no change in the NASH-CRN fibrosis stage (N = 12) the Ph-FCS decreased by a mean of 2.40 (sd 1.43). Pts who underwent GB had a stronger reduction in Ph-FCS than those who underwent SG: 2.64, sd 2.32 vs 1.35, sd 2.4, $p = 0.053$.

Conclusion: AI-assisted quantitative digital pathology provides fibrosis scores that are highly sensitive to liver fibrosis reduction and can uncover fibrosis changes not detectable by manual readings. These technologies have the potential to better identify drug or procedure-induced antifibrotic effects.

WED-263

A machine learning approach to identify patient features associated with metabolic dysfunction-associated steatohepatitis from the United Kingdom biobank

Jörn M Schattenberg¹, Amalia Gastaldelli², Harmeet Malhi³, Alina M Allen⁴, Mazen Nouredin⁵, Umesh Karamchandani⁶, Jonathon Romero⁷, Peter Henstock⁸, Birol Emir⁹, Arun J Sanyal¹⁰. ¹Saarland University Medical Center, Homburg, Germany; ²National Research Council, Institute of Clinical Physiology, Pisa, Italy; ³Mayo Clinic, Rochester MN, United States; ⁴Mayo Clinic, Rochester, MN, United States; ⁵Houston Methodist Hospital, Houston Research Institute, Houston TX, United States; ⁶University of Illinois Urbana-Champaign, Champaign, IL, United States; ⁷Syneos Health, Morrisville, NC, United States; ⁸Pfizer Inc., Andover, MA, United States; ⁹Pfizer Inc., New York, NY,

POSTER PRESENTATIONS

United States; ¹⁰Virginia Commonwealth University, Richmond, VA, United States
Email: joern.schattenberg@uks.eu

Background and aims: Diagnosis of metabolic dysfunction-associated steatohepatitis (MASH) requires an invasive liver biopsy that is prone to sampling errors. Therefore, it is important to identify factors predictive of patients at risk. Using a machine learning (ML) approach applied on data from the UK Biobank, this study aimed to identify variables that have the highest predictive potential for MASH.

Method: This study included UK Biobank data of patients with MASH, defined as those having liver fat >5%. A combined set of features including biomarkers (e.g., alanine aminotransferase [ALT]), demographics and patient clinical characteristics were included. Time, date and features that had less than 10,000 patients with non-null values (29%) were excluded. Missing data (21% of all values) were imputed by assigning a '0' value, using the k-nearest neighbour method, and ML algorithms that can handle missing values. All three approaches generated similar results and the 0 value was used for imputation. Predictive modelling was initially performed on the resulting full dataset (split 75/25 for cross-validation/testing) using classification models to predict the threshold output (5.5) and regression models to predict the continuous values. From comparisons of multiple ML models ranked in order of predictive value, random forest (RF) and CatBoost (CB) proved the best. Using feature importance, a subset of key features was selected for the final models. To identify additional features, a 'fat-free' model excluding fat-related features and a Boruta analysis were applied.

Results: The full dataset consisted of 5917 features from 34,560 individuals. Consistent features were identified using RF and CB, despite these algorithms being fundamentally different. The fat-associated features were most predictive, particularly visceral adipose tissue and android fat tissue. The fat-free analysis identified sex hormone binding globulin, ALT, C-reactive protein and gamma-glutamyl transferase as the most predictive. Area under the curve values for RF and CB classification were 0.86 vs 0.88, respectively, for the top feature set, and 0.84 vs 0.85 for the fat-free feature set. Mean squared error values for RF and CB regression were 0.297 vs 0.286 for the top feature set, and 0.345 vs 0.318 for the fat-free feature set. The Boruta analysis also identified insulin-like growth factor 1, cystatin C and apolipoprotein B as features related to MASH.

Conclusion: CB and RF achieved accurate predictions and identified consistent features. These included measures of fat, its distribution and additional potential biomarkers predictive of MASH outcomes. ML could support the non-invasive identification of at-risk patients. New models will help the field and will need to be validated in non-population-based cohorts.

WED-266

Age impacts the diagnostic ability of the enhanced liver fibrosis test for advanced fibrosis in MASLD

Katrina Pekarska¹, Alexander Hinkson¹, Ian Rowe¹, Richard Parker¹.

¹Leeds Teaching Hospitals NHS Trust, St James's University Hospital, Leeds, United Kingdom

Email: katrina.pekarska@gmail.com

Background and aims: Metabolic dysfunction associated liver disease (MASLD) has become one of the most frequent causes of chronic liver disease. Without appropriate management MASLD can progress to fibrosis and cirrhosis. Detection of liver fibrosis is an important diagnostic step, and several non-invasive fibrosis scores, including enhanced liver fibrosis test (ELF), have been introduced and are widely utilised to identify/exclude advanced fibrosis in patients with MASLD. It is noteworthy that ELF test has been validated in patients aged between 35 and 60 years where a reading ≥ 9.8 indicates a significant fibrosis. The aim of this study was to assess the effect of age on the performance of ELF test in MASLD.

Method: Patients who underwent a liver biopsy for diagnosis or staging of MASLD in routine practice at a single centre were included.

The cohort was divided into four age-based groups: <40 (n = 52), 40–49 (n = 61), 50–59 (n = 111), and ≥ 60 years (n = 81). The performance of ELF test for advanced fibrosis stage (stage F3 and F4) for each age group was assessed using liver biopsy as the standard and using the area under the receiver operating characteristics (AUROC) curve. Statistical analysis was done in R.

Results: In total 305 patients had available data regarding age, ELF test and histopathology and were included in analysis. The median BMI was 35 kg/m² (IQR 31–40) and 60% of patients were male. Diabetes mellitus was present in 160 (52%) and hypercholesterolaemia in 133 (48%). The median age was 54 years (IQR 44–60). Advanced fibrosis was present in 120 patients. Overall, the ELF test in this cohort performed well to predict advanced fibrosis: AUROC 0.74. The performance of the ELF test was particularly good in patients aged >40: AUROC 0.93. However, the performance of the ELF test was worse in other age groups: 40–49 years, AUROC 0.70; 50–59 years, AUROC 0.68; and aged over ≥ 60 AUROC 0.72. The sensitivity (sens.) of the ELF test in all age groups was below 70% and dropped to 42% in those aged 40–49. Optimal cut offs for each age group were calculated: the optimal ELF test cut point increased from younger to older patients: 9.3 for patients aged <40 (sens. 100%), 9.34 for patients aged 40–49 (sens. 73%), 10 for patients aged 50–59 (sens. 69%) and 10.3 for the oldest patients aged over 60 (sens. 75%).

Conclusion: The ELF test has excellent performance to diagnose advanced fibrosis in those aged under 40 years, however the diagnostic performance falls with age. Clinicians should be mindful of this when treating patients of various age groups. New ELF test thresholds for advanced fibrosis are proposed in various age groups to improve ELF test sensitivity and therefore reduce the number of positive cases missed.

WED-267

The FAP Index: A statistical model aiding the detection of advanced liver fibrosis in people with diabetes, obesity or metabolic dysfunction-associated steatosis using a marker of activated stellate cells and myofibroblasts

Ziqi Vincent Wang¹, Badwi Boumelhem¹, William Bachovchin², Geraldine Ooi³, Jacob George⁴, Mohammed Eslam⁴, Leon Adams⁵, Hui Zhang⁴, Geoff McCaughan⁶, Avik Majumdar⁴, Mark Gorrell^{7,8}.

¹Centenary Institute, The University of Sydney, Newtown, Australia;

²Tufts University, Boston, United States; ³Monash University, Melbourne, Australia; ⁴The University of Sydney, Sydney, Australia; ⁵The University of Western Australia, Perth, Australia; ⁶Centenary Institute, Sydney, Australia; ⁷Centenary Institute, The University of Sydney, Newtown; ⁸The University of Sydney, Centenary Institute, Newtown, Australia

Email: v.wang@centenary.org.au

Background and aims: Metabolic dysfunction-associated steatotic disease (MASLD) drives chronic liver injury leading to fibrosis, which is the major correlate of adverse health outcomes. The non-invasive tests (NITs) for liver fibrosis must accurately discriminate fibrosis severity while minimising indeterminate results. Accurate NITs are especially needed for primary screening in general practice and diabetes and obesity clinics. Almost all current NITs are a multi-marker statistical model/algorithm based on markers of hepatocyte damage rather than products of the activated mesenchymal cells (stellate cells and fibroblasts) that create and regulate fibrosis. We previously showed that fibroblast activation protein (FAP) digests collagens and TGF β precursors and is strongly and specifically expressed by myofibroblasts and activated stellate cells in human cirrhosis. We investigated the utility of circulating FAP (cFAP) to detect fibrosis in MASLD.

Method: The FAP shed from cell surfaces as an active enzyme is stable in human serum and plasma. We applied our quantitative, specific, rapid, one-step FAP enzyme assay to sera from a bariatric cohort (training cohort P, n = 160, 36% diabetic; n = 182, 23% diabetic) and a bariatric/MASLD cross-validation cohort (n = 150).

Results: Both insulin resistance and fibrosis were associated with cFAP in the MASLD cohort ($p < 0.05$). We coin the term FAP Index for a multi-variate model that was developed combining cFAP with age, diabetes status and ALT to evaluate liver fibrosis risk, especially in individuals who had an indeterminate result of an NFS or FIB4 test. The training cohort AUROC was 0.875 with a negative prediction value of 92% and a positive prediction value of 95%, indicating high accuracy. The cross-validation cohort AUROC was 0.84, with 98.5% specificity and 55% sensitivity. By serial application of NFS or FIB4 then the FAP Index, the proportion of indeterminate results more than halved, to $<15\%$. Therefore, applying cFAP measurement as a reflex test following an indeterminate FIB4 or NFS would likely have economies of time and expense, and lower the demand for obesity-specialised secondary testing.

Conclusion: We present a novel, inexpensive diagnostic tool for assessment and triage of individuals with diabetes, steatosis or obesity. We suggest that an advantage of including FAP Index in clinical fibrosis assessments is that FAP is strongly expressed by liver cell types that regulate the extracellular matrix.

WED-268

Natural history and expected change over time for MRI derived cT1: Data from clinical trials and the UK Biobank

Charlie Diamond¹, Cayden Beyer², Elizabeth Shumbayawonda¹, John McGonigle¹, Tim Rolph³, Kitty Yale³, Rajarshi Banerjee¹, Helena Thomaides Brears¹, Andrea Dennis¹, Michele Pansini^{4,5}, Naim Alkhouri⁶. ¹Perspectum Ltd., Oxford, United Kingdom; ²Perspectum Inc., Dallas, United States; ³Akero Therapeutics Inc., South San Francisco, United States; ⁴Clinica Di Radiologia EOC, Istituto Di Imaging Della Svizzera Italiana (IIMSI), Lugano, Switzerland; ⁵John Radcliffe Hospital, Oxford University Hospitals NHS Foundation Trust, Oxford, United Kingdom; ⁶Fatty Liver Program, Arizona Liver Health, Chandler, AZ, United States
Email: charlie.diamond@perspectum.com

Background and aims: Evaluation of the efficacy of new treatments in clinical trials in individuals with metabolic dysfunction-associated steatotic liver disease (MASLD) has been hampered by relatively high rates of histological changes in the placebo arms partly due to inconsistencies in pathologists' readings. Iron-corrected T1 (cT1) is an established, highly repeatable MRI biomarker of chronic liver disease activity, which strongly correlates with metabolic dysfunction-associated steatohepatitis (MASH) pathology and associates with liver and cardiovascular outcomes. A minimum detectable change in cT1 has previously been determined as >46 ms, while a change of >80 ms is associated with a 2-point change in NAFLD activity score (clinically meaningful). Using data acquired from volunteers in the UK Biobank (UKBB) imaging study and placebo controlled MASLD trials, we sought to measure change in liver disease activity based on cT1 over time in adults with and without MASLD.

Method: Paired clinical and imaging data from 2325 volunteers from the UKBB (application 9914) and 31 volunteers who served as placebo subjects in 3 interventional clinical MASLD trials, were analysed. All participants were scanned at baseline and follow-up; 115 weeks apart for UKBB and 18–52 weeks for the pooled clinical trial data. Liver MRI scans were analysed using LiverMultiScan (for fat (MRI-PDFF), iron concentration (MRI-LIC) and disease activity (iron corrected T1 mapping, cT1)). MRI criterion for definition of MASLD was of liver fat $\geq 5\%$, and criteria for MASH were liver fat $\geq 5\%$ and cT1 ≥ 800 ms, both with cardiometabolic risk factors. Statistical comparisons across timepoints were performed using Wilcoxon rank sum tests for continuous variables and Fishers exact tests for categorical variables.

Results: In the UKBB (mean age 63 (SD 7) years, 48% male, mean BMI 26 (SD 4) kg/m², 15% obese, 4.1% self-reported diabetic, 18% MASLD and 2.5% MASH), the participants cT1 increased significantly by a mean of 5ms (SD 32; $p < 0.001$) over an average 115-week period. For the 410 individuals with MASLD at baseline, the change in cT1 over

time was negligible (0ms (SD 40)). For the pooled clinical trial placebo cohort (mean age 56 (SD 8) years, 58% male, BMI 35 (SD 7) kg/m², 72% obese, 65% diabetic, 90% MASLD and 81% MASH), cT1 decreased by -7 ms (SD 84) over 18–52 weeks. In both cohorts the average change over time was considerably less than the reported minimal detectable change of 46ms, suggesting the observed changes are not clinically meaningful.

Conclusion: In both UKBB and placebo cohorts cT1 did not meaningfully change over time. These longitudinal datasets provide evidence of the stability of quantitative MRI liver biomarker cT1 in both healthy and MASLD populations. This information can be used to help power future studies and monitor disease over time in patients.

WED-269

Simultaneous assessment of skeletal muscle mass and handgrip strength to identify patients with NAFLD at high risk of advanced liver fibrosis

David Kim¹, Jae Seung Lee², Mi Na Kim², Beom Kyung Kim², Jun Yong Park², Do Young Kim², Sang Hoon Ahn², Nikolaos T. Pyrsopoulos¹, Hye Won Lee², Seung Up Kim². ¹Rutgers New Jersey Medical School, Newark, United States; ²Yonsei University College of Medicine, Seoul, Korea, Rep. of South
Email: dsk143@njms.rutgers.edu

Background and aims: Sarcopenia diagnosis depends on various diagnostic criteria based on different diagnostic modalities. We aimed to identify the predictors of discordance between appendicular skeletal muscle mass (ASM) measured by bioimpedance analysis (BIA) and handgrip strength (HGS) in diagnosing sarcopenia and investigate whether their combined use can identify a subgroup of patients with non-alcoholic fatty liver disease (NAFLD) at high risk for advanced liver fibrosis.

Method: Between 2018 and 2023, NAFLD patients whose ASM was measured by BIA and HGS were recruited. Sarcopenia was diagnosed when ASM/body mass index (BMI) was <0.882 in men or <0.582 in women or when HGS was <28.9 kg in men or <16.8 kg in women. Advanced liver fibrosis was defined as a liver stiffness value by transient elastography of >9.6 kPa.

Results: Among 2,044 patients, 794 (38.8%) and 200 (10.8%) patients had sarcopenia according to BIA and HGS, respectively. In multivariate analysis, male sex (odds ratio [OR] = 1.3) and BMI (OR = 1.2) were independent predictors of discordance between ASM- and HGS-diagnosed sarcopenia ($p < 0.05$). Patients with sarcopenia according to both BIA and HGS and those with sarcopenia according to BIA only demonstrated a significantly higher probability of advanced liver fibrosis than patients without sarcopenia according to both BIA and HGS (all $P < 0.001$).

Conclusion: In NAFLD patients, male sex and BMI were independently associated with discordance in diagnosing sarcopenia via ASM by BIA and HGS. Moreover, the combined use of the methods helped identify those at high risk of advanced liver fibrosis.

WED-270

Clinical profile of patients considered at-risk for MASH with fibrosis identified through an ongoing global screening program with genetics

Samuel Daniels¹, Karin Nelander², John Eriksson², Jelena Saillard³, Lutz Jeremut⁴, Federica Tavaglione⁵, Joao-Filipe Raposo⁶, Marco Arrese⁷, Alma Laura Ladrón de Guevara⁸, Umberto Vespasiani Gentilucci⁹, Naim Alkhouri⁹, Jenny Blau¹⁰. ¹Early Clinical Development, Early CVRM, AstraZeneca, Cambridge, United Kingdom; ²AstraZeneca, Early Biometrics and Statistical Innovation, Data Science and Artificial Intelligence, Gothenburg, Sweden; ³AstraZeneca, Clinical Operations CVRM, BioPharmaceuticals RandD, Gaithersburg, United States; ⁴AstraZeneca, Research, Cardiovascular, Renal and Metabolism, BioPharmaceuticals RandD, Cambridge, United Kingdom; ⁵Clinical Medicine and Hepatology, Fondazione Policlinico

POSTER PRESENTATIONS

Universitario Campus Bio-Medico and Università Campus Bio-Medico di Roma, Rome, Italy; ⁶Associação Protectora dos Diabéticos de Portugal (APDP), Lisbon, Portugal; ⁷Departamento de Gastroenterología, Escuela de Medicina, Pontificia Universidad Católica de Chile, Santiago, Chile; ⁸Centro de Investigación y Gastroenterología S. C., Mexico City, Mexico; ⁹Department of Hepatology, Arizona Liver Health, Chandler, United States; ¹⁰Early Clinical Development, Early CVRM, AstraZeneca, Gaithersburg, United States
Email: samuel.daniels@astrazeneca.com

Background and aims: Chronic liver disease is a rising public health issue with significant contributions from steatotic liver diseases (SLD) such as MASH. Community screening, including blood testing, genetics and imaging such as elastography are important for patient identification for clinical trials. The FAST score is useful to identify those at-risk of progressive MASH with fibrosis. Herein, we investigated the clinical profile of patients screened within hepatology and general medicine clinical trial centres and utilized FAST to risk-stratify for MASH, including evaluating genetic profiles.

Method: The ALIGN screening study is an ongoing multicenter global prospective cohort study aimed at identifying individuals with a high likelihood of MASLD/MASH by collecting blood and genetic samples and using non-invasive imaging. The FAST score is a composite score derived from FibroScan® (Echosens, Paris, France) and AST composed to identify MASH with active disease (NAS ≥ 4), and fibrosis (F ≥ 2). Patients were stratified into risk groups according to published cut-offs (low risk <0.35, intermediate between 0.35–0.67, high risk >0.67) and evaluated using their clinical and genetic profile. Continuous variables presented as mean with standard deviation [SD].

Results: Out of n = 1,328 participants screened, 68.1%, 26%, 5.9% had low, intermediate and high risk FAST scores denoted by <0.35, >0.35–0.67; and >0.67, respectively. Individuals with high risk FAST score had a worse metabolic profile compared to those with low risk FAST, indicated by higher BMI (37.2 kg/m² [7.6] vs 32.6 kg/m² [6.1]), waist circumference (118 cm [16.7] vs 106.7 cm [12.2]), triglycerides (198.4 mg/dL [216.9] vs 149.7 mg/dL [111]) and a greater proportion living with type 2 diabetes (58.2% vs 29.6%). ALT was ~3-fold higher within the high risk FAST risk group compared to low risk FAST risk (93.2 IU/L [65] vs 31.9 IU/L [16.3]). Within the genotyped subgroup (n = 317) the proportion of PNPLA3 rs738409 risk alleles did not differentiate across FAST risk groups (GG prevalence was 21.3%, 33.6%, 22.9% for low, intermediate and high FAST).

Conclusion: FAST score is an important tool to screen for fibrotic MASH in individuals interested in participating in clinical trials. Within ALIGN, participants with a higher FAST had a worse metabolic profile and had elevated ALT compared to those with lower FAST. Within ALIGN, the FAST score had limited ability to stratify risk according to PNPLA3 genetic profile.

WED-271

Circulating vesicle microRNAs for metabolic dysfunction-associated steatotic liver disease (MASLD) staging and progression towards liver cancer

Laura Izquierdo-Sánchez^{1,2,3}, Ainhoa Lapitz^{1,2}, André Simão³, Santiago Iturbe-Rey¹, Marco Arrese⁴, Claudia P. Oliveira^{5,6}, Ignacio Aguirre Allende^{1,7}, Ainhoa Echeveste⁷, Raul Jimenez-Aguero^{1,7}, Emma Eizaguirre^{1,7}, Jorge Arnold⁴, Carmen M. Del Prado Alba⁸, María Luz Martínez-Chantar^{9,10}, Kristina Schoonjans¹¹, Patricia Aspichueta^{2,12,13}, María Jesús Perugorria^{1,2,14}, Luis Bujanda^{1,2,14,15}, Pedro M. Rodrigues^{1,2,16}, Jesus Maria Banales^{1,2,16,17}. ¹Department of Liver and Gastrointestinal Diseases, Biogipuzkoa Health Research Institute, Donostia University Hospital, University of the Basque Country (UPV/EHU), San Sebastian, Spain; ²Carlos III National Institute of Health, Centre for the Study of Liver and Gastrointestinal Diseases (CIBERehd), Madrid, Spain; ³Research Institute for Medicines (iMed.Ulisboa), Universidade de Lisboa, Faculty of Pharmacy, Lisbon, Portugal;

⁴Pontificia Universidad Católica de Chile, Gastroenterología, Escuela de Medicina, Santiago de Chile, Chile; ⁵Instituto do Cancer do Estado de São Paulo, Liver Cancer Group, São Paulo, Brazil; ⁶School of Medicine, Hospital das Clinicas, University of São Paulo, Department of Gastroenterology, Division of Clinical Gastroenterology and Hepatology, São Paulo, Brazil; ⁷Hospital Universitario Donostia, Servicio de Cirugía General y Digestiva, San Sebastian, Spain; ⁸Hospital Universitario Virgen del Rocío, Pathological Anatomy, Sevilla, Spain; ⁹Liver Disease Lab, Center for Cooperative Research in Biosciences (CIC bioGUNE), Basque Research and Technology Alliance (BRTA), Derio, Spain; ¹⁰Carlos III National Institute of Health, Centre for the Study of Liver and Gastrointestinal Diseases (CIBERehd), Madrid, Spain; ¹¹Institute of Bioengineering, School of Life Sciences, Ecole Polytechnique Fédérale de Lausanne, Lausanne, Switzerland; ¹²University of the Basque Country, Department of Physiology, Faculty of Medicine and Nursing, Leioa, Spain; ¹³Biobizkaia Health Research Institute, Barakaldo, Spain; ¹⁴University of the Basque Country, Department of Medicine, Faculty of Medicine and Nursing, Leioa, Spain; ¹⁵Hospital Universitario Donostia, Servicio de Aparato Digestivo, San Sebastian, Spain; ¹⁶IKERBASQUE, Basque Foundation for Science, Bilbao, Spain; ¹⁷University of Navarra, Department of Biochemistry and Genetics, School of Sciences, Pamplona, Spain
Email: jesus.banales@biodonostia.org

Background and aims: Non-invasive biomarker-driven algorithms are urgently needed for classifying Metabolic Dysfunction-Associated Steatotic Liver Disease (MASLD) and monitoring its progression to Steatohepatitis (MASH) and Hepatocellular Carcinoma (HCC). In this study, we investigated microRNAs (miRs) present in serum extracellular vesicles (EVs) that may serve as diagnostic and prognostic biomarkers.

Method: EV-associated miRNAs from obese adults without Steatotic Liver Disease (SLD), lean or obese with simple steatosis, MASH with and without fibrosis (determined by liver biopsy), as well as in patients with MASLD-associated HCC were isolated following the exoRNeasy Midi kit (Qiagen). The small RNA transcriptome on EVs was sequenced following the QIAseq miRNA Library kit (Qiagen) workflow.

Results: A total of 71 individuals were clinically categorized into eight study groups (n = 9 individual per group): Obese without SLD, with simple steatosis, MASH-F0/F1 or MASH-F2-F3, lean with SLD, MASHF0/F1 or MASH-F2-F3, and MASLD-HCC. In total, 1,461 EV-miRs were identified. Notably, the EV levels of 8 miRs were found to be dysregulated in MASH compared to simple steatosis, irrespective of the degree of liver fibrosis and BMI, with individual areas under the receiver operating curve (AUC) values over 0.8. Additionally, the EV levels of 6 miRs were associated with fibrosis scores (F0-F1 vs. F2-F3) regardless of BMI, with AUC values over 0.83. Finally, a total of 130 miRs were found to be dysregulated in serum EVs from patients with MASLD-HCC compared to MASLD, regardless of age, biological sex, and BMI, with some of them exhibiting maximal diagnostic AUC values (e.g., miR-629-5p, miR-488-5p, miR-4732-5p).

Conclusion: This study underscores the potential of EV-miRs as diagnostic tools for staging MASLD and its association with HCC. Ongoing work on logistic models that combine miRs will be valuable for future international validation efforts.

WED-272

A self-testing index for detecting hepatic steatosis and prognostication in the general population

Chuan Liu¹, Shanhao Liu², Jie Shen³, Jie Li⁴, Jingli Gao⁵, Heng Wan³, Qun Zhang⁶, Donghan Su⁷, Hao Liu⁸, Yi Dong⁹, Jia Li¹⁰, Lan Liu³, Shan Wang⁵, Guangjian Li⁵, Yiling Li¹¹, Yu Jun Wong¹², Qing-Lei Zeng¹³, Zhihui Li⁷, Shenghong Ju¹⁴, Wenhong Zhang¹⁵, Michael Pavlides¹⁶, Vincent Wai-Sun Wong^{17,18}, Gao-Jun Teng¹⁹, Xiaolong Qi²⁰. ¹Center of Portal Hypertension, Department of Radiology,

Zhongda Hospital, Medical School, Southeast University, Nanjing;
²Center of Portal Hypertension, Department of Radiology, Zhongda Hospital, Medical School, Southeast University, Nanjing, China;
³Department of Endocrinology and Metabolism, Shunde Hospital, Southern Medical University (The First People's Hospital of Shunde), Foshan, China; ⁴Department of Infectious Diseases, Nanjing Drum Tower Hospital, Affiliated Hospital of Medical School, Nanjing University, Nanjing, China; ⁵Kailuan General Hospital, Tangshan, China;
⁶Department of Infectious Disease, Affiliated Zhongda Hospital of Southeast University, Nanjing, China; ⁷Vanke School of Public Health, Tsinghua University, Beijing, China; ⁸Department of Surgery, University of Pittsburgh Medical Center, Pittsburgh, United States; ⁹Department of Ultrasound, Xinhua Hospital, Shanghai Jiao Tong University, Shanghai, China; ¹⁰Department of Ultrasound, Zhongda Hospital, Medical School, Southeast University, Nanjing, China; ¹¹Department of Gastroenterology, the First Affiliated Hospital of China Medical University, Shenyang, China; ¹²Department of Gastroenterology and Hepatology, Changi General Hospital, Duke-NUS Medical School, Singapore, Singapore;
¹³Department of Infectious Diseases and Hepatology, The First Affiliated Hospital of Zhengzhou University, Zhengzhou, China; ¹⁴Department of Radiology, Zhongda Hospital, School of Medicine, Southeast University, Basic Medicine Research and Innovation Center of Ministry of Education, Zhongda Hospital, Southeast University, Nanjing, China; ¹⁵Department of Infectious Diseases, Shanghai Key Laboratory of Infectious Diseases and Biosafety Emergency Response, Huashan Hospital, Fudan University School of Medicine, Shanghai, China; ¹⁶Oxford NIHR Biomedical Research Centre; Radcliffe Department of Medicine; Translational Gastroenterology Unit, University of Oxford, Oxford, United Kingdom;
¹⁷Medical Data Analytics Centre, The Chinese University of Hong Kong, State Key Laboratory of Digestive Disease, Institute of Digestive Disease, The Chinese University of Hong Kong, Hong Kong, China; ¹⁸Department of Medicine and Therapeutics, The Chinese University of Hong Kong, Hong Kong, China; ¹⁹Center of Interventional Radiology and Vascular Surgery, Department of Radiology, Zhongda Hospital, Medical School, Southeast University, Basic Medicine Research and Innovation Center of Ministry of Education, Zhongda Hospital, Southeast University, Nanjing, China; ²⁰Center of Portal Hypertension, Department of Radiology, Zhongda Hospital, Medical School, Southeast University, Basic Medicine Research and Innovation Center of Ministry of Education, Zhongda Hospital, Southeast University, Nanjing, China
 Email: liuchuan101z@163.com

Background and aims: Hepatic steatosis may result in metabolic dysfunction-associated steatohepatitis (MASH), hepatocellular carcinoma (HCC), and mortality. We aimed to develop and validate a self-testing index to detect hepatic steatosis, and stratify risk of HCC and all-cause mortality in the general population.

Method: This prospective population-based study included 210,679 participants from six cohorts. A prospective derivation (N = 7,000), a prospective test (N = 2,027), a prospective magnetic resonance imaging proton density fat fraction (N = 296), and an NHANES (N = 7,436) cross-sectional cohorts were enrolled to develop and validate a new index for hepatic steatosis. The ability of prognostication stratified by the new index was evaluated in Chinese (N = 142,505) and NHANES (N = 51,415) follow-up cohorts.

Results: In the derivation cohort, three factors for hepatic steatosis were identified, including Age, body mass Index, and Diabetes mellitus, and fitted to develop the "AID" index (web calculator at https://chess.nuist.edu.cn/consult/gzconsult/aid_index). The AID index performed better ($p < 0.05$) capability in predicting hepatic steatosis than other methods in four cross-sectional cohorts. The hepatic steatosis risk was best stratified by the cut-off values at 0 and 2.11. The cumulative incidences of HCC at 15 years in the high-risk group were significantly higher (0.37% vs. 0.29%, $P = 0.034$) than that of the low-risk group in the Chinese follow-up cohort. Notably, the AID index also effectively identified individuals at risk of all-cause mortality in Chinese and NHANES follow-up cohorts.

Conclusion: The AID index that can be self-tested easily demonstrates strong capabilities in diagnosing hepatic steatosis, and stratifying risk of HCC and all-cause mortality in the general population.

WED-273

The performance of the enhanced liver fibrosis test by cardiometabolic risk factors in patients with metabolic dysfunction-associated steatotic liver disease

Kazuhito Kawata¹, Hirokazu Takahashi², Taeang Arai³, Yuya Seko⁴, Takeshi Chida¹, Hidenao Noritake¹, Hidenori Toyoda⁵, Hideki Hayashi⁶, Kanji Yamaguchi⁴, Michihiro Iwaki⁷, Masato Yoneda⁷, Toshihide Shima⁸, Hideki Fujii⁹, Asahihiro Morishita¹⁰, Kengo Tomita¹¹, Miwa Kawanaka¹², Yuichi Yoshida¹³, Tadashi Ikegami¹⁴, Kazuo Notsumata¹⁵, Satoshi Oeda¹⁶, Masanori Atsukawa³, Yoshihiro Kamada¹⁷, Yoshio Sumida¹⁸, Hideaki Fukushima¹⁹, Eiji Miyoshi²⁰, Shinichi Aishima²¹, Takeshi Okanoue²², Yoshito Itoh²³, Atsushi Nakajima²⁴. ¹Hamamatsu University School of Medicine, Hamamatsu, Japan; ²Saga University, Saga, Japan; ³Nippon Medical School, Tokyo, Japan; ⁴Kyoto Prefectural University of Medicine, Kyoto, Japan; ⁵Ogaki Municipal Hospital, Ogaki, Japan; ⁶Gifu City Hospital, Gifu, Japan; ⁷Yokohama City University Graduate School of Medicine, Yokohama, Japan; ⁸Saiseikai Suita Hospital, Suita, Japan; ⁹Osaka Metropolitan University Graduate School of Medicine, Osaka, Japan; ¹⁰Kagawa University Faculty of Medicine, Takamatsu, Japan; ¹¹National Defense Medical College, Tokorozawa, Japan; ¹²Kawasaki Medical School, Kawasaki Medical Center, Okayama, Japan; ¹³Suita Municipal Hospital, Suita, Japan; ¹⁴Tokyo Medical University Ibaraki Medical Center, Ibaraki, Japan; ¹⁵Fukui-ken Saiseikai Hospital, Fukui, Japan; ¹⁶Saga University Hospital, Saga, Japan; ¹⁷Osaka University, Osaka, Japan; ¹⁸Graduate School of Healthcare Management, International University of Healthcare and Welfare, Tokyo, Japan; ¹⁹Siemens Healthcare Diagnostics K.K., Tokyo, Japan; ²⁰Osaka University Graduate School of Medicine, Osaka, Japan; ²¹Kyushu University, Fukuoka, Japan; ²²Saiseikai Suita Hospital, Suita, Japan; ²³Kyoto Prefectural University of Medicine, Kyoto, Japan; ²⁴Yokohama City University Graduate School of Medicine, Yokohama, Japan
 Email: kawata@hama-med.ac.jp

Background and aims: The Enhanced Liver Fibrosis (ELF) test, a non-invasive test derived from serum biomarkers, is valuable for predicting liver fibrosis in chronic liver diseases. However, the impact of positive factors and the positive number in the cardiometabolic risk factors of metabolic dysfunction-associated steatotic liver disease (MASLD) on ELF tests is unknown. We aimed to evaluate the accuracy of the ELF test, according to the positive factors and the positive number in the cardiometabolic risk factors, comparing with the Fibrosis-4 (FIB-4) index and non-alcoholic fatty liver disease fibrosis score (NFS) in patients with MASLD.

Method: In this retrospective study, a total of 1038 patients with biopsy-proven SLD having at least one of five cardiometabolic risk factors were enrolled. The diagnostic performance of the ELF test, the FIB-4 index, and NFS for predicting advanced fibrosis ($\geq F3$ and $F4$) by the positive factor or the positive number in the cardiometabolic risk factors were compared.

Results: The median value of the ELF test, the FIB-4 index, and NFS were 9.9, 1.84, and -0.654, respectively. The patient number of fibrosis stages (F) 0, 1, 2, 3, and 4 were 180, 350, 276, 196, and 36, respectively. The area under the curve (AUROC) of the ELF test for predicting advanced fibrosis was significantly higher than that of the FIB-4 index and NFS (ELF, 0.833; FIB-4, 0.753; NFS, 0.757). The diagnostic performances of the ELF test were significantly greater, regardless of the positive or negative for each cardiometabolic risk factor, although there was no difference in MASLD patients without type 2 diabetes. Furthermore, the AUROC of the ELF test was significantly higher than that of the FIB-4 index and NFS in MASLD patients with two or more positive cardiometabolic risk factors (ELF, FIB-4, and NFS; 0.832, 0.835, and 0.708 at 1 positive factor, 0.868,

POSTER PRESENTATIONS

0.789, and 0.792 at 2 positive factors, 0.832, 0.762, and 0.761 at 3 positive factors, 0.817, 0.725, and 0.732 at 4 positive factors, 0.818, 0.732, and 0.706 at 5 positive factors).

Conclusion: The ELF test showed high diagnostic performance for predicting advanced fibrosis compared with the FIB-4 index and NFS in patients with MASLD, regardless of the positive factor and the positive number in the cardiometabolic risk factors.

WED-274

Impact of sex, body mass index, elevated liver enzymes, and diabetes mellitus on risk-stratification of a large cohort of patients with MASLD

Abdel-Aziz Shaheen¹, Elizabeth Baguley¹, Wendy Schaufert², Alexandra Frolkis¹, Mark G. Swain¹, Juan G. Abraldes³. ¹University of Calgary, Calgary, Canada; ²Alberta Health Services, Calgary, Canada; ³University of Alberta, Edmonton, Canada
Email: az.shaheen@ucalgary.ca

Background and aims: The need to develop and implement clinical care pathways to risk-stratify patients with metabolic dysfunction-associated steatotic liver disease (MASLD) is growing. We aimed to assess risk-stratification of patients with MASLD in primary care and evaluate role of sex, body mass index (BMI), elevated alanine aminotransferase (ALT) and diabetes mellitus (DM) on risk-stratification.

Method: Patients with confirmed MASLD diagnosis from the Calgary MASLD pathway in primary care (n = 10, 844) and Calgary MASLD clinic (n = 806) were included in our study. We compared performance of fibrosis marker FIB-4 to shearwave elastography (SWE) among 7, 738 patients with available FIB-4. Among patients assessed in MASLD clinic, we compared performance of FIB-4, Transient Elastography (TE), SWE to liver biopsy (n = 359) to identify significant ($\geq F2$) or advanced fibrosis ($\geq F3$) according to our exposure variables of interest.

Results: In the MASLD primary care cohort (n = 7, 738), morbid obesity and DM were associated with higher probability of SWE ≥ 8 kPa while elevated ALT and sex had minimal impact on this association. Within the MASLD clinic, female patients with FIB-4 ≥ 1.30 had higher risk of advanced fibrosis compared to men (77.1% vs. 64%, $p = 0.044$). Patients with elevated ALT had two folds increase in advanced fibrosis (58.6% vs. 28.8%, $p < 0.001$). While morbid obesity did not affect risk stratification using FIB-4 as first step, patients with DM had double rates of advanced fibrosis (62.5% vs. 32.3%, $p < 0.001$). Independent predictors of significant fibrosis were age (adj OR 1.03, 95%CI: 1.00–1.06), female sex (adj OR: 2.42, 95%CI: 1.28–4.57), aspartate aminotransferase [AST] (adj OR: 1.03, 1.02–1.05) and DM (adj OR: 6.72, 3.64–12.39). Independent predictors of advanced fibrosis were age (adj OR 1.03, 95%CI: 1.01–1.06), female sex (adj OR: 2.60, 95%CI: 1.44–4.69), aspartate aminotransferase [AST] (adj OR: 1.02, 1.01–1.03) and DM (adj OR: 3.87, 2.04–7.35).

Conclusion: Future clinical care pathways should be designed to prioritize risk-stratification among women, patients with elevated liver enzymes or DM.

WED-275

Understanding barriers to adoption of clinical guidelines for metabolic dysfunction-associated steatotic liver disease among hepatologists in Europe

Laurent Castera¹, William Alazawi², Elisabetta Bugianesi³, Cyrielle Caussy⁴, Massimo Federici⁵, Manuel Romero-Gómez⁶, Jörn M. Schattenberg⁷, Ron Basuroy⁸, Dmitrii Estulin⁹, Jeffrey V. Lazarus¹⁰. ¹Department of Hepatology, Beaujon University of Paris, AP-HP, University of Paris, Clichy, France; ²Barts Liver Center, Queen Mary University of London, London, United Kingdom; ³Department of Medical Sciences, University of Torino, Torino, Italy; ⁴Lyon 1 University and Lyon South Hospital, Lyon, France; ⁵Department

of Systems Medicine, University of Rome Tor Vergata, Rome, Italy; ⁶Virgen Del Rocio University Hospital, Institute of Biomedicine of Seville (CSIC/HUVR/US). University of Seville, Seville, Spain; ⁷Department of Internal Medicine II, Saarland University Medical Center, Homburg, Germany; ⁸Novo Nordisk A/S, Copenhagen, Denmark; ⁹Novo Nordisk Health Care AG, Zurich, Switzerland; ¹⁰Barcelona Institute for Global Health (ISGlobal), Hospital Clinic, University of Barcelona, Barcelona, Spain
Email: laurent.d.castera@gmail.com

Background and aims: The global burden of metabolic dysfunction-associated steatotic liver disease (MASLD) and metabolic dysfunction-associated steatohepatitis (MASH) is high and rising. Clinical practice guidelines (CPGs) advise that patients with suspected MASLD and MASH be assessed for risk based on comorbidities, screened using non-invasive tests, referred to hepatologists when necessary, and offered appropriate interventions. This study aimed to understand attitudes and behaviours toward CPGs, as well as their use in diagnosing and managing MASLD/MASH among physicians in five European countries.

Method: A real-world, cross-sectional study was conducted in France, Germany, Italy, Spain, and the United Kingdom among hepatologists and gastroenterologists with a subspecialty in hepatology, grouped as “hepatologists” for the analysis. Data were collected from March to September 2023 using an online quantitative survey, which participants completed anonymously, and 45-minute qualitative interviews with physicians from each country. Descriptive statistics were used to analyse the data.

Results: 250 hepatologists in the study cared for an average of 116.3 patients per month diagnosed with MASLD/MASH, which they estimated represented 37.4% of their total patient population. Hepatologists reported that 32% of their patients with MASH were confirmed through liver biopsy. To profile patients suspected of MASH, hepatologists reported using vibration-controlled transient elastography (VCTE) (76%), ultrasound (76%), and liver biopsy (64%) most frequently. To confirm diagnosis, liver biopsy was used by 68% of hepatologists; however, 34% of hepatologists stated that liver biopsy was not necessary to confidently diagnose MASH. Hepatologists were most aware of EASL 2021 (55%), AASLD 2023 (44%) and AASLD 2018 (42%) clinical guidelines. A small proportion of hepatologists stated, even when prompted with a list, that they were not aware of any clinical guidelines for MASH (4%), did not follow any guidelines for the diagnosis of MASH (5%) and did not follow any guidelines for the treatment and management of MASH (7%). Among 25 hepatologists who participated in qualitative interviews, most (n = 15) had heard of the new MASLD/MASH nomenclature, and n = 15 also believe it will not change anything for their practice.

Conclusion: This study found that a number of barriers to adoption of CPGs exist, which may drive variation in hepatologists' approach to diagnosing and managing patients with MASH. The findings emphasise the need to continuously embed CPGs into routine care to address the implementation gap and to thereby optimise care for patients with MASH.

WED-278

MASLD assessment using a novel point of care device the Hepatoscope™ in diabetes and obesity clinics

Cyrielle Caussy¹, Bruno Vergès², Rouland Alexia³, Bérénice Ségrestin¹, Dominique Delaunay⁴, Sybil Charrière⁵, Emmanuel Disse¹, Philippe Moulin⁶, Jean-Michel Petit⁷. ¹Hospices Civils de Lyon, Pierre-Bénite, France; ²Dijon University Hospital, Dijon, France; ³Dijon University Hospital, Dijon, France; ⁴Hospices Civils de Lyon, Lyon, France; ⁵Hospices Civils de Lyon, Bron, France; ⁶Hospices Civils de Lyon, Bron, France; ⁷Dijon University Hospital, Dijon, France
Email: cyrielle.caussy@gmail.com

Background and aims: The screening for metabolic dysfunction-associated steatotic liver disease (MASLD) and liver fibrosis is currently recommended in patients with type 2 diabetes (T2D) and

obesity. We aimed at evaluating the correlation of liver fibrosis and steatosis parameters between a FibroScan® and a new ultrasound imaging point-of-care device: Hepatoscope™.

Method: This is an interim analysis from a prospective multicenter study including participants with T2D and/or obesity and MASLD age 40–80 years, BMI <40 kg/m² enrolled in 3 diabetes clinics in France between Dec 2022 and Dec 2023 (ancillary study NCT04435054). All participants underwent the same day liver stiffness measurement using vibration controlled transient elastography (VCTE) by FibroScan®, 2D-measurements of shear wave speed (2DTE) by Hepatoscope™, hepatic fat content assessment using controlled attenuation parameter (CAP) by FibroScan® and ultrasound attenuation (ATT) and backscattering coefficient (BSC) by Hepatoscope™. An exploratory subgroup of 18 participants underwent also magnetic resonance imaging proton density fat fraction (MRI-PDFF). The spearman correlation coefficients and mean bias between VCTE and 2DTE were assessed in participants with both valid VCTE and 2DTE (interquartile range/median ratio ≤0.30). In addition, correlation between CAP or MRI-PDFF and CAP, ATT or BSC were also assessed.

Results: 148 participants were included in the analysis: 64.9% male, 87.8% with T2D, 70.3% with obesity and with mean age: 61.8 ± 9.4 years, BMI: 32.1 ± 3.8 kg/m² and median 2DTE of 6.1 kPa ± 4.3 kPa versus median VCTE: 6.4 ± 4.2 kPa, $p = 0.947$. VCTE and 2DTE were significantly correlated r_2 : 0.46, $p < 0.001$ with a mean bias of -0.2, (95%CI: -5.86–5.37). The median CAP was: 311 ± 52 dB/m versus ATT: 310 ± 42 dB/m, $p = 0.151$ and the median BSC was -22.8 ± -5.4. Both ATT and BSC correlated significantly with CAP: r_2 : 0.55, $p < 0.001$ and r_2 : 0.59, $p < 0.001$, respectively. CAP, ATT and BSC were also significantly correlated with MRI-PDFF: r_2 : 0.80, 0.78 and 0.88, respectively, all $p < 0.001$.

Conclusion: These preliminary data indicate that the Hepatoscope™ 2DTE is significantly correlated with VCTE. It provides the proof of concept that the Hepatoscope™ could be used for the assessment of liver fibrosis and steatosis in patients with MASLD. Further studies in larger cohort are needed to determine the cut-offs and diagnostic performance of the Hepatoscope™ in diabetes and obesity clinics.

WED-279

Landscape of the steatotic liver disease and its risk factors in the point-of-care liver screening program SIRIUS

Tomas Koller¹, Svetlana Adamcova Selcanova², Natalia Kubanek², Daniel Jan Havaj², Karolina Sulejova², Daniela Žilinčanová², Sylvia Dražilová³, Martin Janičko³, Marek Rac⁴, Maria Szantova⁵, Lubomir Skladany². ¹Comenius University Faculty of Medicine in Bratislava, University Hospital Bratislava, Bratislava, Slovakia; ²FD Roosevelt Hospital, Banská Bystrica, Slovakia; ³Louis Pasteur University Hospital, Kosice, Slovakia; ⁴Faculty Hospital Nitra, Nitra, Slovakia; ⁵Comenius University Faculty of Medicine in Bratislava, Bratislava, Slovakia

Email: tomas.koller@fmed.uniba.sk

Background and aims: Metabolic syndrome and alcohol are the most common risk factors for liver disease worldwide. The recent global consensus on steatotic liver disease (SLD) detailed its definition into more etiology-specific categories. We aimed to map the landscape of both risk factors, liver steatosis, and their possible combinations among participants of the liver screening program.

Method: The point-of-care arm of the SIRIUS program has operated in Slovakia since 2022 and visited more than 25 sites. Free-of-charge screening for liver disease is offered to local community-dwelling adults. Inclusion criteria were age >18 y, cases with a history of chronic liver disease or incapacitating severe systemic disease were excluded. The screening procedure included questionnaires on medical history, AUDIT-C, quality of life, food habits, basic anthropometric measurements, blood drop analysis for aminotransferases and blood lipids, and liver stiffness and CAP (Fibroscan by Echosense). Steatosis was defined according to EASL by CAP >275 db/m. The

metabolic syndrome (MS) was defined as at least one component according to the recent consensus and at-risk alcohol consumption (AUD) by AUDIT-C score ≥4 in women (F) or ≥5 in men (M).

Results: We included 1585 participants with a median (25–75 percentile) age of 53 y (44–64), M/F ratio 974/611, BMI 26, 9 (23, 9–30, 4), waist circumference M 101, F 91 cm, with 6, 3% having diabetes, 16, 7% of active smokers, 7, 8% having a history of unspecified liver disease. Steatosis was diagnosed in 31, 2% (M 39, 8, F 25, 9%). From the risk factors, we observed MS in 68, 8% (M72, 2, F66, 7%), and AUD in 15, 4% (M 21, 4, F 11, 4%). In males and females respectively, we observed no risk factors in 18, 3 and 26, 2%, elevated ALT in 33, 7 and 12, 2%, AUD alone in 4, 4 and 4, 6%, MS alone in 28, 3 and 39, 2%, AUD and MS in 9, 2 and 4, 1%, steatosis alone in 4, 3 and 2, 3%, steatosis and AUD (ALD) in 0, 8 and 0, 2%, steatosis and MS (MASLD) in 27, 7 and 20, 7% and steatosis, MS and alcohol (Met-ALD) in 7, 0 and 2, 7%.

Conclusion: Liver disease risk factors are frequently found in the screening program generating a substantial pool of patients eligible for preventive interventions. We observed a slight male predominance in the abnormal ALT, alcohol, and subgroups of steatotic liver disease.

WED-280

Spectroscopy of blood plasma has the potential to differentiate metabolic dysfunction-associated steatohepatitis from steatosis

Barbora Nováková¹, Ondřej Vrtělká², Kateřina Králová², Kateřina Žížalová³, Václav Šmíd⁴, Karel Dvořák⁵, Jaromír Petrátl⁶, Libor Vítek⁷, Martin Leníček³, Vladimír Setnická², Radan Bruha⁶. ¹4th Department of Internal Medicine, First Faculty of Medicine and General University Hospital in Prague, Charles University, 12808 Prague, Czech Republic, Institute of Medical Biochemistry and Laboratory Diagnostics, First Faculty of Medicine and General University Hospital in Prague, Charles University, 12108 Prague, Czech Republic, Prague, Czech Republic; ²Department of Analytical Chemistry, University of Chemistry and Technology Prague, Technická 5, 166 28 Prague 6, Czech Republic, Prague, Czech Republic; ³Institute of Medical Biochemistry and Laboratory Diagnostics, First Faculty of Medicine and General University Hospital in Prague, Charles University, 12108 Prague, Czech Republic, Prague, Czech Republic; ⁴4th Department of Internal Medicine, First Faculty of Medicine and General University Hospital in Prague, Charles University, 12808 Prague, Czech Republic, Prague, Czech Republic; ⁵Regional Hospital Liberec, 460 01 Liberec, Czech Republic, Institute of Medical Biochemistry and Laboratory Diagnostics, First Faculty of Medicine and General University Hospital in Prague, Charles University, 12108 Prague, Czech Republic, Prague, Czech Republic; ⁶4th Department of Internal Medicine, First Faculty of Medicine and General University Hospital in Prague, Charles University, 12808 Prague, Czech Republic, Prague, Czech Republic; ⁷Institute of Medical Biochemistry and Laboratory Diagnostics, First Faculty of Medicine and General University Hospital in Prague, Charles University, 12108 Prague, Czech Republic, 4th Department of Internal Medicine, First Faculty of Medicine and General University Hospital in Prague, Charles University, 12808 Prague, Czech Republic, Prague, Czech Republic
Email: cizkova.barbora@gmail.com

Background and aims: Searching for disease-specific blood spectral patterns was suggested to be a promising advanced experimental diagnostic approach that may provide a characteristic “fingerprint” that can be used diagnostically in the field of hepatology. We aimed to test the potential of spectroscopic analysis of blood plasma for distinguishing different stages of metabolic dysfunction-associated steatotic liver disease (MASLD).

Method: We analyzed blood plasma samples using a combination of conventional and advanced spectroscopic methods (Fourier-transform infrared (FTIR) spectroscopy, Raman spectroscopy, and Electronic circular dichroism (ECD)) in an exploratory group of seven patients with biopsy confirmed metabolic dysfunction-associated steatohepatitis (MASH) and six patients with simple steatosis. Pilot results were validated on 29 patients with MASH and

POSTER PRESENTATIONS

24 patients with steatosis. Further, we tested these methods in the identification of MASH with moderate-to-advanced fibrosis (F2-3; $n = 15$) compared to MASH/steatosis with no/mild fibrosis (F0-1, $n = 29$). Finally, we wanted to differentiate patients with fibrosis ($n = 39$) from those with steatosis ($n = 14$), regardless of the presence of MASH. The presence or absence of MASH was biopsy-proven, as well as the fibrosis grade. The spectra were processed and compared between groups using PCA-LDA method with leave-one-out cross-validation in the exploratory group, and by PLS-DA algorithm with a repeated 10-fold cross-validation, complemented by permutation test in the validation cohort.

Results: The pilot study showed the potential of spectroscopic methods to identify MASH, as the classification accuracy reached up to 77% for the combination of the individual methods. The validation study showed that the combination of FTIR and Raman spectroscopy together with ECD discriminated MASH with a sensitivity of 90% and a specificity of 82% (AUROC 0.93), $p < 0.001$. Furthermore, the same combination of methods showed the ability to identify MASH with moderate-to-advanced fibrosis compared to MASH/steatosis with no/mild fibrosis F0-1 with a sensitivity of 83% and specificity of 82% (AUROC 0.90), $p < 0.001$. Apart from MASH, these methods also identified fibrosis (of any grade) from steatosis with a sensitivity of 80% and specificity of 90% (AUROC 0.91), $p < 0.001$.

Conclusion: Blood plasma spectroscopy seems to have the potential to differentiate patients with MASH or MASH with moderate-to-severe fibrosis, although external validation is necessary. Supported by: MH CZ-DRO-VFN00064165 and by AZV MHCZ NU23-01-00288.

WED-281-YI

A non-invasive score model for prediction of significant fibrosis and fibrotic metabolic dysfunction-associated steatohepatitis based on serum biomolecules

Nateneal Beyene¹, Wilhelmus J Kwanten², Lotte Schoenmakers³, Jolien Derdeyn³, Toon Steinhauer³, Thomas Vanwolleghem², Ann Driessen³, Sven Francque², Luisa Vonghia². ¹University of Antwerp, Antwerp University Hospital, Wilrijk, Belgium; ²Antwerp University Hospital, University of Antwerp, Edegem, Belgium; ³Antwerp University Hospital, Edegem, Belgium
Email: natenealtamerat.beyene@uantwerpen.be

Background and aims: Metabolic dysfunction-associated steatohepatitis (MASH) with significant fibrosis (i.e., $\geq F2$ fibrosis) has a higher risk of developing advanced liver disease. The gold standard for identifying MASH and liver fibrosis remains a histological evaluation via liver biopsy, an invasive and costly procedure. Hence, blood biomarkers based prediction scores may provide an improved option. This study aims to generate serum based score model to predict significant fibrosis in metabolic dysfunction-associated steatotic liver disease (MASLD) patients.

Method: The study includes 120 subjects that underwent a liver biopsy for a suspicion of MASLD at the Antwerp University Hospital. The MASLD activity score system was used to determine the histological MASLD features. Besides standard serum biochemistry, concentrations of bio-molecules cytokeratin-18 (CK-18 M30), tissue inhibitors of metalloproteinases-1 (TIMP1), vascular cell adhesion molecule-1 (VCAM1), and fasting insulin (FI) were measured. Independent predictors of $F \geq 2$ identified by multivariate logistic regression, and the predicted probabilities used to generate prediction models with area under the receiver operating characteristic curves (AUROC). The AUROC of models compared using DeLong test in R via pROC package. $p < 0.05$ considered statistically significant.

Results: Histology revealed that 31 of the 120 subjects had no MASL, 31 had MASL, and 58 had MASH; 48 patients had fibrosis $F \geq 2$, 34 of them had MASH. First, Model-B (combining TIMP1, VCAM1, CK18 and FI) predicted $F \geq 2$ fibrosis with an AUROC of 0.95 (CI, 0.91–99, cut-off = 0.22) with 92% sensitivity and 85% specificity. Model-B predicted fibrotic MASH with an AUROC 0.91 (CI, 0.85–96, cut-off = 0.20) with 86% sensitivity and 83% specificity. Secondly, Model-E

(comprising Gamma-glutamyl transpeptidase, aspartate aminotransferase, alanine transaminase and age) predicted $F \geq 2$ with an AUROC of 0.88 (CI, 0.82–94, cut-off = 0.378) with 81% sensitivity and 79% specificity. Model-E predicted fibrotic MASH with an AUROC of 0.80 (CI, 0.72–88, cut-off = 0.205) with 82% sensitivity and 65% specificity. Thirdly, after computing FIB4 index, model-FIB4 predicted $F \geq 2$ with an AUROC of 0.83 (CI, 0.76–91, cut-off = 0.911) with 81.3% sensitivity and 71.8% specificity. Model-FIB4 also predicted fibrotic MASH with an AUROC of 0.71 (CI, 0.61–81, cut-off = 1.00) with 71% sensitivity and 66% specificity. Model-B outperformed Model-FIB4 in $F \geq 2$ prediction ($p = 0.006$), while there was no difference compared to Model-E ($p = 0.054$). Regarding fibrotic MASH prediction, Model-B was superior to Model-FIB4 and Model-E, $p = 0.001$ and, $p = 0.032$, respectively.

Conclusion: Serum biomolecule based composite score outperformed scores based on routinely available parameters to predict fibrotic MASH. This novel model might be a valuable diagnosis tool, after validation in an external cohort.

WED-282

Prevalence of Low Fibrosis-4 Score in Patients with MASLD-related Hepatocellular Carcinoma: Results from a Multicentre Cohort Study

Benedix Sim¹, Nobuharu Tamaki², Beom Kyung Kim³, Karn Wijarnpreecha⁴, Darren Jun Hao Tan⁵, Majd Aboona⁴, Claire Faulkner⁴, Ken Liu⁶, Wen Hui Lim⁵, Nicholas Syn⁵, Cheng Han Ng¹, Daniel Tung¹, Benjamin Tay¹, Yi Qing Tey¹, John Mok¹, Benjamin Nah¹, Maureen da Costa⁷, Shridhar Iyer⁷, Glenn Bonney⁷, Alfred Kow⁷, Mark Muthiah¹, Margaret Teng¹, Anand Kulkarni⁸, Sung Won Lee³, Rohit Loomba⁹, Daniel Huang¹. ¹Division of Gastroenterology and Hepatology, Department of Medicine, National University Hospital, Singapore, Singapore, Singapore, Singapore; ²Department of Gastroenterology and Hepatology, Musashino Red Cross Hospital, Tokyo, Japan, Tokyo, Japan; ³Division of Gastroenterology and Hepatology, Department of Internal Medicine, College of Medicine, The Catholic University of Korea, Seoul, Republic of Korea, Seoul, Korea, Rep. of South; ⁴Division of Gastroenterology and Hepatology, Department of Medicine, University of Arizona College of Medicine, Phoenix, Arizona, USA, Phoenix, United States; ⁵Yong Loo Lin School of Medicine, National University of Singapore, Singapore, Singapore, Singapore; ⁶AW Morrow Gastroenterology and Liver Centre, Royal Prince Alfred Hospital, Sydney, New South Wales, Australia, Sydney, Australia; ⁷Division of Hepatobiliary and Pancreatic Surgery, Department of Surgery, National University Hospital, Singapore, Singapore, Singapore, Singapore; ⁸Department of Hepatology, Asian Institute of Gastroenterology, Hyderabad, Telangana, India, Hyderabad, India; ⁹NAFLD Research Center, Division of Gastroenterology, University of California at San Diego, La Jolla, CA, United States, La Jolla, United States
Email: benedix.sim@mohh.com.sg

Background and aims: The fibrosis-4 (FIB-4) index has been incorporated in major guidelines as a non-invasive method to risk stratify patients with metabolic dysfunction-associated steatotic liver disease (MASLD). Patients with FIB-4 < 1.3 are considered to be at low risk of advanced fibrosis and are not recommended for follow-up with a hepatologist. However, previous studies have found limitations affecting the accuracy of FIB-4 including older age and diabetes. Hence, we aimed to evaluate the factors associated with falsely low FIB-4 in patients with MASLD-related hepatocellular carcinoma (HCC).

Method: We included adult patients diagnosed with MASLD-related HCC from January 2008 to August 2023 at six academic centers in India, Japan, South Korea, Singapore, and the United States. We compared patient and disease characteristics between patients with FIB-4 < 1.3 versus ≥ 1.3 . Predictors associated with FIB-4 < 1.3 were also investigated with multivariate logistic regression models. p values < 0.05 were considered statistically significant. All analyses were conducted in RStudio 2021.09.0.

Results: We included 538 patients with MASLD-related HCC, of which 38 patients (7.25%) had FIB-4 <1.3. In multivariate analysis adjusting for male sex, presence of cirrhosis, diabetes, obesity, and Barcelona Clinic Liver Cancer (BCLC) staging, diabetes (OR 0.44, 95%CI 0.21–0.90, $p=0.025$) and cirrhosis (OR 0.23, 95%CI 0.10–0.51, $p<0.001$) were associated with decreased odds of FIB-4 <1.3. Obesity was associated with increased odds of FIB-4 <1.3 (OR 2.11, 95%CI 1.00–4.41, $p=0.049$) (Figure 1). Subgroup analysis of patients without cirrhosis was conducted due to the high reported prevalence of HCC in the absence of cirrhosis in patients with MASLD. In subgroup analysis of 229 patients with MASLD-related HCC without cirrhosis, 29 patients had FIB-4 <1.3 (12.66%). Multivariate analysis found that obesity continued to be associated with increased odds of FIB-4 <1.3 in patients without cirrhosis (OR 2.85, 95%CI 1.16–6.92, $p=0.021$).

Conclusion: Obesity was associated with increased likelihood of FIB-4 <1.3 in patients with MASLD-related HCC, regardless of the presence of cirrhosis. Further studies are required to evaluate the effectiveness of FIB-4 as a risk stratification tool in the general population for patients with obesity.

WED-283

The distribution of fibrosis-4 index and vibration-controlled transient elastography-derived liver stiffness measurement for patients with metabolic dysfunction associated steatotic liver disease in the general population

Yuji Ogawa¹, Wataru Tomeno², Imamura Yasushi³, Masaru Baba⁴, Takato Ueno⁵, Takashi Kobayashi⁶, Michihiro Iwaki⁶, Asako Nogami⁶, Takaomi Kessoku⁷, Yasushi Honda⁶, Kento Imajo⁸, Miwa Kawanaka⁹, Mitsuru Hisatomi¹⁰, Mamiko Takeuchi¹¹, Takashi Honda¹², Miwa Tatsuta¹³, Asahiro Morishita¹⁴, Shigeru Mikami¹⁵, Ken Furuya⁴, Noriaki Manabe⁹, Tomoari Kamada⁹, Takumi Kawaguchi¹⁶, Masato Yoneda⁶, Satoru Saito¹⁷, Atsushi Nakajima⁶. ¹NHO Yokohama Medical Center, Yokohama, Japan; ²International University of Health and Welfare Atami Hospital, Atami, Japan; ³Kagoshima Kouseiren Hospital, Kagoshima, Japan; ⁴JCHO Hokkaido Hospital, Sapporo, Japan; ⁵Kurume University, Kurume, Japan; ⁶Yokohama City University Graduate School of Medicine, Yokohama, Japan; ⁷International University of Health and Welfare Narita Hospital, Narita, Japan; ⁸Shin-yurigaoka General Hospital, Kawasaki, Japan; ⁹Kawasaki Medical School General Medical Center, Okayama, Japan; ¹⁰Tsushima city hospital, Tsushima, Japan; ¹¹Anjo Kosei hospital, Anjo, Japan; ¹²Nagoya University Graduate School of Medicine, Nagoya, Japan; ¹³KKR Takamatsu Hospital, Takamatsu, Japan; ¹⁴Kagawa University, Kita-gun, Japan; ¹⁵Kikkoman General Hospital, Noda, Japan; ¹⁶Kurume University School of Medicine, Kurume, Japan; ¹⁷Sanno Hospital, Tokyo, Japan
Email: yuji.ogawa01@gmail.com

Background and aims: The multisociety consensus nomenclature has introduced steatotic liver disease (SLD) with diverse subclassifications which are metabolic dysfunction associated steatotic liver disease (MASLD), metabolic dysfunction and alcohol associated steatotic liver disease (MetALD), alcohol-associated liver disease (ALD), specific etiology, and cryptogenic. We investigated their prevalence, as per the new definition, in the general population. Additionally, we analyzed the distribution of fibrosis-4 (FIB-4) index and vibration-controlled transient elastography (VCTE)-derived liver stiffness measurement (LSM) for MASLD.

Method: In this cross-sectional study, 6, 530 subjects undergoing health check-ups were included. Conventional B-mode ultrasound was performed on all 6, 530 subjects, and those with MASLD were performed VCTE.

Results: The prevalence of SLD was 39.5%, comprising MASLD 28.7%, MetALD 8.6%, ALD 1.2%, specific etiology SLD 0.3%, cryptogenic SLD 0.7%. Subjects with VCTE-derived LSM ≥ 8 kPa constituted 2.1%. FIB-4 ≥ 1.3 showed that the sensitivity, specificity, positive predictive value (PPV), and negative predictive value (NPV) for diagnosing VCTE-derived LSM ≥ 8 kPa were 60.6%, 77.0%, 5.3%, and 98.9%, respectively. The referral rate to specialists was 23.8% using FIB-4 ≥ 1.30 . “FIB-4

≥ 1.3 in subjects <65 years and FIB-4 ≥ 2.0 in subjects ≥ 65 years” showed higher PPV (6.7%) and lower referral rate (17.1%) compared with FIB-4 ≥ 1.3 , but the sensitivity (54.5%) of that was not adequate diagnostic capability as non-invasive test for diagnosing VCTE-derived LSM ≥ 8 kPa.

Conclusion: Acknowledging the selection bias in hepatology centers, we conducted this prospective general population-based study. While the FIB-4 index proves to be a convenient marker, it might not perform well as a primary screening for liver fibrosis in the general population. UMIN Clinical Trials Registry No. UMIN000035188.

WED-284-YI

The Fatty Liver Index (FLI) is more accurate than FIB-4 for detection of advanced liver fibrosis in patients with type-2 Diabetes Mellitus (T2DM) in Primary Care

Ruth Nadal¹, Adrià Juanola^{1,2,3}, Jordi Hoyo⁴, Sara Martínez⁴, Ana Carvelli⁵, Anna Soria^{2,3,5}, Maria Sanz-Rodríguez⁶, Marta Carol^{1,3,6}, Martina Perez-Guasch², Marta Cervera¹, Ana Belen Rubio Garcia^{2,7}, Miriam Pellon^{1,2}, Marife Alvarez⁴, Marina Gigante Lopez⁴, Yolanda Herreros⁴, Cristina Pozo⁴, Carlota Riba¹, Maria Jose Moreta², Jordi Gratacós-Ginès^{1,2,3}, Elisa Pose^{1,2,3,7}, Isabel Graupera^{1,2,3,7}, Pere Ginès^{1,2,3,7}, Núria Fabrellas^{1,3,6,8}. ¹Fundació de Recerca Clínic Barcelona-Institut d'Investigacions Biomèdiques August Pi i Sunyer (FRCB-IDIBAPS), Barcelona, Spain; ²Liver Unit, Hospital Clínic de Barcelona, Barcelona, Spain; ³Centro de Investigación Biomédica en red de enfermedades hepáticas y digestivas, Barcelona, Spain; ⁴Centre d'Atenció Primària Numància, Institut Català de la Salut (ICS), Barcelona, Spain; ⁵de Recerca Clínic Barcelona-Institut d'Investigacions Biomèdiques August Pi i Sunyer (FRCB-IDIBAPS), Barcelona, Spain; ⁶Faculty of Nursing, University of Barcelona, Barcelona, Spain; ⁷Faculty of Medicine and Health Sciences, University of Barcelona, Barcelona, Spain; ⁸Centre d'Atenció Primària La Marina, Institut Català de la Salut (ICS), Barcelona, Spain
Email: runadal@recerca.clinic.cat

Background and aims: The prevalence of advanced fibrosis (AF) in patients with T2DM may be as high as 20% due to the high prevalence of metabolic-associated steatotic liver disease (MASLD). Non-invasive tests, particularly FIB-4, have been proposed as the first step for early identification of AF in this population. This is mainly based on studies performed in cohorts from secondary care or specialized units. However, little information exists on prevalence of AF and usefulness of FIB-4 in the diagnosis of AF in patients with T2DM from Primary Care. The aim of this study was to assess the prevalence of AF in patients with T2DM from Primary Care as well as investigate the usefulness of FIB-4 in the diagnosis of AF.

Method: Cross-sectional study performed in a Primary Care practice in Barcelona. Patients were randomly identified from the center's database and invited to participate through telephone contact. Patients who accepted (54.7%) had a visit by a study nurse with collection of demographic and clinical data, anthropometric measurements, standard lab tests, and transient elastography to measure liver stiffness (LS). Patients with FIB-4 >1.3 (2.0 if age >65 years) or with LS ≥ 8 kPa were referred to the Hospital for a specialized visit.

Results: 430 patients were recruited, 64% men, with a mean age of 69 (SD ± 10) years. The most frequent comorbidity was arterial hypertension (72%), followed by dyslipidemia (69%), obesity (31%), and high-risk alcohol consumption (7%; >21 SU/w in men or >14 in women). The prevalence of AF, defined as LS >10 kPa, was of 4.7%. Mean LS in these patients was 12.2 kPa (SD ± 2.52). Etiologies of liver disease in these patients were MASLD and MetALD. Factors associated with an increased risk of AF were obesity [9% vs 3%, in patients with and without obesity, respectively; $p=0.004$; OR = 3.35 (95%CI 1.39–8.04)] and high-risk alcohol consumption [15% vs 4%, respectively, $p=0.005$; OR = 4.15 (95%CI 1.42–12.11)]. FIB-4 identified correctly only 32% of patients with LS >10 kPa. On the other hand, 104 patients

POSTER PRESENTATIONS

with elevated FIB-4 had $LS \leq 10$ kPa (Se = 32%, Sp = 75%, PPV = 6%, NPV = 95%). By contrast, Fatty Liver Index (FLI), a score that estimates the degree of hepatic steatosis, identified correctly 86% of patients with AF (Se = 86%, Sp = 43%, PPV = 8%, NPV = 98%). The accuracy of FLI for the diagnosis of AF, as estimated by the ROC curve, was greater than that of FIB-4 [FLI = 0.77 (0.66–0.87) vs FIB-4 = 0.54 (0.39–0.70); $p = 0.034$].

Conclusion: The prevalence of AF in patients with T2DM in Primary Care was 4.7%, a value lower than that reported in cohorts from specialized care. Obesity and alcohol risk consumption were risk factors of AF. The accuracy of FIB-4 in identifying AF was only modest. FLI outperformed FIB-4 for identification of patients with AF. These results suggest that FLI but not FIB-4 should be used as the first step of assessment of liver fibrosis in patients with T2DM in Primary Care.

WED-285

Predicting significant hepatic steatosis from routine biochemistry in people with and without type 2 diabetes (T2D)

Magdalena Nowak¹, Andrea Dennis¹, Helena Thomaidis Brears¹, Rajarshi Banerjee¹, Kenneth Cusi², Naim Alkhouri³, Daniel Cuthbertson⁴. ¹Perspectum Ltd., Oxford, United Kingdom; ²University of Florida, Gainesville, FL, United States; ³Arizona Liver Health, Chandler, Arizona, United States; ⁴University of Liverpool, Liverpool, United Kingdom
Email: magdalena.nowak@perspectum.com

Background and aims: Quantifying liver fat content (LFC) using MRI and assessing LFC change in response to therapy has been widely used as a primary end point in early-phase clinical trials of therapeutic agents for metabolic dysfunction-associated liver disease (MASLD). Identifying individuals with LFC of 8% or higher is typically used as an inclusion criterion and various blood-based biomarkers have been proposed, but their value has not been extensively studied in T2D. We aimed to identify the optimal combination of anthropometric and routinely available biochemical tests to better identify patients with high LFC.

Method: Data from participants with suspected MASLD were pooled from three clinical studies; with T2D (N = 173, 41% female, median age: 60y, mean: LFC = 11%, BMI 31 kg/m²) and without T2D (N = 114, 46% female, median age: 55 y, mean: LFC = 12%, BMI 31 kg/m²). Additional validation datasets were analysed: with T2D (N = 305, 43% female, median age: 58 y, mean: LFC = 16%, BMI 34 kg/m²) and without (N = 452, 51% female, median age: 49 y, mean: LFC = 10%, BMI 30 kg/m²). LFC was measured using either magnetic resonance imaging (proton-density fat fraction) or proton magnetic resonance spectroscopy. The diagnostic accuracy was evaluated using Area Under the Receiver Operating Characteristic curve (AUROC). Stepwise logistic regression was performed to select the optimal combination of continuous predictor variables. The Fatty Liver Index (FLI), Hepatic Steatosis Index (HSI) and controlled attenuation parameter (CAP) measured by Fibroscan were also assessed, where available.

Results: LFC ($\geq 8\%$) was most effectively predicted by a simple combination of serum ALT and triglycerides. This model showed good diagnostic accuracy, in both training and validation datasets, in individuals with T2D (Training: AUC 0.78, CI: 0.68–0.88; PPV = 0.86; Validation: AUC: 0.83, CI: 0.78–0.88, PPV = 0.88) and without (Training: AUC: 0.83, CI: 0.73–0.93; PPV = 0.88; Validation: AUC: 0.86, CI: 0.82–0.90, PPV = 0.7). Addition of waist circumference did not significantly increase AUC (0.82–0.87; DeLong test $p > 0.05$). The accuracy of FLI and HSI was less consistent across both T2D and non-T2D groups (FLI, AUC range: 0.73–0.82, PPV range = 0.53–0.9; HSI, AUC range: 0.72–0.76, PPV range = 0.57–0.86). In T2D, the CAP score was less accurate (AUC: 0.71, CI: 0.58–0.83; PPV = 0.77).

Conclusion: This study demonstrates that the combination of ALT and triglycerides accurately identifies patients with LFC of 8% or higher. The integration of such models into the patient recruitment process in hepatology and endocrinology clinics could effectively reduce screen failure rates in clinical trials for MASLD.

WED-286

Identification of serum metabolome signatures associated with hepatocellular carcinoma in metabolic dysfunction-associated steatohepatitis

Atsumasa Komori¹, Kosuke Matsumoto¹, Yuki Kugiyama¹, Tomoyuki Suehiro¹, Yasuhide Motoyoshi¹, Akira Saeki¹, Shinya Nagaoka¹, Kazumi Yamasaki¹, Hiroshi Yatsuhashi¹. ¹NHO Nagasaki Medical Center, Omura, Japan
Email: atsuri1027@yahoo.co.jp

Background and aims: As the incidence of hepatocellular carcinoma (HCC) that arose in metabolic dysfunction-associated steatohepatitis (MASH) is increased worldwide, establishing an effective risk assessment and early diagnosis of HCC among MASH is much anticipated. On the other hand, not only genetic alterations, but also inflammatory humoral factors, that show causal relationship to hepatocarcinogenesis in MASH are still elusive. Serum metabolome is a promising candidate for the non-invasive monitoring of various disease status, reflecting host primary metabolites, gut microbiome, and dietary factors, all of which are likely associated with outcomes of disease. The aim of the study is to identify the serum metabolites in MASH that are associated with the occurrence of HCC.

Method: We profiled serum metabolites of patients with MASH with (n = 11) and without HCC (n = 21: Control) using a comprehensive non-targeted metabolomics approach with LC-MS/CE-MS. Differentially detected metabolites (DDMs) in those with HCC were defined statistically significant with $p < 0.05$ (t-test) and $q < 0.1$ (FDR). All HCC were diagnosed primary as a solitary lesion in pathology-proven MASH patients (Brunt stage 4; n = 5/3; n = 3/2; n = 2/1; n = 1, male n = 9/female n = 2, mean age 73.5), with 31mm of mean diameter (range: 20–37 mm). The demographics of Control patients were as follows: Brunt stage 4; n = 0/3; n = 3/2; n = 12/1; n = 6, male n = 8/female n = 13, mean age 64.5).

Results: 28 DDMs were demonstrated among 336 metabolites being identified by LC-MS/CE-MS. Top two significantly increased metabolites in HCC patients were 3-Methyladipic acid ($p = 5.2 \times 10^{-5}$) and 2-hydroxybutyric acid ($p = 5.1 \times 10^{-5}$), whereas top two in decrease were TG (58:9) and PE (40:4). Levels of 3-Methyladipic acid, a surrogate of omega-oxidation of free fatty acid (FFA), were not differed according to fibrosis stage and were significantly correlated with those of 2-hydroxybutyric acid ($r = 0.7222$, $p < 0.0001$), cortisol ($r = 0.7306$, < 0.0001), and progesterone ($r = 0.7861$, < 0.0001). PUFA-rich TG, e.g. TG (58:7), TG (58:9), and TG (58:10), were significantly decreased in HCC patients ($p = 0.002$, $p = 0.00029$, and $p = 0.00098$, respectively), whereas TG with saturated FFA, e.g. TG (46:0) and TG (48:0) were not ($p = 0.41$ and $p = 0.41$, respectively).

Conclusion: Our metabolome analysis exploratory identified the serum metabolite features of MASH patients with HCC, some of which may potentially be biomarkers for MASH-associated hepatocarcinogenesis.

WED-287

Sequential approach using combination of newly developed HOMA2-IR-ALT-TE-MASH (HALT-M) score and magnetic resonance elastography for non-invasive identifying at-risk metabolic dysfunction-associated steatohepatitis in obese subjects

Seung Kak Shin¹, Yoonseok Lee¹, Oh Sang Kwon¹, Yun Soo Kim¹, Ju Hyun Kim¹, Dae Ho Lee². ¹Division of Gastroenterology and Hepatology, Department of Internal Medicine, Gachon University College of Medicine, Gil Medical Center, Incheon, Korea, Rep. of South; ²Division of Endocrinology, Department of Internal Medicine, Gachon University College of Medicine, Gil Medical Center, Incheon, Korea, Rep. of South
Email: drhormone@naver.com

Background and aims: Presence of metabolic dysfunction-associated steatohepatitis (MASH) and significant fibrosis are associated with increased risk of disease progression and poor clinical outcomes in metabolic dysfunction-associated steatotic liver disease (MASLD) patients. Insulin resistance has been suggested to play a crucial role in

the pathogenesis of MASH. However, this has been given little consideration in most of the non-invasive markers for identifying at-risk MASH. This study aimed to develop the non-invasive sequential approach using combination of HOMA2-IR-ALT-TE-MASH (HALT-M) score and magnetic resonance elastography (MRE) for diagnosis of borderline/definite MASH [MASLD activity score (MAS) ≥ 4] and at-risk MASH (MAS ≥ 4 and fibrosis stage ≥ 2).

Method: Obese (BMI ≥ 25 kg/m²) MASLD patients were prospectively enrolled at Gachon University Gil Medical Center between March 2018 and January 2023. All patients underwent histological confirmation. Newly developed HALT-M score consists of three risk factors: 1) presence of HOMA2-IR ≥ 2.35 or DM, 2) increased ALT (men ≥ 35 U/L, women ≥ 25 U/L), 3) transient elastography (TE) > 8.0 kPa. The three factors were given a score of 1 point each, and a score of 0–3 was calculated and used for non-invasive diagnosis of borderline/definite MASH or at-risk MASH. And combination of HALT-M score and MRE (HALTME index) was used for non-invasive diagnosis of at-risk MASH. Diagnostic performance was evaluated based on the areas under the receiver operating characteristic curve (AUCs).

Results: A total 84 patients (mean age of 35 ± 11 years; 79.8% of female; mean BMI of 37.6 ± 6.1 kg/m²; 35.7% of DM; 84.5% of bariatric surgery) were finally enrolled. At histological confirmation, 43 (51.2%) and 16 (19.0%) patients were diagnosed with borderline/definite MASH and at-risk MASH, respectively. The sensitivity, specificity, PPV, and NPV of HALT-M score ≥ 2 for diagnosis of borderline/definite MASH were 91%, 60%, 71%, 86%, respectively (AUC 0.753; 95% CI 0.645–0.862, $p < 0.001$). The sensitivity, specificity, PPV, and NPV of HALT-M score ≥ 2 for diagnosis of at-risk MASH were 100%, 41%, 29%, 100%, respectively (AUC 0.709; 95% CI 0.594–0.824, $p < 0.001$). The sensitivity, specificity, PPV, and NPV of HALTME index (HALT-M score ≥ 2 plus MRE ≥ 3.6 kPa) for diagnosis of at-risk MASH were 80%, 90%, 63%, 95%, respectively (AUC 0.849; 95% CI 0.723–0.974, $p < 0.001$).

Conclusion: Newly developed HALT-M score including HOMA2-IR, ALT and TE demonstrated high sensitivity in diagnosis of borderline/definite MASH and at-risk MASH. The sequential addition of MRE value increased the specificity for diagnosis of at-risk MASH, showing good diagnostic performance. A large-scale validation study is warranted.

WED-290

Assessment of transient elastography (FibroScan) in obesity patients with non-alcoholic fatty liver disease: a meta-analysis

Ziping Lin¹, Taoyuan Li¹, Jieying Li¹, Yi Liu¹, Xujing Liang¹. ¹The First Affiliated Hospital of Jinan University, Guangzhou, China
Email: lxjlxj@163.com

Background and aims: Obesity is strongly associated with non-alcoholic fatty liver disease (NAFLD). Among the non-invasive tests, controlled attenuation parameter (CAP) and liver stiffness measurement (LSM) have shown better diagnostic performance in NAFLD. However, the accuracy of Fibroscan in patients with obesity (body mass index (BMI) ≥ 30 kg/m²) is not well-defined. This meta-analysis aimed to evaluate the performance of CAP and LSM for assessing steatosis and fibrosis in NAFLD patients with obesity.

Method: We searched the PubMed, Web of Science, Cochrane Library, and Embase databases for relevant articles published up to November 16th, 2023, and selected obese patients with NAFLD diagnosed by liver biopsy. Then we pooled sensitivity (SE), specificity (SP), and area under receiver operating characteristic (AUROC) curves. Quality of the included studies was assessed with the QUADAS-2 tool. Stata 17 and MetaDisc1.4 were used to meta-analyze.

Results: A total of 19 articles were included which consisted of 2349 patients with NAFLD (BMI ≥ 30 kg/m²). The AUROC of FibroScan in identifying the stage of steatosis for $\geq S1$ was 0.85 (sensitivity:80%; specificity:78%), that for $\geq S2$ was 0.80 (sensitivity:80%; specificity:66%) and that for $S3$ was 0.79 (sensitivity:87%; specificity:68%). The AUROC of FibroScan in identifying the stage of fibrosis for $\geq F2$ was 0.82 (sensitivity:80%; specificity:73%), that for $\geq F3$ was 0.77

(sensitivity: 75%; specificity:85%), and that for $F4$ was 0.97 (sensitivity: 97%; specificity:90%). The average values of the optimal cutoff values by fibroscan for $S \geq 1$, ≥ 2 , and $= 3$ are 295 dB/m, 314 dB/m, 331 dB/m, respectively. The average values of the optimal cutoff values by fibroscan for $F \geq 2$, ≥ 3 , and $= 4$ are 8.1 kPa, 9.9 kPa, and 13.1 kPa, respectively.

Conclusion: FibroScan still be reliable for quantifying and staging hepatic steatosis and fibrosis in patients with obesity (BMI ≥ 30 kg/m²). The diagnostic performance of CAP decreased with the severity of liver steatosis. The average value of the optimal cutoff value for CAP was relatively high in obese patients. LSM has shown good accuracy in assessing significant liver fibrosis (AUC = 0.82), advanced liver fibrosis (AUC = 0.77), especially liver cirrhosis (AUC = 0.97) in obese patients. Further studies are needed to explore the result.

WED-291

New optimal cut-points for vibration controlled transient elastography and MR elastography for advanced fibrosis in hispanic versus non-hispanic adults with metabolic dysfunction-associated steatotic liver disease

Monica Tincopa¹, Ricki Bettencourt¹, Egbert Madamba¹, Harris Siddiqi¹, Lisa Richards¹, Rohit Loomba¹. ¹UCSD, San Diego, United States

Email: mtincopa@health.ucsd.edu

Background and aims: Cut-points for non-invasive tests (NITs) in metabolic dysfunction-associated steatotic liver disease (MASLD) were derived from predominantly non-Hispanic populations. The aim of this study is to assess the performance characteristics of current NIT-based risk stratification cut-points to identify advanced fibrosis among Hispanic patients with biopsy-proven MASLD and to identify if alternative cut-points can improve NIT performance.

Method: This prospective cohort enrolled 244 well-characterized adults with biopsy-proven MASLD. Those with significant alcohol use, other causes of liver disease, and decompensated cirrhosis were excluded. Patients underwent a clinical research visit with vibration controlled transient elastography (VCTE), and MR elastography (MRE). Biopsies were read by one experienced hepatopathologist blinded to clinical data. We assessed the performance of currently recommended cut-points for VCTE and MRE to identify advanced ($F \geq 3$) fibrosis (VCTE 9.7, MRE 3.63) among Hispanic versus non-Hispanic individuals. We identified alternative cut-points that optimized VCTE and MRE performance for Hispanic individuals using Youden's J analysis.

Results: The mean age was 52.6 years, with 43% males, mean body-mass-index 31.6 kg/m² with 40% with diabetes and 31% (N = 75) Hispanic. Overall, 78 (32%) had significant fibrosis and 50 (20.4%) had advanced fibrosis on biopsy (40% and 28% among Hispanics, respectively). For advanced fibrosis, VCTE had an area under the receiving operator curve (AUROC) of 0.79 (0.66–0.92) vs 0.93 (0.89–0.98) ($p = 0.04$) and MRE had an AUROC of 0.90 (0.83–0.97) vs 0.96 (0.93–0.99) ($p = 0.12$) in Hispanic vs non-Hispanic adults, respectively. In Hispanic individuals, the cut-points for advanced fibrosis for 90% sensitivity for VCTE and MRE was > 4.4 and > 2.77 kPa, and for 90% specificity was > 11.9 and > 3.58 kPa, respectively. Using Youden's J analysis, the optimal cut-point for advanced fibrosis in Hispanic individuals for VCTE was 8.8 kPa and 2.73 kPa for MRE.

Conclusion: In a well-characterized cohort of adults with biopsy-proven MASLD, Hispanic individuals had higher prevalence of significant and advanced fibrosis. Currently recommended cut-points for VCTE and MRE for advanced fibrosis in MASLD had inferior performance among Hispanic compared to Non-Hispanic individuals. Given higher disease burden and more advanced disease, our analyses suggest that implementing lower cut-points for VCTE and MRE for advanced fibrosis may optimize screening and risk stratification for Hispanic individuals with MASLD.

WED-292

Non-invasive diagnosis of significant portal hypertension based on prealbumin proteomics model

Xiaoyan Wang¹, Chuan Liu², Jianhong Wang¹, Yunfang Liu¹, Dong Wang¹, Xiaoqing Guo³, Ying Guo⁴. ¹Department of Hepatology, The Third People's Hospital of Taiyuan, Taiyuan, China; ²Center of Portal Hypertension, Department of Radiology, Zhongda Hospital, Medical School, Southeast University, Nanjing, China; ³Department of Hepatology, The Third people's Hospital of Taiyuan, Taiyuan, China; ⁴Department of Hepatology, The Third People's Hospital of Taiyuan, Taiyuan, China
Email: taiyanguoying001@163.com

Background and aims: The clinical significant portal hypertension (CSPH) is associated with the increased risk of decompensated cirrhosis in patients. However, the gold standard for its diagnosis, the measurement of hepatic venous pressure gradient (HVPG) is invasive, expensive, and requires a certain level of technical expertise from the operator. This study aims to explore the diagnostic value of a non-invasive model based on prealbumin (PA) proteomics for CSPH in patients with cirrhosis.

Method: This is a Retrospective study. A total of 176 patients with compensated cirrhosis who underwent HVPG measurement were included in this study. They were admitted to the Third People's Hospital of Taiyuan from January 2022 to December 2022. According to the results of HVPG, they were divided into CSPH group (n = 104) and Non-CSPH group (n = 72). CSPH was defined as the threshold of HVPG measurement above 10 mmHg.

Results: There were significant differences in PA, MELD score, and Child-Pugh Class between the two groups (p < 0.05); Serum PA levels were negatively correlated with HVPG in all patients (r = -0.592, P < 0.05); Ordered Logistic regression analysis showed that serum PA (OR = 0.99, 95% CI: 0.98–1.00), PLT (OR = 0.99, 95% CI: 0.98–1.00), and INR (OR = 184.01, 95% CI: 4.19–8088.42) were independent risk factors for CSPH. In the diagnosis of CSPH, the AUC value of PA was 0.80 (0.73–0.87) (p < 0.05), and the optimal critical value was 141.00 mg/L. Its sensitivity was 69.2%, specificity was 81.9%, positive predictive value was 84.7%, and negative predictive value was 64.8%.

Conclusion: Based on the serum prealbumin, the established non-invasive assessment model is simple and feasible, and it has good predictive value for CSPH.

The Corresponding authors: Ying Guo (taiyanguoying001@163.com);

WED-293

Effectiveness of on different models of care based on Fibrosis-4 and/or liver stiffness measurement for the screening of patients with type 2 diabetes mellitus at risk of advanced liver disease

Gian Paolo Cavaglia¹, Arianna Ferro¹, Angelo Armandi^{1,2}, Roberta D'Ambrosio³, Pietro Lampertico^{3,4}, Giulia Periti⁵, Luca Valenti⁵, Carlo Ciccioli⁶, Grazia Pennisi⁶, Salvatore Petta⁶, Lucia Brodosi^{7,8}, Maria Letizia Petroni^{7,8}, Francesca Marchignoli^{7,8}, Loris Pironi^{7,8}, Alessandra Sagripanti⁹, Maria Eva Argenziano⁹, Gianluca Svegliati-Baroni⁹, Gabriella Gruden¹, Elisabetta Bugianesi¹. ¹Department of Medical Sciences, University of Turin, Torino, Italy; ²Metabolic Liver Disease Research Program, I. Department of Medicine, University Medical Center of the Johannes Gutenberg-University, Mainz, Germany; ³Foundation IRCCS Ca' Granda Ospedale Maggiore Policlinico, Division of Gastroenterology and Hepatology, Milano, Italy; ⁴CRC "A. M. and A. Migliavacca" Center for Liver Disease, Department of Pathophysiology and Transplantation, University of Milan, Milano, Italy; ⁵Department of Transfusion Medicine and Haematology, Fondazione IRCCS Ca' Granda Ospedale Maggiore Policlinico, Milano, Italy; ⁶Section of Gastroenterology and Hepatology, Dipartimento Di Promozione Della Salute, Materno Infantile, Medicina Interna e Specialistica Di Eccellenza (PROMISE), University of Palermo, Palermo, Italy; ⁷Department of Medical and Surgical Sciences, University of Bologna, Bologna, Italy;

⁸Clinical Nutrition and Metabolism Unit, IRCCS AOUBO, Bologna, Italy;

⁹Liver Disease and Transplant Unit, Polytechnic University of Marche, Ancona, Italy

Email: elisabetta.bugianesi@unito.it

Background and aims: Patients with type 2 diabetes mellitus (T2DM) are at increased risk of advanced liver fibrosis and should be entered into risk stratification pathways for appropriate referral to hepatologists. An optimal model of care should allow the identification of the largest proportion of high-risk patients without overwhelming hepatology clinical services. In a cohort of patients with T2DM consecutively referred by diabetes Units, we aimed to investigate the efficacy of different models of care based on Fibrosis-4 (FIB-4) and/or vibration controlled transient elastography (VCTE) for the identification of patients needing referral to hepatology clinic.

Method: From April 2021 to October 2023, a total of 706 consecutive T2DM patients at their first referral to 6 different diabetology clinics were prospectively enrolled. All patients underwent liver stiffness measurement (LSM) by VCTE and liver steatosis assessment by controlled attenuation parameter (Fibroscan, Echosens, France). A LSM cut-off value of 8.0 kPa was used to rule out advanced liver fibrosis. Patients were stratified according to FIB-4 values <1.30, 1.30–2.67, and >2.67.

Results: Patients' median age was 59 (IQR 53–65) years and 411 (58.2%) of them were males; 370 (52.4%) patients were obese (BMI ≥30 kg/m²) and 446 (64.3%) had arterial hypertension. Median LSM was 5.3 (IQR 4.3–6.5) kPa; 111 (14.6%) of patients had LSM ≥8.0 kPa. Median FIB-4 value was 1.05 (IQR 0.80–1.40); 490 (69.4%) patients had FIB-4 <1.30, 197 (27.9%) had FIB-4 between 1.30 and 2.67, while 19 (2.7%) patients showed FIB-4 values ≥2.67. In our cohort of T2DM patients, a 2-tier screening for advanced liver fibrosis by FIB-4 followed by VCTE would have led to 50 (7.1%) patients referred to the hepatologist, despite a false negative rate of 8.6% (n = 61). A single tier screening based on FIB-4 ≥1.3 would have resulted in an overflow of patients (n = 216; 30.6%) to hepatology clinic, while a FIB-4 >2.67 would have caused a disproportionate rate of false negative patients (n = 103; 14.6%). Finally, a first line screening based on VCTE would have resulted in a referral rate to hepatologists of 14.6% (n = 111) with a low probability of missing patients at risk of advanced liver fibrosis. However, first-line screening with VCTE could be unfeasible in resource-limited settings.

Conclusion: In diabetology clinics, the most appropriate screening approach for the identification of high-risk patients that require hepatologist's referral should be determined according to local health-care resources. This research was supported by Gilead Sciences, Inc (study ID: IN-IT-989-5790).

WED-294

The use of the FibroScan-AST score and AST to pre-identify metabolic dysfunction-associated steatohepatitis patients with active fibrogenesis in a Phase 1b open-label clinical trial

Mazen Noureddin¹, Eric Lawitz², Naim Alkhoury³, Zeid Kayali⁴, Madhavi Rudraraju⁵, Edward Mena⁶, Rohit Loomba⁷, Tarek Hassanein⁸, Parvez Mantry⁹, Mohammad Siddiqui¹⁰, Kathryn Jean Lucas¹¹, Garry Reiss¹², Oni Aneiros¹³, Dawn Farno¹³, Shawna Differding¹³, Debbie Marshall¹³, Jaime Biracree¹³, Bruno Devadas¹⁴, Praveena Reddy¹⁴, Chetna Patel¹⁴, Jennifer Tsau¹⁴, Michael Chen¹⁴, Michelle Mendoza¹⁴, Scott Butler¹⁴, Holly Oakley¹⁴, Wendi Lichtenberger¹⁴, Shannon Hambridge¹⁴, Pares Shakkher¹⁴, Haakon Wennbo¹⁴, Peter Nagy¹⁴, Zoltan Dordak¹⁴. ¹Houston Research Institute, Houston, TX, United States; ²Texas Liver Institute, University of Texas Health San Antonio, San Antonio, TX, United States; ³Arizona Liver Health, Chandler, AZ, United States; ⁴Jubilee Clinical Research, Rialto, CA, United States; ⁵Pinnacle Clinical Research, San Antonio, TX, United States; ⁶California Liver Research Institute, Pasadena, CA, United States; ⁷University of California San Diego School of Medicine, La Jolla, CA, United States; ⁸Southern California Research Center, Coronado, CA,

United States; ⁹Methodist Dallas Medical Center, Dallas, TX, United States; ¹⁰Virginia Commonwealth University, Richmond, VA, United States; ¹¹Lucas Research, Morehead City, NC, United States; ¹²Tandem Clinical Research, LLC, Marrero, LA, United States; ¹³ICON Clinical Research, Blue Bell, PA, United States; ¹⁴Takeda Pharmaceuticals, Cambridge, MA, United States
Email: zoltan.derdak@takeda.com

Background and aims: Identifying patients with active fibrogenesis in proof-of-concept studies is an unmet need. We assessed screening data from an internal Phase 1b open-label clinical trial that is aimed to enroll patients with active fibrogenesis. Elevated Pro-C3 (≥ 12.6 ng/ml) and enhanced liver fibrosis (ELF) score ≥ 7.7 are active fibrogenesis markers and were used as key inclusion criteria in this study. We aimed to establish a pre-identification strategy that would make qualification on Pro-C3 and ELF more likely based on clinical parameters. We have assessed these clinical parameters and their cut-offs to help identifying patients with active fibrogenesis.

Method: Up to January 01, 2024, we have screened 114 patients with presumed fibrotic MASH. In 103 cases Pro-C3 and ELF values were available (both measured at Nordic Bioscience). All patients with qualifying Pro-C3 also qualified on ELF, therefore assessments focused on correlations between Pro-C3 and clinical parameters. Based on our findings, we performed Pearson's correlation tests between Pro-C3 and AST, liver stiffness measurement (LSM), Controlled Attenuation Parameter (CAP), and the overall FibroScan-AST (FAST) score. We stratified screened patients based on Pro-C3 qualification, determined the difference in AST, LSM, and FAST, and identified thresholds in AST and FAST that increased the likelihood of qualifying on Pro-C3.

Results: Pro-C3 statistically significantly ($p < 0.0001$) correlated with AST ($r = 0.4301$) and the FAST score ($r = 0.5071$). The correlation with CAP was low but reached statistical significance ($r = 0.1986$, $p = 0.0499$). The correlation with LSM was not significant ($r = 0.1034$, $p = 0.3109$). Those with qualifying Pro-C3 had statistically significantly higher mean AST (53.12 vs 33.13 U/L), FAST (0.6413 vs 0.3432) and CAP values (336.6 vs 314.5 kPa) but there was no statistically significant difference in LSM (12.12 vs 10.82 kPa, $p = 0.3144$). 77.27% of patients with AST < 35 U/L and 86.67% of patients with FAST < 0.35 failed on Pro-C3. Patients with qualifying Pro-C3 were more likely to have an AST ≥ 35 U/L (68.97%) and FAST ≥ 0.35 (67.68%). The Area Under the Receiver Operating Characteristic curve (AUROC) value describing the performance to distinguish patients with qualifying vs non-qualifying Pro-C3 was 0.7936 for AST and 0.8068 for FAST.

Conclusion: There have been limited stratification of MASH patients who have active fibrogenesis as evidenced by elevated Pro-C3/ELF levels. Commonly available clinical data can be used to increase the likelihood of qualification based on Pro-C3/ELF. This data may include AST and FAST that reflect the activity of steatohepatitis-a driver of fibrogenesis-and correlate with Pro-C3 levels. This finding highlights that fact that focusing on patients with FAST ≥ 0.35 and AST ≥ 35 U/L will increase the chance of providing direct biochemical evidence for active fibrogenesis.

WED-295-YI

Unmasking racial disparities of MASLD screening guidelines: underdiagnosis of MASLD among black patients with obesity

Gres Karim¹, Navim Mobin¹, Pratishtha Singh¹, Sara Hasan², Saamia Faruqui¹, Ilan Weisberg¹, Amreen Dinani³. ¹New York Presbyterian Brooklyn Methodist Hospital, Brooklyn, United States; ²New York Presbyterian Brooklyn Methodist Hospital, Brooklyn, United States; ³New York Presbyterian Brooklyn Methodist Hospital, Brooklyn, United States
Email: karimgres@gmail.com

Background and aims: Metabolic dysfunction-associated steatotic liver disease (MASLD) is rapidly increasing globally and is often underdiagnosed and undertreated. While considered to be less prevalent with a less aggressive course in the black population,

evidence shows higher risk for all-cause mortality including HCC outcomes emphasizing the need for urgent awareness. The fibrosis 4 index (FIB-4) has been proposed as the initial non-invasive test (NIT) to screen for fibrosis, however its performance is varied, possibly leading to misrepresentation of disease burden in certain populations. We aimed to understand the disease burden in a cohort of black individuals with obesity (body mass index [BMI] > 30 kg/m²) and undiagnosed MASLD, while also investigating disparities in the early detection of MASLD through the diagnostic performance of the FIB-4 and NAFLD Fibrosis score (NFS).

Method: Patients with a diagnosis of obesity (BMI > 30 kg/m²) without documented chronic liver diseases (CLD) or MASLD were identified using electronic medical record (EMR) from a tertiary care gastroenterology clinic between 01/2019 to 01/2020. Demographic information, markers of liver inflammation and synthetic function, medical conditions, and imaging were recorded. FIB-4 and NFS were calculated to determine the stage of liver fibrosis. Outcomes including cirrhosis, development of hepatocellular carcinoma (HCC) and liver-related mortality were noted.

Results: 1082 patients with a BMI > 30 kg/m² and no diagnosis of CLD or MASLD were identified. We identified 236 (22%) black patients, of which majority were female (78%), mean age was 57 years (SD 13), mean BMI was 36.3 kg/m² (SD 16.3), 73 were diabetic, 135 had hypertension, and 14 had coronary artery disease. Average AST and ALT were 22.7 and 22.8 U/L, respectively. 130 patients had class I obesity (BMI 30–34.9), 62 had class II obesity (BMI 35–39.9) and 44 had class III obesity (BMI > 40). Mean FIB-4 was 1.20 and mean NFS was 0.69. While increased NFS was seen with increase in BMI (-0.082 in class I obesity; 1.26 in class III obesity), an inverse association was detected with increasing obesity class and FIB-4 (1.29 in class I obesity; 0.95 in class III obesity). In this cohort, 22 patients developed cirrhosis, 10 developed HCC and 4 died from liver-related causes. FIB-4 and NFS were higher in patients who developed cirrhosis.

Conclusion: In a cohort of black patients with obesity and undiagnosed MASLD, two NITs produced widely discordant results; mean FIB-4 was 1.20, suggesting F0-F1 fibrosis, while mean NFS was 0.69, indicative of advanced fibrosis. Based on current recommendations, relying on FIB-4 alone overlooked 45% of black patients who could benefit from secondary fibrosis assessment, delaying diagnosis in a vulnerable and often underdiagnosed group. Further studies are needed to ascertain if NFS performs better than FIB-4 in screening black patients for MASLD.

WED-296

PLIN2 is a specific marker for liver related disease

Giulia Angelini¹, Sara Russo¹, Federico Biscetti², Andrea Flex², Jérôme Boursier³, Sven Francque⁴, Aldo Trylesinski⁵, Stephen A. Harrison⁶, Geltrude Mingrone¹. ¹Università Cattolica del Sacro Cuore, Rome, Italy; ²Fondazione Policlinico Universitario A. Gemelli IRCCS, Rome, Italy; ³Angers University Hospital, Angers, France; ⁴Antwerp University Hospital, Edegem, Belgium; ⁵Metadep, London, United Kingdom; ⁶Radcliffe Department of Medicine, University of Oxford, UK, Oxford, United Kingdom
Email: giulia.angelini@unicatt.it

Background and aims: Metabolic dysfunction-associated steatohepatitis (MASH) represents the leading cause of chronic liver disease worldwide. Among those with MASH, cardiovascular disease (CVD) is the most common cause of mortality. MASH was also shown to be associated with the development of atherosclerosis and subclinical CVD. Monocytes can accumulate large amounts of lipids, transform into foam cells and drive atherogenesis. The same process of accumulation of lipid-loaded monocytes is also observed in MASH. PLIN2 is a major lipid droplets-associated protein in monocytes that has been linked to both atherosclerosis and MASH. Indeed, several studies report high levels of PLIN2 in MASH and atherosclerosis. This study aims to compare the levels of PLIN2 in subjects with MASH

POSTER PRESENTATIONS

with/without CVD as well as in subjects with CVD alone to assess whether PLIN2 is a specific biomarker for liver related disease.

Method: We analyzed 50 subjects with histologically proven MASH who underwent carotid intima-media thickness (CIMT), a marker of subclinical atherosclerosis to assess co-existing CVD. These patients were compared to 50 subjects with CVD assessed by coronary angiography from the cardiovascular unit who had normal liver tests as a proxy for the absence of liver disease.

PLIN2 was measured by ELISA (Abbexa, Cambridge Science Park, UK). To compare the expression of plasma PLIN2 between MASH and CVD subjects, we used Mann-Whitney U test. In the MASH population we performed a linear regression analysis to assess the correlation between PLIN2 and carotid intima-media thickness (CIMT), a marker of subclinical atherosclerosis.

Results: Fourteen % of individuals with MASH exhibited early atherosclerosis, as determined by CIMT. Within the MASH group, there was no differences in PLIN2 expression between those with and without early atherosclerosis (3.80 ± 0.38 vs. 4.25 ± 0.24 ; $p = 0.37$). Linear regression analysis of PLIN2 showed no correlation between PLIN2 and CIMT (left CIMT $R = 0.04$; $P = 0.14$; right CIMT $R = 0.0001$; $P = 0.95$). There was, however, a significantly higher PLIN2 expression in MASH patients compared to those with CVD (0.75 ± 0.09 vs. 3.61 ± 0.55 ng/ml; $p < 0.0001$).

Conclusion: Plasma PLIN2 is significantly higher in subjects with MASH compared to subjects without MASH but with confirmed CVD. In the MASH population PLIN2 was not able to discriminate subjects with early atherosclerosis, hence PLIN2 did not come out as a marker of CVD. Hepatic biomarkers such as PLIN2 may be used for non-invasive testing and as targets for MASH pharmacological treatment.

WED-297-YI

Characterization of the evolution of liver elasticity in a real-life population with metabolic dysfunction-associated steatotic liver disease: a prospective study

Joyce Scholtens¹, Stéphanie André-Dumont¹, Guillaume Henin^{1,2}, Géraldine Dahlqvist¹, Nicolas Lanthier^{1,2}. ¹Service d'Hépatogastroentérologie, Cliniques universitaires Saint-Luc, UCLouvain, Brussels, Belgium; ²Laboratory of Hepatogastroenterology, Institut de Recherche Expérimentale et Clinique, UCLouvain, Brussels, Belgium
Email: nicolas.lanthier@saintluc.uclouvain.be

Background and aims: MASLD is very common and its course is variable, but there is little prospective data on the long-term follow-up of these patients. The aim of our study is to evaluate the evolution of liver disease using hepatic elastometry by identifying patients who will improve or progress over time.

Method: Transient elastography was conducted at baseline (Y0) and then reassessed at one year (Y1) and three years (Y3) in this prospective single-center study. Regression or progression of liver disease was determined by a decrease (improvers, I) or increase (progressors, P) in liver elasticity exceeding 1.5 kPa compared to the baseline value. Patients with elasticity changes ≤ 1.5 kPa were classified as stable (S).

Results: 229 patients were included (126 women and 103 men) with a mean age of 52 years, mean body mass index (BMI) of 33.9 kg/m^2 and mean waist circumference of 114 cm. 38% were treated for type 2 diabetes. The mean baseline elasticity was 10.5 kPa and the mean controlled attenuation parameter (CAP) was 331.1 dB/m. 44% were classified as F0-F1, 28% as F2, 19% as F3 and 10% as F4. Most patients received lifestyle advice by the hepatologist (69%), others underwent bariatric surgery (13%), were either included in an interventional clinical trial for MASLD/MASH (9%) or referred to the dietitian (8%). 146 patients (64%) and 110 patients (48%) underwent follow-up elastography at Y1 and Y3 respectively. Mean liver elasticity (Y0: 10.5, Y1: 7.8, Y3: 7.9 kPa; $p = 0.0008$) and CAP (Y0: 331.1, Y1: 307.1, Y3: 317.4 dB/m; $p = 0.0007$) decreased over time. At Y1 and Y3 respectively, a minority of patients were P (18–19%), 49–39% remained S and 34–42% were I. Compared with P or S patients, I at Y1 exhibit a more

severe condition at Y0, characterized by higher BMI (I: 34.6, S: 31.7, $P = 32.5 \text{ kg/m}^2$; $p = 0.05$), waist circumference (I: 116, S: 108, $P = 110 \text{ cm}$; $p = 0.0048$), fasting glucose, low HDL, high elasticity (I: 12.2, S: 6.6, $P = 7.5 \text{ kPa}$; $p < 0.0001$) and CAP values. The same is also true for Y3 vs. Y0. At Y1, I are characterized by a significant BMI reduction (-3.7 kg/m^2 ; -9%) compared with S patients (-1.1 kg/m^2 , -2.6%) and P (-0.1 kg/m^2 , -0.4%) ($p = 0.0003$), as well as a reduction in waist circumference, ALT (I: -36% , S: -15% , $P = +5\%$; $p = 0.0036$) and GGT values (I: -31% , S: -12% , $P = -9\%$; $p = 0.0133$). At Y3, I also experienced a notable decrease in BMI (-6%) compared to S patients (-1.7%) and P ($+1.7\%$) ($p = 0.0005$). All the patients who underwent bariatric surgery demonstrated disease regression at either Y1 or Y3.

Conclusion: These are the first prospective data on the evolution of liver elasticity in MASLD patients. Hepatological management has a beneficial effect on liver stiffness and CAP, particularly among patients with initial severe MASLD. A reduction in BMI by 6 to 9% is correlated with a reduction in hepatic elasticity. A fifth of the population are patients who are progressing, characterised by the absence of weight loss.

WED-298-YI

Myosteatosis is associated with metabolic-associated steatotic liver disease (MASLD) but not liver fibrosis-Results from an Indian cohort

Dinesh Walia¹, Samagra Agarwal², Sumaira Qamar³, Shila Patel², Rajni Yadav², Kumble S Madhusudhan², Deepak Gunjan⁴, Anoop Saraya⁵. ¹All India Institute of Medical Sciences, Gastroenterology and Human Nutrition Unit, New Delhi, India; ²All India Institute of Medical Sciences, New Delhi, India; ³All Institute of Medical Sciences, New Delhi, India; ⁴All India Institute of Medical Sciences, New Delhi, India; ⁵Institute of Liver and Biliary Sciences, New Delhi, India
Email: dineshwalia.jul21@aiims.edu

Background and aims: Skeletal muscle alterations are seen in MASLD due to complex metabolic derangements in the liver-adipose-muscle axis. Data on the relationship between muscle alterations, specifically muscle fat infiltration (myosteatosis) and MASLD is scarce. Herein, we aimed to study the association of muscle fat infiltration with histological MASLD activity including fibrosis in obese Asian population, and test whether myosteatosis can be a non-invasive biomarker of MASLD.

Method: 124 cases of MASLD (mean age 40.7 ± 10.3 years, 73% males) and 30 healthy renal donors (mean age 45.8 ± 7.9 years, 23% males) as controls were recruited. All patients underwent biochemical tests, transient elastography (TE), bioelectrical impedance (BIA), computed tomography (CT) to measure the psoas muscle density, skeletal muscle fat index of psoas (SMFI Psoas), skeletal muscle index (SMI), visceral adipose tissue index (VATI), hand grip dynamometry for muscle strength assessment and 4-meter gait speed to assess muscle function. Liver biopsy was done for MASLD patients to assess histological activity (NAS-CRN score) and fibrosis stage. SMFI psoas was compared to other non-invasive tests (NITs) to detect 'at risk fibrosis' (F2-F4) among MASLD patients on ROC analysis.

Results: Compared to controls, patients with MASLD had higher muscle mass (CT-SMI 47.48 ± 8.37 vs $43.32 \pm 8.72 \text{ cm}^2/\text{m}^2$, $p = 0.01$) with similar muscle function and strength. However, patients with MASLD had a higher skeletal muscle fat content than healthy controls (CT-SMFI psoas 87.00 ± 33.41 vs 51.63 ± 21.84 , $p = 0.0001$) and a higher visceral fat content per muscle mass (CT-VATI/SMI of 276.21 ± 105.91 vs $154.26 \pm 102 \text{ cm}^2/\text{m}^2$, $p = 0.0001$). SMFI psoas values were significantly higher among MAFL with no fibrosis (F0), MASH with mild fibrosis (F1), and MASH with 'at risk fibrosis' (F2-F4) when compared to healthy controls (75.06 ± 30.93 , 89.74 ± 36.02 , 91.07 ± 32.47 vs 51.63 ± 21.85 , $p < 0.001$). However, when compared within MASLD, patients with MAFL-F0, MASH-F1, and MASH-F2 to F4 (at risk fibrosis) showed a statistically non-significant trend of increasing SMFI psoas values with progressive fibrosis i.e. 75.06 ± 30.93 , 89.74 ± 36.02 and 91.07 ± 32.47 , $p = 0.087$, respectively. When compared to

NITs to detect 'at risk fibrosis' (F2-F4), SMFI psoas (AUROC-0.587) was inferior to liver stiffness-TE (AUROC- 0.844, $p=0.0001$) but was comparable to FIB-4 (AUROC-0.686, $p=0.15$), NAFLD Fibrosis score (AUROC-0.664, $p=0.29$) and APRI (AUROC-0.646, $p=0.41$). SMFI psoas had a diagnostic accuracy of 61.29% with a sensitivity and specificity of 64.62% and 57.63% respectively, at a cut-off of 79.54 to distinguish between 'at risk' from no to mild fibrosis in MASLD patients.

Conclusion: Myosteatosis is associated with MASLD independent of the degree of liver fibrosis.

WED-299

Utility of ultrasound attenuation imaging in the detection and grading of hepatic steatosis severity as compared to magnetic resonance imaging proton density fat fraction

Angus Patterson¹, Ross Apostolov², Darren Wong², Numan Kutaiba², Paul Gow², Mathis Grossmann², Marie Sinclair². ¹University of Melbourne, Heidelberg, Australia; ²Austin Health, University of Melbourne, Heidelberg, Australia
Email: ajpatterson@student.unimelb.edu.au

Background and aims: Ultrasound attenuation imaging (US-ATI) is a relatively new method of non-invasive quantification of hepatic steatosis. This study aimed to investigate the discriminatory capabilities of US-ATI to detect different grades of hepatic steatosis as quantified by magnetic resonance imaging proton density fat fraction (MRI-PDFF).

Method: We analysed 115 matched MRI-PDFF and US-ATI pairs in 82 male patients (mean age 51.9 years, standard deviation 12.3 years). All patients had non-alcoholic fatty liver disease (NAFLD) and were enrolled in the testosterone for NAFLD (TNT) randomised controlled trial (ACTRN 12619000701123). US-ATI imaging was performed by an experienced sonographer, using a Canon Aplio i800 ultrasound system. Hepatic steatosis was graded into grade 0 (<5.5% on MRI-PDFF), grade 1 steatosis (5.5% to <15.5%), grade 2 steatosis (15.5% to <20.5%), and grade 3 steatosis ($\geq 20.5\%$). Pearson's r was used to examine the correlation between US-ATI values and MRI-PDFF percentage. A receiver operating characteristic (ROC) analysis was undertaken, with the area under the ROC curve (AUROC) used to assess the diagnostic performance of US-ATI for each grade of steatosis.

Results: 103 of 115 US-ATI and MRI-PDFF pairs were performed on the same day and all scans were performed within 4 weeks of each other. The median US-ATI values for grades 0, 1, 2 and 3 steatosis were 0.64 (interquartile range (IQR): 0.61–0.81), 0.83 (IQR: 0.75–0.9), 0.88 (IQR: 0.85–1.01), 0.92 (IQR: 0.82–1.05) dB/cm/MHz, respectively. The correlation coefficient between US-ATI and MRI-PDFF was of moderate strength with $r=0.43$ (95% confidence interval (CI): 0.26–0.56, $p<0.001$). The median US-ATI values of all steatosis grades showed statistically significant differences between each grade ($p\leq 0.02$), with the exception of grade 2 to 3 steatosis ($p=0.8$). The AUROC of US-ATI for grades 0, 1, 2 and 3 steatosis was 0.77 (CI: 0.56–0.98), 0.62 (CI: 0.52–0.73), 0.62 (CI: 0.5–0.75) and 0.67 (CI: 0.56–0.78) respectively.

Conclusion: US-ATI had acceptable diagnostic utility for the exclusion of significant hepatic steatosis, which contrasted with poorer performance for the diagnosis of increasing grades of moderate and severe steatosis. Further studies with larger sample sizes are required to compare its diagnostic utility to other non-invasive techniques for measurement of hepatic steatosis such as controlled attenuation parameter measurement from transient elastography, as well as its ability to monitor changes in steatosis longitudinally.

WED-302-YI

A data-driven approach to determine minimum re-testing interval in persons with metabolic dysfunction associated steatotic liver disease

Richard Parker¹, Callum Wood¹, Ian Rowe^{1,2}. ¹Leeds Liver Unit, St James's University Hospital, Leeds, United Kingdom; ²Leeds Institute for Medical Research, University of Leeds, Leeds, United Kingdom
Email: callum.wood5@nhs.net

Background and aims: Metabolic Dysfunction Associated Steatotic Liver Disease (MASLD) is notable for its significant and increasing prevalence. There are no licensed drug therapies for MASLD; the mainstay of treatment is lifestyle modification. However, it is not clear that patients can make significant lifestyle changes or modify disease trajectory without targeted support. This study assesses MASLD disease progression in a tertiary hepatology service in the UK.

Methods: We extracted liver stiffness measurement data from outpatient and community FibroScan machines in a single tertiary centre, encompassing data from December 2017 to November 2023. Incomplete data was completed from electronic patient records. Data was analysed using R. Analysis included descriptive statistics and exploration of progression of fibroscan results.

Results: 21 925 scans were extracted, representing 13 635 individual patients.

The modal specific indication for fibroscan was MASLD (5 301 scans representing 3 434 patients). CAP was available for 2 323 scans. 937 persons with MASLD underwent follow-up scan after their index examination. The mean time between exams was 507 days (Interquartile range, IQR 364–815). Their mean age was 58.8 years (SD 13.8). The median result for LSM was 8.8 kPa (IQR 6.2–12.9) and (where available) 324 dB/m (IQR 283–360) for CAP. The change in CAP and LSM was calculated for each patient with MASLD and at least one follow-up exam. The median change in LSM was -0.1 kPa (IQR -2.7 to $+1.8$). The median change in CAP was 0 dB/m (IQR ± 27). The median rate of change in CAP was 0 dB/m/year and in LSM was -0.06 kPa/year. Focusing on the 411 patients who had a baseline fibroscan suggestive of at least moderate fibrosis (LSM >10 kPa), 49 (11.9%) had an increase in LSM of at least 20%. Conversely, 113 patients (27.5%) had a decrease in LSM of at least 20%. The median follow-up interval was 489 days (IQR 344–794). 526 patients had a baseline exam showing LSM <10 kPa. Of these, 81 (15.4%) had a subsequent fibroscan showing LSM >10 kPa, suggestive of at least moderate fibrosis. The median follow-up period for these patients was 587 days. 70% of increases in LSM were identified at scans within 18 months of index scan.

Conclusion: In this dataset of 937 follow-up examinations, there was no overall change in liver stiffness. However, there was evidence of progression to clinically significant fibrosis in approximately 1 in 7 patients starting with LSM <10 kPa. This progression in fibrosis contrasts with a larger proportion of patients with elevated LSM at baseline apparently improving. Longitudinal changes in LSM can guide intervals for repeat testing but there is a need to define the magnitude of change that demands modifications to management.

WED-303

Assessment of the correlation and concordance between ELF and VCTE in the AASLD algorithm for MASLD severity assessment

Siham Abdelgani¹, Rida Nadeem², Yasmeen Fallouh², Phillip Leff², Aarya Patel², Manal Chughtai², Sahasraara Hemant³, Shray Patel², Anushka Dharia², Gagana Ameneni², Helena Katchman⁴, Naim Alkhouri². ¹Tel Aviv Medical center, Tel Aviv, Israel; ²Arizona liver health, phoenix, United States; ³Arizona Liver Health, Phoenix, United States; ⁴Tel Aviv Medical Center, Tel Aviv, Israel
Email: naim.alkhouri@gmail.com

Background and aims: Recently, the AASLD published an algorithm to assess the severity of MASLD and identify patients at risk for advanced disease. The algorithm recommends sequential testing starting with FIB4 followed by either enhanced liver fibrosis (ELF) or

POSTER PRESENTATIONS

vibration controlled transient elastography (VCTE). It was assumed that ELF and VCTE can be used interchangeably based on availability but the correlation and concordance between ELF and VCTE has not been evaluated.

Method: Consecutive patients with MASLD that were referred to a tertiary hepatology clinic and had laboratory tests to calculate FIB4 and ELF + VCTE done within a 3-month period were included. The AASLD algorithm was applied. Spearman's correlation coefficient was used to assess correlations.

Results: 263 patients were included with a mean age of 57 ± 14 years, 62% were female, mean BMI 34.73 ± 9.3 , 48% had type 2 diabetes. 134 (51%) had $FIB4 \geq 1.3$, the mean ELF was 9.91 ± 1.24 and the mean VCTE was $13.5 \text{ kPa} \pm 10.6$ indicating a prevalence of advanced fibrosis consistent with specialty care. Overall, there was a significant but weak correlation between ELF and VCTE (Spearman correlation coefficient 0.38, p value <0.01 , Kappa coefficient = 0.17). Importantly, in patients with FIB4 between 1.3–2.67 ($n = 97$) where the AASLD algorithm recommends sequential testing with a second test, ELF was >7.7 in 89 (91%) and VCTE $>8 \text{ kPa}$ in 66 (68%). ELF and VCTE showed concordant results in 65.5% and discordance in 34.5% with a spearman's correlation coefficient of 0.293 indicating poor association. In patients with FIB4 >2.67 ($n = 37$), ELF was >7.7 in 35 (94.5%) and VCTE $>8 \text{ kPa}$ in 24 (64.5%). ELF and VCTE showed concordant results in 68.5% and discordance in 31.5% with a significant spearman's correlation coefficient of 0.611 indicating high association.

Conclusion: Using ELF and VCTE interchangeably as part of the AASLD algorithm may lead to substantial misclassification of patients. Furthermore, in patients with FIB4 between 1.3 and 2.67, there is poor correlation between ELF and VCTE, emphasizing the need for a more refined approach in utilizing these tests for better risk stratification in this group.

WED-304

Accuracy of the recommended algorithm using Fib4 Score and fibroscan to identify MASLD patients with low risk for advanced liver fibrosis in "real world" practice

Inbal Zuckerman¹, Orly Azulay², Eli Zuckerman². ¹Carmel Medical Center, Haifa, Israel; ²Carmel Medical Center, Haifa
Email: elizuc56@gmail.com

Background and aims: Global guidelines summarise that Fib4 Score and fibroscan can be used for assessment of hepatic fibrosis. The negative predictive value is 0.9 with cut-off of 1.3 to rule out significant fibrosis in patients with Metabolic Associated Steatotic Fatty Liver Disease (MASLD).

The aim was to assess the accuracy of the practical algorithm using Fib4 as the initial step to distinguish NAFLD patients with low-risk from patients with moderate-high risk for liver fibrosis trying to identify clinical parameters indicating significant hepatic fibrosis despite low fib4 score.

Method: Included 828 patients with MASLD and Fib4 score less than 1.3 who were referred from primary care clinics from January 2021 to June 2023. All patients underwent fibroscan examination (Echosense). Statistical analysis: For multivariate analysis, a stepwise discriminant analysis model, successfully validated by the leave one out method was used. The true independent variables and their regression coefficients were used in order to build a discriminant score (DS) formula. ROC curves were separately built for the individual independent predictors as well as for their combination in the DS formula. Two tailed P values of 0.05 or less were considered to be statistically significant. Statistical analysis was performed using the IBS SPSS version 26. In parallel to the statistical model, an artificial intelligence (AI) based neural network (NNET) model was developed in order to test for higher predictive values of FIB4. This feedforward backpropagation algorithm was used to train the model. The AI based NNET model was developed using the Matlab 2015a version (MathWorks).

Results: Mean age of this group was 47.5 years old and 396 were males (47%). Mean Fib4 score was 0.84. In 97 patients (11%) fibroscan reading was not reliable. Fibroscan in 153 of 731 patients (21%) showed fibrosis score F2 or more [F2 130 (85%), F3–4 23 (15%)]. 120 of 153 patients underwent liver biopsy showing fibrosis score F3–4 in 21 patients, F2 in 15 and F0–1 in 84. Older age, higher ALT and higher ferritin level were significantly more prevalent in the group with high fibrosis score (despite low Fib4 score).

Conclusion: Fib4 score is highly accurate in distinguishing patients with low risk of fibrosis from those with moderate-high risk in real world clinical practice, missing approximately 5–7% of patients with significant liver fibrosis. Older age, high ALT level and high serum ferritin may indicate need for further investigation with fibroscan and/or liver biopsy in patients with low Fib4 score.

WED-305

Comparison of two non-invasive models for advanced fibrosis (AF) detection in patients with type 2 diabetes (T2D) and MASLD using LiverSTAT, FIB-4 and liver stiffness measurement (LSM) with transient elastography (TE)

Mona Ismail^{1,2}, Abdulrahman Alabdulgader^{3,4}, Abdulnaser Barmou⁵, Mona Munteanu⁶. ¹Division of Gastroenterology, Department of Internal Medicine, King Fahd Hospital of the University, Al-Khobar, Saudi Arabia; ²College of Medicine, Imam Abdulrahman bin Faisal University, Dammam, Saudi Arabia; ³Division of Gastroenterology, Department of Internal Medicine, King Fahd Hospital of the University, Al-Khobar, Al-Khobar, Saudi Arabia; ⁴College of Medicine, Imam Abdulrahman bin Faisal University, Dammam, Saudi Arabia; ⁵Department of Internal Medicine King Fahd Hospital of the University Al-Khobar, Al-Khobar, Saudi Arabia; ⁶Fibronostics, Medical Affairs, Florida, United States
Email: monai4@hotmail.com

Background and aims: Metabolic dysfunction-associated liver disease (MASLD) affects 24% of the population and can progress undetected from simple steatosis to advanced fibrosis (AF) and cirrhosis, especially in patients with type 2 diabetes (T2D). This underscores the importance of early detection and hepatology referrals, as patients with AF are identified late. Given the limitations of liver biopsy and the scarce availability of TE, there is a growing need for non-invasive, cost-effective blood-based tests for liver fibrosis assessment. Clinical care pathways integrating AI-based blood tests like LiverSTAT (LST) offer a promising approach to identifying AF in pts with T2D. These pathways can streamline the diagnostic process, facilitating early detection and intervention. This study evaluated the efficacy of using LST and LSM in identifying advanced fibrosis among patients with T2D and MASLD comparatively to FIB-4 and LSM.

Method: In this retrospective study, we reviewed pts diagnosed with T2D and MASLD with various demographic and clinical factors attending the diabetes clinics at a tertiary university hospital. Cut-offs for AF were those recommended by AASLD clinical practice guidelines: for LSM 12 kPa and for FIB-4 1.3 and 2.67 to rule out and rule in AF; LST used a cut-off of 0.59. We used logistic regression to identify predictors of advanced fibrosis.

Results: We identified 359 T2D pts, 349 pts were included with applicable LSM and complete biomarkers [46.7% males, median age 55 yrs, LSM 5.6 kPa, CAP 302 dB/m, ALT28 U/L, AST21 U/L, FIB-4 0.87, BMI 32.3 Kg/m²]. 309 (88.5%) had LSM and LST that agreed: 23 (6.6%) had presumed AF and 286 (81.9%) had no presumed AF; 40 (11.5%) disagreed, with presumed AF in 16 and 24 as per LST and LSM, respectively. 254 (72.8%) had LSM and FIB-4 that agreed: 12 (3.4%) had presumed AF and 242 (69.3%) had no presumed AF; 25 (7.2%) disagreed, with presumed AF in 7 and 18 pts as per FIB-4 and LSM, respectively. 70 (20.1%) pts had indeterminate FIB-4 results (1.3–2.67), among them, 19 and 17 had presumed AF with LST and LSM, respectively, 11 (15.7%) agreed for AF and 45 (64.3%) agreed for non-AF. In a model including LST biomarkers, LSM, FIB-4, platelets, lipid panel, liver enzymes, glucose, age, and BMI, only age, LST and LSM

were independent predictors of AF. 273 (78%) and 316 (90.5%) had ALT and AST <50 U/l, respectively. ALT decreased significantly with age range while prevalence of AF and mean LST fibrosis scores increased with age range.

Conclusion: In pts with T2D, LST outperformed FIB-4 when combined with LSM for the detection of MASLD-related AF. Liver specific biomarkers should be used instead of liver enzymes as ALT that lack sensitivity for AF detection, especially in aged patients.

WED-306-YI

Prevalence of metabolic-dysfunction associated steatotic liver disease among diabetic and non-diabetic patients in a dutch cohort: evaluation of hepatic steatosis and fibrosis using Fibroscan™

Alina Saidi¹, Willy Theel¹, Vivian de Jong², Diederick Grobbee³, Femme Dirksmeier-Harinc⁴, Manuel Castro Cabezas¹. ¹Franciscus Gasthuis and Vlietland, Department of Internal Medicine, Rotterdam, Netherlands; ²Julius Center for Health Science and Primary Care, Utrecht, Netherlands; ³Julius Center for Health Sciences and Primary Care, Utrecht, Netherlands; ⁴Franciscus Gasthuis and Vlietland, Department of Gastroenterology and Hepatology, Rotterdam, Netherlands
Email: a.saidi@franciscus.nl

Background and aims: Metabolic-dysfunction associated steatotic liver disease (MASLD) often coexists with metabolic disorders, such as type 2 diabetes mellitus (T2DM) and cardiovascular disease (CVD). We investigated the prevalence of MASLD among individuals visiting the cardiometabolic outpatient clinic in our hospital in a diabetic versus non-diabetic population.

Method: The study population consisted of 545 subjects attending the cardiometabolic outpatient clinic of Franciscus Hospital in Rotterdam (78 T1DM, 160 T2DM and 307 non-diabetics). Hepatic steatosis and fibrosis were assessed and graded using transient elastography (Fibroscan®). MASLD was defined as a Controlled Attenuation Parameter (CAP) ≥275 dB/m. Significant fibrosis was defined as a Transient Elastography (TE) value ≥8.1 kPa.

Results: 246 Women and 299 men were included (mean age 54 ± 14 years, mean BMI 29.7 ± 6.6 kg/m²). 39.4% (n = 215) had MASLD and 29.0% (n = 158) had significant fibrosis. The prevalence of MASLD among individuals with T1DM, T2DM, and in those without diabetes was 19.2%, 56.3%, and 35.8%, respectively (p < 0.001). Significant fibrosis was observed in 9.0%, 33.8%, and 31.9% of the individuals, respectively (p < 0.001). Male subjects showed a significantly higher prevalence of significant fibrosis than females (35.0% vrs. 21.6%; p < 0.001).

In the overall population, a positive correlation was found between liver steatosis and liver fibrosis (Spearman's rho = 0.220; p < 0.001). This was also the case for each of the 3 subgroups (T1DM rho = 0.244, p = 0.032; T2DM rho = 0.307, p < 0.001; non-diabetics rho = 0.115, p = 0.044). However, in non-diabetics, when TE was above 8 kPa, the correlation between CAP and TE was lost.

Conclusion: The prevalence of MASLD and significant fibrosis in this Dutch cohort was higher among patients with T2DM compared to patients with T1DM and subjects without diabetes. Significant fibrosis was more prevalent in males. Interestingly, significant fibrosis was equally prevalent in T2DM and in non-diabetics attending the cardiovascular outpatient clinic. Why the association between CAP and TE was lost in these subjects with TE >8.1 kPa, is still unclear.

WED-314-YI

Head-to-head comparison of two different ultrasound systems to measure the liver attenuation parameter

Laura De Rosa^{1,2}, Simone Cappelli³, Giovanni Petralli⁴, Antonio Salvati⁵, Gabriele Ricco⁵, Filippo Oliveri⁵, Barbara Coco⁵, Piero Colombatto⁵, Ferruccio Bonino⁶, Maurizio Brunetto^{3,5,6}, Francesco Faita¹. ¹Institute of Clinical Physiology, National Research Council, Pisa, Italy; ²Department of Information Engineering and Computer Science, University of Trento, Trento, Italy; ³Department of

Clinical and Experimental Medicine, Pisa University, Pisa, Italy;

⁴Department of Surgical Medical, Molecular and Critical Area Pathology, University of Pisa, Pisa, Italy; ⁵Hepatology Unit, Pisa University Hospital, Pisa, Italy; ⁶Institute of Biostructure and Bioimaging, National Research Council, Naples, Naples, Italy

Email: laura.derosa.95@gmail.com

Background and aims: The liver ultrasound attenuation parameter is widely used for estimating the liver fat content (LFC) and its measurement is provided by commercial clinical scanners. In this study, we compared two different technologies currently used to assess LFC in a large cohort of patients (pts) with chronic liver disease (CLD) in order to study the agreement between two commercially available liver fat measurement devices.

Method: This single center study included 777 consecutive CLD pts enrolled at the Hepatology Unit of the University Hospital of Pisa from May 2022 to December 2023 whose LFC was assessed at with two different diagnostic systems: FibroScan® (Echosens, France) equipped with M or XL probe and FT9000 (Hisky Medical, China) equipped with a single convex probe. We compared the values of Controlled Attenuation Parameter (CAP, Fibroscan) and Ultrasound Attenuation Parameter (FT9000) obtained during the same single visit of each patient. Pearson correlation coefficients (R) and Bland-Altman analyses (BAA) were used to study the agreement between CAP and UAP overall and after stratification for BMI ≥25 kg/m². Correlations with biochemical variables (AST, ALT, AST/ALT, GGT) and platelets counts (PLTs) were evaluated also.

Results: Correlation coefficients of CAP and UAP were 0.48 overall, 0.30 in lean pts (BMI <25 kg/m²), and 0.47 in overweight/obese pts (p < 0.001 for all). Overall, BAA showed a significant bias between CAP and UAP (-12 dB/m) and 95% limits of agreement (LoA) ranging from -130 to 100 dB/m; there was not any significant bias (-1.6 dB/m) in lean pts, whereas the bias was significant (-28 dB/m) in pts with BMI ≥25 kg/m². Both CAP and UAP did not correlate significantly with ALT, AST, GGT and PLTs overall and after stratifying with BMI. Both CAP and UAP correlated with the AST/ALT ratio significantly, but with poor coefficients both overall (r = -0.22 and r = -0.15, respectively) and in overweight/obese pts (r = -0.22 and r = -0.20, respectively); no significant correlation was found considering lean pts only.

Conclusion: Despite an overall acceptable and significant correlation between the attenuation parameter measurements provided by the two devices, a consistent bias and wide LoAs in BAA suggest that the two devices have a limited interchangeability, independently from body size, at least in this cohort of pts. Further comparative studies are needed using Magnetic Resonance as reference standard to explore the agreement between the two devices, as well as to define technology-specific cut-offs for fatty liver content quantification in clinical practice.

WED-315

Validation of Fibrosis-6, a novel machine learning non-invasive score to rule out advanced fibrosis and cirrhosis in patients with metabolic-associated fatty liver disease

Mona Ismail^{1,2}, Riham Soliman^{3,4}, Nabiel Mikhail⁵, Gamal Shiha^{3,6}.

¹Division of Gastroenterology, Department of Internal Medicine, King Fahd Hospital of the University, Alkhuab, Saudi Arabia; ²College of Medicine, Imam Abdulrahman bin Faisal University, Dammam, Saudi Arabia; ³Gastroenterology and Hepatology Department, Egyptian Liver Research Institute and Hospital (ELRIAH), Sherbin, El Mansoura, Egypt; ⁴Tropical Medicine Department, Faculty of Medicine, Port Said University, Egypt; ⁵Biostatistics and Cancer Epidemiology Department, South Egypt Cancer Institute, Assiut University, Assiut, Egypt; ⁶Hepatology and Gastroenterology Unit, Internal Medicine Department, Faculty of Medicine, Mansoura University, El Mansoura, Egypt
Email: monai4@hotmail.com

Background and aims: There is an urgent need for simple, blood-based, and non-invasive tests (NITs) to rule out advanced fibrosis/cirrhosis (F3 and F4) in metabolic-associated fatty liver disease. We

POSTER PRESENTATIONS

previously developed and validated the Fibrosis-6 (FIB-6) score, a novel non-invasive diagnostic score, through machine learning with a random forest algorithm. Originally validated for chronic hepatitis C, the FIB-6 score predicts liver fibrosis stages. This study evaluated the accuracy of the FIB-6 score in identifying advanced fibrosis/cirrhosis in patients with metabolic-associated fatty liver disease.

Method: In this retrospective cohort study, we included patients with metabolic-associated fatty liver disease following at the Hepatology clinics at a tertiary university hospital (KFHU) between April 1st, 2021, and April 30, 2022 (Before the new nomenclature). Patients with secondary causes of hepatic steatosis were excluded. Clinical and demographic data were collected. Transient elastography (FibroScan 502 touch, Echosens, Paris, France) was the reference standard for liver fibrosis. The diagnostic accuracy and performance of the FIB-6 score were compared against three established NITs: The fibrosis-4 index (FIB-4) and the aspartate aminotransferase-to-platelet ratio index (APRI), the aspartate aminotransferase (AST)/alanine aminotransferase (ALT) (AAR) ratio.

Results: The study included 406 patients, and the FIB-6 score was more effective in ruling out F3 and F4 stages of fibrosis compared to FIB-4, APRI, and AAR. The FIB-6 score showed a higher sensitivity (96.3%) and negative predictive value (NPV) (90.3%) in ruling out F3 and F4 stages of fibrosis in patients with metabolic-associated fatty liver disease (Table 1). In comparison, the sensitivity of FIB-4 was 43.9%, APRI was 23.2%, and AAR was 29.2%. Additionally, FIB-4, APRI, and AAR had lower NPVs of 86.2%, 83.3%, and 81.9%, respectively.

Conclusion: The FIB-6 score is an accurate and simple non-invasive test for ruling out advanced fibrosis and cirrhosis in patients with metabolic-associated fatty liver disease, surpassing the performance of existing NITs such as FIB-4, APRI, and AAR. This highlights its potential as a valuable diagnostic aid in clinical care pathways.

WED-316

Gadoxetic acid-enhanced MRI enables detection of fibrosis and inflammation in MASLD/MASH

Edvin Johansson¹, Salem Alsaqal², Paul Hockings¹, Håkan Ahlström³, Johannes Hulthe¹, Lars Johansson¹, Charlotte Ebeling Barbier⁴, Fredrik Rorsman⁵, Johan Vessby⁶. ¹Antaros Medical, Mölndal, Sweden; ²Department of Surgical Sciences, Uppsala University, Uppsala, Sweden; ³Department of Surgical Sciences, Uppsala University, Uppsala, Sweden; ⁴Department of Surgical Sciences, Section of Radiology, Uppsala University, Uppsala, Sweden; ⁵Uppsala University Hospital, Uppsala University, Uppsala, Sweden; ⁶Dept of Gastroenterology and Hepatology, Uppsala University Hospital, Uppsala, Sweden
Email: paul.hockings@antarosmedical.com

Background and aims: There is a need for non-invasive biomarkers to measure fibrosis and inflammation in subjects with metabolic dysfunction associated steatotic liver disease (MASLD) or steatohepatitis (MASH). Gadoxetic acid-enhanced Magnetic Resonance Imaging (GA-MRI) can quantify hepatocellular function and potentially identify dysfunction. The purpose of this study was to evaluate the ability of various parameters obtained using GA-MRI to measure fibrosis and inflammation and to assess repeatability.

Method: The study population consisted of 68 participants with biopsy-proven MASLD or MASH (40 male, 28 female) with a mean age of 54.5 years and a mean body mass index of 31 kg/m². Histopathology found 39 participants had fibrosis stage F0–1, and 29 had F2–4, while 15 participants had activity score 0–1 and 53 had activity scores of 2–4. Participants fasted for 6 hours before MRI with a 3.0 T Signa scanner (GEHC). Dynamic contrast-enhanced MRI (DCE-MRI) was performed for a total of 22 minutes (90 timeframes). After 2 minutes of baseline imaging, a bolus of 0.025 ml/kg (25% of the standard dose) of gadoxetate (Primovist, Bayer) was injected intravenously. 30 participants were invited back for a rescans 2–4 weeks after their initial scan to estimate repeatability of the imaging parameters. A tracer-kinetic model was used to estimate flow (F), extracellular volume fraction (V_e) and hepatocyte uptake rate of

gadaxetate (k_{he}) from the DCE-MRI. Liver relative enhancement (RE), the percent change in liver signal from baseline to the hepatobiliary phase (20 min), is also reported.

Results: Fibrosis stage: F0–1 could be distinguished from F2–4 by the flow parameter (AUROC 0.67, p 0.015). Flow also correlated with the histopathological fibrosis stage (Rs –0.30, p 0.01). Similarly, RE could separate F0–1 from F2–4 (AUROC 0.66, p 0.02) and had Rs –0.29, p 0.02. Activity grade: k_{he} correlated with activity grade (Rs –0.29, p 0.02) but failed to separate grade 0–1 from 2–4 (AUROC 0.63, p 0.11). For the same tests, RE performed better (Rs –0.34 p 0.006 and AUROC 0.73 p 0.007). Repeatability: The ICC for repeatability of flow was 0.63, k_{he} was 0.74, and RE was 0.88.

Conclusion: This relatively small study of MASLD/MASH subjects showed that the flow and k_{he} tracer-kinetic parameters derived from gadaxetate MRI correlated with fibrosis and inflammation, respectively. RE at 20 min also correlated with fibrosis and inflammation and importantly has excellent repeatability, however it lacks specificity to distinguish fibrosis from inflammation. Together these parameters provide information about MASLD/MASH disease state, fibrosis, and inflammation without invasive biopsy. This could also have utility in longitudinal monitoring of MASLD/MASH subjects.

WED-317

Guided Vibration-Controlled Transient Elastography, a new vibration-guided FibroScan examination

Jean-Pierre Bronowicki¹, Christiane Stern², Stéphane Audié³, Julie Fouquier³, Cécile Bastard³, Anne Llorca³, Céline Fournier-Poizat³, Véronique Mietté³, Laurent Sandrin³, Cyrielle Caussy⁴. ¹Nancy University Hospital, Nancy, France; ²Hôpital Beaujon, Clichy, France; ³Echosens, Paris, France; ⁴Hospices Civils de Lyon-CHU de Lyon, Lyon, France
Email: cyrielle.caussy@chu-lyon.fr

Background and aims: FibroScan (FS) medical device allow assessment of liver stiffness measurement using Vibration-Controlled Transient Elastography (LSM by VCTE™). A new technology named “Guided VCTE” was developed to help operators localize an optimal region of interest for LSM in a simple and reliable way. The aims of this study were to compare the examination time of LSM by Standard versus Guided VCTE and to demonstrate the equivalence of LSM values between both methods.

Method: This is a prospective study including patients with all causes of chronic liver diseases recruited in 3 expert Hepatology Centers in France between November 2022 and March 2023. For each patient, LSM was performed by expert operators using Standard and Guided VCTE consecutively, with alternating the examination order from a patient to another. Time needed to obtain the first and 10th valid LSM after the operator places the probe on the patient were compared with log-rank tests. LSM equivalence between Standard and Guided VCTE was evaluated in patients with at least 10 valid LSM and Interquartile Range (IQR)/Median ≤30% with both methods. LSM values by Standard and Guided VCTE were compared using a Wilcoxon signed-rank test. The agreement between both methods was assessed using mean bias, Spearman correlation coefficient (rho) and intraclass correlation coefficient (ICC). Estimates are presented with their 95% confidence intervals (CI) and two-sided p < 0.05 are considered statistically significant.

Results: Sixty-six participants (38% female, mean BMI: 33.9 ± 10.0 kg/m², mean age: 55.8 ± 15.4 years) were included in the analysis of the LSM examination time. Time needed to obtain the first valid LSM was significantly lower using Guided VCTE (median survival times 7.3 s [6.0;11.7]) compared to Standard VCTE (22.4 s [10.1;44.8]) with p < 0.0001. Moreover, time needed to reach the 10th valid LSM measurement was also significantly lower with Guided VCTE (33.6 s [28.1–38.8]) compared to Standard VCTE (50.2 s [45.3–70.3]) with p = 0.00012. Fifty-seven participants (42% female, mean BMI: 33.0 ± 9.1 kg/m², mean age: 54.9 ± 15.2 years) were included in the equivalence analysis. There was no significant difference between

the LSM obtained by both methods ($p=0.778$). The mean bias between LSM by both methods was -0.6 kPa $[-2.3;1.1]$ therefore not significantly different from 0. Rho and ICC were 0.92 [0.87;0.95] and 0.88 [0.80;0.93], respectively, highlighting a strong correlation and a good agreement.

Conclusion: Guided VCTE significantly reduces the time needed to obtain the first and 10th valid LSM compared to Standard VCTE. Furthermore, LSM obtained by Standard and Guided VCTE were strongly correlated and in agreement, reflecting an equivalence of LSM between both methods. Therefore, LSM cut-off values derived in the literature using Standard VCTE are applicable using Guided VCTE. Further studies are needed to confirm these results.

WED-318-YI

Steatotic liver disease in diabetic patients: more serious diabetes mellitus, more serious liver disease

Zülal İstemihan¹, Fatih Bektaş², Ali Emre Bardak³, Cansu Kızıltaş³, Gamze Kemeç³, Kanan Nuriyev¹, Aynure Rüstemzade¹, Sezen Genç Uluççen¹, Hülya Hacışahinoğulları², Kubilay Karşıdağ², Bilger Çavuş¹, Asli Çiçibasi Örmeci¹, Filiz Akyuz¹, Kadir Demir¹, Fatih Beşişik¹, Sabahattin Kaymakoglu¹. ¹Istanbul University, Istanbul Faculty of Medicine, Department of Internal Medicine, Division of Gastroenterology, Istanbul, Turkey; ²Istanbul University, Istanbul Faculty of Medicine, Department of Internal Medicine, Division of Endocrinology and Metabolism Diseases, Istanbul, Turkey; ³Istanbul University, Istanbul Faculty of Medicine, Department of Internal Medicine, Istanbul, Turkey
Email: kaymakoglus@hotmail.com

Background and aims: It was aimed to investigate the frequency of metabolic dysfunction-associated steatotic liver disease (MASLD) in patients with type 1 diabetes mellitus (T1DM) and type 2 diabetes mellitus (T2DM) and to reveal the relationship between complications of diabetes and steatotic liver and fibrosis.

Method: In a single-center study conducted at a tertiary university hospital, MASLD was prospectively evaluated with non-invasive scoring based on biochemical tests and FibroScan® in adult patients with T1DM and T2DM and without other causes of liver disease. In FibroScan® measurements, a CAP score of ≥ 275 dB/m was considered as steatosis and ≥ 8.0 kPa was considered as clinically significant fibrosis (F2). Demographic information, waist circumference, weight and height, biochemistry, non-invasive scoring, and FibroScan® measurements of the patients were recorded.

Results: 504 (83%) of a total of 605 diabetic patients had T2DM. 267 (44%) of the patients were male, the mean age was 56.22 ± 14.68 years, and the mean body mass index was 29.02 ± 6.02 kg/m². The frequency of steatotic liver and clinically significant fibrosis was higher in T2DM patients than in T1DM patients ($p < 0.05$). Clinically significant fibrosis was more common in patients with hypertension (HT) and microalbuminuria ($p = 0.01$). As the severity of liver steatosis increased, the rate of clinically significant fibrosis increased ($p = 0.01$). The grade of liver steatosis was higher in diabetic patients with microvascular complications ($p < 0.05$). Considering the lipid profiles, the degree of significant fibrosis and steatosis was higher in patients with low HDL levels ($p = 0.003$, $p = 0.001$, respectively). 30% ($n = 153$) of T2DM had clinically significant fibrosis, and only 23.5% of them ($n = 36$) had ALT > 45 U/L. 5% ($n = 5$) of T1DM had clinically significant fibrosis, and only 1 patient had ALT > 45 U/L. FIB-4 score was ≥ 1.3 in 60 (23.8%) of 252 patients with T2DM and SLD, and the rest had FIB-4 < 1.3 . Liver stiffness was found ≥ 8 kPa in 32.8% of those with FIB-4 score < 1.3 .

In all patients, 'FIB-4' had the strongest correlation with liver stiffness measurement, and 'fatty liver index' had the strongest correlation with CAP score.

Conclusion: Steatotic liver and fibrotic liver are more common in patients with T2DM than in T1DM. As the severity of liver steatosis

increases, fibrosis progresses. Concomitant hypertension, microalbuminuria, microvascular complications, and dyslipidemia in diabetic patients are associated with significant fibrosis and increased steatosis in the liver. The non-invasive tests that correlate best with FibroScan® measurements are FIB-4 and 'fatty liver index'. According to the results of our study, 40% of patients with T2DM and SLD need to be referred to gastroenterologists because they have clinically significant fibrosis.

WED-319

AI digital pathology unmasked the "No Change" in conventional pathological assessment of MASLD patients with one year lifestyle intervention in a prospective cohort study

Xiaoxue Zhu¹, Aruhan Yang¹, Wen Wang¹, Hong Zhang¹, Guoyue Lv¹, Yanhua Ding¹, Qiang Yang², Xiao Teng³. ¹The First Hospital of Jilin University, Changchun, China; ²Hangzhou Choutu Technology Co.Ltd., Hangzhou, China; ³HistoIndex Pte Ltd, Singapore, Singapore
Email: zhuxiaoxue@jlu.edu.cn

Background and aims: At present, there is no medication approved for the treatment of metabolic dysfunction-associated steatotic liver disease (MASLD). Lifestyle interventions that result in weight loss are considered to offer some improvement in MASLD. Pathology serves as the benchmark for evaluating their effectiveness. This study aimed to assess the efficacy of lifestyle interventions in patients with MASLD with the help of AI digital pathology.

Method: This prospective cohort study involved 31 patients who were diagnosed with MASLD based on histological and clinical criteria, then they received monthly lifestyle intervention guidance for one year. The conventional pathology was assessed using the NASH-CRN Histologic Scoring System, while finer evaluation of hepatic steatosis and fibrosis was used AI digital pathology based on SHG/TPEF technology. Clinical markers and pathology changes were analyzed by Pearson Correlation. A p value of < 0.05 was considered statistically significant.

Results: Regarding steatosis, the conventional discrete readings indicated that the numbers of patients with progression, no change, and regression were 3 (9.7%), 17 (54.8%), and 11 (35.5%), respectively. While the continuous measurement from the AI digital pathology changed the numbers to 15 (48.4%), 1 (3.2%) and 15 (48.4%), respectively. Regarding fibrosis, the conventional readings indicated that 6 (19.4%) patients experienced progression, 19 (61.3%) showed no change, and 6 (19.4%) showed regression. While AI digital pathology revealed the numbers were 21 (67.7%) with progression, 3 (9.7%) with no change and 7 (22.6%) with regression. For steatosis assessment, the same trends in MRI-PDFF changes were observed in 14 (45.2%) and 18 (58.1%) individuals with conventional pathology and AI digital pathology, respectively. The numbers of individuals with CAP changes that were consistent with the two pathology methods were 14 (45.2%) and 17 (54.8%), respectively. Stronger statistically significant correlations were found between clinical markers (MRI-PDFF, CAP and weight changes) and AI pathology vs conventional pathology ($r = 0.468$ vs 0.308 , 0.428 vs 0.363 , 0.578 vs 0.530). For fibrosis assessment, the same trends in LSM changes were observed in 10 (32.2%) and 12 (38.7%) individuals with conventional pathology and AI digital pathology, respectively. No statistically significant correlation could be found between NITs (LSM, FIB-4, and FAST) and either conventional or AI pathology.

Conclusion: Continuous measurement from AI digital pathology unmasked the "No Change" in pathological assessment. Changes in other clinical indicators were more consistent with the changes revealed by AI digital pathology, which may provide a more sensitive assessment of lifestyle intervention effectiveness and potentially even therapeutic efficacy in MASLD patients.

WED-320

Optimizing non-alcoholic fatty liver disease care using mac-2 binding protein glycosylation isomer and correlations with advanced diagnostics

Thu Thuy Pham Thi¹, Dat Ho Tan², Chanh Pham Cong³, Boi Hoan Phan Huu⁴, Thai Bieu Phu Dung³, Toan Nguyen Bao³, Khue Nguyen Minh³. ¹Medic Medical Center Ho Chi Minh City, Ho Chi Minh, Viet Nam; ²Medic Medical Center Ho Chi Minh, Ho Chi Minh, Viet Nam; ³Medic Medical Center Ho Chi Minh City, Ho Chi Minh, Viet Nam; ⁴Medic Medical Center, Ho Chi Minh, Viet Nam
Email: drthuthuypham@gmail.com

Background and aims: The escalating prevalence of non-alcoholic fatty liver disease (NAFLD) in Vietnam necessitates early detection. This study aims to establish precise mac-2 binding protein glycosylation isomer (M2BPGi) cut-offs for NAFLD fibrosis stages, evaluating correlations with existing diagnostic methods. Secondary objectives explore variations in M2BPGi levels based on age, gender, and diabetes, providing insights into NAFLD across diverse demographics.

Method: In our Hepatology department, 301 individuals meeting strict inclusion criteria, aged 18 and above, were enrolled with confirmed fatty liver diagnosis via Ultrasound or Fibroscan. Participants, treatment-naïve or having ceased treatment for over 6 months, were included based on MRE suitability. Stratification by fibrosis stage (F0/1, F2, F3, F4) was conducted, excluding co-infection with Hepatitis B or C, pregnancy, underlying cancers, excessive alcohol intake, and end-stage renal disease. Standardized routine tests and imaging, including MRE, were performed. The primary analysis aimed to establish M2BPGi cut-offs for each fibrosis stage, assessing correlations with MRE, Fibroscan, and FIB-4. Sub-population analysis considered age groups, diabetes, and gender for nuanced insights into NAFLD across diverse demographics.

Results: The accuracy of M2BPGi was ascertained through stratified fibrosis cases analyzed using Magnetic Resonance Elastography (MRE). In early NAFLD cases (F0–1), the mean cutoff for M2BPGi was 0.69 with a standard error of the mean (SEM) of 0.039. Similarly, for F2–3 cases, the mean cutoff was 0.77 with SEM 0.031, while F4 cirrhotic cases exhibited a mean cutoff of 1.0 with SEM 0.121. The observed results demonstrated statistical significance between early liver disease and cirrhotic study groups. Notably, significant gender-based differences were observed across all fibrosis stages, with males exhibiting lower M2BPGi levels than females. In terms of age groups, patients aged >65 years demonstrated the highest detected M2BPGi levels. Furthermore, within the cirrhotic group, those with diabetes exhibited significantly higher M2BPGi levels, whereas the differences observed in other groups were statistically non-significant.

Conclusion: This study in Vietnam aims to define precise M2BPGi cut-offs for NAFLD fibrosis stages, improving early detection. Results show significant M2BPGi differences between early NAFLD and cirrhotic groups, with notable gender and age variations. These findings emphasize M2BPGi's potential for nuanced NAFLD characterization and early detection in diverse demographics.

WED-321

Association between psoriasis severity and steatosis measured by artificial intelligence-based algorithm (LIVERFAST)

Sabrina Ab Wahab¹, Rafiz Abdul Rani¹, Liyana Dhamirah Aminuddin¹, Tarita Taib¹. ¹Universiti Teknologi MARA, Sungai Buloh, Malaysia
Email: sabrinaabwahab@gmail.com

Background and aims: Psoriasis is a chronic, inflammatory skin disease often associated with steatotic liver disease. Non-invasive diagnostic tests may assist in detecting liver disease without a liver biopsy, especially in psoriasis patients who require systemic treatment. LIVERFAST (Fibronostics) is an artificial intelligence (AI) technology that uses surrogate blood-serum biomarkers to assess steatosis, fibrosis and activity scores. This study aims to explore the association between psoriasis severity and steatosis by utilising LIVERFAST.

Method: A cross-sectional study was conducted on patients ≥18 years old with chronic plaque psoriasis in the Dermatology Clinic, Universiti Teknologi MARA (UiTM) Medical Specialist Centre, Sungai Buloh, Malaysia. We assessed psoriasis severity measured by psoriasis area and severity index (PASI) scores <10 (mild) and ≥10 (moderate-to-severe) after excluding other liver diseases. We evaluated the relationship with steatosis by comparing PASI scores with steatosis, fibrosis, and activity scores measured by LIVERFAST. Serum biomarkers performed, including alpha-2 macroglobulin, haptoglobin, apolipoprotein A1, total bilirubin, gamma-glutamyl transferase, fasting glucose, total cholesterol, triglycerides, alanine aminotransferase, and aspartate aminotransferase, as well as age, sex, height, and weight were entered into LIVERFAST algorithms to analyse the scores.

Results: A total of 50 patients with chronic plaque psoriasis had a mean PASI of 8.7 ± 6.3 , and body surface area (BSA) was 7.0 [interquartile range (IQR) 9)]% with disease duration of 5.5 years (IQR 11.38). Based on the PASI score, the proportions of mild and moderate-to-severe subjects were 28 (56.0%) and 22 (44.0%), respectively. The proportions of steatosis in the overall cohort were 36%, which was higher in the moderate-to-severe group (40.9%), with no significant difference compared to the mild group (32.1%), $p = 0.565$. Steatosis scores were higher among patients with moderate-to-severe group vs mild group [0.30 (IQR 0.48) vs (0.23 (IQR 0.42)], $p = 0.145$. Mild and moderate-to-severe psoriasis patients differed significantly in the duration of disease ($p = 0.033$) and age ($p = 0.040$). Fibrosis was detected in 16.7% of patients with steatosis detected by LIVERFAST. Psoriatic patients with steatosis were older, with a median of 47.0 (IQR 25) years and had a longer disease duration, with a median of 9 years (IQR 20.25). Waist circumferences were significantly correlated with the PASI score ($r = 0.285$, $p = 0.045$).

Conclusion: Both steatosis scores and proportion were higher in the moderate-to-severe psoriasis group. LIVERFAST, an AI-based blood algorithm, is convenient for screening steatosis, particularly in psoriasis patients. Early detection of fibrosis is also recommended.

WED-322

Sequential diagnostic approach utilizing FIB-4 and ELF for predicting advanced fibrosis in metabolic-associated steatotic liver disease

Yeo Wool Kang¹, Yang-Hyun Baek¹, Sang Yi Moon¹. ¹Department of Internal Medicine, Dong-A University College of Medicine, 32 Daeshingongwonro, Seo-gu, Busan, Korea, Rep. of South
Email: p100100@dau.ac.kr

Background and aims: Hepatic fibrosis is a critical predictor of liver-related mortality in patients with liver diseases. Various screening non-invasive tests (NITs) are available, and the American Association for the Study of Liver Diseases (AASLD) proposed a two-step approach, focusing on diagnostic accuracy, cost, and accessibility. This study aims to evaluate the diagnostic accuracy of fibrosis in metabolic-associated steatotic liver disease (MASLD) patients by utilizing the previously proposed two-step approach, starting with the serum-based fibrosis-4 index (FIB-4) and subsequently employing the Enhanced Liver Fibrosis (ELF) test.

Method: This clinical data and liver biopsies were used for MASLD patients between 2018 and 2023. Various NITs were utilized. The degree of fibrosis was determined based on the results of the liver biopsy. The diagnostic performance of these NITs was assessed using the Area Under the Receiver Operating Characteristic curve (AUROC). Moreover, the diagnostic performance of each test, both when used independently and within the two-step strategy using FIB-4 following ELF, was further analyzed using sensitivity, specificity, accuracy, positive predictive value (PPV), and negative predictive value (NPV).

Results: A total of 150 MASLD patients were included, with a mean age of 46.6 years (median 48 years), 53.3% being male, and 27.3% having type 2 diabetes. The performance of the NITs in identifying advanced fibrosis was as follows: The AUROC of the

aminotransferase-to-platelet ratio index, FIB-4, Non-Alcoholic Fatty Liver Disease (NAFLD) fibrosis score, and ELF for advanced fibrosis ($\geq F3$) were 0.799 (95% CI, 0.726–0.860), 0.732 (95% CI, 0.656–0.803), 0.662 (95% CI, 0.528–0.796), and 0.812 (95% CI, 0.740–0.871), respectively. The combination of FIB-4 ≥ 1.30 and ELF score ≥ 7.7 showed a sensitivity of 76.0%, specificity of 72.0%, PPV of 53.77%, NPV of 87.5%, and accuracy of 73.2% in predicting the diagnosis of advanced fibrosis. Additionally, the combination of FIB-4 ≥ 1.30 and ELF score ≥ 9.8 demonstrated a sensitivity of 56.0%, specificity of 89.6%, PPV of 69.8%, NPV of 82.6%, and accuracy of 79.5% in predicting the diagnosis of advanced fibrosis. This approach allowed the exclusion of 28 individuals (71.8%) from unnecessary liver biopsies.

Conclusion: Our study demonstrated that applying NITs previously used in NAFLD to MASLD patients for predicting fibrosis levels did not show inferiority. Therefore, it revealed that implementing a two-step strategy for MASLD patients at primary healthcare facilities, following the AASLD clinical guidelines, can early predict advanced fibrosis. Consequently, this suggests that adopting the diagnostic approach previously utilized for NAFLD patients in MASLD cases can lead to a reduction in unnecessary referrals or biopsies.

WED-323

Diagnostic performances of FIB-4 and NFS in metabolic dysfunction-associated steatotic liver disease in primary care clinic of Asia

Eileen Yoon¹, Jihyun An², Ha IL Kim³, Joo Hyun Sohn³, Bo-Kyeong Kang⁴, Eun Chul Jang⁵, Huiyul Park⁶, Hye-Lin Kim⁷, Sang Bong Ahn⁸, Joo Hyun Oh⁸, Hyo Young Lee⁹, Dae Won Jun².

¹Department of Internal Medicine, Hanyang University College of Medicine, Seoul, Korea, Rep. of South; ²Department of Internal Medicine, Hanyang University College of Medicine, Seoul, Korea, Rep. of South;

³Department of Internal Medicine, Hanyang University College of Medicine, Guri, Korea, Rep. of South; ⁴Department of Radiology, Hanyang University College of Medicine, Seoul, Korea, Rep. of South; ⁵Department of Occupational and Environmental Medicine, Soonchunhyang University College of Medicine, Chun An, Korea, Rep. of South;

⁶Department of Family Medicine, Myoungji Hospital, Hanyang University College of Medicine, Goyang si, Korea, Rep. of South; ⁷College of Pharmacy, Sahmyook University, Seoul, Korea, Rep. of South;

⁸Department of Internal Medicine, Nowon Eulji Medical Center, Eulji University, College of Medicine, Seoul, Korea, Rep. of South; ⁹Department of Internal Medicine, Kangbuk Samsung Hospital, Sungkyunkwan University School of Medicine, Seoul, Korea, Rep. of South

Email: noshin@hanyang.ac.kr

Background and aims: We aimed to explore extent to which individuals previously diagnosed with non-alcoholic fatty liver disease (NAFLD) meet the criteria fulfilled with the new nomenclature, metabolic dysfunction-associated steatotic liver disease (MASLD), within an Asian primary care cohort. Additionally, we assessed the reliability of the diagnostic performance of FIB-4 and NFS for MASLD within the primary care clinic cohort.

Method: This retrospective cross-sectional study included participants who underwent 6,740 magnetic resonance elastography (MRE) and abdominal ultrasonography during their health checkups at nationwide health promotion centers.

Results: The prevalence rates of NAFLD and MASLD diagnosed based on ultrasonography results were 36.7% and 38.0%, respectively. Notably, 96.8% of patients in the NAFLD cohort fulfilled the new criteria for MASLD. A small proportion of patients with NAFLD ($n = 80$, 3.2%) did not meet the MASLD criteria. Additionally, 168 patients (6.6%) were newly added to the MASLD group. The areas under the receiver operating characteristic curves for diagnosing advanced hepatic fibrosis for FIB-4 (0.824 in NAFLD vs. 0.818 in MASLD, $p = 0.891$) and NFS (0.803 in NAFLD vs. 0.781 in MASLD, $p = 0.618$) were comparable between the MASLD and NAFLD. Furthermore, the sensitivity, specificity, positive and negative predictive value of FIB-

4 and NFS for advanced fibrosis in MASLD were also comparable to those in NAFLD.

Conclusion: Almost patients (96.8%) previously diagnosed with NAFLD fulfilled the new criteria for MASLD in an Asian primary care cohort. Diagnostic performance of FIB-4 in the primary care MASLD cohort demonstrated satisfactory results.

WED-324

Use of FIB4 as a screening test in the bariatric population instead of the NAFLD fibrosis score reduces referral rate to hepatology without reducing identification of significant fibrosis: a retrospective audit

Michael Carbonell¹, Craig Lennie¹, Nuala Davison¹, Naim Fakhri Gomez¹, Veronica Greener¹, R. Daniel Abeles^{1,2}. ¹Chelsea and Westminster Hospital NHS Foundation Trust, London, United Kingdom; ²Division of Digestive Diseases, Imperial College London, London, United Kingdom

Email: michael.carbonell2@nhs.net

Background and aims: Identification of significant metabolic dysfunction-associated liver disease (MASLD) is important for risk stratification prior to bariatric surgery. In our institution prior to 2020, a NAFLD Fibrosis score (NFS) >0.676 triggered referral to Hepatology from the Bariatric service. From 2021 a FIB4 >1.3 was used. This study aims to compare the use of NFS with FIB4 for identifying bariatric patients with significant fibrosis.

Method: Consecutive new patients referred to the bariatric service with calculable NFS and FIB4 at time of referral from Jan-Dec 2017 ($n = 296$, cohort A) and from Jan 2021-Dec 2022 ($n = 406$, cohort B) were included. Data including demographics, enhanced liver fibrosis (ELF) test and transient elastography (Fibroscan) at Hepatology appointment were recorded. A median liver stiffness measurement (LSM) >8 kPa identified significant fibrosis. Microsoft Excel 2016 was used for data collection and statistical analysis. Categorical variables were compared using chi-squared test, continuous variables using Mann-Whitney U-test.

Results: Cohort A had a significantly higher body mass index (BMI) (45.4 vs 44, $p = 0.028$), higher rate of hypertension (HTN) (40.9% vs 26.9%, $p < 0.01$), type 2 diabetes (T2DM) (29.5% vs 23.4%, $p < 0.01$), and higher median NFS (-0.35 vs -0.86 , $p < 0.01$), and FIB4 (0.81 vs 0.68, $p < 0.01$) than cohort B. A significantly higher proportion of patients in Cohort A were referred to Hepatology compared to Cohort B (14.9% vs 6.9%, $p < 0.01$). However, a lower (but not significant) proportion of referred patients in Cohort A had significant fibrosis (20.5% vs 28.6%, $p = 0.43$). Compared to Cohort B, patients in cohort A referred to Hepatology had a significantly higher BMI (44.2 vs 50.5, $p = 0.02$), but there was no significant difference in the presence of HTN (42.9% vs 50%, $p > 0.5$) or T2DM (39.3% vs 50%, $p > 0.5$). There was a higher failure rate of Fibroscan in cohort A (38% vs 5%, $p = 0.01$). Of the 44 patients who underwent a Fibroscan, a FIB4 cut-off of 1.3 had a Sensitivity of 0.65 and Specificity of 0.375, whilst a NFS of 0.676 had a Sensitivity of 0.75 and Specificity of 0.33 for detecting significant fibrosis. In patients with a qualifying NFS or FIB4, an ELF cut-off of 10.51 had a Sensitivity of 0.27 and Specificity of 0.94 for significant fibrosis, with an AUROC of 0.49.

Conclusion: Use of a FIB4 of >1.3 compared to a NFS of >0.676 in the bariatric population reduces the number of referrals to Hepatology but does not reduce identification of patients with significant fibrosis. This may be due to the inclusion of BMI in the NFS over-predicting fibrosis in this population. In this population standard biomarkers, including ELF, did not perform particularly well in identifying significant fibrosis, and even Fibroscan may not function as a gold-standard. Therefore, further studies are warranted to optimize the identification of significant fibrosis in this at risk population.

WED-325-YI

Non-invasive assessment of hepatic steatosis by ultrasound-derived fat fraction (UDFF) in individuals at high-risk for metabolic dysfunction-associated steatotic liver disease

Federica Tavaglione^{1,2}, Valentina Flagiello^{1,2}, Francesca Terracciani^{1,2}, Paolo Gallo^{1,2}, Emma Capparelli¹, Chiara Spiezia³, Antonio De Vincentis^{4,5}, Andrea Palermo^{6,7}, Sara Scriccia⁸, Giovanni Galati², Nicola Napoli^{6,7}, Samuel Daniels⁹, Jenny Blau¹⁰, Björn Carlsson¹¹, Yeganeh Khazrai^{3,12}, Raffaele Antonelli Incalzi^{4,5}, Antonio Picardi^{1,2}, Umberto Vespasiani-Gentilucci^{1,2}. ¹Research Unit of Clinical Medicine and Hepatology, Department of Medicine and Surgery, Università Campus Bio-Medico di Roma, Rome, Italy; ²Operative Unit of Clinical Medicine and Hepatology, Fondazione Policlinico Universitario Campus Bio-Medico, Rome, Italy; ³Research Unit of Food Science and Human Nutrition, Department of Science and Technology for Sustainable Development and One Health, Università Campus Bio-Medico di Roma, Rome, Italy; ⁴Research Unit of Internal Medicine, Department of Medicine and Surgery, Università Campus Bio-Medico di Roma, Rome, Italy; ⁵Operative Unit of Internal Medicine, Fondazione Policlinico Universitario Campus Bio-Medico, Rome, Italy; ⁶Research Unit of Metabolic Bone and Thyroid Disorders, Department of Medicine and Surgery, Università Campus Bio-Medico di Roma, Rome, Italy; ⁷Operative Unit of Metabolic Bone and Thyroid Disorders, Fondazione Policlinico Universitario Campus Bio-Medico, Rome, Italy; ⁸Check-up Center, Fondazione Policlinico Universitario Campus Bio-Medico, Rome, Italy; ⁹Research and Early Development, Cardiovascular, Renal and Metabolism, BioPharmaceuticals R&D, AstraZeneca, Cambridge, United Kingdom; ¹⁰Research and Early Development, Cardiovascular, Renal and Metabolism, BioPharmaceuticals R&D, AstraZeneca, Gaithersburg, United States; ¹¹Translational Science and Experimental Medicine, Research and Early Development, Cardiovascular, Renal and Metabolism, BioPharmaceuticals R&D, AstraZeneca, Gothenburg, Sweden; ¹²Operative Unit of Nutrition and Prevention, Fondazione Policlinico Universitario Campus Bio-Medico, Rome, Italy
Email: fede.tavaglione@gmail.com

Background and aims: Given the increasing number of individuals developing metabolic dysfunction-associated steatotic liver disease (MASLD) and the low rate of those with progressive liver disease, there is a pressing need to conceive simple and affordable biomarkers to assess MASLD in general population settings. Herein, we aimed to investigate the performance of the recently developed ultrasound-derived fat fraction (UDFF) for hepatic steatosis in high-risk individuals.

Method: A total of 302 individuals with obesity, type 2 diabetes, or clinical history of hepatic steatosis were included in the analyses. Clinical, laboratory, and imaging data were collected using standardized procedures during a single screening visit in Rome, Italy. Hepatic steatosis was defined either by controlled attenuation parameter (CAP) ≥ 263 dB/m or ultrasound-based Hamaguchi's score ≥ 2 . UDFF performance for hepatic steatosis was estimated by the area under the receiver operating characteristic curve (AUC).

Results: Overall, median (IQR) UDFF was 12% (7–20). UDFF was positively correlated with CAP ($\rho = 0.73$, $p < 0.0001$) and Hamaguchi's score ($\rho = 0.79$, $p < 0.0001$). Independent predictors of UDFF were circulating triglycerides, alanine aminotransferase (ALT), and ultrasound-measured visceral adipose tissue (VAT). UDFF AUC was 0.89 (0.85–0.93) and 0.92 (0.88–0.95) for CAP- and ultrasound-diagnosed hepatic steatosis, respectively. UDFF AUC for hepatic steatosis was higher than those of fatty liver index (FLI), hepatic steatosis index (HSI), and ALT ($p < 0.0001$). Lower age, ALT, and VAT were associated with discordance between UDFF and ultrasound.

Conclusion: UDFF may be a simple and accurate tool to detect hepatic steatosis and to monitor changes in hepatic fat content over time or in response to therapeutic interventions beyond clinical trial settings.

WED-326

Effects of weight loss on overweight or obese MASLD patients after six months of dieting

Pietro Torre¹, Luigi Schiavo¹, Benedetta Maria Motta¹, Marco Aquino¹, Federica Belladonna¹, Mario Masarone¹, Marcello Persico¹. ¹Department of Medicine, Surgery and Dentistry, "Scuola Medica Salernitana", University of Salerno, Baronissi (SA), Italy, Baronissi, Italy
Email: pietrotorre90@gmail.com

Background and aims: MASLD is a multifactorial disease for which there are no approved pharmacological therapies and for which lifestyle changes still represent the most effective remedy. Nutritional studies could be essential to increase knowledge and assess causality in the field of MASLD. Our aim is to monitor patients diagnosed with MASLD who attend a weight-loss program at our Hepatology Unit, through repeated measurements of clinical parameters, transient elastography (TE), controlled attenuation parameter (CAP), and blood tests. The interaction between genetics and TE/CAP is also considered.

Method: Overweight or obese MASLD patients, aged ≥ 18 , without decompensated cirrhosis or active cancer, were proposed to start a low-glycemic index, nutritionist-guided diet. Weight, BMI, TE/CAP, and blood tests recorded at baseline were compared with the same measurements obtained after 6 months. Weight loss was categorized into classes of weight change compared to baseline ($< 5\%$, 5% – 10% , $> 10\%$). A genetic risk score (GRS) was calculated for each patient and related to changes in TE/CAP results.

Results: Among the 131 patients who underwent the first nutritional visit, 50 attended the 6-months control visit to date. At this time-point, as we previously observed in earlier follow-up visits, a significant difference compared to baseline was found in weight, BMI, and CAP (respectively -7.47 kg [-8.10%], -2.67 Kg/m², and -45.88 dB/m; all $p < 0.0001$). The latter improved proportionally to the extent of weight loss; mean liver stiffness, on the contrary, remained almost unchanged, but it decreased in the $> 10\%$ weight reduction class. Patients with high GRS experienced a greater decrease in TE/CAP values after 6 months of diet. Liver biochemistry also improved.

Conclusion: Diet-induced weight loss has beneficial effects on MASLD, and liver disease improves proportionally to its extent. Genetics appear to modulate change in liver disease severity in patients on diet. Weight loss data represent the backbone of our ongoing studies on changes in metabolomics and gut microbiota for these patients, aimed at further investigate the pathophysiology of the disease.

WED-327

Utility of transient elastography in inflammatory bowel disease

Arun Vaidya¹, Vaibhav Padole¹, Chetan Saner², Jitendra Yadav², Shubham Gupta¹, Ankita Singh², Sidharth Harindranath², Biswa Ranjan Patra¹, Leela Shinde², Apurva Kubal², Mayur Satai², Love Garg², Michael Kuruthukulangara², Nitish Patwardhan², Akash Shukla². ¹KEM Hospital, Mumbai, Mumbai, India; ²KEM hospital, Mumbai, Mumbai, India
Email: arunvaidyagastro@gmail.com

Background and aims: Inflammatory bowel disease (IBD) is associated with various extraintestinal manifestations including hepatic involvement. Hepatic fibrosis and steatotic liver disease (SLD) is an emerging cause of concern in this population. The reported prevalence of SLD in IBD varies from 1.5% to 55%. Transient elastography (TE) is a non-invasive diagnostic tool to measure liver stiffness, splenic stiffness and controlled attenuation parameter (CAP) and has been validated in a variety of clinical populations. We performed this study to explore the utility of TE in patients with IBD.

Method: This was a prospective cohort study including patients with IBD above 18 years of age. Patients with pre-existing liver disease, chronic kidney disease, alcohol abuse and pregnancy were excluded. Consecutive patients underwent Fibroscan (ECHOSENS 630 Xpert)

after written informed consent and CAP value, liver stiffness measurement (LSM), splenic stiffness measurement (SSM) was performed. F1/F2, F3 and F4 fibrosis was defined as LSM values 6–8 kPa, 8.1–12.5 kPa and >12.5 kPa respectively. Advanced fibrosis was considered when LSM value was >8 kPa. Steatosis severity: S1 (mild), S2 (moderate) and S3 (severe) was defined as CAP values 238–260 dB/m, 261–290 dB/m and ≥ 291 dB/m respectively.

Results: A total of 80 IBD cases [Ulcerative colitis (UC): 62, Crohn's disease (CD): 18] were included, of which 37 (46.3%) were females. Mean age of cohort was 39.3 ± 10.8 years. Among patients with IBD, F1/F2, F3 and F4 fibrosis was seen in 13 (16.3%), 6 (7.5%) and 5 (6.3%) respectively. In UC, F1/F2, F3 and F4 fibrosis was seen in 12 (19.4%), 4 (6.5%) and 4 (6.5%) cases respectively and in CD, F1/F2, F3 and F4 fibrosis was seen in 1 (5.6%), 2 (11.1%) and 1 (5.6%) cases respectively. Among IBD cases, S1, S2 and S3 steatosis was seen in 12 (19.4%), 8 (10%) and 5 (6.3%) respectively. In UC, S1, S2 and S3 steatosis was seen in 7 (11.3%), 7 (11.3%) and 2 (3.2%) patients respectively and in CD, S1, S2 and S3 steatosis was seen in 5 (27.8%), 1 (5.6%) and 3 (16.7%) respectively. Steatosis was significantly more common in CD as compared to UC [9/18 (50%) vs 16/62 (25.8%), $p = 0.05$]. Three patients with IBD had concomitant metabolic syndrome and among them, only one had steatosis and advanced fibrosis. SSM was elevated (>40 kPa) in 7 cases, of which only one patient had advanced fibrosis and rest had normal LSM values. Of those 7 cases with increased SSM, 3 patients were subsequently diagnosed with portal hypertension on cross sectional imaging and/or endoscopy. Two patients diagnosed with portal hypertension were on azathioprine for more than 3 years. **Conclusion:** Based on TE findings, there is an increased risk of advanced hepatic fibrosis and steatosis in IBD, even in the absence of metabolic syndrome. SLD occurs more commonly in CD than UC.

WED-330

Description of a cohort of patients with metabolic dysfunction-associated steatotic liver disease followed at an urban liver centre (Toronto liver centre), high prevalence of extrahepatic conditions Elizaveta Shpilevaia¹, Jason Xu¹, Josh Rais¹, Eva Pavic¹, Eva Fragoso¹, Farah Imdad Ali¹, Mehrdad Modarresi¹, Aleena Ghafoor¹, Anish Jammu¹, Marzena Magnes¹, Magdy Elkhatab¹. ¹Toronto Liver Centre, Toronto, Canada
Email: eshpilevaia@tlccure.com

Background and aims: Non-alcoholic fatty liver disease which is now named as metabolic dysfunction associated steatotic liver disease (MASLD) is considered a systemic disorder encompassing a spectrum of hepatic and extrahepatic conditions. The most common cause for morbidity and mortality among patients with MASLD is cardiac events and extrahepatic malignancies. This study aims to characterize a cohort of patients with MASLD evaluated at an Urban Liver Centre shading light on demographic, MASLD-associated comorbidities and extrahepatic manifestations.

Method: A comprehensive analysis was conducted on cohort of 406 patients diagnosed with metabolic dysfunction associated steatotic liver disease (MASLD) utilizing a complete data set. Demographic information, MASLD-associated comorbidities, FibroScan parameters (fibrosis and steatosis) and extrahepatic conditions were recorded.

Results: The cohort demonstrated a diverse age distribution with the majority falling within 50–69 age range (58.1%). Gender distribution were almost equal with female patients constituting 52% of the cohort. Associated common metabolic comorbidities included obesity (38.2%), hypertension (30.5%), dyslipidemia (26.6%) and type 2 diabetes (28.6%). Severe steatosis, as measured by CAP (Controlled Attenuation Parameter), was reported in 52.7%. Moderate fibrosis (F2), as measured by transient elastography, was reported in 19.5%, F3 was reported in 14% and F4 (cirrhosis) in 17.5%. Common extrahepatic conditions included depression (6.2%), coronary artery disease (1.7%), obstructive sleep apnea (2.5%), gastro-esophageal reflux disease (10.3%), irritable bowel syndrome (4.9%)

and hypothyroidism (8.1%). The most common extrahepatic malignancy was breast cancer in 1.7% of female patients.

Conclusion: Non-alcoholic fatty liver disease, now named as MASLD, is a systemic disorder associated with a broad range of extrahepatic conditions. Patients with MASLD should be evaluated and followed by a multidisciplinary team approach to optimally manage disease-associated metabolic comorbidities and extrahepatic conditions. This comprehensive approach to patient care can be a crucial step in preventing major morbidities and reducing high risk of mortality.

WED-331-YI

Subclinical myocardial fibrosis is related to disease severity in patients with metabolic dysfunction-associated steatotic liver disease (MASLD)

Puria Nabilou¹, Signe Wiese¹, Liv Hetland¹, Mikkel Werge¹, Mira Thing¹, Elias Rashu¹, Anders Junker¹, Mads Barløse^{2,3}, Hartwig Siebner^{2,3}, Søren Møller^{2,3}, Flemming Bendtsen^{1,3}, Lise Lotte Gluud^{1,3}, Jens Hove^{3,4}. ¹Gastro Unit, Medical Division, Copenhagen University Hospital Hvidovre, Hvidovre, Denmark; ²Dept. Clinical Physiology and Nuclear Medicine, Centre of Functional and Diagnostic Imaging and Research, Copenhagen University Hospital Hvidovre, Hvidovre, Denmark; ³Dept. of Clinical Medicine, Faculty of Health and Medical Sciences, Copenhagen University, Copenhagen, Denmark; ⁴Dept. of Cardiology, Copenhagen University Hospital Hvidovre, Hvidovre, Denmark
Email: purianabilou@hotmail.com

Background and aims: Myocardial extracellular volume (ECV), derived from advanced cardiac magnetic resonance imaging (CMR), reflects connective tissue in the myocardium. Quantification of myocardial ECV is based on T1 mapping technique with comparison between the pre- and post-contrast T1 relaxation times. An increase in ECV may signify increased fibrosis in the myocardium. We assessed myocardial ECV in metabolic dysfunction associated steatotic liver disease (MASLD) which is increasingly being recognised as a systemic fibroinflammatory disease and which is associated with increased cardiovascular morbidity.

Method: We included 39 patients with histologically verified MASLD without a history of cardiac disease and 11 healthy controls. All participants underwent contrast enhanced CMR with T1 mapping and quantification of myocardial ECV. The patients were extensively characterized including non-invasive biomarkers of liver fibrosis: FibroScan, Fibrosis-4 index (FIB-4), Enhanced Liver Fibrosis Test (ELF), and Pro-C3.

Results: The FibroScan showed that 16 patients had advanced fibrosis with a median value of ≥ 12.5 kPa and that these patients had an increased myocardial ECV suggesting myocardial fibrosis (28% vs. 27% $p = 0.031$). Similar results were found for patients ($n = 12$) with increased ELF score (29% vs. 26%, $p = 0.036$) and Pro-C3 ($n = 11$, 29% vs. 27%, $p = 0.015$). Patients with abnormal myocardial ECV, defined as ECV >27% had significant alterations in structural cardiac parameters including native T1 and T2 relaxation times (1216 vs. 1179, $p = 0.032$ and 41 vs. 39 ms, $p = 0.006$) and functional parameters including increased end-diastolic volume ($p = 0.034$), and cardiac index ($p = 0.010$).

Conclusion: Myocardial ECV values as well as other structural and functional parameters may have prognostic implications that could be used for risk stratification in MASLD, and our findings suggest that CMR could be considered in the monitoring of patients and possibly in the assessment of pharmacological treatments.

WED-332

FAST and Agile-the MASLD Drift: validation of Agile 3+, Agile 4 and FAST scores in 246 biopsy-proven MASLD patients of prevalent caucasian origin

Madalina-Gabriela Taru^{1,2,3,4}, Cristian Tefas^{3,4}, Lidia Neamti^{3,4}, Iulia Minciuna^{3,4}, Vlad Taru^{3,4,5}, Anca Maniu⁴, Ioana Rusu⁴, Bobe Petrushev⁴, Lucia Maria Procopciuc³, Dan-Corneliu Leucuta³, Bogdan Procopet^{3,4}, Silvia Ferri¹, Horia Ștefănescu⁴

POSTER PRESENTATIONS

Monica Lupsor-Platon^{3,4}. ¹Division of Internal Medicine, Hepatobiliary and Immunoallergic Diseases, IRCCS Azienda Ospedaliero-Universitaria di Bologna, Bologna, Italy; ²Department of Medical and Surgical Sciences, University of Bologna, Bologna, Italy; ³Faculty of Medicine, "Iuliu Hatieganu" University of Medicine and Pharmacy, Cluj-Napoca, Romania; ⁴Regional Institute of Gastroenterology and Hepatology "Octavian Fodor", Cluj-Napoca, Romania; ⁵Division of Gastroenterology and Hepatology, Department of Medicine III, Medical University of Vienna, Vienna, Austria
Email: madalinagabrielataru@gmail.com

Background and aims: Metabolic dysfunction-associated steatotic liver disease (MASLD) is a prevalent chronic liver condition with substantial clinical implications. This study aimed to assess the effectiveness of three new, elastography-based, scoring systems for advanced fibrosis $\geq F3$ (Agile 3+), cirrhosis F4 (Agile 4), and fibrotic MASH: MASH + NAS ≥ 4 + F ≥ 2 (FAST score), in a cohort of biopsy-proven MASLD patients of prevalent Caucasian origin. Our secondary aim was to compare their diagnostic performances with those of other fibrosis prediction tools, such as liver stiffness measurement by vibration-controlled transient elastography (LSM-VCTE) alone, Fibrosis-4 Index (FIB-4), AST to Platelet Ratio Index (APRI).

Method: We conducted a single-center, retrospective study, in our tertiary medical center from Cluj-Napoca, Romania, on consecutive patients with baseline laboratory tests, liver biopsy, and reliable LSM-VCTE measurements performed within a maximum timeframe of 3 weeks. The discrimination between tests was evaluated by analyzing the AUROCs. Dual cut-off approaches were applied to rule-out and rule-in $\geq F3$, F4 and fibrotic MASH, respectively. We tested previously reported cut-off values and provided our best thresholds to achieve Se $\geq 85\%$, Se $\geq 90\%$, and Sp $\geq 90\%$, Sp $\geq 95\%$. The DeLong test was used for comparison of diagnostic performance between Agile scores, LSM only, FIB-4, and APRI. The statistical significance was considered for p values < 0.05 for all tests.

Results: Among 246 patients, 113 (45.9%) were women, and 75 (30.5%) presented diabetes. The median age at baseline was 52 years (IQR, 20) and median BMI was 29.0 kg/m² (IQR, 5.1). Agile 3+ and Agile 4 demonstrated excellent performance in identifying $\geq F3$ and F4, achieving AUROCs of 0.909 [0.866–0.942] and 0.968 [0.937–0.986], while the FAST score yielded acceptable results in distinguishing fibrotic MASH, with an AUROC of 0.679 [0.594–0.757]. By using Agile 3+ standard cut-off values for $\geq F3$, 0.451 and 0.679, and LSM-VCTE standard cut-off values for $\geq F3$, 8 kPa and 12 kPa, the proportion of patients that were left unclassified were 12.6% and 21.9%, respectively (McNemar's exact test p = 0.003). By using Agile 4 standard-cut-off values for F4, namely 0.251 and 0.565, and the LSM-VCTE cut-offs of 8 kPa and 20 kPa, then 10 kPa and 20 kPa, the proportion of patients that were left unclassified were 11.4%, 39.4% and 26.8%, respectively (McNemar's exact test p < 0.0001 for both scenarios).

Conclusion: This study validates Agile 3+ and Agile 4 as reliable, non-invasive tests for identifying advanced fibrosis or cirrhosis in MASLD patients, while FAST score demonstrated only moderate performance in identifying fibrotic MASH. Importantly, we showed that Agile scores show better classification of patients with advanced fibrosis or cirrhosis compared to LSM-VCTE, as they significantly reduce the number of patients left in the "grey zone."

WED-333

Assessment of clinical and biochemical parameters and polygenic risk score in a metabolic steatosis population of southern Italy

Benedetta Maria Motta¹, Mario Masarone¹, Pietro Torre¹, Marco Aquino¹, Federica Belladonna¹, Marcello Persico¹. ¹Internal Medicine and Hepatology Division, Department of Medicine, Surgery and Dentistry, "Scuola Medica Salernitana", University of Salerno, Baronissi (Salerno), Italy
Email: bmotta@unisa.it

Background and aims: Metabolic Associated Steatotic Liver Disease (MASLD) is the leading cause of liver diseases, ranging from simple steatosis to steatohepatitis. Environmental and genetic factors have been demonstrated to influence the susceptibility to MASLD development. The gold standard for diagnosis and staging of MASLD is liver biopsy, however, it is an invasive procedure, subject to sampling errors and inter-observer variability. Several non-invasive methods aim at diagnosing hepatic steatosis and predicting significant/advanced fibrosis. GWAS studies identified genetic risk factors, which have been analyzed to develop genetic risk scores (GRS) for liver disease risk stratification. MASLD susceptibility is highly associated with four genetic variants: *PNPLA3* rs738409, *TM6SF2* rs58542926, rs641738 close to *MBOAT7* locus, *GCKR* rs1260326. Our aim was to evaluate how a polygenic risk score based on these variants correlate with liver steatosis and biochemical phenotypes in our dysmetabolic population of Southern Italy.

Method: We enrolled 103 patients attending our Hepatology Unit department, which were genotyped for rs738409, rs58542926, rs641738, rs1260326 by TaqMan 5'-nuclease assays. We used a weighted polygenic risk score (PRS), calculated by multiplying the effect size (beta-coefficient) on steatosis by respective risk alleles and summing the products. Anthropometric data and blood test results were collected.

Results: The effect of the 4 variants on the risk of developing more severe liver disease was evaluated in our population by a weighted PRS, which increased from simple steatosis to MASH/MASH-cirrhosis subjects (p = 0.03).

The effect of the 4 variants together was evaluated by PRS also in biochemical parameters. ALT (p = 0.01), AST (p = 0.003), total cholesterol, and triglycerides levels increase proportionally with PRS, while LDL levels decrease (p = N.S.).

Subjects with high PRS (≥ 0.532) show a significant higher level of ALT (p = 0.04) and an increased AST level (p = N.S.).

Conclusion: This study shows that in our population, the polygenic risk score correlates with biochemical and clinical parameters, identifying the most dysmetabolic subjects.

WED-334

Comparison of Hepatoscope® and FibroScan® for non-invasive assessment of hepatic steatosis and fibrosis among mexican immigrant adults along the southern Arizona United States/Mexico border

Edgar Villavicencio¹, Adriana Maldonado¹, Estefania Ochoa Mora², Ana Gonzalez¹, Naim Alkhouri³, David Garcia¹. ¹University of Arizona, Mel and Enid Zuckerman College of Public Health, Health Promotion Sciences, Tucson, Arizona, United States; ²University of Arizona, Clinical Translational Sciences, University of Arizona Health Sciences, Tucson, Arizona, United States; ³Arizona Liver Health, Chandler, Arizona, United States

Email: evillavicencio@arizona.edu

Background and aims: Mexican-origin adults have one of the highest rates of metabolic dysfunction-associated steatotic liver disease (MASLD) in the United States (U.S.). Given the costs and invasiveness of liver biopsy as the gold standard assessment, transient elastography (TE) by FibroScan® (Echosens, France) has emerged as the non-invasive reference tool for hepatic steatosis and fibrosis within clinical care. However, as other point-of-care non-invasive tests (NITs) for TE are introduced to the commercial market, it is important to assess the comparisons of such methods. Therefore, this study compares a new commercially available TE (Hepatoscope®) and FibroScan® for the non-invasive assessment of hepatic steatosis and fibrosis among Mexican immigrant adults along the Southern Arizona U.S./Mexico border.

Method: Paired sample t-tests were conducted to analyze data from an ongoing prospective cross-sectional community-based sample of 138 Mexican-origin adults (women = 101; men = 37). Hepatic steatosis is assessed via FibroScan® and Hepatoscope® using continuous

attenuation parameter (CAP) values measured in decibels per meter (dB/m). MASLD was identified as having a CAP score ≥ 288 dB/m. Liver stiffness measurements (LSM) in kilopascals (kPa) indicate fibrosis values.

Results: Based on FibroScan[®] results, 51 participants (37%) were identified with MASLD, including 23% of women and 14% of men. Whereas Hepatoscope[®] results indicated that 28 participants (20%) had MASLD, including 50% of women and 50% of men. FibroScan[®] and Hepatoscope[®] steatosis ($r=0.51$, $p<0.001$) and fibrosis levels ($r=0.42$, $p<0.001$) were positively correlated. CAP scores were higher for FibroScan[®] (mean = 269.3 dB/m \pm 49 dB/m) compared to Hepatoscope[®] (mean = 250.9 dB/m \pm 43 dB/m). More specifically, an 18.4-point difference ($SD = \pm 45.8$ dB/m) between FibroScan[®] and Hepatoscope[®] was observed (95% CI = 10.7, 40.9, $p<0.001$) for CAP scores. While fibrosis levels were slightly higher for Hepatoscope[®] (mean = 5.6 kPa \pm 2.5 kPa) than for FibroScan[®] (mean = 5.2 kPa \pm 2.7 kPa), there were no statistically significant differences between screening methods (95% CI = -0.8, 0.1, $p=0.1$).

Conclusion: Our results indicate hepatic steatosis levels are underestimated via Hepatoscope[®] in comparison to FibroScan[®]; however, liver fibrosis levels are comparable between screening methods. This study expands on the critical need for the continued availability of reliable and cost-effective NITs for the assessment of liver disease, particularly among high-risk underrepresented populations.

WED-335

Fibrosis detection in MASLD: A two steps comparative study

Carmen Lara-Romero¹, Inmaculada Dominguez², Filomeno Martínez¹, Maria Isabel Ojeda¹, Maria Nieto³, Inmaculada Gabaldon⁴, Maria del Carmen Rico⁵, Manuel Romero-Gómez¹. ¹Liver and Digestive Diseases Unit. Virgen del Rocío University Hospital, SeLiver Group, Biomedicine Institute of Seville (HUVR/CSIC/US), Medicine Department, University of Seville; CIBEREHD, Seville, Spain; ²Department of Clinical Analysis. University Hospital Virgen del Rocío, Seville, Spain; ³Liver and Digestive Diseases Unit. Virgen del Rocío University Hospital, SeLiver Group, Biomedicine Institute of Seville (HUVR/CSIC/US), Medicine Department, University of Seville, CIBEREHD, Seville; ⁴Las Palmeritas Primary Health Care Centre, Seville, Spain; ⁵Liver and Digestive Diseases Unit. Virgen del Rocío University Hospital, SeLiver Group, Biomedicine Institute of Seville (HUVR/CSIC/US), Medicine Department, University of Seville, CIBEREHD, Seville, Spain
Email: carmenlararomero@gmail.com

Background and aims: Metabolic-Associated Steatotic Liver Disease (MASLD) is an overwhelming burden for the health care system. Accurate algorithms are needed to select patients at risk of progression better.

Method: We included patients with MASLD at risk of fibrosis referred from primary care. One-hundred and nineteen patients (65 males and 54 females; 68% with T2DM) showing at least one NIT altered: FIB4 > 1.3; Hepamet Fibrosis Score (HFS) > 0.12 or NAFLD Fibrosis Score (NFS) > 1.455 were included in a two steps algorithm comparing TE (Fibroscan[®]) and ELF[®] (Siemens) as reflex test. Fibrosis stage was confirmed by MRE. Significant fibrosis was defined by MRE ≥ 3.14 kPa and when not available: TE > 10 kPa + ELF > 11.3 + combined score = 3. Combined score was calculated adding 1 point if FIB-4 > 1.3; NFS > 1.455; HFS > 0.12 or zero when under the cut-off scoring from 0 to 3. Age: 63 \pm 10; BMI: 30.4 \pm 6 kg/m²; HbA1c: 6.4 \pm 1.2%; FIB4: 1.90 \pm 1.64; HFS: 0.19 \pm 0.17; NFS: -0.25 \pm 2.9 and combined score: 1p: 69 (50%); 2p: 33p (28%); 3p: 26p (22%). VCTE: 9.19 \pm 11.41 kPa; CAP: 276 \pm 55; ELF: 10.24 \pm 1.01.

Results: NITs alteration was found: FIB4: 78/118 (66%); HFS: 63/118 (53%); NFS: 99 (84%); VCTE > 8 kPa: 35/118 (30%) and ELF: 78/118 (66%). Significant fibrosis in 20.7% (24/116). ELF > 9.8 was found in 49 patients with VCTE < 8 kPa and VCTE > 8 kPa was found in 6 patients with ELF < 9.8; $p<0.018$. Just 1 patient with VCTE < 8 kPa showed significant fibrosis at MRE and just one too with ELF > 9.8 but

VCTE < 8 kPa showed fibrosis. Sensitivity (S), specificity (Sp) and diagnostic accuracy (DA) were calculated: FIB-4 (S: 0.88, Sp: 0.39; DA: 0.49); HFS (S: 0.67; Sp: 0.51; DA: 0.54), NFS (S: 0.88, Sp: 0.16, DA: 0.31), TE (S: 0.96; Sp: 0.87, DA: 0.88), ELF (S: 0.72, Sp: 0.41, DA: 0.52), combining ELF > 9.8 + VCTE > 8 kPa (S: 0.88, Sp: 0.91, DA: 0.9). A Sankey diagram showed in clear difference between both algorithms.

Conclusion: Referral rate using just freely available NITs seems suboptimal. Combining NITs + VCTE or ELF significantly reduced referral rate, but the combination of both altered VCTE and ELF could better select patients at risk of advanced fibrosis and save unnecessary referral. These results confirmed available data on AGA and AASLD Clinical Practice Guidelines recommending VCTE or ELF respectively after FIB-4.

WED-336

RESIST-NASH: a regional network for identification and referral of masld patients at risk for liver fibrosis

Grazia Pennisi¹, Silvio Buscemi², Gaetano Bertino³, Lucia Frittitta³, Francesco Purrello⁴, Giovanni Raimondo⁵, Fabio Cartabellotta⁶, Maurizio Russello⁷, Giuseppe Malizia⁸, Antonio Carroccio², Antonino Tuttolomondo⁹, Salvatore Camilleri¹⁰, Giovanni Magni¹¹, Anna Licata^{12,13}, Angelo Baldassare Cefalù², Marco Distefano¹⁴, Carla Giordano¹⁵, Chiara Iaria¹⁶, Ignazio Scalisi¹⁷, Prestileo Tullio¹⁸, Maria Luisa Arpi¹⁹, Vito Di Marco¹, Calogero Camma²⁰, Salvatore Petta²⁰. ¹Section of Gastroenterology and Hepatology, Dipartimento Di Promozione Della Salute, Materno Infantile, Medicina Interna e Specialistica Di Eccellenza (PROMISE), University of Palermo, Italy, Palermo, Italy; ²Dipartimento di Promozione della Salute, Materno-Infantile, Medicina Interna e Specialistica di Eccellenza (PROMISE), University of Palermo, I-90100 Palermo, Italy, Palermo, Italy; ³Gastroenterology and Hepatology Unit, University Hospital Policlinico Vittorio Emanuele, Catania, Italy, Catania, Italy; ⁴Department of Clinical and Experimental Medicine, Internal Medicine, Garibaldi-Nesima Hospital, University of Catania, 95122 Catania, Italy, Catania, Italy; ⁵Division of Medicine and Hepatology, University Hospital of Messina, Italy, Department of Clinical and Experimental Medicine, University of Messina, Italy, Messina, Italy; ⁶UOC Medicina Interna, Ospedale Buccheri La Ferla, Palermo, Italy; Palermo, Italy; ⁷Liver Unit, Azienda di Rilievo Nazionale ed Alta Specializzazione (ARNAS) Garibaldi-Nesima, Catania, Italy, Catania, Italy; ⁸Gastroenterology Unit, Azienda Ospedaliera Ospedali Riuniti Villa Sofia-Cervello, Palermo, Italy, Palermo, Italy; ⁹Internal Medicine and Stroke Care Ward, Department of Health Promotion, Maternal and Infant Care, Internal Medicine and Medical Specialties (ProMISE) "G. D'Alessandro", University of Palermo, Piazza delle Cliniche n.2, 90127 Palermo, Italy, Palermo, Italy; ¹⁰Gastroenterology and Endoscopy Unit, "S. Elia-, Raimondi" Hospital, Caltanissetta, Italy, Caltanissetta, Italy; ¹¹Division of Gastroenterology, Ospedale di Acireale, Azienda Sanitaria Provinciale di Catania, Italy, Acireale, Italy; ¹²Medicina Interna ed Epatologia, Dipartimento di Promozione della Salute, Materno-Infantile, di Medicina Interna e Specialistica "G. D'Alessandro", PROMISE, University of Palermo, Via del Vespro 141, 90127, Palermo, Italy, Palermo, Italy; ¹³Medicina Interna ed Epatologia, Dipartimento di Promozione della Salute, Materno-Infantile, di Medicina Interna e Specialistica "G. D'Alessandro", PROMISE, University of Palermo, Palermo; ¹⁴Infectious Diseases Unit Umberto Primo Hospital, Siracuse, Italy, Siracusa, Italy; ¹⁵Section of Endocrinology and Diabetology, Health Promotion, Department of Health Promotion, Mother and Childcare, Internal Medicine and Medical Specialties "G. D'Alessandro", PROMISE, University of Palermo, 90127 Palermo, Italy, Palermo, Italy; ¹⁶Infectious Diseases Unit, ARNAS Civico-Di Cristina-Benfratelli Hospital, 90127 Palermo, Italy, Palermo, Italy; ¹⁷UOC Medicina Interna, Ospedale di Mazzara del Vallo, ASP, Trapani, Italy, Trapani, Italy; ¹⁸Infectious Diseases Unit, ARNAS Civico Hospital, Palermo, Italy, Palermo, Italy; ¹⁹University of Catania, Department of Clinical and Experimental Medicine, Endocrinology Unit, Garibaldi-Nesima Hospital, Catania, 95122, Italy, Catania, Italy; ²⁰Section of Gastroenterology and Hepatology, Dipartimento Di Promozione Della Salute, Materno Infantile, Medicina Interna e Specialistica Di Eccellenza (PROMISE),

POSTER PRESENTATIONS

University of Palermo, Italy, Palermo, Italy
Email: graziapennisi901@gmail.com

Background and aims: The epidemic of metabolic-dysfunction associated steatotic liver disease (MASLD) and its related hepatic and extrahepatic complications, mostly observed in patients with advanced liver fibrosis, raise concerns about the lack of standardized approaches for case finding and linkage to care. The overall goal is the building of a regional network -RESIST-NASH- using standardized models for identification and referral of MASLD patients at risk for liver fibrosis.

Method: Networking Sicilian specialists in gastroenterology, internal medicine and diabetology. Building a web-based platform for the standardized recording of data about patients with MASLD and/or metabolic risk factors. Automatical elaboration of the FIB-4 score, and according to Italian AISF/SID/SIO guidelines, only patients with a FIB-4 >1.3 are further evaluated by performing FibroScan and by recording further data. The platform allows a direct booking of FibroScan test and of hepatological evaluation across centers. Follow-up visits recording clinical events are also allowed.

Results: From 1th April 2023 to 31th October 2023 thirty-eight centers were activated across the Sicily, and twenty-one actively recruited patients with MASLD and/or metabolic risk factors. Nine FibroScan devices were available across the Sicily and shared among centers. Data on 1,424 patients were recorded. Mean age was 58.9 years, 55.2% were male, 47.6% obese, 45.9% were affected by diabetes. Fifty-six percent of patients had a FIB-4 <1.3 and were not worthy of further assessment, while 31.7% were at intermediate risk (FIB-4 1.3–2.67) and 12.3% at high risk (FIB-4 >2.67) of advanced liver fibrosis. Elaboration of data of liver stiffness measurement in patients with at risk FIB-4 and characteristics of this population are ongoing.

Conclusion: RESIST-NASH network can allow a systematic approach to patients with NAFLD and/or with metabolic comorbidities, leading to the correct identification and early referral of patients with liver disease worthy of a specialistic follow-up and management.

WED-337

The non-invasive assessment of liver fibrosis in metabolic dysfunction associated steatotic liver disease (MASLD) in the chinese population: a scoping review

Lai Wei^{1,2}, Di Cao³, Xuan Qi³, Ying Wang³, Yuemin Nan⁴.

¹Hepatopancreatobiliary Center, Beijing Tsinghua Changgung Hospital, Beijing, China; ²School of Clinical Medicine, Tsinghua University, Beijing, China; ³Novo Nordisk (China) Pharmaceuticals Co., Ltd, Beijing, China; ⁴Department of Traditional and Western Medical Hepatology, Hebei Medical University Third Hospital, Shijiazhuang, China
Email: weelai@163.com

Background and aims: Non-invasive tests (NITs)-based risk stratification pathways have been recommended in growing numbers of MASLD guidelines. However, the current guidelines in China do not include the aforementioned pathways, and the awareness, acceptance and clinical practice of NITs among Chinese physicians are relatively low. Therefore, we carried out a scoping review to evaluate the sufficiency of NITs related evidence in China, scrutinize their performance and identify potential data gap.

Method: We followed the Arksey and O'Malley framework for scoping reviews. A search was conducted in 3 English and 4 Chinese databases from Jan 2012 to Mar 2023. Eligible studies must target liver fibrosis assessment in Chinese patients with MASLD (previously known and studied as NAFLD or MAFLD), use liver biopsy as the gold standard, and report at least AUROC for diagnostic performance.

Results: Out of 12,714 retrieved articles, 81 studies were included, involving 35,260 subjects. The majority of the studies (66) focused on the general MASLD population, one on children, and the remaining 14 investigated MASLD patients with comorbidities such as chronic hepatitis B, diabetes/prediabetes, or obesity. Furthermore, several confounders of the diagnostic performance have been tested,

including BMI, age, the degree of hepatic steatosis, HBV infection, AST level, genetic polymorphism of PNPLA3 and the diabetes status. Advanced fibrosis ($\geq F3$) is generally recommended to be screened as the high-risk stage. 35 studies reported diagnostic performance in identifying advanced fibrosis in general MASLD population. 15 studies reported imaging diagnostic methods, 9 of which included evidence of transient elastography (TE), AUROC ranging 0.71–0.94. In 3 with more substantial sample sizes in China (>200), AUROCs was reported to be 0.78–0.94. MRE had the best AUROC of 0.937–0.95, but only 2 studies were identified with relatively small sample sizes (72 and 77 respectively). 25 studies reported evidence for serological biomarkers, scoring tools or algorithms in identifying advanced fibrosis in general MASLD population, among which FIB-4, NFS, and APRI (≥ 15 studies for each) had the most abundant evidence, but a highly scattered distribution of AUROC. However, when using the recommended cut-off value, FIB-4 had high negative predictive value (range: 89.6%–91.5%, cut-off value 1.3) in ruling out advanced fibrosis, as well as NFS (NPV range: 88%–94.8%, cut-off value -1.455). Similar analysis has been conducted for significant fibrosis ($\geq F2$) and cirrhosis (F4).

Conclusion: FIB-4, NFS and TE have been extensively studied in the Chinese population. The performance of FIB-4 and NFS as ruling out tools and TE as a diagnostic tool was similar to that reported in the Western population. The risk stratification pathway recommended by western guidelines might also be applicable to the Chinese population.

WED-338

Transcriptomic analysis reveals novel biomarkers and PI3K-AKT signaling pathway findings of at-risk metabolic dysfunction-associated steatohepatitis

Wen Wang¹, Xiaoxue Zhu¹, Aruhan Yang¹, Yanhua Ding², Guoyue Lv³.

¹Department of Phase I Clinical Trial Center, The First Hospital of Jilin University, Changchun, Jilin, China, changchun, China; ²Department of Phase I Clinical Trial Center, The First Hospital of Jilin University, Changchun, Jilin, China, Department of Phase I Clinical Trial Center, The First Hospital of Jilin University, Changchun, Jilin, China, China; ³The First Hospital of Jilin University, Changchun, Jilin, China, changchun, China
Email: dingyanhua2003@126.com

Background and aims: At-risk metabolic dysfunction-associated steatohepatitis (NASH), which NAFLD activity score ≥ 4 and significant fibrosis ≥ 2 , lacks systematic research on the genes and potential novel biomarker. 24 patients liver biopsy RNA-seq distinguishes differential gene expression between Healthy, MASL and at-risk MASH, clarifies the relationship between these differences and changes in clinical indicators in order to screen out at-risk NASH and reveal the genetic susceptibility mechanism of at-risk MASH.

Method: 24 liver biopsy samples were classified into Healthy (N=8), MASL (N=8), and at-risk MASH (N=8) according to the NAFLD Activity Score (NAS). The multiple groups comparisons were based on Generalized Linear Model (GLM, adjusted p value <0.05 corrected by BH). The Gene set enrichment analysis (GSEA) was based on the Kyoto Encyclopedia of Genes and Genomes (KEGG) database. The transcriptomic and clinical data integrated network analysis were performed by Weighted correlation network analysis (WGCNA) method. The correlation between gene expression module and clinical phenotypes were calculated by Pearson's correlation. Subsequently, the functional enrichment analysis for each co-expressed gene module were based on over-representation analysis, the co-expression network analysis were based on string database.

Results: 786 potential biomarkers were identified among Healthy (10), MASL (49), and at-risk MASH (727) which were highly expressed based on transcriptomic analysis. The gene set enrichment analysis (GSEA) revealed the MASLD pathway were activated whereas the PI3K-AKT signaling pathway was inhibited in at-risk MASH ($p_{adj} < 0.001$). The biosynthesis of co-factors and protein processing pathway related genes were down regulated at Healthy and MASL.

The WGCNA analysis indicated 3 gene modules related to at-risk NASH is not only highly correlated with Metabolic syndrome (TG, $r^2=0.56$, $p_{adj}<0.05$; HbA1C, $r^2=0.50$, $p_{adj}<0.01$; UA, $r^2=0.65$, $p_{adj}<0.001$) but also MRI-PDFF ($r^2=0.83$, $p_{adj}<0.001$), LSM ($r^2=0.62$, $p_{adj}=0.001$). Spontaneously, ALT ($r^2=0.88$, $p_{adj}<0.001$), AST ($r^2=0.75$, $p_{adj}<0.001$) and ferritin ($r^2=0.58$, $p_{adj}=0.003$) are highly related to. Those genes mainly related to fatty acid biosynthesis as well as PARP signaling pathway ($p_{adj}=0.03$). Additionally, fabp4 and ccl22 genes were located in this cluster, which could be considered as biomarker of MASH.

Conclusion: This study systematically described novel biomarkers at-risk MASH, which provide potential drug target and suggest the genetic susceptibility mechanism of at-risk MASH.

WED-339

MASLD patients with liver cirrhosis have an increased early cardiovascular risk measured by epicardial adipose tissue

Marta Hernández Conde¹, Elba Llop Herrera², Christie Perelló³, Susana Mingo⁴, Marta López-Gómez², Javier Abad Guerra², José Luis Martínez Porras², Natalia Fernández Puga², Jesús Rivera², José Luis Calleja Panero². ¹Hospital Universitario Puerta de Hierro Majadahonda, Madrid, Spain; ²Hospital Universitario Puerta de Hierro Majadahonda, Madrid, Spain; ³Hospital Universitario Puerta de Hierro Majadahonda, Madrid, Spain; ⁴Hospital Puerta de Hierro Majadahonda, Madrid, Spain

Email: marta.hernandez.conde@gmail.com

Background and aims: Epicardial adipose tissue (EAT) has been related to a higher risk of cardiovascular events. Its presence is related to excess visceral fat. The relationship between MASLD and the presence of EAT is unknown. We aimed to evaluate the association of liver fibrosis in MASLD patients with TAE.

Method: Cross-sectional observational study of 65 patients with MASLD diagnosed by liver biopsy at the Puerta de Hierro University Hospital between 2016 and 2023 and without a history of previous cardiovascular events.

Results: Regarding baseline characteristics: Most patients (70.8%) have metabolic syndrome. According to liver fibrosis: 30.6% of patients have liver cirrhosis and 37.5% have advance fibrosis. Mean BMI is 32.8 kg/m². Elevated EAT (>9.5 mm men; >7.5 mm women) is presented in 15% of patients. The EAT has good correlation with excess body fat (VAT: $r=0.36$, $p=0.003$; BMI: $r=0.35$, $p=0.005$; CAP through Fibroscan[®]: $r=0.30$, $p=0.018$). Furthermore, patients with Metabolic syndrome have more EAT (7.6 vs. 6.1; $p=0.009$), although it is not associated with the number of metabolic risk factors ($p=0.169$). In our study, a direct association between liver fibrosis and EAT is evident (Kwallis; $p=0.049$; Image). Patients with liver cirrhosis have more EAT (8 vs 6.8; $p=0.06$). Furthermore, elevated EAT is more common among patients with cirrhosis (31.5% vs. 10.2%; $p=0.043$).

Conclusion: Liver fibrosis in patients with MASLD is associated with higher EAT. Therefore, MASLD staging could help identify patients at cardiovascular risk.

WED-340

Agreement between two-dimensional shear wave elastography and transient elastography in metabolic dysfunction-associated steatotic liver disease: implications for primary care screening

Shelley Keating¹, Kanishk Chaudhary², Nicolette Gale³, Thomas Lloyd⁴, Graeme Macdonald². ¹The University of Queensland, School of Human Movement and Nutrition Sciences, Brisbane, Australia; ²Princess Alexandra Hospital, Department of Gastroenterology and Hepatology, Woolloongabba, Australia; ³Princess Alexandra Hospital, The Medical Imaging Department, Woolloongabba, Australia; ⁴Princess Alexandra Hospital, Department of Radiology, Woolloongabba, Australia

Email: s.keating@uq.edu.au

Background and aims: Current practice guidance (AASLD 2023) recommend screening patients with metabolic dysfunction-associated steatotic liver disease (MASLD) for advanced liver disease for

specialist referral. Algorithms currently rely on vibration-controlled transient elastography (VCTE) and blood-based tests. In Australia and elsewhere, access to VCTE in the community is limited. However, other elastography modalities such as two-dimensional shear wave elastography (SWE) are being incorporated into ultrasound services available to primary care. The utility of SWE in evaluating MASLD is not known. We examined the agreement between SWE and VCTE in patients referred from primary care to a specialist service.

Method: Participants were patients referred from primary care to a MASLD clinic. All participants had VCTE and SWE. Agreement between these were evaluated by Bland-Altman plots and/or Passing-Bablok regression analysis. Systematic bias (via one-sample t-test and examination of $y=0$) and proportional bias (via linear regression) were determined. Variables impacting agreement between the methods were examined via multiple regression. The McNemar test determined differences in the proportions of participants correctly identified by SWE with VCTE result of >8 kPa.

Results: 72 patients (54 ± 14 years, 43 % male, BMI 34.0 ± 7.1 kg/m²) were recruited, but in 12 the VCTE and/or the SWE study were of poor quality and their data not further analysed. The remaining 60 patients had a median VCTE of 5.5 [3.4 to 7.7 kPa], with a IQR centile of 6.0 [2.3 to 9.8 %]. The mean difference between VCTE and SWE was 0.93 kPa (95 % CI, 0.06 to 1.80 kPa; Lower to Upper Limit of Agreement 5.69 to 7.55 kPa), with systematic and proportional bias present. Increasing VCTE interquartile range (IQR) centile (adjusted for age, controlled attenuation parameter and alanine aminotransferase) was the only factor identified that correlated with the discrepancy between methods ($\beta=0.9$, $p<0.001$). Every one-centile increase in VCTE IQR was associated with an increase in the difference between VCTE and SWE of 0.9 kPa. The predictive performance of SWE to identify patients with a VCTE of >8 kPa was evaluated at SWE of 7 kPa (based on the observation that SWE underreporting VCTE by ~1 kPa), with specificity 25 %, sensitivity 94 %, and positive and negative predictive powers of 50 % and 83 % respectively. A SWE cut-off of 6 kPa improved sensitivity to 42 % with specificity at 80 %.

Conclusion: On average, SWE underestimated liver stiffness compared with VCTE by 0.93 kPa. The discrepancy between VCTE and SWE increases as VCTE and VCTE IQR increase. SWE has the potential to be used in the evaluation of patients with MASLD where VCTE is not readily available in the community.

WED-341

EUS-guided assessment of steatotic liver disease in bariatric surgery patients

Paula Fernandez Alvarez¹, Rafael Romero Castro¹, Maria Tous Romero¹, Alvaro Gutierrez Dominguez¹, Félix Conde Martín¹, Juan José Ríos Martín¹, Victoria Alejandra Jiménez García¹, Eduardo Dominguez Adame¹, Patricia Cordero Ruiz¹, Francisco Luis Bellido Muñoz¹, Manuel Rodríguez Téllez¹, Angel Caunedo Alvarez¹, Isabel Carmona Soria¹. ¹Virgen Macarena University Hospital, Seville, Spain

Email: paulafer7@gmail.com

Background and aims: Bariatric surgery patients have a higher prevalence of metabolic dysfunction-associated liver disease (MASLD). Percutaneous liver biopsy has technical difficulties and non-invasive markers are not very accurate in this population. The aim was to evaluate the efficacy and safety of EUS-guided bilobar liver biopsy plus EUS-guided portal pressure gradient measurement in diagnosing MASLD and its correlation with non-invasive test patients undergoing bariatric surgery.

Method: An observational, prospective and single-center study was carried out. Patients with suspected of MASLD by liver ultrasound or fatty liver index (FLI) score >60 were included. Demographic, anthropometrics, blood test, non-invasive serological markers (FLI, NAFLD, HEPAMET, APRI, FIB-4) and transient elastography (TE) with XL probe variables were evaluated.

POSTER PRESENTATIONS

Results: A total of 48 patients were evaluated between August 2022 and June 2023. Finally, 33 patients were included (10 refused to participate, 4 were excluded, 1 due to technical difficulties). The prevalence of MASLD was 68.8%, of metabolic dysfunction-associated steatohepatitis (MASH) was 54.5%, and of fibrosis (F1-F2) was 12.6%. EUS-guided portal pressure gradient median was 4.25 mmHg. Remarkably, 9/33 (27.7%) patients had a portal pressure gradient >6 mmHg. MASLD patients showed higher levels of fibrosis determined by transient elastography (TE), steatosis evaluated by coefficient attenuated parameter (CAP) and portal vein pressure, although they were not statistically significant. No differences were detected in FIB-4, NAFLD and HEPAMET scores according to MASLD patients. The quality of liver biopsies was deemed adequate with a median of 7 portal spaces. Adverse events were observed in 2 patients after procedure. One patient suffered mild abdominal pain and the other was diagnosed of atrial fibrillation with rapid ventricular that was successfully reversed with medical therapy.

Conclusion: The prevalence of MASLD and MASH was high in morbid obesity patients. EUS-guided portal pressure gradient and EUS-guided liver biopsies in one-step seem safe and accurately in evaluating the presence of portal hypertension and the underlying steatotic liver disease.

WED-342

Can we define MASLD in liver outpatient clinics? Keeping up with the changing nomenclature

Mercy Karoney¹, Riham Soliman², Mzamo Mbelle³, Ashley Barnabas⁴.

¹Institute of Liver Studies, King's College Hospital, London, United Kingdom; ²Institute of Liver Studies, King's College Hospital, London, United Kingdom; ³Institute of Liver Studies, King's College Hospital, London, United Kingdom; ⁴Institute of Liver Studies, King's College Hospital, London, Kenya

Email: karoneymercy@gmail.com

Background and aims: Metabolic dysfunction-associated steatotic liver disease (MASLD) remains the most common chronic liver disease which affects one third of the adult global population. A multi-society Delphi consensus introduced the new nomenclature MASLD which was previously termed Non-Alcoholic Fatty liver disease (NAFLD) in July 2023. This new nomenclature is considered less stigmatizing, more affirmative, and adequately reflects the role of metabolic dysfunction in the disease spectrum. While NAFLD was based on the exclusion of any other liver disease, MASLD is defined by evidence of hepatic steatosis and at least 1 out of 5 cardiometabolic risk factors. Additionally, the updated nomenclature added MetALD which is a distinct subtype that considers weekly alcohol consumption more than 140 grams or 210 grams for women and men respectively. This change in terminology calls for reclassification of patients previously labelled NAFLD and some discrepancy is expected. The aim of this project was to describe how a cohort of already defined NAFLD patients fit into the newly defined criteria for MASLD and the subtype MetALD.

Method: This was an audit project on NAFLD patients attending the outpatient liver service of King's College Hospital, London. We collected data from records of patients previously diagnosed as NAFLD by the presence of fatty liver on ultrasound, controlled attenuation parameter of FibroScan (Echosens, Paris), or liver biopsy. The collected data was evaluated against the 2023 MASLD criteria.

Results: A total of 201 patients were included in the final analysis, the mean age was 57.4 years, range of 19.7 to 87.6 years, majority of the patients were male 112/201 (55%). Most of the patients, 156/201 (77.6%) had at least one cardiometabolic risk factor out of the five required in the definition for MASLD. The most common cardiometabolic risk factor present was Diabetes 47.8%, followed by Dyslipidaemia in 40.3%. Alcohol use was recorded in 25% (95%CI 8.21 to 17.8%), out of those who reported alcohol consumption, 46% had excess weekly consumption of alcohol. Other liver comorbidities were present in 22% of the patients including Hepatitis B, Hepatitis C,

alcohol related liver disease, autoimmune liver disease, Haemochromatosis and Alpha one antitrypsin deficiency. Out of the total 201 patients, those who met the criteria for MASLD were 89%, Met-ALD was 9% while only 3% did not fit the MASLD criteria.

Conclusion: The new nomenclature, though simple with easily measurable parameters might have some discrepancy with previously defined terminologies as demonstrated here. The use of this nomenclature should be adopted in clinical practice as it eliminates the heterogeneity observed with the previous definition. It is important to check for all the cardiometabolic risk factors as they may indicate a higher risk of fibrosis.

WED-343

Transducer reproducibility in liver ultrasound-derived fat fraction measurements

Reinhard Kubale¹, Guenther Schneider¹, Paul Lessenich¹, Arno Buecker¹, Sebastian Wassenberg², Gabriela Torres³, Arati Gurung³, Timothy Hall⁴, Yassin Labyed³. ¹Universität des Saarlandes, Homburg, Germany; ²punkt05, Düsseldorf, Germany; ³Siemens Healthineers, Issaquah, United States; ⁴University of Wisconsin Madison, Madison, United States
Email: kubale@mac.com

Background and aims: Ultrasound-Derived Fat Fraction (UDFF) is an emerging, multiparametric imaging tool used for non-invasive quantification of liver fat content. This technique shows promise in the evaluation of Metabolic Associated Steatotic Liver Disease (MASLD). The reproducibility of UDFF measurements remains a key determinant of its wider clinical application and potential. Our study aims to assess the reproducibility of liver UDFF measurements across different transducers.

Method: This study included adult subjects with clinical indication for ultrasound examination. 25 participants were scanned using the Siemens SEQUOIA Ultrasound System (software revision, VA30), with three different transducers: DAX (Deep Abdominal Transducer), 5C1, and 9C2. The DAX transducer, designed for high BMI subjects, was used alongside the more broadly used 5C1 and the 9C2, which is typically used for lower BMI individuals and children. For each subject, five UDFF measurements were obtained using each transducer. These measurements were acquired intercostally, targeting approximately the same liver region, about 1.5 cm below the liver capsule. Transducer reproducibility was evaluated using the Intraclass Correlation Coefficient (ICC). The agreement in UDFF measurement among the three transducers was assessed through Bland-Altman Analysis, and the linearity with the Pearson Correlation Coefficient (r).

Results: The study demonstrated good agreement between UDFF measurements using the DAX and 5C1 transducers, with a mean difference of 0.94% (95% CI -0.7–2.6) and 95% limits of agreement ranging from -7.5% (95% CI -9.8–-5.2) to 9.6% (95% CI 7.9–11.3). The Pearson correlation coefficient and ICC for agreement between DAX and 5C1 were $r=0.81$ (95% CI: 0.39–0.87) and 0.81 (95% CI: 0.62–0.91) respectively. Likewise, the mean difference between DAX and 9C2 transducers was -1.14% (95% CI -2.5–2.2), with 95% limits of agreement from -7.9% (95% CI -9.3–-6.6) to 5.6% (95% CI 4.3–7.0); the Pearson correlation coefficient $r=0.88$ (95% CI: 0.49–0.93) and ICC was 0.87 (95% CI: 0.73–0.94). When comparing the 5C1 and 9C2 transducers, the mean difference was -2.0% (95% CI -3.5–0.7), with 95% limits of agreement from -9.1% (95% CI -10.5–-7.7) to 4.9% (95% CI 3.5–6.3). The Pearson correlation coefficient and ICC for agreement between 5C1 and 9C2 were $r=0.87$ (95% CI: 0.55–0.88) and 0.84 (95% CI: 0.60–0.93).

Conclusion: This study demonstrates good reproducibility of UDFF measurements with various transducers on the Siemens SEQUOIA Ultrasound System. The findings suggest the potential benefit of a correction factor to minimize differences between transducers. Future research is needed to understand and mitigate confounding

factors to further optimize UDF clinical protocols and expand its clinical relevance.

WED-347

Diagnosis of advanced liver fibrosis: the synergy of open data, synthetic data generation, CatBoost, and feature engineering

Athanasios Angelakis^{1,2,3}, ¹Amsterdam University Medical Centers, Amsterdam, Netherlands; ²Amsterdam Public Health Research Institute, Amsterdam, Netherlands; ³University of Amsterdam-Data Science Center, Amsterdam, Netherlands
Email: a.angelakis@amsterdamumc.nl

Background and aims: In the landscape of liver disease management, accurately predicting advanced liver fibrosis is crucial yet challenging. This study illuminates the transformative role of synthetic data generation, advanced machine learning algorithms like CatBoost, and sophisticated feature engineering in enhancing the prediction of advanced fibrosis using the FIB-4 score.

Method: Leveraging open MASLD datasets from China (540 patients), Malaysia (147 patients), and India (97 patients), our study introduces a novel approach combining CatBoost—a potent gradient boosting algorithm—with intricate feature engineering on the components of the FIB-4 score. A distinguishing aspect of our methodology is the use of CTGAN for synthetic data generation, a cutting-edge technique that synthesizes realistic and diverse tabular data, addressing issues of data scarcity and imbalance. The training dataset, comprising data from China and India (637 patients), was enriched with a synthetic dataset of 802 instances (originally 1000, with negative values removed) generated via CTGAN. This resulted in a robust and augmented training set of 1517 instances, providing a more comprehensive representation of the patient spectrum.

Results: The inclusion of synthetic data proved pivotal. The ROC-AUC on the test set (Malaysia) for the standard FIB-4 score was 0.7514. Our ML model, which intricately utilizes the FIB-4 score parameters (ML-FIB4), achieved a ROC-AUC of 0.7857. Remarkably, the model enriched with synthetic data augmentation (DA-ML-FIB4) further elevated the ROC-AUC to 0.7944. These results underscore the significant impact of synthetic data generation in enhancing the model's predictive capability and generalizability to diverse patient populations.

Conclusion: The integration of CTGAN-generated synthetic data, coupled with the predictive power of the CatBoost algorithm and innovative feature engineering, marks a substantial advancement in the field of liver fibrosis prediction. This study not only demonstrates improved diagnostic accuracy but also paves the way for leveraging synthetic data in medical research, particularly in scenarios of limited or unbalanced datasets.

WED-348

High prevalence of liver fibrosis and cirrhosis among cohort of patients referred to an urban liver centre for evaluation of metabolic dysfunction-associated steatotic liver disease (utility of transient elastography)

Anish Jammu¹, Jason Xu¹, Josh Rais¹, Elizaveta Shpilevaia¹, Aleena Ghafoor¹, Farah Imdad Ali¹, Eva Pavic¹, Eva Fragos¹, Mehrdad Modarresi¹, Marzena Magnes¹, Magdy Elkhatab¹. ¹Toronto Liver Centre, Toronto, Canada
Email: anishjammu@live.ca

Background and aims: Metabolic dysfunction associated steatotic liver disease (MASLD) is a prevalent liver disorder worldwide. It encompasses a spectrum of conditions ranging from simple steatosis to advanced fibrosis and cirrhosis. Metabolic dysfunction associated steatohepatitis (MASH) is a potentially progressive form of MASLD that can lead to liver fibrosis and cirrhosis. To date, MASH diagnosis is only done through liver biopsy which is an invasive procedure. Transient elastography is a non-invasive tool that can stratify fibrosis stage in order to identify a subgroup of patients who may benefit from having a liver biopsy.

Method: A total of 406 patients were evaluated with a full liver profile to rule out other associated liver diseases. Only patients with pure MASLD were included and stratified with transient elastography to assess the degree of liver fibrosis and steatosis. Patients who had moderately elevated liver stiffness of 8.5 kPa and above were considered for liver biopsy to diagnose MASH. Biopsy results were available in 93.3% of the eligible patients.

Results: The cohort demonstrated a diverse age distribution, with the majority falling within the 50–69 age range (58.1%). The female-to-male ratio was almost equal, with females constituting 52% of the cohort. Common associated comorbidities included obesity (38.2%), hypertension (30.5%), dyslipidemia (26.6%), and type 2 diabetes (28.6%). Transient elastography results demonstrated stage 2 fibrosis (F2 in 19.5%), stage 3 fibrosis (F3 in 14% of the patients), and cirrhosis (F4 in 17.5% of patients). Among patients eligible for liver biopsy, MASH was reported in only 30.5% of cases by the liver pathologist.

Conclusion: Transient elastography is a valuable non-invasive technology for stratifying the severity of liver fibrosis among patients with MASLD referred for liver evaluation. While liver biopsy is still considered to be the gold standard for diagnosing MASH, it has demonstrated significant limitations even when interpreted by a qualified liver pathologist. There is a pressing need for new non-invasive serological markers/technologies to identify patients with MASH who are at greatest risk of developing liver fibrosis and cirrhosis.

MASLD – Experimental and pathophysiology

TOP-228-YI

CD36-mediated hepatocyte-macrophage coordination drives hepatic fibrosis in MASLD

Zhe Dai¹, Yijin Wang², ¹Southern University of Science and Technology, Shenzhen, China; ²Southern University of Science and Technology, Shenzhen, China
Email: wangyj3@sustech.edu.cn

Background and aims: In the context of metabolic dysfunction-associated liver disease (MASLD), a progressive replacement of resident Kupffer cells (ResKCs) by a distinct population of macrophages known as lipid-associated macrophages (LAMs), characterized by CD36 upregulation occurs. However, the precise roles and underlying mechanisms of the CD36-expressing LAMs involved in MASLD pathogenesis remains to be elucidated.

Method: We first investigated the characteristics of LAMs through single-cell RNA sequencing (scRNA-seq) data. Oleic acid (OA)-pretreated THLE-2 cells were co-cultured with macrophages to mimic LAMs to further investigate their functional properties *in vitro*. We explored the molecular regulatory mechanism for SPP1 (encoding osteopontin, OPN) upregulation using chromatin immunoprecipitation sequencing (ChIP-seq) datasets. Lastly, to identify the potential role of CD36 inhibitor in metabolic dysfunction-associated steatohepatitis (MASH) treatment, we employed high-fat diet (HFD)- and high-fat methionine-restriction choline-deficient diet (HFMRC)-induced mouse models.

Results: The findings from scRNA-seq analysis demonstrated an enhanced CD36 expression in LAMs, which correlates with a distinct immunosuppressive phenotype. By utilizing the co-culture system, we were able to confirm that the increased expression of CD36 in LAMs facilitated a more efficient uptake of lipids from hepatocytes with steatosis, subsequently triggering the release of SPP1 through the peroxisome proliferator-activated receptor gamma (PPAR-γ) signaling pathway. ChIP-seq data revealed a PPAR-γ binding site in the SPP1 transcript region, which was further confirmed by chromatin immunoprecipitation-quantitative real-

POSTER PRESENTATIONS

time PCR (ChIP-qPCR) experiments, indicating the direct regulatory interaction between PPAR- γ and SPP1. Furthermore, the stimulation of hepatic stellate cells (HSCs) by SPP1 was demonstrated by the upregulation of α -smooth muscle actin (α -SMA) and collagen type I α 1 (COL1A1) in LX-2 cells, ultimately contributing to the progression of liver fibrosis. The knockdown or inhibition of CD36 in LAMs effectively impedes lipid uptake and SPP1 release, leading to alleviation of fibrosis. These promising effects have been observed in both in vitro cell models and in mice. Notably, the combination of a CD36 inhibitor and pioglitazone exhibits a synergistic effect in effectively inhibiting the progression of liver fibrosis in MASH murine models.

Conclusion: CD36 serves as a facilitator for the transfer of lipids from hepatic cells to LAMs, thereby initiating the activation of hepatic stellate cells and promoting the progression of liver fibrosis. The identification of CD36 as a potential therapeutic target offers promising prospects for the treatment of advanced liver fibrosis associated with MASLD.

TOP-229-YI

The E2F2 target glycerophosphodiester phosphodiesterase domain containing 3 is involved in MASLD progression to HCC and related dyslipidemias

Maider Apodaka-Biguri¹, Nerea Muñoz-Llanes¹, Francisco Gonzalez-Romero¹, Igor Aurrekoetxea¹, Beatriz Gómez Santos¹, Igotz Delgado¹, Xabier Buque^{1,2}, Ane Nieva-Zuluaga¹, Mikel Ruiz de Gauna¹, Idoia Fernández-Puertas¹, Paul Gomez-Jauregui¹, Natalia Sainz-Ramírez¹, Kendall Alfaro-Jiménez¹, Estibaliz Castillero¹, Daniela Mestre Congregado¹, Ashwin Woodhoo^{3,4}, Marta Varela-Rey⁵, Amaia Lujambio⁶, Ana Zubiaga⁷, Patricia Aspichueta^{1,2,8}. ¹Department of Physiology University of the Basque Country UPV/EHU, Faculty of Medicine and Nursing, Leioa, Spain; ²Biocruces Bizkaia Health Research Institute, Cruces University Hospital, Barakaldo, Spain; ³Center for Cooperative Research in Bioscience (CIC bioGUNE), Santiago de Compostela, Spain; ⁴Ikerbasque, Basque Foundation for Science, Bilbao, Spain; ⁵Liver Disease Laboratory, Center for Cooperative Research in Biosciences (CIC bioGUNE), Derio, Spain; ⁶Icahn School of Medicine at Mount Sinai, New York, United States; ⁷Department of Genetic, Physical Anthropology and Animal Physiology, Faculty of Science and Technology, University of Basque Country UPV/EHU, Leioa; ⁸National Institute for the Study of Liver and Gastrointestinal Diseases (CIBERehd, Carlos III Health Institute), Madrid, Spain
Email: patricia.aspichueta@ehu.es

Background and aims: Hepatocellular carcinoma (HCC) is the most common primary liver cancer, which is the fourth leading cause of cancer-related mortality worldwide. Metabolic dysfunction-associated steatotic liver disease (MASLD), and related dyslipidemias are risk factors for HCC development. The role of Glycerophosphodiester phosphodiesterase domain containing 3 (GDPD3) promoting hepatosteatosis has been described; however there is no information about a specific role in promoting dyslipidemias or progression to HCC. Thus, the aims were 1) to identify the role of GDPD3 in the metabolic dysregulation of progressive-MASLD. 2) to investigate the mechanism involved in modulation of GDPD3 expression in progressive MASLD and HCC.

Method: To induce MASLD-related HCC, diethylnitrosamine (DEN) was administered to 14-day-old mice (WT), and fed a high-fat diet (HFD) until sacrificed at 3 and 9 months. HCC was also induced by the sleeping beauty technique (*Myc;sg-Pten* plasmids) combined with feeding a high-fat-diet (HFD). *Gdpd3* was specifically overexpressed in liver with adeno-associated viruses-serotype 8 (AAV8). *E2f2*^{-/-} mice were also used. Hepatic and serum lipidomic and apolipoprotein (Apo) profile was assessed, serum lipoproteins were separated using an ACTA-FPLC. ChIP and gene expression assays were also performed. TCGA-LIHC cohort data were used.

Results: *Gdpd3* overexpression in mice induced hepatosteatosis and a remodeling in serum lipidome reflected in several species of fatty acids, triglycerides (TG) and cholesterol esters, which were increased when compared with the corresponding controls. Accordingly, an increased number of circulating VLDL particles and decreased number of HDL were found, as levels in ApoB and apoE showed. The dyslipidemia was more pronounced in a lipid-rich environment induced by feeding a HFD, where the FPLC analysis showed that *Gdpd3* overexpression in liver increased levels of TG in VLDL particles and cholesterol levels in VLDL and LDL particles. Overexpression of *Gdpd3* in the *Myc;sg-Pten* mice model promoted MASLD-related HCC increasing the number of tumors. Our data showed that GDPD3 was upregulated in human HCC livers within the TCGA-LIHC cohort and that correlated positively with *E2F2*. Hepatic *Gdpd3* and *E2f2* were also increased in preclinical models of MASLD-related HCC where *E2F2* bound directly to the *Gdpd3* promoter at two different sites. In *E2f2*^{-/-} DEN-HFD mice, protected from MASLD-related HCC, *Gdpd3* levels were decreased and its overexpression by AAV8 resulted on partial loss of this protection.

Conclusion: *Gdpd3* is a target of E2F2 in MASLD-related HCC and promotes dyslipidemia and disease progression. Thus, GDPD3 arises as a novel target for treatment.

TOP-240-YI

Hepatic mitochondrial reductive stress predicts liver mortality in the UK biobank

Juho Asteljoki^{1,2,3,4}, Fredrik Åberg⁵, Jagadish Vangipurapu⁶, Katri Kantojärvi⁷, Mari J. Jokinen^{1,2,3}, Jaakko T. Leinonen⁴, Nina Mars⁴, Ville Männistö⁸, Annamari Lundqvist⁷, Veikko Salomaa⁷, Antti Jula⁷, Satu Männistö⁷, Markus Perola⁷, Markku Laakso⁶, Taru Tukiainen⁴, Panu K. Luukkonen^{1,2,3}. ¹Minerva Foundation Institute for Medical Research, Helsinki, Finland; ²Department of Internal Medicine, University of Helsinki, Helsinki, Finland; ³Abdominal Center, Helsinki University Hospital, Helsinki, Finland; ⁴Institute for Molecular Medicine Finland (FIMM), HiLIFE, University of Helsinki, Helsinki, Finland; ⁵Transplantation and Liver Surgery, Helsinki University Hospital and University of Helsinki, Helsinki, Finland; ⁶Internal Medicine, Institute of Clinical Medicine, University of Eastern Finland, Kuopio, Finland; ⁷Public Health and Welfare, Finnish Institute for Health and Welfare, Helsinki, Finland; ⁸Departments of Medicine, University of Eastern Finland and Kuopio University Hospital, Kuopio, Finland
Email: panu.luukkonen@helsinki.fi

Background and aims: Metabolic dysfunction-associated steatotic liver disease (MASLD) is the most common chronic liver disease which can progress to cirrhosis and eventually death. Recent studies have shown that histological severity of MASLD associates with hepatic mitochondrial reductive stress as determined by plasma beta-hydroxybutyrate-to-acetoacetate ratio (bOHB/AcAc). However, it is unclear whether hepatic mitochondrial reductive stress associates with clinically relevant end points. Here, we aimed to investigate whether bOHB/AcAc predicts liver-related mortality in a large prospective cohort. Furthermore, we aimed to identify genetic factors that regulate bOHB/AcAc and whether genetically determined bOHB/AcAc predicts liver-related mortality.

Method: In the prospective UK Biobank data, we excluded participants with liver diagnosis before or at baseline or chronic viral disease at any time. Cases were defined using registry-based causes of death. We assigned participants without liver diagnoses at any time as controls. We matched the cases to controls for age, sex, waist-to-hip ratio, BMI, type 2 diabetes, smoking, and alcohol use in a 1:4 ratio. Plasma bOHB and AcAc concentrations were determined using the Nightingale NMR metabolomics platform. We used Cox regression to evaluate the association between baseline bOHB/AcAc and liver-related mortality. We performed a genome-wide association analysis (GWAS) using REGENIE in the UK Biobank (n = 94, 092), FINRISK and Health 2000 (n = 17, 229), and METSIM cohorts (n = 9, 607). The GWAS results were meta-analysed using the fixed-effects model with

PLINK v1.9. We constructed a genome-wide polygenic risk score (PRS) from high-quality variants using PRSice2 for the unrelated UKB participants (n = 250, 357), whom we did not consider in the initial GWAS. We used Cox regression to evaluate the association between the PRS and liver-related mortality.

Results: Baseline bOHB/AcAc predicted liver-related mortality (HR = 1.16 per 1-SD, p = 0.022) during a median follow-up time of 13.1 years (IQR 11.9–14.2). Amongst distinct causes of liver-related death, baseline bOHB/AcAc predicted particularly cirrhosis-related mortality (HR = 1.27 per 1-SD, p = 0.019). In the GWAS, we identified 18 significant loci associated with bOHB/AcAc (p ≤ 5E-8). Most of these loci annotated to genes that encode for mitochondria-specific proteins (e.g. MPC1 and DHODH) or genes known to modify the risk of MASLD (e.g. GCKR, APOE, and PPP1R3B). Similar to the observed bOHB/AcAc, the PRS predicted cirrhosis-related mortality (HR = 1.19 per 1-SD, p = 0.010).

Conclusion: Both the observed and genetically determined bOHB/AcAc predict liver mortality, particularly cirrhosis-related mortality, independent of common risk factors. These data suggest mitochondrial reductive stress as a possible causal factor in the pathogenesis of liver disease.

THURSDAY 06 JUNE

THU-194

Semaglutide links with improved survival and liver outcomes in MASLD patients, a large multicenter retrospective real-world cohort study

Mohammed Suki¹, Yael Milgrom¹, Mohamad Masarowah¹, Wadiaa Hazo¹, Yariv Tiram², Ofer Perzon³, Esther Forkosh¹, Joseph Sackran¹, Johnny Amer¹, Achraf Imam¹, Abed Khakayla⁴, Rifaat Safadi⁵. ¹Liver institute, Hadassah Hebrew University Hospital, Jerusalem, Israel; ²Liver institute, Hadassah Hebrew University, Jerusalem, Israel; ³Livei institute, Hadassah Hebrew University Hospital, Jerusalem, Israel; ⁴Liver institute, Hadassah Hebrew University Hospital, Jerusalem, Israel; ⁵Liver Insititute, Hadassah Hebrew University Hospital, Jerusalem, Israel
Email: johnnyamer@hotmail.com

Background and aims: Semaglutide (SEMA) has potential benefits in Metabolic dysfunction-associated steatotic liver disease (MASLD). In this large real-world study, SEMA effect on MASLD patients evaluated.

Method: TriNetX is a global research platform de-identified database that spanning 135 million patients across 112 healthcare organizations worldwide. We analyzed electronic medical records of MASLD patients according ICD9 Diagnosis. Following propensity score matching based on 34 variables (demographics, comorbidities, laboratory tests and medication history), SEMA treated (n = 18, 473) correlated with non-SEMA (n = 18, 473) cases. Exclusion criteria: ALT and ALP levels >4 UNL, advanced liver disease (ALD), liver transplant and cancer, past anticoagulation and non-MASLD etiologies. Assessed outcomes were survival, biochemical, hematologic, AFP, metabolic and cardiovascular (CV), ALD, abnormal synthetic function and poor metabolic markers. ALD defined according to ICD9 diagnosis (Portal hypertension, Chronic passive congestion of liver, Ascites, Esophageal/Gastric varices, Hepatic encephalopathy, Hepatorenal/Hepatopulmonary syndromes, Spontaneous bacterial peritonitis, Hepatic failure, Other and unspecified cirrhosis), blood tests (Ammonia >50 umol/L, Platelets <100 k/uL, Bilirubin >2 mg/dL, Albumin <2.80 g/dL) and specific treatments (Neomycin, Rifaximin, Propranolol, Carvedilol, spironolactone >100 mg). Abnormal synthetic function defined by either albumin <2.8, bilirubin >2 or INR>1.7. Poor metabolic markers defined either LDL>130, HDL<40, TG>200 or HBA1c>8%.

Results: Following matching, both cohorts were well-balanced, except of higher BMI in SEMA group; 36.7 ± 6.3 vs. 34.9 ± 7.1 kg/m².

Otherwise, rest parameters were well matched, including mean age 51.1 ± 12.8 vs. 51.4 ± 13.5 years, females in 59.9 vs. 60%, white background in 68.5 vs. 67.5%, diabetes in 61.2 vs. 62.2%, respectively. After one year, the SEMA group demonstrated ~1 BMI point reduction, but kept with significantly higher BMI increase 35.6 ± 6.4 vs. 34 ± 6.9 (p < 0.0001). LDL, triglycerides, and HbA1c levels significantly improved by SEMA, that also reflected by decrease in rates of poor metabolic markers (31.2% vs. 34.4%, p < 0.0001). The SEMA group showed higher survival rates (99.3% vs. 98.1%, p < 0.0001), fewer cardiovascular events (4 vs. 5.4%, p < 0.0001), and reduced progression rates to advanced liver disease (4.098 vs. 9.133%, p < 0.0001), reduced rates of abnormalities in liver enzymes (33.411 vs. 39.419%, p < 0.0001) and liver synthetic function markers (1.4 vs. 6%, p < 0.0001).

Conclusion: In this large real-world cohort, SEMA use in MASLD patients was associated with significantly improved 1-year survival, cardiovascular and liver-related outcomes. Though BMI changes were small in magnitude, potential mechanisms for SEMA's benefits warrant further study.

THU-195

Synergistic effects of thyroid hormone treatment and mitochondrial thyroid receptor p43 overexpression on regression of metabolic dysfunction-associated steatotic liver disease in mice by improving key mitochondrial quality markers

Raghu Ramanathan^{1,2}, Sarah Johnson^{1,2}, Jamal Ibdah^{1,2,3}. ¹Division of Gastroenterology and Hepatology, University of Missouri, Columbia, Missouri 65212, USA, Columbia, United States; ²Harry S. Truman Memorial Veterans Medical Center, Columbia, Missouri 65212, USA, Columbia, United States; ³Department of Medical Pharmacology and Physiology, University of Missouri, Columbia, Missouri 65212, USA, Columbia, United States
Email: raghu.ramanathan@health.missouri.edu

Background and aims: Metabolic dysfunction-associated steatotic liver disease (MASLD) is a major public health problem affecting 30% of the world's population. Mitochondrial dysfunction plays an important role in development and progression of MASLD. Thyroid hormone (TH), notably triiodothyronine (T₃), plays a vital role in regulating mitochondrial metabolic activity. T₃ binds to nuclear thyroid receptor (TR) isoforms and within mitochondria, a truncated TR_{alpha} isoform known as p43 serves as a mitochondrial TR (mTR). The function of mTR is not fully understood and its potential role in MASLD is not known. This study aims to: 1) explore whether mTR overexpression has beneficial effects on MASLD regression in mice; and 2) characterize mTR overexpression effects on key mitochondrial quality markers.

Method: 3-month-old male mice with C57BL/6 background (n = 32) were fed western diet (Research Diets Inc, D12451, 45% kcal fat, 1% cholesterol) for a period of 16-weeks to develop MASLD. Adenoviruses, either Ad-mTRp43 or Ad-beta-gal, at a concentration of 1 × 10¹⁰ viral particles per mouse, diluted in saline, were administered through the tail vein to induce expression in the liver. Three days post-injection, the mice underwent a 7-day intraperitoneal injection treatment with 25 µg of T₃ per 100 g body weight, or a vehicle control (saline). The mice (n = 8 for each treatment group) were then sacrificed for histological and gene expression studies.

Results: Mice overexpressing beta-gal treated with T₃ and mice overexpressing mTR treated with saline demonstrated significant reduction in hepatic steatosis compared to mice overexpressing beta-gal treated with saline, however mice overexpressing mTR treated with T₃ demonstrated a maximal effect on MASLD regression compared to other groups with histological resolution of hepatic steatosis. Mice overexpressing mTR treated with T₃ had 2-fold upregulation of Opa1 (p < 0.001) and Mfn1 (p < 0.05) gene expression and 2-fold reduction in Drp1 gene expression (p < 0.001) compared to other groups. Further, mice overexpressing mTR treated with T₃ demonstrated marked increases in gene expression of AMPK-alpha

POSTER PRESENTATIONS

($p < 0.001$), Nrf1 ($p < 0.05$), and PPAR- α ($p < 0.05$) compared to other groups. These results indicate that combination of mTR overexpression and T₃ treatment enhances markers of both mitochondrial dynamics and mitochondrial biogenesis. Similarly, mice overexpressing mTR treated with T₃ demonstrated significant increases in gene expression of the mitophagy markers Pink ($p < 0.01$) and Bnip-3 ($p < 0.05$) compared to other groups.

Conclusion: Overexpression of mitochondrial thyroid receptor (mTR-p43) in mice synergises thyroid hormone effects on regression of MASLD likely by improving mitochondrial quality markers. Further studies are needed to fully understand the underlying mechanisms for this synergy. (Supported by VA Merit 1BX 004710).

THU-196

Targeting lysyl-tRNA synthetase alleviates metabolic dysfunction-associated steatohepatitis through inhibition of monocyte-derived macrophages in preclinical models

Junghyun Kim¹, Hyeree Kim¹, Kang Soo Lee¹, Hyuk-Sang Kwon², Nam Hoon Kim², Sunghoon Kim^{2,3,4,5}, Yeup Yoon^{1,6}, Wonseok Kang^{1,7}.

¹Samsung Advanced Institute for Health Sciences and Technology (SAIHST), Sungkyunkwan University, Seoul, Korea, Rep. of South; ²Zymedi Co., Ltd., Incheon, Korea, Rep. of South; ³Institute of Artificial Intelligence and Biomedical Research, Medicinal Bioconvergence Research Center, College of Pharmacy, Yonsei University, Incheon, Korea, Rep. of South; ⁴College of Medicine, Gangnam Severance Hospital, Yonsei University, Seoul, Korea, Rep. of South; ⁵Institute for Convergence Research and Education in Advanced Technology, Yonsei University, Incheon, Korea, Rep. of South; ⁶Samsung Medical Center, Seoul, Korea, Rep. of South; ⁷Samsung Medical Center, Sungkyunkwan University School of Medicine, Seoul, Korea, Rep. of South

Email: wonseok1202.kang@samsung.com

Background and aims: Metabolic dysfunction-associated steatohepatitis (MASH) is characterized by steatosis and hepatic inflammation, where macrophages play a pivotal role in the pathogenesis. Although Lysyl-tRNA synthetase (KRS) is known as an enzyme that catalyzes the attachment of lysine to the cognate tRNA during protein synthesis, recent reports have drawn attention toward its non-canonical role for the control of macrophage migration. The goal of the study was to address whether inhibition of monocyte-derived macrophages (MoMFs) by targeting KRS could ameliorate steatohepatitis in preclinical models of MASH. In addition, the single-cell transcriptome analysis was performed on the leukocyte population in early inflammation stage to analyze the dynamic changes in MoMFs.

Method: A specific inhibitor of KRS was administered in various animal models of MASH, including methionine-choline-deficient (MCD) diet model, western diet model combined with carbon tetrachloride administration (WD/CCl₄), and choline-deficient, L-amino acid-defined, high-fat diet (CDAHFD) model. Hepatic steatosis, fibrosis and inflammation were assessed by immunohistochemistry, triglyceride (TG) assay, and flow cytometry. For a high-dimensional characterization of MoMFs, scRNA-seq was performed for intrahepatic CD45⁺ cells isolated from the non-diseased (chow fed) and MASH (MCD-diet) mice treated with or without KRS-specific inhibitor. The cells were identified based on the differentially expressed genes (DEGs) and their expression of a set of standard cell identity genes.

Results: Administration of KRS-specific inhibitor significantly reduced hepatic inflammation and fibrosis in MCD diet-induced model as well as in CDAHFD and WD/CCl₄-induced MASH models, as demonstrated by the reduction of serum alanine and aspartate transaminases, hepatic TG content, and NAFLD activity score. Flow cytometry showed an enrichment of intrahepatic Ly6C^{hi} monocytes in vivo, where it was significantly diminished upon administration of KRS-specific inhibitor. Unsupervised clustering of scRNA-seq revealed 38 distinct cell clusters, including 12 distinct clusters of myeloid cell populations. Among the myeloid cell populations, four clusters representing the MoMFs were significantly diminished in the

KRS-specific inhibitor-treated group, whereas the KC clusters were modestly affected. DEGs and Kyoto Encyclopedia of Genes and Genomes (KEGG) analysis demonstrated that the suppression of MoMFs was related to downregulation of NF- κ B and TNF signaling pathways.

Conclusion: Specific inhibition of KRS is associated with reduced steatohepatitis and fibrosis in preclinical models of MASH through inhibition of MoMF recruitment, suggesting KRS as a potential target for therapeutic intervention.

THU-197

Restoration of natural killer cell antifibrotic activity via a novel immune target; the Neuroligin-4/ β -Neurexin pathway

Johnny Amer¹, Ahmad Salhab¹, Rifaat Safadi¹. ¹Liver institute, Hadassah Hebrew University Hospital, Jerusalem, Israel
Email: johnnyamer@hotmail.com

Background and aims: Several studies demonstrated a cross talk between hepatic stellate cells (HSCs, the source of fibrotic tissue) and Natural Killer (NK) cells. Deterioration in NK cells functionality was described in advanced liver injury of liver fibrosis and metabolic dysfunction-associated liver disease (MASLD). In this study, we aimed to investigate for a novel immune checkpoint that contributes to NK cell impairment and HSCs activations in MASLD with advanced liver fibrosis by assessing neuroligin-4 (NLGN4X) and β -neurexin (β -Nrxn; NLGN4X ligand) expressions, respectively.

Results: Human peripheral and liver tissue-resident NK (trNK) cells as well as primary HSCs from liver biopsies from adult patients (age ≥ 18 years) of histologically documented MASLD with different Metavir scores were obtained. Our data showed 1.8-fold elevated trNK cells expressions of NLGN4X (NK^{NLGN4X+}) in Metavir scores of F3/F4 as compared to their F1/F2 counterparts. NK^{NLGN4X+} subpopulations were associated with impaired function associated with reduced activity of activity related pathway of survival and proliferation as well as inhibited of cytoskeleton protein of F-actin. Moreover, these subpopulations showed an increase in exhaustion markers indicating reduced cytotoxic activity. On the other hand, activated HSCs exhibited elevated β -Nrxn expression, and induced an increase in NLGN4X expression in NK cells, which inhibited their cytotoxic effects. Disruption of the NLGN4X/ β -Nrxn immune axis via NLGN4X knockdown or anti-NLGN4X neutralizing antibodies, promoted reductions in the NK^{NLGN4X+} population to levels similar to those in healthy donors and restored trNK cell survival marker expression and the cytotoxic effects of NK cells against activated HSCs. NLGN4X^{-/-} mice displayed protection against CCl₄-induced liver fibrosis and kept a restored trNK cell activity. Moreover, NLGN4X neutralizing antibody administered to naive mice model with CCl₄ induction reduced NLGN4X expressions on sorted trNK^{NLGN4X+} cells accompanied with elevated AKT, ERK and P70S6 K phosphorylation while inhibited liver fibrosis outcome. Moreover, adoptive transfer of trNK^{NLGN4X-} cells into immunodeficient recipient mice with liver fibrosis resulted in delayed disease progression compared to mice receiving trNK^{NLGN4X+} cells.

Conclusion: These findings describe a novel NLGN4X/ β -Nrxn axis with dual immunotherapeutic potential target approach of NK cells and HSCs in delaying liver fibrosis and attenuating disease progressions.

THU-198

In vitro and in vivo pharmacological characterization of human PNPLA3-targeting short interfering RNA molecules for the treatment of metabolic dysfunction-associated steatohepatitis

Jieun Song¹, Jerome Deval¹, Lillian Adame¹, Ruchika Jaisinghani¹, Emily Tso², Daniel Lin², Aneerban Bhattacharya¹, Antitsa Stoycheva¹, Jacquelyn Sousa¹, Craig Parish², Saul Martinez Montero¹, Vivek Rajwanshi¹, Shane Daguison¹, Vikrant Gohil¹, Qingling Zhang¹, Toni Williamson², Sushmita Chanda¹, Saswata Talukdar², David Smith¹, Leonid Beigelman¹, Julian Symons¹, Yingjiang Zhou²,

Xuan Luong¹. ¹Aligos Therapeutics, Inc., South San Francisco, United States; ²Merck and Co., Inc., Rahway, United States
Email: xluong@aligos.com

Background and aims: Patatin-like phospholipase domain-containing protein 3 (PNPLA3), specifically the single nucleotide polymorphism rs738409[G] (I148M) variant, is a strong genetic risk factor for the development and progression of metabolic dysfunction-associated steatotic liver disease (MASLD) into the more severe metabolic dysfunction-associated steatohepatitis (MASH). While there is still no approved treatment for MASLD/MASH, the field of oligonucleotide-based therapeutics has been rapidly advancing in recent years, with several drugs achieving market approval and many more in clinical trials for metabolic indications. The aim of our studies was to characterize short interfering RNA (siRNA) molecules that effectively silence the expression of PNPLA3 and could be used as potential therapies for MASLD/MASH.

Method: A luciferase reporter assay in COS-7 cells and RT-qPCR assay in Huh-7 cells were used to initially screen proprietary human PNPLA3-targeting siRNAs in vitro for effective silencing of PNPLA3 gene expression. Select compounds were then tested in vivo in PK/PD studies using human PNPLA3 knock-in mice and a subset of molecules was then characterized in MASH efficacy studies using GAN diet-induced obese (DIO), human PNPLA3 knock-in mice. End points included target quantification via RT-qPCR and Western blot analysis, blood liver enzyme levels, and liver histology.

Results: In the luciferase reporter assay, compounds of interest showed target inhibition greater than 50% inhibition at concentrations of 5 to 50 nM. In the RT-qPCR assay, compounds inhibited the endogenous expression of PNPLA3 with half maximal effective concentrations (EC₅₀) ranging between 1 and 60 pM. Select siRNAs demonstrated robust, dose-dependent knockdown of the human RNA target in PK/PD studies using human PNPLA3 knock-in mice. These effects were observed after a single dose at concentrations as low as 0.1 mg/kg and gene expression silencing could be sustained for up to 28 days post-dose. Furthermore, repeat dosing of compounds in DIO mice led to robust target RNA and protein knockdown; one select compound was shown to also decrease in liver enzyme levels, improve MAFLD Activity Score (NAS) score, and reduce liver fibrosis and necrosis/apoptosis in this model.

Conclusion: We discovered several siRNA molecules that effectively silence human PNPLA3 gene expression in vitro and in vivo and repeat dosing of a select compound in a DIO mouse model ultimately led to the improvement of MASH end points. The data generated in these studies allowed for the selection of a lead compound for progression into late-stage preclinical studies.

THU-199

Role and therapeutic potential of miR-22 in MAFLD and obesity: from mouse model to human relevance

Riccardo Panella^{1,2}, Simone Tomasini¹, Anna Altieri³, Francesco Margiotta⁴, Philip Vonschallen⁵, Ulrik Scheele³, Lei Cai⁶, Ryan Temel⁷, Sakari Kauppinen³. ¹Aalborg University, Center for RNA Medicine, Copenhagen SV; ²Resalis Therapeutics, Torino, Italy; ³Aalborg University, Center for RNA Medicine, Copenhagen SV, Denmark; ⁴Dipartimento di Neuroscienze, Psicologia, Area del Farmaco e Salute del Bambino (NEUROFARBA), University of Florence, Florence, Italy; ⁵InSphero, Schlieren, Switzerland; ⁶University of Kentucky, Saha Cardiovascular Research Center, Lexington, United States; ⁷University of Kentucky, Saha Cardiovascular Research Center, Lexington, United States

Email: riccardop@dcm.aau.dk

Background and aims: Non-coding RNAs (ncRNAs) role in MAFLD and their potential for being therapeutic targets is very little explored but it could have a very high impact on patient outcomes. We identified miR-22 as a crucial regulator of hepatic lipid homeostasis using multiple genetic models, and we confirmed its involvement in metabolism and MASH progression. In human subject we found a

positive correlation between miR-22 level and disease progression. Moreover, we developed an antisense oligonucleotide (ASO) based on LNA to inhibit miR-22 pharmacologically. We tested our therapeutic approach in different mouse models, non-human primate (NHP) and primary human samples to demonstrate that miR-22 inhibition has a great protective effect toward hepatic lipid accumulation, inflammation, fibrosis and weight lost.

Method: Genetic engineered mouse (GEM) models, overexpressing miR-22 or knock-out for miR-22 were used to demonstrate the role of miR-22 in metabolism. A dataset from 127 patients with different stages of NASH was used to confirm the role of miR-22 in humans. To prove the therapeutic effect of miR-22 inhibition we used diet induced obesity (DIO) mouse models, the biopsy-confirmed Gubra Amylin (GAN) model, NHP fed with a fast-food diet and human derived liver organoids.

Results: We found that over-expression of miR-22 leads to an obese phenotype and a strong liver steatosis around 10 months of age, in mice fed with normal chow. miR-22 null mice fed with High Fat Diet (HFD) were unable to increase their body weight and their liver were protected from steatosis and inflammation. We designed and tested an anti-sense oligonucleotide (ASO) based on LNA chemistry able to target miR-22 and inhibit its function and we tested it in DIO and GAN mice, as well as in a 24 weeks long experiment with non-human primates and in a 3D model of human liver organoids. We detected a strong and consistent effect of our anti-miR-22 therapy on triglyceride levels, body weight and hepatic collagen deposition, demonstrating the efficacy of miR-22 inhibition in MAFLD and obesity.

Conclusion: We demonstrate the central role of miR-22 in liver metabolism and obesity. miRNA-22 influences the expression of genes involved in lipid biogenesis, energy expenditure, hepatic inflammation and fibrosis. By modulating its levels with an ASO that we designed and tested, we have been able to simultaneously impact different pathways that all contributes to the insight and the progression of systemic diseases like obesity and MASH. We tested our therapy in multiple mouse models, as well as in NHP and primary human organoids, providing extensive evidence that miR-22 role is conserved and that its pharmacological inhibition is an effective therapy to address MASH. Our data are paving the way for a new pharmacological approach to one of the most serious diseases of our time, with an innovative approach based on targeting a non-coding RNA.

THU-200-YI

Clearance of senescent cells alleviates metabolic dysfunction-associated steatohepatitis

Nilofer Sayed¹, Suet Yen Chong¹, Hui Jun Ting¹, Ziyang Zhang², Phyllis Gan Xiu Li³, Shakti Nagpal², Michelle Siying Tan¹, De En Tan⁴, Nicholas Syn⁵, Mark Muthiah⁶, Yock Young Dan⁶, Gert Storm⁷, Jiong Wei Wang⁸. ¹Department of Surgery, Yong Loo Lin School of Medicine, National University of Singapore, Singapore, Singapore; ²Department of Pharmacy, Faculty of Science, National University of Singapore, Singapore, Singapore; ³Department of Pharmacology, Yong Loo Lin School of Medicine, National University of Singapore, Singapore, Singapore; ⁴Temasek Polytechnic, Singapore, Singapore; ⁵Department of Biomedical Informatics, Yong Loo Lin School of Medicine, National University of Singapore, Singapore, Singapore; ⁶National University Hospital, Singapore, Singapore; ⁷Department of Pharmaceuticals, Faculty of Science, Utrecht University, Singapore, Singapore; ⁸Department of Surgery, Yong Loo Lin School of Medicine, Singapore, Singapore

Email: surwang@nus.edu.sg

Background and aims: Metabolic dysfunction-associated steatohepatitis (MASH) is a severe form of fatty liver disease, characterized by hepatic steatosis, inflammation, and fibrosis. Recent reports have shown positive correlation between accumulation of senescent cells in the liver of MASH patients and poor prognosis. These cells are resistant to apoptosis, exhibit a pro-inflammatory secretome, have dysfunctional mitochondria, limit tissue regeneration, and further

POSTER PRESENTATIONS

induce senescence in neighbouring cells. Hence in this study we aim to clear the senescent cells in the liver to alleviate MASH progression.

Method: A senolytic agent was encapsulated within polymer-based nanoparticles (nano-senolytic) and characterized using dynamic light scattering and transmission electron microscopy. These particles were administered intravenously to C57BL/6J mice fed with methionine choline deficient diet or western diet with weekly injection of low dose carbon tetrachloride. One week after the last dose, the liver was harvested, and senescent cells in the liver were analyzed using flow cytometry. Liver steatosis was assessed by Oil red O (ORO) staining and hepatic triglyceride levels. Hepatic inflammation was determined by measurement of inflammatory cytokines and immunofluorescence staining of CD68. Oxidative stress was measured using dichlorodihydrofluorescein diacetate staining and the mitochondria function was tested using the seahorse assay.

Results: The nanoparticles synthesized were around 100 nm in size with a neutral surface charge. Nano-senolytic showed better efficacy in reducing senescent cells in the liver ($p < 0.05$) as compared to the free drug after 4 weeks of treatment. Clearance of senescent cells by nano-senolytic resulted in a significant reduction in steatosis ($p < 0.001$). Moreover, compared to the control group, nano-senolytic treatment reduced macrophages (CD68 staining positive area) by 25%. Biochemical analysis showed a marked reduction in expression of inflammatory cytokines in the liver, including IL-1a ($p < 0.001$), IL-1b ($p < 0.001$), IL-6 ($p < 0.001$), IFN- γ ($p < 0.01$), MCP-1 ($p < 0.001$) and TNF- α ($p < 0.001$). In contrast, the anti-inflammatory cytokines IL-10 ($p < 0.05$) and IL-13 ($p < 0.001$) were upregulated, indicating a reparative microenvironment in the liver after clearing of senescent cells. Furthermore, we observed a reduction in oxidative stress and restoration of mitochondria function, which contribute to the reduction in steatosis.

Conclusion: Our findings suggest that senescent cell clearance restores liver tissue function by reducing hepatic steatosis and inflammation. Encapsulation of the senolytic drug into nanoparticles achieves higher drug concentration at the diseased organ and thereby improving therapeutic efficacy.

THU-201-YI

Artificial intelligence-assisted multiomics depicting the immunometabolism landscape of steatotic livers undergoing bariatric surgery

Shuai Chen¹, Qinghe Zeng^{2,3}, Jiaming Xue¹, Xiurong Cai^{4,5}, Peng Song¹, Liming Tang¹, Christophe Klein³, Frank Tacke⁶, Adrien Guillot⁶, Hanyang Liu^{1,6}. ¹Nanjing Medical University, Changzhou Medical Center, Changzhou, China; ²Université Paris Cité, Laboratoire d'Informatique Paris Descartes (LIPADE), Paris, France; ³Université Paris Cité, Centre d'Histologie, d'Imagerie et de Cytométrie (CHIC), Centre de Recherche des Cordeliers, INSERM, Sorbonne Université, Paris, France; ⁴Charité-Universitätsmedizin Berlin, Department of Hematology, Oncology and Tumor Immunology, Berlin, Germany; ⁵The Jackson Laboratory, Bar Harbor, United States; ⁶Charité-Universitätsmedizin Berlin, Department of Hepatology and Gastroenterology, CCM/CVK, Berlin, Germany
Email: hanyang.liu@charite.de

Background and aims: Metabolic dysfunction-associated steatotic liver disease (MASLD) is a highly prevalent chronic liver disease worldwide. MASLD encompasses a spectrum of steatosis, inflammation, and fibrosis. Evidence suggests that weight loss can lead to remission of hepatic steatosis alone or steatosis and inflammation, respectively. Therefore, weight loss approaches such as dietary intervention (DI) and bariatric surgery (BS) represent therapeutic options for MASLD. It is currently unclear how these interventions affect the hepatic immune mechanisms in MASLD. This study aims to elucidate the intricate immunometabolism landscape of steatotic livers following DI and BS.

Method: This study employed the sleeve gastrectomy (a typical BS procedure) and comparable food intake after sham surgery on a rat

model of MASLD induced by high-fat diet (HFD) feeding for 12 weeks. Circulating markers and in situ pathological alterations were assessed respectively on serum and liver tissue. Simultaneously, single-cell (sc) and single-nuclei (sn) transcriptome analysis were performed on freshly acquired liver cells, and spatial metabolomics analysis was conducted on cryo-sectioned liver. Furthermore, artificial intelligence (AI)-based image analysis was employed to identify the relevant cell type contributions on HandE-stained liver tissue sections. In a translational human study, 18 patients with obesity and liver steatosis were evaluated within 6 months after BS.

Results: In experimental MASLD in rats, both DI and BS attenuated serum triglyceride levels, as well as liver steatosis and fibrosis. The expression of Ppara, Cyp2e1 and Cyp7a1 were increased on hepatocytes upon DI and BS, while BS broadly upregulated lipid metabolism on cholangiocytes, monocytes, macrophages and neutrophils. In contrast, cholangiocytes appear more interactive with other cells upon BS. Additionally, two distinct types of hepatocytes were identified and associated with hepatic zonation characteristics, indicating an explicit loss of periportal features upon DI. In addition, metabolomics analysis suggested enhanced metabolite enrichments on fatty acid and cholesterol metabolism upon BS. AI-based image analysis illustrated the differential infiltration levels of myeloid cells in the liver, leading to metabolic differences among regions. Lastly, serum data from patients as well as in the rat model elucidated a significant increase of FGF-19 levels upon BS.

Conclusion: BS facilitates PPAR α -related metabolic enhancement on hepatocytes and intrahepatic myeloid cells. In addition, the gut-derived signal (FGF-19) may be a key metabolic regulator induced by BS. This study provides the first insight into the immunometabolic dynamics of steatotic livers undergoing BS, thereby shedding light on the pathogenic consequences of this procedure.

THU-202

Prophylactic and therapeutic hepatoprotective effects of the dual FXR/TGR5 agonist INT-767 in the GAN diet-induced ob/ob mouse model of advanced MASH with progressive fibrosis

Jacob Nøhr-Meldgaard¹, Susanne Pors², Rebecca Wendelbo Olsen³, Henrik B. Hansen³, Michael Feigh⁴. ¹Gubra A/S, Hørsholm; ²Gubra A/S, Hørsholm, Denmark; ³Gubra A/S, Hørsholm, Denmark; ⁴Gubra AS, Hørsholm, Denmark
Email: jnm@gubra.dk

Background and aims: The farnesoid X receptor (FXR) and G protein-coupled receptor (GPCR) TGR5 have been implicated in the pathogenesis of metabolic dysfunction-associated steatohepatitis (MASH). Here, we evaluated the efficacy of the dual FXR/TGR5 agonist INT-767 on metabolic, biochemical and histological outcomes in a genetically obese mouse model of accelerated GAN diet-induced MASH with progressive fibrosis.

Method: Male leptin-deficient male B6.V-Lepob/JRj (ob/ob) mice were fed GAN diet high in fat, fructose, and cholesterol for total of 12-weeks or 24-weeks. GAN ob/ob-MASH mice received treatment from the first day of GAN diet feeding (prophylactic treatment) or after 12-weeks of GAN diet feeding (therapeutic treatment). Animals were randomized into treatment groups according to body weight prior to study start. Animals received daily oral dosing with INT-767 (10 mg/kg, $n = 14-16$) or vehicle ($n = 14$) for 12-weeks. Terminal end points included plasma biomarkers, liver biochemistry, NAFLD Activity Score (NAS), fibrosis stage and quantitative liver histology.

Results: Prophylactic and therapeutic INT-767 intervention had no effect on body weight while both improving hepatomegaly. Both interventions reduced plasma ALT/AST, and plasma/liver triglyceride and total cholesterol concentrations, as well as liver hydroxyproline levels. Furthermore, both interventions promoted a significant reduction in NAS, supported by reduced quantitative histological markers of steatosis (liver lipid, number of hepatocytes with lipid droplets) and inflammation (number of inflammatory foci, galectin 3). Prophylactic, but not therapeutic, INT-767 treatment improved

fibrosis stage. In contrast, both interventions significantly reduced histological markers of fibrosis (PSR, Col1a1) and stellate cell activation/fibrogenesis (α -SMA).

Conclusion: The dual FXR/TGR5 agonist INT-767 improves hallmarks of MASH in the GAN ob/ob-MASH mouse model in settings of both prophylactic and therapeutic treatment, respectively. Greater anti-fibrotic effects of INT-767 were attained by prophylactic treatment. These findings suggest the potential utility of dual FXR/TGR5 activation as disease intervention strategy in MASH. Furthermore, it highlights the GAN ob/ob-MASH mouse as an accelerated obese mouse model of advanced MASH with progressive fibrosis, thus having significant utility in preclinical drug discovery for MASH.

THU-203

Integrated spatial transcriptomics and machine learning derived histopathology measurements in steatotic liver disease unmasks biological heterogeneity of steatosis

Carlo Sala Frigerio¹, Crysthiane Ishiy¹, Ali Ebrahimi², Matthew Bronniman³, Qasim Wani³, John Glickman³, Jacqueline Brosnan-Cashman³, Lara Murray³, Robert Brockett³, Jake Mallon¹, Jan Roger¹, Sanjay Kumar², Stephen Atkinson¹.
¹GlaxoSmithKline, Stevenage, United Kingdom; ²GlaxoSmithKline, Collegeville, United States; ³PathAI, Boston, United States
Email: stephen.8.atkinson@gsk.com

Background and aims: Steatotic liver disease (SLD) is a common cause of chronic liver disease characterised by steatosis, inflammation and fibrosis on biopsy. Biological heterogeneity of SLD is unable to be fully captured by classical histopathological evaluation. Traditional transcriptomic approaches require tissue homogenization or dissociation and thus lack the ability to map spatial gene expression specifically to localized pathological features. We integrated machine learning (ML) based measurement of SLD histological features with high-resolution spatial transcriptomics (ST) to overcome these limitations, demonstrating that transcriptomic features can be mapped to specific SLD histopathology at scale.

Method: Human liver tissues preserved by formalin fixation and paraffin embedding (FFPE) were obtained from subjects with healthy livers (n = 8) or SLD (n = 8). ST was performed using 10X Genomics Visium for FFPE which has 55 μ m capture spots. AIM-NASH (PathAI, Boston, MA) was deployed on high-resolution scans of hematoxylin and eosin stained samples on Visium Capture slides and adapted to facilitate per-spot analysis. Transcriptomic and image data were analysed in R and python using pipelines to i) train ML classifiers to predict inflammation or steatosis from gene expression data, and ii) define unsupervised gene expression based clusters.

Results: AIM-NASH-derived features associated with steatosis and inflammation were extracted for each spot. Gene expression could predict the presence of inflammation or severe steatosis. Predictive gene sets contained previously proposed biomarkers and therapeutic targets for inflammation (*HLA-DRA*, *CD74*, *CD63* and *IL32*) and steatosis (*APOC1*, *APOA1*, *APOE*, *ATF5* and *FGF21*). Clustering of transcriptomic data identified nine distinct cellular niches variously enriched for gene markers of hepatocytes, pericentral zonation, hepatic stellate cells and plasma cells. Two niches were associated with significant steatosis identified by AIM-NASH yet expressed distinct gene sets (lipid uptake and metabolism vs. inflammation and immune response). Ingenuity Pathway Analysis inferred lipopolysaccharide, TGF β 1 and IFN γ and inhibition of PPAR γ as potential drivers of these disparate profiles. These results suggest multiple distinct local responses to steatosis occur in SLD.

Conclusion: This study demonstrates the feasibility and power of applying two cutting-edge techniques (spatial transcriptomics and ML-based histological feature prediction) to the same single FFPE tissue section. Integrated data analysis of spatially resolved transcriptomic and high-resolution ML based histopathology data directly links transcriptomic patterns to the local steatosis burden in SLD, revealing dynamic and complementary responses to disease.

THU-206

Deep learning-based predictive modeling of patatin-like phospholipase domain-containing protein 3 variant carriers using magnetic resonance imaging data

Yazhou Chen¹, Benjamin P.M. Laevens¹, Carola Dlugosch¹, Jan Clusmann¹, Teresa Lemaingue², Gustav Anton Müller-Franzes², Daniel Truhn², Carolin V. Schneider¹. ¹Uniklinik RWTH Aachen Medizinische Klinik III, Aachen, Germany; ²Uniklinik RWTH Aachen Klinik for Diagnostic and Interventional Radiology, Aachen, Germany
Email: yachen@ukaachen.de

Background and aims: Steatotic liver disease (SLD) affects 30% of western population due to environmental, lifestyle but also to genetic factors especially the patatin-like phospholipase domain-containing protein 3 (PNPLA3) gene, with its most prominent variant rs738409_G. Identification of variant carriers, based on genome analysis, is expensive. Therefore, we propose a novel deep learning-based approach to discern rs738409_G carriers utilizing magnetic resonance imaging (MRI) data of the liver.

Method: Our study cohort was constructed by selecting patient samples from the UK Biobank for which both data on PNPLA3 rs738409_G status and MRI data were present. To extract the liver fat content, we reconstructed fat fraction maps via r2*-corrected water and fat images based on the IDEAL post-processing water fat separation technique. We extracted liver regions from MRI magnitude images using liver-specific masks, which provide pixel-level segmentation delineating the liver region. Liver masks were segmented by a UNet segmentation model, which was trained with 600 ground truths manually segmented by a medical professional. These segmented liver areas and corresponding variant labels were subsequently utilized as input for the Vision Transformer classification model. The dataset was split into an 8:2 ratio for training and validation purposes respectively.

Results: Firstly, we divided the study cohort into individuals with SLD and without SLD. Within each of these groups, we re-balanced the samples such that a 50:50 ratio was obtained for homozygous and non-carriers. This was achieved by undersampling the majority class (the non-carriers). The SLD group (N_homozygotes = 1018, N_non_carriers = 1018) achieved an AUROC of 0.63 on the validation set. In comparison, the healthy group (N_homozygotes = 803, N_non_carriers = 803) achieved a lower AUROC of 0.55 on the validation set. These results provide first evidence that features on MRI could be present that allow for a better differentiation between homozygous carriers and non-carriers in the SLD group.

Conclusion: In this study, we demonstrated a novel deep learning-based approach to identify PNPLA3 rs738409_G carriers utilizing MRI image data from a well-characterized large cohort. Our method presents an innovative and streamlined technique for identifying genetic variant carriers, offering significant potential for advancing diagnostics in SLD and contributing to the evolution of personalized healthcare.

THU-207-YI

Brain dysfunction is prevented by alpha 2A adrenergic receptor antagonism in a rodent model of diet-induced metabolic dysfunction-associated steatotic liver disease

Anne Catrine Dugaard Mikkelsen¹, Kristoffer Kjærgaard¹, Cecilie Bay-Richter², Abeba Habtesion³, Alexandra Phillips³, Olivia Greenham³, Stephen Hamilton-Dutoit⁴, Anna Hadjihambi⁵, Karen Louise Thomsen^{1,3}, Rajeshwar Prosad Mookerjee^{1,3}.
¹Department of Hepatology and Gastroenterology, Aarhus University Hospital, Aarhus, Denmark; ²Translational Neuropsychiatry Unit, Department of Clinical Medicine, Aarhus, Denmark; ³Institute for Liver and Digestive Health, University College London, London, United Kingdom; ⁴Department of Pathology, Aarhus University Hospital, Aarhus, Denmark; ⁵The Roger Williams Institute of Hepatology, London, United Kingdom
Email: ancami@clin.au.dk

POSTER PRESENTATIONS

Background and aims: Cognitive dysfunction is a common and recognised complication of metabolic dysfunction-associated steatotic liver disease (MASLD) but there are still no approved treatments. We have previously shown that antagonising the alpha 2A adrenergic receptor (ADRA2A) modulates inflammation and MASLD progression. This study aims to investigate the potential of ADRA2A as a novel target also for treating brain dysfunction in MASLD.

Method: Male Sprague Dawley rats received a high-fat, high-cholesterol diet (HFHC—an established MASLD model) or standard diet (controls) for 16 weeks. Half of the HFHC rats received treatment with the ADRA2A antagonist Yohimbine in the drinking water, for the final 10 weeks. Memory was studied with the novel object recognition (NOR) test and depression-like behaviour with the Porsolt's Swim test (PST). Mean arterial pressure was measured in the carotid artery, and partial pressure of oxygen (PtO₂) was assessed in the somatosensory cortex of the brain to quantify tissue oxygen availability. At termination, blood was obtained to examine ammonia concentrations and biochemistry. The liver was collected for histological scoring.

Results: ADRA2A antagonism significantly ameliorated inflammation in the liver, reduced NAS score, and prevented high plasma cholesterol levels induced by the HFHC diet. The HFHC animals exhibited impaired memory in the NOR test (NOR ratio 46 ± 15% versus 79 ± 10%, $p < 0.0001$) and depression-like behaviour in the PST (floating 72 ± 25 versus 39 ± 18 seconds, $p < 0.05$), which was prevented by ADRA2A antagonism (NOR ratio 66 ± 11%, floating 55 ± 20 seconds). Mean arterial pressure was similar between groups, whilst the cortical PtO₂ was reduced by HFHC diet (26 ± 2 versus 21 ± 2 mmHg, $p < 0.0001$) and restored to control levels by ADRA2A antagonism (27 ± 2 mmHg). PtO₂ positively correlated with the performance in the NOR test ($r = 0.6$, $p = 0.002$). The HFHC diet elevated blood ammonia levels compared to control animals (29 ± 6 versus 51 ± 15 µmol/L, $p = 0.001$), and remained unchanged after ADRA2A antagonism (55 ± 7 µmol/L).

Conclusion: Ten weeks of ADRA2A antagonism in a rodent model of MASLD reduced liver inflammation, prevented impaired memory and depression-like behaviour, and maintained oxygen availability in the brain cortex, without impacting on hyperammonaemia. This paves the way for further mechanistic studies and consideration of future clinical translation in MASLD patients at risk of cognitive dysfunction.

THU-208

Clinical translatability of the GAN diet-induced obese and biopsy-confirmed mouse model of MASH

Michael Feigh¹, Maja Andersen¹, Nicolas Eskesen², Denise Oró², Henrik B. Hansen², ¹Gubra, Hørsholm; ²Gubra, Hørsholm, Denmark
Email: mfe@gubra.dk

Background and aims: The Gubra-Amylin NASH (GAN) diet-induced obese (DIO) mouse is an industry-standard model of metabolic dysfunction-associated steatohepatitis (MASH) with progressive fibrosis. The present study aimed to assess liver histopathological effects of 6 late-stage clinically drugs in the GAN DIO-MASH mouse with reference to primary end points in corresponding clinical trials in NASH patients with liver fibrosis.

Method: Male C57BL/6J mice were fed the GAN diet (40 kcal-% fat, 22% fructose, 10% sucrose, 2% cholesterol) for ≥34 weeks. Only mice with biopsy-confirmed NAFLD Activity Score (NAS≥5) and fibrosis (≥stage F1) were included. GAN DIO-MASH mice (n = 14–18 per group) were administered resmetirom (THR-β agonist, 3 mg/kg, QD, PO), semaglutide (GLP-1 receptor agonist, 30 nmol/kg, SC, QD), obeticholic acid (FXR agonist, 30 mg/kg, PO, QD), lanifibranor (pan-PPAR agonist, 30 mg/kg, PO, QD), elafibranor (PPAR-α/δ agonist, 30 mg/kg, PO, QD), (PPAR-δ agonist, 10 mg/kg, PO, QD), firsocostat (ACC inhibitor, 5 mg/kg, PO, QD), or vehicle for 12 weeks.

Histopathological pre-to-post individual assessment of NAS and fibrosis stage was performed and evaluated against FDA/EMA-accepted co-primary/secondary histological end points (resolution of NASH with no worsening of liver fibrosis; ≥1-stage fibrosis improvement without worsening of NASH).

Results: Histological outcomes in GAN DIO-MASH mice were comparable to corresponding clinical trials for resmetirom (MAESTRO-NASH), semaglutide (Newsome *et al.* NJEM 2020), and lanifibranor (NATIVE). Obeticholic acid reversed NASH but not fibrosis in GAN DIO-MASH mice, being line with the FLINT trial, whereas the opposite effect has been reported the pivotal REGENERATE trial. Elafibranor only resolved NASH, being consistent with the GOLDEN-505 trial but contrasting no histological benefits in the pivotal RESOLVE-IT trial. Firsocostat improved both NASH and fibrosis, although these end points were not met in the ATLAS trial.

Conclusion: GAN DIO-MASH mice faithfully reproduce histological outcomes of several compounds profiled in clinical trials for MASH, highlighting clinical translatability and utility of the model in preclinical drug development.

THU-209

Effect of inhibition of the protein tyrosine phosphatase 1B in liver progenitor cells under an steatohepatitis environment in mice

Pilar Valdecantos¹, Silvia Calero Pérez², Alma Astudillo³, Jesús Balsinde³, David Sebastian⁴, Laura Herrero⁵, Angela Martinez Valverde⁶. ¹IIBm Alberto Sols Morreale (CSIC-UAM), Madrid, Spain; Centro de Investigación Biomédica en Red de Diabetes y enfermedades metabólicas (CIBERDEM), Instituto de Salud Carlos III, Madrid, Spain., Madrid, Spain; ²IIBm Alberto Sols-Morreale. CSIC-UAM, CIBERDEM (ISCIII), Spain, Madrid, Spain; ³Instituto de Biología y Genética Molecular (CSIC-UVA), Valladolid, Spain, Valladolid, Spain; ⁴Department of Biochemistry and Physiology, School of Pharmacy and Food Sciences, Institut de Biomedicina de la Universitat de Barcelona (IBUB), Universitat de Barcelona, Barcelona, Spain., Barcelona, Spain; ⁵Department of Biochemistry and Physiology, School of Pharmacy and Food Sciences, Institut de Biomedicina de la Universitat de Barcelona (IBUB), Universitat de Barcelona, Barcelona, Spain, Centro de Investigación Biomédica en Red de Fisiopatología de la Obesidad y la Nutrición (CIBEROBN), Instituto de Salud Carlos III, Madrid, Spain, Barcelona, Spain; ⁶IIBm Alberto Sols-Morreale. CSIC/UAM, Centro de Investigación Biomédica en Red de Diabetes y enfermedades metabólicas (CIBERDEM), Instituto de Salud Carlos III, Madrid, Spain, Madrid, Spain
Email: pvaldecantos@iib.uam.es

Background and aims: Oval cells (OCs) are hepatic progenitor cells with differentiation capacity towards hepatocytes or cholangiocytes under damage. However, the impact of the lipoinflammatory environment of non-alcoholic steatohepatitis (NASH) in the OC niche has not been characterized in depth. Inhibition of protein tyrosine phosphatase 1B (PTP1B) is a pharmacological strategy against metabolic liver damage. The aim of this study was to analyze the role of *Ptpn1* in the plasticity of OCs in mice with NASH and to characterize the interactome between immune and OCs.

Method: *Ptpn1*^{+/+} mice were fed a choline-deficient L-amino acid defined high fat (CDAA-HF) diet for 3 weeks, time at which *Ptpn1*^{+/+} or *Ptpn1*^{-/-} OCs were transplanted. Mice continued under CDAA-HFD diet for 5 weeks. A lipoinflammatory conditioned medium (CM) generated from macrophages treated with palmitate/LPS (PA/LPS) was used to stimulate OCs. Mitochondrial respiration, transcriptomic and lipidomic profiles were also analyzed.

Results: *Ptpn1*^{+/+} mice fed a CDAA diet presented NASH features with expansion of OCs surrounded by inflammatory cells. *Ptpn1*^{+/+} mice transplanted with *Ptpn1*^{-/-} OCs showed higher *Krt19* expression pointing to OC expansion during NASH. Transcriptomic analysis revealed upregulation of hepatocyte, cholangiocyte and

proliferation-related genes in *Ptpn1*^{-/-} OCs. Treatment with PA/LPS-CM for 24 h induced apoptosis in OCs but it was attenuated in the absence of *Ptpn1* concurrently with a higher proliferation rate. Interestingly, PA/LPS-CM collected from *Ptpn1*^{-/-} OCs after 16 h contained less proinflammatory mediators suggesting their utilization to activate proinflammatory cascades that have been shown to prime hepatocyte proliferation in liver regeneration. In fact, stimulation of OCs with PA/LPS-CM rapidly phosphorylated STAT3, p65-NFκB, AKT and ERK together with IκBα degradation and p65-NFκB nuclear translocation, responses exacerbated in *Ptpn1*^{-/-} OCs. Under NASH-like conditions, basal/maximal respiration, ATP production and proton link were higher in *Ptpn1*^{-/-} OCs concurrently with an upregulation of antioxidant defences.

Conclusion: OC expansion concurs with inflammatory features in NASH. The in vitro studies revealed that *Ptpn1* deletion in oval cells favors survival/proliferation under a lipoinflammatory milieu concurrently with higher mitochondrial function and antioxidant capacity, opening therapeutic perspectives to preserve OC plasticity under damage associated to NASH.

THU-210

Dysfunctional activation of the DNA damage response is associated with MASLD progression through an E2F2-dependent mechanism

Beatriz Gómez Santos¹, Idoia Fernández-Puertas¹, Paul Gomez-Jauregui¹, Natalia Sainz-Ramírez¹, Kendall Alfaro-Jiménez¹, Estibaliz Castillero¹, Ane Nieva-Zuluaga¹, Maider Apodaka-Biguri¹, Igor Aurrekoetxea^{1,2}, Igotz Delgado¹, Aritz Lopategi¹, Ainhoa Iglesias³, Lorena Mosteiro González², Gaizka Errazti Olarteoetxea², Sonia Gaztambide⁴, Luis A. Castaño González⁴, Luis Bujanda⁵, Jesus Maria Banales⁵, Xabier Buque¹, Ana Zubiaga³, Patricia Aspichueta^{1,6}. ¹Department of Physiology, Faculty of Medicine and Nursing, University of the Basque Country UPV/EHU, Leioa, Spain; ²Biobizkaia Health Research Institute, Hospital Universitario Cruces, Barakaldo, Spain; ³Department of Genetics, Physical Anthropology and Animal Physiology, Faculty of Science and Technology, University of Basque Country UPV/EHU, Leioa, Spain; ⁴Biobizkaia Health Research Institute, Hospital Universitario Cruces, CIBERDEM/CIBERER, Endo-ERN, Barakaldo, Spain; ⁵Department of Liver and Gastrointestinal Diseases, Biogipuzkoa Health Research Institute-Donostia University Hospital, University of the Basque Country (UPV/EHU), Ikerbasque, Basque Foundation for Science, San Sebastián, Spain; ⁶Biobizkaia Health Research Institute, Hospital Universitario Cruces, Barakaldo, Spain
Email: patricia.aspichueta@ehu.eus

Background and aims: The DNA damage generated as a response to lipotoxicity is a feature often observed in the progression of Metabolic dysfunction-associated steatotic liver disease (MASLD), where E2F transcription factors are overexpressed. However, if the activation of DNA damage response (DDR) could be beneficial in preventing MASLD-related metabolic dysregulation remains unclear. Aims: 1) Identify the relationship between DNA damage, DDR activation and E2F2 overexpression in MASH; 2) Investigate if the activation of DDR is impaired when E2F2 is overexpressed, contributing to metabolic dysregulation.

Methods: In a cohort of patients with obesity, individuals were classified as MASH or no-MASH based on liver biopsy. Hepatic levels of pH2AX (DNA damage marker), Ser15-p53 (a DDR activation marker) and E2F2 were analyzed. Hepatic and serum parameters and the activity of liver mitochondrial complexes were evaluated. *E2f2*^{-/-} and their control mice injected with DEN and fed a high-fat diet were used to induce progressive DNA damage-related MASLD. Primary hepatocytes were exposed to UV or palmitic acid (PA) to induce DNA

damage, *E2f2* was overexpressed with adenovirus, and AZD6738 was used to inhibit DDR.

Results: MASH patients that exhibited higher liver DNA damage displayed increased liver triglyceride and diglyceride levels, coupled with an inefficient fatty acid oxidation (FAO). These findings were corroborated in mouse models, indicating that DNA damage contributes to metabolic rewiring impeding FAO. Levels of E2F2, a FAO regulator, correlated positively with pH2AX in MASH. *E2f2*^{-/-} mice were protected from DNA damage induced by DEN and lipotoxic diets. Concordantly, overexpressing *E2f2* in hepatocytes led to increased DNA damage when exposed to PA or UV, leading to elevated lipid accumulation and an unresponsive FAO. Moreover, MASH patients with higher damage but incomplete DDR activation (reduced Ser15 p-p53) exhibited a more adverse inflammation than those with complete DDR. In *E2f2*-overexpressing hepatocytes, blocking DDR with AZD6738 upon damage resulted in an ineffective increase in FAO that did not reduce the lipid levels, indicating that a dysfunctional DDR further disrupts metabolism when *E2f2* is overexpressed. Specifically, MASH patients with high E2F2 and dysfunctional DDR showed elevated liver damage levels. The results suggest that higher E2F2 levels in MASH increase the extent to which a deficient DDR leads to metabolic disruption and vulnerability to progression. Notably, in MASH, elevated levels of both E2F2 and pH2AX were associated with faster disease progression.

Conclusion: In MASH patients with higher DNA damage, overexpression of E2F2 and deficient DDR activation are linked to altered FAO and increased liver damage. Thus, DDR activation might be beneficial to prevent the MASLD-related metabolic dysregulation, especially in patients with high E2F2 levels.

THU-211

Hepatoprotective effects of a HSD17b13 inhibitor in the CDAA-HFD mouse model of advanced MASH with progressive fibrosis

Joo Hyun Park¹, Denise Oró¹, Henrik B. Hansen¹, Rick Dewey², Katie Gammon², Michael Feigh¹. ¹Gubra, Hørsholm, Denmark; ²Foresite Labs, San Francisco, United States
Email: mfe@gubra.dk

Background and aims: Metabolic dysfunction-associated steatohepatitis (MASH) has emerged as a major challenge for public health because of high global prevalence and lack of evidence-based drug therapies. The newly identified liver-enriched, hepatocyte-specific and lipid droplet-associated protein 17-beta-hydroxysteroid dehydrogenase 13 (17beta-HSD13, encoded by *HSD17B13*) is strongly associated with the development and progression of MASH and liver fibrosis. The present study aimed to evaluate treatment effects of HSD17B13 inhibitor (M5475) in the non-obese, choline-deficient, L-amino-acid defined, high-fat diet (CDAA-HFD) mouse model of advanced MASH with progressive fibrosis.

Method: C57BL/6J mice were fed chow or CDAA-HFD (45 kcal% fat, 0.1% methionine, 1% cholesterol, 28 kcal% fructose) for 3 weeks prior to treatment start (before onset of liver fibrosis) and throughout the treatment period. Animals were randomized into treatment groups based on body weight. A CDAA-HFD baseline group (n = 12) was terminated prior to treatment start. CDAA-HFD fed mice (n = 10–12 per group) were orally administered vehicle or M5475 (30 or 100 mg/kg) for a total of 9 weeks. Chow-fed mice (n = 8) served as normal controls. Terminal end points included plasma/liver biochemistry, AI-assisted histopathological scoring (NAFLD Activity Score (NAS), fibrosis stage), quantitative liver histology and RNA sequencing.

Results: M5475 (100 mg/kg) reduced body weight and liver weight in CDAA-HFD mice compared to vehicle controls. While M5475 dose-dependently reduced hepatic cholesterol levels, other biomarkers (plasma transaminases/PIINP/TIMP-1, liver triglycerides) were unaffected by treatment. M5475 (100 mg/kg) significantly improved

POSTER PRESENTATIONS

fibrosis stage, but not NAS. In contrast, M5475 dose-dependently reduced quantitative markers of liver inflammation (number of inflammatory foci, %-area of galectin-3), but not steatosis. The antifibrotic efficacy of M5475 was supported by dose-dependent reductions in quantitative fibrosis markers (hydroxyproline, %-area of PSR, collagen-1a1, α -smooth muscle actin). M5475 treatment increased several gene expression markers of hepatic lipid and carbohydrate handling in combination with suppression markers of the immune system and extracellular matrix organization. M5475 significantly downregulated hepatic *HSD17B13* expression, indicative of target engagement.

Conclusion: M5475 improves biochemical and histological markers of inflammation and fibrosis in the non-obese CDAA-HFD mouse model of advanced MASH with progressive fibrosis, suggesting therapeutic potential of targeting *HSD17B13* in MASH.

THU-213

Exploring the role of FXR activation in mitigating ceramides-driven lipotoxicity and endoplasmic reticulum stress in metabolic dysfunction associated steatohepatitis

Basma Abdelrahman¹, Rasha Tawfiq¹, Olfat Hammam², Yasmeen Attia¹. ¹Department of Pharmacology, Faculty of Pharmacy, The British University in Egypt, Cairo, Egypt; ²Pathology Department, Theodor Bilharz Research Institute, Giza, Egypt
Email: Basma.alaa@bue.edu.eg

Background and aims: The disruption in ceramides (CER)/sphingolipids balance precipitating lipotoxicity can induce endoplasmic reticulum (ER) stress, thereby contributing to the incidence and progression of metabolic dysfunction associated steatohepatitis (MASH). The impact of the hepatic nuclear farnesoid x receptor (FXR) activation on CER synthesis and the associated ER stress remains to be elucidated. Given the favourable metabolic regulatory impact of FXR in MASH, targeting the FXR/CER axis can be sought as a possible avenue for the alleviation of CER-induced lipotoxicity and inflammatory events in the liver. This has led us to investigate the potential influence of the FXR agonist, obeticholic acid (OCA), in modulating CER synthesis and the associated ER stress in experimental MASH.

Method: Dietary high-fat diet (HFD) model was adopted in the present study to induce MASH. Male C57BL/6 mice were allocated into 3 groups as follows: (I) Normal group that was kept on normal chow, (II) Control group (HFD) that was kept on HFD and received drug vehicle, and (III) OCA-treated group that was kept on HFD and received OCA at a dose of 5 mg/kg/day, p.o. Treatment started after 8 weeks of induction for 4 weeks. Livers were harvested for histopathological evaluation and subsequent analyses. Gene expression of sterol regulatory element binding protein-1c (SREBP1c) and small heterodimer partner-1 (SHP-1) was measured using qRT-PCR. Protein levels of bile acid synthesis rate-limiting enzyme CYP7A1 were also measured by ELISA. Catabolic and salvage CER synthesis pathways were investigated by assessing hepatic levels of sphingosine-1 phosphate (S1P) and acid sphingomyelinase (ASMase), respectively, using ELISA. Hepatic ER stress key regulators, 78-kDa glucose-regulated protein (GRP78) and protein kinase RNA-like endoplasmic reticulum kinase (PERK), as well as the apoptotic marker, C/EBP homologous protein (CHOP), were also measured using ELISA.

Results: Upon histopathological examination, OCA alleviated MASH hallmarks observed in the HFD-fed mice that included macro steatosis and lymphocyte aggregates. OCA treatment resulted in SHP-1 upregulation and SREBP1c downregulation implying the likely reduction of lipogenesis by FXR activation. To further attest to FXR activation, it was observed that CYP7A1 was 79% lower with OCA compared to HFD. Moreover, S1P and ASMase levels were reduced by

63.5% and 49.1% in OCA-treated mice compared to their untreated counterparts, respectively. In line with CER synthesis repression, ER stress markers, GRP78 and PERK, were curtailed by 55.3% and 76.1% in the OCA-treated group when compared to the HFD group, respectively. Analogously, OCA curbed CHOP protein levels by 60.5%.

Conclusion: These findings might imply that FXR activation by OCA can mitigate CER-induced lipotoxicity and the ensuing ER stress in MASH.

THU-214

Spatiotemporal non-invasive characterization of the hepatic microenvironment during metabolic dysfunction-associated liver disease progression

Rallia Velliou¹, Aigli-Ioanna Legaki¹, Aikaterini Avdi¹, Polyxeni Nikolakopoulou¹, Antonios Chatzigeorgiou¹. ¹Department of Physiology, Medical School, National and Kapodistrian University of Athens, Athens, Greece
Email: rvelliou@med.uoa.gr

Background and aims: Metabolic dysfunction-associated liver disease (MASLD) is a growing health concern, with an estimated prevalence of 25% and is strongly linked to metabolic syndrome components. Among MASLD patients, 30% will advance to the more severe stage of metabolic dysfunction-associated steatohepatitis (MASH); a multiparametric disease characterized by hepatic steatosis, inflammation and fibrosis. Despite its prevalence and severity, there is no MASLD-specific therapy available and existing treatments only tackle MASLD-associated pathologies. A limiting factor affecting prompt diagnosis and monitoring of MASLD, is insufficiency in characterizing the hepatic microenvironment and disease scoring in a spatiotemporal non-invasive manner. Thus, this study aimed towards a longitudinal analysis of MASLD progression at three distinct disease stages by performing a multi-stage phenotypic characterization.

Method: A diet-induced MASLD mouse model was utilized to investigate using in vivo micro-CT (μ CT) imaging techniques as a non-invasive method for assessing MASLD progression. Spatiotemporal changes in liver morphology, ECM structure, and inflammation were analyzed, focusing on the hepatic vascular endothelium and hepatic vascular network, since they are implicated in MASLD-related hepatic dysregulation. Liver steatosis, functional tissue uptake/lipid (chylomicron) transfer, portal vein diameter and vascular network density were assessed via μ CT at three distinct stages. Steatosis, fibrosis, inflammation and angiogenesis were evaluated via histology and qPCR at the equivalent timepoints.

Results: Findings show that a longitudinal analysis of important disease markers can be performed to assess MASLD progression. μ CT analysis revealed that liver steatosis and functional tissue uptake/lipid (chylomicron) transfer were higher for pathological compared to control mice and progressively elevated along with disease advancement. Similarly, pathological mice had an increasingly larger portal vein diameter at all timepoints, a structural alteration linked to portal hypertension. Total hepatic vascular network volume was elevated in pathological mice and progressively increased following MASLD progression. Results were validated using basic laboratory approaches. Liver steatosis, inflammation, fibrosis and angiogenesis were assessed via qPCR and histology, confirming disease progression at three stages.

Conclusion: Our work provides valuable insights into spatiotemporal dynamics of MASLD/MASH advancement and highlights the potential of μ CT imaging to support MASLD preclinical research with a cutting-edge, non-invasive method to monitor disease progression, which can pave the way towards more efficient and reproducible approaches to MASLD research and contribute to the development of novel therapies targeting disease progression.

THU-215

Artificial intelligence-derived granular histological markers of fibrosis from hematoxylin and eosin-stained whole slide images associate with non-invasive tests of fibrosis and prognosis to cirrhosis in patients with metabolic dysfunction-associated steatohepatitis

Neel Patel¹, Lara Murray¹, Adam Stanford-Moore¹, Victoria Mountain¹, Jun Xu², Lisa Boyette², Benjamin Glass¹, Timothy R. Watkins², Andrew N. Billin², Ylaine Gerardin¹, Robert Egger¹. ¹PathAI, Inc., Boston, United States; ²Gilead Sciences, Inc., Foster City, United States
Email: neel.patel@pathai.com

Background and aims: Certain non-invasive tests (NITs) are predictive of progression to liver related events (LRE) in MASLD/MASH; however, there is an incomplete understanding of the relationship between NITs and liver histopathology across the spectrum of MASH disease states. NASH Explore™ is a suite of machine learning models that identifies liver cell, tissue, histological landmarks, and fibrosis subtypes in HandE-stained whole slide images (WSIs). Over a thousand human interpretable features (HIFs) are extracted from these model predictions, which quantitatively describe the spatial organization of these substances in relation to one another on a granular level. Here we have deployed NASH Explore to better understand which specific MASH histologies: (i) have the strongest correlations with common NITs and (ii) are associated with progression to cirrhosis and LRE.

Method: We deployed NASH Explore on 4454 HandE WSIs from 3 clinical datasets (STELLAR 3 and STELLAR 4, trials of selonsertib on MASH patients with F3 or F4 fibrosis, respectively, and ATLAS, a trial testing combinations of selonsertib, cilofexor, and firsocosat in F4 MASH patients). We performed correlation analysis of NASH Explore HIFs with fibrosis related NITs (ELF, FIB-4, NFS and FibroScan). Strength of association was measured using Pearson's rho and the effect HIFs on progression to cirrhosis and LRE in STELLAR 3 patients was estimated using Cox proportional hazards regression.

Results: Across time points in all three trials (baseline [BL] and end of study), the fraction of pathological fibrosis area over all tissue positively correlated with fibrosis related NITs (Pearson's rho-ELF: 0.43–0.48; FIB-4: 0.32–0.41; FibroScan: 0.45–0.48; NFS: 0.35–0.36). Nodular fibrosis related HIFs demonstrated the highest positive correlation; additionally, a positive correlation existed between the fraction of nodular fibrosis area over pathological fibrosis and all examined NITs (Pearson's rho-ELF: 0.40–0.49; FIB-4: 0.31–0.37; FibroScan: 0.32–0.37; NFS: 0.38–0.43). The value of these features at BL was prognostic for progression to cirrhosis or LRE (fraction of pathological fibrosis area over tissue HR: 1.59 [1.01–2.47], fraction of nodular fibrosis area over all pathological fibrosis HR: 1.71 [1.19–2.60]). Prognostic value was higher compared to all fibrosis NITs apart from ELF (ELF HR: 2.34 [1.66–3.42], FIB-4 HR: 1.23 [0.99–1.52], FibroScan HR: 1.38 [1.18–1.66], NFS HR: 1.51 [1.0–2.19]).

Conclusion: Using NASH Explore HIFs, we showed that relative areas of pathological and nodular fibrosis positively associate with non-invasive measurement of fibrosis severity and prognosis. Further research is required to validate the association between NITs and granular histological features, which may support the assessment of MASH disease progression or regression through non-invasive surrogates of liver histopathology.

THU-218

A novel role for the epigenetic regulator SUV420H1 in MASLD and its complications

Alessia Pagani¹, Letizia Bavuso Volpe¹, Mariateresa Pettinato¹, Francesco Malvestiti², Valeria Furiosi³, Rossana Carleo¹, Antonella Nai³, Luca Valenti⁴, Laura Silvestri¹. ¹IRCCS San Raffaele Scientific Institute, Milan, Italy; ²Università degli Studi di Milano, Milan, Italy; ³IRCCS San Raffaele Scientific Institute, Milan; ⁴Fondazione IRCCS Ca' Granda Ospedale Maggiore Policlinico, Milan, Italy
Email: silvestri.laura@hsr.it

Background and aims: Several factors contribute to MASLD development and worsening, including deregulated iron metabolism, but the molecular mechanisms involved are still unknown. Notably, a genomic region encompassing the histone methyltransferase Suv420h1 has been associated with iron-dependent hepatic steatosis in mice, suggesting that epigenetic remodelling may play a role in linking lipid and iron metabolism.

Method: To determine whether Suv420h1 might play a role in MASLD, we compared the differentially expressed pathways in the liver of bariatric patients stratified for Suv420h1 expression (High = 42 vs Low = 44) accounting for age, gender and the carriage of the PNPLA3 I148M at-risk variant. Then, we generated mice lacking Suv420h1 in hepatocytes (h1-LCKO) and characterized them after 16 weeks of a NASH-inducing diet (FPC).

Results: In bariatric patients, Suv420h1 positively correlated with inflammatory response, NF-κB-mediated TNFα and IL-6/JAK/STAT3 signalling, IFNγ response, and EMT, independently of other confounders. Additionally, overrepresentation analysis indicated enrichment in genes involved in extracellular matrix and collagen fibril organization, leukocyte migration, proliferation and migration, in patients expressing higher levels of Suv420h1. h1-LCKO mice were born in the expected Mendelian ratios and developed without problems. Body weight was comparable to that of control mice at a young age, while adult mice had a lower body weight compared to controls. The FPC diet resulted in mild overweight and hepatomegaly in ctrl mice, while h1-LCKO mice were protected. Hepatic inactivation of h1 counteracted hepatomegaly and reduced white adipose tissue hypertrophy. This was associated with a reduced number and size of lipid droplets in the hepatocytes, decreased monocyte recruitment and collagen deposition. Consistently, triglycerides and transaminases in the liver were also reduced. Compared to FPC-treated ctrl mice, FPC-treated h1-LCKO mice showed improved glucose tolerance and increased insulin sensitivity. MASLD is often associated with impaired iron metabolism, which may contribute to disease progression. Mice fed the FPC diet showed increased serum iron and decreased expression of hepcidin, the key hormone regulating iron metabolism. Interestingly, deletion of h1 in hepatocytes also improved iron metabolism by decreasing serum iron and increasing hepcidin on FPC diet. Pharmacologic targeting of h1 in the liver, when hepatostasis is already established, is ongoing.

Conclusion: Inactivation of Suv420h1 in the liver counteracts MASLD development and progression and improves iron metabolism. Thus, Suv420h1 can be considered a promising therapeutic target for MASLD and its complications, including deregulated iron metabolism. Further studies are underway to decipher the signalling pathway modulated by Suv420h1 in hepatocytes.

THU-219

Inhibition of HSD17B13 by INI-822 phenocopies the hepatic lipidomic profile of humans with the protective allele

Cindy McReynolds¹, Michael Carleton¹, Chuhan Chung¹, Heather Hsu¹. ¹Inipharm, Bellevue, WA, United States
Email: hhsu@inipharm.com

Background and aims: HSD17B13 is an oxidoreductase associated with lipid droplets in hepatocytes. HSD17B13 polymorphisms that result in inactive enzyme protect against MASH, cirrhosis, and liver cancer. Analysis of human liver tissue from subjects with metabolic syndrome demonstrated increased hepatic phosphatidylcholines (PC) in individuals with inactive HSD17B13 (Luukkonen 2020 JCI Insight). In this work, we hypothesized that INI-822, a selective HSD17B13 small molecule inhibitor, could replicate lipidomic changes found in humans carrying the inactive HSD17B13 gene.

Method: INI-822 was dosed orally once daily in obese Zucker rats on a normal chow (NC), high fat, high cholesterol atherogenic diet (HFCD) and choline deficient, amino acid defined high fat diet (CDAA-HFD), n=4/group. Changes in liver transaminase levels, circulating and hepatic lipids (GC/MS, LC/MS) were measured.

POSTER PRESENTATIONS

Statistical significance was evaluated by ANOVA followed by a Bonferroni multiple comparison test for liver transaminases, mean \pm SD. The lipidomics were evaluated by multiple unpaired t-tests with adjustment for a false discovery rate of $<1\%$, significance reported for $p < 0.01$.

Results: INI-822 treatment of Zucker obese rats led to a decrease in ALT in animals on the challenge diets compared to vehicle control with the largest change in rats on the CDAA-HFD with a $49 \pm 10\%$ decrease with treatment ($p < 0.05$ for all diets). INI-822 treatment did not result in hepatic lipidomic changes in Zucker rats consuming normal chow. Hepatic PCs were elevated in a dose-dependent manner with INI-822 treatment in rats on the CDAA-HFD with 12 PCs elevated vs. controls more than two-fold. PCs were also enriched in rats on HFHCD with 4 PCs elevated >1.7 -fold. These included PC 36:2e and PC 34:3 which have been shown to be elevated in liver biopsies from patients with inactive HSD17B13 alleles. In INI-822-treated animals on the CDAA-HFD, circulating lipids demonstrated a decrease in overall PCs; however levels of specific long chain, polyunsaturated PCs including >10 -fold increases in PC 38:4e, PC 40:5 and 42:3e increased in the HFHCD animals. Plasma levels of esterified hydroxy-lipid HSD17B13 substrates increased while free fatty acids of these same substrates decreased.

Conclusion: HSD17B13 inhibition with INI-822 decreased liver transaminases and led to increased hepatic PC content in Zucker rats on metabolic diets. HSD17B13 inhibition led to lipidomic changes consistent with those found in patients with the loss-of-function protective allele.

THU-220

ATM, guardian of genome integrity, is a new player in NAFLD pathogenesis by modulating mitochondrial metabolism

Pierre Cordier¹, Christelle Kabore¹, Irene Portoles-Plaza¹, Marie Lagouge¹, Alice Verdier¹, Ivan Nemazany², Romain Donne³, Jean-Pierre Couty¹, Fatima Mechta-Grigoriou⁴, Géraldine Gentric⁵, Severine Morizur¹, Chantal Desdouets¹. ¹Centre de Recherche des Cordeliers, INSERM U1138, Paris, France; ²InsERM US 24-CNRS UMS 3633, Platform for Metabolic Analyses, Structure Fédérative de Recherche Necker, Paris, France; ³Icahn school of medicine at Mount Sinai, New York, United States; ⁴Institut Curie, Stress and Cancer Laboratory, Inserm U830, Paris, France; ⁵Institut Curie, Stress and Cancer Laboratory, Inserm, U830, Paris, France
Email: chantal.desdouets@inserm.fr

Background and aims: The incidence of non-alcoholic fatty liver disease (NAFLD) and its progressive form non-alcoholic steatohepatitis (NASH) have become the most prevalent chronic liver disease and a terrifyingly health problem. Key molecular mechanisms behind this sequence have to be still clarified. Based on observations reported by us and others, we propose that Replication Stress (RS) conjointly to an underperforming DNA Damage Response (DDR) might be involved in the progression of NAFLD development.

Method: We analyzed publicly available RNA-seq datasets from patients with NAFLD. We also used mice with targeted hepatocyte ablation of ATM expression and fed them with Choline Deficient High Fat Diet mimicking to induce NASH. Non targeted RNA seq, lipidomic, metabolomic and targeted energy metabolomic analyses as well as cellular and molecular approaches were performed.

Results: First, we exploited a publicly available liver RNA-seq dataset from a cohort of biopsy-proven NAFLD patients to analyze the expression of RS and other DDR genes covering all major DNA repair pathways. Strikingly, we identified RS as the most prominently upregulated DDR pathways, appearing as early as the NAFL state and maintained in NASH-F3 stage. Furthermore, we demonstrated that escalating genotoxicity accompanies progression to fibrosing NASH with cell cycle checkpoint activation, mediated by the ATM-p53 axis,

and exemplified by the upregulation of various DNA double-strand break (DSB) responsive genes. We investigated whether inhibition of ATM in a preclinical mouse model of NAFLD could favour disease progression. We demonstrated that ATM deficiency in NAFLD livers enhances liver tissue damage and liver fibrosis independently of its potential role in regulating compensatory proliferation. In fact, ATM deletion exacerbates toxic lipids accumulation and induces reprogramming of central carbon metabolism as well as nucleotide pool imbalance with underlying liver energy deficit. Mechanistically, we observed that ATM regulates mitochondria function in steatotic hepatocytes by acting on Tricarboxylic acid (TCA) cycle and purine/pyrimidine biosynthesis.

Conclusion: Altogether, our findings shed new light on the mechanism by which an under-performing DDR promotes NAFLD disease progression.

THU-221

Association of non-invasive tests (NITs) with genetic polymorphism in patients with metabolic dysfunction-associated steatotic liver disease (MASLD)

Zobair Younossi^{1,2}, James M. Estep^{1,3}, Zohal Zekrya¹, Sean Felix¹, Brian Lam^{1,3}, Zaid Younossi^{1,4}, Andrei Racila^{1,3}, Maria Stepanova^{1,3,4}. ¹Beatty Liver and Obesity Research Program, Inova Health System, Falls Church, VA, United States; ²The Global NASH Council, 2411 I Street, Washington, DC, United States; ³The Global NASH Council, Washington, DC, United States; ⁴Center for Outcomes Research in Liver Diseases, Washington, DC, United States
Email: zobair.younossi@cldq.org

Background and aims: Genetic risk factors have been linked to advanced histologic stage of fibrosis among patients with MASLD. The association of the genetic factors with non-invasive biomarker-based tests (NITs) or liver stiffness measurement (LSM) by transient elastography (TE) has not been well established.

Method: Clinical, laboratory (Enhanced Liver Fibrosis, FIB-4), liver biopsy and TE data were collected from consented patients with MASLD. Genomic DNA was extracted from the whole blood [QIAamp DNA Blood Mini Kit (Qiagen)] and used for determination of minor allele frequency for genomic loci rs641738 (MBOAT7), rs58542926 (TM6SF2), rs738409 (PNPLA3), rs62305723 (HSD1713B) using CFX96 (BioRad). Individual alleles were evaluated for association with high ELF (≥ 11.3), high FIB-4 (≥ 3.25), high LSM (≥ 10 kPa), and histologic fibrosis (stage 3 or 4 vs. stages 0–2).

Results: We included 1915 MASLD patients [52 ± 14 years, 47% male, BMI 36.9 ± 10.4 , 28% type 2 diabetes (T2D)]. Of these patients, 1.9% had high ELF, 3.4% had high FIB-4; of those with TE ($n = 638$), 15% had high LSM, and of those with a biopsy ($n = 580$), 15% had advanced histologic fibrosis (F3 or F4). Of 4 studied SNPs, only PNPLA3-rs738409 (51% CC, 39% CG, 10% GG) was significantly associated with higher NIT scores: high ELF 0.9% in CC vs. 2.9% in CG/GG, high FIB-4 2.3% in CC vs. 4.7% in CG/GG, high LSM 10% vs. 19%, respectively, and advanced histologic fibrosis 10% in CC vs. 19% in CG/GG (all $p < 0.01$). Similar associations of PNPLA3-rs738409 with NITs were observed in a subgroup of MASLD patients with T2D ($n = 536$): high ELF 2.5% in CC vs. 5.5% in CG/GG, high FIB-4 4.1% in CC vs. 9.1% in CG/GG, high LSM 20% in CC vs. 39% in CG/GG, advanced histologic fibrosis 21% in CC vs. 42% in CG/GG (all $p < 0.05$). In multivariate analysis adjusted for age, sex, BMI and T2D, having PNPLA3-rs738409 CG/GG genotype was independently associated with having high ELF and FIB-4 scores, high LSM, and advanced histologic fibrosis: odds ratio (OR) = 3.53 (1.39–8.99) for high ELF; OR = 2.24 (1.26–4.00) for high FIB-4, OR = 2.56 (1.53–4.27) for high LSM, and OR = 1.99 (1.18–3.37) for advanced histologic fibrosis (all $p < 0.01$).

Conclusion: In patients with MASLD, the polymorphism rs738409 in the PNPLA3 gene is not only associated with advanced histologic

fibrosis but also independently associated with commonly used NITs such as liver stiffness by transient elastography, ELF and FIB-4 scores.

THU-222-YI

The exercise-induced metabokine beta-aminoisobutyric acid regulates hepatic lipid metabolism and reduces hepatic metabolic dysfunction and fatty liver in a dietary obese mouse model

Shaimaa Gad¹, Helene Daou², Amanda MacCannell², Nicole Watt², Laetitia Lichtenstein², David Beech², Scott Bowen³, Lee Roberts².
¹Leeds Institute of Cardiovascular and Metabolic Medicine (LICAMM), School of Medicine, University of Leeds, Faculty of Medicine, Mansoura University, Egypt, Leeds, United Kingdom; ²Leeds Institute of Cardiovascular and Metabolic Medicine (LICAMM), School of Medicine, University of Leeds, Leeds, United Kingdom; ³Faculty of Biological Sciences, University of Leeds, Leeds, United Kingdom
Email: s.a.gad@leeds.ac.uk

Background and aims: Obesity is a common pathology arising from energy disbalance which increases the risk of metabolic and cardiovascular disease. Exercise is an effective intervention, decreasing obesity and associated cardiometabolic risks. Beta-aminoisobutyric acid (BAIBA), a skeletal muscle metabokine regulated by exercise and the transcriptional coregulator Pgc1 α mediates muscle-liver-adipose crosstalk. BAIBA enhances hepatic fatty acid beta oxidation (Fa β O) and browning of fat. The effects and signals of BAIBA on hepatic tissue are poorly elucidated. We hypothesize that BAIBA regulates and can improve hepatic metabolism to treat dietary obesity induced fatty liver.

Method: 8-week-old male C57BL/6J mice were either fed chow diet {CD} \pm BAIBA (100 mg/kg/day water-added) for 6 weeks (A), 14 weeks (B) or high fat diet {HFD} \pm BAIBA for 14 weeks (C) (n = 10/group). We investigated hepatic 1) Metabolism: mitochondrial density (citrate synthase {CS} assay) and function (carnitine palmitoyl transferase {CPT} activity and high resolution mitochondrial respirometry analysis); 2) Molecular phenotype: gene (RT-qPCR) and protein (immunoblotting) expression for Fa β O, mitochondrial, lipid and carbohydrate metabolic markers; 3) Histomorphological analysis. Nominal Significance, p < 0.05 using GraphPad Prism software.

Results: Hepatic tissue from CD 6-week BAIBA treated mice (A) was characterised by significantly: 1) lower acetyl CoA carboxylase alpha (Acaca) gene and protein expression. 2) greater expression of Cpt1a gene and protein as well as peroxisome proliferator activated receptor alpha (Ppara) gene and protein. 3) increased mitochondrial density, total CPT activity and CPT1 activity (identifying increased fatty acid oxidation). 4) enhanced mitochondrial Fa β O. 5) higher gene expression of fatty acid transporter 2, hepatic and monoacylglycerol lipases and fasting induced adipose factor with lower triglycerides. Analysis of hepatic tissue from 14-week BAIBA treated mice under CD (B) and HFD (C) revealed significantly: 1) raised total CPT functional activity. 2) enhanced Acaca protein expression driven by HFD which was reduced with BAIBA treatment. 3) higher expression of Cpt1a, Ppara and gluconeogenic genes with BAIBA treatment under chow conditions. 4) reduced the expression of HFD-induced denovo lipogenesis (DNL) genes including Acaca, diacylglycerol acyltransferase2, stearoyl CoA desaturase1 and elongas6 lipogenic genes. 5) decreased plasma cholesterol in both CD and HFD fed mice. 6) decreased hepatic fat accumulation and decreased fibrosis (collagen I) (n = 5) in BAIBA-treated mice.

Conclusion: BAIBA has beneficial metabolic effects in the livers of lean and obese mice, enhancing hepatic Fa β O, mitochondrial energetics and decreasing DNL leading to reduced hepatic fat accumulation and fibrosis.

THU-223

A novel circular RNA therapy expressing a long-acting FGF21 analog protein reversed obesity, insulin resistance, and steatosis in mouse models

Rui Cao¹, Haitao Wan¹, Jing Zeng¹, Lu Gao². ¹Therorna Shanghai Co., Ltd., Shanghai, China; ²Therorna Inc., Beijing, China
Email: lu.gao@therorna.com

Background and aims: Fibroblast growth factor 21 (FGF21) is a promising therapeutic target for the treatment of metabolic dysfunction-associated steatotic liver disease (MASLD). However, the clinical development of FGF21 analogs were challenging, due to their short half-life *in vivo*. Here we report a novel circular RNA circRNA-0222 expressing long-acting FGF21-fusion protein *in vivo* and investigated its therapeutic effect on glycaemic control, weight loss and steatosis in MASLD mouse models.

Method: Murine 3T3-L1 preadipocytes was stimulated with cultured medium from circRNA-0222 lipid nanoparticle (LNP) transduced cells. Cell lysates were subjected to immunoblot analysis for extracellular signal-regulated kinase 1/2 (ERK) activation. To evaluate the activity of FGF21 analog, luciferase reporter assays were performed in 293 T cells stably transfected with human Beta-Klotho. Expression pharmacokinetics were measured by ELISA post intravenous injection in C57BL/6 mice and cynomolgus monkeys. Oral glucose tolerance test (OGTT) was conducted in male BKS wild-type mice. In the chow diet fed BKS-db/db obese model, body weight, body composition and insulin resistance were measured upon weekly circRNA-0222 administration (n = 6) for 4 weeks. Biomarkers of liver function, blood sugar and steatosis were analyzed in the western-diet induced BKS-db/db mice.

Results: circRNA-0222 rapidly induced phosphorylation of ERK upon stimulation in 3T3-L1 cells. Particularly, circRNA-0222-expressed FGF21 analog (EC50 = 45.3 ng/ml) showed significantly better potency than that of the recombinant FGF21 analog (EC50 = 470 ng/ml). Upon intravenous injection of circRNA-0222 LNP, FGF21 analog became detectable in mouse sera at 2 h post dosing and decayed slowly over 3 weeks. The FGF-21 analog expressed from circRNA-0222 exhibited longer half-life (54–80 h) compared with that of reported recombinant proteins (11–18 h) in mice. In the OGTT study, administration of circRNA-0222 significantly reduced the blood glucose level in a dose-dependent manner. In the BKS-db/db mice, weekly administration of 0.1, 0.25, 0.5 mg/kg circRNA-0222 for 4 weeks resulted in the bodyweight reduction of 9.7%, 14%, 18%, respectively. Surprisingly, the weight reduction was mainly from the loss of fat mass, but not the lean mass. circRNA-0222 led to improvement of insulin secretion at 0.25 mg/kg (p < 0.001). Moreover, circRNA-0222 significantly attenuated circulating ALT, LDL-C, total cholesterol, triglycerides and HbA1c in the western diet-fed BKS-db/db mice. Confirmed with histopathological evaluation, circRNA-0222 significantly improved hepatic steatosis (p < 0.05).

Conclusion: Administration of circRNA-0222 LNP prevented the development of obesity and improved liver disease hallmarks in mouse disease models. Such finding supports further clinical investigation of circRNA-0222 for the treatment of MASLD.

THU-224

CRISPR/Cas9-mediated somatic gene editing in adult mice reveals hepatic KLB as a regulator of bile acid synthesis and hepatic lipid metabolism

Alexandra Aaldijk¹, Dicky Struik¹, Cristy Verzijl¹, Rick Havinga¹, Milaine Hovingh¹, Nicolette Huijman¹, Marieke Smit¹, Bart van de Sluis¹, Johan Jonker¹. ¹Department of Pediatrics, University Medical Center Groningen (UMCG), Groningen, Netherlands
Email: alexandraaldijk@outlook.com

Background and aims: Fibroblast growth factor (FGF) 19 and 21-based drugs have emerged as powerful new biologicals for treating metabolic dysfunction-associated steatotic liver disease (MASLD) due

POSTER PRESENTATIONS

to their ability to lower liver fat in preclinical models and humans. Rodent studies have revealed that the activity of these drugs is strictly dependent on the expression of the transmembrane protein beta-klotho (KLB) in the adipose tissue and the brain, while its role in the liver remains unclear. To date, only germline mouse models have been used to study the function of KLB, demonstrating an effect on body weight, bile acid metabolism, and cholesterol metabolism. However, these models are confounded by various developmental abnormalities. Therefore, we aim to explore hepatic KLB function in adult mice by applying liver-specific Cas9-mediated somatic gene editing.

Method: Liver-specific Cas9-transgenic mice on a C57BL/6J background were injected intravenously with 0.5×10^{11} adeno-associated virus particles containing three single guide RNAs (sgRNAs) targeting exon 1 of the mouse Klb gene to induce a liver-specific knock-down of KLB or a matched viral dose containing scaffold sgRNA as a control. Mice were maintained on a chow diet for 4 weeks after virus injection, followed by extensive phenotypic characterization.

Results: Liver-specific somatic knock-down of Klb led to a 2.6-fold increase in hepatic Cyp7a1 mRNA expression ($p = 0.008$), suggesting increased bile acid synthesis. In line with this, we identified a 3-fold increased fecal bile acid concentration and excretion ($p = 0.008$) despite an unaltered bile flow. Hepatic Klb deficiency also altered bile acid composition as reflected by the increased percentage of unconjugated bile acids in the bile and feces ($p = 0.008$). Finally, hepatic Klb deficiency resulted in a 41% decrease in plasma triglyceride levels ($p = 0.008$) and a 37% increase in hepatic triglyceride levels ($p = 0.016$).

Conclusion: Through applying liver-specific Cas9-mediated somatic gene editing in mice, we provide new insights into the function of KLB during adulthood, independent of developmental effects, and reveal a direct role for hepatic KLB in the regulation of bile acid synthesis and hepatic lipid metabolism. In addition, our findings identify hepatic KLB as a potential target in FGF19- and FGF21-based treatment of MASLD.

THU-225

GDF15 activates AMPK and inhibits gluconeogenesis and fibrosis by attenuating SMAD3 phosphorylation

Javier Jurado-Aguilar^{1,2,3}, Emma Barroso^{1,2,4}, Maribel Bernard Montuenga^{1,2,3}, Meijian Zhang¹, Mona Peyman¹, Patricia Rada^{2,5}, Angela Martinez Valverde^{2,5}, Walter Wahli^{6,7,8}, Xavier Palomer^{1,2,3}, Manuel Vázquez-Carrera^{1,2,3}. ¹Department of Pharmacology, Toxicology and Therapeutic Chemistry, Faculty of Pharmacy and Food Sciences and Institute of Biomedicine of the University of Barcelona (IBUB), University of Barcelona, Barcelona, Spain; ²Spanish Biomedical Research Center in Diabetes and Associated Metabolic Diseases (CIBERDEM)-Instituto de Salud Carlos III, Madrid, Spain; ³Pediatric Research Institute-Hospital Sant Joan de Déu, Esplugues de Llobregat, Spain; ⁴Pediatric Research Institute-Hospital Sant Joan de Déu, Esplugues de Llobregat, Spain; ⁵Instituto de Investigaciones Biomédicas Alberto Sols (CSIC/UAM), Madrid, Spain; ⁶Center for Integrative Genomics, University of Lausanne, Lausanne, Switzerland; ⁷Lee Kong Chian School of Medicine, Nanyang Technological University Singapore, Singapore, Singapore; ⁸ToxAlim (Research Center in Food Toxicology), Toulouse, France
Email: javierjuradoaguilar@ub.edu

Background and aims: The metabolic sensor AMP-activated protein kinase (AMPK) has been reported to be reduced via unknown mechanisms in the liver of mice deficient in growth differentiation factor 15 (GDF15). This is a stress response cytokine that regulates energy metabolism mainly by reducing food intake through its central receptor GFRAL.

Method: Wild-type and *Gdf15*^{-/-} mice, the human hepatic cell line Huh-7, and primary mouse hepatocytes, we examined how GDF15 regulates AMPK.

Results: *Gdf15*^{-/-} mice exhibited glucose intolerance and reduced hepatic phosphorylated AMPK levels that were accompanied by an increase in the phosphorylated levels of the mediator of the fibrotic response mothers against decapentaplegic homolog 3 (SMAD3), together with increased gluconeogenesis and fibrosis. Recombinant (r)GDF15 increased AMPK activation and reduced phosphorylated SMAD3 and the levels of markers of gluconeogenesis and fibrosis in mouse primary culture of hepatocytes, indicating that these effects were independent of GFRAL, and in the liver of mice. Pharmacological inhibition of SMAD3 phosphorylation in *Gdf15*^{-/-} mice prevented glucose intolerance, the deactivation of AMPK and the increase in the levels of proteins involved in gluconeogenesis and fibrosis.

Conclusion: The overactivation of the SMAD3 pathway is responsible for the metabolic alterations in *Gdf15*^{-/-}. Overall, these findings indicate that GDF15 activates AMPK and inhibits gluconeogenesis and fibrosis by attenuating the SMAD3 pathway.

THU-226

CAMSAP1 aggravates liver fibrosis in metabolic dysfunction-associated steatohepatitis by promoting microtubule acetylation

Zhiping Wan¹, Xiaolan Yang¹, Xiaoquan Liu¹, Xiaoman Chen¹, Hong Deng². ¹The Third Affiliated Hospital of Sun Yat-sen University, Guangdong Key Laboratory of Liver Disease Research, Guangzhou, China; ²The Third Affiliated Hospital of Sun Yat-sen University, Guangzhou, China
Email: wanzhp@mail2.sysu.edu.cn

Background and aims: Liver fibrosis is a worrisome feature of metabolic dysfunction-associated steatohepatitis (MASH), and its central event is the activation of hepatic stellate cells (HSCs). Calmodulin-regulated spectrin-associated protein 1 (CAMSAP1)-mediated microtubule acetylation is related to HSCs activation, but the specific mechanism remains unclear. We aimed to explore the role and mechanism of CAMSAP1 in HSCs activation and MASH liver fibrosis.

Method: The CAMSAP1 expression was analyzed in MASH patient livers, MASH rat livers, and activated HSCs. SD rats were fed a high-fat and high-cholesterol diet (HFHCD) for 16 weeks to construct a MASH rat model. A plasmid overexpressing CAMSAP1 was constructed and transfected into HSCs to upregulate the expression of CAMSAP1. RNA sequencing was used to analyze gene expression profiles after upregulation of CAMSAP1.

Results: We found that the expression of CAMSAP1 was not only increased in the livers of MASH patients and MASH rats, but also in activated HSCs. Besides, the level of CAMSAP1 was positively correlated with the degree of liver fibrosis. Upregulation of CAMSAP1 in HSCs increased expression of alpha smooth muscle actin (α SMA), collagen type I alpha 1 (COL1A1), collagen type III alpha 1 (COL3A1) and acetylated α -tubulin (Ac- α -Tub). Moreover, alpha tubulin acetyltransferase (ATAT1) was confirmed to be regulated by CAMSAP1, and CAMSAP1 promoted its expression. Importantly, upregulation of ATAT1 in HSCs also promoted microtubule acetylation and activation of HSCs.

Conclusion: CAMSAP1 is increased in MASH progression. CAMSAP1 upregulates the expression of ATAT1 to promote microtubule acetylation, thereby activating HSCs and aggravating liver fibrosis in MASH.

THU-227

Macrophage phenotype is affected by longitudinal treatment with Zalferrin in a model of metabolic dysfunction-associated steatohepatitis

Benedicte Kapel¹, Dora Hancz¹, Cesar Medina², Maria Dermit², Lise Flyger Walther Jensen¹, Sanne Skovgård Veidal³, Jenny Egecioglu Norlin⁴, Anouk Oldenburger³, Birgitte Andersen¹,

Dominik Pfister¹. ¹Liver Biology Novo Nordisk A/S, Måløv, Denmark;
²Novo Nordisk Research Centre Oxford, Oxford, United Kingdom;
³Obesity and Liver Pharmacology Novo Nordisk A/S, Måløv, Denmark;
⁴Translational Medicine Novo Nordisk A/S, Måløv, Denmark
 Email: DRPF@novonordisk.com

Background and aims: Obesity and diabetes are on a steady global rise and together with genetic predisposition, this increases the risk of Metabolic Dysfunction-Associated Steatohepatitis (MASH). Hallmarks of MASH are chronic necro-inflammation and hepatic fibrosis potentially resulting in liver failure or cancer. There is currently no approved pharmaceutical treatment for MASH thus there is a large unmet medical need to develop effective and safe medication. To increase our understanding of disease progression as well as mode of action (MoA) of pharmacological intervention we aimed to generate longitudinal liver treatment data using a murine model of diet-induced MASH treated with long acting GLP1 or FGF21 analogues.

Method: Disease induction was performed in male C57BL/6J mice fed the Gubra Amylin NASH (GAN) diet, high in fat, fructose, and cholesterol, for 34 weeks. In addition, a chow-fed group was included as a control. Upon disease induction, the mice were randomized into four treatment regimens: 1. vehicle (control), 2. Semaglutide, a long-acting GLP-1 (SC q.d.; 30 nmol/kg) 3. Zalfenmin, a long-acting FGF21 agonist (SC q.d.; 0, 24 mg/kg) or 4. diet intervention by reversal to chow feeding for two, eight, and sixteen weeks. Besides histological and serological assessment, flow cytometry and single-cell RNA sequencing (scRNA-seq) of hepatic tissue were performed.

Results: MASH phenotype (steatosis, inflammation, and fibrosis) was induced, and all treatments (chow reversal, Semaglutide and Zalfenmin) lowered body weight, plasma ALT, liver total cholesterol, and liver triglycerides. Zalfenmin lowered liver lipids more than Semaglutide in this model. Histological analyses indicate in the treatment groups a stop of fibrosis progression (PSR, Col1a1), a decrease in fibrosis activity (a-SMA), and reduction of myeloid staining (CD11b). To investigate disease progression and treatment MoA at a single-cell transcriptomic level, we generated a scRNA-seq dataset of more than 393200 hepatic cells. The dataset included data from more than 166800 myeloid cells and 74500 hepatocytes among other cell types. The data confirmed changes in myeloid cells upon MASH induction, as previously reported in literature. Furthermore, the data revealed that all treatments affected myeloid cell abundance and transcriptome. Noteworthy, longitudinal treatment with Zalfenmin increased abundance of macrophages to a larger degree compared to Semaglutide.

Conclusion: The data support changes in myeloid cells upon MASH disease development and suggest a role for myeloid cells in treatment MoA. The scRNA-seq data will in the future be expanded with single-nucleus RNA sequencing (snRNA-seq) of the same liver samples to support and validate our findings. Furthermore, future analysis will explore the translative value to human sc- and snRNA-seq datasets of MASH patients including clinical perturbations.

THU-230

Human embryonic stem cell-derived mesenchymal stem cells improve mitochondrial oxidative dysfunction in metabolic dysfunction-associated liver disease via the AMPK pathway

Min Kyung Park¹, Yun Bin Lee², Se-Mi Jung², Yoo-Wook Kwon³, Jung-Hwan Yoon². ¹Seoul National University Bundang Hospital, Department of Medicine, Seongnam-si, Gyeonggi-do, Korea, Rep. of South; ²Seoul National University College of Medicine, Department of Internal Medicine and Liver Research Institute, Seoul, Korea, Rep. of South; ³Seoul National University Hospital, Biomedical Research Institute, Seoul, Korea, Rep. of South
 Email: alsrud627@snu.ac.kr

Background and aims: Metabolic dysfunction-associated liver disease (MASLD) is one of the most common chronic liver diseases and is associated with a high disease burden. Nonetheless, there is no approved pharmacological treatment option for it. This study aimed to investigate the therapeutic potential of embryonic stem cell-derived mesenchymal stem cells (ESC-MSCs) for mitochondrial dysfunction and hepatic steatosis using cellular and mouse models of MASLD.

Method: HepG2 cells were treated with palmitic acid (PA) and then co-cultured with ESC-MSCs. C57BL/6 mice were chronically fed a choline-deficient, L-amino acid-defined, high-fat diet (CDAHFD) or normal diet for 24 weeks. At 20 weeks, ESC-MSCs or phosphate-buffered saline was injected into mice via the tail vein. Lipid accumulation was measured through oil red O staining in both cellular and animal models. Mitochondrial mass, reactive oxygen species (ROS), and the activity of antioxidant enzymes were measured to assess mitochondrial oxidative functions.

Results: In the cellular model, PA-induced intracellular lipid accumulation was attenuated by co-culture with ESC-MSCs. Functional mitochondrial mass was reduced by PA treatment and then recovered after co-culture with ESC-MSCs. Increased cellular ROS production mediated by PA treatment was attenuated after co-culture with ESC-MSCs. The activity of superoxide dismutase (SOD) and the ratio of reduced/oxidized glutathione were decreased after PA treatment and restored via co-culture with ESC-MSCs. The expression levels of phosphorylated AMP-activated protein kinase (AMPK) and peroxisome proliferator-activated receptor gamma coactivator-1 (PGC1α) were significantly increased following co-culture with ESC-MSCs. Severe hepatic steatosis was observed in the liver tissues of CDAHFD-fed mice, which ameliorated following the transplantation of ESC-MSCs. Decreased mitochondrial DNA content in the liver tissues of CDAHFD-fed mice was reinstated to near-control levels after the transplantation of ESC-MSCs. Augmented hepatic ROS accumulation caused by CDAHFD was attenuated after the transplantation of ESC-MSCs, with dynamic changes in the activity of SOD and the ratio of glutathione. Furthermore, the transplantation of ESC-MSCs into CDAHFD-fed mice significantly augmented the expression levels of phosphorylated AMPK and PGC1α in the liver tissues.

Conclusion: ESC-MSCs could ameliorate hepatic steatosis in cellular and animal models of MASLD by reducing ROS and restoring mitochondrial oxidative functions through activating the AMPK pathway. This study suggests the therapeutic potential of ESC-MSCs for MASLD.

THU-231

Combination of fatty acid synthase (FASN) inhibitor and thyroid hormone receptor beta (THRb) agonist, resmetirom, improved markers of NASH and cardiovascular health in LDL receptor knockout NASH mice

Wen-Wei Tsai¹, Eveline Gart², Martine C. Morrison², Geurt Stokman², Eduardo Martins¹, George Kembel¹, Marie O'Farrell¹. ¹Sagimet Biosciences, San Mateo, United States; ²TNO Metabolic Health Research, Leiden, Netherlands
 Email: wen-wei.tsai@sagimet.com

Background and aims: Increased *de novo* lipogenesis (DNL) drives the development of NASH and FASN is the key enzyme in the DNL pathway. FASN inhibition not only reduces liver fat but also acts directly on immune and hepatic stellate cells (HSCs) reducing inflammation and fibrosis. Denifanstat (TVB-2640), an oral FASN inhibitor, has demonstrated improvements in liver fat and biomarkers associated with inflammation and fibrosis in NASH trials. THRb agonists increase lipid oxidation which decreases liver fat and resmetirom recently demonstrated significant NASH resolution and fibrosis improvement in the phase 3 trial. We hypothesized that the

POSTER PRESENTATIONS

combination of FASN inhibitor and resmetirom may increase efficacy for NASH treatment based on complementary mechanisms of liver fat reduction and the direct anti-fibrotic effect of FASN inhibitor. This study was designed to evaluate FASN inhibitor alone and in combination with resmetirom on plasma biomarkers and liver histology in LDL receptor knockout (*Ldlr*^{-/-}) NASH mice. Denifanstat and resmetirom were also evaluated *in vitro* in HSCs for direct anti-fibrotic effects.

Method: Male *Ldlr*^{-/-} mice were fed with fast-food diet (FFD) for 18 weeks to induce NASH features and treated with either TVB-3664 (a surrogate FASN inhibitor for denifanstat, 5 mg/kg, PO, QD) or THRb agonist resmetirom (MGL-3196, 3 mg/kg, PO, QD) alone or in combination for 10 weeks. End points included liver enzymes, lipids and liver histology (pending). Primary human HSCs were stimulated by TGF- β 1 and treated with denifanstat or resmetirom at various concentrations.

Results: FFD feeding significantly increased plasma ALT/AST, total cholesterol and triglycerides in *Ldlr*^{-/-} mice. TVB-3664 or resmetirom alone rapidly reduced plasma ALT/AST, total cholesterol and triglycerides with 4 weeks treatment and these reductions were sustained until end of the study (10 weeks); importantly, combination of TVB-3664/resmetirom showed further additive improvements compared to either agent alone. Lipoprotein analysis showed that LDL-C and VLDL-C were highly induced by FFD and both were strongly reduced by TVB-3664 or resmetirom alone and further reduced by the combination. In primary human HSCs, TGF- β 1-stimulated collagen production and plasminogen activator inhibitor 1 secretion were decreased by denifanstat, but not resmetirom, in a dose-dependent manner.

Conclusion: Combination of FASN inhibitor and THRb agonist resmetirom showed further ALT/AST improvement and lipid lowering compared to either agent alone in a mouse model of dyslipidaemia and NASH. *In vitro*, denifanstat, but not resmetirom, directly reduced collagen production. These results suggest that complementary MOAs of denifanstat (DNL inhibition and direct anti-fibrotic effect) and resmetirom (lipid burning) combined could provide added benefit and support future clinical evaluation of this combination for NASH.

THU-232

Additive hepatoprotective effects of DA-1241, a novel GPR119 agonist, in combination with semaglutide in the GAN diet-induced obese and biopsy-confirmed mouse model of MASH

Monika Lewinska¹, Malte H. Nielsen², Susanne Pors³, Henrik B. Hansen³, Il Hoon Jung⁴, Hyung Heon Kim⁵, Michael Feigh³, Mi-Kyung Kim⁶. ¹Gubra A/S, Hørsholm; ²Gubra A/S, Hørsholm, Denmark; ³Gubra, Hørsholm, Denmark; ⁴Dong-A, Yongin-Si, Korea, Rep. of South; ⁵NeuroBo Pharmaceuticals Inc, Cambridge, United States; ⁶Dong-A ST Co., Ltd., Yongin-Si, Korea, Rep. of South
Email: mle@gubra.dk

Background and aims: The G protein-coupled receptor 119 (GPR119) and glucagon-like peptide-1 receptor (GLP1R) is promising therapeutic targets for metabolic dysfunction-associated steatohepatitis (MASH). The aim of this study was to evaluate the effects of DA-1241 (GPR119 agonist) and semaglutide (GLP-1R agonist) combination therapy in the GAN diet-induced obese and biopsy-confirmed mouse model of MASH with moderate-severe liver fibrosis.

Method: Male C57BL/6J mice were fed the GAN diet for 36 weeks before treatment initiation. Only biopsy-confirmed GAN DIO-MASH mice (steatosis score = 3, lobular inflammation score ≥ 2 , fibrosis stage F2-F3) were stratified to treatment (n = 14–15 per group). GAN DIO-MASH mice received once daily treatment with vehicle, DA-1241 (100 mg/kg, PO) or semaglutide (30 nmol/kg, SC) alone or in

combination for 8 weeks. Within-subject comparisons (pre vs. post treatment) were performed for liver biopsy histopathological NAFLD Activity Score (NAS) and Fibrosis Stage. Terminal quantitative end points included plasma/liver biochemistry, liver histomorphometry and RNA sequencing.

Results: DA-1241 was weight-neutral and did not influence liver weight. In contrast, semaglutide robustly reduced body weight by approx. 25% and improved hepatomegaly in GAN DIO-MASH mice with or without combination treatment. There was no additional weight loss in the combination group compared to semaglutide alone. Each monotherapy ameliorated plasma transaminases and liver cholesterol levels, with combination therapy providing further improvement compared to monotherapies. DA-1241 and semaglutide monotherapy each improved NAS (≥ 2 -point) in 21% of mice, whereas combination treatment led to marked improvements (≥ 2 -point in 80% of mice and ≥ 1 -point in all mice), driven by reduction in steatosis and lobular inflammation scores. Correspondingly, combination therapy synergistically promoted quantitative histology for steatosis (%-area of liver lipids, % lipid-laden hepatocytes) compared to monotherapies. While treatments did not significantly influence quantitative markers of fibrosis (PSR, Col1a1), DA-1241 and semaglutide monotherapy lowered α -SMA levels with further improvement in combination treatment, suggesting additive inhibitory effects on fibrogenesis.

Liver transcriptome analysis demonstrated a significant increase in the number of differential expressed genes (DEGs) with prominent signature changes in lipid metabolism, chemokine signaling, and fiber proteins following combination therapy compared to monotherapies.

Conclusion: DA-1241 and semaglutide demonstrate more than additive effects on metabolic, biochemical, and histological end points in GAN DIO-MASH mice, highlighting the therapeutic potential of dual targeting GPR119 and GLP1R function in MASH with liver fibrosis.

THU-233

External validation of machine learning model (MASML) adjusted for prevalence for determining the histologic severity of MASLD in a large cohort of patients with biopsy-proven disease

Naim Alkhouri¹, Joseph Rubinsztain², Karen Taub², Stephen A. Harrison³, Devon Y. Chang⁴, Mazen Nouredin⁵. ¹Arizona Liver Health, Chandler, AZ, United States; ²Pulsar Diagnostics, LLC, Sunrise, FL, United States; ³Pinnacle Clinical Research, Oxford University, San Antonio, TX, United States; ⁴Stanford University, Palo Alto, CA; ⁵Houston Research Institute, Houston, Texas, United States
Email: nalkhouri@azliver.com

Background and aims: Recently, a machine learning model to predict the severity of MASLD was developed using a balanced cohort from 3 tertiary hepatology centers in the U.S. The aim of this study was to 1) externally validate this model in an independent cohort of patients with biopsy-proven MASLD and high-prevalence of advanced disease, 2) compare its performance to FIB-4 and VCTE, and 3) determine the impact of disease prevalence in the model's performance.

Method: Consecutive patients who presented to tertiary hepatology clinics in the US between 2019–2023 were included. Participants were referred by their primary care doctor or gastroenterologist for consideration for clinical trials. VCTE was performed by experienced operators and the NASH CRN scoring system was used to assess histologic severity on liver biopsy. MASML was applied to a cohort of patients with 62.16% prevalence of significant fibrosis stages F2 through F4 (high prevalence cohort). The high-prevalence MASML was then applied to a patient population with the following fibrosis

prevalence: F0-F1: 58.72%, F2: 13.63%, F3: 14.4%, F4: 13.25% (balanced cohort). Descriptive statistics and diagnostic accuracy measures, such as false positive or negative rates, were used.

Results: 1068 patients with biopsy-proven MASLD and VCTE/laboratory tests within a 3-months period were included in this analysis. The median age was 54 years (IQR 17), median BMI was 37.6 kg/m² (IQR 8.09), 62.93% were female, 37.41% were diabetics. The median platelet count was 234 (IQR 75.06), median ALT 49 (IQR 34.49), median AST 42 (IQR 21.96) and median LSM on VCTE was 11.8 kPa (IQR 8). The high-prevalence MASML model had good accuracy for predicting significant fibrosis, advanced fibrosis, and cirrhosis with AUROC for the high-prevalence MASML versus FibroScan and FIB-4 for \geq F2, \geq F3, and F4 being (0.77 vs. 0.59, 0.61), (0.87 vs. 0.67, 0.61), and (0.82 vs. 0.76, 0.56), respectively (p value <0.01 for all). In external validation, the balanced-prevalence MASML model had good intrinsic performance for detecting significant fibrosis with AUROC of 0.88, sensitivity 0.78, specificity 0.82, PPV 0.76 and NPV 0.84.

Conclusion: The MASML model performed better than FIB-4 and VCTE in the high-prevalence patient cohorts. This model has the potential to be used in clinical trials to decrease the screen failure rate due to histology. The MASML model trained with a high-prevalence cohort performed well in the external validation balanced cohort. Additional testing should be performed to improve model performance for primary care, tertiary care and research patient cohorts.

THU-234

Development of a new mouse model combining rapid and robust MASH, liver fibrosis and atherosclerosis: time- and sex-dependent effects

Fanny Lalloyer¹, Eric Baugé¹, Doriane Henry¹, Bart Staels¹. ¹Univ. Lille, INSERM, CHU Lille, Institut Pasteur de Lille, U1011-EGID, Lille, France
Email: fanny.lalloyer@univ-lille.fr

Background and aims: Metabolic dysfunction-associated steatotic liver disease (MASLD) prevalence is the leading cause of chronic liver disease, affecting 2 out of 5 persons worldwide. MASLD patients are at increased risk for cardiovascular diseases. In MASLD patients, the expression of the nuclear receptor peroxisome proliferator-activated receptor- α (PPAR α) is decreased in the liver, suggesting an important role of PPAR α de-activation in MASLD development. In the current study, we developed a new genetic and diet-induced mouse model combining MASLD and atherosclerosis, and investigated the diet- and genetic-induced responses in addition to sex-dependent effects on both pathologies.

Method: Male and female low-density lipoprotein receptor knockout (LDLRKO) mice, deficient (LDLRKO PPAR α ko) or not (LDLRKO PPAR α WT) for PPAR α , were fed a chow or a high-fat (HF) diet during 12 and 18 weeks. Plasma biochemical markers of liver damage (alanine transaminase (ALT) and aspartate transaminase (AST)) were measured. Histological analysis of metabolic dysfunction-associated steatohepatitis (MASH) and fibrosis development was performed in the liver. Atherosclerosis development was quantified in the aortic sinus.

Results: Plasma ALT and AST levels significantly increased in all LDLRKO mice at 12 and 18 weeks of HF diet, with higher levels in both male and female PPAR α ko compared to PPAR α WT mice. At the histological level, LDLRKO mice develop all the characteristics of human MASLD, ie liver steatosis, inflammation and ballooning, as well as liver fibrosis. Interestingly, compared to PPAR α WT mice, PPAR α deficiency aggravated MASLD progression overtime with higher MASH development and liver fibrosis in both male and female PPAR α ko mice. Interestingly, whereas male LDLRKO PPAR α ko mice developed more rapidly MASH (at 12 weeks of HF diet, presence of MASH in 100% of male LDLRKO PPAR α ko), female LDLRKO PPAR α ko mice exhibited the more liver fibrosis at

12 and 18 weeks of HF diet, and developed more pronounced atherosclerosis at 18 weeks, compared to male mice or PPAR α WT mice.

Conclusion: Our new mouse model highlights the importance of PPAR α down-regulation as a key factor in MASH development, liver fibrosis and atherosclerosis, with sex-specific differences in pathological phenotypes. Given the development of robust and progressive MASLD with all histological characteristics of the human disease in a relatively short period of time (12 to 18 weeks), this model will enable to test new drugs for the treatment of MASH and liver fibrosis and their impact on cardiovascular function.

THU-235

Bridging hepatic pathologies: protein expression dynamics in metabolic dysfunction-associated liver disease (MASLD), benign liver tumours and hepatocellular carcinoma

Saima Ajaz¹, Kosh Agarwal¹. ¹King's College Hospital, London, United Kingdom

Email: saima.ajaz@nhs.net

Background and aims: Liver diseases, ranging from benign tumors and metabolic dysfunction-associated steatotic liver disease (MASLD) to hepatocellular carcinoma (HCC), present diverse molecular complexities. This study aims to thoroughly investigate the proteome of liver tissues and blood samples from patients with MASLD, benign liver tumors, and HCC, focusing on mitochondrial, metabolic, and liver disease proteins. Understanding these molecular details is vital for enhancing liver disease diagnosis and treatment, especially given the global variations in severity and etiology.

Method: This cross-sectional study included subjects divided into four groups: Group 1 (Healthy controls, n = 20), Group 2 (Patients with mild liver fibrosis, n = 40), Group 3 (Patients with moderate to advanced liver fibrosis, n = 40), and Group 4 (Patients with diagnosed HCC, n = 30). Liver tissue was collected from subjects with MASLD, HCC, and benign liver tumors. Proteins were extracted for liquid chromatography-mass spectrometry (LC-MS) analysis from a subset of these groups. Additionally, mitochondrial function was assessed using the Seahorse XFp analyzer.

Results: A total of 3417 proteins were analyzed in the HCC samples and corresponding normal tissue samples. 125 proteins showed significant variation (p < 0.001) with the 10 most significant proteins related to mitochondria. Key findings include the lower expression of Fat Acid Synthase (FASN) in HCC samples compared to controls, indicating a limitation in HCC-induced lipid synthesis pathways. Guanine Nucleotide-Binding Protein Subunit Beta-4 (GNB4) was highly expressed in HCC tissues. Albumin, a marker of liver function, was consistent in controls but decreased in HCC samples. Glutamate Dehydrogenase 1 (GDH1) and Carbamoyl Phosphate Synthetase I (CPS1) also showed notable expression patterns, indicating changes in energy metabolism pathways. Mitochondrial functional studies showed significantly reduced maximal respiration in HCC (275 pmol/min) versus HC (327 pmol/min). Substrate reliance test showed decrease in maximal respiration (500 pmol/min versus 380 pmol/min) on blocking glucose in HCC samples highlighting dependence on glucose utilisation in these samples.

Conclusion: This study highlights the intricate protein expression profiles associated with liver diseases, particularly in mitochondrial and metabolic functions. The predominance of carbohydrate-metabolizing proteins in HCC is notable. Cancer is characterized by increased glycolysis, known as the Warburg effect. These proteins imply HCC cells may use glucose differently. By speeding up energy production and biosynthesis, glycolysis can help cancer cells thrive. Understanding HCC's metabolic adaptations, especially glucose metabolism regulation, is essential for creating targeted therapeutics that exploit these vulnerabilities.

POSTER PRESENTATIONS

THU-236-YI

Oxysterol treatment causes indirect stellate cell activation: a potential mechanism linking steroid metabolising enzyme dysregulation with fibrosis

Hamish Miller^{1,2}, Patricia Garrido¹, Wenhao Li³, Raju Kumar¹, Iris Gines⁴, Nikolaos Nikolaou⁵, Tom Potter^{2,6}, Maíra Bailey^{2,6}, Fredrik Karpe², Matthew Neville², Márta Korbonits⁷, William Griffiths⁸, Yuqin Wang⁸, William Alazawi¹, Jeremy Tomlinson². ¹Barts Liver Centre, Blizard Institute, Queen Mary University of London, London, United Kingdom; ²Oxford Centre for Diabetes, Endocrinology and Metabolism, University of Oxford, Oxford, United Kingdom; ³Blizard Institute, Queen Mary University of London, Immunobiology, London, United Kingdom; ⁴Department of Biochemistry and Biotechnology, Universitat Rovira, Tarragona, Spain; ⁵Definigen Ltd, Babraham Research Campus, Cambridge, United Kingdom; ⁶Department of Biological and Medical Sciences, Oxford Brookes University, Oxford, United Kingdom; ⁷Centre for Endocrinology, William Harvey Research Institute, Barts and the London School of Medicine and Dentistry, Queen Mary University of London, London, United Kingdom; ⁸Swansea University Medical School, Swansea, United Kingdom
Email: hamish.miller@nhs.net

Background and aims: Metabolic dysfunction-associated steatotic liver disease (MASLD) is the hepatic manifestation of the metabolic syndrome and affects 30% of the population worldwide. Steroid metabolising enzymes activity and expression become dysregulated as MASLD progresses and advanced liver fibrosis has a specific urinary steroid metabolite signature. As a specific example, aldo-keto reductase family 1 member D1 (AKR1D1) is downregulated as liver fibrosis progresses, leading to the accumulation of an oxysterol substrate, 7- α -hydroxy-3-oxo-4-cholestenic acid (7-HOCA). Here we hypothesise that 7-HOCA itself contributes to fibrosis through stellate cell activation in vitro, as measured by expression of collagen type 1 α 1 (COL1A1).

Method: Hepatocyte-like cells (HepG2) were treated with fatty acids (oleic acid 1000 micromolar and palmitic acid 500 micromolar, 24 hours) and steroid metabolising enzyme mRNA expression was quantified using qPCR. HepG2 cells were treated with 7-HOCA (25 micromolar, 24 hours) and RNA-Seq analysis performed. Stellate-like cells (LX-2) were treated with 7-HOCA directly or with conditioned media from 7-HOCA-treated HepG2 cells and activation was measured using qPCR for COL1A1. 7-HOCA levels were measured using mass-spectrometry based platforms in serum samples from patients with MASLD cirrhosis (and matched controls) (n = 20) and in a large cohort of patients (n = 2251) who had undergone detailed metabolic phenotyping including body composition analysis with dual energy x-ray absorptiometry.

Results: Using in vitro models, fatty acid treatment downregulated AKR1D1 by 40% (p = 0.005). We have previously shown that AKR1D1 genetic knock down leads to 7-HOCA accumulation. Analysis of RNA-Seq data from 7-HOCA-treated HepG2 cells compared to untreated control cells showed that TGF- β regulation of extracellular matrix was the most upregulated pathway (p = 3×10^{-6}). We therefore investigated the effect of 7-HOCA on stellate cell activation. 7-HOCA did not cause direct activation of LX-2 cells. However, when the media from 7-HOCA-treated HepG2 cells was added to LX-2 cells, we observed a 25% upregulation of COL1A1 when compared to control treated cells, consistent with stellate cell activation. Consistent with these observations, 7-HOCA levels were elevated in patients with cirrhosis (p = 0.0024) and correlated positively with BMI (r = 0.1584, p < 0.0001) and with central adiposity (r = 0.2179, p < 0.0001).

Conclusion: Fatty acid treatment leads to down regulation of AKR1D1 with the consequent potential for 7-HOCA accumulation. 7-HOCA is elevated in patients with metabolic disease, and indirectly (via its action on hepatocytes) activates stellate cells to drive a pro-fibrotic phenotype in the liver. These data underscore the novel finding of a significant association between dysregulation of AKR1D1 and the progression of fibrosis in MASLD.

THU-238

Peripheral natural cytotoxic cells are associated with development of non-alcoholic liver fatty disease (NAFLD) in children

Małgorzata Wiese¹, Aldona Wierzbicka², Lidia Gackowska¹, Wojciech Janczyk², Zbigniew Kułaga², Jacek Michalkiewicz², Piotr Socha². ¹Nicolaus Copernicus University Collegium Medicum, Bydgoszcz, Poland; ²The Children's Memorial Health Institute, Warszawa, Poland
Email: mwiese@cm.umk.pl

Background and aims: NAFLD is characterized by chronic, low grade systemic inflammation and changes in distribution of different peripheral immune cell subsets play a role in the development of NAFLD in experimental models and in adults. The aim of the study was to establish which types of lymphocytes are associated with early stages on NAFLD development (as observed in children).

Method: We recruited 45 obese children with NAFLD (diagnosis based on Fibroscan CAP value >250 suggestive of liver steatosis in general pediatric population- Ferraioli G, BioMed Central 2017) aged 15 \pm 1.45 years and 30 aged matched controls. Using multicolor flow cytometry the frequency of the whole blood lymphocyte subsets were assessed including, CD4+, Th1 (CCR6-/CCR4-/CXCR3+), Th2 (CCR6-/CCR4+/CXCR3-), TH17 (CCR6+/CCR4+/CXCR3-), Th17.1 (CCR6-/CCR4-/CXCR3+), CD8+ and CD8+ with granzyme B, perforin or CD161 expression, mucosal associated invariant CD8+ T cells (MAIT) and NK, iNKT, NKT (with or without granzyme B and perforin expression).

Results: NAFLD children compared to controls presented with a) increase in frequency of memory CD45RO bearing CD4+ T cells (45 \pm 14% vs 36 \pm 6%, p = 0.03), b) elevation of granzyme B or perforin expressing NK cells (68 \pm 21% vs 49 \pm 26%, p = 0.02, and 75 \pm 23% vs 57 \pm 30%, p = 0.02, respectively), c) increase in proportion of CD8+/CD161int + T cells (9 \pm 3% vs 7 \pm 3%, p = 0.02), d) decrease of frequency of CD8+/CD161 (-) T cells (82 \pm 8% vs 87 \pm 5%, p = 0.02). The following correlations with clinical parameters were obtained: 1) CAP vs % perforin expressing CD8+ T cells (r = 0.287, p = 0.021) and CAP vs granzyme B (r = 0.291, p = 0.019,) and perforin (r = 0.294, p = 0.018) expressing NK cells, 2) ALT vs granzyme B (r = 0.392, p = 0.013) and perforin (r = 0.308, p = 0.014,) expressing NK cells, 3) GGTP vs perforin bearing iNKT cells (r = 0.278, p = 0.034), 4) TG vs granzyme B expressing NK cells (r = 0.326, p = 0.008), 5) glucose levels vs NKT (r = 0.857, p = 0.013) and vs granzyme (r = 0.787, p = 0.03,) or perforin (p = 0.787, p = 0.03,) bearing NKT cells, 6) HDL-C levels vs granzyme B bearing NK cells (r = 0.342, p = 0.006), 7) insulin levels vs TH1/TH2 cells (r = 0.557, p = 0.010), 8) RWT vs TH1/TH2 (r = 0.262, p = 0.039) and iNKT (p = 0.293, 0.029), 8) IMTR vs iNKT (r = 0.239, p = 0.007), 9) c IMT vs % of iNKT (p = 0.01, r = 0.314).

Conclusion: Proportions of peripheral, natural cytotoxic cells including NK and iNKT expressing granzyme B or perforin may be predictors of NAFLD progress and metabolic disturbances of obesity in early stages of this condition in the pediatric patients. At this stage of NAFLD development innate immunity seems to play a major role. Supported from the National Science Center grant UMO-2018/31/B/NZ5/02735.

THU-239-YI

Metabolic dysfunction-associated steatotic liver disease (MASLD) modeling with hepatocyte-like cells derived from adult liver stem cells via air-liquid interface

Soe Einsy Lynn^{1,2}, Jian Hui Low¹, Yee Siang Lim¹, Chwee Tat Koe¹, Tiffany Woo¹, Junyu Zhao¹, Ganakirathan Kalpenath Rajah¹, Wee Jug Teow¹, Royston Kwok¹, Cheng Peow Bobby Tan¹, Lai Ping Yaw¹, Torsten Wuestefeld¹, Mei Chin Lee¹, Huck Hui Ng^{2,3}. ¹Genome Institute of Singapore, Singapore, Singapore; ²National University of Singapore, Singapore, Singapore; ³Agency for Science, Technology and Research, Genome Institute of Singapore, Singapore, Singapore
Email: e0744034@u.nus.edu

Background and aims: Metabolic dysfunction-associated steatotic liver disease (MASLD) is the most common liver disease worldwide estimated to affect about 38% of the world's population and is the leading cause of liver-related mortality. Therefore, the development of non-invasive diagnosis methods and novel treatments is of priority to manage the disease. To create a robust MASLD target identification and validation system, our laboratory aims to develop an *in vitro* hepatocyte-like cell model that can faithfully recapitulate the disease.

Method: Our laboratory has developed a reproducible method to isolate self-renewable adult liver stem cells (LSC) from donor tissues. Isolated LSC can be differentiated into hepatocyte-like cells (HLC) when cultured via the air-liquid interface (ALI) under defined media culture conditions. The HLC were treated with free fatty acid (FFA) to induce steatosis condition and metabolic dysfunction-associated steatohepatitis (MASH) -inducing compounds to induce MASH-like phenotype. Subsequently, these treated cells were exposed to drugs such as diacylglycerol acyltransferase (DGAT) and acetyl-CoA carboxylase (ACC) inhibitors for observation of drug response.

Results: Differentiated HLCs were validated to express hepatocyte markers and displayed hepatic functionality *in vitro*. Transcriptomic profiling of HLC reveals hepatocyte-specific gene signatures similar to primary human hepatocytes (PHH). FFA-treated HLCs are found to be responsive to drug treatments with DGAT and ACC inhibitors treatment.

Conclusion: Isolated LSC are renewable sources of cells that can generate HLC upon differentiation via ALI under defined media culture conditions. Differentiated HLCs are functionally and transcriptionally similar to primary human hepatocytes, indicating their likeness to hepatic cells. The drug-treated HLC successfully demonstrated the reversal of steatosis, suggesting these cells as reliable cell resources for MASLD modeling.

THU-242

Comparison of machine learning model (MASML), VCTE, and FIB-4 scores for predicting the presence of MASLD in a large cohort of patients in the U.S. using the NHANES database

Mazen Nouredin¹, Joseph Rubinsztain², Karen Taub³, Devon Y. Chang⁴, Stephen A. Harrison⁵, Naim Alkhouri⁶. ¹Houston Research Institute, Houston, TX, United States; ²ChronWell, Inc., Pulsar Diagnostics, LLC, Sunrise, United States; ³Pulsar Diagnostics, LLC, Sunrise, United States; ⁴Stanford University, Palo Alto, CA, United States; ⁵Pinnacle Clinical Research, Oxford University, San Antonio, TX, United States; ⁶Arizona Liver Health, Chandler, AZ, United States
Email: mnh86@hotmail.com

Background and aims: Recently, a machine learning model to predict the severity of MASLD was developed using a cohort from 3 tertiary hepatology centers in the U.S. with a balanced learning set for fibrosis stages F0 through F4. The aim of this study was to compare the performance of this model to FIB-4, and VCTE in a large cohort of patients in the NHANES database from 2018–2020.

Method: Patients stored in the NHANES US database between 2018–2020 that included age, gender and BMI and laboratory values for platelets, AST, ALT and HgA1C + VCTE were included. Those with excessive alcohol consumption or viral hepatitis were excluded. FAST and Agile 3+ scores were applied as the gold standard (given the lack of liver biopsy data) to determine indeterminate and high probability of at-risk MASH and fibrosis stage 3 or higher, respectively. Descriptive statistics and diagnostic accuracy measures, such as false positive or negative rates, were used.

Results: 5,130 patients with sufficient values were included in this analysis. The median age was 52 (IQR 31), median BMI was 27.8 (IQR: 7.95) kg/m², 51.91% were female, 12.01% were diabetics. The median platelet count was 236 (IQR: 79.75), median ALT 18 (IQR: 12), median AST 19 (IQR: 8) and CAP on VCTE was 158 db/M (IQR: 96), median LSM was 4.8 kPa (IQR: 2.3).

7.39% of patients were predicted to have at-risk MASH (MASH with F2–F4) using FAST and 9.02% of patients were predicted to have

fibrosis stage 3 or higher using the Agile 3+ score. The MASML model had good accuracy for predicting at-risk MASH based on the FAST score (AUROC of 0.72) and advanced fibrosis based on AGILE3+ (AUROC of 0.76). Surprisingly, both VCTE and FIB-4 demonstrated low AUROC for advanced fibrosis (0.55 and 0.63 respectively) using AGILE3+ as the gold standard. All models demonstrated a high NPV for advanced fibrosis (>90%), but only FIB-4 demonstrated a moderate PPV (0.69).

Conclusion: MASML outperformed VCTE and FIB4 in predicting at-risk MASH and advanced fibrosis in a representative U.S. cohort with low prevalence of advanced MASLD. MASML relies on readily available clinical and laboratory characteristics avoiding the need for expensive VCTE machines which may facilitate large scale screening at the general population level.

THU-243

Macrophage driven fibrosis resolution assessed by a cross-linked and MMP degraded type III collagen fragment (CTX-III) declines with age and is prognostic for survival in chronic liver disease

Alejandro Mayorca Guiliani¹, Peder Frederiksen², Emilie Skovgaard², Ida Lønsmann², Morten Karsdal³, Flemming Bendtsen⁴, Julie Steen Pedersen⁵, Jonel Trebicka⁶, Diana Leeming². ¹Nordic Bioscience, Herlev, Denmark; ²Nordic Bioscience A/S, Herlev, Denmark; ³Nordic Bioscience A/S, Herlev; ⁴University Hospital, Hvidovre, Hvidovre, Denmark; ⁵Copenhagen University Hospital Hvidovre, Hvidovre, Denmark; ⁶Universitätsklinikum Münster (UKM), Muenster, Germany
Email: amg@nordicbio.com

Background and aims: A wave of unsuccessful antifibrotic drugs for chronic liver disease has created an urgent need for biomarkers to understand the pharmacodynamic effects on fibrogenesis and fibrolysis. Here, we describe how CTX-III, a crosslinked and matrix metalloproteinase-degraded fragment of collagen type III, works as a systemic biomarker of ECM degradation and fibrosis resolution.

Method: An automated platform (IDS-i10, UK) quantifies CTX-III using a sandwich ELISA. First, we detected CTX-III in healthy (n = 1) and fibrotic (F2–3; n = 5) human livers. We then modeled CTX-III production *in vitro*, culturing hepatic stellate cells to generate an ECM and then culturing macrophages (MAC) on this matrix, measuring CTX-III in conditioned medium before and after 8 days of MAC culturing. Furthermore, we established the CTX-III healthy reference in persons of different age groups: 19–29 yrs (n = 23), 30–39 yrs (n = 22), 40–49 yrs (n = 12) and 50–59 yrs (n = 10), as well as in a cohort of MAFLD patients undergoing bariatric surgery (n = 70), and in cirrhotic patients with transjugular intrahepatic portosystemic shunts (TIPS) (n = 86) along with the N-terminal pro-peptide of collagen type III (PRO-C3, a biomarker of fibrogenesis).

Results: CTX-III could be extracted from human fibrotic livers. Non polarized MAC 0 (M0) produced MMPs and generated CTX-III, thus degrading the HSC-produced matrix. CTX-III in serum of healthy adults (median 14.49 ng/ml) CTX-II decreased with age (18.64 ng/ml in 19–29 y.o, 13.6, 10.48 and 8.215 ng/ml in subsequent decades- non sig.) In cirrhotic patients, CTX-III further decreased to a median of 2.5 ng/ml. In bariatric surgery CTX-III begins at a median of 4.91 ng/ml prior to surgery, 4.934 ng/ml after 3 months, 4.730 ng/ml after 6 months and 5.21 after 12 months. CTX-III and PRO-C3 in TIPS patients revealed that patients with high CTX-III and low PRO-C3 survive a significantly longer time than vice versa (p = 0.0348).

Conclusion: CTX-III was detected in human fibrosis tissue. *In vitro* experiments suggest that CTX-III may be the result of immune-mediated degradation and released by macrophages. In healthy humans, CTX-III decreases with age, and decreases even further during diseases such as MAFLD and cirrhosis. This potentially suggests that the ability to degrade crosslinked collagen type III is characteristic of homeostasis and youth. Progressing (MAFLD) and terminal (cirrhosis) fibrosis depress CTX-III production, pointing to impaired ECM degradation as a factor in fibrosis progression along with ECM deposition. This imbalance may be associated with a

POSTER PRESENTATIONS

defective immune response. A combination of CTX-III and PRO-C3 could become a biomarker of healthy ECM balance, fibrosis resolution and prognosis in liver fibrosis.

THU-244

Synergistic hepatoprotective effects of semaglutide and resmetirom combination therapy in the GAN diet-induced obese and biopsy-confirmed mouse model of MASH

Kristoffer Voldum-Clausen¹, Jenny Egecioglu Norlin², Sanne Skovgård Veidal², Denise Oró¹, Line Nilsson¹, Henrik B. Hansen³, Michael Feigh⁴. ¹Gubra A/S, Hørsholm, Denmark; ²Novo Nordisk, Måløv, Denmark; ³Gubra A/S, Hørsholm, Denmark; ⁴Gubra A/S, Hørsholm, Denmark
Email: kvc@gubra.dk

Background and aims: Semaglutide (glucagon-like receptor-1 (GLP-1R) agonist) and resmetirom (THR- β receptor agonist) are both in late-stage clinical development for treatment of metabolic dysfunction-associated steatohepatitis (MASH). The present study aimed to compare metabolic, biochemical, and histological effects of semaglutide and resmetirom as mono- and combination treatment in a translational GAN diet-induced obese and biopsy-confirmed mouse model of MASH with liver fibrosis.

Method: C57BL/6J mice were fed the GAN diet high in saturated fat, fructose, and cholesterol for 38 weeks before treatment start. Only animals with biopsy-confirmed MASH (NAFLD Activity Score, NAS \geq 5) and moderate fibrosis (stage \geq F2) were included and stratified into treatment groups. GAN DIO-MASH mice (n=17–18 per group) received vehicle (SC), semaglutide (30 nmol/kg, SC), resmetirom (3 mg/kg, PO) or resmetirom (3 mg/kg, PO) + semaglutide (30 nmol/kg, SC) once daily for 12 weeks. Vehicle-dosed (SC) chow-fed controls (n=10) served as healthy controls. Within-subject comparisons (pre- vs. post-treatment) were performed for NAS and fibrosis stage. Terminal quantitative end points included plasma/liver biochemistry and quantitative liver histology.

Results: While resmetirom was weight-neutral, semaglutide significantly reduced body weight (28%) and combination treatment led to further weight loss (37%) in GAN DIO-MASH mice. Both monotherapies and combination treatment reduced plasma transaminases and plasma/liver markers of inflammation (MCP-1) and fibrogenesis (TIMP-1). Combination treatment improved hepatomegaly and liver lipid levels greater than individual monotherapies. NAS (pre-post) was significantly improved by semaglutide (\geq 2-point, 28% of mice) and resmetirom (\geq 2-point, 17% of mice) and combination treatment led to synergistic reductions in NAS (\geq 2-point, 71% of mice) largely driven by improved steatosis scores, being further supported by quantitative histology. Only semaglutide significantly reduced quantitative histological markers of inflammation (galectin-3) and fibrogenesis (α -SMA). Treatments did not improve fibrosis stage and quantitative histological markers of fibrosis (PSR, Col1a1).

Conclusion: Both semaglutide and resmetirom improve biochemical and histological hallmarks of MASH in GAN DIO-MASH mice. Further therapeutic benefits are achieved by combination treatment, demonstrating the feasibility of combined stimulation of GLP-1R and THR- β receptor function to improve outcomes in MASH.

THU-245

Assessing the diagnostic accuracy of ChatGPT-4 in the histopathological evaluation of liver fibrosis in metabolic dysfunction-associated steatotic liver disease (MASLD)

Reha Akpınar^{1,2}, Thiyaphat Laohawetwanit^{2,3}, Davide Panzeri⁴, Camilla De Carlo^{1,2}, Vincenzo Belsito¹, Luigi Terracciano^{1,2}, Alessio Aghemo^{2,5}, Nicola Pugliese^{2,5}, Julien Calderaro⁶, Laura Sironi⁴, Luca Di Tommaso^{2,7}. ¹Department of Pathology, IRCCS Humanitas Research Hospital, Milan, Italy; ²Department of Biomedical Sciences, Humanitas University, Milan, Italy; ³Division of Pathology, Chulabhorn International College of Medicine, Thammasat University, Pathum Thani, Thailand; ⁴Department of Physics, University of Milano Bicocca, Milan,

Italy; ⁵Division of Internal Medicine and Hepatology, Department of Gastroenterology, IRCCS Humanitas Research Hospital, Milan, Italy; ⁶Université Paris Est Créteil, INSERM, IMRB, Créteil, France; ⁷Department of Pathology, IRCCS Humanitas Research Hospital, Department of Biomedical Sciences, Humanitas University, Milan, Italy
Email: drrehaakpinar@gmail.com

Background and aims: Data on ChatGPT's ability to evaluate liver fibrosis histopathology is limited. This study aims to assess ChatGPT-4's diagnostic accuracy in evaluating liver fibrosis in metabolic dysfunction-associated steatohepatitis (MASH) by comparing its performance to that of pathologists.

Method: A total of 59 consecutive MASH tissue specimens using Sirius red-stained slides were digitized and evaluated by ChatGPT-4 and four pathologists using the NAS CNR system. The process included converting whole slide images (WSIs) to a compatible format for ChatGPT-4, employing various magnifications, and extracting random fields of view. The diagnostic accuracy of ChatGPT-4 was compared with pathologists' evaluations, complemented by a collagen proportionate area (CPA) quantification for additional insight.

Results: On selected by pathologist images, ChatGPT-4 demonstrated an overall diagnostic accuracy of 81%. Its accuracy dropped to 63% when using randomly cropped images. ChatGPT-4 performed comparably to a liver pathologist on F1, F2 and F3 stages. However, ChatGPT's diagnostic accuracy for F4 (40%) was lower than that of every pathologist. The study also found a moderate to strong correlation between ChatGPT's fibrosis staging and a quantitative evaluation of collagen in the liver biopsy.

Conclusion: ChatGPT can be used to stage liver fibrosis in MASH, if diagnostic areas are selected by expert pathologists. However, even with selected images, F4 stage accuracy is low: a finding suggesting the impossibility of prefiguring the presence of nodules if they are not clearly present in the biopsy. On the other hand, ChatGPT seems to recognize different nuances of fibrosis progression.

THU-247-YI

Multi-tissue profiling of oxylipins reveal a conserved up-regulation of epoxide: diol ratio that associates with white adipose tissue inflammation and liver steatosis in obesity

Charlotte Hateley¹, Antoni Olona², Laura Halliday¹, Matthew Edin³, Jeong-Hun Ko¹, Roberta Forlano¹, Ximena Terra⁴, Fred Lih³, Raul Beltran-Debon⁵, Pinelopi Manousou¹, Sanjay Purkayastha⁶, Krishna Moorthy¹, Mark R Thursz¹, Guodong Zhang⁷, Robert D. Goldin¹, Darryl Zeldin³, Enrico Petretto⁸, Jacques Behmoaras². ¹Imperial College London, London, United Kingdom; ²Duke-NUS Medical School, Singapore, Singapore; ³NIEHS/NIH, North Carolina, United States; ⁴Universitat Rovira i Virgili, Tarragona, United Kingdom; ⁵Universitat Rovira i Virgili, Tarragona, Spain; ⁶Imperial College London NHS, London, United Kingdom; ⁷College of Agriculture and Environmental Sciences, Davis, United Kingdom; ⁸Duke-NUS Medical School, Institute for Big Data and Artificial Intelligence in Medicine, Singapore, Singapore
Email: c.hateley@ic.ac.uk

Background and aims: Obesity drives maladaptive changes in the white adipose tissue (WAT) which can progressively cause insulin resistance, type 2 diabetes mellitus (T2DM) and metabolic dysfunction associated liver disease (MASLD). Obesity-mediated loss of WAT homeostasis can trigger liver steatosis through dysregulated lipid pathways such as those related to polyunsaturated fatty acid (PUFA)-derived oxylipins. However, the exact relationship between oxylipins and liver steatosis remain elusive and cross-tissue dynamics of oxylipins remains ill-defined.

Method: We quantified PUFA-related oxylipin species in the omental WAT, liver biopsies and plasma of 88 patients undergoing bariatric surgery and 9 patients undergoing upper gastrointestinal surgery, using UPLC-MS/MS. We integrated oxylipin abundance with WAT phenotypes (adipogenesis, adipocyte hypertrophy, macrophage

infiltration, type I and VI collagen remodelling) and the severity of MASLD (steatosis, ballooning, inflammation, fibrosis) quantified in each biopsy. The integrative analysis was subjected to (i) adjustment for known risk factors and, (ii) control for potential drug-effects through UPLC-MS/MS analysis of metformin-treated fat explants *ex vivo*.

Results: We reveal a generalized down-regulation of cytochrome P450 (CYP)-derived diols during obesity conserved between the WAT and plasma. Notably, epoxide:diol ratio, indicative of soluble epoxide hydrolyse (sEH) activity, increases with WAT inflammation/fibrosis, hepatic steatosis and T2DM. Increased 12, 13-EpOME:DiHOME in WAT and liver is a marker of worsening metabolic syndrome in patients with obesity.

Conclusion: These findings suggest a dampened sEH activity and a possible role of fatty acid diols during hepatic steatosis and T2DM. They also have implications in view of the clinical trials based on sEH inhibition for metabolic syndrome.

THU-248

Unraveling the interplay of FGF21 and GLP1 analogue in metabolic dysfunction-associated steatohepatitis in vivo

Anouk Oldenburger¹, Birgitte Björkenberg¹, Henning Hvid², Matthew Gillum¹, Dominik Pfister³, Sanne Skovgård Veidal¹, Birgitte Andersen³. ¹Obesity and Liver Pharmacology, Novo Nordisk A/S, Måløv, Denmark; ²Pathology and Imaging, Novo Nordisk A/S, Måløv, Denmark; ³Liver Biology, Novo Nordisk A/S, Måløv, Denmark
Email: auog@novonordisk.com

Background and aims: FGF21 and GLP-1 are under clinical investigation for the treatment of metabolic dysfunction-associated steatohepatitis (MASH). Both FGF21 and GLP-1 analogues have been shown to resolve MASH and prevent fibrosis. Mice lacking FGF21 (FGF21 knockout mice) has been shown to accelerate metabolic induced liver injury in mice and the use of FGF21 KO mouse model presents an opportunity to investigate whether the beneficial effects of a GLP1 analogue on body weight (BW) and MASH parameters are dependent on FGF21 signaling.

Method: Male wildtype (WT) and FGF21 KO were fed chow (Altromin 1324) or choline deficient high fat diet (CDHFD) (Research Diets, A16092003) for 6 weeks. After 6 weeks on CDHFD, the mice were treated with vehicle or a long acting GLP1 analogue (NNC'2220, s.c., q. d., 5 nmol/kg) for an additional 6 weeks (n = 15). Body weight (BW) was recorded during the study and terminal plasma (TG and FFA) and liver were collected. MASH-related (HE, CD45, CD11b, αSMA and PSR staining) parameters were accessed by histology.

Results: The CDHFD did not affect BW in wild type mice nor the FGF21 KO mice but induced a MASH phenotype in both WT and FGF21 KO mice. No difference in inflammation was seen between genotypes while the FGF21 KO mice have significantly more stellate cell activation measured by αSMA staining. Oppositely, liver fibrosis was comparable between WT and FGF21 KO mice. The long acting GLP1 analogue NNC'2220 induced a 18% body weight loss in wild type CDHFD fed mice while the body weight loss was significantly blunted in the FGF21 KO CDHFD fed mice. GLP-1 treatment did not reduce hepatic steatosis in the CDHFD fed mice, while an increase in steatosis was observed in GLP-1 treated FGF21 KO mice. The GLP1 analogue showed a reduction in liver CD45 levels in both WT and FGF21 KO mice. Hence, FGF21 is not required for the inhibitory effect of GLP1 on the abundance of CD45. Furthermore, GLP1 showed a trend towards reduced CD11b, a marker for monocyte recruitment in WT but not in FGF21 KO mice. In terms of fibrotic markers, no significant effect of GLP-1 was observed of PSR staining in neither WT nor FGF21 KO mice and no reduction in αSMA was observed in response to GLP-1 treatment WT nor FGF21 KO mice.

Conclusion: In this study no major difference in MASH parameters induced by CDAHFD diet were observed between WT and FGF21 KO mice. However, a significant increase in αSMA in the FGF21 KO mice was observed. In this model the GLP-1-induced BW loss and the GLP-

1 induced decrease in CD11b recruitment were blunted in the FGF21 KO mice. In conclusion, the use of FGF21 KO mouse model showed that markers like BW and potentially CD11b are affected by GLP-1 via FGF21.

THU-249

The role of the ferroptosis brake glutathione peroxidase 4 in a preclinical model of metabolic dysfunction-associated steatohepatitis

Cédric Peleman^{1,2}, Geraldine Veeckmans^{3,4,5}, Behrouz Hassannia^{3,4,5}, Lieve Vits^{1,2}, Emily Van San^{3,4,5}, Joris De Man^{1,2}, Annelies Van Eyck^{1,2}, Wilhelmus J. Kwanten^{1,2}, Luisa Vonghia^{1,2}, Ann Driessen⁶, Benedicte De Winter^{1,2}, Christophe Van Steenkiste^{1,2}, Sven Francque^{1,2}, Tom Vanden Berghe^{3,4,5}. ¹Laboratory of Experimental Medicine and Pediatrics, Infla-Med Centre of Excellence, University of Antwerp, Antwerp, Belgium; ²Department of Gastroenterology and Hepatology, Antwerp University Hospital, Antwerp, Belgium; ³Laboratory of Pathophysiology, University of Antwerp, Antwerp, Belgium; ⁴Department of Biomedical Molecular Biology, Ghent University, Ghent, Belgium; ⁵VIB-UGent Center for Inflammation Research, Ghent, Belgium; ⁶Department of Pathology, Antwerp University Hospital, Antwerp, Belgium
Email: cedric.peleman@uantwerpen.be

Background and aims: Evidence is accumulating for a recently discovered type of cell death in metabolic dysfunction-associated steatohepatitis (MASH), i.e. ferroptosis. This cell death occurs when uncontrolled peroxidation of polyunsaturated fatty acids overrides physiologic ferroptosis defenses. One prominent ferroptosis brake is glutathione peroxidase 4 (GPX4) which uses reduced glutathione (GSH) as cofactor. In the present study we examined the role of GPX4 in a preclinical MASH model using transgenic mice with whole body GPX4 overexpression or conditional hepatocyte-specific GPX4 knockout.

Method: Male C57BL/6J mice were sacrificed after 1, 2, 3, 4, or 6 weeks on the choline-deficient L-amino acid-defined high-fat diet (CDAHFD) or standard diet (SD) and levels of ferroptosis marker malondialdehyde (MDA) and GPX4 were measured. Whole body GPX4 overexpressing male animals (Gpx4Tg/+) and wild-type littermates were fed CDAHFD or SD for 4 weeks. Likewise, male mice with tamoxifen-inducible hepatocyte-specific GPX4 knockout (Gpx4fl/fl AlbCreERT2Tg/+) and wild-type littermates were fed the CDAHFD or SD for a maximum of eight weeks. After 4 weeks on their respective diets, tamoxifen was administered to induce hepatocyte-specific knockout. Hepatic ferroptosis defenses, vitamin E and ferroptosis-suppressor protein 1 (FSP1) levels, were measured with mass spectrometry and real-time quantitative PCR (RT-qPCR), respectively.

Results: Livers from CDAHFD fed animals displayed MASH already after 1 week and a significant increase in hepatic MDA after 4 weeks (p < 0.01), compared to SD. Immunohistochemistry showed a panlobular increase in GPX4 after 4 weeks CDAHFD, while this epitope was limited to the pericentral region in SD. No increase was noted in GPX4 levels on western blot and RT-qPCR at the same timepoint. Overexpression of GPX4 had no effect on histological lesions of MASH induced by CDAHFD, failed to lower hepatic MDA and did not alter hepatic GSH levels. Gpx4fl/fl AlbCreERT2Tg/+ animals fed SD suffered from acute liver failure and mortality by day 12 after tamoxifen. Unexpectedly, CDAHFD protected Gpx4fl/fl AlbCreERT2Tg/+ animals from mortality (log-rank test: p < 0.01). GPX4 loss after tamoxifen was confirmed on a protein level. Serum vitamin E and FSP1 mRNA expression were significantly higher in Gpx4fl/fl AlbCreERT2Tg/+ on CDAHFD, compared to those on SD (p < 0.001 and p < 0.01, respectively).

Conclusion: CDAHFD induces hepatic cell death with ferroptosis breakdown products and panlobular GPX4 expression. GPX4 overexpression has no effect on liver lesions in CDAHFD. In normal livers, hepatocyte-specific GPX4 knockout is incompatible with life and

POSTER PRESENTATIONS

associated with a drop of other ferroptosis defenses. MASH induced by CDAHFD protects against hepatocyte-specific loss of GPX4, compensated by other ferroptosis defenses that render GPX4 dispensable.

THU-250-YI

Untargeted lipidomics unveils distinct signature of metabolic dysfunction-associated steatohepatitis in the context of obesity

Alina-Iuliana Ono¹, Vicente Cambra-Cortes², Andrea Jiménez-Franco¹, Cristina Placed-Gallego³, Juan Manuel Jiménez-Aguilar¹, Cristian Martínez-Navidad⁴, Helena Castañé⁵, Jordi Camps⁶, Jorge Joven⁷. ¹Universitat Rovira i Virgili, Unitat de recerca biomèdica, Reus, Spain; ²Universitat Rovira i Virgili, Centre de recerca biomèdica, Reus, Spain; ³Universitat Rovira i Virgili, Unitat de recerca biomèdica, Reus, Spain; ⁴Fundació Institut d'Investigació Sanitària Pere Virgili, Unitat de recerca biomèdica, Reus, Spain; ⁵Institut d'Investigació Sanitària Pere Virgili, Unitat de recerca biomèdica, Reus, Spain; ⁶Hospital Universitari Sant Joan de Reus, Unitat de recerca biomèdica, Reus, Spain; ⁷Hospital Universitari Sant Joan de Reus, Unitat de recerca biomèdica, Reus, Spain
Email: alinaonoiu@hotmail.com

Background and aims: Obesity and metabolic dysfunction-associated liver disease (MASLD) are two closely related diseases characterized by an excessive accumulation of fat and an alarming and increasing prevalence. Type 2 diabetes mellitus, cardiovascular problems, dyslipidemia, and cancer are commonly associated with obesity. On the other hand, MASLD can progress negatively to metabolic dysfunction-associated steatohepatitis (MASH), characterized by a dangerous proinflammatory and fibrotic state that can lead to liver dysfunction. Lipid metabolism is altered in these pathologies; however, it is still unknown which role the different lipid species play. **Method:** A non-directed lipidomic analysis by UHPLC-ESI/TOF-MS was performed to assess the concentration of lipid species through liver biopsies from the participants. Group comparisons were made between the 110 obese patients (BMI ≥ 35 kg/m²) classified into nonMASH (n = 50), MASH (n = 50) and uncertain MASH (n = 10) groups.

Results: Obese patients with MASH had a higher lipid concentration of all species except Phosphatidylcholines (PCs), with cholesteryl ester (ChoEs) being the most different compared to non-MASH. From significantly different lipids, ChoE 18:2, ChoE 22:6 and diglyceride (DG) 40:4 were highlighted by multivariate analysis. Histological parameters (NAS, steatosis, ballooning, lobular inflammation, and fibrosis) were analyzed together with the lipid classes, but they did not show a clearly specific behavior in any parameter. Contrarily, ChoE 18:2 and ChoE 22:6 showed a positive tendency as steatosis, lobular inflammation and ballooning increased, while DG 40:4 behaved contrarily.

Conclusion: MASH caused a specific lipid signature in the liver, causing increased ChoEs and diminished PCs. ChoE 18:2, ChoE 22:6 and DG 40:4 were highlighted by the multivariate analysis. Lipid classes were not associated with any histological parameter, although ChoE 18:2 and 22:6 correlated positively with steatosis, inflammation, and ballooning, while DG 40:4 correlated negatively with these same parameters.

THU-251-YI

Liver sinusoidal endothelial cells induce senescence in activated hepatic stellate cells via extracellular vesicles

Junyu Wang¹, Jia Li¹, Manon Buist-Homan¹, Martin Harmsen¹, Han Moshage¹. ¹University Medical Center Groningen, University of Groningen, Groningen, Netherlands
Email: j.wang03@umcg.nl

Background and aims: Liver sinusoidal endothelial cells (LSECs) are considered as key gatekeepers in maintaining hepatic stellate cells (HSCs) homeostasis. The intricate intercellular crosstalk between HSCs and LSECs plays a fundamental role in modulating HSC

quiescence and activation. Previous studies have identified LSEC-derived extracellular vesicles (EVs) as primary mediators in this regulatory process. However, the mechanisms through which LSECs and their EVs modulate the activated phenotype of HSCs (aHSCs) remain unclear. This study aims to investigate the molecular mechanisms of LSECs-mediated modulation of HSC phenotype.

Method: Primary rat LSECs and HSCs were isolated from male Wistar rats. EVs were isolated from the conditioned medium (CM) through differential centrifugation and characterized by nanoparticle tracking analysis, transmission electron microscopy, and marker determination. EVs were added to target cells for 24–72 hours. A primary cell co-culture system was also established to dissect the intercellular signaling mechanisms. Gene expression was determined by qPCR and protein expression by Western blot and immunofluorescence and proliferation of cells by Xcelligence and BrdU assay.

Results: LSEC-derived EVs induced increased expression of inflammation and senescence markers in aHSCs, including IL-1 and senescence-associated β -galactosidase activity and decreased aHSC proliferation. Furthermore, LSEC-derived EVs activated the TLR4/NF- κ B and AKT signaling pathways in aHSCs. The observations with LSEC-derived EVs were replicated in the LSEC-aHSC transwell co-culture system.

Conclusion: LSECs induce aHSC senescence by secreting EVs, which depends on the activation of the TLR4/NF- κ B and AKT pathways. Our results show the importance of LSECs in determining the HSC phenotype.

THU-254-YI

Differential gene expression profiles of liver tissue, subcutaneous and visceral adipose tissue delineates severity of MASLD in heavily obese patients

Lina Jegodzinski¹, Darko Castven¹, Diana Becker², Juliana Marques Affonso¹, Alvaro Mallagaray de Benito³, Lorena Rudolph³, Ashok Kumar Rout³, Matthias Laudes^{4,5}, Rainer Günther⁴, Stefan Schreiber⁴, Svenja Meyhöfer^{1,6}, Friedhelm Sayk¹, Thomas Becker⁷, Jan Henrik Beckmann⁷, Ulrich L. Günther⁸, Witigo von Schönfels⁷, Jens U. Marquardt¹. ¹Department of Medicine I, University Medical Center Schleswig-Holstein, Lübeck, Germany; ²Department of Medicine, University Medical Center, Mainz, Mainz, Germany; ³Institute of Chemistry and Metabolomics, University of Lübeck, Lübeck, Germany; ⁴Department of Medicine I, University Medical Center Schleswig-Holstein, Kiel, Germany; ⁵Institute of Diabetes and Clinical Metabolic Research, Kiel, Germany; ⁶German Center for Diabetes Research (DZD), Neuherberg, Germany; ⁷Department of General, Visceral, Thoracic, Transplantation, and Pediatric Surgery, University Medical Center Schleswig-Holstein, Kiel, Germany; ⁸Institute of Chemistry and Metabolomics, Lübeck, Germany
Email: lina.jegodzinski@uksh.de

Background and aims: Metabolic Dysfunction Associated Steatotic Liver Disease (MASLD) is characterized by heterogeneous clinical traits. The presence of metabolic disturbances, predominantly obesity, plays an important pathophysiological role. Herein, regional predominance of fat accumulation in different adipose tissues are characterized by distinct phenotypic and molecular properties tightly associated with MASLD severity. Importantly, the underlying mechanisms and differential impact of signals from visceral and subcutaneous adipose tissue in this process, as well as the molecular hallmarks, remain to be fully elucidated.

Method: Serum metabolomic and tissue transcriptomic profiles of liver tissue, subcutaneous (SC) and visceral (VF) adipose tissue from patients undergoing bariatric surgery as well as controls were obtained (n = 40) and subdivided according to histological presence of steatotic liver diseases. All tissue samples were subjected to RNA sequencing and corresponding serum samples were analyzed by NMR spectroscopy.

Results: Significant differences in gene expression were observed between all four groups (control, healthy obese, simple steatosis and steatohepatitis (MASH)) and reflected in all analyzed tissues (liver, subcutaneous and visceral adipose tissue), respectively. Interestingly, overlap in gene expression profiles in steatotic liver tissue and MASH showed higher concordance than livers from healthy obese patients. In contrast expression profiles of both VF and SC were highly distinct between all three groups. Interestingly, phenotypic differences across the groups were associated with a significant increase in serum VLDL and IDL particles from healthy obese to MASH patients.

Conclusion: Differences in transcriptomic and metabolomic profiles of heavily obese patients with healthy liver, steatotic liver or steatohepatitis can be recapitulated in expression profiles of adipose tissues from VF and SC, confirming an important role in the development and progression of MASLD. Surprisingly, profiles of adipose tissue display a clear separation of the three groups, suggesting a pathophysiological role in MASLD progression which could be of diagnostic value in the future. Further work is needed to elucidate the exact mechanisms and the relationship to the observed differences in serum lipoprotein metabolism.

THU-255

Calcitriol modulates intestinal AMPK/SIRT1 signaling towards alleviating compromised barrier integrity in MASH: a potential autophagy-dependent role

Andrew Hakeem¹, Basma Abdelrahman^{1,2}, Olfat Hammam³, Mahmoud Khattab⁴, Aiman El-Khatib⁴, Yasmeen Attia¹

¹Pharmacology Department, Faculty of Pharmacy, The British University in Egypt, Cairo, Egypt; ²Faculty of Pharmacy, The British University in Egypt, Department of Pharmacology, Cairo, Egypt; ³Pathology Department, Theodor Bilharz Research Institute, Giza, Egypt; ⁴Pharmacology and Toxicology Department, Faculty of Pharmacy, Cairo University, Cairo, Egypt

Email: andrew.hakeem@bue.edu.eg

Background and aims: The roaring global prevalence of metabolic dysfunction-associated steatotic liver disease (MASLD) in tandem with the lack of approved therapeutic modalities addressing this ailment raises an alarming unmet health need. Failure of the gut barrier integrity is a critical pathological event driving the progression of MASLD towards its more aggressive form, metabolic dysfunction-associated steatohepatitis (MASH). Prior research alludes to an intricate interplay between AMPK/SIRT1 signaling and autophagy in preserving intestinal homeostasis against a plethora of pathological settings. We and others have reported the gut-protective effects of calcitriol (CAL) and its cognate intracellular vitamin D receptor (VDR). However, whether and if CAL-mediated activation of VDR could potentially modulate the crosstalk between AMPK/SIRT1 signaling axis and autophagy alleviating barrier dysfunction triggered by metabolic insults in MASH remains to be explored.

Method: In this study, we utilized a diet-induced MASH model in male C57BL/6 mice randomly allocated into four experimental groups: (I) a normal standard chow diet group, (II) a group fed with a high-fat diet (HFD), (III) a group treated with CAL at 5 ng/gm/day i.p. twice a week, and (IV) a group that received both CAL and hydroxychloroquine (HQ; an autophagy inhibitor), at a dosage of 60 mg/kg/day, p.o. Interventions were initiated after 12 weeks of MASH induction and mice were sacrificed at the end of week 16. VDR and p62 genes expression were assessed using qRT-PCR. Ileal IL-10, AMPK, and SIRT1 were estimated using ELISA.

Results: HandE-stained liver sections of HFD-fed mice showed hepatocyte ballooning and inflammatory cell infiltration, effects that were ameliorated in HFD+CAL mice. HandE-stained ileal sections displayed mucosal atrophy and distorted villous-crypt ratios. Meanwhile, ileal sections from CAL-treated mice showed amelioration of intestinal inflammation that was abolished upon HQ treatment. Expression of VDR was reduced in HFD-fed mice ileums that paralleled augmented expression of p62, the latter suggesting

impaired autophagy. In contrast, VDR ileal levels surged upon treatment with CAL while significantly lowering p62. Additionally, levels of the anti-inflammatory cytokine IL-10 significantly decreased in HFD-fed mice alongside an 84% and 64% decline in AMPK and SIRT1 ileal levels, respectively. Treatment with CAL, however, led to a significant 6-fold surge in IL-10 levels and augmented the expression of both ileal AMPK and SIRT1 compared to the HFD group which was negated upon treatment with the autophagy inhibitor HQ.

Conclusion: The present study findings suggest the capacity of CAL to improve barrier function and curb intestinal inflammation in MASH partly through augmenting AMPK/SIRT1 signaling in an autophagy dependent manner.

THU-256

Without effect on weight loss, semaglutide does not improve MASLD in a dietary mice model for MASLD

Katharina Luise Hupa-Breier¹, Janine Dywicky¹, Björn Hartleben², Michael P. Manns³, Heiner Wedemeyer¹, Fatih Noyan¹, Matthias Hardtke-Wolenski¹, Elmar Jaeckel⁴. ¹Hannover Medical School, Department of Gastroenterology, Hepatology, Infectious Disease and Endocrinology, Hannover, Germany; ²Hannover Medical School, Institute of Pathology, Hannover, Germany; ³Hannover Medical School, Department of Gastroenterology, Hepatology, Infectious Disease and Endocrinology, Hannover, Germany; ⁴University of Toronto, Toronto, Canada

Email: hupa.katharina@mh-hannover.de

Background and aims: Metabolic dysfunction-associated steatotic liver disease (MASLD) is currently one of the most common causes of chronic liver disease with the metabolic syndrome with the central pathogenic factor. As weight loss is a central treatment aspect, GLP1-agonists- as recently established anti-obesity treatments- are also promising treatments of MASLD. The aim of this study was to investigate the effect of GLP1-agonist semaglutide in a new dietary mice model for MASLD with a polygenetic background for the metabolic syndrome and obesity.

Method: TALLYHO/Jngl (TH) mice received 16 weeks of high-fat/high-carbohydrate (HF-HC) diet with a surplus of cholesterol. After 12 weeks of HF-HC, mice were treated with semaglutide.

Results: After 16 weeks of HF-HC treatment, TH mice developed obesity, hyperglycemia and histological proven MASLD (median NAS = 5). Treatment with semaglutide led to a significant improvement of hyperglycemia and dyslipidemia. However, it has interestingly no effect neither on body weight nor on body fat composition in this mice model, which is known to develop obesity by increased food intake due to changes in the central hypothalamus. Furthermore, no significant clinical or histological improvement of MASLD were detectable. Significant reduction of CD36, Srebf1, TNF and Col1a1 reveals mild anti-inflammatory, anti-fibrotic and anti-lipogenic effects on gene level. Nevertheless, intrahepatic CD4+ (p = 0, 018) and Tregs (p = 0, 047) as well as pro-inflammatory macrophages (p = 0, 023) were significantly reduced after semaglutide treatment.

Conclusion: By testing semaglutide in a new polygenetic mouse model of obesity and MASLD, we could demonstrate that semaglutide reduces intrahepatic cellular inflammation. Nevertheless, semaglutide has no significant clinical effects on MASLD, if significant weight loss could not be achieved. Therefore, this data supports the central role of significant weight loss in the therapeutic strategy of MASLD.

THU-257

Metabolic profiling of adipose tissues in metabolic dysfunction-associated steatohepatitis (MASH): insights from lipidomic, proteomic, and epigenetic analyses in morbidly obese patients undergoing bariatric surgery

Cristina Placed-Gallego¹, Juan Manuel Jiménez-Aguilar², Alina-Iuliana Onoiu³, Vicente Cambra-Cortes¹, Andrea Jiménez-Franco¹, Cristian Martínez-Navidad⁴, Helena Castañé⁵, Jordi Camps⁶, Jorge Joven⁶. ¹Universitat Rovira i

POSTER PRESENTATIONS

Virgili, Unitat de Recerca Biomèdica, Reus, Spain; ²Universitat Rovira i Virgili, Unitat de recerca biomèdica, Reus, Spain; ³Universitat Rovira i Virgili, Unitat de recerca biomèdica, Reus, Spain; ⁴Fundació IISPV, Unitat de Recerca Biomèdica, Reus, Spain; ⁵Institut d'Investigació Sanitària Pere Virgili, Unitat de Recerca Biomèdica, Reus, Spain; ⁶Hospital Universitari Sant Joan de Reus, Unitat de recerca biomèdica, Reus, Spain
Email: crisplaced@hotmail.com

Background and aims: Obesity is a complex disease whose prevalence has been observed to be growing exponentially in recent years. Obesity is associated with other diseases such as type 2 diabetes mellitus, respiratory diseases, and cardiovascular diseases, including Metabolic Dysfunction-Associated Steatohepatitis (MASH), which is a severe form of liver disease that poses a global health threat due to its potential to progress to advanced fibrosis, leading to cirrhosis and liver cancer. These diseases are related to adipose tissue, which is primarily responsible for storing triglycerides in adipocytes. Depending on morphology and location, different types of adipose tissue are found, including subcutaneous adipose tissue (SAT) and visceral adipose tissue (VAT).

Method: The study has been conducted with samples from morbidly obese patients who have undergone bariatric surgery. Firstly, a lipidomic study of visceral and subcutaneous adipose tissues was conducted in patients with Metabolic Dysfunction-Associated Steatohepatitis (MASH) (n=49) and without MASH (n=51). Subsequently, a proteomic study of visceral and subcutaneous adipose tissues was conducted in patients with MASH (n=49) and without MASH (n=51). For both studies, both univariate and multivariate statistical analyses were performed.

Results: In visceral adipose tissue, a higher presence of proteins related to the extracellular matrix has been observed, indicating potential changes in the tissue microenvironment. On the other hand, lipidomics reveals a decrease in the quantity of phospholipids, which could have implications for the integrity of cell membranes and intracellular signaling. It is interesting to note that, despite the observed changes in VAT, no significant alterations have been recorded in SAT. This suggests heterogeneity in metabolic responses between tissues, which could have important implications in terms of MASH treatment and management. In an additional analysis, DNA methylation was performed, revealing no significant changes in either VAT or SAT, although the sample size was small.

Conclusion: All those findings highlight the need to address metabolomics to gain a more comprehensive understanding of metabolic changes in MASH. Currently, metabolomics is underway, and it is expected to provide valuable information about the underlying biochemical processes. The DNA methylation finding suggests epigenetic stability amidst the observed metabolic alterations, raising intriguing questions about the interplay between genetics and the environment in the pathogenesis of MASH.

THU-258-YI

Altered liver vascular biology occurring in early stages of metabolic dysfunction-associated steatotic liver disease is significantly improved by the pan-peroxisome proliferator-activated receptor agonist lanifibranor, associating with improved liver histology

Shivani Chotkoe^{1,2}, Guillaume Wettstein³, Luisa Vonghia^{1,2}, Denise van der Graaff², Joris De Man¹, Benedicte De Winter^{1,2}, Pierre Broqua³, Jean-Louis Junien³, Wilhelmus Kwanten^{1,2}, Sven Francque^{1,2}. ¹University of Antwerp, Laboratory of Experimental Medicine and Paediatrics, Wilrijk, Belgium; ²University Hospital Antwerp, Gastroenterology and Hepatology, Edegem, Belgium; ³Inventiva Pharma, Daix, France
Email: shivani.chotkoe@uantwerpen.be

Background and aims: The pan-peroxisome proliferator-activated receptor agonist lanifibranor normalized the intrahepatic vascular resistance (IHVR), the related endothelial dysfunction and liver histology in a methionine-choline-deficient diet rat model of early

metabolic dysfunction-associated steatotic liver disease (MASLD) (EASL 2023; S776). We studied the effects of lanifibranor in the Zucker fatty rat (ZFR) to exclude model specificity, to test a model considered a more clinically relevant representation of MASLD and to examine the effects at the stage of steatohepatitis rather than isolated steatosis.

Method: Male ZFR (8 weeks old, n=6–8/group) were fed a high-fat high-fructose diet (HFHFD) and compared to Zucker lean rats (ZLR, 8 weeks old, n=6–8/group) fed a control diet for 8 weeks. ZFR and ZLR were treated orally with either lanifibranor (100 mg/kg/d) or placebo preventively during the complete 8 weeks of HFHFD. *In vivo* liver and systemic haemodynamics were measured, followed by *in situ ex vivo* liver perfusion in the same animal to assess baseline transhepatic pressure gradient (THPG) at different perfusion flows (10–50 ml/min). Dose-response curves were generated with vasoconstrictor methoxamine (Mx) and vasodilator acetylcholine (ACh) after Mx pre-contraction. Haematoxylin-eosin and Sirius red staining were performed on liver tissue for histology.

Results: In vehicle-treated groups, the livers of ZFRs showed prominent ballooning, mild steatosis and some lobular inflammation compatible with a diagnosis of metabolic dysfunction-associated steatohepatitis. Fibrosis was absent. In ZFRs the mean arterial blood pressure (MABP) was significantly elevated (159.1 ± 2.49 vs. 132.8 ± 2.7 mmHg, $p < 0.0001$), portal pressure *in vivo* (7.07 ± 0.24 vs. 4.86 ± 0.29 mmHg, $p < 0.0001$) was significantly higher as well as THPG *ex vivo* with $p < 0.001$. The ZFRs were not hyperreactive to Mx, but there was hyporeactivity to ACh in comparison with ZLRs. In ZLR, lanifibranor induced no changes in *in vivo* and *ex vivo* haemodynamics. In ZFRs, however, it normalized the MABP (from 159.1 ± 2.49 to 132.6 ± 3.03 mmHg, $p < 0.0001$), strongly decreased the portal pressure *in vivo* (from 7.07 ± 0.24 to 5.2 ± 0.23 mmHg, $p < 0.001$) and normalized THPG *ex vivo* at all flows ($p < 0.001$). Lanifibranor further decreased reactivity to Mx and normalized hyporeactivity to ACh in ZFRs. This was associated with a decrease in ballooning and steatosis on histology.

Conclusion: This study, performed in a dietary model more reflective of human MASLD, confirms that lanifibranor significantly improves portal pressure and associated functional intrahepatic vascular changes, alongside histological improvement. These findings support the role of intrahepatic vascular alterations in the development of MASLD-related portal hypertension, the progression to MASH, and the potential of lanifibranor as an efficacious treatment for MASH.

THU-259

Non-invasive staging of liver disease in C57BL/6NTac mice preconditioned on the modified-Amylin NASH diet using automated shear wave elastography

Laura Griffin¹, Steven Yeung², Sridhar Radhakrishnan², Christopher Moore³, Juan Rojas³, Brian Velasco⁴, Paul Dayton⁴, Tomek Czernuszewicz³. ¹Taconic Biosciences, Rensselaer, United States; ²Research Diets, Inc, New Brunswick, United States; ³Revvity, Inc, Durham, United States; ⁴University of North Carolina Chapel Hill, Chapel Hill, United States
Email: laura.griffin@taconic.com

Background and aims: C57BL/6 mice on a modified Amylin NASH (GAN) diet demonstrates SLD and more closely recapitulate human MASLD compared to other preclinical models. While translatable, this model is characterized by variation which can be addressed through liver biopsies to assess disease stage. However, biopsies are invasive and labor intensive. While non-invasive techniques like liver elastography for humans exist, there is a need for translatable, non-invasive, and high-throughput alternatives for preclinical models. The study goal was to determine whether a non-invasive, automated shear wave elastography (SWE) imaging instrument could accurately determine the progression of SLD in GAN-diet fed C57BL/6NTac (NASH B6) mice.

Method: Commercially available (NASH B6 mice conditioned for 12, 23, 31, or 34 weeks on diet (D09100310, Research Diets, $n = 8/\text{group}$) and age-matched C57BL/6NTac controls ($n = 4/\text{group}$) were shipped by Taconic Biosciences to the University of North Carolina Chapel Hill (UNC) and acclimated for 3 weeks. Liver stiffness, volume, and echogenicity was assessed in each animal via 3D B-mode and SWE imaging (Vega, Revvity, Inc.). Livers were manually segmented from 3D image datasets and median stiffness and echogenicity were quantified by mouse. A separate cohort of NASH B6 mice ($n = 8$; 12 weeks on diet) and age-matched C57BL/6NTac mice were shipped to UNC and acclimated for 1 week. Liver stiffness was assessed longitudinally every 3 weeks up to 24 weeks on diet. Non-invasive ultrasound measurements from all cohorts were compared to histological data to assess correlation with fibrosis scores.

Results: Liver volume ($1.4 \pm 0.2 \text{ cm}^3$ vs. $1.9 \pm 0.4 \text{ cm}^3$, $p = 0.028$) and liver echogenicity ($27.2 \pm 6.7 \text{ a.u.}$ vs. $62.4 \pm 21.6 \text{ a.u.}$, $p = 0.048$) were significantly increased in NASH B6 mice, suggesting hepatomegaly and the presence of moderate to advanced steatosis. Liver stiffness was not statistically different between groups ($4.0 \pm 0.5 \text{ kPa}$ vs. $3.9 \pm 0.5 \text{ kPa}$, $p = 0.570$), suggesting no onset of MASH and/or fibrosis after 12 weeks on diet in the longitudinal cohort. These results are in close agreement with histopathological data which demonstrated substantial liver weight increase at 12 weeks, but no fibrosis onset until 26 weeks or later. Additionally, imaging detected two mice that could be classified as “slow responders” to GAN feeding due to low echogenicity, indicating a lack of steatosis (26 a.u. and 31 a.u., respectively). Further longitudinal and cross-sectional imaging will determine if these mice are indeed outliers or if phenotype will normalize across the cohort.

Conclusion: Our data present the potential of ultrasound to assess SLD progression in a clinically translatable preclinical model in a non-invasive and high-throughput manner. This allows for an improved study design targeting specific SLD stages and reduced model variability in the pursuit of SLD drug discovery.

THU-260

Serum thrombospondin-2 and insulin-like growth factor binding protein 7 predict liver fibrosis and fibrosis regression in patients with MASLD post bariatric surgery

Rambabu Surabattula¹, Pierre Bel Lassen^{2,3}, Sudha Rani Myneni¹, Aron-Wisniewsky Judith^{2,3}, Laurent Genser³, Jean-Daniel Zucker⁴, Karine Clément^{2,3}, Detlef Schuppan^{1,5}. ¹Institute of Translational Immunology, University Medical Center Mainz, Mainz, Germany; ²INSERM, Nutrition and Obesities: Systemic Approaches Research Group (NutriOmics), Sorbonne Université, Paris, France; ³APHP, Nutrition and surgery departments, Pitié-Salpêtrière hospital, Paris, France; ⁴UMMISCO, Unité de Modélisation Mathématique et Informatique des Systèmes Complexes, IRD, Sorbonne Université, Bondy, France; ⁵Harvard Medical School, Beth Israel Deaconess Medical Center, Boston, MA, United States
Email: rasuraba@uni-mainz.de

Background and aims: The prevalence of MASLD in patients eligible for bariatric surgery (BS) can reach 75%-100%. BS usually leads to significant weight loss and often to metabolic normalization. This is accompanied by liver histological improvement in some but not all patients. We established and assessed novel serum markers of fibrogenesis in follow-up of a well-defined cohort of patients with obesity and MASLD undergoing bariatric surgery.

Method: We established sandwich ELISAs measuring the matricellular fibrosis marker thrombospondin-2 (TSP2) and the metabolism/fibrosis-related marker insulin-like growth factor binding protein-7 (IGFBP7) using combinations of recombinant proteins, commercial and self-produced monoclonal and polyclonal antibodies. Sensitivity and specificity were optimized, with intra- and inter assay variations for serum or plasma below 10% and 15%, resp. 132 severely obese patients with matched liver biopsies were included. 74 patients showed fibrosis stage F0-1 and 54 patients intermediate to advanced

fibrosis stage F2-4. Apart from baseline determinations, the evolution of the serum fibrosis markers post-bariatric surgery was analyzed from a subset of 51 subjects with follow-up at 3 and 12 months BS.

Results: Patients with F2-4 fibrosis displayed significantly higher baseline levels of the two markers vs patients with fibrosis F0-1 at baseline for TSP2 (88.6 vs 53.9) and IGFBP7 (208.8 vs 128 ng/ml). TSP2 and IGFBP7 were significantly higher in patients with severe fibrosis F3-4 (mean values 114.4 and 234.5 ng/ml, resp.) indicating more rapid fibrosis progression compared to fibrosis F0-2 (means 62 and 152.3 ng/ml, resp.). The AUROC values to distinguish fibrosis F2-4 or F3-4 from F0-1 or F0-2 were 0.74 and 0.84 for TSP2, and; 0.84 and 0.78 for IGFBP7. The AUROC value to distinguish fibrosis F2-4 from F0-1 was significantly increased for the combination of TSP2 and IGFBP7 (0.86), reaching the range of a perfect test in view of biopsy sampling error. Serum levels of both markers could further differentiate between the presence vs absence of type 2 diabetes. There was a significant correlation of 2 markers with liver enzymes and insulin resistance, while these parameters had a low predictive value. Levels of TSP2 decreased significantly 3 months and remained at a low level at 12 months after BS in patients with baseline F2-4 fibrosis, but not in patients with F0-1 fibrosis supporting its prominent role in liver fibrogenesis, while IGFBP7 was related to fibrogenic inflammation.

Conclusion: The matricellular serum markers TSP2 and IGFBP7 reflect liver fibrogenesis and fibrogenesis combined with metabolic inflammation in a unique cohort of patients undergoing BS. TSP2 alone showed the currently highest predictive value for fibrosis F2-4 and the combination of both markers uniquely predicted response to BS.

THU-261

Artificial intelligence models deployed at scale on hematoxylin and eosin-stained whole slide images reveal stage-dependent collagen composition in metabolic dysfunction-associated steatohepatitis

Ylaine Gerardin¹, Neel Patel¹, Lara Murray¹, Adam Stanford-Moore¹, Jacqueline Brosnan-Cashman¹, Jun Xu², Lisa Boyette², Benjamin Glass¹, Timothy R. Watkins², Andrew N. Billin², Robert Egger¹. ¹PathAI, Inc., Boston, United States; ²Gilead Sciences, Foster City, United States
Email: ylaine.gerardin@pathai.com

Background and aims: Diagnosis and staging of metabolic dysfunction-associated steatohepatitis (MASH; formerly NASH) requires manual pathologist identification of fibrotic structures on collagen-stained slides. The qualitative assessment of these structures makes MASH staging prone to inter-rater variability. Granular, quantitative histopathologic assessment could inform the understanding of fibrosis progression and regression in MASH. We developed AI models to detect and quantify fibrotic features from scanned hematoxylin and eosin-stained (HandE) whole slide images (WSI) at scale and used the results to characterize fibrosis composition in MASH biopsies.

Method: NASH Explore models were deployed on HandE-stained liver biopsies from the STELLAR-3 and STELLAR-4 trials of selonsertib, which enrolled MASH patients with bridging fibrosis or compensated cirrhosis, respectively. Quality filtering was performed to remove WSI with low amounts of analyzable liver tissue (final $n = 3198$). Quantitative features were extracted from each WSI, describing the proportionate areas of 5 pathological fibrosis types (periportal, perisinusoidal, incomplete septal, complete septal, and nodular) and 4 non-pathological collagen types (structural, portal, and non-specific collagen; perivenular fibrosis). These HandE-based features were compared to pathologist-assessed CRN fibrosis stages and sub-ordinal fibrosis scores derived from previously reported AIM-NASH algorithm deployed on paired trichrome-stained slides.

POSTER PRESENTATIONS

Results: AI-based fibrosis quantification revealed increased total collagen, pathological fibrosis, and advanced fibrosis with CRN fibrosis stage. Collagen at lower stages was mainly composed of structural collagen and non-pathogenic fibrosis types, incomplete septal fibrosis peaked at intermediate stages (F2–F3), and the F4 stage was dominated by nodular fibrosis. Dimensionality reduction revealed nodular fibrosis driving the first component of greatest variation across the samples, separating out F4 at the highest extreme and F3 samples at intermediate values. Manually-staged F0, F1, and F2 subpopulations were highly overlapping in the first two principal components, which accounted for 67% of total sample variation.

Conclusion: Characterization of pathological fibrosis and non-pathological collagen features via AI digital pathology yields an understanding of MASH fibrosis progression beyond the resolution provided by CRN scoring. The presence of expected associations, such as nodular fibrosis in F4, provides biological support for empirically-validated AI fibrosis staging. Quantifying fibrosis directly from scanned HandE images with NASH Explore requires no custom microscopy and is scalable for applications in drug development, enhancing understanding of therapeutic mechanisms for anti-fibrotic drugs, and potentially use in clinical care.

THU-262

Targeting macrophage BTK, a potential therapeutic strategy for metabolic dysfunction-associated steatohepatitis

Shiwei Chen¹, Cheng Zhou², Yanbo Wang², Guohua Lou², Min Zheng².

¹The First Allied Hospital, College of Medicine, Zhejiang University, Hang Zhou, China; ²The First Allied Hospital, College of Medicine, Zhejiang University, Hang Zhou, China

Email: minzheng@zju.edu.cn

Background and aims: Metabolic dysfunction-associated steatohepatitis (MASH) is a severe inflammatory liver disease without available pharmacological treatment currently. Bruton's tyrosine kinase (BTK) is a crucial mediator in immune response which plays an important role in various inflammatory diseases. However, the effect of BTK on MASH still remains unknown. This study aimed to investigate the role and mechanism of BTK in methionine and choline deficient (MCD) diet-induced mice MASH.

Method: In our study, mice MASH was induced by MCD diet feeding. The BTK phosphorylation and expression levels were detected in the livers of MASH mice. BTK inhibitor, BTK knockout and myeloid-conditional BTK knockout were applied to explore the effect of BTK in mouse MASH. Further, the molecular mechanism of BTK in MASH was investigated with gain or loss of function approaches in vitro and vivo experiments. Flow cytometry, western blot, ELISA, immunohistochemistry, qPCR, RNA-seq were used in our research.

Results: Our study found that BTK was markedly activated and upregulated in MASH mice fed by MCD diet. Both BTK inhibitor and BTK knockout were able to alleviate mice MASH, and BTK from macrophages and granulocytes were proved to play the key role through BTK phosphorylation detection in multiple immune cell subtypes. Moreover, our results indicated that BTK knockout in myeloid cells could also attenuated mice MASH progression. In terms of mechanism, we found that BTK inhibitor could downregulate phosphatidylinositol-3-kinase (PI3 K)/Akt/forkhead Box Protein O1 (FoxO1) signaling pathway, further suppressed macrophage polarization towards the M1 phenotype, as well as reduced macrophage infiltration in the liver.

Conclusion: Our results proved that BTK inhibition could protect against MASH progression, partially by suppressing PI3 K/Akt/FoxO1 signaling pathway in macrophages. Therefore, macrophage BTK might be a potential therapeutic target for the treatment of MASH.

THU-263-YI

Significance of adipose tissue fibrosis and adipocyte in the progression of metabolic dysfunction-associated steatohepatitis in severe obesity patients

Andrea Jiménez-Franco¹, Marina Ramirez-Baños², Cristina Placed-Gallego¹, Juan Manuel Jiménez-Aguilar¹, Cristian Martínez-Navidad³, Helena Castañé⁴, Alina-Iuliana Onoiu¹, Vicente Cambra-Cortes¹, Jordi Camps⁵, Jorge Joven⁶. ¹Universitat Rovira i Virgili, Unitat de Recerca Biomèdica, Reus, Spain; ²Universitat Rovira i Virgili, Universitat Rovira i Virgili, Reus, Spain; ³Fundació IISPV, Unitat de Recerca Biomèdica, Reus, Spain; ⁴Institut d'Investigació Sanitària Pere Virgili, Unitat de Recerca Biomèdica, Reus, Spain; ⁵Hospital Universitari Sant Joan, Unitat de Recerca Biomèdica, Reus, Spain; ⁶Hospital Universitari Sant Joan de Reus, Unitat de Recerca Biomèdica, Reus, Spain

Email: andreafranco99@gmail.com

Background and aims: Obesity stands as the primary risk factor for the development of metabolic dysfunction-associated steatotic liver disease (MASLD), with an increasing prevalence of both conditions. Adipose tissue dysfunction is considered a critical factor in the development of obesity-related comorbidities, closely tied to tissue morphology. When the capacity to store lipids in adipose tissue is surpassed, it can lead to hypertrophy, hyperplasia, hypoxia, apoptosis, and inflammation. This cascade may result in ectopic lipid deposition, altered adipokine secretion, and the progression of MASLD into metabolic dysfunction-associated steatohepatitis (MASH). However, not all severely obese patients develop MASH, emphasizing the need to study adipose tissue morphology and function for a comprehensive understanding of MASLD development.

Method: A total of 163 patients with severe obesity undergoing bariatric surgery provided liver, subcutaneous adipose tissue (SAT), and visceral adipose tissue (VAT) biopsies, along with blood samples. Of these, 71 were diagnosed with MASH, and 92 were non-MASH. Plasma concentrations of adiponectin, leptin, and FGF21 were assessed using enzyme-linked immunosorbent assay. Histological analysis of SAT and VAT included FAT score evaluation and adipocyte area measurement using ImageJ. Preliminary Western blot analysis of TIMP-4 and MMP-12 expression in VAT and SAT was conducted.

Results: Fatty tissue fibrosis and SAT adipocyte area did not differ between MASH and non-MASH patients. Both groups exhibited larger SAT adipocyte areas compared to VAT adipocyte areas. MASH patients displayed a greater VAT adipocyte area, unrelated to VAT fibrosis, while the opposite was observed in non-MASH patients. Lower adiponectin and higher FGF21 concentrations were found in MASH patients. Adipose tissue histological features were associated with blood concentrations of adiponectin and leptin.

Conclusion: Differences in VAT, but not SAT, histology were observed between MASH and non-MASH patients with severe obesity. Varied blood concentrations of adipokines were noted between these groups, with associations identified between adipokine concentrations and adipose tissue histological features. Our findings suggest a potential influence of adipose tissue on the liver's health status in MASH and non-MASH patients.

THU-266

S100A11 is a pro-inflammatory lipotoxic damage associated molecular pattern in metabolic dysfunction-associated steatohepatitis

Gopanandan Parthasarathy¹, Amy Mauer¹, Harmeet Malhi¹. ¹Mayo Clinic, Rochester, United States

Email: malhi.harmeet@mayo.edu

Background and aims: The endogenous damage associated molecular pattern S100A11 is upregulated on lipotoxic hepatocytes in vitro and is enriched on extracellular vesicles (EVs) in metabolic dysfunction associated steatohepatitis (MASH). Its cognate receptor-receptor for advanced glycation endproducts (RAGE) is upregulated on proinflammatory macrophages in MASH and RAGE

inhibition is associated with amelioration of MASH in a diet induced mouse model. We hypothesized that hepatocyte derived S100A11 enriched EVs promote proinflammatory signalling in macrophages via RAGE activation. To test this hypothesis, we performed in silico and in vitro analyses to confirm hepatocyte specific upregulation of S100A11 and its secretion in EVs in murine and human MASH.

Method: In vitro, EVs released from human and mouse hepatocyte cell lines were analysed for upregulation of S100A11 by unbiased proteomics and confirmed by western blotting and immunogold electron microscopy. To corroborate this, we analysed publicly available whole liver bulk RNA sequencing and single cell RNA sequencing datasets to confirm hepatocyte upregulation of S100A11 in MASH. Interaction between S100A11 and RAGE was assessed by immunofluorescence microscopy and western blotting.

Results: S100A11 was enriched on lipotoxic EVs from human Huh7, mouse AML-12 and primary mouse hepatocytes. S100A11 lacks a transmembrane domain and was found to be bound to annexin A2 by co-immunoprecipitation, and furthermore, both annexin A2 and S100A11 were enriched on lipotoxic hepatocyte-derived EVs. In scRNA sequencing of whole mouse livers, S100a11 and Anxa2 were respectively 11.5- and 9.9 fold upregulated in MASH compared to chow mice. Specifically on hepatocytes, expression of S100a11 and Anxa2 were increased by 36- and 95 fold after 34 weeks of a high fat-high fructose diet. In humans, expression of S100A11 and ANXA2 were significantly increased in bulk RNA sequencing of whole livers from patients with NASH compared to healthy controls. We confirmed in vitro that S100A11 enriched EVs led to RAGE oligomerization and activation of bone marrow derived macrophages and macrophage cell lines.

Conclusion: We have demonstrated that hepatocyte derived S100A11 is a lipotoxic DAMP and along with Annexin A2 is significantly upregulated and enriched on lipotoxic EVs. These S100A11 enriched EVs activate RAGE signalling suggesting that in vivo hepatocyte derived EVs could mediate an intercellular signalling axis via RAGE activation on recruited macrophages.

THU-268

Differential transcriptomic profile in platelet-derived extracellular vesicles in patients with Metabolic Dysfunction-Associated Steatotic Liver Disease (MASLD)

Sheila Gato-Zambrano^{1,2}, Rocío Muñoz-Hernández^{1,2,3}, Antonio Gil-Gómez^{1,2}, Ángela Rojas Álvarez-Ossorio^{1,2}, Vanessa García-Fernández¹, Rocío Gallego-Durán^{1,2}, Rocío Montero-Vallejo^{1,2}, Douglas Maya^{1,2}, Raquel Millán-Domínguez^{1,2,4}, M. Carmen Rico^{1,2,4}, Isabel Fernández-Lizaranzu¹, Javier Ampuero^{1,2,4}, Manuel Romero-Gómez^{1,2,4}. ¹SeLiver Group. Instituto De Biomedicina De Sevilla (IBiS), Hospital Universitario Virgen Del Rocío/CSIC/ Universidad De Sevilla., Sevilla, Spain; ²Centro De Investigación Biomédica En Red De Enfermedades Hepáticas y Digestivas (CIBEREHD), Madrid, Spain; ³Departamento de Fisiología. Facultad de Biología. Universidad de Sevilla., Sevilla, Spain; ⁴UGC de Enfermedades Digestivas, Hospital Universitario Virgen Del Rocío., Sevilla, Spain
Email: sgato-ibis@us.es

Background and aims: Extracellular vesicles (EVs) released under activation and apoptosis conditions contain genetic and protein material from the originating cell. They act as vectors for intercellular communication, contributing to the initiation, pathogenesis, and progression of numerous liver diseases. Both platelets and platelet-derived EVs interact with liver cells, contributing to hepatic damage.

Objectives: (i) To determine the use of platelet-derived EVs as biomarkers for the severity of MASLD, (ii) to determine the differential miRNA profile contained in platelet-derived EVs in patients with different severity degrees.

Method: A total of 97 biopsy-proven MASLD patients were recruited. They were classified into steatosis (n = 23) or steatohepatitis (n = 70) based on the SAF score. EVs quantification was performed by flow

cytometry (LRS Fortessa) using Annexin V-PE and CD41-FITC antibodies. Isolation of EVs was carried out on the FACS Aria Fusion cell sorter (Becton Dickinson) in plasma from 8 patients with steatohepatitis and 4 patients with steatosis. Total RNA enriched in miRNAs was extracted using the miRNeasy Mini Kit (Qiagen), and the differential expression profile of microRNAs was determined by microarray (GeneChip miRNA 4.0 Assay Affymetrix, ThermoFisher CA, USA).

Results: CD41+ EVs levels were significantly elevated in patients with steatohepatitis compared to those with steatosis (1511 ± 268 vs. 28882 ± 542.5; p = 0.04). The results of the differential analysis showed that 9 microRNAs were upregulated in platelet-derived EVs from patients with steatohepatitis (fold change >2, p value <0.05): miR-16, miR-4486, miR-5035p, miR-6727, miR-4498, miR-4708, miR-7855, and miR-6790; and one downregulated: miR-6085.

Conclusion: Platelet-derived EVs are elevated in patients with steatohepatitis, suggesting they could be used as biomarkers for the severity of the pathology. Furthermore, these preliminary data indicate a differential miRNA profile within platelet-derived EVs. However, further studies are needed to elucidate their potential contribution to hepatic damage.

THU-269-YI

Effects of semaglutide, Peptide YY3-36 and empagliflozin on metabolic dysfunctions-associated fatty steatotic liver disease in diet-induced obese rats with chronic nitric oxide synthase-inhibition

Niklas Geiger¹, Simon Kloock¹, Jana Gerner², Aisha-Nike Landthaler², Alexander Georg Nickel², Michael Kohlhaas², Andreas Geier³, Martin Fassnacht¹, Ulrich Dischinger^{1,2}. ¹University Hospital Wuerzburg, Department of Internal Medicine, Division of Endocrinology and Diabetes, Wuerzburg, Germany; ²University Hospital Wuerzburg, Comprehensive Heart Failure Center, Wuerzburg, Germany; ³University Hospital Wuerzburg, Hepatology, Wuerzburg, Germany
Email: Geiger_N1@ukw.de

Background and aims: Metabolic dysfunction-associated steatotic liver disease (MASLD) is a common comorbidity of obesity. In this study, we sought to determine hepatic metabolic and mitochondrial effects of the Glucagon-like Peptide-1-agonist semaglutide, the sodium-glucose linked transporter 2-inhibitor empagliflozin and Peptide YY₃₋₃₆ in diet-induced obese rats with additional chronic inhibition of nitric oxide synthase via N^ω-nitro-L-arginine methyl ester (L-NAME), to induce accelerated liver injury.

Method: Following an eight-week feeding period with a high-fat/fructose-diet (HFD) and L-NAME, male wistar rats were randomized into the following treatment groups: semaglutide, empagliflozin, PYY₃₋₃₆, semaglutide in combination with empagliflozin or PYY₃₋₃₆, a food restricted body weight matched group (BWM) and saline control. After an additional 8 weeks, qRT-PCR was performed to quantify hepatic mRNA expression of metabolic and inflammatory marker genes. Serum was analysed for insulin, glucose, adiponectin and leptin levels. Moreover, in isolated mitochondria, mitochondrial respiration in different states using Oroboros O2K-FluoRespirometer was examined.

Results: In the liver, the de-novo lipogenesis regulating genes MLXIP and SREBF-1 were downregulated in the BWM, semaglutide and PYY₃₋₃₆ mono groups and significantly lower in the semaglutide + PYY₃₋₃₆ group (p < 0.05) compared to saline treated controls. HOMA-index was significantly lower in PYY-mono treated animals (p < 0.05) and in the semaglutide+empagliflozin group (p < 0.05), adiponectin-leptin-ratio was significantly higher in semaglutide + PYY₃₋₃₆ (p < 0.01) and BWM treated animals in comparison to saline (p < 0.01). Moreover, there was a significant downregulation of IL-1b mRNA in the semaglutide-mono treated group (p < 0.05). In the semaglutide+empagliflozin treated group, TNF-alpha-levels were lower compared to saline. Regarding mitochondrial respiration, fatty acid-dependent state 3 respiration, empagliflozin (p < 0.001)

POSTER PRESENTATIONS

as well as semaglutide+empagliflozin ($p < 0.05$) decreased O_2 -consumption significantly in comparison to controls. In the uncoupled state, empagliflozin and PYY₃₋₃₆ mono-treatment decreased the O_2 -rate significantly ($p < 0.05$) compared to saline control. Moreover, semaglutide in combination with PYY₃₋₃₆ or empagliflozin lowered O_2 -consumption.

Conclusion: In summary, the presented data indicate a strong improvement of insulin sensitivity shown by presented metabolic parameters and associated genes. O_2 -consumption of the respiratory chain in mitochondria is decreased in semaglutide, PYY₃₋₃₆, and empagliflozin treated rats, supposing reduced metabolic stress in these groups. The strongest effect was detected in semaglutide+PYY₃₋₃₆ treated animals, which points towards PYY₃₋₃₆ as a promising additive substance in the treatment of MASLD.

THU-271-YI

Brain inflammation and cognitive impairment is not mitigated by a low-fat dietary intervention in ageing mice with MASLD

Matthew Siddle^{1,2}, Deepika Goel², Christos Konstantinou^{1,2}, Rajiv Jalan³, Nathan Davies³, Lindsey Edwards^{4,5}, Debbie L. Shawcross¹, Anna Hadjihambi^{1,2}. ¹King's College London, London, United Kingdom; ²The Roger Williams Institute of Hepatology, London, United Kingdom; ³University College London, London, United Kingdom; ⁴Institute of Liver Studies, King's College London, Department of Inflammation Biology, School of Immunology and Microbial Sciences, Faculty of Life Sciences and Medicine, London, United Kingdom; ⁵Centre for Host Microbiome Interactions, King's College London, Faculty of Dentistry, Oral and Craniofacial Sciences, London, United Kingdom
Email: matthew.siddle@kcl.ac.uk

Background and aims: Metabolic dysfunction-associated steatotic liver disease (MASLD) is linked to cognitive decline, brain hypoxia and inflammation, accelerated ageing, and neurodegeneration. Here, we assessed a low-fat diet (LFD) as a potential neuroprotective intervention in ageing mice.

Method: 6-week-old male C57BL/6NTac mice were fed either a control diet (CD) or a high-fat high-cholesterol diet (HFHC) for 26 weeks to induce MASLD. Half the mice in each group were then placed on the LFD and aged to 18-months. Steatosis was confirmed by histology. All mice were subjected to a battery of behavioural tests. Cortical partial pressure of oxygen (PO₂) and tissue saturation (SO₂) at baseline and in response to systemic hypercapnia (10% CO₂) were monitored under anaesthesia by optical fluorescence and optoacoustic tomography, respectively. CD31 staining was used to assess cortical vasculature. Brain inflammation was evaluated in the cortex and hippocampus using microglial immunofluorescence (Iba-1), with 3D reconstruction and morphological assessment.

Results: Both HFHC and HFHC-LFD mice exhibited anxiety-like behaviour; whilst only aged CD-LFD and HFHC-LFD mice exhibited memory impairment. HFHC, HFHC-LFD, and CD-LFD mice exhibited lower baseline PO₂ and SO₂ but preserved cerebrovascular reactivity. No changes were observed in cortical vascular morphology. HFHC and HFHC-LFD mice showed increased cortical microglia density, coverage, and volume, indicating reactive microglia. Only HFHC-LFD mice exhibited microglial alterations in the hippocampus.

Conclusion: LFD was not sufficient to counteract MASLD progression and its associated brain alterations in ageing mice. Both reduced brain oxygenation and increased inflammation may be contributing to the increased risk of neurodegeneration.

THU-272-YI

MASH-associated endothelial dysfunction in mice: is there no effect?

Justine Lallement¹, Sebastian Bott², Hrag Esfahani³, Dessy Chantal⁴, Isabelle Leclercq⁵. ¹Institute of Experimental and Clinical Research (Laboratory for Hepato-gastroenterology and Pole of Pharmacology and Therapeutics), Université Catholique de Louvain, Brussels, Belgium; ²Institute of Experimental and Clinical Research (Laboratory of Hepato-

Gastroenterology and Pole of Pharmacology and Therapeutics), Université Catholique de Louvain, Brussels, Belgium; ³Institute of Experimental and Clinical Research (Integrated physiology platform), Université Catholique de Louvain, Brussels, Belgium; ⁴Institute of Experimental and Clinical Research (Pole of Pharmacology and Therapeutics), Université Catholique de Louvain, Brussels, Belgium; ⁵Institute of Experimental and Clinical Research (Laboratory of Hepato-Gastroenterology), Université Catholique de Louvain, Brussels, Belgium
Email: justine.lallement@uclouvain.be

Background and Aims: Metabolic dysfunction-associated steatohepatitis (MASH) confers a superimposed risk to develop cardiovascular disease (CVD). Although numerous clinical studies have demonstrated a robust association between MASH and CVD, independent of cardiometabolic risk factors, the pathogenic mechanisms supporting a liver-to-CVD axis remain unknown. Endothelial dysfunction is characterized by an imbalanced endothelium-production of protective (among which nitric oxide (NO) is the most prominent) vs deleterious factors that promote a pro-constrictive phenotype. It is the earliest feature of atherosclerosis and hypertension contributing to the development of major CV events. This study aims to characterize the vascular system with a special focus on endothelial function in a murine model of MASH disease.

Method: Male Foz mice fed with high fat diet (HFD) for 24 weeks were used as a model of MASH. HFD-fed littermates are used as dysmetabolic controls (no MASH). Blood pressure was monitored over 24 h using telemetry and the presence of aortic atherosclerotic plaques was investigated through red oil staining. Endothelial function was evaluated in the first-order mesenteric arteries by wire myograph measurements. Blood nitrosylated hemoglobin (HbNO) was quantified by electron paramagnetic resonance. Asymmetric dimethylarginine (ADMA), an endogenous inhibitor of NO production, was measured using ELISA. Western blot analysis and qPCR were conducted to investigate the NO pathway.

Results: Despite the absence of atherosclerotic plaques and hypertension, HFD-fed Foz mice (FH) exhibit endothelium-dependent impaired relaxation compared to the dysmetabolic controls. We demonstrated reduced NO-dependent vasodilatation in response to carbachol in FH compared to controls. Consistent with these findings, our results indicate reduced expression and activation of endothelial NO synthase (eNOS), as measured by Ser¹¹⁷⁷ phosphorylation level, in the aorta of FH. This is associated with higher plasma ADMA. However, there is no difference in blood HbNO level between the two groups. The hepatic expression of inducible NO synthase (iNOS), induced by inflammation as seen in MASH liver, is significantly increased in FH (fold change 15).

Conclusion : Our results demonstrate that mice with MASH but not the dysmetabolic controls present endothelial dysfunction characterized by impaired NO-dependent vasodilation. This dysfunction may be attributed to lower expression and activation of eNOS and elevated plasma ADMA level. Our data further suggest that the inflamed liver could contribute to the disruption of NO balance by the upregulation of iNOS expression, thereby disturbing systemic NO production. These findings underscore the importance of unraveling the liver-vessel-heart crosstalk to better understand the pathophysiological substratum for MASH-driven increase in CV risk.

THU-273

Distinct gut microbiome and intestinal permeability biomarker in patients with lean MASLD without type 2 diabetes

Nathaya Chuaypen¹, Thananya Jinato¹, Pisit Tangkijvanich¹. ¹Center of Excellence in Hepatitis and Liver Cancer, Faculty of Medicine, Chulalongkorn University, Bangkok, Thailand
Email: pisittkvn@yahoo.com

Background and aims: An altered gut microbiome has been linked to the development of metabolic dysfunction-associated liver disease (MASLD). However, data regarding gut dysbiosis and the mechanistic

insight in Asian patients with lean MASLD (BMI<23 kg/m²), particularly among non-diabetic individuals, are not well defined.

Method: This study included 16 Thai healthy individuals and 100 patients with MASLD without type 2 diabetes (8 lean and 92 non-lean patients). Hepatic steatosis was identified by transient elastography (controlled attenuation parameter >248 dB/m). The 16S rRNA sequencing in fecal samples and bioinformatics analysis were performed for gut microbiome composition. The differential abundance of bacterial composition between groups was analyzed by the DESeq2 method. Plasma intestinal fatty acid-binding protein (I-FABP) and lipopolysaccharide-binding protein (LBP) were analyzed to determine intestinal permeability and bacterial translocation, respectively.

Results: The alpha and beta diversities of the gut microbiome were significantly different between patients with MASLD and healthy subjects. However, the diversities did not differ between the lean and non-lean MASLD ($p = 0.077$ for Shannon index, and PERMANOVA = 0.217 for beta-diversity). Compared to non-lean individuals, patients with lean MASLD revealed significant enrichment of pro-inflammatory bacteria including *Escherichia-Shigella*. Moreover, significant reduction of short-chain fatty acids (SCFAs)-producing bacteria such as *Lachnospira* and *Subdoligranulum* were observed in the lean patients. Combined analysis of these bacterial genera based on a logistic regression model was able to differentiate between lean and non-lean MASLD with a high diagnostic performance (AUC of 0.82). There was a marginally significant increase in I-FABP levels in lean patients when compared to the non-lean individuals [median (95% CI); 544.2 (152.8–1, 330) versus. 261.8 (269.2–377.1) pg/ml, $P = 0.054$]. However, there was no difference in LBP levels between these subgroups of patients [10, 972 (6, 535–16, 525) versus. 12, 437 (11, 429–13, 721) ng/ml, $P = 0.541$].

Conclusion: Non-diabetic patients with lean MASLD exhibited distinct bacterial composition and a trend toward higher circulating intestinal permeability levels than their non-lean counterparts. These findings suggest the role of gut dysbiosis, particularly the decrease of SCFAs-producing bacteria, and increased intestinal barrier disruption that might contribute to the pathogenesis and disease severity of lean MASLD.

THU-274

Targeting mitochondrial complex I modulates lipid metabolism, inflammation and hepatic fibrosis in a MCD-diet model of benign steatosis

Francesca Protopapa¹, Laura Giuseppina Di Pasqua¹, Michelangelo Trucchi¹, Erica Scotti¹, Peng Sun², Stefan Günther Kauschke³, Mariapia Vairretti¹, Anna Cleta Croce⁴, Andrea Ferrigno¹. ¹Department of Internal Medicine and Therapeutics, University of Pavia, Pavia, Italy; ²Boehringer Ingelheim Pharma GmbH and Co. KG, Biberach an der Riss, Germany; ³Boehringer Ingelheim Pharma GmbH and Co. KG, Biberach an der Riss, Germany; ⁴Institute of molecular genetics, Italian National Research Council (CNR), Pavia, Italy Email: francesca.protopapa@unipv.it

Background and aims: MASLD affects 25% of the global population, rising up to 75% in obese or diabetic people. The transition from simple steatosis to MASH is driven by oxidative stress and mitochondrial dysfunction. ROS promote pro-inflammatory cytokine release and chronic inflammatory response, along with HSC activation and hepatic fibrosis development. Mitochondrial complex I is the main ROS producer in MASLD progression, so this study aims to investigate whether the selective inhibition of complex I could contribute to reducing lipid accumulation, regulating specific lipid-related pathways, and mitigating hepatic fibrosis.

Method: male Wistar rats fed a Methionine and Choline deficient (MCD) diet or a Control diet for 6 weeks were orally administered (3 weeks) with complex I modulator (CIM, Boehringer Ingelheim) 10 mg/Kg/day or vehicle, starting from the 4th week. Lipid peroxidation and ROS production were evaluated using TBARS and DCHF-DA

methods. Nitrate/Nitrite concentration was established. Total lipid content was measured using Nile Red dye. The area of lipid droplets and the rate of inflammatory cell infiltration were calculated on HandE stained liver sections. Changes in the expression of factors involved in lipid metabolism (PPAR- α , SREBP1c and mTOR) were analyzed by Western Blot. Collagen deposition was calculated on Sirius Red stained liver sections.

Results: TBARS increased in MCD rats versus Control rats, without changes after CIM administration. ROS increased in MCD groups, but a significant reduction in CIM-treated Controls was detected, compared with untreated ones. Nitrate/Nitrite were reduced in CIM-treated MCD rats compared with untreated ones. Hepatic total lipid content was significantly decreased in CIM-treated MCD rats compared with untreated ones. A significant decrease in lipid droplet areas was observed in CIM-treated MCD rats, compared with untreated ones. Inflammatory cell infiltration was reduced in MCD rats treated with CIM, together with a significant reduction in collagen deposition in Control rats treated with CIM and in CIM-treated MCD rats, compared with untreated groups. Nuclear expression of PPAR- α significantly increased in MCD rats treated with CIM, compared with untreated ones. Nuclear SREBP1c expression was reduced in CIM-treated control and MCD rats, although not significantly. The same trend, significant for Controls, was observed for the ratio P-mTOR/mTOR. Lastly, AST and ALT were decreased in CIM-treated Controls, compared to untreated ones.

Conclusion: this study demonstrates for the first time that administration of complex I modulator could be a feasible strategy to counteract lipid accumulation, inflammation and collagen deposition in a MCD model of steatosis. Although further investigations are needed, these data suggest a promising role of CIM in the modulation of lipid metabolism in a model of benign steatosis.

THU-275

Interleukin 10 reduces fat accumulation and promotes fatty acid degradation and intracellular glucose maintenance in a high-fat-diet mouse model of metabolic dysfunction-associated steatotic liver disease

Akira Kado^{1,2}, Kazuya Okushin¹, Takeya Tsutsumi¹, Kazuhiko Ikeuchi¹, Kyoji Moriya³, Hiroshi Yotsuyanagi⁴, Kazuhiko Koike^{1,5}, Mitsuhiro Fujishiro¹. ¹The University of Tokyo, Tokyo, Japan; ²Health Service Promotion, The University of Tokyo, Tokyo, Japan; ³Tokyo Health Care University, Tokyo, Japan; ⁴Medical Science, The University of Tokyo, Tokyo, Japan; ⁵Kanto Central Hospital, Tokyo, Japan Email: monteruterubest@gmail.com

Background and aims: Metabolic dysfunction-associated steatotic liver disease (MASLD) has been increasing globally, and causes fatty acid and glucose metabolism dysregulation; several MASLD cases are difficult to treat. Interleukin (IL) 10 is immunologically an anti-inflammatory cytokine, whereas it is previously shown to affect intracellular homeostasis, especially autophagy; its cytoprotective effect may be also expected. IL10 is more expressed in peripheral immune cells and liver tissues of patients with advanced MASLD than with relatively mild MASLD. Although the detailed effects of IL10 have not been elucidated, its cytoprotective effect may improve MASLD progression. In this study, we used a high-fat diet (HFD) mice to assess changes in hepatic fat accumulation, and fatty acid and glucose metabolism induced by IL10; these changes were also assessed in vitro.

Method: Six-week-old male C57BL/6J mice were fed with either normal diet (ND) or HFD for 6 weeks. Mice fed with both the ND and HFD were treated with or without IL10 (50 μ g/kg) once every two days for a week before sacrifice. Body weight (BW), liver weight (LW)/BW ratio, blood biochemistry, and liver histology were evaluated. Changes in fatty acid and glucose metabolism were also evaluated in mRNA and protein levels using real-time PCR and western blotting. Furthermore, these changes were evaluated in vitro in normal human

POSTER PRESENTATIONS

hepatocytes using palmitic acid (PA) and various concentrations of IL10.

Results: In the HFD group, LW/BW ratio and serum ALT level were significantly decreased in the IL10-treatment group. Histological analysis revealed that IL10 treatment led to a significant reduction of hepatic steatosis and lobular inflammation; no histological findings of ballooning and fibrosis were observed. The IL10-treatment group showed a significant decrease in fatty acid synthase (FAS) and a significant increase in fatty acid degrading enzyme [carnitine palmitoyltransferase (CPT) 1/2] and glucose metabolism-related enzymes [glucose transporter (GLUT) 2, glycogen synthase (GS), phosphoenolpyruvate carboxykinase (PCK) 1] compared to the non-treatment. In the ND group, few significant changes were observed between these two groups. Focused on the IL10 non-treatment groups, the HFD mice showed a significant increase in FAS, CPT 1/2, GLUT2, and GS, and a significant decrease in PCK1 compared to the ND. These results suggested that fatty acid synthesis upregulated by HFD was reduced by IL10, and fatty acid degradation and intracellular glucose maintenance were promoted. Furthermore, in the presence of PA, similar results were observed in normal hepatocytes by IL10 treatment in vitro.

Conclusion: These results indicate that IL10 can reduce hepatic fat accumulation and promote intracellular glucose uptake and energy maintenance; IL10 offers the potential as a novel therapy for MASLD.

THU-278

Digital pathology with artificial intelligence analysis provides insight to the efficacy of anti-fibrotic compounds in human 3D MASH model

Radina Kostadinova¹, Simon Ströbel¹, Li Chen², Katia Fiaschetti-Egli¹, Jana Gadiant¹, Agnieszka Pawlowska Pawlowska¹, Louis Petitjean², Manuela Bieri¹, Eva Thoma¹, Mathieu Petitjean^{2,3}. ¹InSphero AG, Schlieren, Switzerland; ²PharmaNest, Princeton, United States; ³PharmaNest, Inc, Princeton, United States
Email: radina.kostadinova@insphero.com

Background and aims: Metabolic dysfunction-associated steatohepatitis (MASH) is a severe liver disease characterized by lipid accumulation, inflammation and fibrosis. The development of MASH therapies has been hindered by the lack of human translational models and limitations of analysis techniques for fibrosis. Here we aimed to establish an algorithm for automated phenotypic quantification of fibrosis of Sirius Red stained histology sections of MASH hLiMTs model using a digital pathology quantitative single-fiber artificial Intelligence FibroNest image analysis platform.

Method: The MASH hLiMT model consists of primary human hepatocytes, Kupffer cells, liver endothelial cells and hepatic stellate cells. Upon exposure to defined lipotoxic and inflammatory stimuli such as free fatty acids and LPS in media containing high levels of sugar and insulin the 3D MASH model displayed key disease pathophysiological features within 10 days of treatment. Quantifiable markers were established for drug efficacy testing such as secretion of pro-collagen type I/III and TIMPs/MMPs as well as quantification of fibrosis using FibroNest platform based on the Sirius Red staining of histology slides. Next generation sequencing was used for the assessment of the gene expression changes.

Results: The FibroNest algorithm for MASH hLiMTs was validated using anti-fibrotic reference compounds with different therapeutic modalities-ALK5i and anti-TGF-beta antibody. The phenotypic quantification of fibrosis demonstrated that both reference compounds decreased the deposition of fibrillated collagen in alignment with effects on the secretion of pro-collagen type I/III, tissue inhibitor of metalloproteinases-1 and matrix metalloproteinase-3 and pro-fibrotic gene expression. In contrast, clinical compounds, Firsocostat and Selonsertib, alone and in combination showed strong anti-fibrotic effects on the deposition of collagen fibers, however less pronounced on the secretion of pro-fibrotic biomarkers.

Conclusion: In summary, the phenotypic quantification of fibrosis of MASH hLiMTs combined with secretion of pro-fibrotic biomarkers and transcriptomics represents a promising drug discovery tool for assessing anti-fibrotic compounds.

THU-279

Time-restricted feeding alleviates metabolic associated fatty liver disease via PPAR-related lipid metabolism signaling pathway

Jiang Deng¹, Yikai Wang¹, Xiongtao Liu¹, Xiaoli Jia², Shuangso Dang¹, Juanjuan Shi¹. ¹the Second Affiliated Hospital of Xi'an Jiaotong University, Xi'an, China; ²the Second Affiliated Hospital of Xi'an Jiaotong University, Xi'an, China
Email: juanjuan_shi@xjtu.edu.cn

Background and aims: Specific drugs for treating metabolic associated fatty liver disease (MAFLD) are lacking. In this study, we analyzed the efficacy and mechanism of time-restricted feeding (TRF) and caloric restriction (CR) to provide a theoretical basis for the treatment and prevention of MAFLD.

Method: Fifty Sprague-Dawley (SD) rats were randomly divided into the normal group (10 kcal% fat, n = 12) and the MAFLD group (60 kcal % fat, n = 38) for 10 weeks. The MAFLD group was randomly divided into the TRF group (4 h TRF=feeding at 18:00–22:00), the caloric intake (CR) group (60% CR=the food intake per unit body weight of normal control rats was multiplied by 60%), the TRF+CR group (feeding at 18:00–22:00 and 60% CR) and the model group (free eating), which were fed normal diet (10 kcal% fat) for 14 weeks. Body weight, daily food intake, liver lipid content and biochemical indices were measured, differentially abundant metabolites were screened using liquid chromatography tandem mass spectrometry (LC-MS/MS), and the related molecular mechanism was analyzed using Kyoto Encyclopedia of Genes and Genomes (KEGG) analysis and RT-PCR.

Results: After the high-fat diet was discontinued, the lipid content of the liver of MAFLD rats was significantly reduced, but the weight was not significantly changed. The body weight in the model group were heavier than those in the other four groups ($p < 0.01$). Triglyceride (TG) levels were higher in the TRF+CR group than in the model group ($p < 0.01$); however, there were no significant differences among the other groups. The average daily food intake of the individuals in the normal group, the TRF group, the CR group, the TRF+CR group and the model group were significant differences compared with those in the normal group ($p < 0.001$), and 4 h TRF restricted approximately 29% of the daily food intake. KEGG pathway enrichment indicated that the mechanism of liver lipid clearance involved the PPAR signaling pathway, AMPK signaling pathway, metabolic pathway, etc. Importantly, we observed differences in SIRT1 mRNA levels among the five groups ($p = 0.003$). Compared with those in the normal group, the SIRT1 mRNA levels in the other four groups were significantly increased only in the CR group and the model group ($p < 0.05$). The mRNA expression levels of PPAR α and SIRT1 in the TRF+CR group were lower than those in the TRF, CR and model groups.

Conclusion: We observed that 4 h TRF, 60% CR and 4 h TRF+60% CR significantly reduced body weight and liver lipid content in MAFLD rats, 4 h TRF+60% CR significantly increased serum TG levels, and 4 h TRF improved MAFLD without restricting food intake. These findings may be related to PPAR-related lipid metabolism signaling pathway.

THU-280

DC-SIGN+ macrophages alleviates non-alcoholic steatohepatitis by modulating inflammatory cytokine secretion

Jinxia Liu¹, Haifeng Wu², Xiaojun Zhang², Qin Jin², Huoyan Ji², Lishuai Qu², Rajiv Jalan³, Chunhua Wan⁴. ¹Affiliated Hospital of Nantong University, Nantong, China; ²Affiliated Hospital of Nantong University, Nantong, China; ³UCL Institute for Liver and Digestive Health, London, United Kingdom; ⁴Nantong University, Nantong, China
Email: chwan@ntu.edu.cn

Background and aims: The modulation of immune responses by innate immune receptors plays a crucial role in the progression of

non-alcoholic steatohepatitis (NASH). In this study, we aim to comprehensively investigate the involvement and mechanisms by which the C-type lectin receptor DC-SIGN modulates macrophage inflammatory responses and NASH progression.

Method: Histological analyses were utilized to investigate DC-SIGN expression profile in patients with NASH and healthy subjects. Additionally, immunofluorescence was employed to examine specific cell types expressing DC-SIGN. Adeno-associated viruses (AAV) carrying human DC-SIGN or control viruses were administered via tail vein injection to mice fed with either a high-fat and high-cholesterol (HFHC) diet or a normal chow diet (NCD). Moreover, THP1-differentiated macrophages were employed as an in vitro macrophage model to investigate the molecular mechanism by which DC-SIGN participates in inflammatory regulation.

Results: The expression of DC-SIGN was decreased in the liver tissues from NASH patients and HFHC-fed mice, as well as macrophages stimulated with LPS or PA. Remarkably, the transduction of human DC-SIGN into the livers of HFHC-fed mice notably ameliorated liver lipotoxicity, hepatic steatosis, inflammation, and fibrosis. Additionally, DC-SIGN facilitates macrophage TLR4 endocytosis via direct TLR4 binding, leading to the attenuation of pro-inflammatory environments during NASH progression.

Conclusion: Overall, our findings highlight an active crosstalk between DC-SIGN and TLR4 within hepatic macrophages, demonstrating a protective effect of DC-SIGN in NASH progression. Collectively, this study highlights a promising potential of manipulating macrophage DC-SIGN expression as a novel therapeutic strategy for NASH.

THU-281

Gut dysbiosis is associated with the severity of liver fibrosis assessed by magnetic resonance elastography in patients with MAFLD

Thananya Jinato¹, Nantawat Sathawiwat¹, Natthaya Chuaypen¹, Pisit Tangkijvanich¹. ¹Center of Excellence in Hepatitis and Liver Cancer, Faculty of Medicine, Chulalongkorn University, Bangkok, Thailand
Email: pisittkvn@yahoo.com

Background and aims: The gut microbiome might affect the severity of metabolic dysfunction-associated steatotic liver disease (MASLD), however, data regarding their association in Asian populations are limited. We analyzed the differences in gut microbial composition in Thai patients with MASLD according to the severity of liver fibrosis assessed by magnetic resonance (MR) imaging.

Method: This cross-sectional study included 157 patients with MASLD (51% male, mean age 56 ± 10 years). Liver steatosis grades ≥1 were identified by MR-proton density fat fraction (PDFF) ≥5.2%. Based on MR-elastography (MRE) at the cut-off of 2.97 kPa, there were 131 and 26 patients with mild fibrosis (F01) and significant fibrosis (F234), respectively. Fecal specimens were sequenced targeting the V4 region of the 16S rRNA gene and analyzed using the nf-core amplicon bioinformatics pipeline. Differential analysis of individual taxa between two groups was conducted through linear discriminant analysis effect size (LEFSe), employing a cut-off of LDA Effect Size >2 and a significance level of p < 0.05.

Results: There was no significant difference in alpha-diversities (Chao1, Shannon, and Simpson indices) between patients with F01 and F234. However, the beta diversity significantly differed between the two groups (p = 0.012). A high abundance of *Fusobacterium*, a pathogenic bacteria contributing to the inflammatory process and carcinogenesis, was significantly detected in fecal samples of patients with F234 compared with the F01 group (OR = 3.31, 1.30–8.42, p = 0.012). Additionally, enriched *Fusobacterium* significantly correlated with MRE (kPa) (r = 0.235, p = 0.003). In contrast, the abundance of *Lachnospira*, a short-chain fatty acid-producing bacterium, was significantly lower in patients with F234 compared with the F01 group (OR = 0.38, 0.15–0.93, p = 0.033). The enrichment of

Lachnospira was also negatively correlated with MRE (r = -0.206, p = 0.010).

Conclusion: In an analysis of the gut microbiome of Thai patients with MASLD, we found that gut dysbiosis was correlated with the severity of liver disease. Specifically, the greater abundance of bacterial genera involving inflammatory processes and lower enrichment of beneficial bacteria was significantly associated with fibrosis severity in patients with MASLD. Thus, an altered gut microbiome might contribute to the pathogenesis of MASLD and could be used as biomarkers of disease severity.

THU-282

Evaluation of performance of a cellular profiling technique for quantification of inflammation and steatosis in liver biopsies of patients with MASH

Adi Lightstone^{1,1}, Li Chen¹, Dmitri Fedorov², Mathieu Petitjean¹.

¹PharmaNest, Princeton, United States; ²ViQi, Santa Barbara, United States

Email: adi.lightstone@pharmanest.com

Background and aims: The gold standard for assessment of liver inflammation and steatosis is through pathologist analysis of MASH biopsies. Using a new AI cellular detection, classification, and quantification method trained on pathologist annotations of individual cells and validating the results on pathologist classification of the overall tissue we can generate a quantitative continuous score based on single cell analysis. This is an asset to RandD, diagnosis, as well as addressing limitations of current histological nomenclatures and methods (doi:10.1002/hep.32475).

Method: This retrospective study included 87 NASH liver biopsies diagnosed by a pathologist for histologic assessment resulting in lobular inflammation grades of 0 (N = 7), 1 (68), and 2 (12), and steatosis grades of 0 (N = 2), 1 (40), 2 (30) and 3 (14). Quantitative image analysis of these biopsies stained with HandE detects cell nuclei (~20 k per biopsy) and quantify their morphometric and local surroundings in 86 parameters. A subset of 18 images (~260 K nuclei) was used to develop a machine learning (ML) model using 34.8 K annotations (respectively 7.3 K, 12 K, 7.8 K, 5.4 K, 2.3 K) for steatotic hepatocytes, normal hepatocytes, inflammatory cells (all kinds), liver specialized cells (all kinds), and “debris” (degraded cellular bits). Once the cells were classified, the density (count/mm²) and relative cell count (%) for each cell type were calculated. Macro-steatosis Area Ratio was calculated through vacuole detection as a secondary method (the first being comparison of the cell detection to pathologist definition). Clusters of inflammatory cells were segmented into “small,” “medium,” and “Large” foci.

Results: The cell classification accuracy (error) of the ML model ranged from 65.2% (28%) for specialized cells to 91.1% (11.7%) for inflammatory cells. The steatotic hepatocytes count ratio (detected from ML from pathologists’ annotations) correlates well with Steatosis Area Ratio (R² = 0.5989). The Inflammatory cell ratio (percent of cells that are inflammatory) corresponds well with the Inflammation grades (p 0v1 = 0.12, p 0v2 = 0.015), count of small inflammation foci clusters (p 0v1 = 0.053, p 0v2 = 0.015) moderately corresponds to the histological grades, which is attributed to the histological definition of inflammatory clusters and their assessment.

Conclusion: Quantitative digital pathology can automatically generate tissues panels from HandE stained biopsies. While the scores extracted from these tissue panels correspond to NASH-CRN histological stages, they present the benefit of being quantitative and translational, and not sensitive to liver tissue variation due to swelling, fat invasion, or other various artifacts. The marked improvement from previous work by PharmaNest also demonstrates that the field is improving, and more work can be done to further advance AI digital pathology methods.

POSTER PRESENTATIONS

THU-283

Characterisation of peptidylprolyl isomerase C as a novel player in the pathogenesis of chronic liver disease

Isabel Fuster-Martínez^{1,2}, Ana Benedicto^{2,3}, Cristina Benavides^{1,2}, José Català-Senent⁴, Marta Hidalgo⁴, Francisco García-García⁴, Joan Tosca⁵, Cristina Montón⁵, Juan V. Esplugues^{1,2,6}, Nadezda Apostolova^{1,2,6}, Ana Blas-García^{2,6,7}. ¹Departamento de Farmacología, Universitat de València, Valencia, Spain; ²FISABIO (Fundación para el Fomento de la Investigación Sanitaria y Biomédica de la Comunidad Valenciana), Valencia, Spain; ³Departamento de Farmacología, Universitat de València, Valencia, Spain; ⁴Bioinformatics and Biostatistics Unit, Príncipe Felipe Research Center, Valencia, Spain; ⁵Departamento de Medicina Digestiva, Hospital Clínico Universitario de Valencia, Valencia, Spain; ⁶CIBERehd (Centro de Investigación Biomédica en Red de Enfermedades Hepáticas y Digestivas), Spain, Spain; ⁷Departamento de Fisiología, Universitat de València, Valencia, Spain
Email: isabel.fuster-martinez@uv.es

Background and aims: Pan-cyclophilin inhibitors have been proposed as a strategy for the treatment of metabolic dysfunction-associated steatotic liver disease (MASLD). Although some members of this enzyme family are described to participate in MASLD pathogenesis, little is known about peptidylprolyl isomerase C (PPIC), whose expression was found to be increased in the liver of patients with chronic liver disease (CLD). Our aim was to characterise its role in this pathology.

Method: Gene expression of *PPIC* was analysed in different experimental models of liver injury: *in vivo*, in a meta-analysis from published transcriptomic studies of liver samples of murine models of high fat diet (HFD), with and without anti-steatotic treatments, and in murine models of CCl₄ and Bile Duct Ligation (BDL); and *in vitro*, in fatty acid (FA)-overloaded human hepatoma cells (Hep3B) and TGFβ1-stimulated human hepatic stellate cells (HSCs) (LX-2 cell line). Plasmatic PPIC levels in MASLD patients and healthy controls were measured by ELISA. Furthermore, we examined the effect of silencing *PPIC* in Hep3B and LX-2 cells, analysing cell viability (MTT and phosphatase activity assays), RNA and protein expression (qPCR and Western blotting, respectively), and reactive oxygen species (ROS) levels (CM-H₂DCFDA assay).

Results: Hepatic expression of *Ppic* was significantly increased in all the mouse models of liver injury studied (HFD, CCl₄ and BDL) and reversed by the anti-steatotic treatments investigated in the meta-analysis. It was also upregulated in FA-overloaded Hep3B cells and TGFβ1-stimulated HSCs. In addition, plasma levels of PPIC were significantly increased in MASLD patients (n = 12) compared to healthy donors (n = 11). When *PPIC* was silenced in Hep3B cells, cell viability was not changed, but there was an induction of the IRE1α-XBP1 pathway (involved in the ER stress response) and a reduction in NF-κB phosphorylation and the expression of the chemokines CXCL9 and CXCL10. In LX-2 cells, *PPIC* silencing did not alter cell viability, but showed a tendency to increase ROS levels. Moreover, it triggered pathways associated with the ER stress response (IRE1α-XBP1 and PERK/eIF2α) and promoted the pro-fibrotic state of these cells, since it increased mRNA and protein levels of collagens and α-SMA. It also downregulated the gene expression of the NLRP3-inflammasome components in these cells.

Conclusion: PPIC may be a marker of CLD since it was elevated in the liver of several experimental models and in the plasma of patients with MASLD. However, its role in CLD may be pleiotropic, as silencing of PPIC downregulated some pro-inflammatory mediators in a hepatoma cell line and induced a cellular stress response together with a pro-fibrotic effect in a HSCs cell line.

THU-284

Prediction of MASH features from liver biopsy images using a pre-trained self-supervised learning model

Yang Wang¹, Saurabh Vyawahare¹, Carson McNeil¹, Jessica Loo¹, Marc Robbins¹, Roman Goldenberg¹. ¹Verily Life Sciences, South San Francisco, United States
Email: wayang@verily.com

Background and aims: Using neural networks to identify medically relevant features from histology slide images has greatly increased recently. However, as adoption of the technique becomes available for more diseases, the demand for and expense of training data rises as well. Digital pathology images are gigapixel (s) in size, and a single slide can contain many features. These features are both very time consuming for human annotations due to size alone, and need trained experts, making annotations extremely expensive. To address this problem, self-supervised pathology foundation models trained on existing corpuses of unlabeled training data, such as The Cancer Genome Atlas (TCGA) can be used. These foundation models can serve as a module in the network architecture, reducing the labeled data requirement.

Method: We take an SSL model based on vision transformers (*arXiv preprint arXiv:2310.13259* 2023), which is trained on hematoxylin and eosin (H&E) slides. The SSL model takes as input a 224 × 224 × 3 image patch and outputs an embedding vector. We apply this model to predict features relevant to metabolic dysfunction-associated steatohepatitis (MASH), including inflammation, steatosis, and ballooning. The MASH-labeled data is from the CENTAUR study (*Hepatology*, 72 (3), pp.892–905) which we previously analyzed (in *Modern Pathology* 37.2 (2024): 100377) using fully supervised models. Note that the original SSL model was not trained on the images from this dataset. To apply the SSL model, we perform a two-stage process. First, we use the SSL model as a component in an architecture trained on the smaller set of labeled images to produce a patch classification. Second, the patch classifications are aggregated over a slide to make a slide-level prediction.

Results: While use of the SSL model produced patch-level results similar to previous work on this dataset (*Modern Pathology* 37.2 (2024): 100377), superior results were obtained for grading of ballooning and lobular inflammation slide level scores. Our model had an AUC improved from 0.77 to 0.88 for ballooning, and 0.76 to 0.85 for lobular inflammation. Steatosis performance remained high and consistent. We believe this reflects better generalizability of the model, and increased resilience to messy patch-level labels. We also show that the amount of data needed to segment features of MASH on liver biopsy images is reduced, and in addition, training is made simpler and faster.

Conclusion: Self-supervised foundation models can improve machine learning performance in digital pathology, including for liver diseases. These models can lead to better downstream generalization, and allow training using smaller labeled datasets.

THU-285

Low nonpsychedelic dosed of psilocybin for the therapy of MASLD

Martina Colognesi¹, Daniela Gabbia¹, Andrea Rinaldi², Luciano Cascione², Ilaria Zanotto¹, Stefano Comai³, Katia Sayaf⁴, Andrea Mattarei¹, Marco Banzato¹, Gianfranco Pasut³, Franco Folli⁵, Lucia Centofanti⁵, Sergio Traversa⁶, Marco Pappagallo⁶, Paolo Manfredi⁶, Sara De Martin¹. ¹Department of Pharmaceutical and Pharmacological Sciences, University of Padova, Padova, Italy; ²Genomic Facility, IOR Institute of Oncology Research, Università della Svizzera Italiana, Bellinzona, Switzerland; ³Department of Pharmaceutical and Pharmacological Sciences, University of Padova, Padova; ⁴Department of Surgery, Oncology and Gastroenterology, University of Padova, Padova, Italy; ⁵Department of Health Science, Università degli Studi di Milano, Milano, Italy; ⁶Relmada Therapeutics Inc., Miami, United States
Email: sara.demartin@unipd.it

Background and aims: Psilocybin, an alkaloid of *Psilocybe* mushrooms known for its psychedelic activity after its dephosphorylation to the active compound psilocin, is an agonist of the serotonin receptor 2A isoform (5-HT_{2A}R) and has been shown to reduce weight gain in animal models, although the relevance and mechanism of this effect is controversial. No data are available on the effect of psilocybin in MASLD, which is often associated to obesity. The aim of this study is to assess the activity, toxicity, and mechanism of psilocybin in mice with MASLD induced by a diet rich of fat and fructose (HFHFD).

Method: The effect of psilocybin was tested on 20 C57BL/6 male mice fed with HFHFD for 17 weeks. The treatment group (n = 10) received daily 0.05 mg/Kg*bw psilocybin orally, while the control group (n = 10) received vehicle. Standard diet-fed mice (n = 10) were used as healthy controls. Body weight and food intake were assessed twice weekly. The oral glucose tolerance test (OGTT) and a selection of behavioral studies were performed before sacrifice. MASLD was histologically evaluated by HandE and ORO staining. Blood immunophenotyping was performed by FACS. Alterations in the global hepatic transcriptome were evaluated by RNA sequencing. The expression of proteins involved in insulin signaling was assessed by western blot and immunohistochemistry. Mechanistic studies were performed in HepG2 cells treated with palmitic and oleic acid (1:2, 0.1 mM).

Results: In MASLD mice, psilocybin did not cause central detrimental effects, but a reduction of anxiety-like behavior, $p < 0.05$. Body weight gain, hepatic fat deposition, fasting glucose and plasma triglycerides ($p < 0.05$) were significantly reduced by the treatment. Gene ontology analysis (GO-Biological Processes, GOBP) on mRNA-seq data revealed that psilocybin restored the basal hepatic expression of the gene sets involved in the localization and organization of lipid droplets, and the catabolic processes of lipids, which are dysregulated in MASLD mice. The improvement of insulin sensitivity observed in the OGTT ($p < 0.05$) was confirmed by the normalization of the hepatic insulin signaling, since the protein expression of insulin receptor and IRS-1 was increased vs untreated mice ($p < 0.05$). Immune function was also affected, since psilocybin reverted the increase of PD-1-expressing exhausted NK cells, which was present in MASLD mice ($p < 0.01$). The pivotal role of hepatic 5HT_{2A}R in the metabolic effects of psilocin was confirmed since the pharmacological inhibition of ketanserin abrogated the psilocin-induced reduction of lipid accumulation in HepG2 cells.

Conclusion: Low, nonpsychedelic doses of psilocybin significantly ameliorate MASLD features in experimental models, by a 5-HT_{2A} mediated pleiotropic action. Psilocybin may be considered as a candidate drug for MASLD and associated metabolic disorders.

THU-286

PNPLA3 p.I148M variant affects lipid droplets number and size in patient-derived liver organoids

Elia Casirati¹, Alessandro Cherubini¹, Laura Cerami¹, Fabrizia Carli², Amalia Gastaldelli², Daniele Prati¹, Daniele Dondossola³, Luca Valenti⁴. ¹Fondazione IRCCS Ca' Granda Ospedale Maggiore Policlinico; Transfusion Medicine and Hematology, Milano, Italy; ²National Research Council (CNR), Institute of Clinical Physiology (IFC), Pisa, Italy; ³Fondazione IRCCS Ca' Granda Ospedale Maggiore Policlinico, Hbp Surgery and Liver Transplantation Unit, Milano, Italy; ⁴Fondazione IRCCS Ca' Granda Ospedale Maggiore Policlinico; Transfusion Medicine and Hematology, Università Degli Studi di Milano; Department of Pathophysiology and Transplantation, Milano, Italy
Email: e.casirati@gmail.com

Background and aims: PNPLA3 rs738409 C>G p.I148M variant is the main genetic determinant of metabolic dysfunction-associated steatotic liver disease (MASLD). To this day, this association still lacks a molecular characterization, due to the lack of comprehensive human models. To overcome this gap in knowledge, we generated patient-derived human liver organoids (HLOs) and studied lipid accumulation across different PNPLA3 genotypes.

Method: We generated HLOs from 49 surgical specimens (14 I/I, 24 I/M and 11 M/M for PNPLA3 p.I148M). HLOs were differentiated toward a hepatocyte-like phenotype (Hep-HLO) and exposed to 300 μ M Palmitic and Oleic fatty acids (FAs) for 72 h. Lipid droplets (LDs) average size and number (normalized for nuclei) were quantified by NileRed staining and compared between PNPLA3 Hep-HLOs (n = 3 for each genotype). Finally, lipidomics were conducted on 3 wild-type and 3 homozygous Hep-HLO lines, treated or not with 300 μ M Palmitic and Oleic Acid for 3 days.

Results: As a propaedeutic step, we ascertained that Hep-HLO retain PNPLA3 expression before evaluating its genotype impact on LDs. Untreated organoids displayed LDs average sizes of $0.51 \pm 0.26 \mu\text{m}^2$ (I/I), $0.51 \pm 0.23 \mu\text{m}^2$ (I/M) and $1.31 \pm 1.41 \mu\text{m}^2$ (M/M). While FAs did not impact on average LD size, M/M Hep-HLOs displayed larger LDs ($p = 0.002$ of I/I vs M/M, $p = 0.0002$ for I/M vs MM). Conversely, LDs number were 7.28 ± 5.16 , 21.17 ± 12.40 and 53.14 ± 60.2 in I/I, I/M, M/M respectively, and increased to 18.61 ± 9.31 , 47.68 ± 30.16 and 81.46 ± 54.59 upon exposure to FAs. After ANOVA testing, 23.9% of variability in LDs number can be attributed to genotype and 6.9% to FAs ($p < 0.0001$ for both). Lipidomic analyses highlighted an enrichment of sphingomyelins, lysophosphatidylcholines and ceramides in PNPLA3 M/M Hep-HLO, which was exacerbated by FAs administration. These lipid species are associated with cellular damage, inflammation, Insulin resistance, oxidative stress and MASH development. The opposite trend was observed for phosphatidylcholines, which are essential for LDL loading and triacylglycerols export from the liver and whose levels drop during MASLD development.

Conclusion: Regardless of FA treatment, M/M Hep-HLOs show increased LDs size when compared to I/M and I/I. Conversely, LDs number showed direct correlation with the number of mutated alleles, suggesting that the p.I148M substitution promotes the formation of new LDs, which was exacerbated by exposure to FAs. Preliminary lipidomic analyses highlight an unbalance towards lipid species that are proinflammatory and pro-apoptotic in Hep-HLO homozygous for PNPLA3 rs738409. Overall, these data corroborate the robustness of Hep-HLO as a preclinical in vitro model for genetic predisposition for MASLD. We are now developing siRNAs specific for silencing PNPLA3 rs738409 transcripts to examine the impact on LD phenotypes.

THU-287

Dysregulation of ureagenesis and glutaminolysis in DIAMONDTM mice played a major role in MASLD progression

Rocío Gallego-Durán^{1,2}, Douglas Maya^{1,2}, Lucía López-Bermudo^{3,4}, M^a José Robles-Frias⁵, Blanca Escudero-López^{3,4}, Antonio Cárdenas-García^{3,4}, Rocío Montero-Vallejo^{1,2}, Sheila Gato-Zambrano^{1,2}, Vanessa García-Fernández¹, Ángela Rojas Álvarez-Ossorio^{1,2}, Rocío Muñoz-Hernández^{1,2}, Antonio Gil-Gómez^{1,2}, Francisco Javier Cubero^{2,6}, Javier Vaquero^{2,7}, Jordi Gracia-Sancho^{2,8}, Rafael Bañares^{2,7}, Franz Martin-Bermudo^{3,4}, Javier Ampuero^{1,2,9}, Manuel Romero-Gómez^{1,2,9}. ¹Seliver Group, Instituto De Biomedicina De Sevilla (IBiS), Hospital Universitario Virgen Del Rocío/Csic/Universidad De Sevilla, Sevilla, Spain; ²Centro De Investigación Biomédica En Red De Enfermedades Hepáticas y Digestivas (CIBEREHD), Madrid, Spain; ³Centro Andaluz de Biología Molecular y Medicina Regenerativa-CABIMER, Universidad Pablo de Olavide, Universidad de Sevilla, Consejo Superior de Investigaciones Científicas (CSIC), Sevilla, Spain; ⁴CIBERDEM-, Centro de Investigación Biomédica en Red de Diabetes y Enfermedades Metabólicas Asociadas, Sevilla, Spain; ⁵Pathology Department, Hospital Universitario Virgen del Rocío, Sevilla, Spain; ⁶Departamento de Inmunología, Oftalmología y ORL, Facultad de Medicina, Universidad Complutense de Madrid, Madrid, Spain; ⁷HepatoGastro Lab, Servicio de Ap. Digestivo del HGU Gregorio Marañón, Instituto de Investigación Sanitaria Gregorio Marañón, Spain Centro Nacional de Investigaciones Cardiovasculares (CNIC), Madrid, Spain; ⁸Liver Vascular Biology Research Group, IDIBAPS Biomedical Research Institute, Barcelona, Spain; ⁹UCM Digestive Diseases. Hospital

POSTER PRESENTATIONS

Universitario Virgen Del Rocío, Sevilla, Spain
Email: mromerogomez@us.es

Background and aims: The main aim of our study was to evaluate the implication of ammonia metabolism on MASLD progression in a DIAMOND™ preclinical model under different dietary interventions.

Method: DIAMOND mice (Sanyal Biotechnology, n=28) were randomized to three dietary regimens with different lengths: high-fat diet supplemented with fructose/glucose in drinking water (HF-HFD), choline-deficient high-fat diet model supplemented with 0.1% methionine (CDA-HFD) or standard diet, which was used as a control. HF-HFD and control animals were sacrificed after 21 or 30 weeks of diet intake and CDA-HFD animals were sacrificed after 12 weeks. Oral glutamine challenge (OGC) was performed by gavage administering glutamine (0.5 g/kg) in n=14 animals, and ammonia levels were evaluated at 0, 30, 60, 90, 120, 180 and 240 minutes. AUROC was calculated in microg/dl/h. Liver damage characterization included markers for fibrosis (collagen deposition and COL3A1, COL1A1, and α -SMA expression levels) and inflammation (TNF- α and IL-6 expression). An anatomopathologist blinded to provenance of samples calculated liver fibrosis and NAS Score. UCEs and glutaminase-1 (GLS-1) expression levels were evaluated by qRT-PCR.

Results: Both dietary interventions promoted a general upregulation of fibrotic and inflammatory markers, especially marked in CDA-HFD animals when compared to controls: COL3A1 (17.6 fold [CI95% 12.8–22.4] vs. 1 fold [CI95% 0.67–1.3]; p=0.001) and TNF- α (21.5 fold [CI95% 12.8–30.2] vs. 1 fold [CI95% 0.3–1.9]; p=0.002). CDA-HFD animals showed higher NAS Score rates than both 30w controls (6.8 ± 0.4 vs. 0.33 ± 0.52 ; p<0.001) and HF-HFD (6.2 ± 1.5 ; p=ns). Transcriptomic evaluation of UCEs revealed a significant mRNA downregulation in carbamoyl phosphate synthetase-1 (CPS1) and ornithine transcarbamylase (OTC1) in both CDA-HFD and HF-HFD animals versus controls, together with an increase in GLS1 expression in all groups of animals. Further, GLS1 was correlated with hepatic α -actin (r=0.792; n=28; p<0.001) and TNF- α (r=0.876; n=28; p<0.001). CDA-HFD animals showed increased ammonia levels when compared to controls (54.3 ± 19.23 mcg/dl/h) vs. controls (29.5 ± 2.2 mcg/dl/h; p<0.05), and HF-HFD animals showed an increased trend that did not reach statistical significance (51.87 ± 29.95 mcg/dl/h; p=ns). OGC was found altered in 4/5 CDA-HFD and all HF-HFD mice; $\chi^2 = 10, 73$; p<0.005. A positive correlation was found between ammonia and weight gain (r=0.543; n=14; p<0.045). Multiple linear regression revealed that both GLS-1 and weight gain were independent predictors for liver fibrosis progression.

Conclusion: Ammonia metabolism was found impaired in both production and detoxification in DIAMOND mice. OGC dysregulation were correlated with weight gain and a higher expression of GLS-1. These alterations could play a key role in the development and progression of MASLD.

THU-290-YI

Single nucleotide polymorphism analysis for predicting metabolic-associated fatty liver disease development in patients with severe obesity (types II and III)

Juan Manuel Jiménez-Aguilar¹, Andrea Jiménez-Franco², Helena Castañé³, Alina-Iuliana Onoiu², Vicente Cambra-Cortes², Cristina Placed-Gallego², Cristian Martínez-Navidad³, Jordi Camps⁴, Jorge Joven⁴. ¹Universitat Rovira i Virgili, Unitat de recerca Biomèdica, Reus, Spain; ²Universitat Rovira i Virgili, Unitat de recerca biomèdica, Reus, Spain; ³Fundació IISPV, Unitat de recerca biomèdica, Reus, Spain; ⁴Hospital Universitari Sant Joan de Reus, Unitat de recerca biomèdica, Reus, Spain
Email: juanmaaguilar106@gmail.com

Background and aims: Genome-wide Association Studies (GWAS) have revolutionized genetic exploration, providing crucial insights into complex disease mechanisms. This newfound genetic understanding holds immense promise for enhancing diagnostics and treatment strategies. This progress has proven especially invaluable

in Metabolic-Associated Fatty Liver Disease (MAFLD). GWAS approaches have revealed a multitude of Single Nucleotide Polymorphisms (SNPs) associated with MAFLD. However, the escalating prevalence of MAFLD driven by obesity underlines a pressing healthcare challenge. MAFLD's progression to severe stages like Metabolic-Associated Steatohepatitis (MASH) and advanced liver diseases emphasizes the urgent need for non-invasive diagnostic tools, early detection methods, and treatment strategies. The objective of this study was to determine if genetic variants identified through GWAS can serve as predictive indicators of MAFLD development in patients with obesity types II and III.

Method: The Open Array platform was utilized to genotype 25 specific SNPs from plasma samples. The study cohort comprised 1719 individuals, meticulously divided into the control group (n=415) and the severe obesity group (n=1313). The latter encompassed three subgroups: MAFL (n=137), MASH (n=532), and individuals without MAFLD (n=405). We subsequently conducted an extensive analysis to evaluate the correlation, significance, and strength of the identified SNPs across the various groups while assessing their predictive power for disease progression.

Results: Four significant SNPs (rs58542926, rs1800629, rs8107974, and rs5982) were discovered to be correlated with disease progression within the subset of severely obese patients. Among these, rs5982 (F13A1) exhibited dual significance in both MAFLD and obesity, with a stronger association observed for the disease. Notably, rs58542926 (TM6SF2) significantly affected steatosis scores, while rs1800629 (TNFA) correlated with inflammation scores. All identified SNPs presented weak associations and held little predictive power for disease progression.

Conclusion: The identified SNPs showed significant correlations with MAFLD progression in severely obese patients with obesity types II and III. However, these associations do not translate into robust predictive power for MAFLD progression assessment.

THU-291-YI

Cellular senescence is a common hallmark in diverse models of steatotic liver diseases

Charalampos Pavlidis¹, Mohsin Hassan¹, Marlene Kohlhepp¹, Juan Wang¹, Frank Tacke¹, Tobias Puengel¹, Pavitra Kumar¹, Cornelius Engelmann¹. ¹Charité-Universitätsmedizin Berlin, corporate member of Freie Universität Berlin and Humboldt-Universität zu Berlin, Berlin, Germany
Email: charalampos.pavlidis@charite.de

Background and aims: Senescence involves irreversible cell cycle arrest, triggering specific alterations while sustaining cellular viability. Cellular stress, injury, or disease conditions such as steatotic liver disease (SLD) are associated with an accumulation of senescent hepatocytes. This study seeks to elucidate the evolving role of cellular senescence in the progression of metabolic dysfunction-associated steatotic liver disease (MASLD) and metabolic alcohol-related liver disease (metALD), aiming to identify potential therapeutic targets for disease-modifying interventions.

Method: MASLD was induced in wild-type C57BL6/J mice using a choline-deficient, L-amino acid-defined, high-fat diet (CDAHFD) and a Western Diet (WD). We analyzed the effects of dietary interventions at different time points: CDAHFD: 8 and 12 weeks; WD 4, 7 and 16 weeks. Experimental metALD was induced by a combination of WD and 10% ethanol in drinking water for 4 weeks, followed by an ethanol binge (6 g/kg), and then sacrificed after 24 hours. To dissect the role of senescence in our independent models, we employed Western blot (WB), multiplex immunofluorescence (mIF), and senescence-associated beta-galactosidase (SA-beta-gal) focusing on senescence-associated markers (p53, p21, Lamin B1, ph-RB, Ki67, gamma-H2A.X).

Results: CDAHFD models showed steatosis and inflammation but no fibrosis, while in WD less steatosis and mild inflammation with no fibrosis were observed. Senescence-associated markers p53 (p<0.02), p21 (p<0.02), and gamma-H2A.X were markedly elevated in

CDAHFD models at 8 weeks, intensifying at 12 weeks (p53: $p < 0.03$; p21: $p < 0.008$). Lamin B1 ($p < 0.001$), ph-RB ($p < 0.02$), and Ki67 exhibited reduced expression at 8 weeks for CDAHFD, further decreasing at 12 weeks (Lamin B1: $p < 0.02$; ph-RB: $p < 0.02$). WD models displayed similar senescence trends at 4, 7, and 16 weeks for p53, p21, gamma-H2A.X, Lamin B1, ph-RB, and Ki67, confirmed by mIF as well as by heightened SA-beta-gal levels. Histologically, metALD models showed moderate to high amounts of overall cell death (TUNEL), but mild fibrosis with accumulated adipocytes. In addition, metALD models showed heightened p21 ($p < 0.03$) and p53 but reduced Lamin B1 ($p < 0.006$) and ph-RB in WB. These findings were corroborated by elevated SA-beta-gal levels and by mIF, which showed elevated levels of gamma-H2A.X and reduced levels of Ki67. CDAHFD group showed higher senescence after 12 weeks of WD than at 16 weeks. MetALD models had lower p21 expression and a smaller decrease in ph-RB than MASLD models.

Conclusion: MASLD and metALD induced senescence in hepatocytes, while overall increased senescent cell accumulation correlated with disease severity. CDAHFD accelerates the onset of senescence compared to the WD, highlighting the importance of dietary factors, when determining optimal timing for therapeutic interventions, including senolytics.

THU-292

Genome-wide association study identifies PTPRD associated with metabolic dysfunction-associated steatotic liver disease in South Korea

Dong Yun Kim¹, Heon Yung Gee², Jung Il Lee³, Jun Yong Park¹.

¹Division of Gastroenterology, Department of Internal Medicine, Yonsei University College of Medicine, Seoul, Korea, Rep. of South; ²Department of Pharmacology, Yonsei University College of Medicine, Seoul, Korea, Rep. of South; ³Department of Internal Medicine, Gangnam Severance Hospital, Yonsei University College of Medicine, Seoul, Korea, Rep. of South

Email: jlkyy@yuhs.ac

Background and aims: Numerous single nucleotide polymorphisms (SNPs) related to metabolic dysfunction-associated steatotic liver disease (MASLD) have been identified individually by Genome-Wide Association Studies (GWASs) in Western countries. However, there remains a persistent unmet need to conduct GWAS research exploring the genetic background of MASLD in non-Western populations. Our study aimed to identify genetic variants in patients with MASLD in South Korea.

Method: We performed a GWAS in a discovery group of 414 biopsy proven MASLD patients, alongside a control group of 1,064 healthy control. A replication analysis was conducted in a cohort of 1,246 participants. Additionally, we investigated the associations of SNPs related to MASLD, previously identified in a GWAS on Western populations, within our own cohort.

Results: Nine SNPs in *PTPRD* on chromosome 9p23 and one SNP in *RUNX3* on chromosome 1p36.11 showed a significant association with MASLD at genome-wide significance ($p = 5.0 \times 10^{-8}$). The nine variants in *PTPRD* were all successfully replicated in the replication cohort ($p < 0.0001$). In our cohort, we also observed significant associations with previously reported GWAS signals, such as *PNPLA3* at 22q13 and *SAMM50* at 22q13.31.

Conclusion: Our study discovered novel associations between *PTPRD* at 9p23 and MASLD in Korean patients. These findings enhance our understanding of the genetic pathophysiology of MASLD in non-European populations.

THU-293

Non-invasive assessment of liver inflammation in metabolic dysfunction-associated steatohepatitis (MASH) using MRI cytometry

Xiaoyu Jiang¹, Manhal Izzy¹, Kay Washington¹, John Gore¹, Junzhong Xu¹. ¹Vanderbilt University Medical Center, Nashville, United States

Email: xiaoyu.jiang@vumc.org

Background and aims: The current diagnostic gold standard for Metabolic dysfunction-associated steatohepatitis (MASH) involves invasive biopsy to assess steatosis, lobular inflammation, and ballooning. A non-invasive imaging method that can distinguish MASH from simple hepatic steatosis would reduce risks to patients and allow improved resource allocation. While MRI-based Proton Density Fat Fraction (PDFF) and elastography reliably quantify steatosis and fibrosis, respectively, there is a notable lack of non-invasive methods for assessing inflammation in MASH. As liver inflammation involves smaller-sized inflammatory cells ($< 10 \mu\text{m}$) distinct from hepatocytes ($15\text{--}25 \mu\text{m}$), we aim to demonstrate the capability of MRI cytometry to non-invasively quantify changes in non-fat cell volume and density associated with inflammation.

Method: MRI cytometry integrates water diffusion rate measurements over various timescales, corresponding to probing cellular properties at different distances. The size range of most relevance in the liver is $5 \mu\text{m}$ to $25 \mu\text{m}$, which corresponds to diffusion times of about 5–70 ms. A combination of OGSE (oscillating gradient spin echo) and PGSE (pulsed gradient spin echo) measurements sample this range of diffusion times. Non-fat cell volumes and densities are extracted by fitting diffusion signals to a three-compartment model (blood, intra and extracellular water). Histology-based simulation: MRI cytometry analysis was conducted on simulated PGSE and OGSE signals using segmented histological images of normal human liver tissue, steatosis, and stroma, at three signal-to-noise (SNR) levels (10, 20, and 50). In vivo imaging: MRI cytometry was conducted in three healthy subjects and a MASH patient using a Philips Ingenia CX 3 T scanner. The fat fraction was measured by a clinical standard mDixon sequence.

Results: Simulation: MRI-derived average cell sizes, and densities in stroma significantly exceed those in steatosis and normal liver tissues at all SNR levels, with variations increasing at lower SNRs. In vivo: The fitted average cell size and density for healthy subjects were about $19 \mu\text{m}$, and $15 \times 10^4/\text{mm}^3$, respectively, consistent with existing literature. The MASH liver displayed uniformly high fat content, inhomogeneous high cell densities, and small cell sizes. Two cell populations in the MASH liver were identified: one with cell sizes of $12 \pm 2.4 \mu\text{m}$ and low cell density ($< 106/\text{mm}^3$) and another with cell sizes of $7 \pm 1.9 \mu\text{m}$ and high cell density ($> 106/\text{mm}^3$), likely associated with fatty hepatocytes and inflammatory cells, respectively.

Conclusion: We demonstrate that MRI cytometry can quantify changes in cell size and density associated with inflammation using clinical 3 T scanners in under 12 minutes. These findings establish a solid foundation for future studies into the role of non-invasive assessment of liver cellular characteristics in diagnosing MASH.

THU-294

Resmetirom protects against diet-induced MASLD and reduces atherogenic risk factors in obese Ldlr-/-Leiden mice

Eveline Gart¹, Geurt Stokman¹, Robert Kleemann², Martine C. Morrison¹. ¹TNO, Leiden, Netherlands; ²TNO, Leiden, Netherlands

Email: eveline.gart@tno.nl

Background and aims: The thyroid hormone receptor- β agonist MGL-3196 (Resmetirom) is expected to become the first approved drug for metabolic dysfunction-associated steatotic liver disease (MASLD). Since resmetirom was found to lower plasma LDL cholesterol levels in clinical trials, it may also affect obesity-associated cardiovascular disease (CVD), which is the primary cause

POSTER PRESENTATIONS

of mortality in MASLD patients. The Ldlr^{-/-}.Leiden mice have previously been compared with biopsy-confirmed MASLD patients, which demonstrated that patients with a high risk of developing CVD are particularly well reflected by the Ldlr^{-/-}.Leiden mouse model. In the present study we studied the effect of resmetirom on progression of atherosclerotic CVD, in addition to its effects on MASLD-associated liver fibrosis.

Method: Ldlr^{-/-}.Leiden mice underwent an initial 18-week period of fast-food diet (FFD) feeding to establish early stages of MASLD and atherosclerosis. After this run-in period, one group of mice was terminated as a start-of-treatment reference. The remaining mice were maintained on FFD and received vehicle (FFD + vehicle controls) or 3 mg/kg resmetirom (FFD + Res) by oral gavage for an additional 10 weeks after which they were terminated at t = 28 weeks. Chow-fed mice were included as a healthy reference group. Plasma parameters, liver, adipose and heart tissues, were analyzed in the study.

Results: FFD fed mice developed obesity, dyslipidemia as confirmed by elevated plasma cholesterol and triglycerides levels, and MASLD associated liver fibrosis as compared to chow-fed controls. Therapeutic treatment with resmetirom significantly reduced plasma cholesterol and triglycerides compared to FFD + vehicle-treated controls. Plasma lipoprotein profiles demonstrated that the FFD-induced increase in plasma TGs can mainly be ascribed to an increase in VLDL lipoprotein particles and the increase in plasma cholesterol to an increase in (V)LDL-sized particles. Resmetirom lowered atherogenic risk factors, i.e. TG in VLDL and cholesterol in (V)LDL-sized particles. Subsequent effects on atherosclerosis will be presented (analysis ongoing). Notably, all effects were observed independent of changes in body weight, adiposity, and food intake, as resmetirom did not impact these factors. Furthermore, FFD-induced circulating liver injury markers ALT and AST were significantly reduced upon resmetirom treatment, and reduced to that in the chow-fed group. Consistent with this data, MASLD-associated liver fibrosis was attenuated with resmetirom relative to the FFD control group, as hepatic collagen content corrected for total liver weight was significantly reduced with resmetirom.

Conclusion: Our findings demonstrate that in Ldlr^{-/-}.Leiden mice, treatment with resmetirom has additional protective effects on CVD risk factors and possibly on the extent of atherosclerosis, on top of its effects on MASLD.

THU-295

miR-4449-merlin-TAZ axis modulates fibrosis progression in MASH

Young-Sun Lee¹, Yoonseok Lee², Seong Hee Kang¹, Young Kul Jung¹, Ji Hoon Kim¹, Yeon Seok Seo¹, Hyung Joon Yim¹, Jong Eun Yeon¹.

¹Korea University, Seoul, Korea, Rep. of South; ²Gachon University Gil Medical Center, Incheon, Korea, Rep. of South
Email: lys810@korea.ac.kr

Background and aims: While the majority of metabolic dysfunction-associated steatotic liver disease (MASLD) patients experience benign clinical courses, those with metabolic dysfunction-associated steatohepatitis (MASH) accompanied by fibrosis show poorer prognoses in comparison to patients with simple steatosis or MASH without fibrosis. This study aims to examine the involvement of miR-4449 in the progression of MASH-related fibrosis.

Method: Liver tissue and sera were obtained from MAFLD patients who underwent liver biopsies at Korea University Guro Hospital. MicroRNA sequencing was conducted on sera, while mRNA sequencing was performed on liver tissue from patients with biopsy-confirmed MAFLD. In vitro lipotoxicity was induced in hepatocyte cell lines (HepG2 and Huh7 cells) by treating them with palmitic acids (PA). To investigate the impact of miR-4449 during lipotoxicity, hepatocytes were transfected with either miR-4449 mimic or inhibitor.

Results: A total of 24 MAFLD patients were enrolled, with 15 patients exhibiting simple steatosis or MASH without fibrosis, while nine

patients had MASH with fibrosis. In the miRNA sequencing analysis, 31 miRNA sequences displayed significant differences in expression levels between the two groups. Notably, miR-4449 exhibited the highest expression among the miRNAs showing increased levels in the MASH-fibrosis group compared to the simple steatosis or MASH without fibrosis group. Palmitic acid (PA) treatment elevated the expression of miR-4449 in both the supernatant and hepatocytes. Conversely, the expression of merlin, a potential target of miR-4449, decreased in PA-treated hepatocytes compared to vehicle-treated hepatocytes. Furthermore, merlin expression significantly decreased in MASH patients with fibrosis compared to simple steatosis and MASH patients without fibrosis. Hepatocytes transfected with the miR-4449 mimic displayed decreased merlin expression but increased phosphorylated TAZ expression. In contrast, hepatocytes transfected with the miR-4449 inhibitor exhibited increased merlin expression but decreased phosphorylated TAZ expression.

Conclusion: Patients with MASH-fibrosis exhibited elevated expression of miR-4449. miR-4449 regulates merlin expression and TAZ phosphorylation in hepatocytes during lipotoxicity. Thus, miR-4449 may serve as a promising therapeutic target in the treatment of MASH-fibrosis.

THU-296

Identification and assessment of new circulating serological biomarkers for the evaluation of liver disease severity in MASLD patients

Douglas Maya^{1,2}, Rocío Gallego-Durán^{1,2}, Luis Ibañez-Samaniego^{2,3,4}, Rocío Aller^{5,6}, Juan Manuel Pericás^{2,7}, Rocío Montero-Vallejo^{1,2}, Isabel Payeras³, Anabel Fernández-Iglesias^{2,8}, Rocío Infantes-Fontán⁹, Carmen Carnicero¹⁰, Inmaculada Dominguez⁹, Alba Jiménez-Massip⁷, María Peña-Chilet¹¹, Sheila Gato-Zambrano^{1,2}, Francisco Javier Cubero^{2,3,4}, Antonio Gil-Gómez^{1,2}, Rocío Muñoz-Hernández^{1,2}, Ángela Rojas Álvarez-Ossorio^{1,2}, Victor Arroyo-López^{5,6}, Rebeca Sigüenza^{5,6}, Sergio Muñoz Martínez⁷, Joaquín Dopazo¹¹, Jordi Gracia-Sancho^{2,8}, Rafael Bañares^{2,3,4}, Javier Ampuero Herrojo^{1,2,12}, Manuel Romero-Gómez^{1,2,12}. ¹Seliver Group. Instituto De Biomedicina De Sevilla (IBiS), Hospital Universitario Virgen Del Rocío/Csic/Universidad De Sevilla, Sevilla, Spain; ²Centro De Investigación Biomédica En Red De Enfermedades Hepáticas y Digestivas (CIBEREHD), Madrid, Spain; ³Servicio de Medicina del Aparato Digestivo, Hospital General Universitario Gregorio Marañón, Madrid, Spain; ⁴Facultad de Medicina, Universidad Complutense de Madrid, Madrid, Spain; ⁵BioCritic, Group for Biomedical Research in Critical Care Medicine/Department of Medicine, Dermatology and Toxicology, Universidad de Valladolid/Gastroenterology Unit, Hospital Clínico Universitario de Valladolid, Valladolid, Spain; ⁶Centro de Investigación Biomédica en Red de Enfermedades Infecciosas (CIBERINFEC), Instituto de Salud Carlos III, Madrid, Spain; ⁷Liver Unit, Vall d'Hebron University Hospital, VHIR, Universitat Autònoma de Barcelona, Barcelona, Spain; ⁸Liver Vascular Biology Research Group, IDIBAPS, Barcelona, Spain; ⁹Servicio de Bioquímica Clínica, Hospital Virgen del Rocío, Sevilla, Spain; ¹⁰Institute of Health Sciences of Castilla y Leon (IECSCYL), Soria, Spain; ¹¹Área de Bioinformática. Fundación Progreso y Salud. Junta de Andalucía/Centro de Investigación Biomédica en Red. Área de Enfermedades Raras (CIBERER), Sevilla, Spain; ¹²UCM Digestive Diseases. Hospital Universitario Virgen Del Rocío, Sevilla, Spain
Email: mromerogomez@us.es

Background and aims: First-line Non-Invasive Tests (NITs), such as FIB-4, are valuable for detecting, particularly excluding, advanced liver disease. However, their modest sensitivity and specificity result in many undiagnosed cases and unnecessary hospital referrals due to the absence of powerful confirmatory tests like TE in key screening locations, such as primary and endocrine units. Identifying new biomarkers easily assessable in them is essential to enhance patient selection for Hepatology Unit referrals.

Method: Two-step meta-analysis identified candidates based on gene expression in MASLD patient liver biopsies, using significant

fibrosis as readout. Four Fibrosis Inducible Circulating Elements (FICEs) were selected from cohorts analyzed by Microarray (139 F0-F1 vs. 47 F2-F4) and RNA-seq (234 F0-F1 vs. 197 F2-F4). Circulating levels were measured in a Spanish cohort of biopsy-proven MASLD patients (N = 201).

Results: FICE 2-4 levels (a) increase in the liver (1st 2nd panel) and the bloodstream (3rd panel) of patients with significant fibrosis (F2+), advanced fibrosis (F3+) and at-risk MASH. Logistic regression favoured a score combining FICE2 and FICE4 circulating levels (FICE24; AUC_{95%CI} F2+: 0.78 [0.70–0.85]; F3+: 0.80 [0.73–0.87]; at-risk: 0.80 [0.72–0.88]). Incorporating age with standard analytes (named hereafter as FICE-24C) significantly improved its diagnostic accuracy (FICE24C; AUC_{95%CI} F2+: 0.88 [0.83–0.93]; F3+: 0.86 [0.80–0.92]; at-risk: 0.82 [0.75–0.90]) (b). Diagnostic performance analysis suggests a slight (FICE24) or clear (FICE24-C) superiority of both when compared against primary NITs (FIB4, NFS, HFS, APRI) (c) or confirmatory tests (TE, ELF or FAST) (d). Comparative analyses with common derivation pathways based on FIB-4 and TE indicate that FICE24-C can be used as a confirmatory test and improve the identification of true positive cases (e).

Conclusion: FICE24 and FICE24C, which can be easily assessed by ELISA, show a higher diagnostic accuracy than most primary risk assessment tools and a similar (FICE24) or higher (FICE24C) accuracy than well-established secondary risk assessment tools like TE and ELF. Validation in a separate independent cohort is on its way.

THU-297

Treatment with the CCR2/CCR5 antagonist Cenicriviroc does not affect MASH and fibrosis development in Ldlr-/-Leiden mice, translational to clinical phase 3 trial results

Martine C. Morrison¹, Eveline Gart¹, Wim van Duyvenvoorde¹, Jessica Snabel¹, Aswin L. Menke¹, Anita M. van den Hoek¹, Robert Kleemann¹. ¹The Netherlands Organisation for Applied Scientific Research (TNO), Department of Metabolic Health Research, Leiden, Netherlands
Email: martine.morrison@tno.nl

Background and aims: Cenicriviroc (CVC) is a dual CCR2/CCR5 antagonist that was developed for the treatment of metabolic dysfunction-associated steatohepatitis (MASH) and associated fibrosis. While it showed antifibrotic potential in the phase 2B CENTAUR trial, the phase 3 AURORA trial was terminated at the 1-year interim analysis due to lack of efficacy on improvement of fibrosis. In contrast with these results in humans, many preclinical studies have shown anti-inflammatory and anti-fibrotic efficacy of CVC-which brings into question the translational value of these models for human MASH. Here we studied the effects of CVC treatment in the Ldlr-/-Leiden mouse model for obesity-associated MASH and liver fibrosis, to investigate if this model can more accurately predict treatment effects in MASH patients.

Method: Male Ldlr-/-Leiden mice were fed a MASH and fibrosis-inducing high-fat diet (HFD) for 20 weeks, after which the 14-week treatment with CVC (20 mg/kg BW, provided as dietary admix) was started in one group of mice (HFD+CVC) and another group of mice was kept on HFD as an untreated control. A chow-fed group was included as an aging reference. All mice were terminated at t = 34 weeks for histological and biochemical analysis of MASH and fibrosis development as well as analysis of MASH and fibrosis-related biomarkers.

Results: Twenty weeks of HFD feeding induced obesity, hyperinsulinemia and atherogenic hyperlipidemia with increased plasma LDL cholesterol and triglyceride levels relative to chow. Treatment with CVC did not affect body weight or food intake. CVC significantly lowered fasting blood glucose with a concomitant increase in plasma insulin towards the end of the study. Fasting plasma cholesterol was not affected by CVC treatment while fasting plasma triglycerides were significantly increased. Histologically, CVC treatment did not affect macrovesicular or microvesicular steatosis in the liver. In

addition, CVC had no effect on hepatic inflammation or fibrosis as measured histologically. This lack of anti-fibrotic effect was further corroborated by biochemical analysis of hepatic collagen content and the plasma markers PIIINP, TIMP-1 and CK18-M30, none of which were reduced by CVC treatment.

Conclusion: While many preclinical models have shown efficacy of CVC that contrasts clinical observations, CVC treatment (at a translational dose that did show efficacy in other preclinical models) in the HFD-fed Ldlr-/-Leiden mouse did not reduce hepatic fibrosis-in line with the outcome of the phase 3 AURORA trial. These findings underline the importance for validation of preclinical MASH models not only with treatments that have been found to have clinical efficacy, but also with treatments that have failed clinically.

THU-298

Evaluation of performance of AI digital pathology on the reproducibility and repeatability of fibrosis phenotyping in MASH liver biopsies

Li Chen¹, Nathan Aist¹, Louis Petitjean², Mathieu Petitjean².
¹PharmaNest, Princeton, United States; ²Pharmanest, Princeton, United States
Email: li.chen@pharmanest.com

Background and aims: Metabolic dysfunction-associated steatohepatitis (MASH) is a chronic liver disease characterized by inflammation, steatosis, and fibrosis. The inter-observer and intra-observer variability in diagnosing MASH, especially liver fibrosis staging, by pathologist has long been a concern. This concern is transcended to AI based quantitative image analysis and the generation of fibrosis continuous scores. In this study, we demonstrate the precision of the phenotypic analysis of fibrosis using the FibroNestTM digital pathology platform (PharmaNest Inc, USA).

Method: Three liver biopsies with MASH conditions, each visually determined to have a low, mid, or high fibrosis and steatosis, were stained with Masson's Trichrome for collagen and imaged at 40X with Aperio Microscopy. Three operators (image analysts) independently performed the precision study using FibroNestTM, an AI-based digital pathology quantitative image analysis tool that generates a Phenotypic Fibrosis Composite Scores (Ph-FCS) as a biomarker for fibrosis disease progression. Each operator applied their own perceived full tissue selection and a color normalization step to "extract" collagen stains and remove staining artifacts. Analysis of the three liver biopsies by three different operators is conducted once daily for 5 consecutive days. Coefficient of variation (CoV), calculated using standard deviation divided by the average, is used to determine the inter-observer and intra-observer variability.

Results: For the repeatability performance, the CoV% of the intra-observer variability for the Ph-FCS fibrosis severity is 0.47%, 0.21%, and 0.29% for the low, mid, and high fibrosis samples, respectively. For the reproducibility performance, the CoV% of the intra-observer variability for the Ph-FCS fibrosis severity is 11.53%, 4.95%, and 3.33% for low, mid, and high fibrosis samples, respectively.

Conclusion: As the result for the CoV% are very low, the reproducibility and repeatability performance by the FibroNestTM digital pathology platform to provide fibrosis severity scores is acceptable. This is important as it indicates the precision and consistency of the analysis tool. FibroNestTM is a reliable tool to investigate potential anti-fibrotic drug efficacy for treatment of MASH.

THU-299

A 4-week mouse model allows the rapid evaluation of resmetirom and tirzepatide benefits on metabolic dysfunction-associated steatohepatitis

Francois Briand¹, Natalia Breyner¹, Estelle Grasset¹, Thierry Sulpice¹.
¹Physiogenex, Escalquens, France
Email: f.briand@physiogenex.com

Background and aims: There is currently no marketed drug for the treatment of metabolic dysfunction-associated steatohepatitis

(MASH). To expedite preclinical drug development, we have developed a mouse model fed a high fat/cholesterol/cholic acid diet with cyclodextrin in drinking water (HFCC+CDX diet) to promote hepatocyte cholesterol loading, liver inflammation and MASH within 4 weeks. For future head-to-head comparison or drug combinations studies with incretin-based therapies, we evaluated the efficacy of resmetirom, a thyroid hormone receptor- β agonist, and tirzepatide, a dual gastric inhibitory polypeptide receptor and glucagon-like peptide-1 receptor agonist.

Method: Male, 8-week-old, C57BL/6J mice were fed the HFCC+CDX diet for 4 weeks. After 2 weeks of diet, animals were randomized based on their plasma transaminases levels and body weight. Mice were kept on the same diet and were treated once daily with vehicle, resmetirom 3 mg/kg p.o. or tirzepatide 3 μ g/kg s.c. for 2 weeks. At the end of the treatment period, blood and liver samples were collected for biochemistry and histology analysis.

Results: Resmetirom did not alter plasma transaminases levels but significantly reduces plasma total cholesterol and LDL-cholesterol levels (-27% and -37% respectively, both $p < 0.001$ vs. vehicle). This LDL-lowering effect was associated with higher LDL-receptor ($+39\%$) and lower apolipoprotein B (-17%) hepatic gene expression (both $p < 0.01$). Resmetirom reduced hepatic triglycerides content (-25% , $p < 0.01$) and significantly reduced NAFLD activity score through lower inflammation score ($p < 0.01$), as well as lower IL-6 and IL-1 β hepatic gene expression (both $p < 0.05$). Resmetirom also showed anti-fibrotic effects as shown by a significantly lower % Sirius Red labelling. As expected, tirzepatide induced body weight loss, leading to a 13% lower body weight after 2 weeks of treatment, as compared to vehicle ($p < 0.001$). Although it did not alter plasma transaminases levels significantly, tirzepatide significantly lowered the hepatic gene expression of IL-1 β and IL-6 (both $p < 0.05$ vs. vehicle). It also reduced liver triglycerides content by 18% and hepatic inflammation score ($p < 0.05$ vs. vehicle).

Conclusion: Resmetirom and tirzepatide both improve MASH in our 4-week diet-induced mouse model. This preclinical model will be useful to expedite preclinical drug development for the treatment of MASH.

THU-302

Suitability of non-invasive tests in the evaluation of liver fibrosis in patients with metabolic dysfunction-associated steatotic liver disease

Álvaro Yagüe Parada¹, Andrés Felipe Castañeda Agredo¹, Rocío Calvo Hernandez¹, Agustina Gonzalez Guirado¹, Andres Varela Silva¹, Marta Morán Ortiz de Solorzano¹, Michelle Casanova Cabral¹, Benjamin Polo Lorduy¹. ¹Hospital Universitario Fundación Jiménez Díaz, Madrid, Spain
Email: alvaro.yague@quironsalud.es.

Background and aims: Metabolic dysfunction-associated steatotic liver disease (MASLD) is the main cause of liver disease in our environment and its incidence is raising due to the outbreak of metabolic syndrome and obesity. The spectrum ranges from simple steatosis to steatohepatitis, cirrhosis and hepatocellular carcinoma. It is essential to stratify patients with MASLD according to the degree of liver fibrosis, since its presence and progression determines the prognosis of the disease. Liver biopsy is the gold standard for the diagnosis of cirrhosis and staging of fibrosis. However, it is an invasive procedure with many drawbacks. Non-invasive markers have been developed for the evaluation of liver fibrosis. The aim of this study is to analyze the usefulness of FibroScan, NFS, APRI and FIB-4 indexes in evaluating presence and severity of liver fibrosis in MASLD, using liver biopsy as the reference standard.

Method: The case records of 210 patients who underwent liver biopsy from March 2019 until January 2023 were retrospectively reviewed, selecting for the study those who had undergone FibroScan measurements and blood samples simultaneously or with a maximum difference of three months from liver biopsy. Patients

without histological confirmation of hepatic steatosis (defined as a liver fat content $\geq 5\%$ on biopsy) were later excluded. Non-alcoholic fatty liver disease fibrosis score (NFS), fibrosis-4 index (FIB-4) and AST to platelet ratio index (APRI) were calculated. In all markers, indeterminate results were discarded. Liver fibrosis stage was determined using the METAVIR system.

Results: 194 patients were initially examined, detecting the presence of hepatic steatosis on biopsy in 44.3% of them, who were selected for the study. These patients had a mean age of 54.5 ± 10.6 years, being women the majority of them (76.7%). FibroScan liver stiffness results ranged from 2.6 to 45 kPa (mean: 8.6 kPa). Serological marker values ranged from -5.2 to 1.3 (mean: -2.1) for NFS, from 0.2 to 9.3 (mean: 1.8) for FIB-4 and from 0.1 to 6.1 (mean: 0.9) for APRI. In liver biopsy, 73.3% of the patients presented F0-1, while mild fibrosis ($F \geq 2$) was found in the remaining 26.8%. For the detection of advanced fibrosis (F3-F4), FibroScan showed a sensitivity of 64.3% and a specificity of 87.3% with a positive predictive value of 50% and a negative predictive value of 92.5%. Its degree of concordance with the biopsy was moderate (kappa index: 0.46). NFS showed low sensitivity (25%) and high specificity (98.2%), with a kappa index of 0.3. Regarding FIB-4 and APRI, both showed high sensitivity (85.7% for FIB-4 and 75% for APRI) and specificity (86.1% for FIB-4 and 81.2% for APRI), with a kappa index of 0.55 and 0.36, respectively.

Conclusion: FibroScan and FIB-4 are comparable to liver biopsy with a moderate degree of agreement, being useful tools for the non-invasive detection of advanced fibrosis among patients with MASLD.

THU-303

Elevated SIRT1 levels in arterial hypertension patients with a heightened risk of non-alcoholic fatty liver disease

Anastasiia Radchenko¹, Olena Kolesnikova¹. ¹L.T. Malaya Therapy National Institute of the National Academy of Medical Sciences of Ukraine, Kharkiv, Ukraine
Email: kolesnikova1973@gmail.com

Background and aims: Sirtuin 1 (SIRT1) is associated with the aging process and has been found to have protective effects on the liver due to its ability to regulate lipid metabolism and reduce inflammation. However, some studies suggest that SIRT1 levels may increase in the context of non-alcoholic fatty liver disease (NAFLD) and with older age as a result of compensatory processes. Arterial hypertension (AH) is closely associated with metabolic alterations and is believed to be strongly linked to NAFLD. Nonetheless, the relationship between SIRT1 levels and the risk of NAFLD in patients with AH remains unclear.

Method: Our study involved 86 AH patients with a mean age of 49.1 [40.3;54.6] years (63% women), divided into groups based on the Fatty Liver Index (FLI): group 1- <30 ($n = 38$), group 2-30-60 ($n = 30$), group 3- >60 ($n = 18$), matched for age and gender. Each group was further divided by age: <45 years ($n = 12$, $n = 15$, $n = 3$ respectively) and 45-59 years ($n = 26$, $n = 15$, $n = 15$). Body mass index, waist and hip circumferences, carbohydrate and lipid profiles, liver and kidney blood tests, C-reactive protein (CRP), and SIRT1 were evaluated in all patients.

Results: The levels of SIRT1 were significantly lower in group 1 compared to group 2 ($p = 0.004$) and group 3 ($p = 0.010$). Among patients of younger age (<45 years), no significant difference was found between groups 1 and 2, and group 3 was not compared due to an insufficient number of cases. In the middle-aged patient group, SIRT1 levels were also the lowest in group 1 compared to group 2 ($p = 0.004$) and group 3 ($p = 0.039$). Correlation analysis indicated that in the middle-aged group, SIRT1 was associated with alanine aminotransferase (ALT) ($r = 0.419$, $p = 0.001$), HOMA-IR ($r = 0.412$, $p = 0.002$), low-density lipoprotein cholesterol (LDL-C) ($r = -0.355$, $p = 0.009$), high-density lipoprotein cholesterol (HDL-C) ($r = -0.398$, $p = 0.003$), uric acid (UA) ($r = 0.538$, $p = 0.0001$), glomerular filtration rate (GFR) ($r = 0.620$, $p = 0.0001$), and C-reactive protein (CRP) ($r = 0.377$, $p = 0.039$).

Conclusion: Among middle-aged patients with AH, but not among the younger ones, moderate and high risk of NAFLD according to FLI values were associated with higher levels of SIRT1 compared to patients at low NAFLD risk. This could be a result of complex compensatory mechanisms. Probable factors contributing to these changes include increased insulin resistance, levels of liver enzymes, pro-inflammatory processes, and the development of dyslipidemias, supported by the correlation between SIRT1 and HOMA-IR, ALT, CRP, HDL-C levels. However, middle-aged patients with AH may still benefit from the positive impact of SIRT1 on LDL-C, GFR-both recognized as risk factors for AH and NAFLD-and on UA, often associated with an extended lifespan.

THU-304

Performance of non-invasive indexes in the assessment of metabolic dysfunction-associated steatotic liver disease

Álvaro Yagüe Parada¹, Andrés Felipe Castañeda Agredo², Rocío Calvo Hernández², Agustina González Guirado¹, Andrés Varela Silva¹, Marta Morán Ortiz de Solorzano¹, Michelle Casanova Cabral¹, Benjamin Polo Lorduy². ¹Hospital Universitario Fundación Jiménez Díaz, Madrid, Spain; ²Hospital Universitario Fundación Jiménez Díaz, Madrid, Spain
Email: alvaro.yague@quironsalud.es

Background and aims: Metabolic dysfunction-associated steatotic liver disease (MASLD) includes a spectrum of liver diseases ranging from steatosis to steatohepatitis, fibrosis and cirrhosis. Its prevalence increases with age and obesity, and it is associated with metabolic syndrome and an increased risk of cardiovascular and malignant diseases. Liver biopsy is the gold standard for the diagnosis of MASLD. However, it is and invasive and inaccurate technique with many drawbacks. In order to overcome the limitations of liver biopsy, a number of non-invasive markers have been developed for the evaluation of hepatic steatosis. The aim of this study is to evaluate the ability of CAP, HSI and TyG indexes to predict hepatic steatosis using liver biopsy as the reference standard.

Method: The case records of 210 patients who underwent liver biopsy from March 2019 until January 2023 were retrospectively reviewed. Those patients who had undergone CAP measurements and blood samples simultaneously or with a maximum difference of three months from liver biopsy were included in the study, with a final number of 194 patients. Hepatic Steatosis Index (HSI: sex, body mass index [BMI], alanine aminotransferase [ALT], aspartate aminotransferase [AST], diabetes) and TyG (triglycerides, glucose) were calculated. In all markers, indeterminate results were discarded. Biopsies were performed percutaneously using Tru-cut 16/18G needles. Hepatic steatosis was diagnosed if liver fat content was 5% or greater on biopsy.

Results: 194 patients with a mean age of 51.9±13.5 years were examined, being women the majority of them (73.2%). CAP results ranged from 100 to 400 dB/m (mean: 242.9 dB/m), while serological marker values ranged from 22.8 to 57.2 (mean: 38.7) for HSI and from 7.1 to 11.9 (mean: 8.6) for TyG. In liver biopsy, 44.3% of the patients presented hepatic steatosis, being 59 of them S1 (68.6%), 19 S2 (22.1%) and 8 S3 (9.3%). For the detection of hepatic steatosis, CAP showed a sensitivity of 74.4% and a specificity of 75.3% with a positive predictive value of 71.8% and a negative predictive value of 77.7%. Its degree of concordance with the biopsy was moderate (kappa index: 0.495). Regarding HSI and TyG, both showed high sensitivity (98.5% for HSI and 91.8% for TyG) and low specificity (4% for HSI and 59.3% for TyG), with a kappa index of 0.029 and 0.49, respectively.

Conclusion: Although liver biopsy is the reference standard for the diagnosis of hepatic steatosis, CAP and TyG are accurate and comparable to liver biopsy with a moderate degree of agreement. As CAP needs a specific device and a trained health practitioner that might not be available in some cases, TyG could represent the first step in the diagnosis of MASLD.

THU-305

Evaluation of the performance of AI digital pathology method (FibroNest) on subsections of biopsies to assess performance variability due to region selection

Adi Lightstone¹, Li Chen¹, Mathieu Petitjean¹. ¹PharmaNest, Princeton, United States

Email: adi.lightstone@pharmanest.com

Background and aims: The gold standard for assessment of liver fibrosis and steatosis is using MASH biopsies, though there has often been concern that the disease may present differently in different liver lobes (particularly in early stages). This concern is magnified when using quantitative or AI based digital pathology techniques, as depending on the algorithm, small changes in structure (e.g. the presence of veins) can have large impacts on results. Additionally, when using a digital pathology analysis technique, the computational costs and time are magnified greatly with increased biopsy size. The goal of this study is to analyze the phenotypic fibrosis scores generated by our FibroNest™ Digital Pathology platform on subsections of wedge-shaped biopsies (large biopsies from liver transplants) and see how the results may vary within the wedge.

Method: This study included 17 wedge shaped biopsies from the LITMUS MASH cohort (a large set of biopsies funded by the Innovative Medicines Initiative for the purpose of finding novel biomarkers) stained with Mason's Trichrome and imaged at 20x. Each wedge was sectioned into between 4 and 7 smaller portions; in cases where the staining was inconsistent the subsections were placed such that the stain had a similar pattern throughout. The biopsies were then processed and analyzed using FibroNest™ which calculated and extracted a total of 335 Quantitative Fibrosis traits. The most biologically relevant of these traits were then used to generate a Phenotypic Fibrosis Composite Score (Ph-FCS) which indicates the progression of fibrotic diseases. The scores from each biopsy were then used to generate an overall Coefficient of Variation (CoV) by taking the standard deviation from each section within a wedge biopsy and dividing it by the mean. Allowing us to understand how different sectioning methods may impact the calculated fibrosis score.

Results: Of the 17 wedge biopsies, only 4 of the Ph-FCS scores had a Coefficient of Variation above 15%, of those only 3 were greater than 20% and none were above 26%. 7 had a variation of 10% or below, and the 6 remaining were between 10 and 15%. The biopsy with the greatest variations in the subsections (one with a Ph-FCS of 2.3, another with that of 5.4) was bisected with a large break and included a vein in only one of the subsections.

Conclusion: Barring a few outliers, the low variation in the overall result from a digital pathology measurement of fibrosis in biopsy subsections indicates that the technique works well. With an acceptable CoV below 15%, the intra observer variability results from the FibroNest™ platform show completely acceptable levels for the purposes of scoring and analysis. It also shows that larger biopsies can be cropped down when doing digital pathology, provided a representative portion is selected, to allow for large savings in both time and cost.

THU-306

Study of alternative splicing changes during metabolic dysfunction-associated liver disease development and progression

Eirini Giannousi^{1,2}, Zoi Erpapazoglou², Antonios Chatzigeorgiou¹, Panagiota Kafasla². ¹Department of Physiology, Medical School, National and Kapodistrian University of Athens, Athens, Greece;

²Institute for Fundamental Biomedical Research, B.S.R.C. "Alexander Fleming", Vari, Athens, Greece

Email: eirinigiannousi@hotmail.com

Background and aims: Alternative splicing (AS) is a fundamental molecular mechanism during which exons are joined into different combinations resulting in different mRNA transcripts and producing

POSTER PRESENTATIONS

proteins with distinct structures and functions. An association between AS and liver diseases has been reported, but the exact mechanism is yet to be elucidated. Metabolic dysfunction-associated liver disease (MASLD) is a burgeoning health problem, affecting 25% of the global population, and is strongly associated with the dramatic increase of metabolic syndrome. It ranges from simple steatosis to metabolic dysfunction-associated steatohepatitis (MASH), which is a more severe form, and can lead to fibrosis, cirrhosis, and, ultimately, hepatocellular carcinoma (HCC). Studies have reported a significant correlation between the dysregulated expression of several spliceosome components and splicing factors with the development of MASLD and transition to MASH and HCC. The main goal of this study was to conduct an initial investigation on the alternative splicing changes during MASLD development and progression by focusing on a key player in splice site recognition and AS regulation, the hnRNPM protein. Firstly, hnRNPM expression was examined in various murine and cellular MASH models and then hnRNPM-dependent alternative splicing changes were evaluated across different disease stages.

Method: Murine models mimicking MASLD and MASH development were utilized, namely mice on high-fat diet (HFD) and HFD-high fructose corn syrup 55 (HFCS), mice on TACONIC diet and mice on a combined western diet (WD) and carbon tetrachloride (CCL4) injections. Moreover, HepG2 cells were either treated with palmitate acid to induce steatosis or were silenced for hnRNPM. In the forementioned models, the gene and protein levels of hnRNPM were evaluated by qPCR and immunohistochemistry respectively. Furthermore, examination of the alternative isoform expression of selected, based on a literature search, AS events regulated by hnRNPM was performed with PCR followed by acrylamide gel electrophoresis.

Results: The hnRNPM mRNA and protein levels in the *in vivo* models and the HepG2 steatosis cellular model revealed their progressive decrease during MASLD development. The evaluation of the alternative isoform expression of the chosen hnRNPM-dependent AS events both in the *in vivo* and *in vitro* MASH models did not reveal any major alterations.

Conclusion: This study suggests that hnRNPM expression is significantly altered in three well established murine models that resemble MASLD and MASH progression at different stages. A more comprehensive analysis of hnRNPM-dependent AS-derived isoform is required to address the role of hnRNPM deregulation during disease development.

THU-314

Evaluation of suitable *in vitro* and *in vivo* models for metabolic dysfunction-associated steatotic liver disease

Anja Geisler¹, Lisa Börnel¹, Yvonne Hupfer¹, Lara Zoe Preisner¹, Stefan Lorkowski¹, Maria Wallert¹. ¹Friedrich Schiller University, Jena, Germany

Email: anja.geisler@uni-jena.de

Background and aims: To understand development and progression of metabolic dysfunction-associated steatotic liver disease (MASLD), elucidating the molecular mechanisms is of utmost importance. Due to the high metabolic activity of the liver, the selection of appropriate cell models is a challenge. Primary human hepatocytes are the gold standard. However, primary cells are limited due to a lack of availability, ethical concerns, as well as complex and time-limited culture. Therefore, immortalized cell lines from different sources are often used. Because *in vitro* studies are not sufficient to cover the complex conditions of a living organism, mice are widely used as a model organism. In mice, MASLD can be induced chemically or by diet. Due to the high heterogeneity of the study designs, obtained data are difficult to compare. It is of note that the expression of liver-specific enzymes can differ depending on species (murine vs. human) and model (*in vitro* vs. *in vivo*).

Method: For comparing different *in vitro* models, HepG2, HepaRG, and AML-12 cells as well as primary murine hepatocytes (PMH) were

used. Basal gene expression of liver-specific and metabolism involved genes (albumin (alb), pregnane X receptor (PXR), glutathione S-transferase (GST) α , cytochrome P450 (CYP) 2E1, CYP3A4, CYP4F2) were analyzed by RT-qPCR. To characterize the different stages of MASLD *in vivo* C57BL/6 mice are fed with a high-fat and high-fructose diet (HFFD). In addition to body weight, organ weight and histology, phenotypic markers (e.g. liver inflammation markers) and lipid mediators in blood and liver are determined.

Results: Initial *in vitro* studies revealed that the human hepatic cell line HepG2 and the murine liver cell line AML-12 are of limited use due to the low expression of metabolic key enzymes. Comparative studies of HepG2, HepaRG and AML-12 cells as well as PMH revealed the following differences: mRNA expression of alb, GST α , CYP2E1 and CYP3A4 is significantly higher in PMH than in AML-12. HepaRG cells show higher CYP2E1 and GST α expression levels than HepG2. The studied liver cell models differ significantly in their metabolic activity. HepaRG cells are metabolically more active cells than HepG2 and AML-12 but are not comparable to PMH in the expression of several liver- and inflammation-specific genes.

Conclusion: These results demonstrate the importance of a comprehensive characterization and application-oriented selection of existing hepatic and MASLD model systems.

THU-336

Combination of fatty acid synthase (FASN) inhibitor and thyroid hormone receptor beta (THRb) agonist resmetirom shows synergistic improvement of NAFLD activity score (NAS) within 6-weeks in diet-induced obese mice with biopsy-confirmed MASH

Wen-Wei Tsai¹, Malte H. Nielsen², Michael Feigh², Eduardo Martins¹, George Kemble¹, Marie O' Farrell¹. ¹Sagimet Biosciences, San Mateo, United States; ²Gubra ApS, Horsholm, Denmark

Email: wen-wei.tsai@sagimet.com

Background and aims: Increased *de novo* lipogenesis (DNL) drives the development of MASH, and FASN is the rate-limiting enzyme in the DNL pathway. In preclinical studies, denifanstat (TVB-2640) directly blocks endogenous FASN in stellate cells, immune cells and hepatocytes, thereby directly inhibiting fibrosis, inflammation and steatosis. Denifanstat, an oral FASN inhibitor, has demonstrated significant improvements in MASH resolution and fibrosis improvement in the Ph2b MASH study, FASCINATE-2, as well as decreased liver fat and biomarkers of inflammation and fibrosis. THRb agonists increase lipid oxidation which decreases liver fat; resmetirom (RES) recently demonstrated significant MASH resolution or fibrosis improvement in Phase 3 and is FDA approved for the treatment of MASH with moderate to advanced liver fibrosis. We hypothesized that the combination of a FASN inhibitor and RES may increase efficacy for MASH treatment based on complementary mechanisms of liver fat reduction and the FASN inhibitor's direct anti-fibrotic effect. This study was designed to evaluate a FASN inhibitor alone and in combination with RES on liver histology in biopsy-confirmed MASH mice.

Method: Male C57BL/6J GAN-diet-induced obese mice with histologically confirmed NAS ≥ 5 and fibrosis stage F1-F3 were randomized and treated with either vehicle, TVB-3664 (a surrogate FASN inhibitor for denifanstat, 5 mg/kg, PO, QD) or RES (3 mg/kg, PO, QD) individually or in combination for 6 weeks (n = 10-12 for each group).

Results: After a 6-week treatment, the response rate (RR) for reduction of NAS by 2 or more points was 33% for TVB-3664, 25% for RES, 0% for vehicle and 80% for the combination. Notably, 100% of combination-treated mice showed at least 1-point reduction in NAS, and 30% had 3 or more points of NAS reduction. For steatosis, the RR for 1-point reduction was 17% for TVB-3664, 50% for RES and 100% for the combination, with a 2-point reduction in 80% of combination-treated animals. This was consistent with significant reduction of % hepatocytes with lipid droplets and % area of liver lipids in drug-treated groups. For lobular inflammation, the 1-point RR was 42% for TVB-3664, 8% for RES, and 10% for the combination although these

10% combination-treated animals all had a 2-point reduction. Some ballooning hepatocytes (ballooning score 1) were present before initiation of treatment and all treatments decreased the ballooning score to 0.

Conclusion: Combination of FASN inhibitor and THR β agonist RES had a synergistic effect on histological improvement of NAS compared to single agents within 6-weeks in a mouse model of MASH. These results suggest that the complementary mechanisms of action of denifanstat (directly decrease lipid synthesis, inflammation and fibrosis) and RES (increase lipid oxidation) combined could provide added benefit and support future clinical evaluation of this combination for MASH.

MASLD – Therapy

TOP-193

Consumption of a mediterranean diet with high-polyphenol content extra-virgin olive oil (EVOO) in patients with MASLD: effects on clinical parameters and gene expression on peripheral blood mononuclear cells (PBMCs)

Aurelio Seidita¹, Alessandra Cusimano², Roberto Citarrella¹, Antonina Azzolina³, Roberta Chianetta⁴, Ida Muratori¹, Rosalia Caldarella⁵, Antonino Terranova¹, Anna Licata^{6,7,7}, Antonio Carroccio¹, Juan Iovanna⁸, Melchiorre Cervello³, Maurizio Soresi¹, Lydia Giannitrapani¹. ¹Department of Health Promotion Sciences, Maternal and Infant Care, Internal Medicine and Medical Specialties (PROMISE), University of Palermo, Palermo, Italy; ²Department of Biological, Chemical and Pharmaceutical Science and Technology (STEBICEF), University of Palermo, Palermo, Italy; ³Institute for Biomedical Research and Innovation (IRIB), CNR, Palermo, Italy; ⁴Department of Health Promotion Sciences, Maternal and Infant Care, Internal Medicine and Medical Specialties (PROMISE), University of Palermo, Palermo; ⁵UOC Laboratory Medicine-CORELAB, University Hospital, Palermo, Italy; ⁶Department of Health Promotion Sciences, Maternal and Infant Care, Internal Medicine and Medical Specialties (PROMISE), University of Palermo, Dipartimento di Promozione della Salute, Materno-Infantile, di Medicina Interna e Specialistica "G. D'Alessandro", PROMISE, University of Palermo, Palermo; ⁷Medicina Interna ed Epatologia, Dipartimento di Promozione della Salute, Materno-Infantile, di Medicina Interna e Specialistica "G. D'Alessandro", PROMISE, University of Palermo, Palermo; ⁸INSERM U624, Marseilles, France
Email: lydiagiannitp@gmail.com

Background and aims: The term metabolic dysfunction-associated steatotic liver disease (MASLD) has been introduced to indicate the involvement of liver in Metabolic Syndrome (MetS). Extra Virgin Olive Oil (EVOO), could be the added value of Mediterranean Diet (MD) in the dietary intervention for this condition. We evaluated the efficacy of a high-polyphenol content EVOO (HPPE) on clinical and laboratory parameters of liver function and on expression levels of genes related to endoplasmic reticulum (ER) stress and lipid metabolism, in two groups of MetS/MASLD patients.

Method: Sixty consecutive MetS/MASLD patients were enrolled at Internal Medicine Unit of University Hospital of Palermo and randomized, in a single-center double-blind prospective study, to add HPPE or standard EVOO (SE) (40 ml/daily for 6 months) to the MD. Anthropometric measures, liver function, metabolic status, flow mediated dilatation (FMD), liver ultrasound and abdominal fat features, were analyzed at baseline (T0) and after 6 months (T6). We analyzed the gene expression pattern of some metabolic pathways involved in ER and oxidative stress, lipidic metabolism and development of steatosis, by extraction and subsequent amplification of the RNA from PBMCs

Results: The dietary intervention was well accepted by patients who showed high compliance. From T0 to T6, waist circumference (WC), glycated hemoglobinemia (HbA1C), subcutaneous and visceral fat thickness significantly improved in both HPPE ($p < 0.0001$, $p < 0.03$, $p < 0.0001$, $p < 0.04$ respectively) and SE ($p < 0.0001$, $p < 0.04$, $p < 0.0001$, $p < 0.03$ respectively) group. Insulinemia, HOMA-IR, AST and FMD improved only in HPPE group ($p < 0.03$, $p < 0.03$, $p < 0.01$, $p < 0.001$ respectively). At US evaluation, we observed a trend in reduction in both groups, especially in moderate to severe stages. A significant reduction in the expression of TRB3 (gene involved in ER stress), FASN, SREBP1, PPAR α , PPAR γ and CPT1a (involved in lipid metabolism) was observed from T0 to T6 in the HPPE group, while a significant increase in the expression of TRB3 and FASN was observed in the SE group. We analyzed PNPLA3 (rs738409), TM6SF2 (rs58542926), PCSK9 (LOF) (rs1159114), PCSK9 (GOF) (rs505151) and GSKR (rs1260326) polymorphisms, proving that the minor allele frequency (MAF) in both HPPE and SE group are equivalent to general population.

Conclusion: MD plus EVOO intake for 6 months can improve metabolic and cardiovascular parameters in MetS/MASLD subjects, reducing both anthropometric and insulin resistance indexes, and improving endothelial dysfunction. A trend in reduction has been observed for liver steatosis, consistent to the reduction of FASN and SREBP1 expression. This suggest that MD plus EVOO intake might influence the pathways involved in liver steatosis development and that a longer duration of this dietary intervention might reduce the degree of liver steatosis in a more significant way.

TOP-204

Inhibition of sodium-glucose cotransporter-2 and liver-related complications in diabetic patients

Sung Won Chung^{1,2}, Hyunjae Shin¹, Jaeyeon Park¹, Moon Haeng Hur¹, Min Kyung Park¹, Yun Bin Lee¹, Su Jong Yu¹, Jung-Hwan Yoon¹, Jeong-Hoon Lee¹, Yoon Jun Kim¹. ¹Department of Internal Medicine and Liver Research Institute, Seoul National University College of Medicine, Seoul, Korea, Rep. of South; ²Division of Gastroenterology, Liver Center, Asan Medical Center, University of Ulsan College of Medicine, Seoul, Korea, Rep. of South
Email: pindra@empal.com

Background and aims: No medication has been found to reduce the liver-related events. We evaluated the effect of sodium-glucose cotransporter-2 inhibitor (SGLT2i) on liver-related outcomes.

Method: Single nucleotide polymorphisms (SNPs) associated with SGLT2 inhibition were identified, and a genetic risk score (GRS) was computed using the UK Biobank (UKB) data ($n = 337, 138$). Two-sample Mendelian randomization (MR) was conducted using the FinnGen ($n = 218, 792$) database and UKB data. In parallel, a nationwide population-based study using the Korean National Health Insurance Service (NHIS) database was conducted. The development of liver-related complications (i.e., hepatic decompensation, hepatocellular carcinoma, liver transplantation, and death) was compared between individuals with type 2 diabetes mellitus and steatotic liver diseases treated with SGLT2i ($n = 13, 208$) and propensity score-matched patients treated with dipeptidyl peptidase-4 inhibitor (DPP4i) ($n = 70, 342$).

Results: After computing GRS with six SNPs (rs4488457, rs80577326, rs11865835, rs9930811, rs34497199, and rs35445454), GRS-based MR showed that SGLT2 inhibition (per 1 SD increase of GRS, 0.1% lowering of HbA1c) was negatively associated with cirrhosis development (adjusted odds ratio = 0.83, 95% confidence interval [CI] = 0.70-0.98, $P = 0.03$). When the individuals of UKB population were divided based on GRS and compared the risk of liver-related complications between the upper 5% and the lower 95% of individuals, the top 5% of individuals had substantially fewer liver-related complications than the bottom 95% of individuals (adjusted hazard ratio [aHR] = 0.60, 95% CI = 0.37-0.97, $P = 0.038$). This was consistent in two-sample MR (odds ratio = 0.73, 95% CI = 0.60-0.90, $P = 0.003$). In the Korean NHIS database, the risk of liver-related

POSTER PRESENTATIONS

complications was significantly lower in the SGLT2i group than in the DPP4i group (adjusted hazard ratio [aHR] = 0.88, 95% CI = 0.79–0.97, $P = 0.01$), and this difference remained significant (aHR = 0.75–0.88, all $P < 0.05$) across various sensitivity analyses.

Conclusion: Both Mendelian randomizations using two European cohorts and a Korean nationwide population-based cohort study suggest that SGLT2 inhibition is associated with a lower risk of liver-related events.

TOP-205

Effect of a physical exercise program on the cerebral hemodynamics of patients with metabolic dysfunction-associated steatotic liver disease

Berenice M. Román-Calleja¹, Fernando Martinez Cabrera¹, Regina Romo¹, Carlos Cantu Brito², Carlos Aguilar Salinas³, Ricardo Macías-Rodríguez¹, Astrid Ruiz Margáin¹. ¹Department of Gastroenterology, Instituto Nacional de Ciencias Médicas y Nutrición Salvador Zubirán, Mexico City, Mexico; ²Department of Neurology, Instituto Nacional de Ciencias Médicas y Nutrición Salvador Zubirán, Mexico City, Mexico; ³Direction of Investigation, Instituto Nacional de Ciencias Médicas y Nutrición Salvador Zubirán, Mexico City, Mexico
Email: astrid.ruizm@incmnsz.mx

Background and aims: In patients with obesity and metabolic conditions, microvascular changes can be found, leading to early cognitive impairment. Impairment in the normal cerebral blood flow and cognition have been described in patients with liver steatosis. Physical exercise is beneficial for patients with metabolic dysfunction-associated steatotic liver disease (MASLD) and can potentially help with cognitive function and cerebral hemodynamics, however this has not been explored. Therefore, we aimed to evaluate the effects of a physical exercise program on cerebral hemodynamics in patients with MASLD.

Methods: This was a 16-week randomized open clinical trial. Control group ($n = 20$) received diet with caloric restriction of 20% of energy needs by indirect calorimetry and the Intervention group ($n = 20$) received diet (same as control) + exercise; exercise intervention consisted of walking and gradually increasing 5000 steps, monitored by an activity tracker combined with resistance exercise. All patients received printed book as a cognitive exercise. Body composition, controlled attenuation parameter, liver stiffness, neurocognitive tests, and transcranial doppler ultrasound were obtained at baseline and final evaluations. Patients received weekly text messages to assess compliance and had monthly in-person visits.

Results: 57% of patients were female with a mean age of 46 ± 7 years and BMI of 35.9 ± 5.0 kg/m². Adherence to the intervention was >85%. In the exercise group, the number of steps increased from 6177 (4881–9187) to 11190 (10533–15767) ($p < 0.01$) vs 6339 (4982–8166) to 7341 (6104–9111) ($p = 0.180$) in controls. In both groups, patients had significant reduction in waist circumference and BMI (3.4% and 4.2% intervention $p < 0.05$ vs 2.8% and 3.1% in controls $p < 0.05$). Exercise group showed improvement in: cerebral hemodynamics [Resistance index 0.76 (0.51–0.98) to 0.56 (0.43–0.73), $p = 0.033$, pulsatility index in 0.99 (0.98–1.01) to 0.74 (0.68–0.90), $p = 0.012$] and Breath Holding Index 0.65 (0.54–0.72) to 0.71 (0.63–0.89), $p = 0.096$, cognitive function [Addenbrooke 84 (82–87) to 96 (92–98), $p = 0.002$], steatosis (CAP 362 ± 31 to 304 ± 35 dB/m, $p = 0.031$). Fat mass was reduced in the intervention group ($4.6 \pm 1.2\%$, $p = 0.018$) while muscle mass increased ($1.9 \pm 0.7\%$, $p = 0.033$). The proportion of patients having >7% reduction in body weight loss were also significantly higher in the intervention (55%) compared to control group (30%), $p = 0.023$.

Conclusion: Exercise improves cerebral hemodynamics and cognitive function, as well as body composition in patients with MASLD.

TOP-216

The three strain probiotics for metabolic dysfunction-associated steatotic liver disease improvement: a parallel, double-blind, randomized, placebo-controlled trial

Sung-Min Won^{1,1}, Sang Jun Yoon¹, Jin-Ju Jeong¹, SatyaPriya Sharma¹, Ki Kwang Oh¹, Dong Hoon Yang¹, Hyun Joon Park¹, Sang Gyune Kim², Moon Young Kim³, Ki Tae Suk⁴. ¹Institute for Liver and Digestive Diseases, Hallym University, Chuncheon, Korea, Rep. of South; ²Soonchunhyang University Hospital, Bucheon, Korea, Rep. of South; ³Department of Internal Medicine, Division of Gastroenterology and Hepatology, Yonsei University Wonju College of Medicine, Wonju, Korea, Rep. of South; ⁴Hallym University College of Medicine, Chuncheon, Korea, Rep. of South
Email: ktsuk@hallym.ac.kr

Background and aims: metabolic dysfunction-associated steatotic liver disease (MASLD) is associated with an dysbiosis in the gut microbiota. We evaluated whether probiotic treatment affected liver function parameters and stool microbiome in patients with MASLD.

Method: We performed a double-blind parallel trial of 110 patients with MASLD. Participants (mean age, 47.0 ± 13.6 years; 61% men) were randomly assigned to groups given the probiotics (*Lactobacillus lactis* CKDB001, LL001; *Lactobacillus helveticus* CKDB001, LH001; *Pediococcus pentosaceus* KID7, PPKID7; 1 capsule: 9.0×10^9 CFU, 3 capsule per day; $n = 85$) or placebo ($n = 25$) for 8 weeks. Stool and blood samples were collected at the start and end point of the study. The stool microbiome was analyzed by 16S ribosomal DNA sequencing.

Results: After 8 weeks, in the probiotic group, LL001 treatment improved ALT (87.3 ± 8.2 to 71.1 ± 6.0 , $p = 0.01$) and AST levels (64.9 ± 4.9 to 50.0 ± 3.5 U/L, $p = 0.001$), LH001 treatment improved body weight (78.4 ± 3.0 to 77.2 ± 2.8 kg, $p = 0.01$), and PPKID7 treatment improved total cholesterol levels (186.1 ± 7.0 to 178.0 ± 7.9 mmol/L, $p = 0.03$). Additionally, LH001 treatment significantly decreased PT and INR. In the 16S sequencing analysis, probiotic treatment decreased the abundance of Proteobacteria, and in particular, an increase in the abundance of family Ruminococcaceae and Lachnospiraceae was observed in the LL001 group after 8 weeks. In the pre- and post-comparison of probiotic treatment at the level of the top 20 genera, a tendency was observed to decrease genera Haemophilus and Ruminococcus_g2, while increasing genus Bifidobacterium.

Conclusion: In a randomized clinical trial of patients with MASLD, 8 weeks of treatments of three probiotics were associated with changes in the stool microbiome and improvements in blood biochemical parameters of MASLD (ClinicalTrials.gov, Number: NCT04555434).

TOP-217

A randomized, placebo-controlled phase Ib/IIa trial to evaluate the safety, tolerability, and efficacy of BGT-002, an adenosine triphosphate citrate lyase inhibitor in patients with NAFLD: interim analysis

Yue Hu¹, Hong Zhang¹, Guoyue Lv¹, Fajun Nan², Jingya Li², Yangming Zhang², Dandan Wu¹, Yanhua Ding³, Junqi Niu¹. ¹The First Hospital of Jilin University, Changchun, China; ²Burgeon Therapeutics Co., Ltd., Shanghai, China; ³The First Hospital of Jilin University, Changchun, China
Email: dingyanhua2003@126.com

Background and aims: The prevalence and incidence rate of NAFLD are increasing, which has become a serious public health burden, but the treatment options are limited worldwide. The primary aim of this clinical trial is to evaluate the safety, pharmacokinetics, and efficacy of BGT-002 that is an adenosine triphosphate citrate lyase inhibitor in NAFLD patients.

Method: This is a double-blind and randomized phase Ib/IIa study in 48 NASH patients (aged 18–65 years), the study is consisted of four multiple ascending dose cohorts (50 mg, 75 mg, 100 mg and 150 mg) in which twelve participants were enrolled for every cohorts of which nine received BGT-002 and three received placebo orally once daily

for 28 days. The patients who met the following major criteria: ALT $>1 \times \text{ULN}$ within 3 months without other reasons; BMI $\geq 25 \text{ kg/m}^2$; MRI-PDFF $\geq 10\%$ during screening and baseline and body weight gain or loss $\leq 5\%$ within 4–8 weeks prior to administration were enrolled.

Results: A total of 42 NAFLD patients were enrolled, 36 patients completed the study and 12 patients are undergoing treatment. 36 NAFLD patients were evaluated for safety up to now. 18 of 36 (50%) patients experienced at least one adverse drug reaction (ADR). Most ADRs were grade 1–2. No drop-outs, no SAE. BGT-002 was safe and well-tolerated in this study. After the consecutive administration of BGT-002 50 mg QD, 75 mg QD and 100 mg for 28 days, the plasma concentration reached steady state on the third day, with a T_{max} of 1.056 to 1.537 h, respectively. The mean C_{max} and AUC_{tau} were 22577.78–48955.56 ng/ml and 423943.6–913589.4 ng·h/ml respectively. The mean half-life of BGT-002 was 30 h. The accumulation ratio of drug plasma exposure was 4.876–5.690. LFC was measured by MRI-PDFF at baseline and day 29. LFC have been significantly decreased after a 28-day therapy. The patients receiving BGT-002 or placebo 50 mg, 75 mg or 100 mg once daily had a mean relative reduction from baseline in LFC of -26.6% ($n = 12$), -27.0% ($n = 12$) and -28.5% ($n = 12$). The mean absolute reduction of the LFC in three cohorts were -5.1% , -4.0% and -6.4% from baseline at the end of the treatment. $\geq 30\%$ LFC reduction relative to baseline was measured in 4 (33.3%), 5 (41.7%) and 6 (50.0%) in the 50 mg QD, 75 mg QD and 100 mg QD cohort, respectively. There were 10 (10/36) patients whose LFC level less than 10% on day 29. The biomarker of lipids such as TC, LDL-C and TG declines of varying degrees were observed, especially the decrease in LDL-C was more significant. The level of liver enzyme were evaluated throughout the study. And the improvement of ALT, AST and GGT was observed, especially the GGT level showed a significantly decrease during treatment.

Conclusion: The findings from interim analysis of this study, it was observed that a significant reduction in LFC, lipids and GGT level of NAFLD patients enrolled after 28-days treatment. BGT-002 is safe and well-tolerated. And it might be a promising for NAFLD.

SATURDAY 08 JUNE

SAT-194

Effect of statin therapy in patients with obesity and cirrhosis secondary to metabolic dysfunction-associated steatotic liver disease (MASLD) on pre-liver transplant mortality

Ami Patel¹, Katherine Cooper², Alessandro Coletta², Deepika Devuni².
¹UMass Chan Medical School, Worcester, United States; ²UMass Chan Medical School, Worcester, United States
Email: ami.patel@umassmemorial.org

Background and aims: There is increasing data to suggest that statin medications have beneficial effects in patients with liver disease. In our previous work, we demonstrated that statins reduced pre-liver transplant (LT) mortality in patients with metabolic dysfunction associated liver disease/steatohepatitis (MASLD). In this study we analyzed the impact of statins on pre-LT mortality in patients based on disease etiology and BMI.

Method: We performed a single-center retrospective review of patients evaluated for LT between January 1, 2018–June 30, 2021. Demographic and clinical data were collected through review of electronic medical records. Patients were categorized by statin prescription (statin vs. no statin), liver disease etiology (Metabolic dysfunction-associated steatohepatitis (MASH) vs. non-MASH), and body mass index (BMI >40 vs. BMI <40). The primary outcome was pre-LT death. Variables were assessed for association using chi-squared and t-tests.

Results: A total of 623 patients were included, of which 115 were on a statin medication. Patients on a statin were significantly more likely to have cirrhosis secondary to MASH (53% vs. 15%, $p < 0.001$), have a BMI >40 (15% vs. 8%, $p = 0.020$) and have a prior cardiac diagnosis

(39% vs. 17%, $p < 0.001$). Patients with BMI >40 experienced higher pre-LT mortality compared to patients with a BMI <40 (36.4% vs. 17.3%, $p < 0.001$). In patients prescribed a statin medication, there was no significant relationship between BMI and pre-LT mortality (16.7% vs. 17.2%, $p = 0.958$) or MASH and pre-LT mortality (13.1% vs. 21.4%, $p = 0.180$). In patients not on a statin, BMI >40 was associated with higher pre-LT mortality (44.7% vs. 17.2%, $p < 0.001$) and MASH was also associated with pre-LT mortality in this subgroup (28.6% vs. 17.9%, $p = 0.023$). Interestingly, statins had the largest impact on pre-transplant mortality in patients with combined diagnoses of MASH and a BMI >40 (8.3% vs. 60%, $p = 0.004$). Cardiac history was associated with death in the non-statin group ($p = 0.014$) but not in the statin group ($p = 0.349$).

Conclusion: In this analysis, we found that patients with MASH cirrhosis and patients with a BMI >40 who were taking a statin medication at the time of their LT evaluation were less likely to die on the waitlist compared to patients with MASH or BMI >40 who were not prescribed a statin medication. Our results may suggest that statins confer protective benefits to patients with MASH cirrhosis and patients with BMI >40 , especially when in combination. These findings may be related to optimization of cardiac health in LT candidates.

SAT-195

Effects of icosabutate, a dual free fatty acid receptor-1 and -4 agonist, on elevated non-invasive markers of liver injury, fibrosis and glycemic control in type 2 diabetic MASH patients and F1-F3 fibrosis

Naim Alkhoury¹, David A. Fraser², Hilde Steineger³,
Mazen Nouredin⁴, Quentin M. Anstee⁵, Stephen A. Harrison^{6,7}.
¹Arizona Liver Health, Chandler, United States; ²Northsea Therapeutics, Amste, Netherlands; ³Northsea Therapeutics, Amsterdam, Netherlands; ⁴Houston Research Institute and Houston Methodist Hospital, Houston, United States; ⁵Newcastle University, Translational and Clinical Research Institute, Faculty of Medical Science, Newcastle, United Kingdom; ⁶Radcliffe Department of Medicine, University of Oxford, Oxford, United Kingdom; ⁷Pinnacle Clinical Research, San Antonio, United States
Email: david.fraser@northseatherapeutics.com

Background and aims: Icosabutate (ICO) is a novel, oral, once-daily, liver-targeted, dual free fatty acid receptor (FFAR) -1 and -4 agonist. In the 52 wk phase 2B ICONA study comparing 300 mg or 600 mg ICO therapy with placebo in subjects with MASH and F1–F3 fibrosis, a significant histological response was identified in patients with type 2 diabetes (T2D) treated with 600 mg ICO for both MASH resolution with no worsening of fibrosis and ≥ 2 -point decrease in NAS (effect size 31%, $p = 0.007$) and for ≥ 1 -stage improvement in fibrosis with no worsening of MASH (effect size 19%, $p = 0.02$). These findings were seen in conjunction with a placebo-corrected decrease in HbA1c of $\sim 1\%$ ($p < 0.05$) in subjects with poor glycemic control (baseline HbA1c $\geq 6.5\%$). The aim of this study was to assess the effects of ICO therapy on cases with elevated baseline non-invasive markers of liver injury and fibrosis (NITs), along with concordance between fibrosis response and decreases in ALT and enhanced liver fibrosis score (ELF).

Method: Liver chemistries (ALT, AST) and markers of fibrosis (neoepitope-specific, N-terminal pro-peptide of collagen Type III collagen [PRO-C3], ELF score and amino terminal of type III procollagen peptide (P3NP) and fasting plasma glucose (FPG) were assessed in T2D MASH with baseline and week 52 biopsies receiving 300 mg ICO ($n = 39$), 600 mg ICO ($n = 40$) or placebo ($n = 35$). Treatment effect versus baseline was established using ANCOVA in subjects with elevated baseline levels (ALT $>40 \text{ U/L}$; AST $>34 \text{ U/L}$; PRO-C3 $\geq 12.6 \text{ ng/ml}$; ELF ≥ 9.8 ; P3NP $\geq 10 \text{ ng/ml}$; FPG $\geq 126 \text{ mg/dl}$).

Results: Sixty-eight percent of all T2D subjects were identified with elevated baseline ALT, with corresponding values of 57% (AST), 76% (PRO-C3), 55% (ELF) and 64% for both P3NP and FPG. Treatment with 600 mg ICO induced pronounced and significant (all $p < 0.0001$ vs baseline) reductions in mean ALT (-40 U/L [-50%]), AST (-30 U/L

POSTER PRESENTATIONS

[−50%]) and P3NP (−6.5 ng/ml [−40%]). Significant reductions were also observed in mean PRO-C3 (−6.1 ng/ml [−30%], $p=0.0002$) and ELF score (−0.63 units, $p=0.008$). A similar, but more attenuated, effect was observed in the 300 mg ICO treatment arm for all biomarkers (range −19 to −28% versus baseline), whereas the placebo arm showed no significant change in any variable (range −7 to +3% versus baseline). In alignment with the observed decrease in HbA1c, ICO treatment reduced mean FPG by 21% ($p=0.01$) and 20% ($p=0.007$) versus baseline for 300 mg and 600 mg respectively (placebo unchanged). Irrespective of T2D status, 82% (9/11) of fibrosis in the 600 mg treatment arm had a combined decrease in ALT of >17 U/L and ELF score >0.5 units versus 13% in non-responders.

Conclusion: Once-daily, oral therapy with 600 mg ICO induces pronounced reductions in multiple elevated markers of liver injury and fibrosis in T2D MASH patients. Furthermore, a simultaneous decrease in ALT and ELF score may help identify histological responders to ICO therapy.

SAT-196

A significant decrease in steatosis using non-invasive measurements during monitoring for life style changes in patients with MASLD: interim 6 m results of a monocentric study

Wouter Robaey^{1,2,3}, Leen Heyens^{4,5,6,7}, Struyve Mathieu^{8,9}, Gert Stockmans¹⁰, Kirsten Cardone¹¹, Joop Arends^{4,12}, Ger Koek^{13,14}, Geert Robaey⁹, Joris Penders^{8,9}, Sven Francque^{15,16,17}. ¹Hasselt University, Faculty of Medicine and Life Sciences, Diepenbeek, Belgium; ²Ziekenhuis Oost Limburg, Department of Gastroenterology and Hepatology, Genk, Belgium; ³Ziekenhuis Oost Limburg, Department of Limburg Clinical Research Center, Genk, Belgium; ⁴Maastricht University, Maastricht, Netherlands; ⁵Hasselt University, Hasselt, Belgium; ⁶Ziekenhuis Oost Limburg, department of Gastroenterology and Hepatology, Genk, Belgium; ⁷Ziekenhuis Oost Limburg, department of Limburg Clinical Research Center, Genk, Belgium; ⁸Ziekenhuis Oost Limburg, Genk, Belgium; ⁹Hasselt University, Diepenbeek, Belgium; ¹⁰Ziekenhuis Oost Limburg (Maas en Kempen), Maaseik, Belgium; ¹¹Ziekenhuis Oost Limburg, Department of Limburg Clinical Research Center, Genk, Belgium; ¹²Maastricht University Medical Center, Maastricht, Netherlands; ¹³Maastricht University, Faculty of Health, Medicine and Life Sciences, Maastricht, Belgium; ¹⁴Maastricht University Medical Center, Department of Internal Medicine division Gastroenterology and Hepatology, Maastricht, Netherlands; ¹⁵University of Antwerp, Antwerp, Belgium; ¹⁶Translational Sciences in Inflammation and Immunology, Laboratory of Experimental Medicine and Paediatrics, Faculty of Medicine and Health Sciences, Antwerp, Belgium; ¹⁷Antwerp University Hospital, Department of Gastroenterology and Hepatology, Edegem, Belgium
Email: wouter.robaey@uhasselt.be

Background and aims: Metabolic Dysfunction-Associated Steatotic Liver Disease (MASLD) is an important cause of chronic liver disease. Currently, the cornerstone of therapy is lifestyle modification (diet and exercise). Using paired liver biopsy studies, a weight reduction of more than 5% of body weight (BW) might be sufficient to reduce steatosis (at least one stage). This study investigates the outcome of a reduction of more than 5% of body weight (BW) on steatosis in patients with MASLD using non-invasive methods.

Method: In this ongoing, monocentric (Ziekenhuis Oost Limburg, Genk, Belgium), prospective study patients with MASLD (Controlled Attenuation Parameter CAPTM ≥215 dB/m) are consecutively included since October 2022 to receive lifestyle intervention during 1 year. After 6 months (M6) and 1 year they are re-evaluated (clinical and biochemical evaluation, as well as liver stiffness measurement (LSM) by transient elastography (FibroScan[®]) and CAPTM).

Results: From October 2022 until December 2023, 297 patients were included. Their mean age was 52 ± 12 years, 47 % were female, 9 % had type 2 diabetes, 40 % metabolic syndrome, 53 % were living with obesity, 20 % were known with arterial hypertension. As of the 31st of December 2023, 111 patients presented at the M6 control visit: 41 (37

%) of the patients lost of more than 3 % of BW, 23 (21 %) more than 5 % of BW, 13 (12 %) more than 7 % of BW, and 3 (3 %) more than 10 % of BW. Eight percent ($n=9$) of the patients demonstrated a complete resolution of steatosis using the CAPTM criterion. In 66 % of them this occurred only after a weight reduction of more than 7 % of BW. In patients with a weight loss of more than 5 % of BW a significant reduction in Hepatic Steatosis Index (HSI), Fatty Liver Index (FLI) and CAPTM (M-probe) was observed ($p<0.001$, $p=0.001$, $p=0.02$, resp.), but not in FIB-4 and LSM. The change in Body Mass Index (BMI) explained 65% of the variation in HSI change but only 15% in FLI change. After addition of other variables in the HSI and FLI formula to the regression model only ALAT explained extra 12% of the variation in HSI. Biochemically, there was a significant decrease in alanine transferase (ALAT) ($p=0.04$), HbA1c ($p<0.001$) and triglycerides (TG) ($p=0.02$), but not in aspartate transferase (ASAT), total serum cholesterol, HDL-cholesterol, LDL-cholesterol, Homeostatic model for insulin resistance (HOMA-IR) value and glycaemia.

Conclusion: A significant reduction in steatosis and liver biochemistry, as well as HbA1c and TG was seen already after 6 months using non-invasive blood-based measurements (HSI and FLI) and CAPTM in patients decreasing more than 5% of BW. The change in BMI only partly explained the variation in HSI and to a lesser extent FLI change, suggesting they can be used as markers of steatosis improvement. To achieve a resolution of MASLD a significant weight loss of more than 7% of BW is needed in most of the patients.

SAT-197-YI

Higher serum vitamin D levels is associated with lower MASLD prevalence and incidence: the Rotterdam study

Ibrahim Ayada¹, Yasir J. Abozaid^{2,3}, Jesse Pustjens¹, Laurens van Kleef¹, Robert J. de Knegt¹, Willem Pieter Brouwer¹, Mohsen Ghanbari².

¹Department of Gastroenterology and Hepatology, Erasmus MC, University Medical Center, Rotterdam, The Netherlands, Rotterdam, Netherlands; ²Department of Epidemiology, Erasmus MC, University Medical Center, Rotterdam, The Netherlands, Rotterdam, Netherlands; ³Department of Microbiology and Pathology, College of Veterinary Medicine, University of Duhok, Iraq, Duhok, Iraq
Email: i.ayada@erasmusmc.nl

Background and aims: Metabolic dysfunction associated steatotic liver disease (MASLD) affects around 30% of adults worldwide and there is no approved therapy yet. Therefore, it remains pivotal to identify risk factors impacting this global healthcare burden. Emerging evidence indicates a potential link between vitamin D deficiency and the development of MASLD and progression towards fibrosis. However, the evidence is conflicting, longitudinal assessments are lacking and data on MASLD severity is scarce. Therefore we investigated the associations between vitamin D and MASLD and its severity in a longitudinal cohort study.

Method: We included participants from the prospective population-based Rotterdam study with data on serum concentration of 25-hydroxyvitamin D and FLI. MASLD was assessed by fatty liver index (FLI) at baseline. Associations between vitamin D and MASLD were investigated by logistic regression models that were adjusted for demographics, indicators for metabolic dysfunction, season and kidney function. Longitudinal analysis included associations between vitamin D and incident MASLD based on FLI and on ultrasound obtained 5 to 10 years after baseline. Sensitivity analysis included incident MASLD with ALT>35 or high liver stiffness defined as LSM ≥8 kPa.

Results: We included 7921 participants (age 62.8 (7.9), 57% female) and MASLD was prevalent in 34.1% at baseline. Vitamin D was significantly associated with MASLD at baseline (aOR 0.83, 95%CI 0.75-0.91, per 1 increase of log Vitamin D). Of the 5217 participants that did not have MASLD at baseline, 3102 (age 59.2 (6.06), 65% female) were included for longitudinal analysis and 13.7% developed incident MASLD based on FLI. Additionally, 3204 participants had follow-up data on ultrasound (age 59.3 (6.1), 65% female) and 21.8%

developed incident MASLD). In line with the cross-sectional analysis, vitamin D was significantly associated with incident MASLD, for both MASLD based on FLI (aHR 0, 84, 95% CI 0, 72–0, 98, per 1 increase of log Vitamin D) and ultrasound (aHR 0, 88 95% CI 0, 78–0, 99, per 1 increase of log Vitamin D). Results were consistent across both sexes. Similar directions of effect were obtained when focusing on incident MASLD with elevated ALT (aHR 0, 74 95% CI 0, 53–1, 03, per 1 increase of log Vitamin D) and incident MASLD with high liver stiffness (aHR 0, 87, 95% CI 0, 64–1, 17, per 1 increase of log Vitamin D), though not reaching statistical significance.

Conclusion: In this study, higher serum vitamin D concentration demonstrated significant association with lower prevalence and incidence of MASLD, and potentially linked with reduced MASLD severity. While the exact mechanisms are unknown, maintaining adequate vitamin D levels may have an impact on the development and progression of MASLD, particularly in individuals at risk of or diagnosed with MASLD.

SAT-198

ASC41, a selective THR β agonist significantly reduces liver fat and ALT in biopsy-confirmed MASH patients after 12-week treatment: an interim analysis of a 52-week serial liver biopsy study

Jiangao Fan¹, Junping Shi², Hong Wang³, Ming-Hua Zheng⁴, Jinjun Chen⁵, Yao Xie⁶, Fangfang Lv⁷, Sikui Wang⁸, Ling Yang⁹, Qing Xie¹⁰, Yueqiu Gao¹¹, Chuanwu Zhu¹², Xuebing Yan¹³, Qiya Huang¹⁴, Bin Xu¹⁵, Fei Liu¹⁶, Honglian Bai¹⁷, Hong Deng¹⁸, Airong Hu¹⁹, Xin Gao²⁰, Guoxin Hu²¹, Hong You²², Hong Tang²³, Min Zhang²⁴, Xiaoling Chi²⁵, Qin Du²⁶, Xiaoping Wu²⁷, Hongzhou Lu²⁸, Yuguo Zhang²⁹, Guizhou Zou³⁰, Huanwei Zheng³¹, Yujuan Guan³², Yue Chen³³, Hua Ye³⁴, Tianhuang Liu³⁵, Yuemei Yan³⁶, Jinji J. Wu³⁶. ¹Xinhua Hospital Affiliated to Shanghai Jiaotong University School of Medicine, Shanghai, China; ²The Affiliated Hospital of Hangzhou Normal University, Hangzhou, China; ³Affiliated Zhejiang Hospital, Zhejiang University School of Medicine, Hangzhou, China; ⁴The First Affiliated Hospital of Wenzhou Medical University, Wenzhou, China; ⁵Nanfang Hospital, Southern Medical University, Guangzhou, China; ⁶Beijing Ditan Hospital Capital Medical University, Beijing, China; ⁷Sir Run Run Shaw Hospital, Zhejiang University, Hangzhou, China; ⁸Liaocheng people's hospital, Liaocheng, China; ⁹Union Hospital, Tongji Medical College, Huazhong University of Science and Technology, Wuhan, China; ¹⁰Ruijin Hospital, Shanghai Jiaotong University School of Medicine, Shanghai, China; ¹¹Shanghai University of Traditional Chinese Medicine Shuguang Hospital, Shanghai; ¹²Suzhou no.5 people's Hospital, Suzhou, China; ¹³The Affiliated Hospital of Xuzhou Medical University, Xuzhou, China; ¹⁴Qingyuan People's Hospital, Qingyuan, China; ¹⁵Beijing Youan Hospital Capital Medical University, Beijing, China; ¹⁶Xiangya Hospital, Central South University, Changsha, China; ¹⁷The First People's Hospital of Foshan, Foshan, China; ¹⁸The Third Affiliated Hospital, Sun Yat-Sen University, Guangzhou, China; ¹⁹Ningbo No. 2 Hospital, Ningbo, China; ²⁰Zhongshan Hospital, Fudan University, Shanghai, China; ²¹Peking University Shenzhen Hospital, Shenzhen, China; ²²Beijing Friendship Hospital, Capital Medical University, Beijing, China; ²³West China Hospital Of Sichuan University, Chengdu, China; ²⁴The Second Xiangya Hospital of Central South University, Changsha, China; ²⁵The Second Affiliated Hospital of Guangzhou University of Chinese Medicine, Guangzhou, China; ²⁶the Second Affiliated Hospital, School of Medicine, Zhejiang University, Hangzhou, China; ²⁷The First Affiliated Hospital of Nanchang University, Nanchang, China; ²⁸Shenzhen Third People's Hospital, Shenzhen, China; ²⁹The First Hospital Of Hebei Medical University, Shijiazhuang, China; ³⁰The Second Hospital of Anhui Medical University, Hefei, China; ³¹Shijiazhuang Hospital of Traditional Chinese Medicine, Shijiazhuang, China; ³²Guangzhou Eighth People's Hospital, Guangzhou, China; ³³Taihe Hospital, Hubei University of Medicine, Shiyan, China; ³⁴Ningbo Medical Center Lihuili Hospital, Ningbo, China; ³⁵Meizhou People's Hospital, Meizhou, China; ³⁶Gannex Pharma Co., Ltd., Shanghai, China
Email: corresponding@ascletis.com

Background and aims: ASC41 is a liver-targeting small molecule agonist. Oral, once-daily ASC41 tablet was developed using proprietary formulation technology. ASC41-A, an active metabolite from ASC41, is highly potent and selective against THR β . Three phase I or Ib studies were completed in healthy or obese subjects with elevated LDL-C >110 mg/dL. A U.S. Phase I study demonstrated no clinically significant drug-drug interactions between ASC41/ASC41-A and most frequently used antidepressants and statins as well as no significant difference in drug exposure between Americans and Chinese at the same dose. We reported here a pre-specified interim analysis.

Method: ASC41-202 (NCT05462353) is a randomized, double-blind, placebo-controlled and multi-center Phase II clinical study, which enrolls approx. 180 liver biopsy-confirmed MASH patients ($\geq 7.5\%$ liver fat, NAS ≥ 4 , F1 (<15%), F2, F3) in 3 cohorts of ASC41 tablet (2 mg or 4 mg), once-daily and placebo (1:1:1) for 52-week treatment. Primary end point is a histological reduction in NAS ≥ 2 points that results from reduction of necro-inflammation without worsening fibrosis. Pre-specified interim analysis was conducted when 42 patients completed 12-week treatment.

Results: Mean baseline liver fat content was 18.2%, 17.8% and 18.9% for placebo (n=14), 2 mg (n=13) and 4 mg ASC41 (n=15), respectively. At week 12, mean relative changes from baseline (CFBs) in liver fat were -13.1%, -55.0% (p=0.0001 vs placebo) and -68.2% (p<0.0001 vs placebo) for placebo, 2 mg and 4 mg ASC41, respectively. Percentages of patients achieving $\geq 30\%$ and $\geq 50\%$ relative reduction in liver fat from baseline were 21.4% and 21.4%, 92.3% (p=0.0002) and 46.2% (p=0.24), 93.3% (p<0.0001) and 86.7% (p=0.0004) for placebo, 2 mg and 4 mg ASC41. Percentages of patients achieving normalized liver fat ($\leq 5\%$ absolute liver fat) were 0.0%, 30.8% (p=0.16) and 66.7% (p=0.0017) for placebo, 2 mg and 4 mg ASC41. Mean baseline ALT was 77.6, 65.9 and 84.8 U/L for placebo, 2 mg and 4 mg ASC41. At week 12, mean relative CFBs in ALT were 5.2%, -8.5% (p=0.61) and -32.6% (p=0.0051) for placebo, 2 mg and 4 mg ASC41. Percentages of patients achieving mean ALT decrease >17 U/L were 21.4%, 30.8% (p=0.68) and 73.3% (p=0.0052) for placebo, 2 mg and 4 mg ASC41. Statistically significant reduction in AST was also observed for 4 mg ASC41. Statistically significant mean relative CFBs in LDL-C, TC and TG were observed for both 2 and 4 mg ASC41 vs placebo. AEs were grade 1 in majority across all cohorts. Among patients receiving ASC41 treatment, only two patients (2/28, 7.1%) reported drug-related grade 2 TEAEs. No drug-related grade 3 or higher TEAEs or SAEs were observed in patients receiving ASC41 treatment. ASC41 demonstrated excellent GI tolerability.

Conclusion: Significant reductions in Liver fat, ALT, AST and lipids at week 12 warrant further clinical studies for ASC41 tablet.

SAT-199

Long term outcomes of Saroglitazar in metabolic-dysfunction associated steatotic liver disease related cirrhosis-a prospective cohort study

Rakhi Maiwall¹, Neha Chauhan¹, Priyanka Sharma¹. ¹Institute of Liver and Biliary Sciences, Delhi, India
Email: rakhi_2011@yahoo.co.in

Background and aims: Saroglitazar (SARO), a peroxisome proliferator-activated receptor agonists (PPAR) agonist has shown efficacy in metabolic-dysfunction associated steatotic liver disease (MASLD), however, the data is limited in patients with cirrhosis. We aimed to investigate the efficacy of SARO in improving outcomes in patients with MASLD-related cirrhosis.

Method: Prospective cohort study wherein patients treated with SARO were compared to controls managed with standard of care (SOC). Liver (LSM) and spleen stiffness measurements (SSM) were performed for all patients using transient elastography (reported in KPa) at enrolment, at the time of drug initiation and last follow-up. Response was defined as reduction in LSM by 20% or a decrease in SSM by 10% from the baseline

Results: A total of 182 patients with MASLD-cirrhosis, 44% biopsy-proven, mean age 50.3 ± 10.2 years, 77% males, 79% morbidly obese, 30% with diabetes were enrolled. The mean controlled attenuation parameter (CAP) was 252 ± 49.4, LSM 34.5 ± 18.7, SSM 51.6 ± 24.3, HOMA-IR 2.95 ± 2.62, hepatic venous pressure gradient (HVPG), n = 80) 13.3 ± 4.6 mm of Hg, and CTP score was 6.3 ± 1.6 and all these patients were followed for median 399 days. Of the total patients, 6% had a family history, 51% with patatin-like phospholipase domain-containing 3 (PNPLA3 rs738409) GG-genotype, and 73 (40%) received SARO. A significant correlation of HVPG was seen with LSM ($p < 0.001$, $r = 0.45$) and SSM ($p < 0.001$, $r = 0.41$). Patients treated with SARO were significantly more morbidly obese, worse lipid profile, and LSM and C-reactive protein (CRP) levels compared to SOC group ($p < 0.05$). The LSM and SSM response on the SARO was observed in 25 (34%) and 43 (60%) while 15 (20.5%) had response in both parameters at median of 8 (IQR 9–13) months. A significant reduction was observed in the LSM [(29.5 ± 16.1) vs (26.9 ± 14.9); $p = 0.032$], CAP [(255.2 ± 48.2) vs. (237.4 ± 45.6); $p = 0.008$], HOMA-IR [(2.76 ± 2.43 vs. (2.08 ± 1.02); $p = 0.01$], LDL-cholesterol [(96.4 ± 1.6) vs. (83.9 ± 36.6); $p = 0.07$], HBA1C [(6.1 ± 1.6) vs. (5.7 ± 1.10); $p = 0.04$] and SSM [(50.1 ± 23.3) vs. 42.9 ± 22.28]; $p < 0.001$] pre and post SARO respectively. On the contrary, only a significant reduction in SSM [(52.7 ± 25.1 to 47.6 ± 21.9); $p < 0.001$] and HBA1C [(6.01 ± 1.90 to (5.5 ± 1.4); $p = 0.002$] was observed in the SOC group. Adverse events were mild and reversed with drug discontinuation in 8%.

Conclusion: Almost one in five patients of MASLD-related cirrhosis showed response in both LSM and SSM after saroglitazar. Reduction in SSM was seen in 60% and 30% had LSM response. Improvement in surrogate parameters of fibrosis, portal hypertension and insulin resistance could be achieved after long-term treatment with saroglitazar in patients with MASLD-related cirrhosis without any major adverse events.

SAT-200-YI

Statin use is associated with liver fibrosis regression in the general population: a longitudinal analysis of The Rotterdam Study

Jesse Pustjens¹, Laurens van Kleef¹, Ibrahim Ayada¹, Harry L.A. Janssen^{1,2}, Maryam Kavousi³, Layal Chaker^{3,4}, Arfan Ikram³, Robert J. de Knecht¹, Bruno Stricker³, Bettina E. Hansen^{1,2,3,5}, Willem Pieter Brouwer¹. ¹Department of Gastroenterology and Hepatology, Erasmus MC, University Medical Centre, Rotterdam, Netherlands; ²Toronto Centre for Liver Disease, Toronto General Hospital, University Health Network, Toronto, Canada; ³Department of Epidemiology, Erasmus MC University Medical Centre, Rotterdam, Netherlands; ⁴Department of Internal Medicine, Erasmus MC University Medical Centre, Rotterdam, Netherlands; ⁵IHPME, University of Toronto, Toronto, Canada
Email: j.pustjens@erasmusmc.nl

Background and aims: Liver fibrosis is a growing public health concern, especially due to the increasing prevalence of steatotic liver disease. There are no approved therapeutic options that target fibrosis progression. Recently, statins have demonstrated possible protective effects in cross-sectional studies. Here we assess the effects of incident statin use on liver stiffness changes through longitudinal analyses.

Method: We analyzed participants from the Rotterdam Study, a large prospective population-based cohort study, who underwent serial liver stiffness measurements (LSM) by FibroScan. Participants with an unreliable Fibroscan, viral hepatitis, excessive alcohol use (>60 g/day in males, or >50 g/day in females), or those already on statin treatment, were excluded. To diminish confounding and assess the potential therapeutic effect of statin use, inverse probability of treatment weighting (IPTW) was used in combination with linear and logistic regression analyses. Covariates included in the propensity score model were age, sex, baseline LSMlg10, body mass index, waist circumference, serum lipid-profile, (pre-)diabetes, steatotic liver disease, smoking status and alcohol intake, and weights were

truncated at the 99th percentile. Only those without statin use at baseline were included in the analyses to avoid adjusting for mediators in the causal pathway. Primary end points were difference in LSM compared to baseline (delta LSM) and significant LSM increase ($\geq 20\%$ from baseline). Additional sensitivity analyses were performed in at-risk groups with group-specific weights.

Results: In total, 595 statin-naïve participants with two separate valid LSM were included with a median follow-up of 4 years [4.0; 4.0], median age 70 [68; 72], 42% male, 29.2% MASLD, 6.4% diabetes mellitus type 2. At follow-up there were 157 (26%) incident statin users. At baseline, median LSM was 4.8 [4.0; 8.9] kPa and 5.1 [4.3; 6.1] kPa at follow-up. The median delta LSM was 0.2 [−0.7; 1.3], 33.1% had a clinically significant LSM increase, and 17.1% had a significant decrease. By IPTW analysis, there was a significant protective effect of statin use (delta LSM $\beta = -0.39$ 95% CI: −0.69; −0.88, $p = 0.012$). In sensitivity analysis the strength of the association proved stronger the (pre-)diabetic (delta LSM $\beta = -0.64$ 95% CI: −1.12; −0.17, $p = 0.008$) and overweight (delta LSM $\beta = -0.54$ 95% CI: −0.93; −0.15, $p = 0.007$) population. Moreover, within a median follow-up of 4 years, statin use may reduce the risk of significant LSM progression in the (pre-)diabetic population (aOR 0.56 95% CI 0.30; 1.03, $p = 0.06$).

Conclusion: Statin use is associated with a protective effect on LSM progression in the general population, which was especially prominent within the (pre-)diabetic population. Our findings support the use and study of statins among those patients deemed at risk of clinically significant liver fibrosis.

SAT-201

Phase 3 randomised, placebo-controlled ESSENCE trial of semaglutide 2.4 mg in participants with non-cirrhotic non-alcoholic steatohepatitis: baseline characteristics, impact of new metabolic dysfunction-associated steatotic liver disease criteria and non-invasive tests

Philip N. Newsome¹, Elisabetta Bugianesi², Vlad Ratziu³, Mary E. Rinella⁴, Michael Roden^{5,6,7}, Kristiane A. Engebretsen⁸, Iris Kliers⁸, Laura Østergaard⁸, Denise Vanni⁸, Jeppe Zacho⁸, Arun J. Sanyal⁹. ¹National Institute for Health Research, Birmingham Biomedical Research Centre at University Hospitals Birmingham NHS Foundation Trust, Centre for Liver and Gastrointestinal Research, Institute of Immunology and Immunotherapy, University of Birmingham, Birmingham, United Kingdom; ²Department of Medical Sciences, University of Turin, Turin, Italy; ³Sorbonne Université, Institute for Cardiometabolism and Nutrition, Hospital Pitié-Salpêtrière, INSERM UMRs 1138 CRC, Paris, France; ⁴Department of Medicine, University of Chicago, Chicago, IL, United States; ⁵Department of Endocrinology and Diabetology, Medical Faculty and University Hospital Düsseldorf, Heinrich Heine University Düsseldorf, Düsseldorf, Germany; ⁶German Center for Diabetes Research, Partner Düsseldorf, München-Neuherberg, Germany; ⁷Institute for Clinical Diabetology, German Diabetes Center, Leibniz Center for Diabetes Research at Heinrich Heine University Düsseldorf, Düsseldorf, Germany; ⁸Novo Nordisk A/S, Copenhagen, Denmark; ⁹Stravitz-Sanyal Institute for Liver Disease and Metabolic Health, VCU School of Medicine, Richmond, VA, United States
Email: p.n.newsone@bham.ac.uk

Background and aims: We report the baseline characteristics of participants randomised in the Phase 3 ESSENCE trial of the glucagon-like peptide-1 analogue, semaglutide 2.4 mg subcutaneous once weekly (OW) for non-cirrhotic metabolic dysfunction-associated steatohepatitis (MASH).

Method: ESSENCE (NCT04822181) is an ongoing 247-week Phase 3, randomised trial. Following a 14-week screening phase, 800 participants (part 1) of 1200 planned (part 2) with MASH and fibrosis stages 2/3 (F2/F3) were randomised 2:1 to receive semaglutide 2.4 mg subcutaneous OW or placebo OW added to standard of care. In part 1, the two primary end points at 72 weeks are resolution of steatohepatitis and no worsening of liver fibrosis, and improvement in liver fibrosis and no worsening of steatohepatitis. Based on a

central pathologist evaluation, inclusion criteria were histological presence of steatohepatitis stages F2/F3 per the Non-alcoholic Steatohepatitis Clinical Research Network classification, and a non-alcoholic fatty liver disease activity score (NAS) of ≥ 4 , with a score of ≥ 1 in steatosis, lobular inflammation and hepatocyte ballooning.

Results: 800 participants (250 F2; 550 F3) were randomised. Mean (SD) age was 56 (11.6) years; 57.1% were female; $\geq 99\%$ had ≥ 1 cardiometabolic risk factor (s) in accordance with the metabolic dysfunction-associated steatotic liver disease (MASLD) definition. Mean (SD) NAS was 5.05 (0.95), and higher in F3 versus F2 (5.11 [0.95] vs 4.92 [0.93], respectively). Notably, participants with a higher NAS had more cardiometabolic risk factors for MASLD (52.9% with NAS ≥ 5 vs 45.3% with NAS 4). Similarly, a greater proportion of participants with F3 had all five cardiometabolic risk factors versus F2 (52.9% vs 44.8%, respectively). Although cardiometabolic comorbidities were highly prevalent, 44.5% of participants did not have type 2 diabetes (T2D), and 27.3% did not have obesity. Normal liver transaminases were observed in 26.3% of participants (28% F2; 26% F3). Mean (SD) FibroScan liver stiffness was 12.8 (6.9) kPa, and values of < 8 kPa were observed in 15.3% of participants. Mean (SD) controlled attenuation parameter value was 329 (46) dB/m; mean (SD) enhanced liver fibrosis (ELF) score was 10.0 (1.0), and 43.5% of participants had an ELF score of < 9.8 . Overall, 8.8% and 9.0% of participants with/without T2D did not meet any of the following non-invasive criteria: Fibrosis-4 index ≥ 1.3 , vibration-controlled transient elastography ≥ 8.1 , or ELF ≥ 9.8 , and more participants with F2 (14.7–16.4%) did not meet these criteria versus F3 (4.5–6.7%).

Conclusions: The ESSENCE baseline population includes participants with significant fibrosis (F2 and F3) and approximately 91% of the trial population had ≥ 1 positive diagnostic non-invasive test. Cardiometabolic risk factors were found in $\geq 99\%$ of participants, and in increased numbers in those with higher NAS and fibrosis stages.

SAT-202

TERN-501, a highly selective thyroid hormone receptor β agonist, significantly improved MRI-PDFF, cT1, and liver volume in clinically relevant patient populations with presumed MASH: subgroup analyses from a 12-week phase 2a trial

Stephen A. Harrison¹, Naim Alkhoury², Mazen Nouredin³, Eric Lawitz⁴, Kris V. Kowdley⁵, Rohit Loomba⁶, Lois Lee⁷, Christopher Jones⁷, Erin Quirk⁷. ¹Pinnacle Clinical Research, San Antonio, United States; ²Arizona Liver Health, Tucson, United States; ³Houston Methodist Hospital, Houston Research Institute, Houston, United States; ⁴Texas Liver Institute, University of Texas Health, San Antonio, United States; ⁵Liver Institute Northwest, Elson S. Floyd College of Medicine, Washington State University, Seattle, United States; ⁶NAFLD Research Center, University of California at San Diego, La Jolla, United States; ⁷Terns Pharmaceuticals, Foster City, United States
Email: sharrison@pinnacleclresearch.com

Background and aims: In a dose ranging Ph2a MASH study, TERN-501, a highly selective thyroid hormone receptor β (THR- β) agonist, demonstrated significant, dose-dependent reductions in magnetic resonance imaging proton density fat fraction (MRI-PDFF) and corrected T1 (cT1), meeting all primary and secondary end points. TERN-501 showed a favorable safety profile with similar incidences of adverse events across all doses and placebo with no gastrointestinal or cardiovascular safety signals and no evidence of central thyroid axis effects, demonstrating its high selectivity for THR- β . Here we evaluated efficacy of TERN-501 6 mg, the highest dose tested in the study, using clinically relevant MR based assessments in key patient (pt) subgroups relevant to MASH.

Method: This was a 12 wk, randomized, double-blind, placebo-controlled study in pts with presumed MASH. Changes in liver fat by PDFF, fibro-inflammation by cT1, and liver volume (LV) were assessed at 12 wks using MRI in the following subgroups: pts with 1)

cT1 > 875 msec at baseline; 2) obesity; 3) hypertension; 4) dyslipidemia; 5) type 2 diabetes mellitus (T2DM); and 6) Hispanic ethnicity.

Results: Of the 162 pts equally randomized to 7 arms in the study, 22 and 21 pts were randomized to TERN-501 6 mg and placebo, respectively. After 12 wk once daily dosing of TERN-501 6 mg, -45% mean PDFF, -72 msec mean cT1, and -20% mean LV changes were observed vs. -4% , 4 msec, and 1% in placebo, respectively (all $p < 0.001$). In pts with cT1 > 875 msec at baseline, indicating at-risk MASH pts, -47% mean PDFF ($p < 0.001$), -82 msec mean cT1 ($p < 0.01$), and -22% mean LV ($p < 0.001$) changes were observed vs. -9% , -15 msec, and 0% in placebo, respectively. For pts with obesity, hypertension, dyslipidemia, or Hispanic ethnicity, a statistically significant improvement in mean PDFF, cT1, and LV was observed in all TERN-501 6 mg subgroups vs. placebo (all $p < 0.01$). The small sample size of diabetic pts limited the analysis results despite considerable reduction in all three assessments observed in TERN-501 6 mg vs. placebo ($n = 6$ in TERN-501 6 mg). Notably, the placebo subgroups with obesity, hypertension, dyslipidemia, or T2DM, all of which are metabolic risk factors associated with MASH, showed worse cT1 outcomes than the overall placebo group whereas TERN-501 6 mg in these subgroups showed comparable cT1 improvement vs. the overall TERN-501 6 mg group. Overall, TERN-501 6 mg given once daily for 12 wks consistently demonstrated improvement in PDFF, cT1, and LV in all the key pt subgroups vs. placebo.

Conclusion: 12 wk treatment of TERN-501 6 mg, the highest dose tested in this Ph2a study significantly improved liver fat, cT1, and LV in at-risk MASH pts including those with comorbid conditions or risk factors associated with MASH. With the favorable safety profile of TERN-501 observed in the study, these analyses results support further investigation of TERN-501 in MASH pts.

SAT-203

Pegozafermin added to background GLP-1 therapy in patients with metabolic dysfunction-associated steatohepatitis with F2/F3 fibrosis: ENLIVEN 48-week extension data

Arun J. Sanyal¹, Manal F. Abdelmalek², Kris V. Kowdley³, Naim Alkhoury⁴, Stephen A. Harrison⁵, Jörn M. Schattenberg⁶, Mildred D. Gottwald⁷, Shibao Feng⁸, Germaine D. Agollah⁹, Cynthia L. Hartsfield¹⁰, Hank Mansbach¹⁰, Maya Margalit¹¹, Rohit Loomba¹². ¹Virginia Commonwealth University, Richmond, United States; ²Mayo Clinic, Rochester, United States; ³Liver Institute Northwest, Seattle, United States; ⁴Arizona Liver Health, Chandler, United States; ⁵Pinnacle Clinical Research, San Antonio; ⁶Saarland University Medical Center, Homburg, Germany; ⁷89bio, San Francisco, United States; ⁸89bio, San Francisco; ⁹89bio, San Francisco; ¹⁰89bio, San Francisco, United States; ¹¹89bio, Rehovot, Israel; ¹²University of California San Diego School of Medicine, La Jolla, United States
Email: cindy.hartsfield@89bio.com

Background and aims: Pegozafermin (PGZ), a long-acting fibroblast growth factor 21 (FGF21) analog, was evaluated for efficacy and safety in the Phase 2b ENLIVEN trial in metabolic dysfunction-associated steatohepatitis (MASH) patients with biopsy-proven F2/F3 fibrosis. PGZ 30 mg QW and 44 mg Q2W demonstrated statistically significant improvements in histology (primary end points) and improvement in markers of hepatic and extrahepatic metabolic health. Co-morbidities such as obesity and T2DM are common in patients with MASH and may be treated with glucagon-like peptide-1 receptor agonists (GLP-1 therapy). We previously showed that for patients on stable background GLP-1 therapy, PGZ provided additional improvement in non-invasive tests (NITs) of liver steatosis, fibrosis, inflammation, and metabolic markers compared to GLP-1 therapy alone in a post-hoc analysis at week 24. Following the main study, these patients entered a 24-week extension phase allowing analyses of 48-week data.

Method: In this placebo-controlled, blinded, 24-week extension phase of the Phase 2b ENLIVEN study, patients continued with their assigned treatment arm. The GLP-1 therapy population included 36 patients who received a GLP-1 during the study with the majority

POSTER PRESENTATIONS

having baseline utilization of ≥ 6 months. Most received semaglutide (53%) or dulaglutide (36%) along with additional T2DM medications. Twenty-six patients received PGZ (30 mg QW or 44 mg Q2W) and 10 patients received placebo. Changes at 48 weeks were assessed for NITs of liver steatosis, fibrosis and inflammation, metabolic effects, safety, and tolerability.

Results: In the GLP-1 therapy subgroup, patients had comparable baseline characteristics between placebo and treatment arms. Relative to the full study population, patients on background GLP-1 therapy were more likely to be female (72%) and have T2DM (94%). At week 48, patients on PGZ and GLP-1 combination therapy maintained greater benefits in markers of liver steatosis (MRI-PDFF), fibrosis (ELF and ProC3), and inflammation (ALT) compared to those on background GLP-1 alone. There was also an additional reduction in the FAST score for those receiving PGZ. Metabolic benefits seen at week 48 include a sustained reduction in triglycerides in conjunction with greater reduction of LDL-C compared to GLP-1 therapy alone. Combination of GLP-1 and pegozafermin therapy retained acceptable safety and tolerability with no treatment-related AE discontinuations.

Conclusion: In MASH patients with F2/F3 fibrosis who were receiving background GLP-1 therapy, addition of PGZ demonstrated additional and sustained improvement in markers of liver and metabolic health compared to GLP-1 therapy alone. Confirmatory phase 3 studies are planned to begin in 2024 and will include patients on background incretin therapies per local standard of care.

SAT-206

Improvements in MACK-3, a diagnostic test for active metabolic dysfunction-associated steatohepatitis, parallel response to lanifibranor therapy

Michael Cooreman¹, Sven Francque², Philippe Huot-Marchand³, Lucile Dzen⁴, Martine Baudin³, Jean-Louis Junien³, Pierre Broqua³, Manal F. Abdelmalek⁵, Jerome Boursier⁶. ¹Inventiva, New York, United States; ²University Hospital Antwerp, Edegem; ³Inventiva, Daix, France; ⁴Inventiva, Daix; ⁵Mayo Clinic, Rochester, United States; ⁶CHU Angers, Angers, France
Email: michaelcooreman@msn.com

Background and aims: The pan-PPAR agonist lanifibranor has shown efficacy on histological 'MASH resolution and fibrosis improvement' and on non-invasive markers of cardiometabolic health (CMH), MASH activity and fibrosis-including MACK-3, adiponectin and Pro-C3-in the NATIVE phase 2b study. MACK-3 has been validated against histology as a diagnostic marker for active MASH with fibrosis. Its components (AST, HOMA-IR, and CK-18) reflect the spectrum of MASH biology. We therefore evaluated the correlation of MACK-3 response with improvement of liver histology and CMH markers with treatment.

Method: NATIVE evaluated lanifibranor 800 and 1200 mg/d versus placebo in 247 patients with non-cirrhotic MASH for 24 weeks of treatment. MACK-3, liver histology, adiponectin (ADP), and Pro-C3 (as a marker of fibrogenesis) were evaluated at baseline (BL) and at end of treatment (EOT). Correlations between MACK-3 and ADP, Pro-C3 and histological components according to NASH-CRN and SAF activity (SAF-A) scoring were assessed using Spearman's rank (Rs) among all randomized patients at BL and at EOT. Change in MACK-3 between histological responders and non-responders in the pooled lanifibranor arms were compared using Wilcoxon test.

Results: At BL, MACK-3 correlated with histological fibrosis stage (Spearman Rs = 0.25, $p < 0.001$), disease activity (CRN-NAS: Rs = 0.22, $p < 0.001$; SAF-A: Rs = 0.16, $p = 0.015$) and circulating biomarkers (ADP: Rs = -0.18, $p = 0.006$; Pro-C3: Rs = 0.50, $p < 0.001$). At EOT, MACK-3 still correlated with histological fibrosis stage (Rs = 0.23, $p = 0.01$), disease activity (CRN-NAS: Rs = 0.54, $p < 0.001$; SAF-A: Rs = 0.50, $p < 0.001$) and circulating markers (ADP: Rs = -0.44, $p < 0.001$; Pro-C3: Rs = 0.29, $p < 0.001$). Decrease in MACK-3 value at EOT from BL was significantly higher among lanifibranor-treated histological

responders vs non-responders for 'MASH resolution and fibrosis improvement' (-62% vs -51%, $p = 0.006$), for 'Fibrosis improvement without worsening of MASH' (-60% vs -50%, $p = 0.05$), and for 'MASH resolution without fibrosis worsening' (-63% vs -46%, $p < 0.001$). Similar results were observed for improvement of CRN-NAS of at least 2 points (-61% vs -39%, $p = 0.001$), SAF-A (-59% vs -30%, $p = 0.007$), and individual liver lesions: steatosis (-62% vs -40%, $p < 0.001$), CRN-lobular inflammation (-61% vs -46%, $p = 0.004$), and CRN-ballooning (-60% vs -28%, $p = 0.002$). With lanifibranor, decrease in MACK-3 score at EOT from BL was also correlated with ADP increase (Rs = -0.48, $p < 0.001$) and Pro-C3 decrease (Rs = 0.23, $p = 0.01$).

Conclusion: MACK-3 is a practical diagnostic algorithm for fibrotic MASH that also shows good correlation with improvement of histological disease activity and fibrosis, as well as with improvement of non-invasive biomarkers following therapy with lanifibranor, and thus warrants further study as a potential marker for evaluation of treatment response.

SAT-207

Safety and efficacy outcomes of endoscopic sleeve gastroplasty and lifestyle intervention in post-orthotopic liver transplant patients: A single-center, prospective pilot study

Jaclyn Tuck¹, David M. H. Chascsa¹, Blanca Lizaola-Mayo¹, Justin Potter¹, Alexis Baughman¹, Brian Arizmendi¹, Jaxon Quillen¹, Katie Kunze¹, Abraham Neena¹, Rahul Pannala¹. ¹Mayo Clinic, Phoenix, United States
Email: tuck.jaclyn@mayo.edu

Background and aims: Patients that are post-orthotopic liver transplantation (p-OLT) for metabolic dysfunction-associated steatotic liver disease (MASLD) are at risk for developing recurrent steatosis, fibrosis and complications from chronic liver disease. Obesity management can be challenging in this population as some patients may have contraindications to bariatric surgery. We hypothesized that endobariatric therapy (EBT), particularly endoscopic sleeve gastroplasty (ESG), and lifestyle intervention, in the framework of a protocol-based, multidisciplinary care pathway can be an effective, less invasive treatment option for obesity in these patients. In a single-center, prospective, pilot study, we evaluated the safety and efficacy outcomes of a tailored EBT approach in p-OLT for MASLD and recurrent steatosis.

Method: P-OLT patients with recurrent steatosis and obesity were considered for EBT. ESG (Overstitch, Apollo Endosurgery) was the preferred intervention. A multidisciplinary evaluation and follow-up protocol were established a priori and patient selection was based on performance status, preoperative cardiopulmonary assessment, BMI, and patient readiness for lifestyle change. Demographic and clinical data were collected prospectively. Data were analyzed using R (V 4.2.2) to examine descriptive statistics and graphical representations.

Results: Five patients (male, $n = 4$) underwent ESG. Mean BMI at enrollment was 35.5 kg/m². BMI range was 32–41.3 kg/m². Two patients (40%) had either class 2 or class 3 obesity. The median percent total body weight loss (%TBWL) was 15.14 (range 4–19.6; 1–6 months). A pre- and post-ESG fibroscan and liver biopsy was collected on one patient which showed reduction in liver fibrosis F3–4 to F2–3. There was also substantial histologic improvement with steatohepatitis, NAFLD activity score 6/8 to 4/8, macrosteatosis 35% to 5%, and a rejection activity index 3/9 to no rejection noted. Four patients had initial improvement in their HbA1c, however, 3 eventually had a post-ESG HbA1c that either returned to or was higher than pre-ESG. One patient was able to stop insulin. None of the patients were on GLP-1 agonists at the time of ESG. Blood pressure (BP) was stable for 4 patients. Three patients had improvement in triglycerides. Four patients had improvement in HDL. One patient did not have post-ESG HbA1c, BP or lipid data. 3/5 patients (60%) had improvement in their transaminases. There were no procedural adverse events.

Conclusion: ESG combined with lifestyle intervention and multidisciplinary care, may be an effective and safe obesity treatment option in complex p-OLT patients with recurrent steatosis. We found that patients had significant %TBWL with improvement in triglycerides and HDL following ESG. Future studies should evaluate predictors of efficacy and safety and optimal care frameworks specifically for this patient population.

SAT-208

Sex hormone binding globulin as an effective predictor of treatment response to TERN-501, a potent, highly selective thyroid hormone receptor β agonist: post-hoc analyses from a 12-week phase 2a trial

Naim Alkhour¹, Stephen A. Harrison², Eric Lawitz³, Kris V. Kowdley⁴, Rohit Loomba⁵, Lois Lee⁶, Christopher Jones⁶, Erin Quirk⁶, Mazen Nouredin⁷. ¹Arizona Liver Health, Tucson, United States; ²Pinnacle Clinical Research, San Antonio, United States; ³Texas Liver Institute, University of Texas Health, San Antonio, United States; ⁴Liver Institute Northwest, Elson S. Floyd College of Medicine, Washington State University, Seattle, United States; ⁵NAFLD Research Center, University of California at San Diego, La Jolla, United States; ⁶Terns Pharmaceuticals, Foster City, United States; ⁷Houston Methodist Hospital, Houston Research Institute, Houston, United States
Email: nalkhour@azliver.com

Background and aims: In a 12-week, randomized, double-blind, placebo-controlled phase 2a study in patients with presumed MASH, TERN-501, a highly selective thyroid hormone receptor β (THR- β) agonist, showed significant, dose-dependent decreases in MRI-PDFF (PDFF) and cT1 with a favorable safety profile. Sex hormone binding globulin (SHBG), a protein produced in the liver in response to THR- β agonism, also significantly increased in a dose-dependent manner, demonstrating robust target engagement. Here we evaluated the potential clinical utility of SHBG, a simple blood-based marker, in predicting TERN-501 efficacy measured by PDFF.

Method: PDFF and SHBG were measured at baseline, Week 6 and Week 12 of the study. Receiver operating characteristic (ROC) curve was built to identify an optimal SHBG increase threshold associated with $\geq 30\%$ PDFF reduction, a response criterion that has been linked to histologic improvement in MASH, using pooled data from the TERN-501 3 mg and 6 mg groups at Week 12. The proportion of patients with $\geq 30\%$ PDFF reduction at Week 12 was then assessed using the optimal SHBG increase threshold identified from the ROC curve. The proportion of responders with $\geq 30\%$ PDFF reduction at Week 12 was also assessed using a previously reported SHBG increase threshold of $\geq 120\%$. Finally, the performance of SHBG measured at Week 6 was evaluated as a predictor of PDFF response at Week 12.

Results: At Week 12, 39% ($p < 0.01$) and 64% ($p < 0.001$) of patients in the TERN-501 3 mg and 6 mg groups, respectively, achieved $\geq 30\%$ PDFF reduction vs. 4% of the patients in placebo. SHBG increase $\geq 70\%$ was identified as an optimal threshold associated with $\geq 30\%$ PDFF reduction at Week 12 (sensitivity = 80.7%; specificity = 85.7%; AUROC = 0.84). Majority (86%) of the patients with $\geq 70\%$ SHBG increase at Week 12 achieved $\geq 30\%$ PDFF reduction at Week 12 compared to only 17% of patients with $< 70\%$ SHBG increase. At a higher SHBG increase threshold of $\geq 120\%$, while all patients with $\geq 120\%$ SHBG increase at Week 12 achieved $\geq 30\%$ PDFF reduction at Week 12, 44% of patients with $< 120\%$ SHBG increase still achieved $\geq 30\%$ PDFF reduction at Week 12. Of the patients with $\geq 70\%$ SHBG increase at Week 6, 74% achieved $\geq 30\%$ PDFF reduction at Week 12. Impressively, 93% of the patients with $\geq 120\%$ SHBG increase at Week 6 achieved $\geq 30\%$ PDFF reduction at Week 12 compared to 30% of patients with $< 120\%$ SHBG increase.

Conclusion: Treatment response to TERN-501 in MASH may be effectively predicted or monitored with SHBG, potentially as early as Week 6. Patients achieving a high SHBG increase with TERN-501 treatment may not require MR-based demonstration of liver fat reduction.

SAT-209-YI

A Markov model unveiling the impact of Resmetirom on the natural history of MASLD patients with baseline significant or severe liver fibrosis

Grazia Pennisi¹, Gabriele Di Maria², Marco Enea², Marco Vaccaro³, Carlo Ciccio¹, Ciro Celsa¹, Giuseppe Infantino¹, Adele Tulone¹, Vito Di Marco¹, Calogero Camma¹, Salvatore Petta¹. ¹Section of Gastroenterology and Hepatology, Dipartimento Di Promozione Della Salute, Materno Infantile, Medicina Interna e Specialistica Di Eccellenza (PROMISE), University of Palermo, Italy, Palermo, Italy; ²Dipartimento Di Promozione Della Salute, Materno Infantile, Medicina Interna e Specialistica Di Eccellenza (PROMISE), University of Palermo, Italy, Palermo, Italy; ³Dipartimento di Scienze Economiche, Aziendali e Statistiche, University of Palermo, 90133 Palermo, Italy, Palermo, Italy
Email: grazia.pennisi901@gmail.com

Background and aims: The MAESTRO-NASH phase 3 trial reported that 52-week treatment of Resmetirom is effective in improving fibrosis and MASH in patients with metabolic-dysfunction associated steatotic liver disease (MASLD) with F2 or F3 fibrosis, while data on the impact on 5-year and long-term clinical outcomes are still lacking. Moreover, data about the full spectrum of the natural history of MASLD patients with F2 or F3 fibrosis are scarce and fragmentary. We simulated the transition probabilities of disease progression in MASLD patients with F2 or F3 fibrosis, and the effect of Resmetirom treatment on clinical outcomes.

Method: Data from 12 studies and individual sources on MASLD subjects formed transition matrices for fibrosis stages and complications, defined as compensated (CC) and decompensated cirrhosis (DC), hepatocellular carcinoma (HCC) and mortality-liver-related mortality (LR-M), cardiovascular mortality (CV-M) and extra-hepatic cancer mortality (EHC-M). Markov model was developed to depict the F2 and F3 fibrosis stage progression towards the complications and to evaluate the effect of Resmetirom treatment on the natural history of MASLD.

Results: We estimated the five-year probability of Resmetirom-treated and untreated MASLD patients with baseline F2 fibrosis of developing CC (5.16 vs 6.82, respectively), DC (0.25 vs 0.3, respectively), HCC (0.25 vs 0.32, respectively) and mortality (0.15 vs 0.16 for LR-M; 1.02 vs 1.1 for CV-M; 1.07 vs 1.2 for EHC-M, respectively). Similarly, we estimated the five-year probability of Resmetirom-treated and untreated MASLD patients with baseline F3 fibrosis of developing CC (17.12 vs 21.34, respectively), DC (1.1 vs 1.47, respectively), HCC (1.21 vs 1.73, respectively) and mortality (0.59 vs 0.91 for LR-M, 1.92 vs 2.14 for CV-M and 1.04 vs 1.14 for EHC-M, respectively). Comparable results were obtained extending these probabilities to a lifetime horizon for both F2 and F3 MASLD patients. Sensitivity analyses considering changes in transition probabilities, treatment efficacy and treatment duration are ongoing.

Conclusion: Resmetirom decreases the 5-year and lifetime Markov-model estimated risk of CC, DC, HCC, and liver-related and extra-hepatic mortality in patients with MASLD and F2 or F3 fibrosis.

SAT-210

Role of Saroglitazar in the treatment of metabolic dysfunction-associated steatohepatitis (MASH) in nondiabetic patients: a prospective observational study

Jata Shankar Kumar¹, Priyanshu Bhardwaz², Premashis Kar³. ¹Max Superspeciality Hospital, Ghaziabad, India; ²Max Hospital, Vaishali, Ghaziabad, India; ³Max Superspeciality Hospital, Ghaziabad, India
Email: jata.shankar.dr@gmail.com

Background and aims: Metabolic dysfunction-associated steatohepatitis (MASH) is a metabolic disorder characterized by the accumulation of fat and significant inflammation in the liver. MASLD encompasses patients who have hepatic steatosis and have at least one of five cardiometabolic risk factors. MASH is diagnosed when examination of the liver tissue with a microscope shows fat accumulation in hepatocytes along with inflammation and damage to

POSTER PRESENTATIONS

liver cells. Saroglitazar is a dual PPAR (proliferator peroxisome activated receptor) agonist. Aim of this study is to discuss the role of Saroglitazar in the medical management of MASH in nondiabetic patients.

Method: It was a prospective observational study in a tertiary care center in north India. The study followed the principles of declaration of Helsinki and good clinical Practice as laid down by Indian council of medical research. Total 51 nondiabetic MASH patients (Males or females, 18–75 year of age, body mass index >23 kg/m², nondiabetics) were included in this study. Diagnosis of MASH was done on the basis of liver fibroscan (CAP score >238, LSM value >7 kPa) along with raised liver enzymes (SGOT, SGPT >upper value of normal limits). All of these 51 patients received 4 milligram once daily dose of Saroglitazar for the treatment of MASH. In our study standard treatment protocol were used. ANOVA test and Multiple regression analysis was used to assess the percentage changes in Aspartate transaminase (AST), Alanine transaminase (ALT), Alkaline phosphatase (ALP), Triglyceride (TG), Low density lipoprotein (LDL) and Liver stiffness measurement (LSM) with Controlled attenuation Parameter (CAP).

Results: All of 51 patients who were treated with 4 mg daily dose of Saroglitazar for 24 weeks. 72.5% of these patients were male and 27.5% were female (male: female ratio of 2.6). The mean age of patients was 51 ± 13.13 years. Pretreatment and post treatment values of different parameters were compared. Pretreatment Mean values of ALT and AST were 93.83 ± 6.16 U/L and 76.13 ± 4.1 U/L respectively while their post treatment mean values were 32.97 ± 2.15 U/L and 34.57 ± 1.65 respectively (p value for AST and ALT were <0.001). Pretreatment mean values of fibroscan in terms of LSM and CAP were 16.2 ± 1.57 kPa (kilopascal) and 297.80 ± 37.38 dB/m (decibel/meter) and post treatment Mean values were 7.67 ± 0.23 kPa and 264.80 ± 6.81 dB/m respectively (p values for LSM and CAP were <0.001 and 0.049 respectively). Pretreatment and post treatment value of LDL were 122.1 ± 4.84 and 93.51 ± 4.12 respectively (p < 0.001).

Conclusion: Saroglitazar; a PPAR agonist, was found to be effective in medical management of metabolic dysfunction-associated steatohepatitis (MASH). It reduces the liver stiffness and decreases the elevated liver enzymes (SGOT/SGPT) as well as serum LDL level over duration of 6 months.

SAT-212

Real-world use of Glucagon-like peptide 1 receptor agonists in patients with MASLD: a cross-sectional analysis from TARGET-NASH

A. Sidney Barritt, IV¹, Andrea Mospan², Heather Morris², Anthony Perez², Rohit Loomba³, Michael Fried², Arun J. Sanyal⁴, Philip N. Newsome⁵. ¹UNC Liver Center, University of North Carolina, Chapel Hill, United States; ²Target RWE, Durham, United States; ³Division of Gastroenterology, Department of Medicine, University of California at San Diego, San Diego, United States; ⁴Virginia Commonwealth University, Richmond, United States; ⁵University of Birmingham, Birmingham, United Kingdom
Email: sid_barritt@med.unc.edu

Background and aims: Glucagon-like peptide 1 receptor agonists (GLP-1 RA) are approved in the United States for diabetes and obesity. There is considerable interest in using this class of medications in patients with metabolic dysfunction associated steatotic liver disease (MASLD). Clinical trials have shown these drugs are well tolerated, but real-world data from larger cohorts are lacking. This study aims to describe characteristics of patients with MASLD who are prescribed GLP-1 RA including duration of use and tolerance.

Method: TARGET-NASH is a real-world patient cohort designed to follow patients with MASLD in routine clinical settings. In part, the study aims to gain insights into use of off-label drugs in usual clinical care. Patients are enrolled in TARGET-NASH based on a treating physician's diagnosis of MASLD.

Results: In a cohort of 5,361 TARGET-NASH US adult participants, 603 (11%) were on one or more GLP-1 RA including with MASL (n = 109), MASH (n = 269), and cirrhosis (n = 225). Median age among users was 59 years, 99% type 2 diabetes, 76% obese (BMI >30 kg/m²). Insurance coverage was similar across users vs nonusers. Age differed significantly with GLP-1 RA users disproportionately centered in the 40–64 age group compared to non-GLP-1RA. Relative to Non-Hispanic Whites, Asians (OR = 0.16, p < 0.001) and those with other race/ethnicity (OR = 0.46, p < 0.01) had significantly lower odds of GLP-1 RA use. Across the spectrum of disease severity, patients were more likely to receive a GLP-1 RA when being treated at an academic vs. community site, female, and with obesity class II/III (all p < 0.0001). Comorbidities were more common among GLP-1 RA users including type 2 diabetes, cardiovascular disease, hyperlipidemia, hypertension, autoimmune/rheumatological conditions, anxiety/depression, and arthritis. Duration of GLP-1 treatment was similar across disease severity with a median duration of 2.4 years. Treatment discontinuation, temporary disruptions, or treatment modifications among the 770 patient exposures occurred in 256 (42%) cases overall, 36 (33%) MASL cases, 130 (48%) MASH cases, and 90 (40%) MASH cirrhosis cases. The majority of treatment disruptions (215/256 or 83%) were for non-medical reasons including cost/insurance constraints, temporary pauses, dosage modifications, supply shortages, and various patient/provider decisions. Only 41 (8%) patient-exposures actually stopped following medical events such as GI intolerance.

Conclusion: In TARGET-NASH, 11% of participants were prescribed a GLP-1 RA. Most users were Caucasian women from age 40–64; despite drug access concerns, insurance type did not differ between users and non-users. This real-world population had significant comorbid conditions, including cardiovascular disease and cirrhosis. Despite this, GLP-1 RA were well tolerated with the majority of discontinuations due to non-medical reasons.

SAT-213

Postbiotic supplementation for metabolic dysfunction-associated steatotic liver disease

Maryana Savitska¹, Olena Baka², Elina Manzhali³, Dmytro Kyriienko⁴, Tetyana Falalyeyeva⁵, Maksym Zhayvoronok⁶, Oleksandr Kovalchuk⁷, Nataliya Deresh⁸, Fedir Grygoriev⁹, Nazarii Kobyljak¹⁰. ¹Danylo Halytsky Lviv National Medical University, Lviv, Ukraine; ²Center for Innovative Medical Technologies of the National Academy of Sciences of Ukraine, Kyiv, Ukraine; ³Bogomolets National Medical University, "Verum-expert" Clinic, Kyiv, Ukraine; ⁴Kyiv City Clinical Endocrinology Center, Kyiv, Ukraine; ⁵Taras Shevchenko National University of Kyiv, Medical Laboratory CSD, Kyiv, Ukraine; ⁶Shupyk National Healthcare University of Ukraine, Medical Scientific and Practical Association "MedBud", Kyiv, Ukraine; ⁷Taras Shevchenko National University of Kyiv, Kyiv, Ukraine; ⁸Lifescan Clinic, Kyiv, Ukraine; ⁹MirImmunoPharm LLC, Kyiv, Ukraine; ¹⁰Bogomolets National Medical University, Kyiv, Ukraine
Email: nazariikobyljak@gmail.com

Background and aims: The current study aim was to conduct placebo-controlled randomize clinical trial (RCT) to assess the short-term efficacy and safety of postbiotics on hepatic fat content as measured by magnetic resonance imaging (MRI)-estimated proton density fat fraction (PDFF) and ultrasonography in patients with metabolic dysfunction-associated steatotic liver disease (MASLD).

Method: A total of 39 patients met the criteria for inclusion. The study includes 2 periods. Screening period of up to 1 week to assess the eligibility to inclusion/exclusion criteria. Treatment period for 3 months where the participants receive a twice daily oral dose of postbiotics (cell lysate and DNA fragments of the probiotic strain *L. rhamnosus* DV-NRRLB-68023) at the assigned dose of 100 mg or placebo in capsules. The primary main outcomes were the change of MRI-PDFF in % and ultrasound-based attenuation coefficient measurement (ACM) and hepatorenal index (HRI). Secondary outcomes

were the changes in serum lipid content, anthropomorphic variables, and liver stiffness (LS) measured by Shear Wave Elastography (SWE). ANCOVA was used to assess the difference between groups. Trial registration: NCT05804422

Results: We observed significant decrease in hepatic fat content using both modalities only in postbiotic group: MRI-PDFF (15.02 ± 2.33 to 10.84 ± 2.63 %; $p = 0.045$), ACM (2.63 ± 0.07 to 2.54 ± 0.06 dB/cm; $p = 0.043$) and HRI (1.33 ± 0.05 to 1.24 ± 0.04 ; $p = 0.011$) respectively. In placebo group slight insignificant reduction of MRI-PDFF (10.84 ± 2.13 to 7.88 ± 2.34 %; $p = 0.283$) and ACM (2.60 ± 0.08 to 2.54 ± 0.08 dB/cm; $p = 0.250$) was found. In parallel intervention with placebo was associated with increase of HRI (1.22 ± 0.05 to 1.24 ± 0.04 ; $p = 0.429$) and LS measured by SWE (4.76 ± 0.21 to 4.87 ± 0.21 ; $p = 0.046$). As compared to placebo group LS decreased insignificant in postbiotic group (5.51 ± 0.38 to 5.39 ± 0.36 ; $p = 0.222$). In secondary outcomes analysis significant changes were found only in postbiotic group.

Conclusion: To our knowledge its first RCT which demonstrate that postbiotic supplementation can reduce hepatic fat content in MASLD patients. Modulation of the gut microbiota represents a new treatment for MASLD and should be tested in larger studies.

SAT-214

Using machine learning models to predict baseline fibrosis stage in patients from phase 3 resmetirom trials (MAESTRO-NAFLD and MAESTRO-NASH)

Jörn M. Schattenberg^{1,2}, Quentin M. Anstee³, Stephen A. Harrison⁴, Mazen Noureddin⁵, Rebecca Taub⁶, Dominic Labriola⁶, Jan Priel⁷, Krishna Padmanabhan⁸. ¹Metabolic Liver Research Program, I. Department of Medicine, University Medical Center of Johannes Gutenberg University Mainz, Mainz, Germany; ²The Department of Internal Medicine II, Saarland University Medical Center, Homburg, Germany; ³The Translational and Clinical Research Institute, Faculty of Medical Sciences, Newcastle University, Newcastle-upon-Tyne, United Kingdom; ⁴Pinnacle Clinical Research, San Antonio, TX, United States; ⁵Houston Methodist Hospital, Houston Research Institute, Houston, TX, United States; ⁶Madrigal Pharmaceuticals, Inc., West Conshohocken, PA, United States; ⁷Cytel, Inc., Berlin, Germany; ⁸Cytel, Inc., Waltham, MA, United States

Email: joern.schattemberg@uks.eu

Background and aims: MAESTRO-NASH (NCT03900429) is an ongoing 54-month, randomized, double-blind, placebo-controlled Phase 3 trial evaluating the efficacy of resmetirom in patients with biopsy-confirmed NASH/MASH and fibrosis (F1B-F3 and exploratory F1). MAESTRO-NAFLD-1 (NCT04197479) is a completed, randomized, placebo-controlled trial Phase 3 trial evaluating resmetirom safety and its effects on biomarkers in patients with NASH without a biopsy confirmation. 180 patients with well-compensated NASH cirrhosis were enrolled in an open label arm of MAESTRO-NAFLD-1. 1813 patients had baseline or historic biopsy spanning stage F0-F4 with multiple non-invasive biomarker and imaging measures of NASH with fibrosis.

Method: Adults with ≥ 3 metabolic risk factors were screened. Pts with FibroScan VCTE, liver stiffness ≥ 8.5 kPa, MRI-PDFF $\geq 8\%$, biopsy-confirmed F1B-F3 NASH, NAS ≥ 4 , were eligible for MAESTRO-NASH. MAESTRO-NAFLD-1 included pts with non-invasive measures of NASH (MRI-PDFF $\geq 8\%$, Fibroscan VCTE ≥ 5.5) or well-compensated NASH cirrhosis. Machine learning models evaluated the relative importance of patients' intrinsic characteristics and screening/baseline biomarkers. The Random Forest (RF) model was selected due to its predictive performance. The Full model (FM) included 36 possible explanatory variables, and the lean model (LM) had 21 predictors more likely to be used in clinical practice. LM was based on 1765 patients with non-missing data compared to 607 pts in FM.

Among the potential predictors assessed were demographic characteristics, T2DM, liver tests, MRI-PDFF, MRE, Fibroscan CAP and VCTE, FAST, MAST, FIB-4, Pro-C3, ELF, M30, thyroid hormones, SHBG, and liver and spleen volumes.

Results: Baseline characteristics excluding the population with liver biopsies included: 207 = F0, 271 = F1a or c, 156 = F1b (designated F2-equivalent), 395 = F2, 605 = F3, 131 = F4 (Cirrhosis). The RF model was used to classify patients: F0/F1a/F1c (Early) vs. F1b/F2/F3 (At-risk) vs. F4, a 3-class model. AUC and classification error rates were assessed in repeated cross-validation. The variables that most impacted classification (FM) included: MRE, Fibroscan VCTE, MRI-PDFF, MAST, SHBG and Platelet count; for LM: Fibroscan VCTE, FIB-4, Pro-C3, FAST, GGT, Platelets, AST and Fibroscan CAP. In the FM, mean (SD) AUROC for F0/F1A/1C vs Rest = 0.804 (0.055); F1B/F2/F3 = 0.776 (0.047); F4 vs Rest = 0.930 (0.031). In the LM AUROC for F0/F1A/1C vs Rest = 0.854 (0.017); F1B/F2/F3 = 0.815 (0.018); F4 vs Rest = 0.89 (0.028)

Conclusion: In a population selected for high baseline metabolic risk factors, liver stiffness and liver fat, both FM and LM were able to accurately identify early NASH pts versus those with more significant fibrosis. FM and LM accurately discriminated F4 (cirrhosis) from all others. LM, based on commonly collected biomarkers and lab tests, performed as well as FM.

SAT-215

Healthcare cost and resource utilization among patients with non-alcoholic steatohepatitis (NASH), stratified by glucagon-like peptide 1 receptor agonist (GLP-1) use in real world data

Yestle Kim¹, Jesse Fishman¹, Elliot Tapper², Dave Lewandowski³, Taylor Marlin³, Alina Bogdanov³, Machaon Bonafede³. ¹Madrigal Pharmaceuticals, Inc., West Conshohocken, United States; ²University of Michigan, Ann Arbor, United States; ³Veradigm, Chicago, United States
Email: ykim@madrigalpharma.com

Background and aims: Non-alcoholic steatohepatitis (NASH, also known as metabolic-dysfunction associated steatohepatitis [MASH]), is a progressive condition associated with cirrhosis, liver failure, and hepatocellular carcinoma. GLP-1 s are currently approved for type 2 diabetes (T2D) and obesity. This study aims to characterize GLP-1 use among patients with NASH and summarize healthcare costs and resource utilization.

Method: Adults ≥ 18 years at index with a NASH diagnosis code were identified in electronic health records or claims between 7/1/2018 and 8/31/2022 in the Veradigm Integrated Dataset. Patients with viral hepatitis, alcohol-use disorder or alcoholic liver disease, opioid disorders, cirrhosis, type 1 diabetes, gestational diabetes, or bariatric surgery were excluded. Patients were required to have ≥ 12 months of continuous claims enrollment pre- (baseline) and post- index (follow-up), and not have any GLP-1 claims in the baseline period. Patients were stratified into 3 cohorts based on GLP-1 use (≥ 1 prescription) in the follow-up period: no GLP-1, high-dose GLP-1, and low-dose GLP-1. Duration of GLP-1 use was not analyzed for this abstract. High and low doses of GLP-1 s were determined based on the drug prescribing information; T2D-indicated GLP-1 doses were used as the thresholds for high/low categories. We summarized baseline patient characteristics and costs during the 12-month follow-up period.

Results: We identified 56,756 patients with NASH, 50,094 of whom had no GLP-1 at follow-up, 348 had a high-dose GLP-1, and 2,315 had low-dose GLP-1. Mean (SD) age was 53.8 (14.4), 48.1 (12.0), and 53.1 (11.9) years for no GLP-1, high-dose GLP-1, and low-dose GLP-1 cohorts, respectively. Among those with BMI reported in the baseline period, 16.9% of the no GLP-1 cohort had BMI of 40+, compared to 38.9% in the high-dose GLP-1 cohort and 33.5% in the low-dose GLP-1 cohort. Of the patients with HbA1c measurement during the baseline period, the mean (SD) HbA1c values were 6.4% (1.3%), 6.8% (1.3%), and 7.5% (1.7%) for the no GLP-1, high-dose GLP-1, and low-dose GLP-1 cohorts, respectively. During the follow-up period, 11.0% of no GLP-1 cohort had an inpatient admission, with mean inpatient costs of \$4,

POSTER PRESENTATIONS

516, compared with 6.6% of the high-dose GLP-1 cohort (\$9,472) and 11.4% of the low-dose GLP-1 cohort (\$3,877). Mean emergency department costs were \$1,073 for the no GLP-1 cohort, \$1,222 for the high-dose GLP-1 cohort, and \$1,373 for the low-dose GLP-1 cohort. After excluding costs in the top 1%, mean unadjusted total follow-up costs were \$12,265 for the no GLP-1 cohort, \$17,140 for the high-dose GLP-1 cohort, and \$18,860 for the low-dose GLP-1 cohort.

Conclusion: Compared with patients with no GLP-1 utilization, patient costs with both high- and low-dose GLP-1 utilization were higher; this trend was not explained by expected costs from more medication use.

SAT-218

Liver fibrosis and obesity associated with stroke in an elderly population: protected effect by pravastatin

Willy Theel^{1,2,3}, Vivian de Jong^{4,5}, Diederick Grobbee^{5,6}, J. Wouter Jukema⁷, Stella Trompet⁷, Manuel Castro Cabezas^{5,8,9}.
¹Franciscus Gasthuis and Vlietland, Rotterdam, Netherlands; ²Centrum Gezond Gewicht, Rotterdam, Netherlands; ³Erasmus University Medical Center, Rotterdam, Netherlands; ⁴Julius Global Health, University Medical Center Utrecht, Utrecht, Netherlands; ⁵Julius Clinical, Zeist, Netherlands; ⁶Julius Global Health, University Medical Center Utrecht, Utrecht, Netherlands; ⁷Leiden University Medical Center, Leiden, Netherlands; ⁸Franciscus Gasthuis and Vlietland, Rotterdam, Netherlands; ⁹Erasmus Medical Center, Rotterdam, Netherlands
Email: w.theel@franciscus.nl

Background and aims: Liver fibrosis, as part of the Metabolic dysfunction Associated Steatotic Liver Disease (MASLD) in subjects with obesity may increase cardiovascular risk. A recent meta-analysis demonstrated that statins could be beneficial in the MASLD population. Nevertheless, the effect of statins on cardiovascular disease in elderly subjects with obesity and liver fibrosis remains understudied.

Method: The PROspective Study of Pravastatin in the Elderly at Risk (PROSPER) database was used for this analysis. PROSPER evaluated the effect of pravastatin on major adverse cardiovascular events in an elderly population (>70 years). We divided the study group into three subgroups based on their body mass index (BMI): healthy (<25 kg/m²), overweight (25–29, 9 kg/m²) and obese (≥30 kg/m²). In each group we calculated for all participants the FIB4 score which reflects liver fibrosis using age-adjusted cutoffs: low risk of advanced fibrosis (FIB-4 <2.0), intermediate risk (2.0 ≤ FIB-4 ≤ 2.66) and high risk (FIB-4 ≥ 2.67). Time-to-event data were analyzed using the Cox proportional hazards model for the placebo and pravastatin groups separately and adjusted for sex.

Results: In total 5244 subjects were included. Compared to the reference group with low FIB4 and healthy BMI, the hazard ratio for a (non) fatal stroke was significantly higher (HR 2.58–95%CI 1.14–5.84) in the highest risk group (high FIB4 score and obesity) on placebo. In the pravastatin groups, the differences disappeared, suggesting that pravastatin protects against (non) fatal stroke in elderly subjects with obesity and liver fibrosis. Pravastatin did not influence other cardiovascular end points in this elderly population when analyzed based on different BMI levels and different grades of liver fibrosis.

Conclusion: Elderly people with obesity and liver fibrosis have an increased risk of (non) fatal stroke when compared to a reference population and treatment with pravastatin has a protective effect.

SAT-219

Discovering 1-piperidine propionic acid inhibiting effect on protease activated receptor 2 and serpinb3 as a new therapeutic strategy for metabolic dysfunction-associated steatohepatitis

Monica Chinellato¹, Gianmarco Villano¹, Erica Novo², Cristian Turato³, Santina Quarta¹, Mariagrazia Ruvoletto¹, Alessandra Biasiolo¹, Andrea Martini¹, Stefania Cannito², Camilla Mazzucco¹, Matteo Gasparotto¹, Francesco Filippini¹, Luca Spiezia¹, Laura Cendron¹, Maria Guido¹, Roberto Vettor¹, Maurizio Parola²,

Patrizia Pontisso¹. ¹University of Padova, Padova, Italy; ²University of Torino, Torino, Italy; ³University of Pavia, Pavia, Italy
Email: monica.chinellato@phd.unipd.it

Background and aims: The serine protease inhibitor SerpinB3 has a pivotal role in liver fibrosis and its involvement in MASH development and insulin resistance has been described recently. Conversely, Protease Activated Receptor 2 (PAR2) is a well well-established regulator of inflammatory cascade and it has been proposed as novel target for metabolic liver disease. Recently a small molecule, 1-Piperidine Propionic Acid (1-PPA), has been reported to inhibit inflammatory processes involving SerpinB3. In this work we aim to investigate the pathway involving both proteins to find new therapeutic strategy for MASH treatment.

Method: The effect of 1-PPA has been evaluated with a wide approach, including: a) Biophysical studies to determine the interaction with PAR2; b) Cellular models using cell lines with different extent of expression of SerpinB3, to explore the downstream effects on SerpinB3 and other inflammation and fibrosis genes transcriptional levels; c) mice transgenic or KO for in experimental MASH models.

Results: 1-PPA stabilization effects observed by cellular thermal shift assay and in-silico investigations revealed a putative site of interaction within PAR2 molecule, determining its inactivation. Functional studies showed indeed its antagonist effect on MAPKs signalling. A parallel reduction of the synthesis of SerpinB3 was also observed both in vitro and in vivo in presence of 1-PPA and this effect was associated with the inhibition of lipids accumulation, inflammation and fibrosis in experimental MASH.

Conclusion: 1-PPA has been identified as a novel PAR2 regulator, that was able to inhibit the PAR2-SerpinB3 axis in inflammatory condition. Its effects can protect from MASH development and progression, supporting the potential use of a similar approach for a targeted therapy of this pathological condition.

SAT-220-YI

Efruxifermin treatment improved collagen biomarkers consistent with remodelling of the extracellular matrix in patients with F2-F3 fibrosis due to MASH

Erik Tillman¹, Doreen Chan¹, Reshma Shringarpure¹, Diana Leeming², Morten Karsdal², Stephen A. Harrison³, Andrew Cheng¹, Kitty Yale¹, Tim Rolph¹. ¹Akero Therapeutics, South San Francisco, United States; ²Nordic Bioscience, Herlev, Denmark; ³Pinnacle Clinical Research, San Antonio, United States
Email: erik@akerotx.com

Background and aims: Efruxifermin (EFX) is a long-acting, bivalent Fc-FGF21 analogue in phase 3 clinical trials for the treatment of liver fibrosis due to metabolic dysfunction-associated steatohepatitis (MASH). Across multiple phase 2 studies in patients with moderate-to-severe (F2–F3) fibrosis or compensated cirrhosis (F4) due to MASH, EFX significantly improved markers of liver injury, fibrosis, and fibrogenesis. In the phase 2b HARMONY study in F2–F3 MASH fibrosis, 28 mg and 50 mg EFX improved fibrosis without MASH worsening in significantly more patients than pbo, while also leading to substantially higher rates of MASH resolution without worsening fibrosis after 24 weeks. Here, we aimed to assess the effects of EFX on markers of various components of the extracellular matrix (ECM) to understand EFX pharmacology and the relationship between hepatic ECM remodelling and fibrosis improvement.

Method: We undertook a *post hoc* analysis of biomarkers of fibrogenesis and fibrolysis of collagens associated with pathological fibrosis (types III, VI, and VIII) and components of the basement membrane (type IV collagen). Pro-C3, Pro-C4, Pro-C6, and Pro-C8 are markers of collagen synthesis, while CTX-III and C4M are markers of collagen degradation, Pro-C3/CTX-III or Pro-C4/C4M ratios indicate the balance between fibrogenesis and fibrolysis. Pro-C6, also known as endotrophin, has both *in vitro* and *in vivo* pro-fibrotic activity, and is associated with adipose tissue dysfunction and risk of clinical

outcomes in patients with heart failure with preserved ejection fraction.

Results: After 24 weeks, we identified significant EFX-related shifts towards a potentially beneficial ECM remodelling endotype, with decreased type-III collagen fibrogenesis relative to fibrolysis (suggesting resorption of type-III collagen), with mean reductions in Pro-C3/CTX-III ratio of 16%* and 13%* for 28 mg and 50 mg EFX, respectively, compared to a 7% increase for pbo. EFX also significantly reduced Pro-C8, with mean reductions of 2% and 9%* for 28 mg and 50 mg EFX, compared to a 5% increase for pbo. We observed a trend toward increased type-IV collagen fibrogenesis relative to fibrolysis (suggesting regeneration of type-IV collagen), with mean increases in Pro-C4/C4M ratio of 6% and 11% for 28 mg and 50 mg EFX, respectively, compared to a 2% increase for pbo. EFX significantly reduced Pro-C6, with mean reductions of 11%*** and 12%*** for 28 mg and 50 mg EFX, compared to a 9% increase for pbo. We observed associations between ECM remodelling and improvements in liver pathology, including both fibrosis improvement and MASH resolution [* $p < 0.05$, *** $p < 0.001$ vs pbo].

Conclusion: Together, these results suggest overall beneficial remodelling of the ECM and modulation of markers of pathological fibrosis consistent with improvements in metabolic health, liver health, and suppression of fibrogenesis following EFX treatment.

SAT-221

Effectiveness of Polyene phosphatidylcholine in metabolic-associated fatty liver disease treatment : a real-world study in China

Yi Pan¹, Feng Xue¹, Shanshan Wang², Shuangqing Gao², Lai Wei¹.
¹Beijing Tsinghua Changgung Hospital, School of Clinical Medicine, Tsinghua University, Beijing, China; ²Beijing North Medical and Health Economic Research Center, Beijing, China
Email: weelai@163.com

Background and aims: Metabolic-associated fatty liver disease (MAFLD) has increasingly become the primary cause of liver transplantation and cirrhosis globally. To date, there is no approved pharmacotherapy for MAFLD in the world. Previous studies showed that polyenyl phosphatidylcholine (Essentiale capsule, Ess) could be used for MAFLD due to its action of accelerating liver cell membrane regeneration. We conducted a retrospective observational study based on multicenter real-world data to evaluate the effectiveness of Ess in Chinese MAFLD patients.

Method: MAFLD patients (aged ≥ 18) were identified from the tertiary public hospital between January 1st 2020 and December 31st 2022 following APASL 2020 guideline. Propensity score matching (PSM) was used to match Ess monotherapy group and control (non-hepatoprotective-treated) group. The primary end point was the changes of fibrosis-4 index (FIB-4) from baseline to 24 weeks between the two groups. Changes of liver biochemistry from baseline also were compared between the two groups at 4 weeks, 12 weeks, and 24 weeks of the treatment. In MAFLD patients with hyperlipidemia, between-group differences in changes of blood lipids parameters were compared.

Results: A total of 82, 908 MAFLD patients were identified from 11 hospitals. The median age was 53 (43–63) years old and 64.3 % were male. 7, 093 of MAFLD patients were treated with Ess and those whose test parameters could be available during the follow-up were included in the analysis. After PSM analysis matching for age, sex, type 2 diabetes (T2DM), hypertension, hyperlipidemia, and cardiovascular disease (CVD), there was a statistical difference in the reduction of FIB-4 at 24 weeks between the two groups (-0.12 ± 0.62 for Ess vs. 0.11 ± 0.50 for control, $p = 0.034$). There was a significant difference in the changes of aspartate transaminase from baseline to 12 weeks between the two groups (-6.25 ± 15.18 for Ess vs. -2.41 ± 15.40 for control, $p = 0.0392$). The significant difference between Ess and control group was also observed in the changes of alkaline phosphatase from baseline to 4 weeks (-6.46 ± 60.62 for Ess vs. 2.45

± 28.12 for control, $p = 0.0269$). Between-group differences in changes of total bilirubin from baseline to 4, 12, 24 weeks were significant (4 weeks: -2.80 ± 5.59 for Ess vs. -0.10 ± 7.92 for control, $p = 0.0063$; 12 weeks: -1.97 ± 5.93 for Ess vs. 0.23 ± 6.12 for control, $p = 0.0122$; 24 weeks: -3.39 ± 5.65 for Ess vs. 1.24 ± 3.94 for control, $p = 0.0010$). In the subgroup of MAFLD patients with hyperlipidemia, low-density lipoprotein cholesterol was significantly decreased in Ess-treated group than control group after 12 weeks of treatment (-0.23 ± 0.71 for Ess vs. 0.13 ± 0.67 for control, $p = 0.0442$).

Conclusion: This study found that, in MAFLD patients, Ess treatment could improve liver function and might have beneficial effects on reducing the risk of fibrosis and improving lipid disorders.

Funding: Sanofi.

SAT-224

Pharmacokinetics of the selective glucocorticoid receptor modulator miricorilant in healthy volunteers and patients with presumed metabolic dysfunction-associated steatohepatitis (MASH)

Joseph M. Custodio¹, Kirsteen Donaldson², Jeevan Kunta¹, Kavita Juneja¹, Naim Alkhouri³, Hazel J. Hunt¹. ¹Corcept Therapeutics Incorporated, Menlo Park, CA, United States; ²Jade Consultants (Cambridge) Limited, Cambridge, United Kingdom; ³Arizona Liver Health, Tucson, AZ, United States
Email: jcustodio@corcept.com

Background and aims: Miricorilant (MIRI) is an oral, nonsteroidal selective glucocorticoid receptor (GR) modulator (SGRM) that acts as a mixed agonist/antagonist of the GR and a modest antagonist of the mineralocorticoid receptor. MIRI is in development for the treatment of metabolic dysfunction-associated steatohepatitis (MASH). Over 450 patients (pts) and healthy volunteers (HVs) have received MIRI in clinical trials to date. Here, we describe the pharmacokinetics (PK) and metabolism of MIRI in several non-clinical and phase 1 clinical development trials.

Method: Tissue distribution of oral [¹⁴C]-MIRI 50 mg/kg was assessed in albino mice. Study 850 (NCT03315338) was a first-in-human, double-blind, randomized, placebo-controlled study testing multiple ascending doses (150–900 mg) of oral MIRI for 14 days in fasted HVs; PK was assessed. Study 851 (NCT03878264) evaluated the absorption, distribution, metabolism, and excretion (ADME) and mass balance of a single oral dose of [¹⁴C]-MIRI 150 mg in fed HVs. Study 854 (NCT05553470) was an open-label, adaptive design study of single-dose MIRI 600 mg given under fed conditions in pts with moderate hepatic impairment compared to HVs with normal hepatic function; PK was assessed. Study 861 (NCT05117489) was a phase 1b, open-label trial of adult pts with presumed MASH that included 11 cohorts of pts who received MIRI doses ranging from 30–200 mg intermittently or daily for 12 or 24 weeks; efficacy and PK were assessed. Safety was assessed in all trials.

Results: High levels of radioactivity were present in the liver 1 and 4 hours following oral administration of [¹⁴C]-MIRI in mice. In study 850, systemic concentrations increased with repeated dosing with MIRI 150 mg daily for 14 days in HVs ($n = 9$). Steady state plasma exposures were achieved by Day 7, resulting in an overall accumulation ratio from Days 1 to 14 of 1.68 for C_{max} and 2.17 for $AUC_{(0-\tau)}$, with an elimination half-life of 21.6 hours. MIRI was generally well tolerated in HVs. In study 851, following administration of a single oral dose of [¹⁴C]-MIRI 150 mg to HVs ($n = 6$), 89.1% of the total radioactivity was recovered in the feces, with minimal recovery in the urine ($<5\%$), suggesting that the predominant route of elimination is hepatic. MIRI accounted for $>50\%$ of the total radioactivity in plasma based on $AUC_{(0-\infty)}$, indicating that parent MIRI was the main circulating species in plasma. In study 854, there was no apparent difference in plasma exposures in pts with moderate hepatic impairment ($n = 10$) compared to HVs ($n = 10$) with normal hepatic function. In study 861, MIRI plasma PK behaved in an approximately

POSTER PRESENTATIONS

dose proportional manner across the range of MIRI doses and dosing regimens evaluated in pts with MASH (n = 71).

Conclusion: The presented studies characterize the PK/ADME of MIRI in HVs and pts with MASH. A phase 2b study (MONARCH, NCT06108219) of MIRI 100 mg twice weekly in MASH is underway.

SAT-225

Berberine Ursodeoxycholate (HTD1801) provides a unique therapeutic approach for patients with metabolic diseases and severe insulin resistance

Leigh MacConell¹, Alexander Liberman¹, Abigail Flyer², Kui Liu³.

¹HighTide Therapeutics, Rockville, United States; ²Pacific Northwest

Statistical Consulting, Woodinville, United States; ³HighTide

Therapeutics, Shenzhen, China

Email: lmacconell@hightidetx.com

Background and aims: Hyperinsulinemia is a significant risk factor for several metabolic diseases. HTD1801 is a gut-liver anti-inflammatory metabolic modulator with a unique molecular structure which has been shown to significantly reduce liver fat content (LFC; via MRI-PDFF) and important cardiometabolic end points in an 18-Week, placebo (PBO)-controlled Phase 2 study in patients with MASH and T2DM. HTD1801 is hypothesized to activate AMPK, increasing cellular utilization of glucose and fat, thereby alleviating the effects induced by high insulin. Based on this hypothesis, HTD1801 evaluated post hoc based on baseline insulin levels.

Method: 100 patients were randomized and treated with HTD1801 1000 mg BID, HTD1801 500 mg BID, or PBO for 18 weeks. Patients were then analyzed by subgroups defined by baseline fasting insulin (FIN) levels: ≤ 40 $\mu\text{IU/ml}$ (HTD1801 1000 mg BID: n = 19, HTD1801 500 mg BID: n = 22, PBO: n = 20) vs >40 $\mu\text{IU/ml}$ (HTD1801 1000 mg BID: n = 8, HTD1801 500 mg BID: n = 7, PBO: n = 12).

Results: 27/100 patients had severe insulin resistance (baseline FIN >40 $\mu\text{IU/ml}$). Baseline characteristics were generally similar across insulin subgroups. Across the primary end point (LFC) and key cardiometabolic parameters, dose dependent improvements were observed irrespective of baseline insulin levels with HTD1801 compared to PBO after 18 weeks.

LFC (%)

FIN ≤ 40 $\mu\text{IU/ml}$; HTD1801 1000 mg BID: -4.0, HTD1801 500 mg BID: -2.8, PBO: -2.6

FIN >40 $\mu\text{IU/ml}$; HTD1801 1000 mg BID: -6.9, HTD1801 500 mg BID: -3.7, PBO: -0.6

HbA1c (%)

FIN ≤ 40 $\mu\text{IU/ml}$; HTD1801 1000 mg BID: -0.4, HTD1801 500 mg BID: -0.4, PBO: 0.03

FIN >40 $\mu\text{IU/ml}$; HTD1801 1000 mg BID: -0.9, HTD1801 500 mg BID: -0.3, PBO: 0.2

Weight (kg)

FIN ≤ 40 $\mu\text{IU/ml}$; HTD1801 1000 mg BID: -1.6, HTD1801 500 mg BID: -1.2, PBO: -1.1

FIN >40 $\mu\text{IU/ml}$; HTD1801 1000 mg BID: -8.0, HTD1801 500 mg BID: -2.7, PBO: -1.0

However, in the HTD1801 1000 mg BID group, substantially greater improvements were observed across parameters in patients with elevated baseline insulin compared to patients with lower baseline insulin

Conclusion: These data, while limited to a small number of subjects, suggest that HTD1801 can alleviate the metabolic inhibitory effects caused by hyperinsulinemia, leading to greater metabolic benefits and therefore may offer a unique therapeutic approach for individuals with metabolic diseases and elevated insulin levels. HTD1801 continues to be evaluated in the ongoing Phase 2b study in patients with MASH and T2DM.

SAT-226

Statin prescriptions and progression to a high-risk for advanced fibrosis in primary care patients with metabolic dysfunction-associated steatotic liver disease (MASLD)

Andrew Schreiner¹, Jingwen Zhang¹, Mulugeta Gebregziabher¹.

¹Medical University of South Carolina, Charleston, United States

Email: schrein@musc.edu

Background and aims: Statin medications reduce the risk of cardiovascular events, an important consideration in patients with metabolic dysfunction-associated steatotic liver disease (MASLD). Statins may also reduce the risk of fibrosis progression in MASLD and other chronic liver diseases. We aimed to determine the association of statin prescriptions, and the intensity of statin prescriptions, with progression to a high-risk for advanced fibrosis in primary care patients with low-risk MASLD.

Method: This retrospective cohort study of primary care electronic health record data from 2012 to 2021 included patients with MASLD and an initial low- or indeterminate-risk for advanced fibrosis, determined by Fibrosis-4 Index score (FIB-4 <2.67). Patients were followed from the index FIB-4 score until the primary outcome of a FIB-4 at high-risk for advanced fibrosis (FIB-4 ≥ 2.67). Prescription for a statin during follow-up, treated as a fixed and time-varying covariate, was the primary exposure of interest. We developed Cox regression models for the time to a high-risk FIB-4 score with statin therapy as the primary covariate and adjusting for advanced fibrosis risk at baseline, demographic, and comorbidity variables during follow-up.

Results: The cohort included 1,238 patients with MASLD and a mean age of 54 years and a mean body mass index of 33 kg/m². Of included patients, 64% and 36% had low- and indeterminate-risk FIB-4 scores at baseline. During follow-up of a mean 3.3 (± 2.5) years, 47% (586) of patients received a prescription for a statin, and 18% (220) of patients progressed to a FIB-4 at high-risk for advanced fibrosis. In the fully adjusted Cox regression model with statin prescription as a time-fixed covariate, statins were associated with a lower risk (HR 0.60; 95%CI 0.45–0.80) of progressing to a FIB-4 ≥ 2.67 . In the fully adjusted Cox model with statin prescription as a time-varying covariate, statins were not associated with time to high-risk for advanced fibrosis (HR 0.89; 95%CI 0.67–1.18).

Conclusion: Though evidence from the analysis of statin prescription as a time-fixed covariate demonstrates a protective association with progression to advanced fibrosis, the Cox model with statin prescriptions as a time-varying covariate showed no association between statin prescription and progression of advanced fibrosis risk.

SAT-227

Evaluation of efficacy of Berberine Ursodeoxycholate (HTD1801) compared to ongoing use of GLP-1 receptor agonists in patients with MASH and T2DM

Stephen A. Harrison¹, Guy Neff², Nadege Gunn³, Abigail Flyer⁴, Leigh MacConell⁵. ¹Pinnacle Clinical Research, San Antonio, United States; ²Covenant Metabolic Specialists, Sarasota, United States; ³Impact Research Institute, Waco, United States; ⁴Pacific Northwest Statistical Consulting, Woodinville, United States; ⁵HighTide Therapeutics, Rockville, United States

Email: lmacconell@hightidetx.com

Background and aims: HTD1801 is a gut-liver anti-inflammatory metabolic modulator with a unique molecular structure which has been shown to significantly reduce liver fat content (LFC) as determined by MRI-PDFF and important cardiometabolic end points in an 18-Week, placebo (PBO)-controlled Phase 2 study in patients with MASH and T2DM (NCT03656744). GLP-1 receptor agonists (RA) are widely used for the treatment of T2DM and obesity and are under investigation for treatment of MASH. The purpose of this post-hoc analysis was to evaluate ongoing GLP-1RA use compared to newly initiated HTD1801 treatment alone.

Method: 100 patients were randomized and treated with HTD1801 1000 mg BID (n = 34), HTD1801 500 mg BID (n = 33), or PBO (n = 33) for 18 weeks. The primary end point was change in LFC. This analysis included patients who were randomized to HTD1801 and were not treated concomitantly with GLP-1RA (HTD1801 1000 mg BID: n = 28; HTD1801 500 mg BID: n = 27) or PBO randomized patients who were receiving ongoing GLP-1RA (n = 13).

Results: At baseline, 39% of PBO patients were utilizing GLP-1RA compared with 18% of patients randomized to HTD1801. Baseline characteristics were balanced across groups with the exception of ALT (HTD1801 1000 mg BID: 62.7 U/L; HTD1801 500 mg BID: 46.2 U/L; GLP-1RA: 43.1 U/L). Dose-dependent improvements were observed at Week 18 with HTD1801 treatment in LFC (HTD1801 1000 mg BID: -4.5%; HTD1801 500 mg BID: -3.2%; GLP-1RA: -2.9%), ALT (HTD1801 1000 mg BID: -16.7 U/L; HTD1801 500 mg BID: -4.6 U/L; GLP-1RA: -4.5 U/L), HbA1c (HTD1801 1000 mg BID: -0.4%; HTD1801 500 mg BID: -0.4%; GLP-1RA: 0%), and weight (HTD1801 1000 mg BID: -3.7 kg; HTD1801 500 mg BID: -1.4 kg; GLP-1RA: -1.9 kg). Furthermore, reductions in each of these parameters were greater with HTD1801 1000 mg BID vs ongoing GLP-1RA.

Conclusion: This data suggests newly initiated HTD1801 provides greater benefit than ongoing GLP-1RA use. Utilization of GLP-1RA continues to grow and may be confounding in studies of MASH. This has resulted in their exclusion from some new studies of MASH which is unlikely to be reflective of real-world use. In order to address this concern, GLP-1RA utilization is a stratification factor in the ongoing Phase 2b study of HTD1801.

SAT-230

Effect of omega 3 fatty acid supplementation on hepatic steatosis and liver stiffness in patients with non-alcohol-related fatty liver disease

Muhammad Abedur Rahman Bhuyan¹, Eshita Ashab², Shahinul Alam³, Mamun Al-Mahtab⁴. ¹Shaheed Syed Nazrul Islam Medical College Hospital, Kishorganj, Bangladesh; ²Shaheed Syed Nazrul Islam Medical College Hospital, Kishorganj, Bangladesh; ³Department of Hepatology, Bangabandhu Sheikh Mujib Medical University, Dhaka, Bangladesh; ⁴Department of Interventional Hepatology, Bangabandhu Sheikh Mujib Medical University, Dhaka, Bangladesh
Email: drabedurrahmanzimi@gmail.com

Background and aims: Non-alcoholic fatty liver disease (NAFLD) describes a spectrum of clinicopathological changes in liver extending from simple steatosis through non-alcoholic steatohepatitis (NASH) to fibrosis. NAFLD is an increasingly prevalent disease, there is a lack of approved therapies for it. Omega-3 fatty acids (OMG-3 FA) are beneficial in the treatment of hypertriglyceridaemia. OMG-3 FA treatment might be beneficial to decrease liver triglyceride. OMG-3 FA have a beneficial effect: a) on bioactive metabolites involved in inflammatory pathways, b) on alteration of nuclear transcription factor activities such as peroxisome proliferator-activated receptors, sterol regulatory element-binding protein 1c and carbohydrate-responsive element-binding protein, involved in inflammatory pathways and liver lipid metabolism. OMG-3 FA treatment in patients with NAFLD would be beneficial in treating hepatic steatosis and possibly also in ameliorating inflammation. To evaluate the efficacy of supplementation of OMG-3 FA on hepatic steatosis and liver stiffness in NAFLD patients.

Method: This was a six months randomized open level clinical trial. Study was done in Department of Hepatology Bangabandhu Sheikh Mujib Medical University. 100 patients with sonographic evidence of Fatty liver, who fitted the inclusion and exclusion criteria were enrolled. All the included patients were randomized into OMG-3 FA group (case group) and control group in 1:1 ratio. Transient Elastography (TE) was done in all patients. After six months of follow-up patients underwent biochemical and TE follow-up. All data was presented as mean \pm SD and analyzed by SPSS (version 23). Qualitative data was analyzed by Chi-square test and quantitative

data was analyzed by student's t-test. A statistically significant result was considered when P value was less than 0.05.

Results: Hepatic steatosis improvement was significant in the case group. Controlled attenuation parameter (CAP) in case group (baseline 305.9 \pm 38.8 dB/m, after treatment 284.4 \pm 47.1 dB/m, p = 0.005) and in control group (baseline 279.3 \pm 52.9 dB/m, after treatment 288.4 \pm 49.8, p = 0.144). Fibrosis improvement was insignificant in both groups, Liver stiffness measurement (LSM) in case group was (6.06 \pm 2.5 vs 6.07 \pm 2.6 kPa p = 0.977) and LSM in control group was (7.1 \pm 8.6 vs 7.2 \pm 8.3 kPa, p = 0.826). In Comparative analysis of anthropometric, biochemical and TE changes between baseline and after intervention in OMG-3 FA group ALT improvement was significant (64.2 \pm 57.8 vs 37.4 \pm 21.9 U/L, p = 0.003).

Conclusion: NAFLD and NASH are well recognized causes of progressive chronic liver disease leading to cirrhosis and hepatocellular carcinoma. To date, no therapy provided evidence of significant efficacy. This study has demonstrated that OMG-3 FA supplementation may improve steatosis and ALT but not stiffness.

SAT-231

GL0034 (Utregrlutide), a long acting, glucagon-like peptide-1 receptor agonist, improves body weight loss, lipid and liver injury markers in individuals with obesity: A phase 1 multiple ascending dose study

Rajamannar Thennati¹, Vinod Burade¹, Muthukumaran Natarajan¹, Pradeep Shahi¹, Ravishankara Nagaraja¹, Sudeep Agrawal¹, Bernard Jandrain², Thierry Duvauchelle³, Richard E. Pratley⁴, Bernard Thorens⁵, Tina Vilsbøll⁶, Rohit Loomba⁷. ¹High Impact Innovations-Sustainable Health Solutions (HISHS), Sun Pharmaceutical Industries Limited, Vadodara, India; ²Former MD, Clinical Pharmacology Unit, ATC Co, and Division of Diabetes, Nutrition and Metabolic Disorders, Academic Hospital of Liège, Liège, Belgium; ³Phaster1, Paris, France; ⁴AdventHealth Translational Research Institute, Orlando, United States; ⁵Center for Integrative Genomics, University of Lausanne, Lausanne, Switzerland; ⁶Clinical Research, Steno Diabetes Center Copenhagen, Herlev, University of Copenhagen, Copenhagen, Denmark; ⁷University of California San Diego School of Medicine, La Jolla, CA, United States
Email: rajamannarthennati@yahoo.com

Background and aims: GL0034 (Utregrlutide) is a potent glucagon-like peptide-1 receptor agonist (GLP-1 RA) under development for the treatment of metabolic disorders and metabolic dysfunction-associated steatotic liver disease (MASLD). GL0034 (GL) has demonstrated significant reductions in body weight (BW) up to Day 22 in a single ascending dose study in individuals with obesity. Here, we present safety and MASLD-relevant pharmacodynamic (PD) results of a multiple ascending dose (MAD) phase 1 study in individuals with obesity.

Method: A randomized, double-blind, placebo (PBO)-controlled study was conducted to evaluate the safety, tolerability and PD of MAD study. Individuals with BMI \geq 28 kg/m² (n = 12) were randomized (9:3) to subcutaneous GL increasing doses (680, 900, 1520, 2000 μ g) or placebo, once weekly for four weeks. Biomarker measurements included, body weight, lipid profile (triglycerides (TG), total cholesterol (TC) and low-density lipoprotein (LDL)) and liver enzymes (alanine aminotransferase (ALT), aspartate aminotransferase (AST), gamma-glutamyl transferase (GGT)), free fatty acids (FFA), homeostatic model assessment-insulin resistance (HOMA-IR), and leptin.

Results: Most common adverse events (AE) were gastrointestinal (GI) with dose-dependent nausea, decreased appetite and vomiting. One individual with a GI related serious AE rapidly recovered upon treatment with intravenous rehydration. BMI (kg/m²) at baseline was 32.4 \pm 4.6 for GL treatment group and 27.9 \pm 1.3 for PBO. Reduction in body weight (kg) from baseline (BL) was significant on day 29 [GL: -4.6 \pm 1.5 (p < 0.001); PBO: 0.0 \pm 0.9]. Similarly, on day 23 significant reduction in TG (mg/dL) [GL: -47.1 \pm 54.2 (p < 0.05); PBO -16.7 \pm

POSTER PRESENTATIONS

28.7] was noted from BL. TC (mg/dL) [GL: -20.0 ± 26.8 ; PBO 8.7 ± 26.9] and LDL (mg/dL) [GL: -5.7 ± 23.9 ; PBO 11.3 ± 19.6] also reduced from BL. A trend towards lower ALT, AST and GGT from BL was observed [ALT (U/L)-GL: -9.1 ± 13.9 ; PBO: 6.3 ± 43 and AST (U/L)-GL: -2.7 ± 4.2 ; PBO: 1.7 ± 18.7]. The reduction in GGT (U/L) from BL was significant on day 23 [GL: -4.2 ± 2.4 ($p < 0.001$); PBO 4.3 ± 15.3]. There was no change in the free fatty acid levels from BL in GL and PBO. In the treatment group an improved HOMA-IR was observed on day 23 and day 50 [BL value of 2.3 ± 1.2 to 1.7 ± 1.0 , 1.7 ± 0.4 vs. PBO BL 3.2 ± 0.5 to 2.1 ± 0.1 and 2.6 ± 0.9 , respectively]. A decrease was observed in leptin, on day 23 and day 50 for GL group [Day 23 GL: -5.7 ± 5.9 ; PBO: -3.7 ± 5.3 , Day 50 GL: -4.5 ± 10.2 ; PBO: 5.1 ± 16.4].

Conclusion: GL0034, a potent, long-acting GLP-1RA, was safe, well tolerated and with significant body weight reduction as well as improvements in lipids, liver injury and metabolic biomarkers in individuals with obesity. The observed PD effects suggest potential therapeutic benefits in MASLD patients.

SAT-233

Clinical pharmacokinetics of INI-822, a small molecule inhibitor of HSD17B13

Chuhan Chung¹, Kelly Regal¹, Greg Coulter¹, Paul Pearson¹, Heather Hsu². ¹Inipharma, Bellevue, WA, United States; ²Inipharma, Bellevue, United States
Email: cchung@inipharma.com

Background and aims: Human genetic validation studies identify inactive variants of HSD17B13 as protective against the development of MASH, MASH and alcohol-related cirrhosis, and hepatocellular carcinoma. INI-822, a selective small molecule inhibitor of HSD17B13, was developed to be a once daily oral inhibitor of HSD17B13 for the treatment of chronic liver disease. Nonclinical pharmacokinetic/pharmacodynamic studies measuring plasma levels of bioactive lipid substrates and products demonstrated target engagement with an ED_{50} of 5.4 ± 2.2 mg/kg in rats and an EC_{50} for C_{trough} of 56 ng/ml (abstract McReynolds 2023 J Hepatology). The objective of these studies was to evaluate the pharmacokinetics (PK) of INI-822 in nonclinical and clinical settings.

Method: INI-822 was orally administered to mice (10 mg/kg, $n = 3$ /group, sparse sampling), rats (30 mg/kg, $n = 3$) and dogs (10 mg (~ 1 mg/kg), $n = 6$). Blood was collected, processed to plasma at timed intervals and INI-822 plasma concentrations were determined by LC/MS-MS. In a first-in-human study, PK was determined in a Phase 1, placebo-controlled study of INI-822 in healthy volunteers ($n = 6$ /cohort) following a single oral dose of INI-822. Noncompartmental PK parameters were calculated. Data was presented as mean \pm SD.

Results: INI-822 exposure (AUC_{0-24}) was 17,500 ng \cdot h/ml for 10 mg/kg in mice, $22,200 \pm 5480$ ng \cdot h/ml for 30 mg/kg in rats and $10,600 \pm 3390$ ng \cdot h/ml for 10 mg in dogs. The resulting oral bioavailability (F%) was 44%, 36% and 97% in mice, rats and dogs, respectively. In humans, exposure increased in an approximately dose-proportional manner. The mean C_{max} increased from 289 ± 80 , 569 ± 92 and 1040 ± 337 ng/ml for 25, 50 and 100 mg, respectively. The mean AUC_{0-inf} increased from 3590 ± 1060 , 6930 ± 1920 and 10400 ± 4210 ng \cdot h/ml for 25, 50 and 100 mg, respectively. The mean half-life in these clinical cohorts were amenable to once daily dosing with means ranging from 18.9 to 27.2 h. The estimated steady state AUC and C_{trough} values for the 25 mg dose level exceeded those for the ED_{50} for the rat pharmacokinetic/pharmacodynamic assessment of bioactive lipid substrates and products.

Conclusion: The small molecule HSD17B13 inhibitor, INI-822, achieved clinical plasma exposures that exceeded concentrations projected to inhibit HSD17B13 based on preclinical models. Single ascending dose PK in healthy subjects appeared to achieve dose-proportional maximal plasma concentrations and exposure (AUC). The half-life of INI-822 is suitable for once daily dosing in future clinical trials of MASH subjects. A Phase 1 study, to include evaluation

of multiple doses of INI-822 in healthy volunteers and patients with liver disease, is ongoing.

SAT-236

Efficacy and safety of incretin-based therapies in patients with metabolic dysfunction-associated steatotic liver disease complicated by type 2 diabetes mellitus

Tadamichi Kawano¹, Taeang Arai¹, Masanori Atsukawa¹, Toshifumi Tada², Tsunekazu Oikawa³, Akihito Tsubota³, Kentaro Matsuura⁴, Toru Ishikawa⁵, Hiroshi Abe⁶, Keizo Kato⁶, Asahiro Morishita⁷, Joji Tani⁷, Tomomi Okubo⁸, Katsuhiko Iwakiri¹. ¹Nippon Medical School, Tokyo, Japan; ²Japanese Red Cross Society Himeji Hospital, Himeji, Japan; ³The Jikei University School of Medicine, Tokyo, Japan; ⁴Nagoya City University Graduate School of Medical Sciences, Nagoya, Japan; ⁵Saiseikai Niigata Hospital, Niigata, Japan; ⁶Shinmatsudo Central General Hospital, Chiba, Japan; ⁷Kagawa University, Kagawa, Japan; ⁸Nippon Medical School Chiba Hokusoh Hospital, Chiba, Japan
Email: taeangpark@yahoo.co.jp

Background and aims: The aim of this study was to evaluate the efficacy and safety of oral semaglutide (Sema), a GLP-1 receptor agonist, and tirzepatide (TZP), a dual GIP/GLP-1 receptor agonist, in patients with metabolic dysfunction-associated steatotic liver disease (MASLD) complicated by type 2 diabetes mellitus (T2DM).

Method: Verification 1; multi-institutional prospective study. Eighty-three patients with MASLD who received Sema for T2DM were included. Sema was initiated at a dose of 3 mg once daily, and the dose was gradually increased, while being monitored for any adverse events. Verification 2; single-center prospective pilot study. Thirteen patients with MASLD who received TZP for T2DM were included. TZP was initiated at a dose of 2.5 mg once weekly and was increased to a maintenance dose of 5.0 mg once weekly at week 4.

Results: Verification 1; Sema treatment resulted in significant improvements in glycemic control, liver transaminases, and lipid profiles with weight loss at week 12. These significant improvements were maintained at week 24: glycemic control (plasma glucose 132 mg/dL to 107 mg/dL, HbA1c 7.0% to 6.0%), liver transaminases (ALT 61 U/L to 37 U/L, γ -GTP 63 U/L to 43 U/L), and lipid profiles (LDL-cho 116 mg/dL to 110 mg/dL, TG 133 mg/dL to 116 mg/dL). In 43 patients after 48 weeks of treatment, controlled attenuation parameter (315 dB/m to 296 dB/m) and each non-invasive test for liver fibrosis decreased significantly from baseline (Wisteria floribunda agglutinin-positive Mac-2-binding protein 0.82 to 0.64, type IV collagen 7 s 4.0 ng/ml to 3.4 ng/ml, fibrosis-4 index 1.29 to 0.93, liver stiffness measurement 7.0 kPa to 6.5 kPa). A number of gastrointestinal disorders, including grade 1–2 nausea, were observed during the observation period. Verification 2; TZP treatment resulted in a decrease in body weight (-4.6 kg) at week 12, together with improvements in glycemic control (plasma glucose 134 mg/dL to 100 mg/dL, HbA1c 6.7% to 5.6%), liver transaminases (ALT 61 U/L to 32 U/L, γ -GTP 100 U/L to 41 U/L), and TG (165 mg/dL to 130 mg/dL). Gastrointestinal disorders such as grade 1–2 nausea and constipation were frequently observed in the early phase of treatment. The subsequent course of treatment is being followed.

Conclusion: Both Sema and TZP treatments offered a favorable effect on MASLD as well as improving diabetic status and reducing body weight.

SAT-237

Efficacy and safety of FGF21 analogues in the treatment of metabolic dysfunction-associated steatohepatitis: an updated systematic review and meta-analysis

Fabiana Dolovitsch de Oliveira¹, Emmily Daiane Buarque de Santana Sato², Samira Mohamad Khalil³, Matheus Souza⁴, Gilmaria Coelho Meine⁵. ¹Universidade Federal de Ciências da Saúde de Porto Alegre, Porto Alegre, Brazil; ²Pontifícia Universidade Católica de Campinas, Campinas, Brazil; ³Universidad de

Buenos Aires, Buenos Aires, Argentina; ⁴Universidade Federal do Rio de Janeiro, Rio de Janeiro, Brazil; ⁵Universidade Feevale, Novo Hamburgo, Brazil
Email: gilmara@feevale.br

Background and aims: Fibroblast growth factor 21 (FGF21) regulates energy homeostasis, as well as lipid and glucose metabolism. The FGF21 analogues are believed to benefit patients with metabolic dysfunction-associated steatohepatitis (MASH), but their efficacy and safety are not yet established. Therefore, we aimed to perform a systematic review and meta-analysis to assess the efficacy and safety of FGF21 analogues in the treatment of MASH.

Method: We searched PubMed, Embase, and Cochrane Library databases for randomized controlled trials (RCTs) comparing FGF21 analogues to placebo for the treatment of patients with biopsy-confirmed MASH, reporting at least one of the outcomes of interest. Primary outcomes: fibrosis improvement ≥ 1 stage without worsening of MASH and MASH resolution without worsening of fibrosis. Secondary outcomes: relative reduction $\geq 30\%$ of the hepatic fat fraction (HFF) measured by magnetic resonance imaging derived proton density fat fraction (MRI-PDFF) and adverse events (AEs). We compared binary outcomes using risk ratio (RR), with 95% confidence interval (CI). Heterogeneity was assessed using Cochran's Q test and I^2 statistics. We performed subgroup analyses by the grade of fibrosis (F1–F3 vs. F4) for all outcomes, provided there were at least two studies in each subgroup.

Results: 7 RCTs were included, encompassing 886 obese patients. Among them, 3 studies used Efruxifermin (238 patients), 3 used Pegbelfermin (426 patients) and 1 used Pegzofermin (222 patients). The overall analysis showed significantly higher probability of fibrosis improvement ≥ 1 stage without worsening of MASH (RR 1.74; CI 95% 1.22, 2.46; $p = 0.002$; $I^2 = 0\%$), MASH resolution without worsening of fibrosis (RR 2.29; CI 95% 1.06, 4.94; $p = 0.04$; $I^2 = 49\%$), and reduction $\geq 30\%$ in the HFF by MRI-PDFF (RR 3.03; CI 95% 2.12, 4.33; $p < 0.00001$, $I^2 = 0\%$) with FGF21 analogues in comparison to placebo. Moreover, FGF21 showed no significant difference in the risk of overall AEs (RR 1.04; CI 95% 0.95, 1.14, $p = 0.37$; $I^2 = 44\%$) and serious AEs (RR 0.8; CI 95% 0.50, 1.28; $p = 0.035$; $I^2 = 0\%$) compared to placebo. Regarding the subgroup analysis by the stage of fibrosis: (1) patients with fibrosis stages F1–F3 presented higher fibrosis improvement ≥ 1 stage without worsening of MASH, MASH resolution without worsening of fibrosis, reduction of $\geq 30\%$ in the HFF by MRI-PDFF, and overall AEs with FGF21 analogues compared to placebo, but the risk of serious AEs was similar between both; (2) patients with fibrosis stage F4 showed a non-significant difference in the probability of fibrosis improvement ≥ 1 stage without worsening of MASH, overall AEs, and serious AEs between FGF21 analogues and placebo.

Conclusion: FGF21 analogues seem effective and safe in obese patients with biopsy-confirmed MASH, but the clinical benefit may be restricted to non-cirrhotic patients. New RCTs are necessary establish FGF21 analogues as a therapy for MASH.

SAT-238

Statins are not associated with an increased risk of decompensated cirrhosis in patients with type 2 diabetes mellitus

Jonathan Tjerkaski¹, Emilie Toresson Grip², Anthony Matthews¹, Hannes Hagström¹. ¹Karolinska Institutet, Stockholm, Sweden; ²Karolinska Institutet, Quantify research, Stockholm, Sweden
Email: jonathan.tjerkaski@ki.se

Background and aims: The prevalence of type 2 diabetes mellitus (T2DM) is increasing. T2DM is a major risk factor for atherosclerotic cardiovascular disease (ASCVD). Furthermore, T2DM is also associated with Metabolic dysfunction-Associated Steatotic Liver Disease (MASLD), a major contributor to liver-related morbidity and mortality worldwide. Statins are frequently used to prevent ASCVD in T2DM patients by treating hypercholesterolemia, an important risk factor for ASCVD. Although some studies suggest that statins may protect against liver disease, statins have also been associated with

hepatotoxicity. Statin-induced hepatotoxicity might be particularly harmful in T2DM patients, due to their elevated risk of liver disease. Therefore, the aim of this study was to examine the association between statin therapy and liver disease in T2DM patients.

Method: The participants of this observational cohort study were T2DM patients who did not have any known liver disease or history of alcohol use disorder at the time of inclusion. Data on baseline characteristics and patient outcomes was obtained from electronic health records and nationwide quality registers. We carried out sequential emulated target trials with three-month intervals between 2007 and 2020 to examine the effect of statin therapy on the outcome of decompensated liver cirrhosis, a composite of bleeding esophageal varices, hepatorenal syndrome, ascites, portal hypertension, hepatic encephalopathy and liver transplantation. Marginal structural models were used to compute the effect estimates.

Results: This study included 7837 T2DM patients who were treated with statins and 19359 controls. The adjusted 10-year cumulative risk of developing decompensated liver cirrhosis was 2.7% in the statin group and 2.0% among the controls (risk difference 0.6 [95% confidence interval -2.2 – 3.3]; risk ratio 1.3 [95% confidence interval 0.44 – 3.23]).

Conclusion: We found that statin therapy was not associated with a significantly increased risk of developing decompensated liver cirrhosis in this cohort of T2DM patients.

SAT-239

A phase 4, multicenter, open-label, single-arm study to evaluate the safety and efficacy of saroglitazar 4 mg in patients with non-alcoholic fatty liver disease with obesity, type 2 diabetes mellitus, dyslipidemia, or metabolic syndrome

Deven Parmar¹, Arun J. Sanyal², Kevin Kansagra³, Rahul Shrivastava³. ¹Zydus Therapeutics, Pennington, United States; ²Virginia Commonwealth University, Richmond, VA, United States; ³Zydus Research Center Zydus Lifesciences Ltd, Ahmedabad, India
Email: dparmar@zydustherapeutics.com

Background and aims: Non-alcoholic fatty liver disease (NAFLD) is a common disease, with a prevalence of 13–32% globally and 5–28% in Asian countries, including India.^{1,2} NAFLD is a hepatic component of the metabolic syndrome, which is a clinical syndrome characterized by obesity, dyslipidemia, type 2 diabetes mellitus (T2DM), and hypertension. Saroglitazar is a dual peroxisome proliferator-activated receptor (PPAR) α/γ agonist and is approved in India for the treatment of NAFLD and non-cirrhotic non-alcoholic steatohepatitis (NASH). In EVIDENCES I and III clinical studies, Saroglitazar Mg demonstrated improvement in liver enzymes and liver fat content in patients with NAFLD. However, the impact of saroglitazar in real-world setting in Asian population with NAFLD and comorbidities remains unclear. Here, we describe the design and plan of a study that aims to evaluate the safety and efficacy of saroglitazar 4 mg in patients with NAFLD with comorbidities (obesity, dyslipidemia, T2DM, and metabolic syndrome) in India in real-world settings.

Method: This Phase 4, non-randomized, multicenter, open-label, single-arm study will be conducted at multiple centers in India with approximately 1500 patients. The study consists of a screening period of up to 4 weeks, a treatment period of 52 weeks, and end of the study assessment on completion of 364 days/52 weeks of the treatment. The primary safety and efficacy end points include frequency and severity of treatment-emergent adverse events/serious adverse events and change in liver stiffness measurement (LSM) performed by transient elastography from baseline to week 52, respectively.

Results: At present, more than 200 patients have been enrolled at various centers across India in this study. The mean (\pm SD) age, BMI, and waist circumference of first 50 enrolled patients were 47 ± 11 years, 29 ± 3.7 kg/m², and 91 ± 25 , respectively, and the men to women ratio was 37:13. Further, enrolled patients had LSM ≥ 8 kPa and/or serum ALT ≥ 45 U/L. The enrolled patients with NAFLD also had obesity, T2DM, dyslipidemia, and/or metabolic syndrome. In addition to efficacy, the safety data of large-scale population will

POSTER PRESENTATIONS

further establish the safety of saroglitazar Mg 4 mg dose in patients with NAFLD.

Conclusion: This ongoing study is currently recruiting patients actively. The study will prove the efficacy and safety of saroglitazar Mg 4 mg in patients with NAFLD with different comorbidities.

SAT-242

Efficacy and safety of FGF-analogues for the treatment of MASH: a systematic review and meta-analysis

Maria Viana¹, Arthur Braga¹, Dermeval Neto¹, Junior Samuel Menezes², Luis Felipe Silva³, Antônio Ricardo Cardia Ferraz de Andrade². ¹Bahiana School of Medicine and Public Health, Salvador, Brazil; ²Federal University of Bahia, Salvador, Brazil; ³Federal Fluminense University, Niterói, Brazil
Email: mariaviana21.1@bahiana.edu.br

Background and aims: Metabolic dysfunction-associated steatohepatitis (MASH), an intermediary stage of metabolic dysfunction-associated fatty liver disease (MAFLD), denotes a serious liver condition marked by hepatic steatosis, inflammation, and injury that can lead to cirrhosis. Currently, there is no specific treatment for MASH, with FGF-19 analogs being a possible contender to combat this ailment. We aimed to perform a meta-analysis comparing a novel FGF-19 analog, Aldafermin, to placebo, in patients with MASH.

Method: PubMed, Cochrane Library and EMBASE were systematically searched for RCT comparing FGF-19 analogs to placebo in patients with MAFLD. Statistical analysis was performed using RevMan 5.4 and the PRISMA framework was followed. Outcomes of interest were ELF score, C4 concentration, liver fat content, fibrosis improvement with no worsening of MASH, MASH resolution with no worsening of fibrosis, PRO C3. Safety measures were pooled regarding drug-related side effects (PROSPERO register: CRD42023482818).

Results: From an initial pool of 931 studies, 4 were included comprising 413 patients, of whom 137 received Aldafermin 1 mg, 125 Aldafermin 3 mg, and 151 received placebo; 63% were females and 260 patients were diagnosed with type II diabetes. The mean follow-up period was 5.5 weeks. In the pooled analysis, both Aldafermin 1 mg and 3 mg had significant reduction of ELF score (MD 0.1; 95% CI 0.07–0.13; $p < 0.01$), (MD 0.6; 95% CI 0.01–0.51; $p = 0.04$) respectively, liver fat content and C4. In addition, Aldafermin 1 mg achieved statistical significance in regards to MASH resolution without worsening of fibrosis (OR 0.3; 95% CI 0.11–0.82; $p = 0.02$). In regards to safety measures, Aldafermin 1 mg and 3 mg did not demonstrate significant abdominal pain, nausea, and no serious adverse events, but 3 mg significantly increased the incidence of diarrhea when compared to placebo (OR 0.4; 95% CI 0.22–0.72; $p < 0.01$), with the 1 mg dosage not displaying any significant side effects.

Conclusion: The results of our meta-analysis suggest that in patients with MASH, Aldafermin is associated with a decrease of ELF score, liver fat content, and C4. Notably, only Aldafermin 1 mg displayed an increase in MASH resolution with no worsening of fibrosis and no significant side effects compared to placebo. Further studies with larger sample size and extended follow-up are essential for comprehensively assessing the sustained efficacy and safety of the drug.

SAT-243

Time course of onset, incidence and prevalence of gastrointestinal adverse events with HTD1801 (Berberine Ursodeoxycholate) in patients with MASH and T2DM

Guy Neff¹, Stephen A. Harrison², Nadege Gunn³, Abigail Flyer⁴, Kui Liu⁵, Alexander Liberman⁶. ¹Covenant Metabolic Specialists, Sarasota, United States; ²Pinnacle Clinical Research, San Antonio, United States; ³Impact Research Institute, Waco, United States; ⁴Pacific Northwest Statistical Consulting, Woodinville, United States; ⁵HighTide Therapeutics, Shenzhen, China; ⁶HighTide Therapeutics, Rockville, United States
Email: aliberman@hightidetx.com

Background and aims: HTD1801 is a gut-liver anti-inflammatory metabolic modulator consisting of an ionic salt combination including berberine and ursodeoxycholic acid. The unique molecular structure has been shown to significantly reduce liver fat content (LFC) as determined by MRI-PDFF. Clinically, HTD1801 has improved multiple cardiometabolic end points in an 18-Week, placebo-controlled Phase 2 study in patients with metabolic dysfunction-associated steatohepatitis (MASH) and type 2 diabetes (T2DM) (NCT03656744). The most commonly occurring adverse events (AEs) in studies of HTD1801 across several indications have been mild to moderate gastrointestinal (GI) AEs, primarily diarrhea and nausea. The purpose of this post-hoc analysis is to present time course and severity of GI AEs in patients with MASH and T2DM treated with HTD1801 for 18 weeks.

Method: One hundred patients were randomized and treated with HTD1801 1000 mg BID ($n = 34$), HTD1801 500 mg BID ($n = 33$), or placebo ($n = 33$) for 18 weeks. Onset was defined as the first occurrence of an event for each subject; incidence was defined as any new event within a visit window; and prevalence was defined as any new or ongoing event within a visit window. As AEs can occur at any time, they are assigned to scheduled visits using the following windows based on the study day: Day 0: Day 0; Week 2: Day 1–28; Week 6: Day 29–56; Week 10: Day 57–84; Week 14: Day 85–112; Week 18: Day 113 onward.

Results: Treatment with HTD1801 resulted in significant reductions in LFC, HbA1c, weight, and liver biochemistry compared to placebo. GI AEs were experienced by 10%, 42%, and 56% of patients randomized to placebo, HTD1801 500 mg BID and HTD1801 1000 mg BID, respectively; all of which were mild or moderate in severity. Four subjects in the HTD1801 1000 mg BID group and 1 subject in the HTD1801 500 mg BID group discontinued study drug due to a GI AE. The incidence of GI AEs peaks within the first 4 weeks of treatment (Week 2: HTD1801 1000 mg BID: 29%; HTD1801 500 mg BID: 21%; PBO: 15%) and then rapidly declines with ongoing treatment with HTD1801 (Week 6: HTD1801 1000 mg BID: 9%; HTD1801 500 mg BID: 9%; PBO: 6%). Furthermore, the prevalence of GI AEs also declines with ongoing treatment (HTD1801 1000 mg BID: Week 2: 41%; Week 18: 28%). Diarrhea and nausea were the most commonly occurring GI AEs and follow a consistent trend with all GI AEs; they are early onset, mild or moderate in severity, with a decreasing incidence and prevalence over the course of treatment.

Conclusion: HTD1801 was found to be generally safe and well tolerated in this study. Although most commonly occurring AEs in studies involving HTD1801 are GI related, these events are typically mild to moderate in severity with decreasing incidence over time. Furthermore, these data indicate that tolerability to HTD1801 improves over the course of treatment.

SAT-244

FGF-19 analogues for the treatment of metabolic dysfunction-associated steatohepatitis: a systematic review and meta-analysis

Samira Mohamad Khalil¹, Matheus Souza², Fabiana Dolovitsch de Oliveira³, Emmily Daiane Buarque de Santana Sato⁴, Gilmar Coelho Meire⁵. ¹Universidad de Buenos Aires, Buenos Aires, Argentina; ²Universidade Federal do Rio de Janeiro, Rio de Janeiro, Brazil; ³Universidade Federal de Ciências da Saúde de Porto Alegre, Porto Alegre, Brazil; ⁴Pontifícia Universidade Católica de Campinas, Campinas, Brazil; ⁵Universidade Feevale, Novo Hamburgo, Brazil
Email: gilmar@feevale.br

Background and aims: Metabolic dysfunction-associated steatohepatitis (MASH) is characterized by steatosis, inflammation, and cellular injury, with or without fibrosis. Preclinical models with fibroblast growth factor 19 (FGF19) analogues demonstrated anti-steatotic, anti-inflammatory, and anti-fibrotic activities. Therefore, we aimed to perform a systematic review and meta-analysis to assess

the efficacy and safety of FGF19 analogues for treating patients with MASH.

Method: We searched Embase, PubMed, and Cochrane databases for randomized controlled trials (RCTs) comparing FGF19 analogues to placebo for the treatment of patients with biopsy-confirmed MASH, reporting at least one of the outcomes of interest. Primary outcomes: (1) fibrosis improvement by at least one stage with no worsening of MASH, and (2) MASH resolution with no worsening of fibrosis. Secondary outcomes: (1) change in hepatic fat fraction (HFF) by magnetic resonance imaging derived proton density fat fraction (MRI-PDFF) >30%; (2) change in hepatic enzymes alanine aminotransferase (ALT) and aspartate aminotransferase (AST); (3) changes in fibrogenesis markers (neoepitope-specific N-terminal propeptide of type III collagen [Pro-C3] and Enhanced Liver Fibrosis [ELF] score); and (4) rate of adverse events. We used random-effects model to calculate the pooled risk ratio (RR) for dichotomous variables and mean difference (MD) for continuous variables, with corresponding 95% confidence interval (CI). Heterogeneity was assessed using Cochran's Q test and I² statistics.

Results: We included 4 RCTs (491 patients). All patients were obese adults and received Aldafermin (also known as NGM282), with daily dosages of 0.3 mg, 1 mg, 3 mg, or 6 mg. Mean follow-up ranged from 12 to 48 weeks. The probability of MASH resolution with no worsening of fibrosis (RR 2.74; 95% CI 1.06–7.04; $p = 0.04$; $I^2 = 0\%$) and reduction in HFF by MRI-PDFF >30% (RR 2.69; 95% CI 1.63–4.43; $p < 0.0001$; $I^2 = 29\%$) were higher with FGF-19 analogues compared to placebo. Additionally, FGF19 analogues showed higher reduction in ELF score (MD -0.19 ; 95% CI -0.33 , -0.06 ; $p = 0.006$; $I^2 = 0\%$), ALT (MD -17.70 ; 95% CI -23.33 – -12.06 ; $p < 0.0001$; $I^2 = 32\%$), AST (MD -11.18 ; 95% CI -15.18 , -7.18 ; $p < 0.00001$; $I^2 = 0\%$) and Pro-C3 (MD -4.56 ; 95% CI -7.22 , -1.90 ; $p = 0.0008$; $I^2 = 21\%$). There was no significant difference between the groups in terms of fibrosis improvement by at least one stage with no worsening of MASH (RR 1.50; 95% CI 0.94–2.38; $p = 0.09$; $I^2 = 0\%$), overall adverse events (RR 1.02; 95% CI 0.94, 1.12; $p = 0.58$; $I^2 = 0\%$) and serious adverse events (RR 0.96; 95% CI 0.43, 2.15; $p = 0.92$; $I^2 = 0\%$).

Conclusion: FGF19 analogues might be a safe and effective treatment option for patients with biopsy-confirmed MASH. However, new large RCTs with long-term follow-up are needed to confirm these findings.

SAT-245

Semaglutide for type 2 diabetes control in metabolic dysfunction-associated steatotic liver disease (MASLD): a two-way effect?

Giovanni Petralli¹, Antonio Salvati², Simone Cappelli³, Gabriele Ricco², Lidia Surace², Ranka Vukotic², Piero Colombaro², Francesco Raggi¹, Anna Solini¹, Maurizia Brunetto^{2,3}. ¹Department of Surgical, Medical, Molecular and Critical Area Pathology, Pisa, Italy; ²Hepatology Unit, Pisa University Hospital, Pisa, Italy; ³Department of Clinical and Experimental Medicine, Pisa, Italy
Email: g.petralli94@gmail.com

Background and aims: Therapeutic options for MASLD burden in T2D patients are scanty. GLP1-receptor agonists (GLP1-ra) are clearly indicated for T2D treatment and Semaglutide was shown to induce the steatohepatitis resolution at high daily dosage. In consecutive MASLD-GLP1-ra naïve diabetic patients we studied the impact on liver disease of Semaglutide introduction for glycemic control indication using non-invasive surrogate markers of liver steatosis and fibro-inflammation.

Method: In 62 consecutive overweight/obese T2D pts with MASLD (age 61.4 ± 11.3 yrs, females 32%, BMI 31.4 ± 5.0 kg/m²), anthropometric, bio-humoral and transient elastography (TE) data were collected before (t0) and after 6.4 (6.1–6.6) months (t1) from the 1st injective/oral Semaglutide prescription. GIP, GLP1, Glucagon, Insulin, fasting glucose, glycated hemoglobin, AST, ALT and GGT were measured in t0-t1 serum samples. FibroScan CAP and liver stiffness

(LS) were used as non-invasive markers of liver steatosis and fibro-inflammation involvement, respectively.

Results: BMI (-1.4 ± 0.2 kg/m²), Waist Circumference (-3 ± 1 cm), AST (-10 ± 3 UI/L), ALT (-18 ± 5 UI/L), GGT (-33 ± 15 UI/L), glycol-metabolic parameters [fasting glucose (-40 ± 6 mg/dl) and glycated hemoglobin (-12 ± 1 mmol/mol)], CAP (-25 ± 8 dB/m), and LS (-0.8 ± 0.4 kPa) t0-t1 reductions were significant ($p < 0.006$), while GLP1 ($+95.9$ pM, $p < 0.0001$) increased. Variations of serum ALT and GGT levels associated with glycated hemoglobin reduction ($r = 0.340$, $p = 0.0196$ and $r = 0.368$, $p = 0.0210$, respectively), but not with change in serum concentration of incretin hormones. CAP declined in association with BMI reduction ($r = 0.391$, $p = 0.0035$) and GLP1 increase ($r = -0.415$, $p = 0.0251$). In a multivariate model adjusted for all above mentioned variations, only the GLP1 increase was associated with CAP reduction ($p = 0.0468$).

Conclusion: Semaglutide treatment for T2D in MASLD pts associates with a significant decline of non-invasive surrogate markers of liver steatosis and fibro-inflammation. While glycemic optimization correlated with a reduction of transaminases, an independent effect of GLP1 increase was associated with a reduction of the steatosis.

SAT-248

Liver stiffness improvement with pioglitazone in brazilian patients with metabolic dysfunction-associated steatohepatitis: a multicentric pilot study

Mário Pessoa¹, Isabel Veloso Alves Pereira¹, Patricia Momoyo Zitelli¹, Mísia Joyner de Sousa Dias Monteiro², Cláudia Alves Couto², Juliana Souza de Oliveira¹, Renato Altikes¹, Ana Luiza Gomes Reis¹, Lais Arrivabene Barbieri³, Nathalie Leite³, Cristiane Villela-Nogueira⁴, Claudia P. Oliveira¹. ¹Laboratório de Gastroenterologia Clínica e Experimental LIM-07, Division of Clinical Gastroenterology and Hepatology, Hospital das Clínicas HCFMUSP, Department of Gastroenterology, Faculdade de Medicina, Universidade de São Paulo, São Paulo, Brazil, São Paulo-SP, Brazil; ²Federal University of Minas Gerais, Belo Horizonte-MG, Brazil; ³School of Medicine, Clementino Fraga Filho University Hospital, Federal University of Rio de Janeiro, Rio de Janeiro-RJ, Brazil; ⁴School of Medicine, Clementino Fraga Filho University Hospital, Federal University of Rio de Janeiro, Rio de Janeiro-RJ, Brazil
Email: mgpessoa@usp.br

Background and aims: Pioglitazone, an agonist of peroxisome proliferator-activated receptor gamma, demonstrated efficacy in ameliorating indirect markers of liver steatosis, inflammation and fibrosis as well as addressing systemic and adipose tissue insulin resistance in patients with type 2 diabetes and metabolic dysfunction-associated steatotic liver disease. This study aims to evaluate whether sustained pioglitazone consumption over a period of 12-24 months can improve liver stiffness in individuals diagnosed with metabolic dysfunction-associated steatohepatitis (MASH).

Method: Retrospective data from thirty-six (36) biopsy-proven MASH patients, receiving pioglitazone treatment for 12–24 months were gathered from three public hospitals in Brazil. Vibration-controlled transient elastography parameters pre- and post-pioglitazone treatment were evaluated, as a non-invasive method to monitor the disease progression. Additionally, a thorough analysis of both laboratory and clinical data was undertaken.

Results: The study population was equally divided into male and female subjects (50%, $n = 18$), with a mean age of $65.7 (\pm 11.37)$ and a mean BMI of $31.4 (\pm 6.05)$. At baseline, participants mostly had hypertension (75%, $n = 27$), type II diabetes (75%, $n = 27$), and dyslipidemia 75% ($n = 27$). During the second evaluation, the number of subjects with comorbidities increased to 83.3% ($n = 30$) for hypertension, 77.8% ($n = 28$) for diabetes, and 83.3% ($n = 30$) for dyslipidemia. Furthermore, 58.8% ($n = 20$) of patients were using antihypertensive drugs, and 69.4% ($n = 25$) were using lipid-lowering drugs. At baseline, the liver stiffness measurement (LSM) median was 8.10 (IQR = 5.42) and 9.50 (IQR = 8.38) at the second evaluation.

Prolonged pioglitazone treatment demonstrated LSM attenuation in 47.2% of cases (n = 17), resulting in an absolute reduction ranging from 0.1 to 15.4 kPa and a relative reduction ranging from 1.67% to 62.9% (p = 0, 0002), with no difference in the CAP parameter. In the reduction group, we also observed a decrease in ALT ($56.06 \pm 48.9/38.4 \pm 8.5$, p = 0.01) and AST ($39.5 \pm 6.2/31.44 \pm 5.4$, p = 0.05), with no changes in weight, BMI, FA, GGT, platelets, LDL, HDL, cholesterol, serum glucose, and glycated hemoglobin.

Conclusion: The administration of pioglitazone led to an improvement in liver stiffness among MASH patients although there was no difference in metabolic conditions, indicating its potential advantages in managing both diabetes and MASH.

Non-invasive assesment of liver disease except MASLD

TOP-006

Development and validation of a home-based score to detect advanced liver fibrosis and long-term liver-related outcomes in the general population: a multicohort study

Shanghao Liu¹, Jie Shen², Victor W. Zhong³, Qing-Lei Zeng⁴, Heng Wan², Yuping Chen⁵, Xuanwei Jiang⁶, Jiawei Zhang⁵, Chuan Liu⁷, Gao-Jun Teng⁸, Xiaolong Qi⁹. ¹Center of Portal Hypertension, Department of Radiology, Zhongda Hospital, School of Medicine, Southeast University, Nanjing, China, Basic Medicine Research and Innovation Center of Ministry of Education, Zhongda Hospital, Southeast University, Nanjing, China; ²Department of Endocrinology and Metabolism, Shunde Hospital, Southern Medical University (The First People's Hospital of Shunde), Foshan, China; ³Department of Epidemiology and Biostatistics, School of Public Health, Shanghai Jiao Tong University School of Medicine, Shanghai, China; ⁴Department of Infectious Diseases and Hepatology, The First Affiliated Hospital of Zhengzhou University, Zhengzhou, China; ⁵Center of Portal Hypertension, Department of Radiology, Zhongda Hospital, Medical School, Southeast University, Basic Medicine Research and Innovation Center of Ministry of Education, Zhongda Hospital, Southeast University, Nanjing, China; ⁶Department of Epidemiology and Biostatistics, School of Public Health, Shanghai Jiao Tong University School of Medicine, Shanghai, China; ⁷Center of Portal Hypertension, Department of Radiology, Zhongda Hospital, Medical School, Southeast University, Basic Medicine Research and Innovation Center of Ministry of Education, Zhongda Hospital, Southeast University, Nanjing, China; ⁸Basic Medicine Research and Innovation Center of Ministry of Education, Zhongda Hospital, Southeast University, Center of Interventional Radiology and Vascular Surgery, Department of Radiology, Zhongda Hospital, Medical School, Southeast University, Nanjing, China; ⁹Center of Portal Hypertension, Department of Radiology, Zhongda Hospital, School of Medicine, Southeast University, Basic Medicine Research and Innovation Center of Ministry of Education, Zhongda Hospital, Southeast University, Nanjing, China
Email: qixiaolong@vip.163.com

Background and aims: Liver fibrosis and its subsequent cirrhosis are major global health burden, and early screening and identification is critical; although several tools are available to stratify individuals at risk of liver fibrosis, they are all hospital- or clinic-based. We aimed to develop a simply free home-based score to identify general population at risk of advanced liver fibrosis and liver-related outcomes.

Method: The LiverHome score was derived from a prospective Chinese cohort including the general population who underwent liver fibrosis evaluation by transient elastography. The score's discriminatory accuracy was validated in two prospective cohorts containing Chinese and American general population. Moreover, we

determined the prognostic value of the score in the prediction of all-cause and liver-related outcomes in the NHANES and UK Biobank follow-up cohorts. Advanced fibrosis was defined as liver stiffness measurement ≥ 10 kPa.

Results: We enrolled 410,428 participants: 6,174 in the derivation cohort, 2,646 in the Chinese validation cohort, 7,394 in the American validation cohort, 16,010 in the NHANES prognosis cohort (median follow-up of 2.0 years), and 378,204 in the UK Biobank prognosis cohort (median follow-up of 14.7 years). The new LiverHome score (free online calculator: <https://sourl.cn/ED9GSD>) included waist circumference, diabetes, and viral hepatitis history, and low-risk (LiverHome score <0) and high-risk (LiverHome score ≥ 0) groups were created. The LiverHome score was superior to fibrosis-4 index in identifying advanced fibrosis as measured by area under the receiver-operating characteristics curve (AUC), i.e., 0.77 (0.72–0.82) vs. 0.61 (0.56–0.67), 0.77 (0.70–0.84) vs. 0.68 (0.61–0.76), and 0.83 (0.81–0.85) vs. 0.65 (0.62–0.68), in the derivation, Chinese and American validation cohorts, respectively. In the subgroup analysis from American validation cohort (n = 3, 647), the LiverHome score is superior to the LiverRisk score for detecting advanced fibrosis (0.83 [0.80–0.87] vs. 0.77 [0.74–0.81], p = 0.016). Furthermore, compared to the low-risk group, the high-risk group had a higher risk of all-cause mortality (hazard ratio [HR] = 1.87 [1.60–2.19], p < 0.001) in the NHANES prognosis cohort. Similarly, in the high-risk group, the HR for all-cause mortality was 2.47 (2.40–2.54), and the subdistribution HRs for incident cirrhosis, incident liver cancer, and liver-related mortality were 5.55 (5.02–6.14), 7.07 (5.49–9.12), 5.64 (4.96–6.41) compared with the low-risk group in the UK Biobank prognosis cohort.

Conclusion: The home-based free LiverHome score can accurately predict advanced liver fibrosis and development of all-cause and liver-related outcomes in the general population, and might be used for the most primary screening of risk individuals before the blood- or machine-based stratifications.

TOP-012

Validation of transient elastography and the enhanced liver fibrosis test as prognostic biomarkers across the spectrum of steatotic liver disease

Nikolaj Torp^{1,2}, Mads Israelsen^{1,2}, Stine Johansen^{1,2}, Camilla Dalby Hansen¹, Emil Deleuran Hansen^{1,2}, Ellen Lyngbeck Jensen^{1,2}, Katrine Thorhauge^{1,2}, Johanne Kragh Hansen^{1,2}, Ida Falk Villesen¹, Katrine Tholstrup Bech¹, Charlotte Wernberg^{1,3}, Peter Andersen¹, Katrine Lindvig¹, Maja Thiele^{1,2}, Aleksander Krag^{1,2}. ¹Centre for Liver Research, Department of Gastroenterology and Hepatology, Odense University Hospital, Odense, Denmark; ²Department of Clinical Research, University of Southern Denmark, Odense, Denmark; ³Institute for Regional Health Science, Liver Research Group, Department of Gastroenterology and Hepatology, Hospital of South Denmark, Esbjerg, Denmark
Email: nikolaj.christian.torp@rsyd.dk

Background and aims: Steatotic liver disease (SLD) provides a consensus-driven approach to clinically phenotype patients with hepatic steatosis. As this was not data-driven, the prognostic value of existing non-invasive test cut-offs across the new subgroups needs validation. Therefore, we aimed to validate the prognostic performance of transient elastography (TE) and the enhanced liver fibrosis (ELF) test in patients with SLD.

Method: We included patients from an observational cohort (n = 446) with information on hepatic steatosis, cardiometabolic risk factors and self-reported alcohol intake. All patients had a historic alcohol intake of ≥ 36 g/day for men and ≥ 24 g/day for women for ≥ 1 year, with no prior hepatic decompensation. We classified patients with SLD if they had: 1) ultrasonographic or histological signs of steatosis, 2) CAP > 290 dB/m or 3) $\geq F2$ fibrosis on biopsy attributable to SLD. We used the alcohol intake from the preceding three months to

subclassify into metabolic dysfunction-associated steatotic liver disease (MASLD), metabolic and alcohol-related liver disease (MetALD) and alcohol-related liver disease (ALD). We stratified patients according to the TE ≥ 15 kPa and ELF ≥ 9.8 cut-offs. By review of medical records, we identified hepatic decompensation (Baveno VII) and deaths occurring during follow-up.

Results: In total, 308 patients with TE and ELF measurements, fulfilled the SLD criteria and were subclassified as MASLD (n = 143), MetALD (n = 75) and ALD (n = 90). Average alcohol intake the previous three months were MASLD = 0 g/day (IQR: 0–0), MetALD = 48 g/day (IQR: 36–51) and ALD = 96 g/day (IQR: 69–252). Median TE was 9.3/7.9/8.7 kPa and ELF 9.7/9.5/9.2 (MASLD/MetALD/ALD). During a median follow-up of 61 months (IQR: 50–88), 28 MASLD, 13 MetALD and 15 ALD patients experienced hepatic decompensation. Adjusting for age and sex, the TE ≥ 15 cut-off predicted decompensation in MASLD (HR = 23.1; 95% CI: 6.8–78.1), MetALD (HR = 34.2; 95% CI: 7.3–161.1) and ALD (HR = 9.8; 95% CI: 3.1–31.1). ELF ≥ 9.8 exhibited comparable prognostic performance across all three subgroups. Majority (79%) of decompensations developed in patients with concordant TE ≥ 15 kPa and ELF ≥ 9.8 results. Death occurred in 80 patients, with hepatic decompensation preceding the event in 39 (49%) cases. ATE ≥ 15 kPa was an independent predictor of all-cause mortality in all subgroups (MASLD HR = 4.9; 95% CI: 2.4–10.0, MetALD HR = 7.0; 95% CI: 2.7–18.2 and ALD HR = 4.1; 95% CI: 1.8–9.3). Stratifying by the ≥ 9.8 cut-off, ELF predicted mortality in MASLD (HR = 3.6; 95% CI: 1.7–7.6) and ALD (HR = 6.8; 95% CI: 2.7–17.1) but not MetALD (HR = 1.6; 95% CI: 0.6–4.2).

Conclusion: Our study validates the TE ≥ 15 kPa and ELF ≥ 9.8 cut-offs in patients across the SLD spectrum, demonstrating their effectiveness in predicting hepatic decompensation and all-cause mortality. These findings affirm the utility of TE and ELF test thresholds in clinical practice.

FRIDAY 07 JUNE

FRI-008

Association of elevated liver biochemistries and clinical outcomes within strata of alkaline phosphatase levels in patients with primary biliary cholangitis

David W. Victor, III¹, Joanna P. MacEwan², Jennifer Hernandez², Radhika Nair³, Mustafa Kamal³, Darren Wheeler³, Jing Li³, Leona Bessonova³, Christopher Gasink³, Kris V. Kowdley^{4,5}. ¹Houston Methodist Hospital, Houston, United States; ²Genesis Research Group, Hoboken, United States; ³Intercept Pharmaceuticals, Inc., Morristown, United States; ⁴Washington State University Elon S. Floyd College of Medicine, Spokane, United States; ⁵Liver Institute Northwest, Seattle, United States

Email: dwvictor@houstonmethodist.org

Background and aims: In patients (pts) with primary biliary cholangitis (PBC), elevated liver biochemical tests and the duration of elevation are correlated with increased risk of negative clinical outcomes. We assessed the relationship between the degree of elevation of liver biochemical tests (aspartate aminotransferase [AST] and alanine aminotransferase [ALT]) and 2 fibrosis scores (fibrosis-4 [FIB-4] and AST/platelet ratio index [APRI]) within different strata of alkaline phosphatase (ALP).

Method: Pts ≥ 18 years old with ≥ 1 inpatient or ≥ 2 outpatient PBC diagnosis claims separated by ≥ 30 days between July 2014 and February 2022 were identified from the US Komodo Healthcare Map™ merged with national lab data; the date of the first claim was the index date. Included pts had ≥ 1 biochemistry measurement of ALP, total bilirubin, ALT, and AST during the pre-index period (6 months before and including index date) and ≥ 1 post-index measurement. Pts with a history of hepatic decompensation, liver transplant, significant comorbidities, or prescribed obeticholic acid or fibrates pre-index were excluded. Pts were stratified into 3 groups

based on baseline ALP levels: ALP \leq upper limit of normal (ULN), ALP $>ULN$ to $\leq 1.67 \times ULN$, and ALP $>1.67 \times ULN$. Within each ALP strata, a multivariable Cox proportional hazards model with time-varying covariate was used to assess the association between ALT, AST, FIB-4, and APRI with the composite end point (hospitalization for hepatic decompensation, liver transplant, or death). Within each ALP strata, a separate model was run for each biomarker and fibrosis score. Pts were censored at initiation of second-line therapy, end of insurance enrollment, or end of follow-up.

Results: A total of 3974 pts were stratified into 3 groups: ALP $\leq ULN$ (n = 1443), ALP $>ULN$ to $\leq 1.67 \times ULN$ (n = 1279), and ALP $>1.67 \times ULN$ (n = 1252). Regardless of ALP strata, pts with FIB-4 ≥ 3.25 and APRI >0.5 had consistently increased risk of negative hepatic outcomes compared to pts with FIB-4 <1.3 and APRI ≤ 0.5 , respectively (hazard ratio (HR) range: 5.0 [95% CI, 2.3–11.1] to 7.0 [95% CI, 3.4–14.3] and 1.6 [95% CI, 1.0–2.6] to 17.4 [95% CI, 9.1–33.4]). Compared to pts with AST $<ULN$, those with AST $\geq 1.5 \times ULN$ generally had increased risk of negative hepatic outcomes regardless of ALP strata (HR range: 2.6 [95% CI, 1.6–4.3] to 5.6 [95% CI, 3.2–9.8]). Among pts with baseline ALP $\leq 1.67 \times ULN$, pts with ALT $\geq 2 \times ULN$ had higher risk of negative hepatic outcomes compared to pts with ALT $<ULN$ (HR range: 2.9 [95% CI, 1.0–8.2] to 3.2 [95% CI, 1.2–8.2]).

Conclusion: Across ALP strata, even when ALP is $<ULN$, elevated liver biochemical tests and fibrosis scores were associated with increased risk of hospitalization for hepatic decompensation, liver transplant, or death, highlighting the importance of comprehensive and timely monitoring and treatment of pts with PBC. ©2023 Komodo Health, Inc. All rights reserved. Used with permission.

FRI-009-YI

Diagnostic and prognostic performance of the LiverRisk score in tertiary care

Georg Semmler¹, Lorenz Balcar¹, Benedikt Simbrunner¹, Lukas Hartl¹, Mathias Jachs¹, Michael Schwarz¹, Benedikt Hofer¹, Laurenz Fritz¹, Anna Schedlbauer¹, Katharina Stopfer¹, Daniela Neumayer¹, Jurij Maurer¹, Sophie Gensluckner², Bernhard Scheiner¹, Elmar Aigner², Michael Trauner¹, Thomas Reiberger¹, Mattias Mandorfer¹. ¹Medical University of Vienna, Department of Medicine III, Division of Gastroenterology and Hepatology, Vienna, Austria; ²Paracelsus Medical University Salzburg, First Department of Medicine, Salzburg, Austria
Email: georg.semmler@meduniwien.ac.at

Background and aims: The LiverRisk score has been developed as blood-based tool to estimate liver stiffness measurement (LSM) in the general population (i.e., in subjects without known chronic liver disease (CLD), and thus, detect compensated advanced chronic liver disease (cACLD; LSM ≥ 10 kPa) and stratify their risk of liver-related events. Notably, its utility in other settings is unclear as a one-size-fits-all blood-based test. We aimed to evaluate its diagnostic/prognostic performance in patients referred to specialized hepatology outpatient clinics (i.e., tertiary care).

Method: Subjects with known/suspected CLD at first LSM (cohort-I, n = 5897) or first referral and LSM (cohort-II, n = 1558) were retrospectively included. Calibration/agreement of the LiverRisk score with LSM was assessed as well as its diagnostic accuracy for LSM-defined cACLD compared to FIB-4/APRI. Finally, its predictive performance for hepatic decompensation was evaluated.

Results: In cohort-I/II, mean age was 48.3/51.8 years, 44.2%/44.7% were female, predominant etiologies were viral hepatitis (51.8%)/MASLD (63.7%), median LSM was 6.9 [5.1–10.9]/5.8 [4.5–8.8] kPa, and 1690 (28.7%)/322 (20.7%) had cACLD. Despite a moderate correlation (Pearson's r: 0.325/0.422), the LiverRisk score systematically underestimated LSM (mean difference according to the Bland-Altman-Method: $-2.9/-1.8$ points \pm kPa). Variation of observed differences was considerable (95%CI of agreement: 39.4 and 35.2 points \pm kPa), and showed a clear pattern towards larger disagreement at higher values with lower LiverRisk score values than corresponding LSM.

POSTER PRESENTATIONS

The diagnostic accuracy of the LiverRisk for cACLD (AUROC: 0.757 [95%CI: 0.744–0.770]/0.790 [95%CI: 0.762–0.819]) was comparable to FIB-4 (0.769/0.813) and APRI (0.747/0.765). The cut-off of 10points \pm kPa yielded an overall accuracy of 74.2%/81.2%, high specificity (91.9/93.4%), but low negative predictive value (76.6/84.5%) with false-negative results in 20.0%/13.5% in cohort-I/II, respectively. In cohort-I, 208 (3.5%) patients developed hepatic decompensation (median follow-up: 4.7 years). The LiverRisk score showed a reasonable accuracy for predicting hepatic decompensation within 2 years (AUROC: 0.817); however, it was inferior to LSM (0.891, $p < 0.001$) and FIB-4 (0.912, $p < 0.001$). The strata of LiverRisk score (and of LSM/FIB-4) discriminated patient groups of distinct risks for hepatic decompensation.

Conclusion: While being a major step forward for screening subjects without known liver disease in primary care, the LiverRisk score was not superior (vs. FIB-4) for diagnosis of cACLD or (vs. FIB-4/LSM) for prediction of hepatic decompensation in a tertiary care setting, i.e., in cohorts with a higher pre-test probability of cACLD.

FRI-010

A non-invasive predictive model based on CT radiomics for hepatic venous pressure gradient in liver cirrhosis

Xu Guo¹, Wuque Cai², Huan Tong¹, Tingrui Han¹, Jiayi He², Hongze Sun², Guiying Zhang², Xin Quan¹, Shuaijie Qian¹, Ying Li¹, Bo Wei¹, Yang Tai¹, Daqing Guo², Hao Wu¹. ¹Department of Gastroenterology and Hepatology, West China Hospital, Sichuan University, Chengdu, China; ²School of Life Science and Technology, University of Electronic Science and Technology, Chengdu, China
Email: hxxhwh@163.com

Background and aims: Hepatic venous pressure gradient (HVPG) is used to quantitatively reflect the level of portal vein pressure and HVPG in the different interval could predict the occurrence of end point events in cirrhotic portal hypertension, thus making accurate prognosis judgments and treatment decisions for patients with liver cirrhosis. However, the measurement of HVPG is an invasive, costly, and requires specialized personnel and equipment, resulting in limitation in routine clinical practice. Thus, the study aimed to develop a predictive model based on CT imaging data combined with artificial intelligence (AI) algorithms as a non-invasive, accurate and convenient method to assess HVPG.

Method: A total of 359 patients with cirrhosis, who had both HVPG measurement and contrast-enhanced CT within 14 days prior to the catheterization were collected in the study from July 2016 to June 2022. We selected 4 major levels of CT image for each patient including the first hepatic hilum, second hepatic hilum, intersection of splenic vein and portal vein, and the largest cross-sectional area of the spleen. Then the region of interest (ROI) in each level was performed by manual delineation and sampled into training and testing cohort to develop the predictive model. The predictive performance was evaluated by the area under receiver operating characteristic curves (AUC).

Results: The overall prediction accuracy of the model for HVPG was over 85%. In the training cohort, the AUC value for HVPG > 5 mmHg, ≥ 10 mmHg, ≥ 12 mmHg, ≥ 16 mmHg, ≥ 20 mmHg, were 0.990 (95%CI, 0.986–0.994), 0.993 (95%CI, 0.989–0.996), 0.991 (95%CI, 0.987–0.995), 0.981 (95%CI, 0.976–0.986), 0.978 (95%CI, 0.972–0.984) respectively. In the testing cohort, the AUC value for HVPG > 5 mmHg, ≥ 10 mmHg, ≥ 12 mmHg, ≥ 16 mmHg, ≥ 20 mmHg, were 0.894 (95%CI, 0.868–0.919), 0.852 (95%CI, 0.828–0.876), 0.872 (95%CI, 0.852–0.893), 0.790 (95%CI, 0.765–0.815), 0.797 (95%CI, 0.772–0.823) respectively.

Conclusion: The predictive model showed relatively accurate results of HVPG classification and performed well in the prediction of clinically significant portal hypertension (CSPH, HVPG ≥ 10 mmHg) and esophagogastric variceal bleeding (EGVB, HVPG ≥ 12 mmHg), which provided a non-invasive and rapid method for predicting complications of decompensated liver cirrhosis when HVPG

measurement is not available. Besides, multi-center and large sample tests should be carried out in the future to improve the model.

FRI-014

Comparison of two ultrasound diagnostic systems for measuring liver stiffness in clinical practice

Simone Cappelli¹, Giovanni Petrali², Laura De Rosa^{3,4}, Antonio Salvati⁵, Filippo Oliveri⁵, Barbara Coco⁵, Gabriele Ricco⁵, Piero Colombatto⁵, Ferruccio Bonino⁶, Francesco Faita³, Maurizia Brunetto^{1,5,6}. ¹Department of Clinical and Experimental Medicine, Pisa University, Pisa, Italy; ²Department of Surgical, Medical, Molecular and Critical Area Pathology, Pisa, Italy; ³Institute of Clinical Physiology, National Research Council, Pisa, Italy; ⁴Department of Information Engineering and Computer Science, University of Trento, Trento, Italy; ⁵Hepatology Unit, Pisa University Hospital, Pisa, Italy; ⁶Institute of Biostructure and Bioimaging, National Research Council, Naples, Italy

Email: cappellisimone14@gmail.com

Background and aims: The values of liver stiffness by transient elastography using different ultrasound systems could differ and jeopardize the patients' clinical management. Our aim was to compare the results of two different technologies for liver stiffness measurement in a large cohort of chronic liver disease (CLD) patients (pts).

Method: In 777 consecutive CLD pts admitted at Hepatology Unit of University Hospital of Pisa from May 2022 to December 2023 liver stiffness was at the same time with two different diagnostic systems: FibroScan® (Echosens, France) equipped with M or XL probe and FT9000 (Hisky Medical, China) equipped with a single probe liver stiffness measurement (LSM_{Fibroscan}/LSM_{FT9000}). Pearson correlation coefficients and Bland-Altman analyses (BAA) were conducted to study the agreement between LSM_{Fibroscan}/LSM_{FT9000}. Delta FT9000-FibroScan® LSM (D) associations with CLD clinical parameters was observed too. AST/SGT and platelets counts/portal veins caliper/spleen long axis were used as proxies of necro-inflammatory activity and portal hypertension-vascular congestion.

Results: Overall LSM_{Fibroscan} was strongly correlated with LSM_{FT9000} ($r = 0.77$, $p < 0.001$). LSM correlation varied among BMI classes (normal weight $r = 0.84$, overweight $r = 0.75$, obese $r = 0.65$, $p < 0.001$). LSMs obtained with the two devices showed a bias of 0.52 kPa ($p = 0.01$) with-11/12 kPa 95% LoA, with a clear trend for higher values measured by LSM_{FT9000} for LSM < 10 kPa and vice versa for LSM > 10 kPa. In fact, D was equal to zero for LSM_{Fibroscan} 9.6 kPa. In LSM_{Fibroscan} > 10 kPa cohort D significantly correlated with AST, GGT, portal vein caliper, spleen long axis, and platelets ($r = -0.22$, $r = -0.17$, $r = -0.189$, $r = -0.287$, and $r = 0.031$, respectively). In a bivariate analysis D correlated with LSM_{Fibroscan} and AST ($\beta = 0.002$, $p = 0.001$) with a p of interaction equal to 0.018 and D was also associated with spleen long axis ($\beta = 0.033$, $p = 0.027$) and platelets count ($\beta = -0.008$, $p = 0.018$, respectively), with a significant interaction of both with LSM_{Fibroscan} ($p < 0.001$).

Conclusion: LSM_{Fibroscan} and LSM_{FT9000} measures showed a limited agreement across different dynamic ranges with a good agreement only around 10 kPa. The discrepancies associated with anthropometry and necro-inflammatory activity and vascular congestion proxies. LSM_{FT9000} provides higher values than LSM_{Fibroscan} below 10 kPa whereas LSM_{Fibroscan} higher values, with wider dynamic range, over 20 kPa. Comparative studies using as gold standard reference liver histology and porto-systemic gradient will help to better understand the reasons for the discrepancies. Whether these results will be confirmed, method specific cut-offs in clinical practice will be required.

FRI-015

Stabilization of enhanced liver fibrosis and liver stiffness measures in the open-label extension of the phase 3 POISE trial of obeticholic acid for the treatment of primary biliary cholangitis

Robert G. Gish¹, Darren Wheeler², Jing Li², Christopher Gasink², Alan Bonder³, ¹Robert G. Gish Consultants, LLC, San Diego, United States; ²Intercept Pharmaceuticals, Inc., Morristown, United States; ³Division of Gastroenterology and Hepatology, Beth Israel Deaconess Medical Center, Harvard Medical School, Boston, United States
Email: rgish@robertgish.com

Background and aims: Transient elastography (TE) is a non-invasive alternative to biopsy to determine liver stiffness and indirectly assess fibrosis, which can be predictive of adverse outcomes in patients (pts) with primary biliary cholangitis (PBC). Enhanced liver fibrosis (ELF) is a blood test that consists of an algorithm of 3 fibrosis markers and is a well-validated measure of fibrosis. Obeticholic acid (OCA) was approved for the treatment of PBC based on biomarker improvement in POISE, a 12-month randomized, double-blind (DB), placebo-controlled phase 3 study. Here, we report the results from a post hoc analysis of the impact of OCA on ELF and TE in pts from POISE.

Method: Pts with PBC who could not tolerate or had an inadequate response to first-line ursodeoxycholic acid were randomized to receive placebo, OCA 5–10 mg (OCA titration), or OCA 10 mg daily in the DB phase. During the 5-year open-label extension (OLE), all pts were initially treated with OCA 5 mg daily for 3 months, after which the dose could be titrated based on response and tolerability. ELF was assessed at baseline (BL) and each year after OCA initiation, using an algorithm based on hyaluronic acid, type III procollagen peptide, and tissue inhibitor of metalloproteinase 1 levels. Liver stiffness was measured by TE at BL and each year after OCA initiation at sites where FibroScan was the available form of TE. For pts who received placebo in the DB phase, BL measures were the last assessment before the first OLE OCA dose. If pts received OCA in the DB phase, their BL measures were from the DB BL period. Data points after pts titrated to >10 mg OCA in the OLE were excluded from the analysis.

Results: OCA stabilized ELF over 24 months in pts with evidence of moderate (ELF score ≥ 7.7 and < 9.8) or severe (≥ 9.8 and < 11.3) fibrosis or cirrhosis (≥ 11.3) at BL. The mean ELF scores were 9 at BL (n = 98), 9.19 at month 12 (n = 86), and 9.31 at month 24 (n = 51) in pts with moderate fibrosis. In pts with severe fibrosis, mean ELF scores were 10.35 at BL (n = 62), 10.36 at month 12 (n = 50), and 10.56 at month 24 (n = 31), and in pts with cirrhosis, mean ELF scores were 11.92 at BL (n = 26), 11.54 at month 12 (n = 16), and 11.35 at month 24 (n = 11). In pts with lower liver stiffness (TE < 10 kPa) at BL, the mean TE measures were 6.09 (n = 47) at BL, 6.37 at month 12 (n = 41), and 5.86 at month 24 (n = 31). The mean TE measures in pts with higher liver stiffness (TE ≥ 10 kPa) were 19.27 at BL (n = 32), 18.39 at month 12 (n = 23), and 17.37 at month 24 (n = 19). ELF and TE values after month 24 were similar to those observed from BL to month 24, although the number of pts with TE and ELF measurements decreased over time through month 72.

Conclusion: These results suggest that OCA stabilized fibrosis over time regardless of severity at BL, although interpretability of the data is limited after 24 months because of decreasing sample size over time. Pts with PBC may benefit from OCA treatment early before PBC progresses and fibrosis worsens.

FRI-016

PT-LIFE model for the diagnosis of pediatric liver fibrosis after pediatric liver transplantation

Hao Feng¹, Zicheng Lv¹, Qiang Xia¹. ¹Shanghai Jiaotong Uni aff. Renji Hospital, Shanghai, China
Email: lyuzicheng@163.com

Background and aims: Pediatric liver transplantation is now considered a curative treatment for children with chronic end-stage liver diseases and specific metabolic defects, and has become very successful with high survival rate. Prevalence of fibrosis as high as

65% at 5 years and 69% at 10 years after pediatric liver transplantation has been reported. The gold standard to assess the stage of liver fibrosis is liver biopsy. However, liver biopsies are invasive and can occasionally cause severe morbidity and even mortality. Thus, we aimed to develop and validate a blood-based diagnostic multivariate index test that is specifically designed to rule in and rule out allograft fibrosis in the pediatric liver transplantation recipients.

Method: The discovery cohort included 150 pediatric patients underwent liver graft biopsy in our tertiary liver transplantation department from Aug 2022 to Feb 2023 were prospectively recruited. a logistic bootstrap-based stepwise regression process was done in the discovery cohort to identify a biomarker-based model.

Results: From Aug 2022 to Aug 2023, 262 liver biopsy specimens were prospectively collected in our tertiary liver transplantation department, and 250 of them were eligible and enrolled. The PT-LIFE model showed higher discriminatory accuracy to identify pediatric liver transplantation recipients with moderate to severe fibrosis (LAFSc 3–6) compared with individual components of the score. The AUROC for PT-LIFE in the discovery set was 0.92 (95% CI 0.88–0.97). To enable real-world clinical use, a lower cutoff was established at less than 0.12 to provide a rule-out decision with 90.7% sensitivity, and 94.7% NPV. In addition, an upper cutoff was established at 0.29 or higher to enable a rule-in decision with 76.7% specificity, 90.6% sensitivity, and 76.7% PPV. The so-called grey or indeterminate zone comprised 32 (21.3%) of 150 patients in the discovery cohort, indicating the PT-LIFE test yielded actionable clinical results in 118 (78.7%) patients.

Conclusion: PT-LIFE significantly outperformed other non-invasive fibrosis diagnostics, including APRI, GPR, FIB-4, Forns index, AGILE3+ and AGILE 4 score for the identification of allograft fibrosis in the pediatric liver transplantation recipients. In addition, although PT-LIFE was not developed to specifically identify the subpopulation of recipients with LAFSc ≥ 5 , performance was also significantly better than other non-invasive fibrosis diagnostics (all $p < 0.05$).

FRI-017

Fibrosis activity versus disease stage: systemic markers of fibrosis activity have better prognostic performance than the liver biopsy in patients with alcohol-related liver disease

Stine Johansen^{1,2}, Mads Israelsen^{1,2}, Katrine Lindvig¹, Katrine Thorhauge^{1,2}, Johanne Kragh Hansen^{1,2}, Camilla Dalby Hansen¹, Ida Ziegler Spedtsberg^{1,2}, Helle Schnefeld¹, Peter Andersen¹, Ida Falk Villesen¹, Katrine Tholstrup Bech^{1,2}, Nikolaj Torp^{1,2}, Diana Leeming³, Torben Hansen⁴, Morten Karsdal^{3,5}, Maja Thiele^{1,2}, Aleksander Krag^{1,2}. ¹Centre for Liver Research, Odense University Hospital, Odense, Denmark; ²Department of Clinical Research, Faculty of Health Sciences, University of Southern Denmark, Odense, Denmark; ³Nordic Bioscience A/S, Herlev, Denmark; ⁴Novo Nordisk Foundation Center for Basic Metabolic Research, University of Copenhagen, Copenhagen, Denmark; ⁵Department of Molecular Medicine, Faculty of Health Sciences, University of Southern Denmark, Odense, Denmark
Email: stine.johansen@rsyd.dk

Background and aims: Excessive alcohol consumption is the most significant risk factor for fibrosis progression in patients with steatotic liver disease. As liver fibrosis screening becomes more widespread, patients are identified at varying fibrosis stages, necessitating stage-specific clinical outcome predictions. Consequently, there is a need for prognostic, non-invasive tests that are effective at all fibrosis levels. We aimed to evaluate if the active fibrogenesis marker PRO-C3 can predict clinical outcomes in alcohol-related liver disease (ALD) patients, independent of their baseline liver fibrosis stage, and compare its prognostic accuracy to the established blood-based fibrosis markers Enhanced Liver Fibrosis test (ELF) and Fibrosis-4 Index (FIB-4).

Method: We conducted a prospective cohort study of patients with a prior or current excessive alcohol intake (men: ≥ 36 g/day, women:

POSTER PRESENTATIONS

≥24 g/day for more than 1 year), and no previous decompensation. At baseline, we performed liver biopsies and assessed non-invasive fibrosis tests, along with clinical investigations. During follow-up, we manually reviewed patients' electronic healthcare records for decompensations, all-cause mortality, and reports of alcohol intake. We defined decompensation according to the Baveno VII recommendations.

Results: We followed 458 patients with ALD for median 5.9 years (IQR 4.5–7.8). Mean age was 57 ± 10 years, 76% were males, with fibrosis stages F0–1/F2/F3–4 = 261/107/91 at baseline. During follow-up, 67 patients decompensated, and 100 patients died. In all Kleiner fibrosis stages, PRO-C3 added prognostic value on top of fibrosis stage as a predictor of later decompensation, both for patients with no to moderate fibrosis, F0–2 (hazard ratio, HR_{PRO-C3} 1.05; 95% CI 1.03–1.07, $p < 0.001$), and for patients with advanced fibrosis, F3–4 (HR_{PRO-C3} 1.01; 95% CI 1.00–1.02, $p = 0.027$). In a head-to-head comparison between PRO-C3 (<15.6 ng/ml vs ≥15.6) and Kleiner fibrosis stage (F0–2 vs F3–4) both baseline markers independently predicted later decompensation, though PRO-C3 was a better predictor of the outcome (HR_{PRO-C3} 7.09; 95% CI 3.21–15.68, $p < 0.001$ and HR_{Kleiner} 5.16; 95% CI 2.98–8.94, $p < 0.001$). In a multivariable regression including Kleiner fibrosis stage (F0–2 vs F3–4), PRO-C3 (<15.6 ng/ml vs ≥15.6), ELF (<9.8 vs ≥9.8) and FIB-4 (<1.3 vs ≥1.3) only Kleiner fibrosis stage and PRO-C3 were independent predictors of decompensation.

Conclusion: In alcohol-related liver disease, patients' prognoses are predicted by both baseline markers of disease stage and fibrosis activity. PRO-C3, a marker of fibrosis activity, was a better prognostic marker than Kleiner fibrosis stage, and predicted decompensation in all stages of fibrosis.

FRI-018

Procalcitonin as a predictive marker of incident liver disease

Amanda Finnberg-Kim¹, Mats Pihlgård², Kristina Önnérhag³, Sofia Enhörning². ¹Department of Clinical Sciences in Malmö, Lund University, Malmö, Sweden; ²Perinatal and Cardiovascular Epidemiology, Lund University Diabetes Centre, Department of Clinical Sciences in Malmö, Malmö, Sweden; ³Dept of Gastroenterology and Hepatology Skåne University Hospital Malmö, Malmö, Sweden
Email: amanda.finnberg-kim@med.lu.se

Background and aims: Previous studies have shown that procalcitonin (PCT) concentration can be elevated in patients with liver disease without evidence of ongoing bacterial infection. The relationship between elevated PCT and liver damage is not completely understood. We aimed to investigate the association between elevated PCT and future risk of liver disease.

Method: PCT was measured in individuals without prevalent liver disease in the Malmö Diet and Cancer Cardiovascular Cohort (MDC-CC) and in a sample of the Malmö Preventive Project cohort (MPP). Complete data was available in 3897 individuals in MDC-CC and 3854 individuals in MPP. According to Swedish National Patient Registers which cover almost all hospital-based care in Sweden, 70 subjects in MDC-CC and 49 subjects in MPP developed non-viral liver disease during a median follow-up of 27.1 and 14.8 years respectively. Cox proportional hazards models were used to analyse risk of incident liver disease by PCT levels. We performed our analyses in a pooled sample of both the MPP and MDC-CC cohorts as well as separate analyses for each cohort.

Results: PCT was strongly and independently associated with incident non-viral liver disease of any type during follow-up. In multivariate adjusted models (age, gender, body mass index, hazardous alcohol consumption, total cholesterol, low-density lipoprotein cholesterol, high-density lipoprotein cholesterol, triglycerides, lipid lowering treatment, prevalent diabetes, creatinine, prevalent hypertension and smoking) in the pooled sample, individuals with high PCT (>0.05 ng/ml) had a significantly increased risk of developing liver disease compared to subjects with PCT

concentrations below the cutoff (hazard ratio (HR) 3.4, 95% confidence interval (CI) 2.06–5.61, $p < 0.001$). The HR per standard deviation increase of log-transformed PCT was 1.56 (95% CI 1.32–1.85, $p < 0.001$) in multivariate adjusted models. Separate cohort-specific sensitivity analyses, out of which the cohort-specific analysis of MDC-CC was additionally adjusted for C-reactive protein, showed similar effect estimates as the pooled analyses.

Conclusion: PCT is an independent predictive marker of future diagnosis-verified non-viral liver disease. In selected patients, these findings could have implications for risk assessment leading to earlier detection of liver disease and in turn earlier treatment of the underlying cause of liver injury. Our results also highlight the possibility of PCT as a direct cause of hepatocyte damage.

FRI-020

Validation of FIB-6 Score in assessment of liver fibrosis in chronic hepatitis B

Khalid A. Alswat¹, Riham Soliman², Nabil Mikhail³, Necati Ormeci⁴, George Dalekos⁵, Moutaz F.M. Derbala⁶, Said Ahmed Salim Al Busafi⁷, Waseem Hamoudi⁸, Gamal Shiha⁹. ¹Liver Disease Research Centre, College of Medicine, King Saud University, Riyadh, Saudi Arabia; ²Gastroenterology and Hepatology Department, Egyptian Liver Research Institute and Hospital (ELRIAH), El Mansoura, Egypt, Tropical Medicine Department, Faculty of Medicine, Port Said University, Egypt; ³Gastroenterology and Hepatology Department, Egyptian Liver Research Institute and Hospital (ELRIAH), El-Mansoura, Egypt, Biostatistics and Cancer Epidemiology Department, South Egypt Cancer Institute, Assiut University, Egypt; ⁴Department of Gastroenterology, Ankara University School of Medicine, Ankara, Turkey; ⁵Department of Medicine and Research Laboratory of Internal Medicine, National Expertise Center of Greece in Autoimmune Liver Diseases, General University Hospital of Larissa, Larissa, Greece; ⁶Gastroenterology and Hepatology Department, Hamad Hospital, Doha, Qatar; ⁷Department of Medicine, Division of Gastroenterology and Hepatology, College of Medicine and Health Sciences, Sultan Qaboos University, Muscat, Oman; ⁸Internal Medicine Department, Al-Bashir Hospital, Amman, Jordan; ⁹Gastroenterology and Hepatology Department, Egyptian Liver Research Institute and Hospital (ELRIAH), Sherbin, El-Mansoura, Egypt, Hepatology and Gastroenterology Unit, Internal Medicine Department, Faculty of Medicine, Mansoura University, El-Mansoura, Egypt
Email: kalswat@ksu.edu.sa

Background and aims: We recently developed a simple novel index called fibrosis 6 (FIB-6) using machine learning data analysis. We aimed to evaluate its performance in diagnosis liver fibrosis and cirrhosis in CHB.

Method: Retrospective observational analysis of data obtained from seven sites (Egypt, KSA, Turkey, Greece, Oman, Qatar, and Jordan) of CHB patients. The inclusion criteria include receiving an adequate liver biopsy and a complete biochemical and hematological data. Diagnostic performance analysis of the FIB-6 index was conducted and compared with other non-invasive scores.

Results: 603 patients were included for analysis; the AUROC for FIB-6 for the discrimination of patients with cirrhosis (F4), cACLD (F3 and F4), and significant fibrosis (F2–F4), were 0.854, 0.812, and 0.745, respectively. Analysis using the optimal cut-offs of FIB-6 showed sensitivity of 70.9%, specificity of 84.1%. PPV = 40.3% and NPV = 95.0% for diagnosis of cirrhosis. For diagnosis of cACLD, the results were 71.5%, 69.3%, 40.8% and 89.2% respectively, while for diagnosis of significant fibrosis, the results were 68.3%, 67.5%, 59.9% and 75.0%. When compared with those of FIB-4, APRI, and AAR, the AUROC for the performance of FIB-6 was higher than those of FIB-4, APRI, and AAR in all fibrosis stages. FIB-6 gave the highest sensitivity and NPV (89.1% and 92.4%) in ruling out compensated advanced liver disease (cACLD) and cirrhosis, as compared to FIB-4 (63.8% and 83.0%), APRI (53.9% and 86.6%), and AAR (47.5% and 82.3%) respectively.

Conclusion: The FIB-6 index could be used in ruling out cACLD, fibrosis, and cirrhosis with good reliability.

FRI-021

An integrative machine learning method enhances postoperative liver failure risk assessment with preoperative indicators

Zongkun Zhang¹, Haoyu Wu¹, Hongxuan Li^{2,3}, Bin Shu^{2,3}, Xiaojuan Wang^{2,3}, Yongfeng Huang¹, Shizhong Yang^{2,3}. ¹Department of electronic engineering, Tsinghua University, Beijing, China; ²Hepatopancreatobiliary Center, Beijing Tsinghua Changgung Hospital, Key Laboratory of Digital Intelligence Hepatology (Ministry of Education), School of Clinical Medicine, Tsinghua University, Beijing, China; ³Research Unit of Precision Hepatobiliary Surgery Paradigm, Chinese Academy of Medical Sciences, Beijing, China
Email: ysza02008@btch.edu.cn

Background and aims: Post-hepatectomy liver failure (PHLF) is a severe complication and leading cause of death during the peri-operative period. Presently, the hepatectomy decision-making is mainly based on preoperative ICG-R15 tests and the liver remnant volume assessment. Nevertheless, it is still difficult to completely avoid PHLF. This study aims to develop a comprehensive method that utilizes preoperative indicators to optimize the PHLF risk evaluation using machine learning techniques.

Method: A two-step framework was employed to analyze clinical data. At first, unsupervised learning clustering algorithms were used to identify potential risk levels, forming the basis. Then, supervised models were used to verify the replicability and usefulness of the risk levels. Based on this, the T-test was employed to compare the magnitude of differences between risk levels, and interpretative analysis of the logistic regression classifier was utilized to summarize a practical risk-scoring formula.

Results: The study incorporated the clinical data of 197 patients who underwent hepatectomy, comprising a development cohort (n = 118) and a validation cohort (n = 79). Within the development cohort, two critical risk levels were identified using the k-means cluster Method: a high-risk group (n = 15, PHLF rate = 20.0%) and a low-risk group (n = 103, PHLF rate = 1.9%). The incidence of PHLF showed significant differences between these groups (p = 0.001). Several key preoperative indicators, such as Child score (p = 5.12e-25), DBIL (p = 1.55e-13), TBIL (p = 5.62e-8), and ICG-R15 (p = 2.00e-4), exhibited significant disparities between the two risk groups. Furthermore, a supervised classifier, trained in the development cohort using risk levels as labels, was applied to stratify risk in the validation cohort. In the validation cohort, the high-risk group (n = 9, PHLF rate = 22.2%) and the low-risk group (n = 70, PHLF rate = 4.2%) demonstrated a significant difference in the incidence of PHLF (p = 0.037). The indicators such as Child score (p = 1.55e-10), DBIL (p = 2.03e-09), TBIL (p = 1.34e-07), and ICG-R15 (p = 0.012) still showed substantial differences, thereby confirming the robustness of the risk levels. Moreover, through interpretative analysis of the supervised classifier, we identified the importance of each clinical indicator in risk assessment and developed a risk-scoring formula. Compared to ICG-R15 (AUC = 0.67), the risk-scoring formula (AUC = 0.82) demonstrated superior predictive capability for PHLF.

Conclusion: This study utilizes the superiority of machine learning algorithms to accurately detect possible clinical risk factors and their connections from the data structure itself, providing insight into the impact of preoperative clinical indicators on the risk of PHLF. Moreover, a risk assessment formula is proposed to be used as a reference to optimize surgical decision-making.

FRI-022

N-terminal type III collagen propeptide, golgi protein 73 and their combination accurately assess significant and advanced fibrosis in chronic hepatitis B patients

Qianqian Chen¹, Yee Hui Yeo², Xinyu Hu³, Li Zhu⁴, Fajuan Rui¹, Shengxia Yin⁵, Chuanwu Zhu⁴, CHao Wu⁶, Mindie Nguyen⁷, Jie Li⁶. ¹Nanjing Drum Tower Hospital Clinical College of Nanjing University of Chinese Medicine, Nanjing, China; ²Cedars-Sinai Medical Center, Los Angeles, United States; ³Shandong Provincial Hospital, Ji'nan, China;

⁴The Fifth People's Hospital of Suzhou, Suzhou, China; ⁵Nanjing Drum Tower Hospital, Affiliated Hospital of Medical School, Nanjing University, Nanjing, China; ⁶Nanjing Drum Tower Hospital, Affiliated Hospital of Medical School, Nanjing, China; ⁷Stanford University Medical Center, Palo Alto, United States
Email: lijier@nju.edu.cn

Background and aims: There is an urgent need for non-invasive biomarkers to detect the progression of liver fibrosis in patients with chronic hepatitis B (CHB). PRO-C3, N-terminal type III collagen propeptide, has shown potential as a serum biomarker for diagnosing significant fibrosis in patients with non-alcoholic fatty liver disease. Similarly, GP73, Golgi protein 73, has been suggested as a marker for liver fibrosis progression in CHB patients. However, the diagnostic efficacy of PRO-C3, GP73, and their combination in CHB-related liver fibrosis remains uncertain. Therefore, we aim to assess the performance of these three biomarkers in diagnosing significant and advanced fibrosis in CHB patients.

Method: This study included treatment-naïve CHB patients who underwent simultaneous liver biopsy and blood testing at two tertiary centers. Liver fibrosis was assessed using the Scheuer scoring system (S0-S4). The cohort was divided into groups based on fibrosis stages: S0-1 versus S2-4, and S0-2 versus S3-4. Serum levels of PRO-C3 and GP73 were measured using ELISA. The diagnostic accuracy of PRO-C3, GP73, PRO-C3 combined with GP73, FIB-4, and APRI in identifying fibrosis related to CHB was evaluated using receiver operating characteristic (ROC) curves. The significance of the area under the curves (AUCs) was determined using the Delong test.

Results: A total of 324 individuals with matched liver biopsies were enrolled in this study, with 167 of them undergoing transient elastography (TE). Significant elevation of PRO-C3 and GP73 levels was observed in patients with fibrosis stages S2-4 and S3-4 compared to those with stages S0-1 and S0-2 (p < 0.001). After adjusting for sex, age, body mass index, liver enzymes, and HBV DNA level, PRO-C3 was identified as an independent predictor for significant (OR 1.04, 95% CI: 1.03-1.06) and advanced fibrosis (OR 1.04, 95% CI: 1.03-1.05). In the overall cohort, PRO-C3 combined with GP73 (AUC = 0.84 [0.77-0.89]) outperformed LSM (AUC = 0.74 [0.67-0.81], p = 0.049), FIB-4 (AUC = 0.64 [0.56-0.71], p < 0.001), and APRI (AUC = 0.72 [0.64-0.78], p = 0.007) in detecting significant fibrosis. When used individually, PRO-C3 and GP73 demonstrated comparable diagnostic performance to LSM and outperformed or showed similar performance to APRI and FIB-4 in both diagnoses.

Conclusion: Our findings indicate that PRO-C3, GP73, and their combination are the most effective blood tests for identifying significant and advanced fibrosis in CHB patients, with diagnostic accuracy comparable to TE. This suggests a novel, cost-effective, and accurate option for monitoring fibrosis progression in CHB and guiding clinical decision-making.

FRI-023

Effect of obeticholic acid on reduction and normalization of alanine aminotransferase and aspartate aminotransferase in the phase 3 POISE trial in primary biliary cholangitis

Robert G. Gish¹, Darren Wheeler², Jing Li², Christopher Gasink², David W. Victor, III³. ¹Robert G. Gish Consultants, LLC, San Diego, United States; ²Intercept Pharmaceuticals, Inc., Morristown, United States; ³Houston Methodist Hospital, Houston, United States
Email: rgish@robertgish.com

Background and aims: Obeticholic acid (OCA) is a potent farnesoid X receptor agonist with accelerated approval for primary biliary cholangitis (PBC) based on improvement in alkaline phosphatase (ALP) and total bilirubin (TB) levels in the randomized, double-blind, placebo-controlled phase 3 POISE study. In addition to ALP and TB, elevated alanine aminotransferase (ALT) and aspartate aminotransferase (AST) are associated with an increased risk of negative clinical outcomes in patients with PBC. Herein, we evaluate the effect of OCA on ALT and AST, including the proportion of patients attaining normal

POSTER PRESENTATIONS

levels (defined as ALT ≤ 41 U/L and AST ≤ 34 U/L) among patients with abnormal levels at baseline (BL).

Method: In the POISE study, PBC patients with inadequate response or intolerance to ursodeoxycholic acid were randomized 1:1:1 to receive placebo (PBO), OCA titration (OCA 5 mg daily with option to titrate to 10 mg after 6 months), or OCA 10 mg daily for 12 months. Serum ALT and AST levels were assessed at all visits. The Cochran-Mantel-Haenszel method was used to assess the association between OCA treatment and normalization of ALT or AST among patients with elevated levels at BL.

Results: Among the intention-to-treat (ITT) population, mean BL values for ALT were 56.0 U/L for PBO, 61.6 U/L for OCA titration, and 56.3 U/L for OCA 10 mg. Baseline AST levels were 48.8, 52.3, and 50.5 U/L for PBO, OCA titration, and OCA 10 mg, respectively. Among the 61% of patients with ALT >41 U/L at BL, 16% (7/45) receiving PBO normalized at Month 6 vs 55% (26/47) on OCA 5 mg and 53% (21/40) on OCA 10 mg ($p \leq 0.001$ for both). As early as Week 2, 3 to 4 times more patients had normalized ALT in both OCA groups (both $p < 0.01$ vs PBO). Among the 71% of patients with AST >34 U/L at BL, normalization rates at Month 6 were 12% (6/51) in the PBO arm, 30% (16/53) in the OCA 5-mg arm, and 31% (15/49) in the OCA 10-mg arm ($p < 0.05$ for both). The proportions of patients normalizing ALT and AST on OCA were similar at Month 12. Overall reductions in ALT and AST in the ITT population were significant for both OCA groups vs PBO at all visits (all $p < 0.001$) as early as Week 2, with least-squares mean changes from BL for ALT of -6.6 U/L for PBO, -18.9 U/L for OCA 5 mg, and -22.0 U/L for OCA 10 mg, and -3.8 U/L, -10.6 U/L, and -12.2 U/L for AST, respectively.

Conclusion: OCA significantly reduced ALT and AST as early as Week 2 in both OCA treatment groups, and by Month 6, normalized ALT in $>50\%$ and AST in almost 33% of patients with elevated levels at BL. These data suggest that in addition to reductions in ALP, OCA meaningfully reduces ALT and AST below thresholds that are prognostic for improved clinical outcomes. Additional research is required to understand how measuring ALT and AST levels contributes to a more complete assessment of PBC treatment response in order to minimize the risk of disease progression.

FRI-026

Longitudinal association of magnetic resonance elastography with liver-related events and cardiovascular events in chronic hepatitis

Nobuharu Tamaki¹, Mayu Higuchi¹, Yutaka Yasui¹, Kaoru Tsuchiya¹, Hiroyuki Nakanishi¹, Namiki Izumi¹, Masayuki Kurosaki¹. ¹Musashino Red Cross Hospital, Tokyo, Japan
Email: nobuharu.tamaki@gmail.com

Background and aims: Magnetic resonance elastography (MRE) is a non-invasive modality for liver fibrosis and has a high diagnostic accuracy, but the association between MRE and the risk of complications including liver-related events and cardiovascular events (CVD) remains unclear. In this study, we investigated the longitudinal association between MRE and the risk of complications.

Method: This retrospective study included 2373 consecutive patients with chronic liver disease. The primary outcome was the risk of liver-related events and CVD for MRE. In the subgroup of chronic hepatitis B, the association between MRE and hepatocellular carcinoma (HCC) was also investigated.

Results: In the whole cohort, the adjusted hazard ratios (aHR) (95% confidence interval [CI]) of each 1-kPa increase in liver stiffness for HCC, decompensation, and CVD were 1.28 (1.2–1.4), 1.34 (1.3–1.4), and 0.96 (0.9–1.1), respectively. Similarly, the aHR (95% CI) for HCC, decompensation, and CVD were 4.20 (2.2–8.2), 67.5 (9.2–492), and 0.83 (0.4–1.7), respectively, in patients with cirrhosis (>4.7 kPa) compared to those with minimal fibrosis (<3 kPa). In the subgroup of 504 chronic hepatitis B, the 1-, 3-, and 5-year cumulative incidence of HCC in patients with liver stiffness ≥ 3.6 kPa and those with liver stiffness <3.6 kPa were 3.8%, 7.0%, and 22.9%, and 0%, 0.9%, and 1.5%,

respectively ($p < 0.001$). In the multivariable analysis, MRE-based liver stiffness (per 1 kPa) or liver stiffness ≥ 3.6 kPa was an independent factor for HCC development with an aHR (95% CI) of 1.61 (1.3–2.0) or aHR of 8.22 (2.1–31).

Conclusion: Increased MRE-associated liver stiffness was associated with increased risk for HCC, and decompensation in a dose-dependent fashion and may be used for the early prediction of liver-related events and determination of indications for treatment.

FRI-027

Fibroblast activity kills-circulating endotrophin (PRO-C6) is prognostic for liver-related events in patients with cirrhosis from chronic hepatitis C

Thomas Møller^{1,2}, Emilie Skovgaard³, Diana Leeming¹, Morten Karsdal¹, Keyur Patel⁴. ¹Nordic Bioscience A/S, Herlev, Denmark; ²University of Copenhagen, Department of Biomedical Sciences, Copenhagen, Denmark; ³Nordic Bioscience A/S, University of Copenhagen, Herlev, Denmark; ⁴University Health Network, Toronto, Canada

Email: twm@nordicbio.com

Background and aims: Prognostic markers for patients with compensated cirrhosis at increased risk of developing liver-related events are required. Endotrophin, a potential driver of fibroblast activation and mediator of fibroinflammatory disease, may be assessed non-invasively using PRO-C6. Blood-based collagen extracellular matrix remodeling markers may provide novel prognostic information to identify patients with cirrhosis at higher risk of developing a liver-related event. Here we aimed to investigate the ability of PRO-C6 to predict liver-related events in The Hepatitis C Antiviral Long-Term Treatment Against Cirrhosis Trial (HALT-C) (ClinicalTrials.gov #NCT00006164).

Method: A subgroup of 151 patients with cirrhosis and serum samples from the HALT-C cohort, were included in this study. NordicPRO-C6TM was assessed in serum using a fully validated competitive enzyme-linked immunosorbent assay. Between groups comparison of biomarker levels was performed using Mann-Whitney U test. Patients were stratified above and below a 15.0 ng/ml cut-off of baseline PRO-C6. Cox proportional hazards regression was used to analyze the prognostic value of serum PRO-C6 to identify patients at risk of developing liver-related events. Data provided by NIDDK CR, a program of the National Institute of Diabetes and Digestive and Kidney Diseases.

Results: 69% of the included 151 patients were male. The median (Q1, Q3) age and BMI were 50 (47, 55) years and 29.3 (26.7, 32.6) kg/m², respectively. 47 (31%) of the patients had a liver related outcome over median follow-up (Q1, Q3) of 755 days (371, 1098). PRO-C6 was significantly elevated at baseline in patients who had a liver-related event ($p = < 0.001$). When stratifying the patients above and below the cut-off of 15 ng/ml (high versus low level), the hazard ratio for having a liver related outcome was 3.56 times higher (SD = 0.30, 95% CI = [1.48, 5.52], $p = < 0.001$) in the group with high serum PRO-C6 at baseline, compared to low serum PRO-C6.

Conclusion: PRO-C6, a biomarker of circulating endotrophin was associated with an increased risk of developing a liver-related event, in cirrhotic patients with chronic hepatitis C (CHC). PRO-C6 may be a potential monitoring blood-based marker that may provide prognostic information on cirrhosis patients at higher risk of developing a liver-related event. Comparison with other collagen neo-epitopes and clinical outcome predictor models is ongoing, but validation of PRO-C6 as prognostic marker following sustained virologic response in CHC, and for other compensated advanced chronic liver disease is still required.

FRI-028

Spleen stiffness measurement improves non-invasive prediction of clinically significant portal hypertension in patients with compensated advanced chronic liver disease of mixed etiology

Giulia Francesca Manfredi^{1,2}, Angelo Strada¹, Mattia Lotto¹, Valentina Romano¹, Vincenzo Bonafede³, Michela Burlone⁴, Rosalba Minisini³, Mario Pirisi¹, Cristina Rigamonti¹. ¹Department of Translational Medicine, Università del Piemonte Orientale and Division of Internal Medicine, AOU Maggiore della Carità, Novara, Italy; ²Department of Surgery and Cancer, Imperial College London, Hammersmith Hospital, Du Cane Road, London, United Kingdom; ³Department of Translational Medicine, Università del Piemonte Orientale, Novara, Italy; ⁴Division of Internal Medicine, AOU Maggiore della Carità, Novara, Italy
Email: cristina.rigamonti@uniupo.it

Background and aims: Recently, non-invasive assessment of clinically significant PH (CSPH) in compensated advanced chronic liver disease (cACLD) has been refined by adding spleen stiffness measurement (SSM) to liver stiffness measurement (LSM). We aimed at evaluating the role of SSM in patients with cACLD of mixed etiology in identifying CSPH.

Method: Monocentric prospective study of 149 patients with cACLD (defined as LSM ≥ 10 kPa) out of 309 who consecutively underwent both liver stiffness measurement (LSM) and SSM by vibration-controlled transient elastography (FibroScan[®] 630, Echosens, Paris) at University Hospital in Novara between December 2023 and November 2023. Esophagogastroduodenoscopy (EGDS) was performed according to Baveno VI guidelines and in all patients with SSM >40 kPa. The Baveno VII criteria (BVII) for assessing CSPH using LSM alone [LSM ≤ 15 kPa + platelets (PLTs) $\geq 150000/\text{mmc}$ to rule out CSPH; LSM >25 kPa to rule in CSPH] were compared with the BVII for CSPH incorporating both LSM and SSM (at least 2 out of 3 between LS ≤ 15 kPa, PLTs $\geq 150000/\text{mmc}$, SSM ≤ 40 kPa to rule out CSPH; at least 2 out of 3 between LS >25 kPa, PLT $<150000/\text{mmc}$, SSM >40 kPa to rule in CSPH) to evaluate their ability to identify patients with CSPH.

Results: Among the 149 patients, etiology of liver disease was viral hepatitis (16%), alcohol (31%), metabolic associated steatotic liver disease (15%) or cholestatic/autoimmune disease (21%) or mixed (17%). Eighty-nine were male (60%), median age was 66 years (IQR 22–86), median LSM 19.5 kPa (IQR 13.7–31.7), median SSM 43.6 kPa (IQR 29.5–54.8), median platelet count 128000/mmc (IQR 90000–173000/mmc), median albumin 4.1 g/dl (IQR 3.8–4.4), median total bilirubin 1.1 mg/dl (IQR 0.8–1.8). Sixty-four (43%) patients had any size varices, 18 (12%) had high-risk varices. Considering the BVII assessing only LSM, 21 patients (14%) belonged to rule out zone for CSPH, 51 (34%) belonged to rule in zone, 77 (52%) were in the grey zone. According to the BVII incorporating both LSM and SSM, 45 patients (30%) belonged to rule out zone for CSPH, 53 patients to rule in (35%), while 51 patients (34%) belonged to the grey zone. Diagnostic performance of BVII with LSM alone was: sensitivity 94% (LR- 0.31) for ruling out CSPH and specificity 70% (LR 1.38) for ruling in CSPH. Diagnostic performance of BVII for CSPH incorporating both LSM and SSM was sensitivity 87% (LR- 0.29) for ruling out CSPH and specificity 71% (LR 1.49) for ruling in CSPH. SSM ≤ 40 kPa alone identified patients without any size varices with 80% sensitivity (LR- 0.38) and those without high-risk varices with 89% sensitivity (LR- 0.26).

Conclusion: The combined use of SSM with LSM helped in reducing the proportion of patients in the grey zone for ruling in and ruling out CSPH. Moreover, SSM ≤ 40 kPa alone confirmed its potential role in excluding CSPH in cACLD patients.

FRI-029

Shear wave elastography predicts risk categories in patients with cirrhosis, PANDORA study

Jorge Poo¹, José Raúl Izaguirre², Frida Gasca-Díaz¹, Juan Ramón Aguilar¹, Carlos Ramírez-Castillo¹, Javier Lizardi¹,

Juan Francisco Rivera-Ramos¹, Juan Alfredo Tamayo¹, Carina Zapata², Carolina Treviño-García², Miroslava Hernández², Ilsa López², Graciela Tapia³, Paula Cordero-Pérez², Linda Elsa Muñoz-Espinosa². ¹Grupo Mexicano para el Estudio de las Enfermedades Hepáticas, Ciudad de México, Mexico; ²Hospital Universitario "Dr. José E. González," UANL, Monterrey, Nuevo León, Mexico; ³Facultad de Medicina Veterinaria y Zootecnia, Universidad Nacional Autónoma de México, Ciudad de México, Mexico

Email: consultorio.jpoo@gmail.com

Background and aims: Several non-invasive studies have demonstrated a good correlation between hepatic and/or splenic elastography values and risk categories, including the size of esophageal varices (EV). However, few Latin American studies have described their experience with this non-invasive methodology. The objective was to evaluate the predictive value of shear wave elastography (SWE) to identify patients with cirrhosis and different risk categories related to esophageal varices, Child-Pugh liver function class and/or type of hepatic decompensation.

Method: 3016 patients were evaluated (site 1 = 1606, site 2 = 1410); 137 participants with IQR/median values $>30\%$ were excluded (4.5%); the remaining 2879 subjects had a mean age of 57 ± 14 years; 57% were women; 307 were F0 as a control group (10.7%), 1224 with chronic liver disease F1–F3 (42.5%) and 1348 with cirrhosis (46.8%); the etiology was metabolic in 45.9%, HCV 19.0%, AILD 19.6%, alcohol related 11.4%, HBV 2.1%, DILI 1.0% and idiopathic 0.9%. 2D SWE was evaluated with an Aixplorer ultrasound (Supersonic Imagine) with an SXC 6–1 convex transducer using shear wave (SW) technology. Median and IQR measurements were obtained and the degree of liver stiffness was estimated according to a semiquantitative system. The reliability criterion of SWE was IQR/median less than 30%. In patients with cirrhosis, Child-Pugh and MELD were calculated and endoscopy was performed and EV was classified according to Baveno 7 criteria. Non-parametric Kruskal-Wallis and Mann-Whitney U tests and linear regression were used.

Results: Stiffness scores (median \pm SE (kPa)) were lower in the control group (4.3 ± 0.03) and in patients with chronic liver disease (7.6 ± 0.05) than in patients with cirrhosis (34.8 ± 0.53 , $p < 0.001$) and the following differences were found using Child-Pugh Category: A (22.3 ± 0.7), B (37.2 ± 1.2), C (49.5 ± 2.6) ($p < 0.001$). Cirrhotic patients with and without the following categories of decompensation were significantly different: variceal hemorrhage (39.8 ± 1.8 vs. 29.1 ± 0.9 , $p < 0.05$); ascites (41.7 ± 1.3 vs. 23.1 ± 0.7 , $p < 0.001$); encephalopathy (40.8 ± 2.0 vs. 25.7 ± 0.7 , $p < 0.001$), liver cancer (49.5 ± 4.6 vs. 27.3 ± 0.6 , $p < 0.05$), respectively. Liver stiffness was also different according to endoscopic findings: without EV 16.5 ± 0.4 , small EV 24.0 ± 1.3 , and large EV 32.1 ± 1.6 kPa ($p < 0.001$), and significantly correlated with Child-Pugh score, ascites, and BMI ($r = 0.45$, $p < 0.001$).

Conclusion: The shear wave elastography methodology clearly identifies patients with different risk categories, whether related to liver function, type of liver decompensation or size of esophageal varices, which could be an excellent diagnostic support tool in outpatient clinics dedicated to liver care.

FRI-030

Evaluation of aspartate aminotransferase to platelet ratio index and fibrosis-4 index stabilization in the phase 3 POISE trial of obeticholic acid for the treatment of primary biliary cholangitis

Alan Bonder¹, Darren Wheeler², Jing Li², Christopher Gasink², Robert G. Gish³. ¹Division of Gastroenterology and Hepatology, Beth Israel Deaconess Medical Center, Harvard Medical School, Boston, United States; ²Intercept Pharmaceuticals, Inc., Morristown, United States; ³Robert G. Gish Consultants, LLC, San Diego, United States
Email: abonder@bidmc.harvard.edu

Background and aims: Recent studies suggest that APRI and FIB-4 index predict fibrosis progression in liver disease, but these measures have not been validated in patients (pts) with primary biliary cholangitis (PBC). Obeticholic acid (OCA) was approved for the

POSTER PRESENTATIONS

treatment of PBC based on biomarker improvement in POISE, a 12-month randomized, double-blind (DB), placebo (PBO)-controlled phase 3 study. Here, we report the results from a post-hoc analysis of the impact of OCA on APRI and FIB-4 index in pts from the POISE study.

Method: In the DB phase of POISE, pts with PBC who were intolerant of or had an inadequate response to first-line ursodeoxycholic acid were randomized to receive PBO, OCA 5–10 mg (OCA titration), or OCA 10 mg daily. During the 5-year open-label extension (OLE), all pts were initially treated with OCA 5 mg daily for 3 months, after which the dose could be titrated based on response and tolerability. APRI and FIB-4 were calculated at baseline (BL) and each year during the DB phase and OLE, including based on low vs high BL APRI (<0.5 vs ≥ 1.5) or FIB-4 (<1.45 vs ≥ 2.67). Summary statistics for APRI and FIB-4 for all pts who received OCA (≤ 10 mg), either in the DB phase or OLE, were generated starting from OCA initiation.

Results: In the DB phase, mean APRI scores increased in the PBO group for pts with low or high APRI at BL (0.37 at BL [n = 15] vs 0.38 [n = 15] at month 12 and 2.76 at BL [n = 12] vs 3.37 at month 12 [n = 11], respectively) but decreased in the OCA 5–10 mg group for pts with low or high APRI at BL (0.37 at BL [n = 10] vs 0.32 [n = 10] at month 12 and 2.50 at BL [n = 14] vs 2.16 at month 12 [n = 14], respectively). Mean FIB-4 increased in the PBO group for pts with low or high FIB-4 at BL (1.04 at BL [n = 32] vs 1.22 [n = 31] at month 12 and 4.62 at BL [n = 16] vs 5.43 at month 12 [n = 15], respectively). FIB-4 values in the OCA 5–10 mg group were lower than those in the PBO group at the end of the DB phase for pts with low or high FIB-4 at BL (1.08 at BL [n = 30] vs 1.04 [n = 26] at month 12 and 4.20 at BL [n = 15] vs 4.60 at month 12 [n = 14], respectively). Among OCA-treated pts with low BL APRI, mean APRI scores were 0.39 at BL (n = 45) and 0.36 at month 60 (n = 23). In OCA-treated pts with high APRI at BL, mean APRI scores were 2.74 at BL (n = 35) and 2.48 at month 60 (n = 15). In OCA-treated pts with low FIB-4 at BL, mean FIB-4 values were 1.06 at BL (n = 91) and 1.20 at month 60 (n = 41). In OCA-treated pts with high FIB-4 at BL, mean FIB-4 values were 4.45 at BL (n = 45) and 5.65 at month 60 (n = 20). The sample size for APRI and FIB-4 substantially decreased at month 72, limiting interpretability of the data at this time point.

Conclusion: The data suggest that OCA prevents fibrosis or mitigates worsening of fibrosis in pts with no or low risk at BL through the surrogates APRI and FIB-4, and OCA stabilized fibrosis during the OLE in pts with moderate-to-severe fibrosis at BL. The findings imply that it may be beneficial to treat pts with OCA early before PBC progresses and risk of fibrosis increases.

FRI-033

Enhancing MRCP precision: a comprehensive analysis of intramuscular glucagon administration impact on biliary visualization

Fadi Abu Baker¹, Oren Shibolet², Mohamad Garra¹, Randa Taher¹, Amani Beshara¹, Saif Abu Mouch¹, Michael Oster¹, Abdel-Rauf Zeina¹.

¹Hillel Yaffe medical center, Hadera, Israel; ²Tel Aviv medical center, Tel Aviv, Israel

Email: Fa_fd@hotmail.com

Background and aims: Magnetic resonance cholangiopancreatography (MRCP) has continuously evolved to enhance visualization capabilities, yet the diagnosis of primary sclerosing cholangitis (PSC) remains challenging, especially in its early stages. This study explores the impact of intramuscular glucagon (IMG) administration on final image quality and biliary ductal system diameter in MRCP.

Method: Forty patients (57.5% female; average age 34.45 ± 8.2) with suspected inflammatory bowel disease (IBD) referred for Magnetic Resonance Enterography (MRE) underwent MRCP before and 8–12 minutes after IMG administration. Coronal T2-weighted fast spin-echo high-resolution 3D MRCP images were analyzed quantitatively and qualitatively by two independent MRI specialists. Quantitative assessments included measurements of predefined biliary ductal

segments (distal, mid, and proximal common bile duct (CBD), right hepatic duct (RHD), left hepatic duct (LHD), and gallbladder volume). Qualitative evaluation used a five-point Likert-type scale (1 = perfect visualization; 5 = not visible). Interobserver variation was assessed using Intraclass Correlation Coefficient (ICC) and R-Pearson correlation.

Results: IMG administration led to significant increases in mean bile duct diameters compared to pre-injection. Combined pre- and post-IMG mean diameters were: distal CBD (3.079 ± 1.16 vs. 3.621 ± 1.05), Mid CBD (3.596 ± 1.46 vs. 4.207 ± 1.41), proximal CBD (3.736 ± 2.23 vs. 4.283 ± 1.90), RHD (2.227 ± 1.25 vs. 2.953 ± 0.91), and LHD (2.672 ± 1.30 vs. 3.392 ± 0.81). The differences were statistically significant ($p < 0.01$) for all measurements. Interobserver agreement was strong (ICC 0.798 to 0.931, R 0.731 to 0.939).

IMG administration improved visualization scores significantly (2.65 ± 0.80 vs. 1.67 ± 0.68 ; $P < 0.01$), with a moderate-strong interobserver agreement (ICC 0.655 to 0.829). Additionally, IMG increased gallbladder volume (20.45 ml pre-IMG vs. 38.81 ml post-IMG; $P < 0.01$). Two PSC-associated biliary duct changes showed significant improvement post-IMG.

Conclusion: IMG administration enhances MRCP imaging parameters, increasing ductal diameters, improving biliary tree visualization, and aiding in the detection of associated pathologies, emphasizing its potential utility in early and improved PSC detection.

FRI-034

Radiomics based on MRI for predicting microvascular invasion at edge of hepatic alveolar echinococcosis

Wenya Liu¹. ¹The First Affiliated Hospital of Xinjiang Medical University, Urumqi, China

Email: 13999202977@163.com

Background and aims: To observe the value of radiomics model based on MR T2WI for predicting microvascular invasion at the edge of hepatic alveolar echinococcosis (HAE).

Method: Preoperative MRI data of 89 patients with HAE confirmed by pathology after surgical resection were retrospectively analyzed, including 32 cases with and 57 without microvascular invasion at the lesions edges. Then radiomics features of lesions were extracted based on T2WI, and both variance selection method and univariate selection method were used for screening the optimal features. Three classifiers, including random forest (RF), extreme gradient enhancement tree (XGBoost) and Logistic regression (LR) were used to construct machine learning (ML) models for predicting microvascular invasion at the edge of HAE lesions. Then 89 patients were divided into training set (n = 70) and test set (n = 19) at the ratio of 8:2. The corresponding receiver operating characteristic (ROC) curves were drawn, and the areas under the curves (AUC) were calculated, and the predictive performance of each ML model was observed.

Results: A total of 1409 radiomic features were extracted, and 7 optimal radiomic features were screened out by feature dimension reduction to construct machine learning models. ROC curve showed that XGBoost model performed well in both training set and testing set, with AUC of 0.96 and 0.89, respectively.

Conclusion: Radiomics XGBoost ML model based on MR T2WI could effectively predict microvascular invasion at the edge of HAE lesions.

FRI-035

Development of a non-invasive machine learning-based model for predicting hepatic steatosis in patients with chronic hepatitis B

Zhiyi Zhang¹, Li Zhu², Yiguang Li³, Jian Wang^{4,5}, Shaoqiu Zhang⁴, Fei Cao¹, Juan Xia⁴, Renling Yao⁴, Xingxiang Liu⁶, Jie Li^{1,4,5}, Chuanwu Zhu², Yuanwang Qiu³, Rui Huang^{1,4,5}, Hao Wu^{1,4,5}.

¹Department of Infectious Diseases, Nanjing Drum Tower Hospital Clinical College of Nanjing University of Chinese Medicine, Nanjing, China; ²Department of Infectious Diseases, The Affiliated Infectious Diseases Hospital of Soochow University, Suzhou, China; ³Department of

Infectious Diseases, The Fifth People's Hospital of Wuxi, Wuxi, China;
⁴*Department of Infectious Diseases, Nanjing Drum Tower Hospital, Affiliated Hospital of Medical School, Nanjing University, Nanjing, China;*
⁵*Institute of Viruses and Infectious Diseases, Nanjing University, Nanjing, China;*
⁶*Department of Clinical Laboratory, Huai'an No. 4 People's Hospital, Huai'an, China*
 Email: dr.wu@nju.edu.cn

Background and aims: The incidence of chronic hepatitis B (CHB) combined with hepatic steatosis (HS) is increasing. However, the screening of individuals using liver biopsy and expensive imaging modalities does not appear to be cost-effective for most primary hospitals. This study aimed to develop a non-invasive machine learning-based model for predicting HS in treatment-naïve CHB patients.

Method: Eight hundred and fifty consecutive CHB patients who underwent liver biopsy from four medical centers were retrospectively included. HS was assessed by Brunt classification. The patients were randomly divided into a training set and a test set with a ratio of 7:3. Nine machine learning (ML) models were built, including logistic regression, support vector machine, k-nearest neighbors, random forest (RF), extreme gradient boosting, gradient boosting, adaboost, decision tree, and naive bayes. The best model was selected based on the highest area under the receiver operating characteristic curves (AUC). The performance of the selected model was compared with the hepatic steatosis index (HSI). SHapley Additive exPlanation (SHAP) analysis was used for model explanation.

Results: The median age was 40.0 years and male gender accounted for 63.3%. Among the nine models, RF exhibited a superior predictive performance with an AUC of 0.810 (95% confidence interval: 0.739–0.881) in the test set, significantly higher than HSI (AUC: 0.659, $p = 0.003$). The decision curve analysis showed that the net benefit of the RF model surpassed HS under a wide range of threshold probabilities. SHAP analysis lists the feature importance ranking, and serum uric acid was the most important predictive variable of HS.

Conclusion: This study developed a novel cost-effective, non-invasive RF model to evaluate the presence of HS, which can be used as a promising tool to identify HS in patients with CHB, especially in primary hospitals.

THURSDAY 06 JUNE

Nurses and Allied Health Professionals

THU-008

Does the use of liver frailty index in liver transplant assessment aid clinical decision making and correlate with patient outcomes?

Thomas Crame¹, Rachel Edwards¹, Rachel Howarth¹, Rachel Thomson¹, Emily Bonner¹, Preya Patel². ¹*Liver Unit, Freeman Hospital, The Newcastle upon Tyne Hospitals NHS Foundation Trust, Newcastle Upon Tyne, United Kingdom;* ²*Liver Unit, Freeman Hospital, The Newcastle upon Tyne Hospitals NHS Foundation Trust, Newcastle upon Tyne, United Kingdom*
 Email: thomas.crame1@nhs.net

Background and aims: Frailty is associated with adverse outcomes in cirrhosis and liver transplantation (LT) and has an independent association with mortality. EASL guidelines recommend measurements of frailty, in addition to sarcopenia, when assessing patients with chronic liver disease. The Liver Frailty Index (LFI) is widely used in patients being assessed for LT. We aimed to review the use of LFI in liver transplant assessments at our institution, its role in clinical decision making and correlation with patient outcomes.

Method: A retrospective review of a prospectively maintained database of liver transplant assessments performed at a single liver unit (Freeman Hospital, Newcastle Upon Tyne, UK) was undertaken. Combined organ and super urgent transplants were excluded from analysis. Dietetic assessment of patients included anthropometry, SARC-F (Strength, Assistance in walking, Rise from a chair, Climb stairs, and Falls) and LFI which incorporates 3 measurements: balance, hand grip strength and five timed chair stands.

Results: 268 individuals were assessed by a specialist dietitian between 19/9/2019 to 30/11/23. The median age was 59 years (range 19–73) and 66.8% were male. The predominant aetiologies were alcohol-related liver disease (40%) and metabolic dysfunction-associated steatotic liver disease (MASLD) (24%). On the LFI, 10.9% were classified as robust, 76.4% were pre-frail, and 12.7% were frail. There was a significant, moderately negative correlation between LFI and anaerobic threshold (Spearman's Rho -0.351 $p < 0.001$), and a moderately positive correlation between SARC-F and LFI (Spearman's Rho 0.465 $p < 0.001$). 121 patients were listed for liver transplant with 90 undergoing transplant in the follow-up period. According to LFI, frail patients were significantly less likely to be listed for transplant (5%) compared to robust patients (14.9% $p < 0.001$). Post liver transplant, those classed as pre-frail had a longer time to discharge (mean 18.43 days ± 11.6 days) than those who were robust (mean 14.5 ± 5.1 days), however this was not statistically significant ($p = 0.231$).

Conclusion: LFI has added depth to liver transplant assessment at our institution. LFI correlates well with other commonly used pre transplant assessments of sarcopenia and anaerobic threshold testing. Our data corroborates published data supporting LFI as an effective tool to predict liver transplant outcomes, including likelihood of being listed for transplant and duration of post transplant inpatient stay. Further work is needed to assess whether targeted interventions to optimise patients pre transplant LFI could improve post transplant outcomes.

THU-009

Implementation of food insecurity screening within outpatient hepatology services: a clinical audit

Rachel Howarth¹, Thomas Crame¹, Stuart McPherson^{1,2}, Quentin M. Anstee^{1,2}, Laura Haigh^{1,2}. ¹*Newcastle NIHR Biomedical Research Centre, Newcastle upon Tyne Hospitals, NHS Trust, Newcastle upon Tyne, United Kingdom;* ²*Translational and Clinical Research Institute, Faculty of Medical Sciences, Newcastle University, Newcastle upon Tyne, United Kingdom*
 Email: racheljean.howarth@nhs.net

Background and aims: Liver disorders disproportionately affect the most economically disadvantaged, exacerbating health inequalities. Across Europe, the prevalence of food insecurity (FI) has increased by 130% since 2019, affecting 8.2% of the general population. Evidence indicates a paradox wherein FI contributes to both obesity and compromised nutritional status. FI may also influence the adoption of recommended diet lifestyle advice. We aimed to assess the extent of FI and its associated factors among patients with liver disease in a northern European population.

Method: A prospective audit was undertaken assessing consecutive patients attending hepatology outpatient services between October to December 2023. Food security status was assessed using validated tools (Hunger Vital Signs Two-Item Screener and United States Department of Agriculture, Food and Nutrition Service Six-Item Food Security Survey). Brief advice/signposting was offered to individuals identified as food insecure. Descriptive statistics were conducted, and Chi-square or Fisher's exact tests were performed, as appropriate.

Results: 227 patients (mean age 59 years [range 25–85]; 56% male and 80% white British) completed FI screening. Metabolic dysfunction-associated steatotic liver disease (MASLD) (46%) predominated, followed by alcohol-related liver disease (16%), viral hepatitis (16%) and other diagnoses (17%). 50 patients (22%) were identified as food

POSTER PRESENTATIONS

insecure. Comparing food insecure and secure groups, FI was more prevalent in those with MASLD (52% vs 45%, $p=0.036$), type 2 diabetes (56% vs 41%, $p=0.002$), hypertension (58% vs 53%, $p=0.04$), depression (22% vs 11%, $p=0.012$), mixed anxiety and depression (20% vs 12%, $p=0.04$) and psoriasis (18% vs 10%, $p=0.037$). No significant differences were observed between groups in relation to age, gender, ethnicity, smoking status, presence of cirrhosis, HbA1c, alcohol intake or body mass index.

Conclusion: FI was higher amongst patients with liver disease attending hepatology outpatient services than in the background population, and our results suggest that FI was associated with MASLD and metabolic syndrome features. FI presents an important barrier to implementation of diet lifestyle advice. Healthcare professionals should consider FI within holistic patient assessment to optimise outcomes and attenuate inequalities.

THU-010

Screening for liver disease in alcohol use disorder-is it worthwhile?

Marie Archibald¹, Lynsey Corless¹, Thomas Phillips². ¹Hull University Teaching Hospitals, Hull, United Kingdom; ²University of Hull, Hull, United Kingdom

Email: lynsey.corless@nhs.net

Background and aims: Alcohol Use Disorder (AUD) is a major risk factor for alcohol-related liver disease (ArLD). Screening for ArLD in AUD may offer an opportunity for earlier detection or intervention. We sought to determine the burden of liver disease in a cohort of patients with suspected AUD referred for assessment to our hospital Alcohol Care Team (ACT).

Method: Universal screening for AUD is performed for all admissions to our hospital using electronic entry of FAST (modified AUDIT) score alongside initial observations. ACT referrals are generated automatically on a virtual dashboard for FAST 5+ (i.e. possible alcohol dependence), or if a person is already known to ACT. Referrals can also be made where staff suspect AUD regardless of FAST. Following review, Enhanced Liver Fibrosis (ELF) test is advised for those with suspected AUD followed by Transient Elastography (TE) for those with non-reassuring result. We performed a case note review to identify the proportion of those with AUD who ultimately required 2-stage fibrosis testing, severity of ArLD identified, and reason for admission.

Results: All unique admissions referred to ACT from 1/11/22 to 30/6/23 were reviewed ($n=857$). 112 (13.1%) required 2-stage fibrosis assessment and were further analysed. The cohort was 63.4% male, mean age 56 (23–82)-representative of our AUD population. Mean FAST score was 9.4 (SD 5.1), indicating high levels of alcohol dependence. There was no direct correlation between FAST score and ArLD stage by ELF/TE, suggesting alcohol severity does not reliably predict ArLD severity. Mean ELF was 10.1 (7.7–17.2), and was >9.8 in 51.8% ($n=58$), demonstrating a high level of suspected advanced ArLD in the cohort. Mean TE was 11.3 (2.2–75 kPa). 38.4% ($n=43$) had abnormal TE (>7 kPa), with 24 (21.4%) suggestive of advanced fibrosis (>11 kPa). 62% of the group had normal TE, emphasising the opportunity ACT can offer for ArLD prevention, even in severe AUD. The 20.1% ($n=23$) admitted primarily due to alcohol were younger (mean age 52.8 vs 56) with higher FAST (11 vs 9.4), but there was no significant difference in ArLD severity versus rest of cohort. 53.6% ($n=60$) were admitted for non-alcohol/gastroenterology reasons and were identified at risk of ArLD only as a result of universal screening. Most frequent reasons for admission were falls ($n=17$; 15.8%) and abdominal pain ($n=13$; 11.6%) but we identified 19 admission triggers overall, including elective surgery.

Conclusion: We identified high rates of advanced ArLD in our AUD cohort, showing the potential value of screening in this group to give opportunities to modify ArLD trajectory via specialist AUD/ArLD management. As AUD severity did not directly correlate with ArLD extent, screening should be considered for all presenting with AUD.

Universal screening identified many people who would not otherwise have had ArLD screening or AUD support, and broader adoption should be encouraged.

THU-015-YI

Feasibility of a digital lifestyle intervention (VITALISE) to support self-management in patients with metabolic dysfunction-associated steatotic liver disease

Hollie Smith¹, Leah Avery^{1,2}, Stuart McPherson^{2,3,4}, Rebecca Livingston⁵, Kate Hallsworth^{2,3,4}. ¹Centre for Rehabilitation, School of Health and Life Sciences, Teesside University, Middlesbrough, United Kingdom; ²Translational and Clinical Research Institute, Faculty of Medical Sciences, Newcastle University, Newcastle upon Tyne, United Kingdom; ³NIHR Newcastle Biomedical Research Centre, Newcastle upon Tyne Hospitals NHS Foundation Trust, Newcastle upon Tyne, United Kingdom; ⁴Liver Unit, Newcastle upon Tyne Hospitals NHS Foundation Trust, Newcastle upon Tyne, United Kingdom; ⁵School of Social Sciences, Humanities and Law, Teesside University, Middlesbrough, United Kingdom

Email: h.a.smith@tees.ac.uk

Background and aims: Metabolic dysfunction-associated steatotic liver disease (MASLD) is defined as the presence of hepatic steatosis in conjunction with one cardiometabolic risk factor and no other discernible cause. MASLD is directly linked to overweight and obesity, often caused by dietary excess and inactivity/sedentary behaviour. Weight loss, achieved through lifestyle behaviour change, is the recommended management approach. However, many patients find this challenging. Using intervention mapping we developed a MASLD-specific digital intervention (VITALISE) with tele-coaching support to target changes in dietary and physical activity behaviours. This study aimed to assess the feasibility and acceptability of delivering VITALISE in routine secondary care.

Method: VITALISE is a single-centre, one-arm feasibility study for patients aged ≥ 18 with MASLD. Primary outcomes relate to feasibility (recruitment rate, intervention uptake, engagement/adherence, follow-up rate) and acceptability (patient views via semi-structured interview). Secondary outcomes include clinical measures (body weight, blood pressure, liver stiffness, lipid profile, liver enzymes, glycaemic control), non-invasive measures (QRISK3, FIB-4, NFS), physical activity levels (accelerometry) and patient empowerment (Patient Activation Measure (PAM)).

Results: From November 2022 to May 2023, 35/59 patients eligible to participate were recruited (recruitment rate 59%; mean age 54 ± 13 years; 69% male; 43% with Type 2 Diabetes). 29/35 activated their VITALISE account (intervention uptake 83%) and, of those, 22/29 provided data at 6-month follow-up (follow-up rate 76%; 3/29 patients awaiting follow-up). Interviews are underway, with early data ($n=12$) indicating acceptability of the intervention. There were significant improvements in body weight (-4.3 kg, $p<0.001$), liver stiffness (-3.7 kPa, $p=0.046$), liver enzymes (ALT -29.7 IU/L, $p=0.016$; AST -13.9 IU/L, $p=0.044$; GGT -21.1 IU/L, $p=0.040$) and HbA1c (-2.3 mmol/mol, $p=0.023$) from pre- to post-intervention. Blood pressure, lipid profile, and non-invasive measures did not significantly differ from pre- to post-intervention. Sedentary time significantly decreased (-332 mins/week, $p<0.001$), time spent in light exercise significantly increased ($+183$ mins/week, $p=0.002$) and time spent in moderate exercise showed no change (-5 mins/week, $p=0.443$) from pre- to post-intervention. Early indications of patient empowerment ($n=15$) show no change in PAM score or level from pre- to post-intervention.

Conclusion: Delivery of a digital lifestyle intervention for patients with MASLD in routine secondary care is feasible and acceptable. Significant reductions in body weight and improvements in liver health were achievable. These findings will be used to inform optimisation and larger-scale evaluation of VITALISE.

THU-016

A meta-ethnographic review of experiences and perceptions of physical activity and exercise in people with metabolic dysfunction-associated steatotic liver disease

Shelley Keating¹, Carla Dreyer¹, Kate Hallsworth^{2,3,4}, Jonathan Stine^{5,6,7,8}, Ingrid Hickman⁹. ¹The University of Queensland, School of Human Movement and Nutrition Sciences, Brisbane, Australia; ²Newcastle Upon Tyne Hospitals NHS Foundation Trust, NIHR Newcastle Biomedical Research Centre, Newcastle Upon Tyne, United Kingdom; ³Newcastle Upon Tyne Hospitals NHS Foundation Trust, Liver Unit, Newcastle Upon Tyne, United Kingdom; ⁴Newcastle University, Translational and Clinical Research Institute, Faculty of Medical Sciences, Newcastle Upon Tyne, United Kingdom; ⁵The Pennsylvania State University-, Milton S. Hershey Medical Center, Division of Gastroenterology and Hepatology, Department of Medicine, Hershey, United States; ⁶The Pennsylvania State University-, College of Medicine, Department of Public Health Sciences, Hershey, United States; ⁷The Pennsylvania State University-, Milton S. Hershey Medical Center, Liver Center, Hershey, United States; ⁸The Pennsylvania State University-, Milton S. Hershey Medical Center, Cancer Institute, Hershey, United States; ⁹The University of Queensland, The University of Queensland ULTRA Team, Clinical Trials Capability, Centre for Clinical Research, Herston, Australia
Email: s.keating@uq.edu.au

Background and aims: International guidelines have recently been published for physical activity (PA)/exercise in people with metabolic dysfunction-associated steatotic liver disease (MASLD), which have highlighted broad benefits for MASLD management. However, <20% of people with MASLD meet recommended PA targets. We aimed to review published data on the lived experiences and perceptions of PA and exercise in people with MASLD to inform strategies for increasing the uptake and adherence to exercise in clinical practice.

Method: A meta-ethnographic synthesis was utilised to systematically review articles published in English relating to the experiences and perceptions of PA/exercise in people with MASLD. Databases (PubMed, Embase, Web of Science) were searched from inception to November 2023. Two researchers (CD, SK) independently screened titles and extracted data. Data (study-level themes and subthemes) were coded, translated into third-order concepts, and themed using the validated Noblit and Hare model. Study quality was assessed using the Critical Appraisal Skills Programme checklist.

Results: A total of 1538 articles were screened, with seven studies included (n = 161 participants across six countries; mainly recruited via purposive sampling; overall study quality rated 'high'). Data collection was predominantly via semi-structured interviews and focus groups. Key findings encompassed barriers to PA/exercise uptake and maintenance including: lack of awareness of MASLD and its health impact, which lowered risk perception; lack of information provision regarding the role and importance of PA/exercise for MASLD management; lack of resources, tailored exercise plans or referrals to exercise professionals; multiple comorbidities and symptoms including obesity, musculoskeletal conditions, pain and fatigue; ambivalence of perceived exercise capabilities and low exercise-related self-efficacy; lack of time and competing priorities. Reported enablers of PA/exercise included: accountability to themselves (e.g., habit forming) and to the healthcare professional overseeing their care; social support from family, friends, and healthcare providers; the experience of symptom relief and holistic benefits.

Conclusion: This study translated firsthand experiences and perceptions of PA and exercise for people with MASLD. To improve uptake and maintenance of regular PA/exercise, interventions should focus on increasing awareness of MASLD and its impact on cardiometabolic and liver health and the role of exercise in its management. Appropriate referral to exercise professionals and logistical and behavioural support for personalised exercise care is critical for long-term adherence and sustainability of health benefit.

THU-017-YI

Development of a nurse-led out-patient service to support earlier diagnosis and management of liver disease

Amy Thatcher¹, Vernujaa Nagandiram¹, Vijay Grover¹. ¹The Hillingdon Hospital, London, United Kingdom
Email: amy.thatcher@nhs.net

Background and aims: Hillingdon Hospital is a district general hospital serving a population of 350, 000, with one consultant Hepatologist, two Clinical Nurse Specialists (CNS) and a junior Hepatology Assistant Practitioner (HAP). We streamlined processes for diagnosis and management of liver disease, with limited healthcare resources by using a blended workforce, seeking to minimise the number of formal consultant reviews.

Method: HAP employed in June 2023 with independent Fibroscan[®] clinics from August 2023. Data collected on suspected aetiology of liver disease, Fib4 score, Fibroscan result, Diabetic status and BMI for 523 patients attending a first out-patient appointment in the CNS/HAP clinic where a Fibroscan[®] was performed (March 2022–October 2023). Retrospective analysis of waiting times, compared three months prior and post-employment of a HAP. Outcomes analysed for patients who were independently reviewed by the HAP (with virtual oversight from Consultant/CNS).

Results: 85% of 523 referrals were received from General Practitioners (GP) and all non-invasive liver screens were reviewed by the Hepatologist or CNS prior to acceptance. 265 patients had Metabolic Associated Steatotic Liver Disease (MASLD). Fib4 scores triaged against local guidelines ('low' cut off <1.3). Advice is that patients with a Fib4 >1.3 are referred for a Fibroscan[®] for liver fibrosis assessment. However, some 'lows' were referred and accepted due to abnormal liver imaging- ultrasound suggesting coarse echotexture/nodular outline. Of these 265 patients, 67% were non-fibrotic (Fibroscan[®] <8.1 kPa), 19% fibrotic, 14% cirrhotic (>12 kPa). Of the 62 patients with MASLD and a low fib4 who were accepted for a Fibroscan[®], 22% had at least advanced liver fibrosis (Fibroscan[®] >8.1 kPa). Between August–October 2023, HAP reviewed 47 new patients independently, all patients received brief intervention. 49% patients with normal Fibroscans[®] were reassured and safely discharged back to GP at initial review, 47% required CNS follow-up and 2% required an interval Fibroscan[®] with HAP. Waiting times decreased from an average of 121 days in July 2023 prior to employment of HAP, compared to 48 days in November.

Conclusion: Implementation of an innovative service delivery model for Hepatology outpatients has led to faster diagnosis and access to specialty care, whilst reducing the need for formal consultant review. This model supports patients and clinicians to address and manage health issues at an earlier stage, ensuring appropriate and timely interventions to reduce complications. An interesting observation was that a cohort of MASLD patients with a low Fib4, had advanced liver fibrosis.

THU-020-YI

Evolution of health-related quality of life in liver transplantation patients in relation to acceptance and metabolic liver disease

Janne Suykens^{1,2}, Louis Onghena^{2,3,4,5}, Frederik Berrevoet⁵, Hans Van Vlierberghe^{2,3}, Xavier Verhelst^{2,3}, Sarah Raevens^{2,3}, Eric Hoste⁶, Sander Lefere^{2,3}, Anja Geerts^{2,3}, Carine Poppe^{2,6}. ¹Liver Research Center Ghent, Ghent University, Ghent University Hospital, Ghent, Belgium; ²Department of Internal Medicine and Paediatrics, Hepatology Research Unit, Ghent University, Ghent, Belgium; ³Liver Research Center Ghent, Ghent University, Ghent University Hospital, Ghent, Belgium; ⁴Department for Human Repair and Structure, Department of Gastrointestinal Surgery, Ghent University Hospital, Ghent, Belgium; ⁵Department of General and HPB Surgery and Liver Transplantation, Ghent University Hospital, Ghent, Belgium; ⁶Department of Transplantation, Ghent University Hospital, Ghent, Belgium
Email: janne.suykens@ugent.be

POSTER PRESENTATIONS

Background and aims: The parallel between obesity and metabolic dysfunction-associated steatotic liver disease (MASLD) is remarkable, with potentially harmful effects post-liver transplantation (LT). Illness cognitions regarding helplessness and acceptance are known to play a role in health-related quality of life (HRQoL) of LT patients. We aimed at investigating the evolution of these constructs in relation to specific indications for LT.

Method: A cohort of liver transplantation patients received follow-up from the moment of listing to two years post-LT. We used self-report questionnaires to measure HRQoL, illness cognitions (acceptance, helplessness, disease benefits), depression, anxiety, and stress respectively at different time frames: pre-LT, 1- and 2-years post-LT.

Results: The study included 56 patients with consecutive evaluations, 76.8% were male with a mean age of 51 ± 12.1 at time of diagnosis. Mental HRQoL (MQoL), acceptance and disease benefits increased significantly over time compared to pre-LT with significant attenuation of helplessness, depression, and stress. Alcohol-related liver disease (ALD) listed patients exhibited higher HRQoL, perceived disease benefits and acceptance pre-LT as well as attenuated levels of depression, anxiety, and stress post-LT_{1and2y}. Patients listed for MASLD exhibited significantly lower acceptance when compared to ALD and metabolic and ALD (metALD) listed patients ($p = 0.05$). Acceptance ($p = 0.015$) and MQoL ($p = 0.032$) were higher post-LT_{2y} when patients were transplanted due to ALD, contrary to MASLD transplanted patients.

Conclusion: Acceptance of health status in liver transplantation is dynamic and seems to be an important parameter for HRQoL and follow-up. Considering the hedonistic reflex involved in obesity, MASLD should not be underestimated as an indicative pathology of LT where acceptance of the disease and HRQoL is and remains low after LT, requiring broad preventive societal education and interventions focusing on coping strategies and illness cognitions.

THU-021

Outcomes from a nurse-led home-based care program for patients with liver cirrhosis

Catherine Yu¹, Kendall Fitzpatrick¹, Vanessa Lowen¹, Kristen Peake¹, Mayur Garg¹, Diana Lewis¹, Siddharth Sood¹. ¹Northern Health, Epping, Australia

Email: yucatherineyu@gmail.com

Background and aims: Hospitalised patients with cirrhosis have high readmission rates. Home-based nursing programs for conditions such as heart failure have shown reduced readmission rates, yet similar programs rarely exist for cirrhosis. Liver at Home (LAH) is a new, state-funded 3-month program providing at-home, liver specialist nurse-led care for cirrhotic patients following a hospital admission. Reviews occur in-person or via telehealth. We aim to demonstrate reduced readmission rates in enrolled patients for the duration of the program.

Method: Cirrhotic patients admitted under Gastroenterology were referred to LAH between 1/03/2023–31/09/2023. Patients with at least 90 days of follow-up were included. An admission within 7 days of discharge from the index admission was considered a failed discharge; admission between 8–90 days was considered a readmission. LAH patients were compared to referred, but non-enrolled patients (non-LAH) as an intention to treat analysis. Cox proportional hazard ratios were calculated for all-cause and liver-related first readmission.

Results: There were 27 LAH patients and 16 non-LAH patients ($n = 6$ declined, $n = 6$ resided outside hospital catchment areas, $n = 4$ other reasons). LAH and non-LAH patients were similar in age (59 v 62 years old, $p = 0.50$), gender (66.7% v 62.5% male, $p = 0.88$), cirrhosis aetiology (77.8% v 62.5% alcohol-related [$p = 0.29$]) and severity (median Child-Pugh score: 8 v 8). LAH patients had a similar risk of all-cause readmission compared to non-LAH (40.7% [$11/27$] v 56.3% [$9/16$] respectively; HR 0.68 , 95% CI = 0.28 – 1.6 [$p = 0.38$]). LAH patients appeared less likely to have liver-related admissions in the

first 90 days compared to non-LAH patients (25.9% [$7/27$] v 50% [$8/16$] respectively, HR 0.47 95% CI = 0.17 – 1.30 [$p = 0.14$]). There were a total 10 liver-related admissions for LAH patients and 13 liver-related admissions for non-LAH patients. Infection and hepatic encephalopathy were the main reason for LAH patient admissions, though this was not significantly different to non-LAH patients (Infection: 50% [$5/10$] in LAH v 7.7% [$1/13$] in non-LAH, $p = 0.05$; Hepatic encephalopathy: 30% [$3/10$] v 15.4% [$2/13$], $p = 0.6$). There were no admissions for ascites in the LAH group ($0/10$ v 38.5% [$5/13$], $p = 0.04$). Other causes of readmission in non-LAH group were too low to accurately perform statistical analysis.

Conclusion: Cirrhotic patients enrolled in a 3-month liver specialist nurse-led, at-home care program had a trend towards being less likely to be readmitted for a liver-related reason. No LAH patients were readmitted for ascites, suggesting a primary benefit of the program in managing fluid balance. More data will be required to evaluate program success rates in preventing readmissions.

THU-022

Impact of a joint clinical nurse specialist and dietitian clinic on health related quality of life outcomes for patients with decompensated liver disease

Leah Cox¹, Katie Ballesteros¹, Vikram Sharma¹. ¹Royal London Hospital, Barts Health NHS Trust, London, United Kingdom

Email: leah.cox3@nhs.net

Background and aims: It is well documented that chronic liver disease, particularly decompensated liver disease is associated with poor health related quality of life (HrQoL). A joint Clinical Nurse Specialist (CNS) and Dietitian outpatient clinic was established to provide holistic advice for patients with decompensated liver disease. The interventions provided included disease education, diuretic management, medication review and nutritional assessment. Patients requiring support with alcohol abstinence were referred to the Alcohol Care Team. We aimed to review the clinical outcomes and patient reported HrQoL for patients who attended a newly established joint CNS and Dietitian outpatient clinic.

Method: HrQoL was assessed using the Eq5D-5L questionnaire. All patient's HrQoL was assessed on initial assessment, and repeated at a time frame between 4–6 months. Clinical outcomes were assessed at the same time frame. All patients included in this review attended at least 3 appointments over a 4–6 month period.

Results: The aetiology of liver disease was 82% alcohol related, 9% metabolic dysfunction-associated steatohepatitis, 9% cryptogenic. 55% were males. 27% were Asian and 50% Caucasian. 23% were from other ethnic backgrounds. The median age was 60. Ascites was the main cause of decompensation for 82%. 86% were managed with diuretics. 27% required enteral feeding for nutritional optimisation. 75% had a Child Pugh score of B. The mean MELD score was 12.5. The average number of appointments attended was 3.8. Due to improved nutritional status, 27% re-compensated and did not require a TIPSS procedure as previously planned. 9% are now optimised for consideration for liver transplantation. 13% are now palliative and for conservative management. A comparison of baseline HrQoL scores compared to review at 4–6 months demonstrated an improvement for the majority of patients. 42% had improved mobility, 63% had improved ability to wash and dress themselves, 57% had improved ability to carry out usual activities, such as working and shopping, 68% reported improvement in pain and discomfort and 57% reported improvement in anxiety and depression. Average overall HrQoL scores improved from an average of 48% to 68% over a 4–6 month period. 32% of patients reported an overall improvement in HrQoL of between 30–55%.

Conclusion: A combined nursing and dietetic outpatient review has demonstrated the ability to improve clinical outcomes for patients with decompensated liver disease, in particular inducing recompensation with diuretic management, nutritional optimisation and abstinence support. Close monitoring, and a combined, holistic

assessment has also proven beneficial for patients in relation to HrQoL scores. Analysis should be undertaken to evaluate the cost-effectiveness of this specialist multi-disciplinary clinic as part of a hepatology outpatient service.

THU-027-YI

A pilot pharmacist led carvedilol titration service leads to sustained doses of high dose carvedilol in patients with clinically significant portal hypertension

Yun Jung Kim¹, Din He Tan^{2,3,3}, Kathryn L Nash⁴, Salim I Khakoo⁵, Mark Wright⁴, Ryan M Buchanan⁶. ¹University Hospital Southampton NHS Foundation Trust, Pharmacy, Southampton, United Kingdom; ²University of Southampton, Southampton, United Kingdom; ³University of Southampton Highfield Campus, Medical Student BM5, Southampton, United Kingdom; ⁴University Hospital Southampton NHS Foundation Trust, Southampton, United Kingdom; ⁵University of Southampton, School of Clinical and Experimental Sciences, Faculty of Medicine, Southampton, United Kingdom; ⁶University of Southampton, School of Primary Care, Population Sciences, and Medical Education, Faculty of Medicine, Southampton, United Kingdom
Email: yun.kim@uhs.nhs.uk

Background and aims: Non-selective beta blockers (NSBBs) reduce the risk of hepatic decompensation in patients with cirrhosis and clinically significant portal hypertension (CSPH). However, prescribed doses in real-world practice are frequently below those used in clinical studies and sub-therapeutic doses risk beneficial effects not manifesting as improved clinical outcomes for patients. To address this implementation challenge, we set up a pharmacist led supervision service to initiate and carefully titrate carvedilol to therapeutic doses.

Method: Eligible patients included those meeting the Baveno VII criteria for CSPH without contraindications to NSBB who were on a dose of carvedilol of <25 mg per day. Patients who needed NSBB as secondary prophylaxis for variceal haemorrhage or with decompensated liver disease (defined as Child-Pugh (CP) >B7 or C) were not eligible and remained in the consultant led service. Patients were seen at a single face to face appointment where eligibility was confirmed or reassessed. Blood pressure (BP) and pulse were measured. Patients were followed up with 1–2 weekly telephone calls to assess adverse events and review ambulatory BP and pulse monitoring results. Statistical analysis was performed using Wilcoxon signed-rank test and paired t-test.

Results: In 12 weeks (September to December 2023) 29 patients were reviewed face to face at a community hepatology clinic in Southampton (UK). Mean Age was 59 (standard deviation 11), 69% were male, and MASLD was the most common underlying aetiology (58%). All patients met criteria for CSPH with the following biochemical values (mean \pm SD): platelet count ($157.2 \pm 75.3 \times 10^9/L$), liver stiffness (37.7 ± 22.8 kPa), ELF (11.4 ± 1.1). 4 (14%) were CPB7 the remainder were CPA. 22 (76%) completed dose optimisation. Median time to maximum tolerated dose was 2 weeks (range 1–6). Median dose at the first appointment was 6.25 mg (range, 0–25 mg) with 10 (38%) not taking any carvedilol as baseline. Only 1 (3%) was not started on carvedilol due to a persistently low pulse <55 beats per minute. Post follow-up dose (median = 25 mg, range 6.25–25 mg), was significantly higher than pre-intervention dose (median = 6.25 mg, range 0–25 mg) (Wilcoxon, $p < 0.001$). No significant change was observed for mean arterial pressure ($p = 0.13$) or pulse rate ($p = 0.162$) before and after dose optimisation. 4 experienced fatigue, but no significant adverse events requiring treatment cessation occurred.

Conclusion: Our pharmacist led carvedilol optimisation service was well attended by patients. The clinic achieved rapid, sustained, and safe titration of carvedilol dosing. Although NSBBs are not universally recommended, wherever the practice is implemented we must ensure doses match trials as closely as possible. An intensive pharmacist led service is a feasible approach to achieve this.

THU-028

Usefulness of an educational activity through an informatic tool in participants with chronic hepatitis B infection

Judit Romero-Vico^{1,2}, Anna Feliu-Prius^{1,3}, Ester Sánchez-Gavilán⁴, Marc Ribó⁴, Adriana Palom^{5,6}, Juan Carlos Ruiz-Cobo^{1,3,7}, Elena Vargas-Accarino¹, Núria Fabrellas⁸, Mar Riveiro^{1,3,7,9}, Maria Buti^{1,3}. ¹Research group of liver diseases, Vall Hebron Research Institute, Barcelona, Spain; ²Department of Nursing and Health, University of Barcelona, Barcelona, Spain; ³Department of Medicine, Universitat Autònoma of Barcelona, Barcelona, Spain; ⁴Neurology Department, Vall d'Hebron University Hospital, Barcelona, Spain; ⁵Research group of liver diseases, Vall Hebron Research Institute, Barcelona, Spain; ⁶Biomedical Research Networking Centre for Hepatic and Digestive Diseases, Madrid; ⁷Department of Hepatology, Vall d'Hebron University Hospital, Barcelona, Spain; ⁸Department of Nursing and Health, University of Barcelona, Barcelona, Spain; ⁹Biomedical Research Networking Centre for Hepatic and Digestive Diseases, Madrid, Spain
Email: judviro1630@gmail.com

Background and aims: Low linkage to care rate is a major issue in the management of people living with hepatitis B virus (HBV). This can be attributed to several factors, such as the asymptomatic nature of the infection until advanced stages and the lack of awareness of the potential consequences of the infection. The aim of this study was to assess the knowledge on HBV among patients with chronic HBV infection and to evaluate the performance of an educational activity.

Method: Prospective study including people living with HBV from the outpatient clinics. Through a phone application, the subjects answered a self-response questionnaire designed to assess HBV knowledge. This included aspects related to disease transmission, prevention, treatment, and complications of hepatitis B. The questionnaire comprised 16 dichotomous questions, requiring “yes” or “no” responses. A scoring system from 0 (lowest) to 10 (highest) was used to evaluate the participants' level of knowledge. After completing the questionnaire, an app alert notifies the patients to view an educational video, followed by an invitation to repeat the initial questionnaire.

Results: A total of 92 participants responded to the first questionnaire. Baseline characteristics were: 72% male, mean age 50.2 years (± 12.6), 67% Caucasian, and 40% undergoing treatment for HBV. Regarding their education levels, 7.6% had no basic education, 33.7% basic education, 50% superior education, and 8.7% declined to answer. The questionnaires revealed that the lowest scores were observed for questions related to treatment, while the highest scores were related to transmission pathways. The mean score from the first survey was 8.1 (± 1.6). Following the educational video, 40 (43%) participants completed the second questionnaire. Among them, the initial score was 8.4 (± 1.0) and after the educational activity the score rose to 9.0 (± 1.0), resulting in a significant increase ($p = 0.05$). No other differences were observed in sociodemographic characteristics or educational levels between the patients who responded only to the first or both tests.

Conclusion: These results demonstrate that an educational activity through an application is a useful tool for enhancing participants' knowledge of chronic HBV infection. Therefore, a phone application is a supportive tool in educating patients with this infection.

THU-029

Nurse-led hepatocellular cancer surveillance in district general hospital

Kate Pingoy¹, Areeb Zar¹, Karen Street¹, Karen Raiton¹, Abhishek Ray¹, Prayman Sattianayagam¹, Kunchana Thebuwana¹, Gayatri Chakrabarty¹. ¹Surrey and Sussex NHS Trust, Redhill, United Kingdom
Email: kate.pingoy@nhs.net

Background and aims: Hepatocellular carcinoma (HCC) surveillance is recommended by the National Institute for Health and Care

POSTER PRESENTATIONS

Excellence (NICE) for at-risk patients with 6-monthly liver ultrasound scans (USS). A nurse-led surveillance pathway was introduced at Surrey and Sussex Healthcare NHS Trust (SaSH) in April 2021 to manage patients eligible for surveillance. This study aims to identify the scale of the demand on this service, and scope for improvement.

Method: Patients eligible for surveillance were identified from the existing database. A search of electronic patient records via Discern Reporting Portal in Cerner identified patients who had USS requested from April 2021 to November 2023 under Gastroenterology and Hepatology. Keywords used for search were 'HCC, liver lesions, liver cancer, Hepatoma'. Suspected or confirmed cases of HCC were obtained from regional multidisciplinary meeting (MDM) records. Liver surveillance nurse had access to a dedicated mobile phone which allowed easy access to patient and arranged patients' appointments. A random selection of 30 patients who failed to attend their last ultrasound or clinic appointments were contacted via phone to understand reasons for non-attendance.

Results: In total 344, 381, and 441 patients on the database were for eligible for HCC screening in 2021, 2022 and 2023 respectively. In 2021, 376 USS were requested of which 296 (78.7%) were completed. In 2022, 464 requested and 361 completed (77.8%). In 2023, 690 were requested, and 428 completed so far. From 2021 to 2023, scan requests increased by 83.5%. In 2021 there was 1 case of suspected HCC, 10 in 2022 and 21 in 2023. There were 4 confirmed cases of HCC in 2022 and 9 (7 are Barcelona Clinic Liver Cancer stage 0/A, and 2 stage D) in 2023. 30 selected patients who were contacted via phone for non-attendance had underlying Alcohol-related liver disease (ArLD) or Hepatitis C. 22 of 30 patients attended their appointments after the phone contact. It was highlighted that single hospital visit allowing for same day scan, clinic review with blood tests may improve patient compliance. We recognise some limitations in the nurse-led surveillance pathway. The service requires a high level of data management and patient contact. A dedicated staff to manage patient booking and patients having easy access to liver team via phone has shown better patient engagement.

Conclusion: Since introduction of nurse-led surveillance, there has been an annual increase in the number of scan requests, completed scans, and detection of liver cancer. Patients with ArLD and hepatitis C are more likely to not attend for USS, and requires higher engagement with the team to maintain compliance. There is an increased demand on the service which requires adequate staffing.

THU-032

"Ama il tuo Fegato" program: screening for hepatic fibrosis using liver stiffness measurement (LSM)

Paolo Scivetti¹, Martina Costanzo², Daniela Ferrari³, Anna Lisa Gandolfi⁴, Stefano Pisu⁴, Pietro Raco⁴, Lorena Zanchetta⁵.
¹hepatology clinic, Department of Internal Medicine, ASLBI, Biella, Italy, Ponderano, Italy; ²Liver Team, ASLBI, Biella, Italy, Ponderano, Italy; ³Liver Team, ASLBI, Biella, Italy, Ponderano; ⁴Liver Team, ASLBI, Biella, Italy, Ponderano, Italy; ⁵Liver Team, ASLBI, Biella, Biella, Italy
Email: paolo.scivetti@aslbi.piemonte.it

Background and aims: The "AMA IL TUO FEGATO" program at ASLBI explores the potential of Liver Stiffness Measurement (LSM) as a screening tool for hepatic fibrosis in the general population. While LSM is well-established for chronic liver disease assessment, its application in seemingly healthy individuals remains underexplored. The aim is to understand whether LSM can be effectively used to identify early-stage liver fibrosis in individuals without apparent symptoms of liver disease. The program seeks to contribute to the prevention and timely treatment of liver fibrosis through a broader assessment of the population, thereby expanding the possibilities for early intervention and improving overall liver health management within the community.

Method: In the year 2023, a comprehensive initiative was undertaken, involving 981 participants aged over 40 who responded to an open invitation to participate in the "AMA IL TUO FEGATO" program at

ASLBI. The program was meticulously executed by professional nurses who conducted Liver Stiffness Measurement (LSM) adhering to rigorous international standards. This standardized approach ensures the reliability and accuracy of the gathered data, laying the foundation for a robust analysis of liver health in the studied population.

Results: Results revealed that 81.8% exhibited normal LSM values (<6 kPa), 16.9% exceeded 6 kPa, and 1.6% had stiffness surpassing 14 kPa. Analysis indicated correlations between LSM values and diabetes, BMI, and alcohol intake. Among those with normal LSM, 4.26% were diabetics, 31.85% had a BMI over 26, and 23.33% reported alcohol intake exceeding 2 units/day. For LSM values over 6 kPa, 20.22% were diabetics, 45.95% had a BMI over 26, and 37.84% reported alcohol intake exceeding 2 units/day. In cases exceeding 14 kPa, 20.72% were diabetics, 40% had a BMI over 26, and 20% reported alcohol intake exceeding 2 units/day. Subjects with LSM >6 kPa were referred to their GP for further investigation, and those exceeding 14 kPa were scheduled for Hepatology clinic visits.

Conclusion: The "AMA IL TUO FEGATO" program not only underscores the significance of Liver Stiffness Measurement (LSM) as an efficient tool for the early detection of hepatic fibrosis in seemingly healthy individuals but also accentuates the critical role it plays in preventing the progression of liver diseases. Early identification through LSM is paramount, as it facilitates timely surveillance for potential complications, including hepatocellular carcinoma. Furthermore, the program serves as a noteworthy example, demonstrating the practicality and effectiveness of involving nursing staff in the implementation of LSM.

THU-033

Early evaluation of a pharmacist-led clinic for the management of patients with chronic hepatitis B on antiviral treatment

Aya Al-Hasani¹, David Sherman¹, Uchu Meade¹, Jayshri Shah¹. ¹London North West University Healthcare NHS Trust, London, United Kingdom
Email: jayshri.shah@nhs.net

Background and aims: Between 2020 and 2022, the COVID-19 pandemic resulted in unprecedented service pressures affecting hepatology outpatient clinics in our institution due to various staff and patient factors. Chronic hepatitis B (CHB) patients experienced appointment delays and rescheduling, partly due to prioritisation of new or more urgent referrals. In 2023, we found that 35% of patients requiring monitoring of antiviral therapy for CHB had breached service targets. In addition, due to the high prevalence of CHB in our catchment area in inner North West London, implementation in April 2022 of the National Health Service (NHS) initiative for testing blood borne viruses within emergency departments (ED) resulted in an additional 30 new referrals per month. To support increases in service pressures, a pharmacist-led clinic for the management of patients with CHB was introduced. We aimed to evaluate the achievements of this clinic in its first year.

Method: A protocol for the pharmacist-led clinic was written outlining inclusion criteria: those with a confirmed diagnosis of CHB, who were already stabilised on oral antiviral treatment. Exclusion criteria: new patients referred with diagnosis of CHB, those not on antiviral treatment, patients with decompensated cirrhosis, patients co-infected with hepatitis C, hepatitis D or HIV, patients diagnosed with hepatocellular carcinoma (HCC) and patients who have received liver transplant. In this retrospective study we analysed patient attendance rates, medication adherence and pharmacist interventions between December 2022 to December 2023. Interventions offered included lifestyle advice, referral for HCC screening as per EASL guidelines, checking for co-infection with HIV, hepatitis C and hepatitis D where this had not been previously checked in initial assessment, medication adherence support, and drug-drug interactions (DDIs).

Results: 108 patients were offered appointments in the pharmacist-led clinic. 81% (n = 88) attended their appointment. Lifestyle advice

was given to 64% (n = 57) of patients with concomitant risk factors for chronic liver disease. 24% (n = 21) met the criteria for HCC screening, with some patients with no ultrasound imaging for up to seven years. 24% (n = 21) were screened for co-infection with HIV, hepatitis C or hepatitis D. 17% (n = 15) were non-adherent with antiviral medication. 41 patients were on concomitant medications, 90% (n = 37) were screened for DDIs.

Conclusion: Specialist pharmacists are well positioned to support hepatologists in the management of patients with CHB. With increasing demand and capacity issues, the introduction of a pharmacist-led clinic helps free up consultant time. The service can be delivered safely and effectively as demonstrated. Further studies will need to be carried out with larger patient numbers, including qualitative data on the patient's experience.

THU-034-YI

Dietary composition in individuals with primary sclerosing cholangitis-high prevalence of inadequate fat-soluble vitamin intake

Catarina Lindqvist¹, Michael Ingre², Annika Bergquist³. ¹Unit of Gastroenterology and Rheumatology, Department of Medicine Huddinge, Karolinska Institutet, Medical Unit Clinical Nutrition, Karolinska University Hospital, Stockholm, Sweden; ²Unit of Gastroenterology and Rheumatology, Department of Medicine Huddinge, Karolinska Institutet, Stockholm, Sweden; ³Unit of Gastroenterology and Rheumatology, Department of Medicine Huddinge, Karolinska Institutet, Karolinska University Hospital, Stockholm, Sweden
Email: catarina.lindqvist.1@ki.se

Background and aims: Individuals with primary sclerosing cholangitis (PSC) express a demand for more information about lifestyle and its potential impact on their disease. Despite this, limited research has explored the dietary habits of individuals with PSC. The aim of this study is to compare the dietary intake of individuals with PSC in Sweden to the Estimated Average Requirement according to the Nordic Nutrition Recommendations 2023.

Method: A cross-sectional assessment of dietary intake was performed using a food-frequency questionnaire among 120 individuals with PSC enrolled in PISCATIN (Effect of Simvastatin on the Prognosis of Primary Sclerosing Cholangitis), an ongoing, randomized placebo controlled multicenter study. Macro- and micronutrient intake was compared to The Nordic Nutrition Recommendations 2023. A dietary quality index developed by the National Food Agency in Sweden was used to determine dietary quality. The index considers factors such as fiber, fat, and discretionary foods, as well as adherence to dietary recommendations concerning the consumption of fruits, vegetables, fish, and whole grain bread.

Results: The median age was 47 (IQR 18) and body mass index 25.2 (IQR 5.9) kg/m². Eight persons (10%) had a BMI <20 and 16 (13%) a BMI >30. The median daily energy intake was 1762 (IQR 1132) kilocalories (95% CI 1759–2067). The percentages of energy from different nutrients were as follows: fat 36%, saturated fat 15%, polyunsaturated fat 4.6%, protein 17%, and carbohydrate 43%. On average, participants consumed 18 grams (IQR 18) of fibre. Consumption of low amounts of carbohydrates, fiber, and polyunsaturated fats, along with a high intake of saturated fats, signifies an imbalanced diet. More than 50% of the subjects had suboptimal intake of zinc, selenium and vitamins C, D, and K. In addition, >30% had suboptimal intakes of other micronutrients such as vitamins A, B6, E, niacin, folate, potassium, magnesium, and iron. A substantial proportion of participants (41%) were classified as having a poor dietary quality.

Conclusion: Individuals with PSC, despite the majority having a normal BMI, do not meet the recommended levels of intake for polyunsaturated fat and many of the micronutrients. The high prevalence of low intake of fat-soluble vitamins warrants further exploration in this population where malabsorption is frequent.

THU-039-YI

Educational intervention in cirrhotic outpatients with hepatic encephalopathy secondary to constipation

Martina Perez-Guasch^{1,2}, Alba Martinez¹, Gloria De Prada¹, Ana Alonso¹, Carmen Cierco¹, Eva Lopez-Benages¹. ¹Liver Unit, Hospital Clínic of Barcelona, Barcelona, Spain; ²Fundació de Recerca Clínic Barcelona-Institut d'Investigacions Biomèdiques August Pi i Sunyer (FRCB-IDIBAPS), Barcelona, Spain
Email: maperezgu@clinic.cat

Background and aims: Hepatic encephalopathy (HE) represents one of the most limiting complications in end stage liver diseases (ESLD). Its presence makes patients incapable of self-care, reducing their quality of life and survival. HE precipitating factors include constipation and being a transjugular portosystemic shunt (TIPS) carrier. Part of the treatment of HE is non-absorbable disaccharides rectal administration form. Currently, there is a lack of patients and caregiver's educational program focused on HE management at home, as well as there's an absence of specific devices for efficient and autonomous rectal enema administration. Consequently, most HE episodes are treated either in emergencies or through hospital admissions. The aims of this study are to evaluate the educational program impact, in the need of hospital admissions, emergency visits and in the quality of life.

Method: Pilot interventional study, spanning 6 months of follow-up, conducted at the Hepatology Service of Hospital Clínic of Barcelona between 2017 and 2019. Patients with ESLD, having at least one prior hospital admission for HE either spontaneous or related to TIPS, participated in an educational program. The educational intervention involved an initial visit providing information on HE (diet, treatment, early symptom detection) and training on enema device usage. Six follow-up visits reinforced HE management monthly. All visits were individual and had an approximate duration of 60 minutes. To assess treatment adherence and quality of life, Morisky-Green and SF-12 questionnaires have been used at the beginning and at the end of the study. The remaining data has been retrospectively extracted from the patient's medical history.

Results: 17 subjects were included, mostly male (88%), mean age 63 years. Most subjects were married (77%), lived with the primary caregiver (100%), mainly their partner (82%). The most common cause of ESLD was alcohol consume and Non-Alcoholic Steatohepatitis (24%), followed by Hepatitis C Virus (24%). The average MELD-Na Score was 14 and 10 patients were TIPS carriers. After the intervention, hospital admissions/emergency visits related to constipation-induced HE significantly decreased from a median (interquartile range) of 1 (0.5–3) admissions pre-study to 0 (0–2) during the study. Although the trend is clear, this reduction does not reach statistical significance (p < 0.060). Quality of life assessment did not show statistically significant results in any questions.

Conclusion: The implementations of educational program focus on patients with recurrent HE episodes show a clear tendency to reduce hospital admissions and emergency visits. The nursing care aims to empower patients with knowledge necessary for effective disease management, could positively influencing various aspects of their health and well-being.

THU-040-YI

Establishment of the Irish hepatology nurses association: an association for nurses working in liver disease in Ireland

Michèle Bourke¹, Anne Brennan², Shauna Davitt¹, Edel Dolan², Aileen Murphy², Joanne Murphy². ¹St. Vincent's University Hospital, Dublin 4; ²St. Vincent's University Hospital, Dublin 4, Ireland
Email: mbourke02@gmail.com

Background and aims: In the early 2000's a group of liver nurses with a special interest in hepatitis C, began meeting biannually to discuss their practice. In recent years, this group has expanded. The attendees share a common goal-to improve the care of patients with liver disease in Ireland. The growth in personnel attending the

POSTER PRESENTATIONS

meetings coupled with the diversification of sub-specialties within liver nursing, gave way to a natural progression to formalise the group's structures and develop its scope.

Method: The organising committee developed a survey to assess the opinions of attendees on current practices and expectations for the future. The survey was circulated via email. It comprised questions relating to respondent demographics, perceived objectives of the group in its current state, thoughts on future aims, opinions on formalising a national association with a committee structure, and the payment of an annual membership fee. Responses were returned via email within a 2 month period. The results were collated and presented at the next scheduled meeting. A vote was then conducted to adopt the findings, or not.

Results: 51 eligible participants were identified and contacted via email. A 37% response rate was achieved (n = 19). 1 (5%) Advanced Nurse Practitioner, 17 (90%) Clinical Nurse Specialists (or equivalent level), 1 (5%) Staff Nurses. 13 (68%) worked in a tertiary hospital and 6 (32%) were community based. 6 (32%) worked in general hepatology, 9 (47%) specialised in viral hepatitis, 3 (16%) in hepatocellular carcinoma and 1 (5%) in liver transplant. 2 (10%) of the group were founding members, the remaining 17 (90%) joined in subsequent years. 10 (53%) have been members for 0–5 years, 3 (16%) 6–10 years and 6 (31%) >11 years. Themes identified for current objectives; (i) education, (ii) peer support. Themes identified for future aims; (i) education, (ii) research opportunities, (iii) career development pathways, (iv) promotion of liver nursing (v) networking. 10 (52%) in favour of formalising an association and electing a board to achieve these objectives. 10 (52%) willing to be a board member. 19 (100%) willing to pay a membership fee.

Conclusion: The survey results were presented to the group. In June 2023, the Irish Hepatology Nurses Association (IHNA) was established. A board was elected comprising a Chairperson, Secretary, Treasurer, plus 4 board members. Terms of reference were devised, agreed and adopted by the association. There are 36 paid memberships. The 1st official IHNA meeting organized by the elected board was held in December 2023. A social media presence has been generated to advertise the IHNA to all nurses working within the hepatology field in Ireland and abroad. Works are underway to identify a timeline and processes for achieving the identified future aims.

THU-044

Global subjective assessment and global leadership initiative on malnutrition as predictors of mortality in patients with cirrhosis

Valesca Dall'Alba¹, Nairane Boaventura¹, Larissa Maffini¹, Camila Saueressig², Vittoria Zambon Azevedo³. ¹Universidade Federal do Rio Grande do Sul, Hospital de Clínicas de Porto Alegre, Porto Alegre, Brazil; ²Universidade Federal do Rio Grande do Sul, Hospital de Clínicas de Porto Alegre, Porto Alegre, Brazil; ³Universidade Federal do Rio Grande do Sul (UFRGS), Porto Alegre, Brazil
Email: camilasaueressig@gmail.com

Background and aims: The prevalence of malnutrition in patients with cirrhosis varies widely, ranging from 10 to 100%. The pathogenesis of malnutrition in chronic liver disease is multifactorial and there is not a gold standard nutritional assessment. Taking this into account the objective of this study was to evaluate the prevalence of malnutrition in hospitalized patients with cirrhosis using Subjective Global Assessment (SGA) and Global Leadership Initiative on Malnutrition (GLIM) and their ability to predict mortality in one year.

Method: A cross-sectional study was conducted with adult hospitalized patients with cirrhosis at the Hospital de Clínicas in Porto Alegre, Brazil. BMI, mid-arm muscle circumference (MAMC), weight loss, physical examination, dietary intake, functional capacity metabolic demand, and CRP were used to assess nutritional status by SGA and GLIM. Cox regression model was performed, adjusted for sex and age to evaluate the mortality risk in one year. This study was

approved by the Research Ethics Committee (CAAE: 395078201300153527).

Results: A total of 100 patients were evaluated (60.1 ± 10.4 years, 63% men, 80% white, 61% Child_Pugh B and 30% Child_Pugh C). Regarding the etiology of cirrhosis, HCV and alcohol were the most prevalent (32% and 23%), 33% had diabetes mellitus and 35% hypertension. The prevalence of malnutrition according to the GLIM criteria was 59.8% and according to the SGA (B or C) was 69%. The presence of malnutrition (SGA and GLIM) was an independent risk factor for one-year mortality (HR: 3; 95% CI 1.5–6; p = 0.02, HR: 2.2; 95% CI 1.1–4.1; p = 0.01, respectively).

Conclusion: Both tools (SGA and GLIM) identified a high prevalence of malnutrition and proved to be predictors of mortality. Carrying out early nutritional assessment is important to implement the most assertive dietary therapy approach.

THU-045

Medicines optimisation in patients admitted with hepatic encephalopathy in UK centres

Connor Thompson^{1,2,3}, Arron Jones^{1,4}, Alison Boyle^{1,5}, Niamh Forde^{1,6}, Fiona Rees^{1,2}, Alban Clareburt⁵. ¹British Hepatology Pharmacy Group (BHPG), London, United Kingdom; ²University Hospitals Sussex NHS Foundation Trust, Brighton, United Kingdom; ³Medicines Use Research Group (MURG), University of Brighton, Brighton, United Kingdom; ⁴Barts Health NHS Trust, London, United Kingdom; ⁵NHS Greater Glasgow and Clyde, Glasgow, United Kingdom; ⁶The Royal Liverpool Hospital, Liverpool University Hospitals NHS Foundation Trust, Liverpool, United Kingdom

Email: C.Thompson3@brighton.ac.uk

Background and aims: Hepatic encephalopathy (HE) occurs in up to 40% of people with advanced chronic liver disease and has been estimated to affect 200,000 people in Europe. Medication management for these patients is critical in reducing events and hospital admissions, as well as some medicines being implicated in worsening HE. Optimising medications is an important intervention in improving care of these patients. EASL recommends optimised lactulose dosing as first line followed by rifaximin in recurrence within 6 months of first presentation. We aimed to assess medication use in patients admitted to hospital against medication prescribed at discharge to understand whether there are opportunities for optimisation.

Method: A retrospective service evaluation of inpatients admitted with documented HE was conducted by hepatology specialist pharmacists between April to July 2022 in 4 UK centres. Patient records were used to review prescribed medications at admission and discharge, with focus on medicines frequently prescribed in decompensated cirrhosis, as well as antibiotics and proton pump inhibitors (PPIs). Decompensation history was also recorded. Those with same-day discharge, condensed or missing discharge summaries, who remained an inpatient during the data collection period, or who died during their stay were excluded from data collection.

Results: A total of 31 patients met the inclusion criteria with an average hospital stay of 19 days. With 61% (n = 19) male and a mean age of 61 years. Nine patients had their first presentation with HE. The most common underlying aetiology was alcohol-related liver disease (ArLD) (n = 20). For those with the first presentation of HE, all (n = 9) patients were discharged on lactulose and 44% (n = 4) were discharged on rifaximin. For those with a history of HE, 86% (n = 19/22) were prescribed lactulose on admission. Of the 3 who were not, 1 patient was subsequently started during admission, 1 was prescribed alternative laxatives and the other had no laxatives prescribed on discharge. 36% (n = 8/22) of patients with a history of HE were prescribed rifaximin on admission. This increased to 73% (n = 16/22) at discharge. Overall, there was an increase in lactulose dose from 49 ml/day (n = 23) on admission to 62 ml/day (n = 27) on discharge. There was a 25% (n = 5) reduction in the number of patients on PPIs on discharge.

Conclusion: We found that the majority of patients were prescribed lactulose therapy and this was up-titrated as required. There was an increase in rifaximin prescriptions at discharge compared with admission, although there is potential for further optimisation. There is scope to review other medicines which may contribute to worsening HE, including PPIs. Further work is planned to increase data collection to more centres in the UK and gain evidence of pharmacists' role within these interventions, especially in centres with hepatology specialist pharmacists.

THU-046

Exploring the feasibility of ultrasound liver imaging reporting and data system (US LI-RADS) and visualisation score in clinical application

Dorothy Seng¹, Albert Low², Azizah Afif¹, Denise Lau¹, Teo Simin¹, Pei-Yuan Chang¹. ¹Radiography department, Singapore general hospital, Singapore; ²Division of radiological sciences, Singapore general hospital, Singapore
Email: usdoro@gmail.com

Background and aims: Routine surveillance is highly recommended for patients at risk of developing hepatocellular carcinoma (HCC). The American College of Radiology (ACR) developed an Ultrasound Liver Imaging Reporting and Data System (US LI-RADS) to standardise the imaging technique, interpretation, reporting and data collection for surveillance of ultrasound exams for this group of patients. The US LI-RADS comprises of two components: Ultrasound (US) Category and Visualisation Score (VS). The US Category comprises of 3 scores: US-1 Negative, US-2 Subthreshold, and US-3 Positive. The US VS has 3 ratings: A-No or minimal limitations, B-Moderate limitations, and C-Severe limitations. This study aims to determine the clinical applicability of US LI-RADS during clinical observations and if VS is affected by age, gender body-mass index (BMI) and type of liver diseases.

Method: This is a retrospective, single-centre clinical audit review study. All patients who underwent US Abdomen or Hepatobiliary system for HCC surveillance between May to July 2023 were identified through an anonymised data depository of US clinical audit cases. All US examinations using 3 US machines: Philips Epiq, Canon Aplio, and GE Logiq, using standard institution scanning protocol, were included. Demographic and clinical data, including US category, VS, age, gender, BMI and type of liver diseases were retrieved from the existing data depository. Patients with previously diagnosed or treated HCC were excluded. Data was analysed by IBM SPSS Version 26. Descriptive statistics and Fisher exact tests were performed to test the association between VS and the patient demographics.

Results: A total of 160 patient records were retrieved from the data repository. The mean age of these patients was 62.2 ± 13.3 years. Among them, 69 (43.1%) were male, while 91 (56.9%) were female and the patients' mean BMI was 24.2 ± 4.3 . Majority of patients, 137 (85.6%) were classified as US-1, 14 (8.8%) as US-2, and 9 (5.6%) as US-3. Among the US-3 cases, 3 were subjected to further imaging, leading to 2 cases identified as HCC. The HCC outcomes were associated with the US category observations ($p = 0.033$). VS revealed that 112 (70.0%) cases were assigned VS-A, 43 (26.9%) cases were VS-B, and 5 (3.1%) cases were VS-C. A weak positive correlation existed between age and VS, $R^2 = 0.210$ ($p = 0.008$). However, VS exhibited no significant correlation with BMI, gender, or the specific type of comorbidities. Among the factors affecting VS, poor beam penetration emerged as the primary factor contributing to insufficient visualisation of the liver (17/42, 10.6%).

Conclusion: Our study concluded that US LI-RADS is useful for screening patients at risk. Apart from age, VS has no association between patient demographics and type of liver diseases. It may be feasible to implement US LI-RADS at our institution for more consistent recommendations and standardised reporting.

Public Health – Except viral hepatitis

TOP-445

Associations of food insecurity and healthcare access with the prevalence and mortality of metabolic dysfunction-associated steatotic liver disease (MASLD): a global study of the United Nations and the global burden of disease data

Zobair Younossi^{1,2}, Shira Zelber-Sagi^{1,3}, Carina Kugelman^{1,4}, Jeffrey V. Lazarus^{1,5}, Annette Paik^{1,6}, Leyla Deavila^{1,6,7}, Lynn Gerber^{1,6}, James M. Paik^{1,6}. ¹The Global NASH Council, Washington DC, United States; ²Beatty Liver and Obesity Liver Research Program, Falls Church, VA, United States; ³School of Public Health, University of Haifa, Haifa, Israel; ⁴Denver Health Medical Center, Denver, United States; ⁵Barcelona Institute for Global Health (ISGlobal), Hospital Clinic, University of Barcelona, Barcelona, Spain; ⁶Beatty Liver and Obesity Research Program, Falls Church, United States; ⁷The Center for Outcomes Research in Liver Disease, Washington DC, United States Minor Outlying Islands
Email: zobair.younossi@cldq.org

Background and aims: Food insecurity and lack of healthcare access are important social determinants of health contributing to global MASLD burden. We assessed the impact of food insecurity and healthcare access on the prevalence and mortality of MASLD, globally. **Method:** This ecological study linked surrogates of food security and nutrition data from the Food and Agriculture Organization (FAO) of the United Nations (2016–2019) with MASLD prevalence, MASLD mortality, Socio-Demographic Index (SDI), and Healthcare Access and Quality (HAQ) index data from the Global Burden of Disease Study-2019. High vs low MASLD prevalence ($\geq 22\%$ vs $< 22\%$) and SDI (≥ 0.67 vs < 0.67) were determined according to the median of country-level rates. FAO defines a healthy diet as providing both adequate calories and adequate levels of all essential nutrients/food groups needed for active and healthy life. Amount of calories insufficient to cover energy requirement for an active and healthy life indicated undernourishment (hunger).

Results: In 204 countries, the mean prevalence of MASLD, MASLD-related liver death rate, HAQ and SDI scores were 24.08%, 0.39 per 100,000, 54.7 and 0.64. MASLD prevalence was similar between high and low SDI countries (24.56% vs. 23.60%, $p = 0.668$). In both high and low SDI countries, T2D and obesity were associated with higher prevalence of MASLD ($p < 0.001$). Among high SDI countries, those with high MASLD prevalence experienced higher prevalence of severe food insecurity (6.46% vs. 1.86%), higher cost of a healthy diet (\$3.43 vs \$3.08 per person per day), higher percentage of inability to afford a healthy diet (19.24% vs. 3.99%) and higher rates of MASLD-related liver deaths (0.38 vs. 0.27 per 100,000) as compared to high SDI countries with low MASLD prevalence ($p < 0.02$). In contrast, high SDI countries with low MASLD prevalence had higher HAQ index (78.25 vs. 61.09, $p < 0.001$). Among high SDI countries, generalized linear regression (GLM) models showed that increased MASLD prevalence was associated with severe food insecurity [2.43% increase (95% CI: 0.73–4.17%)] and inability to afford a healthy diet [0.76% increase (0.20–1.31%)], while a higher HAQ index was associated with decreased MASLD prevalence [1.48% reduction, (–1.97 to –1.02%)]. A higher HAQ index was the only parameter inversely associated with MASLD-related deaths [0.91% risk reduction, (–1.49 to –0.32%)]. In similar analyses among the low SDI countries, the opposite patterns were observed where higher food insecurity, undernourishment/hunger and HAQ index were associated with lower MASLD prevalence ($p < 0.03$).

Conclusion: Surrogates of food insecurity are major drivers of MASLD prevalence in high SDI countries while higher access to healthcare is protective against both MASLD prevalence and death. A different pattern was observed in low SDI countries suggesting different factors (poverty, hunger) playing an important role.

POSTER PRESENTATIONS

SATURDAY 08 JUNE

SAT-424

The impact of air pollution on the occurrence of steatotic liver disease in Korea

Jae Moon Yun¹, Su Hwan Cho², Jin-ho Park¹. ¹Seoul National University Hospital, Seoul, Korea, Rep. of South; ²Seoul National University Hospital, Family Medicine, Korea, Rep. of South
Email: iwsby@naver.com

Background and aims: Previous studies investigating the impact of air pollution (AP) on the occurrence of steatotic liver disease (SLD) faced significant challenges in general applicability, primarily due to issues related to the reliability of measuring concentrations of air pollutants and the variability in air pollutant levels between the country of study and most other nations. To address these limitations, we evaluated the association between the prevalence of SLD and long-term AP exposure in a Korean population, using a more accurate method for calculating AP exposure.

Method: We conducted a cross-sectional study of 20,553 participants who had undergone of a health screening program carried out at the Seoul National University Hospital Health Promotion Center between January 2015 and December 2019. SLD was diagnosed through ultrasound in cases exhibiting hepatic steatosis, specifically defined to include only those satisfying at least one cardio-metabolic criteria, obesity, elevated blood glucose, elevated blood pressure, or dyslipidemia. 250 administrative districts-specific levels of air pollutants, including particulate matter (PM) 2.5, PM 10, nitrogen dioxide (NO₂), sulfur dioxide (SO₂), and carbon monoxide (CO), were estimated by validated Community Multiscale Air Quality (CMAQ) modeling system. The odds ratios of SLD according to AP exposure was evaluated using a multiple logistic regression analysis, after adjustments for age, sex, body mass index, presence of abdominal obesity, lifestyle, and comorbidities. SLD was classified as metabolic dysfunction-associated steatotic liver disease (MASLD), MASLD and increased alcohol intake (MetALD), and Alcohol-related liver disease (ALD) based on alcohol consumption. To investigate the influence of AP on SLD in relation to these alcohol-related classifications, stratified analyses were conducted.

Results: Increased the 5-year average exposure levels of PM 2.5, PM10, NO₂, CO were significantly associated with an increased odds of SLD, with odds ratios (ORs) of 1.04 (95% CI 1.01–1.07), 1.06 (1.01–1.11), 1.10 (1.04–1.16), and 1.07 (1.02–1.12) for each 1 interquartile range (IQR) increase in PM 2.5, PM 10, NO₂, and CO, respectively. For SO₂, there was no significant association observed between the increase in average AP exposure concentration and SLD. In stratified analysis targeting subgroups based on alcohol consumption, for each 1 IQR increase in PM2.5, there was a significant increase in the odds of MetALD (OR 1.12, 1.01–1.24), while no significant association was observed in the case of MASLD and ALD.

Conclusion: This study suggests that long-term exposure to ambient PM2.5, PM10, NO₂ and CO may increase the odds of SLD. These effects suggest that the impact of air pollution on the occurrence of fatty liver due to metabolic abnormalities may vary depending on the level of alcohol consumption.

SAT-425

Food swamps and easy access to unhealthy food increases the risk of metabolic dysfunction-associated steatotic liver disease (MASLD) mortality in the United States (U.S.)

Annette Paik^{1,2}, Linda Henry^{1,2}, Leyla Deavila^{1,2}, Saleh Alqahtani^{1,3,4}, Fatema Nader^{1,2,5}, James M. Paik^{1,2,6}, Zobair Younossi^{1,7}. ¹The Global NASH Council, Washington DC, United States; ²Beatty Liver and Obesity Research Program, Falls Church, United States; ³Liver Transplant Center, King Faisal Specialist Hospital, Research Center, Riyadh, Saudi Arabia, Division of Gastroenterology and Hepatology, Riyadh, Saudi Arabia; ⁴Division of Gastroenterology and Hepatology, Johns Hopkins University, Baltimore, United States; ⁵The Center for Outcomes Research in Liver

Disease, Washington DC, United States; ⁶Center for Outcomes Research in Liver Disease, Washington DC, United States; ⁷Beatty Liver and Obesity Research Program, Falls Church, United States
Email: zobair.younossi@cldq.org

Background and aims: Environmental factors such as living in neighborhoods with easy access to poor quality food may increase the risk of MASLD. We assessed the association of food deserts and food swamps with MASLD-related mortality in US.

Method: In this population-based study, MASLD-related deaths were obtained from the National Vital Statistics System (NVSS) (2010–2020). These data were merged with food environment factor from US Department of Agriculture (USDA) Food Environment Atlas (FEA) data (2012, 2014, 2015, 2017, and 2020) by Federal Information Processing System code. Food desert is a proportion of county's total population having both low income and low grocery store access. Retail food environment index (REFI), indicative of food swamps, is a county's ratio of the number of fast-food restaurants and convenience stores to the number of retail healthy food outlets. High mortality was based on ≥ 75 percentiles of US country-level score vs low (<75 percentiles).

Results: Of the eligible 2,400 counties in US (2010–2020), the median (range) of age-adjusted MASLD-related mortality was 19.50 (5.60–122.30) per 100,000 population. Compared to counties with low age-adjusted MASLD-related mortality rate, counties with high age-adjusted MASLD-related mortality rate had higher percentage of elderly residents (≥ 65 years, 16.54% vs. 14.64%), adult type 2 diabetes (T2D) (13.0% vs. 11.10%), and adult obesity (33.00% vs. 32.10%). These counties experienced higher poverty rates (20.25% vs. 15.10%), higher food desert rates (7.90% vs. 5.93%) and higher REFI (ratio, 4.83 vs. 4.38) with lower median household income (\$38,758 vs. \$48,063) and lower Supplemental Nutrition Assistance Program (SNAP) participation among eligible population (78.18% vs. 86.27%), (all p values <0.01). Multivariable logistic regression model showed people living in counties with higher REFI score (4th quartile) had higher odds of MASLD-related mortality (Odds Ratio [OR] = 2.27, 95% CI, 1.36–3.80) compared to those living in counties with lower REFI score (1st quartile). The strongest risk factors for higher MASLD-related mortality were T2D (OR = 1.30, 1.21–1.46), obesity (OR = 1.07, 1.01–1.13), poverty (OR = 1.20, 1.16–1.24) and percentage of Hispanic residents (OR = 1.05, 1.03–1.07), while SNAP participation among eligible population (OR = 0.95, 0.93–0.97), number of available fitness center (per 100,000) (OR = 0.91, 0.87–0.95), and increase change in the number of community supported agriculture farm (OR = 0.997, 0.996–0.999) were protective against MASLD-related deaths. In contrast, there were no associations of food desert with MASLD-related deaths.

Conclusion: Having more access to fast-food restaurants and convenience stores in relation to retail healthy food outlets is associated with increased MASLD related mortality. Efforts must continue to evolve to provide easily accessed healthy food options.

SAT-426-YI

Prevalence and association between chronic kidney disease and steatotic liver disease in a nationally representative sample in the United States

Mason Lai¹, Jennifer Lai¹, Andrew S. Allegretti², Kavish Patidar³, Giuseppe Cullaro¹. ¹University of California, San Francisco, San Francisco, United States; ²Massachusetts General Hospital, Boston, United States; ³Baylor College of Medicine and Michael E. DeBakey Veterans Affairs Medical Center, Houston, United States
Email: mason.lai@ucsf.edu

Background and aims: Steatotic liver disease (SLD) and chronic kidney disease (CKD) are common conditions that are strongly associated. Yet, there is a paucity of data regarding the prevalence of this overlap and the factors that may drive its occurrence.

Method: Using the National Health and Nutrition Examination survey, we examined trends among adult participants from 2005–

2020 that defined SLD with the Fatty Liver Index in the United States. Next, we completed correlative analyses that defined SLD using fibrosis based on the liver stiffness measure among participants from 2017–2020 who underwent FibroScan. We utilized multivariable survey-weighted binomial generalized linear models to determine the factors that were associated with CKD, defined as eGFR <60 or urine albumin-creatinine-ratio >30.

Results: Among the 76,496 participants included in the trend analyses, the estimated prevalence of CKD was 15.7% (95CI 15.2–16.2%) and SLD was 42.3% (95CI 41.4–43.2%). As compared to those without SLD, those with SLD had a significantly higher estimated prevalence of CKD (SLD: 15.7%, 95CI 14.9–16.5% v. No SLD 11.2%, 95CI 10.7–11.7%). As compared to those without SLD (estimated prevalence 11.2%, 95% CI 10.7–11.8%), we found that those with SLD and no to minimal fibrosis had similar levels of CKD (estimated prevalence 10.1%, 95% CI 9.4–10.8%) and those with SLD and advanced fibrosis (estimated prevalence 31.3%, 95% CI 29.6–33.1%) had higher estimates of CKD. In multivariate analyses of 3,824 participants who underwent FibroScan and had SLD by Fatty Liver Index, adjusting for control and presence of DM, HTN, and HLD, compared to those with normal liver stiffness, those with moderate scarring (F2) had similar odds of CKD (1.42, 95CI 0.91–2.20), those with severe scarring (F3) had higher odds of CKD (1.95, 95CI 1.09–3.49), and those with cirrhosis had higher odds of CKD (1.90, 95CI 1.04–3.47).

Conclusion: Our findings highlight that CKD is common among patients with SLD and that higher degrees of hepatic fibrosis are independently associated with CKD, independent of other comorbidities of the metabolic syndrome.

SAT-427-YI

Hepatocellular carcinoma surveillance in the United Kingdom: a multi-centre study assessing uptake and inequalities

Maria Qurashi¹, Varsha Chaitanya-Bhide¹, Shahid Khan², Kate Hyams³, Pamela Rice⁴, Nina Stafford³, Jayshri Shah³, Zinu Philipose⁴, Hooshang Izadi⁵, Rohini Sharma¹. ¹Imperial College London, London, United Kingdom; ²Imperial College Healthcare NHS Trust, London, United Kingdom; ³London North West University Hospitals NHS Trust, London, United Kingdom; ⁴Croydon University Hospitals NHS Trust, London, United Kingdom; ⁵Oxford Brookes University, Oxford, United Kingdom
Email: maria.qurashi09@imperial.ac.uk

Background and aims: Biannual ultrasound surveillance for hepatocellular carcinoma (HCC) in patients with cirrhosis is recommended by international professional bodies. Previous studies in American and Asian cohorts suggest fewer than 25% of patients receive surveillance at recommended intervals; however, there is a paucity of research on HCC surveillance uptake in the United Kingdom (UK). We aimed to quantify HCC surveillance uptake across a multi-centre cohort in the UK and examine socio-demographic factors affecting surveillance attendance.

Method: A multi-centre retrospective review of 869 patients eligible for HCC surveillance at five hospitals in the UK from March 2021–March 2023 was conducted. Attendance at surveillance was categorised as regular (biannual, in line with European Association of Study of the Liver (EASL) guidance), infrequent (received some surveillance, not at recommended intervals) or non-attendance (no surveillance received). We collected data on socio-demographic factors (age, gender, aetiology of liver disease, socio-economic status, hospital site, distance from hospital). Multivariate logistic regression analysis was undertaken to examine if factors were associated with reduced attendance at surveillance.

Results: 16.5% of patients received regular surveillance; 73.1% of patients were in receipt of infrequent surveillance and 10.4% received no surveillance over the two year study period. On multivariate analysis, low socio-economic status (OR 2.8, CI 1.3–6.2, $p=0.01$) and being under the care of a non-specialist hospital (OR 5.3, CI 2.9–9.5, $p<0.001$) were both associated with reduced attendance. Ages 45–75

were a protective factor (OR 0.3, CI 0.1–0.7, $p=0.004$) for non-attendance at surveillance. There was no association between aetiology of liver disease or gender and attendance at surveillance.

Conclusion: This is the first multi-centre study assessing HCC surveillance and its determinants in the UK. HCC surveillance uptake is universally low, with patients of low socio-economic status and those under the care of non-specialist centres most at risk of reduced attendance at surveillance. Our findings highlight the urgent need to address low HCC surveillance uptake in the UK.

SAT-428

Identifying treatment naïve and undiagnosed primary biliary cholangitis patients using a novel case finding database and treatment pathway

Timothy Jobson¹, Christina Owen¹, Almuthana Mohamed¹, Sarah Gormley¹. ¹Somerset NHS Foundation Trust, Musgrove Park Hospital, Taunton, United Kingdom
Email: timothy.jobson@somersetft.nhs.uk

Background and aims: Primary Biliary Cholangitis (PBC) is a chronic, yet under-diagnosed condition with treatment available that can avoid progression to end stage disease or transplantation. In the Somerset Liver Improvement Project (SLIP) we developed a unique case-finding tool (covering >0.5 M patients) enabling rapid longitudinal analysis of blood test results by clinicians to identify cohorts at risk of developing liver disease. We aimed to a) identify patients who had blood markers suggestive of PBC, b) develop a recall treatment pathway co-designed with our public and patient reference group without overloading primary and secondary care and c) offer a clinical review and treatment where appropriate.

Method: Blood test results from 2005 to 2020 were analysed to a) identify the overall number of patients who had ever had a positive mitochondrial antibody (AMA) test b) find those that had AMA reversal on last testing from positive to negative AMA (reverted) and c) identify patients aged 18–70 years with persistent positive AMA and Alkaline Phosphatase (ALP) above 130 U/L to call to clinic. Patients unknown to our service were sent postal letters inviting them to attend a liver clinic. All communication materials were developed with patient and public involvement aiming to maximise response rates. Patients who attended clinic had a clinical assessment performed and confirmatory blood tests taken.

Results: Our database showed 267 males with positive AMA at some point with 31 having reverted AMA on their last test. 951 females had a positive AMA at some point with 107 having reverted AMA on their last test. Overall, 40 patients (9 M, 31 F) met the criteria for clinic invitation. 20 (50%) responded to the invitation and were seen face to face in clinic with 18 having repeat blood tests (2 patients had already been started on treatment in another clinical encounter or setting). 4 of those attending were patients who had been lost to follow-up or previously discharged. Of the 18 patients to have repeat bloods, 10 had a positive AMA on repeat testing and 8 had reverted. 1 patient had reverted twice over time with the last result being negative. 10 patients were considered treatment naïve and started on Ursodeoxycholic acid.

Conclusion: Our novel case finding database can be used to identify treatment naïve and undiagnosed PBC patients. Using our co-designed recall pathway we achieved a 50% response rate leading to clinical review of patients with PBC who were commenced on treatment where appropriate. Variability in AMA status and liver enzyme levels emphasises the importance of longitudinal analysis of past blood results. The AMA reversion rate seen here has not been previously reported in the scientific literature to our knowledge. We demonstrated a powerful methodology for identifying and engaging treatment naïve patients with clear benefits for prognosis, and potentially for clinical trial recruitment.

SAT-429

Impact of body mass index on non-invasive test accuracy for the diagnosis of at-risk metabolic dysfunction-associated steatohepatitis

Paula Iruzubieta¹, Rebeca Mayo², Itziar Mincholé Canals², Ibon Martínez-Arranz², Maria Teresa Arias Loste³, Luis Ibañez-Samaniego⁴, Cristina Alonso², José Luis Calleja Panero⁵, Manuel Romero-Gómez⁶, Rocío Aller⁷, Mazen Noureddin⁸, Javier Crespo¹. ¹Gastroenterology and Hepatology Department, Marqués de Valdecilla University Hospital, Clinical and Translational Research in Digestive Diseases, Valdecilla Research Institute (IDIVAL), Santander, Spain; ²OWL Metabolomics, Derio, Spain; ³Gastroenterology and Hepatology Department, Marqués de Valdecilla University Hospital, Clinical and Translational Research in Digestive Diseases, Valdecilla Research Institute (IDIVAL), Santander, Spain; ⁴Department of Gastroenterology and Hepatology, Gregorio Marañón General University Hospital, Madrid, Spain; ⁵Gastroenterology Department, Hepatology Unit, Puerta de Hierro University Hospital, IDIPHISA, Madrid, Spain; ⁶Department of Digestive Diseases, Virgen del Rocío University Hospital, Clinical and Translational Research Group in Liver and Digestive Diseases, Biomedicine Institute of Sevilla, Sevilla, Spain; ⁷Gastroenterology Department, Centro de Investigación de Endocrinología y Nutrición, Centro de Investigación Biomédica en Red de Enfermedades Infecciosas (CIBERINF), Facultad de Medicina, University of Valladolid, Hospital Clínico de Valladolid, Valladolid, Spain; ⁸Houston Research Institute, Houston, TX, USA, Houston, United States
Email: p.iruzubieta@gmail.com

Background and aims: The prevalence of metabolic dysfunction-associated steatotic liver disease (MASLD) worldwide in obese population is around 75% and the prevalence of metabolic dysfunction-associated steatohepatitis (MASH) about 33%. This study aimed to determine the accuracy of metabolomics-advanced steatohepatitis fibrosis score (MASEF), liver stiffness measurement (LSM) by vibration-controlled transient elastography (VCTE), and FibroScan-AST (FAST) for the evaluation of at-risk MASH (MASH with NAFLD Activity Score (NAS) ≥ 4 and significant fibrosis) according to the body mass index (BMI).

Method: The study included 265 biopsy-proven MASLD patients from tertiary care centers. MASEF score, FAST and LSM by VCTE (Fibroscan) performances were compared to biopsy for the assessment of at-risk MASH. Performances were evaluated by means of area under de curve (AUC) in the different BMI groups.

Results: Patients included in the study had a mean age of 56.9 (± 9.5) years, 46.8% females and 68.7% with type 2 diabetes. 151 patients had a BMI < 35 kg/m², 75 patients (28.3%) had a BMI between 35 and 40 kg/m², and 39 patients (14.7%) had a BMI ≥ 40 kg/m². Prevalence of at-risk MASH was 47.0% (BMI < 35 kg/m²), 42.7% (BMI 35–40 kg/m²) and 33.3% (BMI ≥ 40 kg/m²). MASEF score, FAST and VCTE performances were, respectively: BMI < 35 kg/m², AUC = 0.78/0.75/0.78; BMI between 35 and 40 kg/m², AUC = 0.77/0.74/0.75; BMI ≥ 40 kg/m², AUC = 0.79/0.75/0.65. Not statistical differences were found among the three methods, except for LSM that showed statistically lower AUC in the BMI ≥ 40 kg/m² group, (MASEF vs. FAST: $p = 0.17$, FAST vs. LSM: $p < 0.01$, MASEF vs. LSM: $p < 0.01$).

Conclusion: Our study suggests that MASEF and FAST scores show acceptable accuracy for the detection of at-risk MASH in patients with grade 2 and 3 obesity. MASEF and FAST outperformed VCTE accuracy in morbid obese patients.

SAT-430

Vaccir study: evaluation of vaccination coverage against diphtheria-tetanus-poliomyelitis, pneumococcus, hepatitis A and B, influenza and SARS-COV2 in cirrhotic patients in 17 french general hospitals

Aurore Baron¹, Jean-François Cadranel^{2,3}, Mourad Medmoun⁴, Jacques Arnaud Seyrig⁵, François Xavier Laborne⁶, Florence Skinazi⁷, Xavier Causse⁸, Lemaître Caroline⁹, Serge Bellon¹⁰,

Juliette Verlynde¹¹, Isabelle Rosa¹², Florent Ehrhard¹³, Gilles Macaigne¹⁴, Arnaud Boruchowicz¹⁵, Guillaume Allard¹⁶, Paul Strock¹⁷, Stéphanie De Montigny-Lenhardt¹⁸, Mathilde Petiet Dumont¹⁹, Frederick Moryoussef²⁰, Bénédicte Lambare²¹. ¹Centre Hospitalier Sud Francilien, Corbeil Essonnes, France; ²CH Creil, Creil, France; ³GHP SO, Liver and Digestive Diseases Department, Creil, France; ⁴CH Creil, Creil, France; ⁵Hôpital de Pontivy, Pontivy, France; ⁶CHSF, Corbeil Essonnes, France; ⁷CH SAINT DENIS, Saint Denis, France; ⁸CHR La Source, Orléans, France; ⁹CH le havre, Le Havre, France; ¹⁰Avignon Hospital, Avignon, France; ¹¹CH Dunkerque, Dunkerque, France; ¹²CHI Creteil, Créteil, France; ¹³CH Lorient, Lorient, France; ¹⁴CHI Montfermeil, Montfermeil, France; ¹⁵CH Valenciennes, Valenciennes, France; ¹⁶Centre Hospitalier du Pays d'Aix, Aix en provence, France; ¹⁷Centre Hospitalier de Carcassonne, Carcassonne, France; ¹⁸Centre Hospitalier Edmond Garcin, Aubagne, France; ¹⁹Grand Hôpital de l'Est Fracilien-, Site de Meaux, Meaux, France; ²⁰Centre Hospitalier Intercommunal Poissy Saint-Germain-en-Laye, Poissy, France; ²¹Centre Hospitalier Sud francilien, Corbeil Essonnes, France
Email: aurore.baron@chsf.fr

Background and aims: Cirrhosis exposes patients to an increased risk of serious infections, leading to decompensation of liver disease and death. Vaccination is a simple and effective preventive measure. In France, vaccination against pneumococcus, seasonal influenza, SARS COV2, hepatitis A and B is recommended for all patients with liver disease. Few recent data on vaccination coverage in cirrhotic patients in the world are available but they suggest that it is low. The aim of this study was to estimate, the vaccination coverage of cirrhotic patients, against DTpolio, Pneumococcus, HAV, HBV, influenza, and SARS COV2 in France.

Method: It is a French, prospective, multicentric study, conducted between 09/27/2021 and 12/27/2022. The vaccination coverage of cirrhotic patients, followed for more than six months, in 17 general hospital was estimated via a questionnaire. Patients with vaccination contra-indication or additional immunosuppressive therapy unrelated to their liver disease were excluded. Subgroups were compared according to cirrhosis severity, psychosocial or precariousness risks. Factors associated with incomplete vaccination status were analyzed using a uni- and multivariate logistic regression model. Cases of infection were collated according to vaccination status in order to estimate efficacy.

Results: 728 cases were analyzed comprising 70% men (n = 511), with 58.2 years median age. Cirrhosis was more often caused by alcohol (63% n = 461), mostly non-severe child A (79% n = 549). At the time of diagnosis, rates of vaccination against DTP, HAV, HBV, Influenza and Pneumococcus were 51%, 3%, 12%, 22% and 4% respectively. The rates of de novo vaccinations more than six months after diagnosis were low for DTP 38% (n = 274), HAV 6% (n = 30/481), HBV 10% (on the population eligible for the vaccine) (n = 45/468) with only 50% of complete vaccinations, Pneumococcus 19% (n = 141) with 79% complete vaccination; vaccination rates were better for Influenza 69% (n = 503), and SARS COV2 94% (n = 686). Serological controls were exceptional for HAV or HBV. The main reason for non-vaccination against HAV, HBV and Pneumococcus was non-prescription. Among the non-vaccinated, infections were not rare with 4 HAV, 3 HBV, 16 influenza, 27 COVID cases. In uni and multivariate analyses, vaccination coverage did not differ according to severity of cirrhosis. Precariousness was associated with poorer access to DTP and SarsCOV2 vaccines, and better access to pneumococcal vaccines.

Conclusion: Vaccination coverage of cirrhotic patients against pneumococcus, HAV and HBV is highly inadequate in France, causing frequent and sometimes severe infections, whereas coverage against SARS COV2 and influenza is satisfactory because of strong vaccine incentive from the health authorities. The hepatologist must be aware of the importance of vaccination and become the major conductor of an effective vaccination policy.

SAT-431-YI

Exploring liver vitamin A status and histopathological associations in a Guatemalan cohort: insights into prolonged consumption of vitamin A fortified sugar

Giorgio Cazzaniga^{1,2}, Eric Boy³, Anthony Oxley⁴, Francisco Chew⁵, Keyla Castellanos⁶, Roberto Orozco⁷, Zarina Guzmán⁸, Augusto Rodas⁸, Elmar González⁸, Georg Lietz⁹, Dina Tiniakos^{2,10}.
¹Department of Medicine and Surgery, Pathology, Fondazione IRCCS San Gerardo dei Tintori, University of Milano-Bicocca, Monza, Italy; ²Dept of Pathology, Aretaieion Hospital, National and Kapodistrian University of Athens, Athens, Greece; ³HarvestPlus/IFPRI, Washington D.C., United States; ⁴Fera Science Ltd, Sand Hutton, United Kingdom; ⁵Ministry of Health Guatemala/INCAP, Guatemala City, Guatemala; ⁶Universidad del Valle de Guatemala, Guatemala City, Guatemala; ⁷Departamento Patología Hospital General San Juan de Dios, Guatemala City, Guatemala; ⁸Instituto Nacional de Ciencias Forenses de Guatemala, Guatemala City, Guatemala; ⁹Newcastle University, Newcastle upon Tyne, United Kingdom; ¹⁰Translational and Clinical Research Institute, Newcastle University, Newcastle upon Tyne, United Kingdom
 Email: giorgio9cazzaniga@gmail.com

Background and aims: Guatemala's successful elimination of vitamin A (VA) deficiency is credited to a four-decade-long mandatory sugar fortification initiative. Despite proven effectiveness, concerns have risen regarding the risk of chronic hypervitaminosis A, a recognized cause of liver toxicity. We aimed to evaluate VA status in a cohort of Guatemala City residents, exposed to VA-fortified sugar throughout their lives, and to investigate the associated liver histopathological changes.

Method: This cross-sectional study involved examination of 95 anonymised autopsy liver tissue samples from 95 adolescents and adults without cardiometabolic disease or alcohol toxicity. Informed consent was provided by the family representative. Liver samples were collected within 24 hours of demise due to fatal injuries. Liver VA concentration was measured in all cases. Histology sections were stained with haematoxylin eosin, Masson trichrome and reticulin histochemical stains and were evaluated by two pathologists in consensus. Histological features related to architectural abnormalities, steatosis, inflammation, and vascular changes were semi-quantified. Fibrosis was staged according to Kleiner et al, 2005 and hypertrophic hepatic stellate cells (HSC) were counted per 10 high power fields (HPF, x40) in each acinar zone.

Results: The study cohort included 85 (89%) males (median age 26, range 10–76 years). Thirtyfour (37%) were overweight or obese and 13 (14%) underweight. The mean liver VA concentration was 1.5 µmol/g; 61% samples had liver VA >1 µmol/g and 11% >3 µmol/g. Liver VA values were lower in the 20–39 year age group (mean ± SEM 1.09 µmol/g ± 0.11 µmol/g). One case did not undergo histological scoring due to marked autolysis. Histological changes included: nodular regenerative hyperplasia 16 (17%), steatosis 36 (38%), more than minimal inflammation 4 (4%), more than mild sinusoidal congestion/dilatation 22 (23%), peliosis 4 (4%), and fibrosis stage 1 39 (41%), 2 12 (13%), 3 2 (2%) and 4 1 (1%). In 72 (78%) cases, HSC were <8/10 HPF, while in the remaining 22 (24%) were increased (mean 5, range 0–36/10 HPF). VA concentration was significantly correlated with HSC count (Pearson correlation coefficient $r = 0.24$, $p = 0.02$) and hepatocyte nuclear glycogenation ($r = 0.23$, $p = 0.03$) and was inversely correlated with the extent of steatosis ($r = -0.30$, $p < 0.01$). In samples with increased VA, HSC hyperplasia showed a tendency for zone 2–3 predilection (zone 1 $r = 0.18$ vs zone 2–3 $r = 0.26$) and panzonal steatosis ($r = 0.13$, $p = 0.23$).

Conclusion: The mean liver VA concentration in a Guatemala City cohort surpasses the threshold for hypervitaminosis A. One quarter of affected individuals shows HSC hyperplasia, a histological hallmark of VA liver toxicity. Increased VA appears to affect HSC zonal distribution and hepatic steatosis topography indicating a possible retinol-related pathogenetic mechanism.

SAT-432

A multi-channel educational communication campaign to improve liver disease screening and awareness for clinical care in Southern Arizona along the United States/Mexico border

David Garcia¹, Adriana Maldonado¹, Edgar Villavicencio¹, Naim Alkhouri², Joy Mockbee³, Doug Spegman³. ¹University of Arizona, Mel and Enid Zuckerman College of Public Health, Tucson, United States; ²Arizona Liver Health, Chandler, United States; ³El Rio Health, Tucson, United States
 Email: davidogarcia@arizona.edu

Background and aims: An estimated 25% (~84 million) of adults in the United States (U.S.) have metabolic dysfunction-associated steatotic liver disease (MASLD), an emerging risk factor for liver cancer. In Southern Arizona, liver disease and liver cancer are among the leading causes of death. Thus, there is a critical need to improve liver disease health literacy and promote screenings to increase awareness for clinical care to reduce the disparities experienced among this population. This study aims to implement a multi-channel educational communication campaign along the U.S./Mexico border.

Method: The study team worked with a media firm to create content that is specific to increasing awareness of MASLD risk factors (e.g., obesity, type 2 diabetes) and non-invasive testing (FibroScan®) in both English and Spanish. The 6-month multi-channel educational communication campaign began October 2023 and includes display advertisements in local convenience stores, social media (Facebook and Tik Tok), radio/television (including streaming ads), animated story boards, and testimonial commercials. All advertisements direct individuals interested in a FibroScan® to a website developed by a federally qualified health center (FQHC), in partnership with an academic program developed to foster community-engaged research collaborations, service, and education to advance health equity. All interested individuals can receive a FibroScan® and one-on-one educational sessions about liver disease. High risk individuals identified by FibroScan® are referred to a hepatology clinic.

Results: From October 2023–December 2023 (3 months), over 4.29 million impressions (count of total number of times digital advertisements) have been shown throughout the Southern Arizona region. Paid social media resulted in 2.46 million impressions. Notably, 505, 710 impressions came from TikTok in English and 349, 780 in Spanish. In addition, there were approximately 1.0 million impressions from display advertisements in English and 916, 230 in Spanish. In total, 252, 000 impressions were from English television streaming ads. Overall, 5, 930 individuals went to the study website to learn more about MASLD and 556 completed a request to complete a FibroScan® with over 350 scans completed to date with 25% of the study sample referred to a hepatology clinic for follow-up care.

Conclusion: The on-going multi-channel educational communication campaign has resulted in increased MASLD screenings and awareness of liver disease in Southern Arizona. Future efforts will focus on the process evaluation to gather ongoing feedback about the execution and evolution of the educational campaign to inform the development of a clinical care pathway model.

SAT-433

Transient elastography identifies previously undiagnosed advanced liver disease among those presenting with alcohol dependence

Rachel Edwards¹, Lorraine Hussain¹, Stuart McPherson^{1,2}, Steven Masson^{1,2}. ¹Liver Unit, Freeman Hospital, The Newcastle Upon Tyne Hospital Trust, Newcastle Upon Tyne, United Kingdom; ²Translational and Clinical Research Institute, Newcastle University, Newcastle Upon Tyne, United Kingdom
 Email: rachelmedwards72@gmail.com

Background and aims: Alcohol-related liver disease (ARLD) is the major cause of liver-related morbidity in Europe. EASL recommends screening for the presence of fibrotic liver disease in people drinking

POSTER PRESENTATIONS

alcohol at higher-risk levels. We aimed to assess the uptake of fibrosis testing with Transient Elastography (TE) liver stiffness measurement (LSM), and determine the prevalence of clinically significant fibrosis, among people with alcohol dependence admitted to our institution. This was part of an NHS quality improvement initiative, with a target of inviting $\geq 35\%$ of those admitted with alcohol dependence for fibrosis testing.

Method: All admissions to the Newcastle upon Tyne Hospitals Trust between April 2022 and March 2023 were reviewed prospectively to identify adults admitted for ≥ 1 night with a primary or secondary diagnosis of alcohol dependence. Exclusion criteria were known cirrhosis, already attending liver services, LSM within previous 12 months, life-limiting comorbidity, or lived out of area. Those eligible were invited for TE with FibroScan[®]. TE was considered reliable if at least 10 measurements were performed, and the IQR/median ratio was $\leq 30\%$. LSM < 8 kPa excluded clinically significant fibrosis. LSM > 15 kPa indicated probable advanced fibrosis/cirrhosis. Those with a LSM ≥ 11.5 kPa were offered liver clinic review and those with LSM 8–11.4 kPa were offered 2 year follow-up TE. Data on self-reported alcohol intake was collected.

Results: There were 981 admissions amongst 696 people with alcohol dependence, 100 of whom were known to have cirrhosis. 324 (54% of eligible) individuals were invited for TE, of which 159 (49%) attended. The median age of attendees was 50 years [IQR 38–58], 64% were male and the median weekly alcohol consumption was 140 units [IQR 84–252]. The median LSM was 5.4 kPa [IQR 4.4 to 7 kPa]. 5 had unreliable TE. Overall, 20% ($n=31$) had a LSM of ≥ 8 kPa (significant fibrosis) and 6% ($n=10$) had LSM ≥ 15 kPa (advanced fibrosis/cirrhosis). In total, 79% of those referred to clinic attended. Of these, 55% reported abstinence from alcohol and a further 27% reduced their intake. Among those with LSM > 15 kPa, there was a reduction in alcohol related hospital admissions by 94% in the following 6 months, compared with the 12 months preceding TE.

Conclusion: In a cohort of people with alcohol dependence, half of those offered fibrosis testing attended, identifying clinically significant fibrosis in 20% and cirrhosis in 6%. Most people with cirrhosis were already known to services. Reduction in alcohol consumption was observed in those with advanced fibrosis/cirrhosis identified through this work. Therefore, more proactive fibrosis assessment to identify advanced liver disease may promote behaviour change and reduce alcohol consumption in this high-risk cohort.

SAT-434

Use of FibroScan[®] to assess hepatic steatosis and fibrosis in community-based settings to promote clinical care linkages along the Southern Arizona United States/Mexico border

David Garcia¹, Adriana Maldonado¹, Edgar Villavicencio¹, Rosi Vogel¹, Caitlin Baird¹, Alejandra Cervantes¹, Ana Gonzalez¹, Estefania Ochoa Mora², Naim Alkhouri³. ¹University of Arizona, Mel and Enid Zuckerman College of Public Health, Tucson, United States; ²University of Arizona, Clinical Translational Sciences, University of Arizona Health Sciences, Tucson, United States; ³Arizona Liver Health, Chandler, United States
Email: davidogarcia@arizona.edu

Background and aims: Early detection and screening for metabolic dysfunction-associated steatotic liver disease (MASLD) is needed for at-risk populations. In comparison to other highly prevalent non-communicable chronic conditions (e.g., obesity, type 2 diabetes, and cardiovascular disease), MASLD has received little attention from a public health perspective with global health strategies characterized as inadequate and fragmented. There is a general lack of knowledge around effective screening methods, particularly in community-based settings for high-risk populations. This often leads to a late diagnosis and worse health outcomes for individuals with MASLD. In collaboration with local community partners, we implemented MASLD screenings in community-based settings as part of an ongoing community engaged research study. The purpose of this

study is to assess the use of FibroScan[®] for hepatic steatosis and fibrosis in community-based settings to promote clinical care linkages for liver disease among adults along the Southern Arizona United States/Mexico border.

Method: We used a combination of MASLD screening with FibroScan[®] and educational and behavioral strategies (e.g., handouts and brief counseling) specific to liver health. Continuous attenuation parameter (CAP) values are measured in decibels per meter (dB/m). MASLD is identified as having a CAP score ≥ 288 dB/m. Liver stiffness measurements (LSM) in kilopascals (kPa) indicate fibrosis values. Individuals with a ≥ 280 CAP and ≥ 6 kPa or ≥ 8 kPa alone were referred to a clinical care partner (hepatology clinic).

Results: To date, 1,070 adults (mean age: 52.0 ± 14 years; 37.9% female; 90% Mexican-origin descent) in Southern Arizona have been screened for MASLD. Overall, the prevalence of MASLD is 38%, including 58% men and 42% women ($X^2 = 5.5$, $df = 1$, $p = 0.02$). Of the total sample 25% ($n = 266$) of participants have been referred to hepatology clinic for clinical care follow-up (mean LSM: 10.9 kPa \pm 8.6 kPa). Further, in a subsample of participants ($n = 623$); 79% reporting hearing about fatty liver disease before, primarily from a doctor or media source. Most participants (88%) report that they believe fatty liver disease is preventable; however, 36% are unaware if treatment is available.

Conclusion: MASLD screening with the FibroScan[®] combined with educational information appears to be a viable strategy to initiate community-based screening efforts as a part of a clinical care pathway model. However, it is necessary to ensure these screening efforts are cost-effective, scalable and a “closed loop” system is developed for the referral process for those seeking clinical care.

SAT-435

Benefits and harms of post-treatment surveillance in patients with early-stage of HCC after curative ablation

Awassada Yangcharoen¹, Supot Nimanong¹, Tawesak Tanwandee¹, Watcharasak Chotiayaputta¹, Phunchai Charatcharoenwiththaya¹, Siwaporn Chainuvati¹. ¹Division of Gastroenterology, Department of Medicine Faculty of Medicine, Siriraj Hospital, Mahidol University, Bangkok, Thailand
Email: supotgi@gmail.com

Background and aims: The recurrent rate of HCC after ablation is high. There is no consensus recommendation of post-treatment surveillance. We aimed to investigate benefits and harms of CT/MRI as tools for post-treatment surveillance in patients with early-stage of HCC after curative ablation.

Method: We conducted a retrospective cohort study in HCC BCLC stage 0/A patients, who received curative ablation and underwent CT/MRI over 5-year follow-up. Benefits were rate of recurrent HCC within Milan criteria and received curative treatment. Non-severe harms included number of additional sessions of CT/MRI without recurrent HCC and decline in eGFR while severe harms were contrast injury or invasive procedures.

Results: Among 204 enrolled patients, 88.7% had cirrhosis, 84.3% had single HCC with mean size of 2 cm. The 5-year overall survival rate were 81%. The cumulative 1st-, 2nd-, 5th- year recurrent rate were 25.9%, 41.6% and 55.3% respectively. Rate of recurrent HCC within Milan criteria and received curative treatment were 84% and 73.5%, not significantly different between < 120 days and 120–180 days interval groups. Twenty eight percent of patients underwent additional CT/MRI without recurrent HCC, and no severe harms was recorded. Multivariate analysis revealed frequent sessions of CT/MRI (5–8 sessions in 2-years) were predictors of significant decline in eGFR.

Conclusion: CT/MRI are effective tools for post-treatment surveillance in patients with early-stage HCC after curative ablation. However, frequent imaging sessions (< 6 -months interval in first 2-year) do not increase detection rate of small HCC and are associated with significant decline of eGFR.

SAT-436

Age and sex differences in the incidence of cirrhosis caused by metabolic dysfunction associated steatohepatitis in Manitoba, Canada: a population-based study

Nabiha Faisal¹, Lisa Lix¹, Randy Walld², Alexander Singer², Harminder Singh², Eberhard Renner², Alyson Mahar³. ¹University of Manitoba, Winnipeg; ²University of Manitoba, Winnipeg, Canada; ³Queen's University, Kingston, Canada
Email: nabiha.faisal@umanitoba.ca

Background and aims: Metabolic dysfunction associated steatohepatitis (MASH) has emerged as a predominant cause of cirrhosis, closely linked to the global surge in obesity, diabetes, and metabolic syndrome. The dynamic evolution of cirrhosis risk factors necessitates ongoing efforts in prevention and management. To facilitate the development of these strategies, we aim to investigate the temporal trends in MASH cirrhosis incidence in Manitoba, Canada, and assess changes in cirrhosis rates across age groups and between males and females.

Method: We performed a retrospective population-based cohort study in Manitoba, Canada, using linked administrative healthcare data housed in Manitoba Centre of Health Policy. Patients aged at least 18 years with incident cirrhosis (2010–2020) were identified by use of a validated case finding algorithm (defined as at least one inpatient or outpatient visit with a diagnosis of cirrhosis or related complications), and MASH was defined using a validated hierarchical algorithm (3, 4). Annual cirrhosis incidence rate per 100,000 person-years was calculated using a generalized linear model and generalized estimating equations with a negative binomial distribution adjusting for age and sex. Linear trends of incidence by calendar year, overall and by age and sex, were tested using linear regression models.

Results: Between 2010 and 2020, 31,147 individuals with MASH cirrhosis were identified. MASH constituted 69% of all cirrhosis cases in 2020. The incidence of cirrhosis caused by MASH increased approximately by 35% during the study period. The age and sex adjusted incidence of MASH rose from 208/100,000 (95% CI 192.9–224.7) in 2010 to 281/100,000 (95% CI 261.4–301.8) in 2020. The mean age at diagnosis was 49.7 years (SD 15.9), with 50.1% being men, 31% having diabetes, and 62% hypertension. Females exhibited a greater increase in incidence compared to males (females: 1.6, 95% CI 1.4–1.8; males: 1.1, 95% CI 0.9–1.3). In terms of age groups, the younger age group (18–44) exhibited a higher increase in incidence compared to those aged 65 and above (18–44: 1.5, 95% CI 1.2–1.8; 65+: 1.1, 95% CI 0.9–1.4). On average MASH Cirrhosis incidence increased annually by 4%.

Conclusion: The incidence of MASH cirrhosis has increased significantly since 2010, with age, and sex disparity. Public health action is required to implement an effective multi-faceted approach and public awareness efforts to reverse these trends.

SAT-437-YI

MAF-5 improves the detection of advanced and significant fibrosis in FIB-4 underserved individuals in a United States general population

Laurens van Kleef¹, Jesse Pustjens¹, Harry L.A. Janssen¹, Willem Pieter Brouwer¹. ¹Erasmus MC, University Medical Center, Rotterdam, Netherlands
Email: l.vankleef@erasmusmc.nl

Background and aims: The FIB-4 is the cornerstone of referral pathways as proposed by the EASL, AASLD and AGA, despite concerns regarding the diagnostic accuracy in populations aged <35 years or ≥65 years old or individuals with diabetes (DM). Recently three new scores have been developed: steatosis associated fibrosis estimator (SAFE), LiverRisk score (LRS) and metabolic dysfunction associated fibrosis (MAF-5). Whether these scores can benefit these FIB-4 underserved populations remains to be determined.

Method: We used data from the NHANES 2017–2020 cycle, a United States population-based cohort with data on liver stiffness measurements (LSM). We selected patients with metabolic dysfunction according to the guidelines referral pathways with complete data on LSM and the SAFE, LRS and MAF-5. AUC analysis, detection rate, referral rate and NPV were used to assess its diagnostic accuracy regarding LSM ≥8 and ≥12 kPa, which is suggestive of significant or advanced fibrosis. Three FIB-4 underserved populations were analysed: (1) aged <35 years (2) aged ≥65 years and (3) those with DM.

Results: This first cohort comprised 1437 participants aged <35 (age 26 [22–31], 50% male) among which 5.7% and 1.7% had LSM ≥8 and ≥12 kPa. The AUC for detecting LSM ≥8 kPa by the SAFE, LRS and MAF-5 was 0.72, 0.73 and 0.83, all significantly better than the FIB-4 with an AUC of 0.50. Similarly, FIB-4 was outperformed for LSM ≥12 kPa with an AUC of 0.77 (SAFE), 0.67 (LR) and 0.93 (MAF-5) compared to 0.58 (FIB-4). Additionally, we analyzed 1444 participants aged ≥65 (age 72 [68–78], 50% male) among which 13.1% and 4.4% had LSM ≥8 and ≥12 kPa. The AUC for LSM ≥8 kPa of the SAFE, LRS and MAF-5 was 0.69, 0.68 and 0.75 compared to 0.54 for FIB-4. In this elderly population, results were consistent for LSM ≥12 kPa, with an AUC of 0.76, 0.73 and 0.78 for SAFE, LRS and MAF-5, versus 0.61 for FIB-4. Finally, we focussed on 1191 participants with diabetes (age 61 [43–70], 52% male) among which 22% and 7.3% had LSM ≥8 and ≥12 kPa. Again the AUC for detecting LSM ≥8 kPa was better for SAFE, LRS and MAF-5 with 0.65, 0.61 and 0.77 compared to FIB-4 with 0.55, as well as for LSM ≥12 kPa with 0.74, 0.64 and 0.81 for SAFE, LRS and MAF-5 compared to 0.62 for FIB-4. Implementing these scores in referral strategies to detect LSM ≥8 kPa in these FIB-4 underserved populations combined would result in the detection of 81% of cases with the SAFE score (cut-off 0: referral 55%, NPV 95%), 53% of cases by LRS (cut-off 6: referral 27%, NPV 92%) and 84% with MAF-5 (cut-off 0: referral 46%, NPV 96%), detection rates increased to 86%, 60% and 91% for LSM ≥12 kPa with the SAFE, LRS and MAF-5, respectively.

Conclusion: The FIB-4 was outperformed by the recently developed scores in detecting advanced liver disease in FIB-4 underserved populations. The MAF-5, an age-independent score, had the best performance among the FIB-4 underserved populations and should be considered in referral strategies.

SAT-438

Fatigue is an Important Driver of Work Productivity Loss and Impairment of Patient-Reported Outcomes (PROs) among Patients with Metabolic Dysfunction-Associated Steatotic Liver Disease (MASLD)

Zobair Younossi^{1,2}, Yusuf Yilmaz^{3,4}, Ming-Lung Yu^{3,5}, Vasily Isakov^{3,6}, Marlen Ivon Castellanos Fernández^{3,7}, Vincent Wai-Sun Wong^{3,8}, Yuichiro Eguchi^{3,9}, Manuel Romero-Gómez^{3,10}, Nahum Méndez-Sánchez^{3,11}, Ajay Kumar Duseja^{3,12}, Caglayan Keklikkiran^{3,13}, Jacob George^{3,14}, Elisabetta Bugianesi^{3,15}, Ashwani K. Singal^{3,16}, Saeed Sadiq Hamid^{3,17}, Khalid A. Alswat^{3,18}, Wah-Kheong Chan^{3,19}, Jiangao Fan^{3,20}, George Papatheodoridis^{3,21}, Stuart C. Gordon^{3,22}, Mohamed El-Kassas^{3,23}, Stuart Roberts^{3,24}, Brian Lam^{3,25}, Andrei Racila²⁶, Linda Henry³, Saleh Alqahtani^{3,27}, Maria Stepanova^{3,28}. ¹The Global NASH Council, Washington DC; ²Beatty Liver and Obesity Research Program, Falls Church, United States; ³The Global NASH Council, Washington DC, United States; ⁴Liver Research Unit, Institute of Gastroenterology, Marmara University, Istanbul, Turkey; ⁵School of Medicine and Doctoral Program of Clinical and Experimental Medicine, College of medicine and Center of Excellence for Metabolic Associated Fatty Liver Disease, National Sun Yat-Sen University, Hepatobiliary Division, Department of Internal Medicine, Kaohsiung Medical University Hospital, Kaohsiung, Taiwan; ⁶Chief of Gastroenterology and Hepatology at Institute of Nutrition, Moscow, Russian Federation; ⁷Institute of Gastroenterology, University of Medical Sciences of Havana, Havana, Cuba; ⁸Department of Medicine and

POSTER PRESENTATIONS

Therapeutics, The Chinese University of Hong Kong, Hong Kong, Hong Kong; ⁹Locomedical General Institute, Locomedical Medical Cooperation, Saga, Japan; ¹⁰Digestive Diseases Department, Virgen del Rocio University Hospital, Institute of Biomedicine, Seville, Spain; ¹¹Liver Research Unit, Medica Sur Clinic and Foundation, National Autonomous University of Mexico, Mexico City, Mexico; ¹²Department of Hepatology, Postgraduate Institute of Medical Education and Research, Chandigarh, India; ¹³Department of Gastroenterology, School of Medicine, Recep Tayyip Erdogan University, Rize, Turkey; ¹⁴Storr Liver Centre, Westmead Institute for Medical Research, Westmead University of Sydney, Sydney, Australia; ¹⁵Division of Gastroenterology, Department of Medical Sciences, University of Torino, Torino, United States; ¹⁶University of Louisville School of Medicine, Louisville, United States; ¹⁷Department of Medicine, Aga Khan University, Karachi, Pakistan; ¹⁸Liver Disease Research Center, Department of Medicine, College of Medicine, King Saud University, Riyadh, Saudi Arabia; ¹⁹Gastroenterology and Hepatology Unit, Department of Medicine, Faculty of Medicine, University of Malaya, Kuala Lumpur, Malaysia; ²⁰Department of Gastroenterology, Xinhua Hospital, Shanghai Jiao Tong University School of Medicine, Shanghai, China; ²¹National and Kapodistrian University of Athens, Athens, Greece, ²²Henry Ford Hospital System, Department of Hepatology and Gastroenterology, Detroit, United States, ²³Endemic Medicine Department, Faculty of Medicine, Helwan University, Cairo, United States; ²⁴The Alfred, Department of Hepatology and Gastroenterology, Melbourne Victoria, Australia; ²⁵Beatty Liver and Obesity Research Program, Falls Church, United States; ²⁶The Global Nash Council, Washington DC, United States; ²⁷Organ Transplant Center of Excellence, King Faisal Specialist Hospital and Research Center, Division of Gastroenterology and Hepatology, Johns Hopkins University, Baltimore, MD, USA, Riyadh, Saudi Arabia; ²⁸Center for Outcomes Research in Liver Disease, Washington DC, United States
Email: zobair.younossi@cldq.org

Background and aims: MASLD is associated with fatigue which can have negative impact on clinical outcomes and PROs. We assessed fatigue among MASLD patients seen in real-world practices.

Method: We used data [demographics, medical history, FIB-4 scores, liver stiffness by transient elastography and PRO scores (FACIT-F, CLDQ-NASH, WPAI)] collected by the Global NASH Registry™. Presence of clinically overt fatigue was determined from medical history (MH-based fatigue) or using Fatigue Scale of FACIT-F PRO instrument (FS<30 on a 0–52 scale; PRO-based fatigue).

Results: We included 6783 MASLD patients from 18 countries (Australia, China, Cuba, Egypt, Greece, Hong Kong, India, Italy, Japan, Saudi Arabia, Malaysia, Mexico, Pakistan, Russia, Spain, Taiwan, Turkey, USA): age 51 ± 13 years old, 44% male, 47% employed, 68% obese, 41% type 2 diabetes (T2D), 51% hypertension, 19% with advanced fibrosis (biopsy or transient elastography ≥ 9.5 kPa or FIB-4 ≥ 2.67), 24% history of depression, 29% sleep apnea, 20% abdominal pain. Of all patients, 39% had MH-based fatigue and 26% had PRO-based fatigue by FACIT-F. Concordance between the two fatigue definitions was 68%, with 44% of those with MH-based fatigue also having PRO-based fatigue (vs. 9% among those without MH-based fatigue). Regardless of the definition, MASLD patients with fatigue were younger (50 vs. 52 years), more commonly female (67% vs. 49%), obese (75% vs. 64%) with T2D (45% vs. 38%), depression (34% vs. 17%) and abdominal pain (33% vs. 10%) (all $p < 0.05$). Patients with fatigue also reported a substantial impairment in other PRO scores: total CLDQ-NASH score 4.49 (SD 1.08) vs. 5.51 (0.96) in patients with vs. without MH-based fatigue (impairment of -1.02 , or -17% of range size), compared to 3.83 (0.91) vs. 5.44 (0.89) in those with vs. without PRO-based fatigue (impairment -1.61 , or -27% of range size); similarly total FACIT (4 generic domains of FACIT-F) was -11% by MH-based fatigue and -20% by PRO-based fatigue, and excessive work productivity impairment (WPI) was -13% by the presence of MH-based fatigue and -25% by PRO-based fatigue. After adjustment for clinico-demographic confounders, association of lower PRO scores with fatigue remained significant for all studied PRO scores, with the

effect size again being greater for PRO-based fatigue than MH-based fatigue: -20% vs. -10% for total CLDQ-NASH, -16% vs. -6% for FACIT-F, and -21% vs. -7% for WPI (all $p < 0.0001$). Other predictors of lower PRO scores in MASLD included younger age, female sex, advanced fibrosis, non-hepatic comorbidities, and lack of regular exercise ($p < 0.05$).

Conclusion: MASLD patients experience substantial fatigue burden that is partially captured by medical history and more accurately asserted by a fatigue-specific PRO instrument (FACIT-F). Fatigue is associated with a significant impairment of other PROs and work productivity with its negative economic impact.

SAT-439-YI

Socioeconomic deprivation is independently associated with hepatocellular carcinoma mortality in a western european country with single-payer healthcare

Massih Ningarhari^{1,2}, Alexandre Lacour³, Simon Dauchy³, Michael Genin¹, Amelie Bruandet³, Stéphane Cattan³, Line Carolle Ntandja Wandji^{2,3}, Elise Lemaître³, Valérie Canva³, Alexandre Louvet^{2,4}, Philippe Mathurin^{2,3}, Sébastien Dharancy^{3,5}, Guillaume Lassailly^{2,3}. ¹CHU Lille, Maladies de l'Appareil Digestif, Lille, France; ²Université de Lille, INSERM, Infinite, Lille, France; ³CHU Lille, Lille, France; ⁴CHU Lille, Lille; ⁵Université de Lille, INSERM, Infinite, Lille
Email: massih.ningarhari@chu-lille.fr

Background and aims: Socioeconomic deprivation (SED) has been associated with mortality from hepatocellular carcinoma (HCC) in North America. Determinants of this association such as type of health insurance may differ in Europe. Data on the impact of SEP on HCC survival in countries with universal single-payer healthcare system are scarce.

Method: Retrospective study of all consecutive patients discussed for a first diagnosis of HCC in the regional multidisciplinary tumor board (MTB) of a French tertiary center between 01/01/2019 and 31/12/2019. Demographics, distances to the referral center, dates of diagnosis, referral, MTB, and treatment, patient and tumor characteristics, and treatment were collected. SED was inferred for each patient using the FDep score based on residence's postcode. Overall survival (OS) from the date of diagnosis was calculated using the Kaplan-Meier method, and the association between SED and overall survival was analysed using a Cox model.

Results: We included 318 patients: median age 67 years, alcohol-related liver disease 71%, cirrhosis 81%, Child A 65%, HCC diagnosed by screening 47%, maximal tumour size 3 cm (IQR 2–5.5), median AFP 10 ng/ml (IQR 4–100). The median time between first imaging suggestive of HCC and first discussion in MTB was 27 days (14–50). The median distance between patient's residence and the regional referral centre was 28 km (IQR 16–55). Median OS from the date of diagnosis was 20.1 months (95% CI 16.1–25.1). Patients in the fourth quartile (Q4) of the FDep score, the most deprived, had a significantly poorer OS (HR 1.44, CI95% 1.06–1.97, $p = 0.02$) in univariate analysis. Patients in the Q4 lived farther from the referral centre ($p = 0.006$), were more frequently obese ($p = 0.04$), had more frequently history of liver decompensation ($p = 0.004$), ascites ($p = 0.001$) and larger tumour size ($p = 0.02$) at diagnosis. There was no statistically significant association between belonging to Q4 and excessive alcohol consumption ($p = 0.49$), presence of diabetes ($p = 0.58$), cirrhosis ($p = 0.87$), time between diagnosis and treatment ($p = 0.4$). There was a trend towards lower access to curative treatments (29% vs 37%, $p = 0, 07$). In multivariate analysis, belonging to the Q4 remained significantly associated with increased overall mortality from the date of diagnosis (HR 1.71, CI95% 1.07–2.72, $p = 0, 03$).

Conclusion: Socioeconomic deprivation was independently associated with poorer overall survival in patients with a diagnosis of HCC, even in a Western European country with single-payer universal healthcare system. Studies are needed to optimize public health strategies targeting patients at risk of HCC.

SAT-440

Risk factors for future development of cirrhosis in UK primary care patients with elevated ALT: a survival analysis of the optimum patient care research database

Kris Bennett¹, Victoria Carter², Derek Skinner², William Henley³, David Price^{2,4}. ¹South West Liver Unit, University Hospitals Plymouth NHS Trust, Plymouth, United Kingdom; ²Observational and Pragmatic Research Institute, Midview City, Singapore; ³Department of Health and Community Sciences, University of Exeter Medical School, Exeter, United Kingdom; ⁴Centre of Academic Primary Care, Division of Applied Health Sciences, University of Aberdeen, Aberdeen, United Kingdom
Email: kbennett6@nhs.net

Background and aims: Elevated alanine transaminase (ALT) blood tests are common in primary care and may be the first indication of previously unrecognised steatotic liver disease (SLD). Current non-invasive tests primarily focus on detection of advanced fibrosis or cirrhosis. Stratifying risk earlier in the natural history, when preventative strategies are likely to be most effective, remains an important challenge. This study aimed to identify risk factors for earlier development of cirrhosis in patients with elevated ALT in a primary care population.

Method: A historical cohort study of eligible adults with ALT 50–1000 between January 2000 and December 2020 using the Optimum Patient Care Research Database (www.opcrd.co.uk). Index date was the earliest recorded ALT abnormality. Patients were followed up until primary outcome, death or last data extraction. The primary outcome was a diagnosis of cirrhosis or a proxy-condition (e.g. complication of cirrhosis). Patients with pre-existing cirrhosis, baseline bilirubin >50, prior alcohol misuse, malignancy or non-SLD aetiologies were excluded. Data was analysed using Python with multiple imputation of missing lifestyle/biochemical variables. A multivariate, Cox proportional hazards (Cox-PH) model was fit on 80% of the data using comorbidities, lifestyle factors and biochemical results as predictors. Backwards elimination of predictors was performed using the Akaike Information Criterion. 20% of the data was reserved for internal validation.

Results: 1.04 million patients with an ALT of 50–1000 were included, with 11,478 (1.1%) progressing to cirrhosis. 61% were male, with a median age 49 years and median follow-up 7.1 years. The Cox-PH model identified 13 predictors of cirrhosis, with GLP1-receptor agonist (GLP1-RA) usage (HR=2.34), smoking (HR=2.21) and diabetes (HR=1.68) the strongest predictors. Statin use predicted a lower risk of cirrhosis (HR=0.73) and this association persisted when controlling for cardiovascular disease, diabetes and smoking. Model performance was good (c-index=0.7) with similar performance on unseen test data. Inclusion of markers of alcohol misuse after index ALT abnormality improved model performance further (c-index=0.81).

Conclusion: This study of >1 million primary care patients with abnormal ALT, identifies 13 factors associated with future progression to cirrhosis. GLP1-RA usage is associated with the highest risk which probably serves as a marker of diabetes severity. Statin use is associated with reduced cirrhosis risk. Further observational and randomized studies are warranted to improve prediction of future cirrhosis risk in primary care and identify factors which may slow progression to cirrhosis.

SAT-441-YI

Who doesn't turn up? Exploring patient characteristics associated with non-adherence with regular hepatocellular carcinoma surveillance: a systematic review and meta-analysis

Hannah MacCarthy¹, Ryan M. Buchanan^{1,2}, Dankmar Böhning³, Kate Glyn-Owen¹. ¹University of Southampton, Southampton, United Kingdom; ²University Hospital Southampton, Southampton, United Kingdom; ³Southampton Statistical Sciences Research Institute, University of Southampton, Southampton, United Kingdom
Email: hmm1g19@soton.ac.uk

Background and aims: In 2020, hepatocellular carcinoma (HCC) was the sixth most diagnosed cancer and had the third highest mortality globally. Five-year survival is around 18%, stressing the importance of routine six-monthly surveillance, which increases the likelihood of early detection and receipt of curative treatment. Surveillance adherence is around 52%. HCC disproportionately affects socio-economically deprived and under-served groups, and these groups also have low uptake of population screening programmes. We aimed to explore characteristics associated with non-adherence with regular surveillance for HCC.

Method: This study updated a previous systematic review and meta-analysis of HCC patients, to include recent studies and to explore alternative outcomes in relation to attendance at regular surveillance. Ovid and Embase databases were searched from July 2020–November 2023, in addition to the original searches from January 2014. We included cohort studies of patients with diagnosed HCC, which reported data on prior attendance in a surveillance programme. Data were extracted on attendance, sociodemographic characteristics, risk factors for liver disease and underlying aetiology of disease. Data were analysed using STATA, meta-analysis was conducted where appropriate and sensitivity analyses were conducted excluding studies with high risk of bias. Likelihood of surveillance attendance was reported using odds ratios with 95% confidence intervals (CI).

Results: Overall, 36 studies with a total of 1,398,994 HCC patients were included in the meta-analysis. Of these, 51.6% attended regular surveillance, and 48.4% did not. Male patients had significantly lower odds of attending surveillance compared to females (OR=0.73, 95% CI 0.66–0.82). Former and current smokers had significantly lower odds of attending surveillance compared to non-smokers (OR=0.79, 95% CI 0.68–0.92). Patients with HBV had significantly lower odds of attending regular surveillance compared to patients with HCV (OR=0.62, 95% CI 0.50–0.77). Patients with HCV also had significantly higher odds of attending regular surveillance when compared against other aetiologies (OR=2.34, 95% CI 1.84–2.96). Patients with MASLD had significantly lower odds of attending surveillance when compared with other aetiologies (OR=0.62, 95% CI 0.43–0.91).

Conclusion: Amongst patients with a diagnosis of HCC, the following were less likely to have been attending a regular HCC surveillance programme: Male patients, patients with HBV or MASLD and current/former smokers. This suggests potential targets for interventions aiming to increase surveillance uptake. More research is required to understand why these groups are not attending compared to other groups, such as those with HCV.

SAT-442

Fibro-Predict risk score for liver cirrhosis from nationwide electronic health records

Iris Kalka¹, Rawi Hazzan², Nancy-Sarah Yacovzada¹, Saleh Igbaria², Eran Segal¹, Ziv Neeman³, Adina Weinberger¹. ¹Weizmann Institute of Science, Rehovot, Israel; ²Emek Medical Center, Afula, Israel; ³Emek Medical Center, Rappaport Faculty of Medicine, Technion-Israel Institute of Technology, Afula, Israel
Email: iris.kalka@weizmann.ac.il

Background and aims: Liver diseases, notably cirrhosis, pose a substantial global health challenge, resulting in millions of annual deaths. Existing diagnostic methods primarily target high-risk groups, leaving a significant portion of patients undiagnosed. This study's objective is to develop an accurate screening approach, utilizing nationwide electronic health records (EHR), to identify individuals at risk of cirrhosis within the general population.

Method: A liver cirrhosis diagnostic framework was constructed by analyzing EHR data from 2,255,580 samples. This framework is centered on Fibro-Predict, a machine-learning model capable of predicting five-year disease diagnosis trajectories based on routine blood tests. We conducted a retrospective temporal-validation of the model and an external prospective validation in clinical settings, employing transient elastography.

POSTER PRESENTATIONS

Results: The temporal-validation of Fibro-Predict demonstrated a promising c-index of 0.80 (95% CI 0.80 ± 6E-5) in the training cohort and 0.79 (95% CI 0.79 ± 9E-5) during validation. In a clinical context, our framework exhibited an impressive True Positive Rate (TPR) of 36.8% (28/76) when comparing predicted risk to observed outcomes, surpassing the gold-standard FIB-4 with a TPR of only 3.7% (1/27).

Conclusion: Fibro-Predict, relying solely on routine blood tests, emerges as a valuable tool for cost-effective patient prioritization in cirrhosis screening within the general population. Leveraging nationwide EHR data, we can efficiently identify individuals in need of clinical follow-ups and expedite cirrhosis diagnosis. This approach holds the potential to significantly improve the early detection of cirrhosis and subsequently reduce its associated morbidity and mortality, particularly within underserved populations.

SAT-443

FIB-4 based referral pathways to identify advanced liver disease have poor clinical utility in a United States general population

Laurens van Kleef¹, Jesse Pustjens¹, Harry L.A. Janssen¹, Willem Pieter Brouwer¹. ¹Erasmus MC, University Medical Center, Rotterdam, Netherlands

Email: l.vankleef@erasmusmc.nl

Background and aims: The fibrosis-4 index (FIB-4) is the cornerstone of the referral pathways provided by the AASLD, EASL and AGA that aim at identifying advanced liver disease among low-prevalence populations. Although the diagnostic accuracy of FIB-4 is acceptable in SLD patients who underwent liver biopsy, its clinical utility in these pathways beyond its intended populations remains to be proven.

Method: We used data from the NHANES 2017–2020 cycle, a United States population-based cohort with data on liver stiffness and FIB-4. Participants at risk for advanced liver disease were selected based on the presence of metabolic dysfunction (a constellation of overweight/obesity, dyslipidaemia and impaired glycaemic control) following the AASLD, EASL and AGA referral pathways. Significant (LSM ≥ 8 kPa) and advanced fibrosis (LSM ≥ 12 kPa) prevalence is set out against fibrosis risk estimated with the FIB-4. A general cut-off of 1.3 was used to estimate fibrosis risk. Lastly, the AUROC of the FIB-4 is investigated in the overall population and subgroups.

Results: The cohort comprised 6,191 participants with metabolic dysfunction (aged 52 [36–64] years, 49% male), of them 46% had MASLD, 10.1% significant fibrosis and 3.2% advanced fibrosis. According to the FIB-4-based algorithm, advanced liver disease was ruled out in 72.7% and further work-up was required in 27.3%. However, among those considered to have no advanced liver disease, significant fibrosis was still present in 9.0% and advanced fibrosis in 2.2%. This results in missing out on 59.5% and 48.0% of cases, respectively. When using FIB-4 >2.0 among those aged ≥65 years, even more cases were missed (70.7% of significant fibrosis and 2.4% of advanced fibrosis), but fewer people required further work-up (17.1%). Next, we excluded patients aged <35 years, in which the FIB-4 is known to have poor performance. The proportion that now required further investigation increased to 35.3% and among those considered at low risk of advanced liver disease, still 10.4% had significant and 2.4% advanced fibrosis. The AUROC in the overall population to detect significant fibrosis was 0.61 and for subgroups aged <35, 35–65 and >65 0.50, 0.60 and 0.54 respectively. For advanced fibrosis results were slightly better with an AUROC of 0.67 in the overall population and 0.58, 0.67 and 0.61 in subgroups aged <35, 35–65 and >65 respectively. Diagnostic accuracy did not improve among participants with MASLD.

Conclusion: FIB-4-based referral pathways to identify advanced liver disease among the general population with metabolic dysfunction have poor diagnostic accuracy. Particularly worrisome is the high rate of missing out on significant and advanced fibrosis (up to 70% and 60% respectively). There is an urgent need for a dedicated test that is

specifically developed to identify individuals in the general population who may benefit from hepatologist referral.

SAT-444

Large-scale community outreach Fibroscan program to detect advanced fibrosis and cirrhosis for early detection of liver cancer

Basil Ahmad¹, Helen Boothman², Michael Tolentino², Laura Letham², James Attridge-Smith², Nina van Zyl², Fergus Daly², Daniel Forton¹. ¹St George's University Hospitals NHS Foundation Trust, London, United Kingdom; ²St George's University Hospitals NHS Foundation Trust, London, United Kingdom

Email: daniel.forton@nhs.net

Background and aims: Hepatocellular carcinoma (HCC) is mostly diagnosed at a late stage in the UK.

Advanced fibrosis and cirrhosis are the main risk factors, yet profound inequalities in access to healthcare affect many populations at risk. National Health Service England (NHSE) commissioned pilot projects to identify advanced fibrosis and cirrhosis in patients in community settings, using liver stiffness measurements (LSM) from Fibroscan as the primary screening method. We set up an outreach team that delivered services in a mobile clinic van and other remote locations to offer LSM, targeting groups in local drug and alcohol services, community diabetic retinopathy services, hostels, prisons and other community locations in SW London. Our aim was to evaluate the effectiveness of this approach in identifying subjects for ultrasound HCC surveillance.

Method: We extracted data from our program database covering scans from July 2022 to December 2023. We examined LSMs from 2892 persons (1829 Male : 1055 Female : 8 transgender), with heavy alcohol consumption in 1735, type II diabetes in 280, previous/current viral hepatitis in 96, known metabolic dysfunction-associated steatotic liver disease (MASLD) in 516 and other indications in 266. LSM ≥ 11.5 kPa was used as a cut-off for advanced fibrosis. We utilised peer support workers to increase engagement and to accompany patients to subsequent hospital appointments. Food vouchers were used as incentives as necessary.

Results: 209/2892 subjects (7.2%) had LSM ≥ 11.5 kPa across the overall cohort. The highest prevalence amongst our targeted populations was in current/previous viral hepatitis (10/96; 10.4%), followed by persons with heavy alcohol consumption (161/1735; 9.3%), type II diabetics (15/280; 5.4%), and MASLD (18/516; 3.5%). All patients with LSM ≥ 11.5 kPa were referred to their local hospital for further hepatology review and investigation, including ultrasound HCC surveillance. In a subgroup analysis of 91 persons referred to one hospital, 65 (71%) have attended their first appointment to date.

Conclusion: Targeted outreach community Fibroscan is successful at detecting advanced fibrosis and cirrhosis (7.2% prevalence of LSM ≥ 11.5 kPa) in populations that would not otherwise access liver services, but it is a resource-heavy undertaking. The use of dedicated community Fibroscan technicians, a mobile clinic, peer workers and food vouchers facilitated the engagement of persons who do not readily access healthcare. The initial peer-led transition to specialist hospital assessment and ultrasound surveillance appears to be successful but the necessary long-term sustainability of this arrangement is yet to be determined.

SAT-446

Metabolic risk factors and disease risk in patients with metabolic dysfunction-associated steatotic liver disease: findings from an electronic health record biobank

Longgang Zhao¹, Xinyuan Zhang², Yun Chen², Michelle Lai³, Xuehong Zhang². ¹Brigham and Women's Hospital and Harvard Medical School, Boston, United States; ²Brigham and Women's Hospital and Harvard Medical School, Boston, United States; ³Beth Israel Deaconess Medical Center, Boston, United States

Email: nhlon@channing.harvard.edu.

Background and aims: The long-term prognosis of patients with metabolic dysfunction-associated steatotic liver disease (MASLD) is limited. We aimed to evaluate the difference in baseline characteristics of steatotic liver diseases (SLD) subcategories and further explore the associations between the number of metabolic factors and clinical outcomes.

Method: The Harvard Mass General Brigham Biobank is a health system-based study that incorporates electronic health records and lifestyle data. We included 6,134 patients diagnosed with SLD via medical records and further grouped them into four subcategories, namely MASLD, MetALD, alcohol-related liver disease (ALD), and cryptogenic SLD. Metabolic factors included obesity, prediabetes or diabetes, hypertension, hyperlipidemia, and low high-density lipoprotein level. Disease outcomes were collected from medical records. We compared the differences in demographics, lifestyles, genetics, clinical biomarkers, and body composition between four SLD subcategories. To assess the associations between numbers of metabolic factors and ~40 types of incident disease outcomes among patients with MASLD, we employed Cox proportional hazard regression models to estimate hazard ratios (HR) and their corresponding 95% confidence intervals (CIs) adjusting for multiple covariates.

Results: Compared with ALD (n=745), patients with MASLD (n=4388) were younger, more likely to be female and never smokers. They have higher levels of glucose and HbA1c, but lower levels of cholesterol and low-density lipoprotein. After a median follow-up of ~5 years, the number of metabolic risk factors were associated with higher risk of circulatory disease (HR ≥3 vs 1 factor = 2.37, 95% CI = 1.84–3.06), including atrial fibrillation (HR = 1.76, 95% CI = 1.30–2.39), coronary heart disease (HR = 1.44, 95% CI = 1.20–1.72), ischemic heart diseases (HR = 1.75, 95% CI = 1.39–2.19), heart failure (HR = 1.87, 95% CI = 1.40–2.50), ischemic stroke (HR = 1.52, 95% CI = 1.10–2.11), myocardial infarction (HR = 1.68, 95% CI = 1.13–2.49), and stroke (HR = 1.51, 95% CI = 1.19–1.93). Metabolic factors were also positively associated with hypertension (HR = 2.38, 95% CI = 1.93–2.93), depression (HR = 1.26, 95% CI = 1.05–1.52) and type 2 diabetes (HR = 2.16, 95% CI = 1.77–2.64). Those associations were robust and stable when we excluded the cases that occurred in the first year of follow-up.

Conclusion: Our results indicate that individuals with MASLD exhibited worse glucose but better lipids profiles when compared to those with ALD. Metabolic factors were positively associated with increased risk of adverse health outcomes, including circulatory diseases, hypertension, depression, and type 2 diabetes. These findings underscore the potential importance of metabolic health in patients with MASLD to enhance overall health.

SAT-447

Community liver health champion support can optimise the engagement of underserved patients with hepatocellular cancer surveillance—results of a 1 year regional pilot

Tanya Walker¹, Kate Glyn-Owen², Chris Saison³, Mhukti Perumal⁴, Kelly Gardner³, Wendy Wilson³, Heather Parsons², Ryan Buchanan².
¹Hepatitis C Trust, London, United Kingdom; ²University of Southampton, Southampton, United Kingdom; ³University Hospital Southampton, Southampton, United Kingdom; ⁴NHS England, National Cancer Programme, London, United Kingdom
Email: rmb1d14@soton.ac.uk

Background and aims: Hepatocellular carcinoma (HCC) is an important complication of chronic liver disease and HCC is expected to become the 3rd most common cause of cancer death world-wide by 2030. Incident HCC and death from HCC are skewed towards marginalized and socio-economically deprived populations. Engagement with HCC cancer surveillance in these populations is poor.

The aim of the project was to develop and implement a community champions programme to support under-served patients access HCC surveillance.

Method: The programme was funded by NHS England and implemented in 3 acute hospital trusts in Wessex (UK). Each trust appointed an HCC service navigator, and three liver health champions to work across trusts in the community. Champions had a lived experience of marginalisation or working with under-served populations and were tasked with maximising attendance at ultrasound appointments.

Eligible patients were enrolled into the programme if they were 1) known to need HCC surveillance but had not had a scan for >12 months, 2) highlighted at diagnosis by the clinical team as likely to need support to attend or 3) had a recent record of not attending an appointment with the Hepatology service.

Descriptive statistics were calculated using independent samples t-test and chi-squared tests in SPSS for mac version 28.0.1.14.

Results: Across two acute trusts, 299 eligible patients were added to the Champions programme in 9 months. Due to data governance and staffing challenges the 3rd hospital did not commence the programme in this time frame. The majority were enrolled due to non-attendance at liver US for >12 months prior (n = 158, 53%). Most patients were male (n = 193, 65%) and the mean age was 56 years (SD 12). The most common underlying aetiology was alcohol (n = 94, 31%).

Navigator contact was made with 189 (63%) patients. 180 (95%) of these patients attended for a scan in a mean follow-up of 4 months. 66 patients were referred for community champion support and 41/180 (23%) only attended with their direct input. The 119/299 patients who did not have a scan were significantly more likely to be from an ethnicity other than white British (p < 0.01; 17% vs 11%) but there was no significant difference in index of multiple deprivation, age, sex, or aetiology.

Champions overcame barriers including language, health literacy and homelessness. Their detailed mechanism of effect is subject to an ongoing qualitative study. Referral for champion support was significantly associated with a diagnosis of HCV (p < 0.01).

Conclusion: A programme to support underserved patients attend HCC surveillance imaging can be implemented at a regional level and leads to high rates of attendance in patients previously disengaged from care. Further evidence describing the sustainability of benefit and cost-effectiveness is important to support the implementation of a national service.

SAT-448

The prevalence of steatotic liver disease in young adults: applying the new nomenclature to a UK birth cohort

Ann Archer^{1,2}, Hannah Donnelly^{3,4}, Jon Heron³, Fiona Gordon⁵, Matthew Hickman³, Kushala Abeysekera^{3,5}.
¹Population Health Sciences, University of Bristol, Bristol, United Kingdom; ²University Hospitals Bristol and Weston NHS Foundation Trust, Bristol, United Kingdom; ³Population Health Sciences, University of Bristol, Bristol, United Kingdom; ⁴University Hospital Bristol and Weston NHS Foundation Trust, Bristol, United Kingdom; ⁵University Hospitals Bristol and Weston NHS Foundation Trust, Bristol, United Kingdom
Email: k.abeysekera@bristol.ac.uk

Background and aims: The new steatotic liver disease (SLD) nomenclature provides an overarching term reflecting the overlap between alcohol related liver disease (ALD), metabolic dysfunction associated steatotic liver disease (MASLD), introducing another term—MASLD with greater alcohol consumption (MetALD). In 2019, the Avon Longitudinal Study of Parents and Children (ALSPAC) birth cohort presented the results to EASL of >4000 FibroScan liver stiffness measurements (LSM) on participants (aged 24 years), determining 1 in 5 had steatosis and 1 in 40 had fibrosis. We sought to apply the new nomenclature to our cohort, along with updated thresholds for LSM and controlled attenuation parameter (CAP) to evaluate SLD prevalence in young adults.

Method: 4018 participants had a FibroScan using Echosens 502 Touch. LSMs with an interquartile range/median ratio (IQR/M) >30%

POSTER PRESENTATIONS

were excluded. Cardiometabolic risk was assessed with waist circumference and body mass index; blood pressure; triglyceride, high density lipoprotein, fasting glucose levels. Cut-offs for cardiometabolic risk were taken from published SLD nomenclature statements. Alcohol consumption was trichotomized into normal/hazardous/harmful based on AUDIT-C questionnaires and alcohol use questionnaires. Hazardous alcohol consumption was an AUDIT-C score >5, with harmful alcohol consumption reflecting DSM-V criteria for alcohol use disorder. Statistical analysis was performed using Stata MP 18.0.

Results: Mean age was 24 years (± 0.8). 3765 valid CAP measurements were recorded. Using the EASL CAP cut-off of 275 dB/m, 11.1% of the cohort had steatosis. 3598 valid LSMs were recorded. 89 participants, aged 24 years, had a LSM ≥ 8 kPa (2.4%), of which 8 had LSM ≥ 12 kPa. 13.1% ($n = 470/3599$) participants met DSM-V criteria for alcohol use disorder. 37.2% ($n = 1327/3565$) of participants had a BMI ≥ 25 kg/m². Applying full SLD nomenclature was possible for 1765 participants with complete data available. 10.5% ($n = 186/1765$) met criteria for MASLD of which 7 had fibrosis. 7.3% ($n = 128/1765$) met criteria for MetALD with <5 having fibrosis. 3.4% ($n = 60/1751$) met criteria for ALD with 30% ($n = 18/60$) having fibrosis (>8 kPa).

Conclusion: Based on changing CAP and LSM thresholds the proportion of patients with steatosis fell but estimates for fibrosis prevalence were largely unchanged. Amongst those that fulfilled SLD criteria, the commonest cause of fibrosis was ALD. This is in the context that almost 1 in 8 participants met criteria for alcohol use disorder. ALSPAC will repeat a further 4000 fibroscans with our participants now 30 years old to understand the progression of their SLD.

SAT-449

Prevalence of advanced liver fibrosis in the general population of the Paris region according to FIB 4 scores and liver risk score (Cerbafib)

Henri Tran¹, Patrick Ingiliz¹, Vincent Leroy¹, Stefano Caruso¹, Anne Laure Mazialivou^{1,2}, Adrien Ko², Odile Rousselet³, Cecile Fargeat³. ¹CHU Henri Mondor, Créteil, France; ²Biokortex, Paris, France; ³Cerba Healthcare, Paris, France
Email: henri.tran@aphp.fr

Background and aims: Screening for advanced hepatic fibrosis in the general population may help to identify patients at risk for negative hepatic outcome. However, no perfect non-invasive marker exists. Current guidelines (EASL 2021) recommend to use the low rule-out threshold of the FIB-4 score (1.3) as primary screening tool, but low specificity may lead to a large number of potentially false-positives in need for specialists' referral. Recently, the liver risk score (LRS) has been suggested to more accurately identify at-risk patients. The aim of this study was to compare the two markers in a large cohort from the general population.

Method: Cerbafib is a prospective cohort derived from a collaboration with laboratories situated all over the Paris region. The prevalence of advanced liver fibrosis was assessed by applying the non-invasive FIB 4 score (ALT, AST, age, platelets) with a cut-off of 2.67 (rule-in) and 1.3 (rule-out), and the LRS with a cut-off of 6 (low risk), 10 (medium risk) and 15 kPa (high risk). The correlation between the two scores was studied.

Results: Between January and April 2023, 179 865 patients were included into the cohort. The mean age was 52 years, 45% were men. FIB-4 identified 55 376 (31%) individuals in need for specialists' referral (>1.3), and 4 002 patients (2.2%) with suspected advanced fibrosis. LRS identified 38 175 (21%) patients with estimated liver stiffness >6 kPa, 1 933 patients (1%) >10 kPa, and 35 (0.02%) patients >15 kPa. There was a significant while poor correlation between both tests ($r = 0.45$, $p < 0.01$). The concordance between the two tests was as follows: No fibrosis with FIB 4 <1.3 : 86% have a minimal risk (<6 kPa), 13% low risk (6–10 kPa), 0.6% medium risk (10–15 kPa) and 0.004% high risk (>15 kPa) according to LRS ($r = 0.31$) Inconclusive

result with FIB 4 between 1.3 and 2.67: 64% have a minimal risk, 13% low risk, 1.4% medium risk and 0.02% high risk according to LRS ($r = 0.21$) Fibrosis with FIB >2.67 : 26% have a minimal risk, 64% low risk, 10% medium risk and 0.4% high risk according to LRS ($r = 0.35$).

Conclusion: The Liver Risk Score identifies a population in need for further hepatological investigation. Its use as a mass screening test in the general population may help to identify more accurately those at-risk for advanced liver disease. The well-established FIB-4 test only partially identifies this subgroup and might generate more false-positive patients and increase the need of confirmatory resources. Indeed, among patients with indication of further investigations according to FIB 4, around 60% are in the minimal risk of fibrosis with the LRS. Further studies with clinical end points are needed to confirm these results.

SAT-450

Exploring racial, ethnic, and demographics representativeness in MASH clinical trials: combined data from multiple therapeutic trials including more than 10, 000 patients

Jörn M. Schattenberg¹, Naim Alkhouri², Mazen Nouredin³, Vlad Ratziu⁴, Michael Charlton⁵, Julie Dubourg⁶, Stephen A. Harrison⁷. ¹Saarland University Medical Center, Homburg, Germany; ²Arizona Liver Health, Phoenix, United States; ³Houston Research Institute, Houston, United States; ⁴Sorbonne Université, Institute for Cardiometabolism and Nutrition, Hospital Pitié-Salpêtrière, INSERM UMRs 1138 CRC, Paris, France; ⁵University of Chicago, Chicago, United States; ⁶Summit Clinical Research, San Antonio, United States; ⁷Radcliffe Department of Medicine, University of Oxford, Oxford, United Kingdom
Email: jdubourg@summitclinicalresearch.com

Background and aims: Racial, ethnic and demographic representativeness in metabolic dysfunction-associated steatohepatitis (MASH) is not well-known. We aimed to investigate potential disparities in trial participation by characterizing participants of MASH clinical trials.

Method: We combined screening data from 10 industry-funded MASH phase 2 trials. The participation-to-prevalence ratio (PPR) was calculated by dividing the percentage of white and racialised participants in each trial by the percentage of white and racialised participants with metabolic dysfunction-associated steatotic liver disease (MASLD), respectively, in the United States. By convention, a PPR of less than 0.8 or greater than 1.2 indicates under-representation or over-representation, respectively. We also calculated the PPR for age groups (20–29, 30–39, 40–49, 50–59, 60–69, 70–79, ≥ 80 years) and gender.

Results: We identified 10, 528 participants across 10 industry-funded phase 2 MASH trials. The mean age was 54.7 years (SD 11.6). 58% were female, 89% were white and 41% were Hispanics or Latino. Mean BMI, AST, ALT, and HbA1c were 36.4 kg/m² (SD 9.0), 36.7 IU/L (26.4), 47.1 IU/L (35.7), and 6.5% (SD 1.4). Men and female were adequately represented with a PPR of 0.92 and 1.07, respectively. Participants aged 40–49 and 50–59 years were over-represented with a PPR of 1.41 and 1.37, respectively, while participants aged from 70–79 and ≥ 80 years were under-represented with a PPR of 0.41 and 0.02, respectively. Other age-groups were appropriately represented in the 10 included MASH clinical trials. In regard to race and ethnicity, the White and African American population appeared to be adequately represented with a PPR of 1.41 and 1.37, respectively. However, the Hispanic population was over-represented in this group of MASH clinical trials with a PPR of 4.10.

Conclusion: In the setting of industry-funded MASH clinical trials, racialized participants appear to be either adequately or over-represented. The elderly population appears as under-represented as expected from common inclusion/exclusion criteria in clinical trials. Strategies to improve recruitment and enrolment into randomized controlled trial of under-represented population are needed. Further studies are warranted to assess the appropriate

representativeness of the population in MASH clinical trials as a reflect of the disease population.

SAT-451

Characteristics and waitlist outcomes of liver transplant candidates at high risk for food insecurity

Therese Bittermann¹, David Goldberg², Elena Byhoff³. ¹University of Pennsylvania Perelman School of Medicine, Penn Transplant Institute, Philadelphia, United States; ²University of Miami Miller School of Medicine, Division of Digestive Health and Liver Diseases, Miami, United States; ³University of Massachusetts Medical School, Department of Medicine, Worcester, United States
Email: therese.bittermann@pennmedicine.upenn.edu

Background and aims: Studies have shown that neighborhood-level social determinants of health influence pre- and post-transplant outcomes. To date, no studies have evaluated food insecurity (FI) risk in the liver transplant (LT) population. This study evaluates the characteristics and waitlist outcomes of candidates at high risk for FI and compare these to patients at high risk of broad socioeconomic deprivation, as measured by the Social Deprivation Index (SDI).

Method: This was a retrospective cohort study of LT candidates listed between 1/1/2018–12/31/2021 using national registry data from the Organ Procurement and Transplantation Network, linked to county-level FI data and to county-level SDI, a validated composite measure of socioeconomic deprivation. The correlation between county-level percent FI and SDI was assessed. Multivariable logistic regression was used to evaluate patient characteristics associated with home residence in the ≥90th percentile for FI. Covariates were compared to those associated the ≥90th percentile for SDI. Adjusted time-to-event models evaluated the association of county-level FI and SDI with waitlist mortality.

Results: There were 50, 627 LT candidates listed during the study period. The cohort was 62.3% male with median age 58 years (IQR 49–64), and was 69.7% White, 13.4% Hispanic, 7.1% Black, 4.2% Asian. The most common causes of liver disease were: 37.7% alcohol-associated liver disease (ALD), 22.2% metabolic dysfunction-associated steatotic liver disease (MASLD) and 11.2% hepatitis C virus (HCV). The median county-level percent FI for the cohort was 10.9% (IQR 9.0–13.1), while the median SDI score was 49 (IQR: 27–73). There was overall good correlation between county-level percent FI and SDI (Spearman rho 0.682; $p < 0.001$). Race/ethnicity was associated with both high percent FI and high SDI ($p < 0.001$ for both), but the latter relationship was stronger (e.g., aOR 2.98 for Black/SDI and 1.56 for Black/FI). In contrast, liver disease factors were more strongly associated with percent FI than SDI. For example, patients with MASLD were more likely to live in high FI areas (aOR 1.42 versus ALD; $p < 0.001$ overall), while higher albumin was associated with lower odds of being at risk for FI (aOR 0.79; $p < 0.001$). Percent FI was not associated with adjusted waitlist mortality ($p = 0.119$), while SDI had only a modest effect (aHR 1.07; $p = 0.033$).

Conclusion: The link between MASLD and residence in a high percent FI area may be relevant to disease evolution and also to achieving optimal post-LT outcomes, while that between low albumin and county-level FI may lead to added barriers for waitlisted candidates to overcome malnutrition. Neither county-level social determinants of health measure had a substantial impact on waitlist mortality. Further studies are needed to better understand the potential role of FI on outcomes among LT candidates and recipients.

SAT-452

Evolving patterns in the clinical burden of liver cirrhosis: comprehensive analysis from a leading german tertiary center

Julian Pohl¹, Nirbaanot Walia¹, Matthias Reinhardt¹, Frank Tacke¹, Cornelius Engelmann¹. ¹Gastroenterology and Hepatology, Charité-Universitätsmedizin Berlin, Berlin, Germany
Email: julian.pohl@charite.de

Background and aims: Emerging evidence is highlighting the changes in the burden of cirrhosis. This study aimed to describe the trends in hospitalizations, inpatient mortality and complications of liver cirrhosis in a large tertiary hospital, and comparing this to other major chronic health conditions while taking into account the possible impact of the COVID-19 pandemic. The aim of this study was to derive implications on future patient management in cirrhosis.

Method: The data was acquired retrospectively from the Charité Berlin University hospital's electronic record system from 2011–2022. Included were all patients discharged with an ICD-10 diagnostic code corresponding to cirrhosis (and its complications), and other chronic diseases as control groups (chronic obstructive pulmonary disease, chronic renal failure, ischemic heart disease, chronic heart failure, malignancies, and diabetes). Between 2011–2022 1,181,478 (incl. 24,567 cirrhosis) patient cases were included. To assess the possible impact of the COVID-19 pandemic, mortality trends were compared against the incidence of COVID-related deaths in Germany.

Results: Cirrhosis patients were the youngest of all health conditions assessed, with a median age of 62 (interquartile range 53–70). Since 2017, their total admission numbers decreased, while their in-hospital mortality increased from 6.3 to 8.8%. Ascites and bacterial infections remained the most common acute complications among cirrhosis patients. Proportions of these complications increased during the observational period from 24 to 30% and 23 to 32%. Clear trends in rising mortality of ascites, hepatorenal syndrome and variceal hemorrhage were observed between 2011–2022. Alcohol-related liver disease was the most common etiology of cirrhosis (42%) in each year. Hepatitis C admissions decreased from 14 to 2%, while hepatitis B admissions decreased from 5% (2011) to 1% (2015) and increased from 2016 again to 3%. From 2016, the proportion of admissions for hepatocellular carcinoma increased from 19 to 23% among cirrhosis patients. Compared to other chronic diseases, cirrhosis patients had the second highest likelihood of re-hospitalization after malignancies. There was a sharp rise in mortality in December 2020 for all chronic health conditions (15.2% for cirrhosis patients, which was the second highest rate). Since then, patients with cirrhosis surpassed heart failure as the disease with the highest in-hospital mortality at the Charité hospital.

Conclusion: Although total cirrhosis-related hospital admissions were falling, a higher proportion of cases experienced complications including in-hospital mortality, more than for any other of chronic health conditions assessed. Trends in mortality further aggravated during the COVID pandemic. These results underscore the need for risk stratification and adapted management strategies in cirrhosis.

SAT-453

Diagnostic accuracy of the LiverRisk score to detect significant and advanced fibrosis among a United States general population and important subgroups

Laurens van Kleef¹, Jesse Pustjens¹, Harry L.A. Janssen^{1,2}, Willem Pieter Brouwer¹. ¹Erasmus MC, University Medical Center, Rotterdam, Netherlands; ²Toronto Center for Liver Disease, University Health Network, Toronto, Canada
Email: l.vankleef@erasmusmc.nl

Background and aims: The LiverRisk score (LRS) has recently been proposed as a novel score to predict liver fibrosis and the future development of liver-related outcomes in the general population and may be used in referral strategies. Besides simple laboratory parameters, this score includes age, which may hamper its diagnostic accuracy among young and old populations as has been reported for other non-invasive scores that rely on age.

Method: We used data from the NHANES 2017–2020 cycle, a United States population-based cohort with data on liver stiffness and LRS. We assessed the diagnostic accuracy by AUC and detection rates of LSM ≥8 and ≥12 kPa at proposed thresholds of the LRS. Performance was tested both among the entire general population and clinically relevant subgroups. Sensitivity analyses were performed in

POSTER PRESENTATIONS

participants with metabolic dysfunction (MD), for whom the EASL, AASLD and AGA referral pathways recommend non-invasive testing for the presence of advanced liver disease.

Results: The cohort comprised 7025 participants, aged 49 [33–63] and 49% were male. Among them 9.7% had LSM ≥ 8 and 3.2% LSM ≥ 12 kPa. The AUC in the overall population was 0.73 (95%CI 0.71–0.75) and 0.78 (95%CI 0.74–0.81) to detect LSM ≥ 8 and ≥ 12 kPa. It significantly outperformed the FIB-4 (AUC 0.62 and AUC 0.68 to detect LSM ≥ 8 and ≥ 12 kPa). The LRS however performed differently amongst participants aged 18–40, 40–60 and 60–80: the AUC to detect LSM ≥ 8 kPa was 0.68, 0.73 and 0.68 and the AUC to detect LSM ≥ 12 kPa was 0.73, 0.79 and 0.73, respectively. The score had consistent performance among white, Hispanic and Asian participants, however, the AUC was significantly lower among black participants (AUC 0.74 in white vs 0.66 in black for LSM ≥ 8 kPa). Performance remained comparable across sex or in patients with metabolic dysfunction. Interestingly, the score had excellent predictive value amongst those without MD (thus excluding those with MD), reflected by an AUC of 0.86 and 0.96 in the detection of LSM ≥ 8 and ≥ 12 kPa. Despite the adequate performance as reflected in the AUC, its clinical utility at the suggested cut-offs for very low risk (LRS 6) and low risk (LRS 10) is suboptimal. In the overall population (regardless of MD), 53% of participants with an LSM ≥ 8 kPa had LRS < 6 and 91% LRS < 10 , resulting in a poor sensitivity of 47% and 9%. Detection of LSM ≥ 12 kPa is slightly better with 60% sensitivity at LRS 6 and 14% sensitivity at LRS 10. Performance differed per subgroup. Particularly worrisome is the low sensitivity among participants aged 18–40, with only 21% for LSM ≥ 8 kPa and 34% LSM ≥ 12 kPa at LRS 6.

Conclusion: The LRS score is a promising new tool to predict liver fibrosis, however, its diagnostic accuracy attenuates among patients aged < 40 or ≥ 60 years old, as well as among black individuals. Further studies are required on whether it can be implemented in referral strategies, in which subgroups, and what cut-offs should be utilized.

SAT-454-1Y

Non-housing related socioeconomic factors increase risk of liver fibrosis in screening of an urban population with steatotic liver disease

Huw Purrsell¹, Stephanie Landi^{1,2}, Lucy Bennett³, Oliver Street¹, Jennifer Scott¹, Christopher Mysko^{1,2}, Neil Guha⁴, Karen Piper Hanley^{1,5}, Neil Hanley^{1,6}, Varinder Athwal^{1,2}. ¹University of Manchester, Manchester, United Kingdom; ²Manchester University NHS Foundation Trust, Manchester, United Kingdom; ³NIHR Nottingham Biomedical Research Centre (BRC), Nottingham University Hospitals NHS Foundation Trust and Nottingham University, Nottingham, United Kingdom; ⁴NIHR Nottingham Biomedical Research Centre (BRC), Nottingham University Hospitals NHS Trust and University of Nottingham, Nottingham, United Kingdom; ⁵Wellcome Trust Centre for Cell-Matrix Research, The University of Manchester, Manchester, United Kingdom; ⁶University of Birmingham, Birmingham, United Kingdom
Email: Huw.Purrsell@doctors.org.uk

Background and aims: Socioeconomic deprivation is associated with increased risk of steatotic liver diseases and increased risk of advanced disease. Socioeconomic deprivation is multi-faceted and it is unclear which specific factors predispose to risk of significant liver disease. Healthcare access is also dependent on deprivation and case finding using clinical risk factors improves identification in asymptomatic populations and reduces disparity. We aimed to assess impact of deprivation and its specific aspects on the detection of liver fibrosis in a population screening study.

Method: Patients were recruited to the ID LIVER project in Manchester, UK. Patients were assessed in Community Liver Assessment clinics with risk factors for liver disease including Type 2 diabetes (T2DM), Body Mass Index > 30 kg/m², alcohol consumption > 280 / > 400 grams in females/males per week, abnormal ALT or hepatic steatosis. Patients underwent a clinical history, full non-invasive blood based liver aetiological screen and transient

elastography (TE). Fibrosis was assessed with FIB-4 score and TE. Fibrosis risk was determined by a liver stiffness measurement (LSM) > 8.0 kPa and FIB-4 > 1.3 . Socio-economic deprivation was assessed by domain and sub-domain of the Index of Multiple Deprivation (IMD) at an individual and ward level.

Results: 1249 patients were recruited to the ID LIVER project. 866 (69.3%) patients were identified as MASLD, 133 (10.9%) MetALD and 162 (13.0%) patients had alcohol related liver disease. 260 (20.8%) patients had a LSM > 8.0 kPa. 34 wards across Greater Manchester were assessed and split into quartiles based on the fibrosis incidence. Although there was no correlation at an individual level between IMD score and LSM ($r^2 = 0.01$), wards in the highest quartile for fibrosis detection had a significantly higher IMD score than wards in the lowest quartile (38.01 vs 19.25 ($p = 0.022$, 95% CI 3.10–34.43)). Multivariate analysis, adjusted for T2DM, harmful alcohol consumption and obesity, of the subdomains of the IMD score showed that fibrosis detection correlated with income ($r^2 = 0.29$, $p = 0.005$), employment ($r^2 = 0.31$, $p = 0.003$), education and skills ($r^2 = 0.25$, $p = 0.01$), health and disability ($r^2 = 0.28$, $p = 0.006$), crime ($r^2 = 0.33$, $p = 0.002$) and barriers to housing and services subdomains ($r^2 = 0.22$, $p = 0.02$). Although there was no significant correlation with the living environment subdomain ($p = 0.210$), wards in the lowest quartile of fibrosis detection had a significantly better air quality (0.52 vs 0.79 ($p = 0.049$; 95% CI 0.00–0.54)). 3 year mortality was 1.68% ($n = 21$), of which 15 (71.4%) patients came from areas of high deprivation.

Conclusion: Indoor living environment is the only factor of socioeconomic deprivation not associated with increased risk of liver fibrosis in an urban population with steatotic liver disease.

SAT-455

The rise of metabolic dysfunction-associated steatotic liver disease (MASLD) among adults in Canada between 2012 and 2018

Jessica Burnside¹, Felice Cinque², Giada Sebastiani², Sahar Saeed¹. ¹Queen's University, Kingston, Canada; ²McGill University Health Centre, Montreal, Canada
Email: jessica.burnside@queensu.ca

Background and aims: Metabolic Dysfunction-Associated Steatotic Liver Disease (MASLD) is a highly prevalent yet largely under-appreciated liver condition, absent from public health agendas. A recent study suggested substantial improvements in epidemiological assessments would be necessary to improve national preparedness. Based on the lack of routine ultrasounds and the paucity of transient elastography across Canada, serum biomarkers are the only option to identify steatosis at a population scale. To address this need for routine surveillance, the NAFLD Ridge Score (NRS) was developed using a machine-learning approach and validated against proton magnetic resonance spectroscopy with a sensitivity of 92% and specificity of 90%. Our purpose is to estimate the prevalence of MASLD using a pan-Canadian cohort between 2012–2018.

Method: We used data from the Canadian Longitudinal Study on Aging (CLSA), which prospectively follows community-dwelling adults (45 to 85 years old) from 11 sites (7 provinces) across Canada. The CLSA collects sociodemographic, lifestyle, and clinical data every three years. We estimated the annual prevalence of MASLD (steatosis + one cardiometabolic risk factor) as well as MetALD (140–350 g alcohol/week (F) and 210–420 g alcohol/week (M)). Steatosis was identified by an NRS > 0.44 , which utilizes seven components: serum ALT, high-density lipoprotein cholesterol, triglycerides, hemoglobin A1c, leukocyte count, and the presence of hypertension. We compared the prevalence of MASLD using the NRS score to a non-specific measure of liver damage, ALT (> 40 U/L).

Results: 30 079 CLSA participants were included in the analysis. At baseline, 51% were female (F), with a median age of 62 years (IQR: 54–71 years), and median ALT was 21 U/L (IQR: 16–27 U/L). 83% met at least one of five MASLD cardiometabolic criteria, the most common being 70% BMI > 25 kg/m²; 41.5% having high triglycerides

≥ 1.70 mmol/L; 33% HbA1c $\geq 5.7\%$; 30% with hypertension; and 25% having high HDL ≤ 1.0 mmol/L (Males) or ≤ 1.3 mmol/L (F). There was a significant rise in MASLD prevalence from 32.3% (95%CI 32.2, 32.5%) in 2012 to 39.1% (95%CI: 39.0–39.3%) in 2018. MetALD prevalence varied over time, ranging from 2.2% (95%CI: 2.2–2.2%) in 2016 to 3.5% (95%CI: 3.4–3.5%) in 2012. Males had an average 1.9 times higher prevalence of MASLD and 2.6 times higher prevalence of MetALD compared to females. Only 7.6% (95%CI: 7.5–7.6%) of the cohort had elevated ALT (>40 U/L) and at least one of the cardiometabolic factors.

Conclusion: This is the first Canadian study to estimate MASLD and MetALD prevalence which exceeds previous modelling estimations. Prevalence was consistently significantly greater amongst men. ALT alone vastly underestimated the prevalence of MASLD. Further studies are underway to elicit phenotypes at the greatest risk of MASLD and the bidirectional relationship between liver and metabolic diseases.

SAT-456

A review of lifestyle management guidelines for metabolic dysfunction-associated steatotic liver disease

Dana Ivancovsky Wajcman¹, Christopher Byrne², John F. Dillon², Paul N. Brennan^{2,3}, Marcela Villota-Rivas¹, Zobair Younossi^{3,4}, Alina M. Allen⁵, Javier Crespo⁶, Lynn H. Gerber^{3,4}, Jeffrey V. Lazarus^{1,3,7}. ¹Barcelona Institute for Global Health (ISGlobal), Hospital Clinic, University of Barcelona, Barcelona, Spain; ²Division of Molecular and Clinical Medicine, Ninewells Hospital and Medical School, University of Dundee, Dundee, United Kingdom; ³The Global NASH Council, Washington DC, United States; ⁴Beatty Liver and Obesity Research Program, Inova Health System, Falls Church, United States; ⁵Division of Gastroenterology and Hepatology, Mayo Clinic, Rochester, United States; ⁶Valdecilla Research Institute (IDIVAL), Marqués de Valdecilla University Hospital, Santander, Spain; ⁷CUNY Graduate School of Public Health and Health Policy (CUNY SPH), New York, United States Email: danaivanc@gmail.com

Background and aims: Several clinical management guidelines on metabolic dysfunction-associated steatotic liver disease (MASLD) have been published. We aimed to summarise the lifestyle interventions recommended in these guidelines.

Method: We searched PubMed/MEDLINE, the Cochrane Library, and the Cumulative Index to Nursing and Allied Health Literature (CINAHL) for MASLD clinical management guidelines published from 1 January 2013 to 31 July 2023. Identified documents were thoroughly reviewed for statements regarding weight loss, dietary patterns or habits, dietary supplements, alcohol consumption, physical activity, tobacco smoking, sleeping habits, behaviour change techniques (BCTs), mental health, digital health interventions (DHI), and social, and environmental determinations of health. The authors developed a framework of 8 pre-defined questions that guided the document evaluation, synthesis, and analysis. A statement was considered as a recommendation if: 1) it noted an action would be beneficial and suitable for the patient; and 2) it was repeated in ≥ 3 guidelines. Recommendations were categorised into six domains: weight reduction, physical activity, diet, dietary supplements, alcohol, and smoking. A recommendation was defined as strong if recommended in a two-thirds majority of the guidelines.

Results: The search identified 33 MASLD management guidelines. 27 recommendations were identified. Six recommendations were considered as strong: increase physical activity ($n=33$); achieve a weight reduction of 7–10% to improve steatohepatitis and/or fibrosis ($n=31$); consider bariatric surgery for non-cirrhotic patients with obesity ($n=28$); achieve a weight reduction of ≥ 3 –5% to reduce liver steatosis ($n=24$); exercise 150–300 minutes/week of moderate-intensity or 75–150 minutes/week of vigorous-intensity ($n=24$); and decrease consumption of commercially produced fructose ($n=23$). In contrast, mental health, psychological or CBT treatment, DHIs or additional BCTs, and social or environmental determinants of health were rarely (in ≤ 8 guidelines) mentioned in guidelines, and when

they were, it was in broad statements lacking specific recommendations.

Conclusion: Most MASLD clinical guidelines include recommendations regarding healthy eating, physical activity, and weight management, as these have proven positive effects on health outcomes when sustained. However, our review reveals substantial gaps concerning statements and recommendations regarding mental health and the social and environmental determinants of MASLD. To improve adherence, we recommend that scientific associations develop comprehensive guidelines encompassing social support, environmental factors, and mental health. Additionally, we propose exploring BCTs and DHIs to optimise behavioural modifications. Further research on recommendation implementation is needed.

SAT-457-YI

A community-based pilot for proactive screening of high-risk groups for chronic liver disease can lead to sustained healthcare engagement of people diagnosed with cirrhosis

Ann Archer^{1,2}, Sally Tilden², Jane Gitahi², Grace Cameron², Rosemary King'ori², Becky Knight², James Hawken², Fiona Gordon², Matthew Hickman¹, Kushala Abeysekera^{1,2}. ¹Population Health Sciences, University of Bristol, Bristol, United Kingdom; ²University Hospitals Bristol and Weston NHS Trust, Bristol, United Kingdom Email: ann.archer@uhbw.nhs.uk

Background and aims: The *Alright My Liver?* service was developed in collaboration with service users to screen for advanced liver fibrosis from alcohol, viral hepatitis and metabolic syndrome in the South West of England. The service aims to reach the most high-risk populations for liver disease and those most likely to experience health inequalities. This study aims to report on markers of engagement for those identified as having cirrhosis by the pilot service.

Method: Liver health screening events were co-located with drug and alcohol services, primary care services in areas with a high index of deprivation, weight loss events and with Caafi Health, an organization providing health outreach to black and ethnic minority communities in the region. Clients identified with advanced fibrosis were booked into hepatology clinic and ultrasound with an offer of funded transport and telephone reminders. Routine data has been analysed here, with index of multiple deprivation calculated based on postcode where recorded, and set to 1 if the patient was living in a prison or hostel.

Results: Of 3191 people screened for liver disease, 228 had liver stiffness measurement (LSM) >11.5 kPa and were referred for further assessment. This cohort was ethnically diverse relative to the local population, 78% white British or other (baseline population 84%). The cohort median index of multiple deprivation (IMD) decile was 3, with 20% reporting experience of homelessness. Attendance at first liver ultrasound was 89% ($n=152/170$), rising to 93% ($n=158/170$) including those who attended when offered a second attempt. Attendance at 6-month surveillance ultrasound was 76% ($n=41/54$), rising to 87% ($n=47/54$) including those upon second attempt. For outpatient clinic, 80% ($n=106/132$) attended on first opportunity, rising to 84% ($n=111/132$) when including those who attended on a second invitation. These compare favourably to baseline attendance of 80% locally for both clinic and ultrasound for hepatology patients. A chi-squared test of independence revealed no association between first clinic attendance and AUDIT-C score ≤ 4 , IMD decile ≤ 5 or screening setting. All patients diagnosed with active hepatitis C by the pilot service have been commenced on antiviral therapy ($n=6$). 4% ($n=10/228$) of patients with LSM >11.5 kPa died during the study period. All had suspected ArLD and none had reached their initial appointment date prior to death. Cause of death data was unavailable.

Conclusion: The pilot service is successful in engaging a patient group with their ongoing care despite the presence of potential barriers to attendance including substance dependence, unstable housing and socioeconomic deprivation. The proactive engagement

POSTER PRESENTATIONS

approach in this pilot could have broader utility in hepatology to support an underserved population and prevent emergency admissions.

SAT-458

Impacts of smoking on alcoholic associated liver disease: a nationwide cohort study

Sang Gyune Kim¹, Jeong-Ju Yoo¹, Jae Young Jang², Log Young Kim³.
¹Soonchunhyang University Bucheon Hospital, Bucheon, Korea, Rep. of South; ²Soonchunhyang University Seoul Hospital, Seoul, Korea, Rep. of South; ³Department of Big Data Strategy, National Health Insurance Service, Wonju, Korea, Rep. of South
Email: mcnulty@schmc.ac.kr

Background and aims: Smoking is a preventable risk factor for morbidity and mortality in patients with liver disease. This study aims to explore the additional risks of smoking in the development of alcoholic associated liver disease (ALD), cirrhosis, and hepatocellular carcinoma (HCC) in high-risk drinkers.

Method: Data from the National Health Insurance Service, including claims and health check-up information spanning 2011 to 2017, were used. The overall alcohol consumption was calculated, and ALD was defined based on ICD-10 codes. High-risk drinking was defined as 7 or more drinks for men and 5 or more for women, twice weekly.

Results: Half of the high-risk drinkers were smokers, decreasing in men but stable at 20% for women. ALD prevalence was 0.97% in high-risk drinkers and 1.09% in high-risk drinkers who smoked, higher than 0.16% in social drinkers. ALD incidence over 3-years was highest in high-risk drinkers who smoked (2.35%), followed by high-risk drinkers (2.03%) and social drinkers (0.35%). Cirrhosis and HCC followed similar patterns, with prevalence and incidence was highest in drinkers who smoked. 3-year mortality was 0.65% in high-risk drinkers who smoked, compared to 0.50% in high-risk drinkers and 0.24% in social drinkers. Smoking increased the incidence of ALD, cirrhosis, and HCC by 1.30, 1.50, and 1.45 times, respectively.

Conclusion: Women's risk ratio for ALD, cirrhosis, and HCC increased more significantly with smoking compared to men. Smoking significantly raises the risk of ALD, cirrhosis, and HCC in high-risk drinkers, particularly impacting women more than men. Hence, smoking cessation is crucial for female ALD patients.

SAT-459

Assessments of health utilities in patients with metabolic dysfunction-associated steatohepatitis (MASH): cross-walk between CLDQ-NASH, SF-6D, and the EuroQol EQ-5D

Zobair Younossi^{1,2}, Maria Stepanova^{1,2}, Jesse Fishman³, James Dodge³, Dominic Labriola³, Rebecca Taub³, Fatema Nader^{1,2,4}.
¹The Global NASH Council, Washington, DC, United States; ²Beatty Liver and Obesity Research Program, Inova Health System, Falls Church, VA, United States; ³Madrigal Pharmaceuticals, West Conshohocken, PA, United States; ⁴Center for Outcomes Research in Liver Disease, Washington, DC, United States
Email: zobair.younossi@cldq.org

Background and aims: Non-alcoholic steatohepatitis (NASH), renamed as MASH, is a progressive liver disease which can negatively impact the health-related quality of life (HRQL) and health utilities (HU). EQ-5D is a commonly used measure of HU to calculate quality-adjusted life years (QALYs). For the clinical trials that use Chronic Liver Disease Questionnaire-NASH (CLDQ-NASH) or Short Form-36 (SF-36), ability to convert the HRQL scores (CLDQ-NASH or SF-36) to EQ-5D scores provides a valuable method to estimate HU. Using baseline HRQL data from MAESTRO-NASH Phase 3 trial, we aimed to estimate EQ-5D scores using 2 methods in patients with NASH and different stages of fibrosis.

Method: Baseline data of non-cirrhotic NASH patients were used in this study. The HRQL was assessed using CLDQ-NASH (36 items in 6 domains) and Short Form-36 (SF-36; 36 items). We used two cross-walk algorithms to estimate EQ-5D scores. The first algorithm used 6

domains of CLDQ-NASH in a fractional logistic model to yield EQ-5D estimates (Fishman 2023). The other algorithm included calculation of SF-6D utility scores from SF-36 items (Kharroubi 2007) which were further fed into a generalized regression model that estimated EQ-5D scores from the SF-6D scores (Younossi 2019). The two EQ-5D estimates were evaluated for correlation with each other and then in pre-defined clinical subgroups.

Results: There were 883 NASH patients with CLDQ-NASH and SF-36 data: 25% aged ≥ 65 years, 44% male, 80% obese (BMI >30), 67% type diabetes (T2D), 62% F3 fibrosis and 38% F1b or F2 fibrosis. The mean estimated EQ-5D scores in the total sample were 0.851 (SD = 0.146) according to CLDQ-NASH-based algorithm and 0.853 (SD 0.097) according to the SF-36-based algorithm. The correlations between the two estimated EQ-5D scores were +0.704 (Pearson's) and +0.739 (Spearman's). Similar to the total sample, the differences between the mean EQ-5D estimates using either calculation method did not exceed 0.012 in all studied subgroups (by age, sex, obesity, T2D, fibrosis stage). Using the CLDQ-NASH-based algorithm, EQ-5D scores in those subgroups were as follows [mean (SD)]: 0.871 (0.114) in ≥ 65 years, 0.844 (0.154) in <65 years, 0.884 (0.132) in male, 0.824 (0.151) in female, 0.845 (0.148) in obese, 0.876 (0.136) in non-obese, 0.847 (0.144) in T2D, 0.859 (0.150) in non-T2D, 0.852 (0.138) in F3, and 0.849 (0.158) in F1b or F2. For comparison, the historic EQ-5D estimates for NASH with advanced fibrosis (Younossi 2019) were as follows: 0.835 (0.139) in F3, 0.819 (0.148) in compensated cirrhosis (F4).

Conclusion: Both cross-walk algorithms for calculation of the EQ-5D utility scores in NASH patients were estimable with CLDQ-NASH or SF-36 instruments. A high positive correlation was seen between the total score and subgroup estimates using either method; this improves confidence in their use to calculate quality-adjusted outcomes for cost-effectiveness models.

SAT-462-YI

The interplay between steatotic liver disease and viral infections: systematic review, meta-analysis and data synthesis

Jiajing Li¹, Jiahua Zhou¹, Yining Wang¹, Jaffar A. Al-Tawfiq^{2,3,4}, Willem Pieter Brouwer¹, Pengfei Li¹, Robert J. de Knecht¹, Maikel P. Peppelenbosch¹, Maarten F. M. Engel⁵, Ming-Hua Zheng^{6,7}, Ziad A. Memish^{8,9,10}, Mohammed Eslam¹¹, Harry L.A. Janssen^{1,12}, Ibrahim Ayada¹, Qiuwei Pan¹.
¹Department of Gastroenterology and Hepatology, Erasmus MC-University Medical Center, Rotterdam, Netherlands; ²Infectious Disease Unit, Specialty Internal Medicine, Johns Hopkins Aramco Healthcare, Dhahran, Saudi Arabia; ³Division of Infectious Diseases, Indiana University School of Medicine, Indianapolis, United States; ⁴Division of Infectious Diseases, Johns Hopkins University, Baltimore, United States; ⁵Medical Library, Erasmus MC-University Medical Center, Rotterdam, Netherlands; ⁶MAFLD Research Center, Department of Hepatology, the First Affiliated Hospital of Wenzhou Medical University, Wenzhou, China; ⁷Key Laboratory of Diagnosis and Treatment for the Development of Chronic Liver Disease in Zhejiang Province, Wenzhou, China; ⁸Research and Innovation Center, King Saud Medical City, Ministry of Health and College of Medicine, Al Faisal University, Riyadh, Saudi Arabia; ⁹Hubert Department of Global Health, Rollins School of Public Health, Emory University, Atlanta, United States; ¹⁰Kyung Hee University, Seoul, Korea, Rep. of South; ¹¹Storr Liver Centre, Westmead Institute for Medical Research, Westmead Hospital and University of Sydney, Sydney, Australia; ¹²Toronto Center for Liver Disease, Toronto General Hospital, University of Toronto, Toronto, Canada

Email: j.li.1@erasmusmc.nl

Background and aims: Steatotic liver disease (SLD) affects approximately 30% of adults globally, while the prevalence of viral diseases continues to pose a threat to the global population. This study aims to comprehensively investigate the relationship between SLD and major viral diseases.

Method: A systematic search of Medline, Embase, Web of Science and Cochrane Library databases was conducted from inception to July 8, 2022. Cross-sectional and longitudinal observational studies for adults and published in English with full text available were included, if they provided data on the occurrence of SLD events in viral-infected population. Meta-analysis was performed using random-effects (DerSimonian and Laird) models.

Results: The search identified 47,194 records, and a total of 621 eligible studies involving 390,728 individuals from 55 countries were included. Among patients with mono-infections, the highest SLD prevalence was observed in those infected with hepatitis C virus (HCV) (49%, 95% confidence interval [CI]: 46%–52%), followed by human immunodeficiency virus (HIV) (40%, 36%–45%), hepatitis B virus (HBV) (38%, 34%–41%) and SARS-CoV-2 (37%, 32%–42%). Coinfection with HCV-HIV (44%, 38%–49%) or HBV-HIV (53%, 38%–68%) was associated with higher prevalence of SLD compared to HIV mono-infection. The prevalence of SLD was 53% (38%–68%) in HCV-HBV co-infected populations. Further analysis showed a positive association between SLD and SARS-CoV-2 infection (odds ratio [OR] 2.13, 95% CI [1.06–4.29]), and a negative association between HBV infection and SLD (OR 0.69, 95% CI [0.58–0.83]). No significant association was found between SLD and HIV or HCV infection. The pooled prevalence of steatohepatitis in all viral-infected populations was 17% (14%–20%), with the highest rate observed in HIV-infected (29%, 20%–37%), followed by HCV-infected (21%, 14%–27%) and HBV-infected (8%, 5%–12%) patients. Hepatic steatosis was significantly associated with an increased risk of developing chronic liver disease and hepatocellular carcinoma in HCV- and/or HIV-infected but not in HBV-infected individuals. Importantly, SLD was identified as a risk factor for severe outcomes in SARS-CoV-2-infected patients and for the diagnosis of AIDS in HIV carriers. In HBV and HCV patients who received antiviral therapy, SLD was significantly associated with lower sustained virologic response.

Conclusion: SLD is highly prevalent in viral-infected populations, and the reciprocal interactions between SLD and viral diseases worsen both conditions, leading to poorer patient outcomes. Therefore, increased awareness and the development of intervention strategies are needed to address the burden of SLD in populations with viral infections.

SAT-463

Association between air pollution and heat stress exposome and liver enzymes in NYC runners

Nicholas DeFelice¹, Aman Patel¹, Anthony Lin¹, Nayab Baloch¹, Andrew Moon². ¹Icahn School of Medicine at Mount Sinai, New York, United States; ²UNC Gastroenterology and Hepatology, Chapel Hill, United States

Email: nicholas.defelice@mssm.edu

Background and aims: Chronic and repeated acute heat stress exposures and air pollution can result in damage to the liver, heart, kidney, and muscles. Here, we assessed acute recurrent air pollution and heat stress exposures (internal body temperature, sweat rate, heart rate, etc) in a cohort of long-distance runners to better understand how the natural environment impacts liver function.

Method: During the summer of 2023, 20 athletes provided consent to participate in the study. Subjects were recruited to run 20 km through New York City three times. Prior to the run, participants provided urine and blood, including a comprehensive metabolic panel (CMP), complete blood count (CBC) with differential, and spot creatinine. Approximately a week after the initial blood draw and a week after each run, participants ran 20 km in Manhattan with several environmental sensors to capture individual-level exposures of ambient temperature, humidity, internal core temperature, volume loss, sodium loss, minute ventilation, heart rate variability, and air pollution exposure. After each run, blood and urine samples were collected. We report descriptive data on heat stress and air pollution exposure and subsequent changes to liver enzymes.

Results: Eight men and seven women (of the 20 total enrolled) completed the three 20 km runs in New York City. Environmental exposures while running were highly variable with PM 2.5 air pollution total mass inhaled on a run being 119.0 ug per run (9.8–561.6 ug). Prior to running, all participants' CMP, CBC, and creatinine were within normal ranges. After a 20 km run, one runner had two runs during which AST and ALT increased from a baseline of 19 to 44 and 43 U/L for AST and 24 to 86 and 74 U/L for ALT for runs 1 and 3, respectively. For Run 2, there was no increase in for AST (19 to 20 U/L) or ALT (24 to 24 U/L). For this athlete, we saw no difference in sweat rate or internal body temperature. However, there was a significant difference in PM2.5 air pollution exposure with levels increased above the EPA good air quality for run 1 (217.8 ug) and run 3 (145.2 ug) but normal air pollution levels during run 2 (132.5 ug). Additionally, 3 other runners had an increase in total bilirubin greater than 1.5 times their baseline blood draw and total bilirubin was classified as above normal. Two of the three runs occurred during high air pollution days in which the PM_{2.5} exposure was 3 to 8 times greater than their other run days.

Conclusion: We observed abnormal elevation of ALT, AST, and total bilirubin were more likely to occur in the context of high pollution exposures. It is likely that an increase in AST, ALT, and total bilirubin could reflect muscle breakdown and/or hemolysis. However, this is in line with accumulating literature showing an association between air pollutants exposure and increased liver enzyme levels. These data may be instructive for public health interventions.

SAT-464-YI

Transaminases and older adults: distribution and associations with all-cause mortality

Daniel Clayton-Chubb¹, Ammar Majeed¹, Stuart Roberts¹, Hans Schneider¹, Jessica Fitzpatrick¹, Robyn Woods², Monira Hussain², Natassia Tan¹, Isabella Commins³, John Lubel¹, Cammie Tran², Alex Hodge⁴, John McNeil², William Kemp¹. ¹Alfred Health, Monash University, Melbourne, Australia; ²Monash University, Melbourne, Australia; ³Alfred Health, Melbourne, Australia; ⁴Eastern Health, Monash University, Box Hill, Australia
Email: chubb.daniel@gmail.com

Background and aims: Alanine aminotransferase (ALT) and aspartate aminotransferase (AST) are commonly ordered tests in general medical practice. However, their distribution and significance in older adults is understudied. As such, we aimed to evaluate the gender-stratified distribution of both ALT and AST in older adults, and to assess for any associations of transaminase levels with mortality.

Method: This study is a post-hoc analysis of the Aspirin in Reducing Events in the Elderly (ASPREE) randomised, placebo-controlled trial of daily low-dose aspirin for relatively healthy older persons. Baseline associations were explored with univariate analysis and ordinal logistic regression. Cox regression and restricted cubic splines were used to examine hazard ratios between transaminase levels and mortality.

Results: Of the 11853 participants with both ALT and AST levels recorded, 1054 (8.9%) deaths were recorded over a median of 6.4 (IQR 5.4–7.6) years. All values were above the Australian harmonised reference lower limit of normal. Males and females in the lowest quintile of ALT had an increased hazard of mortality (HR 2.09 [95% CI 1.60–2.74] and HR 1.99 [95% CI 1.49–2.67] respectively). However, for AST, only males in the lowest quintile had an increased hazard of mortality (HR 1.47 [95% CI 1.16–1.87]). These associations remained significant when adjusting for covariates including age, frailty, diabetes, and kidney disease, and when removing outliers.

Conclusion: Low ALT levels independently confer an increased hazard of mortality for older males and females; only low AST impacts older male survival. Further evaluation of mechanism would be worthwhile, and reevaluating the lower limit of normal for ALT in older adults should be considered.

POSTER PRESENTATIONS

SAT-465

Increasing awareness among primary care physicians about MASLD reduced unnecessary referral rates and an increased cardiovascular evaluation

Eileen Yoon¹, Jihyun An¹, Ha Il Kim², Joo Hyun Sohn², Bo-Kyeong Kang³, Eun Chul Jang⁴, Huiyul Park⁵, Hye-Lin Kim⁶, Sang Bong Ahn⁷, Joo Hyun Oh⁷, Hyunwoo Oh⁸, Hyo Young Lee⁹, Dae Won Jun¹. ¹Department of Internal Medicine, Hanyang University College of Medicine, Seoul, Korea, Rep. of South; ²Department of Internal Medicine, Hanyang University College of Medicine, Guri, Korea, Rep. of South; ³Department of Radiology, Hanyang University College of Medicine, Seoul, Korea, Rep. of South; ⁴Department of Occupational and Environmental Medicine, Soonchunhyang University College of Medicine, Cheon An, Korea, Rep. of South; ⁵Department of Family Medicine, Myoungji Hospital, Hanyang University College of Medicine, Goyang si, Korea, Rep. of South; ⁶College of Pharmacy, Sahmyook University, Seoul, Korea, Rep. of South; ⁷Department of Internal Medicine, Nowon Eulji Medical Center, Eulji University, College of Medicine, Seoul, Korea, Rep. of South; ⁸Department of Internal Medicine, Kangbuk Samsung Hospital, Sungkyunkwan University School of Medicine, Seoul, Korea, Rep. of South; ⁹Department of Internal Medicine, Sanggye Paik Hospital, Inje University College of Medicine, Seoul, Korea, Rep. of South
Email: noshin@hanyang.ac.kr

Background and aims: The revised definition of metabolic dysfunction-associated steatotic liver disease (MASLD) is anticipated to enhance awareness among primary care physicians and diminish stigma among patients. This study aimed to assess the impact of an online educational program on MASLD for physicians and its influence on modifying their clinical practice patterns.

Method: A total of 869 physicians [72 physicians at referral centers and 797 primary care physicians (PCPs)], who consented to receive educational materials on MASLD, participated in this study. They completed an initial survey regarding their clinical practices for patients with MASLD, followed by a second online survey eight weeks after receiving a series of seven weekly educational materials on MASLD.

Results: Frequency of utilizing non-invasive tests for liver fibrosis, used as the first tier evaluation in both physicians at referral centers and PCPs, was low at 6.9% and 6.9%, respectively, and there was no difference between the two groups. Regarding barriers to the management of MASLD, specialists in referral centers considered the 'short consultation time' as the primary challenge, while PCPs cited the 'the absence of a fee for this service' as the major barrier. Additionally, the proportion of PCPs considering non-invasive tests testing for patients in the 'at-risk group' increased significantly for those with diabetes (32.6% to 38.5%), cardiovascular disease (9.2% to 16.1%), and ischemic stroke (8.4% to 11.5%). After education, the percentage of PCPs who immediately referred patients to a specialist after a MASLD diagnosis decreased from 15.4% to 12.3% (P value = 0.042).

Conclusion: Increasing awareness among PCPs about MASLD reduced unnecessary referral rates and an increased cardiovascular evaluation.

SAT-466

The association of perceived neighborhood violence and allostatic load with metabolic dysfunction-associated steatotic liver disease in mexican-origin migrant and seasonal farmworkers along the southern Arizona United States/Mexico border

Adriana Maldonado¹, Emma Torres², Melissa Flores³, Edgar Villavicencio¹, Alejandra Hernandez¹, Estefania Ochoa Mora⁴, Ana Gonzalez¹, Julio Loya³, Rogelio Torres², Idolina Castro², Felicitas Torres², Naim Alkhouri⁵, David Garcia¹. ¹University of Arizona, Mel and Enid Zuckerman College of Public Health, Tucson, Arizona, United States; ²Campesinos sin Fronteras, Somerton, Arizona, United States; ³University of Arizona, Tucson, Arizona, United States;

⁴University of Arizona, University of Arizona Health Sciences, Tucson, Arizona, United States; ⁵Arizona Liver Health, Chandler, Arizona, United States

Email: adrianamaldonado@arizona.edu

Background and aims: In the Southern Arizona United States (U.S.)/Mexico border region, estimates indicate that the overall prevalence of MASLD among Mexican-origin adults is 50%; however, studies exploring MASLD risk among Mexican-origin migrant and seasonal farmworkers (MSFWs) do not exist. This is surprising as MSFWs experience high rates of hypertension, type 2 diabetes, hypercholesterolemia, and obesity. In addition, while it has been found that the social and built environment affect individuals' health outcomes, including allostatic load (AL); to date, the impact of neighborhood context on farmworkers' MASLD risk has not been explored. Using a community-based participatory approach, we aimed to examine the association between perceived neighborhood violence (PNV), AL, and MASLD in a cross-sectional sample of MSFWs. We also examined whether AL was a mediator between perceived violence and MASLD. **Method:** Data were collected from a community-based sample of 151 MSFWs (women = 59.6%; men = 40.4%; mean age = 49.7 years \pm 14.1 years; mean BMI = 31.9, \pm 6.5) residing in the Southern Arizona U.S./Mexico border region. Self-reported data on PNV was collected. PNV was assessed by summing scores across four, 4-point Likert scale dimensions where respondents indicated prevalence levels from 1 (never) to 4 (often). Allostatic load, calculated as an index of physiologic dysregulation, included systolic and diastolic blood pressure, body mass index (BMI), total cholesterol, HDL cholesterol, total/HDL cholesterol ratio, C-reactive protein, albumin, and creatinine clearance. Hepatic steatosis and fibrosis were assessed by liver stiffness measurements (LSM) and controlled attenuation parameter (CAP) scores via FibroScan[®]. MASLD was identified as having a CAP score of \geq 288 dB/m. Relevant covariates including age, sex, nativity, and acculturative stress were included in all models.

Results: The mean CAP score was, M = 265.81 \pm 60.97, ranging from 100.0 to 399.0 with 41.1% of the sample being identified with MASLD. The average PNV was reported as M = 5.42 \pm 2.22, ranging from 0 to 13. The mean AL score was M = 4.76 \pm 1.33, ranging from 1.5 to 7.5. PNV was not associated with MASLD status, however, contrary to our expectations, was negatively associated with AL, (b = 0.13, SE = 0.05, 95% CI (-0.01, -0.02)). AL was positively associated with MASLD status, (OR = 2.22, 95% CI (1.58, 3.12)). Lastly, AL was a negative mediator between PNV and MASLD status (average mediated effect = -0.02, 95% CI (-0.03, -0.01)).

Conclusion: This is one of the first studies to explore PNV and AL in the context of MASLD for MSFWs. While study findings highlight potential areas of focus for MASLD-risk reduction interventions, additional research is needed to fully understand the mechanistic pathways through which AL influences MSFWs' risk for MASLD.

SAT-467

Prioritisation of research to tackle stigma in alcohol-related liver disease: results from the ARMS-Hub partnership

Ashwin Dhanda^{1,2}, Victoria Allgar¹, Neeraj Bhala³, Lynne Callaghan¹, Joana Castro⁴, Shilpa Chokshi⁵, Amanda Clements⁴, Ewan H. Forrest⁶, Lesley Manning⁷, Richard Parker⁸, Debbie L. Shawcross⁹, Jennifer Towey¹⁰. ¹University of Plymouth, Plymouth, United Kingdom; ²University Hospitals Plymouth NHS Trust, South West Liver Unit, Plymouth, United Kingdom; ³University of Nottingham, Nottingham, United Kingdom; ⁴University Hospitals Plymouth NHS Trust, Plymouth, United Kingdom; ⁵Roger Williams Institute of Hepatology, London, United Kingdom; ⁶Greater Glasgow and Clyde NHS, Glasgow, United Kingdom; ⁷Not affiliated (public member), Plymouth, United Kingdom; ⁸Leeds Teaching Hospital NHS Trust, Leeds, United Kingdom; ⁹King's College London, London, United Kingdom; ¹⁰University Hospitals Birmingham, Birmingham, United Kingdom
Email: ashwin.dhanda@nhs.net

Background and aims: Despite the high disease burden from alcohol-related liver disease (ALD), there is disproportionately low research activity in the field. Reasons for inattention to ALD are multifactorial but certainly include stigma and lack of engagement and inclusion of people with lived experience (PWLE) in developing and participating in research. We developed an ALD multistakeholder hub (ARMS-Hub) of experts and PWLE/carers with an aim to identify the research priorities to tackle stigma and low research and patient engagement in ALD.

Method: Existing clinical and research networks were mapped and stakeholder members identified across disciplines and settings including hepatology, addictions, biomedical science, community services and charities. Patient and public involvement and engagement (PPIE) members were recruited via the British Liver Trust and through charities and support groups. In-person members were recruited through community alcohol services in Plymouth. 5 virtual stakeholder meetings and 3 virtual and 3 in-person PPIE meetings took place between July and December 2023. Discussions focused on stigma, and inclusion and engagement in research. Major themes and sub-themes were identified from written notes and transcripts. Following the discussions, themes were prioritised by ranking at the fifth stakeholder meeting and research questions generated and reviewed by all stakeholders.

Results: The PPIE in-person group consisted of 31 participants (7 female; median age 45–54; 42% living in the most deprived decile), while our virtual PPIE group was composed of 9 participants (3 female; median age 45–54; 11% living in the most deprived decile). 31 experts attended 5 virtual stakeholder meetings (39% senior clinicians 26% senior nurses, 19% allied health professionals, 10% voluntary sector workers and 6% academics). Major themes were identified and ranked by the attendees: 1) education and awareness, 2) accessibility, 3) language and 4) culture. Sub-themes were also discussed and ranked. The following three subthemes were prioritised: 1) the disconnect between liver and mental health services, 2) preconceptions from healthcare professionals and 3) lack of knowledge of alcohol harms. The ARMS-Hub project team generated overarching research questions relating to each prioritised area and obtained consultation from stakeholders and PPIE members. The final 3 research questions are: 1) How can mental health services best be integrated into liver services? 2) Can an educational package be used to reduce stigma in healthcare professionals? 3) Can we design and implement a diverse educational package around the wider harms of alcohol?

Conclusion: A diverse group of stakeholders, PWLE and carers have prioritised three research areas to tackle stigma and engagement in ALD. Research questions and proposals are being developed to address these crucial issues.

SAT-468

Changing from MAFLD to the new nomenclature: new opportunities to understand the role of alcohol and metabolism to adverse outcomes

Chenlu Yang¹, Shuohua Chen², Shouling Wu², Li Wang¹. ¹*Institute of Basic Medical Sciences, Chinese Academy of Medical Sciences, Peking Union Medical College, Peking, China;* ²*Kailuan General Hospital, Tangshan, China*
Email: liwang@ibms.pumc.edu.cn

Background and aims: In June 2023, steatotic liver disease (SLD) was introduced as an overarching term to replay metabolic dysfunction-associated fatty liver disease (MAFLD) to cover the various etiologies of steatosis. This study aims to explore the distinction of long-term outcomes between the subtypes of SLD and MAFLD.

Method: We included 152, 139 adults diagnosed with ultrasonography from the Kailuan Cohort in China between June 2006 and April 2014. The Cox regression or Fine Gray competitive risk models were used to compare the risk of adverse outcomes in the cross-definition grouping of SLD subtypes and MAFLD. Individuals without viral

hepatitis and excessive alcohol consumption were included in this analysis. In addition, we compared the risk of adverse outcomes under different alcohol consumption levels based on the definition of SLD.

Results: The prevalence of SLD and MAFLD was 32.1% and 31.3%, respectively. The proportion of MetALD-MAFLD, MetALD-only (lean SLD with moderate alcohol consumption and metabolic abnormalities), MASLD-MAFLD, MASLD-only (lean SLD with light alcohol consumption and metabolic abnormalities), and cryptogenic SLD (lean SLD without metabolic abnormalities) was 7.7%, 0.2%, 89.9%, 1.0%, and 1.2%. Compared to non-SLD individuals, MetALD-only and MASLD-only still had higher risks of mortality (HR_{MetALD-only} = 2.14, 95% CI: 1.39, 3.28; HR_{MASLD-only} = 1.55, 95% CI: 1.21, 1.98) and cancers (HR_{MetALD-only} = 2.63, 95% CI: 1.45, 4.79; HR_{MASLD-only} = 1.55, 95% CI: 1.06, 2.26), but MetALD-MAFLD and MASLD-MAFLD subjects were more prone to CVD (HR_{MetALD-MAFLD} = 1.31, 95% CI: 1.20, 1.43; HR_{MASLD-MAFLD} = 1.51, 95% CI: 1.45, 1.56) and CKD (HR_{MetALD-MAFLD} = 1.48, 95% CI: 1.28, 1.72; HR_{MASLD-MAFLD} = 1.72, 95% CI: 1.62, 1.82). Cryptogenic SLD did not show an increased risk for adverse outcomes. Based on the classification of alcohol consumption in SLD, ALD has the highest mortality risk (HR_{ALD vs. MetALD} = 2.19, 95% CI: 1.91, 4.02; HR_{ALD vs. MASLD} = 2.05, 95% CI: 1.12, 3.75). In comparison to MASLD, the MetALD population has an elevated risk of developing cancers (HR = 1.17, 95% CI: 1.01, 1.35) but a lower risk of CVD (HR = 0.87, 95% CI: 0.80, 0.96) and CKD (HR = 0.86, 95% CI: 0.74, 1.00).

Conclusion: The SLD definition can identify individuals with fatty liver who are lean with metabolic abnormalities and at a higher risk of adverse outcomes, which are overlooked by the MAFLD definition. ALD, MetALD, and MASLD may indicate different outcome risks, and it is recommended to manage them separately.

SAT-471

Relationship between steatotic liver disease, all-cause mortality and cardiovascular related outcomes-20 year follow-up of a longitudinal cohort study

Oyekoya Ayonrinde^{1,2,3}, Raj Uchila², John Olynyk^{2,3}, Chrianna Bharat⁴, Kevin Murray¹. ¹*The University of Western Australia, Perth, Australia;* ²*Fiona Stanley Hospital, Murdoch, Australia;* ³*Curtin University, Bentley, Australia;* ⁴*University of New South Wales, Sydney, Australia*
Email: oyekoya.ayonrinde@uwa.edu.au

Background and aims: Steatotic liver disease (SLD) is the most prevalent chronic liver disease globally and has been associated with increased mortality. We examined the longitudinal relationship between the severity of hepatic steatosis, and subsequent mortality and emergence of cardiovascular disease (CVD) in adults participating in the Busselton Health Study, a population-based longitudinal cohort study in Western Australia.

Method: SLD was diagnosed using fatty liver index (FLI), calculated from body mass index, waist circumference, serum triglycerides and gamma glutamyl transferase. Cox proportional hazards models were used to investigate the relationship between FLI and (a) all-cause mortality, (b) CVD mortality, and (c) CVD-related events. Participants were followed for up to 20 years, i.e. from the date of survey (1994/1995) until the date of death or end of follow-up (2014). Restricted cubic splines were used to investigate nonlinear relations between FLI and outcomes of interest, with hazard ratios (HR) and 95% confidence intervals (CI) derived. FLI quintiles were derived and HR estimates reported for the median FLI in each quintile, using the median FLI in quintile 5 as the reference. Models adjusting for age, sex, and history of CVD (model A); age, sex, history of CVD, smoking, diabetes, blood pressure treatment, systolic blood pressure, total cholesterol, and high-density lipoprotein (HDL) cholesterol (model B); and adjusted for all covariates in model B plus alcohol intake (model C) were used in all analyses. Associations were stratified by sex and age <50 vs. 50+ years.

Results: There were 4, 382 participants (56% female) with mean age 51 (SD 17) years recruited in the original cohort. In follow-up there

POSTER PRESENTATIONS

were 974 (22.2%) deaths, 408 (9.3%) CVD-related deaths, and 1018 (23.2%) CVD events. We found a non-linear association between FLI and all-cause mortality ($p < 0.01$), seen in both sexes. After multi-variable adjustment, participants in quintile 1 had a 28% lower risk of all-cause mortality compared with participants in quintile 5 (HR 0.72, 95% CI 0.55–0.94). CVD deaths and events increased with increasing FLI (model A), but this was less apparent after further adjustments (models B and C). There was no association observed between FLI and mortality or CVD outcomes among participants aged < 50 years of age. By contrast, in those aged 50+ years there was an increased risk of all-cause mortality in quintile 3 (HR 1.30, 95% CI 1.08–1.563) and in quintile 4 (HR 1.26, 95% CI 1.09–1.458) of FLI, respectively, and HR 1.29, 95% CI 1.11–1.49 for CVD-related events in quintile 3 ($p < 0.05$ for all), compared to quintile 5.

Conclusion: Severity of SLD was associated with all-cause mortality and CVD-related events, particularly in people aged 50+ years. The relationship between SLD and CVD outcomes was attenuated by other CVD risk factors.

Public Health – Viral hepatitis

TOP-460-YI

Progression of hepatitis B virus (HBV)-related liver disease in immune-tolerant, inactive, and grey zone phases: a systematic review and meta-analysis

Zakary Warsop^{1,2}, Arthur Rakeover², Daniela Yucuma², Yu Ri Im^{2,3}, Si Emma Chen², Rukmini Jagdish^{2,4}, Roger Chou⁵, Philippa Easterbrook⁶, Yusuke Shimakawa². ¹Imperial College London, London, United Kingdom; ²Institut Pasteur, Paris, France; ³Nuffield Department of Medicine, University of Oxford, Oxford, United Kingdom; ⁴St George's Hospital, London, United Kingdom; ⁵Oregon Health and Science University, Portland, United States; ⁶World Health Organisation, Geneva, Switzerland

Email: zakary.warsop18@imperial.ac.uk

Background and aims: The global burden of chronic hepatitis B virus (HBV) (CHB) infection is a major public health challenge. Antiviral therapy is effective in reducing HBV viral load and the risk of developing cirrhosis and hepatocellular carcinoma (HCC), but not all individuals currently require antiviral therapy as only a subset of untreated patients will develop liver-related complications. To improve our understanding of the natural history of CHB in people not currently indicated for treatment across most professional societies' guidelines, a systematic review and meta-analysis was conducted to assess the risk of liver complications at the inactive carrier, grey zone (GZ) and immune tolerant stages of HBV infection.

Method: We searched PubMed, Embase, Web of Science and the Cochrane Library for cohort studies published up to 6 February 2023. Two reviewers independently reviewed titles, abstracts and extracted data from full-text articles. Outcomes included HCC, cirrhosis, all-cause and liver-related mortality and HBsAg sero-clearance. The incidence rates of each outcome were pooled using a generalized linear mixed model according to the different phases of the natural history. Inactive phase (HBeAg-negative chronic infection) was defined as HBeAg-negative, HBV DNA $< 2,000$ IU/ml, and ALT $<$ upper limit of normal (ULN). Immunotolerant phase (HBeAg-positive chronic infection) was defined as HBeAg-positive, HBV DNA $> 20,000$ IU/ml, and ALT $<$ ULN. Patients in the GZ phase were subcategorized into GZ1: HBV DNA $< 2,000$ IU/ml and ALT $1-2 \times$ ULN, GZ2: HBV DNA $2,000-20,000$ and ALT $<$ ULN, and GZ3: HBV DNA $2,000-20,000$ and ALT $1-2 \times$ ULN.

Results: Of 13,124 studies identified and screened, 36 were included. Two (5.6%) of these were from the African World Health Organisation region. There were 4 studies included in each of the GZ and immune

tolerant groups and 15 studies in the inactive carrier group. The pooled incidence rates (per 100 person-years) for developing HCC were: 0.327 (95% CI: 0.258–0.413); 0.390 (0.249–0.611); 0.475 (0.183–1.232) and 0.563 (0.207–1.529) in the GZ1, GZ2, GZ3 and immune tolerant groups respectively. These were significantly higher than in the inactive carrier phase: 0.100 (95% CI 0.064–0.157) ($p < 0.01$). Similar results were found for other outcomes. Studies with a single assessment of viral load and ALT at baseline appeared to show a higher risk than those with multiple assessments.

Conclusion: Patients in the immune tolerant and grey zone phases have a higher risk of developing HBV-related complications. Further trials are needed to confirm the efficacy of treatment in these populations.

TOP-461-YI

Retreating the off-Nuc clinical relapse with Pegylated interferon much increased HBsAg seroclearance-a propensity score matching study

Yu-Ting Kao¹, Yen-Chun Liu², Rong-Nan Chien², Rachel Wen-Juei Jeng². ¹Department of Gastroenterology and Hepatology, Chang Gung Memorial Hospital, Linkou branch, Taoyuan, Taiwan, Taoyuan, Taiwan; ²Chang Gung Memorial Hospital, Linkou branch, Taiwan, Taoyuan, Taiwan
Email: rachel.jeng@gmail.com

Background and aims: HBsAg seroclearance is significantly elevated in HBeAg-negative chronic hepatitis B (CHB) patients upon discontinuation of nucleos(t)ide analogue (NUC) therapy comparing to that during long-term viral suppression. The immune response after stopping Nuc may be modulated by the re-appearance of viral antigen which facilitate the HBsAg seroclearance. This study aims to investigate if retreating off-Nuc clinical relapse (CR) patients with pegylated interferon would enhance the likelihood of achieving functional cure.

Method: From the CGMH off-Nuc cohort, 25 HBeAg-negative CHB off-Nuc CR patients retreated with Peg-IFN (Rx-Peg-IFN) and 980 off-Nuc CR patients retreated with Nuc (Rx-Nuc) were enrolled. Propensity score matching (PSM) was employed, adjusting for age, gender, ALT, HBV DNA, and HBsAg levels at retreatment, between off-Nuc CR patients Rx-Peg-IFN and Rx-Nuc at a 1 to 3 ratio. Kaplan-Meier analysis and log-rank tests compared the cumulative HBsAg loss rate among these three groups.

Results: After PSM, there were 25 and 75 patients in Rx-Peg-IFN and Rx-Nuc arms, respectively. The mean age was 50 of all both arms ($p = 0.63$), 96% (Rx-Peg-IFN) and 86% (Rx-Nuc) were male ($p = 0.31$). The median ALT level of Rx-Peg-IFN and Rx-Nuc were 156 and 162 U/L ($p = 0.29$), HBV DNA levels were 5.7 and 6.0 log₁₀ IU/ml ($p = 0.14$), and HBsAg level was 2.8 and 3.3 log₁₀ IU/ml ($p = 0.62$), respectively. The HBsAg reduction during the 1st year of retreatment was -1.14 versus -0.46 log₁₀ IU/ml, respectively, ($p = 0.0061$). During a median follow-up of 7.1 years (from start of retreatment), 10 and 4 patients lost HBsAg in Rx-Peg-IFN and Rx-Nuc groups, respectively. The cumulative HBsAg seroclearance rates (from start of retreatment) at 1, 2, 5, and 10 years were 12%, 20.2%, 25.5%, and 45.0% in Rx-Peg-IFN arm, versus 0%, 0%, 2.7%, and 4.6% in Rx-Nuc arm, respectively (log rank test, $P < 0.0001$).

Conclusion: Retreatment with Peg-IFN in HBeAg-negative chronic hepatitis B (CHB) patients experiencing clinical relapse (CR) resulted in a significantly elevated HBsAg loss rate (by end of Rx-Peg-IFN treatment: 12%, 1-year post EOT of Rx-Peg-IFN: 20.2%). This underscores the potential strategy of enhancing functional cure by boosting the off-Nuc immune response.

WEDNESDAY 05 JUNE

WED-422

Screening for viral hepatitis in the emergency department-the methodology to automate a feasible, acceptable and effective solution

Julia Di Girolamo^{1,2}, David Prince^{1,2,3}, Basheer Alshiwanna^{1,2,3}, Robert Porritt⁴, David Thomas⁴, Shahida Bakridi⁴, Hung Tran⁴, Sophie Gryllis⁴, Maria Tigla⁴, Rebecca Haack⁴, Kristian Peralta⁴, Melissa Bagatella¹, Irena Petrovski⁵, Julie Doan⁶, Richard Cracknell⁷, Jeremy Lawrence⁸, Michael Maley⁴, Hong Foo⁴, Nathan Jones⁹, Gregory Dore^{3,10}, Miriam Levy^{1,2,3}. ¹Department of Gastroenterology and Liver, Liverpool Hospital, Sydney, Australia; ²Ingham Institute for Applied Medical Research, Sydney, Australia; ³The University of New South Wales, Sydney, Australia; ⁴NSW Health Pathology, Sydney, Australia; ⁵Department of Gastroenterology and Liver, Campbelltown Hospital, Sydney, Australia; ⁶Clinical Reporting and Analytics, Liverpool Hospital, Sydney, Australia; ⁷Department of Emergency Medicine, Campbelltown Hospital, Sydney, Australia; ⁸Department of Emergency Medicine, Fairfield Hospital, Sydney, Australia; ⁹Liverpool Hospital, Sydney, Australia; ¹⁰The Kirby Institute, UNSW, Sydney, Australia
Email: julia.digirolamo@health.nsw.gov.au

Background and aims: Australian guidelines recommend risk factor screening for viral hepatitis in priority populations. Barriers to testing exist in culturally and linguistically diverse (CALD) and Indigenous populations particularly, who may acquire hepatitis via non-injecting use routes. A universal testing strategy may serve hard to reach populations, but implementation remains an issue. We reported Screening of Emergency Admissions at Risk of Chronic Hepatitis (SEARCH) pilot clinical service in Emergency Department (ED) screening of priority populations, efficacy, cost utility, and acceptability. This report describes the methodology required for automation and broad implementation.

Method: A novel pilot clinical service (SEARCH 3X) was developed to automatically test adult ED patient blood specimens for hepatitis B surface antigen (HBsAg) and hepatitis C antibody (HCVAb). A computer algorithm was developed such that at laboratory specimen reception in appropriate specimens, hepatitis serology would be automatically added, directing the specimen through the biochemistry analyser for testing. Positives were confirmed by routine supplementary tests. A re-test order within seven days was automatically denied. The feasibility of reflexive HCV RNA testing on positive HCVAb specimens was examined. Test cancellation mechanism due to patient or clinician request, was developed. Design included the automatic reporting of positive results to the clinical team to precipitate linkage to care. Clinician and patient education resources were developed to promote awareness of viral hepatitis and the testing service, in the form of videos, posters, pamphlets and website including translation into languages for local CALD communities.

Results: Six Australian EDs were identified in metropolitan or rural locations based on feasibility and unmet need. Executive and clinical stakeholders were consulted, and a governing steering committee formed. An initial pilot of 5000 patients per site was set. The automated methodology was successfully implemented in the first two sites with minimal impact on ED services. Ninety-nine percent (n = 10, 204) of eligible patients were successfully tested. The combined HBsAg and HCVAb seroprevalence was 2.5%. Eighty six percent of positive patients were successfully linked to care. No patient or staff complaints were received, nor did any patient decline testing. The proportion of patients tested more than once was 10.5%, of which 80%, were tested twice, 15% tested thrice and remainder 5% tested four to six times.

Conclusion: Automation allows testing of 99% of the target population with no increased work for ED services. The hepatitis seroprevalence justifies the testing and linkage to care is strong. Repeat testing is an issue but may be reduced by optimising the

algorithm. Work is underway to test a further 20, 000 patients at 4 other sites during 2024.

WED-423

Estimation of the prevalence of hepatitis delta virus infection in the European Union

Hugh Watson^{1,2}, Letizia Nidiaci³, Andrea Nizzardo³, James Alexander⁴. ¹Evotec ID, Medical Development and Translational Science, Lyon, France; ²Department of Clinical Medicine, Aarhus University, Aarhus, Denmark; ³Aptuit Srl, Verona, Italy; ⁴Alexander Pharma Consulting, Cary, NC, United States
Email: hugh.watson@evotec.com

Background and aims: Hepatitis delta virus (HDV) prevalence in the general population of the European Union (EU) is unknown. HDV prevalence among HBsAg+ patients referred to hospital hepatology and infectious disease clinics has been described in several EU countries, but there is little information on the prevalence of HDV in the HBsAg+ population not referred to hospital clinics. We aimed to estimate overall prevalence of viraemic HDV in the EU by incorporating data-driven assumptions for the non-referred HBsAg+ population.

Method: Data on HDV prevalence was searched in public databases. Extrapolating from clinic-population estimates of HDV prevalence to estimates of national HDV prevalence required assumptions for (1) the proportion of the HBsAg+ population referred to hospital clinics, and (2) the difference in HDV-RNA prevalence between referred and non-referred patients. The proportion of HBsAg+ patients referred to hospital clinics was derived from literature. As surrogates for non-referred patients, prevalence amongst patients classified as having "inactive disease" and community patients were considered. Corresponding adjustments were made to prevalence estimates derived from hospital clinics. Assumptions were validated by comparison of adjusted estimates from clinic populations with prevalence determined directly in general populations, where available. EU-wide prevalence of HDV was then derived from national HBsAg+ prevalence data using appropriate meta-analytical statistical methods and imputing values for countries lacking data. Sensitivity analyses utilizing alternative assumptions generated a plausible range of prevalence estimates.

Results: 62 estimates of HDV prevalence were identified from 16/27 EU countries. 74% of prevalence estimates were based on hospital clinic HBsAg+ populations. The most likely scenario estimated the proportion of HBsAg+ patients referred to hospitals at 32%, while prevalences of anti-HDV Ab and HDV-RNA in non-referred patients were estimated respectively at 0.28 × and 0.13 × those in referred HBsAg+ patients. Comparison of HDV prevalence derived from clinic and general population samples validated these assumptions. We estimated HDV-RNA prevalence ranging from <1 to 27 in 10, 000 in national populations with an overall figure of 2.9 in 10, 000 (plausible range 2.2 to 4.0) for the EU after imputing values for missing countries.

Conclusion: A general population estimate of HDV-RNA prevalence was obtained for the whole EU with some uncertainty due to the small evidence base for key assumptions.

WED-424

Cost-effectiveness of antiviral therapy in patients with chronic hepatitis B in the high viremic gray zone

Suk-Chan Jang¹, Won-Mook Choi², Gi-Ae Kim³, Hye-Lin Kim⁴, Young-Suk Lim². ¹School of Pharmacy, Sungkyunkwan University, Suwon, Gyeonggi-do, Korea, Rep. of South; ²Department of Gastroenterology, Liver Center, Asan Medical Center, University of Ulsan College of Medicine, Seoul, Korea, Rep. of South; ³Department of Internal Medicine, Kyung Hee University School of Medicine, Seoul, Korea, Rep. of South; ⁴College of Pharmacy, Sahmyook University, Seoul, Korea, Rep. of South
Email: limys@amc.seoul.kr

POSTER PRESENTATIONS

Background and aims: Accumulating evidence indicates that high viremic gray zone patients with low ALT levels have a higher hepatocellular carcinoma (HCC) risk than low viremic individuals with high ALT levels. Recent research shows a not linear but parabolic relationship between HBV DNA levels and HCC risk in gray zone patients. We aimed to assess the cost-effectiveness of initiating antiviral therapy in the gray zone, particularly for patients with HBV DNA levels between 4 and 8 log₁₀ IU/ml associated with a high risk of HCC.

Method: We conducted a cost-utility analysis using a Markov model to compare the expected costs and quality-adjusted life-years (QALYs) of starting antiviral therapy at the gray zone phase (treated gray zone group) compared to delaying treatment until the immune-active phase (untreated gray zone group). The hypothetical cohort of 10,000 patients with CHB in the gray zone phase (60% male, HBV DNA levels 4–8 log₁₀ IU/ml, ALT levels <40 IU/L, HBeAg-positive 50%) was simulated over a 10-year horizon. Transition probabilities and costs were mainly obtained from a multicentre historical cohort study including adult CHB patients without cirrhosis at five tertiary referral hospitals in South Korea. The incremental cost-effective ratio (ICER) using QALY was calculated between the treated gray zone and the untreated gray zone group from the healthcare system and societal perspective.

Results: In the base-case analysis (serum HBV DNA levels of 4–8 log₁₀ IU/ml and all age groups), the ICER was USD 12,630/QALY, indicating cost-effectiveness under the willingness-to-pay threshold of USD 25,000/QALY. Stratified analyses by HBV DNA levels demonstrated the highest cost-effectiveness for levels of 6–7 log₁₀ IU/ml with ICER of USD 2,418/QALY, followed by 5–6 (USD 7,726/QALY), 7–8 (USD 20,390/QALY), and 4–5 (USD 25,375/QALY) log₁₀ IU/ml, which order was consistent with HCC risk by HBV DNA levels. Age-stratified analyses showed the ICER increased as age decreased; initiating treatment for patients over 40 years old was cost-effective. From a societal perspective considering productivity loss, the treat gray zone strategy was dominant (ICER <0), suggesting that this strategy incurred less cost and had a superior effect.

Conclusion: Initiating antiviral therapy in the high viremic gray zone is cost-effective compared to delaying treatment to the immune-active phase. This study suggests that commencing antiviral therapy in the high viremic gray zone phase should be considered, accounting for both clinical and economic burdens.

WED-425

Effects of direct-acting antivirals on end-stage liver disease and mortality among Florida Medicaid beneficiaries with chronic hepatitis C

Pei-Lin Huang¹, Shao-Hsuan Chang¹, Roniel Cabrera², Debbie Wilson¹, Haesuk Park¹. ¹University of Florida College of Pharmacy, Gainesville, United States; ²University of Florida College of Medicine, Gainesville, United States
Email: hpark@cop.ufl.edu

Background and aims: Despite current availability of effective direct-acting antivirals (DAA) therapies, treatment uptake has been suboptimal in the United States (US). Medicaid beneficiaries are known to have the lowest treatment initiation rate due to fewer financial resources and prior authorization policies. We assessed the effects of DAA treatment on the risk end-stage liver disease (i.e., decompensated cirrhosis [DCC], hepatocellular carcinoma [HCC]) and mortality among Medicaid beneficiaries.

Method: We conducted a retrospective cohort study of 2013–2019 Florida Medicaid data of beneficiaries aged 18–64 years with a diagnosis with hepatitis C (HCV). Patients were categorized as those who received DAA therapy and those who did not. The index date was defined as the first DAA initiation date in the DAA group. For each untreated patient, we randomly assigned a hypothetical index date using the distribution of treated patients. The incidence rates of DCC, HCC and all-cause mortality after the index date (i.e., number of

events/person-year) were compared between the DAA and untreated groups, stratified by liver severity (with and without cirrhosis). We used inverse probability of treatment weighted multivariable Cox proportional hazards regression modeling to estimate adjusted hazard ratios (aHR) and 95% confidence intervals (CI). We conducted a sensitivity analysis to define outcome events occurring ≥3 months after the index date and a subgroup analysis for patients receiving ≥8 weeks of DAA treatment.

Results: Among 32,409 Medicaid beneficiaries with HCV (mean age = 45.78, 43% men, 15% Black), 13% received DAAs. Among beneficiaries without cirrhosis DAA treatment was associated with significantly decreased risk of DCC (aHR, 0.46; 95% CI, 0.35–0.60), HCC (aHR, 0.42; 95% CI, 0.22–0.79), and mortality (aHR, 0.16; 95% CI, 0.12–0.21) compared to no treatment. Similarly, among beneficiaries with cirrhosis, DAA treatment was associated with significantly decreased risks of DCC (aHR, 0.33; 95% CI, 0.24–0.45), HCC (aHR, 0.53; 95% CI, 0.32–0.89), and mortality (aHR, 0.17; 95% CI, 0.12–0.25). The findings from sensitivity and subgroup analyses were consistent with the base case analysis.

Conclusion: This cohort study suggests that DAA treatment was associated with decreased risk of DCC, HCC, and mortality among Medicaid beneficiaries with HCV. Despite these promising results, this study demonstrates that only 13% of Florida Medicaid beneficiaries with HCV received DAA treatment. To reach the global health goal of eliminating hepatitis by 2030 in the US, Medicaid programs need to consider offering less-restrictive requirements for HCV treatment and further overcome barriers to the treatment that still exist for vulnerable Medicaid beneficiaries.

WED-426

From kitchen to table: unravelling hepatitis E virus inactivation in pork meat products

Tatjana Locus^{1,2,3}, Michael Peeters³, Ellen Lambrecht¹, Steven Van Gucht³, Thomas Vanwolleghem². ¹Flanders Research Institute for Agriculture, Fisheries and Food, Melle, Belgium; ²Antwerp University Hospital, Edegem, Belgium; ³Sciensano, Brussels, Belgium
Email: tatjana.locus@ilvo.vlaanderen.be

Background and aims: Hepatitis E virus (HEV) infection through the consumption of pork and wild boar meat is a significant public health concern, and is recognized as the primary cause of acute viral hepatitis in Europe (ECDC, 2019). Theoretical analyses focusing on HEV contamination and exposure, performed by our research team revealed that ready-to-eat pork products pose the highest risk of HEV contamination (Locus et al., 2023a). However, the impact of diverse meat processing methods on the infectivity of the virus remains poorly understood. Consequently, there is an urgent need to investigate the influence of these methods in relevant matrices. This study aims to elucidate the effects of common meat processing techniques, including heating, drying, and pH reduction, on the inactivation of HEV in pork meat products.

Method: The impact of different core temperatures (68°C, 72°C, 80°C, and 99°C) on the integrity of HEV were assessed by spiking raw liver and pork fat with cell culture produced HEV and preparing pork liver pâtés according to a standard recipe. In a subsequent series of experiments, we prepared both standard and pH-reduced (achieved by adding DL-Lactic acid until pH 4.1) dried pork sausages. These sausages were initially refrigerated for 24 hours and then transferred to a biosafety cabinet for additional drying. At intervals of two, seven, and fourteen days, we assessed the sausages for weight, pH, water activity, and the presence of HEV. Detection of infectious HEV particles was carried out through immunostaining, complemented by in-house proxy methods to evaluate HEV capsid and genome integrity (Locus et al., 2023b) in both sets of experiments.

Results: Significant reductions in HEV particles with intact capsids were observed in pâtés heated to 68°C, 72°C, and 80°C (1.3, 1.3, and 1.5 logs, respectively) compared to unheated controls (p < 0.001 ***). No viral RNA was detected at 99°C (more than 3.5 logs reduction, p <

0.001 ***). No intact HEV genomes were detected, except in two out of three pâtés heated to 68°C. In standard and pH-reduced dried pork sausages, significant reductions in HEV particles with intact capsids were evident after 14 days ($p < 0.001$ ***), but complete reduction did not occur (2.2 and 1.2 logs, respectively). After seven days, intact genomes were detected in one and two out of three standard and pH-reduced sausages, respectively. After 14 days, intact genomes were found in one of three pH-reduced sausages.

Conclusion: Our findings suggest that existing meat processing methods may not be entirely effective in disintegrating Hepatitis E virus (HEV) particles in high-risk food products. The experimental framework and assays designed to assess viral capsid and genome integrity provide valuable insights. Further research is warranted to identify and implement optimal meat processing techniques that can significantly reduce the risk of foodborne HEV infections.

WED-427

Progress towards achieving hepatitis C elimination in the country of Georgia, April 2015–November 2023

Tengiz Tsertsvadze^{1,2}, Akaki Abutidze^{1,2}, Lali Sharvadze^{2,3}, Maia Butsashvili⁴, Jaba Zarkua⁵, Rania Tohme⁶, Shaun Shadaker⁶, Ekaterine Adamia⁷, Tamar Gabunia⁷. ¹Infectious Diseases, AIDS and Clinical Immunology Research Center, Tbilisi, Georgia; ²Ivane Javakhishvili Tbilisi State University, Tbilisi, Georgia; ³Hepatology clinic HEPA, Tbilisi, Georgia; ⁴Health Research Union, Tbilisi, Georgia; ⁵Medical Center Mrcheveli, Tbilisi, Georgia; ⁶Division of Viral Hepatitis, Centers for Disease Control and Prevention, Atlanta, United States; ⁷Ministry of IDPs from the Occupied Territories, Labour, Health and Social Affairs of Georgia, Tbilisi, Georgia
Email: tt@aidcenter.ge

Background and aims: The country of Georgia launched the world's first national hepatitis C elimination program in April 2015. Key strategies include nationwide screening, active case finding, linkage to care, decentralized care, and provision of treatment for all persons with hepatitis C virus (HCV) infection, along with effective prevention interventions. The elimination program aims to achieve the following targets by 2025: a) diagnose 90% of HCV-infected persons, b) treat 95% of those diagnosed, and c) cure 95% of those treated (90–95–95 targets). We report progress toward these HCV elimination targets in Georgia.

Method: The estimated number of persons with HCV infection was based on a 2015 population-based national seroprevalence survey, which showed that 5.4% of the general adult population had current HCV infection (approximately 150,000 persons). We analyzed data in the national HCV screening and treatment databases during April 2015–November 2023.

Results: As of November 30, 2023, 162,089 adults screened reactive for HCV antibodies. Of those, 135,547 (83.6%) received HCV RNA or core antigen testing, of whom 105,328 (77.7%) had current HCV infection, and 84,928 (80.6%) of them initiated treatment. Of 59,663 persons who were evaluated for sustained virologic response (SVR) after treatment completion, 59,055 (99.0%) had no detectable HCV RNA. Based on the 90–95–95 program goals, Georgia has diagnosed 78.0% of the target 135,000 (90% of the estimated 150,000 adults with current HCV infection), treated 66.2% of the target 128,250 (95% of 135,000), and cured 48.5% of the target 121,837 (95% of 128,250). Treatment effectiveness was comparable among persons with advanced fibrosis (elastography score F3–F4 or FIB-4 >3.25) with 98.4% achieving SVR, and among patients with mild or no liver fibrosis (elastography score ≤F2 or FIB-4 <1.25), SVR = 99.2%, $p < 0.0001$.

Conclusion: Georgia has made substantial progress towards eliminating hepatitis C. More than 70% of persons with current HCV infection have been diagnosed, and most have initiated treatment and experienced high cure rates regardless of fibrosis status. Challenges remain in identifying and linking to care persons with current HCV infection in Georgia. Scaling up the integrated,

decentralized model of HCV treatment, which is already implemented in many locations, to cover more sites will be critical to improve linkage to care and close gaps in the HCV cascade of care.

WED-428-YI

Patient, provider, and neighborhood-level factors associated with hepatitis delta testing in an academic health system

Lauren Alpert¹, Anna Mageras¹, Rachel Smith², Xiaotao Zhang¹, Tatyana Kushner¹. ¹Icahn School of Medicine at Mount Sinai, New York, United States; ²UPMC Children's Hospital of Pittsburgh, Pittsburgh, United States
Email: lauren.alpert@icahn.mssm.edu

Background and aims: International guidelines recommend screening all hepatitis B surface antigen (HBsAg) positive patients for hepatitis delta virus (HDV) antibody (Ab) and all HDV Ab positive patients for HDV RNA. However, studies have shown heterogeneous HDV testing patterns worldwide. We evaluated the demographic, clinical, and social determinants of HDV testing among HBsAg positive patients in an academic health system.

Method: All patients with a positive HBsAg test between 7/2021 and 7/2023 were identified. Within this cohort, HDV Ab and RNA testing rates were determined. Community deprivation index (CDI), a marker of neighborhood resources based on American Community Survey data, was used to estimate socioeconomic and environmental disparities in the study population. Multivariable logistic regression analysis was performed to determine factors associated with HDV Ab testing.

Results: 2,495 HBsAg positive patients were identified, among whom 1,348 (54%) received HDV Ab testing; 44 (3%) were HDV Ab positive. Thirty-two (73%) HDV Ab positive patients received HDV RNA testing; 12 (38%) were HDV RNA positive. Those tested for HDV Ab were median age of 50; 60% male, 31% Asian, 25% Black, and 10% Hispanic. Patients with HDV Ab testing were more likely to be younger and Asian, have an active patient portal linked to the electronic health record (EHR), receive their most recent HBsAg test in a liver clinic, have a hepatitis B virus (HBV) diagnosis code in the EHR, receive hepatitis C virus (HCV) Ab or HIV testing, and receive HBV treatment ($p < 0.05$). The mean CDI for those with HDV Ab testing was higher than for those without, indicating more resource scarcity among tested individuals. On multivariable logistic regression analysis, the following were associated with higher odds of HDV Ab testing: white (OR = 1.39, 95% CI: 1.04, 1.86) and Black (OR = 1.76, 95% CI: 1.37, 2.27) compared to Asian race, HBV diagnosis code in the EHR (OR = 1.39, 95% CI: 1.14, 1.71), HCV Ab (OR = 2.54, 95% CI: 2.01, 3.21) and HIV (OR = 1.31, 95% CI: 1.08, 1.59) testing, HBV treatment (OR = 1.65, 95% CI: 1.36, 2.01), and residence in a high CDI ZIP code (OR = 1.36, 95% CI: 1.13, 1.64). Patients were least likely to receive HDV Ab testing in primary care, inpatient, and emergency room settings; they were most likely to receive testing in liver clinics, followed by gastroenterology, OB/GYN, and infectious disease clinics ($p < 0.05$).

Conclusion: In an academic health system, only about half of HBsAg positive patients were tested for HDV Ab. Liver specialty care and comprehensive HBV management were associated with higher odds of HDV Ab testing. Resource scarcity did not decrease the likelihood of HDV testing, suggesting that provider factors had more influence on testing rates than social factors. Efforts to test patients less engaged in the health system and provide HDV education to non-liver providers will be critical to improve HDV screening rates.

WED-429

Hepatitis B virus care cascade in Rwanda: a population based-study

Jean Damascene Makuza¹, Dahn Jeong², Marie Paul Nisingizwe³, Phymar Soe⁴, Richard Morrow⁵, Georgine Cua⁵, Héctor Alexander Velásquez García⁶, Albert Tuyishime⁷, Michael Law⁸, Alnoor Ramji⁹, Naveed Janjua¹⁰. ¹University of British

POSTER PRESENTATIONS

Columbia, School of Population and Public Health, Rwanda Biomedical Centre, Kigali, Rwanda, Vancouver, Canada; ²University of British Columbia, School of Population and Public Health, British Columbia Center for Disease Control, Vancouver, Canada; ³University of British Columbia, Vancouver, Canada; ⁴University of British Columbia, School of Population and Public Health, Vancouver, Canada; ⁵University of British Columbia, School of Population and Public Health, British Columbia Center for Disease Control, Vancouver, Canada; ⁶University of British Columbia, School of Population and Public Health, British Columbia Center of Disease Control, Vancouver, Canada; ⁷Rwanda Biomedical Center, IHDP Department, Kigali, Rwanda; ⁸University of British Columbia, School of Population and Public Health, Vancouver, Canada; ⁹University of British Columbia, Division of Gastroenterology, Vancouver, Canada; ¹⁰British Columbia Center for Disease Control, University of British Columbia, School of Population and Public Health, Vancouver, Canada

Email: makorofr@gmail.com

Background and aims: The global burden of viral hepatitis B (HBV) is substantial, and monitoring progress across the care cascade is essential for effective elimination strategies. In Sub-Saharan Africa, data on the HBV care cascade are limited. We aimed to quantify the HBV care cascade in Rwanda among diagnosed with HBV infection individuals from 2016 to 2023.

Method: In this population-based retrospective cohort study, we used routinely collected data from the District Health Information System 2, which included 4.5 million people screened for HBV from January 2016 to June 2023. During this period, individuals were included if they were >2 years old. The HBV care cascade was analysed across five stages: (1) lifetime prevalence, (2) diagnosis, (3) enrolled in care, (4) treatment initiation, and (5) treatment continuation. Infections were identified by having at least one reactive antigen or nucleic acid test, and lifetime prevalence was estimated as the sum of diagnosed and estimated undiagnosed cases. Multivariable logistic regression was used to identify progression-related factors through the different cascade stages.

Results: Among the 4, 604, 468 persons screened, 55, 820 tested positive for HBsAg (HBV infection diagnosed). Of these individuals, 51, 065 (91.5%) had HBV mono-infection, and 4, 755 (8.5%) had HBV/HIV co-infection. Among all individuals identified with chronic HBV infection, 21, 182 (38.0%) were enrolled in care, 5, 966 (28.2%) were eligible for HBV treatment, 4, 746 (79.6%) initiated treatment, and 4, 621 (97.4%) continued treatment at 1-year post-initiation. Individuals enrolled at district hospitals were more likely to be engaged in care (adjusted odds ratio [aOR], 2.09; 95% CI, 1.93, 2.26), eligible for HBV treatment (aOR: 1.82; 95% CI, 1.61, 2.07), initiate HBV treatment (aOR: 2.41; 95% CI, 1.85, 3.14), and be retained in care (aOR: 5.85; 95% CI, 2.74, 12.49), compared to those followed up at health centers. Compared to those living at ≤30-minute distance, those living at >1 hour to reach a facility were more likely to be engaged with care, eligible for HBV treatment, and initiate treatment, while they were less likely to be retained in care. Individuals living with HIV were more likely to be engaged in care but less likely to initiate HBV treatment.

Conclusion: Overall, engagement with care was low among individuals diagnosed with chronic HBV infection. Individuals followed at district hospitals were more likely to be engaged in care, eligible and initiate the HBV treatment, and retained in care, highlighting the need for strengthening decentralization and integration of HBV services to lower-level health facilities by increasing well-trained healthcare providers, and infrastructure for prevention and treatment of HBV at health centre level.

WED-430

Epidemiological changes and clinical events in the HepCoVe hepatitis C positive cohort. The viral elimination after availability of new antiviral therapies through a 20-year observational study

Luisa Cavalletto¹, Liliana Chemello². ¹University Hospital, Dept of Medicine DIMED, Padova, Italy; ²University Hospital, Dept of Medicine DIMED, Padova, Italy

Email: luisa.cavalletto@unipd.it

Background and aims: Since 2000, the HepCoVe network, by a shared web patient-individual-record among liver units in the Veneto region of Italy, has recruited a cohort of cases with chronic hepatitis C (CHC) and supported the implementation of screening programs and antiviral treatments, with the objectives of: a) comparing the characteristics of the cohort in cases with parenteral risk reported before or after 1995, the date of the mandatory application of anti-HCV testing in Italy, and b) tracking the changes induced by antiviral therapies, by the use previous of interferon (IFN) and then of the direct antiviral therapy (DAA).

Method: A data-set of 3397 cases, with CHC prospectively collected from January 2000 underwent to an accurate report of risk-infection and clinical events, lab and virologic tests, the staging of liver fibrosis with biopsy (Ishak score) or measuring the liver (LS), and the spleen stiffness (SS), to diagnose portal hypertension (PH) by VCTE (Fibroscan®). All cases were genotyped and had a viremia tested by PCR at baseline and at 12-week after therapy to define sustained virologic response (SVR). Mortality and HCC occurrence was analysed by KM curves in cases with and without SVR.

Results: At baseline, the profile of 1949, respect to 978 cases, with parental risk reported before or after 1995, showed higher infection of HCV1b or 2a/c (73.1 vs. 62.8%) and lower HCV1a, 3a and 4c/d (27.2 vs. 37.2%) and higher rate of transfusion (36 vs. 4%). Moreover they were older (56 vs. 53 yrs) and with advanced fibrosis or cirrhosis (24 vs 10%) (all, $p < 0.01$). During a 20.2 ± 5.4 yrs follow-up, we analysed the SVR rate in the IFN-RBV (2000–2014) and in the DAA-era (2015–2023), respectively 60 vs 95% ($p < 0.01$). In the latter only 24 cases, 83% with advanced fibrosis or cirrhosis, had a relapse viremia, while twenty-nine (6, 1%) cases developed a de novo HCC, 82% within 24-month after stopping DAA therapy. By a multivariate analysis we identified: LS (HR 2.04; CI 1, 8–2.3), virologic relapse (7.71; 2.2–26.8), signs of PH (3.8; 1.5–9.9) and bilirubin levels (1.1; 0.8–1.8) as variables associated to HCC occurrence (all, $p < 0.01$). At 20-year analysis the risk of HCC occurrence in our cohort was of 0.81 and 3.75 per person/yr in cases with or without SVR ($p < 0.001$).

Conclusion: This 20-year cohort study confirmed the presence of at least 2 epidemiological outbreaks period of HCV exposition in Italy, the first characterized by HCV1b or 2a/c infection, mainly link to transfusions and with a more advanced liver disease, and the second with higher prevalence of genotypes HCV-1a, 3a and 4c/d, related to drug addiction, in younger population. DAA therapy induced pangenotypic HCV eradication, attaining 95% of cases with SVR, however without removing the de-novo HCC risk. Nowadays, the LS and SS measurements remain a pivotal tool for management of cases with advanced liver disease and residual risk of HCC.

WED-431

Testing practice and prevalence of hepatitis delta virus (HDV) among patients with chronic hepatitis B (CHB): a large canadian population-based study

Abdel-Aziz Shaheen¹, Meng Wang², Bing Li², Carla Coffin¹. ¹University of Calgary, Calgary, Canada; ²Alberta Health Services, Calgary, Canada
Email: az.shaheen@ucalgary.ca

Background and aims: Patients with chronic hepatitis B (CHB) and hepatitis delta virus (HDV) coinfection have worse clinical outcomes compared to HBV mono-infected individuals. Recent studies estimating the burden of HDV have reported significant heterogeneity of HDV prevalence due to study designs or testing practices. Therefore, we aim to report HDV antibody (anti-HDV) testing, HDV prevalence

rates and identify predictors of testing as well as anti-HDV positivity in a large Canadian population-based study.

Method: We used the Alberta Provincial Laboratory database to identify patients with CHB (≥ 2 positive HBsAg or HBeAg; or positive testing and negative HBe IgM for ≥ 6 months) as well as anti-HDV screening and positive result from April 1st, 2012–March 31st, 2022, in Alberta, Canada (population ~ 4.6 million). We linked HBV monoinfected or HBV/HDV coinfecting patients with Alberta ambulatory, inpatient, and pharmacy databases. We compared patient demographics, laboratory, clinical, and HBV therapy in individuals with or without anti-HDV testing and anti-HDV positivity. Adjusted logistic regressions were used to identify predictors of anti-HDV screening and anti-HDV positivity among all CHB patients that were tested.

Results: Over ~ 10 year period (2012–2022), 11,000 patients with CHB were identified in Alberta. Anti-HDV testing was reported among 1,737 patients (15.8%) of which 73 were anti-HDV positive (4.2%). Anti-HDV screening increased between 2012–2020 (11.9%–23.3% with an annual increase of 8.7%, $p < 0.001$), then declined to 16.8% post COVID-19 pandemic. Anti-HDV testing was more common in younger CHB patients (median age 38 vs. 42 years, $p < 0.001$), male sex (63.4% vs. 53.4%, $p < 0.001$), with elevated ALT (58.8% vs. 43.6%, $p < 0.001$), and less likely in anti-HBV treated patients (24.2% vs. 26.6%, $p = 0.037$). In those who were screened, patients with positive anti-HDV had similar age (median: 40 vs. 42 years, $p = 0.148$), male sex (74.7% vs. 64.5%, $p = 0.059$), ALT (68.5% vs. 59.3%, $p = 0.146$), as well as receiving CHB treatment (30.8% vs. 23.7%, $p = 0.156$). The main independent predictors for anti-HDV testing were age (aOR: 0.98; 95%CI: 0.97–0.98), male sex (aOR 1.58: 1.38–1.80), elevated ALT (aOR 1.76: 1.54–1.99), and CHB treatment (aOR 0.56: 0.49–0.65). However, none of the latter predictors were associated with HDV coinfection.

Conclusion: In this large population-based study, HDV testing and positivity rates among patients with CHB are lower than previously reported in Canada. Universal HDV screening along with reflex HDV RNA testing in anti-HDV positive patients, particularly among older and female patients living with CHB are needed to understand the true epidemiology of HBV/HDV coinfection.

WED-432

Systematic review and meta-analysis of barriers and enablers to hepatitis C direct-acting antiviral treatment initiation

Kathleen Bryce^{1,2}, Fiona Burns^{1,2}, Colette Smith², Alison Rodger^{1,2}, Douglas Macdonald^{1,3}. ¹Royal Free London NHS Foundation Trust, London, United Kingdom; ²Institute for Global Health, University College London, London, United Kingdom; ³Institute of Liver and Digestive Health, University College London, London, United Kingdom
Email: kathleenbryce@doctors.org.uk

Background and aims: Despite the successes of the direct-acting antiviral (DAA) programme for hepatitis C virus (HCV) infection, many groups still experience challenges to accessing care. We aimed to determine the barriers and enablers associated with hepatitis C DAA initiation and their relative impact.

Method: We performed a systematic review and meta-analysis of the barriers and enablers to HCV treatment initiation in the DAA era in high income settings with free universal healthcare. We searched eight bibliographic databases for studies published between 2014 and May 2022 using pre-defined keywords. We included quantitative studies investigating positive or negative associations with DAA treatment initiation. Data were extracted into a standardised form and a random-effects meta-analysis was conducted to pool the effects of variables on treatment initiation. The I^2 statistic was used to measure heterogeneity across studies.

Results: Of 5198 articles identified, 42 studies conducted in Australia, Canada and Europe were included. Overall quality was 'fair' or 'good' in 37. Significant negative associations with DAA treatment included: unstable housing (14 studies, pooled odds ratio (OR) 0.48, 95% confidence interval (CI) 0.40–0.58, $I^2 = 21.1\%$); active injecting drug

use (OR 0.54, CI 0.39–0.74, $I^2 = 97.5\%$); low income or socioeconomic status (seven studies, OR 0.75, CI 0.60–0.94, $I^2 = 73.7\%$) and female gender (26 studies, OR 0.78, CI 0.69–0.89, $I^2 = 89.9\%$). Positive associations included: increasing age (17 studies, OR 1.76, 95% CI 1.30–2.40, $I^2 = 95.4\%$); previous HCV treatment (nine studies, OR 2.20, CI 1.45–3.34, $I^2 = 85.8\%$); fibrosis stage (13 studies, OR 1.80, CI 1.15–2.79, $I^2 = 95.6\%$) and opioid substitution in people who inject drugs (12 studies, OR 1.54, 95% CI 1.15–2.05, $I^2 = 65.9\%$). There was no overall effect of high-risk alcohol use on treatment initiation when compared with lower (or no) alcohol use (13 studies, OR 0.91, 95% CI 0.64–1.27, $I^2 = 98.3\%$).

Conclusion: The most impactful factors associated with DAA treatment initiation were socioeconomic and fixed demographic or disease characteristics. This should enable pre-emptive identification and intervention in those at risk of disengagement before treatment. Active injecting drug use was the only behavioural characteristic consistently associated with lower treatment initiation but this is significantly mitigated by opiate substitution therapy.

WED-433

Combatting blood-borne viral syndemics with automated electronic based screenings of HBV, HCV, HDV and HIV in a hospital

Su Wang^{1,2}, Ruth Brogden¹, Jaymie Yango¹, Aryana Velez¹, Nandanie Budhoo¹, Eric Handler¹, Stephen Omahony³. ¹Cooperman Barnabas Medical Center, Livingston NJ, United States; ²Hepatitis B Foundation, Doylestown, United States; ³RWJBarnabas Health, West Orange, United States
Email: suwang8@gmail.com

Background and aims: Achieving hepatitis B (HBV) and C (HCV) elimination will require integration into health care systems as part of routine care. A syndemic approach is also important to address other blood-borne viruses (BBV) such as HIV and hepatitis delta (HDV). HDV is believed to be underdiagnosed with an estimated 12 million people with HDV infection. Establishing HBV reflex testing to HDV testing protocols is one way increase testing. In a 597-bed community hospital with an Emergency Department (ED) of 100,000 yearly visits, an electronic medical record (EMR) based automated screening algorithm was implemented to scale up HCV, HBV, HDV and HIV screening and linkage to care (LTC).

Method: In March 2018, the EMR was modified at Cooperman Barnabas Medical Center (CBMC) in the Emergency Department (ED) and inpatient units to implement automated HCV (HCVAb reflex to HCV RNA) and HBV (HBsAg) screening. In 2020 screening criteria was expanded to follow CDC recommendations for universal HCV screening. To capture the intersection of the opioid epidemic and viral hepatitis, urine/serum toxicology and peer recovery specialist orders also led to automatic hepatitis orders. In 2021, an automated HIV screening was developed for at-risk patients, and in 2022, hepatitis delta (HDVAb) reflex testing from all positive HBsAg tests was implemented. Positive screening tests for all viruses were sent to patient navigator (PN) in real-time who initiated LTC for evaluation and treatment.

Results: Since the beginning of the program, 100,950 HCV screenings have been conducted with 407 (0.4%) current HCV infection and 343 (84%) LTC. Since 2021, the at-risk HIV screenings totalled 7,313 with 102 (1.4%) infected and 98 (96%) LTC. Patients screened for HBV totalled 44,172 with 395 (0.9%) infected and 330 (84%) LTC. Since August 2022, when HDV reflex testing began, 9,191 HBsAg tests were performed, with 58 HBsAg positive. There were 53 reflex HDVAb tests performed, with 3 (5.9%) HDVAb positive. Only one HDV RNA test was successfully performed because the patient who was still hospitalized and was a negative test. The other 2 patients were lost to follow-up and HDV RNA test was not performed.

Conclusion: Automating EMR based screening for HBV, HCV, HIV and HDV has been a successful approach to integrating and scaling up BBV screening in a community hospital. A pilot reflex HDV testing algorithm was effective for completing HDV Ab tests, but obtaining

POSTER PRESENTATIONS

manual HDV RNA testing which was not as successful. This emphasizes the need for double reflex HDV testing. Integrating automated EMR testing across blood borne viruses will be critical to reduce liver cancer rates and address public health burden of syndemics.

WED-434

Cost-effectiveness analysis of hepatitis B vaccination policy for newborns in Taiwan

Chia Ling Hsieh¹, Vivian Chia-Rong Hsieh², Meng Lun Hsieh³. ¹China Medical University, Taichung City, Taiwan; ²China Medical University, Taichung, Taiwan; ³Taichung Veterans General Hospital, Taichung City, Taiwan

Email: morganpolo@gmail.com

Background and aims: Taiwan was the first in the world to implement universal hepatitis B vaccination for newborns, with proven success in reducing hepatitis B virus (HBV) seroprevalence and childhood hepatocellular carcinoma. However, children born to highly infectious mothers still have a 10% chance of becoming HBV carriers. In 2019, the vaccination policy was revised to administer the first dose of HBV vaccination and hepatitis B immunoglobulin (HBIG) within 24 hours after birth for babies born to hepatitis B surface antigen (HBsAg)-positive mothers. Infants born to HBsAg-negative mothers would still receive the first dose of HBV vaccination. This study seeks to assess the cost-effectiveness of the 2019 HBV vaccination policy (for HBsAg-positive mothers) in comparison to the prior policy, which involved administering HBIG and the first vaccine dose within 24 hours only in HBsAg-positive and hepatitis B e antigen (HBeAg)-positive mothers.

Method: From the payer perspective, a cost-effectiveness model was developed using a decision-tree followed by Markov cohort analysis. The decision-tree captured the different vaccination scenarios based on the infection status (HBeAg and HBsAg) of pregnant mothers and babies under the two vaccination policies. Those that moved through the decision-tree were simulated until 81 years of age with each cycle representing one year. Parameter values were extracted from published literature, including vaccine coverage, effectiveness, and transition probabilities between health states. Our main outcome measures included the incremental cost-effectiveness ratio (ICER) and incremental cost-utility ratio (ICUR), utilizing life-years (LYs) and quality-adjusted life years (QALYs), respectively. Discount rate of 3% was used on both costs and effectiveness measures. One-way and probabilistic sensitivity analyses were performed to test the robustness of model results. TreeAge Pro 2019 version 1.1 (TreeAge Software Inc.) was used to develop the model and simulate the results.

Results: Our findings suggest that compared with the prior policy, the current policy had 248 more susceptible (uninfected) HBV cases, 16 more immune tolerant cases, 3 more cases of inactive carrier, 4 more chronic hepatitis B cases, and 6 more deaths. Baseline ICER value was -USD702.49 per LY gained and baseline ICUR value was -USD1, 393.14 per QALY gained. Sensitivity analysis revealed that results were most sensitive to vaccine effectiveness and coverage in newborns born to HBsAg-positive and HBeAg-negative mothers in the previous policy. Monte Carlo analysis showed that 100% of ICERs fell in the fourth quadrant and below the willingness-to-pay threshold of USD25, 933.59.

Conclusion: The current HBV vaccination policy for newborns may offer better value for money compared to the previous policy with more targeted population.

WED-435

Prevalence of active hepatitis delta infection among new diagnoses of hepatitis B in the Barcelona metropolitan area

Jesús Trejo Zahinos¹, Francisco Rodríguez-Frías^{2,3}, Marcos Belsol⁴, Susana Bernalte¹, Ricard Riel⁵, Camila Picchio⁶, Maria Francesca Cortese^{1,7,8}, David Tabernero^{1,7,8}, Maria Buti^{7,8}, Ariadna Rando-Segura^{1,2,8}. ¹Department of Microbiology, Vall d'Hebron University Hospital, Barcelona, Spain; ²Centro de Investigación Biomédica en Red de Enfermedades Hepáticas y Digestivas (CIBERehd), Instituto de Salud Carlos III, Madrid, Spain; ³Liver Unit, Vall d'Hebron University Hospital, Barcelona, Spain; ⁴Department of Microbiology, Vall d'Hebron University Hospital, Barcelona, Spain; ⁵Primary Care Barcelona, Barcelona, Spain; ⁶Barcelona Institute for Global Health (ISGlobal), Clinic Hospital, Barcelona, Spain; ⁷Centro de Investigación Biomédica en Red de Enfermedades Hepáticas y Digestivas (CIBERehd), Instituto de Salud Carlos III, Madrid, Spain; ⁸Liver Unit, Vall d'Hebron University Hospital, Barcelona, Spain

Email: ariadna.rando@vallhebron.cat

Background and aims: The WHO estimates that hepatitis D virus (HDV) affects approximately 5% of individuals with chronic Hepatitis B virus (HBV) infection worldwide. However, this prevalence may be higher especially in certain geographical areas where the availability of serological tests for the detection of anti-HDV may be limited. The aim of this study was to estimate the prevalence of HDV and the proportion of patients with active HDV infection among new HBV diagnoses.

Method: Descriptive study conducted in the clinical laboratories of Vall d'Hebron Hospital (which serves 75% of the Barcelona metropolitan area) between January 2022 and November 2023. Throughout this period, all newly diagnosed HBV cases underwent reflex serological screening for HDV antibodies (LIAISON[®]XL MUREX Anti-HDV), and if positive, a determination of HDV RNA (in-house PCR, lower limit of quantification 5.75×10^2) was performed.

Results: A total of 704 individuals with a newly diagnosed HBV case were detected (323 cases in primary healthcare, 361 in hospital healthcare and 20 in addiction centers and prisons). Serological screening for HDV was performed in 96.3% (678/704) of them. The overall prevalence of anti-HDV positivity in newly diagnosed HBV cases was 5.3%, and globally 1.6% had an active HDV infection (RNA HDV+, 30.5% if considering the only HDV patients). However, the prevalence was not homogeneous across healthcare levels being higher in addiction centers and prisons (16, 7%, 3/18 anti-HDV tested cases) and hospital healthcare (5.4%, 19/349) than primary healthcare (4.5%, 14/311).

Conclusion: The prevalence of HDV among new diagnoses of HBV in the Barcelona city area was 5.3% (as globally estimated by the WHO), with 30.5% of anti-HDV with active HDV infection (HDV RNA +). However, the prevalence varies depending on the healthcare center considered. More newly diagnosed cases had to be included to confirm the results. Study supported by the Gilead-AEEH Grant for Microelimination Projects in Hepatitis C and Hepatitis D Epidemiology, Code: GLD2023/52.

WED-436

HCV reinfection among people who use drugs (PWUD) treated for HCV infection: a long-term view

Brian Conway^{1,2}, Rossitta Yung¹, Shawn Sharma¹, Shana Yi¹, Saina Beitari¹. ¹Vancouver Infectious Diseases Centre, Vancouver, Canada; ²Simon Fraser University, Burnaby, Canada

Email: brian.conway@vidc.ca

Background and aims: Comprehensive programs of care for priority populations such as PWUD are needed to eliminate HCV infection as a public health concern by 2030. A primary challenge associated with such initiatives is the need for effective strategies to mitigate the risk of reinfection. Meta-analyses suggest a reinfection rate of approximately 5 per 100 person-years (py) among key populations. The objective of this analysis is to assess reinfection rates among

populations of PWUD successfully treated for HCV infection and subsequently maintained in long-term follow-up within a multidisciplinary program of care.

Method: In our program, we provide HCV therapy to PWUD within the context of a comprehensive, multidisciplinary program addressing all medical, social, mental health and addiction-related needs with strategies designed to maximize adherence. Once HCV cure has been documented, patients continue to be integrated in care. This includes individualized addiction care, provision of safe supply and education about safer practices to reduce the risk of reinfection. HCV RNA testing is repeated annually, or more frequently if clinically indicated. We conducted an ongoing, prospective evaluation of the last 305 successful courses of HCV therapy administered to PWUD in our center to determine the rate of HCV reinfection and its correlates.

Results: The inception cohort consisted of 291 individuals who were cured of HCV infection between 03/19–10/23. We document median age 47 (22–83) years, 28.2% female, 20.1% identifying as indigenous, 41.2% unstably housed, and 92.2% continuing active drug use (mostly fentanyl). We documented 10 cases of reinfection with a rate of 3.3 cases per 100 person-years. Of these 10 reinfected patients, 2 were female, 2 identified as indigenous, and all were experiencing unstable housing and ongoing drug use.

Conclusion: Even within a very vulnerable group of individuals with a high risk of HCV reinfection, our program with systematic and comprehensive approaches to reduce the risk of reinfection are associated with rates below 5/100 py. As we treat increasing numbers of individuals who are more vulnerable, strategies such as the ones we have implemented will be important in maximizing the benefits of HCV therapy in these priority populations.

WED-437

Viral hepatitis elimination: scale up now to avert the worst yet to come

Devin Razavi-Shearer¹, Ivane Gamkrelidze¹, Kathryn Razavi-Shearer¹, Alexis Voeller¹, Samantha Hall¹, Homie Razavi¹. ¹Center for Disease Analysis Foundation, Lafayette, United States
Email: dravishearercdafound.org

Background and aims: We aim to estimate the impact of all countries meeting the WHO 2030 programmatic targets of 90% diagnosis rate, 80% treated, 90% three-dose coverage, and 90% birth dose coverage on morbidity and mortality due to hepatitis B virus (HBV) and hepatitis C virus (HCV) at the global level through 2050.

Method: The results of a literature review and Delphi process were integrated into country-specific ProGRESs and Bright Models for the HBV and HCV analyses respectively. These Markov models utilize country specific inputs to estimate the natural history of the disease and future burden. Where prevalence data were unavailable, regional averages were applied to the total population of a country. The elimination scenario was developed for each country, assuming a major scale up in diagnosis, treatment and vaccination would start in 2024.

Results: 170 country level HBV and 117 HCV models were available. In 2015, it was estimated that there were 2.79 million new HBV and HCV chronic infections, with 51% due to HBV; 989,000 incident cases of hepatocellular carcinoma (HCC), with 81% due to HBV, and 1.27 million deaths due to HBV and HCV, with 80% of them being due to HBV. If current trends in diagnosis and treatment continue, incidence is projected to decrease through 2050, with 2.20 new infections in 2030 and 2.23 million in 2050. The share of incident cases due to HBV is expected to decrease to 19.4% by 2050 as a result of current vaccination programs. Without additional interventions the incident number of cases of HCC are expected to increase through 2050, 1.27 million in 2030 and 1.35 million in 2050. The share of incident HCC due to HBV is expected to increase to 84.6% by 2050. Similarly, deaths will increase to 1.61 million in 2030 and 1.76 million in 2050, with HBV's share increasing to 83.8% in 2050. Deaths due to HBV and HCV are expected to peak at 1.82 million in 2043. If the 2030

programmatic targets are met, we estimate that through 2050 there will be 47.5 million new chronic cases averted, 29.7% due to HBV; 13.2 million incident cases of HCC averted, 69.0% due to HBV; and 20.6 million lives saved, 71.6% due to HBV.

Conclusion: We have a relatively short window, 20 years, to save the greatest number of lives from HBV and HCV. While prevention is an integral part of elimination, most people dying in this timespan were infected decades ago. This study further highlights the immediate need to drastically scale up diagnosis and treatment along with vaccination in areas where it remains suboptimal.

WED-438-YI

Real-world based cost effectiveness analysis of entecavir versus tenofovir on prognosis of hepatitis B virus-related hepatocellular carcinoma after curative hepatectomy

Chun-Ting Ho¹, Chien-Wei Su², Elise Chia-Hui Tan³, Yi-Hsiang Huang^{4,5}, Ming-Chih Hou^{4,6}, Jaw-Ching Wu⁷. ¹Taipei Veterans General Hospital, Taipei, Taiwan; ²Department of General Medicine, Department of Medicine, Taipei Veterans General Hospital, Taipei, Taiwan; ³Department of Health Service Administration, College of Public Health, China Medical University, Taichung, Taiwan; ⁴Division of Gastroenterology and Hepatology, Department of Medicine, Taipei Veterans General Hospital, Taipei, Taiwan; ⁵School of Medicine, College of Medicine, National Yang Ming Chiao Tung University, Taipei, Taiwan; ⁶School of Medicine, College of Medicine, National Yang Ming Chiao Tung University, Taipei, Taiwan; ⁷Institute of Clinical Medicine, School of Medicine, National Yang Ming Chiao Tung University, Taipei, Taiwan
Email: elisetam.g@gmail.com

Background and aims: For patients with hepatitis B virus (HBV) related hepatocellular carcinoma (HCC), antiviral therapies could reduce the risk of recurrence and improve overall survival (OS) after resection. Entecavir (ETV), tenofovir disoproxil fumarate (TDF), and tenofovir alafenamide (TAF) are currently recommended as first-line antiviral agents in clinical practice guidelines for patients with CHB. However, there is still controversy about whether TAF, TDF and ETV have different effects on clinical outcomes and costs. We aimed to compare the cost and effectiveness among ETV, TDF, and TAF treatment for patients with HBV-related HCC after hepatectomy.

Method: This was a retrospective cohort study compared TAF, TDF and ETV in terms of cost and effectiveness in real-world setting. Patients received either ETV, TDF or TAF at least 28 defined daily dose (DDD) and continued their initial treatment regimen during the study period without change. The liver-related direct medical costs, life-years (LYs), quality-adjusted life-years (QALYs) and Incremental cost-effectiveness ratio (ICER) were estimated. We took the perspective of healthcare payer in Taiwan.

Results: A total of 1,494 patients were identified during 2010–2020 and the median follow-up was 2.15 years (IQR: 1.39–2.94). After adjusted baseline characteristics, compared to ETV, HCC patients who received TDF (HR: 0.99; 95% CI: 0.72–1.35) or TAF (adj-HR: 0.97; 95% CI: 0.67–1.41) had similar risk of recurrence after hepatectomy. However, compared to ETV, patients who received TAF had a lower risk of all-cause death (adj-HR: 0.50; 95% CI: 0.28–0.80). TAF (US\$11,516 ± 14,537) had significant lower direct medical cost, compared to ETV (US\$12,882 ± 18,496) and TDF (US\$13,146 ± 15,185).

Compared to TAF, patients used ETV and TDF had higher health benefit in terms of LYs and QALY and increased medical cost. The ICER per QALY gained were US\$3,538 for ETV and US\$5,405 for TDF. When using US\$9,000 as the WTP threshold, the probability of ETV and TDF being cost-effectiveness was 100% and 96.1%, respectively. Both ETV, TDF, and TAF showed the similar health benefits in terms of RFS. However, TAF had better OS. The cost-effectiveness analysis found, compared to TAF, ETV and TDF have the ICERs of US\$3,160 and US\$5,405 for the treatment of HCC patient after hepatectomy in Taiwan.

Conclusion: Both ETV and TDF could be considered the cost-effective option, although they had a poorer OS compared to TAF therapy. Compared with previous trial-based CE studies, the results could

POSTER PRESENTATIONS

reflect the value of antiviral therapy in a real-world setting which can improve the shared decision-making of clinicians and patients.

WED-439

Linkage of anti-HCV reactive persons to HCV care and treatment services in Georgia

Vladimer Getia¹, Rania Tohme², Sophia Surguladze³, Shaun Shadaker², Maia Tsereteli¹, Ekaterine Adamia¹, Amiran Gamkrelidze⁴, Irina Tskhomelidze³. ¹National Center for Disease Control and Public Health (NCDC), Tbilisi, Georgia; ²Centers for Disease Control and Prevention, Atlanta, United States; ³The Task Force for Global Health, Tbilisi, Georgia; ⁴University of Georgia, School of Health Sciences, Tbilisi, Georgia
Email: irinkatskhomelidze@gmail.com

Background and aims: As of October 31, 2023, 78.6% (approximately 2.23 million) of Georgia's adult population has been screened for hepatitis C virus (HCV) infection. However, linkage to care remains a challenge; approximately 13% of individuals who tested reactive for anti-HCV have not undergone viremia testing. Furthermore, 15% of individuals with confirmed current HCV infection have not initiated treatment. In light of this, the National Center for Disease Control implemented a program to promote linkage to care for persons who have been lost to follow-up before receiving viremia testing or HCV treatment. The program aimed to link $\geq 70\%$ of individuals who tested anti-HCV reactive to viremia testing and $\geq 50\%$ of those with current infection to treatment.

Method: Key strategies of this initiative included the distribution of reminder text messages, the formation of mobile teams for conducting home-based blood collection, and the provision of lists to healthcare facilities to expedite the treatment process for those who have not yet started. Adults (age ≥ 18 years) who had not been linked to care more than three months after a reactive antibody or viremia test were contacted by patient navigators via text messaging and phone calls or home visits, guiding them towards HCV viremia testing or treatment. A maximum of two contact attempts were made per person. Navigators received incentives for successfully linking patients to care.

Results: During October 2021–October 2023, a total of 20,497 adults were identified who had a reactive anti-HCV test but were not linked to viremia testing within 3 months of screening, 18,063 (88.1%) had valid phone numbers in the HCV screening database, and of those 14,180 (78.5%) could be reached. The remaining 3,883 could not be reached, had moved, or emigrated. Of those contacted, 3,790 (26.7%) presented for viremia testing, including 868 reached by mobile blood collection teams. Overall, 1,881 (49.6%) of those tested were positive for HCV RNA or core antigen, and 1,122 (59.6%) of them initiated HCV treatment. From that same period, 14,397 adults previously diagnosed with current HCV infection were not linked to treatment. Of them, 13,076 (90.8%), had valid phone numbers, of whom 6,989 (53.4%) could be reached and 1,604 (23.0%) initiated treatment. An additional 2,422 (34.7%) of those reached agreed to be treated but did not enroll in the program.

Conclusion: While the efforts to combat hepatitis C in Georgia have led to significant progress, these results highlight the need for more effective strategies to link diagnosed individuals to care. Developing more engaging patient outreach programs, using novel strategies and clearly communicating the importance of treatment are essential steps towards achieving hepatitis C elimination targets in Georgia.

WED-440

Community-based interventions to increase hepatitis B virus and hepatitis C virus infections screening among at-risk migrant and refugee populations in Italy, Greece, and Spain: 1-year results of the VH-COMSAVAC project

Camila Picchio^{1,2}, Aina Nicolàs Olivé¹, George Kalamitsis³, Ioanna Liatsou⁴, Niki Panera⁴, Ignacio Peña Ruiz⁵, Cristina Arcas⁵, Sandra Chamorro-Tojeiro^{6,7}, José A. Pérez Molina^{6,7},

Guiseppa Colucci^{8,9}, Angelo Pezzullo¹⁰, Domenico Pascucci¹¹, Ana Requena¹², Jeffrey V Lazarus^{12,13}. ¹Barcelona Institute for Global Health (ISGlobal), Hospital Clínic, University of Barcelona, Barcelona, Spain; ²Drexel University Dornsife School of Public Health, Department of Community Health and Prevention, Philadelphia, United States; ³Hellenic liver patient association "Prometheus", Athens, Greece; ⁴Hellenic Liver Patients Association "Prometheus", Athens, Greece; ⁵Salud Entre Culturas, National Referral Unit for Tropical Diseases, Infectious Diseases Department, University Hospital Ramón y Cajal, Madrid, Spain; ⁶National Referral Unit for Tropical Diseases, Infectious Diseases Department, University Hospital Ramón y Cajal, IRYCIS, Madrid, Spain; ⁷Centro de Investigación Biomédica en Red de Enfermedades Infecciosas (CIBERINFEC), Instituto de Salud Carlos III, Madrid, Spain; ⁸Division of Gastroenterology and Hepatology, Fondazione IRCCS Ca' Granda Policlinico, Milan, Italy; ⁹Policlinico of Milan, Gastroenterology and Hepatology, Milano, Italy; ¹⁰Section of Hygiene, Department of Life Sciences and Public Health, Università Cattolica del Sacro Cuore, Rome, Italy; ¹¹Department of Life Sciences and Public Health, Università Cattolica del Sacro Cuore, Rome, Italy; ¹²Barcelona Institute for Global Health (ISGlobal), Hospital Clínic, University of Barcelona, Barcelona, Spain; ¹³CUNY Graduate School of Public Health and Health Policy (CUNY SPH), New York, United States
Email: camila.picchio@isglobal.org

Background and aims: Migrants residing in Europe and originating from regions with a mid/high prevalence of hepatitis B (HBV) and hepatitis C (HCV) might be unaware of their status due to the inadequacy of testing and vaccination in their home countries or complicated care pathways in their host countries. Additionally, they can suffer structural and legal barriers to accessing healthcare which leads to an underutilization of services. Viral hepatitis Community Screening, Vaccination, and Care (VH-COMSAVAC) is an ongoing EU co-funded project in Italy, Greece, and Spain which aims to scale-up and implement community-based HBV and HCV testing models of care among migrants and refugees with documented mid/high incidence and prevalence using simplified diagnostic tools and person-centred referral processes.

Method: Between 11/2022–12/2023, viral hepatitis testing was offered to 470 people across four locations (Athens, Barcelona, Madrid, and Milan). Testing in community settings used HBV surface antigen (HBsAg) and anti-HCV rapid lateral flow tests. Each setting structured their care pathways according to operational and legal feasibility. In Barcelona, direct referral for positive cases and whole blood sample collection using a plasma separation cards were provided during community screenings. In Madrid, Milan and Athens, participants were referred for follow-up at collaborating centers to ensure linkage to care, regardless of their status. Community health workers and intercultural mediators supported screening interventions in Spain.

Results: 470 participants were included for analysis, with a median age of 39 years (IQR = 28–49). They were primarily male (71.3%) from Ghana (29.2%), Guinea (8.7%) and Albania (8.3%), and 41.7% arrived to the EU <5 years ago. Most participants had never been tested for HBV nor HCV (58.3%). 8.3% of participants reported being fully vaccinated against HBV. Less than half (43.0%) knew what HBV and/or HCV was. HBsAg+ prevalence was 7.0% (95% CI: 4.7%–9.3%) and anti-HCV+ prevalence was 2.6% (95% CI: 1.3%–4.4%). Migrants residing in Italy showed the highest HBsAg+ prevalence (10.0%), followed by Spain (7.1%), and Greece (6.3%). No anti-HCV+ cases were observed in Italy and three in Spain (1.1%), whereas Greece reported a prevalence of 5.7%. HBsAg+ prevalence was not associated with any risk factor, but anti-HCV+ was associated with multiple sex partners, drug use and unprotected sex ($p < 0.05$).

Conclusion: Community based strategies which are culturally and linguistically appropriate and offer viral hepatitis screening, provide effective models for identifying and providing care to migrant and refugee populations at high risk of HBV and HCV infections who may

otherwise not engage in care, which aligns with the 2030 WHO hepatitis elimination goal.

WED-441-YI

Precise estimation of national HBV prevalence: the importance of double hepatitis B surface antigen and hepatitis B core antibody testing in low endemic countries

Arno Furquim d'Almeida¹, Erwin Ho¹, Christian Schüttler², Philippe Beutels³, Pierre Van Damme⁴, Niel Hens^{3,5}, Heidi Theeten⁴, Thomas Vanwolleghem^{1,6}. ¹Viral Hepatitis Research Group, Laboratory of Experimental Medicine and Pediatrics, University of Antwerp, Antwerp, Belgium; ²Institute of Medical Virology, National Reference Center for Hepatitis B Viruses and Hepatitis D Viruses, Justus Liebig University, Giessen, Germany; ³Centre for Health Economics Research and Modelling of Infectious Diseases (CHERMID), Vaccine and Infectious Disease Institute (VAXINFECTIO), University of Antwerp, Antwerp, Belgium; ⁴Centre for the Evaluation of Vaccination, Vaccine and Infectious Disease Institute (VAXINFECTIO), University of Antwerp, Antwerp, Belgium; ⁵Data Science Institute, Interuniversity Institute for Biostatistics and statistical Bioinformatics (I-BioStat), University of Hasselt, Hasselt, Belgium; ⁶Department of Gastroenterology and Hepatology, Antwerp University Hospital, Antwerp, Belgium
Email: arno.furquimdalmeyda@uantwerpen.be

Background and aims: In light of the WHO viral hepatitis elimination targets set for 2030, robust and repetitive age-specific HBV prevalence studies are needed. Previous HBV prevalence studies reported a hepatitis B surface antigen (HBsAg) prevalence of 0.7% (1993/1994) and 0.66% (2003) in Belgium. However, automated HBsAg assays are typically designed to be oversensitive and might result in an overestimation of the HBV prevalence. Here, we examine the Belgian HBV seroprevalence in adults and investigate the difference in HBV seroprevalence estimates using either HBsAg positivity alone or hepatitis B core antibodies (anti-HBc) HBsAg double positivity as criterium for HBV infection.

Method: 3840 residual serum samples were collected from adult ambulatory patients in 10 private diagnostic laboratories-geographically representing the whole country-during Q2/Q3 2020 (outside the COVID-19 lockdown). The number of samples in each laboratory was stratified per region, age group (10-year age bands) and sex. HBsAg and anti-HBc were analyzed on automated analyzers (Abbott Alinity I). For HBsAg positive anti-HBc negative samples, anti-HBc confirmatory assays were performed by an independent laboratory. The samples were weighted by comparing the sample and population frequencies by sex, 10-year age band and province.

Results: HBsAg was detected in 27/3840 samples, resulting in a weighted HBsAg seroprevalence of 0.69% (95% CI 0.43%–1.04%). However, 15/27 HBsAg positive samples were anti-HBc negative and thus serodiscordant. Independent hepatitis B core antigen neutralization assays revealed that all 15 serodiscordant samples were truly anti-HBc negative, thereby confirming a significant HBsAg false positivity rate for HBV infections of 55.6%. Therefore, a weighted national HBV seroprevalence, based on HBsAg and anti-HBc double positivity, of 0.27% (95% CI 0.13%–0.49%) was obtained. The weighted age-specific seroprevalence ranged from 0.20% (95% CI 0.01%–0.87%) in the 40–49 age group to 0.91% (95% CI 0.32%–1.97%) in the 60–69 age group. There were no double positive samples in the age groups 20–29, 30–39, 80–89 and >90. Although, 8/12 (66.7%) of the double positive samples originated from males, there was no statistically significant difference between sexes ($p = 0.07$). Since 164/3840 (4.27%) samples were anti-HBc positive, we estimate that 4.37% (95% CI 3.65%–5.18%) of the Belgian population had a past HBV exposure.

Conclusion: This population-based nationwide study estimates a Belgian HBV seroprevalence, based on HBsAg and anti-HBc double positivity, of 0.27% (95% CI 0.13%–0.49%) in 2020. Our results illustrate that HBV prevalence based on HBsAg positivity alone overestimates the number of infections due to a high false positivity of automated

HBsAg assays. In low-endemic countries, confirmatory anti-HBc testing is therefore advocated to correctly assess the HBV prevalence.

WED-442

Decreasing trend of hepatitis C in homeless people between 2019–2023: a retrospective study in Madrid, Spain

Daniel Sepúlveda-Crespo^{1,2}, Pablo Ryan^{2,3,4,5}, Jorge Valencia^{3,6}, Rafael Amigot-Sánchez¹, Helena Codina¹, Guillermo Cuevas³, Jeffrey V Lazarus^{7,8}, Felipe Pérez-García^{2,9,10}, Isidoro Martínez^{1,2}, Salvador Resino García^{1,2}. ¹Unidad de Infección e Inmunidad, Centro Nacional de Microbiología, Instituto de Salud Carlos III, Madrid, Spain; ²Centro de Investigación Biomédica en Red en Enfermedades Infecciosas (CIBERINFEC), Instituto de Salud Carlos III, Madrid, Spain; ³Hospital Universitario Infanta Leonor, Madrid, Spain; ⁴Universidad Complutense de Madrid (UCM), Madrid, Spain; ⁵Instituto de Investigación Sanitaria Gregorio Marañón (IiSGM), Madrid, Spain; ⁶Unidad de Reducción de Daños "SMASD", Madrid, Spain; ⁷Barcelona Institute for Global Health (ISGlobal), Hospital Clínic, Universidad de Barcelona, Barcelona, Spain; ⁸CUNY Graduate School of Public Health and Health Policy (CUNY SPH), New York, United States; ⁹Hospital Universitario Príncipe de Asturias, Asturias, Spain; ¹⁰Universidad de Alcalá, Madrid, Spain
Email: danisecre@hotmail.com

Background and aims: Micro-elimination strategies for hepatitis C, targeting high-risk populations such as people who are homeless, aim to efficiently prevent and treat the disease, contributing to national elimination goals by addressing specific risk factors and barriers to medical care. Implementation of point-of-care HCV RNA testing is key to testing and treatment programs, evaluating cures, and monitoring hepatitis C reinfection. The objective of this study was to estimate the prevalence, associated risk factors, and temporal trend of HCV active infection among the homeless population in Madrid, Spain.

Method: A retrospective study was conducted in Madrid, Spain, spanning from 2019 to 2023 and involving 2,709 homeless individuals. Participants were recruited through a mobile screening unit with consecutive enrollment based on the order of appearance. The inclusion of homeless people was carried out on the street or in homeless shelters. Screening involved a rapid HCV antibody test followed by HCV RNA testing using Xpert HCV VL Fingerstick. Data were analyzed using logistic regression, and p values were adjusted for multiple testing using the false discovery rate (q -values).

Results: The prevalence of HCV active infection during the study period was 6.3% (from 7.2% in 2019 to 3.4% in 2023; p value = 0.039). The main risk factors for active HCV infection included being an injecting drug user (IDU), encompassing both non-active IDU (adjusted odds ratio (aOR) = 13.1; q -value < 0.001) and active IDU in the last year (aOR = 31; q -value < 0.001), having no economic income (aOR = 1.8; q -value = 0.015), and alcohol consumption (aOR = 1.8; q -value = 0.004). From 2019 to 2023, there was a significant decrease in the prevalence of HCV active infection across the entire population (from 7.2% to 3.4%, p value = 0.039), among IDU (from 25.3% to 9.4%, p value = 0.040), alcohol consumers (from 12.2% to 6.4%, p value < 0.001), and those with no economic income (from 7.0% to 4.4%, p value = 0.033).

Conclusion: Among homeless individuals, IDU was highlighted as the primary risk factor for active HCV infection, followed by other significant factors such as lack of economic income and alcohol consumption. The significant decline in HCV infection rates across the entire population and among major risk groups during the study period suggests the effectiveness of preventive policies in reducing the prevalence of HCV among the homeless population.

POSTER PRESENTATIONS

WED-443-YI

Usability and acceptability of blood-based hepatitis C virus self-testing (HCVST) among the urban slum population in northern India

Ajeet Bhadoria¹, Kathirvel Selv², Rajesh Somvanshi³, Amrita Mehndiratta⁴. ¹All India Institute of Medical Sciences Rishikesh, Near Barrage, RISHIKESH, India; ²PGI Chandigarh, Chandigarh, India; ³District Viral Hepatitis Management Unit, Haridwar, India; ⁴All India Institute of Medical Sciences Rishikesh, Rishikesh, India
Email: ajeetsinghbhadoria@gmail.com

Background and aims: People living in urban slums are disproportionately affected by hepatitis C virus (HCV) infection and many remain undiagnosed. World Health Organization (WHO) has recommended Hepatitis C virus self-testing (HCVST) as an additional testing strategy that could help to expand access to HCV testing. We conducted a study to document the usability and acceptability of blood-based HCVST among the general population residing in urban slums in Northern India.

Method: We conducted a cross-sectional study nested within a Cluster Randomized Control Trial (CTRI/2023/07/054590) between July–Dec 2023 at urban slums of Haridwar district in Northern India. As a secondary objective we evaluated the feasibility of blood-based HCV self-testing among lay users in two urban primary health centers (UPHCs). The study assessed ease of use (usability) by measuring error rates, user-reported difficulties, and agreement between self-interpretations and interpretations by trained personnel (inter-reader concordance) and between self-tests and tests performed by trained personnel (inter-operator concordance). Acceptability was assessed through a semi-structured interview examining participants' responses to contrived test results ("positive", "negative", and "invalid").

Results: Among 392 participants with mean age 39.7 ± 15.9 years, 56% were females, 23% had education up to primary school or lower and 70% were married. Blood-based HCVST proved highly acceptable among people living in urban slums. While some timekeeping and reading mistakes within the allotted time occurred, most participants successfully performed the tests. There was a strong association between lower education level and observed errors (95% vs 72%; $p < 0.001$). The vast majority, however, expressed high acceptability: 98.3% said they'd use HCV self-testing again, and 97.9% would recommend it to others. Inter-reader and inter-operator concordance were 96.9% (kappa: 0.91) and 98.7% (kappa: 0.94), respectively.

Conclusion: Our study demonstrates that blood-based HCVST are highly acceptable among the general population living in urban slums with satisfactory ability to conduct the tests and interpret the results and TR could be a very useful additional testing strategy with current testing options. However, more research is needed to determine the most effective way to integrate it with existing facility-based testing to improve access to HCV diagnosis across the country.

WED-444

The burden of chronic hepatitis delta in Italy: potential impacts and effects of bulevirtide through cost of illness and cost consequence analysis

Andrea Marcellusi¹, Martina Paoletti¹, Francesco Saverio Mennini¹, Loreta Kondili², Nicola Coppola³, Barbara Coco⁴, Alessandra Mecozzi⁵, Sara Mollea⁶, Chong Kim⁷, Marvin Rock⁷. ¹Economic Evaluation and HTA (EEHTA-CEIS), Centre for Economic and International Studies, Faculty of Economics, University of Rome "Tor Vergata", Rome, Italy; ²Center for Global Health, Istituto Superiore di Sanità, Rome, Italy; ³Infectious Diseases Unit, Department of Mental Health and Public Medicine, University of Campania Luigi Vanvitelli, 80138, Naples, Italy; ⁴Hepatology Unit and Laboratory of Molecular Genetics and Pathology of Hepatitis Viruses, Reference Center of the Tuscany Region for Chronic Liver Disease and Cancer, Department of Medical Specialties, University Hospital of Pisa, Via Paradisa 2, 56124, Pisa, Italy; ⁵Hospital pharmacy

director, Hospital S. Eugenio-CTO, Rome, Italy; ⁶Gilead Sciences Srl, Milan, Italy; ⁷Gilead Sciences, Inc., Foster City, United States
Email: andrea.marcellusi@uniroma2.it

Background and aims: Chronic hepatitis delta virus (HDV) causes the most severe form of viral hepatitis in humans. The purpose of the study was to determine the costs incurred by the National Health Service (NHS) and society due to HDV in Italy, as well as to understand the costs and effects of the introduction of bulevirtide for the treatment of Chronic Hepatitis Delta.

Method: The economic impact of HDV infection was estimated through a cost of illness analysis (COI), while the costs and effects of the introduction of bulevirtide for the treatment of chronic HDV were estimated via a cost-consequence analysis (CCA). The analyses were carried out on a hypothetical cohort of 1000 adult patients with compensated liver disease and a mean age of 45 years over a 10 year time horizon. For the cost consequence analysis, bulevirtide vs no bulevirtide scenarios were compared; pegylated interferon-alpha and best supportive care (BSC) were included in the treatment mix. The analyses were conducted from the NHS perspective and societal perspective. Both direct and indirect costs were included in the model: direct costs considered were healthcare resource utilization costs, monitoring costs and adverse events costs, while indirect costs included total loss of productivity caused by HDV infection. Health outcomes included life years (LYs), quality-adjusted life years (QALYs) and deaths avoided. A discount rate of 3 percent was applied for both costs and health outcomes.

Results: The COI estimated a 10 year economic burden of 27,455,757 euros for the management of patients with HDV in Italy. The estimated cost saving of introducing bulevirtide was 1,557,994 euros, for a total expenditure of 25,897,763 euros. In terms of changes in health outcomes over the 10 years, LYs gained increased by 6.6 percent, QALYs gained increased by 8.7 percent, and the number of deaths were reduced by 12 percent.

Conclusion: Over 10 years, the estimated economic burden of HDV infection for 1000 adult patients was approximately 27 million euros. However, the introduction of bulevirtide resulted in a cost reduction, associated with an increase in LYs and QALYs and a significant decrease in death rate. This study's assessment of burden incurred by the NHS and society in managing HDV infection in Italy indicates that investing in bulevirtide appears to significantly alleviate the clinical and economic burden associated with HDV infection, while increasing morbidity and mortality.

WED-446

Safety of direct-acting antivirals for hepatitis C infection and direct oral anticoagulants co-administration: an italian multicentric study

Valerio Rosato¹, Marcello Dallio², Angiola Spinetti³, Alessia Ciancio⁴, Michele Milella⁵, Piero Colombatto⁶, Giuseppe D'Adamo⁷, Elena Rosselli Del Turco⁸, Paolo Gallo⁹, Nicola Pugliese¹⁰, Roberta D'Ambrosio¹¹, Elisa Colella¹², Maurizia Brunetto⁶, Andrea Falcomatà⁹, Umberto Vespasiani-Gentilucci⁹, Stella De Nicola¹⁰, Alessio Aghemo¹⁰, Pietro Lampertico^{11,13}, Alessandro Soria¹², Antonio Izzi¹⁴, Alessandro Federico², Davide Mastrocinque¹, Ernesto Claar¹. ¹Ospedale Evangelico Betania, Naples, Italy; ²University of Campania "Luigi Vanvitelli", Naples, Italy; ³ASST Spedali Civili di Brescia, Brescia, Italy; ⁴University of Turin, Turin, Italy; ⁵Policlinico di Bari, Bari, Italy; ⁶Azienda Ospedaliera Universitaria Pisana, Pisa, Italy; ⁷Umberto I Hospital, Nocera, Italy; ⁸IRCCS Azienda Ospedaliero-Universitaria di Bologna, Bologna, Italy; ⁹Università Campus Bio-Medico di Roma, Rome, Italy; ¹⁰Humanitas Research Hospital IRCCS, Rozzano, Italy; ¹¹Fondazione IRCCS Cà Granda Ospedale Maggiore Policlinico, Milan, Italy; ¹²Azienda Ospedaliera San Gerardo Monza, Monza, Italy; ¹³CRC "A. M. and A. Migliavacca" Center for Liver Disease, University of Milan, Milan, Italy; ¹⁴Ospedale "Domenico Cotugno", Naples, Italy
Email: valeriosato@gmail.com

Background and aims: Direct oral anticoagulants (DOACs) are generally recommended for the management of thrombosis and atrial fibrillation. As substrates of cytochrome P450 (CYP) 3A4 and/or P-glycoprotein, they are implicated in potential co-medication drug-drug interactions. NS5A/NS5B inhibitors are hepatitis C direct-acting agents (DAAs) that exert a mild inhibition of p-glycoprotein without effects on CYP3A4, but, theoretically, may lead to an increased risk of bleeding. On this purpose, we retrospectively evaluated the risk of vascular adverse events (bleeding and thrombosis) among HCV patients under DOACs/DAAs therapy.

Method: Patients receiving sofosbuvir-based HCV regimens and DOAC between May 2017 and April 2023 in 12 Italian medical centers were consecutively enrolled. Baseline characteristics, especially on bleeding risk and liver function, were collected. Primary end point of the study was the occurrence of bleeding events, classified as major and minor, thromboembolic events and DAAs viral outcomes. Finally, the DOAC/DAA group was compared with a cohort of patients, matched by demographic characteristics (age and sex), that switched to warfarin during antiviral treatment.

Results: Of 104 total patients, 38 (36, 5%) were cirrhotic, diagnosed by liver stiffness or, when not possible, by clinical characteristics. Sofosbuvir/velpatasvir (78, 8%) was the most commonly prescribed DAA and rivaroxaban (35, 6%) most frequent DOAC, followed by apixaban (26, 9%), dabigatran (19, 2%) and edoxaban (18, 3%). The main indication for anticoagulant therapy was atrial fibrillation (76%). All patients were already receiving DOACs before the start of DAAs. No major bleeding events were recorded. On the contrary, four minor bleeding events occurred during concomitant DOAC/DAA treatment, but none caused DAA or DOAC discontinuation. In order to evaluate the risk factors associated to bleeding events an univariate analysis was performed. The antiplatelet therapy was the only additional risk factors statistically related to bleeding events with a hazard ratio (HR) of 13-fold higher. Moreover, the antiplatelet therapy, evaluated by LOGIT binomial analysis with demographic characteristics, remained statistically associated to bleeding events, leading to a HR of 20-fold higher.

By comparing the main population with the warfarin switched matched cohort, composed by 104 patients matched for demographic characteristics, no significant differences were found in the rate of clinical relevant bleeding. A single major bleeding-event leading to anticoagulation and DAAs discontinuation was reported.

Conclusion: In our study, the concomitant use of NS5A/NS5B inhibitors with DOAC showed a good safety, highlighting the concomitant antiplatelet therapy as the only risk factor associated to bleeding events. These findings support the use of DOAC during sofosbuvir-based HCV treatment.

WED-447

Age at incident cirrhosis among individuals with hepatitis C virus infection: a United States administrative claims analysis

Laura Telep¹, Catherine Frenette¹, Amanda Singer¹, Sundaresan Murugesan¹, Anand Chokkalingam¹, Bruce Kreter¹, Steven Flamm². ¹Gilead Sciences, Foster City, United States; ²Rush University Medical Center, Chicago, United States
Email: laura.telep@gilead.com

Background and aims: The United States (US) Centers for Disease Control and Prevention (CDC) reports that the incidence of hepatitis C virus (HCV) infection has increased substantially since 2013, due largely to injection drug use. Given that the development of cirrhosis is associated with cumulative exposure to HCV infection, it may be less likely to occur in younger individuals with HCV. Pre-treatment requirements of cirrhosis assessment in this population may serve as a barrier to treatment initiation. The goal of this study is to examine the incidence and age distribution of cirrhosis in a large US administrative claims dataset among in people with HCV to support the simplification of pre-treatment requirements for those in younger age groups.

Method: A retrospective observational cohort study was conducted with the IQVIA PharMetrics PlusTM database which contains adjudicated medical and pharmacy claims for commercially insured individuals in the US. Index date, the first inpatient or first of two outpatient claims for HCV at least 30 days apart, occurred between 2016 and 2022. Included individuals were adults (18+ years) with continuous enrollment for 365 days prior and at least 1 day of follow-up after the index date, and no evidence of cirrhosis, liver decompensation, or direct-acting antiviral (DAA) treatment at baseline. The incidence rate (IR) of cirrhosis with 95% confidence intervals (CI) was calculated for individuals stratified by index date age group (in 5-year strata). In addition, the age distribution at time of incident cirrhosis was examined by study year, and over the whole study period. Important sub-populations including people who inject drugs (PWID), have evidence of alcohol abuse, or are coinfecting with HBV or HIV were also examined.

Results: Among 68,744 individuals with HCV who met all inclusion/exclusion criteria, 10,678 (15.5%) were under 35 years. Over the entire study period, 9,471 claims for incident cirrhosis were recorded. The IR in all age group strata <35 years ranged from 0.8–1.5 per 100 person years (PY), compared to 2.4–10.6 per 100 PY in strata ≥35 years. Each year from 2017 to 2022, the proportion of individuals <35 years with incident cirrhosis was ≤3.5% (range 1.9–3.5%). Over the entire study period, 2.4% of incident claims occurred in this group. The proportion of patients <35 years with cirrhosis claims was similarly low in subgroups of patients with alcohol abuse (4.6%), HBV coinfection (3.0%), and HIV coinfection (0%) in 2017–2019, with similar proportions during the pandemic 2020–2022. The proportion of PWID <35 years with cirrhosis claims was slightly higher at 9.9% in 2017–2019 and 5.5% in 2020–2022.

Conclusion: Cirrhosis in individuals <35 years was uncommon and occurred most frequently in PWID. Due to the benefits of DAA regimens, treatment of younger individuals should be considered without evaluation of cirrhosis status to increase treatment uptake.

WED-448

Peak mortality is on the horizon: will we flatten the curve?

Devin Razavi-Shearer¹, Ivane Gamkrelidze¹, Kathryn Razavi-Shearer¹, Alexis Voeller¹, Samantha Hall¹, Homie Razavi¹. ¹Center for Disease Analysis Foundation, Lafayette, United States
Email: drazavishearer@cdafound.org

Background and aims: This study aims to estimate liver related deaths due to hepatitis B virus (HBV) and hepatitis C virus (HCV) at the global level through 2050 if current trends in diagnosis and treatment continues. Secondly, a scenario was developed to examine the impact of all countries meeting the 2030 targets of 90% diagnosis rate and 80% of those diagnosed being on treatment.

Method: Historical number of HCC and cirrhosis cases attributed to HBV and HCV were collected when available. In the remaining countries ProGrEsS and Bright Markov models were used to estimate historical viral hepatitis morbidity and associated mortality. The models utilized country specific inputs to estimate the natural history of the disease and future burden (2022–2050). The results were reviewed with national experts to check the absolute number forecasts and trends. Where HCV and HBV prevalence data were unavailable, regional averages were applied to the total population of the country. The elimination scenario was developed for each country, assuming a major scale up in diagnosis and treatment starting in 2024 to meet the WHO 2030 elimination targets.

Results: 170 country level HBV and 117 HCV models were available. In 2015, it was estimated that there were 1.27 million deaths due to HBV and HCV, with 79.5% of them being due to HBV. Total deaths are expected to increase until 2043 when deaths will peak at 1.82 million with 84.4% due to HBV. After this point, deaths attributed to HBV begin to decline as a result of global vaccination programs and all-cause mortality. Deaths due to HCV declined from 2015 to 2020, but this was largely driven by the Egyptian elimination program. Without

POSTER PRESENTATIONS

additional intervention HCV deaths are expected to increase through 2050. If the programmatic targets are met by 2030, we estimate that there will be 5.8 million lives saved among people living with HCV, and 14.7 million lives saved among people living with HBV.

Conclusion: We have a relatively short window, 20 years, to save the greatest number of lives from HBV and HCV. While prevention is an integral part of elimination, the majority of people dying in this timespan were infected decades ago. This study further highlights the immediate need to drastically scale up diagnosis and treatment.

WED-449

Advancing HCV elimination: emergency department screening beyond risk factors

Anny Camelo Castillo¹, Teresa Maria Jordan Madrid¹, Antonio Duarte Carazo¹, Manuel Rodriguez Maresca¹, Teresa Cabezas Fernandez¹, Alba Carrodegua², José Luis Vega Sáenz¹, Marta Casado-Martin¹. ¹Torrecedenas University Hospital, Almería, Spain; ²Gilead Sciences, Madrid, Spain
Email: anjo134@gmail.com

Background and aims: Spain may be one of the first countries to achieve the World Health Organization's goal of eliminating viral hepatitis C by 2030. A serosurvey by the Spanish Ministry of Health 2017–2018 estimated a 0.22% hepatitis C virus (HCV) active infection prevalence among the general population and the guideline recommends hepatitis C screening only in people with exposures or risk situations for Hepatitis C Virus (HCV) infection. However, we know that many of the people who were infected years ago do not meet the screening criteria, so following these guidelines recommendations, many patients with HCV infection would remain undiagnosed. We aimed to evaluate HCV screening efficacy in the Emergency Department (ED) of Torrecedenas University Hospital (Almería, Spain) and identify the prevalence of exposures and risk situations for HCV infection in patients with active HCV infection.

Method: We implemented opportunistic HCV screening in the ED (FOCUS Program), using existing infrastructure and staff since August 2021. With the "one-step strategy", HCV antibodies were detected in adults (between 18 and 69 years old) who needed blood-work for any reason, and then viral RNA was quantified in positive anti-HCV patients. We contacted positive patients to ensure linkage to care, recording any previous history of exposures or situations of risk of HCV infection.

Results: We screened 19110 patients from August 2021 to December 2023, finding 310 anti-HCV positive patients (average age 56 ± 8 y.o, 75% male) and 69 HCV RNA positive patients (83% males).

With these data, the seroprevalence rate in the population attending our hospital's emergency department is 1.62%, and the active infection rate is 0.36%. Of the total number of patients with active infection, 56 (81%) were linked to care and 36 (52%) of these started antiviral treatment. A large percentage of viremic patients had stage F3–F4 liver cirrhosis, indicating a late diagnosis in the course of their HCV infection. We identified exposures or risk situations in 50% of the medical records of viremic patients. The most common were injecting or inhaling drug use (44%), immigrant status (9%), a history of incarceration (8%), and HIV/HBV co-infection (2%) were the main ones. 78% of patients with active HCV infection had a previous visit to the ED and 89% had a previous visit to primary care.

Conclusion: Undocumented HCV infection among our population is higher than estimated in the Spanish population. Half of the patients diagnosed in our ED do not report exposures or risk situations for HCV infection, so following the recommendations of the current screening guideline they would never have been diagnosed. Therefore, Hepatitis C screening in EDs beyond the criteria set out in the screening guideline should be reconsidered as an effective strategy to increase the rate of diagnosis for the elimination of Hepatitis C.

WED-450

Long term outcome among HCV-infected people who use drugs (PWUD) successfully treated for HCV infection with Glecaprevir/Pibrentasvir (G/P)

Brian Conway^{1,2}, Rossitta Yung¹, Shawn Sharma³, Shana Yi⁴, Saina Beitari⁴. ¹Vancouver Infectious Diseases Centre, Vancouver, Canada; ²Simon Fraser University, Burnaby, Canada; ³Vancouver Infectious Diseases Centre, Vancouver, Canada; ⁴Vancouver Infectious Diseases Centre, Vancouver, Canada
Email: brian.conway@vidc.ca

Background and aims: An increasing number of studies have demonstrated the efficacy of HCV therapy in all priority populations, including active PWUD. Within our GRAND PLAN study, we documented a cure rate of 97.3% (108/111 participants) among a population of active PWUD consisting largely of fentanyl users with unstable housing. There is an interest in determining if the benefit of therapy is preserved over time in this population of vulnerable individuals at high risk of adverse outcomes, including reinfection and death, the latter in the context of an opioid crisis with 6–7 deaths/day in the most affected population in our community.

Method: The inception cohort consisted of 108 individuals cured within the GRAND PLAN study. After HCV cure was achieved participants were maintained in follow-up within a multidisciplinary program of care, to attend to medical, social, mental health and addiction-related needs. This includes systematic monitoring for reinfection, provision of opiate agonist therapy and safe supply and education about safer drug use practices. The outcome of this analysis was survival and rate of reinfection.

Results: Among 108 subjects, we note: median age 47 (22–75) years, 27.8% female, 21.3% Indigenous, 97.2% active drug use, 46.7% with unstable housing. Over a follow-up of 30 (12–60) months, 104 (96.3%) remained alive, and 4 individuals died of an opioid overdose (rate 1.7/100 py). Of the 104 remaining participants, 6 (5.8%) were re-infected (rate 1.8/100 py). All 6 have recently initiated therapy and outcomes of repeat therapy are pending.

Conclusion: Beyond our ability to successfully treat HCV infection in vulnerable inner-city populations, there is a need to maximize the benefit of therapy after a cure has been achieved, especially in the setting of the opioid crisis. Our data suggests that by maintaining these individuals in care post-SVR, our program leads to a reduction in overdose deaths, a systematic detection of reinfection events and prompt re-initiation of HCV therapy when it is required.

WED-451-YI

Characterizing hepatitis B virus infection in children and household contacts in the Democratic Republic of Congo to inform elimination efforts in a resource-limited setting

Camille Morgan¹, Kimberly Powers¹, Jessie Edwards¹, Marcel Yotebieng², Michael Emch¹, Stane Bijou¹, Upasana Devkota¹, Gavin Cloherty³, Feng-Chang Lin¹, Jérémie Muwonga⁴, Melchior Kashamuka⁵, Antoinette Tshetu⁵, Sylvia Becker-Drepps¹, Jonathan B. Parr¹, Peyton Thompson¹. ¹University of North Carolina at Chapel Hill, Chapel Hill, United States; ²Albert Einstein College of Medicine, Bronx, United States; ³Abbott Diagnostics, Abbott Park, United States; ⁴Programme National de Lutte Contre le SIDA, Kinshasa, Congo, Dem. Republic of (formally known as Zaire); ⁵École de Santé Publique, Université de Kinshasa, Kinshasa, Congo, Dem. Republic of (formally known as Zaire)
Email: camille_morgan@med.unc.edu

Background and aims: Despite global reductions in hepatitis B virus (HBV) prevalence, an estimated 6.3 million children are infected globally, two-thirds of whom live in Africa. In the Democratic Republic of Congo (DRC), HBV prevalence of all ages is 3 to 5%, implying an estimated 3–5 million chronic infections where hepatology care is virtually inaccessible. The three-dose infant HBV vaccine was first introduced in DRC in 2007 (now within the pentavalent vaccine) and remains one of the only nationally

programmed HBV prevention measures. To inform elimination efforts in resource-constrained settings like the DRC, an improved understanding of HBV epidemiology, particularly among children, is needed.

Method: Using the most recent (2013–14) nationally representative Demographic and Health Survey in DRC, we analysed >8,000 biospecimens and associated survey data to characterize HBV surface antigen (HBsAg) prevalence and associated factors among children 0–5 years old. HBsAg testing using dried blood spots (DBS) was performed on the Abbott ARCHITECT platform. We also performed HBsAg testing on all adult samples from all households of HBsAg-positive children and on adults in a random 3:1 selection of households without HBsAg-positive children.

Results: We analysed DBS and survey data from 7,036 children and 1,091 household members. Among children 0–5 years, weighted HBsAg prevalence was 1.3% (95% CI: 1.0%, 1.6%), with substantial regional variation of 0% to 6% across 26 provinces. HBsAg prevalence among boys (1.8%; 95% CI: 1.2%, 2.6%) was double that of girls (0.8%, 95% CI: 0.5%, 1.4%). HBsAg prevalence did not decrease with decreasing age, counter to what might be expected with improved vaccine roll-out. HBV prevalence was higher among children with *Plasmodium falciparum* malaria compared with children without (1.7% vs 1.1%). Negative tetanus antibodies (proxy for pentavalent vaccination), male sex, rural locale, lower household wealth, and living in nearly all regions outside the capital city's province, Kinshasa, were statistically significantly associated with higher HBsAg prevalence among children. Adults living with HBsAg-positive children had 14.7 (95% CI: 3.5, 25.8) more HBsAg cases per 100 persons compared with those not living with HBsAg-positive children.

Conclusion: DRC remains far from HBV elimination goals of 0.1% prevalence among children, with no evidence of decreasing HBsAg prevalence with declining age, and prevalence above 6% in large rural regions of DRC. Higher prevalence in rural areas and remote provinces could suggest challenges with widespread vaccine implementation. Higher prevalence in boys indicates biological or social factors (e.g. circumcision) for follow-up investigation. This study highlights specific groups and areas for targeted HBV prevention efforts in DRC.

WED-452

Implementing a hepatitis C virus patient search identification tool in primary care settings

Amber Copeland¹, Sarah Montague¹, Stephen D Ryder¹. ¹Nottingham University Hospitals NHS Trust, Queen's Medical Centre, Nottingham, United Kingdom

Email: amber.copeland@nuh.nhs.uk

Background and aims: For England to declare hepatitis C (HCV) elimination by 2025, prevalence in Primary Care must be established. A Patient Search Identification (PSI) tool organised and funded by Merck, Sharp and Dohme (UK) (MSD), to support NHS England's (NHSE) HCV Elimination Strategy, uses a pre-installed search tool on general practice (GP) systems to identify patients coded as positive or at risk for HCV. This enables Operational Delivery Networks (ODNs) to find the estimated 81,000 missing patients.

Method: Management of this project required one full time post who worked with MSD and a Primary Care Network (PCN) to demonstrate the tool, arrange Data Sharing Agreements, search lists and run testing. The ODN compared PCN HCV positive lists (PL) to hospital records and the national HCV treatment registry to confirm previous treatment, clearance and who needed confirmatory testing. 105 patients from the PL (36.21%) did not need a test. Due to large volumes of patients on the at-risk list (ARL), risks identifying patients as less likely to have ever had a test were prioritised into 'phase 1'. Patients needing a test in the PL and those in 'phase 1' were offered testing, via letter, at their GP and directed to the NHSE/PreventX online testing portal for home-test. Online survey feedback was requested from staff and patients.

Results: In a PCN population (7 GPs) of 65,807,290 patients were recorded as HCV positive and 11,205 at risk. To date 2 of 7 GP's hosted 2 testing events each. 41 patients from HCV PL and 670 from the ARL were invited. Of 711 invited, 68 (9.5%) received a Blood Borne Virus (BBV) screen, 2 of which unsuccessfully tried using a home-test. Results showed; 1 HCV RNA Positive (Lost to Care) (LTC), 1 HIV Ab Positive, 4 HBsAg Positive (1 LTC, 1 false positive). Uptake of GP testing was largest in the ethnicity risk group (83.8%). 643 (90.5%) patients did not attend their GP for a test. It is unknown how many used the home-test. Feedback suggests patients ($N = 25$) were unsure why they had been offered a test. They were hesitant to take a home test, but were satisfied with testing at the GP. Staff ($N = 1$) reported high levels of satisfaction. These actions resulted: 99 patient records required updating due to improper coding and two system search errors were fixed by the MSD team. Concerns around information sharing had prevented other PCN's running the tool. An information governance document to allay concerns was created by NHSE/ODN detailing direct care.

Conclusion: The PSI tool was deployed in a PCN of 7 GP's. The tool is implementable at scale and has an important potential yield as we aim for elimination by enabling the ODN to engage a new group of patients and find those previously LTC. Though quick to run, analysis and recall of patients is time consuming but led to innovative use of technology to save time and increase reach, e.g. text invites. Phase 2 of inviting ARL patients and testing in the remaining GPs will be implemented.

WED-453

Reasons patients with hepatitis B and C declined linkage to care and strategies for re-engaging this reachable cohort

Jihae Jeon¹, Francina Collado¹, Anna Mageras², Aura Blanco¹, Tasnim Bhuiyan¹, Lidia Funes¹, Daryin Hummel¹, Daemena Leocadio¹, De Shaunda Page-Cook¹, Lismeiry Paulino¹, Douglas T Dieterich¹.

¹Icahn School of Medicine at Mount Sinai, New York, United States;

²Icahn School of Medicine at Mount Sinai, Division of Liver Diseases, New York, United States

Email: jihae.jeon@mssm.edu

Background and aims: In our large, urban hospital system, we identified patients who declined linkage to viral hepatitis care. Few studies have examined pre-appointment declines in detail, especially drawing on direct conversations. We aimed to describe reasons for and analyze factors associated with declining linkage to care in our system.

Method: From 1/2019 to 12/2023, our patient navigators received lists of patients who engaged with our health system the week prior and whose most recent HCV RNA result was positive. From 9/2022 to 12/2023, they also reached out to patients who were HBsAg-positive. Navigators contacted patients by phone and patient portal to offer liver appointments and documented their encounters and outcomes in REDCap. We summarized this data and, using multivariable logistic regression, assessed factors (age, sex, race, ethnicity, active patient portal, and Medicaid insurance) for possible association with declined care.

Results: Among 186 HBsAg+ patients contacted, 142 (76%) were linked, 28 (15%) lost to follow-up, and 16 (9%) declined, reasons being: upset about outreach (6), unknown (4), not a priority (3), deferring care (1), negative interaction with health system (1). Patient navigators reached out to 1,834 patients with an HCV RNA+ result. Of these, 430 (24%) were linked to a first liver visit, 542 (30%) had no/incorrect contact information, 538 (29%) did not respond, 130 (7%) stopped responding after initial contact, and 194 (11%) declined linkage. Reasons for declining were: deferring care (48), not a priority (35), old/too ill from other conditions (30), upset over outreach (29), unknown (24), finances (11), did not recall screening visit (6), transportation (5), negative interaction with health system (5), bad experience with interferon (1). Persons who declined HCV linkage had higher odds than those who accepted care of being female (OR =

POSTER PRESENTATIONS

1.70, 95% CI: 1.16, 2.51), being commercially insured (OR = 2.34; 95% CI: 1.58, 3.48), and having no patient portal (OR = 2.28; 95% CI: 1.49, 3.49). Black patients had almost half the odds of whites of declining care (OR = 0.53; 95% CI: 0.32, 0.87).

Conclusion: Potential explanations for regression results include women prioritizing caretaker responsibilities and commercially insured patients' concerns about copays. For patients with long-past diagnoses, navigator scripts should explain delayed follow-up and include details of the screening visit to reduce patient anger. We plan to follow-up with patients who were upset about phone outreach via letter/patient portal, in case they are more receptive to these media, and include information about financial assistance and new drugs. Mental health support for navigators can reduce burnout from fraught conversations. We also plan to deploy novel education approaches, including videos in multiple languages. We re-open cases after 6 months in case patient priorities have shifted.

WED-454-YI

Accessing healthcare: perspectives of people who use drugs

Zoi Papalamprakopoulou^{1,2}, Elisavet Ntagianta³, Vasiliki Triantafyllou³, George Kalamitsis³, Arpan Dhar¹, Suzanne Dickerson⁴, Angelos Hatzakis^{2,5}, Andrew Talal¹, ¹Division of Gastroenterology, Hepatology, and Nutrition, Jacobs School of Medicine and Biomedical Sciences, University at Buffalo, Buffalo, NY, United States; ²Hellenic Scientific Society for the Study of AIDS, Sexually Transmitted and Emerging Diseases, Athens, Greece; ³Hellenic Liver Patient Association "Prometheus", Athens, Greece; ⁴Division of Biobehavioral Health and Clinical Science, School of Nursing, University at Buffalo, Buffalo, NY, United States; ⁵Department of Hygiene, Epidemiology and Medical Statistics, National and Kapodistrian University of Athens, Athens, Greece
Email: zoipapal@buffalo.edu

Background and aims: People who use drugs (PWUD) have the highest hepatitis C virus (HCV) incidence and prevalence. This population should be prioritized in HCV elimination programs. PWUD typically avoid conventional healthcare settings due to stigma and shunning. We aimed to comprehend how PWUD in Athens, Greece access healthcare by exploring their experiences, attitudes, and beliefs related to their interactions with the healthcare system. We also sought to identify barriers and facilitators in the process of accessing and navigating conventional healthcare settings. **Method:** Between May and September 2023, we conducted nine focus group discussions (FGDs) in Athens, Greece each comprised of 4 to 9 participants (N = 57) recruited through purposive sampling. Inclusion criteria required age at least 18 years, a history of injection drug use, internet access, Greek verbal fluency, and the ability to provide informed consent. The FGDs were conducted using a semi-structured interview guide, audio-recorded, transcribed, translated into English, and de-identified. We analyzed FGD transcripts using grounded theory.

Results: Participants' mean (SD) age was 47.9 (8.9) years, 89.5% (51/57) were male, 91.2% (52/57) were of Greek origin, and 61.4% (35/57) had attended at least 10 years of school. Three main themes emerged from the FGDs: (1) seeking care after an individuals' rapid health decline, (2) encountering barriers when seeking healthcare, and (3) recommending processes to build trust in healthcare providers and institutions. Participants shared personal experiences of rapid deterioration in their health and disclosed a variety of approaches used to access healthcare. Encountering barriers when seeking medical care included delayed access to healthcare, facing stigma in healthcare settings, mistrusting the healthcare system, and addressing competing priorities, such as homelessness, poor mental health, and substance use withdrawal. Building trust in healthcare was facilitated by stigma minimization, empathy encountered in the patient-provider relationship, and engagement of community organizations.

Conclusion: PWUD in Athens, Greece, described healthcare access challenges due to stigma, mistrust of the healthcare system, and competing priorities. Important considerations for building trust in healthcare settings are the curtailment of stigma, an empathetic medical approach, and the engagement of community organizations in healthcare delivery. Addressing these issues is critical to increase healthcare access among PWUD to ultimately enhance HCV elimination efforts.

WED-455

Sex disparities in initiation of direct-acting antivirals for hepatitis C treatment: data from the French national healthcare database (2014–2022, ANRS FANTASIO 2 study)

Clémence Ramier¹, Cécile Brouard², Vincent Di Beo¹, Yoann Allier³, Abbas Mourad¹, Morgane Bureau¹, Philippe Sogni^{4,5,6}, Sylvie Deuffic-Burban⁷, Marc Bourliere^{1,8}, Patrizia Carrieri¹, Camelia Protopopescu¹, Benjamin Rolland^{9,10,11,12}, Fabienne Marcellin¹. ¹Aix Marseille Univ, Inserm, IRD, SESSTIM, Sciences Economiques and Sociales de la Santé et Traitement de l'Information Médicale, ISSPAM, Marseille, France; ²Santé publique France, Saint Maurice, France; ³ANRS | Maladies Infectieuses Emergentes, Paris, France; ⁴Université Paris Descartes, Paris, France; ⁵INSERM U1223, Institut Pasteur, Paris, France; ⁶Service d'Hépatologie, hôpital Cochin, Assistance Publique-Hôpitaux de Paris, Paris, France; ⁷Université Paris Cité et Université Sorbonne Paris Nord, Inserm, IAME, Paris, France; ⁸Hôpital St Joseph, Service d'Hépatogastroentérologie, Marseille, France; ⁹PSYR, CNRL, INSERM U1028, CNRS UMR5292, UCBL1, Bron, France; ¹⁰Université Claude Bernard Lyon 1, Lyon, France; ¹¹Centre Hospitalier Le Vinatier, Bron, France; ¹²Service Universitaire d'Addictologie de Lyon (SUAL), HCL, CH Le Vinatier, Lyon, France
Email: clemence.ramier@inserm.fr

Background and aims: Eradication of hepatitis C by 2025 is a national public health objective in France. To achieve this target, universal access to direct-acting antivirals (DAA) was set up in August 2017 in the country. National surveillance data showed sex disparities in both hepatitis C screening and prevalence, with more women undergoing screening tests and less women diagnosed with chronic hepatitis C. Sex disparities were also found in access to hepatitis C treatment for specific populations, such as people who inject drugs, with less women initiating therapy. Using data from the French national healthcare database (SNDS), we explored potential sex disparities in DAA initiation before and after universal access.

Method: The study population included all adult individuals with chronic hepatitis C residing in metropolitan France between January 2014 (date of DAA arrival) and December 2022 (up-to-date records in the SNDS). Analyses were performed separately on two study periods: before August 2017 (period 1) and after August 2017 (period 2). The study outcome was defined as the time between the baseline of each period and DAA initiation (i.e., first delivery of DAA recorded in the SNDS). Incidence rates of DAA initiation were compared between men and women in the two periods. Cox proportional hazards models were used to test for potential sex disparities in DAA initiation in both periods, after adjustment for age, social vulnerability (benefiting from free complementary health insurance or state medical assistance), as well as disease stage and comorbidities justifying eligibility to DAA treatment before 2017. Comorbidities were identified using standard algorithms developed by the French national health insurance fund (Cnam).

Results: The study population included 152,165 individuals (38.4% of women, 75.7% aged 30 to 64 years) of whom 100,313 initiated DAA treatment between 2014 and 2022 (39.5% of women, 78.4% aged 30 to 64 years). The incidence rate of DAA initiation [95% confidence interval (CI)] was significantly lower in women than in men in period 1 (30.8 [30.4–31.2] vs 33.1 [32.8–33.5] per 100 person-years (PY)) and significantly higher in women than in men in period 2 (22.3 [22.0–22.6] vs 18.6 [18.4–18.8] per 100 PY). Multivariable models showed significant sex disparities in DAA initiation, with adjusted hazard

ratios [95% CI] for women (ref. men) at 0.91 [0.89–0.92] for period 1, and 1.06 [1.04–1.08] for period 2.

Conclusion: DAA initiation was delayed for women before universal access in France, but significantly improved after removal of eligibility criteria for treatment initiation. Differences between men and women in both risk factors of disease progression and use of healthcare services may partially explain these findings. Further research is needed to document potential sex disparities in DAA initiation in specific subpopulations of individuals with chronic hepatitis C.

WED-456

Implementation of an Electronic Medical Record-Based Automatic Alert System for the Care Cascade of Hepatitis-C-Virus Infection in Patients Undergoing Elective Surgery

Jae Seung Lee¹, Ho Soo Chun², Hye Won Lee¹, Mi Na Kim¹, Beom Kyung Kim¹, Jun Yong Park¹, Do Young Kim¹, Sang Hoon Ahn¹, Seung Up Kim¹. ¹Yonsei University College of Medicine, Department of Internal Medicine, Seoul, Korea, Rep. of South; ²Ewha Womans University College of Medicine, Department of Internal Medicine, Seoul, Korea, Rep. of South
Email: ksukorea@yuhs.ac

Background and aims: The care cascade for hepatitis C virus (HCV) faces a significant obstacle due to poor awareness, especially in patients undergoing elective surgery. To address this issue, we introduced an electronic medical record (EMR)-based automatic alert system in 2021 to enhance the awareness among surgical healthcare providers regarding HCV screening and referral rates.

Method: Implemented in a tertiary medical center in South Korea, the system alerts surgeons to order preoperative anti-HCV antibody tests, and if needed, consult hepatologists at discharge for patients undergoing elective surgery.

Results: After implementation, the system significantly increased HCV screening rate for 76, 310 patients, compared with 129, 065 patients undergoing surgery between 2016 and 2020 (82.8–96.8%, $P < 0.001$). Out of 73, 834 patients who were tested for anti-HCV antibody, the system alerted 12, 048 (16.3%) patients. However, out of 463 patients who tested positive for anti-HCV antibody after system implementation, only 42 (15.3%) out of 275 (59.4%) who required consultation were referred to hepatologists. Linkage failure was associated with other surgery departments than hepatobiliary and transplant surgery departments (odds ratio [OR] = 5.940, 95% confidence interval [CI], 3.080–12.410, $P < 0.001$) and shorter hospitalization duration (OR = 0.980, 95% CI, 0.950–0.990, $P = 0.012$).

Conclusion: Although EMR-based automatic alert system was effective in increasing HCV screening for patients undergoing elective surgery; however, it could not link them to care cascade in surgery departments. Combining more proactive approaches, such as reflex testing or a call-back strategy, would be beneficial.

WED-457-YI

Eliminating hcv infection from prisons in Sicily: the sintesi project (*)

Lorenza Di Marco^{1,2,3}, Fabio Cartabellotta^{4,5}, Fabio Santangelo³, Fabrizio Scalici^{3,6}, Rosario Insinna^{3,6}, Tullio Prestileo^{3,7}, Maria Giovanna Minissale^{3,4}, Vincenza Calvaruso^{3,8}, Antonio Craxi³, Vito Di Marco^{3,8}. ¹Department of Oncology and Hematology, Azienda Ospedaliero-Universitaria di Modena, Modena, Italy; ²Clinical and Experimental Medicine PhD Program, University of Modena and Reggio Emilia, Modena, Italy; ³Sicilian Network for Therapy, Epidemiology and Screening In Hepatology (SINTESI), Palermo, Italy; ⁴Department of Medicine Buccheri -La Ferla Hospital, Palermo, Italy; ⁵Sicilian Network for Therapy, Epidemiology and Screening In Hepatology (SINTESI), Palermo, Italy; ⁶Medical Area of the "Pagliarelli-Lorusso" Prison, Palermo, Italy; ⁷UOSD Infectious Pathologies of Vulnerable Populations, ARNAS-Civico Hospital, Palermo, Italy; ⁸Department of Health

Promotion, Mother and Child Care, Internal Medicine and Medical Specialties (PROMISE), University of Palermo, Palermo, Italy
Email: vito.dimarco@unipa.it

Background and aims: In all countries HCV among prisoners has a higher prevalence than in the general population. Specific models of screening and linkage to care are needed to improve the care cascade.

Method: The Sicilian Network for Therapy, Epidemiology and Screening In Hepatology (SINTESI) run an HCV point-of-care project in all 23 prisons of Sicily. All prisoners received information on HCV screening and the possibility of receiving treatment with Direct Acting Antiviral (DAA) while incarcerated. HCV status was assessed by screening all subjects for anti-HCV by rapid oral test (OraQuick HCV) and immediate reflex testing for HCV-RNA (GeneXpert-HCV Viral Load, Cepheid). HCV RNA positive subjects received DAA therapy within 72 hours of screening. All prisoners signed an informed consent to use personal data. Chi-square test was used to analyze differences between groups.

Results: Among 5, 912 prisoners (98% of entire prison population) informed of the screening project, 4, 911 (83%) accepted to undergo HCV testing. The mean age was 42 years (range 18–86) and 95.8% was males. Non-Italian origin accounted for 12.2% of prisoners (3.7% other EU countries, 7.5% Africa, 0.6% Asia and 0.2% South America). Overall, 245 subjects (5%) testes anti HCV positive, with a prevalence of 4.9% among males and 6.7% among females ($p = 0.25$). We evaluated the risk of drug addiction in subjects with HCV infection in a prison. A prevalence of 25% (25/99) was found among PWUDs on opioid substitution, as compared to 2.9% (30/1, 040) in non-PWUDs ($p < 0.0001$). Among 245 anti HCV positive prisoners, 20 refused to be tested for HCV-RNA, 100 tested negative (80 had a history of viral clearance under previous DAA treatment while 20 did not report previous therapy for HCV) and 125 were HCV-RNA positive. Twelve of the latter refused treatment, while 113 started a cycle of DAAs while incarcerated. Among 56 subjects assessable for SVR, 55 (98%) obtained HCV clearance.

Conclusion: In Sicily, HCV infection is 4 times more common among people in prison than in the general population mostly due to parenteral drug use. Half of the prisoners with a positive screening were unaware of their HCV status and only 32% had received DAAs previously. A one-shot HCV test-and-treat point-of-care approach is highly effective in this setting. (*) The project was approved by the Regional Department of Health and the Regional Department of Prisons and was funded by HCV STAT (Simplification and Test and Treat Strategies toward HCV Elimination) program of Gilead Sciences.

WED-458

Low testing rates but high prevalence of hepatitis delta virus in Saudi Arabia

Faisal M Sanai¹, Khalid A Alswat², Mohammed A Babatin³, Duna Barakeh⁴, Majed Almaghrabi¹, Ahmed Saati¹, Adnan Alzanbagi⁵, Faisal Abaalkhail⁴, Mona H Ismail⁶, Hani Tamim⁷, Abdullah S Alghamdi⁸, Jabir A Alzaidi³, Asma AlNajjar⁴, Abdulaziz Tashkandi⁵, Waleed K Al-Hamoudi⁴, Norah Jamal Alromaih⁶, Habeeb I.A. Razack², Saleh A Alqahtani⁴. ¹King Abdulaziz Medical City, Jeddah, Saudi Arabia; ²King Saud University, Riyadh, Saudi Arabia; ³King Fahd General Hospital, Jeddah, Saudi Arabia; ⁴King Faisal Specialist Hospital and Research Centre, Riyadh, Saudi Arabia; ⁵King Abdullah Medical City, Makkah, Saudi Arabia; ⁶King Fahd Hospital of the University, AlKhobar, Saudi Arabia; ⁷Alfaisal University, Riyadh, Saudi Arabia; ⁸King Fahad General Hospital, Jeddah, Saudi Arabia
Email: drsaleh.a.alqahtani@gmail.com

Background and aims: Hepatitis delta virus (HDV) significantly impacts public health, often co-infecting with hepatitis B virus (HBV) or superinfecting chronic HBV carriers. Despite its clinical importance, there is a lack of comprehensive data on HDV prevalence, particularly in the Middle East and specifically in Saudi Arabia (SA). This study aimed to fill this gap by investigating the prevalence of

POSTER PRESENTATIONS

HDV in SA, evaluating HDV testing practices in clinical settings, and exploring the clinicodemographic profile of affected patients.

Method: This retrospective, observational study involved the chart review of consecutive, adult or adolescent (>14 years) patients positive for anti-HBsAg across six medical centers in SA from 2012 to 2022. We assessed anti-HDV seroprevalence in these patients and evaluated various risk factors, comorbidities liver biochemistry (serum biomarkers), and fibrosis stages (by transient elastography).

Results: Among the 2173 HBV-infected patients (mean age 48.3 ± 14.6 years and 60.9% male), 794 (36.5%) patients were tested for anti-HDV. The prevalence of HDV was 8.8% (68 out of 776) among HBsAg-positive patients. Of those who tested positive for anti-HDV, 47.1% (32 out of 68) underwent HDV RNA testing, with 32% (10 out of 32) testing positive. Age, gender, alkaline phosphatase, and albumin level were significantly associated with anti-HDV positivity (all $p < 0.05$). However, no significant correlation was observed with comorbidities like hypertension, diabetes, or dyslipidemia. Notably, HDV co-infected patients exhibited higher rates of advanced fibrosis (stages $\geq F3$) compared to those with HBV mono-infection (26.9% vs. 15.0%, $p = 0.028$).

Conclusion: The study reveals a relatively high prevalence of anti-HDV among tested patients in SA, with HDV co-infected individuals exhibiting more severe liver disease than those with HBV mono-infection. These findings underscore the need to enhance HDV serological testing, including reflex testing for HDV RNA, across SA to improve the diagnosis and management of this infection.

WED-459-YI

Opt-out hepatitis B testing in urban emergency departments, linkage to healthcare and clinical outcomes

Jonathan Durban¹, Shiny Jaimes¹, Sally Thomas¹, Nina van Zyl¹, Noeleen Bennett¹, Hannah Hesketh¹, Helen Boothman¹, Nick Tatman¹, Markus Gess², Sarah Clark¹, Daniel Forton¹. ¹St George's University Hospitals NHS Foundation Trust, London, United Kingdom; ²KINGSTON Hospital NHS Foundation Trust, London, United Kingdom
Email: daniel.forton@nhs.net

Background and aims: Chronic hepatitis B infection (CHB) remains an underdiagnosed condition in the UK. In 2022 the national health service (NHS) in England commissioned opt out emergency department (ED) testing for blood borne viruses (HIV and hepatitis B and C) in regions with a high prevalence of HIV. We report the initial clinical outcomes for hepatitis B (HBV) testing in the 5 EDs in SW London.

Method: All adults undergoing blood tests in EDs had BBV testing, including HBV surface antigen (HBsAg) unless they opted out. Testing information was displayed using widely positioned posters in EDs. The only change to patient flow in the ED was an additional vial of blood taken for BBV testing. All reactive HBsAg results were managed by the SW London Hepatitis Network. We analyzed all data for testing and follow-up between November 2022 and October 2023, as the 5 EDs commenced testing sequentially.

Results: There were 356, 204 adult ED attendances during the testing periods in the 5 EDs. 211, 438 adults had blood tests. 106, 624 adults were tested for HBsAg and 620 had reactive tests giving a CHB prevalence of 0.58% in the tested population. Of these 232 were new diagnoses, 213 were known cases under care, 101 were known but lost to follow-up (LTFU) and 74 remain unknown as contact has not been made. A dedicated team have made successful contact with 540/620 patients (236 at second attempt, 136 at third). 204 of the new diagnoses have now had diagnostic counselling and an assessment by an HBV nurse specialist and 186 (111 M; 75 F) have had medical review. 177/186 (95%) have a country of birth outside of the UK (38% Africa, 18% South Asia, 10% other Asia, 22% South and East Europe, 6% other Europe). The median age was 52 in men, 49 in women, range (19–88) years. 180 patients (97%) were eAg-ve, only 2 patients eAg+ve and 4 were false positives. The median viral load was 611 IU/ml (Q1 25–78, Q2 78–611, Q3 611–370, Q4 370– 12×10^6). The median liver stiffness was 5.1kPa (Q1 2.5–4.2, Q2 4.2–5.1, Q3 5.1–6.1, Q4 5.1–20)

and CAP was 242 dB/m² (Q1 100–212, Q2 212–242, Q3 242–281, Q4 281–392). 30% had a CAP > 275, indicating a high prevalence of concomitant steatosis. 51 patients (27%) were judged to have eAg-ve chronic HBV with a treatment indication and 41 commenced nucleotide therapy. There were no incident cases of hepatocellular carcinoma, 3 patients had positive delta serology. Overall linkage to care for new and LTFU patients was 76%.

Conclusion: In this urban population, at least 37% of detected CHB were new diagnoses in a very mixed ethnic population, with a high proportion having a treatment indication. ED testing is a highly effective method to increase HBV diagnoses and re-engage LTFU patients but requires significant dedicated resource for testing, diagnostic counselling, clinical assessment, and maintenance of engagement. Culturally sensitive, community-based arrangements for ongoing engagement with this cohort will be required.

WED-462

Characteristics of a prospective cohort undergoing assessment for hepatitis C treatment in London and time to treatment initiation

Kathleen Bryce^{1,2}, Amy Teague¹, Fiona Burns^{1,2}, Colette Smith², Alison Rodger^{1,2}, Douglas Macdonald^{1,3}. ¹Royal Free London NHS Foundation Trust, London, United Kingdom; ²Institute for Global Health, University College London, London, United Kingdom; ³Institute of Liver and Digestive Health, University College London, London, United Kingdom

Email: kathleenbryce@doctors.org.uk

Background and aims: The characteristics of individuals living with untreated hepatitis C in the UK have not been well-described and this limits the ability of clinical teams to address barriers to care. We aimed to characterise a cohort of people undergoing assessment for hepatitis C direct-acting antiviral (DAA) treatment and measure time to treatment initiation.

Method: We conducted a prospective cohort study including individuals attending a nurse-led assessment in drug services and hospital clinics in North London between May and December 2022. Baseline questionnaires were self-completed on paper or electronically via a tablet device on the day of assessment and follow-up (by linkage to a clinical patient management system) was for at least three months. Questionnaires collected data on socioeconomic status, drug and alcohol use and mental health, previous experiences of accessing hepatitis C care, beliefs about DAA treatment and experiences of stigma. A descriptive analysis was performed.

Results: Clinic non-attendance was 48% (54/113) but study acceptance was high at 86% (43 of 50 individuals approached to participate). Of the 39 study participants who returned a questionnaire, 67% were male, mean (range) age was 52 (27–86) years, 56% were UK-born, 23% unstably housed, 56% did not always have money for basic needs and 59% of these were severely food insecure (by the Household Food Insecurity Access Scale). Over half (56%) had a mental health diagnosis, 43% had PHQ9 scores consistent with depression and 38% had GAD7 scores in keeping with anxiety. 16% had an AUDIT score suggestive of higher risk drinking. Almost a third (31%) were diagnosed via ED opt-out testing and 21% had previously missed an appointment or declined hepatitis C treatment. 41% reported perceived stigma relating to hepatitis C. Over 90% believed that DAA treatment would be of benefit but 66% thought that it would have side effects and 54% that treatment would require a liver biopsy. The majority (87%) started DAA treatment during follow-up and the median time from assessment to treatment start was 47.5 days (IQR 41, range 13–184). Almost all (97%) of these completed treatment and (of those who had at least three months of follow-up available after completion), 55% (11/20) had a recorded sustained virological response (SVR) check, all with viral cure.

Conclusion: This small cohort demonstrates that factors previously shown to be associated with disengagement from hepatitis C care are highly prevalent in those attending assessment for treatment. Subsequent treatment initiation and completion rates in participants

were high, highlighting the inherent ascertainment bias that complicates prospective studies of patient disengagement. The high non-attendance rate emphasises that greater efforts are needed to enable engagement with care amongst people experiencing barriers to access.

WED-463

Implementation of the educate, test, and treat outreach model in Shabu village, Nigeria: lessons learned

Riham Soliman¹, Ibrahim Alhassan², Ruth Bello³, Akpan Nse⁴, Ayman Hassan⁵, Ahmed Farahat⁶, Ahmed Salem⁶, Amr Taha⁷, Ramy Sabry⁶, Ahmed Geith⁶, Ahmed Elshawaf⁶, Nabel Mikhail⁸, Gamal Shiha⁹. ¹Tropical Medicine Dept., Faculty of Medicine, Port Said University, Egyptian Liver Research Institute and Hospital (ELRIAH), Mansoura, Egypt; ²Department of Public Health, Ministry of Health, Nasrwa, Nigeria; ³Dalhatu Araf specialist Hospital, Lafia, Nasrwa, Nigeria; ⁴Department of Public Health, Ministry of Health, Nasarawa state, Nasarawa, Nigeria; ⁵Egyptian Liver Research Institute and Hospital (ELRIAH), Higher Institute of Applied Medical Sciences, Mansoura, Egypt; ⁶Egyptian Liver Research Institute and Hospital (ELRIAH), Mansoura, Egypt; ⁷Egyptian Liver Research Institute and Hospital (ELRIAH), Mansoura; ⁸Egyptian Liver Research Institute and Hospital (ELRIAH), Biostatistics and Cancer Epidemiology Department, South Egypt Cancer Institute, Assuit University, Mansoura, Egypt; ⁹Hepatology and Gastroenterology Unit, Internal Medicine Department, Faculty of Medicine, Mansoura University, Egyptian Liver Research Institute and Hospital (ELRIAH), Mansoura, Egypt
Email: g_shiha@hotmail.com

Background and aims: More than 90% of people living with hepatitis B and C in Africa lack much needed care with at least 200 000 deaths a year [1] Our aim was to assess the feasibility of application of the “Educate, Test and Treat” outreach model in an African village setting [2].

Method: This work was done from 6th to 17th December 2023 in Shabu Village, Nasarawa State, Nigeria, as a collaborative work between Association of Liver Patients Care (ALPC), African Liver Patients’ Association (ALPA), African Scientific, Research and Innovation Council (ASRIC) and Nasarawa State Health Authorities. The village was divided into enumerated segments, assigning each resident a distinct identification number ranging from 1 to 3002. Concurrently, individuals were scheduled for a specific date to undergo Hepatitis screening. This community-based Educate, test-and-treat project consisted of community mobilisation facilitated by a network of village promoters and establishment of partnerships; an educational campaign to raise awareness, comprehensive testing, diagnosis, and treatment. For the educational campaign, we used public awareness events, and promotional materials (e.g., booklets). Risk factors were assessed using a detailed questionnaire covering medical history, household practices, and local cultural procedures potentially contributing to hepatitis transmission. Comprehensive testing, linkage to care, and treatment was offered to all eligible villagers. Testing was done by use of HCV antibody and hepatitis B surface antigen (HBsAg) rapid diagnostic tests, with HCV-RNA PCR confirmation of positive cases, and staging of liver disease by use of transient elastography.

Results: Of 3,002 eligible individuals, 2532 (84.3%) were screened for HCV antibody and HBsAg by Rapid Diagnostic Test (RDT). 333 (13.1%) were found positive for HCV antibodies and 781 (30.8%) for HBsAg. 96.9% of HCV antibody positive patients were RNA positive and 84.5% of HBsAg positive patients were DNA positive. 12.3% of HCV antibody positive patients and 8.1% of HBsAg positive patients were cirrhotic as indicated by FibroScan. Several practices were identified that may significantly contribute to the risk of Hepatitis transmission, including scarification tattoos utilizing unsterile tools, group male circumcision with non-sterile equipment and unsafe practices by street barbers. HCV-RNA-positive participants were offered a 12-week course of sofosbuvir (400 mg orally, daily) and Daclatsvir

(60 mg orally, daily). CHB patients were offered Tenofovir 245 mg mg and 2000 subjects were vaccinated against HBV.

Conclusion: In this work, we demonstrated the feasibility of a community-based “educate, test and treat” program as a model for the elimination of hepatitis infection in rural communities in Africa. This approach could be an important strategy for adoption towards the elimination of hepatitis.

WED-464

Dried blood spot self-collection for hepatitis B, C, and COVID-19 antibodies

Ahreni Saunthar¹, Sarah Sousa Tran¹, Agustina Crespi¹, Aaron Vanderhoff¹, Anne Claude Gingras², Karen Colwill², Tony Mazzulli³, Camelia Capraru¹, Mia Biondi¹, Jordan J. Feld¹. ¹University Health Network, Toronto, Canada; ²Mount Sinai Hospital, Toronto, Canada; ³Mount Sinai Hospital/University Health Network, University of Toronto, Toronto, Canada
Email: ahreni.saunthar@uhn.ca

Background and aims: Limited access to healthcare providers, particularly in rural/remote areas, hampers diagnosis and serosurveillance of hepatitis C virus (HCV) and hepatitis B virus (HBV). While dried blood spot collection enables testing for multiple infections from a fingerprick, it still requires interaction with the healthcare system. We aimed to evaluate contactless, mail-based self-collection dried blood spot (scDBS) testing, to increase accessibility and flexibility in HCV and HBV testing compared to conventional phlebotomy-based testing.

Method: Participants were recruited from a tertiary care hepatology clinic and a large academic family practice in Toronto, Canada. The study included participants seropositive for HCV, HBV, and COVID-19, and those with unknown serostatus. Interested participants were mailed an scDBS collection kit, with paper instructions, a QR-code to video instructions, a demographic questionnaire, and an acceptability survey. A prepaid return envelope was included to return the DBS card and questionnaire.

Results: Of 390 recruited participants, 39.2% (n = 153) completed the study. Results have been analyzed for a subset of 77 participants (33F, 44M, mean age 54). Of the 77 paired serum and DBS samples, 7 were HCV antibody positive, 16 were HBsAg positive, and 54 had unknown serostatus.

By scDBS, HBsAg detection occurred in all known positive samples (n = 16), with no false positive results (n = 61); and therefore sensitivity was 100% (95% CI 79.4–100.0) and specificity was also 100% (95% CI 94.1–100.0). Of those who tested HCV antibody positive in serum, sensitivity for 7 samples was 85.7% (95% CI 42.1–99.6) with 1 false negative. Not surprisingly, the false negative resulted from a very low signal-to-cut-off ratio (S/CO) observed in serum. The specificity for 70 known negative samples was 97.1% (95% CI 90.0–99.7) with 2 false positives. There was 100% concordance between serum and scDBS COVID-19 antibody results. Participants highly recommended mail-based testing (n = 72, 96.0%); most rated the process as excellent/good (n = 69, 95.5%); 52.0% (n = 39) reported collection as very easy/easy, and 81.9% (946/1155) of required spots were completed perfectly.

Conclusion: scDBS allowed for collection and testing for HCV, HBV, and COVID-19 exposure without the need for interaction with the healthcare system. High scDBS concordance and simplicity drive scalable disease screening, compensating for the marginal reduction in DBS sensitivity and specificity. Overall, the approach was acceptable to patients and could offer a strategy for reaching groups with structural or geographic barriers to care.

POSTER PRESENTATIONS

WED-465

Increasing hepatitis C screening rates at a New York City primary care clinic: a continuation

Jake Debroff^{1,2}, Piya Kositangool², Carolina Villarroel², Gres Karim³, Anna Mageras⁴, Desiree Chow². ¹Mount Sinai Beth Israel, New York, United States; ²Mount Sinai Beth Israel, New York, United States;

³New York Presbyterian Brooklyn Methodist Hospital, Brooklyn, United States; ⁴Icahn School of Medicine at Mount Sinai, Liver Diseases, New York, United States

Email: jake.debroff@mountsinai.org

Background and aims: According to the Centers for Disease Control (CDC), Hepatitis C virus (HCV) infection has continuously increased in incidence since 2013. The New York City (NYC) Department of Health (DOH) reports that 86,000 people in NYC are living with chronic HCV. Given the severe complications of chronic HCV infection, including cirrhosis and hepatocellular carcinoma, the DOH is targeting a 50% improvement in HCV screening rates by 2030. Although current screening guidelines recommend a one-time screening test for HCV in all adults aged 18 to 79, the impediment to achieving improved detection rates appears to be rooted in the need for improved provider education. Our quality improvement study aims to increase HCV screening rates by performing stepwise educational interventions at a NYC primary care clinic.

Method: The second iteration of a Plan-Do-Study-Act (PDSA) approach was initiated in August 2023 among a team of internal medicine residents, primary care physicians, and a viral hepatitis program manager. Prior interventions, such as a best practice alert within the electronic medical record (EMR) instituted in 2022, were continued throughout the study period. A cohort of 35 internal medicine residents underwent an educational HCV presentation designed to better their understanding of the current guidelines regarding HCV testing as well as the significance of screening to prevent adverse liver outcomes. This second phase of the intervention emphasized detailed provider education and involved ancillary staff such as nurses and patient care assistants. Following education, all clinic staff were encouraged to place HCV screening orders as appropriate during each patient intake.

Results: Brief surveys to assess provider knowledge were collected before and 4–6 weeks after an educational presentation regarding HCV screening was given to all resident providers. After receiving the educational session, there was a 10% rise in correct responses regarding the population to be screened, with 92.6% of residents answering correctly. An increase of 17.8% was observed for correctly identifying the appropriate screening test. Following the initiation of the comprehensive education program, HCV screening rates were shown to improve steadily over the course of five months to 28 percent. Notably, screening rates were more than double the reported average for primary care clinics throughout the hospital system (28% vs 13%).

Conclusion: The implementation of an educational plan focused on up-to-date screening guidelines and patient awareness was shown to improve screening rates over a 5 month period at a NYC primary care clinic. Furthermore, there was a significant enhancement in the knowledge of internal medicine residents, enabling patient education and ultimately promoting higher compliance with HCV screening to prevent adverse long-term liver outcomes.

WED-466

The cost of HBV and HCV elimination in Ethiopia based on the current disease burden

Alexis Voeller¹, Hailemichael Desalegn², Devin Razavi-Shearer¹, Ivane Gamkrelidze¹, Homie Razavi¹. ¹Center for Disease Analysis Foundation, Lafayette, United States; ²St. Paul's Hospital Millennium Medical College, Addis Ababa, Ethiopia

Email: avoeller@cdafound.org

Background and aims: Based on their current trajectory, Ethiopia will not meet the WHO elimination targets for hepatitis B (HBV) or

hepatitis C (HCV) without increasing preventative measures. This study aims to evaluate the current and future disease burden for HBV and HCV along with the economic burden to estimate what the necessary steps are to achieve the elimination of viral hepatitis as a public health threat. This will result in the outline of potential paths forward for Ethiopia.

Method: To complete this analysis, we utilized a literature review, conducted a Delphi process with Ethiopian experts and used mathematical modelling to estimate HBV and HCV disease and economic burden within the country. Two modelling scenarios were created for each disease: 2023 Base (reporting the empirical data through 2023); WHO elimination (estimating the number of patients who need to be screened, diagnosed, and treated to reach set targets). For HBV, an additional scenario was created to estimate the prophylaxis coverage needed meet the $\leq 0.1\%$ prevalence in ≤ 5 -year-olds.

Results: If Ethiopia were to introduce a universal birth dose program in 2024, healthcare providers would be vaccinating 3.9 million infants each year. This intervention alone combined with continued high levels of three dose coverage would meet the WHO prevalence elimination target ($\leq 0.1\%$ in ≤ 5 -year-olds) by 2043 while averting 6,800–8,600 new HBV infections per year. To implement this program, Ethiopia would need an annual budget of 39.0 million Birrs. The cost per infection averted could reach up to 8,630 Birrs if introduced. To achieve HBV elimination, an estimated 892,000 patients would need to be diagnosed annually along with 821,400 patients treated. Birth dose vaccination coverage would also need to increase to at least 90% while maintaining a 96% three dose coverage. These number of patients are based on a 2022 estimate of 7.8 million HBV infections with less than 10% of those being diagnosed and less than 1% of the eligible diagnosed population treated. In order to work towards elimination targets for HCV, Ethiopia would need to expand screening and treatment to 74,000 individuals per year. This is due to the fact that by 2022, there were an estimated 690,000 viremic HCV infections with less than 6% being diagnosed and less than 1% being treated. To meet the HCV targets Ethiopia will require an annual budget of up to 678 million Birrs until 2032, decreasing to less than 113 million Birrs in 2035 for screening, lab tests and treatment.

Conclusion: If Ethiopia moves forward on the path towards hepatitis elimination, an upfront investment will need to be made to support screening, diagnosis and treatment along with HBV vaccination. By 2035, the HBV interventions will be cost-effective saving 79,500 lives whereas, by 2036, HCV interventions will be cost saving, sparing 46,300 lives, and ensuring better health for all Ethiopians.

WED-467-YI

HBV and HCV screening and linkage-to-care in vulnerable people permanently or temporarily living in Tuscany

Monica Monti¹, Teresita Caruso^{1,2}, Alice Castellaccio³, Laura Carraresi⁴, Renato Brunetti⁵, Sara Irene Bonelli³, Donatella Aquilini⁶, Alessandro Nerli⁶, Elisabetta Lorefice⁷, Pierluigi Blanc³, Francesco Cipriani^{5,8}, Anna Linda Zignego¹, Laura Gragnani². ¹University of Florence, MaSVE Center, Department of Experimental and Clinical Medicine, Florence, Italy; ²University of Pisa, Department of Translational Research and New Technologies in Medicine and Surgery, Pisa, Italy; ³San Jacopo Hospital, Infectious Disease Unit, Pistoia, Italy; ⁴University of Florence, Department of Neurosciences, Psychology, Drug Research and Child Health, Florence, Italy; ⁵Epidemiology Unit, Department of Prevention, Central Tuscany Health Authority, Florence, Italy; ⁶“Santo Stefano” Hospital, Infectious Disease Unit, Prato, Italy; ⁷“San Giuseppe” Hospital, Gastroenterology Unit, Empoli, Italy; ⁸Tuscany Regional Centre for Work-Related Injuries and Diseases (CeRIMP), Florence, Italy

Email: laura.gragnani@unipi.it

Background and aims: The health issue of vulnerable groups is of increasing interest for public health and health inequalities. Accessible healthcare and treatment are essential for improving

living conditions and stopping the spread of infectious diseases. WHO's global hepatitis strategy has the goal to eliminate HBV and HCV infection in the next future. Therefore, we aimed at performing HBV and HCV screenings at different charities supporting migrants and marginal people, to reveal residual and hidden infections and link-to-care positive subjects.

Method: The screenings were conducted with an on-site strategy at meal centers and shelters for migrants. After an explanatory interview and the informed consent procedure, positivity to anti-HCV and HBsAg was tested with rapid finger-prick tests. The positive subjects were immediately referred to the closest outpatient clinic.

Results: From January 2021 to November 2023, 1,195 subjects were tested, 950 (79%) males (M), mean age: 36 years. 49/1195 (4.1%) subjects were HBsAg+, 42 M (95%), mean age 28 years; 32/1195 (2.7%) were anti-HCV+, 28, 87.5% M, mean age 50 years. While HBsAg positivity was not associated to particular risk factors, anti-HCV positivity was linked to injection drug use (83%) and unprotected sex (50%). On the total 80 positive subjects (one was coinfect), 20 (25%) were lost, 56 (70%, 41 HBsAg+ and 15 anti-HCV+) were linked to care, 4/80 (5%) previously treated subjects refused the appointment. 11/41 (27%) HBsAg+ patients initiated an antiviral treatment while 21/41 (51%) are monitored and 9/41 (22%) have scheduled appointments. Liver evaluation showed an F0-F1 in 88%, F2 in 6% and F3 in 6%. The HBsAg- subjects were referred to the disease control and prevention centers to receive a vaccine. Among the 15 anti-HCV+ linked to care patients, 8/15 (53%) were previously treated SVR patients as confirmed by a negative viremia while all the remaining 7 (100%) were HCV-RNA+ and underwent ATV (4 SVR, 3 still ongoing). Liver evaluation was available for 3 patients (1 F0-F1, 1 F2 and 1 F4).

Conclusion: Compared to the latest national prevalences, our study showed a percentage 5 times higher for HBsAg (4.1% vs 0.8%) and almost 4 times higher for the anti-HCV (2.7% vs 0.74%). Adherence and linkage to care rates are very successful considering the particular setting and the fact that participation did not imply an economic reward. The most alarming data is the young age of HBsAg+ subjects prevalently coming from areas where the vaccination is not universal. Thus, the geographical origin emerged as the main risk factor. Mean age and risk factors for the anti-HCV+ are similar to those described on the general population. The results stress the need to implement the screening of marginal groups to reveal and treat the residual "pockets" of HBV and HCV infection with a benefit for the individual and for the entire community, also limiting disparities in healthcare.

WED-468

Progress in hepatitis C screening as part of the hepatitis C elimination program in Georgia

Maia Tsereteli¹, Vladimer Getia¹, Ekaterine Adamia¹, Irina Tskhomelidze², Sophia Surguladze², Amiran Gamkrelidze³, Shaun Shadaker⁴, Nancy Glass⁴, Rania Tohme⁴. ¹National Center for Disease Control and Public Health, Tbilisi, Georgia; ²The Task Force for Global Health, Tbilisi, Georgia; ³University of Georgia, School of Health Sciences, Tbilisi, Georgia; ⁴Centers for Disease Control and Prevention, Atlanta, United States
Email: mtsereteli2002@yahoo.com

Background and aims: In 2015, Georgia initiated the National Hepatitis C Elimination Program which aimed to reduce the prevalence of chronic hepatitis C virus (HCV) infection among adults by 90% by providing free-of-charge hepatitis C testing and treatment to all citizens. This program was a response to the high burden of chronic HCV infection in Georgia which was estimated to have 150,000 persons (5.4% prevalence) with HCV infection in 2015 based on a nationally representative serosurvey. Since then, significant progress has been achieved. In 2021, the estimated number of people having HCV infection had dropped to 48,600 (1.8% prevalence). This study aims to assess HCV antibody (anti-HCV) screening coverage among Georgia's adult population.

Method: We used Georgia's national HCV screening registry data, which collects data from the HCV elimination program utilizing patients' national identification numbers (ID), to determine the number of adults screened for HCV infection during April 28, 2015–November 30, 2023. To calculate the screening coverage in the 2023 adult population, we used the 2023 adult population data from the Georgian National Statistics Office. For the calculation of HCV screening coverage by age and sex, we excluded persons screened anonymously at harm reduction sites (n = 162,026) to avoid possible duplications and those who had a documented death date in vital statistics as of November 30, 2023.

Results: During April 28, 2015–November 30, 2023, 2,460,887 Georgian adults have been screened for anti-HCV (87% of the average annual adult population during those years). After excluding persons who died (n = 231,756), we estimated that 2,229,131 (79%) of the 2.84 million Georgian adult population in 2023 were screened for HCV infection. Screening coverage was 76% for men and 81% for women. Among men, screening rates were above 60% in all age groups; those aged ≥70 years had the highest screening coverage at 87%. The lowest screening coverage in males was 68% among those aged 18–29 years. In the adult female population, screening coverage was above 70% in all age groups ranging from a high of 92% among those aged 30–39 years to a low of 74% among those aged 18–29 years.

Conclusion: Nearly 80% of the 2023 adult population in Georgia has been screened for hepatitis C. However, younger age groups have the lowest screening rates. Innovative approaches to encourage screening in younger age groups such as conducting screening at universities and primary healthcare centers could help identify persons with HCV infection and ultimately achieve HCV elimination goals in Georgia.

WED-469

Investigating household hepatitis B transmission using whole-genome sequencing and serological analysis in Kinshasa Province, Democratic Republic of Congo

Camille Morgan¹, Patrick Ngimbi², Sarah Ntambua², Jolie Matondo², Jeansy Mavinga², Bienvenu Tukebana², Martine Tabala³, Nana Mbonze³, Melchior Kashamuka³, Linda James⁴, Mark Anderson⁵, Gavin Cloherty⁶, Chris Hennelly¹, Josh Quick⁷, Nick Loman⁸, Christopher Kent⁷, Samuel Wilkinson⁷, Elizabeth Waddilove⁹, Marion Delphin⁹, George Airey¹⁰, Sheila Lumley¹⁰, Philippa C Matthews¹¹, Marcel Yotebieng¹², Samuel Mampunza², Jonathan B. Parr¹, Peyton Thompson¹.
¹University of North Carolina at Chapel Hill, Chapel Hill, United States; ²Université Protestante au Congo, Kinshasa, Congo, Dem. Republic of (formally known as Zaire); ³École de Santé Publique, Université de Kinshasa, Kinshasa, Congo, Dem. Republic of (formally known as Zaire); ⁴University of North Carolina at Chapel Hill, Université Protestante au Congo, Kinshasa, Congo, Dem. Republic of (formally known as Zaire); ⁵Abbott Laboratories, Abbott Diagnostics, North Chicago, United States; ⁶Abbott Laboratories, Abbott Diagnostics, Woodstock, United States; ⁷University of Birmingham, Birmingham, United Kingdom; ⁸University of Birmingham, Birmingham, United Kingdom; ⁹The Francis Crick Institute, London, United Kingdom; ¹⁰University of Oxford, Oxford, United Kingdom; ¹¹The Francis Crick Institute, University College London, London, United Kingdom; ¹²Albert Einstein College of Medicine, Bronx, United States
Email: camille_morgan@med.unc.edu

Background and aims: The Democratic Republic of Congo (DRC) has a hepatitis B virus (HBV) prevalence of 3–5% but minimal HBV prevention or advanced hepatology care. Limited HBV research in Africa suggests more frequent horizontal transmission than other regions, but regional epidemiology and clinical features remain poorly understood. We sought to characterize HBV transmission within households using whole-genome sequencing (WGS) and serological assays to inform much-needed prevention strategies in DRC.

POSTER PRESENTATIONS

Method: Building on the largest household study of HBV in DRC, we conducted a sub-study of households with known HBV infections. We performed point-of-care (POC) HBV surface antigen (HBsAg) testing (Abbott DETERMINE II), collected medical histories, and collected venous blood samples for HBV sequencing and serological analyses. Serological analysis was performed using the Abbott ARCHITECT, and included infection markers HBsAg Next (LOD; 0.005 IU/ml) and HBV viral load (VL) with Abbott RealTime HBV DNA (LLOQ; 20 IU/ml). WGS was performed on an Oxford Nanopore MinION using venous samples and dried blood spots (DBS).

Results: Among 25 households comprising 139 participants (80 female, 59 male) with samples collected in Kinshasa, median age was 15 years (IQR: 7, 29); thirty-five (25%) were born outside Kinshasa Province. Median household size was 6 (IQR: 4, 7). Concordance across HBV infection markers (POC, VL, Next) was limited: 35 (25%) participants were POC-positive, 25 (71%) of whom were Next-positive and 23 (66%) of whom had detectable HBV VL. Five of 104 (4%) POC-negative participants had detectable VL and 10 POC HBsAg-negative (10%) were Next-positive. Eight of 28 viremic participants (29%) had VLs $\geq 20,000$ IU/ml and eight (29%) were HBeAg-positive, seven of which had both. Five participants reported HIV coinfection and on tenofovir-based therapy, with undetectable HBV DNA. Of 69 children born since the three-dose infant HBV vaccination was introduced in 2007, 30 (43%) had isolated anti-HBs reactivity; eight (12%) were HBV-positive on at least one infection marker and 7 (10%) had detectable anti-HBc. Initial analysis of sequencing data from 33 samples (25 serum; 8 DBS) yielded 25 (76%) full or majority length genomes and confirmed infection by HBV genotypes A, D, and E in this cohort. Within five households with >1 infection fully sequenced, four had highly similar HBV sequences among individuals; however, one household cluster had infections with two distinct genotypes, strongly suggestive of multiple HBV introductions in the household.

Conclusion: Our findings highlight unique HBV transmission and clearance patterns within households in Kinshasa, and provide the first evidence of HBV genotype D circulating in the DRC. These and ongoing analyses will improve our understanding of HBV epidemiology in populations in the WHO Africa region and can be used to inform elimination efforts.

WED-470

Screening emergency admissions at risk of chronic hepatitis 3 extension (SEARCH 3X)-universal is better than risk-based screening for viral hepatitis

Basheer Alshiwanna^{1,2,3}, Miriam Levy^{2,3,4}, Julia Di Girolamo^{2,3}, Melissa Bagatella¹, Irena Petrovski⁵, Robert Porritt¹, David Thomas¹, Shahida Bakridi¹, Hung Tran⁶, Sophie Gryllis¹, Maria Tigla⁷, Rebecca Haack⁵, Kristian Peralta⁵, Julie Doan¹, Jeremy Lawrence⁸, Richard Cracknell⁵, Michael Maley¹, Hong Foo¹, Nathan Jones⁵, Gregory Dore^{3,9}, David Prince^{1,3}. ¹Liverpool Hospital, Sydney, Australia; ²Ingham Institute for Applied Medical Research, Sydney, Australia; ³The University of New South Wales, Sydney, Australia; ⁴Liverpool Hospital, Liverpool, Sydney, Australia; ⁵Campbelltown Hospital, Sydney, Australia; ⁶NSW Health Pathology, IT Services, Sydney, Australia; ⁷Fairfield Hospital, Sydney, Australia; ⁸Fairfield Hospital, Sydney, Australia; ⁹The Kirby Institute, Sydney, Australia
Email: b.shiwanna@gmail.com

Background and aims: Viral hepatitis remains an important public health concern globally. Despite effective therapies for cure of hepatitis C (HCV) and suppression of hepatitis B (HBV), a significant proportion of Australians remain undiagnosed or not linked with care. We evaluate the use of universal, automated hepatitis screening in the emergency department (ED) and assess diagnosis rates and linkage to care (LTC) success.

Method: A novel pilot clinical service utilizing automated universal hepatitis screening in the ED, "SEARCH 3X" (Screening of Emergency Admissions at Risk of Chronic Hepatitis Third Extension) was implemented across two metropolitan hospitals in Sydney,

Australia. A computer algorithm solution automatically added Hepatitis B surface antigen (HBsAg) and Hepatitis C antibody (HCV Ab) tests when an adult underwent routine biochemistry testing in ED. Data was collected on patient demographics, overall prevalence of viral hepatitis and effectiveness of LTC (defined as successful contact by the SEARCH team).

Results: 10, 204 unique patients were tested using the SEARCH 3X algorithm. Positive serology for HBsAg and/or HCV Ab was detected in 92 (0.9%) and 170 (1.7%) patients respectively, equating to 259 (2.5%) unique patients overall (3 with HBV-HCV co-infection). The median age of the population tested was 58 years old (IQR 45–66), with a relatively even gender distribution (M:F; 44%:56%). The prevalence of positive HBsAg and/or HCV Ab in Indigenous Australians was 8.0% (3 HBV and 28 HCV from 375 tested), in non-indigenous Australians 1.9% (6 HBV and 79 HCV from 4384 tested), and in Overseas-born (OB) patients 2.7% (83 HBV and 63 HCV from 5445 tested). Of the 259 total positive patients, 251 were eligible for follow-up (too unwell n = 5, deceased n = 3) and 224 (86%) were successfully LTC. HCV diagnosis was new in 16/170 (9%) patients. HCV Ab positive patients were more often male (62% vs 44%; $p < 0.001$) and Indigenous (16.5% vs 3.5%; $p < 0.001$) compared with HCV Ab negative patients. HCV RNA was available in 134/170 HCV patients. RNA test was positive in 16 patients (12%) and negative in 118 (88%). Of RNA negative patients, 77/118 (65%) had previous HCV treatment, 28/118 (24%) had no previous treatment but had a risk factor for blood-borne virus; 13/118 (11%) treatment status and/or risk factor unknown. HBV diagnosis was new in 23/92 (25%) patients. Of those with known diagnosis, only 24/69 (39%) were receiving guideline-based care. HBsAg positive patients were more often OB (90% vs 53%; $p < 0.001$) and non-English speaking (39% vs 15%; $p < 0.001$) compared to HBsAg negative patients.

Conclusion: Opportunistic universal testing in ED represents an effective strategy for identifying cases of viral hepatitis and linking them to care. A substantial proportion of patients with viral hepatitis were previously undiagnosed. To achieve elimination, novel enhanced testing strategies will be required.

WED-471

Retrospective analysis of longitudinal data for UK adults living with chronic HBV: characteristics of the population on dual therapy

Cedric Tan^{1,2}, Tingyan Wang^{3,4}, Jakub Jaworski⁵, Ben Glampson⁶, Dimitri Papadimitriou^{6,7}, Luca Mercuri⁸, Christopher R Jones^{7,9}, Stacy Todd¹⁰, Karl McIntyre¹¹, Andrew Frankland¹¹, Hizni Salih^{4,12}, Gail Roadknight^{4,12}, Stephanie Little^{4,12}, Theresa Noble^{4,12}, Kinga A Várnai^{4,12}, Cori Campbell^{4,13}, Cai Davis¹⁴, Ashley I Heinson¹⁴, Michael George¹⁴, Florina Borca¹⁴, Louise English¹⁵, Luis Romão¹⁵, David Ramlakhan¹⁵, William Frisby¹⁶, John Taylor¹⁶, Kerrie Woods⁴, Jim Davies⁴, Eleni Nastouli¹⁷, Salim I Khakoo¹⁸, Alexander J Stockdale¹⁰, Nicholas Easom¹⁶, Graham S Cooke⁶, William Gelson¹⁹, Eleanor Barnes^{3,4}, Philippa C Matthews^{12,13,20,21,22}. ¹UCL Genetics Institute, University College London, London, United Kingdom; ²The Francis Crick Institute, London, United Kingdom; ³Nuffield Department of Medicine, Oxford, United Kingdom; ⁴NIHR Oxford Biomedical Research Centre, Oxford, United Kingdom; ⁵Cambridge University Hospitals NHS Foundation Trust, Cambridge, United Kingdom; ⁶NIHR Health Informatics Collaborative, Imperial College Healthcare NHS Trust, London, United Kingdom; ⁷NIHR Imperial Biomedical Research Centre, London, United Kingdom; ⁸NIHR Health Informatics Collaborative, Imperial College Healthcare NHS Trust, NIHR Imperial Biomedical Research Centre, London, United Kingdom; ⁹Department of Infectious Disease, Imperial College London, London, United Kingdom; ¹⁰Tropical Infectious Diseases Unit, Royal Liverpool Hospital, Liverpool University Hospitals NHS Trust, Liverpool, United Kingdom; ¹¹Liverpool Clinical Laboratories, Liverpool University Hospitals NHS Trust, Liverpool, United Kingdom; ¹²NIHR Health

Informatics Collaborative, Oxford University Hospitals NHS Foundation Trust, Oxford, United Kingdom; ¹³Nuffield Department of Medicine, University of Oxford, Oxford, United Kingdom; ¹⁴Southampton Emerging Therapies and Technologies Centre, University Hospital Southampton NHS Foundation Trust, Southampton, United Kingdom; ¹⁵NIHR University College London Hospitals Biomedical Research Centre, London, United Kingdom; ¹⁶Hull University Teaching Hospitals NHS Trust, Hull, United Kingdom; ¹⁷Department of Infection, Immunity and Inflammation, UCL Great Ormond Street Institute of Child Health, London, United Kingdom; ¹⁸School of Clinical and Experimental Sciences, Faculty of Medicine, University of Southampton, Southampton, United Kingdom; ¹⁹Cambridge Liver Unit, Cambridge University Hospitals NHS Foundation Trust, Cambridge, United Kingdom; ²⁰The Francis Crick Institute, London, United Kingdom; ²¹Division of Infection and Immunity, University College London, London, United Kingdom; ²²Department of Infectious Diseases, University College London Hospital, London, United Kingdom
Email: cedric.tan@crick.ac.uk

Background and aims: The treatment landscape for hepatitis B virus (HBV) is changing as clinical guidelines for use of nucleos(tide) analogue (NA) agents move towards simplified assessment and broader treatment eligibility. Dual treatment may be prescribed for people living with HBV who are HIV coinfecting, who are accessing Pre-Exposure Prophylaxis (PrEP) to protect against HIV acquisition, and in individuals in whom HBV viraemia is not suppressed on monotherapy. In many global settings, dual therapy is also more widely available and affordable than monotherapy. It is therefore important to explore outcomes of dual therapy, and to consider its impact on outcomes, cost and accessibility.

Method: We analysed routinely-collected longitudinal clinical records from >14000 adults with chronic HBV infection across six secondary care centres in the UK, as part of the National Institute for Health and Care Research (NIHR) Health Informatics Collaborative (HIC) programme to characterise those receiving dual therapy.

Results: In this cohort, 2, 688/14, 587 (18%) individuals had a record of NA treatment, among whom 230/2, 688 (9%) were on dual therapy for at least a year. The most common dual regimens were Entecavir-Tenofovir (93/230) and Lamivudine-Tenofovir (82/230). Males accounted for the majority of individuals on both dual therapy, (158/230, 69%), and monotherapy group (1, 546/2, 458, 63%) ($p = 0.086$). There were no significant differences in median HBV viral load during mono- or dual therapy, after excluding the first six months of therapy ($p = 0.74$). There were also no significant differences between the proportion of patients with abnormal ALT levels (>40 IU/ml), or APRI scores, for patients undergoing mono versus dual therapy both at baseline, and at the last recorded timepoint during therapy (ALT: $p = 1$, $p = 0.65$; APRI: $p = 0.4$, $p = 0.25$). However, patients on dual therapy had significantly higher FIB-4 scores than those on monotherapy, both at baseline ($p = 0.0043$) and at the last timepoint ($p = 0.0082$).

Conclusion: Our finding that 9% of adults receiving HBV therapy in the UK are on dual agents highlights a need for more data collection to characterise this group. In particular, more data are needed to focus on those with HIV coinfection who may be under the care of sexual health services rather than hepatology clinics. Most outcome markers for dual and monotherapy are comparable, however Fib-4 scores may point to a disadvantage in the dual therapy group, with advanced disease potentially being the indication for adding a second agent.

WED-472

Female, mild steatosis, low baseline hepatitis B surface level and over 11.35 months of treatment facilitate clinical cure with interferon therapy in chronic hepatitis B patients

Lili Liu¹, Daqiong Zhou¹, Jiangyu Liu¹, Xinyue Chen², Zhenhuan Cao¹.
¹The Third Unit, Department of Hepatology, Beijing Youan Hospital, Capital Medical University, Beijing, China, Beijing, China; ²The First Unit,

Department of Hepatology, Beijing Youan Hospital, Capital Medical University, Beijing, China, Beijing, China
Email: caozhenhuanyu@mail.ccmu.edu.cn

Background and aims: Hepatitis B surface antigen (HBsAg) clearance is a desired functional cure for hepatitis B, which is harder to achieve clinically. Identifying effective predictive markers, especially the impact of hepatic steatosis on achieving a functional cure with interferon therapy, is crucial.

Method: A retrospective cohort from Beijing You'an Hospital spanning 2008–2023, involved chronic hepatitis B (CHB) patients who had received at least 6 months of interferon therapy and underwent Fibroscan examination within one year prior to treatment. Univariate and multivariate logistic regression analysis methods were used to investigate the factors influencing HBsAg clearance.

Results: A total of 1397 CHB patients (median age 36.0 years, 65.4% male) were enrolled and 152 patients (10.88%) achieved HBsAg clearance, with 1-and 2-year cumulative HBsAg clearance rates of 13.36% and 32.34%, respectively. Multivariate logistic regression analysis demonstrated that male (odds ratio [OR] 0.566; 95%CI 0.364–0.880; $p = 0.011$) was adverse to HBsAg clearance. HBsAg<1000 IU/ml (OR 8.731; 95%CI 4.024–18.946; $p < 0.001$), HBsAg<100 IU/ml (OR 43.005; 95%CI 19.295–95.855; $p < 0.001$), mild steatosis (OR 1.830; 95%CI 1.038–3.229; $p = 0.037$) and prolonged interferon therapy (OR 1.147; 95%CI 1.101–1.195; $p < 0.01$) facilitated HBsAg clearance. Cumulative HBsAg clearance was significantly higher in patients with combined mild steatosis than those without combined steatosis ($p = 0.0069$).

Conclusion: Controlled attenuation parameter (CAP) values have a good predictive value in patients on initial interferon therapy and combined mild steatosis facilitates achieving clinical cure. Furthermore female, baseline HBsAg <1000 IU/ml, and longer interferon therapy were strong predictors of HBsAg clearance.

WED-473

Assessing the burden and knowledge, attitudes, and practices of hepatitis B and hepatitis C among dentists in the country of Georgia

Lika Karichashvili¹, Maia Tsereteli¹, Maia Alkhazashvili¹, Nazibrola Chitadze¹, Sophia Surguladze², Irina Tskhomelidze², Shaun Shadaker³, Tsira Merabishvili⁴, Anna Khoperia⁴, Francisco Averbhoff⁵, Gavin Cloherty⁵, Ketevan Gogilashvili⁶, Zurab Alkhanishvili⁷, Rania Tohme⁸.
¹National Centre for Disease Control and Public Health, Tbilisi, Georgia, Tbilisi, Georgia; ²Task Force for Global Health, Tbilisi, Georgia, Tbilisi, Georgia; ³Division of Viral Hepatitis, Centres for Disease Control and Prevention, Atlanta, USA, Atlanta, United States; ⁴National Centre for Disease Control and Public Health, Tbilisi, Georgia, Tbilisi, Georgia; ⁵Abbott Diagnostics, Abbott Park, Illinois, USA, Illinois, United States; ⁶Tbilisi State Medical University, Tbilisi, Georgia, Tbilisi, Georgia; ⁷Ivane Javakishvili Tbilisi State University, Tbilisi, Georgia; ⁸Division of Viral Hepatitis, Centres for Disease Control and Prevention, Atlanta, USA, Atlanta, United States
Email: lika.karichashvili@gmail.com

Background and aims: In 2021, a nationally representative serosurvey revealed a hepatitis C virus (HCV) infection prevalence of 1.8% and a hepatitis B virus (HBV) infection prevalence of 2.7% among adults in Georgia. Healthcare-related HCV and HBV transmission is still a major problem in developing countries, including Georgia. However, limited data are available on the prevalence and awareness of hepatitis B and hepatitis C among dentists and dental health professionals (collectively, dental healthcare workers [DHCW]). We assessed the prevalence, knowledge, attitudes, and practices (KAP) of HBV and HCV infection among DHCWs in Georgia.

Method: We conducted a facility-based survey using a multi-stage cluster design. Using probability-proportional-to-size sampling, we selected 214 dental facilities from the largest cities, Tbilisi, Kutaisi, Batumi, Zugdidi, and Telavi, followed by random selection of

POSTER PRESENTATIONS

participants in each facility using the Kish Grid. KAP data were obtained through a self-reported questionnaire, and blood samples were collected and tested for HCV antibody (anti-HCV), HCV RNA, Total hepatitis B core antibody (Total anti-HBc), and HBV surface antigen (HBsAg). Analyses were conducted using STATA 17.

Results: Among 519 participants (100% response rate), 81% were in Tbilisi, 76% were dentists, 84% were female, and the median age was 40 years [IQR 33–47 years]. While 44% of DHCW reported a past needlestick injury, only 10% and 8% of participants knew the correct probability of HBV and HCV infection after a single contaminated needlestick, respectively. Most (78%) were aware that hepatitis B is vaccine preventable but 83% thought it is curable. More than half (57%) thought that HCV is vaccine preventable and 80% knew that HCV can be cured. More than 90% believed healthcare workers are at high risk for HBV and HCV exposure. Most (70%) knew the optimal method for pre-sterilizing and aseptically storing instruments. Of 519 participants, 83% and 91% reported previously being screened for HBV and HCV, respectively, and 30% reported being vaccinated against hepatitis B. Among 517 participants who provided blood samples, 12.2% were Total anti-HBc reactive, 0.6% were HBsAg positive, 0.8% were anti-HCV reactive, and none were positive for HCV RNA.

Conclusion: The study revealed limited awareness among DHCWs in Georgia regarding HBV and HCV transmission after a contaminated needlestick injury. Although DHCW demonstrated awareness of hepatitis B vaccination and recognized their occupational risk, less than a third had been vaccinated. However, the prevalence of hepatitis B and hepatitis C was low. Continuous education and training on infection control practices and on viral hepatitis are crucial to enhance DHCW awareness and prevent occupational exposures.

WED-474

Population-based hepatitis C screening in Lithuania: 18-month results of the program and scenarios for achieving WHO elimination targets

Limas Kupcinskas¹, Egle Ciupkeviciene², Alexis Voeller³, Viaceslavas Zaksas⁴, Ligita Jancoriene⁵, Edita Kazenaite⁶, Viktorija Basyte-Basevice¹, Devin Razavi-Shearer³, John Ward⁷, Gediminas Urbonas⁸, Janina Petkeviciene⁹. ¹Department of Gastroenterology, Lithuanian University of Health Sciences, Kaunas, Lithuania; ²Department of Preventive Medicine, Lithuanian University of Health Sciences, Kaunas, Lithuania; ³Center for Disease Analysis Foundation, Lafayette, Colorado, United States; ⁴National Health Insurance Fund under the Ministry of Health, Vilnius, Lithuania; ⁵Clinic of Infectious Diseases and Dermatovenerology, Vilnius University, Kaunas, Lithuania; ⁶Clinic of Gastroenterology, Nephrourology and Surgery, Vilnius University, Vilnius, Lithuania; ⁷Coalition for Global Hepatitis Elimination, Decatur, United States; ⁸Department of Family Medicine, Lithuanian University of Health Sciences, Kaunas, Lithuania; ⁹Health Research Institute, Lithuanian University of Health Sciences, Kaunas, Lithuania
Email: l.kupcinskas@gmail.com

Background and aims: Lithuanian HCV screening program started on May, 2022. State health authorities pay general practitioners (GPs) a special promoting fee for performing serological tests for HCV antibodies: 1. For the population born in 1945–1994 (once per life) and 2. For people who inject drugs (PWID) or are HIV-infected (annual HCV testing). Such an initiative is the first in Central and Eastern Europe. This study aimed to evaluate the results of the first 18-month of the program and different scenarios to achieve WHO 2030 targets.

Method: GPs invited people to perform a serum blood test for HCV antibodies. Anti-HCV positive patients were referred to a gastroenterologist or infectologist for HCV RNA testing, and if result was positive, direct-acting antiviral (DAA) therapy was prescribed. Information about patients was obtained from the database of the National Health Insurance Fund. The Markov disease progression

model elaborated by the CDA Foundation was used to assess HCV elimination progress. The data from the 2022–2023 screening were used as inputs. Three scenarios were developed: the 'Base' scenario—return to pre-screening program level in 2023 and 2 scenarios with different extents of treatment.

Results: At the beginning of 2022, about 1.8 million people born in 1945–1994 lived in Lithuania. Between May 5, 2022 and October 31, 2023 from this population 1026268 people (57, 7%) were tested for HCV antibodies. Positive test results were found in 1.23% of cases. In the risk group, 8751 PWID and HIV+ people were screened, of whom 30, 3% were seropositive. All seropositive patients were referred to specialists. Viremia was detected in 58%. During 18-month period 4068 patients were treated with DAA. Treatment delay for 54% of HCV patients was related to organizational problems (consultation waiting line, some treatment restrictions, delay in drugs supply). Solving organizational challenges, by the end of 2024 we expect to perform HCV antibody testing in 80% of the target population and treatment of 80% of RNA-positive individuals, further aiming to cure all infected patients by 2030. The Markov disease progression model to assess HCV elimination progress showed the following scenarios: Scenario 1: if the same number of patients are treated as before the screening, the WHO targets will not be reached. Scenario 2: treating 70% of infected patients will meet most but not all WHO targets. Scenario 3: by treating all infected patients by 2030, the WHO target will be met by saving 150 lives and preventing 90 new cases of decompensated cirrhosis and 120 cases of hepatocellular carcinoma.

Conclusion: Our data show that in European country with moderate HCV seroprevalence, a population-based screening program can be feasible, screening near 60% (more than 1 million) of the population born between 1945 and 1994 during the first 18 months of the program. We hope that WHO 2030 goals can be achievable in Lithuania.

WED-475

Optimal strategies for eliminating mother-to-child transmission of hepatitis B in Burkina Faso

Andréa Gosset¹, Shevanthi Nayagam^{2,3}, Sylvie Boyer¹, Alice N. Guingané⁴, Nora Schmit², Abdoul Salam Eric Tiendrebeogo⁵, Dramane Kania⁶, Patrizia Carrieri¹, Yusuke Shimakawa⁷, Timothy B. Hallett². ¹Aix Marseille University, INSERM, IRD, SESSTIM, Sciences Economiques and Sociales de la Santé and Traitement de l'Information Médicale, ISSPAM, 13005 Marseille, France, Marseille, France; ²MRC Centre for Global Infectious Disease Analysis, School of Public Health, Imperial College London, London, United Kingdom, London, United Kingdom; ³Department of Surgery and Cancer, Imperial College London, London, United Kingdom, London, United Kingdom; ⁴Hepatogastroenterology Department, Bogodogo University Hospital Center, Ouagadougou, Burkina Faso, Ouagadougou, Burkina Faso; ⁵Laboratoire Mixte International de Vaccinologie (LAMIVAC), Bobo-Dioulasso, Burkina Faso, Bobo-Dioulasso, Burkina Faso; ⁶Centre Muraz, Institut national de santé publique, Bobo-Dioulasso, Burkina Faso, Bobo-Dioulasso, Burkina Faso; ⁷Unité d'Epidémiologie des Maladies Emergentes, Institut Pasteur, 75015 Paris, France, Paris, France
Email: andrea.gosset@inserm.fr

Background and aims: High prevalence of hepatitis B (HBV) in West Africa (6%–17%) requires new strategies to prevent mother-to-child transmission (MTCT). Despite current recommendations for tenofovir prophylaxis in pregnant women with HBV DNA $\geq 200,000$ IU/ml or HBe antigen (HBeAg) positivity, coverage remains low, mainly due to the lack of HBV screening in antenatal care and the high cost of HBV DNA test. We evaluated the impact on the HBV epidemic and MTCT elimination as well as the cost-effectiveness of four alternative strategies to select pregnant women for tenofovir prophylaxis in antenatal care at primary healthcare centres (PHCs) in Burkina Faso: 1) HBV DNA $\geq 200,000$ IU/ml, 2) HBeAg-positive, 3) HB core antigen (HBcAg)-positive using rapid diagnostic test, and 4) all HBsAg-positive women (Treat All).

Method: We used a deterministic compartmental dynamic model stratified by age, sex, and transmission mode. We assessed costs from the perspective of the Burkina Faso government health system. We used a micro-costing approach to determine the costs of implementing each strategy during routine antenatal visits at PHCs. We included costs of HBV vaccination (HepB3), birth dose (HepB-BD), and care costs for patients with advanced liver disease. An epidemiological model simulated the strategies from 2024 to 2124, while a cost-effectiveness analysis considered a one-year strategy implementation (in 2024) with a lifetime health and cost impact assessment. The baseline strategy was the current situation in Burkina Faso where HepB-BD is administered alongside HepB3. We assumed 90% HBsAg screening coverage among pregnant women, 90% second test coverage among HBsAg-positive women, and 90% TDF prophylaxis coverage among eligible women. We considered a cost-effectiveness threshold of 0.5 times Burkina Faso's per capita GDP in 2022 (US \$416.5). We discounted health outcomes and costs using a 3% discount rate. We conducted deterministic and probabilistic sensitivity analyses.

Results: In the cost-effectiveness model, the Treat All strategy dominated the other strategies and the status quo scenario, with an incremental cost-effectiveness ratio of US\$14.1 per DALY averted corresponding to an 81.2% probability of being cost-effective. This finding was most sensitive to transition rates to decompensated cirrhosis and HepB-BD efficacy in mothers with high viral load. Implementing the Treat All strategy from 2024 to 2124 could eliminate HBV MTCT by 2034, and reduce chronic HBV cases, deaths, and DALYs attributable to MTCT by 12.1% [4.9%; 13.9%], 10.0% [4.1%; 13.2%], and 11.4% [5.6%; 16.0%], respectively.

Conclusion: The Treat All strategy emerged as the dominant and cost-effective strategy for implementation in antenatal care, with the potential to eliminate HBV MTCT by 2034. However, further research is needed to assess the acceptability and feasibility of this strategy in real-world settings.

WED-476

Sofosbuvir/Velpatasvir (S/V) for the treatment of HCV infection among vulnerable inner-city residents: extending the results of the SIMPLIFY study

Brian Conway^{1,2}, Rossitta Yung¹, Shawn Sharma¹, Shana Yi¹, Saina Beitari¹. ¹Vancouver Infectious Diseases Centre, Vancouver, Canada; ²Simon Fraser University, Burnaby, Canada
Email: brian.conway@vidc.ca

Background and aims: The combination of Sofosbuvir/Velpatasvir (S/V) is approved for the treatment of chronic HCV infection. In the SIMPLIFY study of active drug users, 97/103 HCV-infected individuals were cured with a 12-week course of S/V administered as one pill once a day, with no virologic failures. We aimed to extend the results of the SIMPLIFY study, evaluating the safety and efficacy of S/V in a prospective study of HCV-infected inner-city residents enriched for risk behaviors for non-adherence to therapy, including problematic drug use and unstable housing.

Method: Through dedicated outreach events, we identified HCV-infected patients who were not currently engaged in health care and who were eligible to receive government-funded antiviral therapy for HCV infection. We enrolled in a multidisciplinary program of care to address medical, psychological, social, and addiction-related needs, and provided S/V therapy in this context, with enhanced supervision of adherence. The primary end point of this analysis was the achievement of cure, defined as an undetectable HCV RNA 12 or more weeks after the completion of therapy.

Results: In this ongoing study, we have identified 256 eligible subjects, median age 46 (20–81) years, 28.9% female, mostly genotypes 3A/or 1A (46.2%, 43.8%) and 22.7% with advanced fibrosis (F3/F4), 70.3% with unstable housing and 97.6% active drug users, usually fentanyl and/or amphetamines (98%, 74.3%). Of the 256, HCV treatment has been started in 231 cases (within a median 6 weeks of

engagement in care), with 22 awaiting treatment and 3 opioid overdose deaths before its initiation. Of 231, 6 discontinued prematurely (all within the first week of treatment), 3 died on treatment (opioid overdoses), 213 have completed treatment and 9 remain on treatment. Of the 213, 24 are in follow-up and await evaluation of outcome, with 184/189 (97.4%) cured with 5 virologic relapses.

Conclusion: Taken together, our data support the efficacy of S/V in populations even more challenging than those enrolled in the SIMPLIFY study with HCV therapy administered within comprehensive multidisciplinary programs such as ours. This information will be essential to the development of strategies to eliminate HCV therapy in all priority populations, including the demographic evaluated in this study.

WED-477-YI

Semi-quantitative interviews with chronic hepatitis B patients to determine their knowledge of hepatitis B, personal experiences and views on decentralisation of care in London, United Kingdom

Alexander Cole^{1,2}, Thi Thuan Nguyen³, Yusuke Shimakawa⁴, Ameet Dhar^{1,2}, Belinda Smith^{1,2}, Shevanthi Nayagam¹, Ashley Brown^{1,2}, Koen Peters³, Maud Lemoine^{1,2}. ¹Imperial College London, London, United Kingdom; ²Imperial College Healthcare NHS Trust, London, United Kingdom; ³University of Antwerp, Antwerp, Belgium; ⁴Institut Pasteur, Paris, France
Email: alexander.cole@nhs.net

Background and aims: The World Health Organisation (WHO) hepatitis B elimination plan aims for increased detection and treatment of chronic hepatitis B (CHB) by 2030. Decentralisation of patient care is an important consideration for CHB management. We conducted interviews with CHB patients to determine their knowledge of hepatitis B infection, personal experiences of living with CHB, experiences of consultant-hepatologist led outpatient clinics and potential acceptability of decentralised outpatient care pathways.

Method: Semi-quantitative interviews conducted with 29 CHB patients attending outpatient hepatology clinics between 1st June 2022 and 1st July 2023 at St Mary's Hospital, London. A random sampling method was used to select participants. Individual interviews were conducted face-to-face or via telephone covering the domains of patient knowledge, quality of life (QOL), outpatient clinics at St Mary's Hospital and views of decentralised care pathways.

Results: Patients were able to correctly identify modes of hepatitis B transmission: mother-to-child (79%), sexual intercourse (86%), intravenous drug use (79%), blood transfusions (86%) and tattoos or body piercings (72%). CHB negatively impacted QOL across multiple domains including mental health (62%), employment (41%) and personal relationships (41%). 31% of participants felt stigmatised for having CHB including experiences with friends and employers. At St Mary's Hospital, 93% of participants were satisfied with the level of care provided in outpatient hepatology clinics. For decentralised care, 76% of participants would agree to be seen by a nurse specialist, 69% by a pharmacist and 79% by their local general practitioner (GP) for CHB management. 72% of participants had an overall preference to see a hospital doctor for regular CHB management.

Conclusion: Patients had good knowledge of hepatitis B transmission. CHB negatively impacted patients' QOL across multiple domains and many patients experienced stigma. Patients were satisfied overall with outpatient hepatology clinics at St Mary's Hospital. Most participants would accept clinical reviews by nurse specialists, pharmacists and general practitioners in a decentralised care model. Patients had a preference to receive care from hospital doctors for ongoing CHB management.

POSTER PRESENTATIONS

WED-478

Telehealth accessibility and acceptability among people who use drugs

Zoi Papalamprakopoulou^{1,2}, Sotirios Roussos³, Elisavet Ntagianta⁴, Vasiliki Triantafyllou⁴, George Kalamitsis⁴, Arpan Dharia¹, Vana Sypsa³, Angelos Hatzakis^{2,3}, Andrew Talal¹. ¹Division of Gastroenterology, Hepatology, and Nutrition, Jacobs School of Medicine and Biomedical Sciences, University at Buffalo, Buffalo, NY, United States; ²Hellenic Scientific Society for the Study of AIDS, Sexually Transmitted and Emerging Diseases, Athens, Greece; ³Department of Hygiene, Epidemiology and Medical Statistics, National and Kapodistrian University of Athens, Athens, Greece; ⁴Hellenic Liver Patient Association "Prometheus", Athens, Greece
Email: zoipapal@buffalo.edu

Background and aims: Hepatitis C virus (HCV) elimination programs should prioritize the inclusion of people who use drugs (PWUD), a medically underserved population that often faces stigma and geographical barriers when accessing healthcare. Recent data indicate that telehealth is highly effective in expanding access to HCV care among PWUD. We aimed to investigate telehealth accessibility and acceptability among PWUD in Athens, Greece.

Method: We recruited 162 PWUD through respondent-driven sampling to undergo an interviewer-administered, 109-item, structured questionnaire. Eligibility criteria required age at least 18 years, a history of injection drug use, Greek verbal fluency, and the ability to provide informed consent. Main study outcomes included internet access, computer access, use of social media, and willingness to receive healthcare through telemedicine in an opioid agonist treatment (OAT) program. We employed logistic regression to assess the impact of sociodemographic characteristics and injection drug use (IDU) on these outcomes.

Results: Participants' mean (SD) age was 45.9 (8.8) years, 84.0% (136/162) were male, 90.1% (146/162) were of Greek origin, 77.8% (126/162) reported IDU in the past 12 months, 85.2% (138/162) were not currently linked to an OAT program, and 50.0% (81/162) were experiencing homelessness. Among participants, 66.0% (107/162) and 31.5% (51/162), respectively, reported current internet and computer access. Compared to those with secure housing, participants experiencing homelessness reported decreased internet (50.6% vs 81.5%, $p < 0.001$) and computer access (11.1% vs 51.9%, $p < 0.001$). Multivariable analyses revealed that increasing age (per 1-year increase: odds ratio [OR] = 0.94, 95% confidence interval [CI], [0.89, 0.99], $p = 0.032$), IDU within the past 12 months (0.29 [0.10, 0.88], $p = 0.028$), and homelessness (0.29 [0.13, 0.65], $p = 0.003$) were associated with a lower odds of internet access. Homelessness (0.17 [0.07, 0.41], $p < 0.001$) and unemployment (0.25 [0.07, 0.98], $p = 0.046$) were associated with a lower odds of computer access. Despite limited (1.9%, 3/162) participant experience with telemedicine, 84.0% (136/162) expressed willingness to receive healthcare through telemedicine in an OAT program.

Conclusion: Homelessness is associated with restricted internet and computer access among PWUD in Athens, Greece and poses challenges to expanding healthcare access through telehealth. Among PWUD with secure housing, access to infrastructure is permissive for telehealth interventions. These data should inform telehealth policy and practice for HCV care among PWUD.

WED-479

Improved social outcomes after integrated hepatitis C and opioid use disorder treatment

Andrew Talal¹, Raktim Mukhopadhyay², Valentina Veronesi³, Arpan Dharia¹, Giovanni Saraceno³, Marianthi Markatou³. ¹University at Buffalo, Jacobs School of Medicine and Biomedical Sciences, Buffalo, United States; ²University at Buffalo, CDSE, Buffalo, United States; ³University at Buffalo, Department of Biostatistics, Buffalo, United States
Email: ahtalal@buffalo.edu

Background and aims: Integrated treatment for hepatitis C virus (HCV) and opioid use disorder (OUD) is widely advocated, although few studies have simultaneously evaluated the outcomes for each entity. Using data obtained from participants in opioid treatment programs (OTPs) that dispense methadone, we explored the associations between OUD and HCV treatment uptake and substance use and social factors.

Method: We utilized administrative data including demographics, social, and substance use factors collected from 522 OTP participants. We evaluated the cumulative percentage change during the initial 5 years after methadone initiation. We subsequently performed factor analysis for mixed-type data, a dimensionality reduction technique used also to investigate the contribution of individual variables. We next used k-means clustering to identify participant subgroups. We used random forests to identify the most important variables that predict HCV treatment initiation.

Results: Data from 522 participants (62.3% male, 46.6% White, 22.8% Black, 30.7% other races, 31.8% Hispanic, median age 49.0 years) revealed cumulative percentage improvements in primary, secondary, and tertiary illicit substance use after 3–4 years on methadone. We also found increased participation in education, employment, and decreases in criminal justice involvement. Through factor analysis, we identified that variables encompassing basic needs (i.e., food, clothing, utilities, healthcare, phone, and childcare) explain 10.4% of the variation. The second most important categorization were variables related to substance use and frequency that explain 8.6% of the variation. Cluster 1 had the greatest improvements in substance use, substance use frequency, residence type, and employment. Demographic characteristics were well balanced over the four subgroups except clusters 2 and 3 that contained a slightly higher proportion of non-Hispanic, White, and unmarried individuals. The random forest application to predict HCV treatment initiation among participants revealed that demographic (e.g., age, sex), treatment group (i.e., facilitated telemedicine, offsite referral), substance use, and social (e.g., housing, marital status) variables had the highest predictive capacity.

Conclusion: We quantified improvements in substance use and social factors after integration of HCV treatment into OTPs through telemedicine. Factor analysis identified social and substance use factors that explain 19.1% of the variation. K-means clustering permitted categorization of individuals on improvements in variables of interest. The random forest approach identifies important demographic, treatment group, substance use, and social variables for predicting HCV treatment initiation. The ability to classify participants could improve patient-centered care delivery for integrating HCV and OUD treatment.

WED-480-YI

Maternal health progression: EMR system's contribution to understanding hepatitis prevalence in Uzbekistan

Samantha Hall¹, Shakhlo Sadirova², Erkin Musabaev³, Homie Razavi¹. ¹Center for Disease Analysis, Lafayette, United States; ²Center for Disease Analysis, Tashkent, Uzbekistan; ³Research Institute of Virology, Tashkent, Uzbekistan

Email: shall@cdafound.org

Background and aims: As countries work towards the elimination of mother to child transmission of HIV, syphilis and hepatitis B virus (HBV), it is imperative to assess which strategies can strengthen national programs. In Uzbekistan, there are over 600, 000 births annually, necessitating extensive testing of pregnant women. This study examined the impact of implementing an electronic medical record (EMR) system designed to centralize test results for pregnant women across four regions of Uzbekistan. The primary objective is to demonstrate the utility of this EMR system in efficiently gathering and analyzing data, specifically focusing on estimating the prevalence of infections such as hepatitis B (HBV) and hepatitis C (HCV), by age and region.

Method: Over a 12-month period, 60 trained nurses at 60 maternity hospitals in Tashkent, Samarkand, Surkhandarya, and Syrdarya utilized the Research Electronic Data Capture (REDCap) system to enter test results recorded in patients' medical history files. A total of 81,017 pregnant women, aged 15–45, were screened for HBsAg and anti-HCV. Manual extraction and entry of test results into REDCap were conducted during patients' visits to maternity hospitals, utilizing a convenient sampling approach. Crude and age-adjusted prevalence were calculated with a 95% confidence interval (CI) for both markers. Associations with HBV and HCV were investigated using Chi-squared analysis and Poisson regression for age group and region.

Results: Among the pregnant women, the overall prevalence of HBsAg stood at 1.36%, with an age-adjusted prevalence of 1.19%. For anti-HCV, the overall prevalence was 0.36%, with an age-adjusted prevalence of 0.33%. The chi-squared analysis revealed a significant association between region and both HBV ($X^2 = 1487$, $p < 0.001$) and HCV ($X^2 = 114$, $p < 0.001$). Similarly, a significant association was found between age group and both HBV ($X^2 = 114$, $p < 0.001$) and HCV ($X^2 = 28$, $p < 0.001$). The highest age-adjusted prevalence was observed among 25- to 29-year-olds for both HBV (1.47%) and HCV (0.39%). Samarkand exhibited the highest prevalence of the sampled regions for both HBV (4.49%) and HCV (0.85%). Regression analyses demonstrated lower rates of both HBV and HCV infection in younger age groups, as compared to 25- to 29-year-olds ($p < 0.01$), and higher rates in residence of Samarkand ($p < 0.001$).

Conclusion: Implementing an EMR system for centralizing test results has proven effective in estimating the prevalence of HBV and HCV infections among pregnant women in Uzbekistan. The findings highlight regional and age-specific variations in infection rates, emphasizing the importance of targeted public health interventions. The study emphasizes the potential of this open access EMR system to streamline data collection, allowing for evidence-based policy decisions and reducing unnecessary testing costs for this vulnerable population.

WED-481

Elimination days-How good clinical practice can contribute to the elimination of hepatitis C

Pedro Lages Martins¹, Mário Jorge Silva¹, João Silva¹, Daniela Rabaça¹, Cláudia Pereira², Filipe Mendes³, Margarida Alves⁴, Paulo Caldeira⁵, Rita Corte-Real¹, Filipe Calinas¹. ¹Unidade Local de Saúde São José, Lisboa, Portugal; ²Ares do Pinhal-Associação de Recuperação de Toxicodependentes, Lisboa, Portugal; ³Equipa de Tratamento de Xabregas-Divisão de Intervenção nos Comportamentos Aditivos e nas Dependências, Lisboa, Portugal; ⁴IN-Mouraria-Grupo de Atividades em Tratamentos, Lisboa, Portugal; ⁵Ares do Pinhal-Associação de Recuperação de Toxicodependentes, Lisboa, Portugal
Email: pb.lages.martins@gmail.com

Background and aims: With the ongoing conventional clinical practice, it seems unlikely that the goal of eliminating hepatitis C by 2030 will be achieved in many countries. We presume that there are diagnosed hepatitis C patients who have lost hospital follow-up without receiving treatment. With this initiative, we aim to identify those patients who were once under our care and bring them back into medical care, including treatment for HCV infection.

Method: Results of HCV RNA tests requested between 01/2010 and 3/2023 by clinicians from a tertiary hospital service were examined. We identified the patients with detectable HCV viral load in the most recent assessment. Among these, patients currently alive without records of maintained follow-up (at our hospital or other institutions) nor scheduled/initiated treatment at any point were identified. Patients were contacted by mail, phone, and/or email for evaluation in hospital consultations and/or decentralized clinics. Confirmation of active infection was conducted, as well as treatment, and post-treatment follow-up when indicated.

Results: Analyzing the results of 7168 HCV viral loads, 473 patients with detectable HCV RNA in the most recent assessment were identified. Of these, 44 were under specialized care follow-up (37 at our hospital and 7 at other institutions), 147 had initiated treatment (with unknown completion status and/or outcome), and 162 had passed away. We successfully contacted 90 (75%) out of the 120 patients who presumably had never initiated HCV treatment. Sixty-nine percent (62/90) of these patients were reassessed, 55 in hospital consultations and 7 in decentralized clinics. Treatment for hepatitis C was initiated in 56 patients.

Conclusion: This "relink" strategy, which is nothing more than good clinical practice, allows for the recovery of a significant number of previously known hepatitis C patients back into clinical care and their treatment.

WED-482

Local elimination programs leading to global action in HCV (LEGA-C): implementation science studies in Europe aiming to streamline the HCV care pathway

Candido Hernández¹, Julian Elrayes², Marinela Mendez³, Francesca Frigerio⁴, Louise Missen⁵, Audrey Le Blevet⁶, Mehtap Guendogdu⁷, Kyung min Kwon², Stacey Scherbakovsky², Kim Vanstraelen⁸, Bruce Kreter². ¹Gilead Sciences, Madrid; ²Gilead Sciences, Foster City, United States; ³Gilead Sciences, Madrid, Spain; ⁴Gilead Sciences, Milan, Italy; ⁵Gilead Sciences, London, United Kingdom; ⁶Gilead Sciences, Paris, France; ⁷Gilead Sciences, Munich, Germany; ⁸Gilead Sciences, Brussels, Belgium
Email: candido.hernandez@gilead.com

Background and aims: Since 2016 Gilead Sciences, Inc., has supported over 120 studies in more than 30 countries focused on hepatitis C virus (HCV) elimination under the LEGA-C (Local Elimination programs leading to Global Action in HCV) initiative. In 2020, EASL released the last recommendations on treatment of hepatitis C and identified patients who will benefit from a more streamlined care pathway (e.g., people who inject drugs-PWID, prisoners, homeless individuals, migrants, patients living with mental health or substance use disorders, men who have sex with men, or sex workers). Here we aim to comprehensively describe the studies run under the LEGA-C umbrella in European countries, specifically focusing on populations historically less engaged in healthcare.

Method: We identified the LEGA-C studies performed in European region, and extracted information on the following variables: country, type of population included (as mentioned per EASL 2020 Guidelines), number of patients/individuals reached, use of a simplified care pathway (e.g., simple monitoring, test and treat approach), year of communication/publication, and the impact factor (IF).

Results: 32 (27%) of the studies were conducted in Europe across 12 European countries (Austria, France, Denmark, Georgia, Germany, Greece, Italy, Netherlands, Portugal, Spain, Switzerland, and UK) as of July 2022. In these 32 studies, 25 (73%) focused on special populations with more than 8,935 individuals reached, including persons who use/inject drugs ($n = 13$ studies), men who have sex with men ($n = 7$), prison residents ($n = 5$), migrants ($n = 4$), homeless patients ($n = 2$), psychiatric patients ($n = 1$), and sex workers ($n = 1$). At the time of the analysis, 19 out of the 32 studies were presented or published: 6 studies in 2018–19, 2 in 2020, and 11 in 2021–22. During 2021–2022, there was an increase in studies that included patients who were homeless, sex workers, in prison, and PWID. There were 6 studies involving special populations that were cited a total of 48 times with a mean IF of 4.02 (3.00–6.86). Among the 32 studies, the test and treat approach ($n = 18$) was the most frequent, followed by the screening and monitoring simplification approach ($n = 9$). Notably, both approaches witnessed an increase in studies during the years 2021 to 2022 compared to 2018 to 2020.

POSTER PRESENTATIONS

Conclusion: Since 2016, the LEGA-C initiative has supported 32 studies conducted in Europe, with 25 out of the 32 focused on streamlining the care pathway for a variety of populations with HCV infection. The findings highlight the value of multi-stakeholder collaboration reaching nearly 9, 000 individuals who were mostly underserved and difficult to reach. These patients play a crucial role in the goal of achieving the elimination of HCV in Europe.

WED-483

Performance comparison of four hepatitis E antibodies detection methods

Ana Avellon Calvo¹, Milagros Muñoz Chimento², Nazaret Diaz-Sanchez², Lucía Morago², Alejandra García-Lugo², María Isabel Zamora Cintas³, María Mateo³, María Simón³, Monica Sanchez-Martinez³. ¹National Center of Microbiology CIBERESP, Hepatitis Unit, Majadahonda (Madrid), Spain; ²National Center of Microbiology, Instituto de Salud Carlos III, Majadahonda (Madrid), Spain; ³Hospital General de la Defensa, Madrid, Spain
Email: aavellon@isciii.es

Background and aims: Hepatitis E virus antibody detection constitutes the main screening test for Hepatitis E infection. Anti HEV IgM is used as first line detection test for acute infection while anti HEV IgG represents the main tool to assess seroprevalence. Sensitivity and specificity of marketed techniques have been under discussion. The aim of this study is to compare sensitivity and specificity of four of the more widely used techniques in Europe.

Method: Sample panels used for comparison were configured according to immunoblot (Recomline, Mikrogen) (IB) results. They were as follows: Panel I (immediate acute HEV infection) included 21 samples positive to anti-HEV IgM by IB and positive HEV-RNA. Panel II (acute HEV infection in early convalescence phase) included 71 samples positive to anti-HEV IgM by IB and negative for HEV-RNA. Panel III (past HEV infection) included 100 samples positive to anti-HEV IgG. Panel IV (HEV IgM negative) included 101 samples and Panel V (HEV IgG negative) another 100 samples. Compared techniques were: LIAISON[®] MUREX DiaSorin anti-HEV immunoglobulin (Ig) G and anti-HEV IgM assays (Liaison); Wantai HEV IgM and IgG ELISA (Wantai); VIDAS[®] BioMérieux anti-HEV IgM and IgG tests (Vidas) and Hepatitis E VIRCLIA[®] VirCell IgM and IgG monostests (Virclia). Test sensitivity and specificity, Cohen's kappa coefficient (k) for qualitative results and Pearson's correlation coefficient (PS) for concentrations were estimated.

Results: Anti HEV IgM acute phase sensitivity (Panel I) (confident interval (CI) 95%) was 100% for all techniques, while acute and convalescence phase sensitivity (Panel I+II) was 96.74 (93.11–100.37) for Liaison; 82.60 (74.86–90.35) for Wantai; 88.04 (81.41–94.67) for Vidas and 80.90 (72.73–89.07) for Virclia. Anti HEV IgM specificity (Panel IV) was calculated for Liaison and Virclia reaching 100% in both cases. Anti HEV IgM Wantai agreed with Vidas and Virclia with moderate K (0.404 and 0.472). Pearson correlation of quantitative results was higher when comparing anti HEV IgM Liaison-Vidas (0.783) and Wantai-Virclia (0.767) Anti HEV IgG past infection sensitivity (Panel III) (CI 95%) was 100% for Liaison, Vidas and Virclia and 99 (96.07–101.26) for Wantai. Specificity (Panel V) was calculated for Liaison and Virclia reaching 97.17 (94.01–100.33) for Liaison and 90.57 (82.65–94.71) for Virclia.

Conclusion: Anti HEV IgM sensitivity was excellent in acute phase for all techniques, decreasing when including the convalescence phase, as after several days of infection, sensitivity of techniques differs being the highest Liaison (96.74%) and Vidas (88.04%). Anti HEV IgM specificity of Liaison and Virclia was optimal. Anti HEV IgG sensitivity was 100% for Liaison, Vidas and Virclia, being slightly lower for Wantai (99.0%). Anti HEV IgG specificity was higher in Liaison (97.17%) than in Virclia (90.57%).

WED-484

Hepatitis C virus and HIV infection among persons who inject drugs in six sites in Tajikistan, 2022

Aziz Nabadzhonov¹, Rezeda Ashurova², Farkhod Saydullaev³, Patrick Nadol⁴, Bolot Kalmyrzaev⁵, Hieremila Haile⁶, Shaun Shadaker⁶, Rania Tohme⁶, Safarhon Sattorov⁷, Senad Handanagic⁶. ¹US Centers for Disease Control and Prevention in Tajikistan, Dushanbe, Tajikistan; ²US Centers for Disease Control and Prevention, Dushanbe, Tajikistan; ³US Centers for Disease Control and Prevention, Dushanbe, Tajikistan; ⁴US Centers for Disease Control and Prevention, Bishkek, Kyrgyz Republic; ⁵US Centers for Disease Control and Prevention, Atlanta, United States; ⁶US Centers for Disease Control and Prevention, Atlanta, United States; ⁷Tajikistan National AIDS center, Dushanbe, Tajikistan
Email: wk9@cdc.gov

Background and aims: Modeling estimates indicate that 3% of people in Tajikistan could be infected with hepatitis C virus (HCV) and 0.2% with HIV. The risk of HCV and HIV infection is higher among persons who inject drugs (PWID). In 2022, the estimated PWID population size in Tajikistan was 18, 000. Persons receiving medication for opioid use disorders receive free testing for anti-HCV, but viremia testing and treatment must be paid out of pocket unless there is support from donor agencies. We estimate the prevalence of exposure and infection and testing history for HCV and HIV among PWID in Tajikistan.

Method: Respondent-driven sampling was used to recruit PWID from six sites in Tajikistan in 2022: Dushanbe, Khujand, Khorog, Kulob, Penjikent and Vahdat. Inclusion criteria included ≥ 18 years old, self-reported injecting drugs in the past 30 days, and residing in a defined survey area. Participants self-reported demographic and risk behaviors and were offered HIV and HCV rapid testing (RT). Those with reactive HCV RT were tested for viremic infection (HCV RNA). We report unweighted aggregated and city-specific ranges.

Results: We recruited 1, 714 PWID, of whom 95% were >30 years-old (median = 42; Q1–Q3:35–49), 94% were male, 39% were unemployed, 41% injected drugs for ≥ 11 years, 30% reported injecting drugs at least once daily, and 11% reported sharing a needle or syringe in the past 6 months. Heroin was the most frequently injected drug (71%). The aggregated HIV prevalence was 12% (n = 199; range by city 6–21%); anti-HCV prevalence was 28% (n = 472; range 17–43%) and viremic HCV prevalence was 18% (n = 301; range 10–27%). Among 199 PWID with HIV, 72% (n = 143; range 39–90%) were reactive for anti-HCV, and 34% (n = 68; range 17–90%) tested positive for HCV RNA. In total, 53% (n = 869; range 28–85%) of PWID reported ever being tested for HCV, and 87% were ever tested for HIV (n = 1499; range 76–99%). Among PWID who were anti-HCV reactive, 47% (n = 217; range 26–83%) were unaware of their status.

Conclusion: A substantial percentage of PWID were exposed to HCV, almost one in five had viremic HCV infection, and more than one in ten had HIV infection. Only half of PWID reported ever being tested for anti-HCV. Expansion of screening for HCV among PWID is needed. HCV infection was more common among people living with HIV. Integrating prevention, screening and treatment for hepatitis C with harm reduction and HIV services could help reduce the HCV burden among PWID in Tajikistan.

WED-485

Uptake in viral hepatitis screening, vaccination and linkage to care among at-risk migrants in Catalonia, Spain: three years of a community-based intervention

Camila Picchio^{1,2}, Aina Nicolàs Olivé¹, Daniel K Nomah³, Ariadna Rando-Segura^{4,5}, Maria Buti^{5,6}, Sabela Lens^{5,7}, Xavier Forns^{5,7}, Mireia Miquel^{5,8,9}, Sergio Rodríguez-Tajes^{5,7}, Francisco Javier Pamplona Portero¹⁰, Carmen López Núñez¹¹, Francisco Rodríguez-Frías¹², Jeffrey V Lazarus^{1,13}. ¹Barcelona Institute for Global Health (ISGlobal), Hospital Clínic, University of Barcelona, Barcelona, Spain; ²Department of Community Health and Prevention,

Dornsife School of Public Health, Drexel University, Philadelphia, United States; ³Center for Epidemiological Studies on Sexually Transmitted Infections and HIV/AIDS in Catalonia (CEEISCAT), Department of Health, Generalitat de Catalunya, Badalona, Spain; ⁴Microbiology Department, University Hospital Vall d'Hebron, Barcelona, Spain; ⁵CIBER Hepatic and Digestive Diseases (CIBERehd), Instituto Carlos III, Madrid, Spain; ⁶Hospital Campus, Liver Unit, University Hospital Vall d'Hebron, Barcelona, Spain; ⁷Liver Unit, Hospital Clínic, IDIBAPS, University of Barcelona, Barcelona, Spain; ⁸Hepatology Unit, Digestive System Service, University Hospital Parc Taulí, Research and Innovation Institute I3PT, Universitat Autònoma de Barcelona, Sabadell, Spain; ⁹Medicine Department, Universitat de Vic-Universitat Central de Catalunya (UVic-UCC), Vic, Spain; ¹⁰Department of Digestive Diseases, Hospital de Santa Caterina, Salt, Spain; ¹¹Department of Digestive Diseases, Hospital Trueta, Girona, Spain; ¹²Liver Pathology Unit, Biochemistry and Microbiology Service, Hospital Universitari Vall d'Hebron, Barcelona, Spain; ¹³CUNY Graduate School of Public Health and Health Policy (CUNY SPH), New York, United States
Email: camila.picchio@isglobal.org

Background and aims: Chronic viral hepatitis infections remain a major public health challenge. Migrants from countries with mid/high hepatitis B (HBV) and hepatitis C (HCV) prevalence are disproportionately affected by these infections in Europe. Additionally, they often encounter additional barriers to access and comprehend their host health system, which exacerbate their timely diagnosis. This ongoing study aims to scale-up a community-based model of HBV/HCV screening, HBV vaccination, and linkage to care among migrants born in countries with mid/high HBV/HCV prevalence in Catalonia, Spain.

Method: A total of 48 community-based screening interventions were conducted between 11/2020 and 12/2023 in Catalonia, Spain. Participants were offered HBV and HCV screening through rapid diagnostic tests and simplified blood sample collection using plasma separation cards. Screening for anti-HCV screening was offered from 06/2022. Community health workers were responsible for the recruitment of migrants at risk. All participants were offered linkage to care, including direct referral to a liver specialist for positive cases, the first dose of HBV vaccination administered in the community, or post-test counselling (PTC) to report a past resolved infection. Data were analysed using standard descriptive statistics with Stata v14.0.

Results: 829 and 381 people were tested for HBV and HCV, respectively. Participants were primarily from Ghana (77%) and Senegal (14.2%). Most were men (64.1%) with a mean age of 42 years (SD ± 10.8). Almost half (48.4%) had finished secondary school but had no higher studies and 24.2% were recently arrived migrants (≤5 years). Most reported never having been tested for HBV/HCV before (70.3% and 79.6%, respectively) and 10.2% reported being fully vaccinated against HBV. Prevalence of HBsAg+ was 9.53% (95% CI 7.5–11.5%) and anti-HCV+ was 0.53% (95% CI 0.06–1.89, n=2) and none had detectable HCV RNA. The prevalence of resolved HBV infection (HBsAg-/anti-HBc+) was 39.5%. The overall linkage to care rate was 59.9%; with 70.9% of those HBsAg+ attending a specialist visit. Among those requiring vaccination/PTC, 58.7% had results communicated, and 76 people (10.4%) are awaiting communication of results due to the second scheduled visit scheduled for a future time. Of those who required vaccination, 60.6% were informed and 82.7% of those offered the first dose of the HBV vaccine in the community received it.

Conclusion: This community-based model of care has proven effective in increasing viral hepatitis screening among migrants in Catalonia by using simplified diagnostic tools and direct referral pathways. Successful linkage to care is expected to increase due to second community visits scheduled in the upcoming months. Community health workers have played a crucial role in minimizing cultural and linguistic barriers often encountered by this at-risk population.

WED-486-YI

Material deprivation is associated with liver stiffness measurement and liver-related events in people with HIV

Felice Cinque^{1,2}, Clara Long³, Dana Kablawi⁴, Dong Kim⁴, Thierry Tadjou⁴, Wesal Elgretli⁵, Luz Ramos Ballesteros⁶, Amanda Lupu⁴, Michael Nudo⁴, Bertrand Lebouche⁷, Nadine Kronfli⁷, Joseph Cox^{7,8}, Cecilia Costiniuk⁷, Alexandra De Pokomandy⁷, Jean-Pierre Routy⁷, Marina B. Klein^{7,8}, Frederic Lamonde⁹, Raman Agnihotram⁹, Sahar Saeed¹⁰, Giada Sebastiani^{11,12}. ¹Division of Gastroenterology and Hepatology, McGill University Health Centre, Chronic Viral Illness Service, McGill University Health Centre, Montreal, Canada; ²SC-Medicina Indirizzio Metabolico, Fondazione IRCCS Ca' Granda Ospedale Maggiore Policlinico of Milan, Department of Pathophysiology and Transplantation, University of Milan, Italy, Milan, Italy; ³Division of Gastroenterology and Hepatology, McGill University Health Centre, Chronic Viral Illness Service, Division of Infectious Diseases, Department of Medicine, McGill University Health Centre, MONTREAL, Canada; ⁴Division of Gastroenterology and Hepatology, McGill University Health Centre, Chronic Viral Illness Service, Division of Infectious Diseases, Department of Medicine, McGill University Health Centre, Montreal, Canada; ⁵Division of Experimental Medicine, McGill University, Montreal, Canada, Montreal, Canada; ⁶Division of Gastroenterology and Hepatology, McGill University Health Centre, Montreal, Canada; ⁷Chronic Viral Illness Service, Division of Infectious Diseases, Department of Medicine, McGill University Health Centre, Montreal, Canada; ⁸Department of Epidemiology, Biostatistics and Occupational Health, McGill University, Montreal, Canada; ⁹Research Institute, McGill University Health Centre, Montreal, Canada; ¹⁰Department of Public Health Sciences, Queens University, Kingston, Canada; ¹¹Division of Gastroenterology and Hepatology, McGill University Health Centre, Montreal, Chronic Viral Illness Service, Division of Infectious Diseases, Department of Medicine, McGill University Health Centre, Montreal, Canada; ¹²Division of Experimental Medicine, McGill University, Montreal, Canada
Email: cinque.felice@gmail.com

Background and aims: Socioeconomic status drives health disparities in people with HIV (PWH). The effect of material deprivation on hepatic outcomes in PWH has not been assessed. Aim: to evaluate the association between material deprivation and liver fibrosis, metabolic dysfunction-associated steatotic liver disease (MASLD) and clinical outcomes in PWH.

Method: We included consecutive PWH from the LIVER disease in HIV (LIVEHIV) cohort with available Fibroscan. MASLD was defined as presence of hepatic steatosis by controlled attenuation parameter (CAP) ≥ 248 dB/m and at least one metabolic abnormality. Significant liver fibrosis was defined as liver stiffness measurement (LSM) ≥ 8. Socioeconomic status was assessed by the Pamplon Material Deprivation Index (MDI). PWH with MDI quintiles 4 and 5 were classified as "deprived" while PWH with MDI quintiles 1 and 2 as "privileged". Multivariable linear regression analysis investigated associations of MDI with LSM and CAP. Incidence of liver outcomes (ascites, variceal bleeding, hepatic encephalopathy, hepatocellular carcinoma, liver transplantation), extrahepatic outcomes (cancer, cardiovascular disease) and overall mortality were evaluated through survival analysis.

Results: Among the 768 PWH included (median age 54 years, 76% male, 25% HBV coinfect, 10% HCV coinfect, 23% with significant liver fibrosis and 33% with MASLD), 40% were materially privileged while 47% were materially deprived. At baseline, materially deprived PWH were more frequently female and of Black ethnicity and had higher prevalence of metabolic comorbidities. After adjustments, material deprivation was associated with increased LSM at baseline ($\beta = 1.858$, 95% CI 0.53–3.17; $p = 0.006$) but not with CAP ($\beta = 6.469$, 95% CI –5.55–18.49; $p = 0.291$). In the survival analysis, during a median follow-up of 3.8 years, the incidence of liver-related events was significantly higher in materially deprived PWH compared to

POSTER PRESENTATIONS

materially privileged PWH (log rank $p = 0.04$), while there was no difference in extrahepatic events or all-cause mortality.

Conclusion: Material deprivation, reflecting socioeconomic status, is associated with liver fibrosis and liver-related events in PWH. Future strategies should assess whether improved material security improves liver outcomes.

WED-487

Geographic variability in harm reduction uptake, risk behaviors, and network characteristics among people who inject drugs in Kenya: a key hurdle to hepatitis C elimination

Hannah Manley¹, Lindsey Riback¹, Mercy Nyakowa², Chenshu Zhang³, Rose Wafula², Nazila Ganatra², Matthew Akiyama³. ¹Albert Einstein College of Medicine, New York, United States; ²Kenya Ministry of Health, Nairobi, Kenya; ³Albert Einstein College of Medicine, New York, United States

Email: makiyama@montefiore.org

Background and aims: Hepatitis C (HCV) is highly concentrated among people who inject drugs (PWID). In Kenya, there is a strong gradation in HCV prevalence from the Coastal region moving inland. This gradation has been attributed to the introduction of heroin in the Coast in the 1980s; however, regional differences in HCV-related risk behaviors, networks, and harm reduction coverage are not well characterized. We assessed factors associated with HCV among PWID located in the Coastal region and Nairobi.

Method: We are recruiting 3500 PWID from needle and syringe program (NSP) sites in Kenya using respondent driven sampling. Participants complete biobehavioral surveys and receive testing for HCV, hepatitis B (HBV), and HIV. We conducted this analysis using chi-squared tests or t-tests when appropriate.

Results: Thus far, among 2508 participants enrolled in Nairobi (33.0%), Coast (48.8%), and Western (17.7%) region, participants are mainly male (89.9%) and 34.6 years old on average (SD = 8.6). One-fifth (19.8%, N = 496) are HCV antibody positive (HCV+). Regional prevalence is highest in the Coast (25.4%, N = 311/1223), followed by Nairobi (22.1%, N = 183/828), and the Western region (0.5%, N = 2/443). HCV+ participants in Coast were more likely to have injected in the last 30 days than those in Nairobi (96.5% v. 72.1%, $p < 0.001$) and injected more times on average (86.8 v. 64.3, $p < 0.001$) in the same timeframe. HCV+ individuals from Coast were more likely to have reused another person's needle (25.1% v. 0%, $p < 0.001$) or injection equipment (e.g., cookers, cotton, water/solution; 27.3% v. 6.6%, $p < 0.001$) at last injection when compared to those in Nairobi. Those with HCV in Coast were less likely to have previously accessed HCV testing (64.3% v. 77.6%, $p = 0.002$), NSP (78.1% v. 98.4%, $p < 0.001$), and opioid agonist therapy (OAT) (50.8% v. 84.2%, $p < 0.001$). In looking at social network characteristics, HCV+ participants in Coast knew more PWID (by face or name) in Kenya on average than those in Nairobi (15.6 v. 9.6, $p < 0.001$) and more individuals who are HCV+ (0.7 v. 0.2, $p < 0.001$). They also identify a greater proportion of their named network members as injection partners (90.1% v. 5.2% of members seen in last 30 days, $p < 0.001$), and injected with a greater proportion of their named network members in the same timeframe (90.7% v. 40.5%, $p < 0.001$). HCV+ participants living in Coast are more likely to report having ever been incarcerated than those in Nairobi (66.9% v. 32.2%, $p < 0.001$).

Conclusion: While data are preliminary, higher risk behaviors and lower NSP and OST uptake may be drivers of the higher HCV prevalence in Coastal Kenya. Social network characteristics also highlight how injection networks may contribute to higher HCV prevalence in Coastal Kenya as compared to Nairobi. Due to differing risk factors for HCV, once size fits all intervention may not be optimal and targeted, regional approaches may be needed.

WED-490

Optimizing a hepatitis C screening model for general population using easily accessible data

Chi Zhang¹, Yi-Qi Liu¹, Hong Zhao¹, Gui-Qiang Wang¹. ¹Peking University First Hospital, Beijing, China

Email: zhangcdoctor@126.com

Background and aims: Globally, an estimated 58 million chronic hepatitis C virus (HCV) infections. Direct-acting antiviral medicines (DAAs) can cure more than 95% of persons with HCV infection, but access to diagnosis (20%) and treatment (15%) was low. We aimed to develop screening algorithms that accurately identifies HCV infection using easily accessible demographic parameters.

Method: We obtained data from population-based cohorts National Health and Nutrition Examination Survey (NHANES 1990–2020), and divided them into training (6-cycles; $n = 46243$) and testing (5-cycles; $n = 37060$) cohort. Then, we applied logistic regression to calculate the odds ratio (OR) of 4 demographic factors (sex, ethnicity, blood transfusion history, birth year) for diagnosing HCV infection. Next, we developed and compared 9 machine learning (ML) algorithms to diagnose HCV infection in training cohort. Finally, we adopted the selected algorithm to establish the diagnostic model and test the performances.

Results: The overall cohort ($n = 83303$) was 49.0% male; 37.9% White, 23.2% Black, 29.0% Hispanic, and 10.0% other; 8.8% of participants had a history of blood transfusion; with a mean birth year of 1972 ± 23 . The positive rates of anti-HCV and HCV RNA among studied population were 1.3% and 0.8% (unweighted). In multivariate analysis, all four parameters were significantly correlated with HCV infection: male sex (OR 2.01; $P < 0.001$); Black versus White (OR 1.96; $P = 0.008$); blood transfusion history (OR 2.14; $P < 0.001$); born 1970 and before (OR 8.98; $P < 0.001$). Comparing the AUC values of 9 ML algorithms in the training cohort, XGBoost was selected as the best prediction model. The AUC of the XGBoost model for diagnosing HCV infection was 0.891 (95%CI 0.880–0.903) for the training set. In the testing set, the AUC was 0.843 (0.827–0.858), and the sensitivity, specificity, PPV and NPV were 0.78, 0.78, 0.288 and 0.967, respectively.

Conclusion: To predict HCV infection in general population, only 4 easily obtained demographic features are needed using our ML model.

WED-491

Understanding barriers and enablers to hepatitis C treatment initiation: a systematic review of qualitative studies

Kathleen Bryce^{1,2}, Fiona Burns^{1,2}, Colette Smith¹, Alison Rodger^{1,2}, Douglas Macdonald^{2,3}. ¹Institute for Global Health, University College London, London, United Kingdom; ²Royal Free London NHS Foundation Trust, London, United Kingdom; ³Institute of Liver and Digestive Health, University College London, London, United Kingdom

Email: kathleenbryce@doctors.org.uk

Background and aims: Many factors associated with disengagement from care between hepatitis C diagnosis and treatment initiation have been identified in the direct-acting antiviral (DAA) era. We aimed to better understand and contextualise these factors by undertaking a systematic review of qualitative studies on DAA treatment initiation.

Method: We performed a systematic review of the barriers and enablers to hepatitis C DAA treatment initiation, in high income settings with free publicly-funded universal healthcare provision. We searched eight bibliographic databases for studies published between 2014 and May 2022 using pre-defined keywords. We included provider and patient interview-based qualitative studies investigating positive (enablers) or negative (barriers) associations with DAA treatment initiation. The Capability, Opportunity, Motivation, Behaviour (COM-B) framework was used to synthesise our findings.

Results: Of 5198 articles identified, 21 studies conducted in Australia, Canada and Europe were included. Overall quality was good. Barrier

themes included: lack of knowledge of DAA availability and effectiveness, poor mental and physical health and deferral to stabilise drug use first (Capability); previous negative healthcare experiences including stigma, competing priorities and resource limitations of the patient (such as housing) as well as of the provider and healthcare context (Opportunity); and beliefs about consequences of hepatitis C and of DAA treatment (Motivation). Enabler themes included: peer advocate-led awareness-raising and education (Capability); building trusting patient-provider relationships, simplified integrated/co-located multidisciplinary care services to address multiple needs (Opportunity); and changing beliefs about consequences and individual capabilities (Motivation).

Conclusion: Interview-based studies of barriers and enablers to DAA treatment explain multiple factors associated with lower treatment uptake borne out in quantitative analyses, such as low socioeconomic status, insecure housing, active drug use, disease stage, age and treatment experience. By identifying an individual's Capability, Opportunity and Motivation barriers, pre-emptive supportive interventions can be tailored to efficiently enable engagement with DAA treatment.

WED-492

Evaluation of hepatitis C treatment and care model in primary healthcare centers in the country of Georgia

Akaki Abutidze^{1,2}, Tengiz Tsertsvadze^{1,2}, Lali Sharvadze^{2,3}, Rania Tohme⁴, Shaun Shadaker⁴, Ekaterine Adamia⁵, Tamar Gabunia⁵.
¹Infectious Diseases, AIDS and Clinical Immunology Research Center, Tbilisi, Georgia; ²Ivane Javakhishvili Tbilisi State University, Tbilisi, Georgia; ³Hepatology clinic HEPA, Tbilisi, Georgia; ⁴Division of Viral Hepatitis, Centers for Disease Control and Prevention, Atlanta, United States; ⁵Ministry of IDPs from the Occupied Territories, Labour, Health and Social Affairs of Georgia, Tbilisi, Georgia
Email: akakiabutidze@yahoo.com

Background and aims: In April 2015, with a partnership with Gilead Sciences and technical assistance from the US Centers for Disease Control and Prevention, Georgia launched the world's first hepatitis C elimination program. By the end of November 2023, more than 85,000 patients with current hepatitis C virus (HCV) infection initiated treatment, with 99% cure rates among those tested for sustained virologic response (SVR). Broad access to direct acting antivirals (DAAs) resulted in rapid increase in treatment uptake in 2016, which has since declined due to barriers in diagnosis and linkage to care. To address this issue, Georgia initiated service decentralization in 2018 by integrating HCV screening and treatment in primary healthcare centers (PHCs). We report preliminary results of an integrated model of hepatitis C care in PHCs.

Method: By November 30, 2023, a total of 10 PHCs were providing hepatitis C care services throughout the country. The integrated model was based on "one stop shop" approach, where patients receive all HCV screening, treatment, and care services in selected PHCs. PHCs provided care to HCV treatment-naïve patients with no or mild fibrosis (FIB-4 score < 1.45) using simplified diagnostics and a treatment monitoring approach, while persons with advanced liver fibrosis/cirrhosis were referred to specialized clinics. Patients were treated with Sofosbuvir/Ledipasvir and/or Sofosbuvir/Velpatasvir for 12 weeks. SVR was defined as undetectable HCV RNA at 12–24 weeks after end of therapy. The Extension for Community Healthcare Outcomes (ECHO) telemedicine model was used to train and support primary healthcare providers. Regular teleECHO videoconferencing was conducted to provide primary care providers with advice and clinical mentoring.

Results: Overall, 1,881 persons with current HCV infection were evaluated for FIB-4 score at PHCs as of November 30, 2023. A total of 1,238 persons initiated treatment, and of them 1,162 (93.9%) had completed treatment at the time of analysis. Of 1,134 persons eligible for SVR testing (12–24 weeks post treatment completion), 889 (78.4%) had been tested, and 874 (98.3%) achieved SVR.

Conclusion: Our analysis shows the effectiveness of integrating a simplified HCV diagnosis and treatment model in PHCs. Countrywide expansion of this model is warranted to bridge the gaps in the hepatitis C care continuum and ensure high rates of treatment uptake, enabling Georgia to achieve hepatitis C elimination.

WED-493-YI

Direct-acting antivirals in women of reproductive age infected with hepatitis C virus

Krystyna Dobrowolska¹, Małgorzata Pawłowska², Dorota Zarębska-Michaluk³, Piotr Rzymński⁴, Ewa Janczewska⁵, Magdalena Tudrujek-Zdunek⁶, Hanna Berak⁷, Włodzimierz Mazur⁸, Jakub Klapaczynski⁹, Beata Lorenc¹⁰, Justyna Janocha-Litwin¹¹, Anna Parfieniuk-Kowerda¹², Dorota Dybowska², Piekarska Anna¹³, Rafał Krygier¹⁴, Beata Dobracka¹⁵, Jerzy Jaroszewicz¹⁶, Robert Flisiak¹².
¹Collegium Medicum, Jan Kochanowski University, Kielce, Poland; ²Department of Infectious Diseases and Hepatology, Faculty of Medicine, Collegium Medicum Bydgoszcz, Nicolaus Copernicus University, Toruń, Poland; ³Department of Infectious Diseases and Allergology, Jan Kochanowski University, Kielce, Poland; ⁴Department of Environmental Medicine, Poznań University of Medical Sciences, Poznań, Poland; ⁵Department of Basic Medical Sciences, School of Public Health in Bytom, Medical University of Silesia, Katowice, Poland; ⁶Department of Infectious Diseases, Medical University of Lublin, Lublin, Poland; ⁷Outpatient Clinic, Hospital for Infectious Diseases in Warszawa, Warszawa, Poland; ⁸Clinical Department of Infectious Diseases in Chorzów, Medical University of Silesia, Katowice, Poland; ⁹Department of Internal Medicine and Hepatology, The National Institute of Medicine of the Ministry of Interior and Administration, Warszawa, Poland; ¹⁰Pomeranian Center of Infectious Diseases, Medical University, Gdańsk, Poland; ¹¹Department of Infectious Diseases and Hepatology, Wrocław Medical University, Wrocław, Poland; ¹²Department of Infectious Diseases and Hepatology, Medical University of Białystok, Białystok, Poland; ¹³Department of Infectious Diseases and Hepatology, Medical University of Łódź, Łódź, Poland; ¹⁴Outpatients Hepatology Department, State University of Applied Sciences, Konin, Poland; ¹⁵MedicalSpec Medical Center, Wrocław, Poland; ¹⁶Department of Infectious Diseases and Hepatology, Medical University of Silesia in Katowice, Bytom, Poland
Email: krystyna.dobrowolska98@gmail.com

Background and aims: Eliminating hepatitis C virus (HCV) infection in the population of women of reproductive age is important not only for the health of women themselves, but also for the health of their children. The aim of the analysis is to evaluate the effectiveness of contemporary therapy in a large cohort of women of childbearing age from routine clinical practice and identify the factors reducing therapeutic success in hopes of achieving the goal of complete virus elimination in this group.

Method: The analyzed population consisted of 7,861 patients with chronic hepatitis C treated with direct-acting antiviral drugs (DAAs) between 2015 and 2022 at 26 hepatology centres, including 3,388 women aged 15–49 years as defined as reproductive age by the World Health Organization. The comparison group was a population of 4,473 men of the corresponding age. Data were collected retrospectively using the nationwide EpiTer-2 database.

Results: Females were significantly less often infected with HCV genotype (GT) 3 compared to males (11.2% vs 15.7%, $p < 0.001$). They also had less frequent comorbidities (40.5% vs. 44.2%, $p = 0.001$) and were less likely to use concomitant medications (37.2% vs. 45.2%, $p < 0.001$). Hepatocellular carcinoma and a history of liver transplantation were significantly less frequently documented in women, as were HIV and HBV co-infections. Men were more likely than women to be treatment-experienced (17.4% vs. 13.5%, $p < 0.001$). In both genders, previous antiviral therapy was predominantly IFN-based regimens, significantly more common used in women (94.5% vs. 82.8%, $p < 0.001$). In the current treatment, women were more likely to receive a genotype-specific regimen (55.4%), while there was a slight predominance of pangenotypic options for men (50.5%). The

POSTER PRESENTATIONS

overall effectiveness in intent-to-treat and per protocol analysis in the female population was 96.3% and 98.8%, respectively, while a 92.9% and 96.8% cure rate was documented in men, $p < 0.001$. Regardless of the treatment type, GT and the advancement of liver fibrosis, women were significantly more likely to achieve the sustained virologic response as compared to men. GT3 and cirrhosis were independent factors increasing the risk of treatment failure irrespective of gender. Women more frequently reported adverse events as compared to men, with the most common weakness/fatigue (6.9% vs. 5.5%, $p = 0.01$) and headache (4.4% vs. 2.4%, $p < 0.001$). Adverse events were mostly mild in nature; deaths occurred in 0.3% of men and 0.1% of women ($p = 0.03$), and none were considered by the treating physician to be therapy-related.

Conclusion: We have demonstrated an excellent efficacy and safety profile for the treatment of HCV infection in women of reproductive age. This gives hope for the micro-elimination of HCV infections in this population, translating into a reduced risk of severe disease in both women and their children.

WED-494

Local Hepatitis Elimination and Prevention (LHEAP)-Doorstep Model for Elimination of Hepatitis B and Hepatitis C in Rawalpindi, Pakistan

Nida Ali¹, John Ward², Ehsan Ghani³, Qaiser Hussain⁴, Muhammad Irfan⁴. ¹The Task force for Global Health, Coalition for Global Hepatitis Elimination, Decatur, United States; ²Coalition for Global Hepatitis Elimination, The Task Force for Global Health, Decatur, United States; ³District Health Authority, Rawalpindi, Pakistan; ⁴Local Hepatitis Elimination and Prevention, District Health Authority, Rawalpindi, Pakistan
Email: nida.ali4883@gmail.com

Background and aims: It is estimated that 5 million people are infected with Hepatitis B Virus (HBV) and 10 million are infected by Hepatitis C Virus (HCV) in Pakistan. This makes Pakistan the highest burden country in terms of HCV cases and 9th highest burden country in terms of HBV cases globally. Thousands of new patients are added every year. The service delivery is centralized with little to no access for marginalized and high-risk communities. Also, the centralized hepatitis care system does not offer the comprehensive services for prevention, testing and treatment.

Ministry of Primary and Secondary Healthcare of Punjab Province, in coordination with the Coalition for Global Hepatitis Elimination USA launched Local Hepatitis Elimination and Prevention (LHEAP) project in June 2023. LHEAP is a 3-year implementation research project providing full menu of essential hepatitis prevention, testing and treatment services at the community doorstep. The overall aim of the project is to generate the evidence for feasibility of HBV and HCV micro-elimination through implementation of decentralized community healthcare model. In the first phase, we intend to test-run the doorstep hepatitis elimination model.

Method: LHEAP is implemented in Rawalpindi district in a population of 100, 000 persons. The trained frontline workers go from door to door to do the following: 1) HBV and HCV Rapid Diagnostic Test (RDT), 2) Reflex testing i.e., on spot blood draw for PCR, 3) Hepatitis B adult vaccination, 4) Treatment for HBV and HCV, 5) Active follow-up to support individuals through the treatment, 6) Referral services for decompensated cases, 7) Follow-up testing for HBV and HCV.

Results: At the end of the first phase of testing, 34445 persons of all age groups were screened in 7 weeks of implementation. Among those 147 (0.43%) were found to be positive for HBsAg. 105 (71.4%) persons received confirmatory viral load testing and 68 (64.8%) tested positive. Treatment with tenofovir was initiated for 7 (10%) patients. Of the 34445, 619 (1.8%) were positive for Anti-HCV. 404 persons received viral load testing and 218 (54%) were found to have active viremia. Of those, treatment was started for 138 (63.3%) patients.

Frontline teams vaccinated 14326 adults with the first and then second dose of Hepatitis B vaccine.

Conclusion: The prevalence in the general population of is found to be lower than expected. This may be attributed to the fact that all age groups were included in the sample. Moreover, the population is settled in the urban households with predominant risk of interaction with the healthcare settings and open access to frequent therapeutic injections. Treatment initiation of HBV remain a challenge. Visit to primary care is required after confirmatory testing and the guidelines do not favor inclusive approach.

WED-495

The impact of integration and decentralization of HBV services on enhancing the HBV care continuum: an interrupted time series

Jean Damascene Makuza¹, Dahn Jeong², Marie Paul Nisingizwe², Phymar Soe², Richard Morrow³, Georgine Cua³, Héctor Alexander Velásquez García⁴, Janvier Serumondo⁵, Albert Tuyishime⁶, Joseph Puyat⁷, Alnoor Ramji⁸, Naveed Janjua⁴. ¹Rwanda Biomedical Center, University of British Columbia, School of Population and Public Health, Vancouver, Canada; ²University of British Columbia, School of Population and Public Health, Vancouver, Canada; ³University of British Columbia, School of Population and Public Health, British Columbia Center for Disease Control, Vancouver, Canada; ⁴British Columbia Center for Disease Control, University of British Columbia, School of Population and Public Health, Vancouver, Canada; ⁵Rwanda Biomedical Center, Kigali, Rwanda; ⁶Rwanda Biomedical Centre, Kigali, Rwanda; ⁷University of British Columbia, Vancouver, Canada; ⁸University of British Columbia, Faculty of Medicine, Division of Gastroenterology, Vancouver, Canada
Email: makorofr@gmail.com

Background and aims: Rwanda adopted decentralization and integration of hepatitis B virus (HBV) services into existing health services in July 2019. However, the impact of these changes has not been explored. Therefore, we assessed the impact of decentralization and integration of HBV diagnosis, treatment, and follow-up services into existing services on the HBV care cascade in Rwanda, including engagement in care, treatment initiation and continuation.

Method: We used data from the District Health Information System 2 data that included 4.5 million individuals screened for HBV in Rwanda between January 2016 and June 2023. We included individuals aged >2 years and analysed the proportion of individuals enrolled in care among those diagnosed, those who initiated the treatment among those who were eligible for HBV treatment, and those who were retained on treatment. We conducted interrupted time series (ITS) analysis overall and stratified by sex and age categories using a segmented linear regression model to assess the impact of decentralization of HBV services and included first-order autocorrelation terms to control for data correlation.

Results: Among the 4, 604, 468 persons included, 55, 820 (pre-policy: 21, 641 vs. post-policy: 34, 179) were diagnosed with HBV infections. Of those, 21, 182 (37.9%) [pre-policy: 5, 034 (23.3%) vs. post-policy: 16, 148 (47.2%)] were engaged in care, 5, 966 (28.2%) [pre-policy: 2, 435 (48.4%) vs. post-policy: 3, 531 (21.9%)] were eligible for HBV treatment, 4, 746 (79.6%) [pre-policy: 1, 950 (80.1%) vs. post-policy: 2, 796 (79.2%)] initiated treatment, and 4, 621 (97.4%) [pre-policy: 1, 942 (99.6%) vs. post-policy: 2, 679 (95.8%)] continued treatment at one-year post-initiation. ITS results showed that the proportion of individuals enrolled in care increased in level by 12.28 [95% confidence interval (CI): 4.46, 33.02] in July 2019 and remained stable since then. The proportion of individuals who retained in care decreased in trend (-2.46 , with 95% CI: -3.30 , -2.10). In our stratified analyses, we observed these changes in care enrollment in under 55 years old age categories and among males. We found no significant level nor trend change for the proportions of individuals who initiated HBV treatment.

Conclusion: Our findings indicate that decentralization of HBV services had a significant impact on engagement with care but did

not improve treatment initiation. Further investigations and strategic adaptations such as training of more health care providers on HBV management as well as intensive mentorship may be required to optimize the effectiveness of the HBV care continuum post-decentralization.

WED-496

Defining the data requirement to achieve the hepatitis C elimination in the United Kingdom: the Somerset liver improvement project

Emma Saunbury¹, Almuthana Mohamed¹, Christina Owen¹, Timothy Jobson¹. ¹Somerset NHS Foundation Trust, Taunton, United Kingdom
Email: almuthana700@gmail.com

Background and aims: Despite treatment initiatives to meet the World Health Organisation target of eliminating hepatitis C virus (HCV) by 2030, many patients with HCV in the United Kingdom (UK) are not yet linked to specialist services or treated. Using a novel case finding database in Somerset (609, 474 individuals), we aimed to identify unknown and untreated HCV patients, and determine the impact of deprivation on this patient population by refining the methodology to identify HCV patients for treatment.

Method: The database was configured to identify two groups of patients: those with persistently abnormal liver function tests (LFTs) and no HCV test; and a second group with positive HCV antibody (Ab) between 2004–2023 (age 18–70). Clinical records and 'high-cost drug' records were reviewed to determine treatment status, spontaneous HCV clearance, and/or sustained virological response (SVR) post-treatment. Postcodes were used to determine patients' Index of Multiple Deprivation (IMD) comparing most deprived deciles (IMD 1–2) with the rest (IMD 3–10) in line with the NHS Core20Plus5 programme. The cohort requiring treatment was queried for overlap with the 'lost positives' (NHS England programme) from 2018.

Results: 14, 525 had persistently abnormal LFTs (ALT>40; 90 days). However, 67% of them had never had HCV Ab tests. 1001 patients were identified with positive HCV Ab (current or prior), significantly weighted towards deprived areas (0.63% in IMD1–2; 0.21% in IMD3–10; $p < 0.0001$). HCV exposure was strongly associated with early mortality. The mortality of HCV Ab positive patients was significantly higher in deprived areas (25.2% in IMD1–2, 18.6% in IMD3–10; $P = 0.045$). Median age at death was 49 years. Overall, 687 alive HCV Ab positive patients were identified. Of them, 442 were either HCV PCR negative or treated. 120 identified as requiring treatment and 132 needed further investigation. Concerningly, 11% (75 patients) had never had HCV PCR test and further 74 had failed to engage with our service (although neither of these groups were associated with IMD). Of the patients requiring treatment now only 13% were also seen in the local 'Lost Positives' cohort identified from the NHS England Programme (2018).

Conclusion: Our data suggests that finding and treating the majority of cases requires a systematic approach to a) ensure all patients with abnormal LFTs have HCV Ab status checked; b) ensuring all HCV Ab positive patients have PCR status checked, and confirmed where negative; c) data across multiple geographies (patients with missing results may have had them elsewhere) and d) regular data refresh and an iterative approach, as while there have been successful prior initiatives, new untreated populations arise. Further work is underway to offer investigation and/or treatment to the relevant patients in Somerset.

WED-497

Presentations of acute hepatitis C in London, focussed in men who have sex with men (MSM)

Maeve Barlow¹, Indrajit Ghosh¹, Angieszka Kemper¹, Philippa C Matthews^{1,2}, Stuart Flanagan¹. ¹Central and North West London NHS Foundation Trust, Mortimer Market Centre, London, United Kingdom; ²The Francis Crick Institute, London, United Kingdom
Email: maeve.barlow1@nhs.net

Background and aims: WHO Elimination targets for HCV are dependent on early diagnosis and treatment. Since 2020 we have noted an increase in cases of acute HCV infection in North Central London (NCL). We characterised affected individuals to inform future strategies for testing and treating.

Method: We undertook a retrospective clinical audit to identify cases of acute HCV from 1 Jan 2020 to 31 Dec 2023 in individuals aged over 18 years. We identified cases through the NCL Hepatitis database and information was gathered from the Electronic Patient Record. Acute HCV was defined as: a negative HCV antigen result in the 6 months prior to a positive test, a significant risk event had occurred.

We used Stata (v17, StataCorps, Texas, USA) to conduct descriptive and frequency analyses.

Results: 20, 933 HCV antigen tests and 6491 HCV RNA tests were performed in our services during the 4-year period. We identified 35 adults with acute HCV. 5/35 (14.3%) occurred in 2020, 6 (17.1%) in 2021, 10 (28.6%) in 2022 and 14 (40.0%) in 2023. Median age was 37 years (range 22–58), 34/35 (97.1%) identified as male and 15/35 (42.9%) were born in the United Kingdom followed by Brazil (14.3%) and Columbia (8.6%), with 12/35 (34.3%) of cases reporting 12 other countries of birth. Most cases (28/35, 80.0%) were detected in the sexual health clinic setting, followed by hospital (8.6%) and primary care (5.7%). 33/35 (94.3%) were MSM, and the most identified risk factor for HCV acquisition was unprotected anal intercourse (UAI) in 32/35 (91.4%). Other risk factors included recreational drug use (62.9%), injecting drug use (37.1%) and fisting/sex toy use (14.3%). All individuals had at least one identifiable risk factor, and 22/35 (62.9%) reported multiple risk factors. 21/35 (60%) HCV cases arose in people living with HIV (PLWH), with a median CD4 count of 740 cells/mm³ (range 340 to 950), all on antiretroviral therapy. Of those eligible, 8/13 (61.5%) were on pre-exposure prophylaxis (PrEP). At HCV diagnosis, of those tested, 16/28 (57.1%) had a concurrent sexually transmitted infection (STI), the most common of which was gonorrhoea (35.7%), then chlamydia (21.4%) and syphilis (21.4%). 3/28 (10.7%) individuals had more than one STI identified. HCV infection was recurrent in 10/35 (28.6%). The most common genotype was 1a (19/35, 54.3%). 34/35 patients were commenced on Direct Acting Antivirals (DAA) and all 34 had completed DAA treatment by 31 Dec 2023, of whom none had detectable HCV RNA at end of treatment. Of those attending for their 12- or 24-week follow-up ($n = 23$), 100% had achieved SVR. Since completing treatment, there have been no known reinfections.

Conclusion: We highlight acute HCV infections in London primarily in MSM living with HIV infection, with UAI the most common risk factor. Targeted testing and intervention is essential to make prompt diagnoses. Ongoing active monitoring will guide screening and prevention interventions.

WED-498

Impact of direct-acting antiviral market access policy barriers and restrictions in patients with hepatitis C virus: A database analysis of US claims from states with and without Medicaid restrictions

Nancy S Reau¹, Krithika Rajagopalan², Dilip Makhija³, Fatema Turkistani², Caroline Burk², Marvin Rock³, Michelle Martin⁴. ¹Rush University, Chicago, United States; ²Anlitiks, Inc., Windermere, United States; ³Gilead Sciences, Inc., Foster City, United States; ⁴University of Illinois at Chicago, Chicago, United States
Email: nancy_reau@rush.edu

Background and aims: Market access policy barriers to direct-acting antivirals (DAAs) among patients with hepatitis C virus (HCV)

POSTER PRESENTATIONS

infection in public health insurance programs (e.g., Medicaid in the US) may result in undesirable outcomes among the vulnerable HCV patient population. While many state Medicaid plans have implemented sobriety restriction policies that require evidence of sobriety before DAAs are prescribed, no studies have examined the real-world consequences of such restrictions. This claims database analysis was conducted to examine the health care resource utilization (e.g., inpatient hospitalizations) impact of sobriety restrictions to DAAs among Medicaid patients with HCV infection in the United States.

Method: Data from the Anlitiks All Payor Claims data, an open-source data representing data from all 50 state Medicaid from January 2020 to June 2022 was used. Patients initiating DAAs (i.e., index date) between January to December 2021 were categorized based on their "state of residence" on index date into States with no sobriety restrictions (S/no-SR) and States with sobriety restrictions (S/SR). All eligible patients had ≥ 12 months pre-index, ≥ 6 months of post-index follow-up, and continuous medical enrollment (i.e. ≥ 1 medical claim during follow-up). Proportion of patients with ≥ 1 all-cause medical (inpatient, ER, outpatient, office) visits by type for S/no-SR vs S/SR cohort were examined. Cohort differences were analysed using unadjusted and adjusted (i.e., controlling for confounders) logistic regression models and reported as odds ratios (OR) and adjusted odds ratios (AOR) and associated 95% confidence intervals (CI), respectively.

Results: A total of 4,623 (S/no-SR) and 2,295 (S/SR) patients were eligible for analysis. The S/no-SR cohort had a mean age of 43.0 (SD = 11.51) years, 58.1% (n = 2,686) were male, and 59.68% (n = 2,759) had substance use history. The S/SR cohort had a mean age of 45.0 (SD = 12.02) years, 50.28% (n = 1,154) were male, and 44.1% (n = 1,012) had substance use history. All-cause medical visits by type were: 18.14% vs. 22.02% (inpatient), 37.44% vs. 42.34% (ER), 55.39% vs. 62.53% (outpatient), and 69.06% vs. 76.43% (office) for S/no-SR vs. S/SR cohorts, respectively. Unadjusted OR showed that all differences were significant and AOR demonstrated significantly ($p < 0.05$) higher odds of inpatient [AOR 2.09 (1.59–2.73)] and outpatient visits [AOR 1.52 (1.28–1.82)] for S/SR cohort compared to S/no-SR cohort.

Conclusion: In this analysis, Medicaid patients initiating DAAs in S/SR were 2 times and 1.5 times more likely to have inpatient and outpatient visits, respectively. Findings suggest that restricting DAA access in the vulnerable Medicaid HCV population may be associated with adverse HCRU consequences and potentially impede WHO's 2030 HCV global elimination goals.

WED-499

Predictors of treatment initiation for hepatitis C virus among pregnant and postpartum individuals using health administrative data from Ontario, Canada from 1999 to 2021

Andrew Mendlowitz^{1,2,3}, Jennifer Flemming^{4,5}, Tatyana Kushner⁶, William WL Wong^{2,7,8}, Zoe Greenwald^{8,9,10}, Camelia Capraru¹, Bo Chen¹, Wenbin Li³, Chelsea Masterman¹¹, Jordan J. Feld¹, Mia Biondi^{1,12}. ¹Toronto Centre for Liver Disease/Viral Hepatitis Care Network (VIRCAN), University Health Network, Toronto, Canada; ²Toronto Health Economics and Technology Assessment (THETA) Collaborative, University Health Network, Toronto, Canada; ³ICES, Queen's University, Kingston, Canada; ⁴ICES, Queen's University, Kingston, Canada; ⁵Departments of Medicine and Public Health Sciences, Queen's University, Kingston, Canada; ⁶Division of Liver Diseases, Icahn School of Medicine at Mount Sinai, New York, United States; ⁷School of Pharmacy, University of Waterloo, Waterloo, Canada; ⁸ICES, Toronto, Canada; ⁹Dalla Lana School of Public Health, University of Toronto, Toronto, Canada; ¹⁰Centre on Drug Policy Evaluation, MAP Centre for Urban Health Solutions, Li Ka Shing Knowledge Institute, St. Michael's Hospital, Toronto, Canada; ¹¹School of Nursing, University of Western Ontario, London, Canada; ¹²School of Nursing, York University, Toronto, Canada
Email: andrew.mendlowitz@mail.utoronto.ca

Background and aims: With the ongoing overdose epidemic, hepatitis C virus (HCV) prevalence has increased among younger individuals, including women of childbearing potential. Prior work has documented maternal complications and poor post-delivery linkage-to-care among those infected. Understanding factors associated with treatment initiation before, during, and after pregnancy may help develop strategies to enable HCV care for this population.

Method: We performed a population-based retrospective cohort study, linking individuals with pregnancy records (2003 to 2021) and positive HCV RNA test results (1999 to 2021) to provincial health administrative data in Ontario, Canada. Pregnancies were identified as early loss (<20 weeks), induced abortion and live/still births >20 weeks. HCV treatment was identified using outpatient prescription claims or HCV RNA test records. Individuals were followed from first RNA positive, until treatment initiation or censored at earliest date of death, emigration, HCV RNA negative, or end of study. Time-dependent Cox regression was used to evaluate associations between variables and treatment initiation, estimating crude (HR) and adjusted hazard ratios (aHR).

Results: We identified 6,928 individuals with HCV RNA positive test (s) and ≥ 1 pregnancy (18,822 pregnancies in total: 13,776 (73.0%) prior to first RNA positive, 3,458 (18.3%) during follow-up, and 1,628 (8.6%) after treatment initiation). After a median follow-up of 5.93 (95%CI:5.59–6.26) years, 3,878 people (44.0%) initiated treatment. Median age at RNA positivity was 30 years (IQR:26–36). In crude models, older age (HR 1.02, 95%CI:1.02–1.03), prior pregnancy (HR 1.50, 95%CI:1.39–1.63), substance use (HR 1.21, 95%CI:1.13–1.30), and initiating opioid agonist therapy (OAT) (HR 1.33, 95%CI:1.25–1.42) were associated with increased likelihood of treatment initiation. Number of pregnancies after RNA positive was associated with lower likelihood of treatment initiation (HR 0.90, 95%CI:0.86–0.95). Relative to pre-2012, treatment initiation was more likely among those with their first RNA positive from 2012 to 2017 (HR 2.27, 95%CI: 2.09–2.47) or post-2017 (HR 4.90, 95%CI:4.43–5.43). In a multivariable model stratified by prior pregnancy and era of first RNA positive, treatment initiation was associated with age >30 years at RNA positive, initiating OAT (aHR 1.10, 95%CI:1.01–1.20) and substance use diagnosis (aHR 0.80, 95%CI:0.72–0.88).

Conclusion: Among people who are diagnosed with chronic HCV and experience pregnancy, those of older age at diagnosis were more likely to initiate treatment. In addition, while people with diagnosis of substance use were less likely to initiate treatment, likelihood increased for those engaged in OAT. Additional strategies are needed to improve linkage after diagnosis, but prior to pregnancy; especially if not engaged in drug treatment.

WED-500

Exploring the underlying causes of disengagement from hepatitis C care

Kathleen Bryce^{1,2}, Fiona Burns^{1,3}, Colette Smith⁴, Alison Rodger^{1,3}, Douglas Macdonald^{1,5}. ¹Royal Free London NHS Foundation Trust, London, United Kingdom; ²Institute for Global Health, University College London, London, United Kingdom; ³Institute for Global Health, University College London, London, United Kingdom; ⁴Institute for Global Health University College London, University College London, London, United Kingdom; ⁵Institute of Liver and Digestive Health, University College London, London, United Kingdom
Email: kathleenbryce@doctors.org.uk

Background and aims: Despite established hepatitis C test-to-cure pathways in the community, some people have been unable to engage with treatment. We undertook an interview-based exploration of the barriers and enablers to hepatitis C direct-acting antiviral (DAA) treatment initiation in a key population of people who had delayed treatment.

Method: We conducted semi-structured interviews with individuals who had delayed (for at least six months with one appointment missed) or declined DAA therapy, as well as service providers.

Participants were identified using peer support and outreach networks. The topic guide was informed by a systematic review of barriers and enablers to treatment initiation. Responses were structured within the Capability, Opportunity, Motivation, Behaviour (COM-B) model by reflexive thematic analysis.

Results: Fourteen participants with hepatitis C (two women) were interviewed at drug treatment services, in their place of residence or clinical settings between November 2022 and January 2023. They were aged between 32–66 and diagnosed with hepatitis C between 1–30 (median 7) years ago. Nine participants were of White ethnicity and UK-born, 13 had a mental health diagnosis or concern and 11 had physical comorbidity, five of whom had severely reduced mobility. Six were currently homeless. Ten providers (clinical and allied health professionals, peer advocates and outreach team members) were interviewed in person or online. We identified four themes. “Once bitten, twice shy”: negative earlier life experiences and interactions with health and social care were barriers to subsequent engagement with DAA treatment (Opportunity). Previous difficulty navigating the healthcare system and experiencing enacted stigma led to the expectation of poor care again next time, with resultant avoidance. “This is a relief”: positive interactions with services, however, had the potential to repair damaged relationships and build trust through addressing the individual’s priorities first (Capability, Opportunity). “You can’t make plans”: lack of service adaptability and patient-provider ‘fit’ was a barrier to accessing treatment when life circumstances were unpredictable (Capability, Opportunity). “Stepping stones”: stability (individually defined) was needed to enable treatment uptake (Capability, Opportunity and Motivation). Most participants wanted treatment but felt a strong aversion to the possibility of ‘failing’ therapy and so deferred until they felt ready to complete it.

Conclusion: These themes provide a useful starting point and guide for exploring individual beliefs and behaviours surrounding hepatitis C treatment. Understanding the underlying capability, opportunity and motivational causes beneath apparently “chaotic” interactions with care providers might facilitate tailored intervention and support through treatment.

WED-501

“I go as much and to as many doctors I can trust to not be stigmatised”: factors in the experience of hepatitis B that affect linkage to care and treatment

Myliisa Vu¹, Sylvester Okeke², Robyn Horwitz², Elena Cama², Loren Brenner², Thomas Tu¹. ¹The Westmead Institute for Medical Research, Sydney, Australia; ²UNSW, Sydney, Australia
Email: myliisa.vu@wimr.org.au

Background and aims: The WHO 2030 elimination targets for hepatitis B include reducing new hepatitis infections by 90% and hepatitis B related deaths by 65%. Achieving these targets is impossible without expanding diagnosis, linkage to care, and treatment. Understanding the experiences of those not currently engaged in clinical monitoring and barriers to treatment and care is vital to improving these rates. This study aims to understand the experiences of people living with hepatitis B including barriers to post-diagnosis clinical monitoring and treatment.

Method: An online survey co-designed with members of the affected community was developed to understand engagement in treatment and monitoring among people living with hepatitis B. Participants were recruited from a global online community support group HepBCommunity.org. In contrast to clinically led studies, this approach allowed us to access a population of people who had been diagnosed, but not necessarily linked to care. Survey data included structured and open-ended questions and was collected through Qualtrics. Quality assurance measures were adopted to screen out suspicious responses. Quantitative data were analysed using simple frequency counts while open responses were coded into NVivo and thematically analysed.

Results: A total of 77 responses were received between May and November 2023 with the most responses (34.5%) from people residing in Australia. About a third of participants (33.8%) reported non-regular engagement in care (>1 year interval since last check-up) or had not engaged in care at all. About 50% of the participants disclosed that they have delayed or cancelled monitoring appointments to avoid stigma, with ~3 in 5 participants (57%) reporting having experienced stigma at their health service. Regarding barriers to treatment, two thirds of participants (64%) reported a negative medication experience. For those not taking medication, 50% cited fear of side effects and 33% reported unsatisfactory health provider services as primary reasons. Thematic analysis of responses to open-ended questions found that clinical monitoring and treatment are influenced by access to (i) affordable services; (ii) social networks; (iii) friendly, confidential, and stigma-free services; and (iv) trusted healthcare providers and pharmaceutical companies.

Conclusion: Our study shows that HepBCommunity.org can be used to assess the needs and experiences of the affected community who are not linked to care, a key demographic for engagement and elimination efforts. Our interim results highlight the negative effect of stigma in linkage to care and suggest that the fear of adverse experiences with the medication itself or the interactions with the health system act as barriers to treatment. Our work highlights specific areas where public health measures could be most impactful to facilitate global elimination of hepatitis B.

WED-502

Simplified criteria for antiviral initiation in patients with chronic HBV infection: an economic evaluation and budget impact analysis in Thailand

Pisit Tangkijvanich¹, Ratree Sawangjit², Maneerat Chayanupatkul³, Unchalee Permsuwan⁴, Piyameth Dilokthornsakul⁴. ¹Center of Excellence in Hepatitis and Liver Cancer, Faculty of Medicine, Chulalongkorn University, Bangkok, Thailand; ²Department of Clinical Pharmacy, Faculty of Pharmacy, Mahasarakham University, Mahasarakham, Thailand; ³Department of Physiology, Faculty of Medicine, Chulalongkorn University, Bangkok, Thailand; ⁴Department of Pharmaceutical Care, Faculty of Pharmacy, Chiang Mai University, Chiang Mai, Thailand
Email: pisittkvn@yahoo.com

Background and aims: Current criteria for initiating antiviral treatment in patients with chronic hepatitis B virus (HBV) infection are complex and difficult to implement. Simplified criteria could allow general practitioners to start antivirals for eligible patients in the general population to reduce liver-related complications, particularly hepatocellular carcinoma (HCC). However, the expansion of criteria might increase the overall financial burden. Thus, this study aimed to determine the cost-effectiveness of two simplified antiviral treatment initiation criteria among Thai patients with chronic HBV infection, who were naïve to antiviral treatment and aged ≥30 years old.

Method: A hybrid model of the decision tree and Markov model was developed. Two simplified antiviral treatment initiation criteria were (1) the Expanded criteria, defined as treating patients with HBsAg-positive and HBV DNA ≥2,000 IU/ml regardless of alanine transaminase (ALT) level, and patients with cirrhosis by tenofovir alafenamide (TAF) as the first-line drug, and (2) the Test-and-Treat criteria, defined as treating patients with HBsAg-positive and detectable HBV DNA regardless of ALT level, and patients with cirrhosis by TAF. PubMed was searched from its inception to July 2023 to identify input parameters. Best supportive care was chosen for patients who were ineligible for TAF. Incremental cost-effectiveness ratio (ICER) per quality-adjusted life year (QALY) was calculated.

Results: Our data demonstrated that both criteria could improve total patients’ life-year and QALY, but they increase total cost. Specifically, the Expanded criteria and Test-and-Treat criteria could improve 0.164 life-years and 0.152 QALYs compared to current practice. Moreover,

POSTER PRESENTATIONS

both criteria could reduce 4, 846 new cases of HCC per 100, 000 patients. The ICERs for the Expanded criteria and Test-and-Treat criteria were 24, 838 Thai baht (THB) (approximately 711 USD)/QALY and 163, 060 THB (4, 665 USD)/QALY, respectively. Budget impacts of the Expanded criteria and Test-and-Treat criteria for fully implemented after five years were 1, 549 million THB (44 million USD) and 4, 326 million THB (124 million USD), respectively.

Conclusion: At the current willingness-to-pay of 160, 000 THB (4, 578 USD)/QALY, the Expanded criteria were considered a cost-effective strategy. However, the Test-and-Treat criteria might not be cost-effective for initiating antiviral treatment in patients with chronic HBV in Thailand at the current threshold. In this context, health policy decision-makers might consider implementing the simplified criteria based on cost-effectiveness information and budget impacts.

WED-503

Liver stiffness measurement before and after antiviral treatment for hepatitis C: results from an OST-based hepatology service facility

Nikolaos Papadopoulos¹, Ioannis Braimakis², Sofia Vasileiadis³, Eleni-Myrto Trifylli⁴, Iosif Galinos¹, Anastasia Drimousi⁵, Melanie Deutsch³. ¹2nd Department of Internal Medicine, 401 General Army Hospital of Athens, Athens, Greece; ²Department of Gastroenterology, 417 Army Share Fund Hospital, Athens, Greece; ³2nd Department of Internal Medicine, Medical School of National and Kapodistrian University of Athens, Hippokraton General Hospital of Athens, Athens, Greece; ⁴1st Department of Internal Medicine, 417 Army Share Fund Hospital, Athens, Greece; ⁵Emergency Assistance and Support Unit, Organization Against Drugs (OKANA), Athens, Greece
Email: nipapmed@gmail.com

Background and aims: Direct Acting Antivirals (DAAs) have improved efficacy and tolerability in the treatment of chronic hepatitis C virus (HCV) infection in people who inject drugs (PWIDs). However, data regarding the impact of anti-HCV treatment with DAAs in liver fibrosis is lacking in this group of patients. We determined the stages of liver fibrosis before and after anti-HCV treatment with DAAs in an opiate substitution therapy (OST)-based hepatology service facility in Athens, Greece.

Method: We retrospectively enrolled 122 HCV patients (M/F: 109/13, mean age: 46 ± 8.6) treated for chronic hepatitis C (CHC) with no signs of reinfection. All of them were evaluated with liver stiffness measurement (LSM) before and after complete treatment between September 2018 and December 2023. The following stages of fibrosis were defined: F0–1: <7, F2: 7–8.9, F3: 9–11.9, and F4: ≥12 kPa.

Results: 15/122 (12.5%) were treatment-experienced, 1/122 (0.8%) were HBsAg positive, and 3/122 (2.5%) were HIV positive. Genotype distribution: G1: 18%, G3: 43.4%, G4: 10.7%, HCV RNA positive/no genotype determination: 27.9%. Before treatment, liver fibrosis classification according to LSM was: F0/F1: 20/122 (16.4%), F2: 48/122 (39.3%), F3: 14/122 (11.5%), F4: 40/122 (32.8%), while after treatment was: F0/F1: 60/122 (49.2%), F2: 32/122 (26.2%), F3: 11/122 (9%), F4: 19/122 (15.6%). The mean LSM re-evaluation period was 22.5 ± 10.4 months after the end of the treatment. Two F0/F1 patients (10%) were deteriorated to F2 stage after treatment. One F2 patient (2.1%) deteriorated to the F3 stage after treatment, 13 patients (27.1%) remained in the F2 stage, while 34 patients (70.8%) improved to F0/F1. Two (14.3%) F3 patients were stable after treatment, while 12 (85.7%) were improved. Finally, 19 (47.5) of the F4 patients were stable, while 21 (52.5%) improved. Multivariate analysis demonstrated that the pre-treatment stage of advanced fibrosis/cirrhosis was associated with LSM improvement after treatment (Chi-Square: 48.246, p < 0.005).

Conclusion: The liver fibrosis stage, according to LSM, improves significantly after HCV treatment with DAAs in PWIDs, especially in those with advanced fibrosis or cirrhosis before treatment.

WED-513

Automatic opportunistic age screening for hepatitis C virus. A public health strategy in Galicia, Spain. Project 2023

Elena Cruz-Ferro¹, Susana Miras-Carballal¹, Marta Piñeiro-Sotelo¹, Sonia Touceda-Taboada¹, Ignacio Díaz-Vázquez², Javier Cereijo-Fernández³, Juan Turnes Vázquez⁴. ¹General Directorate of Public Health, Santiago, Spain; ²Preventive medicine service of the University Hospital Complex of A Coruña, A Coruña, Spain; ³General Directorate of Public Health, Santiago, Spain; ⁴Pontevedra University Hospital Complex, PONTEVEDRA, Spain
Email: elena.cruz.ferro@sergas.es

Background and aims: Hepatitis C virus (HCV) is a main cause of liver disease worldwide. All countries, following WHO recommendations, must establish programs to achieve the goal of its elimination as a public health problem by 2030. Galicia is a region with a low prevalence of HCV infection, and it is estimated that 85% of cases are concentrated in the 40–69-year-old cohort, which would mean 3, 864 cases of undiagnosed active infection. For this reason, following the recommendations of the WHO, it has drawn up a strategy to address its elimination. One of its main features is the active recruitment of ≥45% of patients aged 40–69 in three years, since in this group the prevalence of unknown active infection is estimated at 0.33%. The aim of this study is to present the results of the screening and the opportunistic of the cohort of 50–59 years carried out in 2023, the estimated prevalence of active infection is 0.50%.

Method: Descriptive retrospective study Source: Epidemiological Surveillance System (VIXÍA). Scope: Galicia. Period: year 2023. Variables: cohort of 50–59 years, health area (HA), population, start date.

Procedure: automatic request for HCV-RNA analysis to any person in the age group who is requested for an analysis for any reason. Determination of HCV viral load using the sample pooling strategy (pooling of 100 samples).

Results: Opportunistic age screening was progressively implemented throughout Galicia in 2023, reaching 53.26% of the target population. 107, 238 samples were analyzed, with 148 positive results (0.14% active infections). The start date and results are indicated for each HA: - Santiago de Compostela and Barbanza (27/01/2023): 25, 240 samples analyzed (75.66% of the population); 24 positive results; 0.10% active infections. - A Coruña and Cee (20/03/2023): 24, 255 samples analyzed (58.53% of the population); 43 positive results; 0.18% active infections. - Lugo, A Mariña and Monforte de Lemos (12/04/2023): 12, 969 samples analyzed (52.92% of the population); 18 positive results; 0.14% active infections. - Pontevedra and O Salnés (08/05/2023): 14, 689 samples analyzed (63.95% of the population); 20 positive results; 0.14% active infections. - Ferrol (19/06/2023): 5, 298 samples analyzed (37.99% of the population); 5 positive results; 0.09% active infections. - Ourense, Verín and O Barco de Valdeorras (28/06/2023): 8, 400 samples analyzed (37.85% of the population); 12 positive results; 0.14% active infections. - Vigo (05/07/2023): 16, 387 samples analyzed; 26 positive results (38.16% of the population); 0.16% active infections.

Conclusion: The objective of studying 45% of the target population in Galicia and in the HA that started before June was met. A percentage of active infection lower than estimated was observed.

WED-514

High rates of hepatitis C RNA positivity and engagement in care from community pharmacies with a high intensity test and treat (HITT) model

Samuel Uveges¹, Edward Nicholson², Clinton Askew³, Sarah Montague², Stephen D Ryder². ¹Trust Pharmacy, Queen's Medical Centre, Nottingham, United Kingdom; ²Nottingham University Hospitals NHS Trust, Queen's Medical Centre, Nottingham, United Kingdom; ³The Hepatitis C Trust, London, United Kingdom
Email: samuel.uveges2@nuh.nhs.uk

Background and aims: Community pharmacies providing Opioid Substitution Therapy (OST) are a potentially important site for Hepatitis C Virus (HCV) testing and treatment as they interact with patients who may not have undergone testing at, or do not attend, addiction services. We aim to demonstrate the yield of introducing a HITT model in 12 community pharmacies, testing patients on OST prescriptions and not.

Method: Raise awareness of hepatitis C elimination at Local Pharmaceutical Committee and community pharmacy level by providing Continuous Professional Development (CPD) educational sessions to all staff and offering shadowing opportunities with the Operational Delivery Network (ODN) team. An ODN team consisting of Specialist Pharmacy Technician, Viral Hepatitis Clinical Nurse Specialist and Hepatitis C Trust Peer ran the events utilising the pharmacies consultation room to complete the test. The team used dried blood spot tests and provided a £5 incentivisation for patients on OST. Any patient who requested a test was tested regardless of OST status.

Results: Between July 2022 and July 2023, 21 testing events were held at 12 different community pharmacy locations. 252 individuals were tested. 51 were HCV abs positive and 13 were HCV RNA positive. 10 patients have been referred for treatment, 9 have commenced DAA treatment. 4 have achieved SVR12. 1 was HCV RNA negative on retest, 2 have yet to engage in care. 120 patients were in receipt of an OST prescription of which 13 were HCV RNA positive; 10.8% HCV RNA positivity. No HCV RNA positives were found in people not on OST. 36 of 52 HCV Ab positive patients had been treated previously. Of which 8 patients had been lost to follow-up and required an overdue SVR12 blood test. 4 of which were still HCV RNA+. 12 education sessions were delivered to between 2 and 10 people per site prior to the testing sessions commencing. Standardised feedback forms were sent to 11 locations and were completed by 8. Feedback suggests this testing model had minimal impact upon the day-to-day running of the pharmacy, all found CPD sessions beneficial and that their knowledge of hepatitis was improved.

Conclusion: The HITT model found patients who were registered with addiction services that had not received BBV testing and/or had not been referred to the ODN for DAA treatment. The data confirms that this group has a high HCV RNA positivity rate in those on OST. Feedback data suggests that this model is acceptable to community pharmacy teams and has helped to foster closer working between the ODN and community pharmacies.

WED-515

Identifying barriers of hepatitis C linkage to care among beneficiaries of harm reduction centers in Georgia

Maia Butsashvili¹, Lasha Gulbiani¹, George Kamkamidze¹, Ketevan Stvilia², Maia Tsereteli², Shaun Shadaker³, Rania Tohme⁴.

¹Health Research Union, Tbilisi, Georgia; ²National Center for Disease Control and Public Health, Tbilisi, Georgia; ³Centers for Disease Control and Prevention, Atlanta, United States; ⁴US Centers for Disease Control and Prevention, Atlanta, United States
Email: maibutsashvili@gmail.com

Background and aims: Georgia has one of the highest proportions of people who inject drugs (PWID) representing 2.23% of the adult population, and PWID represent 25% of persons with hepatitis C virus (HCV) infection in Georgia. Despite extensive screening of PWID at harm reduction (HR) centers, a substantial proportion of people with HCV infection are not aware of their status and therefore not linked to care. According to the integrated bio-behavioral survey conducted in 2022 among PWID, 58.1% were HCV antibody reactive and 32.1% had chronic HCV infection. The aim of this study was to identify barriers of HCV linkage to care among HR beneficiaries.

Method: We implemented a cross-sectional study to collect socio-demographic, risk behavior, HCV testing and treatment data among beneficiaries of HR centers in Batumi and Zugdidi cities in Western Georgia. Convenience sampling was used for recruitment. We conducted face-to-face interviews with PWID who had documented

detectable HCV virus and assessed their characteristics based on linkage to HCV care. Linked participants were defined as those being enrolled in HCV treatment. Non-linked participants were HCV RNA or HCV core antigen positive individuals without a history of HCV treatment. Bivariate analysis was conducted to elucidate factors associated with linkage to care.

Results: A total of 123 PWID with detectable HCV virus participated in the study, of whom 65.9% (n = 81) were linked and 34.1% (n = 42) were non-linked to HCV care. Age, education level, and employment status were not significantly associated with linkage to HCV care. Linked participants were more likely than non-linked participants to think that HCV treatment is important (97.5% vs. 88.1%, p = 0.04). Non-linked participants were more likely than linked participants to report that they needed more information about hepatitis C (75.0% vs. 53.1%, p = 0.03), and that improving awareness regarding the HCV pre-treatment procedures (e.g. what laboratory tests are needed before treatment, where to receive these services, etc.) was necessary (67.9% vs. 40.5%, p = 0.01), and that receiving more information regarding long-term complications of untreated hepatitis C is important (89.3% vs 64.6%; p = 0.01).

Conclusion: Implementing educational interventions among PWID focusing on the importance of HCV treatment and possible health outcomes of untreated HCV infection are needed to improve linkage to hepatitis C care among beneficiaries of harm reduction centers. Scaling up treatment among PWID is important for the achievement of elimination of hepatitis C in Georgia.

WED-516

Novel approach to re-engage untreated patients with chronic active HCV

Ana Fuentes^{1,2,3}, Lucía Chaves-Blanco¹, Alberto Vázquez¹, Marta Illescas¹, Lucía Pérez-Rodríguez¹, Fernando García García¹, Federico García García^{1,2,4}. ¹Hospital Universitario Clínico San Cecilio, Granada, Spain; ²Ibs. Granada, Granada, Spain; ³CIBERINFEC, Granada, Spain; ⁴CIBERINFEC, Madrid, Spain
Email: anafuenteslop@gmail.com

Background and aims: The World Health Organization (WHO) acknowledges hepatitis C as a significant public health challenge. Identifying and addressing untreated patients with chronic active Hepatitis C Virus (HCV) infection is a critical step towards achieving elimination. Existing strategies have largely been ineffective in reconnecting these patients to care. In this study, we introduce and discuss the outcomes of an "opportunistic" approach for re-engaging chronic active HCV diagnosed patients who have not received treatment.

Method: This prospective study was conducted at the San Cecilio University Clinical Hospital. It involved reviewing laboratory data and medical records of patients with serum or plasma samples submitted for routine analysis. An automated system in the Laboratory Information System (LIS) generated daily reports of patients with prior positive anti-HCV tests. We reviewed LIS data and medical records daily to check for evidence of antiviral treatment, sustained viral response (SVR), or risk-factors for re-infection. If no data was found, we tested samples for HCV-RNA. Positive results were communicated to the referring physician, and the patients were referred to the hepatology unit for treatment evaluation.

Results: The results cover the period from 22 May to 31 December 2023. We identified 1428 HCV-positive patients with available serum samples for unrelated reasons. Upon review, 91% (1296 out of 1428) showed SVR and lacked re-infection risk factors. Among the remaining 132 patients, 42 (2.9% of the total and 32% of those with no previous information) were viremic. Of these, 24 (57%) were engaged in care, 21 (87%) commenced antiviral treatment, 2 declined treatment due to advanced age and comorbidities, 1 were advised to cease alcohol consumption before treatment, and 2 are not attend an appointment.

POSTER PRESENTATIONS

Conclusion: Our study describes an effective “opportunistic” approach to re-engage untreated patients with chronic active HCV. This strategy leverages the fact that these patients are already in contact with healthcare services, making reintroduction into the hepatitis C care continuum more efficient than other re-engagement strategies. We recommend this approach as a significant advancement towards eliminating hepatitis C.

Rare liver diseases (including paediatric and genetic) – Basic

TOP-145

p.Pro871Arg variant in JAG1 demonstrates a common manifestation of Alagille's syndrome

Preeti Sharma¹, Joanne Mushi¹, Jake Mann¹. ¹University of Birmingham, Birmingham, United Kingdom
Email: jpmann.gsy@gmail.com

Background and aims: Large studies of exome sequencing have demonstrated the existence of common manifestations of severe monogenic disease. These are yet to be described for liver disease. Alagille Syndrome (ALGS), a multisystem monogenic disorder caused by mutations in the JAG1-NOTCH2 pathway. It's hepatic manifestations are characterised by cholestasis, fibrosis, and frequently necessitates transplantation.

Method: Here, we used genome-wide association study summary statistics to identify common variants in JAG1 associated with liver-related traits in otherwise healthy adults. We found genome-wide significant associations ($p < 5 \times 10^{-8}$) between variants (e.g single nucleotide polymorphisms) and liver biochemistry (ALT, bilirubin, GGT, ALP) in $n = 1,654,950$ participants from the Common Metabolic Disease Portal and $n = 394,841$ from UK BioBank. Candidate variants were studied using AlphaFold protein modelling and *in silico* saturation mutagenesis of JAG1. Finally, we curated a database of all known human pathogenic JAG1 variants.

Results: We found rs35761929G>C, encoding p.Pro871Arg in JAG1 to be significantly associated with ALT ($p = 4.2e-10$) and bilirubin ($p = 9.7e-10$). This is a common variant (effect allele frequency = 0.05) and not reported to be associated with ALGS. It is predicted to affect protein stability however is classified as benign according to AlphaMissense (pathogenicity score = 0.09, where 1 = pathogenic and 0 = benign). p.Pro871Arg variant is found within the cysteine-rich extracellular domain of JAG1. Utilising In-Silico Saturation Mutagenesis, this region was found to be generally tolerant of mutations (median pathogenicity score = 0.24 (IQR 0.12–0.70)), similar to the intracellular domain (median pathogenicity score = 0.25 (IQR 0.14–0.45)), but in contrast to the DSL domain (median pathogenicity score = 0.95 (IQR 0.67–0.99)). This was validated by generating a database of all known JAG1 human variants, through which 671 unique pathogenic variants associated with ALGS were identified. Stop codons at position 871 were linked to ALGS but no other pathogenic missense mutations were found.

Conclusion: These findings underscore the implication of the NOTCH2-JAG1 pathway in common liver diseases such as metabolic dysfunction-associated steatotic liver disease (MASLD) and alcohol-related liver disease (ALD). Deciphering the functional alterations caused by the p.Pro871Arg variant in JAG1 can provide valuable insight for therapeutic interventions, and allow targeting of the NOTCH2-JAG1 pathway.

TOP-146

Activation of the HIF-1alpha pathway in cholangiocytes of patients with biliary atresia and its association with cilia disruption

Patricia Quelhas¹, Rui Oliveira², Jorge Luiz dos Santos¹. ¹CICS-UBI-Health Sciences Research Centre, University of Beira Interior, Covilhã, Portugal; ²Institute for Clinical and Biomedical Research (iCBR), Serviço de Anatomia Patológica, Centro Hospitalar e Universitário, Universidade de Coimbra (SAP-CHUC), Coimbra, Portugal
Email: patriciaasquelhas@gmail.com

Background and aims: Biliary atresia (BA) is a progressive hepatic disorder starting in infancy, often leading to liver failure and transplantation. Ischemic cholangiopathy constitutes a biliary disruption resulting from poor arterial blood supply by the peribiliary vascular plexus (PVP). In previous studies, our group demonstrated the presence of an ischemic cholangiopathy in a specific subset of patients with isolated BA, which showed activation of the HIF-1alpha pathway in cholangiocytes. It has been previously demonstrated that ciliopathy occurs in BA, both in syndromic and non-syndromic forms, similar to what happens in polycystic kidney diseases with ductal plate malformation, isolated neonatal cholangitis (DCDC2), and choledochal cyst. Considering that hypoxia can disrupt biliary epithelial cilia thus leading to an ischemic cholangiopathy, we hypothesized that hypoxia may be correlated with absence of cholangiocyte cilia in the subset of BA patients presenting HIF-1alpha pathway activation in the liver. This study aims to unveil whether HIF-1alpha nuclear positivity in cholangiocytes of BA patients correlates with absence of apical cilia and/or alterations in the cellular immunolocalization of Tubulin-4alpha acetylated (TUBA4A).

Method: Using immunofluorescence analysis on liver samples from biliary atresia patients and controls with neonatal cholestasis, this study looked for nuclear HIF-1alpha signals, associated with hypoxia, and TUBA4A signals for cilia analysis in cholangiocytes. Portal spaces, parenchyma, fibrovascular septa and extra-portal ductular reaction were analyzed. At the initial step, cholangiocytes with nuclear HIF1 alpha-positive samples were identified. The presence of cilia in biliary structures was observed through TUBA4A labeling and correlated with the HIF1A positivity status.

Results: A tendency was noted between HIF-positive and HIF-negative samples concerning the number of ducts with cilia, with HIF-positive samples showing a lower number of cilia. It was also observed that when tubulin is expressed in the cytoplasmic form, differences exist between controls and BA in the intensity of tubulin labeling, with higher intensity in BA. Moreover, when comparing BA patients who died within two years post-portoenterostomy with those who did not die or died after the initial two years, those exhibiting weak or moderate cytoplasmic tubulin intensity showed a higher mortality rate during the specified period.

Conclusion: The activation of the HIF1 alpha pathway appears to affect the morphology or presence/absence of cilia in intra- and extra-portal ducts. There also seems to be a difference in the cytoplasmic expression of tubulin in Biliary Atresia, and this alteration seems to worsen the early post-portoenterostomy prognosis, with decreased cytoplasmic tubulin expression being associated with higher early mortality.

FRIDAY 07 JUNE

FRI-151

RNA editing for the treatment of Alpha-1 antitrypsin deficiency

Prashant Monian¹, Genliang Lu¹, Chikdu Shivalila¹, Keith Bowman¹, Marissa Bylsma¹, Michael Byrne¹, Megan Cannon¹, Jigar Desai¹, Alyse Faraone¹, Frank Favaloro¹, Anamitra Ghosh¹, Jack Godfrey¹, Nidia Hernandez¹, Olivia Huth¹, Naoki Iwamoto¹,

Tomomi Kawamoto¹, Jayakanthan Kumarasamy¹, Pachamuthu Kandasamy¹, Anthony Lamattina¹, Amber Lindsey¹, Fangjun Liu¹, Richard Looby¹, Khoa Luu¹, Jake Metterville¹, Ik-Hyeon Paik¹, Qianli Pan¹, Erin Purcell-Estabrook¹, Jeanette Rheinhardt¹, Mamoru Shimizu¹, Kuldeep Singh¹, Stephany Standley¹, Carina Thomas¹, Snehlata Tripathi¹, Hailin Yang¹, Ryan Yordanoff¹, Benny Yin¹, Hui Yu¹, Cynthia Caracta¹, Padma Narayanan¹, Paloma Giangrande¹, Chandra Vargeese¹. ¹Wave Life Sciences, Cambridge, United States
Email: pmonian@wavelifesci.com

Background and aims: Alpha-1 antitrypsin (AAT) is an acute-phase protein synthesized by hepatocytes and secreted into circulation, where it protects the lungs from protease-induced damage. A point mutation in the *SERPINA1* gene (Z allele) is the most common cause for AAT deficiency (AATD). The resulting Z-AAT protein misfolds and aggregates in hepatocytes, decreasing functional AAT in circulation. Homozygous ZZ mutation carriers are at risk for severe AATD, which can lead to progressive liver injury and/or chronic obstructive pulmonary disease. Current standard of care addresses only lung disease and aims to restore serum AAT levels to an anticipated therapeutic threshold ($\geq 11 \mu\text{M}$) by weekly intravenous AAT from human plasma. Approaches in development address only a subset of patient needs (e.g., silencing approaches to reduce liver aggregates) or do not restore wild-type AAT (e.g., small-molecule approaches). We aim to decrease Z-AAT in liver and restore wild-type AAT in circulation by correcting Z mRNA with AIMers—chemically modified oligonucleotides that direct A-to-I RNA editing by recruiting endogenous ADAR enzymes. To facilitate hepatocyte delivery, AIMers are conjugated to N-Acetylgalactosamine (GalNAc-AIMers). This approach is designed to preserve physiological regulation of AAT while protecting the lungs and decreasing Z-AAT aggregation in liver.

Method: NSG-PiZ mice, expressing a human *SERPINA1* Z transgene, were treated with 10 mg/kg GalNAc-AIMER by subcutaneous injection for 13 weeks. Total serum AAT was quantified by ELISA, and the proportion of Z-AAT and M-AAT in serum was measured by mass spectrometry. Human iPSC-derived hepatocytes (ZZ genotype) were treated with GalNAc-AIMER *in vitro*. RNA editing was quantified by Sanger sequencing. The diameter of PAS-D-positive globules in hepatocytes was measured, and lobular inflammation was semi-quantitatively graded. AAT aggregates were quantified *in vitro* using an antibody specific to polymeric AAT.

Results: In NSG-PiZ mice, GalNAc-AIMers direct ~50% editing of the Z mRNA in liver and durably increased serum AAT levels ($\geq 33 \text{ mM}$ at 13 weeks). Secreted AAT had the expected wild-type amino acid sequence. Treated mice showed a significant decrease in liver inflammation and hepatocyte turnover, and a reduction in the size of PAS-D-positive globules. GalNAc-AIMers corrected the expression of genes inappropriately upregulated in the NSG-PiZ mouse liver and effectively cleared pre-existing AAT aggregates in human ZZ iPSC-derived hepatocytes *in vitro*.

Conclusion: These findings highlight the potential of GalNAc-AIMers to address both liver and lung manifestations of AATD. Wave Life Sciences is advancing WVE-006, an investigational GalNAc-AIMER, into clinical trials for the treatment of AATD. This clinical program (RestorAATion) is designed to provide proof of concept for the first RNA editing therapy in humans.

FRI-152-YI

Gene editing to treat liver metabolic disorders: harnessing paired Cas9-Nickases for efficient and safe treatment of primary hyperoxaluria type 1

Laura Torella¹, Martin Bilbao-Arribas², Julia Klermund³, Geoffroy Andrieux⁴, África Vales Aranguren², Cristina Olague Micheltorena², Julen Torrens-Baile², Eduardo Salido⁵, Toni Cathomen³, Nerea Zabaleta⁶, Gloria González-Aseguinolaza². ¹CIMA University of Navarra, Pamplona, Spain; ²Center for Applied

Medical Research (CIMA), University of Navarra, Pamplona, Spain; ³Institute for Transfusion Medicine and Gene Therapy, Medical Center-University of Freiburg, Center for Chronic Immunodeficiency (CCI), Medical Center-University of Freiburg, Freiburg, Germany; ⁴Institute of Medical Bioinformatics and Systems Medicine, Medical Center-University of Freiburg, Faculty of Medicine, University of Freiburg, Freiburg, Germany; ⁵Hospital Universitario de Canarias, Universidad La Laguna, CIBERER, Tenerife, Spain; ⁶Grousbeck Gene Therapy Center, Schepens Eye Research Institute, Mass Eye and Ear, Harvard Medical School, Boston, United States
Email: ltorella@alumni.unav.es

Background and aims: Primary hyperoxaluria type 1 (PH1) is a rare metabolic disorder with excessive oxalate production in the liver, leading to kidney toxicity. Currently, severe PH1 treatment involves RNA interference to reduce glycolate oxidase (GO) expression, raising concerns about therapy compliance and long-term efficacy. CRISPR-Cas9-mediated gene disruption offers a potential one-time therapeutic strategy. However, nuclease editors pose off-target risks, and adeno-associated vectors (AAV) for CRISPR delivery present challenges due to genome integration into CRISPR-mediated double-strand breaks (DSBs). Investigating paired Cas9 nickases (nCas9) aims to enhance safety by minimizing off-target events and achieving accurate gene disruption.

Method: Comparing paired nCas9, single or paired Cas9 nucleases (wtCas9) with the same guide RNAs (gRNAs), we examined *in vivo* disruption of the *Hao1* gene (GO encoding gene). AAV8 vectors delivered editing tools to PH1 mouse livers, restricting Cas9 expression to hepatocytes using a liver-specific promoter. Molecular and biochemical analyses assessed the efficiency, accuracy, and safety of the editing approaches, along with therapeutic efficacy.

Results: Paired nCas9, delivered via two AAV vectors, were as effective as individual or paired wtCas9 in reducing GO. Single nicks failed to disrupt *Hao1*, while DSBs induced by paired nCas9, likely repaired via the microhomology-mediated end-joining pathway, led to modifications of variable sizes. Single wtCas9-induced DSBs were primarily repaired through the non-homologous end-joining pathway, generating small insertions and deletions, whereas paired wtCas9 consistently resulted in a precise deletion of the sequence between the two cuts in most cases. Investigating AAV integration at the on-target site revealed existing tools consistently underestimated integration frequency. The application of a custom pre-processing pipeline to the analysis showed paired nCas9 significantly reduced AAV integration compared to individual or paired wtCas9. Disparities may be attributed to observed differences in repair mechanisms following nCas9 and wtCas9 editing. An all-in-one AAV vector for nCas9-mediated cleavage maintained editing efficiency with a reduced injected dose, resulting in a significant therapeutic effect while reducing AAV integration dose-dependently. Assessment of gRNA specificity through CIRCLE-seq, CAST-Seq, and long-read nanopore sequencing revealed no off-target activity or chromosomal translocations.

Conclusion: Paired nCas9 demonstrates promise for *in vivo* gene disruption, achieving efficiency comparable to wtCas9. This approach shows therapeutic efficacy, reduces on-target AAV integration frequency, and the risk for off-targets, representing a positive step toward developing a safe and effective long-term treatment for PH1 patients.

FRI-153

High prevalence of steatotic liver disease and systemic inflammation in hereditary fructose intolerance (HFI) patients independent of age, BMI and the presence of metabolic syndrome

Teresa Cardoso Delgado^{1,2,3}, Ainara Cano⁴, Maria Mercado-Gómez², Xabier Buque⁵, Cristina Alonso⁶, Marina Serrano-Macia², Carlos Alcalde⁷, Amaya Belanger-Quintana⁸, Elvira Cañedo-Villarroya⁹, Leticia Ceberia Hualde¹⁰, Silvia Chumillas-Calzada¹¹, Patricia Correcher¹²,

POSTER PRESENTATIONS

Dolores García-Arenas¹³, Igor Gómez¹⁴, Tomás Hernández¹⁵, Elsa Izquierdo-García¹⁶, Dámaris Martínez Chicano¹³, Montserrat Morales¹¹, Consuelo Pedrón-Giner⁹, Estrella Petrina Jáuregui¹⁷, Luis Peña¹⁸, Paula Sánchez-Pintos¹⁹, Juliana Serrano-Nieto²⁰, María Unceta Suárez^{21,22}, Isidro Vitoria Miñana¹², Jose Alejandro Larena²³, María Luz Couce¹⁹, María Luz Martínez-Chantar^{2,24}, Patricia Aspichueta^{5,22,24}, Javier de las Heras Montero^{25,26,27}, ¹IIS BioBizkaia, Barakaldo, Bizkaia, Spain; ²Liver Disease Lab, Center for Cooperative Research in Biosciences (CIC bioGUNE), Basque Research and Technology Alliance (BRTA), Derio, Spain; ³IKERBASQUE, Basque Foundation for Science, Bilbao, Spain; ⁴IIS Biobizkaia, Barakaldo, Bizkaia; ⁵Department of Physiology, Faculty of Medicine and Nursing, University of the Basque Country UPV/EHU, Leioa, Spain; ⁶RUBIÓ METABOLOMICS, S.L.U., Derio, Spain; ⁷Paediatrics Unit, Río Hortega University Hospital, Valladolid, Spain; ⁸Metabolic Diseases Unit, Department of Paediatrics, Ramón y Cajal Hospital, Madrid, Spain; ⁹Department of Metabolism Diseases and Nutrition, Niño Jesús University Children's Hospital, Madrid, Spain; ¹⁰Internal Medicine Service, Cruces University Hospital, Barakaldo, Spain; ¹¹12 de Octubre University Hospital, CIBERER, MetabERN, Madrid, Spain; ¹²Nutrition and Metabolic Diseases Unit, La Fe University Hospital, Valencia, Spain; ¹³Department of Paediatric Gastroenterology, Hepatology and Nutrition, Sant Joan de Déu Hospital, Barcelona, Spain; ¹⁴Araba University Hospital, Vitoria, Spain; ¹⁵Paediatric Service, Albacete University Hospital, Albacete, Spain; ¹⁶Pharmacy Department, Infanta Leonor University Hospital, Albacete, Spain; ¹⁷Clinical Nutrition Section, Navarra University Hospital, Pamplona, Spain; ¹⁸Pediatric Gastroenterology, Hepatology and Nutrition Unit, Complejo Hospitalario Universitario Insular Materno Infantil, Las Palmas de Gran Canaria, Spain; ¹⁹Unit of Diagnosis and Treatment of Congenital Metabolic Diseases, Department of Pediatrics, IDIS-Health Research Institute of Santiago de Compostela, CIBERER, MetabERN, Santiago de Compostela, Spain; ²⁰Paediatric Service, Málaga Regional University Hospital (HRU), 29010, Málaga, Spain; ²¹Biochemistry Laboratory, Metabolism Area, Cruces University Hospital, Barakaldo, Spain; ²²Biochemistry Laboratory, Metabolism Area, Cruces University Hospital, Barakaldo, Spain; ²³Ostak, Hospital Galdakao-Usansolo, Galdakao, Spain; ²⁴Centro de Investigación Biomédica en Red de Enfermedades Hepáticas y Digestivas (CIBERehd), Carlos III National Health Institute, Madrid, Spain; ²⁵Biocruces Bizkaia Health Research Institute, Barakaldo, Spain; ²⁶Division of Paediatric Metabolism, CIBERER, MetabERN, Cruces University Hospital, Barakaldo, Spain; ²⁷Department of Paediatrics, University of the Basque Country (UPV/EHU), Leioa, Spain
Email: teresadejesus.cardosodelgado@bio-bizkaia.eus

Background and aims: Hereditary Fructose Intolerance (HFI) is an autosomal recessive inborn error of metabolism characterized by pathological loss-of-function variants of the aldolase B (ALDOB) gene. Although fructose, sucrose and sorbitol (FSS)-restricted diet halts HFI acute life-threatening complications, HFI patients on lifelong FSS-restricted diet are susceptible to a series of metabolic manifestations.

Method: A cohort of HFI patients on long-term FSS-restricted diet (n = 32) was compared to a group of age, gender- and body weight-matched controls (n = 28) in a cross-sectional study. Serum lipidomics profiling by LC/MS was carried out to better understand altered metabolic processes in HFI patients, together with NMR-based serum glycoprotein/lipoprotein analysis, serum amino acids and acylcarnitines profiling and assessment of hepatic steatosis by MRS/MRI. Moreover, silencing of ALDOB and treatment with metformin was evaluated in cultured hepatocytes by measuring lipid content followed by assessment of de novo lipogenesis (DNL) and fatty acid oxidation (FAO).

Results: HFI patients are characterized by a distinct serum lipidomics signature highlighting alterations in inflammation and liver lipid metabolism. Indeed, HFI patients present elevation of serum inflammation markers such as GlycA, early marker of systemic inflammation as well as increased cardiovascular disease (CVD) risk. In agreement, increased serum cholesterol, altered serum lipoprotein profile, mildly increased arterial blood pressure is reported in HFI patients. Also, HFI patients are characterized by marked hepatic steatosis associated with increased DNL index and reduced surrogates of FAO (altered serum b-hydroxybutyrate, plasma acylcarnitines and valine amino acid levels). Likewise, silencing of ALDOB in cultured hepatocytes increases lipid cell content by augmenting DNL and diminishing FAO. Liver steatosis in HFI patients is not associated with age, BMI, the amount of ingested fructose and is also unrelated to the presence of metabolic syndrome.

Conclusion: Systemic inflammation and liver steatosis are common chronic complications in long-term FSS-restricted HFI patients independent of classical risk factors for MASLD. HFI patients with higher GlycA, an early marker of systemic inflammation, present a distinct serum lipidomic and lipoprotein profile predicting augmented cardiovascular disease risk. Further studies are necessary to assess the risk of fibrosis progression in HFI patients.

FRI-154

Copper overload promotes steatosis in Wilson disease by inhibiting peroxisome proliferator activated receptor alpha-fatty acid binding protein 1- glutathione peroxidase 4 signaling and inducing ferroptosis

Chen Liang¹, Li Bai², Shan Tang³, Sujun Zheng⁴. ¹Beijing YouAn Hospital, Capital Medical University, Beijing Key Laboratory of Liver Failure and Artificial Liver Treatment Research, Beijing, China; ²Beijing YouAn Hospital, Capital Medical University, Beijing Key Laboratory of Liver Failure and Artificial Liver Treatment Research, Beijing, China; ³Beijing YouAn Hospital, Capital Medical University, Beijing, China; ⁴Beijing YouAn Hospital, Capital Medical University, Beijing, China
Email: zhengsujun@ccmu.edu.cn

Background and aims: ATP7B Arg778Leu is most common mutation in Asian patients with Wilson disease (WD), a disorder of copper excretion. Mild to moderate hepatic steatosis is the most common nonspecific change in WD pathology. Blocking hepatic steatosis early is important for preventing the development of WD and ensuing sequelae. However, the molecular mechanism underlying this phenomenon needs to be elucidated. Herein, we addressed this issue using ATP7B Arg778Leu HepG2 cell model, patient samples and bioinformatics analysis.

Method: The levels of steatosis and ferroptosis were assessed in ATP7B Arg778Leu HepG2 treated with CuSO₄ and/or liver tissues from WD patients. The relationship between steatosis and ferroptosis was determined by the administration of ferroptosis inhibitor fer-1. Bioinformatics analysis was performed to screen out hub genes and signaling pathways related to WD steatosis. The regulation among peroxisome proliferator-activated receptor alpha (PPARα), fatty acid binding protein 1 (FABP1), glutathione peroxidase 4 (GPX4) and ferroptosis was analyzed using PPARα inducer fenofibrate (FN) and inhibitor GW6471 (GW) as well as FABP1 recombinant (FABP1rp). The interaction among PPARα, FABP1 and GPX4 was determined using correlation analysis, immunofluorescence staining and CO-IP experiment. Finally, the expression of GPX4, PPARα and FABP1 was detected and compared in the liver tissues from WD patients with or without steatosis and healthy individuals.

Results: The levels of steatosis and ferroptosis indicators were obviously changed in ATP7B Arg778Leu HepG2 treated with CuSO₄ and/or liver tissues from WD patients. Inhibiting ferroptosis alleviated steatosis. PPARα and FABP1 were screened out as potential regulators for steatosis according to bioinformatics analysis. The administration of FN led to up-regulated PPARα, FABP1 and GPX4 expression, conversely, GW treatment resulted in down-regulated

expression of these three proteins. In addition, the administration of rFABP1 brought about elevated FABP1 and GPX4, but not PPAR α . Moreover, PPAR α , FABP1 and GPX4 were co-localization and interacted. The expression of GPX4, PPAR α and FABP1 was reduced in liver tissues from WD patients with steatosis compared with that in WD liver tissues without steatosis.

Conclusion: Copper overload promotes ferroptosis and steatosis in WD by down-regulating PPAR α -FABP1-GPX4 signaling. Therefore, up-regulating PPAR α and FABP1 expression to block ferroptosis is a potential target to prevent steatosis and delaying disease progression in WD patients.

FRI-155

Introduction of class I-III mutations of CFTR in isogenic human iPSCs-derived cholangiocytes and 3D organoids provides pathophysiological information relevant for treatment of cystic fibrosis-related liver disease (CFLD)

Shakila Taleb¹, Saif Zaman¹, Zehra Syeda¹, Mario Strazzabosco¹, Romina Fiorotto¹. ¹*Yale School of Medicine, New Haven, United States*
Email: romina.fiorotto@yale.edu

Background and aims: Cystic Fibrosis-associated liver disease (CFLD) causes significant morbidity and mortality in patients with CF. Using CF animal models and human induced pluripotent stem cells (iPSC)-derived cholangiocytes bearing the DF508 mutation, we showed that CFTR-defective biliary cells present changes in secretion, cell polarity and innate immune responses. However, the impact of different CFTR mutations on CFLD phenotype and response to therapies remains unclear. In this study, we aimed to generate human cholangiocyte carrying different CFTR mutations using gene editing of iPSC and study the effects of these mutations on biliary cell physiology.

Method: Isogenic iPSC lines bearing the following CFTR mutations W1282X (class I), DF508 (class II) and G551D (class III) were generated using CRISPR/Cas9 gene editing. iPSC lines were differentiated to cholangiocytes and cultured in monolayers or 3D biliary organoids were generated along the differentiation process using Matrigel. Cholangiocyte specification was verified by RT-PCR and IHC. Bulk-RNA-seq was performed in monolayers. Using forskolin-induced swelling (FIS) organoids were tested for differences in CFTR baseline function and response to CFTR modulators.

Results: iPSCs-derived biliary organoids maintained morphological and functional properties of mature biliary epithelium similar to tissue-derived biliary organoids. iPSC-organoids with different CFTR mutations show no or minimal response to FIS (W1282X<DF508<G551D). CFTR modulators (ETI) (3 μ M) treatment improved FIS in DF508 and G551D but not W1282X organoids. Immunolabeling for β -catenin and ZO-1 showed disarrangement of cellular polarity in all CF organoids. Transcriptome analysis, identified 11 differentially expressed genes (DEGs) in common among all mutations, compared to isogenic controls. Enrichment of DEGs related to cytoskeletal components were present in all CFTR mutated lines compared to the control line. A strongly reduced gene and protein expression of NLRP2, a relatively uncharacterized component of the inflammasome and a negative regulator of TNF-mediated NF- κ B signaling, was found in all the CF lines. Decreased expression of NLRP2 in CFTR-mutated cholangiocytes might be mechanistically related to the pro-inflammatory phenotype described in CF cholangiocytes.

Conclusion: Using gene editing of iPSC we have generated human cholangiocytes and organoids carrying mutations that impact CFTR function at different levels. CFTR dysfunction affects the morphology, transcriptome and secretory function of cholangiocytes in a mutation-specific way. Biliary organoids with CFTR mutations with residual protein production respond to CFTR modulators used in the clinic. This iPSC-based platform will be useful to identify new therapeutics.

FRI-158-YI

The cyst microenvironment is spatially patterned to promote polycystic liver disease

Scott Waddell¹, Yuelin Yao², Luke Boulter³. ¹*MRC Human Genetics Unit, Institute of Genetics and Cancer, University of Edinburgh, Edinburgh, United Kingdom*; ²*MRC Human Genetics Unit, School of Informatics, University of Edinburgh, Edinburgh, United Kingdom*; ³*MRC Human Genetics Unit, Institute of Genetics and Cancer, University of Edinburgh, Edinburgh, United Kingdom*

Email: scott.waddell@ed.ac.uk

Background and aims: Polycystic liver diseases (PLDs) are a group of genetically heterogeneous conditions characterised by the presence of multiple fluid-filled cysts within the liver. Cyst growth results in hepatomegaly (liver enlargement), leading to abdominal pain, shortness of breath and malnutrition, and consequently, patients suffer from an extremely poor quality of life. Additionally, cysts are at risk of rupture and infection, which leads to sepsis if left untreated. There are currently no widely approved pharmaceutical treatments for PLD patients and despite several dysregulated molecular targets having been previously identified within cyst cells, none of these have been translated for clinical practice. Cyst epithelial cells are surrounded by a complex cyst microenvironment (CME), which is instructed by the cyst epithelia. Very little work, however, has focused on how non-epithelial cells within the CME contribute to cyst growth within the liver, particularly in human disease, nor whether modulation of the CME represents a therapeutic strategy to target the formation of cysts in patients. In cancer, therapies that target the microenvironment, namely immunotherapy, have revolutionised patient care; *could taking a similar approach and targeting the CME in PLD yield similar clinical successes?* We hypothesise that the formation of a unique CME in PLD offers a number of candidate targets for therapeutic intervention and aim to 1. Spatially map the CME in PLD patients and 2. Identify targetable processes which could reduce cystic growth.

Method: Using patient PLD tissue, we have used GeoMx spatial transcriptomics and Akoya fusion high-plex immunophenotyping to spatially map the formation and composition of the CME in PLD. We have then used a combination of human ductular organoid cultures and mouse models of PLD to identify novel molecular processes that can be pharmacologically manipulated to limit cyst formation.

Results: By combining single cell RNA sequencing from PLD tissue with a forward-phase cytokine arrays from human PLD organoids, we have found that cystic cells significantly increase the expression of a range of cytokines, including *Ccl20*, *Tgfb* and *Tnf*. These data indicate that cystic cells actively recruit an immune infiltrate to cystic lesions thereby promoting cystogenesis. Using spatial mapping technologies enables us to define where within the PLD CME different cells are found and we can show that T cells are the most abundant immune cell type within the cyst microenvironment in human PLD. Furthermore, T cells within the PLD CME express PD-1, suggesting that these T cells are in an exhausted state and susceptible to anti-PD-1 therapeutics.

Conclusion: Cyst cells recruit and pattern immune cells within the CME. These immune cells are largely made up of exhausted, PD-1⁺ T cells, which represent an immunotherapy candidate for pharmaceutical intervention in human PLD.

FRI-159

The whole genome sequence and transcriptome study on the HCCs derived from patients with Fontan-associated liver disease

Taiji Yamazoe¹, Eiji Kakazu¹, Michitaka Matsuda¹, Taizo Mori¹, Sachiyo Yoshio¹, Tatsuya Kanto¹. ¹*The Research Center for Hepatitis and Immunology, Ichikawa, Japan*

Email: lb-19yamazoe@hospk.ncgm.go.jp

Background and aims: The Fontan-associated liver disease (FALD) is characterized by a congestive hepatopathy and developed liver cirrhosis and hepatocellular carcinoma (HCC) after 15–20 years

POSTER PRESENTATIONS

after the Fontan procedure. The prognosis of FALD-HCC patients is significantly worse compared to non-HCC FALD patients, thus indicating the importance of the understanding of genomic and transcriptomic signature of FALD hepatocarcinogenesis. To this end, we performed the analysis of the whole genome sequences (WGS) together with RNA sequences.

Method: We sequenced four paired tumor and nontumor of the surgically resected specimens. The samples were prepared with TruSeq DNA PCR Free kit or NEBNext Poly (A) mRNA Magnetic Isolation/Ultra II Directional RNA Library Prep Kit, and sequenced up to 300G base or 6G base with NovaSeq6000. We used BWA to map to hg38, and executed the pipeline of GATK BaseRecalibrator, Mutect2 and Funcotator. The maf data were analysed by maftools in R software.

Results: The age of patients were 22–43 year old. The tumor subtype of HCC were poor differentiated or mixed hepatocellular cholangiocarcinoma. We identified 3514 nonsynonymous mutations in total. Of them, 2882 (82.0%) were single nucleotide variation, and 315 were indel. The majority of mutations were missense mutations (2804), followed by splice site mutations (377). The variant allele frequency was 0.0926 ± 0.0984 (mean \pm SD). The number of mutations were relatively high (878.5 \pm 173.0). There was no mutations of TERT promoter, TP53, CTNNB1 or ARID1A, but mutations of PTEN and AXIN1. The affected oncogenic signaling pathways were Hippo, PI3 K, NOTCH, RTK-RAS and WNT pathway. The transversions were significantly higher than the transitions (56.0 ± 0.71 vs 44.0 ± 0.71). The base substitution of C to T was predominant, followed by T to C, C to A, which is similar to other etiological HCC and CCA. The COSMIC signatures were COSMIC 5 and 3 (SBS40, 5, 3). These data indicates that the mutational signatures were different from other etiological HCC but their oncogenic mutations were related on the common tumorigenic pathways. The pathway analysis with the upregulated genes compared to virus-related and non-viral HCC (Riken Japanese HCC database in ICGC) showed the high score in VEGFA-VEGFR2 signaling and G1 to S cell cycle control. These data indicate the rapid tumor growth phenotype of FALD HCC.

Conclusion: We performed WGS and RNAseq of four paired samples derived from HCC patients with FALD. The findings suggested that disease specific phenotype, which is different from the HCC with other etiologies. We are sequencing another four paired samples including one Focal Nodular Hyperplasia to draw the genomic mutation landscape of FALD HCC.

FRI-160-YI

Endoplasmic reticulum stress in biliary atresia: unravelling cholangiocyte dysfunction through organoid-based RNA sequencing

Yara Hamody¹, Adi Har-Zahav², Keren Danan³, Irit Gat-Viks⁴, Raanan Shamir², Orith Waisbourd-Zinman². ¹Felsenstein Medical Research Center, Faculty of Medicine, Tel-Aviv University, Tel-Aviv, Israel, Tel Aviv, Israel; ²Schneider Children's Medical Center of Israel, Petach Tikva, Israel; ³Tel Aviv University, Tel Aviv, Israel; ⁴Tel Aviv University, Tel Aviv University, Israel
Email: yarahamody@gmail.com

Background and aims: Biliary atresia (BA) represents a significant form of biliary fibrosis, identified predominantly in neonates under three months, characterized by obstruction of extrahepatic bile ducts and advancing liver fibrosis. The etiology remains elusive. Building on our prior discovery where BA-derived human cholangiocyte organoids (HCOs) exhibited anomalous morphological characteristics compared to controls, we conducted an RNA sequencing analysis. The aim was to delineate the pathways contributing to cholangiocyte injury in BA, with a particular focus on the Endoplasmic Reticulum (ER) stress and the Unfolded Protein Response (UPR) pathways already implicated in various liver disorders.

Method: In this study, we cultivated human cholangiocyte organoids derived from both BA patients and non-BA controls. These organoids

underwent comprehensive RNA sequencing to identify key pathways and gene expressions associated with BA. We employed reverse transcription polymerase chain reaction (RT-PCR) to validate the RNA-seq findings and to ensure the functional significance of the identified genes. Subsequent experiments included western blotting and immunofluorescence staining, which were utilized to examine the expression levels of proteins involved in ER stress and to assess the integrity of epithelial cell polarity. Additionally, we investigated the specific involvement of cytochrome P450 enzymes in ER stress within the context of BA, particularly focusing on their role in drug metabolism.

Results: Our RNA sequencing analysis revealed a distinctive expression profile in BA-derived HCOs, implicating numerous biological pathways, prominently ER stress, UPR, and drug metabolism. Key findings include the identification of PERK, an essential UPR regulator, and BiP/GRP78, a heat shock protein, both critical for ER homeostasis, as being markedly upregulated in BA HCOs compared to controls. Immunofluorescent staining confirmed significantly elevated levels of both PERK and BiP/GRP78 in BA samples. Further, our Western blot and RT-PCR analyses corroborated the increased presence of BiP/GRP78 in BA-afflicted organoids. In addition, we examined cytochrome P450 (CYP450) enzymes for their role in ER stress and drug metabolism. Notably, the CYP4A isoforms were found to be overexpressed in BA patients relative to control subjects. The chemical inhibitor HET0016, targeting CYP4A activity, demonstrated a reduction in ER stress markers, with a notable decrease in PERK levels, upon application to BA HCOs, suggesting a possible therapeutic angle through modulation of CYP450 activity.

Conclusion: Our findings suggest that ER stress and the UPR significantly contribute to cholangiocyte damage in BA. These results pave the way for further investigation into targeted therapeutic strategies that may ameliorate ER stress in BA, potentially altering the disease course.

FRI-161

Correlation of non-invasive tests with histological features and intrahepatic Z-alpha-1 antitrypsin burden in patients with alpha-1 antitrypsin deficiency-associated liver disease

Jen-Chieh Chuang, Ruixue Hou¹, Feng Hong¹, Maria D. Paraskevopoulou¹, Jie Cheng¹, Susana Gonzalez¹, Nirav K. Desai, Paresh Thakker¹, Thomas Schluep², Javier San Martin², Rohit Loomba³, Pavel Strnad⁴. ¹Takeda Development Center Americas, Inc., Cambridge, MA, United States; ²Arrowhead Pharmaceuticals, Inc., Pasadena, CA, United States; ³University of California San Diego School of Medicine, La Jolla, CA, United States; ⁴University Hospital RWTH Aachen, Aachen, Germany
Email: jen-chieh.chuang@takeda.com

Background and aims: Alpha-1 antitrypsin deficiency (AATD) is a genetic disease characterized by low levels of serum alpha-1 antitrypsin (AAT), a liver-derived serine protease inhibitor (Pi) that maintains the protease-antiprotease balance in the lungs. The Pi*ZZ genotype produces misfolded AAT (Z-AAT), resulting in hepatic AAT aggregates and reduced antiprotease activity in the lungs. Fibrosis and chronic liver disease (LD) may develop owing to increased cellular stress, apoptosis, inflammation and fibrogenesis. No pharmacological treatments exist and reliable non-invasive tests (NITs) are limited for AATD-associated LD (AATD-LD). We aimed to leverage data from two clinical trials to investigate the correlations of NITs with LD burden in patients (pts) with AATD-LD.

Method: Baseline serum and histology samples from phase 2 AROAAT-2001 (NCT03945292) and AROAAT-2002 (NCT03946449) trials of fazirsiran or placebo in pts with AATD-LD were used. Baseline correlations of NITs (ALT, APRI, AST, FIB-4, LSM via transient elastography, Pro-C3 and serum Z-AAT) and total intrahepatic Z-AAT to histological features (METAVIR fibrosis stage, portal inflammation and PAS-D globule burden) were evaluated by Spearman correlation analysis. Serum and total intrahepatic Z-AAT were

analyzed by LC-MS. Further methodological details are described in Strnad *et al*, *NEJM*, 2022. The performance of individual NITs on the identification of pts with AATD-LD and significant ($\geq F2$) or advanced ($\geq F3$) fibrosis were evaluated by AUROC analysis.

Results: Of 56 pts from the AROAAT-2001 ($n = 40$) and AROAAT-2002 ($n = 16$) studies, 40 pts had recorded METAVIR fibrosis stage at baseline: F0, 4 (7%); F1, 11 (20%); F2, 17 (30%); F3, 6 (11%); and F4, 2 (4%). ALT, AST, Pro-C3, LSM, APRI and serum Z-AAT correlated with METAVIR fibrosis stage ($p < 0.05$); AST, Pro-C3, FIB-4 and serum Z-AAT correlated with portal inflammation ($p < 0.05$); and LSM, FIB-4 and serum Z-AAT correlated with PAS-D globule burden ($p < 0.05$). Total intrahepatic Z-AAT correlated with METAVIR fibrosis stage, portal inflammation and PAS-D globule burden ($p < 0.05$). ALT, AST, Pro-C3 and LSM had AUROC scores ≥ 0.75 for the identification of pts with $\geq F2$ fibrosis. LSM and serum Z-AAT had AUROC scores ≥ 0.80 for the identification of pts with $\geq F3$ fibrosis.

Conclusion: The study identified correlations of NITs (ALT, APRI, AST, FIB-4, LSM, Pro-C3, serum Z-AAT) and total intrahepatic Z-AAT to histological features (METAVIR fibrosis stage, portal inflammation and PAS-D globule burden). ALT, AST, Pro-C3, LSM and serum Z-AAT demonstrated adequate-good discriminatory performance in the identification of pts with $\geq F2$ and $\geq F3$ fibrosis. Clinical utilities of these NITs in the identification of pts with AATD-LD and in monitoring treatment responses will require validation in larger studies.

Acknowledgements: Writing assistance provided by E L Wescott, PhD, of Oxford PharmaGenesis.

FRI-162

Analysis of cellular crosstalk in fibrocystic liver disease (PKHD1-/- mouse) reveals a central role for cholangiocytes, neutrophils and chronic biliary infection in disease pathogenesis

Zehra Syeda¹, Tory Bauer-Pisani¹, Shakila Taleb¹, Romina Fiorotto¹, Mario Strazzabosco¹. ¹Yale School of Medicine, New Haven, United States

Email: mario.strazzabosco@yale.edu

Background and aims: Caroli disease (CD) and Congenital hepatic fibrosis (CHF) are caused by mutation in Polycystic kidney hepatic disease 1 gene (PKHD1) and lead to biliary malformations, cholangiocyte dysfunction, portal inflammation, portal fibrosis and episodes of cholangitis. PKHD1 encodes for fibrocystin (FPC), a protein expressed in cilia, plasma membrane and centromeres of cholangiocytes. FPC is involved in multiple cellular functions from polarity and cell matrix interactions to differentiation. This study was designed to investigate the relationships among the cell types present in the pericycystic infiltrate in Pkhd1-KO mice at single cell level.

Method: We isolated single cells from portal tract of 3 months old Pkhd1-KO and WT mice ($n = 2$). Single cell transcriptomic profiling of 18,492 single cells, allowed the identification of the cell types present in the samples. Dataset was analyzed by Seurat and CellChatDB. Cystic area, inflammation, fibrosis was scored histologically (Ck19, CD45 and Sirius red staining), before and after antibiotic treatment. Aerobic and anaerobic microbial cultures and antibiograms were performed.

Results: scRNA-seq analysis revealed 9 distinct cell populations in the portal tract of WT and Pkhd1-KO. Cholangiocytes in Pkhd1-KO have higher expression of the Cxcl1 and Cxcl5 chemokines. Gene ontology analysis of cholangiocytes from Pkhd1-KO showed an enrichment of genes involved in the recruitment of neutrophils and activation of innate immune responses to microbial components. CellChatDB analysis showed a strong connection between Cxcl1/Cxcl5 and the Cxcr2 receptor present in neutrophils, consistent with their recruitment by cholangiocytes. As predicted by transcriptomic analysis, Wright Giemsa staining showed presence of microbial component inside several cysts, identified as *Enterococcus spp.* Treatment of Pkhd1-KO (4 weeks old) for 8 weeks with Sulfamethoxazole/trimethoprim (SMZ/TMP) diet (based on the antibiogram) resulted in the eradication of *Enterococcus*.

Immunohistochemistry staining after antibiotics treatment showed statistically significant decrease in inflammation, cystic area and fibrosis in treated Pkhd1-KO mice when compared to untreated Pkhd1-KO mice. scRNA-seq was repeated after antibiotic treatment and confirmed the decrease in inflammatory signaling.

Conclusion: This study shows a complex signaling network originating from cholangiocytes and amplified by the recruited neutrophils. The biliary colonization aligns well with the natural history of disease as patients with fibrocystin deficiency suffer from recurrent cholangitis. Further studies are ongoing to clarify if and how neutrophils interact with cholangiocytes non-destructively and their role in the progression of the disease.

FRI-163-YI

Pronounced vasculature phenotypes in new mouse models with ALGS and BA-associated mutations in Jag1

Anna Maria Frontino¹, Daniel V. Oliveira¹, Eliška Trampotová¹, Mitra Tavakoli², Noémi K. M. Van Hul³, Oren Gozlan⁴, Emma Andersson³, Gabriela Pavlinková², David Sprinzak⁴, Jan Mašek¹. ¹Department of Cell Biology, Faculty of Science, Charles University, Prague, Czech Republic; ²Laboratory of Molecular Pathogenesis, Institute of Biotechnology, CAS, Vestec, Czech Republic; ³Department of Cell and Molecular Biology, Karolinska Institutet, Stockholm, Sweden; ⁴School of Neurobiology, Biochemistry and Biophysics, George S. Wise Faculty of Life Sciences, Tel Aviv University, Tel Aviv, Israel

Email: frontina@natur.cuni.cz

Background and aims: Biliary atresia (BA) and Alagille (ALGS) syndrome are the two most common pediatric cholangiopathies typically resulting in liver transplantation. Loss-of-function mutations in the Notch ligand *Jagged1* (*Jag1*) have been associated with ~94% of ALGS cases, but intriguingly, other *Jag1* mutations were found in patients with BA. Missense mutations linked to ALGS (R1097W), and BA (R1213Q) target conserved, intracellular regions of *Jag1*, thus likely pointing at physiologically relevant domains. To test these functions *in vivo*, we recapitulated the missense mutations in C57BL/6 mice.

Results: Using CRISPR/Cas9, we generated two new mouse models with missense mutations in *Jag1* intracellular domain (*Jag1*^{RW/RW} and *Jag1*^{RQ/RQ}). Not triggered by any hepatotoxic insult, *Jag1*^{RW/RW} and *Jag1*^{RQ/RQ} mice manifested more significant and contrasting effects on neonatal liver vasculature than biliary morphogenesis. *Jag1*^{RW/RW} mutants exhibit bile ducts (BDs) with disrupted, yet functional morphology accompanied by 50% ($p < 0.05$) decrease in hepatic artery (HA) quantity. In contrast, *Jag1*^{RQ/RQ} mutants had hypertrophic and increased HA numbers along highly hypoplastic portal veins, with no impact on BDs at P10 and P30. Furthermore, collagen deposition was significantly higher ($p < 0.05$) in *Jag1*^{RQ/RQ} animals at P30, suggesting emerging fibrosis, which was not present in *Jag1*^{RW/RW} and control mice. The progressive liver damage was further illustrated by a ~2-fold increase in blood serum levels of Aspartate Aminotransferase in the *Jag1*^{RQ/RQ} mutants at P30 stage. Ultrasound analysis revealed portal vein dilation in *Jag1*^{RQ/RQ} mutants, indicating systemic vascular or blood pressure alterations. Finally, JAG1-NOTCH2 transactivation, monitored via reporter assay, was not altered in cell lines expressing JAG1 RW and JAG1 RQ.

Conclusion: To our knowledge, we have produced the first mouse models recapitulating the exact ALGS and BA mutations found in humans. Our findings from *Jag1*^{RQ/RQ} mice reveal unaltered biliary morphogenesis accompanied by aberrant HA outgrowth, in contrast to *Jag1*^{RW/RW} mice, which exhibit disrupted biliary morphogenesis and HA loss. Based on our data, *Jag1*^{RW/RW} mutants represent a "mild" ALGS model, a condition that can be potentiated with simultaneous deletion of one allele of *Jag1*, while *Jag1*^{RQ/RQ} mice open possibilities for further investigation, particularly in exploring responses to hepatotoxins like biliary atresia. Our data indicate that the vasculature and potentially periportal mesenchyme are more sensitive to *Jag1*

POSTER PRESENTATIONS

activity than the BDs; further research is needed to uncover if this is a mouse-specific feature or a shared trait between mice and humans. Our ongoing transcriptomics analysis of the *Jag1^{RW/RW}*, and *Jag1^{RQ/RQ}* liver tissue aims to elucidate the different signaling activities originating from the ALGS- and BA-associated mutations.

FRI-164

Proteomic analysis identified fazirsiran treatment-responsive protein biomarkers in patients with alpha-1 antitrypsin deficiency-associated liver disease

Jen-Chieh Chuang, Ruixue Hou¹, Feng Hong¹, Jie Cheng¹, Maria D. Paraskevopoulou¹, Nirav K. Desai, Paresh Thakker², Javier San Martin³, Thomas Schlupe³, Pavel Strnad⁴, ¹Takeda Development Center Americas, Inc., Cambridge, MA, United States; ²Takeda Development Center Americas, Inc., Cambridge, United States; ³Arrowhead Pharmaceuticals, Inc., Pasadena, CA, United States; ⁴University Hospital RWTH Aachen, Aachen, Germany
Email: jen-chieh.chuang@takeda.com

Background and aims: Alpha-1 antitrypsin deficiency (AATD) is a rare genetic disease characterized by low levels of serum alpha-1 antitrypsin (AAT), primarily affecting the lungs and/or liver. Patients with the protease inhibitor (Pi)*ZZ genotype express misfolded AAT, resulting in hepatic AAT aggregates and reduced antiprotease activity in the lungs. Fibrosis and chronic liver disease may develop owing to cellular stress, inflammation and apoptosis. Currently no pharmacological treatments for AATD-associated liver disease (AATD-LD) exist. Fazirsiran is an investigational N-acetylgalactosamine-conjugated small interfering RNA undergoing phase 3 development in patients with AATD-LD. Proteomics data to identify biomarkers relevant for therapeutic targeting and to elucidate disease pathophysiology are limited. This study aimed to detect treatment-responsive protein biomarkers and cellular pathways by leveraging a novel platform for proteomic discovery from the sera of patients with AATD-LD treated with fazirsiran.

Method: Olink, a dual-antibody-based proteomics platform, was utilized for proteomic discovery. Serum samples were assessed from adults with AATD, a Pi*ZZ genotype, and biopsy-proven liver fibrosis participating in AROAAT-2002 (NCT03946449), a phase 2, open-label trial of fazirsiran (100 or 200 mg) for 24 or 48 weeks. Olink data were integrated with single nucleus RNA-sequencing (Snucseq) data to map expressed proteins to potential source cells in the liver. A mixed effects model was applied to measure biomarker change from baseline over time and false discovery rate-adjusted p value was used to select the top biomarkers. Differentially expressed protein (DEP) and pathway analyses were also conducted.

Results: The concentrations of 3072 proteins were measured in 16 patients with AATD-LD. Fazirsiran treatment resulted in continuous and sustained DEPs in the serum through 48 weeks. DEPs were primarily mapped to hepatocytes, cholangiocytes, immune cells (T cells and macrophages), mesenchymal cells and endothelial cells. Of the liver mesenchymal cell-enriched proteins, many were components of the extracellular matrix associated with hepatic stellate cell activation and liver damage. Pathway analysis showed that fazirsiran-induced proteomic changes were linked to the reduced activity of molecular pathways that promote cellular stress, inflammation, apoptosis and fibrosis.

Conclusion: This study leveraged a novel platform for proteomic discovery in patients with AATD-LD, identified candidate biomarkers reflecting disease severity, and demonstrated potential benefit of fazirsiran treatment in reducing cellular stress, inflammation and damage. Biomarkers identified in these analyses may have clinical utility but require validation in larger studies.

Acknowledgements: Writing assistance provided by R Tooze, PhD, of Oxford PharmaGenesis.

FRI-165

SarsCov2 vaccine does not increase the risk of autoimmune liver disease

Stanislas Pol^{1,2}, Charlotte Mouliade^{1,2}, Lucia Parlatti^{1,2}, Samir Bouam³, Vincent Mallet^{1,2}, ¹AP-HP Centre Université Paris Centre, Groupe Hospitalier Cochin Port Royal, DMU Cancérologie et spécialités médico-chirurgicales, Service des Maladies du foie, Paris, France; ²Université Paris Cité, F-75006, Paris, France; ³AP-HP Centre Université de Paris, Groupe Hospitalier Cochin Port Royal, DMU PRIM, Service d'Information Médicale, Paris, France
Email: stanislas.pol@aphp.fr

Background and aims: The European Association for the Study of the Liver (EASL) conference in London, 2021, highlighted a potential link between SarsCov2 vaccines and autoimmune liver diseases, specifically autoimmune hepatitis and primary biliary cholangitis. To explore this further, we conducted a population-level investigation in France. We studied the incidence of autoimmune liver diseases before and after the rollout of SarsCov2 vaccines, which began on December 27, 2020 in France. By October 17, 2021, approximately 75.8% of the French population (50,889,053 individuals) had received at least one vaccine dose, and 73.8% (49,551,532 people) had completed the initial vaccine series, which typically consisted of two doses.

Method: We selected from the National French Hospital Discharge Database spanning 2013–2022, all adult patients discharged with diagnoses of autoimmune hepatitis (ICD-10: K754) or primary biliary cirrhosis (ICD-10: K743) (N = 10,869). Severe autoimmune liver disease was defined as hepatic or extrahepatic organ failure within 4 weeks after autoimmune liver disease onset. To examine the incidence of autoimmune liver diseases in relation to the SarsCov2 vaccine rollout, an Interrupted Time Series Analysis (ITSA) was conducted with January 1, 2021 as the reference date, this being the closest date to the vaccine rollout commencement on December 27, 2020. A 3-year washout period (2013–2015) was included to ascertain the measurement of incident cases.

Results: The sample comprised 7,844 patients with a median age of 58 years (IQR 44–69), of whom 26.6% were male. Approximately 13% progressed to severe autoimmune liver disease and 5.8% either died or underwent liver transplantation, within 12 weeks post-onset. The median (range) incidence of autoimmune liver disease and of severe autoimmune liver disease were 90 (43–125) and 13 (5–21) cases per month, respectively. No statistically significant changes were observed in the incidence of both autoimmune liver disease (p = 0.83) and severe autoimmune liver disease (p = 0.33) pre- and post-vaccination. Higher age (p = 0.034), and significant comorbidities (p < 0.001) were more prevalent in patients with autoimmune liver disease onset during the COVID-19 vaccine period. Older age (p = 0.003 in multivariate analysis) was the sole risk factor linked to the severity of autoimmune liver disease.

Conclusion: The rollout of SarsCov2 vaccines did not correlate with an increase in the incidence of autoimmune liver disease, including both general cases and those classified as severe, in French hospitals.

FRI-166

Impaired nuclear glycogen metabolism affects liver homeostasis in Argininosuccinic aciduria

Leandro Soria¹, Alfonso D'Alessio¹, Paola Arena¹, Elena Polishchuk¹, Claudia Perna¹, Angela De Angelis¹, Sonam Gurung², Dany Perocheau², Rossella De Cegli¹, Youngmok Lee³, Samira Safarikia⁴, Marco Spada⁴, Carlo Dionisi-Vici⁴, Julien Baruteau², Nicola Brunetti-Pierri¹, ¹Telethon Institute of Genetics and Medicine, Pozzuoli, Italy; ²UCL Great Ormond Street Institute of Child Health, London, United Kingdom; ³UCONN Health Center, Farmington, United States; ⁴Bambino Gesù Children Hospital, Rome, Italy
Email: brunetti@tigem.it

Background and aims: Glycogen is synthesized *de novo* in the nucleus, and nuclear glycogenolysis provides a carbon pool for histone acetylation. Abnormal nuclear glycogen catabolism has been

associated with epigenetic changes in gene expression and lung cancer progression. We found abundant hepatic nuclear glycogen storage in *Asl^{Neo/Neo}* mice, a mouse model of Argininosuccinic Aciduria (ASA), an inherited urea cycle disorder due to argininosuccinate lyase (ASL) deficiency. In *Asl^{Neo/Neo}* mice we investigated underlying mechanisms of aberrant nuclear glycogen storage and its consequences on liver homeostasis.

Method: Nuclear glycogen storage in hepatocytes was investigated by electron microscopy on liver sections. Enzymes and acetylated histones were determined by Western Blot on nuclear purified fractions. Hepatic gene expression profiling was performed by QuantSeq analysis. Survival of *Asl^{Neo/Neo}* mice was investigated following intravenous administration of adeno-associated virus vectors encoding the human glycogen phosphorylase (PYGL), the rate-limiting enzyme in glycogenolysis, and after intraperitoneal injections of vorinostat, a pan-Histone Deacetylase (HDAC) inhibitor.

Results: Consistent with *Asl^{Neo/Neo}* mice, nuclear glycogen storage was observed in a liver specimen of an ASA patient. In the nuclei of *Asl^{Neo/Neo}* mouse livers, quantification of glycogen metabolizing enzymes suggested increased glycogen synthesis and reduced glycogenolysis. These nuclei also showed reduced acetyl-CoA content, and a marked decrease in lysine acetylation of several histones, especially H3K9. Notably, neither nuclear glycogen accumulation nor reduced histone acetylation were observed in various murine models of defective glycogen metabolism (including PYGL deficiency) or ureagenesis (other urea cycle disorders). Transcriptomic analysis of *Asl^{Neo/Neo}* mouse livers revealed H3K9-dependent changes. Moreover, increased histone acetylation, by means of hepatocyte-specific PYGL overexpression or HDAC inhibition, improved *Asl^{Neo/Neo}* mice survival.

Conclusion: Defective hepatic nuclear glycogen mobilization and histone hypoacetylation result in global transcriptomic changes in hepatic gene expression and reduced survival in ASA mice. These findings may have implications for development of improved therapies for liver disease in ASA and potentially, other liver disorders with aberrant nuclear glycogen storage.

FRI-167-YI

Modelling wolman disease using genetically engineered human liver organoids

Davide Selvestrel¹, Beatrice Anfusio¹, Suresh Velnati², Luca Fava³, Giovanni Sorrentino^{2,4}. ¹International Centre for Genetic Engineering and Biotechnology (ICGEB), Equal Contribution, Trieste (TS), Italy; ²International Centre for Genetic Engineering and Biotechnology (ICGEB), Trieste (TS), Italy; ³University of Trento, Trento, Italy; ⁴University of Trieste-Dipartimento di Scienze Mediche, Chirurgiche e della Salute, Università Degli Studi di Trieste, Trieste, Italy
Email: giovanni.sorrentino@icgeb.org

Background and aims: Wolman disease (WD) is a rare inherited autosomal recessive disease caused by mutations in the lysosomal acid lipase (LAL) gene and characterized by the accumulation of cholesteryl esters and triglycerides in lysosomes, leading to severe liver and visceral dysfunction. There is currently no cure for this devastating disease, and treatments are limited to supportive care. In this project, we aim to develop an in vitro model of WD using liver organoids derived from human induced pluripotent stem cells (iPSCs).

Method: To this aim, we implemented a reproducible method to derive multi-cellular human liver 3D organoids composed of hepatocyte-, stellate-, biliary- and Kupffer-like cells that exhibit gene expression and functions similar to in vivo-derived tissues.

Results: Upon free fatty acid treatment, these organoids recapitulate key features of WD, including steatosis, inflammation, and fibrosis, in a multi-step manner. To design a patient-specific organotypic model of WD, we used CRISPR-Cas9 gene editing to introduce mutations in the LAL gene in iPSCs, and we are currently characterizing the hepatic

organoids derived from these cells to assess their capability to model disease-associated phenotypes.

Conclusion: This innovative platform has the potential to recapitulate pathophysiological features of WD, in vitro, including personalized response to therapy, and will offer a new approach for studying the molecular mechanisms underlying development and progression of this disease, thus facilitating the discovery of effective treatments.

FRI-170

Impact of helminth infection on the efficacy of COVID-19 mRNA vaccine in mice

Jinpeng Su^{1,2}, Youssef Hamway^{2,3,4}, Julia Schluckebier^{3,4}, Bo-Hung Liao¹, Zhe Xie¹, Clarissa Prazeres da Costa^{2,3,4}, Ulrike Protzer^{1,2}. ¹Institute of Virology, Technical University of Munich/Helmholtz Munich, Munich, Germany; ²German Center for Infection Research (DZIF), Munich partner site, Munich, Germany; ³Institute for Medical Microbiology, Immunology and Hygiene, Technical University of Munich, Munich, Germany; ⁴Center for Global Health, Technical University of Munich, Munich, Germany
Email: protzer@tum.de

Background and aims: *Schistosoma* are helminth parasites that infect around 250 million humans. The parasite matures in the liver, causes liver damage, and influences host immune responses. The effectiveness of mRNA vaccines, as a newly emerging vaccine type of global importance, in populations with *Schistosoma* infections is uncertain. Here, we aimed to explore how the immunogenicity of the mRNA-based COVID-19 vaccine Comirnaty was influenced by an underlying helminth infection using an experimental *Schistosoma mansoni*-infection model.

Method: Naïve mice and mice chronically infected with *S. mansoni* were vaccinated intramuscularly with 1 µg or 5 µg of Comirnaty and boosted after four weeks. Vaccine-induced humoral and cellular immune responses were evaluated one week after boost immunization by quantifying and subtyping spike-specific IgG responses, assessing SARS-CoV-2 virus-neutralizing activity of sera, and performing intracellular cytokine staining on splenocytes re-stimulated with spike-specific peptide pool.

Results: The titers of spike-specific IgG antibodies were comparable in naïve and helminth-infected mice following low- and high-dose Comirnaty immunization and the sera showed similar SARS-CoV-2 infection-neutralization capacity. Despite this, spike-specific IgG subclasses revealed distinct patterns. Immunization of naïve mice primarily induced the IgG_{2c} subclass associated with a Th1 response, while in helminth-infected mice, a predominance of the IgG₁ subclass was observed, indicative of a Th2-prone response. Comirnaty immunization of helminth-infected mice stimulated strong, dose-dependent spike-specific IFN-gamma+ CD4 T-cell responses comparable to those in the respective naïve mice. By contrast, spike-specific IFN-gamma+ CD8 T-cell responses in helminth-infected mice were significantly lower than those in naïve mice. Moreover, helminth infection remarkably altered the poly-functionality of vaccine-induced CD8 T cells, as evidenced by a significant decrease in spike-specific IFN-gamma+ TNF-alpha+ IL-2+ CD8 T cells. Of note, the suppression of CD8 T-cell responses caused by helminth infection persisted even if higher vaccine doses were applied.

Conclusion: Chronic infection with a helminth that elicits mainly liver and intestinal inflammation surprisingly altered the characteristics of antibody responses and substantially decreased the magnitude and functionality of CD8 T-cell responses elicited by a COVID-19 mRNA-based vaccine.

FRI-171

Paediatric solid organ transplant recipients (SOTR) demonstrate greater serological response to initial SARS-CoV-2 vaccination than adult SOTR, and comparable rates of antibody degradation

María Pilar Ballester¹, Tobias Laue², Lilianeleny Meoli³, Eva Uson⁴, Frauke Mutschler⁵, Carl Grabitz⁶, Valérie McLin⁷, Lorenzo D'Antiga⁸, Montserrat Pujadas⁴, Ângela Carvalho-Gomes⁹, Iván Sahuco¹⁰, Ariadna Bono¹¹, Federico D'Amico¹², Raffaella Viganò¹³, Elena Diago Sempere¹⁴, Beatriz Tormo¹⁵, Elvira Inglese¹⁶, Dani Martinez¹⁷, Antonio Riva¹⁸, Rajni Sharma¹⁸, Hio Lam Phoebe Tsou¹⁸, Nicola Harris¹⁸, Annelotte Broekhoven¹⁹, Marjolein Kikkert¹⁹, Shessy Morales¹⁹, Sebenzile Myeni¹⁹, Mar Riveiro Barciela²⁰, Adriana Palom²¹, Nicola Zeni²², Alessandra Brocca²², Annarosa Cussigh²³, Sara Cmet²³, Desamparados Escudero-García²⁴, Matteo Stocco¹, Leonardo Natola²⁵, Donatella Ieluzzi²⁵, Veronica Paon²⁵, Angelo Sangiovanni²⁷, Elisa Farina²⁷, Clara Di Benedetto²⁸, Yolanda María Sanchez-Torrijos²⁹, Ana Lucena Valera³⁰, Eva Roman³¹, Elisabet Sanchez³¹, Rubén Sánchez-Aldehuelo³², Julia López-Cardona³³, Itzel Canas-Perez³⁴, Christine Jackson³⁴, Dhaarica Jeyanesan³⁵, Alejandro Esquivel Morochó³⁶, Simone Di Cola³⁷, Lucia Lapenna³⁸, Giacomo Zaccherini³⁹, Deborah Bongiovanni³⁹, Paola Zanaga⁴⁰, Katia Sayaf⁴², Sabir Hossain⁴¹, Javier Crespo⁴², Mercedes Robles-Díaz⁴³, Antonio Madejón¹⁴, Helena Degroote⁴⁴, Javier Fernández⁴⁵, Marko Korenjak⁴⁶, Xavier Verhelst⁴⁷, Francisco Javier García-Samaniego⁴⁸, Raul J. Andrade⁴⁹, Paula Iruzubieta⁵⁰, Gavin Wright⁴¹, Paolo Caraceni³⁹, Manuela Merli⁵¹, Vishal C. Patel¹⁸, Amir Gander³⁴, Agustín Albillos³³, German Soriano³¹, Maria Francesca Donato⁵², David Sacerdoti²⁵, Pierluigi Toniutto²³, Maria Buti⁵³, Christophe Duvoux⁵⁴, Paolo Antonio Grossi⁵⁵, Thomas Berg⁵⁶, Wojciech Polak⁵⁷, Massimo Puoti⁵⁸, Anna Bosch⁴, Luca Saverio Belli¹², Patrizia Burra⁵⁹, Francesco Paolo Russo⁶⁰, Minneke Coenraad¹⁹, José Luis Calleja Panero⁶¹, Giovanni Perricone¹², Shilpa Chokshi¹⁸, Marina Berenguer⁶², Joan Clària⁴⁵, Richard Moreau⁶³, Vicente Arroyo⁶⁴, Paolo Angeli⁶⁵, Cristina Sanchez⁶⁶, Javier Ampuero⁶⁷, Salvatore Piano⁶⁸, Emanuele Nicastro⁶⁹. ¹Hospital Clínico Universitario de Valencia, Valencia, Spain; ²Medical School Hannover, Hannover, Germany; ³Institute of Liver Studies, London, United Kingdom; ⁴EF Clif, Barcelona, Spain; ⁵MH Hannover, Hannover, Germany; ⁶MH hannover, Hannover, Germany; ⁷University Hospitals Geneva, Geneva, Switzerland; ⁸Papa Giovanni XXIII Hospital, Bergamo, Italy; ⁹IS La Fe Health Research Institute, Valencia, Spain; ¹⁰La Fe University Hospital, Valencia, Spain; ¹¹La Fe Health Research Institute, Valencia, Spain; ¹²ASST Grande Ospedale Metropolitano Niguarda, Milan, Italy; ¹³ASST GOM Niguarda, Milan, Italy; ¹⁴Hospital Universitario La Paz, Madrid, Spain; ¹⁵HU Puerta de Hierro, Madrid, Spain; ¹⁶Niguarda Hospital, Milan, Italy; ¹⁷Hospital Universitario Valle Hebrón, Barcelona, Spain; ¹⁸Foundation for Liver Research, London, United Kingdom; ¹⁹Leiden University Medical Center, Leiden, Netherlands; ²⁰Hospital Universitario Vall d'Hebron, Barcelona, Spain; ²¹Vall d'Hebron University Hospital, Barcelona, Spain; ²²University of Padova, Padova, Italy; ²³Azienda Sanitaria Universitaria Integrata, Udine, Italy; ²⁴Clinic University Hospital of Valencia, Valencia, Spain; ²⁵University of Verona, Verona, Italy; ²⁶University and Azienda Ospedaliera Universitaria Integrata of Verona, Verona, Italy; ²⁷Foundation IRCCS Cà Granda Ospedale, Milan, Italy; ²⁸Foundation IRCCS Ca' Granda Ospedale Maggiore Policlinico, Milan, Italy; ²⁹Virgen del Rocío Hospital, Seville, Spain; ³⁰HOSP GENERAL VIRGEN DEL ROCIO, Seville, Spain; ³¹Hospital de la Santa Creu i Sant Pau, Barcelona, Spain; ³²Hospital Universitario Ramon y Cajal, Madrid, Spain; ³³Hospital Universitario Ramón y Cajal, Madrid, Spain; ³⁴Royal Free London NHS Foundation Trust, London, United Kingdom; ³⁵King's College Hospital, London, United Kingdom; ³⁶King's College London, London, United Kingdom; ³⁷Sapienza University of Rome, Rome, Italy; ³⁸Sapienza University, Rome, Italy;

³⁹University of Bologna, Bologna, Italy; ⁴⁰Azienda Ospedale-Università Padova, Padova, Italy; ⁴¹Mid and South Essex NHS Foundation Trust, Basildon, United Kingdom; ⁴²Valdecilla Research Institute (IDIVAL), Santander, Spain; ⁴³University Hospital Virgen de la Victoria, Malaga, Spain; ⁴⁴UZ Gent, Gent, Belgium; ⁴⁵Hospital Clinic Barcelona, Barcelona, Spain; ⁴⁶European Liver Patients' Association, Brussels, Belgium; ⁴⁷Ghent University Hospital, Ghent, Belgium; ⁴⁸La Paz University Hospital, Madrid, Spain; ⁴⁹Virgen de la Victoria University Hospital, Malaga, Spain; ⁵⁰Hospital Valdecilla, Santander, Spain; ⁵¹Università degli Studi di Roma Sapienza, Roma, Italy; ⁵²Foundation IRCCS Ca' Granda Ospedale Maggiore Policlinico, Milan, Italy; ⁵³Hospital Universitari Vall d'Hebron, Barcelona, Spain; ⁵⁴Henri Mondor Hospital APHP, Paris Est University, Creteil, France; ⁵⁵UNIVERSITY OF INSUBRIA, Varese, Italy; ⁵⁶University Hospital Leipzig, Leipzig, Germany; ⁵⁷Erasmus MC, University Medical Center Rotterdam, Rotterdam, Netherlands; ⁵⁸University of Milano-Bicocca, Milan, Italy; ⁵⁹Padova University Hospital, Padova, Italy; ⁶⁰University Hospital Padua, Padua, Italy; ⁶¹Hospital Puerta de Hierro, Majadahonda, Spain; ⁶²La Fe University and Polytechnic Hospital, Valencia, Spain; ⁶³Inserm and Université de Paris, Paris, France; ⁶⁴European Foundation for the Study of Chronic Liver Failure, Barcelona, Spain; ⁶⁵University Hospital of Padova, Padova, Italy; ⁶⁶EF-Clif, Barcelona, Spain; ⁶⁷Hospital Universitario Virgen del Rocío, Seville, Spain; ⁶⁸University and Hospital of Padova, Padova, Italy; ⁶⁹Hospital Papa Giovanni XXIII Bergamo, Bergamo, Italy
Email: mapibafe@gmail.com

Background and aims: The Covid-19 pandemic has disproportionately affected solid organ transplant recipients (SOTR). Adult patients have decreased responsiveness to SARS-CoV-2 vaccination and higher incidence of infection. The aim of this study was to determine serological response to SARS-CoV-2 vaccination in paediatric liver- and kidney-transplant (LT, KT) recipients, and undertake comparative analyses with adult SOTR patients.

Method: COBALT is a European, prospective, multi-centre, case-control study of SARS-CoV-2 vaccine responses in adult and paediatric patients. For this nested study, samples were taken at 7- and 32-weeks following initial Covid-19 vaccination. Serological end points were measured by ELISA, presented as geometric mean (IU) and 95% CI, and comparative analyses were performed with Mann-Whitney testing.

Results: A total of 42 paediatric SOTR were recruited, from whom serological data were available for 28 participants (9 post-LT and 19 post-KT). Data from 125 adult SOTR were included (all post-LT); these data have been previously published (PMID: 37870985). All paediatric participants received mRNA vaccines and 117 (93.6%) adult participants received mRNA vaccines. Paediatric SOTR patients had significantly higher anti-Spike IgG levels than adult participants at week 7 [121, 130 (57, 584–254, 804) vs 9, 676 (6, 330–14, 792) AU/ml, test $p < 0.0001$] and week 32 [76, 947 (13, 586–435, 803) vs 7, 917.7 (3, 4890–17, 964) AU/ml, $p = 0.0084$]. No significant difference in week 7 anti-Spike IgG response was found between paediatric LT and KT recipients (126, 459 (34, 292–466, 346) vs 118, 685 (44, 022–319, 984) AU/ml, $p = 0.8838$). No differences were seen between children and adults in the rate of decline of anti-Spike IgG between week 7 and 32 ($p = 0.4928$). No factors were significantly associated with week 7 anti-Spike IgG levels in the paediatric group.

Conclusion: Consistent with data from healthy children, paediatric SOTR demonstrate greater SARS-CoV-2 vaccine responses than comparable adult SOTR patients. These data support efficacy of SARS-CoV-2 vaccination in child SOTR, and may alleviate vaccine hesitancy in this patient group.

FRI-172

Primary adult hepatocytes-derived organoids to characterize intrahepatic cholestasis

Benedetta Blarasin^{1,2}, Gabriele Codotto^{1,3,4}, Marco Stebel², Claudio Tiribelli¹, Cristina Bellarosa¹. ¹Italian Liver Foundation, Liver Brain Unit, Trieste, Italy; ²University of Trieste, Department of Life Sciences, Trieste, Italy; ³University of Ferrara, Department of Life Sciences and Biotechnology, Ferrara, Italy; ⁴AREA Science Park, Genomics and Epigenomics Platform, Trieste, Italy
Email: benedetta.blarasin@fegato.it

Background and aims: Intrahepatic cholestasis is an impairment of bile flow involving the bile canaliculi. There are still clinically diagnosed cholestasis that remain without a definition of the molecular mechanisms involved. It is necessary to find an *in vitro* model able to maintain liver cells architecture and polarity and to self-renew. Adult Hepatocytes-derived organoids (Hep-Orgs) model is based on reproducing the environment occurring during liver regeneration upon liver hepatectomy. The main benefits of this model are their long-term culture and the cell maturity. Hepatocytes can be sourced directly from the patient. This study aims to obtain and characterize Hep-Orgs to study the molecular mechanisms involved in intrahepatic cholestasis.

Method: Mouse liver perfusion and digestion were developed to isolate primary adult hepatocytes according to Charni-Natan (DOI: 10.1016/j.xpro.2020.100086). Adult hepatocytes were then plated in Matrigel droplets and cultured according to Peng (DOI: 10.1016/j.cell.2018.11.012). Hep-Orgs growth was followed morphologically. EdU proliferation assay and albumin release by ELISA were performed. To induce intrahepatic cholestasis Hep-Orgs were treated with 10 μ M Cyclosporine A (CsA) for 24 hours and with 50 μ M CsA for 4 hours. The biliary excretion after treatment with CsA was observed using Dichlorofluorescein (DCF, 0, 5 μ M for 2 hours) and DCF clearance was evaluated by Nikon A1 MP microscope. Bile canaliculi deformations were analyzed by rhodamine-phalloidin staining of pericanalicular F-actin and localization of the junctional ZO-1 protein. Immunofluorescence images were captured with Nikon Eclipse Ti-E epifluorescence microscope.

Results: After 10 days organoids showed 100 μ m dimensions and, at day 32, they reached 250 μ m showing a typical "bunch- of-grape" shape. Organoids were kept in culture for a maximum of 63 days. Hep-Orgs maintained a high proliferation rate at day 34 and albumin release increased over time (days 15, 30, 45, and 55). CsA caused a buildup of cytoplasmic DCF and altered the F-actin cytoskeletal distribution. In untreated Hep-Orgs, a predominant pericanalicular distribution of F-actin around bile canaliculi was observed, while in the CsA-treated a less intense staining was present.

Conclusion: The Hep-Orgs were satisfying in terms of growth and long-term expansion, and maintained the morphological features and a high proliferative potential, with high levels of albumin released in the medium. The treatment with CsA was able to reproduce the cytoskeletal modifications that happen during intrahepatic cholestasis, indicating that this model is suitable for studying the molecular mechanisms involved in intrahepatic cholestasis.

FRI-173

Mutational profile and correlation with Leipzig score in Wilson disease-a comprehensive analysis

Anand Kulkarni¹, V. V. Ravikanth¹, Govardhan Bale¹, Mithun Sharma¹, Sowmya Iyengar¹, Shantanu Venishetty¹, Manasa Alla¹, Rajesh Gupta¹, Nagaraja Padaki¹, Nageshwar Reddy¹. ¹AIG Hospitals, Hyderabad, India
Email: anandvk90@gmail.com

Background and aims: The Leipzig score is an excellent tool for diagnosis of Wilson disease (WD). However, mutational analysis is not available widely and most rely on clinical and laboratory diagnosis of WD. We aimed to assess the role of mutational analysis in WD in the Indian population.

Method: Consecutive WD patients being treated with chelation therapy were included. DNA was isolated from 2 ml of whole blood and amplified with primer pools to generate the complete exonic and untranslated regions (UTRs; 3' and 5') of *ATP7B* gene (Ion AmpliSeq Designer; Thermo Fisher Scientific). Primary objective was to describe the mutational analysis and then compare the same among probable (Leipzig score 2–3) and high likely WD (Leipzig score >3) assessed through clinical features and lab tests.

Results: A total of 136 patients (median age-19 years; females-35.3%; Leipzig score-4; Nazer score-5 and NWI-5) being treated as WD were included in this analysis. Ninety-two patients underwent genetic analysis. Of them, 56.5% had no pathogenic variants, 21.7% had two pathogenic variants (homozygous-11 and compound heterozygous-9), and 21.7% had one heterozygous pathogenic variant. Of these 20 patients with one pathogenic variant, 13 patients had variants of unknown significance (VUS) and/or other pathogenic conflicting variants and seven had no other variants. Of the 52 patients with no pathogenic variants, 30 had no other variants, while 22 had other VUS/pathogenic conflicting variants. Of these 22 patients, 13 had homozygous or compound heterozygous mutations, while the other nine had only one variant. In total, 50% of patients (46/92) could be genetically labeled as WD, while 16 had one pathogenic variant with no other variants or only one VUS or another pathogenic variant. While 32.6% (n=30) had no mutations at all. The most common pathogenic variant was p.Gly1061Glu followed by p.Cys271Ter. Of the 59 patients with Leipzig clinical scores 2–3 (probable WD based on clinical and lab parameters), 43 underwent genetic tests, and of the 77 patients with Leipzig clinical scores >3 (high likely WD based on clinical and lab parameters), 49 underwent genetic tests. Of the 43 probable WD, 44.2% (n=19) had confirmed mutation, while seven had a single variant and 17 had none. Similarly, for patients with high likely WD, 27 (55.1%) had confirmed WD through mutational analysis, nine had one variant, and 13 had none.

Conclusion: Only 50% of patients with proven WD have classical genetic variants of the disease. Expanding the genetic testing to regulatory and other genome regions in the heterozygous carriers and in patients with no variants may uncover newer variants.

FRI-174

Spectrum of UGT1A1 variations in chinese patients with Gilbert's syndrome

Wenting Tan¹, Wenyan Zhang¹, Yan Zhu¹, Yunjie Dan¹, Xiaomei Xiang², Xiuhua Wang², Yi Zhou¹, Yanzhi Guo¹, Jie Xia¹, Guohong Deng¹. ¹Southwest Hospital, Chongqing, China; ²Southwest Hospital, Chongqing, China
Email: tan_wenting@126.com

Background and aims: Gilbert syndrome (GS) is an inherited abnormality characterized by moderate unconjugated hyperbilirubinemia without hemolysis. This rare autosomal recessive condition is caused by mutation in *UGT1A1* gene encoding for the UDP-glucuronosyl transferase. The spectrum of *UGT1A1* variations varies markedly between different ethnic populations. In this study, we aimed to investigate genetic causes and related characters for this condition in Chinese population.

Method: Totally, 425 patients with idiopathic jaundice who visited our hospital between Oct 2017 to Nov 2023 were included in this study. All patients were deeply sequenced by targeted next-generation sequencing panel in which 43 disease-causing genes known to be associated with genetic liver disease were involved in, including those resulting in unconjugated (*UGT1A1*) and conjugated hyperbilirubinemia (*ABCC2*, *SLCO1B1* and *SLCO1B3*).

Results: Among the cohort, 213 patients were diagnosed as GS (151 males) with age of 30.9 \pm 14.2 years old. Sixteen of them were self-reported with early-onset under 18 years old, 128 of them were adult-onset (median 27.5 yrs, range 18–68 yrs) while 69 of them remains unclear. All of them had unconjugated hyperbilirubinemia with a median IBIL level of 42.1 μ mol/L (range 28.5–59.9 μ mol/L) and total

POSTER PRESENTATIONS

bilirubin levels of 54.0 $\mu\text{mol/L}$ (range 38.1–77.4 $\mu\text{mol/L}$), meanwhile with normal liver enzyme (with average ALT level 24.1 IU/L, range 14.1–43.0 IU/L), kidney and coagulation function. Thirty-three percent of them developed visible yellowish discoloration of the skin and/or mucous membranes. Two hundred and seven patients (97.2%) harbored pathogenic/affected variations on *UGT1A1* gene, top frequent sites are c.-3275T>G and c.-1352A>C (both with MAF 57.9%) located on phenobarbital-responsive enhancer module (PBREM) and distal element respectively, followed by c.221G>A (p.Gly71Arg, MAF 26.7%), c.-54_-53dupAT (24.0%), c.686C>A (p.Pro229Gln, 6.25%), c.1091C>T (p.Pro364Leu, 5.5%) and c.1456T>G (p.Tyr486Asp, 2.4%). Totally, we detected 31 *UGT1A1* allelic variants, 9 of them are novel, including harmful nonsense and frameshift variant which finally resulted in protein translation stop (c.715C>T, p.Gln239*; c.655C>T, p.Gln219*; c.1047delG, p.Ile350fsX). Forty-one patients (19.2%) carried homozygous pathogenic variants and 166 patients (77.9%) showed multiple sites of variants in *UGT1A1*; however, no significant association have been found between variant (type, number or region) and bilirubin levels ($p > 0.05$).

Conclusion: We described here the spectrum of *UGT1A1* variants and nine novel *UGT1A1* mutations in our DS cohort. Polymorphisms in the enhancer, promoter and coding region of *UGT1A1* were commonly observed in southwestern Chinese GS patients. Our findings expand on the spectrum of *UGT1A1* mutations and provide additional evidence between *UGT1A1* and hyperbilirubinemia.

Rare liver diseases (including paediatric and genetic) – Clinical

TOP-139

Combination of liver steatosis and premenopausal is a risk factor for DILI due to cyclin-dependent kinase 4/6 inhibitors as first-line treatment for metastatic breast cancer

Kreina Sharela Vega-Cano¹, Lourdes Ruiz-Ortega², Pau Mascaró Baselga¹, Paula Esteban², Oriol Mirallas Viñas¹, Francesca Filippi-Arriaga³, Laia Joval Ramentol⁴, Juan Carlos Ruiz-Cobo², Pau Benito Buch¹, Jesus Yaringaño¹, Gaspar Joaquin Molina¹, Diego Gomez Puerto¹, Lucia Sanz Gómez¹, Esther Zamora Adelantado¹, Maria Buti^{2,5}, Meritxell Bellet Ezquerra¹, Mar Riveiro Barciela^{2,5}. ¹Medical Oncology department, Vall d'Hebron University Hospital and Vall d'Hebron Institute of Oncology (VHIO), Barcelona, Spain, Barcelona, Spain; ²Liver Unit, Internal Medicine Department, Hospital Universitari Vall d'Hebron, Barcelona, Spain, Barcelona, Spain; ³Clinical Pharmacology Department, Hospital Universitari Vall d'Hebron, Barcelona, Spain, Barcelona, Spain; ⁴Data Science, Vall d'Hebron Institute of Oncology (VHIO), Barcelona, Spain, Barcelona, Spain; ⁵CIBERehd, Madrid, Spain
Email: mar.riveiro@gmail.com

Background and aims: the estimated rate of drug-induced liver injury (DILI) by cyclin-dependent kinase 4/6 inhibitors (CDKi) in clinical trials was 13%, although there are limited data on its characteristics and risk factors in clinical practice. We aimed to assess the incidence, characteristics and risk factors for CDKi-associated DILI.

Method: retrospective study including all patients who received CDKi from 2018 to 2022. Characteristics of DILI \geq grade 2 (CTCAE) were described. A case-control study (1:3) was also performed to investigate associated risk factors.

Results: 472 women were treated with CDKi and 26 (5.5%) developed DILI: 11 (42%) grade-2, 13 (50%) grade-3 and 2 (8%) grade-4, in a median follow-up of 218 days (IQR 37–399). No one developed severe hepatitis. Incidence of DILI related to CDKi: ribociclib 11.6%, abemaciclib 8%, palbociclib 3%, Median age was 61 years and 54%

were premenopausal women. 11.5% had risk alcohol intake and 27% metastatic disease. After CDKi discontinuation, DILI was resolved in 88.5% in a median of 44 days (IQR 26–61). CDKi was restarted in 15 (58%) women, 61.5% of whom experienced a recurrence of toxicity. No risk factor was found in the case-control study, although liver steatosis showed a trend to increase DILI rate ($p = 0.08$). The combination of liver steatosis and premenopause (9 patients) was associated with a higher risk of DILI (67% vs. 19%, $p = 0.004$; OR 8.6, 95%CI 2.1–43.6), as was the combination of steatosis and baseline ALT > 35 IU/ml (57% vs. 21%, $p = 0.04$; OR 5.15, 95%CI 1.07–27.8). An exploratory analysis showed a lower progression-free survival in the DILI group (22.2 vs 36 months, $p = 0.03$; HR 1.84, 95% CI 1.06–3.22).

Conclusion: 5.5% of patients treated with CDKi experienced DILI, the majority grade-3 and associated with ribociclib therapy. CDKi-DILI was most common among premenopausal women with steatosis and it could be associated with a lower progression-free survival, though these results need to be confirmed prospectively.

TOP-140

Evolution of clinical presentation, treatment and prognosis of patients with alveolar echinococcosis treated at the university hospital Zurich: a 50-year experience

Ansgar Deibel¹, Yannick Kindler¹, Rubens Mita², Soleen Ghafoor³, Cordula Meyer zu Schwabedissen¹, Alexander Schweiger⁴, Felix Grimm⁵, Michael Reinehr⁶, Achim Weber⁷, Căcilia Reiner³, Andreas E. Kremer¹, Henrik Petrowsky⁸, Pierre-Alain Clavien⁸, Peter Deplazes⁵, Stefanie von Felten⁹, Beat Müllhaupt¹. ¹Department of Gastroenterology and Hepatology, University Hospital Zurich, University of Zurich, Zurich, Switzerland; ²Master Program in Biostatistics, University of Zurich, Zurich, Switzerland; ³Institute of Diagnostic and Interventional Radiology, University Hospital Zurich, University of Zurich, Zurich, Switzerland; ⁴Department of Infectious Diseases, Cantonal Hospital Zug, Zug, Switzerland; ⁵Institute of Parasitology, University of Zurich, Zurich, Switzerland; ⁶Department of Pathology and Molecular Pathology, University Hospital Zurich, University of Zurich, Zurich, Switzerland; ⁷Department of Pathology and Molecular Pathology, University Hospital Zurich, University Hospital Zurich, Zurich, Switzerland; ⁸Department of Visceral and Transplant Surgery, University Hospital Zurich, University of Zurich, Zurich, Switzerland; ⁹Institute of Epidemiology, Biostatistics and Prevention, University of Zurich, Zurich, Switzerland
Email: rudolfansgar.deibel@usz.ch

Background and aims: Alveolar echinococcosis (AE) is an orphan zoonotic liver disease of increasing concern in Europe and other endemic areas across the globe. AE mimics a malignant tumor with infiltrative growth and occasional metastatic spread. Without adequate treatment, the disease has a 90% 10-year-mortality. The mainstay of treatment is surgical resection and medical treatment with benzimidazoles (BMZ). The majority of cases is unresectable due to advanced disease stage at diagnosis. Long-term BMZ therapy is highly effective in stabilizing the disease course for unresectable cases. The study aim was to evaluate the evolution in the presentation, treatment, and prognosis of AE patients over the past 50 years.

Method: Retrospective cohort study of 334 AE patients who were treated at the University Hospital Zurich between 1973–2022. Analysis included patient demographics, symptomatology at diagnosis, AE stage according to PNM classification, treatment strategy (curative or palliative surgical resection; long-term BMZ treatment), treatment outcome, overall survival and causes of death. In order to analyze changes over time, variables were stratified by decade of diagnosis. Overall survival was compared to the general Swiss population through relative survival analysis. Risk of AE-associated death was compared between curatively resected patients and non-

resected participants, propensity-score-matched by PNM-classification.

Results: Over the decades, there was no change in patient demographics. The median age at diagnosis is 58 years with a slight female predominance. Since 2000, a steady increase in new diagnosis of AE was observed, with an increasing proportion attributable to incidental diagnosis. This was accompanied by a stage migration towards earlier AE stages. Nevertheless, fewer patients underwent surgical resection. In total, 126 patients (38%) underwent curative resection, of which 20 patients (16%) suffered disease recurrence. Ninety patients (27%) died but causes of death were predominantly non-AE related. AE-related death occurred after a median of 159 months. Median age at death of any cause was 79 years. The 15-year overall survival was 73% and did not differ by decade of diagnosis or disease stage. Relative survival of AE patients was similar to that of the general Swiss population over the first 13 years after diagnosis. Risk of AE-related death was very low in both resected and matched non-resected cases and similar over 13 years.

Conclusion: Annual AE cases are rising, with considerable changes in clinical presentation, stage of the disease and pursued treatment strategy. Survival is limited primarily by non-AE-related causes of death and similar to the general Swiss population over the first 13 years. Risk of AE-related death was similar over the first 13 years after diagnosis between curatively resected patients and matched non-resected patients.

TOP-141

Longitudinal assessment of individuals with homozygous alpha-1 antitrypsin deficiency (Pi*ZZ genotype) provides evidence for clinical patient management

Malin Fromme¹, Audrey Payancé², Mattias Mandorfer³, Katrine Thorhaug^{4,5}, Monica Pons^{6,7}, Marc Miravittles⁸, Jan Stolk⁹, Bart van Hoek¹⁰, Guido Stirnimann¹¹, Soňa Fraňková¹², Jan Sperl¹², Andreas E. Kremer¹³, Christina Schrader¹, Lorenz Balcar³, Benedikt Schaefer¹⁴, Joanna Chorostowska-Wynimko¹⁵, John Ryan¹⁶, Christian Trautwein¹, Heinz Zoller¹⁴, Michael Trauner³, Joan Genesca^{6,7}, William J. H. Griffiths¹⁷, Virginia C. Clark¹⁸, Aleksander Krag^{4,5}, Alice Turner¹⁹, Noel G. McElvaney²⁰, Pavel Strnad¹. ¹Medical Clinic III, Gastroenterology, Metabolic Diseases and Intensive Care, University Hospital RWTH Aachen, Aachen, Germany; ²AP-HP, service d'hépatologie, Hôpital Beaujon, AP-HP, Clichy, France, DMU Digest, Centre de référence des Maladies Vasculaires du foie, FILFOIE, Clichy, France, Université Paris Cité, Paris, France; ³Division of Gastroenterology and Hepatology, Department of Internal Medicine III, Medical University of Vienna, Vienna, Austria; ⁴Department of Gastroenterology and Hepatology, Odense University Hospital, Odense C, Denmark; ⁵Department of Clinical Research, Faculty of Health Sciences, University of Southern Denmark, Odense C, Denmark; ⁶Liver Unit, Hospital Universitari Vall d'Hebron, Vall d'Hebron Institute of Research (VHIR), Vall d'Hebron Barcelona Hospital Campus, Universitat Autònoma de Barcelona, Barcelona, Spain; ⁷Centro de Investigación Biomédica en Red de Enfermedades Hepáticas y Digestivas (CIBERehd), Instituto de Salud Carlos III, Madrid, Spain; ⁸Pneumology Department, Hospital Universitari Vall d'Hebron, Vall d'Hebron Institut de Recerca (VHIR), Vall d'Hebron Barcelona Hospital Campus, CIBER de Enfermedades Respiratorias (CIBERES), Barcelona, Spain; ⁹Department of Pulmonology, Leiden University Medical Center, Leiden, Netherlands; ¹⁰Department of Gastroenterology and Hepatology, Leiden University Medical Center, Leiden, Netherlands; ¹¹University Clinic for Visceral Surgery and Medicine, University Hospital Inselspital and University of Bern, Bern, Switzerland; ¹²Department of Hepatogastroenterology, Institute for Clinical and Experimental Medicine, Prague, Czech Republic; ¹³Department of Gastroenterology and Hepatology, University Hospital Zürich, University of Zürich, Zürich, Switzerland; ¹⁴Department of Internal Medicine I, Medical University Innsbruck, Innsbruck, Austria; ¹⁵Department of Genetics and Clinical Immunology, National Institute of Tuberculosis and Lung Diseases, Warsaw, Poland; ¹⁶Hepatology Unit,

Beaumont Hospital, RCSI University of Medicine and Health Sciences, Dublin, Ireland; ¹⁷Department of Hepatology, Cambridge University Hospitals NHS Foundation Trust, Cambridge, United Kingdom; ¹⁸Division of Gastroenterology, Hepatology, and Nutrition, University of Florida, Gainesville, Florida, United States; ¹⁹Institute of Applied Health Research, University of Birmingham, Birmingham, United Kingdom; ²⁰Irish Centre for Genetic Lung Disease, Royal College of Surgeons in Ireland, Beaumont Hospital, Dublin, Ireland
Email: mfromme@ukaachen.de

Background and aims: Homozygous Pi*Z mutation in *SERPINA1* confers a strong predisposition to lung and liver-related mortality. Current therapeutic approaches address either the pulmonary loss-of-function or the hepatic gain-of-function mechanism. We evaluated the disease course and non-invasive surrogates for the development of hepatic and pulmonary end points in an international, multicenter Pi*ZZ cohort with available longitudinal follow-up.

Method: In cohort 1, 737 Pi*ZZ subjects from 25 centers received a standardized clinical, laboratory, and elastographic assessment. At least six months afterwards, a follow-up interview was performed focusing on liver- and lung related end points. Hepatic end points were defined as first hepatic decompensation/liver transplantation or liver-related death, pulmonary end points comprised (listing for) lung transplantation or lung-related death. Cohort 2 consisted of 135 Pi*ZZ adults without significant liver fibrosis, who received a baseline and follow-up examination at least two years later, both including liver stiffness measurement (LSM).

Results: During 2634 patient-years of follow-up, 39 individuals died, with liver and lung being responsible for 46% and 36% of deaths, respectively (cohort 1). 41 Pi*ZZ subjects that developed a hepatic end point, presented with higher liver fibrosis markers at baseline, i.e., LSM (24 vs. 5 kPa, $p < 0.001$), AST-to-platelet ratio index (APRI, 1.1 vs. 0.3 units, $p < 0.001$) and fibrosis-4 index (FIB-4, 3.8 vs. 1.2, $p < 0.001$). Hepatic end points within five years were most accurately predicted by LSM (AUC 0.95) followed by APRI (0.92) and FIB-4 (0.90). Baseline lung parameters displayed only a moderate predictive utility for lung-related end points (FEV1 AUC 0.76). Notably, out of 540 Pi*ZZ individuals with LSM < 7.1 kPa, nobody developed a hepatic end point despite over 1900 follow-up years, while such end points were rare among subjects with APRI < 0.5 /FIB-4 < 1.3 units. An increase in all non-invasive liver fibrosis scores coincided with an increased occurrence of hepatic end points. Similarly, there was an increased incidence of lung end points in subgroups with lower FEV1 values. Interestingly, a Pi*ZZ subject with mild-to moderate pulmonary function impairment/increases in liver stiffness (i.e., FEV1 50–70% vs. LSM 7.1–10 kPa) displayed a three times higher risk of liver- vs. lung-related end points. In cohort 2, 8.9% showed a fibrosis progression based on LSM (≥ 7.1 kPa). Progressors displayed higher BMI (27.3 vs. 23.9 kg/m², $p = 0.004$), baseline LSM (6.1 vs. 4.6 kPa, $p = 0.002$) and APRI (0.44 vs. 0.28 $p < 0.001$).

Conclusion: Non-invasive surrogates of liver fibrosis were able to stratify hepatic decompensation risk in Pi*ZZ adults. Interestingly, liver risk was higher in those with mild-to moderate increases in liver stiffness, as compared to lung risk in those with mild-moderately impaired pulmonary function.

TOP-142-YI

Safety and efficacy of direct oral anticoagulants in cirrhotic and non-cirrhotic splanchnic vein thrombosis

Lucia Giuli¹, Rosa Talerico¹, Silvia Betti¹, Francesca Bartolomei¹, Elena Rossi¹, Antonio Gasbarrini¹, Maurizio Pompili², Valerio De Stefano¹, Roberto Pola¹, Maria Pallozzi¹, Brigida Eleonora Annicchiarico¹, Francesca Romana Ponziani¹, Francesco Santopaolo¹. ¹Fondazione Policlinico Universitario Agostino Gemelli IRCCS, Rome, Italy; ²Fondazione Policlinico Universitario Agostino Gemelli IRCCS, Rome, Italy
Email: lucia.giuli92@gmail.com

POSTER PRESENTATIONS

Background and aims: Splanchnic vein thrombosis (SVT) is a potentially life-threatening disease that can occur in cirrhotic and non-cirrhotic patients. Anticoagulation with heparins and vitamin K antagonists (VKA) is the mainstay of treatment. Recent studies have suggested that direct oral anticoagulants (DOACs) may offer a viable alternative in these settings. However, data on the safety and efficacy of DOACs are still limited, especially in cirrhotic patients. The aim of our study is to prospectively define the incidence of progression/recurrence of thrombosis and of major bleeding events during therapy with DOACs in patients with SVT.

Method: We conducted a prospective, single-centre, observational study. Consecutive cirrhotic and non-cirrhotic patients with either recent (<6 months) or chronic SVT who started DOACs at therapeutic dose were enrolled between June 2022 and June 2023. At one, three and six months patients were evaluated for clinical manifestation of venous thromboembolism and major bleeding events according to ISTH criteria. At six months a CT scan was performed to assess progression or recurrence of SVT.

Results: Of the 48 patients enrolled (mean age 59, 52% males, 38% cirrhotic), 21 had a recent SVT (43.8%). Of the 27 patients with chronic SVT, 19 (70%) had a cavernous transformation. Of the 18 cirrhotic patients, 83% were Child A and 17% Child B. 24 patients (50%) started rivaroxaban, 22 apixaban (45%) and 2 edoxaban (5%). All patients had received a previous treatment with heparins or VKA. Cirrhotic patients more frequently had varices ($p=0.002$) and previous episodes of variceal bleeding ($p=0.002$). Cirrhotic patients were older (67 vs 55, $p=0.0003$), had lower mean level of platelets (87444 vs 285466, $p=0.00003$) and higher mean level of bilirubin ($p=0.01$). At six months follow-up all patients were alive and there were two asymptomatic episodes of recurrence/progression of SVT (4.2%) and one episode of major bleeding (2.1%). No differences in the cumulative incidence of these events were found among cirrhotic and non-cirrhotic patients. Concerning recanalization, 8 patients presented complete recanalization (16.7%), 28 patients presented stability (58.3%) and 10 partial regression of SVT (20.8%). Complete recanalization was significantly more frequent in patients with recent SVT ($p=0.0009$).

Conclusion: DOACs appear to be a safe and effective alternative for the treatment of SVT in cirrhotic and non-cirrhotic patients.

TOP-143-1Y

Porto-sinusoidal vascular disease among patients undergoing surgery for liver metastases: prevalence, non-invasive diagnosis, and burden on surgical outcomes

Elton Dajti¹, Matteo Serenari¹, Deborah Malvi², Gerti Dajti¹, Federico Ravaioli¹, Luigi Colecchia¹, Giovanni Marasco³, Federica Odaldi⁴, Matteo Renzulli⁵, Amanda Vestito⁶, Francesco Azzaroli⁷, Giovanni Barbara¹, Matteo Ravaioli¹, Davide Festi³, Maria Antonietta D'Errico¹, Matteo Cescon⁸, Antonio Colecchia⁹. ¹University of Bologna, Bologna, Italy; ²Sant'Orsola-Malpighi Hospital, University of Bologna, Bologna, Italy; ³University of Bologna, Italy, Bologna, Italy; ⁴General Surgery and Transplant Unit, IRCCS, Azienda Ospedaliero-Universitaria di Bologna, Bologna, Italy; ⁵IRCCS AOUBO di Bologna, Bologna, Italy; ⁶Gastroenterology Unit, IRCCS S. Orsola Hospital, Bologna, Italy, Bologna, Italy; ⁷IRCCS Azienda Ospedaliero-Universitaria di Bologna Policlinico di Sant'Orsola, Bologna, Italy; ⁸Alma Mater Studiorum-University of Bologna, Bologna, Italy; ⁹POLICLINICO DI MODENA, Modena, Italy Email: e_dajti17@hotmail.com

Background and aims: Oxaliplatin has been associated with porto-sinusoidal vascular disease (PSVD), but scarce data is available. We aimed to i) describe PSVD prevalence among patients undergoing resection for liver metastases; ii) assess whether pre-operative liver (LSM) and spleen stiffness measurements (SSM) by transient elastography could diagnose PSVD and predict post-operative complications.

Method: This is a prospective single center study enrolling consecutive patients undergoing hepatic resection for metastases at a tertiary center. For each patient we evaluated previous exposure to chemotherapy, co-morbidities, elastography, type of surgery, histological features at the resection specimen, morbidity (post-hepatectomy liver failure (PHLF), major complications according to Clavien-Dindo), and overall survival.

Results: We included 68 patients in the analysis: 34 (50%) were female, 49 (72%) had a primary colon cancer, and 60 (88%) had undergone previous chemotherapy. At histology, 29 (44%) of the patients had a diagnosis PSVD (of whom 10 with non-specific signs of portal hypertension, PH), and 5 (8%) had steatohepatitis. SSM <21 kPa (NPV 87%) and >40 kPa (PPV 100%) could accurately rule-out and rule-in PSVD; none of the patients with PH signs had SSM <21 kPa. PSVD was associated with a significantly higher need for transfusions (0 vs 14%), incidence of PHLF (22 vs 45%), major complications (11 vs 31%), 90-day mortality (0 vs 14%). Pre-operative LSM was associated with the development of clinically significant PHLF (OR: 1.491, 95%-CI: 1.114–1.996), major complications (OR: 1.346, 95%-CI: 1.063–1.704), and mortality (HR: 1.379, 95%-CI: 1.122–1.696). The cut-offs of <4.5 kPa and >8 kPa were able to stratify for the risk of clinically significant (CS)-PHLF (0%, 11%, and 33% in LSM <4.5 kPa, 4.5–8 kPa, >8 kPa) and major complications (0%, 25%, 44% in LSM <4.5 kPa, 4.5–8 kPa, >8 kPa). The combination of LSM with SSM (LSM <4.5 kPa or LSM 4.5–8 kPa, but SSM <21 kPa) increased the subgroup of patients at low risk of complications (0% CS-PHLF, 3.2% major complications).

Conclusion: PSVD is a very common finding among patients undergoing liver surgery for metastases and it is associated with increased morbidity and mortality. LSM and SSM can correctly identify patients with PSVD and those at risk of clinically relevant post-operative complications. The non-invasive evaluation could improve risk stratification of patients undergoing surgery.

TOP-144-1Y

Heterozygosity for rare Apolipoprotein B variants predispose to severe metabolic associated steatotic liver disease

Matteo Mureddu¹, Serena Pelusi², Luisa Ronzoni², Francesco Malvestiti³, Vittoria Moretti², Hadi Eigadeh², Giorgio Soardo⁴, Alessandro Federico⁵, Francesco Paolo Russo⁶, Anna Ludovica Fracanzani⁷, Umberto Vespasiani-Gentilucci⁸, Luca Miele⁹, Elisabetta Bugianesi¹⁰, Roberta D'Ambrosio¹¹, Salvatore Petta¹², Mirella Fraquelli¹¹, Daniele Prati², Luca Valenti¹³. ¹Università degli Studi di Milano, Milan, Italy; ²Transfusion Medicine Unit, Fondazione IRCCS Ca' Granda Ospedale Maggiore Policlinico, Milan, Milan, Italy; ³Department of Pathophysiology and Transplantation, Università degli Studi di Milano, Milan, Italy; ⁴Clinica Medica, Department of Medicine, European Excellence Center for Arterial Hypertension, University of Udine, Udine, Italy; ⁵Department of Precision Medicine, University of Campania "Luigi Vanvitelli," Naples, Italy; ⁶Department of Surgery, Oncology and Gastroenterology, University Hospital Padua, Padua; ⁷Medicine and Metabolic Diseases, Fondazione IRCCS Ca' Granda Ospedale Maggiore Policlinico, Milan, Department of Pathophysiology and Transplantation, Università degli Studi di Milano, Milan, Italy; ⁸Clinical Medicine and Hepatology Unit, Department of Medicine and Surgery, Campus Bio-Medico University of Rome, Rome, Italy; ⁹Dipartimento Universitario Medicina e Chirurgia Traslazionale, Università Cattolica del Sacro Cuore, Rome, Area Medicina Interna, Gastroenterologia e Oncologia Medica, Fondazione Policlinico A. Gemelli IRCCS, Rome, Rome, Italy; ¹⁰Department of Medical Sciences, Division of Gastroenterology, University of Turin, Turin, Italy; ¹¹Gastroenterology and Hepatology Unit, Fondazione IRCCS Ca' Granda Ospedale Maggiore Policlinico, Milan, Milan, Italy; ¹²Section of Gastroenterology, Di.Bi.M.I.S Policlinico Paolo Giaccone Hospital, University of Palermo, Palermo, Italy; ¹³Department of Pathophysiology and Transplantation, Ca' Granda IRCCS Foundation, Policlinico Hospital, University of Milan, Transfusion Medicine Unit, Fondazione IRCCS Ca' Granda Ospedale Maggiore Policlinico, Milan, Milan, Italy Email: matteo.mureddu@studenti.unimi.it

Background and aims: Apolipoprotein B (ApoB) is fundamental to guarantee stability and secretion of Very Low-Density Lipoprotein (VLDL) from the liver. Loss-of-function mutations of APOB gene predispose to Familial Hypobetalipoproteinemia (FHBL) and steatotic liver disease (SLD). However, whether heterozygosity for rare protein coding APOB variants contribute to sporadic cases of severe MASLD with advanced fibrosis and/or hepatocellular carcinoma (HCC) is still disputed.

Aim of this study was to evaluate the prevalence of rare APOB mutations in a cohort of patients with advanced metabolic or cryptogenic SLD.

Method: 510 patients with liver disease were examined through Whole Exome Sequencing (WES) or Target Sequencing (TS) and 50 healthy controls.

SLD was defined by the availability of at least one among: 1) Controlled attenuation parameter (CAP) of at least 275 dB/m at Fibroscan; 2) Liver steatosis at ultrasonography, computed tomography or magnetic resonance imaging 3) Histological evidence of liver steatosis.

Rare variants were selected considering a Maximum Allelic Frequency (MAF) of 1%. All stop gained and frameshift mutations were considered in the analysis. Missense mutations were considered only if had CADD_Phred greater than 20. Missense mutations, splicing variants, splicing donor variants, 5' and 3' UTR variants, duplications and non-frame deletions were included if located in exons 1–26 or introns 1–25 and predicted by ClinVar and/or Franklin Genox to be pathogenic or likely pathogenic.

Results: Out of 510 subjects, 12 (2%) harbored APOB rare variants and 320 (62%) had evidence of steatosis. No mutation respecting selection criteria was found among controls.

The mutated subjects displayed lower LDL-C ($p = 0.009$), suggesting impaired VLDL secretion, and lower platelets count ($p = 0.01$) and a higher prevalence of FIB-4 > 2.67 ($p = 0.03$), irrespective of age and sex, suggesting more severe liver damage.

In the overall cohort, APOB variants were not associated with HCC, but after stratification for cirrhosis, HCC was more prevalent in the mutated than non-mutated patients without overt cirrhosis (OR 5.6 for HCC, 95% CI 1.09–8.7; $p = 0.02$ in the mutated versus non mutated patients in the absence of overt cirrhosis).

Conclusion: This study further supports the notion that heterozygous APOB variants predispose to severe SLD and HCC, and the importance of integrating genetic analysis in the management of patients with MASLD and cryptogenic liver disease.

WEDNESDAY 05 JUNE

WED-129

Abdominal surgery in patients with chronic noncirrhotic extra hepatic portal vein obstruction: a multicenter retrospective case-control study

Laure Elkrief¹, Corentin Denecheau-Girard¹, Marta Magaz², Michael Praktijn³, Nicola Colucci⁴, Isabelle Ollivier-Hourmand⁵, Jérôme Dumortier⁶, Macarena Simón-Talero⁷, Luis Téllez⁸, Florent Artru⁹, Magdalena Meszaros¹⁰, Xavier Verhelst¹¹, Nicolas Tabchouri¹, Francisca Beires¹², Irene Andaluz², Massimo Leo¹², Mara Diekhöner¹³, Safi Dokmak¹², Yilliam Fundora², Judit Vidal Gonzalez¹⁴, Christian Toso⁴, Aurélie Plessier¹², Juan Carlos García-Pagán², Pierre-Emmanuel Rautou¹². ¹Tours University Hospital, Tours, France; ²Hospital Clinic de Barcelona, Barcelona, Spain; ³University Hospital Münster, Münster, Germany; ⁴Geneva University Hospital, Geneva, Switzerland; ⁵CHU de Caen, Caen, France; ⁶Hôpital Edouard Herriot, Lyon, France; ⁷Hospital Vall d'Hebron, Barcelona, Spain; ⁸Hospital Universitario Ramón y Cajal, Madrid, Spain; ⁹CHUV, Lausanne, Switzerland; ¹⁰CHU Montpellier,

Montpellier, France; ¹¹Ghent University Hospital, Ghent, Belgium; ¹²Hôpital Beaujon, Clichy, France; ¹³University Hospital Bonn, Bonn, Germany; ¹⁴Hospital Universitari Vall d'Hebron, Barcelona, Spain
Email: laure_elkrief@yahoo.fr

Background and aims: In patients with noncirrhotic chronic extra-hepatic portal vein obstruction (EHPVO), data on morbi-mortality of abdominal surgery unrelated to portal hypertension are scarce.

Method: We retrospectively analyzed the charts of patients with EHPVO undergoing abdominal surgery within the VALDIG and the FILFOIE network. Cox univariate and multivariate regressions analyses were performed to identify factors associated with complications or death. We also compared the cumulative incidence of complications or death after surgery in patients with noncirrhotic EHPVO with matched controls without EHPVO who had similar surgical interventions.

Results: Seventy-six patients with EHPVO (58% male, median age 53 years) were included. Twenty-three (30%) patients had a history of ascites and 34 (45%) a strong risk factor for thrombosis. Seventy-eight interventions were performed, including 14 wall surgeries, 20 cholecystectomies, and 44 other surgeries. Fourteen (14%) had ≥ 1 major bleeding. Sixteen (21%) patients had ≥ 1 Dindo-Clavien grade ≥ 3 postoperative complication within 1 month after surgery. Emergency procedure and surgery other than wall or cholecystectomy were the main factors associated with major bleeding and with Dindo-Clavien grade ≥ 3 postoperative complications. Twelve (15%) patients had ≥ 1 portal hypertension related complication within 3 months after surgery, with a favorable outcome under medical therapy in 11/12 patients. Three (4%) patients died within 12 months after surgery. Six-month cumulative risk of death was higher in patients with serum creatinine ≥ 100 $\mu\text{mol/L}$ at surgery (20%, vs. 1%, $p = 0.004$). An unfavorable outcome (i.e. either complication or death) occurred in 29 (37%) patients and was associated to the presence of history of ascites and surgery other than wall surgery or cholecystectomy: 17% of the patients with none of these features had an unfavorable outcome, vs. 48% and 100% when one or both features were present, respectively. As compared to 126 matched control patients without EHPVO, incidence of both major bleeding ($p < 0.001$) and portal-hypertension related complication ($p < 0.001$) was significantly higher in patients with EHPVO but not that of neither grade ≥ 3 post-operative complication nor death within 12 months after surgery.

Conclusion: Patients with EHPVO are at high-risk of major bleeding and surgical complications, especially in those with history of ascites and/or undergoing surgery other than wall surgery or cholecystectomy.

WED-130

Prevalence and predictors of porto-sinusoidal vascular disorder in patients with persistent and unexplained gamma-glutamyl transferase elevation: a multicenter study

Nicola Pugliese¹, Francesca Romana Ponziani², Federica Cerini³, Luca Di Tommaso⁴, Federica Turati⁵, Marco Maggioni⁶, Matteo Angelo Manini⁷, Francesco Santopaulo⁸, Cristiana Bianco⁹, Chiara Masetti¹⁰, Maria Cristina Giustiniani¹¹, Carlo La Vecchia¹², Luca Valenti¹³, Luigi Terracciano¹⁴, Mauro Viganò¹⁵, Alessio Aghemo¹⁶. ¹Department of Biomedical Sciences, Humanitas University, Pieve Emanuele (MI), Italy; ²Division of Internal Medicine and Hepatology, Department of Gastroenterology, IRCCS Humanitas Research Hospital, Rozzano, MI, Italy, Rozzano (Milano), Italy; ³Hepatology Unit, CEMAD Centro Malattie dell'Apparato Digerente, Medicina Interna e Gastroenterologia, Fondazione Policlinico Universitario Gemelli IRCCS, 00168 Rome, Italy; ⁴Dipartimento di Medicina e Chirurgia Traslazionale, Università Cattolica del Sacro Cuore, 00168 Rome, Italy, Roma, Italy; ⁵Hepatology Division San Giuseppe Hospital, MultiMedica IRCCS, Università degli Studi di Milano, Via San Vittore 12, 20123 Milan, Italy, Milan, Italy; ⁶Humanitas University, Milan, Italy; ⁷Laboratory of Medical

POSTER PRESENTATIONS

Statistics, Biometry and Epidemiology "G.A. Maccacaro, Department of Clinical Sciences and Community Health, University of Milan, Italy, Milan, Italy; ⁶Fondazione IRCCS Ca' Granda Ospedale Maggiore Policlinico, Department of Pathology, Milan, Italy, Milano, Italy; ⁷Hepatology Unit, Humanitas Gavazzeni, Bergamo, Italy, Bergamo, Italy; ⁸Fondazione Policlinico Universitario Agostino Gemelli IRCCS, Roma, Italy; ⁹Fondazione IRCCS Ca' Granda Ospedale Maggiore Policlinico Milano, Milano, Italy; ¹⁰Humanitas Research Hospital IRCCS, Rozzano (Milano), Italy; ¹¹Fondazione Policlinico A. Gemelli, Roma; ¹²Laboratory of Medical Statistics, Biometry and Epidemiology "G.A. Maccacaro, Department of Clinical Sciences and Community Health, University of Milan, Italy, Milano, Italy; ¹³University of Milan, Milano, Italy; ¹⁴Humanitas Research Hospital, Milano, Italy; ¹⁵MultiMedica IRCCS, Università degli Studi di Milano, Milan, Italy; ¹⁶Department of Biomedical Sciences, Humanitas University, Pieve Emanuele (MI), Italy, Milan, Italy
Email: nicola.pugliese@live.com

Background and aims: Porto-sinusoidal vascular disorder (PSVD) is a group of vascular disorders characterized by lesions involving portal venules and sinusoids, irrespective of the presence of portal hypertension (PH). Liver biopsy (LB) is essential for diagnosis. In a single-center study, we demonstrated high rates of PSVD in patients with persistently elevated gamma-glutamyl transferase (GGT). This multicenter study aims to establish PSVD prevalence in a larger dataset of individuals with persistent and unexplained GGT elevation, and to identify associated risk factors.

Method: The study included all patients who underwent LB for persistent and unexplained GGT elevation in five Italian Hepatology Units between March 2015 and December 2021.

Results: 144 patients met the inclusion criteria. The majority were males (76/144, 52.8%) and mean age was 51.9 years (range 19–74). Twelve (8.3%) had liver stiffness measurements (LSM) >12 kPa, only 7 (4.8%) had ultrasound PH evidence. Histological findings were consistent with PSVD in 96 patients (67%). Alternative diagnoses were metabolic dysfunction-associated steatohepatitis (MASH) in 13 (9%), sarcoidosis in 3 (2%) and congenital hepatic fibrosis in 3 (2%). Histological examination couldn't provide a diagnosis in 29 (20%) patients. Male sex (odds ratio, OR = 2.60, 95% confidence interval, CI: 1.13–5.99), LSM <12 kPa (OR = 11.05, 95% CI: 2.16–56.66) and GGT <200 U/L (OR = 2.69, 95% CI: 1.22–5.98) were associated with histological findings of PSVD.

Conclusion: PSVD is the main cause of persistent and unexplained elevation of GGT. Male sex, LSM <10 kPa and GGT <200 U/L are associated with PSVD. These findings highlight the role of LB in elucidating the underlying pathology and aiding in the diagnosis of patients with persistent and unexplained GGT elevation.

WED-131-YI

Von Willebrand factor antigen reflects portal hypertension severity in porto-sinusoidal vascular disorder and predicts liver-related outcomes

Lorenz Balcar¹, Georg Semmler¹, Michael Schwarz¹, Emina Halilbasic¹, Albert Friedrich Stättermayer¹, Michael Trauner¹, Mattias Mandorfer¹, Thomas Reiberger¹, Bernhard Scheiner¹.

¹Medical University of Vienna, Vienna, Austria
Email: lorenz.balcar@meduniwien.ac.at

Background and aims: Von Willebrand factor antigen (VWF-Ag) reflects endothelial dysfunction and is a versatile non-invasive marker correlating with portal hypertension severity as well as outcomes in patients with cirrhosis. Patients with porto-sinusoidal vascular disorder (PSVD) are at risk to develop portal hypertension and associated complications, yet no study has so far evaluated the properties of VWF-Ag as a marker for portal hypertension or predictor of complications in PSVD.

Method: Patients with established diagnosis of PSVD at the Medical University of Vienna and available VWF-Ag at the diagnosis of PSVD were retrospectively included. VWF-Ag cut-offs predicting the

presence of specific clinical signs of portal hypertension as well as identifying patients at risk for liver-related outcomes (first/further hepatic decompensation + liver-related death) were developed.

Results: One-hundred and eighteen patients were included (mean age 48 ± 16 years; 64% female, 36% male). Forty-seven patients (40%) had a history of decompensation and 22 (19%) a portal vein thrombosis at diagnosis (mean MELD 9 ± 3, mean CTP 6 ± 1 points). Overall, 72% had specific, whereas 88% had unspecific signs of portal hypertension. Mean VWF-Ag was 221 ± 90%, median platelet count (PLT) was 122 (IQR: 71, 192 G/L) and median VITRO score (VWF-Ag/PLT) was 1.6 (IQR: 0.9, 3.1).

VWF-Ag and VITRO score were significantly higher in patients with specific signs of portal hypertension (VWF-Ag: 233 ± 87 vs. 192 ± 94; p = 0.027; VITRO: 2.2 [IQR: 1.1–3.7] vs. 1 [IQR: 0.5–1.9]; p = 0.002), whereas PLT, albumin, Child-Pugh-score or MELD score were not different among both groups. During a median follow-up of 3.8 years, 22 (19%) patients developed one or more liver-related complications. After adjusting for age, MELD, and history of decompensation, VWF-Ag was significantly associated with the outcome of interest (log, per 10; aHR: 2.94 [95%CI: 1.08–8.05]; p = 0.036). A VWF-Ag cut-off at ≥174% identified patients with considerable risk of developing liver-related outcomes during follow-up (at 3 years: 21% vs. 0%). Accordingly, this cut-off also stratified compensated patients at baseline with distinct risk (at 5 years: 17% vs. 0%).

Conclusion: VWF identifies PSVD patients with portal hypertension and associated liver-related outcomes independently of and superior to established prognostic markers.

WED-132

Role of transient elastography in diagnosis and prognosis of Fontan-associated liver disease

Marta Cuadros¹, Marta Abadía¹, Consuelo Froilán¹, Nerea Gonzalo¹, Miriam Romero¹, Araceli García-Sánchez¹, Francisco Javier García-Samaniego¹, Antonio Oliveira¹, José Carlos Erdozaín¹, José Ruiz-Cantador¹, Elvira Ana González-García¹, Inés Ponz¹, Pablo Merás¹, Carlos Merino¹, Adriana Rodríguez-Chaverri¹, Enrique Balbacid¹, Maria Dolores Martin-Arranz^{1,2,3}, Pilar Castillo¹. ¹Hospital Universitario La Paz, Madrid, Spain; ²Instituto de Investigación Hospital Universitario La Paz (IdiPAZ), Madrid, Spain; ³Universidad Autónoma de Madrid, Madrid, Spain
Email: cuadrosmartinez@gmail.com

Background and aims: Fontan-associated liver disease (FALD) is an emerging entity that affects patients with single-ventricle physiology who undergo the Fontan procedure. Recently, a definition of advanced FALD (A-FALD) has been proposed by the European Association for the Study of the Liver (EASL) and the European Reference Network (ERN) on Rare Liver Diseases, based on portal hypertension criteria. In FALD, liver congestion increases liver stiffness. Thus, liver stiffness measurement (LSM) by transient elastography (TE) may have a role in the diagnosis and prognosis of this disease.

Method: Retrospective study in a single-center, Hospital Universitario La Paz (Madrid, Spain). Laboratory data, ultrasound (US) findings (Canon Aplio i800), and LSM by TE (FibroScan[®]) were collected. FALD was defined by US criteria (hepatomegaly, liver surface nodularity, parenchymal heterogeneity, hyperechoic lesions, splenomegaly, or collaterals), and A-FALD, based on the EASL-ERN definition (oesophageal varices, portosystemic shunts, ascites, or splenomegaly).

Results: Between January 2017 and November 2023, 91 patients with Fontan surgery were included: mean age 33.3 ± 8.2 years, mean time since Fontan surgery 24.3 ± 7.7 years, 55/91 (60.4%) male. LSM by TE was associated with FALD and A-FALD in univariate and multivariate analysis (p < 0.05). LSM was significantly higher in patients with FALD than those without, median LSM 27.7 kPa (21.9–34.3 kPa) vs 14.6 kPa (11.4–18.5 kPa) (p < 0.001). The area under the receiver

operating characteristic (AUROC) of LSM for FALD was 0.905 (95% CI: 0.814–0.997) ($p < 0.001$). The optimal cut-off point for FALD was 19 kPa (sensitivity 92.3%, specificity 80.0%). The cut-off point to rule-out FALD was 15 kPa (sensitivity 96.9%). The cut-off point to rule-in FALD was 25 kPa (specificity 100%). Patients with A-FALD had higher LSM compared with those without, median LSM 29.5 kPa (22.4–36.6 kPa) vs 20.2 kPa (14.6–27.7 kPa) ($p = 0.001$). The AUROC of LSM for A-FALD was 0.764 (95% CI: 0.624–0.905) ($p = 0.001$). The optimal cut-off point for A-FALD was 25 kPa (sensitivity 69.6%, specificity 68.4%). The cut-off point to rule-out A-FALD was 19 kPa (sensitivity 95.7%). The cut-off point to rule-in A-FALD was 39 kPa (specificity 94.8%). LSM correlated with clinically relevant events (need for heart or heart-liver transplantation, hepatocellular carcinoma and death), with statistically significant differences in multivariate analysis (odds-ratio: 1.07; 95% CI: 1.01–1.13; $p = 0.03$). Regarding mortality, LSM values were significantly higher in patients who died, median LSM 44.6 kPa (34.6–62.9 kPa) vs 25 kPa (20.2–32.2 kPa) ($p = 0.006$). **Conclusion:** In patients with Fontan surgery, liver stiffness measurement by TE correlates with FALD and clinically relevant events (need for heart or heart-liver transplantation, hepatocellular carcinoma, and death).

WED-133

Quality of life in adults with Wilson disease: a study from the international Wilson disease registry

Claus Niederau¹, Aurélie Poujois², George Alex³, Anil Dhawan⁴, Caroline Roatta⁵, C. Omar Kamlin⁶, Timothy Jenkins⁶, Pramod Mistry⁷. ¹Katholische Kliniken, Oberhausen, Germany; ²Hôpital Fondation Adolphe de Rothschild, Paris, France; ³Murdoch Children's Institute, Parkville, Australia; ⁴Liver Institute, London, United Kingdom; ⁵Bernard Pepin Institute, Service Neurologie Hôpital Lariboisière, Paris, France; ⁶Orphan SA, London, United Kingdom; ⁷Yale School of Medicine, New Haven, United States
Email: pramod.mistry@yale.edu.au

Background and aims: Wilson disease is a prototype inborn error of metabolism that results in a wide spectrum of liver disease and neuropsychiatric symptoms. Multiple therapeutic options are available, however, chronic disease management, may be limited by impaired health related quality of life (HRQoL). Due to extreme heterogeneity of WD, real-world data on HRQoL are needed to harness maximal potential of therapies.

Method: The International Wilson Disease (iWD) registry was established in 2021 (NCT05239858). Patients aged 18 years or greater at first visit, completed a 12-Item Short-Form Health Survey (SF-12), a validated multipurpose indicator of health status. Data were analysed using SPSS v29. Correlations between continuous variables were estimated using Spearman's correlation and between quantitative variables and two or more groups using Mann-Whitney Kruskal-Wallis tests respectively.

Results: Between 29/06/2022 and 30/11/2023, 334 subjects were enrolled, of whom 322 met age eligibility criteria from Germany (76), Belgium (15), Spain (83), Poland (44), UK (47), and France (57). SF-12 was completed by 314/322 (97.5%). Of the 322, 50.6% (163) were female, mean (SD) age of 39.1 (14.6) years. Clinical phenotypes were reported in 298 (hepatic [166], neurologic [72], asymptomatic [48], psychiatric [7], mixed [5] respectively. WD therapy was documented in 318; d-penicillamine (135), zinc salts (79), trientine tetrahydrochloride (52), trientine dihydrochloride (43), chelator plus zinc (9). The majority (222/314; 71%) rated their general health as either good or very good, with only 10/314 (3%) reporting this as poor. The mean (SD) physical health composite summary (PCS) and the mental health composite summary (MCS) for this cohort were 42.8 (4.6) and

45.8 (5.5), respectively. No differences were seen by gender, class of therapy or country. MCS but not PCS was significantly lower with psychiatric phenotype vs other phenotypes.

Conclusion: In a European cross-sectional survey of adults with WD, whilst self-reported general health was rated high in many patients, mean physical and mental health scores were lower than US reference values. These data highlight areas for improvement in HRQoL and underscore the need for research to develop WD specific instruments to address these data gaps (*abstract submitted on behalf of the International Wilson Disease (iWD) Registry Collaborators*).

WED-134

Treatment adherence and associated clinical outcomes for Wilson disease patients: a real-world, retrospective, multinational survey

Niall Hatchell¹, Nathan Ball¹, Kieran Wynne-Cattanach¹, Emily Quinones¹, Jennifer Mellor¹. ¹Adelphi Real World, Bollington, United Kingdom
Email: niall.hatchell@adelphigroup.com

Background and aims: Wilson disease (WD) is a rare, multisystemic disease caused by dysfunctional copper excretion, with hepatic and neuropsychiatric presentation. Prescription of copper-binding medication ensures copper is serum ceruloplasmin-bound and excreted. Complete adherence is key to improving clinical outcomes, however it is unknown to what extent in WD patients. We investigated real-world clinical outcomes for patients with varying adherence to WD treatment, and drivers of adherence.

Method: Data were drawn from the Adelphi Wilson Disease Specific Programme™, a cross-sectional survey of physicians and their consulting patients in Australia, Brazil, Canada, France, Germany, Italy, Spain, and the United Kingdom from June 2022–March 2023. Physicians reported patient demographics, clinical outcomes (including disease presentation via Unified Wilson Disease Rating Scale, UWDRS), treatment, and adherence. Physicians reported patients as “not at all,” “a little,” “somewhat,” “mostly” or “completely” adherent to taking their medication exactly as agreed, and responses were grouped into “patients with complete adherence” (pCA) or “patients with suboptimal adherence” (pSA). Comparisons between groups were made using Fisher's Exact test or t-test. Logistic regression was used to assess the association between outcomes and the likelihood of having “complete adherence.” Odds ratios (OR) were calculated.

Results: Data were analysed for 615 WD patients (from 210 WD treating physicians) with known adherence levels, of whom 51% were pCA. Mean (standard deviation; SD) age was 33.4 (14.35) years and 67% were male. Patients' mean (SD) time since diagnosis was 5.9 (6.35) years. D-penicillamine was the most prescribed treatment (68% of patients), and mean (SD) time on any treatment was 4.1 (4.57) years. WD patients experienced a mean (SD) of 8.1 (6.79) symptoms, with pSA experiencing more symptoms, 10.0 (7.28) compared to pCA, (6.4 (5.79)) ($p < 0.0001$). Total mean (SD) UWDRS scores were higher for pSA, 39.8 (43.12) compared to pCA, 20.6 (27.98; $p < 0.01$). pSA had higher hepatic, psychiatric and neurologic UWDRS domain scores than pCA, 10.4, 13.4 and 25.5, compared to 2.2, 3.9, and 5.1 respectively (all $p < 0.01$). Side effects of current WD regimen were more common among pSA (19%) than pCA (42%) ($p < 0.01$). Significant associations were observed between experiencing side effects (OR 0.37; $p < 0.01$) and total UWDRS score (OR 0.98; $p < 0.01$) with likelihood of being adherent.

Conclusion: pSA were experiencing more symptoms and greater impairment across all UWDRS domains. Our findings suggest side effects of currently approved WD treatments had an association with suboptimal adherence in these patients. This indicates a need for newer WD treatment options with more manageable side effect profiles to improve adherence and outcomes.

WED-135-YI

Impact of metabolic alterations on liver phenotype of patients with homozygous alpha-1 antitrypsin deficiency (Pi*ZZ)

Christina Schrader¹, Malin Fromme¹, Audrey Payancé², Matthias Mandorfer³, Katrine Thorhauge^{4,5}, Monica Pons^{6,7}, Marc Miravittles⁸, Jan Stolk⁹, Bart van Hoek¹⁰, Guido Stirnimann¹¹, Soňa Fraňková¹², Jan Sperl¹², Andreas E. Kremer¹³, Lorenz Balcar³, Benedikt Schaefer¹⁴, Joanna Chorostowska-Wynimko¹⁵, Christian Trautwein¹, Heinz Zoller¹⁴, Michael Trauner³, Joan Genesca^{6,7}, William J. H. Griffiths¹⁶, Virginia C. Clark¹⁷, Aleksander Krag^{4,5}, Noel G. McElvaney¹⁸, Alice Turner¹⁹, Pavel Strnad¹. ¹Medical Clinic III, Gastroenterology, Metabolic Diseases and Intensive Care, University Hospital RWTH Aachen, Aachen, Germany; ²AP-HP, service d'hépatologie, Hôpital Beaujon, AP-HP, Clichy, France; ³DMU Digest, Centre de référence des Maladies Vasculaires du foie, FILFOIE, Clichy, France; ⁴Université Paris Cité, Clichy, France; ⁵Division of Gastroenterology and Hepatology, Department of Internal Medicine III, Medical University of Vienna, Vienna, Austria; ⁶Department of Gastroenterology and Hepatology, Odense University Hospital, Odense, Denmark; ⁷Department of Clinical Research, Faculty of Health Sciences, University of Southern Denmark, Odense, Denmark; ⁸Liver Unit, Hospital Universitari Vall d'Hebron, Vall d'Hebron Institute of Research (VHIR), Vall d'Hebron Barcelona Hospital Campus, Universitat Autònoma de Barcelona, Barcelona, Spain; ⁹Centro de Investigación Biomédica en Red de Enfermedades Hepáticas y Digestivas (CIBERehd), Instituto de Salud Carlos III, Madrid, Spain; ¹⁰Pneumology Department, Hospital Universitari Vall d'Hebron, Vall d'Hebron Institut de Recerca (VHIR), Vall d'Hebron Barcelona Hospital Campus, CIBER de Enfermedades Respiratorias (CIBERES), Barcelona, Spain; ¹¹Department of Pulmonology, Leiden University Medical Center, Leiden, The Netherlands; ¹²Department of Gastroenterology and Hepatology, Leiden University Medical Center, Leiden, Netherlands; ¹³University Clinic for Visceral Surgery and Medicine, University Hospital Inselspital and University of Bern, Bern, Switzerland; ¹⁴Department of Hepatogastroenterology, Institute for Clinical and Experimental Medicine, Prague, Czech Republic; ¹⁵Department of Gastroenterology and Hepatology, University Hospital Zürich, University of Zürich, Zürich, Switzerland; ¹⁶Department of Internal Medicine I, Medical University Innsbruck, Innsbruck, Austria; ¹⁷Department of Genetics and Clinical Immunology, National Institute of Tuberculosis and Lung Diseases, Warsaw, Poland; ¹⁸Department of Hepatology, Cambridge University Hospitals NHS Foundation Trust, Cambridge, United Kingdom; ¹⁹Division of Gastroenterology, Hepatology, and Nutrition, University of Florida, Gainesville, United States; ¹⁸Irish Centre for Genetic Lung Disease, Royal College of Surgeons in Ireland, Beaumont Hospital, Dublin, Ireland; ¹⁹Institute of Applied Health Research, University of Birmingham, Birmingham, United Kingdom
Email: christina.schrader@rwth-aachen.de

Background and aims: Pi*ZZ genotype is responsible for the majority of severe alpha-1 antitrypsin deficiency cases and confers a genetic susceptibility to lung emphysema and liver fibrosis. We analyzed the significance of metabolic factors in the European Pi*ZZ cohort.

Method: A multicenter international cohort consisted of 1160 PiZZ individuals at baseline, 590 of them completed a follow-up assessment at least 6 months later. Inclusion criteria comprised no additional liver comorbidities, an at most moderate alcohol consumption and no liver decompensation prior to baseline. Baseline liver examinations included clinical and laboratory work-up, along with non-invasive liver fibrosis assessment via AST-to-platelet ratio index (APRI). During follow-up interviews, a need for liver transplantation, liver-associated death, the development of decompensated cirrhosis (i.e., ascites, hepatorenal syndrome, or hepatic encephalopathy) were counted as liver end points.

Results: At baseline, 198 participants were obese (BMI ≥ 30 kg/m²) and 39 had diabetes. The latter displayed more often than non-diabetic individuals elevated AST and ALT values as well as diminished platelets (OR 2.8–4.2, $p < 0.01$ for all comparisons). APRI suggestive of significant (≥ 0.5 units) and advanced liver fibrosis (≥ 1.0 units) was also more common (OR 2.7 and 7.7; $p < 0.01$ for both). Compared to non-obese subjects, obese individuals had more often elevated AST and ALT values and diminished platelets (OR 1.3–2.1, $p < 0.01$ for all comparisons). Over a median follow-up time of 3.54 years, 127 subjects passed away and 41 individuals experienced a hepatic end point. Pi*ZZ individuals with a hepatic end point demonstrated a significantly higher BMI (28.2 vs. 24.8 kg/m², $p < 0.001$), were more often male (73.2% vs. 52.3%, $p = 0.01$), and had more frequently diabetes mellitus (15.4% vs. 3.1%, $p < 0.001$). Diabetes (HR 5.1, $p < 0.001$) and obesity (HR 2.7, $p = 0.008$) conferred a higher risk of hepatic end points during follow-up, whereas the impact of male gender was less pronounced (HR 2.2, $p = 0.022$).

Conclusion: In Pi*ZZ subjects, diabetes and obesity are associated with elevated liver injury/fibrosis markers at baseline and an increased risk of hepatic decompensation during follow-up. These factors should be considered in the clinical management of these subjects.

WED-136

Comorbidity burden associated with fatigue or pruritus in patients with primary biliary cholangitis in the United States: a matched case-control study

Nisreen Shamseddine¹, Hongbo Yang², Su Zhang², Sonal Kumar³. ¹Ipsen Biopharmaceuticals, Inc, Cambridge, United States; ²Analysis Group, Inc., Boston, United States; ³Weill Cornell Medical College, New York, United States
Email: nisreen.shamseddine@ipsen.com

Background and aims: Primary biliary cholangitis (PBC) is a chronic rare cholestatic liver disease with adverse health outcomes including end-stage liver disease. Pruritus and fatigue are common conditions associated with PBC. This study assessed the additional comorbidity burden of PBC-associated pruritus or fatigue in patients living in the United States.

Method: This retrospective study used IQVIA PharMetrics® Plus data (2016–2022). Patients with PBC and pruritus, and those with PBC and fatigue were separately selected as cases. Patients with PBC and neither pruritus nor fatigue were eligible as controls; controls were selected by matching to cases at a 1:1 ratio on the parameters of sex, insurance type, region, PBC duration, and postindex follow-up duration. Index date was defined as a random date for the pruritus/fatigue diagnosis after the initial PBC diagnosis for cases and a random medical visit for controls. The number of comorbidities per patient by 1, 3, and 5 years postindex was compared between cases and matched controls. For each individual comorbidity, the cumulative incidence by 1, 3, and 5 years postindex were compared between cases and matched controls and the hazard ratio of developing the comorbidity in cases vs. controls was estimated.

Results: 760 pruritus cases and matched controls (median follow-up: 23.3 month) and 1839 fatigue cases and matched controls (median follow-up: 21.5 month) were included. At baseline (the 1-year period before index), the mean number of comorbidities per patient was 1.1 for pruritus cases vs 0.5 for controls ($p < 0.001$) and 1.1 for fatigue cases vs 0.5 for controls ($p < 0.001$). The number of comorbidities by 1, 3, and 5 years postindex were significantly higher for cases vs controls: 1.9 vs 0.8, 2.3 vs 1.0, and 2.7 vs 1.0, respectively ($p < 0.001$ for all) for pruritus groups; 1.7 vs 0.7, 2.2 vs 0.9, and 2.5 vs 1.0 ($p < 0.001$ for all) for fatigue groups. The most common comorbidities were fatigue, anxiety, and urinary tract infection (UTI) in patients with pruritus, and anxiety, UTI, and depression in patients with fatigue. The hazard ratio of developing individual comorbidities ranged from 1.5–2.8 for pruritus cases relative to controls ($p < 0.001$ for all), and 1.3–4.0 for fatigue cases relative to controls ($p < 0.01$ for all).

Conclusion: This analysis suggests that patients with PBC with pruritus and fatigue experience a significant comorbidity burden. The findings highlight an unmet need for PBC treatments that reduce the adverse health outcomes associated with PBC.

WED-137-YI

Reviewing the largest experience of liver transplantation for Wilson's disease in the UK: single centre review of patient and graft outcomes and long term survival

James Liu Yin¹, Claire Kelly¹, Adrian Bomford¹, Rosa Miquel², Niloufar Safinia¹, Alberto Sanchez-Fueyo¹, Marianne Samyn³, Deepak Joshi¹, Michael Heneghan¹, Kosh Agarwal¹, Abid Suddle¹, Varuna Aluvihare¹, Krishna Menon¹, Anil Dhawan⁴, Nigel Heaton⁵, Aftab Ala¹. ¹Institute of Liver Studies, King's College Hospital, London, United Kingdom; ²Liver Histopathology, King's College Hospital, London, United Kingdom; ³Paediatric Liver, Gastroenterology and Nutrition Centre, King's College Hospital, London, United Kingdom; ⁴Paediatric Liver, King's College Hospital, Paediatric Liver, GI and Nutrition Centre, London, United Kingdom; ⁵King's College Hospital, London, United Kingdom
Email: aftab.ala1@nhs.net

Background and aims: Wilson's disease (WD) is a genetic metabolic liver condition caused by mutation of the ATP7B transporter leading to accumulation of copper particularly in brain and hepatic tissue resulting in liver failure. Clinically this presents acutely but may be a cause of chronic liver failure. Transplantation is often necessary in those who present with acute liver failure or decompensated chronic liver disease. King's College Hospital, London (KCH) has a large cohort of WD patients. We aim to review the outcomes from liver transplantation performed in our institution.

Method: We reviewed clinical, genetic and biochemical data for all patients transplanted for WD at KCH from 1990 to 2023. Data was collected from current electronic records. Statistical analysis was performed using Microsoft excel and Graphpad Prism.

Results: There were 65 patients transplanted for a clinical diagnosis of WD since 1990 (38F:27M). Age range was from 7 to 56 years (yr) with median age of 20 yr. Listing for transplant was 41 (63%) as super urgent, 16 (25%) as chronic (3 listed as priority) and 12% with unavailable data. 57 transplants were with whole livers, 7 received left lobes and 1 right lobe. There were 61 DBD grafts, 3 DCD (listed for chronic) and 1 living un-related donor. 52% of patients were on single agent immunosuppression, 38% on dual and 10% on three. 5% had graft loss within 90 days and overall 17% required multiple transplants (2Tx: 10 patients, 3Tx:1 patient). Reasons for graft loss were cholangiopathy (2), acute rejection, nodular regenerative hyperplasia, early and late hepatic artery thrombosis, multifactorial graft dysfunction, chronic rejection (3), and de-novo autoimmune hepatitis. Patient survival was 94% at 1 yr, 91% at 5 yr and 91% at 10 yr. Graft survival was 94% at 1 yr, 86% at 5 yr and 82% at 10 yr. For patients listed as super-urgent, survival was 90% at 1 yr and 88% at 5 yr. No statistical significance in graft survival was found between genetic mutations (none/heterozygous/compound/homozygous $p = 0.40$), listing criteria (super urgent/chronic $p = 0.09$) or blood type (A/B/AB/O $p = 0.66$). Using linear regression analysis with length of survival and graft survival as dependent variables comparing age, MELD, UKELD, urinary copper level and tissue copper level, there was no statistically significant result.

Conclusion: This is the largest reported experience of liver transplantation for WD in the UK. Overall survival after transplant for WD was comparable to the national average at 1 yr, but was considerably higher at 5 and 10 yr. Similarly for super-urgent transplants, 1 yr survival was comparable, but at 5 yr was higher. While this may be explained by the younger median age of patients, transplant for WD remains an effective treatment for acute liver failure caused by WD. Further collaborative work at scale is needed to understand outcomes and contributing factors over short and long term periods.

WED-138

Patients with alpha-1-antitrypsin deficiency and the risk of developing liver events: a longitudinal cohort study

Pavel Strnad¹, Tina Landsvig Berentzen², Louise Maymann Nitze², Klaus Kaas Andersen², Michael Soliman³, Kamal Kant Mangla², Mohamed Tawfik², Alice Turner⁴. ¹University Hospital RWTH Aachen, Aachen, Germany; ²Novo Nordisk A/S, Copenhagen, Denmark; ³Novo Nordisk, Boston, United States; ⁴Institute of Applied Health Research, University of Birmingham, Birmingham, United Kingdom
Email: pstrnad@ukaachen.de

Background and aims: Alpha-1-antitrypsin (AAT) deficiency (AATD) is a rare genetic disorder that manifests as lung and/or liver disease, but the progression to severe liver disease remains poorly understood. The aim of this study was to characterise a population with AATD at the time of diagnosis and to estimate the subsequent risk of developing severe liver disease.

Method: This longitudinal cohort study included patients with a diagnosis of AATD aged ≥ 18 years and registered in the Clinical Practice Research Datalink after 1 April 1997, with no alcohol-related disorders, viral, biliary or autoimmune liver diseases or prescriptions of drugs inducing liver disease before or on the date of their AATD diagnosis (index date). Patients were characterised at the index date and followed until time of first severe liver event or 31 March 2021, whichever came first. Events were defined as liver-related hospitalisation or death from hepatocellular carcinoma, liver transplant, chronic liver failure, liver cirrhosis, portal hypertension, or hepatic decompensation recorded in the Hospital Episodes Statistics or Office for National Statistics Death Registration. Aalen-Johansen cumulative incidence functions were estimated and a reference population was matched according to birth year and sex.

Results: In total, 3402 eligible patients had an AATD diagnosis, of whom 74 with a severe liver event before their AATD diagnosis were excluded. In the 3328 patients with no prior liver event, 50.9% were male and median age was 49 years. Few (33%) had serum AAT measured at the index date: median (5%, 95%) 0.80 (0.20, 1.14) g/L. Liver function tests in the AATD vs reference population were: median aspartate aminotransferase (AST) 28 vs 23 u/L, alanine aminotransferase (ALT) 33 vs 22 u/L, gamma-glutamyl transferase (GGT) 53 vs 28 u/L and platelet count 252 vs 251×10^9 /L. During a median follow-up of 5.7 years, 122 incident liver events occurred, with cirrhosis ($n = 43$), hepatic decompensation ($n = 37$) and portal hypertension ($n = 20$) being the most common. The cumulative incidence of a liver event at 10 years post-index date was 5.1% and 1.3% in the AATD and reference population ($p < 0.001$), respectively. In patients with AATD with low AAT (< 57 mg/dL) or low platelet count ($< 150,000$), or high levels of AST (> 40 U/L), ALT (> 40 U/L) or GGT (> 30 IU/L) at the index date, the cumulative incidence of a liver event at 10 years was 11%, 45%, 19%, 10% and 9%, respectively.

Conclusion: In this real-world population of patients with AATD registered in general practice, the risk of developing a severe liver event was significantly higher than in the reference population. In patients with AATD with a low level of serum AAT or abnormal liver function tests, the risk of developing severe liver events was even higher. These results highlight a strong unmet medical need for monitoring and treatment of liver-related complications in patients with AATD.

WED-151

Routine cholestasis genetic testing in patients with intrahepatic cholestasis of pregnancy reveals high prevalence of genetic variants of bile acid transport defects

Kelly Dale¹, Anita Kohli², Rida Nadeem¹, Naim Alkhoury². ¹Arizona Liver Health, Phoenix, United States; ²Arizona Liver Health, Phoenix, United States
Email: kdale@azliver.com

Background and aims: Intrahepatic cholestasis of pregnancy (ICP) is a condition unique to pregnancy causing pruritus, elevated liver

POSTER PRESENTATIONS

enzymes, and elevated serum bile acids. It has been associated with complications including stillbirth and preterm delivery. Some women continue to experience cholestasis often with pruritus that occurs outside of pregnancy. Genetic predisposition is often implicated in ICP specifically with mutations in the ATP8B1, ABCB11, and ABCB4 genes that are associated with progressive familial intrahepatic cholestasis (PFIC). The aim of this study was to assess the utility of routine cholestasis genetic testing in patients with ICP.

Method: Consecutive patients that presented to a tertiary hepatology clinic for history of cholestasis and ICP were tested prospectively for causes of genetic cholestasis with the cholestasis panel that tests for 77 genes. Routine clinical and laboratory parameters were collected. The severity of liver disease was assessed with vibration controlled transient elastography (VCTE). Descriptive statistics were used to characterize the cohort.

Results: Seven patients with history of ICP were tested. The mean age was 41.3 ± 13.9 years and the mean BMI was 28 ± 3.6 kg/m². Laboratory parameters were as follows: ALT 45 ± 20.7 U/L, AST 35 ± 18.5 , alkaline phosphatase 120.4 ± 51 , GGT 59.4 ± 54 , bilirubin 0.44 ± 0.11 , and platelet count 326.7 ± 57.4 k/uL. The mean liver stiffness on VCTE was 4.9 ± 1.0 kPa and the mean controlled attenuation parameter was 243.4 ± 62 dB/m indicating no significant liver fibrosis. Genetic testing revealed that 5/7 (71.4%) of patients were heterozygote for a genetic variant in the ABCB4 gene typically associated with PFIC type 3. One patient was heterozygote for a genetic variant of MYO5B associated with PFIC 10. One patient was heterozygote for 3 genetic variants including CC2D2A, NPHP3, and UGT1A1. 6/7 (85.7%) of patients had recurrent episodes of pruritus that continued to occur outside of pregnancy. 4/7 (57.1%) were on ursodeoxycholic acid.

Conclusion: Cholestasis genetic testing in patients presenting to hepatology clinic for history of cholestasis and ICP revealed high prevalence of ABCB4 variants. To our knowledge, the association between MYO5B and ICP is novel. The role of other genetic variants for cholestasis other than PFIC genes needs to be better understood.

WED-152

Design and study population of MITIGATE: the first multinational randomized controlled clinical trial in IgG4 related disease, evaluating the efficacy and safety of the CD19 B cell depleting agent inebilizumab

John Stone¹, Emma Culver², Arezou Khosroshahi³, Wen Zhang⁴, Emanuel Della Torre⁵, Kazuichi Okazaki⁶, Yoshiya Tanaka⁷, Matthias Lohr⁸, Nicolas Schleinitz⁹, Lingli Dong¹⁰, Hisanori Umehara¹¹, Marco Lanzillotta⁹, Zachary Wallace¹, Mikael Ebbo⁹, George Webster¹², Yanping Wu¹³, Daniel Cimbora¹³, Nishi Rampal¹³. ¹Massachusetts General Hospital, Harvard Medical School, Boston, United States; ²John Radcliffe Hospital, University of Oxford, Oxford, United Kingdom; ³Emory University School of Medicine, Atlanta, United States; ⁴Peking Union Medical College, Beijing, China; ⁵San Raffaele Hospital, Milan, Italy; ⁶Kansai Medical University Kori Hospital, Osaka, Japan; ⁷University of Occupational and Environmental Health, Kitakyushu, Japan; ⁸Karolinska Institutet, Stockholm, Sweden; ⁹Hôpital de la Timone, AP-HM, Aix-Marseille Université, Marseille, France; ¹⁰Tongji Medical College, Huazhong University of Science and Technology, Shanghai, China; ¹¹Nagahama City Hospital, Shiga, Japan; ¹²University College Hospital, London, United Kingdom; ¹³Amgen, Inc., Thousand Oaks, United States
Email: jhstone@mgh.harvard.edu

Background and aims: The roles of B cells in the pathophysiology of IgG4 Related Disease (IgG4-RD) and existing clinical experience suggest that B cell depletion may be an effective therapeutic avenue. Inebilizumab is a humanized, glycoengineered CD19 monoclonal antibody that effectively and selectively depletes B cells. The Phase 3 MITIGATE trial (NCT04540497) is a randomized, double-blinded,

placebo-controlled trial that aims to demonstrate the efficacy and safety of inebilizumab monotherapy in IgG4-RD.

Method: MITIGATE is being conducted at 80 sites in 22 countries, enrolling IgG4-RD patients who meet the ACR/EULAR Classification Criteria for IgG4-RD with a score of at least 20 as determined by an Eligibility Committee (EC). Eligibility criteria included a history of multiorgan disease and active disease at the time of screening to increase the risk of flares for the primary end point. Subjects were stratified based on newly diagnosed (46%) vs. recurrent (54%) disease to control for differences in flare risk. The primary end point is time to first Adjudication Committee-determined and investigator-treated IgG4-RD flare during the 12-month randomized controlled period. The study is event-driven and is powered on the accrual of 39 disease flares. To permit evaluation of inebilizumab as monotherapy, other immunosuppressive agents are prohibited and glucocorticoids are discontinued at the end of study week 8.

Results: Enrolment completed in April 2023 with 135 subjects enrolled. The mean age was 58.2 years and 65% were male. Time since diagnosis ranged from 0.1 to 20.5 years (median 0.9 years). Baseline ACR/EULAR Classification Criteria scores ranged from 20 to 74. The number of organs affected by IgG4-RD up to the time of enrolment varied from 2 to 13, with 2–3 organs affected in 41% of subjects and ≥ 6 organs affected in 24% of subjects. The pancreas, bile ducts, and liver were affected in 52%, 31%, and 7% of subjects respectively. Hepatobiliary disease was accompanied by pancreatic involvement in 95% of cases, but only 59% of those with pancreatic involvement also had hepatobiliary disease. The submandibular, lacrimal, and parotid glands, lymph nodes, kidney, sinuses, and lungs were each affected in at least 20% of the study population. These findings suggest that the study population carries substantial hepatobiliary disease burden and is representative of real-world IgG4-RD cohorts.

Conclusion: MITIGATE enrolled a representative IgG4-RD population in terms of both number and distribution of organs affected. More than half of participants had hepato-pancreato-biliary disease, and hepatobiliary disease without pancreatic involvement was rare. Trial results are expected in 2024 and aim to establish the safety and efficacy of CD19-targeted B cell depletion by inebilizumab in IgG4-RD, potentially leading to the first approved treatment for this disease.

WED-153

Advances in the diagnosis of cholestatic liver diseases with the implementation of exome sequencing

Ignasi Olivas^{1,2,4}, Meritxell Jodar³, Helena Hernández Evole^{1,2}, Pínelopi Arvaniti^{1,2,4}, Anna Pocurull^{1,2}, Zoe Mariño^{1,2,5}, Celia Badenas³, María Carlota Londoño^{1,2,5}, Sergio Rodríguez-Tajes^{1,2}. ¹Liver Unit, Hospital Clínic Barcelona, Barcelona, Spain; ²Institut d'Investigacions Biomèdiques August Pi i Sunyer (FRCB-IDIBAPS), Barcelona, Spain; ³Biochemistry and Molecular Genetics Department, Hospital Clínic Barcelona, Barcelona, Spain; ⁴Department of Medicine and Research Laboratory of Internal Medicine, Expertise Center of Greece in Autoimmune Liver Diseases, ERN RARE-LIVER, University Hospital of Larissa, Larissa, Greece; ⁵Centro de Investigación Biomédica en Red de Enfermedades Hepáticas y Digestivas (CIBERehd), Instituto de Salud Carlos III, Madrid, Spain
Email: ignasiolivasalberch@gmail.com

Background and aims: Clinical practice guidelines recommend performing a genetic testing in patients with chronic idiopathic cholestasis (CIC) after ruling-out common causes of cholestasis. The implementation in clinical practice of techniques of next generation sequencing (NGS) has facilitated the study of genes related to cholestasis. Our aim is to determine the usefulness of genetic study using NGS in the diagnosis of CIC in adults.

Method: Thirty-nine adults with CIC underwent NGS (filtered by a panel of 35 genes associated with cholestasis) in blood samples. Genetic variants were classified according to the American College of

Medical Genetics and Genomics criteria as follows: pathogenic (PV), likely pathogenic (LPV) and variant of uncertain significance (VUS).

Results: Twenty-six patients were women (66%), with a median age of 46 years (IQR 39–53), ALP $1.2 \times \text{ULN}$ (IQR 0.8–1.5), GGT 102 U/L (IQR 54–216), bilirubin 0.7 mg/dL (IQR 0.6–1). Twenty-one percent had pruritus, 23% cholestasis of pregnancy, seven (18%) low phospholipid-associated cholelithiasis (LPAC) syndrome and 10% drug-induced liver injury (DILI). Four patients (10%) had a family history of cholestasis and 6 had been previously misdiagnosed. Nineteen (49%) presented a genetic variant in heterozygosis. In 8 patients, we identified a PV or LPV that explained their symptoms: 5 had heterozygous variants in the *ABCB4* gene, 4 of them with LPAC syndrome and one with DILI; one patient had an heterozygous variant in *PRKCSH* gene with a polycystic liver disease, and two patients had a microdeletion of chromosome 17q12 in heterozygosis that contains *HNF1B* gene presenting diabetes mellitus, hypomagnesaemia and alteration of liver enzymes. A VUS was detected in 5 patients, 4 in the *ABCB4* gene and one in *NOTCH2*, which after functional or family segregation studies could be associated with patient symptoms. Finally, six patients had a PV, LPV or VUS in *PKHD1*, *ABCC2*, *HNF1B* and *ATP7B* genes but with unknown correlation to patients' symptoms.

Conclusion: A high percentage of patients with CIC presented variants in genes related to cholestasis, which may explain their symptoms. Given the therapeutic implications for patients and families, patients with CIC should undergo genetic testing to rule-out the presence of genetic cholestasis.

WED-154

Evaluation of secondary sarcopenia and Fontan circulatory failure in post-Fontan hepatic complications

Yohei Koizumi^{1,2}, Hirooka Masashi³, Yoshiko Nakamura⁴, Yano Ryo¹, Makoto Morita⁵, Yuki Okazaki⁶, Yusuke Imai⁵, Takao Watanabe¹, Osamu Yoshida¹, Yoshio Tokumoto¹, Masanori Abe¹, Yoichi Hiasa¹.

¹Department of Gastroenterology and Metabology, Ehime University Graduate School of Medicine, Toon, Ehime, Japan; ²Saiseikai Matsuyama Hospital, Department of Internal Medicine, Matsuyama, Ehime, Japan; ³Department of Gastroenterology and Metabology, Ehime University Graduate School of Medicine, Toon Ehime, Japan; ⁴Department of Gastroenterology and Metabology, Ehime University Graduate School of Medicine, TOon, Ehime, Japan; ⁵Department of Gastroenterology and Metabology, Ehime University Graduate School of Medicine, Toon, EHime, Japan; ⁶Department of Gastroenterology and Metabology, Ehime University Graduate School of Medicine, Toon, EHime, Japan

Email: shachiyo2@yahoo.co.jp

Background and aims: A reduction in skeletal muscle mass (sarcopenia) is a known risk factor affecting long-term prognosis and life expectancy of adult cirrhosis cases; however, it has not been previously reported whether sarcopenia is a prognostic factor in patients with Fontan-associated liver disease (FALD). This study aimed to elucidate the relationship between FALD and sarcopenia.

Method: Among 105 post-Fontan procedure cases diagnosed using imaging from January 2012 to December 2022 at our department, 62 cases aged ≥ 18 years were selected, along with a control group of 50 adults matched for age. Diagnosis of sarcopenia was assessed by measuring skeletal muscle mass using the psoas muscle index at the L3 level.

Results: Among the 62 FALD cases, 38 were diagnosed with sarcopenia. The median skeletal muscle mass was significantly lower in the FALD group compared to that in the control group for both males (7.12 cm²/m² vs. 5.89 cm²/m²) and females (5.42 cm²/m² vs. 4.05 cm²/m²) ($p < 0.001$). Multivariate Cox hazard analysis was conducted to assess factors related to Fontan circulatory failure and revealed that a New York Heart Association functional classification ≥ 3 , B-type natriuretic peptide levels, and skeletal muscle mass were predictive factors. Furthermore, two cases of heart failure-related deaths were observed among the 62 cases, and both cases matched

the diagnosis of sarcopenia. Additionally, liver stiffness values measured using vibration-controlled transient elastography were significantly higher in the sarcopenia group (21.5 kPa) compared to that in the non-sarcopenia group (13.2 kPa) ($p = 0.0014$).

Conclusion: Sarcopenia is considered a predictive factor for Fontan circulatory failure and a risk factor for the progression of liver fibrosis due to FALD. The evaluation of skeletal muscle mass may serve as a comprehensive screening tool for multi-organ failure in cases of Fontan circulation.

WED-155

A ratio of exchangeable copper below 15% accurately excludes Wilson disease and may be useful for the first-line etiologic work-up within a liver unit

Zoe Mariño¹, Clàudia García-Solà¹, Anna Soria¹, Sabela Lens¹, Adrià Juanola¹, Jordi Gratacós-Ginès¹, Elisa Pose¹, María Carlota Londoño¹, Sergio Rodríguez-Tajes¹, Isabel Graupera¹, Xavier Fornés¹, Mercè Torra². ¹Liver Unit, Hospital Clínic Barcelona, CIBERehd, IDIBAPS, ERN-RARE Liver, Universitat de Barcelona, Barcelona, Spain; ²Biochemistry and Molecular Genetics Department, Hospital Clínic Barcelona, IDIBAPS, Universitat de Barcelona, Barcelona, Spain
Email: zmarino@clinic.cat

Background and aims: Diagnosis of Wilson disease (WD) is complex. Exchangeable copper (CuEX) arisen some years ago as a biomarker reflecting the free copper systemic pool; its ratio referred to total copper (REC) was shown to be useful for WD diagnosis and has progressively been extended across Europe. REC $\geq 18\%$ identifies new WD cases (El Balkhi S et al, 2011) whereas WD patients on follow-up usually present REC $> 15\%$. Moreover, carriers and healthy individuals present REC $< 15\%$. Data on REC values among patients with other liver diseases is scarce. Our aim was to evaluate the usefulness of REC since its availability in our center.

Method: Retrospective unicentric analysis of CuEX/REC indications in clinical practice. CuEX ($\mu\text{g/dL}$) and REC (%) quantification were performed locally by inductively plasma coupled to mass spectrometry (ICP-MS) since December 2021. In those patients with more than one assessment, only one was considered; among WD patients, one measurement at diagnosis and one in follow-up were retained. Variables were expressed in median (IQR) and statistical analysis was done with SPSS V27.

Results: Up to 341 patients [54% male, median age 47] had a CuEX/REC measurement; most of them were patients followed at the Liver Unit (95.6%). Most cases (275, 80.6%) were classified as non-wilsonian patients, 60 WD cases (17.6%) and 6 carriers of one *ATP7B* mutation (1.8%). Median age at sample extraction was significantly lower among WD patients (38 years) compared to non-WD and carriers [Kruskal-Wallis, $p = 0.003$]. Reasons for REC evaluation were: chronic liver tests and/or imaging abnormalities (54%), WD diagnosis or follow-up (17.3%), acute hepatitis (14.4%), chronic cholestasis (6.2%), high ferritin levels (3.2%), neuro-psychiatric symptoms (2.1%) or copper abnormalities (2.1%). Ceruloplasmin (Cp) levels were significantly lower and urinary copper excretion (UCE) was significantly higher among WD patients compared to non-wilsonian and carrier individuals [Kruskal-Wallis, $p < 0.01$]. However, their negative predictive values (NPV) for excluding WD were suboptimal: 47% for Cp levels $< 0.2 \text{ g/L}$ and 81% for UCE $< 100 \mu\text{g}/24\text{hs}$ (available in 149). REC was significantly higher among WD patients when compared to carriers and non-wilsonian patients [23.3% (IQR 12.7–39.5%) vs 5% (IQR 4.1–6.4%) vs 4.9% (IQR 3.9–5.9%), Kruskal-Wallis, $p < 0.01$]. REC $\geq 18\%$ identified 36/60 WD patients (sensitivity = 60%) improving to 70% if REC was $> 15\%$. The NPV for excluding WD with a REC value below 18% was 90.1% which improved to 93.4% when REC was below 15%. Only one non-wilsonian patient presented REC values above 15%, corresponding to a female patient with an acute autoimmune hepatitis and REC 47%. All carriers showed REC $< 15\%$.

POSTER PRESENTATIONS

Conclusion: REC quantification is an accurate tool for excluding WD at a liver Unit and could be used at the first-line diagnostic biomarker upon validation in larger cohorts.

WED-158-YI

Disease experience and care expectations in european patients with immune-mediated liver disease

Pierre-Antoine Soret¹, Bert Tomsin², José A. Willemse³, Martine Walmsley⁴, Victorio Gnutti⁵, Wiebke Papenthin⁶, Natalie Uhlenbusch⁷, Tom J. G. Gevers⁸, Nora Cazzagon⁹, Christoph Schramm¹⁰, Pierre Corret¹¹, Sara Lemoine¹, Angela Leburgue¹². ¹Sorbonne University, Reference Center for Inflammatory Biliary Diseases and Autoimmune Hepatitis, European Reference Network on Hepatological Diseases (ERN Rare-Liver), Saint-Antoine Hospital, Assistance Publique-Hôpitaux de Paris, Sorbonne University, INSERM, Saint-Antoine Research Center (CRSA), Paris, France; ²Mijnlever Patient Association Rare Liver Disease, Belgium, Overijse, Belgium; ³Patient Organisation, Dutch Liver Patients Association, Hoagland, Netherlands; ⁴PSC Support, Banbury, United Kingdom; ⁵AMAF Monza Onlus, Muggio, Italy; ⁶Morbus Wilson e.V., Kleinmachnow, Germany; ⁷University Medical Center Hamburg-Eppendorf, Hamburg, Germany; ⁸Maastricht University Medical Center, Maastricht, Netherlands; ⁹University of Padua, Padova, Italy; ¹⁰Department of Medicine, University Medical Centre Hamburg-Eppendorf, Hamburg, Germany; ¹¹ALBI Patient Association, Versailles, France; ¹²ALBI Patient Association, Versailles, France
Email: pierre.soret@aphp.fr

Background and aims: In the context of rare immune-mediated liver diseases, gaps between a physician's perception and patient's experience can mask patients' unmet needs. To identify and reduce those gaps appears crucial to improve patient management, adherence to treatments and quality of life.

Method: We conducted an observational international study based on an online survey, with the participation of Belgian, French, Italian, Dutch, and British patient organisations dealing with immune-mediated liver diseases (on behalf of ERN RARE-LIVER). Patients had to describe their 3 main symptoms and impact of the disease on daily life, provide suggestions to improve their well-being, and rate their overall satisfaction with care, from 0 to 10 (mean \pm standard deviation).

Results: 560 patients were included: 256 with primary biliary cholangitis [PBC], 98 with primary sclerosing cholangitis [PSC], 150 with autoimmune hepatitis [AIH] and 56 with overlap AIH-PBC/PSC. The most frequent symptoms declared were fatigue (73%), digestive issues (23%) and itch (19%). 72% of patients reported troubles in daily life mostly due to fatigue (34%), and restrictions in personal (35%) and professional life (19%). 250 patients (44%) declared that they had never asked for or never had satisfactory answers about specific aspects of their disease, in particular regarding the course of the disease (33%), care (29%) and stage of the disease (15%). Out of the 258 patients (46%) who expressed detailed suggestions to improve their well-being, 39% wanted global care (not limited to their liver disease alone but to include comorbidities, symptom management, psychological support), 34% asked for a better dialogue with their doctor and 12% were looking for closer medical follow-up and more empathy. Based on 544 patients, global satisfaction with care was 7.51 (\pm 2.10). No significant difference was observed in answers between PBC, PSC, AIH and overlap patients.

Conclusion: Patients with immune-mediated liver diseases were satisfied overall with their medical care. Nevertheless, improvements in symptom management, better consideration of alterations to quality of life and a more empathic dialogue were identified as needed by patients in order to improve the management of their disease. The burden in the different diseases was equivalent, and underscores a need for a global care approach.

WED-159

Usefulness of serological scores in the diagnosis of Fontan-associated liver disease

Marta Cuadros¹, Marta Abadía¹, Consuelo Froilán¹, Nerea Gonzalo¹, Miriam Romero¹, Araceli García-Sánchez¹, Francisco Javier García-Samaniego¹, Antonio Oliveira¹, José Carlos Erdozaín¹, José Ruiz-Cantador¹, Elvira Ana González-García¹, Pablo Merás¹, Carlos Merino¹, Inés Ponz¹, Adriana Rodríguez-Chaverri¹, Enrique Balbacid¹, Maria Dolores Martin-Arranz^{1,2,3}, Pilar Castillo¹. ¹Hospital Universitario La Paz, Madrid, Spain; ²Universidad Autónoma de Madrid, Madrid, Spain; ³Instituto de Investigación Hospital Universitario La Paz (IdiPAZ), Madrid, Spain
Email: cuadrosmartinez@gmail.com

Background and aims: Fontan-associated liver disease (FALD) is often described in adult patients with Fontan correction of single-ventricle congenital heart disease. The assessment of the severity of FALD through non-invasive methods is challenging and serological scores have not been validated in this setting. We aim to evaluate the role of non-invasive serological scores in the diagnosis of FALD.

Method: Retrospective study in a single-center, Hospital Universitario La Paz (Madrid, Spain). Serological scores of liver fibrosis were evaluated: Forns index, FIB4, and AST-to-platelet ratio index (APRI). FALD was defined by ultrasound (US) criteria (hepatomegaly, liver surface nodularity, parenchymal heterogeneity, hyper-echoic lesions, splenomegaly, or collaterals), and A-FALD, based on the EASL-ERN definition (oesophageal varices, portosystemic shunts, ascites, or splenomegaly).

Results: Between January 2017 and November 2023, 91 patients with Fontan surgery were included: mean age 33.3 ± 8.2 years, mean time since Fontan surgery 24.3 ± 7.7 years, 55/91 (60.4%) male. The prevalence of FALD was 81/91 (89.0%). A-FALD was detected in 52/73 (71.2%). Forns index showed statistically significant relationship with FALD and A-FALD in univariate and multivariate analysis. Forns index was significantly higher in patients with FALD, median score 5.8 (interquartile-range 5.0–6.9), compared to patients without FALD, median score 4.5 (interquartile-range 3.5–5.2) ($p = 0.005$). This difference was observed as well in patients with A-FALD, median score 6.3 (interquartile-range 5.4–7.2), compared to patients without A-FALD, median score 5.0 (interquartile-range 4.3–5.6). The area under the receiver operating characteristic (AUROC) of the Forns index score for FALD was 0.772 (95% CI: 0.620–0.924, $p = 0.005$). The cut-off point to rule-out FALD was 4.04 (sensitivity 91.9%). The AUROC of the Forns index score for A-FALD was 0.773 (95% CI: 0.662–0.884, $p < 0.001$). The cut-off point to rule-out A-FALD was 4.00 (sensitivity 96.2%). FIB4 and APRI were associated with FALD and A-FALD in univariate analysis, but not in multivariate analysis.

Conclusion: The relationship between Forns index and FALD in our study suggests that this score may be a useful non-invasive tool in the evaluation of patients with Fontan surgery.

WED-160

Autoantibody diagnostics in pediatric non-viral liver diseases: a multicenter retrospective head-to-head comparison of immunofluorescence- and enzyme-linked immunosorbent assay-based testing

Theresa Kirchner¹, Alejandro Campos-Murguía¹, Norman Junge², Muhammed Yuksek^{3,4}, Wojciech Janczyk⁵, Claudine Lalanne⁶, Kalliopi Zachou^{7,8}, Ye Htun Oo⁹, Jérôme Gournay¹⁰, Simon Pape¹¹, Joost PH Drenth¹¹, Amédée Renand¹², George Dalekos^{7,8}, Luigi Muratori⁶, Piotr Socha⁵, Cigdem Arkan⁴, Yun Ma³, Heiner Wedemeyer¹, Ulrich Baumann², Bastian Engel¹, Richard Taubert¹. ¹Department of Gastroenterology, Hepatology, Infectious Diseases and Endocrinology, Hannover Medical School, Hannover, Germany; ²Division of Pediatric Gastroenterology and Hepatology, Department of Pediatric Nephrology, Hepatology and Metabolic Disorders, Hannover Medical School, Hannover, Germany;

³Institute of Liver Studies, King's College Hospital, Department of Inflammation Biology, School of Immunology and Microbial Sciences, King's College London, London, United Kingdom; ⁴Koç University Research Centre for Translational Medicine (KUTTAM)-Liver Immunology Lab, Istanbul, Istanbul, Turkey; ⁵Department of Gastroenterology, Hepatology, Nutritional Disorders and Pediatrics, The Children's Memorial Health Institute, Warsaw, Poland; ⁶Department of Medical and Surgical Sciences, University of Bologna, Bologna, Italy; ⁷Institute of Internal Medicine and Hepatology, Larissa, Greece; ⁸Department of Medicine and Research Laboratory of Internal Medicine, National Expertise Center of Greece in Autoimmune Liver Diseases, General University Hospital of Larissa, Larissa, Greece; ⁹Centre for Liver and Gastro Research, National Institute of Health Research Birmingham Biomedical Research Centre, Institute of Immunology and Immunotherapy, The Medical School, Birmingham, United Kingdom; ¹⁰Nantes Université, CHU Nantes, Institut des Maladies de l'Appareil Digestif (IMAD), Hépatogastro-Entérologie, Inserm CIC 1413, Nantes, France; ¹¹Department of Gastroenterology and Hepatology, Radboud University Medical Center, Nijmegen, Netherlands; ¹²Nantes Université, Inserm, Center for Research in Transplantation and Translational Immunology, UMR 1064, F-44000 Nantes, Nantes, France
Email: kirchner.theresa@mh-hannover.de

Background and aims: Due to heterogeneous clinical presentation diagnosing pediatric autoimmune hepatitis (pAIH) is challenging. Traditional diagnosis includes immunofluorescence testing (IFT) of antinuclear (ANA) and smooth muscle antibodies (SMA) on rodent tissue sections. Recently polyreactive immunoglobulin G (pIgG) was suggested as a new and more accurate biomarker in adult and pediatric AIH. The aim of this retrospective multicenter study was to assess the diagnostic value of enzyme-linked immunosorbent assay-(ELISA)-based ANA testing in treatment naïve pAIH in comparison with traditional IFT as gold standard according to actual guidelines and scoring systems and the evaluation of diagnostic accuracy for different cut-offs of IFT.

Method: In this multicenter retrospective study three commercial ANA, one anti F-actin ELISA, IFT on rodent tissue sections and HEP-2 cells as well as pIgG measured using a home-made HIP1R/BSA ELISA were performed. Sixty-nine pAIH and 136 non-AIH liver disease patients were included from existing biorepositories. All ELISA and IFT for ANA and SMA were performed centrally in a head-to-head comparison with the performer being blinded to clinical data.

Results: Area under the curve (AUC) to predict pAIH for ANA ELISAs was 0.641 (95% CI 0.558–0.724) to 0.739 (95% CI 0.669–0.810) with higher AUC for ELISA with HEP-2 extracts. AUC for ANA (rodent tissue and HEP2 cells) and SMA in IFT was 0.749 (95% CI 0.676–0.822), 0.757 (95% CI 0.687–0.826) and 0.720 (95% CI 0.637–0.802) respectively. The highest AUCs were achieved by F-actin ELISA (0.831, 95% CI 0.771–0.892) and pIgG (0.846, 95% CI 0.785–0.906). Sensitivities were 24.6 to 62.3% for ANA ELISAs, 89.9% for ANA in IFT on rodent tissue (with recommended cut-off $\geq 1:20$), 95.7% for ANA on HEP2 cells (with recommended cut-off $\geq 1:20$), 61.5% for SMA in IFT (with recommended cut-off $\geq 1:20$), 73.9% for F actin ELISA, and 78.3% for pIgG. Specificities were 66.2 to 90.4% for ANA ELISAs, 26.6% for ANA in IFT on rodent tissue (with recommended cut-off $\geq 1:20$), 18.4% for ANA on HEP2 cells, 39.7% for SMA in IFT, 73.5% for F actin ELISA, and 83.1% for pIgG. Sensitivity in ANA ELISA could be improved by adjusted pediatric cut offs but with no further improvement of overall accuracies (66.8%–69.3%). However, accuracy in IFT could be improved from 47.8 to 73.7% (ANA rodent tissue), from 44.4 to 73.2% (ANA HEP-2) and from 43.7 to 80.3% (SMA) by an adjusted cut off of 1:320. Accuracy of F-actin and pIgG was 81.0% and 80.0% with adjusted pediatric cut-offs.

Conclusion: F-actin and pIgG ELISA exhibited the highest accuracies off all analyzed autoantibodies tests for the prediction of pAIH in pediatric non-viral liver disease. Furthermore, the study suggests an increase of the currently employed diagnostic cut-off values for ANA and SMA in IFT in children for best prediction of pAIH.

WED-161-YI

Liver steatosis and fibrosis in children with diabetes mellitus type 1: single-center analysis including MASLD-associated genetic variants

Jolanta Swiderska¹, Wiktor Smyk², Sebastian Więckowski³, Susanne N. Weber⁴, Piotr Milkiewicz^{5,6}, Elżbieta Moszczyńska¹, Piotr Socha³, Marcin Krawczyk^{4,7}. ¹Department of Endocrinology and Diabetology, The Children's Memorial Health Institute, Warsaw, Poland; ²Department of Gastroenterology and Hepatology, Medical University of Gdansk, Gdańsk, Poland; ³Department of Gastroenterology, Hepatology and Nutrition Disorders, The Children's Memorial Health Institute, Warsaw, Poland; ⁴Department of Medicine II, Saarland University Medical Center, Saarland University, Homburg, Germany; ⁵Liver and Internal Medicine Unit, Department of General, Transplant and Liver Surgery, Medical University of Warsaw, Warsaw, Poland; ⁶Translational Medicine Group, Pomeranian Medical University, Szczecin, Poland; ⁷Laboratory of Metabolic Liver Diseases, Department of General, Transplant and Liver Surgery, Medical University of Warsaw, Warsaw, Poland
Email: marcin.krawczyk@uks.eu

Background and aims: Diabetes is a recognized metabolic risk factor for excessive hepatic fat accumulation. While the association between type 2 diabetes mellitus (DM2) and metabolic dysfunction-associated steatotic liver disease (MASLD) is well established, data on the incidence of MASLD in the setting of type 1 diabetes mellitus (DM1) is scarce. Here, we investigate an exhaustive cohort of children with DM1 for the presence of fatty liver and liver scarring in conjunction with common genetic polymorphisms associated with MASLD.

Method: Prospectively, we recruited 162 children (71 girls, mean age 14 ± 3 years) with DM1. Liver stiffness measurement (LSM) and controlled attenuation parameter (CAP) were performed to non-invasively evaluate liver fibrosis and steatosis, respectively. Liver function tests, biochemical and metabolic parameters were assessed concurrently with LSM and CAP. Genotyping of the three genetic variants known to influence liver injury (i.e., *PNPLA3* p.I148M, *TM6SF2* p.E167K, and *MBOAT7* p.G17E) was performed using TaqMan assays with fluorescence detection and compared to the frequencies in Polish adult individuals.

Results: The mean CAP was 208 ± 33 dB/m and values above 249 dB/m, i.e., suggestive of liver steatosis (Ferraioli et al., *BMC Gastroenterol* 2017), were present in 10% of patients. Mean LSM was 4.6 ± 1.1 kPa, and 1% of patients had LSM above 8.6 kPa indicative of advanced fibrosis (Lee et al., *J Pediatr*. 2013). Most of the recruited children with DM1 (91%) exhibited normal AST and ALT activities. The median BMI z-score was 0.18 (range -2.7 – 2.3). Multivariate linear regression showed that CAP positively correlated with BMI z-score ($\beta = 13.8$, $p < 0.001$) and HbA1c ($\beta = 3.1$, $p = 0.001$), and inversely with age ($\beta = -1.9$, $p = 0.037$). LSM positively correlated with BMI ($\beta = 0.6$, $p = 0.019$). The minor allele frequencies (MAF) for *PNPLA3*, *TM6SF2*, and *MBOAT7* variants were 0.20, 0.10, and 0.47, respectively, aligning with data for the general Polish population (all $p > 0.05$ for genotype distribution comparison). Notably, no significant association was found between the analyzed genetic variants and liver phenotypes in uni- or multivariate models.

Conclusion: Children with DM1 have a low risk of developing significant hepatic steatosis or fibrosis, especially in the absence of metabolic risk factors. These phenotypes do not appear to be significantly influenced by a pro-MASLD genetic predisposition. These findings emphasize the importance of managing metabolic syndrome components in DM1 patients to mitigate the risk of progressive liver injury risks.

WED-162

Performance of transient elastography, Fib4 and APRI in the diagnosis of severe liver fibrosis in patient with HFE hemochromatosis

Lise Trubert¹, Oumnia Masrouj², Morcet Jeff², Laine Fabrice³, Turlin Bruno², Edouard Bardou-Jacquet². ¹CHU Rennes, Rennes, France; ²CHU Rennes, Rennes, France; ³CHU Rennes, Rennes, France
Email: edouard.bardou-jacquet@chu-rennes.fr

Background and aims: Liver fibrosis and cirrhosis are the main determinant of death in patients with HFE hemochromatosis (HH). Current EASL guidelines recommend screening for liver fibrosis in all HH patients at the time of diagnosis. While non-invasive tests are preferred, limited evidence exists comparing transient elastography (TE), Fib-4, and APRI to liver biopsy in this context. Our study aimed to evaluate the diagnostic performance of these tests in detecting liver fibrosis in HH patients.

Method: We included HH patients from our database (2005–2023) who underwent both liver biopsy and TE within a year of diagnosis. Patients with TE >7.1 kPa and IQR >0.3 were excluded. Clinical and demographic data were recorded. The diagnostic performance of TE, Fib-4, and APRI was assessed using ROC curves for severe liver fibrosis (Metavir F3F4).

Results: A total of 127 patients (81.9% male, age 49.5 ± 11.3, BMI 25.9 ± 4) were included. Diabetes and excessive alcohol consumption were present in 10.2% and 7.9%, respectively. Ferritin levels were 1508 µg/L ± 1321, and transferrin saturation was 85% ± 14.6. Liver iron content (available for 63 patients) had a mean value of 290 µmol/g ± 108 by magnetic resonance imaging. Fibrosis stage prevalence was F0F1 = 48.1%, F2 = 25.2%, F3 = 7.9%, and F4 = 18.9%. Mean TE was 9.8 kPa ± 8.8, Fib-4 was 1.45 ± 0.83, and APRI was 0.69 ± 0.48. AUC for severe fibrosis diagnosis by ferritin, TE, Fib-4, and APRI were 0.92 (0.86–0.96), 0.94 (0.88–0.97), 0.85 (0.77–0.91), and 0.83 (0.75–0.90) respectively. Cutoff value at a fixed sensitivity of 90% were ferritin: 1853 µg/L, TE: 8.6 kPa, Fib-4: 1.18, and APRI: 0.53. Cutoff value at a fixed specificity of 90% were ferritin: 2224 µg/L, TE: 9.9 kPa, Fib-4: 2.04, and APRI: 0.87. Using ferritin cutoffs, 81 (64%) patient were correctly classified and 12 (9.4%) patient would have required liver biopsy. Using TE cutoffs 104 (81%) patients were correctly classified and 10 (7%) would have required a liver biopsy. Combining both criteria resulted in correct classification of 82 (64%) patients, without false negatives/positives. However, 32 (25%) had discrepant results, and 12 (9%) were in the intermediate zone requiring liver biopsy.

Conclusion: Our findings suggest that the ferritin criterion for liver biopsy in HH could be increased to 1800 µg/L while maintaining high sensitivity. APRI and Fib-4 exhibited lower performance compared to ferritin and TE in assessing liver fibrosis in HH patients. We propose TE cutoffs of 8.6 kPa to rule out severe fibrosis and 9.9 kPa to confirm it. Overall, combining non-invasive tests could significantly reduce the need for liver biopsy in HH patients based on previous biopsy criteria while maintaining excellent diagnostic performance.

WED-163

Non-invasive testing reveals fibrosis risk in heterozygous Alpha-1 Antitrypsin deficiency

George Marek¹, Harmeet Malhi¹. ¹Division of Gastroenterology and Hepatology, Mayo Clinic, Rochester, United States
Email: marek.george@mayo.edu

Background and aims: Alpha 1 antitrypsin deficiency (AATD) is caused by proteotoxic alleles of the SERPINA1 gene. The disease is codominant and up to 1:2000 individuals are homozygous (ZZ) and 4% of the population are carriers (MZ). The Z allele is associated with steatotic liver disease in recent GWAS studies. Liver stiffness measurements by transient elastography of UK biobank cohort suggest that there is an increased liver stiffness in MZ. However, the clinical significance of MZ in the outpatient clinical setting is not well understood. In this study, we sought to determine if MZ

phenotype is associated with increased fibrosis or steatosis on initial non-invasive testing.

Method: We retrospectively evaluated patients phenotyped for AATD who had transient elastography evaluation of their native liver. Data was collected from separate sites across the Mayo Clinic health system in Minnesota, Wisconsin, Arizona, and Florida. Elastography reports were extracted using Mayo Data Explorer. Statistical comparisons including Shapiro-Wilk testing for normality, Mann-Whitney U testing, and Pearson's Chi-squared testing to compare categorical groups R version 4.3.2. The activities in this study were approved by an institutional review board (IRB) at the Mayo Clinic in Rochester Minnesota.

Results: We abstracted 5461 individual readings from 2259 individuals with a known AAT phenotype. 1858 were MM, 132 were MZ, 6 ZZ, and 81 had rare variants. We compared MM and MZ patients and found the ages at initial elastography were similar 54 (41–64) and 58 (45–64) p = 0.2. The proportion of patients with kPa values >9.5 suggesting advanced fibrosis or cirrhosis was greater in MZ individuals 48 (37%) vs. MM 526 (28%) p = 0.048. Baseline CAP values were 276 (220–329), 269 (229–318) p = 0.3. We compared longitudinal changes for 389 individuals who had at least one year of follow-up. The median (IQR) follow-up was 2.17 (1.41–3.36) years for MM and 1.95 (1.36–3.23) for MZ p = 0.4. The change per year in LSM was –0.15 kPa/yr (–0.95–0.59) for MM and –0.43 (–0.80–1.29) for MZ p = 0.8 likewise, the change in CAP was similar between groups –6 (–21–10) and –1 (–13–14) dB/m/yr p = 0.7.

Conclusion: MM and MZ patients began non-invasive monitoring at similar ages but a higher proportion of MZ individuals had evidence of advanced disease. The prevalence and severity of steatosis was similar amongst MM and MZ individuals. MM and MZ individuals had similar changes in LSM and CAP. This is not a natural history cohort and presumably, after initial evaluation, patients with longitudinal follow-up also had appropriate medical counseling and access to treatment of comorbid conditions. Our data suggest that patients with longitudinal follow-up in both groups showed modest improvements in both steatosis and fibrosis over time. Early identification of liver disease in people with MZ may be useful in preventing advanced disease.

WED-164

Interim safety results of the ongoing international phase I/II GATEWAY gene therapy trial with VTX-801 conducted in adult patients with Wilson disease

Thomas Damgaard Sandahl¹, William M. Lee², Aftab Ala³, Regino P. Gonzalez-Peralta⁴, Valentina Medici⁵, Fred Askari⁶, Sean Rudnick⁷, Ulrich Lauer⁸, Hartmut Schmidt⁹, Sonia Valero¹⁰, Gloria Gonzalez¹⁰, Jean Philippe Combal¹⁰, Lorenzo D'Antiga¹¹, Bernard Benichou¹⁰, Michael Schilsky¹². ¹Department of Hepatology and Gastroenterology, Aarhus University Hospital, Aarhus, Denmark; ²Division of Digestive and Liver Diseases, University of Texas Southwestern Medical Center, Dallas, United States; ³The Royal Surrey County Hospital, Guilford, United Kingdom; ⁴AdventHealth for Children, AdventHealth Transplant Institute, Orlando, United States; ⁵Division of Gastroenterology and Hepatology, University of California Davis, Sacramento, United States; ⁶Department of Medicine, University of Michigan, Ann Arbor, United States; ⁷Department of Internal Medicine, Section on Gastroenterology and Hepatology, Atrium Health Wake Forest Baptist, Winston-Salem, United States; ⁸Department of Medical Oncology and Pneumology, Virotherapy Center Tübingen (VCT), Medical University Hospital, Tübingen, Germany; ⁹Klinik für Gastroenterologie, Hepatologie und Transplantationsmedizin, Universitätsklinikum Essen, Essen, Germany; ¹⁰Vivet Therapeutics, Paris, France; ¹¹Department of Pediatric Hepatology, Gastroenterology, Transplantation, ASST Papa Giovanni XXIII Hospital, Bergamo, Italy; ¹²Department of Medicine, Section of Digestive Diseases, and Department of Surgery, Section of Transplant and Immunology, Yale School of Medicine, New Haven, United States
Email: bbenichou@vivet-therapeutics.com

Background and aims: Wilson Disease (WD) is a rare, inherited, debilitating, life-threatening disorder of Cu homeostasis due to pathogenic variants in the ATP7B copper-transporter. Impaired ATP7B function leads to decreased biliary Cu excretion, tissue Cu accumulation, and reduced circulating ceruloplasmin (Cp) levels. Limitations of current management include late diagnosis, constraining life-long treatment with chelators and/or zinc, side effects, and poor adherence affecting long-term outcomes, including survival. VTX-801 is a recombinant adeno-associated viral vector (rAAV) carrying a shortened ATP7B gene under the control of a liver-specific promoter. Previous studies with a single VTX-801 injection in 6-week-old WD mice demonstrated the restoration of biliary excretion of iv-injected ⁶⁴Cu, the restoration of Cu homeostasis and Cp levels the preservation of liver integrity and function, and 100% long-term animal survival.

Method: GATEWAY is an international phase I/II, open-label, 5-year follow-up, single dose-escalation study of VTX-801 in adult patients with WD (NCT04537377). This first-in-human clinical study is assessing the safety, pharmacodynamics and efficacy of VTX-801; standard of care treatment may be withdrawn in VTX-801 responders at 3 months post-infusion based upon ⁶⁴Cu assessments.

Results: VTX-801 Cohort 1 (low dose) dosing has been completed (N = 2 patients), and no SAE has been reported at time of abstract submission. Both patients experienced mild, transient ALT increase (maximum 95 and 97 IU) following VTX-801 infusion without affecting liver function. One patient experienced a non-serious infusion-associated reaction (chills and fever, rigors, right arm tingling, headache) successfully managed with symptomatic treatment, as well as a self-resolving, transient worsening of low lymphocyte counts; he also experienced a delayed, mild ALT elevation (maximum 104 IU) managed with a course of oral steroid treatment, like what has been reported with other systemic AAV treatments. Collection of pharmacodynamic data is ongoing and will be presented.

Conclusion: Treatment of patients of the GATEWAY Cohort 1 (low dose) has been completed. No serious adverse events have been reported. Follow-up of treated patients and enrolment of Cohort 2 (intermediate dose) are underway. The investigational gene therapy product VTX-801 may provide in the future a valuable alternative to existing treatments by addressing unmet medical needs.

WED-165

Long-term clinical outcomes of patients with acute hepatic porphyria who were not attack-free after 6 months of givosiran treatment in a subgroup analysis of the phase 3 ENVISION study

Paolo Ventura¹, Encarna Guillén-Navarro^{2,3}, Bruce Wang⁴, Weiming Du⁵, Ana Camejo⁵, Manish Thapar⁶. ¹Internal Medicine Unit, University of Modena and Reggio Emilia, Modena, Italy; ²Medical Genetics Section, Virgen de la Arrixaca University Hospital, IMIB Pascual Parrilla, University of Murcia (UMU), Murcia, Spain; ³CIBERER-ISCIII, Madrid, Spain; ⁴UCSF Health, San Francisco, United States; ⁵Alnylam Pharmaceuticals, Cambridge, United States; ⁶Thomas Jefferson University, Philadelphia, United States
Email: paoloven@unimore.it

Background and aims: Acute hepatic porphyria (AHP) is a group of rare, chronic, multisystem disorders characterized by acute attacks, chronic symptoms, progressive elements, and long-term complications requiring proactive management. Givosiran is an RNAi therapeutic approved for AHP treatment. In ENVISION (NCT03338816), givosiran treatment led to sustained reductions in annualized attack rate (AAR). Among patients who completed the study through month (M) 36, 58% were attack-free after their first 6M of givosiran treatment for the duration of the trial. In this analysis, we examined treatment outcomes in patients who were not attack-free after their first 6M of givosiran treatment.

Method: Eligible patients had AHP, were aged ≥12 years, and had experienced ≥2 attacks requiring hospitalization, urgent care, or

intravenous (IV) hemin at home within 6 M before study enrollment. A 6M placebo-controlled double-blind (DB) period was followed by a 30 M open-label extension (OLE) period in which all patients received givosiran. This post hoc, descriptive analysis included patients who were randomized in the DB period and completed the OLE period. Subgroups were defined based on patient attack frequency after the first 6 M of givosiran treatment (0 attacks, Group A; ≥1 attack, Group B).

Results: 94 patients were randomized, and 79 completed ENVISION; 46 (58%) and 33 (42%) were in Groups A and B, respectively. In Group B, the mean percentage reduction in composite AAR (attacks requiring hospitalization, urgent care, or IV hemin at home) per 6 M interval were 57% after >6–12 M of givosiran treatment and 85% after >30–36 M, relative to historical composite AAR (mean [SD], 12.8 [9.6]). Quality of life improved in both groups: after 6M and 36M of treatment, mean SF-12 version 2 Physical Component Summary scores increased from baseline by 7.3 and 8.3 points (Group A) and 4.1 and 9.1 (Group B); EQ-VAS scores increased by 6.9 and 19.9 points (Group A) and 2.2 and 17.5 points (Group B). After 6 M and 36 M of givosiran treatment, median percentage reductions from baseline in aminolevulinic acid levels were 88% and 93% (Group A) and 85% and 92% (Group B), and median percentage reductions from baseline in porphobilinogen levels were 88% and 97% (Group A) and 86% and 93% (Group B).

Conclusion: Both patient groups had reduced attacks and other treatment-related improvements within the first 6 M of givosiran treatment. Those who were not attack-free after the first 6 M of treatment experienced further attack reductions and quality of life improvements with longer-term givosiran treatment.

WED-166

Efficacy and safety of odevixibat in a subgroup of adult patients with progressive familial intrahepatic cholestasis in the PEDFIC 2 study

Henkjan J. Verkade¹, Kathleen M. Loomes², Janis M. Stoll³, Tao Gu⁴, Anthony Loizides⁵, Christof Maucksch⁶. ¹Pediatric Gastroenterology – Hepatology, University of Groningen, Beatrix Children's Hospital, University Medical Center Groningen, Groningen, Netherlands; ²Children's Hospital of Philadelphia, Philadelphia, Pennsylvania, United States; ³Department of Pediatrics, Washington University School of Medicine, St. Louis, Missouri, United States; ⁴Albireo Pharma, an Ipsen Company, Cambridge, Massachusetts, United States; ⁵Albireo Pharma, an Ipsen Company, Cambridge, Massachusetts, United States; ⁶Ipsen Pharma GmbH, Munich, Germany
Email: h.j.verkade@umcg.nl

Background and aims: Progressive familial intrahepatic cholestasis (PFIC) is a group of rare genetic liver diseases that present with a range of phenotypes. Although PFIC symptoms typically present in infancy, symptom onset may not occur until adulthood. The safety and efficacy of odevixibat, an ileal bile acid transporter inhibitor, were evaluated in patients with PFIC in the phase 3 PEDFIC 1 and PEDFIC 2 studies (NCT03566238; NCT03659916). To investigate treatment effects of odevixibat in adults with PFIC, we examined its efficacy and safety in an adult subgroup from PEDFIC 2.

Method: PEDFIC 2 is an ongoing, 72-week, open-label extension study evaluating odevixibat 120 µg/kg once daily in patients of any age with any type of PFIC. This analysis spans from patients' first dose of odevixibat to a data cut-off of 31 July 2022. Patient-reported pruritus scores (range, 0–4; higher scores indicate worse symptoms), serum bile acid (sBA) levels, hepatic parameters (total bilirubin and alanine aminotransferase [ALT] levels), and treatment-emergent adverse events (TEAEs) were evaluated.

Results: Overall, 5 adult patients with PFIC (PFIC1, n = 3; PFIC2, n = 2) enrolled in PEDFIC 2 (mean [range] age, 23.3 [19.5–26.0] years; 40% female; mean [range] odevixibat exposure, 56.5 [24.0–90.4] weeks). At baseline, all patients had elevated sBAs and moderate-to-severe pruritus. At the data cut-off, 4 patients were ongoing in the study and

POSTER PRESENTATIONS

1 patient had discontinued the study due to withdrawal of consent. sBA levels ranged from 213–433 $\mu\text{mol/L}$ at baseline and 11–446 $\mu\text{mol/L}$ at last assessment; 4 of the 5 patients had reductions in sBA levels from baseline. Four patients had reductions in pruritus score from baseline to weeks 21–24; reductions in those 4 patients ranged from 0.2–2.5 points. Four patients who had elevated total bilirubin at baseline (range, 26–1004 $\mu\text{mol/L}$) experienced reductions by last assessment (range, 14–568 $\mu\text{mol/L}$). Elevated baseline ALT was observed in 4 patients (range, 64–136 U/L); 3 of these patients experienced reductions by last assessment (range, 51–128 U/L). At least 1 TEAE was reported in 4 of the 5 patients (80%); most were mild to moderate in severity. Two patients experienced serious TEAEs: 1 patient reported streptococcal septic arthritis, and 1 patient with a history of pancreatitis reported acute pancreatitis. None of the TEAEs were considered drug related, and no patient discontinued due to TEAEs.

Conclusion: Most of the adult patients with PFIC enrolled in the ongoing PEDFIC 2 study appeared to experience clinical benefits with odevixibat, including reductions in sBAs, pruritus, and/or improvements in hepatic parameters. Most TEAEs with odevixibat in adults with PFIC were mild or moderate in severity, and none were considered to be drug related. These findings suggest that odevixibat treatment in adult patients with PFIC warrants further clinical investigation.

WED-167

Recanalization for Budd-Chiari syndrome and development of a prognostic score: a multicentre study of 834 cases from China

Qiuhe Wang¹, Bohan Luo², Dongdong Xia³, Chunqing Zhang⁴, Ke Xu⁵, Kewei Zhang⁶, Mingsheng Li⁷, Qingrong Fan⁸, Wei Bai², Guohong Han². ¹National Clinical Research Centre for Digestive Disease and Xijing Hospital of Digestive Diseases, Fourth Military Medical University, Xi'an, China, Xi'an, China; ²Department of Liver Diseases and Interventional Radiology, Digestive Diseases Hospital, Xi'an International Medical Center Hospital, Northwest University, Xi'an, China, Xi'an, China; ³National Clinical Research Centre for Digestive Disease and Xijing Hospital of Digestive Diseases, Fourth Military Medical University, Xi'an, China, Xi'an, China; ⁴Shandong Provincial Hospital affiliated to Shandong University, Jinan, China; ⁵Department of Radiology, First Affiliated Hospital of China Medical University, Shenyang 110001, China, Shenyang, China; ⁶Henan Provincial People's Hospital, Zhengzhou, China; ⁷Department of Vascular Surgery, The First Affiliated Hospital of Zhengzhou University, Zhengzhou 450052, China, Zhengzhou, China; ⁸Department of Interventional Radiology, Heze Municipal Hospital, Heze 274000, China, Heze, China
Email: hangh@fmmu.edu.cn

Background and aims: Large cohort studies on recanalization for Budd-Chiari syndrome (BCS) are lacking. We conducted this multicentre retrospective study to depict characteristics and treatment allocation of Chinese BCS patients; to intensively explore the outcome of recanalization; and to develop a recanalization-specific prognostic score.

Method: A total of 834 BCS patients undergoing recanalization from January 2010 to May 2019 were included from 6 Chinese centres. Cox regression was used to develop the prognostic score.

Results: Recanalization was performed in 83.1% of all screened patients, while inferior vena cava (IVC) obstruction is seen in 87.1% of recanalized patients. Median follow-up was 58.0 (35.2–84.9) months, and 5-year orthotopic liver transplantation (OLT)-free survival was 91.1% (89.0–93.3%). Compared to angioplasty alone, initial stenting significantly reduced 5-year restenosis (11.2% [7.0–15.3%] vs. 24.1% [20.1–27.8%], HR 0.50 [0.34–0.73], log-rank $p < 0.001$) and symptom recurrence (13.7% [9.0–18.2%] vs. 20.5% [16.7–24.1%], HR 0.62 [0.43–0.91], log-rank $p = 0.014$), but did not improve 5-year OLT-free survival (90.2% [86.4–94.1%] vs. 91.6% [89.1–94.3%], HR 1.11 [0.70–1.78], log-rank $p = 0.647$). The results remained consistent after propensity score matching and across subgroups. The BCS-

recanalization score for outcome prediction and risk stratification was developed and internally validated, and its performance was superior to existing models.

Conclusion: Being representative of Chinese BCS patients, the current cohort reported the universality of IVC obstruction and the predominance of recanalization. The substantial benefits of stenting are robust. BCS-recanalization score could be used for outcome prediction and risk stratification. Future validations are needed.

WED-170

TRISTAN-Retrospective real world data in management of Wilson disease therapies in Germany

Isabelle Mohr¹, Christian Hartmann², Johannes Wiegand³, Thomas Lang⁴, Peter Buggisch⁵, Michael Praktikjnjo⁶, Karl Heinz Weiss⁷, Frank Tacke⁸, Verena Aliane⁹, Annette Athari⁹, Carlot Kruse⁹. ¹Universitätsklinikum Heidelberg, Zentrum für Innere Medizin, Medizinische Klinik IV für Gastroenterologie und Hepatologie, Heidelberg, Germany; ²Medizinische Fakultät und Universitätsklinikum Düsseldorf, Heinrich-Heine-Universität Düsseldorf, Klinik für Neurologie, Düsseldorf, Germany; ³Universitätsklinikum Leipzig, Klinik und Poliklinik für Onkologie, Gastroenterologie, Hepatologie und Pneumologie, Leipzig, Germany; ⁴Klinikum Starnberg, Klinik für Kinder- und Jugendmedizin, Starnberg, Germany; ⁵MVZ Ifi-Institut Hamburg, Hamburg, Germany; ⁶Universitätsklinikum Münster, Medizinische Klinik B (Gastroenterologie, Hepatologie, Endokrinologie, Klinische Infektiologie), Münster, Germany; ⁷Krankenhaus Salem, Innere Medizin, Heidelberg, Germany; ⁸Charité-Universitätsmedizin Berlin, Department für Hepatologie und Gastroenterologie, Campus Virchow-Klinikum (CVK) und Campus Charité Mitte (CCM), Berlin, Germany; ⁹Univar Solutions B.V., Rotterdam, Netherlands
Email: isabelle.mohr@med.uni-heidelberg.de

Background and aims: Wilson disease (WD) is a rare autosomal recessively inherited disorder of the copper metabolism with pathological copper accumulation mainly in the liver and brain. In Germany D-penicillamine (D-Pen) and zinc salts are approved as first-line treatment. Trientine (Trientine dihydrochloride (TETA-2HCl) and Trientine tetrahydrochloride (TETA-4HCl)) are both available for patients who are intolerant to D-Pen. Data on therapy management of patients, specifically with respect to switch of therapeutic regimen, are sparse. We retrospectively assessed real-world data of patients who were treated with Trientine at least once, regarding the diagnostic and therapeutic management, duration, sequence and dosing of the different therapeutic options in specialized WD centres in Germany.

Method: Anonymized data from WD patients receiving Trientine therapy at least once during their course of treatment was included. Data was collected during 1st of January 2012 and 31st of December 2021 with one or more documented follow-up visits. Data collection included centre structure, WD diagnosis, and therapeutic standards as well as disease and therapy history. This includes all previous and current treatments, switching between therapies, and duration of treatments. Data analysis was exploratorily analyzed (descriptive analysis/graphical display).

Results: In total we included 6 German WD centres and a total of 143 patients (range 5 to 85 years old, 68 males, 75 females), eight of these patients were paediatric (<18 years). The median age at diagnosis was slightly higher for males (18.0 years) compared to females (14.5 years). Most patients showed hepatic symptoms at time of diagnosis ($n = 78$) while neurologic ($n = 39$) and other symptoms ($n = 35$) were less frequent. The neurological patients were diagnosed at a later stage (median 25.0 years) than patients without neurologic symptoms (median 14.5 years). 109 patients revealed with full documentation of therapy switch. From these patients, 50% were switched from D-Pen to Trientine after 7 years of D-Pen therapy with the latest switch observed after 48 years. Dose conversion factors between different chelators or formulations in mg were reported for D-Pen to

TETA-2HCl as 0.75, D-Pen to TETA-4HCl as 0.60, TETA-2HCl to TETA-4HCl as 0.84 and TETA-4HCl to TETA-2HCl as 1.27.

Conclusion: This data helps to understand therapy management of WD patients in German specialized WD centres. Furthermore, this data gives an interesting insight into the real-life dosing of chelators when switching between drugs or formulations and thus might support physicians in future therapy and dosing decisions.

WED-171

Spleen stiffness and VWF-based non-invasive tests reflect severity of prehepatic and presinusoidal portal hypertension

Lorenz Balcar¹, Georg Semmler¹, Michael Schwarz¹, Nina Dominik¹, Benedikt Hofer¹, Katharina Stopfer¹, Anna Schedlbauer¹, Can Hopp¹, David Bauer¹, Lukas Hartl¹, Mathias Jachs¹, Benedikt Simbrunner¹, Albert Friedrich Stättermayer¹, Behrang Mozayani¹, Matthias Pinter¹, Michael Trauner¹, Mattias Mandorfer¹, Thomas Reiberger¹, Bernhard Scheiner¹. ¹Medical University of Vienna, Vienna, Austria
Email: lorenz.balcar@meduniwien.ac.at

Background and aims: Non-cirrhotic portal vein thrombosis (NCPVT) and porto-sinusoidal vascular disorder (PSVD) are frequent causes of prehepatic and/or presinusoidal portal hypertension (PH) in the absence of cirrhosis. However, diagnosis is often delayed as it requires cross-sectional imaging or liver biopsy. Liver stiffness measurement (LSM) is useful to differentiate PSVD from cirrhosis. Spleen stiffness measurement (SSM), von Willebrand factor-antigen (VWF) and its ratio to platelet count (VITRO) may detect prehepatic/presinusoidal PH.

Method: Consecutive patients with established diagnosis of PSVD/NCPVT and controls with compensated cirrhosis with available and valid VCTE-SSM data at the outpatient clinic of the Medical University of Vienna between 08/2022–08/2023 were included. VCTE-LSM, -SSM, PLT, VWF, and VITRO were analysed regarding their potential in differentiating between PSVD, NCPVT, and cirrhosis including subgroups of patients with clinical suspicion of PH.

Results: One-hundred fifty-seven patients were included: 55 with prehepatic/presinusoidal PH (PSVD n = 27, NCPVT n = 25, PSVD+PVT n = 3) and 102 with cirrhosis (mainly alcohol n = 46 and metabolic n = 25 aetiology). Comparing patients with prehepatic/presinusoidal PH vs. cirrhosis, no significant differences regarding Child-Pugh stage (87% vs. 87% stage A), PLT (128 vs. 112 G/L; p = 0.183), or splenomegaly (86% vs. 74%; p = 0.087) were evident. LSM was significantly lower in patients with prehepatic/presinusoidal PH (8.1 vs. 29.7 kPa; p < 0.001); however, SSM was significantly higher (74.3 vs. 50.5 kPa; p < 0.001) leading to an SSM/LSM ratio which differentiated prehepatic/presinusoidal from sinusoidal PH (7.5 vs. 1.63; p < 0.001). VWF (222 ± 74 vs. 260 ± 81; p = 0.005) and VITRO score (1.5 vs. 2.2; p = 0.012) also were lower in prehepatic/presinusoidal PH. Results were similar when only including patients with clinical signs of PH (LSM: 8.3 vs. 30.5 kPa; p < 0.001; SSM: 74.9 vs. 51.3 kPa; p < 0.001; SSM/LSM ratio: 7.56 vs. 1.64; p < 0.001; VWF: 227 ± 73 vs. 259 ± 79%; p = 0.016; VITRO: 1.61 vs. 2.37; p = 0.011). In binomial regression analysis, log-transformed SSM was associated with the presence of specific signs of PH in prehepatic/presinusoidal PH (B: 4.928 ± 2.345; p = 0.036). When sub-stratifying patients with prehepatic/presinusoidal PH, patients with NCPVT had higher SSM (86 vs. 50.2 kPa; p = 0.019) and SSM/LSM ratios (10 vs. 5.14; p = 0.006) compared to PSVD patients. Other NITs were comparable among prehepatic/presinusoidal PH aetiologies.

Conclusion: VCTE-SSM and VWF provide potentially more relevant information on the severity and aetiology of PH (prehepatic/presinusoidal vs. sinusoidal) as compared to LSM and PLT alone, especially when combined with PLT (VITRO) and LSM (SSM/SSM ratio).

WED-172

Transaminase Pattern Over Time Is Not Associated with a More Aggressive Hepatic Evolution: Results from the AEEH Wilson Registry

Marina Berenguer¹, Luis García-Villarreal², Antonio Olveira³, Esther Molina⁴, Jose María Moreno Planas⁵, Marta Romero-Gutiérrez⁶, Jose Pinazo Bandera⁷, Helena Masnou⁸, Paula Iruzubieta⁹, Maria Luisa Gonzalez Dieguez¹⁰, Javier Ampuero¹¹, José Ramón Fernández¹², Carolina Muñoz Codoceo¹³, Ana Arencibia Almeida¹⁴, Sara Lorente¹⁵, Manuel Delgado¹⁶, Diego Burgos Santamaria¹⁷, Víctor Manuel Vargas Blasco¹⁸, Alba Cachero¹⁹, Manuel Hernández Guerra²⁰, Judith Gómez-Camarero²¹, Julia Morillas²², María Lázaro Ríos²³, Isabel Carmona Soria²⁴, Gemma Carrión²⁵, Ariadna Bono²⁶, Anna Miralpeix²⁷, Pablo Alonso Castellano², Zoe Mariño²⁷. ¹Hospital Universitari i Politècnic La Fe, IISLaFe, Ciberehd, Valencia, Valencia, Spain; ²Servicio Digestivo, Complejo Hospitalario Universitario Insular Materno Infantil (CHUIMI), Las Palmas de Gran Canaria, Spain; ³Hospital Universitario La Paz, Madrid, Spain; ⁴Hospital Clínico de Santiago, Santiago de Compostela, Spain; ⁵Servicio de Aparato Digestivo, Complejo Hospitalario Universitario de Albacete, Facultad de Medicina Universidad de Castilla La Mancha, Albacete, Spain; ⁶Hospital Universitario de Toledo, Toledo, Spain; ⁷Unidad de Hepatología, Unidad de Gestión Clínica de Aparato Digestivo, Hospital Universitario Virgen de la Victoria, Instituto de Investigación Biomédica de Málaga-Plataforma Bionand, Málaga, Spain; ⁸Unitat Hepatologia, Servei Aparell Digestiu, Hospital Universitari Germans Trias i Pujol, Badalona, Spain; ⁹Hospital Universitario Marqués de Valdecilla, Santander, Spain; ¹⁰Hospital Universitario Central de Asturias, Oviedo, Spain; ¹¹Hospital Universitario Virgen del Rocío, Sevilla, Spain; ¹²Hospital Universitario de Cruces, Barakaldo, Spain; ¹³Hospital Universitario 12 de Octubre, Madrid, Spain; ¹⁴Hospital Universitario Nuestra Señora de La Candelaria, Santa Cruz de Tenerife, Spain; ¹⁵Unidad de Hepatología y Trasplante Hepático, Hospital Clínico Lozano Blesa de Zaragoza, IIS Aragón, Zaragoza, Spain; ¹⁶Hospital Universitario A Coruña, A Coruña, Spain; ¹⁷Hospital Ramón y Cajal, Madrid, Spain; ¹⁸Servicio de Hepatología, Hospital Vall d'Hebron, Universitat Autònoma Barcelona, CIBERehd, Barcelona, Spain; ¹⁹Hospital Universitari de Bellvitge, Hospitalet de Llobregat, Spain; ²⁰Hospital Universitario de Canarias, Santa Cruz Tenerife, Spain; ²¹Hospital Universitario de Burgos, Burgos, Spain; ²²Hospital Universitario Virgen de la Luz, Cuenca, Spain; ²³Hospital Universitario Miguel Servet, Zaragoza, Spain; ²⁴Hospital Virgen Macarena, Sevilla, Spain; ²⁵Hospital Universitario Infanta Leonor, Madrid, Spain; ²⁶Hospital Universitari i Politècnic La Fe, IISLaFe, Ciberehd, Valencia, Spain; ²⁷Servicio de Hepatología, Hospital Clínic, CIBERehd, IDIBAPS, ERN-RARE Liver, Universitat de Barcelona, Barcelona, Spain
Email: marina.berenguer@uv.es

Background and aims: The prognosis in Wilson's disease (WD) depends on early diagnosis and adequate compliance with chronic treatment. Copper homeostasis parameters help determine stability in WD, but they do not always correlate with liver enzymes or prognosis. Our aim was to determine the predictive value of transaminases in WD.

Method: Patients with confirmed WD diagnosis (Leipzig Score >3) with hepatic and/or mixed presentation and ≥1 year of follow-up from diagnosis were included in the Registry. Demographic data, phenotype, severity at diagnosis, treatment and compliance, analytical, histological, and elastographic parameters were collected. Patients were stratified by hepatic severity at diagnosis: mild group 1 (without cirrhosis) vs severe group 2. The transaminase pattern during follow-up was analyzed (stable: always normal AST and ALT vs fluctuating: AST and/or ALT >ULN or fluctuating normal/elevated). "Aggressive evolution" was defined as histological or elastographic progression or clinical decompensation, including the need for transplantation or death from liver-related causes.

Results: A total of 228 patients were included (mild group 1, n = 160, 70%; severe group 2, n = 68, 30%). The median follow-up time was 16

POSTER PRESENTATIONS

years. Group 2 patients were older at diagnosis, had a higher proportion of mixed presentations, a lower proportion of zinc treatment (both at initiation and first year post-treatment), and a lower proportion of patients with elevated ALT at diagnosis ($p < 0.05$). One-third of group 1 patients had an aggressive evolution, mainly due to elastographic worsening, compared to 50% in group 2 ($p = 0.016$), especially due to decompensation and increased hepatic stiffness. A fluctuating or high transaminase pattern was not associated with worse evolution. In group 1, 31% of patients with this pattern progressed compared to 45% of patients with persistently normal transaminases ($p = 0.71$). These percentages were higher in group 2, where 50% of “high/fluctuating transaminases” had a poor prognosis compared to 67% of patients with normal transaminases ($p = 0.47$). Overall, 38% had aggressive progression, which was associated with older age at diagnosis, normal-range transaminases at diagnosis, chelation therapy, and belonging to group 2. A stable transaminase pattern was associated with aggressive progression without reaching statistical significance. Only age at diagnosis remained statistically significant in multivariable analysis.

Conclusion: Aggressive progression in WD patients was not associated with a high/fluctuating transaminase pattern. The type of treatment, its modifications, and adherence may have influenced these results. Early diagnosis, and therefore a high index of suspicion, is essential for a favourable prognosis.

WED-173

Clinical, radiological and demographic characteristics of a female cohort of polycystic liver disease patients from the United Kingdom

Avisnata Das¹, Aleksandra Trojak¹, Benjamin Giles¹, Aqeel Jamil¹, Joanna Dowman¹, Andrew Fowell¹, Richard Aspinall¹. ¹Portsmouth Hospitals University NHS Trust, Portsmouth, United Kingdom
Email: avisnata@gmail.com

Background and aims: Polycystic liver disease (PLD) is a rare genetic disease of the liver that can significantly affect quality of life (QoL) of patients and cause serious complications. PLD-specific questionnaire score (PLD-Q score) (ranging from 0 to 100) can objectively assess severity of PLD-related symptoms. Female sex is known to be a significant factor contributing to severe PLD. We hereby report PLD-related findings in an exclusively female cohort of patients in terms of symptom severity, radiological characteristics, influence of estrogen use and pregnancy, nature of co-morbidities and complications.

Method: We interrogated registry data from a single large secondary care centre regarding 30 women with PLD in terms of PLD-Q scores, age of diagnosis, Qian's grade of liver cysts, presence of dominant cyst (size > 8 cm), profile of co-morbidities and complications.

Results: The PLD-Q scores in 30 women ranged from 9 to 83 with a mean of 41.1 and median of 39.5. The age of PLD diagnosis ranged from 14 to 73 years with a mean of 48 years. 4 patients (15%) had Qian's grade 2 disease (11–20 liver cysts), 13 (48%) had Grade 3 liver cysts (> 20 cysts), 10 (37%) had Grade 4 liver cysts (> 20 cysts with hepatomegaly symptoms). 17 (63%) patients had no dominant cyst while 10 (37%) patients had ≥ 1 dominant cyst. Out of 20 patients with relevant data, 12 (60%) patients had received estrogen-containing compounds (either as oral contraception or as hormone replacement) for at least a year and this group had a mean PLD-Q score of 41.25 which was higher than the mean PLD-Q score of 36.0 in the group of 8 (40%) patients who had not used estrogen in any form. The difference in mean scores was however not statistically significant. Mean PLD-Q score in the group of 6 patients who had never been pregnant was 38.50 and lower than the mean score (41.77) in the group of 13 patients with one or more pregnancies, though the difference was again not statistically significant. 26 (86.7%) women had at least one co-morbidity while 4 (13.3%) had none. Hypertension (14 patients), Diabetes mellitus (4 patients) and End-stage renal disease (4 patients) were the commonest co-morbidities. 18 women (60%) had at least one PLD-related complication while 12 (40%) had none.

Abdominal hernias (7 patients) and cyst infections (3 patients) were the two commonest complications in this cohort. 5 out of the 7 patients needed surgical repair of hernia.

Conclusion: The data demonstrated that the average woman in our cohort was diagnosed with PLD towards end of fifth decade of life and is likely to have more severe symptoms if there is history of estrogen use and previous pregnancy. Hypertension was the commonest co-morbidity and abdominal hernia the commonest complication.

WED-174

Next-generation sequencing for non-cirrhotic portal thrombosis and its impact on portal hypertension

Ilias Kounis^{1,2,3,4}, Laurence Legros⁵, Erica Nicola Lynch^{4,6}, Clementine Roger⁴, Anne Spraul⁷, Eleonora De Martin^{1,2,3,8}, Rodolphe Sobesky^{1,2,3,4}, Oriana Ciacio^{1,2,3,4}, Daniel Azoulay^{1,2,3,4}, Didier Samuel^{1,2,3,4}, Cyrille Feray^{1,2,3,4}, Audrey Coilly^{1,2,3,4}. ¹France FHU HepatinoV, Villejuif, France; ²Université Paris-Saclay, Inserm, Physiopathogénèse et traitement des maladies du Foie, Villejuif, France; ³Inserm, Université Paris-Saclay, UMR-S 1193, Villejuif, France; ⁴AP-HP Hôpital Paul-Brousse, Centre Hépatobiliaire, Villejuif, France; ⁵AP-HP, université PARIS-Saclay, Kremlin Bicêtre, France; ⁶Gastroenterology Research Unit, Department of Experimental and Clinical Biomedical Sciences “Mario Serio,” University of Florence, Florence, Italy; ⁷Biochemistry Unit, DMU15, Bicêtre Hospital, AP-HP, Paris-Saclay University, Kremlin Bicêtre, France; ⁸AP-HP Hôpital Paul Brousse, Centre Hépatobiliaire, Villejuif, France
Email: ilias.kounis@aphp.fr

Background and aims: Myeloproliferative neoplasms (MPNs) stand out as the leading cause of non-tumoral non-cirrhotic splanchnic vein thrombosis. Next-generation sequencing (NGS) enables the simultaneous assessment of multiple genes implicated in myeloid clonal pathology. This study aims to explore the potential of NGS in elucidating the etiology of portal thrombosis and its role in the development of portal hypertension.

Method: This retrospective monocenter study included all adult patients diagnosed with non-cirrhotic portal thrombosis at our unit from 2020 to 2023. These patients underwent a comprehensive diagnostic evaluation, including NGS, within the hematology department. Diagnosis and follow-up non-cirrhotic portal vein thrombosis adhered to the European Association for the Study of the Liver (EASL) guidelines. Cox regression analysis identified independent risk predictors (HR 95% CI) for the development of portal hypertension.

Results: The study enrolled 46 patients with non-cirrhotic portal thrombosis over a median follow-up period of 3.9 [2.4, 8.7] years. NGS findings were obtained from 36 (78.2%) patients, revealing a total of 19 mutations. Among the cohort, 22 (47.8%) developed portal hypertension. One patient (2.2%) underwent liver transplantation, and four patients (8.7%) underwent mesentericocaval anastomosis. Liver biopsy was performed in 13 (28.3%) patients, with seven meeting the VALDIG criteria for porto-sinusoidal vascular disease. Identified mutations included IDH2, CSF3R, ETV6, JAK2 non V617F, EZH2, TET2, and JAK2 V617F. In the multivariate analysis of portal hypertension development, the combination of JAK2 + non-JAK2 mutation, or the presence of non-JAK mutation showed no statistically significant association with portal hypertension, with hazard ratios of 2.52 (0.99, 6.48) and 1.52 (0.51, 4.52) respectively, and p values of 0.14 and 0.53 respectively.

Conclusion: NGS identified JAK2-exon12 mutations previously undetected by conventional techniques. However, these patients do not seem to have a higher risk of developing portal hypertension.

WED-175

Intrauterine blood transfusion causes dose- and time-dependent signal alterations in the liver and the spleen on fetal magnetic resonance imaging

Michael Schwarz¹, Victor Schmidbauer², Nikolaus Nowak², Patric Kienast², Martin Watzenboeck², Marlene Stuempflen², Caroline Schwarz¹, Dieter Bettelheim³, Christina Haberl³, Julia Binder³, Herbert Kiss³, Thomas Reiberger¹, Daniela Prayer², Gregor Kasprian². ¹Division of Gastroenterology and Hepatology, Department of Medicine III, Medical University of Vienna, Vienna, Austria; ²Department of Biomedical Imaging and Image-guided Therapy, Medical University of Vienna, Vienna, Austria; ³Department of Obstetrics and Gynecology, Division of Obstetrics and Feto-Maternal Medicine, Medical University of Vienna, Vienna, Austria
Email: victor.schmidbauer@meduniwien.ac.at

Background and aims: Intrauterine transfusions (IUTs) are life-saving interventions in fetal anemia—a rare but potentially fatal complication in pregnancy. However, with each transfusion iron bypasses iron uptake regulation in the maternal liver and placenta and accumulates in fetal organs, predominantly in the liver and spleen. Unlike other imaging modalities, magnetic resonance imaging (MRI) is capable of non-invasively assessing fetal liver disease and iron overload. For this study we analyzed the effect of IUTs on prenatal MRI of the fetal liver and spleen.

Method: Eight fetuses who received IUTs and fetal MRI between 2014 and 2023 were retrospectively included in this analysis. Fetuses were gestational age-matched with other fetuses, who also underwent fetal MRI for other indications, but did not receive IUTs. Imaging assessment was performed on T1-/T2-weighted MR data. For all fetuses, volumetry of the liver and spleen as well as signal intensity (SI) measurements in these organs were performed.

Results: Fetuses who received IUTs had significantly larger liver (71.9 vs. 45.1 cm³ p = 0.003) and spleen (5.5 vs. 2.4 cm³, p = 0.029) organ volumes compared to age-matched controls. In the IUT cohort, T1-weighted SI for both livers (p = 0.018) and spleens (p = 0.026) was significantly lower. The reduction of T1-weighted SI of the fetal liver showed an inverse correlation with the number of IUTs received (Spearman's rho = -0.63, p = 0.009). Regarding T2-weighted SI of the liver, we observed a positive correlation with number of days elapsed between transfusion and MRI (rho = 0.86, p = 0.011). Similar, but less pronounced SI changes were found for fetal spleens on both T1- (rho = -0.54, p = 0.029) and T2-weighted (rho = 0.57, p = 0.150) imaging.

Conclusion: We observed significant dose-dependent changes in SI of both fetal livers and spleens for T1-weighted imaging that increased with number of transfusions received. For T2-weighted imaging, reduction in hepatic SI following IUT decreased in a time-dependent manner. Furthermore, hepatosplenomegaly was commonly found following IUT. Awareness of these temporary changes following IUTs allows for a better discrimination from other causes of fetal iron overload or splenomegaly with distinct prognosis.

WED-176

Early predictors of successful Kasai portoenterostomy for biliary atresia

Nishant Wadhwa¹, Arjun Maria², Sonia Badwal³, Satish Aggarwal³, Alpna Prasad¹. ¹Sir Ganga Ram Hospital, New Delhi, India; ²Sir Ganga Ram Hospital, Pediatric Surgery, New Delhi, India; ³Sir Ganga Ram Hospital, New Delhi, India
Email: arjunmaria@hotmail.com

Background and aims: To identify factors associated with successful Kasai Portoenterostomy (KPE).

Method: Retrospective analysis of 49 infants who underwent KPE between January 2018 to October 2023. Successful KPE was defined as total bilirubin <1 mg/dl by 6 months of age. None of the patients received post KPE steroids and none were tested for concomitant CMV.

Results: The median age at KPE was 71 (59–83) days, with 21 (42.9%) less than 65 days. Median follow-up was of 11 (6–36) months with native liver survival in 27 (55.1%). Thirty six (73.5%) were type III biliary atresia and 2 (4%) were associated with other congenital anomalies. Successful KPE was in 22 (44.9%). Age less than 65 days at the time of KPE was significantly associated with successful KPE (42.9% vs 57.1%, OR 5, 95% CI 1.472–16.988, p = 0.009). Weight (p = 0.932), total bilirubin (p = 0.907), direct bilirubin (p = 0.667), AST (p = 0.837), ALT (p = 0.937), Total protein (p = 0.051), albumin (p = 0.201) and INR (p = 0.220) at the time of surgery did not affect outcome. Ishak fibrosis grade (p = 0.267) and inflammation grade (p = 0.743) were not associated with outcome. Post surgery, lower total bilirubin (7.95 mg/dl vs 10.1 mg/dl, MD 0.07 to 4.66, p = 0.043) and direct bilirubin (4.92 mg/dl vs 6.5 mg/dl, MD 0.16 to 3.03, p = 0.03) by post operative day 7 were associated with a successful outcome. Parameters like ascites for more than 7 days (p = 0.071), albumin (p = 0.431), AST (p = 0.091), ALT (p = 0.108) and INR (p = 0.241) at 7 days post KPE did not affect the outcome. Seventeen patients suffered from complications post KPE with sepsis in 17, bowel perforation in 3 and biliary ascites in 2. Presence of complications post KPE did not affect the outcome (p = 0.825). Twenty (40.8%) patients suffered from a median of 1 (1–3) cholangitis episodes. However, cholangitis was not associated with outcome (p = 0.374). On logistic regression analysis age less than 65 days (OR 8.024, 95% CI 1.865 to 34.530, p = 0.005) and lower total bilirubin at day 7 post KPE (OR 0.789, 95% CI 0.642 to 0.970, p = 0.028) were found to be significantly associated with successful KPE increasing the correctness of classification of model from 55.1% to 73.5%.

Conclusion: There is a 8 folds increase in successful outcome if KPE is done at less than 65 days of age. Bilirubin at post operative day 7 is an early predictor of successful KPE.

WED-177

Determination of liver biopsy quality criteria for the diagnosis of porto-sinusoidal vascular disorder (PSVD)

Chloé De Broucker^{1,2}, Valérie Paradis^{2,3}, Miguel Albuquerque^{2,3}, Audrey Payancé^{1,2}, Aurélie Plessier^{1,2}, Francois Durand⁴, Paul Emile Zafar^{2,3}, Pierre-Emmanuel Rautou^{1,2}. ¹AP-HP, Hôpital Beaujon, Service d'Hépatologie, DMU DIGEST, Centre de Référence des Maladies Vasculaires du Foie, FILFOIE, ERN RARE-LIVER, Clichy, France; ²Université Paris-Cité, Inserm, Centre de recherche sur l'inflammation, UMR 1149, Paris, France; ³Pathology, Hopital Beaujon, Clichy, France; ⁴Hepatology and Liver Intensive Care, Hospital Beaujon, University Paris Cité, Paris, France
Email: c.debroucker@gmail.com

Background and aims: Baveno VII guidelines defined porto-sinusoidal vascular disorder (PSVD) as clinical or radiological signs of portal hypertension, or histological signs typical for PSVD in the absence of cirrhosis on a liver biopsy. These guidelines arbitrarily defined 20 mm as the minimal size of liver biopsy for the diagnosis of PSVD. This study aimed to establish evidence-based liver biopsy quality criteria to rule out cirrhosis in patients with signs of portal hypertension.

Method: Twenty-four liver explants from patients with cirrhosis or PSVD were selected. Among the twelve patients with cirrhosis, Laennec score was evenly distributed into 4A, 4B and 4C; four patients had hepatocellular carcinoma. Causes of cirrhosis were related to alcohol use disorder (n = 6), metabolic-dysfunction (n = 6), HBV (n = 2) and HCV (n = 2) infections (some had several causes). Among the twelve patients with PSVD, histological lesions included obliterative portal venopathy (n = 11), nodular regenerative hyperplasia (n = 5) and incomplete septal cirrhosis (n = 5) (some had several histological lesions). Slides were stained with picosirius and Masson's trichrome. 31 200 virtual liver biopsies were generated from these 24 explants, including various lengths (5, 10, 15, 20 and 25 mm) and widths (572 µm corresponding to a transjugular biopsy and 1000 µm corresponding to a percutaneous biopsy). All 31 200

POSTER PRESENTATIONS

virtual biopsies were classified as “cirrhosis” or “no cirrhosis” by an expert pathologist, who had no information on the clinical data.

Results: Overall sensitivity of percutaneous biopsies for the diagnosis of cirrhosis was 85% (95% confidence interval: 84–85%). Sensitivity was significantly higher with picosirius [86% (85–87%)] than with Masson's trichrome staining [83% (82–84%)] ($p < 0.001$). Sensitivity increased with the length of percutaneous biopsies, reaching a plateau at 15 mm, at which point sensitivity was 89% (88–91%) for picosirius and 86% (84–88%) for Masson's trichrome.

When focusing on biopsies longer than 15 mm, sensitivity was significantly higher for percutaneous biopsies [89% (88–90%)] than for transjugular biopsies [84% (84–86%)] ($p < 0.001$). A plateau was also observed from 15 mm for transjugular biopsies.

Specificity, corresponding to the number of correctly diagnosed PSVD, was 89% (88–89%) for percutaneous biopsies, and 87% (86–89%) for transjugular biopsies. Out of the four explants for which specificity was below 90%, irrespective of biopsy size, three had incomplete septal cirrhosis.

Conclusion: For the diagnosis of PSVD, the minimum liver biopsy length to exclude cirrhosis is 15 mm. Picosirius staining should be preferred. Sensitivity of transjugular is slightly lower than percutaneous, but the transjugular route offers other useful information, including hepatic venous pressure gradient and the presence or not of hepatic vein-to-vein collaterals.

WED-178

Enhanced liver phenotyping in unexplained chronic liver disease: the LIPHE algorithm

Anna Sessa^{1,2}, Edouard Reizine^{2,3}, Giuliana Amaddeo^{2,4}, Mélanie Simoes⁵, Jeremy Augustin⁵, Stefano Caruso⁶, Julien Calderaro⁷, Alain Luciani^{2,5}, Vincent Leroy^{2,7}. ¹Paris Est University UPEC, Henri Mondor Hospital, Créteil, France; ²Inserm U955, Créteil, France; ³Henri Mondor University Hospital, Créteil, France; ⁴Henri Mondor University Hospital, Créteil, France; ⁵Henri Mondor Hospital, Créteil, France; ⁶Inserm U 955, UPEC Paris Est University, Créteil, France; ⁷Henri Mondor Hospital, UPEC Paris Est University, Créteil, France

Email: asessa1990@gmail.com

Background and aims: Chronic elevation of liver tests is associated with long-term hepatic events and an increased risk of mortality. In nearly 10% of cases, these abnormalities remain unexplained despite a specialized etiological assessment. Our aim was to evaluate the diagnostic performance of dedicated liver phenotyping (LIPHE) using a combination of innovative techniques.

Method: This is an ongoing real-life monocentric prospective cohort study. Consecutive patients referred to our centre by gastroenterologists for unexplained chronic elevation of liver tests after a comprehensive work-up including viral serologies, iron and copper evaluation, auto-immunity, ultrasound, CT and/or MRI were included. The LIPHE algorithm consisted of step 1: standardized questionnaire, laboratory tests (auto-antibodies according to reference methods, A1AT, REC, biliary acids, Nt-ProBNP, HOMA) and multi-parametric magnetic resonance imaging (LIPHE-MRI) including fat and iron assessment, T1 dixon, T2 TSE FS, T2 HASTE, diffusion, vMRE, T1 mapping, T1 VIBE with dynamic vascular phases and hepato-biliary phase and 3D cholangio-MRI; step 2: liver biopsy; step 3 genetic or shotgun metagenomic analysis.

Results: The 1-year interim analysis included 72 patients (median age: 53 years, male: 39%). Liver enzymatic profiles were cytolysis in 20 (28%) patients (median ALT: 65 IU/l), cholestasis in 34 patients (median ALP: 162 IU/l), and mixed pattern or others in 18 patients. Cirrhosis was present in 12 patients (17%). Step 1 was performed in all patients, step 2 in 44 and step 3 in 12 patients. Definite diagnosis was made in 52 patients (72%), and probable diagnosis in 13 patients (18%). Definite diagnosis were distributed as follow: MAFLD ($n = 5$) not fulfilling classical criteria, porto-sinusoidal vascular disease ($n = 5$), primary biliary cholangitis ($n = 5$), primary sclerosing cholangitis

($n = 5$), congestive cardiac liver ($n = 4$), drug induced liver injury ($n = 4$), auto-immune hepatitis ($n = 4$), hyperthyroidism ($n = 3$), ABCB4 related genetic cholestasis ($n = 3$), alpha1 antitrypsin deficiency ($n = 2$), biliary hamartomatosis ($n = 2$), benign cyst/tumors ($n = 2$), miscellaneous ($n = 8$). The main diagnostic contributors were liver biopsy in 23 cases (32%), LIPHE MRI in 21 cases (29%), laboratory tests in 10 cases (14%) and anamnesis in 5 cases (7%). The diagnosis remained not identified in 7 (10%) patients.

Conclusion: The LIPHE algorithm may bring etiologic diagnosis in the majority of patients with non-elucidated liver disease who present with a large spectrum of rare and complex liver diseases. A combination of standardized questionnaire, laboratory tests, and multi-parametric MRI may avoid liver biopsy in 40% of cases and appears to be a promising first-line approach.

WED-179-YI

Liver fibrosis status and circulating polymers in alpha-1 antitrypsin deficiency patients with a Z/rare genotype

Naomi Kappe¹, Jan Stolk¹, Bart van Hoek¹. ¹Leiden University Medical Center, Leiden, Netherlands

Email: b.van_hoek@lumc.nl

Background and aims: Alpha-1 antitrypsin deficiency (AATD) is a hereditary condition caused by mutations in SERPINA1. The Z mutant (Glu342Lys) is a common AATD-deficient allele. Retention of polymerized Z alpha-1 antitrypsin (Z-AAT) in the liver causes hepatocyte damage. Z-AAT polymers in circulation are positively associated with liver injury. Patients with a partial deficiency (MZ genotype, M codes for the wild-type allele) have a small absolute increased risk of developing liver disease compared to healthy controls. It is unknown if patients with a Z allele and a rare deficiency allele (not known to cause AAT polymers) (Z/rare genotype) are at greater risk for the development of liver fibrosis. In this study, we investigated liver fibrosis status and Z-AAT polymer levels in Z/rare individuals. A cohort of MZ individuals, matched according to age and sex, served as the control group.

Method: In this cohort study, clinical data and serum and plasma samples were collected from patients aged ≥ 18 years with a confirmed Z/rare or MZ AAT genotype who visited the Gastroenterology and Hepatology outpatient clinic at the Leiden University Medical Center (LUMC) in the Netherlands. The samples were retrieved from the LUMC CuraRata Biobank. The groups were matched for age and sex. Liver fibrosis status was assessed by transient elastography, Aspartate aminotransferase to Platelet Ratio Index, fibrosis-4, and the Enhanced Liver Fibrosis test.

Results: 15 individuals with the Z/rare genotype and 15 individuals with a MZ genotype were included. BMI, Diabetes Mellitus type 2, and daily alcohol consumption did not differ between the two groups. Liver fibrosis status did not vary significantly between Z/rare and MZ individuals. All patients had no or very mild fibrosis. The median Z-AAT polymer level in Z/rare individuals was 519.5 $\mu\text{g/ml}$ [432.5–1370.8] compared to 727.7 $\mu\text{g/ml}$ [538.7–1313.8] in MZ individuals ($p = 0.23$).

Conclusion: This study showed no or very mild liver fibrosis in AATD patients with a Z/rare genotype. There was no significant difference between the liver fibrosis status and the presence of Z-AAT polymers between the Z/rare and MZ groups. Although not significantly different, the median polymer level of the MZ cohort was numerically higher than that of the Z/rare cohort, which might suggest an even lower risk of liver disease in Z/rare individuals than in MZ individuals.

WED-180

Clinical profile and outcomes of Wilson's disease in the young and adult population

Anand Kulkarni¹, Mithun Sharma¹, Rajesh Gupta¹, Manasa Alla¹, Sowmya Iyengar¹, Shantanu Venishetty¹, Nagaraja Padaki¹, Nageshwar Reddy¹. ¹AIG Hospitals, Hyderabad, India

Email: anandvk90@gmail.com

Background and aims: Wilson's disease (WD) can present with hepatic, neurological, or psychiatric symptoms. There are few studies reporting clinical patterns of WD from Asia; however, none in the recent decade have eluded this aspect in a large cohort of patients, which we aimed to report.

Method: Retrospective data of WD patients from our tertiary care liver hospital from June 2020 to January 2024 were included. The primary objective was to describe the clinical and laboratory characteristics, course, and outcomes of patients with WD and secondary was to compare the same among young (<19 years) and adult (≥ 19 years) population. Data was analyzed using SPSS ver.29 and most variables are expressed as median (minimum-maximum).

Results: 136 proven WD (females-35.3%) with a median age of 19 years (2–57) with a median Leipzig score of 4; Nazer score and New Wilson Index score of 5 were included. The median ceruloplasmin level, 24-hour urinary copper levels, and liver copper levels ($n = 49$) were 14.5 (2–39) mg/dl, 135 (13–3467) $\mu\text{g/day}$, and 98 (55–252) $\mu\text{g/g}$, respectively. None of the patients had liver copper levels less than 50 $\mu\text{g/g}$, while only one had liver copper levels $>250 \mu\text{g/g}$. The most common type of presentation in the cohort was decompensated cirrhosis (25%), followed by acute-on-chronic liver failure (ACLF) in 18.4% and acute liver failure (ALF) in 15.4%. Neurological symptoms (tremors-5; dysarthria-2; ataxia-2; chorea-1; cramps-1 in varying combinations) were present in 6.6% of patients, Kayser-Fleischer (KF) ring in 44.1% of patients, and hemolytic jaundice in 22.8%. After a median duration of 20.5 months follow-up, 108 patients (79.4%) were alive, and 18 (13.2%) had undergone living donor liver transplantation (LDLT). Ten patients (7.4%) had died within 45 days of diagnosis, of which eight were diagnosed with ALF, and two were diagnosed with ACLF. Of the 18 patients (ACLF-10, DCLD-5, ALF-3) who underwent LDLT, two died of sepsis and graft failure, and rest were alive. When we assessed according to age, most patients in younger population presented as ACLF/ALF (48.5%; 32/66), while the most common type of presentation in adults (≥ 19 years) was decompensated cirrhosis (31.4%, 22/70). Mean ceruloplasmin levels and liver copper levels were similar among the two groups. However, 24 h urine copper levels were higher in the younger population (199.4 [14–3467] mg/d) than the adult population (129 [13–1406] $\mu\text{g/d}$; $P = 0.01$). Neurological symptoms were more common in adults (11.4% vs. 1.5%; $P = 0.03$), while KF ring were more common in young populations (53% vs. 35.7%; $P = 0.03$). Transplant-free survival was 72.7% in the young population compared to 85.7% in adults ($p = 0.06$). **Conclusion:** WD presents as a severe disease in the younger population, and a trend towards poorer transplant-free survival was noted in the younger population.

WED-181

Use of metallothionein 1 as an ancillary tool for the diagnosis of Wilson disease

Clàudia García-Solà¹, Gabriela Caballero², Anna Soria¹, Octavi Bassegoda¹, Anna Pocurull¹, Xavier Forn¹, Isabel Graupera¹, Alba Díaz², Zoe Mariño¹. ¹Liver Unit, Hospital Clínic of Barcelona, IDIBAPS, CIBERehd, ERN-RARE Liver, Universitat de Barcelona, Barcelona, Spain; ²Pathology Department, Centre de Diagnòstic Biomèdic, Hospital Clínic of Barcelona, IDIBAPS, CIBERehd, Universitat de Barcelona, Barcelona, Spain
Email: zmarino@clinic.cat

Background and aims: Histological findings of Wilson disease (WD) are nonspecific and can be confused with more prevalent liver diseases, such as metabolic-dysfunction associated steatotic liver disease (MASLD). Classical histochemical stains (orcein, rhodanine) have low sensitivity, whereas intrahepatic copper quantification is only performed with high clinical suspicion, given its low availability and high cost. In 2021, Rowan *Dj et al* suggested the use of a novel immunohistochemical staining for metallothionein-1 (MT-1) (main intrahepatic copper chelator) as a good strategy for differentiating WD from other liver diseases and this was also recently shown by

Wiethoff *et al* (2023). Our objective was to evaluate the usefulness of this staining between WD patients and a lean-MASLD group, where differential diagnosis could be more difficult.

Method: Blinded histological evaluation by 2 anatomical pathologists using Ishak/CRN classification of liver biopsies from 20 patients with WD (WD group) and 29 MASLD patients with a BMI $<31 \text{ kg/m}^2$ (LEAN group). MT-1 was scored according to Rowan *et al*. Clinical and analytical variables were collected from both groups. Variables were expressed as medians/IQR_{25–75} or percentages. For statistical analysis, Chi²/U-Mann-Whitney was used, and the kappa index was used for inter-observer agreement.

Results: WD patients were significantly younger than those in the LEAN group (37.5 vs 70 years, $p < 0.01$) whereas LEAN patients were more frequently diabetic and dyslipemic ($p < 0.05$). AST and GGT (but not ALT) at the time of liver biopsy were significantly higher in the LEAN group (56 vs 35 IU/L; 104 vs 46 IU/L in WD respectively, $p < 0.05$). Liver biopsies were mainly performed during follow-up in WD patients (median time after diagnosis: 13 years) due to liver test impairment or suspected comorbidities (50%). Conversely, $>70\%$ of liver biopsies in the LEAN group were performed at diagnosis, as part of the etiological study or due to suspected advanced disease. No significant differences were observed in the stage of portal/lobular inflammation, fibrosis, or steatosis (grade, type or distribution) between both groups. In WD biopsies, more glycogenated nuclei were observed (50 vs 20.7%, $p = 0.033$) whereas steatohepatitis was only seen in LEAN patients (41 vs 0%, $p < 0.01$). Up to 70% of WD biopsies were positive for MT-1 vs 0% in LEAN biopsies ($p < 0.01$), with an H score of 205 (IQR_{25–75} 137.5–242.5) vs 0 in LEAN ($p < 0.01$). Interobserver agreement was excellent (kappa = 0.896). MT-1 scoring was not different among WD patients according to time since diagnosis, treatment received (chelator vs zinc), ceruloplasmin levels or intrahepatic copper (available only in 8).

Conclusion: MT-1 staining could be a good strategy for histological differentiation between WD and MASLD and could be easily incorporated in the diagnostic work-up of patients with liver disease.

WED-182

The enhanced liver fibrosis test in alpha-1 antitrypsin deficiency patients homozygous for the Z-allele

Naomi Kappe¹, Jan Stolk¹, Bart van Hoek¹. ¹Leiden University Medical Center, Leiden, Netherlands
Email: b.van_hoek@lumc.nl

Background and aims: Alpha-1 antitrypsin deficiency (AATD) is a hereditary condition caused by mutations in the SERPINA1 gene. Alpha-1 antitrypsin (AAT) is primarily synthesized in the liver. A common AATD deficiency allele is the Z mutant (Glu342Lys). Homozygous carriage of the Z mutant (ZZ genotype) predisposes to liver fibrosis due to the accumulation of Z-AAT in the liver. Common indirect serum fibrosis markers, such as fibrosis-4 (FIB-4) and aspartate aminotransferase Platelet Ratio Index (APRI), have been analyzed in AATD. The sensitivity and specificity of these markers are too low to be used independently for the assessment of liver fibrosis. The enhanced liver fibrosis test (ELF) is a direct serum biomarker of liver fibrosis with increasing popularity and has not yet been validated in AATD. With transient elastography (TE, FibroScan) we assessed the performance of ELF in the evaluation of fibrosis status in homozygous Z patients. We also assessed APRI and FIB-4 to evaluate whether the ELF test exceeded the performance of these fibrosis serum markers in our cohort.

Method: In this cohort study, clinical data and serum samples were collected from patients with a ZZ genotype who visited the Gastroenterology and Hepatology outpatient clinic at the Leiden University Medical Center (LUMC) in the Netherlands. Samples were retrieved from the LUMC CuraRata biobank. Included patients had a valid TE assessment, and were aged ≥ 18 years. Patients were excluded if they had any extrahepatic fibrotic disorder or any other liver disease (except for metabolic dysfunction-associated steatotic liver disease)

POSTER PRESENTATIONS

and if they reported pathological alcohol consumption. The Area under the ROC (AUROC) was calculated to assess the accuracy of the serum fibrosis markers in detecting either significant or advanced fibrosis (≥ 7.1 kPa and ≥ 10.0 kPa, respectively as assessed by TE).

Results: 50 patients were included in the study. The cohort was fairly healthy with a mean BMI just above the upper limit of normal, low daily alcohol consumption, and only two patients had diabetes mellitus type 2. APRI had the highest AUROC for the detection of both fibrosis stages, with an AUROC of 0.854 (95% confidence interval (CI) 0.749–0.958) for significant fibrosis and 0.922 (95% CI 0.847–0.998) for advanced fibrosis. For significant fibrosis FIB-4 had the second highest AUROC of 0.790 (95% CI 0.643–0.938), for advanced fibrosis the ELF test had the second highest AUROC of 0.859 (95% CI 0.719–0.998). For significant fibrosis the ELF test had an AUROC of 0.768 (0.629–0.908).

Conclusion: In our cohort, the ELF test did not perform better than the cheaper and more accessible APRI or FIB-4 for the assessment of significant and advanced fibrosis status in homozygous Z AATD patients. Further validation of the ELF test and other fibrosis- and fibrogenesis-markers, preferably with liver biopsy results and longitudinal follow-up, is required.

WED-183-YI

Neurodegeneration in aceruloplasminemia and carriers of heterozygous ceruloplasmin variants: brain atrophy or iron toxicity?

Marlene Panzer^{1,2}, Christoph Birk^{3,4}, Elisabetta Indelicato⁵, Bernhard Glodny⁴, Benedikt Schaefer¹, Christoph Scherfler⁵, Elke Gizewski^{3,4}, Herbert Tilg¹, Heinz Zoller^{1,2}. ¹Department of Medicine I, Medical University of Innsbruck, Innsbruck, Austria; ²Christian Doppler Laboratory for Iron and Phosphate Biology, Medical University of Innsbruck, Innsbruck, Austria; ³Neuroimaging Research Core Facility, Medical University of Innsbruck, Innsbruck, Austria; ⁴Department of Neuroradiology, Medical University of Innsbruck, Innsbruck, Austria; ⁵Department of Neurology, Medical University of Innsbruck, Innsbruck, Austria
Email: marlene.panzer@i-med.ac.at

Background and aims: The autosomal recessive disease Aceruloplasminemia is caused by mutations in ceruloplasmin and characterized by progressive iron accumulation in the brain, liver and pancreas. Early signs include low ceruloplasmin, hyperferritinemia and low transferrin saturation. First neurological manifestations are typically reported between 40 and 60 years of age. The aim of this study is to describe neurodegeneration in aceruloplasminemia and assess the effect of heterozygous ceruloplasmin variants on brain iron.

Method: Clinical and radiological features of neurodegeneration were assessed in four homozygous or compound heterozygous and three single heterozygous patients. Patient records were reviewed to collect demographic, biochemical and clinical parameters. Neurological impairment was quantified by the Unified Wilson Disease Rating Scale. Magnetic Resonance Imaging (MRI) was performed on a 3 Tesla scanner including R2* relaxometry for iron quantification. R2*-values were analyzed in deep gray matter structures segmented using FSL first. Brain Volumetric measurements were performed using MRI parameters and were compared to sex- and age-matched healthy controls.

Results: Plasma ceruloplasmin concentrations were below the lower limit of normal in all patients included. Three homozygous patients had elevated ferritin and reduced transferrin saturation. Homozygous patients presented with a spectrum of symptoms ranging from mild tremor to severe neurologic impairment. All heterozygous patients were asymptomatic. Significantly increased R2*-values indicating iron overload in thalamus, caudate nuclei and putamen were measured in homozygous patients compared to heterozygous carriers and healthy controls. Increased R2* was also observed in the white matter of homozygous patients. Total

intracranial volume differed numerically between homozygous and heterozygous patients and healthy controls.

Conclusion: This study indicates that iron not exclusively accumulates in basal ganglia, dentate nuclei and thalamus as previously described but might also affect white matter. Brain iron accumulation does not prevent automated volume segmentation of subcortical brain regions. Quantitative MRI is feasible in patients with aceruloplasminemia and allows assessment of neurodegeneration.

WED-184

Evaluation of routine outpatient assessment methods for post-Fontan procedure liver complications

Yohei Koizumi^{1,2}, Hirooka Masashi¹, Yoshiko Nakamura¹, Yano Ryo¹, Makoto Morita¹, Yuki Okazaki¹, Yusuke Imai¹, Takao Watanabe¹, Osamu Yoshida¹, Yoshio Tokumoto¹, Masanori Abe¹, Yoichi Hiasa³. ¹Department of Gastroenterology and Metabology, Ehime University Graduate School of Medicine, Toon City, Japan; ²Saiseikai Matsuyama Hospital, Department of Internal Medicine, Matsuyama, Ehime, Japan; ³Department of Gastroenterology and Metabology, Ehime University Graduate School of Medicine, Toon, Ehime, Japan
Email: shachiyo2@yahoo.co.jp

Background and aims: Non-invasive ultrasound technique for liver fibrosis and cardiac function assessment in Fontan-associated liver disease (FALD) is needed to evaluate real-time disease progression. However, it is still unclear how to optimally monitor FALD in outpatient settings. We conducted a prospective follow-up study to examine adult cases who underwent the Fontan procedure.

Method: A total of 69 cases out of 105 Fontan postoperative cases who underwent imaging diagnosis at our department from January 2012 to December 2022 were included in this study. Blood test results, liver stiffness measurements, and cardiac ultrasound examinations were performed at the time of follow-up initiation and at one and five years later. Clinical end points (venous aneurysms, hepatocellular carcinoma, Fontan circulatory failure, and death) were set and evaluated.

Results: Among the 69 FALD cases, two cases had hepatocellular carcinoma. There was no significant difference in liver stiffness values at the time of observation initiation and five years later ($p = 0.214$). Univariate analysis revealed that patients with clinical end points were associated with low platelet counts ($p = 0.011$), the presence of liver nodules ($p = 0.052$), ventricular dysfunction ($p = 0.013$), and the number of years after the Fontan procedure. Multivariate analysis showed a correlation between the number of years after the Fontan procedure and liver stiffness values ($p = 0.007$). However, these associations were not significant when adjusted for Fontan type, age at the beginning of observation, cardiac function, and MELD-XI score.

Conclusion: The ideal monitoring approach for patients with FALD remains uncertain. Liver stiffness measurement is a useful non-invasive secondary indicator for cirrhosis, and it may help capture patients who require more frequent continuous monitoring for hepatocellular carcinoma. However, our study did not result in a clear benefit to periodically conducting liver stiffness measurements as there was no significant difference over time in adult cases.

WED-185

Frequency of ATP8B1, ABCB11 and ABCB4 gene mutations in adult patients with idiopathic chronic cholestasis

Paulo Bittencourt¹, Liana Codes², Antônio Ricardo Cardia Ferraz de Andrade³, Raimundo Gama⁴, Livia Falcao⁴, Raimundo Parana⁵, Maria Lucia Ferraz⁴, Gilda Porta⁶. ¹Bahiana School of Medicine and Public Health, Unit of Gastroenterology and Hepatology, Portuguese Hospital, Salvador, Bahia, Salvador, Brazil; ²Bahiana School of Medicine and Public Health, AMO Oncology Clinic, Salvador, Brazil; ³Federal University of Bahia, Salvador, Brazil; ⁴Federal University of Sao Paulo, Sao Paulo, Brazil; ⁵Hospital Aliança, Instituto

D'Or de Pesquisa e Ensino, University Hospital of Salvador, Bahia, Brazil, Salvador, Brazil; ⁶Hospital Sirio Libanes, Sao Paulo, Brazil
Email: plbbr@uol.com.br

Background and aims: Several bile transporter gene mutations have been associated with progressive familial intrahepatic cholestasis (PFIC) types 1 to 6 in children as well as to intrahepatic cholestasis of pregnancy (ICP) and low phospholipid associated cholelithiasis (LPAC) in adults. The purpose of the present study was to assess frequency of those mutations in adults with idiopathic cholestatic chronic liver disease (CLD).

Method: All patients with cholestatic CLD of unknown cause followed in three different reference centers in Brazil were genotyped for ABCB11, ABCB4, ABCC2, ATP8B1, CFTR, JAG1, KIF12, LSR, MYO5B, NR1H4, PPM1F, serpin1, TJP2, USP53, VIPAS39, VPS33B, PEX26 and WDR83OS gene mutations using Illumina NovaSeq 6000 Sequencing. Primary biliary cirrhosis, primary sclerosing cholangitis as well as other causes for cholestatic CLD were excluded in all patients.

Results: 35 patients (69% males, median age at disease onset 28 [14–70] years) were included in the study. Eighteen (51%) had cirrhosis and 7 (20%) had been submitted to liver transplantation. Only one had hepatocellular carcinoma. Twenty-eight (80%) patients were either heterozygous (n = 13), compound heterozygous (n = 11) or homozygous (n = 4) for ABCB4 (n = 24), serpin 1 (n = 3), ABCB11 (n = 1), ABCC2 (n = 1) and PEX26 (n = 1) gene mutations. All but 15 patients exhibited known pathogenic (49%) or likely pathogenic (16%) mutations.

Conclusion: More than half of the Brazilian patients with cholestatic CLD of unknown cause were shown to exhibit pathogenic or likely pathogenic mutations in bile transporter genes, particularly ABCB4. Genotyping may identify most of those subjects as late-onset PFIC III patients.

WED-186

Exchangeable copper quantification falls below normal range in a high proportion of patients with Wilson disease during follow-up

Zoe Mariño¹, Clàudia García-Solà¹, Ariadna Bono², Sonia García-García², Anna Miralpeix¹, Rocio Andreu³, Cristina Aguado³, Xavier Forn¹, Mercè Torra⁴, Marina Berenguer².
¹Liver Unit, Hospital Clínic Barcelona, IDIBAPS, CIBERehd, ERN-RARE Liver, Universitat de Barcelona, Barcelona, Spain; ²La Fe University Hospital, Hepatology and Liver Transplantation Unit, IIS La Fe, Hospital Universitario y Politécnico La Fe, Valencia, Spain; ³Biochemistry Department La Fe, Hospital UP La Fe, Valencia, Spain; ⁴Biochemistry and Molecular Genetics Department, Hospital Clínic Barcelona, IDIBAPS, Universitat de Barcelona, Barcelona, Spain
Email: zmarino@clinic.cat

Background and aims: Defining copper biomarkers for adequate follow-up in Wilson disease (WD) is still a matter for discussion. International recommendations are based on the combination of urinary copper excretion (UCE) and non-specific liver parameters (ALAT) depending on therapy and time from diagnosis. Exchangeable copper (CuEX) arises as a novel biomarker reflecting the free copper pool and was expected to be a good tool assessing copper homeostasis. Although its ratio (REC) was shown to be very useful for diagnosis (when >18%), no recommendation has been published to date for its use during follow-up. Our aim was to define CuEX utility and behavior on clinical follow-up.

Method: Real-life retrospective assessment of serum CuEX quantification performed during a 2-year period among WD patients followed in 2 large tertiary centers in Spain. Patients were considered stable (group 1, G1) if diagnosis had been achieved >1 year before, were compliant to medication and were on stable drug doses; otherwise, they were classified as non-stable and included in group 2 (G2). Serum samples were obtained as required by clinical practice and CuEX/REC were measured by inductively plasma coupled to mass spectrometry (ICP-MS). Reference intervals were set between 4.1–7.1 µg/dL, as published by El Balkhi et al, 2009. UCE was measured by

atomic spectroscopy and was considered “adequate” when copper quantification was 200–500 µg/24 h under chelation therapy or <100 µg/24 h when zinc salts were used. Statistical analysis was performed with SPSS-V27.

Results: Ninety-one WD patients were included (median age 38; median years from diagnosis: 19.3): 39 patients (43%) in G1 and 52 (57%) in G2, with no differences in terms of sex, age, therapy or time elapsed from diagnosis. Serum CuEX was quantified in 199 samples (median: 2 times/patient; 35.2% of samples from G1 vs 64.8% in G2). Median CuEX concentrations were not significantly different between G1/G2, with a delta-change <0.5 µg/dL between timepoints. Only 70 (35.2%) samples were within the pre-defined “normal range,” with up to 115 (57.8%) being below and 14 (7%) above. Distribution of CuEX was not different between groups, regardless of clinical stability or not, but all samples above 7.1 µg/dL (n = 14, 10.8%) corresponded to patients in G2. No correlation was observed between CuEX and UCE; at baseline only 17 (23%) patients had CuEX and UCE aligned (both being below/within or above their normal ranges). ALAT levels (but not ASAT) were significantly lower among patients with CuEX below normality, when compared to patients with CuEX within or above normality (p = 0.015).

Conclusion: CuEX levels were below normality in more than half of our real-life WD patients and seems an unreliable biomarker for assessing copper homeostasis. It should be used with caution and combined with other parameters. Reference CuEX target ranges should be re-defined for WD patients.

WED-187-YI

Clinical and biochemical characteristics of a Danish and Turkish cohort of incident and prevalent patients with primary biliary cholangitis

Hasan Eruzun¹, Lars Bossen², Dilara Turan Gökçe³, İlkey Ergenç^{4,5}, Zekiye Nur Harput⁶, Neslihan Güneş Aydemir⁷, Meral Akdoğan Kayhan³, Hasan Basri Yavıcı⁸, Peter Holland-Fischer⁹, Jesper Bach Hansen⁹, Yusuf Yilmaz^{10,11}, Orhan Sezgin⁶, Haydar Adanir⁷, Ahmet Bektaş¹², Henning Grønbaek¹³.
¹Ondokuz Mayıs University, Department of Gastroenterology, Samsun, Turkey; ²Department of Hepatology and Gastroenterology, Aarhus University Hospital and Clinical Institute, Aarhus University, Department of Internal Medicine, Regional Hospital Horsens, Horsens, Denmark, Aarhus, Denmark; ³Ankara Bilkent City Hospital, Department of Gastroenterology, Ankara, Turkey; ⁴Institute of Liver Studies, King's College Hospital, London, United Kingdom; ⁵Department of Gastroenterology, School of Medicine, Marmara University, İstanbul, Turkey; ⁶Mersin University, Department of Gastroenterology, Mersin, Turkey; ⁷Akdeniz University, Department of Gastroenterology, Antalya, Turkey; ⁸Marmara University, School of Medicine, Department of Internal Medicine, İstanbul, Turkey; ⁹Department of Gastroenterology and Hepatology, Aalborg University Hospital, Aalborg, Denmark; ¹⁰Department of Gastroenterology, School of Medicine, Recep Tayyip Erdoğan University, Rize, Turkey; ¹¹Department of Gastroenterology, School of Medicine, Marmara University, İstanbul, Turkey; ¹²Ondokuz Mayıs University, Department of Gastroenterology, Samsun, Turkey, ¹³Department of Hepatology and Gastroenterology, Aarhus University Hospital and Clinical Institute, Aarhus University, Aarhus, Denmark
Email: hasaneruzun@gmail.com

Background and aims: Primary biliary cholangitis (PBC) is a progressive chronic inflammatory liver disease. Environmental triggers, individual genetic predisposition, and epigenetic factors influence disease development and progression. Although it is observed in all races and regions, the incidence and prevalence show geographical variation. In our study, we compared cohorts of Danish and Turkish PBC patients with different genetic backgrounds.

Method: We compared basic demographic and biochemical data of four cohorts: 1) 155 prevalent Danish patients, 2) 77 incident Danish patients, 3) 103 prevalent Turkish patients, and 4) 101 incident Turkish patients. We evaluated liver disease severity and response

POSTER PRESENTATIONS

rates to ursodeoxycholic acid (UDCA) treatment in prevalent PBC patients.

Results: More than 90% of the included patients were female, except in the Danish incident cohort with 75% female. Turkish patients had lower median age in the prevalent cohort compared to Danish patients. Median albumin levels were higher in the Turkish cohorts than in the Danish, when comparing incident with incident and prevalent with prevalent, respectively; and more patients were AMA positive in the Turkish cohorts. Other biochemical data were similar between cohorts. Around 15% of the patients in all the cohorts had cirrhosis. More patients in the Turkish prevalent cohort were complete responders to UDCA than in the Danish prevalent cohort.

Conclusion: Turkish and Danish patients have similar age at diagnosis, and the same proportion have cirrhosis, but Turkish patients have higher AMA positivity rates than Danish. More Turkish than Danish patients have a complete response to UDCA treatment.

WED-188

Diagnosis and monitoring pathways using non-invasive tests in patients with alpha-1 antitrypsin deficiency-associated liver disease: results from an expert Delphi panel

Virginia C. Clark¹, Mark A. Price², Jon Russo², Rohit Loomba³, Alice Turner⁴, Pavel Strnad⁵. ¹University of Florida, Gainesville, FL, United States; ²RTI Health Solutions, Research Triangle Park, Durham, NC, United States; ³University of California San Diego School of Medicine, La Jolla, CA, United States; ⁴University of Birmingham, Birmingham, United Kingdom; ⁵University Hospital RWTH Aachen, Aachen, United States

Email: virginia.clark@medicine.ufl.edu

Background and aims: Alpha-1 antitrypsin deficiency (AATD) is a rare genetic condition and the severe protease inhibitor (Pi)*ZZ genotype increases the risk of liver disease (AATD-LD) and/or lung disease. Liver biopsy is the gold standard for assessing AATD-LD, but because of its invasiveness, high cost and sample/reader variability, it is infrequently used in real-world practice. Despite availability of non-invasive tests (NITs), there is a lack of consensus and guidelines for the diagnosis and monitoring of AATD-LD. We conducted a Delphi panel study to address this need.

Method: Healthcare providers with relevant specialties from the USA, Canada, EU and UK who managed at least two patients with AATD-LD in the past two years were recruited for the Delphi panel. Two iterative surveys were developed and administered, with the second survey clarifying the results from the first with an opportunity to provide deeper feedback. Following the surveys, a real-time consensus-building exercise focused on topics lacking consensus from the surveys. Controlled feedback was anonymous, and panellists were able to review individual/aggregated responses and qualify/change their responses.

Results: In total, 20 experts (in hepatology [n = 9], pulmonology [n = 6], transplant hepatology [n = 3], gastroenterology [n = 1] and hepatology and transplant hepatology [n = 1]) completed the study. Consensus was achieved on the topics of usage and evaluation of NITs, risk stratification and monitoring. All panellists agreed that vibration-controlled transient elastography (VCTE) is the preferred NIT for the initial assessment of AATD-LD owing to its accessibility and reliability. Magnetic resonance elastography and enhanced liver fibrosis tests were also considered by all as valuable tools following VCTE. Most (85%) agreed that VCTE <8 kPa could indicate no or mild fibrosis and VCTE ≥8 kPa could indicate clinically significant fibrosis, which may correspond to F2 or higher on the meta-analysis of histological data (METAVIR) scale. Most (85%) agreed that VCTE ≥13 kPa may indicate cirrhosis; however, two panellists suggested different values for this category, and one was unsure. Most (≥85%) also agreed that, to improve disease monitoring, the most important risk stratification for AATD-LD is at the F1 to F2 transition on the METAVIR scale.

Conclusion: Utilizing the Delphi technique, this study identified a clinically applicable framework for diagnosis and monitoring of

AATD-LD. A high level of agreement emerged regarding preferred NITs and their usage, risk stratification and monitoring in the context of AATD-LD management. The results provide a foundation for future efforts into NIT validation, further refinement of consensus, and the development of clinical guidelines for AATD-LD.

Acknowledgements: Writing assistance provided by E Sugrue, PhD, of Oxford PharmaGenesis.

WED-189

Patient survey of Wilson's disease patients in the United Kingdom

William J. H. Griffiths¹, Nick Probert², Catherine Stewart³, Valerie Wheeler⁴, Elaine Kamara⁵. ¹Addenbrooke's Hospital, Cambridge University Hospitals NHS Foundation Trust, Cambridge, United Kingdom; ²Orphanan, London, United Kingdom; ³University Hospitals Birmingham NHS Foundation Trust, Birmingham, United Kingdom; ⁴Wilson's Disease Support Group (WDSG), Cambridge, United Kingdom; ⁵Orphanan, Medical, London, United Kingdom
Email: bill.griffiths@nhs.net

Background and aims: Wilson's disease (WD) is a rare disease requiring lifelong therapy. Challenges with long term treatment are well recognised with a risk of increased morbidity, mortality, and liver transplantation in those poorly adherent to therapy. We designed an online survey for WD patients to better understand their needs.

Method: The UK Wilson's Disease Support Group (WDSG) partnered with Orphanan to develop a patient questionnaire hosted on the WDSG website and Facebook page. The domains covered in 35 questions were demographics, presentation, diagnosis, current and past treatments, monitoring, adherence and living with WD. Respondents were given multiple choices to answer or free text as appropriate. Anonymised data were analysed.

Results: Between 1st November 2023 and 11th January 2024, 41 subjects registered and of these 8 were disqualified (parental response [1], not living in UK [3] and less than 50% completed [4]); 33 subject responses were thus analysed. Participants were predominantly female (58%) and white (94%) with 21 (64%) completing all questions. Median (range) age was 43 (14–70) and time since diagnosis was 22 (1–59). Themes from the survey identified a desire for more local laboratory testing, improvement in time to diagnosis and more monitoring of drug tolerability. Data on current and past medication and reasons for changing were provided by 29/33 (88%), of whom 18/29 (62%) were on D-penicillamine (DPA) with majority (75%) continuing since diagnosis and 6 switched (3 intolerant to zinc and 3 declared problems with trientine). 10/29 (34%) of patients were on trientine (6 on branded trientine-2HCl, 3 on trientine-4HCl and 1 generic trientine-2HCl). Only 2 patients were on zinc (1 in combination with trientine-4HCl). Subjects reported experiencing (unspecified) ongoing adverse reactions (9/29; 5 DPA, 2 trientine-4HCl, 1 zinc and 1 trientine-4HCl plus zinc). Inconveniences to therapy were reported by 29/33 and included pill size, taste, losing medication, breaking bottle, remembering and most commonly food restrictions (14/29). Frequency of dosing, timing with food, taste, adverse reactions, and difficulty swallowing medications were recorded as challenges to adherence, with 10% of respondents admitting to missing a dose frequently, defined either as daily or up to 4 times a week.

Conclusion: This is the first online survey of WD patients in the UK which we are aware of. It gives a snapshot of the demographics, challenges, and adherence of UK patients with WD. Unmet needs identified in this survey include patient reported inconveniences to therapy, monitoring and identification of ongoing adverse reactions. All have the potential to impact adherence and further real world data are needed to confirm findings of this survey and to investigate interventions to improve health related quality of life of patients with WD.

WED-190

Elevated hepatic copper content in porto-sinusoidal-vascular disorder: leading down a wrong track

Lorenz Balcar¹, Nina Dominik¹, Behrang Mozayani¹, Georg Semmler¹, Michael Schwarz¹, Emina Halilbasic¹, Michael Trauner¹, Mattias Mandorfer¹, Thomas Reiberger¹, Bernhard Scheiner¹, Albert Friedrich Stättermayer¹. ¹Medical University of Vienna, Vienna, Austria

Email: lorenz.balcar@meduniwien.ac.at

Background and aims: Porto-sinusoidal vascular disorder (PSVD) is a rare vascular liver disorder characterised by clinical evidence of portal hypertension and specific histological findings in the absence of cirrhosis, which is poorly understood in terms of pathophysiology. While elevated hepatic copper content serves as diagnostic hallmark in Wilson disease (WD) and may also be present in cholestasis, there are no data on copper and PSVD so far. Therefore, the objective of this study was to systematically evaluate the prevalence of elevated hepatic copper content and to determine the clinical implications of these pathomechanistic changes in patients with PSVD.

Method: Patients with an established diagnosis of PSVD at the Medical University of Vienna and available hepatic copper content at the time of diagnosis of PSVD were retrospectively included. Elevated hepatic copper content was analysed for liver-related outcomes (first/further hepatic decompensation/liver-related death) in a multistate model.

Results: Overall, 92 patients were included into this study (mean age 49 ± 16 ; 57% male, 44% female; 40% decompensated; median hepatic copper content 30 [IQR: 18–55] $\mu\text{g/g}$) of whom 25 (29%) had mildly ($\geq 50 \mu\text{g/g}$) and 4 (4%) severely ($\geq 250 \mu\text{g/g}$) elevated hepatic copper content. Of the patients with mildly elevated hepatic copper content, 14 (15%) had evidence of cholestasis, but 15 (16%) had not.

Elevated levels of hepatic copper content were associated with younger age in multivariable linear regression analysis. During a median follow-up of 3.6 years, 21 (23%) patients developed one or more liver-related complications. After adjusting for age, Child-Pugh score, and decompensation status, hepatic copper content was significantly associated with the outcome of interest (per 10, log-transformed; aHR: 1.63 [95%CI: 1.19–2.24]; $p = 0.002$). A cut-off based on maximal rank-tests at $\geq 90 \mu\text{g/g}$ identified patients with considerable risk of developing liver-related outcomes during follow-up (at 2 years: 51% vs. 12%; $p = 0.007$).

Conclusion: Elevated hepatic copper levels may be frequently observed in patients with PSVD in the absence of cholestasis, especially in young patients, which might possibly steer the diagnosis into a wrong direction in sense of WD. Since patients yielding elevated hepatic copper content had higher risks of liver-related complications, the specific pathomechanisms and potential therapeutic consequences remain yet to be explored.

WED-191

The impact on adherence and patient satisfaction following a switch to trientine tetrahydrochloride for the maintenance therapy in Wilson's disease

Massimo Zuin¹, Valentina Medici², Nora Cazzagon³, Alberto Civolani⁴, Fabio Tedone⁵, Stefania Lopatriello⁵, Andrea Crosignani⁶, Pier Maria Battezzati⁷. ¹University of Milan, Milan, Italy; ²University of California Davis, Sacramento, United States; ³University of Padua, Padua, Italy; ⁴AOU Cagliari, Policlinico di Monserrato, Cagliari, Italy; ⁵Helaglobe srl, Firenze, Italy; ⁶Polo universitario San Paolo, Milano, Italy; ⁷University of Milan, Milano, Italy

Email: massimo.zuin@gmail.com

Background and aims: Wilson disease (WD), an inherited disorder of copper transport resulting in copper accumulation in the liver and brain. WD can be managed effectively if patients adhere to therapy. All therapies have food restrictions, require multiple daily dosing and side effects are common. We aimed to obtain patient reported data on

adherence, satisfaction, and health related quality of life (HQoL) before and after a switch to trientine tetrahydrochloride (TETA4).

Method: An Italian multicenter, retrospective (RP) prospective (P) observational study of WD adults prescribed TETA4 (Orphalan SA, France). Demographic data, 24-hour urinary copper excretion (UCE), posology and pill count at each visit were collected. Patient reported outcomes were obtained from Morisky Medication Adherence Scale (MMAS-4/8), Patient Experiences and Satisfaction with Medication questionnaire (PESaM) and HQoL questionnaire (SF36). Data were collected at two-time points; baseline (T0) and first visit (minimum 3 months) after switching to TETA4 (T1).

Results: Of the 25 patients enrolled, 9 and 16 were in the RP and P cohort respectively and 14 were female. Median (IQR) age and time from diagnosis was 43 (30, 52) and 24 (14, 30) years, respectively. The majority were employed (18/25) and 8/25 had co-morbidities. Pre-switch therapies were zinc (13), penicillamine (6), trientine dihydrochloride (TETA2; 4) and combination TETA2/zinc (2). At both T0 and T1, proportion of UCE outside recommended therapeutic range was unchanged (15; 60%). Mean (range) of pills of TETA4 prescribed was 4 (2–6). Based on returned pills at first follow-up, 16/23 were adherent, 6/23 moderately- and 1/23 non-adherent. In RP cohort, baseline adherence was 33% (MMAS-4) rising to 89% at T1 and in P cohort (MMAS-8), 25% self-reported as very adherent at T0 rising to 50% at T1. Overall patient satisfaction to therapy was high and unchanged. Median scores on 5-point scale in 4/6 domains of perceived effectiveness, satisfaction, impact of adverse events, ease of use and overall satisfaction were 4 at T0 and T1; only change, an increase from 4 to 5 in ease of use. Median (range) scores on a 0–100 scale (SF36) were overall high and unchanged at T0 and T1, with the exception, increasing for general health 56.2 (15–87.5) to 62.5 (6.25–81.3), energy 46.6 (13.3–100) to 60 (20–80) and social function 75 (25–100) to 87.5 (25–100). Statistically significant changes were seen in 2 domains; physical function and role limitations due to emotional state.

Conclusion: Patient reported adherence improved with TETA4 compared with previous therapy. Patient satisfaction and HQoL following switch to TETA4 improved through perceived ease of use (PESaM) and domains of energy, social functioning and general health (SF36) respectively. UCE values are unreliable to assess adherence. Long term data to assess continued adherence and HQoL are needed.

WED-192

Raising awareness of long term chelation therapy challenges in Wilson's disease-Potential implications of monitoring and developing skin and vascular complications

James Liu Yin¹, Jon Salisbury², Aftab Ala¹. ¹Institute of Liver Studies, King's College Hospital, London, United Kingdom; ²Histopathology, King's College Hospital, London, United Kingdom

Email: aftab.ala1@nhs.net

Background and aims: Wilson's disease (WD) is a genetic metabolic liver condition that results in excessive copper being retained in the body. Long term penicillamine (DPA), the most commonly used chelator for the treatment of WD, has a recognised association with connective tissue disorders (CTD) such as elastosis perforans serpiginosa and cutis laxa (CL). Crucially, it is not known whether this is directly due to the medication itself, from over treatment leading to copper deficiency or both. There is an additional potential risk of vascular issues due to disruption in the formation of collagen fibres by lysyl oxidase whose action requires copper. The response to treatment and monitoring of WD is assessed with the calculated non-caeruloplasmin bound copper (cNCC) and 24 hr urinary copper excretion (UCE). These inaccurate methods can be hard to clinically interpret and may potentiate over treatment.

Method: We reviewed patients with newly identified skin conditions within our WD cohort at King's College Hospital, London. We used our electronic patient records system including histopathology and

POSTER PRESENTATIONS

imaging records to review the clinical course of our patients, medication prescribed and biochemical markers.

Results: We identified 4 patients with WD, on long term treatment with chelation therapy and with acquired CL, 1 patient had a biopsy to confirm the diagnosis and the others were made clinically. 2 patients had echocardiograms performed, 1 patient had aortic root dilatation confirmed with a MRI aorta, whilst the other had no abnormalities detected. Patients' ages ranged from 37–57 years (3M: 1F) and years of treatment from 19–45 years. Treatment regime was mostly with DPA but 1 patient had only zinc and trientine. On review our patients had results for less than 1 UCE per year and that inter and intra patient results varied greatly (2–46 $\mu\text{mol}/24\text{ hr}$). The median value of cNCC for each patient was 0.11, –1.65, 3.95 and 0.5 (normal <1.6 $\mu\text{mol}/\text{L}$). Of note, 44% of cNCC values were negative in value and therefore not clinically interpretable (inaccurate due to inherent issues with cNCC formula).

Conclusion: There is a growing cohort of patients who have been exposed to copper chelation for a significant period of time. It is crucial to raise awareness, investigate and understand side effects of medication which may have potential long term serious complications.

Although a small cohort, our data showed wide variations in UCE, regularly un-interpretable cNCC results, skin changes in a patient without DPA use and a significant vascular issue. It highlights the need to develop accurate monitoring of copper to guide medication dosing, understand the mechanism and vascular complications of CTD and to investigate the consequences of over treatment in WD. International prospective studies are necessary to answer these important questions with further mechanistic studies to understand the underlying pathophysiology.

Viral Hepatitis – Experimental and pathophysiology

TOP-353

An mRNA vaccine exhibits anti-viral activity in mouse model of persistent hepatitis B infection

Aditi Deshpande¹, Aileen Rubio¹, Bharat Dixit¹, Pooja Tiwari², Lei Qiugang³, Sun Ya³. ¹ClearB Therapeutics, Concord, United States; ²Arnav Biotech Corp., Atlanta, United States; ³Wuxi AppTech, Shanghai, China
Email: adeshpande@clearbtherapeutics.com

Background and aims: We previously reported declines in serum HBsAg levels and concomitant clearance of infected hepatocytes after administration of a therapeutic subunit adjuvanted vaccine, CLB-3000 which consists of two modified HBsAg variants displaying clearance profile (CP) associated loop 1 and 2 epitopes identified from patients who achieve functional cure (EASL 2021 poster 853, AASLD 2021 poster 829). We have developed eight mRNA vaccine candidates with two coding sequences; loop1 (40X) and loop 2 (50X) in combination with different 5' UTRs (US Patent Application #20190314493; Stadler, C. et al, Nat Med 23, 815–817 (2017); Cao, J., et al, Nat Commun. 12, 4138 (2021)). Two candidates for each coding sequence were selected based on in vitro expression and were formulated into lipid nanoparticles and assessed for anti-viral activity in murine model of persistent Hepatitis B infection.

Method: 8 template DNA sequences were designed for two candidate vaccines, 40X and 50X, using combinations of four 5' UTRs. The eight mRNA candidates (1–40X, 2–40X, 3–40X, 4–40X, 1–50X, 2–50X, 3–50X, 4–50X) were synthesized by in-vitro transcription using N¹-1-methyl pseudouridine. Two 5' UTRs (1, 3) were prioritized based on protein expression level of candidates 1–40X, 3–40X, 1–50X and 3–50X in A549 and U937 cell lines assessed by western blot. These candidates

were formulated in lipid nanoparticles and tested for efficacy in the Hydrodynamic tail vein injection (HDI) model of persistent Hepatitis B infection [Chou H-H et al 2015. PNAS 112 (7) pp2175]. CBA/CaJ mice were given three biweekly intramuscular (IM) injections at a total mRNA dose level of 5 μg and monitored over time for serological markers of HBsAg, HBV DNA and liver HBcAg immunohistochemistry at end of study.

Results: mRNA candidates 1–40X, 3–40X, 1–50X and 3–50X demonstrated robust expression of HBsAg protein of appropriate molecular weight in A549 and U937 cell lines. Treatment of mice in the HDI model with 5 μg total mRNA dose displayed an average reduction of 2.6 log HBsAg from baseline to five weeks post last dose across all treatment groups, with the combination of all four candidates 1–40X +3–40X+1–50X+3–50X displaying the highest reduction of 3 log HBsAg compared to two mRNA candidates 3–40X+1–50X giving a 2.4 log reduction. The HBV DNA had similar trend in reduction as HBsAg in plasma. Liver compartment analysis confirmed clearance of HBcAg positive cells following serum HBsAg clearance. In comparison to mice in the treatment groups, persistent infection was maintained in placebo mice through the study duration.

Conclusion: An mRNA therapeutic vaccine was highly efficacious in a murine model of persistent HBV infection with rapid plasma HBsAg decline and clearance, and clearance of infected hepatocytes. These findings further support the development of an mRNA based therapeutic vaccination approach in chronic hepatitis B patients.

TOP-354

Potent and sustainable HBsAg clearance by a liver-targeting PD-L1 siRNA in mice

Zhiwei Yang¹, Nan Liu¹, Hongli Zhang¹, Ping Chen¹, Hui Chen¹. ¹Suzhou Siran Biotechnology Co., Ltd., Suzhou, China
Email: yangzhiwei@siranbio.com

Background and aims: The efficacy of PD-1/PD-L1 checkpoint antibodies has been proven in chronic hepatic B (CHB) clinical studies. CHB patients with low HBsAg baseline showed HBsAg loss and seroconversion, suggesting that immunomodulatory approach is effective for CHB treatment. However, systemic PD-L1 inhibition may result in intolerable immune response, and its efficacy need to be further improved to increase functional cure ratio. SA012, a N-acetylgalactosamine (GalNAc) conjugated siRNA therapeutic agent, which targets the mRNA of PD-L1 gene, has been developed for the treatment of CHB. Here, we report its pre-clinical data.

Method: hPD-1/PD-L1 AAV-HBV mice have been used in the following studies: 1) SA012 alone was injected subcutaneously at 7.5 mg/kg QW for 8 doses. 2) VIR-2218 (a siRNA targeting HBV-X gene) 1 mg/kg Q4W was injected subcutaneously for 2 doses and SA012 was injected at 7.5 mg/kg QW for 8 doses. Serum HBsAg, HBV DNA and HBsAb were detected at different time points till the end of study at Day 98. Additionally, the safety profile of biochemistry, routine blood test and histopathology were assessed in rat toxicity studies with SA012 100 mg/kg Q2W for 3 doses.

Results: 1) In SA012 monotherapy study, continuous HBsAg reduction was observed. 1/7 mice achieved HBsAg clearance after Day 49, and 4/7 mice achieved HBV DNA detection limit (LLOQ). 5/7 mice achieved HBsAb over 40 mIU/ml. 2) When SA012 was combined with VIR-2218, it showed much faster and higher HBsAg clearance ratio: 4/8 in the combo group compared to 1/7 in SA012 monotherapy group. Meanwhile, no mice showed HBsAg clearance in VIR-2218 monotherapy group. When SA011 (a GalNAc-conjugated siRNA developed by SiranBio, targeting HBV-X gene) was added sequentially to SA012+VIR2218 combo treatments, the highest HBsAg clearance ratio (6/8 mice, 75%) and HBV DNA clearance ratio (8/8 mice, 100%) were achieved. No rebound was observed in HBsAg clearance mice during the entire study. No significant abnormality was observed in rat tox studies.

Conclusion: SA012 has shown potent and sustainable HBsAg and anti-HBV activity in pre-clinical studies when used alone or

combined with VIR-2218/SA011. SA012 monotherapy can elicit prolonged reduction of HBsAg and HBV DNA in mice, and induced high levels of HBsAb. When combined with VIR-2218, faster and higher ratio of HBsAg clearance (50%) was achieved. When SA011 was added to the combo therapy, it showed the highest ratio of HBsAg clearance (75%) and HBV DNA elimination (100%). No viral rebound was observed during our entire studies. These results support further clinical development of SA012. The orthogonal mechanism of SA012 provides many possibilities for combo therapies with other modalities to reach the goal of CHB functional cure.

TOP-355-YI

T cells expressing HBV-specific chimeric antigen receptors harboring a Fab fragment control HBV infection in mice

Zhe Xie¹, Oliver Quitt², Anna D. Kosinska², Lisa Wolff², Elfriede Nöbner², Ulrike Protzer^{2,3}. ¹Institute of Virology, Technical University of Munich, Munich, Germany; ²Institute of Virology, Technical University of Munich/Helmholtz Munich, Munich, Germany; ³German Center for Infection Research (DZIF), partner site Munich, Munich, Germany
Email: zhe.xie@tum.de

Background and aims: Chimeric-antigen-receptors (CARs) are synthetic receptors designed to drive antigen-specific activation of T cells upon binding to cognate antigen. CAR-T cells are used in cancer therapy but are also interesting for chronic viral infections. Our study aimed to generate novel CARs that target the hepatitis B virus envelope protein (HBVenv) on the membrane of HBV-infected cells using an antigen binding fragment (Fab) consisting of heavy and light chains instead of a variable single-chain fragment. The aim of this study was to overcome functional alterations of the new format, and to study the antiviral efficacy of FabCAR-engrafted T cells in vitro and in vivo.

Method: We constructed novel CARs containing the Fab fragment of HBVenv-specific monoclonal antibodies as binding domains and CD3 as well as CD28 intracellular signaling domains. We characterized the FabCAR T-cell function by T-cell activation upon HBsAg stimulation and elimination of HBVenv-transgenic hepatoma cells. The antiviral effect was accessed by coculturing FabCAR-T cells with HBV infected HepG2-NTCP cells. To study in vivo efficacy, CD45.1 murine T cells expressing FabCAR were transferred to CD45.2 AAV-HBV infected, HBV-carrier Rag1 knock-out mice.

Results: Multifunctional FabCAR-T cells could be induced via HBsAg stimulation. FabCAR-T cells specifically eliminated HBV envelop protein transgenic cell lines Huh7S and HepG2SML. Elimination of target cells was accompanied by secretion of interferon-gamma, tumor necrosis factor, and granzyme B. FabCAR-T cells showed antiviral activity by significantly decreasing the level of viral antigen, intracellular HBV DNA, and HBV cccDNA in HBV-infected HepG2-NTCP cells. In HBV-carrier mice, after adoptive transfer, FabCAR-T cells proliferated and localized to the liver, resulting in target cell killing indicated by ALT flare and an antiviral effect by HBsAg and HBeAg reduction.

Conclusion: T cells stably transduced with our FabCARs are polyfunctional and could efficiently eliminate HBVenv-positive cells in an antigen-dependent manner in cell culture and in a preclinical animal model. Thus, FabCAR-T cells are promising candidates for treating chronic hepatitis B and HBV-associated hepatocellular carcinoma.

TOP-356

Combination treatment of a TLR7/8 dual agonist with an antisense oligonucleotide bepirovirsen and entecavir leads to additive HBsAg decline in the AAV-HBV mouse model

Ke Qiu¹, Zhiling Deng¹, Taiyu He¹, Zhi-wei Chen¹, Taichang Yuan², Guozhi Tang², Ming-Li Peng¹, Hong Ren¹. ¹Key Laboratory of Molecular Biology for Infectious Diseases (Ministry of Education), Institute for Viral Hepatitis, the Second Affiliated Hospital of Chongqing Medical

University, Chongqing, China; ²Shanghai Visonpharma Co., LTD, Shanghai, China
Email: renhong0531@vip.sina.com

Background and aims: Achieving high levels of functional cure of chronic hepatitis B (CHB) will likely require a combination regimen that blocks viral replication, reduces antigen load, and activates host immune responses to control residual virus. Bepirovirsen is a promising antisense oligonucleotide (ASO) against HBV which can significantly reduce hepatitis B surface antigen (HBsAg) but the duration is limited. TLR7 and TLR8 agonists induced durable antiviral efficacy in preclinical studies. However, the effect of single-acting TLR agonists in reducing HBsAg in clinical studies is limited. Recently, TLR7/8 dual acting agonists have been reported can induce broad cytokines which may provide novel opportunities towards functional HBV cure. This current work describes the investigation of combinations of a TLR7/8 dual acting agonist (VE03702) with bepirovirsen (ASO) and entecavir (ETV) in a mouse model of HBV infection. Sequential and concomitant treatment of these agents were explored and the results may inform future clinical combination trial design.

Method: C57BL/6 mice infected with rAAV8-1.3HBV were treated ETV and ASO for three weeks then stopped treatment or switched to VE03702 or Peg-IFN treatment for four weeks. ETV was orally administered at 0.1 mg/kg daily, and ASO was dosed at 50 mg/kg, subcutaneously once a week. VE03702 was dosed at 0.05 mg/kg, subcutaneously once a week, and Peg-IFN was dosed at 30 g/kg, subcutaneously twice a week. HBsAg was the key viral end point measured for these studies. Additionally, two potential clinical treatment paradigms were tested where both ASO and Peg-IFN were administered concurrently or ASO preceding treatment with Peg-IFN sequentially.

Results: In the first three weeks, concomitant treatment of ASO and ETV resulted in an up to 1.67 log reduction in HBsAg levels. After stopping treatment of ASO, serum HBsAg rapidly rebounded to pretreatment levels within 4 weeks while HBV DNA was still below the lower detection limit. When switching to VE03702 treatment after stopping ASO administration, additional decreases reaching 4.5 logs in HBsAg were observed. After 4 doses of VE03702, HBsAg loss was observed and anti-HBs antibodies in the serum were detected. For the sequential treatment of ASO followed by Peg-IFN, rapid rebound in HBsAg occurred after discontinuation of ASO resulting in no added benefit in this regimen. There is no significant difference between the sequential and concurrent treatment paradigms of Peg-IFN and ASO.

Conclusion: Combinations of a TLR7/8 dual agonist (VE03702) and bepirovirsen (ASO) and ETV provide additional reduction in HBsAg when dosed sequentially in the AAV-HBV mouse model of HBV. VE03702 showed more effectiveness than Peg-IFN in terms of avoiding HBsAg rebound after ASO discontinuation, suggesting the potential for clinical translation.

TOP-357

Second generation HBV siRNAs with novel chemistries demonstrate improved profiles compared with ALG-125755 and other clinical stage siRNAs

Jin Hong¹, Vivek Rajwanshi¹, Saul Montero², Min Luo¹, Kellan Passow¹, Cheng Liu¹, Hyunsoon Kang¹, Jacquelyn Sousa¹, Dana Cho¹, John Cortez¹, Shane Daguison¹, Kusum Gupta¹, Hua Tan², Vera Huang², Dawei Cai², Rostom Ahmed-Belkacem¹, Lawrence Blatt¹, David Smith¹, Leonid Beigelman², Julian Symons¹. ¹Aligos Therapeutics, Inc., South San Francisco, United States; ²Previous Employee of Aligos Therapeutics, Inc., South San Francisco, United States
Email: jhong@aligos.com

Background and aims: Hepatitis B virus (HBV) siRNAs have been shown to effectively reduce HBsAg in chronic hepatitis B (CHB) subjects. When combined with interferon or a TLR7 agonist, a significant portion of patients demonstrate HBsAg loss. ALG-125755 is an HBV siRNA currently in Phase I. Single doses have been evaluated

POSTER PRESENTATIONS

in healthy volunteers and virologically suppressed HBsAg negative CHB subjects. ALG-125755 was well tolerated with a favorable PK profile and viral kinetic data indicated evidence of HBsAg lowering at all dose levels evaluated. In this study, a multi-pronged approach was taken to further improve the potency, stability, hepatocyte-specific delivery and safety of ALG-125755 with the aim of developing a best-in-class HBV siRNA.

Method: In vitro inhibition of HBsAg release by siRNA was performed in the HepG2.2.15 cell line after transfection. Secreted HBsAg was quantified by ELISA. The stability of HBV siRNAs was profiled in mouse liver homogenates. Off target activity was evaluated by RNAseq in HepG2.2.15. The binding of different GalNAc moieties to the asialoglycoprotein receptor (ASGR) was measured in human and mouse liver microsomes. In the AAV-HBV mouse model, HBV siRNAs conjugated with GalNAc were administered subcutaneously (SC) with serial blood collections for HBsAg and ALT assessment.

Results: By applying novel sugar stabilization chemistry at the ALG-125755 antisense strand (AS) 3' region, 100% of the AS was maintained after 48-hour incubation in mouse liver homogenate, compared with 72% for the parent. Novel acyclic nucleoside chemistry was introduced into the seed region. This improved safety with a total off target reduction of 97% in an RNAseq assay. Surprisingly this also improved efficacy in reducing HBsAg by an additional 1.8 log₁₀ IU/ml compared with parent after a single dose of 5 mg/kg in AAV-HBV mouse model. An optimized GalNAc was assessed for binding to human and mouse ASGRs and exhibited a Kd of 13.6 and 5.9 nM respectively, while parental GalNAc showed a Kd of 97.9 and 15.5 nM respectively. ALG-125839 is a 2nd generation HBV siRNA incorporating some of these novel chemistries. Compared head-to-head with an ALG-125755 analog and another Phase 2 (Ph2) clinical stage HBV siRNA in the AAV-HBV mouse model after 6 repeat doses of 5 mg/kg, every two weeks, ALG-125839 showed an average additional 0.5 log₁₀ IU/ml HBsAg reduction over the ALG-125755 analog across multiple timepoints both during and post treatment. When compared to the Ph2 siRNA, the ALG-125839 HBsAg nadir was 1.5 log₁₀ IU/ml deeper. ALG-125839 was more durable than the Ph2 siRNA with HBsAg nadir maintained for 12 weeks in the follow-up period while HBsAg in Ph2 siRNA group returned to baseline.

Conclusion: ALG-125839 with novel chemistries demonstrated improved activity and potential safety when compared with ALG-125755 and a Ph2 siRNA. Further studies of this novel compound are warranted.

TOP-358-YI

Non-HAP CAM-A ALG-006746 and ALG-006780 induce rapid HBsAg reductions in AAV-HBV mice and have favorable pharmacokinetic profiles

Hannah Vanrusselt¹, Jordi Verheyen¹, Kusum Gupta², Lars Degrauwe¹, Cheng Liu², Abel Acosta Sanchez³, Mélanie Bollier³, Jean-Boris Nshimyumuremyi³, Benjamin Verburgh³, Clovis Peter³, Qingling Zhang⁴, Lawrence Blatt², Leonid Beigelman², Julian Symons², Sushmita Chanda², David Smith⁵, Andreas Jekle², Sandrine Vendeville¹, David McGowan¹, Yannick Debing¹. ¹Aligos Belgium BV, Leuven, Belgium; ²Aligos Therapeutics, Inc., South San Francisco, United States; ³Novalix, Leuven, Belgium; ⁴Aligos Therapeutics, Inc., South San Francisco, United States; ⁵Aligos Therapeutics, Inc., South San Francisco, Belgium
Email: hvanrusselt@aligos.com

Background and aims: Hepatitis B virus (HBV) capsid assembly is an attractive target for the treatment of chronic hepatitis B (CHB). Class A capsid assembly modulators (CAM-A) induce HBV core protein (HBc) aggregation and sustained HBsAg reduction in CHB mouse models. We recently presented data on the first non-heteroaryldihydropyrimidine (HAP) CAM-A with sustained in vivo HBsAg declines. Here we present two novel non-HAP CAM-A with rapid HBsAg reductions in AAV-HBV mice and favorable pharmacokinetic (PK) profiles.

Method: HBV DNA antiviral activity was determined in HepG2.117 cells using quantitative PCR, with and without 40% human serum. Effects on cccDNA establishment were assessed in HBV-infected primary human hepatocytes (PHH). Further characterization was performed using electron microscopy visualization and immunofluorescent HBc staining. HBc-dependent CAM-A-induced cell death (CCD) was assessed in HBc-expressing cells. PK properties were evaluated in rat, beagle dog and cynomolgus monkey, whereas in vivo antiviral efficacy was assessed in the adeno-associated virus (AAV)-HBV mouse model.

Results: ALG-006746 and ALG-006780 potently inhibited HBV DNA production in HepG2.117 cells with EC₅₀/EC₉₀ values of 10.6/45.0 nM and 7.76/31.6 nM respectively. Inclusion of 40% human serum resulted in modest 2.3- and 1.7-fold shifts in antiviral activity, respectively. Evaluation in PHH demonstrated pronounced inhibition of cccDNA establishment at higher concentrations. Both compounds induced the formation of aberrant viral capsids, as observed by electron microscopy, and small nuclear HBc aggregates, confirming their CAM-A "tiny" (CAM-A_t) subtype. Similar to other CAM-A, ALG-006746 and ALG-006780 induced CCD in HBc-expressing cells upon extended incubation. Both compounds showed low to moderate plasma clearance and moderate volume of distribution in three different species. Following a single oral administration of each compound in rat and dog, good bioavailability (79–91%) was achieved. Both compounds showed the expected immediate declines in HBV DNA in AAV-HBV-transduced mice but also reduced HBsAg with unexpectedly rapid kinetics compared to previously described CAM-A_t molecules. ALG-006746 induced a sharp decline from day 35 on, whereas ALG-006780 reduced HBsAg levels already at day 14, reaching a 1.5 log₁₀ IU/ml reduction by day 35, similar to HAP CAM-A RG7907.

Conclusion: With rapid in vivo HBsAg declines and favorable PK profiles, ALG-006746 and ALG-006780 are promising CAM-A candidates for further development.

TOP-359-YI

Development of a replication-competent Vesicular Stomatitis Virus (VSV) vector for therapeutic hepatitis B vaccination

Jinpeng Su^{1,2}, Anna D. Kosinska^{1,2}, Susanne Miko¹, Edanur Ates-Öz¹, Dorothee von Laer³, Janine Kimpel³, Ulrike Protzer^{1,2}. ¹Institute of Virology, Technical University of Munich/Helmholtz Munich, Munich, Germany; ²German Center for Infection Research (DZIF), Munich partner site, Munich, Germany; ³Institute of Virology, Medical University of Innsbruck, Innsbruck, Austria
Email: jinpeng.su@tum.de

Background and aims: Eliciting robust immune responses against hepatitis B virus (HBV) through therapeutic vaccination holds significant promise to cure chronic hepatitis B. We have developed a heterologous prime-boost clinical vaccine candidate, *TherVacB*, employing a protein-prime with recombinant HBV surface and core antigens (HBsAg, HBcAg), and a vector-boost with recombinant Modified Vaccinia virus Ankara vector (MVA) expressing HBV antigens. In this study, we aimed to use a replication-competent chimeric Vesicular Stomatitis Virus vector (VSV-GP) known to induce both B- and T-cell responses as an alternative viral vector. We evaluated different regimens incorporating this new vector alongside the original *TherVacB* regimen.

Method: AVSV-GP vector encoding HBsAg and HBcAg (VSV-GP-HBs/c) has been constructed. The new recombinant vector was evaluated for the encoded antigen expression through Western blot and immunofluorescence staining and its immunogenicity and antiviral efficacy were tested in both HBV-naïve and HBV-carrier mice.

Results: In vitro analyses demonstrated that the VSV-GP-HBs/c vector was successfully generated, and the encoded antigens were properly expressed. A single immunization with VSV-GP-HBs/c vector could induce HBV-specific immune responses, albeit at a very low level. When the VSV-GP-HBs/c vector was employed to substitute the

protein for prime in *TherVacB* regimen, the resulting immunization induced modest HBV-specific immune responses. It led to minor antiviral effects in HBV-carrier mice. In contrast, utilizing the VSV-GP-HBs/c vector to replace the MVA-HBs/c for boosting in *TherVacB* elicited robust HBV-specific antibody and T-cell responses. Furthermore, the approach resulted in a significant 3-log decrease in serum HBsAg levels, as well as a substantial 60%–70% reduction in the numbers of HBV-positive hepatocytes, intrahepatic HBV-DNA and HBV-RNA in the liver. The efficacy of the heterologous protein-prime/VSV-GP-boost approach was comparable to that of the classical *TherVacB* regimen, highlighting the importance of including protein in the priming phase of therapeutic hepatitis B vaccines. Of note, using a second viral vector, whether homologous or heterologous, after the protein-prime/viral vector-boost regimen did not further enhance vaccine-induced responses.

Conclusion: The protein-prime/vector-boost strategy stands as a promising and optimal therapeutic vaccine approach to cure chronic hepatitis B, in which VSV-GP-HBs/c could efficiently serve as a boost viral vector.

TOP-360-1Y

Hepatitis B Spliced-generated Protein (HBSP): a key factor of viral escape

Pierre Bablon¹, Hoan Nguyen Dang¹, Céline Goy¹, Jules Sotty¹, Aurélie Schnuriger², Lynda Aoudjehane³, Jeremy Augustin⁴, Chiara Guerrera⁵, Valérie Soulard⁶, Jonathan Pol⁷, Camille Sureau⁸, Patrick Soussan². ¹Centre de Recherche de Saint-Antoine (CRSA), Inserm/Sorbonne Université, Paris, France; ²Centre de Recherche de Saint-Antoine (CRSA), Inserm/Sorbonne Université/APHP, Paris, France; ³Institut de Cardiometabolisme et Nutrition (ICAN), Paris, France; ⁴Hôpital Henri Mondor, Inserm/APHP, Paris, France; ⁵SFR Necker, Inserm/Université Paris Cité, Paris, France; ⁶Centre d'Immunologie des Maladies Infectieuses (CIMI), Inserm/Sorbonne Université, Paris, France; ⁷Centre de Recherche des Cordeliers (CRC), Inserm/Sorbonne Université/Université Paris Cité, Paris, France; ⁸Université de Tours, CNRS, Tours, France

Email: pierre.bablon@inserm.fr

Background and aims: Hepatitis B Virus (HBV) infection leads to one million death per year, almost by cirrhosis and cancer. In contrary, *in vitro* efficient HBV infection remains stealthy. The main role of host immune response in pathogenesis was largely reported but remained unable to cure HBV during decades. Alternative splicing of viral transcripts induces the expression of Hepatitis B Splice-generated Protein (HBSP). On one hand, upregulation of this splicing activity has been reported during liver injury, and on the other hand, HBSP modulates TNF-alpha signaling pathway. Considering that HBSP-transgenic mice were less susceptible to liver inflammation and fibrosis, our study aimed to investigate its contribution when expressed in the context of HBV.

Method: HBSP-invalidated HBV (HBV-HBSPko) or wildtype HBV (HBVwt) viruses and AAV2/8 containing HBV-HBSPko or HBVwt whole genome were used to infect primary human hepatocytes (PHH) cultivated in 2D and 3D models and C57Bl6/J male mice, respectively. Liver cells culture and mouse tissues were analyzed by ELISA, Western Blot, immunofluorescence/immunohistochemistry, (RT) qPCR, RNAseq, proteomic and FACS.

Results: Transcriptomic analysis of HBVwt-infected PHH in 2D, compared to non-infected (NI), confirmed the stealth effect on infection (only 16/13554 differentially expressed genes (DEGs)). Infection of 3D PHH partially abrogated the stealthy effect of HBVwt (78/13615 DEGs, compared to NI). Surprisingly, infection with HBV-HBSPko increased the number of DEGs (up to 7-fold), in 2D and 3D models). Gene set enrichment of DEGs between HBV-HBSPko and HBVwt infection in 3D PHH showed that they were notably involved in cytokine-receptor interactions ($p = 0.009$) and cytokines signaling pathways ($p = 0.01$). These data led us to study the impact of HBSP invalidation on antiviral activity in AAV-HBV infected mice. Seven

weeks post-infection, a striking 12-fold reduction of intra-hepatic HBc positive cells was observed in mice infected with AAV-HBV-HBSPko, compared to AAV-HBVwt (confirmed by WB), with no impact on other viral parameters (HBsAg expression, viral transcription and viral load). Decrease in HBc expression was related to an activation of type I interferon (IFN) in the liver of HBV-HBSPko-infected mice. In contrary, HBVwt infection failed to induce a type I IFN response, strengthening the key role of HBSP in viral immune escape. Intra-hepatic immune cells (flow cytometry) and prime-boost assays are under study in this model.

Conclusion: For the first time, our data demonstrated the major role of HBSP in the stealth effect of viral infection. Targeting the immune escape mechanisms developed by HBV, through HBSP expression, could open new strategies for curing the chronic infection.

TOP-368

Detection of HBV-, HDV- and human mRNAs in archival FFPE tissues by spatial transcriptomics

Sangeetha Mahadevan¹, Ricardo Ramirez¹, Anjali Rao¹, Christina Moon¹, Andrew James¹, Rosanna Win¹, Edith Vaquero¹, Subhra Chaudhuri¹, Kai-Hui Sun¹, Meghan Holdorf¹, Lauri Diehl¹. ¹Gilead Sciences, Foster City, United States

Email: sangeetha.mahadevan1@gilead.com

Background and aims: Chronic infection with both hepatitis delta virus (HDV) and hepatitis B virus (HBV) results in the most severe form of viral hepatitis affecting 12–60 million people worldwide. While spatial transcriptomics (ST) is capable of spatially resolved, genome-wide RNA profiling, querying both viral and human mRNAs on FFPE tissue has not been evaluated to-date. Understanding the consequences of HBV/HDV co-infection on the host and characterizing the regional heterogeneity of each virus could potentially enable development of new therapies. In this study, we designed HBV- and HDV-specific probes to enable human and viral RNA co-detection in liver biopsy samples from a small cohort of HBV mono-infected, and HBV/HDV co-infected patients.

Method: FFPE sections from liver biopsies of 8 individuals (2 Healthy; 5 HBV mono-infected, and 1 HBV/HDV co-infected) were obtained from commercial sources. We designed 17 probes spanning HBV which recognize Surface, X and Core open reading frames (ORF). In addition, we designed probes against the DR1 sequence and anti-sense DNA to decipher between HBV-integration and cccDNA. For HDV, we designed sample specific probes which recognize HDAG ORF (HDAG mRNA, HDV anti-genome), HDV genome, HDV anti-genome from a non-coding region. These probes were spiked into the Human Transcriptome V2 probe set and applied to FFPE sections using the 10X Genomics Visium CytAssist Spatial Gene Expression workflow. A multiplex immunofluorescence (IF) stain detecting Hepatitis B surface antigen (HBsAg), Hepatitis B core antigen (HBcAg) and Hepatitis Delta antigen (HDAG) was performed on a serial section. Chromogenic *In Situ* Hybridization (CISH) from Advanced Cell Diagnostics using custom designed sense- and anti-sense Basescope probes was performed on a serial section to validate the signal from ST.

Results: There was a striking concordance between RNA signal from ST and CISH as well as protein signal from IF, validating the sensitivity and specificity of the ST approach. Areas that were positive for HBsAg and/or HBcAg by IF had a positive signal for their respective ST probes. HBsAg+, HBcAg- areas by IF had positive ST signal from Surface and X-ORFs, but not Core-ORF or DR1 probe, consistent with HBV integration. The HDV co-infected sample lacked both HBcAg (IF and ST) and cccDNA (ST) suggesting all HBsAg+ cells were a result of HBV integration. We identified evidence of cells containing only HDV markers suggestive of HDV-monoinfection, as well as cells containing both markers for HBsAg and HDV suggestive of HDV replication in HBV-integrated cells.

Conclusion: We successfully demonstrated that custom probe spike-ins can enable detection of HBV DNA/RNA, HDV RNA and human

POSTER PRESENTATIONS

mRNA in archival FFPE tissue. Future efforts will focus on applying this assay to larger sample sets with matched clinically relevant metadata.

TOP-369

HEV replication and genomic diversification in the human kidney

André Gömer¹, Avista Wahid², Lucas Hueffner², Martina Friesland², Katja Dinkelborg², Elmira Aliabadi², Fenja Laue², Saskia Janshoff¹, Markus Cornberg³, Benjamin Maasoumy³, Sven Pischke⁴, Tobias Müller⁵, Birgit Bremer³, Julian Schulze zur Wiesch⁴, Julia Benckert⁵, Rainer Ulrich⁶, Svenja Hardtke³, Petra Dörge³, Florian Vondran³, Ansgar Lohse⁴, Michael P. Manns³, Daniel Todt¹, Heiner Wedemeyer³, Thomas Pietschmann², Eike Steinmann¹, Patrick Behrendt². ¹Molecular and Medical Virology, Ruhr University Bochum, Bochum, Germany; ²TWINCORE, Hannover, Germany; ³Hannover Medical School, Hannover, Germany; ⁴University Medical Centre Hamburg-Eppendorf, Hamburg, Germany; ⁵Charité Berlin, Berlin, Germany; ⁶Friedrich-Loeffler-Institut, Greifswald, Germany
Email: andre.goemer@rub.de

Background and aims: Hepatitis E virus (HEV) is a widespread zoonotic virus that can cause acute fulminant as well as chronic hepatitis and has been associated with a range of extrahepatic manifestations. Among these, renal injuries have been reported, including membranoproliferative glomerulonephritis with or without cryoglobulinemia and membranous glomerulonephritis. However, it remains unclear whether a productive infection of kidney related cells causes tissue pathology. We here aim to dissect whether HEV can infect kidney cell in vitro. In addition, we evaluate whether in patients HEV shows mutational signatures that correlate with compartmentalization.

Method: We here use state-of-the-art HEV cell culture models based on HEV-3 Kernow-C1 p6 to study the full replication cycle of HEV in renal cell lines and primary renal cells. In addition, we evaluate the efficacy of commonly used direct acting antivirals. Moreover, we quantify renal biomarkers as proxy for kidney damage in patients with chronic HEV infection (Trial Number NCT03282474). Subsequently, we tested these patients for HEV RNA in urine, stool and blood and analysed sequence composition of viral populations to get insights into intra-host diversity and compartmentalization.

Results: Nine out of nine tested human kidney cell lines allow viral entry, replication and production of infectious progeny particles, indicating that HEV can propagate in kidney-derived cell lines. In addition, more authentic primary kidney cells also support HEV infection. Interestingly, in these cells and cell lines the broad-spectrum antiviral ribavirin was less effective in inhibiting HEV replication. We then identified patients with chronic infection and elevated renal biomarkers who tested positive for HEV RNA in blood, stool, and urine. Following, we performed phylogenetic analysis and mutational fingerprinting which showed diversification into sample specimen. In particular, urine-derived virus was divergent from blood- and faecal-derived virus.

Conclusion: In conclusion, renal cells support HEV propagation in vitro with reduced ribavirin sensitivity. In addition, HEV showed compartmentalisation into distinct clusters that correlated with sample type. Taken together, these data suggest extrahepatic replication of HEV, which may clinically serve as a reservoir for patient relapse.

TOP-384-YI

Macrophage-augmented organoids recapitulate the complex pathophysiology of viral diseases affecting the liver and devise advanced treatment strategies

Kuan Liu^{1,2}, Yining Wang¹, Jiajing Li¹, Jiahua Zhou¹, Ana Maria Gonçalves³, Zhe Dai⁴, Rick Schraauwen⁵, Kimberley Ober-Vliegen², Martin van Royen⁵, Monique M.A. Versteegen², Yijin Wang⁴, Harry L.A. Janssen^{1,6}, Maikel P. Peppelenbosch¹, Pengfei Li¹, Amaro Nunes Duarte-Neto³,

Luc van der Laan², Qiuwei Pan¹. ¹Department of Gastroenterology and Hepatology, Erasmus MC-University Medical Center, Rotterdam, Netherlands; ²Department of Surgery, Erasmus MC Transplant Institute, University Medical Center, Rotterdam, Netherlands; ³Departamento de Patologia, Faculdade de Medicina, Universidade de São Paulo, São Paulo, Brazil; ⁴School of Medicine, Southern University of Science and Technology, Shenzhen, Guangdong, China; ⁵Department of Pathology, Erasmus MC-University Medical Center, Rotterdam, Netherlands; ⁶Toronto Center for Liver Disease, Toronto General Hospital, University of Toronto, Toronto, Canada
Email: k.liu@erasmusmc.nl

Background and aims: The liver is a preferential site for hepatotropic and non-hepatotropic virus invasions. The pathophysiology of viral diseases is complex and often evokes strong inflammatory responses. Currently available in vitro models mainly recapitulate the viral life cycle per se, but fail to model immune cells (such as macrophages) mediated pathogenesis. This study aims to build macrophage-augmented organoids (MaugOs) that simultaneously recapitulate viral infection and the resulting inflammatory response, and to devise advanced treatment strategies.

Method: Human intrahepatic cholangiocyte organoids (ICOs) and hepatic macrophages were isolated from healthy donor tissues, and liver donor organ preservation fluid, respectively. Primary macrophages and THP-1 macrophages were derived from peripheral blood mononuclear cells and THP-1 monocyte cells, respectively. Organoids and different types of macrophages were integrated to form MaugOs. Two RNA viruses—hepatitis E virus (HEV) and SARS-CoV-2, and one DNA virus—monkeypox virus (MPXV), either primarily or secondarily affecting the liver, were taken as disease modalities.

Results: Time-lapse confocal showed ICOs and macrophages migrated and integrated into spheroids within 24 hours to form MaugOs. Immunofluorescent staining identified HEV transmission from initially infected ICOs to macrophages. A panel of inflammatory genes were activated in HEV-infected MaugOs. Integration of M1 (versus M0 or M2) polarized macrophages into HEV-infected organoids resulted in the strongest inflammatory response. This led to the effective killing of infected organoids and release of viruses into supernatant. In MaugOs, treatment of human bile inhibited HEV replication through the farnesoid X receptor and reduced inflammatory response partially through Takeda G protein-coupled receptor 5. The combination of NLRP3 inflammasome inhibitor and antiviral compound ribavirin simultaneously inhibited HEV replication and IL-1 beta production in MaugOs. Assessing the liver of a patient died from monkeypox, we observed MPXV infected hepatocytes, cholangiocytes and macrophages, triggering focal hepatitis. Consistently, hepatocyte differentiated and undifferentiated ICOs robustly supported productive infection of MPXV, which spread virus to macrophages and triggered inflammatory responses in MaugOs. Similarly, MaugOs were susceptible to SARS-CoV-2 infection and triggered a moderate inflammatory response.

Conclusion: MaugOs support the productive infections of these three viruses, which in turn triggered inflammatory responses. MaugOs can capture the multi-dimensions of viral pathophysiology, and enable the development of advanced treatment strategies aiming at simultaneously targeting the virus and inflammation.

SATURDAY 08 JUNE

SAT-337

Serum levels of IgA inform on the transcriptomic architecture of the liver and predict hepatocellular carcinoma in chronic viral hepatitis patients

Nicolaas Van Renne¹, Stijn Van Hees¹, Bart Cuypers², Arno Furquim d'Almeida¹, Axelle Vanderlinden¹, Pieter Meysman³, Jordan J. Feld⁴, Paloma Sangro⁵, Stefan Bourgeois⁶, Dirk Sprengers⁷, Geert Robaey⁸, Luisa Vonghia⁹, Peter Michiels¹⁰, Sven Francque¹⁰,

Bruno Sangro¹¹, Owen Cain¹², Ahmed M Elsharkawy¹³, Robert A. de Man¹⁴, Andre Boonstra¹⁴, Harry Janssen¹⁵, Ann Driessen¹⁶, Kris Laukens³, Thomas Vanwolleghem¹⁰. ¹Viral Hepatitis Research Group, Laboratory of Experimental Medicine and Pediatrics, Antwerp University, Antwerp, Belgium; ²Department of Biomedical Sciences, Institute of Tropical Medicine, Department of Computer Science, University of Antwerp, Antwerp, Belgium; ³Department of Computer Science, University of Antwerp, Antwerp, Belgium; ⁴Toronto Center for Liver Disease, Toronto General Hospital, University Health Network, Toronto, Canada; ⁵Liver Unit, Clínica Universidad de Navarra and CIBEREHD, Pamplona, Spain; ⁶Department of Gastroenterology and Hepatology, Antwerp University Hospital, Department of Gastroenterology and Hepatology, ZNA Stuivenberg, Antwerp, Belgium; ⁷Department of Gastroenterology and Hepatology, GZA Antwerp, Antwerp, Belgium; ⁸Hasselt University, Faculty of Health and Life Sciences, Hasselt, Belgium; ⁹Viral Hepatitis Research Group, Laboratory of Experimental Medicine and Pediatrics, Antwerp University, Department of Gastroenterology and Hepatology, Antwerp University Hospital, Antwerpen, Belgium; ¹⁰Viral Hepatitis Research Group, Laboratory of Experimental Medicine and Pediatrics, Antwerp University, Department of Gastroenterology and Hepatology, Antwerp University Hospital, Antwerp, Belgium; ¹¹Liver Unit, Clínica Universidad de Navarra and CIBEREHD, Pamplona, Belgium; ¹²Department of Cellular Pathology, University Hospitals Birmingham, Birmingham, United Kingdom; ¹³NIHR Birmingham Biomedical Research Centre, University Hospitals Birmingham, Liver Unit, Queen Elizabeth Hospital Birmingham, Birmingham, United Kingdom; ¹⁴Department of Gastroenterology and Hepatology, Erasmus Medical Center, Rotterdam, Netherlands; ¹⁵Toronto Center for Liver Disease, Toronto General Hospital, University Health Network, Toronto, Canada; ¹⁶Department of Pathology, Antwerp University Hospital, Antwerp, Belgium
Email: nicolaasvanrenne@hotmail.com

Background and aims: Chronic viral hepatitis B and C (HBV and HCV) associated hepatocellular carcinoma (HCC) requires early detection for curative treatment. Unfortunately, HCC surveillance with abdominal ultrasound frequently misses early HCC cases. Our goal was to discover biomarkers for determining personalized HCC risk.

Method: Using semi-supervised machine learning, an HCC risk signature was devised from RNA-seq data of liver biopsies from two international nested case-control cohorts of precancerous HBV and HCV patients (training cohort: n = 56, validation cohort n = 51). All patients underwent strict HCC surveillance, with median observation times of 8.5 years (IQR: 5.9–12.2) and 9.5 years (IQR: 6.3–14.6) respectively. An explainable AI-approach leveraged scRNA-seq and RNA-seq deconvolution to elucidate the cellular components defining HCC risk. Immunohistochemistry staining and spatial transcriptomics localized their distribution in the liver. Paired liver transcriptome and clinical data was queried for additional risk factors. A serum protein was measured in a consecutive patient cohort (n = 188, median follow-up 5.9 years, IQR: 3.1–9.3).

Results: In the training cohort, a Cox score capturing HCC risk was calculated for every gene. A leave-one-out-cross-validation retained a 557 gene risk signature. High-risk stratified patients were at higher risk of HCC compared to low-risk patients ($p = 1.82 \times 10^{-9}$, $p = 0.017$ and $p = 0.048$ in the respective training cohort, the validation cohort, and an external microarray cohort of HCV patients). HCC patients with a high-risk profile in non-tumoral adjacent tissue in two external cohorts (n = 82 and n = 228) were also more likely to develop HCC recurrence than low-risk patients ($p = 0.025$ and 0.030). The risk signature reflects the expansion of fibrovascular tissue, a decline in hepatocytes, and higher transcriptional activity of IgA plasma cells localized in the portal areas of the liver.

A paired liver transcriptome and serum IgA analysis showed that serum IgA is a proxy for the liver transcriptome, and a separate cohort (n = 188) demonstrated serum IgA predicts HCC. Patients aged ≥ 40 with advanced fibrosis and serum IgA ≥ 400 mg/dL had a risk of 22.5% of HCC within 3 years, ~3-fold higher than patients with serum IgA

150–400 mg/dL. Patients with serum IgA < 150 mg/dL were free from HCC. Notably, repetitive serum sampling in 62 patients showed serum IgA was stable within these thresholds over a median of 3.7 years (IQR: 1.4–8.0) of follow-up.

Conclusion: In chronic viral hepatitis, intrahepatic IgA plasma cells associate with future HCC development. Serum IgA is a stable, non-invasive HCC risk stratifier that can be integrated into a convenient personalized HCC risk assessment. When coupled to more sensitive imaging techniques, it may improve early detection and patient survival.

SAT-338-YI

Using retrieval augmented generation to increase large language models accuracy: a proof-of-concept pipeline on european hepatitis C virus (HCV) guidelines

Mauro Giuffrè¹, Simone Kresovic², Saveria Lory Croce³, Dennis Shung¹. ¹Department of Internal Medicine (Digestive Diseases), Yale School of Medicine, Connecticut, USA, New Haven, United States; ²Department of Engineering and Architecture, University of Trieste, Italy, Trieste, Italy; ³Department of Medical, Surgical, and Health Sciences, University of Trieste, Italy, Trieste, Italy
Email: gff.mauro@gmail.com

Background and aims: Large Language Models (LLMs) can potentially improve adherence to evidence-based medicine by providing clinical decision support. However, LLM responses to clinical questions are unstable and inaccurate. We propose a retrieval augmented generation (RAG) and prompt architecture pipeline to provide relevant and accurate responses based on published clinical guidelines regarding managing Hepatitis C Virus (HCV) infection.

Method: We created 15 questions about management recommendations for HCV derived from guideline text and non-text sources (i.e., graphical tables). We present an ablation study to demonstrate the differences in accuracy with each of the design choices in the pipeline and compare them to baseline GPT-4-Turbo using RAG based on the European Association for the Study of the Liver (EASL) guidelines on HCV with a structured format and accompanying custom prompt engineering and conversion of tables to lists. Our primary outcome is accuracy from text and non-text sources (i.e., digital image processing, DIP), with answers being graded as completely accurate vs. inaccurate by two expert hepatologists. The secondary outcome is to assess quantitatively the text similarity between expert-provided answers and LLM-provided answers using the OpenAI Score.

Results: The sole assessment of GPT-4 DIP performances initially resulted in 16% overall accuracy in extracting information from non-text sources. The customized LLM pipeline achieved 98.7% overall accuracy, which was significantly better than the GPT-4-Turbo alone (98.7% vs. 50.7%; $P < 0.001$). Incorporating in-context guidelines improved accuracy (72% vs. 50.7%; $P = 0.02$). When the in-context guidelines were cleaned, and tables were converted from images to csv files, accuracy improved to 80% (vs. 50.7%; $P < 0.001$); after the guidelines were formatted with a consistent structure and tables were re-formatted to lists, accuracy improved further to 92% (vs. 50.7%; $P < 0.001$). Finally, adding custom prompt engineering led to an improvement in accuracy of 98.7% (vs. 50.7%; $P < 0.001$), with no further improvement despite few-shot learning with 54 question-answer pairs. We also found systematic statistically significant differences in similarity metrics when the outputs of the in-context experiments were compared to the baseline outputs, as reported in (0.959 vs. 0.0945, $P < 0.001$). At the same time, we did not find any statistically significant difference when comparing similarity metrics across all the in-context experiments, not reflecting a discrepancy in accuracy when outputs were qualitatively graded by the experts.

Conclusion: Our study demonstrates the potential of LLMs to provide accurate clinical responses based on clinical guidelines. Our pipeline highlights the importance of appropriate guideline formatting for effective LLM integration in future clinical decision support systems.

SAT-339

Sequential administration of siRNA with an mRNA encoding clearance profile associated variants of HBsAg exhibits significant antiviral activity in AAV/HBV mouse model

Aditi Deshpande¹, Bharat Dixit¹, Aileen Rubio¹, Lei Qiugang², Sun Ya³.
¹ClearB Therapeutics, Concord, United States; ²Wuxi AppTech, Shanghai, China; ³Wuxi Apptech, Shanghai, China
 Email: adeshpande@clearbtherapeutics.com

Background and aims: We previously reported declines in serum HBsAg levels after administration of an mRNA vaccine comprised of two modified HBsAg sequences encoding functional cure epitopes [EASL 2024 poster #1450] in the Hydrodynamic tail vein injection (HDI) model of persistent Hepatitis B infection. It has been shown in preclinical studies that the effectiveness of therapeutic vaccines can be increased through the knockdown of HBsAg expression via siRNA (Michler, T., et al. 2020. *Gastroenterology* 158, pp1762–1775). In this study, the bivalent mRNA vaccine in combination with siRNA AD66810 (WO2018/195165; which targets the X gene expression in the HBV genome) was assessed for efficacy in AAV/HBV murine model.

Method: Male C57BL/6 mice were infected with AAV8 virus carrying 1.3 copies of the HBV genome (genotype D, serotype ayw) at 5×10^{10} viral genome equivalents to establish a stable infection of $\sim 4 \log$ IU/ml HBsAg (Yang D, et al 2014 *Cell Mol Immunol* 11 pp718). A single dose of siRNA AD66810 at 3 mg/Kg was given on day 0, followed by three biweekly intramuscular (IM) injections of mRNA vaccine given on days 14, 28 and 42 at dose levels of 1, 5 and 20 μ g. Mice were monitored over time for serological markers of HBsAg, HBV DNA and cellular immune response at end of study.

Results: Mice in the AAV/HBV model treated with siRNA AD66810 at 3 mg/Kg followed by 1, 5 or 20 μ g dose levels of mRNA displayed 1.2, 1.6 and 1.2 \log IU/ml HBsAg reduction respectively from baseline one-week post-last dose compared to 0.7 \log IU/ml HBsAg reduction seen in siRNA monotherapy group. The HBV DNA had similar trend in reduction as HBsAg in plasma. The mice in the placebo group resulted in no significant change in plasma HBsAg and HBV DNA levels over the study duration. The cellular immune response tested by ELISPOT demonstrated significantly higher splenocyte cells expressing IFN- γ compared to the siRNA monotherapy group.

Conclusion: Sequential administration of a single dose of siRNA AD66810 followed by therapeutic vaccination using mRNA encoding two modified HBsAg sequences was highly efficacious in an AAV/HBV murine model compared to siRNA monotherapy. These findings further support the development of combination therapy of anti-viral siRNA and therapeutic mRNA vaccination in Chronic Hepatitis B patients.

SAT-340-YI

Human intestinal enteroids as a new in vitro model to study hepatitis E virus

Nanci Santos-Ferreira¹, Xin Zhang¹, Johan Neyts¹, Suzanne J.F. Kaptein¹, Joana Rocha-Pereira¹. ¹KU Leuven-Department of Microbiology, Immunology and Transplantation, Rega Institute, Laboratory of Virology and Chemotherapy, Leuven, Belgium
 Email: nanci.ferreira@kuleuven.be

Background and aims: Hepatitis E virus (HEV) is an emerging viral pathogen responsible for acute viral hepatitis globally. No specific vaccines or antivirals against HEV (besides ribavirin) are available to date. This is partly due to fundamental limitations of its *in vitro* cultivation, a shared feature with other hepatotropic and enteric viruses. While HEV is an enteric virus transmitted fecal-orally and shed in high titers in the stool, little attention has been given to the role and contribution of the gut compartment in HEV-induced disease. HEV replication in primary intestinal cells and human liver-derived organoids has been reported (PMID: 31727684; 35044825). Viral dissemination between the gut and liver is poorly understood, and whether the gut functions as an HEV reservoir is unknown. To

tackle this and other knowledge gaps in HEV research, we developed an infection model for HEV using Human Intestinal Enteroids (HIEs). HIEs are tissue-derived non-transformed *in vitro* 3D cell cultures arranged in a crypt-villus structure that incorporate the physiological features of the intestinal epithelium, including the presence of different cell populations (enterocytes, goblet cells, enteroendocrine and Paneth cells).

Method: Human fetal ileum 3D-HIEs were used for infection with HEV gt 1 Sar55/S17, HEV gt 3 Kernow-C1 p6 (HEV-p6) strain or p6-G1634R (HEV-p6-R) that contains a fitness-enhancing mutation. HEV infection was performed employing: a) differentiated 3D-HIEs; b) differentiated 2D-HIEs in a transwell system; and c) electroporation of HIEs with full-length HEV capped RNA or HEV-p6-luciferase (luc) subgenomic RNA.

Results: Infection of 3D-HIEs with HEV-p6-R resulted in a $1 \log_{10}$ increase in HEV RNA up to 7 days post-infection (dpi) in an MOI-dependent manner, with replication peaking at 1 dpi. Infection of HIEs in transwell yielded similar replication levels, with shedding mainly to the apical side of the intestinal epithelial layer. Importantly, electroporation of HIEs with full length genome of HEV-p6 or HEV-p6-R resulted in a sustained increase in viral load over time, reaching 3.1×10^5 and 5.5×10^5 vRNA copies/ml, respectively, at 11 days post electroporation (dpe). Likewise, electroporation of HEV-p6-luc resulted in a 20-fold increase in luciferase signal at 11 dpe; a 5-fold increase was observed upon electroporation of HEV gt1 Sar55/S17-luc. Immunostainings of infected HIEs with a capsid-targeting antibody showed a strong presence of viral antigens.

Conclusion: We here successfully established an HEV cultivation model in HIEs, with electroporation being the most efficient method. We are now determining which specific intestinal cell types are infected. Our next goal is to establish a gut-liver axis model using an organ-on-chip system to gather information on HEV dissemination and host-pathogen interactions, which may advance the discovery of novel HEV therapeutics.

SAT-341

Discovery of a pan-genotypic hepatitis E virus replication inhibitor

Xin Zhang¹, Mara Klöhn², Sivi Ouwerkerk-Mahadevan³, Michelle Jagst⁴, Liesbeth Vereyken³, Peter Verboven³, Daniel Todt², Tim H.M. Jonckers³, Lotte Coelmont¹, Helen Fletcher⁵, Kirandeep Samby⁵, Anil Koul⁵, Johan Neyts¹, Eike Steinmann², Suzanne J.F. Kaptein¹. ¹KU Leuven Department of Microbiology, Immunology and Transplantation, Rega Institute for Medical Research, Laboratory of Virology and Chemotherapy, Leuven, Belgium; ²Department of Molecular and Medical Virology, Ruhr University Bochum, Bochum, Germany; ³Janssen Research and Development, Janssen Pharmaceutica N.V., Beerse, Belgium; ⁴Department of Molecular and Medical Virology, Ruhr University Bochum, Institute of Virology, University of Veterinary Medicine Hannover, Bochum/Hannover, Germany; ⁵Janssen Global Public Health, Janssen Pharmaceutica, Beerse, Belgium
 Email: xin.zhang@kuleuven.be

Background and aims: Hepatitis E virus (HEV; *Orthohepevirinae* subfamily within the *Hepeviridae* family) constitutes a substantial public health burden with around 20 million human infections annually, including 3.3 million symptomatic cases. Most importantly, appropriate treatment options for HEV-infected pregnant women and immunocompromised patients are lacking, underscoring the pressing requirement for the development of safe and efficacious pan-genotypic therapies to combat HEV.

Method: Different luciferase-based HEV subgenomic replicon systems were used to screen a small library of pre-selected molecules from an antiviral program at Janssen Pharmaceutica. Quantitative assessment of viral RNA replication was achieved by measuring the Gaussia luciferase (GLuc) reporter in cell culture supernatant. The antiviral effect of the selected hit compound on HEV infection was

corroborated by measuring viral antigens and viral RNA. Subsequently, the prophylactic and therapeutic efficacy of the compound was assessed in the athymic nude rat HEV infection model by assessing the viral kinetics in feces and the viral load in different tissues.

Results: We report on the identification of JNJ-64779117 which exerts nanomolar, pan-genotype antiviral activity against HEV in different cell types, including primary human hepatocytes (PHH). JNJ-64779117 is a nucleoside analogue and is assumed to target the viral polymerase as its 5'-triphosphate form. JNJ-64779117 has a promising pharmacokinetic and safety profile in both rats and dogs. In addition, the compound exhibited strong antiviral activity in the nude rat HEV infection model. Remarkably, initiating treatment 5 or 10 days after infection led to a rapid and significant reduction in viral load within 4 days. Moreover, at the highest dose, suppression of viral RNA levels in feces and liver tissue was effectively maintained until the end of the study at day 17 or 22 after treatment discontinuation. An additive effect was observed *in vitro* when combining JNJ-64779117 with ribavirin, a drug that is used off-label for the treatment of HEV infections.

Conclusion: Altogether, these results clearly illustrate the potential of JNJ-64779117 as a potent inhibitor of HEV across genotypes and the *Orthohepevirinae* subfamily. JNJ-64779117 may be an interesting candidate for the treatment of HEV infections.

SAT-342-YI

PegIFN α treatment in NUC-suppressed HBV/HDV-infected mice with high numbers of HDV-monoinfected cells reduces HDV infection below the limit of quantification

Annika Volmari^{1,2}, Tassilo Volz^{1,2}, Lena Allweiss^{1,2}, Marc Luetgehm^{2,3}, Simon Fletcher⁴, Meghan Holdorf⁴, Robert Muench⁴, Maura Dandri^{1,2}. ¹University Medical Center Hamburg-Eppendorf, I. Medical Department, Center for Internal Medicine, Hamburg, Germany; ²German Center for Infection Research (DZIF), Hamburg-Lübeck-Borstel-Riems site, Germany; ³University Medical Center Hamburg-Eppendorf, Institute of Microbiology, Virology and Hygiene, Hamburg, Germany; ⁴Gilead Sciences, Foster City, California, United States
Email: a.volmari@uke.de

Background and aims: Treatment of patients with chronic hepatitis D (CHD) remains challenging. The relative amounts and intrahepatic distribution of HBV+ and HDV+ cells may vary significantly. To which extent viral distribution is affected by current treatments and whether the intrahepatic virological landscape may also impact drug efficacy remain unclear. Nucleos(t)ide analogs (NUCs) suppress HBV replication and limit intrahepatic spread but do not target HDV, and it remains uncertain whether NUCs also affect HDV spread within the liver. PegIFN α is often used to treat CHD patients, and studies in immunodeficient humanized mice have demonstrated the ability of pegIFN α to suppress patient-derived HDV strains (Giersch, *JHEPRep* 2023). This study aimed to investigate how treatment with NUCs and pegIFN α impact HDV intrahepatic dissemination, replication activity, and persistence *in vivo* using human liver chimeric mice.

Method: Treatment of humanized mice with the NUC lamivudine (LAM, 0.4 mg/ml in drinking water) was started 3 weeks after HBV/HDV coinfection during the ramp-up phase of viral spreading. After 4 weeks of NUC treatment, one group of mice additionally received pegIFN α (i.p., 25 ng/g body weight) twice a week for 8 weeks, while the control group continued to receive LAM. Virological parameters were analyzed using qPCR and immunofluorescence (IF) staining. Mice stably infected with HBV and superinfected with HDV received 8 weeks pegIFN α for comparison.

Results: LAM treatment initiated during the spreading phase of both viruses reduced HBV DNA in the serum (Δ 1.2 log₁₀ in 4w) and slowed down the intrahepatic spread of HBV but had no effect on the ramp-up phase of HDV viremia (Δ 2.9 log₁₀; median HDV RNA 9×10^6 copies/ml). IF imaging showed strong HDV dissemination, resulting in large

areas harboring mono-infected HDV+ cells. ALT levels transiently increased during HDV spread and strongly correlated with HDV RNA in the serum ($r = 0.8047$; $p < 0.0001$). Adding pegIFN α reduced all HDV markers in serum and liver below the LLOQ by 8 weeks of treatment, while levels of intrahepatic HDV RNA did not decrease in animals not receiving pegIFN α (12w LAM). In contrast, 8-week pegIFN α treatment in HDV superinfected mice, where most human hepatocytes are HBV/HDV co-infected, only reduced intrahepatic HDV RNA by 0.5 log₁₀. Expression of human interferon-stimulated genes was enhanced during HDV spread in LAM-suppressed mice (ISG15 1.5 log₁₀) compared to pretreatment and increased further upon treatment with pegIFN α (ISG15 0.7 log₁₀).

Conclusion: NUC treatment in HBV/HDV co-infected mice during the viral ramp-up phase limits HBV intrahepatic spread but does not hinder further HDV dissemination. In a setting where HDV largely persisted in the absence of HBV co-infection, pegIFN α treatment profoundly impacted HDV, nearly clearing HDV infection.

SAT-343

Impact of hepatitis C virus direct acting antivirals on hepatocellular carcinoma evolution

Stanislas Pol^{1,2}, Laurent Lam³, Charlotte Mouliade^{1,2}, Fabrice Carrat^{3,4}. ¹AP-HP Centre Université Paris Centre, Groupe Hospitalier Cochin Port Royal, DMU Cancérologie et spécialités médico-chirurgicales, Service des Maladies du foie, Paris, France, Paris, France; ²Université Paris Cité, F-75006, Paris, France; ³Sorbonne Université, INSERM, Institut Pierre Louis d'Épidémiologie et de Santé Publique, IPLESP, Paris, France; Sorbonne Université, Department of Public Health, Paris, France; ⁴Sorbonne Université, Department of Public Health, Assistance Publique-Hôpitaux de Paris, Hôpital Saint-Antoine, Paris, France, Paris, France
Email: stanislas.pol@aphp.fr

Background and aims: The clinical impact of direct-acting antivirals (DAA) in patients with HCV-related hepatocellular carcinoma (HCC) remains unknown. We aimed to determine the potential benefits of DAA in patients with HCV-related HCC.

Method: We analyzed the French national health insurance system (Système National des Données de Santé-SNDS) which covers more than 99% of the French population. We identified patients with HCV-related HCC between 2013 and December 2021. The impact of DAA exposure after HCC diagnosis on overall mortality, liver transplantation (LT), and HCC recurrence after curative therapy were quantified using marginal structural models and inverse probability of treatment weighting (IPTW) accounting for time dependent exposure and confounders.

Results: Among the 4760 patients with HCV-related HCC, 2585 deaths (54.3%) occurred during the follow-up. The incidence and risk of mortality was reduced after DAA exposure (incidence rate (IR) of 306/1000 person-years (PY) before DAA exposure and 184/1000 PY after DAA exposure, adjusted hazard-ratio (aHR) 0.81; 95% CI 0.74–0.88; $p < 0.001$). A total of 418 LT (8.8%) was performed during the follow-up (IR of 35/1000 PY before DAA exposure and 34/1000 PY after DAA exposure, aHR 0.99; 95% CI 0.78–1.25; $p = 0.93$). DAA exposure was associated with a significant reduction of HCC recurrence in patients undergoing a curative therapy for HCC (aHR 0.53; 95% CI 0.28–0.98; $p = 0.04$). HCC relapse after HCC-related LT occurred in 52 patients out of 225 patients with LT after HCC and naive for HCV treatment. The incidence rates of HCC relapse after LT were 77/1000 PY of DAA exposure and 55/1000 PY of no DAA exposure (aHR 1.30, 95% CI 0.73, 2.33; $p = 0.37$).

Conclusion: After a first diagnosis of HCV-related HCC, DAA treatment, compared to no DAA treatment, was associated with a reduced risk of mortality in patients with HCV-related HCC and a reduced risk HCC recurrence after curative therapy for HCC. DAA exposure did not limit access to transplantation in patients with HCV-related HCC and was not found associated with an increased risk of HCC recurrence after LT. Our findings support the recommendation of DAA therapy in all cases of HCV-related HCC.

SAT-348-YI

Hepatitis B virus-induced collagen VI expression by hepatocytes contributes to liver fibrosis by promoting stellate cell activation

Zakaria Boulahtouf¹, Alessia Virzi¹, Lea Girard¹, Emma Gerdes¹, Julien Moehlin¹, Laura Heydmann¹, Sarah Durand¹, Marine Oudot¹, Fabio Giannone^{1,2,3}, Patrick Pessaux^{1,2,3}, Eloi Verrier¹, Thomas Baumert^{1,2,4}, Joachim Lupberger¹. ¹Institute for Translational Medicine and Liver Disease (ITM), Inserm U1110, Université de Strasbourg, Strasbourg, France; ²Pôle Hépatologie-digestif, Strasbourg University Hospitals, Strasbourg, France; ³Institut Hospitalo-Universitaire (IHU), Université de Strasbourg, Strasbourg, France; ⁴Institut Universitaire de France (IUF), Paris, France
Email: joachim.lupberger@unistra.fr

Background and aims: Chronic infection with hepatitis B virus (HBV) is a main cause of the progression of chronic liver disease from fibrosis to cirrhosis and cancer. Despite an efficient control of HBV infection by antivirals, liver disease can progress in patients. Whereas the HBV life cycle is well characterized, the understanding of virus-induced fibrosis and HCC is still only partially understood. Stellate cell activation to myofibroblasts differentiation is a hallmark of liver fibrosis characterized by collagen I and IV deposition to the extracellular matrix. Here we aimed to identify the molecular mechanisms of HBV-induced liver fibrosis and to uncover new therapeutic concepts targeting liver disease progression.

Method: Proteomic analyses of HBV-infected HepG2-NTCP cells were performed using liquid chromatography tandem mass spectrometry. Results were validated in primary human hepatocytes and studied mechanistically using cell culture, primary human stellate cells and hepatocytes and liver transcriptomics from HBV patients. The impact of viral proteins on signaling pathways and stellate cell activation were studied using lentiviral expression vectors, FACS and immunoblotting.

Results: Genome-wide proteomic analyses in infected cells revealed a dysregulation of signaling associated with extracellular matrix (ECM) remodeling during HBV infection. Among these we identified collagen VI being upregulated in HBV-infected hepatocytes (HepG2 and primary human hepatocytes) and secreted to the medium. Notably, COL6A1 silencing attenuated viral transcription, suggesting an immediate pro-viral role for collagen VI. By studying the effect of signaling inducers with link to chronic liver disease we revealed a functional link between Akt/mTOR signaling and collagen VI expression in hepatocytes. Studying the individual viral proteins, we found that predominantly HBs-expressing cells stimulated collagen VI expression. In HBV-infected patients, liver transcriptomic data showed significantly increased collagen VI levels associated with the severity of liver fibrosis. As collagens promote myofibroblast differentiation, we demonstrate that both, recombinant collagen VI and supernatants of hepatocytes overexpressing collagen VI activated patient-derived stellate cell isolates emphasizing the role of collagen VI in promoting hepatic fibrosis.

Conclusion: HBV infection of hepatocytes and HBsAg expression directly triggers Akt signaling and collagen VI secretion that contributes to stellate cell activation in the liver. Our proteomic atlas reveals a previously unrecognized role for collagen VI in HBV pathogenesis and disease biology. The understanding of these mechanisms will contribute to unravel novel therapeutic candidate targets for liver fibrosis and attenuation of cancer risk.

SAT-361

Generation and characterization of hepatitis D virus specific antisera with respect to the recognized epitopes

Keerthihan Thiyagarajah^{1,2}, Nirmal Adeel¹, Sascha Hein¹, Younes Husria³, Jan Raupach³, Johannes Miller³, Jonel Trebicka⁴, Sandra Ciesek⁵, Eberhard Hildt¹, Kai-Henrik Peiffer⁶. ¹Paul-Ehrlich Institute, Langen, Germany; ²J. W. Goethe University, Frankfurt am Main, Germany; ³Paul-Ehrlich-Institute, Langen, Germany;

⁴Universitätsklinikum Münster (UKM), Münster, Germany; ⁵Institute for Medical Virology, German Centre for Infection Research, External Partner Site Frankfurt, University Hospital, Goethe University Frankfurt am Main, Frankfurt am Main, Germany; ⁶Uniklinikum Münster, Münster, Germany
Email: keerthihan.thiyagarajah@pei.de

Background and aims: Hepatitis D virus (HDV), a defective RNA virus with estimated 60 million global infections induces the most severe form of viral hepatitis. To this day, many steps of the HDV life cycle remain enigmatic and diagnostic screenings are suboptimal leading to underestimation. Highly sensitive HDV-specific antibodies are urgently needed for research and diagnosis. Despite the necessity, only limited research is conducted on characterizing HDV specific antibodies. Thus, we first generated highly sensitive HDV-specific polyclonal antibodies and ultimately aimed to characterize the obtained antibodies with respect to the recognized epitopes.

Method: Since HDV only encodes for two protein isoforms termed S- and L-HDAg, which differ by a C-terminal extension in L-HDAg, we immunized two rabbits with purified S-HDAg either in its native or in a denatured form. Epitope mapping of obtained hyperimmune sera was performed using peptide arrays with 15 amino acid long overlapping synthetic peptides covering the full-length S-HDAg protein.

Results: Epitope mapping using the obtained hyperimmune sera revealed several highly reactive B-cell epitopes in S-HDAg. Interestingly, antisera obtained by immunization with denatured S-HDAg were more polyclonal as reflected by more recognized epitopes. For instance, one epitope localized within the oligomerization domain of S-HDAg was exclusively recognized during immunization with the denatured protein. Projection of this epitope into a 3D model of S-HDAg revealed steric shielding of the epitope in the native octameric state of the protein likely preventing recognition of the epitope by B-cells in the native state. In contrast to this, one epitope within the second arginine rich motif was also recognized during immunization with native S-HDAg, likely due to less steric hindrance and higher accessibility in the oligomeric state as reflected by the 3D model.

Conclusion: We identified highly immunogenic S-HDAg epitopes, which are accessible in the native conformation of S-HDAg and therefore are promising target sequences for the generation of highly sensitive HDAg-specific monoclonals useable for diagnosis and research. Synthetic/recombinant variants of these epitope sequences can even be used as potent vaccine candidates. Furthermore, the well characterized sera obtained in this study can be used for CLSM-based analysis of HDV life cycle and for Western blot and ELISA based quantitative analysis of HDAg.

SAT-362

Identification of IGF2BP1 as a novel host factor in regulating HBV RNA stability via N6-methyladenosine modification dependent manner

Deyao Li¹, Jing Ning², Xiangmei Chen³. ¹School of Basic Medical Sciences, Peking University Health Science Center, Beijing, China; ²Peking University Third Hospital, Beijing, China; ³School of Basic Medical Sciences, Peking University Health Science Center, Beijing, China
Email: xm_chen6176@bjmu.edu.cn

Background and aims: Hepatitis B virus (HBV) infection is the primary cause of chronic hepatitis B, cirrhosis, and hepatocellular carcinoma world widely. During HBV replication, HBV RNA undergoes post-transcriptional regulation by host cells which primarily relies on various host RNA binding proteins. However, the detailed mechanisms underlying post-transcriptional regulation of HBV RNA remain unknown. Herein, we investigated the role of RNA binding protein IGF2BP1 in the process of HBV replication.

Method: The host proteins associated with HBV Dane particles was analyzed by mass spectrometry. Gene silencing and ectopic over-expression were used to detect the function of IGF2BP1 in regulating

HBV replication. RNA turnover, RNA pull-down, and RNA immunoprecipitation assays were used to investigate the stability and binding between IGF2BP1 and HBV RNAs.

Results: Our study identified IGF2BP1 as an RNA binding protein that can be encapsulated into HBV Dane particles. According to the HBV replication cell model, the HBV infection cell model, and the HBV replication mouse model, we confirmed that IGF2BP1 promotes HBV replication. To elucidate the underlying mechanism, we found that IGF2BP1 enhanced the stability of all five HBV RNAs through its KH domain. IGF2BP1 recognized and bound to m6A modification sites on HBV RNAs, consequently promoted HBV RNA expression. This increased HBV RNA expression led to elevated protein expression and the formation of rcDNA, ultimately enhancing HBV replication.

Conclusion: Our study demonstrated IGF2BP1 as a critical host factor in enhancing the stability of HBV RNAs and facilitating HBV replication which provided a novel target for the development of anti-HBV drugs.

SAT-363

Hepatocellular carcinoma development post hepatitis C virus cure is associated with distinct changes in the dynamics of the soluble inflammatory milieu

Moana Witte^{1,2,3,4}, Carlos Oltmanns^{1,2,3,4}, Jan Tauwaldt^{1,2,3,4}, Hagen Schmaus^{1,2,3,4}, Jasmin Mischke^{1,2,3,4}, Leon Kalix^{5,6}, Gordon Grabert^{5,6}, Mara Bretthauer^{5,6}, Katja Deterding¹, Benjamin Maasoumy¹, Heiner Wedemeyer¹, Tim Kacprowski^{5,6}, Anke R.M. Kraft^{1,2,3,4}, Markus Cornberg^{1,2,3,4}. ¹Department of Gastroenterology, Hepatology, Infectious Diseases and Endocrinology, Hannover Medical School, Hannover, Germany; ²TWINCORE Center of Experimental and Clinical Infection Research, Hannover, Germany; ³German Center for Infection Research (DZIF), Hannover, Germany; ⁴Center for Individualized Infection Medicine (CiIM), Hannover, Germany; ⁵Braunschweig Integrated Centre for Systems Biology (BRICS), Technische Universität Braunschweig, Braunschweig, Germany; ⁶Division Data Science in Biomedicine, Peter L. Reichertz Institute for Medical Informatics of Technische Universität Braunschweig and Hannover Medical School, Braunschweig, Germany
Email: witte.moana@mh-hannover.de

Background and aims: Chronic hepatitis C virus (HCV) infection can lead to cirrhosis and an increased risk of developing hepatocellular carcinoma (HCC). Despite successful viral elimination by direct-acting antiviral therapy (DAA), some individuals may still experience sequelae such as HCC. In a previous study, we have demonstrated persistent changes in the inflammatory milieu in chronic HCV patients that are closely related to cirrhosis and the extent of liver damage (EASL 2023). In our current study, we aim to further decipher the role of inflammatory milieu changes and direct interactions in the development of HCC after viral elimination.

Method: The study cohort comprises 92 chronic HCV patients treated with DAA therapy at the Hannover Medical School and studied over several time points. 31 of the 92 patients developed HCC during (n = 3) or after DAA therapy (26/31 male, mean age 59, elastography 24.7 ± 18 kPa) and were compared to 61 propensity score-matched patients who did not develop HCC (52/61 male, mean age 58, mean elastography 33.5 ± 19 kPa). Plasma samples were available at baseline, end of treatment and long-term follow-up (median: 96 weeks), and plasma levels of 92 soluble immune mediators (SIM) were measured by Olink proteomics. 39 inactive HBsAg+ carriers served as controls to validate previous results.

Results: In both cohorts, over 25 SIM remained altered at follow-up compared to HBsAg+ carriers, confirming previous findings. Compared to patients who did not develop HCC, 14 SIM were significantly altered in patients who developed HCC (adjusted p value <0.05). 12 of the 14 SIM were elevated in patients who developed HCC, including hepatocellular growth factor (HGF), the interleukins IL6 and IL8 and the protease uPA, while SCF was decreased. A network analysis demonstrated close interactions between 9 out of the 14 SIM

and linked them to pathways in cancer or transcriptional misregulation in cancer (KEGG hsa05202, hsa05200). Patients who developed HCC after viral elimination showed different dynamics for HGF and IL8. Levels remained high during all time points in the HCC group, while patients who did not develop HCC showed a significant decrease over time (adjusted p value <0.05).

Conclusion: Our study validates prior data indicating that individuals with chronic HCV and cirrhosis maintain increased levels of various soluble immune mediators compared to controls. Specifically, the sustained persistence or absence of dynamics in plasma levels of HGF and IL8, recognized for their association with carcinogenesis, in patients developing HCC post HCV cure underscores the potential impact of the soluble inflammatory milieu on HCC risk following viral elimination.

SAT-364

Mathematical modeling of hepatitis B and D viral kinetics during coinfection in humanized mice suggests differences in their infectivity

Ashish Goyal¹, Takuro Uchida², Grace N Makokha³, Hiromi Abe-Chayama⁴, Yuji Ishida⁵, Chise Tatenos⁵, Harel Dahari¹, Kazuaki Chayama^{3,6}. ¹The Program for Experimental and Theoretical Modeling, Division of Hepatology, Department of Medicine, Stritch School of Medicine, Loyola University Chicago, Maywood, IL, United States; ²Department of Gastroenterology, Faculty of Medicine, Oita University, Yufu, Japan; ³Hiroshima Institute of Life Sciences, Hiroshima, Japan; ⁴Medical Specialist Graduate Education and Research, Hiroshima University, Hiroshima, Japan; ⁵PhoenixBio Co., Ltd., Hiroshima, Japan; ⁶RIKEN Center for Integrative Medical Sciences, Yokohama, Japan
Email: harel.dahari@gmail.com

Background and aims: Understanding of hepatitis D virus (HDV) and hepatitis B virus (HBV) dynamics during acute co-infection in humans is lacking due to the uncertainty of the exact time of infection and sparse kinetic data. We aim to provide insights into HDV/HBV acute co-infection by studying frequently sampled kinetic data in uPA/SCID mice with humanized livers from inoculation to steady state using a mathematical modeling approach.

Method: 4 mice were inoculated with co-infected serum of HDV RNA (6.0 log cp/ml) and HBV DNA (6.0 log cp/ml). HBV DNA and HDV RNA levels were frequently measured from blood samples up to 12 weeks post infection. Using the model selection theory, we identified a mathematical model that best reproduced the observed serum HBV and HDV kinetics. The model incorporated four different states of human hepatocytes (termed cells), (i) uninfected, (ii) HBV mono-infected, (iii) HDV mono-infected, and (iv) HBV/HDV co-infected. Cells were allowed to transition into infectious states by one virus at a time. Furthermore, in HBV and HBV/HDV infected cells, intracellular processes leading to the production of HBV virions was described as in [Hepatology 2023, 78 (Suppl.1): S530–S531]. This intracellular model included saturation in pre-genomic RNA (pgRNA) production from covalently closed circular DNA (cccDNA), and linear production rates of relaxed circular DNA (rcDNA) from pgRNA and rcDNA secretion. In contrast, HDV virions were assumed to be produced by co-infected cells at a constant rate. Several models exploring the impact on intracellular HBV processes by HDV in co-infected cells as well as differences in infectivity for different cell-infection status were tested. We fit the models to the observed serum viral data using a population, nonlinear mixed-effects approach.

Results: The serum kinetics of HBV and HDV in all 4 humanized mice was successfully recapitulated using the best model which assumed different infectivity based on virus and cell type. HDV infectivity of uninfected cells ($2 \times 10^{-11} \text{ day}^{-1} \cdot \text{copies}^{-1}$) is estimated to be ~40-fold lower compared to HBV infectivity of uninfected cells ($8 \times 10^{-10} \text{ day}^{-1} \cdot \text{copies}^{-1}$). Moreover, HBV infectivity of HDV mono-infected cells ($1.7 \times 10^{-3} \text{ day}^{-1} \cdot \text{copies}^{-1}$) is estimated to be many-fold higher compared to HDV infectivity of HBV mono-infected cells ($2.6 \times 10^{-9} \text{ day}^{-1} \cdot \text{copies}^{-1}$). Analysis also suggests that due to the

POSTER PRESENTATIONS

presence of HDV, cccDNA per infected cell accumulates to a lower level in co-infected cells (~1.9 copies) compared to HBV mono-infected cells (~5 copies). All parameters were identifiable in the best model.

Conclusion: Modeling suggests that different HBV and HDV infectivity of uninfected and mono-infected cells plays a pivotal role in reproducing the observed viral kinetics from infection to steady state in humanized mice.

SAT-365

Hepatitis B virus mutations associated with hepatocellular carcinomas are regulated by HLA genotype

Aiko Sakai¹, Masaya Sugiyama¹. ¹National Center for Global Health and Medicine, Ichikawa, Japan

Email: msugiyama@hosp.ncgm.go.jp

Background and aims: Several viral mutations have been reported as predictors of the risk of developing hepatocellular carcinoma (HCC) in chronic hepatitis B. In particular, the C1653T and A1762T/G1764A mutations in the core promoter region have been largely reported, but these mutations have sometimes not been reproduced, depending on study reports. The causes of the uncertain reproducibility remain unclear, in part because it is unclear whether it is due to differences in patient populations between studies. On the other hand, in GWAS-based analyses, several groups including ours have reported genetic polymorphisms in the HLA-DPB1 region in patients with HCC development, and the importance of HLA genotypes has attracted attention. In this study, patients were classified according to their HLA-DPB1 genotypes, and the patterns of HBV mutations associated with hepatocarcinogenesis were analysed.

Method: A total of 2996 cases were enrolled in this multicentre study in Japan. These included 408 cases of CHB, 307 cases of HCC and 2281 healthy subjects. In this study, among the HLA-DPB1 genotypes, we focused on HLA-DPB1*05:01 (about 40%) and HLA-DPB1*02:01 (about 20%), which are commonly carried by Japanese, and established four groups of homo- and heterozygotes of each. Within these four groups, HBV sequence comparisons were made between CHB and HCC matched for age, sex and HBV genotype.

Results: In the analysis of the patient carrying HLA-DPB1*05:01 as homozygote, the A1762T/G1764A mutation in the core promoter region was significantly detected in the HCC population compared to the CHB population ($p < 0.001$, OR = 8.8; 95%CI 4.4–17.8). In addition, the C1653T mutation was significantly detected in the HCC population with heterozygous HLA-DPB1*05:01 compared to the CHB population ($p < 0.001$, OR = 4.4; 95%CI 2.0–9.6). In contrast, analysis of the homozygous HLA-DPB1*02:01 population revealed a significant C129T mutation in the PreS2 region ($p < 0.02$, OR = 23.8; 95%CI 4.5–119.8). Similarly, analysis of the HLA-DPB1*02:01 heterozygote population revealed a significant C129T mutation in the PreS2 region ($p < 0.01$, OR = 33.1; 95%CI 11.3–96.5). The C129T mutation of the HBV genome in the PreS2 region was novel.

Conclusion: The pattern of HBV mutations associated with HCC development varies according to HLA genotype. Stratification using human disease-related genes partly explains why viral mutations differ between individuals. This stratification approach to risk assessment may lead to useful prognostication.

SAT-366

Immune correlates of HDV clearance in chronic HDV infected patients

Arshi Khanam¹, Abutaleb Ameer², Alip Ghosh³, Furkan Kaysin⁴, Cihan Yurdaydin⁵, Shyamasundaran Kottilil³. ¹Institute of Human Virology University of Maryland School of Medicine, Baltimore, United States; ²GW School of Medicine and Health Sciences, Washington DC, United States; ³Institute of Human Virology, University of Maryland

School of Medicine, Baltimore, United States; ⁴Koc University School of Medicine, Istanbul, Turkey; ⁵Koc University School of Medicine, Istanbul, Turkey

Email: akhanam@ihv.umaryland.edu

Background and aims: Chronic hepatitis delta (CHD) virus infection causes the most severe form of viral hepatitis due to rapid progression towards end-stage liver disease. In the presence or absence of antivirals, very few patients resolve CHD. An enhanced understanding of what derives the resolution of CHD infection is critical to project future therapeutic strategies. We aimed to investigate hepatitis D virus (HDV)-specific T cell responses to determine the immune correlates of HDV cure.

Method: We examined peripheral blood transcriptomic profiles of patients who are chronically infected with HBV and HDV (CHB/CHD-coinfection, $n = 39$) and compare them with those who cleared CHD (CHD-resolved, $n = 11$) and who cleared both CHB and CHD (CHB/CHD-resolved, $n = 3$) to identify molecular signatures that can predict the correlates of viral clearance and disease severity. Virus-specific (HBV and HDV) functions of peripheral T lymphocytes (CD4 and CD8 T cells) were also tested by flow cytometry.

Results: Transcriptomic profile revealed that MERTK, CDKN1C, RIPK3, and MECOM genes were significantly upregulated in CHB/CHD-coinfection likely contributing to inflammation, fibrosis and tumor development in these patients. While, patients with resolved CHD had upregulated gene expressions of immune recovery such as T cell receptor repertoire, HLA-DRA, CD28, and CD69, implying improved T cell functions associated with HDV clearance. Investigation of virus-specific T cell responses further revealed improved HDV-specific CD4/CD8 T cell functions in terms of IFN- γ (CD4: $p = 0.001$, CD8: $p = 0.0003$), TNF- α (CD4: $p = 0.0001$, CD8: $p = 0.0008$) and IL-21 (CD4: $p = 0.02$, CD8: $p = \text{ns}$) secretion in CHD-resolved patients than CHD-viremic individuals. The functional recovery of virus-specific T cells in CHD-resolved patients was primarily attributed to the presence of higher effector cells with reduced expression of exhaustion markers PD-1 and TIM-1 in CD4/CD8 T cells along with improved T cell proliferation. Patients with resolved CHB/CHD were also enriched in HBs and HDV-specific T cell functions. However, the recovery was lower than HDV-specific responses and seemed inadequate to clear CHB; suggesting robust HDV-specific T cell functions may have secondary response helping in CHB clearance. HDV-specific polyfunctional responses among CD4/CD8 T cells coproducing IFN- γ , TNF- α , IL-2 and IL-21, along with cytotoxic granules perforin and granzymeB were profound in CHB/CHD-resolved patients while a very few with resolved CHD had polyfunctional T cells.

Conclusion: HDV clearance is associated with presence of higher effector T cells producing robust HDV-specific polyfunctional cytokines while reflecting a transcriptional profile implying a broad anti-HDV peripheral immunity. Hence, these results may guide distinct correlates that define HDV functional cure with antiviral therapeutics.

SAT-367

HBV promotes viral replication and autophagic secretion through HBx down-regulation of HDAC6 expression

Lili Wu¹, Huiying Yu¹, Zhiliang Gao¹, Bingliang Lin¹. ¹Third Affiliated Hospital of Sun Yat-sen University, Guangzhou, China

Email: wulli23@mail.sysu.edu.cn

Background and aims: HDAC6 is an enzyme important for regulating microtubule protein deacetylation and participating in autophagic transport, and its role in HBV replication and autophagic secretion needs to be further elucidated.

Method: Twenty-eight patients with chronic hepatitis B who underwent liver puncture, 12 of them obtained HBsAg <0.05 IU/ml after treatment with pegylated interferon- α (PEG-IFN) combined with nucleotide analogs (NAs), 4 patients had HBsAg levels between 0.05–300 IU/ml after the same regimen, and 14 treatment-naïve

patients had HBsAg levels >300 IU/ml. HepG2, HepG2.2.15 cell line was used for experimental studies.

Results: The level of serum HBsAg was negatively correlated with the expression of HDAC6 in the liver tissue of the patients, in which the higher the level of serum HBsAg, the lower the level of HDAC6 in the liver of patients. HBV could significantly down-regulate HDAC6 expression by up-regulating the methylation level of the HDAC6 promoter region, and the results suggested that it was HBx rather than HBsAg or HBeAg that was involved in the above process. HBV inhibited viral autophagic degradation and promote viral autophagic secretion by up-regulating P62 and Rab11 levels, whereas HDAC6 overexpression was able to reverse the above results. Transcription of virus-associated RNA and replication of HBV DNA were found to be significantly enhanced after the use of HDAC6 selective inhibitor (ACY1215). HDAC6 may be a potential target for HBV antiviral therapy.

Conclusion: HBV promotes viral replication and autophagic secretion through HBx down-regulation of HDAC6 expression.

SAT-370

PRO-C3 determined active fibrogenesis is a predictor of liver-related outcomes in patients with chronic hepatitis C

Emilie Skovgaard^{1,2}, Thomas Møller^{1,3}, Morten Karsdal¹, Diana Leeming⁴, Keyur Patel⁵. ¹Nordic Bioscience A/S, Herlev, Denmark; ²Department of Biomedical Sciences, University of Copenhagen, Denmark, Copenhagen, Denmark; ³University of Copenhagen, Department of Biomedical Sciences, København N, Denmark; ⁴Nordic Bioscience A/S, Herlev; ⁵University Health Network, Toronto, Canada
Email: esk@nordicbio.com

Background and aims: Patients with untreated chronic hepatitis C (CHC) infection are at increased risk of developing a liver related outcome. Despite the availability of simplified direct acting antiviral therapy, the prevalence of CHC remains unchanged in many industrialized countries. Biomarkers that can predict which chronic liver disease patients with inflammatory injury are at greatest risk of developing a clinical outcome are required. In a study population from The Hepatitis C Antiviral Long-Term Treatment Against Cirrhosis Trial (HALT-C) (ClinicalTrials.gov #NCT00006164), we investigated the ability of PRO-C3 as a marker of active fibrogenesis to predict liver-related outcomes compared to METAVIR fibrosis stage on biopsy in patients with hepatitis C virus (HCV) who were non-responders to prior interferon-based standard-of-care.

Method: Serum levels of the fibrogenesis marker, nordicPRO-C3TM, was measured in stored serum samples using a competitive ELISA. Fibrosis stage was assessed by liver biopsy at baseline and end-of-study. Cox proportional hazard regression analysis was employed for investigation of the association between baseline PRO-C3 levels or METAVIR stage and risk of clinical outcome. Kaplan-Meier analysis was employed to examine the event-free survival probability when stratifying PRO-C3 into below and above the lower quartile (Q1 = 27.6 ng/ml) and METAVIR stage (F1-F2 vs F3-F4). Data provided by NIDDK CR, a program of the National Institute of Diabetes and Digestive and Kidney Diseases.

Results: This study population included a subgroup of 340 patients from the HALT-C cohort with a median age of 50 years, BMI of 29.4 kg/m², and 65% of the patients were male. Sixty-seven patients (20%) had a liver-related outcome over median follow-up 839 days (Q1-Q3: 474–1132). When dividing patients into baseline PRO-C3 above and below the Q1 cut-off, the Hazard Ratio (HR) for having an outcome was 3.71 times higher (95% CI = [1.60–8.57], $p < 0.01$) in patients with high baseline PRO-C3. For biopsy-determined fibrosis stage, the HR for having an outcome was 3.20 times higher (95% CI = [1.71–5.98], $p < 0.001$) in patients with F3–F4 compared to F1–F2. For METAVIR stage, F2–4, patients have an estimated HR of appr. 2% per ng/ml change in PRO-C3 for a liver-related outcome. No events occurred in patients with F1 at baseline.

Conclusion: Fibrosis activity, represented by the level of type III collagen formation (PRO-C3), is associated with an increased risk of

developing a liver-related outcome in patients with untreated HCV infection. PRO-C3 provided a higher risk predictor for outcomes than advanced fibrosis on biopsy. Pro-fibrogenic markers such as PRO-C3 could provide prognostic utility in other chronic liver disease patients with ongoing inflammatory injury.

SAT-371

No amino acid substitution in HBV PreS1, HDAG, or NTCP associated with suboptimal response to bulevirtide in combination with pegylated interferon alfa-2a treatment in participants with chronic hepatitis delta: results from MYR204 a phase 2b study

Yang Liu¹, Silvia Chang², Simin Xu², Ross Martin², Thomas Aeschbacher², Savrina Manhas², Roberto Mateo², Lindsey May³, Dong Han³, Tahmineh Yazdi³, Caleb Marceau³, Christopher Richards³, Pui Yan Ho³, Chunfeng Li³, Clarissa Martinez³, nadine peinovich³, Andrew Lopez³, Dmitry Manuilov³, Renee-Claude Mercier³, Audrey H. Lau³, Tarik Asselah⁴, Fabien Zoulim⁵, Evguenia Maiorova², Hongmei Mo². ¹Gilead Sciences, Foster City, United States; ²Gilead Sciences, foster city, United States; ³gilead, foster city, United States; ⁴Hôpital Beaujon AHPH, Université de Paris, INSERM, Clichy, France; ⁵Hospital Croix Rousse HCL, INSERM, Université Claude Bernard Lyon 1, Lyon, France
Email: yang.liu@gilead.com

Background and aims: Bulevirtide (BLV) is a novel entry inhibitor that binds to the HDV entry receptor, sodium taurocholate cotransporting polypeptide (NTCP), and is approved for the treatment of compensated chronic hepatitis D (CHD) in the EU. Although BLV is a highly potent HDV inhibitor, some patients have suboptimal virologic response likely due to viral and/or host mechanisms. Here, we describe virologic analysis results for participants with suboptimal response to BLV in a recently completed Phase 2b study MYR204 (NCT03852433), which evaluated finite treatment with BLV with or without peginterferon alfa-2a (PegIFN) in patients with CHD.

Method: A total of 174 participants with CHD were randomized (1:2:2:2) to receive (A) PegIFN for 48 weeks (W); (B) BLV 2 mg + PegIFN for 48 W; (C) BLV 10 mg + PegIFN for 48W, then BLV 2 mg (B) or 10 mg (C) monotherapy for 48 W; or (D) BLV 10 mg for 96 W. Participants were followed for 48 W after end of treatment (EOT). Virologic resistance analysis population (RAP) included on-treatment virologic non-responders (NR; HDV RNA decrease <1 log₁₀ IU/ml from baseline [BL] through EOT), participants with virologic breakthrough (VB; a ≥1 log₁₀ increase from nadir for ≥2 consecutive visits through EOT; or ≥2 consecutive HDV RNA ≥LLOQ if previously <LLOQ), participants with unconfirmed VB at EOT (EOT Blip), participants with persistent viremia with HDV RNA >100 IU/ml through EOT (PV), participants with post-treatment viral relapse (undetectable HDV RNA at EOT and detectable HDV RNA at follow-up Week 48 [FU48]) or viral rebound (detectable HDV RNA at EOT and ≥2 log₁₀ IU/ml increase in HDV RNA from EOT). Resistance testing included deep sequencing of HBV PreS1 and HDV hepatitis delta antigen (HDAG) coding regions, phenotypic analysis, and host NTCP polymorphism analysis.

Results: Resistance analysis was performed for 30 participants (NR, n = 1; VB, n = 25; EOT Blip, n = 4; PV, n = 6) through Week 96 (EOT) and 53 participants (relapse, n = 23; rebound, n = 30) at FU48 in Arms B/C/D. No amino acid substitutions at HBV PreS1 BLV region or HDV HDAG associated with reduced susceptibility to BLV were identified from any RAP participants from BL through FU48. The BL amino acid substitutions or emerged substitutions during treatment were also observed in virologic responders (VR; undetectable HDV RNA or a decline in HDV RNA ≥2 log₁₀ IU/ml from BL at EOT) and remained sensitive to BLV in vitro. The BLV EC₅₀ values from n = 124 BL samples in this study were similar across NRs, VBs, EOT Blips, PVs, and VRs. Three NTCP synonymous nucleotide changes were detected in RAP participants but were not associated with treatment outcome.

POSTER PRESENTATIONS

Conclusion: Suboptimal on-treatment response to BLV in combination with PegIFN as well as post-treatment viral relapse or rebound were not associated to amino acid substitutions in HBV PreS1, HDAg, or NTCP.

SAT-372

Study on the correlation between HLA-DR+CD38+CD8+ T cell changes and efficacy in the treatment of hepatitis B virus with interferon

Yanjie Lin¹, Shiyu Wang², Liu Yang², Xiaoyue Bi², Yao Xie³, Minghui Li³
¹Department of Hepatology Division 2, Peking University Ditan Teaching Hospital, Beijing, China; ²Department of Hepatology Division 2, Beijing Ditan Hospital, Capital Medical University, Beijing, China; ³Department of Hepatology Division 2, Peking University Ditan Teaching Hospital, Department of Hepatology Division 2, Beijing Ditan Hospital, Capital Medical University, Beijing, China
Email: wuhm2000@sina.com

Background and aims: Interferon (IFN) plays a dual role of direct antiviral and immune regulation in anti-hepatitis B virus (HBV) therapy. Some patients can obtain early hepatitis B surface antigen (HBsAg) response in the early stage of IFN treatment, but the decline of HBsAg level stagnates in the later stage, and the antiviral effect cannot be continued even if IFN treatment is continued. Currently, how to further explain the cause of this phenomenon from the immunological level is still a problem to be solved. Thus, we aim to investigate changes in phenotype and function of CD8⁺ T lymphocytes in chronic hepatitis B (CHB) patients undergoing IFN and correlation with clinical response.

Method: CHB patients were divided into three groups according to antiviral treatment. Peg-IFN α was then administered to Naïve group and nucleos (t) ide analogues (NAs)-treated group. For Plateau group, whose HBsAg decline reached a plateau, IFN therapy was stopped and was resumed after an interval. Peripheral blood samples were collected to detect clinical indexes, and T lymphocyte related phenotypes and functions using flow cytometry at corresponding detection points of three groups.

Results: A prospective cohort of 151 CHB patients participated in this study. During IFN treatment, HLA-DR⁺CD38^{dim} subset of CD8⁺ T cells increased and then markedly decreased, while the HLA-DR⁺CD38^{hi} subgroup increased significantly in both Naïve and NAs-treated groups (p all <0.0001). For Plateau group, the HLA-DR⁺CD38^{dim}CD8⁺ T cells increased significantly and the HLA-DR⁺CD38^{hi}CD8⁺ T cells greatly decreased after IFN intermittent treatment (p all <0.0001). The changes of HLA-DR⁺CD38^{dim} and HLA-DR⁺CD38^{hi} subsets during IFN intermittent treatment were strongly positively correlated with the changes of HBsAg during IFN retreatment, respectively ($r=0.4843$, $p=0.0066$; $r=0.4588$, $p=0.0315$). Compared with activated HLA-DR⁺CD38^{dim}CD8⁺ T cells, HLA-DR⁺CD38^{hi} subgroup expressed lower level of co-stimulatory molecules and killing ability.

Conclusion: IFN treatment made activated HLA-DR⁺CD38^{dim}CD8⁺ T cells gradually differentiated into HLA-DR⁺CD38^{hi} subset that indicated impaired killing function. IFN intermittent therapy can reverse this trend and help restore antiviral efficacy of IFN.

SAT-373

Intrahepatic sodium taurocholate co-transporting polypeptide gene transcript and membrane-localized protein expression changes in chronic hepatitis D patients following 48 weeks of treatment with Bulevirtide

Wildaliez Nieves¹, David Pan¹, Abhishek Aggarwal¹, Shiva Zabolli¹, Christina Moon¹, Lauri Diehl¹, Liyun Ni¹, Savrina Manhas¹, Hongmei Mo¹, Lena Allweiss², Dmitry Manuilov¹, Grace M. Chee¹, Renee-Claude Mercier¹, Jeffrey Wallin¹, Maura Dandri-Petersen²
¹Gilead Sciences, Inc., Foster City, United States; ²Department of Internal

Medicine, Center for Internal Medicine, University Medical Center Hamburg-Eppendorf, German Center for Infection Research (DZIF), Hamburg, Germany
Email: wildaliez.nieves@gilead.com

Background and aims: Bulevirtide (BLV), is an N-terminally myristoylated, Hepatitis B virus large envelope protein-derived, synthesized lipopeptide that binds specifically to the sodium taurocholate co-transporting polypeptide (NTCP) and acts as a potent, highly selective entry inhibitor of hepatitis D virus (HDV) into hepatocytes. We investigated whether 48 weeks (W48) of BLV treatment affects NTCP gene and protein expression.

Method: Participants from the ongoing MYR301 Phase 3 study were randomized in a 1:1:1 ratio to receive BLV 2 or 10 mg/day or no treatment (control) for W48. Bile acids (BA), alanine transaminase (ALT), and HDV RNA were assessed at all time points including baseline (BL) and W48. Virologic responders (VR) were defined as those with undetectable HDV RNA (<LLOQ, target not detected) or a decline in HDV RNA from BL of $\geq 2 \log_{10}$ IU/ml. A liver biopsy was performed at the screening visit in a subset of patients with a follow-up biopsy at W48. Approximately one-third of the biopsy was immersed in a tissue stabilizer at -20° C until processing for RNAseq ($n=48$). The remaining biopsy was formalin-fixed and paraffin embedded following standard procedures for a multiplex immunofluorescence assay including NTCP, sodium-potassium ATPase for cell membrane location and DAPI nuclear stain ($n=162$, BL and W48 matched). The image analysis, limited to hepatocytes, measured the median intensity of the NTCP membrane signal.

Results: Transcriptomics did not reveal any differences in NTCP gene expression between treatment arms ($p=0.42$) or response groups ($p=0.29$) at W48 compared to BL. The NTCP protein expression was similar between arms at W48. However, in participants treated with 2 mg (mean fold-change (FC) = 1.32; $p=0.030$) and 10 mg BLV (mean FC = 1.35; $p=0.016$), NTCP protein expression was elevated at W48 compared to BL as opposed to the control where no significant change was observed. When assessed by viral response subgroups, change from BL remained significant in the BLV-treated VR group ($p=0.0012$, $n=44$), but there were too few BLV-treated non-responders ($n=10$) to allow for a meaningful comparison. Furthermore, there was no observable difference in the \log_{10} fold-change in median NTCP protein expression for the two categories of ALT normalization at W48: (i) participants with ALT \leq ULN and (ii) those that had ALT > ULN. When correlating baseline, W48, and \log_{10} FC of BA levels, HDV RNA levels, and ALT normalization with NTCP protein expression, no significant correlations were observed.

Conclusion: Our results suggest that BLV treatment does not alter NTCP gene expression but may increase NTCP protein levels in the plasma membrane of hepatocytes. BL NTCP and changes in NTCP protein levels do not appear to be a predictor of HDV viral load or BA and ALT changes over W48 of treatment. Further analysis is needed to confirm these findings and determine the potential impact, if any, on clinical outcome.

SAT-374-YI

IL-15 plus anti-PDL-1 restores CD8 T-cell response against core but not against polymerase in chronic hepatitis B with extreme exhaustion-associated factors

Henar Calvo Sánchez^{1,2,3}, Julia Peña Asensio⁴, Joaquín Míquel^{2,4}, Eduardo Sanz-de Villalobos^{5,6}, Alberto Delgado⁴, Miguel Torralba^{4,7,8}, Alejandro González Praetorius^{4,9}, Juan Ramón Larrubia^{2,5,8}. ¹Group of Research in Translational Cellular Immunology (GITIC). IDISCAM, Guadalajara, Spain; ²Section of Gastroenterology and Hepatology. Guadalajara University Hospital, Guadalajara, Spain; ³Departament of Medicine and Medical Specialties. University of Alcalá, Alcalá de Henares, Spain; ⁴Group of Research in Translational Cellular Immunology (GITIC). IDISCAM, Guadalajara, Spain; ⁵Group of Research

in Translational Cellular Immunology (GITIC). IDISCAM., Guadalajara, Spain; ⁶Section of Gastroenterology and Hepatology, Guadalajara University Hospital., Guadalajara, Spain; ⁷Service of Internal Medicine, Guadalajara University Hospital., Guadalajara, Spain; ⁸Department of Medicine and Medical Specialties, University of Alcalá, Alcalá de Henares, Spain; ⁹Section of Microbiology, Guadalajara University Hospital., Guadalajara, Spain
Email: henarcs@hotmail.com

Background and aims: Restoring the functionality of proliferative progeny (PP) in e-Ag (-) chronic hepatitis B (CHBe (-)) could be achieved by rebalancing energy supply and demand in activated progenitor (AP) HBV-specific CD8 T-cells. IL-15 could readjust cellular metabolism, potentially aiding in achieving a functional cure. The aim of the study was to evaluate the ability of IL-15 combined with anti-PD-L1 to restore the functionality of HBV-specific CD8 T-cell response as a function of the degree of cellular exhaustion estimated by a predictive model using clinical variables (Peña Asensio et al, Aliment Pharmacol 2023).

Method: The predictive model estimated the exhaustion level of HBV-specific CD8 cells in CHBe (-) patients treated with nucleos (t)ide (NUC) analogues. HBV-specific CD8 cells were visualized by pentameric technology. After Ag-specific stimulation, AP and PP were detected by TCF1 staining and forward scatter level. Analysis included the metabolic profile, memory phenotype, and mTORC1 activation in APs. The effector capacities in PP (proliferation, interferon- γ , tumour necrosis factor- α and CD107a) were evaluated. The role of IL-15 \pm anti-PD-L1 in remodelling the metabolic profile and enhancing effector function was assessed. Analyses were performed by flow cytometry.

Results: The quiescent progenitor (PQ [TCF1+/FSClow]) HBV-specific CD8+ cells showed a memory-like phenotype. After Ag encounter, the generated AP [TCF1+/FSChigh] subset maintained the PD1+/CD127+ phenotype and gave rise to PP ([TCF1-/FSChigh]). In AP cells, IL-15 compared to IL2 decreased the initial mTORC1 boost, but maintained its activation longer, linked to a catabolic profile that correlated with functional improvement of PP. In CHBe (-) cases treated with NUC, the AP subset showed an anabolic phenotype associated with dysfunctional PP. In CHBe (-) cases with low probability of restoration of HBV-specific CD8 cells during NUC treatment, IL-15/anti-PD-L1 treatment restored reactivity of the HBV-core but not HBV-polymerase-specific CD8 T-cell response, whereas cases with high probability of restoration recovered functionality spontaneously during treatment.

Conclusion: In patients with poor prognosis factors for HBV-specific CD8 T-cell response restoration, combined IL-15 and anti-PD-L1 treatment could improve the energy balance of the PA pool, associated with recovery of PP against core but not against polymerase. CHBe (-) patients with favorable prognostic factors for restoration spontaneously recover this effector response during treatment.

SAT-375

Proteomic analysis of plasma exosomes: a novel method to identify potential therapeutic targets for chronic hepatitis B

Meng Zhao¹, Saisai Zhang¹, Danny Ka-Ho Wong¹, Lung-Yi Mak^{1,2}, Judy Wai-Ping Yam³, Cherlie Lot-Sum Yeung³, Rex Wan-Hin Hui¹, Man-Fung Yuen^{1,2}, Wai-Kay Seto^{1,2}. ¹Department of Medicine, School of Clinical Medicine, The University of Hong Kong, Hong Kong, China; ²State Key Laboratory of Liver Research, The University of Hong Kong, Hong Kong, China; ³Department of Pathology, School of Clinical Medicine, The University of Hong Kong, Hong Kong, China
Email: mengz014@connect.hku.hk

Background and aims: Chronic hepatitis B (CHB) is characterized by an exhausted immune response against the virus. A possible mechanism is communication between hepatitis B virus (HBV)-infected hepatocytes and the host's immune system via exosomes, contributing to immune-dysregulation in CHB. However, studies of the role of exosomes in CHB are scarce and do not consider the

different CHB disease phases. We aimed to investigate the changes in plasma proteome in CHB patients and healthy controls.

Method: We recruited treatment-naïve CHB patients of different disease phases and healthy controls. Exosomes were isolated from plasma using ultracentrifugation method (Optima XL-80 K, Beckman Coulter, United States). Data-independent acquisition (DIA) mass spectrometry was performed to detect the dynamic profiles of exosome proteins. Bioinformatics and annotation analyses of top differentially expressed proteins (DEPs) were performed using Gene ontology (GO) Enrichment Analysis and Kyoto Encyclopedia of Genes and Genomes (KEGG) Analysis. The types and proportions of infiltrating immune cells were detected by immune filtration analysis using CIBERSORT.

Results: In this interim analysis involving 10 healthy controls and 30 CHB patients (10 HBeAg-positive, 10 HBeAg-negative, and 10 CHB patients with hepatitis B surface antigen [HBsAg] seroclearance), 2142 exosome proteins were identified, of which 128 proteins were significantly altered in CHB vs. healthy controls (fold change >2 or <0.5, all $p < 0.05$). The most significant DEPs were observed with CIT, KRTDAP, KRT16 and HM13 (fold change = 176.422, 13.774, 0.123 and 0.078 respectively, $p < 0.05$). When comparing HBsAg-positive patients with CHB patients achieving HBsAg seroclearance, 95 significant DEPs (87 downregulated and 8 upregulated proteins) were detected. GO analyses revealed these DEPs to be enriched in multiple immune-related processes; KEGG analyses showed their involvement in the estrogen signaling pathway ($p = 0.002$). When compared to HBsAg-positive patients, CHB patients with HBsAg seroclearance, had a significantly increased fraction of activated dendritic cells (0.006 ± 0.010 vs. 0.028 ± 0.027 , $p = 0.026$) and eosinophils (0 vs. 0.002 ± 0.004 , $p = 0.047$), while resting dendritic cells were significantly decreased (0.041 ± 0.019 vs. 0.024 ± 0.021 , $p = 0.045$). No significant difference was observed between patients with HBsAg seroclearance and healthy controls through immune infiltration.

Conclusion: Plasma exosomes of CHB patients contain proteins associated with host immune response. The estrogen signaling pathway may potentially be associated with HBsAg seroclearance. Annotation of plasma exosomes can potentially identify serum markers in different CHB disease phases and effectors that trigger immunity against HBV. This can be a potential method of identifying novel CHB therapeutic targets.

SAT-376

Hepatitis C virus specific CD8+ T cells of patients with acute and chronic HCV infection display high expression of CD96 and other co-inhibitory molecules

Maximilian Knapp¹, Christin Ackermann^{2,3}, Leon Cords¹, Tim Westphal⁴, Julian Schulze zur Wiesch^{5,6}. ¹University Medical Center Hamburg-Eppendorf, I. Department of Medicine, Gastroenterology and Infectious Diseases Unit, Hamburg, Germany; ²Institute of Hematopathology Hamburg (HpH), Hamburg, Germany; ³University Medical Center Hamburg-Eppendorf, I. Department of Medicine, Gastroenterology and Infectious Disease Unit, Hamburg, Germany; ⁴University Medical Center Hamburg Eppendorf, Hamburg, Germany; ⁵University Medical Center Hamburg-Eppendorf, I. Department of Medicine, Gastroenterology and Infectious Diseases Unit, Hamburg, Germany; ⁶Deutsches Zentrum für Infektionsforschung (DZIF), Braunschweig, Germany
Email: knapp_maximilian@t-online.de

Background and aims: The Hepatitis C virus-specific T cell response exhibits significant differences in function and phenotype during acute and chronic as well as in spontaneously resolved, and successfully DAA-treated HCV infection. It was previously described that levels of soluble CD96, a surface protein that was first described as a late activation marker, but also as a marker of leukemic stem cells and a target of oncological antibody therapies, were increased in patients with chronic Hepatitis B and cirrhosis (Gong et al., Clin Exp

POSTER PRESENTATIONS

Immunol, 2009). Furthermore, CD96 shares CD155 as a ligand with TIGIT, an inhibitory co-receptor also expressed on HCV-specific T cells. The current study aimed to define the characteristics of HCV-specific (HCVs) CD8⁺ T cells with a focus on the CD96-CD155-TIGIT axis at different stages of infection.

Method: Research was undertaken using class I MHC tetramers on CD8⁺ T cells specific to HCV in 38 individuals with HLA-A*01:01, *02:01, and *24:02 genotypes. A 21-color flow cytometry panel was used to evaluate the expression patterns of surface proteins CD3, CD4, CD8, CD28, CD38, CD39, CD62L, CD69, CD73, CD96, CD127, TIGIT, PD-1, Slamf6, and transcription factors T-bet, TCF1, NR2F6, TOX and IRF4. Flow cytometry data were analysed using FlowJo10. Data were clustered using UMAP and FlowSOM. GraphPad Prism10 was used for statistical analysis.

Results: Frequencies of HCVs CD8⁺ T cells expressing PD-1 (mean 27.7% vs. 51.5%, $p < 0.001$) and TIGIT (mean 45.1% vs. 57.1%, $p = 0.0014$) were elevated compared to bulk CD8⁺ T cells. Moreover, HCV-specific CD8⁺ T cells also showed significantly higher frequencies of CD96-expressing cells compared to bulk CD8⁺ T cells (mean 10.8% vs. 41.0%, $p < 0.001$) irrespective of the disease stage. Analysing the frequencies of functional subsets within HCVs CD8⁺ T cells of CD96⁺ and CD96⁻ populations revealed significant differences of CD62L⁻ CD127⁻ effector (mean: 26, 5% vs. 29, 7%, $p = 0.0243$) and CD62L⁺ CD127⁻ intermediate (mean: 4, 4% vs. 13, 5%, $p < 0.001$) subsets. Moreover, CD96⁺ HCVs CD8⁺ T cells showed higher frequencies of IRF4⁺ (mean: 98, 4% vs. 94, 3%, $p = 0.0002$), TCF1⁺ (mean: 29, 7% vs. 20%, $p < 0.0001$) and TOX⁺ (mean: 26, 3% vs. 20, 8%, $p = 0.0001$) cells compared to CD96⁻ HCVs CD8⁺ T cells. Within the HCVs CD8⁺ T cells, diverse clusters were identified, with CD96 standing out as a distinctly expressed marker of HCV-specific T cells with exhaustive phenotype. **Conclusion:** Our study reveals a significant increase of CD96⁺ HCVs CD8⁺ T cells with co-expression of known co-inhibitory markers. Furthermore, we measured different frequencies of IRF4⁺, TCF1⁺ and TOX⁺ T cell subsets between CD96⁺ and CD96⁻ HCVs CD8⁺ T cells. CD96⁺ is potentially an additional druggable co-inhibitory checkpoint of exhausted T cells in human viral and oncological diseases with therapeutic potential.

SAT-377

CRISPR-Cas13b-mediated suppression of hepatitis B surface antigen-pre-clinical investigations of a new therapeutic approach

Laura McCoullough^{1,2}, Mohamed Fareh^{3,4}, Wenxin Hu^{3,4}, Vitina Sozzi¹, Christina Makhoul¹, Yianni Droungas^{1,2}, Chee Leng Lee¹, Hans Netter¹, Mina Takawy^{1,5}, Sharon Lewin^{5,6,7}, Damian Purcell², Jacinta Holmes⁸, Joseph Trapani^{3,4}, Margaret Littlejohn^{1,5}, Peter Revill^{1,5} ¹Victorian Infectious Diseases Reference Laboratory, Royal Melbourne Hospital, at the Peter Doherty Institute for Infection and Immunity, Melbourne, Australia; ²Department of Microbiology and Immunology, University of Melbourne, at the Peter Doherty Institute for Infection and Immunity, Melbourne, Australia; ³Cancer Immunology Program, Peter MacCallum Cancer Centre, Melbourne, Australia; ⁴Sir Peter MacCallum Department of Oncology, The University of Melbourne, Melbourne, Australia; ⁵Department of Infectious Diseases, University of Melbourne at the Peter Doherty Institute for Infection and Immunity, Melbourne, Australia; ⁶Victorian Infectious Diseases Service, Royal Melbourne Hospital at the Peter Doherty Institute for Infection and Immunity, Melbourne, Australia; ⁷Department of Infectious Diseases, Alfred Hospital and Monash University, Melbourne, Australia; ⁸Department of Gastroenterology, St. Vincent's Hospital, Melbourne, Australia
Email: laura.mccoullough@mh.org.au

Background and aims: Low hepatitis B surface antigen (HBsAg) levels are associated with better clinical outcomes, and may be key to achieving a HBV functional cure. The HBV RNAs represent a potential target for new treatments to reduce HBsAg, which has been highlighted by RNA interference and antisense oligonucleotide studies.

CRISPR-Cas13b endonuclease, naturally used by bacteria to target and suppress bacteriophage RNAs, has been repurposed to target RNAs in mammalian cells. Cas13b has high specificity due to its 30-nucleotide guide RNA (gRNA) which reduces the possibility of off-target effects. Here, in a world first study, we targeted the HBV RNAs using CRISPR-Cas13b to reduce HBsAg *in vitro* and *in vivo*.

Method: gRNAs were designed to target either the 5' or 3' end of the HBV pregenomic RNA (pgRNA). HepG2 cells were transfected with WT HBV clones of multiple genotypes, and plasmids expressing Cas13b-BFP and gRNAs. The replication phenotype of WT HBV was determined five days post-transfection. HepAD38 cells were transfected with Cas13b-BFP and gRNA plasmids and secreted HBeAg and HBsAg was measured. In a pilot experiment, WT HBV, Cas13b and gRNA plasmids were simultaneously hydrodynamically injected into CBA mice and sera HBsAg was measured one week post-HDI.

Results: Cas13b strongly suppressed HBV replication and significantly reduced secreted HBeAg and HBsAg by 95% in HepG2 cells. The effect was pan-genotypic. Despite low transfection efficiency, Cas13b reduced secreted HBsAg in HepAD38 cells. Finally, the *in vivo* pilot experiment showed that sera HBsAg was transiently reduced by ~50% when Cas13b was co-injected with WT HBV.

Conclusion: The HBV RNAs were successfully targeted and degraded using CRISPR-Cas13b to significantly reduce HBsAg in cell culture and *in vivo*, demonstrating its potential as a novel treatment option for chronic HBV infection.

SAT-378

Association between occult hepatitis B virus infection and parenchymal renal cell carcinoma

Daniele Lombardo¹, Marta Rossanese², Cristina Musolino³, Giuseppina Raffa⁴, Giuseppe Caminiti⁵, Carlo Saitta⁶, Giuseppe Mucciardi², Michele Chiappetta⁶, Maurizio Martini⁶, Antonio Ieni⁶, Vincenzo Ficarra¹, Giovanni Raimondo⁷, Teresa Pollicino⁸ ¹University Hospital G. Martino Messina, Messina, Italy; ²University Hospital G. Martino Messina, Messina, Italy; ³University Hospital "G. Martino" Messina, Messina, Italy; ⁴University Hospital "G. Martino" of Messina, Messina, Italy; ⁵University of Messina, Messina, Italy; ⁶University Hospital of Messina, Messina, Italy; ⁷Division of Medicine and Hepatology, University Hospital of Messina, Messina, Italy; ⁸University Hospital "G. Martino" of Messina, Messina, Italy
Email: tpollicino@unime.it

Background and aims: There is increasing evidence of an association between chronic kidney disease and HBV infection, including cases of occult HBV infection (OBI), which refers to the long-term persistence of HBV genome in individuals who test negative for HBsAg. In addition, an increased incidence of renal cell carcinoma (RCC) has been observed in HBsAg-positive individuals, although data on the prevalence of RCC in OBI individuals remain unexplored. The aims of this study were (1) to determine the prevalence of OBI in patients diagnosed with RCC, and (2) to investigate the molecular characteristics of HBV in both tumour and non-tumour renal tissues.

Method: We conducted a prospective study that included consecutive HBsAg-negative patients who underwent nephrectomy for malignant kidney tumours at the Department of Urology, University Hospital of Messina, from April 2019 to May 2021. For comparison, we included a control group (CG) of patients who underwent nephrectomy for benign kidney tumours. At the end of each surgery, we collected paired samples of tumour and adjacent non-tumour kidney tissue. These samples were then divided; one part was used for histological examination and the other was immediately frozen and stored for molecular analysis. Serum samples were also collected from each patient and stored at -80°C. The study was approved from the local ethics committee. Informed consent was obtained from each participant to the study. To detect and characterise HBV infection in tissue samples, we used highly sensitive PCR approaches to detect total HBV, HBV cccDNA and HBV

RNA. High-throughput hepatitis B virus integration sequencing (HBIS) was also used to investigate HBV DNA integration.

Results: The study recruited 83 HBsAg-negative patients, including 54 with renal cell carcinoma (RCC) and 29 with benign kidney tumours (CG). None of these patients showed clinical, biochemical, or ultrasound signs of liver disease. OBI was found in 19/54 (35.2%) RCC patients and in 1/29 (3.4%) CG patients ($p=0.001$). OBI was not detected in any serum samples from either RCC or CG patients. Among the RCC cases, 36/54 had clear cell renal cell carcinoma (ccRCC), and 18/54 had either papillary or chromophobe RCC. OBI occurred in 9/36 (25%) ccRCC cases and in 10/18 (55.5%) non-ccRCC cases ($p=0.03$). Further molecular investigations revealed the presence of both the HBV cccDNA and integrated HBV DNA in renal tissues from patients with OBI.

Conclusion: Occult HBV infection (OBI) shows a significant association with renal cell carcinoma (RCC), particularly with non-clear cell RCC (non-ccRCC) histotypes. The identification of replication-competent HBV cccDNA and integrated HBV DNA in both tumour and non-tumour renal tissues suggests the potential for HBV replication within renal cells.

SAT-379

Immune checkpoint proteins are associated with persistently elevated liver stiffness after successful HCV therapy in people with HIV

Rubén Martín-Escolano¹, Ana Virseda-Berdeses¹, Juan Berenguer², Juan Gonzalez², Oscar Brochado-Kith¹, Amanda Fernández Rodríguez¹, Cristina Díez², Víctor Hontañón³, Salvador Resino García¹, María Ángeles Jiménez Sousa¹. ¹Instituto de Salud Carlos III, Centro Nacional de Microbiología, Majadahonda, Madrid, Spain; ²Hospital General Universitario "Gregorio Marañón," Madrid, Spain; ³Hospital Universitario La Pa, Madrid, Spain
Email: r.martin@isci.es

Background and aims: Hepatic cirrhosis remain the main complication of hepatitis C virus (HCV) infection despite the novel direct-acting antiviral (DAA) therapy, being accelerated by the human immunodeficiency virus (HIV). Alternatively, several immune checkpoint proteins are upregulated and correlated with cirrhosis progression. Here, we aimed to evaluate the association of plasma immune checkpoint proteins one year after successful completion of HCV treatment with persistently elevated liver stiffness (liver stiffness measurement (LSM) ≥ 12.5 kPa) five years after HCV treatment in people with HIV (PWH).

Method: We performed a retrospective study in 39 HIV/HCV-coinfected patients with advanced fibrosis or cirrhosis who achieved sustained virologic response (SVR). Plasma samples were collected one year after treatment, and immune checkpoint proteins and inflammatory biomarkers were analyzed using a Luminex 200TM analyzer. The statistical association analysis used Generalized Linear Models (GLM) with gamma distribution. Correlation between significant immune checkpoint proteins and inflammatory biomarkers was performed using the Spearman correlation test.

Results: There was a downward trend in the value of LSM years after the completion of successful HCV treatment, but it was not significant because there was wide variability among PWH. In this regards, 61.5% of patients showed persistently high liver stiffness five years after HCV treatment. Higher plasma baseline levels of BTLA (aAMR = 1.49; $q=0.022$), PD-1 (aAMR = 1.49; $q=0.022$), and TIM-3 (aAMR = 1.28; $q=0.039$) one year after successful treatment was associated with persistently elevated liver stiffness five years after HCV treatment. These significant immune checkpoints were correlated to inflammatory biomarkers in PWH who had persistently elevated liver stiffness. BTLA and PD-1 correlated negatively with IL-1RA ($p=0.018$ and $p=0.049$, respectively), PD-1 correlated positively with IP-10 ($p=0.028$), and TIM-3 correlated positively with IL-8 ($p=0.018$).

Conclusion: Elevated plasma levels of immune checkpoint proteins were associated with persistently elevated liver stiffness five years

after HCV eradication, particularly BTLA, PD-1, and TIM-3, suggesting a potential immunopathological role in persistently elevated liver stiffness after HCV eradication in PWH.

SAT-380

Burden of acute hepatitis A in France-a 10-year nationwide study

Charlotte Mouliade^{1,2}, Anne Marie Roque-Afonso³, Lucia Parlato^{1,2}, Nathalie Goutte⁴, Samir Bouam⁵, Philippe Sogni^{1,2}, Stanislas Pol^{1,2}, Vincent Mallet^{1,2}. ¹AP-HP, Centre Université Paris Centre, Groupe Hospitalier Cochin Port Royal, DMU Cancérologie et spécialités médico-chirurgicales, Service des Maladies du foie, Paris, France; ²Université Paris Cité, F-75006, Paris; France; ³Université Paris Saclay, INSERM U1193; AP-HP, Hôpital Paul Brousse, National Reference Center for Hepatitis A, Villejuif, France; ⁴INSERM U1193; APHP, Hôpital Paul Brousse, Direction des soins, Villejuif, France; ⁵AP-HP, Centre Université de Paris, Groupe Hospitalier Cochin Port Royal, DMU PRIME, Service d'Information Médicale, PARIS, France
Email: charlotte.mouliade@aphp.fr

Background and aims: Data regarding the severity and mortality rate of acute hepatitis A (AHA) in France, especially following the 2017 global AHA outbreak, remain limited. This study aimed to assess the burden of AHA-related hospitalizations from 2013 to 2022 in France and to identify factors contributing to its severity and mortality.

Method: Cases of AHA were identified as primary discharge diagnoses in the French National Uniform Hospital Discharge Data Set from 2013 to 2022 using ICD-10 codes B150 or B159. The study evaluated associations with death/liver transplantation and AHA severity (defined as death/liver transplantation or hepatic/extrahepatic organ failure within 12 weeks post-admission) using adjusted odds ratios (aOR) in both original and propensity-matched samples. AHA cases were categorized as pre- or post-outbreak based on a threshold date of June 15, 2017, the midpoint of 2017.

Results: Among the 6,734 patients identified (61% male, median age 31.0 years [IQR: 19–49]), 1.6% ($n=108$) experienced death or liver transplantation, and 28.7% ($n=1,931$) presented with severe AHA. Independent risk factors for AHA death/liver transplantation included post-outbreak AHA (aOR 1.83, 95% CI: 1.19–2.87, $p=0.007$), cirrhosis (aOR 4.75, 95% CI: 2.27–9.78, $p<0.001$), and severe comorbidities (aOR 6.31, 95% CI: 3.26–12.5, $p<0.001$ for a Charlson comorbidity index ≥ 3). Factors influencing AHA severity were post-outbreak AHA (aOR 1.19, 95% CI: 1.07–1.33, $p=0.002$), older age (aOR 1.19 per decade, 95% CI: 1.14–1.24, $p<0.001$), male sex (aOR 1.44, 95% CI: 1.29–1.62, $p<0.001$) cirrhosis (aOR 1.54, 95% CI: 1.07 to 2.23, $p=0.021$), and HIV infection (aOR 1.34, 95% CI: 1.04–1.72, $p=0.022$). Propensity-matched samples showed increased risks of AHA mortality (aOR 1.57, 95% CI: 1.03–2.45, $p=0.043$) and severity (aOR 1.18, 95% CI: 1.05–1.32, $p=0.004$) post-AHA outbreak.

Conclusion: The severity and mortality of AHA in France have notably increased over the past decade. These findings underscore the importance of promoting hepatitis A virus vaccination, particularly among older and comorbid patients.

SAT-381

Low diversity of the TCRbeta repertoire in patients with chronic hepatitis D

Maria Francesca Cortese^{1,2}, Adriana Palom^{3,4}, Beatriz Pacín Ruiz^{1,5}, Francesc Rudilla^{6,7}, Emma Enrich Randé^{6,7}, Mireia Antón Iborra⁶, Juan Carlos Ruiz-Cobo⁴, Mar Riveiro Barciela^{4,5}, David Tabernero^{1,2,8}, Ariadna Rando-Segura^{1,5,9}, Maria José Herrero^{6,7}, Maria Buti^{2,4,10}. ¹Department of microbiology, Liver Unit, Vall d'Hebron Institut de Recerca (VHIR), Vall d'Hebron Barcelona Hospital Campus, Barcelona, Spain; ²Carlos III Health Institute, Network Center For Biomedical Research in Hepatic and Digestive Diseases (CIBERehd), Madrid, Spain; ³Carlos III Health Institute, Network Center For Biomedical Research in Hepatic and Digestive Diseases (CIBERehd), Madrid, Spain; ⁴Department

POSTER PRESENTATIONS

of Hepatology, Vall d'Hebron Hospital Universitari, Vall d'Hebron Barcelona Hospital Campus, Barcelona, Spain; ⁵Carlos III Health Institute, Network Center For Biomedical Research in Hepatic and Digestive Diseases (CIBERehd), Barcelona, Spain; ⁶Histocompatibility and Immunogenetics Laboratory, Banc de Sang i Teixits, Barcelona, Spain; ⁷Transfusional Medicine Group, Vall d'Hebron Research Institute, Universitat Autònoma de Barcelona, Barcelona, Spain; ⁸Liver Disease, Viral hepatitis laboratory, Vall d'Hebron Institut de Recerca (VHIR), Vall d'Hebron Barcelona Hospital Campus, Barcelona, Spain; ⁹Department of Microbiology, Vall d'Hebron Hospital Universitari, Vall d'Hebron Barcelona Hospital Campus, Barcelona, Spain; ¹⁰Universitat autonoma de Barcelona (UAB), Barcelona, Spain
Email: mariafcortese@gmail.com

Background and aims: The hepatitis delta virus (HDV) causes a chronic infection and a limited percentage of chronic hepatitis delta patients (CHD, anti-HDV positive) can achieve spontaneous or treatment-related control of HDV replication and/or normalization of ALT levels. The function of T cells is controlled by the activation of the T cell receptor (TCR). Its genetic diversity is essential to recognize the viral antigens and induce the immune response. The interrelation between HDV infection and the TCR repertoire is still unknown. The aim of the present study is to analyze the TCR repertoire diversity in CHD patients versus healthy donors and in relation to the presence of HDV RNA and ALT levels for predicting disease progression.

Method: Peripheral blood mononuclear cells (PBMCs) were obtained from 25 adult patients with CHD (15 with detectable and 10 with undetectable HDV RNA). A group of 27 healthy adult donors was used as control. Biochemistry and virological parameters were collected. T cells (CD3+) were isolated from the PBMC by using an immunomagnetic positive selection commercial kit (Stemcell). T cells' DNA was isolated and the variable (TRBV), diversity (TRBD) and joining (TRBJ) gene rearrangements of the beta chain of the TCR were studied by next-generation sequencing (Miseq, Illumina). The diversity of the TCR repertoire (normalized Shannon Wiener index, SnW, and inverted Simpson index, S) in CHD patients was compared to the healthy group and in the same HDV group considering variables such as HDV RNA detectability or ALT levels (ALT above or below 50 U/L). Moreover, the frequency in using the different TRBV and TRBJ among the HDV patients was also determined.

Results: From the 25 anti-HDV included patients, 16 (64%) presented elevated ALT levels and 8 (32%) had liver cirrhosis. HDV patients presented a lower diversity of the TCR beta repertoire (both SnW and S indices) than healthy donors ($p < 0.05$). No difference in terms of diversity was observed when comparing patients with detectable or undetectable HDV RNA or normal or elevated ALT levels. When we considered the frequency of use of the TCR beta chain gene segments among HDV patients with detectable or undetectable viremia as well as ALT levels, we observed that patients with undetectable HDV RNA or normal ALT presented a higher frequency of use of the TRBV28 segment than patients with detectable HDV RNA or elevated ALT ($p = 0.057$ and 0.031 respectively).

Conclusion: CHD patients presented a lower diversity of the TCR repertoire than healthy donors probably suggesting a kind of enrichment in some clonotypes due to the infection. Patients with undetectable HDV RNA or normal ALT levels presented a high usage of a specific variable genetic segment. These results need to be further evaluated in a larger cohort of patients. Grant PI23/01065, funded by Instituto de Salud Carlos III and co-funded by European Union (ERDF, "A way to make Europe").

SAT-382

Ethanol exposure exacerbates HBV-infection pathogenesis: possible mechanisms and treatment targets

Natalia Osna¹, Murali Ganesan¹, Grace Bybee¹, Ashrafi Sultana¹, Carol Casey², Kusum Kharbada², Howard Gendelman¹, Larisa Poluektova¹, Benson Edagwa¹. ¹University of Nebraska Medical Center, Omaha, United States; ²University of Nebraska Medical Center, VA Medical Center, Omaha, United States
Email: nosna@unmc.edu

Background and aims: About 250 million people suffer from hepatitis B (HBV) infection, with an annual rate of cell death up to 800,000. The frequency of chronic hepatitis B (CHB) and detrimental outcomes are higher in patients with alcohol use disorders (AUD). However, the mechanisms under these events as well as therapeutic targets are not clear yet and their identification is the main purpose of this study. While HBV replicates only in hepatocytes, the activation of non-permissive macrophages by HBV supports hepatitis persistence. Here, we hypothesized that the protective crosstalk between macrophages and hepatocytes regulates innate immunity in infected hepatocytes and this protection is disrupted by exposure to ethanol. **Method:** The study was performed in HBV-expressing hepatocyte-like cells, HepG2.2.15 or HepAD38 and monocyte-derived macrophages (MDMs) exposed or not to acetaldehyde-generating system (AGS) to mimic ethanol metabolism. For in vivo experiments, we used Tg05 HBV-replicating mice.

Results: In vitro experiments, we found that the expression of HBV DNA, HBV RNA and HBcAg was elevated in AGS-treated hepatocytes due to suppression of Interferon-stimulated genes (ISGs), ISG15, APOBEC 3G and OAS1. HBV-containing supernatants from these cells activated mRNAs of inflammasome receptors, NLRP3 and AIM 2 as well as IL-1b and IL-18 in MDMs and suppressed the induction of ISGs in response to IFN type 1. Extracellular vesicles (EVs) mediated the hepatocyte-MDM crosstalk, which was blocked by the EV inhibitor, GW4869. Supernatants collected from these HBV-activated ethanol-non-exposed MDMs diminished the effects of ethanol on ISGs in hepatocytes and decreased the expression of HBV markers in hepatocytes, which was reversed by MDM exposure to ethanol. The increase in HBV marker expression accompanied by suppression of ISGs and inflammasome activation in liver cells were confirmed in vivo on ethanol-fed Tg05 mice. In attempts to reduce an inflammation in the liver, we tested the ability of the immunomodulatory drug, tizoxanide (TIZ) to control inflammasome activation in HBV-exposed MDMs. TIZ is an active metabolite of FDA-approved nitazoxanide (NTZ) with low bioavailability that was transformed into hydrophobic lipophilic crystalline prodrug to obtain long-acting properties. We observed that the treatment of activated MDMs with TIZ suppressed AIM2, IL-1b, IL-18 mRNAs and increased IFN α mRNA, indicating that TIZ can downregulate the inflammatory component in HBV-infection.

Conclusion: In conclusion, ethanol suppresses ISG in hepatocytes thereby increasing the expression of HBV. EV-mediated delivery of HBV to macrophages causes activation of inflammasome and hepatitis. This inflammation can be attenuated by the long-acting immunomodulator, TIZ to serve as an additional component of HBV-infection treatment along with the direct anti-viral drugs.

SAT-383

Rapid analysis of HBV-specific T cell secretomes reveals distinct antiviral immune profiles among chronic HBV patients

Nina Le Bert¹, Apostolos Koffas², Anthony Tan¹, Rajneesh Kumar³, Lung-Yi Mak², Tizong Miao², Yu Lei², Smrithi Hariharaputran¹, Shou Kit Hang¹, Yifei Guo¹, Qi Chen¹, Upkar Gill², Wan Cheng Chow³, Antonio Bertoletti¹, Patrick Kennedy². ¹Programme in Emerging Infectious Diseases, Duke-NUS Medical School, Singapore, Singapore; ²Barts Liver Center, Barts and The London School of Medicine and Dentistry, Queen Mary University of London, London, United Kingdom;

³Gastroenterology and Hepatology, Singapore General Hospital, Singapore, Singapore
Email: nina@duke-nus.edu.sg

Background and aims: Clinical management of chronic HBV (CHB) patients relies exclusively on assessing virological and biochemical biomarkers despite the importance of HBV-specific T cells in viral control. We developed a robust and rapid whole blood assay (WBA) to measure the functional secretome of HBV-specific T cells. We tested the WBA in a large cohort of CHB patients, across all disease phases, to characterize their T cell immune profile in relation to virological and biochemical parameters.

Method: We sampled a total of 240 CHB patients (20 HBeAg⁺ infection, 25 HBeAg⁺ hepatitis, 85 HBeAg⁻ infection, 10 HBeAg⁻ hepatitis, 60 HBeAg⁻ on NUC, 40 HBeAg⁻) and 30 healthy HepB vaccinees. 20 patients (10 HBeAg⁺ under NUC, 10 HBeAg⁻) were tested monthly over 3 time points. A small volume of whole blood (2 ml) was aliquoted and stimulated with 6 customized peptide pools covering all HBV proteins of 4 genotypes (A, B, C, and D). Supernatants were collected at 16hr for cytokine quantification (IFN- γ , IL-2, granzyme B, TNF- α , IL-4) with ELISA. In parallel, PBMCs were isolated from selected patients to perform ex-vivo and in-vitro expansion ELISpot assays. To identify patients with distinct immune profiles, machine learning algorithms such as UMAP were applied for dimensionality reduction, visualization, and clustering of the secretome data from the >1450 whole blood HBV-T cell assays performed.

Results: Secretion of cytokines in response to HBV-peptide pool stimulation was detected in over 90% of all CHB patients. Parallel ex-vivo IFN- γ ELISpot analysis frequently failed to detect HBV-specific T cell responses, except in those with strong cytokine release in the WBA, suggesting a superior sensitivity. Substantial variability was observed in cytokine quantity (pg/ml), quality (different cytokines), and reactivity towards distinct HBV-proteins (different peptide pools) across all CHB patients, irrespective of their clinical classification. Yet, longitudinal analysis revealed stable profiles within patients. Machine learning algorithms separated CHB patients within similar clinical phases into clusters with distinct HBV-specific immune profiles.

Conclusion: A rapid HBV-specific T cell test, performed in a small volume of blood, can identify CHB patients with distinct immune profiles. The ability to distinguish patients within similar clinical disease phases based on their antiviral T cell function will provide a novel biomarker for interpreting host-viral interactions and can signpost the selection of novel immunotherapies.

SAT-386-YI

Characterization of intrahepatic immune microenvironment in liver biopsies across different phases of untreated HBeAg-negative patients

Maria Stella Franzè^{1,2,3}, Pascale Maille^{1,2,4}, Stefano Caruso^{1,2,4}, Julien Calderaro^{1,2,4}, Yasmine Bouda^{1,2}, Anna Sessa^{1,2,5}, Stéphane Chevaliez^{1,2,6}, Patrick Ingiliz^{1,5}, Teresa Pollicino³, Giovanni Raimondo³, Jean-Michel Pawlotsky^{1,2,6}, Vincent Leroy^{1,2,5}, Giuliana Amadeo^{1,2,5}. ¹Team "Viruses, Hepatology, Cancer", Institut Mondor de Recherche Biomédicale, INSERM Unit U955, Créteil, France; ²Université Paris-Est Créteil, Créteil, France; ³Department of Clinical and Experimental Medicine, University of Messina, Messina, Italy; ⁴Department of Pathology, Henri Mondor University Hospital, Assistance Publique-Hôpitaux de Paris, Créteil, France; ⁵Department of Hepatology, Henri Mondor University Hospital, Assistance Publique-Hôpitaux de Paris, Créteil, France; ⁶Department of Virology, National Reference Center for Viral Hepatitis B, C, and D, Henri Mondor University Hospital, Assistance Publique-Hôpitaux de Paris, Créteil, France
Email: mariastellafranze@gmail.com

Background and aims: Chronic hepatitis B virus (HBV) infection is characterized by multiple interplays between virus and host immune response that define distinct clinical phases that were defined

arbitrarily. We aimed to characterize the intrahepatic immune microenvironment by evaluating gene expression profiles in a large cohort of untreated HBeAg negative patients to decipher the immune activation profiles according to biochemical, virological and histological characteristics.

Method: Ninety-eight HBeAg positive HBeAg negative patients who underwent liver biopsy at Henri Mondor Hospital between 2005 and 2020 were included. Data were collected for each patient at time of biopsy and during follow-up. According to EASL guidelines, patients were classified as HBeAg negative chronic HBV infection and HBeAg negative chronic hepatitis B (CHB). RNA sequencing was performed for each case.

Results: Seventy-six patients (77.6%) were male, with a median age of 40 (33–52) years. Thirty-seven subjects (38%) had a chronic infection (14 with HBV DNA <2,000 IU/ml, 23 with >2,000 IU/ml but <20,000 IU/ml) and 61 (62%) a CHB. Fibrosis was F0/F1 in 84 patients (85.7%), F2/F3 in 11 (11.2%), F4 in 3 (3.1%). Histological activity was A0/A1 in 75 cases (76.5%) and A2/3 in 23 (23.5%). RNA sequencing analysis by unsupervised hierarchical clustering identified two clusters of patients with differentially expressed genes (DEGs) profiles: 18 cluster 1 (C1) and 80 cluster 2 (C2). C1 was associated to higher age ($p = 0.023$), fibrosis ($p < 0.001$), activity ($p < 0.001$), HBV DNA ($p < 0.001$) and ALT levels ($p < 0.001$) compared to C2. C1 contained only CHB patients ($p = 0.001$). By Microenvironment Cell Populations counter method, we identified an intrahepatic immune infiltrate enriched of fibroblasts, monocytes, cytotoxic lymphocytes, and endothelial, myeloid dendritic, natural killer, B, T, CD8⁺ T cells in C1 vs C2. Supervised analysis for DEGs showed 1265 genes significantly down and 539 up-regulated in C2 vs C1. Gene set enrichment analysis with Molecular Signatures Database performed with a hypergeometric test showed that C1 was associated with gene sets pathways mainly involved in immune response. A sensitivity analysis by unsupervised hierarchical clustering was performed in subgroup of 71 patients that were F0/1-A0/1 and identified again 2 distinct clusters. Immune infiltrate profiles were significantly different for presence of CD8⁺ T cells and immune pathways activation.

Conclusion: Our analysis of liver immune microenvironment revealed differences in gene profiles of HBeAg negative patients, with immune related pathways in CHB and in a subgroup of HBVs without markers of active infection. These results suggest the need to well characterize HBV patients for identifying those at risk of liver disease progression and requiring early antiviral treatment.

SAT-387

Use of capillary Samples for hepatitis B Virus Load Quantification Using Xpert (R) HBV

Gora Lo¹, Ambroise Ahouidi², Mame matar Diop², Pape Omar Thiaw³, Abdoulaye Souaré², Lamine Faye³, Etienne Grovogui³, Nafissatou Leye², Cyrille Diédhiou², Ndeye Aminata Diaw², Jean Daveiga³, Souleymane Mboup². ¹Institut de Recherche en Santé, de Surveillance Épidémiologique et de Formations, Université Cheikh Anta de Diop, Dakar, Senegal; ²Institut de Recherche en Santé, de Surveillance Épidémiologique et de Formations, Dakar, Senegal; ³Hôpital saint Jean de Dieu, Thiès, Senegal
Email: gora.lo@iressef.org

Background and aims: HBV DNA Quantification in whole venous blood or plasma viral load is a key element in the management of chronic hepatitis B, allows a more direct and reliable measurement of viral replication and monitoring of the virological response to therapy. Collecting venous blood for diagnostic purposes, especially in infants and young children, could be challenging in many situations. Alternative solutions using capillary blood (finger stick test) for HBV genome quantification will improve the diagnosis and treatment of HBV, mainly in resource-limited countries, by increasing accessibility to diagnosis and improving disease surveillance. The aim of the current study was to optimize and evaluate the performance of

POSTER PRESENTATIONS

Xpert® in HBV viral load quantification using capillary blood and plasma.

Method: This is a descriptive cross-sectional study carried out at IRESSEF, Senegal from July to December 2023. Capillary blood and plasma samples were collected from chronic HBV carriers HBV and used for HBV viral load determination with the Xpert® HBV VL test cartridge and Abbott real-time HBV PCR (m2000®) as a gold standard. For capillary blood, sample was diluted 1 in 10 before testing with Xpert® HBV VL assay. Statistical analysis using Meth Val® software focused on determining correlation and concordance.

Results: A total of 95 patients with chronic HBV (37 men and 58 women) were enrolled in the study. The median age was 35 years [20–81]. The mean HBV Xpert® viral load on capillary blood and plasma was 3, 05 and 3, 12 log UI/ml, respectively. Viral load Xpert® measurements between capillary blood and plasma correlated strongly with a correlation coefficient of $r^2 = 0.903$ ($p < 0.001$). Mean (SD) difference of Xpert® viral load values between plasma and capillary blood was -0.236 log UI/ml. There was a high correlation between viral load results in plasma and in Capillary blood/plasma, tested by m2000 and the Xpert® respectively ($r^2 = 0.93$ and 0.88 respectively, $p < 0.001$). Overall, Xpert® viral load values in Capillary blood and plasma tended to be lower than m2000® viral load in plasma with mean (SD) differences of 0.06 log UI/ml for Capillary blood and of 0.29 log UI/ml for plasma. Compared to the plasma tested by Xpert® and m2000, the sensitivity, the specificity were 88, 100% and 83 and 97% respectively.

Conclusion: Capillary blood provided results highly correlated to the plasma values. High detection rate was obtained with Capillary Blood when viral load was >2.0 log UI/ml. Capillary blood collection may provide a reliable method for HBV DNA quantification using Xpert® HBV VL assay.

SAT-388

Comprehensive analysis of CHB concurrent with NAFLD: a proteomics report based on clinical liver samples

Xin Tong¹, Shengxia Yin², Fajuan Rui³, Chao Wu⁴, Jie Li⁴. ¹Department of infectious diseases, Nanjing Drum Tower Hospital, Affiliated Hospital of Medical School, Nanjing University, Nanjing, China; ²Department of Infectious Diseases, Nanjing Drum Tower Hospital, The Affiliated Hospital of Nanjing University Medical School, Nanjing, China; ³Nanjing Drum Tower Hospital Clinical College of Nanjing University of Chinese Medicine, Nanjing, China; ⁴Nanjing Drum Tower Hospital, Affiliated Hospital of Medical School, Nanjing University, Nanjing, China
Email: tongxin5694@126.com

Background and aims: In recent years, NAFLD has become more prevalent in patients with chronic hepatitis B as the prevalence of obesity and metabolic syndrome has increased. Both diseases can lead to liver fibrosis and even HCC, but the pathogenesis of each disease and CHB concurrent with NAFLD have not been fully elucidated.

Method: We characterized the protein expression in liver tissues among four groups of people with healthy control ($n = 6$), CHB ($n = 8$), NAFLD ($n = 7$), and CHB concurrent with NAFLD ($n = 10$) by using proteomic profiling. Based on the obtained DEPs results, further bioinformatics analysis was performed. We also verified the expression of some DEPs in the livers of patients and model mice.

Results: Compared with the CHB group, a total of 109 proteins were differentially expressed in the group of CHB patients combined with NAFLD (73 upregulated and 36 downregulated). Further KEGG analysis showed that the differences in various metabolism-related pathways in the liver of patients with CHB concurrent with fatty liver were more pronounced than in single CHB patients, especially the abnormal activation of cholesterol metabolic pathways, which is consistent with the characteristics of fatty liver disease. In addition, we found that accelerated viral clearance in HBV-infected patients with concurrent fatty liver might be associated with an inflammatory response and activation of a large number of metabolic reactions in

the organism. These changes were mainly associated with differential enrichment of proteins such as KRT24, SERPINB3, CDSN, S100A7, SYPL1, AGXT, and PGC1- α . Compared with the NAFLD group, a total of 221 proteins were differentially expressed in the group of CHB patients combined with NAFLD (22 upregulated and 199 down-regulated). Including metabolism of xenobiotics by cytochrome P450, IL-17 signaling pathway, retinol metabolism and 36 major down regulated pathways, including Glycolysis/Gluconeogenesis, fatty acid degradation, PPAR signaling pathway, Fat digestion and absorption. This results suggested that metabolic pathways were inhibited when CHB concurrent NAFLD, which provided a new perspective on the mechanism of interaction between these two diseases.

Conclusion: The prognosis of CHB complicated with NAFLD may not be optimistic compared with that of hepatitis B and NAFLD alone, which is closely related to the differential expression of certain proteins in the liver after the complication of the two diseases. Our study provides new insights into the disease development and clinical mechanisms of CHB and NAFLD.

SAT-389

HBV and HBsAg strongly reshape the phenotype, function and metabolism of DCs according to patients' clinical stage

Lucile Dumolard¹, Gerster Théophile^{2,3}, Florent Chuffart¹, Thomas Decaens^{1,2}, Marie-Noëlle Hilleret^{1,2}, Sylvie Larrat⁴, Philippe Saas^{1,3}, Evelyne Jouvin-Marche¹, David Durantel⁵, Patrice N Marche¹, Zuzana Macek Jilkova^{1,2}, Caroline Aspord^{1,3}. ¹Univ. Grenoble Alpes, Inserm U 1209, CNRS UMR 5309, Institute for Advanced Biosciences, Grenoble, France; ²Hepato-Gastroenterology and Digestive Oncology Department, CHU Grenoble Alpes, Grenoble, France; ³Etablissement Français du Sang Auvergne-Rhône-Alpes, RandD Laboratory, Grenoble, France; ⁴Univ. Grenoble Alpes, Laboratoire de Virologie, CHU Grenoble Alpes, Grenoble, France; ⁵INSERM, U1111, Centre International de Recherche en Infectiologie (CIRI), University of Lyon (UCBL1), CNRS UMR_5308, ENS de Lyon, Lyon, France
Email: zuzana.mjilkova@gmail.com

Background and aims: Hepatitis B is a liver infection caused by the Hepatitis B virus (HBV). Infected individuals, who fail to control the viral infection, develop chronic hepatitis B (CHB) and are at risk to develop life-threatening liver diseases, such as cirrhosis or liver cancer. Dendritic cells (DCs) play important roles in the immune response against HBV, but are functionally impaired in CHB patients. The underlying mechanisms involved in HBV-induced DC dysfunctions remain to be elucidated.

Method: We explored DC modulations by HBV and Hepatitis B surface antigen (HBsAg) by exposing blood-derived cDC1s, cDC2s and pDCs from healthy donors to HBV or HBsAg, and stimulating them with TLR-L. Their phenotypic and functional features, as well as their metabolic profile, were analysed through multiparametric flow cytometry and multiplex assays, and further explored on patients' samples.

Results: We found that HBV deeply reshaped DC secretome in response to TLR-L. Strikingly, we observed that HBV-exposed DCs secrete high levels of CX3CL1 (fractalkine), a chemokine responsible for attracting antiviral effectors to the site of infection. HBsAg exposure favored DC activation while drastically altering TRAIL expression in response to TLR-L and increasing the secretion of cytokines/chemokines involved in immune tolerance. HBsAg further dampened the metabolism of DC subsets while driving metabolic switches. Notably, relevance of CX3CL1/CX3CR1 axis, TGF- β and metabolic disturbances was demonstrated within intrahepatic DC subsets in patients according to disease stage.

Conclusion: Our work brings new insights into the immunomodulation induced by HBV on DCs, which contribute to impaired antiviral responses and progression towards chronicity.

SAT-390

Nonclinical phenotypic evaluation of clinically identified baseline and treatment-emergent hepatitis B Virus variants that contain single nucleotide polymorphisms in the bepirovirsen binding site

Alexander Koenig¹, Michael Savarese¹, Elise Turk¹, Chi Lau¹, Nicholas Galwey², Jerome Bouquet¹, Robert Elston², Dickens Theodore³, Melanie Paff¹, Shihyun You¹, Christine Livingston¹.
¹GSK, Collegeville, United States; ²GSK, Stevenage, United Kingdom; ³GSK, Durham, United States

Email: christine.m.livingston@gsk.com

Background and aims: Bepirovirsen (GSK3228836, BPV) is an antisense oligonucleotide under Phase 3 investigation for treatment of Chronic Hepatitis B. BPV targets a highly conserved 20 nucleotide sequence common among HBV pgRNA and mRNA transcripts, where HBx and HBV pol open reading frames overlap. SNPs in the BPV binding site of HBV genomes from B-Clear Phase 2b (NCT04449029) samples were previously reported among a minority of pre- and post-treatment isolates. Clinically identified baseline (BL) HBV variants were previously evaluated nonclinically for their susceptibility to the GalNAc-conjugated form of BPV, GSK3389404, in primary human hepatocytes (PHH) and to BPV in the case of HBV variant C9A using the RNA Launch model. In this study, we evaluated the susceptibility of BL variants (C9A, T10A, T10G, C20T) and treatment emergent (TE) variants (C9A, G8A, C15T) to BPV in PHH. HBV variant fitness and susceptibility to BPV compared with WT HBV were assessed by the levels of secreted HBsAg and HBeAg.

Method: HBV variant stocks containing clinically identified SNPs in the BPV binding site were generated by transfection of HepG2 cells with 1.3X HBV variant genome plasmids. PHH were infected with WT or HBV variant stocks for 7 days, followed by BPV treatment every 3–4 days totaling 4 sequential doses. After 15 days of BPV treatment, culture supernatant was collected for HBsAg and HBeAg quantification. The susceptibility of HBV variants to BPV compared with WT HBV was determined using dose-response analysis. Mid and high fitness variants were defined as those displaying HBsAg and HBeAg levels of 20–60% or >60% relative to WT HBV, respectively.

Results: HBV variant fitness and susceptibility to BPV were largely consistent between HBsAg and HBeAg readouts. HBV variants exhibited varying levels of fitness, with C9A, T10A, T10G, C20T being high fitness variants, and G8A and C15T being low fitness variants compared with WT HBV. C9A exhibited the lowest susceptibility to BPV compared to WT HBV (about 4.1-fold and 3.6-fold reduction in EC50 as indicated by secreted HBsAg and HBeAg levels, respectively). T10G exhibited approximately 2–3-fold reduction in susceptibility across both readouts. C15T and G8A exhibited approximately 2–3-fold reduction as determined by HBsAg levels and nearly 2-fold reduction as determined by HBeAg levels. T10A and C20T exhibited less than 2-fold reduction across HBsAg and HBeAg readouts.

Conclusion: Using our two-step system of HepG2 and PHH, we evaluated the susceptibility of clinically identified HBV BL and TE variants containing SNPs in the BPV site to BPV. The biological basis for varying levels of fitness of each variant, through potential impact of SNPs on HBx and HBV DNA polymerase function, is under evaluation. While the frequency of these HBV variants is very low, the relevance of the *in vitro* phenotypic data to clinical outcome is subject to further investigation.

SAT-391

Investigation of HBV cccDNA Methylation by Bisulfite sequencing for therapeutic targeting in liver biopsies from hepatitis B patients

Purnima Tyagi^{1,1}, Akhilesh Saini¹, Jitendra Kumar¹, Shiv Kumar Sarin¹, Vijay Kumar¹.
¹Institute of Liver and Biliary Sciences, New Delhi, India
 Email: vijaykumar98@gmail.com

Background and aims: There is a growing need to study novel therapeutics that particularly target cccDNA (covalently closed

circular) in hepatitis B virus (HBV), since its eradication may lead to the elimination of chronic hepatitis B (CHB). There is an urgent need to better understand the methylation status of HBV cccDNA throughout the infection, and also the role it plays in viral replication. Thus, identifying novel CpG sites of methylation and demethylation in cccDNA in patients with high and low viral replication may aid in the finding of new targets against cccDNA.

Method: Liver biopsies (n = 20) from CHB patients were collected and were sub-grouped on basis of HBeAg negative (n = 13) and HBeAg positive (n = 7), serum HBsAg positive [\log_{10} IU/ml 3.53 ± 1.04 >6 months], serum HBV DNA [\log_{10} IU/ml 4.3 ± 1.33] and serum HBeAg positive [\log_{10} IU/ml 2.52 ± 0.81]. Isolated cccDNA was treated with Bisulfite treatment and PCR was done of CpG island I, island II, and island III region by using BSP (Bisulfite-specific primers) followed by the sanger sequencing. The HBV DNA level was quantified by qPCR.

Results: The methylation sites in CpG island II, and III were significantly higher in HBeAg⁺ patients (p < 0.01) as compared to HBeAg⁺ patients. CpG island I (1–236) region cytosines at positions 74, 94, 157, and 161 were found to be in a demethylated state in both patient groups and cytosines at 1201, 1579, 1689, 1698, 1750, and 1774 were frequently methylated in the CpG II island (1126–1804) region in HBeAg⁺ patients. Furthermore, cytosines at positions 2555, 2597, and 2601 in CpG III island (2497–2642) were found to be in a methylated state in the HBeAg⁺ group whereas these sites were observed in a demethylated state in the HBeAg⁺ group. No significant correlation was found between methylation status and HBV DNA levels in the CpG island I (p > 0.01). The degree of CpG island II (p < 0.05) and CpG island III (p < 0.01) methylation was significantly higher in patients with low HBV DNA titer (\log_{10} HBV DNA >4) than that with high HBV DNA titer (\log_{10} HBV DNA <4).

Conclusion: CpG I in the HBV genome was seldom methylated whereas, CpG II and III regions appeared to be the hot spots for methylation in the HBV genome. CpG island III of the HBV cccDNA showed a higher methylation levels in patients associated with lower serum HBV DNA levels indicating that hypermethylation of CpG island II and III contributes to the reduced HBV DNA levels. Thus, our findings suggest cccDNA methylation in CpG island II and III correlates with reduced viral mRNA transcription, which in turn could lower the serum HBV DNA loads. However, there was no significant association was found between CpG islands methylation density and ALT/AST levels. Nevertheless, association between cccDNA methylation and viral replication has provided the basis for developing innovative therapeutic strategies of silencing cccDNA and eventually depleting the cccDNA reservoir.

SAT-392

Perturbed pathways of lipid metabolism in patients with chronic hepatitis B infection after cessation of long term nucleos (t)ide analogue

Fengge Zhu¹, Rex Wan-Hin Hui¹, Liqiong Yang¹, Saisai Zhang¹, Jiaqi Wang¹, Xue Li¹, Tsz Yan Kwok¹, James Fung¹, Wai-Kay Seto¹, Man-Fung Yuen¹, Lung Yi Loey Mak¹.
¹The University of Hong Kong, Hong Kong, China

Email: loeymak@gmail.com

Background and aims: The ‘stop-to-cure’ approach is a potential strategy to achieve finite duration of nucleoside analogue (NUC) in patients with chronic hepatitis B (CHB) infection. We examined the serial serum metabolomic profiles among flare compared to non-flare CHB patients who had stopped NUCs, followed by *in silico* data mining to identify relevant pathways.

Method: Patients with HBeAg-negative non-cirrhotic CHB on ≥ 3 years of NUC were recruited. NUCs were stopped and they were prospectively followed up every 6 weeks for virological relapse (VR: serum HBV DNA rise from undetectable to >2000 IU/ml) \pm clinical flare (VR plus alanine aminotransferase [ALT] >2 times upper limit of normal), with serial blood sampling for metabolomic profiling at week 0, at NUC resumption (for flare patients, or non-flare patients

POSTER PRESENTATIONS

with VR or HBeAg sero-reversion), and at ALT normalization following NUC resumption among flare patients. A total of 8 patients (4 flare [among which 2 developed subsequent HBsAg seroclearance, SC], 4 VR or HBeAg sero-reversion) were included in this interim analysis. Serum metabolomics data was acquired with 1D 1H-Nuclear magnetic resonance spectroscopy. Metabolomics data was analysed with MetaboAnalyst 6.0. GEO datasets was analyzed with GEO2R.

Results: Metabolites involved in lipid metabolism (triglyceride and total fatty acid) were significantly downregulated in flare patients compared to non-flare patients at NUC resumption. Among flare patients, succinic acid is significantly downregulated in those who subsequently achieved SC compared to flare-no-SC patients upon ALT normalization. Dimethylsulfone involved in triacylglycerol degradation is upregulated in flare patients with SC, compared to flare-no-SC and non-flare patients, at all timepoints. Compartment specific *in silico* data mining based on GEO DataSets showed genes involved in fatty acid synthesis (FAR1, FASN), fatty acid elongation in mitochondria (NDUFAB1), fatty acid elongation in endoplasmic reticulum (ELOVL1, ELOVL5) were significantly increased in the liver of CHB patients (GSE230397) compared to control, but not in peripheral blood CD8 T cells (GSE217838), indicating a compartment specific imbalance of lipid metabolism. In CHB patients with severe flare, fatty acid beta-oxidation associated genes ACAT1, ACSL1 and ACSL4 were significantly downregulated in the PBMCs of the survival group compared to patients who died (GSE168049).

Conclusion: We demonstrated alterations of lipid metabolism pathways in CHB patients with post-NUC cessation flare that were associated with clinical outcomes. Fatty acid metabolism is perturbed in patients with CHB and is inferred to be associated with survival in those with severe HBV flare based on *in silico* datasets analysis. Our work reveals an imbalance in lipid metabolism in CHB both in spatial location and molecular signature.

SAT-393

Profile of miRNAs in chronic hepatitis D patients with or without viral replication

Maria Francesca Cortese^{1,2}, Beatriz Pacín Ruiz^{1,3}, Adriana Palom^{2,4}, Selene García-García^{2,5}, Javier Perez Garreta⁵, David Tabernero^{2,5,6}, Ariadna Rando-Segura^{2,5,7}, Juan Carlos Ruiz-Cobo⁴, Mar Riveiro Barciela^{2,4}, Maria Buti^{2,4,8}. ¹Department of microbiology, Liver Unit, Vall d'Hebron Institut de Recerca (VHIR), Vall d'Hebron Barcelona Hospital Campus, Barcelona, Spain; ²Carlos III Health Institute, Network Center For Biomedical Research in Hepatic and Digestive Diseases (CIBERehd), Madrid, Spain; ³Carlos III Health Institute, Network Center For Biomedical Research in Hepatic and Digestive Diseases (CIBERehd), Barcelona, Spain; ⁴Department of Hepatology, Vall d'Hebron Hospital Universitari, Vall d'Hebron Barcelona Hospital Campus, Barcelona, Spain; ⁵Department of microbiology, Liver Unit, Vall d'Hebron Institut de Recerca (VHIR), Vall d'Hebron Barcelona Hospital Campus, Barcelona, Spain; ⁶Liver Unit, Liver Disease, Viral Hepatitis Laboratory, Vall d'Hebron Institut de Recerca (VHIR), Vall d'Hebron Barcelona Hospital Campus, Barcelona, Spain; ⁷Department of Microbiology, Vall d'Hebron Hospital Universitari, Vall d'Hebron Barcelona Hospital Campus, Barcelona, Spain; ⁸Universitat Autònoma de Barcelona, Bellaterra, Spain
Email: mariafcortese@gmail.com

Background and aims: A limited percentage of chronic hepatitis D (CHD) patients can achieve spontaneous or treatment-related control of hepatitis delta virus (HDV) replication (undetectable HDV RNA), however the mechanism behind this virological control is still unclear. The microRNAs (miRNAs) are small RNAs involved in several biological processes, including the host response to a viral infection. The aim of this study was to analyze the circulating miRNAs profile of CHD patients to identify potential biomarkers that differentiate controllers from non-controllers (HDV patients with respectively undetectable and detectable HDV RNA).

Method: Thirty CHD patients (anti-HDV positive) were included in the study: 15 controllers (with undetectable HDV RNA in at least two consecutive samples) and 15 non-controllers (persistent detectable HDV RNA). Biochemistry values and virological parameters were collected. The small RNAs (including miRNAs, miRNAs precursors and small nucleolar RNA- snoRNA) were isolated from the CHD plasma samples and their profile was analyzed by microarray (Affimetrix, miRNA array). The differentially expressed miRNAs were identified by adjusting a linear model with empirical Bayes moderation of the variance. The main miRNA targets were catalogued by using different databases (miRecords, miRtarbase, tarbase), and their most represented biological roles were evaluated by enrichment analysis (Gene Ontology-MF and Reactome pathway).

Results: More than 6300 small RNA sequences were included in the differential expression study. Among them, 20 small RNAs were differentially expressed between the two groups (non-adjusted p value <0.05; absolute log2FC >1) mainly targeting genes implicated in DNA transcription and pathways involved in intracellular signaling. When considering an adjusted p value (BH-adjusted p <0.25, absolute log2FC >1 and B-statistic >0 or average expression >1.5), 6 miRNAs were differently expressed between the groups. The HDV controllers (undetectable HDV RNA) showed 5/6 down-regulated (miR-23b-3p, miR-194-5p, miR-122-5p, miR-192-5p and miR-26a-5p with a log2FC of respectively -3.13, -2.62, -4.07, -1.54 and -2.7) and 1/6 (miR-33a-5p; log2FC of 0.29) up-regulated miRNAs in comparison to subjects with detectable HDV RNA.

Conclusion: A different miRNAs profile can be observed in chronic hepatitis D patients that can control the HDV replication or not. The most differentially expressed miRNAs could regulate target genes involved in cellular transcription and intracellular signaling pathway. Further studies are needed to inspect the specific mechanism associated with miRNAs expression, their activity on cellular gene expression and their role in HDV replication. Study supported by the grants PI20/01692 and PI23/01065, funded by Instituto de Salud Carlos III and co-funded by European Union (ERDF, "A way to make Europe").

SAT-394

HBV genotyping: grasping a new window of opportunity?

Marion Delphin¹, Ka Chun Li², Elizabeth Waddilove¹, Cedric Tan¹, Jacqueline Martin³, Catherine De Lara⁴, Eleanor Barnes⁵, Jose Lourenco⁶, Philippa C Matthews^{1,7}. ¹the francis crick institute, london, United Kingdom; ²university college london, london, United Kingdom; ³John Radcliffe Hospital, oxford, United Kingdom; ⁴Medawar Building for Pathogen Research, University of Oxford, oxford, United Kingdom; ⁵Department of Hepatology, John Radcliffe Hospital, oxford, United Kingdom; ⁶BioISI (Biosystems and Integrative Sciences Institute), Faculty of Sciences, University of Lisbon, lisbon, Portugal; ⁷University college london, london, United Kingdom
Email: marion.delphin@crick.ac.uk

Background and aims: The Hepatitis B Virus (HBV) accounts for chronic infection in 316 million people worldwide, in spite of a safe and efficient vaccine since the 1990's. Incomplete immunisation coverage, poor diagnosis and treatment, and high prevalence of infection make HBV a leading contributor to hepatocellular carcinoma and cirrhosis. Ten HBV genotypes have been described (from A to J), defined by >8% divergence in nucleotides. Each has specific geographic distribution, transmission patterns, pathophysiology, treatment outcomes and resistance profiles, however genotyping is still not part of routine testing for people living with HBV (PLWHB). The current gold standard, HBV full genome sequencing and phylogenetic analysis, requires resources, time and expertise, which are not widely accessible in many clinical settings. Other methods have been described, but with varying sensitivity in discriminating between the ten genotypes.

Method: To identify the optimum window for distinguishing between genotypes we used public data from 9, 777 HBV sequences

(representing genotypes A to H; I and J excluded due to recombination). Sequences were aligned, numbered (HBV X02763 reference sequence) and fitted in a Random Forest Algorithm, with a sliding window approach across the viral genome. We identified a window of 450 bp in the HBV polymerase gene (nucleotides 642–1092), which confidently distinguishes between genotypes with the lowest error. We designed PCR primers specific to this window (5' GGG-TCA-CCA-TAT-TCY-TGG-GAA-CAA-G 3' and 5' CTG-TAA-CAC-GAG-AAG-GGG-TCC-TAG 3') and performed PCR, followed by Sanger sequencing, to two sample sets, (i) A dilution series of plasmids of known sequence/genotypes containing HBV genomes (genotype A, B, C, D, E, F, H, J provided by the Revill lab) or produced using a similar design by GenArt (genotype G and I). (ii) 10 Serum samples obtained from PLWHB (genotype A, B, C, D, E and G), enrolled at Oxford University Hospitals, UK (ethics ref.N17/01/013).

Results: We validated our new PCR primers to amplify the optimum genotyping window, showing that the method works on HBV plasmid genotypes of viral genome equivalent (VGE) down to 10^3 /ml. When comparing the known genotype of each plasmid, with the one identified with our method, an accuracy of 100% was observed for all genotypes except HBV-I (identified as HBV-A). Serum samples of PLWHB were then used to further confirm our technique.

Conclusion: We developed an HBV genotyping method capable of distinguishing all major genotypes with a low rate of errors, at high sensitivity (down to 10^3 VGE/ml) using standard techniques that could be deployed in broad settings. This rapid and affordable approach could overcome the existing barriers to implementing HBV genotyping in routine services, contributing to insights into epidemiology, disease outcomes, evaluation of novel therapeutics, and personalised medicine.

SAT-395

ROS-dependent activation of JAK2/STAT3 pathway contributes to HBV-induced liver inflammation

Rui Song¹, Shasha Yu¹, Wenhui Peng¹, Jinglin Tang², Min Chen¹.
¹Department of Infectious Diseases, the Second Affiliated Hospital of Chongqing Medical University, Chongqing, China; ²Department of Laboratory, the People's Hospital of Chongqing, Chongqing, China
Email: mchen@hospital.cqmu.edu.cn

Background and aims: Recent studies suggested that hepatitis B virus (HBV) might induce mitochondrial dysfunction, resulting in increased reactive oxygen species (ROS) production. However, very little is known about whether ROS is responsible for the occurrence of hepatic inflammation during chronic HBV infection.

Method: An HBV-replicating mouse model was established by performing HBV-expressing plasmids pAAV-HBV1.2 hydrodynamic injection. Levels of intrahepatic ROS, oxidative stress and liver inflammation grade were dynamically evaluated. Meanwhile, inflammation-related cytokines production, immune cell infiltration, and signal pathway activation in liver tissue were examined by RT-PCR, WB, and FACS. Moreover, in vivo antioxidant treatment was applied to explore the potential mechanisms of the occurrence of hepatic inflammation mediated by ROS.

Results: Significantly increased ROS fluorescence intensity and decreased ratio of reduced to oxidized glutathione (GSH/GSSG) were observed in liver tissue from mice at 4 weeks after injection of pAAV-HBV1.2 plasmids. Simultaneously, these mice displayed remarkably higher liver inflammation grade and elevated serum ALT levels with prominent upregulation of inflammatory cytokines production (IL-6 and IL-8) and immune cell infiltration (monocytes). Meanwhile, enhancement of Nrf2 expression and activation of JAK2/STAT3 signaling pathway were found in these mice. Furthermore, ROS scavenging with N-acetylcysteine attenuated activation of JAK2/STAT3 pathway and liver inflammation.

Conclusion: This study revealed that HBV-induced ROS overproduction activates the JAK2/STAT3 pathway and contributes to the liver

inflammation. Our findings provide a new look at the key factor to trigger hepatic inflammation during chronic HBV infection.

SAT-396

Differences in the intrahepatic expression of immune checkpoint molecules on T cells and natural killer cells in chronic HBV patients

Lucile Dumolard¹, Marie-Noëlle Hilleret¹, Gerster Théophile², Charlotte Costentin^{1,2}, Thomas Decaens^{1,2}, Evelyne Jouvin-Marche¹, Patrice N Marche¹, Zuzana Macek Jilkova^{1,2}. ¹Univ. Grenoble Alpes, Inserm U 1209, CNRS UMR 5309, Team Epigenetics, Immunity, Metabolism, Cell Signaling and Cancer, Institute for Advanced Biosciences, Grenoble, France; ²Service d'hépatogastroentérologie, Pôle Digidune, CHU Grenoble Alpes, La Tronche, France
Email: zuzana.mjilkova@gmail.com

Background and aims: Patients with chronic hepatitis B virus (HBV) infection are characterised by impaired immune response that failed to eliminate HBV. Nucleos(t)ide analogs (NUC) are antiviral treatments representing the standard of care, but rarely lead to HBsAg clearance. Future therapies focus on the use of immunotherapies in combination with NUC to remodel the host immune response. Immune checkpoint molecules (ICM) control the amplitude of the activation and function of immune cells, that makes them the key regulators of the immune response.

Method: Here, we performed a multiparametric flow cytometry analysis of ICM and we determined their expression on intrahepatic lymphocyte subsets in untreated and in treated patients with HBV in comparison with non-pathological liver tissue.

Results: Liver of untreated inactive carriers as well as immune active HBV patients exhibited high accumulation of PD-1+CD8+ T cells while the frequencies of TIM-3+CD8+ T cells, 4-1BB+ T cells and 4-1BB+NK cells were highest in immune active phase. Our findings showed that the HBeAg status is linked to a distinct immune phenotype of intrahepatic CD8+ T cells and NK cells characterised by high expression of ICM, particularly 4-1BB. Importantly, antiviral treatment partially restored the normal expression of ICM in the liver compartment in NUC-treated HBV patients. Finally, we described important differences in ICM expression between intrahepatic and circulating NK cells in chronic HBV patients.

Conclusion: Our study shows clear differences in the intrahepatic expression of ICM on NK cells and T cells in chronic HBV patients depending on their clinical stage.

SAT-397

Transcriptomic analysis and high-throughput hepatitis B virus integration sequencing of HepaD38 cells

Cristina Musolino¹, Daniele Lombardo², Valeria Chines³, Giuseppina Raffa⁴, Domenico Giosa⁵, Riccardo Aiese Cigliano⁶, M'homed Aguenoz³, Giovanni Raimondo³, Teresa Pollicino⁷.
¹University Hospital "G.Martino" Messina, Messina; ²University Hospital "G. Martino" Messina, Messina, Italy; ³University Hospital "G. Martino" of Messina, Messina, Italy; ⁴University Hospital "G. Martino" of Messina, Messina, Italy; ⁵University of Messina, Messina, Italy; ⁶Sequentia Biotech SL, Barcelona, Barcelona, Spain; ⁷University Hospital G Martino of Messina, Messina, Italy
Email: tpollicino@unime.it

Background and aims: Hepatitis B virus (HBV) infection is a major cause of hepatocellular carcinoma (HCC) development worldwide. One key carcinogenic mechanism of HBV involves the integration of its DNA into the host genome. Recent findings have revealed that mitochondrial DNA (mtDNA) may also be a target for HBV integration. This suggests a novel potential mechanism whereby the integration of HBV into mtDNA could play a role in liver damage and the progression of HCC. The objectives of this study included: (1) Conducting a comprehensive analysis of HBV integration into mtDNA of the HepaD38 cell line, which is derived from HepG2 cells and supports tetracycline (Tet)-off inducible HBV replication; (2)

POSTER PRESENTATIONS

Assessing the mitochondrial function in HepaD38 cells during HBV replication.

Method: We employed a high-throughput Hepatitis B Virus Integration Sequencing (HBIS) method alongside RNA sequencing (RNASeq) to explore HBV integration within mitochondria isolated from HepaD38 cells, following Tet removal for a period of seven days. Concurrently, at this same time point, we assessed the mitochondrial function of HepG2 and HepaD38 cells using the Seahorse XFP Analyzer.

Results: Seven days post Tet removal, the average quantities of HBV DNA and HBV RNA in HepaD38 cells were $1.1 \times 10^3 \pm 6.0 \times 10^2$ and $1.0 \times 10^1 \pm 5.9 \times 10^{-1}$ copies per cell, respectively. Concurrently, the mean levels of HBV DNA and HBsAg in the cell supernatants were $2 \times 10^6 \pm 2.7 \times 10^4$ copies/ml and $4.1 \times 10^3 \pm 7.2 \times 10^2$ IU/ml, respectively. At the same time point, HBIS revealed an average of 81 ± 11.9 HBV integration sites in the mtDNA of $\sim 1.5 \times 10^5$ HBV-replicating HepaD38 cells. Notably, these integration sites were predominantly found in the COX1, RNR2, and ND2 mitochondrial genes. Additionally, RNASeq analysis revealed a substantial presence (average \pm S.D.: 635 ± 143.7) of HBV-mitochondrial transcript fusions within the same number of HBV-induced HepaD38 cells. We found multiple instances of chimeric transcripts resulting from HBV integration into mtDNA with flanking mitochondrial sequences most frequently corresponding to the COX1, RNR2, ND2, ND4, and ND6 genes. Interrupted HBV open reading frames (ORFs) were common in the surface gene (HBs), X gene (HBx), and between X and core (HBc) regions. Functional analysis of the mitochondria demonstrated that, in comparison to HepaD38 cells without HBV replication and viral integration, those replicating HBV exhibited a two-fold decrease in basal respiration, ATP-linked respiration, and maximal respiration.

Conclusion: The results of this study indicate that: (1) HBV can integrate into the mtDNA of HepaD38 cells during HBV replication; (2) the mtDNA site of HBV insertion may be transcriptionally active; and (3) the replication of HBV and its integration into mtDNA may contribute to mitochondrial dysfunction.

SAT-398

Rapid establishment of enterically-transmitted hepatitis viruses animal model by using lipid nanoparticle-based viral RNA delivery system

Tianxu Liu¹, Lin Wang². ¹Peking university health science center, Beijing, China; ²School of Basic Medical Sciences, Beijing, China
Email: lin_wang@pku.edu.cn

Background and aims: HAV and HEV are currently the most common causative agent of acute viral hepatitis in humans. Wild-type HAV and HEV has long been extremely difficult to culture in cells and only limited cell-adapted strains can be used for in vitro culture. The viral stocks used to infect animals are usually prepared directly from feces or liver homogenates collected from infected animals or feces. Using reverse generic system, either after many days or weeks in culture to collect adequate titers of infectious viral stocks or direct injection of in vitro transcribed (IVT) full-length viral genomic RNA (vRNA) into the liver is required to establish animal infection. These procedures are either time-consuming or warrant invasive operation which impede the efficiency, uniformity and quality control of the establishment of a tractable animal model. Therefore, a culture-free, robust and rapid approach for the establishment of in vivo infection is urgently warranted.

Method: By using this innovative LNP-based RNA delivery platform and full-length viral genome RNA (vRNA) system, we successfully encapsulated the full-length viral genome RNAs (vRNAs) of HAV and HEV into LNP, and established the corresponding animal models by intravenous injection of these LNP-vRNA formulations. The effect of the model was evaluated by detecting fecal detoxification, urine antigen, liver tissue HE staining, immunohistochemistry, transcriptome analysis and other experimental methods.

Results: We rationally prepared Lipid nanoparticle (LNP)-encapsulated full-length genomic RNA (vRNA) of HAV and HEV, and establishment of HAV and HEV infection was achieved after intravenous injection in susceptible animals. Upon LNP-vRNA injection, HAV and HEV Infection resulted in rise of viral RNA in feces, liver or bile samples, or viral antigen in urine. 10 μ g HEV RNA could induce successful infection in individual rabbit. Liver showed inflammatory infiltration and active transcriptional response against acute HEV infection. The antiviral efficacy of ribavirin and in vivo function of HEV genome mutation and deletion were validated in our model.

Conclusion: By using this innovative LNP-based RNA delivery platform and full-length viral genome RNA (vRNA) system, we successfully encapsulated the full-length viral genome RNAs (vRNAs) of HAV and HEV into LNP, and established the corresponding animal models by intravenous injection of these LNP-vRNA formulations. This novel approach enables rapid and efficient establishment of HAV and HEV in vivo infection in multiple animals, providing a powerful tool to investigate the pathogenesis of these enterically-transmitted hepatitis viruses as well as to evaluate specific countermeasures.

SAT-399

Immune profiling of HBsAg-specific B cells in CHB patients with HBsAg loss

Yifei Guo¹, Yue Guo¹, Yide Kong¹, Haoxiang Zhu¹, Jiming Zhang¹.

¹Department of Infectious Diseases, Shanghai Key Laboratory of Infectious Diseases and Biosafety Emergency Response, National Medical Center for Infectious Diseases, Huashan Hospital, Fudan University, Shanghai, China

Email: yfguo21@m.fudan.edu.cn

Background and aims: HBsAg loss, namely, the functional cure, is the optimal end point of current antiviral therapies. However, little is known about the frequency, phenotype and class-switching of HBsAg-specific B cells in chronic hepatitis B (CHB) patients with HBsAg loss. Here, we compare the HBsAg-specific memory B cells (HBs⁺ Bm cells) of CHB patients with and without HBsAg loss, as well as functional cure CHB patients with different anti-HBs levels.

Method: We included 42 treatment-naïve CHB patients without HBsAg loss (chronic HBsAg⁺), 94 interferon-treated CHB patients with HBsAg loss (chronic HBsAg⁻), and 20 healthy controls with or without HBsAg-vaccinated. Detailed characterization of memory B cell responses in peripheral blood was determined through high-dimensional flow cytometry. HBs⁺ Bm cells were identified and examined using fluorescently labeled HBsAg bait.

Results: No statistically differences in frequency were observed among vaccinated controls (median 0.09%), chronic HBsAg⁺ (median 0.14%), and chronic HBsAg⁻ (median 0.14%) patients. Similarly, the frequency did not differ significantly across all clinical phases of chronic HBV infection. Of note, we observed that the increased frequency of HBs⁺ Bm cells was accompanied by concordant elevation of anti-HBs levels, even though there was a trend, not statistical significance, towards elevated frequencies in patients with $10 \leq \text{anti-HBs} < 500$ IU/L compared with anti-HBs < 10 IU/L. A composite sample was generated by merging FCM results of HBs⁺ Bm cells with non-HBs⁺ Bm cells from CHB patients. The UMAP showed a clear segregation of HBs⁺ Bm cells from non-HBs⁺ Bm cells, indicating the distinct immune profiles of HBs⁺ Bm cells. Furthermore, compared with global memory B cells, a range of expression of inhibitory markers, including BTLA, CD11c, PD-1, CD22, and FcRL5 were increased, which were consistent with preliminary studies on impaired HBsAg-specific B cell function. When comparing the differences of HBs⁺ Bm cells in chronic HBsAg⁺ and chronic HBsAg⁻ patients, there were not significant differences in frequency of resting (CD21⁺CD27⁺), activated (CD21⁺CD27⁺), atypical (CD21⁺CD27⁻), and intermediate (CD21⁺CD27⁻) HBs⁺ Bm cells. Of note, expressions of T-bet and CXCR5 were decreased in chronic HBsAg⁻ patients. Analysis of class-switching of HBs⁺ Bm cells detected a trend towards elevated

proportion IgG⁺ HBs⁺ Bm cells in chronic HBsAg- compared with chronic HBsAg+ patients. For chronic HBsAg- patients, HBs⁺ Bm cells in patients with anti-HBs ≥ 500 IU/L exhibited lower expression of CXCR5 and higher proportion of IgG⁺ than other two groups (10 \leq anti-HBs <500 IU/L and anti-HBs <10 IU/L).

Conclusion: HBs⁺ Bm cells exhibit a distinct immune profile compared to global memory B cells. Low expression of CXCR5 in HBs⁺ Bm cells might be associated with restored function and a favorable outcome.

SAT-402

Bemnifosbuvir is a potent HCV NS5B inhibitor with a favorable antiviral profile and high resistance barrier

Qi Huang¹, Dawei Cai¹, Steven Good¹, Nancy Agrawal¹, Jean-Pierre Sommadossi¹. ¹Atea Pharmaceuticals, Inc., Boston, United States

Email: huang.qi@ateapharma.com

Background and aims: Bemnifosbuvir (BEM), an oral prodrug of a guanosine nucleotide analog, has demonstrated highly potent, pan-genotypic, best-in-class *in vitro* antiviral activity against all hepatitis C virus (HCV) genotypes (GTs 1–5) tested. Viral resistance has emerged as an important consideration for direct-acting antivirals (DAAs) as it may impact efficacy of HCV infection treatment. The antiviral activity of BEM was profiled against a panel of sofosbuvir (SOF) non-structural protein 5B (NS5B) resistance-associated variants (RAVs) selected *in vitro* or identified in HCV patients. *In vitro* resistance selection was performed using HCV GT-1a and –1b replicon cells to identify NS5B RAVs potentially impacting BEM antiviral activity.

Method: *In vitro* resistance selection was conducted in the presence of G418 and gradually-increasing concentrations of AT-511 (free base of BEM). Cells from each passage were collected for genotypic analysis. Emerging NS5B substitutions (single or linked) were selected for phenotyping in transient replicon assays.

Results: Resistance selection in GT1b replicons identified C223H as the primary substitution that confers resistance to AT-511, which is the same mutant identified in GT-2a (JFH-1) replicons cultured in the presence of PSI-352938 or PSI-353661, two HCV nucleotide analogs that also generate the same active tri-phosphate AT-9010, in previous studies (Lam, JVI, 2011). C223H substitution requires two nucleotide mutations, which confers a higher barrier to resistance. Additional substitutions were identified in GT-1a (C316F, N444D, F574V, I585T) and GT-1b (F54I, N206S, E237G, T344I, Y586C). Phenotypic evaluation of both GT-1a and –1b mutations indicated that single amino acid changes did not significantly reduce AT-511 activity (up to 1.7-fold). However, a combination of amino acid changes in GT-1b (F54I, C223H, E237G, T344I, Y586C) conferred higher levels of resistance (up to 5.9-fold). In addition, SOF did not show cross-resistance to C223H, and only conferred weak resistance to the linked mutants.

Conclusion: BEM is at least 10-fold more potent than SOF across all genotypes tested and is not resistant to SOF RAVs (S282T, L159F/S282T). C223H was found to be the primary BEM RAV in GT-1b and multiple substitutions at other NS5B regions were required to confer meaningful resistance, suggesting a very high barrier to resistance for BEM. BEM is currently being evaluated in combination with ruzasvir (RZR), a highly potent pan-genotypic NS5A inhibitor, in a Phase 2 clinical trial (NCT05904470). Based upon the data demonstrated to date, it is expected that the BEM/RZR combination should have a more compelling antiviral profile against major HCV NS5A RAVs than current standard of care.

SAT-403

Vitamin D supplementation accelerated reduction of HBsAg levels in patients with chronic hepatitis B requiring treatment and in inactive carrier phase

Thitaporn Roongrawee¹, Sirinporn Suksawatamnuay², Panarat Thaimai², Prooksa Ananchuensook³, Supachaya Sriphoosanaphan⁴, Kessarin Thanapirom⁵, Piyawat Komolmit⁶. ¹Division of Gastroenterology, Department of Medicine, Faculty of Medicine, King Chulalongkorn Memorial Hospital, Bangkok, Thailand; ²Division of Gastroenterology, Department of Medicine, Faculty of Medicine, Chulalongkorn University and King Chulalongkorn Memorial Hospital, Thai Red Cross Society, Bangkok, Thailand, Chulalongkorn University and King Chulalongkorn Memorial Hospital, Bangkok, Thailand; ³Chulalongkorn University, Division of Gastroenterology, Department of Medicine, Bangkok, Thailand; ⁴Institute for Liver and Digestive Health, University College London, London, United Kingdom; ⁵Division of Gastroenterology, Department of Medicine, Faculty of Medicine, Bangkok, Thailand; ⁶Division of Gastroenterology, Department of Medicine, Faculty of Medicine, Chulalongkorn University and King Chulalongkorn Memorial Hospital, Bangkok, Thailand
Email: thitagitfr@gmail.com

Background and aims: Low levels of vitamin D are prevalent among individuals with chronic hepatitis B (CHB) infection. Vitamin D is known to modulate the immune system and potentially influence the immune response to hepatitis B viral replication, as indicated by the quantitative hepatitis B surface antigen (qHBsAg)-a marker of viral replication and predictive indicator for functional cure. Previous studies established a correlation between vitamin D levels and qHBsAg levels. However, the direct impact of vitamin D supplementation on qHBsAg levels remains a subject of ongoing investigation.

Method: Retrospective data from HBV inactive carriers and CHB patients undergoing antiviral treatment with initially low vitamin D levels were analyzed. Quantification of qHBsAg levels before and after vitamin D supplementation over an 18-month period was conducted.

Results: Among 1069 CHB cases follow-up at King Chulalongkorn Memorial Hospital's liver clinic, complete data for qHBsAg and vitamin D levels were available for 203 patients. Of these, 88 were inactive carriers, and 115 were CHB patients. Vitamin D insufficiency (vitamin D levels 20–30 ng/ml) was observed in 77 patients, while 97 patients had vitamin D deficiency (vitamin D levels below 20 ng/ml). Pre-supplementation vitamin D levels averaged 19.5 \pm 4.8 ng/ml and significantly increased to 36.69 \pm 14.58 ng/ml post-supplementation ($p < 0.01$). Most patients received weekly vitamin D supplements at a dosage of 40,000 IU/week (N 145; 71.43%), followed by 60,000 IU/week (N 43; 21.18%) and 20,000 IU/week (N 15; 7.38%), respectively. The average interval between qHBsAg measurements before starting vitamin D was 10.6 months and the average time after vitamin D initiation was 11.1 months. The level of qHBsAg demonstrated an 11.23% decrease before vitamin D supplementation, significantly reducing further to 18.20% post-supplementation ($p = 0.032$). Subgroup analysis revealed a significant decline of qHBsAg level in 88 inactive carriers (–9.23% vs –19.30%; $p = 0.028$) and in 79 patients with qHBsAg levels more than 1,000 IU/ml (0.53% vs –14.30%; $p = 0.009$). However, CHB patients on antiviral treatment and patients with qHBsAg levels between 100 and 1,000 IU/ml showed substantial reduction but lacked statistical significance (–12.77% vs –17.35%; $p = 0.422$, –13.77% vs –18.31%; $p = 0.257$, respectively).

Conclusion: This study demonstrates a significant decrease in qHBsAg levels following vitamin D supplementation, particularly prominent in individuals with high qHBsAg levels exceeding 1,000 IU/ml and inactive carriers. These findings imply a potential enhancement of qHBsAg decline facilitated by vitamin D. The implications warrant further exploration if vitamin D's role in managing chronic hepatitis B, presenting avenues for future research.

SAT-404

The Lipidome in phenotyping hepatitis B infection ('LiPHe-B'): preliminary results from our pilot study

Marion Delphin¹, Susana Palma-Duran^{1,2}, Mariana Silva dos Santos¹, Emily Martyn¹, Elizabeth Waddilove¹, Emma Wall¹, Tongai Gibson Maponga³, Jacqueline Martin⁴, Catherine De Lara⁵, Paul Klenerman⁵, Eleanor Barnes⁵, James Macrae¹, Philippa C Matthews^{1,6}. ¹*the francis crick institute, london, United Kingdom*; ²*Department of Food Science, Research Center in Food and Development A.C, Hermosillo, Mexico*; ³*Division of Medical Virology, Stellenbosch University/National Health Laboratory Service Tygerberg Business Unit, cape town, South Africa*; ⁴*Department of Hepatology, John Radcliffe Hospital, oxford, United Kingdom*; ⁵*Nuffield Department of Medicine, Medawar Building for Pathogen Research, University of Oxford, oxford, United Kingdom*; ⁶*University College London, london, United Kingdom*

Email: marion.delphin@crick.ac.uk

Background and aims: Chronic Hepatitis B infection (CHB) kills 1 million people per year, due to liver fibrosis, cirrhosis, and hepatocellular carcinoma (HCC). Hepatitis B Virus (HBV) has been described as a 'metabovirus' for its close connection with host metabolism and lipids, but current biomarkers are blunt tools for risk assessment, and guidelines do not account for host and viral genetics, metabolic risk factors, and environmental influences contributing to liver disease. There is a need for improved risk-stratification that accounts for these parameters and can inform patient-stratified approaches. The liver is one of the most important organs in energy metabolism, and the origin of most blood lipids, potentially explaining why host lipid profiles could impact or reflect the antiviral immune response and HCC progression. We set out a pilot study to optimize methods and establish proof-of-principle for this approach in HBV, and to determine whether profiles differed between people living with HBV (PLWHB) vs healthy controls.

Method: Serum samples were obtained from PLWHB, enrolled at Oxford University Hospitals, UK (n = 60) (ethics ref.N17/01/013) and age and sex-matched healthy non-infected adults, from the Legacy Study, London UK (n = 60) (ethics ref.21/YH/0222). Meta-data were recorded at the time of recruitment, supported by Electronic Patient Records where available. Lipids were extracted using a modified Bligh-Dyer extraction method followed by Liquid Chromatography-Mass Spectrometry (LC-MS) analysis for lipidome profile. Data processing and statistical analysis were performed using Xcalibur (Thermo Scientific), MS-DIAL (v 5.1.230517), KniMet pipeline for MS-based and SIMCA 17 (Sartorius, Germany). Principal component analysis (PCA) and orthogonal partial least square-discriminant analysis (OPLS-DA) models were used to explore the differences in the lipidome between CHB and controls.

Results: Comprehensive lipid profiles were obtained for a pilot subset of 40/120 serum samples. Initial multivariate analyses revealed clear differences in the lipidomes of non-infected and infected individuals. Detected features were initially annotated by comparison of molecular and associated fragment ions to compound libraries (both in-house and commercial). Further lipid extraction and identification is currently ongoing, along with additional clustering analysis based on liver disease progression in patients.

Conclusion: Adults living with HBV have a distinct lipidome profile that distinguishes them from matched adult controls. Developing insights into lipid biomarkers may enhance our understanding of the mechanisms that determine infection outcomes and treatment response, support better patient-stratification risk assessment and guide evidence-based interventions.

SAT-405

Differential expression and sequence variants of sodium taurocholate cotransporting polypeptide (NTCP) do not affect HDV inhibition by Bulevirtide (BLV)

Simin Xu¹, Thomas Aeschbacher¹, Savrina Manhas¹, Chunfeng Li¹, Ross Martin¹, Yang Liu¹, Evguenia Maiorova¹, Hongmei Mo¹, Roberto Mateo¹. ¹*Gilead Sciences Inc, Foster City, United States*
Email: simin.xu@gilead.com

Background and aims: The bile acid transporter sodium taurocholate cotransporting polypeptide (NTCP) is a transmembrane protein expressed on the surface of hepatocytes in the liver. NTCP is also an entry receptor for hepatitis B virus (HBV) and its satellite hepatitis D virus (HDV). The HDV entry inhibitor bulevirtide (BLV) specifically binds NTCP and blocks HDV from entering hepatocytes. The goal of this study was to investigate the role of NTCP expression level and polymorphisms on BLV inhibition of HDV.

Method: Public data were analyzed to identify NTCP single nucleotide polymorphisms (SNPs) with a Minor Allele Frequency (MAF) >1% in United States (US) and global racial groups (White, Black, Asian, Latino). In addition, NTCP whole exon sequencing was performed on primary human hepatocytes (PHHs) from 50 US donors. These were further evaluated for NTCP expression, mRNA levels and HDV sensitivity to BLV in an in vitro phenotyping assay. PHHs from 33 PHH donors carrying identified NTCP SNPs and various expression NTCP levels were evaluated for HDV sensitivity to BLV in an in-vitro phenotyping assay.

Results: Six NTCP SNPs were observed in the public dataset with MAFs >1% in one or more racial group. Of these SNPs, 2 were non-synonymous (C800T, T668C) and 4 were synonymous (G225A, T627C, C960A, C111T). C800T (aaS267F) was found with a MAF of 3.6% in the Asian racial group in the global dataset. T668C (aaI223T) was found in the Black racial group in the US and global datasets with MAFs of 1.6% and 4.1%, respectively. Four NTCP variants were detected in the 50 PHH donors from the US. C800T (aaS267F) and T668C (aaI223T) non-synonymous SNPs were detected in PHHs from an Asian and Black donor, respectively. Synonymous SNPs G225A and T627C were detected in 4 donors (Black, n = 2; Latino, n = 1; White, n = 1) and 2 Black donors, respectively. NTCP surface protein levels varied 5.8-fold and mRNA levels varied 391-fold among the 50 PHH donors. BLV remained active against HDV on PHHs expressing all levels of NTCP and all NTCP SNPs observed in the 50 US donors.

Conclusion: BLV potently inhibits HDV regardless of naturally occurring NTCP sequence variants and differential NTCP expression levels.

SAT-406-YI

HBV dominance is associated with a distinct inflammatory milieu in HBV/HCV coinfection

Carlos Oltmanns^{1,2,3}, Moana Witte^{1,2,3}, Anika Wranke¹, Katja Deterding¹, Heiner Wedemeyer^{1,4,5}, Christine Falk⁶, Anke R.M. Kraft^{1,2,3,4,5}, Steffen Wiegand⁷, Markus Cornberg^{1,2,3,4,5}.

¹*Department of Gastroenterology, Hepatology, Infectious Diseases and Endocrinology, Hannover Medical School (MHH), Hannover, Germany*;

²*Centre for Individualised Infection Medicine (CiiM), a joint venture between the Helmholtz Centre for Infection Research (HZI) and Hannover Medical School (MHH), Hannover, Germany*;

³*TWINCORE, a joint venture between the Helmholtz-Centre for Infection Research (HZI) and the Hannover Medical School (MHH), Hannover, Germany*;

⁴*Cluster of Excellence Resolving Infection Susceptibility (RESIST; EXC 2155), Hannover Medical School, Hannover, Germany*;

⁵*German Centre for Infection Research (DZIF), partner site Hannover-Braunschweig, Hannover, Germany*;

⁶*Institute of Transplant Immunology, IFB-Tx, Hannover Medical School, Hannover, Germany*;

⁷*Department of Anesthesiology and Intensive Care Medicine, Hannover Medical School, Hannover, Germany*

Email: oltmanns.carlos@mh-hannover.de

Background and aims: Hepatitis B (HBV) and C (HCV) virus coinfection is linked to a higher risk of cirrhosis and hepatocellular carcinoma (HCC) compared to mono-infection. Despite this, data is limited, and further investigation is needed to understand the underlying mechanisms. While patients are classified based on dominance patterns, the impact on the immune system remains largely unknown. It is recognized that HBV reactivation may occur following HCV clearance. This study aims to explore the potential immune interactivity between HCV and HBV by analyzing patterns of soluble immune mediators (SIM).

Method: Fifty-nine soluble immune mediators were measured in serum or plasma samples of 49 patients chronically infected with hepatitis B and hepatitis C virus. Patients were classified based on dominance patterns: HBV dominance (n = 8), HCV dominance (n = 22), HBV and HCV codominance (n = 11) and no dominance (n = 8).

Results: SIM expression was distinct based on different dominance patterns. HBV activity induced higher SIM expression and altered the soluble inflammatory milieu (22 SIM altered, $p < 0.05$). Altered pathways included JAK-STAT pathway ($p = 1.36 \times 10^{-20}$), IL-17 signaling ($p = 2.47 \times 10^{-13}$) and Th17 ($p = 1.69 \times 10^{-9}$) cell differentiation. CTACK ($r = -0.69$, $p = 7.02 \times 10^{-6}$) and SDF-1 α ($r = -0.55$, $p = 0.002$) correlated inversely with HCV-RNA.

Conclusion: Serologically classifying dominance patterns in HBV and HCV coinfection may manifest in a distinct soluble inflammatory milieu. Elevated HBV activity correlates with an increased expression of soluble immune mediators, particularly influencing the alteration of key signaling pathways such as JAK-STAT and the TH17/IL-17 axis. These changes play a crucial role in the development of liver fibrosis.

SAT-407

Long-term sustained decline of anti-HCV neutralizing antibodies in HIV/HCV-coinfected patients after therapy-induced HCV clearance

Daniel Sepúlveda-Crespo^{1,2}, Camilla Volpi^{1,3}, Rafael Amigot-Sánchez¹, Marta Quero-Delgado¹, María Yélamos⁴, Cristina Díez^{2,5,6}, Julián Gómez⁴, Víctor Hontañón^{7,8}, Juan Berenguer^{2,5,6}, Juan González^{2,7,8}, Rubén Martín-Escolano^{1,2}, Salvador Resino García^{1,2}, Isidoro Martínez^{1,2}. ¹Unidad de Infección Viral e Inmunidad, Centro Nacional de Microbiología, Instituto de Salud Carlos III, Madrid, Spain; ²Centro de Investigación Biomédica en Red en Enfermedades Infecciosas (CIBERINFEC), Instituto de Salud Carlos III, Madrid, Spain; ³Dipartimento di scienze farmaceutiche e biomolecolari, Università degli Studi di Milano, Milan, Italy; ⁴Departamento de Bioquímica y Biología Molecular, Facultad de Ciencias Químicas, Universidad Complutense, Madrid, Spain; ⁵Unidad de Enfermedades Infecciosas/VIH; Hospital General Universitario Gregorio Marañón, Madrid, Spain; ⁶Instituto de Investigación Sanitaria del Gregorio Marañón (IISGM), Madrid, Spain; ⁷Unidad de VIH; Servicio de Medicina Interna, Hospital Universitario La Paz, Madrid, Spain; ⁸Instituto de Investigación Hospital Universitario La Paz, (IdIPAZ), Madrid, Spain
Email: danisecre@hotmail.com

Background and aims: Cross-reactive neutralizing antibodies against hepatitis C virus (HCV), primarily targeting the E2 glycoprotein, play a crucial role in controlling and clearing HCV infection and protecting against HCV reinfection. This study aimed to evaluate the titers and the amplitude of anti-E2 antibodies (anti-E2-Abs) and neutralizing antibodies against HCV (anti-HCV-nAbs) in HIV/HCV-coinfected patients over five years after the sustained viral response (SVR) following IFN-based therapy (PEG-IFN α /RBV or PEG-IFN α /RBV/DAA) or IFN-free DAA therapy.

Method: We followed 76 HIV/HCV-coinfected patients for five years after antiviral therapy-induced SVR. Plasma levels of anti-E2-Abs and anti-HCV-nAbs against five HCV genotypes (Gt1a, Gt1b, Gt2a, Gt3a, and Gt4a) were determined using ELISA and microneutralization assays, respectively. Statistical analyses comparing the three follow-up time points (baseline, one-year, and five-year post-HCV

treatment) were performed using Generalized Linear Mixed Models. p values were adjusted using the False Discovery Rate (q-value).

Results: Compared to baseline, plasma anti-E2-Abs titers decreased at one year (1.9 to 2.3-fold, q-value < 0.001) and five years (3.4 to 9.1-fold, q-value < 0.001) post-HCV treatment. Plasma anti-HCV-nAbs decreased 2.9 to 8.4-fold (q-value < 0.002) at one year and 17.8 to 90.4-fold (q-value < 0.001) at five years post-HCV treatment. HCV-nAbs titers against Gt3a were consistently the lowest. Low anti-E2-Abs nonresponse rates were observed throughout the follow-up, while anti-HCV-nAbs nonresponse rates increased. At baseline, anti-HCV-nAb were undetected in 4.0–5.3% of patients. At the five-year post-HCV treatment, nonresponse rates increased 1.8 to 13.5-fold (q-value < 0.05), with the highest nonresponse rate for Gt3a.

Conclusion: An overall decline in humoral responses against HCV (anti-E2-Abs and anti-HCV-nAbs) among HIV/HCV-coinfected patients at one- and five-years post-HCV treatment was observed, regardless of the analyzed HCV genotype. However, this decline was more pronounced for the anti-HCV-nAbs, particularly in the Gt3.

SAT-408

Molecular and functional analysis of a hepatitis B virus genotype C infection in a vaccinated individual

Maëlen Delcourt¹, Peter Gowland², Christoph Niederhauser³, Daniel Candotti¹. ¹Dept of Virology-Henri Mondor Hospital-Paris-Est University-INSERM U955-IMRB-Team 18, Creteil, France; ²Interregional Blood Transfusion SRC, Laboratory Diagnostics and RandD Diagnostics, Berne, Switzerland; ³Interregional Blood Transfusion SRC, Laboratory Diagnostics and RandD Diagnostics, Berne, Switzerland
Email: daniel.candotti@inserm.fr

Background and aims: Global hepatitis B virus (HBV) vaccination is key to the WHO objective to eradicate hepatitis B by 2030. The present study investigates an acute HBV infection in a regular blood donor from Switzerland with a complete vaccination course (Engerix B; 2001/2002).

Method: HBV infection was monitored by testing for serological markers and HBV DNA in a 6-months follow-up. PreS/S region was sequenced after viral particle concentration. S amino acid substitutions-related phenotype was investigated by site directed mutagenesis and in vitro functional analysis.

Results: At index time, HBV DNA (6 IU/ml) was detected in the presence of anti-HBs (500 mIU/ml) as only serological marker. Anti-HBs level was 14 mIU/ml and all HBV markers were negative in the donation collected six months earlier. HBV subgenotype C1 strain supported recent HBV exposure in Thailand. Follow-up showed transient HBV viraemia, anti-HBs level increase (> 1 000 mIU/ml), and no HBsAg and anti-HBc seroconversion. PreS/S amino acid sequence was identical to a consensus sequence from HBV_C-infected Asian donors. The S protein had 19 aa substitutions, including 8 within MHR, compared to a HBV_{A2} consensus sequence. Substitutions S114T, T126I, N131T, and T143S were observed at positions previously associated with immune escape. Quasispecies distribution showed 6 sequences differing by only one aa (W35R, Q51Stop, L89P, I195R, and G202E x2) from the dominant sequence. W35R and I195R were associated with significantly lower HBsAg production and cellular retention. A sW36R substitution resulted in a similar HBsAg production phenotype. The potential function of this conserved WW motif in the S cytosolic domain was investigated further by replacing sW35 with aa carrying positive (H, K, and R) or negative (E) charged lateral, uncharged polar lateral (Q), and hydrophobic side chain (A, M, F, and W). W35K and W35Q lead to intracellular retention of HBsAg. W35K was associated to reduced HBsAg production and W35F substitution leads to no phenotypic change. Results of W35H, E, A, M are pending.

Conclusion: HBV genotype C infection was confirmed in a fully vaccinated individual and was associated with an efficient secondary anti-HBs response leading to transient viraemia without HBsAg and

POSTER PRESENTATIONS

anti-HBc seroconversion over six months. This supported previous study suggesting that anti-HBs-only occult HBV infection was associated to vaccine escape. Infection may be related to low level of anti-HBs at the time of virus contact and aa variability in S epitopes between HBV_C strain and HBV_{A2}-derived vaccine. In vitro neutralization analysis is ongoing for confirmation. Unusual mutations in S cytosolic domain were associated to HBsAg reduced production and intracellular retention. Further investigations are needed to clarify the potential function of the conserved sW35sW36 motif in HBsAg production and viral replication.

SAT-409

Whole-genome hepatitis B virus sequencing at low viral loads from serum and dried blood spot using a multiplexed tiled amplicon approach

Sheila Lumley¹, Christopher Kent², Samuel Wilkinson², Camille Morgan³, Elizabeth Waddilove⁴, Marion Delphin⁴, George Airey¹, James Campbell⁴, Catherine De Lara¹, Jacqueline Martin⁵, Patrick Ngimbi⁶, Jonathan B. Parr³, Peyton Thompson³, Eleanor Barnes¹, Azim Ansari¹, Nick Loman², Josh Quick², Philippa C Matthews⁴. ¹University of Oxford, Oxford, United Kingdom; ²University of Birmingham, Birmingham, United Kingdom; ³University of North Carolina at Chapel Hill, North Carolina, United States; ⁴Francis Crick Institute, London, United Kingdom; ⁵Oxford University Hospitals NHS Foundation Trust, Oxford, United Kingdom; ⁶Université Protestante au Congo, Kinshasa, Congo, Dem. Republic of (formally known as Zaire)
Email: sheila.lumley@trinity.ox.ac.uk

Background and aims: Hepatitis B Virus (HBV) sequencing can be used to investigate viral transmission, evolution and polymorphisms linked to adverse outcomes such as resistance associated mutations (RAMs) and vaccine escape mutations (VEMs). However currently it is not possible to sequence full HBV genomes from approximately half of people with detectable HBV viral loads (VL), due to low median VL v.s. relatively high VLs required for full genome sequencing, high host background, genome structure and viral diversity. For the first time, we utilised an amplicon sequencing approach based on the ARTIC SARS-CoV-2 sequencing protocol for targeted full-genome HBV sequencing. We sequenced eight overlapping 500 bp amplicons to generate high quality consensus genomes from a range of VLs, including low VL samples, which it was previously not possible to sequence.

Method: HBV-specific primers were designed using a developmental version of PrimalScheme3. A multiple sequence alignment was generated from 2001 genomes and from this 94 primers were selected for each amplicon in order to cover the diversity present, resulting in the amplification of 8 amplicons generating a theoretical 100% genome coverage due to the circular genome. Plasma and dried blood spot (DBS) clinical samples with HBV VL 1.5–8.4 log (10) IU/ml from the UK and Democratic Republic of Congo were sequenced. Amplification and library preparation were performed by adapting the nCoV-2019 LoCost v3 sequencing protocol (Quick et al. 2020); 12 UK and 35 DRC samples multiplexed per run. Samples were sequenced on an Oxford Nanopore MinION with flowcell chemistry v10.4.1. Data were basecalled and demultiplexed using guppy (6.5.7). To enable compatibility with artic fieldbioinformatics (1.2.4), which generated the draft consensus genomes, primer.bed files were modified using primalhelper (1.0.0). We calculated genome coverage (at 20x depth) using samtools and bedtools.

Results: 47 clinical samples were sequenced. For samples with VL above 3 log (10) IU/ml, full length HBV genomes were recovered (100% coverage). For samples with VL as low as 1.5 log (10) IU/ml we were still able to achieve 90% genome coverage; the reduction in % coverage was due to lower sequencing depth of one amplicon. Genotypes A-E were identified, and data demonstrated distinct transmission patterns between households. We were able to call polymorphisms at sites of previously reported RAMs and VEMs.

Conclusion: We developed a simple, inexpensive targeted sequencing method to generate full-length HBV genomes at low VLs, which have previously been challenging to sequence. This method is readily deployable in resource-limited settings due to use of the MinION, and can also be easily adapted to other sequencing platforms. This data was used to call genotypes, RAMs, VEMs and perform phylogenetic analysis in previously difficult to sequence samples.

SAT-410

Establishment of a highly effective in vitro model for HBV genotype E infection

Rodrigue Kamga Wouambo¹, Felix Lehmann², Maria Pfefferkorn¹, Madlen Matz-Soja^{1,3}, Thomas Berg¹, Dieter Glebe⁴, Florian van Bömmel¹. ¹Division of Hepatology, Department of Medicine II, Leipzig University Medical Center, Leipzig, Germany; ²Charité-Universitätsmedizin Berlin, corporate member of Freie Universität Berlin and Humboldt-Universität zu Berlin, Institute of Virology, Berlin, Germany; ³Rudolf-Schönheimer-Institute for Biochemistry, Leipzig, Germany; ⁴Institute for Medical Virology, National Reference Centre for Hepatitis B viruses and Hepatitis D viruses, Justus Liebig University Giessen, Giessen, Germany
Email: rodrigue.kamgawouamba@medizin.uni-leipzig.de

Background and aims: Hepatitis B virus genotype E (HBV-E) is highly prevalent in Africa and associated with a higher viral replication and higher risk of hepatocellular carcinoma development compared to other HBV genotypes. Although Africa has a disproportionately high burden of hepatitis B, studies concerning this genotype are still under-represented. Our project aims at establishing an effective in vitro model for HBV-E to better understand its biomarker production and pathogenesis.

Method: The 1.1 and 1.5mer overlength HBV DNA constructs were engineered by fast cloning as previously described (Li et al. 2011). In brief, the primers for insert amplification were designed with insert-specific sequences and additional 15–17 bases overlapping with the vector-ends. The 1.5mer was generated from the 1.1mer template and the plasmids were transfected with variable ratios to the transfection reagent (2:1; 3:1; and 4:1) into HepG2-hNTCP cells to produce HBV-E viral particles. Viral particles were concentrated by ultrafiltration using Vivaspin® 20, 300, 000 MWCO PES (Sartorius) and thereafter tested for infectivity in vitro. HBV DNA, HBV RNA, HBeAg and HBsAg composition were quantified from supernatant collected either every 2 or 7 days during transfection or infection experiments.

Results: Transfection of both HBV-E plasmids resulted in successful secretion of HBeAg and HBsAg, with a higher expression from the 1.5mer plasmid. Transfecting 1.5mer at different ratios (2:1; 3:1 and 4:1) revealed similar mean levels of HBV DNA (8.7; 8.19; 8.02 [log10cp/ml]), HBV RNA (5.05; 4.4; 4.8 [log10cp/ml]) and total HBsAg (45.92 ± 7.2; 40.94 ± 3.16; 46.9 ± 4.02 [ng/ml]) at 8 dpi. Interestingly, mean LHBs levels and proportions of secreted HBsAg in supernatant were 3-fold higher using transfection ratio 3:1 (2.7 ng/ml and 6.32%) compared to 2:1 (0.79 ng/ml and 1.68%) and 4:1 (0.72 ng/ml and 1.64%). In vitro infection with the generated HBV-E viruses (Week 5, MOI=200) lead to de novo infection; HBV DNA and RNA levels decreased from input (7.30 and 4.89 log10cp/ml) to wash-out (3.89 and 0 log10cp/ml) and showed a stable increase to 5.25 and 3.16 log10cp/ml after 10 dpi follow by a sustained expression until 22 dpi.

Conclusion: The newly engineered HBV-E plasmids can be transfected in cell culture and used to generate infectious and replicating HBV-E viruses for in vitro analysis. Our model is ready-for-use in further studies on HBV replication and drug efficacy testing concerning HBV-E.

SAT-411

Absorption, distribution, metabolism, and excretion of [14C]-Bemnifosbuvir in the rats

Alex Vo¹, Steven Good¹, Nancy Agrawal¹, Jean-Pierre Sommadossi¹.
¹Atea Pharmaceuticals, Inc., Boston, United States
 Email: vo.alex@ateapharma.com

Background and aims: Bemnifosbuvir (BEM), a phosphoramidate oral prodrug of a unique, 6-modified guanosine nucleotide with potent antiviral activity against the RNA-dependent polymerase (RdRP) of several single stranded RNA viruses, is currently in development for the treatment of COVID-19 and HCV (in combination with the NS5A inhibitor ruzasvir). The mass balance, excretion, and metabolism of [14C]-BEM were characterized in normal and bile-duct cannulated (BDC) rats after a single oral dose.

Method: Male SD and LE rats received a single dose of [14C]-BEM at 60 mg/kg (200 µCi/kg). Urine and feces were collected through 168 h post-dose while plasma was collected for up to 48 h post-dose in normal rats. Urine and feces were collected for up to 96 h post-dose in BDC rats. Radioactivity was quantified by liquid scintillation counting. Tissue distribution was determined by quantitative whole-body autoradiography.

Results: The primary route of elimination of radioactivity was in the urine (50%) and feces (41%) in normal rats, and in the urine (43%), feces (35%), and bile (19%) in BDC rats, with total recovery of radioactivity of 91% in normal rats and 97% in BDC rats. BEM was widely distributed, with quantifiable levels present in many tissues through 24 h. In general, levels in tissues were similar to or lower than those in blood. Relatively high tissue levels were observed in the kidneys, liver, thymus, and small intestine. Low tissue levels were observed in brain, spinal cord, and bone. Concentrations in the eye lens were below the level of quantification. In general, the average elimination half-life for most tissues was <18 hr with no evidence for long-term retention or irreversible binding in skin or eye (uvea). BEM undergoes multistep metabolic activation to its active triphosphate (TP) metabolite AT-9010, which is found intracellularly. The major plasma circulating metabolites were AT-229 and AT-273. In urine, the major components were AT-229, AT-273, and AT-219. In bile, the major metabolite was AT-551. In feces, the major components were AT-229 and AT-273.

Conclusion: Following a single oral dose in rats, BEM has favorable overall ADME properties, including good bioavailability (>60%) and wide distribution to tissues with low penetration into the brain. BEM was highly and rapidly metabolized to the metabolite AT-273, which was a surrogate for the intracellular pharmacologically active TP.

SAT-412

Low risk of drug-drug interactions for Ruzasvir based upon in vitro metabolism and transporter interaction studies

Alex Vo¹, Jocelyn Yabut², Michael Hafey³, Hui Wan², Nancy Agrawal¹, Jean-Pierre Sommadossi¹.
¹Atea Pharmaceuticals, Inc., Boston, United States; ²Merck and Co., Inc., West Point, United States; ³Merck and Co., Inc., Rahway, United States
 Email: vo.alex@ateapharma.com

Background and aims: Ruzasvir (RZR), a potent small molecule inhibitor of hepatitis C nonstructural protein 5A (NS5A), is currently being developed for the treatment of hepatitis C virus (HCV) in combination with bemnifosbuvir, a potent nucleotide prodrug inhibitor of the RNA-dependent RNA polymerase (RdRp) of HCV. The potential of RZR to mediate drug-drug interactions (DDIs) via cytochrome P450 (CYP) metabolizing enzymes and transporters was evaluated *in vitro*.

Method: RZR was incubated *in vitro* with human liver microsomes, hepatocytes, and transporter transfected cells or membrane vesicles to evaluate its interaction with relevant enzymes/transporters.

Results: *In vitro* CYP reaction phenotyping suggested that CYP3A was the primary enzyme involved in the hepatic oxidative metabolism of RZR; however, the extent of CYP-mediated metabolism was observed

to be very low *in vivo*. RZR did not exhibit direct nor time-dependent inhibition of any major CYP450 enzymes at concentrations up to 10 µM. In human hepatocytes, RZR did not significantly induce CYP1A2, CYP2B6, or CYP3A4 mRNA. RZR inhibited P-gp-mediated digoxin transport and BCRP-mediated methotrexate uptake with an IC₅₀ of 0.049 µM and 0.27 µM, respectively. RZR inhibited uptake of pitavastatin and sulfobromophthalein mediated by OATP1B1 and OATP1B3 with an IC₅₀ of 0.092 µM and 0.052 µM, respectively. RZR also inhibited BSEP transporter with IC₅₀ of 0.37 µM. RZR did not exhibit any inhibition on OAT1, OAT3, and OCT2 transporters.

Conclusion: Based on *in vitro* data and static DDI risk assessment models, RZR has low potential to be a perpetrator of DDI via inhibition or induction of CYP450. Likewise, it has low potential to inhibit OATP1B1 and OATP1B3. The relevance of BSEP inhibition to DDIs is limited. However, RZR may be a perpetrator of DDI with P-gp and BCRP, which warrants further investigation *in vivo*.

SAT-413

Hepatitis B virus seroepidemiology in the Vukuzazi population programme, KwaZulu Natal, South Africa

Motswedi Anderson¹, Tongai Gibson Maponga², Gregory Jording-Jespersen³, Janine Upton⁴, Dickman Gareta⁴, Malcolm Ellapen⁵, Elizabeth Waddilove⁶, Lusanda Mazibuko⁴, Stephen Olivier⁷, Jacob Busang⁸, Gloria Sukali⁹, Marion Delphin⁶, Resign Gunda⁴, Emily Wong⁴, Mark Seidner¹⁰, Thandeka Khoza⁷, Thumbi Ndungu⁷, Kathy Baisley⁷, Khanyi Msomi¹¹, Theresa Smit⁷, Collins Iwuji¹², Philippa C Matthews⁶.
¹Africa Health Research Institute, KwaZulu Natal, South Africa; ²Tygerberg Hospital and Stellenbosch University, Stellenbosch, South Africa; ³Stellenbosch, South Africa; ⁴Africa Health Institute Partnership (AHRI), Durban, South Africa; ⁵Africa Health Research Institute (AHRI), Durban, South Africa; ⁶National Health Laboratory Service, Albert Luthuli Hospital, Durban, South Africa; ⁷The Francis Crick Institute, London, United Kingdom; ⁸Africa Health Research Institute, Durban, South Africa; ⁹Africa Health Institute Partnership, Durban, South Africa; ¹⁰Africa Health Research Institute, Division of Infectious Diseases, Massachusetts General Hospital, Durban, South Africa; ¹¹National Health Laboratory Service, Albert Luthuli Hospital, Durban, South Africa; ¹²Africa Health Research Institute, Durban, South Africa
 Email: philippa.matthews@crick.ac.uk

Background and aims: There are approximately 80 million people living with chronic Hepatitis B virus (HBV) in the WHO Africa region, but few seroepidemiology data to guide public health and clinical management strategies in African populations, for whom HBV elimination goals are still far from reach. We set out to investigate HBV infection markers in a rural population in South Africa.

Method: The EVOLVE-HBV ('Evaluation of Vukuzazi LiVER disease') study used stored samples and biometric data collected by the Vukuzazi programme in KwaZulu Natal, South Africa. Vukuzazi enrolled participants who were ≥15 years old between May 2018 and March 2020. We selected 500 participants, stratified by sex, HIV status and age, to include adolescents and younger adults (born after routine HBV vaccine roll out started in South Africa from 1995 onwards). We screened plasma samples (according to availability) for HBV surface antigen (HBsAg), HBV core antibodies (anti-HBc) and HBV surface antibodies (anti-HBs). Two-tail significance tests were run at a 95% confidence interval using ANOVA and T-tests to determine differences in HBV biomarkers by age, sex and HIV status.
Results: Among 500 individuals in this study, 277 (55.4%) were female, 231 (46.2%) were living with HIV infection, and the median age was 31 years (IQR: 25–50). HBV infection (HBsAg) was present in 25/491 (5.1%) samples tested. Of the 25 participants who were HBsAg positive, 15/25 (60%) were male, median age was 46 years (IQR 28–55), 10/25 (40%) were HIV positive, and anti-HBc was present in 17/23 (73.9%). HBsAg was more likely to be positive in older participants (p = 0.004).

POSTER PRESENTATIONS

The overall prevalence of anti-HBc was 155/479 (32.4%), highlighting a high rate of exposure in this population. In this group, 84/155 (54.2%) were female, 75 (48.4%) HIV positive and median age was 50 years (39–61). Anti-HBc was more likely to be positive in older participants ($p < 0.001$).

There were 171/493 (34.7%) participants with anti-HBs titre > 10 mIU/ml, of whom 101/171 (59.1%) were female, 86 (50.3%) were HIV positive, and median age was 46 years (IQR 28–57). Vaccine-mediated immunity could be inferred in those with anti-HBs > 10 mIU/ml but HBsAg and anti-HBc negative; this serostatus was present in only 44/493 (8.9%) although our cohort was selected to include a cross-section of the population who should have received routine immunisation. Anti-HBs status was more likely to be positive in older participants ($p < 0.001$).

HBsAg, anti-HBc and anti-HBs were not associated with sex or HIV status ($p > 0.05$ for all).

Conclusion: In this population previously neglected by HBV research and clinical services, exposure to HBV is high, but only a minority of participants had evidence of vaccine-mediated immunity. Rapid scale-up of vaccination, diagnosis and treatment of HBV infection will be needed to make progress towards 2030 elimination goals.

SAT-414

Hepatitis B virus particles in serum contain minus strand DNA and degraded pregenomic RNA of variable and inverse lengths

Johan Ringlander¹, Sebastian Malmström¹, Anders Eilard¹, Lucia Gonzales Strömberg¹, Joakim Stenbäck¹, Maria Andersson¹, Simon B. Larsson¹, Michael Kann¹, Staffan Nilsson¹, Kristoffer Hellstrand¹, Gustaf Rydell¹, Magnus Lindh¹. ¹Sahlgrenska Academy, University of Gothenburg, Gothenburg, Sweden
Email: johan.ringlander@gu.se

Background and aims: Quantification of hepatitis B virus (HBV) RNA in serum has emerged as a complementary clinical marker, in particular for the monitoring of the effect of antiviral therapy. However, the nature of RNA particles and their composition of RNA remains incompletely known.

Method: We have used droplet digital PCR (ddPCR) assays that target three gene segments to quantify HBV RNA and HBV DNA in serum samples from 75 patients with chronic HBV infection.

Results: The HBV RNA levels were higher in the core than in the S and X regions (median 7.20 vs. 6.80 and 6.58 log copies/ml; $p < 0.0001$), whereas HBV DNA levels showed an inverse gradient (7.71 vs. 7.73 and 7.77 log copies/ml, $p < 0.001$). By quantification in core on average 80% of the nucleic acid was DNA. The core DNA/RNA ratio was associated with viral load and genotype. In individual patients with paired samples, the relationships between core, S and X RNA levels were stable over time ($n = 29$; $p = 0.006$).

Conclusion: The results suggest that pregenomic RNA is completely reverse transcribed to minus DNA in $\approx 75\%$ of the virus particles, whereas the remaining 25% contain both RNA and DNA of lengths that reflect variable progression of the polymerase.

SAT-415

Metabolic alteration linked to antiviral treatment response in 3D in-vitro model system of hepatitis B virus infection

Abhishak Gupta¹, Nupur Sharma², Sadam H Bhat¹, Jaswinder Maras¹. ¹Institute of Liver and Biliary Sciences, New Delhi, India; ²Institute of Liver and Biliary sciences, New Delhi, India
Email: abhigupta78@gmail.com

Background and aims: Hepatitis B virus (HBV) infection is a global health concern. Metabolic alterations during HBV antiviral reflect the treatment response in liver/hepatocytes remains unclear. Delineation of the metabolic changes in 3D in-vitro model system could help in characterization of cellular metabolic response and clearance of HBV infection. The primary aim was to develop a 3D model system using HepG2.2.15 and metabolic alteration during anti-viral treatment.

Method: 3D in-vitro model was developed for HepG2.2.15 by culturing them for 3 days. ETV at a dose of 1 and 10 micromolars was used for treatment and analyzed post 24, 48 or 72 hrs for the metabolic changes and viral markers. HBsAg, HBeAg and HBV DNA quantification were performed. Secretory metabolites from supernatants were extracted and analyzed using UPLC-HRMS based on comparative metabolomics coupled with pattern recognition methods and network pathway. Significant changes in the secretome were identified using WMCNA and the metabolite module specific to treatment response (temporal) or HBV infection was subjected to pathway analysis and correlation to ETV treatment dynamics.

Results: A 3D in-vitro model system was established with approx 20 K cells/organoids. ETV treatment both at 1 and 10 micromolars significantly lowered antigen secretion, virion production and HBV DNA synthesis without affecting cell viability in HepG2.2.15 organoids. HBsAg, HBeAg, and HBV DNA secretion were decreased temporally from 24 to 72 hrs ($p < 0.05$). WMCNA of the secretome led to the identification of 5 metabolite modules. ETV treatment temporally down regulated 83 metabolites linked to inflammatory Tryptophan metabolism (5-Hydroxy-N-formylkynurenine; Indolepyruvate), Sphingolipid metabolism, Arachidonic acid metabolism, Amino-acid metabolism and Lipid metabolism and others ($FC > 1.5$, $FDR < 0.01$, $p < 0.05$). Metabolites significantly increased and linked with treatment response were mainly involved in vitamin metabolism (Pantothenate and CoA biosynthesis, riboflavin, ascorbate and others), amino acid metabolism (Arginine, proline, glycine and others), Taurine and hypotaurine metabolism, and energy metabolism (pentose phosphate pathways) and others ($p < 0.05$). Secretome analysis showed that HBV infection induced inflammatory and oxidative metabolic pathways were significantly hampered. Further, increase in energy and amino acid metabolism post ETV treatment correlates with the inhibition of HBsAg/HBeAg expression and HBV replication.

Conclusion: 3D in-vitro model reflects changes in the secretory metabolite correlate to anti-viral treatment response and could be used for monitoring HBV replication/infection and development strategies for antiviral.

SAT-418

Prevalence of hepatitis C virus infection in a nursing home: a frequently overlooked submerged population

Paolo Gallo¹, Giulia Di Pasquale², Valentina Flagiello², Antonio De Vincentis², Francesca Terracciani², Antonio Picardi², Umberto Vespasiani-Gentilucci², Raffaele Antonelli Incalzi². ¹Fondazione policlinico universitario Campus bio-medico, Rome, Italy; ²Fondazione Policlinico Universitario Campus Bio-Medico, Rome, Italy
Email: paolo.gallo@policlinicocampus.it

Background and aims: Despite the therapeutic success achieved through direct-acting antiviral agents, a significant number of individuals with undiagnosed hepatitis C virus (HCV) infection, often referred to as the “submerged” population (comprising institutionalized aged subjects living in nursing homes), persists. The objective of this study is to assess the prevalence of HCV antibodies and infection among patients residing in the Italian Hospital Group (IHG) Nursing Home in Guidonia Montecelio, Rome.

Method: The study was conducted across Extensive and Intensive Care Unit, Alzheimer Unit, Geriatric Unit, and Psychiatric Disorders Unit. All participants provided written consent to participate. Collected data encompassed patients' sociodemographic details, blood test results, and risk factors for HCV infection. Anti-HCV testing was done with Advanced Quality Rapid capillary test, followed by confirmation through a serum test. Anti-HCV positive testing has been followed by an HCV-RNA test. Descriptive statistics were employed to present the data, and logistic regressions were applied to assess risk factors for anti-HCV positivity.

Results: 434 patients were included. Both capillary and serum anti-HCV positivity were identified in 13 patients (3%), while the

prevalence of infection was 2.3%. Notably, positive patients exhibited a predominance of males and a younger age compared to their anti-HCV negative counterparts. The Psychiatric unit displayed the highest prevalence, with 46% of the cases (6 out of 13 patients). Logistic regression analysis identified several significant associations with anti-HCV positivity. Age (OR 0.96, 95% CI 0.93–0.99, $p = 0.01$), sex (OR 0.26, 95% CI 0.06–0.88, $p = 0.04$), hepatitis B virus (HBV) infection (OR 20.75, 95% CI 3.95–91.7, $p < 0.001$), dementia (OR 0.14, 95% CI 0.02–0.55, $p = 0.01$), smoking (OR 6.50, 95% CI 2.09–22.8, $p < 0.001$), and injection drug use (OR 10.5, 95% CI 1.59–51.09, $p = 0.005$) were all identified as significantly associated with anti-HCV positivity. Multivariate analysis confirmed only HBV infection (OR 13.7, 95% CI 1.82–94.8, $p = 0.008$) and smoke (OR 6.23, 95% CI 1.12–40.5, $p = 0.04$) as independently associated with the positivity.

Conclusion: Our findings reveal a 2.3% prevalence of HCV infection among people living in the Nursing Home; anti-HCV positivity was negatively associated with age and positively associated with dementia. Notably, the highest prevalence was observed in psychiatric patients, who not only exhibited increased susceptibility to HCV infection but were also younger compared to the general Nursing Home population. These preliminary data advocate that institutionalized (particularly psychiatric) patients should be included in HCV infection screening program in the submerged populations.

SAT-419

Transcriptomics reveals the regulation mechanism of the Chinese herbal TiaoGanJianPijieDu formula on inhibiting hepatitis B virus replication in mice

Ningyi Zhang¹, Xu Cao¹, Hening Chen¹, Jiaxin Zhang², Xiaoke Li², Xiaobin Zao³, Yong'an Ye². ¹Dongzhimen Hospital, Beijing University of Chinese Medicine, Beijing, China; ²Dongzhimen Hospital, Beijing University of Chinese Medicine, Beijing University of Chinese Medicine, Liver Diseases Academy of Traditional Chinese Medicine, Beijing, China; ³Dongzhimen Hospital, Beijing University of Chinese Medicine, Key Laboratory of Chinese Internal Medicine of Ministry of Education and Beijing, Dongzhimen Hospital, Beijing University of Chinese Medicine, Beijing, China
Email: ningyi0202@163.com

Background and aims: Chronic Hepatitis B (CHB) is a chronic inflammatory liver disease caused by hepatitis B virus (HBV) infection. The Chinese herbal TiaoGanJianPijieDu formula (TGJP), a representative formula of traditional Chinese medicine (TCM) “immune incubation” therapy, has been widely used in the clinic and proved to be effective in the treatment of CHB. However, the underlying mechanism of TGJP is still unclear and needs to be further explored, which is the purpose of this study.

Method: HBV replicating mice was applied for animal model and treated with intragastric administration of distilled water (1 ml/10 g) or TGJP solution (0.33 g/ml) for 16 weeks. The therapeutic effect of TGJP on CHB was examined by serum HBV biomarker assay, Immunohistochemical (IHC) and qPCR. Hepatic tissue transcriptomic analysis was used to investigate the anti-HBV mechanism of TGJP on CHB. Gene Ontology (GO) and Kyoto Encyclopaedia of Genomes (KEGG) were used for further functional enrichment analysis.

Results: We established a mouse model by hyperbaric hydrodynamic injection (HDI) of 1.2-fold HBV plasmid DNA into the tail vein. Serum HBsAg was measured 48 hours after modelling, and serum HBsAg-positive animals were considered successfully modelling. Compared to the model, the serum HBsAg and HBeAg level were significantly decreased in the TGJP group after 5-week TGJP treatment. Hepatic HBV antigens IHC staining and qPCR showed that TGJP significantly enhanced clearance of hepatic HBsAg and HBeAg deposition and significantly inhibited the relative expression of total HBV DNA and HBV RNA, as compared with the model group. From the second week of TGJP treatment, serum ALT and AST levels in the TGJP group were significantly higher than those in the model group and remained elevated until the fifth week. The decline in serum HBsAg and HBeAg

levels followed the elevation of liver transaminases, suggesting finite liver inflammation may promote HBV clearance. Transcriptome analysis showed that there were 275 differentially expressed genes (DEGs) being identified between model group and TGJP group, including 128 up-regulated genes and 296 down-regulated genes. Heatmap suggested that there were significant differences in HBV-replicating mice liver after TGJP treatment compared with the model group. GO enrichment analysis showed that the top 20 enriched functions were mainly related to the activation and migration of immune cells. KEGG enrichment analysis of DEGs showed that the top 3 enriched pathways were mainly involved in the interaction between viral proteins and cytokines and their receptors, cytokine-cytokine receptor interactions, chemokine signalling pathways, which were closely related to the regulation of innate immunity.

Conclusion: Transcriptomics analysis showed that TGJP exerts an inhibition effect on HBV replicating in mice by regulating host immune function, especially innate immune.

SAT-420

The Chinese herbal TiaoGanJianPijieDu formula exerts an inhibition effect on hepatitis B virus replication by regulating hepatic CCL2-CCR2 signaling pathway and inducing immune-inflammatory response

Ningyi Zhang¹, Hening Chen¹, Xu Cao¹, Xiaobin Zao², Yong'an Ye³. ¹Dongzhimen Hospital, Beijing University of Chinese Medicine, Beijing, China; ²Dongzhimen Hospital, Beijing University of Chinese Medicine, Key Laboratory of Chinese Internal Medicine of Ministry of Education and Beijing, Dongzhimen Hospital, Beijing University of Chinese Medicine, Beijing, China; ³Dongzhimen Hospital, Beijing University of Chinese Medicine, Beijing University of Chinese Medicine, Liver Diseases Academy of Traditional Chinese Medicine, Beijing, China
Email: ningyi0202@163.com

Background and aims: Chronic hepatitis B (CHB) are a chronic inflammatory liver disease with host immune dysfunction caused by hepatitis B virus (HBV) infection. The Chinese herbal TiaoGanJianPijieDu formula (TGJP) has been widely used in clinical practice and has performed well in the treatment of CHB. However, the underlying mechanism of the TGJP for CHB remains to be studied. In this study, we aimed to explore the mechanism of TGJP in CHB treatment and to explore the targets and pathways of TGJP in modulating immunity.

Method: HBV-replicating mouse was applied as animal model, given TGJP gavage for 16 weeks. Ultra performance liquid chromatography-mass spectrometry/mass spectrometry (UPLC-MS/MS) identified the major components of TGJP. Transcriptomic was used for TGJP mechanism further study. The key pathways and putative targets of TGJP were obtained by network pharmacology analysis and transcriptomic. We validated the putative targets and key pathways of TGJP by immunohistochemistry (IHC), enzyme-linked immunosorbent assay (ELISA) and qPCR.

Results: We identified 174 active components of TGJP by UPLC-MS/MS, then screened 1043 targets of TGJP and 10019 CHB disease targets via public databases. Transcriptomics screened 275 differentially expressed genes in the livers of model and TGJP mice. We intersected above targets and obtained 14 key targets of TGJP in CHB treatment. Based on network pharmacology and transcriptomics analysis, we selected CCL2 as the key gene and CCL2/CCR2 axis as the key pathway for further research. GEO dataset validates the critical role of CCL2 in CHB. Animal experiments confirmed that compared with the model group, the serum and liver CCL2 levels of HBV replicating mice in the TGJP group were significantly higher than those in the model group, and the relative expression of *Ccl2* and *Ccr2* in liver tissues of mice were significantly higher. IHC results showed a significant increase of CD68⁺ and CCR2⁺ macrophages count in the liver tissue of the TGJP group compared with the model and control groups. Macrophages performs the role of inducing immune-inflammatory responses and activating adaptive immunity. By gene

POSTER PRESENTATIONS

set enrichment analysis, we found that TGJP upregulated inflammatory and immune response signalling pathways, which was confirmed by qPCR. Compared with the model group, TGJP up-regulated the expression of inflammatory factors such as *Cxcl10*, *Il33* and *Ifnlr1*, and down-regulated the expression of *Il10*. IHC also showed that CD8⁺ T cells were significantly increased in the TGJP group compared with the model group and the control group, suggesting that adaptive immunity was activated.

Conclusion: TGJP plays an anti-HBV role by upregulating the intrahepatic CCL2-CCR2 signalling pathway, promoting macrophage chemotaxis to the liver, inducing hepatic immune-inflammatory responses, and activating adaptive immunity.

SAT-421

Hepatitis B core related antigen in South Africa and the United Kingdom-does one size fit all?

Louise Downs¹, Marion Delphin², Tingyan Wang³, Cori Campbell³, Catherine De Lara³, Sheila Lumley⁴, Sue Wareing⁵, Polly Fengou⁵, Tongai Gibson Maponga⁶, Marije Van Schalkwyk⁷, Shiraaz Gabriel⁸, Susan Hugo⁹, Monique Andersson^{10,11}, Jacqueline Martin¹⁰, Elizabeth Waddilove¹², Kosh Agarwal¹³, Geoffrey Dusheiko¹³, Ivana Carey¹³, Wolfgang Preiser¹⁴, Eleanor Barnes¹⁵, Gavin Kelly¹², Philippa C Matthews¹⁶. ¹Nuffield Department of Medicine, University of Oxford, Department of Infectious Diseases and Microbiology, Oxford University Hospitals NHS Foundation Trust, Oxford, United Kingdom; ²The Francis Crick Institute, London, United Kingdom; ³Nuffield Dept of Medicine, University of Oxford, UK, Oxford, United Kingdom; ⁴Nuffield Dept of Medicine, University of Oxford, Department of Infectious Diseases and Microbiology, Oxford University Hospitals NHS Foundation Trust, Oxford, United Kingdom; ⁵Department of Infectious Diseases and Microbiology, Oxford University Hospitals NHS Foundation Trust, Oxford, UK, Oxford, United Kingdom; ⁶Division of Medical Virology, Stellenbosch University, Faculty of Medicine and Health Sciences, Tygerberg, Cape Town, South Africa; ⁷Division of Infectious Diseases, Department of Medicine, Stellenbosch University/Tygerberg, Cape Town, South Africa; ⁸Division of Gastroenterology, Department of Medicine, Stellenbosch University/Tygerberg Academic Hospital, Cape Town, South Africa; ⁹Division of Infectious Diseases, Department of Medicine, Stellenbosch University/Tygerberg Academic Hospital, Cape Town, South Africa; ¹⁰Department of Infectious Diseases and Microbiology, Oxford University Hospitals NHS Foundation Trust, Oxford, United Kingdom; ¹¹Radcliffe Department of Medicine, University of Oxford, Oxford, United Kingdom; ¹²The Francis Crick Institute, 1 Midland Road, London, United Kingdom; ¹³Institute of Liver Studies, King's College Hospital, London, United Kingdom; ¹⁴Division of Medical Virology, Stellenbosch University, Faculty of Medicine and Health Sciences, Tygerberg, National Health Laboratory Service, Tygerberg Business Unit, Tygerberg, Cape Town, South Africa; ¹⁵Nuffield Dept of Medicine, University of Oxford, Oxford, United Kingdom; ¹⁶The Francis Crick Institute, 1 Midland Road, University College London Hospitals, London, United Kingdom
Email: louise.downs@exeter.ox.ac.uk

Background and aims: Hepatitis B core related antigen (CrAg) has been associated with disease outcomes in chronic hepatitis B infection (CHB). To date, only the PROLIFICA study (Gambia), has assessed CrAg in Africa and no studies have compared CrAg in different continents. Here we aimed to examine how CrAg varies between cohorts in South Africa (SA) and the United Kingdom (UK) and investigate the association between CrAg and liver outcomes.

Method: Serum samples and clinical metadata were obtained from adults with CHB at Oxford University Hospitals, UK (n = 142), and Tygerberg Hospital in Cape Town, SA (n = 121) (ref. 09/H0604/20 and N17/01/013 respectively). HBV DNA, CrAg, HBsAg, HBeAg and ALT were measured. Liver health was assessed using APRI, Fib-4 and elastography. Associations between liver health and CrAg in the two cohorts were interrogated using complete-case logistic regression

with CrAg (linear) and cohort (binary) as covariates against (binary) liver health indicators.

Results: The UK and SA cohorts were of similar age (median 40 and 39 years respectively, p = 0.2) and sex (46% and 45% female respectively, p = 0.8). Comparing UK and SA cohorts, CrAg levels were lower in the UK (3.4 vs 3.8 log₁₀ IU/ml, p < 0.002), fewer people in the UK were HBeAg positive (12% vs 35%, p < 0.001) and fewer UK patients were on nucleoside analogue (NA) treatment (31% vs 65%, p < 0.001). HBV DNA was overall higher in the UK cohort, but more people in the SA cohort had HBV DNA >200,000 IU/ml (26% vs 5.6%, p < 0.001). By univariate analysis, CrAg was significantly correlated with HBV DNA in both cohorts (p < 0.0001) but there was no significant difference in CrAg between those on and off NA therapy in each cohort. We derived heatmaps to explore the extent to which CrAg correlated with markers of liver outcome within each cohort. Within the UK cohort, there was no significant correlation between CrAg and any liver parameter. Within the SA population, there was a significant positive correlation between CrAg and liver inflammation (ALT, p < 0.05). The strength of any association of CrAg with liver disease outcome did not significantly vary between cohorts.

Conclusion: Despite similar age and sex structures, HBV characteristics and CrAg distribution significantly differed between cohorts from the UK and SA. We observed no significant correlation between liver fibrosis or cirrhosis and CrAg, although liver inflammation by ALT was positively correlated with CrAg in SA. Associations may be influenced by HIV infection and other genetic, immunological or environmental factors. This novel comparison between geographical settings identifies knowledge gaps in interpretation of CrAg in different population groups.

SAT-422

E-selectin levels in patients with chronic hepatitis C

Petr Husa, Jr.^{1,2}, Svatava Snopkova^{1,2}, Jiřina Zavřelová³, Filip Zlámál⁴, Radek Svačina^{1,2}, David Vydřák^{1,2}, Petr Husa, Sr.^{2,5}. ¹Department of Infectious Diseases, University Hospital Brno, Brno, Czech Republic; ²Faculty of Medicine, Masaryk University, Brno, Czech Republic; ³Department of Hematology, University Hospital Brno, Brno, Czech Republic; ⁴Research Centre for Toxic Compounds in the Environment, Masaryk University, Brno, Czech Republic; ⁵Department of Infectious Diseases, University Hospital Brno, Brno, Czech Republic
Email: husa.petr2@fnbrno.cz

Background and aims: Selectins (cluster of differentiation, CD62) are a family of transmembrane glycoproteins expressed on the surface of different cells. E-selectin (ES) is primarily present in membranes of endothelial cells. Inflammatory cytokines like tumor necrosis factor alpha or interleukin 1 beta stimulate ES expression. ES binds with CD15 s on the surface of neutrophils, allowing reversible adhesion of leucocytes and their rolling movement on endothelial cells. By the described mechanism, ES plays a fundamental role at the beginning of the physiological inflammatory response. Elevated ES levels are associated with different diseases like atherosclerosis, rheumatoid arthritis, HIV, or chronic hepatitis C (CHC). Aim of the study was to assess ES concentrations in the group of patients with CHC in comparison with the control group (CG).

Method: A total of 36 patients with CHC treated with direct acting antivirals (DAA) was included in study group (SG). The control group consisted of 40 healthy individuals. ES levels were detected in venous blood using a conventional sandwich ELISA test-Human sE-selectin Platinum ELISA (eBioscience, San Diego, USA). Testing was performed at baseline (BS), at the end of antiviral treatment (ET) and 12 weeks after the last dose of DAA (SVR12). The Mann-Whitney U test was used for comparison of ES levels between two groups.

Results: The median of ES concentration in CG was 6.2 (1.6–13.3) ng/ml, in SG 76.7 (27.8–179.3) ng/ml at BS, 69.9 (21.7–167.4) ng/ml at ET and 57.8 (20.5–120.2) ng/ml at SVR12. The difference between CG and SG at BS, ET, and SVR 12 was statistically significant (p < 0.001). All patient with CHC achieved a sustained virological response.

Conclusion: ES concentrations were significantly higher in SG at BS and remained elevated at SVR12 although the decrease during the study was also substantial ($p < 0.001$ between BS and ET as well as between ET and SVR12). The basis of the increased concentration in SG is a systemic inflammatory reaction that persists even after achieving SVR.

SAT-423

Highly expressed CTLA4 on B cells defected BCR signal to inhibit the secretion of anti-HBs in CHB patients

Shengxia Yin¹, Xin Tong¹, Chao Wu¹, Jie Li¹. ¹Nanjing Drum Tower Hospital, Affiliated Hospital of Medical School, Nanjing University, Nanjing, China
Email: att717@163.com

Background and aims: The generation of anti-HBs is lacking in CHB patients. The cause is controversial. B cells activation state has a crucial effect on the secretion level of antibodies. Therefore, B cell status deserves more attention.

Method: Single-Cell RNA-seq analysis was performed in peripheral B cells. Peripheral and liver infiltrated B cells were characterized by flow cytometry. BCR signaling was tested by Ca²⁺ flow and WB assay. Aimed to explore the inhibiting role of CTLA4, we did CTLA4-blocking test in vitro. Further, B6-Ighm-KO mice were injected with HBsAg preimmunized CTLA4-/- B cell after establishing HBV transduction model and HBV serological indicators were detected. CO-IP assay and proteome analysis was made to explore the downstream proteins of CTLA4.

Results: CTLA4 was highly expressed in B cells of CHB patients and more obviously in HBsAg-specific B cells. Moreover, CTLA4 was highly expressed in about 50% of the infiltrating HBsAg-specific B cells. CTLA4+HBsAg+B cells tended to show activated markers. GO analysis, Ca²⁺ flow and WB assay showed that BCR signaling of CTLA4+B cells was defected. Moreover, CTLA4 blocking could partly restore the deflection and make B cells secreted more anti-HBs. In mice model, B6-Ighm-KO mice injected with CTLA4-/- B cells showed decreased level of HBV serological indicators. Proteome assay showed SHIP-1 was the down stream of CTLA4.

Conclusion: The circulating and liver infiltrating B cells increased the expression of CTLA4 to defected the BCR signal which might contribute to the deficiency of viral specific humoral response during CHB course.

WEDNESDAY 05 JUNE

Viral hepatitis AE – Clinical aspects

WED-420

Evaluation of molnupiravir as an antiviral against hepatitis E virus infection

Siddharth Sridhar¹, Shusheng Wu¹, Jianwen Situ², Estie Hon-Kiu Shun², Nicholas Foo-Siong Chew². ¹Department of Microbiology, School of Clinical Medicine, LKS Faculty of Medicine, The University of Hong Kong, Hong Kong, Hong Kong; ²Department of Microbiology, School of Clinical Medicine, LKS Faculty of Medicine, The University of Hong Kong, Hong Kong, Hong Kong
Email: sid8998@hku.hk

Background and aims: Hepatitis E virus (HEV) is an important cause of chronic hepatitis in immunocompromised persons. There are few effective treatment options for patients with chronic hepatitis E who are intolerant or unresponsive to ribavirin. Drug repurposing efforts are required to identify new treatment options for this condition. Molnupiravir is a prodrug of a broad-spectrum antiviral nucleoside

analogue (N-hydroxycytidine) that induces lethal mutagenesis in viral populations. This drug has recently been licensed globally for treatment of Coronavirus Disease 2019 (COVID-19). This study aimed to evaluate activity of molnupiravir against HEV.

Method: *In vitro* cytotoxicity and antiviral efficacy of varying concentrations of molnupiravir were assessed using infectious cDNA clones (pSK-HEV-2) and patient derived HEV isolates in Huh7 and PLC/PRF/5 cells respectively. Rats were immunosuppressed with a combination of prednisolone, tacrolimus, and mycophenolate mofetil administered by oral gavage. These are commonly used immunosuppressants in organ transplant recipients and are proven to prolong HEV infection in rats (Sridhar S et al, JHEP Reports, 2022). Immunosuppressed rats were infected with HEV for one week and then treated with molnupiravir (dosed at either 250 mg/kg/day or 400 mg/kg/day), ribavirin 50 mg/kg/day, or left untreated. Antiviral effectiveness in clearing HEV in serum, faeces, and liver tissue was compared to control and ribavirin-treated rats over 28 days. Liver histology and immunohistochemistry was assessed.

Results: Molnupiravir demonstrated low cytotoxicity and dose-dependent reduction in supernatant RNA load in both infectious cDNA clone and wildtype HEV cell culture models. In the animal model, untreated animals harbored prolonged HEV infection until end of experiment. The higher dose of molnupiravir (400 mg/kg/day) rapidly reduced viral shedding in serum and stool compared to other treatment groups. A majority of rats treated at the 400 mg/kg/day molnupiravir dose level cleared infection in both compartments by week 4 of treatment. Liver tissue showed improved histology and decreased immunohistochemical staining in the molnupiravir group together with lower viral loads at end of treatment.

Conclusion: Molnupiravir, a licensed antiviral for COVID-19, shows promise against HEV in *in vivo* and *in vitro* models. Further work is required to translate molnupiravir into a clinical solution for ribavirin-refractory chronic hepatitis E.

WED-421

Hepatitis E in Japan: a nationwide survey 2012–2017

Takeshi Matsui¹, Jong-Hon Kang², Kazunari Tanaka², Hiroaki Okamoto³. ¹Center for Gastroenterology, Teine-Keijinkai Hospital, Sapporo, Japan; ²Center for Gastroenterology, Teine Keijinkai Hospital, Sapporo, Japan; ³Jichi Medical University School of Medicine, Shimotsuke, Japan
Email: mtake0402@gmail.com

Background and aims: In Japan, testing for hepatitis E virus (HEV) has been covered by the medical insurance system since November 2011. Since then, the diagnosis of HEV infection has rapidly expanded in clinical practice throughout the country. These changing circumstances have encouraged us to conduct a nationwide investigation of HEV infection.

Method: To 525 medical facilities, we requested a survey to investigate the medical record for the patients with HEV infection diagnosed from 2012 to 2017. The questionnaire included baseline characteristics, clinical course and virologic aspects of the patients.

Results: A total of 503 cases (407 males, average age of 56.6 years) were registered from 155 medical facilities across Japan. In Eastern Japan, 324 cases were collected from 69 facilities (4.7 cases/facility), and 179 cases were gathered from 86 (2.1 cases/facility) in Western Japan. Among them, 273 patients had habitual alcohol consumption of 30 g/day or more. Pre-existing liver disease was present in 93 patients, hypertension in 84, diabetes mellitus in 82, and dyslipidemia in 93, respectively. The average Body Mass Index (BMI) at onset was 23.9 kg/m². Except for four cases, none had traveled to HEV endemic areas. Ninety patients had consumed pork meat within the past two months, 87 had ingested pork offal, 13 had consumed venison, and 18 had eaten wild boar meat. Transfusion transmission of HEV was suspected in 4 patients. For the diagnosis of HEV infection, 468 (98.5%) of 475 patients underwent an anti-HEV IgA test, certified by insurance in Japan, and were positive. HEV RNA was

detected in 222 patients using PCR. Among 178 patients whose HEV genotypes were determined, genotype 3 was identified in 123 patients (69.1%), genotype 4 in 51 (28.7%), and genotype 1 in 4 (2.2%) patients who had traveled to endemic areas. Of the 503 patients, 346 (68.8%) were hospitalized, and 52 (10.3%) developed ALF. Six patients (1.2%) presented with hepatic coma, 2 (0.4%) received liver transplantation, and 4 (0.8%) died. ALF was associated with male gender, alcohol consumption, BMI, genotype 4, and pre-existing liver disease or diabetes. AHE shifted to chronic hepatitis in 6 patients (1.2%). They had undergone organ transplantation or had underlying diseases including hematological disorders, respectively. Extrahepatic manifestations such as neurological disorders including Guillain-Barré syndrome, were observed in six patients.

Conclusion: AHE in Japan was autochthonous with rare exceptions, and genotype 3 of HEV was the dominant strain. A higher incidence in Eastern Japan might be observed compared to the Western area. Whereas AHE was self-limited in almost 90% of patients, ALF developed in 10%, and 1% had a fatal course. This may be the first nationwide study to examine the clinical picture of HEV infection throughout Asian countries including Japan.

Viral hepatitis B and D – Clinical aspects

TOP-400

Impact of bulevirtide given with or without nucleos (t)ide analogues on 48-week virologic outcomes in patients with chronic hepatitis delta virus infection

Pietro Lampertico^{1,2}, Maurizio Brunetto^{3,4}, Maria Buti^{5,6}, Soo Aleman⁷, Pavel Bogomolov⁸, Vladimir Chulanov⁹, Nina Mamonova¹⁰, Viacheslav Morozov¹¹, Olga Sagalova¹², Tatyana Stepanova¹³, John F. Flaherty¹⁴, Mingyang Li¹⁴, Dmitry Manuilov¹⁴, Ben L. Da¹⁴, Renee-Claude Mercier¹⁴, Grace M. Chee¹⁴, Markus Cornberg¹⁵, Heiner Wedemeyer¹⁵, Tarik Asselah¹⁶. ¹Division of Gastroenterology and Hepatology, Fondazione IRCCS Ca' Granda Ospedale Maggiore Policlinico, Milan, Italy; ²Department of Pathophysiology and Transplantation, CRC "A. M. and A. Migliavacca" Center for Liver Disease, Department of Pathophysiology and Transplantation, University of Milan, Milan, Italy; ³Hepatology Unit, Reference Center of the Tuscany Region for Chronic Liver Disease and Cancer, University Hospital of Pisa and Department of Clinical and Experimental Medicine, University of Pisa, Pisa, Italy; ⁴Department of Clinical and Experimental Medicine, University of Pisa, Pisa, Italy; ⁵Hospital Universitario Vall d'Hebron, Barcelona, Spain; ⁶CIBERED del Instituto Carlos III, Madrid, Spain; ⁷Department of Infectious Diseases, Karolinska University Hospital/Karolinska Institutet, Stockholm, Sweden; ⁸State Budgetary Institution of Health Care of Moscow Region "Moscow Regional Research Clinical Institute Named After M.F. Vladimirovsky," Moscow, Russian Federation; ⁹FSBI National Research Medical Center for Phthiopulmonology and Infectious Diseases of the Ministry of Health of the Russian Federation, Moscow, Russian Federation; ¹⁰FSBI National Research Medical Center for Phthiopulmonology and Infectious Diseases of the Ministry of Health of the Russian Federation, Moscow, Russian Federation; ¹¹LLC Medical Company "Hepatolog," Samara, Russian Federation; ¹²South Ural State Medical University, Chelyabinsk, Russian Federation; ¹³LLC Clinic of Modern Medicine, Moscow, Russian Federation; ¹⁴Gilead Sciences, Inc., Foster City, United States; ¹⁵Medizinische Hochschule Hannover, Klinik für Gastroenterologie, Hepatologie und Endokrinologie, Hannover, Germany; ¹⁶Hôpital Beaujon APHP, Université de Paris-Cité, INSERM UMR1149, Clichy, France
Email: ben.da@gilead.com

Background and aims: Hepatitis delta virus (HDV) causes the most severe form of viral hepatitis. While nucleos (t)ide analogues (NAs)

are first line treatments for chronic hepatitis B virus (HBV) infection, they have shown no impact on HDV RNA levels in chronic HDV (CHD) patients. Recent HDV guidelines recommend use of NAs in CHD patients with cirrhosis or those without cirrhosis and HBV DNA ≥ 2000 IU/ml. We evaluated virologic outcomes associated with bulevirtide (BLV) over 48 weeks when given with vs. without concomitant NAs.

Method: Data from 3 studies (MYR203, MYR204, MYR301) were pooled for participants receiving BLV 2 mg/d or 10 mg/d as monotherapy, or no anti-HDV treatment (MYR301 control arm). In MYR204 and MYR301, NA use was allowed based on HBV guidelines. HDV outcomes (virologic response [VR], defined as undetectable HDV RNA or $\geq 2 \log_{10}$ IU/ml decrease from baseline [BL], ALT normalization, and combined response [CR], defined as VR and ALT normalization), and HBV outcomes (% with undetectable HBV DNA, defined as $< \text{LLOQ}$ [10 IU/ml], target not detected), change from BL in HBV DNA and in HBsAg levels in participants with HBV DNA $\geq \text{LLOQ}$ at BL) were assessed over 48 weeks (W) in those receiving vs. not receiving NAs. **Results:** 280 participants were included in 4 groups: BLV 2 mg/d (n = 64), BLV 10 mg/d (n = 165), total BLV (n = 229), and no anti-HDV treatment (control; n = 51). Overall, NAs were used concomitantly in 160 participants (57%; group ranges: 48%–63%). BL characteristics were comparable except the proportion with cirrhosis and mean liver stiffness were higher (50% and 14.7 kPa) in those on NAs vs. no NAs (29% and 13.7 kPa). Tenofovir-based therapy was most used (87% [139/160]). For the total BLV group, CR, VR, and ALT normalization with vs. without NAs at W48 were: 45% vs. 47%, 83% vs. 73%, and 50% vs. 58%, respectively; these responses were 3% vs. 0%, 6% vs. 0%, and 9% vs. 16% for controls, respectively. Mean changes from BL in HBV DNA at W48 with and without NAs were -1.37 vs $-0.71 \log_{10}$ IU/ml for the total BLV group, and -0.81 vs $-0.15 \log_{10}$ IU/ml for control. For the total BLV group, 24% (30/126) and 36% (45/124) receiving concomitant NAs had undetectable HBV DNA at BL and W48, respectively, while 13% (13/100) and 21% (20/97) of participants not receiving concomitant NAs had undetectable HBV DNA at these times. For controls, 25% (8/32) and 41% (13/32) on NAs and 21% (4/19) and 11% (2/18) not on NAs had undetectable HBV DNA at BL and W48, respectively. BLV given with or without NAs had no impact on HBsAg levels.

Conclusion: NAs given with BLV for 48 weeks had no impact on HDV responses, while greater reductions in HBV DNA levels were seen when BLV and NAs are combined compared to BLV alone.

TOP-401-YI

Improvement of liver stiffness during nucleo (s)tide analogue treatment in patients with chronic hepatitis B and advanced fibrosis is not associated with a reduction in hepatocellular carcinoma risk

Lesley A. Patmore¹, Yan Liang², Mai Kilany³, Arno Furquim d'Almeida⁴, Vincent Wai-Sun Wong², Thomas Vanwolleghem⁴, Pieter Honkoop⁵, Hans Blokzijl⁶, Ozgur Koc⁷, Harry L.A. Janssen^{1,3}, Matthijs Kramer⁷, Joep de Bruijne⁸, A. Kaewdech⁹, Robert A. de Man¹, R. Bart Takkenberg¹⁰, Grace Lai-Hung Wong², Jordan J. Feld³, Milan J. Sonneveld¹. ¹Erasmus MC, University Medical Center, Rotterdam, Netherlands; ²The Chinese University of Hong Kong, Hong Kong, Hong Kong; ³Toronto Centre for Liver Disease, Toronto General Hospital, University of Toronto, Toronto, Canada; ⁴Antwerp University Hospital, University of Antwerp, Edegem, Belgium; ⁵Albert Schweitzer Hospital, Dordrecht, Netherlands; ⁶University Medical Center Groningen, University of Groningen, Groningen, Netherlands; ⁷Maastricht University Medical Center, Maastricht, Netherlands; ⁸University Medical Center Utrecht, University of Utrecht, Utrecht, Netherlands; ⁹Prince of Songkla University, Songkhla, Thailand; ¹⁰Amsterdam University Medical Centers, Amsterdam, Netherlands
Email: l.patmore@erasmusmc.nl

Background and aims: Chronic hepatitis B (CHB) patients with advanced fibrosis are at high risk for hepatocellular carcinoma (HCC)

and other adverse liver outcomes. Since liver stiffness correlates with severity of fibrosis in untreated patients, an improvement in liver stiffness measurement (LSM) by vibration-controlled transient elastography is used as a surrogate marker for fibrosis regression in patients on antiviral therapy. However, the association between on-treatment LSM with adverse liver-related outcomes is yet unknown. **Method:** We conducted an international multicenter retrospective cohort study of mono-infected CHB patients with advanced fibrosis ($\geq F3$ based on liver biopsy or LSM ≥ 9.0 kPa) and with available on-treatment LSM after at least 3 years of follow-up, at sites in Belgium, Canada, Hong Kong, the Netherlands, and Thailand. On-treatment LSM was categorized into <6 kPa, $6-9$ kPa and >9 kPa. We assessed the association between on-treatment LSM with HCC development, as well as liver-related events (first of HCC, liver transplantation and liver-related mortality).

Results: We analyzed 512 patients with a median age at baseline of 50 years, 76% were male. Median baseline HBV DNA was $5.6 \log_{10}$ IU/ml. At baseline 40.8% had F3 and 59.2% had F4, 71.7% was based on LSM (median 12.7 kPa, IQR 10.5–17.6). All patients initiated antiviral therapy with nucleos(t)ide analogue and 93% had undetectable HBV DNA at on-treatment LSM. The median time between baseline assessment and on-treatment LSM was 4.5 years and median on-treatment LSM was 6.9 kPa (IQR 5.1–10.3). The on-treatment LSM was <6 kPa in 196 (38.3%) patients, $6-9$ kPa in 156 (30.5%) patients and >9 kPa in 160 (31.2%) patients. During a median follow-up of 6.8 years after the on-treatment LSM, 53 patients developed HCC. In univariable analysis, on-treatment LSM was not associated with HCC development (hazard ratio [HR] 1.01, $p = 0.607$). The 5-year cumulative HCC incidence was comparable across on-treatment LSM strata; 4.7% for <6 kPa, 6.2% for $6-9$ kPa and 4.3% for >9 kPa ($p = 0.454$). In multivariable analysis adjusting for age, sex, platelet count, ALT and HBV DNA, only older age (adjusted HR [aHR] 1.056, $p < 0.001$) and platelet count (aHR 0.992, $p = 0.011$) were significantly associated with HCC development, whereas on-treatment LSM was not (aHR 1.027, $p = 0.833$). Findings were consistent for patients with F3 ($p = 0.512$) or F4 at baseline ($p = 0.249$). The risk of liver-related events was also comparable across LSM strata (4.7% for <6 kPa, 6.2% for $6-9$ kPa and 5.9% for >9 kPa ($p = 0.184$)).

Conclusion: The majority of CHB patients with advanced fibrosis decreases in LSM during antiviral therapy. Unfortunately, this improvement is not associated with a clinically relevant reduction in the risk of HCC and liver-related events. On-treatment LSM should therefore not be used to guide HCC surveillance strategies, nor as a surrogate end point in clinical trials.

TOP-416-YI

High frequency of liver cirrhosis in european patients with hepatitis D: first data from a large multicentre study (D-SOLVE and HDV-1000 consortia)

Anika Wranke^{1,2,3}, Habiba Kamal^{3,4,5}, Zillah Cargill⁶, Monica Radu^{3,7}, Elisabetta Degasperis^{3,8,9}, Karin Lindahl^{3,4,5}, Petra Dörge^{1,3,10}, Julia Kahlhöfer^{1,3,10,11}, Kosh Agarwal⁶, Pietro Lampertico^{3,8,9}, Florin Alexandru Caruntu^{3,7}, Heiner Wedemeyer^{1,2,3,12}, Soo Aleman^{3,4,5}, Ivana Carey⁶, Lisa Sandmann^{1,3,12}. ¹Department of Gastroenterology, Hepatology, Infectious Diseases and Endocrinology, Hannover Medical School, Hannover, Germany; ²German Center for Infection Research (DZIF), Hannover/Braunschweig, Germany; ³D-SOLVE: EU-funded Network on individualized management of hepatitis D, Germany; ⁴Department of Infectious Diseases, Karolinska University Hospital, Stockholm, Sweden; ⁵Department of Medicine Huddinge, Infectious Diseases, Karolinska Institute, Stockholm, Sweden; ⁶Institute of Liver Studies, King's College Hospital, London, United Kingdom; ⁷Institutul de Boli Infectioase, Bucharest, Romania; ⁸Division of

Gastroenterology and Hepatology, Foundation IRCCS Ca' Granda Ospedale Maggiore Policlinico, Milan, Italy; ⁹CRC "A. M. and A. Migliavacca" Center for Liver Disease, Department of Pathophysiology and Transplantation, University of Milan, Milan, Italy; ¹⁰German Center for Infection Research (DZIF), HepNet Study-House/German Liver Foundation, Hannover, Germany; ¹¹Centre for Individualized Infection Medicine (CiiM), Helmholtz Centre for Infection Research/Hannover Medical School, Hannover, Germany; ¹²Excellence Cluster RESIST, Excellence Initiative Hannover Medical School, Hannover, Germany Email: sandmann.lisa@mh-hannover.de

Background and aims: Infection with the hepatitis D virus (HDV) can lead to hepatitis delta, which is associated with a high risk of developing liver-related complications, including hepatic decompensation and hepatocellular carcinoma (HCC). The global epidemiology and disease severity of hepatitis delta is highly heterogeneous and disease presentation has changed over the last decades. There is limited knowledge on disease pathophysiology and host-virus interactions explaining the large inter-individual variability in the course of the disease. We aim to screen a large multicentre cohort of well-defined HDV-infected patients from different European countries to better understand not only the epidemiology but also to identify individual factors that determine the outcome of infection, thus providing the basis for an individualised treatment approach.

Method: We report first findings from an observational, non-interventional, cross-sectional multicentre cohort with the aim of enrolling 1000 European HDV-infected patients from England, France, Italy, Germany, Romania and Sweden. Patients with detectable anti-HDV for at least 6 months can be included. Retrospective data is obtained from databases and patient records for each patient's most recent visit that is eligible for inclusion (index visit). Available biosamples are used for virological and immunological analyses.

Results: To date, 561 patients have been included (England 27%, Italy 9%, Germany 19%, Romania 11%, Sweden 34%). The majority of patients is male (55%) with a mean age of 48 ± 12 years. The top three countries of birth were Romania (17%), Mongolia (15%) and Sierra Leone (8%). Two out of five patients were classified as having cirrhosis at the index visit (39%, 216/560), of whom 14% (29/211) and 31% (65/207) presented with ascites or esophageal varices while only few patients had signs of hepatic encephalopathy (4%, 9/211). A history of previous hepatic decompensation was documented in 11% (57/518) of patients. HCC was reported for only 29 patients (5%) at the index visit. Regarding antiviral treatment, 40% (223/560) of patients had a history of interferon (IFN)-based treatment, while only 3% were receiving IFN-based treatment at the index visit. Nucleos(t)ide analogues were used in 53% of patients and bulevirtide (BLV) in 6% (34/561). The latter is likely to underestimate the number of patients actually treated with BLV, as patients included in other registries and/or clinical trials were excluded. Anti-HCV antibodies were present in 8% of cases, while HCV RNA was not detected in any of the patients. HDV RNA was detected in 47% of patients, respectively.

Conclusion: This study has the potential to elucidate HDV epidemiology, disease burden and cascades of HDV care in a large multicentre cohort. Data collection is still ongoing and the results from the updated dataset will be presented at the conference.

TOP-417

Machine learning can improve prediction of hepatitis B surface antigen seroclearance: A large multicentre cohort study in the United Kingdom

Tingyan Wang^{1,2}, Jakub Jaworski³, Ben Glampson^{4,5}, Dimitri Papadimitriou^{4,5}, Luca Mercuri^{4,5}, Christopher R. Jones^{5,6}, Stacy Todd⁷, Karl McIntyre⁸, Andrew Frankland⁸, Hizni Salih^{1,9}, Gail Roadknight^{1,9}, Stephanie Little^{1,9}, Theresa Noble^{1,9}, Kinga A. Várnai^{1,9}, Cori Campbell^{1,2}, Cai Davis^{10,11}, Ashley I. Heinson^{10,11}, Michael George^{10,11}, Florina Borca^{10,11}, Louise English¹², Luis Romão¹², David Ramlakhan¹², William Frisby¹³, John Taylor¹³, Kerrie Woods^{1,9}, Jim Davies^{1,14}, Eleni Nastouli^{15,16},

POSTER PRESENTATIONS

Salim I. Khakoo¹⁷, Alexander J. Stockdale^{7,18}, Nicholas Easom^{13,19}, Graham S. Cooke^{4,5,20}, William Gelson²¹, Philippa C. Matthews^{2,9,22,23,24}, Eleanor Barnes^{1,2,9}. ¹NIHR Oxford Biomedical Research Centre, Oxford, United Kingdom; ²Nuffield Department of Medicine, University of Oxford, Oxford, United Kingdom; ³Cambridge University Hospitals NHS Foundation Trust, Cambridge, United Kingdom; ⁴NIHR Health Informatics Collaborative, Imperial College Healthcare NHS Trust, London, United Kingdom; ⁵NIHR Imperial Biomedical Research Centre, London, United Kingdom; ⁶Department of Infectious Disease, Imperial College London, London, United Kingdom; ⁷Tropical Infectious Diseases Unit, Royal Liverpool Hospital, Liverpool University Hospitals NHS Trust, Liverpool, United Kingdom; ⁸Liverpool Clinical Laboratories, Liverpool University Hospitals NHS Trust, Liverpool, United Kingdom; ⁹NIHR Health Informatics Collaborative, Oxford University Hospitals NHS Foundation Trust, Oxford, United Kingdom; ¹⁰Southampton Emerging Therapies and Technologies Centre, University Hospital Southampton NHS Foundation Trust, Southampton, United Kingdom; ¹¹Clinical Informatics Research Unit, Faculty of Medicine, University of Southampton, Southampton, United Kingdom; ¹²NIHR University College London Hospitals Biomedical Research Centre, London, United Kingdom; ¹³Hull University Teaching Hospitals NHS Trust, Hull, United Kingdom; ¹⁴Department of Computer Science, University of Oxford, Oxford, United Kingdom; ¹⁵Department of Infection, Immunity and Inflammation, UCL Great Ormond Street Institute of Child Health, London, United Kingdom; ¹⁶Department of Virology, UCLH, London, United Kingdom; ¹⁷School of Clinical and Experimental Sciences, Faculty of Medicine, University of Southampton, Southampton, United Kingdom; ¹⁸Department of Clinical Infection, Microbiology and Immunology, Institute of Infection, Veterinary and Ecological Sciences, University of Liverpool, Liverpool, United Kingdom; ¹⁹Hull York Medical School, University of Hull, Hull, United Kingdom; ²⁰Faculty of Medicine, Department of Infectious Disease, Imperial College London, London, United Kingdom; ²¹Cambridge Liver Unit, Cambridge University Hospitals NHS Foundation Trust, Cambridge, United Kingdom; ²²The Francis Crick Institute, London, United Kingdom; ²³Division of Infection and Immunity, University College London, London, United Kingdom; ²⁴Department of Infectious Diseases, University College London Hospital, London, United Kingdom
Email: tingyan.wang@ndm.ox.ac.uk

Background and aims: Prediction of hepatitis B surface antigen (HBsAg) seroclearance in individuals with chronic hepatitis B (CHB) is challenging but crucial for understanding outcomes of infection and to support the evaluation of novel therapies aiming at functional cure. **Method:** We studied a large ethnically diverse cohort of CHB adults (on or off antiviral treatment) from 7 secondary care centres in England with longitudinal laboratory and clinical monitoring, established by the National Institute for Health and Care Research Health Informatics Collaborative (NIHR HIC) from electronic health records (EHRs), representing data between 1992–2022. HBsAg seroclearance was determined by a negative HBsAg test, confirmed by at least one follow-up negative. Follow-up duration was defined as the interval between the date of CHB diagnosis and the date of HBsAg seroclearance or last HBsAg measurement. We excluded individuals with followed up duration <6 months, or liver transplantation. We conducted univariate analyses to explore the characteristics of individuals with vs without HBsAg seroclearance. Data were randomly split into training and test sets (90% vs 10%). We applied 10 machine learning (ML) models for HBsAg seroclearance prediction based on the most predictive variables selected by univariate analyses. We derived the relative feature importance based on the ML models of best performance, evaluated by area under the receiver operating characteristics curve (AUC).

Results: We included 4,448 adults who were followed up for 21,589 person years (median follow-up of 4 years per patient). 55% were male, and the median age was 39 (interquartile range (IQR): 32–49) years, 37% on treatment, comprising 37% Asian, 21% Black, 29% White, and 13% other ethnicities. 304 patients (1.4%) achieved HBsAg

seroclearance (226 confirmed with a follow-up result, 1.0%). On univariate analysis, individuals who were older at baseline, male, of White ethnicity, untreated, and had lower baseline HBV viral load (VL) and HBsAg, higher alkaline phosphatase (ALP), lower haemoglobin (Hb), HCV/HBV coinfection, and longer follow-up, were more likely to have HBsAg seroclearance (all $p < 0.05$). The five best predictive ML models (AUC ≥ 0.80) confirmed that baseline age, ethnicity, follow-up duration, baseline HBV VL, ALP, Hb, bilirubin, deprivation score, treatment status, and creatinine, are consistently the top 10 important factors contributing to the prediction performance.

Conclusion: In addition to well-known predictors, we identified ethnicity, deprivation score, and several routine laboratory parameters for HBsAg seroclearance prediction. Big data analytics and ML by utilising large EHRs datasets can be promising to identify individuals with the highest chance of HBsAg loss which is relevant to determining immune-mediated clearance and functional cure using new therapeutic agents.

FRIDAY 07 JUNE

FRI-361

Burden of liver disease progression in patients with chronic HDV infection: a population-based study for France

Lucia Parlati¹, Charlotte Mouliade², Samir Bouam³, Philippe Sogni², Stanislas Pol², Vincent Mallet². ¹AP-HP, Centre Université Paris Centre, Groupe Hospitalier Cochin Port Royal, DMU Cancérologie et spécialités médico-chirurgicales, Service des Maladies du foie, Paris, France, Université Paris Cité, F-75006, Paris, France, Paris, France; ²AP-HP, Centre Université Paris Centre, Groupe Hospitalier Cochin Port Royal, DMU Cancérologie et spécialités médico-chirurgicales, Service des Maladies du foie, Paris, France, Université Paris Cité, F-75006, Paris, France, Paris, France; ³AP-HP, Centre Université de Paris, Groupe Hospitalier Cochin Port Royal, DMU PRIM, Service d'Information Médicale, Paris, France, Paris, France
Email: lucia.parlati85@gmail.com

Background and aims: The burden of liver disease progression to hepatocellular carcinoma or decompensated cirrhosis associated with chronic hepatitis D virus (HDV) infection remains largely unquantified at the population level.

Method: We conducted a retrospective analysis using data from the French National Diagnosis Related Group Database (2014–2023), focusing on cases of chronic HDV infection (ICD-10 code B180) recorded in French hospitals over the past decade. Our objective was to estimate the Population Attributable Fraction (PAF) of alcohol use disorders, non-HDV related chronic liver diseases, type-2 diabetes mellitus, and obesity, in relation to the risk of liver disease progression. We used logistic regression models adjusted for sex, age at censoring, deprivation and major comorbidities, to compute the probability of liver disease progression under both actual conditions and counterfactual scenarios—the latter representing a hypothetical absence of specific risk factors. The PAFs were determined by comparing these probabilities to quantify the contribution of each risk factor to liver disease progression.

Results: Of 5,954 individuals (median [IQR] age at inception 48 [36–61] years, 54% men), 14% ($n = 832$) were recorded with liver disease progression (7.2% with hepatocellular carcinoma, 10.5% with decompensated cirrhosis). The median age at the time of liver disease progression was 54 (44–62) years, with an overwhelmingly (76%) male predominance. Among patients with liver disease progression, the prevalence of alcohol use disorders, non-HDV related chronic liver diseases, obesity, and type-2 diabetes mellitus was 41.6%, 28.8%, and 37%, respectively. Key risk factors of liver disease progression ($p < 0.01$) were male sex [aOR 2.2 (95% CI: 1.82 to 2.67)], alcohol use disorders [aOR 4.97 (4.09 to 6.04)], non-HDV related chronic liver diseases [aOR 5.37 (3.73 to 7.70)], type-2 diabetes mellitus [aOR 1.57

(1.23 to 1.99), and obesity [1.47 (1.16 to 1.86)]. Severe comorbidities [aOR 0.42 (0.33 to 0.53)], and deprivation [aOR 0.84 (0.71 to 1.00)] were not association with liver disease progression. The PAF (95% CI) for alcohol use disorders, type-2 diabetes mellitus, non-HDV related chronic liver diseases, and obesity were 28.1% (26.7%–29.4%), 6.4% (6.0%–6.8%), 5.5% (4.6%–6.3%), and 5.4% (5.1%–5.7%), respectively.

Conclusion: Approximately 45% of the liver disease burden linked to chronic HDV infection in France from 2014 to 2023 was found to be attributable to modifiable, non-HDV-related risk factors.

FRI-362-YI

Hepatitis B surface antigen (HBsAg) seroclearance following discontinuation of nucleos (t)ide analogues (NA) treatment has comparable durability to HBsAg seroclearance achieved during NA therapy

Terry Cheuk-Fung Yip^{1,2,3}, Mandy Sze-Man Lai^{1,2}, Jimmy Che-To Lai^{1,2,3}, Yee-Kit Tse^{1,2,3}, Henry L.Y. Chan^{2,4}, Vincent Wai-Sun Wong^{1,2,3}, Grace Lai-Hung Wong^{1,2,3}. ¹Department of Medicine and Therapeutics, The Chinese University of Hong Kong, Hong Kong, Hong Kong; ²Medical Data Analytics Centre (MDAC), The Chinese University of Hong Kong, Hong Kong, Hong Kong; ³Institute of Digestive Disease, Faculty of Medicine, The Chinese University of Hong Kong, Hong Kong, Hong Kong; ⁴Department of Internal Medicine, Union Hospital, Hong Kong, Hong Kong
Email: tcfyip@cuhk.edu.hk

Background and aims: The durability of hepatitis B surface antigen (HBsAg) seroclearance achieved after nucleos (t)ide analogues (NA) therapy cessation is not well defined. We compared the cumulative rate of HBsAg seroreversion and seroconversion in patients who developed HBsAg loss after stopping NA, during NA therapy, after interferon (IFN) treatment, or spontaneously.

Method: Adult patients with chronic hepatitis B mono-infection who cleared HBsAg from 2000–2022 were identified from a territory-wide database in Hong Kong. Patients with liver transplantation, cancer, or use of immunosuppressants before HBsAg loss were excluded. Time-dependent cause-specific hazard (CSH) models were used to compare different forms of HBsAg loss on the development of HBsAg seroreversion and seroconversion and examine the factors linked to these outcomes.

Results: Of 6,028 patients with HBsAg loss (mean age 58 ± 13 years; 38.6% female; 3.8% cirrhosis), 259 (4.3%), 865 (14.3%), 100 (1.7%), and 4,804 (79.7%) lost HBsAg after NA therapy cessation, during NA therapy, after IFN treatment, and spontaneously respectively; their corresponding mean age at HBsAg loss was 54, 56, 50, and 58 years; 30.1%, 28.3%, 23.0%, and 41.3% were female respectively. Most patients had normal liver function at HBsAg loss. In patients who cleared HBsAg after NA therapy cessation, during NA therapy, after IFN treatment, and spontaneously, 9 (3.5%), 51 (5.9%), 4 (4.0%), and 261 (5.4%) developed HBsAg seroreversion at a median (25th–75th percentile) follow-up of 4.9 (2.5–8.3) years. The 10-year overall cumulative risk (95%CI) of HBsAg seroreversion was 9.6% (7.8%–11.6%). Compared to patients with HBsAg loss during NA therapy, those with HBsAg loss after NA therapy cessation (adjusted CSH ratio [aCSHR] [95%CI] 0.58 [0.29–1.19], $p=0.14$), after IFN treatment (0.65 [0.23–1.81], $p=0.41$), or spontaneously (0.81 [0.59–1.10], $p=0.18$) had a comparable rate of HBsAg seroreversion. Male gender (aCSHR [95%CI] 0.76 [0.61–0.95]) and positive anti-HBs (0.44 [0.30–0.64]) were associated with a lower rate of HBsAg seroreversion, while diagnosis of cancer (3.03 [1.89–4.84]) and immunosuppressant use (1.79 [1.17–2.74]) during follow-up were associated with more HBsAg seroreversion. Among 3,449 patients with antibody to HBsAg (anti-HBs) measurement, the 10-year cumulative incidence (95%CI) of positive anti-HBs was 53.6% (51.7%–55.5%). Patients who achieved HBsAg loss after NA therapy cessation (aCSHR [95%CI] 1.00 [0.77–1.29]), after IFN treatment (1.19 [0.86–1.65]), or spontaneously (0.98 [0.86–1.13]) had a similar rate of developing positive anti-HBs compared to those with HBsAg loss during NA therapy.

Conclusion: HBsAg seroclearance achieved after NA therapy cessation is similarly durable to those achieved during NA therapy, after IFN treatment, and spontaneously, with a comparable chance of HBsAg seroconversion over time.

FRI-363-YI

Association between metabolic dysfunction, severity of liver fibrosis and fibrosis progression in patients with chronic hepatitis B-an individual patient data meta-analysis

Lisa M. van Velsen¹, Lesley A. Patmore¹, Jordan J. Feld², Henry L.Y. Chan³, Teerha Piratvisuth⁴, Rong-Nan Chien⁵, Edo J. Dongelmans¹, Vedran Pavlovic⁶, Leland J. Yee⁷, Willem Pieter Brouwer¹, Audrey H. Lau⁷, Bettina E. Hansen¹, Maria Buti^{8,9}, Qing Xie¹⁰, Keyur Patel², Scott K. Fung², Harry L.A. Janssen^{1,2}, Milan J. Sonneveld¹. ¹Erasmus University Medical Center, Rotterdam, Netherlands; ²Toronto Centre for Liver Disease, University of Toronto, Toronto, Canada; ³The Chinese University of Hong Kong, Hong Kong, China; ⁴Prince of Songkla University, Hat Yai, Thailand; ⁵Chang Gung Memorial Hospital, Linkou Branch, Taiwan, College of Medicine, Chang Gung University, Taiwan, Taipei, Taiwan; ⁶Roche Products Ltd, Welwyn Garden City, United Kingdom; ⁷Gilead Sciences, Foster City, United States; ⁸Liver Unit, Hospital Universitari Vall d'Hebron, Barcelona, Spain; ⁹CIBER Hepatic and Digestive Diseases (CIBERehd), Instituto Carlos III, Madrid, Spain; ¹⁰Ruijin Hospital, Shanghai Jiaotong University School of Medicine, Shanghai, China
Email: l.vanvelsen@erasmusmc.nl

Background and aims: Presence of metabolic comorbidities (ie. overweight, diabetes mellitus [DM], hypertension [HT], and dyslipidemia [DL]) has been associated with a higher risk of liver-related outcomes in chronic hepatitis B (CHB) patients. We studied the association between presence of metabolic comorbidities with severity of liver fibrosis before and during antiviral therapy (AVT).

Method: We analyzed data from the SONIC-B database, which comprises data of CHB patients who underwent liver biopsy in two tertiary clinics in the Netherlands and Canada, or as part of 8 global clinical trials. We analyzed the association between the presence of metabolic comorbidities with severity of liver fibrosis in currently untreated patients, and with fibrosis regression (decrease of ≥ 1 METAVIR class in patients with baseline METAVIR $\geq F2$) and fibrosis progression (increase from METAVIR F0–2 at baseline to METAVIR F3–4) in biopsies taken at 48–72 weeks after initiation of AVT. Comparisons were performed using the Chi-square test and multi-variable logistic regression.

Results: We analysed biopsies from 2821 currently untreated CHB patients. Median age was 37 years, 53% HBeAg positive, with median HBV DNA of 7.17 log IU/ml. Overweight, HT, DM and DL were present in 51%, 6.8%, 4.3% and 3.9% of patients, and 25.4% had advanced fibrosis (METAVIR F3–4). Presence of overweight (30.8 vs 19.8%; $p < 0.001$), HT (39.3 vs 24.4%, $p < 0.001$), DM (42.5 vs 24.7%, $p < 0.001$) and DL (46.8 vs 24.6%, $p < 0.001$) was associated with a higher risk of advanced fibrosis. The highest risk of advanced fibrosis was seen in patients with multiple comorbidities (19.4% if no metabolic comorbidities, 27.9% with 1 comorbidity, 43.6% if ≥ 2 comorbidities, $p < 0.001$). Findings were consistent in multivariable analysis (adjusted odds ratio [aOR] for 1 comorbidity: 1.135, aOR for ≥ 2 comorbidities: 1.566, $p = 0.022$). Follow-up biopsy was available for 1307 patients, 757 treated with NUC monotherapy and 550 with PEG-IFN \pm NUC. Fibrosis regression was observed in 261 (39.4%) patients, and was more often observed in patients without metabolic comorbidities (49.8%), when compared to patients with 1 (33.9%) or ≥ 2 metabolic comorbidities (28.0%, $p < 0.001$). Findings were consistent in multivariable analysis (aOR for 1 comorbidity: 0.646, aOR for ≥ 2 comorbidities: 0.463, $p = 0.020$). Finally, progression to advanced fibrosis during AVT was predominantly seen in patients with metabolic comorbidities: the risk was 4.6% in patients without metabolic comorbidities, compared to 9.8% and 14.3% in patients with 1 or ≥ 2 metabolic comorbidities ($p = 0.001$).

POSTER PRESENTATIONS

Conclusion: Presence of metabolic comorbidities in untreated patients with CHB is associated with more severe liver fibrosis. Furthermore, in patients on AVT, presence of metabolic comorbidities is associated with less fibrosis regression, and even a significant risk of fibrosis progression.

FRI-364

Baseline and reduction at 1 year of hepatitis B surface antigen level predicts functional cure and low HBsAg titer: A long-term kinetics of hepatitis B surface antigen

Soon Kyu Lee¹, Jung Hyun Kwon¹, Soon Woo Nam¹. ¹Division of Hepatology, Department of Internal Medicine, Incheon St. Mary's Hospital, College of Medicine, The Catholic University of Korea, Seoul, Korea, Rep. of South
Email: doctorkwon@catholic.ac.kr

Background and aims: Long-term nucleos (t)ide analogue (NA) therapy is usually mandatory in patients with chronic hepatitis B (CHB) infection. In the stopping rule, a low HBsAg titer (<2 log IU/ml) has been suggested as the cut-off level for stopping NA therapy. However, the long-term kinetics of quantitative HBsAg levels and their predictive role in functional cure or stopping NA strategy remain unclear.

Method: We consecutively enrolled 1661 patients with chronic hepatitis or liver cirrhosis who started NA therapy between 2006 and 2020. Finally, 852 patients (entecavir, n = 287; tenofovir, n = 565), who were serially checked annually for HBsAg levels, were analyzed in our study. Patients were classified into three groups according to the quantitative HBsAg levels: the low HBsAg group (HBsAg <2 log IU/ml), the intermediate HBsAg group (2 log ≤ HBsAg <3 log IU/ml), and the high HBsAg group (HBsAg ≥ 3 log IU/ml). The primary outcome was the identification of the rate and predictive factors of functional cure and achievement of low HBsAg titer during NA treatment. Moreover, we also evaluated the long-term kinetics of HBsAg levels and the development of hepatocellular carcinoma (HCC).

Results: During a mean follow-up of 6.3 ± 3.6 years, the rate of functional cure after NA treatments was 2.28% (n = 19), and 108 patients (12.9%) achieved a low HBsAg group. The rate of the low HBsAg and intermediate group increase from 6.5% and 15.3% at baseline to 7.7% and 17.9% at the first year, and 14.2% and 39.6% at 8 years, respectively. The changes in the mean levels of HBsAg showed a steep reduction in the first year of NA therapy than after the first year in both functional and non-functional cure groups. The HBeAg (+) group demonstrated a higher baseline HBsAg titer and a greater reduction at one year compared to the HBeAg (−) group. Among patients with HBeAg (+), the chronic hepatitis group showed a significant reduction at one year. In multivariate Cox-regression analysis, lower baseline HBsAg titer (<1000 IU/ml), and the presence of reduction in the 1 year of HBsAg titer were both identified as predictive factors for an achievement of functional cure and low HBsAg titer after NA therapy. During follow-up, there was no development of HCC in patients achieving functional cure.

Conclusion: Our study demonstrated the rapid reduction in HBsAg titer in the first year of NA therapy and an increase in low HBsAg group during NA therapy. Moreover, lower baseline HBsAg titer and a decrease in the first year of HBsAg titer may predict functional cure and low HBsAg titer during NA treatments.

FRI-365-1Y

Limited use of established risk scores for the prediction of hepatocellular carcinoma in patients with chronic hepatitis D virus infection

Robin Iker^{1,2}, Anika Wranke^{1,2}, Hannah Schneider¹, Heiner Wedemeyer^{1,2,3,4}, Helenie Kefalakes^{1,2,3,4}, Lisa Sandmann^{1,3,4}. ¹Department of Gastroenterology, Hepatology, Infectious Diseases and Endocrinology, Hannover Medical School, Hannover, Germany; ²German

Center for Infection Research (DZIF), Hannover/Braunschweig, Hannover, Germany; ³D-SOLVE: EU-funded Network on individualized management of hepatitis D, Hannover, Germany; ⁴Excellence Cluster RESIST, Excellence Initiative Hannover Medical School, Hannover, Germany
Email: iker.robin@mh-hannover.de

Background and aims: Hepatocellular carcinoma (HCC) is a major health burden and one of the leading causes of cancer-related deaths worldwide. Patients with chronic HDV infection (CHD) are at risk of developing HCC. In chronic HBV or HCV infection, risk scores are commonly used to predict HCC, but none has been validated in CHD. Here, we aim to validate existing HCC risk scores for their predictive potential in patients with CHD.

Method: Data from patients with CHD and a minimum follow-up (FU) of 6 months were retrospectively collected at Hannover Medical School from 1990 to 2023. Patients with HCC development (CHD-HCC) during FU were identified and matched to patients without HCC development (CHD-non-HCC) based on sex, age, INR, and bilirubin in a 1:2 ratio. Time points for data collection were first visit to the clinic (BL), 12 (HCC-12) and 6 months (HCC-6) prior to HCC development, as well as at HCC diagnosis (HCC). Comparable time points were selected for the matched CHD-non-HCC cohort with the last one defined as the last available visit. Validated HCC risk scores were calculated and compared between the cohorts. The following scores were analyzed: PAGE-B (platelets, age, sex), aMAP (age, sex, albumin/bilirubin, platelets), Toronto HCC Risk Index (age, etiology, sex, platelets), REAL-B (age, sex, alcohol, cirrhosis, diabetes, platelets, alpha-fetoprotein (AFP)), CAMD (cirrhosis, age, sex, diabetes), AASL (age, albumin, sex, cirrhosis) and ADRES-HCC (sex, FIB-4 index, AFP).

Results: We retrospectively identified 251 CHD patients of whom 14% (36/251) were diagnosed with HCC during FU. At BL, the majority of CHD-HCC patients were male (75%), cirrhosis was present in 89% of patients and median time to HCC diagnosis was 3.42 years (IQR 1.4–6.96). The prevalence of liver cirrhosis, hepatic comorbidities and prior interferon treatment was similar to the matched 72 CHD-non-HCC patients. When comparing HCC prediction scores between the cohorts, overall test performance was poor. At BL, the REAL-B score reached the highest AUC with 0.655, followed by CAMD (AUC = 0.61) and aMAP (AUC = 0.61). Slightly weaker test performance was detected at HCC-12, with the three best performing tests being REAL-B (0.61), CAMD (AUC = 0.59) and ADRES-HCC (AUC = 0.56). At HCC-6, ADRES-HCC (AUC = 0.69), REAL-B (AUC = 0.66) and aMAP (AUC = 0.62) performed best. At HCC diagnosis, ADRES-HCC (AUC = 0.68) and aMAP (AUC = 0.66) were the two best scores to distinguish between patients with and without HCC. Interestingly, AFP alone outperformed all scores at every time point with an AUC of 0.69, 0.64, 0.75, and 0.78 at BL, HCC-12, HCC-6 and HCC respectively.

Conclusion: In our cohort, none of the analyzed scores predicted HCC development with sufficient accuracy and consistency. However, HCC risk stratification is essential for the management of CHD patients. Thus, the development of a valid HCC risk score should be addressed in future studies.

FRI-366

HBV DNA thresholds and immune tolerance: unveiling new insights from cross-sectional hepatic histology data in hepatitis B

Xiaoke Li¹, Tingyu Zhang², Xin Sun², Daqiao Zhou³, Xiaoling Chi⁴, Yueqiu Gao⁵, Yong-an Ye¹. ¹Dongzhimen Hospital, Beijing University of Chinese Medicine, Beijing, China; ²Beijing University of Chinese Medicine, Beijing, China; ³Shenzhen Traditional Chinese Medicine Hospital, Shenzhen, China; ⁴The Second Affiliated Hospital of Guangzhou University of Chinese Medicine, Guangzhou, China; ⁵Shuguang Hospital Affiliated to Shanghai University of Traditional Chinese Medicine, Shanghai, China
Email: lixiaoke@bucm.edu.cn

Background and aims: Immune tolerance (IT) is pivotal in HBV persistence. Current guidelines, constrained by liver biopsy

limitations, use high HBV viral loads and normal liver enzymes as surrogate IT markers. Yet, defining 'high viral load' lacks uniformity across regional guidelines. Furthermore, the definition of a quasi-immune tolerance phase in HBeAg-negative patients remains a contentious issue. This cross-sectional study in China seeks to clarify the relationship between serum HBV DNA levels and hepatic inflammation grades (from liver biopsy) in untreated chronic hepatitis B patients. It aims to uncover high viral load patterns with concurrent low hepatic inflammation in various infection statuses and to determine a more accurate HBV DNA threshold for IT identification.

Method: Our study encompassed 1,275 nucleos(t)ide analogue-naïve chronic HBV patients from China, including 568 HBeAg-negative and 707 HBeAg-positive subjects. The cohort was stratified based on HBeAg status, following which we delved into the relationship between hepatic inflammation (assessed through biopsy) and serum HBV DNA levels. Spearman's correlation analysis and a stepwise looping algorithm were employed for the precise determination of optimal HBV DNA cut-off values for assessing hepatic inflammation.

Results: The study identified distinct correlations within groups defined by HBV DNA thresholds. In HBeAg-negative patients, a threshold of 6.45 log₁₀ IU/ml was set, showing Spearman correlation coefficients of 0.40 ($p < 0.01$) and -0.32 ($p = 0.036$) below and above this level, respectively. In HBeAg-positive patients, an 8.92 log₁₀ IU/ml threshold resulted in coefficients of -0.10 ($p < 0.01$) and -0.63 ($p < 0.01$). These findings suggest a nuanced, non-linear connection between viral load and liver inflammation in both HBeAg-defined categories, with variable patterns across HBV DNA levels.

Conclusion: This study highlights the diverse relationship between HBV DNA viral load and hepatic inflammation in chronic hepatitis B patients at different DNA levels. Generally, elevated HBV DNA levels correlate with increased liver inflammation, but this trend reverses at higher levels. Interestingly, similar patterns are observed in both HBeAg-positive and -negative groups, albeit with lower HBV DNA thresholds in the latter. These findings challenge the traditional view that immune tolerance is exclusive to HBeAg-positive individuals, introducing the possibility of a quasi-immune tolerance state in HBeAg-negative patients. This revelation suggests a possible shift in our understanding of immune tolerance in chronic hepatitis B and underscores the need for a reevaluation of treatment strategies for these patients, potentially impacting their clinical management.

FRI-367

Prediction of hepatocellular carcinoma risk and liver-related events in chronic hepatitis D, an international retrospective cohort study (RIDE)

Lesley A. Patmore¹, Michelle Spaan¹, Kosh Agarwal², Ozgur Koc³, Hans Blokzijl⁴, Samantha Brouwer⁵, Hanneke van Soest⁶, Astrid van Hulzen⁷, Harry L.A. Janssen¹, Jolanda Lammers⁷, Louis Jansen⁸, Mark Claassen⁹, Robert A. de Man¹, R. Bart Takkenberg¹⁰, Remco van Dijk¹¹, Dirk Posthouwer³, Jurriën Reijnders^{1,5}, Ivana Carey², Milan J. Sonneveld¹. ¹Erasmus MC, University Medical Center, Rotterdam, Netherlands; ²King's College Hospital, London, United Kingdom; ³Maastricht University Medical Center, Maastricht, Netherlands; ⁴University Medical Center Groningen, University of Groningen, Groningen, Netherlands; ⁵Haga Hospital, The Hague, Netherlands; ⁶Haaglanden Medical Center, The Hague, Netherlands; ⁷Isala Hospital, Zwolle, Netherlands; ⁸OLVG, Amsterdam, Netherlands; ⁹Rijnstate Hospital, Arnhem, Netherlands; ¹⁰Amsterdam University Medical Centers, Amsterdam, Netherlands; ¹¹Leiden University Medical Center, Leiden, Netherlands
Email: l.patmore@erasmusmc.nl

Background and aims: Chronic hepatitis D (CHD) is the most severe form of chronic viral hepatitis, with a high risk of developing hepatocellular carcinoma (HCC) and other liver-related events. Risk

stratification is urgently needed to guide HCC surveillance strategies and to prioritize treatment with novel antiviral agents.

Method: We conducted a multicenter retrospective cohort of all consecutive anti-HDV positive patients managed at 10 academic and non-academic sites in the Netherlands and the United Kingdom. We excluded patients with current or past hepatitis C or HIV infection. The PAGE-B score was calculated at first visit as previously published based on platelet count, age and sex, and patients were categorized as low (<10), intermediate (10–17) and high risk (>17) for HCC development. We studied the cumulative incidence of HCC and liver-related events, defined as the first of a composite of HCC, liver transplantation and liver-related mortality, in the overall study population, and across PAGE-B risk strata.

Results: We analyzed 269 patients; 58% was male with a median age of 38 years (inter quartile range [IQR] 32–47) at enrolment. At enrolment, 35.5% had cirrhosis and 45% were HDV RNA positive. In 66.5% of patients antiviral therapy was started with either a nucleos(t)ide analogue ($n = 164$) and/or (pegylated) interferon ($n = 41$) during follow-up. During a median follow-up of 4.3 years (IQR 1.5–6.4), a total of 47 first events were recorded (HCC: $n = 13$, liver transplantation: $n = 34$, liver-related death: $n = 13$). The 5-year cumulative incidence of HCC and liver-related events were 3.8% (95% confidence interval [CI] 1.05–6.5), and 15.6% (95% CI 10.5–20.7). The 5-year cumulative incidence of HCC was 0% among patients with a low PAGE-B score ($n = 115$, 44% of cohort), compared to 3.2% in the intermediate risk group ($n = 121$, 46% of cohort) and 25.4% in the high risk group ($n = 26$, 10% of cohort; $p < 0.001$). The 5-year cumulative incidence of liver-related events was 2.1% among patients with a low PAGE-B score, compared to 21.1% in the intermediate risk group and 45.5% in the high risk group ($p < 0.001$). Findings were consistent in patients with cirrhosis at baseline; the 5-year cumulative HCC incidence was 0% in the low PAGE-B group, and 9.1% and 32.4% in the intermediate and high risk groups ($p < 0.001$). Among HDV RNA positive patients, the 5-year cumulative HCC incidence was 0% in the low PAGE-B group compared to 6.8% and 32.5% in the intermediate and high risk groups ($p < 0.001$).

Conclusion: Patients with CHD are at high risk of adverse liver-related outcomes. PAGE-B predicts the risk of HCC development and other liver related events, and can therefore be used to guide HCC surveillance strategies and treatment prioritization.

FRI-370

Bulevirtide efficacy and safety in chronic hepatitis delta patients on liver transplant waiting list

Magdalena Meszaros¹, Marie-Noëlle Hilleret^{2,2}, Jérôme Dumortier³, Louis Dalteroche⁴, Armand Aberge⁵, Marianne Latournerie⁶, Teresa Antonini⁷, Filomena Conti⁸, Patrick Borentain⁹, Nassim Kamar¹⁰, Camille Besch¹¹, Claire Francoz¹², Maryline Debette-Gratien¹³, Sébastien Dharancy¹⁴, Georges-Philippe Pageaux¹. ¹CHU Montpellier, Montpellier, France; ²CHU Grenoble Alpes, Grenoble, France; ³Hopital Edouard Erriot, Lyon, France; ⁴CHU Tours, Tours, France; ⁵CHU de Clermont-Ferrand, Clermont-Ferrand, France; ⁶CHU Dijon, Dijon, France; ⁷Hopital de la Croix Rousse, Lyon, France; ⁸APHP, Paris, France; ⁹CHU Timone, Marseille, France; ¹⁰CHU Toulouse, Toulouse, France; ¹¹CHU Strasbourg, Strasbourg, France; ¹²Beaujon Hospital, Clichy, University Paris Cité, Clichy, France; ¹³CHU dupuytren, Limoges, France; ¹⁴CHRU Lille, Lille, France
Email: m-meszaros@chu-montpellier.fr

Background and aims: Bulevirtide (BLV), a breakthrough antiviral inhibiting hepatitis Delta virus (HDV) cell entry, received European Medicine Agency approval in 2020 for HDV chronic infection in compensated liver disease patients. Its use in patients on liver transplant (LT) waiting list (for decompensated liver disease or hepatocarcinoma (HCC) remains underexplored. This study aims to gather real-life data on BLV usage in patients awaiting LT or undergoing LT candidacy evaluation.

POSTER PRESENTATIONS

Method: Consecutive HDV-infected cirrhotic patients being on liver transplant waiting list or undergoing pretransplant evaluation in whom BLV (2 mg daily) was prescribed were included.

Clinical, biological, and virological characteristics were collected at baseline, week 24 and week 48, and at LT. Liver-related events (HCC, LT) and adverse events were documented. Virological response was defined by HDV RNA undetectable or ≥ 2 -log decline vs. baseline, virologic non-response: HDV-RNA decline < 1 log vs baseline and biochemical response: ALT normalization vs baseline.

Results: Fourteen patients from six French LT centers were included. The mean age was 52 ± 9.4 years, 71.4% were men. At BLV initiation 12 patients were Child A (85.8%), 1 (7.1%) Child B and 1 (7.1%) Child C. Four (28.5%) patients received concomitant PEG IFN α 180 μ g/week. Mean MELD score was 9.14 ± 2.74 . Median platelet count 78 (26–350) $\times 10^9/L$, liver stiffness measurement (LSM) 17.4 (10–50) kPa, alanine aminotransferase (ALT) 87.5 (32–139) U/L, HBsAg 4402 (315–13899) IU/ml, HDV RNA 6 (2.23–7.4) log IU/ml. Large gastroesophageal varices were present in 9 (64%) patients. Seven (50%) patients had active HCC: 3 (43%) were BCLC-0, 3 (43%) BCLC-B and 1 (14%) BCLC-A. Eleven (78%) patients received 48 weeks (W) of BLV therapy. At W48 HDV RNA declined by a median of 2.56 (IQR 3.02) log IU/ml ($p < 0.001$) vs. baseline, becoming undetectable in 6 (54%) patients. A virological response at W48 was seen in 8 (72.7%) patients and a non-response in 1 (10%) patient. At W48 median ALT decreased to 34 (8–93) U/L ($p < 0.001$ vs baseline). Biochemical response at W48 was 72.8%. Combined response (at W48 was 54, 5%. Median MELD score was unchanged at W48. No significant changes in HBsAg concentrations were observed between W0 vs W24. No symptomatic adverse event was observed. 9 (64%) patients underwent LT after a mean waiting time of 12 (6–20) months. At LT, HDV RNA declined by a median of 1.81 (1.34) log IU/ml ($p < 0.004$) vs. baseline and was undetectable in 4 (44.4%) patients. Two patients died, one from cholangiocarcinoma and another of HCC progression. None of them were attributed to BLV.

Conclusion: BLV demonstrates safety and efficacy in patients on LT waiting list for decompensated liver disease or HCC. A 48-week course of therapy leads to significant virological and biochemical responses, providing valuable insights for the management of chronic hepatitis Delta in the LT setting.

FRI-371

Undetectable HDV RNA at 24 weeks of treatment with combination therapy is an important predictor of maintained response off-therapy

Fabien Zoulim¹, Vladimir Chulanov², Pietro Lampertico^{3,4}, Heiner Wedemeyer⁵, Adrian Streinu-Cercel^{6,7}, Victor Pantea⁸, Stefan Lazar⁹, George Sebastian Gherlan^{7,9}, Pavel Bogomolov¹⁰, Tatyana Stepanova¹¹, Viacheslav Morozov¹², Vladimir Syutkin¹³, Olga Sagalova¹⁴, Dmitry Manuilov¹⁵, Renee-Claude Mercier¹⁵, Lei Ye¹⁵, Grace M. Chee¹⁵, Ben L. Da¹⁵, Audrey H. Lau¹⁵, Anu Osinusi¹⁵, Marc Bourliere¹⁶, Vlad Ratziu¹⁷, Stanislas Pol¹⁸, Marie-Noëlle Hilleret¹⁹, Tarik Asselah²⁰. ¹Hospital Croix Rousse, Lyon, France; ²Sechenov University, Moscow, Russian Federation; ³Department of Pathophysiology and Transplantation, CRC “A. M. and A. Migliavacca” Center for Liver Disease, University of Milan, Milan, Italy; ⁴Division of Gastroenterology and Hepatology, Foundation IRCCS Ca’ Granda Ospedale Maggiore Policlinico, Milan, Italy; ⁵Medizinische Hochschule Hannover, Klinik für Gastroenterologie, Hepatologie und Endokrinologie, Hannover, Germany; ⁶Matei Bals National Institute of Infectious Diseases, Bucharest, Romania; ⁷“Carol Davila” University of Medicine and Pharmacy, Bucharest, Romania; ⁸Infectious Clinical Hospital “T. Ciorba,” Chisinau, Moldova; ⁹Dr. Victor Babes Foundation, Bucharest, Romania; ¹⁰M.F. Vladimirovsky Moscow Regional Research and Clinical Institute, Moscow, Russian Federation; ¹¹LLC Clinic of Modern Medicine, Moscow, Russian Federation; ¹²LLC Medical Company “Hepatolog,” Samara, Russian Federation; ¹³Institute of Emergency Medicine n.a. NV Sklifosovskiy, Moscow, Russian Federation; ¹⁴South Ural State Medical

University, Chelyabinsk, Russian Federation; ¹⁵Gilead Sciences, Inc., Foster City, United States; ¹⁶Hôpital Saint Joseph, Marseille, France; ¹⁷CH Pitié-Salpêtrière, Paris, France; ¹⁸Hôpital Cochin, Paris, France; ¹⁹Centre Hospitalier Universitaire Grenoble Alpes, Grenoble, France; ²⁰Hôpital Beaujon APHP, Université de Paris-Cité, INSERM UMR1149, Clichy, France Email: renee-claude.mercier@gilead.com

Background and aims: Bulevirtide (BLV) is a first-in-class entry inhibitor approved in the EU for the treatment of chronic hepatitis delta (CHD). In MYR204, a Phase 2b study evaluating finite treatment with BLV with or without pegylated interferon alfa-2a (PegIFN), combination treatment resulted in higher post-treatment virologic response rates compared with either monotherapy regimen. Here we present the predictors of on-treatment and post-treatment responses with combination treatment.

Method: 174 patients with CHD were randomized (1:2:2:2) and stratified based on cirrhosis status to receive (A) PegIFN for 48 weeks (W); or (B) BLV 2 mg + PegIFN, or (C) BLV 10 mg + PegIFN for 48W followed by 48W of monotherapy with BLV 2 mg or 10 mg, respectively; or (D) BLV 10 mg for 96W. All patients were followed up to 48W (FU-48) post-end of treatment (EOT). In this sub-analysis, the univariate logistic regression model was used to examine whether any baseline or on-treatment clinical characteristics predicted responses at EOT and FU-24, and sustained HDV RNA undetectability at FU-48 with combination therapy (arms B and C). The assessed end points included undetectable HDV RNA (target not detected) and composite end point (undetectable HDV RNA and ALT normalization). Predictors with a p value < 0.05 was considered significant.

Results: Baseline (BL) characteristics were similar between all arms. BL predictors of undetectable HDV RNA and composite end point at EOT with combination therapy included absence of cirrhosis (odds ratio (OR) 3.6, 4.2; $p \leq 0.006$), HDV RNA $<$ median 5.54 log₁₀ IU/ml (OR 2.6, 2.5; $p = 0.03$), and LS < 11.1 kPa (OR 3.8, 6.1; $p \leq 0.003$). The BL predictors of responses at FU-24 included HDV RNA $<$ median (OR 4.5, 4.0; $p \leq 0.002$), no interferon experience (only for undetectable HDV RNA, OR 2.4; $p = 0.04$), LS < 11.1 kPa (OR 2.4, 3.2; $p \leq 0.04$) and lower HBsAg (OR 0.4, 0.4; $p \leq 0.02$). In patients who achieved undetectable HDV RNA at EOT ($n = 51$), sustained HDV RNA undetectability at FU-48 was significantly predicted by BL HDV RNA level $<$ median 5.09 log₁₀ IU/ml (OR 4.0; $p = 0.0294$), earlier onset to HDV RNA undetectability ($p = 0.0030$), and longer duration of HDV RNA undetectability ($p = 0.0029$). Importantly, achieving undetectable HDV RNA at W24 after treatment initiation predicted maintained viral suppression at FU-48 (OR 19.1; $p = 0.0005$). In patients who were undetectable at both W24 and EOT, 92% maintained treatment response at FU-48 while only 38% of patients who had positive HDV RNA at W24 and undetectable HDV RNA at EOT maintained the response at FU-48.

Conclusion: In patients with CHD treated with combination therapy with BLV + PegIFN, absence of cirrhosis, lower HDV RNA and liver stiffness at BL were identified as significant predictors of undetectable HDV RNA and composite end point at EOT. Achievement of early undetectable HDV RNA at on-treatment W24 is an important predictor of long term off-treatment viral response.

FRI-372

The effect of age and pregnancy on transition into Immune Active disease in Immune Tolerant patients-a retrospective cohort study of 245 patients

Mai Kilany¹, Edo J. Dongelmans², Jordan J. Feld³, Milan J. Sonneveld⁴, Bettina E. Hansen⁴, Harry L.A. Janssen⁵. ¹Toronto Centre for Liver Disease-University of Toronto, Toronto, Canada; ²Erasmus University Medical Center, Rotterdam, Netherlands; ³Toronto Center for Liver Disease, Toronto, Canada; ⁴Erasmus MC University Medical Center, Rotterdam, Netherlands; ⁵Erasmus MC-University Medical Center, Rotterdam, Netherlands Email: mai.kilany@uhn.ca

Background and aims: It remains unclear whether starting anti-viral therapy (AVT) in Immune Tolerant (IT) chronic hepatitis B (CHB) patients is beneficial. Patients are likely to transition into Immune Active (IA) disease over time, and is unknown whether AVT could prevent this. We longitudinally followed IT-CHB patients to identify risk factors associated with phase transition to IA and the rates of adverse outcomes (cirrhosis, hepatic decompensation and HCC).

Method: This is a retrospective single center observational study of all IT-CHB patients who were diagnosed between 1990–2020. Strict criteria for IT-disease were used: HBeAg positive, HBV DNA ≥ 6 log and if ALT ≤ 40 U/ml. IA disease was defined as ALT ≥ 80 , or >40 for two visits (in the absence of other causes of ALT elevation) or presence of $\geq F2$ on liver biopsy or non-invasive tests. KM- and Cox-method (including start of AVT as time-dependent covariate) were used for cumulative incidences and identifying predictors, in which first visit with lab was defined as baseline.

Results: In total, 245 patients were included with a median age of 29.6 [24–38] years; 68% were female and 89% were Asian. Median baseline ALT and HBV DNA were 25 [21–32] U/ml and 8.6 [8.2–9.1] log₁₀ U/ml. Those above age 40 at baseline had higher median ALT 31 [24–36] vs. 24 [20–31] U/ml ($p < 0.001$) of those <40 , but there were no differences in baseline HBV DNA level (8.7 vs. 8.6 log₁₀ U/ml, $p = 0.49$).

The median follow-up time was 142 [99–181] months. The 5- and 10 year cumulative incidences of IA transition were 38% and 61%, with a median time of 7.0 [3.2–13.8] years. 143 (58%) patients started AVT, of which IA disease was the most common indication (54%). IA transition was more common in patients with increased ALT levels at baseline (aHR 1.08, 95%CI 1.05–1.11, $p < 0.001$) and women who received short-term nucleos(t)ide analogue (NA) therapy during pregnancy (aHR 3.76; 95%CI 0.86–16.35, $p = 0.08$). For the latter group, median time between NA withdrawal and IA transition was 36 [8.2–75.1] months, excluding post-partum flares. Notably, increased age at baseline seemed not associated with a higher risk for phase transition (aHR 1.01; 95%CI 0.99–1.02, $p = 0.89$). Furthermore, changes in ALT- and HBV-DNA levels at 1- and 5-year were equal among different age groups ($<25/25-34/35-44/>45$ years, all $p > 0.05$). Regarding liver-related adverse events, four patients (1.6%) developed cirrhosis, one patient (0.4%) developed HCC approximately 6 years after transition, two patients (0.8%) achieved HBsAg-loss and no patients decompensated. All events occurred after IA phase transition.

Conclusion: A majority of IT patients transition into IA-disease within 10 years. IA transition rates were higher in patients with increased baseline ALT-levels and after short-term NA therapy during pregnancy. Interestingly, no effect of baseline age was seen.

FRI-373

Impact of pregnancy on global and HBV-specific B-cell immunity

Anna Pocurull¹, Mireia García-López¹, Cristina Collazos¹, Thais Leonel¹, Marta López², Simon Fletcher³, Elena Perpinan⁴, Georgios Koutsoudakis¹, Patricia Huelin⁵, Carlos Aracil⁵, Juan Carlos Hurtado¹, Xavier Forns¹, Mala Maini⁶, Sofia Pérez-del-Pulgar¹, Sabela Lens¹. ¹Liver Unit, Hospital Clínic Barcelona. IDIBAPS. University of Barcelona, CIBEREHD, Barcelona, Spain; ²Gynaecology and Obstetrics, Hospital Clínic Barcelona, IDIBAPS, Barcelona, Spain; ³Gilead Sciences, Foster City, United States; ⁴Institute of Liver Studies, King's College Hospital, School of Immunology and Microbial Sciences, Faculty of Life Sciences and Medicine, King's College London, London, UK, London, United Kingdom; ⁵Arnau Vilanova University Hospital, Lleida, Spain; ⁶Division of Infection and Immunity, University College of London (UCL), London, United Kingdom
Email: pocurull@recerca.clinic.cat

Background and aims: Pregnancy represents a particular immunological state induced by the presence of the fetus. However, the role of B-cell immunity, especially regarding virus-specific B cells, has been poorly characterized, and its influence on the virological control of

chronic hepatitis B (CHB) during pregnancy remains unclear. We aimed to characterize both the global and specific humoral immunity to Hepatitis B Virus (HBV) during pregnancy and postpartum among patients with CHB. As postpartum ALT flares in HBV suggest alterations of immunity during this transition we aimed to analyze the correlates of B-cell immunity.

Method: We longitudinally collected peripheral blood mononuclear cells (PBMC) from pregnant women diagnosed with CHB (PrandHBV, $n = 22$) at multiple intervals during pregnancy (2nd and 3rd trimesters) and postpartum (weeks 6, 16, and 48), analyzing them by spectral flow cytometry. Controls included pregnant patients without HBV (Pr, $n = 9$) and non-pregnant women with CHB (HBV, $n = 9$). We studied global and memory B cells (MBC) and characterized viral antigen-specific MBC (HBsAg-MBC and HBcAg-MBC) using fluorochrome-labeled baits. Additionally, we examined follicular T cells (Tfh) and regulatory B cells (B regs). ALT flare after delivery was defined by a two-fold increase from the baseline value.

Results: In terms of global B-cell immunity, pregnancy was associated with a reduced frequency of Bregs and Tfh in both groups ($p < 0.05$). However, the percentage of atypical or dysfunctional MBC phenotype (CD21-CD27-) was higher in PrandHBV compared to Pr patients (5% vs. 3%, $p = 0.02$). The frequencies of Tfh and MBC increased after delivery, indicating a potential restoration of T cell-B cell interaction. Regarding virus-specific immunity, the frequency of HBcAg-MBC in PrandHBV patients increased post-delivery (0.4 vs. 0.9%; $p < 0.05$) whereas the frequency of HBsAg-MBC remained stable. Interestingly, PrandHBV patients who developed a postpartum ALT flare ($n = 5$), had a higher frequency of atypical HBcAg-MBC during pregnancy (5% vs 0%; $p = 0.01$).

Conclusion: While global immunity experiences changes during pregnancy, our study sheds light on the specific B-cell responses directed against HBV. The identification and characterization of virus-specific MBCs, specifically those targeting HBcAg, reveal dynamic changes post-delivery. The increased frequency of HBcAg-MBCs suggests a potential boost in the immune response following childbirth. The changes observed in HBcAg-MBC subpopulations could serve as potential indicators for predicting postpartum ALT flares. However, further studies are essential to comprehensively understand the involvement of these cells in the immunological and virological changes induced by pregnancy.

FRI-374-YI

The UK experience of liver transplantation for HBV: excellent clinical outcomes despite a significant burden of HBV/Delta disease and wide variation in hepatitis B immunoglobulin prophylaxis practices-time for a consistent approach?

Almuthana Mohamed¹, Maria Guerra Veloz¹, Silke François², Gemma Botterill³, Rachel Smith⁴, Muhammad Salman⁵, Lindsay Greenland¹, Lucy Turner⁶, Stuart McPherson⁵, Andrew Bathgate⁷, Douglas Thorburn², William Gelson⁴, Mark Aldersley⁶, Ahmed M. Elsharkawy³, Kosh Agarwal¹. ¹Institute of Liver Studies, King's College Hospital, London, United Kingdom; ²Royal Free London NHS Foundation Trust, London, United Kingdom; ³University Hospitals Birmingham NHS Foundation Trust, Birmingham, United Kingdom; ⁴Cambridge University Hospitals NHS Foundation Trust, Cambridge, United Kingdom; ⁵The Newcastle Upon Tyne Hospitals NHS Foundation Trust, Newcastle, United Kingdom; ⁶Leeds Teaching Hospitals NHS Trust, Leeds, United Kingdom; ⁷Royal Infirmary of Edinburgh NHS Lothian, Edinburgh, United Kingdom
Email: almuthana700@gmail.com

Background and aims: Hepatitis B immunoglobulin (HBIG) along with high genetic barrier Nucleos(t)ide analogues (NUCs) are currently the standard care for prophylaxis against Hepatitis B (HBV) recurrence post liver transplantation (LT). Retrospective data from Italy suggests lifelong use of HBIG for high-risk HBV patients post-LT. However, indefinite HBIG therapy remains controversial, with heterogeneity in dosage and duration protocols in LT centres. We

POSTER PRESENTATIONS

audited the current management of HBV post-LT and outcomes within the UK for the past decade using LT centre's data.

Method: A retrospective, multicentre study was conducted by the British Association for the Study of Liver (BASL), including all patients who had LT for HBV between 2010–2023 in the 7 UK LT centres. Clinical and LT data were collected. HBV recurrence defined by reappearance of HBsAg and/or detectable HBV DNA. Multivariate regression analysis was used to identify predictors of HBV recurrence and survival.

Results: 299 patients were included (78.6% male; median age 52 years). 23.4% had HBV/Hepatitis D (HDV) coinfection. Common indications for HBV LT were decompensated cirrhosis (44.8%) and hepatocellular carcinoma (HCC) (43.5%). At the time of LT, 64.2% had undetectable HBV DNA and 69% with HBV/HDV coinfection had detectable HDV RNA. All patients with available data (96.3%) had NUCs post-LT and 81% received HBIG post-LT regardless of HBV DNA at the time of LT. However, there was heterogeneity in HBIG doses in the first week (range 0 to 10 HBIG doses) and maintenance dosing following LT (51.8% had maintenance HBIG doses, range 1 week to >10 years). During a median follow-up of 5 years, only 15 patients (5%) had HBV recurrence. Of them, 86.7% (n=13) had high-risk of recurrence pre-LT; 4 had HBV/HDV coinfection, 5 had HCC, and 4 had fulminant HBV. Out of 43 patients (14.4%) who did not receive HBIG post-LT; only 1 patient had HBV recurrence (HBsAg positive at 6 months), and 1 patient died due to non-HBV related graft failure. The median survival post-LT was 54 months (range 0–159 months), and 38 patients died with only 2 deaths related to HBV recurrence. Multivariate regression analysis showed no significant association between number of HBIG doses in the first week post-LT, maintenance HBIG and HBV recurrence ($p=0.192$, 0.619 respectively) or mortality ($p=0.301$, 0.437 respectively).

Conclusion: UK data confirms that HBV recurrence and survival are not influenced by HBIG use and that survival post-LT, including a significant component of HBV/HDV coinfection, is excellent. However, most patients had prolonged maintenance HBIG doses post-LT. Almost all patients who did not receive HBIG post-LT (as per centre protocol) had no recurrence or increase in mortality. Early withdrawal or HBIG-free prophylaxis should be a strategy for most patients in a risk stratified manner, and this should be robustly reflected in clinical practice guidelines.

FRI-375

The coinfection of hepatitis C virus or human immunodeficiency virus in chronic hepatitis B in South Korea: A population-based study using the Korean Health Insurance Review and Assessment Service database

Jae Yoon Jeong¹, Won Sohn², Hyunwoo Oh^{2,3}, Hyo Young Lee⁴, Yeonjae Kim¹, Seong Woo Nam¹. ¹National Medical Center, Seoul, Korea, Rep. of South; ²Kangbuk Samsung Hospital, Sungkyunkwan University School of Medicine, Seoul, Korea, Rep. of South; ³Uijeongbu Eulji Medical Center, Uijeongbu, Korea, Rep. of South; ⁴Inje University Sanggye Paik Hospital, Seoul, Korea, Rep. of South
Email: jyjeong76@hanmail.net

Background and aims: Concurrent infections such as hepatitis C virus (HCV) and human immunodeficiency virus (HIV) in patients with chronic hepatitis B virus (HBV) infection were associated with the development of liver cirrhosis and hepatocellular carcinoma (HCC). However, there have been few studies for on the prevalence, clinical characteristics, use of antivirals and development of liver related complications such as liver cirrhosis and HCC in HBV/HCV or HBV/HIV coinfection. This study aimed to evaluate the prevalence, comorbidities, treatment patterns and liver related complications of patients with HBV/HCV or HBV/HIV coinfection in South Korea.

Method: A retrospective, cross-sectional study was conducted using the nationwide claims data from the Health Insurance Review and Assessment Service from 2014 to 2021 in South Korea. In this study, the number of chronic hepatitis B (CHB) patients increased annually,

starting at 327, 041 individuals (221, 143 men) in 2014 and reaching 473, 811 (269, 981 men) by 2021. These patients were classified into HBV mono-infection, HBV/HCV coinfection, and HBV/HIV coinfection groups, and comparisons were made among these groups annually.

Results: The prevalence of HBV/HCV coinfection among CHB patients between 2014 and 2021 ranged from 0.76% (2, 505/327, 041 in 2014) to 1.00% (4, 053/407, 310 in 2016), while HBV/HIV coinfection prevalence ranged from 0.055% (180/327, 041 in 2014) to 0.067% (308/462, 098 in 2020). The proportion of male gender in HBV mono-infection or HBV/HCV coinfection was approximately 60%, but HBV/HIV coinfection was predominantly observed in males (over 90%). The proportion of patients aged 50 and above among CHB patients consistently increased over time (52.0% in 2014 → 65.6% in 2021), with a higher prevalence observed in the following order: HBV/HCV coinfection (70.1% in 2014 → 81.0% in 2021), HBV mono-infection (51.9% in 2014 → 65.5% in 2021), and HBV/HIV coinfection (39.4% in 2014 → 57.2% in 2021). The presence of liver-related outcomes was higher in HBV/HCV coinfection followed by HBV mono-infection and then HBV/HIV coinfection. The proportion of liver cirrhosis in HBV/HCV coinfection, HBV mono-infection and HBV/HIV coinfection was 7.4%, 5.4%, and 5.1%, respectively ($p < 0.001$ in 2021). Also, the proportion of HCC in HBV/HCV coinfection, HBV mono-infection and HBV/HIV coinfection was 10.6%, 6.3%, and 5.1%, respectively ($p < 0.001$ in 2021). Cirrhosis demonstrated a decreasing trend over time (8.5% in 2014 → 5.4% in 2021), while the development of HCC showed no significant changes (6.3% in 2014 → 6.3% in 2021).

Conclusion: Patients with HBV/HCV coinfection are older than HBV mono-infection while those with HBV/HIV coinfection was younger than HBV mono-infection in South Korea. The prevalence of liver related complications among CHB patients was highest in HBV/HCV coinfection, followed by HBV mono-infection, and then HBV/HIV coinfection.

FRI-376

The impact of alanine aminotransferase fluctuation on the hepatocellular carcinoma risk in chronic hepatitis B patients

Yongsu Park¹, Hyunjae Shin¹, Jeong-Hoon Lee¹. ¹Department of Internal Medicine and Liver Research Institute, Seoul National University College of Medicine, Seoul, Korea, Rep. of South
Email: pindra@empal.com

Background and aims: High alanine aminotransferase (ALT) levels are well-established risk factors for hepatocellular carcinoma (HCC) development in chronic hepatitis B (CHB) patients. However, the impact of ALT fluctuation around normal margin on the development of HCC remains unclear.

Method: Patients with CHB, whose ALT levels were measured at least 4 times for the first two years, were enrolled. Based on the tertiles of coefficient of variation (CV, standard deviation divided by mean) of serial ALT levels, patients were divided into low-, intermediate-, or high-fluctuation groups. The primary outcome was HCC occurrence. Baseline characteristics were balanced using the inverse probability of treatment weighting (IPTW).

Results: Among 4, 413 patients, 76 (1.7%) developed HCC during a median follow-up of 12.6 (interquartile range [IQR] = 6.9–18.7) years. The median CV values of the low-, intermediate-, and high-fluctuation groups were 0.15, 0.30, and 0.71, respectively. Because baseline ALT levels were significantly higher in the high-fluctuation group than the other groups, we focused on the comparison between the low-fluctuation (n = 1, 471) and intermediate-fluctuation groups (n = 1, 471). Before balancing the baseline characteristics, the risk of HCC was significantly higher in the intermediate-fluctuation group compared to the low-fluctuation group (hazard ratio [HR] = 2.15, 95% confidence interval [CI] = 1.18–3.90, $P = 0.01$). After applying IPTW, the intermediate-fluctuation group maintained a significantly higher risk of HCC than the low-fluctuation group (HR = 1.99, 95% CI = 1.07–3.68, $P = 0.03$). Sensitivity analyses conducted with various

definitions of ALT fluctuation also reaffirmed the consistent result of the main analysis.

Conclusion: In CHB patients without antiviral treatment, fluctuating ALT, is associated with an increased risk of HCC. Further studies are warranted to evaluate if antiviral treatment for patients with ALT fluctuation could reduce the HCC risk.

FRI-377

Decline of Serum HBV RNA level During the First Week of Nucleos(t)ide Analogues Therapy Is Associated with Liver Injury and More Efficient Clearance of Hepatitis B Virus

Liandong Wu¹, Zhenggang Yang¹, Min Zheng¹. ¹State Key Laboratory for Diagnosis and Treatment of Infectious Diseases, The First Affiliated Hospital, Zhejiang University School of Medicine, National Clinical Research Center for Infectious Diseases, National Medical Center for Infectious Diseases, Collaborative Innovation Center for Diagnosis and Treatment of Infectious Diseases, Hangzhou, China
Email: minzheng@zju.edu.cn

Background and aims: Chronic hepatitis B (CHB) is a major global health problem. Although nucleos(t)ide analogues (NAs) are effective in controlling hepatitis B virus (HBV) infection, viral eradication remains unattainable due to the persistence of covalently closed circular DNA (cccDNA). Serum HBV RNA is a non-invasive biomarker directly reflecting cccDNA transcriptional activity. It was previously demonstrated that extracellular/serum HBV RNA levels increased after NAs treatment in HBV-producing cell lines and HBV transgenic mice, while serum HBV RNA levels declined under persistent NAs therapy in CHB patients. Early change of serum HBV RNA level after NAs therapy and its influencing factors remain unclear, as well as the clinical significance.

Method: 131 treatment-naïve CHB patients were included in this prospective cohort study with 12-week follow-up. Serum HBV RNA levels at baseline and within the first week of NAs therapy were measured, and patients were divided into three cohorts according to changes in serum HBV RNA levels within the first week of NAs therapy. In cohort A (n=45), serum HBV RNA levels increased $>0.5 \log_{10}$ copies/ml; in cohort B (n=41), serum HBV RNA levels changed $<0.5 \log_{10}$ copies/ml; in cohort C (n=45), serum HBV RNA levels decreased $>0.5 \log_{10}$ copies/ml.

Results: Using ordinal logistic regression, alanine aminotransferase (ALT) was found to be associated with the decreasing trend of serum HBV RNA levels within the first week of NAs therapy (odds ratio = 1.25, $P < 0.001$). Area under receiver operating characteristic curve (AUC) for ALT to predict patients in cohort A was 0.841 ($p < 0.001$); AUC to predict cohort B was 0.607 ($p = 0.048$); AUC to predict cohort C was 0.902 ($p < 0.001$). Δ HBV RNA was calculated by difference between serum HBV RNA levels from baseline to different time points under NAs therapy (posttreatment level minus baseline level). Median Δ HBV RNA of week 2 among cohorts A, B, and C were 0.55, -0.33, and -1.82 \log_{10} copies/ml, respectively ($p < 0.001$); median Δ HBV RNA of week 4–6 were -0.16, -0.61, and -3.18 \log_{10} copies/ml ($p < 0.001$); median Δ HBV RNA of week 8–12 were -0.73, -1.07, and -4.01 \log_{10} copies/ml ($p < 0.001$). Similarly, median Δ HBV DNA of week 1 were -1.16, -1.65, and -2.17 \log_{10} IU/ml ($p = 0.013$); median Δ HBV DNA of week 2 were -2.21, -2.37, and -3.02 \log_{10} IU/ml ($p = 0.033$); median Δ HBV DNA of week 4–6 were -3.15, -3.17, and -4.15 \log_{10} IU/ml ($p = 0.015$); median Δ HBV DNA of week 8–12 were -3.54, -4.19, and -5.29 \log_{10} IU/ml ($p = 0.073$). Median Δ HBsAg of week 4–6 were 0.02, 0.04, and -0.62 \log_{10} IU/ml ($p = 0.012$); median Δ HBsAg of week 8–12 were -0.03, -0.05, and -0.93 \log_{10} IU/ml ($p = 0.004$).

Conclusion: Serum HBV RNA levels were more likely to decline within the first week of NAs therapy in patients with more severe liver injury. Patients whose serum HBV RNA levels declined significantly within the first week of NAs therapy exhibited higher efficiency of viral clearance.

FRI-378

Effect of diabetes on the risk of fibrosis progression in patients with chronic hepatitis B

Mi Na Kim^{1,2}, Jae Seung Lee^{1,2}, Hye Won Lee^{1,2}, Beom Kyung Kim^{1,2}, Seung Up Kim^{1,2}, Jun Yong Park^{1,2}, Do Young Kim^{1,2}, Sang Hoon Ahn^{1,2}. ¹Department of Internal Medicine, Yonsei University College of Medicine, Seoul, Korea, Rep. of South; ²Yonsei Liver Center, Severance Hospital, Seoul, Korea, Rep. of South
Email: ahnsh@yuhs.ac

Background and aims: Diabetes is associated with a higher risk of hepatocellular carcinoma in patients with chronic hepatitis B (CHB). However, there are limited data regarding fibrosis progression in CHB patients with diabetes compared with those without diabetes. We investigated the effect of diabetes on the risk of fibrosis progression in patients with CHB.

Method: We recruited 3,450 patients with CHB who performed transient elastography from 2012 through 2020. The primary cross-sectional outcome was the prevalence of advanced fibrosis. The primary longitudinal outcome was fibrosis progression. Advanced fibrosis was defined, according to guidelines, as a liver stiffness measurement greater than 9.0 kilopascals. Fibrosis progression was defined as incident advanced fibrosis at 3-year of follow-up.

Results: The prevalence of advanced fibrosis in our cohort was 27.4% at baseline. A higher proportion of patients with diabetes had advanced fibrosis than those without diabetes (37.3% vs 24.8%; $p < 0.001$). In multivariate analysis, diabetes was significantly associated with advanced fibrosis (odds ratio [OR], 1.49; 95% confidence interval [CI], 1.24–1.78). The longitudinal analysis was done in 2,504 patients with fibrosis stage of F0–2 at baseline. Diabetes was significantly associated with a higher risk of fibrosis progression after multivariate-adjustment (OR, 1.98; 95% CI, 1.48–2.65). The independent association of diabetes and the risk of fibrosis progression remained in each cohort of patients without antiviral therapy (OR, 1.83; 95% CI, 1.22–2.75), and those with antiviral therapy (OR, 2.15; 95% CI, 1.42–3.27).

Conclusion: In a large, well-characterized cohort study of patients with CHB, diabetes was associated with advanced fibrosis, and a higher risk for progression to advanced fibrosis.

FRI-379

Feasibility of aMAP combined with liver stiffness assessed using transient elastography for prediction of hepatocellular carcinoma development in patients with chronic hepatitis B

Hye Yeon Chon^{1,2}, Hyung Joon Yim³, Su Jong Yu⁴, Ja Kyung Kim^{1,2}, Sang Hoon Ahn^{1,5}, Sang Gyune Kim⁶, Yeon Seok Seo⁷, Seung Up Kim^{1,5}. ¹Yonsei University College of Medicine, Seoul, Korea, Rep. of South; ²Yongin Severance Hospital, Yongin, Korea, Rep. of South; ³Korea University Ansan Hospital, Korea University College of Medicine, Ansan, Korea, Rep. of South; ⁴Seoul National University College of Medicine, Seoul, Korea, Rep. of South; ⁵Yonsei Liver Center, Severance Hospital, Seoul, Korea, Rep. of South; ⁶Soonchunhyang University College of Medicine Bucheon Hospital, Bucheon, Korea, Rep. of South; ⁷Korea University College of Medicine, Seoul, Korea, Rep. of South
Email: skukorea@yuhs.ac

Background and aims: The age-male-albumin-bilirubin-platelet (aMAP) score combined with liver stiffness (LS) assessed using transient elastography was recently suggested to be helpful for estimating fibrotic burden in patients with chronic hepatitis B (CHB). We evaluated the performance of the aMAP score combination with LS for predicting HCC development.

Method: We retrospectively reviewed 944 patients with CHB who initiated antiviral therapy in five tertiary hospitals of Korea between May 2005 and July 2021.

Results: Most patients were male (n = 527, 55.8%), and the median age was 50 years. During the follow-up period (median 47.7 months), 44 patients developed HCC. The aMAP score (66.3 vs. 60.1), aMAP-LSM_{advanced fibrosis} (aMAP_{af}; 97.4 vs. 72.7), and aMAP-LSM_{cirrhosis} (aMAP_c;

91.0 vs. 55.7) were significantly higher in patients who developed HCC than those who did not (all $P < 0.05$). Similarly, the PAGE-B score (16.0 vs. 12.0) and modified PAGE-B (mPAGE-B) score (12.5 vs. 10.0) were significantly higher in patients who developed HCC than those who did not (all $P < 0.05$). In multivariate analysis, an increased aMAP (hazard ratio [HR], 1.125; 95% confidence interval [CI], 1.003–1.225), aML_{af} (HR, 1.049; 95% CI, 1.005–1.095), and aML_C (HR, 1.039; 95% CI, 1.008–1.071) were independently associated with the increased risk of HCC development ($p < 0.05$). The PAGE-B score (HR, 1.163; 95% CI, 1.028–1.315) and mPAGE-B score (HR, 1.205; 95% CI, 1.006–1.445) maintained their predictive significance after adjustment ($p < 0.05$). The areas under the curve (AUROCs) at 3 years of antiviral therapy were 0.843 for aML_{af}, 0.839 for aML_C, 0.790 for aMAP, 0.764 for mPAGE-B, and 0.752 for PAGE-B, respectively. The AUROCs at 5 years of antiviral therapy were 0.802 for aML_{af}, 0.799 for aML_C, 0.752 for aMAP, 0.718 for PAGE-B, and 0.716 for mPAGE-B, respectively. The AUROCs of aML_{af} and aML_C at 3 and 5 years of antiviral therapy were significantly higher than those of the PAGE-B and mPAGE-B scores ($p < 0.05$).

Conclusion: The aMAP score combined with LS helped to predict HCC development, and its performance was superior to that of PAGE-B and mPAGE-B.

FRI-380

HBV-specific T cell specificity and functionality can be influenced by stage of chronic HBV disease, antigen levels and age

An De Creus¹, Thierry Verbinen^{1,1}, Bart Fevery¹, Simon Verheijden¹, Michael Biermer¹, Sandra De Meyer¹, Oliver Lenz¹. ¹Janssen Pharmaceutica NV, Beerse, Belgium
Email: adecreus@its.jnj.com

Background and aims: To aid the development of immunomodulatory treatments for chronic hepatitis B (CHB) patients, it is essential to better understand HBV-specific T cell immune responses at different stages of CHB infection. Therefore, we investigated breadth and functionality of HBV-specific T cells at different stages of HBV disease.

Method: Peripheral blood mononuclear cells (PBMCs) were isolated from CHB patients: not currently treated (NCT) HBeAg positive (N = 51, of which 21 were immune tolerant (IT)), NCT HBeAg-negative (N = 36), virologically suppressed (VS) HBeAg-positive (N = 25), and VS HBeAg-negative (N = 120). PBMCs were analyzed for T cell responses against peptides covering HBV core, polymerase, and surface antigens using qualified ex vivo overnight IFN γ ELISpot. ELISpot values \geq positivity threshold (PT) were considered detectable responses, values $>3 \times PT$ were considered strong responses. Association of T cell responses with viral serum markers and patient characteristics were assessed.

Results: Overall, 148/232 (64%) patients had detectable responses to at least one antigen and 8% had responses to all 3 antigens. The percentage of patients with detectable responses to surface/envelope (15%) was lower compared to core (34%) and polymerase (52%). The percentage of patients with detectable core responses was 0% in IT, low in HBeAg-positive (23% for NCT and 17% for VS) and higher in HBeAg-negative patients (44% for both NCT and VS). Overall, the percentage of patients with detectable core responses was inversely correlated with serum HBcrAg levels (51% vs 9% for $<3.0 \log U/ml$ and $\geq 7.0 \log U/ml$ respectively). For HBeAg-negative patients with HBcrAg levels $<4 \log_{10} U/ml$, strong core responses were more prevalent (22%) than in HBeAg-negative patients with $>4 \log_{10} U/ml$ (11%). Other factors that influenced frequency of detectable core responses were HBsAg levels (42% vs 22% for $\geq 10,000 IU/ml$ and $<10,000 IU/ml$ respectively) and age (39% vs 15% for ≥ 30 years and <30 years respectively). Age impacted percentage of patients with detectable surface responses, with trend in decreasing responses from 20% to 7% as age increased from <30 to ≥ 60 years, with no apparent impact on percentage of patients with strong surface responses. HBsAg, HBcrAg levels and HBeAg status did not correlate

with detectable surface responses. Detectable polymerase responses were not associated with disease stage, viral markers, or age.

Conclusion: This evaluation of breadth and functionality of HBV-specific T-cell responses in 232 CHB patients showed that HBV-specific T cells are detectable ex vivo in most patients across all disease stages, with differences in specificity and strength of the T cell responses by disease state, HBeAg status, HBcrAg and HBsAg levels, and age.

FRI-381

Detection of functional HBV-specific CD8+ response is associated with significant decrease of HBsAg level after treatment withdrawal in eAg (-) chronic hepatitis B

Henar Calvo Sánchez^{1,2,3}, Julia Peña Asensio⁴, Joaquín Míquel^{2,5}, Eduardo Sanz-de Villalobos^{2,4}, Alberto Delgado⁴, Miguel Torralba^{1,6,7}, Alejandro González Praetorius^{1,8}, Juan Ramón Larrubia^{1,7,9}. ¹Group of Research in Translational Cellular Immunology (GITIC), IDISCAM, Guadalajara, Spain; ²Section of Gastroenterology and Hepatology, Guadalajara University Hospital, Guadalajara, Spain; ³Departament of Medicine and Medical Specialties, University of Alcalá, Alcalá de Henares, Spain; ⁴Group of Research in Translational Cellular Immunology (GITIC), IDISCAM, Guadalajara, Spain; ⁵Group of Research in Translational Cellular Immunology (GITIC), IDISCAM, Guadalajara, Spain; ⁶Service of Internal Medicine, Guadalajara University Hospital, Guadalajara, Spain; ⁷Departament of Medicine and Medical Specialties, University of Alcalá, Alcalá de Henares, Spain; ⁸Section of Microbiology, Guadalajara University Hospital, Guadalajara, Spain; ⁹Section of Gastroenterology and Hepatology, Guadalajara University Hospital, Guadalajara, Spain
Email: henarcs@hotmail.com

Background and aims: Loss of hepatitis B virus surface antigen (HBsAg) is the goal upon discontinuation of nucleos (t)ide analogues (NUCs) treatment in e-antigen negative (eAg (-)) chronic hepatitis B. However, there are no clear predictive factors defining the population that will experience HBsAg loss after discontinuation of NUCs. The study aim was to evaluate the presence of a decrease in HBsAg level greater than 50% of the baseline level after discontinuation of NUC treatment according to the presence of hepatitis B virus (HBV)-specific CD8+ response against core or polymerase epitopes upon discontinuation of treatment in a 3-year follow-up.

Method: A cohort of 12 patients HLA-A2+ with eAg (-) chronic hepatitis B treated with NUCs for a mean duration of 82 months (95% CI: 64–103), 70% male, with a mean age of 46 years (95% CI 40–53) and with fibrosis $<F3$ were enrolled. At the time of suspension, the proliferative capacity of CD8+ T cells specific against core18-27 and polymerase455-63 was assessed after 10 days of antigen-specific in-vitro stimulation. HBV-specific CD8+ cells were visualized by flow cytometry after labelling with multimeric complexes and anti-CD3/anti-CD8 antibodies. Interferon- γ (IFN γ) and tumor necrosis factor- α (TNF α) production in culture supernatants were assessed using ELISA. The HBsAg level was quantified at baseline and quarterly after discontinuation of treatment. Patients were followed for 3 years. Kaplan-Meier curves for the presence of a greater than 50% decrease in HBsAg level during follow-up were compared between the cohort with and without functional HBV-specific CD8+ cells. The number of cases that reached functional cure was recorded.

Results: 58% (7/12) of cases had CD8+ T cells specific against core and/or polymerase with proliferative capacity. The supernatants of these cultures showed significantly higher IFN γ and TNF α levels than in the non-proliferating cases (Core cultures: IFN γ $p < 0.01$; TNF α $p < 0.05$. Polymerase cultures: IFN γ $p < 0.01$; TNF α $p < 0.01$). 71% (5/7) of cases with functional HBV-specific CD8+ cells had a greater than 50% decrease in baseline HBsAg level, whereas this occurred in only 20% (1/5) of cases without functional cells, with significantly different Kaplan-Meier survival curves ($p < 0.05$). 42% (3/7) of cases with functional cells achieved functional cure, while no cases in the cohort

without functional HBV-specific CD8⁺ cells lost HBsAg during follow-up.

Conclusion: The presence of functional HBV-specific CD8⁺ T cells at the time of NUC discontinuation could select the population of patients with eAg (-) chronic hepatitis B likely to clear HBsAg.

FRI-382

The predictive value of serum HBV RNA level in chronic hepatitis B patients treated with nucleos (t)ide analogues

Yuxuan Song¹, Yandi Xie², Xiaojing Zhang³, Rongkuan Li⁴, Sujun Zheng⁵, Shuyun Zhang⁶, Ping Li⁷, Erhei Dai⁸, Xuefei Duan⁹, Juan Liu¹⁰, Bo Feng², Fengmin Lu¹¹. ¹Peking University People's Hospital, Beijing, China; ²Peking University People's Hospital, Peking University Hepatology Institute, Beijing, China; ³Hangzhou Xixi Hospital, Hangzhou, China; ⁴The Second Affiliated Hospital of Dalian Medical University, Dalian, China; ⁵Beijing You'an Hospital, Capital Medical University, Beijing, China; ⁶The Second Hospital of Harbin Medical University, Harbin, China; ⁷Tianjin Second People's Hospital, Tianjin, China; ⁸Shijiazhuang Fifth Hospital, Shijiazhuang, China; ⁹Beijing Ditan Hospital, Capital Medical University, Beijing, China; ¹⁰Research Center for Technologies in Nucleic Acid-Based Diagnostics, Hunan, China; ¹¹Peking University People's Hospital, Peking University Hepatology Institute, School of Basic Medicine, Peking University Health Science Center, Beijing, China
Email: xieyandee@163.com

Background and aims: Serum hepatitis B virus (HBV) RNA may serve as an important indicator for evaluating the efficacy of antiviral treatment and the activity of HBV in liver tissue. However, further research is needed to ascertain its accuracy and reliability. This study primarily explores the correlation between HBV RNA and other HBV markers, as well as evaluates its predictive ability on virologic response (VR), hepatitis B e antigen (HBeAg) seroconversion and hepatitis B surface antigen (HBsAg) reduction.

Method: A multicenter prospective study was conducted over a 48-week period in HBeAg-positive chronic hepatitis B (CHB) patients who were either undergoing or about to start nucleos (t)ide analog. The correlation between serum HBV RNA and dynamic changes in HBV DNA and HBsAg was described using Spearman correlation analysis. Cox regression analysis was performed to assess the predictive ability of HBV RNA on VR, HBeAg seroconversion and HBsAg reduction.

Results: A total of 427 patients from eight hospitals were enrolled who were divided into the high-viral-load group (n=214) and the low-viral-load group (n=213) based on baseline HBV RNA levels. Patients in the low-viral-load group had lower HBV DNA (p=0.009) and HBsAg (p<0.001) levels compared to those in the high-viral-load group. Serum HBV RNA levels were positively correlated with serum HBsAg levels at baseline, 24 weeks, and 48 weeks (r=0.193, p=0.008; r=0.336, p=0.004; r=0.480, p<0.001) and with HBV DNA levels at 12 weeks during follow-up (r=0.318, p=0.008). Stratified analysis revealed that these correlations were more pronounced in the high-viral-load group at baseline. During the follow-up period, 294 patients (68.9%) remained HBV RNA positive after achieving HBV DNA undetectable. A total of 162 patients (38.0%) experienced HBV RNA seroclearance with a median time of 12 weeks. Serum HBV RNA serves as an independent indicator for predicting VR (AUC=0.852, p=0.024), the seroconversion of HBeAg (AUC=0.826, p=0.003) and HBsAg reduction (AUC=0.801, p=0.002). Patients with HBV RNA below 9.12 log₁₀ copies/ml (sensitivity=0.7, specificity=0.8) at 12 weeks of treatment were more likely to be VR. Patients with HBV RNA below 4.31 log₁₀ copies/ml (sensitivity=0.8, specificity=0.8) prior to treatment were more likely to achieve HBeAg seroconversion.

Conclusion: HBeAg-positive CHB patients with higher initial HBV RNA levels have higher HBV replication capacity compared to those with lower initial HBV RNA levels. Serum HBV RNA can serve as a complementary indicator to HBsAg for better evaluation of whether patients have achieved functional cure. It can also be used as a

substitute for HBV DNA in the early stages of treatment to predict VR, particularly in patients with initially high levels of HBV RNA. Pre-treatment HBV RNA levels can predict HBeAg seroconversion during treatment.

FRI-383

Unique characteristics and risk of liver-related events among individuals with hepatitis D virus infection with and without concurrent hepatitis C virus infection: a United States administrative claims analysis

Laura Telep¹, David Wyles², Grace M. Chee¹, Anand Chokkalingam¹, Amanda Singer¹, Tatyana Kushner³. ¹Gilead Sciences, Foster City, United States; ²Denver Health Medical Center, Denver, United States; ³Icahn School of Medicine at Mount Sinai, Division of Liver Diseases, New York, United States
Email: laura.telep@gilead.com

Background and aims: Infection with hepatitis delta virus (HDV), an incomplete RNA virus that occurs only in the presence of hepatitis B virus (HBV), is associated with rapid progression to advanced liver disease including compensated and decompensated cirrhosis (CC, DC) and hepatocellular carcinoma (HCC). While some prior United States (US)-based population studies have cited high rates of HCV infection among individuals with HDV, data on the natural history of HDV/HCV infection are limited. This study characterizes the prevalence of HCV infection among individuals with HDV and examines the risk of liver-related events associated with HDV infection with and without HCV.

Method: A retrospective cohort study was conducted using the HealthVerity dataset from 2015 to 2022 that includes medical and pharmacy claims and electronic health records for more than 100 million individuals living in the US. Those included were ≥18 years at cohort entry with one year of prior continuous insurance enrollment and at least one day of available follow-up and one inpatient or two outpatient International Classification of Diseases codes for HDV and HCV. A propensity score (PS) model was constructed using baseline demographics, clinical characteristics, and treatment history, and was used to estimate hazard ratios (HRs) with 95% confidence intervals (CI) comparing risk of advanced liver disease events (CC, DC, HCC, liver transplant [LTx]) among individuals with HDV infection with and without HCV.

Results: From 2015–2022, 9,632 individuals with HDV infection met inclusion criteria, including continuous enrollment, among which 30% (n=2,885) had claims indicating concurrent HCV infection. Those with HCV were older (mean age 54.7 vs 51.5 years), more likely to be male (61.4% vs 44.3%), had more claims for severe liver disease at baseline (CC: 38.5% vs 7.1%; DC: 26.2% vs 5.4%; HCC: 7.7% vs 1.7%; and LTx: 3.7% vs 0.7%) and were more likely to have initiated treatment with hepatitis B nucleos (t)ide analogues (32.7% vs. 19.9%) or interferon (0.6% versus 0%), all with p<0.01. Approximately 25% of individuals with HCV had dispensing claims for direct acting antiviral (DAA) treatment. Baseline evidence of smoking, alcohol and substance abuse, and mental health issues was significantly higher in individuals with vs without HCV (p<0.01). After PS weighting and excluding individuals with evidence of advanced liver disease at baseline, those with HCV had a significant increased risk of developing CC (HR: 4.0, CI: 3.2–5.1). Among those with CC at baseline the risk of developing DC, HCC, or LTx was also increased with concurrent HCV: HR: 2.4, CI: 1.3–4.4.

Conclusion: Among individuals with HDV, concurrent HCV infection was not uncommon (~30%) and was associated with a notably increased risk of developing advanced liver disease. DAA treatment uptake and HDV treatment among HDV/HCV patients is needed to optimize disease outcomes.

FRI-386

Optimizing HDV diagnosis algorithm in Israel: reflex testing, prevalence of HDV seropositive individuals identified in Maccabi HealthCare services and assessment of three commercially available HDV viral load assays

Yael Gozlan¹, Rachel Shirazi², Orna Mor³, Licitia Schreiber⁴. ¹Ministry of Health, Ramat Gan, Israel; ²Ministry of Health, Tel HaShomer, Israel; ³Tel Aviv University, Tel Aviv, Israel; ⁴Maccabi MEGA lab, Maccabi Healthcare Services, Rehovot, Israel

Email: yael.gozlan@sheba.health.gov.il

Background and aims: EASL 2023 guidelines call for testing of anti HDV antibodies in all HBsAg positive cases, to identify chronic hepatitis D (HDV). Moreover, quantitation of HDV RNA viral load is highly suggested, but a significant variability between different assays does exist.

We compared the efficiency of anti-HDV reflex testing to previously performed approach in identifying individuals positive for anti HDV antibodies (HDV-Abs), determined the prevalence of HDV-RNA positives in our cohort and evaluated the results of three commercial HDV viral load assays.

Method: We reviewed HDV results in all cases tested for HBsAg in Maccabi virology laboratory since November 2021. HDV viral loads were compared between EuroBioplex, Robogene and Altona RealStar Kits.

Results: Between 1 November 2021 and 31 October 2022, 144, 512 individuals were tested for HBsAg; 1% (1276) were HBsAg positive. Only 28% (356) cases were tested for anti HDV-Abs of which 38 were anti HDV-Abs positive. Between November 2022 and 31 October 2023, after implementation of anti-HDV reflex testing, 151, 594 were tested for HBsAg; 1%, 1428, were HBsAg positive. Anti-HDV reflex testing was performed in all cases (1428, 100%) of which 77 were anti HDV-Abs positive. HDV-RNA was assessed in 97 of all these HDV-Abs positive samples and 61% (59) were found to be HDV-RNA positive. EuroBioplex, Robogene and Altona viral load assays demonstrated consistent inter-assay results, their overall agreement was high, and the average and standard deviation (\pm) Cq values were comparable (22 ± 7 , 23 ± 8 and 24 ± 9 , for the three assays, respectively). However, the average and standard deviation of viral loads quantified by each of them were different (7 ± 1.3 , 5.4 ± 1.8 and 5.9 ± 1.7 , respectively) with EuroBioplex giving the highest IU/ml values.

Conclusion: Anti-HDV reflex testing increased the number of HDV-Abs positive patients by \sim two-fold, and should be implemented in clinical practice. The majority of such patients are HDV-RNA positive presenting with high viral loads. HDV-RNA quantitation should be consistently performed with a single viral load assay, to enable accurate comparison between longitudinal viral load results.

FRI-387

Similarly low risk of hepatocellular carcinoma and cirrhotic complications in patients in the HBeAg-negative indeterminate phase compared with chronic infection

Vicki Wing-Ki Hui^{1,2,3}, Terry Cheuk-Fung Yip^{3,4,5}, Yee-Kit Tse^{3,4,6}, Jimmy Che-To Lai^{3,4,6}, Henry L.Y. Chan^{4,7}, Vincent Wai-Sun Wong^{3,4,6}, Grace Lai-Hung Wong^{3,4,6}. ¹Medical Data Analytics Centre, Hong Kong; ²Department of Medicine and Therapeutics, The Chinese University of Hong Kong, Hong Kong; ³State Key Laboratory of Digestive Disease, The Chinese University of Hong Kong, Hong Kong; ⁴Medical Data Analytics Centre, The Chinese University of Hong Kong, Hong Kong; ⁵Department of Medicine and Therapeutics, The Chinese University of Hong Kong, Hong Kong; ⁶Department of Medicine and Therapeutics, The Chinese University of Hong Kong, Hong Kong; ⁷Department of Internal Medicine, Union Hospital, Hong Kong

Email: 1155063467@link.cuhk.edu.hk

Background and aims: Patients with chronic hepatitis B virus (HBV) infection in the indeterminate phase are not covered by the current management guidelines for antiviral treatment. We aimed to

evaluate the risk of cirrhotic complications and hepatocellular carcinoma (HCC) in these patients.

Method: All non-cirrhotic patients who were negative for hepatitis B e antigen (HBeAg) at baseline were identified and classified into three HBV phases according to EASL criteria based on their first observed HBV phase: a. immune active phase (alanine aminotransferase [ALT] ≥ 40 IU/L and HBV DNA $\geq 2,000$ IU/ml), indeterminate phase (ALT ≥ 40 IU/L and HBV DNA $< 2,000$ IU/ml; or ALT < 40 IU/L and HBV DNA $\geq 2,000$ IU/ml), and inactive phase (ALT < 40 IU/L and HBV DNA $< 2,000$ IU/ml). Time-dependent crude incidence rates were used to compare the risk of cirrhotic complications and HCC across different HBV phases.

Results: We identified 55,012 HBeAg-negative patients (mean age 54 years, 51% male). At study entry, 12,325 (22.4%), 18,871 (34.3%), and 23,816 (43.3%) patients were classified into chronic hepatitis, indeterminate phase, and chronic infection respectively. Baseline HBV DNA, ALT, and FIB-4 in indeterminate group were 3.5 [1.9, 4.3] log₁₀ IU/ml, 35 [24, 58] U/L, and 1.3 [0.8, 2.1], respectively. During a median follow-up of 2.8 [1–6.4] years, there were on average 1.68 phase transitions for each patient, with around 18,000 patients having transitioned to the indeterminate phase. The time-dependent crude incidence rates of cirrhotic complications and HCC were highest in the chronic hepatitis group (18.9 and 14.0 per 1,000 person-years, $P < 0.001$ compared with the other two phases), while the rates were not significantly different between patients in the indeterminate and chronic infection phases (cirrhotic complications: 10.3 vs. 10.4, $P = 0.9$; HCC: 4.3 vs. 3.8, $P = 0.6$).

Conclusion: The risks of developing cirrhotic complications and HCC of patients in the indeterminate and inactive phases were similarly low compared to immune active phase.

FRI-388

Clinically significant liver stiffness decrease, as defined by the Baveno VII consensus, is associated with improved long-term prognosis in chronic hepatitis B patients with compensated advanced chronic liver disease

Rex Wan-Hin Hui¹, Lung Yi Loey Mak¹, Trevor Kwan-Hung Wu¹, James Fung¹, Man-Fung Yuen¹, Wai-Kay Seto¹. ¹The University of Hong Kong, Hong Kong, Hong Kong

Email: huirex@connect.hku.hk

Background and aims: The Baveno VII consensus introduced the term “clinically-significant liver stiffness (LS) decrease,” yet also highlighted that the criterion required validation. We assessed the long-term implications of clinically-significant LS decrease in chronic hepatitis B (CHB) patients with compensated advanced chronic liver disease (cACLD).

Method: We recruited CHB patients with ACLD (LS ≥ 10 kPa) and without history of clinical liver decompensation (variceal bleeding, hepatic encephalopathy or ascites) from Queen Mary Hospital, Hong Kong. Vibration controlled transient elastography (VCTE) and comprehensive blood tests were performed at baseline and year 2. Clinically-significant liver stiffness (LS) decrease was defined as LS reduction by $\geq 20\%$ with LS < 20 kPa or any LS decrease to < 10 kPa, in accordance with Baveno VII. Patients were monitored for liver-related events (hepatocellular carcinoma [HCC], decompensation, or liver-related mortality).

Results: This analysis included 317 patients (Mean baseline age 60.0 \pm 10.4, 65.3% male, 75.7% on nucleos(t)ide analogues [NUCs] at baseline for a median of 53.4 [22.6–87.3] months). The median baseline LS was 13.6 (11.5–18.8) kPa. The baseline Child-Pugh score was 5, 6 and 7 in 298 (94.0%), 16 (5.0%) and 3 (0.9%) patients respectively. In baseline treatment-naïve patients ($n = 77$), 60 patients (77.9%) were started on NUCs in subsequent follow-up, 12 patients (15.6%) refused NUCs, and 5 patients (6.5%) were not treated due to undetectable HBV DNA. VCTE was performed at an interval of 2.3 (1.9–2.7) years. The median LS at interval VCTE was 11.9 (8.8–16.9) kPa, with 155 patients (48.9%) achieving clinically-significant LS

decrease. NUC initiation in treatment-naïve patients (OR 1.945, 95% CI 1.052–3.594, $p=0.034$) and lower baseline LS (OR 0.971, 95% CI 0.944–0.999, $p=0.040$) were independent predictors of clinically-significant LS decrease. After median follow-up for 5.9 (3.3–7.8) years, 58 (18.3%) patients developed liver-related events, with 39 (12.3%), 25 (7.9%) and 16 (5.0%) patients developing HCC, decompensation, and liver-related mortality respectively. Clinically-significant LS decrease was an independent protective factor of liver-related events (14 events in patients with LS decrease vs 44 events in patients without; RR 0.201, 95% CI 0.063–0.647, $p=0.007$), whereas smoking (RR 4.443, 95% CI 1.299–15.200, $p=0.017$) was associated with increased risk. When assessing liver-related events separately, clinically significant LS decrease independently predicted lower HCC risk (RR 0.256, 95% CI 0.066–0.990, $p=0.048$), but was not associated with decompensation or liver-related mortality (both $p>0.05$).

Conclusion: Clinically-significant LS decrease is achievable in CHB-related cACLD with NUC therapy, and is associated with improved long-term outcomes, primarily through reducing HCC risk.

FRI-389

Hepatitis delta virus infection is associated with significantly greater incidence of cirrhosis and hepatic decompensation in U.S. veterans with chronic hepatitis B

Robert Wong¹, Zeyuan Yang², Janice Jou³, Binu John⁴, Joseph K. Lim⁵, Ramsey C. Cheung¹. ¹Veterans Affairs Palo Alto Health Care System, Stanford University School of Medicine, Palo Alto, United States; ²Veterans Affairs Palo Alto Health Care System, Palo Alto, United States; ³Oregon Health and Sciences University, Portland, United States; ⁴Miami VA Medical System, University of Miami Miller School of Medicine, Miami, United States; ⁵Yale University School of Medicine, New Haven, United States

Email: rwong123@stanford.edu

Background and aims: Hepatitis delta virus (HDV) infection in patients with chronic hepatitis B (CHB) is associated with significantly greater risks of liver-related morbidity and mortality. However, data on the natural history of HDV are limited, and it remains unclear the magnitude of increased risks of cirrhosis or hepatic decompensation associated with HDV. We aim to evaluate the long-term incidence of cirrhosis or hepatic decompensation among a national cohort of U.S. Veterans with CHB with vs. without concurrent HDV infection.

Method: Using longitudinal data on all U.S. Veterans receiving care within Veteran health systems from 2010 to 2023, we identified patients with CHB with concurrent HDV infection based on laboratory testing (HDV antibody, HDV RNA, HDV antigen). Patients with cirrhosis or hepatocellular carcinoma (HCC) at time of HDV diagnosis or within 6 months were excluded. Patients with HDV were 1:2 propensity score matched to CHB patients without HDV. Incidence (per 100,000 person-years) of cirrhosis, hepatic decompensation, or HCC (censoring for death) between CHB patients with vs. without HDV were calculated using competing risks Nelson-Aalen methods for estimating cumulative hazards and compared using log-rank testing and the z-statistic as appropriate.

Results: Among 27,548 CHB patients identified, overall, 16.1% completed HDV testing and 3.25% were positive for HDV. After excluding patients with cirrhosis or HCC at baseline, 71 patients with HDV were included (95.8% male, 47.9% African American, 31.0% non-Hispanic white, 15.5% Asian, mean age 55.4 ± 12.6 years, 16.9% concurrent diabetes, 16.9% reporting high risk alcohol use), who were propensity score matched to 140 CHB patients without HDV. Compared to CHB patients without HDV, those with concurrent HDV had significantly greater incidence of cirrhosis (4.39 vs. 1.30 per 100,000 person-years, $p<0.01$) and hepatic decompensation (2.18 vs. 0.41 per 100,000 person-years, $p=0.01$). The risk of HCC in patients with HDV trended higher compared to CHB patients without HDV,

but did not reach statistical significance (1.28 vs. 0.41 per 100,000 person-years, $p=0.11$).

Conclusion: Among a national cohort of Veterans with CHB in the U.S., patients with concurrent HDV infection had more than three times greater risk of cirrhosis and more than five times greater risk of hepatic decompensation compared to CHB patients without HDV. These data highlight the importance of implementing timely and appropriate HDV screening in patients with CHB to ensure early diagnosis and linkage to HDV care and management to reduce long-term risks of liver disease progression and complications.

FRI-390

Off-treatment outcomes after discontinuing tenofovir-based treatment in hepatitis B e antigen-positive and hepatitis B e antigen-negative patients with chronic hepatitis B virus

Maria Buti^{1,2}, Henry L.Y. Chan³, Scott K. Fung⁴, Cheng-Yuan Peng⁵, Frida Abramov⁶, Dana Tedesco⁶, Hongyuan Wang⁶, Leland J. Yee⁶, John F. Flaherty⁷, Edward J. Gane⁸, Young-Suk Lim⁹, Harry L.A. Janssen^{10,11}, Kosh Agarwal¹². ¹Hospital Universitario Vall d'Hebron, Barcelona, Spain; ²CIBEREHD del Instituto Carlos III, Madrid, Spain; ³Faculty of Medicine, the Chinese University of Hong Kong, Hong Kong, China; ⁴University of Toronto, Department of Medicine, Toronto, Canada; ⁵School of Medicine, China Medical University, Taichung, Taiwan, and Division of Hepatogastroenterology, Department of Internal Medicine, China Medical University Hospital, Taichung, Taiwan; ⁶Gilead Sciences, Inc., Foster City, United States; ⁷Gilead Sciences, Inc., Foster City, United States; ⁸Auckland Clinical Studies, Auckland, New Zealand; ⁹Asan Medical Center, University of Ulsan College of Medicine, Seoul, Korea, Rep. of South; ¹⁰Toronto Centre for Liver Disease, Toronto General Hospital, University Health Network, Toronto, Canada; ¹¹Department of Gastroenterology and Hepatology, Erasmus MC, University Medical Center, Rotterdam, Netherlands; ¹²Institute of Liver Studies, King's College Hospital NHS Foundation Trust, London, United Kingdom

Email: frida.abramov@gilead.com

Background and aims: Treatment guidelines permit stopping nucleos (t)ide (NA) therapy with appropriate monitoring in patients with undetectable hepatitis B virus (HBV) DNA who are non-cirrhotic and hepatitis B e antigen (HBeAg)-negative, with the aim of potentially achieving functional cure (hepatitis B s antigen [HBsAg] loss) or maintaining virological remission. This analysis characterises outcomes in the subset of patients enrolled in trials of tenofovir alafenamide (TAF) who discontinued NA therapy after up to 8 years of treatment.

Method: Patients with chronic hepatitis B (CHB), enrolled in 2 Phase 3 studies (HBeAg-negative [NCT01940341] and HBeAg-positive [NCT01940471] patients, respectively) of TAF vs tenofovir disoproxil fumarate, who discontinued study treatment for reasons other than HBsAg seroconversion after up to 8 years of treatment, and did not immediately initiate NA therapy, were required to enter a treatment-free follow-up (TFFU) phase for up to 24 weeks. During TFFU, patients were assessed at the end of their treatment (TFFU baseline [BL]) and monitored every 4 weeks for safety, including alanine aminotransferase (ALT) elevation (defined as ALT >2 -fold TFFU BL or >10 -fold upper limit of normal [ULN; central laboratory cutoff]) or ALT flare (defined as ALT elevation occurring at 2 consecutive visits), and for changes in HBV serology, HBV DNA, and ALT levels.

Results: Of 1298 patients enrolled in the 2 studies, 251 (19%) entered TFFU (96 [38%] were HBeAg-positive and 155 [62%] were HBeAg-negative at TFFU BL); 144 (57%) completed 24 weeks of monitoring (median [quartile (Q)1, Q3] duration, 24.0 [12.3, 24.6] weeks). Of the 107 patients who discontinued from TFFU before 24 weeks, 98 (92%) had resumed NA treatment. By missing-equals-excluded analysis in the subset who completed 24 weeks of TFFU, 31% and 63% had HBV DNA <29 IU/ml and ALT $<ULN$, respectively, compared with 89% and 82%, respectively, at TFFU BL. Overall, 2 patients had HBsAg loss (1 with anti-HBs seroconversion); both were HBeAg-negative at TFFU baseline. A total of 60/251 (24%) patients experienced a post-

POSTER PRESENTATIONS

treatment adverse event (AE), of which 6% were Grade ≥ 3 , and 2% were serious AEs (hepatitis exacerbation [n = 5], head injury [n = 1], and plica syndrome [n = 1]). Overall, 31% had a Grade ≥ 3 laboratory abnormality, the majority being increases in aminotransferases. A total of 35/251 (14%) and 8/251 (3%) experienced ALT elevation or ALT flare, respectively. However, 69% of patients with ALT elevation could not be retested to assess flare due to lack of further follow-up. No deaths or hepatic decompensation events occurred during TFFU.

Conclusion: After up to 24 weeks of stopping NAs, viral and biochemical recurrences were frequent, and few patients achieved HBsAg loss. While severe outcomes were uncommon, close monitoring and timely resumption of NA therapy are both important to avoid adverse outcomes.

FRI-391

Relapse incidence and severe flares in chronic hepatitis B patients with lymphoma post rituximab-based chemotherapy versus HBeAg-negative hepatitis B patients without cancer after nucleos(t)ide analogue cessation

Yen-Chun Liu^{1,2}, Yu-Jia Shih², Rachel Wen-Juei Jeng¹, Chao-Wei Hsu^{1,2}, Rong-Nan Chien^{1,2}. ¹Chang Gung Memorial Hospital, Linkou branch, Taoyuan, Taiwan; ²College of Medicine, Chang Gung University, Taoyuan, Taiwan
Email: rachel.jeng@gmail.com

Background and aims: Rituximab-based chemotherapy (R-CHOP) elevates the risk of reactivation compared to solid tumor regimens, and severe flares may persist post-prophylactic nucleos(t)ide analogue (Nuc) cessation. This study investigates differences in off-Nuc clinical relapse incidence, severity, and HBsAg loss between CHB patients with lymphoma on R-CHOP and HBeAg-negative CHB patients who completed finite Nuc treatment.

Method: Non-cirrhotic HBeAg-negative CHB patients with lymphoma, HBsAg-positive, treated with R-CHOP, ceased prophylactic Nuc after >12-week post-chemotherapy extension, forming the lymphoma-CHB cohort. Their off-therapy clinical relapse, severity, and HBsAg seroclearance rates were compared with HBeAg-negative CHB patients who stopped Nuc per APASL rules (Off-Nuc cohort). Clinical relapse (CR) was defined as HBV DNA ≥ 2000 IU/ml with ALT $> 2 \times$ ULN. Severe hepatitis criteria included ALT ≥ 1000 U/L or T.Bil ≥ 3.5 mg/dL, or flares with hepatic decompensation (HD). HD was defined as T.Bil ≥ 2 mg/dL and INR ≥ 1.5 , with or without ascites or hepatic encephalopathy. Kaplan-Meier and log-rank tests compared cumulative incidence. 1:1 Propensity Score Matching (PSM) adjusted age, gender, Nuc types, pretherapy HBV DNA, and end-of-treatment HBsAg for sensitivity analysis.

Results: The lymphoma-CHB cohort (117 patients), discontinuing prophylactic Nuc post-R-CHOP, and the off-Nuc cohort (940 patients) treated with finite Nuc therapy were compared. Lymphoma patients, older (57 vs. 52 years, $P < 0.001$), less male (53% vs. 82%, $P < 0.001$), with lower HBV DNA (3.2 vs. 6.3 log₁₀ IU/ml, $P < 0.001$), and ALT levels (19 vs. 167 U/L, $P < 0.001$) at treatment initiation. Off-Nuc CR incidence was comparable at 1-year (33% vs. 37%), but 2-year cumulative incidence was lower in lymphoma (34% vs. 59%, $P = 0.001$). However, off-Nuc severe flare incidence was significantly higher in lymphoma at both 1- and 2-years (24% and 24% vs. 7% and 11%). The lymphoma arm had much higher annual HBsAg loss incidence than non-cancer off-Nuc patients (4.1% vs. 1.4%, $P = 0.011$). Cox regression indicated a higher risk for severe flare in lymphoma off-Nuc patients (adjusted hazard ratio: 2.36, $P < 0.001$). Propensity score-matched cohorts (61 patients each) showed comparable CR at 1- and 2-years ($p > 0.5$), but relapse severity appeared greater in the lymphoma arm (ALT: 1315 vs. 265 U/L). The 2-year cumulative severe flare incidence remained much higher in the lymphoma group (33% vs. 10%, $P = 0.002$). Time to relapse timing also appeared shorter in the lymphoma off-Nuc patients (23 vs. 32 weeks, $P = 0.019$).

Conclusion: HBeAg-negative CHB patients with lymphoma, who stopped Nuc post-R-CHOP, showed earlier CR onset and higher off-

Nuc severe flare risk. B cell immunity changes may contribute. Stringent off-therapy monitoring is crucial for CHB patients with Rituximab-based lymphoma regimens.

FRI-392-YI

Chronic HDV coinfection (CHD) is characterized by a more elevated production of Middle and Large HBsAg than HBV mono-infection, that parallels HDV replicative and cytolytic activity

Lorenzo Piermatteo¹, Stefano D'Anna¹, Antonella Olivero², Leonardo Duca³, Giulia Torre¹, Carlotta Castelli¹, Elisabetta Teti⁴, Andrea Di Lorenzo⁴, Vincenzo Malagnino⁴, Marco Iannetta⁴, Leonardo Baiocchi⁵, Simona Francioso⁵, Ilaria Lenci⁵, Francesca Ceccherini Silberstein³, Michele Milella⁶, Annalisa Saracino⁶, Alessia Ciano², Loredana Sarmati⁴, Pietro Lampertico^{7,8}, Mario Rizzetto², Gian Paolo Caviglia², Valentina Svicher¹, Romina Salpini¹. ¹University of Rome "Tor Vergata," Department of Biology, Rome, Italy; ²University of Turin, Department of Medical Sciences, Turin, Italy; ³University of Rome "Tor Vergata," Department of Experimental Medicine, Rome, Italy; ⁴University of Rome "Tor Vergata," Department of Systems Medicine, Rome, Italy; ⁵"Tor Vergata" University Hospital, Hepatology Unit, Rome, Italy; ⁶University of Bari "Aldo Moro," Department of Biomedical Sciences and Human Oncology, Clinic of Infectious Diseases, Bari, Italy; ⁷Foundation IRCCS Ca' Granda Ospedale Maggiore Policlinico, Division of Gastroenterology and Hepatology, Milan, Italy; ⁸University of Milan, CRC "A. M. and A. Migliavacca" Center for Liver Disease, Department of Pathophysiology and Transplantation, Milan, Italy
Email: lorenzo.piermatteo@uniroma2.it

Background and aims: HBV surface proteins (HBsAg) enable HBV and HDV entry and morphogenesis. Total HBsAg comprises 3 different forms: Large- (L-HBs), Middle- (M-HBs) and Small-HBs (S-HBs) with L-HBs found in virions and not in subviral particles. Here, we investigate HBs forms levels in the setting of chronic HBV mono-infection (CHB) and HDV coinfection (CHD).

Method: 262 plasma samples from HBeAg-negative patients were included: 143 CHD and 119 CHB. Total HBsAg is measured by COBAS HBsAg II assays (Roche Diagnostics), HBs forms by ad hoc designed ELISAs (Beacle Inc) and HDV RNA by RoboGene HDV RNA Quantification Kit 2.0.

Results: CHD and CHB patients have a comparable age (median [IQR]: 54 [44–60] and 53 [39–64] years; $P = 0.8$) and rate of Nuc treatment (41.2% and 34.5%, $P = 0.3$). CHD have lower HBV DNA (median [IQR]: 1.3 [0.0–2.3] vs 1.6 [1.2–3.4] log₁₀ IU/ml, $P = 0.002$) and higher ALT (median [IQR]: 79 [50–113] vs 36 [22–63] U/L, $P < 0.001$) and total HBsAg levels (median [IQR]: 5206 [827–8555] vs 1776 [354–6936] IU/ml, $P = 0.008$). Median (IQR) HDV RNA is 5.2 (3.4–6.0) log₁₀ IU/ml. Notably, HBs forms composition varies between CHD and CHB with remarkably higher M-HBs and L-HBs in CHD (median [IQR]: 1127 [145–2301] vs 142 [25–707] and 2.0 [0.2–6.3] vs 0.06 [0.2–0.5] ng/ml, $P < 0.001$) despite similar S-HBs levels in the two groups (median [IQR]: 3221 [587–6497] vs 1039 [239–5438] ng/ml). Multivariable analysis confirms CHD as an independent factor associated with higher levels of M-HBs and L-HBs (OR [95%CI]: 4.7 [1.7–12–4] and 6.2 [2.2–17.9], $P < 0.002$ for both). Among CHD, the HBs forms positively correlate with HDV RNA levels (Rho = 0.48, 0.49 and 0.43 for S-, M- and L-HBs; $P < 0.001$ for all) while, in CHB, milder correlation with HBV DNA levels is observed only for L-HBs (Rho = 0.29, 0.02). Furthermore, patients with highly-replicating HDV (HDV RNA > 3 log IU/ml) show significantly higher levels of all HBs forms than lowly-replicating HDV (median [IQR] ng/ml: 4431 [1251–6950] vs 274 [25–2640] for S-HBs; 1404 [191–2484] vs 127 [4–1242] for M-HBs; 3.3 [0.2–7.8] vs 0.3 [0.04–1.1] for L-HBs, $P < 0.001$ for all). Focusing on lowly-replicating HDV patients, 43.5% have altered ALT (median [IQR]: 75 [55–93] U/L). Notably, in this set of patients, M-HBs > 200 ng/ml is the best cut-off predicting altered ALT (70% of patients with M-HBs > 200 ng/ml vs 30% with M-HBs < 200 ng/ml has ALT > 40 U/L; PPV = 70%, NPV = 76.9%; $P = 0.04$), supporting the role of M-

HBs in reflecting cytolitic activity in the setting of low HDV replication.

Conclusion: The composition of HBs forms varies in CHD and CHB patients, with CHD characterized by more elevated M-HBs and L-HBs production paralleling HDV replicative activity. This could reflect a variation in the proportion of circulating viral and subviral particles between CHD and CHB.

Overall, HBs forms can play a role in identifying patients more prone to liver disease progression, in whom treatment could be prioritized.

FRI-393

Healthcare resource utilisation and costs of hepatitis delta virus infection vs hepatitis B virus monoinfection across disease states among hospitalised adults in Italy

Pietro Lampertico^{1,2}, Valentina Perrone³, Luca Degli Esposti³, Melania Leogrande³, Chong Kim⁴, Marvin Rock⁴. ¹Foundation IRCCS Ca' Granda Ospedale Maggiore Policlinico, Division of Gastroenterology and Hepatology, Milan, Italy; ²CRC "A. M. and A. Migliavacca" Center for Liver Disease, Department of Pathophysiology and Transplantation, University of Milan, Milan, Italy; ³CliCon S.r.l. Società Benefit, Health, Economics and Outcomes Research, Bologna, Italy; ⁴HEOR-Global Value and Access, Gilead Sciences, Inc., Foster City, United States
Email: chong.kim9@gilead.com

Background and aims: Hepatitis delta virus (HDV) infection occurs in individuals with hepatitis B virus (HBV) monoinfection and leads to the most severe form of viral hepatitis. In this retrospective analysis, healthcare resource utilisation (HCRU) and costs were compared between patients with HDV infection vs HBV monoinfection (HBV only) across levels of disease severity among hospitalised adults in Italy.

Method: The administrative databases of local health units in Italy (covering approximately 12 million individuals) were screened for patients aged 18 years or older who had at least 1 HDV or HBV hospitalisation discharge diagnosis (using *International Classification of Diseases, 9th Edition, Clinical Modification* codes) between 1 Jan 2009 and 30 Jun 2022. Included patients had an HDV or HBV-only diagnosis between 1 Jan 2010 and 30 Jun 2022 (identification period), no previous diagnosis, and at least 12 months of continuous enrolment before and after diagnosis. Patients' first diagnosis was used as their index date, and baseline demographics and clinical characteristics were assessed 12 months prior to the index date. Comparisons of mean per patient per year (PPPY) all-cause HCRU and costs between subgroups of liver disease severity were performed using the Mann-Whitney U test, and descriptive statistics were summarised.

Results: Of 15,628 hospitalised patients, 14,238 were screened for HDV infection or HBV only, and 9,945 were included in this analysis (HDV cohort, n = 556; HBV cohort, n = 9,389). The mean (standard deviation) age (55.8 [15.6] vs 56.8 [16.5] years, p = 0.157) and percentage of patients that were male (66.0% vs 63.6%, p = 0.248) were similar between those with HDV vs HBV only. Compared to patients with HBV only at baseline, a greater proportion of patients with HDV had compensated cirrhosis (CC; 19.6% [HDV] vs 11.5% [HBV], p < 0.001), decompensated cirrhosis (DCC; 10.4% vs 8.0%, p = 0.043), hepatocellular carcinoma (HCC; 7.6% vs 4.0%, p < 0.001), and liver transplantation (LT; 4.9% vs 0.8%, p < 0.001). Patients with HDV spent fewer months in each liver disease state than patients with HBV only. Mean (95% confidence interval) length of hospital stay (days) PPPY was significantly longer for patients with HDV vs HBV only among those with CC (92.7 [48.71–136.67] vs 48.8 [40.37–57.20], p = 0.011) and DCC (113.0 [49.22–176.75] vs 52.2 [44.57–59.77], p = 0.041). Mean total and inpatient costs PPPY were significantly higher for those with HDV vs HBV only who had CC, DCC, HCC, or LT. These costs numerically increased with disease state severity.

Conclusion: In Italy, the mean inpatient length of stay and total healthcare costs were higher for patients with HDV vs HBV only and increased with greater liver disease severity among hospitalised

adults. These findings highlight the need for early screening, diagnosis, and treatment of HDV to help reduce the clinical and economic burden of disease.

FRI-394

High burden of cirrhosis and increasing response rates to bulevirtide-based regimens: insights from the austrian prospective hepatitis D registry

Michael Schwarz¹, Caroline Schwarz^{1,2}, David Bauer^{1,2}, Marlene Panzer³, Michael Strasser⁴, Silvia Reiter⁵, Livia Dorn⁶, Andreas Maieron⁶, Alexander Moschen⁵, Elmar Aigner⁴, Michael Trauner¹, Albert Friedrich Stättermayer¹, Mattias Mandorfer¹, Heinz Zoller³, Michael Gschwantler², Thomas Reiberger¹, Mathias Jachs¹. ¹Division of Gastroenterology and Hepatology, Department of Medicine III, Medical University of Vienna, Vienna, Austria; ²Department of Internal Medicine IV, Klinik Ottakring, Vienna, Austria; ³Department of Internal Medicine I, Medical University of Innsbruck, Innsbruck, Austria; ⁴First Department of Medicine, Paracelsus Medical University, Salzburg, Austria; ⁵Department of Internal Medicine 2, Johannes Kepler University Linz, Linz, Austria; ⁶Department of Internal Medicine 2, Gastroenterology and Hepatology and Rheumatology, Karl Landsteiner University of Health Sciences, University Hospital of St. Pölten, Sankt Pölten, Austria
Email: thomas.reiberger@meduniwien.ac.at

Background and aims: Chronic hepatitis D (CHD) is the most severe form of viral hepatitis, characterized by a rapid progression towards liver cirrhosis. Bulevirtide (BLV) has been approved for the treatment of CHD patients with compensated liver disease, but real-world data regarding predictors for treatment are limited. This study aimed to comprehensively characterize the Austrian cohort of CHD patients and to analyze their response to BLV treatment.

Method: CHD patients who visited one of the six participating Austrian hospitals from 2020 onwards were prospectively included. Demographic, clinical, laboratory data, liver stiffness measurement (LSM), biomarkers of systemic inflammation and single nuclear polymorphisms (SNPs) in the interleukin 28B (IL28B), Patatin-like phospholipase domain-containing protein 3 (PNPLA3), SERPINA1, and sodium-taurocholate cotransporting polypeptide (NTCP) genes were assessed in a subset of patients. Patients receiving BLV were assessed for the end points "virological response" (VR) defined as HDV-RNA decline of ≥ 2 log and for "combined response" (CR) defined as VR with ALT normalization at week (W)24, W48, and W96.

Results: We included 84 patients with positive HDV antibodies (median age 46 years [IQR 37–56], 57.1% male) and 59 (70.2%) had detectable HDV-RNA. LSMs available in 67 patients were: F0/1 n = 17 (25.4%), F2 n = 10 (14.9%), F3 n = 9 (13.4%), and F4 n = 31 (46.3%). Nine (10.7%) had already progressed to decompensated cirrhosis. There was no association between PNPLA3 genotype and liver disease severity (G/C or G/G: 14 [58.3%] in cirrhosis vs. 11 [68.8%] without cirrhosis, p = 0.505). BLV treatment was initiated in 50 out of 59 HDV-RNA viremic patients (F3/F4: 70.0%) and median treatment duration was 17 (8–24) months. Pegylated interferon alfa-2a (PEGIFN) was added to BLV treatment in 13 (26%) patients after a median of 10 (7–18) months. VR rates were at W24 63.0% (29/46), W48 68.4% (26/38), and W96 71.2% (16/21). CR was achieved at W24 in 19.6% (9/46), at W48 in 42.1% (16/38), and at W96 in 42.9% (9/21). We found no baseline demographic (age, sex, body mass index) nor laboratory parameters (ALT, CRP, IL-6, HDV RNA, HBV DNA, HBs antigen levels) that were predictive of VR or CR. Polymorphisms in IL28B (distribution among patients with available data: C/C: 16/33, C/T: 16/33, T/T: 1/33) as well as PNPLA3 (C/C: 13/36, C/G: 20/36, G/G: 3/36) were not associated with VR/CR to BLV at W24, W48 nor W96, respectively. No polymorphisms were found for NTCP or SERPINA1.

Conclusion: Within this prospectively characterized cohort of Austrian CHD patients we found >50% with advanced fibrosis and >10% with decompensated cirrhosis. BLV was initiated in 50 patients and increasing VR and CR rates were seen under BLV treatment for up

POSTER PRESENTATIONS

to two years. PEGIFN was added to BLV in thirteen patients. No laboratory or clinical parameters were found to predict response to BLV treatment.

FRI-395

HDV infection in Israel: epidemiology and co-morbidities

Hisham Sholy¹, Hedy Rennert², Eli Zuckerman¹. ¹Carmel Medical Center, Haifa, Israel; ²Carmel Medical Center, Haifa
Email: elizuc56@gmail.com

Background and aims: About 1–5% of people with chronic HBV infection are co-infected with HDV, however global reports from many regions are inaccurate. Epidemiological data of hepatitis D virus infection (HDV) in Israel is limited as large population-based studies have not performed so far. The aim of this study was to collect epidemiological, co-morbidities and natural history data of HDV infection in the largest population-based study performed in Israel.

Method: Data were obtained from the computerized records and database of Clalit Health Services (CHS). The database contains information regarding demographic parameters, laboratory tests and pharmacy records, hospitalization and primary care physician records and death-related data.

Results: Through 1.2002–10.2022, 1, 995, 911 out of 4, 376, 447 (45.6%) CHS insured individuals were tested for HBsAg. Of 28, 448 positive for HBsAg (1.43%), 10, 667 (37.5%) were tested for HDV-Ab and of them, 728 were tested positive (7.01%). Only 369 HDV-Ab positive individuals were tested for HDV-RNA by PCR (50.6%) and of those, 138 (37%) were HDV-RNA positive (qualitative testing). Of 28, 448 HBsAg+ individuals, 1931 (6.8%) were younger than 20 y/o. Co-infected patients were older than HBV mono-infection (mean age 46.4 ± 14 vs. 42.5 ± 16 y/o, $p < 0.01$). The largest number of HDV-positive patients were born in Russia (28.4%) followed by Israel (23.7%), Ethiopia (19.3%), Uzbekistan (5.3%), and Morocco (4.2%). The prevalence of co-infected patients was higher in Jews compared with Arabs (3.2% vs 1.3%, $p < 0.001$). Alcohol abuse was more prevalent in the co-infection than in the mono-infection group (5.5% vs 2.5%, $p < 0.001$). As expected, the rate of liver transplantation was significantly higher in the co-infected than the mono-infected group: 39/728 (5.4%) vs only 165/27720 (0.6%) ($p < 0.001$, OR 9.4). Those with positive RNA were more likely to undergo liver transplantation than those with negative RNA (10.1% vs 0.4%, OR 25). The prevalence of cirrhosis and HCC were significantly higher among co-infected (24% vs 4.7%, $p < 0.001$, OR 6.5 for cirrhosis, 8.1% vs 1.9%, $p < 0.001$, OR 4.4 for HCC). FIB4 was calculated and reveals more significant liver fibrosis (Fib4 > 1.45) in the co-infection group (43.3% vs 23.9%). HBV-DNA was undetectable in 23.5% of positive RNA patients compared with 16.1% of RNA negative patients (NS).

Conclusion: This is the largest epidemiological study on HDV infection performed in Israel. The estimated rate of HDV infection among HBsAg-positive individuals is 7.01%. Co-infection is significantly associated with poor prognosis and higher prevalence of cirrhosis, HCC, and liver transplantation. More efforts should be directed to increase diagnosis rate and the number of treated patients.

FRI-396

Risk of hepatocellular carcinoma decreases after antiviral therapy-induced HBsAg seroclearance

Han Ah Lee¹, Hyun Woong Lee², Dong Hyun Sinn³, Sang Hoon Ahn², Beom Kyung Kim², Seung Up Kim². ¹Ewha Womans University, Seoul, Korea, Rep. of South; ²Yonsei University College of Medicine, Seoul, Korea, Rep. of South; ³Samsung Medical Center, Seoul, Korea, Rep. of South
Email: amelia86@naver.com

Background and aims: Antiviral therapy (AVT) reduces the risk of hepatitis B virus-related hepatocellular carcinoma (HCC). The difference in risk of HCC development after hepatitis B surface antigen (HBsAg) seroclearance to the AVT status was explored.

Method: Patients with chronic hepatitis B who achieved HBsAg seroclearance between 2003 and 2022 were retrospectively evaluated. The primary outcome was the development of HCC after HBsAg seroclearance.

Results: Of the study population, 1, 280 (84.2%) and 241 (15.8%) patients achieved HBsAg seroclearance without (spontaneous clearance group) and with AVT (AVT-induced clearance group), respectively. During follow-up (median 4.3 years), 37 (2.4%) patients developed HCC after HBsAg seroclearance. HCC cumulative incidence was comparable between the two groups (hazard ratio [HR] = 0.461; $P = 0.150$; log-rank test, $P = 0.197$), whereas it was significantly lower in the AVT-induced HBsAg clearance group than in the spontaneous HBsAg clearance group in the inverse probability of treatment weighting analysis (HR = 0.442; $P = 0.005$; log-rank test, $P = 0.004$). In multivariate analysis, spontaneous HBsAg clearance, albumin-bilirubin (ALBI) grade ≥ 2 , liver cirrhosis, and platelet count $< 50 \times 10^9/L$ were independently associated with the increased risk of HCC development. The newly established antiviral therapy, cirrhosis, ALBI, and platelet count (ACAP) scores had a C-index of 0.765, and the time-dependent areas under the curve of HCC prediction at 5 and 8 years were 0.774 and 0.823, respectively. The predictive model exhibited good discriminative performance in internal validation and sensitivity analysis.

Conclusion: The risk of HCC differed according to the AVT status after HBsAg seroclearance. The ACAP model may help clinicians implement timely interventions and surveillance strategies.

FRI-397

A machine learning model to predict liver-related outcomes after the functional cure of chronic hepatitis B

Moon Haeng Hur¹, Seung Up Kim², Hyun Woong Lee², Han Ah Lee³, Hyung-Chul Lee¹, Sang Hoon Ahn², Beom Kyung Kim², Hwi Young Kim³, Yeon Seok Seo⁴, Hyunjae Shin¹, Jaeyeon Park¹, Yunmi Ko¹, Youngsu Park¹, Yun Bin Lee¹, Su Jong Yu¹, Yoon Jun Kim¹, Jung-Hwan Yoon¹, Jeong-Hoon Lee¹. ¹Seoul National University College of Medicine, Seoul, Korea, Rep. of South; ²Yonsei University College of Medicine, Seoul, Korea, Rep. of South; ³Ewha Womans University College of Medicine, Seoul, Korea, Rep. of South; ⁴Korea University College of Medicine, Seoul, Korea, Rep. of South
Email: pindra@empal.com

Background and aims: The risk of hepatocellular carcinoma (HCC) and hepatic decompensation persists after hepatitis B surface antigen (HBsAg) seroclearance. This study aimed to develop and validate a machine learning model to predict the risk of liver-related outcomes (LROs) following HBsAg seroclearance.

Method: A total of 2, 046 consecutive patients who achieved HBsAg seroclearance between 2000 and 2022 were enrolled from 6 centers in South Korea: the training and validation cohorts consisted of 944 and 1, 102 patients, respectively. A new model (designated as PLAN-C) was developed using variables based on the results of multivariable Cox analysis and a gradient-boosting machine algorithm. The primary outcome was the development of any LRO, including HCC, cirrhosis-related complications, and liver-related death.

Results: During a median follow-up of 55.2 (interquartile range = 30.1–92.3) months, 123 LROs were confirmed (1.1%/person-year). The PLAN-C was constructed using 6 variables: age, sex, diabetes, alcohol consumption, cirrhosis, and platelet count. Compared to previous HCC prediction models, the PLAN-C showed significantly superior predictive accuracy in both the training (c-index: 0.85 vs. 0.63–0.70, all $P < 0.001$) and the validation (0.84 vs. 0.61–0.81; all $P < 0.05$ except for CU-HCC, $P = 0.09$) cohorts. The calibration plots demonstrated a close correlation between the predicted and observed risks of LRO (Hosmer-Lemeshow test $P > 0.05$ in both cohorts). When entire patients were divided into 3 groups according to the risk predicted by PLAN-C, the low-risk group had a significantly lower 5-year incidence of LRO (0.8%), compared to the intermediate-risk (4.0%) and high-risk (22.8%) groups (both $P < 0.001$).

Conclusion: This novel machine learning model consisting of 6 variables provides reliable risk prediction of LRO after HBsAg seroclearance that can be used for personalized surveillance.

FRI-398

Targeted capture single-cell sequencing provides new insights into persistent hepatitis B virus (HBV) infection

Yanfang Huang¹, Hongyuan Xue¹, Yongping Liu², Miaoqu Zhang¹, Qiran Zhang¹, Jinhang He¹, Ning Jiang³, QuanBao Zhang¹, Zhengxin Wang¹, Chao Qiu⁴, Wenhong Zhang¹. ¹Huashan Hospital, Fudan University, Shanghai, China; ²Hangzhou Xixi Hospital, Hangzhou, China; ³School of Life Sciences, Fudan University, Shanghai, China; ⁴Institutes of Biomedical Sciences, Fudan University, Shanghai, China
Email: zhangwenhong@fudan.edu.cn

Background and aims: At the single-cell level, viral infections show significant heterogeneity. To study these infections, a technique called single-cell transcriptome sequencing which captures polyadenylated transcripts using oligo (dT) is usually used. However, this method is not very effective in capturing viral sequences as the host cellular transcriptome overwhelms, leaving only a small fraction of the viral part. To improve the detection rate of the viral sequence, we have designed five additional HBV-specific probes alongside the oligo (dT) probe to specialize in capturing HBV mRNA or DNA.

Method: Targeted capture single-cell RNA sequencing was utilized to assess the performance of the assay on a mixture of HBV-positive human HepAD38 and HBV-negative mouse 3T3. Fourteen human liver tissues were analyzed, including two healthy donors, four individuals with antiviral-naïve chronic hepatitis B, 2 HBV-associated decompensated cirrhosis, and 6 HBV-associated liver failure. In addition, humanized chimeric URG (Tet-uPA-Rag2 null-γc null) mice (Hu-URG mice) treated with antivirals, including saline solution (used as a control, n = 2), Entecavir (n = 3) and peg-interferon (n = 2), were examined. The hepatocytes were directly observed for HBV replication and transcriptional activity using in situ hybridization.

Results: Hepatocytes that are infected with HBV have high expression of plasma proteins, lipoproteins, and coagulation-related proteins. This suggests that actively synthesizing and metabolizing hepatocytes are more supportive of HBV replication. Multiple splicing factors such as DDX5, DDX17, SRSF2, SRSF5, HNRNP1, etc. are down-regulated in HBV-positive hepatocytes and liver failure and up-regulated in Hu-URG mice after anti-viral treatment.

Conclusion: We have developed a specialized method to detect the presence of HBV mRNA or DNA in liver cells at a single-cell resolution.

FRI-399

Hepatitis B core-related antigen is a good predictor for high risk of mother to child transmission in chronic hepatitis B

Ivana Carey¹, Mark Anderson², James Lok¹, Zillah Cargill¹, Gavin Cloherty², Geoffrey Dusheiko¹, Kosh Agarwal¹. ¹Institute of Liver Studies, King's College Hospital, London, United Kingdom; ²Department of Infectious Diseases, Abbott Diagnostics, North Chicago, United States
Email: ivana.kraslova@kcl.ac.uk

Background and aims: HBV mother to child transmission (MTCT) is preventable by HBsAg screening of all pregnant women at 1st trimester, followed by appropriate prophylaxis. WHO guidelines advise treating all HBsAg+ women with HBV DNA >200000 IU/ml from 2nd trimester together with birth dose vaccination and HBIg. While HBV DNA test is available in developed countries, access to molecular testing is sparse in resource-limited countries. Hepatitis B core-related antigen (HBcrAg) is a composite pan-genotypic serological marker, which correlates with HBV DNA levels and could be utilised in resource-limited setting. We aimed to compare HBcrAg plasma levels with other virological (HBV DNA and pre-genomic RNA) and serological markers (HBeAg status and quantitative HBsAg) in a single centre cohort of HBsAg+ pregnant patients tested at the 2nd trimester and evaluate if HBcrAg can assess the risk of HBV MTCT (HBV DNA >200000 IU/ml = high risk).

Method: Plasma samples from the 2nd trimester (median gestation 22 wks) of 1028 HBsAg+ pregnant patients with post-partum follow-up >1 year and information about their infants HBV infection status were collected between 1.1.2012–31.12.2022. We measured levels of HBV DNA by TaqMan PCR [IU/ml], quantitative HBsAg by Abbott Architect® [IU/ml], HBcrAg by CLEIA Fujirebio [log₁₀ IU/ml] and pgRNA by Abbott Diagnostics dual-target real-time-PCR assay [LLOQ = 0.49 log₁₀ IU/ml]. The results were compared according to the risk of HBV MTCT stratified by HBV DNA >200000 IU/ml = high risk vs HBV DNA <200000 IU/ml = low risk).

Results: From 1028 enrolled patients (median age 30 yrs): 668 (65%) patients were aware of HBV infection before pregnancy with 165 (16%) already on tenofovir. 144 (14%) patients were HBeAg+ and 175 (17%) had HBV DNA >200000 IU/ml. HBeAg+ patients had predominantly high HBV DNA, but there were 55 (5%) HBeAg-negative patients with HBV DNA >200000 IU/ml. Although HBsAg levels were high (>10000 IU/ml) in 360 (35%) patients, only 102 (10%) patients with high HBsAg had high HBV DNA (>200000 IU/ml). HBcrAg levels were significantly higher in patients with high viral load (7.0 vs. 3.2, p < 0.05) irrespective of HBeAg status and all patients with high HBV DNA had HBcrAg levels above 6 log₁₀ IU/ml. All high viral load patients had high levels of pgRNA >4.5 log₁₀ IU/ml. There were only 4 patients with low HBV DNA with pgRNA >4.5 log₁₀ IU/ml. All patients with high HBV DNA started on tenofovir at the 2nd trimester and all had pre-delivery HBV DNA levels <200000 IU/ml. No case of MTCT was reported in our cohort. ROC analysis confirmed that HBcrAg and pgRNA were able to predict more accurately high risk of HBV MTCT than HBsAg (HBcrAg AUROC = 1.0, pgRNA AUROC = 0.98 vs. HBsAg AUROC = 0.68).

Conclusion: Pregnancy plasma HBcrAg levels are more accurate than HBeAg and HBsAg levels to assess HBV MTCT risk. HBcrAg levels >6 log₁₀ IU/ml predict a high MTCT risk and offers a serological alternative for maternal testing.

FRI-402

The unique role of hepatitis B virus enhancer 1 in unevenly activating preS1 and preS2 promoters of integrated HBV DNA which impacts HBsAg secretion efficiency

Fengmin Lu¹, Zhiqiang Gu¹. ¹Department of Microbiology and Infectious Disease Center, School of Basic Medical Sciences, Peking University, Beijing, China, Beijing, China
Email: lu.fengmin@hsc.pku.edu.cn

Background and aims: The achievement of a “functional cure” for chronic hepatitis B (CHB) remains a formidable challenge. As another source of HBsAg, HBV DNA integration limits the achievement of a functional cure. Thus, uncovering the unique characteristics of HBsAg derived from integrated HBV DNA will shed new light on strategies for achieving a functional cure.

Method: Using clinical cohorts, animal and cell models simulating integrated HBV DNA, we explored the expression and secretion characteristics of HBsAg derived from integrated HBV DNA and the underlying mechanism.

Results: A semi-quantitative analysis of intrahepatic HBsAg protein level in 563 treatment-naïve patients revealed that, in contrast to the significantly lower serum HBsAg levels, no significant decrease of intrahepatic HBsAg protein was observed in the HBeAg-negative patients, as compared to that in HBeAg-positive patients. *In vitro* studies of integrated HBV DNA mimic and long-read RNA sequencing of liver biopsy from patients revealed that, the lower HBsAg secretion efficiency seen in HBeAg-negative patients might be attributed to a relative increased proportion of 2.4 kb HBV RNA derived from integrated HBV DNA than covalently closed circular DNA (cccDNA), which resulted in L-HBsAg over-expression and the subsequent impaired HBsAg secretion. Mechanistically, the change of 2.4 kb HBV

POSTER PRESENTATIONS

RNA proportion was caused by retargeting and uneven activation on preS1 (SP1) than preS2 (SP2) promoters by HBV enhancer 1 (Enh1) element, largely due to the loss of core promoter (CP) in integrated HBV DNA.

Conclusion: The secretion of HBsAg originated from integrated HBV DNA was impaired. Mechanistically, functional deficiency of CP leads to the promoter (s) retargeting of Enh1 and uneven activation of SP1 over SP2, resulting in an increase in proportion of L-HBsAg.

FRI-403

Evaluation of a novel hepatitis B DNA test from fingerstick capillary blood at the point-of-care as a tool to enhance clinical management

Behzad Hajarizadeh¹, Jacob George², Miriam Levy³, Ian Wong⁴, Jess Howell⁵, Gesalit Cabrera¹, Elise Tu¹, Marianne Martinello¹, Tanya Applegate¹, Gail Matthews⁶. ¹The Kirby Institute, University of New South Wales (UNSW), Sydney, Australia; ²Storr Liver Centre, Westmead Hospital, University of Sydney, The Westmead Institute for Medical Research, University of Sydney, Sydney, Australia; ³Liverpool Hospital, University of New South Wales (UNSW), South Western Clinical School, University of New South Wales (UNSW), Sydney, Australia; ⁴Blacktown Hospital, Sydney, Australia; ⁵The Burnet Institute, St Vincent's Hospital, Melbourne, Australia; ⁶The Kirby Institute, University of New South Wales (UNSW), St Vincent's Hospital, Sydney, Australia
Email: bhajarizadeh@kirby.unsw.edu.au

Background and aims: HBV DNA tests are essential to guide HBV clinical management, including antiviral treatment eligibility and effectiveness. Standard of care HBV DNA tests are expensive and need central laboratory infrastructure, limiting access while delayed time to result may interrupt continuity of care. This study evaluated the diagnostic performance of the Xpert® HBV Viral Load assay (Cepheid), using fingerstick capillary blood at the point-of-care compared to standard of care HBV DNA testing using venipuncture whole blood.

Method: Participants diagnosed with chronic HBV infection were enrolled from six hospital-based hepatitis clinics in Australia. Participants provided fingerstick capillary blood samples diluted 1 in 10 and tested for quantitative HBV DNA using Xpert® HBV Viral Load assay (adjusted lower limit of quantification: 100 IU/ml). The standard of care assay (gold standard) was Roche COBAS® AmpliPrep/COBAS® TaqMan® HBV DNA Test, using plasma from venipuncture whole blood samples. Sensitivity and specificity of the Xpert® HBV Viral Load for HBV DNA quantification were compared with the gold standard. A Bland-Altman difference plot was used to assess bias and agreement measurements.

Results: To date, 178 participants have been enrolled (recruitment ongoing, total sample size n = 300). Participants included 46% female, 19% HBeAg positive, 44% on HBV treatment, and 6% with cirrhosis, with a median age of 46 years. As measured by the gold standard test, HBV DNA was undetected in 58 participants (33%), detected <100 IU/ml in 38 (21%), and detected ≥100 IU/ml in 82 (46%; viral load range: 110 to >180 million IU/ml). Sensitivity and specificity of the Xpert® for HBV DNA ≥100 IU/ml (vs. <100 or undetected) was 96.3% (95%CI: 93.6, 99.1) and 89.6% (95%CI: 85.1, 94.1), respectively. Among 13 participants whose HBV viral loads fell in different categories between the Xpert® and gold standard assays, the difference in viral loads detected by two assays ranged from 38 to 388 IU/ml. The Bland-Altman difference plot demonstrated that HBV viral loads detected by the Xpert® were a mean of 0.18 log IU/ml (standard deviation 0.28) higher than those measured by the gold standard. The limits of agreement indicated that 95% of the differences between the two assays were between -0.37 and 0.74 log IU/ml.

Conclusion: This interim analysis showed minimal difference in HBV viral loads detected by the Xpert® compared to the gold standard assay. Among participants with inconsistent HBV viral loads between assays, the difference was not sufficient to impact clinical decision making. If validated, this fingerstick assay has the potential to

simplify clinical care for people living with HBV, particularly hard-to-reach population, and those in remote and resource limited settings.

FRI-404

To establish the threshold for transient elastography indicating advanced fibrosis in patients with chronic hepatitis B and hepatic steatosis

Fajuan Rui¹, Yee Hui Yeo², Xiaoming Xu¹, Wenjing Ni¹, Liang Xu³, Jie Li⁴. ¹Nanjing Drum Tower Hospital Clinical College of Nanjing University of Chinese Medicine, Nanjing, China; ²Cedars-Sinai Medical Center, California, United States; ³Tianjin Second People's Hospital, Tianjin, China; ⁴Nanjing Drum Tower Hospital, Affiliated Hospital of Medical School, Nanjing University, Nanjing, China
Email: lijier@sina.com

Background and aims: Transient elastography (TE) is widely recognized as an effective, non-invasive technique for diagnosing liver fibrosis by assessing liver stiffness. Although specific threshold values have been proposed separately for chronic hepatitis B (CHB) and hepatic steatosis (HS), no such recommendations exist for patients with both CHB and HS. With the rising occurrence of HS in individuals with CHB, it's increasingly important to establish a definitive TE threshold for best clinical outcomes. This study employs a substantial cohort of patients with both CHB and HS, who have undergone liver biopsy and FibroScan, to identify the precise TE threshold for detecting advanced fibrosis.

Method: The study included sequential patients with CHB and HS, who had biopsy data from 2016 to 2021 at Tianjin Second People's Hospital. The Youden index was used to find the ideal TE cutoff for patients with both CHB and HS. We calculated the Area Under the Curve (AUC) for the existing 9.7 kPa TE cutoff for patients with CHB or HS and the new optimal cutoff, comparing them using the DeLong test. Additionally, we compared AUCs for both cutoffs in subgroups with body mass indexes (BMI) below and above 25 kg/m².

Results: A total of 613 patients participated in the study, with a median age of 36. Of these, 72% (442) were male, and 12% (74) exhibited advanced fibrosis. The study determined an optimal Transient Elastography (TE) cutoff value at 8.8 kPa, which showed an AUC of 0.733. This was significantly more accurate than the AUC of 0.681 obtained using the recommended TE cutoff of 9.7 kPa (p = 0.015). In a subgroup of patients with a BMI <25 kg/m², the optimal cutoff yielded an AUC of 0.708, surpassing the AUC of 0.566 for the contemporary cutoff value (p = 0.003). The sensitivity (SE) of the optimal cutoff was higher than that of the contemporary cutoff in both the overall cohort and the BMI subgroup analysis (overall cohort: 70.27 vs. 55.41; BMI <25 kg/m²: 56.00 vs. 24.00; BMI <25 kg/m²: 77.55 vs. 71.42). However, the specificity (SP) of the optimal cutoff was lower than that of the contemporary cutoff (overall cohort: 76.25 vs. 80.71; BMI <25 kg/m²: 85.64 vs. 89.23; BMI <25 kg/m²: 70.93 vs. 75.87).

Conclusion: The optimal TE cutoff for assessing advanced fibrosis in patients with CHB and concurrent HS is 8.8 kPa, lower than the 9.7 kPa for CHB patients without HS. The optimal TE cutoff offers superior SE, making it more effective at ruling in advanced fibrosis. It's more appropriate for screening patients with advanced fibrosis, ensuring they receive the appropriate medical care. For those with both CHB and HS, a stricter (lower) TE value is needed for more accurate assessment, reflecting the unique interaction between CHB and HS and its impact on liver response and fibrosis progression.

FRI-405

Heterogeneity in the diagnostic performances of HDV-RNA quantification assays used in clinical practice in Italy: results from a national quality control multicenter study

Romina Salpini¹, Lorenzo Piermatteo¹, Gian Paolo Caviglia², Ada Bertoli^{3,4}, Maurizia Brunetto^{5,6}, Bianca Bruzzone⁷, Annapaola Callegaro⁸, Cinzia Caudai⁹, Daniela Cavallone¹⁰, Nicola Coppola¹¹, Nunzia Cuomo¹², Stefano D'Anna¹,

Mariantonietta Di Stefano¹³, Leonardo Duca³, Floriana Facchetti¹⁴, Claudio Farina¹⁵, Donatella Ferraro¹⁶, Elisa Franchin¹⁷, Daniela Francisci¹⁸, Silvia Galli¹⁹, AnnaRosa Garbuglia²⁰, William Gennari²¹, Valeria Ghisetti²², Pietro Lampertico^{14,23}, Nadia Marasco²⁴, Stefano Menzo²⁵, Valeria Micheli²⁶, Grazia Anna Niro²⁷, Antonella Olivero², Pierpaolo Paba⁴, Concetta Ilenia Palermo²⁸, Orazio Palmieri²⁹, Stefania Paolucci³⁰, Mariantonietta Pisaturo¹¹, Teresa Pollicino³¹, Giuseppina Raffa³¹, Giulia Torre¹, Ombretta Turriziani³², Sergio Uzzau³³, Maria Linda Vatteroni³⁴, Maurizio Zazzi³⁵, Antonio Craxi³⁶, Francesca Ceccherini Silberstein³, Valentina Svicher³⁷. ¹University of Rome "Tor Vergata," Department of Biology, Rome, Italy; ²University of Turin, Department of Medical Sciences, Turin, Italy; ³University of Rome "Tor Vergata," Department of Experimental Medicine, Rome, Italy; ⁴Tor Vergata Polyclinic Foundation, Unit of Virology, Rome, Italy; ⁵University of Pisa, Dept of Clinical and Experimental Medicine, Pisa, Italy; ⁶Pisa University Hospital, Hepatology Unit and Laboratory of Molecular Genetics and Pathology of Hepatitis Viruses, Pisa, Italy; ⁷University of Genoa, Genoa, Italy; Department of Health Sciences, Genoa, Italy; ⁸ASST Bergamo Est, Medicina di Laboratorio, Bergamo, Italy; ⁹Siena University Hospital, Microbiology and Virology Unit, Siena, Italy; ¹⁰University Hospital of Pisa, Hepatology Unit and Laboratory of Molecular Genetics and Pathology of Hepatitis Viruses, Pisa, Italy; ¹¹University of Campania Luigi Vanvitelli, Department of Mental Health and Public Medicine, Section of Infectious Diseases, Caserta, Italy; ¹²Federico II University, Department of Neurosciences and Reproductive and Odontostomatological Sciences, Napoli, Italy; ¹³University Hospital "Riuniti" of Foggia, Clinical and Surgical Sciences, Section of Infectious Diseases, Foggia, Italy; ¹⁴Foundation IRCCS Ca' Granda Ospedale Maggiore Policlinico, Division of Gastroenterology and Hepatology, Milan, Italy; ¹⁵ASST "Papa Giovanni XXIII," Microbiology and Virology Unit, Bergamo, Italy; ¹⁶University of Palermo, Section of Microbiology and Clinical Microbiology, Department of Health Promotion, Mother and Child Care, Internal Medicine and Medical Specialties, PROMISE, Palermo, Italy; ¹⁷University of Padova, Department of Molecular Medicine, Padova, Italy; ¹⁸Santa Maria della Misericordia Hospital, Infectious Diseases Laboratory, Perugia, Italy; ¹⁹IRCCS S. Orsola-Malpighi University Hospital, Operative Unit of Clinical Microbiology, Bologna, Italy; ²⁰"Lazzaro Spallanzani" National Institute for Infectious Diseases, IRCCS, Laboratory of Virology, Rome, Italy; ²¹Azienda Ospedaliero Universitaria di Modena, Department of Laboratory Medicine and Pathological Anatomy, Molecular Microbiology and Virology Unit, Modena, Italy; ²²Amedeo di Savoia Hospital, ASL Città di Torino, Laboratory of Microbiology and Virology, Turin, Italy; ²³University of Milan, CRC "A. M. and A. Migliavacca" Center for Liver Disease, Department of Pathophysiology and Transplantation, Milan, Italy; ²⁴"Magna Graecia" University, Department of Health Sciences, Unit of Microbiology, Catanzaro, Italy; ²⁵Università Politecnica Delle Marche, Department of Biomedical Sciences and Public Health, Ancona, Italy; ²⁶Ospedale Sacco, Laboratory of Clinical Microbiology, Virology and Bioemergencies, Milan, Italy; ²⁷Fondazione IRCCS "Casa Sollievo della Sofferenza," Division of Gastroenterology and Endoscopy, San Giovanni Rotondo, Italy; ²⁸Azienda Ospedaliero-Universitaria Policlinico "G. Rodolico-S.Marco," Catania, Italy; ²⁹Fondazione IRCCS "Casa Sollievo Sofferenza," Gastroenterology Unit, San Giovanni Rotondo, Italy; ³⁰Fondazione IRCCS Policlinico San Matteo, Microbiology and Virology Unit, Pavia, Italy; ³¹University Hospital "G. Martino" Messina, Department of Clinical and Experimental Medicine, Messina, Italy; ³²Sapienza University of Rome, Department of Molecular Medicine, Rome, Italy; ³³University of Sassari, Department of Biomedical Sciences, Sassari, Italy; ³⁴Pisa University Hospital, Virology Unit, Pisa, Italy; ³⁵University of Siena, Department of Medical Biotechnology, Siena, Italy; ³⁶University of Palermo, Section of Gastroenterology and Hepatology, Department of Health Promotion, Mother and Child Care, Internal Medicine and Medical Specialties, PROMISE, Palermo, Italy; ³⁷University of Rome "Tor Vergata," Department of Biology, Rome, British Indian Ocean Territory

Email: rsalpini@yahoo.it

Background and aims: A reliable quantification of serum hepatitis D virus (HDV) RNA is of paramount importance for a proper monitoring of patients under antiviral therapy. This quality control study aimed at comparing the diagnostic performances of different quantitative HDV RNA assays, used in clinical practice.

Method: Two HDV RNA sample panels were quantified at 29 Italian labs by 6 commercial assays defined as #1 (RoboGene 2.0, N = 9 labs), #2 (Eurobio on In/BeGenius ELITech platform, N = 7), #3 (Altona RealStar, N = 5), #4 (Anatolia Bosphore, N = 3), #5 (Dia.Pro.Dia., N = 2), #6 (Nuclear Laser Medicine, N = 1) and 2 in-house assays defined as #7 (N = 2). Panel A comprised 8 serial dilutions of WHO HDV genotype 1 standard from 5 to 0.5 logIU/ml, while Panel B included 20 clinical serum samples with HDV RNA from 6 to 0.5 logIU/ml. Participating labs quantified each dilution of Panel A and B 9 and 5 times, respectively (3 independent runs). Panel A was used to define assay sensitivity by estimating the 95%LOD (limit of detection). Panel B was used to evaluate assay precision by calculating the intra-run and inter-run coefficient of variation (CV). Lastly, the accuracy was assessed by calculating the differences between expected and observed values at each HDV RNA load for both Panels.

Results: By analysing Panel A, 95%LOD varied across the assays highlighting different sensitivities. In particular, #3 had the lowest median 95%LOD (10 [min-max: 3–316] IU/ml), followed by #1 (31 [3–316] IU/ml), #6 (31 IU/ml) and #2 (100 [100–316] IU/ml). The remaining 3 assays had a median 95%LOD ranging from 316 to 1000 IU/ml. Moreover, 5 assays showed a <0.5 logIU/ml difference between expected and observed HDV-RNA values for all dilutions, with #1 showing the best accuracy (Median [IQR]: 0.0 [–0.2–0.0] logIU/ml). Conversely, for #5 and #6 these differences exceeded 0.5 logIU/ml (median [IQR]: –0.7 [–0.7–0.6] and –1.3 [–1.6–1.1] logIU/ml), highlighting substantial HDV RNA underestimation. With Panel B, different reproducibility levels were observed across the assays. Indeed, #2 and #3 had a median intra-run CV <10% (median [IQR]: 8.0% [6.5–11.2%] and 9.9% [6.8–12.3%]) while assays #1, #4 and #7 showed a median intra-run CV from 10% to 15% and #5 and #6 of 18.9% and 26.2%. Inter-run CV depicted a similar scenario with the highest reproducibility for #2 and #3. For samples with HDV RNA <5.0 logIU/ml, five assays exhibited a <0.5 logIU/ml difference between expected and observed HDV RNA. Conversely, for HDV RNA >5.0 logIU/ml, an underestimation >1 logIU/ml was observed for most assays (N = 5).

Conclusion: This study underlines different levels of sensitivities, that could hamper the proper quantification of low level HDV RNA. There is a need to improve the accuracy in HDV RNA quantification at high viral load for most assays. These results should be carefully considered for the proper monitoring of virological response to anti-HDV drugs.

FRI-406

Real world outcomes of hepatitis delta patients with mild or moderate fibrosis

Sabela Lens¹, Habiba Kamal², Arno Furquim d'Almeida³, Segolene Brichler⁴, Margarita Papatheodoridis⁵, Adriana Palom⁶, Marta Casado-Martin⁷, Stefan Bourgeois⁸, Moises Diago⁹, Karin Lindahl¹², Marta Hernández Conde¹⁰, Manuel Rodríguez¹¹, Christophe Moreno¹², Alvaro Giráldez-Gallego¹³, Francisco Javier Garcia-Samaniego¹⁴, Thomas Sersté¹⁵, Joaquin Cabezas¹⁶, JeAn Delwaide¹⁷, Maria Buti¹⁸, George Papatheodoridis⁵, Dominique Roulot¹⁹, Thomas Vanwolleghem²⁰, Victor de Ledinghen²¹, Soo Aleman², José Luis Calleja Panero¹⁰. ¹Liver Unit, Hospital Clinic, FCRB/IDIBAPS, CIBERehd, University of Barcelona, Barcelona, Spain; ²Dept of Infectious Diseases, Karolinska University Hospital, Stockholm, Sweden; ³Viral Hepatitis Research Group, Laboratory of Experimental Medicine and Pediatrics, University of Antwerp, Antwerp, Belgium; ⁴Departement of Microbiology, Assistance Publique-Hopitaux de Paris, Hopital Avicenne, Bobigny, Université Sorbonne Paris Nord, Bobigny, France; ⁵Academic Department of Gastroenterology, Medical School of National and

POSTER PRESENTATIONS

Kapodistrian University of Athens, General Hospital of Athens "Laiko," Athens, Greece; ⁶Liver Unit, Internal Medicine Department, Hospital Universitari Vall d'Hebron, Vall d'Hebron Barcelona Hospital Campus, Barcelona, Spain; ⁷Liver Unit, Hospital Universitario Torrecárdenas, Almería, Spain; ⁸Department of Gastroenterology, ZNA Antwerp, Antwerp, Belgium; ⁹Liver Unit, Hospital General Universitario Valencia, Valencia, Spain; ¹⁰Liver Unit, University Hospital Puerta del Hierro, Madrid, CIBERehd, University Autónoma de Madrid, Madrid, Spain; ¹¹Liver Unit, Hospital Universitario Central de Asturias, Oviedo, Spain; ¹²Department of Gastroenterology, Hepatopancreatology and Digestive Oncology, CUB Hôpital Erasme, Université Libre de Bruxelles, Brussels, Belgium; ¹³Digestive Diseases Unit, Virgen del Rocío University Hospital, Sevilla, Spain; ¹⁴Liver Unit, University Hospital La Paz, IDIPAZ, CIBERehd, Madrid, Spain; ¹⁵Department of Hepato-Gastroenterology, CHU Saint-Pierre, Brussels, Belgium, Brussels, Belgium; ¹⁶Gastroenterology and Hepatology Department, Marqués de Valdecilla University Hospital, IDIVAL, Santander, Spain; ¹⁷Department of Hepato-Gastroenterology, CHU Sart-Tilman, Université de Liège, Liège, Belgium; ¹⁸Liver Unit, Internal Medicine Department, Hospital Universitari Vall d'Hebron, Vall d'Hebron Barcelona Hospital Campus, CIBERehd, Barcelona, Spain; ¹⁹Département of Hepatology, Assistance Publique-Hopitaux de Paris, Hôpital Avicenne, Bobigny, Université Sorbonne Paris Nord, Bobigny, France; ²⁰Department of Gastroenterology and Hepatology, Antwerp University Hospital, Antwerp, Belgium; ²¹Department of Hepatology, University Hospitals of Bordeaux, Bordeaux, France
Email: joseluis.calleja@uam.es

Background and aims: Hepatitis Delta is considered the most severe form of viral hepatitis. New therapeutic options are now available and, in some countries, therapy prioritization is recommended. We aimed to evaluate the real world outcomes of HDV-infected patients with mild or moderate fibrosis in order to identify risk factors for fibrosis progression.

Method: Multicenter international retrospective study of adult patients with active HDV infection (HDV-RNA+) and absence of advanced fibrosis at diagnosis. Baseline demographical, clinical and virological variables were collected. Cirrhosis development and liver-related events (decompensation, HCC) were recorded. Patients were followed until last follow-up (FU) visit, liver transplantation (LT) or death.

Results: The cohort included 170 adult patients with mild/moderate fibrosis assessed histologically (45%) and/or non-invasively [median (IQR) age at first visit: 37 (31–45) years, males: 53%]. Most patients were Caucasians (55%) or Asians (21%), <5% were coinfecting with HIV or HCV and <15% had comorbidities (obesity, diabetes, hypertension). At baseline, only 36% of patients had ALT >2xULN. In 102 cases with LSM within year-1, median (IQR) values were 7.6 (6–9) kPa. During the study period, 33% of patients received Interferon, 36% NA and only 8% bulevirtide therapy. After a median (IQR) follow-up of 62 (21–108) months, 31 (18%) patients developed cirrhosis; of them, 5 developed liver decompensation and 2 HCC. One patient underwent LT and one patient with HCC died. Median LSM (IQR) of patients at cirrhosis diagnosis was 16 (10–17) kPa. By multivariate analysis, higher LSM at baseline (model 1) and albumin and platelet levels (model 2 excluding LSM) were the only independent predictors for cirrhosis development. The best cut-off for LSM value at baseline for cirrhosis development was 7.6 kPa (Se 84%). Neither baseline qHDV-RNA levels nor ALT influenced on cirrhosis development. In addition, 17 (10%) patients achieved HDV-RNA clearance during FU (6 after IFN therapy and 11 spontaneously) with only 1/17 patients developing cirrhosis during FU.

Conclusion: Some patients with active HDV replication and mild-moderate fibrosis may have a benign course, but up to 18% of such patients progress to cirrhosis within 5 years having increased risk for liver-related complications. LSM seems to be a reliable non-invasive predictor, as patients with LSM <7.6 kPa have a low probability of progression to cirrhosis. Dissecting the factors associated with

fibrosis progression may be useful to prioritize the need of new antiviral therapies.

FRI-407

Screening rates, prevalence, and natural history of hepatitis B/ delta virus co-infection vs. hepatitis B mono-infection: data from a large US integrated healthcare system

Varun Saxena^{1,2,3}, Lue-Yen Tucker², Xiaoran Li¹, Krisna Chai¹, Suk Seo¹, Nizar Mukhtar¹, Grace M. Chee⁴, Kyung Min Kwon⁴, Sreepriya Balasubramanian¹, Brock Macdonald¹, Julie Schmitt², ¹Kaiser Permanente Northern California, Oakland, United States; ²Kaiser Permanente Northern California Division of Research, Oakland, United States; ³University of California San Francisco, San Francisco, United States; ⁴Gilead Sciences Inc., Foster City, United States
Email: varun.saxena@kp.org

Background and aims: Hepatitis delta virus (HDV) among patients with chronic hepatitis B virus (HBV) is the most severe form of viral hepatitis. Despite this, HBV/HDV co-infection prevalence in the United States (US) remains uncertain. In this study, we aim to demonstrate screening rates of HDV, estimates of HBV/HDV prevalence, and natural history data of HBV/HDV vs. HBV alone from a large US integrated healthcare system.

Method: In this retrospective cohort study from Kaiser Permanente Northern California, an integrated healthcare system with over 4.6 million patients, all adult HBV infected patients identified from January 2009 to December 2018 were included. Proportions of anti-HDV testing, positive anti-HDV, HDV RNA testing, and detectable HDV RNA were studied. Three groups were identified: HBV mono-infected (included those without anti-HDV testing), HBV with anti-HDV positive (included those without HDV RNA testing) and HBV/HDV co-infected (those with detectable HDV RNA). Groups were followed until outcome of interest, insurance loss or study termination at end of 2022. Outcomes of interest included fibrosis progression (at least 1 fibrosis stage increase between serial transient elastography measurements), cirrhosis, decompensated cirrhosis, hepatocellular carcinoma (HCC), liver transplantation and all-cause mortality.

Results: We identified 17,794 HBV infected patients, of which 10,461 (59%) underwent anti-HDV testing. 83 of 10,461 patients (0.8%) were anti-HDV positive; 73 of 83 (88%) had HDV RNA tested and 11 of 73 (15%) were HDV RNA detectable. Among the HBV mono-infected (n = 17,700) vs. HBV with anti-HDV positive (n = 83) vs. HBV/HDV (n = 11) patients, baseline characteristics showed highest proportion of female in HBV mono-infected (47%), median age youngest in HBV/HDV (44 years) and highest BMI in HBV/HDV (27 kg/m²) (all p < 0.05). For comorbidities, diabetes and hypertension were highest in HBV with anti-HDV positive (23% and 13% respectively) with active tobacco users highest in HBV/HDV (10%) (all p < 0.05). The HBV/HDV had the highest proportion of patients with baseline cirrhosis at 45% (p < 0.05). HBV/HDV (vs. HBV with anti-HDV positive vs. HBV mono-infected) showed the most fibrosis progression (100% vs. 15% vs. 11%), cirrhosis development (75% vs. 18% vs. 7%), decompensation development (30% vs. 7% vs. 0.6%), liver transplantation (18% vs. 6% vs. 0.4%), and mortality (18% vs. 11% vs. 6%) (all p < 0.05). HCC development was most common in HBV with anti-HDV positive at 11% vs. 9% in HBV/HDV vs. 2% in HBV mono-infected (p < 0.01).

Conclusion: From this large US HBV cohort, HDV screening rate was 59%, revealing <1% anti-HDV positive rate and 0.1% HBV/HDV prevalence. The findings support the aggressive nature of HDV infection and that of HDV exposure as well. Controlled cox-regression analysis will be presented to confirm HDV as the cause for the more severe natural history.

FRI-408

Statins in untreated chronic HBV link with improved survival, liver outcome and inflammation: a large multicenter retrospective real-world cohort study

Mohammed Suki¹, Tamer Safadi², Yael Milgrom¹, Mohamad Masarowah¹, Wadiaa Hazo¹, Yariv Tiram¹, Johnny Amer¹, Abed Khakayla¹, Ashraf Imam¹, Esther Forkosh¹, Joseph Sackran¹, Ofer Perzon¹, Ahmad Salhab¹, Sylvia Drazilova², Peter Jarčuška², Rifaat Safadi¹. ¹Liver institute, Hadassah Hebrew University Hospital, Jerusalem, Israel; ²2nd Department of Internal Medicine, University Hospital and Faculty of Medicine, Pavol Jozef Šafárik University, Košice, Slovakia
Email: johnnyamer@hotmail.com

Background and aims: Statins link to antiviral and immunomodulatory properties that could benefit chronic hepatitis B virus (HBV) infection. However, clinical data remains restricted to small-scale unmatched trials. This large real-world retrospective cohort study assessed long term outcomes of statins in chronic HBV patients without anti-viral.

Method: TriNetX is a global research platform de-identified database that spanning 135 million patients across 112 healthcare organizations worldwide. We analyzed electronic medical records of 11569 HBV mono-infected adults (18–90 years) during 2003–2023 from the TriNetX network. Patients defined as detectable HBV DNA >10 IU/ml, never treated with HBV anti-viral (at index event and along 15 follow-up years), either started statins only at index event or never treated with statins. Exclusion criteria were ALT and ALP levels >4 UNL, liver transplants, HCC, and past anticoagulation therapy. Outcomes assessed over 1, 5, 10 and 15 years; including mortality and survival, laboratory data (biochemical, hematologic, AFP), manifestations and complications of cirrhosis, viral load trajectories, as well as metabolic and cardiovascular (CV) outcomes. Advanced liver disease and complications of cirrhosis were defined according to ICD9 terms, blood tests (albumin, bilirubin, INR, Platelets) and specific treatments (NSBB, ammonia lowering agents and spironolactone).

Results: Following an extensive matching of 44 clinical and laboratory parameters, propensity score matching created 2 balanced groups for analysis, statin-exposed (n=935) and unexposed (n=935). Despite extensive matching, LDL remained significantly higher in the statin group, with a non-significant trend of higher TG and HBA1c at baseline. Statin group demonstrated a significant improvement in mortality and survival (p < 0.005), as well as manifestations of advanced liver disease (p < 0.05), but not HCC and neither liver transplant. Although BMI remained similar in both groups, the statin group exhibited a significant LDL and AST improvements and HBA1c worsening, while CV events equalized. Interestingly, viral load kept similar in both groups in all tested time points.

Conclusion: This long-term real-world study in HBV patients suggests effectiveness of statins on survival and liver outcomes despite the higher metabolic risks at baseline (lipid profile) and along follow-up (HBA1c worsening). Statins improved LDL and equalized CV events despite higher metabolic risks, suggesting survival improvement because of the liver alleviation. Ongoing similar viral load in both groups and AST decline in statin group suggesting an anti-inflammatory mechanism but not a direct viral effect.

FRI-409

Enhancing hepatitis delta diagnosis in southern Spain: efficacy and cost-effectiveness of double reflex testing

Ana Fuentes^{1,2,3}, Adolfo de Salazar^{2,3,4}, Lucía Chaves-Blanco⁴, Elena Ruiz-Escorlano⁴, Natalia Montiel⁵, Manuel Macías⁶, Valle Odero⁷, Juan Cristobal Aguilar⁷, Ana Belén Pérez⁸, Pilar Barrera⁸, Teresa Cabezas Fernandez⁹, Anny Camelo Castillo¹⁰, Begoña Palop¹¹, Rocio González-Grande¹², Aurora García-Barrionuevo¹³, Jose María Pinazo-Bandera¹⁴, Fernando Fernández Sánchez¹⁵, María Carmen Lozano Domínguez¹⁶, Álvaro Giraldez¹⁶, María del Carmen Domínguez¹⁷, Carlota Jimeno-Maté¹⁷,

Encarnación Ramirez Arellano¹⁸, Patricia Cordero¹⁸, Francisco Franco Álvarez De La Luna¹⁹, Pilar del Pino²⁰, Alberto De La Iglesia Salgado²¹, Carmen Sendra-Fernández²¹, Antonio Sampedro²², M. Ángeles López-Garrido²², M. Pilar Luzón-García²³, Carmen Molina-Villalba²⁴, Joaquin Salas²⁵, Carolina Roldan²⁶, Laura Castillo-Molina²⁷, Fernando García García²⁸, Carolina Freyre²⁹, Germán Santamaría-Rodríguez³⁰, José María Rosales¹⁵, Raquel Domínguez-Hernández³⁰, Marta Casado-Martin³¹, Federico Garcia Garcia^{2,3,32}. ¹University Hospital Clinic San Cecilio, Ibs. Granada, Granada, Spain; ²Ibs. Granada, Granada, Spain; ³CIBERINFEC, Madrid, Spain; ⁴University Hospital Clinic San Cecilio, Granada, Spain; ⁵Hospital Puerta del Mar, Cádiz, Spain; ⁶Hospital Puerta del Mar, Cádiz; ⁷Hospital del S.A.S de Jerez de la Frontera, Jerez de la Frontera, Spain; ⁸Hospital Universitario Reina Sofía, Córdoba, Spain; ⁹Hospital Universitario Torrecardenas, Almería, Spain; ¹⁰TorreCardenas University Hospital, Almería, Spain; ¹¹Complejo Hospitalario Regional de Málaga, Málaga, Spain; ¹²Hospital Universitario Regional de Málaga, Málaga, Spain; ¹³Hospital Clínico Universitario Virgen de la Victoria, Málaga; ¹⁴Hospital Clínico Universitario Virgen de la Victoria, Málaga, Spain; ¹⁵Hospital Costa del Sol, Marbella, Spain; ¹⁶Hospital Universitario Virgen del Rocío, Sevilla, Spain; ¹⁷Hospital Universitario Nuestra Señora de Valme, Sevilla, Spain; ¹⁸Hospital Universitario Virgen Macarena, Sevilla, Spain; ¹⁹Hospital Juan Ramón Jiménez, Huelva, Spain; ²⁰Hospital Juan Ramón Jiménez, Huelva, Spain; ²¹Hospital Infanta Elena, Huelva, Spain; ²²Hospital Universitario Virgen de las Nieves, Granada, Spain; ²³Hospital de Poniente, El Ejido, Spain; ²⁴Hospital de Poniente, El Ejido, Spain; ²⁵Hospital de Poniente, Almería, Spain; ²⁶Complejo Hospitalario ciudad de Jaén, Jaén, Spain; ²⁷Hospital Universitario Ciudad de Jaén, Jaén, Spain; ²⁸Hospital Universitario Clínico San Cecilio, Granada, Spain; ²⁹Hospital Universitario Puerto Real, Puerto Real, Spain; ³⁰Hospital Puerto Real, Puerto Real, Spain; ³¹Hospital Torrecardenas, Almería, Spain; ³²Hospital Universitario Clinico San Cecilio, Granada, Spain
Email: anafuenteslop@gmail.com

Background and aims: Hepatitis delta is a significant global health concern, affecting an estimated 15 to 20 million people worldwide. With the recent introduction of Bulevirtide, the first antiviral specifically for hepatitis delta, and forthcoming new antivirals targeting hepatitis B virus, there are now more therapeutic options. These developments could enhance elimination strategies. Our study focuses on assessing the prevalence of undiagnosed hepatitis delta in Southern Spain (Andalusia) and evaluating the feasibility and cost-effectiveness of reflex testing for hepatitis delta.

Method: We conducted an ambispective (both retrospective and prospective) multicentre study across 17 hospitals in Andalusia. During the retrospective phase (January 2018 to June 2022), we analyzed the hepatitis delta diagnostic process, focusing on patients positive for HBsAg. We identified those tested for anti-delta antibodies and those who underwent HDV RNA testing, extracting data from the Laboratory Information Systems (LIS) of participating centers. From October 2022 to March 2023, all centers began the prospective phase, implementing reflex testing for hepatitis delta (testing for anti-HDV in all HBsAg-positive patients who hadn't been previously tested). We evaluated the cost-effectiveness of implementing reflex testing in the prospective phase population versus non-implementation, considering only direct healthcare costs (screening and diagnosis), excluding treatment costs.

Results: In the retrospective phase, we analyzed 18, 583 HBsAg-positive patients. Of these, 3436 (18%) underwent anti-HDV testing, with 205 (6%) testing positive. HDV RNA testing was conducted on 158 patients, identifying 69 (1.9%) as HDV-RNA positive. In the prospective phase, of 3, 370 HBsAg-positive patients, 986 had prior anti-HDV testing. Of the remaining 2, 384, 2, 293 (96%) were tested for anti-HDV, with 109 (4.7%) testing positive. HDV RNA was tested in 97 of these 109 patients (89%), resulting in 30 patients (1.3% of all HBsAg-positive, 31.6% of HDV-RNA tested) being identified as HDV-RNA positive. In the cost-effectiveness analysis, we observed a cost

POSTER PRESENTATIONS

saving of €132 per HBsAg positive screened of anti-HDV patient and €6, 246 per patient diagnosed with a positive HDV viral load.

Conclusion: Our retrospective analysis reveals an under-diagnosis of HDV in Southern Spain, with only a fifth of HBsAg-positive patients screened for anti-HDV from 2018 to early 2022. Implementing double reflex HDV testing has proven feasible and significantly increases the detection of chronic HDV infection. This approach is crucial in identifying “missing” hepatitis delta patients. Furthermore, our findings suggest that reflex testing for HDV in HBsAg-positive patients is an efficient strategy.

FRI-410

Mitochondrial dysfunction and metabolic plasticity in the hepatitis B virus specific immune response: new insights and implications for hepatitis B virus cure

Saima Ajaz¹, Riham Soliman¹, James Lok¹, Kosh Agarwal¹. ¹Institute of liver studies, King's College Hospital NHS Foundation Trust, London, United Kingdom

Email: saima.ajaz@nhs.net

Background and aims: Hepatitis B virus (HBV) is a leading cause of cirrhosis and hepatocellular carcinoma. Chronic infection is characterized by an exhausted adaptive immune response in which there is reduced proliferative capacity and altered ATP biogenesis. Our aim was to explore the metabolic profile of these immune cells in more detail, including amongst those treated with nucleos(t)ide analogues (NUC).

Method: For this cross-sectional study, adult subjects were divided into three groups: Group 1 (healthy controls, HC, n = 10), Group 2 (chronic HBV infection, NUC suppressed, n = 16) and Group 3 (chronic HBV infection, not currently treated, n = 6). Peripheral blood mononuclear cells were extracted from whole blood using density gradient centrifugation and 300, 000 cells/well were selected for downstream analysis. Oxygen consumption rate (OCR; basal, ATP-linked, and maximal), extracellular acidification rate (ECAR) and reserve capacity were assessed using the Seahorse XFp analyzer (Agilent Technologies). Dependency of mitochondrial respiration for different substrates was explored using the XFp Cell Mito Stress Test Kit, including selective inhibition of glucose, glutamine, and long chain fatty acid pathways.

Results: Subjects were matched for key demographic characteristics, including age (45.5 ± 9.9), sex (male: female ratio of 12:10) and BMI (29 ± 6.5 kg/m²). HBV-infected individuals demonstrated greater reliance on glucose for ATP generation, irrespective of their treatment status; however, they were significantly less efficient at oxidative phosphorylation when compared to healthy controls (ATP-linked respiration rate 14.6 ± 5.7 vs 87.8 ± 47 pmol/min, p = 0.006). Inhibition of glucose pathway led to an increase in maximal respiration rate amongst HBV patients who were not currently treated (315 pmol/min versus 221 pmol/min); this indicates metabolic flexibility and the potential to activate alternative pathways. Similar compensatory mechanisms were not observed in the NUC-suppressed population, as shown by a reduction in maximal respiration after glucose interference (202 pmol/min versus 312 pmol/min). The same cohort also demonstrated a lower basal respiration rate (93.5 ± 22 pmol/min, p < 0.05), compared with HC (193.5 ± 38 pmol/min) and individuals not on NUCs (192.4 ± 45 pmol/min).

Conclusion: In chronic HBV infection, the adaptive immune response preferentially upregulates glycolysis at the expense of oxidative phosphorylation. This phenomenon, which is reminiscent of the Warburg effect, may contribute to their exhausted phenotype and ultimately HBV persistence. We demonstrate that these immune cells are adaptable and can promote alternative metabolic pathways under the right conditions; manipulation of their metabolic profile, perhaps in combination with checkpoint modulation, represents a viable therapeutic strategy.

FRI-411-YI

Proportions of indeterminate phase of patients with chronic hepatitis B virus infection according to different international guidelines

Shaoqiu Zhang¹, Chao Jiang², Jian Wang^{1,3}, Zhiyi Zhang⁴, Fei Cao⁴, Li Zhu⁵, Ye Xiong⁴, Tao Fan⁴, Xiaomin Yan¹, Yuxin Chen⁶, Chuanwu Zhu⁵, Xingxiang Liu⁷, Jie Li^{1,3,4}, Chao Wu^{1,3,4}, Rui Huang^{1,2,3,4}. ¹Department of Infectious Diseases, Nanjing Drum Tower Hospital, Affiliated Hospital of Medical School, Nanjing University, Nanjing, China; ²Department of Infectious Diseases, Nanjing Drum Tower Hospital Clinical College of Jiangsu University, Nanjing, China; ³Institute of Viruses and Infectious Diseases, Nanjing University, Nanjing, China; ⁴Department of Infectious Diseases, Nanjing Drum Tower Hospital Clinical College of Nanjing University of Chinese Medicine, Nanjing, China; ⁵Department of Infectious Diseases, The Affiliated Infectious Diseases Hospital of Soochow University, Suzhou, China; ⁶Department of Laboratory Medicine, Nanjing Drum Tower Hospital, Affiliated Hospital of Medical School, Nanjing University, Nanjing, China; ⁷Department of Hepatology, Huai'an No. 4 People's Hospital, Huai'an, China

Email: doctor_hr@126.com

Background and aims: Definitions of natural phases of chronic hepatitis B virus (HBV) infection vary among international hepatitis B guidelines. A considerable number of patients with chronic HBV infection do not fit into usual phases and were classified into “indeterminate phase.” We compared the proportions of indeterminate phase among different international guidelines.

Method: A total of 9, 694 treatment-naïve patients with chronic HBV infection were included from three medical centers. Patients were classified as different natural phases according to guidelines by the 2018 American Association for the Study of Liver Diseases (AASLD), the 2017 European Association for the Study of the Liver (EASL) and the 2015 World Health Organization (WHO). Patients fall outside the defined phases by international guidelines were defined as indeterminate phase. Each natural phase has its corresponding indeterminate phase and thus the indeterminate phase was further divided into four subcategories. Significant liver fibrosis was estimated by non-invasive tests.

Results: The proportion of indeterminate phase of patients with chronic HBV infection was highest according to the definitions by WHO guidelines (36.93%), followed by AASLD guidelines (27.69%) and EASL guidelines (25.96%). The proportion of patients with indeterminate phase increased significantly with age. With regards to different indeterminate phase subtypes, the proportion of indeterminate phase corresponding to HBeAg-negative CHB (HBeAg-negative chronic hepatitis B) was highest according to WHO guidelines (76.54%) followed by EASL (54.43%) and AASLD (38.22%) guidelines (p < 0.001). The proportion of significant liver fibrosis in patients with indeterminate phase were comparable among different international guidelines (EASL: 15.92%; AASLD: 15.21%; WHO: 13.79%, p = 0.117). However, patients with indeterminate phase corresponding to HBeAg-negative CHB had a higher rate of significant fibrosis in EASL guidelines (19.38%) compared to AASLD guidelines (16.91%) and WHO guidelines (14.48%) (p = 0.006).

Conclusion: The proportion of indeterminate phase in chronic HBV-infected patients varied among international hepatitis B guidelines and was lowest according to the definition by EASL guidelines. There is no significant difference in the rates of significant liver fibrosis in patients with indeterminate phase among three guidelines. However, patients in the indeterminate phase corresponding to HBeAg-negative CHB had higher proportion of significant liver fibrosis according to EASL guidelines.

FRI-412

Quantification of plasma hdv rna in untreated and bulevirtide-treated patients with chd: a comparison between robogene 2.0, eurobioplex and altostar

Maria Paola Anolli¹, Sara Uceda Renteria², Elisabetta Degasperi¹, Floriana Facchetti¹, Dana Sambarino¹, Marta Borghi¹, Riccardo Perbellini¹, Roberta Soffredini¹, Sara Monico¹, Ferruccio Ceriotti¹, Pietro Lampertico^{1,3}. ¹Division of Gastroenterology and Hepatology, Foundation IRCCS Ca' Granda Ospedale Maggiore Policlinico, Milan, Italy; ²Virology Unit, Foundation IRCCS Ca' Granda Ospedale Maggiore Policlinico, Milan, Italy; ³CRC "A. M. and A. Migliavacca" Center for Liver Disease, Department of Pathophysiology and Transplantation, University of Milan, Milan, Italy
Email: sara.ucedarenteria@policlinico.mi.it

Background and aims: Accurate HDV-RNA quantification is crucial for diagnosis and management of chronic hepatitis Delta, yet a significant variability between assays do exist. We compared three methods to quantify HDV-RNA levels in untreated and Bulevirtide (BLV)-treated CHD patients.

Method: Frozen plasma from untreated and BLV-treated CHD patients were tested in a single-center retrospective study: Robogene HDV-RNA Quantification Kit 2.0 (Roboscreen GmbH; LOD 6 IU/ml on 7500 Fast Real-Time PCR System [Applied Biosystem]), EurobioPlex HDV PCR quantitative (Eurobio Scientific, LOD 100 IU/ml) on CFX96™ real-time PCR detection system [Bio-Rad] and AltoStar HDV RT-PCR Kit 1.5 (Altona Diagnostics; RUO test, estimated LOD <10 IU/ml).

Results: Overall, 429 plasma samples from 130 CHD (69 untreated and 61 BLV-treated) patients were studied. Median HDV-RNA were higher with Robogene than EurobioPlex [3.78 (0.70–7.99) vs. 4.69 (2.00–8.19) Log IU/ml, $p < 0.0001$]. Compared to Robogene 2.0, EurobioPlex reported similar HDV-RNA ($\Delta \pm 0.5$ Log) in 66 (28%) patients but higher >0.5 Log in 160 (69%). Viremia was lower with Robogene than AltoStar [3.32 (0.70–7.37) vs. 3.91 (0.19–7.54) Log IU/ml, $p < 0.0001$]. AltoStar reported HDV-RNA levels >0.5 Log in 127 (52%). Virological response at week 24 (Robogene vs. Eurobio and AltoStar) and 48 (Robogene vs. AltoStar) did not differ. HDV-RNA undetectability rates at week 24 were 11% vs. 33% with Robogene vs. EurobioPlex, and 11% vs. 3% Robogene vs. AltoStar. At week 48, 47 samples collected at on treatment week 48 were analyzed with the three tests: HDV-RNA levels were 3.04 (0.70–6.20) IU/ml vs. 3.62 (2.00–7.12) vs. 3.37 (0.28–6.45) IU/ml with Robogene vs. EurobioPlex vs. AltoStar, respectively ($p = 0.36$). At week 72 HDV-RNA was undetectable in 42%, 83% and 25% of patients, respectively.

Conclusion: HDV-RNA levels quantified by EurobioPlex and Altostar were 1 and 0.5 logs higher than Robogene 2.0, respectively. HDV-RNA undetectability rates during BLV differed according to the method.

FRI-413

Prevalence, fate and implication of gray zone on the trajectory of hepatitis B surface antigen in treatment-naïve young adults with chronic hepatitis B infection

Lung Yi Loey Mak¹, Apostolos Koffas², Grace Dolman², Yu Lei³, Anna Riddell², Upkar Gill², Patrick Kennedy². ¹The University of Hong Kong, Queen Mary University of London, Hong Kong, China; ²Queen Mary University of London, London, United Kingdom; ³Chongqing Medical University, Queen Mary University of London, London, United Kingdom
Email: loeymak@gmail.com

Background and aims: Chronic hepatitis B (CHB) patients designated in the grey zone (GZ) are currently excluded from treatment. We aimed to characterize the prevalence of GZ patients and the dynamic profiles of quantitative hepatitis B surface antigen (qHBsAg) in young adults under long-term follow-up.

Method: Treatment-naïve CHB patients aged ≤ 30 were prospectively recruited with serum qHBsAg (in IU/ml), hepatitis B virus (HBV) DNA (in IU/ml) and alanine aminotransferase (ALT, in U/L) longitudinally

monitored. Disease phases were classified according to EASL guidelines, while GZ was defined when the hepatitis B e antigen (HBeAg)-ALT-DNA profile does not fall into any phases, i.e., GZ-A: HBeAg+, ALT ≤ 40 , HBV DNA $< 1 \times 10^6$; GZ-B: HBeAg+, ALT > 40 , HBV DNA $< 2 \times 10^4$; GZ-C: HBeAg-, ALT ≤ 40 , HBV DNA > 2000 ; GZ-D: HBeAg-, ALT > 40 , HBV DNA ≤ 2000 .

Results: A total of 250 patients were recruited (median age 26 years [interquartile range 22–29], 46.4% male, predominant genotype D, 36% White/43.2% Black/17.6% Asian/3.2% unknown). At baseline, 24% were HBeAg-positive, with 28.4% falling into the GZ (A: 2.4%, B: 0.8%, C: 22.8%, D: 2.4%). Over a median follow-up (FU) of 56.5 months, median qHBsAg decreased from 8255 to 7138 ($p < 0.001$). Interestingly, at long-term FU, 29.2% patients experienced an increase in qHBsAg from baseline, more commonly observed in patients with higher qHBsAg levels at 12 months (OR 2.257, 95% CI 1.120–4.500) and patients showing increase in qHBsAg at 12 months compared to baseline (OR 7.556, 95% CI 2.412–23.667). HBsAg seroclearance was observed in 3.8%. After censoring 13 patients started on nucleoside analogues during FU, the proportion of GZ patients reduced to 19.9% (A: 2.2%, B: 0%, C: 12.9%, D: 4.3%). Proportion of patients achieving qHBsAg < 100 and qHBsAg < 1000 increased from 6.4% to 10.4%, and 15.6% to 21.7%, respectively, at long-term FU. Male gender (OR 2.702, 95% CI 1.031–7.080), baseline qHBsAg (OR 0.015, 95% CI 0.002–0.114), serial change in qHBsAg level (OR 0.036, 95% CI 0.005–0.246) and GZ at 12 months (OR 0.103, 95% CI 0.013–0.833) were associated with achieving qHBsAg < 1000 at long-term FU.

Conclusion: More than 25% of young treatment-naïve CHB patients were designated as GZ and the prevalence declined with age, together with a general decline in qHBsAg. A subset of patients demonstrated serial increase in serum qHBsAg levels over long-term FU. GZ and dynamic increase in qHBsAg were associated with higher qHBsAg levels and should be considered for treatment.

FRI-414

Hepatitis B treatment in Africa: experiences from a scale-up program in Ethiopia

Lasse Rossvoll¹, Hailemichael Desalegn², Fikadu Girma Gudissa³, Dawit Birhanu⁴, Ahmed Hussien⁵, Waqtola Cheneke⁶, Asiya Jeylan³, Esayas Gudina⁶, Nega Berhe⁷, Asgeir Johannessen¹. ¹Vestfold Hospital Trust, Tønsberg, Norway; ²St. Paul's Hospital Millennium Medical College, Addis Ababa, Ethiopia; ³Adama Comprehensive Specialized Hospital Medical College, Adama, Ethiopia; ⁴Dubti General Hospital, Dubti, Ethiopia; ⁵Jigjiga University Sheikh Hassan Yabare Comprehensive Specialized Hospital, Jigjiga, Ethiopia; ⁶Jimma University, Jimma, Ethiopia; ⁷Addis Ababa University, Addis Ababa, Ethiopia
Email: lasse.rossvoll@gmail.com

Background and aims: In sub-Saharan Africa treatment for chronic hepatitis B (CHB) is rarely available, and data on the management of CHB from this region is scarce. In 2021/22 we set up a scale-up CHB treatment program at four regional hospitals in Ethiopia. Here we present early experiences from this public-sector scale-up program.

Method: A total of 5,863 HIV-negative adults with CHB were enrolled between December 2021 and December 2023. The patients were assessed with laboratory tests, including viral markers and liver enzymes. The treatment eligibility criteria were: i) clinically diagnosed cirrhosis, ii) aspartate aminotransferase to platelet ratio index (APRI) ≥ 0.7 , iii) alanine aminotransferase (ALT) > 40 U/L and HBV DNA $> 2,000$ IU/ml, and iv) hepatocellular carcinoma in first-degree relative and HBV DNA $> 2,000$ IU/ml. Tenofovir disoproxil fumarate was the preferred antiviral drug and was provided free of charge.

Results: The median age was 30 years (interquartile range 25–38) and 2,861 (48.8%) patients were women. Coinfection with HCV was uncommon ($n = 92$; 1.6%). Most patients had normal (≤ 40 U/L) ALT ($n = 4,277$; 72.9%) and low (≤ 0.5) APRI ($n = 4,399$; 75.0%). At inclusion, 3,697 (63.1%), 986 (16.8%) and 1,052 (17.9%) had HBV DNA $< 2,000$ IU/ml, 2000–19,999 IU/ml and $\geq 20,000$ IU/ml, respectively.

POSTER PRESENTATIONS

Overall, 2,954 (50.4%) patients were classified as inactive carriers, defined as HBV DNA <2,000 IU/ml and ALT ≤40 U/L. 1,002 (17.1%) patients had APRI ≥0.7, suggestive of cirrhosis. Male sex (adjusted odds ratio (AOR) 3.45; 95% CI 2.93–4.07) and HBV DNA >2,000 (AOR 3.13; 95% CI 2.70–3.62) were independently associated with cirrhosis. In total, 1,571 (26.8%) patients were eligible for treatment at baseline evaluation.

Conclusion: Roughly 25% of the patients were eligible for treatment at enrollment, highlighting the importance of improved access to CHB treatment in sub-Saharan Africa. Another 25% were indeterminate and would need longitudinal follow-up to determine treatment eligibility. The remaining 50% were classified as inactive carriers and could probably have less intensive follow-up.

FRI-415

Hepatitis B virus genotype and some baseline characteristics, but not race, affect HBsAg kinetics during nucleos (t)ide analogue therapy

Rachel Wen-Juei Jeng^{1,2}, Margarita Papatheodoridis³, Yen-Chun Liu^{1,2}, Emilia Hadziyannis⁴, Spiros Manolakopoulos⁴, Rong-Nan Chien^{1,2}, George Papatheodoridis³. ¹Chang Gung Memorial Hospital, Linkou Medical Center, Department of Gastroenterology and Hepatology, Taoyuan, Taiwan; ²Chang Gung University, College of Medicine, Taoyuan, Taiwan; ³National and Kapodistrian University of Athens, General Hospital of Athens "Laiko," Department of Gastroenterology, Athens, Greece; ⁴National and Kapodistrian University of Athens, General Hospital of Athens "Hippokratio," 2nd Department of Internal Medicine, Athens, Greece

Email: gepapath@med.uoa.gr

Background and aims: In a previous multicenter cohort study including chronic hepatitis B (CHB) patients with mixed HBeAg status (89% Asians), there was little impact of ethnicity on HBsAg seroclearance during nucleos (t)ide analogue (NA) therapy (crude hazard ratio: 0.8, Hsu YC et al JID 2021), but the potential impact of ethnicity/race on HBsAg kinetics during NAs remains unclear. We assessed potential differences in HBsAg kinetics between Taiwanese and Greek HBeAg-negative CHB patients.

Method: Non-cirrhotic HBeAg-negative CHB patients (n = 806) from Taiwan (n = 541) and Greece (n = 265) receiving entecavir (ETV) or tenofovir (TDF) were recruited. Baseline host and viral characteristics and NA type were compared between those with and without rapid on-NA HBsAg decline (>0.5 log₁₀ IU/ml/year). Logistic regression identified predictors and a 1:1 propensity score matching for HBV genotypes (GT) B and C/D was performed for sensitivity analysis.

Results: Compared to the Greek, the Taiwanese cohort had greater proportion of males (81% vs. 68%, P < 0.001) and history of past treatment (63% vs. 41%, P < 0.001), increased utilization of ETV (75% vs. 42%, P < 0.001), higher ALT (192 vs. 63 U/L, P < 0.001) and HBV DNA levels (6.5 vs. 5.1 log₁₀ IU/ml, P < 0.001), lower HBsAg levels (3.2 vs. 3.5 log₁₀ IU/ml, P < 0.001) at NA onset, and shorter follow-up (3 vs. 3.9 years, P < 0.001). Multivariate logistic regression identified past treatment history [adjusted Odds Ratio (aOR): 2.03, P = 0.006], ALT > 5x ULN (aOR: 2.18, P = 0.003) and higher HBsAg levels at NA onset (aOR: 3.58, P < 0.001) as independent predictors for on-NA rapid HBsAg decline, while ethnicity/race did not reach statistical significance (aOR: 2.1, P = 0.07). Univariate analysis indicated that patients with GT-C (crude OR: 0.47, P = 0.072) or D (crude OR: 0.23, P < 0.001) compared to GT-B were less likely to experience on-NA rapid HBsAg decline. In the PS-matched cohort, adjusting for characteristic differences between GT-B vs. C/D patients, multivariate logistic regression showed that patients with HBV GT-C/D infection were less likely to have rapid on-NA HBsAg decline (aOR: 0.4, P = 0.02). The predominant impact of HBV GT on HBsAg kinetics occurred in the first year of NA therapy (GT-B vs. GT-C/D: HBsAg reduction: -0.35 vs. -0.12 log₁₀ IU/ml/year, P < 0.001), even after adjusting for ALT, HBV DNA, and HBsAg levels at NA onset. The cumulative incidence of on-

NA HBsAg loss was comparable between different ethnicity/race (log-rank test, P = 0.4) and HBV GTs (log rank test, P = 0.2).

Conclusion: On-NA HBsAg kinetics are mostly affected by HBV GT and baseline characteristics like high ALT and low HBsAg levels, but not by ethnicity/race. HBV GT influences HBsAg reduction primarily within the first year of NA therapy.

FRI-418

10-year clinical outcomes in chronic hepatitis B patients treated with tenofovir in The Gambia, West Africa

Erwan Vo Quang¹, Gibril Ndow², Sulayman Bah³, Rohey Bangura³, Lamin Bojang³, Bakary Dibba³, Sainabou Drammeh³, Alhagie Touray³, Kitabu Jammeh³, Isabelle Chemin⁴, Amie Ceesay³, Gavin Cloherty⁵, Umberto D'Alessandro³, Mark R. Thursz³, Yusuke Shimakawa⁶, Maud Lemoine³. ¹Medical Research Council Unit, London School of Hygiene and Tropical Medicine, Fajara, Gambia; ²Medical Research Council Unit The Gambia, London School of Hygiene and Tropical Medicine, Banjul, The Gambia, Fajara, Gambia; ³Medical Research Council Unit The Gambia, London School of Hygiene and Tropical Medicine, Banjul, The Gambia, Fajara, Gambia; ⁴International Agency for Research on Cancer, Lyon, France, Lyon, France; ⁵Abbott USA, USA, United States; ⁶Institut Pasteur, Paris, France, Paris, France

Email: erwan.voquang@gmail.com

Background and aims: Effectiveness and safety of long-term tenofovir disoproxil fumarate (TDF) in people with chronic hepatitis B virus infection (CHB) has been inadequately documented in Africa. From the longitudinal PROLIFICA study, we evaluated the long-term clinical outcomes of CHB patients treated with TDF in The Gambia.

Method: In this prospective cohort study, we followed-up participants who were consecutively diagnosed with CHB without HCC between 2012 and 2015 in The Gambia. CHB participants eligible to treatment (EASL guidelines) were initiated on TDF, 300 mg daily. The primary outcome was the overall survival in untreated and treated patients.

Results: From December 2011 to October 2015 1,117 treatment naïve CHB participants were recruited, including 141/1,117 (12.6%) initiated on TDF. Treated patients were mainly males (84%) with baseline median age at 35 (IQR: 28–39), median Fibroscan 8.9 (7.0–14.0), including 54/121 (45%) cirrhosis, 3.0% and 7.2% of HCV or HDV coinfections, median HBV DNA 3,474 (IQR: 142–263,720) and eAg positive in 37/131 (28%). During a median follow-up of 6.8 (5.6–8.6) years, 62/1117 (4.3%) died of any cause, including 35/141 (24%) on TDF. Deaths were mostly driven by end-stage liver disease (87.5%) followed by HCC (12.5%). The 1-, 6- and 10-year cumulative survival probabilities in treated patients without cirrhosis, with compensated or with decompensated cirrhosis at baseline were 100%, 95% and 92%; 100%, 97% and 96%, 88%, 63% and 57%; respectively (p < 0.01). The mortality rate among non-cirrhotic patients on TDF was similar to that of untreated and ineligible patients (p = 0.28). Cirrhosis (HR: 8.3, 95%CI 1.6–42.7) and ascites (HR 4.7, 1.4–16.0) were independent predictive factors of mortality at baseline among patients on TDF. Proportion of treated patients with undetectable HBV DNA and ALT normalisation were 66% and 45% at year 6, 93% and 88% at year 10. 31/80 (38%) and 11/25 (44%) had significant liver fibrosis regression at year 6 (p < 0.01) and 10 (p = 0.04), including 17/25 (68%) and 5/6 (83%) of cirrhosis regression, respectively. Adherence to TDF was very good in most patients (70% and 87% at year 6 and 10, respectively). Kidney impairment on TDF was observed in only 2/138 (1.4%) patients and was comparable the rate 10 of 503 untreated CHB patients (2.0%). Bone mass analysis in treated and untreated patients is in progress.

Conclusion: In non-cirrhotic patients, TDF is associated with an excellent safety profile and an overall survival at 10 years, comparable to the survival observed in untreated CHB patients who are ineligible for AVT. The suboptimal survival among cirrhotic patients reflects the lack of early diagnosis of cirrhosis in Africa.

FRI-419

Epidemiological characteristics of hepatitis D virus infection in patients with hepatitis B related hepatocellular carcinoma

Tangnuer Talafu¹, Xinting Li¹, Li Yang¹, Rongjiong Zheng¹, Xiaobo Lu¹.
¹Xinjiang Clinical Research Center for Infectious Disease (Viral Hepatitis), Center for Infectious Disease and Hepatology of the First Affiliated Hospital of Xinjiang Medical University, Urumqi, China
 Email: xjykdLuxiaobo@126.com

Background and aims: The objective of this study was to explore the seroepidemiological features of hepatitis D virus (HDV) infection among individuals diagnosed with HBV-associated primary hepatocellular carcinoma (HCC) at a singular medical center in Xinjiang.

Method: This study employed a single-center, cross-sectional analysis, enrolling 180 patients with HBV-associated HCC hospitalized between December 2021 to May 2023 at the Center for Infectious Disease and Hepatology of the First Affiliated Hospital of Xinjiang Medical University. All patients underwent Anti-HDV IgM, anti-HDV IgG and HDV Ag tests to investigate the epidemiological traits of co-infected HDV in HBV-associated HCC patients, as well as the correlation between HDV and HBV virologic and serologic markers.

Results: Out of the 180 patients, with a mean age of 56.67 ± 9.50 years and 156 (86.67%) being male, 23 (12.78%) were HDV seropositive (HDV-IgM and/or HDV-IgG and/or HDV-Ag) individuals. Epidemiological analysis of HDV seropositive patients indicated a mean age of 56.17 ± 12.90 years, with 19 (82.60%) being males, median ALT of 29 U/L and AST of 44.57 U/L. Vertical transmission accounted for 85% of HBV infections, with no history of intravenous drug use. Stratifying by HBV DNA loads revealed HDV seropositivity rates of 15.7%, 10.3% and 5.6% for HBV DNA <20 IU/ml, 20–2000 IU/ml, and >2000 IU/ml, respectively. Correlation analysis suggested an inverse trend between HDV seropositivity and HBV DNA levels ($p > 0.05$), that is the lower the level of HBV DNA, the higher the rate of HDV seropositivity. Grouping by HBsAg levels (HBsAg <0.05 IU/ml, 0.05–250 IU/ml and >250 IU/ml) showed HDV seropositivity rates of 4%, 7.7% and 18.9% respectively, with a significant positive correlation between HDV seropositivity and HBsAg levels ($p < 0.05$), that is the higher the level of HBsAg, the higher the HDV seropositivity rate. Analysis of disease duration, biochemical indices, and coagulation function and other laboratory indicators revealed no statistically significant differences between HDV seropositivity and negative patients ($p > 0.05$).

Conclusion: The seroprevalence of HDV among patients with HBV-associated HCC at a single center in Xinjiang was found to be 12.78%, indicating a notable prevalence. This underscores the importance of emphasizing the role of HDV in the etiology of hepatocellular carcinoma and suggests potential implications for the strategy of hepatocellular carcinoma prevention.

FRI-420

Serum HBsAg rather than HBV DNA reflects liver HBV transcript levels of hepatitis B patients treated by nucleoside analogues

Wenhua Zhang¹, Haitao Tang¹, Qinghua Lu², Tingxia Chao³, Haifang Cao², Hongfei Zhang⁴, Feng Ren⁵.
¹Gansu Wuwei Tumour Hospital, Wuwei, China; ²The 4th People's Hospital of Qinghai Province, Xining, China; ³Gansu Wuwei Tumour Hospital, Wuwei, China; ⁴Jumei Doctor Group Medical (Shenzhen) Co., Ltd, Shenzhen, China; ⁵Beijing Youan Hospital, Capital Medical University, Beijing, China
 Email: 925944468@qq.com

Background and aims: The therapeutic goal of CHB is to achieve a “functional” cure, which is characterized by sustained HBsAg loss and HBV DNA levels below the lower limit of detection. However, it is almost impossible to achieve sustained HBsAg loss with nucleoside analogues (NAs) treatment. It is poor treatment efficacy and low HBsAg conversion rate for antiviral treatment of CHB patients with high HBsAg levels, although serum HBV DNA levels were below the lower limit of detection or undetectable. Here, we evaluated serum HBsAg and serum HBV DNA, which is better for evaluating HBV

transcriptional activity in liver tissue of hepatitis B patients treated by NAs.

Method: This study was derived from the “Excellence” project-HBV cohort, which consisted of 20 CHB patients (male/11, female/9) with NAs (ETV/TDF/TAF) treatment for a median interquartile range (IQR) of 36 (4–240) months, whose aged 27–58 years and admitted to the hospital from May 2023 to October 2023. Liver histologic biopsy was performed immediately after admission. Intrahepatic HBV covalent closed loop DNA (cccDNA) was quantified by droplet digital PCR (ddPCR), and intrahepatic HBV DNA was quantified by quantitative real-time PCR (qRT-PCR). Intrahepatic HBV cccDNA and HBV DNA parameters were analyzed in relation to serum HBsAg and HBV DNA levels, respectively.

Results: Serum HBsAg levels of all CHB patients with antiviral treatment were greater than 1500 IU/ml, but serum HBV DNA were already at very low or undetectable levels. Interestingly, for CHB patients with no HBV DNA detection in serum, their liver tissues have high levels of HBV DNA (4.880 ± 0.894 , log₁₀ IU/ml) and HBV cccDNA (3.967 ± 0.695 , log₁₀ copies/μL) with significantly positive correlation ($r = 0.772$, $P < 0.0001$). Serum HBsAg level was positively correlated with intrahepatic HBV cccDNA level ($r = 0.673$, $P = 0.0011$), and positively correlated with intrahepatic HBV DNA level ($r = 0.728$, $P = 0.0003$). The serum HBsAg and serum HBeAg level had good correlation ($r = 0.618$, $P = 0.0037$), however, serum HBV DNA and serum HBeAg level were no correlated with intrahepatic HBV cccDNA level and intrahepatic HBV DNA level.

Conclusion: In CHB patients with NAs treatment, serum HBsAg rather than HBV DNA reflects liver HBV transcript levels of hepatitis B patients. It is serum HBsAg level, not HBV DNA level that may comprehensively reflect HBV replication activity and help evaluation of antiviral therapeutic efficacy.

FRI-423

Early treatment of patients with indeterminate HBV viraemia does not improve retention in care and risks overtreating patients who may spontaneously clear HBsAg

Sharon Macleod¹, Fiona Marra², Alison Boyle², Erica Peters³, Rachael Swann³, Ewan H. Forrest⁴, Stephen Barclay⁴.
¹NHS Greater Glasgow and Clyde, Glasgow Royal Infirmary, Pharmacy Department, Glasgow, United Kingdom; ²NHS Greater Glasgow and Clyde, Gartnavel General Hospital, Glasgow, United Kingdom; ³NHS Greater Glasgow and Clyde, Queen Elizabeth Hospital, Glasgow, United Kingdom; ⁴NHS Greater Glasgow and Clyde, Walton Liver Clinic, Glasgow Royal Infirmary, Glasgow, United Kingdom
 Email: sharon.macleod2@ggc.scot.nhs.uk

Background and aims: Current HBV treatment guidelines include recommendations to observe patients with indeterminate viraemia, and/or ALT elevations to establish their true phase of infection. Recent evidence suggests however that many patients persist in the indeterminate phase of infection, leaving the best course of action unclear. We sought to examine the outcomes of patients with indeterminate viraemia with regards to phase of infection, investigation, and initiation of treatment, along with HBsAg loss.

Method: Samples tested for HBV DNA in our health board with a unique patient identifier between 2009 and 2022 were identified from a virology database, and each individual's first and last HBV DNA identified. Viraemia was classed as indeterminate if between 2,000 iu/ml and 20,000 iu/ml and low or high if below or above this range respectively. Adults with indeterminate viraemia, and a minimum of 1 quantifiable viral load at 12 months or later underwent case note interrogation. Data was recorded on demographics, ALT, DNA, liver biopsy, treatment status, HBsAg loss and retention in care. Patients were considered retained in care if they attended their last appointment prior to December 2023, or if relevant discharge, death or transfer out of area. Patients were excluded if case note review demonstrated treatment prior to first recorded DNA.

POSTER PRESENTATIONS

Results: 26, 522 DNA samples relating to 3, 422 individuals were identified. Of these 1, 1615 had two samples ≥ 12 m apart (median 59 m, IQR 67), of which 236 (14.6%) were indeterminate (996 (61.7%) low 383 (23.7%) high). 14 indeterminate cases were excluded (13 prior treatment, 1 paediatric). Of the remaining 222, 145 (65.3%) were male, with a median age of 34. 30 (13.5%) also had indeterminate ($1-2 \times$ ULN) ALT and 10 (4.5%) high ALT. 11 were born in the UK, with Asia (89) and Africa (67) the most common regions of origin. At 12 months low/indeterminate/high viral loads were seen in 96 (43.2%), 84 (37.8%) and 18 (9.9%) respectively, whilst 22 (9.9%) had commenced treatment. 24 (10.8%) underwent liver biopsy at some point during assessment, of whom 11 received treatment. At last assessment viral loads were high/indeterminate/low or undetectable in 11 (5) %, 61 (27.6%) and 93 (42.1%), including 15 patients (6.8%) who had HBsAg loss. 56 patients (25.3%) received treatment by end of follow-up, 28 within 18 months and 28 beyond. Retention in care was not influenced by starting treatment by 18 months (71.4% vs 69.6%, $p = 0.84$).

Conclusion: In this cohort 1:4 individuals with initial indeterminate DNA required treatment per current guidelines. Earlier treatment of those with indeterminate HBV DNA levels will simplify care and may avoid liver biopsy, though the minority underwent this. 42% of patients had low level viraemia at the end of follow-up including 6.8% with HBsAg loss who would be overtreated. Early treatment did not appear to influence retention in care.

FRI-424

Effectiveness of immunoprophylaxis for preterm infants of mothers having chronic hepatitis B virus infection: a retrospective study

Guanlun Zhou¹, Guorong Han¹, Yuhao Ju¹, Yan Chen¹, Chao Chen¹. ¹The Second Hospital of Nanjing, Nanjing, China
Email: gl270408@163.com

Background and aims: The long-term effectiveness of immunoprophylaxis for preterm infants delivered by mothers with hepatitis B virus (HBV) infection remains unclear. This study aimed to investigate the effectiveness and indicators of immunoprophylaxis in preterm infants.

Method: 2238 infants delivered by HBsAg-positive mothers were enrolled, including 175 preterm infants and 2063 full-term infants. Preterm infants were administered 10 μ g of hepatitis B vaccine immediately after birth and at one, two and seven months while full-term infants received vaccine immediately after birth and at one and six months. All infants were followed up till 24 months. Effectiveness of immunoprophylaxis in preterm infants was analyzed by comparing the dynamics of HBV mark (HBV-M) and responsible factors were investigated using multivariate regression analysis.

Results: The differences in the HBsAb titers between groups were not statistically significant at 7–12 and 24 months of age ($p > 0.05$), but the titers in the preterm group were lower relative to the full-term group. There were no significant differences ($p > 0.05$) between the two groups for medium-to-high responses of HBsAb at 7–12 and 24 months. Multivariate logistic regression analysis showed that Apgar score at one minute (2.687 [1.116, 6.472]) was a predictor of medium-to-high response of HBsAb at 7–12 month.

Conclusion: HBsAb titers in preterm infants delivered by HBV-infected mothers who were vaccinated following the “0–1–2–7” immunoprophylaxis protocol were similar to those in full-term infants, thereby indicating good outcomes. One-minute Apgar score could be used to predict HBsAb levels in preterm infants at 7–12 months of age after completion of the immunoprophylaxis regimen.

FRI-425

Hepatitis B core-related antigen (HBcrAg) in a prospective French hospital database on chronic hepatitis B (HBVbiomark)

Erwan Vo Quang¹, Stéphane Chevaliez¹, Scoazec Giovanna², Varaut Anne², Giuliana Amaddeo², Amal Boukraa², Mélanie Simoes²,

Anne Laure Mazialivoua², Alexandre Soulier¹, Valérie Ortonne¹, Olivia Garrigou¹, Jean-Michel Pawlotsky¹, Vincent Leroy², Patrick Ingiliz². ¹INSERM U955, Creteil, France; ²Hopital Henri-Mondor, Creteil, France

Email: patrick.ingiliz@aphp.fr

Background and aims: Hepatitis B core-related antigen (HBcrAg) is a composite marker consisting of HBcAg, HBeAg and p22cr, suggested to be used in clinical practice in order to predict hepatitis B virus (HBV) disease stages or outcomes. HBcrAg is a translational product of viral transcription, and may be used in addition to such as ALAT, viral load, HBeAg or quantitative HBsAg (qHBsAg) to characterize eAg-negative patients. Here, we assessed HBcrAg levels in a French mono-centric eAg-negative HBV database.

Method: HBVbiomark is a prospective cohort of HBV patients followed-up in the outpatient department of the Henri-Mondor Hospital in Créteil, France. After informed consent, patients clinical, virological and treatment data are captured on an annual basis, and blood samples are stored for investigation of novel biomarkers. HBcrAg is measured by chemiluminescence method using the automatic Lumipulse G600 II analyzer (Fujirebio Inc, Japan) according to the manufacturer's instructions. HBsAg-positive/HBeAg-negative subjects were classified according to EASL guidelines as: chronic hepatitis B (CHB), e-negative infection (ENI) and grey zone (GZ, -viral load >2000 IU/ml and normal ALT, or viral load <2000 IU/ml and elevated ALT).

Results: Since May 2023, 348 patients have been included and 233 were eAg negative. The median age is 46 years (IQR: 37–58), and 70% are male. 91% of patients were born outside France, most of which (63%) in sub-Saharan Africa. The median ALT level is 27 U/L, the median liver stiffness value is 5 kPa (IQR 4.3–6.2), the median HBV DNA level is 25 U/L (IQR 10–695 IU/ml), the median HBsAg level is 2746 IU/ml (583–11988 IU/ml) and the median HBcrAg level 2.5 (IQR 2.0–3.3) log U/ml. About half of the patients (44%) were on antiviral treatment. 90/233 (74.6%) were classified as ENI, 104/233 (45%) as CHB, and 39/233 (17%) as GZ. HBcrAg levels were 2.3, 2.75, and 2.6 log IU/ml in ENI, CHB, and GZ respectively ($p = 0.08$), and treatment duration did not change HBcrAg levels. Proportion of patients with HBcrAg levels above 3 log IU/ml was different across CHB, ENI and GZ, with 44%, 26% and 31%, respectively ($p = 0.03$). No correlation was found with HBV viral load and quantitative HBsAg levels.

Conclusion: HBcrAg may help to define disease stages more accurately, especially for the so-called grey zone in e-negative patients, and the inactive carrier state in patients from Sub-Saharan Africa. Our cohort will further study the relation of novel biomarkers and disease progression.

FRI-426

Comparing the impact of Interferon-based and direct-acting agents therapies on HBsAg seroclearance rates in patients with hepatitis B and hepatitis co-infection

Cheng Er Hsu¹, Yen-Chun Liu¹, Rachel Wen-Juei Jeng¹, Ya-Ting Cheng¹, Yi-Chung Hsieh¹, Wei Teng¹, Rong-Nan Chien¹, I-Shyan Sheen¹, Chun-yen Lin¹. ¹Chang Gung Memorial Hospital, Linkou Branch, Taiwan, Taoyuan, Taiwan
Email: rachel.jeng@gmail.com

Background and aims: The treatment approach for chronic hepatitis C (CHC) has shifted from interferon-based regimens (IFN) to direct-acting agents (DAAs) due to enhanced tolerance and increased sustained virological response (SVR) rates. While pegylated interferon remains a primary therapy for chronic hepatitis B, it is unclear whether HBsAg seroclearance rates in coinfecting HBV/HCV patients in an HBV-endemic country, where most HBV infections are acquired perinatally, are higher with IFN-based regimens compared to DAAs, which specifically target HCV. This study aims to compare HBsAg seroclearance rates in HBV/HCV coinfecting patients treated with IFN-based or DAA regimens.

Method: Retrospective analysis was conducted on two cohorts from Chang Gung Memorial Hospital, Linkou branch: the IFN-based CHC cohort (July 2002–January 2017) and the DAA CHC cohort (March 2015–December 2019). The study focused on CHC patients with a pre-therapy HBsAg seropositive status, including those with available follow-up HBsAg serostatus and achieved SVR. Cox regression analysis identified independent factors for HBsAg seroclearance. Propensity score matching (PSM) addressed heterogeneity between the IFN and DAA groups, adjusting for age, gender, ALT levels, and qHBsAg levels at start of anti-HCV treatment. Kaplan-Meier analysis and log-rank tests compared the cumulative HBsAg seroclearance incidence between the two groups.

Results: Among 356 HBV/HCV coinfecting patients achieving SVR, 130 received IFN-based treatment, and 226 received DAA treatment. The IFN group was younger age (51.3 vs. 59.9 years, $p < 0.001$), predominantly male (69% vs. 54%, $p = 0.0067$), and higher baseline ALT levels (89.5 vs. 50.0 U/L, $p < 0.001$), and longer follow-up (median: 10.3 vs. 4.3 years, $p < 0.001$), had comparable pretherapy HBsAg levels (185 vs. 103 IU/ml, $p = 0.17$). During follow-up, 57 IFN-based and 27 DAA patients achieved HBsAg loss. The 5-year cumulative HBsAg seroclearance rate was numerically higher in IFN than DAA (19% vs. 12%, $p = 0.194$). Multivariate Cox regression identified pre-therapy qHBsAg < 100 IU/ml (aHR: 2.85, $p < 0.001$) and post-therapy qHBsAg < 100 IU/ml (aHR: 3.54, $p < 0.001$) as independent factors for HBsAg loss, while IFN treatment did not reach significance (crude HR: 1.12, $p = 0.67$). After PSM (59 patients in each arm), age, male proportion, and pre-therapy HBsAg level were comparable. The 5-year cumulative HBsAg seroclearance was numerically higher in the IFN arm (28% vs. 13%, $P = 0.172$) but did not achieve statistical significance.

Conclusion: In an HBV-endemic country with HBV/HCV coinfection, IFN-based therapy did not significantly increase the HBsAg loss rate compared to the DAA regimen. This could be attributed to the initially low HBsAg levels in these patients. Lower HBsAg levels at the beginning or end of anti-HCV treatment are independent factors for post-anti-HCV treatment HBsAg loss.

FRI-427

Chronic hepatitis delta with normal ALT and hepatitis D viremia: unravelling its natural history

Muge Ozari Gulnar¹, Habiba Kamal², Adriana Palom³, Sena Arici⁴, Rafael Esteban⁵, Esra Tunç⁶, Onur Keskin⁷, Ramazan Idilman⁴, Maria Buti⁸, Soo Aleman⁹, Cihan Yurdaydin¹⁰. ¹Koc University School of Medicine, Department of Gastroenterology, Istanbul, Turkey; ²Dept of Infectious Diseases, Karolinska University Hospital, Stockholm, Sweden; ³Vall d'Hebron University Hospital, Barcelona, Spain; ⁴Ankara University School of Medicine, Ankara, Turkey; ⁵Hospital Universitari Vall d'Hebron, Barcelona, Spain; ⁶Ankara University School of Medicine Department of Gastroenterology, Ankara, Turkey; ⁷Hacettepe University School of Medicine, Ankara, Turkey; ⁸Hospital Universitari Vall d'Hebron, Barcelona, Spain; ⁹Department of Infectious Diseases, Karolinska University Hospital/Karolinska Institutet, Stockholm, Sweden; ¹⁰Koc University School of Medicine, Department of Gastroenterology, Istanbul Email: muge.ozari@gmail.com

Background and aims: Chronic hepatitis delta (CHD) represents the most severe form of chronic viral hepatitis and the main cause of liver-related mortality due to suboptimal therapy. However, CHD may run a less severe course than in the past (Rosina et al, Gastro 1999, Kamal et al, Hepatology 2020). We had previously described patients with persistent normal ALT and hepatitis D viremia (PNAV) (Arici et al, EASL 2021). The aim of the current study was to increase the size of this patient population and to unravel the natural history of PNAV.

Method: PNAV were arbitrarily defined as patients with normal ALT and hepatitis D viremia on at least three determinations, 3 to 12 months apart within a duration of 2 years among patients who had never received interferon and/or bulevirtide based treatment for CHD. Such patients have been collected between 2014–2023 from the

databases of 2 academic hospitals in Turkey, one in Spain and one in Sweden. A total of 44 PNAV are described. Follow-up was 18 months to 12 years.

Results: The centers in Sweden, Spain and two centers in Turkey contributed a total of 20, 12, 8 and 4 patients from database cohorts of 157, 60, 250 and 50, respectively. Cirrhosis was reported in 12 patients based on imaging studies, and FibroScan or liver biopsy. Endoscopy was performed in 20 patients, small varices were detected in one case only. On long term follow-up two type of patient scenarios evolve: one group of patients continue with normal ALT and viremia, in the other group HDV RNA levels tend to decrease or even became undetectable. The 2 groups did not differ in terms of age, gender, ALT, AST, GGT or platelet count (214 ± 86 [$x \pm SD$] [$n = 25$] vs. 237 ± 81 [$n = 18$], $p = 0.372$) but patients displaying low or undetectable HDV RNA levels (< 1000 IU/ml) appear to have significantly lower qHBsAg levels (7378 ± 5722 vs. 987 ± 1402 , $p = 0.0073$). HDV RNA levels were similar (3.60 ± 1.11 vs. 4.23 ± 1.43 IU/ml). Liver biopsy was available in 10 patients. Histologic activity index and fibrosis stage were lower in PNAVs vs controls (8 [3–13] vs 10 [8–14] and 2 [0–4] vs 3 [2–6], $p = 0.05$ and $p = 0.014$, respectively). In the PNAV group, 2 patients had fibrosis stage 3 and 4 according to Ishak et al and one patient had cirrhosis on biopsy. Three additional patients had clinical or radiologic evidence of cirrhosis. On long-term follow-up patients normal ALT persisted. HDV RNA became undetectable in one patient.

Conclusion: The study suggests that a subgroup of CHD patients present with normal ALT and hepatitis D viremia. The proportional weight of this subgroup in chronic hepatitis D cohorts needs careful assessment. PNAV do not necessarily imply milder disease and advanced fibrosis/cirrhosis may be observed, though clinically significant portal hypertension appears to be rare. Further, 18 (40%) patients developed low levels of viremia and even cleared HDV. The role of qHBsAg levels to predict this latter group needs serious consideration.

FRI-428

Evaluating the effectiveness and safety of tenofovir alafenamide fumarate for preventing mother-to-child transmission of hepatitis B virus

Malipati Aierkenjiang¹, Li Yang², Xiaofeng Sun³, Xiaobo Lu⁴. ¹Infectious Disease and Hepatology No.1 Department, The First Affiliated Hospital of Xinjiang Medical University, Urumqi, China; ²Infectious Disease and Hepatology Department, The First Affiliated Hospital of Xinjiang Medical University, Urumqi, China; ³Infectious Disease and Hepatology No.1 Department, The First Affiliated Hospital of Xinjiang Medical University, Urumqi, China; ⁴Infectious Disease and Hepatology Department, The First Affiliated Hospital of Xinjiang Medical University, Urumqi, China Email: 387663581@qq.com

Background and aims: This investigation addressed the paucity of data on tenofovir allafenamide fumarate's (TAF) utility in preventing mother-to-child transmission (MTCT) of hepatitis B virus (HBV) among infected pregnant women. The study's purpose was to assess the effectiveness and safety of both TAF and tenofovir disoproxil fumarate (TDF) in preventing HBV MTCT.

Method: This single-center retrospective study totally enrolled 97 HBV-infected pregnant women with HBsAg-positive, HBeAg-positive and HBV DNA levels exceeding 200,000 IU/ml. Participants received treatment with either TAF or TDF at 18–24 weeks of gestation at the Center for Infectious Diseases and Hepatology Department of the First Affiliated Hospital of Xinjiang Medical University from September 2018 to September 2021. Follow-up extended to 7 months postpartum. Standardized immunoprophylaxis was administered to infants within 12 hours of birth and at 1 and 6 months of age. The primary end point was the safety of mothers and infants throughout the treatment and follow-up, with secondary end points focusing on the MTCT rate at 7 months postpartum and virologic decline.

POSTER PRESENTATIONS

Results: TAF was administered to 43 pregnant women, while TDF was given to 54; there were 43 and 54 live-born infants respectively, with all mothers and infants completing the 7-month follow-up. After delivery, 87 subjects continued TAF or TDF treatment, and both groups were well-tolerated, without treatment discontinuation due to adverse events. The primary adverse events were puerperal anemia (23%) in the TAF group and perinatal rupture of membranes (16%) in the TDF group, unrelated to the therapeutic agents. Laboratory tests showed no alanine transaminase (ALT) flares during treatment and follow-up. No congenital malformations or defects were reported in infants at birth, and their growth parameters remained within the normal range at 7 months of age, no statistically significant differences were observed between the TAF and TDF groups ($P > 0.05$). Maternal HBV DNA levels exhibited a significant reduction from baseline at delivery, decreasing from 6.44 ± 0.88 to 3.33 ± 1.14 IU/ml in the TAF group, and from 6.57 ± 0.76 to 3.77 ± 0.95 IU/ml in the TDF group, with no statistically significant distinction in the magnitude of reduction between the group ($P > 0.05$). Infants from both groups tested negative for HBsAg, HBeAg, and HBV DNA at 7 months, displaying no statistical variance between the two groups ($P > 0.05$).

Conclusion: The effectiveness and safety of TAF in preventing mother-to-child transmission among HBV-infected pregnant women was similar to that of TDF. This was accompanied by a favorable safety and tolerability profile, and both groups achieved 0% HBV MTCT rate. These findings propose TAF as a viable option for future use in the prevention of mother-to-child transmission of HBV.

FRI-429

Detectable HDV RNA is associated with worse outcome in patients infected with HBV and HDV: results from a meta-analysis

Jackie Bitton¹, Laura Weichselbaum², Christophe Moreno², Pierre Deltenre^{2,3}. ¹Clinique Saint-Luc, Bouge, Belgium; ²CUB Hôpital Erasme, Brussels, Belgium; ³Clinique St-Luc, Bouge, Belgium
Email: pierre.deltenre01@gmail.com

Background and aims: Patients with chronic hepatitis B who are co- or super-infected with hepatitis delta virus (HDV) usually have a more aggressive liver disease than mono-infected hepatitis B virus (HBV) patients. However, whether HDV RNA status is associated with increased risk of liver events in patients with both HBV and HDV infection has not been precisely assessed. We aimed to synthesize the available evidence on whether HDV RNA status is associated with an increased risk of liver-related events in patients infected with HBV and HDV.

Method: Meta-analysis of trials evaluating liver-related events in patients with HBV and HDV infection according to the presence or the absence of detectable HDV RNA. Random effects model was used to obtain a summary estimate of primary outcomes among patients who had detectable HDV RNA vs. those who had undetectable HDV RNA. Differences between groups were expressed as odds ratios (ORs) with 95% CIs. Primary end points were the development of cirrhosis, hepatic decompensation, hepatocellular carcinoma and death or liver transplantation. Heterogeneity was assessed using Cochran's Q test and the I^2 statistic.

Results: Six studies with 1391 HBsAg and HDV antibody positive patients were included. 1089 patients had detectable HDV RNA and 302 had undetectable HDV RNA. Median age ranged between 30 and 49 years and 66% of patients were males. Age and sex ratio did not seem to differ between patients who had detectable HDV RNA and those who had undetectable HDV RNA. The median follow-up ranges between 36 and 233 months. Data on cirrhosis was available for 647 patients, data on decompensation for 702 patients, data on hepatocellular carcinoma for 770 patients and data on death or liver transplantation for 773 patients. Compared to patients with undetectable HDV RNA, patients with detectable HDV RNA had a higher risk of cirrhosis (OR = 4.3, 95% CI = 2.1–8.8, $p < 0.01$) with high heterogeneity between studies ($p = 0.01$, $I^2 = 71\%$), a higher risk of decompensation (OR = 3.2, 95% CI = 1.7–6.1, $p < 0.01$) with moderate

heterogeneity between studies ($p = 0.15$, $I^2 = 43\%$), a higher risk of hepatocellular carcinoma (OR = 2.0, 95% CI = 1.2–3.6, $p = 0.01$) with low heterogeneity between studies ($p = 0.2$, $I^2 = 27\%$) and a higher risk of death or liver transplantation (OR = 3.9, 95% CI = 2.7–5.6, $p < 0.01$) with no heterogeneity between studies ($p = 0.6$, $I^2 = 0\%$).

Conclusion: Patients infected with HBV and HDV who have detectable HDV RNA have a higher risk of liver disease progression including death or the need for liver transplantation than patients with undetectable HDV RNA.

FRI-430

Efficacy and safety of Tenofovir Amibufenamide in the treatment of chronic hepatitis B: a real-world multicenter clinical study

Yaping Li¹, Hongmei Zu², Yongmei Lin³, Guoe Gou¹, Xiaohong Gao⁴, Guang-Hua Xu⁴, Dandan Cui¹, Shuangso Dang¹. ¹The Second Affiliated Hospital of Xi'an Jiaotong University, Xi'an, China; ²The Fourth People's Hospital of Qinghai Province, Xining, China; ³Hanzhong 3201 Hospital, Hanzhong, China; ⁴Affiliated Hospital of Yan'an University, Yan'an, China

Email: dang212@126.com

Background and aims: The clinical profile of Tenofovir Amibufenamide (TMF) in patients with chronic hepatitis B (CHB) requires further clarification. This study evaluates the real-world effectiveness and safety of TMF and compares it to tenofovir disoproxil fumarate (TDF) in a CHB cohort.

Method: In this multicenter, prospective, real-world cohort study, we recruited 183 eligible patients with CHB who attended the outpatient clinic of the Department of Infection of the 4 sites from August 2021 to August 2022. 183 subjects were stratified into TMF ($n = 94$) and TDF ($n = 89$) groups, as well as treatment-naïve (TN) and treatment-experienced (TE) subgroups. We monitored virological response (VR, defined as HBV DNA < 20 IU/ml), alanine transaminase (ALT) normalization rates, renal function markers, and lipid profiles.

Results: In the TN cohort, virological response (VR) rates at weeks 24 and 48 for the TMF group were 42.86% and 90.48%, respectively, compared to 60.00% and 83.33% for the TDF group. The differences in VR rates between TMF and TDF were not statistically significant ($\chi^2 = 3.615$, $p = 0.057$; $\chi^2 = 1.386$, $p = 0.239$). ALT normalization rates for the TMF group were 84.85% and 90.91% according to local laboratory standards, and 56.82% and 70.45% per AASLD 2018 standards. Corresponding rates for the TDF group were 92.59% and 96.30% (local laboratory standards), and 61.90% and 78.57% (AASLD 2018 standards). These differences were also not statistically significant ($\chi^2 = 0.230$, $p = 0.631$; $\chi^2 = 0.744$, $p = 0.388$). Among the treatment-experienced (TE) group, VR rates at weeks 24 and 48 were 65.71% and 82.86%, respectively. The ratios of ALT normalization for the TE group based on local laboratory standards were 86.67% and 93.33%, and according to AASLD 2018 standards, they were 66.67% and 76.67%. The TE group showed a statistically significant difference in ALT normalization following AASLD 2018 standards ($z = -2.822$, $p = 0.005$). VR rates for high-level viremia were similar between TMF and TDF groups ($\chi^2 = 1.635$, $p = 0.201$; $\chi^2 = 0.601$, $p = 0.438$), however, the TMF group showed a more marked reduction in viral load after 24 weeks. Additionally, TMF was associated with improved renal safety over TDF, with no significant difference observed in blood lipid levels between the two treatments.

Conclusion: TMF is comparable to TDF in the efficacy of CHB treatment with no adverse impact on renal function or lipid levels. For TE patients, transitioning to TMF from other antiviral therapies does not compromise antiviral efficacy.

FRI-431

The underestimated burden of hepatitis D among people living with chronic hepatitis B in the Gambia

Erwan Vo Quang¹, Patrick Ingiliz², Amie Ceesay³, Isabelle Chemin⁴, Sainabou Drammeh³, Stéphane Chevaliez⁵, Rohey Bangura³, Jean-Michel Pawlotsky⁵, Bakary Dibba⁶, Kitabu Jammeh⁷,

Vincent Leroy⁸, Sulayman Bah⁷, Lamin Bojang⁶, Mark R. Thursz⁹, Umberto D'Alessandro⁶, Yusuke Shimakawa¹⁰, Maud Lemoine¹¹, Gibril Ndow⁶. ¹Medical Research Council Unit, London School of Hygiene and Tropical Medicine, Fajara, Gambia; ²Hepatology Department, Henri-Mondor University Hospital, INSERM U955, Créteil, France, Créteil, France; ³Medical Research Council Unit The Gambia, London School of Hygiene and Tropical Medicine, Banjul, The Gambia, Banjul, Gambia; ⁴Cancer Research Centre, INSERM, Lyon, France, Lyon, France; ⁵National Reference Center for Viral Hepatitis B, C and delta, Department of Virology, Hôpital Henri Mondor, Université Paris-Est, Créteil, France, Créteil, France; ⁶Medical Research Council Unit The Gambia, London School of Hygiene and Tropical Medicine, Banjul, The Gambia, Fajara, Gambia; ⁷Medical Research Council Unit The Gambia, London School of Hygiene and Tropical Medicine, Banjul, The Gambia, Fajara, Gambia; ⁸National Reference Center for Viral Hepatitis B, C and delta, Department of Virology, Hôpital Henri Mondor, Université Paris-Est, Créteil, France, Créteil, France; ⁹Department of Metabolism, Digestion and Reproduction, Division of Digestive Diseases, Imperial College London, London, UK, London, United Kingdom; ¹⁰Unité d'Épidémiologie des Maladies Émergentes, Institut Pasteur, Paris, France, Paris, France; ¹¹Medical Research Council Unit The Gambia, London School of Hygiene and Tropical Medicine, Banjul, The Gambia, Banjul, Gambia
Email: erwan.voquang@gmail.com

Background and aims: Hepatitis Delta virus (HDV) infection and its clinical impact in people living with chronic hepatitis B virus infection (CHB) have not been well documented in Africa. From a large-scale population-based and hospital-based cohort of CHB patients, we assessed the long-term clinical outcomes of CHB patients with positive HDV serology in The Gambia.

Method: We analyzed CHB patients who were prospectively enrolled in the PROLIFICA cohort study in The Gambia following a large-scale community- and blood bank-based screening intervention and new referral of CHB diagnosis to our liver clinic. All participants had a comprehensive liver assessment including fasting Fibroscan, HBV DNA measurement (GeneXpert, Cepheid) and HDV serology (Diasorin, Italy). The primary end point was the survival probability, and the secondary end point was the proportion of patients who had liver disease progression (≥ 1 stage increase by Fibroscan compared to baseline).

Results: From November 2012 to April 2024, 3, 074 CHB participants were recruited and 2, 504 were screened for HDV. At enrolment, median age was 33 (IQR: 32–45) and 68/2, 504 (12.6%) patients were tested positive for HDV. HDV-positive patients were mainly male (72%), baseline median age 38 (IQR: 32–50), median HBV DNA 176 (10–1, 732), median Fibroscan 8 kPa (5–28), including 34/80 (42.5%) and 17/86 (20%) with cirrhosis and HCC at enrolment, respectively; 6.0% and 3.5% were coinfecting with HIV and HCV. Completion of HDV analysis and genotyping are in progress. Multivariate analysis identified positive HDV serology, male sex, HBeAg positivity, HBV DNA >2000 IU/ml and APRI >2 as risk factors associated with cirrhosis (odds ratio: 8.2 (95%CI: 4.1–16.1, $p < 0.01$; odds ratio: 2.6 (CI: 1.6–4.2, $p < 0.01$; odds ratio: 2.6 (CI: 1.4–4.5, $p < 0.01$; odds ratio: 2.4 (CI: 1.6–3.6); $p < 0.01$; odds ratio: 39.4 (CI: 23.2–70.0); $p < 0.01$, respectively). Of 2, 504 patients, 1, 466 patients (58.5%) attended at least 2 follow-up visits. During a median follow-up of 6.0 (range: 2.1–7.5) years, 72 (4.9%) of the 1, 466 patients died of any cause. The 1-, 5- and 7-year cumulative survival probabilities were lower in HDV positive patients (92%, 84%, 84%, respectively) compared to HDV-negative participants (99%, 96% and 94%) ($p < 0.01$). In the whole cohort of CHB patients, age >40 years (HR 8.90, 2.67–29.71), positive HDV serology (HR 6.42, 2.16–19.14) and HCC (hazard ratio [HR] 27.07, 95% CI 9.25–79.24), were independent predictive factors of overall mortality. Compared to HDV-negative patients, development of cirrhosis but not liver fibrosis progression was more frequently observed in HDV-positive patients ($p < 0.02$).

Conclusion: Positive-HDV serology is frequently observed in individuals living with CHB in The Gambia and is associated with a poor

prognosis, highlighting urgent efforts for screening and care of HDV infection in Africa.

FRI-432

The concentration of HDV-RNA correlates with the probability of developing clinical events in patients with chronic hepatitis D

Adriana Palom^{1,2}, Sergio Rodriguez-Tajes^{2,3}, Ariadna Bono⁴, Antonio Madejón⁵, Ariadna Rando-Segura⁶, Sabela Lens^{2,3}, Marina Berenguer^{2,4}, Francisco Javier Garcia-Samaniego⁵, Juan Carlos Ruiz-Cobo¹, Ángela Carvalho-Gomes^{2,4}, Elena Vargas-Accarino⁷, Mar Riveiro Barciela^{1,2}, Rafael Esteban¹, Maria Buti^{1,2}. ¹Liver Unit, Hospital Universitari Vall d'Hebron, Barcelona, Spain; ²Centro de Investigación Biomédica en Red en Enfermedades Hepáticas y Digestivas, Madrid, Spain; ³Liver Unit, Hospital Clínic de Barcelona, IDIBAPS, Barcelona, Spain; ⁴Hepatology and Liver Transplant Department, Hospital Universitario y Politécnico La Fe, Valencia, Spain; ⁵Liver Unit, Hospital Universitario La Paz, IdiPAZ, Madrid, Spain; ⁶Microbiology Department, Clinical Analysis Laboratory, Hospital Universitari Vall d'Hebron, Barcelona, Spain; ⁷Liver Unit, Hospital Universitari Vall d'Hebron, Barcelona, Spain
Email: mariabutiferret@gmail.com

Background and aims: In patients with hepatitis D, the presence of HDV-RNA in serum is associated with disease progression and the development of clinical events. However, it has not been established whether serum HDV-RNA concentrations could predict clinical events, as is the case with hepatitis B. Our aim was to evaluate the relationship between HDV-RNA concentrations and the risk of developing liver events.

Method: Multicenter retrospective-prospective study including all adult anti-HDV positive patients followed for more than 1 year. HDV-RNA was quantified in an initial sample using an in-house PCR technique with a lower limit of detection (LLD) of 600 IU/ml in a centralized laboratory. Patients were visited every 6 months as per normal practice, and clinical events (decompensation, hepatocellular carcinoma, liver transplant, or liver-related death) were collected during follow-up.

Results: A total of 151 subjects were included; 60.9% male, median age 44 (IQR 36–52) years, all HDV untreated, HDV-RNA 15, 000 (IQR 0–518, 000) IU/ml, ALT 48 (IQR 29–87) IU/ml, and 32 (21%) with liver cirrhosis at inclusion. During a median follow-up of 5.5 (2.2–7.0) years, 25 patients (16.5%) experienced at least one clinical event. Baseline HDV-RNA levels were stratified based on a 1-log increase from the LLD of 600 IU/ml. The studied groups were: <600 IU/ml, between 600–6, 000, >6, 000–60, 000, >60, 000–600, 000, and >600, 000 IU/ml, and clinical events were observed in 4% (1/51), 12% (3/18), 20% (5/19), 24% (6/34), and 40% (10/29) of the patients, respectively ($p = 0.003$). Therefore, HDV-RNA concentrations were positively correlated to the presence of clinical events ($p < 0.001$). However, the rate of subjects with normal ALT was negatively correlated with the HDV-RNA concentrations ($p < 0.001$): 82.4% (42/51), 47.1% (8/17), 33.3% (6/18), 26.5% (9/34), and 21.4% (6/28).

When clustering groups comparing those with HDV-RNA between 600–600, 000 IU/ml and those with HDV-RNA >600, 000 IU/ml, the first group was less likely to present clinical events than the latter (14/71 vs 10/29) ($p = 0.097$). Among the 69 patients without liver cirrhosis, no differences in clinical events were observed between patients with HDV RNA 600–600, 000 vs >600, 000 (5/50 vs 4/19, $p = 0.203$) or normal ALT vs increased ALT (19/49 vs 5/19, $p = 0.250$). From the 24 patients with detectable HDV RNA without cirrhosis and normal ALT, those with 600–600, 000 IU/ml presented less clinical outcomes than those with >600, 000 IU/ml (0/19 vs 2/5) ($p = 0.036$).

Conclusion: The initial concentrations of HDV-RNA positively correlate with the development of clinical events, so their quantification would help predict the risk of clinical outcomes during subsequent follow-up. Moreover, in non-cirrhotic patients with normal ALT, those with initial HDV-RNA levels <600, 000 IU/ml are less likely to present clinical events than those with higher viraemias.

FRI-433

Metabolic dysfunction-associated steatotic liver disease is not independently associated with complete response to oral antiviral treatment in chronic hepatitis B

Juseok Lee¹, Byung Seok Kim¹, Changhyeong Lee¹, Jeong Eun Song¹.

¹Department of Internal Medicine, Daegu Catholic University School of Medicine, Daegu, Korea, Rep. of South
Email: ssong3004@naver.com

Background and aims: The impact of dysfunction-associated steatotic liver disease (MASLD) on treatment response following nucleos (t)ide analogue (NA) treatment for chronic hepatitis B (CHB) patients has not been clearly elucidated. The aim of this study is to investigate the impact of MASLD on complete viral response (CVR) and biochemical response in CHB patients who received NA treatment.

Method: We retrospectively recruited CHB patients receiving NA therapy from January 2014 to December 2020. CHB patients with decompensated cirrhosis or hepatocellular carcinoma were excluded. All patients were divided into CHB group and CHB with MASLD group according to MASLD diagnostic criteria. Therapeutic response related data were recorded and compared at multiple time points. Kaplan-Meier and Cox regression analyses were utilized to estimate the impact of MASLD on complete virological response (CVR).

Results: A total of 460 patients were enrolled (356 CHB without MASLD, 104 CHB with MASLD). The majority of patients were male (55.3%) and HBeAg-positive (55.2%). In comparison to non-MASLD patients, those with MASLD were more likely to be HBeAg-positive (65.4% vs. 52.2%, $p=0.018$), have hypercholesterolemia (22.9% vs. 12.5%, $p=0.009$), and present with a higher mean HBV DNA titer (6.56 ± 1.45 vs. 6.26 ± 1.47 , $p=0.064$). They also had a higher mean BMI (25.3 ± 3.4 vs. 22.9 ± 4.5 kg/m², $p<0.001$) at baseline. Both groups achieved similar rates of ALT normalization (MASLD vs non-MASLD; 100% vs 99.7%, $p=0.588$), and HBsAg seroclearance (2.9% vs 3.7%, $p=0.707$) during the follow-up of up to 65 months. However, MASLD group had lower cumulative rates of CVR at week 96, compared with non-MASLD patients (81.1% vs 91.3%, $p=0.001$). In multivariate analyses, MASLD was not independently associated with CVR outcomes, but higher baseline HBV DNA and HBeAg positivity at baseline was negatively associated with achieving CVR.

Conclusion: The presence of MASLD did not negatively affect CHB treatment outcomes of complete virologic response or biochemical response.

FRI-434

High levels of anti-HBc are associated with higher rates of immune control after 48 weeks of treatment with PegIFN alfa-2a in patients with HBeAg-positive chronic hepatitis B

Maria Pfefferkorn¹, Simon Handrick¹, Melanie Maier², Cynthia Wat³, Thomas Berg¹, Florian von Bömmel¹. ¹Division of Hepatology, Department of Medicine II, Leipzig University Medical Center, Leipzig, Germany; ²Institute of Medical Microbiology and Virology, Leipzig University Medical Center, Leipzig, Germany; ³Roche Products Ltd, Welwyn, United Kingdom

Email: Maria.pfefferkorn@medizin.uni-leipzig.de

Background and aims: The clinical relevance of quantitative antibody levels to HBV core antigen (anti-HBc) as a new biomarker for chronic hepatitis B (CHB) was investigated, but observations on the relationship between anti-HBc levels and treatment response were contradictory. We aimed to investigate the association of anti-HBc levels with other HBV biomarkers and with treatment response to PegIFN alfa-2a.

Method: A total of 132 patients with HBeAg-positive chronic hepatitis B treated with 180 mg/week PegIFN alfa-2a for 48 weeks in three prospective multicenter studies (WV16240, WV16241 and WV19432; Hoffmann-La Roche) were retrospectively analyzed. Patients were analyzed according to week 72 treatment response in three different subgroups: I) patients with ($n=63$) or without ($n=69$)

serological response (SR; defined by HBeAg SC), II) patients with ($n=69$) or without ($n=69$) virological response (VR; HBV DNA levels <2000 IU/ml) and III) patients with ($n=50$) or without ($n=82$) combined response (HBeAg SC and HBV DNA levels <2000 IU/ml). Levels of anti-HBc were measured in samples collected at BL, week 12, 24, 48, and 72 using the anti-HBc II Abbott Architect system and the WHO anti-HBc standard.

Results: Patients with anti-HBc titers >4.0 log IU/ml at baseline had in comparison to patients with anti-HBc titers <4.0 log IU/ml a higher chance of achieving SR (59.1% vs. 43%) VR (72.7% vs. 38.2%) and CR (54.5% vs. 28.0%) while significantly lower probabilities (0% for SR, 28.6% for VR and 0% for CR) were demonstrated for low anti-HBc titers at BL (<2.0 log IU/ml). Interestingly, considering the threshold of 2.5 log IU/ml anti-HBc at BL, in patients with higher anti-HBc (>2.5 log IU/ml at BL) HBV RNA levels were significantly lower at week 48 and 72 (5.4 vs. 7.3 logcp/ml at week 72; $p<0.001$), respectively.

Conclusion: In line with previous studies, HBeAg-positive patients benefit from higher anti-HBc levels at the beginning of PegIFN alfa-2a therapy and low levels (<2.0 log IU/ml) of anti-HBc might be a marker for a low immune response. The association of anti-HBc levels and response to treatment needs to be investigated for other treatments for chronic hepatitis B.

FRI-435

Serological and nucleic acid testing laboratory screening rates for hepatitis delta virus among adult patients in the United States

Robert Wong^{1,2}, Robert G. Gish³, Chong Kim⁴, Gary Leung⁵, Ira Jacobson⁶, Joseph K. Lim⁷, Marvin Rock⁴. ¹Stanford University School of Medicine, Stanford, United States; ²VA Palo Alto Healthcare System, Palo Alto, United States; ³Hepatitis B Foundation, Doylestown, United States; ⁴HEOR-Global Value and Access, Gilead Sciences, Inc., Foster City, United States; ⁵RWE-Epidemiology, Gilead Sciences, Inc., Foster City, United States; ⁶NYU Grossman School of Medicine, New York, United States; ⁷Yale University School of Medicine, New Haven, United States

Email: chong.kim9@gilead.com

Background and aims: Limited data exist regarding hepatitis delta virus (HDV) testing patterns. This study investigated real-world HDV laboratory screening and follow-up nucleic acid testing (NAT) rates among adult patients in the United States (US).

Method: Quest Diagnostics national laboratory data were used to identify US adults who completed at least one anti-HDV test without prior HDV RNA (RNA) testing from 1/1/2015 to 31/12/2022, in order to describe patterns of follow-up RNA testing and repeat anti-HDV testing. More specifically, among patients who tested positive for anti-HDV (anti-HDV-pos), we: a) identified the proportion of patients who completed follow-up RNA testing; b) examined results of RNA testing from patients who completed two rounds of follow-up RNA testing; and c) identified the proportion of patients who completed follow-up anti-HDV testing and had anti-HDV pos or anti-HDV negative (anti-HDV-neg) results.

Results: A total of 49, 272 patients completed anti-HDV testing without prior RNA testing, among whom 917 (1.9%) then completed an RNA test. Among 908 anti-HDV-pos patients, 268 (29.5%) completed follow-up RNA testing, of whom 95 (35.4%) had detectable RNA. Among the anti-HDV-pos patients with detectable RNA, a subsequent 51 (53.7%) patients had at least one additional RNA test, of whom 47 (92.2%) had detectable RNA and 4 (7.8%) had undetectable RNA. Among the 173 anti-HDV-pos patients with undetectable RNA, a subsequent 41 (23.7%) patients had at least one additional RNA test. Among 48, 364 patients who first tested negative for anti-HDV, 649 patients completed follow-up RNA testing, of whom 5 (0.8%) had detectable RNA. Moreover, of the 908 patients who were anti-HDV-pos on their initial anti-HDV test, 227 (25%) completed a second anti-HDV test of whom 127 (55.9%) tested positive and 100 (44.1%) tested

negative. All 4, 134 anti-HDV-neg patients who completed a second anti-HDV test remained negative.

Conclusion: Analyses of laboratory data from 2015 to 2022 showed that among anti-HDV-pos patients, follow-up HDV RNA testing rates are suboptimal. These data emphasise the utility and importance of NAT testing following anti-HDV results.

FRI-436

Are healthcare professionals appropriately screening for hepatitis delta virus in patients with chronic hepatitis B? Results from an interactive decision support app

Sarah Anderson¹, Jacqueline Meredith¹, Zachary Schwartz¹, Maria Buti². ¹Clinical Care Options, Reston, United States; ²Hospital Universitario Vall d'Hebron, CIBEREHD del Instituto Carlos III, Madrid, Spain, Barcelona, Spain
Email: sanderson@clinicaloptions.com

Background and aims: Patient variables that inform hepatitis B virus (HBV) and hepatitis delta virus (HDV) treatment candidacy and selection are complex and interconnected. In deciding whether and how to treat or monitor HBV, healthcare professionals (HCPs) must consider variables including HBeAg, HBV DNA, ALT, fibrosis, bone and renal alterations. In addition, EASL guidelines recommend that *all* people with HBV should be screened for HDV. To aid HCPs in aligning their management decisions with practice guidance, we developed an interactive decision support tool: an app called *Hep B Consult*. In this analysis, we used app results to examine whether HCPs who wanted to follow the EASL guidelines were appropriately working up patients for HBV and HDV.

Methods: In March 2023, Clinical Care Options (CCO) released the *Hep B Consult* app, available as a mobile app and on our website platform. The app enables HCPs to enter patient variables—if known—related to HBV and HDV infection. After the HCP specifies their intended approach, the app presents management recommendations specific to that patient case based on HCP-selected AASLD, APASL, or EASL practice guidance. To determine whether HCPs looking for EASL guidance were properly working up patients with HBV infection and screening for HDV according to EASL guidelines, we examined cases entered between March 3, 2023, and December 8, 2023. In cases where these HCPs marked any patient variables as “unknown” (HBeAg, HBV DNA, ALT, fibrosis, bone and renal alterations, HDV antibodies, HDV RNA), we considered the HCP's workup incomplete. We measured how often HCPs had an incomplete workup and which variables HCPs failed to include.

Results: During the study period, 206 HCPs entered 419 cases after choosing EASL as their preferred HBV guidance. Of the cases entered by HCPs, most were entered by physicians (72.3%), followed by advanced practice nurses (2.4%), and pharmacists (1.2%). Of these cases entered by HCPs who identified their country (n = 212), 61.3% (n = 130) were entered by HCPs from Europe. The highest proportion of cases were entered by HCPs from the United Kingdom (20.8%), followed by Italy (8.0%) and Portugal (6.1%). None of the 419 cases entered was missing HBeAg, HBV DNA, ALT, fibrosis assessment, or bone or renal data. However, *HDV antibodies* were not screened in 25.2% (106/419) of cases. Of the cases entered by HCPs from European countries, HDV antibodies were not screened in 14.6% (19/130). Of the 78 cases where the patient was HDV antibody positive, 8.9% did not have follow-up screening for *HDV RNA*.

Conclusion: HCPs who used the *Hep B Consult* app to enter a patient case demonstrated a comprehensive patient workup *with the exception of HDV status*. This behavior is not aligned with the EASL HDV guidelines, which recommend screening all people who are HBsAg positive for HDV at least once. HCPs need education on the importance of screening all people with HBV for HDV.

FRI-437

Poor Performance of FIB-4 in Fibrosis Prediction for Chronic Hepatitis B Patients with Metabolic Dysfunction-Associated Liver Disease in Daily Clinical Practice

Fadi Abu Baker¹, Saif Abu Mouch¹, Dorin Nicola¹, Randa Taher¹.
¹Technion Faculty of Medicine, Haifa, Israel
Email: Fa_fd@hotmail.com

Background and aims: The coexistence of chronic hepatitis B (CHB) and metabolic dysfunction-associated liver disease (MASLD) has gained recognition, but the diagnostic accuracy of non-invasive markers in this context remains underexplored. This study aimed to evaluate the utility of the FIB-4 index for fibrosis prediction in CHB patients and investigate its performance in the distinct subgroup of CHB-MASLD.

Method: A prospective study from 2021 to 2022 included 109 CHB and 64 CHB-MASLD patients. All underwent liver stiffness measurement via ShearWave Elastography (SWE) and FIB-4 calculation. MASLD criteria were defined, creating CHB-alone and CHB-MASLD groups. Statistical analyses included t-tests, ROC curves, and correlation assessments.

Results: No significant age, gender, or ethnicity differences were observed between CHB and CHB-MASLD groups. CHB-MASLD patients exhibited higher BMI, increased prevalence of obesity, dysglycemia, and dyslipidemia. HBeAg negativity and nucleoside/tide treatment rates were comparable. FIB-4 and APRI scores were elevated in CHB-MASLD. ROC analysis revealed an AUC of 0.86 for FIB-4 in CHB, with an optimal cutoff of 1.95. Subgroup analysis by BMI showed consistent FIB-4 performance. In CHB-MASLD, the ROC curve showed an AUC of 0.61 (p = 0.12) indicating non-significance.

Conclusion: Our study affirms FIB-4's robust performance in predicting fibrosis for CHB patients across varied BMI profiles. Yet, challenges surface when applying FIB-4 to those with concurrent CHB and MASLD. These limitations stress the urgency for refined fibrosis prediction tools, essential for navigating the complex interplay of viral and metabolic factors in the CHB-MASLD population.

FRI-438

Real-world clinical data-driven modelling on the initiation time of peripartum antiviral prophylaxis among pregnant women with chronic hepatitis B virus infection

Naijuan Yao¹, Shihao He², Jing Wang¹, Wenting Zhong¹, Mingwang Shen², Tianyan Chen¹. ¹Department of Infectious Disease, The First Affiliated Hospital of Xi'an Jiaotong University, Xi'an, Shaanxi, China; ²China-Australia Joint Research Center for Infectious Diseases, School of Public Health, Xi'an Jiaotong University Health Science Center, Xi'an, Shaanxi, China
Email: chentianyan@xjtu.edu.cn

Background and aims: Recommendations for when to initiate antiviral prophylaxis for pregnant women with chronic hepatitis B virus (HBV) infection vary in the guidelines. We aim to explore the timing of antiviral prophylaxis for interrupting mother-to-child transmission (MTCT) of HBV in pregnant women with high viral loads using a mathematical model.

Method: We collected the real-world clinical data of 328 treated pregnant women with chronic HBV infection from July 2010 to December 2020 in the First Affiliated Hospital of Xi'an Jiaotong University. We developed a mathematical model to describe the viral kinetics of how HBV DNA levels decrease after antiviral prophylaxis. We calculated how long it would take exactly to decrease maternal viral load below a threshold of 5.3 log₁₀ IU/ml, at which the MTCT risk was negligible (0.04%), to avoid the usually overestimated time needed due to less frequent DNA testing. We derived the prophylaxis initiation time by using the childbirth gestational week of each woman to subtract the above time needed to reach the threshold value. We performed a sensitivity analysis to explore how a lower threshold of 4.0 log₁₀ IU/ml (corresponding to a 0.0% risk of MTCT) would affect the results.

POSTER PRESENTATIONS

Results: The median time for all 328 pregnant women with chronic HBV infection to reduce HBV DNA levels below the threshold of $5.3 \log_{10}$ IU/ml was 4.16 (range: 0.18–12.81) weeks, and it should be initiated to prophylaxis no later than 35.14 (range: 25.19–41.42) weeks. Particularly, prophylaxis initiation time should be no later than 33.93 (range: 25.19–39.45), 35.51 (range: 28.59–39.80), and 36.16 (range: 28.25–41.42) weeks for those women with viral loads $>8.0 \log_{10}$ IU/ml, >7.0 to $\leq 8.0 \log_{10}$ IU/ml, and >5.3 to $\leq 7.0 \log_{10}$ IU/ml, respectively. If the threshold value decreased to $4.0 \log_{10}$ IU/ml, the prophylaxis initiation time should be no later than 33.16 (range: 21.69–39.25) gestational weeks.

Conclusion: It is recommended that pregnant women with high HBV DNA level $>8.0 \log_{10}$ IU/ml should initiate antiviral prophylaxis no later than 25.19 gestational weeks to ensure enough safety. To further prevent MTCT of HBV infection and avoid immunoprophylaxis failures for these women, antiviral prophylaxis should be initiated no later than 21.69 gestational weeks.

FRI-439

An online web-based calculator accurately diagnoses immune tolerant phase in chronic HBV-infected patients

Chi Zhang¹, Yi-Qi Liu¹, Hong Zhao¹, Gui-Qiang Wang¹. ¹Peking University First Hospital, Beijing, China
Email: zhangdoctor@126.com

Background and aims: There were different antiviral treatment strategies and prognoses between immune tolerant (IT) and non-IT in chronic hepatitis B (CHB) patients. However, existing non-invasive diagnostics were not precision. We aimed to explore new non-invasive models for diagnosing IT and assessed the risk of hepatocellular carcinoma (HCC) in IT patients.

Method: We included treatment-naïve CHB patients with liver biopsy who serological met the diagnostic criteria of IT (HBeAg-positive, HBV DNA >5 lgIU/ml, normal ALT). This study included four parts: in step 1, we described the clinical characteristics of IT patients. In step 2, we evaluated the value of non-invasive markers recommended by the guidelines for the diagnosis of IT. In step 3, a new model for the diagnosis of IT with non-invasive markers were developed and validated. In step 4, to assess the risk of developing HCC using 15 HCC prediction models for IT and non-IT.

Results: According to the criteria for the diagnosis of IT by WHO 2015 guidelines, 196 patients were finally included in this study, of which 83 were liver biopsy-proven IT. In the IT group age, qAnti-HBc, ALT, AST and LSM were lower. While, HBV DNA and HBsAg were higher. The risk of non-IT increased 1.2-fold and 3.92-fold in patients aged 30–40 (95%CI 1.00–4.81, $P=0.049$) and >40 years (95%CI 2.28–10.60, $P<0.001$), respectively, compared to those aged <30 years. Compared to HBV DNA >8 lg IU/ml, the risk of non-IT was increased 4.33-fold and 9.96-fold in patients 7–8 lg IU/ml ($p=0.001$) and <8 lg IU/ml ($p<0.001$), respectively. The accuracy of non-invasive marker combinations for the diagnosis of IT did not exceed 0.800, whether in accordance with EASL2017/APASL2015, AASLD2018 or CHINA2019 criteria (0.709, 0.658 and 0.765, respectively). Using univariate analysis, LASSO regression and multivariate analysis, we created a CALA model (qAnti-HBc, LSM, AST, ALP) to diagnosing IT. The AUROC of CALA model reached 0.890 and 0.892 in training and validation sets, respectively, which were significantly higher than APRI, FIB-4 and LSM. For clinical convenience, we have made CALA model in an online web-based calculator and QR code. We included 15 hepatitis B related HCC prediction models (REACH-B, mREACH-BI, mREACH-BII, GAG-HCC, CU-HCC, LSM-HCC, PAGE-B, mPAGE-B, NGM1-HCC, NGM2-HCC, CAMD, RWS-HCC, AASL-HCC, REAL-B, aMAP) by searching the PubMed database. The risk of HCC was significantly lower in biopsy-proven IT than in biopsy-proven non-IT population (all $P<0.01$). Subsequently, the CALA model was used to differentiate IT and the same results were obtained as those confirmed by liver biopsy (all $P<0.01$, except CU-HCC model $P=0.066$).

Conclusion: Online web-based calculator of CALA model can accurately and conveniently diagnose IT. Patients with liver biopsy or CALA model-proven IT were at a lower risk of developing HCC.

FRI-440

HBV precore and basal core promoter mutations exert direct cytopathic effect in humanized mice

Fengmin Lu¹, Guixin Li², Danli Yang¹, Hongsong Chen². ¹Department of Microbiology and Infectious Disease Center, School of Basic Medical Sciences, Peking University, Beijing, China, Beijing, China; ²Peking University People's Hospital, Peking University Hepatology Institute, Beijing Key Laboratory of Hepatitis C and Immunotherapy for Liver Disease, Beijing International Cooperation Base for Science and Technology on NAFLD Diagnosis, Beijing, China, Beijing, China
Email: lu.fengmin@hsc.pku.edu.cn

Background and aims: Basal core promoter (BCP, A1762T/G1764A) and precore (PC, G1896A) combined mutations occur increasingly with age in chronic HBV-infected patients. The association of the combined mutations and disease progression remains ambiguous. This study aimed to explore the effects of BCP+PC combined mutations on pathogenicity.

Method: Human hepatocyte chimeric mice were infected HBV by tail-vein injection with wild-type or BCP + PC mutant viral suspension. Liver samples of mice were collected at pre-designed point. Paraffin liver sections were used either for Hematoxylin and eosin (HandE) or immunohistochemistry (IHC) staining techniques. Total RNA of the liver tissues was extracted and RNA sequencing or RT-qPCR was conducted.

Results: HandE staining revealed that infection with HBV harboring BCP + PC mutations induced more extensive and severe degeneration of hepatocytes, as well as cytoplasmic vacuolation, paralleled with enhanced accumulation of core proteins. However, no significant change of intrahepatic HBsAg was observed in BCP + PC group. Next, transcriptomic analysis was carried out using RNA-Seq to differentiate the molecular characteristics in livers infected with WT and BCP + PC mutant strains. Gene set enrichment analyses implied that BCP + PC mutants might exacerbate hepatocyte injury by inducing endoplasmic reticulum (ER) stress, unfolded protein response, and activating tumor necrosis factor pathway. We also found that the intrahepatic mRNA level of glucose-regulated protein 78, XBP1, activating transcription factor 4, C/EBP-homologous protein, growth arrest and DNA damage 34, ER sulfhydryl oxidase 1 were potentially increased in chimeric mice infected with BCP + PC mutants, suggesting the enhanced ER stress and reactive oxygen species production. Moreover, IHC staining of 8-hydroxyguanine (8-OHdG), a marker of oxidative DNA damage, demonstrated the presence of 8-OHdG-positive cells in BCP + PC groups, whereas few were detected in the WT group.

Conclusion: BCP and PC combined mutations might induce severe hepatocyte damage via aberrant core protein expression in human hepatocyte chimeric mice.

FRI-441

Metabolic dysfunction-associated steatotic liver disease (MASLD) evaluation in HBeAg negative chronic hepatitis B patients: italian cross-sectional observational study

Livio Criscuolo¹, Riccardo Nevola², Alfredo Caturano³, Rosa Cotugno⁴, Martina Di Capua³, Raffaele Galiero³, Marco La Montagna³, Luca Rinaldi⁵, Ernesto Claar⁶, Ferdinando Carlo Sasso³, Grazia Anna Niro⁷, Aldo Marrone³. ¹Ospedali Riuniti Area Stabiese, Internal Medicine and Hepatology Unit, Castellammare di Stabia-Gragnano, Italy; ²AORN San Giuseppe Moscati, Department of Internal Medicine, Avellino, Italy; ³University of Campania Luigi Vanvitelli, Department of Advanced Medical and Surgical Sciences, Naples, Italy; ⁴IRCCS "Casa Sollievo della Sofferenza," Liver Unit, San Giovanni Rotondo, Italy; ⁵University of Molise, Department of Medicine and

Health Sciences, Campobasso, Italy; ⁶Ospedale Evangelico Betania, Liver Unit, Naples, Italy; ⁷IRCCS Casa Sollievo della Sofferenza, Gastroenterology Unit, San Giovanni Rotondo, Italy
Email: aldo.marrone@unicampania.it

Background and aims: Concomitant occurrence of HBV infection and metabolic dysfunction-associated steatotic liver disease (MASLD) has increased worldwide. Patients with chronic hepatitis B (CHB) and MASLD potentially have different pathophysiological conditions than those with MASLD alone. Experimental data suggest that MASLD may inhibit viral replication; conversely, the virus may exert effects on glycid and lipid metabolism. We aimed to evaluate the prevalence of MASLD in patients with CHB and analyze the associated factors.

Method: We conducted a cross-sectional observational study on HBeAg negative CHB Italian patients, enrolled in 2021–2023. The exclusion criteria were HCV and HDV coinfections, significant alcohol consumption, history or active hepatocellular carcinoma, decompensated cirrhosis, contraindications to transient elastography. Demographic, anthropometric, metabolic, laboratory and virological parameters were evaluated in the population. Liver fibrosis was evaluated non-invasively by FibroScan[®] and Fibrosis-4 Index, while SLD was assessed by ultrasonography and controlled attenuation parameter (CAP). Population was divided into two groups setting a threshold at CAP ≥ 248 dB/m to define hepatic steatosis. Logistic regression model was used to identify determinants associated with MASLD. Regression analysis of steatosis based on CAP score and quantitative HBV DNA was performed in HBeAg negative chronic infection subgroup, using Pearson's method.

Results: Study included 149 patients: 58.4% males, with an average age of 57.5 ± 12.3 years; 102/149 (68%) receiving antiviral therapy, among these 48% entecavir and 52% tenofovir. MASLD was observed in 48.3%; impaired fasting blood glucose or diabetes were present in 38.9%. Univariable analysis demonstrated a positive association of several metabolic parameters with MASLD (triglycerides, metabolic syndrome, fasting blood glucose, diabetes, obesity, body mass index-BMI), while inverse relationship between female sex, cirrhosis, HBeAg negative chronic infection and MASLD was revealed. At multivariable logistic regression analysis female gender was linked to a diminished likelihood of MASLD (OR: 0.14; 95% CI: 0.05–0.40; $p = 0.0003$), while both higher BMI (OR 1.41; 95% CI: 1.21–1.65; $p < 0.0001$) and diabetes (OR 6.81, 95% CI: 1.28–36.1, $p = 0.024$) was correlated with an elevated likelihood of MASLD. Regression analysis didn't show a statistically significant correlation between CAP score and HBV-DNA in HBeAg negative chronic infection subgroup ($r = -0.23$; $p = 0.13$).

Conclusion: The prevalence of MASLD by CAP evaluation in patients with CHB observed in our study was similar to that reported by previous studies. Diabetes and BMI represent the only metabolic factors associated with MASLD. MASLD in CHB patients is influenced more by obesity, insulin resistance and female sex hormones than by viral features.

FRI-442

Disease progression and persistent alanine aminotransferase elevation in HCV/HIV persons after DAA-related eradication: role of HBV and HDV co-infections

Roberto Rossotti¹, Alessandro Tavelli², Vincenzo Malagnino³, Valentina Svicher⁴, Eugenia Quiros-Roldan⁵, Alessandra Bandera⁶, Francesco Maria Fusco⁷, Marco Rivano Capparuccia⁸, Giovanni Battista Gaeta⁹, Valentina Mazzotta¹⁰, Massimo Puoti^{11,12}, Antonella D'Arminio Monforte². ¹ASST Grande Ospedale Metropolitano Niguarda, Milan, Italy; ²ICONA Foundation, Milan, Italy; ³Department of Medicine of Systems, University of Rome Tor Vergata, Rome, Italy; ⁴Department of Experimental Medicine, University of Rome Tor Vergata, Rome, Italy; ⁵University of Brescia and ASST Spedali Civili di Brescia, Department of Infectious and Tropical Diseases, Brescia, Italy; ⁶Infectious Disease Unit, Department of Internal Medicine, Fondazione IRCCS Ca, Granda, Ospedale Maggiore Policlinico, Department of Pathophysiology

and Transplantation, University of Milano, Milan, Italy; ⁷UOC Infezioni Sistemiche e dell'Immunodepresso, AORN Ospedali dei Colli, P.O. "D. Cotugno," Naples, Italy; ⁸Infectious and Tropical Disease Unit, Policlinico Umberto I, Department of Public Health and Infectious Diseases, Sapienza University, Rome, Italy; ⁹University L. Vanvitelli, Infectious Diseases Unit, Naples, Italy; ¹⁰Clinical Infectious Diseases Department, National Institute for Infectious Diseases Lazzaro Spallanzani IRCCS, Rome, Italy; ¹¹Infectious Diseases Unit, ASST Grande Ospedale Metropolitano Niguarda, Milan, Italy; ¹²School of Medicine and Surgery, University of Milan-Bicocca, Milan, Italy
Email: roberto.rossotti@ospedaleniguarda.it

Background and aims: Direct-acting antivirals (DAA) allow to achieve sustained virological response (SVR) also in HIV and especially HBV co-infection, whose replication is generally suppressed by HCV with consequent risks of HBV reactivation after eradication. Few data are available about triple/quadruple HIV/HCV/HBV \pm HDV co-infected individuals (3/4CoInf-i) with SVR. Aim of this study is to compare ALT normalization and severe liver-related events in HIV/HCV co-infected vs. HIV/HCV with occult B infection (OBI) vs. 3/4CoInf-i after HCV eradication.

Method: Study population: all HIV/HCV co-infected individuals with available HBV serology enrolled in ICONA/HepalCONA cohorts who achieved SVR after DAAs. Standard survival analysis was used to estimate ALT normalization (i.e., two consecutive values below 42 for men and 30 U/L for females) and two composite clinical outcomes: the first included liver-related events (hepatocellular carcinoma, hepatic decompensation, transplantation, death) in individuals with and without cirrhosis (CO1); the second evaluated only non-cirrhotics who developed a FIB4 increase >3.25 in addition to CO1 (CO2). Univariate/multivariable Cox regression analyses were performed to assess variables associated to these outcomes.

Results: The analysis included 1,182 individuals: 476 HIV/HCV, 650 HIV/HCV + OBI, 56 3/4CoInf-i (HDV serology was available for 33 subjects with 15 positivity). The 3/4CoInf-i had significantly higher proportion of cirrhotics (38.3%) and lower CD4 count (589 cell/mm³, IQR 409–867) and all received ART regimens with anti-HBV activity. This group was associated with lower likelihood to normalize ALT (aHR 0.67, 95%CI 0.47–0.97, $p = 0.035$) but, when HDV co-infection was included in the model, only the quadruple infection retained significance (aHR 0.20, 95%CI 0.05–0.82, $p = 0.025$).

We observed 54 events for CO1 and 104 for CO2. The adjusted models found that age and male sex were positively associated to both CO1 and CO2, while CD4 count was protective for the two outcomes. The 3/4CoInf-i group was not associated with CO1 or CO2.

Conclusion: Age, male sex and CD4 have an impact on disease progression greater than the presence of triple or quadruple infection under active anti-HBV regimens. The 3/4CoInf-i group achieves normal ALT values less commonly after SVR, but this outcome is mediated by HDV. A wide antiviral combination is essential to maintain liver function.

FRI-443

Compassionate use of REP 2165-Mg in chronic HBV/HDV patients with progressive liver disease and failure to previous pegIFN therapy

Gheorghe Placinta¹, Victor Pantea¹, Lilia Cojuhari¹, Valentin Cebotarescu¹, Michel Bazinet², Andrew Vaillant². ¹Nicolae Testemitanu State University of Medicine and Pharmacy, Chişinău, Moldova; ²Replicor Inc., Montreal, Canada
Email: avalliant@replicor.com

Background and aims: REP 2165 is an analog of REP 2139 no longer in development with identical activity to REP 2139 in HBV and HDV in clinical studies (achieving HBV functional cure and HDV cure) but with weaker liver accumulation. REP 2165-Mg drug product from the REP 401 study is being deployed to meet international demand for compassionate access to NAP therapy.

POSTER PRESENTATIONS

Method: Prior to REP 2165-Mg treatment, two chronic HBV/HDV Caucasian patients (1: female 46 y.o. and 2: male 51 y.o.) with rapid progression of liver disease (F3 fibrosis) received therapy with TDF + pegIFN. Patient 1 completed 48 weeks of pegIFN with HDV RNA TND (no HBsAg response) with HDV rebound after removal of pegIFN. After 50 weeks of pegIFN, patient 2 had only achieved a 1 log decline in HDV RNA (no HBsAg response). Existing TDF therapy in both patients was supplemented with weekly IV infusion of 500 mg REP 2165-Mg and 180 µg of pegIFN (pegIFN was uninterrupted in patient 2) scheduled for 48 weeks. Safety and biochemical response were monitored weekly and virologic response every 4 weeks using standard assays for quantitative HBsAg (LLOQ 0.05 IU/ml) and anti-HBs (cutoff for seroconversion 10 mIU/ml), HBV DNA (LLOQ 10 IU/ml) and HDV RNA (LLOQ 10 IU/ml).

Results: Patients 1 and 2 have completed 28 and 30 weeks of combination therapy. IV infusion of REP 2165-Mg in both patients was accompanied by fever and chills requiring supportive therapy for the first 4 weeks. REP 2165-Mg dosing was reduced to 250 mg QW after week 12 due to rapid elimination of HDV RNA. Administration since week 4 was asymptomatic with no supportive therapy and no other AEs have been observed. Patient 1 has experienced three discrete ALT flares during therapy (3× baseline) and patient 2 experienced ALT elevation starting at week persisting at 3× baseline from week 12 onward. ALT flares were otherwise asymptomatic with no changes in liver synthetic function. Patient 1 achieved HDV RNA loss persistent since week 12. HBsAg has declined 1.79 log from baseline (currently 136 IU/ml). Anti-HBs seroconversion has persisted since week 16 (currently 130 mIU/ml). Patient 2 achieved HDV RNA loss persistent since week 8. HBsAg has declined 4.5 log from baseline (currently 0.14 IU/ml). Anti-HBs seroconversion has persisted prior to week 12 (currently 130 mIU/ml).

Conclusion: Although REP 2165-Mg is no longer in clinical development, it demonstrates excellent safety and efficacy against HBV and HDV infection in patients with advanced liver disease with prior pegIFN failure. These results confirm previous clinical data, expand the database of NAP compassionate use and inform on the design of upcoming phase IIA studies.

FRI-444

An initial study of geospatial approach for molecular epidemiology of hepatitis B virus in Indonesia: tale from two regions

Sri Jayanti¹, Turyadi Turyadi¹, Nu'man AS Daud^{2,3}, AM Luthfi Parewangi^{2,3}, Rini Rachmawarni Bachtiar^{2,3}, Irda Handayani⁴, Rina Masadah⁵, Agustiningih Agustiningih¹, Korri Elvanita El Khobar¹, Muhammad Nasrum Massi⁶, David Handojo Muljono^{3,7}, Caecilia Sukowati^{1,8}. ¹Eijkman Research Centre for Molecular Biology, National Research and Innovation Agency of Indonesia, Jakarta, Indonesia; ²Department of Internal Medicine, Dr. Wahidin Sudirohusodo Hospital, Makassar, Indonesia; ³Department of Internal Medicine, Faculty of Medicine, Hasanuddin University, Makassar, Indonesia; ⁴Department of Clinical Pathology, Faculty of Medicine, Hasanuddin University, Makassar, Indonesia; ⁵Department of Pathology Anatomy, Faculty of Medicine, Hasanuddin University, Makassar, Indonesia; ⁶Department of Microbiology, Faculty of Medicine, Universitas Hasanuddin, Makassar, Indonesia; ⁷Faculty of Medicine and Health, University of Sydney, New South Wales, Australia; ⁸Hepatocellular Carcinoma Unit, Italian Liver Foundation ONLUS, Trieste, Italy
Email: srijayanti.arsan@gmail.com

Background and aims: The complexity of the Hepatitis B Virus (HBV) genetic makeup shows variations across different geographical regions, and specific HBV genotypes are associated with distinct clinical implications and treatment responses. While previous studies have identified predominant genotypes, there is a notable lack of a comprehensive geospatial evaluation of hepatitis B genotypes in Indonesia. This emphasizes the need for thorough investigations into

the prevalence of hepatitis B categorized by genotype in different regions.

Method: In our study, we utilized a geospatial approach to analyze the regional molecular epidemiology of HBV genotypes in addition to the determination of HBV subtypes and phylogenetic analysis of genotypes. Two hundred and seventy-eight HBV isolates and their clinical data were obtained from chronic hepatitis B patients located in two distant regions, DKI Jakarta and South Sulawesi, representing western and eastern parts of Indonesia, respectively. HBV surface antigen subtypes (*adw*, *adr*, *ayw*, or *ayr*) were determined using deduced amino acid sequences 122 and 160 in the 'a' determinant region. HBV genotype was determined from DNA sequences of the S gene of HBV DNA subjected to phylogenetic analysis using standard reference sequences. Patients' data were characterized according to demographics, genotype likelihood phylogeny, and geospatial hotspot analysis using Getis-Ord Gi* statistics.

Results: Demographic data showed in Jakarta, the predominant HBV subtypes were 73.7% *adw*, 24.2% *adr*, and 2.1% *ayw*, with no detection of *ayr*. In South Sulawesi, the subtype distribution is more balanced, with 42.9% *adr*, 32.1% *adw*, 21.4% *ayw*, and a minor presence of 3.6% *ayr*. HBV isolates from DKI Jakarta were dominated by genotype B while South Sulawesi was genotype C ($p < 0.0001$). Geospatial analysis uncovered a higher prevalence of genotype C in the northern area of DKI Jakarta, contrasting with a more evenly spread occurrence of genotype B. Meanwhile, the distribution of HBV genotypes B and C in South Sulawesi was largely distributed across the region. Among these two regions, North Jakarta and Makassar appeared as significant hotspot cities for both genotype B and genotype C.

Conclusion: This early study indicates the distinct pattern in hepatitis B molecular epidemiology, emphasizing the necessity for a thorough study of the geospatial distribution of HBV genotypes in Indonesia.

WEDNESDAY 05 JUNE

Viral Hepatitis B and D – Current therapies

WED-390

Efficacy and safety of tenofovir alafenamide fumarate in preventing HBV vertical transmission in high maternal viral load: a multi-centre, prospective cohort study

Xingfei Pan¹, Fang He², Xujing Liang³, Jiangxia Qin⁴, Yanqiu Li⁵, Xueting Ou¹, Zicong Liang¹, Panpan Zhai¹, Liyang Zhou¹, Xiaoping Tang⁶. ¹The Third Affiliated Hospital of Guangzhou Medical University, Guangzhou, China; ²The Third Affiliated Hospital of Guangzhou Medical University, Guangzhou, China; ³The First Affiliated Hospital of Jinan University, Guangzhou, China; ⁴Huadu Maternal and Child Health Hospital of Guangzhou, Guangzhou, China; ⁵Panyu Maternal and Child Care Service Centre of Guangzhou, Guangzhou, China; ⁶Guangzhou Eighth People's Hospital, Guangzhou Medical University, Guangzhou, China
Email: panxf0125@163.com

Background and aims: Prevention of mother-to-child transmission (MTCT) is a key intervention to reduce the prevalence and burden of HBV. Few efficacy and safety data are published regarding tenofovir alafenamide fumarate (TAF) administered during pregnancy. We designed a multi-centre, prospective cohort study to evaluate efficacy and safety of TAF in pregnant women with chronic HBV infection during mid to late pregnancy.

Method: We enrolled pregnant women with HBV DNA levels >200 000 IU/ml. They were randomized to receive TAF or tenofovir disoproxil fumarate (TDF) from 24–35 weeks of gestation until

delivery. All infants received HBV immune prophylaxis as planned. Primary end points were maternal HBV DNA reduction at delivery and infant's hepatitis B surface antigen (HBsAg) positivity at 7 months. Secondary end points were rates of adverse events and defects in infants.

Results: From 1 June 2021 to 31 January 2023, 168 mothers were enrolled from the Third Affiliated Hospital of Guangzhou Medical University, the First Affiliated Hospital of Jinan University, Huadu Maternal and Child Health Hospital of Guangzhou, and Panyu Maternal and Child Care Service Centre of Guangzhou. Baseline characteristics were comparable between 2 groups. In TAF group, 88 mothers were enrolled and 94 infants were born (six pairs of twins). Mean maternal age, gestational age, alanine aminotransferase (ALT) level and HBV DNA load at baseline were 30.2 ± 4.3 years, 28.6 ± 2.4 weeks, 22.4 ± 15.6 U/L and 7.0 ± 1.1 log₁₀ IU/ml, respectively. Twenty (22.7%) cases were of in vitro fertilization, 20 (22.7%) cases had anemia, and 5 cases (5.7%) had gestational diabetes. In TDF group, 80 mothers were enrolled and 83 infants were born (one set of triplets and one pair of twins). Mean maternal age, gestational age, ALT level and HBV DNA load were 30.5 ± 4.4 years, 28.3 ± 2.3 weeks, 31.3 ± 47.6 U/L and 7.1 ± 1.0 log₁₀ IU/ml, respectively. Eleven (13.8%) cases were of in vitro fertilization, 18 (22.5%) cases had anemia, and 4 (5%) cases had gestational diabetes. The median duration of treatment was 10 (1–16) and 11 (3–15) weeks in TAF and TDF groups, respectively. The serum HBV DNA load was reduced by 3.5 ± 1.1 and 3.6 ± 1.2 log₁₀ IU/ml at delivery in TAF and TDF groups with no statistical difference between groups ($p = 0.644$). None of infants were HBsAg positive at 7 months of age. Neither mothers nor infants experienced any serious adverse events during following-up. Seventeen (19.3%) maternal complications (mainly preterm labor and premature rupture of membranes) in TAF group and 12 (15%) in TDF's ($p = 0.460$). Five (5.3%) TAF and 5 (6.0%) TDF cases had fetal intrauterine distress ($p = 0.839$). None of the babies had any congenital defects. There was 1 case of delayed fetal growth and development in both groups and 1 case of slow fetal growth in TDF group during the follow-up.

Conclusion: TAF is as effective and safe as TDF in interrupting MTCT in both mothers and infants.

WED-391

Long-term virological and clinical outcomes of patients with HDV-related compensated cirrhosis treated with bulevirtide monotherapy for up to 120 weeks: a retrospective multicenter european study (save-d)

Elisabetta Degasper¹, Maria Paola Anolli¹, Mathias Jachs², Thomas Reiberger², Victor de Lédighen³, Sophie Metivier⁴, Giampiero D'Offizi⁵, Francesco De Maria⁵, Christoph Schramm⁶, Hartmut Schmidt⁶, Caroline Zöllner⁷, Frank Tacke⁷, Christopher Dietz-Fricke⁸, Heiner Wedemeyer⁸, Margarita Papatheodoridi⁹, George Papatheodoridis⁹, Ivana Carey¹⁰, Kosh Agarwal¹⁰, Florian van Bömmel¹¹, Maurizia Brunetto¹², Mariana Cardoso¹³, Gabriella Verucchi¹⁴, Alessia Ciano¹⁵, Fabien Zoulim¹⁶, Soo Aleman¹⁷, Nasser Semmo¹⁸, Alessandra Mangia¹⁹, Marie-Noëlle Hilleret²⁰, Alessandro Loglio²¹, Uta Merle²², Teresa Santantonio²³, Nicola Coppola²⁴, Adriano Pellicelli²⁵, Bruno Roche²⁶, Xavier Causse²⁷, Louis Dalteroché²⁸, Jérôme Dumortier²⁹, Nathalie Ganne-Carrié³⁰, Frederic Heluwaert³¹, Isabelle Ollivier-Hourmand³², Dominique Roulot³³, Alessandro Federico³⁴, Francesca Pileri³⁵, Monia Maracci³⁶, Matteo Tonnini³⁷, Jean-Pierre Arpurt³⁸, Karl Barange³⁹, Eric Billaud⁴⁰, Stanislas Pol⁴¹, Anne Gervais⁴², Anne Minello Franza⁴³, Isabelle Rosa⁴⁴, Massimo Puoti⁴⁵, Pietro Lampertico^{1,46}. ¹Division of Gastroenterology and Hepatology, Foundation IRCCS Ca' Granda Ospedale Maggiore Policlinico, Milan, Italy; ²Division of Gastroenterology and Hepatology, Department of Internal Medicine III, Medical University of Vienna, Vienna, Austria; ³Hepatology Department, Haut-Lévêque Hospital, Bordeaux, France;

⁴Hepatology Unit, CHU Rangueil, Toulouse, France; ⁵Division of Infectious Diseases-Hepatology, Department of Transplantation and General Surgery, Istituto Nazionale per le Malattie Infettive "L. Spallanzani" IRCCS, Rome, Italy; ⁶Department of Gastroenterology, Hepatology and Transplant Medicine, Medical Faculty, University of Duisburg-Essen, Essen, Germany; ⁷Department of Hepatology and Gastroenterology, Charité Universitätsmedizin Berlin, Berlin, Germany; ⁸Department of Gastroenterology, Hepatology, Infectious Diseases and Endocrinology at Hannover Medical School, Hannover, Germany; ⁹Department of Gastroenterology, General Hospital of Athens "Laiko", Medical School of National and Kapodistrian University of Athens, Athens, Greece; ¹⁰Institute of Liver Studies, King's College Hospital, London, United Kingdom; ¹¹Division of Hepatology, Department of Medicine II, Leipzig University Medical Center, Laboratory for Clinical and Experimental Hepatology, Leipzig, Germany; ¹²Department of Clinical and Experimental Medicine, University of Pisa and Hepatology Unit, University Hospital of Pisa, Pisa, Italy; ¹³Gastroenterology Department, Hospital Prof. Doutor Fernando Fonseca, Amadora, Amadora, Portugal; ¹⁴Department of Medical and Surgical Sciences, Unit of Infectious Diseases, "Alma Mater Studiorum" University of Bologna, S. Orsola-Malpighi Hospital, Bologna, Italy; ¹⁵Department of Medical Sciences, University of Turin, Gastroenterology Division of Città della Salute e della Scienza of Turin, University Hospital, Turin, Italy; ¹⁶Lyon Hepatology Institute, Université Claude Bernard Lyon 1; Hospices Civils de Lyon, INSERM Unit 1052-CRCL, Lyon, France; ¹⁷Infectious Disease Clinic, Karolinska University Hospital, Stockholm, Sweden; ¹⁸Department of Visceral Surgery and Medicine, Inselspital, Bern University, Switzerland, Bern, Switzerland; ¹⁹Liver Unit, Fondazione IRCCS "Casa Sollievo della Sofferenza", San Giovanni Rotondo, Italy; ²⁰Service d'hépatogastro-entérologie, CHU Grenoble-Alpes, Grenoble, France; ²¹Gastroenterology, Hepatology and Transplantation Division, ASST Papa Giovanni XXIII, Bergamo, Italy; ²²Department of Internal Medicine IV, Gastroenterology and Hepatology, Heidelberg University Hospital, Heidelberg, Germany; ²³Department of Medical and Surgical Sciences, Infectious Diseases Unit, University of Foggia, Foggia, Italy; ²⁴Department of Mental Health and Public Medicine-Infectious Diseases Unit, University of Campania Luigi Vanvitelli, Naples, Italy; ²⁵Liver Unit, San Camillo Hospital, Department of Transplantation and General Surgery, Rome, Italy; ²⁶Hepato-Biliary Center, AP-HP Hôpital Universitaire Paul Brousse, Paris-Saclay University, Research INSERM-Paris Saclay Unit 1193, Villejuif, France; ²⁷Hôpital de la Source Orleans, Orleans, France; ²⁸Service d'Hépatogastro-entérologie CHU de Tours, Tours, France; ²⁹Department of Digestive Diseases, Hospices Civils de Lyon, Edouard Herriot hospital, Claude Bernard Lyon 1 University, Lyon, France; ³⁰AP-HP, Avicenne Hospital, Hepatology Department, F-93000 Bobigny, Bobigny, France; ³¹Centre Hospitalier Annecy Genevois, 74000 Annecy, Annecy, Italy; ³²Department of Hepatogastroenterology, CHU de Caen Normandie, Caen, France; ³³AP-HP, Avicenne hospital, Liver Unit, Sorbonne Paris Nord University, Bobigny, France; ³⁴Division of Hepatogastroenterology, Department of Precision Medicine, Università della Campania "Luigi Vanvitelli", Naples, Italy; ³⁵Division of Internal Medicine and Center for Hemochromatosis, University of Modena and Reggio Emilia, Modena, Italy; ³⁶Institute of Infectious Diseases and Public Health, Università Politecnica delle Marche, Ancona, Italy; ³⁷Division of Internal Medicine, Hepatobiliary and Immunoallergic Diseases, IRCCS Azienda Ospedaliero-Universitaria di Bologna, Bologna, Italy; ³⁸Department of Gastroenterology, CH d'Avignon, Avignon, France; ³⁹Department of Gastroenterology, Toulouse University Hospital, Toulouse, France; ⁴⁰Université de Nantes, INSERM UIC 1413, Department of Infectious Diseases, CHU Hôtel Dieu, Nantes, France; ⁴¹Université Paris Cité; Assistance Publique des Hôpitaux de Paris, Hôpital Cochin, Hepatology/Addictology Department, Paris, France; ⁴²Assistance Publique des Hôpitaux de Paris, Hôpital Bichat Claude Bernard, Service des Maladies Infectieuses et Tropicales, Paris, France; ⁴³CHU Dijon, Service d'Hépatogastro-entérologie et oncologie digestive, Inserm EPICAD LNC-UMR1231, Université de Bourgogne-Franche Comté, Dijon, France; ⁴⁴Service d'Hépatogastro-entérologie, Centre Hospitalier Intercommunal, Créteil, France; ⁴⁵School of Medicine and Surgery

POSTER PRESENTATIONS

University of Milano Bicocca, Milan, Italy; ⁴⁶CRC “A. M. and A. Migliavacca” Center for Liver Disease, Department of Pathophysiology and Transplantation, University of Milan, Milan, Italy
Email: elisabetta.degasperi@policlinico.mi.it

Background and aims: Bulevirtide (BLV) has been approved for treatment of chronic hepatitis D virus (HDV) infection in Europe in 2020, however, long-term real-life effectiveness and safety data in large cohorts of HDV patients with cirrhosis treated beyond week 48 are lacking.

Method: Consecutive HDV patients with compensated cirrhosis starting BLV 2 mg/day sc since September 2019 were included in a retrospective multicenter real-life European study (SAVE-D). Clinical, biochemical, virological features and liver-related events were collected. Virological (HDV-RNA undetectable or ≥ 2 -log decline vs. baseline), biochemical (ALT < 40 U/L), combined response (biochemical + virological) and adverse events were assessed. HDV-RNA was quantified locally.

Results: 243 patients receiving BLV monotherapy up to 120 weeks [median follow-up: 72 (range 24–120) weeks] were included: age 49 (IQR 39–58) years, 60% men, ALT 80 (55–130) U/L, liver stiffness measurement (LSM) 18.2 (13.0–26.2) kPa, platelets 94 (68–146) G/L, 100% CPT score A, 52% with varices, 10% HIV-positive, 11% with a history of ascites, 6% with active HCC, 92% on NUC. Baseline HDV-RNA and HBsAg levels were 5.3 (3.4–4.1) log IU/ml and 3.8 (4.1–6.5) log IU/ml, respectively. Virological responses at W24, W48, W72, W96, W120 were 52%, 66% 70%, 77% and 90%, respectively, while HDV RNA undetectability was achieved by 18%, 31%, 42%, 47%, and 52% of patients. Biochemical and combined responses were 53%, 62%, 63%, 65%, 71%, and 33%, 45%, 50%, 51% and 67%, respectively. Patients with < 1 log HDV-RNA decline vs. baseline declined from 23% at W24 to 7% at W96. Responses were similar in HIV positive and negative patients. AST, GGT, albumin, IgG and LSM values significantly improved throughout treatment (LSM baseline 18.2 kPa \diamond 10.0 kPa W120). Lower baseline HDV-RNA was the only predictor of HDV-RNA undetectability at week 48 (HR 0.75; 95% CI 0.60–0.94, $p = 0.01$). Bile acids significantly increased, 8% patients reported mild and transient pruritus, 3% injection site reactions. Overall, 19 (8%) patients discontinued treatment for the following reasons: grade 3 maculopapular rash ($n = 1$), non-compliance ($n = 1$), long-term HDV-RNA undetectability ($n = 2$), virological non-response ($n = 3$), lost to follow-up ($n = 7$); in additional 5 patients, add-on PegIFN to BLV monotherapy was performed. The W120 cumulative incidence of de-novo HCC and decompensation was 4.2% (95% CI 2–7%) and 3.4% (95% CI 1–6%), respectively. 11 patients underwent liver transplantation (HCC $n = 9$; decompensation $n = 2$) and 4 died of BLV-unrelated causes (sepsis, pneumonia, HCC, intestinal infarction).

Conclusion: BLV 2 mg/day monotherapy up to 120 weeks was safe and effective in patients with HDV-related compensated cirrhosis. Virological and clinical responses continued to increase during long-term BLV therapy. Liver-related complications were rare.

WED-392

Improvement in liver histology is observed in most patients with chronic hepatitis delta after 48 weeks of bulevirtide monotherapy

Pietro Lampertico^{1,2}, Soo Aleman³, Pavel Bogomolov⁴, Tatyana Stepanova⁵, Markus Cornberg⁶, Sandra Ciesek⁷, Annemarie Berger⁷, Dmitry Manuilov⁸, Mingyang Li⁸, Audrey H. Lau⁸, Ben L. Da⁸, Grace M. Chee⁸, Maurizia Brunetto^{9,10}, Stefan Zeuzem¹¹, Heiner Wedemeyer⁶. ¹Division of Gastroenterology and Hepatology, Foundation IRCCS Ca' Granda Ospedale Maggiore Policlinico, Milan, Italy; ²Department of Pathophysiology and Transplantation, CRC “A. M. and A. Migliavacca” Center for Liver Disease, University of Milan, Milan, Italy; ³Department of Infectious Diseases, Karolinska University Hospital/Karolinska Institutet, Stockholm, Sweden; ⁴State Budgetary Institution of Health Care of Moscow Region “Moscow Regional Research Clinical Institute Named After M.F. Vladimirovsky,” Moscow, Russian Federation; ⁵LLC Clinic of Modern Medicine, Moscow, Russian

Federation; ⁶Medizinische Hochschule Hannover, Klinik für Gastroenterologie, Hepatologie und Endokrinologie, Hannover, Germany; ⁷Institute for Medical Virology, German Centre for Infection Research, External Partner Site Frankfurt, University Hospital, Goethe University Frankfurt am Main, Frankfurt am Main, Germany; ⁸Gilead Sciences, Inc., Foster City, United States; ⁹Hepatology Unit, Reference Center of the Tuscany Region for Chronic Liver Disease and Cancer, University Hospital of Pisa and Department of Clinical and Experimental Medicine, University of Pisa, Pisa, Italy; ¹⁰Department of Clinical and Experimental Medicine, University of Pisa, Pisa, Italy; ¹¹University Hospital Frankfurt, Department of Medicine, Frankfurt am Main, Germany
Email: ben.da@gilead.com

Background and aims: Patients with chronic HDV (CHD) treated with bulevirtide (BLV) in the Phase 3 study MYR301 showed superior responses at week (W) 48 vs controls based on the combined response end point of virologic response (VR; ≥ 2 log₁₀ IU/ml decline from baseline [BL] or undetectable HDV RNA) and ALT normalization. Recent sub analyses has shown that ALT improvement often occurs discordant of VR with BLV. We now explore the relationship between virologic, biochemical, and histologic change through 48W in MYR301.

Method: In MYR301, patients were randomized 1:1:1 to 144W of BLV 2 mg or 10 mg or control (48W no BLV followed by 96W of BLV 10 mg), with an additional 96W of follow-up after the end of treatment. Liver biopsy was performed per study protocol at BL and W48 in the absence of contraindications. This analysis focused on the patients with paired biopsies. Viral response categories at W48 included VR, partial response (PR; ≥ 1 but < 2 log₁₀ IU/ml) or non-response (NR; < 1 log₁₀ IU/ml). Histologic parameters included histologic activity index (HAI; 0–18), HAI category (0–4), and Ishak fibrosis score (0–6). Improvement in HAI or fibrosis was defined as ≥ 1 point. Histological improvement was defined as ≥ 2 point improvement in HAI with no worsening of fibrosis. The evolution and correlation of laboratory, virologic, and histologic parameters across groups was examined.

Results: Of the 150 randomized patients, 83 (55%) had paired biopsy data: 25-BLV 2 mg, 31-BLV 10 mg, and 27-control. At BL ($n = 83$), mean age 42 years, 52% males, 84% White, 33% with compensated cirrhosis and 61% were on concomitant nucleos(t)ide analogue therapy. Mean HDV RNA and median ALT, HAI, and Ishak fibrosis score was 5.1 log₁₀ IU/ml, 92 U/L, 9, and 2. At W48, 80% (45/56), 11% (6/56), and 9% (5/56) of patients treated with BLV achieved VR, PR, and NR while no control achieved VR. Similar median change in ALT U/L was observed across viral response groups: VR, –51; PR, –56; NR, –64; which was superior compared to control, –11. ALT normalization occurred in most with VR (69%, 31/45) and PR (67%, 4/6) but also occurred in 1 with NR (20%, 1/5) and 2 control (7%, 2/27). Decrease in ALT was observed in 89% (50/56) of BLV treated patients (including all patients with PR ($n = 6$) and NR ($n = 5$)); of those with ALT decrease, 80% (40/50) also had HAI improvement. A higher likelihood of improvement in HAI category and a greater decrease in median HAI from BL was observed with VR: 69% (31/45), –4 and PR: 83% (5/6), –3 compared to NR: 20% (1/5), 0 and control: 30% (8/27), –1. ALT normalization did not have a clear correlation with the degree of HAI improvement. Improvement in fibrosis occurred in VR: 58% (26/45), PR: 33% (2/6), NR: 25% (1/4), and control: 30% (8/27). Histological improvement occurred in VR: 69% (31/45), PR: 83% (5/6); NR: 25% (1/4); and control: 33% (9/27).

Conclusion: Improvement in liver histology is observed in most patients with CHD after 48 weeks of BLV monotherapy.

WED-393

Association between post-treatment ALT elevation and subsequent hepatitis B surface antigen seroclearance in chronic hepatitis B patients stopping nucleos (t)ide analogue therapy

Yao-Chun (Holden) Hsu¹, Ying-Nan Tsai², Jia-Ling Wu³, Cheng-Hao Tseng⁴, Yi-Ling Wu², Shang-Chen Tseng², Chih-Lung Hung², Jaw-Town Lin². ¹E-Da Hospital, Kaohsiung; ²E-Da Hospital, Kaohsiung, Taiwan; ³National Cheng Kung University, Tainan, Taiwan; ⁴E-Da Cancer Hospital, Kaohsiung
Email: holdenhhsu@gmail.com

Background and aims: Serum alanine aminotransferase (ALT) frequently rises after chronic hepatitis B (CHB) patients discontinue nucleos (t)ide analogue (NA). ALT elevation was presumed to be conducive of hepatitis B surface antigen (HBsAg) seroclearance but supporting or refuting evidence was lacking. We aimed to clarify the association between ALT elevation and HBsAg seroclearance following NA cessation.

Method: This is a retrospective, multi-center cohort study based on reviewing all CHB patients who had discontinued NA after being treated for one year or longer between April 01, 2004 and May 24, 2022. Patients with malignancy, hepatic insufficiency, viral coinfections, or organ transplantation were excluded. The primary outcome was the association between ALT flares, defined as ALT >5 times the upper limit of normal (ULN) and HBsAg seroclearance after NA cessation. The incidence of HBsAg seroclearance was estimated using the competing risk analysis to account for informative censoring by retreatment. Time-dependent sub-distribution hazard models were developed to clarify the association of ALT elevation with subsequent HBsAg seroclearance.

Results: A total of 850 patients were eligible (74.5% male, with a median age of 53.2 years). During a median post-treatment follow-up of 3.7 years (IQR, 1.4–6.3), HBsAg seroclearance occurred in 47 patients, at an average annual rate of 1.37% (95% confidence interval [CI], 1.01–1.83%) and a cumulative incidence of 13.2% (95% CI, 9.59–17.39%) at 10 years. Peak serum ALT level post-NA cessation was significantly lower in patients achieving HBsAg seroclearance (median, 77 U/L; IQR, 42–136) compared to those who did not achieve HBsAg seroclearance (median, 127 U/L; IQR, 47–341; $p < 0.0001$). Post-treatment ALT flare was associated with a lower incidence of HBsAg seroclearance (sub-distribution hazard ratio, 0.27; 95% CI, 0.12–0.63). The inverse association between ALT elevation and HBsAg seroclearance was consistently observed in the sensitivity tests with ALT threshold set at $2 \times$ ULN or $1 \times$ ULN. Among the subset of 399 patients with quantitative HBsAg data available at end of treatment (EOT), the association between elevated ALT and HBsAg seroclearance was no longer significant after adjusting for EOT HBsAg levels. In this subgroup analysis, a lower EOT HBsAg level was associated with a higher incidence of HBsAg seroclearance regardless of ALT elevation during the follow-up.

Conclusion: Following NA cessation, patients who experienced ALT elevation, whether the threshold was set at 5-, 2-, or 1-fold ULN, had a significantly lower incidence of subsequent HBsAg loss. No independent association between ALT elevation and HBsAg clearance was noted in the subgroup analyses adjusted for EOT qHBsAg. Our data refutes post-treatment ALT elevation may aid in clearing HBsAg and suggest NA cessation be avoided in patients at risk of ALT flares.

WED-394

Hepatic flares after nucleos (t)ide analogue cessation in HBeAg-negative hepatitis B: results from the Nuc-Stop study

Marte Holmberg^{1,2}, Olav Dalgard^{2,3}, Soo Aleman⁴, Nega Berhe^{1,5,6}, Hailemichael Dessalegn^{5,7}, Nina Weis^{8,9}, Lars Heggelund^{10,11}, Lars Normann Karlsen¹², Pascal Brugger-Synnes¹³, Hans Erling Simonsen¹⁴, Dag Henrik Reikvam^{2,6}, Asgeir Johannessen^{1,2,6}. ¹Vestfold Hospital Trust, Department of Infectious Diseases, Tønsberg, Norway; ²University of Oslo, Faculty of Medicine, Institute of Clinical Medicine, Oslo, Norway; ³Akershus

University Hospital, Department of Infectious Diseases, Lørenskog, Norway; ⁴Karolinska University Hospital, Department of Infectious Diseases, Stockholm, Sweden; ⁵Addis Ababa University, Aklilu Lemma Institute of Pathobiology, Addis Ababa, Ethiopia; ⁶Oslo University Hospital, Department of Infectious Diseases, Oslo, Norway; ⁷St. Paul's hospital Millennium Medical College, Addis Ababa, Ethiopia; ⁸Copenhagen University Hospital, Hvidovre, Department of Infectious Diseases, Hvidovre, Denmark; ⁹University of Copenhagen, Faculty of Health and Medical Sciences, Department of Clinical Medicine, Copenhagen, Denmark; ¹⁰Vestre Viken Hospital Trust, Drammen Hospital, Drammen, Norway; ¹¹University of Bergen, Faculty of Medicine, Department of Clinical Sciences, Bergen, Norway; ¹²Stavanger University Hospital, Department of Gastroenterology, Stavanger, Norway; ¹³Ålesund Hospital, Department of Medicine, Ålesund, Norway; ¹⁴Bodø Hospital, Department of Medicine, Bodø, Norway
Email: marte.holmberg@online.no

Background and aims: Hepatic flares are frequently reported after nucleos (t)ide analogue (NA) cessation and can be detrimental leading to liver injury, hepatic decompensation or even death. We aimed to describe flares and predictive factors for flares after NA cessation in a prospective trial.

Method: This was a sub-analysis of the Nuc-Stop Study, a prospective, randomized, multicenter trial where 127 HBeAg-negative patients, virally suppressed for at least 24 months, stopped NA treatment and were followed up for 36 months. Flares were defined as ALT increase above $2 \times$ upper limit of normal (ULN) and divided into three groups: mild (ALT $2-5 \times$ ULN), moderate (ALT $5-20 \times$ ULN), and severe (ALT $>20 \times$ ULN). The timing and severity of flares were described. Kruskal Wallis tests were used to compare groups. Logistic regression was used to identify predictors of flares.

Results: A flare was observed in 60 (47.2%) patients. The flare was mild in 28 (22.1%), moderate in 22 (17.3%), and severe in 10 (7.9%) patients. Of these, early flares within 3 months after NA cessation, were observed in 33 (55.0%) patients, whereas 8 (13.3%) had a flare between 3 and 6 months, 5 (8.3%) between 6 and 12 months, and 14 (23.3%) after 12 months. Most of the patients had been treated with tenofovir (97, 76.4%), the remaining with entecavir. The median time from treatment stop to first flare was significantly shorter for patients who stopped tenofovir (2.1 months, IQR 1.9–8.4) than for those who stopped entecavir (5.8, IQR 5.1–12.2) ($p = 0.01$). Genotype was known in 115 (90.6%) patients, 35 (27.6%) had genotype B or C and 80 (63.0%) had other genotypes (A, D, E). Median time in months from treatment stop to flare was 5.7 (IQR 2.0–12.2) for patients with genotype B or C and 2.8 (IQR 1.9–6.5) for patients with other genotypes. Median time to severe flares was 2.1 (IQR 1.8–3.0) months; all except one were observed within 6 months after NA cessation. All 10 patients with severe flares had been treated with tenofovir, the median peak ALT was 1403 (range 874–2600) U/L. Median peak HBV DNA was 20 300 000 (IQR 2 300 000–260 000 000) IU/ml, and most commonly occurred on the last visit before peak ALT. ALT declined to normal levels and HBV DNA was fully suppressed after restart of NA therapy. No patients developed decompensated liver disease. Age (per 1-year increment; adjusted odds ratio 1.07; 95% CI 1.02–1.12) and qHBsAg at the time of NA cessation (per 1 log₁₀ IU/ml increment; adjusted odds ratio 1.96; 95% CI 1.12–3.43) were independent predictors of flares.

Conclusion: Flares occurred in half of the patients after NA cessation and were associated with age and qHBsAg level. Severe flares were uncommon, primarily occurred within 6 months, and normalized quickly after restart of NA therapy.

WED-395

Undetectable hepatitis delta virus RNA at the end of treatment with bulevirtide and pegylated interferon alpha-2a is an important predictor of 48 weeks sustained virologic response in chronic hepatitis delta

Fabien Zoulim¹, Tarik Asselah², Vladimir Chulanov³, Adrian Streinu-Cercel^{4,5}, George Sebastian Gherlan^{5,6}, Pavel Bogomolov⁷, Tatyana Stepanova⁸, Viacheslav Morozov⁹, Olga Sagalova¹⁰, Renee-Claude Mercier¹¹, Lei Ye¹¹, Dmitry Manuilov¹¹, Audrey H. Lau¹¹, Grace M. Chee¹¹, Ben L. Da¹¹, Marc Bourliere¹², Heiner Wedemeyer¹³, Pietro Lampertico^{14,15}. ¹Hospital Croix Rousse, Lyon, France; ²Hôpital Beaujon APHP, Université de Paris, INSERM UMR1149, Clichy, France; ³Sechenov University, Moscow, Russian Federation; ⁴Matei Bals National Institute of Infectious Diseases, Bucharest, Romania; ⁵"Carol Davila" University of Medicine and Pharmacy, Bucharest, Romania; ⁶Dr. Victor Babes Foundation, Bucharest, Romania; ⁷M.F. Vladimirovsky Moscow Regional Research and Clinical Institute, Moscow, Russian Federation; ⁸LLC Clinic of Modern Medicine, Moscow, Russian Federation; ⁹LLC Medical Company "Hepatolog," Samara, Russian Federation; ¹⁰South Ural State Medical University, Chelyabinsk, Russian Federation; ¹¹Gilead Sciences, Inc., Foster City, United States; ¹²Hôpital Saint Joseph, Marseille, France; ¹³Medizinische Hochschule Hannover, Klinik für Gastroenterologie, Hepatologie und Endokrinologie, Hannover, Germany; ¹⁴Division of Gastroenterology and Hepatology, Foundation IRCCS Ca' Granda Ospedale Maggiore Policlinico, Milan, Italy; ¹⁵Department of Pathophysiology and Transplantation, CRC "A. M. and A. Migliavacca" Center for Liver Disease, University of Milan, Milan, Italy
Email: renee-claude.mercier@gilead.com

Background and aims: Chronic hepatitis delta (CHD) infection is the most severe form of viral hepatitis. Bulevirtide (BLV), 2 mg, is approved for the treatment of compensated CHD in the European Union. Currently, the clinical relevance of target not detected (TND) versus below the lower limit of quantification (<LLOQ) for HDV RNA levels is unknown. The Phase 2b study MYR204 (NCT03852433) evaluated finite treatment with BLV with or without pegylated interferon alfa-2a (PegIFN) in patients with CHD. Here we compared the ability to maintain the post-treatment virologic response based on achieving undetectable (<LLOQ with TND) HDV RNA or <LLOQ with target detected (<LLOQ, TD) at end of treatment (EOT).

Method: Patients were randomised (N = 174; 1:2:2:2) and stratified based on the absence or presence of compensated cirrhosis to receive (A) PegIFN for 48 weeks (W), (B) BLV 2 mg + PegIFN, (C) BLV 10 mg + PegIFN for 48W followed by 48W of monotherapy with BLV 2 mg or 10 mg, respectively; or (D) BLV 10 mg for 96W. All patients were followed for up to 48W after EOT (FU-48). The primary end point was the proportion of patients who achieved undetectable HDV RNA at 24W post-EOT. HDV RNA levels were determined by RT-qPCR using RoboGene 2.0 (LLOQ 50 IU/ml, limit of detection 6 IU/ml). Virologic response rates at FU-48 were compared between patients with undetectable HDV RNA and those with HDV RNA <LLOQ, TD at EOT.

Results: Demographics and baseline characteristics were similar across groups: male (71%), White (87%), and mean (SD) age 41 (8.7) yrs. Overall, 34% had compensated cirrhosis, 48% received concomitant nucleos (t)ide analogue therapy, and 48% had prior interferon experience. Mean (SD) HDV RNA, alanine aminotransferase, and liver stiffness were 5.3 (1.2) log₁₀ IU/ml, 114 (95) U/L, and 13.1 (7.7) kPa, respectively. At EOT, 42% (73/174) achieved undetectable HDV RNA: A: 21% (5/24), B: 44% (22/50), C: 70% (35/50), and D: 22% (11/50). Additionally, 19% (33/174) were <LLOQ, TD: A: 4% (1/24), B: 18% (9/50), C: 16% (8/50), and D: 30% (15/50). Of the patients with undetectable HDV RNA at EOT, 60% (44/73) maintained undetectable HDV RNA at FU-48: A: 100% (5/5), B: 55% (12/22), C: 60% (21/35), and D: 55% (6/11). Moreover, 29% (21/73) had HDV RNA >LLOQ: B: 27% (6/22), C: 31% (11/35), and D: 36% (4/11). Four patients (5%; 4/73) became <LLOQ, TD, and 5% (4/73) discontinued early by FU-48. Of those who were <LLOQ, TD at EOT, only 6% (2/33) had undetectable HDV RNA (1 each

in groups B and C) and 9% (3/33) remained <LLOQ, TD at FU-48, while 73% (24/33) had HDV RNA >LLOQ; A: 100% (1/1), B: 56% (5/9), C: 63% (5/8), and D: 87% (13/15); 4 discontinued early.

Conclusion: In patients with compensated CHD, achieving on-treatment undetectable HDV RNA with TND is a predictor of undetectable HDV RNA in the post-treatment period. The majority of patients with HDV RNA <LLOQ, TD at EOT had virologic rebound at FU-48.

WED-396

Changes in metabolic parameters after switching from tenofovir disoproxil fumarate to tenofovir alafenamide among chronic hepatitis B patients: a randomized, open-label controlled trial

Titinan Veerachit-O-larn^{1,2}, Thanapat Atthakitmongkol³, Wanwarang Teerasamit⁴, Supot Nimanong³, Siwaporn Chainuvati³, Phunchai Charatcharoenwithaya³, Tawesak Tanwandee³, Watcharasak Chotiyaputta³. ¹Division of Gastroenterology, Department of Medicine, Faculty of Medicine Siriraj Hospital, Mahidol University, Bangkok, Thailand; ²Division of Gastroenterology, Department of Medicine, Siriraj Hospital, Mahidol University, Bangkok, Thailand; ³Division of Gastroenterology, Department of Medicine, Faculty of Medicine Siriraj Hospital, Mahidol University, Bangkok, Thailand; ⁴Division of Diagnostic Radiology, Department of Radiology, Faculty of Medicine Siriraj Hospital, Mahidol University, Bangkok, Thailand
Email: watcharagi@gmail.com

Background and aims: Tenofovir alafenamide (TAF) is increasingly preferred over Tenofovir disoproxil fumarate (TDF) due to its lower nephrotoxicity and bone loss. However, the current data have shown controversy regarding metabolic outcomes among patients treated with TAF compared to those treated with TDF. The aim of this study is to evaluate the effect of TAF and TDF on metabolic parameters in chronic hepatitis B (CHB) patients.

Method: A total of ninety CHB patients treated with TDF were enrolled and randomly assigned to either switch to TAF (TAF group, n = 46) or continue TDF (TDF group, n = 44). Metabolic profiles were assessed at baseline, 24-week, and 48-week intervals through biochemical laboratory tests. Carotid Doppler Ultrasonography was conducted by a single radiologist who was blinded to the study group, evaluating carotid intima-media thickness (CMT) at baseline and at the end of the study. All patients received advice from the dietician nurse and underwent continuous diet monitoring for one year in order to avoid high lipid and high hyperglycemic diets. The primary outcome was the change in lipid profile from baseline.

Results: The mean age of the patients was 59.4 ± 8.2 years, with a male predominance of 63.0%, and the mean body mass index (BMI) was 23.5 ± 4.1 kg/m². The baseline characteristics including BMI, fasting blood sugar (FBS), glycated hemoglobin (HbA1c), total cholesterol (TC), triglyceride (TG), high-density lipoprotein (HDL), low-density lipoprotein (LDL), CMT, and co-morbidities were similar between both groups. At the end of the study, there were significant changes between the TDF and TAF groups in TC (173.6 ± 34.9 and 196.9 ± 37.4 mg/dL, respectively, p = 0.003) and TG (83.2 ± 38.5 and 118.8 ± 78.3 mg/dL, respectively p = 0.007). Significant increases in TC and TG levels were observed in the TAF group compared to the TDF group after 48 weeks of follow-up (p = 0.024 and p = 0.033, respectively). After 48-week, the percentage changes in FBS and HbA1c were significantly greater in the TAF group [FBS; TAF 6.4 ± 10.5% vs TDF 0.6 ± 12.2% (p = 0.017) and HbA1c; TAF 2.1 ± 4.5% vs TDF - 0.03 ± 3.7% (p = 0.015)]. However, no significant differences in HDL and LDL were observed between the groups over 48 weeks. Regarding CMT, both groups had a slight decrease in mean common carotid artery (CCA) thickness and maximum internal carotid artery (ICA) thickness from baseline [CCA thickness; TAF - 5.6 ± 7.3% vs TDF - 2.5 ± 25.1% (p = 0.416) and maximum ICA thickness; TAF - 7.1 ± 18.3% vs TDF - 9.6 ± 18.5% (p = 0.517)]; however, the differences between the two groups were not statistically significant.

Conclusion: Patients with CHB treated with TAF demonstrated a significant increase in metabolic parameters, including TC, TG, FBS, and HbA1c compared to those treated with TDF. However, no differences were observed in HDL, LDL, and CIMT over the 48 weeks of follow-up. (Trial registration number: TCTR20220209003).

WED-397

Tenofovir-based antiviral therapy reduces long-term incidence of hepatocellular carcinoma in chronic hepatitis B patients

W. Ray Kim¹, Young-Suk Lim², Harry L.A. Janssen^{3,4}, Sang Hoon Ahn⁵, Ira Jacobson⁶, Masashi Mizokami⁷, Grace Wong⁸, Frida Abramov⁹, Leland J. Yee⁹, Hongyuan Wang⁹, Catherine Frenette^{9,10}, John F. Flaherty⁹, Scott K. Fung¹¹, Patrick Marcellin¹², Wai-Kay Seto¹³, Kosh Agarwal¹⁴, Jinlin Hou¹⁵, Seng Gee Lim¹⁶, Jia-Horng Kao¹⁷, Maria Buti¹⁸. ¹Mayo Clinic College of Medicine, Rochester, United States; ²Asan Medical Center, Seoul, Korea, Rep. of South; ³Erasmus MC University Hospital, Rotterdam, Netherlands; ⁴Toronto Centre for Liver Disease, Toronto, Canada; ⁵Yonsei University College of Medicine, Seoul, Korea, Rep. of South; ⁶NYU Langone Health, New York, United States; ⁷National Center for Global Health and Medicine, Ichikawa, Japan; ⁸The Chinese University of Hong Kong, Hong Kong, Hong Kong; ⁹Gilead Sciences, Foster City, United States; ¹⁰Scripps Clinic, La Jolla, United States; ¹¹University of Toronto, Toronto, Canada; ¹²Hôpital Beaujon, Clichy, France; ¹³The University of Hong Kong, Hong Kong, Hong Kong; ¹⁴Kings College Hospital, London, United Kingdom; ¹⁵Nanfeng Hospital of Southern Medical University, Guangzhou, China; ¹⁶National University Hospital, Singapore, Singapore; ¹⁷National Taiwan University Hospital, Taipei, Taiwan; ¹⁸Hospital General Universitari Vall d'Hebron, Ciberehd del Instituto Carlos III, Barcelona, Spain
Email: wrkim@stanford.edu

Background and aims: Chronic hepatitis B (CHB) is a leading cause of hepatocellular carcinoma (HCC). Antiviral therapy with nucleot (s)ide analogues (NAs) has been shown to reduce HCC risk. This pooled analysis of four phase 3 studies (GS-US-174-0102 [Study 102], GS-US-174-0103 [Study 103], GS-US-320-0108 [Study 108], and GS-US-320-0110 [Study 110]) aimed to assess impact of tenofovir (TFV)-based NAs on long term HCC risk in CHB patients, utilizing three validated risk prediction algorithms.

Method: Studies 102 and 103 randomized patients 2:1 to double-blind (DB) treatment with tenofovir disoproxil fumarate (TDF) or adefovir dipivoxil (ADV) for 48 weeks, then open-label (OL) TDF, whereas Studies 108 and 110 randomized patients 2:1 to DB treatment with tenofovir alafenamide (TAF) or TDF for up to 144 weeks, then OL TAF. All patients were assessed over 384 weeks (8 years). HCC risk was estimated using the following models: Risk Estimation for HCC in Chronic Hepatitis B (REACH-B); modified Platelet Age Gender-HBV (mPAGE-B); and age-Male-ALBI-Platelets (aMAP). Primary outcomes included: HCC incidence (via standardized incidence ratios [SIRs] of HCC based on ratio of observed vs. model-predicted cases [REACH-B]); and the proportions of patients who shifted from baseline risk categories (aMAP and mPAGE-B).

Results: In total, 1,939 (n = 641 from 102/103 and n = 1,298 from 108/110) patients were included in the pooled analysis. By Year 8, 41 (2.1%) patients had developed HCC. By multivariate analysis, older age, male sex, and cirrhosis at baseline were associated with HCC development. By REACH-B, the SIR was 0.39 (95% confidence interval: 0.29, 0.53; p < 0.0001), indicating the observed incidence to be 61% lower than the predicted incidence; for patients with cirrhosis, the SIR was 46% lower. By aMAP and mPAGE-B models, most patients were at low- or medium-risk for HCC development at baseline, and either stayed the same or shifted to a lower risk category at Year 8, while most high-risk patients had shifted to at least medium-risk by Year 8.

Conclusion: In this large dataset of prospectively followed CHB patients, HCC risk was significantly impacted with long-term TFV-based treatment in CHB patients with and without cirrhosis.

WED-398

HBsAg loss in inactive chronic hepatitis B carriers is dependent on level of qHBsAg and interferon response: a randomised control trial

Seng Gee Lim¹, Guan Huei Lee², Yock Young Dan³, Yin Mei Lee⁴, Htet Htet Toe Wai Khine⁵, Yuh Ling Amy Tay⁶, Cindy Seah⁷, Liang Shen⁵, Edwin, Shih-Yen Chan⁸, Martin Hibberd⁹. ¹National University Health System, Yong Loo Lin School of Medicine, Singapore, Singapore; ²National University Health System, Singapore; ³National University Health System, Yong Loo Lin School of Medicine, Singapore, Singapore; ⁴National University Health System, Singapore, Singapore; ⁵Yong Loo Lin School of Medicine, Singapore, Singapore; ⁶Yong Loo Lin School of Medicine, Singapore, Singapore; ⁷National University Health System, Singapore, Singapore; ⁸Singapore Clinical Research Institute, Duke-NUS Medical School, Singapore, Singapore; ⁹London School of Hygiene and Tropical Medicine, London, United Kingdom
Email: mdclimsg@nus.edu.sg

Background and aims: Peginterferon therapy of Chronic Hepatitis B (CHB) carriers how mixed results for HBsAg loss, but its unclear whether low qHBsAg (<1000 IU/ml) or low HBV DNA (<2000 IU/ml) are more important.

Method: This was a 3-arm RCT of peginterferon alpha2a (PEG) (pegasys, Roche) 180mcg weekly randomised 1:1:1 to 24 weeks (PEG24), 48 weeks (PEG48) or no treatment (C) in CHB carriers (clinicaltrials.gov:NCT02992704). Patients were randomly assigned based on: HBsAg (+)>6months, HBeAg (-), normal ALT, HBV DNA $\leq 2 \times 10^4$ IU/ml or qHBsAg ≤ 1000 IU/ml; absence of cirrhosis, treatment naive, absence of HCV/HDV/HIV coinfection. The primary end point was HBsAg loss 24weeks after treatment, and study size of 90 patients had 80% power to detect a 25% difference between any PEG arm and control. Data analysis was performed using SPSSv20 based on ITT analysis. Baseline and on-treatment variables and multivariate analysis were used to predict HBsAg loss at end-of-treatment (EOT) and end of 24weeks followup (FU24). PAXgene transcriptome analysis was performed on relevant patients.

Results: Baseline characteristics were similar between groups. HBsAg loss occurred in a total of 7/30 (23.3%) in PEG48, 9/30 (30%) in PEG24 and 0/30 (0%) in C at the EOT (p = 0.007) but 5/30 (16.7%) in PEG48, 5/30 (16.7%) in PEG24 and 1/30 (3.4%) in C at FU24 (p = 0.093). Baseline predictors of HBsAg loss at FU24 showed qHBsAg and ALT were significant by logistic regression with backwards model selection (p = 0.002, and p = 0.04 respectively). ROC curve analysis showed AUROC 0.896 (95% CI 0.806–0.986), with threshold of qHBsAg <76 IU/ml, had 100% sensitivity and 62% specificity for HBsAg loss at FU24. There were three distinct patterns (clusters) of interferon response despite qHBsAg <76 IU/ml, based on their HBsAg reduction at week 12. Cluster 1 had a HBsAg reduction of 2.19logIU/ml, cluster 2 had a mean reduction of 1logIU/ml and cluster 3 had a mean reduction of 0.05logIU/ml. Responders (HBsAg loss) occurred in 2/2 in cluster 1, 7/13 in cluster 2 and 5/15 in cluster 3. We examined responders and non-responders using PAXgene transcriptome analysis and found that responders had 55 differentially expressed genes of which 37 were upregulated. The most significantly upregulated was MMP8 and a cluster of 13 genes which were enriched in the neutrophil degranulation pathway (p = 5.59×10^{-12}). There were 282 adverse events mostly interferon related (90%). There were 4 Serious Adverse Events but no deaths.

Conclusion: HBsAg loss with PEG in inactive carriers leads to 16.7% HBsAg loss with low baseline qHBsAg and interferon responsiveness driving HBsAg loss but not HBV DNA. A novel neutrophil enriched pathway was found in responders based on transcriptome analysis.

WED-399-YI

The composition of HBsAg along with HDV-RNA predicts virological response in chronic hepatitis delta patients treated with bulevirtide for 48 weeks

Stefano D'Anna¹, Romina Salpini², Elisabetta Degasper³, Leonardo Duca¹, Maria Paola Anolli³, Lorenzo Piermatteo², Dana Sambarino³, Marta Borghi³, Floriana Facchetti³, Francesca Ceccherini Silberstein¹, Riccardo Perbellini³, Pietro Lampertico^{3,4}, Valentina Svicher². ¹Department of Experimental Medicine, University of Rome "Tor Vergata", Rome, Italy; ²Department of Biology, University of Rome "Tor Vergata", Rome, Italy; ³Division of Gastroenterology and Hepatology, Foundation IRCCS Ca' Granda Ospedale Maggiore Policlinico, Milan, Italy; ⁴CRC "A. M. and A. Migliavacca" Center for Liver Disease, Department of Pathophysiology and Transplantation, University of Milan, Milan, Italy
Email: stefanodanna26@gmail.com

Background and aims: HDV exploits HBV surface protein (HBsAg) for releasing of progeny and entry into hepatocytes. HBsAg consists of 3 different forms: Large- (L-HBs), Middle- (M-HBs) and Small-HBsAg (S-HBs). L-HBs is predominantly present in virions and mediates binding to NTCP receptor, while the lack of M-HBs production is known to favour the release of replication-competent virions. Here, we investigate the kinetics of HBs forms under bulevirtide treatment (BLV).

Method: 28 consecutive patients with HDV-related compensated cirrhosis starting BLV 2 mg/day monotherapy were enrolled in this retrospective/longitudinal study, all under effective NUC treatment at entry. L-HBs, M-HBs and S-HBs were quantified by *ad-hoc* ELISAs in baseline and week 48 (W48) samples (Beacle). HDV RNA was quantified by Robogene 2.0. Virological response was defined as HDV RNA undetectable or >2log decline compared to baseline, biochemical response as ALT normalization.

Results: At baseline, median (IQR) age was 53 (40–63) years, liver stiffness 19.4 (15.4–32.9) kPa, ALT 106 (77–147) U/l, serum HDV RNA 5.4 (4.4–6.0) log IU/ml and HBsAg levels 3.7 (3.4–4.9) log IU/ml. Pre-treatment median (IQR) levels of S-HBs, M-HBs and L-HBs were 3999 (1482–7184), 1032 (305–2222) and 6 (2–14) ng/ml, respectively. At W48, serum HDV RNA declined by 3.1 (1.8–3.7) log IU/ml while virological and biochemical responses were observed in 71% and 75% of patients, respectively. A >10% decrease of S-HBs, M-HBs and L-HBs levels was observed in 57%, 54% and 39% of patients with a median (IQR) decline of 1095 (839–2403), 145 (39–350) and 10 (4–15) ng/ml, respectively. Baseline HDV RNA <5 log IU/ml was associated with HDV RNA <100 IU/ml at W48 (75% with vs 25% without, $P = 0.02$). A similar correlation was observed for baseline L-HBs <9 ng/ml (62.5% with vs 25% without, $P = 0.05$). The combination of pre-treatment L-HBs <9 ng/ml + HDV RNA <5 log IU/ml was the best predictor for achieving HDV RNA <100 IU/ml (PPV:87.5%, NPV:70%; $P = 0.01$). This combination showed also the best diagnostic accuracy for predicting HDV RNA <100 IU/ml plus ALT normalization (PPV:75%, NPV:75%; $P = 0.03$). A different scenario was observed for M-HBs. Patients with baseline M-HBs >500 ng/ml had a significantly greater virological response than those with baseline M-HBs <500 ng/ml (HDV RNA decline of 3.4 [2.5–3.8] vs 1.6 [1.2–3.2] log IU/ml, $P = 0.03$). Baseline M-HBs >500 ng/ml predicted the achievement of virological response at W48 of BLV (PPV: 88.8%, NPV: 60%; $P = 0.01$). Superimposable results were observed in a subgroup of 12 patients with serum HDV RNA <5 log IU/ml at baseline (PPV: 100%, NPV: 57%; $P = 0.038$).

Conclusion: Quantification of L-HBs and M-HBs along with serum HDV RNA may reflect the burden of circulating infectious or replication-competent virions in the setting of HBV/HDV co-infection, possibly providing a new tool to identify patients more likely to respond to BLV monotherapy.

WED-402

Risk of hepatocellular carcinoma after curative treatment when switching from Tenofovir Disoproxil Fumarate or Entecavir to Tenofovir Alafenamide: a real-world multicenter cohort study

Hyunjae Shin¹, Yunmi Ko¹, Youngsu Park¹, Yoon Jun Kim¹. ¹Seoul National University Hospital, Seoul, Korea, Rep. of South
Email: yoonjun@snu.ac.kr

Background and aims: Antiviral treatment reduce the risk of developing hepatocellular carcinoma (HCC) in patients with chronic hepatitis B (CHB). However, there is a lack of high-quality evidence regarding the preventive effects of TAF on HCC. We evaluated the impact of TAF use after curative treatment on HCC recurrence.

Method: Patients who underwent surgery or radiofrequency ablation as a curative treatment for HCC were selected. Those patients who continued antiviral treatment with NAs (entecavir [ETV] or tenofovir disoproxil fumarate [TDF]) or switched to TAF were included. The primary outcome was HCC recurrence, and the time-varying effect of NA use on HCC recurrence was analyzed using various statistical methods.

Results: Among 2,794 consecutive patients with CHB who received curative treatment for HCC, 199 subsequently switched from ETV or TDF to TAF. After a median of 3.0 years, 1,303 patients (46.6%) experienced HCC recurrence. After propensity score matching (ratio 1:10), switching to TAF was not associated with an increased HCC recurrence (hazard ratio [HR], 1.00 [95% CI, 0.68–1.47]; $p = 1.00$) by time-varying Cox analysis. Switching to TAF was not associated with HCC recurrence in subgroups of NA (HR, 1.06 [95% CI, 0.67–1.67]; $p = 0.81$ for TDF, and 1.09 [95% CI, 0.51–2.33]; $p = 0.82$ for ETV). Kaplan-Meier analysis showed comparable HCC recurrence-free survival between patients who switched to TAF and those who continued with their NA ($p = 0.08$). Time-varying Cox analyses in various subgroups confirmed the primary findings.

Conclusion: TAF is as effective as TDF and ETV in preventing HCC recurrence after curative treatment.

WED-403

HELlenic multicenter ReAl-life CLInical Study for bulevirtide therapy in chronic hepatitis D (HERACLIS_BLV_D)

Margarita Papatheodoridi¹, Vasilios Sevastianos², Kalliopi Zachou³, Dimitrios Christodoulou⁴, Ioannis Koskinas⁵, Melanie Deutsch⁶, Alexandra Alexopoulou⁷, Ioannis Elefsiniotis⁸, Christos Triantos⁹, Eleni Gigi¹⁰, Theodoros Androutsakos¹¹, Dimitrios Karagiannakis¹, Iliana Mani¹², Dimitrios Dimitroulopoulos¹³, Maria Mela¹⁴, Emmanouil Sinakos¹⁰, Spyridon Michopoulos¹⁵, Konstantinos Mimidis¹⁶, Nikolaos Papadopoulos¹⁷, Athanasios Kontos¹⁸, Christos Veteranos¹⁹, Dimitrios Lymberopoulos²⁰, George Giannoulis²¹, Vasilios Papadimitropoulos²², Evdokia Avramopoulou²³, Spyridon Pantzios²⁴, Larisa Vasileva²², Hariklia Kranidioti⁵, Emmanouil Koullias⁵, Nikolaos Psychos²⁵, Paraskevi Fytilli¹¹, Ioannis Vlachogiannakos¹, Evangelos Cholongitas¹¹, Spiliotis Manolopoulos²², Ioannis Goulis²⁶, George Dalekos²¹, George Papatheodoridis¹. ¹General Hospital of Athens "Laiko", Medical School of National and Kapodistrian University of Athens, Athens, Greece; ²General Hospital of Athens "Evangelismos", Athens, Greece; ³General University Hospital of Larissa, Larisa, Greece; ⁴University General Hospital of Ioannina, Ioannina, Greece; ⁵General Hospital of Athens "Hippokratio", Medical School of National and Kapodistrian University of Athens, Athens, Greece; ⁶General Hospital of Athens "Hippokratio", Athens, Greece; ⁷General Hospital of Athens "Hippokratio", Athens, Greece; ⁸General and Oncology Hospital of Kifisia "Agioti Anargyroi", Athens, Greece; ⁹University Hospital of Patras, Patras, Greece; ¹⁰General Hospital of Thessaloniki "Hippokratio", Aristotle University of Thessaloniki, Thessaloniki, Greece; ¹¹General Hospital of Athens "Laiko", Athens, Greece; ¹²General Hospital of Athens "Hippokratio", Medical School of National and Kapodistrian University of Athens, Athens, Greece; ¹³Agios Savvas Hospital of Athens, Athens,

Greece; ¹⁴General Hospital of Athens "Evangelismos, Athens, Greece; ¹⁵General Hospital of Athens "Alexandras," Athens, Greece; ¹⁶University General Hospital of Alexandroupolis, Alexandroupolis, Greece; ¹⁷401 General Army Hospital of Athens, Athens, Greece; ¹⁸Agios Savvas Hospital, Athens, Greece; ¹⁹General Hospital of Athens "Evangelismos", Athens, Greece; ²⁰General Hospital of Athens "Evangelismos," Athens, Greece; ²¹General University Hospital of Larissa, Larissa, Greece; ²²General Hospital of Athens "Hippokratio", Athens, Greece; ²³University General Hospital of Patras, Patras, Greece; ²⁴General and Oncology Hospital of Kifisia "Agioi Anargyroi," Athens, Greece; ²⁵General University Hospital of Ioannina, Ioannina, Greece; ²⁶General Hospital of Thessaloniki "Hippokratio," Athens, Greece
Email: gepapath@med.uoa.gr

Background and aims: Bulevirtide (BLV) has received conditional approval by the European Medicine Agency for the treatment of compensated chronic hepatitis D (CHD) in 2020 and has started to be used in some European countries including Greece, but there are limited real-life data to date. The aim of this study is to assess the efficacy and safety of BLV in CHD patients treated at Greek liver centers.

Method: All adult (>16 years old) patients with CHD followed at any of the participating centers who started BLV before the approvals (05-11/2023) of the HERACLIS_BLV_D study (NCT05928000) were included. All patients were treated with daily BLV subcutaneous injections of 2 mg, with or without concomitant use of a nucleos (t) ide analogue (NA). Patients' monitoring was based on standard clinical practice according to the current recommendations for treatment of CHD. A predefined case report form was used for data collection. Serum HDV RNA during the study was determined by a polymerase chain reaction assay at a central lab (sensitivity: 100 IU/ml).

Results: In total, 76 patients were included; mean age: 50 ± 12 years, males: 37 (49%), born in Greece: 21 (28%), mean BMI: 25.4 ± 3.9 kg/m², mean liver stiffness (LS): 15.9 ± 9.5 kPa, cirrhosis: 45 (59%) (decompensated cirrhosis: 6/45), (peg-)interferon (IFN) in the past: 32 (42%) cases. No patient received combination of BLV with pegIFN; BLV alone was given in 9 (12%) and BLV plus a NA in 67 (88%) patients (ETV: 29, TDF: 35, TAF: 3). At 6 months, virological response (VR: serum HDV RNA undetectable or decline ≥2 log₁₀ IU/ml) was observed in 43 (24+19) (70.5%), biochemical response (BR: ALT ≤40 IU/L) in 43 (70.5%) and combined VR+BR in 32 (52.5%) of 61 patients. At 12 months, VR was observed in 40 (31+9) (83%), BR in 35 (73%) and combined VR+BR in 28 (58%) of 48 patients. Of the patients with no or partial VR (serum HDV RNA decline <1 or 1–<2 log₁₀ IU/ml), 11/18 and 7/8 cases achieved BR at 6 and 12 months, respectively; all cases without BR had reduced ALT and/or HDV RNA levels. Response rates did not differ between cirrhotic and non-cirrhotic patients. There was no drug-related serious adverse event and no patient discontinued BLV.

Conclusion: BLV therapy with or without NA is safe and effective in the treatment of CHD in real-life at Greek liver centers offering VR and BR rates even higher than those reported in clinical trials perhaps due to different patient characteristics.

WED-404

Comparable outcomes between Besifovir and other antiviral therapies in hepatocellular carcinoma development among patients with chronic hepatitis B

Jae Seung Lee¹, Sung Won Lee², Sang Gyune Kim³, Yeon Seok Seo⁴, Su Jong Yu⁵, Hyung Joon Yim⁶, Hye Won Lee¹, Mi Na Kim¹, Beom Kyung Kim¹, Jun Yong Park¹, Do Young Kim¹, Sang Hoon Ahn¹, Seung Up Kim¹. ¹Yonsei University College of Medicine, Department of Internal Medicine, Seoul, Korea, Rep. of South; ²Bucheon St. Mary's Hospital, The Catholic University of Korea School of Medicine, Department of Internal Medicine, Bucheon, Korea, Rep. of South; ³Soonchunhyang University Bucheon Hospital, Soonchunhyang University College of Medicine, Department of Internal Medicine,

Bucheon, Korea, Rep. of South; ⁴Korea University Anam Hospital, Korea University College of Medicine, Department of Internal Medicine, Seoul, Korea, Rep. of South; ⁵Seoul National University College of Medicine, Department of Internal Medicine and Liver Research Institute, Seoul, Korea, Rep. of South; ⁶Korea University Ansan Hospital, Korea University College of Medicine, Department of Internal Medicine, Division of Gastroenterology and Hepatology, Ansan, Korea, Rep. of South
Email: ksukorea@yuhs.ac

Background and aims: Besifovir dipivoxil maleate (BSV), an acyclic nucleotide phosphonate, has potent antiviral efficacy against chronic hepatitis B (CHB), similar to other antiviral agents, such as entecavir (ETV), tenofovir disoproxil fumarate (TDF), and tenofovir alafenamide (TAF). This study compares outcomes between BSV and the other antiviral agents in hepatocellular carcinoma (HCC) development among patients with CHB.

Method: We conducted a retrospective cohort of 2,684 treatment-naïve patients with CHB who started their first-line antiviral therapy (AVT) between May 2017 and April 2022 with ETV (n = 840), TAF (n = 706), TDF (n = 666), or BSV (n = 472) at six tertiary medical institutions in South Korea. The incidence and hazard ratio (HR) were calculated using Kaplan-Meier and Cox regression analyses, respectively. Selection bias was minimized using inverse probability of treatment weighting (IPTW) and propensity score matching (PSM).

Results: Compared to the patients with other antiviral agents, BSV users showed a higher proportion of male patients (61.2% vs. 50.1–56.2%), alcohol intake >20 g/day (12.1% vs. 5.5–11.2%), and cirrhosis (37.9% vs. 30.5–34.3%). The incidence of HCC in BSV users (n = 6, 4.4 per 1000 person-years [PYs]) was similar to that in TAF users (8.5 per 1000 PYs, log-rank P = 0.111, HR 2.098, 95% confidence interval [CI] 0.827–5.324), however, significantly lower than those in ETV (n = 38, 12.7 per 1000 PYs, log-rank P = 0.026, HR 2.603, 95% CI 1.087–6.233) and TDF users (12.7 per 1000PYs, log-rank P = 0.035, HR 2.539, 95% CI 1.034–6.234). After applying 1:1:1 IPTW, the incidence of HCC in BSV users (n = 7 of 591, 3.8 per 1000 PYs) was similar to that in TAF users (n = 17 of 713, 8.6 per 1000 PYs, adjusted HR [aHR] 2.324, 95% CI 0.894–6.043), however, significantly lower than in ETV (n = 32 of 706, 12.4 per 1000 PYs, aHR 2.795 (95% CI 1.138–6.866, E-value 5.035) and TDF users (n = 34 of 674, 14.6 per 1000 PYs, aHR 3.322 (95% CI 1.334–8.274, E-value 6.099). Following separated 1:1 PSM (all 472 pairs), the incidence of HCC in BSV users (n = 6, 4.4 per 1000 PYs) was similar to that in TAF users (n = 12, 8.6 per 1000 PYs, log-rank P = 0.782, aHR 1.167, 95% CI 0.392–3.471), however, significantly lower than in ETV (n = 27, 15.2 per 1000 PYs, log-rank P = 0.025, aHR 2.978, 95% CI 1.024–8.659, E-value 5.404), and TDF users (n = 27, 16.6 per 1000 PYs, log-rank P = 0.025, aHR 3.000, 95% CI 1.090–8.254, E-value 5.449).

Conclusion: BSV showed comparable outcomes in HCC development among patients with CHB compared to TAF, ETV, and TDF. Given the small number of events and the relatively short follow-up duration observed in BSV users, further long-term analysis is warranted.

WED-405

Tenofovir disoproxil fumarate and tenofovir alafenamide interruption in hepatitis B and human immunodeficiency virus co-infected individuals in the United States: monitoring practices and incidence of hepatitis B reactivation or hepatitis flare

Douglas T. Dieterich¹, Laurence Brunet², Ricky Hsu^{3,4}, Karam Mounzer⁵, Gerald Pierone⁶, Michael Wohlfeiler⁷, Jennifer Fusco², Megan Dunbar⁸, Joshua Gruber⁸, Leland J. Yee⁸, Catherine Frenette⁸, Gregory Fusco². ¹Icahn School of Medicine at Mount Sinai, New York, United States; ²Epividian, Raleigh, United States; ³AIDS Healthcare Foundation, New York, United States; ⁴NYU Langone Medical Center, New York, United States; ⁵Philadelphia FIGHT, Philadelphia, United States; ⁶Whole Family Health Center, Vero Beach, United States; ⁷AIDS Healthcare Foundation, Miami, United States; ⁸Gilead Sciences, Inc., Foster City, United States
Email: laurence.brunet@epividian.com

POSTER PRESENTATIONS

Background and aims: Among HBV core antibody positive (cAb+) people with HIV, suppressive HBV treatment including either tenofovir disoproxil fumarate or tenofovir alafenamide (TDF/TAF) is recommended to prevent HBV reactivation. We describe TDF/TAF interruptions and HBV monitoring practices in the United States as well as assess the incidence of HBV reactivation and hepatitis flares during TDF/TAF interruptions in the OPERA cohort.

Method: All TDF/TAF interruptions among HBV surface antigen positive (sAg+) and/or cAb+ people with HIV were categorized by risk of reactivation (high: sAg+; moderate: sAg-/cAb+/HBV surface antibody negative [sAb-]; low: sAg-/cAb+/sAb+). Presence of HBV DNA, sAg and alanine transaminase (ALT) testing was assessed before (within ≤ 12 months) and during the interruption. Incidence of HBV reactivation and hepatitis flares (AASLD definitions) was assessed with Poisson regression.

Results: Of 31,241 HBV/HIV co-infected people, 4,901 (16%) had ≥ 1 interruption, for a total of 5,643 interruptions (11% high, 19% moderate, 69% low risk); median duration: 83 weeks (IQR: 28–202). There were no DNA tests before (high: 55%, moderate: 97%, low: 97%) or during interruptions (high: 49%, moderate: 92%, low: 95%). There was no sAg test in 75% of high, 70% of moderate and 72% of low risk interruptions. HBV reactivation occurred in 103 high risk interruptions (16% overall; 32% of those with DNA tests) for an incidence rate [IR] of 9.59 per 100 person-years (95% CI: 7.91, 11.64). Reactivation occurred in 18 moderate risk interruptions (2% overall; 5% of those with DNA and/or sAg tests); IR: 0.58 (95% CI: 0.36, 0.91). Only 5 low risk interruptions resulted in HBV reactivation (0% overall; 0% of those with DNA and/or sAg tests); IR: 0.04 (95% CI: 0.02, 0.11). ALT tests were available before (high: 90%, moderate: 91%, low: 93%) and during interruptions (high: 98%, moderate: 100%, low: 99%). Hepatitis flares occurred in 60 (9%) high-risk interruptions (IR per 100 person-years: 5.28; 95% CI: 4.10, 6.80), 52 (5%) moderate-risk interruptions (IR: 1.72; 95% CI: 1.31, 2.26), and 132 (3%) low-risk interruptions (IR: 1.22; 95% CI: 1.03, 1.45).

Conclusion: In this large US cohort of sAg+ and/or cAb+ people with HIV receiving care in primary or HIV care clinics, TDF/TAF interruptions were common and lengthy, and HBV lab monitoring was sub-optimal, suggesting that primary and HIV care providers tend to be unaware of HBV status or overlook HBV monitoring and management in people with co-infection. While sAg+ individuals had the highest HBV reactivation and hepatitis flare risk, all were at-risk regardless of serology. Given infrequent testing, many reactivations were likely missed. Primary and HIV care providers need to incorporate HBV monitoring in their standard of care and proceed with caution if considering a TDF/TAF interruption for people with HBV/HIV co-infection.

WED-406

DARING-B study: 5-year outcomes after nucleos (t)ide analogue (NA) cessation in Caucasian non-cirrhotic patients with HBsAg-negative chronic hepatitis B (CHBe-)

Margarita Papatheodoridi¹, Eirini Rigopoulou², Kalliopi Zachou², Emilia Hadziyannis³, Nikolaos Gatselis⁴, Ioannis Vlachogiannakos⁵, Spilios Manolakopoulos³, George Dalekos², George Papatheodoridis⁴.

¹Department of Gastroenterology, Medical School of National and Kapodistrian University of Athens, General Hospital of Athens "Laiko," Athens, Greece; ²Department of Medicine and Research Laboratory of Internal Medicine, Thessaly University Medical School, Larissa, Greece; ³2nd Department of Internal Medicine, Medical School of National and Kapodistrian University of Athens, General Hospital of Athens "Hippokratio," Athens, Greece; ⁴Department of Gastroenterology, Medical School of National and Kapodistrian University of Athens, General Hospital of Athens "Laiko," Athens, Greece; ⁵Medical School of National and Kapodistrian University of Athens, General Hospital of Athens "Laiko," Athens, Greece
Email: gepapath@med.uoa.gr

Background and aims: Cessation of long-term NA therapy has been regarded lately as a potential strategy that may increase the probability of functional cure, ie. HBsAg loss, in CHBe- patients, who should remain under close monitoring after stopping NA. The outcomes within 1–2 years post-NA have been well studied, but there are few data about longer outcomes. We aimed to assess the 5-year outcomes of our non-cirrhotic CHBe- patients included in the DARING-B study.

Method: DARING-B study prospectively enrolled 57 Caucasian patients (mean age: 58 ± 10 years, males: 37) without cirrhosis before NAs from 2 tertiary liver centers in Greece from 12/2015 to 03/2016. Patients with coinfection, cirrhosis, cancer or liver transplantation were excluded. Patient and treatment characteristics before and at end of NA therapy (EOT) were recorded. After NA cessation, patients were followed monthly for the first 3 months, every 2–3 months until completion of the first year and every 6 months thereafter. Predefined criteria for retreatment were used. Study end points were death or liver transplantation, liver decompensation, hepatocellular carcinoma (HCC), virological relapse (VR: HBV DNA > 2000 IU/ml), clinical relapse (CR: HBV DNA $> 2,000$ and ALT $> 2 \times$ ULN), retreatment and HBsAg loss.

Results: Median follow-up (FUP) was 5 (IQR: 3.6–6.5) years after EOT; only 4 patients were lost to FUP (< 24 months). No patient died, required liver transplantation, developed liver decompensation or jaundice. Only one patient developed HCC diagnosed at 11 months (cumulative 1-year and 5-year incidence: 1.8%). At 1, 2, 3, 5 and 6 years post-NA, cumulative rates of VR were 70%, 74%, 75%, 75% and 75%, of CR were 33%, 35%, 39%, 39% and 39% and of retreatment were 26%, 30%, 38%, 45% and 45%, respectively. In total, 17/57 (30%) patients achieved HBsAg loss (2 after retreatment) with 1-, 2-, 3-, 5- and 6-year post-NA cumulative rates of 16%, 20%, 21%, 27% and 37%, respectively. EOT HBsAg ≤ 100 IU/ml was associated with more frequent HBsAg loss (HR: 6.7, $P < 0.001$) and less frequent VR (HR: 0.35, $P = 0.045$), whereas EOT HBsAg ≤ 1000 IU/ml was also associated with more frequent HBsAg loss (HR: 16.7, $P = 0.007$) and less frequent CR (HR: 0.44, $P = 0.057$) and retreatment (HR: 0.33, $P = 0.009$).

Conclusion: Functional cure rates increase over the first 5–6 years after NA cessation in non-cirrhotic Caucasian patients with CHBe-, while risk of CR is mainly observed during the first year substantially decreasing thereafter.

WED-407

Characterization of hepatitis D virus RNA and hepatitis B surface antigen kinetics during pegylated interferon-alpha monotherapy: The D-LIVR study

Leeor Hershkovich¹, Harel Dahari¹, Scott Cotler¹, Ingrid Choong², Colin Hislop², Theo Heller³, Christopher Koh³, Jeffrey Glenn⁴, Tarik Asselah^{5,6}, Saeed Sadiq Hamid⁷, Ohad Etzion⁸. ¹Program for Experimental and Theoretical Modeling, Division of Hepatology, Department of Medicine, Stritch School of Medicine, Loyola University Chicago, Maywood, IL, United States; ²Eiger BioPharmaceuticals, Palo Alto, CA, United States; ³Liver Disease Branch, NIDDK, NIH, Bethesda, MD, United States; ⁴Division of Gastroenterology and Hepatology, Departments of Medicine, Microbiology and Immunology, Stanford School of Medicine, Stanford, CA, United States; ⁵Hôpital Beaujon, APHP, Clichy and the University of Paris-Cité, Paris, France; ⁶INSERM UMR1149, Paris, France; ⁷Aga Khan University, Karachi, Pakistan; ⁸Soroka University Medical Center, Beersheva, Israel
Email: harel.dahari@gmail.com

Background and aims: Current understanding of the kinetic profiles of hepatitis D virus (HDV) and hepatitis B surface antigen (HBsAg) during pegylated-interferon- α -2a (pegIFN) monotherapy is based on a 24-week analysis in 12 treated patients with HDV [Hepatology 2014;60:1902–1910]. We analyzed data from the Phase 3 D-LIVR study to further characterize HDV and HBsAg kinetics in patients treated with pegIFN alone.

Method: 52 participants in the D-LIVR study (NCT03719313) were treated with pegIFN and oral placebo for 48 weeks. HDV RNA was measured by Quest laboratories (lower limit of quantification, LLOQ <40 IU/ml; target not detected, TND <4 IU/ml) and HBsAg by Abbott Diagnostics at baseline, Weeks 1, 2, and 4 of therapy, and then every 4 weeks until end of therapy (EOT) and at 24 weeks of follow-up (EOFU). We defined monophasic (MP) pattern as a single HDV decline, biphasic (BP) pattern as an initial rapid decline followed by a slower decline, and triphasic (TP) pattern as two decline phases separated by an intermediary plateau. MP, BP, or TP patterns that were followed by a plateau (\geq LLOQ), termed flat partial response (FPR), biphasic FPR (BFPR), and staircase, respectively. A ≥ 2 -fold change in slope was used to distinguish between decline phases.

Results: 28 patients were excluded from analysis: 11 discontinued therapy, 9 had poor adherence or dose reductions, and 8 were non-responders (<1.6 log decline from baseline). Of the remaining 24 patients, 22 experienced an average delay of 8.0 ± 9.7 days before HDV declined from baseline, while 2 experienced very long delays of 20 and 28 weeks. Thereafter, we identified 6 HDV kinetic patterns: MP (n = 3), BP (n = 2), TP (n = 4) which were associated with reaching TND (n = 7), and those who plateaued above TND: FPR (n = 7), BFPR (n = 4), and staircase (n = 4). 12 (50%) patients had HDV rebound (>1.5 log IU/ml increase from nadir) after MP (n = 2/3), BP (n = 1/2), TP (n = 1/4), FPR (n = 4/7), BFPR (n = 3/4), and staircase (n = 1/4) declines, 23 ± 14 weeks into therapy. HDV rebound was not associated with HDV decline patterns. While HBsAg remained at baseline levels (3.6 ± 0.6 log IU/ml) for most patients (19/24), 5 patients (1MP, 1BP, 2TP, and 1 staircase who had a transient rebound before reaching TND) experienced a >1.5 log decline from baseline, all of whom achieved sustained TND until EOFU. Another patient (FPR) was HDV detectable at EOT but achieved TND at EOFU, while HBsAg remained at baseline level. A decline of >1.5 log in HBsAg from baseline by Week 36 had a 100% positive predictive value and a 95% negative predictive value for reaching HDV TND at EOFU.

Conclusion: Complex HDV decline patterns including triphasic and staircase were observed under pegIFN, that were not previously reported. The longer kinetic analysis (48 vs 24 weeks) identified on treatment HDV rebound in 50% of patients who initially responded to pegIFN. A >1.5 log HBsAg decline from baseline by Week 36 was associated HDV TND at EOFU.

WED-408

Factors influencing HBsAg clearance in children with chronic hepatitis B undergoing antiviral therapy: significance of age at treatment onset and HBeAg titer dynamics

Byung-Ho Choe¹, Sukjin Hong². ¹Kyungpook National University Children's Hospital, Daegu, Korea, Rep. of South; ²Daegu Catholic University Medical Center, Daegu, Korea, Rep. of South
Email: bhchoi@knu.ac.kr

Background and aims: This study aims to investigate the characteristics and determinants of HBsAg clearance in paediatric patients with HBeAg-positive chronic hepatitis B undergoing antiviral treatment in Korea, where genotype C is predominant.

Method: We enrolled 145 children diagnosed with chronic hepatitis B for antiviral therapy. Eligible patients had a history of HBsAg positivity for at least six months, elevated ALT levels more than twice the upper normal limit for six months or longer, or confirmation through liver biopsy. Treatment with nucleos (t)ide analogues (NA) was continued beyond complete remission (normalization of ALT levels, undetectable HBV DNA levels, and HBeAg seroconversion), followed by an additional NA consolidation therapy, at least 1 year. The duration of consolidation therapy was extended by the revision of EASL and APASL guideline to over 3 years, which was further extended if HBsAg titer decrease rapidly, in the expectation of achieving functional cure. Exclusion criteria included HBeAg-negative hepatitis B, spontaneous HBeAg seroconversion, or acute exacerbation of chronic hepatitis B from other causes. The study

analyzed various factors such as gender, pre-treatment ALT and HBV DNA levels, age at the initiation of treatment, and duration of treatment until complete remission, to identify variables that significantly influence HBsAg clearance. Additionally, we assessed the impact of the decrement velocity of HBeAg titer during NA treatment, categorizing the slope of the titer decrease into tertiles, and employing chi-square and logistic regression for analysis.

Results: In the study group of 145 patients, consisting of 80 males (55.2%) and 65 females (44.8%), with an average age of 8.0 ± 5.3 years (mean \pm SD) at the start of treatment, 35 (24%) achieved HBsAg clearance. The average duration from treatment initiation to clearance was 32.2 ± 39.2 months (mean \pm SD). Identified factors influencing HBsAg clearance included gender, pretreatment ALT levels, and age at the onset of treatment. Notably, female patients (p = 0.047) and those with higher pretreatment ALT levels (p = 0.046) showed better outcomes. Children under six years exhibited a significantly higher rate of clearance (p = 0.011), with a more rapid decrease in HBeAg titer also being a contributing factor (p = 0.015). All patients achieving HBsAg clearance eventually developed anti-HBs. No patient who had achieved functional cure has relapsed after discontinuation of NA.

Conclusion: In the treatment of HBeAg-positive chronic hepatitis B with NA, preschoolers or those demonstrating a rapid decline in HBeAg titer during NA treatment are more likely to achieve HBsAg clearance. For patients with Genotype C, particularly those younger than 6 years, a rapid decline in HBeAg titer may indicate the potential benefit of considering an extension of treatment until HBsAg loss is achieved.

WED-409

Improved HBV-RNA quantification by HBV-RNA reverse transcription droplet digital PCR

Bernhard Kleter¹, Sanne Gils¹, Joël Meyboom¹, Thierry Verbinnen², Oliver Lenz³, Leen-Jan Doorn¹. ¹Viroclinics-DDL, Rijswijk, Netherlands; ²Janssen Research and Development, Beerse, Belgium; ³Janssen Pharmaceutica, Beerse, Belgium, Beerse, Belgium
Email: bernhard.kleter@cerbaresearch.com

Background and aims: HBV-RNA is used as an exploratory biomarker in chronic HBV infection. HBV-RNA can be specifically detected in plasma, often even when HBV DNA is completely suppressed by e.g. nucleos (t)ide analogue treatment. The limit of detection (LOD) of the Viroclinics-DDL in-house fully validated HBV-RNA high sensitivity RT-qPCR assay is 25 copies/ml and a lower limit of quantification (LLOQ) 869 copies/ml (158 copies/qPCR). A HBV-RNA RT droplet digital PCR (ddPCR) assay was developed to improve sensitivity and extend the lower quantifiable range as ddPCR is most effective at low copy numbers of target.

Method: A comparison between our validated HBV-RNA high sensitivity RT-qPCR assay using 500 μ L of plasma and the HBV RNA RT-ddPCR test was performed using 133 plasma samples from patients with chronic hepatitis B participating in Janssen clinical trials, JADE (NCT03361956), OCTOPUS (NCT05275023) and PENGUIN (NCT04667104). HBV-RNA RT-ddPCR was performed with a plasma sample volume of 400 μ L in 81 samples and the remaining 52 samples were tested with 200 μ L due to sample volume shortage. From the OCTOPUS and PENGUIN studies baseline samples from virologically suppressed patients were tested (HBV DNA <20 IU/ml detected or negative). Samples from JADE were used to assess longitudinal HBV-RNA, HBV-DNA, HBsAg and HBeAg profiles in 13 patients. In the JADE series, 28 samples were virologically suppressed.

Results: Based on HBV *in vitro* transcribed pregenomic RNA testing by RT-ddPCR the limit of blank is 0.73 copies/RT-ddPCR using Armbruster's approach. When testing 400 μ L plasma samples the 95% LOD by probit analysis was 2.7 copies/RT-ddPCR, corresponding to 16 copies/ml. The LLOQ was determined according to FDA-guidelines at 23.6 copies/RT-ddPCR, corresponding to 141 copies/

ml. In the panel of 133 samples concordant results by both assays were found in 74 (56%) samples. The qPCR and ddPCR assays scored below LOD in 65 (49%) and 39 (29%) samples, respectively. Four of the 39 samples were between LOD and LLOQ in the qPCR assay. By ddPCR, 49 samples were in the range between LOD and LLOQ. By qPCR, 24 of these 49 cases were also in the range between LOD and LLOQ and the remaining 25 samples were below LOD. In the quantifiable range of both assays, far more samples were found quantifiable by the ddPCR assay than by the qPCR assay, 45 (34%) and 15 (11%) respectively. All 15 qPCR quantifiable samples were also quantifiable by the ddPCR assay. Even 5 of them were quantifiable when testing 200 μ L plasma in the ddPCR assay.

Conclusion: Results show a clearly improved sensitivity and quantification of HBV RNA by the HBV-RNA RT-ddPCR assay. Due to the higher sensitivity in quantification of low HBV RNA concentrations, the response to treatment can be assessed for a longer period. This makes the HBV-RNA RT-ddPCR assay highly suitable for monitoring patients during antiviral treatment in clinical trials.

WED-410

Sustained virological response after treatment with Bulevirtide in HDV patients. Data from the french multicenter real-life cohort

Victor de Lédighen¹, Karine Lacombe², Stanislas Pol², Laurent Alric³, Caroline Lascoux-Combe², Dulce Alfaia⁴, Marie-Noëlle Hilleret⁵, Nathalie Ganne-Carrié⁶, Jérôme Gournay⁷, Veronique Loustaud-Ratti⁸, Miroslava Subic-Levrero⁴, Fatoumata Coulibaly⁹, Estelle Le Pabic¹⁰, Christelle Tual¹⁰, Segolene Brichler⁶, Fabien Zoulim⁴. ¹CHU Bordeaux, pessac, France; ²APHP, Paris, France; ³CHU Toulouse, Toulouse, France; ⁴CHU Lyon, Lyon, France; ⁵CHU Grenoble, Grenoble, France; ⁶APHP, Bobigny, France; ⁷CHU Nantes, Nantes, France; ⁸CHU Limoges, Limoges, France; ⁹ANRS, Paris, France; ¹⁰CHU Rennes, Rennes, France
Email: victor.deledighen@chu-bordeaux.fr

Background and aims: Bulevirtide (BLV) has been approved for the treatment of patients with HDV infection. However, the long-term efficacy is unknown. The aim of this analysis was to evaluate the prevalence and factors associated with sustained virological response (SVR) in patients treated with BLV 2 mg daily with or without PEG-IFN α 2a in the French ANRS Buledelta cohort.

Method: Out of the 271 patients enrolled in the BuleDelta cohort, 30 patients with chronic HDV infection who stopped antiviral therapy were included in this analysis. Their characteristics were as follows: male 53.3%, mean age 45.7 \pm 11.5 years, mean liver stiffness measurement 12.2 \pm 8.3 kPa, cirrhosis 76.7%, median HDV-RNA 5.88 [Interquartile Range (IQR): 5.07; 6.56] log₁₀ (IU/ml), median qHBsAg 3544 [IQR: 878.8; 9356.0] UI/ml. Patients received 16.8 \pm 7.7 months of BLV 2 mg QD SC alone (N = 11) or in combination with PEG-IFN α once weekly (N = 19) according to physician's choice. All patients had undetectable or unquantifiable HDV RNA when stopping treatment. SVR was defined as persistently undetectable or unquantifiable HDV-RNA during their follow-up (FU).

Results: During the first 48 weeks FU, 17 patients (56.7%) experienced a relapse (quantifiable HDV RNA). Relapse was observed in 9/17 patients (52.9%) within the first 12 weeks FU. For the other 8, 5 relapsed at FU24 and 3 at FU36. None of the following factors was associated with SVR: age, gender, BLV duration, pegIFN treatment, cirrhosis, HDV RNA viral load, normal ALT at the end of treatment, time between the first unquantifiable HDV RNA and discontinuation of treatment, time between the start of treatment and the first unquantifiable HDV RNA. Three patients had qHBsAg below 100 IU/ml at the end of treatment (68.5, 66.6, 84.0, respectively). Among them, 2 experienced a relapse.

Conclusion: In patients who stopped treatment with BLV with or without pegIFN, SVR was observed in 43.3%. No factor was identified to be associated with SVR. Relapse was observed in more than 50% of patients during the first 12 weeks FU. Larger studies are needed to identify baseline or on-treatment predictive factors of SVR.

WED-411

The large (LHBs) and middle (MHBs) hepatitis B surface antigen are associated with response to bulevirtide or PEG-IFN α treatment in patients with chronic hepatitis Delta (CHD)

Maria Pfefferkorn¹, Jonathan Seltsmann¹, Romy Winkler¹, Rodrigue Kamga Wouambo², Sara Sopena Santistevé^{3,4}, Madlen Matz-Soja^{1,5}, Maria Buti^{3,6,7}, Heyne Renate⁸, Pietro Lampertico^{9,10}, Thomas Berg¹, Florian van Bömmel¹. ¹Division of Hepatology, Department of Medicine II, Leipzig University Medical Center, Leipzig, Germany; ²Division of Hepatology, Department of Medicine II, Leipzig University Medical Center, Germany, Germany; ³Centro de Investigación Biomédica en Red de Enfermedades Hepáticas y Digestivas (CIBERehd), Instituto de Salud Carlos III, Madrid, Spain; ⁴Liver Pathology Lab, Biochemistry and Microbiology Departments (Clinical Laboratories), Hospital Universitari Vall d'Hebron, Vall d'Hebron Barcelona Hospital Campus, Barcelona, Spain; ⁵Rudolf-Schönheimer-Institute for Biochemistry, Leipzig, Germany; ⁶Universitat Autònoma de Barcelona (UAB), Department of Medicine, Barcelona, Spain; ⁷Liver Unit, Internal Medicine Department, Hospital Universitari Vall d'Hebron, Vall d'Hebron Barcelona Hospital Campus, Barcelona, Spain; ⁸Liver and Study Center Checkpoint, Berlin, Germany; ⁹Division of Gastroenterology and Hepatology, Foundation IRCCS Ca' Granda Ospedale Maggiore Policlinico, Milan, Italy; ¹⁰CRC "A. M. and A. Migliavacca" Center for Liver Disease, Department of Pathophysiology and Transplantation, University of Milan, Milan, Italy
Email: Maria.pfefferkorn@medizin.uni-leipzig.de

Background and aims: CHD can be treated with the entry inhibitor bulevirtide (BLV) or with the immune modulator PEG-IFN α , but predicting treatment response remains uncertain. The composition of hepatitis B surface antigen (HBsAg), including large (L), middle (M), and small (S) forms, has been associated with HBsAg loss in hepatitis B virus (HBV) mono-infection. This study aimed to evaluate HBsAg composition in the natural course of CHD and its association with treatment response.

Method: 42 CHD patients receiving either 180 mg/week PEG-IFN α (n = 30) or 2 mg/day BLV (+ TDF 245 mg/day; n = 12) from 4 European centers (Leipzig, Berlin, Barcelona and Milan) were observed for a mean duration of 33.4 (12–156) months. Patients were divided according to their treatment response (decreases of HDV RNA or undetectability) after 12 months: I) Nonresponse defined as a <2 log decline in HDV RNA levels (NR; n = 17), II) partial response: a \geq 2 log IU/ml decline (n = 4), III) complete response: undetectable HDV RNA levels (n = 13) and VI) functional cure with HBsAg loss (n = 4). Six additional patients who underwent liver transplantation (after a mean time of 60 (2–72) months), with (2 with PEG-IFN and 2 with TDF treatment) or without (n = 1) treatment, were included. HBsAg composition, HDV RNA and HBV DNA were quantified in serum samples at time points BL, 6, 12, 18, and 24 months.

Results: Prior to treatment initiation, all groups showed similar levels of HDV RNA (6.5 log₁₀ IU/ml), total HBsAg (4.1 log₁₀ ng/ml), LHBs (2.8 log₁₀ ng/ml) and MHBs (2.9 log₁₀ ng/ml). Patients with subsequent transplantation or NR receiving either PEG-IFN α or BLV showed the highest proportions of MHBs (%) and LHBs (%) and showed no changes in either HBsAg levels, MHBs (%) and LHBs (%) during treatment (after 6 to 24 months), respectively. In contrast, patients with complete virologic response exhibited a decrease in MHBs (%) from 10.9 (6.9–26.5)% at BL to 2.1 (0–3.1)% after 12 months with PEG-IFN α (n = 7; p = 0.016) and from 10.5 (3.3–19.4)% at BL to 2.9 (2.3–3.5)% after 12 months with BLV (n = 6). Furthermore, establishing a BL-Cutoff for MHBs % and LHBs % showed that patients with <8% MHBs or <4.8% LHBs at the start of either PEG-IFN or BLV treatment had significantly higher likelihood to achieve a complete virologic response during treatment (60% vs. 14.3%; p < 0.005 for MHBs and 83% vs. 16% for LHBs; p < 0.005).

Conclusion: MHBs and LHBs may serve as valuable markers for monitoring treatment response to PEG-IFN α and BLV in patients with

CHD. However, these findings require validation in a larger patient cohort.

WED-412

Functional cure and prediction analysis of pegylated interferon alpha-2b in HBeAg negative chronic hepatitis B patients with normal ALT (Ice-breaking Project in China): an interim analysis update

Chong Zhang¹, Dawu Zeng², Dachuan Cai³, Xiulan Xue⁴, Lingyi Zhang⁵, Baojun Song⁶, Yufeng Gao⁷, Yan Huang⁸, Jia Shang⁹, Xiaofeng Wu¹⁰, Ying Zhang¹¹, Hua Jin¹², Hui Chen¹³, Hong Tang¹⁴, Xiaobo Lu¹⁵, Yujuan Guan¹⁶, Feng Min¹⁷, Liang Xu¹⁸, Gang Li¹⁹, Zhengguang Wang²⁰, Xiaoguang Dou¹. ¹Shengjing Hospital of China Medical University, Shenyang, China; ²The First Affiliated Hospital of Fujian Medical University, Fuzhou, China; ³The Second Affiliated Hospital of Chongqing Medical University, Chongqing, China; ⁴The First Affiliated Hospital of Xiamen University, Xiamen, China; ⁵Lanzhou University Second Hospital, Lanzhou, China; ⁶The Sixth People's Hospital of Fushun, Fushun, China; ⁷The First Affiliated Hospital of Anhui Medical University, Hefei, China; ⁸Xiangya Hospital Central South University, Changsha, China; ⁹Henan Provincial People's Hospital, Zhengzhou, China; ¹⁰The Sixth People's Hospital of Shenyang, Shenyang, China; ¹¹Dalian Public Health Medical Center, Dalian, China; ¹²The Sixth People's Hospital of Benxi, Benxi, China; ¹³Hepatobiliary Hospital of Jilin, Changchun, China; ¹⁴West China Hospital of Sichuan University, Chengdu, China; ¹⁵The First Affiliated Hospital of Xinjiang Medical University, Urumchi, China; ¹⁶Guangzhou Eighth People's Hospital Guangzhou Medical University, Guangzhou, China; ¹⁷Army Seventy-three Army Hospital, Xiamen, China; ¹⁸Tianjin Second People's Hospital, Tianjin, China; ¹⁹Liaohu Oilfield General Hospital, Panjin, China; ²⁰Anshan City Hospital For Infectious Disease, Anshan, China
Email: zhangchong_83@163.com

Background and aims: In China, the proportion of Hepatitis B e antigen (HBeAg) negative chronic hepatitis B (CHB) patients is gradually increasing, which is related to the pre-C region mutation of long-term HBV infection. The disease progression of HBeAg negative CHB patients is fast, a large proportion of them have moderate or advanced liver inflammation or fibrosis, even if alanine aminotransferase (ALT) is normal, which requires timely antiviral treatment. The purpose of this study was to analyse the efficacy of pegylated interferon alpha-2b (PegIFN α -2b) in HBeAg negative CHB patients with normal ALT, and to explore the predictive factors of virological and serological responses. Preliminary data was presented at EASL2023 and here we update the latest results of this project.

Method: This is a multi-center, prospective, non-interventive, real-world clinical study conducted in China, involving 20 hospitals in 12 provinces or municipalities, which enrolled CHB patients with age of 18–60 years, Hepatitis B surface antigen (HBsAg) positive for more than 6 months, HBeAg negative, HBV DNA >20 IU/ml and normal ALT, without antiviral treatment history. PegIFN α -2b 180 μ g/week was applied on a voluntary basis. Examinations were performed every 12 weeks during treatment to monitor antiviral efficacy and adverse effects. The treatment strategy is adjusted according to the virological and serological response every 24 weeks, the total treatment course is not exceeded 96 weeks.

Results: A total of 249 patients were currently enrolled, and statistical analysis only be performed on 120 patients who completed PegIFN α -2b treatment. 72 (60.0%) were male, with an average age of 39.76 \pm 8.28 years (21–60 years). The median baseline HBV DNA and HBsAg were 6.87 $\times 10^2$ IU/ml (1.00 $\times 10^1$ ~ 7.62 $\times 10^6$) and 297.91 IU/ml (0.12 ~ 32828.22) respectively. The mean duration of PegIFN α -2b treatment was 12.78 months. 43 patients (35.83%) achieved HBsAg loss, and their baseline HBsAg levels were significantly lower than those who did not achieve HBsAg loss (381.29 \pm 827.18 vs. 1872.31 \pm 4102.32, $p < 0.001$). 23 patients achieved HBsAg loss after a short course of 6–9 months, with lower baseline HBsAg levels compared to those achieved HBsAg loss after a course of ≥ 12 months (96.34 \pm

141.54 vs. 708.98 \pm 1130.47, $p < 0.001$). Furthermore, HBsAg loss rate increased to 52.38% in patients with baseline HBV DNA <1000 IU/ml and HBsAg <500 IU/ml, and 66.67% in those with baseline HBV DNA <100 IU/ml and HBsAg <100 IU/ml. These patients all experienced functional cure with a short course of PegIFN α -2b treatment.

Conclusion: HBeAg negative CHB patients with normal ALT can achieve a high rate of functional cure by PegIFN α -2b therapy, especially for those with low baseline HBV DNA and HBsAg levels, only a short course of PegIFN α -2b treatment is required.

WED-413

10-year results under tenofovir disoproxil fumarate and entecavir in chronic hepatitis B; HBV clearance rare, disease outcomes good

Züla İstemihan¹, Gamze Kemeç², Timurhan Cebeci², Okan Cetin², Sezen Genç Uluçen¹, Aynure Rüstemzade¹, Kanan Nuriyev¹, Bilger Çavuş¹, Asli Çifcibasi Örmeci¹, Filiz Akyuz¹, Kadir Demir¹, Fatih Beşik¹, Sabahattin Kaymakoglu¹. ¹Istanbul University, Istanbul Faculty of Medicine, Department of Internal Medicine, Division of Gastroenterohepatology, Istanbul, Turkey; ²Istanbul University, Istanbul Faculty of Medicine, Department of Internal Medicine, Istanbul, Turkey
Email: kaymakoglus@hotmail.com

Background and aims: This study aims to investigate antiviral effectiveness, side effects, and disease outcomes in patients who have been using oral antivirals for a long-term in chronic hepatitis B (CHB).

Method: Patients with CHB who had been using tenofovir disoproxil fumarate (TDF) or entecavir (ETV) for at least 10 years were included in this retrospective study. Co-infected patients, those receiving immunosuppressive therapy, and transplant patients were excluded.

Results: Of the total 173 patients (baseline mean age 43.44 \pm 11.74 years) in the study, 110 (63.6%) were men. 33 (19.1%) patients were cirrhotic, and HBeAg was negative in 131 (75.7%) patients at the beginning of treatment. 94 (54.3%) patients were treatment-naïve. 92 (53.2%) patients used TDF and 81 (46.8%) patients used ETV for a mean of 156.76 \pm 21.60 (120–204) months. HBV-DNA negativity (<10 IU/ml) was achieved in 100% of those who received ETV and in 95.5% of those who received TDF, and there was no statistical difference between them ($p = 0.06$). Patients who remained HBV-DNA positive were non-compliant with treatment. HBsAg became negative in only 4 (2.3%) patients, 2 of them developed anti-HBs. In the total group ALT normalization (<42 U/L) was observed in 96.8% of patients with elevated baseline ALT. 13 (39.4%) of 33 patients who were cirrhotic at baseline regressed to the noncirrhotic stage, in this group, platelets were significantly high (>150 $10^3/\mu$ l) before the treatment ($p < 0.05$). 8 (5.7%) of 140 noncirrhotic patients at baseline progressed to the cirrhotic stage. 7 (4%) of all patients decompensated. In the total group, FIB-4 and APRI scores decreased significantly under treatment ($p = 0.009$ and $p = 0.000$, respectively). Hepatocellular carcinoma (HCC) developed in 9 (5.2%) patients. All HCCs occurred after the 5th year of treatment. PAGE-B score was significantly higher in those who developed HCC ($p = 0.009$). HCC was significantly more common in treatment-naïve patients ($p = 0.033$). The age at HBV diagnosis was significantly higher in HCC patients ($p = 0.023$), but the most important risk factor for the development of HCC was cirrhosis at baseline. Cirrhosis increased the risk of HCC by 7.8 times. 8 (4.6%) patients died in the follow-up, and 2 were due to liver disease and the remaining non-liver disease. During follow-up, nephropathy (GFR <60 ml/min) developed in 13 (7.5%) patients, and hypophosphatemia ($p < 2.5$ mg/dL) developed in 19 (11%) patients. The rate of side effects in TDF recipients was significantly higher ($p = 0.018$).

Conclusion: At the end of 10 years, HBV-DNA negativity was achieved in almost all patients, and HBsAg sero-clearance was rarely achieved. Treatment-related side effects were more common in TDF. Nearly half of cirrhotic patients regressed to the noncirrhotic stage. Very few patients developed HCC and the 10-year mortality rate was similar to the general population.

WED-414

Demographic, virological and clinical features of patients with chronic hepatitis delta treated with bulevirtide: a multicenter Italian study (d-shield)

Maria Paola Anolli¹, Elisabetta Degasperis¹, Giampiero D'Offizi², Alessia Rianda², Alessandro Loglio³, Mauro Viganò³, Alessia Ciano⁴, Yulia Troshina⁴, Maurizia Brunetto⁵, Barbara Coco⁵, Serena Zaltron⁶, Pierluigi Toniutto⁷, Letizia Marinaro⁸, Andrea Gori⁹, Alessandro Federico¹⁰, Teresa Santantonio¹¹, Gabriella Verucchi¹², Filomena Morisco¹³, Alessandra Mangia¹⁴, Stella De Nicola¹⁵, Monia Maracci¹⁶, Antonietta Romano¹⁷, Pietro Gatti¹⁸, Rosa Zampino¹⁹, Marcello Persico²⁰, Pietro Pozzoni²¹, Adriano Pellicelli²², Nicola Coppola²³, Francesca Pileri²⁴, Matteo Tonnini²⁵, Massimo Puoti²⁶, Pietro Lampertico^{1,27}. ¹Division of Gastroenterology and Hepatology, Foundation IRCCS Ca' Granda Ospedale Maggiore Policlinico, Milan, Italy; ²Division of Infectious Diseases-Hepatology, Department of Transplantation and General Surgery, Istituto Nazionale per le Malattie Infettive "L. Spallanzani" IRCCS, Rome, Italy; ³Gastroenterology, Hepatology and Transplantation Division, ASST Papa Giovanni XXIII, Bergamo, Italy; ⁴Department of Medical Sciences, University of Turin, Gastroenterology Division of Città della Salute e della Scienza di Turin, University Hospital, Turin, Italy; ⁵Department of Clinical and Experimental Medicine, University of Pisa and Hepatology Unit, University Hospital of Pisa, Pisa, Italy; ⁶Infectious Disease Department, Spedali Civili Brescia, Brescia, Italy; ⁷Hepatology and Liver Transplantation Unit, Academic Hospital, University of Udine, Udine, Italy; ⁸SCDU Infectious Diseases, Amedeo di Savoia Hospital, ASL Città di Torino, Turin, Italy; ⁹Infectious Disease Unit II, Ospedale Luigi Sacco, ASST Fatebenefratelli Sacco, Milan, Italy; ¹⁰Division of Hepatogastroenterology, Department of Precision Medicine, Università della Campania "Luigi Vanvitelli", Naples, Italy; ¹¹Department of Medical and Surgical Sciences, Infectious Diseases Unit, University of Foggia, Foggia, Italy; ¹²Department of Medical and Surgical Sciences, Unit of Infectious Diseases, "Alma Mater Studiorum" University of Bologna, S. Orsola-Malpighi Hospital, Bologna, Italy, Bologna, Italy; ¹³Department of Clinical Medicine and Surgery, Diseases of the Liver and Biliary System Unit, University of Naples "Federico II", Naples, Italy; ¹⁴Liver Unit, Fondazione IRCCS "Casa Sollievo della Sofferenza", San Giovanni Rotondo, Italy; ¹⁵Division of Internal Medicine and Hepatology, Department of Gastroenterology, IRCCS Humanitas Research Hospital, Rozzano, Italy; ¹⁶Institute of Infectious Diseases and Public Health, Università Politecnica delle Marche, Ancona, Italy; ¹⁷Unit of Internal Medicine and Hepatology (UIMH), Department of Medicine, University of Padova, Padova, Italy; ¹⁸Internal Medicine Unit, Brindisi General Hospital, Brindisi, Italy; ¹⁹Department of Advanced Medical and Surgical Sciences, University of Campania Luigi Vanvitelli, Naples, Italy; ²⁰Department of Medicine, Surgery and Dentistry, University of Salerno, Baronissi, Italy; ²¹Department of Internal Medicine, Liver Unit, ASST Lecco, Lecco, Italy; ²²Liver Unit, San Camillo Hospital, Department of Transplantation and General Surgery, Rome, Italy; ²³Department of Mental Health and Public Medicine-Infectious Diseases Unit, University of Campania Luigi Vanvitelli, Naples, Italy; ²⁴Division of Internal Medicine and Center for Hemochromatosis, University of Modena and Reggio Emilia, Modena, Italy; ²⁵Division of Internal Medicine, Hepatobiliary and Immunoallergic Diseases, IRCCS Azienda Ospedaliero-Universitaria di Bologna, Bologna, Italy; ²⁶School of Medicine and Surgery University of Milano Bicocca, Milano, Italy; ²⁷CRC "A. M. and A. Migliavacca" Center for Liver Disease, Department of Pathophysiology and Transplantation, University of Milan, Milan, Italy
Email: pietro.lampertico@unimi.it

Background and aims: Bulevirtide (BLV) is the only approved drug for patients with chronic hepatitis delta (CHD). In Italy this drug has been available since 2021, but no studies so far have addressed the demographic, virological and clinical features of patients treated with BLV monotherapy or in combination.

Method: Consecutive HDV patients with chronic hepatitis Delta (CHD) starting BLV 2 mg/day as monotherapy or in combination with pegIFNalpha were included in a multicenter real-life Italian study (D-SHIELD). Patients' characteristics before and during BLV treatment were collected. Virological, biochemical, clinical features were assessed.

Results: 257 patients with CHD from 26 centers were enrolled in this ongoing study. 99% received BLV 2 mg/day monotherapy: median age was 53 (28–81) years, 55% men, 96% of European origin, 83% with cirrhosis, 7% HIV-coinfected. Among patients with cirrhosis, 40% had varices, 10% had a history of HCC (active in 7%), 11% had a history of ascites (5% persistent), 3% with previous varices hemorrhage, 6% had decompensated (CPT-B) cirrhosis. At BLV start, median ALT were 79 (18–1, 074) U/L, liver stiffness measurement (LSM) 14.1 (4.0–68.1) kPa, platelets 112 (14–362) × 10³/mm³, 97% patients were on NUC therapy, 89% HBeAg negative. Median HDV RNA was 5.3 (1.5–8.2) log IU/ml and HBsAg 3.7 (0.6–4.7) log IU/ml. Patients with cirrhosis had lower HDV RNA values compared to non-cirrhotic patients (5.21 vs. 5.69 Log IU/ml, p=0.03), while no differences were observed concerning HBsAg (3.69 vs. 3.83 Log IU/ml, p=0.2) and ALT levels (80 U/L vs. 75, p=0.4).

Conclusion: D-SHIELD is the largest single country study on BLV treatment for CHD in Europe. Almost all Italian patients starting this new treatment option have been treated with 2 mg/day monotherapy. Most patients were European-born, with advanced liver disease, high viral load and elevated ALT levels.

WED-415

Effectiveness and safety analysis of switching to tenofovir alafenamide after entecavir or tenofovir treatment

Xue Liu¹, Zhihao Zhao¹, Xianggen Kong², Shiyu Cui², Xuemei Jiang².

¹Shandong university, Jinan, China; ²Shandong public health clinical center, Jinan, China

Email: shdixm@163.com

Background and aims: To investigate the effectiveness and safety of switching to tenofovir alafenamide (TAF) in patients with chronic viral hepatitis B after taking entecavir (ETV) or tenofovir (TDF) in a real-life setting.

Method: A total of 149 patients with chronic viral hepatitis B who had impaired renal function or were potentially at risk, or chronic viral hepatitis B with low viral load, were enrolled in the study from January 1, 2013 to May 1, 2023 by Shandong Public Health Clinical Center. The patients were divided into G1: ETV-TAF (61 patients) and G2: TDF-TAF (88 patients). All patients were followed up for at least 48 weeks. During the follow-up period, HBV DNA levels, HBsAg quantitative levels, liver function, renal function and blood lipids were collected, analyzed and compared between the two groups.

Results: At baseline, there were no statistical differences between the two groups in the rate of complete virologic response, quantitative HBsAg levels, or ALT levels. At 48 weeks of switching to TAF, both groups had significantly higher rates of complete virological response (G1: 54.1% vs. 67.2%, $\chi^2 = 48.865$, P=0.000; G2: 63.6% vs. 77.3%, $\chi^2 = 3.931$, P=0.047) and significantly lower quantitative HBsAg levels (G1: z = -4.879, p=0.000; G2: z=3.174, p=0.002) and lower mean ALT values (G1: z=2.237, p=0.000; G2: z= -2.571, p=0.010) compared to baseline. In the both groups, eGFR levels increased compared with baseline, but there was no statistically difference at weeks 48. At baseline, 16 and 33 patients in the ETV-TAF group and TDF-TAF group, had an eGFR of less than 90 ml/min/1.73 m², and after 48 weeks of switching to TAF therapy, 6 patients in each group had an eGFR of greater than 90 ml/min/1.73 m². Median urinary beta-2 microglobulin levels improved significantly from baseline in both groups after 48 weeks of switching to TAF (G1: z= -2.785, p=0.005; G2: z= -4.008, p=0.000). There were no significant differences in triglyceride, LDL, total cholesterol, and HDL levels compared to

baseline at 24 and 48 weeks after switching in the ETV-TAF group, whereas in the TDF-TAF group at 48 weeks after switching, LDL and total cholesterol levels were higher compared to baseline, but there was no statistically difference in the proportion of patients with dyslipidaemia after 48 weeks of switching to TAF treatment in both the ETV-TAF group and the TDF-TAF group compared to baseline.

Conclusion: In patients with impaired renal function or potentially at risk for chronic hepatitis B, or chronic viral hepatitis B with low viral load, switching from ETV or TDF to TAF resulted in sustained enhancement of virologic response, sustained reduction in surface antigen levels, and improvement in ALT. Notably, patients experienced improvements in glomerular function and tubular markers.

WED-418

A national multicenter study on initial antiviral treatment preferences on chronic hepatitis B: Entecavir versus Tenofovir disoproxil fumarate

Tansu Yamazhan¹, Esra Zerdali², Yusuf Onlen³, Selma Tosun⁴, Özgür Günel⁵, Ayşe Batirel⁶, İmran Hasanoğlu⁷, Tuba Turunç⁸, Umay Balcı⁹, Sibel Yıldız Kaya¹⁰, Oğuz Karabay¹¹, İlknur Esen Yıldız¹², Lütüye Nilsun Altunal¹³, Deniz Cevahir Ozkaya¹⁴, Selçuk Kaya¹⁵, Ayşe İnci¹³, Sevil Alkan¹⁶, Dilek Yıldız¹³, Tayibe Bal¹⁷, Esma Aslıhan Aydemir¹⁸, Nurullah Eser¹⁹, Serhat Uysal²⁰, Fehmi Tabak¹⁰, Rahmet Güner²¹. ¹Ege University Infectious Diseases and Clinical Microbiology, İzmir, Turkey; ²Sağlık Bilimleri University, İstanbul, Turkey; ³Mustafa Kemal University, Hatay, Turkey; ⁴Sağlık Bilimleri University, İzmir, Turkey; ⁵Samsun University, Samsun, Turkey; ⁶Sağlık Bilimleri University, İstanbul, Turkey; ⁷Sağlık Bilimleri University, Ankara, Turkey; ⁸Sağlık Bilimleri University, Adana, Turkey; ⁹Sağlık Bilimleri University, Antalya, Turkey; ¹⁰Cerrahpaşa University, İstanbul, Turkey; ¹¹Sakarya University, Sakarya, Turkey; ¹²Recep Tayyip Erdoğan University, Rize, Turkey; ¹³Sağlık Bilimleri University, İstanbul, Turkey; ¹⁴Sağlık Bilimleri University, İzmir, Turkey; ¹⁵Onsekiz Mart University, Çanakkale, Turkey; ¹⁶Onsekiz Mart University, Çanakkale, Turkey; ¹⁷Abant İzzet Baysal University, Bolu, Turkey; ¹⁸Samsun University, Samsun, Turkey; ¹⁹Sağlık Bilimleri University, İstanbul, Turkey; ²⁰Fırat University, Elazığ, Turkey; ²¹Sağlık Bilimleri University, Ankara, Turkey Email: tansuyamazhan@gmail.com

Background and aims: No current medications for chronic HBV treatment aim at eradicating the virus; therefore, the main goal of successful therapy is achieving functional cure through long-term or lifelong treatments. In selecting the initial antiviral drug, identifying comorbidities and monitoring possible long-term side effects are key considerations outlined in national and international guidelines. This study investigates whether there are statistically significant differences/differences in patient or disease parameters when a physician initiates entecavir (ETV) or tenofovir disoproxil fumarate (TDF) in a chronic HBV patient.

Method: Patient data was recorded by "electronic patient follow-up form. Treatment naïve, >18 years old, diagnosed with chronic HBV for at least 1 year since 2010 and initiated on antiviral therapy were included. Patients' data, including age and gender, age at diagnosis and treatment initiation, body mass index (BMI), the presence of comorbidities, liver disease activity, liver biopsy results, presence of cirrhosis and/or hepatic steatosis, the status of the virus via HBeAg positivity result, HBV-DNA levels; host factors including renal functions, cholesterol, triglyceride levels and basal bone mineral density (BMD), assessed using dual-energy X-ray absorptiometry (DEXA) test.

Results: The study involved 31 centers from Türkiye. Data from a total of 2,259 (1,391 were male (61.6%)) patients were analyzed. Among the participants, with 1,270 patients (56.22%) initially opting for TDF

and 989 (43.78%) for ETV. ETV was preferred in males, while TDF was chosen more in females ($p = 0.005$). The mean of ages at diagnosis and treatment initiation for ETV were $40, \pm 13$, and $44, \pm 13$ and for TDF they were $36, \pm 13$, and $40, \pm 12$ ($p < 0.001$). TDF was more often chosen as the initial treatment in patients with lower BMI (median 25.7 versus 26.2 $p = 0.001$). The median initial creatinine level for TDF and ETV was 0.75 and 0.80 respectively ($p < 0.001$). The situation is similar for eGFR, where the median for the ETV group was 94.37, TDF group was 101.12. In patients with an initial eGFR value < 60 ($n = 36$), upon reevaluation, physicians favored ETV as the initial drug choice ($p < 0.001$). BMD was assessed in 365 (16.3%) patients prior to treatment. DEXA tests were conducted in 116 (11.8%) and 249 (19.8%) patients who were to start ETV and TDF, respectively ($p < 0.001$).

Conclusion: Our study is an important national multicenter study with a broad patient series that clearly outlines the factors considered by infectious disease and hepatology specialists when initiating treatment for chronic HBV. Patient-related parameters; gender, age at diagnosis and treatment initiation of the disease, baseline renal functions, and the status and stage of the virus or liver disease have been found to be more important than the disease itself in drug selection.

WED-419

Comparative efficacy of standard and low-dose peginterferon-alpha2a in chronic delta hepatitis: a retrospective controlled study

Asim Qurbanov¹, Elvan Isik², İlker Turan², Galip Ersoz², Fulya Günsar², Zeki Karasu², Ulus Akarca². ¹Ege University, Faculty of Medicine, Department of Internal Medicine, İzmir, Turkey; ²Ege University, Faculty of Medicine, Department of Gastroenterology, İzmir, Turkey Email: ulusakarca@gmail.com

Background and aims: Chronic delta hepatitis represents the most severe form of viral hepatitis, yet therapeutic options remain limited. While interferon-based therapies have been the cornerstone of treatment, their use is hampered by substantial side effects and marginal efficacy. This study assesses the effectiveness and tolerability of standard-dose versus low-dose peginterferon-alpha2a in patients with compensated chronic delta hepatitis.

Method: We conducted a retrospective analysis of patients treated with peginterferon-alpha2a at our center from 2000 to 2020. Patients receiving low-dose therapy (135 or 90 ug per week) over the past 5 years were compared with those treated with the standard dose (180 ug per week). End points included alanine aminotransferase (ALT) normalization and Delta RNA clearance.

Results: Our cohort comprised 45 patients, predominantly male (73%) with a mean age of 45.2 years. Treatment distribution was 20 patients on standard dose and 25 on low dose. Pretreatment transaminase levels, platelets counts, prothrombin time, renal functions, HBV DNA and HDV RNA levels, rates of cirrhosis and prior interferon use were comparable. Cirrhosis was present in 38%, and 36% had prior interferon therapy. Median treatment durations in regular and low dose groups were 13 and 12 months, respectively. The complete response rates at 6, 12, and 18 months for standard and low-dose groups were 35%, 45%, 30% and 20%, 24%, 28%, respectively, with no significant differences. Side effect profiles were similar, though less hematological toxicity was noted in the low-dose group.

Conclusion: Low-dose peginterferon-alpha2a demonstrates comparable efficacy to the standard dose in chronic delta hepatitis, with a trend toward a better side effect profile. This approach may offer a cost-effective alternative in managing this challenging condition.

WEDNESDAY 05 JUNE

Viral Hepatitis B and D – New therapies, unapproved therapies or strategies

WED-361

Dosing with the Capsid Assembly Modulator ALG-000184 in Untreated HBeAg Negative CHB Subjects Results in Potent Antiviral Effects Including Suppression of HBV DNA/RNA and Declines in HBcrAg Levels

Kosh Agarwal¹, Edward J. Gane², Man-Fung Yuen³, Christian Schwabe⁴, Alina Jucov⁵, Alexei Hacetean⁵, Min Wu⁶, Kha Le⁶, Maida Maderazo⁶, Lawrence Blatt⁶, Sushmita Chanda⁶, Tse-I Lin⁶, Matt McClure⁶. ¹King's College Hospital, Institute of Liver Studies, London, United Kingdom; ²Faculty of Medicine, University of Auckland, Auckland, New Zealand; ³Department of Medicine, School of Clinical Medicine, The University of Hong Kong, Hong Kong, China; ⁴New Zealand Clinical Research Limited, Auckland, New Zealand; ⁵ARENIA Exploratory Medicine, Republican Clinical Hospital and Nicolae Testemitanu State University of Medicine and Pharmacy, Chisinau, Moldova; ⁶Aligos Therapeutics, Inc., South San Francisco, United States Email: kosh.agarwal@kcl.ac.uk

Background and aims: ALG-000184 is a prodrug of ALG-001075, a potent chronic hepatitis B (CHB) capsid assembly modulator-empty (CAM-E) that inhibits viral replication and cccDNA establishment in vitro.

Method: ALG-000184-201 is a multi-part, multi-center, double-blind, randomized, placebo-controlled study (NCT04536337). In Part 4 Cohort B, eligible treatment naïve or currently-not-treated HBeAg+ and HBeAg- CHB subjects are receiving open-label daily doses of 300 mg ALG-000184 alone × ≤96 weeks. Previously, we reported that HBeAg+ subjects treated for ≤48 weeks in this cohort experienced potent antiviral effects as seen by declines in HBV DNA, RNA and multiple antigen levels (Yuen et al., AASLD 2023). Here we report for the first time antiviral and safety data in HBeAg- subjects who received 300 mg ALG-000184 monotherapy × ≤40 weeks.

Results: 11 HBeAg- subjects were enrolled with a mean age of 48 years; they were 55% male, 73% non-Asian and had a mean (SEM) BMI of 26 (1.1) kg/m². Subjects were infected with HBV genotype D (n = 7, 64%), B (n = 2, 18%), C (n = 1, 9%) and A (n = 1, 9%). At baseline, mean (SEM) viral marker values were: 4.3 (0.2) log₁₀ IU/ml for DNA, 2.0 (0.3) log₁₀ copies/ml for RNA, 3.5 (0.2) log₁₀ IU/ml for HBsAg and 3.1 (0.3) log₁₀ IU/ml for HBcrAg. During 300 mg ALG-000184 monotherapy, all subjects achieved undetectable HBV DNA (<10 IU/ml) within 20 weeks and RNA (<10 copies/ml) levels within 42 days. No viral breakthroughs have occurred. HBcrAg levels (iTACT-HBcrAg assay, LLOQ: <1.8 log₁₀ IU/ml) declined rapidly in the first 28 days of treatment followed by a slower downward trend. The maximum mean (SEM) and individual HBcrAg reductions through Week 40 were 0.5 (0.2) log₁₀ IU/ml and 0.7 log₁₀ IU/ml, respectively. HBcrAg reductions ≥0.5 log₁₀ IU/ml have been observed in 40% of subjects and one additional subject (with a low baseline level) became undetectable at Day 28, which has been maintained throughout treatment. No clinically significant decline was observed in HBsAg. The ALG-000184 safety profile remains favorable with no serious adverse events or discontinuations due to treatment-emergent adverse events (TEAEs) reported. Grade ≥3 TEAEs were reported in 2 subjects: an asymptomatic cholesterol and triglycerides increase (n = 1), which has been improving despite continued dosing, and one asymptomatic liver transaminase elevation (n = 1), which resolved despite continued dosing and was without clinically significant changes of liver synthetic function. This event was assessed as not being related to drug toxicity by an independent safety committee.

Conclusion: Consistent with its in vitro antiviral properties, dosing with ALG-000184 demonstrated dual antiviral effects in untreated HBeAg- CHB subjects: complete suppression of HBV DNA and RNA, suggesting inhibition of HBV replication, as well as reducing HBcrAg levels, indicating inhibition of cccDNA establishment/replenishment.

WED-362

Rapid hepatitis B surface antigen reduction in chronic hepatitis B virus infection: preliminary results from a phase I b study evaluating multiple ascending doses of HT-102, a neutralizing antibodies against hepatitis B surface antigen in chronic hepatitis B patients

Dong Wang¹, Shanzhong Zhang¹, Yanqin Ma¹, Lijuan Ding¹, Zhipeng Zhang¹, Ying Qu², Lungen Lu². ¹Suzhou Hepa Thera Biopharmaceutical Co.Ltd., Shanghai, China; ²Department of Gastroenterology, Shanghai General Hospital, Shanghai, China Email: wangdong@hepathera.com

Background and aims: HT-102 is a human monoclonal antibody targeting the conserved antigenic loop of hepatitis B surface antigen (HBsAg) with the potential to functions as 1) inhibition of hepatitis B virus (HBV) entry into cells, 2) elimination of virions and sub-viral particles for the treatment of chronic HBV infection. Single dose of HT-102 up to 600 mg were well tolerated in healthy subjects. Here, we reported preliminary Phase Ib data in subjects with chronic HBV infection.

Method: This was a randomized, double-blind, placebo-controlled, phase Ib, multiple ascending doses study of HT-102 administered via subcutaneous (SC) injection to subjects with chronic HBV infection. The 1b part enrolled subjects who were on nucleos (t)ide reverse transcriptase inhibitor (NRTI) therapy ≥2 months and had HBsAg >200 IU/ml, <3, 000 IU/ml with hepatitis B e antigen (HBeAg) negative at screening and HBV DNA <2, 000 IU/ml within 3 months before screening. Eligible patients were assigned to 50 mg, 150 mg, or 300 mg group to receive 5 SC HT-102 doses, every week for 4 weeks. Eight subjects per cohort were randomized (6:2) to receive HT-102 or placebo. All patients received NRTI treatment throughout the study. Patients were followed-up to Day 70 after the first HT-102 or placebo dosed. The protocol conformed to the Declaration of Helsinki guidelines and was approved by appropriate institutional review committee (s). Written informed consent was obtained prior to study procedures. Preliminary blinded data for the ongoing cohort evaluating 50 mg and 150 mg were presented.

Results: Sixteen subjects were enrolled in 50 mg, 150 mg of HT-102 or placebo and 12 subjects were randomized to receive 5 SC doses of HT-102, and 4 to receive placebo. Demographic and baseline characteristics were well balanced across cohorts (baseline HBsAg: 2.96 ± 0.35 log₁₀ IU/ml for 50 mg group; 2.82 ± 0.24 log₁₀ IU/ml for 150 mg group). In 50 mg group six subjects rapidly achieved mean 2.1 log₁₀ IU/ml decline in HBsAg from baseline at nadir and in 150 mg group six subjects achieved mean HBsAg decreases 2.4 log₁₀ IU/ml at nadir with sustained HBsAg declines for 4 weeks post last dose (4 subjects without HBsAg reduction were excluded in two cohorts). So far, all patients showed good safety and tolerability. All adverse event (AE)s were grade 1 or 2. No serious AEs or discontinuations due to AEs were reported. No subjects developed clinical or laboratory evidence of immune complex disease. Additional follow-up is ongoing.

Conclusion: Multiple doses of HT-102 50 mg or 150 mg was associated with rapid HBsAg reductions in the majority of subjects and greater HBsAg decline with longer sustained duration was observed in 150 mg group. Preliminary safety data suggested that HT-102 is generally well tolerated in CHB patients with NRTI. These early data support further evaluation of HT-102 as a potential functional cure for patients with chronic HBV infection.

WED-363

Promising preliminary data on preclinical efficacy with an innovative plasmid-launched live attenuated virus vaccine for chronic hepatitis B

Frederik Pauwels¹, Goele Bosmans¹, Sarah Provost¹, Thomas Vercruysse¹, Joeri Auwerx¹, Gregory Fanning¹, Mathieu Peeters¹, Wilfried Dalemans¹, Hanne Callewaert¹. ¹AstriVax, Leuven, Belgium
Email: frederik.pauwels@astrivax.com

Background and aims: AstriVax is developing a vaccine platform technology that is suitable for prophylactic and therapeutic applications and is based on a plasmid-launched live attenuated virus (PLLAV) encompassing flaviviruses, like yellow fever virus (YFV) 17D vaccine strain that can carry foreign antigens. The YFV vaccine is one of the most effective vaccines available, inducing long-lived humoral responses as well as strong cellular immunogenicity. With the therapeutic potential of our platform, we initiated development of a potential best-in-class vaccine for chronic hepatitis B infection, where the induction of effective and long-lasting CD8 T-cell responses is considered key in eliminating infected hepatocytes.

Method: The hepatitis B virus (HBV) core (HBc) was used as a model antigen to insert into the polyprotein encoding YFV 17D. The ability of this recombinant live-attenuated virus (LAV) to induce cellular immune responses against HBc was evaluated preclinically in a mouse model permissive for YFV replication (deficient in interferon (IFN) signaling). Given the complexity of the animal models that can be used with this platform we performed an initial assessment of the effect of the induced HBc-specific T-cells on viral parameters in AAV-HBV transduced C57BL/6 mice by adoptive transfer ± liver micro-environment modulation using a toll-like receptor (TLR) 9 agonist.

Results: Single injection of YFV-HBc PLLAV induced YFV and HBc specific T-cell responses in uninfected permissive mice. Similarly, an immunization with PLLAV-derived YFV-HBc LAV resulted in the detection of comparable numbers of IFN-gamma spot-forming cells upon stimulation with peptides for YFV and HBc antigen. Adjuvanted HBc protein prime followed by YFV-HBc LAV vaccination 15 days later increased the number of IFN-gamma secreting HBc-specific T-cells compared to YFV-HBc LAV only vaccination. Isolated splenocytes were then used for passive immunization of C57BL/6 mice with established AAV-HBV infection and high surface antigen (HBsAg) baseline (>4 log IU/ml), resulting in significant decreases in serum HBsAg, transient transaminase increase and a reduction in transduced hepatocytes positive for HBc when combined with a TLR9 agonist.

Conclusion: We found that a YFV PLLAV carrying an HBc antigen induced robust T-cell responses against HBc in a YFV-permissive mouse model. Furthermore, we were able to show that adoptive transfer of heterologous prime-boost generated T-cells resulted in a sustained decline of HBV persistence, despite high baseline HBsAg levels. These promising early efficacy data demonstrate the potential of YFV-vectored vaccines in inducing strong and effective T-cell responses, and warrant further preclinical characterization of the vaccine platform in direct vaccination settings and evaluation in human studies as part of therapeutic regimen for chronic hepatitis B.

WED-364

High-dimensional analysis of flow cytometry data reveals differences in post-treatment frequencies of naïve B cells, CD56dim natural killer cells, and terminally differentiated effector memory CD8+ T cells in responders versus non-responders to bepirovirsen

Thea Hogan¹, Eduardo Gomez Castaneda¹, Esther Perez Garcia¹, Ruth Barnard¹, Avijit Ray², Melanie Paff², Dickens Theodore³, Jennifer M. Singh². ¹GSK, Stevenage, United Kingdom; ²GSK, Collegeville, PA, United States; ³GSK, Durham, United States
Email: jennifer.m.singh@gsk.com

Background and aims: Bepirovirsen (BPV) is an unconjugated antisense oligonucleotide in development for the treatment of chronic hepatitis B virus (HBV) infection. In the Phase 2b B-Clear study, 9–10% of participants (pts) with chronic HBV infection who received BPV 300 mg for 24 weeks achieved the primary outcome (hepatitis B surface antigen and HBV DNA loss sustained for 24 weeks off-treatment). This post hoc investigation used high-dimensional analysis of flow cytometry data to understand the immunological landscape in pts who received BPV in B-Clear and determine whether cell frequencies and/or phenotypes differ with treatment time and/or response.

Method: Flow cytometric analysis was performed on 114 peripheral blood mononuclear cell samples from 47 pts using a 30-colour deep immunophenotyping panel. Cells were visualised in a reduced dimensionality space (UMAP) and metaclustered using FlowSOM. Metaclusters showing differential abundance according to the pts off-treatment response (e.g. primary outcome responder, null responder) or change in abundance relative to baseline (ARB) at 3 post-treatment timepoints (off-treatment Day 1, 78 and 162) were further evaluated for phenotypic annotation. Analyses were descriptive. Selection was made based on sample availability.

Results: Baseline demographics and disease characteristics were similar between those who had flow analysis and those that did not. The UMAP space revealed unique cell clusters between primary outcome responders and null responders. FlowSOM analysis identified 17 B cell, 18 natural killer (NK) cell and 14 T cell metaclusters. Two B cell metaclusters showed increased ARB in primary outcome responders versus null responders at all post-treatment timepoints; both metaclusters had a phenotype consistent with naïve B cells. One NK cell metacluster showed increased ARB at later timepoints (off-treatment Day 78 and 162) in primary outcome responders versus null responders, with a phenotype consistent with CD56dim NK cells. One T cell metacluster showed increased ARB at all post-treatment timepoints in primary outcome responders versus null responders, with phenotypes consistent with the terminally differentiated effector memory (TEMRA) CD8+ T cell subset (Granzyme B+ and T cell factor 1+) and T cells expressing Valpha 7.2+ T cell receptor.

Conclusion: This high-dimensional analysis revealed increases in the post-treatment abundance of naïve B cells, CD56^{dim} NK cells and TEMRA CD8+ T cells in responders versus non-responders to BPV in B-Clear. This analysis provides a first glance at the immunological landscape in pts treated with BPV. These data will shape analyses that will be applied to subsequent clinical trials to further elucidate the immune response in BPV-treated pts.

Funding: GSK (study 209668).

WED-365

Extended treatment of HBeAg+ CHB subjects with the Capsid assembly modulator ALG-000184 with or without Entecavir is associated with reductions in viral markers and favorable anti-HBeAb trends

Man-Fung Yuen¹, Edward J. Gane², Kosh Agarwal³, Junqi Niu⁴, Hong Ren⁵, Yanhua Ding⁴, Xieer Liang⁶, Xian Yu⁵, Jia Xu⁴, Alina Jucov⁷, Alexei Haceatrea⁸, Min Wu⁹, Kha Le⁹, Maida Maderazo⁹, Lawrence Blatt⁹, Sushmita Chanda⁹, Tse-I Lin⁹, Matt McClure⁹, Jinlin Hou⁶. ¹The University of Hong Kong, Hong Kong, China, ²University of Auckland, Auckland, New Zealand; ³King's College Hospital, Institute of Liver Studies, London, United Kingdom; ⁴The First Hospital of Jilin University, Changchun, China; ⁵The Second Affiliated Hospital of ChongQing Medical University, Chongqing, China; ⁶Nanfeng Hospital, Southern Medical University, Guangzhou, China; ⁷RENSIA Exploratory Medicine, Republican Clinical Hospital and Nicolae Testemitanu State University of Medicine and Pharmacy, Moldova, Chisinau, Moldova; ⁸ARENSIA Exploratory Medicine, Republican Clinical Hospital and Nicolae Testemitanu State University of Medicine and Pharmacy, Chisinau, Moldova; ⁹Aligos Therapeutics, Inc., South San Francisco, United States
Email: jlhoumu@163.com

Background and aims: ALG-000184 is a prodrug of ALG-001075, a potent chronic hepatitis B (CHB) capsid assembly modulator-empty that inhibits viral replication and cccDNA establishment in vitro.

Method: ALG-000184-201 is a multi-part, multi-center, double-blind, randomized, placebo-controlled study (NCT04536337). In Part 4, eligible treatment naïve or currently-not-treated HBeAg+ CHB subjects were either randomly assigned (3:1) to receive oral daily doses of 300 mg ALG-000184 or placebo + entecavir (ETV) × 12 weeks followed by open-label treatment with 300 mg ALG-000184 + ETV × ≤96 weeks (Cohort 2); or receive open-label daily doses of 300 mg ALG-000184 alone × ≤96 weeks. Previously, we reported data of up to 48 weeks of treatment from these 2 cohorts, which showed greater reductions in HBV DNA/RNA and HBV antigens for ALG-000184 ± ETV vs. ETV alone. Here we report data after receiving 300 mg ALG-000184 ± ETV × ≤64 weeks.

Results: 22 HBeAg+/HBeAb- subjects were enrolled and received ≥12 weeks of treatment with ALG-000184 + ETV (n = 12) or ALG-000184 alone (n = 10). Mean (SEM) baseline viral marker values were HBV DNA 8.0 (0.2) log₁₀ IU/ml; HBV RNA 6.0 (0.3) log₁₀ copies/ml; HBSAg 4.3 (0.1) log₁₀ IU/ml; HBeAg 2.4 (0.1) log₁₀ PEI U/ml and HBcrAg 8.3 (0.1) log₁₀ U/ml. After receiving 300 mg ALG-000184 ± ETV × ≤64 weeks, maximum (max) mean (SEM) reductions of HBV DNA and RNA were 7.1 (0.4) log₁₀ IU/ml and 4.7 (0.7) log₁₀ copies/ml. Of these subjects, 55% (n = 12) and 100% (n = 22) achieved <LLOQ for HBV DNA and RNA. No viral breakthrough has been observed in subjects receiving ALG-000184 alone. Mean (SEM) and max reductions in HBSAg, HBeAg, and HBcrAg were: 1.2 (0.4) and 2.1 log₁₀ IU/ml, 1.8 (0.2) and 2.2 log₁₀ PEI U/ml, 2.3 (0.3) and 2.7 log₁₀ IU/ml, respectively. In parallel to HBeAg declines, mean (SEM) cut-off index (COI) of ROCHE Elecsys HBeAb assay (≤1 COI indicates anti-HBe positive) trended favorably, i.e. declining from baseline 5.2 (0.7) to 1.4 (0.1), suggestive of more non-HBeAg bound circulatory HBeAb. Two subjects have achieved HBeAb COI <1 along with substantial qHBeAg declines, which may suggest an ongoing transition to HBeAg seroconversion. Safety data continue to indicate ALG-000184 is well tolerated: no serious adverse events or discontinuations due to treatment-emergent adverse events (TEAEs) have been reported; Grade ≥3 TEAEs were reported in 7 subjects: uric acid increase (n = 1), eGFR decrease (n = 1), neutropenia (n = 1), cholesterol, triglycerides increase (n = 1) and ALT/AST elevations (n = 5). All resolved, improved or stabilized despite continued ALG-000184 dosing and were assessed by an independent safety committee as not being related to drug toxicity.

Conclusion: Treatment of HBeAg+ CHB subjects with ALG-000184 ± ETV continues to be well tolerated and lowers key viral markers over time. In parallel, an immunologic response may be emerging as evidenced by favorable trends for anti-HBeAb levels.

WED-366

Characterization of BJT-778, an anti-HBsAg neutralizing monoclonal antibody for treatment of hepatitis B virus and hepatitis D virus infections

Hilario Ramos¹, Ronald Alcala^{2,3,4}, Maud Michelet^{2,3,4}, Emmanuel Combe^{2,3,4}, Jerome Deval¹, Roy Grecko¹, Kevin Lin¹, Nancy Shulman¹, Fabien Zoulim^{2,3,4,5}, Keting Chu¹, Barbara Testoni^{2,3,4}, Hassan Javanbakht¹. ¹Bluejay Therapeutics, San Mateo, United States; ²INSERM U1052, CNRS UMR-5286, Cancer Research Center of Lyon (CRCL), Lyon, France; ³University of Lyon, Université Claude-Bernard (UCBL), Lyon, France; ⁴Hepatology Institute of Lyon, Lyon, France; ⁵Department of Hepatology, Croix Rousse Hospital, Hospices Civils de Lyon, Lyon, France
Email: hramos@bluejaytx.com

Background and aims: Chronic hepatitis B (CHB) is a major health problem around the world, impacting millions of people. Compared to CHB infection alone, co-infection with Hepatitis D Virus (HDV) is associated with more severe liver disease, causing faster progression to cirrhosis, hepatocellular carcinoma, and liver failure. In this

context, we have characterized BJT-778, a potent, pan-genotypic, fully human immunoglobulin G1 (IgG1) monoclonal antibody (mAb) with anti-HBsAg neutralizing properties, demonstrating its potential for the treatment of CHB and Chronic Hepatitis D (CHD).

Method: The binding affinity of BJT-778 to HBsAg was assessed using surface plasmon resonance. An enzyme-linked immunosorbent assay (ELISA) was used to assess the BJT-778 binding profile with representative HBsAg isolates from the major genotypes of HBV. The specificity of BJT-778 was evaluated using a Retrogenix human plasma membrane protein binding cell array, which includes 4, 955 overexpressed human membrane proteins. Furthermore, in vitro neutralization was determined against HBV and HDV enveloped with HBsAg representing major HBV genotypes. The in vivo efficacy of BJT-778 was also investigated in a humanized Fah/Rag2/IL-2rγ triple knockout (FRG) mouse model of chronic HBV infection.

Results: BJT-778 is a potent, selective, fully human IgG1-neutralizing mAb that targets the antigenic loop present in all forms of HBsAg proteins. It binds with high affinity to the HBsAg protein, with K_d values ranging from 0.22 to 0.39 nM. BJT-778 demonstrates effective binding to HBsAg proteins across major HBV genotypes, with half-maximal inhibitory concentration (IC₅₀) values ranging from 0.02 to 0.07 nM. It neutralizes both HBV and HDV infections in vitro, exhibiting picomolar half-maximal effective concentration (EC₅₀) values. Furthermore, its neutralization activity is pan-genotypic, as evidenced by tests conducted with HDV enveloped with HBsAg from major genotypes. Additionally, BJT-778 is highly specific for HBsAg and did not show significant binding to any of the 4, 955 tested human membrane proteins at a concentration of 2 µg/ml. In a humanized FRG mouse model, a 20 mg/kg dose of BJT-778 demonstrated rapid depletion of HBsAg from serum, achieving a reduction of 2.88₁₀ logs within 30 minutes post-antibody administration. In contrast, the IgG control, a negative control antibody, exhibited minimal activity against HBsAg in this model.

Conclusion: BJT-778 is a potent, selective, fully human IgG1-neutralizing mAb that can neutralize HBV and HDV infections in vitro and clear HBsAg-containing particles from serum in a humanized mouse model. BJT-778 is currently undergoing clinical evaluation in subjects with CHB and CHD infections.

WED-367

Viral sequence analysis of chronic hepatitis B (CHB) patients treated with the silencing RNA (siRNA) JNJ-3989 in the REEF-1 and REEF-2 clinical studies

Thierry Verbinen^{1,1}, Erkki Lathouwers¹, John Jerzowski², Michael Biermer¹, Craig Grant³, Kosh Agarwal⁴, Man-Fung Yuen⁵, Sandra De Meyer¹, Oliver Lenz¹. ¹Janssen Pharmaceutica NV, Beerse, Belgium; ²Janssen Research and Development, LLC, Titusville, United States; ³Janssen RandD, High Wycombe, United Kingdom; ⁴Institute of Liver Studies, King's College Hospital, London, United Kingdom; ⁵Department of Medicine, The University of Hong Kong, Hong Kong, China
Email: tverbinn@its.jnj.com

Background and aims: JNJ-3989 is an siRNA composed of 2 triggers targeting the HBsAg and HBx protein open reading frame. Baseline (BL) polymorphisms in the target region complementary to positions 2–18 of the S- and X-trigger, considered potentially relevant for binding and activity, were present in 10% and 2.4% of not currently treated (NCT) REEF-1 patients, respectively, with no impact on JNJ-3989 induced HBsAg decline.

Here, viral sequence changes in the S-/X-trigger target regions were evaluated in patients with virologic relapse (VR; at least transient off-treatment increase in HBV DNA to >200 IU/ml from <LLOQ) after discontinuation of all treatment in REEF-1 (NCT03982186) and REEF-2 (NCT0412954).

Method: HBV DNA/RNA was extracted from on- and off-treatment plasma samples with sufficiently high HBV DNA/RNA levels and HBV genome was sequenced using Illumina sequencing. Nucleotide (nt)

variants were defined as changes versus the universal HBV reference sequence (sequence read frequency >15%).

Results: In REEF-1, VR occurred in 30/37 (81%) JNJ-3989 treated virologically suppressed (VS) patients stopping all treatment in REEF-2, in 54/77 (70%) JNJ-3989 treated and 39/40 (98%) NA-control arm patients, respectively. Across both studies 114/123 (93%) VS patients with VR had off-treatment HBV sequence data available. Variants at X-trigger target region positions of interest (POI) were more frequently observed off-treatment in JNJ-3989 treated VS patients than in NA-control arm VS patients with VR (56% and 5.7%, respectively). Variants at X-trigger target region POI 1794, 1785, and 1784 were observed off-treatment with a prevalence of 43%, 18% and 6.5%, respectively, which is higher than the prevalence of these variants off-treatment in either NA-only treated patients with VR (range: 0%–2.9%) or observed at baseline in REEF-1 NCT patients (range: 0%–1.2%). Variants at S-trigger target region POI were present off-treatment in 33% of JNJ-3989- and 19% of NA-only treated VS patients with VR and majority had variant at S-trigger POI 273, also frequently (10%) observed as at baseline in REEF-1 NCT patients. To assess if these variants observed during off-treatment follow-up were selected on-treatment, EOT samples from 30 NCT JNJ 3989-treated patients were evaluated using HBV RNA based sequencing and no emerging variants at S- or X-trigger target POI were detected. Off-treatment HBsAg kinetics did not differ between JNJ-3989 treated patients with and without variants in S-/X-trigger target POI observed during VR.

Conclusion: In JNJ-3989-treated patients who discontinued all treatment and experienced VR, variants within the X-trigger target region were frequently observed during VR but were not selected on-treatment, suggesting that these X-trigger variants developed off-treatment in JNJ-3989 treated patients. Presence of these variants did not impact off-treatment HBsAg kinetics.

WED-370

Bepirovirsen immune mechanism of action may potentiate infected hepatocyte killing: indirect evidence from B-together peripheral longitudinal biomarker analysis

Shilpy Joshi¹, Johannes Freudenberger¹, Jennifer M. Singh¹, Leigh Felton², Susan Dixon², Melanie Paff¹, Dickens Theodore³, Jill Walker⁴, ¹GSK, Collegeville, PA, United States; ²GSK, London, United Kingdom; ³GSK, Research Triangle Park, NC, United States; ⁴GSK, San Francisco, CA, United States
Email: shilpy.s.joshi@gsk.com

Background and aims: B-Together assessed efficacy and safety of sequential bepirovirsen (BPV), an unconjugated antisense oligonucleotide, followed by pegylated interferon (PegIFN) in participants (pts) with chronic hepatitis B virus (HBV) infection. Previously, we demonstrated that pts treated with BPV may experience transient alanine transaminase (ALT) increases. We investigated the role of BPV's immune mechanism of action (MoA) with respect to virological response (VR) and surrogate markers associated with hepatocyte cell death using peripheral longitudinal biomarker exploratory analysis.

Method: B-Together was a Phase 2b trial in 108 pts on stable nucleos(t)ide analogues. Pts were randomised (1:1) to receive BPV for 12 or 24 weeks followed by up to 24 weeks of PegIFN. The primary end point was the proportion of pts with hepatitis B surface antigen and HBV DNA below the limit of detection for 24 weeks after end of treatment (tx). Here, peripheral blood mononuclear cells, blood, and serum samples were subjected to flow cytometry, whole blood transcriptomics (WBT) and proteomics analyses, respectively. Relative expression was measured at baseline (BL) and post-BL at multiple timepoints during the BPV, PegIFN and off-tx phases. To determine differential expression, multivariate models were fit that included tx arms and VR subgroups.

Results: By Week 3, BPV led to a significant increase from BL in mean expression of serum proteins, including several cytokines, independent of arms or VR subgroups. These proteins showed enrichment in

immune effector response and apoptotic pathways. After 4 weeks of BPV, upward trends in proliferating activated CD8+ T-cells and B-cells were observed with a significant increase in mean expression from BL of some genes associated with proliferation in WBT independent of arms or response subgroups. After 7 weeks of BPV tx, a subset of proteins including liver and apoptosis-specific proteins showed increased abundance in serum and were more pronounced in BPV responders. Abundance of these proteins was highly correlated with ALT levels, which in turn was sometimes associated with transient low level HBV DNA elevations in serum; indirectly linking the observation to infected hepatocyte death.

Conclusion: BPV led to activation of the immune response in treated pts, providing support for an immune MoA. Three observations provide indirect evidence of a role for BPV in infected hepatocyte death: 1) presence of proliferating, activated adaptive immune cells in all response subgroups before rise in ALT; 2) increases in several liver and apoptosis-specific proteins in the serum concomitant with ALT elevations; 3) intermittent increase in HBV DNA during ALT elevations occurring more frequently in BPV responders than non-responders. Work is ongoing to further elucidate the multiple MoA of BPV and their roles in HBV functional cure.

Funding: GSK [209348/NCT04676724].

WED-371

Imdusiran (AB-729) administered every 8 weeks in combination with 24 weeks of pegylated interferon alfa-2a in virally suppressed, HBeAg-negative subjects with chronic HBV infection leads to HBsAg loss in some subjects at end of IFN treatment

Man-Fung Yuen¹, Jeong Heo², Ronald G. Nahass³, Grace Lai-Hung Wong⁴, Tatiana Burda⁵, Kalyan Ram Bhamidimarri⁶, Tsung-Hui Hu⁷, Tuan T. Nguyen⁸, Young-Suk Lim⁹, Chi-Yi Chen¹⁰, Stuart C. Gordon¹¹, Jacinta Holmes¹², Wan-Long Chuang¹³, Anita Kohli¹⁴, Naim Alkhouri¹⁴, Kevin Gray¹⁵, Emily P. Thi¹⁶, Elina Medvedeva¹⁵, Timothy Eley¹⁵, Sharie C. Ganchua¹⁶, Christina Iott¹⁶, Elizabeth Eill¹⁶, Christine L. Espiritu¹⁶, Mark Anderson¹⁷, Tiffany Fortney¹⁷, Gavin Cloherty¹⁷, Karen D. Sims¹⁵.
¹The University of Hong Kong, Queen Mary Hospital, Hong Kong, China; ²College of Medicine, Pusan National University, Pusan National University Hospital, Busan, Korea, Rep. of South; ³ID Care, Hillsborough, NJ, United States; ⁴The Chinese University of Hong Kong, Prince of Wales Hospital, Hong Kong, China; ⁵Arenia Exploratory Medicine, Chisinau, Moldova; ⁶University of Miami Miller School of Medicine, Miami, FL, United States; ⁷Kaohsiung Chang Gung Memorial Hospital, Kaohsiung, Taiwan; ⁸Research and Education Inc, San Diego, CA, United States; ⁹Asan Medical Center, University of Ulsan College of Medicine, Seoul, Korea, Rep. of South; ¹⁰Chia-Yi Christian Hospital, Chiayi City, Taiwan; ¹¹Henry Ford Hospital, Detroit, MI, United States; ¹²St Vincent's Hospital, University of Melbourne, Melbourne, Australia; ¹³Kaohsiung Medical University Hospital, Kaohsiung City, Taiwan; ¹⁴Arizona Liver Health, Chandler, AZ, United States; ¹⁵Arbutus Biopharma, Clinical Development, Warminster, PA, United States; ¹⁶Arbutus Biopharma, Research, Warminster, PA, United States; ¹⁷Abbott Laboratories, Abbott Diagnostics, Infectious Disease Research, Abbott Park, IL, United States
Email: ksims@arbutusbio.com

Background and aims: Functional cure of CHB will require suppression of viral replication, reduction of HBsAg and use of an immunomodulator such as pegylated interferon alfa-2a (IFN) to enhance HBV-specific immunity. Imdusiran (AB-729) is a GalNAc-conjugated single trigger siRNA that targets all HBV RNA transcripts and reduces all viral antigens including HBsAg. AB-729-201 is an ongoing Phase 2a study assessing 24 weeks of imdusiran followed by 12 or 24 weeks of IFN ± additional imdusiran doses in HBeAg-negative CHB subjects virally suppressed on nucleos(t)ide analogue (NA) therapy. Interim data through the end of the IFN treatment period (EOT) is available for all subjects.

Method: Forty-three subjects received imdusiran 60 mg every 8 weeks (wks) for 24 wks (4 doses) during the lead-in phase. After Wk

POSTER PRESENTATIONS

24, subjects were randomized to 1 of 4 sub-groups: A1 (24 wks IFN + 2 imdusiran doses + NA; N = 12), A2 (24 wks IFN + NA; N = 13), B1 (12 wks IFN + 1 imdusiran dose + NA; N = 8) or B2 (12 wks IFN + NA; N = 10). After completing IFN ± imdusiran treatment, subjects continued NA therapy for 24 wks and stopped NA therapy if ALT < 2 × upper limit of normal, HBV DNA undetectable and HBsAg < 100 IU/ml. Safety, antiviral and immunologic assessments were obtained. HBsAg was assessed via Roche Cobas Elecsys HBsAg II assay (lower limit of quantitation [LLOQ] = 0.05 IU/ml) and results < LLOQ were analyzed by Abbott HBsAg Next assay (sensitivity cutoff = 0.005 IU/ml).

Results: Baseline characteristics were described previously. All subjects have completed IFN dosing, and 18/43 subjects have been assessed for NA discontinuation (d/c) at Wk 76 or 64. In groups A1/A2, 7/25 (28%) subjects had HBsAg ≤ LLOQ at EOT (Wk 52) and 5/7 were confirmed to be non-reactive with the Abbott Next assay. All 7 subjects had concurrent anti-HBs levels > 10 IU/L, and 5/7 had levels > 100 IU/L. In groups B1/B2, 0/18 subjects had HBsAg ≤ LLOQ at EOT (Wk 40), although 2 reached < LLOQ during IFN treatment but subsequently rebounded. Group A1 had more profound HBsAg mean (±SE) log₁₀ change from baseline at EOT than other groups; A1 = -2.85 (0.41) log₁₀, A2 = -1.44 (0.43) log₁₀, B1 = -1.85 (0.38) log₁₀, and B2 = -1.68 (0.17) log₁₀. Imdusiran treatment was well-tolerated with no serious adverse events (AEs) or AEs leading to d/c; IFN-related AEs were like those reported previously. Nine of 18 subjects have stopped NA therapy; 1 subject has HBsAg and HBV DNA < LLOQ after 6 months off NA therapy suggestive of functional cure, and 1 subject restarted therapy after 8 wks due to confirmed HBV DNA > 20,000 IU/ml with normal ALT levels.

Conclusion: HBsAg ≤ LLOQ with detectable anti-HBs was observed at EOT in 28% of subjects who received 4 or 6 doses of imdusiran plus 24 weeks of IFN, but in 0 subjects who received 4 or 5 doses of imdusiran plus 12 weeks of IFN. The study remains ongoing and additional EOT data, durability of EOT HBsAg loss, and preliminary immunology data for a subset of study subjects will be presented.

WED-372

Downregulation of soluble FASLG as a potential mechanism of enhanced immune-related clearance of infected hepatocytes induced by JNJ-73763989 in HBeAg-negative virologically suppressed chronic hepatitis B patients

Simon Verheijden¹, Marianne Tuefferd¹, Marjolein Crabbe¹, Ewoud de Troyer¹, Thomas Vanwolleghem², Harry Janssen³, Michael Biermer⁴, Oliver Lenz¹. ¹Johnson and Johnson Innovative Medicine, Beerse, Belgium; ²Antwerp University Hospital, Edegem, Belgium; ³Centre for Liver Disease, Toronto, Canada; ⁴Johnson and Johnson Innovative Medicine, Neuss, Germany
Email: Sverhei1@its.jnj.com

Background and aims: Persistent exposure to hepatitis B surface antigen (HBsAg) in chronically infected hepatitis B patients can interfere with the host immune response to clear infected hepatocytes. JNJ-73763989 (JNJ-3989), a small interfering RNA (siRNA) targeting all HBV ribonucleic acid (RNA) transcripts resulting in profound HBV surface antigen (HBsAg) reductions, is currently under development for treatment of chronic hepatitis B. Here, we evaluated serum proteome changes during JNJ-3989 treatment across two clinical studies, to evaluate the effect of JNJ-3989 on host responses. **Method:** Serum was collected from HBeAg-negative, virologically suppressed (VS) patients from two phase 2 studies with 48 weeks of JNJ-3989 based treatment: REEF-1 (n = 44) and REEF-2 (n = 35). Soluble serum proteins were evaluated with Olink Explore®, a high-throughput protein biomarker discovery platform used before in chronic hepatitis B studies. A mixed effects model was applied to assess serum protein changes during JNJ-3989 based treatment. Significantly affected proteins were explored by evaluating overlap between both studies and association with HBsAg levels.

Results: 84/1460 (5.8%) proteins (REEF-1) and 669/2943 (22.7%) proteins (REEF-2) were differentially expressed comparing baseline

with on-treatment. 62 proteins were consistently changed under JNJ-3989 based treatment across both studies. Network analysis showed apoptosis (FAS, FASLG, TNFRSF10B, CTSE, CTSL) and glyoxylate/dicarboxylate, sphingolipid and carbohydrate metabolism (AGXT, SHMT1, HAO1, SMPD1, ASAH2, ENPP7) as the main pathways affected during JNJ-3989 treatment. Most of the upregulated proteins (56/62; 90.3%) were liver-enriched cytoplasmic proteins involved in hepatocyte metabolism, suggesting increased hepatocyte death. Soluble Fas Ligand (FASLG), a key protein involved in cell death induced by cytotoxic T/NK cells was downregulated in both studies and at multiple timepoints. Strikingly, we did not observe any association with FASLG levels and HBsAg levels at baseline or on-treatment. Only 1/62 protein (PON2) was associated with HBsAg levels at baseline, whereas 4/62 proteins (AGXT, C19orf12, CTSE, SEZ6L) were negatively associated with HBsAg levels at W48 of treatment, but not at baseline. **Conclusion:** Serum proteomic analyses in VS HBeAg negative patients across two clinical studies showed that JNJ-3989 treatment reduces soluble FASLG and increases serum levels of intracellular hepatocyte proteins, suggestive of increased hepatocyte cell death. As soluble FASLG can interfere with the pro-apoptotic action of cytotoxic T/NK cells through steric hinderance of the membrane bound FAS/FASLG interaction, these data suggest JNJ-3989 treatment might improve clearance of infected hepatocytes by cytotoxic immune cells through restoration of FAS/FASLG mediated apoptotic signaling.

WED-373-YI

Epidemiological data and clinical profiles of hepatitis B surface antigen levels in chronic hepatitis B: implications for novel drug development

Rex Wan-Hin Hui¹, Trevor Kwan-Hung Wu¹, Ryan Hin-Man Leung¹, Lung Yi Loey Mak¹, Danny Ka-Ho Wong¹, James Fung¹, Wai-Kay Seto¹, Man-Fung Yuen¹. ¹The University of Hong Kong, Hong Kong, Hong Kong
Email: huirex@connect.hku.hk

Background and aims: Quantitative hepatitis B surface antigen (qHBsAg) is an important biomarker in the management of chronic hepatitis B (CHB). qHBsAg < 100 IU/ml is associated with spontaneous HBsAg seroclearance, whereas qHBsAg < 1000 IU/ml is associated with improved treatment responses to different novel HBV antivirals. Despite its prognostic role, epidemiological data and clinical profiles of qHBsAg in CHB is not well-defined.

Method: We performed a large cohort study on CHB patients who received qHBsAg testing between 2009 and 2020 in Queen Mary Hospital, Hong Kong. Serum qHBsAg was measured by the Elecsys HBsAg II assay (lower limit of detection: 0.05 IU/ml). Patients with undetectable qHBsAg were excluded from this analysis. Tests for serum HBV DNA, hepatitis B e-antigen (HBeAg) and liver biochemistry were measured on the same samples. We reported proportions of patients with different qHBsAg levels and analysed factors associated with qHBsAg < 1000 and < 100 IU/ml respectively.

Results: This analysis included 4,293 patients (62.5% male; mean age 48.0 ± 12.9; 20.4% HBeAg positive; 45.2% on nucleos(t)ide analogue [NUC]). The median qHBsAg level was 627.2 (interquartile range 117.0–1868.0) IU/ml. The proportion of patients in each qHBsAg strata were 8.3% with qHBsAg < 10 IU/ml, 15.0% with 10–100 IU/ml, 35.5% with 100–1000 IU/ml, 21.5% with 1000–3000 IU/ml, 5.3% with 3000–5000 IU/ml, and 14.4% with ≥ 5000 IU/ml. This corresponds to 58.8% and 23.3% of patients with qHBsAg < 1000 IU/ml and < 100 IU/ml respectively. In treatment-naïve patients (n = 2,354), 47.1%, 23.0% and 10.1% of patients had qHBsAg < 1000 IU/ml, < 100 IU/ml and < 10 IU/ml respectively. In NUC-treated patients (n = 1,939, median NUC duration 5.4 [3.6–8.1] years), 73.0%, 23.7% and 6.1% of patients had qHBsAg < 1000 IU/ml, < 100 IU/ml and 10 IU/ml respectively. Female sex (829.7 vs 518.6 IU/ml in males), treatment-naïve status (1242.0 vs 357.7 IU/ml in NUC-treated patients) and HBeAg-positive status (2398.0 vs 398.2 IU/ml in HBeAg-negative) were associated with higher qHBsAg levels respectively (all p < 0.001). Older age correlated with lower qHBsAg (r = -0.157, p < 0.001). Serum HBV DNA (r = 0.188),

alanine aminotransferase ($r=0.130$) and bilirubin ($r=0.031$) all weakly correlated with qHBsAg (all $p<0.05$). In both treatment-naïve and NUC-treated groups, age and HBeAg status were independent predictors of qHBsAg <1000 IU/ml and <100 IU/ml respectively (all $p<0.001$).

Conclusion: Over 40% of CHB patients have qHBsAg >1000 IU/ml. These patients are unlikely to have spontaneous HBsAg seroclearance, and will also have suboptimal responses to novel HBV antivirals, highlighting a potential treatment gap. Demographic, viral and treatment factors were associated with qHBsAg. Targeted strategies using different combination therapies and treatment durations for patients with specific characteristics should be studied in future clinical trials.

WED-374

Safety, tolerability, and pharmacokinetics of BJT-778, a monoclonal antibody for treatment of chronic hepatitis B and chronic hepatitis D, following single ascending doses in healthy volunteers

Edward J. Gane¹, Christian Schwabe², Patrick Smith³, Courtney Moc Willeford³, Carole Moore⁴, Roy Grecko⁴, Keting Chu⁵, Hassan Javanbakht⁴, Nancy Shulman^{4,4}. ¹University of Auckland, New Zealand Clinical Research, Auckland, New Zealand; ²New Zealand Clinical Research, Auckland, New Zealand; ³Certara, Inc., Princeton, NJ, United States; ⁴Bluejay Therapeutics, Inc., San Mateo, CA, United States; ⁵Bluejay Therapeutics, Inc., San Mateo, Inc, United States
Email: edgane@adhb.govt.nz

Background and aims: BJT-778 is a potent, selective, fully human immunoglobulin G1-neutralizing monoclonal antibody that targets the antigenic loop present in all forms of hepatitis B surface antigen proteins, which are the key viral protein responsible for recognition, binding, and entry of hepatitis B virus (HBV) and hepatitis delta virus (HDV) virions to hepatocytes. In addition to preventing hepatocyte infection, BJT-778 should facilitate both clearance of circulating virions and presentation to antigen presenting cells, thereby enhancing HBV-specific T-cell responses. BJT-778-001 is an ongoing 2-part study evaluating the safety, tolerability, pharmacokinetics (PK), and antiviral activity of BJT-778 in healthy volunteers (HVs) and in subjects with chronic HBV (CHB) including those with chronic HDV (CHD) infection.

Method: Part 1 of the study is a Phase 1a/1b double-blind, randomized, placebo-controlled single-ascending-dose in HVs (Cohort A), CHB and CHD subjects (Cohorts B-D). Subjects were randomized 6:2 to receive a single subcutaneous dose of BJT-778 75 mg, 300 mg, or 900 mg, or placebo. Part 2 of the study is a multicenter, open-label Phase 2a multiple dose study in CHB and CHD subjects. Preliminary data from Cohort A of Part 1 are reported here.

Results: Among the 24 HVs in Cohort A, 18 HVs were randomized to receive BJT-778. Maximum plasma concentrations (C_{max}) of BJT-778 were achieved at 7 days post-dose with mean elimination half-lives of approximately 27 to 37 days across all dose levels. The C_{max} and area under the plasma concentration-time curve from time 0 to infinity (AUC_{inf}) increased proportionally between 75 mg to 900 mg and mean values ranged from 6.74 to 87.1 ug/ml (C_{max}) and 333 to 5070 day*ug/ml (AUC_{inf}). In vitro, the half maximal effective concentration (EC₅₀) values for neutralization of HBV and HDV infections were 0.09 and 0.01 nM, respectively, and plasma concentrations consistently exceeded the EC₅₀ for all doses levels over the 84-day sampling period. Preliminary safety data are still under blinded review. Among the 24 HVs who received either BJT-778 or placebo, six adverse events (AEs) in five subjects were considered as potentially related to treatment. These events include injection site bruising (n=4), injection site swelling (n=1), and fatigue (n=1), all Grade 1 (mild). There were no serious AEs, Grade 3/4 AEs, or significant laboratory abnormalities reported.

Conclusion: The PK of BJT-778 administered subcutaneously increased dose-proportionally up to the highest dose, 900 mg. The long half-life and sustained plasma concentration surpassing the EC₅₀ support the convenient clinical dosing schedules and suggest that dose levels are within the therapeutic range, respectively. All doses were safe and well tolerated. Following these favorable safety and PK results, the proof-of-concept Phase 1b study has been initiated in patients with CHB and CHD.

WED-375

VTP-300 immunotherapeutic, plus low dose PD-1 inhibitor, nivolumab, continues to show meaningful, sustained reductions in HBsAg levels

Dereck Tait¹, Louise Bussey¹, Radka Kolenovska¹, Matt Downs¹, Katie Anderson¹, Antonella Vardeu¹, Man-Fung Yuen², Wan-Long Chuang³, Chun-Jen Liu⁴, Apinya Leerapun⁵, Pisit Tangkijvanich⁶. ¹Barinthus Biotherapeutics, Didcot, Oxford, United Kingdom; ²Queen Mary Hospital, Hong Kong, Hong Kong; ³Kaohsiung Medical University ChungHuo Memorial Hospital, Kaohsiung City, Taiwan; ⁴National Taiwan University Hospital, Taipei City, Taiwan; ⁵Maharaj Nakorn Chiang Mai Hospital, Chiang Mai, Thailand; ⁶King Chulalongkorn Memorial Hospital, Bangkok, Thailand
Email: dereck.tait@barinthusbio.com

Background and aims: Functional cure of chronic hepatitis B (CHB) is considered to be achieved when HBsAg and HBV DNA are undetectable in the blood and the immune system maintains this state. VTP-300 is a targeted immunotherapeutic consisting of two viral vectors, ChAdOx1 and MVA, containing consensus HBV genotype C sequences; full length surface, modified polymerase, and core sequences. Study HBV003 is an ongoing open-label, randomised, Phase 2b study to assess the safety, immunogenicity, and efficacy of different regimens of VTP-300 in combination with low dose nivolumab in participants with non-cirrhotic CHB who are on suppressive therapy with nucleos (t)ide analogues (NUC).

Method: Up to 120 participants with HBsAg ≥ 10 and <4000 IU/ml are being enrolled into three groups in HBV003. The protocol was amended to alter the HBsAg inclusion criteria to ≥ 10 and <200 IU/ml and to exclude participants considered to be at risk of auto-immune thyroiditis. All three groups received ChAdOx1-HBV on Day 1, which was followed by: MVA-HBV and low dose nivolumab on Day 29 in Group 1; MVA-HBV and low-dose nivolumab on Days 29 and 85 in Group 2; MVA-HBV on Days 29 and 85 with low-dose nivolumab administered on Day 36 in Group 3. NUCs may be discontinued if participants meet certain criteria. Safety data, immunology data, and HBV marker data are collected throughout the study to Day 336.

Results: 76 participants have currently been recruited, of whom 24 (32%) have baseline HBsAg levels ≤ 200 IU/ml. Day 169 data, 6 months after first dose of study drug, are currently available from 70 participants. In total, HBsAg log reductions at Day 169 of ≥ 0.5 log and ≥ 1 log in participants with HBsAg ≤ 200 IU/ml were observed in 59% and 27% participants, respectively, compared to 13% and 2% in participants with HBsAg levels >200 IU/ml. 18 participants have met the eligibility criteria for NUC discontinuation and four have discontinued NUCs. Three participants (two in Group 2 and one in Group 1) have undetectable HBV DNA and HBsAg at Day 113, Day 169, and 10 weeks post-NUC discontinuation. One unrelated SAE has been reported, and thyroid dysfunction was reported in seven participants. Further accumulating data, including safety, HBV markers, NUC discontinuation, and immunology data will be presented.

Conclusion: Preliminary safety data suggest that VTP-300 in combination with low dose nivolumab has been generally well tolerated and has resulted in meaningful, sustained HBsAg reductions, particularly in participants with baseline HBsAg levels ≤ 200 IU/ml. We believe that VTP-300 is a promising immunotherapeutic candidate for enhancing CHB functional cure rates. VTP-300 is also being investigated in combination with a siRNA inhibitor, imdusiran.

WED-376

Tobevibart (VIR-3434), a monoclonal antibody, resistance analysis in participants with chronic HBV: Results from a Phase 1 single dose study

Hasan Imam¹, Julia di Iulio¹, Thanh Quach¹, Yi-Pei Chen¹, Sonia Maciejewski¹, Keith Boundy¹, Andre Arizpe¹, Kosh Agarwal², Man-Fung Yuen³, Andrea Cathcart¹, Gregory Camus¹. ¹Vir Biotechnology, Inc., San Francisco, United States; ²King's College Hospital, London, United Kingdom; ³Queen Mary Hospital, The University of Hong Kong, Hong Kong SAR, Hong Kong
Email: gcamus@vir.bio

Background and aims: Tobevibart (VIR-3434) is an investigational Fc-engineered human monoclonal antibody targeting the conserved antigenic loop of HBsAg in development for the treatment of chronic hepatitis B (CHB) and chronic hepatitis D. Here, we report hepatitis B virus (HBV) sequencing results in participants with CHB given a single dose of tobivabart, before and after treatment.

Method: VIR-3434-1002 was a randomized, double-blind, placebo-controlled phase 1 single ascending dose study that evaluated the safety, tolerability, and antiviral activity of tobivabart. In Part D, participants with CHB were not on NRTIs, had baseline HBV DNA ≥ 1000 IU/ml, and received a single dose of 75 or 300 mg of tobivabart subcutaneously. The whole HBV virus genome was sequenced in these viremic participants, both at baseline and following tobivabart treatment. HBV genotypes were determined for each participant based on phylogenetic analysis of the viral sequence data and genotype specific HBV reference sequences. Viral sequences at baseline were aligned to their genotype specific reference sequences to identify substitutions from reference. Viral sequences post-treatment were compared to their corresponding baseline sequences to identify potential emergent substitutions. In vitro phenotypic analysis of substitutions in the tobivabart binding site are underway.

Results: Twelve participants enrolled in Part D received a single dose of either 75 or 300 mg tobivabart, while 4 participants were randomized to the placebo group. HBV sequencing was successful in all 16 participants in the tobivabart treatment or placebo groups at both baseline and postbaseline timepoints. Out of the 16 participants enrolled in Part D, 4, 2, 4, and 6 participants had HBV genotypes A, B, C, and D, respectively. At baseline, 2 participants each in the tobivabart 75 mg, 300 mg, and placebo groups had substitutions in the tobivabart binding site when compared to the relevant genotype reference sequences. No binding site emergent substitutions relative to baseline were identified in any of the 12 participants who received tobivabart. Four of these participants had emergent substitutions in the HBV S gene, outside the tobivabart binding site. All of these emergent substitutions in the S gene were found in only 1 participant each. Phenotypic analysis of the binding site substitutions from reference will be presented.

Conclusion: Viral sequencing analysis of 12 participants who received a single dose of tobivabart showed no treatment-emergent substitutions in the tobivabart binding site, and no emergent substitution in the S gene was found in more than 1 participant at any dose evaluated. These findings suggest no emergence of resistance following a single dose of tobivabart, and support its continued development for functional cure of CHB and treatment of HDV.

WED-377

Preclinical profiling of ABI-6250, a novel orally bioavailable small-molecule therapeutic candidate for the treatment of chronic hepatitis D

Marc P. Windisch¹, Nuruddin Unchwaniwala¹, Jinghu Carl Li¹, Yanhong Zhu¹, Heidi Contreras¹, Dinara Azimova¹, Francielle Tramontini Gomes de Sousa¹, Joseph Tan¹, Kirsten Stray¹, Ariel Tang¹, Peter Haggie¹, Gene Schulze¹, Michael Shen¹, Jiaxin Yu¹, Michel Perron¹, Michael A. Walker¹, William E. Delaney¹, Min Zhong¹.

¹Assembly Biosciences, Inc., South San Francisco, United States
Email: mwindisch@assemblybio.com

Background and aims: Chronic hepatitis D virus infection (cHDV) is the most severe form of viral hepatitis. Bulevirtide (BLV), a peptide preventing the binding of HDV to sodium taurocholate co-transporting polypeptide (NTCP), the viral entry receptor, is approved in Europe for the treatment of cHDV. Clinical trials demonstrated the safety and efficacy of injectable BLV. Here we describe the preclinical profiling of a new therapeutic candidate, ABI-6250, a novel orally bioavailable small-molecule HDV entry inhibitor.

Method: ABI-6250 HDV half-maximal effective concentration (EC₅₀) and protein-adjusted EC₅₀ were determined in pretreated HepG2-NTCP cells by measuring intracellular hepatitis D antigen (HDag) following infection. ABI-6250's competitive inhibition of hepatitis B virus (HBV) preS1 NTCP binding, impact on NTCP-dependent bile acid (BA) uptake, and selectivity against a broad panel of BA transporters were assessed by monitoring fluorescently labeled preS1 binding and BA uptake in human embryonic kidney cells. Metabolic stability was assessed in liver microsomes (LMs) from multiple species. Oral bioavailability was determined in both rodents and non-human primates (NHPs). Dose-escalating pharmacokinetic/pharmacodynamic (PK/PD) and tolerability studies were performed in NHPs and rats, monitoring drug exposure and BA elevations.

Results: ABI-6250 potently inhibits the infection of all tested HDV genotypes (1–3), with HBV genotype B or D envelopes (HDV EC₅₀=5–16 nM), and a protein-adjusted EC₅₀ increase of approximately 35-fold in HDV genotype 3 enveloped with HBV genotype D. ABI-6250 inhibits preS1 binding (half-maximal inhibitory concentration [IC₅₀]=22 nM) and NTCP-dependent BA uptake (IC₅₀=11 nM), demonstrating the target is NTCP. Furthermore, ABI-6250 has >10-fold selectivity for NTCP *in vitro* compared to other evaluated BA transporters, including organic anion-transporting protein (OATP) 1B1 and OATP1B3. ABI-6250 has high metabolic stability in human, NHP, and rat LMs (predicted clearance = 1.0–2.5 ml/min/kg) and good oral bioavailability (F = 100% in mice, rats, and NHPs), with a terminal half-life of 4 to 5 hours in rodents and 15 hours in NHPs. PK/PD studies in NHPs show dose-dependent ABI-6250 plasma exposure and increasing BA levels at low therapeutic doses, between 0.3 and 3 mg/kg, without affecting OATP1B1 and OATP1B3 (demonstrated by monitoring coproporphyrin plasma levels), indicating ABI-6250 effectively and selectively inhibits NTCP *in vivo*. ABI-6250 is well tolerated at exposures above the expected efficacious concentration when orally dosed daily for 7 consecutive days in rats and NHPs.

Conclusion: ABI-6250 is a highly potent, orally bioavailable HDV entry inhibitor with a preclinical profile supporting a once-daily oral therapy for cHDV and is expected to enter Phase 1 clinical studies by the end of 2024.

WED-378

Association of baseline characteristics and plasma ALG-001075 to HBsAg responses in HBsAg+ CHB subjects following ALG-000184 ± ETV treatment

Kha Le¹, Man-Fung Yuen², Edward J. Gane³, Kosh Agarwal⁴, Jinlin Hou⁵, Junqi Niu⁶, Yanhua Ding⁶, Xieer Liang⁵, Alina Jucov⁷, Min Wu¹, Maida Maderazo¹, Lawrence Blatt¹, Tse-I Lin¹, Matt McClure¹, Sushmita Chanda¹. ¹Aligos Therapeutics, Inc., South San Francisco, United States; ²Department of Medicine, School of Clinical Medicine, The University of Hong Kong, Hong Kong, China; ³Faculty of Medicine, University of Auckland, Auckland, New Zealand; ⁴King's College Hospital, Institute of Liver Studies, London, United Kingdom; ⁵Nanfeng Hospital, Southern Medical University, Guangzhou, China; ⁶The First Hospital of Jilin University, Changchun, China; ⁷ARENSIA Exploratory Medicine, Republican Clinical Hospital and Nicolae Testemitanu State University of Medicine and Pharmacy, Chisinau, Moldova
Email: schanda@aligos.com

Background and aims: ALG-000184 is a prodrug of ALG-001075, a potent chronic hepatitis B (CHB) capsid assembly modulator-empty that inhibits viral replication and cccDNA establishment in vitro.

Method: ALG-000184-201 is a multi-part, multi-center, double-blind, randomized, placebo-controlled study (NCT04536337). In Part 4, eligible treatment naïve or currently-not-treated HBeAg+ CHB subjects that enrolled in Cohorts 1 and 2 were randomly assigned (3:1) to receive oral daily doses of 100 and 300 mg ALG-000184, respectively or placebo in combination with entecavir (ETV) × 12 weeks followed by open-label treatment with 100 mg ALG-000184 + ETV × ≤12 weeks and 300 mg ALG-000184 + ETV × ≤96 weeks, respectively. Those enrolled in Cohort B received open-label daily doses of 300 mg ALG-000184 alone × ≤96 weeks. A total of 22 subjects (n = 4, 9, and 9 in Cohorts 1, 2 and B, respectively) with at least 24 weeks of ALG-000184 dosing were included in the analysis. Baseline participant characteristics, including age, sex, ethnicity, HBV genotype, HBsAg, HBeAg, HBcrAg and steady state plasma ALG-001075 exposures, and change from baseline of HBsAg at weeks 24, 36 and 48 were measured. Exploratory linear univariate and multiple regression models were used to determine possible associations between selected baseline variables, plasma ALG-001075 exposures and HBsAg reduction.

Results: Substantial reductions in HBV DNA/RNA and HBV antigens have been noted for ALG-000184 + ETV and ALG-000184 monotherapy. In a multiple regression model, baseline HBsAg (< or ≥4 log10 IU/ml) and steady state plasma ALG-001075 exposure (AUC or Ctrough) statistically significantly predicted change from baseline in HBsAg at week 24 ($p < 0.00018$, $R^2 = 0.65$). Baseline HBsAg of ≥4 log10 IU/ml was a significant predictor of having a HBsAg reduction. Higher plasma ALG-001075 exposures added statistically significantly to the prediction ($p < 0.01$). Baseline HBcrAg (≥4 log10 IU/ml) was a significant predictor of HBsAg reduction based on univariate regression analysis but did not add statistical significance to baseline HBsAg and plasma ALG-001075. Similar results were observed at weeks 36 and 48. There were no statistically significant associations found between age, sex, ethnicity, HBV genotype, baseline HBeAg or ALT and change from baseline in HBsAg. HBeAg+ CHB subjects treated with ALG-000184 had dose related decrease in HBeAg and HBcrAg irrespective of their baseline.

Conclusion: Higher baseline HBsAg (≥4 log10 IU/ml) and plasma ALG-001075 levels appear to be predictors of HBsAg response to ALG-000184 treatment while HBV DNA, RNA, HBeAg and HBcrAg declines are independent of their baseline characteristics.

WED-379

Intrahepatic changes in immunologic and virologic markers during siRNA JNJ-73763989 (JNJ-3989) based treatment of chronic hepatitis B (CHB) patients: imaging mass cytometry (IMC) analyses from the INSIGHT study

Kim Thys¹, Marjolein Crabbe¹, Hans Wils¹, Hinrich Goehlmann¹, Simon Verheijden¹, Pietro Lampertico², Tarik Asselah³, Edward J. Gane⁴, Scott K. Fung⁵, Patrick Kennedy⁶, Thomas Vanwolleghem⁷, Ewa Janczewska⁸, Julian Schulze zur Wiesch⁹, Mark S. Sulkowski¹⁰, Carine Guinard-Azadian¹, Michael Biermer¹, Oliver Lenz¹. ¹Johnson and Johnson Innovative Medicine, Beerse, Belgium; ²Foundation IRCCS Ca' Granda Ospedale Maggiore Policlinico, Division of Gastroenterology and Hepatology, CRC "A. M. and A. Migliavacca" Center for Liver Disease, Department of Pathophysiology and Transplantation, University of Milan, Milan, Italy; ³Université de Paris-Cité, INSERM UMR1149, Department of Hepatology, AP-HP Hôpital Beaujon, Clichy, France; ⁴New Zealand Liver Transplant Unit, University of Auckland, Auckland, New Zealand; ⁵Toronto General Hospital, Toronto Center for Liver Disease, Toronto, Canada; ⁶Barts and The London School of Medicine and Dentistry, London, United Kingdom; ⁷University of Antwerp, Faculty of Medicine and Health Sciences, Laboratory of Experimental Medicine and Pediatrics, Viral Hepatitis Research Group, Antwerp, Belgium; ⁸Medical

University of Silesia in Katowice, Faculty of Public Health in Bytom, Bytom, Poland; ⁹University Medical Center Hamburg-Eppendorf, Hamburg, Germany; ¹⁰Johns Hopkins University, Baltimore, United States

Email: kthys@its.jnj.com

Background and aims: The evaluation of patients with chronic hepatitis B (CHB) focuses primarily on the peripheral compartment due to difficulties obtaining samples directly from the liver, the site of viral infection. In the INSIGHT study, we analyzed intrahepatic changes in CHB patients under JNJ-3989 treatment.

Method: In INSIGHT, CHB patients who were hepatitis B e-antigen (HBeAg) positive and not currently treated (Group 1) or HBeAg-negative and virologically suppressed by nucleos (t)ide analogs (NA) (Group 2) received 48-weeks of siRNA JNJ-3989 + NA ± CAM-E JNJ-6379. Core liver biopsies (CLB) were collected at baseline and week 40 and assessed using Hyperion imaging mass cytometry. This method assessed non-parenchymal and liver immune cells for 30 proteins, including viral HBsAg, Ki67 as a proliferation marker, and several immune markers. All cells were classified into eight distinct phenotypes of lymphocytes/monocytes, hepatocytes, and structural cells using 11 markers: Collagen type1, Pan-keratin, cytokeratin18, CD45, CD20, CD3, CD4, CD8, CD57, CD68, and CD14. HBsAg was used to distinguish infected from non-infected hepatocytes.

Results: Nineteen baseline- and fifteen week 40 CLB samples were assessed. Differential protein abundance analysis showed higher proportions of immune cell markers in infected than non-infected hepatocytes. Nkp46, an activation marker of NK cells, was significantly enriched in infected (5%) vs non-infected hepatocytes (<1%). Also, the proportion of PDL-2-positive cells was significantly higher ($p = 0.003$) among the infected hepatocytes. The proportion of Ki67-positive cells was higher ($p = 0.022$) among the non-infected than the infected hepatocytes. The proportion of HBsAg positive hepatocytes was significantly lower ($p < 0.001$) at week 40 compared to baseline in both cohorts, consistent with the effect of JNJ-3989. The proportion of CD8+ T-cells was significantly lower ($p = 0.002$) at week 40 compared to baseline in Group 1 but not in Group 2. Differential abundance analysis of proteins within the different cell types highlighted Ki67 as significantly reduced ($p < 0.05$) in both infected and non-infected hepatocytes at week 40 compared to baseline in Group 1. In addition, the proportion of PDL-1-positive cells among the infected hepatocytes showed a trend for an increase in both groups during treatment ($p = 0.058$). This effect was absent in the non-infected hepatocytes.

Conclusion: Spatial single-cell profiling of immune and viral markers in the liver from CHB patients demonstrated a decrease in the numbers of infected hepatocytes with a trend towards higher proportions of PDL-1 positive hepatocytes after 40 weeks of treatment with JNJ-3989. Although there was a lower proportion of Ki67-positive cells among the infected hepatocytes, proportions were further reduced in all hepatocytes during treatment, indicating less proliferation.

WED-381

A double-blind, placebo-controlled, single-ascending dose phase I a study to evaluate the safety, tolerability, and pharmacokinetics of HT-102, a neutralizing antibodies against the hepatitis B surface antigen in Chinese healthy volunteers

Mingjian Zhang¹, Dong Wang², Shanzhong Zhang², Yanqin Ma², Lijuan Ding², Zhipeng Zhang², Lungen Lu³, Xueying Ding¹.

¹Department of Clinical Research Center, Shanghai General Hospital, Shanghai, China; ²Suzhou Hepa Thera Biopharmaceutical Co.Ltd., Shanghai, China; ³Department of Gastroenterology, Shanghai General Hospital, Shanghai, China

Email: wangdong@hepathera.com

Background and aims: HT-102, is an investigational monoclonal antibody, targeting the antigenic loop of hepatitis B surface antigen (HBsAg) with the potential to functions as 1) inhibition of hepatitis B

virus (HBV) entry into cells, 2) elimination of virions and sub-viral particles for the treatment of chronic HBV infection. This first-in-human study investigated the safety, tolerability and single-dose pharmacokinetic (PK) profile of HT-102 in Chinese healthy subjects.

Method: The randomized, double-blind, placebo-controlled, single-ascending dose phase I study enrolled 32 healthy subjects. 8 healthy subjects per cohort were randomized (6:2 ratio) to receive a single subcutaneous (SC) dose of HT-102 (50, 150, 300, 600 mg) or placebo. Serum PK samples were collected over 24 hours (day 1), and on days 2 to days 56 across pre to post-dose period. Anti-drug antibody (ADA) was assessed on day1 (pre-dose), days 14, days 28 and days 56. Safety assessments included adverse events (AEs), clinical laboratory tests, vital signs, physical examinations and 12-lead electrocardiograms. Injection-site tolerability assessments were performed pre-dose 30 min, post-dose 30 min, 2 h, D2 and D3 for first dose and pre-dose 30 min, post-dose 30 min, 2 h for other dosage period. Safety and tolerability was assessed based on CTCAE v5.0.

Results: The results showed good safety and tolerability of HT-102 in healthy volunteers. All treatment-emergent adverse events (TEAEs) were grade 1 or 2 in HT-102 group. No SAE or TEAEs led to premature study discontinuation or death were reported in HT-102 group. The most common TEAEs (>10% subjects) included blood uric acid increased and blood fibrinogen decreased. HT-102 was absorbed after SC injection with a median T_{max} of 119.9–312.5 h, and median serum half-life ($t_{1/2}$) of 428.0–528.6 h. Following administration of 50–600 mg HT-102, the maximum concentrations (C_{max}) and area under the concentration-time curve to the time of the last quantifiable concentration (AUC_{0-t}) ranges of healthy subjects were 5373.0–64895.4 ng/ml and 3515241.8–49624629.1 h*ng/ml, respectively. HT-102 exposure including C_{max} and AUC_{0-last} increased in a dose-proportional manner and PK parameters C_{max} , AUC_{0-168h} , AUC_{0-t} , $AUC_{0-\infty}$ showed linear kinetic characteristics across single SC dose range of 50–600 mg. All samples for ADA test were negative except one sample on Day 56 from 150 mg cohort tested ADA positive (titer 3.6) with a negative result for further Nab test.

Conclusion: A single SC dose of HT-102 at 50–600 mg was safe and well tolerated with a favorable PK profile in Chinese healthy subjects. These data support further clinical development of HT-102 for HBV infection treatment.

WED-382

Modeling dual antiviral activity of Isonafarnib to explain hepatitis D virus RNA negativity 24 weeks after end of therapy despite RNA positivity at end of therapy: The D-LIVR study

Adquate Mhlanga¹, Harel Dahari¹, Leeor Hershkovich¹, Scott Cotler¹, Ingrid Choong², Colin Hislop², Theo Heller³, Christopher Koh³, Jeffrey Glenn⁴, Tarik Asselah^{5,6}, Saeed Sadiq Hamid⁷, Ohad Etzion⁸.

¹Program for Experimental and Theoretical Modeling, Division of Hepatology, Department of Medicine, Stritch School of Medicine, Loyola University Chicago, Maywood, IL, United States; ²Eiger BioPharmaceuticals, Palo Alto, CA, United States; ³Liver Disease Branch, NIDDK, NIH, Bethesda, MD, United States; ⁴Division of Gastroenterology and Hepatology, Departments of Medicine, Microbiology and Immunology, Stanford School of Medicine, Stanford, CA, United States; ⁵Hôpital Beaujon, APHP, Clichy and the University of Paris-Cité, Paris, France; ⁶INSERM UMR1149, Paris, France; ⁷Aga Khan University, Karachi, Pakistan; ⁸Soroka University Medical Center, Beersheva, Israel
Email: harel.dahari@gmail.com

Background and aims: Recent in vitro studies indicate a loss of hepatitis D virus (HDV) infectivity upon farnesyl transferase inhibitor treatment. We identified 2 patients in the Phase 3 D-LIVR study who had detectable HDV RNA at the end of therapy (EOT) with Isonafarnib (LNF) + ritonavir for 48 weeks and became HDV RNA negative at the end of 24-week follow-up (EOFU). This observation prompted us to develop a new mathematical model for HDV that considers infectious (V_i) and non-infectious (V_{ni}) virus.

Method: 144 patients in the D-LIVR study (NCT03719313) were treated with LNF+ritonavir for 48 weeks. 4 patients had HDV target not detected (TND) at EOFU. Two of the 4 patients had HDV detected at EOT, including one who had large HDV fluctuations during therapy with an ALT flare during EOT and follow-up and one who had a biphasic HDV decline until Week 12 that was followed by a plateau (~3 log below baseline) until EOT with normal ALT levels from Week 8 until EOFU. The mathematical model assumes that in addition to LNF blocking V_i and V_{ni} production, LNF further enhanced the ratio of V_{ni} to V_i , which led to <1 infectious-virus particle in the total extracellular body fluid (~13, 500 ml) prior to EOT. Since HBsAg remained at baseline level during LNF therapy, the number of infected cells were held constant. We assume that at baseline, 99% of total virus ($V_i + V_{ni}$) is infectious and that V_i and V_{ni} have similar clearance rate constant from blood. Key parameters of the model include the production rate constants for V_i and V_{ni} , the efficacy of LNF in blocking both V_i and V_{ni} production, and a parameter that accounts for LNF increasing the efficacy of blocking V_i production, resulting in a gradual increase of V_{ni} which increases the ratio of V_{ni} to V_i during therapy.

Results: The model was able to reproduce the total HDV kinetic pattern, i.e., a biphasic viral decline that lasted ~12 weeks followed by a viral plateau until EOT. The model predicts that while V_i declined in a biphasic manner until reaching <1 infectious-virus particle in the extracellular body fluid prior to EOT, V_{ni} had a transient decline at the beginning of therapy that was followed by a V_{ni} plateau. Modeling suggests that in addition to LNF blocking V_i and V_{ni} production ($\epsilon \sim 94.4\%$), LNF further enhanced the ratio of V_{ni} to V_i , thus increasing the log (V_{ni}/V_i) from -2 to 6 by EOT, which led to <1 infectious-virus particle in the extracellular body fluid prior to EOT.

Conclusion: This new HDV model can explain why patients, despite having detectable HDV RNA by EOT, subsequently achieved negative HDV RNA status during follow-up. Further research is needed to validate the existence of V_i and V_{ni} dynamics in LNF-treated patients to be able to test and refine our theoretical efforts in understanding LNF antiviral mode of action.

WED-383

Antiviral efficacy of REP 2139-Mg and effects on HVPg in HDV/HBV coinfecting patients with cirrhosis and portal hypertension non-responding to previous bulevirtide treatment

Mathias Jachs^{1,2}, Michael Schwarz^{1,2}, Michel Bazinet³, Matthias Mandorfer^{1,2}, Thomas Reiberger^{1,2}, Andrew Vaillant³.
¹Division of Gastroenterology and Hepatology, Department of Internal Medicine III, Medical University of Vienna, Vienna, Austria; ²Vienna Hepatic Hemodynamic Laboratory, Division of Gastroenterology and Hepatology, Department of Internal Medicine III, Medical University of Vienna, Vienna, Austria; ³Replicor Inc., Quebec, Canada
Email: avalliant@replicor.com

Background and aims: The nucleic acid polymer (NAP) REP 2139-Mg demonstrated safety and antiviral efficacy in patients with hepatitis B/D virus (HBV/HDV) coinfection. We undertook to measure changes in hepatic venous pressure gradient (HVPg) accompanying antiviral response patients with HBV/HDV cirrhosis.

Method: REP 2139-Mg (250 mg SC qW)-available through a named patient use program (NCT05683548)-was administered for 48 weeks together with pegylated interferon (pegIFN, 90 µg SC qW) and concomitant TAF or TDF therapy in 3 HDV/HBV patients, who failed previous bulevirtide therapy. All patients had cirrhosis and clinically significant portal hypertension (CSPH) and thus, also underwent HVPg measurement at baseline (BL), at week (W)12 and W48 (end of therapy, EOT).

Results: Patient 1 (Caucasian male, 69 y.o., Child-A5, large varices, HVPg 17 mmHg) had BL HDV-RNA of 3.28 log₁₀ copies/ml and quantitative HBs antigen (qHBsAg) 1202 IU/ml. By EOT, no antiviral response nor ALT flare was observed despite switching to weekly i.v. administration of REP 2139-Mg week 20 and dose increase to 500 mg

by week 36, but qHBsAg decreased to 760 IU/ml. HVPg at W12 decreased to 14 mmHg (–18%) returned to BL with 17 mmHg (0% from BL) at EOT. Patient 2 (Caucasian female, 51 y.o., Child-A5, large varices, HVPg 14 mmHg) had BL HDV-RNA of 4.97 log₁₀ copies/ml and qHBsAg of 626 IU/ml. The patient developed an ALT flare (max. 683 U/L, max. bilirubin 6.9 mg/dL) at W8, which was also seen with previous pegIFN exposure. After pegIFN discontinuation, ALT and bilirubin steadily declined during continued REP 2139-Mg therapy. HDV-RNA was negative by week 16. The patient was switched to IV administration by week 37. By EOT, HDV-RNA remained negative, qHBsAg was at 0.5 IU/ml, and ALT was normal at 28 U/L. HVPg increased to 17 mmHg (+21%) at week 12 but returned to 14 mmHg (0% from BL) at EOT. Patient 3 (Caucasian male, 38 y.o., Child-A5, large varices, HVPg 22 mmHg) had a BL HDV-RNA of 4.52 log₁₀ copies/ml and a qHBsAg of 922 IU/ml. After an initial ALT flare (max. ALT 659 U/L, bilirubin within normal range) at W7, HDV-RNA was negative by week 27. By EOT, HDV-RNA remained negative, qHBsAg was at 0.18 IU/ml, and ALT 41 U/L. HVPg was 18 mmHg (–18%) at W12 and remained decreased to 19 mmHg (–14%) at EOT. REP 2139-Mg was well tolerated with no severe adverse events. SC injections were accompanied by local and transient grade 1 erythema and itching in patient 2. No adverse events were associated with IV infusion.

Conclusion: Weekly REP 2139-Mg in combination with TDF and low-dose pegIFN appeared safe and effective against HBV/HDV infection in patients with cirrhosis and CSPH. Potential ALT flares should be monitored closely but may reflect an immune response triggering the subsequent decrease/loss of HDV-RNA and of HBsAg-as observed in 2 out of our 3 patients. Portal hypertension may remain controlled despite ALT flares during REP 2139-Mg therapy in patients with CSPH.

WED-386

A double-blind, placebo-controlled, single-ascending dose phase I a study to evaluate the safety, tolerability, and pharmacokinetics of HT-101, an investigational small interfering ribonucleic acid targeting hepatitis B virus in Chinese healthy subjects

Jianxiong Zhang¹, Dong Wang², Shanzhong Zhang², Yanqin Ma², Lijuan Ding², Zhipeng Zhang², Hong Ma³, Jidong Jia³, Ruihua Dong¹.
¹Research Ward, Beijing Friendship Hospital, Capital Medical University, Beijing, China; ²Suzhou Hepa Thera Biopharmaceutical Co. Ltd., Shanghai, China; ³Liver Research Center, Beijing Friendship Hospital, Capital Medical University, Beijing, China
Email: wangdong@hepathera.com

Background and aims: HT-101 is an N-acetylgalactosamine (GalNAc)-conjugated small interfering ribonucleic acid (siRNA) targeting hepatitis B virus. Preclinical studies exhibited a promising potential for the treatment of chronic hepatitis B virus (HBV) infection. This first-in-human study investigated the safety, tolerability and single-dose pharmacokinetic profile of HT-101 in Chinese healthy subjects.

Method: The randomized, double-blind, placebo-controlled, single-ascending dose phase I a study enrolled 50 healthy subjects. Two subjects received a single subcutaneous (SC) dose of HT-101 at 25 mg, and in other six cohorts (n = 8 per cohort), healthy subjects were randomized (6:2) to receive a single SC dose of HT-101 (50~800 mg) or placebo. Blood and urine samples were obtained for pharmacokinetic determination across a 48 h post-dose period. Safety assessments included adverse events (AEs), clinical laboratory tests, vital signs, physical examinations and 12-lead electrocardiograms pre- and post-dosing. Safety and tolerability was assessed based on CTCAE v5.0.

Results: The results showed good safety and tolerability of HT-101 in healthy subjects. No subjects discontinued due to any AE, no serious AE nor death were reported. The most common AEs included increased blood triglycerides, decreased lymphocyte percentage and decreased haemoglobin. HT-101 was rapidly absorbed, with consistent pharmacokinetic parameters observed for both sense strand and antisense strand characterizations. Plasma

pharmacokinetics characterized by functional antisense strand revealed a median time to peak plasma concentration (T_{max}) of 2.5~6.0 h and median plasma half-life (t_{1/2}) of 2.5~6.1 h. Following 25~800 mg SC dose, the maximum concentrations (C_{max}) and area under the concentration-time curve to the time of the last quantifiable concentration (AUC_{0-t}) were 75.3~5120.0 ng/ml and 553~57100 h*ng/ml, respectively. HT-101 exposure increased in a slightly supra-proportional to dose manner following 25~800 mg SC dose, suggesting that at liver target site there might be a saturation mechanism with the dose increasing. After a single SC dose, the average renal clearance rate (CLR) of HT-101 ranged from 4.6 to 6.7 L/h, with fractional excretion (Fe) at 13.1~41.9% and accumulated excretion (Ae) at 3.6~331.0 mg. In 25~200 mg cohorts, Fe was 13~17%, which increased to 30~40% within 400~800 mg cohorts. This shift also suggested saturation of the liver absorption, leading to enhanced urinary excretion. Notably, no metabolites were detected in plasma or urine, aside from the original drug HT-101. The concentration-QTc analysis indicated that risk of prolonged QTc interval was not observed.

Conclusion: A single SC dose of HT-101 at 25~800 mg was safe and well tolerated in Chinese healthy subjects. These data support further clinical development of HT-101 for HBV infection treatment.

WED-387

Study on the role of dendritic cells in CHB patients treated with intermittent Interferon therapy

Liu Yang¹, Tingting Jiang², Shiyu Wang², Ziyu Zhang², Xinxin Li², Yao Xie³, Minghui Li⁴.
¹Department of Hepatology Division 2, Beijing Ditan Hospital, Capital Medical University, Beijing, China; ²Department of Hepatology Division 2, Beijing Ditan Hospital, Capital Medical University, Beijing, China; ³Department of Hepatology Division 2, Beijing Ditan Hospital, Capital Medical University, Department of Hepatology Division 2, Peking University Ditan Teaching Hospital, Beijing, China; ⁴Department of Hepatology Division 2, Peking University Ditan Teaching Hospital, Department of Hepatology Division 2, Beijing Ditan Hospital, Capital Medical University, Beijing, China
Email: wuhm2000@sina.com

Background and aims: To investigate the relationship between the frequency of DCs subsets and the expression of surface co-stimulatory molecules and chemokine receptors in patients with CHB and the plateau of slow decline of HBsAg and the clinical efficacy during IFN intermittent therapy.

Method: CHB patients were divided into IFN initial treatment group (patients with natural history of CHB without any antiviral treatment before, and were given IFN antiviral treatment after admission, namely NH group, NAs treated group (NA group) and IFN treated plateau arriving group (P group). After perfecting the baseline related examination, the patients in the NH group were given IFN alone or in combination with NAs antiviral therapy; patients in the P group were retreated with IFN after 12–24 W of IFN intermission. For patients in the NH group, at baseline before IFN treatment, at 4 W and 12–24 W after IFN treatment; patients in NA group at baseline; patients in P group at baseline when IFN was stopped, 12–24 W of IFN intermission and 12–24 W of IFN retreatment, the viral, serological, biochemical and DC related indicators were collected.

Results: 49 patients in NH group, 47 patients in NA group and 47 patients in the P group were included. At baseline, the percentage of CD141 and CD1c double negative myeloid dendritic cells (DN mDC) subset, the percentage of CD86⁺ cells in DN mDC and the CD86 MFI of CD86⁺ DN mDC, the percentage of CX3CR1⁺ cells in DN mDC and the CX3CR1 MFI of CX3CR1⁺ DN mDC in the P group were significantly lower than those in the NA group and NH group. 35 patients in P group were followed up for 12–24 W of IFN intermission. The percentage of DN mDC increased significantly, and the percentage of CD86⁺ cells in DN mDC, CD86 MFI of CD86⁺ DN mDC, CX3CR1⁺ cells in DN mDC and CX3CR1 MFI of CX3CR1⁺ DN mDC increased significantly; Twelve patients in the P group were followed up until

POSTER PRESENTATIONS

12–24 W of IFN retreatment, and the data of three follow-up points were obtained. It was found that the proportion of DN mDC increased significantly, and the percentage of CD86⁺ cells in DN mDC, CD86 MFI of CD86⁺ DN mDC, CX3CR1⁺ cells in DN mDC and CX3CR1 MFI of CX3CR1⁺ DN mDC all showed a trend of increasing first and then decreasing 11 patients in the NH group were followed up until IFN treatment 12–24 W. It was found that the percentage of DN mDC decreased significantly after 4 W and 12–24 W use of IFN; CD86 MFI of CD86⁺ DN mDC after 4 W and 12–24 W use of IFN were significantly lower than those in baseline; the percentage of CX3CR1⁺ cells in DN mDC after 4 W and 12–24 W use of IFN decreased significantly compared with baseline; The CX3CR1 MFI of CX3CR1⁺ DN mDC after 12–24 W use of IFN was significantly lower than that of baseline.

Conclusion: IFN treatment significantly decreased the percentage of DN mDC subsets, and the percentage of CD86⁺ and CX3CR1⁺ cells in DN mDC and their CD86 and CX3CR1 MFI. In the P group the above indexes recovered to some extent after 12–24 W of IFN intermission.

WED-388

Safety, tolerability, and hepatitis B surface antigen reduction of HT-101 in chronic hepatitis B patients: preliminary results from a phase I b study

Dong Wang¹, Shanzhong Zhang², Yanqin Ma², Lijuan Ding², Zhipeng Zhang², Hong Ma³, Jidong Jia³. ¹Suzhou Hepa Thera Biopharmaceutical Co. Ltd., Shanghai, China; ²Suzhou Hepa Thera Biopharmaceutical Co. Ltd., Shanghai, China; ³Liver Research Center, Beijing Friendship Hospital, Beijing, China
Email: wangdong@hepathera.com

Background and aims: HT-101 is an N-acetylgalactosamine (GalNAc)-conjugated small interfering ribonucleic acid (siRNA) targeting hepatitis B virus. Preclinical studies exhibited a promising potential for the treatment of chronic hepatitis B virus (HBV) infection. Here we reported preliminary data from an ongoing study evaluating the safety, tolerability, and antiviral activity of HT-101 in chronic HBV infection participants with nucleos (t)ide reverse transcriptase inhibitor (NRTI) treatment.

Method: This was a randomized, double-blind, placebo-controlled, phase Ib, multiple ascending doses study of HT-101 administered via subcutaneous (SC) injection to chronic hepatitis B patients who received continuous NRTI therapy for ≥6 months. Participants with non-cirrhosis (<F3) were restricted with HBsAg <5, 000 IU/ml at screening. Participants received two subcutaneous HT-101 injections, 4 weeks apart, of 50, 100, 200 or 400 mg. At each dose level, eight participants were randomly assigned to HT-101 or placebo (6:2 ratio). Follow-up was carried out for 24 weeks post first dose. The protocol conformed to the Declaration of Helsinki guidelines and was approved by appropriate institutional review committee (s). Written informed consent was obtained prior to study procedures.

Results: Thirty-three participants with chronic hepatitis B (including 1 participant prematurely discontinued) were randomly assigned to receive two doses of HT-101 (50, 100, 200 or 400 mg) or placebo, given 4 weeks apart. So far, all patients showed good safety and tolerability. No subjects discontinued due to an adverse event (AE), no serious adverse events (SAE) nor death were reported. The follow-up visit is still ongoing and the data has not been un-blinded. According to preliminary pharmacodynamics data available in 50 mg and 100 mg cohorts: Demographic and baseline characteristics were generally well balanced across treatment groups (baseline HBsAg: $2.85 \pm 0.37 \log_{10}$ IU/ml for 50 mg group; $2.94 \pm 0.37 \log_{10}$ IU/ml for 100 mg group). The mean log reduction in HBsAg level in 50 mg and 100 mg cohort plotted against time was depicted in figure (4 participants without HBsAg reduction exclusive). Higher doses of HT-101 were associated with greater HBsAg reduction. In 100 mg HT-101 group, the mean reduction of HBsAg at Week 12 achieved ($2.28 \pm 0.64 \log_{10}$ IU/ml) and in 50 mg group, the mean reduction of HBsAg at Week 16 achieved ($1.50 \pm 0.51 \log_{10}$ IU/ml).

Conclusion: Two monthly doses of HT-101 administered SC were well safe and tolerated in Chinese patients with chronic HBV infection. Dose-dependent significant reductions from baseline in serum HBsAg levels were achieved through up to 16 weeks post last dose. Higher doses of HT-101 will be evaluated in subsequent cohort. These data support the continued development of HT-101 for treatment of chronic HBV infection.

WED-389

Pharmacokinetics and safety of the monoclonal antibody tobevibart (VIR-3434) administered as monotherapy or in combination with the small interfering RNA elebsiran (VIR-2218) in cirrhotic participants with mild hepatic impairment

Li Wang¹, Sneha Gupta¹, Michael A. Chattergoon¹, Asma El-zailik¹, Cheng Huang¹, George Hristopoulos¹, Maribel Reyes¹. ¹Vir Biotechnology, Inc., San Francisco, United States
Email: liwang@vir.bio

Background and aims: Tobeivibart (VIR-3434) is a human immunoglobulin G1 (IgG1) monoclonal antibody (mAb) that binds to the antigenic loop present in all forms of hepatitis B surface antigen (HBsAg). Elebsiran (VIR-2218) is a N-acetylgalactosamine (GalNAc)-conjugated, double-stranded RNA interference (RNAi) therapeutic that targets the X region of the hepatitis B virus (HBV) genome that is common to all HBV viral RNA transcripts. Here, we report the pharmacokinetics (PK) and safety of tobevibart administered as monotherapy or in combination with elebsiran in cirrhotic participants who have mild hepatic impairment with a Child-Pugh-Turcotte Class-A (CPT-A) score, and in matched healthy volunteers (HV).

Method: VIR-2218-V107 (NCT05484206) is a Phase 1, open-label, single-dose parallel-group study. CPT-A and HV participants were demographically matched. Participants received a single subcutaneous (SC) dose of tobevibart 300 mg or tobevibart 300 mg + elebsiran 200 mg. Blood samples were collected up to 18 weeks post-dose to measure the concentrations of tobevibart, elebsiran and its major metabolite. Safety and tolerability were monitored throughout the study.

Results: Eight cirrhotic CPT-A participants and 8 HV participants (matched by demographics) were enrolled in each cohort (tobeivibart monotherapy and tobevibart/elebsiran combination therapy). Tobeivibart PK exposure was comparable in CPT-A and HV participants. Preliminary geometric mean ratios (GMR) of tobevibart C_{max} and AUC_{inf} in CPT-A to HV participants were 0.96 (90% CI: 0.64–1.42) and 0.94 (90% CI: 0.72–1.23) in tobeivibart monotherapy, and 1.06 (90% CI: 0.71–1.59) and 1.01 (90% CI: 0.73–1.40) in tobeivibart/elebsiran combination therapy, respectively. Tobeivibart PK was similar in mono and combo therapy in both CPT-A and HV participants, indicating no PK drug-drug interaction (DDI) between tobevibart and elebsiran. Exposure of elebsiran was also comparable in CPT-A and HV participants. Preliminary GMR of C_{max} and AUC_{inf} in CPT-A to HV was 0.94 (90% CI: 0.53–1.68) and 1.54 (90% CI: 1.15–2.05), respectively. Tobeivibart and elebsiran were generally well tolerated in cirrhotic CPT-A participants. One SAE of asthma exacerbation was reported in a CPT-A participant who received tobevibart 300 mg monotherapy. The participant has a prior history of asthma flares requiring emergency department management and the SAE was considered unrelated to tobevibart.

Conclusion: Tobeivibart and elebsiran exposures were comparable in CPT-A and HV participants. A single dose of tobevibart 300 mg mono and tobeivibart 300 mg + elebsiran 200 mg combo therapy was well tolerated in CPT-A participants and no drug related SAE was observed. The data supports continued evaluation of the tobevibart 300 mg monotherapy and tobeivibart 300 mg + elebsiran 200 mg combination therapy in patients with HBV and HDV infection with CPT-A hepatic impairment.

Viral Hepatitis C – Clinical aspects including follow up after SVR

TOP-385-YI

Evaluation of liver fibrosis in patients with advanced chronic liver disease due to hcv after 6 years of sustained viral response. study with paired biopsies at 3 and 6 years

Lidia Canillas^{1,2,3}, Dolores Naranjo⁴, Teresa Broquetas^{1,2}, Zoe Mariño^{5,6,7,8}, Xavier Forns^{5,6,7,8}, Jose A. Carrión^{1,2,3,9}. ¹Liver Section, Gastroenterology Department, Hospital del Mar, Barcelona, Spain; ²Hospital del Mar Medical Research Institute (IMIM), Barcelona, Spain; ³Department of Medicine and Life Sciences, Universitat Pompeu Fabra, Barcelona, Spain; ⁴Gastrointestinal and Hepatobiliary Pathology Section, Department of Pathology, Hospital del Mar, Barcelona, Spain; ⁵Liver Unit, Hospital Clínic, Barcelona, Spain; ⁶Institut D'investigacions Biomèdiques August Pi I Sunyer (IDIBAPS), Barcelona, Spain; ⁷Centros de Investigación Biomédica en Red de Enfermedades Hepáticas y Digestivas (CIBERehd), Madrid, Spain; ⁸Department of Medicine, Medicine and Life Sciences School, Universitat de Barcelona, Barcelona, Spain; ⁹Department of Medicine, Universitat Autònoma de Barcelona, Barcelona, Spain
Email: jcarrión@psmar.cat

Background and aims: More than half of hepatitis C virus (HCV) infected patients with advanced chronic liver disease (ACLD) (transient elastography, TE>10 kPa) treated with direct-acting antivirals (DAAs) had cirrhosis (METAVIR = F4) after 3 years of sustained viral response (SVR) (Broquetas et al. Liver Int. 2021 Nov;41 (11):2733–2746). We aimed to evaluate the fibrosis stage in HCV-infected patients with ACLD after 6 years of SVR and to assess the diagnostic reliability of TE to identify cirrhosis and fibrosis regression. **Method:** Prospective and multicentric study in patients with ACLD due to HCV that achieved SVR with DAAs. Fibrosis stage was assessed with liver biopsy after 3 (LB3) and 6 (LB6) years of SVR according to the METAVIR scale. Fibrosis progression was defined as METAVIR increase, regression as METAVIR decrease, and stability as METAVIR without change. The TE's diagnostic reliability (c statistic) was evaluated to identify cirrhosis (F4) and fibrosis regression.

Results: We included 76 patients. We excluded 26 (33%) patients from the analysis for different reasons (death, comorbidities, anticoagulant treatment, etc.). Thus, we analyzed data of 50 (67%) patients with LB6, and 32 (64%) of them had paired biopsies (LB3 and LB6). Among patients with LB6 (N = 50), the median (IQR) age was 54 (49–60) and 72% were men. Before treatment, the median (IQR) of TE was 16.9 (13.1–21.8) kPa. Hence, 29 (57%) patients had TE >15 kPa, and 22 (43%) had TE 10–15 kPa. After 6 years of SVR, the median (IQR) of TE was 9.6 (7.5–13.3) kPa. The LB6 showed fibrosis stage (METAVIR) F2 in 13 (26%), F3 in 21 (43%), and F4 in 15 (31%) patients. Among patients with paired biopsies (LB3 and LB6) (n = 32), fibrosis regression was observed in 6 (19%) patients, progression in 11 (34%), and stability in 15 (47%) patients. Patients with fibrosis progression compared to those with regression or stability of fibrosis had more frequently diabetes (46% vs 29%), obesity (50% vs 29%), hypertension (73% vs 52%), and alcohol consumption of >20–30 g/day (22% vs 5%) without reaching statistical significance (all p = ns). The discrimination capacity (c-statistic) of TE to identify patients with cirrhosis after 6 years of SVR was 0.761 and to identify patients with fibrosis regression was 0.423.

Conclusion: Persistent cirrhosis is frequent, even 6 years after SVR, in patients with advanced chronic liver disease. The diagnostic reliability of transient elastography is not enough to identify patients with persistent cirrhosis after SVR. Fibrosis regression after SVR is slow in patients with advanced chronic liver disease requiring invasive techniques for its recognition.

THURSDAY 06 JUNE

THU-378

Prediction of outcomes in patients with HCV compensated liver cirrhosis after SVR: results from 5-years of follow-up

Filomena Morisco¹, Alessandro Federico², Massimo Marignani³, Flavia L Lombardo⁴, Valentina Cossiga¹, Luisa Ranieri¹, Mario Romeo², Marina Cipullo², Paola Begini³, Federico Gioli³, Tommaso Stroffolini⁵. ¹Department of Clinical Medicine and Surgery, Departmental Program "Diseases of the liver and biliary system", University of Naples "Federico II", Naples, Italy, Naples, Italy; ²Hepato-Gastroenterology Unit, University of Campania Luigi Vanvitelli, Naples, Italy, Naples, Italy; ³Department of Digestive and Liver Disease, S. Andrea University Hospital, Rome, Italy, Rome, Italy; ⁴National Center for Disease Prevention and Health Promotion, Italian National Institute of Health, 00161 Rome, Italy, Rome, Italy; ⁵Department of Tropical and Infectious Diseases, Policlinico Umberto I, Rome, Italy, Rome, Italy
Email: filomena.morisco@unina.it

Background and aims: In cirrhotic patients with HCV infection, the clinical challenge for physicians after achieving sustained virological response (SVR) is to accurately identify the subset of patients at-risk of developing liver-related event (LRE). The aims of our study are to: 1) evaluate incidence of and risk factors for LRE in a cohort of advanced chronic liver disease (ACLD) patients treated with DAA; 2) to evaluate the dynamic changes of liver stiffness in a subgroup of patients with favorable outcomes in 5 years of follow-up.

Method: A prospective multicenter study was conducted in 3 Italian centers. Consecutive patients with HCV-related ACLD starting DAA therapy between September 2014 and June 2018 were enrolled. Patients were followed for a mean period of 4.6 years after achieving SVR12 with regular biannual clinical, laboratoristic and instrumental follow-up. The at-risk period for each subject was defined by the time from the SVR12 until the end of follow-up or the onset of event. Cumulative and separate analysis were made according to the development of LRE.

Results: A total of 575 patients with ACLD achieving SVR12 were followed-up for 5 years. The male/female ratio was 1.1 and the mean age was 64.1 ± 12 years. Nearly all subjects (94.4%) belonged to the Child- Pugh A stage. The mean liver stiffness (LSM) at baseline was 19.2 kPa. Overall, 98 (17%) patients developed any type of events and the mortality rate was of 8.8% (3% for liver-related cause). The HCC was the most frequent LRE (7.1%), followed by ascites (5%). The incidence rate was 1.6 (95%CI 1.2–2.2) per 100 person/year (p/y) for both HCC and liver decompensation. Among pre-treatment variables, LSM≥20 kPa (HR 13.5; 95% CI 5.2–35.3) was the only independent predictor of liver decompensation, while liver stiffness≥20 kPa (HR 9.2; 95% CI 4.0–21.3) and male sex (HR 3.6 95% CI 1.6–8.0) both were independent predictors of HCC development. Overall, 477 subjects did not experience LRE during the follow-up and, among these, paired LSM were available for 341 (71.5%) subjects. In this subgroup, the mean LSM, at SVR12, was 16.9 ± 4.2 kPa and decreased to 13.0 ± 4.0 kPa at the end of follow-up (T60). Overall, any LSM reduction was observed in 314 (92.1%) subjects with a mean reduction of 4.4 kPa. Among these 314 subjects, half of them showed a decrease of LSM ≥20%.

Conclusion: This study shows the relevance of baseline LSM as a tool to stratify patients at risk of developing LRE. The dynamic changes over time of LSM require a continuous long term monitoring of this parameter to update changes in fibrosis degree of subjects after SVR.

THU-379

Artificial intelligence model for predicting liver-related events in non-cirrhotic patients after successful treatment by direct-acting antivirals for chronic hepatitis C

Huapeng Lin^{1,2}, Jimmy Che-To Lai², Hye Won Lee³, Terry Cheuk-Fung Yip², Sang Hoon Ahn³, Grace Lai-Hung Wong², Xiangjun Meng¹, Vincent Wai-Sun Wong², Victor de Lédighen⁴, Seung Up Kim³. ¹Shanghai Jiao Tong University, Shanghai, China; ²The Chinese University of Hong Kong, Hong Kong, Hong Kong; ³Yonsei University, Seoul, Korea, Rep. of South; ⁴Bordeaux University, Bordeaux, France
Email: linhuapeng5@163.com

Background and aims: Current guidelines recommend ultrasound screening every 6 months after sustained virologic response (SVR) in patients with chronic hepatitis C (HCV)-related cirrhosis. Identifying non-cirrhotic patients at higher risk of developing liver-related events (LREs) who could benefit from surveillance programs following HCV eradication are rarely explored. We aimed to develop and validate a machine learning-based model for LREs prediction and risk stratification in non-cirrhotic HCV patients after SVR.

Method: Random Survival Forest model was trained for prediction of LREs in 913 non-cirrhotic HCV patients after SVR in Korea and further tested in a combined cohort from Hong Kong and France (N = 1264, liver stiffness measurement [LSM] <15 kPa and no biopsy diagnosed cirrhosis). Model performance was assessed according to Harrell's C-index and time-dependent receiver operating characteristic (ROC) curve.

Results: We developed the AI-Safe score with LSM, age, sex and other six biochemistry tests. The incidence of LREs and hepatocellular carcinoma (HCC) in the validation cohort were 4.6 and 3.1 per 1000 patient-years, respectively. The C-index of the AI-Safe score in validation cohort was 0.86 (95% confidence interval [CI], 0.82–0.90). The area under ROC curves of the AI-Safe score for LREs in 3 and 5 years were 0.88 (95%CI 0.84–0.92) and 0.79 (95%CI 0.71–0.87) respectively. The C-index of the AI-Safe score for HCC in the validation cohort was 0.87 (95%CI 0.81–0.92). The AUROCs for 3-year and 5-year HCC in the validation cohort were 0.88 (95%CI 0.84–0.93) and 0.82 (95%CI 0.75–0.90). The AI-Safe score had a consistently good performance in patients with LSM <10 or 8 kPa for the predictions of LREs and also HCC. The performance of the AI-Safe score was significantly better than FIB-4, APRI and a Cox regression-based model for the prediction of LREs. Compared with existing HCC risk scores for HCV SVR patients, we could still observe a significantly better performance for AI-Safe score in the predicting of HCC. Using the cutoff of 0.08, the 5-year LREs reached 6.2% in the high-risk group but only 0.6% in the low-risk group. The 5-year HCC rate was 3.5% in the high-risk group, and 0.2% in the low-risk group.

Conclusion: The AI-Safe score is a useful machine learning-based tool to identify non-cirrhotic patients at higher risk of developing LREs.

THU-380-YI

Individualized intervals for streamlined directly observed therapy in PWIDs-a unique approach to continue HCV microelimination throughout the COVID19 pandemic

Caroline Schwarz^{1,2}, Angelika Schütz³, David Bauer^{1,2}, Enisa Gutic², Thomas Reiberger¹, Hans Haltmayer³, Michael Gschwantler^{2,4}. ¹Medical University of Vienna, Vienna, Austria; ²Klinik Ottakring, Vienna, Austria; ³Suchthilfe Wien gGmbH, Vienna, Austria; ⁴Sigmund Freud University, Vienna, Austria
Email: michael.gschwantler@gesundheitsverbund.at

Background and aims: Direct-acting antivirals (DAA) administered via directly observed therapy (DOT) are highly effective for treating HCV in people who inject drugs (PWIDs) on opioid agonist therapy (OAT). Our traditional concept of DOT relied on DAA prescription via a low-threshold facility (LTF) and supervised administration alongside OAT at a pharmacy or LTF. In PWIDs with good adherence, intervals of

DOT distribution may be extended from daily to once weekly, however, the impact of these adjustments on sustained virologic response (SVR) rates remains unknown. While most HCV elimination efforts were interrupted through the COVID19 pandemic, we present an individualized approach for DOT HCV DAA treatment in PWIDs which was successfully maintained throughout the pandemic.

Method: This study compared DOT distribution intervals, SVR rates, and socioeconomic characteristics between two cohorts of PWIDs on OAT. The first cohort consisted of 239 PWIDs on OAT who initiated DOT with DAA between March 16, 2020, and May 2, 2023, defined as the 'COVID period'. The second cohort included 441 PWIDs starting DOT between September 26, 2014, and March 12, 2020, identified as the 'pre-COVID period'.

Results: Pre-COVID, daily DOT was the most frequent approach used in 348 (78.9%) PWIDs, compared to 19 (4.3%) and 74 (16.8%) PWIDs with 2–3 times/week and once weekly OAT/DAA dispensation, respectively. During COVID daily OAT/DAA schedules were observed in only 75 (31.4%) PWIDs, while 60 (25.1%) and 104 (43.5%) were extended to 2–3 times/week and once weekly intervals, respectively (p < 0.001). SVR rates remained high and comparable between groups (167/168 [99.4%] COVID vs. 402/405 [99.3%] pre-COVID according to modified intention-to-treat analysis; p = 0.849), with no significant difference in missed visits (59 [0.8%] COVID vs. 84 [0.4%] pre-COVID; p = 0.239). However, loss of follow-up post-therapy was more frequent in the COVID period (28.5% vs. 7.5% pre-COVID; p < 0.001). Socioeconomic status was equal or even lower during COVID (unemployment: 83.7% vs. 67.3%, p = 0.967; homelessness: 38.5% vs. 35.1%, p = 0.227; habitual alcohol consumption: 29.3% vs. 10.7%, p < 0.001; ongoing intravenous drug use: 64.0% vs. 57.8%, p = 0.616). Importantly, no treatment interruptions or COVID19-related deaths were observed.

Conclusion: The traditional "daily" DOT concept targeted adherence issues in PWIDs related to ongoing substance use, psychiatric comorbidities, and low socioeconomic status. Importantly, our novel "relaxed interval" DOT concept, with individualized, extended OAT/DAA schedules, yielded similar SVR rates. Hence, the effectiveness of DOT hinges on more streamlined linkage to HCV care and simplified DAA access through a single visit at an LTF rather than strict daily surveillance.

THU-381

Prognostic implications of liver stiffness impairment after HCV cure in cACLD patients

Monica Pons^{1,2}, Georg Semmler³, Sonia Alonso Lopez⁴, Sabela Lens^{2,5}, Elton Dajti⁶, Marie Griemsmann⁷, Alberto Zanetto⁸, Lukas Burghart^{9,10}, Stephanie Hametner-Schreil¹¹, Lukas Hartl^{9,12}, Maria Luisa Manzano Alonso¹³, Sergio Rodriguez-Tajes⁵, Paola Zanaga⁸, Michael Schwarz⁹, Maria Luisa Gutierrez¹⁴, Mathias Jachs^{9,12}, Anna Pocurull^{2,5}, Benjamin Polo Lorduy¹⁵, Dominik Ecker¹¹, Beatriz Mateos Muñoz¹⁶, Sonia Izquierdo¹⁷, Yolanda Real Martínez¹⁸, Michael Gschwantler¹⁰, Francesco Paolo Russo⁸, Francesco Azzaroli¹⁹, Benjamin Maasoumy⁷, Thomas Reiberger^{9,12}, Xavier Fornis^{2,5}, Rafael Bañares^{2,4}, Mattias Mandorfer^{9,20}, Joan Genesca^{1,2}. ¹Liver Unit, Vall d'Hebron University Hospital, Vall d'Hebron Institut of Research (VHIR), Vall d'Hebron Barcelona Hospital Campus, Universitat Autònoma de Barcelona, Barcelona, Spain; ²Centro de Investigación Biomédica En Red de Enfermedades Hepáticas y Digestivas (CIBERehd), Instituto de Salud Carlos III, Madrid, Spain; ³Department of Medicine III, Division of Gastroenterology and Hepatology, Vienna, Austria; ⁴Liver Unit, Hospital General Universitario Gregorio Marañón, Instituto De Investigación Sanitaria Gregorio Marañón (IISGM), Universidad Complutense de Madrid, Madrid, Spain; ⁵Liver Unit, Hospital Clínic, Universitat de Barcelona, Barcelona, Spain; ⁶Department of Medical and Surgical Sciences (DIMEC), University of Bologna, IRCCS Azienda Ospedaliero-Universitaria di Bologna, European Reference Network on Hepatological Diseases (ERN RARE-LIVER), Bologna, Italy; ⁷Hannover Medical School,

Department of Gastroenterology, Hepatology and Endocrinology, Hannover, Germany; ⁸Gastroenterology and Multivisceral Transplant Unit, Department of Surgery, Oncology, and Gastroenterology, Padua University Hospital, Padua, Italy; ⁹Division of Gastroenterology and Hepatology, Department of Internal Medicine III, Medical University of Vienna, Vienna, Austria; ¹⁰Department of Internal Medicine IV, Klinik Ottakring, Vienna, Austria; ¹¹Department of Internal Medicine IV, Ordensklinikum Linz Barmherzige Schwestern, Linz, Austria; ¹²Vienna Hepatic Hemodynamic Lab, Division of Gastroenterology and Hepatology, Department of Internal Medicine III, Medical University of Vienna, Vienna, Austria; ¹³Liver Unit, Hospital Universitario 12 De Octubre, Madrid, Spain; ¹⁴Gastroenterology Unit, Hospital Universitario Fundación Alcorcón, Madrid, Spain; ¹⁵Gastroenterology Unit, Hospital Universitario Fundación Jiménez Díaz, Madrid, Spain; ¹⁶Liver Unit, Hospital Universitario Ramón y Cajal, Madrid, Spain; ¹⁷Gastroenterology Unit, Hospital Universitario Clínico San Carlos, Madrid, Spain; ¹⁸Gastroenterology Unit, Hospital Universitario La Princesa, Madrid, Spain; ¹⁹Department of Medical and Surgical Sciences (DIMEC), University of Bologna, Italy; IRCCS Azienda Ospedaliero-Universitaria di Bologna, European Reference Network on Hepatological Diseases (ERN RARE-LIVER), Bologna, Italy; ²⁰Vienna Hepatic Hemodynamic Lab, Division of Gastroenterology and Hepatology, Department of Internal Medicine III, Medical University of Vienna, Vienna, Spain
Email: monica.pons@vhir.org

Background and aims: In patients with hepatitis C (HCV) compensated advanced chronic liver disease (cACLD) cured with oral antivirals, follow-up (FU) liver stiffness measurement (LSM) performed after end of treatment (EOT) helps to stratify the risk of decompensation. However, information regarding prognostic performance of repeated LSM after EOT is still lacking. We aimed to evaluate the risk of liver related events (LRE) using repeated LSM after EOT and explore factors associated with LSM impairment.

Method: We retrospectively analyzed a multicentric European cohort including HCV-cACLD patients cured with oral antivirals with repeated LSM after EOT. We used 3 time-point LSM: after EOT (B-LSM), between 12 months to 36 months after EOT (LSM1) and after 54 months (LSM2). LSM impairment was defined as $\geq 20\%$ increase with respect to B-LSM with a final LSM ≥ 10 kPa. The cumulative incidence of LRE was compared between groups. LRE included decompensation events and hepatocellular carcinoma.

Results: 1052 patients with B-LSM were included. In 815 patients LSM1 was performed and in 646 LSM2 was available (in 466 all three LSM were available). During a median follow-up of 6.3 years, 80 patients developed LRE. 68 LRE occurred after LSM1 (with 23 of LRE occurring after LSM2). In 63 patients (7.7%), LSM1 worsened (increase $\geq 20\%$ with LSM1 ≥ 10 kPa) during FU vs 752 patients. Patients with LSM1 impairment had lower baseline mean platelet count ($140 \times 10^9/L$ vs $166 \times 10^9/L$, $p < 0.001$), higher bilirubin levels (0.8 mg/dL vs 0.7 mg/dL, $p = 0.016$) and higher GGT levels (45 IU/L vs 36 IU/L, $p = 0.056$) compared to patients without LSM1 impairment. No significant difference was found in metabolic risk factors neither in alcohol consumption between both groups. The incidence rate of LRE in patients with LSM1 impairment was 3.9/1000 patient-years compared to 1.9/1000 patient-years ($p = 0.024$). The risk of LRE at 5-year-FU was 20% in the LSM1 impairment group vs 11.6% in the other group ($p = 0.079$). Due to short FU after LSM2 (median 14 months), incidence of LRE related to LSM impairment was not explored.

Conclusion: In HCV-cACLD patients cured with oral antivirals, impairment in LSM during FU is not frequent but associated with a double risk of presenting LRE. Those patients in whom LSM worsens

during FU have a more advanced liver disease. In this cohort, metabolic risk factors did not associate with LSM impairment.

THU-382

Lead-in cohort results from a phase 2 study of a novel 8-week combination regimen of Bepirovir and Ruzasvir in patients with chronic hepatitis C virus infection

Alina Jucov¹, Brian Conway², Laura Iliescu³, Paul Mitru⁴, Simin Florescu⁵, Roxana Cernat⁶, Elena Ermaciov⁷, Shannan Lynch⁸, Marina Majarian⁸, Sergey Izmailyan⁸, Xiao-Jian Zhou⁸, Keith Pietropaolo⁸, Bruce Belanger⁸, Arantxa Horga⁸, Janet Hammond⁸. ¹Arensia Exploratory Medicine GmbH, Chisinau, Moldova, and Nicolae Testemitanu State University of Medicine and Pharmacy, Chisinau, Moldova; ²Vancouver Infectious Diseases Centre, Vancouver, Canada; ³Institutul Clinic Fundeni, Bucharest, Romania; ⁴University of Medicine and Pharmacy, Craiova, Romania; ⁵Spitalul Clinic de Boli Infectioase si Tropicale Dr. Victor Babes, Bucharest, Romania; ⁶Clinical Hospital for Infectious Diseases, "Ovidius" University Constanta, Constanta, Romania; ⁷Arensia Exploratory Medicine GmbH, Chisinau; ⁸Atea Pharmaceuticals, Inc., Boston, United States
Email: alina.jucov@arensia-em.com

Background and aims: Bepirovir (BEM) and ruzasvir (RZR) are potent, pan-genotypic inhibitors of the HCV NS5B polymerase and the NS5A protein, respectively. In previous studies, the combination of BEM and daclatasvir ($n = 10$), and uprifosbuvir and RZR ($n > 400$), were safe, well-tolerated, and each combination achieved high sustained virologic response (SVR) rates in HCV-infected patients. BEM+RZR exhibited synergistic anti-HCV activity *in vitro* with no pharmacokinetic (PK) drug-drug interaction in healthy subjects, prompting evaluation of this novel combination in a phase 2 open-label study assessing efficacy and safety of BEM+RZR administered for 8 weeks in 280 HCV-infected patients (NCT05904470).

Method: In this single arm study, a lead-in cohort ($n = 60$) of treatment-naïve, non-cirrhotic patients with chronic HCV (any genotype) received 550 mg BEM once daily (QD) + 180 mg RZR QD for 8 weeks. Objectives of this preliminary analysis included assessment of safety (reported adverse events [AEs], laboratory abnormalities, serial electrocardiograms [ECGs]) and efficacy (achievement of SVR4). An SVR4 rate of $\geq 90\%$ in the lead-in cohort was needed to proceed with further enrollment. Plasma HCV RNA was evaluated using the Roche cobas[®] HCV quantitative nucleic acid test for use on the cobas[®] 6800/8800 systems, with a lower limit of quantitation (LLOQ) of 15 IU/ml.

Results: The 60 lead-in patients were infected with GT1 ($n = 45$), GT2 ($n = 2$) and GT3 ($n = 13$), and 17% had F3 fibrosis. 57% were male, 95% were Caucasian, with a median age of 47 (range 25–79) years. All patients completed the 8-week treatment period with no premature treatment discontinuations or drug-related serious AEs. AEs were mostly mild; no clinically significant laboratory or ECG abnormalities were observed. Viral load decreased rapidly after treatment initiation, with 90% of patients achieving below LLOQ by week 4 (residual viral loads of the remaining patients were near LLOQ ranging from 16 to 31 IU/ml) and 100% achieving below LLOQ by end of treatment. At the time of this analysis, 58 subjects reached the SVR4 timepoint. Of these, 57 subjects (98%) achieved SVR4.

Conclusion: BEM+RZR for 8 weeks was well tolerated in HCV-infected patients. A high rate of SVR4 (98%) was documented in this preliminary analysis. All patients will continue to be followed to SVR12. Based on these results, the study will continue to enroll an additional 220 patients, including those with compensated cirrhosis.

THU-383

Predictive performance of HCC risk scores in chronic hepatitis C patients with advanced fibrosis after achieving SVR: real-world experience from a tertiary UK centre

Riham Soliman¹, Saima Ajaz¹, James Lok¹, Mercy Karoney¹, Evangelos Chalatsis¹, Ivana Carey¹, Mary D Cannon¹, Kathryn Oakes², Teresa Bowyer¹, Kosh Agarwal¹, Maria Guerra Veloz¹. ¹Institute of Liver Studies, King's College Hospital NHS Foundation Trust, London, United Kingdom; ²Institute of Liver Studies, King's College Hospital NHS Foundation Trust, London, United Kingdom
Email: riham.soliman@nhs.net

Background and aims: Current guidelines recommend biannual hepatocellular carcinoma (HCC) surveillance in patients with chronic hepatitis C (CHC) infection and advanced liver fibrosis. However, this 'one-size-fits-all' strategy places a huge burden on healthcare systems and regression of fibrosis may occur with disease-modifying treatments. Our aim is to compare the discriminative ability of risk prediction scores for HCC development in patients with CHC who have achieved sustained virological response (SVR).

Method: In this retrospective single centre study we compared the predictive performance of the aMAP, THRI and GES scores in a cohort of patients with treated HCV infection (F3–F4) and achieved SVR with direct acting antivirals (DAAs) between 2014 and 2020. Data was collected until HCC occurrence, death or last follow-up visit. Cumulative incidences were calculated using the Kaplan-Meier method and compared using the log-rank test. The performance of each model was assessed further using Harrell's c statistics.

Results: 508 patients were included in the analysis, 70% males with a median age of 58.0 years. The majority (61.4%) were cirrhotic. By applying the GES score, 264 (52.0%), 174 (36.4%), and 70 (13.8%) of the patients were considered at low, intermediate, and high risk for HCC. Cumulative HCC incidence in the three categories were as follows: low-risk cohort (defined as GES score ≤ 6 , cumulative incidence 1.20%, 95% CI 0.65–2.04), intermediate-risk cohort (defined as score > 6 and ≤ 7.5 , incidence 2.26% CI 1.34–3.59), and high-risk cohort (scores > 7.5 , incidence 5.86%, 95% CI 3.47–9.31). For the aMAP score, 41 (8.1%), 204 (40.2%), and 263 (51.8%) of the studied patients were at low, intermediate, and high risk for HCC. Cumulative HCC incidence was 0.73% (95% CI 0.04–3.60) in their low-risk group, 0.65% (95% CI 0.24–1.43) in their intermediate-risk group, and 3.56% (95% CI 2.56–4.84) in their high-risk group. For the THRI score, 105 (20.7%), 352 (69.3%), and 15 (10.0%) of the studied patients were at low, intermediate, and high risk for HCC; cumulative incidences were 0.79% (95% CI 0.20–2.16), 2.05% (95% CI 1.40–2.91) and 6.31% (95% CI 3.42–10.73), respectively. The Harrell's c-statistic for the three scores were 0.646 (GES), 0.6723 (aMAP) and 0.6314 (THRI).

Conclusion: All three scores effectively stratified our patient cohort into low, intermediate, and high-risk groups. Screening can be safely avoided in low risk, potentially improving the cost-effectiveness of our HCC surveillance programmes.

THU-386-YI

Renin-angiotensin inhibitor intake is associated with improved survival in patients with chronic hepatitis C viral infection following SVR-data from the german hepatitis C-registry (DHC-R)

Tammo Lambert Tergast¹, Marie Griemsmann¹, Leyla Valiyeva¹, Peter Buggisch², Stefan Mauss³, Hartwig Klinker⁴, Klaus H.W. Boeker⁵, Christine John⁶, Ralf Link⁷, Stefan Zeuzem⁸, Thomas Berg⁹, Heiner Wedemeyer^{1,10}. ¹Hannover Medical School, Department of Gastroenterology, Hepatology, Infectious Diseases and Endocrinology, Hanover, Germany; ²ifi-Institute for Interdisciplinary Medicine, Hamburg, Germany; ³Center for HIV and Hepatogastroenterology, Düsseldorf, Germany; ⁴University of Würzburg Medical Center, Division of Infectious Diseases, Department of Internal Medicine II; Würzburg, Germany; ⁵Center of Hepatology; Hanover, Germany; ⁶Center of Gastroenterology, Berlin, Germany; ⁷MVZ-

Offenburg GmbH/St. Josefs-Klinik, Offenburg, Germany; ⁸University Hospital Frankfurt, Department of Medicine I, Gastroenterology, Hepatology and Endocrinology, Frankfurt am Main, Germany; ⁹Leipzig University Medical Center, Division of Hepatology, Department of Medicine II, Leipzig, Germany; ¹⁰Leberstiftungs-GmbH Deutschland, Hanover, Germany
Email: tergest.tammo@mh-hannover.de

Background and aims: The role of renin-angiotensin inhibitors (RAS-Inhibitors) on the clinical course of patients with chronic liver disease remains unclear. Antifibrotic effects have been described in animal models and it has been hypothesized that RAS-Inhibitor intake could exert positive effects on the natural history of liver disease, potentially leading to lower rates of hepatocellular carcinoma (HCC), hepatic decompensation (HD) and improved survival. However, clinical data to support this are lacking. This study investigated the impact of RAS-Inhibitor intake on the clinical course of patients with chronic hepatitis C (HCV) in the well-established German Hepatitis C-Registry (DHC-R).

Method: Overall, 10703 patients were included in this study. Patients with malignancies, without sustained virological response (SVR), HIV or history of organ transplantation were excluded. Study end points were mortality, incidence of hepatic decompensation and incidence of HCC, respectively. Survival analysis was conducted via multi-variable Cox-regression, adjusting for important confounding factors such as presence of arterial hypertension, type 2 diabetes mellitus, chronic kidney disease, sex or age.

Results: RAS-Inhibitor intake was present in 2207 (21%) patients. In total, 128 events of hepatic decompensation, 130 deaths and 82 HCCs were documented during follow-up of 18783 patient years. Presence of type 2 diabetes mellitus, presence of dyslipidemia, arterial hypertension, chronic kidney disease or coronary artery disease was significantly more frequent in patients with RAS-Inhibitor intake (18% vs. 5%, $P < 0.001$, 6% vs. 1%, $P < 0.001$, 76% vs. 9%, $P < 0.001$, 6% vs. 1%, $P < 0.001$ and 9% vs. 1%, $P < 0.001$, respectively). Intake of RAS-Inhibitors was not associated with a lower incidence of hepatic decompensation (HR: 0.99, 95%CI: 0.65–1.53, $P = 0.99$) or hepatocellular carcinoma (HR: 0.77, 95%CI: 0.46–1.32, $P = 0.34$). However and importantly, RAS-inhibitor intake was independently associated with improved survival (HR: 0.54, 95%CI 0.33–0.87, $P = 0.01$) irrespective of the higher frequency of metabolic comorbidities.

Conclusion: Although the incidences of HCC or hepatic decompensation is unaffected, the intake of RAS inhibitors was associated with a reduced mortality in patients with HCV following SVR.

THU-387

Safety and efficacy of two pangenotypic direct acting antivirals (sofosbuvir/velpatasvir and glecaprevir/pibrentasvir) for the treatment of hepatitis C in children

Maria Pokorska-Śpiwak¹, Ewa Talarek², Anna Dobrzeńska³, Małgorzata Aniszewska², Magdalena Pluta², Magdalena Marczyńska². ¹Medical University of Warsaw, Regional Hospital of Infectious Diseases, Warsaw, Poland; ²Medical University of Warsaw, Regional Hospital of Infectious Diseases in Warsaw, Warsaw, Poland; ³Regional Hospital of Infectious Diseases in Warsaw, Warsaw, Poland
Email: maria.pokorska-spiwak@wum.edu.pl

Background and aims: The aim of this study was to analyze and compare safety and efficacy of two pangenotypic regimens (sofosbuvir/velpatasvir, SOF/VEL and glecaprevir/pibrentasvir, GLE/PIB) used for treatment of chronic hepatitis C (CHC) in children.

Method: In this single-center study we compared outcomes of CHC treatment in two groups of children: 50 participants aged 6–18 years treated with SOF/VEL in PANDAA-PED Project, and 41 patients aged 5 to 18 years treated with GLE/PIB in POLAC Project. We included all children who had been treated since January 2022, whose evaluation of sustained viral response at 12-week posttreatment (SVR12) was performed until December 31, 2023. In all cases, fixed drug doses adjusted to the patients' weight were used.

Results: Both studied groups (SOF/VEL vs. GLE/PIB) did not differ with respect to sex (46% males in SOF/VEL group, and 51% in GLE/PIB group, $p = 0.62$) and age (10.0 ± 2.5 vs. 9.3 ± 3.2 years, $p = 0.18$). Most children were infected vertically (94% and 93%, $p = 0.8$), mainly with genotype 1 HCV (74% and 61%, $p = 0.31$) followed by genotype 3 and 4. Most children were treatment-naïve (94% vs. 98%, $p = 0.41$). At baseline, median alanine aminotransferase (ALT) levels did not differ: 48 IU/L (IQR 34–65) vs. 47 IU/L (35–68), $p = 0.84$, similarly to the HCV viral load (mean \log_{10} 5.8 ± 0.79 IU/ml vs. 5.9 ± 0.97 IU/ml, $p = 0.36$). One child in SOF/VEL group and 2 in GLE/PIB group presented with significant fibrosis (F2–3 in METAVIR scale). SVR12 was 100% in both groups. At 4-week of treatment, 2/50 (4%) patients in SOF/VEL group and 7/41 (17%) in GLE/PIB group presented with detectable HCV RNA ($p = 0.03$), but all were negative at the end of treatment. The most intense decrease in ALT level occurred during the first 4 weeks of treatment and it was similar in both groups [29 IU/L (14–43) vs. 28 (14–43) IU/L, $p = 0.94$]. Adverse events (AEs) were reported in 40% of patients in SOF/VEL group compared to 41.5% in GLE/PIB group ($p = 0.96$). The most common AEs included headache, abdominal pain, fatigue, asthenia, and somnolence. Asthenia occurred only in the SOF/VEL group (12%, $p = 0.02$), whereas skin itching only in GLE/PIB group (7%, $p = 0.05$).

Conclusion: Both pangenotypic regimens were 100% effective. The prevalence of AEs was similar in both groups. Thus, no superiority of any of the studied regimens for treatment of CHC in children was revealed.

THU-389

Sustained virological response after early discontinuation of HCV treatment

Robert Flisiak¹, Dorota Zarebska-Michaluk², Ewa Janczewska³, Anna Parfieniuk-Kowderda¹, Włodzimierz Mazur⁴, Marek Sitko⁵, Justyna Janocha-Litwin⁶, Rafał Krygier⁷, Beata Lorenc⁸, Anna Piekarska⁹, Barbara Sobala-Szczygieł¹⁰, Krystyna Dobrowolska², Łukasz Socha¹¹, Jerzy Jaroszewicz¹⁰. ¹Medical University of Białystok, Białystok, Poland; ²Jan Kochanowski University, Kielce, Poland; ³ID Clinic, Mysłówice, Poland; ⁴Medical University of Silesia, Chorzów, Poland; ⁵Jagiellonian University, Kraków, Poland; ⁶Wrocław Medical University, Wrocław, Poland; ⁷NZOZ Gemini, Żychlin, Poland; ⁸Medical University of Gdańsk, Gdańsk, Poland; ⁹Medical University of Łódź, Łódź, Poland; ¹⁰Medical University of Silesia, Bytom, Poland; ¹¹Pomeranian Medical University, Szczecin, Poland
Email: robert.flisiak1@gmail.com

Background and aims: So far, the effectiveness of therapy with direct-acting antivirals (DAA) discontinued before 4 weeks has not been analyzed in clinical practice. The aim of this study is to determine to what extent such a short therapy will enable achieving a sustained virological response (SVR) under real-world experience.

Method: Of the 16, 815 patients registered in the EpiTer-2 national database, 195 patients (1.2%) discontinued therapy, of which 97 had both the assessment of SVR and the time of discontinuation of therapy available.

Results: The majority (63.9%) patients discontinued treatment after 4 weeks, but 37 discontinued before the end of 4th week, including 12 within 2 weeks. The most common reason for therapy discontinuation was hepatic decompensation (20.6%) or the patient's personal decision (18.6%), and less frequently increased transaminase activity, cardiovascular or gastrointestinal symptoms, and anemia. Patients who discontinued therapy compared to those who completed treatment as planned were significantly older, more likely to have experienced prior therapy failure, more frequently have cirrhosis, a history of decompensation, and a Child-Pugh classification of B or C. SVR was achieved by 93.5% of patients who discontinued treatment after 4 weeks, 60.9% if discontinued at week 3 or 4 and 33.3% at week 1 or 2. The SVR rate after pangenotypic treatment in patients who discontinued after week 4 (100%) did not differ significantly from that observed in patients who completed the therapy planned (97.4%).

However, SVR after discontinuation before week 4 compared to discontinuation after that time was significantly lower in both pangenotypic (42.9% vs 100%) and genotype-specific (57.1% vs 92.5%) treated patients. The characteristics of four patients who responded to treatment lasting no longer than 2 weeks suggested that the main positive prognostic factor was a low baseline viral load ($<400,000$ IU/ml).

Conclusion: Despite discontinuation of therapy after the 4th week of treatment, the chances of achieving SVR are high and even very early discontinuation of therapy does not exclude therapeutic success, especially in patients with low baseline viral load.

THU-390

Achieving HCV elimination in underserved populations-an austrian initiative for HCV care for homeless people without medical insurance

Caroline Schwarz^{1,2}, Bernadette Becsi³, Stephan Leick³, Stephan Gremmel³, Lena Wien⁴, Enisa Gutic¹, Thomas Reiberger², Hans Haltmayer⁵, Michael Gschwandler^{1,4}. ¹Klinik Ottakring, Vienna, Austria; ²Medical University of Vienna, Vienna, Austria; ³neunerhaus Gesundheitszentrum, Vienna, Austria; ⁴Sigmund Freud University, Vienna, Austria; ⁵Suchthilfe Wien gGmbH, Vienna, Austria
Email: schwarz.caroline1990@gmail.com

Background and aims: Direct-acting antiviral agents (DAA) facilitate excellent sustained virologic response (SVR) rates, yet reaching HCV elimination in Austria remains challenging. People experiencing homelessness (PEH) and/or lack of medical insurance (PELI) are at risk for HCV infection, however, specific elimination projects have not been designed for this population. We present the first Austrian HCV elimination project for PEH and PELI.

Method: The project was based at a low-threshold institution (LTI) providing medical care, social support, and housing for $>5,000$ PEH and PELI in Vienna per year. AntiHCV screening was offered at the LTI or one of its associated 27 housing institutions since 03/2020. AntiHCV (+) blood samples were further tested for HCV-RNA by PCR ("reflex testing"). HCV-viremic persons received DAA via a hepatitis outpatient clinic integrated in the LTI. PEH were provided with housing via the LTI for the duration of therapy, and in PELI treatment was kindly provided by Abbvie® or Gilead®. Adherence to DAA therapy, was supported by social workers of the LTI and in the respective housing facilities.

Results: Between 03/2020 and 07/2023, 601 individuals underwent serologic testing for HCV, and 116 (19.3%) showed antiHCV (+). While in 24/116 (20.7%) persons HCV-RNA PCR remained negative indicating resolved HCV infection, 92 (79.3%) were HCV-viremic. Among these, DAA therapy was initiated in 36/92 (39.1%) so far. At database closure (07/2023), 21/36 (58.3%) persons had completed DAA treatment and SVR was documented in 17 (81.0%), while 4 (19.0%) individuals remained on post-treatment follow-up. No DAA treatment interruptions were observed.

Conclusion: While the COVID19 pandemic limited the number of PEH and PELI reached by our screening effort, a substantial proportion of this underserved population underwent HCV testing through this project. HCV seroprevalence was 19.3%, HCV viremia exceeded expectations with 79.3% (tested) and 15.3% (overall)-underlining the relevance of targeted HCV care for PEH and PELI. Our data show that streamlined treatment with DAA is highly effective in the population of PEH and PELI, however, given that additional supporting measures are taken including social worker assistance and provision of safe housing for the duration of therapy. Future HCV elimination efforts should include the underserved population of PEH and PELI in whom HCV prevalence seems alarmingly high despite the availability of DAA. This study was supported by Abbvie® and Gilead®.

POSTER PRESENTATIONS

THU-391-YI

Impact of hepatitis C cure on outcomes for patients undergoing curative therapy for hepatocellular carcinoma

Alex Wynne¹, Edward J. Gane², Akhilesh Swaminathan³. ¹Auckland City Hospital, Auckland, New Zealand; ²Faculty of Medicine, University of Auckland, Auckland, New Zealand; ³Auckland City Hospital, Liver Unit, Auckland, New Zealand
Email: alexwynne25@gmail.com

Background and aims: Direct-acting antivirals (DAA) with high cure rates have had a dramatic impact on hepatitis C virus (HCV) and its complications, including reduction in incidence of index hepatocellular carcinoma (HCC). However, the impact on outcomes of hepatitis C cure for patients receiving curative intent treatment for their initial HCC is currently not known. Our aim is to assess the impact of hepatitis C cure on incidence of further (recurrent or metachronous) HCC, and on survival, in individuals who have undergone curative intent treatments.

Method: We conducted retrospective analysis of all patients that have received curative intent treatment (surgical resection or ablation) for HCC secondary to HCV in New Zealand between 2003 and 2023. We compared outcomes of those who achieved sustained viral response (SVR) prior to HCC treatment with those who had not achieved SVR prior. We used Kaplan Meier comparison of recurrence free survival and overall survival using Log-Rank and univariable and multivariable analysis using Cox Regression.

Results: Of the 203 patients included in the analysis, 56% had achieved SVR prior to or at the time of their HCC diagnosis. Our analysis showed that achieving SVR prior to initial HCC therapy reduces risk of HCC recurrence compared to never achieving SVR (Hazard Ratio (HR)=0.44, 95% Confidence Interval (CI) 0.26–0.64). Our analysis also showed that patients achieving SVR prior to the initial HCC therapy reduces the risk of death compared to those not having achieved SVR (HR = 0.36, 95% CI 0.21–0.64).

Conclusion: These results demonstrate that eradication of HCV infection in patients who present with their index HCC reduces the risk of recurrent HCC following resection or ablation by almost 60%. In the era of highly effective DAA therapy and limited supply of deceased donors, patients with HCV infection who have been diagnosed with their index HCC should be treated with DAAs and offered resection or ablation rather than transplantation.

THU-394

Improvement of hepatitis C virus care cascade by In-hospital Reflex tEsting ALarm-C (REAL-C) model

Jonggi Choi¹, Kanghee Park¹, Jina Park¹, Ji won Yang¹, Hyeyeon Hong¹, Sung Won Chung¹. ¹Asan Medical Center, Seoul, Korea, Rep. of South
Email: jkchoi0803@gmail.com

Background and aims: World Health Organization (WHO) has set targets to eliminate viral hepatitis, including hepatitis C virus (HCV) infection, by 2030. Achieving these goals necessitates improved rates of diagnosis and treatment. We present the results of the in-hospital Reflex tEsting ALarm-C (REAL-C) model, which incorporates reflex HCV RNA testing and sending alarming messages for physicians.

Method: We conducted a retrospective study at Asan Medical Center in Seoul, Republic of Korea, focusing on 1,730 patients newly testing positive for anti-HCV between March 2020 and June 2023. Three distinct periods were defined: pre-REAL-C (n=696), incomplete REAL-C (n=515), and complete REAL-C model periods (n=519). The primary outcome measured was the rate of HCV RNA testing throughout the study period. Additionally, the referral rate to gastrointestinal (GI) department, linkage time for diagnosis and treatment, and the treatment uptake rate.

Results: The rate of HCV RNA testing increased significantly from 51.0% (pre-REAL-C) to 95.6% (complete REAL-C). This improvement was consistent across clinical departments, regardless of patients' comorbidities. Among patients confirmed with HCV infection, the GI referral rate increased from 57.1% to 81.1% after the implementation of

the REAL-C model. Treatment uptake rates among treatment-eligible patients was 92.4% during the study period. The mean days from anti-HCV positivity to HCV RNA testing decreased from 45.1 to 1.9. The mean days from the anti-HCV positivity to direct-acting antiviral treatment also decreased from 89.5 to 49.5 with the REAL-C model. **Conclusion:** The REAL-C model, featuring reflex testing and alarming messages, effectively increased HCV RNA testing rates and streamlined care cascades. Our model facilitated progress toward achieving the WHO's elimination goals for HCV infection.

THU-395

Is hepatitis C screening based on risk factors enough in primary care setting?

Elena Vargas-Accarino¹, Ariadna Rando-Segura², Ingrid Arcusa³, Eva de Diego⁴, Núria García⁵, Elena Monserrat⁶, Marta Selvi⁷, Maria Asuncion Ubeda Pastor⁴, Imma Valls⁸, Carla Ventosa⁹, Adriana Palom¹, Judit Romero-Vico¹, Juan Carlos Ruiz-Cobo^{1,10,11}, Mar Riveiro Barciela^{1,10,11,12}, Rafael Esteban^{1,10,11,12}, Maria Buti^{1,10,11,12}. ¹Liver Diseases Research Group, Vall d'Hebron Research Institute, Barcelona, Spain; ²Microbiology and Biochemistry Department, Vall d'Hebron University Hospital, Barcelona, Spain; ³CAP Trinitat Vella, Barcelona, Spain; ⁴CAP Horta, Barcelona, Spain; ⁵CAP Río de Janeiro, Barcelona, Spain; ⁶CAP Chafarinas, Barcelona, Spain; ⁷CAP Sant Andreu, Barcelona, Spain; ⁸CAP San Rafael, Barcelona, Spain; ⁹CAP Guineueta, Barcelona, Spain; ¹⁰Liver Unit, Vall d'Hebron University Hospital, Barcelona, Spain; ¹¹Medicine Department, Universitat Autònoma de Barcelona, Barcelona, Spain; ¹²CIBERehd, enfermedades hepáticas y digestivas, Madrid, Spain
Email: mariabutiferret@gmail.com

Background and aims: Most international guidelines recommend HCV screening only for individuals with risk factors or elevated ALT. These recommendations are based on descriptive studies in which it was identified that more than 80% of patients with positive anti-HCV had risk factors. However, screening strategies based on risk factors may be insufficient for eradicating the infection in high-income countries, since the undiagnosed population remains stable. The objective of our study was to evaluate the application of hepatitis C screening guidelines in primary care centers (PCC) in Spain.

Method: Retrospective search in the microbiology database of the anti-HCV+ and HCV-RNA+ patients from 7 primary care centers. Medical records of those patients were reviewed to assess the screening recommendation application and treatment indication.

Results: Of a total of 90,170 different individuals who attended these 7 primary care centers, 9,052 (10%) were screened for hepatitis C between January 2021 and March 2023. Anti-HCV antibodies were detected in 277 (3%) individuals and 48 (7%) were HCV-RNA+, accounting for 0.5% of the screened patients. Medical records of those 277 anti-HCV+ patients were reviewed to analyze their screening criteria. We found that only 38% of anti-HCV+ patients reported risk factors. Of them, 19% were people who inject drugs, 9% had a previous blood transfusion, 4% had tattoos, 4% had sexual risk behavior and 2% were infected by vertical transmission. Analyzed by transaminases levels, 76% had normal transaminases and 24% presented elevated AST or ALT. When analyzed together, we found that 150 (54%) anti-HCV+ patients neither reported risk factor nor presented elevated transaminases. From the 48 HCV-RNA+ patients, only 42% reported risk factors and 31% elevated transaminases; while analyzing it together we found that 22 (46%) of them neither reported risk factors nor elevated transaminases. Anti-HCV+ participants were 55% male, median age 59 years and 70% were born in Spain. Basal median AST and ALT were 29 and 35 IU/L respectively and had FIB-4 and APRI of 2.2 and 0.4 respectively. However, HCV-RNA+ cases were mainly male (60%), older (median age of 69 years) and had higher AST and ALT levels (41 and 47 IU/L respectively) and FIB-4 and APRI of 0.85 and 0.45, respectively. Age and transaminases were significantly higher in individuals with HCV-RNA (p < 0.05).

Conclusion: Only 10% of patients attending primary care centers are screened for hepatitis C, with 0.5% of these patients being viremic. More than a half of anti-HCV+ patients neither reported risk factors nor had elevated transaminases and they would not have been screened for hepatitis C if following current guidelines. Moreover, almost a half of HCV-RNA+ patients would not have been treated. HCV universal screening in PCC could be a good strategy to eliminate hepatitis C.

THU-396

HCV patients achieving sustained virologic response after direct-acting antiviral therapy may still face adverse clinical outcomes: analysis of gene enrichment, marker expression, and clinical outcomes

Daniel Millian¹, Omar Saldarriaga², Esteban Arroyave², Heather Stevenson³, Arvind Rao⁴, Santhoshi Krishnan⁴. ¹University of Texas Medical Branch, Galveston, Texas, United States; ²University of Texas Medical Branch, Galveston, Texas, United States; ³University of Texas Medical Branch, Galveston, Tx, United States; ⁴University of Michigan, Michigan, United States
Email: damillia@utmb.edu

Background and aim: The incidence of HCV in the United States is on the rise, driven by the opioid epidemic, and even though over 95% of HCV patients respond positively to direct-acting antiviral (DAA) therapy they continue to be at risk of re-infection, and chronic liver disease. In this study, we explore the complex aftermath of DAA treatment for Hepatitis C, focusing on the observation where patients achieving sustained virologic response (SVR) may still face adverse clinical outcomes, including portal hypertension and hepatocellular carcinoma. We aim to determine the gene and protein expression of the hepatic microenvironment before and after DAA treatment to identify key biological markers associated with poor outcomes.

Method: Utilizing cutting-edge multispectral imaging, we scrutinize the nuances of intrahepatic macrophage (CD68, CD14, CD16, MAC387, and CD163) and T cells (CD3, CD4, CD8, CD45, and FoxP3) phenotypes. This involves the comparison of liver biopsies collected before (n = 10) and after (n = 10) SVR attainment (5 were paired biopsies from the same patients; total of 15 patients). Employing advanced imaging analysis and machine learning algorithms, we decoded the changes in these pivotal immune cells. Furthermore, our exploration extends to over 700 genes through RNA isolated from liver biopsies using NanoString nCounter and RNA sequencing (SMART-seq). Both platforms were correlated with clinical outcomes.

Results: The pre and post-treatment (Pre-Tx, Post-Tx) fresh liver tissue data from 15 patients were analyzed and correlated with clinical outcomes. We observed that in the post-Tx liver biopsies of patients without inflammation, the liver enzymes aspartate aminotransferase (AST) (Pre-Tx 122 U/L, SD ± 105 and post-Tx 29 U/L, SD ± 10.3, respectively), and alanine aminotransferase (ALT) (Pre-Tx 96 U/L, SD ± 104 and Post-Tx 20 U/L, SD ± 27) returned to baseline compared to Pre-Tx values. This coincides with the multispectral imaging showing a switch from proinflammatory/M1-like to anti-inflammatory/M2-like macrophage phenotypes pre- and post-treatment, respectively. Nanostring gene expression analysis showed an enrichment of inflammatory and interferon-induced antiviral genes in the pre-treatment group when compared to the Post-Tx. However, after treatment, the fibrosis stage of 5 out of 15 patients did not improve or regress to baseline, and 2 out of these 5 patients died from decompensated cirrhosis and one succumbed to cholangiocarcinoma. These results were subsequently confirmed using RNA sequencing.

Conclusion: In summary, this work reveals distinctive gene and marker expression profiles before the administration of DAAs, which undergo notable changes post-treatment. However, patients with advanced fibrosis or with cirrhosis at the initiation of the antiviral therapy may develop poor clinical outcomes even after achieving sustained virologic response.

THU-397-YI

Long-term histological fibrosis evolution following sustained virological response after hepatitis C-recurrence in liver-transplanted patients

Tibo Lemmens¹, Cindy Serdjebi², Guillaume Henin¹, Selda Aydin¹, Pamela Baldin¹, Florine Chandes², Géraldine Dahlqvist¹. ¹Cliniques universitaires Saint Luc, Brussels, Belgium; ²Biocellvia, Marseille, France
Email: tibolemmens123@gmail.com

Background and aims: Hepatitis C (HCV) recurrence after liver transplantation (LT) is universal if HCV-RNA persists at time of LT and progression to fibrosis can occur rapidly. Nowadays, sustained virological response (SVR) is obtained in 97% of HCV-infected patients treated with direct acting antivirals (DAA) after LT. Fibrosis diminishes in HCV patients after SVR but there is paucity of data on fibrosis regression occurring after SVR following LT. In addition, most studies evaluate fibrosis with non-invasive techniques while these are not validated after LT because of LT-specific complications. There are no data evaluating long-term evolution of fibrosis after SVR since the introduction of DAA treatments (>5–10 years). The aim of this study is to histologically evaluate liver fibrosis evolution in short and long term follow-up biopsies after HCV-elimination in LT-patients.

Method: In this retrospective monocentric cohort study, we evaluated 32 patients with SVR after recurrent HCV following LT and treated with IFN (n = 4) or DAA (n = 28). Protocolar liver biopsies were collected between 2011 and 2020. We compared liver biopsies before HCV treatment, with those taken during short-term follow-up (<2 years) and long-term follow-up (≥3 years). Massons' trichrome (MTC) slides were used for METAVIR- and LAF scoring. Picro-Sirius-red (PSR) slides were used for both a semi-quantitative assessment of fibrosis expressed as total fibrosis area (%) and an automated morphometric assessment of fibrosis with artificial intelligence (AI) based technology MorphoQuant.

Results: All 32 patients reached SVR after LT, including 24 with follow-up biopsies. Scoring and AI-based analyses were performed on 19 and 24 patients, respectively. PSR analysis showed a significant reduction in total fibrosis area on the short-term biopsies (−4.9%, p < 0.002) in 73% of patients, which remained stable even after long-term assessment (−4.9%, p < 0.001). MTC based scoring confirmed fibrosis regression in the long-term biopsies, according to either METAVIR (−0.8, p < 0.01) or LAF-Score (−1.5, p < 0.02) but not in the short-term biopsies. AI-based analysis showed a significant reduction of collagen proportionate area in the short-term biopsies after HCV treatment, and a stabilization over time (−3.2%, p < 0.001). This reduction was notably significant in the perivascular area (−2.5%, p < 0.002), but not in the peri-sinusoidal or septal area. Finally, collagen fibres were smaller after short-term evaluation (−0.18%, p < 0.02), which was confirmed in long-term follow-up biopsies.

Conclusion: Achieving SVR after post-LT HCV-recurrence results in swift reduction of fibrosis with stabilization on the long term. AI-based analyses show earlier changes than the classical histological scoring systems.

THU-398

Metabolic factors predict significant liver fibrosis in people who use drugs (PWUD) and general population with HCV infection. Time to re-consider the follow-up strategy in chronic hepatitis C patients

Hariklia Kranidioti¹, Olga Anagnostou², Georgios Kontos¹, Sofia Vasileiadi¹, Anestis Goulas¹, Nikolaos Papadopoulos^{3,4}, Melanie Deutsch¹, Spilios Manolakopoulos¹. ¹2nd Department of Internal Medicine, National and Kapodistrian University of Athens, General Hospital of Athens Hippocratio, Athens, Greece; ²Greek Organization against of Drugs (OKANA), Athens, Greece; ³401 General Army Hospital of Athens, Athens, Greece; ⁴401 General Army Hospital of Athens, 2nd Department of Internal Medicine, Athens, Greece
Email: harakranidioti@yahoo.gr

POSTER PRESENTATIONS

Background and aims: Comorbidities related to metabolic syndrome are associated with liver fibrosis and affect the management and surveillance of patients with HCV infection. The aim of the study was to address the prevalence of metabolic risk factors in HCV patients and their impact on liver stiffness according to the source of infection.

Method: We included patients with detectable HCV RNA who received treatment with DAAs in our outpatient liver clinic from June 2014 to July 2021. Metabolic profile was based on BMI measurement, medical records and prescribed medication for diabetes mellitus (DM), arterial hypertension (AH) and dyslipidemia (DLD) on baseline evaluation. Liver stiffness was evaluated with transient elastography (TE).

Results: 680 patients were analyzed (71% males, 51 ± 12 years old, 57% >50 years old). 422 (62%) patients reported previous history of drug use (PWUD) and 71% was under substitution with buprenorphine or methadone. Regarding metabolic risk factors, 41 (6%) patients presented DM, 215 (32%) AH, 80 (12%) DLD and 275 (40%) had BMI >25 (mean BMI 24.9 kg/m²). Compared with PWUD, patients who had HCV infection from other sources (general population) were older (56 vs 47 years, $p < 10^{-3}$), had higher BMI (26 vs 24 kg/m², $p < 10^{-3}$), and presented more frequently DM (12.7% vs 1.7%, $p < 10^{-3}$), AH (24% vs 12%, $p < 10^{-3}$) and DLD (12.7% vs 1.9%, $p < 10^{-3}$). In total, 327 (51%) patients (43% PWUD vs 61% general population, $p < 10^{-3}$) had significant fibrosis or cirrhosis (liver stiffness >9 kPa). Logistic regression analysis revealed that predictive factors for significant fibrosis were source of infection (general population) ($p < 10^{-3}$), older age ($p < 10^{-3}$), BMI ($p < 10^{-3}$), BMI >25 kg/m² ($p < 10^{-3}$), AH ($p = 0.01$), and the presence of DM ($p < 10^{-3}$). In multivariate analysis, age and BMI were the only independent predictive factors. Sub-cohort analysis for PWUD and general population separately for individuals >or <50 years old, showed that BMI was the only independent predictive factor for significant fibrosis ($p < 10^{-3}$). Liver stiffness addressed an independent positive predictive value ($p = 0.04$) for poor outcome (liver related death or hepatocellular carcinoma).

Conclusion: Our data postulated that metabolic factors could predict significant fibrosis in patients with HCV infection. BMI represents an independent risk factor for significant fibrosis regardless the source of infection and the older age. The presence of metabolic factors should be taken under consideration for the management and follow-up of the chronic HCV patients.

THU-399-Y1

Burden of extrahepatic manifestations after HCV cure: assessing the effect of IFN versus DAA-induced SVR in a large population-based cohort in British Columbia, Canada

Dahn Jeong¹, Stanley Wong², Jean Damascene Makuza¹, Héctor Alexander Velásquez García^{1,2}, Mel Krajden³, Richard Morrow¹, Prince Adu², Sofia Bartlett^{1,2}, Georgine Cua⁴, Amanda Yu², Maria Alvarez², Naveed Janjua^{1,2}. ¹School of Population and Public Health, University of British Columbia, Vancouver, Canada; ²BC Centre for Disease Control, Vancouver, Canada; ³Department of Pathology and Laboratory Medicine, University of British Columbia, Vancouver, Canada; ⁴Faculty of Medicine, University of British Columbia, Vancouver, Canada
Email: dahn.jeong@bccdc.ca

Background and aims: Prior research indicates that hepatic and extrahepatic damage from chronic HCV infection may persist post-virologic cure. While evidence supports HCV treatment benefits in reducing the risk of extrahepatic manifestations (EHMs) among individuals achieving sustained virologic response (SVR) compared to those living with untreated HCV, the burden of EHM after SVR remains unclear. Moreover, differences in health outcomes after interferon (IFN) vs direct-acting antiviral (DAA)-based SVR have been suggested. This analysis assessed the EHM burden among individuals achieving SVR through IFN or DAA treatment in a large, population-based cohort.

Method: We used the British Columbia Hepatitis Testers Cohort (BC-HTC), which includes all individuals diagnosed with HCV from 1990 to 2015, linked with administrative health datasets. Our study sample included individuals receiving IFN or DAA treatment with confirmed SVR. EHM diagnoses were obtained through ICD-9/10 diagnostic and procedure codes in hospitalization and physician billing data, including chronic kidney disease (CKD), type 2 diabetes (DM), major adverse cardiac events (MACE), neurocognitive disorders (NCD) and mood and anxiety disorders (MAAD). We computed incidence rates (IR) of EHMs by treatment type from the date of SVR assessment. To address the differences in baseline sociodemographic and clinical characteristics between people treated with IFN or DAA, we adopted inverse probability of treatment weighting (IPTW) to induce balance across characteristics. Multivariable subdistribution hazard models, weighted with IPTW and accounting for competing mortality risks, were used to estimate risk of incident EHMs.

Results: Study sample included 4,551 persons treated with IFN and 10,819 persons treated with DAA, with confirmed SVR. Those treated with DAA were younger, more likely to have a history of drug and alcohol use disorder, with a greater prevalence of EHMs prior to SVR compared to individuals treated with IFN. Persons treated with DAA had a higher IR of CKD, MACE and NCD compared to those treated with IFN. The IR of DM and MAAD didn't differ between people treated with IFN or DAA. When adjusting for differences in baseline characteristics with IPTW and competing mortality risks, people treated with IFN had reduced risks of CKD, MACE and NCD, but higher risk of DM and MAAD compared to those treated with DAA; adjusted subdistribution hazard ratios: CKD 0.68 (95% CI 0.57–0.80), DM 1.37 (95% CI 1.10–1.69), MACE 0.60 (95% CI 0.53–0.69), NCD 0.56 (95% CI 0.47–0.68) and MAAD 1.49 (95% CI 1.24–1.79).

Conclusion: Individuals who were treated with DAA had higher EHM burden before and after virologic cure compared to those treated with IFN. Given the shift to DAA treatments, further research is needed to understand pre-therapeutic EHM risk factors and the impact of curative therapy on EHMs and overall long-term health outcomes.

THU-402

Higher cardiovascular burden in people living with HIV (PLWH) with metabolic syndrome and history of HCV infection

Alessia Siribelli¹, Michele Bellomo², Camilla Muccini², Riccardo Lolatto², Giulia Morsica², Sara Diotallevi², Nicola Gianotti², Simona Bossolasco¹, Costanza Bertoni¹, Vincenzo Spagnuolo¹, Antonella Castagna³, Hamid Hasson¹. ¹San Raffaele Scientific Institute, Milan, Italy; ²San Raffaele Scientific Institute, Milan, Italy; ³Vita-Salute San Raffaele University, San Raffaele Scientific Institute, Milan, Italy
Email: siribelli.alessia@hsr.it

Background and aims: People living with HIV (PLWH) have higher occurrence of major adverse cardiovascular events (MACE). This study aimed to identify factors associated with MACE in PLWH during a 10-years (yrs) follow-up (FU).

Method: Retrospective study including PLWH followed at San Raffaele Scientific Institute, Italy, between January 2013–December 2023, with at least 3 observations for laboratory data. Metabolic syndrome (MetS) defined according to ATP3 criteria (NCEP). MACE considered were myocardial infarction, unstable angina, stroke, transient ischemic attack, peripheral arterial ischemia, revascularization. Trained binary classification algorithm (simple logistic regression), calculating at each examination the probability of developing at least one MACE within the following year was used. To adjust for residual variability of developing MACE, generalized additive mixed model (GAMM), with random intercept and non-parametric model of variables was used. Continuous variables as age, yrs of MetS, Log HIV viremia and CD4 were modelled with smooth effects, the remaining with standard regression coefficients.

Results: Overall, 5416 PLWH were included: 4363 (81%) were males, 3088 (58%) smokers or ex, 2437 (45%) had MetS, HBV and HCV

coinfection were diagnosed in 377 (7%, of which 1.9% not virologically suppressed) and 1076 (20% of which 1.8% untreated), respectively. During a median FU of 9.7 yrs, 216 (4%) developed at least one MACE. In simple logistic regression, higher occurrence of MACE was significantly associated with age (OR = 1.06; 95%CI = 1.04, 1.07; $p < 0.0001$), male sex (OR = 2.29; 95%CI = 1.64, 3.28; $p < 0.0001$), presence of MetS (OR = 1.72; 95%CI = 1.27, 2.29; $p < 0.0003$), smoking (OR = 2.01; 95%CI = 1.58, 2.56; $p < 0.0001$), co-presence of HCV with MetS (OR = 1.72; 95%CI = 1.09, 2.72; $p = 0.021$), use of protease inhibitors (PI) (OR = 2.1; 95%CI = 1.45, 3.03; $p < 0.0001$) and integrase inhibitors (INSTI) (OR = 1.34; 95%CI = 1.03, 1.73; $p = 0.0274$). In GAMM, age ($p = 0.0001$), male sex (OR = 2.23; 95%CI = 1.46, 3.41; $p = 0.0002$), smoking (OR = 1.91; 95%CI = 1.39, 2.62; $p < 0.0001$), use of PI (OR = 1.65; 95%CI = 1.06, 2.58; $p = 0.0278$) confirmed to increase occurrence of MACE.

Conclusion: In a large cohort of PLWH, during 10-yr of FU, MACE are more likely to occur in people with MetS and history of HCV infection, additionally to traditional factors and specific HIV therapy. Surveillance and appropriate management of MetS, particularly in people coinfecting with HCV-HIV, could help reduce cardiovascular burden.

THU-403

Liver fibrosis and steatosis in children after effective treatment of chronic hepatitis C using direct acting antivirals

Maria Pokorska-Śpiwak¹, Ewa Talarek², Anna Dobrzeniecka³, Małgorzata Aniszewska⁴, Magdalena Pluta¹, Magdalena Marczyńska¹.
¹Medical University of Warsaw, Regional Hospital of Infectious Diseases in Warsaw, Warsaw, Poland; ²Medical University of Warsaw, Warsaw, Poland; ³Regional Hospital of Infectious Diseases in Warsaw, Warsaw, Poland; ⁴Medical University of Warsaw, Regional Hospital of Infectious Diseases in Warsaw, Warsaw, Poland
Email: maria.pokorska-spiwak@wum.edu.pl

Background and aims: In this study we aimed to examine the long-term influence of successful treatment with direct acting antivirals (DAAs) on liver fibrosis and steatosis in children with chronic hepatitis C (CHC).

Method: Of 135 children aged 5 to 18 years who had been treated with DAAs due to CHC in our Department between July 2019 and December 2023 as a part of two projects: PANDAA-PED (12-week treatment with sofosbuvir/velpatasvir, SOF/VEL) and POLAC Project (12/24-week treatment with sofosbuvir/ledipasvir, SOF/LDV, and 8-week with glecaprevir/pibrentasvir, GLE/PIB), we selected successfully treated participants, who completed control evaluation at one-year posttreatment. Liver fibrosis and steatosis were assessed using transient elastography at baseline, 12-week posttreatment, and one-year posttreatment. Significant fibrosis was diagnosed when liver stiffness measurement (LSM) was >7 kPa, cirrhosis when LSM was ≥ 12.5 kPa, and steatosis when controlled attenuation parameter (CAP) was >238 dB/m.

Results: We identified 67 patients (32 boys, 48%) eligible for the study: 49 after SOF/VEL treatment, 9 after GLE/PIB, and 9 after SOF/LDV. At baseline, the mean age was 10.4 ± 2.9 years. There were 62 (93%) patients infected vertically, 58 (87%) were treatment-naïve, 41 (61%) were infected with genotype 1. All children had undetectable HCV RNA at one-year posttreatment. At baseline, 5/67 (7%) participants presented with significant fibrosis, including 2 with cirrhosis. At 12-week posttreatment, only 2 of these patients had LSM >7 kPa, and one-year posttreatment only one cirrhotic patient had abnormal LSM. Mean values of LSM for the study group were 4.9 kPa (95%CI 4.4–5.4) at baseline, 4.8 kPa (3.9–5.8) at 12-week posttreatment, and 4.5 kPa (3.8–5.3) at one-year posttreatment (all $p > 0.05$), whereas corresponding CAP values were 180 dB/m (170–191), 195 dB/m (185–206), and 191 dB/m (180–201), respectively (for the first two values $p = 0.009$). Number of patients with steatosis increased from 4 (6%) at baseline to 7 (10%) at 12-week posttreatment, and to 8 (12%) at one-year posttreatment.

Conclusion: Successful treatment with DAAs leads to regression of significant liver fibrosis in most cases. Increased CAP values after therapy require further analysis on larger groups of patients.

THU-404

Impact of hepatitis C treatment on mortality among liver cancer patients in Georgia-2015–2022

Anna Khoperia¹, Maia Butsashvili², Shaun Shadaker³, Susan Gaweł⁴, Sophia Surguladze⁵, Nazibrola Chitadze¹, Konstantine Kazanjan¹, Vladimer Getia¹, Lasha Gulbiani², Geoff Beckett⁶, Alan Landay⁷, Maia Tsereteli¹, Maia Alkhazashvili¹, Amiran Gamkrelidze⁸, Francisco Averbhoff⁴.
¹National Center for Disease Control and Public Health, Tbilisi, Georgia; ²Health Research Union, Tbilisi, Georgia; ³Centers for Disease Control and Prevention, Atlanta, United States; ⁴Abbott Diagnostics, Illinois, United States; ⁵The Task Force for Global Health, Tbilisi, Georgia; ⁶Centers for Disease Control and Prevention, Retired, Atlanta, United States; ⁷Rush University, Chicago, United States; ⁸University of Georgia, School of Health Sciences, Tbilisi, Georgia
Email: annakhoperia@gmail.com

Background and aims: Chronic hepatitis C virus (HCV) infection can result in hepatocellular carcinoma (HCC), the most common form of primary liver cancer (PLC). The country of Georgia has an HCV elimination program providing testing and treatment since 2015. This study uses data from national registries to assess the association of HCV infection and treatment with mortality in individuals with documented history of liver cancer in Georgia.

Method: We conducted a retrospective registry-based cross-sectional study of adult (≥ 18 years) liver cancer cases in the Georgian Cancer Registry (GCR) during January 2015–December 2022 linked to HCV screening and treatment data using unique national IDs. HCC, defined as ICD-10 of C22.0, was compared to other PLC cases (ICD-10 C22.1–C22.9). Mortality was defined as a recorded death date at the time of analysis. We conducted bivariable and multivariable analyses to compare mortality proportion between the HCC subtype versus other liver cancer subtypes, explore differences in mortality of cases with and without HCV history, and the correlation between HCV treatment and mortality in the HCV-infected subgroup. Logistic regression modeling assessed factors associated with mortality: age, sex (female vs. male), achievement of sustained viral response (SVR) after treatment (yes vs. no), and GCR-assigned liver cancer ICD-10 code (HCC vs. other types of liver cancer). Odds ratios (OR) and 95% confidence intervals (CI) were calculated. Cases with missing vital status were excluded.

Results: Of 1736 adults with PLC, 1388 (79.9%) were deceased at the time of analysis. Although age was associated with increased mortality (OR = 0.7, 95% CI [0.6–0.8]), a statistically significant association was not found between sexes. HCC was reported among 419 (24.1%) PLC cases. Compared to HCC cases, other combined subcategories of liver cancer (OR = 2.1, 95% CI [1.6–2.8]) were associated with increased mortality. Overall, 1393 (80.2%) PLC cases were screened for anti-HCV, and out of 717 (51.5%) tested for viremia, 655 (91.4%) were HCV RNA positive; of those, 495 (75.6%) initiated HCV treatment and 445 (89.9%) completed. No statistically significant differences were observed in mortality between anti-HCV reactive and non-reactive groups with documented PLC. Logistic regression analyses controlling for sex among PLC patients with viremic HCV infection, achievement of SVR (adjusted OR [aOR] = 2.04, 95% CI [1.04–4.17], $p = 0.049$) and having HCC compared to other liver cancers (aOR = 2.59, 95% CI [1.51–4.45], $p < 0.001$) were associated with reduced mortality.

Conclusion: While no statistically significant mortality associations were found between anti-HCV reactive and non-reactive cases with documented PLC, achieving sustained virologic response (SVR) is a potential factor associated with reduced mortality among liver cancer patients with a history of HCV infection.

POSTER PRESENTATIONS

THU-405

Analysis of a decentralized model interdisciplinary for the elimination of HCV in vulnerable population in the province of Huelva (Spain). To continue advancing in the elimination of hepatitis C, it is necessary to establish a clearly defined integrated care plan

Gema Romero¹, Ana Bejarano¹, Francisco Franco¹, Pilar Del Pino¹, María Dolores Santos¹. ¹Hospital Universitario Juan Ramón Jiménez, Huelva, Spain

Email: gemaherrera@hotmail.com

Background and aims: the objective of this study is to evaluate the implementation of a comprehensive strategy of microelimination based on the decentralization of the diagnosis and treatment.

Method: prospective observational study in which screening of the HCV infection through rapid serological tests (saliva or whole blood samples), in settlements of immigrant workers in the agricultural campaign in the province of Huelva and people who go to centers that serve the vulnerable population in Huelva capital (Cáritas, center Red Cross of Torrejón meeting and reception and Virgen de la Cinta social lunchroom). In the detected positive, an "in situ" viremia study was performed (GeneXpert®). In patients viraemic, a comprehensive out-of-hospital assessment was carried out at the same time by the hepatologist with Fibroscan® and abdominal ultrasound with portable devices and dispensing of the antiviral treatment.

Results: 322 people were screened with close to 100% success in participating in each working day. The majority nationalities of the settlement population were Ghanaian (85), Morocco (70) and Romania (56). In the social centers the majority were Spanish population (64). 5 viremic patients were detected (prevalence of 1.5%), 4 being treated, not leading to treatment was carried out on one of the patients because a lesion was detected in the abdominal ultrasound suggestive of hepatocellular carcinoma. Among the viremic patients, the two detected in settlements were of Romanian origin, with an incidence of 3.5% in said population.

Conclusion: decentralization in virological diagnosis, medical care by experts in HCV and the provision of treatment is feasible and eliminates known barriers. It is necessary for them proactive multidisciplinary teams.

THU-406

Knowledge, perceptions and barriers to the diagnosis and treatment of hepatitis C among persons who inject drugs: findings from the Educate-Test-Treat (ETT) programme in Singapore

Alyssa Sim¹, Shann Long¹, Sanchalika Acharyya², Gerard Wong³, Ryan Jia Jie Liew^{1,4}, Kuo Chao Yew¹. ¹Department of Gastroenterology and Hepatology, Tan Tock Seng Hospital, Singapore, Singapore; ²Clinical Research and Innovation Office (CRIO), Tan Tock Seng Hospital, Singapore, Singapore; ³HCSA Highpoint Halfway House, HCSA Community Services, Singapore, Singapore; ⁴Anglo Chinese School (Independent), Singapore, Singapore

Email: alyssasim@gmail.com

Background and aims: The World Health Organization (WHO) has implemented a global elimination strategy, setting a rate of $\geq 90\%$ of chronic hepatitis C (HCV) being diagnosed to achieve eradication target goals by 2030. Its prevalence is high among people who inject drugs (PWID). Despite effective, simple oral Direct-Acting Antivirals (DAA), the uptake of diagnosis and treatment for HCV among PWID has been consistently low. We aimed to identify gaps in knowledge and attitudes in our local cohort and uncover local barriers towards achieving elimination of HCV.

Method: PWID from 4 halfway houses in Singapore were recruited from March 2022–April 2023. Using a structured questionnaire, information was gathered on baseline demographics and socio-economic status. We also assessed HCV awareness, knowledge, attitudes and perceptions regarding pursuit of treatment. Seven items were extracted from the questionnaire which pertained to

'knowledge' and 'attitude', each with a total score of 7 and classified into 'poor' (0–2), 'average' (3–5), or 'good' (6–7) for both domains. Statistical analysis was conducted on SPSS version 27 and statistical significance set at $p = 0.05$.

Results: Out of 198 participants, mean age was 54.0 years and 99% were male. Less than 20% of the participants had completed tertiary education. Participants with lower education levels were at greater risk of HCV infection, and although had poorer knowledge, demonstrated better attitude. 45.9% demonstrated average understanding of HCV. 35.9% were found to have poor understanding. The majority displayed good attitude (79.8%) and average attitude (20.2%). Notably, none displayed poor attitude. From univariate analysis, looking at knowledge and awareness of HCV, poor knowledge was associated with increasing age ($p = 0.018$) and lower education levels ($p = 0.034$). There were no significant differences in terms of these patient factors with regards to attitude. However, on multivariate analysis, increasing age (OR1.05, CI 1.01–1.09) $p = 0.02$ and increased knowledge scores (OR1.21, CI 0.98–1.49) $p = 0.073$ were associated with better attitude. When looking at potential barriers to the diagnosis and treatment of HCV, cost was the most important factor (56.6%), followed by side effects (39.5%) and perceived stigma (4.1%). We also identified venepuncture and saliva to be the preferred testing methods for HCV.

Conclusion: In conclusion, there are evident gaps in knowledge of HCV among PWID. It is essential to develop targeted education strategies in addressing misconceptions about HCV. Efforts to improve linkage to care should address barriers at different levels, and system-level changes are important. Targeting this may help us effectively achieve the HCV elimination goals in Singapore.

THU-407

A new pattern for hepatitis C management in hospital: establishment and effectiveness verification

Dong Yan¹, Siheng Zhu¹, Xiaoting Ye², Heqing Huang³. ¹The First Affiliated Hospital, Zhejiang University School of Medicine, Hangzhou, China; ²Ruian people's Hospital, Ruian, China; ³Zhuji people's Hospital of Zhejiang Province, Zhuji, China

Email: yandonh@zju.edu.cn

Background and aims: Viral hepatitis C is a kind of infectious disease caused by hepatitis C virus (HCV) infection. Statistics have shown that the rates of diagnosis and treatment coverage were not high. This study aims to establish a new management pattern of hepatitis C in hospital and verify whether it can improve the rates of diagnosis and treatment.

Method: A new management pattern of hepatitis C in hospital was established and promoted: First, newly-found HCV antibody positive patients were collected through our infection monitoring system every two weeks and followed regularly, then sorting out and analyzing the data; Second, real-time reminders were set up in the electronic case record system and on the results sheets, urging for specialized diagnosis and treatment; Third, all medical stuff needed to receive training to improve their understanding of hepatitis C infection; Fourth, infectious disease report card of hepatitis C was specially added. The RNA testing rates and the treatment rates of hepatitis C in different periods were then compared.

Results: Before the new pattern, the total HCV-RNA testing rate was 68.79% (3002/4364), with the RNA positive rate of 51.53% (1547/3002), and the treatment rate was 32.35% (764/2362). The RNA testing rate of non-infectious disease departments was 52.89% (1363/2577). Among males, 1715/2441 (70.26%) tested RNA, while among females the rate was 1287/1923 (66.93%). The RNA testing rates in different age groups were as follows: aged 0 to 29–76.40% (437/572), aged 30 to 59–70.97% (1907/2687), aged 60 to 89–59.84% (657/1098), and aged 90 and above–14.29% (1/7). Under the new pattern, the total RNA testing rate increased to 86.84% (409/471), with the RNA positive rate of 78.48% (321/409), and the treatment rate achieved 65.00% (195/300). The RNA testing rate in non-infectious disease

departments reached 201/253 (79.45%). The RNA testing rates for males and females increased to 84.47% (261/309) and 91.36% (148/162) respectively. In the first three age groups, the RNA testing rates all increased, specifically: aged 0 to 29–92.11% (35/38), aged 30 to 59–85.02% (278/327), and aged 60 to 89–91.43% (96/105). Comparing the RNA testing rates and treatment rates before and after the new pattern, there were statistical differences ($p < 0.05$). Cases aged 90 and above had the RNA testing rate of 0. After the new pattern, the lost-to-follow-up cases still accounted for 18.67%, which may be one of the reasons affecting the treatment rate. After being followed up, a total of 302 HCV antibody positive cases agreed to get re-examined, of which 35 cases were RNA positive and 33 received treated. After complete treatments and re-examinations, the complete virological response rate was 100%.

Conclusion: The new management pattern of hepatitis C in hospital effectively reduced the missed diagnosis of hepatitis C and increased the treatment rate, which is worth popularizing.

THU-408

The prognostic influence of toll-like receptor 4 +3725G/C gene polymorphism on biochemical profile among chronic HCV hepatitis patients

Tetiana Bevz¹, Iryna Bondaruk¹, Kiarina Myroniuk-Konstantynovych¹, Larysa Moroz¹, Galyna Martyniuk², Yaroslav Demchyshyn¹. ¹National Pirogov Memorial Medical University, Vinnytsia, Ukraine; ²Central city hospital, Rivne, Ukraine
Email: tasya241@gmail.com

Background and aims: The progression of chronic hepatitis C (CHC) and the development of liver fibrosis appear due to the multifaceted morphological response of the liver to hepatocyte damage. Therefore, the main task during choosing of management approaches of patients with CHC is to assess the degree of necro-inflammatory changes and the stage of liver fibrosis.

Method: We examined 131 patients with CHC (diagnosis confirmation by qualitative and quantitative HCV-RNA determination, HCV-genotyping), age 26–72 yrs (average age 43.8 ± 0.84 yrs). Among examined patients there were 59 females and 72 males.

Results: The ALT level of 116.72 ± 9.31 IU/l was determined in the carriers of the GC genotype, which was 1.79 fold higher ($p < 0.001$) than in the carriers of the GG genotype, and in monozygotic carriers of the C allele (CC-genotype) it was 2.57 fold higher ($p < 0.001$). The level of AST in serum of carriers of genotypes GC/CC was 77.09 ± 7.01 IU/l/100.46 ± 11.79 IU/l, vs. among GG genotype carriers 44.39 ± 2.49 IU/l ($p < 0.001$). LDH level was also significantly higher in patients with the C allele of the TLR4 gene ($p < 0.05$). The level of total bilirubin in carriers of the GC and CC genotypes were 1.55 and 1.68 fold higher ($p < 0.001$), accordingly, than among individuals with the GG genotype. The level of GGT in the CC genotype patients was higher ($p < 0.001$) than in individuals with the GG genotype: 155.53 ± 18.38 IU/l vs. 57.56 ± 3.67 IU/l. The presence of the C allele reliably affected the reduction of total protein and albumin levels. Cholesterol level in patients with genotypes GC and CC was higher in 1.22 fold ($p < 0.001$) than in patients with genotype GG. The assessment of the direction, strength and reliability of correlation relations between CC/GC genotypes of the TLR4 gene and indexes of the functional condition of the liver in patients with CHC had shown a direct correlation of significant strength in the presence of the C allele with the level of ALT ($r = 0.52$; $p < 0.05$) and the level of total bilirubin ($r = 0.56$; $p < 0.05$), a direct correlation of moderate strength with the level of AST ($r = 0.44$; $p < 0.05$), GGT ($r = 0.48$; $p < 0.05$) and cholesterol ($r = 0.44$; $p < 0.05$), moderate strength inverse correlation with the level of total protein ($r = -0.34$; $p < 0.05$) and albumin level ($r = -0.51$; $p < 0.05$). ALT (beta = 0.38; $p = 0.004$), albumin level (beta = -0.2; $p = 0.009$) and total bilirubin (beta = 0.32; $p = 0.0001$) as independent clinical predictors by means of multivariate analysis and a logistic regression model. The factor logistic model was reliable with the coefficient of determination of 52%.

Conclusion: Carriers with CC and GC genotypes of the TLR4 gene rs11536889 +3725G/C have a significantly more severe course of CHC than GG genotype carriers that is showed by the main cytolytic, cholestatic and hepatocellular insufficiency syndromes indexes.

THU-410

Clinical interventions and use of resources for the management of adverse effects associated with multiple drug interactions in the hepatitis C population

Juan Turnes¹, Antonio Garcia Herola², Ramón Morillo Verdugo³, Marinela Mendez⁴, Candido Hernández⁵, Antoni Sicras Mainar⁶. ¹Servicio de Gastroenterología y Hepatología, CHU, Pontevedra, Spain; ²Sección de Medicina Digestiva, Hospital Marina Baixa de Villajoyosa, Alicante, Spain; ³Farmacia Hospitalaria, Hospital de Valme, AGS Sur de Sevilla, Sevilla, Spain; ⁴Medical Affairs, Gilead Sciences S.L., Madrid, Spain, Madrid, Spain; ⁵Medical Affairs, Gilead Sciences S.L., Madrid, Spain; ⁶Health Economics and Outcomes Research, Atrys Health, Barcelona, Spain
Email: jturnesv@gmail.com

Background and aims: Direct-acting antivirals (DAAs) share pharmacokinetic pathways with many comedications commonly administered to patients living with chronic hepatitis C virus (HCV) infection (PLWHCV). Previous studies have analyzed prevalence of potential drug-drug interactions (DDIs) between comedication taken by PLWHC and DAAs, including single and multiple-DDIs (≥2 drug-drug interactions with DAAs) and reported adverse effects (AEs) associated to DDIs. This study aims to evaluate the clinical interventions and resources utilization to manage AEs in patients with multiple-DDIs and the medical specialties that reported AEs.

Method: retrospective observational study, obtained from the BIG-PAC database (Atrys Health), in HCV patients (2017–2020). Potential DDIs treated with DAAs (Sofosbuvir/Velpatasvir [SOF/VEL] and Glecaprevir/Pibrentasvir [GLE/PIB]) were evaluated using the University of Liverpool DDIs database. The AEs, clinical interventions, use of resources for the management of AEs and the specialty that reported AEs were analyzed.

Results: 1620 patients were included (730 treated with SOF/VEL and 890 with GLE/PIB). 27.4% (444/1620) of the total patients who received comedications showed at least ≥1 Potential DDI. About 10% (123/1256) of patients receiving ≥2 comedications had potential multiple-DDIs (52 with SOF/VEL and 71 with GLE/PIB). 18 AEs were reported, of which 16 occurred in patients with potential multiple-DDIs. Therefore, 13% (16/123) of patients with potential multiple-DDIs presented AEs. All AEs required clinical interventions or use of resources for their management. The most frequent interventions were discontinuations (of comedication or DAAs) and reduction of comedication dose, being more frequent in the group treated with GLE/PIB, since this group presented approximately three times more AEs than the group treated with SOF/VEL (18.3% GLE/PIB [13/71] vs 5.8% SOF/VEL [3/52]; $p < 0.05$). There were three DAAs discontinuations in patients treated with GLE/PIB (two associated with atorvastatin and one with quetiapine) and one in the group treated with SOF/VEL (associated with carvedilol). All dose reductions were reported in the group treated with GLE/PIB (associated with paliperidone, enalapril and simvastatin). AEs were reported mostly by primary care physicians (62.5%).

Conclusion: There is an elevated risk of AEs in hepatitis C patients with potential multiple-DDIs treated with DAAs, particularly with cardiovascular and nervous system comedication, especially with DAAs containing protease inhibitor. These AEs may require clinical interventions and the use of resources for their clinical management. This circumstance is especially relevant in the context of treatment simplification, where HCV specialists usually see the patients only at treatment initiation.

THU-411

Long term liver-related events in patients with HCV-related liver disease and advanced fibrosis after sustained virological response with direct-acting antivirals

Jorge Barajas¹, Tomás Artaza¹, Juan José Sánchez-Ruano¹, Marta Romero-Gutiérrez¹, Carolina Delgado¹, Gema De la Cruz¹, Concepción González¹, Raquel Lomas¹, Rafael Gómez Rodríguez¹.

¹Complejo Hospitalario Universitario de Toledo, Toledo, Spain

Email: jorgebarper@gmail.com

Background and aims: Direct-acting antivirals (DAAs) achieve a high rate of sustained virological response (SVR) in patients with hepatitis C virus (HCV) infection. It is not clearly defined whether this SVR is associated with a reduction in liver-related events. We aim to analyze the development of complications related to portal hypertension (PH) as well as de novo hepatocellular carcinoma (HCC) in patients with SVR after DAAs treatment.

Method: An ambispective single-center study included 295 patients with SVR. Patients with HCV-related liver disease and advanced fibrosis treated with DAAs were included. Patients with transient elastography (TE) between 9.5 and 12.5 kPa were classified as F3, while those with TE >12.5 kPa or clinical, analytical, and ultrasound data compatible with cirrhosis were classified as F4. All patients achieved SVR, and consecutive sampling was performed from July 2014 to March 2022. Follow-up was censored at 5 years.

Results: The median age was 60 years and 185 (62.71%) were male. Two hundred thirty-two (78.64%) had cirrhosis. The mean follow-up was 47 months. Thirty-six (12, 2%) had a liver-related event. Complications related to PH were experienced by 20 (6.78%) patients during the first 5 years, all of them F4. Of the 20 patients with PH related complications, 17 (85%) had ascitic decompensation, 4 (20%) had gastrointestinal bleeding and 11 (55%) had hepatic encephalopathy. In our series, de novo HCC was developed by 22 (7.46%) patients. In 21 cases, HCC occurred in patients with F4. The median time to HCC diagnosis was 18 months (95% CI, 0.76–35.23). One patient treated with DAAs had a previous history of HCC and it did not recur. Thirty-four (11.52%) patients died at 5-years, with 12 (35.29%) dying from liver-related events. Among those deceased from liver-related events, 6 died from PH complications, 5 from HCC, and 1 patient died from cholangiocarcinoma. Four (1.36%) patients underwent liver transplantation, 2 for HCC and 2 for decompensated cirrhosis.

Conclusion: The risk of developing liver-related events in patients with advanced fibrosis due to HCV after SVR after DAAs treatment for the first 5 years was significant. In our series, 12.2% had a liver-related event. The most frequent events were the development of HCC (7.46%) and decompensation of liver disease (6.78%). Adequate follow-up in these patients appears crucial to achieve early management of these complications.

THU-412

Hepatitis C lost to follow-up rates in primary care practices in Belgium

Marie Coessens^{1,2}, Jeoffrey Schouten¹, Wim Verlinden^{1,2}. ¹Department of gastroenterology and hepatology, Vitaz, Sint-Niklaas, Belgium;

²Laboratory of Experimental Medicine and Pediatrics (LEMP), University of Antwerp, Wilrijk, Belgium

Email: wim.verlinden@vitaz.be

Background and aims: If we aim to eliminate hepatitis C (HCV) by 2030, resources need to be allocated efficiently. Belgian hospital-based lost to follow-up (LTFU) projects have shown that up to 19% of patients drop out of HCV care, with up to half of them being successfully re-admitted. This is the first project to assess LTFU rates in primary care, while promoting patient re-engagement in HCV care and the prevention of LTFU.

Method: A list was compiled by a non-hospital-based clinical laboratory, containing all positive HCV serology results requested between 2010 and 2023 by a general practitioner (GP) based in Antwerp. A member of the study team went through the patient list

together with the participating GPs, assessing patient status in the HCV care continuum [(a) negative HCV antibody confirmation test, (b) negative HCV antibody confirmation test and HCV RNA negative, (c) positive HCV serology and HCV RNA negative, (d) positive HCV serology without HCV RNA result available, (e) last available HCV RNA positive, (f) negative HCV RNA <12 weeks after end of treatment (EOT), (g) negative HCV RNA ≥ 12 weeks after end of treatment or sustained virological response (SVR), (h) deceased]. The patient was considered LTFU if no action was taken in case of status d, e, or f. GPs were encouraged to re-engage these patients in HCV care and LTFU rates were re-assessed after one year. A risk profile (age, gender, HCV genotype, presence of cirrhosis, HIV status, lifetime drug use, being born abroad) of patients with status e, f or g was developed to identify patients at risk of LTFU who need additional GP counselling for their referral to the hepatologist.

Results: In total, 167 out of 275 (60, 73%) GPs agreed to participate and 363 primary care patients were analysed for their status in the HCV care continuum [(a) 30/363 (8.26%); (b) 63/363 (17.36%); (c) 82/363 (22.59%); (d) 18/363 (4.96%); (e) 32/363 (8.82%); (f) 5/363 (1.38%); (g) 117/366 (32.23%); (h) 16/363 (4.41%)]. The rate of LTFU was 15.51% (55 out of 363). In addition, a liver-related cause of death was documented in 25% of deceased patients. For 9 patients that were initially considered LTFU [(d) 1/9; (e) 5/9; (f) 3/9], status in the HCV care continuum was already re-assessed one year after the project was launched [(e) 3/9; (f) 4/9; (g) 2/9]. Thanks to our intervention, DAA therapy was initiated in 3 out of 5 patients with an untreated chronic HCV infection and an SVR12 was already documented in 2 out of 9 patients. None of the risk factors for LTFU could be retained.

Conclusion: Hepatitis C LTFU rates in primary care are significant and up to half of patients can be successfully re-admitted to care. Given that the LTFU strategy comes without screening costs, this is a feasible and highly cost-effective strategy on the road towards HCV elimination.

THU-413

Baseline gamma-glutamyl transpeptidase levels are associated with aggravation of esophagogastric varix after direct-acting antiviral therapy in cirrhotic patients with hepatitis C virus

Yuki Tahata¹, Hayato Hikita¹, Satoshi Mochida², Akio Ido³, Daiki Miki⁴, Ryotaro Sakamori¹, Hitoshi Yoshiji⁵, Norifumi Kawada⁶, Nobuyuki Enomoto⁷, Taro Yamashita⁸, Masayuki Kurosaki⁹, Hidekatsu Kuroda¹⁰, Yoichi Hiasa¹¹, Kazuhiko Nakao¹², Naoya Kato¹³, Goki Suda¹⁴, Yasunari Nakamoto¹⁵, Hiroshi Yatsushashi¹⁶, Kentaro Matsuura¹⁷, Taro Takami¹⁸, Eiji Kakazu¹⁹, Yoshito Itoh²⁰, Yasuhiro Asahina²¹, Yoshiyuki Ueno²², Ryosuke Tateishi²³, Shuji Terai²⁴, Masahito Shimizu²⁵, Norio Akuta²⁶, Takahiro Kodama¹, Tomohide Tatsumi¹, Tomomi Yamada²⁷, Tetsuo Takehara¹.

¹Department of Gastroenterology and Hepatology, Osaka University Graduate School of Medicine, Suita, Japan; ²Department of Gastroenterology and Hepatology, Saitama Medical University, Saitama, Saitama, Japan; ³Digestive and Lifestyle Diseases, Department of Human and Environmental Sciences, Kagoshima University Graduate School of Medicine and Dental Sciences, Kagoshima, Japan; ⁴Department of Gastroenterology and Metabolism, Graduate School of Biomedical and Health Sciences, Hiroshima University, Hiroshima, Japan; ⁵Department of Gastroenterology, Nara Medical University, Nara, Japan; ⁶Department of Hepatology, Graduate School of Medicine, Osaka Metropolitan University, Osaka, Japan; ⁷First Department of Internal Medicine, Faculty of Medicine, University of Yamanashi, Yamanashi, Japan; ⁸Department of Gastroenterology, Kanazawa University Graduate School of Medicine, Kanazawa, Japan; ⁹Department of Gastroenterology and Hepatology, Musashino Red Cross Hospital, Tokyo, Japan; ¹⁰Division of Gastroenterology and Hepatology, Department of Internal Medicine, Iwate Medical University, Iwate, Japan; ¹¹Department of Gastroenterology and Metabolism, Ehime University Graduate School of Medicine, Ehime, Japan; ¹²Department of Gastroenterology and

Hepatology, Nagasaki University of Graduate School of Biomedical Sciences, nagasaki, Japan; ¹³Department of Gastroenterology, Graduate School of Medicine, Chiba University, chiba, Japan; ¹⁴Department of Gastroenterology and Hepatology, Graduate School of Medicine, Hokkaido University, hokkaido, Japan; ¹⁵Second Department of Internal Medicine, Faculty of Medical Sciences, University of Fukui, fukui, Japan; ¹⁶Clinical Research Center, National Hospital Organization Nagasaki Medical Center, nagasaki, Japan; ¹⁷Department of Gastroenterology and Metabolism, Nagoya City University Graduate School of Medical Sciences, nagoya, Japan; ¹⁸Department of Gastroenterology and Hepatology, Yamaguchi University Graduate School of Medicine, yamaguchi, Japan; ¹⁹The Research Center for Hepatitis and Immunology, National Center for Global Health and Medicine, chiba, Japan; ²⁰Department of Molecular Gastroenterology and Hepatology, Graduate School of Medical Science, Kyoto Prefectural University of Medicine, kyoto, Japan; ²¹Department of Gastroenterology and Hepatology, Department of Liver Disease Control, Tokyo Medical and Dental University, tokyo, Japan; ²²Department of Gastroenterology, Faculty of Medicine, Yamagata University, yamagata, Japan; ²³Department of Gastroenterology, Graduate School of Medicine, The University of Tokyo, tokyo, Japan; ²⁴Division of Gastroenterology and Hepatology, Graduate School of Medicine and Dental Sciences, Niigata University, niigata, Japan; ²⁵Department of Gastroenterology/Internal Medicine, Gifu University Graduate School of Medicine, gifu, Japan; ²⁶Department of Hepatology, Toranomon Hospital, tokyo, Japan; ²⁷Department of Medical Innovation, Osaka University Hospital, suita, Japan
Email: yuki.tahata@gh.med.osaka-u.ac.jp

Background and aims: Direct-acting antiviral (DAA) therapy has enabled viral elimination in almost all cirrhotic patients with hepatitis C virus (HCV). Although some cirrhotic patients undergo aggravation of esophagogastric varix after DAA therapy, the factors associated with aggravation of esophagogastric varix in cirrhotic patients, including decompensated cirrhosis, are unclear.

Method: A total of 478 patients with HCV-related compensated or decompensated cirrhosis were treated with DAA between February 2019 and December 2021 at 31 Japanese hospitals. Among them, 207 patients who could evaluate esophagogastric varix before and after DAA therapy were enrolled in this study. Decompensated cirrhosis was defined as baseline Child-Pugh class B (CP-B) or C, or CP-A with decompensating events before DAA therapy. Sustained virologic response (SVR) was defined as serum HCV-RNA undetectable at 12 or 24 weeks after the end of treatment. The form of esophagogastric varix was evaluated according to Japanese general rules: F1 was straight, small-caliber one; F2 was moderately enlarged, beady one; and F3 was markedly enlarged, nodular or tumor-shaped one (Dig Endosc 2010;22:1–9). Patients without esophagogastric varix or those with F1 were defined as low-risk varix, and patients with F2 or more or with a history of varix rupture were defined as high-risk varix. Aggravation of esophagogastric varix was defined as varix rupture or treatment for varix. We examined the cumulative incidence rate and the factors associated with aggravation of esophagogastric varix after DAA therapy.

Results: The median age was 69 years old, 55% of patients were male, 60% were decompensated cirrhosis, and 28% had high-risk varix at baseline. SVR rates of patients with compensated and decompensated cirrhosis were 98.8% and 96.0%, respectively ($p = 0.228$). During the median observation period of 39.2 months from starting DAA therapy, 22 patients underwent treatment for varix, and three experienced varix rupture. The 3-year rate of aggravation of esophagogastric varix was 11.5%. In multivariate Cox proportional hazard analyses, high-risk varix at baseline ($p < 0.001$), baseline higher gamma-glutamyl transpeptidase (GGT) levels ($p = 0.003$), and virologic response ($p = 0.045$) were significantly associated with aggravation of esophagogastric varix, while alcohol consumption was not. The 3-year rates of aggravation of esophagogastric varix were 27.5% in patients with high-risk varix, 5.9% in those with low-risk

varix, and 23.8% in patients with GGT of 75U/l or more and 8.2% in those with GGT less than 75U/l, respectively.

Conclusion: In cirrhotic patients with HCV treated with DAA, baseline status of esophagogastric varix, baseline GGT levels, and virologic response to DAA were significantly associated with the aggravation of esophagogastric varix.

THU-414

Incidence of hepatocellular carcinoma in patients with hepatitis C treated with direct-acting antiviral agents: results of a long-term prospective study period

Emanuela De Santis¹, Alessandro Caioli¹, Fernando De Angelis¹, Adriano De Santis¹. ¹Sapienza, University of Rome, Rome, Italy
Email: emanuela.desantis@uniroma1.it

Background and aims: Hepatocellular carcinoma (HCC) is the most common primary liver tumor. Liver cirrhosis, whose one of the main etiological agents is hepatitis C virus (HCV) infection, represents the most frequent risk factor. Direct-acting antivirals (DAAs) are associated with a sustained virological response (SVR) rate of more than 95%. Despite viral eradication, however, a residual risk of HCC persists in patients with significant fibrosis, especially in cases with concomitant liver-related comorbidities. Several works in the literature have investigated the incidence of HCC after SVR from DAAs. However, in published cases the follow-up is limited to 3 years. This work aims to evaluate the incidence of HCC in patients with hepatitis C who have achieved SVR after being treated with DAAs considering a follow-up time beyond the three years considered in the literature, and to identify predictive factors for development of hepatocellular carcinoma.

Method: We have examined 452 patients suffering from HCV-related chronic hepatitis and undergoing treatment with DAAs. Anthropometric, anamnestic, laboratory, ultrasound and elastography data have been collected for each patient at three times: T0 (before starting antiviral therapy), T1 (6 months after the end of treatment), T2 (last clinical data relating to the last follow-up visit/date of HCC diagnosis). The total duration of the follow-up has been calculated in all patients.

Results: In our sample, 18 patients (4%) developed hepatocellular carcinoma: 11 (61.1%) had a diagnosis of liver cirrhosis confirmed using elastography and biochemical data, while for the remaining 7 (38.9%), the fibrosis was classified as absent or minimal. A Cox regression model was used to identify predictive factors for the onset of HCC. Variables that were found to be significantly positively associated with the onset of HCC in simple and multiple regression were: AFP levels at T0, APRI levels at T0 and male sex. For the 7 patients in which significant fibrosis had been excluded, histological examination of liver tissue resulted in a diagnosis of liver cirrhosis. In 4 of these individuals, the identification of hepatocarcinoma occurred 5 years after the start of antiviral therapy and in 1 subject more than 7 years later.

Conclusion: In conclusion, in our sample, for 38.8% of the HCC cases the fibrosis stage was underestimated, resulting in the exclusion of these patients from follow-up. Our study demonstrates that AFP and APRI levels at baseline could be useful for selecting patients for whom it is appropriate to continue follow-up despite the absence of significant fibrosis.

THU-418

Screening for chronic hepatitis C in pre-surgical patients

Mercedes Vergara¹, Gemma Solé¹, Isabel Esteve¹, Meritxell Casas², Jordi Sánchez³, Cristina Solé⁴, José Alberto Ferrusquí⁵, Mireia Miquel⁶. ¹Parc Taulí Hospital Universitari. Institut d'Investigació i Innovació Parc Taulí (I3PT-CERCA). Universitat Autònoma de Barcelona., Sabadell, Spain; ²Parc Taulí Hospital Universitari. Institut d'Investigació i Innovació Parc Taulí (I3PT-CERCA), Sabadell, Spain; ³Parc Taulí Hospital Universitari. Institut d'Investigació i Innovació Parc Taulí (I3PT-CERCA). Universitat Autònoma de Barcelona, CIBERehd. Carlos III Insitute,

POSTER PRESENTATIONS

Sabadell, Spain; ⁴Parc Taulí Hospital Universitari. Institut d'Investigació i Innovació Parc Taulí (I3PT-CERCA). Universitat Autònoma de Barcelona, CIBERehd. Carlos III Institute, Sabadell, Spain; ⁵Parc Taulí Hospital Universitari. Institut d'Investigació i Innovació Parc Taulí (I3PT-CERCA). Universitat Autònoma de Barcelona, 08208, Spain; ⁶Parc Taulí Hospital Universitari. Institut d'Investigació i Innovació Parc Taulí (I3PT-CERCA), Departament de Medicina. Universitat de Vic-Universitat Central de Catalunya (UVic-UCC). Vic. CIBERehd, Sabadell, Spain
Email: mvergara@tauli.cat

Background and aims: Since the introduction of direct-acting antivirals for the treatment of chronic hepatitis C, the majority of patients have been treated and cured of the infection. However, the remain undetected patients are crucial to be promptly treated to achieve virtual elimination of the virus by 2030. In Spain, screening is not universal and depends on clinical suspicion based on clinical history. Recent published results on emergency screening near our area reflected bimodal distribution of RNA-VHC in our population: men between 50–60 years old and women under 90. We performed automated screening for hepatitis C antibodies (HCV-Ab) in patients over 50 who were undergoing preoperative analysis for elective surgery, both outpatient and inpatient.

Method: All patients over fifty years' old who underwent preoperative analysis were studied with a HCV-Ab detection in the same blood sample as required by the anaesthetists before surgery. Those who were positive, HCV-RNA was determined with the same sample. If a positive value was confirmed, they were referred to the Hepatology Unit for evaluation and treatment through an alert issued from the laboratory directly to the Unit.

Results: Preliminary results obtained from September 1 to December 31, 2023, a total of 2, 121 patients were evaluated. Forty-five (2.1%) were positive for HCV-Ab, of which 4 (0.18%) were positive for HCV-RNA. Two of them were men aged 54 and 55, one of them with cirrhosis criteria by transitional elastography (17.4 Kpa (IQR med 8%). The patients were not previous aware of de HCV infection. Both patients were treated with direct antiviral agents achieving a sustained virological response without any side effects. The other two were 83 and 89 old women respectively without any signs of significant fibrosis neither analytical, echography or elastography criteria (6, 6 and 7.1 KPa respectively), that denied treatment.

Conclusion: Automated preoperative screening in patients over 50 years old makes it possible to detect patients with HCV-RNA not aware of the infection helping to eradicate the virus. Cost effectiveness study of this strategy is pending but the low cost of VHC-Ab and the QALY gained make its effectiveness highly probable.

THU-419

Regression of hepatic fibrosis in patients with chronic hepatitis C treated with direct-acting antivirals (DAAs). A long-term, prospective, observational study

Evdoxia Avramopoulou¹, Efthymios Tsounis¹, Stavros Kanaloupitis¹, Konstantinos Zisimopoulos¹, Maria Kalafateli^{2,3}, Ioanna Aggeletopoulou¹, Christos Sotiropoulos⁴, Theodora Kafentzi⁴, Georgios Geramoutsos¹, Odysseas Ampazis¹, Georgia Diamantopoulou¹, Angeliki Tsintoni⁵, Konstantinos Thomopoulos¹, Christos Triantos¹. ¹Division of Gastroenterology, Department of Internal Medicine, University Hospital of Patras, Patras, Greece; ²Department of Gastroenterology, General Hospital of Patras, Patras, Greece; ³Patras General Hospital "Agios Andreas", Gastroenterology, Patra, Greece; ⁴Division of Gastroenterology, Department of Internal Medicine, University Hospital of Patras, Patras, Greece; ⁵Department of Internal Medicine, University Hospital of Patras, Patras, Greece
Email: chtriantos@hotmail.com

Background and aims: Successful hepatitis C virus (HCV) treatment with direct-acting antivirals (DAAs) is associated with an improvement in liver fibrosis post-treatment. This study aims to assess the

long-term impact of DAA-based therapy on hepatic fibrosis through extended follow-up (FUP).

Method: Successful HCV treatment with DAAs is associated with an improvement in liver fibrosis post-treatment. This study aims to assess the long-term impact of DAA-based therapy on hepatic fibrosis through extended FUP.

Results: The overall sustained virologic response rate for this cohort was 98.8% (166/168). The median liver stiffness before treatment was 9.9 kPa (IQR: 7.5–18.8) compared to 7.2 kPa (IQR: 5.1–11.6) following DAA-based therapy ($p < 0.001$). In non-cirrhotic patients, the median transient elastography measurements were significantly reduced ($p < 0.001$) from 7.6 kPa (IQR: 6.5–9.2) to 5.8 kPa (IQR: 4.5–7.3). In patients with cirrhosis, the median liver stiffness plummeted from 18.6 kPa (IQR: 12.4–23.7) to 11.6 kPa (IQR: 7.3–17.2) after a FUP period of 31 months (IQR: 12–63.5) ($p < 0.001$). Regression of significant fibrosis (F4 stage) was observed in 18/36 patients (50%) using a cut-off value of 12 kPa. Moreover, the median Child-Pugh (CP) score was decreased from 7 (IQR: 5–7) to 5 (IQR: 5–7) post-treatment ($p = 0.002$). Nine out of 21 (42.9%) patients with baseline Child Pugh (CP) stage B regressed to CP stage A. Regression of liver fibrosis was also evident in various sub-group analyses, including patients with diabetes mellitus [baseline 15.5 kPa (IQR: 10.3–19.1) vs FUP 8.1 kPa (IQR: 5.7–9.9); $p = 0.12$], current intravenous drug user (baseline 9.7 kPa (IQR: 6.2–13.2) vs FUP 6.7 kPa (IQR: 5.2–9.2); $p = 0.049$], and alcohol-abuse [baseline 12 kPa (IQR: 7.7–20.4) vs FUP 7.7 kPa (IQR: 5.4–12); $p < 0.001$].

Conclusion: The current analysis supports a substantial improvement in hepatic fibrosis in HCV across diverse subgroups of HCV patients who received DAA-based treatment during long-term FUP. In cirrhotic patients, treatment with DAAs could lead to cirrhosis regression.

THU-420

Evaluation of LiverRisk score as predictor of liver fibrosis and mortality in patients with HCV-related hepatitis treated with direct acting antivirals

Antonietta Romano¹, Amalia Rita Caspanello^{1,2}, Salvatore Piano¹, Marta Tonon¹, Carmine Gambino¹, Valeria Calvino¹, Anna Barone¹, Nicola Zeni¹, Simone Incicco³, Roberta Gagliardi¹, Paolo Angeli¹. ¹Unit of Internal Medicine and Hepatology, Department of Medicine, University of Padova, Italy, Padova, Italy; ²Department of Clinical and Experimental Medicine, Unit of Medicine and Hepatology, University of Messina, Messina, Italy; ³Unit of Internal Medicine and Hepatology, Department of Medicine, University of Padova, Italy, Padova
Email: antonietta.romano@aopd.veneto.it

Background and aims: The LiverRisk score has been recently developed and validated as a predictor of liver fibrosis and liver-related outcomes in the general population. This score has never been evaluated as predictor of liver fibrosis and outcomes in secondary care, such as in patients with chronic liver diseases. The aim of this study was to evaluate the role of the LiverRisk score as a predictor of liver fibrosis and mortality in patients with HCV-related hepatitis treated with direct acting antivirals (DAA).

Method: patients were enrolled retrospectively, outpatients with chronic hepatitis C treated with DAA between 2015 and 2017 were included consecutively. Patients were followed-up until September 2023. The exclusion criteria were: liver transplantation before DAAs and presence of HCC. Patient characteristics and LiverRisk score were collected before starting the DAA. The data for the calculation of LiverRisk score were collected the same day the fibroscan was performed. The primary end point was a liver stiffness ≥ 10 kPa. Area under the receiver operating characteristic (AUROC) curve was evaluated for assessing the discrimination ability of Liver Risk score. Overall mortality was assessed at the end of follow-up.

Results: in this ongoing study, 136 patients of our center with chronic hepatitis C treated with DAA were enrolled. In this population, 51% were men, the mean age was 65.3 ± 12.2 years, 65.4% were genotype

1, 59.6% had liver cirrhosis, the mean liver stiffness measurement was 15.9 KPa (3.5–48.8), sustained virological response (SVR) was 95.5% and the mean follow-up was of 59 months. Coinfection with hepatitis B virus (HBV) was present in 8.8%. Discrimination ability of the LiverRisk score in the prediction of liver stiffness ≥ 10 KPa was very good as shown by an AUROC of 0.848 (95% confidence interval [CI] = 0.767–0.930; $p = 0.000$). During follow-up 21 patients (15.4%) died. LiverRisk score was associated with the risk of all cause of mortality (Hazard Ratio = 1.154; 95% CI = 1.01–1.318; $p = 0.035$).

Conclusion: the liver risk score is a good predictor of fibrosis and mortality in HCV patients treated with DAA.

THURSDAY 06 JUNE

Viral hepatitis C – Therapy and resistance

THU-362

Ravadasvir in combination with sofosbuvir for 12 or 24 weeks achieved high sustained virological response rates in genotype 3 chronic hepatitis C without or with compensated liver cirrhosis

Soek Siam Tan¹, Caroline Men  tre  ², Isabela Ribeiro², Nicolas Salvadori³, Sabine Yerly⁴, Nicole Ngo-Giang-Huong⁵, Graciela Diap². ¹Hospital Selayang, Dept of Hepatology, Batu Caves, Malaysia; ²DNDi, Geneva, Switzerland; ³AMS-PHPT Research Platform, Muang, Chiang Mai, Thailand; ⁴Hopitaux Universitaires de Gen  ve, Gen  ve, Switzerland; ⁵AMS-BAT Laboratory, Muang, Chiang Mai, Thailand
Email: tanss@selayanghospital.gov.my

Background and aims: Hepatitis C virus (HCV) genotype (GT) 3 is the second most common GT and accounts for approximately 14–17 million of the estimated 58 million HCV cases globally. GT3 is associated with injecting drug use (IDU), the primary mode of HCV transmission, with more severe liver disease and a lower sustained virological response (SVR), especially in patients with cirrhosis, even in the era of direct-acting antiviral therapies. Ravadasvir, a potent NS5A inhibitor with no clinically significant interaction with cytochrome P450 enzymes, was recently added to the WHO Model Lists of Essential Medicines for the treatment of HCV in combination with sofosbuvir, based on the results of the phase 2/3 STORM-C-1 trial. We analysed the GT3 cohort of this trial to report on efficacy in this subpopulation.

Method: An open-label, single-arm phase 2/3 study in people with chronic HCV \pm HIV infections of all GT was conducted in Malaysia and Thailand. Ravadasvir (200 mg) and sofosbuvir (400 mg) were administered once-daily for 12 weeks to patients without cirrhosis and for 24 weeks to those with compensated cirrhosis (CC). The primary efficacy end point was SVR at 12 weeks post-treatment. Patients underwent clinical and laboratory assessments at weeks 1 and 4 and then every 4 weeks during treatment and at 4, 12 and 24 weeks post-treatment.

Results: Of the 603 patients enrolled, 296 (49%) had HCV GT3; of these, 258 (87%) had subtype 3a, 34 (11%) had subtype 3b, and 4 (1%) could not be subtyped. The median age was 48 years (IQR 41–56), 77% were male, 53% had cirrhosis, 23% were interferon \pm ribavirin treatment-experienced, and 49% reported a history of IDU. SVR at 12 and 24 weeks post-treatment (SVR12/24) was 97.6% (289/296), with similar rates between those without cirrhosis, 97.8% (136/139) and those with CC, 97.5% (153/157). The SVR 12/24 for GT3a was 98.1% (253/258) and for GT3b was 97.1% (33/34). In patients with any baseline resistance-associated substitution (RAS), the SVR12/24 was 96.7% (59/61) in GT3a and 97.1% (33/34) in GT3b. Of the 41 patients with GT3a and baseline Y93H RAS, 39 (95.1%) achieved SVR12/24, including all 9 patients with both S62L and Y93H RAS. Three patients

who did not achieve SVR12/SVR24 discontinued treatment early after 2, 3 and 9 doses of study drugs. Virological failure was observed in four of 296 (1.4%) patients. Three had baseline RAS, 93H ($n = 2$) and 30 K + 31 M ($n = 1$), but none had treatment-emergent RAS in NS5A or NS5B. One patient had no baseline RAS results as amplification was not possible.

Conclusion: In chronic GT3 hepatitis C, the combination of ravadasvir and sofosbuvir for 12 weeks in patients without cirrhosis and 24 weeks in patients with CC achieved high SVR12/24 of 97.8% and 97.5%, respectively. There was a minimal impact of the presence of Y93H RAS at baseline on response rates and no evidence of treatment-emergent virologic resistance.

THU-363

Validation of a modified pediatric formulation of Sofosbuvir and Daclatasvir in genotype-4 HCV-infected children weighing 17–35 Kg

Ahmed Farrag¹, Maggie Abbassi¹, Fatma Ebeid², Tim Cressey³, Philippa Easterbrook⁴, Nirmeen Sabry⁵, Manal El-Sayed⁶. ¹Clinical Pharmacy Department, Faculty of Pharmacy, Cairo University, Cairo, Egypt; ²Pediatric Department, Faculty of Medicine, Ain Shams University, Clinical Research Center, Faculty of Medicine Ain Shams University Reserach Institute (MASRI-CRC), Cairo, Egypt; ³AMS-PHPT Research Collaboration, Faculty of Associated Medical Sciences, Chiang Mai University, Chiang Mai, Thailand; ⁴World Health Organisation HQ, Geneva, Switzerland; ⁵Clinical Pharmacy Department, Faculty of Pharmacy, Cairo University, Cairo, Egypt; ⁶Pediatric Department, Faculty of Medicine, Ain-Shams University, Clinical Research Center, Faculty of Medicine Ain Shams University Reserach Institute (MASRI-CRC), Cairo, Egypt
Email: manalhelsayed@yahoo.co.uk

Background and aims: Sofosbuvir (SOF) plus Daclatasvir (DCV) is the regimen of choice in low and middle-income countries (LMICs) for treatment of chronic hepatitis C virus (HCV) infection in adults and adolescents. Based on extrapolation of efficacy, safety and PK data from studies in adults, adolescents or older children and PK simulation studies, in 2022 the World Health Organization (WHO) recommended this regimen to older children (6–11 years and weighing >26 kg) at adult dose (400/60 mg) and in younger children 3–5 years or weighing 14–25 kg at half the adult dose (ie 200/30 mg). However, clinical data on this dose in younger children is still lacking. We conducted a clinical pharmacokinetic study to assess the pharmacokinetics, safety, efficacy, and acceptability of once daily 30 mg DCV plus 200 mg SOF for 12 weeks in treatment-na  ve children weighing 17 to ≤ 35 kg with chronic HCV infection.

Method: This study is an interventional, single centre, single arm, open label clinical trial that included treatment-na  ve children with chronic HCV infection of median age 7 years (range 5–13 years) and weight 17 to ≤ 35 kg. Children who weighed 17 to ≤ 35 kg received once daily oral DCV 30 mg in combination with 200 mg SOF (two small 100 mg tablets new formulation) for 12 weeks. A swallow-ability test was performed before inclusion in the trial. Steady state plasma concentrations were determined. Non-compartmental PK analysis was performed using Pkanalix 2023. Efficacy was assessed using quantitative HCV-PCR at the end of treatment (EOT) and 12 weeks after finishing treatment (SVR12). Patients were followed up for any adverse events. Palatability of the tablets was recorded at each study visit. The study is registered at ClinicalTrials.gov under NCT05854511.

Results: Twelve patients weighing 17 ≤ 35 kg were included. All patients (12/12) completed the 12 weeks course of SOF + DCV. Mean \pm standard deviation for the area under the curve (AUC)₂₄, maximum plasma concentration at steady-state (C_{ssmax}), and minimum plasma concentration at steady-state (C_{ssmin}) were: 11, 082 \pm 5, 168 h.ng.ml⁻¹, 1, 062 \pm 342 ng.ml⁻¹ and 198 \pm 156 ng.ml⁻¹, respectively for DCV; 2, 127 \pm 1, 866 h.ng.ml⁻¹, 952 \pm 579 ng.ml⁻¹ and 18 \pm 21 ng.ml⁻¹, respectively for SOF; 15, 256 \pm 4, 113 h.ng.ml⁻¹, 1605 \pm

POSTER PRESENTATIONS

743 ng·mL⁻¹ and 312 ± 112 ng·mL⁻¹, respectively for its major metabolite GS331007. Results for DCV values are comparable to those achieved by adults. All patients (12/12) achieved SVR12. No serious adverse events were reported. All patients (12/12) could swallow the medication with no difficulty.

Conclusion: A combination of half of the available adult SOF/DAC dose, 30 mg DCV and 200 mg SOF, provides safe and effective drug exposure, and is well-tolerated orally in children weighing 17–35 Kg. This preparation can provide an affordable formulation for treatment of chronic hepatitis C infection in young children to scale up elimination in this special population.

THU-364

Modeling suggests that undetectable HCV at week 2 of DAA therapy could identify patients for shorter treatment duration

Ashish Goyal¹, Ohad Etzion², Kimberly Page³, Tatyana Kushner⁴, Yedidya Saiman⁵, Scott Cotler¹, Harel Dahari¹. ¹Program for Experimental and Theoretical Modeling, Division of Hepatology, Department of Medicine, Stritch School of Medicine, Loyola University Chicago, Maywood, IL, United States; ²Soroka University Medical Center, Beersheva, Israel; ³Division of Epidemiology, Biostatistics and Preventive Medicine, Department of Internal Medicine, University of New Mexico Health Sciences Center, Albuquerque, NM, United States; ⁴Division of Liver Diseases, Icahn School of Medicine at Mount Sinai, New York, NY, United States; ⁵Department of Medicine, Section of Hepatology, Lewis Katz School of Medicine at Temple University, Temple University Hospital, Philadelphia, PA, United States
Email: harel.dahari@gmail.com

Background and aims: The World Health Organization (WHO) calls for identifying predictors of successful treatment with reduced duration of DAA therapy. This objective is particularly important in people who inject drugs (PWID), in whom shorter treatment could improve adherence, decrease loss to follow-up, and reduce cost. In addition, there is a need to minimize DAA duration to reduce DAA exposure and increase acceptance in pregnant women. Here we investigate the feasibility of response-guided therapy (RGT) to reduce length of treatment using a computational modeling approach.

Method: Previous modeling efforts based on ~300 patients receiving DAA (such as sofosbuvir + velpatasvir, elbasvir + grazoprevir, sofosbuvir + ledipasvir, or pibrentasvir + glecaprevir) allowed us to characterize viral-host parameters, DAA efficacy in blocking HCV production, and treatment outcomes [Math Biosci. 2022 Jan;343:108756]. Based on this real-life patient data, parameter distributions were identified and then 20,000 parameter combinations of viral-host and treatment parameters were generated, each representing an *in silico* patient. Next, viral kinetic profile under DAA treatment for each patient was simulated using a multiscale model [Proc Natl Acad Sci U S A. 2013 Mar 5;110 (10):3991–6]. The time to cure (TTC) for each *in silico* patient, defined as the time to reach less than one HCV viral copy in the 15L of extracellular body fluid, i.e. $V = 7 \times 10^{-5}$ IU/mL [Sci Rep. 2020 Oct 20;10 (1):17820], was then estimated using mathematical modeling simulations.

Results: Out of 20,000 *in silico* patients, about 10,000 (~50%) achieved undetectable HCV (<1 IU/mL) by day 14 after initiation of treatment. Modeling suggests that if HCV is undetectable on or before day 14 of DAA therapy, 90% and 98% of HCV-infected individuals can be cured within 4 and 5 weeks of DAA treatment, respectively. The median predicted TTC was ~22 days with ~0.6% reaching TTC as early as 2 weeks. Approximately 8% of these cases also had undetectable viral load at day 7, predicting that 90% and 98% cure rates could be achieved with 3 and 4 weeks of DAA treatment, respectively.

Conclusion: Mathematical modeling of *in silico* patients that reach undetectable HCV by day 14 predicted that >90% cure rates could be achieved with 4–5 weeks of DAA therapy. This RGT could improve treatment access, facilitate HCV elimination, and reduce cost, particularly in patient groups most affected by HCV such as PWID.

THU-365

Real-world effectiveness and safety of 8-week glecaprevir/pibrentasvir for treatment-naïve patients from Taiwan nationwide HCV registry

Chung-Feng Huang^{1,2}, Te-Sheng Chang^{3,4}, Hsing-Tao Kuo⁵, Chien-Wei Huang⁶, Lien-Ray Mo⁷, Chi-Ming Tai^{8,9}, Kuo-Chih Tseng^{10,11}, Ming-Jong Bair^{12,13}, Sih-Ren Wang¹⁴, Ching-Chu Lo¹⁵, Lee-Won Chong^{16,17}, Pin-Nan Cheng¹⁸, Ming-Lun Yeh^{1,19}, Cheng-Yuan Peng^{20,21}, Chien-Yu Cheng²², Jee-Fu Huang^{1,23}, Chih-Lang Lin²⁴, Chi-Chieh Yang²⁵, Tsai-Yuan Hsieh²⁶, Tzong-Hsi Lee²⁷, Pei-Lun Lee²⁸, Wen-Chih Wu²⁹, Chih-Lin Lin³⁰, Wei-Wen Su³¹, Sheng-Shun Yang^{32,33,34}, Chia-Chi Wang³⁵, Jui-Ting Hu³⁶, Chun-Ting Chen^{26,37}, Yi-Hsiang Huang^{38,39}, Chun-Chao Chang^{40,41}, Chia-Sheng Huang⁴², Guei-Ying Chen⁴³, Chien-Neng Kao⁴⁴, Chun-Jen Liu⁴⁵, Mei-Hsuan Lee⁴⁶, Pei-Chien Tsai¹, Chia-Yen Dai¹, Jia-Horng Kao⁴⁵, Han-Chieh Lin^{38,39}, Wan-Long Chuang¹, Chao-Hung Hung⁴⁷, Chi-Yi Chen⁴⁸, Ming-Lung Yu^{1,19,23,47,49}. ¹Hepatobiliary Division, Department of Internal Medicine and Hepatitis Center, Kaohsiung Medical University Hospital, College of Medicine, Kaohsiung Medical University, Kaohsiung, Taiwan; ²Ph.D. Program in Translational Medicine, College of Medicine, Kaohsiung Medical University, Academia Sinica, Kaohsiung, Taiwan; ³Division of Hepatogastroenterology, Department of Internal Medicine, Chang Gung Memorial Hospital, Chiayi, Taiwan; ⁴College of Medicine, Chang Gung University, Taoyuan, Taiwan; ⁵Division of Gastroenterology and Hepatology, Department of Internal Medicine, Chi Mei Medical Center, Yongkang District, Tainan, Taiwan; ⁶Division of Gastroenterology, Kaohsiung Armed Forces General Hospital, Kaohsiung, Taiwan; ⁷Division of Gastroenterology, Tainan Municipal Hospital (Managed By Show Chwan Medical Care Corporation), Tainan, Taiwan; ⁸Department of Internal Medicine, E-Da Hospital, Kaohsiung, Taiwan; ⁹School of Medicine, College of Medicine, I-Shou University, Kaohsiung, Taiwan; ¹⁰Department of Internal Medicine, Dalin Tzu Chi Hospital, Buddhist Tzu Chi Medical Foundation, Chiayi, Taiwan; ¹¹School of Medicine, Tzuchi University, Hualien, Taiwan; ¹²Division of Gastroenterology, Department of Internal Medicine, Taitung Mackay Memorial Hospital, Taitung, Taiwan; ¹³Mackay Medical College, New Taipei, Taiwan; ¹⁴Division of Gastroenterology, Department of Internal Medicine, Yuan's General Hospital, Kaohsiung, Taiwan; ¹⁵Division of Gastroenterology, Department of Internal Medicine, St. Martin De Porres Hospital, Chiayi, Taiwan; ¹⁶Division of Hepatology and Gastroenterology, Department of Internal Medicine, Shin Kong Wu Ho-Su Memorial Hospital, Taipei, Taiwan; ¹⁷School of Medicine, Fu-Jen Catholic University, New Taipei, Taiwan; ¹⁸Division of Gastroenterology and Hepatology, Department of Internal Medicine, National Cheng Kung University Hospital, College of Medicine, National Cheng Kung University, Tainan, Taiwan; ¹⁹Center for Liquid Biopsy and Cohort Research, Kaohsiung Medical University, Kaohsiung, Taiwan; ²⁰Center for Digestive Medicine, Department of Internal Medicine, China Medical University Hospital, Taichung, Taiwan; ²¹School of Medicine, China Medical University, Taichung, Taiwan; ²²Division of Infectious Diseases, Department of Internal Medicine, Taoyuan General Hospital, Ministry of Health and Welfare, Taoyuan, Taiwan; ²³Hepatitis Research Center, College of Medicine, Kaohsiung Medical University, Kaohsiung, Taiwan; ²⁴Liver Research Unit, Department of Hepato-Gastroenterology and Community Medicine Research Center, Chang Gung Memorial Hospital at Keelung, College of Medicine, Chang Gung University, Keelung, Taiwan; ²⁵Department of Gastroenterology, Division of Internal Medicine, Show Chwan Memorial Hospital, Changhua, Taiwan; ²⁶Division of Gastroenterology, Department of Internal Medicine,

Tri-Service General Hospital, National Defense Medical Center, Taipei, Taiwan; ²⁷Division of Gastroenterology and Hepatology, Far Eastern Memorial Hospital, New Taipei, Taiwan; ²⁸Division of Gastroenterology and Hepatology, Department of Internal Medicine, Chi Mei Medical Center, Liouying, Tainan, Taiwan; ²⁹Wen-Chih Wu Clinic, Fengshan, Kaohsiung, Taiwan; ³⁰Department of Gastroenterology, Renai Branch, Taipei City Hospital, Taipei, Taiwan; ³¹Department of Gastroenterology and Hepatology, Changhua Christian Hospital, Changhua, Taiwan; ³²Division of Gastroenterology and Hepatology, Department of Internal Medicine, Taichung Veterans General Hospital, Taichung, Taiwan; ³³Institute of Biomedical Sciences, National Chung Hsing University, Taichung, Taiwan; ³⁴Department of Post-Baccalaureate Medicine, College of Medicine, National Chung Hsing University, Taichung, Taiwan; ³⁵Taipei Tzu Chi Hospital, Buddhist Tzu Chi Medical Foundation and School of Medicine, Tzu Chi University, Taipei, Taiwan; ³⁶Liver Center, Cathay General Hospital, Taipei, Taiwan; ³⁷Division of Gastroenterology, Department of Internal Medicine, Tri-Service General Hospital Penghu Branch, National Defense Medical Center, Taipei, Taiwan; ³⁸Division of Gastroenterology and Hepatology, Department of Medicine, Taipei Veterans General Hospital, Taipei, Taiwan; ³⁹Institute of Clinical Medicine, School of Medicine, National Yang-Ming Chiao Tung University, Taipei, Taiwan; ⁴⁰Division of Gastroenterology and Hepatology, Department of Internal Medicine, Taipei Medical University Hospital, Taipei, Taiwan; ⁴¹Division of Gastroenterology and Hepatology, Department of Internal Medicine, School of Medicine, College of Medicine, Taipei Medical University, Taipei, Taiwan; ⁴²Yang Ming Hospital, Chiayi, Taiwan; ⁴³Penghu Hospital, Ministry of Health and Welfare, Penghu, Taiwan; ⁴⁴National Taiwan University Hospital Hsin-Chu Branch, Hsinchu, Taiwan; ⁴⁵Hepatitis Research Center and Department of Internal Medicine, National Taiwan University Hospital, Taipei, Taiwan; ⁴⁶Institute of Clinical Medicine, National Yang-Ming Chiao Tung University, Taipei, Taiwan; ⁴⁷Division of Hepatogastroenterology, Department of Internal Medicine, Kaohsiung Chang Gung Memorial Hospital, Kaohsiung, Taiwan; ⁴⁸Division of Gastroenterology and Hepatology, Department of Medicine, Dittmanson Medical Foundation Chiayi Christian Hospital, Chiayi, Taiwan; ⁴⁹School of Medicine, College of Medicine, Center of Excellence for Metabolic Associated Fatty Liver Disease, National Sun Yat-Sen University, Kaohsiung, Taiwan
Email: fish6069@gmail.com

Background and aims: The once-daily, oral, fixed-dose, direct-acting antiviral combination of glecaprevir/pibrentasvir (G/P) is indicated for chronic hepatitis C (CHC) infection with HCV genotypes 1–6 in patients with or without compensated cirrhosis (CC). Treatment duration of 8 weeks is recommended in all treatment-naïve (TN) patients. As Taiwan government is committed to eliminating HCV by 2025, this study aimed to measure the real-world evidence for TN patients using 8-week G/P in Taiwan HCV Registry (TACR).

Method: The TACR is an ongoing nationwide registry program organized and supervised by Taiwan Association for the Study of the Liver (TASL), which aims to setup a database and biobank of patients with CHC in Taiwan. Data was analyzed as of 31 May 2023 for CHC patients treated with G/P. Effectiveness reported as sustained virologic response at post-treatment week 12 (SVR12) was assessed by modified intent-to-treat (mITT) populations that excluded patients who lost to follow-up or without SVR12 data. Safety profile was assessed in the ITT population.

Results: Of 8,041 TN patients treated with G/P, 7,246 patients received 8-week regimen (ITT) and 7,204 of which had SVR12 data available (mITT). The overall SVR12 rate was 98.9% (7,122/7,204) in the mITT population. For selected subgroups including patients with compensated cirrhosis, GT3, diabetes, chronic kidney disease, person who inject drugs, and HIV, the SVR12 rate was 98.3% (342/348), 95.1% (272/286), 98.9% (1,084/1,096), 99.0% (1,171/1,183), 97.4% (566/581), and 96.1% (248/258), respectively. Overall, 14.1% (1,021/7,246) of the patients experienced adverse events (AEs) in the ITT population. Twenty-two patients (0.3%) experienced serious adverse events and

fifteen (0.2%) resulted in permanent drug discontinuation. None of them were considered as treatment drug related. The most frequent AEs (>5%) were fatigue (5.6%) and pruritus (5.4%). Laboratory abnormalities of Grade 3 and 4 for bilirubin, AST, and ALT were all 0.2%, respectively.

Conclusion: In this real-world Taiwanese cohort, 8-week G/P therapy was effective and well-tolerated in all TN patients, including general and special populations.

THU-366

Use of proton pump inhibitors among German Hepatitis C patients treated with sofosbuvir/velpatasvir: Data from the German Hepatitis C-Registry (2016–2022)

Markus Cornberg¹, Gerlinde Teuber², Ralf Link³, Uwe Naumann⁴, Hartwig Klinker⁵, Christine John⁶, Candido Hernández^{7,8}, Marianna Schwenken⁹, Christoph Sarrazin¹⁰, ¹Hannover Medical School, Hannover, Germany; ²Private Practice, Frankfurt/Main, Frankfurt am Main, Germany; ³MVZ-Offenburg GmbH, Offenburg, Germany; ⁴UBN/Praxis, Berlin, Germany; ⁵University of Würzburg Medical Center, Würzburg, Germany; ⁶Private Practice of Internal Medicine, Center of Gastroenterology, Berlin, Germany; ⁷Gilead Sciences Europe Ltd, Uxbridge, United Kingdom; ⁸Gilead Sciences, S.L, Madrid, Spain; ⁹Gilead Sciences GmbH, Munich, Germany; ¹⁰Department of Internal Medicine and Liver Center, Wiesbaden, Germany
Email: cornberg.markus@mh-hannover.de

Background and aims: Literature and product labels suggest velpatasvir bioavailability may be reduced when administered concomitantly with a proton pump inhibitor (PPI), based on pharmacokinetic studies. We aimed to determine the clinical relationship between PPI use and sustained virologic response rates (SVR) in patients treated with sofosbuvir/velpatasvir (SOF/VEL) ± ribavirin (RBV) in a real-world, ongoing, noninterventional, multicenter, prospective, observational German Hepatitis C-Registry (DHC-R). The DHC-R is a national multicenter real-world registry including about 18,900 patients.

Method: The present analysis is based on 1,154 patients enrolled between 2016 and 2022 in the DHC-R, as treated with SOF/VEL, split between those receiving and not receiving PPI drugs as comedication. Baseline characteristics (demographics, viral infection, liver status, number and type of PPI drugs) and SVR (patients with SVR available: based on modified intention to treat (mITT), including patients with ITT SVR and ITT relapses) were analyzed. Also, co-use of metamizole was collected, as this comedication shows the same drug-drug interaction (DDI) profile as PPIs (risk of direct acting antiviral (DAA) exposure), thus checking a multi-drug-drug interaction (DDI) scenario.

Results: Patients receiving PPI represented 8.5% (98/1,154) of the total SOF/VEL cohort. Pantoprazole was the most common PPI co-used (78/98 patients; dose per day: 20 mg: 28/78, 40 mg: 29/78, 80 mg: 2/78, unspecified: 19/78 patients), followed by omeprazole (19/98 patients; dose per day: 20 mg: 14/19, 40 mg: 2/19, unspecified: 3/19 patients) and esomeprazole (1/98 patients; dose per day: 80 mg: 1/1), with 9.2% of the SOF/VEL+ PPI group also receiving metamizole. Those patients receiving PPI vs. non-PPI seemed older (≥50 years old (yo): 59% and 37%, respectively), with more females (38% and 27%), less genotype 3 (GT3) (47% and 62%), but with a higher proportion of cirrhosis (compensated cirrhosis (CC): 50% and 32%; decompensated cirrhosis (DC): 17% and 4%). In terms of effectiveness, SVR was similar in both groups, also in cirrhosis (=98%) for all genotypes, and even in the presence of GT3 + CC (both ≥96%). Co-use of metamizole had no impact on SVR (=100%). Besides, no negative PPI dose-dependent SVR trend was noticed with the PPI dose given (20 mg: =96–100%, 40 mg: =91–100%, 80 mg: =100%, unspecified dose: =100%).

Conclusion: PPI co-use in patients under SOF/VEL therapy included in DHC-R did not impact the SVR. Those results were also not impacted by the cirrhotic status, PPI dose or the presence of a multi-DDI scenario.

THU-367-YI

Effectiveness and safety of direct-acting antivirals in the treatment of elderly people infected with HCV

Michał Brzdek¹, Dorota Zarębska-Michaluk², Krzysztof Tomaszewicz³, Magdalena Tudrujek-Zdunek³, Beata Lorenc⁴, Włodzimierz Mazur⁵, Hanna Berak⁶, Justyna Janocha-Litwin⁷, Jakub Klapaczynski⁸, Ewa Janczewska⁹, Dorota Dybowska¹⁰, Anna Parfieniuk-Kowerda¹¹, Piekarska Anna¹², Jerzy Jaroszewicz¹³, Robert Flisiak¹¹. ¹Department of Infectious Diseases and Allergology, Jan Kochanowski University, Kielce 25-317, Poland, Kielce, Poland; ²Department of Infectious Diseases and Allergology, Jan Kochanowski University, Poland, Kielce, Poland; ³Department of Infectious Diseases, Medical University of Lublin, Poland, Lublin, Poland; ⁴Pomeranian Center of Infectious Diseases, Medical University Gdańsk, Poland, Gdańsk, Poland; ⁵Clinical Department of Infectious Diseases, Clinical University of Silesia in Katowice, Poland, Chorzów, Poland; ⁶Daily Department, Hospital for Infectious Diseases in Warsaw, Poland, Warszawa, Poland; ⁷Department of Infectious Diseases and Hepatology, Medical University Wrocław, Poland, Wrocław, Poland; ⁸Department of Internal Medicine and Hepatology, The National Institute of Medicine of the Ministry of Interior and Administration, Poland, Warszawa, Poland; ⁹Department of Basic Medical Sciences, Faculty of Public Health in Bytom, Medical University of Silesia in Katowice, Poland, Bytom, Poland; ¹⁰Department of Infectious Diseases and Hepatology, Faculty of Medicine, Nicolaus Copernicus University, Poland, Bydgoszcz, Poland; ¹¹Department of Infectious Diseases and Hepatology, Medical University of Białystok, Poland, Białystok, Poland; ¹²Department of Infectious Diseases and Hepatology, Medical University of Łódź, Poland, Łódź, Poland; ¹³Department of Infectious Diseases and Hepatology, Medical University of Silesia in Katowice, Poland, Bytom, Poland
Email: michal.brzdek@gmail.com

Background and aims: In the interferon (IFN) era, therapeutic options and their efficacy in treating chronic hepatitis C virus (HCV) infection in elderly patients were severely limited. The introduction of direct-acting antivirals (DAAs) with their effectiveness and safety has revolutionized the approach to treating this population. Nevertheless, elderly patients have often been excluded from participation in clinical trials of DAA drugs, so the results of real-world studies are particularly important in the context of the geriatric population. The current study was conducted among patients over the age of 65, with notable inclusion of those over the age of 85. The study aims to analyze the effectiveness and safety of antiviral DAA treatment in an elderly HCV-infected population.

Method: All consecutive patients aged 65 and above selected from 16,828 individuals with chronic HCV infection from the EpiTer-2 multicenter database were included in the study. The analyzed patients were divided by age into three groups: Group A (65–74 years), Group B (75–84 years) and Group C (85 years or older). Patients started IFN-free therapy at 22 Polish hepatology centers between July 2015 and December 2022. Treatment effectiveness was assessed by sustained virologic response (SVR). Safety data were collected during therapy and at 12-week follow-up.

Results: A total of 3,505 elderly patients were included in the analysis, and they were divided into three groups: 2,501 patients in Group A, 893 in Group B, and 111 in Group C. The studied population, regardless of age group, was predominantly female. Patients had a high prevalence of comorbidities (84.9%, 92.2%, and 93.7%, respectively) as well as a high rate of using concomitant medications. In the per-protocol (PP) analysis, both Groups A and B achieved a similarly high SVR rate of up to 97.9%, and in all patients aged 85 and older SVR was documented. Similarly, high SVR rates exceeding 94% were documented in subgroups based on gender, fibrosis severity, HCV genotype, and prior treatment history.

Conclusion: IFN-free therapies are highly effective and well tolerated by the elderly, including those over 85 years. Age should not be a barrier to treatment, but careful management is necessary.

THU-370

Hepatocellular carcinoma may be a viral reservoir during treatment of hepatitis C with direct-acting antivirals

Mário Jorge Silva^{1,2,3}, Ana Patricia Negrinho², Fatima Oliveira Martins², Antonio Figueiredo^{1,3}, Helena Gloria^{1,3}, Carina Santos^{1,3}, Pedro Lages Martins^{1,2,3}, Vasco Ribeiro^{1,2,3}, Mario Oliveira^{1,3}, Hugo Pinto Marques^{1,2,3}, Silvia Vilares Conde², Filipe Calinas^{1,3}. ¹Centro Clínico Académico de Lisboa, Lisbon, Portugal; ²NOVA Medical School, Lisbon, Portugal; ³Centro Hospitalar Universitário de Lisboa Central/Unidade Local de Saúde São José, Lisbon, Portugal
Email: mariojorgesilva01@gmail.com

Background and aims: Direct-acting antivirals (DAAs) revolutionized the treatment of chronic hepatitis C virus (HCV) infection. Viable hepatocellular carcinoma (HCC) has been identified as one of the few predictors of non-response to hepatitis C treatment with DAAs. However, it is still unclear why patients with HCC have a lower response to DAAs. Several hypotheses have been raised, including the possible role of HCC as a viral reservoir during antiviral treatment. We aim to assess if HCC acts as a viral reservoir for HCV during treatment of hepatitis C with DAAs.

Method: We characterized quantitatively the presence of HCV in liver explant tissue (obtained during transplant surgery) from a cirrhotic patient with viable HCC. The patient was chronically infected with HCV genotype 3 and at the time of surgery was completing his first month of treatment with sofosbuvir/daclatasvir. HCV quantification was performed with immunofluorescence targeting non-structural protein 3 (NS3). Tissue samples were evaluated through widefield microscopy with Zeiss (R) Observer. Intensity of fluorescence was quantified in Fiji (R) program and compared between HCC and non-tumoral liver tissue regions. Statistical analyses were performed using GraphPad (R), and One-way ANOVA between all groups was calculated. Differences were considered statistically significant when $p < 0.05$ (two-sided). This project is approved by the institutional Ethics Committee.

Results: In this patient undergoing treatment with sofosbuvir + daclatasvir for one month, we found significantly higher levels of immunofluorescence for HCV in the viable HCC tissue than in the non-tumoral liver cirrhosis tissue: fluorescence intensity/area was 55.8 ± 31.5 in tumoral tissue vs 0.6 ± 0.3 in non-tumoral tissue ($p < 0.05$)-representing higher density of HCV in HCC tissue than in the remainder cirrhosis non-tumoral tissue.

Conclusion: The present results suggest that HCV clearance is delayed in HCC tissue, compared to non-tumoral cirrhosis liver tissue. HCC may, then, act as viral reservoir for HCV during treatment with DAAs. Further studies are needed to confirm this hypothesis.

THU-371

Impact of a simplified diagnosis-monitoring strategy on Glecaprevir/Pibrentasvir (G/P) treatment initiation and response in patients with chronic hepatitis C virus (HCV) infection receiving opioid substitute therapy in Israel-a real world evidence

Eli Zuckerman¹, Orly Azulay². ¹Liver Unit, Carmel Medical Center, Technion Faculty of Medicine, Haifa; ²Liver Unit, Carmel Medical Center, Haifa, Israel
Email: elizuc56@gmail.com

Background and aims: Although HCV treatment for patients who using drugs (PWIDs) has shown good outcome and is recommended by international guidelines, treatment uptake has remained low. The primary objective was to assess the impact of active intervention model ("simplified") versus conventional approach on treatment initiation and response in patients with chronic HCV infection receiving Opioid-Substitute Therapy (OST) in methadone Clinics in Israel.

Method: The data was collected from one Drug Maintenance Treatment Center (DMTC) in Haifa, containing 324 HCV-Ab-positive patients out of approximately 500 PWIDs treated with OST. Group A

("simplified" approach) included 81 patients tested and prescribed with G/P at the DMTC during 2020–2023. The nurse reviewed the patients' charts, withdrew blood sample included HCV RNA, blood count and chemistry and then performed fibroscan as needed while treatment (G/P) was prescribed by the hepatologist. Follow-up was performed by the Liver Unit staff. Group B- included 50 patients complete all required pre-treatment testing at the community clinics and were referred to the Liver Unit at Carmel Medical Center (up to December 31, 2019).

Results: Mean age was similar in both groups (49.2 and 50.8 years, respectively). Fibrosis assessment either by fibroscan or fib4 score was available in all patients from group A and in 32/50 in group B. The proportion of patients with advanced disease (F3–4) was significantly higher in group A (28% vs 15%, $p < 0.05$). The mean time elapsed from diagnosis of HCV infection to treatment initiation was significantly shorter in Group B (48 vs 126 months, respectively, $p < 0.0001$) and the same applies to the time from diagnosis to the first HCV PCR-negative test (94 vs 136 months, $p < 0.0001$). In Group A, the mean time elapsed from the time of intervention to treatment initiation was 9.25 months (range 0–33 months). In 74 of 81 of Group A (91%) and in 36 of 50 (72%) of group B, PCR results to determine SVR were available. SVR was achieved in 72 patients of group A (97%) and in 32 patients in group B (88%). Seven patients lost to follow-up in group A and fourteen in group B. In intention-to-treat analysis the SVR rate was significantly higher in group A ($p < 0.05$).

Conclusion: "Simplified" model applied in very difficult-to treat OST patients is effective in reducing time of linkage-to-care and of treatment initiation and increasing the rate of SVR. However, even in this model in "real world" setting, we have faced barriers to better management of these patients.

THU-372-YI

Point of care hepatitis C screening and treatment among people who use drugs in new york city addiction centers: barriers and opportunities

Jessica Siguencia¹, Jhané Phanor¹, Anthony Choi¹, Robert S. Brown, Jr¹, Laura Maroldo², ¹Weill Cornell Medicine, New York, United States; ²West Midtown Medical Group, New York, United States
Email: jms4007@med.cornell.edu

Background and aims: Among people who use drugs (PWUDs) in the US, Hepatitis C Virus (HCV) is prevalent in 70% and is often untreated due to limited access to testing and care. The addiction care setting provides a unique opportunity to bridge this accessibility gap by including point-of-care (POC) HCV testing among services used by PWUDs. The AbbVie B20 Study is a randomized study of test, educate, and treat in two drug addiction centers in New York City. Our preliminary results provide lessons on the significant challenges facing HCV screening and treatment in addiction centers.

Method: Patients in addiction care settings were recruited and screened for HCV infection, using HCV antibody with reflex RNA test, and a POC Cepheid HCV Viremia (RNA) test. The ongoing trial randomizes all eligible patients to a video-based patient education and treatment at the drug treatment program versus a standard of care (SOC) referral for Hospital clinic-based HCV therapy.

Results: Out of 12 addiction care locations in New York City contacted, only 2 locations participated, and 21 patients have been screened so far. At site 1, a residential drug and alcohol rehabilitation center, 9 of 148 residents consented. These 9 patients' HCV results came back negative. The most common barriers to participation included unwillingness to interact with a medical team, aversion to undergo phlebotomy, prior negative HCV status, and competing priorities in the rehabilitation center. At site 2, a walk-in addiction treatment center, 11 of 15 patients were screened, seven participants were identified as HCV positive. Three of the seven were randomized to SOC and none came to our clinic. After missing SOC appointments, two of the three SOC patients began medication at the addiction center and have SVR pending. The last SOC patient never began

medication due to competing health priorities, which resulted in an emergency room admission. The remaining four participants were randomized to the test-and-treat arm and could start treatment at the site after completing video-based education. Two out of the four struggled with returning to the site for medication initiation and they have yet to reconnect with the facility. Out of the remaining two test-and-treat participants, one lost and stopped taking medication but returned 4 months later to restart medication. The last participant completed medication and had a confirmed sustained virologic response (SVR).

Conclusion: Substantial barriers exist at the individual patient level to HCV treatment, even when a medical provider provides POC testing and therapy. POC testing, ideally without phlebotomy, and treatment is essential for HCV eradication. Strategies to implement mental health services along with a test-and-treat strategy may allow us to overcome the identified barriers to initiating and completing HCV treatment in this vulnerable population.

THU-373-YI

Quality of etiotropic therapy efficacy of chronic hepatitis C patients in accordance of toll-like receptor 4 +3725G/C gene polymorphisms variety

Tetiana Bevz¹, Larysa Moroz¹, Kiarina Myroniuk-Konstantynovych¹, Iryna Bondaruk¹, Galyna Martyniuk², Yaroslav Demchyshyn¹.

¹National Pirogov Memorial Medical University, Vinnytsia, Ukraine;

²Central City Hospital, Rivne, Ukraine

Email: tasya241@gmail.com

Background and aims: Antiviral therapy is considered to be the only method that can stop the progression HCV infection, the development of hepatocellular carcinoma and death. The end point of antiviral therapy is the achievement of a sustained virologic response (SVR), which in 99% of cases is associated with the possibility of complete elimination of the virus. The aim of our study was to assess the dependence of the frequency of obtaining a SVR to antiviral therapy on the +3725G/C polymorphism of the toll-like receptor 4 (TLR4) gene.

Method: 111 chronic hepatitis C (1b genotype), patients (78 males, 33 females) were observed. All participants received antiviral treatment with Sofosbuvir/Ledipasvir. The duration of antiviral therapy was 12 weeks in patients without cirrhosis and 24 weeks in patients with liver cirrhosis.

Results: The vast majority of treated patients achieved a SVR (91.89%), the antiviral therapy was ineffective for 9 patients (8.11%). The number of non-RSVs was significantly ($p < 0.05$) higher among patients with the +3725C allele of the TLR4 gene (GC and CC genotypes)-77.8% of all those who did not respond to treatment were carriers of this allele. It was established that among patients with the GG genotype, only 2.41% of patients with chronic hepatitis C did not have a SVR. According to the results of the genotypes distribution comparison according to variants of the TLR4 gene +3725G/C allelic polymorphism by the exact two-tailed Fisher test among patients with chronic hepatitis C who had received antiviral therapy, the significantly higher frequency of carriers of the +3725G allele (genotypes GG and GC) was detected ($p < 0.001$) in the group of patients with RSV vs. the group of patients who did not receive a SVR. According to the odds ratio calculations, it was established that individuals carrying the +3725G allele of the TLR4 gene have a 13 fold higher chance of obtaining a SVR during antiviral therapy use (OR = 13.5; CI 2.61, 69.81). It was established that in the vast majority of patients (68.63% [n = 70]) with chronic hepatitis C, whom a SVR was obtained in, absent liver fibrotic changes (F0) or initial stages of liver fibrosis were observed in 2.26 fold higher number of patients vs. ones with liver fibrosis/cirrhosis (F3–F4). Among non-RSV patients, the degree of liver fibrosis F0–F2 were not detected.

Conclusion: Among patients with chronic hepatitis C who did not have a SVR to administered antiviral therapy, there were 3.2 fold higher number of patients with severe liver fibrosis/cirrhosis (F3–F4).

POSTER PRESENTATIONS

Most of the patients (77.8%) who did not achieve a SVR were carriers of the +3725C allele of the TLR4 gene ($p < 0.05$). The odds ratios of achieving a SVR in patients with chronic hepatitis C with the 1b genotype were 13 fold higher among carriers of the +3725G allele of the TLR4 gene than among carriers of the +3725C allele.

THU-374

Description of age, sex, and characteristics of hepatitis C patients in the SVR10 K study: a real-world SOF/VEL analysis performed across five global regions

Soo Aleman¹, Fatima Higuera-de-la-Tijera², Francisco Javier Garcia-Samaniego³, Marta Casado-Martin⁴, Grace Lai-Hung Wong⁵, Mohammed Alzaabi⁶, Habiba Kamal¹, Karin Lindahl¹, Aastha Chandak⁷, Marta Martinez⁸, Artak Khachatryan⁷, Linda Chen⁹, Candido Hernández¹⁰, Kim Vanstraelen¹¹, Ming-Lung Yu¹². ¹Karolinska University Hospital, Stockholm, Sweden; ²Hospital General de México "Dr. Eduardo Liceaga," Mexico DF, Mexico; ³Hospital Universitario La Paz, Madrid, Spain; ⁴Hospital de Torrecárdenas, Almería, Spain; ⁵Prince of Wales Hospital, Hong Kong, Hong Kong; ⁶Zayed Military Hospital, Abu Dhabi, United Arab Emirates; ⁷Certara Inc, Princeton, United States; ⁸Certara Inc, Madrid, Spain; ⁹Gilead Sciences, Foster City, United States; ¹⁰Gilead Sciences, Madrid, Spain; ¹¹Gilead Sciences, Brussels, Belgium; ¹²National Sun Yat-sen University, Kaohsiung, Taiwan
Email: soo.aleman@regionstockholm.se

Background and aims: A previously published real-world data analysis demonstrated high effectiveness of sofosbuvir/velpatasvir (SOF/VEL) in >6,000 HCV patients from 12 clinical cohorts across Australia, Canada, Europe and USA. Irrespective of age, male patients were more likely to have advanced fibrosis and infection with HCV GT 3, and median time to treatment initiation was numerically shorter in male patients across the age spectrum. The aim of this large real-world analysis was to evaluate characteristics of an expanded pool of HCV patients treated with SOF/VEL across regions globally.

Method: This analysis included patients ≥ 18 years treated with SOF/VEL without ribavirin (RBV) for 12 weeks from 7 sites across Hong Kong, Mexico, Sweden, Spain, Taiwan, and the United Arab Emirates. Baseline characteristics, such as age (in categories ≤ 50 yo), sex, being treatment experienced (TE), cirrhosis presence (F4, no decompensated), genotype, coinfections (HBV, HDV, HIV), time to treatment initiation (TTI) from HCV diagnosis were described, along with sustained virology response rates (SVR) (4/12/24).

Results: Among 4,679 patients, 59% (2,760) were males and 41% (1,919) were females, with 73% females vs 64% males being ≥ 50 yo ($p < 0.001$). Coinfections were more prevalent in males (HIV 6.9% vs 1.6% $p < 0.001$; HBV 4.9% vs 3.4%, $p = 0.005$; HDV 0.2% vs 0.1%, $p < 0.001$), they were more often TE (5.9% vs 3.9%, $p = 0.001$) and more often had GT3 (24.2% vs 17.6%, $p < 0.001$); these differences were seen mostly in males ≥ 50 yo. No differences by sex was observed for patients with compensated cirrhosis (19.9% male vs 21.7% female, $p = 0.34$). Time to treatment initiation with the HCV therapy was shorter in females aged ≥ 50 yo, with 23% treated in the first month, as compared to 16% of males above 50 yo ($p < 0.001$). In 4,195 patients with SVR

outcomes (effectiveness population), both sex and age groups had SVR greater than 97%, showing a statistically significant difference between female and male patients aged ≥ 50 yo (99.4% vs 98.5%; $p = 0.0266$).

Conclusion: This new analysis confirms the high effectiveness of using SOF/VEL in diverse populations globally, with real-world SVR higher than 97% across diverse age, sex and geographic groups.

THU-375

When glecaprevir/pibrentasvir ultra-short therapy is enough to eradicate HCV infection

Alberto Grassi¹, Natascia Celli², Silvana Maccariello², Gabriele Donati³, Angela Fabbri², Giorgio Ballardini². ¹Ospedale Cervesi, Cattolica (RN), AUSL della Romagna, Cattolica (RN), Italy; ²Internal Medicine Unit, Infermi Hospital, Rimini, Italy; ³Internal Medicine Unit, State Hospital of San Marino, Borgo Maggiore, San Marino
Email: albgrassi@yahoo.com

Background and aims: There is general agreement about the fact that at least 8 weeks of therapy with direct antiviral agents (DAAs) are necessary to achieve definitive hepatitis C virus (HCV) eradication but, probably, the real impact of DAAs in HCV replication is not yet completely known.

Method: From 2018 to 2023, 302 HCV-RNA+ patients received antiviral treatment with glecaprevir/pibrentasvir (G/P) and completed 12 weeks post-treatment follow-up.

Results: Sustained virological response (SVR) was globally obtained in 297 patients (98.3%). Ten patients prematurely suspended treatment, mainly for light side effects (itching, headache weakness). The main characteristics of patients are the following: median age (years): 63 (40–83); male/female: 7/3; liver fibrosis score (metavir): 3 F 1, 3 F 2, 2 F 3, 2 F 4; genotype (G): 3 G 1, 3 G 2, 3 G 3, 1 G 4; median pre-treatment HCV RNA (log IU): 5 (4–7); median pre-treatment alanine transaminase (ALT) (IU): 54 (6–248); median duration of treatment (days): 7 (4–28). Nine of them (90%) were HCV RNA negative at the end of treatment and six of them (60%) resulted SVR; three (30%) relapsed 12 weeks post the end of treatment and only one (10%) resulted non-responder. SVR patients showed pre-treatment ALT level lower than non SVR patients (IU median values: 39 vs 131, $p = 0.017$). Age, gender, liver fibrosis score, genotype, pre-treatment HCV RNA and duration of therapy were not significantly different in the two groups.

Conclusion: In this tiny series of patients, HCV eradication was obtained in 60% of cases with (even extremely) reduced duration of treatment with G/P. Apparently SVR resulted more probable when pre-treatment degree of HCV related hepatic cytonecrosis was low. More studies about this topic would be important to eventually permit ultra-short scheduled of treatment to eradicate HCV infection. This should strengthen the case for offering treatment with DAAs to all HCV+ people, even to subjects with presumed reduced compliance with therapy (prisoners, drug addicts, etc) in accordance with the World Health Organisation (WHO) program to eliminate HCV infection within 2030.

Author Index

- Aabakken, Lars, S22 ([OS-023-YI](#)), S50 ([OS-076-YI](#))
- Aagaard, Niels Kristian, S236 ([FRI-134](#)), S244 ([SAT-088](#))
- Aaldijk, Alexandra, S573 ([THU-224](#))
- Aamann, Luise, S236 ([FRI-134](#))
- Aba Alkhail, Faisal, S496 ([FRI-291](#))
- Abaalkhail, Faisal, S500 ([FRI-304](#)), S671 ([WED-458](#))
- Abadia, Marta, S398 ([SAT-485](#)), S706 ([WED-132](#)), S712 ([WED-159](#))
- Abasszade, Joshua, S400 ([SAT-492](#))
- Abate, Maria Lorena, S59 ([OS-094](#)), S501 ([FRI-314](#)), S522 ([WED-233-YI](#))
- Abbas, Nadir, S290 ([TOP-147](#)), S308 ([THU-098](#)), S309 ([THU-099-YI](#)), S315 ([THU-111](#)), S321 ([THU-125](#)), S332 ([THU-160](#))
- Abbassi, Maggie, S831 ([THU-363](#))
- Abbas, Zaigham, S158 ([THU-052](#)), S167 ([THU-078](#))
- Abbati, Chiara, S499 ([FRI-299](#))
- Abdelgani, Siham, S547 ([WED-303](#))
- Abdelkader, Nadia Abdelaaty, S30 ([OS-038-YI](#)), S199 ([TOP-062](#)), S200 ([TOP-064-YI](#))
- Abdelmalak, Jonathan, S400 ([SAT-492](#))
- Abdelmalek, Manal F., S72 ([OS-118](#)), S84 ([LBP-014](#)), S95 ([LBP-036](#)), S216 ([FRI-081](#)), S502 ([FRI-316](#)), S607 ([SAT-203](#)), S608 ([SAT-206](#))
- Abdelrahman, Basma, S570 ([THU-213](#)), S583 ([THU-255](#))
- Abdelraouf, Mariam Ismail, S491 ([FRI-273-YI](#))
- Abdo-Francis, Juan Miguel, S140 ([SAT-260](#))
- Abe-Chayama, Hiromi, S42 ([OS-061](#)), S735 ([SAT-364](#))
- Abedin, Nada, S52 ([OS-079-YI](#))
- Abe, Hiroshi, S616 ([SAT-236](#))
- Abeles, R. Daniel, S470 ([FRI-215-YI](#)), S553 ([WED-324](#))
- Abel, Florian, S54 ([OS-082](#))
- Abe, Masanori, S118 ([SAT-319](#)), S711 ([WED-154](#)), S722 ([WED-184](#))
- Abergel, Armand, S41 ([OS-060](#)), S168 ([THU-079](#)), S369 ([SAT-010](#)), S385 ([SAT-048](#)), S423 ([FRI-485](#)), S763 ([FRI-370](#))
- Åberg, Fredrik, S460 ([TOP-308](#)), S514 ([WED-210](#)), S562 ([TOP-240-YI](#))
- Aberle, Judith, S54 ([OS-083](#))
- Aberle, Stephan, S54 ([OS-083](#))
- Abeysekera, Kushala, S647 ([SAT-448](#)), S651 ([SAT-457-YI](#))
- Abid, Reema, S253 ([SAT-118](#))
- Aboona, Majd, S146 ([SAT-278](#)), S478 ([FRI-236-YI](#)), S540 ([WED-282](#))
- Abosheishaa, Hazem, S489 ([FRI-269](#))
- Abow-Mohamed, Ikram, S484 ([FRI-256-YI](#))
- Abozaid, Yasir J., S464 ([FRI-200](#)), S604 ([SAT-197-YI](#))
- Abraham, Michal, S278 ([WED-534](#))
- Abraham, Sameer, S58 ([OS-090](#))
- Abraham, Sunje, S205 ([FRI-043](#)), S309 ([THU-100](#))
- Abraldes, Juan G., S36 ([OS-047-YI](#))
- Abraldes, Juan G., S538 ([WED-274](#))
- Abramov, Frida, S771 ([FRI-390](#)), S797 ([WED-397](#))
- Abrams, Gary, S8 ([LBO-002](#))
- Abril-Fornaguera, Jordi, S411 ([TOP-507-YI](#)), S417 ([FRI-467](#))
- Abubucker, Sahar, S58 ([OS-090](#))
- Abudi, Nathalie, S278 ([WED-534](#))
- Abutidze, Akaki, S659 ([WED-427](#)), S685 ([WED-492](#))
- Accetta, Antonio, S28 ([OS-035-YI](#)), S212 ([FRI-068](#))
- Aceituno, Laia, S36 ([OS-047-YI](#)), S381 ([SAT-037](#)), S381 ([SAT-039](#))
- Acharyya, Sanchalika, S826 ([THU-406](#))
- Acin, Victor, S29 ([OS-037](#))
- Ackerman, Margaret, S131 ([THU-331-YI](#))
- Ackermann, Christin, S739 ([SAT-376](#))
- Acosta, Glen, S58 ([OS-090](#))
- Acosta-López, Silvia, S139 ([SAT-257](#)), S142 ([SAT-267](#))
- Acquaviva, Antonio, S451 ([THU-486-YI](#))
- Acel, Stefan, S502 ([FRI-315](#))
- Adali, Gupse, S167 ([THU-078](#)), S336 ([THU-171](#))
- Adame, Eduardo Dominguez, S559 ([WED-341](#))
- Adame, Lillian, S564 ([THU-198](#))
- Adamia, Ekaterine, S659 ([WED-427](#)), S664 ([WED-439](#)), S675 ([WED-468](#)), S685 ([WED-492](#))
- Adam, Lukas, S340 ([THU-180](#))
- Adam, René, S373 ([SAT-019](#)), S378 ([SAT-029](#)), S452 ([THU-491](#))
- Adams, Alexandre, S302 ([SAT-179](#))
- Adams, Leon, S84 ([LBP-014](#)), S275 ([WED-526](#)), S483 ([FRI-250](#)), S487 ([FRI-263](#)), S534 ([WED-267](#))
- Adang, Rob P.R., S314 ([THU-109](#)), S327 ([THU-138](#))
- Adanir, Haydar, S161 ([THU-058](#)), S336 ([THU-171](#)), S723 ([WED-187-YI](#))
- Adan-Villaescusa, Elena, S287 ([FRI-538](#)), S348 ([FRI-555](#))
- Addy, Carol, S321 ([THU-124](#)), S337 ([THU-174](#))
- Adebayo, Danielle, S209 ([FRI-053](#))
- Adeel, Nirmal, S734 ([SAT-361](#))
- Adelantado, Esther Zamora, S702 ([TOP-139](#))
- Adelmeijer, Jelle, S178 ([WED-068-YI](#))
- Adhoute, Xavier, S447 ([THU-475](#))
- Adlung, Lorenz, S24 ([OS-027-YI](#)), S278 ([WED-534](#))
- Adofina, Lisette, S128 ([THU-320-YI](#)), S281 ([WED-542-YI](#))
- Adori, Csaba, S294 ([SAT-155](#))
- Adorini, Luciano, S124 ([TOP-313](#)), S126 ([THU-316](#))
- Adotti, Valentina, S258 ([SAT-131](#))
- Adrien, Bocquillon, S133 ([THU-335](#))
- Adu, Prince, S40 ([OS-058](#)), S824 ([THU-399-YI](#))
- Adžić, Gordan, S69 ([OS-112-YI](#))
- Aeschbacher, Thomas, S737 ([SAT-371](#)), S750 ([SAT-405](#))
- Affonso, Juliana Marques, S582 ([THU-254-YI](#))
- Affo, Silvia, S24 ([OS-026-YI](#)), S420 ([FRI-474-YI](#))
- Afif, Azizah, S637 ([THU-046](#))
- Afihene, Mary, S395 ([SAT-479-YI](#))
- Afolabi, Seyifunmi, S519 ([WED-225](#))
- Afonso, Natalia, S231 ([FRI-121](#))

*Page numbers for abstracts are followed by the abstract number(s) in parentheses.

Author Index

- Agarwal, Ayush, S201 ([TOP-065](#)), S506 ([TOP-276](#))
- Agarwal, Kosh, S26 ([OS-031](#)), S27 ([OS-033](#)), S75 ([OS-127](#)), S78 ([LBP-001](#)), S79 ([LBP-005](#)), S100 ([LBP-044](#)), S350 ([TOP-553](#)), S388 ([SAT-057](#)), S577 ([THU-235](#)), S709 ([WED-137-YI](#)), S756 ([SAT-421](#)), S759 ([TOP-416-YI](#)), S763 ([FRI-367](#)), S765 ([FRI-374-YI](#)), S771 ([FRI-390](#)), S775 ([FRI-399](#)), S780 ([FRI-410](#)), S793 ([WED-391](#)), S797 ([WED-397](#)), S806 ([WED-361](#)), S807 ([WED-365](#)), S808 ([WED-367](#)), S812 ([WED-376](#)), S812 ([WED-378](#)), S820 ([THU-383](#))
- Agarwal, Samagra, S62 ([OS-098-YI](#)), S208 ([FRI-053](#)), S546 ([WED-298-YI](#))
- Aggarwal, Abhishek, S738 ([SAT-373](#))
- Aggarwal, Arnav, S201 ([TOP-065](#)), S506 ([TOP-276](#))
- Aggarwal, Satish, S719 ([WED-176](#))
- Aggeletopoulou, Ioanna, S830 ([THU-419](#))
- Aghemo, Alessio, S404 ([SAT-502-YI](#)), S406 ([SAT-514](#)), S439 ([THU-447](#)), S470 ([FRI-215-YI](#)), S496 ([FRI-290](#)), S497 ([FRI-294](#)), S500 ([FRI-304](#)), S580 ([THU-245](#)), S666 ([WED-446](#)), S705 ([WED-130](#))
- Agnes, Salvatore, S369 ([SAT-009](#))
- Agnetti, Jean, S432 ([FRI-525](#))
- Agnihotram, Raman, S683 ([WED-486-YI](#))
- Agollah, Germaine D., S72 ([OS-118](#)), S607 ([SAT-203](#))
- Agopian, Vatche, S369 ([SAT-009](#))
- Agrawal, Ankit, S33 ([OS-043](#))
- Agrawal, Nancy, S749 ([SAT-402](#)), S753 ([SAT-411](#)), S753 ([SAT-412](#))
- Agrawal, Sudeep, S615 ([SAT-231](#))
- Agredo, Andrés Felipe Castañeda, S598 ([THU-302](#))
- Aguado, Cristina, S723 ([WED-186](#))
- Aguenoz, M'hommed, S747 ([SAT-397](#))
- Aguilar, Anna, S154 ([SAT-304](#))
- Aguilar, Ferran, S83 ([LBP-012](#)), S157 ([THU-050](#)), S174 ([TOP-073](#)), S188 ([WED-098-YI](#))
- Aguilar, Humberto, S11 ([LBO-006](#))
- Aguilar, Juan Cristobal, S779 ([FRI-409](#))
- Aguilar, Juan Ramón, S627 ([FRI-029](#))
- Aguilar, María Dolores Espinosa, S365 ([TOP-002](#))
- Aguilera Sancho, Victoria, S142 ([SAT-267](#))
- Aguirre Allende, Ignacio, S536 ([WED-271](#))
- Agustiniingsih, Agustiniingsih, S792 ([FRI-444](#))
- Agut, Mireia, S141 ([SAT-262](#))
- Agyei-Nkansah, Adwoa, S395 ([SAT-479-YI](#))
- Ahamada, Aliyya, S222 ([FRI-095](#))
- Ah Lee, Han, S774 ([FRI-397](#))
- Ahl, Liv Grete, S245 ([SAT-090-YI](#))
- Ahlström, Håkan, S550 ([WED-316](#))
- Ahmad, Basil, S523 ([WED-236-YI](#)), S646 ([SAT-444](#))
- Ahmad, Jawad, S114 ([TOP-345](#))
- Ahmed-Belkacem, Rostom, S727 ([TOP-357](#))
- Ahmed, Syed, S62 ([OS-098-YI](#))
- Ahmed, Yeni Ait, S25 ([OS-028](#)), S302 ([SAT-180](#))
- Ahn, Jin Hee, S78 ([LBP-002](#))
- Ahn, Min-Ji, S69 ([OS-113](#))
- Ahn, Richard, S261 ([TOP-564](#))
- Ahn, Sang Bong, S148 ([SAT-284](#)), S473 ([FRI-223](#)), S553 ([WED-323](#)), S654 ([SAT-465](#))
- Ahn, Sang Hoon, S290 ([FRI-545](#)), S481 ([FRI-246](#)), S495 ([FRI-287](#)), S498 ([FRI-296](#)), S535 ([WED-269](#)), S671 ([WED-456](#)), S767 ([FRI-378](#)), S767 ([FRI-379](#)), S774 ([FRI-396](#)), S774 ([FRI-397](#)), S797 ([WED-397](#)), S799 ([WED-404](#)), S818 ([THU-379](#))
- Ahouidi, Ambroise, S743 ([SAT-387](#))
- Aierkenjiang, Malipati, S785 ([FRI-428](#))
- Aigner, Annette, S366 ([TOP-003-YI](#))
- Aigner, Elmar, S500 ([FRI-303](#)), S621 ([FRI-009-YI](#)), S773 ([FRI-394](#))
- Ainora, Maria Elena, S533 ([WED-261-YI](#))
- Ain, Quratul, S263 ([THU-527](#))
- Airey, George, S675 ([WED-469](#)), S752 ([SAT-409](#))
- Airolidi, Aldo, S175 ([TOP-085](#)), S215 ([FRI-078-YI](#)), S376 ([SAT-025](#)), S380 ([SAT-034](#))
- Airolidi, Mario, S451 ([THU-486-YI](#))
- Aishima, Shinichi, S537 ([WED-273](#))
- Aist, Nathan, S474 ([FRI-225](#)), S597 ([THU-298](#))
- Aithal, Guruprasad, S147 ([SAT-280](#)), S148 ([SAT-285-YI](#))
- Ai, Yingjie, S242 ([SAT-081](#)), S275 ([WED-524-YI](#))
- Aizenshtadt, Aleksandra, S294 ([SAT-154-YI](#))
- Ajayi, Omolola, S128 ([THU-320-YI](#))
- Ajaz, Saima, S577 ([THU-235](#)), S780 ([FRI-410](#)), S820 ([THU-383](#))
- Ajdini, Suela, S375 ([SAT-023](#))
- Ajith, Ananya, S353 ([SAT-537](#))
- Akakpo, Jeph, S109 ([FRI-333](#))
- Akamatsu, Nobuhisa, S9 ([LBO-004](#)), S89 ([LBP-026](#)), S374 ([SAT-021](#))
- Akanmu, Alani, S395 ([SAT-479-YI](#))
- Akanni, Wasiu, S48 ([OS-073](#))
- Akarca, Ulus, S80 ([LBP-006](#)), S100 ([LBP-044](#)), S211 ([FRI-067](#)), S805 ([WED-419](#))
- Akarsu, Mesut, S336 ([THU-171](#))
- Akatsuka, Teppei, S123 ([SAT-335](#))
- Akbary, Kutbuddin, S465 ([FRI-203](#)), S515 ([WED-213](#))
- Akhan, Sila, S27 ([OS-033](#))
- Akiyama, Matthew, S684 ([WED-487](#))
- Akpinar, Reha, S19 ([OS-017](#)), S401 ([SAT-494](#)), S438 ([THU-446](#)), S580 ([THU-245](#))
- Aktas, Huseyin, S309 ([THU-100](#))
- Akuta, Norio, S828 ([THU-413](#))
- Akyildiz, Murat, S374 ([SAT-021](#))
- Akyuz, Filiz, S377 ([SAT-028](#)), S551 ([WED-318-YI](#)), S803 ([WED-413](#))
- Ala, Aftab, S709 ([WED-137-YI](#)), S714 ([WED-164](#)), S725 ([WED-192](#))
- Alabdulgader, Abdulrahman, S548 ([WED-305](#))
- AlAhmed, Reem S., S500 ([FRI-304](#))
- Alaimo, Domenico, S252 ([SAT-113](#))
- Alam, Imtiaz, S514 ([WED-211](#))
- Alam, Shahinul, S158 ([THU-052](#)), S167 ([THU-078](#)), S615 ([SAT-230](#))
- Alarcón, Cristina, S453 ([THU-493](#))
- Alarcon, Francisca Cuenca, S329 ([THU-154-YI](#))
- Alard, Berenice, S171 ([THU-088](#))
- Alaswad, Ahmed, S21 ([OS-021-YI](#))
- Álava, Ane, S416 ([FRI-464](#))
- Al-Ayoubi, Jana, S205 ([FRI-044-YI](#))
- Alazawi, William, S528 ([WED-248](#)), S538 ([WED-275](#)), S578 ([THU-236-YI](#))
- Alba, Laura, S489 ([FRI-269](#))
- Albano, Emanuele, S421 ([FRI-479-YI](#))
- Albenmoussa, Ali, S500 ([FRI-304](#))
- Alberzoni, Chiara, S325 ([THU-133-YI](#))
- Albhaisi, Somaya, S209 ([FRI-053](#))
- Albillos, Agustín, S52 ([OS-080](#)), S61 ([OS-096-YI](#)), S157 ([THU-050](#)), S161 ([THU-057-YI](#)), S188 ([WED-098-YI](#)), S189 ([WED-100-YI](#)), S238 ([SAT-069](#)), S277 ([WED-530-YI](#)), S468 ([FRI-211](#)), S700 ([FRI-171](#))
- Albiol, Joaquim, S362 ([WED-016](#)), S364 ([WED-028](#))
- Alblas, Gabrielle, S492 ([FRI-278](#))
- Alborelli, Ilaria, S291 ([TOP-150-YI](#))
- Albrecht, Vincent, S193 ([WED-111](#))
- Albuquerque, Miguel, S412 ([FRI-454](#)), S719 ([WED-177](#))
- Alcala, Ronald, S808 ([WED-366](#))
- Alcalde, Carlos, S693 ([FRI-153](#))
- Alcaraz, Estefania, S46 ([OS-069](#)), S177 ([WED-059](#))
- Aldana, Andres Gomez, S334 ([THU-164-YI](#))
- Aldersley, Mark, S765 ([FRI-374-YI](#))
- Alderslieste, Yasser A., S309 ([THU-100](#))
- Aleksieva, Niya, S186 ([WED-090](#))
- Aleman, Soo, S92 ([LBP-029](#)), S100 ([LBP-044](#)), S758 ([TOP-400](#)), S759 ([TOP-416-YI](#)), S777 ([FRI-406](#)), S785 ([FRI-427](#)), S793 ([WED-391](#)), S794 ([WED-392](#)), S795 ([WED-394](#)), S836 ([THU-374](#))
- Aleman, Merce Roget, S329 ([THU-154-YI](#))
- Alenzi, Maram, S129 ([THU-322-YI](#))
- Alessandria, Carlo, S30 ([OS-038-YI](#)), S157 ([THU-050](#)), S161 ([THU-057-YI](#)), S174 ([TOP-084](#)), S188 ([WED-098-YI](#)), S193 ([WED-112](#)), S199 ([TOP-062](#)), S200 ([TOP-064-YI](#)), S210 ([FRI-056-YI](#)), S215 ([FRI-078-YI](#))
- Alessi, Nicola, S252 ([SAT-113](#))
- Alexander, James, S657 ([WED-423](#))
- Alexandre, Humbert, S49 ([OS-074](#))
- Alex, George, S707 ([WED-133](#))

- Alexia, Rouland, S508 (WED-194), S538 (WED-278)
- Alexopoulos, Theodoros, S208 (FRI-052), S214 (FRI-076)
- Alexopoulou, Alexandra, S208 (FRI-052), S208 (FRI-053), S214 (FRI-076), S798 (WED-403)
- Alfaite, Dulce, S802 (WED-410)
- Alfano, Vincenzo, S280 (WED-540-YI)
- Alfaro-Jiménez, Kendall, S64 (OS-101-YI), S112 (FRI-343-YI), S419 (FRI-472-YI), S562 (TOP-229-YI), S569 (THU-210)
- Alghamdi, Abdullah S, S671 (WED-458)
- Alghamdi, Saad, S496 (FRI-291), S500 (FRI-304)
- Al-Hamoudi, Waleed K, S671 (WED-458)
- Al-Hamoudi, Waleed K., S496 (FRI-291), S500 (FRI-304)
- Al-Hasani, Aya, S634 (THU-033)
- Alhassan, Ibrahim, S673 (WED-463)
- Aliabadi, Elmira, S730 (TOP-369)
- Aliane, Verena, S716 (WED-170)
- Ali, Aya, S418 (FRI-470)
- Alicia, Delorme, S360 (WED-008)
- Ali, Dina, S232 (FRI-123)
- Ali, Farah Imdad, S555 (WED-330), S561 (WED-348)
- Alimenti, Eleonora, S396 (SAT-481-YI), S397 (SAT-482), S401 (SAT-493-YI)
- Ali, Nida, S686 (WED-494)
- Alipour, Zahra, S411 (SAT-530)
- Ali, Sajid, S3 (GS-005)
- Alisi, Anna, S289 (FRI-544)
- Alitti, Clémentine, S441 (THU-459-YI)
- AlJabri, Abdullah, S76 (OS-125)
- Aljuraysan, Ahmed, S172 (THU-090)
- Alkan, Sevil, S805 (WED-418)
- Alkhanishvili, Zurab, S677 (WED-473)
- Alkhazashvili, Maia, S677 (WED-473), S825 (THU-404)
- Alkhouri, Naim, S4 (GS-006), S37 (OS-051), S72 (OS-118), S72 (OS-119), S76 (OS-125), S84 (LBP-014), S88 (LBP-024), S146 (SAT-278), S463 (FRI-198), S464 (FRI-199), S481 (FRI-247), S482 (FRI-249), S504 (TOP-253), S505 (TOP-264), S507 (TOP-300), S510 (WED-199), S511 (WED-200), S511 (WED-201), S511 (WED-202), S515 (WED-212), S518 (WED-223), S522 (WED-234), S535 (WED-268), S535 (WED-270), S542 (WED-285), S544 (WED-294), S547 (WED-303), S556 (WED-334), S576 (THU-233), S579 (THU-242), S603 (SAT-195), S607 (SAT-202), S607 (SAT-203), S609 (SAT-208), S613 (SAT-224), S641 (SAT-432), S642 (SAT-434), S648 (SAT-450), S654 (SAT-466), S709 (WED-151), S809 (WED-371)
- Allabauer, Ida, S356 (SAT-546)
- Allah, Belimi Hibat, S209 (FRI-053)
- Allaire, Manon, S50 (OS-077), S239 (SAT-071), S349 (TOP-552), S367 (TOP-005), S413 (FRI-456), S441 (THU-458), S444 (THU-466)
- Alla, Manasa, S149 (SAT-290-YI), S440 (THU-456), S454 (THU-498), S701 (FRI-173), S720 (WED-180)
- Allam, Dalia, S209 (FRI-053)
- Allan, Richard, S337 (THU-174)
- Allard, Guillaume, S640 (SAT-430)
- Allard, Marc Antoine, S452 (THU-491)
- Allegretti, Andrew S., S30 (OS-038-YI), S199 (TOP-062), S200 (TOP-064-YI), S242 (SAT-082), S638 (SAT-426-YI)
- Allen, Alina M, S504 (TOP-252-YI), S528 (WED-248), S533 (WED-263)
- Allen, Alina M., S470 (FRI-218), S651 (SAT-456)
- Allen, Christopher, S212 (FRI-069)
- Allende, Daniela, S76 (OS-125)
- Aller, Rocío, S71 (OS-116), S596 (THU-296), S640 (SAT-429)
- Allgar, Victoria, S654 (SAT-467)
- Allier, Yoann, S670 (WED-455)
- Allison, Michael, S127 (THU-317), S145 (SAT-274), S147 (SAT-280), S148 (SAT-285-YI)
- Allo, Gabriel, S223 (FRI-100)
- Allsworth, Max, S195 (WED-117)
- Allweiss, Lena, S74 (OS-122), S733 (SAT-342-YI), S738 (SAT-373)
- Almaghrabi, Majed, S671 (WED-458)
- Almahanna, Yousef, S84 (LBP-014)
- Almahroos, Amal, S290 (TOP-147)
- Al-Mahtab, Mamun, S158 (THU-052), S167 (THU-078), S615 (SAT-230)
- Almeida, Ana Arencibia, S318 (THU-118), S717 (WED-172)
- Almeida, Bruna, S128 (THU-320-YI)
- Almeida, Gustavo, S351 (SAT-533)
- Almeida, Mathieu, S159 (THU-053)
- Almholt, Kasper, S79 (LBP-003)
- AlNajjar, Asma, S671 (WED-458)
- AlOmair, Waleed S., S500 (FRI-304)
- Aloman, Costica, S8 (LBO-003)
- Alonso, Ana, S635 (THU-039-YI)
- Alonso, Cristina, S529 (WED-251), S640 (SAT-429), S693 (FRI-153)
- Alonso, Ines, S431 (FRI-521)
- Alonso, Maria Luisa Manzano, S818 (THU-381)
- Alonso-Peña, Marta, S337 (THU-172)
- Alpert, Lauren, S659 (WED-428-YI)
- Alqahtani, Saleh, S472 (FRI-221), S496 (FRI-291), S638 (SAT-425), S643 (SAT-438)
- Alqahtani, Saleh A, S671 (WED-458)
- Alqahtani, Saleh A., S500 (FRI-304)
- Alqedrh, Mohannad, S246 (SAT-093-YI)
- Alric, Laurent, S28 (OS-034), S41 (OS-060), S802 (WED-410)
- Alromaih, Norah Jamal, S671 (WED-458)
- Alsaed, Mohamad, S374 (SAT-021)
- Alsaqal, Salem, S550 (WED-316)
- Al-Shakhshir, Sarah, S309 (THU-099-YI)
- Al-sharif, Aya M., S491 (FRI-273-YI)
- Al-Sharif, Lubna, S483 (FRI-254)
- Alshiwanna, Basheer, S657 (WED-422), S676 (WED-470)
- Alsina, Tania Hernaez, S318 (THU-118)
- Alswat, Khalid A, S671 (WED-458)
- Alswat, Khalid A., S496 (FRI-291), S624 (FRI-020), S643 (SAT-438)
- Altadill, Ariadna, S141 (SAT-262), S233 (FRI-126)
- Altajar, Sarah, S518 (WED-222)
- Al-Tawfiq, Jaffar A., S652 (SAT-462-YI)
- Altekoester, Jannis, S368 (SAT-008)
- Altepeter, Laura, S203 (FRI-039)
- Altieri, Anna, S565 (THU-199)
- Altikes, Renato, S619 (SAT-248)
- Altmann, Philipp, S223 (FRI-098), S224 (FRI-103-YI)
- Altunal, Lütfiye Nilsun, S805 (WED-418)
- Alunni, Gianluca, S475 (FRI-230-YI)
- Aluvihare, Varuna, S388 (SAT-055), S388 (SAT-057), S709 (WED-137-YI)
- Alvarado, Ruben, S391 (TOP-512-YI)
- Alvarado-Tapias, Edilmar, S85 (LBP-016), S238 (SAT-069), S255 (SAT-123), S355 (SAT-543)
- Álvares-da-Silva, Mario, S80 (LBP-006), S83 (LBP-012), S161 (THU-058), S208 (FRI-053), S219 (FRI-088), S334 (THU-164-YI)
- Alvarez-Alvarez, Ismael, S103 (TOP-350-YI)
- Alvarez, Angel Caunedo, S559 (WED-341)
- Álvarez, Ángeles, S266 (THU-539)
- Álvarez-Cancelo, Ana, S337 (THU-172)
- Alvarez, Carolina Almohalla, S377 (SAT-027)
- Álvarez, Juan, S207 (FRI-051)
- Alvarez, Maria, S40 (OS-058), S824 (THU-399-YI)
- Alvarez, Marife, S541 (WED-284-YI)
- Álvarez-Mon, Melchor, S189 (WED-100-YI)
- Álvarez-Ossorio, Ángela Rojas, S587 (THU-268), S593 (THU-287), S596 (THU-296)
- Alvarez, Patricia, S154 (SAT-304)
- Alvarez, Paula Fernandez, S559 (WED-341)
- Alvarez-Silva, Camila, S47 (OS-071-YI), S47 (OS-072-YI), S283 (WED-548)
- Álvarez, Sonia, S398 (SAT-485)
- Alvaro, Domenico, S96 (LBP-038), S175 (TOP-085), S215 (FRI-077-YI), S306 (THU-093), S310 (THU-101), S422 (FRI-481)
- Alves, Alexandre, S416 (FRI-465)
- Alves, Filipe Caseiro, S21 (OS-020)
- Alves, Margarida, S681 (WED-481)
- Alzaabi, Mohammed, S836 (THU-374)
- Alzaidi, Jabir A, S671 (WED-458)
- Alzanbagi, Adnan, S671 (WED-458)
- Amaddeo, Giuliana, S50 (OS-077), S367 (TOP-005), S413 (FRI-456), S444 (THU-466), S453 (THU-494), S456 (THU-503), S720 (WED-178), S743 (SAT-386-YI), S784 (FRI-425)
- Amado, Luis Enrique Morano, S26 (OS-030)
- Amador, Alberto, S29 (OS-037)

Author Index

- Amagase, Hiromasa, S42 ([OS-062](#))
 Amangurbanova, Maral, S522 ([WED-235](#))
 Amara, Suneetha, S443 ([THU-464](#))
 Amato, Fabrizio, S475 ([FRI-230-YI](#)), S480 ([FRI-243](#))
 Ambery, Philip, S238 ([SAT-069](#))
 Ambrosini, Gina, S519 ([WED-225](#))
 Ambros, Raphael, S250 ([SAT-106](#))
 Ambrozkiwicz, Filip, S349 ([FRI-556](#))
 Ameer, Abutaleb, S736 ([SAT-366](#))
 Ameneni, Gagana, S547 ([WED-303](#))
 Amer, Johnny, S63 ([OS-100](#)), S95 ([LBP-035](#)), S268 ([THU-547](#)), S563 ([THU-194](#)), S564 ([THU-197](#)), S779 ([FRI-408](#))
 Amiama, Clara, S398 ([SAT-485](#))
 Amigot-Sánchez, Rafael, S665 ([WED-442](#)), S751 ([SAT-407](#))
 Aminian, Ali, S76 ([OS-125](#))
 Aminuddin, Liyana Dhamirah, S552 ([WED-321](#))
 Amiridze, Natalja, S25 ([OS-028](#))
 Amiri, Ramin, S128 ([THU-320-YI](#))
 Amna, Abichou-Klich, S508 ([WED-194](#))
 Amor, Carmen, S398 ([SAT-485](#))
 Ampazis, Odysseas, S830 ([THU-419](#))
 Ampuero, Javier, S427 ([FRI-501](#)), S587 ([THU-268](#)), S593 ([THU-287](#)), S700 ([FRI-171](#)), S717 ([WED-172](#))
 Anagnostou, Olga, S823 ([THU-398](#))
 Ananchuensook, Prooksa, S196 ([WED-120](#)), S221 ([FRI-093](#)), S749 ([SAT-403](#))
 Anand, Abhinav, S201 ([TOP-065](#))
 Anandanadarajah, Sanjayan, S246 ([SAT-093-YI](#))
 Anand, Anil Chandra, S219 ([FRI-088](#))
 Anastasiy, Igor, S87 ([LBP-020](#))
 Andaluz, Irene, S705 ([WED-129](#))
 Andersen, Birgitte, S574 ([THU-227](#)), S581 ([THU-248](#))
 Andersen, Jesper, S419 ([FRI-472-YI](#)), S426 ([FRI-498-YI](#))
 Andersen, Klaus Kaae, S709 ([WED-138](#))
 Andersen, Maja, S421 ([FRI-478](#)), S568 ([THU-208](#))
 Andersen, Mette Lehmann, S139 ([SAT-255](#))
 Andersen, Peter, S41 ([OS-059](#)), S47 ([OS-072-YI](#)), S77 ([OS-126](#)), S137 ([SAT-250](#)), S139 ([SAT-255](#)), S142 ([SAT-266](#)), S153 ([SAT-298](#)), S205 ([FRI-045](#)), S466 ([FRI-206-YI](#)), S503 ([TOP-241-YI](#)), S510 ([WED-199](#)), S620 ([TOP-012](#)), S623 ([FRI-017](#))
 Anders, Margarita, S9 ([LBO-004](#)), S89 ([LBP-026](#))
 Anderson, Blaire, S231 ([FRI-122](#))
 Anderson, Katie, S26 ([OS-031](#)), S811 ([WED-375](#))
 Anderson, Mark, S675 ([WED-469](#)), S775 ([FRI-399](#)), S809 ([WED-371](#))
 Anderson, Motswedi, S753 ([SAT-413](#))
 Anderson, Sarah, S789 ([FRI-436](#))
 Andersson, Emma, S66 ([OS-107-YI](#)), S697 ([FRI-163-YI](#))
 Andersson, Maria, S754 ([SAT-414](#))
 Andersson, Monique, S756 ([SAT-421](#))
 Andrade, Raul J., S18 ([OS-015](#)), S44 ([OS-066-YI](#)), S103 ([TOP-350-YI](#)), S107 ([FRI-324](#)), S329 ([THU-154-YI](#)), S341 ([THU-182](#)), S344 ([THU-189](#)), S374 ([SAT-021](#)), S700 ([FRI-171](#))
 André da Silva, Rafael, S113 ([FRI-348](#))
 André-Dumont, Stéphanie, S151 ([SAT-293-YI](#)), S473 ([FRI-224](#)), S546 ([WED-297-YI](#))
 Andreichenko, Irina, S268 ([THU-542](#))
 Andreis, Alessandro, S475 ([FRI-230-YI](#)), S480 ([FRI-243](#))
 Andreola, Fausto, S17 ([OS-014-YI](#)), S161 ([THU-057-YI](#)), S179 ([WED-069](#)), S182 ([WED-078](#)), S182 ([WED-080](#)), S188 ([WED-099-YI](#))
 Andreone, Pietro, S80 ([LBP-006](#)), S92 ([LBP-029](#)), S98 ([LBP-040](#)), S310 ([THU-101](#))
 Andres, Duarte Rojo, S219 ([FRI-088](#))
 Andreu, Rocío, S723 ([WED-186](#))
 Andrews, Charles P., S72 ([OS-119](#))
 Andrews, Tallulah, S31 ([OS-040-YI](#))
 Andrieux, Geoffroy, S693 ([FRI-152-YI](#))
 Androutsakos, Theodoros, S798 ([WED-403](#))
 Aneiros, Oni, S544 ([WED-294](#))
 Anfuso, Beatrice, S429 ([FRI-516-YI](#)), S699 ([FRI-167-YI](#))
 Ang, Celina, S51 ([OS-078-YI](#)), S443 ([THU-464](#))
 Angchaisuksiri, Pantep, S221 ([FRI-093](#))
 Angelakis, Athanasios, S561 ([WED-347](#))
 Angel, Dylan, S246 ([SAT-093-YI](#))
 Angel, Enrique, S194 ([WED-113](#))
 Angelico, Roberta, S369 ([SAT-009](#))
 Angelini, Giulia, S516 ([WED-215](#)), S545 ([WED-296](#))
 Angeli, Paolo, S9 ([LBO-004](#)), S28 ([OS-035-YI](#)), S30 ([OS-038-YI](#)), S83 ([LBP-012](#)), S89 ([LBP-026](#)), S157 ([THU-050](#)), S161 ([THU-057-YI](#)), S174 ([TOP-084](#)), S188 ([WED-098-YI](#)), S193 ([WED-112](#)), S199 ([TOP-062](#)), S200 ([TOP-064-YI](#)), S206 ([FRI-047-YI](#)), S212 ([FRI-068](#)), S215 ([FRI-078-YI](#)), S224 ([FRI-101-YI](#)), S243 ([SAT-083-YI](#)), S246 ([SAT-094-YI](#)), S700 ([FRI-171](#)), S830 ([THU-420](#))
 Angelis, Fernando De, S829 ([THU-414](#))
 Angerilli, Valentina, S438 ([THU-446](#))
 Angiolillo, Martina, S451 ([THU-486-YI](#))
 Anglero-Rodriguez, Yessenia, S58 ([OS-090](#))
 Anglicheau, Dany, S372 ([SAT-016](#))
 Angrisani, Debora, S96 ([LBP-038](#)), S306 ([THU-093](#))
 Angulo-Mcgrath, Isabela, S316 ([THU-114](#))
 Anirvan, Prajna, S163 ([THU-067](#)), S248 ([SAT-099-YI](#)), S285 ([WED-554](#)), S488 ([FRI-266-YI](#))
 Aniszewska, Małgorzata, S820 ([THU-387](#)), S825 ([THU-403](#))
 An, Jihyun, S148 ([SAT-284](#)), S152 ([SAT-296](#)), S473 ([FRI-223](#)), S477 ([FRI-234](#)), S553 ([WED-323](#)), S654 ([SAT-465](#))
 Anjum, Syed Muhammad Muneeb, S192 ([WED-109](#))
 An, Kyongman, S82 ([LBP-011](#))
 An, Mahru, S97 ([LBP-039](#)), S261 ([TOP-564](#))
 Anna Niro, Grazia, S310 ([THU-101](#))
 Anna, Piekarska, S685 ([WED-493-YI](#)), S834 ([THU-367-YI](#))
 Anne, Varaut, S784 ([FRI-425](#))
 Annicchiarico, Brigida Eleonora, S703 ([TOP-142-YI](#))
 Anolli, Maria Paola, S73 ([OS-120](#)), S344 ([THU-190](#)), S781 ([FRI-412](#)), S793 ([WED-391](#)), S798 ([WED-399-YI](#)), S804 ([WED-414](#))
 Ansari, Azim, S752 ([SAT-409](#))
 Anstee, Quentin M., S4 ([GS-006](#)), S79 ([LBP-003](#)), S95 ([LBP-036](#)), S467 ([FRI-208](#)), S509 ([WED-196](#)), S603 ([SAT-195](#)), S611 ([SAT-214](#)), S629 ([THU-009](#))
 Anta, Julia Arribas, S238 ([SAT-068](#))
 Antal-Szalmás, Péter, S169 ([THU-080-YI](#)), S313 ([THU-106-YI](#))
 Antoine, Corinne, S369 ([SAT-010](#)), S372 ([SAT-016](#))
 Anton, Aina, S15 ([OS-010](#)), S179 ([WED-070](#))
 Antonelli, Barbara, S388 ([SAT-056](#)), S396 ([SAT-481-YI](#)), S397 ([SAT-482](#))
 Antoniello, Deana, S26 ([OS-031](#))
 Antonini, Teresa, S22 ([OS-022](#)), S168 ([THU-079](#)), S172 ([THU-092](#)), S367 ([TOP-005](#)), S385 ([SAT-048](#)), S763 ([FRI-370](#))
 Antunes, Nuno, S18 ([OS-016](#)), S80 ([LBP-006](#)), S91 ([LBP-028](#)), S312 ([THU-105](#))
 Antwi, Milton, S57 ([OS-089-YI](#)), S278 ([WED-531](#))
 Antwi, Samuel, S396 ([SAT-479-YI](#))
 Anty, Rodolphe, S6 ([GS-010](#)), S61 ([OS-097](#)), S168 ([THU-079](#)), S369 ([SAT-010](#)), S385 ([SAT-048](#)), S444 ([THU-466](#))
 Aoki, Yutaka, S513 ([WED-208](#))
 Aoua, Sherin Al, S528 ([WED-249](#))
 Aoudjehane, Lynda, S729 ([TOP-360-YI](#))
 Apecechea, Nikolas Scheffer, S37 ([OS-052](#)), S464 ([FRI-201](#))
 Apodaka-Biguri, Maider, S64 ([OS-101-YI](#)), S112 ([FRI-343-YI](#)), S419 ([FRI-472-YI](#)), S562 ([TOP-229-YI](#)), S569 ([THU-210](#))
 Apostolova, Nadezda, S266 ([THU-539](#)), S592 ([THU-283](#))
 Apostolov, Ross, S547 ([WED-299](#))
 Appanna, Gautham, S408 ([SAT-521](#))
 Applegate, Tanya, S776 ([FRI-403](#))
 Aprile, Francesca, S376 ([SAT-025](#)), S380 ([SAT-034](#))
 Aqel, Bashar, S43 ([OS-064](#))
 Aquilini, Donatella, S674 ([WED-467-YI](#))
 Aquino, Marco, S554 ([WED-326](#)), S556 ([WED-333](#))

- Aqul, Amal A., S323 (THU-129)
- Arab, Juan Pablo, S30 (OS-038-YI), S84 (LBP-014), S146 (SAT-278), S199 (TOP-062), S200 (TOP-064-YI), S379 (SAT-033)
- Aracil, Carlos, S453 (THU-493), S765 (FRI-373)
- Aracil, Carlos Ferre, S85 (LBP-016)
- Arai, Taeang, S248 (SAT-101), S537 (WED-273), S616 (SAT-236)
- Arai, Yasuaki, S3 (GS-005)
- Aranguren, África Vales, S693 (FRI-152-YI)
- Aras, Nermin, S407 (SAT-519)
- Araujo, Joana Gonçalves, S349 (TOP-552), S415 (FRI-459)
- Aravinthan, Aloysious, S209 (FRI-053)
- Arbelaiz, Ander, S432 (FRI-525)
- Árbol, Luis Ruiz Del, S231 (FRI-121)
- Arcari, Ivan, S497 (FRI-294)
- Arcas, Cristina, S664 (WED-440)
- Archer, Ann, S647 (SAT-448), S651 (SAT-457-YI)
- Archibald, Marie, S630 (THU-010)
- Arcusa, Ingrid, S822 (THU-395)
- Ardevol, Alba, S192 (WED-107)
- Arechederra, Maria, S287 (FRI-538), S348 (FRI-555), S416 (FRI-464)
- Arellano, Encarnación Ramirez, S779 (FRI-409)
- Arena, Ilaria, S332 (THU-161)
- Arena, Paola, S698 (FRI-166)
- Arena, Umberto, S258 (SAT-131)
- Arencibia Almeida, Ana, S329 (THU-154-YI), S330 (THU-155)
- Arends, Joop, S604 (SAT-196)
- Aretxabaleta, Nerea Hernández, S365 (TOP-002)
- Argemí, Josep Maria, S15 (OS-010), S348 (FRI-555), S355 (SAT-543), S455 (THU-501)
- Argenziano, Maria Eva, S544 (WED-293)
- Arias, Ana, S365 (TOP-002)
- Arias-Sánchez, Sara, S337 (THU-172)
- Aricha, Revital, S268 (THU-547), S295 (SAT-158)
- Arici, Sena, S785 (FRI-427)
- Arietti, Natalia, S453 (THU-493)
- Ariño, Silvia, S13 (OS-005-YI), S24 (OS-026-YI), S420 (FRI-474-YI)
- Ariungerel, Nomin, S82 (LBP-011)
- Arizmendi, Brian, S608 (SAT-207)
- Arizpe, Andre, S812 (WED-376)
- Ankan, Cigdem, S54 (OS-083), S374 (SAT-021), S712 (WED-160)
- Armandi, Angelo, S2 (GS-004), S38 (OS-054), S61 (OS-096-YI), S461 (FRI-194-YI), S475 (FRI-230-YI), S480 (FRI-243), S483 (FRI-251-YI), S484 (FRI-255), S496 (FRI-290), S501 (FRI-314), S522 (WED-233-YI), S525 (WED-243-YI), S544 (WED-293)
- Armengol, Carolina, S417 (FRI-466-YI)
- Armisen, Javier, S93 (LBP-031)
- Armstrong, Matthew, S472 (FRI-220-YI)
- Armstrong, Paul, S450 (THU-485-YI)
- Arnaud Seyrig, Jacques, S640 (SAT-430)
- Arnold, Jorge, S536 (WED-271)
- Aron-Wisniewsky, Judith, S493 (FRI-282), S512 (WED-206), S533 (WED-262)
- Aroob, Subas, S192 (WED-109)
- Arora, Anil, S158 (THU-052), S167 (THU-078), S209 (FRI-053), S475 (FRI-231)
- Arora, Jaiveer, S153 (SAT-299)
- Arora, Umang, S506 (TOP-276)
- Arora, Vinod, S158 (THU-052), S164 (THU-070), S167 (THU-078), S177 (WED-057)
- Arpi, Maria Luisa, S557 (WED-336)
- Arpurt, Jean-Pierre, S73 (OS-120), S793 (WED-391)
- Arrabal, Oscar, S455 (THU-500)
- Arrese, Marco, S80 (LBP-006), S83 (LBP-012), S84 (LBP-014), S219 (FRI-088), S535 (WED-270), S536 (WED-271)
- Arroyave, Esteban, S823 (THU-396)
- Arroyo-López, Victor, S71 (OS-116), S596 (THU-296)
- Arroyo, Vicente, S9 (LBO-004), S16 (OS-011), S83 (LBP-012), S89 (LBP-026), S157 (THU-049), S157 (THU-050), S159 (THU-055), S161 (THU-057-YI), S174 (TOP-073), S174 (TOP-084), S177 (WED-059), S185 (WED-087), S188 (WED-098-YI), S193 (WED-112), S203 (FRI-039), S231 (FRI-121), S700 (FRI-171)
- Arslanow, Anita, S41 (OS-059), S503 (TOP-241-YI)
- Arsyad, Nik Ma Nik, S209 (FRI-053)
- Artaza, Tomás, S139 (SAT-257), S142 (SAT-267), S828 (THU-411)
- Arteaga, Mireya, S157 (THU-049)
- Arteaga, Noah, S373 (SAT-019)
- Arteta, Beatriz, S64 (OS-101-YI), S431 (FRI-521)
- Artru, Florent, S53 (OS-081), S116 (SAT-315), S156 (TOP-108), S168 (THU-079), S383 (SAT-043), S705 (WED-129)
- Artusa, Fabian, S52 (OS-079-YI), S442 (THU-463)
- Artyomenko, Alexander, S339 (THU-178)
- Arumugam, Manimozhiyan, S47 (OS-071-YI), S47 (OS-072-YI), S159 (THU-055), S283 (WED-548)
- Arun, J Sanyal, S476 (FRI-231)
- Arvaniti, Pinelopi, S291 (TOP-149-YI), S293 (SAT-153-YI), S710 (WED-153)
- Asada, Shohei, S175 (TOP-096)
- Asahina, Yasuhiro, S828 (THU-413)
- Asati, Pankaj, S476 (FRI-231)
- Asenjo-Lobos, Claudia, S195 (WED-117)
- Asensio, Julia Peña, S738 (SAT-374-YI), S768 (FRI-381)
- Asensio, Maitane, S432 (FRI-523), S433 (FRI-526)
- Aseyiga, Adepeju, S88 (LBP-022)
- Asgharpour, Amon, S1 (GS-001), S2 (GS-004), S38 (OS-054)
- Ashab, Eshita, S615 (SAT-230)
- Ashdhir, Prachis, S239 (SAT-070)
- Ashfaq-Khan, Muhammad, S297 (SAT-164-YI)
- Ashurova, Rezeda, S682 (WED-484)
- Asibey, Shadrack, S395 (SAT-479-YI)
- Asif, Ayma, S360 (SAT-558)
- Askari, Fred, S714 (WED-164)
- Askew, Clinton, S690 (WED-514)
- Askgaard, Gro, S149 (SAT-286-YI)
- Aslan, Rahmi, S161 (THU-058)
- Aspden, Leah, S381 (SAT-039)
- Aspichueta, Patricia, S32 (OS-042-YI), S64 (OS-101-YI), S112 (FRI-343-YI), S419 (FRI-472-YI), S536 (WED-271), S562 (TOP-229-YI), S569 (THU-210), S694 (FRI-153)
- Aspinall, Richard, S718 (WED-173)
- Aspite, Silvia, S258 (SAT-131)
- Aspord, Caroline, S744 (SAT-389)
- Asrani, Sumeet, S30 (OS-038-YI), S161 (THU-058), S163 (THU-060), S199 (TOP-062), S200 (TOP-064-YI)
- Assawasuwannakit, Suraphon, S410 (SAT-529)
- Asselah, Tarik, S1 (GS-002), S26 (OS-030), S27 (OS-033), S41 (OS-060), S75 (OS-127), S737 (SAT-371), S758 (TOP-400), S764 (FRI-371), S796 (WED-395), S800 (WED-407), S813 (WED-379), S814 (WED-382)
- Assenat, Eric, S115 (SAT-306)
- Assy, Prof Nimer, S172 (THU-091)
- Asteljoki, Juho, S562 (TOP-240-YI)
- Astudillo, Alma, S568 (THU-209)
- Atef, Remon, S491 (FRI-273-YI)
- Ates-Öz, Edanur, S6 (GS-008), S351 (SAT-533), S728 (TOP-359-YI)
- Athari, Annette, S716 (WED-170)
- Athwal, Varinder, S67 (OS-109), S650 (SAT-454-YI)
- Atkinson, Stephen, S130 (THU-326), S567 (THU-203)
- Atkinson, Stephen R, S14 (OS-008-YI)
- Atkinson, Stephen R., S127 (THU-317), S145 (SAT-274)
- Atsukawa, Masanori, S248 (SAT-101), S537 (WED-273), S616 (SAT-236)
- Atthakitmongkol, Thanapat, S796 (WED-396)
- Attia, Yasmeen, S418 (FRI-470), S570 (THU-213), S583 (THU-255)
- Attridge-Smith, James, S646 (SAT-444)
- Aubé, Christophe, S68 (OS-110)
- Auch, Benjamin, S46 (OS-070)
- Audière, Stéphane, S550 (WED-317)
- Augustin, Jeremy, S720 (WED-178), S729 (TOP-360-YI)
- Auletta, Salvatore, S173 (TOP-072)
- Aurélié, Vielle-Marchiset, S49 (OS-074)

Author Index

- Auriemma, Alessandra, S51 ([OS-078-YI](#)), S446 ([THU-472-YI](#))
- Aurrekoetxea, Igor, S64 ([OS-101-YI](#)), S112 ([FRI-343-YI](#)), S419 ([FRI-472-YI](#)), S562 ([TOP-229-YI](#)), S569 ([THU-210](#))
- Austin, Andrew, S127 ([THU-317](#)), S145 ([SAT-274](#))
- Autret, Axelle, S109 ([FRI-333](#))
- Auwerx, Joeri, S807 ([WED-363](#))
- Auzinger, Georg, S44 ([OS-065](#))
- Avades, Tamar, S153 ([SAT-299](#))
- Avdi, Aikaterini, S570 ([THU-214](#))
- Averhoff, Francisco, S677 ([WED-473](#)), S825 ([THU-404](#))
- Avery, Leah, S630 ([THU-015-YI](#))
- Avian, Alexander, S383 ([SAT-042](#))
- Avila, Jose Efren Barragan, S65 ([OS-103](#))
- Avila, Matias A., S265 ([THU-533](#)), S287 ([FRI-538](#)), S348 ([FRI-555](#)), S416 ([FRI-464](#)), S417 ([FRI-466-YI](#))
- Avitabile, Emma, S13 ([OS-005-YI](#))
- Avolio, Alfonso, S368 ([SAT-009](#))
- Avramopoulou, Evdoxia, S798 ([WED-403](#)), S830 ([THU-419](#))
- Awad, Reham Awad, S491 ([FRI-273-YI](#))
- Awosika, Nichola, S445 ([THU-471-YI](#))
- Awuku, Yaw, S395 ([SAT-479-YI](#))
- Ayada, Ibrahim, S464 ([FRI-200](#)), S604 ([SAT-197-YI](#)), S606 ([SAT-200-YI](#)), S652 ([SAT-462-YI](#))
- Ayawin, Joshua, S395 ([SAT-479-YI](#))
- Aydemir, Esmâ Aslıhan, S805 ([WED-418](#))
- Aydemir, Neslihan Güneş, S723 ([WED-187-YI](#))
- Aydin, Selda, S823 ([THU-397-YI](#))
- Ayonrinde, Oyekoya, S275 ([WED-526](#)), S483 ([FRI-250](#)), S487 ([FRI-263](#)), S519 ([WED-225](#)), S655 ([SAT-471](#))
- Ayoub, Walid S, S39 ([OS-055](#)), S200 ([TOP-063](#))
- Azaceta, María Del Barrio, S318 ([THU-118](#))
- Azariadis, Kalliopi, S322 ([THU-126](#)), S325 ([THU-134](#))
- Azcon, Javier Ramon, S46 ([OS-069](#))
- Azevedo, Vittoria Zambon, S493 ([FRI-282](#)), S636 ([THU-044](#))
- Azimova, Dinara, S812 ([WED-377](#))
- Aziz, Fatima, S157 ([THU-049](#))
- Aziz, Karim, S520 ([WED-227](#))
- Azkargorta, Mikel, S50 ([OS-076-YI](#))
- Azkona, María, S416 ([FRI-464](#))
- Azoulay, Daniel, S370 ([SAT-011](#)), S378 ([SAT-029](#)), S385 ([SAT-049](#)), S718 ([WED-174](#))
- Azulay, Orly, S548 ([WED-304](#)), S834 ([THU-371](#))
- Azuma, Koichi, S42 ([OS-062](#))
- Azzaroli, Francesco, S238 ([SAT-068](#)), S241 ([SAT-078-YI](#)), S399 ([SAT-490](#)), S704 ([TOP-143-YI](#)), S818 ([THU-381](#))
- Azzolina, Antonina, S601 ([TOP-193](#))
- Baak, L.C., S213 ([FRI-074-YI](#)), S314 ([THU-109](#)), S327 ([THU-138](#))
- Baba, Masaru, S541 ([WED-283](#))
- Babatin, Mohammed A, S671 ([WED-458](#))
- Bablon, Pierre, S729 ([TOP-360-YI](#))
- Babu, Rosmy, S127 ([THU-318](#)), S279 ([WED-535-YI](#))
- Bachovchin, William, S534 ([WED-267](#))
- Bach, Stephane, S109 ([FRI-333](#))
- Bachtiar, Rini Rachmawarni, S792 ([FRI-444](#))
- Badal, Joyce, S403 ([SAT-498](#))
- Badenas, Celia, S710 ([WED-153](#))
- Bader, Gary L., S31 ([OS-040-YI](#))
- Badger, Kerry, S150 ([SAT-291](#))
- Badia-Aranda, Esther, S139 ([SAT-257](#)), S142 ([SAT-267](#))
- Badlani, Disha, S129 ([THU-322-YI](#))
- Badwal, Sonia, S719 ([WED-176](#))
- Baek, Seung-Woo, S68 ([OS-111](#))
- Baek, Yang-Hyun, S501 ([FRI-306](#)), S552 ([WED-322](#))
- Bae, Myung Ae, S78 ([LBP-002](#))
- Baffy, Gyorgy, S518 ([WED-222](#))
- Bagatella, Melissa, S657 ([WED-422](#)), S676 ([WED-470](#))
- Baguley, Elizabeth, S538 ([WED-274](#))
- Bagulho, Luis, S9 ([LBO-004](#)), S89 ([LBP-026](#))
- Bagur, Alexandre Triay, S524 ([WED-238](#))
- Bah, Sulayman, S782 ([FRI-418](#)), S787 ([FRI-431](#))
- Baicus, Cristian, S216 ([FRI-080](#))
- Baiges, Anna, S53 ([OS-081](#)), S240 ([SAT-074](#)), S255 ([SAT-123](#))
- Bai, Honglian, S605 ([SAT-198](#))
- Baik, Soon Koo, S136 ([THU-348](#))
- Bai, Lang, S494 ([FRI-285](#)), S499 ([FRI-302](#))
- Bailey, Máira, S578 ([THU-236-YI](#))
- Bai, Li, S113 ([FRI-347](#)), S694 ([FRI-154](#))
- Bainbridge, Jennifer, S297 ([SAT-165-YI](#))
- Bain, Gerard, S517 ([WED-220](#))
- Baiocchi, Leonardo, S59 ([OS-094](#)), S96 ([LBP-038](#)), S306 ([THU-093](#)), S772 ([FRI-392-YI](#))
- Bairaktari, Eleni, S322 ([THU-126](#)), S325 ([THU-134](#))
- Baird, Caitlin, S642 ([SAT-434](#))
- Bair, Ming-Jong, S74 ([OS-121](#)), S832 ([THU-365](#))
- Baisley, Kathy, S753 ([SAT-413](#))
- Bai, Wei, S447 ([THU-475](#)), S716 ([WED-167](#))
- Bai, Yupan, S422 ([FRI-484](#))
- Bajaj, Jasmohan, S1 ([GS-001](#)), S60 ([OS-095](#)), S159 ([THU-055](#)), S161 ([THU-058](#)), S163 ([THU-060](#)), S197 ([WED-123](#)), S206 ([FRI-046](#)), S208 ([FRI-053](#)), S212 ([FRI-069](#)), S218 ([FRI-086](#)), S219 ([FRI-088](#)), S242 ([SAT-082](#)), S364 ([WED-027](#)), S434 ([FRI-530](#))
- Bajunayd, Amani, S84 ([LBP-014](#))
- Bakala, Adam, S79 ([LBP-005](#)), S100 ([LBP-044](#))
- Baka, Olena, S610 ([SAT-213](#))
- Baker, Fadi Abu, S628 ([FRI-033](#)), S789 ([FRI-437](#))
- Bakken, Sofia Maria, S457 ([THU-514](#))
- Bakridi, Shahida, S657 ([WED-422](#)), S676 ([WED-470](#))
- Balakrishnan, Dinesh, S31 ([OS-039](#))
- Balanesco, Paul, S216 ([FRI-080](#))
- Balaseviciute, Ugne, S417 ([FRI-467](#))
- Balasubramanian, Sreepriya, S778 ([FRI-407](#))
- Balasubramanyam, Aarthi, S97 ([LBP-039](#))
- Balbacid, Enrique, S706 ([WED-132](#)), S712 ([WED-159](#))
- Balcar, Lorenz, S24 ([OS-027-YI](#)), S30 ([OS-038-YI](#)), S69 ([OS-112-YI](#)), S165 ([THU-071](#)), S166 ([THU-075-YI](#)), S199 ([TOP-062](#)), S200 ([TOP-064-YI](#)), S243 ([SAT-086-YI](#)), S250 ([SAT-105](#)), S250 ([SAT-106](#)), S251 ([SAT-111](#)), S253 ([SAT-117](#)), S255 ([SAT-122](#)), S257 ([SAT-128](#)), S436 ([TOP-488-YI](#)), S621 ([FRI-009-YI](#)), S703 ([TOP-141](#)), S706 ([WED-131-YI](#)), S708 ([WED-135-YI](#)), S717 ([WED-171](#)), S725 ([WED-190](#))
- Balci, Deniz, S369 ([SAT-009](#))
- Balci, Umay, S805 ([WED-418](#))
- Baldassarre, Maurizio, S206 ([FRI-047-YI](#)), S215 ([FRI-078-YI](#))
- Baldin, Pamela, S151 ([SAT-293-YI](#)), S823 ([THU-397-YI](#))
- Bale, Govardhan, S701 ([FRI-173](#))
- Balestrieri, Cinzia, S322 ([THU-127-YI](#))
- Balistreri, William, S54 ([OS-082](#))
- Balkhed, Wile, S530 ([WED-255-YI](#)), S532 ([WED-259](#))
- Ballardini, Giorgio, S836 ([THU-375](#))
- Ballester, Jose, S232 ([FRI-125](#))
- Ballester, María Pilar, S202 ([TOP-066-YI](#)), S232 ([FRI-125](#)), S700 ([FRI-171](#))
- Ballesteros, Katie, S632 ([THU-022](#))
- Ballesteros, Luz Ramos, S489 ([FRI-270-YI](#)), S683 ([WED-486-YI](#))
- Ball, Nathan, S707 ([WED-134](#))
- Baloch, Nayab, S653 ([SAT-463](#))
- Balogh, Boglarka, S169 ([THU-080-YI](#)), S313 ([THU-106-YI](#))
- Balsano, Rita, S408 ([SAT-523](#)), S447 ([THU-474-YI](#))
- Balsinde, Jesús, S568 ([THU-209](#))
- Bal, Tayibe, S805 ([WED-418](#))
- Baltzinger, Philippe, S42 ([OS-061](#))
- Balutsch, Nicolas, S243 ([SAT-086-YI](#))
- Balzano, Emanuele, S370 ([SAT-013](#))
- Bampoh, Sally, S395 ([SAT-479-YI](#))
- Banales, Jesus M, S32 ([OS-042-YI](#))
- Bañales, Jesús M., S300 ([SAT-175](#))
- Banales, Jesus Maria, S50 ([OS-076-YI](#)), S64 ([OS-101-YI](#)), S265 ([THU-533](#)), S286 ([WED-558](#)), S295 ([SAT-159-YI](#)), S419 ([FRI-472-YI](#)), S536 ([WED-271](#)), S569 ([THU-210](#))
- Bañares, Juan, S29 ([OS-037](#)), S36 ([OS-047-YI](#))
- Bañares, Rafael, S157 ([THU-050](#)), S188 ([WED-098-YI](#)), S276 ([WED-528-YI](#)), S593 ([THU-287](#)), S596 ([THU-296](#)), S818 ([THU-381](#))

- Banchelli, Federico, S62 ([OS-099-YI](#))
 Bandaria, Jigar, S460 ([TOP-309](#))
 Bandera, Alessandra, S791 ([FRI-442](#))
 Bandera, Jose Pinazo, S103 ([TOP-350-YI](#)), S341 ([THU-182](#)), S717 ([WED-172](#))
 Bandera, José Pinazo, S139 ([SAT-257](#)), S142 ([SAT-267](#))
 Bandi, Juan Carlos, S342 ([THU-185](#))
 Banerjee, Rajarshi, S21 ([OS-020](#)), S511 ([WED-200](#)), S524 ([WED-238](#)), S535 ([WED-268](#)), S542 ([WED-285](#))
 Bangura, Rohey, S782 ([FRI-418](#)), S786 ([FRI-431](#))
 Bansal, Ruchi, S266 ([THU-538](#))
 Bantel, Heike, S334 ([THU-164-YI](#)), S528 ([WED-249](#))
 Banzato, Marco, S592 ([THU-285](#))
 Banz, Vanessa, S373 ([SAT-019](#))
 Bao, Toan Nguyen, S552 ([WED-320](#))
 Bao, Yujie, S422 ([FRI-484](#))
 Barabanchyk, Olena, S530 ([WED-256](#))
 Barabino, Matteo, S428 ([FRI-514](#))
 Barace, Sergio, S15 ([OS-010](#))
 Baracos, Vickie, S231 ([FRI-122](#))
 Barajas, Jorge, S453 ([THU-493](#)), S828 ([THU-411](#))
 Barakeh, Duna, S671 ([WED-458](#))
 Barange, Karl, S73 ([OS-120](#)), S793 ([WED-391](#))
 Barbaglia, Matteo Nazzareno, S409 ([SAT-524](#))
 Barbara, Giovanni, S704 ([TOP-143-YI](#))
 Barbero, Fei-lynn, S382 ([SAT-040](#))
 Barbero, Manuel, S219 ([FRI-088](#))
 Barbier, Charlotte Ebeling, S550 ([WED-316](#))
 Barbieri, Lais Arrivabene, S619 ([SAT-248](#))
 Barbier, Louise, S368 ([SAT-009](#))
 Barbosa, Markus Gregorio, S347 ([FRI-549-YI](#))
 Barciela, Mar Riveiro, S291 ([TOP-149-YI](#)), S318 ([THU-118](#)), S700 ([FRI-171](#)), S702 ([TOP-139](#)), S741 ([SAT-381](#)), S746 ([SAT-393](#)), S787 ([FRI-432](#)), S822 ([THU-395](#))
 Barclay, Stephen, S117 ([SAT-317](#)), S783 ([FRI-423](#))
 Bardak, Ali Emre, S551 ([WED-318-YI](#))
 Bardeesy, Nabeel, S25 ([OS-029](#))
 Bardou-Jacquet, Edouard, S28 ([OS-034](#)), S61 ([OS-097](#)), S383 ([SAT-043](#)), S463 ([FRI-197](#)), S520 ([WED-227](#)), S714 ([WED-162](#))
 Bargallo, Ana, S192 ([WED-107](#))
 Bari, Khurram, S165 ([THU-074](#)), S242 ([SAT-082](#))
 Barišić-Jaman, Mislav, S155 ([SAT-305](#))
 Barletta, Francesca, S134 ([THU-340-YI](#))
 Barløse, Mads, S555 ([WED-331-YI](#))
 Barlow, Maeve, S687 ([WED-497](#))
 Barmou, Abdalnaser, S548 ([WED-305](#))
 Barnabas, Ashley, S560 ([WED-342](#))
 Barnard, Ruth, S807 ([WED-364](#))
 Barnes, Chris N., S97 ([LBP-039](#))
 Barnes, Eleanor, S470 ([FRI-215-YI](#)), S676 ([WED-471](#)), S746 ([SAT-394](#)), S750 ([SAT-404](#)), S752 ([SAT-409](#)), S756 ([SAT-421](#)), S760 ([TOP-417](#))
 Barnes, Mathew, S350 ([TOP-553](#))
 Barnhart, Huiman, S114 ([TOP-345](#))
 Barnhill, Michele S., S152 ([SAT-297](#))
 Bar, Nir, S237 ([FRI-136](#))
 Baron, Aurore, S168 ([THU-079](#)), S444 ([THU-466](#)), S640 ([SAT-430](#))
 Barone, Anna, S28 ([OS-035-YI](#)), S30 ([OS-038-YI](#)), S199 ([TOP-062](#)), S200 ([TOP-064-YI](#)), S212 ([FRI-068](#)), S243 ([SAT-083-YI](#)), S830 ([THU-420](#))
 Barral, Patricia, S282 ([WED-545-YI](#))
 Barreales Valbuena, Mónica, S142 ([SAT-267](#))
 Barrenechea-Barrenechea, Jon Ander, S417 ([FRI-466-YI](#))
 Barrera, Pedro, S453 ([THU-493](#))
 Barrera, Pilar, S779 ([FRI-409](#))
 Barrett, Kimberly, S8 ([LBO-002](#))
 Barrientos, Viviana, S195 ([WED-117](#))
 Barrio, María Del, S142 ([SAT-267](#))
 Barritt, A. SidneyIV, S394 ([SAT-476](#)), S610 ([SAT-212](#))
 Barritt IV, A. Sidney, S472 ([FRI-222-YI](#))
 Barroso, Emma, S574 ([THU-225](#))
 Barroti, Láis, S271 ([THU-556](#))
 Barrufet, Marta, S53 ([OS-081](#))
 Bartel, Claudius, S316 ([THU-113](#))
 Bartels, Amy, S364 ([WED-027](#))
 Bartels, Stephan, S425 ([FRI-492-YI](#))
 Bartlett, Sofia, S40 ([OS-058](#)), S824 ([THU-399-YI](#))
 Bartley, Hollie, S186 ([WED-090](#))
 Bartneck, Matthias, S266 ([THU-538](#))
 Bartolí, Ramon, S192 ([WED-107](#))
 Bartolomei, Francesca, S703 ([TOP-142-YI](#))
 Bartolomeo, Claudia Di, S335 ([THU-167](#))
 Bártulos, Deyanira, S141 ([SAT-262](#))
 Barutcu, Sezgin, S161 ([THU-058](#))
 Baruteau, Julien, S698 ([FRI-166](#))
 Barutta, Federica, S475 ([FRI-230-YI](#)), S483 ([FRI-251-YI](#))
 Basak, Trayambak, S158 ([THU-051](#))
 Basch, Ethan, S394 ([SAT-476](#))
 Bascur, Francisca, S195 ([WED-117](#))
 Baserga, Adriana, S316 ([THU-113](#))
 Basheer, Maamoun, S172 ([THU-091](#))
 Bassaganyas, Laia, S411 ([TOP-507-YI](#))
 Ba-Ssalamah, Ahmed, S250 ([SAT-106](#))
 Bassegoda, Octavi, S378 ([SAT-030](#)), S471 ([FRI-219-YI](#)), S721 ([WED-181](#))
 Bastard, Cécile, S550 ([WED-317](#))
 Bastati, Nina, S250 ([SAT-106](#))
 Basualdo, Jorge, S348 ([FRI-555](#))
 Basuroy, Ron, S37 ([OS-052](#)), S464 ([FRI-201](#)), S538 ([WED-275](#))
 Basyte-Basevice, Viktorija, S678 ([WED-474](#))
 Bataller, Ramon, S13 ([OS-005-YI](#)), S139 ([SAT-257](#)), S142 ([SAT-267](#)), S469 ([FRI-213](#))
 Bateman, Rebecca, S9 ([LBO-004](#)), S89 ([LBP-026](#))
 Bathgate, Andrew, S765 ([FRI-374-YI](#))
 Batirel, Ayse, S805 ([WED-418](#))
 Batra, Anil, S368 ([SAT-008](#))
 Battaglia, Salvatore, S51 ([OS-078-YI](#))
 Battezzati, Pier Maria, S725 ([WED-191](#))
 Battiston, Carlo, S70 ([OS-114](#))
 Batt, Nicholas, S400 ([SAT-492](#))
 Bat-Ulzii, Purevjargal, S82 ([LBP-011](#))
 Baudin, Martine, S608 ([SAT-206](#))
 Bauer, David, S243 ([SAT-086-YI](#)), S251 ([SAT-111](#)), S253 ([SAT-117](#)), S335 ([THU-166](#)), S717 ([WED-171](#)), S773 ([FRI-394](#)), S818 ([THU-380-YI](#))
 Bauer, Michael, S178 ([WED-060-YI](#))
 Bauer-Pisani, Tory, S697 ([FRI-162](#))
 Bauer, Ulrike, S440 ([THU-457](#))
 Baugé, Eric, S577 ([THU-234](#))
 Baugh, Macy, S489 ([FRI-269](#))
 Baughman, Alexis, S608 ([SAT-207](#))
 Baumann, Anja, S132 ([THU-334](#)), S279 ([WED-538-YI](#))
 Baumann, Ulrich, S115 ([TOP-346-YI](#)), S712 ([WED-160](#))
 Baumert, Thomas, S17 ([OS-013](#)), S25 ([OS-029](#)), S31 ([OS-040-YI](#)), S42 ([OS-061](#)), S734 ([SAT-348-YI](#))
 Bauschen, Alina, S182 ([WED-077](#))
 Bâve, Aiva, S312 ([THU-104](#))
 Baven-Pronk, Martine A.M.C., S18 ([OS-015](#))
 Baweja, Sukriti, S177 ([WED-057](#)), S274 ([WED-522-YI](#))
 Bax, Jeroen, S382 ([SAT-040](#))
 Bayer, Katharina, S484 ([FRI-255](#))
 Bayne, David, S219 ([FRI-088](#))
 Bayne, Kendra, S58 ([OS-090](#))
 Bay-Richter, Cecilie, S567 ([THU-207-YI](#))
 Baysal, Sidar, S384 ([SAT-046](#))
 Bayye, Rajkumar, S62 ([OS-098-YI](#))
 Bazán, Cynthia, S15 ([OS-010](#))
 Bazinet, Michel, S28 ([OS-034](#)), S791 ([FRI-443](#)), S814 ([WED-383](#))
 Beaufrère, Aurélie, S412 ([FRI-454](#)), S413 ([FRI-456](#))
 Beccaria, Cristian, S35 ([OS-048](#))
 Becchetti, Chiara, S367 ([SAT-007-YI](#)), S376 ([SAT-025](#)), S380 ([SAT-034](#))
 Beccuti, Guglielmo, S475 ([FRI-230-YI](#)), S483 ([FRI-251-YI](#))
 Bech, Katrine Tholstrup, S41 ([OS-059](#)), S77 ([OS-126](#)), S137 ([SAT-250](#)), S205 ([FRI-045](#)), S466 ([FRI-206-YI](#)), S503 ([TOP-241-YI](#)), S510 ([WED-199](#)), S620 ([TOP-012](#)), S623 ([FRI-017](#))
 Becker, Diana, S582 ([THU-254-YI](#))
 Becker-Drepps, Sylvia, S668 ([WED-451-YI](#))
 Becker, Thomas, S582 ([THU-254-YI](#))
 Beckett, Geoff, S825 ([THU-404](#))
 Beck, Juergen, S23 ([OS-025-YI](#))
 Beckmann, Jan Henrik, S582 ([THU-254-YI](#))
 Becsi, Bernadette, S821 ([THU-390](#))
 Bedossa, Pierre, S4 ([GS-006](#)), S4 ([GS-011](#)), S8 ([LBO-002](#)), S507 ([TOP-289](#)), S512 ([WED-206](#)), S526 ([WED-245](#)), S533 ([WED-262](#))

Author Index

- Bedoya, José Ursic, S9 ([LBO-004](#)),
S28 ([OS-034](#)), S89 ([LBP-026](#)),
S143 ([SAT-269](#)), S156 ([TOP-108](#)),
S376 ([SAT-026](#))
- Beech, David, S573 ([THU-222-YI](#))
- Bee Goh, George Boon, S38 ([OS-054](#))
- Beenen, Amke, S291 ([TOP-150-YI](#))
- Beer, Lucian, S250 ([SAT-106](#))
- Bee, Yong Mong, S525 ([WED-242](#))
- Begini, Paola, S96 ([LBP-038](#)),
S306 ([THU-093](#)), S817 ([THU-378](#))
- Begum, Shahida, S101 ([LBP-046](#))
- Behera, Sanatan, S158 ([THU-052](#)),
S167 ([THU-078](#))
- Behling, Cynthia, S7 ([LBO-001](#)),
S8 ([LBO-002](#))
- Behmoaras, Jacques, S580 ([THU-247-YI](#))
- Behncke, Rose Yinghan, S302 ([SAT-180](#))
- Behrendt, Patrick, S353 ([SAT-538-YI](#)),
S730 ([TOP-369](#))
- Beigelman, Leonid, S564 ([THU-198](#)),
S727 ([TOP-357](#)), S728 ([TOP-358-YI](#))
- Beilin, Lawrence, S275 ([WED-526](#)),
S483 ([FRI-250](#)), S487 ([FRI-263](#))
- Beires, Francisca, S705 ([WED-129](#))
- Beitari, Saina, S662 ([WED-436](#)),
S668 ([WED-450](#)), S679 ([WED-476](#))
- Bejarano, Ana, S826 ([THU-405](#))
- Bekhuis, Youri, S246 ([SAT-092-YI](#))
- Bektaş, Ahmet, S723 ([WED-187-YI](#))
- Bektaş, Fatih, S551 ([WED-318-YI](#))
- Bektas, Hicran, S11 ([OS-001](#))
- Belal, Sophie, S109 ([FRI-333](#))
- Belanger, Bruce, S819 ([THU-382](#))
- Belanger-Quintana, Amaya, S693 ([FRI-153](#))
- Beldi, Guido, S373 ([SAT-019](#))
- Belicova, Lenka, S66 ([SAT-107-YI](#))
- Belkacem, Karima Ben, S5 ([GS-007](#)),
S326 ([THU-136](#))
- Belladonna, Federica, S493 ([FRI-281](#)),
S554 ([WED-326](#)), S556 ([WED-333](#))
- Bellafante, Daniele, S62 ([OS-099-YI](#))
- Bellanti, Francesco, S310 ([THU-101](#))
- Bellarosa, Cristina, S701 ([FRI-172](#))
- Bellec, Claire, S168 ([THU-079](#))
- Bellet, Jonathan, S5 ([GS-007](#))
- Belletini, Matteo, S475 ([FRI-230-YI](#)),
S480 ([FRI-243](#))
- Bellia, Valentina, S70 ([OS-114](#)),
S375 ([SAT-022](#)), S438 ([TOP-506](#)),
S439 ([THU-454](#))
- Belli, Luca Saverio, S9 ([LBO-004](#)),
S89 ([LBP-026](#)), S368 ([SAT-009](#)),
S700 ([FRI-171](#))
- Bello, Arnaud Del, S367 ([TOP-005](#)),
S385 ([SAT-048](#))
- Bellomo, Michele, S824 ([THU-402](#))
- Bellon, Serge, S640 ([SAT-430](#))
- Bello, Ruth, S673 ([WED-463](#))
- Belsito, Vincenzo, S580 ([THU-245](#))
- Belsol, Marcos, S662 ([WED-435](#))
- Beltran-Debon, Raul, S580 ([THU-247-YI](#))
- Beltran, Oscar, S83 ([LBP-012](#))
- Benach, Joan, S154 ([SAT-304](#))
- Bena, James, S76 ([OS-125](#))
- Benali, Souad, S28 ([OS-034](#))
- Benamar, Amal, S452 ([THU-491](#))
- Benavides, Cristina, S266 ([THU-539](#)),
S592 ([THU-283](#))
- Ben Belkacem, Karima, S313 ([THU-107](#))
- Bencardino, Katia, S451 ([THU-486-YI](#))
- Benchimol, Eric, S305 ([TOP-168-YI](#))
- Benckert, Julia, S730 ([TOP-369](#))
- Bendall, Oliver, S250 ([SAT-107-YI](#))
- Bende, Renata, S238 ([SAT-068](#))
- Bendridi, Nadia, S49 ([OS-074](#))
- Bendtsen, Flemming, S47 ([OS-072-YI](#)),
S555 ([WED-331-YI](#)), S579 ([THU-243](#))
- Bendtsen, Kristian, S79 ([LBP-003](#))
- Benedetto, Clara Di, S700 ([FRI-171](#))
- Benedé-Ubieto, Raquel,
S276 ([WED-528-YI](#)), S351 ([SAT-534](#))
- Benedicto, Aitor, S431 ([FRI-521](#))
- Benedicto, Ana, S266 ([THU-539](#)),
S592 ([THU-283](#))
- Benedittis, Carla De, S329 ([THU-153](#))
- Benefield, Thad, S393 ([SAT-472](#))
- Bengsch, Bertram, S23 ([OS-025-YI](#)),
S54 ([OS-083](#)), S69 ([OS-112-YI](#))
- Bengtsson, Tore, S294 ([SAT-155](#))
- Bengus, Andreea, S216 ([FRI-080](#))
- Benichou, Bernard, S714 ([WED-164](#))
- Benitez, Carlos, S83 ([LBP-012](#)),
S209 ([FRI-053](#))
- Benjamin Mauz, Jim, S245 ([SAT-090-YI](#))
- Benmassaoud, Amine, S248 ([SAT-100](#)),
S484 ([FRI-256-YI](#))
- Bennett, Kris, S153 ([SAT-299](#)),
S250 ([SAT-107-YI](#)), S645 ([SAT-440](#))
- Bennett, Lucy, S650 ([SAT-454-YI](#))
- Bennett, Noeleen, S672 ([WED-459-YI](#))
- Benson, Joanne, S504 ([TOP-252-YI](#))
- Benz, Fabian, S259 ([SAT-135](#))
- Benzoubir, Nassima, S432 ([FRI-525](#))
- Beo, Vincent Di, S670 ([WED-455](#))
- Bera, Chinmay, S209 ([FRI-053](#)),
S497 ([FRI-293](#))
- Berak, Hanna, S685 ([WED-493-YI](#)),
S834 ([THU-367-YI](#))
- Berardi, Francesco, S404 ([SAT-502-YI](#)),
S406 ([SAT-514](#))
- Berardi, Giammauro, S369 ([SAT-009](#))
- Berasain, Carmen, S287 ([FRI-538](#)),
S348 ([FRI-555](#)), S416 ([FRI-464](#))
- Berberova, Magda, S485 ([FRI-257](#))
- Berenguer, Juan, S741 ([SAT-379](#)),
S751 ([SAT-407](#))
- Berenguer, Marina, S9 ([LBO-004](#)),
S89 ([LBP-026](#)), S344 ([THU-189](#)),
S361 ([WED-009](#)), S362 ([WED-015](#)),
S377 ([SAT-027](#)), S531 ([WED-257](#)),
S700 ([FRI-171](#)), S717 ([WED-172](#)),
S723 ([WED-186](#)), S787 ([FRI-432](#))
- Berentzen, Tina Landsvig, S709 ([WED-138](#))
- Bergamin, Irina, S502 ([FRI-315](#))
- Berg, Christoph P., S368 ([SAT-008](#)),
S440 ([THU-457](#))
- Berger, Annemarie, S794 ([WED-392](#))
- Berger, Hilmar, S25 ([OS-028](#)),
S57 ([OS-088-YI](#))
- Berggren, Per-Olof, S281 ([WED-543](#))
- Bergheim, Ina, S132 ([THU-334](#)),
S279 ([WED-538-YI](#))
- Berghe, Tom Vanden, S581 ([THU-249](#))
- Bergquist, Annika, S22 ([OS-023-YI](#)),
S312 ([THU-104](#)), S386 ([SAT-050](#)),
S635 ([THU-034-YI](#))
- Bergram, Martin, S532 ([WED-259](#))
- Berg, Thomas, S162 ([THU-059](#)),
S404 ([SAT-501-YI](#)), S700 ([FRI-171](#)),
S752 ([SAT-410](#)), S788 ([FRI-434](#)),
S802 ([WED-411](#)), S820 ([THU-386-YI](#))
- Berhe, Nega, S781 ([FRI-414](#)),
S795 ([WED-394](#))
- Berlakovich, Gabriela, S9 ([LBO-004](#)),
S89 ([LBP-026](#))
- Bermudez, Maria, S192 ([WED-107](#))
- Berná, Genoveva, S71 ([OS-116](#))
- Bernalte, Susana, S662 ([WED-435](#))
- Bernal, Vanesa, S139 ([SAT-257](#)),
S142 ([SAT-267](#)), S453 ([THU-493](#))
- Bernal, William, S9 ([LBO-004](#)),
S44 ([OS-065](#)), S89 ([LBP-026](#)),
S156 ([TOP-108](#)), S178 ([WED-068-YI](#))
- Bernardi, Elisabetta De, S325 ([THU-133-YI](#))
- Bernardi, Mauro, S215 ([FRI-078-YI](#))
- Bernard, Nathalie, S313 ([THU-107](#))
- Bernasconi, Davide, S325 ([THU-133-YI](#)),
S335 ([THU-167](#))
- Bernasconi, Monica, S401 ([SAT-494](#))
- Bernatik, Sophia, S298 ([SAT-166](#))
- Berning, Marco, S238 ([SAT-069](#))
- Bernsmeier, Christine, S292 ([TOP-150-YI](#)),
S341 ([THU-182](#))
- Bernstein, David, S242 ([SAT-082](#))
- Berres, Marie-Luise, S52 ([OS-079-YI](#)),
S356 ([SAT-545](#))
- Berrevoet, Frederik, S371 ([SAT-014-YI](#)),
S386 ([SAT-051](#)), S420 ([FRI-475-YI](#)),
S631 ([THU-020-YI](#))
- Bertazzoni, Arianna, S404 ([SAT-502-YI](#)),
S406 ([SAT-514](#))
- Bertelli, Cristina, S474 ([FRI-226](#)),
S482 ([FRI-248-YI](#))
- Bertetto, Rubina, S329 ([THU-153](#))
- Bertino, Gaetano, S96 ([LBP-038](#)),
S306 ([THU-093](#)), S557 ([WED-336](#))
- Bert, Nina Le, S36 ([OS-050](#)), S81 ([LBP-009](#)),
S742 ([SAT-383](#))
- Bertoldi, Elisa, S210 ([FRI-056-YI](#))
- Bertoletti, Antonio, S36 ([OS-050](#)),
S81 ([LBP-009](#)), S742 ([SAT-383](#))
- Bertoli, Ada, S776 ([FRI-405](#))
- Bertoni, Costanza, S824 ([THU-402](#))
- Bertot, Luis, S275 ([WED-526](#))
- Berzigotti, Annalisa, S61 ([OS-096-YI](#)),
S183 ([WED-081](#)), S183 ([WED-082](#)),
S238 ([SAT-068](#)), S238 ([SAT-069](#)),
S254 ([SAT-121](#)), S373 ([SAT-019](#)),
S392 ([SAT-469](#)), S393 ([SAT-473](#))
- Besch, Camille, S367 ([TOP-005](#)),
S763 ([FRI-370](#))

- Beschi, Riccardo, S533 (WED-261-YI)
 Beshara, Amani, S628 (FRI-033)
 Beşik, Fatih, S377 (SAT-028),
 S551 (WED-318-YI), S803 (WED-413)
 Bessa, Xavier, S207 (FRI-051)
 Bessissow, Ali, S484 (FRI-256-YI)
 Bessone, Fernando, S83 (LBP-012),
 S341 (THU-182)
 Besson, Florent, S50 (OS-077)
 Bessonova, Leona, S314 (THU-110),
 S621 (FRI-008)
 Bettelheim, Dieter, S719 (WED-175)
 Bettencourt, Ricki, S522 (WED-235),
 S543 (WED-291)
 Bettinger, Dominik, S52 (OS-079-YI),
 S52 (OS-080), S187 (WED-094),
 S219 (FRI-088), S443 (THU-464),
 S447 (THU-475)
 Betti, Silvia, S703 (TOP-142-YI)
 Beuers, Ulrich, S5 (GS-007), S204 (FRI-043),
 S296 (SAT-160), S301 (SAT-178-YI),
 S309 (THU-100), S314 (THU-109),
 S317 (THU-115-YI), S319 (THU-120-YI),
 S327 (THU-138)
 Beukema, Menno, S319 (THU-120-YI)
 Beutels, Philippe, S665 (WED-441-YI)
 Beuzit, Luc, S383 (SAT-043)
 Bevez, Tetiana, S827 (THU-408),
 S835 (THU-373-YI)
 Bewick, Gavin, S274 (WED-523)
 Beyene, Nateneal, S540 (WED-281-YI)
 Beyer, Cayden, S21 (OS-020),
 S522 (WED-234), S524 (WED-238),
 S535 (WED-268)
 Bezerra, Lucas, S334 (THU-164-YI)
 Bhadoria, Ajeet, S348 (FRI-554),
 S666 (WED-443-YI)
 Bhadoria, Pooja, S348 (FRI-554)
 Bhala, Neeraj, S654 (SAT-467)
 Bhamidimarri, Kalyan Ram,
 S809 (WED-371)
 Bhandal, Khushpreet, S332 (THU-160)
 Bhandari, Bal Raj, S11 (LBO-006)
 Bhanot, Sanjay, S7 (GS-012), S93 (LBP-031)
 Bharat, Chrianna, S655 (SAT-471)
 Bhardwaj, Manisha, S184 (WED-086),
 S195 (WED-118), S360 (SAT-557-YI)
 Bhardwaz, Priyanshu, S609 (SAT-210)
 Bhaskar, Ashima, S283 (WED-549)
 Bhat, Adil, S294 (SAT-155)
 Bhat, Mamatha, S114 (TOP-344-YI),
 S381 (SAT-037), S381 (SAT-039)
 Bhatnagar, Aishwarya, S177 (WED-058-YI),
 S188 (WED-095-YI)
 Bhat, Sadam H, S103 (TOP-349-YI),
 S108 (FRI-327-YI), S754 (SAT-415)
 Bhat, Sadam H., S125 (TOP-329-YI),
 S127 (THU-318), S134 (THU-339),
 S273 (WED-519-YI), S294 (SAT-155)
 Bhattacharya, Aneerban, S564 (THU-198)
 Bhattacharya, Debashruti, S347 (FRI-550)
 Bhattacharya, Mallika, S476 (FRI-231)
 Bhavani, Ruveena, S158 (THU-052),
 S167 (THU-078), S209 (FRI-053)
 Bhoori, Sherrie, S70 (OS-114),
 S368 (SAT-009), S375 (SAT-022),
 S438 (TOP-506), S439 (THU-454)
 Bhuiyan, Tasnim, S669 (WED-453)
 Bhuyan, Muhammad Abedur Rahman,
 S615 (SAT-230)
 Bhuyan, Pallavi, S285 (WED-554)
 Biagini, Maria Rosa, S342 (THU-184)
 Bianchini, Marcello, S62 (OS-099-YI)
 Bianco, Cristiana, S491 (FRI-275-YI),
 S705 (WED-130)
 Bian, Xiyun, S106 (FRI-323)
 Biasiolo, Alessandra, S612 (SAT-219)
 Bibani, Norsaf, S270 (THU-554)
 Bicknell, Roy, S425 (FRI-493)
 Bieri, Manuela, S590 (THU-278)
 Biermer, Michael, S27 (OS-032),
 S27 (OS-033), S79 (LBP-005),
 S100 (LBP-044), S768 (FRI-380),
 S808 (WED-367), S810 (WED-372),
 S813 (WED-379)
 Biewenga, Maaike, S374 (SAT-021)
 Bigam, David, S231 (FRI-122)
 Biggins, Scott, S161 (THU-058),
 S206 (FRI-046), S218 (FRI-086)
 Bihari, Chhagan, S137 (SAT-249),
 S184 (WED-086), S195 (WED-118),
 S274 (WED-522-YI), S279 (WED-535-YI)
 Bihary, Dóra, S125 (TOP-328-YI)
 Bijou, Stane, S668 (WED-451-YI)
 Bilancio, Giancarlo, S493 (FRI-281)
 Bilbao-Arribas, Martin, S693 (FRI-152-YI)
 Bilbao, Itxarone, S365 (TOP-002)
 Billaud, Eric, S73 (OS-120), S793 (WED-391)
 Billin, Andrew N., S462 (FRI-195),
 S505 (TOP-264), S571 (THU-215),
 S585 (THU-261)
 Bina, Niccolò, S96 (LBP-038),
 S306 (THU-093)
 Bindal, Vasundhra, S103 (TOP-349-YI),
 S108 (FRI-327-YI), S125 (TOP-329-YI),
 S127 (THU-318), S134 (THU-339),
 S273 (WED-519-YI), S283 (WED-549),
 S294 (SAT-155)
 Binder, Julia, S719 (WED-175)
 Bindra, Jas, S118 (SAT-320)
 Bingqing, Yang, S479 (FRI-242)
 Binquet, Christine, S369 (SAT-010)
 biolato, marco, S175 (TOP-085),
 S533 (WED-261-YI)
 Bioletto, Fabio, S522 (WED-233-YI),
 S525 (WED-243-YI)
 Biondi, Mia, S673 (WED-464),
 S688 (WED-499)
 Biquard, Louise, S180 (WED-071),
 S193 (WED-112), S524 (WED-239)
 Biracree, Jaime, S544 (WED-294)
 Birgit, Kohnke-Ertel, S298 (SAT-166)
 Birhanu, Dawit, S781 (FRI-414)
 Biribin, Lara, S258 (SAT-131)
 Biriuchenko, Iryna, S530 (WED-256)
 Birkel, Christoph, S722 (WED-183-YI)
 Birligea, Mihaela, S216 (FRI-080)
 Birrer, Dominique L., S345 (TOP-559)
 Biscetti, Federico, S545 (WED-296)
 Bishop, Rebecca, S9 (LBO-004),
 S89 (LBP-026)
 Bissonnette, Julien, S180 (WED-071)
 Biswas, Sagnik, S201 (TOP-065),
 S506 (TOP-276)
 Biswas, Subhrajit, S184 (WED-086)
 Bitetto, Davide, S206 (FRI-047-YI)
 Bittencourt, Paulo, S83 (LBP-012),
 S254 (SAT-119), S722 (WED-185)
 Bittermann, Therese, S649 (SAT-451)
 Bitton, Jackie, S133 (THU-335),
 S786 (FRI-429)
 Bitzer, Michael, S52 (OS-079-YI)
 Bi, Xiaojuan, S365 (WED-029)
 Bi, Xiaoyue, S355 (SAT-544), S738 (SAT-372)
 Bjerring, Peter Nissen, S115 (TOP-346-YI)
 Björkenberg, Birgitte, S581 (THU-248)
 Björnsson, Einar S., S236 (FRI-133),
 S328 (THU-151), S389 (SAT-059)
 Björnsson, Helgi K, S328 (THU-151)
 Blach, Elzbieta, S70 (OS-115)
 Blair, Brian, S489 (FRI-268)
 Blaise, Lorraine, S441 (THU-458),
 S441 (THU-459-YI), S451 (THU-487-YI)
 Blamire, Andrew, S297 (SAT-165-YI)
 Blanc, Jean-Frédéric, S68 (OS-110),
 S441 (THU-459-YI), S444 (THU-466)
 Blanco, Aura, S669 (WED-453)
 Blanco, Gerardo, S365 (TOP-002)
 Blanco, Jesus Miguens, S46 (OS-070),
 S282 (WED-546)
 Blanco, Maria Rosa, S141 (SAT-262)
 Blanco, Sonia, S329 (THU-154-YI)
 Blanc, Pierluigi, S674 (WED-467-YI)
 Blank, Antje, S92 (LBP-029)
 Blarasin, Benedetta, S701 (FRI-172)
 Blasco, Víctor Manuel Vargas,
 S157 (THU-050), S188 (WED-098-YI),
 S717 (WED-172)
 Blasco, Victor Vargas, S80 (LBP-006),
 S311 (THU-103)
 Blas-García, Ana, S266 (THU-539),
 S592 (THU-283)
 Blasi, Annabel, S15 (OS-010),
 S179 (WED-070)
 Blatt, Lawrence, S727 (TOP-357),
 S728 (TOP-358-YI), S806 (WED-361),
 S807 (WED-365), S812 (WED-378)
 Blau, Jenny, S93 (LBP-031),
 S535 (WED-270), S554 (WED-325-YI)
 Blaumeiser, Andreas, S23 (OS-025-YI)
 Blerk, Sebastian Van, S47 (OS-071-YI)
 Blet, Alice, S22 (OS-022)
 Blevet, Audrey Le, S681 (WED-482)
 Blevins, Christina, S8 (LBO-003)
 Bloch, Guenseli, S223 (FRI-100)
 Bloks, Vincent, S347 (FRI-549-YI)
 Blokzijl, Hans, S286 (TOP-560),
 S758 (TOP-401-YI), S763 (FRI-367)
 Bloom, Patricia, S211 (FRI-059),
 S214 (FRI-075)
 Bloom, Stephen, S338 (THU-177-YI),
 S402 (SAT-496)

Author Index

- Blottière, Hervé, S159 (THU-053)
 Blümel, Sena, S56 (OS-086-YI),
 S440 (THU-457)
 Boano, Valentina, S96 (LBP-038),
 S306 (THU-093)
 Boaventura, Nairane, S636 (THU-044)
 Bobat, Bilal, S161 (THU-058)
 Bobis, Ingrid, S341 (THU-182)
 Bobowski-Gerard, Marie, S171 (THU-088),
 S191 (WED-105)
 Boccaccio, Vincenzo, S96 (LBP-038),
 S306 (THU-093)
 Bodakçi, Emin, S407 (SAT-519),
 S479 (FRI-238)
 Bode, Johannes, S259 (SAT-135)
 Boeckx, Bram, S125 (TOP-328-YI)
 Boeckxstaens, Guy, S16 (OS-012-YI)
 Boeira, Paula, S153 (SAT-299)
 Boeker, Klaus H.W., S820 (THU-386-YI)
 Boe, Maria, S446 (THU-472-YI)
 Boerries, Melanie, S23 (OS-025-YI)
 Boersma, Femke, S314 (THU-109),
 S327 (THU-138)
 Boesch, Markus, S16 (OS-012-YI),
 S125 (TOP-328-YI)
 Boettcher, Katrin, S52 (OS-079-YI)
 Boettcher, Michael, S368 (SAT-008)
 Bofill, Alex, S378 (SAT-030)
 Bogaards, Johannes, S315 (THU-112-YI)
 Bogdanos, Dimitrios, S358 (SAT-551)
 Bogdanov, Alina, S611 (SAT-215)
 Bogomolov, Pavel, S1 (GS-002),
 S92 (LBP-029), S758 (TOP-400),
 S764 (FRI-371), S794 (WED-392),
 S796 (WED-395)
 Böhning, Dankmar, S645 (SAT-441-YI)
 Böing, Elaine, S91 (LBP-028)
 Boix, Loreto, S420 (FRI-474-YI),
 S424 (FRI-491-YI), S425 (FRI-494-YI)
 Boix, Paula, S194 (WED-113)
 Bojang, Lamin, S782 (FRI-418),
 S787 (FRI-431)
 Bojunga, Jörg, S203 (FRI-039)
 Bolis, Francesca, S19 (OS-017)
 Bollier, Mélanie, S728 (TOP-358-YI)
 Bolli, Niccolò, S459 (TOP-301)
 Bollipo, Steven, S400 (SAT-492)
 Bomford, Adrian, S709 (WED-137-YI)
 Bomo, Jérémy, S64 (OS-102)
 Bonacchi, Giacomo, S475 (FRI-230-YI)
 Bonaccorsi, Eliano, S369 (SAT-009),
 S371 (SAT-014-YI)
 Bonafede, Machaon, S611 (SAT-215)
 Bonafede, Vincenzo, S627 (FRI-028)
 Bonaiuto, Emanuela, S318 (THU-117-YI)
 Bonatti, Chiara, S390 (TOP-509-YI)
 Bonazza, Deborah, S429 (FRI-516-YI)
 Bondaruk, Iryna, S827 (THU-408),
 S835 (THU-373-YI)
 Bonder, Alan, S308 (THU-098),
 S340 (THU-181), S374 (SAT-021),
 S623 (FRI-015), S627 (FRI-030)
 Bonelli, Sara Irene, S674 (WED-467-YI)
 Bong Ahn, Sang, S152 (SAT-296)
 Bongini, Marco, S70 (OS-114),
 S369 (SAT-009), S375 (SAT-022),
 S438 (TOP-506), S439 (THU-454)
 Bongiovanni, Deborah, S700 (FRI-171)
 Bongiovanni, Laura, S347 (FRI-549-YI)
 Bonhomme, Marie, S86 (LBP-018)
 Bonino, Ferruccio, S549 (WED-314-YI),
 S622 (FRI-014)
 Bonitz, Katharina, S186 (WED-089-YI),
 S197 (WED-122-YI), S198 (WED-125),
 S267 (THU-540)
 Bonne, Lawrence, S125 (TOP-328-YI),
 S246 (SAT-092-YI)
 Bonner, Emily, S629 (THU-008)
 Bonney, Glenn, S540 (WED-282)
 Bonnier, Dominique, S261 (THU-522)
 Bono, Ariadna, S700 (FRI-171),
 S717 (WED-172), S723 (WED-186),
 S787 (FRI-432)
 Bono, Elisa, S35 (OS-048)
 Bonomo, Mimma, S378 (SAT-031-YI)
 Bonyhay, Luminita, S486 (FRI-259)
 Boodram, Basmattee, S43 (OS-063)
 Boon, Mariëtte, S278 (WED-533)
 Boon, Nathalie, S133 (THU-335)
 Boonstra, Andre, S513 (WED-209),
 S731 (SAT-337)
 Boonstra, Kirsten, S317 (THU-115-YI)
 Boor, Peter, S32 (OS-041-YI),
 S273 (WED-521-YI)
 Boothman, Helen, S646 (SAT-444),
 S672 (WED-459-YI)
 Boot, James, S298 (SAT-167-YI)
 Borca, Florina, S676 (WED-471),
 S759 (TOP-417)
 Borentain, Patrick, S172 (THU-092),
 S763 (FRI-370)
 Borges, Catarina, S115 (TOP-346-YI)
 Borghi, Marta, S73 (OS-120),
 S344 (THU-190), S781 (FRI-412),
 S798 (WED-399-YI)
 Borissova, Julia, S172 (THU-092)
 Bork, Peer, S47 (OS-071-YI),
 S47 (OS-072-YI), S48 (OS-073),
 S203 (FRI-039), S272 (TOP-563)
 Börmel, Lisa, S600 (THU-314)
 Boros, Carina, S451 (THU-487-YI)
 Borràs, Mar, S455 (THU-501)
 Borre, Mette, S236 (FRI-134)
 Boruchowicz, Arnaud, S640 (SAT-430)
 Bosca, Andrea, S377 (SAT-027)
 Bosch, Anna, S9 (LBO-004), S89 (LBP-026),
 S700 (FRI-171)
 Bosch, Jaime, S183 (WED-081),
 S183 (WED-082), S238 (SAT-069),
 S254 (SAT-121)
 Bosch, Miriam, S351 (SAT-533)
 Bos, Daniel, S394 (SAT-474)
 Bo, Simona, S501 (FRI-314),
 S522 (WED-233-YI), S525 (WED-243-YI)
 Bosmans, Goele, S807 (WED-363)
 Bosselmann, Emily, S21 (OS-021-YI)
 Bossen, Lars, S723 (WED-187-YI)
 Bossolasco, Simona, S824 (THU-402)
 Bostjan, Humar, S345 (TOP-559)
 Botero, María Luisa, S15 (OS-010)
 Böttcher, Jan P., S35 (OS-049-YI)
 Böttcher, Katrin, S35 (OS-049-YI)
 Botteaux, Anne, S131 (THU-331-YI)
 Botterill, Gemma, S765 (FRI-374-YI)
 Böttler, Tobias, S70 (OS-115),
 S187 (WED-094)
 Bott, Sebastian, S588 (THU-272-YI)
 Bouam, Samir, S698 (FRI-165),
 S741 (SAT-380), S760 (FRI-361)
 Bouattour, Mohamed, S3 (GS-005),
 S41 (OS-060), S50 (OS-077),
 S68 (OS-110), S69 (OS-112-YI),
 S413 (FRI-456), S444 (THU-466),
 S452 (THU-492)
 Boubaya, Marouane, S50 (OS-077)
 Boucher, Louis-Martin,
 S484 (FRI-256-YI)
 Bouda, Yasmine, S413 (FRI-456),
 S743 (SAT-386-YI)
 Boudes, Pol, S245 (SAT-089)
 Boudjema, Karim, S9 (LBO-004),
 S89 (LBP-026), S383 (SAT-043)
 Bougueon, Matthieu, S64 (OS-102)
 Boukraa, Amal, S784 (FRI-425)
 Boulahtouf, Zakaria, S734 (SAT-348-YI)
 Boulter, Luke, S66 (OS-105-YI),
 S416 (FRI-463-YI), S695 (FRI-158-YI)
 Bouma, Gerd, S18 (OS-015)
 Boumelhem, Badwi, S534 (WED-267)
 Boundy, Keith, S812 (WED-376)
 Bouquet, Jerome, S745 (SAT-390)
 Bourgeois, Stefan, S79 (LBP-005),
 S730 (SAT-337), S777 (FRI-406)
 Bourke, Michèle, S635 (THU-040-YI)
 Bourliere, Marc, S1 (GS-002), S28 (OS-034),
 S41 (OS-060), S444 (THU-466),
 S670 (WED-455), S764 (FRI-371),
 S796 (WED-395)
 Boursier, Jerome, S2 (GS-004),
 S7 (LBO-001), S37 (OS-053),
 S41 (OS-060), S456 (THU-503),
 S519 (WED-224), S520 (WED-227),
 S608 (SAT-206)
 Boursier, Jérôme, S38 (OS-054),
 S545 (WED-296)
 Boussios, Costas, S460 (TOP-309)
 Bouzbib, Charlotte, S207 (FRI-050-YI),
 S218 (FRI-087), S222 (FRI-094-YI),
 S222 (FRI-095), S239 (SAT-071),
 S486 (FRI-259)
 Bovolenta, Elena Rodriguez, S35 (OS-048)
 Bowden, Abi, S339 (THU-178)
 Bowen, David, S380 (SAT-036-YI)
 Bowen, Scott, S573 (THU-222-YI)
 Bowlus, Christopher L., S80 (LBP-006),
 S97 (LBP-039), S98 (LBP-040),
 S312 (THU-105), S325 (THU-132)
 Bowman, Keith, S692 (FRI-151)
 Bowyer, Teresa, S820 (THU-383)
 Bo, Yang, S369 (SAT-009)
 Boy, Eric, S641 (SAT-431-YI)
 Boyer, Sylvie, S678 (WED-475)

- Boyette, Lisa, S462 (FRI-195), S505 (TOP-264), S571 (THU-215), S585 (THU-261)
- Boyle, Alison, S636 (THU-045), S783 (FRI-423)
- Boyle, Billy, S195 (WED-117)
- Bozon-Rivière, Pauline, S376 (SAT-026)
- Bozso, Boglarka, S313 (THU-106-YI)
- Bozward, Amber, S354 (SAT-540-YI), S356 (SAT-546)
- Bozzano, Sergio, S128 (THU-320-YI)
- Bozzarelli, Silvia, S408 (SAT-523), S447 (THU-474-YI)
- Braconi, Chiara, S419 (FRI-472-YI)
- Bradbury, Molly, S408 (SAT-521)
- Braga, Arthur, S618 (SAT-242)
- Brahmania, Mayur, S147 (SAT-280), S148 (SAT-285-YI)
- Braimakis, Ioannis, S690 (WED-503)
- Brancaccio, Giuseppina, S28 (OS-034), S59 (OS-094)
- Brandi, Giovanni, S395 (SAT-477-YI), S446 (THU-472-YI)
- Brandi, Johannes, S278 (WED-534)
- Brandl, Roswitha, S223 (FRI-098), S224 (FRI-103-YI)
- Brand, Stephan, S502 (FRI-315)
- Brandt, Annette, S132 (THU-334), S279 (WED-538-YI)
- Braticevici, Carmen Fierbinteanu, S238 (SAT-068)
- Braun, Felix, S9 (LBO-004), S89 (LBP-026), S368 (SAT-009)
- Bravo, Isabel, S177 (WED-059)
- Bravo, Miguel Ángel Gómez, S377 (SAT-027)
- Brears, Helena Thomaides, S511 (WED-200), S524 (WED-238), S535 (WED-268), S542 (WED-285)
- Breder, Sigurd, S22 (OS-023-YI), S386 (SAT-050)
- Breitkopf-Heinlein, Katja, S33 (OS-043)
- Bremer, Birgit, S730 (TOP-369)
- Brendel, Karl, S321 (THU-124)
- Brener, Loren, S689 (WED-501)
- Brennan, Anne, S635 (THU-040-YI)
- Brennan, Emily, S146 (SAT-279)
- Brennan, Paul, S81 (LBP-007)
- Brennan, Paul N, S528 (WED-248)
- Brennan, Paul N., S651 (SAT-456)
- Bretthauer, Mara, S735 (SAT-363)
- Brevini, Teresa, S81 (LBP-008)
- Breyner, Natalia, S13 (OS-006), S597 (THU-299)
- Briand, Francois, S13 (OS-006), S597 (THU-299)
- Brichler, Segolene, S28 (OS-034), S777 (FRI-406), S802 (WED-410)
- Brígido, Ana, S286 (WED-558)
- Brito, Carlos Cantu, S602 (TOP-205)
- Briz, Oscar, S432 (FRI-523), S433 (FRI-526)
- Brjalin, Vadim, S172 (THU-092)
- Brocca, Alessandra, S157 (THU-050), S224 (FRI-101-YI), S700 (FRI-171)
- Brocco, Silvia, S224 (FRI-101-YI)
- Brochado-Kith, Oscar, S741 (SAT-379)
- Brochhausen, Christoph, S191 (WED-106)
- Brochon-Toiser, Jade, S25 (OS-029)
- Brockett, Robert, S567 (THU-203)
- Brodosi, Lucia, S544 (WED-293)
- Broekhoven, Annelotte, S47 (OS-071-YI), S204 (FRI-043), S700 (FRI-171)
- Brogden, Ruth, S661 (WED-433)
- Brol, Maximilian Joseph, S9 (LBO-004), S47 (OS-072-YI), S89 (LBP-026), S169 (THU-083), S180 (WED-074), S203 (FRI-039), S283 (WED-548), S391 (TOP-511)
- Bronniman, Matthew, S567 (THU-203)
- Bronowicki, Jean-Pierre, S41 (OS-060), S550 (WED-317)
- Brøns, Charlotte, S47 (OS-072-YI)
- Bronzoni, Jessica, S369 (SAT-009), S370 (SAT-013), S383 (SAT-044)
- Brooks, James, S392 (SAT-469)
- Brophy, Mary, S518 (WED-222)
- Broqua, Pierre, S584 (THU-258-YI), S608 (SAT-206)
- Broquetas, Teresa, S207 (FRI-051), S471 (FRI-219-YI), S817 (TOP-385-YI)
- Brosnan-Cashman, Jacqueline, S567 (THU-203), S585 (THU-261)
- Brouard, Cécile, S670 (WED-455)
- Brouwer, Kenneth, S126 (THU-316)
- Brouwer, Samantha, S763 (FRI-367)
- Brouwers, Bram, S7 (LBO-001)
- Brouwer, Willem Pieter, S464 (FRI-200), S503 (TOP-241-YI), S604 (SAT-197-YI), S643 (SAT-437-YI), S761 (FRI-363-YI)
- Brown, Ashley, S470 (FRI-215-YI), S679 (WED-477-YI)
- Browne, Sarah, S515 (WED-212), S517 (WED-219), S529 (WED-251)
- Brown, James, S8 (LBO-003)
- Brown, Richard, S58 (OS-092)
- Brown, Robert S Jr, S835 (THU-372-YI)
- Brown, Robert S Jr., S242 (SAT-082), S314 (THU-110)
- Brown, S. David, S292 (TOP-156)
- Bruandet, Amelie, S644 (SAT-439-YI)
- Brucoleri, Mariangela, S396 (SAT-481-YI)
- Brüggemann, Yannick, S58 (OS-092), S94 (LBP-034)
- Brugger-Synnes, Pascal, S795 (WED-394)
- Bruha, Radan, S539 (WED-280)
- Brûha, Radan, S311 (THU-103)
- Bruix, Jordi, S455 (THU-501)
- Brujats, Anna, S355 (SAT-543)
- Brunet, Laurence, S799 (WED-405)
- Brunet, Mercè, S291 (TOP-149-YI)
- Brunetti-Pierri, Nicola, S698 (FRI-166)
- Brunetti, Renato, S674 (WED-467-YI)
- Brunetto, Maurizia, S27 (OS-033), S73 (OS-120), S79 (LBP-005), S92 (LBP-029), S96 (LBO-038), S306 (THU-093), S310 (THU-101), S549 (WED-314-YI), S619 (SAT-245), S622 (FRI-014), S666 (WED-446), S758 (TOP-400), S776 (FRI-405), S793 (WED-391), S794 (WED-392), S804 (WED-414)
- Brunnbauer, Philipp, S84 (LBP-015)
- Bruno, Benjamin, S10 (LBO-005)
- Bruno, Daniele, S446 (THU-472-YI)
- Bruno, Pillot, S49 (OS-074)
- Bruno, Turlin, S383 (SAT-043), S520 (WED-227), S714 (WED-162)
- Bruns, Tony, S30 (OS-038-YI), S44 (OS-066-YI), S115 (TOP-346-YI), S172 (THU-092), S178 (WED-060-YI), S199 (TOP-062), S200 (TOP-064-YI), S223 (FRI-100), S229 (FRI-116), S259 (SAT-135), S308 (THU-098), S341 (THU-182), S351 (SAT-534), S356 (SAT-545), S357 (SAT-549)
- Brunt, Elizabeth M., S467 (FRI-208)
- Brusilovskaya, Ksenia, S197 (WED-122-YI), S198 (WED-125)
- Brusset, Bleuenn, S444 (THU-466)
- Bruzzzone, Bianca, S776 (FRI-405)
- Bryant, Andy, S297 (SAT-165-YI)
- Bryce, Kathleen, S661 (WED-432), S672 (WED-462), S684 (WED-491), S688 (WED-500)
- Brynjulfson, Lisa R. V., S33 (OS-044-YI)
- Brzdek, Michał, S834 (THU-367-YI)
- Buarque de Santana Sato, Emmily Daiane, S616 (SAT-237)
- Bucci, Daniele, S65 (OS-103)
- Bucci, Laura, S449 (THU-481-YI)
- Buchanan, Ryan, S647 (SAT-447)
- Buchanan, Ryan M, S633 (THU-027-YI)
- Buchanan, Ryan M., S506 (TOP-277), S645 (SAT-441-YI)
- Buch, Pau Benito, S702 (TOP-139)
- Buch, Stephan, S56 (OS-086-YI)
- Buchtele, Nina, S340 (THU-180)
- Bücker, Arno, S560 (WED-343)
- Buckholz, Adam, S138 (SAT-251)
- Bucur, Roxana, S381 (SAT-037)
- Budhoo, Nandanie, S661 (WED-433)
- Budvytyte, Laura, S152 (SAT-297)
- Buechter, Matthias, S238 (SAT-068)
- Bueno-Vélez, Marvin, S154 (SAT-303)
- Buescher, Gustav, S24 (OS-027-YI)
- Bueti, Francesca, S345 (THU-192)
- Buettner, Veronika, S426 (FRI-495)
- Buggisch, Peter, S716 (WED-170), S820 (THU-386-YI)
- Bugianesi, Elisabetta, S2 (GS-004), S4 (GS-006), S7 (LBO-001), S38 (OS-054), S79 (LBP-003), S421 (FRI-479-YI), S459 (TOP-301), S475 (FRI-230-YI), S477 (FRI-233), S480 (FRI-243), S483 (FRI-251-YI), S501 (FRI-314), S522 (WED-233-YI), S525 (WED-243-YI), S538 (WED-275), S544 (WED-293), S606 (SAT-201), S643 (SAT-438), S704 (TOP-144-YI)
- Buhmann, Raymund, S162 (THU-059)
- Buist-Homan, Manon, S582 (THU-251-YI)
- Bujanda, Luis, S32 (OS-042-YI), S50 (OS-076-YI), S64 (OS-101-YI),

Author Index

- S295 ([SAT-159-YI](#)), S536 ([WED-271](#)), S569 ([THU-210](#))
- Bukeirat, Faisal, S249 ([SAT-102](#))
- Bulato, Cristiana, S237 ([TOP-061-YI](#))
- Bumbu, Andreea Livia, S151 ([SAT-294](#))
- Bunck, Mathijs, S7 ([LBO-001](#))
- Buño, Antonio, S398 ([SAT-485](#))
- Bunse, Till, S6 ([GS-008](#))
- Bu, Peili, S100 ([LBP-045](#))
- Buque, Xabier, S32 ([OS-042-YI](#)), S64 ([OS-101-YI](#)), S112 ([FRI-343-YI](#)), S419 ([FRI-472-YI](#)), S562 ([TOP-229-YI](#)), S569 ([THU-210](#)), S693 ([FRI-153](#))
- Burade, Vinod, S615 ([SAT-231](#))
- Burda, Tatiana, S809 ([WED-371](#))
- Burden, Jemima, S298 ([SAT-167-YI](#))
- Bureau, Christophe, S6 ([GS-010](#)), S61 ([OS-097](#)), S168 ([THU-079](#)), S172 ([THU-092](#))
- Bureau, Morgane, S670 ([WED-455](#))
- Burell, Marta, S53 ([OS-081](#))
- Burghart, Lukas, S335 ([THU-166](#)), S341 ([THU-183-YI](#)), S818 ([THU-381](#))
- Burgio, Marco Dioguardi, S50 ([OS-077](#)), S53 ([OS-081](#)), S413 ([FRI-456](#))
- Burkard, Thomas, S58 ([OS-092](#))
- Burk, Caroline, S687 ([WED-498](#))
- Burke, Emma, S101 ([LBP-046](#)), S332 ([THU-160](#))
- Burke, Laura, S260 ([SAT-137](#)), S397 ([SAT-483-YI](#))
- Burkey, Jennifer, S126 ([THU-316](#))
- Burlone, Michela, S409 ([SAT-524](#)), S627 ([FRI-028](#))
- Burlone, Michela Emma, S51 ([OS-078-YI](#)), S451 ([THU-486-YI](#))
- Burns, Fiona, S661 ([WED-432](#)), S672 ([WED-462](#)), S684 ([WED-491](#)), S688 ([WED-500](#))
- Burnside, Jessica, S650 ([SAT-455](#))
- Burra, Patrizia, S237 ([TOP-061-YI](#)), S258 ([SAT-131](#)), S367 ([SAT-007-YI](#)), S368 ([SAT-009](#)), S374 ([SAT-021](#)), S376 ([SAT-024-YI](#)), S700 ([FRI-171](#))
- Burt, Alastair, S507 ([TOP-289](#))
- Burza, Maria Antonella, S374 ([SAT-021](#))
- Burz, Sebastian, S184 ([WED-083](#))
- Busafi, Said Ahmed Salim Al, S624 ([FRI-020](#))
- Busang, Jacob, S753 ([SAT-413](#))
- Buscemi, Silvio, S557 ([WED-336](#))
- Buscher, Konrad, S169 ([THU-083](#)), S198 ([WED-126](#))
- Busek, Mathias, S294 ([SAT-154-YI](#))
- Bush, Brian, S161 ([THU-058](#)), S208 ([FRI-053](#)), S218 ([FRI-086](#)), S219 ([FRI-088](#))
- Busset, Michele Droz Dit, S70 ([OS-114](#))
- Bussey, Louise, S26 ([OS-031](#)), S811 ([WED-375](#))
- Bustamante, Javier, S64 ([OS-101-YI](#))
- Butaye, Emma, S311 ([THU-102-YI](#)), S442 ([THU-463](#))
- Buti, Maria, S27 ([OS-033](#)), S39 ([OS-056-YI](#)), S79 ([LBP-005](#)), S100 ([LBP-044](#)), S407 ([SAT-516](#)), S470 ([FRI-215-YI](#)), S633 ([THU-028](#)), S662 ([WED-435](#)), S682 ([WED-485](#)), S700 ([FRI-171](#)), S702 ([TOP-139](#)), S741 ([SAT-381](#)), S746 ([SAT-393](#)), S758 ([TOP-400](#)), S761 ([FRI-363-YI](#)), S771 ([FRI-390](#)), S777 ([FRI-406](#)), S785 ([FRI-427](#)), S787 ([FRI-432](#)), S789 ([FRI-436](#)), S797 ([WED-397](#)), S802 ([WED-411](#)), S822 ([THU-395](#))
- Butler, Andrew, S81 ([LBP-008](#))
- Butler, Scott, S544 ([WED-294](#))
- Butsashvili, Maia, S659 ([WED-427](#)), S691 ([WED-515](#)), S825 ([THU-404](#))
- Buttler, Laura, S226 ([FRI-107-YI](#)), S226 ([FRI-109](#))
- Büttner, Reinhard, S423 ([FRI-486](#))
- Butt, Saad, S246 ([SAT-093-YI](#))
- Buzzanca, Valerio, S96 ([LBP-038](#)), S306 ([THU-093](#))
- Buzzetti, Elena, S496 ([FRI-290](#))
- Bybee, Grace, S742 ([SAT-382](#))
- Byers, Susan, S400 ([SAT-492](#))
- Byhoff, Elena, S649 ([SAT-451](#))
- Bylsma, Marissa, S692 ([FRI-151](#))
- Byrne, Chris D, S528 ([WED-248](#))
- Byrne, Chris D., S488 ([FRI-267](#)), S506 ([TOP-277](#))
- Byrne, Christopher, S651 ([SAT-456](#))
- Byrne, Michael, S692 ([FRI-151](#))
- Bziezi, Khalid I, S500 ([FRI-304](#))
- Caballería, Joan, S139 ([SAT-257](#)), S142 ([SAT-267](#))
- Caballeria, Llorenç, S503 ([TOP-241-YI](#))
- Caballero, Arantxa, S318 ([THU-118](#)), S330 ([THU-155](#))
- Caballero-Camino, Francisco, S300 ([SAT-175](#))
- Caballero, Gabriela, S721 ([WED-181](#))
- Cabezas, Joaquin, S79 ([LBP-005](#)), S139 ([SAT-257](#)), S142 ([SAT-267](#)), S777 ([FRI-406](#))
- Cabezas, Manuel Castro, S549 ([WED-306-YI](#)), S612 ([SAT-218](#))
- Cabibbo, Giuseppe, S51 ([OS-078-YI](#)), S252 ([SAT-113](#)), S443 ([THU-464](#)), S445 ([THU-471-YI](#))
- Cabibi, Daniela, S19 ([OS-017](#))
- Cable, Edward, S300 ([SAT-175](#)), S301 ([SAT-177](#))
- Cabral, Michelle Casanova, S598 ([THU-302](#)), S599 ([THU-304](#))
- Cabras, Silvia, S302 ([SAT-179](#))
- Cabrera, Araceli Bravo, S219 ([FRI-088](#))
- Cabrera, Fernando Martinez, S602 ([TOP-205](#))
- Cabrera, Gesalit, S776 ([FRI-403](#))
- Cabrera, Maria Cecilia, S30 ([OS-038-YI](#)), S199 ([TOP-062](#)), S200 ([TOP-064-YI](#))
- Cabrera, Roniel, S11 ([LBO-006](#)), S658 ([WED-425](#))
- Cabrera, Tatiana, S484 ([FRI-256-YI](#))
- Caccamo, Gaia, S345 ([THU-192](#)), S345 ([SAT-009](#)), S368 ([SAT-009](#)), S388 ([SAT-056](#))
- Caccia, Riccardo, S227 ([FRI-110](#))
- Cacciatore, Pierluigi, S175 ([TOP-085](#))
- Cacciola, Irene, S345 ([THU-192](#))
- Cáceres, Federico, S139 ([SAT-257](#)), S142 ([SAT-267](#))
- Cachero, Alba, S365 ([TOP-002](#)), S717 ([WED-172](#))
- Cachier, Agnes, S54 ([OS-084-YI](#))
- Cacho-Pujol, Julia, S346 ([FRI-548](#))
- Cadamuro, Luca, S96 ([LBP-038](#)), S306 ([THU-093](#)), S310 ([THU-101](#))
- Cadenas, Cristina, S85 ([LBP-017](#))
- Cadoux, Mathilde, S349 ([TOP-552](#))
- Cadranel, Jean-François, S168 ([THU-079](#)), S640 ([SAT-430](#))
- Caesar, Cornelius, S297 ([SAT-164-YI](#))
- Cahen, Djuna L, S319 ([THU-120-YI](#))
- Cai, Chao, S333 ([THU-163](#))
- Cai, Dachuan, S803 ([WED-412](#))
- Cai, Dawei, S727 ([TOP-357](#)), S749 ([SAT-402](#))
- Cai, Junwei, S526 ([WED-246](#))
- Cai, Lei, S565 ([THU-199](#))
- Caini, Patrizio, S428 ([FRI-502](#))
- Cain, Owen, S423 ([FRI-487](#)), S425 ([FRI-493](#)), S731 ([SAT-337](#))
- Caioli, Alessandro, S829 ([THU-414](#))
- Cai, Qingxian, S100 ([LBP-045](#))
- Cai, Qun, S105 ([FRI-319](#))
- Cai, Shan, S532 ([WED-259](#))
- Cai, Wuque, S622 ([FRI-010](#))
- Cai, Xiurong, S566 ([THU-201-YI](#))
- Cai, Yijing, S219 ([FRI-088](#)), S333 ([THU-163](#))
- Calabrese, Maria Pia, S439 ([THU-447](#))
- Calay, Ediz S., S326 ([LBP-135](#))
- Caldarella, Rosalia, S601 ([TOP-193](#))
- Caldarone, Francesca, S409 ([SAT-524](#))
- Caldeira, Paulo, S681 ([WED-481](#))
- Calderaro, Julien, S19 ([OS-017](#)), S349 ([TOP-552](#)), S413 ([FRI-456](#)), S438 ([THU-446](#)), S453 ([THU-494](#)), S580 ([THU-245](#)), S720 ([WED-178](#)), S743 ([SAT-386-YI](#))
- Calderón, Natalia Martagón, S298 ([SAT-170](#))
- Caldiero, Anthony, S416 ([FRI-465](#))
- Caldonazzi, Nicolás, S19 ([OS-017](#))
- Cales, Paul, S41 ([OS-060](#))
- Calia, Rosaria, S369 ([SAT-009](#))
- Calinas, Filipe, S681 ([WED-481](#)), S834 ([THU-370](#))
- Caliskan, Ali Riza, S374 ([SAT-021](#))
- Calixto, Lesly, S378 ([SAT-030](#))
- Calixto, Zyanya, S468 ([FRI-211](#))
- Callaghan, Lynne, S654 ([SAT-467](#))
- Callegaro, Annapaola, S776 ([FRI-405](#))
- Calleja, Josune Cabello, S159 ([THU-055](#)), S391 ([TOP-511](#))
- Calleri, Alberto, S210 ([FRI-056-YI](#))
- Callewaert, Hanne, S807 ([WED-363](#))
- Callewaert, Nico, S311 ([THU-102-YI](#)), S442 ([THU-463](#))
- Calls, Mallory, S326 ([THU-136](#))

- Calvaruso, Vincenza, S18 ([OS-016](#)), S19 ([OS-017](#)), S61 ([OS-096-YI](#)), S96 ([LBP-038](#)), S175 ([TOP-085](#)), S206 ([FRI-047-YI](#)), S252 ([SAT-113](#)), S306 ([THU-093](#)), S310 ([THU-101](#)), S329 ([THU-153](#)), S671 ([WED-457-YI](#))
- Calvert, Stacey, S44 ([OS-065](#))
- Calvino, Valeria, S28 ([OS-035-YI](#)), S212 ([FRI-068](#)), S224 ([FRI-101-YI](#)), S243 ([SAT-083-YI](#)), S830 ([THU-420](#))
- Calvisi, Diego, S419 ([FRI-472-YI](#))
- Calvo, Ana Avellon, S682 ([WED-483](#))
- Calvo, Henar, S391 ([TOP-512-YI](#))
- Calvo-Orteu, Maria, S120 ([SAT-325](#))
- Cama, Elena, S689 ([WED-501](#))
- Camagni, Stefania, S369 ([SAT-009](#))
- Cambra-Cortes, Vicente, S582 ([THU-250-YI](#)), S583 ([THU-257](#)), S586 ([THU-263-YI](#)), S594 ([THU-290-YI](#))
- Cambridge, William, S354 ([SAT-541](#))
- Camejo, Ana, S715 ([WED-165](#))
- Cameron, Grace, S651 ([SAT-457-YI](#))
- Cameron, Madeline, S19 ([OS-018](#)), S305 ([TOP-169](#)), S320 ([THU-121](#))
- Camilleri, Salvatore, S557 ([WED-336](#))
- Caminiti, Giuseppe, S740 ([SAT-378](#))
- Camma, Calogero, S51 ([OS-078-YI](#)), S62 ([OS-099-YI](#)), S252 ([SAT-113](#)), S310 ([THU-101](#)), S445 ([THU-471-YI](#)), S503 ([FRI-317](#)), S557 ([WED-336](#)), S609 ([SAT-209-YI](#))
- Çamöz, Elif Serteser, S407 ([SAT-518](#))
- Campadello, Paola, S224 ([FRI-101-YI](#))
- Campana, Lara, S186 ([WED-090](#))
- Campani, Claudia, S258 ([SAT-131](#)), S395 ([SAT-477-YI](#)), S426 ([FRI-498-YI](#)), S441 ([THU-458](#)), S446 ([THU-472-YI](#)), S452 ([THU-492](#))
- Campani, Daniela, S365 ([TOP-001](#)), S383 ([SAT-044](#)), S456 ([THU-502](#))
- Campbell, Cori, S676 ([WED-471](#)), S756 ([SAT-421](#)), S759 ([TOP-417](#))
- Campbell, James, S752 ([SAT-409](#))
- Campbell, John, S81 ([LBP-007](#)), S186 ([WED-090](#))
- Campello, Elena, S237 ([TOP-061-YI](#))
- Campigotto, Michele, S332 ([THU-161](#))
- Campinoti, Sara, S128 ([THU-320-YI](#))
- Campion, Daniela, S96 ([LBP-038](#)), S210 ([FRI-056-YI](#)), S306 ([THU-093](#))
- Campos-Murguía, Alejandro, S21 ([OS-021-YI](#)), S44 ([OS-066-YI](#)), S712 ([WED-160](#))
- Campos-Varela, Isabel, S9 ([LBO-004](#)), S89 ([LBP-026](#))
- Campreciós, Genís, S15 ([OS-010](#)), S179 ([WED-070](#))
- Camps, Jordi, S582 ([THU-250-YI](#)), S583 ([THU-257](#)), S586 ([THU-263-YI](#)), S594 ([THU-290-YI](#))
- Camus, Christophe, S116 ([SAT-315](#)), S156 ([TOP-108](#))
- Camus, Gregory, S812 ([WED-376](#))
- Canalis, Chiara, S451 ([THU-486-YI](#))
- Canarutto, Giulia, S280 ([WED-540-YI](#))
- Canas-Perez, Itzel, S700 ([FRI-171](#))
- Cancado, Eduardo, S343 ([THU-188](#))
- Cançado, Guilherme, S320 ([THU-121](#))
- Cancelo, Ana Álvarez, S329 ([THU-154-YI](#))
- Candels, Lena Susanna, S273 ([WED-521-YI](#))
- Candinas, Daniel, S373 ([SAT-019](#))
- Candotti, Daniel, S751 ([SAT-408](#))
- Cañedo-Villarroya, Elvira, S693 ([FRI-153](#))
- Caneglias, Alessandro, S175 ([TOP-085](#))
- Cañete, Nuria, S139 ([SAT-257](#)), S142 ([SAT-267](#)), S207 ([FRI-051](#))
- Canga, Elia, S120 ([SAT-325](#))
- Canillas, Lidia, S207 ([FRI-051](#)), S817 ([TOP-385-YI](#))
- Canini, Valentina, S19 ([OS-017](#))
- Canivet, Clémence M, S2 ([GS-004](#)), S37 ([OS-053](#)), S38 ([OS-054](#)), S519 ([WED-224](#))
- Canivet, Clémence M., S456 ([THU-503](#))
- Cannavò, Maria Rita, S96 ([LBP-038](#)), S306 ([THU-093](#))
- Cannegieter, Suzanne, S204 ([FRI-043](#))
- Cannella, Roberto, S503 ([FRI-317](#))
- Canning, Rachel, S504 ([TOP-252-YI](#))
- Cannito, Stefania, S421 ([FRI-479-YI](#)), S612 ([SAT-219](#))
- Cannon, Mary D, S820 ([THU-383](#))
- Cannon, Megan, S692 ([FRI-151](#))
- Cano, Ainara, S693 ([FRI-153](#))
- Cano, Clara Sánchez, S365 ([TOP-002](#))
- Cano, Susana, S398 ([SAT-485](#))
- Canova, Lorenzo, S344 ([THU-190](#)), S396 ([SAT-481-YI](#)), S397 ([SAT-482](#)), S401 ([SAT-493-YI](#)), S413 ([FRI-456](#))
- Cantafora, Alfredo, S215 ([FRI-077-YI](#))
- Cantiga, Cristiane, S271 ([THU-556](#))
- Cant, Mark, S186 ([WED-090](#))
- Cantó, Elisabet, S355 ([SAT-543](#))
- Canva, Valérie, S644 ([SAT-439-YI](#))
- Cao, Di, S558 ([WED-337](#))
- Cao, Fei, S628 ([FRI-035](#)), S780 ([FRI-411-YI](#))
- Cao, Haifang, S783 ([FRI-420](#))
- Cao, Haixia, S99 ([LBP-043](#))
- Cao, Jie, S387 ([SAT-054](#))
- Cao, Rena, S380 ([SAT-036-YI](#))
- Cao, Rui, S573 ([THU-223](#))
- Cao, Shuya, S403 ([SAT-499](#))
- Cao, Weihua, S344 ([THU-191](#))
- Cao, Xu, S194 ([WED-114](#)), S755 ([SAT-419](#)), S755 ([SAT-420](#))
- Cao, Yaling, S107 ([FRI-325](#))
- Cao, Yuzhe, S390 ([TOP-510](#))
- Cao, Zhenhuan, S227 ([FRI-111](#)), S677 ([WED-472](#))
- Cao, Zhujun, S161 ([THU-058](#)), S208 ([FRI-053](#)), S219 ([FRI-088](#))
- Caparrós, Esther, S194 ([WED-113](#))
- Capel, Jeroen, S206 ([FRI-046](#))
- Capelli, Roberta, S499 ([FRI-299](#))
- Capilla, Alicia, S141 ([SAT-262](#))
- Capinha, Francisco, S52 ([OS-080](#)), S220 ([FRI-090](#)), S405 ([SAT-513](#))
- Capodicasa, Luigi, S252 ([SAT-113](#)), S310 ([THU-101](#))
- Caporali, Cristian, S62 ([OS-099-YI](#))
- Capozza, Thomas, S95 ([LBP-036](#))
- Capparelli, Emma, S554 ([WED-325-YI](#))
- Capparuccia, Marco Rivano, S791 ([FRI-442](#))
- Cappelli, Simone, S549 ([WED-314-YI](#)), S619 ([SAT-245](#)), S622 ([FRI-014](#))
- Cappuyns, Sarah, S411 ([TOP-507-YI](#))
- Capraru, Camelia, S673 ([WED-464](#)), S688 ([WED-499](#))
- Capua, Martina Di, S790 ([FRI-441](#))
- Caraceni, Paolo, S30 ([OS-038-YI](#)), S157 ([THU-050](#)), S161 ([THU-057-YI](#)), S188 ([WED-098-YI](#)), S193 ([WED-112](#)), S199 ([TOP-062](#)), S200 ([TOP-064-YI](#)), S206 ([FRI-047-YI](#)), S215 ([FRI-078-YI](#)), S700 ([FRI-171](#))
- Caracta, Cynthia, S693 ([FRI-151](#))
- Carazo, Antonio Duarte, S668 ([WED-449](#))
- Carbonell-Asins, Juan Antonio, S202 ([TOP-066-YI](#)), S232 ([FRI-125](#))
- Carbonell, Michael, S553 ([WED-324](#))
- Carbonell, Nicolas, S6 ([GS-010](#)), S168 ([THU-079](#))
- Carbone, Marco, S5 ([GS-007](#)), S19 ([OS-017](#)), S96 ([LBP-038](#)), S299 ([SAT-171](#)), S306 ([THU-093](#)), S308 ([THU-098](#)), S310 ([THU-101](#)), S311 ([THU-102-YI](#)), S321 ([THU-125](#)), S325 ([THU-133-YI](#)), S332 ([THU-161](#)), S335 ([THU-167](#))
- Carda-Auten, Jessica, S394 ([SAT-476](#))
- Cardenas, Andres, S240 ([SAT-074](#)), S378 ([SAT-030](#))
- Cárdenas-García, Antonio, S593 ([THU-287](#))
- Cardillo, Massimo, S367 ([SAT-007-YI](#)), S389 ([SAT-058](#))
- Cardinale, Vincenzo, S310 ([THU-101](#))
- Cardinali, Sara, S533 ([WED-261-YI](#))
- Cardone, Kirsten, S604 ([SAT-196](#))
- Cardoso, Filipe Sousa, S115 ([TOP-346-YI](#))
- Cardoso, Joana, S362 ([WED-015](#))
- Cardoso, Mariana, S793 ([WED-391](#))
- Cardoso, Miguel, S358 ([SAT-554-YI](#))
- Carestia, Agostina, S112 ([FRI-342](#))
- Caretti, Anna, S428 ([FRI-514](#))
- Carey, Elizabeth, S10 ([LBO-005](#))
- Carey, Ivana, S756 ([SAT-421](#)), S759 ([TOP-416-YI](#)), S763 ([FRI-367](#)), S775 ([FRI-399](#)), S793 ([WED-391](#)), S820 ([THU-383](#))
- Cargill, Zillah, S759 ([TOP-416-YI](#)), S775 ([FRI-399](#))
- Cariou, Bertrand, S93 ([LBP-032](#)), S508 ([WED-194](#))
- Carla, Cremonese, S203 ([FRI-039](#))
- Carleo, Rossana, S571 ([THU-218](#))
- Carleton, Michael, S571 ([THU-219](#))
- Carlhäll, Carl-Johan, S532 ([WED-259](#))
- Carli, Fabrizia, S593 ([THU-286](#))
- Carlis, Luciano De, S445 ([THU-470-YI](#))
- Carlomagno, Matteo, S466 ([FRI-207-YI](#)), S482 ([FRI-248-YI](#))
- Carlioni, Vinicio, S428 ([FRI-502](#))

Author Index

- Carlos García-Pagán, Juan, S180 ([WED-071](#)), S255 ([SAT-123](#))
- Carlos Ruiz-Cobo, Juan, S787 ([FRI-432](#))
- Carlos, Terra, S83 ([LBP-012](#))
- Carlota Londoño, María, S293 ([SAT-153-YI](#)), S329 ([THU-154-YI](#)), S330 ([THU-155](#)), S336 ([THU-170-YI](#)), S344 ([THU-189](#)), S711 ([WED-155](#))
- Carlsson, Björn, S93 ([LBP-031](#)), S554 ([WED-325-YI](#))
- Carmichael, Elizabeth, S416 ([FRI-463-YI](#))
- Carnevale, Sara, S215 ([FRI-077-YI](#))
- Carnicero, Carmen, S71 ([OS-116](#)), S596 ([THU-296](#))
- Carnì, Paola, S96 ([LBP-038](#)), S306 ([THU-093](#))
- Caro, Antonia, S207 ([FRI-051](#))
- Carole, Cagnot, S41 ([OS-060](#))
- Caroline, Lemaitre, S640 ([SAT-430](#))
- Carol, Marta, S160 ([THU-056](#)), S176 ([WED-055](#)), S503 ([TOP-241-YI](#)), S541 ([WED-284-YI](#))
- Caron de Fromentel, Claude, S280 ([WED-540-YI](#))
- Carone, Livia, S9 ([LBO-004](#)), S89 ([LBP-026](#))
- Carrai, Paola, S370 ([SAT-013](#))
- Carramiñana, Sonia, S154 ([SAT-304](#))
- Carraresi, Laura, S674 ([WED-467-YI](#))
- Carraro, Amedeo, S368 ([SAT-009](#))
- Carrat, Fabrice, S5 ([GS-007](#)), S41 ([OS-060](#)), S733 ([SAT-343](#))
- Carrero, Zunamys, S19 ([OS-017](#))
- Carrieri, Patrizia, S508 ([WED-195](#)), S670 ([WED-455](#)), S678 ([WED-475](#))
- Carrier, Paul, S168 ([THU-079](#)), S387 ([SAT-052](#))
- Carrilho, Flair Jose, S83 ([LBP-012](#)), S157 ([THU-050](#))
- Carrillo, Maria Cortes, S350 ([TOP-553](#))
- Carrión, Gemma, S717 ([WED-172](#))
- Carrión, Jose A., S207 ([FRI-051](#)), S255 ([SAT-123](#)), S471 ([FRI-219-YI](#)), S817 ([TOP-385-YI](#))
- Carroccio, Antonio, S557 ([WED-336](#)), S601 ([TOP-193](#))
- Carrodegas, Alba, S668 ([WED-449](#))
- Carr-Smith, Camilla, S350 ([TOP-553](#))
- Cartabellotta, Fabio, S557 ([WED-336](#)), S671 ([WED-457-YI](#))
- Carter, Victoria, S645 ([SAT-440](#))
- Carucci, Patrizia, S451 ([THU-486-YI](#)), S458 ([THU-517](#))
- Caruntu, Florin Alexandru, S759 ([TOP-416-YI](#))
- Caruso, Stefano, S349 ([TOP-552](#)), S413 ([FRI-456](#)), S648 ([SAT-449](#)), S720 ([WED-178](#)), S743 ([SAT-386-YI](#))
- Caruso, Teresita, S674 ([WED-467-YI](#))
- Carvalho, Sofia, S220 ([FRI-090](#)), S358 ([SAT-554-YI](#)), S405 ([SAT-513](#))
- Carvalho-Gomes, Ângela, S361 ([WED-009](#)), S531 ([WED-257](#)), S700 ([FRI-171](#)), S787 ([FRI-432](#))
- Carvelli, Ana, S541 ([WED-284-YI](#))
- Casabella, Antonio, S29 ([OS-037](#))
- Casado-Carbajo, Julia, S154 ([SAT-303](#))
- Casado-Martin, Marta, S170 ([THU-086](#)), S668 ([WED-449](#)), S777 ([FRI-406](#)), S779 ([FRI-409](#)), S836 ([THU-374](#))
- Casar, Christian, S350 ([SAT-531-YI](#))
- Casari, Federico, S62 ([OS-099-YI](#))
- Casas, Meritxell, S141 ([SAT-262](#)), S233 ([FRI-126](#)), S829 ([THU-418](#))
- Cascione, Luciano, S592 ([THU-285](#))
- Casella, Silvia, S96 ([LBP-038](#)), S306 ([THU-093](#))
- Casey, Carol, S132 ([THU-333](#)), S742 ([SAT-382](#))
- Casillas, Linda, S332 ([THU-160](#)), S472 ([FRI-220-YI](#)), S476 ([FRI-232](#))
- Casirati, Elia, S593 ([THU-286](#))
- Cas, Michele Dei, S428 ([FRI-514](#))
- Caspanello, Amalia Rita, S830 ([THU-420](#))
- Cassard, Anne-Marie, S130 ([THU-327](#)), S136 ([THU-347-YI](#))
- Cassidy, Sophie, S297 ([SAT-165-YI](#))
- Cassinotto, Cristophe, S238 ([SAT-068](#))
- Castagna, Antonella, S824 ([THU-402](#))
- Castagno, Davide, S475 ([FRI-230-YI](#)), S480 ([FRI-243](#))
- Castañeda Agredo, Andrés Felipe, S599 ([THU-304](#))
- Castaneda, Eduardo Gomez, S807 ([WED-364](#))
- Castañé, Helena, S582 ([THU-250-YI](#)), S583 ([THU-257](#)), S586 ([THU-263-YI](#)), S594 ([THU-290-YI](#))
- Castano-Garcia, Andrés, S455 ([THU-500](#))
- Castellaccio, Alice, S674 ([WED-467-YI](#))
- Castellana, Eleonora, S451 ([THU-486-YI](#)), S458 ([THU-517](#))
- Castellaneta, Antonino, S96 ([LBP-038](#)), S306 ([THU-093](#)), S310 ([THU-101](#))
- Castellano, Giancarlo, S24 ([OS-026-YI](#))
- Castellano, Pablo Alonso, S717 ([WED-172](#))
- Castellanos, Keyla, S641 ([SAT-431-YI](#))
- Castelli, Carlotta, S772 ([FRI-392-YI](#))
- Castelli, Florence, S174 ([TOP-073](#)), S184 ([WED-083](#))
- Castelli, Marco, S492 ([FRI-279-YI](#))
- Castell, Javier, S71 ([OS-116](#))
- Castello, Borja, S287 ([FRI-538](#))
- Castello, Inmaculada, S329 ([THU-154-YI](#)), S336 ([THU-170-YI](#))
- Castelnuovo, Gabriele, S475 ([FRI-230-YI](#)), S480 ([FRI-243](#)), S483 ([FRI-251-YI](#)), S501 ([FRI-314](#)), S522 ([WED-233-YI](#)), S525 ([WED-243-YI](#))
- Castelo-Branco, Miguel, S21 ([OS-020](#))
- Castera, Laurent, S2 ([GS-004](#)), S38 ([OS-054](#)), S52 ([OS-080](#)), S84 ([LBP-014](#)), S503 ([TOP-241-YI](#)), S524 ([WED-239](#)), S526 ([WED-245](#)), S528 ([WED-248](#)), S538 ([WED-275](#))
- Castiella, Agustin, S341 ([THU-182](#))
- Castillero, Estibaliz, S562 ([TOP-229-YI](#)), S569 ([THU-210](#))
- Castillo, Anny Camelo, S668 ([WED-449](#)), S779 ([FRI-409](#))
- Castillo-Castañeda, Stephany, S171 ([THU-089](#))
- Castillo, Elisa, S189 ([WED-100-YI](#)), S277 ([WED-530-YI](#))
- Castillo-González, Raquel, S276 ([WED-528-YI](#))
- Castillo, Joaquín Andrés, S160 ([THU-056](#))
- Castillo, Mauricio, S83 ([LBP-012](#)), S208 ([FRI-053](#))
- Castillo-Molina, Laura, S170 ([THU-086](#)), S779 ([FRI-409](#))
- Castillo, Pilar, S398 ([SAT-485](#)), S706 ([WED-132](#)), S712 ([WED-159](#))
- Castoldi, Mirco, S426 ([FRI-495](#))
- Castro, Idolina, S654 ([SAT-466](#))
- Castro, Joana, S654 ([SAT-467](#))
- Castro-Narro, Graciela, S9 ([LBO-004](#)), S89 ([LBP-026](#))
- Castro, Rafael Romero, S559 ([WED-341](#))
- Castro, Raísa Quiñones, S45 ([OS-067](#)), S277 ([WED-529](#))
- Castro, Rui E., S32 ([OS-042-YI](#)), S286 ([WED-558](#)), S358 ([SAT-554-YI](#))
- Castven, Darko, S582 ([THU-254-YI](#))
- Casula, Elisabetta, S232 ([FRI-125](#))
- Casulleras, Mireia, S16 ([OS-011](#)), S185 ([WED-087](#))
- Catalano, Gabriele, S370 ([SAT-013](#))
- Català-Senent, José, S592 ([THU-283](#))
- Catanese, Maria Teresa, S26 ([OS-030](#))
- Catanzaro, Elisa, S318 ([THU-117-YI](#))
- Cathcart, Andrea, S812 ([WED-376](#))
- Cathomen, Toni, S693 ([FRI-152-YI](#))
- Cattan, Stéphane, S444 ([THU-466](#)), S644 ([SAT-439-YI](#))
- Cattel, Francesco, S451 ([THU-486-YI](#)), S458 ([THU-517](#))
- Cattral, Mark S., S381 ([SAT-037](#)), S381 ([SAT-039](#))
- Caturano, Alfredo, S790 ([FRI-441](#))
- Cauchy, Francois, S451 ([THU-487-YI](#))
- Caudai, Cinzia, S776 ([FRI-405](#))
- Causse, Xavier, S73 ([OS-120](#)), S387 ([SAT-052](#)), S640 ([SAT-430](#)), S793 ([WED-391](#))
- Caussy, Cyrielle, S49 ([OS-074](#)), S508 ([WED-194](#)), S528 ([WED-248](#)), S538 ([WED-275](#)), S538 ([WED-278](#)), S550 ([WED-317](#))
- Cavalletto, Luisa, S660 ([WED-430](#))
- Cavalli, Ilaria, S96 ([LBP-038](#)), S306 ([THU-093](#))
- Cavallone, Daniela, S776 ([FRI-405](#))
- Caviglia, Gian Paolo, S59 ([OS-094](#)), S210 ([FRI-056-YI](#)), S371 ([SAT-015-YI](#)), S421 ([FRI-479-YI](#)), S451 ([THU-486-YI](#)), S458 ([THU-517](#)), S475 ([FRI-230-YI](#)), S480 ([FRI-243](#)), S522 ([WED-233-YI](#)), S525 ([WED-243-YI](#)), S544 ([WED-293](#)), S772 ([FRI-392-YI](#))
- Çavuş, Bilger, S377 ([SAT-028](#)), S551 ([WED-318-YI](#)), S803 ([WED-413](#))

- Cazemier, Marcel, S319 (THU-120-YI)
 Cazier, Helene, S412 (FRI-454)
 Cazzagon, Nora, S5 (GS-007),
 S96 (LBP-038), S306 (THU-093),
 S308 (THU-098), S310 (THU-101),
 S318 (THU-117-YI), S321 (THU-125),
 S712 (WED-158-YI), S725 (WED-191)
 Cazzaniga, Giorgio, S19 (OS-017),
 S299 (SAT-171), S641 (SAT-431-YI)
 Cebeci, Timurhan, S803 (WED-413)
 Cebotarescu, Valentin, S791 (FRI-443)
 Ceccherini Silberstein, Francesca,
 S777 (FRI-405)
 Cederborg, Anna, S530 (WED-255-YI)
 Ceesay, Amie, S782 (FRI-418),
 S786 (FRI-431)
 Cefalù, Angelo Baldassare, S557 (WED-336)
 Celada-Sendino, Miriam, S139 (SAT-257),
 S142 (SAT-267)
 Celant, Anna, S35 (OS-048)
 Celik, Ferya, S11 (OS-001)
 Celis-Morales, Carlos, S138 (SAT-254)
 Celli, Natascia, S836 (THU-375)
 Celsa, Ciro, S51 (OS-078-YI), S252 (SAT-113),
 S310 (THU-101), S443 (THU-464),
 S445 (THU-471-YI), S503 (FRI-317),
 S609 (SAT-209-YI)
 Cendron, Laura, S612 (SAT-219)
 Centeno, Delphine, S422 (FRI-485)
 Centofanti, Lucia, S592 (THU-285)
 Centonze, Leonardo, S445 (THU-470-YI)
 Cen, Yelei, S110 (FRI-334)
 Ceola, Stefano, S19 (OS-017)
 Cepic, Sara, S155 (SAT-305)
 Cerami, Laura, S593 (THU-286)
 Cercato, Cintia, S93 (LBP-032)
 Cereijo-Fernández, Javier, S690 (WED-513)
 Ceriani, Roberto, S404 (SAT-502-YI),
 S406 (SAT-514), S439 (THU-447)
 Cerini, Federica, S96 (LBP-038),
 S306 (THU-093), S310 (THU-101),
 S439 (THU-447), S497 (FRI-294),
 S705 (WED-130)
 Cериotti, Ferruccio, S401 (SAT-493-YI),
 S781 (FRI-412)
 Cerisuelo, Miriam Cortes, S388 (SAT-057)
 Cernat, Roxana, S819 (THU-382)
 Cerny, Andreas, S341 (THU-182)
 Cerochi, Orlando, S49 (OS-075-YI)
 Cerpa, Alberto, S398 (SAT-485)
 Cerrito, Lucia, S452 (THU-492)
 Cerutti, Elisabetta, S367 (SAT-007-YI)
 Cervantes, Alejandra, S642 (SAT-434)
 Cervello, Melchiorre, S601 (TOP-193)
 Červenková, Lenka, S349 (FRI-556)
 Cervera, Marta, S160 (THU-056),
 S176 (WED-055), S541 (WED-284-YI)
 Cesarini, Lucia, S376 (SAT-025),
 S380 (SAT-034), S451 (THU-486-YI)
 Cescon, Matteo, S368 (SAT-009),
 S390 (TOP-509-YI), S704 (TOP-143-YI)
 Cespiati, Annalisa, S332 (THU-161),
 S466 (FRI-207-YI), S474 (FRI-226),
 S482 (FRI-248-YI), S497 (FRI-294)
 Cetin, Okan, S803 (WED-413)
 Ceunen, Helga, S157 (THU-049)
 Chae, Eun Hee, S270 (THU-555)
 Chae, Yuna, S264 (THU-531)
 Chai, Krisna, S778 (FRI-407)
 Chainuvati, Siwaporn, S642 (SAT-435),
 S796 (WED-396)
 Chaitanya-Bhide, Varsha, S639 (SAT-427-YI)
 Chaker, Loyal, S606 (SAT-200-YI)
 Chakrabarty, Gayatri, S633 (THU-029)
 Chalatsis, Evangelos, S820 (THU-383)
 Chalaye, Julia, S50 (OS-077),
 S373 (SAT-020), S453 (THU-494)
 Chambers, Jenny, S274 (WED-523)
 Chamorro -Tojeiro, Sandra,
 S664 (WED-440)
 Chamroomkul, Naichaya, S396 (SAT-480-YI),
 S410 (SAT-529)
 Chan, Albert CY, S375 (SAT-023)
 Chandak, Aastha, S836 (THU-374)
 Chanda, Sushmita, S564 (THU-198),
 S728 (TOP-358-YI), S806 (WED-361),
 S807 (WED-365), S812 (WED-378)
 Chandes, Florine, S823 (THU-397-YI)
 Chandler, Christopher, S369 (SAT-009)
 Chan, Doreen, S8 (LBO-002),
 S612 (SAT-220-YI)
 Chandramouli, Abhishek Shankar,
 S477 (FRI-233)
 Chan, Esther Wai Yin, S116 (SAT-314)
 Chang, Chun-Chao, S832 (THU-365)
 Chang, Devon Y., S576 (THU-233),
 S579 (THU-242)
 Chang, Jason Pik Eu, S169 (THU-082),
 S238 (SAT-068), S525 (WED-242)
 Chang, Liuyi, S119 (SAT-321)
 Chang, Michael, S12 (OS-003)
 Chang, Min, S344 (THU-191)
 Chang, Pei-Yuan, S637 (THU-046)
 Chang, Shao-Hsuan, S658 (WED-425)
 Chang, Silvia, S737 (SAT-371)
 Chang, Te-Sheng, S74 (OS-121),
 S832 (THU-365)
 Chang, Wei-Ting, S493 (FRI-280)
 Chang, Yoosoo, S517 (WED-221)
 Chan, Henry L.Y., S510 (WED-198),
 S761 (FRI-362-YI), S761 (FRI-363-YI),
 S770 (FRI-387), S771 (FRI-390)
 Chan, Kun-Ming, S414 (FRI-458)
 Chan, Sally, S250 (SAT-107-YI)
 Chan, Shih-Yen, S797 (WED-398)
 Chan, Stephen, S3 (GS-005)
 Chantal, Dessy, S588 (THU-272-YI)
 Chan, Wah-Kheong, S2 (GS-004),
 S643 (SAT-438)
 Chanwat, Rawisak, S401 (SAT-495)
 Chao, Jessica, S126 (THU-315)
 Chao, Tingxia, S783 (FRI-420)
 Chappell, Katie, S127 (THU-317)
 Charalampous, Themoula,
 S185 (WED-088-YI)
 Charatcharoenwittaya, Phunchai,
 S642 (SAT-435), S796 (WED-396)
 Charbonney, Emmanuel, S187 (WED-092)
 Charchuta, Mikolaj, S272 (WED-517)
 Charlotte, Frederic, S239 (SAT-071),
 S512 (WED-206), S533 (WED-262)
 Charlton, Michael, S37 (OS-051),
 S463 (FRI-198), S464 (FRI-199),
 S467 (FRI-208), S481 (FRI-247),
 S482 (FRI-249), S504 (TOP-253),
 S507 (TOP-300), S511 (WED-201),
 S511 (WED-202), S518 (WED-223),
 S648 (SAT-450)
 Charpy, Flora, S385 (SAT-048)
 Charrière, Sybil, S508 (WED-194),
 S538 (WED-278)
 Chascsa, David M. H., S152 (SAT-297),
 S608 (SAT-207)
 Chassaing, Benoit, S136 (THU-347-YI)
 Chatelier, Emmanuelle Le, S159 (THU-053)
 Chattergoon, Michael A., S75 (OS-127),
 S816 (WED-389)
 Chatzigeorgiou, Antonios, S570 (THU-214),
 S599 (THU-306)
 Chatziioannou, Anastasia Chrysovalantou,
 S275 (WED-525)
 Chatzikosma, Charikleia, S229 (FRI-117)
 Chaudhary, Kanishk, S559 (WED-340)
 Chaudhuri, Subhra, S729 (TOP-368)
 Chauhan, Neha, S164 (THU-068),
 S164 (THU-069), S605 (SAT-199)
 Chauhan, Shivi, S184 (WED-086),
 S195 (WED-118)
 Chaves-Blanco, Lucía, S691 (WED-516),
 S779 (FRI-409)
 Chavez-Pacheco, Juan, S171 (THU-089)
 Chayama, Kazuaki, S42 (OS-061),
 S735 (SAT-364)
 Chayanupatkul, Maneerat, S689 (WED-502)
 Chazouillères, Olivier, S5 (GS-007),
 S41 (OS-060), S313 (THU-107),
 S326 (THU-136)
 Chebaro, Alexandre, S383 (SAT-043)
 Chee, Grace M., S1 (GS-002), S92 (LBP-029),
 S738 (SAT-373), S758 (TOP-400),
 S764 (FRI-371), S769 (FRI-383),
 S778 (FRI-407), S794 (WED-392),
 S796 (WED-395)
 Chegade, Nabil El Hage, S384 (SAT-047)
 Chegade, Nour El Hage, S384 (SAT-047)
 Chelstowska, Sylwia, S328 (THU-152-YI)
 Chemello, Liliana, S660 (WED-430)
 Chemin, Isabelle, S782 (FRI-418),
 S786 (FRI-431)
 Chen, Ao, S419 (FRI-473)
 Chen, Bo, S320 (THU-121), S497 (FRI-293),
 S688 (WED-499)
 Chen, Chao, S784 (FRI-424)
 Chen, Chaobo, S403 (SAT-499)
 Chen, Chao-Long, S375 (SAT-023),
 S445 (THU-470-YI)
 Chen, Chen, S333 (THU-163)
 Chen, Chien-Hung, S74 (OS-121),
 S401 (SAT-495)
 Chen, Chi-Yi, S26 (OS-031), S74 (OS-121),
 S86 (LBP-019), S809 (WED-371),
 S832 (THU-365)

Author Index

- Chen, Chun-Ting, S832 (THU-365)
 Chen, Dongbo, S429 (FRI-515)
 Cheneke, Waqtola, S781 (FRI-414)
 Chen, Ethan, S26 (OS-030)
 Chen, Fen-Fang, S399 (SAT-486)
 Cheng, Andrew, S8 (LBO-002),
 S612 (SAT-220-YI)
 Cheng, Chao, S260 (SAT-136)
 Cheng, Chien-Yu, S832 (THU-365)
 Cheng, Cong, S26 (OS-030)
 Cheng, Franco Wing Tak, S116 (SAT-314)
 Cheng, Guofeng, S86 (LBP-019),
 S99 (LBP-043)
 Cheng, Hong Sheng, S280 (WED-539)
 Cheng, Jie, S696 (FRI-161),
 S698 (FRI-164)
 Cheng, Long, S69 (OS-112-YI)
 Cheng, Pin-Nan, S74 (OS-121),
 S832 (THU-365)
 Chen, Guei-Ying, S832 (THU-365)
 Cheng, Yang, S81 (LBP-009)
 Cheng, Ya-Ting, S784 (FRI-426)
 Cheng, Ya-Yun, S493 (FRI-280)
 Chen, Hao, S100 (LBP-045)
 Chen, Haoqi, S271 (TOP-562),
 S347 (FRI-551), S363 (WED-020)
 Chen, Hening, S755 (SAT-419),
 S755 (SAT-420)
 Chen, Hongsong, S429 (FRI-515),
 S790 (FRI-440)
 Chen, Huazhong, S117 (SAT-318)
 Chen, Hui, S726 (TOP-354),
 S803 (WED-412)
 Chen, Itsuko Chih-Yi,
 S445 (THU-470-YI)
 Chen, Jia, S109 (FRI-331)
 Chen, Jiaxian, S105 (FRI-319),
 S345 (FRI-546)
 Chen, Jinjun, S95 (LBP-037),
 S100 (LBP-045), S117 (SAT-318),
 S209 (FRI-053), S238 (SAT-068),
 S605 (SAT-198)
 Chen, Li, S24 (OS-026-YI), S474 (FRI-225),
 S533 (WED-262), S590 (THU-278),
 S591 (THU-282), S597 (THU-298),
 S599 (THU-305)
 Chen, Liang, S100 (LBP-045)
 Chen, Linda, S836 (THU-374)
 Chen, Lingyan, S135 (THU-343)
 Chen, Lu, S333 (THU-163)
 Chen, Michael, S544 (WED-294)
 Chen, Min, S747 (SAT-395)
 Chen, Mingyue, S86 (LBP-019)
 Chen, Minjun, S148 (SAT-285-YI)
 Chen, Ping, S726 (TOP-354)
 Chen, Qi, S742 (SAT-383)
 Chen, Qianqian, S625 (FRI-022)
 Chen, Qincong, S100 (LBP-045)
 Chen, Qingyu, S111 (FRI-338),
 S111 (FRI-339)
 Chen, Rusi, S395 (SAT-477-YI),
 S499 (FRI-299)
 Chen, Shao-Ting, S124 (SAT-336)
 Chen, Shiwei, S586 (THU-262)
 Chen, Shiyao, S106 (FRI-322),
 S242 (SAT-081), S268 (THU-546),
 S275 (WED-524-YI)
 Chen, Shuai, S362 (WED-017-YI),
 S566 (THU-201-YI)
 Chen, Shuohua, S655 (SAT-468)
 Chen, Si Emma, S656 (TOP-460-YI)
 Chen, Sisi, S121 (SAT-330)
 Chen, Siyuan, S427 (FRI-500-YI)
 Chen, Tao, S158 (THU-052), S167 (THU-078)
 Chen, Tianyan, S19 (OS-018),
 S305 (TOP-169), S789 (FRI-438)
 Chen, Vincent, S84 (LBP-014),
 S146 (SAT-278), S478 (FRI-236-YI)
 Chen, Wei, S121 (SAT-326)
 Chen, Wei-Ting, S414 (FRI-458)
 Chen, Wen-Chi, S490 (FRI-271),
 S493 (FRI-280)
 Chen, Xiangmei, S734 (SAT-362)
 Chen, Xiaofei, S36 (OS-050), S87 (LBP-021)
 Chen, Xiaolong, S271 (TOP-562),
 S347 (FRI-551), S363 (WED-020)
 Chen, Xiaoman, S574 (THU-226)
 Chen, Xiaoxue, S344 (THU-191)
 Chen, Xin, S108 (FRI-330), S300 (SAT-175)
 Chen, Xinyue, S677 (WED-472)
 Chen, Xiong, S433 (FRI-527)
 Chen, Xiyao, S430 (FRI-517),
 S437 (TOP-504)
 Chen, Yajin, S382 (SAT-041)
 Chen, Yan, S784 (FRI-424)
 Chen, Yazhou, S392 (TOP-520),
 S528 (WED-247), S567 (THU-206)
 Chen, Yen-Wen, S300 (SAT-175)
 Chen, Ying, S100 (LBP-045)
 Chen, Yi-Pei, S812 (WED-376)
 Chen, Yi-Yu, S490 (FRI-271), S493 (FRI-280)
 Chen, Yu, S113 (FRI-347), S117 (SAT-318),
 S280 (WED-541)
 Chen, Yue, S605 (SAT-198)
 Chen, Yu-Fu, S256 (SAT-125)
 Chen, Yu-Jen, S256 (SAT-125)
 Chen, Yun, S646 (SAT-446)
 Chen, Yuping, S526 (WED-246),
 S620 (TOP-006)
 Chen, Yuxin, S780 (FRI-411-YI)
 Chen, Zhi-wei, S727 (TOP-356)
 Chen, Zhiwei, S271 (TOP-562),
 S347 (FRI-551), S363 (WED-020)
 Cheon, Gab Jin, S247 (SAT-098)
 Cheon, Jaekyung, S51 (OS-078-YI)
 Cheres, Ioana, S409 (SAT-525)
 Chermak, Faiza, S6 (GS-010),
 S369 (SAT-010), S385 (SAT-048)
 Cherqui, Daniel, S378 (SAT-029)
 Cherry, Roger, S406 (SAT-515)
 Cherubini, Alessandro, S593 (THU-286)
 Chessa, Luchino, S96 (LBP-038),
 S306 (THU-093), S322 (THU-127-YI)
 Chetouani, Mohamed, S207 (FRI-050-YI)
 Cheuk-Fung Yip, Terry, S38 (OS-054),
 S770 (FRI-387)
 Cheung, Angela, S19 (OS-018),
 S305 (TOP-169)
 Cheung, Ching Lung, S116 (SAT-314)
 Cheung, Ka, S289 (FRI-542)
 Cheung, Ramsey C., S150 (SAT-292),
 S154 (SAT-302), S771 (FRI-389)
 Cheung, Tan-To, S424 (FRI-490-YI)
 Cheung, Tanto, S438 (THU-446)
 Chevaliez, Stéphane, S28 (OS-034),
 S743 (SAT-386-YI), S784 (FRI-425),
 S786 (FRI-431)
 Chevallier, Patrick, S68 (OS-110)
 Chevre, Raphael, S133 (THU-338)
 Chew, Francisco, S641 (SAT-431-YI)
 Chew, Nicholas Foo-Siong, S757 (WED-420)
 Chianetta, Roberta, S601 (TOP-193)
 Chiappetta, Michele, S740 (SAT-378)
 Chiara, Francesco De, S46 (OS-069)
 Chicano, Dámaris Martínez, S694 (FRI-153)
 Chi, Chen-Ta, S449 (THU-479)
 Chidambaram, Nachaippan, S10 (LBO-005)
 Chida, Takeshi, S537 (WED-273)
 Chien, Rong-Nan, S656 (TOP-461-YI),
 S761 (FRI-363-YI), S772 (FRI-391),
 S782 (FRI-415), S784 (FRI-426)
 Chien, Yong Chee, S9 (LBO-004),
 S89 (LBP-026)
 Chihab, Kinan, S21 (OS-021-YI)
 Chihiro, Goto, S301 (SAT-176)
 Chimeno, Milagros Muñoz,
 S682 (WED-483)
 Chinaka, Ifechukwuamaka, S432 (FRI-524)
 China, Louise, S248 (SAT-100)
 Chinellato, Monica, S612 (SAT-219)
 Chines, Valeria, S422 (FRI-481),
 S747 (SAT-397)
 Chin, Simone, S380 (SAT-036-YI)
 Chitadze, Nazibrola, S677 (WED-473),
 S825 (THU-404)
 Chi, Xiaoling, S605 (SAT-198),
 S762 (FRI-366)
 Chng, Elaine, S56 (OS-087), S76 (OS-124),
 S465 (FRI-203), S467 (FRI-208)
 Cho, Dana, S727 (TOP-357)
 Chodnicka, Paulina, S328 (THU-152-YI)
 Choe, Byung-Ho, S801 (WED-408)
 Choe, Hun Jee, S487 (FRI-261-YI)
 Cho, Eun Ju, S457 (THU-515),
 S517 (WED-221)
 Choi, Anthony, S835 (THU-372-YI)
 Choi, Gichan, S82 (LBP-011)
 Choi, Gi Hong, S459 (THU-519)
 Choi, Gina, S114 (TOP-345)
 Choi, Jin-Young, S408 (SAT-522)
 Choi, Jonggi, S74 (OS-121), S144 (SAT-272),
 S305 (TOP-157), S822 (THU-394)
 Choi, Jong Young, S264 (THU-530),
 S448 (THU-478)
 Choi, Joon-Il, S448 (THU-478)
 Choi, Nam Joon, S82 (LBP-011)
 Choi, Sung Eun, S132 (THU-332-YI)
 Choi, Won-Mook, S74 (OS-121),
 S305 (TOP-157), S657 (WED-424)
 Choi, Woo Jin, S381 (SAT-037)
 Choi, Yoonjeong, S104 (TOP-351-YI)
 Choi, Yukyung, S283 (WED-547)

- Choi, Yun-Jung, S301 ([SAT-177](#)), S319 ([THU-119](#))
- Cho, Ju-Yeon, S223 ([FRI-099](#))
- Chokkalingam, Anand, S667 ([WED-447](#)), S769 ([FRI-383](#))
- Chokshi, Shilpa, S58 ([OS-091](#)), S128 ([THU-320-YI](#)), S174 ([TOP-084](#)), S178 ([WED-068-YI](#)), S281 ([WED-542-YI](#)), S350 ([TOP-553](#)), S654 ([SAT-467](#)), S700 ([FRI-171](#))
- Cholongitas, Evangelos, S217 ([FRI-083](#)), S798 ([WED-403](#))
- Cho, Nam H., S487 ([FRI-261-YI](#))
- Chong, Bee Yen, S525 ([WED-242](#))
- Chong, Hsu, S337 ([THU-173](#))
- Chong, Lee-Won, S832 ([THU-365](#))
- Chong, Suet Yen, S565 ([THU-200-YI](#))
- Chon, Hong Jae, S51 ([OS-078-YI](#)), S69 ([OS-112-YI](#)), S443 ([THU-464](#)), S445 ([THU-471-YI](#))
- Chon, Hye Yeon, S767 ([FRI-379](#))
- Choo, Jocelyn, S235 ([WED-526](#))
- Choong, Ingrid, S800 ([WED-407](#)), S814 ([WED-382](#))
- Choo-wing, Rayman, S58 ([OS-090](#))
- Chopra, Ishveen, S118 ([SAT-320](#))
- Chorostowska-Wynimko, Joanna, S703 ([TOP-141](#)), S708 ([WED-135-YI](#))
- Cho, Su Hwan, S638 ([SAT-424](#))
- Cho, Sung Woo, S264 ([THU-530](#))
- Chotiprasidhi, Perapa, S395 ([SAT-479-YI](#))
- Chotiayaputta, Watcharasak, S642 ([SAT-435](#)), S796 ([WED-396](#))
- Chotkoe, Shivani, S584 ([THU-258-YI](#))
- Choudhary, Narendra S., S158 ([THU-052](#)), S167 ([THU-078](#)), S475 ([FRI-231](#))
- Choudhary, Nishu, S129 ([THU-321](#)), S181 ([WED-076](#)), S272 ([WED-518-YI](#)), S276 ([WED-527-YI](#))
- Choudhury, Ashok Kumar, S158 ([THU-052](#)), S161 ([THU-058](#)), S164 ([THU-070](#)), S167 ([THU-078](#)), S209 ([FRI-053](#)), S219 ([FRI-088](#))
- Chouhan, Bhavik, S289 ([FRI-542](#))
- Chouhan, Mohd. Imran, S248 ([SAT-099-YI](#))
- Chou, Roger, S656 ([TOP-460-YI](#))
- Chou, Shih-Hsuan, S449 ([THU-479](#))
- Chow, Angela, S497 ([FRI-295](#))
- Chow, Desiree, S674 ([WED-465](#))
- Chowdhury, Debashis, S158 ([THU-052](#))
- Chowdhury, Dr. Debashis, S167 ([THU-078](#))
- Chow, Pierce, S401 ([SAT-495](#))
- Chow, Wan Cheng, S742 ([SAT-383](#))
- Cho, Yong Kyun, S223 ([FRI-099](#))
- Cho, Young Seo, S238 ([SAT-068](#))
- Christen, Lucienne, S373 ([SAT-019](#))
- Christie, Mo, S339 ([THU-178](#))
- Christodoulou, Dimitrios, S798 ([WED-403](#))
- Chua, Damien, S280 ([WED-539](#))
- Chua, Joel, S86 ([LBP-019](#))
- Chuang, Jen-Chieh, S696 ([FRI-161](#)), S698 ([FRI-164](#))
- Chuang, Wan-Long, S26 ([OS-031](#)), S27 ([OS-033](#)), S86 ([LBP-019](#)), S490 ([FRI-271](#)), S493 ([FRI-280](#)), S809 ([WED-371](#)), S811 ([WED-375](#)), S832 ([THU-365](#))
- Chu, Audrey, S126 ([THU-315](#))
- Chuayppen, Natthaya, S434 ([FRI-530](#)), S588 ([THU-273](#)), S591 ([THU-281](#))
- Chuffart, Florent, S744 ([SAT-389](#))
- Chughlay, Farouk, S26 ([OS-030](#))
- Chughtai, Manal, S510 ([WED-199](#)), S547 ([WED-303](#))
- Chui, Celine Sze Ling, S116 ([SAT-314](#))
- Chu, In-Sun, S68 ([OS-111](#))
- Chuken, Yamil Alonso Lopez, S3 ([GS-005](#))
- Chu, Keting, S808 ([WED-366](#)), S811 ([WED-374](#))
- Chulanov, Vladimir, S1 ([GS-002](#)), S92 ([LBP-029](#)), S758 ([TOP-400](#)), S764 ([FRI-371](#)), S796 ([WED-395](#))
- Chumillas-Calzada, Silvia, S693 ([FRI-153](#))
- Chung, Amber, S169 ([THU-082](#))
- Chung, Brian K., S33 ([OS-044-YI](#)), S65 ([OS-104](#)), S262 ([THU-525-YI](#)), S296 ([SAT-163-YI](#))
- Chung, Chuhan, S571 ([THU-219](#)), S616 ([SAT-233](#))
- Chung, Goh Eun, S517 ([WED-221](#))
- Chung, Jin Wook, S447 ([THU-475](#))
- Chung, Matthew Shing Hin, S116 ([SAT-314](#))
- Chung, Minsup, S82 ([LBP-011](#))
- Chung, Moon Jae, S323 ([THU-128](#))
- Chung, Raymond, S17 ([OS-013](#)), S42 ([OS-061](#))
- Chung, Sai, S31 ([OS-040-YI](#))
- Chung, Samuel, S289 ([FRI-542](#))
- Chung, Sung Won, S144 ([SAT-272](#)), S305 ([TOP-157](#)), S601 ([TOP-204](#)), S822 ([THU-394](#))
- Chung, Woo Jin, S457 ([THU-516](#))
- Chung, Yong Eun, S408 ([SAT-522](#))
- Chung, Yooyun, S315 ([THU-111](#))
- Chun, Ho Soo, S671 ([WED-456](#))
- Chun, Su-Kyung, S69 ([OS-113](#))
- Chu-Van, Emeline, S184 ([WED-083](#))
- Chvala, Lubos, S379 ([SAT-033](#))
- Ciacio, Oriana, S718 ([WED-174](#))
- Ciancio, Alessia, S73 ([OS-120](#)), S666 ([WED-446](#)), S772 ([FRI-392-YI](#)), S793 ([WED-391](#)), S804 ([WED-414](#))
- Ciccarelli, Olga, S368 ([SAT-009](#))
- Ciccia, Roberta, S51 ([OS-078-YI](#))
- Ciccioli, Carlo, S503 ([FRI-317](#)), S544 ([WED-293](#)), S609 ([SAT-209-YI](#))
- Cicolani, Nicolò, S289 ([FRI-544](#))
- Cierco, Carmen, S635 ([THU-039-YI](#))
- Ciesek, Sandra, S170 ([THU-087](#)), S734 ([SAT-361](#)), S794 ([WED-392](#))
- Çıfıbaşı Örmeci, Aslı, S377 ([SAT-028](#))
- Çiftçi, Aslı, S407 ([SAT-519](#))
- Cigliano, Riccardo Aiese, S747 ([SAT-397](#))
- Cilla, Marta, S367 ([SAT-007-YI](#))
- Cillo, Umberto, S28 ([OS-034](#)), S59 ([OS-094](#)), S369 ([SAT-009](#)), S375 ([SAT-023](#)), S376 ([SAT-024-YI](#)), S389 ([SAT-058](#))
- Cimbora, Daniel, S710 ([WED-152](#))
- Cinque, Felice, S474 ([FRI-226](#)), S650 ([SAT-455](#)), S683 ([WED-486-YI](#))
- Cintas, María Isabel Zamora, S682 ([WED-483](#))
- Cintra, Luciano, S271 ([THU-556](#))
- Ciocan, Dragos, S130 ([THU-327](#)), S136 ([THU-347-YI](#))
- Cipriani, Francesco, S674 ([WED-467-YI](#))
- Cipullo, Marina, S173 ([TOP-072](#)), S213 ([FRI-070-YI](#)), S817 ([THU-378](#))
- Citarrella, Roberto, S601 ([TOP-193](#))
- Citterio, Davide, S70 ([OS-114](#))
- Cittone, Micol, S329 ([THU-153](#))
- Ciupkeviciene, Egle, S678 ([WED-474](#))
- Cives-Losada, Candela, S433 ([FRI-526](#))
- Civitaresse, Antonio, S91 ([LBP-027](#))
- Civolani, Alberto, S725 ([WED-191](#))
- Claar, Ernesto, S175 ([TOP-085](#)), S666 ([WED-446](#)), S790 ([FRI-441](#))
- Claassen, Marco, S381 ([SAT-037](#))
- Claassen, Mark, S763 ([FRI-367](#))
- Claessen, Guido, S246 ([SAT-092-YI](#))
- Claire, Primot, S508 ([WED-194](#))
- Clareburt, Alban, S636 ([THU-045](#))
- Claria, Joan, S9 ([LBO-004](#)), S83 ([LBP-012](#)), S89 ([LBP-026](#))
- Clària, Joan, S16 ([OS-011](#)), S47 ([OS-071-YI](#)), S48 ([OS-073](#)), S157 ([THU-050](#)), S159 ([THU-055](#)), S161 ([THU-057-YI](#)), S174 ([TOP-073](#)), S174 ([TOP-084](#)), S177 ([WED-059](#)), S184 ([WED-083](#)), S185 ([WED-087](#)), S188 ([WED-098-YI](#)), S193 ([WED-111](#)), S193 ([WED-112](#)), S700 ([FRI-171](#))
- Clark, Annie, S97 ([LBP-039](#))
- Clarke, Lindsey, S450 ([THU-485-YI](#))
- Clark, Sarah, S523 ([WED-236-YI](#)), S672 ([WED-459-YI](#))
- Clarkson, Scott, S58 ([OS-090](#))
- Clark, Virginia C., S703 ([TOP-141](#)), S708 ([WED-135-YI](#)), S724 ([WED-188](#))
- Clasen, Frederick, S182 ([WED-078](#))
- Clasen, Marco, S369 ([SAT-009](#))
- Claudia, Kunst, S191 ([WED-106](#))
- Claudie, Pinteur, S49 ([OS-074](#))
- Claus, Eveline, S125 ([TOP-328-YI](#)), S246 ([SAT-092-YI](#))
- Clavien, Pierre A., S345 ([TOP-559](#))
- Clavien, Pierre-Alain, S702 ([TOP-140](#))
- Clavo, Nataly, S195 ([WED-117](#))
- Clawson, Alicia, S517 ([WED-220](#))
- Clayton-Chubb, Daniel, S653 ([SAT-464-YI](#))
- Clemente, Ana, S139 ([SAT-257](#)), S142 ([SAT-267](#))
- Clément, Karine, S512 ([WED-206](#)), S585 ([THU-260](#))
- Clements, Amanda, S654 ([SAT-467](#))
- Clerick, Jan, S246 ([SAT-092-YI](#))
- Clewe, Oskar, S93 ([LBP-031](#))
- Cloherly, Gavin, S668 ([WED-451-YI](#)), S675 ([WED-469](#)), S677 ([WED-473](#)), S775 ([FRI-399](#)), S782 ([FRI-418](#)), S809 ([WED-371](#))
- Close, Lila, S272 ([TOP-563](#))

Author Index

- Clouston, Andrew D., S467 ([FRI-208](#))
 Clusmann, Jan, S392 ([TOP-520](#)),
 S494 ([FRI-284-YI](#)), S528 ([WED-247](#)),
 S567 ([THU-206](#))
 Cmet, Sara, S700 ([FRI-171](#))
 Cobbold, Jeremy, S135 ([THU-343](#))
 Cobiella, Jose, S4 ([GS-011](#))
 Cocca, Massimiliano, S280 ([WED-540-YI](#))
 Cocchi, Lorenzo, S369 ([SAT-009](#))
 Cocchis, Donatella, S371 ([SAT-015-YI](#)),
 S378 ([SAT-031-YI](#))
 Coco, Barbara, S96 ([LBP-038](#)),
 S306 ([THU-093](#)), S549 ([WED-314-YI](#)),
 S622 ([FRI-014](#)), S666 ([WED-444](#)),
 S804 ([WED-414](#))
 Codes, Liana, S83 ([LBP-012](#)), S254 ([SAT-119](#)),
 S722 ([WED-185](#))
 Codina, Helena, S665 ([WED-442](#))
 Codoceo, Carolina Muñoz, S717 ([WED-172](#))
 Codoni, Greta, S341 ([THU-182](#))
 Codotto, Gabriele, S701 ([FRI-172](#))
 Coelho Meine, Gilmar, S618 ([SAT-244](#))
 Coelmont, Lotte, S732 ([SAT-341](#))
 Coenraad, Minneke, S21 ([OS-020](#)),
 S47 ([OS-071-YI](#)), S159 ([THU-055](#)),
 S184 ([WED-083](#)), S193 ([WED-111](#)),
 S203 ([FRI-039](#)), S205 ([FRI-043](#)),
 S382 ([SAT-040](#)), S492 ([FRI-278](#)),
 S700 ([FRI-171](#))
 Coenraad, Minneke J., S48 ([OS-073](#)),
 S169 ([THU-080-YI](#))
 Coessens, Marie, S828 ([THU-412](#))
 Coffin, Carla, S660 ([WED-431](#))
 Cohen, Gordon, S3 ([GS-005](#))
 Cohen, Yotam, S65 ([OS-103](#))
 Coilly, Audrey, S50 ([OS-077](#)),
 S156 ([TOP-108](#)), S168 ([THU-079](#)),
 S367 ([TOP-005](#)), S369 ([SAT-010](#)),
 S370 ([SAT-011](#)), S378 ([SAT-029](#)),
 S385 ([SAT-048](#)), S385 ([SAT-049](#)),
 S718 ([WED-174](#))
 Cointet, Alix, S524 ([WED-239](#))
 Coirier, Valentin, S116 ([SAT-315](#))
 Cojuhari, Lilia, S791 ([FRI-443](#))
 Colapietro, Francesca, S18 ([OS-015](#)),
 S19 ([OS-017](#)), S96 ([LBP-038](#)),
 S306 ([THU-093](#)), S310 ([THU-101](#)),
 S404 ([SAT-502-YI](#)), S406 ([SAT-514](#)),
 S439 ([THU-447](#)), S497 ([FRI-294](#))
 Cola, Simone Di, S364 ([WED-022](#)),
 S700 ([FRI-171](#))
 Colca, Jerry, S82 ([LBP-010](#))
 Cole, Alexander, S679 ([WED-477-YI](#))
 Colecchia, Antonio, S61 ([OS-096-YI](#)),
 S62 ([OS-099-YI](#)), S238 ([SAT-068](#)),
 S241 ([SAT-078-YI](#)), S389 ([SAT-060](#)),
 S399 ([SAT-490](#)), S704 ([TOP-143-YI](#))
 Colecchia, Luigi, S238 ([SAT-068](#)),
 S241 ([SAT-078-YI](#)), S399 ([SAT-490](#)),
 S704 ([TOP-143-YI](#))
 Colella, Elisa, S666 ([WED-446](#))
 Coletta, Alessandro, S603 ([SAT-194](#))
 Colhoun, Helen, S93 ([LBP-032](#))
 Collado, Francina, S669 ([WED-453](#))
 Collazos, Cristina, S765 ([FRI-373](#))
 Colle, Isabelle, S125 ([TOP-328-YI](#)),
 S321 ([THU-123-YI](#))
 Colli, Agostino, S238 ([SAT-068](#))
 Collienne, Christine, S172 ([THU-092](#))
 Collier, Nicholson, S43 ([OS-063](#))
 Collins, Kate, S338 ([THU-177-YI](#)),
 S400 ([SAT-492](#))
 Coll, Mar, S13 ([OS-005-YI](#)), S160 ([THU-056](#)),
 S176 ([WED-055](#))
 Coll, Susana, S207 ([FRI-051](#))
 Colmenero, Jordi, S365 ([TOP-002](#))
 Colnot, Sabine, S416 ([FRI-465](#))
 Colognesi, Martina, S592 ([THU-285](#))
 Colombain, Lea, S28 ([OS-034](#))
 Colombatto, Piero, S549 ([WED-314-YI](#)),
 S619 ([SAT-245](#)), S622 ([FRI-014](#)),
 S666 ([WED-446](#))
 Colombo, Massimo, S42 ([OS-061](#))
 Colominas-González, Elena, S207 ([FRI-051](#))
 Colsch, Benoit, S423 ([FRI-485](#))
 Colucci, Giuseppe, S664 ([WED-440](#))
 Colucci, Nicola, S705 ([WED-129](#))
 Colwill, Karen, S673 ([WED-464](#))
 Colyn, Leticia, S431 ([FRI-522](#))
 Comai, Stefano, S592 ([THU-285](#))
 Combal, Jean Philippe, S714 ([WED-164](#))
 Combe, Emmanuel, S808 ([WED-366](#))
 Combet, Stephanie, S486 ([FRI-259](#))
 Comito, Tiziana, S406 ([SAT-514](#))
 Commins, Isabella, S653 ([SAT-464-YI](#))
 Conde, Isabel, S318 ([THU-118](#)),
 S330 ([THU-155](#)), S531 ([WED-257](#))
 Conde, Marta Hernández, S559 ([WED-339](#)),
 S777 ([FRI-406](#))
 Conde, Silvia Vilares, S834 ([THU-370](#))
 Conejero, María Dolores Antón,
 S329 ([THU-154-YI](#))
 Conesa, Nalika, S430 ([FRI-519-YI](#))
 Cong, Chanh Pham, S552 ([WED-320](#))
 Congreave, Susan, S350 ([TOP-553](#))
 Congregado, Daniela Mestre,
 S562 ([TOP-229-YI](#))
 Conklin, Jamie, S394 ([SAT-476](#))
 Conti, Filomena, S156 ([TOP-108](#)),
 S168 ([THU-079](#)), S367 ([TOP-005](#)),
 S369 ([SAT-010](#)), S385 ([SAT-048](#)),
 S763 ([FRI-370](#))
 Conti, Giorgio De, S224 ([FRI-101-YI](#))
 Conti, Maria, S322 ([THU-127-YI](#))
 Contreras, Bryan J., S16 ([OS-011](#)),
 S174 ([TOP-073](#)), S185 ([WED-087](#))
 Contreras, Heidi, S812 ([WED-377](#))
 Contreras, Jorge, S195 ([WED-117](#))
 Conway, Brian, S662 ([WED-436](#)),
 S668 ([WED-450](#)), S679 ([WED-476](#)),
 S819 ([THU-382](#))
 Cook, Carl, S87 ([LBP-020](#))
 Cooke, Graham S, S676 ([WED-471](#))
 Cooke, Graham S., S760 ([TOP-417](#))
 Cooney, Rachel, S309 ([THU-099-YI](#))
 Cooper, Katherine, S603 ([SAT-194](#))
 Cooreman, Michael, S608 ([SAT-206](#))
 Copeland, Amber, S669 ([WED-452](#))
 Copil, Francisca, S441 ([THU-458](#))
 Coppa, Jorgelina, S70 ([OS-114](#))
 Coppola, Annachiara, S213 ([FRI-070-YI](#))
 Coppola, Nicola, S73 ([OS-120](#)),
 S666 ([WED-444](#)), S776 ([FRI-405](#)),
 S793 ([WED-391](#)), S804 ([WED-414](#))
 Cordero, Patricia, S779 ([FRI-409](#))
 Cordero-Pérez, Paula, S627 ([FRI-029](#))
 Cordie, Ahmed, S491 ([FRI-273-YI](#))
 Cordier, Pierre, S572 ([THU-220](#))
 Cordova-Gallardo, Jacqueline,
 S30 ([OS-038-YI](#)), S161 ([THU-058](#)),
 S171 ([THU-089](#)), S199 ([TOP-062](#)),
 S200 ([TOP-064-YI](#))
 Cordova, Henry, S378 ([SAT-030](#))
 Cords, Leon, S739 ([SAT-376](#))
 Corless, Lynsey, S232 ([FRI-123](#)),
 S630 ([THU-010](#))
 Cornberg, Markus, S92 ([LBP-029](#)),
 S226 ([FRI-107-YI](#)), S226 ([FRI-109](#)),
 S253 ([SAT-117](#)), S350 ([SAT-532-YI](#)),
 S351 ([SAT-533](#)), S353 ([SAT-538-YI](#)),
 S730 ([TOP-369](#)), S735 ([SAT-363](#)),
 S750 ([SAT-406-YI](#)), S758 ([TOP-400](#)),
 S794 ([WED-392](#)), S833 ([THU-366](#))
 Corona, Mario, S215 ([FRI-077-YI](#))
 Corpechot, Christophe, S5 ([GS-007](#)),
 S80 ([LBP-006](#)), S91 ([LBP-027](#)),
 S98 ([LBP-040](#)), S308 ([THU-098](#)),
 S311 ([THU-102-YI](#)), S313 ([THU-107](#)),
 S315 ([THU-111](#)), S321 ([THU-125](#)),
 S326 ([THU-136](#))
 Corradini, Stefano Ginanni,
 S215 ([FRI-077-YI](#))
 Corrales, Fernando J., S348 ([FRI-555](#))
 Correcher, Patricia, S693 ([FRI-153](#))
 Correia, Luís, S220 ([FRI-090](#)),
 S405 ([SAT-513](#))
 Correll, Todd, S75 ([OS-127](#))
 Correnti, Margherita, S426 ([FRI-498-YI](#))
 Corret, Pierre, S326 ([THU-136](#)),
 S712 ([WED-158-YI](#))
 Corrigall, Douglas, S147 ([SAT-280](#)),
 S174 ([TOP-084](#))
 Corso, Rocco, S325 ([THU-133-YI](#))
 Cortada, Judith, S233 ([FRI-126](#))
 Corte, Cristina Della, S332 ([THU-161](#))
 Cortellini, Alessio, S51 ([OS-078-YI](#)),
 S443 ([THU-464](#))
 Corte-Real, Rita, S681 ([WED-481](#))
 Cortese, Maria Francesca, S662 ([WED-435](#)),
 S741 ([SAT-381](#))
 Cortez, John, S727 ([TOP-357](#))
 Cortez-Pinto, Helena, S220 ([FRI-090](#)),
 S358 ([SAT-554-YI](#)), S405 ([SAT-513](#))
 Cosculluela, Albert, S141 ([SAT-262](#))
 Cosenza, Agostino, S439 ([THU-447](#))
 Cossiga, Valentina, S96 ([LBP-038](#)),
 S306 ([THU-093](#)), S367 ([SAT-007-YI](#)),
 S817 ([THU-378](#))
 Costa, Guido, S401 ([SAT-494](#))
 Costain, Alice, S265 ([THU-535-YI](#))
 Costa, Montserrat, S177 ([WED-059](#)),
 S231 ([FRI-121](#))

- Costanzo, Martina, S96 (LBP-038), S306 (THU-093), S634 (THU-032)
- Costa, Tania, S21 (OS-020)
- Costentin, Charlotte, S37 (OS-053), S50 (OS-077), S54 (OS-084-YI), S168 (THU-079), S444 (THU-466), S747 (SAT-396)
- Costes, Francesc Xavier Belvis, S154 (SAT-304)
- Costiniuk, Cecilia, S683 (WED-486-YI)
- Cotler, Scott, S800 (WED-407), S814 (WED-382), S832 (THU-364)
- Cots, Meritxell Ventura, S139 (SAT-257)
- Cott, Andrew Van, S88 (LBP-022)
- Cotugno, Rosa, S96 (LBP-038), S306 (THU-093), S790 (FRI-441)
- Couce, María Luz, S694 (FRI-153)
- Couffon, Margaux, S466 (FRI-207-YI), S495 (FRI-286)
- Coulibaly, Fatoumata, S802 (WED-410)
- Coulouarn, Cedric, S426 (FRI-498-YI)
- Coulshed, Andrew, S338 (THU-177-YI)
- Coulter, Greg, S616 (SAT-233)
- Coulthard, Helen, S101 (LBP-046)
- Coustal, Cyril, S115 (SAT-306)
- Coutinho, Anelisa, S254 (SAT-119)
- Couto, Cláudia Alves, S83 (LBP-012), S619 (SAT-248)
- Couty, Jean-Pierre, S349 (TOP-552), S415 (FRI-459), S572 (THU-220)
- Cova, Agata, S439 (THU-454)
- Cox, Helen, S274 (WED-523)
- Cox, I. Jane, S281 (WED-542-YI), S364 (WED-027)
- Cox, Joseph, S683 (WED-486-YI)
- Cox, Leah, S632 (THU-022)
- Cozzolongo, Raffaele, S96 (LBP-038), S175 (TOP-085), S215 (FRI-078-YI), S306 (THU-093)
- Crabbe, Marjolein, S810 (WED-372), S813 (WED-379)
- Craciun, Rares, S409 (SAT-525)
- Cracknell, Richard, S657 (WED-422), S676 (WED-470)
- Crame, Thomas, S629 (THU-008), S629 (THU-009)
- Cramp, Matthew, S153 (SAT-299)
- Cransac, Martine Neau, S367 (TOP-005)
- Cratchley, Alyn, S530 (WED-254)
- Craxi, Antonio, S671 (WED-457-YI), S777 (FRI-405)
- Creamer, John, S408 (SAT-521)
- Crespi, Agustina, S673 (WED-464)
- Crespi, Silvia, S397 (SAT-482)
- Crespo, Gonzalo, S15 (OS-010)
- Crespo, Javier, S85 (LBP-016), S142 (SAT-267), S318 (THU-118), S329 (THU-154-YI), S330 (THU-155), S337 (THU-172), S468 (FRI-211), S469 (FRI-213), S640 (SAT-429), S651 (SAT-456), S700 (FRI-171)
- Crespo, Maria, S112 (FRI-343-YI)
- Cressey, Tim, S831 (THU-363)
- Creus, An De, S27 (OS-033), S79 (LBP-005), S768 (FRI-380)
- Crisuolo, Livio, S790 (FRI-441)
- Cristina Morelli, Maria, S332 (THU-161)
- Cristóbal, Mario Romero, S365 (TOP-002)
- Cristoferi, Laura, S19 (OS-017), S299 (SAT-171), S308 (THU-098), S310 (THU-101), S325 (THU-133-YI), S335 (THU-167)
- Crittenden, Daria B., S20 (OS-019), S98 (LBP-040)
- Croce, Anna Cleta, S589 (THU-274)
- Crocè, Lory Saveria, S175 (TOP-085), S429 (FRI-516-YI)
- Croce, Saveria Lory, S238 (SAT-068), S731 (SAT-338-YI)
- Crosignani, Andrea, S725 (WED-191)
- Croteau-Chonka, Damien, S126 (THU-315)
- Crouch, Emilie, S17 (OS-013), S25 (OS-029), S31 (OS-040-YI), S42 (OS-061)
- Cruz-Adalia, Aranzazu, S276 (WED-528-YI)
- Cruz-Ferro, Elena, S690 (WED-513)
- Csarmann, Katja, S132 (THU-334)
- Csillag, Aniko, S169 (THU-080-YI)
- Cuadrado, Antonio, S365 (TOP-002)
- Cuadros, Marta, S398 (SAT-485), S706 (WED-132), S712 (WED-159)
- Cua, Georgine, S659 (WED-429), S686 (WED-495), S824 (THU-399-YI)
- Cubells, Almudena, S361 (WED-009), S362 (WED-015)
- Cubero, Francisco Javier, S112 (FRI-343-YI), S276 (WED-528-YI), S593 (THU-287), S596 (THU-296)
- Cucco, Monica, S376 (SAT-025), S380 (SAT-034)
- Cuccorese, Giuseppe, S96 (LBP-038), S306 (THU-093)
- Cuellar-Partida, Gabriel, S462 (FRI-195)
- Cuerva, Marina Orti, S318 (THU-118)
- Cuevas, Guillermo, S665 (WED-442)
- Cuffari, Biagio, S62 (OS-099-YI), S96 (LBP-038), S306 (THU-093)
- Cui, Dandan, S786 (FRI-430)
- Cui, Jing, S481 (FRI-245)
- Cui, Shiyu, S804 (WED-415)
- Cullaro, Giuseppe, S242 (SAT-082), S638 (SAT-426-YI)
- Culver, Emma, S290 (TOP-147), S302 (SAT-179), S310 (THU-101), S324 (THU-130), S710 (WED-152)
- Cummings, Oscar, S7 (LBO-001)
- Cunha, Beatriz, S254 (SAT-119)
- Cuño-Gómez, Carlos, S425 (FRI-494-YI), S430 (FRI-519-YI)
- Cuomo, Nunzia, S776 (FRI-405)
- Cuperus, Frans J.C., S309 (THU-100), S314 (THU-109), S319 (THU-120-YI), S327 (THU-138)
- Curé-Martin, Audace, S61 (OS-097)
- Curhan, Gary, S460 (TOP-309)
- Currà, Jaqueline, S474 (FRI-226), S482 (FRI-248-YI)
- Currie, Sue, S86 (LBP-018)
- Curto, Armando, S96 (LBP-038), S306 (THU-093)
- Cusi, Giulia, S364 (WED-022)
- Cusi, Kenneth, S79 (LBP-003), S470 (FRI-218), S522 (WED-234), S528 (WED-248), S542 (WED-285)
- Cusimano, Alessandra, S601 (TOP-193)
- Cussigh, Annarosa, S700 (FRI-171)
- Cussons, Claire, S150 (SAT-291)
- Custodio, Joseph M., S613 (SAT-224)
- Cuthbertson, Daniel, S506 (TOP-277), S542 (WED-285)
- Cutsem, Eric Van, S411 (TOP-507-YI)
- Cuyas, Berta, S29 (OS-037)
- Cuyppers, Bart, S730 (SAT-337)
- Czarnecki, Judith, S70 (OS-115)
- Czernichow, Sebastien, S526 (WED-245)
- Czernuszczyk, Tomek, S584 (THU-259)
- Czubkowski, Piotr, S374 (SAT-021)
- Dabbah, Shoham, S166 (THU-076-YI)
- Da, Ben, S8 (LBO-003)
- Da, Ben L., S1 (GS-002), S758 (TOP-400), S764 (FRI-371), S794 (WED-392), S796 (WED-395)
- Da, Binlin, S260 (SAT-136)
- da Costa, Maureen, S540 (WED-282)
- D'Adamo, Giuseppe, S666 (WED-446)
- Dadhigh, Sunil, S158 (THU-052), S167 (THU-078), S476 (FRI-231)
- Dağcı, Gizem, S377 (SAT-028)
- Daguison, Shane, S564 (THU-198), S727 (TOP-357)
- Daha, Ioana, S216 (FRI-080)
- Dahari, Harel, S43 (OS-063), S735 (SAT-364), S800 (WED-407), S814 (WED-382), S832 (THU-364)
- Dahboul, Fatima, S422 (FRI-485)
- Dahiya, Monica, S219 (FRI-088)
- Dahlqvist, Géraldine, S360 (WED-008), S371 (SAT-014-YI), S546 (WED-297-YI), S823 (THU-397-YI)
- Dahlström, Nils, S530 (WED-255-YI), S532 (WED-259)
- Daiane Buarque de Santana Sato, Emmily, S618 (SAT-244)
- Dai, Chia-Yen, S490 (FRI-271), S493 (FRI-280), S832 (THU-365)
- Dai, Erhei, S769 (FRI-382)
- Dai, Qingqing, S263 (THU-527)
- Dai, Shejiao, S235 (FRI-131)
- Dai, Zhe, S561 (TOP-228-YI), S730 (TOP-384-YI)
- Dajani, Khaled, S231 (FRI-122)
- Dajti, Elton, S52 (OS-080), S61 (OS-096-YI), S238 (SAT-068), S241 (SAT-078-YI), S390 (TOP-509-YI), S399 (SAT-490), S704 (TOP-143-YI), S818 (THU-381)
- Dajti, Gerti, S704 (TOP-143-YI)
- Dalal, Nishu, S283 (WED-549)
- Dalbeni, Andrea, S51 (OS-078-YI), S395 (SAT-477-YI), S443 (THU-464), S445 (THU-471-YI), S446 (THU-472-YI),

Author Index

- S474 (FRI-226), S492 (FRI-279-YI), S496 (FRI-290)
- Dalbby Hansen, Camilla, S139 (SAT-255), S142 (SAT-266), S153 (SAT-298)
- Dale, Kelly, S709 (WED-151)
- Dalekos, George, S18 (OS-015), S20 (OS-019), S44 (OS-066-YI), S308 (THU-098), S311 (THU-102-YI), S321 (THU-125), S322 (THU-126), S325 (THU-134), S335 (THU-167), S624 (FRI-020), S712 (WED-160), S798 (WED-403), S800 (WED-406)
- Dalemans, Wilfried, S807 (WED-363)
- D'Alessandro, Umberto, S782 (FRI-418), S787 (FRI-431)
- D'Alessio, Alfonso, S698 (FRI-166)
- D'Alessio, Antonio, S23 (OS-025-YI), S51 (OS-078-YI), S52 (OS-079-YI), S69 (OS-112-YI), S443 (THU-464), S445 (THU-471-YI)
- Dalgard, Olav, S795 (WED-394)
- Dall'Acqua, Stefano, S157 (THU-050)
- Dall'Alba, Valesca, S636 (THU-044)
- Dallio, Marcello, S173 (TOP-072), S213 (FRI-070-YI), S666 (WED-446)
- Dalteroche, Louis, S41 (OS-060), S53 (OS-081), S73 (OS-120), S763 (FRI-370), S793 (WED-391)
- Daly, Fergus, S646 (SAT-444)
- Damadoglu, Ebru, S224 (FRI-104)
- Damascene Makuza, Jean, S686 (WED-495)
- D'Amato, Daphne, S96 (LBP-038), S306 (THU-093), S325 (THU-133-YI), S332 (THU-161)
- Damato, Elio, S215 (FRI-077-YI)
- D'Ambrosio, Francesca, S533 (WED-261-YI)
- D'Ambrosio, Roberta, S401 (SAT-493-YI), S459 (TOP-301), S470 (FRI-215-YI), S544 (WED-293), S666 (WED-446), S704 (TOP-144-YI)
- Dam, Gitte, S236 (FRI-134)
- D'Amico, Federico, S96 (LBP-038), S306 (THU-093), S700 (FRI-171)
- Damien, Leleu, S508 (WED-194)
- Damme, Pierre Van, S665 (WED-441-YI)
- Danan, Keren, S696 (FRI-160-YI)
- Dandri, Maura, S74 (OS-122), S733 (SAT-342-YI)
- Dandri-Petersen, Maura, S738 (SAT-373)
- Danford, Christopher, S10 (LBO-005)
- Dang, Hoan Nguyen, S729 (TOP-360-YI)
- Dang, Shuang suo, S195 (WED-116), S590 (THU-279), S786 (FRI-430)
- Daniel, dos Santos da Rocha Tarciso, S83 (LBP-012)
- Daniele, Bruno, S395 (SAT-477-YI)
- Daniel, P. Vineeth, S134 (THU-341)
- Daniels, Samuel, S535 (WED-270), S554 (WED-325-YI)
- Daniş, Nilay, S336 (THU-171)
- D'Anna, Stefano, S59 (OS-094), S772 (FRI-392-YI), S776 (FRI-405), S798 (WED-399-YI)
- Danneberg, Sven, S214 (FRI-075)
- Danpanichkul, Pojsakorn, S139 (SAT-256), S146 (SAT-278)
- Danse, Etienne, S473 (FRI-224)
- D'Antiga, Lorenzo, S54 (OS-082), S331 (THU-158), S700 (FRI-171), S714 (WED-164)
- Dan, Yock Young, S524 (WED-238), S565 (THU-200-YI), S797 (WED-398)
- Dan, Yock-Young, S147 (SAT-281)
- Dan, Yunjie, S701 (FRI-174)
- Daou, Helene, S573 (THU-222-YI)
- D'Arcangelo, Francesca, S367 (SAT-007-YI)
- Da Rin, David, S313 (THU-107)
- Dasarathy, Srinivasan, S76 (OS-125)
- Das, Avisnata, S718 (WED-173)
- Dashdorj, Arghun, S82 (LBP-011)
- Dashdorj, Naranbaatar, S82 (LBP-011)
- Dashdorj, Naranjargal, S82 (LBP-011)
- Dashenkova, Nataliya, S268 (THU-542)
- Dassetto, Clara, S385 (SAT-048)
- Das, Sudip, S26 (OS-030)
- Dato, Fabiola Di, S198 (WED-124), S359 (SAT-556-YI)
- Datz, Christian, S56 (OS-086-YI), S500 (FRI-303)
- Dauchy, Simon, S644 (SAT-439-YI)
- Daud, Nu'man AS, S792 (FRI-444)
- Davalos, Milagros, S83 (LBP-012)
- Daveiga, Jean, S743 (SAT-387)
- David, Bruna Araujo, S353 (SAT-539-YI)
- Davidov, Yana, S166 (THU-076-YI)
- Davidson, Irwin, S42 (OS-061)
- Davie, Sarah, S523 (WED-236-YI)
- Davies, Jim, S676 (WED-471), S759 (TOP-417)
- Davies, Nathan, S17 (OS-014-YI), S179 (WED-069), S182 (WED-078), S588 (THU-271-YI)
- Davis, Brian, S1 (GS-001)
- Davis, Cai, S676 (WED-471), S759 (TOP-417)
- Davis, Charlotte, S26 (OS-031)
- Davis, Heather, S27 (OS-032)
- Davis, Matthew, S469 (FRI-214), S494 (FRI-283)
- Davison, Nuala, S553 (WED-324)
- Davison, Scott, S208 (FRI-053)
- Davis, Tom, S315 (THU-112-YI)
- Davitte, Jonathan, S126 (THU-315)
- Davitt, Shauna, S635 (THU-040-YI)
- D'Avola, Delia, S355 (SAT-543)
- Dayal, V.M., S158 (THU-052), S167 (THU-078)
- Day, Le, S131 (THU-330)
- Dayton, Paul, S584 (THU-259)
- Daza, Jimmy, S334 (THU-164-YI)
- de Andrade, Cherley, S190 (WED-102)
- De Angelis, Angela, S698 (FRI-166)
- Dear, James W., S145 (SAT-274)
- De, Arka, S129 (THU-324), S152 (SAT-295), S158 (THU-051), S217 (FRI-082), S475 (FRI-231)
- Deavila, Leyla, S472 (FRI-221), S637 (TOP-445), S638 (SAT-425)
- Debaecker, Simon, S191 (WED-105)
- De Benedittis, Carla, S409 (SAT-524)
- de Benito, Alvaro Mallagaray, S582 (THU-254-YI)
- Debes, Jose, S395 (SAT-479-YI)
- Debette-Gratien, Maryline, S387 (SAT-052), S763 (FRI-370)
- Debing, Yannick, S728 (TOP-358-YI)
- de Boer, Wink, S314 (THU-109), S327 (THU-138)
- de Boer, Ynto, S18 (OS-015), S304 (SAT-185), S315 (THU-112-YI)
- Debray, Dominique, S374 (SAT-021)
- Debroff, Jake, S674 (WED-465)
- De Broucker, Chloé, S719 (WED-177)
- de Bruijne, Joep, S758 (TOP-401-YI)
- de Bruin, Gijs J., S213 (FRI-074-YI), S314 (THU-109), S327 (THU-138)
- de Bruyne, Ruth, S57 (OS-089-YI)
- Debzi, Nabil, S219 (FRI-088)
- Decaens, Thomas, S41 (OS-060), S367 (TOP-005), S369 (SAT-010), S413 (FRI-455), S444 (THU-466), S744 (SAT-389), S747 (SAT-396)
- Decaris, Martin, S97 (LBP-039), S261 (TOP-564)
- De Carlis, Luciano, S368 (SAT-009), S376 (SAT-025)
- De Carlis, Riccardo, S368 (SAT-009)
- De Carlo, Camilla, S401 (SAT-494), S438 (THU-446), S580 (THU-245)
- de Carvalho, Luís Abreu, S420 (FRI-475-YI)
- De Cegli, Rossella, S698 (FRI-166)
- Dechaumet, Sylvain, S184 (WED-083)
- de Cid, Rafael, S337 (THU-172)
- Deckmyn, Olivier, S512 (WED-206)
- Declerck, Salomé, S151 (SAT-293-YI), S473 (FRI-224)
- de Diego, Eva, S822 (THU-395)
- de Dios, Olaya, S277 (WED-530-YI)
- Dedoussis, George, S508 (WED-195)
- Defar, Marta, S155 (SAT-305)
- DeFelice, Nicholas, S653 (SAT-463)
- De Ferrari, Gaetano, S475 (FRI-230-YI)
- De Franco, Francesca, S124 (TOP-313)
- Degasperi, Elisabetta, S73 (OS-120), S96 (LBP-038), S306 (THU-093), S329 (THU-153), S332 (THU-161), S344 (THU-190), S401 (SAT-493-YI), S759 (TOP-416-YI), S781 (FRI-412), S793 (WED-391), S798 (WED-399-YI), S804 (WED-414)
- de Gauna, Mikel Ruiz, S32 (OS-042-YI), S64 (OS-101-YI), S419 (FRI-472-YI), S562 (TOP-229-YI)
- de Graaf, Michiel, S382 (SAT-040)
- Degrauwe, Lars, S728 (TOP-358-YI)
- Degré, Delphine, S133 (THU-335)
- Degroote, Helena, S700 (FRI-171)
- de Guevara, Alma Laura Ladrón, S535 (WED-270)
- de Haas, Robbert, S394 (SAT-474)
- Deheragoda, Maesha, S21 (OS-020)
- Dehez, Marion, S321 (THU-124)

- Deibel, Ansgar, S308 (THU-098), S702 (TOP-140)
- Deising, Adam, S384 (SAT-047)
- de Jonge, Hendrik J.M., S314 (THU-109), S327 (THU-138)
- de Jonge, Jeroen, S380 (SAT-035)
- de Jong, Sofie, S304 (SAT-185)
- de Jong, Vivian, S549 (WED-306-YI), S612 (SAT-218)
- Dekervel, Jeroen, S69 (OS-112-YI), S411 (TOP-507-YI)
- de Knecht, Robert J., S380 (SAT-035), S464 (FRI-200), S467 (FRI-209), S503 (TOP-241-YI), S604 (SAT-197-YI), S606 (SAT-200-YI), S652 (SAT-462-YI)
- de Kort, Sander, S319 (THU-120-YI)
- de Laat, Bas, S237 (TOP-061-YI)
- De la Cruz, Gema, S828 (THU-411)
- de Laguiche, Elisabeth, S462 (FRI-196)
- De La Iglesia Salgado, Alberto, S779 (FRI-409)
- De La Luna, Francisco Franco Álvarez, S779 (FRI-409)
- Delamarre, Adèle, S514 (WED-211)
- Delaney, William E., S812 (WED-377)
- de la Peña-Ramirez, Carlos, S9 (LBO-004), S83 (LBP-012), S89 (LBP-026), S174 (TOP-073)
- De Lara, Catherine, S750 (SAT-404), S752 (SAT-409), S756 (SAT-421)
- de la Rosa, Gloria, S365 (TOP-002)
- de las Heras Montero, Javier, S694 (FRI-153)
- Delataille, Philippe, S191 (WED-105)
- de la Torre, Manuel, S355 (SAT-543)
- Delaunay, Dominique, S508 (WED-194), S538 (WED-278)
- de la Viña, Daniela, S342 (THU-185)
- Del Barrio Azaceta, María, S329 (THU-154-YI), S330 (THU-155)
- Del Barrio, María, S337 (THU-172), S469 (FRI-213)
- del Campo, Nuria Pérez Diaz, S522 (WED-233-YI), S525 (WED-243-YI)
- del Campo, Rosa, S277 (WED-530-YI)
- del Carmen Domínguez, María, S779 (FRI-409)
- del Carmen Rico, María, S557 (WED-335)
- del Castillo-Cruz, Alejandro, S346 (FRI-548)
- Delcea, Caterina, S216 (FRI-080)
- DelConte, Anthony, S10 (LBO-005)
- Delcourt, Maëlen, S751 (SAT-408)
- de Lédinghen, Victor, S2 (GS-004), S37 (OS-053), S38 (OS-054), S41 (OS-060), S73 (OS-120), S168 (THU-079), S514 (WED-211), S520 (WED-227), S777 (FRI-406), S793 (WED-391), S802 (WED-410), S818 (THU-379)
- Delehouze, Claire, S109 (FRI-333)
- Delfino, Pietro, S35 (OS-048)
- Delgado, Alberto, S738 (SAT-374-YI), S768 (FRI-381)
- Delgado-Calvo, Kevin, S432 (FRI-523)
- Delgado, Carolina, S828 (THU-411)
- Delgado, Igotz, S64 (OS-101-YI), S112 (FRI-343-YI), S419 (FRI-472-YI), S562 (TOP-229-YI), S569 (THU-210)
- Delgado, Manuel, S717 (WED-172)
- Delgado, Teresa C., S417 (FRI-466-YI)
- Delgado, Teresa Cardoso, S693 (FRI-153)
- Delignette, Marie Charlotte, S22 (OS-022)
- Deliktaş Onur, İlknur, S407 (SAT-518)
- Delire, Bénédicte, S122 (SAT-331)
- Dellinger, Andrew, S114 (TOP-345)
- Delo, Joseph, S352 (SAT-535-YI)
- de los Ríos-Arellano, Ericka, S436 (FRI-535)
- De los Santos Fernández, Romina, S103 (TOP-350-YI)
- Delphine, Arquier, S49 (OS-074)
- Delphine, Degré, S131 (THU-331-YI)
- Delphin, Marion, S675 (WED-469), S746 (SAT-394), S750 (SAT-404), S752 (SAT-409), S753 (SAT-413), S756 (SAT-421)
- del Pino, Pilar, S779 (FRI-409)
- Del Prado Alba, Carmen M., S536 (WED-271)
- del Río-Álvarez, Alvaro, S417 (FRI-466-YI)
- Deltenre, Pierre, S53 (OS-081), S786 (FRI-429)
- De Luca, Chiara, S470 (FRI-215-YI)
- Delugré, Fabian, S298 (SAT-166)
- Delwaide, Jean, S6 (GS-010), S371 (SAT-014-YI), S777 (FRI-406)
- Del Zompo, Fabio, S31 (OS-040-YI), S42 (OS-061)
- De Man, Joris, S584 (THU-258-YI)
- de Man, Robert A., S394 (SAT-474), S731 (SAT-337), S758 (TOP-401-YI), S763 (FRI-367)
- De Martin, Eleonora, S378 (SAT-029)
- De Matthaëis, Nicoletta, S306 (THU-093), S533 (WED-261-YI)
- de Mattos, Kessy Djonis Martins, S439 (THU-447)
- Demchyshyn, Yaroslav, S827 (THU-408), S835 (THU-373-YI)
- de Meijer, Vincent, S286 (TOP-560), S304 (SAT-185)
- De Meyer, Sandra, S808 (WED-367)
- Demidem, Aicha, S423 (FRI-485)
- Demir, Kadir, S377 (SAT-028), S551 (WED-318-YI), S803 (WED-413)
- Demir, Münevver, S259 (SAT-135), S366 (TOP-003-YI)
- De Monte, Sara, S224 (FRI-103-YI)
- Demory, Alix, S441 (THU-459-YI), S451 (THU-487-YI)
- de Mutsert, Renée, S492 (FRI-278)
- De Muyndck, Kevin, S292 (SAT-151-YI)
- Deneau, Mark, S374 (SAT-021)
- Denecheau-Girard, Corentin, S705 (WED-129)
- Denecke, Timm, S404 (SAT-501-YI)
- Deng, Guohong, S701 (FRI-174)
- Deng, Hong, S574 (THU-226), S605 (SAT-198)
- Deng, Huan, S161 (THU-058)
- Deng, Jiang, S590 (THU-279)
- Deng, Sisi, S65 (OS-103)
- Deng, Tianxurun, S526 (WED-246)
- Deng, Wen, S344 (THU-191)
- Deng, Zhiling, S727 (TOP-356)
- den Hoed, Caroline, S9 (LBO-004), S89 (LBP-026), S380 (SAT-035), S464 (FRI-200)
- De Nicola, Stella, S404 (SAT-502-YI), S406 (SAT-514), S439 (THU-447)
- Denk, Gerald, S182 (WED-077)
- Dennis, Andrea, S511 (WED-200), S522 (WED-234), S524 (WED-238), S535 (WED-268), S542 (WED-285)
- Dennis, Claude, S400 (SAT-492)
- den Ouden, Marjolein, S480 (FRI-244)
- Denys, Alban, S53 (OS-081)
- de Oliveira, Fabiana Dolovitsch, S618 (SAT-244)
- Deplazes, Peter, S702 (TOP-140)
- Derbala, Moutaz F.M., S624 (FRI-020)
- Derbel, Haytham, S453 (THU-494)
- Derdak, Zoltan, S544 (WED-294)
- Derdeyn, Jolien, S259 (SAT-134), S540 (WED-281-YI)
- Deresh, Nataliya, S610 (SAT-213)
- Dermit, Maria, S574 (THU-227)
- De Rosa, Antonio, S438 (THU-446)
- De Rosa, Laura, S549 (WED-314-YI)
- DeRoza, Marianne, S169 (THU-082)
- D'Errico, Maria Antonietta, S704 (TOP-143-YI)
- Desai, Amisha, S101 (LBP-046)
- Desai, Jigar, S692 (FRI-151)
- Desai, Nirav K., S696 (FRI-161), S698 (FRI-164)
- de Saint-Loup, Marc, S2 (GS-004), S38 (OS-054)
- de Salazar, Adolfo, S779 (FRI-409)
- Desalegn, Hailemichael, S161 (THU-058), S208 (FRI-053), S219 (FRI-088), S674 (WED-466), S781 (FRI-414)
- de Sárraga, Carla, S233 (FRI-126)
- Desbois-Mouthon, Christèle, S416 (FRI-465)
- Deschenes, Marc, S484 (FRI-256-YI)
- Deschler, Sebastian, S35 (OS-049-YI)
- Desdouets, Chantal, S349 (TOP-552), S415 (FRI-459), S572 (THU-220)
- Desert, Romain, S25 (OS-029)
- Deshmukh, Akhil, S177 (WED-057)
- Deshpande, Aditi, S726 (TOP-353), S732 (SAT-339)
- De Silva H, Janaka, S158 (THU-052), S167 (THU-078)
- De Simone, Paolo, S365 (TOP-001), S368 (SAT-009)
- DeSimone, Paolo, S383 (SAT-044)
- Desjonqueres, Elvire, S456 (THU-503)
- Desmarests, Maxime, S61 (OS-097)
- De Smet, Vincent, S262 (THU-524-YI)
- Desmons, Aurore, S130 (THU-327)
- de Solorzano, Marta Morán Ortiz, S598 (THU-302)
- de Sousa, Raysa, S190 (WED-102)

Author Index

- Dessalegn, Hailemichael, S795 ([WED-394](#))
 De Stefano, Valerio, S703 ([TOP-142-YI](#))
 Desterke, Christophe, S370 ([SAT-011](#)),
 S385 ([SAT-049](#)), S432 ([FRI-525](#))
 de Temple, Brittany, S8 ([LBO-002](#))
 Deterding, Katja, S253 ([SAT-117](#)),
 S735 ([SAT-363](#)), S750 ([SAT-406-YI](#))
 Determann, Madita, S56 ([OS-086-YI](#))
 Detlefsen, Sönke, S32 ([OS-041-YI](#)),
 S41 ([OS-059](#)), S142 ([SAT-266](#)),
 S510 ([WED-199](#))
 de Toni, Enrico, S24 ([OS-027-YI](#)),
 S52 ([OS-079-YI](#)), S440 ([THU-457](#)),
 S458 ([THU-517](#))
 de Troyer, Ewoud, S810 ([WED-372](#))
 Detry, Olivier, S371 ([SAT-014-YI](#)),
 S386 ([SAT-051](#))
 Deuffic-Burban, Sylvie, S670 ([WED-455](#))
 Deutsch, Melanie, S690 ([WED-503](#)),
 S798 ([WED-403](#)), S823 ([THU-398](#))
 Devadas, Bruno, S544 ([WED-294](#))
 Devadas, Krishnadas, S158 ([THU-052](#)),
 S167 ([THU-078](#)), S475 ([FRI-231](#))
 Deval, Jerome, S564 ([THU-198](#)),
 S808 ([WED-366](#))
 Dev, Anouk, S400 ([SAT-492](#))
 Devarbhavi, Harshad, S158 ([THU-052](#)),
 S167 ([THU-078](#))
 de Veer, Rozanne C., S308 ([THU-098](#)),
 S309 ([THU-100](#)), S314 ([THU-109](#)),
 S319 ([THU-120-YI](#)), S327 ([THU-138](#))
 De Venuto, Clara, S215 ([FRI-078-YI](#))
 De Vincentis, Antonio, S306 ([THU-093](#)),
 S554 ([WED-325-YI](#))
 Devisscher, Lindsey, S57 ([OS-089-YI](#)),
 S143 ([SAT-268](#)), S278 ([WED-531](#)),
 S292 ([SAT-151-YI](#)), S311 ([THU-102-YI](#)),
 S321 ([THU-123-YI](#)), S420 ([FRI-475-YI](#)),
 S442 ([THU-463](#))
 Devkota, Upasana, S668 ([WED-451-YI](#))
 De Vos, Zenzi, S292 ([SAT-151-YI](#))
 De Vree, Marleen, S309 ([THU-100](#))
 de Vries, Annemarie, S315 ([THU-112-YI](#))
 de Vries, Elsemieke S., S309 ([THU-100](#)),
 S317 ([THU-115-YI](#))
 Devshi, Dhruti, S174 ([TOP-084](#))
 Devuni, Deepika, S603 ([SAT-194](#))
 de Waart, Rudi, S296 ([SAT-160](#))
 Dewey, Rick, S569 ([THU-211](#))
 De Winter, Benedicte, S584 ([THU-258-YI](#))
 de Wit, Koos, S213 ([FRI-074-YI](#))
 de Wit, Ulrike, S309 ([THU-100](#))
 de Zawadzki, Andressa, S47 ([OS-072-YI](#))
 Dhaliwal, Galvin, S60 ([OS-095](#))
 Dhanda, Ashwin, S153 ([SAT-299](#)),
 S654 ([SAT-467](#))
 Dhanireddy, Kiran, S9 ([LBO-004](#)),
 S89 ([LBP-026](#))
 Dhanjal, Jaspreet, S347 ([FRI-550](#))
 Dhar, Ameet, S679 ([WED-477-YI](#))
 Dharancy, Sebastien, S168 ([THU-079](#)),
 S369 ([SAT-010](#))
 Dharancy, Sébastien, S6 ([GS-010](#)),
 S156 ([TOP-108](#)), S367 ([TOP-005](#)),
 S385 ([SAT-048](#)), S644 ([SAT-439-YI](#)),
 S763 ([FRI-370](#))
 Dharia, Anushka, S547 ([WED-303](#))
 Dharia, Arpan, S670 ([WED-454-YI](#)),
 S680 ([WED-478](#)), S680 ([WED-479](#))
 Dhawan, Anil, S21 ([OS-020](#)),
 S707 ([WED-133](#)), S709 ([WED-137-YI](#))
 Dhiman, Radha Krishan, S158 ([THU-052](#)),
 S167 ([THU-078](#)), S219 ([FRI-088](#))
 Diago, Moises, S777 ([FRI-406](#))
 Diamantopoulou, Georgia,
 S830 ([THU-419](#))
 Diamond, Charlie, S511 ([WED-200](#)),
 S535 ([WED-268](#))
 Diap, Graciela, S831 ([THU-362](#))
 Dias dos Santos, Diego, S113 ([FRI-348](#))
 Dias, Marlon, S190 ([WED-102](#))
 Diaw, Ndeye Aminata, S743 ([SAT-387](#))
 Díaz, Alba, S468 ([FRI-211](#)),
 S721 ([WED-181](#))
 Diaz, Alejandro Armesilla,
 S186 ([WED-090](#))
 Diaz del Campo, Nuria Pérez,
 S475 ([FRI-230-YI](#)), S480 ([FRI-243](#)),
 S483 ([FRI-251-YI](#)), S501 ([FRI-314](#))
 Diaz-Ferrer, Javier, S30 ([OS-038-YI](#)),
 S199 ([TOP-062](#)), S200 ([TOP-064-YI](#))
 Diaz-Gonzalez, Alvaro, S318 ([THU-118](#)),
 S330 ([THU-155](#))
 Diaz-González, Álvaro, S329 ([THU-154-YI](#)),
 S337 ([THU-172](#)), S344 ([THU-189](#))
 Diaz, Ivanna, S483 ([FRI-254](#))
 Diaz, Juan Manuel, S9 ([LBO-004](#)),
 S83 ([LBP-012](#)), S89 ([LBP-026](#)),
 S157 ([THU-049](#))
 Díaz-Lagares, Cándido, S45 ([OS-068](#))
 Diaz, Luis Antonio, S84 ([LBP-014](#))
 Diaz-Muñoz, Mauricio, S436 ([FRI-535](#))
 Díaz, Pedro, S266 ([THU-539](#))
 Diaz-Sanchez, Nazaret, S682 ([WED-483](#))
 Diaz, Vanessa, S391 ([TOP-512-YI](#))
 Díaz-Vázquez, Ignacio, S690 ([WED-513](#))
 Diba, Camellia, S27 ([OS-033](#))
 Dibba, Bakary, S782 ([FRI-418](#)),
 S786 ([FRI-431](#))
 DiBenedetto, Clara, S388 ([SAT-056](#))
 Di Benedetto, Fabrizio, S369 ([SAT-009](#)),
 S389 ([SAT-060](#))
 Dickerson, Suzanne, S670 ([WED-454-YI](#))
 Dickinson, Klara, S308 ([THU-098](#))
 Dickson, Rolland, S43 ([OS-064](#)),
 S152 ([SAT-297](#))
 Dieckmann, Nathan, S12 ([OS-003](#))
 Diédhiou, Cyrille, S743 ([SAT-387](#))
 Dieguez, Maria Luisa Gonzalez,
 S365 ([TOP-002](#)), S717 ([WED-172](#))
 Diehl, Anna Mae, S502 ([FRI-316](#))
 Diehl, Lauri, S729 ([TOP-368](#)),
 S738 ([SAT-373](#))
 Diekhöner, Mara, S705 ([WED-129](#))
 Dierkhising, Ross, S504 ([TOP-252-YI](#))
 Dieterich, Douglas T, S669 ([WED-453](#))
 Dieterich, Douglas T., S799 ([WED-405](#))
 Dietrich, Julie, S80 ([LBP-006](#))
 Dietrich, Peter, S327 ([THU-137](#)),
 S338 ([THU-176](#)), S356 ([SAT-546](#))
 Dietz-Fricke, Christopher, S73 ([OS-120](#)),
 S793 ([WED-391](#))
 Diez, Cristina, S741 ([SAT-379](#)),
 S751 ([SAT-407](#))
 Differding, Shawna, S544 ([WED-294](#))
 Di Girolamo, Julia, S676 ([WED-470](#))
 di Iulio, Julia, S812 ([WED-376](#))
 Dijkgraaf, Marcel, S317 ([THU-115-YI](#))
 Diken, Mustafa, S435 ([FRI-533](#))
 Dileo, Eleonora, S475 ([FRI-230-YI](#)),
 S483 ([FRI-251-YI](#)), S501 ([FRI-314](#)),
 S522 ([WED-233-YI](#)), S525 ([WED-243-YI](#))
 Dille, Matthias, S426 ([FRI-495](#))
 Dill, Michael, S300 ([SAT-174](#))
 Dillon, John F, S14 ([OS-007-YI](#))
 Dillon, John F., S81 ([LBP-007](#)),
 S651 ([SAT-456](#))
 Dilokthornsakul, Piyameth,
 S689 ([WED-502](#))
 Dimanche-Boitrel, Marie-Thérèse,
 S109 ([FRI-333](#))
 Di Marco, Vito, S215 ([FRI-078-YI](#)),
 S310 ([THU-101](#)), S503 ([FRI-317](#)),
 S557 ([WED-336](#)), S609 ([SAT-209-YI](#))
 Di Maria, Gabriele, S310 ([THU-101](#)),
 S503 ([FRI-317](#)), S609 ([SAT-209-YI](#))
 Dimitroulopoulos, Dimitrios,
 S798 ([WED-403](#))
 Dimitrova, Dessislava, S79 ([LBP-005](#))
 Dimitrova, Magdalena Genadieva,
 S172 ([THU-092](#))
 Dimou, Aikaterini, S322 ([THU-126](#)),
 S325 ([THU-134](#))
 Dinani, Amreen, S487 ([FRI-262](#)),
 S545 ([WED-295-YI](#))
 Dincer, Dinc, S219 ([FRI-088](#)),
 S336 ([THU-171](#))
 Dingli, Florent, S193 ([WED-112](#)),
 S524 ([WED-239](#))
 Ding, Lijuan, S806 ([WED-362](#)),
 S813 ([WED-381](#)), S815 ([WED-386](#)),
 S816 ([WED-388](#))
 Ding, Rui, S228 ([FRI-114](#))
 Ding, Xiangchun, S447 ([THU-475](#))
 Ding, Xiaoyan, S344 ([THU-191](#))
 Ding, Xueying, S813 ([WED-381](#))
 Ding, Yanhua, S86 ([LBP-019](#)), S99 ([LBP-043](#)),
 S461 ([TOP-310](#)), S551 ([WED-319](#)),
 S558 ([WED-338](#)), S602 ([TOP-217](#)),
 S807 ([WED-365](#)), S812 ([WED-378](#))
 Dinkelborg, Katja, S730 ([TOP-369](#))
 Dionisi-Vici, Carlo, S698 ([FRI-166](#))
 Diop, Mame matar, S743 ([SAT-387](#))
 Diotallevi, Sara, S824 ([THU-402](#))
 DiPiazza, Amber, S58 ([OS-090](#))
 Dirksmeier-Harinck, Femme,
 S549 ([WED-306-YI](#))
 Di Sandro, Stefano, S389 ([SAT-060](#))
 Dischinger, Ulrich, S587 ([THU-269-YI](#))
 Dispienzieri, Giulia, S376 ([SAT-025](#))
 Disse, Emmanuel, S508 ([WED-194](#)),
 S538 ([WED-278](#))

- Distefano, Marco, S96 ([LBP-038](#)), S175 ([TOP-085](#)), S306 ([THU-093](#)), S557 ([WED-336](#))
- Di Tommaso, Luca, S401 ([SAT-494](#)), S438 ([THU-446](#)), S580 ([THU-245](#)), S705 ([WED-130](#))
- Divita, Taylor, S132 ([THU-333](#))
- Diwakar, Sunidhi, S184 ([WED-086](#)), S195 ([WED-118](#)), S360 ([SAT-557-YI](#))
- Dixit, Bharat, S726 ([TOP-353](#)), S732 ([SAT-339](#))
- Dixit, VK, S475 ([FRI-231](#))
- Dixon, Susan, S809 ([WED-370](#))
- Di Zeo-Sánchez, Daniel E., S18 ([OS-015](#))
- Dlugosch, Carola, S567 ([THU-206](#))
- Doan, Julie, S657 ([WED-422](#)), S676 ([WED-470](#))
- Doban, Vitalii, S326 ([THU-135](#))
- Dobbermann, Henrike, S211 ([FRI-059](#))
- Dobracka, Beata, S685 ([WED-493-YI](#))
- Dobrovic, Alexander, S372 ([SAT-017](#))
- Dobrowolska, Krystyna, S685 ([WED-493-YI](#)), S821 ([THU-389](#))
- Dobryanska, Marta, S78 ([LBP-001](#)), S87 ([LBP-020](#))
- Dobrzyniecka, Anna, S820 ([THU-387](#)), S825 ([THU-403](#))
- Dodge, James, S652 ([SAT-459](#))
- Dotod, Mihai Daniel, S211 ([FRI-058](#))
- D'Offizi, Giampiero, S73 ([OS-120](#)), S793 ([WED-391](#)), S804 ([WED-414](#))
- Dohan, Anthony, S50 ([OS-077](#))
- Dohmen, Kazufumi, S42 ([OS-062](#))
- Dohoczky, David, S155 ([SAT-305](#))
- Dokmak, Safi, S372 ([SAT-016](#)), S705 ([WED-129](#))
- Dokmeci, A. Kadir, S158 ([THU-052](#)), S167 ([THU-078](#))
- Dolan, Edel, S635 ([THU-040-YI](#))
- Dolce, Arianna, S289 ([FRI-543](#))
- Dolman, Grace, S781 ([FRI-413](#))
- Dolovitsch de Oliveira, Fabiana, S616 ([SAT-237](#))
- Dominguez, Alvaro Gutierrez, S559 ([WED-341](#))
- Dominguez-Hernández, Raquel, S779 ([FRI-409](#))
- Dominguez, Inmaculada, S508 ([WED-195](#)), S557 ([WED-335](#)), S596 ([THU-296](#))
- Dominguez, María Carmen Lozano, S779 ([FRI-409](#))
- Dominik, Nina, S156 ([TOP-097-YI](#)), S165 ([THU-071](#)), S166 ([THU-075-YI](#)), S243 ([SAT-086-YI](#)), S250 ([SAT-105](#)), S251 ([SAT-111](#)), S253 ([SAT-118](#)), S255 ([SAT-122](#)), S257 ([SAT-128](#)), S717 ([WED-171](#)), S725 ([WED-190](#))
- Donadon, Matteo, S428 ([FRI-514](#))
- Donakonda, Sainitin, S351 ([SAT-533](#))
- Donaldson, Kirsteen, S613 ([SAT-224](#))
- Donati, Gabriele, S836 ([THU-375](#))
- Donato, Maria Francesca, S368 ([SAT-009](#)), S700 ([FRI-171](#))
- Dondero, Federica, S116 ([SAT-315](#)), S372 ([SAT-016](#)), S451 ([THU-487-YI](#))
- Dondossola, Daniele, S369 ([SAT-009](#)), S593 ([THU-286](#))
- Dongelmans, Edo J., S761 ([FRI-363-YI](#)), S764 ([FRI-372](#))
- Dong, Fuchen, S209 ([FRI-053](#))
- Dongiovanni, Paola, S289 ([FRI-544](#)), S459 ([TOP-301](#)), S516 ([WED-218](#))
- Dong, Jiahong, S395 ([SAT-478](#)), S433 ([FRI-527](#))
- Dong, Lingli, S710 ([WED-152](#))
- Dong, Ruihua, S815 ([WED-386](#))
- Dong, Tang, S526 ([WED-246](#))
- Dong, Yi, S536 ([WED-272](#))
- Dong, Yinuo, S120 ([SAT-324](#)), S122 ([SAT-333](#))
- Do, Nhan, S518 ([WED-222](#))
- Donnelly, Hannah, S647 ([SAT-448](#))
- Donne, Romain, S572 ([THU-220](#))
- Donné, Romain, S415 ([FRI-459](#))
- Donohue, Kathleen, S100 ([LBP-044](#))
- Dooley, Steven, S263 ([THU-526](#)), S287 ([FRI-539](#))
- Doorn, Leen-Jan, S801 ([WED-409](#))
- Dopazo, Joaquín, S596 ([THU-296](#))
- Dorcaratto, Dimitri, S266 ([THU-539](#))
- Dore, Gregory, S657 ([WED-422](#)), S676 ([WED-470](#))
- Dörge, Petra, S730 ([TOP-369](#)), S759 ([TOP-416-YI](#))
- Dorn, Livia, S773 ([FRI-394](#))
- Dosi, Michela, S439 ([THU-454](#))
- Doskey, Luke, S134 ([THU-341](#))
- Douda, Tomas, S311 ([THU-103](#))
- Douglas, Mark, S28 ([OS-034](#))
- Doukas, Michail, S394 ([SAT-474](#))
- Dou, Xiaoguang, S95 ([LBP-037](#)), S803 ([WED-412](#))
- DovaL, Dinesh, S343 ([THU-187](#))
- Dowden, Stephanie, S519 ([WED-225](#))
- Dow, Ellie, S14 ([OS-007-YI](#))
- Dowman, Joanna, S718 ([WED-173](#))
- Downs, Louise, S756 ([SAT-421](#))
- Downs, Matt, S811 ([WED-375](#))
- Doyle, Adam, S161 ([THU-058](#))
- Dragan, Alexandru Victor, S216 ([FRI-080](#))
- Draganov, Ventseslav, S172 ([THU-092](#))
- Dragonì, Gabriele, S88 ([LBP-023](#)), S342 ([THU-184](#))
- Drammeh, Sainabou, S782 ([FRI-418](#)), S786 ([FRI-431](#))
- Drapkina, Oxana, S501 ([FRI-305](#))
- Drasdo, Dirk, S263 ([THU-526](#))
- Drazilova, Sylvia, S29 ([OS-036-YI](#)), S779 ([FRI-408](#))
- Dražilová, Sylvia, S539 ([WED-279](#))
- Drenth, Joost P.H., S20 ([OS-019](#)), S309 ([THU-100](#)), S314 ([THU-109](#)), S319 ([THU-120-YI](#)), S327 ([THU-138](#))
- Drenth, Joost PH, S18 ([OS-015](#)), S317 ([THU-115-YI](#)), S712 ([WED-160](#))
- Dreyer, Carla, S631 ([THU-016](#))
- Driessche, Annelien Van, S321 ([THU-123-YI](#))
- Driessen, Ann, S540 ([WED-281-YI](#)), S581 ([THU-249](#)), S731 ([SAT-337](#))
- Drilhon, Nicolas, S54 ([OS-084-YI](#))
- Drimousi, Anastasia, S690 ([WED-503](#))
- Drossaert, Stans, S480 ([FRI-244](#))
- Drotar, Peter, S29 ([OS-036-YI](#))
- Droungas, Yianni, S740 ([SAT-377](#))
- Duah, Amoako, S395 ([SAT-479-YI](#))
- Duan, Jianzhou, S149 ([SAT-287](#))
- Duan, Xuefei, S769 ([FRI-382](#))
- Duan, Zhongping, S158 ([THU-052](#)), S167 ([THU-078](#))
- Duarte-Neto, Amaro Nunes, S730 ([TOP-384-YI](#))
- Dube, Asha, S333 ([THU-162-YI](#))
- Dubois, Anaëlle, S58 ([OS-091](#))
- Dubois, Remy, S412 ([FRI-454](#))
- Dubourg, Julie, S37 ([OS-051](#)), S84 ([LBP-014](#)), S88 ([LBP-024](#)), S463 ([FRI-198](#)), S464 ([FRI-199](#)), S481 ([FRI-247](#)), S482 ([FRI-249](#)), S504 ([TOP-253](#)), S507 ([TOP-300](#)), S511 ([WED-201](#)), S511 ([WED-202](#)), S515 ([WED-213](#)), S518 ([WED-223](#)), S648 ([SAT-450](#))
- Duca, Leonardo, S772 ([FRI-392-YI](#)), S777 ([FRI-405](#)), S798 ([WED-399-YI](#))
- Ducarmon, Quinten, S47 ([OS-071-YI](#)), S272 ([WED-517](#))
- Ducci, Juri, S365 ([TOP-001](#)), S383 ([SAT-044](#)), S456 ([THU-502](#))
- Duckworth, Adam, S81 ([LBP-008](#))
- Duclos-Vallée, Jean-Charles, S41 ([OS-060](#))
- Ducournau, Gerard, S444 ([THU-466](#))
- Duc, Pham Minh, S261 ([THU-523](#)), S430 ([FRI-518](#))
- Duda, Julia, S57 ([OS-088-YI](#))
- Duduskar, Shivalee, S178 ([WED-060-YI](#))
- Duffy, Austin, S450 ([THU-485-YI](#))
- Dufour, Jean-François, S69 ([OS-112-YI](#)), S393 ([SAT-473](#))
- Du, Guifang, S433 ([FRI-527](#))
- Duhamel, Alain, S6 ([GS-010](#))
- Du, Jing, S526 ([WED-246](#))
- Du, Laijing, S100 ([LBP-045](#))
- Düll, Miriam M., S317 ([THU-116-YI](#)), S327 ([THU-137](#)), S338 ([THU-176](#))
- Dulmage, Keely, S88 ([LBP-022](#))
- Duman, Serkan, S407 ([SAT-519](#)), S479 ([FRI-238](#))
- Dumitrascu, Catalina, S14 ([OS-009-YI](#))
- Dumitru, Radu, S446 ([THU-473](#))
- Dumolard, Lucile, S744 ([SAT-389](#)), S747 ([SAT-396](#))
- Dumont, Mathilde Petiet, S640 ([SAT-430](#))
- Dumortier, Jérôme, S6 ([GS-010](#)), S22 ([OS-022](#)), S73 ([OS-120](#)), S367 ([TOP-005](#)), S369 ([SAT-010](#)), S385 ([SAT-048](#)), S705 ([WED-129](#)), S763 ([FRI-370](#)), S793 ([WED-391](#))
- Dunbar, Megan, S799 ([WED-405](#))
- Dung, Thai Bieu Phu, S552 ([WED-320](#))
- Dunichand-Hoedl, Abha, S231 ([FRI-122](#))

Author Index

- Dunn, Nicholas, S84 ([LBP-014](#))
Dunn, Winston, S84 ([LBP-014](#))
Dupuy, Julie, S514 ([WED-211](#))
Dupuy, Marie, S115 ([SAT-306](#))
Du, Qin, S605 ([SAT-198](#))
Duque, Juan Carlos Rodriguez, S469 ([FRI-213](#))
Durand, Francois, S9 ([LBO-004](#)), S54 ([OS-084-YI](#)), S89 ([LBP-026](#)), S116 ([SAT-315](#)), S180 ([WED-071](#)), S372 ([SAT-016](#)), S451 ([THU-487-YI](#)), S719 ([WED-177](#))
Durand, François, S199 ([TOP-062](#))
Durand, Sarah, S17 ([OS-013](#)), S42 ([OS-061](#)), S734 ([SAT-348-YI](#))
Durand, Stephanie, S422 ([FRI-485](#))
Duran-Güell, Marta, S16 ([OS-011](#)), S174 ([TOP-073](#)), S185 ([WED-087](#))
Duran, Osman Firat, S407 ([SAT-519](#))
Durante, Barbara, S401 ([SAT-494](#)), S438 ([THU-446](#))
Durantel, David, S744 ([SAT-389](#))
Durban, Jonathan, S672 ([WED-459-YI](#))
Durkalski-Mauldin, Valerie, S104 ([TOP-352](#))
Duseja, Ajay Kumar, S84 ([LBP-014](#)), S129 ([THU-324](#)), S152 ([SAT-295](#)), S158 ([THU-051](#)), S158 ([THU-052](#)), S167 ([THU-078](#)), S217 ([FRI-082](#)), S219 ([FRI-088](#)), S475 ([FRI-231](#)), S643 ([SAT-438](#))
Dusheiko, Geoffrey, S756 ([SAT-421](#)), S775 ([FRI-399](#))
Du, Shunda, S99 ([LBP-042](#))
du Sorbier, Aymeric Monegier, S5 ([GS-007](#))
Dutta, Pinaki, S217 ([FRI-082](#))
Duun-Henriksen, Anne, S93 ([LBP-032](#))
Duvauchelle, Thierry, S615 ([SAT-231](#))
Duvoux, Christophe, S6 ([GS-010](#)), S9 ([LBO-004](#)), S89 ([LBP-026](#)), S369 ([SAT-010](#)), S373 ([SAT-020](#)), S385 ([SAT-048](#)), S453 ([THU-494](#)), S700 ([FRI-171](#))
Du, Weiming, S715 ([WED-165](#))
Du, Yu, S83 ([LBP-013](#))
Dvořák, Karel, S311 ([THU-103](#)), S539 ([WED-280](#))
Dwarampudi, Siva, S227 ([FRI-112](#))
Dwarkanathan, Vignesh, S506 ([TOP-276](#))
Dwarkasing, Roy, S315 ([THU-112-YI](#))
Dwivedi, Girish, S483 ([FRI-250](#)), S487 ([FRI-263](#))
Dwivedi, Ved, S283 ([WED-549](#))
Dwyer, Benjamin J, S186 ([WED-090](#))
Dybowska, Dorota, S685 ([WED-493-YI](#)), S834 ([THU-367-YI](#))
Dyson, Jessica, S290 ([TOP-147](#)), S297 ([SAT-165-YI](#)), S315 ([THU-111](#)), S331 ([THU-159-YI](#))
Dywicki, Janine, S583 ([THU-256](#))
Dzen, Lucile, S608 ([SAT-206](#))
Eapen, CE, S158 ([THU-052](#)), S161 ([THU-058](#)), S167 ([THU-078](#))
Easaw, Sue, S84 ([LBP-015](#))
Easom, Nicholas, S676 ([WED-471](#)), S760 ([TOP-417](#))
Easterbrook, Philippa, S656 ([TOP-460-YI](#)), S831 ([THU-363](#))
Ebadi, Maryam, S231 ([FRI-122](#)), S374 ([SAT-021](#))
Ebbo, Mikael, S710 ([WED-152](#))
Ebeid, Fatma, S831 ([THU-363](#))
Ebel, Sebastian, S404 ([SAT-501-YI](#))
Ebert, Matthias, S263 ([THU-526](#)), S287 ([FRI-539](#)), S334 ([THU-164-YI](#))
Ebihara, Takeshi, S506 ([TOP-288](#))
Ebrahimi, Ali, S567 ([THU-203](#))
Eccher, Albino, S438 ([THU-446](#))
Echavarría, Victor, S139 ([SAT-257](#))
Echavarría, Victor, S376 ([SAT-024-YI](#))
Echeveste, Ainhoa, S536 ([WED-271](#))
Eckel, Juergen, S269 ([THU-548-YI](#))
Ecker, Dominik, S818 ([THU-381](#))
Edagwa, Benson, S742 ([SAT-382](#))
Edeline, Julien, S383 ([SAT-043](#)), S411 ([TOP-507-YI](#))
Edin, Matthew, S580 ([THU-247-YI](#))
Edlund, Karolina, S57 ([OS-088-YI](#)), S273 ([WED-521-YI](#))
Edwards, Jessie, S668 ([WED-451-YI](#))
Edwards, Lindsey, S17 ([OS-014-YI](#)), S46 ([OS-070](#)), S182 ([WED-078](#)), S282 ([WED-545-YI](#)), S588 ([THU-271-YI](#))
Edwards, Rachel, S629 ([THU-008](#)), S641 ([SAT-433](#))
Edwin, S797 ([WED-398](#))
Efe, Cumali, S341 ([THU-182](#)), S374 ([SAT-021](#))
Efferth, Thomas, S432 ([FRI-523](#))
Egge, Julius, S205 ([FRI-044-YI](#))
Eggermont, Fabienne, S172 ([THU-092](#))
Egger, Robert, S571 ([THU-215](#)), S585 ([THU-261](#))
Eghtesad, Bijan, S9 ([LBO-004](#)), S89 ([LBP-026](#))
Eguchi, Susumu, S9 ([LBO-004](#)), S89 ([LBP-026](#))
Eguchi, Yuichiro, S643 ([SAT-438](#))
Ehmer, Ursula, S52 ([OS-079-YI](#)), S298 ([SAT-166](#)), S440 ([THU-457](#))
Ehrenbauer, Alena Friederike, S205 ([FRI-044-YI](#)), S245 ([SAT-090-YI](#))
Ehrhard, Florent, S520 ([WED-227](#)), S640 ([SAT-430](#))
Ehrlich, S. Dusko, S159 ([THU-053](#))
Eide, Emma, S22 ([OS-023-YI](#)), S386 ([SAT-050](#))
Eigadeh, Hadi, S704 ([TOP-144-YI](#))
Eilard, Anders, S754 ([SAT-414](#))
Eill, Elizabeth, S26 ([OS-031](#)), S809 ([WED-371](#))
Eischeid-Scholz, Hannah, S423 ([FRI-486](#))
Eizaguirre, Emma, S536 ([WED-271](#))
Ekelik, Merve, S479 ([FRI-238](#))
Eker, Hasan, S420 ([FRI-475-YI](#))
Ekheden, Isabella, S334 ([THU-165](#))
Eklund, Olof, S93 ([LBP-031](#))
Ekser, Burcin, S369 ([SAT-009](#))
Ekstedt, Mattias, S462 ([FRI-196](#)), S530 ([WED-255-YI](#)), S532 ([WED-259](#))
Eksteen, Bertus, S5 ([GS-007](#))
Elangovan, Lavanya, S350 ([TOP-553](#))
Elbasiony, Mohammed, S158 ([THU-052](#)), S167 ([THU-078](#))
Elbeshbeshy, Hany, S98 ([LBP-040](#))
El-domiaty, Nada, S378 ([SAT-029](#))
Elefsiniotis, Ioannis, S454 ([THU-495](#)), S798 ([WED-403](#))
Eley, Timothy, S26 ([OS-031](#)), S809 ([WED-371](#))
Elgretli, Wesal, S683 ([WED-486-YI](#))
Elhanan, Gai, S462 ([FRI-195](#))
Elhan, Atilla, S479 ([FRI-238](#))
Elhence, Anshuman, S201 ([TOP-065](#))
Elia, Chiara, S215 ([FRI-078-YI](#))
Elias, Kathleen, S292 ([TOP-156](#))
Elinav, Eran, S65 ([OS-103](#))
Elisa, Farina, S388 ([SAT-056](#))
Elizalde, María, S416 ([FRI-464](#))
El-Karim, Lima Awad, S49 ([OS-075-YI](#))
El-Kassas, Mohamed, S643 ([SAT-438](#))
Elkhashab, Magdy, S555 ([WED-330](#)), S561 ([WED-348](#))
El Khateeb, Engy, S491 ([FRI-273-YI](#))
El-Khatib, Aiman, S583 ([THU-255](#))
Elkhatib, Hana, S191 ([WED-105](#))
Elkholi, Ayman, S246 ([SAT-093-YI](#))
Elkrief, Laure, S9 ([LBO-004](#)), S53 ([OS-081](#)), S54 ([OS-084-YI](#)), S61 ([OS-097](#)), S89 ([LBP-026](#)), S168 ([THU-079](#)), S238 ([SAT-068](#)), S385 ([SAT-048](#)), S524 ([WED-239](#)), S705 ([WED-129](#))
Ellapen, Malcolm, S753 ([SAT-413](#))
Ellik, Zeynep Melekoğlu, S407 ([SAT-519](#)), S479 ([FRI-238](#))
Elliman, Steven, S101 ([LBP-046](#))
Elliott, Joanne, S300 ([SAT-175](#))
Elliott, Zoe, S227 ([FRI-112](#))
El Maimouni, Cautar, S471 ([FRI-219-YI](#))
Elmazar, Mohamed, S418 ([FRI-470](#))
Elortza, Felix, S50 ([OS-076-YI](#))
Elrayes, Julian, S681 ([WED-482](#))
Elsabaawy, Maha, S238 ([SAT-068](#))
El-Sayed, Manal, S831 ([THU-363](#))
Elsaygh, Jude, S252 ([SAT-114](#))
Elsharkawy, Ahmed M, S731 ([SAT-337](#))
Elsharkawy, Ahmed M., S765 ([FRI-374-YI](#))
Elshawaf, Ahmed, S673 ([WED-463](#))
Elston, Robert, S745 ([SAT-390](#))
Elurbide-Tardio, Jasmin, S287 ([FRI-538](#))
Elwir, Saleh, S374 ([SAT-021](#))
El-zailik, Asma, S816 ([WED-389](#))
Emadali, Anouk, S413 ([FRI-455](#))
Emch, Michael, S668 ([WED-451-YI](#))
Emir, Birol, S533 ([WED-263](#))
Emond, Jean, S375 ([SAT-023](#))
Endo, Kei, S451 ([THU-490](#))
Enea, Marco, S503 ([FRI-317](#)), S609 ([SAT-209-YI](#))
Engebretsen, Kristiane A., S606 ([SAT-201](#))

- Engel, Bastian, S19 ([OS-017](#)),
S21 ([OS-021-YI](#)), S44 ([OS-066-YI](#)),
S341 ([THU-182](#)), S712 ([WED-160](#))
- Engel, Maarten F. M., S652 ([SAT-462-YI](#))
- Engelmann, Cornelius, S9 ([LBO-004](#)),
S89 ([LBP-026](#)), S161 ([THU-057-YI](#)),
S182 ([WED-080](#)), S203 ([FRI-040](#)),
S288 ([FRI-541-YI](#)), S359 ([SAT-555](#)),
S594 ([THU-291-YI](#)), S649 ([SAT-452](#))
- Engesæter, Lise, S22 ([OS-023-YI](#)),
S386 ([SAT-050](#))
- English, Louise, S676 ([WED-471](#)),
S759 ([TOP-417](#))
- Enhörning, Sofia, S624 ([FRI-018](#))
- Enkhjargal, Saruul, S82 ([LBP-011](#))
- Enkhtaivan, Sanjaasuren, S82 ([LBP-011](#))
- Enomoto, Masaru, S430 ([FRI-518](#))
- Enomoto, Nobuyuki, S828 ([THU-413](#))
- Enríquez-Rodríguez, César, S207 ([FRI-051](#))
- Eoh, Hyungjin, S128 ([THU-319](#)),
S288 ([FRI-540](#))
- Epping, Ludger S.M., S319 ([THU-120-YI](#))
- Erasmus, Hans-Peter, S170 ([THU-087](#))
- Erdmann, Joris, S304 ([SAT-185](#)),
S394 ([SAT-474](#))
- Erdozain, José Carlos, S398 ([SAT-485](#)),
S706 ([WED-132](#)), S712 ([WED-159](#))
- Ergenc, Ilkay, S329 ([THU-153](#))
- Ergenc, Ilkay, S723 ([WED-187-YI](#))
- Erhard Uschner, Frank, S159 ([THU-055](#)),
S169 ([THU-083](#)), S170 ([THU-087](#)),
S171 ([THU-088](#)), S184 ([WED-083](#)),
S188 ([WED-098-YI](#)), S193 ([WED-111](#)),
S198 ([WED-126](#))
- Erickson, Mary, S124 ([TOP-313](#)),
S126 ([THU-316](#)), S325 ([THU-132](#))
- Eriksson, John, S535 ([WED-270](#))
- Erinjeri, Joseph, S3 ([GS-005](#))
- Erlacher, Sophia, S35 ([OS-049-YI](#))
- Erler, Nicole S., S309 ([THU-100](#)),
S314 ([THU-109](#)), S319 ([THU-120-YI](#)),
S327 ([THU-138](#))
- Ermaciová, Elena, S819 ([THU-382](#))
- Erminelli, Davide, S246 ([SAT-094-YI](#))
- Ernst, Martha, S191 ([WED-106](#))
- Erpapazoglou, Zoi, S599 ([THU-306](#))
- Er, Ramazan Erdem, S479 ([FRI-238](#))
- Ersoz, Galip, S805 ([WED-419](#))
- Ertl, Hildegund, S86 ([LBP-018](#))
- Eruzun, Hasan, S723 ([WED-187-YI](#))
- Ervolino, Edilson, S271 ([THU-556](#))
- Esarte, Silvia Goñi, S329 ([THU-154-YI](#)),
S344 ([THU-189](#))
- Eschrich, Johannes, S25 ([OS-028](#))
- Escobar, Jose, S3 ([GS-005](#))
- Escobar, Mafalda, S423 ([FRI-486](#))
- Escoda, Ona, S45 ([OS-068](#))
- Escorsell, Àngels, S355 ([SAT-543](#))
- Escudero-García, Desamparados,
S232 ([FRI-125](#)), S469 ([FRI-213](#)),
S700 ([FRI-171](#))
- Escudero-López, Blanca, S71 ([OS-116](#)),
S593 ([THU-287](#))
- Eser, Nurullah, S805 ([WED-418](#))
- Esfahani, Hrag, S588 ([THU-272-YI](#))
- Eskesen, Nicolas, S568 ([THU-208](#))
- Eslam, Mohammed, S534 ([WED-267](#)),
S652 ([SAT-462-YI](#))
- Esmat, Gamal, S491 ([FRI-273-YI](#))
- Espen, Lore Van, S47 ([OS-072-YI](#)),
S272 ([TOP-563](#))
- Espinosa-Escudero, Ricardo A.,
S432 ([FRI-523](#))
- Espinoza, Karina Sato, S395 ([SAT-479-YI](#))
- Espiritu, Christine L., S26 ([OS-031](#)),
S809 ([WED-371](#))
- Esplugues, Juan V., S266 ([THU-539](#)),
S592 ([THU-283](#))
- Esposti, Luca Degli, S773 ([FRI-393](#))
- Esteban-Fabro, Roger, S411 ([TOP-507-YI](#))
- Esteban, Paula, S318 ([THU-118](#)),
S330 ([THU-155](#)), S702 ([TOP-139](#))
- Esteban, Rafael, S785 ([FRI-427](#)),
S787 ([FRI-432](#)), S822 ([THU-395](#))
- Estep, James M., S520 ([WED-230](#))
- Estep, James M., S476 ([FRI-232](#)),
S572 ([THU-221](#))
- Esteve, Isabel, S829 ([THU-418](#))
- Estévez-Vázquez, Olga,
S276 ([WED-528-YI](#))
- Estulin, Dmitrii, S538 ([WED-275](#))
- Estupiñan, Enrique Carrera,
S30 ([OS-038-YI](#)), S199 ([TOP-062](#)),
S200 ([TOP-064-YI](#))
- Etten, Richard Van, S11 ([LBO-006](#))
- Ettorre, Giuseppe Maria, S368 ([SAT-009](#))
- Ettrich, Thomas, S52 ([OS-079-YI](#))
- Etzion, Ohad, S28 ([OS-034](#)),
S800 ([WED-407](#)), S814 ([WED-382](#)),
S832 ([THU-364](#))
- Eugenio, Mélanie Simoes, S109 ([FRI-333](#))
- Evangelista, Andreia, S343 ([THU-188](#))
- Evans, Jennifer, S54 ([OS-082](#))
- Evans, Katie, S88 ([LBP-022](#))
- Evans, Tom, S26 ([OS-031](#))
- Evole, Helena Hernández, S468 ([FRI-211](#)),
S710 ([WED-153](#))
- Evon, Donna, S394 ([SAT-476](#))
- Eyck, Annelies Van, S581 ([THU-249](#))
- Ezurra, Iranzu, S85 ([LBP-016](#))
- Ezquerria, Meritxell Bellet, S702 ([TOP-139](#))
- Fabbri, Angela, S836 ([THU-375](#))
- Faber, Klaas Nico, S304 ([SAT-185](#))
- Fabián, Ondřej, S32 ([OS-041-YI](#))
- Fabregat, Isabel, S287 ([FRI-538](#)),
S303 ([SAT-183](#))
- Fabrellas, Núria, S41 ([OS-059](#)),
S160 ([THU-056](#)), S176 ([WED-055](#)),
S503 ([TOP-241-YI](#)), S541 ([WED-284-YI](#)),
S633 ([THU-028](#))
- Fabrice, Laine, S463 ([FRI-197](#)),
S520 ([WED-227](#)), S714 ([WED-162](#))
- Facchetti, Floriana, S73 ([OS-120](#)),
S401 ([SAT-493-YI](#)), S777 ([FRI-405](#)),
S781 ([FRI-412](#)), S798 ([WED-399-YI](#))
- Fagan, Andrew, S1 ([GS-001](#)),
S364 ([WED-027](#))
- Fagioli, Stefano, S96 ([LBP-038](#)),
S175 ([TOP-085](#)), S215 ([FRI-078-YI](#)),
S306 ([THU-093](#)), S368 ([SAT-009](#)),
S439 ([THU-447](#))
- Faillie, Jean-Luc, S115 ([SAT-306](#))
- Fairchild, Timothy, S519 ([WED-225](#))
- Fairclough, Sarah, S174 ([TOP-084](#))
- Faisal, Nabiha, S219 ([FRI-088](#)),
S643 ([SAT-436](#))
- Faita, Francesco, S549 ([WED-314-YI](#)),
S622 ([FRI-014](#))
- Faitot, François, S369 ([SAT-010](#)),
S385 ([SAT-048](#))
- Faivre, Jamila, S280 ([WED-540-YI](#))
- Fajardo, Javier, S355 ([SAT-543](#))
- Falalyeyeva, Tetyana, S610 ([SAT-213](#))
- Falbo, Elisabetta, S96 ([LBP-038](#)),
S306 ([THU-093](#))
- Falcao, Livia, S722 ([WED-185](#))
- Falcomatà, Andrea, S175 ([TOP-085](#)),
S666 ([WED-446](#))
- Falcone, Gianmarco, S62 ([OS-099-YI](#))
- Faletti, Riccardo, S371 ([SAT-015-YI](#))
- Falgà, M. Àngels, S255 ([SAT-123](#))
- Falk, Christine, S350 ([SAT-532-YI](#)),
S750 ([SAT-406-YI](#))
- Falk Villesen, Ida, S139 ([SAT-255](#)),
S142 ([SAT-266](#)), S153 ([SAT-298](#))
- Fallahzadeh, Mohammad Amin,
S219 ([FRI-088](#))
- Falleni, Monica, S428 ([FRI-514](#))
- Fallon, Michael, S478 ([FRI-236-YI](#))
- Fallouh, Yasmeen, S510 ([WED-199](#)),
S547 ([WED-303](#))
- Fallowfield, Jonathan, S56 ([OS-087](#)),
S81 ([LBP-007](#)), S354 ([SAT-541](#)),
S465 ([FRI-203](#))
- Fang, Hongsheng, S422 ([FRI-484](#))
- Fang, Jianwu, S102 ([LBP-048](#))
- Fang, Jing, S349 ([TOP-552](#)), S415 ([FRI-459](#))
- Fang, Rui, S109 ([FRI-332](#))
- Fan, Jiangao, S2 ([GS-004](#)), S38 ([OS-054](#)),
S523 ([WED-237](#)), S605 ([SAT-198](#)),
S643 ([SAT-438](#))
- Fanning, Gregory, S807 ([WED-363](#))
- Fan, Qingrong, S716 ([WED-167](#))
- Fan, Rong, S95 ([LBP-037](#))
- Fan, Tao, S780 ([FRI-411-YI](#))
- Fan, Weiguo, S263 ([THU-526](#)),
S287 ([FRI-539](#))
- Fan, Zihao, S107 ([FRI-325](#))
- Farahat, Ahmed, S673 ([WED-463](#))
- Faraone, Alyse, S692 ([FRI-151](#))
- Fareh, Mohamed, S740 ([SAT-377](#))
- Fargeat, Cecile, S648 ([SAT-449](#))
- Faria, Flávio, S271 ([THU-556](#))
- Farias, Alberto, S9 ([LBO-004](#)),
S30 ([OS-038-YI](#)), S83 ([LBP-012](#)),
S89 ([LBP-026](#)), S157 ([THU-050](#)),
S161 ([THU-057-YI](#)), S199 ([TOP-062](#)),
S200 ([TOP-064-YI](#)), S208 ([FRI-053](#))
- Farias, Alberto Queiroz, S174 ([TOP-073](#))
- Farid, Gaouar, S5 ([GS-007](#)), S313 ([THU-107](#)),
S326 ([THU-136](#))

Author Index

- Farina, Claudio, S777 ([FRI-405](#))
 Farina, Elisa, S439 ([THU-447](#)),
 S700 ([FRI-171](#))
 Färkkilä, Martti, S5 ([GS-007](#))
 Farmer, Douglas, S354 ([SAT-542](#))
 Farno, Dawn, S544 ([WED-294](#))
 Farrag, Ahmed, S831 ([THU-363](#))
 Faruqui, Saamia, S545 ([WED-295-YI](#))
 Farzi, Mohsen, S530 ([WED-254](#))
 Fassan, Matteo, S438 ([THU-446](#))
 Fassio, Eduardo, S30 ([OS-038-YI](#)),
 S83 ([LBP-012](#)), S199 ([TOP-062](#)),
 S200 ([TOP-064-YI](#))
 Fassnacht, Martin,
 S587 ([THU-269-YI](#))
 Fatta, Erika, S474 ([FRI-226](#)),
 S482 ([FRI-248-YI](#))
 Faulkes, Rosemary, S219 ([FRI-088](#)),
 S423 ([FRI-487](#))
 Faulkner, Claire, S540 ([WED-282](#))
 Faure, Stéphanie, S115 ([SAT-306](#)),
 S143 ([SAT-269](#)), S376 ([SAT-026](#))
 Favaloro, Frank, S692 ([FRI-151](#))
 Fava, Luca, S699 ([FRI-167-YI](#))
 Faviana, Pinuccia, S428 ([FRI-502](#))
 Favier, Laurie, S6 ([GS-010](#))
 Faye, Lamine, S743 ([SAT-387](#))
 Fear, Janine, S101 ([LBP-046](#))
 Fedele, Veronica, S438 ([TOP-506](#))
 Federica, Mirici, S332 ([THU-161](#))
 Federici, Massimo, S538 ([WED-275](#))
 Federico, Alessandro, S73 ([OS-120](#)),
 S173 ([TOP-072](#)), S213 ([FRI-070-YI](#)),
 S332 ([THU-161](#)), S459 ([TOP-301](#)),
 S666 ([WED-446](#)), S704 ([TOP-144-YI](#)),
 S793 ([WED-391](#)), S804 ([WED-414](#)),
 S817 ([THU-378](#))
 Federico, Piera, S395 ([SAT-477-YI](#)),
 S446 ([THU-472-YI](#))
 Fedorov, Dmitri, S591 ([THU-282](#))
 Fedzhaga, Iryna, S499 ([FRI-298](#))
 Feigh, Michael, S421 ([FRI-478](#)),
 S566 ([THU-202](#)), S568 ([THU-208](#)),
 S569 ([THU-211](#)), S576 ([THU-232](#)),
 S580 ([THU-244](#)), S600 ([THU-336](#))
 Feigin, Eugene, S237 ([FRI-136](#))
 Feio-Azevedo, Rita, S125 ([TOP-328-YI](#))
 Feiwen, Deng, S368 ([SAT-009](#))
 Felber, Marco, S117 ([SAT-316](#))
 Feld, Jordan J., S49 ([OS-075-YI](#)),
 S673 ([WED-464](#)), S688 ([WED-499](#)),
 S730 ([SAT-337](#)), S758 ([TOP-401-YI](#)),
 S761 ([FRI-363-YI](#)), S764 ([FRI-372](#))
 Feldman, Theodore, S518 ([WED-222](#))
 Feletti, Valentina, S96 ([LBP-038](#)),
 S306 ([THU-093](#))
 Feliu-Prius, Anna, S633 ([THU-028](#))
 Felix, Sean, S476 ([FRI-232](#)),
 S520 ([WED-230](#)), S572 ([THU-221](#))
 Felli, Emanuele, S25 ([OS-029](#)),
 S369 ([SAT-009](#))
 Felli, Eric, S183 ([WED-081](#)),
 S183 ([WED-082](#))
 Felton, Leigh, S809 ([WED-370](#))
 Fenaille, Francois, S174 ([TOP-073](#)),
 S184 ([WED-083](#))
 Feng, Bo, S230 ([FRI-118](#)), S521 ([WED-231](#)),
 S769 ([FRI-382](#))
 Feng, Dechun, S124 ([TOP-312](#))
 Feng, Hao, S623 ([FRI-016](#))
 Fengou, Polly, S756 ([SAT-421](#))
 Feng, Rilu, S287 ([FRI-539](#))
 Feng, Shibao, S72 ([OS-118](#)),
 S522 ([WED-235](#)), S607 ([SAT-203](#))
 Fenske, Wiebke K., S72 ([OS-119](#))
 Feo, Tullia De, S388 ([SAT-056](#))
 Feray, Cyrille, S6 ([GS-010](#)), S370 ([SAT-011](#)),
 S385 ([SAT-049](#)), S718 ([WED-174](#))
 Ferenc, Anna, S265 ([THU-533](#))
 Féret, Jérôme, S64 ([OS-102](#))
 Ferguson, James, S309 ([THU-099-YI](#)),
 S332 ([THU-160](#)), S337 ([THU-173](#)),
 S397 ([SAT-483-YI](#))
 Fernanda, Fernandes Souza,
 S83 ([LBP-012](#))
 Fernandes, Diogo, S286 ([WED-558](#)),
 S358 ([SAT-554-YI](#))
 Fernandes, Flavia, S238 ([SAT-068](#))
 Fernandes, Wendy, S281 ([WED-542-YI](#))
 Fernandez-Barrena, Maite G.,
 S287 ([FRI-538](#)), S348 ([FRI-555](#)),
 S416 ([FRI-464](#)), S417 ([FRI-466-YI](#))
 Fernández-Carrillo, Carlos, S139 ([SAT-257](#)),
 S142 ([SAT-267](#))
 Fernández, Cristina, S453 ([THU-493](#))
 Fernández-de la Varga, Margarita,
 S329 ([THU-154-YI](#))
 Fernandez-Fernandez, Maria,
 S346 ([FRI-548](#))
 Fernandez-Gordón Sánchez, Flor M.,
 S344 ([THU-189](#))
 Fernández-Iglesias, Anabel,
 S596 ([THU-296](#))
 Fernandez, Javier, S203 ([FRI-039](#))
 Fernández, Javier, S9 ([LBO-004](#)),
 S83 ([LBP-012](#)), S89 ([LBP-026](#)),
 S157 ([THU-049](#)), S157 ([THU-050](#)),
 S177 ([WED-059](#)), S185 ([WED-087](#)),
 S188 ([WED-098-YI](#)), S231 ([FRI-121](#)),
 S700 ([FRI-171](#))
 Fernández, José Ramón, S717 ([WED-172](#))
 Fernández-Lizaranzu, Isabel, S71 ([OS-116](#)),
 S508 ([WED-195](#)), S587 ([THU-268](#))
 Fernández, Marlen Ivon Castellanos,
 S643 ([SAT-438](#))
 Fernández-Martínez, Elisa, S417 ([FRI-467](#))
 Fernández-Martos, Rubén, S398 ([SAT-485](#))
 Fernández, Miguel Angel, S71 ([OS-116](#))
 Fernández-Puertas, Idoia, S64 ([OS-101-YI](#)),
 S112 ([FRI-343-YI](#)), S419 ([FRI-472-YI](#)),
 S562 ([TOP-229-YI](#)), S569 ([THU-210](#))
 Fernández- Rodríguez, Conrado,
 S318 ([THU-118](#)), S330 ([THU-155](#))
 Fernández-Rodríguez, Conrado,
 S139 ([SAT-257](#)), S142 ([SAT-267](#)),
 S391 ([TOP-512-YI](#))
 Fernandez-Simon, Alejandro,
 S378 ([SAT-030](#))
 Fernandez, Teresa Cabezas,
 S668 ([WED-449](#)), S779 ([FRI-409](#))
 Fernández-Vaquero, Mirian, S25 ([OS-029](#))
 Ferrandino, Giuseppe, S195 ([WED-117](#))
 Ferrari, Daniela, S634 ([THU-032](#))
 Ferrari, Gaetano De, S480 ([FRI-243](#))
 Ferraro, Daniele, S369 ([SAT-009](#))
 Ferraro, Donatella, S777 ([FRI-405](#))
 Ferraz de Andrade, Antônio Ricardo Cardia,
 S618 ([SAT-242](#)), S722 ([WED-185](#))
 Ferraz, Maria Lucia, S722 ([WED-185](#))
 Ferreira, Carlos, S315 ([THU-112-YI](#))
 Ferreira, Carlos Noronha, S30 ([OS-038-YI](#)),
 S52 ([OS-080](#)), S199 ([TOP-062](#)),
 S200 ([TOP-064-YI](#))
 Ferreira-Gonzalez, Sofia, S14 ([OS-008-YI](#))
 Ferreira, Alejandra Otero, S365 ([TOP-002](#))
 Ferreira, Elena, S318 ([THU-118](#)),
 S330 ([THU-155](#))
 Ferrer, Ana, S468 ([FRI-211](#))
 Ferrer, Joana, S420 ([FRI-474-YI](#))
 Ferrer, Teresa, S427 ([FRI-501](#)),
 S453 ([THU-493](#))
 Ferri, Flaminia, S215 ([FRI-077-YI](#))
 Ferrigno, Andrea, S589 ([THU-274](#))
 Ferrinho, Diogo, S126 ([THU-315](#))
 Ferri, Silvia, S399 ([SAT-490](#)), S499 ([FRI-299](#)),
 S521 ([WED-232-YI](#)), S555 ([WED-332](#))
 Ferro, Arianna, S475 ([FRI-230-YI](#)),
 S483 ([FRI-251-YI](#)), S544 ([WED-293](#))
 Ferrusquía, José Alberto, S29 ([OS-037](#)),
 S52 ([OS-080](#)), S141 ([SAT-262](#)),
 S233 ([FRI-126](#)), S255 ([SAT-123](#)),
 S829 ([THU-418](#))
 Feshtali, Shirin, S394 ([SAT-474](#))
 Festen, Eleonora, S304 ([SAT-185](#))
 Festi, Davide, S238 ([SAT-068](#)),
 S241 ([SAT-078-YI](#)), S399 ([SAT-490](#)),
 S704 ([TOP-143-YI](#))
 Fevery, Bart, S79 ([LBP-005](#)), S768 ([FRI-380](#))
 Fiancette, Rémi, S354 ([SAT-540-YI](#)),
 S360 ([SAT-558](#))
 Fiaschetti-Egli, Katia, S590 ([THU-278](#))
 Ficarra, Vincenzo, S740 ([SAT-378](#))
 Fichez, Jeanne, S37 ([OS-053](#))
 Fichtner, Alexander, S115 ([TOP-346-YI](#))
 Fierro-Angulo, Oscar M., S115 ([TOP-346-YI](#))
 Figueiredo, Antonio, S362 ([WED-015](#)),
 S834 ([THU-370](#))
 Figueroa, María, S303 ([SAT-183](#))
 Filee, Patrice, S131 ([THU-331-YI](#))
 Filipek, Natalia, S219 ([FRI-088](#))
 Filip, Gabriela Adriana, S409 ([SAT-525](#))
 Filippi-Arriaga, Francesca, S702 ([TOP-139](#))
 Filippi, Massimo, S123 ([SAT-334](#))
 Filippini, Francesco, S612 ([SAT-219](#))
 Fillmore, Nathanael, S518 ([WED-222](#))
 Filomia, Roberto, S345 ([THU-192](#))
 Finkel, Jemima, S248 ([SAT-100](#))
 Finkelmeier, Fabian, S52 ([OS-079-YI](#)),
 S69 ([OS-112-YI](#)), S203 ([FRI-039](#)),
 S411 ([TOP-507-YI](#))
 Finnberg-Kim, Amanda, S624 ([FRI-018](#))
 Finotti, Michele, S369 ([SAT-009](#))

- Fiori, James, S483 (FRI-250), S487 (FRI-263)
 Fiorotto, Romina, S695 (FRI-155),
 S697 (FRI-162)
 Fischer, Katarzyna, S308 (THU-095)
 Fischer, Petra, S61 (OS-096-YI),
 S144 (SAT-273-YI)
 Fischer, Susan, S382 (SAT-040)
 Fishman, Jesse, S469 (FRI-214),
 S494 (FRI-283), S611 (SAT-215),
 S652 (SAT-459)
 Fisseha, Henok, S209 (FRI-053)
 Fite, Gerard Angeles, S254 (SAT-121)
 Fitzpatrick, Chloe, S195 (WED-117)
 Fitzpatrick, Emer, S21 (OS-020)
 Fitzpatrick, Jessica, S653 (SAT-464-YI)
 Fitzpatrick, Kendall, S632 (THU-021)
 Fix, Oren, S394 (SAT-476)
 Firat, Hatice Gülgün, S407 (SAT-518)
 Fjellstrom, Ola, S93 (LBP-031)
 Flagiello, Valentina, S175 (TOP-085),
 S554 (WED-325-YI), S754 (SAT-418)
 Flahault, Cécile, S313 (THU-107)
 Flaherty, John F., S758 (TOP-400),
 S771 (FRI-390), S797 (WED-397)
 Flamm, Maria, S500 (FRI-303)
 Flamm, Steven, S8 (LBO-003),
 S667 (WED-447)
 Flanagan, Stuart, S687 (WED-497)
 Flatley, Sarah, S333 (THU-162-YI)
 Flemming, Jennifer, S19 (OS-018),
 S305 (TOP-168-YI), S305 (TOP-169),
 S688 (WED-499)
 Fletcher, Helen, S732 (SAT-341)
 Fletcher, Simon, S58 (OS-091),
 S733 (SAT-342-YI), S765 (FRI-373)
 Flex, Andrea, S545 (WED-296)
 Flink, Hajo J., S309 (THU-100),
 S314 (THU-109), S319 (THU-120-YI),
 S327 (THU-138)
 Flisiak, Robert, S685 (WED-493-YI),
 S821 (THU-389),
 S834 (THU-367-YI)
 Floreani, Annarosa, S5 (GS-007),
 S96 (LBP-038), S306 (THU-093),
 S318 (THU-117-YI), S374 (SAT-212)
 Flores, Belen Moron, S302 (SAT-179)
 Florescu, Simin, S819 (THU-382)
 Flores, Joan Ericka, S402 (SAT-496)
 Flores, Maria, S70 (OS-114),
 S439 (THU-454)
 Flores, Melissa, S654 (SAT-466)
 Flyer, Abigail, S614 (SAT-225),
 S614 (SAT-227), S618 (SAT-243)
 Focaccia, Enrico, S65 (OS-103)
 Fodor, Andreea, S144 (SAT-273-YI)
 Foerster, Friedrich, S52 (OS-079-YI),
 S411 (TOP-507-YI), S440 (THU-457)
 Foglia, Beatrice, S421 (FRI-479-YI)
 Fogt, Maria, S466 (FRI-206-YI)
 Folie, Patrick, S502 (FRI-315)
 Folli, Franco, S592 (THU-285)
 Folseraas, Trine, S22 (OS-023-YI),
 S50 (OS-076-YI), S386 (SAT-050)
 Fomin, Vladislav, S138 (SAT-251)
 Fondevila, Constantino, S9 (LBO-004),
 S89 (LBP-026), S362 (WED-016),
 S364 (WED-028), S386 (SAT-051)
 Fong, Erica, S8 (LBO-002)
 Fonghoi, Lalita, S396 (SAT-480-YI),
 S410 (SAT-529)
 Fonseca, Daniela, S195 (WED-117)
 Fontana, Robert, S104 (TOP-352),
 S114 (TOP-345)
 Fontela, Fernando Diaz,
 S531 (WED-257)
 Fonte, Stefano, S364 (WED-022)
 Fonvig, Cilius, S47 (OS-072-YI)
 Foo, Hong, S657 (WED-422),
 S676 (WED-470)
 Forbes, Stuart J., S14 (OS-008-YI),
 S186 (WED-090)
 Forbes, Stuart J., S81 (LBP-007),
 S127 (THU-317), S130 (THU-326)
 Forde, Niamh, S470 (FRI-215-YI),
 S636 (THU-045)
 Forkosh, Esther, S563 (THU-194),
 S779 (FRI-408)
 Forlano, Roberta, S282 (WED-546),
 S466 (FRI-207-YI), S470 (FRI-215-YI),
 S495 (FRI-286), S580 (THU-247-YI)
 Forner, Alejandro, S420 (FRI-474-YI),
 S444 (THU-467-YI)
 Forns, Xavier, S39 (OS-056-YI),
 S105 (FRI-321), S120 (SAT-325),
 S682 (WED-485), S711 (WED-155),
 S721 (WED-181), S723 (WED-186),
 S765 (FRI-373), S817 (TOP-385-YI),
 S818 (THU-381)
 Forrest, Ewan H., S219 (FRI-088)
 Forrest, Ewan H., S117 (SAT-317),
 S127 (THU-317), S138 (SAT-254),
 S145 (SAT-274), S147 (SAT-280),
 S148 (SAT-285-YI), S654 (SAT-467),
 S783 (FRI-423)
 Forsgren, Mikael, S530 (WED-255-YI),
 S532 (WED-259)
 Fortea, Jose, S85 (LBP-016)
 Fortea, Jose Ignacio, S61 (OS-096-YI),
 S238 (SAT-068)
 Forte, Paolo, S342 (THU-184)
 Fortin, Davide, S508 (WED-195)
 Fortney, Tiffany, S809 (WED-371)
 Forton, Dan, S352 (SAT-535-YI)
 Forton, Daniel, S523 (WED-236-YI),
 S646 (SAT-444), S672 (WED-459-YI)
 Fortunato, Mariangela, S404 (SAT-502-YI),
 S406 (SAT-514)
 Fortune, Brett, S249 (SAT-102)
 Fortuny, Marta, S444 (THU-467-YI),
 S455 (THU-500)
 Foschi, Francesco, S215 (FRI-078-YI)
 Foster, C. J., S489 (FRI-268)
 Fouad, Yasser, S30 (OS-038-YI),
 S199 (TOP-062), S200 (TOP-064-YI)
 Fouassier, Laura, S432 (FRI-525)
 Fouchard, Isabelle, S456 (THU-503),
 S519 (WED-224)
 Fouquier, Julie, S550 (WED-317)
 Fournier-Poizat, Céline, S2 (GS-004),
 S38 (OS-054), S503 (TOP-241-YI),
 S550 (WED-317)
 Fournot, Tom Stephane, S344 (THU-189)
 Fowell, Andrew, S718 (WED-173)
 Fracanzani, Anna, S497 (FRI-294)
 Fracanzani, Anna Ludovica,
 S289 (FRI-544), S466 (FRI-207-YI),
 S516 (WED-218)
 Fracas, Elia, S397 (SAT-482)
 Fraessdorf, Mandy, S4 (GS-006),
 S72 (OS-119)
 Fragoso, Eva, S555 (WED-330),
 S561 (WED-348)
 Fraitzl, Veronika, S53 (OS-081)
 Francesca Cortese, Maria, S746 (SAT-393)
 Francesca Donato, Maria, S374 (SAT-021),
 S388 (SAT-056)
 Francesca Secchi, Maria, S374 (SAT-021)
 Francesco, Prampolini, S62 (OS-099-YI)
 Francés, Rubén, S194 (WED-113)
 Franchin, Elisa, S777 (FRI-405)
 Francioso, Simona, S59 (OS-094),
 S772 (FRI-392-YI)
 Francisci, Daniela, S777 (FRI-405)
 Franck, Martin, S528 (WED-249)
 Franco, Carmen Cepeda, S365 (TOP-002)
 Franco, Francisco, S826 (THU-405)
 Francois, Silke, S248 (SAT-100)
 François, Silke, S765 (FRI-374-YI)
 Francoz, Claire, S61 (OS-097),
 S116 (SAT-315), S168 (THU-079),
 S200 (TOP-064-YI), S369 (SAT-010),
 S372 (SAT-016), S385 (SAT-048),
 S763 (FRI-370)
 Francque, Sven, S37 (OS-053),
 S61 (OS-096-YI), S80 (LBP-006),
 S259 (SAT-134), S540 (WED-281-YI),
 S545 (WED-296), S581 (THU-249),
 S584 (THU-258-YI), S604 (SAT-196),
 S608 (SAT-206), S730 (SAT-337)
 Frank, Anna Katharina, S294 (SAT-154-YI)
 Frankel, Matthew, S268 (THU-547),
 S295 (SAT-158)
 Frankland, Andrew, S676 (WED-471),
 S759 (TOP-417)
 Fraňková, Soňa, S32 (OS-041-YI),
 S703 (TOP-141), S708 (WED-135-YI)
 Franza, Anne Minello, S73 (OS-120),
 S369 (SAT-010), S793 (WED-391)
 Franzè, Maria Stella, S345 (THU-192),
 S413 (FRI-456), S743 (SAT-386-YI)
 Fraquelli, Mirella, S238 (SAT-068),
 S704 (TOP-144-YI)
 Fraser, Alasdair, S81 (LBP-007)
 Fraser, David A., S603 (SAT-195)
 Frassanito, Gabriella, S389 (SAT-060)
 Frate, Rossella Del, S428 (FRI-502)
 Frazão, Laura, S362 (WED-015)
 Frazer, Monica, S485 (FRI-258)
 Frazzetto, Evelise, S96 (LBP-038),
 S306 (THU-093)
 Frederic, Haedge, S223 (FRI-100)
 Frederiksen, Peder, S579 (THU-243)

Author Index

- Freemantle, Nicholas, S204 (FRI-041), S220 (FRI-089)
- Frei, Anja Laura, S56 (OS-086-YI)
- Freilich, Bradley, S11 (LBO-006)
- Freitag, Angelina, S98 (LBP-041)
- French, Marika, S21 (OS-020)
- Frenette, Catherine, S667 (WED-447), S797 (WED-397), S799 (WED-405)
- Freudenberg, Johannes, S809 (WED-370)
- Freyer, Erich, S350 (SAT-532-YI), S353 (SAT-538-YI)
- Freyre, Carolina, S779 (FRI-409)
- Frey, Vanessa, S500 (FRI-303)
- Frias, Juan P, S8 (LBO-002)
- Frick, Adrian, S436 (TOP-488-YI)
- Fricker, Zachary, S10 (LBO-005)
- Friebe, Andreas, S297 (SAT-164-YI)
- Friederich, Philip W., S213 (FRI-074-YI), S309 (THU-100)
- Friederike Ehrenbauer, Alena, S253 (SAT-117)
- Friedland, Ari, S58 (OS-090)
- Fried, Michael, S610 (SAT-212)
- Friedrich Stättermayer, Albert, S250 (SAT-105), S340 (THU-180), S341 (THU-182), S341 (THU-183-YI)
- Friesland, Martina, S730 (TOP-369)
- Frigerio, Carlo Sala, S567 (THU-203)
- Frigerio, Francesca, S681 (WED-482)
- Frigo, Francesco, S175 (TOP-085), S210 (FRI-056-YI), S458 (THU-517)
- Frings, Alexandra Ginesta, S195 (WED-117)
- Frisancho, Luis, S139 (SAT-257), S142 (SAT-267)
- Frisby, William, S676 (WED-471), S759 (TOP-417)
- Frissen, Mick, S229 (FRI-116), S351 (SAT-534), S357 (SAT-549)
- Frittitta, Lucia, S557 (WED-336)
- Fritz, Laurenz, S621 (FRI-009-YI)
- Fritz, Tanja, S115 (TOP-346-YI)
- Froilán, Consuelo, S706 (WED-132), S712 (WED-159)
- Frolkis, Alexandra, S538 (WED-274)
- Fromme, Malin, S32 (OS-041-YI), S703 (TOP-141), S708 (WED-135-YI)
- Frongillo, Francesco, S369 (SAT-009)
- Frontino, Anna Maria, S697 (FRI-163-YI)
- Fruendt, Thorben, S52 (OS-079-YI)
- Fuchs, Alexander, S435 (FRI-533)
- Fuchs, Claudia, S81 (LBP-008), S296 (SAT-161)
- Fuchs, Michael, S1 (GS-001)
- Fu, Danting, S280 (WED-541)
- Fuentes, Ana, S691 (WED-516), S779 (FRI-409)
- Fuertes, Diana, S29 (OS-037)
- Füglstaller, Désirée, S171 (THU-088)
- Fujii, Hideki, S537 (WED-273)
- Fujimoto, Kentaro, S247 (SAT-095)
- Fujishiro, Mitsuhiro, S393 (SAT-470), S437 (TOP-505), S589 (THU-275)
- Fujiwara, Kisako, S247 (SAT-095)
- Fujiwara, Naoto, S17 (OS-013), S42 (OS-061)
- Fu, Jiwei, S120 (SAT-323)
- Fukumoto, Kenji, S506 (TOP-288)
- Fukushima, Hideaki, S537 (WED-273)
- Fukushima, Masanori, S228 (FRI-113), S234 (FRI-128)
- Fulgenzi, Claudia, S51 (OS-078-YI), S52 (OS-079-YI), S443 (THU-464), S445 (THU-471-YI)
- Fullam, Anthony, S48 (OS-073), S203 (FRI-039), S272 (TOP-563)
- Fumagalli, Valeria, S35 (OS-048)
- Fundora, Yilliam, S15 (OS-010), S179 (WED-070), S377 (SAT-027), S705 (WED-129)
- Funes, Lidia, S669 (WED-453)
- Fung, James, S745 (SAT-392), S770 (FRI-388), S810 (WED-373-YI)
- Fung, Scott K., S27 (OS-033), S761 (FRI-363-YI), S771 (FRI-390), S797 (WED-397), S813 (WED-379)
- Fung, Yan Yue James, S161 (THU-058)
- Funuyet-Salas, Jesús, S71 (OS-116)
- Fu, Rebecca, S58 (OS-092)
- Furiosi, Valeria, S571 (THU-218)
- Furquim d'Almeida, Arno, S665 (WED-441-YI), S730 (SAT-337), S758 (TOP-401-YI), S777 (FRI-406)
- Fürst, Anna, S351 (SAT-533)
- Fürst, Stefan, S229 (FRI-115)
- Furumaya, Alicia, S394 (SAT-474)
- Furusyo, Norihiro, S42 (OS-062)
- Furuya, Ken, S541 (WED-283)
- Fusco, Francesco Maria, S791 (FRI-442)
- Fusco, Gregory, S799 (WED-405)
- Fusco, Jennifer, S799 (WED-405)
- Fuß, Johannes, S350 (SAT-531-YI)
- Fuster, Daniel, S154 (SAT-303), S190 (WED-104)
- Fuster-Martínez, Isabel, S266 (THU-539), S592 (THU-283)
- Fu, Xiao, S440 (THU-455)
- Fytli, Paraskevi, S798 (WED-403)
- Gabaldon, Inmaculada, S557 (WED-335)
- Gabbia, Daniela, S592 (THU-285)
- Gabdulkhakova, Adelya, S299 (SAT-173-YI)
- Gabrielli, Victor, S195 (WED-117)
- Gabriel, Maria Magdalena, S205 (FRI-044-YI)
- Gabriel, Shiraaz, S756 (SAT-421)
- Gabrys, Philipp, S85 (LBP-017)
- Gabunia, Tamar, S659 (WED-427), S685 (WED-492)
- Gackowska, Lidia, S578 (THU-238)
- Gadano, Adrian, S9 (LBO-004), S30 (OS-038-YI), S83 (LBP-012), S89 (LBP-026), S157 (THU-050), S199 (TOP-062), S200 (TOP-064-YI), S208 (FRI-053)
- Gadonne, Cloé, S42 (OS-061)
- Gadient, Jana, S590 (THU-278)
- Gadour, Eyad, S172 (THU-090)
- Gad, Shaimaa, S573 (THU-222-YI)
- Gaeta, Giovanni Battista, S28 (OS-034), S59 (OS-094), S791 (FRI-442)
- Gagliani, Nicola, S278 (WED-534)
- Gagliardi, Roberta, S28 (OS-035-YI), S206 (FRI-047-YI), S212 (FRI-068), S224 (FRI-101-YI), S243 (SAT-083-YI), S830 (THU-420)
- Gahete, Manuel D., S415 (FRI-462-YI)
- Gaia, Silvia, S451 (THU-486-YI), S458 (THU-517)
- Gairing, Simon J., S230 (FRI-120), S249 (SAT-104-YI)
- Gairing, Simon Johannes, S52 (OS-079-YI), S211 (FRI-059), S214 (FRI-075)
- Gairola, Abhishek, S331 (THU-159-YI)
- Galante, Antonio, S30 (OS-038-YI), S199 (TOP-062), S200 (TOP-064-YI)
- Galati, Giovanni, S238 (SAT-068), S554 (WED-325-YI)
- Galati, Joseph, S10 (LBO-005)
- Gale, Nicolette, S559 (WED-340)
- Galhenage, Sam, S26 (OS-031)
- Galiero, Raffaele, S790 (FRI-441)
- Galinos, Iosif, S690 (WED-503)
- Gallagher, Mary Leslie, S1 (GS-001)
- Gallaher, Charles, S388 (SAT-057)
- Gallant, Marie, S321 (THU-123-YI)
- Gallant, Maxime, S11 (LBO-006)
- Gallego-Durán, Rocío, S2 (GS-004), S38 (OS-054)
- Gallego-Durán, Rocío, S427 (FRI-501), S508 (WED-195), S587 (THU-268), S593 (THU-287), S596 (THU-296)
- Gallegos-Orozco, Juan F., S9 (LBO-004), S89 (LBP-026), S118 (SAT-320)
- Galle, Peter R., S51 (OS-078-YI), S52 (OS-079-YI), S211 (FRI-059), S214 (FRI-075), S230 (FRI-120), S249 (SAT-104-YI), S411 (TOP-507-YI), S443 (THU-464), S445 (THU-471-YI), S461 (FRI-194-YI), S484 (FRI-255)
- Galleron, Nathalie, S159 (THU-053)
- Galletti, Simone, S533 (WED-261-YI)
- Galletto, Athena, S453 (THU-494)
- Galli, Andrea, S88 (LBP-023), S96 (LBP-038), S306 (THU-093), S342 (THU-184)
- Galli, Silvia, S777 (FRI-405)
- Gallo, Paolo, S175 (TOP-085), S554 (WED-325-YI), S666 (WED-446), S754 (SAT-418)
- Galgaard, Elisabeth, S79 (LBP-003)
- Galun, Eithan, S278 (WED-534)
- Galwey, Nicholas, S745 (SAT-390)
- Galy-Fauroux, Isabelle, S349 (TOP-552)
- Gamangatti, Shivanand, S201 (TOP-065)
- Gama, Raimundo, S722 (WED-185)
- Gambato, Martina, S318 (THU-117-YI), S376 (SAT-024-YI)
- Gambino, Carmine, S28 (OS-035-YI), S212 (FRI-068), S224 (FRI-101-YI), S243 (SAT-083-YI), S830 (THU-420)
- Gamkrelidze, Amiran, S664 (WED-439), S675 (WED-468), S825 (THU-404)

- Gamkrelidze, Ivane, S663 (WED-437), S667 (WED-448), S674 (WED-466)
- Gammon, Katie, S569 (THU-211)
- Gampa, Anuhya, S51 (OS-078-YI)
- Gananandan, Kohilan, S188 (WED-098-YI)
- Ganatra, Nazila, S684 (WED-487)
- Gan, Can, S241 (SAT-077)
- Ganchua, Sharie C, S26 (OS-031)
- Ganchua, Sharie C., S809 (WED-371)
- Gandelman, Olga, S195 (WED-117)
- Gander, Amir, S700 (FRI-171)
- Gandolfi, Anna Lisa, S634 (THU-032)
- Gandon, Yves, S463 (FRI-197), S520 (WED-227)
- Gane, Edward J., S26 (OS-030), S72 (OS-119), S75 (OS-127), S78 (LBP-001), S79 (LBP-005), S86 (LBP-018), S86 (LBP-019), S87 (LBP-020), S100 (LBP-044), S141 (SAT-261), S771 (FRI-390), S806 (WED-361), S807 (WED-365), S811 (WED-374), S812 (WED-378), S813 (WED-379), S822 (THU-391-YI)
- Ganesan, Murali, S742 (SAT-382)
- Gan, Galvin, S515 (WED-213)
- Ganger, Daniel, S8 (LBO-003), S242 (SAT-082)
- Gani, Rino, S158 (THU-052), S167 (THU-078)
- Ganne-Carrié, Nathalie, S41 (OS-060), S50 (OS-077), S54 (OS-084-YI), S68 (OS-110), S73 (OS-120), S441 (THU-458), S441 (THU-459-YI), S444 (THU-466), S451 (THU-487-YI), S456 (THU-503), S793 (WED-391), S802 (WED-410)
- Ganry, Olivier, S444 (THU-466)
- Gantzel, Rasmus, S244 (SAT-088)
- Gao, Bin, S124 (TOP-312)
- Gao, Bowen, S198 (WED-124)
- Gao, Fei, S390 (TOP-510)
- Gao, Haibing, S209 (FRI-053)
- Gao, Hongbo, S95 (LBP-037)
- Gao, Jingli, S536 (WED-272)
- Gao, Jixian, S100 (LBP-045)
- Gao, Juan, S435 (FRI-532)
- Gao, Lu, S573 (THU-223)
- Gao, Shuangqing, S613 (SAT-221)
- Gao, Xiaohong, S786 (FRI-430)
- Gao, Xin, S605 (SAT-198)
- Gao, Xu, S69 (OS-112-YI)
- Gao, Yanhang, S100 (LBP-045), S209 (FRI-053)
- Gao, Yao, S107 (FRI-325)
- Gao, Youfang, S526 (WED-246)
- Gao, Yuanjiao, S344 (THU-191)
- Gao, Yueqiu, S605 (SAT-198), S762 (FRI-366)
- Gao, Yufeng, S803 (WED-412)
- Gao, Zhiliang, S87 (LBP-021), S161 (THU-058), S736 (SAT-367)
- Garajova, Ingrid, S395 (SAT-477-YI)
- Garajová, Ingrid, S446 (THU-472-YI)
- Gárate-Rascón, María, S416 (FRI-464)
- Garbuglia, AnnaRosa, S777 (FRI-405)
- García, Amaya Redín, S365 (TOP-002)
- García, Ana Belen Rubio, S541 (WED-284-YI)
- García-Arenas, Dolores, S694 (FRI-153)
- García-Barrionuevo, Aurora, S779 (FRI-409)
- García-Calderó, Héctor, S15 (OS-010), S179 (WED-070)
- García-Calonge, Marta, S455 (THU-500)
- García-Criado, María Ángeles, S53 (OS-081), S255 (SAT-123)
- García, David, S556 (WED-334), S641 (SAT-432), S642 (SAT-434), S654 (SAT-466)
- García, Esther Perez, S807 (WED-364)
- García, Federico García, S691 (WED-516), S779 (FRI-409)
- García-Fernández, Vanessa, S427 (FRI-501), S508 (WED-195), S587 (THU-268), S593 (THU-287)
- García, Fernando García, S691 (WED-516), S779 (FRI-409)
- García-García, Alberto, S170 (THU-086)
- García-García, Francisco, S592 (THU-283)
- García-García, Selene, S746 (SAT-393)
- García-García, Sonia, S139 (SAT-257), S142 (SAT-267), S723 (WED-186)
- García-Gavilán, María Carmen, S170 (THU-086)
- García, Héctor Alexander Velásquez, S40 (OS-058), S659 (WED-429), S824 (THU-399-YI)
- García-López, Mirea, S765 (FRI-373)
- García-Lugo, Alejandra, S682 (WED-483)
- García-Luna, Pedro Pablo, S508 (WED-195)
- García, Marta, S29 (OS-037)
- García-Martin, Carmen, S154 (SAT-303)
- García-Mediavilla, María-Victoria, S45 (OS-067), S277 (WED-529)
- García, Núria, S822 (THU-395)
- García-Pagán, Juan Carlos, S15 (OS-010), S53 (OS-081), S61 (OS-096-YI), S85 (LBP-016), S179 (WED-070), S238 (SAT-069), S240 (SAT-074), S705 (WED-129)
- García, Paul, S413 (FRI-455)
- García-Pras, Ester, S105 (FRI-321)
- García-Retortillo, Montserrat, S207 (FRI-051), S291 (TOP-149-YI), S318 (THU-118), S329 (THU-154-YI), S330 (THU-155), S336 (THU-170-YI), S344 (THU-189)
- García-Rioja, Javier, S71 (OS-116)
- García-Sáez, Juan, S303 (SAT-183)
- García, Salvador Resino, S665 (WED-442), S741 (SAT-379)
- García-Samaniego, Francisco Javier, S398 (SAT-485), S700 (FRI-171), S777 (FRI-406), S787 (FRI-432), S836 (THU-374)
- García-Samaniego, Francisco Javier, S706 (WED-132), S712 (WED-159)
- García-Sánchez, Araceli, S398 (SAT-485), S706 (WED-132), S712 (WED-159)
- García-Solà, Clàudia, S711 (WED-155), S721 (WED-181), S723 (WED-186)
- García-Tsao, Guadalupe, S206 (FRI-046), S218 (FRI-086)
- García, Victoria Alejandra Jiménez, S559 (WED-341)
- García-Villarreal, Luis, S717 (WED-172)
- Gardner, Kelly, S647 (SAT-447)
- Gareta, Dickman, S753 (SAT-413)
- Garfinkel, Benjamin, S296 (SAT-161)
- Garg, Love, S554 (WED-327)
- Garg, Mayur, S632 (THU-021)
- Gargouri, Dalila, S270 (THU-554)
- Garg, Pratibha, S129 (THU-324), S152 (SAT-295), S158 (THU-051), S217 (FRI-082)
- Garhy, Naeema El, S491 (FRI-273-YI)
- Garin, Etienne, S383 (SAT-043)
- Garioud, Armand, S168 (THU-079)
- Garitta, Elena, S298 (SAT-167-YI)
- Garlantezec, Ronan, S520 (WED-227)
- Garner, Will, S307 (THU-094), S323 (THU-129), S331 (THU-158)
- Garra, Mohamad, S628 (FRI-033)
- Garreta, Javier Perez, S746 (SAT-393)
- Garrido, Patricia, S578 (THU-236-YI)
- Garrigou, Olivia, S784 (FRI-425)
- Garteiser, Philippe, S524 (WED-239), S526 (WED-245)
- Gart, Eveline, S513 (WED-209), S575 (THU-231), S595 (THU-294), S597 (THU-297)
- Gasbarrini, Antonio, S452 (THU-492), S533 (WED-261-YI), S703 (TOP-142-YI)
- Gasca-Díaz, Frida, S627 (FRI-029)
- Gasche, Christoph, S436 (TOP-488-YI)
- Gasch, Oriol, S29 (OS-037)
- Gasink, Christopher, S325 (THU-132), S621 (FRI-008), S623 (FRI-015), S625 (FRI-023), S627 (FRI-030)
- Gasparotto, Matteo, S612 (SAT-219)
- Gaspar, Rui, S238 (SAT-068)
- Gassama-Diagne, Ama, S432 (FRI-525)
- Gastaca, Mikel, S365 (TOP-002), S368 (SAT-009)
- Gastaldelli, Amalia, S533 (WED-263), S593 (THU-286)
- Gato-Zambrano, Sheila, S427 (FRI-501), S587 (THU-268), S593 (THU-287), S596 (THU-296)
- Gatselis, Nikolaos, S308 (THU-098), S311 (THU-102-YI), S335 (THU-167), S800 (WED-406)
- Gatti, Gemma, S289 (FRI-542)
- Gatti, Pietro, S96 (LBP-038), S306 (THU-093), S804 (WED-414)
- Gattolliat, Olivier, S326 (THU-135)
- Gat-Viks, Irit, S696 (FRI-160-YI)
- Gautam, Misha, S489 (FRI-269)
- Gautam, Shivani, S274 (WED-522-YI)
- Gautier, Jean-François, S526 (WED-245)
- Gavasso, Sabrina, S237 (TOP-061-YI)
- Gavis, Edith, S1 (GS-001)
- Gawel, Susan, S825 (THU-404)

Author Index

- Gawlitzka, Joshua, S213 ([FRI-071](#))
- Gayoso, Rafael, S398 ([SAT-485](#))
- Gazari, Maria Mercedes Rodriguez, S208 ([FRI-053](#))
- Gazda, Jakub, S29 ([OS-036-YI](#))
- Gazelakis, Kathryn, S400 ([SAT-492](#))
- Gaztambide, Sonia, S569 ([THU-210](#))
- Gbadamosi, Semiu, S460 ([TOP-309](#))
- Geary, Richard, S7 ([GS-012](#))
- Gebara, Karim, S143 ([SAT-269](#))
- Gebregziabher, Mulugeta, S614 ([SAT-226](#))
- Gee, Heon Yung, S595 ([THU-292](#))
- Geerts, Anja, S57 ([OS-089-YI](#)), S115 ([TOP-346-YI](#)), S143 ([SAT-268](#)), S278 ([WED-531](#)), S292 ([SAT-151-YI](#)), S311 ([THU-102-YI](#)), S321 ([THU-123-YI](#)), S371 ([SAT-014-YI](#)), S386 ([SAT-051](#)), S420 ([FRI-475-YI](#)), S442 ([THU-463](#)), S631 ([THU-020-YI](#))
- Geervliet, Eline, S266 ([THU-538](#))
- Gefen, Maytal, S278 ([WED-534](#))
- Geffers, Robert, S21 ([OS-021-YI](#))
- Gehring, Adam, S352 ([SAT-536](#))
- Geier, Andreas, S52 ([OS-079-YI](#)), S69 ([OS-112-YI](#)), S223 ([FRI-098](#)), S224 ([FRI-103-YI](#)), S334 ([THU-164-YI](#)), S528 ([WED-249](#)), S587 ([THU-269-YI](#))
- Geiger, Niklas, S587 ([THU-269-YI](#))
- Geisler, Anja, S600 ([THU-314](#))
- Geisler, Fabian, S35 ([OS-049-YI](#)), S298 ([SAT-166](#))
- Geisler, Lukas, S359 ([SAT-555](#))
- Geith, Ahmed, S673 ([WED-463](#))
- Geladari, Eleni, S208 ([FRI-052](#)), S214 ([FRI-076](#))
- Gelson, William, S676 ([WED-471](#)), S760 ([TOP-417](#)), S765 ([FRI-374-YI](#))
- Gelu-Simeon, Moana, S41 ([OS-060](#))
- Gely, Cristina, S355 ([SAT-543](#))
- Genç Uluçeçen, Sezen, S377 ([SAT-028](#))
- Genda, Takuya, S490 ([FRI-272](#))
- Gendelman, Howard, S742 ([SAT-382](#))
- Genesca, Joan, S36 ([OS-047-YI](#)), S471 ([FRI-219-YI](#)), S703 ([TOP-141](#)), S708 ([WED-135-YI](#)), S818 ([THU-381](#))
- Genevieve, Franck, S519 ([WED-224](#))
- Genin, Michael, S644 ([SAT-439-YI](#))
- Gennari, William, S777 ([FRI-405](#))
- Genov, Jordan, S172 ([THU-092](#))
- Genser, Laurent, S512 ([WED-206](#)), S585 ([THU-260](#))
- Gensluckner, Sophie, S500 ([FRI-303](#)), S621 ([FRI-009-YI](#))
- Gentilucci, Umberto Vespasiani, S459 ([TOP-301](#)), S535 ([WED-270](#))
- Gentleman, Eileen, S128 ([THU-320-YI](#))
- Gentric, Géraldine, S572 ([THU-220](#))
- Georgaka, Sokratia, S67 ([OS-109](#))
- George, Jacob, S161 ([THU-058](#)), S208 ([FRI-053](#)), S219 ([FRI-088](#)), S534 ([WED-267](#)), S643 ([SAT-438](#)), S776 ([FRI-403](#))
- George, Michael, S676 ([WED-471](#)), S759 ([TOP-417](#))
- Georges, Bertrand, S529 ([WED-251](#))
- Geramoutsos, Georgios, S830 ([THU-419](#))
- Gerardin, Ylaine, S571 ([THU-215](#)), S585 ([THU-261](#))
- Gerber, David, S394 ([SAT-476](#)), S403 ([SAT-498](#))
- Gerber, Lynn, S637 ([TOP-445](#))
- Gerber, Lynn H., S651 ([SAT-456](#))
- Geremia, Alessandra, S302 ([SAT-179](#))
- Geretti, Anna Maria, S59 ([OS-094](#))
- Gerges, Emma, S734 ([SAT-348-YI](#))
- Germani, Giacomo, S332 ([THU-161](#)), S373 ([SAT-019](#))
- Gerner, Jana, S587 ([THU-269-YI](#))
- Gerolami, René, S168 ([THU-079](#))
- Gerussi, Alessio, S19 ([OS-017](#)), S299 ([SAT-171](#)), S310 ([THU-101](#)), S321 ([THU-125](#)), S325 ([THU-133-YI](#)), S335 ([THU-167](#))
- Gervais, Anne, S54 ([OS-084-YI](#)), S73 ([OS-120](#)), S793 ([WED-391](#))
- Gervais, Stéphane, S519 ([WED-224](#))
- Gess, Markus, S672 ([WED-459-YI](#))
- Gestels, Naomi, S259 ([SAT-134](#))
- Getia, Vladimer, S664 ([WED-439](#)), S675 ([WED-468](#)), S825 ([THU-404](#))
- Gevers, Tom J. G., S712 ([WED-158-YI](#))
- Gevers, Tom J.G., S44 ([OS-066-YI](#)), S309 ([THU-100](#)), S314 ([THU-109](#)), S319 ([THU-120-YI](#)), S327 ([THU-138](#)), S341 ([THU-182](#))
- Gex, Quentin, S189 ([WED-101-YI](#))
- Geybels, Milan, S79 ([LBP-003](#))
- Geyvandova, Natalia, S92 ([LBP-029](#))
- Ghabril, Marwan, S114 ([TOP-345](#))
- Ghafoor, Aleena, S555 ([WED-330](#)), S561 ([WED-348](#))
- Ghafoor, Soleen, S702 ([TOP-140](#))
- Ghait, Mohamed, S178 ([WED-060-YI](#))
- Ghanbari, Mohsen, S464 ([FRI-200](#)), S604 ([SAT-197-YI](#))
- Ghanekar, Anand, S381 ([SAT-037](#)), S381 ([SAT-039](#))
- Ghani, Ehsan, S686 ([WED-494](#))
- Ghani, Leith, S478 ([FRI-236-YI](#))
- Ghantous, Lucy, S278 ([WED-534](#))
- Ghazinyan, Hasmik, S158 ([THU-052](#)), S167 ([THU-078](#))
- Gheorghe, Cristian, S343 ([THU-186](#))
- Gheorghe, Liana, S343 ([THU-186](#))
- Gherlan, George Sebastian, S1 ([GS-002](#)), S764 ([FRI-371](#)), S796 ([WED-395](#))
- Ghinolfi, Davide, S370 ([SAT-013](#))
- Ghioca, Mihaela, S343 ([THU-186](#))
- Ghisetti, Valeria, S777 ([FRI-405](#))
- Ghosh, Alip, S736 ([SAT-366](#))
- Ghosh, Anamitra, S692 ([FRI-151](#))
- Ghosh, Indrajit, S687 ([WED-497](#))
- Ghosh, Sourabh, S346 ([FRI-547-YI](#))
- Giacomello, Emiliana, S429 ([FRI-516-YI](#))
- Giampaolo, Luca, S332 ([THU-161](#))
- Giangrande, Paloma, S693 ([FRI-151](#))
- Giannelli, Valerio, S368 ([SAT-009](#))
- Giannini, Edoardo, S96 ([LBP-038](#)), S306 ([THU-093](#)), S310 ([THU-101](#)), S332 ([THU-161](#))
- Giannitrapani, Lydia, S601 ([TOP-193](#))
- Giannone, Fabio, S17 ([OS-013](#)), S734 ([SAT-348-YI](#))
- Giannou, Anastasios, S64 ([OS-101-YI](#))
- Giannoulis, George, S322 ([THU-126](#)), S325 ([THU-134](#)), S798 ([WED-403](#))
- Giannousi, Eirini, S599 ([THU-306](#))
- Gianotti, Nicola, S824 ([THU-402](#))
- Giardini, Andrea Casadei, S438 ([THU-446](#))
- Gibilisco, Fabio, S19 ([OS-017](#))
- Gibson Maponga, Tongai, S753 ([SAT-413](#)), S756 ([SAT-421](#))
- Gibson, Robert, S219 ([FRI-088](#))
- Giehren, Franziska, S24 ([OS-027-YI](#))
- Giera, Martin, S278 ([WED-533](#))
- Gieswinkel, Alexander, S461 ([FRI-194-YI](#))
- Gigante, Elia, S168 ([THU-079](#))
- Gigi, Eleni, S798 ([WED-403](#))
- Giguët, Baptiste, S116 ([SAT-315](#)), S341 ([THU-182](#)), S383 ([SAT-043](#))
- Giladi, Hilla, S279 ([WED-534](#))
- Gil, Carlos, S289 ([FRI-542](#))
- Gil, Cristiane Damas, S113 ([FRI-348](#))
- Gile, Jennifer, S52 ([OS-079-YI](#))
- Giles, Benjamin, S718 ([WED-173](#))
- Gil-Cómez, Antonio, S427 ([FRI-501](#)), S587 ([THU-268](#)), S593 ([THU-287](#)), S596 ([THU-296](#))
- Gillet, Patrick, S434 ([FRI-530](#))
- Gillum, Matthew, S581 ([THU-248](#))
- Gill, Upkar, S59 ([OS-094](#)), S742 ([SAT-383](#)), S781 ([FRI-413](#))
- Gil-Pitarch, Claudia, S417 ([FRI-466-YI](#))
- Gils, Sanne, S801 ([WED-409](#))
- Gines, Iris, S578 ([THU-236-YI](#))
- Ginès, Pere, S13 ([OS-005-YI](#)), S30 ([OS-038-YI](#)), S41 ([OS-059](#)), S70 ([OS-115](#)), S139 ([SAT-257](#)), S159 ([THU-055](#)), S160 ([THU-056](#)), S176 ([WED-055](#)), S199 ([TOP-062](#)), S200 ([TOP-064-YI](#)), S468 ([FRI-211](#)), S471 ([FRI-219-YI](#)), S503 ([TOP-241-YI](#)), S541 ([WED-284-YI](#))
- Gingras, Anne Claude, S673 ([WED-464](#))
- Gioia, Stefania, S206 ([FRI-047-YI](#)), S214 ([FRI-075](#)), S258 ([SAT-131](#))
- Gioli, Federico, S817 ([THU-378](#))
- Giordano, Carla, S557 ([WED-336](#))
- Giorgi, Alberto De, S458 ([THU-517](#))
- Giorgi, Mauro, S371 ([SAT-015-YI](#)), S378 ([SAT-031-YI](#))
- Giorgio, Angelo Di, S115 ([TOP-346-YI](#))
- Giosa, Domenico, S422 ([FRI-481](#)), S747 ([SAT-397](#))
- Giovanna, Scoazec, S784 ([FRI-425](#))
- Giovanni, Faria Silva, S83 ([LBP-012](#))
- Giovannini, Alice, S88 ([LBP-023](#))
- Girala, Marcos, S30 ([OS-038-YI](#)), S199 ([TOP-062](#)), S200 ([TOP-064-YI](#)), S334 ([THU-164-YI](#))
- Giraldez, Álvaro, S779 ([FRI-409](#))

- Giráldez, Carmen Cárcamo, S24 ([OS-026-YI](#)), S420 ([FRI-474-YI](#))
- Giráldez-Gallego, Alvaro, S777 ([FRI-406](#))
- Girard, Lea, S734 ([SAT-348-YI](#))
- Girard, Muriel, S374 ([SAT-021](#))
- Giraudo, Pablo, S429 ([FRI-516-YI](#))
- Giraudo, Chiara, S224 ([FRI-101-YI](#))
- Giri, Dewan, S487 ([FRI-262](#))
- Girish, Vishnu, S164 ([THU-070](#))
- Girolamo, Julia Di, S657 ([WED-422](#))
- Gisèle, NKontchou, S441 ([THU-459-YI](#)), S451 ([THU-487-YI](#)), S456 ([THU-503](#))
- Gish, Robert G., S325 ([THU-132](#)), S469 ([FRI-214](#)), S494 ([FRI-283](#)), S623 ([FRI-015](#)), S625 ([FRI-023](#)), S627 ([FRI-030](#)), S788 ([FRI-435](#))
- Gispert, Àngels, S45 ([OS-068](#))
- Gitahi, Jane, S651 ([SAT-457-YI](#))
- Gitto, Stefano, S258 ([SAT-131](#)), S456 ([THU-502](#))
- Giuffrè, Mauro, S731 ([SAT-338-YI](#))
- Giuli, Lucia, S52 ([OS-080](#)), S703 ([TOP-142-YI](#))
- Giustiniani, Maria Cristina, S533 ([WED-261-YI](#)), S705 ([WED-130](#))
- Giustini, Leonardo, S35 ([OS-048](#))
- Gizewski, Elke, S722 ([WED-183-YI](#))
- Gjini, Kamela, S475 ([FRI-230-YI](#)), S480 ([FRI-243](#)), S501 ([FRI-314](#))
- Glampson, Ben, S676 ([WED-471](#)), S759 ([TOP-417](#))
- Glapa-Nowak, Aleksandra, S302 ([SAT-179](#))
- Glass, Benjamin, S571 ([THU-215](#)), S585 ([THU-261](#))
- Glass, Nancy, S675 ([WED-468](#))
- Glaus, Jesus, S98 ([LBP-041](#))
- Glavini, Katerina, S26 ([OS-030](#))
- Glebe, Dieter, S752 ([SAT-410](#))
- Gleeson, Dermot, S333 ([THU-162-YI](#))
- Glenn, Jeffrey, S800 ([WED-407](#)), S814 ([WED-382](#))
- Glickman, John, S567 ([THU-203](#))
- Glitscher, Mirco, S170 ([THU-087](#))
- Globke, Brigitta, S366 ([TOP-003-YI](#))
- Glodny, Bernhard, S722 ([WED-183-YI](#))
- Gloria de la Rosa, S377 ([SAT-027](#))
- Gloria, Helena, S834 ([THU-370](#))
- Glover, Alison, S81 ([LBP-007](#))
- Gluud, Lise Lotte, S79 ([LBP-003](#)), S238 ([SAT-069](#)), S513 ([WED-207](#)), S513 ([WED-209](#)), S529 ([WED-250-YI](#)), S555 ([WED-331-YI](#))
- Glyn-Owen, Kate, S506 ([TOP-277](#)), S645 ([SAT-441-YI](#)), S647 ([SAT-447](#))
- Gnutti, Victorio, S712 ([WED-158-YI](#))
- Gobbato, Arianna, S241 ([SAT-078-YI](#)), S399 ([SAT-490](#))
- Godart, Cécile, S416 ([FRI-465](#))
- Godbole, Ira, S23 ([OS-025-YI](#))
- Goddemaer, Griet, S172 ([THU-092](#))
- Godfrey, Jack, S692 ([FRI-151](#))
- Godinho-Santos, Ana, S358 ([SAT-554-YI](#))
- Godin, Laura, S112 ([FRI-342](#))
- Godoy, Maíra, S369 ([SAT-009](#))
- Goediker, Juliana, S258 ([SAT-130](#))
- Goehlmann, Hinrich, S813 ([WED-379](#))
- Goeij, Femke De, S369 ([SAT-009](#))
- Goel, Aparna, S8 ([LBO-003](#)), S98 ([LBP-040](#)), S374 ([SAT-021](#))
- Goel, Ashish, S158 ([THU-052](#)), S167 ([THU-078](#)), S219 ([FRI-088](#))
- Goel, Deepika, S588 ([THU-271-YI](#))
- Goenka, Mahesh, S158 ([THU-052](#)), S167 ([THU-078](#))
- Goffaux, Alexis, S151 ([SAT-293-YI](#)), S473 ([FRI-224](#))
- Goffette, Cécile, S313 ([THU-107](#))
- Gofton, Cameron, S209 ([FRI-053](#))
- Gogia, Sudhanshu, S8 ([LBO-002](#))
- Gogilashvili, Ketevan, S677 ([WED-473](#))
- Gogou, Christiana, S229 ([FRI-117](#))
- Goh, George Boon Bee, S2 ([GS-004](#)), S467 ([FRI-208](#)), S502 ([FRI-316](#)), S525 ([WED-242](#))
- Gohil, Vikrant, S564 ([THU-198](#))
- Goikoetxea-Usandizaga, Naroa, S417 ([FRI-466-YI](#))
- Goitre, Ilaria, S525 ([WED-243-YI](#))
- Gokcan, Hale, S336 ([THU-171](#)), S407 ([SAT-519](#)), S479 ([FRI-238](#))
- Gökçe, Dilara Turan, S336 ([THU-171](#)), S479 ([FRI-238](#)), S723 ([WED-187-YI](#))
- Golabi, Pegah, S472 ([FRI-221](#))
- Goldberg, David, S649 ([SAT-451](#))
- Goldenberg, Daniel, S278 ([WED-534](#))
- Goldenberg, Regina, S190 ([WED-102](#))
- Goldenberg, Roman, S592 ([THU-284](#))
- Goldenberg, Simon, S46 ([OS-070](#))
- Goldin, Robert D., S580 ([THU-247-YI](#))
- Goli, Larissa, S88 ([LBP-024](#))
- Gömer, André, S58 ([OS-092](#)), S730 ([TOP-369](#))
- Gomes de Sousa, Francielle Tramontini, S812 ([WED-377](#))
- Gomez-Cabrero, David, S193 ([WED-112](#))
- Gómez-Cabrero, David, S174 ([TOP-073](#))
- Gómez- Camarero, Judith, S318 ([THU-118](#)), S329 ([THU-154-YI](#)), S330 ([THU-155](#)), S344 ([THU-189](#))
- Gómez-Camarero, Judith, S717 ([WED-172](#))
- Gómez, Carlos, S120 ([SAT-325](#))
- Gómez, Concepción, S469 ([FRI-213](#))
- Gómez-Domínguez, Elena, S318 ([THU-118](#)), S329 ([THU-154-YI](#)), S330 ([THU-155](#)), S344 ([THU-189](#))
- Gómez-Hurtado, Isabel, S194 ([WED-113](#))
- Gómez, Igor, S694 ([FRI-153](#))
- Gomez-Jauregui, Paul, S64 ([OS-101-YI](#)), S112 ([FRI-343-YI](#)), S419 ([FRI-472-YI](#)), S562 ([TOP-229-YI](#)), S569 ([THU-210](#))
- Gómez, Julián, S751 ([SAT-407](#))
- Gómez, Lucia Sanz, S702 ([TOP-139](#))
- Gómez, Mariano, S453 ([THU-493](#))
- Gomez-Martin, Carlos, S455 ([THU-501](#))
- Gomez, Naim Fakhri, S553 ([WED-324](#))
- Gómez-Orellana, Antonio M., S23 ([OS-024](#)), S365 ([TOP-002](#))
- Gonçalves, Ana Maria, S730 ([TOP-384-YI](#))
- Gonçalves, João, S358 ([SAT-554-YI](#))
- Goncalves, Luciana Lofego, S30 ([OS-038-YI](#)), S83 ([LBP-012](#)), S199 ([TOP-062](#)), S200 ([TOP-064-YI](#))
- Gong, Weidong, S447 ([THU-475](#))
- Gonzalès, Emmanuel, S307 ([THU-094](#))
- González, Alejandro Miranda, S277 ([WED-530-YI](#))
- Gonzalez, Ana, S556 ([WED-334](#)), S642 ([SAT-434](#)), S654 ([SAT-466](#))
- González-Aseguinolaza, Gloria, S693 ([FRI-152-YI](#))
- Gonzalez-Carmona, Maria Angeles, S52 ([OS-079-YI](#))
- González, Carolina Jiménez, S468 ([FRI-211](#))
- Gonzalez, Concepción, S828 ([THU-411](#))
- González-Corrales, Carlos, S303 ([SAT-183](#))
- González-Díaz, Irene, S398 ([SAT-485](#))
- Gonzalès, Elmar, S641 ([SAT-431-YI](#))
- González-Gállego, Javier, S45 ([OS-067](#)), S277 ([WED-529](#))
- González-García, Elvira Ana, S706 ([WED-132](#)), S712 ([WED-159](#))
- Gonzalez, Gloria, S714 ([WED-164](#))
- González-Grande, Rocio, S365 ([TOP-002](#)), S779 ([FRI-409](#))
- González-Huezo, Maria Sarai, S83 ([LBP-012](#)), S161 ([THU-058](#))
- González, Javier Martínez, S172 ([THU-092](#)), S189 ([WED-100-YI](#)), S329 ([THU-154-YI](#)), S344 ([THU-189](#))
- González, Jesús M., S329 ([THU-154-YI](#)), S330 ([THU-155](#)), S453 ([THU-493](#))
- Gonzalez, Juan, S741 ([SAT-379](#)), S751 ([SAT-407](#))
- Gonzalez, Judit Vidal, S705 ([WED-129](#))
- González, Lorena Mosteiro, S569 ([THU-210](#))
- González, Luis A. Castaño, S569 ([THU-210](#))
- González-Padilla, Sheila, S232 ([FRI-125](#))
- González-Pascual, Andrea, S318 ([THU-118](#))
- Gonzalez-Peralta, Regino P., S323 ([THU-129](#)), S714 ([WED-164](#))
- González-Robles, Alba, S45 ([OS-067](#)), S277 ([WED-529](#))
- González-Romero, Francisco, S112 ([FRI-343-YI](#)), S562 ([TOP-229-YI](#))
- González-Romero, Francisco, S64 ([OS-101-YI](#)), S419 ([FRI-472-YI](#))
- Gonzalez-Sanchez, Ester, S432 ([FRI-525](#))
- Gonzalez, Susana, S696 ([FRI-161](#))
- Gonzalez, Veronica Enith Prado, S157 ([THU-049](#))
- Gonzalo, Nerea, S706 ([WED-132](#)), S712 ([WED-159](#))
- Goodman, Russell, S131 ([THU-330](#))
- Goodman, Zachary, S467 ([FRI-208](#)), S520 ([WED-230](#))
- Good, Steven, S749 ([SAT-402](#)), S753 ([SAT-411](#))
- Gordien, Emmanuel, S28 ([OS-034](#))
- Gordillo, Noelia, S172 ([THU-092](#))
- Gordon, Fiona, S647 ([SAT-448](#)), S651 ([SAT-457-YI](#))

Author Index

- Gordon, Stuart C, S20 ([OS-019](#))
 Gordon, Stuart C., S98 ([LBP-040](#)),
 S643 ([SAT-438](#)), S809 ([WED-371](#))
 Gore, John, S595 ([THU-293](#))
 Gorgulho, Joao, S24 ([OS-027-YI](#)),
 S69 ([OS-112-YI](#))
 Görgülü, Esra, S170 ([THU-087](#))
 Gori, Andrea, S804 ([WED-414](#))
 Goria, Odile, S54 ([OS-084-YI](#))
 Gormley, Sarah, S639 ([SAT-428](#))
 Gorospe, Emmanuel, S11 ([LBO-006](#))
 Gorrell, Mark, S534 ([WED-267](#))
 Gorsuch, Cassandra, S88 ([LBP-022](#))
 Gosset, Andréa, S678 ([WED-475](#))
 Goto, Juliana, S271 ([THU-556](#))
 Goto, Tatsuya, S512 ([WED-203](#))
 Gottardi, Andrea De, S117 ([SAT-316](#)),
 S238 ([SAT-069](#))
 Gottfredsson, Magnús, S236 ([FRI-133](#))
 Gottwald, Mildred D., S72 ([OS-118](#)),
 S522 ([WED-235](#)), S607 ([SAT-203](#))
 Gougelet, Angélique, S349 ([TOP-552](#)),
 S416 ([FRI-465](#))
 Goughnour, Peter, S78 ([LBP-002](#))
 Gou, Guoe, S786 ([FRI-430](#))
 Goulart, Denis Mariano, S50 ([OS-077](#))
 Goulas, Anestis, S823 ([THU-398](#))
 Goulis, Ioannis, S196 ([WED-121-YI](#)),
 S798 ([WED-403](#))
 Gournay, Jérôme, S6 ([GS-010](#)),
 S41 ([OS-060](#)), S520 ([WED-227](#)),
 S712 ([WED-160](#)), S802 ([WED-410](#))
 Goutte, Nathalie, S370 ([SAT-011](#)),
 S385 ([SAT-049](#)), S741 ([SAT-380](#))
 Govaere, Olivier, S31 ([OS-040-YI](#)),
 S125 ([TOP-328-YI](#))
 Gowland, Peter, S751 ([SAT-408](#))
 Gow, Paul, S547 ([WED-299](#))
 Goyal, Ashish, S735 ([SAT-364](#)),
 S832 ([THU-364](#))
 Goyal, Lipika, S25 ([OS-029](#))
 Goyal, Omesh, S158 ([THU-052](#)),
 S167 ([THU-078](#)), S475 ([FRI-231](#))
 Goy, Céline, S729 ([TOP-360-YI](#))
 Gozlan, Oren, S697 ([FRI-163-YI](#))
 Gozlan, Yael, S770 ([FRI-386](#))
 Grabbe, Stephan, S435 ([FRI-533](#))
 Grabert, Gordon, S735 ([SAT-363](#))
 Grabitz, Carl, S700 ([FRI-171](#))
 Gracia-Sancho, Jordi, S183 ([WED-081](#)),
 S183 ([WED-082](#)), S593 ([THU-287](#)),
 S596 ([THU-296](#))
 Graf, Christiana, S213 ([FRI-071](#))
 Graf, Markus, S213 ([FRI-071](#))
 Gragnani, Laura, S428 ([FRI-502](#)),
 S674 ([WED-467-YI](#))
 Graham, Cat, S81 ([LBP-007](#))
 Grajkowska, Wiesława,
 S328 ([THU-152-YI](#))
 Grajower, Martin M,
 S528 ([WED-248](#))
 Grammatikopoulos, Tassos,
 S198 ([WED-124](#)), S359 ([SAT-556-YI](#))
 Granito, Alessandro, S446 ([THU-472-YI](#))
 Grant, Craig, S808 ([WED-367](#))
 Granz, Diana, S484 ([FRI-255](#))
 Grasset, Estelle, S13 ([OS-006](#)),
 S597 ([THU-299](#))
 Grassi, Alberto, S836 ([THU-375](#))
 Grasso, Maria, S61 ([OS-096-YI](#))
 Grasu, Cristian Mugur, S410 ([SAT-528](#)),
 S446 ([THU-473](#))
 Gratacós-Ginès, Jordi, S13 ([OS-005-YI](#)),
 S139 ([SAT-257](#)), S142 ([SAT-267](#)),
 S160 ([THU-056](#)), S176 ([WED-055](#)),
 S541 ([WED-284-YI](#)), S711 ([WED-155](#))
 Grau, Katrine, S477 ([FRI-233](#))
 Grau, Laia, S233 ([FRI-126](#))
 Graupera, Isabel, S13 ([OS-005-YI](#)),
 S41 ([OS-059](#)), S160 ([THU-056](#)),
 S176 ([WED-055](#)), S468 ([FRI-211](#)),
 S471 ([FRI-219-YI](#)), S503 ([TOP-241-YI](#)),
 S541 ([WED-284-YI](#)), S711 ([WED-155](#)),
 S721 ([WED-181](#))
 Gray, Kevin, S809 ([WED-371](#))
 Gray, Meagan, S8 ([LBO-003](#))
 Grbic, Dusanka, S19 ([OS-018](#)),
 S305 ([TOP-169](#))
 Grecko, Roy, S808 ([WED-366](#)),
 S811 ([WED-374](#))
 Green, Ellen, S393 ([SAT-472](#))
 Greener, Veronica, S553 ([WED-324](#))
 Greenham, Olivia, S567 ([THU-207-YI](#))
 Greenhill, Elysia, S400 ([SAT-492](#))
 Greenland, Lindsay, S765 ([FRI-374-YI](#))
 Greenman, Raanan, S268 ([THU-547](#)),
 S295 ([SAT-158](#))
 Greenwald, Zoe, S688 ([WED-499](#))
 Greig, Robert, S117 ([SAT-317](#))
 Greinert, Robin, S244 ([SAT-087-YI](#))
 Gremmel, Stephan, S821 ([THU-390](#))
 Grewal, Priya, S165 ([THU-074](#))
 Grgas, Katharina, S85 ([LBP-017](#))
 Grgurevic, Ivica, S238 ([SAT-068](#)),
 S503 ([TOP-241-YI](#))
 Grgurević, Ivica, S155 ([SAT-305](#))
 Grieco, Antonio, S533 ([WED-261-YI](#))
 Griemsmann, Marie, S226 ([FRI-107-YI](#)),
 S226 ([FRI-109](#)), S818 ([THU-381](#)),
 S820 ([THU-386-YI](#))
 Griffin, Laura, S584 ([THU-259](#))
 Griffiths, William, S578 ([THU-236-YI](#))
 Griffiths, William J. H., S373 ([SAT-018-YI](#)),
 S703 ([TOP-141](#)), S708 ([WED-135-YI](#)),
 S724 ([WED-189](#))
 Grillo, Marta, S35 ([OS-048](#))
 Grimason, Haley, S88 ([LBP-022](#))
 Grimm, Daniel, S484 ([FRI-255](#))
 Grimmer, Katharine, S4 ([GS-011](#))
 Grimm, Felix, S702 ([TOP-140](#))
 Grimsrud, Marit, S50 ([OS-076-YI](#))
 Gringeri, Enrico, S59 ([OS-094](#)),
 S376 ([SAT-024-YI](#))
 Grip, Emilie Toresson, S37 ([OS-052](#)),
 S464 ([FRI-201](#)), S617 ([SAT-238](#))
 Grisetti, Luca, S429 ([FRI-516-YI](#))
 Gris-Oliver, Albert, S411 ([TOP-507-YI](#)),
 S417 ([FRI-467](#))
 Groba, Sara Noemi Reinartz, S52 ([OS-080](#)),
 S180 ([WED-074](#)), S258 ([SAT-130](#)),
 S391 ([TOP-511](#))
 Groba, Sara Reinartz, S133 ([THU-338](#))
 Grobbee, Diederick, S549 ([WED-306-YI](#)),
 S612 ([SAT-218](#))
 Groen, Roos, S382 ([SAT-040](#))
 Grønbaek, Henning, S172 ([THU-092](#)),
 S244 ([SAT-088](#)), S723 ([WED-187-YI](#))
 Grossar, Lorenz, S311 ([THU-102-YI](#)),
 S321 ([THU-123-YI](#)), S442 ([THU-463](#))
 Grosse, Gerrit M., S205 ([FRI-044-YI](#))
 Große, Karsten, S115 ([TOP-346-YI](#)),
 S229 ([FRI-116](#)), S308 ([THU-098](#)),
 S351 ([SAT-534](#))
 Groß, Finja, S335 ([THU-167](#))
 Grosshennig, Anika, S205 ([FRI-044-YI](#))
 Grossi, Ilaria, S59 ([OS-094](#))
 Grossi, Paolo Antonio, S700 ([FRI-171](#))
 Grossmann, Mathis, S547 ([WED-299](#))
 Grottenthaler, Julia M., S368 ([SAT-008](#)),
 S440 ([THU-457](#))
 Grover, Vijay, S631 ([THU-017-YI](#))
 Grovogui, Etienne, S743 ([SAT-387](#))
 Groza, Adrian, S409 ([SAT-525](#))
 Grube, Julia, S57 ([OS-088-YI](#))
 Gruber, Joshua, S799 ([WED-405](#))
 Gruden, Gabriella, S475 ([FRI-230-YI](#)),
 S483 ([FRI-251-YI](#)), S544 ([WED-293](#))
 Gruevska, Aleksandra, S107 ([FRI-326-YI](#))
 Grün, Dominic, S33 ([OS-043](#))
 Grupper, Ayelet, S237 ([FRI-136](#))
 Gruttadauria, Salvatore, S368 ([SAT-009](#))
 Grygoriev, Fedir, S610 ([SAT-213](#))
 Gryllis, Sophie, S657 ([WED-422](#)),
 S676 ([WED-470](#))
 Grypari, Ioanna Maria, S454 ([THU-495](#))
 Gryspeerdt, Filip, S420 ([FRI-475-YI](#))
 Grzelka, Malgorzata, S354 ([SAT-541](#))
 Grzyb, Krzysztof, S50 ([OS-076-YI](#))
 Grzymiski, Joseph J., S462 ([FRI-195](#))
 Gschwantler, Michael, S335 ([THU-166](#)),
 S773 ([FRI-394](#)), S818 ([THU-380-YI](#)),
 S818 ([THU-381](#)), S821 ([THU-390](#))
 Guan, Jin, S209 ([FRI-053](#))
 Guan, Yujuan, S605 ([SAT-198](#)),
 S803 ([WED-412](#))
 Guan, Yukun, S124 ([TOP-312](#))
 Guariglia, Marta, S475 ([FRI-230-YI](#)),
 S480 ([FRI-243](#)), S483 ([FRI-251-YI](#)),
 S501 ([FRI-314](#)), S522 ([WED-233-YI](#)),
 S525 ([WED-243-YI](#))
 Guarino, Maria, S367 ([SAT-007-YI](#))
 Guarnaccia, Carla, S371 ([SAT-015-YI](#))
 Guasconi, Tomas, S62 ([OS-099-YI](#)),
 S258 ([SAT-131](#))
 Guccione, Ernesto, S417 ([FRI-467](#))
 Gucht, Steven Van, S658 ([WED-426](#))
 Guckenbiehl, Sabrina, S182 ([WED-077](#))
 Gudd, Cathrin L C, S181 ([WED-075-YI](#))
 Gudina, Esayas, S781 ([FRI-414](#))
 Gudissa, Fikadu Girma, S781 ([FRI-414](#))
 Guedes, Ana Luiza Vilar, S343 ([THU-188](#))
 Guelow, Karsten, S191 ([WED-106](#))

- Guendogdu, Mehtap, S681 ([WED-482](#))
 Guennec, Adrien Le, S364 ([WED-027](#))
 Guerra, Javier Abad, S559 ([WED-339](#))
 Guerra, Manuel Hernández, S329 ([THU-154-YI](#)), S344 ([THU-189](#)), S717 ([WED-172](#))
 Guerra, Sara, S345 ([TOP-559](#))
 Guerreiro, Nelson, S26 ([OS-030](#))
 Guerrero, Chiara, S729 ([TOP-360-YI](#))
 Guerrero, Antonio, S255 ([SAT-123](#))
 Guerrero-Misas, Marta, S170 ([THU-086](#)), S531 ([WED-257](#))
 Guerrieri, Francesca, S280 ([WED-540-YI](#))
 Guha, Neil, S503 ([TOP-241-YI](#)), S650 ([SAT-454-YI](#))
 Guichelaar, Maureen, S480 ([FRI-244](#))
 Guichon, Céline, S22 ([OS-022](#))
 Guida, Alice, S88 ([LBP-023](#))
 Guidetti, Cristiano, S389 ([SAT-060](#))
 Guido, Maria, S612 ([SAT-219](#))
 Guidone, Caterina, S516 ([WED-215](#))
 Guidotti, Luca, S35 ([OS-048](#))
 Guijarro, Jorge, S232 ([FRI-125](#))
 Guijo-Rubio, David, S23 ([OS-024](#))
 Guiliani, Alejandro Mayorca, S513 ([WED-207](#)), S579 ([THU-243](#))
 Guillamon-Thiery, Alex, S13 ([OS-005-YI](#)), S176 ([WED-055](#))
 Guillaume, Maeva, S520 ([WED-227](#))
 Guillén-Navarro, Encarna, S715 ([WED-165](#))
 Guillen, Pilar, S141 ([SAT-262](#))
 Guillot, Adrien, S25 ([OS-028](#)), S57 ([OS-088-YI](#)), S298 ([SAT-170](#)), S302 ([SAT-180](#)), S414 ([FRI-457](#)), S566 ([THU-201-YI](#))
 Guinard-Azadian, Carine, S27 ([OS-033](#)), S813 ([WED-379](#))
 Guinart-Cuadra, Albert, S355 ([SAT-543](#))
 Guingané, Alice N., S678 ([WED-475](#))
 Guinovart, Martí, S141 ([SAT-262](#))
 Guirado, Agustina Gonzalez, S598 ([THU-302](#)), S599 ([THU-304](#))
 Guiu, Boris, S50 ([OS-077](#)), S52 ([OS-080](#)), S68 ([OS-110](#))
 Guix, Maria Garcia, S369 ([SAT-009](#))
 Gulamhusein, Aliya, S19 ([OS-018](#)), S98 ([LBP-040](#)), S305 ([TOP-168-YI](#)), S305 ([TOP-169](#)), S320 ([THU-121](#))
 Gulbani, Lasha, S691 ([WED-515](#)), S825 ([THU-404](#))
 Gulden, Lukas, S229 ([FRI-115](#))
 Gulnar, Muge Ozari, S785 ([FRI-427](#))
 Gültan, Merve, S6 ([GS-008](#))
 Gu, Lubing, S149 ([SAT-287](#))
 Gumussoy, Mesut, S407 ([SAT-519](#)), S479 ([FRI-238](#))
 Günal, Özgür, S805 ([WED-418](#))
 Gunasegaran, Bavani, S81 ([LBP-009](#))
 Gunda, Resign, S753 ([SAT-413](#))
 Gundlach, Jan Paul, S369 ([SAT-009](#))
 Gunduz, Feyza, S219 ([FRI-088](#))
 Guner, Rahmet, S805 ([WED-418](#))
 Gungabissoon, Usha, S332 ([THU-160](#)), S472 ([FRI-220-YI](#)), S485 ([FRI-258](#))
 Gunjan, Deepak, S62 ([OS-098-YI](#)), S201 ([TOP-065](#)), S546 ([WED-298-YI](#))
 Gunn, Nadege, S11 ([LBO-006](#)), S614 ([SAT-227](#)), S618 ([SAT-243](#))
 Günsar, Fulya, S211 ([FRI-067](#)), S805 ([WED-419](#))
 Günther, Rainer, S582 ([THU-254-YI](#))
 Günther, Ulrich L., S582 ([THU-254-YI](#))
 Guo, Daqing, S622 ([FRI-010](#))
 Guo, Feng, S161 ([THU-058](#)), S234 ([FRI-129](#))
 Guo, Jiang, S69 ([OS-112-YI](#))
 Guo, Lixin, S527 ([WED-246](#))
 Guo, Shuling, S93 ([LBP-031](#))
 Guo, Tiantian, S119 ([SAT-321](#)), S121 ([SAT-326](#))
 Guo, Wuhua, S260 ([SAT-136](#))
 Guo, Xiaoqing, S544 ([WED-292](#))
 Guo, Xu, S241 ([SAT-077](#)), S622 ([FRI-010](#))
 Guo, Yanzhi, S701 ([FRI-174](#))
 Guo, Yifei, S742 ([SAT-383](#)), S748 ([SAT-399](#))
 Guo, Ying, S544 ([WED-292](#))
 Guo, Yue, S748 ([SAT-399](#))
 Guo, Zhiong, S369 ([SAT-009](#))
 Gupta, Abhishak, S283 ([WED-549](#)), S294 ([SAT-155](#)), S754 ([SAT-415](#))
 Gupta, Digant, S340 ([THU-181](#))
 Gupta, Haripriya, S286 ([WED-557](#))
 Gupta, Kusum, S727 ([TOP-357](#)), S728 ([TOP-358-YI](#))
 Gupta, Priyanka, S55 ([OS-085](#))
 Gupta, Rajesh, S149 ([SAT-290-YI](#)), S701 ([FRI-173](#)), S720 ([WED-180](#))
 Gupta, Rohit, S476 ([FRI-231](#))
 Gupta, Shubham, S554 ([WED-327](#))
 Gupta, Sneha, S816 ([WED-389](#))
 Gurbuz, Burcu, S224 ([FRI-104](#))
 Guruceaga, Elisabet, S416 ([FRI-464](#))
 Gurung, Arati, S560 ([WED-343](#))
 Gurung, Sonam, S698 ([FRI-166](#))
 Gustot, Thierry, S9 ([LBO-004](#)), S83 ([LBP-012](#)), S89 ([LBP-026](#)), S131 ([THU-331-YI](#)), S133 ([THU-335](#)), S157 ([THU-050](#)), S161 ([THU-057-YI](#)), S172 ([THU-092](#)), S188 ([WED-098-YI](#))
 Gu, Tao, S715 ([WED-166](#))
 Gutic, Enisa, S818 ([THU-380-YI](#)), S821 ([THU-390](#))
 Gutierrez, Julio, S384 ([SAT-047](#))
 Gutiérrez, Laura, S29 ([OS-037](#))
 Gutierrez, Maria Luisa, S818 ([THU-381](#))
 Gutiérrez, Maria Luisa, S391 ([TOP-512-YI](#)), S453 ([THU-493](#))
 Gutierrez, Maria Salud García, S194 ([WED-113](#))
 Gutiérrez, Oscar Morales, S161 ([THU-058](#))
 Gutierrez, Pedro, S23 ([OS-024](#))
 Gu, Wenyi, S47 ([OS-071-YI](#)), S159 ([THU-053](#)), S159 ([THU-055](#)), S169 ([THU-083](#)), S170 ([THU-087](#)), S180 ([WED-074](#)), S184 ([WED-083](#)), S193 ([WED-111](#)), S203 ([FRI-039](#)), S259 ([SAT-135](#)), S272 ([TOP-563](#)), S391 ([TOP-511](#))
 Guy, Cynthia D., S467 ([FRI-208](#))
 Gu, Zhiqiang, S775 ([FRI-402](#))
 Guzmán, Zarina, S641 ([SAT-431-YI](#))
 Haack, Rebecca, S657 ([WED-422](#)), S676 ([WED-470](#))
 Haase, Jil, S94 ([LBP-034](#))
 Haas, Victor, S350 ([SAT-531-YI](#))
 Haberl, Christina, S719 ([WED-175](#))
 Haber, Philipp, S411 ([TOP-507-YI](#))
 Habib, Mariam, S350 ([TOP-553](#))
 Habtesion, Abeba, S17 ([OS-014-YI](#)), S179 ([WED-069](#)), S182 ([WED-078](#)), S182 ([WED-080](#)), S188 ([WED-099-YI](#)), S567 ([THU-207-YI](#))
 Hacetarean, Alexei, S806 ([WED-361](#)), S807 ([WED-365](#))
 Hacıhahinoğulları, Hülya, S551 ([WED-318-YI](#))
 Haderer, Marika, S191 ([WED-106](#))
 Hadjihambi, Anna, S110 ([FRI-335](#)), S192 ([WED-110](#)), S567 ([THU-207-YI](#)), S588 ([THU-271-YI](#))
 Hadziyannis, Emilia, S782 ([FRI-415](#)), S800 ([WED-406](#))
 Hafey, Michael, S753 ([SAT-412](#))
 Hagger, Georgina, S181 ([WED-075-YI](#))
 Haggie, Peter, S812 ([WED-377](#))
 Haghnejad, Vincent, S260 ([SAT-137](#)), S397 ([SAT-483-YI](#))
 Hagihara, Atsushi, S430 ([FRI-518](#))
 Hagström, Hannes, S2 ([GS-004](#)), S37 ([OS-052](#)), S38 ([OS-054](#)), S40 ([OS-057-YI](#)), S147 ([SAT-280](#)), S148 ([SAT-285-YI](#)), S462 ([FRI-196](#)), S464 ([FRI-201](#)), S617 ([SAT-238](#))
 Hagymási, Krisztina, S311 ([THU-103](#))
 Hahn, Gareth, S350 ([TOP-553](#))
 Haigh, Laura, S629 ([THU-009](#))
 Hai, Hoang, S261 ([THU-523](#)), S430 ([FRI-518](#))
 Haile, Hieremila, S682 ([WED-484](#))
 Hai Liu, Chang, S499 ([FRI-302](#))
 Haimberger, Friedrich, S243 ([SAT-086-YI](#))
 Hajarizadeh, Behzad, S776 ([FRI-403](#))
 Hajer, Ben Khadhra, S444 ([THU-466](#))
 Hakeem, Andrew, S583 ([THU-255](#))
 Haktaniyan, Busra, S161 ([THU-058](#))
 Hala, Al-Tamimi, S161 ([THU-058](#))
 Haldar, Debashis, S101 ([LBP-046](#))
 Halilbasic, Emina, S335 ([THU-166](#)), S340 ([THU-180](#)), S341 ([THU-183-YI](#)), S706 ([WED-131-YI](#)), S725 ([WED-190](#))
 Halimani, Noreen, S268 ([THU-542](#))
 Hallensleben, Michael, S21 ([OS-021-YI](#))
 Hallen, Stefan, S93 ([LBP-031](#))
 Haller, Alexandre, S42 ([OS-061](#))
 Haller, Dirk, S65 ([OS-103](#))
 Haller, Rosa, S284 ([WED-551](#))
 Hallett, Timothy B., S678 ([WED-475](#))
 Halliday, Anna, S340 ([THU-181](#)), S485 ([FRI-258](#))
 Halliday, Laura, S580 ([THU-247-YI](#))
 Halliday, Neil, S290 ([TOP-147](#)), S315 ([THU-111](#))

Author Index

- Hall, Samantha, S663 (WED-437), S667 (WED-448), S680 (WED-480-YI)
- Hallsworth, Kate, S630 (THU-015-YI), S631 (THU-016)
- Hall, Timothy, S560 (WED-343)
- Hall, Zoe, S107 (FRI-326-YI)
- Halter, Sébastien, S156 (TOP-108)
- Haltmayer, Hans, S818 (THU-380-YI), S821 (THU-390)
- Hambridge, Shannon, S544 (WED-294)
- Hamdan, Nashla, S497 (FRI-293)
- Hamdy, Mona Salah Eldin, S491 (FRI-273-YI)
- Hametner-Schreil, Stephanie, S818 (THU-381)
- Hamid, Saeed Sadiq, S158 (THU-052), S643 (SAT-438), S800 (WED-407), S814 (WED-382)
- Hamilton-Dutoit, Stephen, S567 (THU-207-YI)
- Hamilton, James, S27 (OS-032)
- Hamimi, Akila, S416 (FRI-465)
- Hammad, Seddik, S263 (THU-526), S287 (FRI-539)
- Hammam, Olfat, S418 (FRI-470), S570 (THU-213), S583 (THU-255)
- Hammar, Niklas, S40 (OS-057-YI)
- Hammer, Fabian, S257 (SAT-128)
- Hammond, Janet, S819 (THU-382)
- Hammond, Nigel, S67 (OS-109)
- Hamody, Yara, S696 (FRI-160-YI)
- Hamon, Annaïg, S109 (FRI-333)
- Hamoudi, Waseem, S624 (FRI-020)
- Hampe, Jochen, S56 (OS-086-YI)
- Hamway, Youssef, S699 (FRI-170)
- Ham, Young Lim, S286 (WED-557)
- Hamza, Rania, S491 (FRI-273-YI)
- Hancz, Dora, S574 (THU-227)
- Handanagic, Senad, S682 (WED-484)
- Handayani, Irda, S792 (FRI-444)
- Hand, James, S350 (TOP-553)
- Handjiev, Sava, S14 (OS-007-YI)
- Handler, Eric, S661 (WED-433)
- Han, Dong, S737 (SAT-371)
- Handrick, Simon, S788 (FRI-434)
- Hanemaaijer, Roeland, S513 (WED-209)
- Han, Feng, S65 (OS-103)
- Hanford, Paula, S332 (THU-160)
- Hanf, Remy, S191 (WED-105), S337 (THU-174)
- Hang, Shou Kit, S742 (SAT-383)
- Han, Guohong, S447 (THU-475), S716 (WED-167)
- Han, Guorong, S784 (FRI-424)
- Ha, Nguyen Thi, S261 (THU-523), S430 (FRI-518)
- Hanley, Karen Piper, S67 (OS-109), S265 (THU-535-YI), S650 (SAT-454-YI)
- Hanley, Neil, S67 (OS-109), S650 (SAT-454-YI)
- Han, Ma Ai Thanda, S478 (FRI-236-YI)
- Hannah, Nicholas, S338 (THU-177-YI), S400 (SAT-492)
- Hann, Angus, S369 (SAT-009)
- Han Ng, Cheng, S147 (SAT-281)
- Hansen, Bettina, S19 (OS-018), S305 (TOP-169), S374 (SAT-021)
- Hansen, Bettina E., S49 (OS-075-YI), S305 (TOP-168-YI), S308 (THU-098), S309 (THU-100), S311 (THU-102-YI), S314 (THU-109), S319 (THU-120-YI), S320 (THU-121), S321 (THU-125), S327 (THU-138), S335 (THU-167), S606 (SAT-200-YI), S761 (FRI-363-YI), S764 (FRI-372)
- Hansen, Camilla Dalby, S41 (OS-059), S77 (OS-126), S137 (SAT-250), S205 (FRI-045), S466 (FRI-206-YI), S510 (WED-199), S620 (TOP-012), S623 (FRI-017)
- Hansen, Emil Deleuran, S139 (SAT-255), S142 (SAT-266), S466 (FRI-206-YI), S620 (TOP-012)
- Hansen, Henrik B., S421 (FRI-478), S566 (THU-202), S568 (THU-208), S569 (THU-211), S576 (THU-232), S580 (THU-244)
- Hansen, Jesper Bach, S723 (WED-187-YI)
- Hansen, Johanne Kragh, S41 (OS-059), S47 (OS-072-YI), S77 (OS-126), S137 (SAT-250), S205 (FRI-045), S466 (FRI-206-YI), S503 (TOP-241-YI), S510 (WED-199), S620 (TOP-012), S623 (FRI-017)
- Hansen, Lars, S93 (LBP-031)
- Hansen, Lissi, S12 (OS-003)
- Hansen, Torben, S47 (OS-072-YI), S466 (FRI-206-YI), S623 (FRI-017)
- Han, Seul Ki, S136 (THU-348)
- Han, Sunguck, S82 (LBP-011)
- Han, Tingrui, S622 (FRI-010)
- Han, Yanan, S526 (WED-246)
- Hao, Hongxiao, S344 (THU-191)
- Hao, Jie, S357 (SAT-547)
- Hao, Kunyan, S100 (LBP-045)
- Hao, Miao, S195 (WED-116)
- Hao Tan, Darren Jun, S147 (SAT-281)
- Haraguchi, Masafumi, S228 (FRI-113), S234 (FRI-128)
- Haraldsson, Halldor A., S236 (FRI-133)
- Harder, Lea Mørch, S79 (LBP-003)
- Hardisty, Gareth, S291 (TOP-148)
- Hardtke, Svenja, S730 (TOP-369)
- Hardtke-Wolenski, Matthias, S583 (THU-256)
- Hardwigsen, Jean, S369 (SAT-010)
- Haridy, James, S400 (SAT-492)
- Hariharaputran, Smrithi, S742 (SAT-383)
- Harindranath, Sidharth, S554 (WED-327)
- Haring, Martijn, S394 (SAT-474)
- Harlow, Christopher, S388 (SAT-057)
- Harmsen, Martin, S582 (THU-251-YI)
- Haro, Juan Acevedo, S157 (THU-049), S250 (SAT-107-YI)
- Harputluoglu, Murat, S30 (OS-038-YI), S199 (TOP-062), S200 (TOP-064-YI), S336 (THU-171), S374 (SAT-021)
- Harput, Zekiye Nur, S723 (WED-187-YI)
- Harris, M. Scott, S515 (WED-212), S517 (WED-219), S529 (WED-251)
- Harris, Nicola, S128 (THU-320-YI), S174 (TOP-084), S281 (WED-542-YI), S350 (TOP-553), S700 (FRI-171)
- Harrison, Emily, S88 (LBP-022)
- Harrison, Laura, S333 (THU-162-YI)
- Harrison, Stephen A., S2 (GS-004), S4 (GS-011), S8 (LBO-002), S37 (OS-051), S38 (OS-054), S56 (OS-087), S71 (OS-117), S72 (OS-118), S76 (OS-124), S84 (LBP-014), S88 (LBP-024), S141 (SAT-263), S463 (FRI-198), S464 (FRI-199), S467 (FRI-208), S481 (FRI-247), S482 (FRI-249), S504 (TOP-253), S505 (TOP-265), S507 (TOP-289), S507 (TOP-300), S511 (WED-201), S511 (WED-202), S515 (WED-213), S516 (WED-215), S517 (WED-219), S518 (WED-223), S545 (WED-296), S576 (THU-233), S579 (THU-242), S603 (SAT-195), S607 (SAT-202), S607 (SAT-203), S609 (SAT-208), S611 (SAT-214), S612 (SAT-220-YI), S614 (SAT-227), S618 (SAT-243), S648 (SAT-450)
- Hartleben, Björn, S21 (OS-021-YI), S583 (THU-256)
- Hartl, Johannes, S316 (THU-113)
- Hartl, Lukas, S61 (OS-096-YI), S156 (TOP-097-YI), S165 (THU-071), S166 (THU-075-YI), S242 (SAT-080-YI), S243 (SAT-086-YI), S250 (SAT-105), S251 (SAT-111), S253 (SAT-117), S253 (SAT-118), S255 (SAT-122), S257 (SAT-128), S340 (THU-180), S621 (FRI-009-YI), S717 (WED-171), S818 (THU-381)
- Hartman, Mark, S7 (LBO-001)
- Hartmann, Christian, S716 (WED-170)
- Hartsfield, Cynthia L., S72 (OS-118), S607 (SAT-203)
- Har-Zahav, Adi, S696 (FRI-160-YI)
- Hasanoğlu, İmran, S805 (WED-418)
- Hasan, Sara, S545 (WED-295-YI)
- Haselwanter, Patrick, S340 (THU-180)
- Hashida, Ryuuki, S472 (FRI-221)
- Hashiguchi, Taishi, S434 (FRI-531)
- Hashim, Ahmed, S457 (THU-514), S521 (WED-232-YI)
- Hassan, Ayman, S673 (WED-463)
- Hassan, Cesare, S496 (FRI-290), S500 (FRI-304)
- Hassanein, Tarek, S242 (SAT-082), S544 (WED-294)
- Hassani, Afshar, S75 (OS-127)
- Hassani, Majda El, S229 (FRI-116)
- Hassan, Mohsin, S594 (THU-291-YI)
- Hassannia, Behrouz, S581 (THU-249)
- Hassan, Zeinab, S172 (THU-090)
- Hasselblatt, Peter, S54 (OS-083)
- Hasson, Dan, S417 (FRI-467)
- Hasson, Hamid, S824 (THU-402)
- Hatchell, Niall, S707 (WED-134)

- Hateley, Charlotte, S580 (THU-247-YI)
 Hatem, Ammar, S491 (FRI-273-YI)
 Hatten, Hannes, S431 (FRI-522)
 Hatzakis, Angelos, S670 (WED-454-YI), S680 (WED-478)
 Haupt, Axel, S7 (LBO-001)
 Hauskov, Sara, S153 (SAT-298)
 Havaj, Daniel Jan, S379 (SAT-033), S539 (WED-279)
 Havinga, Rick, S573 (THU-224)
 Hawken, James, S651 (SAT-457-YI)
 Hawkins, Claudia, S395 (SAT-479-YI)
 Hayashi, Hideki, S537 (WED-273)
 Hayashi, Jun, S42 (OS-062)
 Hayashi, Paul, S114 (TOP-345)
 Hayato, Muranaka, S128 (THU-319)
 Haydel, Brandy, S374 (SAT-021)
 Hayes, Peter, S161 (THU-058), S208 (FRI-053), S219 (FRI-088)
 Hay, Ophir, S278 (WED-534)
 Hazard, Octave, S64 (OS-102)
 Hazia, Olha, S284 (WED-551)
 Hazo, Wadiaa, S563 (THU-194), S779 (FRI-408)
 Hazzan, Rawi, S645 (SAT-442)
 Heard, Nicole, S88 (LBP-022)
 Heaton, Nigel, S128 (THU-320-YI), S281 (WED-542-YI), S709 (WED-137-YI)
 Hees, Stijn Van, S730 (SAT-337)
 He, Fang, S792 (WED-390)
 Heger, Zbynek, S417 (FRI-466-YI)
 Heggelund, Lars, S795 (WED-394)
 Hegmar, Hannes, S504 (TOP-252-YI)
 He, Hengqiu, S440 (THU-455)
 Heida, Andries, S347 (FRI-549-YI)
 Heide, Danijela, S65 (OS-103)
 Heij, Lara, S426 (FRI-495)
 Heikenwälder, Mathias, S25 (OS-029), S31 (OS-040-YI), S42 (OS-061), S56 (OS-086-YI), S65 (OS-103), S278 (WED-534), S411 (TOP-507-YI), S426 (FRI-495)
 Heilani, Myriam, S203 (FRI-039)
 Heimanson, Zeev, S212 (FRI-069)
 Heim, Kathrin, S351 (SAT-533)
 Heim, Markus, S292 (TOP-150-YI)
 Heinrich, Bernd, S350 (SAT-532-YI)
 Heinrich, Sophia, S21 (OS-021-YI), S440 (THU-457)
 Hein, Sascha, S734 (SAT-361)
 Heinson, Ashley I, S676 (WED-471)
 Heinson, Ashley I., S759 (TOP-417)
 Heintz, Sarah, S58 (OS-091)
 Hejda, Vaclav, S91 (LBP-027), S311 (THU-103)
 He, Jiayi, S622 (FRI-010)
 He, Jinhang, S775 (FRI-398)
 Heldens, Anneleen, S57 (OS-089-YI), S278 (WED-531)
 Helder, Jeltje, S5 (GS-007)
 Heller, Theo, S800 (WED-407), S814 (WED-382)
 Hellstrand, Kristoffer, S754 (SAT-414)
 Heluwaert, Frederic, S73 (OS-120), S793 (WED-391)
 Hemant, Sahasraara, S510 (WED-199), S547 (WED-303)
 Hemati, Hami, S294 (SAT-155)
 Hemetsberger, Paul, S242 (SAT-080-YI)
 He, Mingfeng, S440 (THU-455)
 Hemmer, Helene, S33 (OS-043)
 Hemming Karlsen, Tom, S296 (SAT-163-YI)
 Hemminki, Kari, S349 (FRI-556)
 Henderson, Louise, S393 (SAT-472)
 Henderson, Neil, S105 (FRI-318-YI), S107 (FRI-326-YI)
 Heneghan, Michael, S80 (LBP-006), S311 (THU-103), S315 (THU-111), S374 (SAT-021), S388 (SAT-057), S709 (WED-137-YI)
 Hengstler, Jan G., S57 (OS-088-YI), S85 (LBP-017), S273 (WED-521-YI)
 Henin, Guillaume, S151 (SAT-293-YI), S473 (FRI-224), S546 (WED-297-YI), S823 (THU-397-YI)
 Henley, William, S645 (SAT-440)
 Hennan, Jim, S509 (WED-196)
 Hennelly, Chris, S675 (WED-469)
 Henninger, Benjamin, S515 (WED-214-YI)
 Henricsson, Marcus, S273 (WED-521-YI)
 Henrique, Mariana Moura, S286 (WED-558), S358 (SAT-554-YI)
 Henry, Doriane, S577 (THU-234)
 Henry, Linda, S465 (FRI-202), S470 (FRI-218), S472 (FRI-221), S638 (SAT-425), S643 (SAT-438)
 Henry, Paulina, S151 (SAT-293-YI)
 Henschler, Reinhard, S162 (THU-059)
 Hens, Niel, S665 (WED-441-YI)
 Henstock, Peter, S533 (WED-263)
 Henze, Lara, S350 (SAT-531-YI)
 Heo, Jeong, S3 (GS-005), S20 (OS-019), S98 (LBP-040), S457 (THU-516), S809 (WED-371)
 Heo, Subin, S437 (TOP-489-YI)
 He, Qiuyan, S415 (FRI-459)
 Herber, Adam, S162 (THU-059), S404 (SAT-501-YI)
 Her, Chris, S261 (TOP-564)
 Hercog, Rajna, S47 (OS-071-YI)
 Hercun, Julian, S19 (OS-018), S305 (TOP-169)
 Herkel, Johannes, S278 (WED-534)
 Hermanbessiere, Paul, S514 (WED-211)
 Hermán-Sánchez, Natalia, S415 (FRI-462-YI)
 Hermans, Greet, S157 (THU-049)
 Hermes, Joy-Marie, S384 (SAT-047)
 Hernaez Alsina, Tania, S330 (THU-155)
 Hernaez, Ruben, S9 (LBO-004), S89 (LBP-026)
 Hernández-Abrego, Andy, S436 (FRI-535)
 Hernandez, Alejandra, S654 (SAT-466)
 Hernández, Candido, S681 (WED-482), S827 (THU-410), S833 (THU-366), S836 (THU-374)
 Hernández-Èvole, Helena, S336 (THU-170-YI)
 Hernández-Gea, Virginia, S15 (OS-010), S85 (LBP-016), S179 (WED-070), S240 (SAT-074), S255 (SAT-123)
 Hernandez, Jennifer, S621 (FRI-008)
 Hernández-Labra, Elia, S140 (SAT-260)
 Hernández, Miroslava, S627 (FRI-029)
 Hernandez, Nidia, S692 (FRI-151)
 Hernández-Quijano, Lizeth Vanessa, S436 (FRI-535)
 Hernandez, Rocio Calvo, S598 (THU-302), S599 (THU-304)
 Hernandez-Rubio, Anna, S154 (SAT-303), S190 (WED-104)
 Hernandez-Tejero, Maria, S203 (FRI-039)
 Hernández-Tejero, María, S157 (THU-049)
 Hernández, Tomás, S694 (FRI-153)
 Herola, Antonio Garcia, S827 (THU-410)
 Heron, Jon, S647 (SAT-448)
 Herraes, Elisa, S432 (FRI-523)
 Herranz, Jose Maria, S287 (FRI-538), S348 (FRI-555)
 Herranz, José María, S265 (THU-533)
 Herrera, Blanca, S303 (SAT-183)
 Herrera, Elba Llop, S2 (GS-004), S38 (OS-054), S61 (OS-096-YI), S85 (LBP-016), S559 (WED-339)
 Herrera, Ronald, S477 (FRI-235), S486 (FRI-260), S509 (WED-197)
 Herrero, Alba, S431 (FRI-521), S435 (FRI-534)
 Herrero, Astrid, S376 (SAT-026)
 Herrero, Jose Ignacio, S348 (FRI-555), S531 (WED-257)
 Herrero, Laura, S568 (THU-209)
 Herreros, Angela Martínez, S329 (THU-154-YI)
 Herreros, Yolanda, S541 (WED-284-YI)
 Herrojo, Javier Ampuero, S329 (THU-154-YI), S596 (THU-296)
 Herr, Winship, S347 (FRI-550)
 Hershkovich, Leeor, S800 (WED-407), S814 (WED-382)
 Hertig, Alexandre, S372 (SAT-016)
 He, Ruiling, S526 (WED-246)
 Hervás, César, S23 (OS-024), S365 (TOP-002)
 Hervieu, Valerie, S508 (WED-194)
 He, Shihao, S789 (FRI-438)
 Hesketh, Hannah, S672 (WED-459-YI)
 Heslop, James, S81 (LBP-008)
 He, Song, S427 (FRI-500-YI)
 Hessheimer, Amelia Judith, S362 (WED-016), S364 (WED-028)
 He, Taiyu, S269 (THU-549), S727 (TOP-356)
 Hetland, Liv, S529 (WED-250-YI), S555 (WED-331-YI)
 Hetland, Liv Eline, S513 (WED-207)
 Hetzer, Jenny, S65 (OS-103)
 Heucke, Niklas, S25 (OS-028)
 Heurgue-berlot, Alexandra, S54 (OS-084-YI), S413 (FRI-456), S444 (THU-466)

Author Index

- Heusler, Hélène, S291 ([TOP-150-YI](#))
Heusner, Carrie, S20 ([OS-019](#)),
S98 ([LBP-040](#))
Hewitt, Katherine, S427 ([FRI-499-YI](#))
Heydmann, Laura, S734 ([SAT-348-YI](#))
Heyens, Leen, S604 ([SAT-196](#))
Heyerick, Lander, S292 ([SAT-151-YI](#)),
S420 ([FRI-475-YI](#))
Heymann, Felix, S353 ([SAT-539-YI](#))
Hiasa, Yoichi, S512 ([WED-203](#)),
S711 ([WED-154](#)), S722 ([WED-184](#)),
S828 ([THU-413](#))
Hiatt, Shirin, S12 ([OS-003](#))
Hibberd, Martin, S797 ([WED-398](#))
Hickman, Ingrid, S631 ([THU-016](#))
Hickman, Matthew, S647 ([SAT-448](#)),
S651 ([SAT-457-YI](#))
Hidalgo, Marta, S592 ([THU-283](#))
Hidam, Ashini, S164 ([THU-068](#)),
S164 ([THU-069](#))
Higashi, Mai, S513 ([WED-208](#))
Higuchi, Mayu, S626 ([FRI-026](#))
Higuera-de-la-Tijera, Fatima,
S140 ([SAT-260](#)), S836 ([THU-374](#))
Higuera, Monica, S407 ([SAT-516](#))
Hikita, Hayato, S506 ([TOP-288](#)),
S828 ([THU-413](#))
Hild, Benedikt, S223 ([FRI-100](#)),
S384 ([SAT-046](#))
Hildebrand, Hannah, S443 ([THU-464](#))
Hiltdt, Eberhard, S170 ([THU-087](#)),
S734 ([SAT-361](#))
Hillaire, Sophie, S54 ([OS-084-YI](#))
Hill, Brandon, S141 ([SAT-263](#))
Hillebrandt, Karl, S84 ([LBP-015](#))
Hilleret, Marie-Noëlle, S1 ([GS-002](#)),
S6 ([GS-010](#)), S73 ([OS-120](#)),
S367 ([TOP-005](#)), S385 ([SAT-048](#)),
S744 ([SAT-389](#)), S747 ([SAT-396](#)),
S763 ([FRI-370](#)), S764 ([FRI-371](#)),
S793 ([WED-391](#)), S802 ([WED-410](#))
Himanshi, Himanshi, S177 ([WED-058-YI](#)),
S188 ([WED-095-YI](#))
Himmelsbach, Vera, S52 ([OS-079-YI](#)),
S69 ([OS-112-YI](#))
Hinkson, Alexander, S136 ([TOP-311-YI](#)),
S534 ([WED-266](#))
Hiraoka, Atsushi, S248 ([SAT-101](#))
Hirata, Yoshihiro, S301 ([SAT-176](#))
Hires, Mate, S29 ([OS-036-YI](#))
Hirode, Grishma, S49 ([OS-075-YI](#))
Hirooka, Masashi, S512 ([WED-203](#))
Hirschfield, Gideon, S311 ([THU-103](#))
Hirschfield, Gideon M., S5 ([GS-007](#)),
S19 ([OS-018](#)), S97 ([LBP-039](#)),
S98 ([LBP-040](#)), S101 ([LBP-046](#)),
S305 ([TOP-168-YI](#)), S305 ([TOP-169](#)),
S308 ([THU-098](#)), S311 ([THU-102-YI](#)),
S320 ([THU-121](#)), S321 ([THU-125](#)),
S374 ([SAT-021](#)), S485 ([FRI-258](#))
Hisatomi, Mitsuru, S541 ([WED-283](#))
Hislop, Colin, S800 ([WED-407](#)),
S814 ([WED-382](#))
Hjorth, Maria, S12 ([OS-002](#))
Ho, Chi-Kung, S490 ([FRI-271](#)),
S493 ([FRI-280](#))
Ho, Chun-Ting, S398 ([SAT-484](#)),
S663 ([WED-438-YI](#))
Hockings, Paul, S550 ([WED-316](#))
Hocquet, Didier, S61 ([OS-097](#))
Ho, Daniel Wai-Hung, S419 ([FRI-473](#))
Hodge, Alex, S653 ([SAT-464-YI](#))
Hodge, Jacqueline, S250 ([SAT-106](#))
Hodson, James, S337 ([THU-173](#))
Hoerning, André, S356 ([SAT-546](#))
Hoeroldt, Barbara, S333 ([THU-162-YI](#))
Ho, Erwin, S665 ([WED-441-YI](#))
Hofer, Benedikt, S156 ([TOP-097-YI](#)),
S165 ([THU-071](#)), S166 ([THU-075-YI](#)),
S186 ([WED-089-YI](#)), S197 ([WED-122-YI](#)),
S198 ([WED-125](#)), S243 ([SAT-086-YI](#)),
S250 ([SAT-105](#)), S251 ([SAT-111](#)),
S253 ([SAT-117](#)), S253 ([SAT-118](#)),
S255 ([SAT-122](#)), S257 ([SAT-128](#)),
S267 ([THU-540](#)), S335 ([THU-166](#)),
S341 ([THU-183-YI](#)), S621 ([FRI-009-YI](#)),
S717 ([WED-171](#))
Höffer, Anne, S21 ([OS-021-YI](#))
Hofmann, Maike, S23 ([OS-025-YI](#)),
S54 ([OS-083](#)), S187 ([WED-094](#)),
S351 ([SAT-533](#))
Ho, Frederick, S138 ([SAT-254](#))
Hofstetter, Thomas, S98 ([LBP-041](#))
Hogan, Thea, S807 ([WED-364](#))
Hogardt, Michael, S203 ([FRI-039](#))
Höhn, Annika, S279 ([WED-538-YI](#))
Holdorf, Meghan, S729 ([TOP-368](#)),
S733 ([SAT-342-YI](#))
Hollande, Clemence, S50 ([OS-077](#)),
S452 ([THU-492](#))
Holland-Fischer, Peter, S723 ([WED-187-YI](#))
Holleboom, Onno, S513 ([WED-209](#))
Holmberg, Marte, S795 ([WED-394](#))
Holmes, Elaine, S127 ([THU-317](#)),
S145 ([SAT-274](#))
Holmes, Jacinta, S42 ([OS-061](#)),
S78 ([LBP-001](#)), S400 ([SAT-492](#)),
S740 ([SAT-377](#)), S809 ([WED-371](#))
Holm, Jens-Christian, S47 ([OS-072-YI](#))
Holm, Louise Aas, S47 ([OS-072-YI](#))
Holterhus, Paul-Martin, S350 ([SAT-531-YI](#))
Holtmann, Theresa, S359 ([SAT-555](#)),
S442 ([THU-463](#))
Homer, Victoria, S101 ([LBP-046](#))
Honda, Takashi, S541 ([WED-283](#))
Honda, Yasushi, S541 ([WED-283](#))
Hong, Feng, S696 ([FRI-161](#)), S698 ([FRI-164](#))
Hong, Hyeyeon, S144 ([SAT-272](#)),
S822 ([THU-394](#))
Hong, Jin, S727 ([TOP-357](#))
Hong Koh, Jia, S147 ([SAT-281](#))
Hong, Sukjin, S801 ([WED-408](#))
Honkoop, Pieter, S758 ([TOP-401-YI](#))
Hontañón, Victor, S741 ([SAT-379](#)),
S751 ([SAT-407](#))
Hoorens, Anne, S278 ([WED-531](#))
Hopp, Can, S717 ([WED-171](#))
Ho, Pui Yan, S737 ([SAT-371](#))
Hoque, Zohan, S58 ([OS-090](#))
Horecki, Marcin, S308 ([THU-095](#))
Horga, Arantxa, S819 ([THU-382](#))
Horhat, Adelina, S144 ([SAT-273-YI](#)),
S151 ([SAT-294](#))
Hornus, Pierre, S326 ([THU-136](#))
Horrillo, Raquel, S46 ([OS-069](#)),
S177 ([WED-059](#)), S231 ([FRI-121](#))
Horslen, Simon P., S331 ([THU-158](#))
Horsmans, Yves, S122 ([SAT-331](#))
Horsthuis, Karin, S315 ([THU-112-YI](#))
Horst, Ludwig J., S265 ([THU-534-YI](#)),
S327 ([THU-137](#))
Horstmeier, Henriette, S186 ([WED-089-YI](#)),
S197 ([WED-122-YI](#)), S198 ([WED-125](#)),
S267 ([THU-540](#))
Horta, Diana, S139 ([SAT-257](#)),
S142 ([SAT-267](#)), S318 ([THU-118](#)),
S329 ([THU-154-YI](#)), S330 ([THU-155](#)),
S336 ([THU-170-YI](#)), S453 ([THU-493](#))
Horta, Gloria, S129 ([THU-322-YI](#))
Hortelano-Hernandez, Nazaret,
S432 ([FRI-523](#))
Horvath, Angela, S229 ([FRI-115](#)),
S284 ([WED-551](#))
Horwitz, Robyn, S689 ([WED-501](#))
Hosgood, Sarah, S81 ([LBP-008](#))
Hoshida, Yujin, S17 ([OS-013](#)), S42 ([OS-061](#))
Ho, Shinn-Ying, S449 ([THU-480](#))
Hosking, Joanne, S250 ([SAT-107-YI](#))
Ho So, Young, S487 ([FRI-261-YI](#))
Hossain, Sabir, S700 ([FRI-171](#))
Hosseini-Tabatabaei, Azadeh, S4 ([GS-006](#)),
S72 ([OS-119](#))
Hoste, Eric, S631 ([THU-020-YI](#))
Ho, Steve, S261 ([TOP-564](#))
Hotho, Daphne M., S309 ([THU-100](#))
Houghton, David, S297 ([SAT-165-YI](#))
Hou, Hypatia, S507 ([TOP-289](#))
Hou, Jinlin, S26 ([OS-030](#)), S86 ([LBP-019](#)),
S95 ([LBP-037](#)), S99 ([LBP-043](#)),
S797 ([WED-397](#)), S807 ([WED-365](#)),
S812 ([WED-378](#))
Hou, Lifang, S395 ([SAT-479-YI](#))
Hou, Ming-Chih, S256 ([SAT-125](#)),
S398 ([SAT-484](#)), S449 ([THU-479](#)),
S663 ([WED-438-YI](#))
Hountondji, Lina, S115 ([SAT-306](#))
Hourri, Inbal, S320 ([THU-121](#))
Hou, Ruixue, S696 ([FRI-161](#)), S698 ([FRI-164](#))
Houssaina, Jlassi, S270 ([THU-554](#))
Houssel-Debry, Pauline, S54 ([OS-084-YI](#)),
S116 ([SAT-315](#)), S369 ([SAT-010](#)),
S383 ([SAT-043](#)), S385 ([SAT-048](#))
Housset, Chantal, S5 ([GS-007](#))
Hove, Jens, S555 ([WED-331-YI](#))
Hovingh, Milaine, S573 ([THU-224](#))
Hov, Johannes R., S22 ([OS-023-YI](#)),
S50 ([OS-076-YI](#))
Howarth, Rachel, S629 ([THU-008](#)),
S629 ([THU-009](#))
Howel, Denise, S297 ([SAT-165-YI](#))
Howell, Jess, S776 ([FRI-403](#))
Howell, Jessica, S402 ([SAT-496](#))

- Howson, Joanna, S135 (THU-343)
Hoylan, Fernandez, S368 (SAT-009)
Hoyle, Henry, S294 (SAT-154-YI)
Hoyo, Jordi, S541 (WED-284-YI)
Hristopoulos, George, S816 (WED-389)
Hruška, Pavel, S134 (THU-340-YI)
Hsieh, Chia Ling, S662 (WED-434)
Hsieh, Meng-Hsuan, S490 (FRI-271), S493 (FRI-280)
Hsieh, Meng Lun, S662 (WED-434)
Hsieh, Ming-Yen, S490 (FRI-271), S493 (FRI-280)
Hsieh, Ping-Han, S256 (SAT-125)
Hsieh, Sen-Yung, S284 (WED-550)
Hsieh, Tsai-Yuan, S832 (THU-365)
Hsieh, Vivian Chia-Rong, S662 (WED-434)
Hsieh, Yi-Chung, S414 (FRI-458), S491 (FRI-274), S784 (FRI-426)
Hsu, Chao-Wei, S26 (OS-031), S772 (FRI-391)
Hsu, Cheng Er, S784 (FRI-426)
Hsu, Heather, S571 (THU-219), S616 (SAT-233)
Hsu, Po-Yao, S490 (FRI-271), S493 (FRI-280)
Hsu, Ricky, S799 (WED-405)
Hsu, Wei-Fan, S51 (OS-078-YI)
Hsu, Yao-Chun (Holden), S74 (OS-121), S79 (LBP-005), S86 (LBP-019), S795 (WED-393)
Htun Oo, Ye, S356 (SAT-546), S360 (SAT-558)
Hu, Airong, S605 (SAT-198)
Hualde, Leticia Ceberia, S693 (FRI-153)
Huang, Ang, S124 (SAT-336)
Huang, Cheng, S816 (WED-389)
Huang, Chia-Sheng, S832 (THU-365)
Huang, Chien-Hao, S158 (THU-052), S167 (THU-078), S414 (FRI-458)
Huang, Chien-Wei, S832 (THU-365)
Huang, Chung-Feng, S490 (FRI-271), S493 (FRI-280), S832 (THU-365)
Huang, Daniel, S139 (SAT-256), S147 (SAT-281), S366 (TOP-004), S478 (FRI-236-YI), S522 (WED-235), S540 (WED-282)
Huang, Emily, S131 (THU-330)
Huang, Fung Yu, S424 (FRI-490-YI)
Huang, Heqing, S826 (THU-407)
Huang, Hongyang, S419 (FRI-473)
Huang, Jee-Fu, S490 (FRI-271), S493 (FRI-280), S832 (THU-365)
Huang, Jian, S121 (SAT-330), S466 (FRI-207-YI), S495 (FRI-286)
Huang, Jianyong, S141 (SAT-261)
Huang, Jinyu, S102 (LBP-048)
Huang, Ming, S447 (THU-475)
Huang, Mingxing, S526 (WED-246)
Huang, Pei-Lin, S658 (WED-425)
Huang, Pinzhu, S129 (THU-322-YI)
Huang, Qi, S749 (SAT-402)
Huang, Qiya, S605 (SAT-198)
Huang, Rui, S135 (THU-343), S230 (FRI-118), S233 (FRI-127), S628 (FRI-035), S780 (FRI-411-YI)
Huang, Shang-Chin, S399 (SAT-486)
Huang, Ting, S66 (OS-107-YI)
Huang, Vera, S727 (TOP-357)
Huang, Xi, S280 (WED-541)
Huang, Xiaohong, S198 (WED-124), S359 (SAT-556-YI)
Huang, Xiaoquan, S106 (FRI-322), S242 (SAT-081), S268 (THU-546), S275 (WED-524-YI)
Huang, Xingyue, S118 (SAT-320)
Huang, Yan, S26 (OS-030), S803 (WED-412)
Huang, Yanfang, S775 (FRI-398)
Huang, Yi-Hsiang, S51 (OS-078-YI), S69 (OS-112-YI), S398 (SAT-484), S443 (THU-464), S445 (THU-471-YI), S449 (THU-479), S449 (THU-480), S663 (WED-438-YI), S832 (THU-365)
Huang, Yi-Wen, S75 (OS-123)
Huang, Yongfeng, S625 (FRI-021)
Huang, Yun, S47 (OS-072-YI)
Hua, Rui, S26 (OS-030)
Huber, Samuel, S24 (OS-027-YI), S64 (OS-101-YI), S278 (WED-534), S350 (SAT-531-YI)
Hubers, Lowiek, S301 (SAT-178-YI)
Hu, Caixia, S357 (SAT-548)
Hucke, Florian, S52 (OS-079-YI)
Hueffner, Lucas, S730 (TOP-369)
Huelin, Patricia, S765 (FRI-373)
Hufnagel, Franziska, S104 (TOP-352), S134 (THU-340-YI)
Hughes, David, S275 (WED-525)
Hughes, Sarah, S523 (WED-236-YI)
Hugo, Susan, S756 (SAT-421)
Huguet-Pradell, Júlia, S411 (TOP-507-YI), S417 (FRI-467)
Hu, Guoxin, S605 (SAT-198)
Huh, Gunn, S323 (THU-128)
Hui, Chee, S92 (LBP-030)
Huijckman, Nicolette, S573 (THU-224)
Hui Lim, Wen, S147 (SAT-281)
Hui, Rex Wan-Hin, S739 (SAT-375), S770 (FRI-388), S810 (WED-373-YI)
Hui, Vicki Wing-Ki, S150 (SAT-292), S770 (FRI-387)
Hu, Jing, S526 (WED-246)
Hu, Jinhua, S158 (THU-052), S167 (THU-078)
Hu, Jinpeng, S526 (WED-246)
Hu, Jui-Ting, S75 (OS-123), S832 (THU-365)
Hu, Leiping, S344 (THU-191)
Hull, Diana, S101 (LBP-046), S332 (THU-160)
Hul, Noémi K. M. Van, S697 (FRI-163-YI)
Hulthe, Johannes, S550 (WED-316)
Hum, Dean, S171 (THU-088), S191 (WED-105)
Hu, Meiqian, S117 (SAT-318)
Hu, Michael, S89 (LBP-025)
Hummel, Daryin, S669 (WED-453)
Hundertmark, Jana, S414 (FRI-457)
Hung, Chao-Hung, S832 (THU-365)
Hung, Chih-Lung, S795 (WED-393)
Hung, Kuo-Chan, S58 (OS-090)
Hung, Ya-Wen, S449 (THU-479)
Hunnicut, Jake, S476 (FRI-232), S485 (FRI-258)
Hunter, Robert W., S145 (SAT-274)
Hunt, Hazel J., S613 (SAT-224)
Hunyady, Peter, S203 (FRI-039)
Huot-Marchand, Philippe, S608 (SAT-206)
Huo, Yong, S100 (LBP-045)
Hupa-Breier, Katharina Luise, S226 (FRI-107-YI), S226 (FRI-109), S583 (THU-256)
Hu, Peng, S87 (LBP-021), S209 (FRI-053)
Hupfer, Yvonne, S600 (THU-314)
Hur, Moon Haeng, S457 (THU-515), S517 (WED-221), S601 (TOP-204), S774 (FRI-397)
Hu, Rong, S87 (LBP-021)
Hurtado, Juan Carlos, S765 (FRI-373)
Husa, Petr Jr, S756 (SAT-422)
Husa, Petr Sr, S756 (SAT-422)
Hu, Sile, S135 (THU-343)
Huskens, Dana, S178 (WED-068-YI)
Husria, Younes, S734 (SAT-361)
Hussain, Lorraine, S641 (SAT-433)
Hussain, Monira, S653 (SAT-464-YI)
Hussain, Nasir, S309 (THU-099-YI), S332 (THU-160), S472 (FRI-220-YI)
Hussain, Qaiser, S686 (WED-494)
Hussain, Samina Ajaz, S4 (GS-006), S72 (OS-119)
Hussain, Sophia, S489 (FRI-269)
Husseini, Kinan El, S54 (OS-084-YI)
Hussen, Ahmed, S781 (FRI-414)
Huth, Olivia, S692 (FRI-151)
Hutsch, Tomasz, S304 (SAT-184)
Hu, Tsung-Hui, S809 (WED-371)
Huu, Boi Hoan Phan, S552 (WED-320)
Hu, Wanchao, S130 (THU-327), S136 (THU-347-YI)
Hu, Weiyue, S531 (WED-258)
Hu, Wenhao, S447 (THU-475)
Hu, Wenxin, S740 (SAT-377)
Hu, Xiaoxiong, S526 (WED-246)
Hu, Xinyu, S459 (TOP-307), S625 (FRI-022)
Hu, Yue, S602 (TOP-217)
Hvid, Henning, S581 (THU-248)
Hwang, Carey, S75 (OS-127)
Hwang, Jae-Seok, S112 (FRI-341)
Hwang, Sangyoun, S457 (THU-516)
Hyams, Kate, S639 (SAT-427-YI)
Hydes, Theresa, S506 (TOP-277)
Hyon Park, Jae, S410 (SAT-526)
Hyun Oh, Joo, S152 (SAT-296)
Hyun Sohn, Joo, S152 (SAT-296), S477 (FRI-234)
Jacob, Razvan, S343 (THU-186)
Jacob, Speranta, S343 (THU-186)
Iacone, Roberto, S25 (OS-029), S31 (OS-040-YI)
Iadanza, Giorgia, S213 (FRI-070-YI)
Iannaccone, Matteo, S35 (OS-048)
Iannetta, Marco, S59 (OS-094), S772 (FRI-392-YI)

Author Index

- Iannone, Giulia, S206 (FRI-047-YI), S215 (FRI-078-YI)
- Iaria, Chiara, S557 (WED-336)
- Iavarone, Massimo, S42 (OS-061), S396 (SAT-481-YI), S397 (SAT-482), S401 (SAT-493-YI), S413 (FRI-456), S438 (THU-446)
- Ibañez-Samaniego, Luis, S70 (OS-115), S596 (THU-296), S640 (SAT-429)
- Ibdah, Jamal, S563 (THU-195)
- Ibidapo-Obe, Oluwatomi, S229 (FRI-116), S351 (SAT-534), S357 (SAT-549)
- Iborra, Ignacio, S192 (WED-107)
- Iborra, Mireia Antón, S741 (SAT-381)
- Ibrahim, Wafaa, S378 (SAT-029)
- Ichaï, Philippe, S156 (TOP-108), S378 (SAT-029)
- Ichart, Xavier, S45 (OS-068)
- Ichiki, Yasunori, S42 (OS-062)
- Ichimoto, Keiko, S118 (SAT-319)
- Idikut, Aytekin, S224 (FRI-104)
- Idilman, Ramazan, S161 (THU-058), S208 (FRI-053), S219 (FRI-088), S336 (THU-171), S407 (SAT-519), S479 (FRI-238), S785 (FRI-427)
- Ido, Akio, S828 (THU-413)
- Iebba, Valerio, S280 (WED-540-YI)
- Iegri, Claudia, S175 (TOP-085)
- Ielasi, Luca, S395 (SAT-477-YI), S446 (THU-472-YI)
- Ieluzzi, Donatella, S96 (LBP-038), S306 (THU-093), S700 (FRI-171)
- Ieni, Antonio, S740 (SAT-378)
- Ierardi, Anna Maria, S396 (SAT-481-YI)
- Igbaria, Saleh, S645 (SAT-442)
- Iglesias, Ainhoa, S112 (FRI-343-YI), S419 (FRI-472-YI), S569 (THU-210)
- Iglesias, Estefania Huergo, S176 (WED-055)
- Iglseder, Bernhard, S500 (FRI-303)
- Ignacio Fortea, Jose, S238 (SAT-069)
- Ignat, Mina, S144 (SAT-273-YI), S151 (SAT-294)
- Ignatova, Simone, S530 (WED-255-YI)
- Ihli, Franziska, S298 (SAT-166)
- Ijzermans, Jan, S394 (SAT-474)
- Ikegami, Tadashi, S537 (WED-273)
- Ikegami, Toru, S374 (SAT-021)
- Iker, Robin, S762 (FRI-365-YI)
- Ikeuchi, Kazuhiko, S589 (THU-275)
- Ikram, Arfan, S606 (SAT-200-YI)
- Iliescu, Laura, S211 (FRI-058), S221 (FRI-092), S324 (THU-131), S410 (SAT-528), S446 (THU-473), S819 (THU-382)
- Il Kim, Ha, S477 (FRI-234)
- Illescas, Marta, S691 (WED-516)
- Iloabachie, Chidi, S403 (SAT-498)
- Ilyas, Sumera I., S52 (OS-079-YI)
- Imade, Godwin, S395 (SAT-479-YI)
- Imai, Yusuke, S711 (WED-154), S722 (WED-184)
- Imajo, Kento, S541 (WED-283)
- Imam, Achraf, S563 (THU-194)
- Imam, Ashraf, S95 (LBP-035), S779 (FRI-408)
- Imam, Hasan, S812 (WED-376)
- Imamura, Michio, S42 (OS-061)
- Imerzoukene, Ghiles, S109 (FRI-333)
- Im, Yu Ri, S656 (TOP-460-YI)
- Incalzi, Raffaele Antonelli, S554 (WED-325-YI), S754 (SAT-418)
- Incicco, Simone, S28 (OS-035-YI), S30 (OS-038-YI), S199 (TOP-062), S200 (TOP-064-YI), S212 (FRI-068), S224 (FRI-101-YI), S243 (SAT-083-YI), S830 (THU-420)
- Indelicato, Elisabetta, S722 (WED-183-YI)
- Inderson, Akin, S317 (THU-115-YI)
- Indulti, Federica, S62 (OS-099-YI), S258 (SAT-131)
- Infantes-Fontán, Rocío, S596 (THU-296)
- Infantino, Giuseppe, S503 (FRI-317), S609 (SAT-209-YI)
- Ingiliz, Patrick, S470 (FRI-215-YI), S648 (SAT-449), S743 (SAT-386-YI), S784 (FRI-425), S786 (FRI-431)
- Inglese, Elvira, S700 (FRI-171)
- Ingravallo, Angelica, S62 (OS-099-YI)
- Ingre, Michael, S312 (THU-104), S635 (THU-034-YI)
- Inkmann, Michael, S245 (SAT-089)
- Innocenti, Tommaso, S342 (THU-184)
- Inoue, Masanori, S123 (SAT-335), S247 (SAT-095)
- Insinna, Rosario, S671 (WED-457-YI)
- Insonere, Jean-Louis-Marie, S47 (OS-071-YI)
- Invernizzi, Federica, S341 (THU-182), S367 (SAT-007-YI), S388 (SAT-056)
- Invernizzi, Pietro, S5 (GS-007), S19 (OS-017), S80 (LBP-006), S96 (LBP-038), S299 (SAT-171), S306 (THU-093), S310 (THU-101), S325 (THU-133-YI), S335 (THU-167), S422 (FRI-481)
- Ioanitorescu, Simona, S211 (FRI-058), S410 (SAT-528), S446 (THU-473)
- Ioannou, George, S147 (SAT-281)
- Iott, Christina, S26 (OS-031), S809 (WED-371)
- Iovanna, Juan, S601 (TOP-193)
- Ippolito, Davide, S325 (THU-133-YI)
- Iqbal, Iffat, S19 (OS-018), S305 (TOP-169)
- Iqbal, Shahed, S462 (FRI-195)
- Iqbal, Tariq, S309 (THU-099-YI)
- Iraola-Guzman, Susana, S337 (THU-172)
- Iredahl, Fredrik, S532 (WED-259)
- Irfan, Muhammad, S686 (WED-494)
- Irigaray-Miramón, Ainara, S287 (FRI-538), S348 (FRI-555)
- Irizar, María Esther, S112 (FRI-343-YI)
- Iruzubieta, Paula, S468 (FRI-211), S469 (FRI-213), S640 (SAT-429), S700 (FRI-171), S717 (WED-172)
- Irving, William, S12 (OS-004)
- Isabel Lucena, Maria, S107 (FRI-324)
- Isac, Teodora, S211 (FRI-058)
- Isakov, Vasily, S643 (SAT-438)
- Iserte, Gemma, S444 (THU-467-YI), S455 (THU-500)
- Ishida, Yuji, S128 (THU-319), S288 (FRI-540), S735 (SAT-364)
- Ishikawa, Toru, S248 (SAT-101), S616 (SAT-236)
- Ishiy, Crysthiane, S567 (THU-203)
- Isik, Elvan, S211 (FRI-067), S336 (THU-171), S805 (WED-419)
- Ismail, Mona, S548 (WED-305), S549 (WED-315)
- Ismail, Mona H, S671 (WED-458)
- Israel, Robert, S212 (FRI-069)
- Israelsen, Mads, S41 (OS-059), S47 (OS-072-YI), S77 (OS-126), S137 (SAT-250), S139 (SAT-255), S142 (SAT-266), S153 (SAT-298), S205 (FRI-045), S466 (FRI-206-YI), S510 (WED-199), S620 (TOP-012), S623 (FRI-017)
- Issoufaly, Tazime, S180 (WED-071)
- İstemihan, Zülal, S336 (THU-171), S377 (SAT-028), S551 (WED-318-YI), S803 (WED-413)
- Istrate, Mircea, S221 (FRI-092), S324 (THU-131), S410 (SAT-528)
- Itoh, Yoshito, S537 (WED-273), S828 (THU-413)
- Ito, Takanori, S118 (SAT-319)
- Ito, Takashi, S368 (SAT-009), S375 (SAT-023)
- Itti, Emmanuel, S453 (THU-494)
- Iturbe-Rey, Santiago, S536 (WED-271)
- Ivanchuk, Oleksandr, S499 (FRI-298)
- Ivanics, Tommy, S381 (SAT-037)
- Ivashkin, Vladimir, S30 (OS-038-YI), S199 (TOP-062), S200 (TOP-064-YI)
- Iv, A. Sidney Barritt, S403 (SAT-498)
- Ivey, Kerry, S275 (WED-526)
- Iwaki, Michihiro, S235 (FRI-130), S537 (WED-273), S541 (WED-283)
- Iwakiri, Katsuhiko, S248 (SAT-101), S616 (SAT-236)
- Iwamoto, Naoki, S692 (FRI-151)
- Iwasa, Motoh, S248 (SAT-101)
- Iwasawa, Kentaro, S302 (SAT-180)
- Iwuji, Collins, S753 (SAT-413)
- Iyengar, Anushree, S326 (THU-135)
- Iyengar, Sowmya, S149 (SAT-290-YI), S440 (THU-456), S454 (THU-498), S701 (FRI-173), S720 (WED-180)
- Iyer, Shridhar, S540 (WED-282)
- Izadi, Hooshang, S639 (SAT-427-YI)
- Izaguirre, José Raúl, S627 (FRI-029)
- Izai, Ryo, S123 (SAT-335)
- Izbéki, Ferenc, S311 (THU-103)
- Izmailyan, Sergey, S819 (THU-382)
- Izquierdo-Bueno, Pedro, S9 (LBO-004), S89 (LBP-026)
- Izquierdo-García, Elsa, S694 (FRI-153)
- Izquierdo-Sánchez, Laura, S286 (WED-558)
- Izquierdo-Sánchez, Laura, S32 (OS-042-YI), S50 (OS-076-YI), S295 (SAT-159-YI), S419 (FRI-472-YI), S536 (WED-271)

- Izquierdo, Sonia, S818 (THU-381)
- Izumi, Namiki, S626 (FRI-026)
- Izzi, Antonio, S96 (LBP-038), S175 (TOP-085), S306 (THU-093), S666 (WED-446)
- Izzy, Manhal, S595 (THU-293)
- Jaber, Samir, S156 (TOP-108)
- Jachs, Mathias, S28 (OS-034), S61 (OS-096-YI), S73 (OS-120), S156 (TOP-097-YI), S165 (THU-071), S166 (THU-075-YI), S242 (SAT-080-YI), S243 (SAT-086-YI), S250 (SAT-105), S251 (SAT-111), S253 (SAT-117), S253 (SAT-118), S255 (SAT-122), S257 (SAT-128), S621 (FRI-009-YI), S717 (WED-171), S773 (FRI-394), S793 (WED-391), S814 (WED-383), S818 (THU-381)
- Jack, Kathryn, S12 (OS-004)
- Jackson, Christine, S700 (FRI-171)
- Jackson, Edward, S524 (WED-238)
- Jacobs, Jon, S131 (THU-330)
- Jacobs, Maria, S373 (SAT-018-YI)
- Jacobson, Ira, S20 (OS-019), S86 (LBP-019), S788 (FRI-435), S797 (WED-397)
- Jacobs, Thomas, S278 (WED-534)
- Jacob, Torid, S258 (SAT-130)
- Jacquemin, Emmanuel, S307 (THU-094)
- Jacques, Carrietta, S58 (OS-090)
- Jacques, Sophie, S432 (FRI-525)
- Jadlowiec, Caroline, S152 (SAT-297)
- Jaekel, Elmar, S21 (OS-021-YI), S44 (OS-066-YI), S381 (SAT-037), S381 (SAT-039), S583 (THU-256)
- Jaekers, Joris, S125 (TOP-328-YI)
- Jaeschke, Hartmut, S109 (FRI-333)
- Jafarian, Ali, S387 (SAT-053)
- Jaffe, Aron, S58 (OS-090)
- Jafri, Syed-Mohammed, S84 (LBP-014), S374 (SAT-021)
- Jafri, Wasim, S158 (THU-052), S167 (THU-078)
- Jagdish, Rukmini, S656 (TOP-460-YI)
- Jagst, Michelle, S732 (SAT-341)
- Jaillais, Anais, S367 (TOP-005)
- Jaimes, Shiny, S672 (WED-459-YI)
- Jain, Harsh, S248 (SAT-099-YI)
- Jain, Swachi, S411 (SAT-530)
- Jaisinghani, Ruchika, S564 (THU-198)
- Jakhar, Deepika, S67 (OS-108-YI), S176 (WED-056), S181 (WED-076)
- Jalal, Prasun, S9 (LBO-004), S89 (LBP-026), S384 (SAT-045)
- Jalan, Rajiv, S9 (LBO-004), S17 (OS-014-YI), S47 (OS-071-YI), S48 (OS-073), S83 (LBP-012), S89 (LBP-026), S157 (THU-050), S159 (THU-055), S161 (THU-057-YI), S174 (TOP-084), S179 (WED-069), S182 (WED-078), S182 (WED-080), S184 (WED-083), S188 (WED-098-YI), S188 (WED-099-YI), S193 (WED-111), S202 (TOP-066-YI), S588 (THU-271-YI), S590 (THU-280)
- James, Andrew, S729 (TOP-368)
- James, Linda, S675 (WED-469)
- Jamil, Aqeel, S718 (WED-173)
- Jamil, Khurram, S118 (SAT-320), S165 (THU-074), S240 (SAT-076)
- Jammeh, Kitabu, S782 (FRI-418), S786 (FRI-431)
- Jammu, Anish, S555 (WED-330), S561 (WED-348)
- Janardhan, Sujit, S240 (SAT-076)
- Jancorienne, Ligita, S678 (WED-474)
- Janczewska, Ewa, S79 (LBP-005), S172 (THU-092), S685 (WED-493-YI), S813 (WED-379), S821 (THU-389), S834 (THU-367-YI)
- Janczyk, Wojciech, S328 (THU-152-YI), S578 (THU-238), S712 (WED-160)
- Jandrain, Bernard, S615 (SAT-231)
- Jang, Byoung Kuk, S112 (FRI-341), S457 (THU-516)
- Jang, Eun Chul, S152 (SAT-296), S473 (FRI-223), S553 (WED-323), S654 (SAT-465)
- Jang, Eun Sun, S74 (OS-121)
- Jang, Heejoon, S532 (WED-260)
- Jang, Helena, S341 (THU-182)
- Jang, Jae Young, S652 (SAT-458)
- Jang, Jeong Won, S264 (THU-530)
- Jang, Suk-Chan, S657 (WED-424)
- Jang, Tyng-Yuan, S490 (FRI-271), S493 (FRI-280)
- Janicko, Martin, S29 (OS-036-YI), S157 (THU-050), S161 (THU-057-YI), S188 (WED-098-YI)
- Janičko, Martin, S539 (WED-279)
- Janik, Maciej, S44 (OS-066-YI), S238 (SAT-068), S328 (THU-152-YI), S335 (THU-167), S338 (THU-175-YI), S374 (SAT-021)
- Janjua, Naveed, S40 (OS-058), S659 (WED-429), S686 (WED-495), S824 (THU-399-YI)
- Jankowska, Irena, S374 (SAT-021)
- Janmohamed, Ashnila, S101 (LBP-046)
- Janocha-Litwin, Justyna, S685 (WED-493-YI), S821 (THU-389), S834 (THU-367-YI)
- Janowski, Kamil, S328 (THU-152-YI)
- Jansen, Christian, S259 (SAT-135)
- Jansen, Louis, S763 (FRI-367)
- Janshoff, Saskia, S730 (TOP-369)
- Janssen, Harry, S731 (SAT-337), S810 (WED-372)
- Janssen, Harry L.A., S49 (OS-075-YI), S308 (THU-098), S309 (THU-100), S314 (THU-109), S319 (THU-120-YI), S327 (THU-138), S464 (FRI-200), S467 (FRI-209), S606 (SAT-200-YI), S643 (SAT-437-YI), S646 (SAT-443), S649 (SAT-453), S652 (SAT-462-YI), S730 (TOP-384-YI), S758 (TOP-401-YI), S761 (FRI-363-YI), S763 (FRI-367), S764 (FRI-372), S771 (FRI-390), S797 (WED-397)
- Jan, Zehnder, S393 (SAT-473)
- Janzen, Juliana, S58 (OS-092)
- Janz, Malte, S203 (FRI-039)
- Jara, Lorena, S391 (TOP-512-YI)
- Jara, Maximilian Kurt, S79 (LBP-003)
- Jarboui, Mohamed Ali, S134 (THU-340-YI)
- Jarčuška, Peter, S29 (OS-036-YI), S779 (FRI-408)
- Jarman, Edward, S416 (FRI-463-YI)
- Jarman, Georgeina L., S373 (SAT-018-YI)
- Jaroszewicz, Jerzy, S685 (WED-493-YI), S821 (THU-389), S834 (THU-367-YI)
- Jarumanokul, Roongrueng, S396 (SAT-480-YI), S410 (SAT-529)
- Jarvis, James, S281 (WED-542-YI)
- Jaster, Alain, S197 (WED-123)
- Jáuregui, Estrella Petrina, S694 (FRI-153)
- Javanbakht, Hassan, S78 (LBP-001), S352 (SAT-536), S808 (WED-366), S811 (WED-374)
- Javed, P, S158 (THU-052), S167 (THU-078)
- Jaworski, Jakub, S676 (WED-471), S759 (TOP-417)
- Jayanti, Sri, S792 (FRI-444)
- Jayasekera, Channa, S152 (SAT-297)
- Jayathilaka, Bishma, S92 (LBP-030)
- Jeanne, Sakina Sayah, S191 (WED-105)
- Jeannin, Sophie, S37 (OS-051), S504 (TOP-253), S518 (WED-223)
- Jeddou, Heithem, S383 (SAT-043)
- Jeff, Morcet, S714 (WED-162)
- Jegodzinski, Lina, S582 (THU-254-YI)
- Jekle, Andreas, S728 (TOP-358-YI)
- Jelleschitz, Julia, S279 (WED-538-YI)
- Jenab, Mazda, S275 (WED-525)
- Jeng, Rachel Wen-Juei, S414 (FRI-458), S491 (FRI-274), S656 (TOP-461-YI), S772 (FRI-391)
- Jenkins, Timothy, S707 (WED-133)
- Jenne, Craig, S112 (FRI-342)
- Jensen, Anne-Sofie Houlberg, S529 (WED-250-YI)
- Jensen, Ellen Lyngbeck, S77 (OS-126), S139 (SAT-255), S142 (SAT-266), S620 (TOP-012)
- Jensen, Lars Juhl, S47 (OS-072-YI)
- Jensen, Lise Flyger Walther, S574 (THU-227)
- Jensen, Morten Daniel, S399 (SAT-487-YI)
- Jensen, Rasmus Tanderup, S47 (OS-072-YI)
- Jeong, Boryeong, S437 (TOP-489-YI)
- Jeong, Dahn, S40 (OS-058), S659 (WED-429), S686 (WED-495), S824 (THU-399-YI)
- Jeong, Heon Se, S323 (THU-128)
- Jeong, Jae Yoon, S223 (FRI-099), S766 (FRI-375)
- Jeong, Jin-Ju, S602 (TOP-216)
- Jeong, Won-il, S132 (THU-332-YI)
- Jeong, Yun Seong, S68 (OS-111)
- Jeon, Jihae, S669 (WED-453)
- Jepsen, Peter, S149 (SAT-286-YI), S236 (FRI-134), S244 (SAT-088), S399 (SAT-487-YI)
- Jerez, Melissa, S195 (WED-117)

Author Index

- Jermutus, Lutz, S535 ([WED-270](#))
 Jerzowski, John, S27 ([OS-033](#)),
 S100 ([LBP-044](#)), S808 ([WED-367](#))
 Jeschke, Matthias, S443 ([THU-465-YI](#))
 Jesús Perugorria, María, S536 ([WED-271](#))
 Jeyanesan, Dhaarica, S185 ([WED-088-YI](#)),
 S227 ([FRI-112](#)), S700 ([FRI-171](#))
 Jeylan, Asiya, S781 ([FRI-414](#))
 Jezequel, Caroline, S383 ([SAT-043](#))
 Jha, Ashish Kumar, S158 ([THU-052](#)),
 S167 ([THU-078](#))
 Jhajharia, Ashok, S239 ([SAT-070](#))
 Jhaveri, Ajay, S219 ([FRI-088](#))
 Jia, Catherine, S505 ([TOP-264](#))
 Jia, Guiquan, S354 ([SAT-541](#))
 Jia, Jidong, S158 ([THU-052](#)), S228 ([FRI-114](#)),
 S815 ([WED-386](#)), S816 ([WED-388](#))
 Jia, Jingquan, S394 ([SAT-476](#))
 Jiang, Chao, S780 ([FRI-411-YI](#))
 Jiang, Jing, S105 ([FRI-319](#)), S108 ([FRI-330](#)),
 S117 ([SAT-318](#)), S345 ([FRI-546](#))
 Jiang, Lei, S102 ([LBP-048](#))
 Jiang, Longfeng, S106 ([FRI-323](#)),
 S354 ([SAT-542](#))
 Jiang, Ning, S775 ([FRI-398](#))
 Jiang, Siyu, S106 ([FRI-322](#))
 Jiang, Tingting, S145 ([SAT-275](#)),
 S344 ([THU-191](#)), S355 ([SAT-544](#)),
 S815 ([WED-387](#))
 Jiang, Wei, S494 ([FRI-285](#)), S499 ([FRI-302](#))
 Jiang, Weimin, S527 ([WED-246](#))
 Jiang, Xiaoyu, S595 ([THU-293](#))
 Jiang, Xuan, S440 ([THU-455](#))
 Jiang, Xuanwei, S620 ([TOP-006](#))
 Jiang, Xuemei, S804 ([WED-415](#))
 Jiang, Yandan, S145 ([SAT-275](#))
 Jiang, Yichong, S235 ([FRI-132](#))
 Jiang, Yiwei, S131 ([THU-331-YI](#))
 Jiang, Yongfang, S219 ([FRI-088](#))
 Jiang, Yue, S403 ([SAT-498](#))
 Jiang, Yuyong, S145 ([SAT-275](#)),
 S344 ([THU-191](#))
 Jiang, Z. Gordon, S128 ([THU-319](#)),
 S129 ([THU-322-YI](#))
 Jiang, Zhenzhou, S111 ([FRI-338](#)),
 S111 ([FRI-339](#))
 Jia, Tingting, S264 ([THU-532](#))
 Jia, Xiaoli, S590 ([THU-279](#))
 Ji, Fanpu, S69 ([OS-112-YI](#))
 Ji, Huoyan, S590 ([THU-280](#))
 Jilkova, Zuzana Macek, S413 ([FRI-455](#)),
 S744 ([SAT-389](#))
 Jiménez, Adrián, S303 ([SAT-183](#))
 Jimenez-Aguero, Raul, S536 ([WED-271](#))
 Jiménez-Aguilar, Juan Manuel,
 S582 ([THU-250-YI](#)), S583 ([THU-257](#)),
 S586 ([THU-263-YI](#)), S594 ([THU-290-YI](#))
 Jiménez, Andrés González,
 S103 ([TOP-350-YI](#))
 Jimenez-Esquivel, Natalia, S160 ([THU-056](#))
 Jiménez-Franco, Andrea,
 S582 ([THU-250-YI](#)), S583 ([THU-257](#)),
 S586 ([THU-263-YI](#)), S594 ([THU-290-YI](#))
 Jiménez-Masip, Alba, S471 ([FRI-219-YI](#))
 Jiménez-Massip, Alba, S468 ([FRI-211](#)),
 S596 ([THU-296](#))
 Jimeno-Maté, Carlota, S779 ([FRI-409](#))
 Jinato, Thananya, S434 ([FRI-530](#)),
 S588 ([THU-273](#)), S591 ([THU-281](#))
 Jindal, Ankur, S6 ([GS-009](#)),
 S164 ([THU-070](#))
 Jing, Jinhua, S234 ([FRI-129](#))
 Jin, Hua, S803 ([WED-412](#))
 Jin, Qin, S590 ([THU-280](#))
 Jin, Xian, S102 ([LBP-048](#))
 Jin, Yanqi, S280 ([WED-541](#))
 Jin, Yi, S182 ([WED-078](#))
 Jirsa, Milan, S335 ([THU-167](#))
 Ji, Xianyou, S100 ([LBP-045](#))
 Ji, Yun, S36 ([OS-050](#))
 Jobson, Timothy, S639 ([SAT-428](#)),
 S687 ([WED-496](#))
 Jochheim, Leonie, S52 ([OS-079-YI](#)),
 S443 ([THU-465-YI](#))
 Jodar, Meritxell, S710 ([WED-153](#))
 Johannes, Chang, S258 ([SAT-130](#))
 Johannessen, Asgeir, S781 ([FRI-414](#)),
 S795 ([WED-394](#))
 Johansen, Pierre, S37 ([OS-052](#)),
 S464 ([FRI-201](#))
 Johansen, Stine, S41 ([OS-059](#)),
 S47 ([OS-072-YI](#)), S77 ([OS-126](#)),
 S137 ([SAT-250](#)), S139 ([SAT-255](#)),
 S142 ([SAT-266](#)), S153 ([SAT-298](#)),
 S205 ([FRI-045](#)), S466 ([FRI-206-YI](#)),
 S510 ([WED-199](#)), S620 ([TOP-012](#)),
 S623 ([FRI-017](#))
 Johansson, Edvin, S550 ([WED-316](#))
 Johansson, Lars, S550 ([WED-316](#))
 John, Binu, S771 ([FRI-389](#))
 John, Christine, S820 ([THU-386-YI](#)),
 S833 ([THU-366](#))
 John, Katharina, S528 ([WED-249](#))
 Johnson, Jeff, S300 ([SAT-175](#)),
 S301 ([SAT-177](#)), S319 ([THU-119](#))
 Johnson, Sarah, S563 ([THU-195](#))
 Jokinen, Mari J., S562 ([TOP-240-YI](#))
 Jokl, Elliot, S67 ([OS-109](#)),
 S265 ([THU-535-YI](#))
 Joly, Dominique, S372 ([SAT-016](#))
 Jonckers, Tim H.M., S732 ([SAT-341](#))
 Jones, Arron, S636 ([THU-045](#))
 Jones, Christopher, S607 ([SAT-202](#)),
 S609 ([SAT-208](#))
 Jones, Christopher R, S676 ([WED-471](#))
 Jones, Christopher R., S759 ([TOP-417](#))
 Jones, David, S80 ([LBP-006](#)), S91 ([LBP-028](#))
 Jones, David E., S91 ([LBP-027](#)),
 S290 ([TOP-147](#)), S297 ([SAT-165-YI](#)),
 S315 ([THU-111](#)), S321 ([THU-125](#)),
 S325 ([THU-132](#))
 Jones, Nathan, S657 ([WED-422](#)),
 S676 ([WED-470](#))
 Jones, Owen, S381 ([SAT-039](#))
 Jones, Pamela, S101 ([LBP-046](#))
 Jones, Rebecca L., S397 ([SAT-483-YI](#))
 Jones, Rhian, S101 ([LBP-046](#))
 Jonigk, Danny, S21 ([OS-021-YI](#))
 Jonker, Johan, S347 ([FRI-549-YI](#)),
 S573 ([THU-224](#))
 Joo, Lucy, S489 ([FRI-268](#))
 Joon Kim, Dong, S167 ([THU-078](#))
 Joo, Saekyung, S532 ([WED-260](#))
 Jopson, Laura, S297 ([SAT-165-YI](#))
 Jördens, Markus S., S33 ([OS-044-YI](#)),
 S262 ([THU-525-YI](#)), S296 ([SAT-163-YI](#))
 Jording-Jespersen, Gregory, S753 ([SAT-413](#))
 Jörg, Vincent, S24 ([OS-027-YI](#)),
 S52 ([OS-079-YI](#))
 Jorquera, Francisco, S45 ([OS-067](#)),
 S277 ([WED-529](#))
 Jose Carrilho, Flair, S161 ([THU-057-YI](#))
 José Herrero, Maria, S741 ([SAT-381](#))
 Joseph Brol, Maximilian, S170 ([THU-087](#)),
 S198 ([WED-126](#))
 Joseph, Merlyn, S400 ([SAT-492](#))
 Jose, Sophie, S406 ([SAT-515](#))
 Joshi, Deepak, S315 ([THU-111](#)),
 S709 ([WED-137-YI](#))
 Joshi, Shilpy, S809 ([WED-370](#))
 Jothamani, Dinesh, S9 ([LBO-004](#)),
 S89 ([LBP-026](#)), S158 ([THU-052](#)),
 S167 ([THU-078](#)), S219 ([FRI-088](#))
 Joubaud, Francoise, S519 ([WED-224](#))
 Jou, Janice, S771 ([FRI-389](#))
 Joung, Hyunhae, S283 ([WED-547](#))
 Jouvin-Marche, Evelyne, S744 ([SAT-389](#)),
 S747 ([SAT-396](#))
 Jovanovic, Emilija, S81 ([LBP-008](#))
 Joven, Jorge, S582 ([THU-250-YI](#)),
 S583 ([THU-257](#)), S586 ([THU-263-YI](#)),
 S594 ([THU-290-YI](#))
 Jover, Ramiro, S45 ([OS-067](#))
 Jowsey-Gregoire, Sheila, S146 ([SAT-279](#))
 Joyner de Sousa Dias Monteiro, Mísia,
 S619 ([SAT-248](#))
 Juanola, Adrià, S13 ([OS-005-YI](#)),
 S30 ([OS-038-YI](#)), S139 ([SAT-257](#)),
 S160 ([THU-056](#)), S176 ([WED-055](#)),
 S199 ([TOP-062](#)), S200 ([TOP-064-YI](#)),
 S503 ([TOP-241-YI](#)), S541 ([WED-284-YI](#)),
 S711 ([WED-155](#))
 Juanola, Oriol, S117 ([SAT-316](#)),
 S194 ([WED-113](#))
 Juan Song, Sherlot, S479 ([FRI-239](#))
 Juárez-Fernández, María, S45 ([OS-067](#)),
 S277 ([WED-529](#))
 Juarez-Rivera, Bibiana Elena, S436 ([FRI-535](#))
 Jucov, Alina, S75 ([OS-127](#)), S78 ([LBP-001](#)),
 S87 ([LBP-020](#)), S806 ([WED-361](#)),
 S807 ([WED-365](#)), S812 ([WED-378](#)),
 S819 ([THU-382](#))
 Judith, Aron-Wisnewskey, S585 ([THU-260](#))
 Juel, Helene Baek, S47 ([OS-072-YI](#))
 Ju, Guomin, S303 ([SAT-181-YI](#))
 Jühling, Frank, S17 ([OS-013](#)), S25 ([OS-029](#)),
 S31 ([OS-040-YI](#)), S42 ([OS-061](#))
 Jukema, J. Wouter, S382 ([SAT-040](#)),
 S492 ([FRI-278](#)), S612 ([SAT-218](#))
 Jula, Antti, S460 ([TOP-308](#)),
 S562 ([TOP-240-YI](#))
 Julian, Judit, S291 ([TOP-149-YI](#))

- Jumat, Nur Halisah Binte, S524 ([WED-238](#))
- Jun, Dae Won, S148 ([SAT-284](#)),
S473 ([FRI-223](#)), S553 ([WED-323](#)),
S654 ([SAT-465](#))
- Juneja, Kavita, S613 ([SAT-224](#))
- Juneja, Pinky, S66 ([OS-106-YI](#)),
S67 ([OS-108-YI](#)), S176 ([WED-056](#)),
S181 ([WED-076](#))
- Jung, Dong-Hwan, S379 ([SAT-032](#))
- Junge, Norman, S712 ([WED-160](#))
- Jung, Il Hoon, S264 ([THU-531](#)),
S576 ([THU-232](#))
- Jung, Jooyi, S468 ([FRI-210](#))
- Jung, Se-Mi, S575 ([THU-230](#))
- Jung, Yong Jin, S487 ([FRI-261-YI](#)),
S532 ([WED-260](#))
- Jung, Young Kul, S596 ([THU-295](#))
- Junien, Jean-Louis, S584 ([THU-258-YI](#)),
S608 ([SAT-206](#))
- Junker, Anders, S513 ([WED-207](#)),
S529 ([WED-250-YI](#)), S555 ([WED-331-YI](#))
- Junker, Lioba, S259 ([SAT-135](#))
- Junot, Christophe, S184 ([WED-083](#))
- Jun Teh, Kevin Kim, S38 ([OS-054](#))
- Jurado-Aguilar, Javier, S574 ([THU-225](#))
- Jura, Jolanta, S265 ([THU-533](#)),
S304 ([SAT-184](#))
- Juran, Brian D., S326 ([THU-135](#))
- Jurgens, Matthias C., S319 ([THU-120-YI](#))
- Jurkiewicz, Elzbieta, S328 ([THU-152-YI](#))
- Jurr, Helen, S169 ([THU-083](#))
- Ju, Shenghong, S536 ([WED-272](#))
- Justo, Mariana, S271 ([THU-556](#))
- Ju, Yuhao, S784 ([FRI-424](#))
- Kabaçam, Gökhan, S374 ([SAT-021](#))
- Kaballo, Moahmmed, S172 ([THU-090](#))
- Kabbaj, Meriam, S171 ([THU-088](#))
- Kabelitz, Martin, S245 ([SAT-090-YI](#))
- Kablawi, Dana, S683 ([WED-486-YI](#))
- Kabore, Christelle, S415 ([FRI-459](#)),
S572 ([THU-220](#))
- Kacprowski, Tim, S735 ([SAT-363](#))
- Kadhefi, Mehdi, S313 ([THU-107](#))
- Kadioglu, Onat, S432 ([FRI-523](#))
- Kado, Akira, S589 ([THU-275](#))
- Kaestner, Klaus, S89 ([LBP-025](#))
- Kaewdech, A., S758 ([TOP-401-YI](#))
- Kaewdech, Apichat, S396 ([SAT-480-YI](#)),
S410 ([SAT-529](#))
- Kafasla, Panagiota, S599 ([THU-306](#))
- Kafentzi, Theodora, S830 ([THU-419](#))
- Kagawa, Tatehiro, S118 ([SAT-319](#))
- Kagbo-Kue, Suaka, S152 ([SAT-297](#))
- Kager, Julianne, S35 ([OS-049-YI](#))
- Kahlhöfer, Julia, S759 ([TOP-416-YI](#))
- Kahl, Sabine, S508 ([WED-195](#))
- Kahn, Steven, S93 ([LBP-032](#))
- Kai, Marco, S358 ([SAT-551](#))
- Kaji, Kosuke, S175 ([TOP-096](#))
- Kajiwara, Eiji, S42 ([OS-062](#))
- Kakazu, Eiji, S695 ([FRI-159](#)),
S828 ([THU-413](#))
- Kakisaka, Keisuke, S118 ([SAT-319](#))
- kakita, naruyasu, S506 ([TOP-288](#))
- Kakrana, Priyanka, S26 ([OS-030](#))
- Kakuda, Thomas, S27 ([OS-033](#)),
S100 ([LBP-044](#))
- Kalafateli, Maria, S830 ([THU-419](#))
- Kalafati, Ioanna-Panagiota,
S508 ([WED-195](#))
- Kalal, Chetan, S158 ([THU-052](#)),
S167 ([THU-078](#))
- Kalamitsis, George, S664 ([WED-440](#)),
S670 ([WED-454-YI](#)), S680 ([WED-478](#))
- Kalista, Kemal Fariz, S158 ([THU-052](#)),
S167 ([THU-078](#))
- Kalix, Leon, S735 ([SAT-363](#))
- Kalka, Iris, S645 ([SAT-442](#))
- Kallenbach, Michael, S392 ([SAT-469](#))
- Kalmyrzaev, Bolot, S682 ([WED-484](#))
- Kalra, Naveen, S152 ([SAT-295](#)),
S217 ([FRI-082](#))
- Kamada, Tomoari, S541 ([WED-283](#))
- Kamada, Yoshihiro, S512 ([WED-203](#)),
S537 ([WED-273](#))
- Kamal, Habiba, S759 ([TOP-416-YI](#)),
S777 ([FRI-406](#)), S785 ([FRI-427](#)),
S836 ([THU-374](#))
- Kamali, Can, S84 ([LBP-015](#))
- Kamal, Mustafa, S621 ([FRI-008](#))
- Kamani, Lubna, S158 ([THU-052](#)),
S167 ([THU-078](#))
- Kamara, Elaine, S724 ([WED-189](#))
- Kamar, Nassim, S763 ([FRI-370](#))
- Kamath, Binita M., S307 ([THU-094](#))
- Kamath, Patrick S., S161 ([THU-058](#)),
S163 ([THU-060](#)), S206 ([FRI-046](#)),
S208 ([FRI-053](#)), S218 ([FRI-086](#)),
S219 ([FRI-088](#))
- Kamimura, Hiroteru, S118 ([SAT-319](#))
- Kaminsky, Elenor, S12 ([OS-002](#))
- Kamkamidze, George, S691 ([WED-515](#))
- Kamlin, C. Omar, S707 ([WED-133](#))
- Kanaloupitis, Stavros, S830 ([THU-419](#))
- Kandasamy, Pachamuthu, S693 ([FRI-151](#))
- Kandulski, Arne, S191 ([WED-106](#))
- Kaneko, Tatsuya, S301 ([SAT-176](#))
- Kang, Beodeul, S69 ([OS-112-YI](#))
- Kang, Bo-Kyeong, S152 ([SAT-296](#)),
S473 ([FRI-223](#)), S553 ([WED-323](#)),
S654 ([SAT-465](#))
- Kang, Hyunsoon, S727 ([TOP-357](#))
- Kang, Jong-Hon, S498 ([FRI-297](#)),
S757 ([WED-421](#))
- Kang, Sang-Hee, S68 ([OS-111](#))
- Kang, Seong Hee, S596 ([THU-295](#))
- Kang, Wonseok, S74 ([OS-121](#)),
S564 ([THU-196](#))
- Kang, Yeo Wool, S501 ([FRI-306](#)),
S552 ([WED-322](#))
- Kania, Dramane, S678 ([WED-475](#))
- Kan, Motoyasu, S301 ([SAT-176](#))
- Kann, Michael, S754 ([SAT-414](#))
- Kannt, Aimo, S104 ([TOP-352](#))
- Kanogawa, Naoya, S123 ([SAT-335](#)),
S247 ([SAT-095](#))
- Kansagra, Kevin, S617 ([SAT-239](#))
- Kansra, Sanjay, S124 ([TOP-313](#)),
S126 ([THU-316](#))
- Kant Mangla, Kamal, S462 ([FRI-196](#)),
S464 ([FRI-201](#)), S477 ([FRI-233](#))
- Kantojärvi, Katri, S562 ([TOP-240-YI](#))
- Kanto, Tatsuya, S695 ([FRI-159](#))
- Kanzaki, Hiroaki, S123 ([SAT-335](#))
- Kao, Chien-Neng, S832 ([THU-365](#))
- Kao, Jia-Horng, S399 ([SAT-486](#)),
S797 ([WED-397](#)), S832 ([THU-365](#))
- Kao, Wei-Yu, S399 ([SAT-486](#))
- Kao, Yu-Ting, S656 ([TOP-461-YI](#))
- Kapel, Benedicte, S574 ([THU-227](#))
- Kaplan, David, S253 ([SAT-116](#))
- Kapoor, Himanshi, S510 ([WED-199](#))
- Kappe, Naomi, S720 ([WED-179-YI](#)),
S721 ([WED-182](#))
- Kappus, Matthew Robert, S219 ([FRI-088](#))
- Kaps, Leonard, S435 ([FRI-533](#)),
S484 ([FRI-255](#))
- Kaptein, Suzanne J.F., S94 ([LBP-034](#)),
S732 ([SAT-340-YI](#)), S732 ([SAT-341](#))
- Karabay, Oğuz, S805 ([WED-418](#))
- Karadağ, Soylu Neşe, S341 ([THU-182](#))
- Karagiannakis, Dimitrios, S798 ([WED-403](#))
- Karakaya, Fatih, S479 ([FRI-238](#))
- Karakulak, Ugur, S224 ([FRI-104](#))
- Kara, Leila, S533 ([WED-262](#))
- Karamchandani, Umesh, S533 ([WED-263](#))
- Karam, Vincent, S373 ([SAT-019](#)),
S386 ([SAT-051](#))
- Karasu, Zeki, S208 ([FRI-053](#)),
S211 ([FRI-067](#)), S336 ([THU-171](#)),
S805 ([WED-419](#))
- Karayel, Sevinc Tugce, S407 ([SAT-519](#)),
S479 ([FRI-238](#))
- Karbannek, Henrik, S244 ([SAT-087-YI](#))
- Karichashvili, Lika, S677 ([WED-473](#))
- Karim, Gres, S252 ([SAT-114](#)),
S487 ([FRI-262](#)), S545 ([WED-295-YI](#)),
S674 ([WED-465](#))
- Karim, Md. Fazal, S158 ([THU-052](#)),
S167 ([THU-078](#))
- Karkossa, Isabel, S104 ([TOP-352](#))
- Karl, Anna, S104 ([TOP-352](#)),
S134 ([THU-340-YI](#))
- Karlen, Vanessa, S338 ([THU-176](#))
- Karlsen, Lars Normann, S795 ([WED-394](#))
- Karlsen, Tom Hemming, S33 ([OS-044-YI](#)),
S50 ([OS-076-YI](#)), S65 ([OS-104](#)),
S294 ([SAT-154-YI](#))
- Karmi, Naomi, S304 ([SAT-185](#))
- Karoney, Mercy, S388 ([SAT-057](#)),
S560 ([WED-342](#)), S820 ([THU-383](#))
- Karpe, Fredrik, S578 ([THU-236-YI](#))
- Kar, Premashis, S609 ([SAT-210](#))
- Kar, Sanjib, S475 ([FRI-231](#)),
S488 ([FRI-266-YI](#))
- Karsdal, Morten, S47 ([OS-072-YI](#)),
S70 ([OS-115](#)), S255 ([SAT-122](#)),
S513 ([WED-207](#)), S579 ([THU-243](#)),
S612 ([SAT-220-YI](#)), S623 ([FRI-017](#)),
S626 ([FRI-027](#)), S737 ([SAT-370](#))
- Karşıdağ, Kubilay, S551 ([WED-318-YI](#))

Author Index

- Karvellas, Constantine, S9 ([LBO-004](#)), S89 ([LBP-026](#)), S156 ([TOP-108](#))
- Kaseb, Ahmed, S68 ([OS-111](#))
- Kaser, Arthur, S81 ([LBP-008](#))
- Kashamuka, Melchior, S668 ([WED-451-YI](#)), S675 ([WED-469](#))
- Kashfi, Farzaneh, S300 ([SAT-174](#))
- Kasi, Phanindra Babu, S349 ([FRI-556](#))
- Kasper, Jonathan, S515 ([WED-212](#)), S517 ([WED-219](#))
- Kasper, Philipp, S223 ([FRI-100](#))
- Kasprian, Gregor, S719 ([WED-175](#))
- Kasraianfard, Amir, S387 ([SAT-053](#))
- Katav, Avi, S268 ([THU-547](#)), S295 ([SAT-158](#))
- Katchman, Helena, S219 ([FRI-088](#)), S237 ([FRI-136](#)), S547 ([WED-303](#))
- Kather, Jakob Nikolas, S19 ([OS-017](#)), S392 ([TOP-520](#)), S427 ([FRI-499-YI](#))
- Katja, Füssel, S5 ([GS-007](#)), S265 ([THU-534-YI](#))
- Kato, Jun, S301 ([SAT-176](#))
- Kato, Keizo, S616 ([SAT-236](#))
- Kato, Naoya, S123 ([SAT-335](#)), S247 ([SAT-095](#)), S301 ([SAT-176](#)), S303 ([SAT-182](#)), S828 ([THU-413](#))
- Katzarov, Krum, S172 ([THU-092](#))
- Katz, Courtney, S17 ([OS-013](#))
- Kauppinen, Sakari, S565 ([THU-199](#))
- Kaur, Amandeep, S340 ([THU-181](#))
- Kaur, Impreet, S66 ([OS-106-YI](#)), S67 ([OS-108-YI](#)), S176 ([WED-056](#))
- Kaur, Parminder, S129 ([THU-324](#)), S152 ([SAT-295](#)), S158 ([THU-051](#)), S217 ([FRI-082](#))
- Kaur, Savneet, S66 ([OS-106-YI](#)), S67 ([OS-108-YI](#)), S176 ([WED-056](#)), S177 ([WED-058-YI](#)), S181 ([WED-076](#)), S188 ([WED-095-YI](#)), S294 ([SAT-155](#)), S346 ([FRI-547-YI](#)), S348 ([FRI-554](#))
- Kaur, Senamjit, S310 ([THU-101](#)), S324 ([THU-130](#))
- Kauschke, Stefan Günther, S197 ([WED-122-YI](#)), S198 ([WED-125](#)), S267 ([THU-540](#)), S589 ([THU-274](#))
- Kaushal, Shruti, S347 ([FRI-550](#))
- Kautz, Achim, S320 ([THU-122](#))
- Kavanagh, Dean, S425 ([FRI-493](#))
- Kavousi, Maryam, S606 ([SAT-200-YI](#))
- Kav, Taylan, S224 ([FRI-104](#))
- Kawada, Norifumi, S261 ([THU-523](#)), S430 ([FRI-518](#)), S828 ([THU-413](#))
- Kawaguchi, Takumi, S147 ([SAT-281](#)), S541 ([WED-283](#))
- Kawai, Hidehiko, S490 ([FRI-272](#))
- Kawamoto, Tomomi, S693 ([FRI-151](#))
- Kawamura, Etsushi, S430 ([FRI-518](#))
- Kawanaka, Miwa, S537 ([WED-273](#)), S541 ([WED-283](#))
- Kawano, Akira, S42 ([OS-062](#))
- Kawano, Tadamichi, S248 ([SAT-101](#)), S616 ([SAT-236](#))
- Kawashima, Keigo, S35 ([OS-048](#))
- Kawata, Kazuhito, S248 ([SAT-101](#)), S537 ([WED-273](#))
- Kaya, Baris, S224 ([FRI-104](#))
- Kayahara, Takahisa, S122 ([SAT-332-YI](#))
- Kayali, Zeid, S544 ([WED-294](#))
- Kaya, Selçuk, S805 ([WED-418](#))
- Kaya, Sibel Yildiz, S805 ([WED-418](#))
- Kayes, Tahrima, S219 ([FRI-088](#))
- Kayhan, Meral Akdogan, S336 ([THU-171](#)), S723 ([WED-187-YI](#))
- Kaymakoglu, Sabahattin, S336 ([THU-171](#)), S377 ([SAT-028](#)), S551 ([WED-318-YI](#)), S803 ([WED-413](#))
- Kaysin, Furkan, S736 ([SAT-366](#))
- Kazanjan, Konstantine, S825 ([THU-404](#))
- Kazennaite, Edita, S678 ([WED-474](#))
- Kazma, Rémi, S26 ([OS-030](#))
- Keating, Shelley, S559 ([WED-340](#)), S631 ([THU-016](#))
- Keaveny, Andrew, S209 ([FRI-053](#))
- Ke, Bibo, S106 ([FRI-323](#)), S354 ([SAT-542](#))
- Kechagias, Stergios, S530 ([WED-255-YI](#)), S532 ([WED-259](#))
- Kedarisetty, Chandan, S158 ([THU-052](#)), S167 ([THU-078](#))
- Keelty, Nigel, S250 ([SAT-107-YI](#))
- Kefalakes, Helenie, S762 ([FRI-365-YI](#))
- Ke, Haoying, S418 ([FRI-471](#))
- Keitel-Anselmino, Verena, S25 ([OS-028](#))
- Keklikkiran, Caglayan, S643 ([SAT-438](#))
- Kelkar, Natasha, S131 ([THU-331-YI](#))
- Keller, Marisa Isabell, S47 ([OS-071-YI](#)), S47 ([OS-072-YI](#)), S48 ([OS-073](#)), S203 ([FRI-039](#)), S272 ([TOP-563](#))
- Kelly, Claire, S388 ([SAT-055](#)), S388 ([SAT-057](#)), S709 ([WED-137-YI](#))
- Kelly, Deirdre, S307 ([THU-094](#))
- Kelly, Gavin, S756 ([SAT-421](#))
- Kelly, Geoff, S281 ([WED-542-YI](#))
- Kelsch, Lara, S187 ([WED-094](#))
- Kemble, George, S4 ([GS-011](#)), S575 ([THU-231](#)), S600 ([THU-336](#))
- Kemeç, Gamze, S551 ([WED-318-YI](#)), S803 ([WED-413](#))
- Kemmer, Nyngi, S9 ([LBO-004](#)), S89 ([LBP-026](#)), S242 ([SAT-082](#))
- Kemper, Angieszka, S687 ([WED-497](#))
- Kempf, Volkhard A. J., S203 ([FRI-039](#))
- Kempt-Kropp, Michael, S314 ([THU-109](#)), S327 ([THU-138](#))
- Kemp, William, S338 ([THU-177-YI](#)), S402 ([SAT-496](#)), S653 ([SAT-464-YI](#))
- Kench, Charlotte, S380 ([SAT-036-YI](#))
- Kendall, Timothy, S56 ([OS-087](#)), S465 ([FRI-203](#))
- Kennedy, James, S219 ([FRI-088](#)), S423 ([FRI-487](#))
- Kennedy, Oliver, S506 ([TOP-277](#))
- Kennedy, Patrick, S59 ([OS-094](#)), S78 ([LBP-001](#)), S350 ([TOP-553](#)), S742 ([SAT-383](#)), S781 ([FRI-413](#)), S813 ([WED-379](#))
- Kenny, Fiona, S128 ([THU-320-YI](#))
- Kent, Christopher, S675 ([WED-469](#)), S752 ([SAT-409](#))
- Kenz, Zackary, S517 ([WED-219](#))
- Ke, Qiao, S260 ([SAT-136](#))
- Keraite, Ieva, S417 ([FRI-467](#))
- Kerbert, Annarein, S161 ([THU-057-YI](#)), S188 ([WED-099-YI](#)), S204 ([FRI-043](#))
- Kerbert-Dreteler, Marjo J., S309 ([THU-100](#))
- Kerins, Caoimhe, S128 ([THU-320-YI](#))
- Kerkar, Nanda, S18 ([OS-015](#))
- Kersten, Remco, S301 ([SAT-178-YI](#))
- Keshi, Eriselda, S84 ([LBP-015](#))
- Keskin, Onur, S224 ([FRI-104](#)), S785 ([FRI-427](#))
- Keski-Rahkonen, Pekka, S275 ([WED-525](#))
- Kessoku, Takaomi, S541 ([WED-283](#))
- Ketkar, Amol, S186 ([WED-090](#))
- Khac, Eric Nguyen, S6 ([GS-010](#)), S61 ([OS-097](#)), S413 ([FRI-456](#)), S444 ([THU-466](#))
- Khachatryan, Artak, S836 ([THU-374](#))
- Khajuria, Rahul, S6 ([GS-009](#))
- Khakayla, Abed, S563 ([THU-194](#)), S779 ([FRI-408](#))
- Khakoo, Salim I, S633 ([THU-027-YI](#)), S676 ([WED-471](#))
- Khakoo, Salim I., S760 ([TOP-417](#))
- Khalailah, Abed, S95 ([LBP-035](#))
- Khaled, Najib Ben, S24 ([OS-027-YI](#)), S52 ([OS-079-YI](#)), S69 ([OS-112-YI](#)), S440 ([THU-457](#)), S458 ([THU-517](#))
- Khalili, Korosh, S49 ([OS-075-YI](#))
- Khalil, Samira Mohamad, S616 ([SAT-237](#))
- Khanam, Arshi, S736 ([SAT-366](#))
- Khan, Muhammad Bilal, S192 ([WED-109](#))
- Khanna, Amardeep, S297 ([SAT-165-YI](#))
- Khan, Pervez Ali, S44 ([OS-065](#))
- Khan, Seema, S216 ([FRI-081](#))
- Khan, Shahid, S406 ([SAT-515](#)), S639 ([SAT-427-YI](#))
- Khan, Sheeba, S5 ([GS-007](#)), S101 ([LBP-046](#))
- Khan, Zaiba, S285 ([WED-554](#))
- Kharbanda, Kusum, S281 ([WED-544](#)), S742 ([SAT-382](#))
- Khattab, Mahmoud, S583 ([THU-255](#))
- Khatua, Chitta Ranjan, S163 ([THU-067](#)), S488 ([FRI-266-YI](#))
- Khazrai, Yeganeh, S554 ([WED-325-YI](#))
- Kheloufi, Lyès, S207 ([FRI-050-YI](#)), S218 ([FRI-087](#)), S222 ([FRI-094-YI](#)), S222 ([FRI-095](#))
- Khemichian, Saro, S242 ([SAT-082](#))
- Kheong, Chan Wah, S38 ([OS-054](#))
- Khine, Htet Htet Toe Wai, S797 ([WED-398](#))
- Khobar, Korri Elvanita El, S792 ([FRI-444](#))
- Khoperia, Anna, S677 ([WED-473](#)), S825 ([THU-404](#))
- Khoruts, Alexander, S1 ([GS-001](#))
- Khosroshahi, Arezou, S710 ([WED-152](#))
- Khoza, Thandeka, S753 ([SAT-413](#))
- Kianmanesh, Reza, S413 ([FRI-456](#))
- Kienast, Patric, S719 ([WED-175](#))
- Kießling, Paul, S33 ([OS-043](#))
- Kijrattanakul, Pitiphong, S221 ([FRI-093](#))
- Kikkert, Marjolein, S700 ([FRI-171](#))
- Kilany, Mai, S758 ([TOP-401-YI](#)), S764 ([FRI-372](#))

- Kilian, Christoph, S278 ([WED-534](#))
 Kiloh, George, S289 ([FRI-542](#))
 Kilpatrick, Alastair M, S14 ([OS-008-YI](#))
 Kilpatrick, Alastair M., S81 ([LBP-007](#)),
 S127 ([THU-317](#)), S130 ([THU-326](#))
 Kim, Aryoung, S402 ([SAT-497](#))
 Kim, Beom Kyung, S290 ([FRI-545](#)),
 S495 ([FRI-287](#)), S498 ([FRI-296](#)),
 S535 ([WED-269](#)), S540 ([WED-282](#)),
 S671 ([WED-456](#)), S767 ([FRI-378](#)),
 S774 ([FRI-396](#)), S774 ([FRI-397](#)),
 S799 ([WED-404](#))
 Kim, Bohyun, S448 ([THU-478](#))
 Kim, Byung Ik, S223 ([FRI-099](#))
 Kim, Byung Seok, S788 ([FRI-433](#))
 Kim, Chang Wook, S167 ([THU-077](#))
 Kim, Chan Yeong, S48 ([OS-073](#))
 Kim, Chong, S666 ([WED-444](#)),
 S773 ([FRI-393](#)), S788 ([FRI-435](#))
 Kim, David, S535 ([WED-269](#))
 Kim, Dong, S683 ([WED-486-YI](#))
 Kim, Donghee, S146 ([SAT-278](#)),
 S478 ([FRI-236-YI](#))
 Kim, Dong Hwan, S448 ([THU-478](#))
 Kim, Dong Joon, S158 ([THU-052](#))
 Kim, Dong-Sik, S459 ([THU-519](#))
 Kim, Dong Yun, S595 ([THU-292](#))
 Kim, Do Young, S290 ([FRI-545](#)),
 S495 ([FRI-287](#)), S498 ([FRI-296](#)),
 S535 ([WED-269](#)), S671 ([WED-456](#)),
 S767 ([FRI-378](#)), S799 ([WED-404](#))
 Kimer, Nina, S513 ([WED-207](#)),
 S529 ([WED-250-YI](#))
 Kim-Fuchs, Corina, S373 ([SAT-019](#))
 Kim, Gi-Ae, S74 ([OS-121](#)), S468 ([FRI-210](#)),
 S657 ([WED-424](#))
 Kim, Gloria, S79 ([LBP-005](#))
 Kim, Ha Il, S148 ([SAT-284](#)), S152 ([SAT-296](#)),
 S473 ([FRI-223](#)), S553 ([WED-323](#)),
 S654 ([SAT-465](#))
 Kim, Hail, S78 ([LBP-002](#))
 Kim, Hee Jin, S323 ([THU-128](#))
 Kim, Hee Yeon, S167 ([THU-077](#)),
 S458 ([THU-518](#))
 Kim, Hong Soo, S247 ([SAT-098](#))
 Kim, Hwi Young, S481 ([FRI-246](#)),
 S774 ([FRI-397](#))
 Kim, Hye-Lin, S152 ([SAT-296](#)),
 S473 ([FRI-223](#)), S553 ([WED-323](#)),
 S654 ([SAT-465](#)), S657 ([WED-424](#))
 Kim, Hyeree, S564 ([THU-196](#))
 Kim, Hyung Heon, S264 ([THU-531](#)),
 S576 ([THU-232](#))
 Kim, Hyung Joon, S74 ([OS-121](#))
 Kim, Hyung Jun, S457 ([THU-516](#))
 Kim, Hyunseok, S39 ([OS-055](#)),
 S200 ([TOP-063](#))
 Kim, In-San, S104 ([TOP-351-YI](#))
 Kim, Ja Kyung, S767 ([FRI-379](#))
 Kim, Jeong Han, S30 ([OS-038-YI](#)),
 S199 ([TOP-062](#)), S200 ([TOP-064-YI](#))
 Kim, Jeong Su, S286 ([WED-557](#))
 Kim, Ji Hoon, S68 ([OS-111](#)), S74 ([OS-121](#)),
 S596 ([THU-295](#))
 Kim, Jin-Wook, S450 ([THU-484](#))
 Kim, Jongman, S379 ([SAT-032](#)),
 S459 ([THU-519](#))
 Kim, Ju Hyun, S542 ([WED-287](#))
 Kim, Jung Hee, S223 ([FRI-099](#))
 Kim, Junghyun, S564 ([THU-196](#))
 Kim, Kang Mo, S305 ([TOP-157](#))
 Kim, Ki-Hun, S459 ([THU-519](#))
 Kim, Kyunghwan, S283 ([WED-547](#))
 Kim, Kyurae, S132 ([THU-332-YI](#))
 Kim, Log Young, S652 ([SAT-458](#))
 Kimmann, Markus, S258 ([SAT-130](#))
 Kim, Mi-Kyung, S112 ([FRI-341](#)),
 S264 ([THU-531](#)), S576 ([THU-232](#))
 Kim, Mi Na, S495 ([FRI-287](#)), S498 ([FRI-296](#)),
 S535 ([WED-269](#)), S671 ([WED-456](#)),
 S767 ([FRI-378](#)), S799 ([WED-404](#))
 Kim, Min Jeong, S132 ([THU-332-YI](#))
 Kim, Min Ju, S286 ([WED-557](#))
 Kim, Moon Young, S136 ([THU-348](#)),
 S602 ([TOP-216](#))
 Kim, Myeong-Jin, S408 ([SAT-522](#))
 Kim, Nam Hoon, S564 ([THU-196](#))
 Kimpel, Janine, S728 ([TOP-359-YI](#))
 Kim, Sang Gyune, S136 ([THU-348](#)),
 S247 ([SAT-098](#)), S602 ([TOP-216](#)),
 S652 ([SAT-458](#)), S767 ([FRI-379](#)),
 S799 ([WED-404](#))
 Kim, Sang Jin, S379 ([SAT-032](#))
 Kim, Sehee, S305 ([TOP-157](#))
 Kim, Seohyun, S104 ([TOP-351-YI](#))
 Kim, Seon-Ok, S437 ([TOP-489-YI](#))
 Kim, Seung Up, S2 ([GS-004](#)), S38 ([OS-054](#)),
 S290 ([FRI-545](#)), S447 ([THU-475](#)),
 S481 ([FRI-246](#)), S495 ([FRI-287](#)),
 S498 ([FRI-296](#)), S535 ([WED-269](#)),
 S671 ([WED-456](#)), S767 ([FRI-378](#)),
 S767 ([FRI-379](#)), S774 ([FRI-396](#)),
 S774 ([FRI-397](#)), S799 ([WED-404](#)),
 S818 ([THU-379](#))
 Kim, Su Ah, S82 ([LBP-011](#))
 Kim, Sung-Eun, S30 ([OS-038-YI](#)),
 S199 ([TOP-062](#)), S200 ([TOP-064-YI](#))
 Kim, Sunghoon, S564 ([THU-196](#))
 Kim, Tae-Hoon, S82 ([LBP-011](#))
 Kim, Tae Hyoung, S264 ([THU-531](#))
 Kimura, Naruhiro, S291 ([TOP-148](#))
 Kimura, Takefumi, S478 ([FRI-237](#))
 Kimura, Takeshi, S513 ([WED-208](#))
 Kim, Won, S487 ([FRI-261-YI](#)),
 S532 ([WED-260](#))
 Kim, W. Ray, S30 ([OS-038-YI](#)),
 S199 ([TOP-062](#)), S200 ([TOP-064-YI](#)),
 S399 ([SAT-486](#)), S797 ([WED-397](#))
 Kim, Ye-Jee, S305 ([TOP-157](#))
 Kim, Yeonjae, S766 ([FRI-375](#))
 Kim, Yestle, S469 ([FRI-214](#)), S494 ([FRI-283](#)),
 S611 ([SAT-215](#))
 Kim, Yoon Jun, S457 ([THU-515](#)),
 S517 ([WED-221](#)), S601 ([TOP-204](#)),
 S774 ([FRI-397](#)), S798 ([WED-402](#))
 Kim, Yunhee, S270 ([THU-555](#))
 Kim, Yun Jung, S633 ([THU-027-YI](#))
 Kim, Yun Soo, S542 ([WED-287](#))
 Kim, Yu Sung, S219 ([FRI-088](#))
 Kinast, Volker, S58 ([OS-092](#))
 Kindler, Yannick, S702 ([TOP-140](#))
 King, Christopher, S106 ([FRI-323](#)),
 S354 ([SAT-542](#))
 King, Leela, S519 ([WED-225](#))
 King'ori, Rosemary, S651 ([SAT-457-YI](#))
 Kingston, Kishanthan, S207 ([FRI-050-YI](#))
 Kirchner, Theresa, S21 ([OS-021-YI](#)),
 S44 ([OS-066-YI](#)), S341 ([THU-182](#)),
 S712 ([WED-160](#))
 Kiremitçi, Saba, S407 ([SAT-519](#)),
 S479 ([FRI-238](#))
 Kirsch, Polly, S39 ([OS-055](#))
 Kirupakaran, Thishana, S495 ([FRI-286](#))
 Kiss, Herbert, S719 ([WED-175](#))
 Kitto, Laura, S105 ([FRI-318-YI](#))
 Kiyono, Soichiro, S123 ([SAT-335](#)),
 S247 ([SAT-095](#))
 Kırımker, Elvan Onur, S369 ([SAT-009](#))
 Kızıldaş, Cansu, S551 ([WED-318-YI](#))
 Kjærgaard, Kristoffer, S567 ([THU-207-YI](#))
 Kjærgaard, Maria, S41 ([OS-059](#)),
 S466 ([FRI-206-YI](#))
 Kjaer, Mette, S79 ([LBP-003](#))
 Kjems, Lise, S242 ([SAT-082](#))
 Klahr, Emma, S278 ([WED-534](#))
 Klapaczynski, Jakub, S685 ([WED-493-YI](#)),
 S834 ([THU-367-YI](#))
 Klarenbeek, Gijs, S206 ([FRI-046](#))
 Kleemann, Robert, S94 ([LBP-033](#)),
 S595 ([THU-294](#)), S597 ([THU-297](#))
 Kleigrew, Karin, S35 ([OS-049-YI](#))
 Klein, Christophe, S566 ([THU-201-YI](#))
 Kleiner, David E, S465 ([FRI-203](#))
 Kleiner, David E., S467 ([FRI-208](#))
 Klein, Marina B., S683 ([WED-486-YI](#))
 Klein, Sabine, S17 ([OS-014-YI](#)),
 S169 ([THU-083](#)), S170 ([THU-087](#)),
 S180 ([WED-074](#)), S182 ([WED-078](#)),
 S198 ([WED-126](#)), S203 ([FRI-039](#)),
 S283 ([WED-548](#))
 Klemm-Kropp, Michael, S213 ([FRI-074-YI](#)),
 S309 ([THU-100](#)), S319 ([THU-120-YI](#))
 Klerner, Paul, S750 ([SAT-404](#))
 Klermund, Julia, S693 ([FRI-152-YI](#))
 Kleter, Bernhard, S801 ([WED-409](#))
 Kliers, Iris, S93 ([LBP-032](#)), S606 ([SAT-201](#))
 Klinker, Hartwig, S820 ([THU-386-YI](#)),
 S833 ([THU-366](#))
 Kloeckner, Roman, S52 ([OS-079-YI](#)),
 S447 ([THU-475](#))
 Klöhn, Mara, S58 ([OS-092](#)), S94 ([LBP-034](#)),
 S732 ([SAT-341](#))
 Kloock, Simon, S587 ([THU-269-YI](#))
 Kloosterhuis, Niels, S347 ([FRI-549-YI](#))
 Klotz, Anton, S436 ([TOP-488-YI](#))
 Knapp, Maximilian, S739 ([SAT-376](#))
 Knetemann, Elisabeth, S435 ([FRI-534](#))
 Kneteman, Norman, S231 ([FRI-122](#))
 Knight, Becky, S651 ([SAT-457-YI](#))
 Knöchel, Jane, S93 ([LBP-031](#))
 Knolle, Percy A., S35 ([OS-049-YI](#)),
 S351 ([SAT-533](#))

Author Index

- Knorr-Klocke, Jana, S359 (SAT-555)
 Knott, Craig, S406 (SAT-515)
 Knox, Ellen, S337 (THU-173)
 Knudsen, Lotte Bjerre, S79 (LBP-003)
 Ko, Adrien, S648 (SAT-449)
 Koay, Tsin Shue, S128 (THU-320-YI)
 Kobayashi, Kazufumi, S123 (SAT-335),
 S247 (SAT-095)
 Kobayashi, Takashi, S235 (FRI-130),
 S541 (WED-283)
 Kobeiter, Hicham, S453 (THU-494)
 Kobus, Zuzanna, S25 (OS-028)
 Kobyliak, Nazarii, S610 (SAT-213)
 Kocheise, Lorenz, S24 (OS-027-YI)
 Koc, Ozgur, S758 (TOP-401-YI),
 S763 (FRI-367)
 Kodama, Takahiro, S506 (TOP-288),
 S828 (THU-413)
 Koduru, Srinivas, S523 (WED-237)
 Koe, Chwee Tat, S578 (THU-239-YI)
 Koek, Ger, S604 (SAT-196)
 Koelzer, Viktor Hendrik, S56 (OS-086-YI)
 Koenig, Aaron, S520 (WED-230)
 Koenig, Alexander, S745 (SAT-390)
 Koester, Leonie, S269 (THU-548-YI)
 Koffas, Apostolos, S59 (OS-094),
 S742 (SAT-383), S781 (FRI-413)
 Koh, Benjamin, S139 (SAT-256),
 S366 (TOP-004)
 Koh, Christopher, S800 (WED-407),
 S814 (WED-382)
 Ko, Hin Hln, S19 (OS-018), S305 (TOP-169)
 Koh, Jia Hong, S139 (SAT-256),
 S366 (TOP-004)
 Kohjima, Motoyuki, S42 (OS-062)
 Kohlhaas, Michael, S587 (THU-269-YI)
 Kohlhepp, Marlene, S25 (OS-028),
 S359 (SAT-555), S414 (FRI-457),
 S594 (THU-291-YI)
 Kohli, Anita, S709 (WED-151),
 S809 (WED-371)
 Koike, Kazuhiko, S589 (THU-275)
 Koizumi, Yohei, S512 (WED-203),
 S711 (WED-154), S722 (WED-184)
 Ko, Jeong-Hun, S580 (THU-247-YI)
 Kojima, Ryuta, S123 (SAT-335),
 S301 (SAT-176)
 Kojima, Takashi, S506 (TOP-288)
 Kolenovska, Radka, S811 (WED-375)
 Kolesnikova, Olena, S598 (THU-303)
 Kolev, Mirjam, S44 (OS-066-YI),
 S341 (THU-182)
 Koller, Tomas, S539 (WED-279)
 Koller, Tomáš, S379 (SAT-033)
 Komiyama, Yasuyuki, S118 (SAT-319)
 Komolmit, Piyawat, S196 (WED-120),
 S221 (FRI-093), S258 (SAT-129),
 S749 (SAT-403)
 Komori, Atsumasa, S542 (WED-286)
 Komuta, Mina, S123 (SAT-335)
 Kondili, Loreta, S666 (WED-444)
 Kondo, Chisa, S248 (SAT-101)
 Kondo, Takayuki, S123 (SAT-335),
 S247 (SAT-095)
 Kondylis, Evangelos, S423 (FRI-486)
 Kong, Defu, S286 (TOP-560)
 Kong, Xianggen, S804 (WED-415)
 Kong, Yide, S748 (SAT-399)
 Königshofer, Philipp, S186 (WED-089-YI),
 S197 (WED-122-YI), S198 (WED-125),
 S267 (THU-540)
 Konings, Joke, S237 (TOP-061-YI)
 Konstantinides, Stavros, S461 (FRI-194-YI)
 Konstantinou, Christos, S110 (FRI-335),
 S192 (WED-110), S588 (THU-271-YI)
 Kontogianni, Meropi, S208 (FRI-052),
 S214 (FRI-076)
 Kontos, Athanasios, S798 (WED-403)
 Kontos, Georgios, S823 (THU-398)
 Koo, Bo Kyung, S487 (FRI-261-YI)
 Kooner, Emily, S246 (SAT-093-YI)
 Koons, Josh, S141 (SAT-261)
 Koop, Paul-Henry, S392 (TOP-520),
 S494 (FRI-284-YI)
 Koo, Yolanda Wei Ling, S280 (WED-539)
 Koppana, Parthu, S58 (OS-090)
 Korbonits, Márta, S578 (THU-236-YI)
 Korenjak, Marko, S700 (FRI-171)
 Korf, Hannelie, S16 (OS-012-YI),
 S125 (TOP-328-YI)
 Kornfehl, Andrea, S156 (TOP-097-YI),
 S242 (SAT-080-YI), S253 (SAT-118)
 Koroki, Keisuke, S123 (SAT-335),
 S247 (SAT-095)
 Korolewicz, James, S52 (OS-079-YI)
 Kosay, Tolga, S161 (THU-058)
 Kosek, David, S66 (OS-107-YI)
 Koshizaka, Takuya, S513 (WED-208)
 Koshy, Abraham, S158 (THU-052),
 S167 (THU-078), S476 (FRI-231)
 Koshy, Anoop, S31 (OS-039)
 Kosinska, Anna D., S6 (GS-008),
 S34 (OS-045), S351 (SAT-533),
 S727 (TOP-355-YI), S728 (TOP-359-YI)
 Kosinski, Mark, S485 (FRI-258)
 Kositangool, Piya, S674 (WED-465)
 Koskinas, Ioannis, S798 (WED-403)
 Kosmoliaptsis, Vassillis, S81 (LBP-008)
 Kostadinova, Radina, S98 (LBP-041),
 S590 (THU-278)
 Kostara, Christina, S322 (THU-126),
 S325 (THU-134)
 Koster, Mirjam, S347 (FRI-549-YI)
 Köster, Sofia, S93 (LBP-031)
 Kotak, Anaya, S489 (FRI-269)
 Kotb, Ahmed, S172 (THU-090)
 Kotelevtsev, Yuri, S268 (THU-542)
 Kotlinowski, Jerzy, S265 (THU-533),
 S304 (SAT-184)
 Kotsiliti, Eleni, S65 (OS-103)
 Kottlilil, Shyamasundaran, S86 (LBP-019),
 S736 (SAT-366)
 Koul, Anil, S732 (SAT-341)
 Koullias, Emmanouil, S798 (WED-403)
 Koul, Roshan, S294 (SAT-155)
 Kounis, Ilias, S370 (SAT-011),
 S385 (SAT-049), S718 (WED-174)
 Koutny, Florian, S500 (FRI-303)
 Koutsoudakis, Georgios, S293 (SAT-153-YI),
 S765 (FRI-373)
 Kovalchuk, Oleksandr, S610 (SAT-213)
 Kovats, Patricia, S169 (THU-080-YI),
 S313 (THU-106-YI)
 Kovoov, Eshwari, S87 (LBP-020)
 Kovynev, Artemiy, S272 (WED-517)
 Kow, Alfred, S147 (SAT-281),
 S540 (WED-282)
 Kowdley, Kris V., S18 (OS-016),
 S72 (OS-118), S80 (LBP-006),
 S91 (LBP-028), S95 (LBP-036),
 S97 (LBP-039), S98 (LBP-040),
 S212 (FRI-069), S308 (THU-098),
 S312 (THU-105), S321 (THU-125),
 S607 (SAT-202), S607 (SAT-203),
 S609 (SAT-208), S621 (FRI-008)
 Koyanagi, Toshimasa, S42 (OS-062)
 Ko, Yunmi, S517 (WED-221),
 S774 (FRI-397), S798 (WED-402)
 Kraemer, Hannah, S368 (SAT-008)
 Kraft, Anke R.M., S350 (SAT-532-YI),
 S353 (SAT-538-YI), S735 (SAT-363),
 S750 (SAT-406-YI)
 Kraft, Felix, S340 (THU-180)
 Krag, Aleksander, S30 (OS-038-YI),
 S32 (OS-041-YI), S41 (OS-059),
 S47 (OS-072-YI), S77 (OS-126),
 S137 (SAT-250), S139 (SAT-255),
 S142 (SAT-266), S153 (SAT-298),
 S159 (THU-055), S199 (TOP-062),
 S200 (TOP-064-YI), S204 (FRI-041),
 S205 (FRI-045), S466 (FRI-206-YI),
 S503 (TOP-241-YI), S510 (WED-199),
 S620 (TOP-012), S623 (FRI-017),
 S703 (TOP-141), S708 (WED-135-YI)
 Kragh Hansen, Johanne, S139 (SAT-255),
 S142 (SAT-266), S153 (SAT-298)
 Krajden, Mel, S40 (OS-058),
 S824 (THU-399-YI)
 Krall, Anja, S69 (OS-112-YI)
 Krall, Christoph, S340 (THU-180)
 Králová, Kateřina, S539 (WED-280)
 Kramer, Georg, S165 (THU-071),
 S186 (WED-089-YI)
 Kramer, Matthijs, S758 (TOP-401-YI)
 Kranidioti, Hariklia, S798 (WED-403),
 S823 (THU-398)
 Krarup, Niels, S477 (FRI-233)
 Krause, Jenny, S24 (OS-027-YI),
 S350 (SAT-531-YI)
 Kraus, Nico, S170 (THU-087)
 Krauss, Stefan, S294 (SAT-154-YI)
 Krawanja, Julia, S250 (SAT-106)
 Krawczyk, Marcin, S339 (THU-179),
 S713 (WED-161-YI)
 Krebs, William, S8 (LBO-003)
 Kremer, Andreas, S374 (SAT-021)
 Kremer, Andreas E., S91 (LBP-028),
 S98 (LBP-040), S308 (THU-098),
 S317 (THU-116-YI), S320 (THU-122),
 S327 (THU-137), S338 (THU-176),
 S440 (THU-457), S702 (TOP-140),
 S703 (TOP-141), S708 (WED-135-YI)

- Kremer, Wolfgang Maximilian, S484 ([FRI-255](#))
- Kremser, Christian, S515 ([WED-214-YI](#))
- Krenn, Katharina, S340 ([THU-180](#))
- Krenzien, Felix, S84 ([LBP-015](#))
- Krešević, Simone, S731 ([SAT-338-YI](#))
- Kreter, Bruce, S667 ([WED-447](#)), S681 ([WED-482](#))
- Krieg, Laura, S104 ([TOP-352](#))
- Krishnamurthy, Jagadeesh, S369 ([SAT-009](#))
- Krishnan, Santhoshi, S823 ([THU-396](#))
- Kriss, Michael, S9 ([LBO-004](#)), S89 ([LBP-026](#))
- Kristic, Antonia, S250 ([SAT-106](#))
- Kroll, Claudia, S335 ([THU-167](#))
- Kromm, Franziska, S132 ([THU-334](#))
- Kronfli, Nadine, S683 ([WED-486-YI](#))
- Kronsten, Victoria, S46 ([OS-070](#)), S388 ([SAT-055](#))
- Kruger, Frederik, S80 ([LBP-006](#))
- Kruk, Beata, S308 ([THU-095](#)), S335 ([THU-167](#)), S339 ([THU-179](#))
- Kruk, Emilia, S369 ([SAT-009](#))
- Kruse, Carlot, S716 ([WED-170](#))
- Krutsenko, Yekaterina, S299 ([SAT-173-YI](#))
- Krygier, Rafal, S685 ([WED-493-YI](#)), S821 ([THU-389](#))
- Kuang, Fu, S99 ([LBP-043](#))
- Kubal, Apurva, S554 ([WED-327](#))
- Kubale, Reinhard, S560 ([WED-343](#))
- Kubaneck, Natalia, S379 ([SAT-033](#)), S539 ([WED-279](#))
- Kubes, Paul, S353 ([SAT-539-YI](#))
- Kubo, Shoji, S430 ([FRI-518](#))
- Kuczyński, Magdalena, S497 ([FRI-293](#))
- Kudo, Masatoshi, S3 ([GS-005](#)), S51 ([OS-078-YI](#)), S69 ([OS-112-YI](#)), S401 ([SAT-495](#)), S443 ([THU-464](#)), S445 ([THU-471-YI](#))
- Kuenzler, Patrizia, S502 ([FRI-315](#))
- Kugelmas, Carina, S637 ([TOP-445](#))
- Kugiyama, Yuki, S542 ([WED-286](#))
- Kuhn, Michael, S47 ([OS-071-YI](#)), S48 ([OS-073](#)), S203 ([FRI-039](#)), S272 ([TOP-563](#))
- Kuijper, Ed J, S47 ([OS-071-YI](#))
- Kuiper, Edith M.M., S309 ([THU-100](#)), S319 ([THU-120-YI](#))
- Kuivenhoven, Jan Albert, S347 ([FRI-549-YI](#))
- Kujundžić, Petra Dinjar, S155 ([SAT-305](#))
- Kułaga, Zbigniew, S578 ([THU-238](#))
- Kulikov, Alexey, S268 ([THU-542](#))
- Kulkarni, Anand, S30 ([OS-038-YI](#)), S149 ([SAT-290-YI](#)), S158 ([THU-052](#)), S161 ([THU-058](#)), S167 ([THU-078](#)), S199 ([TOP-062](#)), S200 ([TOP-064-YI](#)), S440 ([THU-456](#)), S454 ([THU-498](#)), S540 ([WED-282](#)), S701 ([FRI-173](#)), S720 ([WED-180](#))
- Kulle, Alexandra E., S350 ([SAT-531-YI](#))
- Kumada, Takashi, S512 ([WED-203](#))
- Kumakura, Yasuhisa, S513 ([WED-208](#))
- Kumar, Ajay, S158 ([THU-052](#)), S167 ([THU-078](#))
- Kumar, Anil, S283 ([WED-549](#))
- Kumar, Anupam, S184 ([WED-086](#)), S195 ([WED-118](#)), S360 ([SAT-557-YI](#))
- Kumarasamy, Jayakanthan, S693 ([FRI-151](#))
- Kumar, Ashish, S158 ([THU-052](#)), S167 ([THU-078](#)), S219 ([FRI-088](#))
- Kumaraswamy, P, S440 ([THU-456](#))
- Kumar, Deepa, S485 ([FRI-257](#))
- Kumar, Dhananjay, S360 ([SAT-557-YI](#))
- Kumari, Anupama, S129 ([THU-321](#)), S184 ([WED-086](#)), S195 ([WED-118](#)), S273 ([WED-519-YI](#)), S274 ([WED-522-YI](#)), S276 ([WED-527-YI](#)), S294 ([SAT-155](#))
- Kumar, Jata Shankar, S609 ([SAT-210](#))
- Kumar, Jitendra, S274 ([WED-522-YI](#)), S745 ([SAT-391](#))
- Kumar, Karan, S454 ([THU-498](#))
- Kumar, Kopal, S489 ([FRI-269](#))
- Kumar, Lakshmi, S31 ([OS-039](#))
- Kumar, Manoj, S164 ([THU-070](#)), S294 ([SAT-155](#))
- Kumar, Niraj, S283 ([WED-549](#))
- Kumar, Pavitra, S161 ([THU-057-YI](#)), S288 ([FRI-541-YI](#)), S594 ([THU-291-YI](#))
- Kumar, Rahul, S169 ([THU-082](#))
- Kumar, Rajneesh, S742 ([SAT-383](#))
- Kumar, Raju, S578 ([THU-236-YI](#))
- Kumar, Rakesh, S177 ([WED-057](#))
- Kumar, Sandeep, S184 ([WED-086](#)), S195 ([WED-118](#)), S360 ([SAT-557-YI](#))
- Kumar, Sanjay, S567 ([THU-203](#))
- Kumar, Saran, S347 ([FRI-550](#))
- Kumar Sarin, Shiv, S108 ([FRI-327-YI](#)), S177 ([WED-058-YI](#)), S181 ([WED-076](#)), S184 ([WED-086](#)), S195 ([WED-118](#))
- Kumar, Shiva, S219 ([FRI-088](#))
- Kumar, Sonal, S138 ([SAT-251](#)), S314 ([THU-110](#)), S708 ([WED-136](#))
- Kumar, Surendra, S209 ([FRI-053](#))
- Kumar, Vijay, S745 ([SAT-391](#))
- Kumazaki, Shunsuke, S506 ([TOP-288](#))
- Kunos, George, S124 ([TOP-312](#))
- Kunstein, Anselm, S259 ([SAT-135](#))
- Kunta, Jeevan, S613 ([SAT-224](#))
- Kunze, Katie, S608 ([SAT-207](#))
- Kuo, Alexander, S8 ([LBO-003](#)), S9 ([LBO-004](#)), S39 ([OS-055](#)), S89 ([LBP-026](#)), S200 ([TOP-063](#))
- Kuo, Hsing-Tao, S832 ([THU-365](#))
- Kuo, Yu-Lun, S449 ([THU-479](#))
- Kupčinskis, Juozas, S172 ([THU-092](#))
- Kupcinskis, Limas, S341 ([THU-182](#)), S678 ([WED-474](#))
- Kupfer, Jörg, S338 ([THU-176](#))
- Kuppe, Christoph, S33 ([OS-043](#))
- Kuroda, Hidekatsu, S451 ([THU-490](#)), S828 ([THU-413](#))
- Kuromatsu, Ryoko, S512 ([WED-203](#))
- Kurosaki, Masayuki, S478 ([FRI-237](#)), S626 ([FRI-026](#)), S828 ([THU-413](#))
- Kurosugi, Akane, S301 ([SAT-176](#))
- Kuruthukulangara, Michael, S554 ([WED-327](#))
- Kushner, Tatyana, S659 ([WED-428-YI](#)), S688 ([WED-499](#)), S769 ([FRI-383](#)), S832 ([THU-364](#))
- Kutaiba, Numan, S547 ([WED-299](#))
- Kuyvenhoven, Johan P.H., S205 ([FRI-043](#)), S309 ([THU-100](#))
- Kwanten, Wilhelmus, S259 ([SAT-134](#)), S584 ([THU-258-YI](#))
- Kwanten, Wilhelmus J, S61 ([OS-096-YI](#)), S540 ([WED-281-YI](#))
- Kwanten, Wilhelmus J., S581 ([THU-249](#))
- Kwok, Royston, S578 ([THU-239-YI](#))
- Kwok, Tsz Yan, S745 ([SAT-392](#))
- Kwong, Allison, S8 ([LBO-003](#))
- Kwon, Hyuk-Sang, S564 ([THU-196](#))
- Kwon, Jung Hyun, S762 ([FRI-364](#))
- Kwon, Kyung min, S681 ([WED-482](#)), S778 ([FRI-407](#))
- Kwon, Oh Sang, S542 ([WED-287](#))
- Kwon, So Young, S74 ([OS-121](#))
- Kwon, Yoojin, S283 ([WED-547](#))
- Kwon, Yoo-Wook, S575 ([THU-230](#))
- Kwo, Paul Yien, S86 ([LBP-019](#)), S240 ([SAT-076](#))
- Kyranas, Eirini, S198 ([WED-124](#)), S359 ([SAT-556-YI](#))
- Kyriienko, Dmytro, S610 ([SAT-213](#))
- Kyritsi, Vaia, S229 ([FRI-117](#))
- Kyziroglou, Maria, S229 ([FRI-117](#))
- Laakso, Markku, S514 ([WED-210](#)), S562 ([TOP-240-YI](#))
- Labanca, Sara, S96 ([LBP-038](#)), S306 ([THU-093](#))
- Labenz, Christian, S61 ([OS-096-YI](#)), S211 ([FRI-059](#)), S214 ([FRI-075](#)), S230 ([FRI-120](#)), S249 ([SAT-104-YI](#)), S484 ([FRI-255](#))
- Labenz, Joachim, S211 ([FRI-059](#)), S214 ([FRI-075](#))
- Laborne, François Xavier, S640 ([SAT-430](#))
- Labreuche, Julien, S6 ([GS-010](#))
- Labriola, Dominic, S71 ([OS-117](#)), S76 ([OS-124](#)), S141 ([SAT-263](#)), S465 ([FRI-202](#)), S505 ([TOP-265](#)), S509 ([WED-196](#)), S611 ([SAT-214](#)), S652 ([SAT-459](#))
- Labruyere, Marie, S369 ([SAT-010](#))
- Labuhn, Simon, S52 ([OS-079-YI](#))
- Labyed, Yassin, S560 ([WED-343](#))
- Lacaille, Florence, S374 ([SAT-021](#))
- Lacey, Madeleine, S470 ([FRI-215-YI](#))
- Lachenmayer, Anja, S373 ([SAT-019](#))
- Lachiondo-Ortega, Sofia, S417 ([FRI-466-YI](#))
- Lachlan, Neil, S81 ([LBP-007](#))
- Lackner, Carolin, S467 ([FRI-208](#))
- Lackner, Karl, S461 ([FRI-194-YI](#))
- Lacombe, Karine, S802 ([WED-410](#))
- Lacotte, Stéphanie, S189 ([WED-101-YI](#))
- Lacour, Alexandre, S644 ([SAT-439-YI](#))
- Łącz, Joanna, S328 ([THU-152-YI](#)), S338 ([THU-175-YI](#))
- La, Danie, S352 ([SAT-536](#))

Author Index

- Ladrón de Guevara, Alma Laura, S98 ([LBP-040](#))
- Laevens, Benjamin P.M., S392 ([TOP-520](#)), S528 ([WED-247](#)), S567 ([THU-206](#))
- Laffi, Giacomo, S215 ([FRI-078-YI](#))
- LaGasse, Kaitlin, S485 ([FRI-258](#))
- Lagouge, Marie, S572 ([THU-220](#))
- Lagoutte, Isabelle, S416 ([FRI-465](#))
- Lah, Ponan Ponan Claude Regis, S219 ([FRI-088](#))
- Lai, Francisco Tsz Tsun, S116 ([SAT-314](#))
- Lai, Jennifer, S10 ([LBO-005](#)), S206 ([FRI-046](#)), S218 ([FRI-086](#)), S638 ([SAT-426-YI](#))
- Lai, Jimmy Che-To, S154 ([SAT-302](#)), S235 ([FRI-132](#)), S761 ([FRI-362-YI](#)), S770 ([FRI-387](#)), S818 ([THU-379](#))
- Lai, Mandy Sze-Man, S235 ([FRI-132](#)), S510 ([WED-198](#)), S761 ([FRI-362-YI](#))
- Lai, Mason, S638 ([SAT-426-YI](#))
- Lai, Michelle, S2 ([GS-004](#)), S38 ([OS-054](#)), S129 ([THU-322-YI](#)), S646 ([SAT-446](#))
- Laiola, Manolo, S159 ([THU-053](#))
- Lai, Quirino, S368 ([SAT-009](#)), S375 ([SAT-023](#)), S445 ([THU-470-YI](#)), S456 ([THU-502](#))
- Lakhloufi, Dalila, S131 ([THU-331-YI](#))
- Lalanne, Claudine, S712 ([WED-160](#))
- Laleman, Wim, S9 ([LBO-004](#)), S30 ([OS-038-YI](#)), S47 ([OS-071-YI](#)), S48 ([OS-073](#)), S61 ([OS-096-YI](#)), S89 ([LBP-026](#)), S157 ([THU-050](#)), S159 ([THU-055](#)), S161 ([THU-057-YI](#)), S169 ([THU-080-YI](#)), S174 ([TOP-073](#)), S184 ([WED-083](#)), S188 ([WED-098-YI](#)), S193 ([WED-111](#)), S199 ([TOP-062](#)), S200 ([TOP-064-YI](#)), S203 ([FRI-039](#)), S246 ([SAT-092-YI](#)), S272 ([TOP-563](#))
- Lallement, Justine, S588 ([THU-272-YI](#))
- Lalli, Luca, S439 ([THU-454](#))
- Lalloyer, Fanny, S577 ([THU-234](#))
- La Mantia, Claudia, S503 ([FRI-317](#))
- Lamarque, Catherine, S373 ([SAT-020](#))
- Lamattina, Anthony, S693 ([FRI-151](#))
- Lambare, Bénédicte, S640 ([SAT-430](#))
- Lambert Tergast, Tammo, S253 ([SAT-117](#))
- Lamb, Hildo, S21 ([OS-020](#)), S492 ([FRI-278](#))
- Lambrecht, Ellen, S658 ([WED-426](#))
- Lambrechts, Diether, S125 ([TOP-328-YI](#)), S411 ([TOP-507-YI](#))
- Lam, Brian, S476 ([FRI-232](#)), S520 ([WED-230](#)), S572 ([THU-221](#)), S643 ([SAT-438](#))
- Lam, Eileen, S400 ([SAT-492](#))
- Lami, Francesca, S241 ([SAT-078-YI](#)), S399 ([SAT-490](#))
- Lam, Jason, S242 ([SAT-082](#))
- Lam, Laurent, S733 ([SAT-343](#))
- Lammers, Jolanda, S763 ([FRI-367](#))
- Lammers, Twan, S431 ([FRI-522](#)), S435 ([FRI-533](#))
- Lammert, Frank, S244 ([SAT-087-YI](#)), S503 ([TOP-241-YI](#))
- Lamonde, Frederic, S683 ([WED-486-YI](#))
- Lamoureux, Anouck, S115 ([SAT-306](#))
- Lampertico, Pietro, S1 ([GS-002](#)), S73 ([OS-120](#)), S75 ([OS-127](#)), S79 ([LBP-005](#)), S92 ([LBP-029](#)), S100 ([LBP-044](#)), S227 ([FRI-110](#)), S310 ([THU-101](#)), S329 ([THU-153](#)), S344 ([THU-190](#)), S388 ([SAT-056](#)), S396 ([SAT-481-YI](#)), S397 ([SAT-482](#)), S401 ([SAT-493-YI](#)), S470 ([FRI-215-YI](#)), S544 ([WED-293](#)), S666 ([WED-446](#)), S758 ([TOP-400](#)), S759 ([TOP-416-YI](#)), S764 ([FRI-371](#)), S772 ([FRI-392-YI](#)), S773 ([FRI-393](#)), S777 ([FRI-405](#)), S781 ([FRI-412](#)), S793 ([WED-391](#)), S794 ([WED-392](#)), S796 ([WED-395](#)), S798 ([WED-399-YI](#)), S802 ([WED-411](#)), S804 ([WED-414](#)), S813 ([WED-379](#))
- Lampichler, Katharina, S69 ([OS-112-YI](#))
- Lanari, Jacopo, S369 ([SAT-009](#))
- Landais, Paul, S370 ([SAT-011](#)), S385 ([SAT-049](#))
- Landay, Alan, S825 ([THU-404](#))
- Landi, Stephanie, S650 ([SAT-454-YI](#))
- Landthaler, Aisha-Nike, S587 ([THU-269-YI](#))
- Lane, Lindsay, S393 ([SAT-472](#))
- Lange, Christian M., S30 ([OS-038-YI](#)), S115 ([TOP-346-YI](#)), S182 ([WED-077](#)), S199 ([TOP-062](#)), S200 ([TOP-064-YI](#)), S440 ([THU-457](#))
- Lange, Naomi, S134 ([THU-341](#))
- Langenbacher, Diane, S320 ([THU-122](#))
- Langer, Mona-May, S182 ([WED-077](#))
- Langthaler, Patrick, S500 ([FRI-303](#))
- Lang, Thomas, S716 ([WED-170](#))
- Lani, Lorenzo, S446 ([THU-472-YI](#)), S449 ([THU-481-YI](#))
- Lannes, Adrien, S54 ([OS-084-YI](#)), S168 ([THU-079](#)), S172 ([THU-092](#)), S456 ([THU-503](#)), S519 ([WED-224](#))
- Lanthier, Nicolas, S151 ([SAT-293-YI](#)), S360 ([WED-008](#)), S386 ([SAT-051](#)), S473 ([FRI-224](#)), S546 ([WED-297-YI](#))
- Lan, Tian, S298 ([SAT-170](#))
- Lan, Tianwen, S99 ([LBP-043](#))
- Lanzillotta, Marco, S710 ([WED-152](#))
- Laohawetwanit, Thiyaphat, S580 ([THU-245](#))
- Laouenan, Cedric, S524 ([WED-239](#)), S526 ([WED-245](#))
- Laouirem, Samira, S412 ([FRI-454](#))
- Lape, Janel, S88 ([LBP-022](#))
- Lapenna, Lucia, S364 ([WED-022](#)), S367 ([SAT-007-YI](#)), S700 ([FRI-171](#))
- Lapitz, Ainhoa, S50 ([OS-076-YI](#)), S295 ([SAT-159-YI](#)), S536 ([WED-271](#))
- Laquerriere, Patrice, S25 ([OS-029](#))
- Lara, Catherine De, S746 ([SAT-394](#))
- Lara-Romero, Carmen, S2 ([GS-004](#)), S38 ([OS-054](#)), S71 ([OS-116](#)), S508 ([WED-195](#)), S557 ([WED-335](#))
- Larena, Jose Alejandro, S694 ([FRI-153](#))
- Larger, Etienne, S526 ([WED-245](#))
- Largo, Carlota, S364 ([WED-028](#))
- Larrat, Sylvie, S744 ([SAT-389](#))
- Larrea, Emily, S398 ([SAT-485](#))
- Larrey, Dominique, S115 ([SAT-306](#)), S122 ([SAT-331](#))
- Larrubia, Juan Ramón, S391 ([TOP-512-YI](#)), S738 ([SAT-374-YI](#)), S768 ([FRI-381](#))
- Larsson, Simon B., S754 ([SAT-414](#))
- Lasa-Elosegi, Irune, S295 ([SAT-159-YI](#))
- Lasco, Roberta, S371 ([SAT-015-YI](#)), S378 ([SAT-031-YI](#))
- Lascoux-Combe, Caroline, S802 ([WED-410](#))
- Lassailly, Guillaume, S6 ([GS-010](#)), S133 ([THU-335](#)), S644 ([SAT-439-YI](#))
- Lassen, Pierre Bel, S585 ([THU-260](#))
- Lasser, Luc, S172 ([THU-092](#))
- Latasa, Maria U., S287 ([FRI-538](#)), S348 ([FRI-555](#)), S416 ([FRI-464](#))
- Lathouwers, Erkki, S27 ([OS-033](#)), S808 ([WED-367](#))
- Latorre, Raquel, S453 ([THU-493](#))
- Latournerie, Marianne, S168 ([THU-079](#)), S369 ([SAT-010](#)), S385 ([SAT-048](#)), S763 ([FRI-370](#))
- Lau, Audrey, S92 ([LBP-029](#))
- Lau, Audrey H., S1 ([GS-002](#)), S74 ([OS-122](#)), S737 ([SAT-371](#)), S761 ([FRI-363-YI](#)), S764 ([FRI-371](#)), S794 ([WED-392](#)), S796 ([WED-395](#))
- Läubli, Heinz, S292 ([TOP-150-YI](#))
- Lau, Chi, S745 ([SAT-390](#))
- Laucirica, Isabel, S233 ([FRI-126](#))
- Lau, Denise, S637 ([THU-046](#))
- Laudes, Matthias, S582 ([THU-254-YI](#))
- Laue, Fenja, S730 ([TOP-369](#))
- Lauer, Ulrich, S714 ([WED-164](#))
- Laue, Tobias, S115 ([TOP-346-YI](#)), S700 ([FRI-171](#))
- Lau, George, S158 ([THU-052](#)), S167 ([THU-078](#))
- Lau, Jessie, S261 ([TOP-564](#))
- Laukens, Kris, S731 ([SAT-337](#))
- Laura, Chiara, S35 ([OS-048](#))
- Laurence, Duvillard, S508 ([WED-194](#))
- Laurent, Alexis, S453 ([THU-494](#))
- Lauridsen, Mette, S211 ([FRI-059](#)), S214 ([FRI-075](#)), S364 ([WED-027](#))
- Lauterio, Andrea, S380 ([SAT-034](#))
- Lauw, Michael, S141 ([SAT-261](#))
- La Vecchia, Carlo, S705 ([WED-130](#))
- Lavezzo, Bruna, S371 ([SAT-015-YI](#)), S378 ([SAT-031-YI](#))
- Lawitz, Eric, S4 ([GS-006](#)), S4 ([GS-011](#)), S7 ([LBO-001](#)), S72 ([OS-119](#)), S80 ([LBP-006](#)), S86 ([LBP-019](#)), S95 ([LBP-036](#)), S98 ([LBP-040](#)), S544 ([WED-294](#)), S607 ([SAT-202](#)), S609 ([SAT-208](#))
- Lawler, John, S268 ([THU-547](#)), S295 ([SAT-158](#))
- Law, Michael, S659 ([WED-429](#))
- Lawrence, Jeremy, S657 ([WED-422](#)), S676 ([WED-470](#))
- Layani, Shanny, S278 ([WED-534](#))
- Lazaridis, Konstantinos N., S326 ([THU-135](#))
- Lazar, Stefan, S1 ([GS-002](#)), S764 ([FRI-371](#))

- Lazarus, Jeffrey V, S39 ([OS-056-YI](#)), S528 ([WED-248](#)), S664 ([WED-440](#)), S665 ([WED-442](#)), S682 ([WED-485](#))
- Lazarus, Jeffrey V., S470 ([FRI-218](#)), S508 ([WED-195](#)), S538 ([WED-275](#)), S637 ([TOP-445](#)), S651 ([SAT-456](#))
- Lazcanoiturburu, Nerea, S303 ([SAT-183](#))
- Lazzeri-Barcelo, Francesca, S281 ([WED-543](#))
- Leal-Lassalle, Hector, S276 ([WED-528-YI](#)), S351 ([SAT-534](#))
- Leandre, Fanny, S416 ([FRI-465](#))
- Leatherbury, Neil, S88 ([LBP-022](#))
- Lebosse, Fanny, S61 ([OS-097](#)), S122 ([SAT-331](#))
- Lebossé, Fanny, S22 ([OS-022](#))
- Lebouche, Bertrand, S683 ([WED-486-YI](#))
- Lebray, Pascal, S486 ([FRI-259](#))
- Leburgue, Angela, S321 ([THU-125](#)), S326 ([THU-136](#)), S712 ([WED-158-YI](#))
- Leclercq, Isabelle, S2 ([GS-003-YI](#)), S473 ([FRI-224](#)), S588 ([THU-272-YI](#))
- L'écuyer, Sydnée, S187 ([WED-092](#))
- Lee, Ahlim, S458 ([THU-518](#))
- Lee, Amani, S134 ([THU-341](#))
- Lee, Ariel, S36 ([OS-050](#))
- Lee, Changhyeong, S788 ([FRI-433](#))
- Lee, Chee Leng, S740 ([SAT-377](#))
- Lee, Chieh-Ju, S449 ([THU-479](#))
- Lee, Christina, S380 ([SAT-036-YI](#))
- Lee, Christopher, S12 ([OS-003](#))
- Lee, Dae Ho, S542 ([WED-287](#))
- Lee, Dakyung, S350 ([SAT-531-YI](#))
- Lee, Danbi, S305 ([TOP-157](#))
- Lee, Dong Ho, S457 ([THU-515](#))
- Lee, Donghyeon, S532 ([WED-260](#))
- Lee, Eng Sing, S497 ([FRI-295](#))
- Lee, Eva, S419 ([FRI-473](#))
- Lee, Guan Huei, S797 ([WED-398](#))
- Lee, Guan-Huei, S158 ([THU-052](#)), S167 ([THU-078](#))
- Lee, Hae Won, S459 ([THU-519](#))
- Lee, Han Ah, S481 ([FRI-246](#)), S774 ([FRI-396](#))
- Lee, Han Chu, S305 ([TOP-157](#))
- Lee, Hannah, S1 ([GS-001](#))
- Lee, Hwee Khim, S525 ([WED-242](#))
- Lee, Hye Won, S2 ([GS-004](#)), S38 ([OS-054](#)), S290 ([FRI-545](#)), S495 ([FRI-287](#)), S498 ([FRI-296](#)), S535 ([WED-269](#)), S671 ([WED-456](#)), S767 ([FRI-378](#)), S799 ([WED-404](#)), S818 ([THU-379](#))
- Lee, Hyo Young, S148 ([SAT-284](#)), S553 ([WED-323](#)), S654 ([SAT-465](#)), S766 ([FRI-375](#))
- Lee, Hyung-Chul, S774 ([FRI-397](#))
- Lee, Hyun Woong, S774 ([FRI-396](#)), S774 ([FRI-397](#))
- Lee, I-Cheng, S449 ([THU-479](#)), S449 ([THU-480](#))
- Lee, Jae-Jin, S128 ([THU-319](#)), S288 ([FRI-540](#))
- Lee, Jae Myeong, S247 ([SAT-098](#))
- Lee, Jae Seung, S495 ([FRI-287](#)), S498 ([FRI-296](#)), S535 ([WED-269](#)), S671 ([WED-456](#)), S767 ([FRI-378](#)), S799 ([WED-404](#))
- Lee, Jeong-Hoon, S74 ([OS-121](#)), S457 ([THU-515](#)), S517 ([WED-221](#)), S601 ([TOP-204](#)), S766 ([FRI-376](#)), S774 ([FRI-397](#))
- Lee, Jooho, S69 ([OS-113](#))
- Lee, Joon Hyeok, S401 ([SAT-495](#))
- Lee, Joyce Man Fong, S419 ([FRI-473](#))
- Lee, Jung Il, S595 ([THU-292](#))
- Lee, Ju-Seog, S68 ([OS-111](#))
- Lee, Juseok, S788 ([FRI-433](#))
- Lee, Kang Soo, S564 ([THU-196](#))
- Lee, Kyumok, S69 ([OS-113](#))
- Lee, Lois, S607 ([SAT-202](#)), S609 ([SAT-208](#))
- Lee, Mei Chin, S578 ([THU-239-YI](#))
- Lee, Mei-Hsuan, S832 ([THU-365](#))
- Leeming, Diana, S70 ([OS-115](#)), S255 ([SAT-122](#)), S513 ([WED-207](#)), S579 ([THU-243](#)), S612 ([SAT-220-YI](#)), S623 ([FRI-017](#)), S626 ([FRI-027](#)), S737 ([SAT-370](#))
- Lee, Pei-Chang, S51 ([OS-078-YI](#)), S69 ([OS-112-YI](#)), S443 ([THU-464](#)), S449 ([THU-479](#))
- Lee, Pei-Lun, S832 ([THU-365](#))
- Leerapun, Apinya, S811 ([WED-375](#))
- Lee, Seung-Min, S69 ([OS-113](#))
- Lee, Seung Soo, S437 ([TOP-489-YI](#))
- Lee, So-Hee, S112 ([FRI-341](#))
- Lee, Soon Kyu, S762 ([FRI-364](#))
- Lee, Sujin, S264 ([THU-531](#))
- Lee, Sung-Hwan, S68 ([OS-111](#))
- Lee, Sung Won, S540 ([WED-282](#)), S799 ([WED-404](#))
- Lee, Sunyoung, S68 ([OS-111](#))
- Lee, Taesic, S136 ([THU-348](#))
- Lee, Tzong-Hsi, S832 ([THU-365](#))
- Lee, William M., S10 ([LBO-005](#)), S104 ([TOP-352](#)), S714 ([WED-164](#))
- Lee, Wing Yu, S181 ([WED-075-YI](#))
- Lee, Yin Mei, S797 ([WED-398](#))
- Lee, Yoonseok, S542 ([WED-287](#)), S596 ([THU-295](#))
- Lee, Yoon Suk, S270 ([THU-555](#))
- Lee, Youngmok, S698 ([FRI-166](#))
- Lee, Young-Sun, S596 ([THU-295](#))
- Lee, Yun Bin, S74 ([OS-121](#)), S457 ([THU-515](#)), S517 ([WED-221](#)), S575 ([THU-230](#)), S601 ([TOP-204](#)), S774 ([FRI-397](#))
- Lee, Yunjeong, S450 ([THU-484](#))
- Lee, Yun Kyu, S532 ([WED-260](#))
- Lee, Yu Rim, S457 ([THU-516](#))
- Lefaucheur, Carmen, S372 ([SAT-016](#))
- Lefebvre, Eric, S97 ([LBP-039](#))
- Lefebvre, Rémy, S49 ([OS-074](#))
- Lefere, Sander, S57 ([OS-089-YI](#)), S143 ([SAT-268](#)), S278 ([WED-531](#)), S292 ([SAT-151-YI](#)), S311 ([THU-102-YI](#)), S321 ([THU-123-YI](#)), S371 ([SAT-014-YI](#)), S386 ([SAT-051](#)), S420 ([FRI-475-YI](#)), S442 ([THU-463](#)), S631 ([THU-020-YI](#))
- Leff, Phillip, S547 ([WED-303](#))
- Legagneux, Vincent, S64 ([OS-102](#)), S261 ([THU-522](#))
- Legaki, Aigli-Ioanna, S570 ([THU-214](#))
- Legendre, Christophe, S372 ([SAT-016](#))
- Legido-Quigly, Cristina, S47 ([OS-072-YI](#))
- Legros, Laurence, S718 ([WED-174](#))
- Legry, Vanessa, S191 ([WED-105](#))
- Lehmann, Felix, S752 ([SAT-410](#))
- Lehmann-Mühlenhoff, Ulrich, S425 ([FRI-492-YI](#))
- Lehuen, Agnes, S524 ([WED-239](#))
- Leibiger, Barbara, S281 ([WED-543](#))
- Leibiger, Ingo, S281 ([WED-543](#))
- Leicht, Hans Benno, S223 ([FRI-098](#)), S224 ([FRI-103-YI](#))
- Leick, Stephan, S821 ([THU-390](#))
- Leinhard, Olof Dahlqvist, S530 ([WED-255-YI](#)), S532 ([WED-259](#))
- Leinonen, Jaakko T., S562 ([TOP-240-YI](#))
- Leipnitz, Ian, S368 ([SAT-009](#))
- Leite, Nathalie, S619 ([SAT-248](#))
- Leith, Damien, S14 ([OS-007-YI](#)), S208 ([FRI-053](#))
- Lei, Victor, S40 ([OS-058](#))
- Lei, Yu, S742 ([SAT-383](#)), S781 ([FRI-413](#))
- Lekakis, Vasileios, S217 ([FRI-083](#))
- Le, Kha, S806 ([WED-361](#)), S807 ([WED-365](#)), S812 ([WED-378](#))
- Lelouvier, Benjamin, S47 ([OS-071-YI](#))
- Lemainque, Teresa, S567 ([THU-206](#))
- Lemaire, Véronique Grando, S441 ([THU-459-YI](#)), S451 ([THU-487-YI](#))
- Lemaître, Elise, S644 ([SAT-439-YI](#))
- Lembeck, Pia, S180 ([WED-074](#))
- Lembo, Erminia, S516 ([WED-215](#))
- Lemerle, Cyril, S298 ([SAT-167-YI](#))
- Lemmens, Tibo, S823 ([THU-397-YI](#))
- Lemoine, Maud, S470 ([FRI-215-YI](#)), S679 ([WED-477-YI](#)), S782 ([FRI-418](#)), S787 ([FRI-431](#))
- Lemoine, Sara, S5 ([GS-007](#)), S313 ([THU-107](#)), S326 ([THU-136](#)), S712 ([WED-158-YI](#))
- Lenci, Ilaria, S59 ([OS-094](#)), S368 ([SAT-009](#)), S772 ([FRI-392-YI](#))
- Lencioni, Riccardo, S3 ([GS-005](#))
- Leníček, Martin, S539 ([WED-280](#))
- Lennie, Craig, S553 ([WED-324](#))
- Lens, Sabela, S39 ([OS-056-YI](#)), S255 ([SAT-123](#)), S293 ([SAT-153-YI](#)), S351 ([SAT-533](#)), S470 ([FRI-215-YI](#)), S682 ([WED-485](#)), S711 ([WED-155](#)), S765 ([FRI-373](#)), S777 ([FRI-406](#)), S787 ([FRI-432](#)), S818 ([THU-381](#))
- Lenz, Dominic, S115 ([TOP-346-YI](#))
- Lenzen, Henrike, S253 ([SAT-117](#))
- Lenzi, Marco, S18 ([OS-015](#))
- Lenz, Oliver, S27 ([OS-032](#)), S27 ([OS-033](#)), S100 ([LBP-044](#)), S768 ([FRI-380](#)), S801 ([WED-409](#)), S808 ([WED-367](#)), S810 ([WED-372](#)), S813 ([WED-379](#))
- Leocadio, Daemena, S669 ([WED-453](#))
- Leogrande, Melania, S773 ([FRI-393](#))
- Leo, Massimo, S705 ([WED-129](#))

Author Index

- Leonel, Thais, S105 (FRI-321), S291 (TOP-149-YI), S765 (FRI-373)
- Leoni, Simona, S499 (FRI-299)
- León, Raquel Ríos, S329 (THU-154-YI)
- Leó Snorrason, Bjarki, S389 (SAT-059)
- Leow, Wei Qiang, S467 (FRI-208)
- Lepida, Antonia, S133 (THU-335)
- Lepore, Maia, S409 (SAT-524)
- Lepour, Maxence, S360 (WED-008)
- Leppkes, Moritz, S327 (THU-137)
- Leproux, Apolline, S207 (FRI-050-YI), S222 (FRI-094-YI), S222 (FRI-095)
- Lequoy, Marie, S50 (OS-077), S413 (FRI-456), S441 (THU-458), S453 (THU-494), S456 (THU-503)
- Leroy, Vincent, S41 (OS-060), S172 (THU-092), S373 (SAT-020), S413 (FRI-456), S453 (THU-494), S648 (SAT-449), S720 (WED-178), S743 (SAT-386-YI), S784 (FRI-425), S787 (FRI-431)
- Lerut, Jan, S375 (SAT-023)
- Lesage, Candice, S115 (SAT-306)
- Leserre, Federica, S470 (FRI-215-YI)
- Lesi, Olufunmilayo, S395 (SAT-479-YI)
- Lesmana, Laurentius A., S158 (THU-052), S167 (THU-078)
- Lessenich, Paul, S560 (WED-343)
- Lesurtel, Mickael, S368 (SAT-009), S372 (SAT-016), S451 (THU-487-YI)
- Letham, Laura, S646 (SAT-444)
- Letunic, Ivica, S48 (OS-073)
- Leucuta, Dan-Corneliu, S521 (WED-232-YI), S555 (WED-332)
- Leung, Gary, S788 (FRI-435)
- Leung, Kristel, S305 (TOP-168-YI), S320 (THU-121)
- Leung, Kyle, S185 (WED-088-YI)
- Leung, Ryan Hin-Man, S810 (WED-373-YI)
- Levantesi, Fabio, S215 (FRI-078-YI)
- Levesque, Mitchell, S56 (OS-086-YI)
- Levi, Cristina, S180 (WED-071)
- Levine, Alina, S314 (THU-110)
- Levrero, Massimo, S280 (WED-540-YI), S508 (WED-194)
- Levy, Cynthia, S5 (GS-007), S80 (LBP-006), S91 (LBP-028), S97 (LBP-039), S98 (LBP-040), S308 (THU-098), S311 (THU-102-YI), S312 (THU-105), S321 (THU-125), S374 (SAT-021)
- Levy, Francis, S452 (THU-491)
- Levy, Miriam, S657 (WED-422), S676 (WED-470), S776 (FRI-403)
- Lévy, Vincent, S50 (OS-077)
- Lewandowski, Dave, S611 (SAT-215)
- Lewin, Maite, S41 (OS-060), S50 (OS-077)
- Lewin, Sharon, S740 (SAT-377)
- Lewinska, Monika, S421 (FRI-478), S576 (THU-232)
- Lewis, Diana, S632 (THU-021)
- Lewis, Kyle, S302 (SAT-180)
- Lewis, Philip Starkey, S186 (WED-090)
- Lewis, Whitney, S88 (LBP-022)
- Leye, Nafissatou, S743 (SAT-387)
- Leyh, Catherine, S52 (OS-079-YI)
- Leyva, Rina, S95 (LBP-036)
- L'Hermite, Sébastien, S116 (SAT-315), S156 (TOP-108)
- Liachko, Ivan, S46 (OS-070)
- Liang, Chen, S694 (FRI-154)
- Liang, Lilian, S235 (FRI-132)
- Liang, Po-Cheng, S490 (FRI-271), S493 (FRI-280)
- Liang, Wannian, S527 (WED-246)
- Liang, Wanying, S95 (LBP-037)
- Liang, Xi, S105 (FRI-319), S108 (FRI-330), S117 (SAT-318), S119 (SAT-322), S345 (FRI-546)
- Liang, Xiao, S526 (WED-246)
- Liang, Xieer, S26 (OS-030), S99 (LBP-043), S807 (WED-365), S812 (WED-378)
- Liang, Xuan, S526 (WED-246)
- Liang, Xujing, S543 (WED-290), S792 (WED-390)
- Liang, Yan, S758 (TOP-401-YI)
- Liang, Zicong, S792 (WED-390)
- Liao, Bo-Hung, S699 (FRI-170)
- Liao, Siqi, S427 (FRI-500-YI)
- Liaskos, Christos, S358 (SAT-551)
- Liatsou, Ioanna, S664 (WED-440)
- Li, Baiyun, S526 (WED-246)
- Li, Beiling, S161 (THU-058)
- Liberal, Rodrigo, S18 (OS-015)
- Liberman, Alexander, S614 (SAT-225), S618 (SAT-243)
- Li, Bing, S660 (WED-431)
- Li, Bingqi, S345 (FRI-546)
- Li, Bo, S271 (TOP-561)
- Licata, Anna, S557 (WED-336), S601 (TOP-193)
- Li, Chan, S235 (FRI-131)
- Li, Chenghang, S531 (WED-258)
- Lichenstein, Henri, S87 (LBP-020)
- Lichtenberger, Wendi, S544 (WED-294)
- Lichtenstein, Laeticia, S573 (THU-222-YI)
- Li, Chuanjiang, S382 (SAT-041)
- Li, Chunfeng, S737 (SAT-371), S750 (SAT-405)
- Li, Chunming, S87 (LBP-021)
- Li, Dan, S7 (GS-012)
- Li, Debiao, S39 (OS-055)
- Li, Deyao, S734 (SAT-362)
- Li, Dong, S36 (OS-050)
- Liebe, Roman, S263 (THU-526)
- Lieb, Sabine, S52 (OS-079-YI), S404 (SAT-501-YI)
- Lietz, Georg, S641 (SAT-431-YI)
- Liew, Ian Yang, S497 (FRI-295)
- Liew, Ryan Jia Jie, S826 (THU-406)
- Li, Fang, S526 (WED-246)
- Li, Feng, S106 (FRI-322), S268 (THU-546)
- Li, Fenxiang, S526 (WED-246)
- Li, Gang, S803 (WED-412)
- Lightstone, Adi, S474 (FRI-225), S591 (THU-282), S599 (THU-305)
- Li, Gong, S395 (SAT-478), S442 (THU-462)
- Li, Guangjian, S536 (WED-272)
- Li, Guang-Ming, S100 (LBP-045)
- Li, Guangxin, S395 (SAT-478)
- Li, Guixin, S790 (FRI-440)
- Liguori, Antonio, S496 (FRI-290), S516 (WED-215), S533 (WED-261-YI)
- Li, Hai, S219 (FRI-088)
- Li, Hailiang, S447 (THU-475)
- Lih, Fred, S580 (THU-247-YI)
- Li, Hongxuan, S395 (SAT-478), S442 (THU-462), S625 (FRI-021)
- Li, Jia, S536 (WED-272), S582 (THU-251-YI)
- Li, Jiajing, S464 (FRI-200), S652 (SAT-462-YI), S730 (TOP-384-YI)
- Li, Jianjun, S357 (SAT-548)
- Li, Jianping, S87 (LBP-021)
- Li, Jiaping, S447 (THU-475)
- Li, Jiaqi, S119 (SAT-322)
- Li, Jie, S161 (THU-058), S459 (TOP-307), S525 (WED-244), S527 (WED-246), S536 (WED-272), S625 (FRI-022), S628 (FRI-035), S744 (SAT-388), S757 (SAT-423), S776 (FRI-404), S780 (FRI-411-YI)
- Li, Jieying, S543 (WED-290)
- Li, Jing, S314 (THU-110), S325 (THU-132), S447 (THU-475), S621 (FRI-008), S623 (FRI-015), S625 (FRI-023), S627 (FRI-030)
- Li, Jinghu Carl, S812 (WED-377)
- Li, Jingya, S602 (TOP-217)
- Li, Juan, S119 (SAT-321)
- Li, Jun, S105 (FRI-319), S106 (FRI-323), S108 (FRI-330), S117 (SAT-318), S119 (SAT-322), S345 (FRI-546), S354 (SAT-542)
- Li, Ka Chun, S746 (SAT-394)
- Li, Kang, S357 (SAT-548)
- Li, Lanlan, S116 (SAT-314)
- Li, Lequn, S401 (SAT-495)
- Li, Ling, S527 (WED-246)
- Liljeblad, Mathias, S93 (LBP-031)
- Lillie, Katy, S408 (SAT-521)
- Lilly, Leslie, S381 (SAT-037), S381 (SAT-039)
- Lim, Chaeyeon, S144 (SAT-272)
- Li, Meng, S128 (THU-319), S288 (FRI-540)
- Li, Min, S526 (WED-246)
- Li, Minghui, S344 (THU-191), S355 (SAT-544), S738 (SAT-372), S815 (WED-387)
- Li, Mingsheng, S716 (WED-167)
- Li, Mingyang, S92 (LBP-029), S758 (TOP-400), S794 (WED-392)
- Lim, Joseph K., S771 (FRI-389), S788 (FRI-435)
- Lim, Nicholas, S242 (SAT-082)
- Limon-Miro, Ana, S218 (FRI-086)
- L'Imperio, Vincenzo, S19 (OS-017), S299 (SAT-171)
- Lim, Seng Gee, S81 (LBP-009), S797 (WED-397), S797 (WED-398)
- Lim, Wei Yen, S497 (FRI-295)
- Lim, Wen Hui, S139 (SAT-256), S366 (TOP-004), S540 (WED-282)
- Lim, Yee Siang, S578 (THU-239-YI)

- Lim, Young-Suk, S74 ([OS-121](#)),
S305 ([TOP-157](#)), S657 ([WED-424](#)),
S771 ([FRI-390](#)), S797 ([WED-397](#)),
S809 ([WED-371](#))
- Lin, Anthony, S653 ([SAT-463](#))
- Linares, Pedro, S329 ([THU-154-YI](#))
- Lin, Bingliang, S736 ([SAT-367](#))
- Lin, Che, S399 ([SAT-486](#))
- Lin, Cheng, S266 ([THU-538](#))
- Lin, Chih-Lang, S832 ([THU-365](#))
- Lin, Chih-Lin, S75 ([OS-123](#)),
S832 ([THU-365](#))
- Lin, Chun-yen, S51 ([OS-078-YI](#)),
S414 ([FRI-458](#)), S443 ([THU-464](#)),
S445 ([THU-471-YI](#)), S784 ([FRI-426](#))
- Lincoff, A. Michael, S93 ([LBP-032](#))
- Lindh, Karin, S759 ([TOP-416-YI](#)),
S777 ([FRI-406](#)), S836 ([THU-374](#))
- Lin, Daniel, S564 ([THU-198](#))
- Lindemann, Aylin, S327 ([THU-137](#))
- Linden, Daniel, S93 ([LBP-031](#))
- Lindenmeyer, Christina, S9 ([LBO-004](#)),
S89 ([LBP-026](#))
- Lindh, Magnus, S754 ([SAT-414](#))
- Lindqvist, Catarina, S635 ([THU-034-YI](#))
- Lindsey, Amber, S693 ([FRI-151](#))
- Lindström, Lina, S334 ([THU-165](#))
- Lindvig, Katrine, S47 ([OS-072-YI](#)),
S77 ([OS-126](#)), S137 ([SAT-250](#)),
S139 ([SAT-255](#)), S142 ([SAT-266](#)),
S153 ([SAT-298](#)), S205 ([FRI-045](#)),
S466 ([FRI-206-YI](#)), S503 ([TOP-241-YI](#)),
S510 ([WED-199](#)), S620 ([TOP-012](#)),
S623 ([FRI-017](#))
- Lindvig, Katrine Prier, S41 ([OS-059](#))
- Line, Pål Dag, S22 ([OS-023-YI](#)),
S386 ([SAT-050](#))
- Lin, Feng-Chang, S668 ([WED-451-YI](#))
- Lin, Frederic, S172 ([THU-092](#))
- Ling, Danielle Ho Wei, S208 ([FRI-053](#))
- Ling, Ning, S357 ([SAT-547](#))
- Ling, Sophia, S92 ([LBP-030](#))
- Lingvay, Ildiko, S93 ([LBP-032](#))
- Lin, Han-Chieh, S832 ([THU-365](#))
- Lin, Huapeng, S2 ([GS-004](#)), S38 ([OS-054](#)),
S818 ([THU-379](#))
- Li, Ning, S83 ([LBP-013](#))
- Lin, Jaw-Town, S795 ([WED-393](#))
- Linke, Alexandra, S115 ([TOP-346-YI](#))
- Lin, Kevin, S808 ([WED-366](#))
- Link, Frederik, S263 ([THU-526](#)),
S287 ([FRI-539](#))
- Link, Ralf, S820 ([THU-386-YI](#)),
S833 ([THU-366](#))
- Lin, Mandy, S97 ([LBP-039](#))
- Lin, Min, S238 ([SAT-069](#))
- Lin, Minghua, S219 ([FRI-088](#))
- Lin, Po-Ting, S51 ([OS-078-YI](#)),
S414 ([FRI-458](#))
- Lin, Renyong, S365 ([WED-029](#))
- Lin, Ruihe, S411 ([SAT-530](#))
- Lin, Shi-Ming, S3 ([GS-005](#)),
S414 ([FRI-458](#))
- Linton, Kenneth, S298 ([SAT-167-YI](#))
- Lin, Tse-I, S806 ([WED-361](#)),
S807 ([WED-365](#)), S812 ([WED-378](#))
- Lin, WeiQi, S8 ([LBO-003](#))
- Lin, Yanjie, S738 ([SAT-372](#))
- Lin, Yen-Chen, S449 ([THU-480](#))
- Lin, Yi-Hung, S490 ([FRI-271](#)),
S493 ([FRI-280](#))
- Lin, Yongmei, S786 ([FRI-430](#))
- Lin, Yuanbang, S354 ([SAT-542](#))
- Lin, Zhengyu, S447 ([THU-475](#))
- Lin, Ziping, S543 ([WED-290](#))
- Linzmeier, Luise, S56 ([OS-086-YI](#))
- Lionetti, Marta, S459 ([TOP-301](#))
- Li, Peng, S117 ([SAT-318](#))
- Li, Pengfei, S464 ([FRI-200](#)),
S652 ([SAT-462-YI](#)), S730 ([TOP-384-YI](#))
- Li, Phyllis Gan Xiu, S565 ([THU-200-YI](#))
- Li, Ping, S769 ([FRI-382](#))
- Li, Qiang, S395 ([SAT-478](#))
- Lira, Alba, S233 ([FRI-126](#))
- Li, Rong, S361 ([WED-010](#))
- Li, Rongkuan, S119 ([SAT-321](#)),
S769 ([FRI-382](#))
- Li, Shu, S333 ([THU-163](#))
- Lisi, Chiara, S451 ([THU-486-YI](#))
- Li, Size, S194 ([WED-114](#))
- Liška, Václav, S349 ([FRI-556](#))
- Lisman, Ton, S112 ([FRI-342](#)),
S177 ([WED-068-YI](#)), S250 ([SAT-105](#))
- Li, Songming, S369 ([SAT-009](#))
- Lissenberg-Witte, Birgitte, S18 ([OS-015](#))
- Li, Taishun, S260 ([SAT-136](#))
- Li, Taoyuan, S543 ([WED-290](#))
- Littera, Roberto, S322 ([THU-127-YI](#))
- Littlejohn, Margaret, S740 ([SAT-377](#))
- Little, Stephanie, S676 ([WED-471](#)),
S759 ([TOP-417](#))
- Liu, Biyu, S357 ([SAT-548](#))
- Liu, Chang Hai, S494 ([FRI-285](#))
- Liu, Cheng, S727 ([TOP-357](#)),
S728 ([TOP-358-YI](#))
- Liu, Chenghai, S209 ([FRI-053](#))
- Liu, Chengyu, S526 ([WED-246](#))
- Liu, Chenrui, S195 ([WED-116](#))
- Liu, Chenyi, S333 ([THU-163](#))
- Liu, Chien-An, S449 ([THU-480](#))
- Liu, Chuan, S526 ([WED-246](#)),
S536 ([WED-272](#)), S544 ([WED-292](#)),
S620 ([TOP-006](#))
- Liu, Chun-Jen, S75 ([OS-123](#)),
S811 ([WED-375](#)), S832 ([THU-365](#))
- Liu, Cong, S278 ([WED-533](#))
- Liu, Dengxiang, S526 ([WED-246](#))
- Liu, Fangjun, S693 ([FRI-151](#))
- Liu, Fei, S100 ([LBP-045](#)), S605 ([SAT-198](#))
- Liu, Hanyang, S298 ([SAT-170](#)),
S566 ([THU-201-YI](#))
- Liu, Hao, S536 ([WED-272](#))
- Liu, Huiru, S230 ([FRI-119](#)), S405 ([SAT-503](#)),
S454 ([THU-499](#))
- Liu, Jiangyu, S227 ([FRI-111](#)),
S677 ([WED-472](#))
- Liu, Jiao, S531 ([WED-258](#))
- Liu, Jin, S525 ([WED-242](#))
- Liu, Jing, S161 ([THU-058](#))
- Liu, Jinsong, S403 ([SAT-499](#))
- Liu, Jinxia, S590 ([THU-280](#))
- Liu, Jinze, S60 ([OS-095](#))
- Liu, Juan, S769 ([FRI-382](#))
- Liu, Jun, S135 ([THU-343](#))
- Liu, Kaipeng, S230 ([FRI-119](#)),
S405 ([SAT-503](#)), S454 ([THU-499](#))
- Liu, Ken, S9 ([LBO-004](#)), S89 ([LBP-026](#)),
S338 ([THU-177-YI](#)), S380 ([SAT-036-YI](#)),
S540 ([WED-282](#))
- Liu, Kuan, S730 ([TOP-384-YI](#))
- Liu, Kui, S614 ([SAT-225](#)), S618 ([SAT-243](#))
- Liu, Lan, S536 ([WED-272](#))
- Liu, Lili, S227 ([FRI-111](#)), S677 ([WED-472](#))
- Liu, Liwei, S121 ([SAT-326](#))
- Liu, Margaret C., S43 ([OS-064](#)),
S152 ([SAT-297](#))
- Liu, Mei, S121 ([SAT-330](#))
- Liu, Min, S135 ([THU-342](#))
- Liu, Nan, S726 ([TOP-354](#))
- Liu, Qing, S220 ([FRI-091](#))
- Liu, Ruiyang, S418 ([FRI-471](#))
- Liu, Ruyu, S344 ([THU-191](#))
- Liu, Shanghao, S526 ([WED-246](#)),
S536 ([WED-272](#)), S620 ([TOP-006](#))
- Liu, Shi, S95 ([LBP-037](#))
- Liu, Tianhuang, S605 ([SAT-198](#))
- Liu, Tianxu, S748 ([SAT-398](#))
- Liu, Tong, S145 ([SAT-274](#))
- Liu, Weihong, S36 ([OS-050](#)), S87 ([LBP-021](#))
- Liu, Wen-Jie, S75 ([OS-123](#))
- Liu, Wenya, S628 ([FRI-034](#))
- Liu, Wen-Yue, S2 ([GS-004](#)), S38 ([OS-054](#)),
S526 ([WED-246](#))
- Liu, Xiangyu, S505 ([TOP-264](#))
- Liu, Xiaojun, S119 ([SAT-321](#))
- Liu, Xiaoquan, S574 ([THU-226](#))
- Liu, Xing, S526 ([WED-246](#))
- Liu, Xingxiang, S628 ([FRI-035](#)),
S780 ([FRI-411-YI](#))
- Liu, Xionghao, S590 ([THU-279](#))
- Liu, Xuanchen, S230 ([FRI-119](#)),
S400 ([SAT-491](#)), S405 ([SAT-503](#))
- Liu, Xue, S804 ([WED-415](#))
- Liu, Xujie, S102 ([LBP-048](#))
- Liu, Yali, S95 ([LBP-037](#))
- Liu, Yang, S100 ([LBP-045](#)), S737 ([SAT-371](#)),
S750 ([SAT-405](#))
- Liu, Yanning, S110 ([FRI-334](#))
- Liu, Yaozu, S240 ([SAT-075-YI](#)),
S256 ([SAT-124](#))
- Liu, Yen-Chun, S656 ([TOP-461-YI](#)),
S772 ([FRI-391](#)), S782 ([FRI-415](#)),
S784 ([FRI-426](#))
- Liu, Yi, S543 ([WED-290](#))
- Liu, Yihan, S138 ([SAT-251](#))
- Liu Yin, James, S725 ([WED-192](#))
- Liu, Yi-Qi, S684 ([WED-490](#)), S790 ([FRI-439](#))
- Liu, Yiwen, S87 ([LBP-021](#))
- Liu, Yongping, S775 ([FRI-398](#))
- Liu, Yunfang, S544 ([WED-292](#))
- Liu, Yunpeng, S99 ([LBP-042](#))
- Liu, Zhe-Rui, S124 ([SAT-336](#))

Author Index

- Liu, Zhilong, S271 ([TOP-562](#)), S347 ([FRI-551](#)), S363 ([WED-020](#))
- Livia, Bumbu Andreea, S144 ([SAT-273-YI](#))
- Livingston, Christine, S745 ([SAT-390](#))
- Livingston, Rebecca, S630 ([THU-015-YI](#))
- Li, Wang, S390 ([TOP-510](#))
- Li, Wei, S11 ([LBO-006](#)), S99 ([LBP-042](#))
- Li, Wenbin, S305 ([TOP-168-YI](#)), S688 ([WED-499](#))
- Li, Wenhao, S578 ([THU-236-YI](#))
- Li, Xiaoke, S194 ([WED-114](#)), S755 ([SAT-419](#)), S762 ([FRI-366](#))
- Li, Xiaoran, S778 ([FRI-407](#))
- Li, Xingjie, S152 ([SAT-297](#))
- Li, Xinjie, S526 ([WED-246](#))
- Li, Xinting, S783 ([FRI-419](#))
- Li, Xinxin, S355 ([SAT-544](#)), S815 ([WED-387](#))
- Lix, Lisa, S643 ([SAT-436](#))
- Li, Xue, S116 ([SAT-314](#)), S745 ([SAT-392](#))
- Li, Xuefeng, S526 ([WED-246](#))
- Li, Xuejiao, S271 ([TOP-562](#)), S347 ([FRI-551](#)), S363 ([WED-020](#))
- Li, Yang, S21 ([OS-021-YI](#))
- Li, Yangyang, S488 ([FRI-267](#))
- Li, Yanqiu, S792 ([WED-390](#))
- Li, Yaping, S195 ([WED-116](#)), S786 ([FRI-430](#))
- Li, Yiguang, S628 ([FRI-035](#))
- Li, Yiling, S536 ([WED-272](#))
- Li, Ying, S241 ([SAT-077](#)), S622 ([FRI-010](#))
- Li, Yong, S235 ([FRI-131](#))
- Li, Yuecui, S531 ([WED-258](#))
- Li, Yujia, S263 ([THU-526](#)), S287 ([FRI-539](#))
- Li, Yuyu, S234 ([FRI-129](#))
- Lizaola-Mayo, Blanca, S608 ([SAT-207](#))
- Lizardi, Javier, S627 ([FRI-029](#))
- Li, Zhihao, S381 ([SAT-037](#)), S381 ([SAT-039](#)), S445 ([THU-470-YI](#))
- Li, Zhihui, S527 ([WED-246](#)), S536 ([WED-272](#))
- Li, Zhipeng, S109 ([FRI-331](#))
- Li, Zixiang, S447 ([THU-475](#))
- Llarch, Neus, S455 ([THU-500](#))
- Llavall, Anna Clavé, S46 ([OS-070](#))
- Lledó, José Luis, S455 ([THU-501](#))
- Lleo, Ana, S18 ([OS-015](#)), S19 ([OS-017](#)), S96 ([LBP-038](#)), S306 ([THU-093](#)), S308 ([THU-098](#)), S310 ([THU-101](#)), S341 ([THU-182](#)), S404 ([SAT-502-YI](#)), S406 ([SAT-514](#)), S439 ([THU-447](#)), S447 ([THU-474-YI](#))
- Llibre-Nieto, Gemma, S233 ([FRI-126](#))
- Llinás, Margarita Sala, S318 ([THU-118](#))
- Llorca, Anne, S503 ([TOP-241-YI](#)), S550 ([WED-317](#))
- Llorens, Jordi Vengohechea, S362 ([WED-016](#))
- Llovet, Josep, S411 ([TOP-507-YI](#)), S417 ([FRI-467](#))
- Llovet, Laura Patricia, S374 ([SAT-021](#))
- Llovet, Llaura, S5 ([GS-007](#))
- Lloyd, Thomas, S559 ([WED-340](#))
- Lluch-García, Paloma, S232 ([FRI-125](#))
- Lo, Ching-Chu, S832 ([THU-365](#))
- Lo, Chingchu, S74 ([OS-121](#))
- Locus, Tatjana, S658 ([WED-426](#))
- Loew, Damarys, S193 ([WED-112](#)), S524 ([WED-239](#))
- Loey Mak, Lung Yi, S781 ([FRI-413](#))
- Loffredo-Verde, Eva, S34 ([OS-045](#))
- Lo, Gin-Ho, S26 ([OS-031](#))
- Loglio, Alessandro, S73 ([OS-120](#)), S439 ([THU-447](#)), S470 ([FRI-215-YI](#)), S793 ([WED-391](#)), S804 ([WED-414](#))
- Lo, Gora, S743 ([SAT-387](#))
- Lohoues, Marie Jeanne, S208 ([FRI-053](#))
- Lohr, Carolin, S426 ([FRI-495](#))
- Lohr, Matthias, S710 ([WED-152](#))
- Lohse, Ansgar, S730 ([TOP-369](#))
- Lohse, Ansgar W., S5 ([GS-007](#)), S24 ([OS-027-YI](#)), S44 ([OS-066-YI](#)), S265 ([THU-534-YI](#)), S316 ([THU-113](#)), S335 ([THU-167](#)), S350 ([SAT-531-YI](#)), S374 ([SAT-021](#))
- Loinaz, Carmelo, S9 ([LBO-004](#)), S89 ([LBP-026](#))
- Loizides, Anthony, S715 ([WED-166](#))
- Lok, Anna, S214 ([FRI-075](#))
- Lok, James, S775 ([FRI-399](#)), S780 ([FRI-410](#)), S820 ([THU-383](#))
- Lolatto, Riccardo, S824 ([THU-402](#))
- Loman, Nick, S675 ([WED-469](#)), S752 ([SAT-409](#))
- Lomas, Raquel, S828 ([THU-411](#))
- Lombard, Alice, S280 ([WED-540-YI](#))
- Lombardi, Rosa, S466 ([FRI-207-YI](#)), S470 ([FRI-215-YI](#)), S474 ([FRI-226](#)), S482 ([FRI-248-YI](#)), S496 ([FRI-290](#)), S497 ([FRI-294](#))
- Lombardo, Antonino, S206 ([FRI-047-YI](#)), S252 ([SAT-113](#))
- Lombardo, Daniele, S422 ([FRI-481](#)), S740 ([SAT-378](#)), S747 ([SAT-397](#))
- Lombardo, Flavia L, S817 ([THU-378](#))
- Lonardi, Sara, S395 ([SAT-477-YI](#)), S438 ([THU-446](#)), S446 ([THU-472-YI](#))
- Londoño, María Carlota, S98 ([LBP-040](#)), S105 ([FRI-321](#)), S291 ([TOP-149-YI](#)), S308 ([THU-098](#)), S311 ([THU-102-YI](#)), S318 ([THU-118](#)), S468 ([FRI-211](#)), S710 ([WED-153](#))
- Long, Clara, S683 ([WED-486-YI](#))
- Longerich, Thomas, S23 ([OS-025-YI](#)), S273 ([WED-521-YI](#)), S426 ([FRI-495](#))
- Long, Mian, S83 ([LBP-013](#))
- Long, Michelle, S93 ([LBP-032](#))
- Longo, Miriam, S516 ([WED-218](#))
- Long, Shann, S826 ([THU-406](#))
- Lønsmann, Ida, S579 ([THU-243](#))
- Looby, Richard, S693 ([FRI-151](#))
- Loo, Jessica, S592 ([THU-284](#))
- Loomba, Rohit, S4 ([GS-011](#)), S7 ([GS-012](#)), S7 ([LBO-001](#)), S49 ([OS-074](#)), S71 ([OS-117](#)), S72 ([OS-118](#)), S76 ([OS-125](#)), S79 ([LBP-003](#)), S93 ([LBP-031](#)), S95 ([LBP-036](#)), S147 ([SAT-281](#)), S505 ([TOP-264](#)), S505 ([TOP-265](#)), S515 ([WED-212](#)), S522 ([WED-235](#)), S540 ([WED-282](#)), S543 ([WED-291](#)), S544 ([WED-294](#)), S607 ([SAT-202](#)), S607 ([SAT-203](#)), S609 ([SAT-208](#)), S610 ([SAT-212](#)), S615 ([SAT-231](#)), S696 ([FRI-161](#)), S724 ([WED-188](#))
- Loomes, Kathleen M., S715 ([WED-166](#))
- Loosen, Sven H., S259 ([SAT-135](#))
- Loo, Xiu Ying, S497 ([FRI-295](#))
- Lopategi, Aritz, S569 ([THU-210](#))
- Lopatriello, Stefania, S725 ([WED-191](#))
- Lopes, Maykel, S347 ([FRI-550](#))
- Lopez, Andrew, S737 ([SAT-371](#))
- Lopez-Benages, Eva, S635 ([THU-039-YI](#))
- López-Bermudo, Lucía, S71 ([OS-116](#)), S593 ([THU-287](#))
- López-Cánovas, Juan L., S415 ([FRI-462-YI](#))
- López-Cardona, Julia, S700 ([FRI-171](#))
- López-Garrido, M. Ángeles, S779 ([FRI-409](#))
- López-Gómez, Marta, S559 ([WED-339](#))
- López, Guillermo Paz, S103 ([TOP-350-YI](#))
- López, Ilsa, S627 ([FRI-029](#))
- Lopez-Labrador, F. Xavier, S361 ([WED-009](#))
- Lopez, Laia Grau, S141 ([SAT-262](#))
- Lopez, Marina Gigante, S541 ([WED-284-YI](#))
- López, Marta, S765 ([FRI-373](#))
- Lopez-Pascual, Amaya, S287 ([FRI-538](#)), S348 ([FRI-555](#)), S416 ([FRI-464](#))
- López-Sáez, Berta, S141 ([SAT-262](#)), S233 ([FRI-126](#))
- Lopez, Sonia Alonso, S818 ([THU-381](#))
- Lopez-Talavera, Juan Carlos, S517 ([WED-220](#))
- López-Vicario, Cristina, S16 ([OS-011](#)), S174 ([TOP-073](#)), S185 ([WED-087](#))
- Lorduy, Benjamin Polo, S598 ([THU-302](#)), S599 ([THU-304](#)), S818 ([THU-381](#))
- Lorefice, Elisabetta, S674 ([WED-467-YI](#))
- Lorenc, Beata, S685 ([WED-493-YI](#)), S821 ([THU-389](#)), S834 ([THU-367-YI](#))
- Lorente, Sara, S329 ([THU-154-YI](#)), S717 ([WED-172](#))
- Lorenzo, Andrea Di, S59 ([OS-094](#)), S772 ([FRI-392-YI](#))
- Lorenzo, Stefania De, S395 ([SAT-477-YI](#)), S446 ([THU-472-YI](#))
- Lorenzo, Surace, S332 ([THU-161](#))
- Lorkowski, Stefan, S600 ([THU-314](#))
- Lorrai, Michela, S322 ([THU-127-YI](#))
- Losito, Francesco, S96 ([LBP-038](#)), S306 ([THU-093](#))
- Loste, Maria Teresa Arias, S468 ([FRI-211](#)), S640 ([SAT-429](#))
- Lotichius, Maria Hoppe, S375 ([SAT-023](#))
- Lotto, Mattia, S627 ([FRI-028](#))
- Lou, Guohua, S110 ([FRI-334](#)), S586 ([THU-262](#))
- Loumaye, Audrey, S151 ([SAT-293-YI](#)), S473 ([FRI-224](#))
- Lourenco, Jose, S746 ([SAT-394](#))
- Loustaud-Ratti, Veronique, S28 ([OS-034](#)), S41 ([OS-060](#)), S70 ([OS-115](#)), S387 ([SAT-052](#)), S444 ([THU-466](#)), S802 ([WED-410](#))
- Louvet, Alexandre, S6 ([GS-010](#)), S8 ([LBO-003](#)), S61 ([OS-097](#)),

- S91 (LBP-027), S156 (TOP-108), S644 (SAT-439-YI)
- Lovatt, Jessica, S150 (SAT-291)
- Loveridge, Robert, S44 (OS-065)
- Lövgren-Sandblom, Anita, S274 (WED-523)
- Lovley, Andrew, S485 (FRI-258)
- Low, Albert, S637 (THU-046)
- Lowen, Vanessa, S632 (THU-021)
- Low, Jian Hui, S578 (THU-239-YI)
- Loya, Julio, S654 (SAT-466)
- Lozano, Adelina, S83 (LBP-012)
- Lozano, Elisa, S432 (FRI-523), S433 (FRI-526)
- Lubel, John, S338 (THU-177-YI), S400 (SAT-492), S653 (SAT-464-YI)
- Luber, Andrew, S86 (LBP-018)
- Lu, Bingxia, S99 (LBP-043)
- Lubuela, Gwladys, S372 (SAT-016)
- Luca', Martina, S376 (SAT-025)
- Lucà, Martina, S227 (FRI-110)
- Lucantoni, Federico, S266 (THU-539)
- Lucas, Kathryn Jean, S8 (LBO-002), S544 (WED-294)
- Lucatelli, Pierleone, S215 (FRI-077-YI)
- Lucchina, Natalie, S238 (SAT-068)
- Lucena, Felipe, S348 (FRI-555)
- Lucena, Maria Isabel, S18 (OS-015), S103 (TOP-350-YI), S341 (THU-182)
- Lucero, Ignacio, S342 (THU-185)
- Luciani, Alain, S50 (OS-077), S413 (FRI-456), S453 (THU-494), S720 (WED-178)
- Lucia, Pietro Di, S35 (OS-048)
- Lucidi, Valerio, S89 (LBP-026)
- Luckhardt, Sonja, S104 (TOP-352)
- Ludovica Fracanzani, Anna, S470 (FRI-215-YI), S474 (FRI-226), S482 (FRI-248-YI), S704 (TOP-144-YI)
- Ludvigsson, Jonas F, S334 (THU-165)
- Ludwigs, Lina, S273 (WED-521-YI)
- Luedde, Tom, S259 (SAT-135), S296 (SAT-163-YI), S392 (SAT-469), S426 (FRI-495)
- Luetgehmman, Marc, S733 (SAT-342-YI)
- Lu, Fengmin, S769 (FRI-382), S775 (FRI-402), S790 (FRI-440)
- Lu, Genliang, S692 (FRI-151)
- Lugon, Nicolas, S218 (FRI-086)
- Lu, Hongzhou, S605 (SAT-198)
- Luiz dos Santos, Jorge, S692 (TOP-146)
- Lujambio, Amaia, S415 (FRI-459), S562 (TOP-229-YI)
- Lu, Jingyi, S419 (FRI-473)
- Lukasziak, Magdalena, S289 (FRI-542)
- Luketic, Velimir, S1 (GS-001)
- Lu, Liuqiang, S485 (FRI-257)
- Lulli, Matteo, S428 (FRI-502)
- Lu, Lungen, S806 (WED-362), S813 (WED-381)
- Lu, Mingqin, S209 (FRI-053), S333 (THU-163)
- Lumley, Sheila, S675 (WED-469), S752 (SAT-409), S756 (SAT-421)
- Lundberg, Peter, S530 (WED-255-YI), S532 (WED-259)
- Lundqvist, Annamari, S460 (TOP-308), S562 (TOP-240-YI)
- Luni, Camilla, S128 (THU-320-YI)
- Lun, Liou Wei, S209 (FRI-053)
- Luo, Bohan, S716 (WED-167)
- Luo, Jianjun, S240 (SAT-075-YI), S256 (SAT-124)
- Luo, Jiing-Chyuan, S256 (SAT-125), S449 (THU-479)
- Luo, Jinjin, S117 (SAT-318), S119 (SAT-322)
- Luo, Min, S727 (TOP-357)
- Luong, Xuan, S565 (THU-198)
- Luo, Qiumin, S109 (FRI-331)
- Luo, Xinhua, S257 (SAT-126)
- Luo, Xuan, S198 (WED-124), S382 (SAT-041)
- Lupberger, Joachim, S42 (OS-061), S734 (SAT-348-YI)
- Lupsor-Platon, Monica, S521 (WED-232-YI), S556 (WED-332)
- Lupu, Amanda, S683 (WED-486-YI)
- Lupu, Gabriel, S403 (SAT-498)
- Lu, Qinghua, S783 (FRI-420)
- Luque, Natalia, S455 (THU-501)
- Luque, Raul M, S415 (FRI-462-YI)
- Lurje, Georg, S366 (TOP-003-YI)
- Lurz, Eberhart, S54 (OS-083)
- Lu, Shelly C., S39 (OS-055)
- Lusina, Ekaterina, S52 (OS-080), S238 (SAT-068), S501 (FRI-305)
- lusivka-Nzinga, Clovis, S41 (OS-060)
- Luther, Jay, S131 (THU-330)
- Lu, Tingting, S99 (LBP-043)
- Luu, Khoa, S693 (FRI-151)
- Luukkonen, Panu K., S562 (TOP-240-YI)
- Luu, Nguyet, S101 (LBP-046)
- Lu, Wei, S230 (FRI-119), S405 (SAT-503), S454 (THU-499)
- Lu, Wei-Yu, S291 (TOP-148)
- Lu, Wenting, S236 (FRI-135)
- Lu, Xiaobo, S783 (FRI-419), S785 (FRI-428), S803 (WED-412)
- Lu, Xiaomin, S505 (TOP-264)
- Lu, Xingyu, S95 (LBP-037)
- Lu, Yao, S344 (THU-191)
- Lu, Ya-Wen, S124 (SAT-336)
- Luyendyk, James, S112 (FRI-342)
- Lu, Zhi, S362 (WED-017-YI)
- Luzón-García, M. Pilar, S779 (FRI-409)
- Lv, Fangfang, S87 (LBP-021), S526 (WED-246), S605 (SAT-198)
- Lv, Guoyue, S551 (WED-319), S558 (WED-338), S602 (TOP-217)
- Lv, Jianxiang, S36 (OS-050)
- Lv, Jiaojian, S526 (WED-246)
- Lv, Lingchun, S100 (LBP-045)
- Lv, Ruimin, S59 (OS-093)
- Lv, Zicheng, S623 (FRI-016)
- Lyberopoulou, Angeliki, S322 (THU-126), S325 (THU-134)
- Lygoura, Vasiliki, S311 (THU-102-YI)
- Lymberopoulos, Dimitrios, S798 (WED-403)
- Lynch, Erica Nicola, S342 (THU-184), S718 (WED-174)
- Lynch, Kate, S338 (THU-177-YI)
- Lynch, Shannan, S819 (THU-382)
- Lynn, Soe Einsin, S578 (THU-239-YI)
- Lyons, Anabel Martinez, S66 (OS-105-YI)
- Lyra, André Castro, S83 (LBP-012)
- Lytvyak, Ellina, S18 (OS-015), S19 (OS-018), S305 (TOP-169), S308 (THU-098), S315 (THU-111), S374 (SAT-021)
- Lyu, Xueying, S419 (FRI-473)
- Ma, Ann Thu, S30 (OS-038-YI), S199 (TOP-062), S200 (TOP-064-YI)
- Maan, Rael, S30 (OS-038-YI), S199 (TOP-062), S200 (TOP-064-YI), S380 (SAT-035)
- Maarten Vrolijk, Jan, S327 (THU-138)
- Maasoumy, Benjamin, S61 (OS-096-YI), S172 (THU-092), S202 (FRI-038-YI), S204 (FRI-042), S205 (FRI-044-YI), S226 (FRI-107-YI), S226 (FRI-109), S242 (SAT-080-YI), S245 (SAT-090-YI), S253 (SAT-117), S350 (SAT-532-YI), S730 (TOP-369), S735 (SAT-363), S818 (THU-381)
- Mabile-Archambeaud, Isabelle, S168 (THU-079)
- Mabrut, Jean-Yves, S22 (OS-022), S369 (SAT-010)
- Macaigne, Gilles, S640 (SAT-430)
- MacCannell, Amanda, S573 (THU-222-YI)
- Maccariello, Silvana, S836 (THU-375)
- MacCarthy, Hannah, S645 (SAT-441-YI)
- Macchiarulo, Antonio, S126 (THU-316)
- Macchi, Chiara, S491 (FRI-275-YI)
- Maccioni, Luca, S124 (TOP-312)
- MacConell, Leigh, S614 (SAT-225), S614 (SAT-227)
- MacDonald, Andrew, S265 (THU-535-YI)
- Macdonald, Brock, S778 (FRI-407)
- Macdonald, Douglas, S661 (WED-432), S672 (WED-462), S684 (WED-491), S688 (WED-500)
- Macdonald, Graeme, S559 (WED-340)
- Macedo, Guilherme, S18 (OS-015)
- Macek, Celina, S191 (WED-106)
- Macek Jilkova, Zuzana, S747 (SAT-396)
- MacEwan, Joanna P., S314 (THU-110), S621 (FRI-008)
- Machado, Nathália, S271 (THU-556)
- Machaj, Gabriela, S304 (SAT-184)
- Ma, Cheng, S149 (SAT-287)
- Macías, Manuel, S779 (FRI-409)
- Macias, Rocio, S432 (FRI-523), S433 (FRI-526)
- Macias-Rodriguez, Ricardo, S602 (TOP-205)
- Maciejewski, Sonia, S75 (OS-127), S812 (WED-376)
- Macke, Amanda, S132 (THU-333)
- Macleod, Sharon, S783 (FRI-423)
- MacMillan, Mark, S81 (LBP-007)
- Macnaughtan, Jane, S17 (OS-014-YI), S182 (WED-078)
- MacParland, Sonya, S31 (OS-040-YI)

Author Index

- Macpherson, Iain, S14 ([OS-007-YI](#)), S81 ([LBP-007](#))
- MacQuillan, Gerry, S219 ([FRI-088](#))
- Macrae, James, S750 ([SAT-404](#))
- Madaleno, Joao, S30 ([OS-038-YI](#)), S115 ([TOP-346-YI](#)), S199 ([TOP-062](#)), S200 ([TOP-064-YI](#))
- Madamba, Egbert, S522 ([WED-235](#)), S543 ([WED-291](#))
- Madathil, SaiBala, S31 ([OS-039](#))
- Madejón, Antonio, S700 ([FRI-171](#)), S787 ([FRI-432](#))
- Made, Lilian Torres, S208 ([FRI-053](#))
- Maderazo, Maida, S806 ([WED-361](#)), S807 ([WED-365](#)), S812 ([WED-378](#))
- Madhukar, Patel, S368 ([SAT-009](#))
- Madhusudhan, Kumble S, S546 ([WED-298-YI](#))
- Mädler, Sophia, S32 ([OS-041-YI](#))
- Madrid, Teresa Maria Jordan, S668 ([WED-449](#))
- Madsen, Lone, S149 ([SAT-286-YI](#))
- Maeso-Gonzalez, Javier, S197 ([WED-123](#))
- Maestri, Marcello, S428 ([FRI-514](#))
- Maevskaia, Marina, S232 ([FRI-124](#))
- Maffi, Gabriele, S470 ([FRI-215-YI](#))
- Maffini, Larissa, S636 ([THU-044](#))
- Magaz, Marta, S705 ([WED-129](#))
- Ma, Genshan, S100 ([LBP-045](#))
- Mageras, Anna, S659 ([WED-428-YI](#)), S669 ([WED-453](#)), S674 ([WED-465](#))
- Mager, Lukas, S65 ([OS-103](#))
- Maggioni, Marco, S413 ([FRI-456](#)), S438 ([THU-446](#)), S705 ([WED-130](#))
- Maggiore, Giuseppe, S374 ([SAT-021](#))
- Maggs, Daniel, S210 ([LBP-045](#))
- Magistri, Paolo, S389 ([SAT-060](#))
- Magnanensi, Jeremy, S171 ([THU-088](#))
- Magnes, Marzena, S555 ([WED-330](#)), S561 ([WED-348](#))
- Magri, Giovanni, S557 ([WED-336](#))
- Magrofuoco, Maria, S59 ([OS-094](#))
- Magyar, Christian, S373 ([SAT-019](#)), S381 ([SAT-037](#)), S381 ([SAT-039](#))
- Mahadevan, Sangeetha, S729 ([TOP-368](#))
- Ma, Haiyan, S36 ([OS-050](#))
- Mahajan, Shivani, S11 ([LBO-006](#))
- Mahallawi, Waleed, S172 ([THU-090](#))
- Mahapatra, Soumya Jagannath, S201 ([TOP-065](#))
- Mahar, Alyson, S643 ([SAT-436](#))
- Maharshi, Sudhir, S158 ([THU-052](#)), S167 ([THU-078](#)), S225 ([FRI-106-YI](#))
- Maheshwari, Deepanshu, S184 ([WED-086](#)), S195 ([WED-118](#)), S360 ([SAT-557-YI](#))
- Mahgoub, Sara, S2 ([GS-004](#)), S38 ([OS-054](#)), S101 ([LBP-046](#))
- Mahmud, Nadim, S253 ([SAT-116](#))
- Ma, Hong, S95 ([LBP-037](#)), S815 ([WED-386](#)), S816 ([WED-388](#))
- Mai, Ahn, S3 ([GS-005](#))
- Maier, Felix, S54 ([OS-083](#))
- Maier, Melanie, S788 ([FRI-434](#))
- Maieron, Andreas, S500 ([FRI-303](#)), S773 ([FRI-394](#))
- Mai, Jiajia, S99 ([LBP-043](#))
- Maille, Pascale, S413 ([FRI-456](#)), S743 ([SAT-386-YI](#))
- Mailly, Laurent, S17 ([OS-013](#)), S25 ([OS-029](#)), S31 ([OS-040-YI](#))
- Maimaitinijati, Yusufukadier, S433 ([FRI-527](#))
- Maimone, Sergio, S345 ([THU-192](#))
- Maina, Flavio, S303 ([SAT-183](#))
- Mainar, Antoni Sicras, S827 ([THU-410](#))
- Maini, Mala, S765 ([FRI-373](#))
- Maino, Cesare, S325 ([THU-133-YI](#))
- Maio, Giovanni Di, S439 ([THU-454](#))
- Maiorova, Evguenia, S737 ([SAT-371](#)), S750 ([SAT-405](#))
- Maire, Cecile, S24 ([OS-027-YI](#))
- Maisonnette, Patrick, S18 ([OS-015](#))
- Maiwall, Rakhi, S30 ([OS-038-YI](#)), S103 ([TOP-349-YI](#)), S108 ([FRI-327-YI](#)), S125 ([TOP-329-YI](#)), S127 ([THU-318](#)), S158 ([THU-052](#)), S164 ([THU-068](#)), S164 ([THU-069](#)), S164 ([THU-070](#)), S199 ([TOP-062](#)), S200 ([TOP-064-YI](#)), S294 ([SAT-155](#)), S476 ([FRI-231](#)), S605 ([SAT-199](#))
- Majano, Lucía, S329 ([THU-154-YI](#))
- Majarian, Marina, S819 ([THU-382](#))
- Majeed, Ammar, S338 ([THU-177-YI](#)), S402 ([SAT-496](#)), S653 ([SAT-464-YI](#))
- Ma, Jingqin, S240 ([SAT-075-YI](#)), S256 ([SAT-124](#))
- Maji, Prabir, S158 ([THU-052](#)), S167 ([THU-078](#))
- Major, Marian, S43 ([OS-063](#))
- Majumdar, Avik, S23 ([OS-024](#)), S338 ([THU-177-YI](#)), S400 ([SAT-492](#)), S534 ([WED-267](#))
- Ma, Jun, S395 ([SAT-479-YI](#))
- Mak, Anne Linde, S513 ([WED-209](#))
- Makara, Michael, S311 ([THU-103](#))
- Ma, Kevin, S200 ([TOP-063](#)), S216 ([FRI-081](#))
- Makhija, Dilip, S687 ([WED-498](#))
- Makhlouf, Christina, S740 ([SAT-377](#))
- Mak, Lung-Yi, S86 ([LBP-019](#)), S424 ([FRI-490-YI](#)), S739 ([SAT-375](#)), S742 ([SAT-383](#))
- Mak, Lung Yi Loey, S27 ([OS-032](#)), S116 ([SAT-314](#)), S745 ([SAT-392](#)), S770 ([FRI-388](#)), S810 ([WED-373-YI](#))
- Makokha, Grace N, S735 ([SAT-364](#))
- Makowski, Markus, S213 ([FRI-071](#))
- Maksud, Philippe, S50 ([OS-077](#))
- Makuza, Jean Damascene, S40 ([OS-058](#)), S659 ([WED-429](#)), S824 ([THU-399-YI](#))
- Makwana, Hardik, S423 ([FRI-486](#))
- Malagnino, Vincenzo, S59 ([OS-094](#)), S772 ([FRI-392-YI](#)), S791 ([FRI-442](#))
- Malam, Yogeshkumar, S81 ([LBP-008](#))
- Ma, Lan, S526 ([WED-246](#))
- Malayil, George, S31 ([OS-039](#))
- Maldonado, Adriana, S556 ([WED-334](#)), S641 ([SAT-432](#)), S642 ([SAT-434](#)), S654 ([SAT-466](#))
- Malek, Amina, S326 ([THU-136](#))
- Malek, Nisar P., S368 ([SAT-008](#))
- Malenstein, Hannah Van, S125 ([TOP-328-YI](#))
- Maleux, Geert, S125 ([TOP-328-YI](#)), S246 ([SAT-092-YI](#))
- Maley, Michael, S657 ([WED-422](#)), S676 ([WED-470](#))
- Malham, Vanessa Bou, S432 ([FRI-525](#))
- Malhi, Harmeet, S134 ([THU-341](#)), S533 ([WED-263](#)), S586 ([THU-266](#)), S714 ([WED-163](#))
- Ma, Li, S256 ([SAT-124](#))
- Malino, Donald, S341 ([THU-182](#))
- Malinverno, Federica, S19 ([OS-017](#)), S310 ([THU-101](#)), S332 ([THU-161](#))
- Malizia, Giuseppe, S557 ([WED-336](#))
- Mallela, Venkata Ramana, S349 ([FRI-556](#))
- Mallet, Maxime, S61 ([OS-097](#)), S239 ([SAT-071](#))
- Mallet, Vincent, S54 ([OS-084-YI](#)), S470 ([FRI-215-YI](#)), S698 ([FRI-165](#)), S741 ([SAT-380](#)), S760 ([FRI-361](#))
- Mallick, Himel, S138 ([SAT-251](#))
- Mallon, Jake, S567 ([THU-203](#))
- Malmström, Sebastian, S754 ([SAT-414](#))
- Maltman, Jessica, S197 ([WED-123](#))
- Malvestiti, Francesco, S459 ([TOP-301](#)), S491 ([FRI-275-YI](#)), S571 ([THU-218](#)), S704 ([TOP-144-YI](#))
- Malvi, Deborah, S704 ([TOP-143-YI](#))
- Mammone, Simone, S173 ([TOP-072](#)), S213 ([FRI-070-YI](#))
- Mamonova, Nina, S92 ([LBP-029](#)), S758 ([TOP-400](#))
- Mampunza, Samuel, S675 ([WED-469](#))
- Mamutova, Elvira, S501 ([FRI-305](#))
- Manabe, Noriaki, S541 ([WED-283](#))
- Manchon, Pauline, S526 ([WED-245](#))
- Manco, Rita, S2 ([GS-003-YI](#))
- Mandea, Matei, S343 ([THU-186](#))
- Mandorfer, Mattias, S61 ([OS-096-YI](#)), S85 ([LBP-016](#)), S156 ([TOP-097-YI](#)), S165 ([THU-071](#)), S166 ([THU-075-YI](#)), S238 ([SAT-069](#)), S242 ([SAT-080-YI](#)), S243 ([SAT-086-YI](#)), S250 ([SAT-105](#)), S250 ([SAT-106](#)), S251 ([SAT-111](#)), S253 ([SAT-117](#)), S253 ([SAT-118](#)), S255 ([SAT-122](#)), S257 ([SAT-128](#)), S335 ([THU-166](#)), S341 ([THU-183-YI](#)), S621 ([FRI-009-YI](#)), S703 ([TOP-141](#)), S706 ([WED-131-YI](#)), S708 ([WED-135-YI](#)), S717 ([WED-171](#)), S725 ([WED-190](#)), S773 ([FRI-394](#)), S814 ([WED-383](#)), S818 ([THU-381](#))
- Mandot, Ameet, S158 ([THU-052](#)), S167 ([THU-078](#))
- Mandy, Chan, S2 ([GS-004](#)), S38 ([OS-054](#))
- Maneenil, Chongkonrat, S396 ([SAT-480-YI](#)), S410 ([SAT-529](#))
- Manes, Giampiero, S332 ([THU-161](#))

- Manfredi, Giulia, S51 ([OS-078-YI](#)), S443 ([THU-464](#))
- Manfredi, Giulia Francesca, S96 ([LBP-038](#)), S306 ([THU-093](#)), S329 ([THU-153](#)), S445 ([THU-471-YI](#)), S627 ([FRI-028](#))
- Manfredi, Paolo, S592 ([THU-285](#))
- Manfredi, Sylvain, S444 ([THU-466](#))
- Mangia, Alessandra, S73 ([OS-120](#)), S470 ([FRI-215-YI](#)), S793 ([WED-391](#)), S804 ([WED-414](#))
- Mangini, Chiara, S211 ([FRI-059](#)), S214 ([FRI-075](#)), S246 ([SAT-094-YI](#))
- Mangla, Kamal Kant, S37 ([OS-052](#)), S460 ([TOP-309](#)), S709 ([WED-138](#))
- Mangoni, Emanuele Durante, S332 ([THU-161](#))
- Manhas, Savrina, S737 ([SAT-371](#)), S738 ([SAT-373](#)), S750 ([SAT-405](#))
- Manhota, Menisha, S195 ([WED-117](#))
- Mani, Iliana, S208 ([FRI-052](#)), S214 ([FRI-076](#)), S219 ([FRI-088](#)), S798 ([WED-403](#))
- Manini, Matteo Angelo, S705 ([WED-130](#))
- Mani Tripathi, Dinesh, S177 ([WED-058-YI](#)), S181 ([WED-076](#)), S188 ([WED-095-YI](#))
- Maniu, Anca, S555 ([WED-332](#))
- Man, Joris De, S581 ([THU-249](#))
- Manley, Hannah, S684 ([WED-487](#))
- Mannaerts, Inge, S435 ([FRI-534](#))
- Mann, Derek A., S425 ([FRI-493](#))
- Manning, Lesley, S654 ([SAT-467](#))
- Mannini, Antonella, S426 ([FRI-498-YI](#))
- Männistö, Satu, S460 ([TOP-308](#)), S562 ([TOP-240-YI](#))
- Männistö, Ville, S460 ([TOP-308](#)), S514 ([WED-210](#)), S562 ([TOP-240-YI](#))
- Mann, Jake, S432 ([FRI-524](#)), S692 ([TOP-145](#))
- Mann, Matthias, S32 ([OS-041-YI](#)), S47 ([OS-072-YI](#)), S169 ([THU-080-YI](#)), S182 ([WED-078](#)), S193 ([WED-111](#))
- Manns, Michael P., S374 ([SAT-021](#)), S583 ([THU-256](#)), S730 ([TOP-369](#))
- Manolakopoulos, Spiliot, S782 ([FRI-415](#)), S798 ([WED-403](#)), S800 ([WED-406](#)), S823 ([THU-398](#))
- Manousou, Pinelopi, S282 ([WED-546](#)), S466 ([FRI-207-YI](#)), S470 ([FRI-215-YI](#)), S495 ([FRI-286](#)), S580 ([THU-247-YI](#))
- Mansbach, Hank, S72 ([OS-118](#)), S607 ([SAT-203](#))
- Manship, Thomas, S81 ([LBP-007](#))
- Mantovani, Alessandro, S483 ([FRI-254](#)), S496 ([FRI-290](#)), S503 ([FRI-317](#))
- Mantovani, Anna, S474 ([FRI-226](#))
- Mantovani, Giuseppe, S431 ([FRI-521](#))
- Mantovani, Stefania, S428 ([FRI-514](#))
- Mantry, Parvez, S10 ([LBO-005](#)), S514 ([WED-211](#)), S544 ([WED-294](#))
- Manuel Pericàs, Juan, S471 ([FRI-219-YI](#))
- Manuel Sousa-Martin, Jose, S318 ([THU-118](#)), S330 ([THU-155](#))
- Manuilov, Dmitry, S1 ([GS-002](#)), S74 ([OS-122](#)), S92 ([LBP-029](#)), S737 ([SAT-371](#)), S738 ([SAT-373](#)), S758 ([TOP-400](#)), S764 ([FRI-371](#)), S794 ([WED-392](#)), S796 ([WED-395](#))
- Manuli, Chiara, S371 ([SAT-015-YI](#)), S378 ([SAT-031-YI](#))
- Manzhali, Elina, S610 ([SAT-213](#))
- Manzorro, Alvaro Giménez, S336 ([THU-170-YI](#))
- Mao, Shaoshuai, S59 ([OS-093](#))
- Mao, Xianhua, S27 ([OS-032](#))
- Mao, Xudong, S102 ([LBP-048](#))
- Mao, Yimin, S120 ([SAT-324](#)), S122 ([SAT-333](#))
- Maponga, Tongai Gibson, S750 ([SAT-404](#))
- Maracci, Monia, S73 ([OS-120](#)), S793 ([WED-391](#)), S804 ([WED-414](#))
- Marano, Martina, S475 ([FRI-230-YI](#)), S480 ([FRI-243](#))
- Marascio, Nadia, S777 ([FRI-405](#))
- Marasco, Giovanni, S238 ([SAT-068](#)), S241 ([SAT-078-YI](#)), S399 ([SAT-490](#)), S704 ([TOP-143-YI](#))
- Maras, Jaswinder, S103 ([TOP-349-YI](#)), S108 ([FRI-327-YI](#)), S125 ([TOP-329-YI](#)), S127 ([THU-318](#)), S129 ([THU-321](#)), S134 ([THU-339](#)), S164 ([THU-068](#)), S164 ([THU-069](#)), S184 ([WED-086](#)), S272 ([WED-518-YI](#)), S273 ([WED-519-YI](#)), S276 ([WED-527-YI](#)), S283 ([WED-549](#)), S294 ([SAT-155](#)), S754 ([SAT-415](#))
- Marcantonio, Gesualdo, S175 ([TOP-085](#))
- Marceau, Caleb, S737 ([SAT-371](#))
- Marcellin, Fabienne, S670 ([WED-455](#))
- Marcellin, Patrick, S797 ([WED-397](#))
- Marcellusi, Andrea, S666 ([WED-444](#))
- Marchant, Arnaud, S131 ([THU-331-YI](#))
- Marche, Patrice N., S744 ([SAT-389](#)), S747 ([SAT-396](#))
- Marchesi, Julian R., S46 ([OS-070](#)), S282 ([WED-546](#))
- Marchetti, Alfredo, S459 ([TOP-301](#))
- Marchetti, Piero, S365 ([TOP-001](#)), S383 ([SAT-044](#)), S456 ([THU-502](#))
- Marchignoli, Francesca, S544 ([WED-293](#))
- Marciano, Sebastián, S9 ([LBO-004](#)), S30 ([OS-038-YI](#)), S83 ([LBP-012](#)), S89 ([LBP-026](#)), S161 ([THU-057-YI](#)), S174 ([TOP-073](#)), S193 ([WED-112](#)), S199 ([TOP-062](#)), S200 ([TOP-064-YI](#)), S219 ([FRI-088](#))
- Marcille, Théo, S326 ([THU-136](#))
- Marco, Lorenza Di, S389 ([SAT-060](#)), S399 ([SAT-490](#)), S671 ([WED-457-YI](#))
- Marco, Rosanna De, S215 ([FRI-078-YI](#))
- Marco, Vito Di, S206 ([FRI-047-YI](#)), S252 ([SAT-113](#)), S671 ([WED-457-YI](#))
- Marculescu, Rodrig, S251 ([SAT-111](#)), S255 ([SAT-122](#)), S257 ([SAT-128](#))
- Marczyńska, Magdalena, S820 ([THU-387](#)), S825 ([THU-403](#))
- Marek, George, S134 ([THU-341](#)), S714 ([WED-163](#))
- Mareljic, Nikola, S115 ([TOP-346-YI](#))
- Maresca, Manuel Rodriguez, S668 ([WED-449](#))
- Margáin, Astrid Ruiz, S602 ([TOP-205](#))
- Margalit, Maya, S72 ([OS-118](#)), S522 ([WED-235](#)), S607 ([SAT-203](#))
- Margarita, Sara, S491 ([FRI-275-YI](#))
- Margiotto, Francesco, S565 ([THU-199](#))
- Maria, Alexandre, S115 ([SAT-306](#))
- Maria, Arjun, S719 ([WED-176](#))
- Maria da Penha, Zago Gomes, S83 ([LBP-012](#))
- Maria, Francesco De, S793 ([WED-391](#))
- Maria Ierardi, Anna, S397 ([SAT-482](#)), S401 ([SAT-493-YI](#))
- Maria, Nicola De, S389 ([SAT-060](#))
- Maria Saracco, Giorgio, S483 ([FRI-251-YI](#))
- Marie, Essig, S387 ([SAT-052](#))
- Marignani, Massimo, S817 ([THU-378](#))
- Marijuan, Rebeca P., S432 ([FRI-523](#))
- Marí, Montserrat, S424 ([FRI-491-YI](#)), S425 ([FRI-494-YI](#)), S430 ([FRI-519-YI](#))
- Marinaro, Letizia, S804 ([WED-414](#))
- Marín, Eva, S398 ([SAT-485](#))
- Marini, Alberto, S335 ([THU-167](#))
- Marin, Jose J. G., S348 ([FRI-555](#)), S417 ([FRI-466-YI](#)), S432 ([FRI-523](#)), S433 ([FRI-526](#))
- Marino, Mónica, S30 ([OS-038-YI](#)), S199 ([TOP-062](#)), S200 ([TOP-064-YI](#))
- Marino, Patrizia, S508 ([WED-195](#))
- Mariño, Zoe, S710 ([WED-153](#)), S711 ([WED-155](#)), S717 ([WED-172](#)), S721 ([WED-181](#)), S723 ([WED-186](#)), S817 ([TOP-385-YI](#))
- Marin, Renato, S332 ([THU-161](#))
- Markaide, Enara, S32 ([OS-042-YI](#)), S419 ([FRI-472-YI](#))
- Markatou, Marianthi, S680 ([WED-479](#))
- Markezana, Aurelia, S278 ([WED-534](#))
- Mark, Henry E., S528 ([WED-248](#))
- Mark, Henry E., S470 ([FRI-218](#))
- Marlin, Taylor, S611 ([SAT-215](#))
- Marnmana, Sakunkan, S258 ([SAT-129](#))
- Maroldo, Laura, S835 ([THU-372-YI](#))
- Marot, Astrid, S53 ([OS-081](#))
- Marotta, Federico, S48 ([OS-073](#))
- Marquardt, Jens U., S24 ([OS-027-YI](#)), S52 ([OS-079-YI](#)), S211 ([FRI-059](#)), S214 ([FRI-075](#)), S435 ([FRI-534](#)), S582 ([THU-254-YI](#))
- Marques de Alcanatara Barreto, Camila, S83 ([LBP-012](#))
- Marques, Hugo Pinto, S9 ([LBO-004](#)), S89 ([LBP-026](#)), S115 ([TOP-346-YI](#)), S362 ([WED-015](#)), S834 ([THU-370](#))
- Marquet, Pierre, S387 ([SAT-052](#))
- Márquez, Laura, S453 ([THU-493](#))
- Marra, Fabio, S62 ([OS-099-YI](#)), S96 ([LBP-038](#)), S258 ([SAT-131](#)), S306 ([THU-093](#)), S426 ([FRI-498-YI](#)), S452 ([THU-492](#))
- Marra, Fiona, S783 ([FRI-423](#))
- Marra, Paolo, S439 ([THU-447](#))
- Marrone, Aldo, S790 ([FRI-441](#))
- Marrone, Giuseppe, S533 ([WED-261-YI](#))
- Marron, Thomas, S51 ([OS-078-YI](#))
- Marron, Thomas U., S443 ([THU-464](#))

Author Index

- Marschall, Hanns-Ulrich, S273 ([WED-521-YI](#)), S374 ([SAT-021](#))
- Marsche, Gunther, S383 ([SAT-042](#))
- Marshall, Debbie, S544 ([WED-294](#))
- Mars, Nina, S562 ([TOP-240-YI](#))
- Marti-Aguado, David, S139 ([SAT-257](#)), S142 ([SAT-267](#)), S469 ([FRI-213](#))
- Martí, Aina, S29 ([OS-037](#)), S139 ([SAT-257](#))
- Martí Carretero, Aina, S154 ([SAT-304](#))
- Martin-Arranz, Maria Dolores, S706 ([WED-132](#)), S712 ([WED-159](#))
- Martin-Bermudo, Franz, S71 ([OS-116](#)), S593 ([THU-287](#))
- Martin, Carmen Alonso, S365 ([TOP-002](#))
- Martin, Eleonora De, S122 ([SAT-331](#)), S341 ([THU-182](#)), S367 ([TOP-005](#)), S718 ([WED-174](#))
- Martinelli, Caterina, S370 ([SAT-013](#)), S383 ([SAT-044](#))
- Martinello, Marianne, S776 ([FRI-403](#))
- Martin, Eric F, S374 ([SAT-021](#))
- Martín-Escolano, Rubén, S741 ([SAT-379](#)), S751 ([SAT-407](#))
- Martinez, Alba, S635 ([THU-039-YI](#))
- Martínez, Alicia, S13 ([OS-005-YI](#))
- Martínez-Arenas, Laura, S361 ([WED-009](#)), S531 ([WED-257](#))
- Martínez-Arranz, Ibon, S640 ([SAT-429](#))
- Martínez-Cáceres, Eva, S190 ([WED-104](#))
- Martínez-Chantar, María Luz, S417 ([FRI-466-YI](#)), S536 ([WED-271](#)), S694 ([FRI-153](#))
- martinez, clarissa, S737 ([SAT-371](#))
- Martinez, Dani, S700 ([FRI-171](#))
- Martínez, El Hajra Ismael, S330 ([THU-155](#))
- Martínez, Eva, S391 ([TOP-512-YI](#))
- Martínez, Filomeno, S557 ([WED-335](#))
- Martínez-Flórez, Susana, S45 ([OS-067](#)), S277 ([WED-529](#))
- Martínez-García de la Torre, Raquel A, S24 ([OS-026-YI](#))
- Martínez-García de la Torre, Raquel A., S420 ([FRI-474-YI](#))
- Martínez-Gili, Laura, S14 ([OS-008-YI](#)), S127 ([THU-317](#)), S130 ([THU-326](#)), S282 ([WED-546](#)), S470 ([FRI-215-YI](#))
- Martinez, Isabella, S404 ([SAT-500-YI](#))
- Martínez, Isidoro, S665 ([WED-442](#)), S751 ([SAT-407](#))
- Martínez, Ismael El Hajra, S318 ([THU-118](#))
- Martínez, Jorge Carlos, S9 ([LBO-004](#)), S89 ([LBP-026](#))
- Martínez, Lidia, S45 ([OS-068](#))
- Martinez, Marta, S836 ([THU-374](#))
- Martínez, Marta Guindo, S47 ([OS-072-YI](#))
- Martínez-Navidad, Cristian, S582 ([THU-250-YI](#)), S583 ([THU-257](#)), S586 ([THU-263-YI](#)), S594 ([THU-290-YI](#))
- Martinez-Pomares, Luisa, S431 ([FRI-521](#))
- Martínez-Sánchez, Celia, S13 ([OS-005-YI](#)), S176 ([WED-055](#))
- Martinez, Sara, S541 ([WED-284-YI](#))
- Martinez, Sebastian, S194 ([WED-113](#))
- Martínez, Sergio Muñoz, S468 ([FRI-211](#)), S596 ([THU-296](#))
- Martínez, Yolanda Real, S818 ([THU-381](#))
- Martín, Félix Conde, S559 ([WED-341](#))
- Martín, Francisco Javier Atienza, S508 ([WED-195](#))
- Martini, Andrea, S332 ([THU-161](#)), S612 ([SAT-219](#))
- Martini, Maurizio, S740 ([SAT-378](#))
- Martini, Silvia, S368 ([SAT-009](#)), S371 ([SAT-015-YI](#)), S378 ([SAT-031-YI](#))
- Martin, Jacqueline, S746 ([SAT-394](#)), S750 ([SAT-404](#)), S752 ([SAT-409](#)), S756 ([SAT-421](#))
- Martin, Javier San, S696 ([FRI-161](#))
- Martín, Juan José Ríos, S559 ([WED-341](#))
- Martin- Mateos, Rosa, S9 ([LBO-004](#)), S89 ([LBP-026](#))
- Martin-Mateos, Rosa, S139 ([SAT-257](#)), S142 ([SAT-267](#)), S365 ([TOP-002](#))
- Martin, Michelle, S687 ([WED-498](#))
- Martin, Miguel Torres, S24 ([OS-026-YI](#))
- Martino, Beatrice, S466 ([FRI-207-YI](#)), S495 ([FRI-286](#))
- Martino, Vincent Di, S61 ([OS-097](#)), S369 ([SAT-010](#)), S423 ([FRI-485](#)), S481 ([FRI-245](#))
- Martín, Padilla Machaca, S83 ([LBP-012](#))
- Martin, Robert, S300 ([SAT-175](#))
- Martin, Romain, S17 ([OS-013](#))
- Martin, Ross, S737 ([SAT-371](#)), S750 ([SAT-405](#))
- Martin, Sara De, S592 ([THU-285](#))
- Martins, Eduardo, S4 ([GS-011](#)), S575 ([THU-231](#)), S600 ([THU-336](#))
- Martins, Fatima Oliveira, S834 ([THU-370](#))
- Martins, Paulo, S368 ([SAT-009](#))
- Martins, Pedro Lages, S681 ([WED-481](#)), S834 ([THU-370](#))
- Martin, Vanessa, S141 ([SAT-262](#))
- Martró, Elisa, S39 ([OS-056-YI](#))
- Marty, Benjamin, S473 ([FRI-224](#))
- Martyn, Emily, S750 ([SAT-404](#))
- Martyniuk, Galya, S827 ([THU-408](#)), S835 ([THU-373-YI](#))
- Maruzzelli, Luigi, S62 ([OS-099-YI](#))
- Marzano, Alfredo, S175 ([TOP-085](#)), S210 ([FRI-056-YI](#))
- Marzoni, Marco, S96 ([LBP-038](#)), S306 ([THU-093](#)), S310 ([THU-101](#))
- Masadah, Rina, S792 ([FRI-444](#))
- Masarone, Mario, S493 ([FRI-281](#)), S554 ([WED-326](#)), S556 ([WED-333](#))
- Masarowah, Mohamad, S563 ([THU-194](#)), S779 ([FRI-408](#))
- Masashi, Hirooka, S238 ([SAT-068](#)), S711 ([WED-154](#)), S722 ([WED-184](#))
- Mascaró Baselga, Pau, S702 ([TOP-139](#))
- Mascia, Alessia, S322 ([THU-127-YI](#))
- Mašek, Jan, S697 ([FRI-163-YI](#))
- Masellis, Chiara, S439 ([THU-447](#))
- Masetti, Chiara, S404 ([SAT-502-YI](#)), S406 ([SAT-514](#)), S439 ([THU-447](#)), S497 ([FRI-294](#)), S705 ([WED-130](#))
- Ma, Shiwen, S345 ([FRI-546](#))
- Masiero, Lucia, S367 ([SAT-007-YI](#))
- Masi, Gianluca, S51 ([OS-078-YI](#)), S69 ([OS-112-YI](#)), S395 ([SAT-477-YI](#)), S446 ([THU-472-YI](#))
- Maslova, Ganna, S121 ([SAT-327](#))
- Masnou, Helena, S29 ([OS-037](#)), S192 ([WED-107](#)), S717 ([WED-172](#))
- Mason, Andrew L., S19 ([OS-018](#)), S305 ([TOP-169](#)), S308 ([THU-098](#)), S321 ([THU-125](#)), S374 ([SAT-021](#))
- Masood, Ramsha, S24 ([OS-027-YI](#))
- Masood, Zainab, S491 ([FRI-273-YI](#))
- Maspero, Marianna, S70 ([OS-114](#)), S375 ([SAT-022](#)), S438 ([TOP-506](#))
- Masrour, Oumnia, S463 ([FRI-197](#)), S520 ([WED-227](#)), S714 ([WED-162](#))
- Massi, Muhammad Nasrum, S792 ([FRI-444](#))
- Massons, Carme, S141 ([SAT-262](#))
- Masson, Steven, S127 ([THU-317](#)), S145 ([SAT-274](#)), S147 ([SAT-280](#)), S148 ([SAT-285-YI](#)), S641 ([SAT-433](#))
- Masterman, Chelsea, S688 ([WED-499](#))
- Mastrocinque, Davide, S666 ([WED-446](#))
- Mastrotto, Francesca, S431 ([FRI-521](#))
- Masuda, Katsunori, S513 ([WED-208](#))
- Masutti, Flora, S175 ([TOP-085](#))
- Matchett, Kylie, S107 ([FRI-326-YI](#))
- Mate, Carlota Jimeno, S316 ([THU-114](#))
- Mateescu, Bogdan, S216 ([FRI-080](#))
- Mateo, María, S682 ([WED-483](#))
- Mateo, Roberto, S737 ([SAT-371](#)), S750 ([SAT-405](#))
- Mateos Muñoz, Beatriz, S330 ([THU-155](#)), S336 ([THU-170-YI](#))
- Mateos, Rosa María Martín, S468 ([FRI-211](#))
- Matherly, Scott, S1 ([GS-001](#)), S364 ([WED-027](#))
- Mathers, John, S138 ([SAT-254](#))
- Mathew, Babu, S103 ([TOP-349-YI](#)), S108 ([FRI-327-YI](#)), S125 ([TOP-329-YI](#)), S127 ([THU-318](#)), S134 ([THU-339](#)), S273 ([WED-519-YI](#)), S283 ([WED-549](#)), S294 ([SAT-155](#))
- Mathieu, Struyve, S604 ([SAT-196](#))
- Mathurin, Philippe, S6 ([GS-010](#)), S28 ([OS-034](#)), S41 ([OS-060](#)), S644 ([SAT-439-YI](#))
- Matilla, Ana, S453 ([THU-493](#)), S455 ([THU-501](#))
- Matilla, Gonzalo, S103 ([TOP-350-YI](#))
- Matondo, Jolie, S675 ([WED-469](#))
- Matsuda, Michitaka, S695 ([FRI-159](#))
- Matsui, Takeshi, S498 ([FRI-297](#)), S757 ([WED-421](#))
- Matsumoto, Kosuke, S542 ([WED-286](#))
- Matsumoto, Minoru, S519 ([WED-226](#))
- Matsumoto, Takayuki, S451 ([THU-490](#))
- Matsuura, Kentaro, S616 ([SAT-236](#)), S828 ([THU-413](#))
- Matsuzaki, Toshihisa, S512 ([WED-203](#))
- Matta, Heansika, S129 ([THU-322-YI](#))
- Mattalia, Alberto, S96 ([LBP-038](#)), S306 ([THU-093](#))

- Mattana, Marco, S364 (WED-022)
 Mattarei, Andrea, S592 (THU-285)
 Matter, Matthias, S292 (TOP-150-YI)
 Matthaëis, Nicoletta De, S96 (LBP-038)
 Matthews, Anthony, S617 (SAT-238)
 Matthews, Gail, S776 (FRI-403)
 Matthews, Philippa C, S675 (WED-469),
 S676 (WED-471), S687 (WED-497),
 S746 (SAT-394), S750 (SAT-404),
 S752 (SAT-409), S753 (SAT-413),
 S756 (SAT-421)
 Matthews, Philippa C., S760 (TOP-417)
 Matthijnssens, Jelle, S47 (OS-072-YI),
 S272 (TOP-563)
 Mattos, Angelo Z., S30 (OS-038-YI),
 S83 (LBP-012), S89 (LBP-026),
 S157 (THU-050), S161 (THU-057-YI),
 S199 (TOP-062), S200 (TOP-064-YI)
 Matz-Soja, Madlen, S752 (SAT-410),
 S802 (WED-411)
 Maucksch, Christof, S715 (WED-166)
 Mauer, Amy, S134 (THU-341),
 S586 (THU-266)
 Maurel, Pauline, S387 (SAT-052)
 Maurel, Thomas, S486 (FRI-259)
 Maurer, H. Carlo, S35 (OS-049-YI)
 Maurer, Jurij, S621 (FRI-009-YI)
 Mauro, David, S394 (SAT-476),
 S403 (SAT-498)
 Mauro, Ezequiel, S444 (THU-467-YI),
 S455 (THU-500)
 Mauss, Stefan, S820 (THU-386-YI)
 Mauz, Jim Benjamin, S204 (FRI-042),
 S205 (FRI-044-YI), S226 (FRI-107-YI),
 S226 (FRI-109), S242 (SAT-080-YI)
 Mavinga, Jeansy, S675 (WED-469)
 Mawardi, Mohammad, S496 (FRI-291)
 Ma, Wei, S100 (LBP-045)
 Ma, Xiaoyan, S459 (TOP-307)
 Ma, Xiong, S271 (TOP-561)
 Maya, Douglas, S427 (FRI-501),
 S587 (THU-268), S593 (THU-287),
 S596 (THU-296)
 Ma, Yanqin, S806 (WED-362),
 S813 (WED-381), S815 (WED-386),
 S816 (WED-388)
 Mayer, Carlotta, S65 (OS-104)
 May, Lindsey, S737 (SAT-371)
 Mayo, Marilyn J., S80 (LBP-006),
 S91 (LBP-028), S98 (LBP-040),
 S308 (THU-098), S312 (THU-105),
 S374 (SAT-021)
 Mayo, Rebeca, S640 (SAT-429)
 Mayor, Patricia, S398 (SAT-485)
 Ma, Yuk Ting, S423 (FRI-487), S425 (FRI-493)
 Ma, Yun, S198 (WED-124),
 S359 (SAT-556-YI), S712 (WED-160)
 Mazain, Sarah, S337 (THU-174)
 Mazialivou1, Anne Laure, S648 (SAT-449)
 Mazialivoua, Anne Laure, S784 (FRI-425)
 Mazibuko, Lusanda, S753 (SAT-413)
 Ma, Zikun, S119 (SAT-321)
 Mazo, Daniel, S72 (OS-119), S83 (LBP-012)
 Mazurak, Vera C., S231 (FRI-122)
 Mazur, Włodzimierz, S685 (WED-493-YI),
 S821 (THU-389), S834 (THU-367-YI)
 Mazzaferro, Vincenzo, S70 (OS-114),
 S368 (SAT-009), S375 (SAT-022),
 S438 (TOP-506), S439 (THU-454)
 Mazzarelli, Chiara, S175 (TOP-085),
 S376 (SAT-025), S380 (SAT-034),
 S451 (THU-486-YI)
 Mazzoni, Gianluca, S79 (LBP-003)
 Mazzotta, Valentina, S791 (FRI-442)
 Mazzucco, Camilla, S612 (SAT-219)
 Mazzulli, Tony, S673 (WED-464)
 Mbelle, Mzamo, S388 (SAT-057),
 S560 (WED-342)
 Mbonze, Nana, S675 (WED-469)
 Mboup, Souleymane, S743 (SAT-387)
 McCain, Josiah, S43 (OS-064)
 McCaughan, Geoff, S9 (LBO-004),
 S23 (OS-024), S89 (LBP-026),
 S380 (SAT-036-YI), S534 (WED-267)
 McCausland, Kristen, S485 (FRI-258)
 McClure, Matt, S806 (WED-361),
 S807 (WED-365), S812 (WED-378)
 McClure, Tess, S372 (SAT-017)
 McCommis, Kyle, S82 (LBP-010)
 McCoullough, Laura, S740 (SAT-377)
 McCulloch, William, S4 (GS-011)
 McCullough, Arthur, S76 (OS-125)
 McCune, Anne, S147 (SAT-280),
 S148 (SAT-285-YI)
 McDaniel, Matthew, S517 (WED-219)
 McDermott, Eleanor, S485 (FRI-258)
 McDonnell, Neil D., S292 (TOP-156)
 McElvaney, Noel G., S703 (TOP-141),
 S708 (WED-135-YI)
 McGary, Alyssa K., S43 (OS-064),
 S152 (SAT-297)
 McGenity, Clare, S530 (WED-254)
 McGilvray, Ian, S31 (OS-040-YI),
 S381 (SAT-037), S381 (SAT-039)
 McGinty, Gio, S408 (SAT-521)
 McGirr, Ashleigh, S485 (FRI-258)
 McGonigle, John, S511 (WED-200),
 S535 (WED-268)
 McGowan, David, S728 (TOP-358-YI)
 McGowan, Neil, S81 (LBP-007)
 McGrath, Erinn, S450 (THU-485-YI)
 McIntyre, Karl, S676 (WED-471),
 S759 (TOP-417)
 McKeating, Jane, S42 (OS-061)
 McLaughlin, Megan, S332 (THU-160),
 S472 (FRI-220-YI), S476 (FRI-232)
 McLeod, Tina, S101 (LBP-046)
 McLin, Valérie, S700 (FRI-171)
 McNeil, Carson, S592 (THU-284)
 McNeil, John, S653 (SAT-464-YI)
 McPhail, Mark J W, S44 (OS-065),
 S110 (FRI-335), S181 (WED-075-YI),
 S192 (WED-110)
 McPhail, Mark J. W., S127 (THU-317),
 S145 (SAT-274)
 McPherson, Stuart, S629 (THU-009),
 S630 (THU-015-YI), S641 (SAT-433),
 S765 (FRI-374-YI)
 McReynolds, Cindy, S571 (THU-219)
 McWherter, Charles A., S20 (OS-019),
 S98 (LBP-040), S300 (SAT-175),
 S301 (SAT-177), S308 (THU-098),
 S319 (THU-119)
 Meade, Uchu, S634 (THU-033)
 Mechta-Grigoriou, Fatima,
 S572 (THU-220)
 Mecozzi, Alessandra, S666 (WED-444)
 Meda, Clara, S289 (FRI-543)
 Medicis, Joe, S469 (FRI-214), S494 (FRI-283)
 Medici, Valentina, S714 (WED-164),
 S725 (WED-191)
 Medina-Caliz, Inmaculada,
 S103 (TOP-350-YI)
 Medina, Cesar, S574 (THU-227)
 Medina, Jhon, S58 (OS-090)
 Medmoun, Mourad, S640 (SAT-430)
 Medrano, Indhira Perez, S318 (THU-118)
 Medvedeva, Elina, S26 (OS-031),
 S809 (WED-371)
 Meena, Dr Babu Lal, S164 (THU-070)
 Meersseman, Philippe, S157 (THU-049),
 S246 (SAT-092-YI)
 Mega, Andrea, S310 (THU-101),
 S500 (FRI-303)
 Megnien, Sophie Jeannin, S88 (LBP-024)
 Mehdi, Nour-El-Houda, S413 (FRI-455)
 Mehndiratta, Amrita, S666 (WED-443-YI)
 Mehreen, Sania, S192 (WED-109)
 Mehrez, Cyrine Ben, S270 (THU-554)
 Mehta, Anurag, S343 (THU-187),
 S477 (FRI-233)
 Mehta, Ashwini, S8 (LBO-003)
 Mehta, Gautam, S188 (WED-099-YI)
 Mehta, Manu, S475 (FRI-231)
 Mehta, Neil, S445 (THU-470-YI)
 Mehta, Rajiv, S476 (FRI-231)
 Mehta, Shailender, S519 (WED-225)
 Mehta, Shubham, S201 (TOP-065),
 S506 (TOP-276)
 Mehta, Varun, S475 (FRI-231)
 Meier, Jörn Arne, S258 (SAT-130)
 Meine, Gilmaria Coelho, S616 (SAT-237)
 Meiser, Philippa, S35 (OS-049-YI)
 Mei, Tingting, S357 (SAT-548)
 Mejean, Arnaud, S372 (SAT-016)
 Mela, Maria, S798 (WED-403)
 Melandro, Fabio, S369 (SAT-009)
 Melehani, Jason H., S505 (TOP-264)
 Melkebeke, Lukas Van, S16 (OS-012-YI),
 S125 (TOP-328-YI)
 Mello, Debora, S190 (WED-102)
 Mellor, Jennifer, S707 (WED-134)
 Mello, Tommaso, S88 (LBP-023)
 Mello, Vivianne, S254 (SAT-119)
 Mells, George, S310 (THU-101)
 Mells, George F., S290 (TOP-147),
 S321 (THU-125)
 Meloni, Seema T., S326 (THU-135)
 Melton, Phillip, S483 (FRI-250),
 S487 (FRI-263)
 Melum, Espen, S22 (OS-023-YI),
 S33 (OS-044-YI), S262 (THU-525-YI),

Author Index

- S294 ([SAT-154-YI](#)), S296 ([SAT-163-YI](#)), S386 ([SAT-050](#))
- Memish, Ziad A., S652 ([SAT-462-YI](#))
- Memoli, Massimo, S123 ([SAT-334](#))
- Mena, Edward, S404 ([SAT-500-YI](#)), S544 ([WED-294](#))
- Mendes, Filipe, S681 ([WED-481](#))
- Mendes, Liliana Sampaio Costa, S83 ([LBP-012](#))
- Méndez, Isabel, S436 ([FRI-535](#))
- Mendez, Luis, S195 ([WED-117](#))
- Mendez, Marinela, S681 ([WED-482](#)), S827 ([THU-410](#))
- Méndez-Sánchez, Nahum, S171 ([THU-089](#)), S643 ([SAT-438](#))
- Mendizabal, Manuel, S9 ([LBO-004](#)), S83 ([LBP-012](#)), S89 ([LBP-026](#))
- Mendler, Michel, S404 ([SAT-500-YI](#))
- Mendlowitz, Andrew, S688 ([WED-499](#))
- Mendoza, Michelle, S544 ([WED-294](#))
- Mendoza, Yuly, S61 ([OS-096-YI](#))
- Menezes, Maria, S337 ([THU-172](#))
- Menétrey, Caroline, S831 ([THU-362](#))
- Menezes, Junior Samuel, S618 ([SAT-242](#))
- Meng, Fangmin, S240 ([SAT-075-YI](#))
- Meng, Guofeng, S102 ([LBP-048](#))
- Mengozi, Giulia, S342 ([THU-184](#))
- Meng, Xiangjun, S818 ([THU-379](#))
- Meng, Xianmei, S526 ([WED-246](#))
- Meng, Yao, S119 ([SAT-321](#)), S121 ([SAT-326](#))
- Menke, Aswin L., S597 ([THU-297](#))
- Mennini, Francesco Saverio, S666 ([WED-444](#))
- Mennini, Gianluca, S364 ([WED-022](#))
- Menon, Balachandran, S440 ([THU-456](#))
- Menon, Krishna, S128 ([THU-320-YI](#)), S281 ([WED-542-YI](#)), S388 ([SAT-057](#)), S709 ([WED-137-YI](#))
- Mensah, Angelina, S21 ([OS-021-YI](#))
- Menu, Yves, S50 ([OS-077](#))
- Menzo, Stefano, S777 ([FRI-405](#))
- Meoli, Lilianeleny, S46 ([OS-070](#)), S700 ([FRI-171](#))
- Merabet, Yasmina Ben, S444 ([THU-466](#))
- Merabishvili, Tsira, S677 ([WED-473](#))
- Merás, Pablo, S706 ([WED-132](#)), S712 ([WED-159](#))
- Mercado-Gómez, Maria, S417 ([FRI-466-YI](#)), S693 ([FRI-153](#))
- Mercer, Carolyn, S324 ([THU-130](#))
- Mercier-nome, Françoise, S130 ([THU-327](#))
- Mercier, Renee-Claude, S1 ([GS-002](#)), S74 ([OS-122](#)), S737 ([SAT-371](#)), S738 ([SAT-373](#)), S758 ([TOP-400](#)), S764 ([FRI-371](#)), S796 ([WED-395](#))
- Mercuri, Luca, S676 ([WED-471](#)), S759 ([TOP-417](#))
- Mercurio, Francesco, S252 ([SAT-113](#)), S503 ([FRI-317](#))
- Meredith, Jacqueline, S789 ([FRI-436](#))
- Merens, Vincent, S262 ([THU-524-YI](#)), S267 ([THU-541](#))
- Mereu, Caterina, S322 ([THU-127-YI](#))
- Mereu, Elisabetta, S13 ([OS-005-YI](#)), S293 ([SAT-153-YI](#))
- Merino, Carlos, S706 ([WED-132](#)), S712 ([WED-159](#))
- Merlen, Grégory, S348 ([FRI-555](#))
- Merle, Philippe, S41 ([OS-060](#)), S68 ([OS-110](#)), S441 ([THU-459-YI](#)), S444 ([THU-466](#))
- Merle, Uta, S115 ([TOP-346-YI](#)), S300 ([SAT-174](#)), S793 ([WED-391](#))
- Merli, Manuela, S30 ([OS-038-YI](#)), S199 ([TOP-062](#)), S200 ([TOP-064-YI](#)), S364 ([WED-022](#)), S367 ([SAT-007-YI](#)), S700 ([FRI-171](#))
- Meroni, Marica, S289 ([FRI-544](#)), S516 ([WED-218](#))
- Merrick, Blair, S46 ([OS-070](#))
- Mertens, Bart, S204 ([FRI-043](#))
- Mertz, Kirsten, S291 ([TOP-150-YI](#))
- Mesa, Alicia, S455 ([THU-500](#))
- Mesa, Nora, S141 ([SAT-262](#))
- Mesquita, Mariana, S112 ([FRI-343-YI](#))
- Mesropian, Agavni, S411 ([TOP-507-YI](#)), S417 ([FRI-467](#))
- Messina, Vincenzo, S175 ([TOP-085](#))
- Mestre, Anna, S177 ([WED-059](#)), S231 ([FRI-121](#))
- Meszáros, Magdalena, S28 ([OS-034](#)), S52 ([OS-080](#)), S376 ([SAT-026](#)), S385 ([SAT-048](#)), S705 ([WED-129](#)), S763 ([FRI-370](#))
- Metcalfe, W. James, S462 ([FRI-195](#))
- Metin, Olga, S28 ([OS-034](#))
- Metivier, Sophie, S28 ([OS-034](#)), S41 ([OS-060](#)), S70 ([OS-115](#)), S73 ([OS-120](#)), S793 ([WED-391](#))
- Metterville, Jake, S693 ([FRI-151](#))
- Méunier, Alexandre, S61 ([OS-097](#))
- Meunier, Lucy, S61 ([OS-097](#)), S115 ([SAT-306](#)), S122 ([SAT-331](#)), S376 ([SAT-026](#))
- Meuree, Samuel, S131 ([THU-331-YI](#))
- Meuris, Leander, S311 ([THU-102-YI](#)), S442 ([THU-463](#))
- Meyapali, Lauren-Ange Djia, S133 ([THU-335](#))
- Meyboom, Joël, S801 ([WED-409](#))
- Meyer, Bernhard, S242 ([SAT-080-YI](#))
- Meyer, Carsten, S53 ([OS-081](#)), S258 ([SAT-130](#)), S259 ([SAT-135](#))
- Meyer-Herbon, Pamela, S502 ([FRI-315](#))
- Meyer, Jasper, S350 ([SAT-531-YI](#))
- Meyer, Markus, S25 ([OS-029](#))
- Meyer, Sandra De, S768 ([FRI-380](#))
- Meyer, Tim, S411 ([TOP-507-YI](#))
- Meyer zu Schwabedissen, Cordula, S702 ([TOP-140](#))
- Meyhöfer, Sebastian, S93 ([LBP-032](#))
- Meyhöfer, Svenja, S582 ([THU-254-YI](#))
- Meysman, Pieter, S730 ([SAT-337](#))
- Mezzano, Gabriel, S160 ([THU-056](#)), S336 ([THU-170-YI](#))
- Mhlanga, Aduque, S814 ([WED-382](#))
- Miao, Tizong, S742 ([SAT-383](#))
- Michalak, Sophie, S519 ([WED-224](#))
- Michalczyk, Matheus Truccolo, S161 ([THU-058](#))
- Michalkiewicz, Jacek, S578 ([THU-238](#))
- Michalkova, Hana, S417 ([FRI-466-YI](#))
- Michal, Matthias, S461 ([FRI-194-YI](#))
- Michard, Baptiste, S9 ([LBO-004](#)), S89 ([LBP-026](#))
- Michel, Correas Jean, S526 ([WED-245](#))
- Michelet, Maud, S58 ([OS-091](#)), S808 ([WED-366](#))
- Micheli, Valeria, S777 ([FRI-405](#))
- Michel, Maurice, S461 ([FRI-194-YI](#)), S484 ([FRI-255](#))
- Micheltorena, Cristina Olague, S693 ([FRI-152-YI](#))
- Michielsen, Peter, S730 ([SAT-337](#))
- Michl, Patrick, S300 ([SAT-174](#))
- Michopoulos, Spyridon, S798 ([WED-403](#))
- Miclea, Razvan, S394 ([SAT-474](#))
- Micu, Laurentiu, S211 ([FRI-058](#))
- Middelburg, Tim, S315 ([THU-112-YI](#))
- Midha, Vandana, S158 ([THU-052](#))
- Miele, Luca, S368 ([SAT-009](#)), S459 ([TOP-301](#)), S496 ([FRI-290](#)), S516 ([WED-215](#)), S533 ([WED-261-YI](#)), S704 ([TOP-144-YI](#))
- Mieli-Vergani, Giorgia, S341 ([THU-182](#))
- Miethke, Alexander, S323 ([THU-129](#)), S331 ([THU-158](#))
- Miette, Véronique, S550 ([WED-317](#))
- Miglianti, Michela, S96 ([LBP-038](#)), S306 ([THU-093](#)), S322 ([THU-127-YI](#))
- Miglior, Isabel, S369 ([SAT-009](#))
- Mihaila, Alexandra Alina Mihaela, S221 ([FRI-092](#)), S324 ([THU-131](#))
- Mikaelyan, Arsen, S268 ([THU-542](#))
- Mikami, Shigeru, S541 ([WED-283](#))
- Mikhail, Nabil, S549 ([WED-315](#)), S624 ([FRI-020](#)), S673 ([WED-463](#))
- Miki, Daiki, S828 ([THU-413](#))
- Mikkelsen, Anne Catrine Daugaard, S567 ([THU-207-YI](#))
- Mikkelsen, Morten Faarbæk, S528 ([WED-248](#))
- Miko, Susanne, S728 ([TOP-359-YI](#))
- Milan, Alberto, S480 ([FRI-243](#))
- Milardi, Giulia, S447 ([THU-474-YI](#))
- Mildenberger, Philipp, S52 ([OS-079-YI](#))
- Milella, Michele, S666 ([WED-446](#)), S772 ([FRI-392-YI](#))
- Milgrom, Yael, S563 ([THU-194](#)), S779 ([FRI-408](#))
- Millinovich, Alex, S76 ([OS-125](#))
- Milkiewicz, Małgorzata, S308 ([THU-095](#))
- Milkiewicz, Piotr, S44 ([OS-066-YI](#)), S308 ([THU-095](#)), S328 ([THU-152-YI](#)), S335 ([THU-167](#)), S338 ([THU-175-YI](#)), S339 ([THU-179](#)), S374 ([SAT-021](#)), S713 ([WED-161-YI](#))
- Millán-Dominguez, Raquel, S587 ([THU-268](#))
- Millán, Olga, S291 ([TOP-149-YI](#))
- Millan, Raquel, S71 ([OS-116](#))
- Miller, Hamish, S578 ([THU-236-YI](#))

- Miller, Johannes, S734 ([SAT-361](#))
 Miller, Keith, S465 ([FRI-202](#))
 Millian, Daniel, S823 ([THU-396](#))
 Milosevic, Marko, S155 ([SAT-305](#))
 Milton, Yuka, S302 ([SAT-180](#))
 Mimidis, Konstantinos, S798 ([WED-403](#))
 Minami, Tatsuya, S393 ([SAT-470](#)), S437 ([TOP-505](#))
 Miñana, Ainhoa Ferret, S46 ([OS-069](#))
 Miñana, Isidro Vitoria, S694 ([FRI-153](#))
 Mincholé Canals, Itziar, S640 ([SAT-429](#))
 Minciuna, Iulia, S380 ([SAT-035](#)), S555 ([WED-332](#))
 Minerva, Matthew, S8 ([LBO-002](#))
 Min, Feng, S803 ([WED-412](#))
 Mingo, Susana, S559 ([WED-339](#))
 Mingrone, Geltrude, S516 ([WED-215](#)), S545 ([WED-296](#))
 Minguez, Beatriz, S407 ([SAT-516](#)), S411 ([TOP-507-YI](#))
 Minh, Khue Nguyen, S552 ([WED-320](#))
 Minisini, Rosalba, S409 ([SAT-524](#)), S627 ([FRI-028](#))
 Minissale, Maria Giovanna, S671 ([WED-457-YI](#))
 Minocha, Shilpi, S347 ([FRI-550](#))
 Minuz, Pietro, S492 ([FRI-279-YI](#))
 Miquel, Joaquin, S391 ([TOP-512-YI](#))
 Miquel, Joaquin, S738 ([SAT-374-YI](#)), S768 ([FRI-381](#))
 Miquel, Mireia, S141 ([SAT-262](#)), S233 ([FRI-126](#)), S318 ([THU-118](#)), S330 ([THU-155](#)), S453 ([THU-493](#)), S682 ([WED-485](#)), S829 ([THU-418](#))
 Miquel, Rosa, S128 ([THU-320-YI](#)), S281 ([WED-542-YI](#)), S388 ([SAT-057](#)), S709 ([WED-137-YI](#))
 Miraglia, Roberto, S62 ([OS-099-YI](#))
 Miralpeix, Anna, S717 ([WED-172](#)), S723 ([WED-186](#))
 Miranda, Alejandro, S189 ([WED-100-YI](#))
 Miras-Carballal, Susana, S690 ([WED-513](#))
 Miravittles, Marc, S703 ([TOP-141](#)), S708 ([WED-135-YI](#))
 Mischitelli, Monica, S215 ([FRI-077-YI](#))
 Mischke, Jasmin, S735 ([SAT-363](#))
 Mishalian, Inbal, S278 ([WED-534](#))
 Mishra, Ajay, S158 ([THU-052](#)), S167 ([THU-078](#))
 Mishra, Gauri, S402 ([SAT-496](#))
 Missale, Gabriele, S332 ([THU-161](#))
 Missen, Louise, S681 ([WED-482](#))
 Mistry, Pramod, S707 ([WED-133](#))
 Mistry, Sameer, S350 ([TOP-553](#))
 Mita, Rubens, S702 ([TOP-140](#))
 Mitchell, Alice, S274 ([WED-523](#))
 Mitchell, Eoin, S181 ([WED-075-YI](#))
 Mitchell, Mack, S8 ([LBO-003](#))
 Mitchell, Oliver, S523 ([WED-236-YI](#))
 Mitchell-Thain, Robert, S321 ([THU-125](#)), S339 ([THU-178](#))
 Mitrut, Paul, S819 ([THU-382](#))
 Mittal, Ashi, S129 ([THU-321](#)), S181 ([WED-076](#)), S272 ([WED-518-YI](#)), S276 ([WED-527-YI](#))
 Mittal, Ashmit, S177 ([WED-057](#))
 Mitten, Emilie, S518 ([WED-222](#))
 Miuma, Satoshi, S228 ([FRI-113](#)), S234 ([FRI-128](#))
 Miutescu, Bogdan, S172 ([THU-090](#))
 Miwa, Chihiro, S123 ([SAT-335](#))
 Miyaaki, Hisamitsu, S228 ([FRI-113](#)), S234 ([FRI-128](#))
 Miyakami, Yuko, S519 ([WED-226](#))
 Miyoshi, Eiji, S537 ([WED-273](#))
 Mizokami, Masashi, S797 ([WED-397](#))
 Mizuno, Motowo, S122 ([SAT-332-YI](#))
 Mladenovic, Rebecca, S315 ([THU-111](#))
 Mlitz, Veronika, S66 ([OS-106-YI](#)), S296 ([SAT-161](#))
 Moalli, Federica, S35 ([OS-048](#))
 Moal, Valérie, S519 ([WED-224](#))
 Moal, Vanessa Liévin-Le, S136 ([THU-347-YI](#))
 Mobin, Navim, S252 ([SAT-114](#)), S545 ([WED-295-YI](#))
 Mocci, Stefano, S322 ([THU-127-YI](#))
 Mochida, Satoshi, S828 ([THU-413](#))
 Mockbee, Joy, S641 ([SAT-432](#))
 Modarresi, Mehrdad, S555 ([WED-330](#)), S561 ([WED-348](#))
 Moeckli, Beat, S189 ([WED-101-YI](#))
 Moehlin, Julien, S25 ([OS-029](#)), S31 ([OS-040-YI](#)), S734 ([SAT-348-YI](#))
 Moga, Lucile, S52 ([OS-080](#)), S61 ([OS-096-YI](#))
 Moghadamrad, Sheida, S117 ([SAT-316](#))
 Mogler, Carolin, S35 ([OS-049-YI](#)), S54 ([OS-083](#)), S298 ([SAT-166](#))
 Mogul, Douglas B., S307 ([THU-094](#)), S323 ([THU-129](#)), S331 ([THU-158](#))
 Mogyorossy, Sandor, S313 ([THU-106-YI](#))
 Mohamad Khalil, Samira, S618 ([SAT-244](#))
 Mohamad, Merianne, S185 ([WED-088-YI](#))
 Mohamed, Almuthana, S639 ([SAT-428](#)), S687 ([WED-496](#)), S765 ([FRI-374-YI](#))
 Mohamed, Islam, S489 ([FRI-269](#))
 Mohamed, Rahma, S491 ([FRI-273-YI](#))
 Mohamed, Zubair, S31 ([OS-039](#))
 Mohammad, Tabish, S62 ([OS-098-YI](#))
 Mohammed, Merianne, S227 ([FRI-112](#))
 Mohan, Prasad V G, S476 ([FRI-231](#))
 Mohd, Sheeraz, S519 ([WED-225](#))
 Mohkam, Kayvan, S22 ([OS-022](#))
 Mo, Hongmei, S737 ([SAT-371](#)), S738 ([SAT-373](#)), S750 ([SAT-405](#))
 Mohr, Isabelle, S716 ([WED-170](#))
 Mohr, Raphael, S52 ([OS-079-YI](#)), S259 ([SAT-135](#)), S411 ([TOP-507-YI](#)), S442 ([THU-463](#))
 Moiola, Lucia, S123 ([SAT-334](#))
 Moirand, Romain, S6 ([GS-010](#)), S168 ([THU-079](#))
 Mok, John, S540 ([WED-282](#))
 Mol, Bregje, S315 ([THU-112-YI](#)), S317 ([THU-115-YI](#))
 Moles, Anna, S346 ([FRI-548](#))
 Mo, Lien-Ray, S832 ([THU-365](#))
 Molina, Esther, S717 ([WED-172](#))
 Molina, Gaspar Joaquin, S702 ([TOP-139](#))
 Molina, Laura, S299 ([SAT-173-YI](#))
 Molinari, Nicolas, S385 ([SAT-048](#))
 Molinaro, Antonio, S273 ([WED-521-YI](#))
 Molina, Valle, S45 ([OS-068](#))
 Molina-Villalba, Carmen, S779 ([FRI-409](#))
 Moliterni, Camilla, S2 ([GS-003-YI](#))
 Mollea, Sara, S666 ([WED-444](#))
 Møller, Emilie, S244 ([SAT-088](#))
 Möller, Marie, S443 ([THU-465-YI](#))
 Möller, Sören, S205 ([FRI-045](#))
 Møller, Søren, S555 ([WED-331-YI](#))
 Møller, Thomas, S626 ([FRI-027](#)), S737 ([SAT-370](#))
 Molzen, Line, S149 ([SAT-286-YI](#))
 Monache, Guido Delle, S96 ([LBP-038](#)), S306 ([THU-093](#))
 Mondelli, Mario Umberto, S428 ([FRI-514](#))
 Monforte, Antonella D'Arminio, S791 ([FRI-442](#))
 Monga, Satdarshan, S299 ([SAT-173-YI](#))
 Monge, Fanny, S520 ([WED-230](#))
 Monian, Prashant, S692 ([FRI-151](#))
 Monico, Sara, S73 ([OS-120](#)), S470 ([FRI-215-YI](#)), S781 ([FRI-412](#))
 Monllor-Nunell, Teresa, S52 ([OS-080](#))
 Monneret, Guillaume, S22 ([OS-022](#))
 Monsel, Antoine, S156 ([TOP-108](#))
 Monserrat, Elena, S822 ([THU-395](#))
 Monserrat, Jorge, S189 ([WED-100-YI](#))
 Montagna, Marco La, S790 ([FRI-441](#))
 Montagnese, Sara, S211 ([FRI-059](#)), S214 ([FRI-075](#)), S246 ([SAT-094-YI](#)), S332 ([THU-161](#))
 Montague, Sarah, S669 ([WED-452](#)), S690 ([WED-514](#))
 Montal, Robert, S411 ([TOP-507-YI](#))
 Montalto, Michael, S507 ([TOP-289](#))
 Montalvá, Eva, S362 ([WED-015](#)), S531 ([WED-257](#))
 Montañés, Rosa, S15 ([OS-010](#)), S179 ([WED-070](#))
 Montano-Loza, Aldo J, S18 ([OS-015](#)), S19 ([OS-018](#)), S231 ([FRI-122](#)), S305 ([TOP-169](#)), S308 ([THU-098](#)), S315 ([THU-111](#))
 Montano-Loza, Aldo J., S97 ([LBP-039](#)), S374 ([SAT-021](#))
 Montaut, Emilie, S413 ([FRI-455](#))
 Montavoci, Linda, S428 ([FRI-514](#))
 Monte, Enric Redondo, S35 ([OS-049-YI](#))
 Monteiro, Victoria, S190 ([WED-102](#))
 Monte, Maria J., S348 ([FRI-555](#)), S433 ([FRI-526](#))
 Montenegro-Navarro, Nieves, S107 ([FRI-324](#))
 Montero, Jose Luis, S455 ([THU-501](#))
 Montero, Saul, S727 ([TOP-357](#))
 Montero, Saul Martinez, S564 ([THU-198](#))
 Montero-Vallejo, Rocío, S427 ([FRI-501](#)), S587 ([THU-268](#)), S593 ([THU-287](#)), S596 ([THU-296](#))
 Monte, Sara De, S223 ([FRI-098](#))

Author Index

- Montes, Pedro, S30 ([OS-038-YI](#)),
S199 ([TOP-062](#)), S200 ([TOP-064-YI](#))
- Montiel, Natalia, S779 ([FRI-409](#))
- Monti, Gianpaola, S380 ([SAT-034](#))
- Montigny-Lenhardt, Stéphanie De,
S640 ([SAT-430](#))
- Monti, Monica, S674 ([WED-467-YI](#))
- Montironi, Carla, S15 ([OS-010](#)),
S411 ([TOP-507-YI](#))
- Montón, Cristina, S592 ([THU-283](#))
- Montón-Rodríguez, Cristina, S232 ([FRI-125](#))
- Montravers, Françoise, S50 ([OS-077](#))
- Montuenga, Maribel Bernard,
S574 ([THU-225](#))
- Moodley, Prebhashan, S250 ([SAT-107-YI](#))
- Mookerjee, Rajeshwar Prosad,
S157 ([THU-050](#)), S188 ([WED-098-YI](#)),
S567 ([THU-207-YI](#))
- Moon, Andrew, S393 ([SAT-472](#)),
S394 ([SAT-476](#)), S403 ([SAT-498](#)),
S653 ([SAT-463](#))
- Moon, Christina, S729 ([TOP-368](#)),
S738 ([SAT-373](#))
- Moon, Eun Jeong, S448 ([THU-478](#))
- Moon, Joon Ho, S487 ([FRI-261-YI](#))
- Moon, Sang Yi, S501 ([FRI-306](#)),
S552 ([WED-322](#))
- Moore, Carole, S811 ([WED-374](#))
- Moore, Celia, S350 ([TOP-553](#))
- Moore, Christopher, S584 ([THU-259](#))
- Moore, Kevin, S165 ([THU-074](#))
- Moorthy, Krishna, S580 ([THU-247-YI](#))
- Moosburner, Simon, S84 ([LBP-015](#))
- Mora, Alfonso, S112 ([FRI-343-YI](#))
- Mor, Adi, S268 ([THU-547](#)), S295 ([SAT-158](#))
- Moradi, Ali Mohammad, S387 ([SAT-053](#))
- Mora, Estefania Ochoa, S556 ([WED-334](#)),
S642 ([SAT-434](#))
- Morago, Lucía, S682 ([WED-483](#))
- Morais, Maria, S339 ([THU-178](#))
- Morales, Albert, S424 ([FRI-491-YI](#)),
S425 ([FRI-494-YI](#)), S430 ([FRI-519-YI](#))
- Morales, Dalia, S453 ([THU-493](#))
- Morales, Montserrat, S694 ([FRI-153](#))
- Morales-Ruiz, Manuel, S160 ([THU-056](#))
- Morales, Shessy, S700 ([FRI-171](#))
- Morana, Ester, S332 ([THU-161](#))
- Morcet, Jeff, S463 ([FRI-197](#))
- Moreau, Clemence, S37 ([OS-053](#))
- Moreau, Richard, S9 ([LBO-004](#)),
S83 ([LBP-012](#)), S89 ([LBP-026](#)),
S157 ([THU-050](#)), S159 ([THU-055](#)),
S161 ([THU-057-YI](#)), S174 ([TOP-073](#)),
S174 ([TOP-084](#)), S185 ([WED-087](#)),
S188 ([WED-098-YI](#)), S700 ([FRI-171](#))
- Morelli, Olivia, S96 ([LBP-038](#)),
S306 ([THU-093](#))
- Morement, Helen, S406 ([SAT-515](#))
- Morengi, Emanuela, S406 ([SAT-514](#))
- Moreno, Christophe, S6 ([GS-010](#)),
S8 ([LBO-003](#)), S131 ([THU-331-YI](#)),
S133 ([THU-335](#)), S386 ([SAT-051](#)),
S777 ([FRI-406](#)), S786 ([FRI-429](#))
- Moreno, Sarai Romero, S365 ([TOP-002](#))
- Morer, Carla, S154 ([SAT-304](#))
- Moreta, Maria Jose, S139 ([SAT-257](#)),
S160 ([THU-056](#)), S541 ([WED-284-YI](#))
- Moreto, Amanda, S343 ([THU-188](#))
- Moretti, Alessandra, S96 ([LBP-038](#)),
S175 ([TOP-085](#)), S306 ([THU-093](#))
- Moretti, Vittoria, S459 ([TOP-301](#)),
S704 ([TOP-144-YI](#))
- Morgan, Camille, S668 ([WED-451-YI](#)),
S675 ([WED-469](#)), S752 ([SAT-409](#))
- Morgan, Erin, S7 ([GS-012](#))
- Morganti, Elisa, S428 ([FRI-502](#))
- Morgera, Ulrike, S20 ([OS-019](#)),
S98 ([LBP-040](#))
- Moriarty, Aoife, S450 ([THU-485-YI](#))
- Mori, Benedetta, S439 ([THU-447](#))
- Morii, Eiichi, S506 ([TOP-288](#))
- Morillas, Julia, S717 ([WED-172](#))
- Morillas, Rosa M, S192 ([WED-107](#)),
S329 ([THU-154-YI](#)),
S503 ([TOP-241-YI](#))
- Morimoto, Youichi, S122 ([SAT-332-YI](#))
- Morioka, Sho, S288 ([FRI-540](#))
- Morisco, Filomena, S96 ([LBP-038](#)),
S215 ([FRI-078-YI](#)), S306 ([THU-093](#)),
S367 ([SAT-007-YI](#)), S804 ([WED-414](#)),
S817 ([THU-378](#))
- Morishita, Asahiro, S248 ([SAT-101](#)),
S537 ([WED-273](#)), S541 ([WED-283](#)),
S616 ([SAT-236](#))
- Morita, Chie, S42 ([OS-062](#))
- Mori, Taizo, S695 ([FRI-159](#))
- Morita, Makoto, S711 ([WED-154](#)),
S722 ([WED-184](#))
- Mori, Trevor, S275 ([WED-526](#)),
S483 ([FRI-250](#)), S487 ([FRI-263](#))
- Moriya, Kyoji, S589 ([THU-275](#))
- Morizur, Severine, S349 ([TOP-552](#)),
S415 ([FRI-459](#)), S572 ([THU-220](#))
- Morizzo, Erika, S93 ([LBP-031](#))
- Morocho, Alejandro Esquivel,
S700 ([FRI-171](#))
- Moroni, Francesca, S81 ([LBP-007](#))
- Mor, Orna, S770 ([FRI-386](#))
- Moroz, Larysa, S827 ([THU-408](#)),
S835 ([THU-373-YI](#))
- Morozov, Viacheslav, S1 ([GS-002](#)),
S92 ([LBP-029](#)), S758 ([TOP-400](#)),
S764 ([FRI-371](#)), S796 ([WED-395](#))
- Morrell, Nick, S179 ([WED-069](#))
- Morris, Ben, S88 ([LBP-022](#))
- Morris, David, S81 ([LBP-007](#))
- Morris, Heather, S472 ([FRI-222-YI](#)),
S610 ([SAT-212](#))
- Morrison, Martine C., S94 ([LBP-033](#)),
S575 ([THU-231](#)), S595 ([THU-294](#)),
S597 ([THU-297](#))
- Morrison, Mary, S58 ([OS-090](#))
- Morris, Sean, S309 ([THU-099-YI](#))
- Morrow, Richard, S40 ([OS-058](#)),
S659 ([WED-429](#)), S686 ([WED-495](#)),
S824 ([THU-399-YI](#))
- Morsica, Giulia, S824 ([THU-402](#))
- Morsy, Yasser, S56 ([OS-086-YI](#))
- Mortensen, Frank Viborg,
S399 ([SAT-487-YI](#))
- Morton, Jennifer, S419 ([FRI-472-YI](#))
- Moruzzi, Noah, S281 ([WED-543](#))
- Moryoussef, Frederick, S640 ([SAT-430](#))
- Moschen, Alexander, S773 ([FRI-394](#))
- Moshage, Han, S582 ([THU-251-YI](#))
- Mospan, Andrea, S472 ([FRI-222-YI](#)),
S610 ([SAT-212](#))
- Moszczyńska, Elżbieta, S713 ([WED-161-YI](#))
- Motamedrad, Maryam, S231 ([FRI-122](#))
- Motoyoshi, Yasuhide, S542 ([WED-286](#))
- Motta, Benedetta Maria, S554 ([WED-326](#)),
S556 ([WED-333](#))
- Motta, Raffaella, S318 ([THU-117-YI](#))
- Motta, Rodrigo, S302 ([SAT-179](#)),
S324 ([THU-130](#))
- Mouch, Saif Abu, S628 ([FRI-033](#)),
S789 ([FRI-437](#))
- Mould, Andrea, S483 ([FRI-250](#)),
S487 ([FRI-263](#))
- Mouliade, Charlotte, S698 ([FRI-165](#)),
S733 ([SAT-343](#)), S741 ([SAT-380](#)),
S760 ([FRI-361](#))
- Moulin, Philippe, S508 ([WED-194](#)),
S538 ([WED-278](#))
- Moulis, Lionel, S143 ([SAT-269](#))
- Mountain, Victoria, S571 ([THU-215](#))
- Mounzer, Karam, S799 ([WED-405](#))
- Mourad, Abbas, S508 ([WED-195](#)),
S670 ([WED-455](#))
- Moura, Miguel, S358 ([SAT-554-YI](#)),
S405 ([SAT-513](#))
- Mouri, Hirokazu, S122 ([SAT-332-YI](#))
- Mouri, Sarah, S207 ([FRI-050-YI](#)),
S218 ([FRI-087](#)), S222 ([FRI-094-YI](#)),
S222 ([FRI-095](#)), S239 ([SAT-071](#))
- Mourya, Akash Kumar, S66 ([OS-106-YI](#)),
S188 ([WED-095-YI](#)), S346 ([FRI-547-YI](#))
- Mousel, Travis, S1 ([GS-001](#))
- Moylan, Cynthia, S216 ([FRI-081](#))
- Mozayani, Behrang, S717 ([WED-171](#)),
S725 ([WED-190](#))
- Msomi, Khanyi, S753 ([SAT-413](#))
- Mubarak, Abdullah, S11 ([LBO-006](#))
- Mucciardi, Giuseppe, S740 ([SAT-378](#))
- Muccini, Camilla, S824 ([THU-402](#))
- Mücke, Marcus, S203 ([FRI-039](#))
- Mücke, Victoria, S203 ([FRI-039](#))
- Muecke, Marcus Maximilian,
S170 ([THU-087](#))
- Mueller, Sebastian, S134 ([THU-340-YI](#))
- Muench, Robert, S733 ([SAT-342-YI](#))
- Muenzel, Thomas, S461 ([FRI-194-YI](#))
- Mugambwa, Caroline, S58 ([OS-090](#))
- Muga, Robert, S154 ([SAT-303](#)),
S190 ([WED-104](#))
- Muglia, Riccardo, S439 ([THU-447](#))
- Mukewar, Saurabh, S158 ([THU-052](#)),
S167 ([THU-078](#)), S475 ([FRI-231](#))
- Mukewar, Shrikant, S475 ([FRI-231](#))
- Mukherjee, Arpan, S88 ([LBP-022](#))
- Mukherjee, Sumanta, S332 ([THU-160](#)),
S472 ([FRI-220-YI](#)), S476 ([FRI-232](#))

- Mukherji, Atish, S42 ([OS-061](#))
Mukhopadhyay, Raktim, S680 ([WED-479](#))
Mukhtar, Nizar, S778 ([FRI-407](#))
Mulé, Sébastien, S50 ([OS-077](#)),
S373 ([SAT-020](#)), S453 ([THU-494](#))
Muljono, David Handojo, S792 ([FRI-444](#))
Mullen, Eduardo, S342 ([THU-185](#))
Muller, Allison, S61 ([OS-097](#))
Müller, Christian, S25 ([OS-028](#))
Müller, Florian, S65 ([OS-103](#))
Müller-Franzes, Gustav Anton,
S567 ([THU-206](#))
Müller, Johannes, S134 ([THU-340-YI](#))
Muller, Kate, S275 ([WED-526](#))
Müller, Lukas, S52 ([OS-079-YI](#))
Muller, Marion, S25 ([OS-029](#))
Müller, Ralph, S70 ([OS-115](#))
Müller-Reif, Johannes, S193 ([WED-111](#))
Müller-Schilling, Martina,
S115 ([TOP-346-YI](#)), S191 ([WED-106](#))
Müller, Thomas, S54 ([OS-083](#))
Müller, Tobias, S730 ([TOP-369](#))
Müllhaupt, Beat, S702 ([TOP-140](#))
Mullish, Benjamin H., S46 ([OS-070](#)),
S127 ([THU-317](#)), S282 ([WED-546](#)),
S470 ([FRI-215-YI](#)), S495 ([FRI-286](#))
Müllner-Bucsics, Theresa,
S156 ([TOP-097-YI](#)), S242 ([SAT-080-YI](#)),
S253 ([SAT-118](#))
Munker, Stefan, S263 ([THU-526](#))
Muñoz, Beatriz Mateos, S318 ([THU-118](#)),
S818 ([THU-381](#))
Muñoz, Elena, S266 ([THU-539](#))
Muñoz-Espinosa, Linda Elsa, S627 ([FRI-029](#))
Muñoz, Francisco Luis Bellido,
S559 ([WED-341](#))
Munoz-Hernández, Rocío, S71 ([OS-116](#)),
S427 ([FRI-501](#)), S587 ([THU-268](#)),
S593 ([THU-287](#)), S596 ([THU-296](#))
Muñoz, Javier, S362 ([WED-016](#)),
S364 ([WED-028](#))
Munoz, Leticia, S189 ([WED-100-YI](#)),
S277 ([WED-530-YI](#))
Muñoz-Llanes, Nerea, S562 ([TOP-229-YI](#))
Muñoz, Manuel Bernal, S107 ([FRI-324](#))
Muñoz Martínez, Sergio, S471 ([FRI-219-YI](#))
Munteanu, Mona, S514 ([WED-211](#)),
S548 ([WED-305](#))
Murad, Mohamad, S229 ([FRI-116](#))
Murad, Sarwa Darwish, S380 ([SAT-035](#))
Murai, Kazuhiro, S506 ([TOP-288](#))
Muralidharan, Vijayaragavan,
S372 ([SAT-017](#))
Muratori, Ida, S601 ([TOP-193](#))
Muratori, Luigi, S96 ([LBP-038](#)),
S306 ([THU-093](#)), S712 ([WED-160](#))
Muratori, Paolo, S18 ([OS-015](#))
Mura, Vincenzo La, S459 ([TOP-301](#))
Murcia, C., S369 ([SAT-009](#))
Mureddu, Matteo, S704 ([TOP-144-YI](#))
Murgia, Antonio, S195 ([WED-117](#))
Murielle, Verboom, S21 ([OS-021-YI](#))
Murillo Perez, Carla Fiorella,
S308 ([THU-098](#))
Murphy, Aileen, S635 ([THU-040-YI](#))
Murphy, Joanne, S635 ([THU-040-YI](#))
Murphy, Robert, S395 ([SAT-479-YI](#))
Murray, Kevin, S655 ([SAT-471](#))
Murray, Lara, S567 ([THU-203](#)),
S571 ([THU-215](#)), S585 ([THU-261](#))
Murtuza-Baker, Syed, S67 ([OS-109](#))
Murugesan, Sundaresan, S667 ([WED-447](#))
Musabaev, Erkin, S680 ([WED-480-YI](#))
Muscari, Fabrice, S369 ([SAT-010](#))
Muscaritoli, Maurizio, S215 ([FRI-077-YI](#))
Muselli, Marco, S19 ([OS-017](#))
Mushi, Joanne, S692 ([TOP-145](#))
Musolino, Cristina, S422 ([FRI-481](#)),
S740 ([SAT-378](#)), S747 ([SAT-397](#))
Mussetto, Alessandro, S96 ([LBP-038](#)),
S306 ([THU-093](#))
Mustafa, Ghulam, S192 ([WED-109](#))
Muthiah, Mark, S139 ([SAT-256](#)),
S147 ([SAT-281](#)), S366 ([TOP-004](#)),
S478 ([FRI-236-YI](#)), S524 ([WED-238](#)),
S540 ([WED-282](#)), S565 ([THU-200-YI](#))
Mutschler, Frauke, S700 ([FRI-171](#))
Muwonga, Jérémie, S668 ([WED-451-YI](#))
Muzaffar, Mahvish, S443 ([THU-464](#))
Myeni, Sebenzile, S700 ([FRI-171](#))
Myer, Vic, S58 ([OS-090](#))
Myneni, Sudha Rani, S363 ([WED-021](#)),
S585 ([THU-260](#))
Myojin, Yuta, S506 ([TOP-288](#))
Myoteri, Despoina, S454 ([THU-495](#))
Myroniuk-Konstantynovych, Kiarina,
S827 ([THU-408](#)), S835 ([THU-373-YI](#))
Mysko, Christopher, S650 ([SAT-454-YI](#))
Nabidzhonov, Aziz, S682 ([WED-484](#))
Nabilou, Puria, S30 ([OS-038-YI](#)),
S199 ([TOP-062](#)), S200 ([TOP-064-YI](#)),
S513 ([WED-207](#)), S529 ([WED-250-YI](#)),
S555 ([WED-331-YI](#))
Nachit, Maxime, S473 ([FRI-224](#))
Nadalín, Silvio, S9 ([LBO-004](#)),
S89 ([LBP-026](#)), S368 ([SAT-008](#)),
S368 ([SAT-009](#))
Nadal, Ruth, S160 ([THU-056](#)),
S176 ([WED-055](#)), S503 ([TOP-241-YI](#)),
S541 ([WED-284-YI](#))
Nadda, Rohit, S129 ([THU-324](#)),
S152 ([SAT-295](#))
Nadeem, Mahum, S60 ([OS-095](#))
Nadeem, Rida, S84 ([LBP-014](#)),
S510 ([WED-199](#)), S547 ([WED-303](#)),
S709 ([WED-151](#))
Nader, Fatema, S465 ([FRI-202](#)),
S470 ([FRI-218](#)), S476 ([FRI-232](#)),
S496 ([FRI-291](#)), S638 ([SAT-425](#)),
S652 ([SAT-459](#))
Nadim, Al Hajjar, S409 ([SAT-525](#))
Nadinskaya, Maria, S52 ([OS-080](#))
Nadjiri, Jonathan, S213 ([FRI-071](#))
Nadol, Patrick, S682 ([WED-484](#))
Nagandiram, Vernujaa, S631 ([THU-017-YI](#))
Nagao, Chikako, S248 ([SAT-101](#))
Nagaoka, Shinya, S542 ([WED-286](#))
Nagaraja, Ravishankara, S615 ([SAT-231](#))
Nagpal, Leena, S337 ([THU-173](#))
Nagpal, Shakti, S565 ([THU-200-YI](#))
Nagral, Abha, S161 ([THU-058](#)),
S208 ([FRI-053](#)), S475 ([FRI-231](#))
Nagy, Laura, S131 ([THU-330](#))
Nagy, Mohamed, S491 ([FRI-273-YI](#))
Nagy, Peter, S544 ([WED-294](#))
Nahass, Ronald G., S809 ([WED-371](#))
Nah, Benjamin, S139 ([SAT-256](#)),
S366 ([TOP-004](#)), S540 ([WED-282](#))
Nahon, Pierre, S41 ([OS-060](#)), S61 ([OS-097](#)),
S68 ([OS-110](#)), S441 ([THU-459-YI](#)),
S451 ([THU-487-YI](#))
Nai, Antonella, S571 ([THU-218](#))
Naik, Keval, S147 ([SAT-280](#))
Naimi, Sabrine, S136 ([THU-347-YI](#))
Nair, Radhika, S314 ([THU-110](#)),
S621 ([FRI-008](#))
Najafian, Nilofar, S152 ([SAT-297](#))
Najimi, Mustapha, S172 ([THU-092](#)),
S353 ([SAT-537](#))
Nakagawa, Miyuki, S123 ([SAT-335](#))
Nakagawa, Ryo, S301 ([SAT-176](#)),
S303 ([SAT-182](#))
Nakajima, Atsushi, S2 ([GS-004](#)),
S38 ([OS-054](#)), S147 ([SAT-281](#)),
S235 ([FRI-130](#)), S238 ([SAT-068](#)),
S537 ([WED-273](#)), S541 ([WED-283](#))
Nakamoto, Shingo, S123 ([SAT-335](#)),
S247 ([SAT-095](#)), S301 ([SAT-176](#))
Nakamoto, Yasunari, S828 ([THU-413](#))
Nakamura, Makoto, S248 ([SAT-101](#))
Nakamura, Masato, S123 ([SAT-335](#)),
S247 ([SAT-095](#)), S301 ([SAT-176](#))
Nakamura, Yoshiko, S711 ([WED-154](#)),
S722 ([WED-184](#))
Nakamuta, Makoto, S42 ([OS-062](#))
Nakanishi, Hiroyuki, S626 ([FRI-026](#))
Nakao, Kazuhiko, S228 ([FRI-113](#)),
S234 ([FRI-128](#)), S828 ([THU-413](#))
Nakao, Yasuhiko, S228 ([FRI-113](#)),
S234 ([FRI-128](#))
Nakib, Diana, S31 ([OS-040-YI](#))
Nalbant, Bahar, S115 ([TOP-346-YI](#))
Nalpas, Catherine, S27 ([OS-033](#))
Nam, Gi-Hoon, S104 ([TOP-351-YI](#))
Nam, Heechul, S167 ([THU-077](#))
Namisaki, Tadashi, S175 ([TOP-096](#))
Nam, Seong Woo, S766 ([FRI-375](#))
Nam, Soon Woo, S762 ([FRI-364](#))
Nan, Fajun, S602 ([TOP-217](#))
Nan, Yüemin, S558 ([WED-337](#))
Naoumov, Nikolai V., S465 ([FRI-203](#))
Napoli, Nicola, S554 ([WED-325-YI](#))
Napolitano, Carmine, S213 ([FRI-070-YI](#))
Naqash, Abdul Rafah, S443 ([THU-464](#))
Naqvi, Hasan, S242 ([SAT-082](#))
Naranjo, Dolores, S817 ([TOP-385-YI](#))
Narayanan, Padma, S693 ([FRI-151](#))
Narayanawamy, K, S476 ([FRI-231](#))
Nardelli, Silvia, S62 ([OS-099-YI](#)),
S206 ([FRI-047-YI](#)), S214 ([FRI-075](#)),
S215 ([FRI-078-YI](#)), S258 ([SAT-131](#))

Author Index

- Nardone, Gerardo, S96 ([LBP-038](#)), S306 ([THU-093](#))
- Nartey, Yvonne, S395 ([SAT-479-YI](#))
- Nash, Kathryn L, S633 ([THU-027-YI](#))
- Nasr, Patrik, S530 ([WED-255-YI](#)), S532 ([WED-259](#))
- Nassiri-Toosi, Mohssen, S387 ([SAT-053](#))
- Nastouli, Eleni, S676 ([WED-471](#)), S759 ([TOP-417](#))
- Natarajan, Muthukumaran, S615 ([SAT-231](#))
- Nath, Preetam, S488 ([FRI-266-YI](#))
- Natola, Leonardo, S700 ([FRI-171](#))
- Natola, Leonardo Antonio, S51 ([OS-078-YI](#))
- Nault, Jean Charles, S50 ([OS-077](#)), S68 ([OS-110](#)), S168 ([THU-079](#)), S413 ([FRI-456](#)), S441 ([THU-458](#)), S441 ([THU-459-YI](#)), S451 ([THU-487-YI](#))
- Naumann, Uwe, S833 ([THU-366](#))
- Nautiyal, Nidhi, S177 ([WED-057](#)), S184 ([WED-086](#)), S195 ([WED-118](#)), S360 ([SAT-557-YI](#))
- Navarro, Mariana Gutierrez-Zamora, S154 ([SAT-304](#))
- Navarro, Victor, S114 ([TOP-345](#))
- Naviglio, Silvio, S173 ([TOP-072](#))
- Nawrot, Margaux, S49 ([OS-074](#))
- Nayagam, Shevanthi, S678 ([WED-475](#)), S679 ([WED-477-YI](#))
- Nayak, Hemanta, S248 ([SAT-099-YI](#))
- Nazarenko, Dan, S88 ([LBP-022](#))
- İnci, Ayşe, S805 ([WED-418](#))
- Ndow, Gibril, S782 ([FRI-418](#)), S787 ([FRI-431](#))
- Ndungu, Thumbi, S753 ([SAT-413](#))
- Neamti, Lidia, S555 ([WED-332](#))
- Nederveen, Aart, S315 ([THU-112-YI](#))
- Neeman, Ziv, S645 ([SAT-442](#))
- Neena, Abraham, S608 ([SAT-207](#))
- Neff, Guy, S4 ([GS-006](#)), S8 ([LBO-002](#)), S72 ([OS-119](#)), S614 ([SAT-227](#)), S618 ([SAT-243](#))
- Negi, Preeti, S177 ([WED-057](#))
- Neglia, Maria Cristina, S329 ([THU-153](#))
- Negrillo, Ricardo Cabello, S161 ([THU-058](#))
- Negrinho, Ana Patricia, S834 ([THU-370](#))
- Negri, Tiziana, S439 ([THU-447](#))
- Nehme, Zeina, S25 ([OS-029](#))
- Neiryneck, Gauthier, S2 ([GS-003-YI](#))
- Nelander, Karin, S535 ([WED-270](#))
- Nemazanyy, Ivan, S572 ([THU-220](#))
- Nenu, Iuliana, S409 ([SAT-525](#))
- Neria, Fernando, S377 ([SAT-027](#))
- Neri, Sergio, S215 ([FRI-078-YI](#))
- Nerli, Alessandro, S674 ([WED-467-YI](#))
- Nesterchuk, Mikhail, S268 ([THU-542](#))
- Neto, Dermeval, S618 ([SAT-242](#))
- Netter, Hans, S740 ([SAT-377](#))
- Neubauer, Stefan, S21 ([OS-020](#))
- Neumann-Haefelin, Christoph, S28 ([OS-034](#))
- Neumann, Olaf, S23 ([OS-025-YI](#))
- Neumann, Ulf, S426 ([FRI-495](#))
- Neumayer, Daniela, S621 ([FRI-009-YI](#))
- Neurath, Markus F, S317 ([THU-116-YI](#)), S327 ([THU-137](#)), S338 ([THU-176](#)), S356 ([SAT-546](#))
- Neuschwander-Tetri, Brent A., S467 ([FRI-208](#)), S472 ([FRI-222-YI](#))
- Nevens, Frederik, S14 ([OS-009-YI](#)), S16 ([OS-012-YI](#)), S91 ([LBP-027](#)), S125 ([TOP-328-YI](#)), S172 ([THU-092](#)), S308 ([THU-098](#)), S321 ([THU-125](#)), S386 ([SAT-051](#))
- Nevermann, Nora, S425 ([FRI-492-YI](#))
- Neville, Matthew, S578 ([THU-236-YI](#))
- Nevola, Riccardo, S790 ([FRI-441](#))
- Nevzorova, Yulia, S276 ([WED-528-YI](#)), S351 ([SAT-534](#))
- Newell, Evan, S81 ([LBP-009](#))
- Newsome, Philip N., S2 ([GS-004](#)), S4 ([GS-006](#)), S38 ([OS-054](#)), S79 ([LBP-003](#)), S93 ([LBP-032](#)), S101 ([LBP-046](#)), S459 ([TOP-307](#)), S472 ([FRI-220-YI](#)), S472 ([FRI-222-YI](#)), S606 ([SAT-201](#)), S610 ([SAT-212](#))
- Newton, Julia, S297 ([SAT-165-YI](#))
- Neyts, Johan, S94 ([LBP-034](#)), S732 ([SAT-340-YI](#)), S732 ([SAT-341](#))
- Ng, Cheng Han, S139 ([SAT-256](#)), S366 ([TOP-004](#)), S478 ([FRI-236-YI](#)), S540 ([WED-282](#))
- Ng, Huck Hui, S578 ([THU-239-YI](#))
- Ngimbi, Patrick, S675 ([WED-469](#)), S752 ([SAT-409](#))
- Ng, Irene Oi-Lin, S419 ([FRI-473](#))
- Ngo-Giang-Huong, Nicole, S831 ([THU-362](#))
- Ngongang, Norbert, S373 ([SAT-020](#))
- Ngu, Natalie, S400 ([SAT-492](#))
- Nguyen, Brian, S369 ([SAT-009](#))
- Nguyen, Isabelle, S384 ([SAT-047](#))
- Nguyen, Long, S370 ([SAT-011](#)), S385 ([SAT-049](#))
- Nguyen, Mindie, S11 ([LBO-006](#)), S625 ([FRI-022](#))
- Nguyen, Thi Thuan, S679 ([WED-477-YI](#))
- Nguyen, Tuan T., S809 ([WED-371](#))
- Ng, Wee Han, S200 ([TOP-063](#)), S216 ([FRI-081](#))
- Niazi, Mohammad, S93 ([LBP-031](#))
- Niazi, Shehzad, S146 ([SAT-279](#))
- Niaz, Qamar, S192 ([WED-109](#))
- Nicastro, Emanuele, S700 ([FRI-171](#))
- Nicetto, Dario, S354 ([SAT-541](#))
- Nicholls, Stephen, S93 ([LBP-032](#))
- Nicholson, Edward, S690 ([WED-514](#))
- Nicholson-Scott, Louise, S195 ([WED-117](#))
- Nickel, Alexander Georg, S587 ([THU-269-YI](#))
- Nicoara-Farcau, Oana, S144 ([SAT-273-YI](#))
- Nico Faber, Klaas, S286 ([TOP-560](#))
- Nicola, Dorin, S789 ([FRI-437](#))
- Nicola, Francesca De, S280 ([WED-540-YI](#))
- Nicolas, Bertocchini, S49 ([OS-074](#))
- Nicola, Stella De, S497 ([FRI-294](#)), S666 ([WED-446](#)), S804 ([WED-414](#))
- Nicoletti, Paola, S114 ([TOP-345](#))
- Nicoll, Amanda, S8 ([LBO-003](#)), S339 ([THU-177-YI](#)), S400 ([SAT-492](#)), S402 ([SAT-496](#))
- Nidiaci, Letizia, S657 ([WED-423](#))
- Niechcial, Anna, S56 ([OS-086-YI](#))
- Nie, Chunhui, S447 ([THU-475](#))
- Niederau, Claus, S707 ([WED-133](#))
- Niederhauser, Christoph, S751 ([SAT-408](#))
- Nielsen, Elise Jonasson, S211 ([FRI-059](#)), S214 ([FRI-075](#))
- Nielsen, Malte H., S576 ([THU-232](#)), S600 ([THU-336](#))
- Nielsen, Trine, S47 ([OS-072-YI](#))
- Nieto, Maria, S557 ([WED-335](#))
- Nieuwenhove, Yves Van, S143 ([SAT-268](#)), S278 ([WED-531](#)), S371 ([SAT-014-YI](#))
- Nieva-Zuluaga, Ane, S64 ([OS-101-YI](#)), S112 ([FRI-343-YI](#)), S419 ([FRI-472-YI](#)), S562 ([TOP-229-YI](#)), S569 ([THU-210](#))
- Nieves, Wildaliz, S74 ([OS-122](#)), S738 ([SAT-373](#))
- Niewoehner, John, S118 ([SAT-320](#))
- Nijhawan, Sandeep, S476 ([FRI-231](#))
- Nikolakopoulou, Polyxeni, S570 ([THU-214](#))
- Nikolaou, Nikolaos, S289 ([FRI-542](#)), S578 ([THU-236-YI](#))
- Nikolas Kather, Jakob, S392 ([SAT-469](#))
- Nikolov, Ivaylo, S172 ([THU-092](#))
- Nikolov, Petar, S485 ([FRI-257](#))
- Nikooie, Amir, S7 ([LBO-001](#))
- Ni, Liyun, S738 ([SAT-373](#))
- Nilsson, Line, S580 ([THU-244](#))
- Nilsson, Staffan, S754 ([SAT-414](#))
- Nilusmas, Samuel, S41 ([OS-060](#))
- Nimanong, Supot, S642 ([SAT-435](#)), S796 ([WED-396](#))
- Ningarhari, Massih, S367 ([TOP-005](#)), S644 ([SAT-439-YI](#))
- Ning, Jing, S734 ([SAT-362](#))
- Ning, Qin, S158 ([THU-052](#)), S167 ([THU-078](#))
- Niosi, Marco, S173 ([TOP-072](#))
- Niro, Grazia Anna, S96 ([LBP-038](#)), S306 ([THU-093](#)), S777 ([FRI-405](#)), S790 ([FRI-441](#))
- Nishida, Naoshi, S51 ([OS-078-YI](#)), S69 ([OS-112-YI](#)), S443 ([THU-464](#))
- Nishijima, Suguru, S47 ([OS-072-YI](#)), S48 ([OS-073](#))
- Nishikawa, Hiroki, S248 ([SAT-101](#))
- Nisingizwe, Marie Paul, S659 ([WED-429](#)), S686 ([WED-495](#))
- Nissen, Nicholas, S9 ([LBO-004](#)), S89 ([LBP-026](#))
- Nissen, Steven, S76 ([OS-125](#))
- Nistal, Esther, S45 ([OS-067](#)), S277 ([WED-529](#))
- Nitze, Louise Maymann, S79 ([LBP-003](#)), S709 ([WED-138](#))
- Niu, Hao, S103 ([TOP-350-YI](#))
- Niu, Junqi, S86 ([LBP-019](#)), S95 ([LBP-037](#)), S99 ([LBP-043](#)), S602 ([TOP-217](#)), S807 ([WED-365](#)), S812 ([WED-378](#))

- Niu, Lili, S47 ([OS-072-YI](#))
- Ni, Wenjing, S459 ([TOP-307](#)),
S525 ([WED-244](#)), S527 ([WED-246](#)),
S776 ([FRI-404](#))
- Nizzardo, Andrea, S657 ([WED-423](#))
- N'Kontchou, Gisele, S68 ([OS-110](#))
- Nobes, Jennifer, S14 ([OS-007-YI](#))
- Noble, Alexandra, S302 ([SAT-179](#))
- Noble, Theresa, S676 ([WED-471](#)),
S759 ([TOP-417](#))
- Nofit, Eugenia, S19 ([OS-017](#)),
S310 ([THU-101](#))
- Nogami, Asako, S235 ([FRI-130](#)),
S541 ([WED-283](#))
- Nogueira, Gabriel, S254 ([SAT-119](#))
- Nogué, Santiago, S45 ([OS-068](#))
- Nøhr-Meldgaard, Jacob, S566 ([THU-202](#))
- Nojima, Masanori, S513 ([WED-208](#))
- Nomah, Daniel K, S682 ([WED-485](#))
- Nomura, Hideyuki, S42 ([OS-062](#))
- Nordahl, Helene, S460 ([TOP-309](#))
- Nordenvall, Caroline, S312 ([THU-104](#))
- Nordhus, Kathrine Sivertsen,
S262 ([THU-525-YI](#))
- Nordmann, Thierry, S32 ([OS-041-YI](#))
- Noritake, Hiedenao, S537 ([WED-273](#))
- Norlin, Jenny Egecioglu, S79 ([LBP-003](#)),
S574 ([THU-227](#)), S580 ([THU-244](#))
- Norman, Gary, S308 ([THU-095](#))
- Nößner, Elfriede, S727 ([TOP-355-YI](#))
- Notsumata, Kazuo, S537 ([WED-273](#))
- Noureddin, Mazen, S4 ([GS-006](#)),
S37 ([OS-051](#)), S71 ([OS-117](#)), S72 ([OS-119](#)),
S88 ([LBP-024](#)), S146 ([SAT-278](#)),
S147 ([SAT-281](#)), S463 ([FRI-198](#)),
S464 ([FRI-199](#)), S481 ([FRI-247](#)),
S482 ([FRI-249](#)), S504 ([TOP-253](#)),
S505 ([TOP-264](#)), S505 ([TOP-265](#)),
S507 ([TOP-300](#)), S511 ([WED-201](#)),
S511 ([WED-202](#)), S518 ([WED-223](#)),
S528 ([WED-248](#)), S533 ([WED-263](#)),
S544 ([WED-294](#)), S576 ([THU-233](#)),
S579 ([THU-242](#)), S603 ([SAT-195](#)),
S607 ([SAT-202](#)), S609 ([SAT-208](#)),
S611 ([SAT-214](#)), S640 ([SAT-429](#)),
S648 ([SAT-450](#))
- Nousbaum, Jean-Baptiste, S54 ([OS-084-YI](#))
- Nousbaum, JeanB-aptiste, S444 ([THU-466](#))
- Nováková, Barbora, S539 ([WED-280](#))
- Novo, Erica, S612 ([SAT-219](#))
- Nowak, Jan, S302 ([SAT-179](#))
- Nowak, Magdalena, S542 ([WED-285](#))
- Nowak, Nikolaus, S719 ([WED-175](#))
- Nowak, Sebastian, S258 ([SAT-130](#))
- Noyan, Fatih, S583 ([THU-256](#))
- Nozaki, Akito, S248 ([SAT-101](#))
- Nse, Akpan, S673 ([WED-463](#))
- Nshimyumuremyi, Jean-Boris,
S728 ([TOP-358-YI](#))
- Ntagianta, Elisavet, S670 ([WED-454-YI](#)),
S680 ([WED-478](#))
- Ntambua, Sarah, S675 ([WED-469](#))
- Nudo, Michael, S683 ([WED-486-YI](#))
- Nuhn, Lutz, S435 ([FRI-533](#))
- Nulan, Yeldos, S183 ([WED-081](#)),
S183 ([WED-082](#))
- Numit, Amornkan, S396 ([SAT-480-YI](#)),
S410 ([SAT-529](#))
- Nunag, Dominic, S469 ([FRI-214](#)),
S494 ([FRI-283](#))
- Nunes, Joao, S145 ([SAT-274](#))
- Nunes, Tiago, S323 ([THU-129](#)),
S331 ([THU-158](#))
- Núñez, Carmen López,
S682 ([WED-485](#))
- Núñez, Laura, S231 ([FRI-121](#))
- Nuozzi, Giorgia, S237 ([TOP-061-YI](#))
- Nur, Abdulsemed Mohammed,
S30 ([OS-038-YI](#)), S199 ([TOP-062](#)),
S200 ([TOP-064-YI](#))
- Nurcis, Jessica, S421 ([FRI-479-YI](#))
- Nuriyev, Kanan, S377 ([SAT-028](#)),
S551 ([WED-318-YI](#)), S803 ([WED-413](#))
- Nwosu, Zeribe, S263 ([THU-526](#))
- Nyakowa, Mercy, S684 ([WED-487](#))
- Nyam P, David, S161 ([THU-058](#))
- Nychas, Emmanouil, S454 ([THU-495](#))
- Oakes, Kathryn, S820 ([THU-383](#))
- Oakley, Holly, S544 ([WED-294](#))
- Oberti, Frédéric, S61 ([OS-097](#)),
S68 ([OS-110](#)), S444 ([THU-466](#)),
S456 ([THU-503](#)), S519 ([WED-224](#))
- Oberti, Giovanna, S466 ([FRI-207-YI](#)),
S482 ([FRI-248-YI](#))
- Ober-Vliegen, Kimberley,
S730 ([TOP-384-YI](#))
- O'Brien, Alastair, S204 ([FRI-041](#)),
S220 ([FRI-089](#))
- Ochirbat, Enkhnommin, S82 ([LBP-011](#))
- Ochirsum, Byambasuren, S82 ([LBP-011](#))
- Ochoa Mora, Estefania, S654 ([SAT-466](#))
- O'Connor, Ian P, S472 ([FRI-222-YI](#))
- Odaldi, Federica, S704 ([TOP-143-YI](#))
- Odenhal, Margarete, S423 ([FRI-486](#))
- Odero, Valle, S779 ([FRI-409](#))
- O'Donnell, Denise, S470 ([FRI-215-YI](#))
- O'Donoghue, Jennifer, S470 ([FRI-215-YI](#))
- Odorizzi, Roberta, S389 ([SAT-060](#))
- Odrizola, Aitor, S61 ([OS-096-YI](#))
- Odriljin, Tatjana, S517 ([WED-220](#))
- Oeda, Satoshi, S537 ([WED-273](#))
- Oeller, Marc, S32 ([OS-041-YI](#))
- Oezsoy, Adil, S392 ([SAT-469](#))
- O'Farrell, Marie, S575 ([THU-231](#))
- O'Farrell, Marie, S4 ([GS-011](#)),
S600 ([THU-336](#))
- O'Farrelly, Cliona, S450 ([THU-485-YI](#))
- Øgaard, Jonas, S33 ([OS-044-YI](#)),
S262 ([THU-525-YI](#)), S296 ([SAT-163-YI](#))
- Ogasawara, Sadahisa, S123 ([SAT-335](#)),
S247 ([SAT-095](#))
- Ogawa, Chikara, S248 ([SAT-101](#))
- Ogawa, Eiichi, S42 ([OS-062](#))
- Ogawa, Sadanobu, S512 ([WED-203](#))
- Ogawa, Yuji, S541 ([WED-283](#))
- Ogle, Jonathan, S10 ([LBO-005](#))
- O'Hare, Cathy, S126 ([THU-315](#))
- Oh, Hyunwoo, S148 ([SAT-284](#)),
S152 ([SAT-296](#)), S654 ([SAT-465](#)),
S766 ([FRI-375](#))
- Ohira, Masahiro, S9 ([LBO-004](#)),
S89 ([LBP-026](#))
- Oh, Joo Hyun, S148 ([SAT-284](#)),
S473 ([FRI-223](#)), S553 ([WED-323](#)),
S654 ([SAT-465](#))
- Oh, Jun, S115 ([TOP-346-YI](#))
- Oh, Ki Kwang, S602 ([TOP-216](#))
- Oh, Sooyeon, S69 ([OS-113](#))
- Ohtake, Jyunya, S513 ([WED-208](#))
- Ohta, Yuki, S301 ([SAT-176](#))
- Oidosambuu, Odgerel, S82 ([LBP-011](#))
- Oikawa, Tsunekazu, S616 ([SAT-236](#))
- Oi-Lin Ng, Irene, S438 ([THU-446](#))
- Ojeda, Asunción, S52 ([OS-080](#)),
S240 ([SAT-074](#))
- Ojeda, David Guardamino,
S129 ([THU-322-YI](#))
- Ojeda, Maria Isabel, S557 ([WED-335](#))
- Okamoto, Hiroaki, S498 ([FRI-297](#)),
S757 ([WED-421](#))
- O'Kane, Grainne, S445 ([THU-470-YI](#))
- Okanoue, Takeshi, S537 ([WED-273](#))
- Okazaki, Kazuichi, S710 ([WED-152](#))
- Okazaki, Yuki, S118 ([SAT-319](#)),
S711 ([WED-154](#)), S722 ([WED-184](#))
- Okechukwu, Queeny, S298 ([SAT-170](#))
- O'Keeffe, Ayla, S423 ([FRI-487](#))
- Okeke, Edith, S208 ([FRI-053](#)),
S395 ([SAT-479-YI](#))
- Okeke, Sylvester, S689 ([WED-501](#))
- Okpala, Naomi Chioma,
S84 ([LBP-015](#))
- Okubo, Hironao, S248 ([SAT-101](#))
- Okubo, Tomomi, S248 ([SAT-101](#)),
S616 ([SAT-236](#))
- Okushin, Kazuya, S589 ([THU-275](#))
- Olafsson, Sigurdur, S236 ([FRI-133](#)),
S389 ([SAT-059](#))
- Olah, Fruzsina, S313 ([THU-106-YI](#))
- Olaizola, Paula, S66 ([OS-105-YI](#)),
S295 ([SAT-159-YI](#))
- Olartekoetxea, Gaizka Errazti,
S569 ([THU-210](#))
- Olasz, Irina, S141 ([SAT-262](#))
- Olbrich, Anne, S404 ([SAT-501-YI](#))
- Oldak, Natalia, S374 ([SAT-021](#))
- Oldani, Graziano, S189 ([WED-101-YI](#))
- Oldenburger, Anouk, S574 ([THU-227](#)),
S581 ([THU-248](#))
- O'Leary, Jacqueline, S163 ([THU-060](#)),
S206 ([FRI-046](#)), S218 ([FRI-086](#))
- O'Leary, Jacqueline G., S118 ([SAT-320](#))
- Olivas Alberch, Pol, S255 ([SAT-123](#))
- Olivas, Ignasi, S105 ([FRI-321](#)),
S291 ([TOP-149-YI](#)), S293 ([SAT-153-YI](#)),
S336 ([THU-170-YI](#)), S468 ([FRI-211](#)),
S710 ([WED-153](#))
- Olivas, Pol, S15 ([OS-010](#)), S53 ([OS-081](#)),
S240 ([SAT-074](#))
- Olivé, Aina Nicolàs, S39 ([OS-056-YI](#)),
S664 ([WED-440](#)), S682 ([WED-485](#))

Author Index

- Oliveira, Claudia P., S536 (WED-271), S619 (SAT-248)
- Oliveira, Daniel V., S697 (FRI-163-YI)
- Oliveira, Mariana M., S187 (WED-092)
- Oliveira, Mario, S834 (THU-370)
- Oliveira, Pedro, S271 (THU-556)
- Oliveira, Rui, S692 (TOP-146)
- Olivera, Marco, S165 (THU-074)
- Oliveri, Filippo, S549 (WED-314-YI), S622 (FRI-014)
- Olivero, Antonella, S59 (OS-094), S501 (FRI-314), S522 (WED-233-YI), S772 (FRI-392-YI), S777 (FRI-405)
- Olivieri, Simone, S213 (FRI-070-YI)
- Oliviero, Barbara, S428 (FRI-514)
- Olivier, Stephen, S753 (SAT-413)
- Öllinger, Robert, S366 (TOP-003-YI)
- Ollivier-Hourmand, Isabelle, S54 (OS-084-YI), S61 (OS-097), S73 (OS-120), S367 (TOP-005), S444 (THU-466), S705 (WED-129), S793 (WED-391)
- Olona, Antoni, S580 (THU-247-YI)
- Olsen, Kathryn, S337 (THU-173)
- Olsen, Rebecca Wendelbo, S566 (THU-202)
- Oltman, Marian, S311 (THU-103)
- Oltmanns, Carlos, S735 (SAT-363), S750 (SAT-406-YI)
- Olveira, Antonio, S398 (SAT-485), S706 (WED-132), S712 (WED-159), S717 (WED-172)
- Olynyk, John, S275 (WED-526), S483 (FRI-250), S487 (FRI-263), S655 (SAT-471)
- Omahony, Stephen, S661 (WED-433)
- Omar, Heba, S491 (FRI-273-YI)
- Omata, Masao, S167 (THU-078)
- Omeish, Haya A., S84 (LBP-014)
- Omer, Hélène, S65 (OS-103)
- Omer, Muhammad Ovais, S192 (WED-109)
- Onderwater, Susanne L., S314 (THU-109), S327 (THU-138)
- Onea, Mihaela, S25 (OS-029)
- Ong, Charlotte Chung Hui, S147 (SAT-281)
- Ong, Christen, S139 (SAT-256), S366 (TOP-004)
- Ong, Christen En Ya, S147 (SAT-281)
- Ong, Elden, S147 (SAT-281)
- Onghena, Louis, S57 (OS-089-YI), S143 (SAT-268), S278 (WED-531), S371 (SAT-014-YI), S631 (THU-020-YI)
- Ong, John, S81 (LBP-008)
- Oniscu, Gabriel, S369 (SAT-009)
- Onlen, Yusuf, S805 (WED-418)
- Önnerhag, Kristina, S624 (FRI-018)
- Onofrio, Fernanda, S374 (SAT-021)
- Onoiu, Alina-Iuliana, S582 (THU-250-YI), S583 (THU-257), S586 (THU-263-YI), S594 (THU-290-YI)
- Onstein, Julia, S414 (FRI-457)
- Ooho, Aritsune, S42 (OS-062)
- Ooi, Geraldine, S534 (WED-267)
- Ooi, Qing Xi, S321 (THU-124)
- Oo, Ye Htun, S33 (OS-044-YI), S34 (OS-046), S101 (LBP-046), S316 (THU-113), S337 (THU-173), S354 (SAT-540-YI), S374 (SAT-021), S712 (WED-160)
- Opawska, Krystyna, S70 (OS-115)
- Oppert, Jean Michel, S493 (FRI-282), S512 (WED-206)
- Orakov, Askarbek, S48 (OS-073)
- Orasan, Olga, S521 (WED-232-YI)
- Oravilahti, Anniina, S514 (WED-210)
- Ordóñez, Jose-Manuel, S455 (THU-501)
- Oregoni, Alain, S281 (WED-542-YI)
- O'Reilly, Lucy, S117 (SAT-317)
- Orienti, Marco, S533 (WED-261-YI)
- Orlandini, Alessandra, S310 (THU-101)
- Orlent, Hans, S321 (THU-123-YI)
- Orman, Eric, S30 (OS-038-YI), S199 (TOP-062), S200 (TOP-064-YI)
- Örmeci, Asli Çifcibasi, S551 (WED-318-YI), S803 (WED-413)
- Ormeci, Necati, S624 (FRI-020)
- Oró, Denise, S568 (THU-208), S569 (THU-211), S580 (THU-244)
- O'Rourke, Joanne, S423 (FRI-487), S425 (FRI-493)
- Orozco, Roberto, S641 (SAT-431-YI)
- Orr, James, S408 (SAT-521)
- Ortega, Miguel A., S277 (WED-530-YI)
- Orti Cuerva, Marina, S330 (THU-155)
- Ortiz de Solorzano, Marta Morán, S599 (THU-304)
- Ortiz, María Luisa, S365 (TOP-002)
- Ortiz-Rivero, Sara, S433 (FRI-526)
- Ortonne, Valérie, S784 (FRI-425)
- Orts, Lara, S15 (OS-010), S240 (SAT-074), S255 (SAT-123)
- Oscarsson, Jan, S238 (SAT-069)
- Osinusi, Anu, S1 (GS-002), S92 (LBP-029), S764 (FRI-371)
- Osler, Merete, S149 (SAT-286-YI)
- Osna, Natalia, S281 (WED-544), S742 (SAT-382)
- Østergaard, Laura, S606 (SAT-201)
- Oster, Michael, S628 (FRI-033)
- Ostrovskaya, Anna, S232 (FRI-124)
- Ostyn, Tessa, S25 (OS-029), S31 (OS-040-YI), S125 (TOP-328-YI)
- O'Sullivan, Therese, S275 (WED-526)
- Osuna-Gómez, Rubén, S355 (SAT-543)
- Osvely, Mendez, S83 (LBP-012)
- Otani, Tomohiro, S235 (FRI-130)
- Oton, Elena, S365 (TOP-002)
- Ottobrelli, Antonio, S210 (FRI-056-YI), S371 (SAT-015-YI), S378 (SAT-031-YI)
- Otto-Mora, Patricia, S23 (OS-025-YI)
- Oubaya, Nadia, S373 (SAT-020)
- Ouchi, Mayu, S301 (SAT-176), S303 (SAT-182)
- Oude-Elferink, Ronald, S296 (SAT-160)
- Oudot, Marine, S17 (OS-013), S42 (OS-061), S734 (SAT-348-YI)
- Ouwkerk-Mahadevan, Sivi, S732 (SAT-341)
- Ou, Xueting, S792 (WED-390)
- Ouyang, Qin, S121 (SAT-330)
- Ouzan, Denis, S41 (OS-060)
- Ovadia, Caroline, S274 (WED-523)
- Owen, Christina, S639 (SAT-428), S687 (WED-496)
- Owen, Emma, S408 (SAT-521)
- Oxley, Anthony, S641 (SAT-431-YI)
- Ozenne, Violaine, S441 (THU-458)
- Özercan, Abdullah Mübin, S407 (SAT-519), S479 (FRI-238)
- Ozik, Jonathan, S43 (OS-063)
- Ozkaya, Deniz Cevahir, S805 (WED-418)
- Özlem, Elpek Gülsüm, S341 (THU-182)
- Özsezen, Serdar, S513 (WED-209)
- Ozudogru, Talha, S211 (FRI-067)
- Paba, Pierpaolo, S777 (FRI-405)
- Pabic, Estelle Le, S802 (WED-410)
- Pablo Arab, Juan, S147 (SAT-280), S148 (SAT-285-YI)
- Pacenti, Monia, S59 (OS-094)
- Pace Palitti, Valeria, S310 (THU-101)
- Pacheco, Beatriz, S303 (SAT-183)
- Padaki, Nagaraja, S440 (THU-456), S454 (THU-498), S701 (FRI-173), S720 (WED-180)
- Padaki, Nagaraja Rao, S158 (THU-052), S167 (THU-078), S476 (FRI-231)
- Padilla, María, S377 (SAT-027)
- Padilla, Marlene, S468 (FRI-211)
- Padmanabhan, Krishna, S611 (SAT-214)
- Padole, Vaibhav, S554 (WED-327)
- Paez, Antonio, S231 (FRI-121)
- Paff, Melanie, S745 (SAT-390), S807 (WED-364), S809 (WED-370)
- Pagani, Alessia, S571 (THU-218)
- Pagani, Francesca, S24 (OS-027-YI)
- Pagano, Duilio, S369 (SAT-009)
- Pagano, Giulia, S9 (LBO-004), S89 (LBP-026), S365 (TOP-002)
- Pageaux, Georges-Philippe, S6 (GS-010), S41 (OS-060), S50 (OS-077), S68 (OS-110), S115 (SAT-306), S143 (SAT-269), S156 (TOP-108), S168 (THU-079), S172 (THU-092), S369 (SAT-010), S376 (SAT-026), S385 (SAT-048), S444 (THU-466), S763 (FRI-370)
- Page-Cook, De Shaunda, S669 (WED-453)
- Page, Kimberly, S832 (THU-364)
- Pages, Josefina, S9 (LBO-004), S89 (LBP-026)
- Pagès, Laura, S29 (OS-037)
- Pages, Nieves Aparicio, S314 (THU-109), S327 (THU-138)
- Pagni, Fabio, S19 (OS-017), S299 (SAT-171)
- Paik, Annette, S637 (TOP-445), S638 (SAT-425)
- Paik, Ik-Hyeon, S693 (FRI-151)
- Paik, James M., S470 (FRI-218), S472 (FRI-221), S637 (TOP-445), S638 (SAT-425)
- Paik, Woo Hyun, S323 (THU-128)
- Paisley, Sarah, S412 (FRI-454)

- Pais, Raluca, S486 (FRI-259),
S493 (FRI-282), S512 (WED-206),
S533 (WED-262)
- Pajancic, Larissa, S436 (TOP-488-YI)
- Pakseresht, Radin, S497 (FRI-293)
- Palassin, Pascale, S115 (SAT-306)
- Pálek, Richard, S349 (FRI-556)
- Palermo, Andrea, S554 (WED-325-YI)
- Palermo, Concetta Ilenia, S777 (FRI-405)
- Paley, Lizz, S406 (SAT-515)
- Palitti, Valeria Pace, S96 (LBP-038),
S175 (TOP-085), S306 (THU-093)
- Palladino, Simona, S370 (SAT-013)
- Palle, Mads Sundby, S79 (LBP-003)
- Palloni, Andrea, S395 (SAT-477-YI),
S446 (THU-472-YI)
- Pallozzi, Maria, S452 (THU-492),
S703 (TOP-142-YI)
- Palma, Carolina, S286 (WED-558),
S358 (SAT-554-YI)
- Palma-Duran, Susana, S750 (SAT-404)
- Palma, Elena, S58 (OS-091),
S128 (THU-320-YI), S178 (WED-068-YI)
- Palma, Sara De, S35 (OS-048)
- Palmieri, Orazio, S777 (FRI-405)
- Palmisano, Angela, S401 (SAT-494)
- Palmisano, Silvia, S429 (FRI-516-YI)
- Palom, Adriana, S633 (THU-028),
S700 (FRI-171), S741 (SAT-381),
S746 (SAT-393), S777 (FRI-406),
S785 (FRI-427), S787 (FRI-432),
S822 (THU-395)
- Palomer, Xavier, S574 (THU-225)
- Palomino-Echevarria, Sara, S174 (TOP-073),
S176 (WED-055)
- Palop, Begoña, S779 (FRI-409)
- Pamecha, Viniyendra, S294 (SAT-155)
- Panackel, Charles, S158 (THU-052),
S167 (THU-078)
- Panariello, Adelaide, S376 (SAT-025)
- Pan, Cuizhen, S240 (SAT-075-YI)
- Pan, David, S738 (SAT-373)
- Pandey, Sushmita, S103 (TOP-349-YI),
S108 (FRI-327-YI), S125 (TOP-329-YI),
S127 (THU-318), S134 (THU-339),
S273 (WED-519-YI), S283 (WED-549),
S294 (SAT-155)
- Pandiaraja, Dhivya, S400 (SAT-492)
- Pandol, Stephen, S39 (OS-055)
- Pandeyarajan, Vijay, S39 (OS-055)
- Panella, Riccardo, S565 (THU-199)
- Panera, Nadia, S289 (FRI-544)
- Panera, Niki, S664 (WED-440)
- Panero, José Luis Calleja, S2 (GS-004),
S38 (OS-054), S61 (OS-096-YI),
S85 (LBP-016), S469 (FRI-213),
S559 (WED-339), S640 (SAT-429),
S700 (FRI-171), S777 (FRI-406)
- Panigrahi, Manas Kumar, S163 (THU-067),
S248 (SAT-099-YI), S285 (WED-554),
S488 (FRI-266-YI)
- Panio, Angelo, S371 (SAT-015-YI)
- Pan, Ling, S102 (LBP-048)
- Pan, Long, S415 (FRI-459)
- Panman, Lia, S289 (FRI-542)
- Pan, Mei-Hung, S491 (FRI-274)
- Pannala, Rahul, S608 (SAT-207)
- Pannifex, Sally, S523 (WED-236-YI)
- Pan, Qianli, S693 (FRI-151)
- Pan, Qiwei, S464 (FRI-200),
S652 (SAT-462-YI), S730 (TOP-384-YI)
- Pansini, Michele, S522 (WED-234),
S535 (WED-268)
- Pan, Tao, S430 (FRI-517)
- Pant, Asmita, S291 (TOP-150-YI)
- Pantea, Victor, S1 (GS-002), S764 (FRI-371),
S791 (FRI-443)
- Pantel, Solène, S22 (OS-022)
- Pantzios, Spyridon, S454 (THU-495),
S798 (WED-403)
- Pan, Xingfei, S792 (WED-390)
- Pan, Yi, S613 (SAT-221)
- Panzeri, Davide, S580 (THU-245)
- Panzer, Marlene, S722 (WED-183-YI),
S773 (FRI-394)
- Paoletti, Martina, S666 (WED-444)
- Paolini, Erika, S516 (WED-218)
- Paolo Caviglia, Gian, S378 (SAT-031-YI),
S483 (FRI-251-YI), S501 (FRI-314),
S776 (FRI-405)
- Paolo Russo, Francesco, S237 (TOP-061-YI),
S389 (SAT-058)
- Paolucci, Stefania, S777 (FRI-405)
- Paon, Veronica, S700 (FRI-171)
- Papadimitriou, Dimitri, S676 (WED-471),
S759 (TOP-417)
- Papadimitriou, Nikolaos, S275 (WED-525)
- Papadimitropoulos, Vasilios,
S798 (WED-403)
- Papadopoulos, Nikolaos, S690 (WED-503),
S798 (WED-403), S823 (THU-398)
- Papagiouvanni, Ioanna, S196 (WED-121-YI)
- Papalamprakopoulou, Zoi,
S670 (WED-454-YI), S680 (WED-478)
- Papathanasiou, Erofilis, S229 (FRI-117)
- Papatheodori, Margarita,
S470 (FRI-215-YI), S777 (FRI-406),
S782 (FRI-415), S793 (WED-391),
S798 (WED-403), S800 (WED-406)
- Papatheodoridis, George, S73 (OS-120),
S217 (FRI-083), S470 (FRI-215-YI),
S643 (SAT-438), S777 (FRI-406),
S782 (FRI-415), S793 (WED-391),
S798 (WED-403), S800 (WED-406)
- Papenthin, Wiebke, S712 (WED-158-YI)
- Pape, Simon, S712 (WED-160)
- Papini, Dimitri, S88 (LBP-023)
- Pappagallo, Marco, S592 (THU-285)
- Papp, Maria, S30 (OS-038-YI),
S47 (OS-071-YI), S48 (OS-073),
S157 (THU-050), S159 (THU-053),
S159 (THU-055), S161 (THU-057-YI),
S169 (THU-080-YI), S184 (WED-083),
S188 (WED-098-YI), S193 (WED-111),
S199 (TOP-062), S200 (TOP-064-YI),
S272 (TOP-563), S313 (THU-106-YI),
S316 (THU-113), S335 (THU-167)
- Paprottka, Philipp, S213 (FRI-071)
- Parada, Álvaro Yagüe, S598 (THU-302),
S599 (THU-304)
- Paradis, Valérie, S412 (FRI-454),
S524 (WED-239), S526 (WED-245),
S719 (WED-177)
- Parana, Raymundo, S722 (WED-185)
- Paranhos, Bruno, S190 (WED-102)
- Parasar, Anupama, S272 (WED-518-YI)
- Parasiliti-Caprino, Mirko, S501 (FRI-314),
S522 (WED-233-YI)
- Paraskevopoulou, Maria D., S696 (FRI-161),
S698 (FRI-164)
- Pardo, Carlos, S61 (OS-096-YI)
- Pardo, Fernando, S348 (FRI-555)
- Parente, Alessandro, S231 (FRI-122),
S374 (SAT-021)
- Pares, Albert, S5 (GS-007), S374 (SAT-021)
- Parewangi, AM Luthfi, S792 (FRI-444)
- Parfieniuk-Kowerda, Anna,
S685 (WED-493-YI), S821 (THU-389),
S834 (THU-367-YI)
- Parikh, Neehar, S69 (OS-112-YI)
- Parikh, Neehar D., S200 (TOP-063)
- Parikh, Pathik, S158 (THU-052),
S167 (THU-078)
- Parish, Craig, S564 (THU-198)
- Parisi, Alessandro, S51 (OS-078-YI)
- Parisse, Simona, S215 (FRI-077-YI)
- Paritala, Soumith, S42 (OS-061)
- Park, Do Hyun, S323 (THU-128)
- Parker, Craig, S141 (SAT-261)
- Parker, Richard, S136 (TOP-311-YI),
S147 (SAT-280), S148 (SAT-285-YI),
S150 (SAT-291), S260 (SAT-137),
S397 (SAT-483-YI), S530 (WED-254),
S534 (WED-266), S547 (WED-302-YI),
S654 (SAT-467)
- Parker, Susan, S87 (LBP-020)
- Parkes, Julie, S506 (TOP-277)
- Park, Haesuk, S658 (WED-425)
- Park, Huiyul, S148 (SAT-284),
S152 (SAT-296), S473 (FRI-223),
S553 (WED-323), S654 (SAT-465)
- Park, Hyewon, S68 (OS-111)
- Park, Hyun Joon, S602 (TOP-216)
- Park, Jae Hyon, S408 (SAT-522)
- Park, Jeayeon, S457 (THU-515),
S517 (WED-221), S601 (TOP-204),
S774 (FRI-397)
- Park, Jeong Ha, S286 (WED-557)
- Park, Jina, S144 (SAT-272),
S822 (THU-394)
- Park, Jin-ho, S638 (SAT-424)
- Park, Ji Yeon, S112 (FRI-341)
- Park, Jong Geun, S264 (THU-530)
- Park, Joo Hyun, S569 (THU-211)
- Park, Joo Kyung, S323 (THU-128)
- Park, Jun Yong, S290 (FRI-545),
S495 (FRI-287), S498 (FRI-296),
S535 (WED-269), S595 (THU-292),
S671 (WED-456), S767 (FRI-378),
S799 (WED-404)
- Park, Kanghee, S822 (THU-394)
- Park, Kena, S68 (OS-111)

Author Index

- Park, Min Kyung, S575 (THU-230), S601 (TOP-204)
- Park, Mi Suk, S408 (SAT-522)
- Park, Neung Hwa, S74 (OS-121)
- Park, Soo Young, S74 (OS-121), S457 (THU-516)
- Park, Yewan, S468 (FRI-210)
- Park, Young Joo, S457 (THU-516)
- Park, Young Nyun, S408 (SAT-522), S438 (THU-446)
- Park, Youngsu, S517 (WED-221), S766 (FRI-376), S774 (FRI-397), S798 (WED-402)
- Parlak, Erkan, S224 (FRI-104)
- Parlati, Lucia, S470 (FRI-215-YI), S698 (FRI-165), S741 (SAT-380), S760 (FRI-361)
- Parmar, Deven, S617 (SAT-239)
- Parola, Maurizio, S421 (FRI-479-YI), S612 (SAT-219)
- Parr, Jonathan B., S668 (WED-451-YI), S675 (WED-469), S752 (SAT-409)
- Parsons, Heather, S647 (SAT-447)
- Parthasarathy, Gopanandan, S586 (THU-266)
- Partipilo, Tommaso, S369 (SAT-009)
- Pascale, Alina, S41 (OS-060), S452 (THU-491)
- Pascale, Marco Maria, S368 (SAT-009)
- Pasciuto, Tina, S369 (SAT-009)
- Pascual, Sonia, S365 (TOP-002), S453 (THU-493)
- Pascual-Vicente, Teresa, S365 (TOP-002)
- Pascucci, Domenico, S664 (WED-440)
- Pascut, Devis, S429 (FRI-516-YI)
- Pasqua, Laura Giuseppina Di, S589 (THU-274)
- Pasquale, Giulia Di, S175 (TOP-085), S754 (SAT-418)
- Pasquazzi, Caterina, S59 (OS-094)
- Pass, Chloe, S81 (LBP-007)
- Passeri, Daniela, S124 (TOP-313)
- Passow, Kellan, S727 (TOP-357)
- Pastore, Mirella, S426 (FRI-498-YI)
- Pastor, Maria Asuncion Ubeda, S154 (SAT-304), S822 (THU-395)
- Pastrovic, Frane, S155 (SAT-305)
- Pasupuleti, Samba Siva Rao, S158 (THU-052)
- Pasut, Gianfranco, S592 (THU-285)
- Patarak, Michal, S379 (SAT-033)
- Patch, David, S248 (SAT-100)
- Patel, Aarya, S510 (WED-199), S547 (WED-303)
- Patel, Ahsan Shueb, S477 (FRI-233)
- Patel, Aman, S653 (SAT-463)
- Patel, Ami, S603 (SAT-194)
- Patel, Chetna, S544 (WED-294)
- Patel, Darshna, S101 (LBP-046)
- Patel, Harsh, S252 (SAT-114)
- Patel, Isha, S5 (GS-007)
- Patel, Keyur, S381 (SAT-037), S497 (FRI-293), S626 (FRI-027), S737 (SAT-370), S761 (FRI-363-YI)
- Patel, Mahesh, S10 (LBO-005)
- Patel, Neel, S571 (THU-215), S585 (THU-261)
- Patel, Nilang, S60 (OS-095)
- Patel, Preya, S629 (THU-008)
- Patel, Sameer, S44 (OS-065)
- Patel, Shila, S546 (WED-298-YI)
- Patel, Shray, S547 (WED-303)
- Patel, Vaishali, S1 (GS-001)
- Patel, Vishal C, S110 (FRI-335), S178 (WED-068-YI), S185 (WED-088-YI), S192 (WED-110)
- Patel, Vishal C., S46 (OS-070), S127 (THU-317), S145 (SAT-274), S227 (FRI-112), S700 (FRI-171)
- Paternostro, Rafael, S243 (SAT-086-YI)
- Paterson, Anna, S81 (LBP-008)
- Pathak, Piyush, S201 (TOP-065)
- Pathak, Vai, S131 (THU-330)
- Patidar, Kavish, S30 (OS-038-YI), S199 (TOP-062), S200 (TOP-064-YI), S242 (SAT-082), S638 (SAT-426-YI)
- Patil, Avinash, S26 (OS-030)
- Patil, Nilesh, S294 (SAT-155)
- Patmore, Lesley A., S758 (TOP-401-YI), S761 (FRI-363-YI), S763 (FRI-367)
- Patra, Biswa Ranjan, S554 (WED-327)
- Patrikiou, Eleni, S358 (SAT-551)
- Patseas, Dimitrios, S181 (WED-075-YI)
- Patten, Daniel, S423 (FRI-487), S425 (FRI-493)
- Patterson, Angus, S547 (WED-299)
- Patterson, Scott D., S462 (FRI-195)
- Paturel, Alexia, S280 (WED-540-YI)
- Patwardhan, Nitish, S554 (WED-327)
- Patwardhan, Vilas, S308 (THU-098), S374 (SAT-021)
- Patwa, Yashwi Haresh Kumar, S219 (FRI-088)
- Paul, Anna, S31 (OS-039)
- Paule, Lorena, S189 (WED-100-YI), S277 (WED-530-YI)
- Paulino, Lismeiry, S669 (WED-453)
- Paulsen, Vemund, S50 (OS-076-YI)
- Paulusma, Coen, S296 (SAT-160)
- Paulweber, Bernhard, S500 (FRI-303)
- Pauwels, Frederik, S807 (WED-363)
- Pavic, Eva, S555 (WED-330), S561 (WED-348)
- Pavlidis, Michael, S536 (WED-272)
- Pavlidis, Charalampos, S594 (THU-291-YI)
- Pavlinková, Gabriela, S697 (FRI-163-YI)
- Pavlova, Desislava, S172 (THU-092)
- Pavlovic, Vedran, S761 (FRI-363-YI)
- Pawlik, Timothy, S375 (SAT-023)
- Pawlotsky, Jean-Michel, S413 (FRI-456), S743 (SAT-386-YI), S784 (FRI-425), S786 (FRI-431)
- Pawlowska, Agnieszka Pawlowska, S590 (THU-278)
- Pawlowska, Małgorzata, S685 (WED-493-YI)
- Payancé, Audrey, S52 (OS-080), S180 (WED-071), S703 (TOP-141), S708 (WED-135-YI), S719 (WED-177)
- Payawal, Diana, S158 (THU-052), S167 (THU-078)
- Payeras, Isabel, S596 (THU-296)
- Paz, Luis González-de, S120 (SAT-325)
- Pazo-Cid, Roberto, S455 (THU-501)
- Peake, Kristen, S632 (THU-021)
- Pearson, Paul, S616 (SAT-233)
- Pechlivanis, Alexandros, S127 (THU-317)
- Peck-Radosavljevic, Markus, S52 (OS-079-YI), S52 (OS-080), S334 (THU-164-YI)
- Peddu, Praveen, S388 (SAT-057)
- Pedersen, Julie Steen, S47 (OS-072-YI), S579 (THU-243)
- Pedersen, Mark, S312 (THU-105), S374 (SAT-021)
- Pedica, Federica, S123 (SAT-334), S341 (THU-182), S438 (THU-446)
- Pedicini, Vittorio, S404 (SAT-502-YI), S406 (SAT-514)
- Pedret-Dunn, Anna, S337 (THU-174)
- Pedron-Giner, Consuelo, S694 (FRI-153)
- Pedro, Patricia, S274 (WED-523)
- Peeters, Frank, S473 (FRI-224)
- Peeters, Mathieu, S807 (WED-363)
- Peeters, Michael, S658 (WED-426)
- Peiffer, Kai-Henrik, S169 (THU-083), S170 (THU-087), S198 (WED-126), S203 (FRI-039), S734 (SAT-361)
- peinovich, nadine, S737 (SAT-371)
- Peiseler, Moritz, S353 (SAT-539-YI)
- Pei, Xiong, S494 (FRI-285), S499 (FRI-302)
- Peix, Judit, S411 (TOP-507-YI)
- Peixoto, Carolina, S362 (WED-015)
- Pei, Yiyi, S525 (WED-242)
- Pei, Zhaohui, S100 (LBP-045)
- Pekarska, Katrina, S136 (TOP-311-YI), S534 (WED-266)
- Pelaez, Maria De Los Angeles Quiroga, S93 (LBP-032)
- Peled, Amnon, S278 (WED-534)
- Pelegrina, Amalia, S207 (FRI-051)
- Peleman, Cédric, S581 (THU-249)
- Pelizzaro, Filippo, S376 (SAT-024-YI)
- Pellegrini, Elisa, S452 (THU-492)
- Pellegrino, Rossella, S426 (FRI-495)
- Pellegrin, Sophie, S116 (SAT-315)
- Pellicciari, Roberto, S124 (TOP-313), S126 (THU-316)
- Pellicelli, Adriano, S73 (OS-120), S793 (WED-391), S804 (WED-414)
- Pell, Jill, S138 (SAT-254)
- Pellon, Miriam, S541 (WED-284-YI)
- Peloso, Andrea, S189 (WED-101-YI)
- Peltzer, Mona, S273 (WED-521-YI)
- Pelusi, Serena, S459 (TOP-301), S491 (FRI-275-YI), S704 (TOP-144-YI)
- Peña, Andrea, S233 (FRI-126)
- Peña-Chilet, María, S596 (THU-296)
- Peña, Luis, S694 (FRI-153)

- Peña-Ramirez, Carlos de la, S157 (THU-050), S161 (THU-057-YI)
- Peña-Sanfelix, Patricia, S417 (FRI-466-YI)
- Pena, Xuel, S154 (SAT-303)
- Penazza, Sofia, S390 (TOP-509-YI)
- Pencek, Richard, S97 (LBP-039)
- Penders, Joris, S604 (SAT-196)
- Peng, Cheng-Yuan, S26 (OS-030), S74 (OS-121), S771 (FRI-390), S832 (THU-365)
- Peng, Chuanhui, S303 (SAT-181-YI)
- Peng, Feng, S209 (FRI-053)
- Peng, Hong, S257 (SAT-126)
- Peng, Jie, S95 (LBP-037)
- Peng, Liang, S109 (FRI-331), S430 (FRI-517)
- Peng, Ming-Li, S269 (THU-549), S357 (SAT-547), S727 (TOP-356)
- Peng, Wenbo, S59 (OS-093)
- Peng, Weng Chuan, S421 (FRI-480)
- Peng, Wenhui, S747 (SAT-395)
- Penna, Andrea Della, S369 (SAT-009)
- Pennisi, Grazia, S2 (GS-004), S36 (OS-047-YI), S38 (OS-054), S252 (SAT-113), S496 (FRI-290), S497 (FRI-294), S503 (FRI-317), S544 (WED-293), S557 (WED-336), S609 (SAT-209-YI)
- Peppelenbosch, Maikel P., S464 (FRI-200), S652 (SAT-462-YI), S730 (TOP-384-YI)
- Pera, Guillem, S503 (TOP-241-YI)
- Pera, Izabela, S154 (SAT-304)
- Peralta, Kristian, S657 (WED-422), S676 (WED-470)
- Perbellini, Riccardo, S73 (OS-120), S344 (THU-190), S401 (SAT-493-YI), S781 (FRI-412), S798 (WED-399-YI)
- Perciani, Catia, S31 (OS-040-YI)
- Pereira, Cláudia, S681 (WED-481)
- Pereira, Gustavo, S30 (OS-038-YI), S83 (LBP-012), S157 (THU-050), S161 (THU-057-YI), S161 (THU-058), S199 (TOP-062), S200 (TOP-064-YI)
- Pereira, Isabel Veloso Alves, S619 (SAT-248)
- Pereira-Leal, Jose, S362 (WED-015)
- Pereira, Sheila, S365 (TOP-002)
- Perelló, Christie, S469 (FRI-213), S559 (WED-339)
- Pérennès, Hélène, S313 (THU-107)
- Perera, Thamara, S9 (LBO-004), S89 (LBP-026), S369 (SAT-009)
- Pérez, Alba Maria Paar, S258 (SAT-130)
- Pérez, Ana Belén, S779 (FRI-409)
- Perez, Anthony, S610 (SAT-212)
- Perez-Campuzano, Valeria, S240 (SAT-074)
- Pérez-del-Pulgar, Sofia, S105 (FRI-321), S351 (SAT-533), S765 (FRI-373)
- Pérez-García, Felipe, S665 (WED-442)
- Perez-Guasch, Martina, S13 (OS-005-YI), S160 (THU-056), S176 (WED-055), S541 (WED-284-YI), S635 (THU-039-YI)
- Pérez-Hernández, José Luis, S30 (OS-038-YI), S83 (LBP-012), S140 (SAT-260), S199 (TOP-062), S200 (TOP-064-YI), S219 (FRI-088)
- Pérez, Judith, S362 (WED-015)
- Pérez-López, Raquel, S455 (THU-501)
- Pérez, Martina, S29 (OS-037)
- Perez Medrano, Indhira, S329 (THU-154-YI), S330 (THU-155)
- Pérez Molina, José A., S664 (WED-440)
- Pérez-Palacios, Domingo, S316 (THU-114)
- Pérez-Rodríguez, Lucía, S691 (WED-516)
- Pérez-Rojas, Judith, S531 (WED-257)
- Perez, Sara Lorente, S365 (TOP-002), S531 (WED-257)
- Perez-Silva, Laura, S432 (FRI-523)
- Pérez, Silvia Calero, S293 (SAT-152), S568 (THU-209)
- Perez, Valeria, S255 (SAT-123)
- Perfecto, Arkaitz, S369 (SAT-009)
- Pericàs, Juan Manuel, S29 (OS-037), S36 (OS-047-YI), S154 (SAT-304), S468 (FRI-211), S503 (TOP-241-YI), S596 (THU-296)
- Perignon, Claire, S168 (THU-079), S385 (SAT-048)
- Perini, Marcos, S368 (SAT-009)
- Perin, Nicola, S318 (THU-117-YI)
- Periti, Giulia, S491 (FRI-275-YI), S544 (WED-293)
- Perlberg, Vincent, S218 (FRI-087)
- Perlemuter, Gabriel, S130 (THU-327), S136 (THU-347-YI)
- Permsuwan, Unchalee, S689 (WED-502)
- Perna, Claudia, S698 (FRI-166)
- Perna, Cristian, S468 (FRI-211)
- Perocheau, Dany, S698 (FRI-166)
- Perola, Markus, S460 (TOP-308), S562 (TOP-240-YI)
- Peron, Jean Marie, S444 (THU-466)
- Perpinan, Elena, S765 (FRI-373)
- Perra, Andrea, S322 (THU-127-YI)
- Perricone, Giovanni, S9 (LBO-004), S30 (OS-038-YI), S89 (LBP-026), S172 (THU-092), S199 (TOP-062), S200 (TOP-064-YI), S332 (THU-161), S376 (SAT-025), S380 (SAT-034), S700 (FRI-171)
- Perrin, Clara, S453 (THU-494)
- Perrone, Valentina, S773 (FRI-393)
- Perron, Michel, S812 (WED-377)
- Persico, Marcello, S493 (FRI-281), S554 (WED-326), S556 (WED-333), S804 (WED-414)
- Perucchini, Chiara, S35 (OS-048)
- Perugorria, María Jesús, S50 (OS-076-YI)
- Perugorria, Matxus, S32 (OS-042-YI), S295 (SAT-159-YI)
- Perumal, Mhukti, S647 (SAT-447)
- Perumal, Sathish Kumar, S281 (WED-544)
- Perzon, Ofer, S563 (THU-194), S779 (FRI-408)
- Pesatori, Eugenia Vittoria, S96 (LBP-038), S306 (THU-093), S325 (THU-133-YI)
- Pes, Francesco, S322 (THU-127-YI)
- Pessaux, Patrick, S17 (OS-013), S25 (OS-029), S734 (SAT-348-YI)
- Pessoa, Mário, S619 (SAT-248)
- Peta, Valentina, S512 (WED-206)
- Peteers, Koen, S679 (WED-477-YI)
- Petera, Mélanie, S422 (FRI-485)
- Peter, Clovis, S728 (TOP-358-YI)
- Petermann, Fanny, S138 (SAT-254)
- Peters, Erica, S783 (FRI-423)
- Peter, Simon, S425 (FRI-492-YI)
- Petit, Arthur, S441 (THU-459-YI)
- Petitjean, Louis, S474 (FRI-225), S533 (WED-262), S590 (THU-278), S597 (THU-298)
- Petitjean, Mathieu, S533 (WED-262), S590 (THU-278), S591 (THU-282), S597 (THU-298), S599 (THU-305)
- Petit, Jean-Michel, S508 (WED-194), S538 (WED-278)
- Petkeviciene, Janina, S678 (WED-474)
- Petrallii, Giovanni, S549 (WED-314-YI), S619 (SAT-245), S622 (FRI-014)
- Petrenko, Oleksander, S267 (THU-540)
- Petrenko, Oleksandr, S186 (WED-089-YI), S197 (WED-122-YI), S198 (WED-125), S296 (SAT-161)
- Petretto, Enrico, S580 (THU-247-YI)
- Petroni, Maria Letizia, S544 (WED-293)
- Petros, Sirak, S162 (THU-059)
- Petrosyan, Armen, S132 (THU-333)
- Petrovski, Irena, S657 (WED-422), S676 (WED-470)
- Petrowsky, Henrik, S702 (TOP-140)
- Petrtyl, Jaromír, S539 (WED-280)
- Petrucelli, Stefania, S370 (SAT-013)
- Petrucci, Lucrezia, S533 (WED-261-YI)
- Petrushev, Bobe, S555 (WED-332)
- Petryna, Vitalii, S285 (WED-555)
- Petryszyn, Pawel, S238 (SAT-069)
- Petta, Salvatore, S2 (GS-004), S36 (OS-047-YI), S38 (OS-054), S252 (SAT-113), S466 (FRI-207-YI), S496 (FRI-290), S497 (FRI-294), S503 (FRI-317), S544 (WED-293), S557 (WED-336), S609 (SAT-209-YI), S704 (TOP-144-YI)
- Petter, Mathias, S340 (THU-180)
- Pettinato, Mariateresa, S571 (THU-218)
- Petzold, Katja, S66 (OS-107-YI)
- Peviani, Matteo, S318 (THU-117-YI)
- Peyman, Mona, S574 (THU-225)
- Peyton, Adam, S98 (LBP-040)
- Pezzati, Daniele, S370 (SAT-013)
- Pezzato, Francesco, S5 (GS-007), S318 (THU-117-YI)
- Pezzullo, Angelo, S664 (WED-440)
- Pfefferkorn, Maria, S752 (SAT-410), S788 (FRI-434), S802 (WED-411)
- Pfister, Dominik, S575 (THU-227), S581 (THU-248)
- Pfisterer, Larissa, S197 (WED-122-YI), S198 (WED-125), S267 (THU-540)
- Phanor, Jhané, S835 (THU-372-YI)
- Phen, Samuel, S51 (OS-078-YI)
- Philippe de Souza Ferreira, Luiz, S113 (FRI-348)
- Philipose, Zinu, S639 (SAT-427-YI)

Author Index

- Philipp, Alexander, S69 ([OS-112-YI](#))
 Philipp Weltzsch, Jan, S341 ([THU-182](#))
 Phillips, Gino, S411 ([TOP-507-YI](#))
 Phillips, Alexandra, S17 ([OS-014-YI](#)),
 S179 ([WED-069](#)), S182 ([WED-078](#)),
 S567 ([THU-207-YI](#))
 Phillips, Sandra, S58 ([OS-091](#)),
 S350 ([TOP-553](#))
 Phillips, Thomas, S630 ([THU-010](#))
 Phua, Hwee Pin, S497 ([FRI-295](#))
 Piano, Salvatore, S28 ([OS-035-YI](#)),
 S30 ([OS-038-YI](#)), S157 ([THU-050](#)),
 S161 ([THU-057-YI](#)), S188 ([WED-098-YI](#)),
 S199 ([TOP-062](#)), S200 ([TOP-064-YI](#)),
 S206 ([FRI-047-YI](#)), S212 ([FRI-068](#)),
 S215 ([FRI-078-YI](#)), S224 ([FRI-101-YI](#)),
 S243 ([SAT-083-YI](#)), S503 ([TOP-241-YI](#)),
 S700 ([FRI-171](#)), S830 ([THU-420](#))
 Piazza, Silvano, S280 ([WED-540-YI](#))
 Piazzolla, Valeria, S470 ([FRI-215-YI](#))
 Picardi, Antonio, S175 ([TOP-085](#)),
 S554 ([WED-325-YI](#)), S754 ([SAT-418](#))
 Picariello, Lucia, S88 ([LBP-023](#))
 Picchio, Camila, S39 ([OS-056-YI](#)),
 S662 ([WED-435](#)), S664 ([WED-440](#)),
 S682 ([WED-485](#))
 Piccolo, Gaetano, S428 ([FRI-514](#))
 Pichard, Anais Vallet, S526 ([WED-245](#))
 Piedra-Cerezal, Ana Maria, S455 ([THU-500](#))
 Piekarska, Anna, S821 ([THU-389](#))
 Piermatteo, Lorenzo, S59 ([OS-094](#)),
 S772 ([FRI-392-YI](#)), S776 ([FRI-405](#)),
 S798 ([WED-399-YI](#))
 Pierone, Gerald, S799 ([WED-405](#))
 Piessevaux, Hubert, S360 ([WED-008](#))
 Pieter Brouwer, Willem, S467 ([FRI-209](#)),
 S606 ([SAT-200-YI](#)), S646 ([SAT-443](#)),
 S649 ([SAT-453](#)), S652 ([SAT-462-YI](#))
 Pietropaolo, Keith, S819 ([THU-382](#))
 Pietschmann, Thomas, S730 ([TOP-369](#))
 Pihlsgård, Mats, S624 ([FRI-018](#))
 Pikkupera, Laura, S466 ([FRI-206-YI](#))
 Pileri, Francesca, S73 ([OS-120](#)),
 S793 ([WED-391](#)), S804 ([WED-414](#))
 Pilger, Alexander, S166 ([THU-075-YI](#))
 Pillai, Anjana, S51 ([OS-078-YI](#)),
 S445 ([THU-471-YI](#))
 Pilowa, Cara, S75 ([OS-127](#))
 Pinato, David J., S23 ([OS-025-YI](#)),
 S51 ([OS-078-YI](#)), S52 ([OS-079-YI](#)),
 S69 ([OS-112-YI](#)), S443 ([THU-464](#)),
 S445 ([THU-471-YI](#))
 Pinazo-Bandera, Jose María, S779 ([FRI-409](#))
 Pinceaux, Kieran, S116 ([SAT-315](#))
 Pineda, Abraham Ramos, S161 ([THU-058](#))
 Piñeiro-Sotelo, Marta, S690 ([WED-513](#))
 Pingoy, Kate, S633 ([THU-029](#))
 Pinheiro, Tiago, S271 ([THU-556](#))
 Pinkoviezky, Itai, S11 ([LBO-006](#))
 Pino, Pilar Del, S826 ([THU-405](#))
 Pinter, Matthias, S24 ([OS-027-YI](#)),
 S51 ([OS-078-YI](#)), S52 ([OS-079-YI](#)),
 S69 ([OS-112-YI](#)), S166 ([THU-075-YI](#)),
 S250 ([SAT-105](#)), S270 ([THU-550](#)),
 S436 ([TOP-488-YI](#)), S443 ([THU-464](#)),
 S445 ([THU-471-YI](#)), S717 ([WED-171](#))
 Pinto, Elisa, S376 ([SAT-024-YI](#))
 Pinto, Sandra, S416 ([FRI-465](#))
 Pinyol, Roser, S411 ([TOP-507-YI](#)),
 S417 ([FRI-467](#))
 Pinzani, Massimo, S268 ([THU-547](#)),
 S295 ([SAT-158](#))
 Piqué-Gili, Marta, S411 ([TOP-507-YI](#))
 Piqueras, Belén, S453 ([THU-493](#))
 Piquet-Pellorce, Claire, S109 ([FRI-333](#))
 Pirani, Tasneem, S44 ([OS-065](#)),
 S185 ([WED-088-YI](#)), S227 ([FRI-112](#))
 Piratvisuth, Teerha, S396 ([SAT-480-YI](#)),
 S410 ([SAT-529](#)), S761 ([FRI-363-YI](#))
 Pirenne, Jacques, S371 ([SAT-014-YI](#))
 Pirisi, Mario, S51 ([OS-078-YI](#)),
 S329 ([THU-153](#)), S409 ([SAT-524](#)),
 S445 ([THU-471-YI](#)), S451 ([THU-486-YI](#)),
 S627 ([FRI-028](#))
 Pironi, Loris, S544 ([WED-293](#))
 Pirozzi, Angelo, S51 ([OS-078-YI](#)),
 S408 ([SAT-523](#)), S438 ([THU-446](#)),
 S447 ([THU-474-YI](#))
 Pisano, Giuseppina, S466 ([FRI-207-YI](#)),
 S474 ([FRI-226](#)), S482 ([FRI-248-YI](#))
 Pisaturo, Marianonietta, S777 ([FRI-405](#))
 Piscaglia, Fabio, S238 ([SAT-068](#)),
 S390 ([TOP-509-YI](#)), S395 ([SAT-477-YI](#)),
 S445 ([THU-471-YI](#)), S446 ([THU-472-YI](#)),
 S452 ([THU-492](#)), S457 ([THU-514](#)),
 S499 ([FRI-299](#)), S521 ([WED-232-YI](#))
 Pischke, Sven, S730 ([TOP-369](#))
 Piscuoglio, Salvatore, S438 ([THU-446](#))
 Piseddu, Ignazio, S24 ([OS-027-YI](#)),
 S458 ([THU-517](#))
 Pistrenko, Karyna, S35 ([OS-049-YI](#))
 Pisu, Stefano, S634 ([THU-032](#))
 Pitrone, Concetta, S345 ([THU-192](#))
 Pitta, Anais, S61 ([OS-097](#))
 Pivetti, Alessandra, S389 ([SAT-060](#)),
 S399 ([SAT-490](#))
 Pivtorak, Kateryna, S499 ([FRI-298](#))
 Pivtorak, Natalya, S499 ([FRI-298](#))
 Pizzolante, Fabrizio, S96 ([LBP-038](#)),
 S306 ([THU-093](#)), S533 ([WED-261-YI](#))
 Placed-Gallego, Cristina,
 S582 ([THU-250-YI](#)), S583 ([THU-257](#)),
 S586 ([THU-263-YI](#)), S594 ([THU-290-YI](#))
 Placinta, Gheorghe, S791 ([FRI-443](#))
 Plagiannakos, Christina, S19 ([OS-018](#)),
 S305 ([TOP-169](#))
 Plaikner, Michaela, S515 ([WED-214-YI](#))
 Planas, Jose María Moreno,
 S717 ([WED-172](#))
 Planell, Núria, S176 ([WED-055](#))
 Plauth, Mathias, S223 ([FRI-098](#))
 Plebani, Riccardo, S439 ([THU-447](#))
 Plessier, Aurélie, S52 ([OS-080](#)),
 S53 ([OS-081](#)), S54 ([OS-084-YI](#)),
 S705 ([WED-129](#)), S719 ([WED-177](#))
 Pleßow, Olivia, S134 ([THU-340-YI](#))
 Plissonnier, Marie-Laure, S58 ([OS-091](#))
 Plonowski, Artur, S292 ([TOP-156](#))
 Pluta, Magdalena, S820 ([THU-387](#)),
 S825 ([THU-403](#))
 Poca, Maria, S355 ([SAT-543](#))
 Pocheptnia, Svitlana, S250 ([SAT-106](#))
 Pochettino, Paolo, S451 ([THU-486-YI](#)),
 S458 ([THU-517](#))
 Poch, Tobias, S350 ([SAT-531-YI](#))
 Pockros, Paul, S384 ([SAT-047](#))
 Pocurull, Anna, S105 ([FRI-321](#)),
 S120 ([SAT-325](#)), S710 ([WED-153](#)),
 S721 ([WED-181](#)), S765 ([FRI-373](#)),
 S818 ([THU-381](#))
 Podini, Paola, S516 ([WED-218](#))
 Podlesny, Daniel, S48 ([OS-073](#))
 Poetter-Lang, Sarah, S250 ([SAT-106](#))
 Poetz, Oliver, S432 ([FRI-523](#))
 Poggi, Guido, S341 ([THU-182](#))
 Poggiolini, Irene, S475 ([FRI-230-YI](#)),
 S480 ([FRI-243](#))
 Poggio, Paolo Del, S332 ([THU-161](#)),
 S341 ([THU-182](#))
 Pohl, Julian, S161 ([THU-057-YI](#)),
 S203 ([FRI-040](#)), S649 ([SAT-452](#))
 Pohl, Junika, S35 ([OS-049-YI](#))
 Pöhlmann, Doris, S56 ([OS-086-YI](#))
 Poisa, Paolo, S96 ([LBP-038](#)),
 S306 ([THU-093](#))
 Pokharna, Rupesh, S239 ([SAT-070](#))
 Pokomandy, Alexandra De,
 S683 ([WED-486-YI](#))
 Pokorska-Śpiewak, Maria, S820 ([THU-387](#)),
 S825 ([THU-403](#))
 Polak, Wojciech, S9 ([LBO-004](#)),
 S89 ([LBP-026](#)), S368 ([SAT-009](#)),
 S380 ([SAT-035](#)), S700 ([FRI-171](#))
 Pola, Roberto, S703 ([TOP-142-YI](#))
 Polishchuk, Elena, S698 ([FRI-166](#))
 Pol, Jonathan, S729 ([TOP-360-YI](#))
 Pollarsky, Florencia, S508 ([WED-195](#))
 Pollicino, Teresa, S422 ([FRI-481](#)),
 S740 ([SAT-378](#)), S743 ([SAT-386-YI](#)),
 S747 ([SAT-397](#)), S777 ([FRI-405](#))
 Pol, Stanislas, S1 ([GS-002](#)), S41 ([OS-060](#)),
 S50 ([OS-077](#)), S73 ([OS-120](#)),
 S526 ([WED-245](#)), S698 ([FRI-165](#)),
 S733 ([SAT-343](#)), S741 ([SAT-380](#)),
 S760 ([FRI-361](#)), S764 ([FRI-371](#)),
 S793 ([WED-391](#)), S802 ([WED-410](#))
 Poluektova, Larisa, S742 ([SAT-382](#))
 Polvani, Simone, S88 ([LBP-023](#))
 Polverini, Davide, S496 ([FRI-290](#))
 Polychronopoulou, Efstathia,
 S384 ([SAT-045](#))
 Pomej, Katharina, S69 ([OS-112-YI](#)),
 S250 ([SAT-106](#)), S436 ([TOP-488-YI](#))
 Pomfret, Elizabeth, S9 ([LBO-004](#)),
 S89 ([LBP-026](#))
 Pommie, Christelle, S326 ([THU-135](#))
 Pompili, Enrico, S206 ([FRI-047-YI](#)),
 S215 ([FRI-078-YI](#))
 Pompili, Maurizio, S175 ([TOP-085](#)),
 S368 ([SAT-009](#)), S452 ([THU-492](#)),
 S703 ([TOP-142-YI](#))
 Ponce-Alonso, Manuel, S277 ([WED-530-YI](#))

- Ponnaiah, Maharajah, S512 ([WED-206](#))
- Ponsioen, Cyriel, S5 ([GS-007](#)), S304 ([SAT-185](#)), S315 ([THU-112-YI](#)), S317 ([THU-115-YI](#))
- Ponsioen, Cyriel Y., S309 ([THU-100](#)), S314 ([THU-109](#)), S319 ([THU-120-YI](#)), S327 ([THU-138](#))
- Ponsioen, Willemijn, S317 ([THU-115-YI](#))
- Pons, Jose Antonio, S365 ([TOP-002](#))
- Pons, Monica, S36 ([OS-047-YI](#)), S703 ([TOP-141](#)), S708 ([WED-135-YI](#)), S818 ([THU-381](#))
- Ponsolles, Clara, S42 ([OS-061](#))
- Pontisso, Patrizia, S612 ([SAT-219](#))
- Ponziani, Francesca Romana, S452 ([THU-492](#)), S703 ([TOP-142-YI](#))
- Ponz, Inés, S706 ([WED-132](#)), S712 ([WED-159](#))
- Poo, Jorge, S627 ([FRI-029](#))
- Poon, Francis, S399 ([SAT-486](#))
- Popescu, Irinel, S343 ([THU-186](#))
- Pop, Gabriel, S50 ([OS-077](#))
- Pophillat, Céline, S349 ([TOP-552](#)), S415 ([FRI-459](#))
- Popov, Yury, S129 ([THU-322-YI](#))
- Poppe, Carine, S631 ([THU-020-YI](#))
- Poretti, Dario, S406 ([SAT-514](#))
- Porras, Almudena, S303 ([SAT-183](#))
- Porras, José Luis Martínez, S559 ([WED-339](#))
- Porritt, Robert, S657 ([WED-422](#)), S676 ([WED-470](#))
- Pors, Susanne, S421 ([FRI-478](#)), S566 ([THU-202](#)), S576 ([THU-232](#))
- Porta, Gilda, S722 ([WED-185](#))
- Portal, Jean-Jacques, S68 ([OS-110](#))
- Portero, Francisco Javier Pamplona, S682 ([WED-485](#))
- Portlock, Theo, S46 ([OS-070](#))
- Portoles-Plaza, Irene, S572 ([THU-220](#))
- Pose, Elisa, S13 ([OS-005-YI](#)), S139 ([SAT-257](#)), S142 ([SAT-267](#)), S160 ([THU-056](#)), S176 ([WED-055](#)), S503 ([TOP-241-YI](#)), S541 ([WED-284-YI](#)), S711 ([WED-155](#))
- Posligua-Garcia, Joel, S107 ([FRI-324](#))
- Possamai, Lucia A, S181 ([WED-075-YI](#))
- Posthouwer, Dirk, S763 ([FRI-367](#))
- Potente, Michael, S180 ([WED-074](#))
- Potěšil, David, S134 ([THU-340-YI](#))
- Poth, Tanja, S33 ([OS-043](#))
- Potter, Justin, S608 ([SAT-207](#))
- Potter, Tom, S578 ([THU-236-YI](#))
- Poujois, Aurélie, S707 ([WED-133](#))
- Poujol-Robert, Armelle, S54 ([OS-084-YI](#))
- Poulin, Sebastien, S28 ([OS-034](#))
- Powell, Elizabeth E., S467 ([FRI-208](#))
- Powers, Kimberly, S668 ([WED-451-YI](#))
- Power, Sydney, S403 ([SAT-498](#))
- Poyatos-García, Paloma, S232 ([FRI-125](#))
- Poynard, Thierry, S512 ([WED-206](#)), S524 ([WED-239](#))
- Poza, Joaquín, S398 ([SAT-485](#))
- Pozo, Cristina, S541 ([WED-284-YI](#))
- Pozzoni, Pietro, S96 ([LBP-038](#)), S306 ([THU-093](#)), S804 ([WED-414](#))
- Prada, Gloria De, S635 ([THU-039-YI](#))
- Prada, Patricia Olivera, S279 ([WED-538-YI](#))
- Praetorius, Alejandro González, S738 ([SAT-374-YI](#)), S768 ([FRI-381](#))
- Praharaj, Dibya Lochan, S161 ([THU-058](#))
- Praharaj, Dibyalochan, S476 ([FRI-231](#))
- Prajapati, Jiya, S129 ([THU-324](#))
- Prakash, Prem, S177 ([WED-058-YI](#))
- Praktiknjo, Michael, S52 ([OS-080](#)), S53 ([OS-081](#)), S133 ([THU-338](#)), S159 ([THU-055](#)), S170 ([THU-087](#)), S258 ([SAT-130](#)), S259 ([SAT-135](#)), S391 ([TOP-511](#)), S705 ([WED-129](#)), S716 ([WED-170](#))
- Prandoni, Paola, S380 ([SAT-034](#))
- Prasad, Alpna, S719 ([WED-176](#))
- Prasad V G, Mohan, S167 ([THU-078](#))
- Prati, Daniele, S459 ([TOP-301](#)), S491 ([FRI-275-YI](#)), S593 ([THU-286](#)), S704 ([TOP-144-YI](#))
- Pratley, Richard E., S615 ([SAT-231](#))
- Pratschke, Johann, S366 ([TOP-003-YI](#))
- Pratt, Daniel, S98 ([LBP-040](#))
- Prayer, Daniela, S719 ([WED-175](#))
- Prazeres da Costa, Clarissa, S699 ([FRI-170](#))
- Praz, Viviane, S347 ([FRI-550](#))
- Precisi, Arianna, S456 ([THU-502](#))
- Preiser, Wolfgang, S756 ([SAT-421](#))
- Preisner, Lara Zoe, S600 ([THU-314](#))
- Prejac, Juraj, S69 ([OS-112-YI](#))
- Prémaud, Aurélie, S387 ([SAT-052](#))
- Premkumar, Madhumita, S129 ([THU-324](#)), S152 ([SAT-295](#)), S158 ([THU-051](#)), S217 ([FRI-082](#))
- Presa, José, S30 ([OS-038-YI](#)), S61 ([OS-096-YI](#)), S199 ([TOP-062](#)), S200 ([TOP-064-YI](#))
- Pressiani, Tiziana, S51 ([OS-078-YI](#)), S408 ([SAT-523](#)), S438 ([THU-446](#)), S443 ([THU-464](#)), S447 ([THU-474-YI](#))
- Prestileo, Tullio, S671 ([WED-457-YI](#))
- Price, David, S645 ([SAT-440](#))
- Price, Mark A., S724 ([WED-188](#))
- Priel, Jan, S611 ([SAT-214](#))
- Prieto, Fernando, S364 ([WED-028](#))
- Primignani, Massimo, S227 ([FRI-110](#))
- Prince, David, S657 ([WED-422](#)), S676 ([WED-470](#))
- Prió, Alba, S154 ([SAT-304](#))
- Probert, Nick, S724 ([WED-189](#))
- Procopciuc, Lucia Maria, S555 ([WED-332](#))
- Procopet, Bogdan, S61 ([OS-096-YI](#)), S144 ([SAT-273-YI](#)), S151 ([SAT-294](#)), S165 ([THU-071](#)), S186 ([WED-089-YI](#)), S409 ([SAT-525](#)), S521 ([WED-232-YI](#)), S555 ([WED-332](#))
- Procopio, Fabio, S401 ([SAT-494](#))
- Proehl, Sarah, S98 ([LBP-040](#))
- Proels, Markus, S70 ([OS-115](#)), S311 ([THU-103](#))
- Proença, Daniela, S362 ([WED-015](#))
- Prokosch, Sandra, S65 ([OS-103](#))
- Pronicki, Maciej, S328 ([THU-152-YI](#))
- Prosad Mookerjee, Rajeshwar, S161 ([THU-057-YI](#))
- Prosperi, Edoardo, S390 ([TOP-509-YI](#))
- Protopapa, Francesca, S589 ([THU-274](#))
- Protopapa, Nefeli, S196 ([WED-121-YI](#))
- Protopapas, Adonis, S196 ([WED-121-YI](#)), S229 ([FRI-117](#))
- Protopapas, Andreas, S196 ([WED-121-YI](#)), S229 ([FRI-117](#))
- Protopopescu, Camelia, S670 ([WED-455](#))
- Protzer, Ulrike, S6 ([GS-008](#)), S34 ([OS-045](#)), S99 ([LBP-042](#)), S351 ([SAT-533](#)), S699 ([FRI-170](#)), S727 ([TOP-355-YI](#)), S728 ([TOP-359-YI](#))
- Provera, Alessia, S421 ([FRI-479-YI](#))
- Provost, Sarah, S807 ([WED-363](#))
- Prudence, Alexander, S208 ([FRI-053](#))
- Prunier, Delphine, S519 ([WED-224](#))
- Psychos, Nikolaos, S798 ([WED-403](#))
- Puchades, Laura, S469 ([FRI-213](#))
- Puchas, Philip, S300 ([SAT-174](#))
- Puengel, Tobias, S414 ([FRI-457](#)), S594 ([THU-291-YI](#))
- Puente, Angela, S61 ([OS-096-YI](#)), S85 ([LBP-016](#)), S469 ([FRI-213](#))
- Puerto, Diego Gomez, S702 ([TOP-139](#))
- Puga, Natalia Fernández, S559 ([WED-339](#))
- Pugliese, Nicola, S332 ([THU-161](#)), S404 ([SAT-502-YI](#)), S406 ([SAT-514](#)), S439 ([THU-447](#)), S470 ([FRI-215-YI](#)), S496 ([FRI-290](#)), S497 ([FRI-294](#)), S500 ([FRI-304](#)), S580 ([THU-245](#)), S666 ([WED-446](#)), S705 ([WED-130](#))
- Puig-Diví, Valentí, S233 ([FRI-126](#))
- Puigvehí, Marc, S207 ([FRI-051](#))
- Pujadas, Montserrat, S700 ([FRI-171](#))
- Pujos-Guillot, Estelle, S422 ([FRI-485](#))
- Pukitis, Aldis, S172 ([THU-092](#))
- Pulaski, Hanna, S507 ([TOP-289](#))
- Pulixi, Edoardo, S474 ([FRI-226](#)), S482 ([FRI-248-YI](#))
- Pungpapong, Surakit, S43 ([OS-064](#))
- Punukollu, Rachana, S152 ([SAT-297](#))
- Puoti, Francesca, S367 ([SAT-007-YI](#))
- Puoti, Massimo, S73 ([OS-120](#)), S700 ([FRI-171](#)), S791 ([FRI-442](#)), S793 ([WED-391](#)), S804 ([WED-414](#))
- Purcell, Damian, S740 ([SAT-377](#))
- Purcell-Estabrook, Erin, S693 ([FRI-151](#))
- Pureur, Dimitri, S115 ([SAT-306](#))
- Puri, Puneet, S1 ([GS-001](#)), S523 ([WED-237](#))
- Purkayastha, Sanjay, S580 ([THU-247-YI](#))
- Purrello, Francesco, S557 ([WED-336](#))
- Pursello, Huw, S650 ([SAT-454-YI](#))
- Pustjens, Jesse, S467 ([FRI-209](#)), S503 ([TOP-241-YI](#)), S604 ([SAT-197-YI](#)), S606 ([SAT-200-YI](#)), S643 ([SAT-437-YI](#)), S646 ([SAT-443](#)), S649 ([SAT-453](#))
- Putignano, Antonella, S9 ([LBO-004](#)), S131 ([THU-331-YI](#))
- Puyat, Joseph, S686 ([WED-495](#))
- Puybasset, Louis, S218 ([FRI-087](#))
- Puzzi, Debora, S369 ([SAT-009](#))
- Pydyn, Natalia, S265 ([THU-533](#))

Author Index

- Pyles, Kelly, S82 (LBP-010)
- Pyrasopoulos, Nikolaos T., S8 (LBO-003), S30 (OS-038-YI), S199 (TOP-062), S200 (TOP-064-YI), S240 (SAT-076), S242 (SAT-082), S535 (WED-269)
- Qamar, Sumaira, S546 (WED-298-YI)
- Qian, Shuaijie, S241 (SAT-077), S622 (FRI-010)
- Qiao, Wenying, S357 (SAT-548)
- Qin, Jiangxia, S792 (WED-390)
- Qin, Ling, S357 (SAT-548)
- Qin, Shukui, S3 (GS-005)
- Qi, Pan, S442 (THU-462)
- Qiu, Chao, S775 (FRI-398)
- Qiugang, Lei, S726 (TOP-353), S732 (SAT-339)
- Qiu, Ke, S727 (TOP-356)
- Qiu, Mengjie, S65 (OS-103)
- Qiu, Xiao, S99 (LBP-043)
- Qiu, Yuanwang, S628 (FRI-035)
- Qi, Wenying, S194 (WED-114)
- Qi, Xiaolong, S238 (SAT-068), S526 (WED-246), S536 (WED-272), S620 (TOP-006)
- Qi, Xuan, S558 (WED-337)
- Quach, Susanna, S302 (SAT-180)
- Quach, Thanh, S812 (WED-376)
- Quah, Joanne Hui Min, S525 (WED-242)
- Quan, Dongmei, S99 (LBP-042)
- Quang, Erwan Vo, S782 (FRI-418)
- Quantin, Xavier, S115 (SAT-306)
- Quan, Xin, S225 (FRI-105), S241 (SAT-077), S622 (FRI-010)
- Quarta, Santana, S612 (SAT-219)
- Quattrini, Angelo, S516 (WED-218)
- Quehenberger, Peter, S257 (SAT-128)
- Queiroz Farias, Alberto, S193 (WED-112)
- Quelhas, Patricia, S692 (TOP-146)
- Quero-Delgado, Marta, S751 (SAT-407)
- Quiambao, Ronald, S514 (WED-211)
- Quick, Josh, S675 (WED-469), S752 (SAT-409)
- Quillen, Jaxon, S608 (SAT-207)
- Quinones, Emily, S707 (WED-134)
- Quiñones, Marta, S139 (SAT-257), S142 (SAT-267), S391 (TOP-512-YI)
- Quinquis, Benoit, S159 (THU-053)
- Quintini, Cristiano, S369 (SAT-009)
- Quirk, Erin, S607 (SAT-202), S609 (SAT-208)
- Quiros-Rivero, Pablo, S316 (THU-114)
- Quiros-Roldan, Eugenia, S791 (FRI-442)
- Quitt, Oliver, S727 (TOP-355-YI)
- Qu, Lishuai, S590 (THU-280)
- Qumosani, Karim, S19 (OS-018), S305 (TOP-169)
- Qurashi, Maria, S639 (SAT-427-YI)
- Qurbanov, Asim, S377 (SAT-028), S805 (WED-419)
- Qureshi, Raabia, S489 (FRI-269)
- Qu, Xiaoye, S106 (FRI-323), S354 (SAT-542)
- Qu, Xiujuan, S99 (LBP-042)
- Qu, Ying, S806 (WED-362)
- Rababoc, Razvan, S221 (FRI-092), S324 (THU-131), S410 (SAT-528), S446 (THU-473)
- Rabaça, Daniela, S681 (WED-481)
- Rabinowich, Liane, S30 (OS-038-YI), S161 (THU-058), S199 (TOP-062), S200 (TOP-064-YI)
- Rachida, Lebtahi, S50 (OS-077)
- Rachmilewitz, Jacob, S278 (WED-534)
- Racila, Andrei, S101 (LBP-047), S465 (FRI-202), S476 (FRI-232), S520 (WED-230), S572 (THU-221), S643 (SAT-438)
- Rac, Marek, S539 (WED-279)
- Raco, Pietro, S634 (THU-032)
- Rada, Patricia, S574 (THU-225)
- Radchenko, Anastasiia, S598 (THU-303)
- Radenne, Sylvie, S9 (LBO-004), S89 (LBP-026)
- Radhakrishnan, Sridhar, S584 (THU-259)
- Rådholm, Karin, S532 (WED-259)
- Radrezza, Silvia, S65 (OS-104)
- Radu, Monica, S759 (TOP-416-YI)
- Radu, Pompilia, S69 (OS-112-YI), S254 (SAT-121), S373 (SAT-019), S392 (SAT-469), S393 (SAT-473)
- Rae, Colin, S419 (FRI-472-YI)
- Raevens, Sarah, S9 (LBO-004), S30 (OS-038-YI), S54 (OS-084-YI), S57 (OS-089-YI), S89 (LBP-026), S115 (TOP-346-YI), S143 (SAT-268), S199 (TOP-062), S200 (TOP-064-YI), S278 (WED-531), S292 (SAT-151-YI), S311 (THU-102-YI), S321 (THU-123-YI), S420 (FRI-475-YI), S442 (THU-463), S631 (THU-020-YI)
- Rafael, Oliveira Ximenes, S83 (LBP-012)
- Raffaele, Brustia, S413 (FRI-456), S453 (THU-494)
- Raffa, Giuseppina, S422 (FRI-481), S740 (SAT-378), S747 (SAT-397), S777 (FRI-405)
- Raggi, Chiara, S426 (FRI-498-YI)
- Raggi, Francesco, S619 (SAT-245)
- Ragone, Angela, S173 (TOP-072)
- Ragone, Enrico, S175 (TOP-085)
- Rahbari, Nuh, S33 (OS-043)
- Rahematpura, Suditi, S209 (FRI-053)
- Rahimi, Robert, S212 (FRI-069)
- Rahimi, Robert S., S242 (SAT-082)
- Rahmouni, Souad, S432 (FRI-525)
- Rahnenführer, Jörg, S57 (OS-088-YI)
- Railton, Karen, S633 (THU-029)
- Raimondo, Giovanni, S345 (THU-192), S422 (FRI-481), S470 (FRI-215-YI), S557 (WED-336), S740 (SAT-378), S743 (SAT-386-YI), S747 (SAT-397)
- Rainer, Florian, S383 (SAT-042)
- Rais, Josh, S555 (WED-330), S561 (WED-348)
- Rajab, Rawan, S489 (FRI-269)
- Rajagopalan, Krithika, S687 (WED-498)
- Rajah, Ganakirthan Kalpenath, S578 (THU-239-YI)
- Rajan, Vijayraghavan, S164 (THU-070)
- Rajendran, Luckshi, S381 (SAT-039)
- Rajoriya, Neil, S147 (SAT-280), S148 (SAT-285-YI), S209 (FRI-053), S337 (THU-173)
- Raj, Prema, S169 (THU-082)
- Rajwanshi, Vivek, S564 (THU-198), S727 (TOP-357)
- Rakeover, Arthur, S656 (TOP-460-YI)
- Ralmilay, Samonee, S129 (THU-324), S152 (SAT-295), S217 (FRI-082)
- Raluy, Mireia, S477 (FRI-235), S486 (FRI-260), S509 (WED-197)
- Ramachandran, Prakash, S354 (SAT-541)
- Ramachandran, Veena, S185 (WED-088-YI), S227 (FRI-112)
- Ramadass, Balamurugan, S285 (WED-554)
- Ramadori, Eleonora, S52 (OS-079-YI)
- Ramamoorthi, Nandhini, S354 (SAT-541)
- Ramanathan, Raghu, S563 (THU-195)
- Ramasubbu, Kumudha, S252 (SAT-114)
- Ramentol, Laia Joval, S702 (TOP-139)
- Ramier, Clémence, S670 (WED-455)
- Ramirez-Baños, Marina, S586 (THU-263-YI)
- Ramírez-Castillo, Carlos, S627 (FRI-029)
- Ramírez-Mejía, Mariana, S171 (THU-089)
- Ramirez, Ricardo, S729 (TOP-368)
- Ramji, Alnoor, S40 (OS-058), S659 (WED-429), S686 (WED-495)
- Ramlakhan, David, S676 (WED-471), S759 (TOP-417)
- Rammohan, Ashwin, S9 (LBO-004), S89 (LBP-026), S368 (SAT-009)
- Ramos, Hilario, S352 (SAT-536), S808 (WED-366)
- Ramos, Olga, S453 (THU-493)
- Rampal, Nishi, S710 (WED-152)
- Ramsauer, Lukas, S35 (OS-049-YI)
- Rana, K, S343 (THU-187)
- Rana, Randeep, S62 (OS-098-YI)
- Randé, Emma Enrich, S741 (SAT-381)
- Rando-Segura, Ariadna, S662 (WED-435), S682 (WED-485), S741 (SAT-381), S746 (SAT-393), S787 (FRI-432), S822 (THU-395)
- Rangan, Pooja, S146 (SAT-278), S478 (FRI-236-YI)
- Ranieri, Luisa, S817 (THU-378)
- Rani, Rafiz Abdul, S552 (WED-321)
- Ranjan, Piyush, S475 (FRI-231)
- Ran, Qiu Ju, S235 (FRI-131)
- Ranvir, Vikas, S25 (OS-029)
- Rao, Anjali, S729 (TOP-368)
- Rao, Arvind, S823 (THU-396)
- Rao, Chenyi, S268 (THU-546)
- Rao, Huiying, S95 (LBP-037)
- Rao, Padaki Nagaraj, S149 (SAT-290-YI)
- Rao, Qunfang, S219 (FRI-088)
- Rao, Vikram, S261 (TOP-564)
- Rapetti, Rachele, S332 (THU-161)
- Rapin, Alison, S109 (FRI-333)
- Raposo, Joao-Filipe, S535 (WED-270)
- Raschzok, Nathanael, S366 (TOP-003-YI)
- Rasha, Fahmida, S42 (OS-061)

- Rasheed, Muhammad Adil, S192 ([WED-109](#))
- Rashidi-Alavijeh, Jassin, S223 ([FRI-100](#))
- Rashid, Tamir, S298 ([SAT-167-YI](#))
- Rashu, Elias, S513 ([WED-207](#)), S529 ([WED-250-YI](#)), S555 ([WED-331-YI](#))
- Rasineni, Karuna, S281 ([WED-544](#))
- Rastogi, Archana, S137 ([SAT-249](#)), S195 ([WED-118](#)), S346 ([FRI-547-YI](#))
- Rastogi, Mukul, S476 ([FRI-231](#))
- Rastogi, Tashi, S353 ([SAT-539-YI](#))
- Rastovic, Una, S128 ([THU-320-YI](#))
- Raszeja-Wyszomirska, Joanna, S9 ([LBO-004](#)), S89 ([LBP-026](#)), S338 ([THU-175-YI](#))
- Rathinam, Vijay, S178 ([WED-060-YI](#))
- Rathi, Pravin, S158 ([THU-052](#)), S167 ([THU-078](#))
- Rathi, Sahaj, S129 ([THU-324](#)), S152 ([SAT-295](#)), S217 ([FRI-082](#))
- Ratziu, Vlad, S1 ([GS-002](#)), S4 ([GS-006](#)), S8 ([LBO-002](#)), S37 ([OS-051](#)), S79 ([LBP-003](#)), S88 ([LBP-024](#)), S95 ([LBP-036](#)), S141 ([SAT-263](#)), S441 ([THU-458](#)), S463 ([FRI-198](#)), S464 ([FRI-199](#)), S467 ([FRI-208](#)), S481 ([FRI-247](#)), S482 ([FRI-249](#)), S486 ([FRI-259](#)), S493 ([FRI-282](#)), S504 ([TOP-253](#)), S505 ([TOP-265](#)), S507 ([TOP-289](#)), S507 ([TOP-300](#)), S511 ([WED-201](#)), S511 ([WED-202](#)), S512 ([WED-206](#)), S518 ([WED-223](#)), S533 ([WED-262](#)), S606 ([SAT-201](#)), S648 ([SAT-450](#)), S764 ([FRI-371](#))
- Raubenheimer, David, S138 ([SAT-254](#))
- Rau, Monika, S223 ([FRI-098](#)), S224 ([FRI-103-YI](#)), S528 ([WED-249](#))
- Raupach, Jan, S734 ([SAT-361](#))
- Rauschecker, Mitra, S93 ([LBP-031](#))
- Rausch, Lilli, S161 ([THU-057-YI](#))
- Rautou, Pierre-Emmanuel, S52 ([OS-080](#)), S54 ([OS-084-YI](#)), S61 ([OS-096-YI](#)), S174 ([TOP-073](#)), S180 ([WED-071](#)), S193 ([WED-112](#)), S238 ([SAT-068](#)), S524 ([WED-239](#)), S705 ([WED-129](#)), S719 ([WED-177](#))
- Ravaioli, Federico, S52 ([OS-080](#)), S61 ([OS-096-YI](#)), S238 ([SAT-068](#)), S241 ([SAT-078-YI](#)), S390 ([TOP-509-YI](#)), S399 ([SAT-490](#)), S496 ([FRI-290](#)), S499 ([FRI-299](#)), S521 ([WED-232-YI](#)), S704 ([TOP-143-YI](#))
- Ravaioli, Matteo, S369 ([SAT-009](#)), S390 ([TOP-509-YI](#)), S704 ([TOP-143-YI](#))
- Ravikanth, V. V., S701 ([FRI-173](#))
- Ray, Abhishek, S633 ([THU-029](#))
- Ray, Avijit, S807 ([WED-364](#))
- Razack, Habeeb I.A., S671 ([WED-458](#))
- Raza, Mohammed, S172 ([THU-090](#))
- Razavi, Homie, S663 ([WED-437](#)), S667 ([WED-448](#)), S674 ([WED-466](#)), S680 ([WED-480-YI](#))
- Razavi-Shearer, Devin, S663 ([WED-437](#)), S667 ([WED-448](#)), S674 ([WED-466](#)), S678 ([WED-474](#))
- Razavi-Shearer, Kathryn, S663 ([WED-437](#)), S667 ([WED-448](#))
- Razvan-Ioan, Simu, S221 ([FRI-092](#)), S410 ([SAT-528](#))
- Read, Robert W., S462 ([FRI-195](#))
- Reati, Raffaella, S332 ([THU-161](#))
- Reau, Nancy S., S687 ([WED-498](#))
- Reboux, Noemi, S168 ([THU-079](#))
- Recalde, Miriam, S416 ([FRI-464](#))
- Reddick, Traci, S88 ([LBP-022](#))
- Reddy, Gautham, S118 ([SAT-320](#))
- Reddy, K. Rajender, S161 ([THU-058](#)), S163 ([THU-060](#)), S206 ([FRI-046](#)), S218 ([FRI-086](#))
- Reddy, Nageshwar, S149 ([SAT-290-YI](#)), S440 ([THU-456](#)), S454 ([THU-498](#)), S701 ([FRI-173](#)), S720 ([WED-180](#))
- Reddy, Praveena, S544 ([WED-294](#))
- Redeker, Hanna, S425 ([FRI-492-YI](#))
- Reekmans, Ann, S125 ([TOP-328-YI](#))
- Rees, Fiona, S636 ([THU-045](#))
- Reeves, Helen Louise, S411 ([TOP-507-YI](#)), S459 ([TOP-301](#))
- Regal, Kelly, S616 ([SAT-233](#))
- Regnat, Katharina, S186 ([WED-089-YI](#)), S197 ([WED-122-YI](#)), S198 ([WED-125](#)), S267 ([THU-540](#)), S436 ([TOP-488-YI](#))
- Regnault, Hélène, S50 ([OS-077](#)), S413 ([FRI-456](#)), S453 ([THU-494](#)), S456 ([THU-503](#))
- Reiberger, Thomas, S28 ([OS-034](#)), S61 ([OS-096-YI](#)), S73 ([OS-120](#)), S85 ([LBP-016](#)), S156 ([TOP-097-YI](#)), S165 ([THU-071](#)), S166 ([THU-075-YI](#)), S172 ([THU-092](#)), S186 ([WED-089-YI](#)), S197 ([WED-122-YI](#)), S198 ([WED-125](#)), S238 ([SAT-068](#)), S242 ([SAT-080-YI](#)), S243 ([SAT-086-YI](#)), S250 ([SAT-105](#)), S250 ([SAT-106](#)), S251 ([SAT-111](#)), S253 ([SAT-117](#)), S253 ([SAT-118](#)), S255 ([SAT-122](#)), S257 ([SAT-128](#)), S267 ([THU-540](#)), S296 ([SAT-161](#)), S335 ([THU-166](#)), S341 ([THU-183-YI](#)), S621 ([FRI-009-YI](#)), S706 ([WED-131-YI](#)), S717 ([WED-171](#)), S719 ([WED-175](#)), S725 ([WED-190](#)), S773 ([FRI-394](#)), S793 ([WED-391](#)), S814 ([WED-383](#)), S818 ([THU-380-YI](#)), S818 ([THU-381](#)), S821 ([THU-390](#))
- Reichert, Matthias, S244 ([SAT-087-YI](#)), S503 ([TOP-241-YI](#))
- Reichman, Trevor, S381 ([SAT-037](#)), S381 ([SAT-039](#))
- Reich, Maria, S25 ([OS-028](#))
- Reider, Lukas, S156 ([TOP-097-YI](#)), S242 ([SAT-080-YI](#)), S253 ([SAT-118](#))
- Reid, Susan, S242 ([SAT-082](#))
- Reig, María, S420 ([FRI-474-YI](#)), S424 ([FRI-491-YI](#)), S425 ([FRI-494-YI](#)), S455 ([THU-500](#)), S455 ([THU-501](#))
- Reijnders, Jurriën, S763 ([FRI-367](#))
- Reikvam, Dag Henrik, S795 ([WED-394](#))
- Reims, Henrik Mikael, S22 ([OS-023-YI](#)), S50 ([OS-076-YI](#)), S386 ([SAT-050](#))
- Reinders, Jörg, S85 ([LBP-017](#))
- Reinehr, Michael, S702 ([TOP-140](#))
- Reineke-Plaaß, Tanja, S425 ([FRI-492-YI](#))
- Reiner, Cäcilia, S702 ([TOP-140](#))
- Reinhardt, Christian, S249 ([SAT-104-YI](#))
- Reinhardt, Matthias, S203 ([FRI-040](#)), S649 ([SAT-452](#))
- Reis, Ana Luiza Gomes, S619 ([SAT-248](#))
- Reiss, Garry, S544 ([WED-294](#))
- Reissing, Johanna, S259 ([SAT-135](#))
- Reißing, Johanna, S178 ([WED-060-YI](#)), S229 ([FRI-116](#)), S351 ([SAT-534](#)), S356 ([SAT-545](#)), S357 ([SAT-549](#))
- Reiter, Florian P., S52 ([OS-079-YI](#)), S69 ([OS-112-YI](#)), S223 ([FRI-098](#)), S224 ([FRI-103-YI](#))
- Reiter, Florian P., S443 ([THU-465-YI](#))
- Reiter, Silvia, S773 ([FRI-394](#))
- Reitz, Isabella, S43 ([OS-064](#))
- Reizine, Edouard, S373 ([SAT-020](#)), S453 ([THU-494](#)), S720 ([WED-178](#))
- Rejano-Gordillo, Claudia M., S417 ([FRI-466-YI](#))
- Rela, Mohamed, S9 ([LBO-004](#)), S89 ([LBP-026](#)), S368 ([SAT-009](#))
- Rela, Mohd., S158 ([THU-052](#)), S161 ([THU-058](#)), S167 ([THU-078](#))
- Remih, Katharina, S104 ([TOP-352](#)), S134 ([THU-340-YI](#))
- Remon, Pablo, S508 ([WED-195](#))
- Renand, Amédée, S712 ([WED-160](#))
- Renate, Heyne, S802 ([WED-411](#))
- Rendina, Maria, S368 ([SAT-009](#))
- Rendina, Maria Grazia, S332 ([THU-161](#))
- Ren, Feng, S107 ([FRI-325](#)), S121 ([SAT-330](#)), S783 ([FRI-420](#))
- Ren, Hong, S86 ([LBP-019](#)), S99 ([LBP-043](#)), S727 ([TOP-356](#)), S807 ([WED-365](#))
- Rennebaum, Florian, S391 ([TOP-511](#))
- Renne, Nicolaas Van, S730 ([SAT-337](#))
- Renner, Eberhard, S643 ([SAT-436](#))
- Rennert, Hedy, S774 ([FRI-395](#))
- Renne, Salvatore, S438 ([THU-446](#))
- Renne, Thomas, S24 ([OS-027-YI](#))
- Ren, Qiuyang, S442 ([THU-462](#))
- Rensen, Patrick CN, S272 ([WED-517](#)), S278 ([WED-533](#))
- Renteria, Sara Uceda, S401 ([SAT-493-YI](#)), S781 ([FRI-412](#))
- Ren, Weixin, S447 ([THU-475](#))
- Ren, Wenhui, S230 ([FRI-118](#)), S233 ([FRI-127](#))
- Ren, Yayun, S56 ([OS-087](#)), S76 ([OS-124](#)), S465 ([FRI-203](#)), S467 ([FRI-208](#)), S488 ([FRI-267](#))
- Ren, Zhenggang, S3 ([GS-005](#))
- Renzulli, Matteo, S241 ([SAT-078-YI](#)), S399 ([SAT-490](#)), S704 ([TOP-143-YI](#))
- Requena, Ana, S39 ([OS-056-YI](#)), S664 ([WED-440](#))
- Resino Garcia, Salvador, S751 ([SAT-407](#))

Author Index

- Resnick, Murray, S507 ([TOP-289](#))
Reuken, Philipp, S178 ([WED-060-YI](#)),
S229 ([FRI-116](#)), S259 ([SAT-135](#))
Reverter, Enric, S45 ([OS-068](#)),
S115 ([TOP-346-YI](#))
Reviejo, Maria, S433 ([FRI-526](#))
Revill, Peter, S740 ([SAT-377](#))
Reyes, Alfred, S141 ([SAT-262](#))
Reyes, Eira Cerda, S30 ([OS-038-YI](#)),
S199 ([TOP-062](#)), S200 ([TOP-064-YI](#))
Reyes, Maribel, S816 ([WED-389](#))
Reyngoudt, Harmen, S473 ([FRI-224](#))
Reynolds, Helen, S81 ([LBP-008](#))
Rey, Silvia García, S508 ([WED-195](#))
Rezvani, Milad, S298 ([SAT-170](#)),
S302 ([SAT-180](#))
Rhaïem, Rami, S413 ([FRI-456](#))
Rhee, Hyungjin, S408 ([SAT-522](#)),
S410 ([SAT-526](#))
Rheinhardt, Jeanette, S693 ([FRI-151](#))
Riachi, Ghassan, S61 ([OS-097](#)),
S444 ([THU-466](#))
Rialdi, Alex, S417 ([FRI-467](#))
Rianda, Alessia, S804 ([WED-414](#))
Riba, Carlota, S541 ([WED-284-YI](#))
Riback, Lindsey, S684 ([WED-487](#))
Ribaldone, Davide Giuseppe,
S475 ([FRI-230-YI](#)), S480 ([FRI-243](#))
Ribeiro, Andrea, S332 ([THU-160](#)),
S472 ([FRI-220-YI](#)), S476 ([FRI-232](#))
Ribeiro, Isabela, S831 ([THU-362](#))
Ribeiro, Vasco, S834 ([THU-370](#))
Ribera, Jordi, S160 ([THU-056](#))
Ribó, Marc, S633 ([THU-028](#))
Riccardi, Laura, S533 ([WED-261-YI](#))
Ricchiuti, Antony, S459 ([TOP-301](#))
Ricciardi, Federico, S195 ([WED-117](#))
Ricci, Chiara, S96 ([LBP-038](#)),
S306 ([THU-093](#))
Ricciuto, Amanda, S305 ([TOP-168-YI](#))
Rico, Gabriele, S549 ([WED-314-YI](#)),
S619 ([SAT-245](#)), S622 ([FRI-014](#))
Rice, Pamela, S639 ([SAT-427-YI](#))
Richard, Alyson, S275 ([WED-526](#))
Richards, Christopher, S737 ([SAT-371](#))
Richards, Lisa, S522 ([WED-235](#)),
S543 ([WED-291](#))
Richardson, Daniel, S394 ([SAT-476](#))
Richardson, Naomi, S34 ([OS-046](#)),
S356 ([SAT-546](#))
Richardson, Paul, S127 ([THU-317](#)),
S145 ([SAT-274](#)), S470 ([FRI-215-YI](#))
Rich, Nicole, S200 ([TOP-063](#))
Richter, Mathis, S133 ([THU-338](#))
Richter, Nicolas, S204 ([FRI-042](#))
Ricklefs, Franz, S24 ([OS-027-YI](#))
Rico, M. Carmen, S587 ([THU-268](#))
Rico, Naira, S120 ([SAT-325](#))
Riddell, Anna, S781 ([FRI-413](#))
Riddell, Sophie, S524 ([WED-238](#))
Rider, Elora, S231 ([FRI-122](#))
Rider, Patricia, S424 ([FRI-491-YI](#)),
S425 ([FRI-494-YI](#)), S430 ([FRI-519-YI](#))
Ridruejo, Ezequiel, S334 ([THU-164-YI](#))
Riel, Ricard, S662 ([WED-435](#))
Rieusset, Jennifer, S49 ([OS-074](#))
Riff, Arnaud, S22 ([OS-022](#))
Rigamonti, Cristina, S19 ([OS-017](#)),
S51 ([OS-078-YI](#)), S96 ([LBP-038](#)),
S306 ([THU-093](#)), S310 ([THU-101](#)),
S329 ([THU-153](#)), S409 ([SAT-524](#)),
S627 ([FRI-028](#))
Rigaud, Céline, S387 ([SAT-052](#))
Riggio, Oliviero, S30 ([OS-038-YI](#)),
S62 ([OS-099-YI](#)), S199 ([TOP-062](#)),
S200 ([TOP-064-YI](#)), S215 ([FRI-078-YI](#)),
S258 ([SAT-131](#))
Rigopoulou, Eirini, S335 ([THU-167](#)),
S800 ([WED-406](#))
Rill, Aina, S13 ([OS-005-YI](#)),
S293 ([SAT-153-YI](#))
Rimassa, Lorenza, S51 ([OS-078-YI](#)),
S52 ([OS-079-YI](#)), S69 ([OS-112-YI](#)),
S404 ([SAT-502-YI](#)), S406 ([SAT-514](#)),
S408 ([SAT-523](#)), S438 ([THU-446](#)),
S443 ([THU-464](#)), S445 ([THU-471-YI](#)),
S447 ([THU-474-YI](#))
Rimini, Margherita, S438 ([THU-446](#))
Rimola, Jordi, S455 ([THU-500](#)),
S455 ([THU-501](#))
Rinaldi, Andrea, S592 ([THU-285](#))
Rinaldi, Luca, S790 ([FRI-441](#))
Rinaldi, Mauro, S475 ([FRI-230-YI](#))
Rinder, Pierre, S326 ([THU-136](#))
Rinella, Mary E., S95 ([LBP-036](#)),
S467 ([FRI-208](#)), S606 ([SAT-201](#))
Ring, Julian, S94 ([LBP-034](#))
Ringlander, Johan, S754 ([SAT-414](#))
Riordan, Stephen, S161 ([THU-058](#)),
S400 ([SAT-492](#))
Ríos, María Lázaro, S717 ([WED-172](#))
Ripamonti, Ilaria, S325 ([THU-133-YI](#))
Ripoll, Cristina, S244 ([SAT-087-YI](#))
Ristic, Tijana, S350 ([SAT-532-YI](#))
Ritaccio, Gabrielle, S394 ([SAT-476](#))
Ritschl, Paul, S366 ([TOP-003-YI](#))
Ritz, Thomas, S414 ([FRI-457](#))
Rius, Lidia, S141 ([SAT-262](#))
Riva, Antonio, S174 ([TOP-084](#)),
S281 ([WED-542-YI](#)), S700 ([FRI-171](#))
Riveiro Barciela, Mar, S329 ([THU-154-YI](#)),
S330 ([THU-155](#))
Riveiro, Mar, S633 ([THU-028](#))
Rivera-Espinosa, Liliana, S171 ([THU-089](#))
Rivera, Jesús, S469 ([FRI-213](#)),
S559 ([WED-339](#))
Rivera-Ramos, Juan Francisco,
S627 ([FRI-029](#))
Riviere, Benjamin, S115 ([SAT-306](#)),
S143 ([SAT-269](#)), S376 ([SAT-026](#))
Rivoire, Michel, S58 ([OS-091](#))
Rivoltini, Licia, S439 ([THU-454](#))
Rizzato, Mario Domenico, S438 ([THU-446](#))
Rizzetto, Mario, S59 ([OS-094](#)),
S772 ([FRI-392-YI](#))
Roadknight, Gail, S676 ([WED-471](#)),
S759 ([TOP-417](#))
Roatta, Caroline, S707 ([WED-133](#))
Robaey, Geert, S604 ([SAT-196](#)),
S730 ([SAT-337](#))
Robaey, Wouter, S604 ([SAT-196](#))
Robbani, Shahriyar Mahdi, S48 ([OS-073](#))
Robbins, Marc, S592 ([THU-284](#))
Robert, Geffers, S425 ([FRI-492-YI](#))
Robert, Sage, S84 ([LBP-014](#))
Roberts, Carol, S339 ([THU-178](#))
Roberts, Curt, S11 ([LBO-006](#))
Roberts, Lee, S573 ([THU-222-YI](#))
Roberts, Lewis, S396 ([SAT-479-YI](#))
Roberts, M. Scot, S515 ([WED-212](#)),
S517 ([WED-219](#)), S529 ([WED-251](#))
Robertson, Tayla, S497 ([FRI-293](#))
Roberts, Stuart, S26 ([OS-031](#)),
S78 ([LBP-001](#)), S338 ([THU-177-YI](#)),
S400 ([SAT-492](#)), S402 ([SAT-496](#)),
S643 ([SAT-438](#)), S653 ([SAT-464-YI](#))
Robin, Fabien, S383 ([SAT-043](#))
Robins, Deborah, S7 ([LBO-001](#))
Robinson, Chloe, S289 ([FRI-542](#))
Roblero, Juan Pablo, S30 ([OS-038-YI](#)),
S199 ([TOP-062](#)), S200 ([TOP-064-YI](#))
Robles-Díaz, Mercedes, S18 ([OS-015](#)),
S44 ([OS-066-YI](#)), S45 ([OS-067](#)),
S700 ([FRI-171](#))
Robles-Frias, M^a José, S593 ([THU-287](#))
Rocca, Maria Assunta, S123 ([SAT-334](#))
Roccarina, Davide, S238 ([SAT-068](#)),
S258 ([SAT-131](#))
Rocchetti, Adele, S332 ([THU-161](#))
Rocchetto, Simone, S497 ([FRI-294](#))
Rocco, Alba, S96 ([LBP-038](#)), S306 ([THU-093](#))
Rocha-Pereira, Joana, S732 ([SAT-340-YI](#))
Roche, Bruno, S73 ([OS-120](#)),
S793 ([WED-391](#))
Rockey, Don, S8 ([LBO-003](#)), S238 ([SAT-069](#)),
S242 ([SAT-082](#))
Rock, Marvin, S666 ([WED-444](#)),
S687 ([WED-498](#)), S773 ([FRI-393](#)),
S788 ([FRI-435](#))
Rodas, Augusto, S641 ([SAT-431-YI](#))
Rodden, Kathryn, S101 ([LBP-046](#))
Rode, Agnès, S68 ([OS-110](#)),
S441 ([THU-459-YI](#))
Rodén, Michael, S470 ([FRI-218](#)),
S508 ([WED-195](#)), S528 ([WED-248](#)),
S606 ([SAT-201](#))
Roderburg, Christoph, S52 ([OS-079-YI](#)),
S259 ([SAT-135](#)), S426 ([FRI-495](#))
Roderick, Paul, S506 ([TOP-277](#))
Rodger, Alison, S661 ([WED-432](#)),
S672 ([WED-462](#)), S684 ([WED-491](#)),
S688 ([WED-500](#))
Rodrigo, Miguel Angel Merlos,
S417 ([FRI-466-YI](#))
Rodrigo-Torres, Daniel, S14 ([OS-008-YI](#))
Rodrigues, Almir, S271 ([THU-556](#))
Rodrigues, Inês, S220 ([FRI-090](#)),
S405 ([SAT-513](#))
Rodrigues, José, S286 ([WED-558](#))
Rodrigues, Pedro M, S32 ([OS-042-YI](#))
Rodrigues, Pedro M., S295 ([SAT-159-YI](#)),
S536 ([WED-271](#))

- Rodrigues, Pedro Miguel, S50 ([OS-076-YI](#)), S265 ([THU-533](#)), S286 ([WED-558](#)), S419 ([FRI-472-YI](#))
- Rodríguez, Amanda Fernández, S741 ([SAT-379](#))
- Rodríguez-Chaverri, Adriana, S706 ([WED-132](#)), S712 ([WED-159](#))
- Rodríguez-Frías, Francisco, S662 ([WED-435](#)), S682 ([WED-485](#))
- Rodríguez, Juan Carlos Lopez, S282 ([WED-545-YI](#))
- Rodríguez, Luz, S216 ([FRI-081](#))
- Rodríguez, Manuel, S455 ([THU-500](#))
- Rodríguez, Manuel, S777 ([FRI-406](#))
- Rodríguez, Maria, S374 ([SAT-021](#))
- Rodríguez-Perálvarez, Manuel, S23 ([OS-024](#)), S365 ([TOP-002](#)), S415 ([FRI-462-YI](#))
- Rodríguez-Perálvarez, Manuel L., S318 ([THU-118](#)), S330 ([THU-155](#))
- Rodríguez, Rafael Gómez, S453 ([THU-493](#)), S828 ([THU-411](#))
- Rodríguez, Ricardo Ulises Macias, S115 ([TOP-346-YI](#))
- Rodríguez, Sergio Vaquez, S139 ([SAT-257](#))
- Rodríguez-Tajes, Sergio, S291 ([TOP-149-YI](#)), S293 ([SAT-153-YI](#)), S329 ([THU-154-YI](#)), S336 ([THU-170-YI](#)), S344 ([THU-189](#)), S682 ([WED-485](#)), S710 ([WED-153](#)), S711 ([WED-155](#)), S787 ([FRI-432](#)), S818 ([THU-381](#))
- Roehlen, Natascha, S25 ([OS-029](#)), S31 ([OS-040-YI](#))
- Roels, Jana, S292 ([SAT-151-YI](#))
- Roest, Mark, S178 ([WED-068-YI](#)), S237 ([TOP-061-YI](#))
- Roger, Clementine, S718 ([WED-174](#))
- Roger, Jan, S567 ([THU-203](#))
- Rogers, Geraint, S275 ([WED-526](#))
- Rogers, Penelope, S332 ([THU-160](#))
- Roget, Mercé, S291 ([TOP-149-YI](#))
- Roggenbuck, Dirk, S308 ([THU-095](#))
- Rohbeck, Elisabeth, S269 ([THU-548-YI](#))
- Röhlen, Natascha, S51 ([OS-078-YI](#)), S52 ([OS-079-YI](#))
- Rohr-Udilova, Nataliya, S270 ([THU-550](#))
- Roig, Cristina, S85 ([LBP-016](#))
- Rojas, Ángela, S427 ([FRI-501](#))
- Rojas, Juan, S584 ([THU-259](#))
- Rojo, Carla, S416 ([FRI-464](#))
- Rojo, Diego, S207 ([FRI-051](#)), S471 ([FRI-219-YI](#))
- Roldan, Carolina, S779 ([FRI-409](#))
- Roldan, Yasmin, S293 ([SAT-153-YI](#))
- Rolland, Benjamin, S670 ([WED-455](#))
- Rolland, Celine, S519 ([WED-224](#))
- Rolle, Emanuela, S451 ([THU-486-YI](#)), S458 ([THU-517](#))
- Rolle-Kampczyk, Ulrike, S134 ([THU-340-YI](#))
- Rolle, Valentin, S168 ([THU-079](#))
- Rollo, Paolo, S318 ([THU-117-YI](#))
- Rolph, Tim, S8 ([LBO-002](#)), S522 ([WED-234](#)), S535 ([WED-268](#)), S612 ([SAT-220-YI](#))
- Romagnoli, Dante, S399 ([SAT-490](#))
- Romagnoli, Renato, S369 ([SAT-009](#)), S371 ([SAT-015-YI](#)), S378 ([SAT-031-YI](#))
- Romana Ponziani, Francesca, S705 ([WED-130](#))
- Román-Calleja, Berenice M., S602 ([TOP-205](#))
- Roman, Eva, S355 ([SAT-543](#)), S700 ([FRI-171](#))
- Romano, Antonietta, S804 ([WED-414](#)), S830 ([THU-420](#))
- Romano, Valentina, S627 ([FRI-028](#))
- Romanov, Roman, S268 ([THU-542](#))
- Román-Sagüillo, Sara, S45 ([OS-067](#)), S277 ([WED-529](#))
- Romão, Luis, S676 ([WED-471](#)), S759 ([TOP-417](#))
- Rombouts, Krista, S428 ([FRI-502](#))
- Romeo, Mario, S173 ([TOP-072](#)), S213 ([FRI-070-YI](#)), S817 ([THU-378](#))
- Romero, Gema, S316 ([THU-114](#)), S826 ([WED-509](#))
- Romero-Gómez, Manuel, S2 ([GS-004](#)), S38 ([OS-054](#)), S70 ([OS-115](#)), S71 ([OS-116](#)), S344 ([THU-189](#)), S427 ([FRI-501](#)), S508 ([WED-195](#)), S538 ([WED-275](#)), S557 ([WED-335](#)), S587 ([THU-268](#)), S593 ([THU-287](#)), S596 ([THU-296](#)), S640 ([SAT-429](#)), S643 ([SAT-438](#))
- Romero-Grimaldo, Berta, S16 ([OS-011](#)), S174 ([TOP-073](#)), S185 ([WED-087](#))
- Romero-Gutiérrez, Marta, S453 ([THU-493](#)), S717 ([WED-172](#)), S828 ([THU-411](#))
- Romero, Jonathon, S533 ([WED-263](#))
- Romero, Maria Tous, S559 ([WED-341](#))
- Romero, Marta, S432 ([FRI-523](#))
- Romero, Miriam, S398 ([SAT-485](#)), S706 ([WED-132](#)), S712 ([WED-159](#))
- Romero-Vico, Judit, S633 ([THU-028](#)), S822 ([THU-395](#))
- Romo, Regina, S602 ([TOP-205](#))
- Roncalli, Massimo, S438 ([THU-446](#))
- Ronca, Vincenzo, S374 ([SAT-021](#))
- Roncero, Cesáreo, S303 ([SAT-183](#))
- Rondena, Jessica, S491 ([FRI-275-YI](#))
- Ronot, Maxime, S50 ([OS-077](#))
- Ronzoni, Luisa, S459 ([TOP-301](#)), S704 ([TOP-144-YI](#))
- Rooney, Michael, S178 ([WED-060-YI](#)), S263 ([THU-527](#)), S351 ([SAT-534](#))
- Roongrawee, Thitaporn, S196 ([WED-120](#)), S749 ([SAT-403](#))
- Roque-Afonso, Anne Marie, S741 ([SAT-380](#))
- Roque-Cuellar, María C., S508 ([WED-195](#))
- Rorsman, Fredrik, S12 ([OS-002](#)), S550 ([WED-316](#))
- Rosa, Isabelle, S61 ([OS-097](#)), S73 ([OS-120](#)), S168 ([THU-079](#)), S640 ([SAT-430](#)), S793 ([WED-391](#))
- Rosa, Laura De, S622 ([FRI-014](#))
- Rosales, José María, S779 ([FRI-409](#))
- Rosales-Zábal, Jose Miguel, S170 ([THU-086](#)), S316 ([THU-114](#))
- Rosaria, Piras Maria, S332 ([THU-161](#))
- Rosario, Michelle, S350 ([TOP-553](#))
- Rosato, Valerio, S175 ([TOP-085](#)), S666 ([WED-446](#))
- Rose, Christopher F., S187 ([WED-092](#))
- Rose-John, Stefan, S278 ([WED-534](#))
- Roselli, Elena, S376 ([SAT-025](#))
- Rosenberger, Florian, S32 ([OS-041-YI](#)), S169 ([THU-080-YI](#)), S182 ([WED-078](#)), S193 ([WED-111](#))
- Rosenberg, Nofar, S278 ([WED-534](#))
- Rosendaal, Frits, S492 ([FRI-278](#))
- Rosen, Hana, S76 ([OS-125](#))
- Rosenkranz, Susan, S12 ([OS-003](#))
- Rosi, Martina, S258 ([SAT-131](#))
- Roskams, Tania, S25 ([OS-029](#)), S31 ([OS-040-YI](#)), S125 ([TOP-328-YI](#))
- Rosmorduc, Olivier, S367 ([TOP-005](#)), S452 ([THU-491](#))
- Rossanese, Marta, S740 ([SAT-378](#))
- Rossi, Elena, S703 ([TOP-142-YI](#))
- Rossi, Massimo, S364 ([WED-022](#)), S375 ([SAT-023](#))
- Rossi, Pietro, S342 ([THU-184](#))
- Rosso, Chiara, S421 ([FRI-479-YI](#)), S475 ([FRI-230-YI](#)), S480 ([FRI-243](#)), S483 ([FRI-251-YI](#)), S501 ([FRI-314](#)), S522 ([WED-233-YI](#)), S525 ([WED-243-YI](#))
- Rosso, Natalia, S429 ([FRI-516-YI](#))
- Rossotti, Roberto, S791 ([FRI-442](#))
- Ross, Paul, S388 ([SAT-057](#))
- Rossum, Thea Van, S48 ([OS-073](#))
- Rossvoll, Lasse, S781 ([FRI-414](#))
- Rotellar, Fernando, S348 ([FRI-555](#))
- Roth, Dominik, S327 ([THU-137](#))
- Rothermel, Ulrike, S65 ([OS-103](#))
- Roth, Esther, S198 ([WED-126](#))
- Roth, Noam Pinchas Gessler, S246 ([SAT-093-YI](#))
- Rotroff, Daniel, S131 ([THU-330](#))
- Röttele, Felix, S54 ([OS-083](#))
- Roulet, Alain, S47 ([OS-071-YI](#))
- Roulot, Dominique, S41 ([OS-060](#)), S526 ([WED-245](#)), S777 ([FRI-406](#)), S793 ([WED-391](#))
- Rourke, Colm O., S419 ([FRI-472-YI](#))
- Rousseau, Alexandra, S313 ([THU-107](#))
- Rousseau, Annick, S387 ([SAT-052](#))
- Rousselet, Odile, S648 ([SAT-449](#))
- Rousselot, Morgane, S109 ([FRI-333](#))
- Roussos, Sotirios, S680 ([WED-478](#))
- Rout, Ashok Kumar, S582 ([THU-254-YI](#))
- Routy, Jean-Pierre, S683 ([WED-486-YI](#))
- Roux, Charles, S239 ([SAT-071](#))
- Roux, Julie, S50 ([OS-077](#))
- Roux, Marine, S37 ([OS-053](#))
- Roux, Olivier, S30 ([OS-038-YI](#)), S116 ([SAT-315](#)), S372 ([SAT-016](#))
- Rovida, Elisabetta, S426 ([FRI-498-YI](#))
- Rowe, Anna, S101 ([LBP-046](#))
- Rowe, Ian, S136 ([TOP-311-YI](#)), S260 ([SAT-137](#)), S397 ([SAT-483-YI](#)), S530 ([WED-254](#)), S534 ([WED-266](#)), S547 ([WED-302-YI](#))
- Rowe, Melissa, S89 ([LBP-025](#))

Author Index

- Roy, Akash, S158 (THU-052), S167 (THU-078), S209 (FRI-053), S476 (FRI-231)
- Royo, Laura, S417 (FRI-466-YI)
- Roy, Sanchari, S426 (FRI-495)
- Roy, Trinava, S489 (FRI-268)
- Rozpondek, Piotr, S70 (OS-115)
- Rubin, Martina, S123 (SAT-334)
- Rubin, Moises Nevah, S478 (FRI-236-YI)
- Rubinsztain, Joseph, S576 (THU-233), S579 (THU-242)
- Rubio, Aileen, S726 (TOP-353), S732 (SAT-339)
- Rubio, Ana Belén, S13 (OS-005-YI), S160 (THU-056), S176 (WED-055)
- Rubio, Ignacio, S178 (WED-060-YI)
- Rubio, Sonia Albertos, S391 (TOP-512-YI)
- Rudilla, Francesc, S741 (SAT-381)
- Rudler, Marika, S172 (THU-092), S207 (FRI-050-YI), S218 (FRI-087), S222 (FRI-094-YI), S222 (FRI-095), S239 (SAT-071), S486 (FRI-259)
- Rudnick, Sean, S714 (WED-164)
- Rudolph, Lorena, S582 (THU-254-YI)
- Rudraraju, Madhavi, S4 (GS-011), S544 (WED-294)
- Rueda, Francisco Navarrete, S194 (WED-113)
- Rui, Fajuan, S459 (TOP-307), S525 (WED-244), S625 (FRI-022), S744 (SAT-388), S776 (FRI-404)
- Ruiz, Beatriz Pacín, S741 (SAT-381), S746 (SAT-393)
- Ruiz-Blazquez, Paloma, S346 (FRI-548)
- Ruiz-Cantador, José, S706 (WED-132), S712 (WED-159)
- Ruiz-Cobo, Juan Carlos, S633 (THU-028), S702 (TOP-139), S741 (SAT-381), S746 (SAT-393), S822 (THU-395)
- Ruiz de Gauna, Mikel, S112 (FRI-343-YI)
- Ruiz de Zarate, Alma Diaz, S414 (FRI-457)
- Ruiz-Escolano, Elena, S779 (FRI-409)
- Ruiz-Fernández, Gloria, S398 (SAT-485)
- Ruiz, Ignacio Peña, S664 (WED-440)
- Ruiz-Ortega, Lourdes, S702 (TOP-139)
- Ruiz, Pablo, S9 (LBO-004), S89 (LBP-026)
- Ruiz, Patricia Cordero, S316 (THU-114), S559 (WED-341)
- Rukavina, Nadia, S381 (SAT-037)
- Rule, Jody, S104 (TOP-352)
- Ruscica, Massimiliano, S491 (FRI-275-YI)
- Rusie, Adriana, S211 (FRI-058), S324 (THU-131)
- Rusignuolo, Giuseppe, S187 (WED-094)
- Russell, Jennifer, S450 (THU-485-YI)
- Russello, Maurizio, S96 (LBP-038), S175 (TOP-085), S306 (THU-093), S310 (THU-101), S557 (WED-336)
- Russo, Ashley, S178 (WED-060-YI)
- Russo, Francesco Paolo, S376 (SAT-024-YI), S470 (FRI-215-YI), S700 (FRI-171), S704 (TOP-144-YI), S818 (THU-381)
- Russo, Jon, S724 (WED-188)
- Russo, Mark, S8 (LBO-003)
- Russo, Sara, S516 (WED-215), S545 (WED-296)
- Rüstemzade, Aynure, S377 (SAT-028), S551 (WED-318-YI), S803 (WED-413)
- Rusu, Ioana, S144 (SAT-273-YI), S555 (WED-332)
- Ruvoletto, Mariagrazia, S612 (SAT-219)
- Ruz-Zafra, Pilar, S139 (SAT-257), S142 (SAT-267)
- Ryan, John, S703 (TOP-141)
- Ryan, Pablo, S665 (WED-442)
- Rydel, Gustaf, S754 (SAT-414)
- Ryder, Stephen D, S669 (WED-452), S690 (WED-514)
- Ryder, Stephen D., S127 (THU-317), S145 (SAT-274), S350 (TOP-553)
- Rymell, Soubera, S21 (OS-020)
- Ryo, Yano, S711 (WED-154), S722 (WED-184)
- Ryu, Je Ho, S459 (THU-519)
- Ryu, Seungho, S517 (WED-221)
- Rzagalinski, Ignacy, S65 (OS-104)
- Rzymiski, Piotr, S685 (WED-493-YI)
- Saas, Philippe, S744 (SAT-389)
- Saati, Ahmed, S671 (WED-458)
- Saba, Francesca, S483 (FRI-251-YI), S501 (FRI-314), S522 (WED-233-YI), S525 (WED-243-YI)
- Sabbah, Meriam, S270 (THU-554)
- Sabio, Guadalupe, S112 (FRI-343-YI)
- Sabiote, Clara, S468 (FRI-211)
- Sabirov, Marat, S268 (THU-542)
- Saborido, Belen, S455 (THU-500)
- Saborowski, Anna, S69 (OS-112-YI), S425 (FRI-492-YI)
- Sabry, Nirmeen, S831 (THU-363)
- Sabry, Ramy, S673 (WED-463)
- Sacco, Rodolfo, S96 (LBP-038), S175 (TOP-085), S306 (THU-093)
- Sacerdoti, David, S51 (OS-078-YI), S474 (FRI-226), S492 (FRI-279-YI), S700 (FRI-171)
- Sachdeva, Sanjeev, S158 (THU-052), S167 (THU-078)
- Sackran, Joseph, S563 (THU-194), S779 (FRI-408)
- Sadiq Hamid, Saeed, S167 (THU-078)
- Sadirova, Shakhlo, S680 (WED-480-YI)
- Saeed, Anwaar, S51 (OS-078-YI), S69 (OS-112-YI), S443 (THU-464)
- Saeed, Sahar, S650 (SAT-455), S683 (WED-486-YI)
- Saeidinejad, MohammadMahdi, S182 (WED-080)
- Saeki, Akira, S542 (WED-286)
- Saez-Palma, Maria, S58 (OS-091)
- Sáez-Peñataro, Joaquín, S120 (SAT-325)
- Safadi, Rifaat, S63 (OS-100), S95 (LBP-035), S268 (THU-547), S278 (WED-534), S563 (THU-194), S564 (THU-197), S779 (FRI-408)
- Safadi, Tamer, S779 (FRI-408)
- Safarikia, Samira, S698 (FRI-166)
- Saffioti, Francesca, S268 (THU-547), S295 (SAT-158)
- Saffouri, Baker, S95 (LBP-035)
- Safinia, Niloufar, S709 (WED-137-YI)
- Sagalova, Olga, S1 (GS-002), S92 (LBP-029), S758 (TOP-400), S764 (FRI-371), S796 (WED-395)
- Sagar, Sagar, S33 (OS-043)
- Sagasta, Michele, S388 (SAT-056), S497 (FRI-294)
- Sagripanti, Alessandra, S544 (WED-293)
- Sahin, Cennet, S52 (OS-079-YI)
- Sahoo, Biswajit, S248 (SAT-099-YI)
- Sahoo, Manoj, S158 (THU-052), S167 (THU-078)
- Sahuco, Iván, S361 (WED-009), S700 (FRI-171)
- Saibeni, Simone, S332 (THU-161)
- Saidi, Alina, S549 (WED-306-YI)
- Saif, Rimsha, S125 (TOP-329-YI), S127 (THU-318)
- Saigal, Dr Sanjiv, S167 (THU-078)
- Saigal, Sanjeev, S476 (FRI-231)
- Saigal, Sanjiv, S158 (THU-052)
- Saillard, Jelena, S535 (WED-270)
- Saiman, Yedidya, S832 (THU-364)
- Saini, Akhilesh, S745 (SAT-391)
- Sainz-Ramírez, Natalia, S64 (OS-101-YI), S112 (FRI-343-YI), S419 (FRI-472-YI), S562 (TOP-229-YI), S569 (THU-210)
- Saison, Chris, S647 (SAT-447)
- Saithanyamurthi, Hemamala Venugopal, S158 (THU-052), S167 (THU-078)
- Saito, Satoru, S235 (FRI-130), S541 (WED-283)
- Saito, Takeshi, S128 (THU-319), S288 (FRI-540)
- Saitta, Carlo, S96 (LBP-038), S306 (THU-093), S345 (THU-192), S422 (FRI-481), S740 (SAT-378)
- Saitta, Daniel, S400 (SAT-492)
- Sajkowska-Kozielewicz, Joanna, S66 (OS-107-YI)
- Sakai, Aiko, S736 (SAT-365)
- Sakamori, Ryotaro, S828 (THU-413)
- Sakane, Sadatsugu, S506 (TOP-288)
- Sakthivel, Suganya, S55 (OS-085)
- Sala Llinás, Margarita, S329 (THU-154-YI), S330 (THU-155), S336 (THU-170-YI), S344 (THU-189)
- Salamé, Ephrem, S6 (GS-010), S369 (SAT-010), S387 (SAT-052)
- Salas, Joaquin, S779 (FRI-409)
- Salas, Mar, S233 (FRI-126)
- Salcedo, Magdalena, S318 (THU-118), S329 (THU-154-YI), S330 (THU-155), S336 (THU-170-YI)
- Salcedo, MTeresa, S468 (FRI-211)
- Saldanha, Oliver, S19 (OS-017)
- Saldarriaga, Omar, S823 (THU-396)
- Salem, Ahmed, S673 (WED-463)
- Sales, Fernanda, S254 (SAT-119)
- Salgado, Emilio, S45 (OS-068)

- Salhab, Ahmad, S63 (OS-100),
S95 (LBP-035), S268 (THU-547),
S564 (THU-197), S779 (FRI-408)
- Saliba, Faouzi, S9 (LBO-004), S89 (LBP-026),
S156 (TOP-108), S367 (TOP-005),
S378 (SAT-029)
- Salido, Eduardo, S85 (LBP-017),
S693 (FRI-152-YI)
- Salié, Henrike, S23 (OS-025-YI)
- Salih, Hizni, S676 (WED-471),
S759 (TOP-417)
- Salimzadeh, Loghman, S81 (LBP-009),
S352 (SAT-536)
- Salinas, Carlos Aguilar, S602 (TOP-205)
- Salinas, Javier, S362 (WED-016),
S364 (WED-028)
- Salis, Aina, S207 (FRI-051)
- Salisbury, Jon, S725 (WED-192)
- Salman, Muhammad, S765 (FRI-374-YI)
- Salmerón, Javier, S329 (THU-154-YI)
- Salomaa, Veikko, S460 (TOP-308),
S562 (TOP-240-YI)
- Salomone, Federico, S96 (LBP-038),
S306 (THU-093)
- Salpini, Romina, S59 (OS-094),
S772 (FRI-392-YI), S776 (FRI-405),
S798 (WED-399-YI)
- Salsetta, Jeanette, S439 (THU-454)
- Saltini, Dario, S52 (OS-080),
S61 (OS-096-YI), S62 (OS-099-YI),
S258 (SAT-131)
- Salvadori, Nicolas, S831 (THU-362)
- Salvati, Antonio, S549 (WED-314-YI),
S619 (SAT-245), S622 (FRI-014)
- Samaan, Jamil, S200 (TOP-063)
- Samaeng, Maseetoh, S396 (SAT-480-YI),
S410 (SAT-529)
- Samal, Subash, S248 (SAT-099-YI)
- Samant, Hrishikesh, S30 (OS-038-YI),
S199 (TOP-062), S200 (TOP-064-YI)
- Sambarino, Dana, S73 (OS-120),
S781 (FRI-412), S798 (WED-399-YI)
- Samby, Kirandeep, S732 (SAT-341)
- Samonakis, Dimitrios N., S470 (FRI-215-YI)
- Sampaziotis, Fotios, S81 (LBP-008),
S294 (SAT-154-YI)
- Sampedro, Antonio, S779 (FRI-409)
- Samson, Michel, S109 (FRI-333)
- Samuel, Didier, S6 (GS-010), S9 (LBO-004),
S89 (LBP-026), S370 (SAT-011),
S378 (SAT-029), S385 (SAT-049),
S432 (FRI-525), S718 (WED-174)
- Samy, Hadjadj, S508 (WED-194)
- Samyn, Marianne, S709 (WED-137-YI)
- Sanahuja, Josep Marti, S362 (WED-016)
- Sanai, Faisal, S496 (FRI-291)
- Sanai, Faisal M, S671 (WED-458)
- Sanchez, Abel Acosta, S728 (TOP-358-YI)
- Sánchez-Aldehuelo, Rubén, S700 (FRI-171)
- Sánchez, Aránzazu, S303 (SAT-183)
- Sánchez-Azofra, María, S398 (SAT-485)
- Sánchez-Bueno, Francisco, S377 (SAT-027)
- Sánchez-Campos, Sonia, S45 (OS-067),
S277 (WED-529)
- Sanchez, Cristina, S9 (LBO-004),
S83 (LBP-012), S89 (LBP-026),
S157 (THU-049), S157 (THU-050),
S161 (THU-057-YI),
S188 (WED-098-YI), S193 (WED-112),
S700 (FRI-171)
- Sanchez, Elisabet, S700 (FRI-171)
- Sanchez-Fernandez, Norberto,
S231 (FRI-122)
- Sánchez, Fernando Fernández,
S779 (FRI-409)
- Sanchez-Fueyo, Alberto,
S709 (WED-137-YI)
- Sánchez-Gavilán, Ester, S633 (THU-028)
- Sánchez, Henar Calvo, S738 (SAT-374-YI),
S768 (FRI-381)
- Sánchez, Jordi, S29 (OS-037),
S141 (SAT-262), S172 (THU-092),
S233 (FRI-126), S829 (THU-418)
- Sanchez, Lukas Otero, S133 (THU-335)
- Sanchez-Martinez, Monica,
S682 (WED-483)
- Sánchez-Pintos, Paula, S694 (FRI-153)
- Sánchez-Rodríguez, María Belén,
S174 (TOP-073)
- Sánchez-Ruano, JuanJosé, S828 (THU-411)
- Sanchez-Serrano, Jose, S232 (FRI-125)
- Sanchez-Torrijos, Yolanda María,
S170 (THU-086), S508 (WED-195),
S700 (FRI-171)
- Sánchez, Victor, S132 (THU-334)
- Sanchez, William, S8 (LBO-002)
- Sancho-Bru, Pau, S24 (OS-026-YI),
S139 (SAT-257), S142 (SAT-267),
S420 (FRI-474-YI)
- Sancho-Temiño, Lucía, S276 (WED-528-YI)
- Sancho, Victoria Aguilera, S139 (SAT-257),
S361 (WED-009), S365 (TOP-002)
- Sandahl, Thomas Damgaard,
S341 (THU-182), S714 (WED-164)
- Sandell, Therése, S93 (LBP-031)
- Sandmann, Lisa, S61 (OS-096-YI),
S245 (SAT-090-YI), S253 (SAT-117),
S759 (TOP-416-YI), S762 (FRI-365-YI)
- Sandrin, Laurent, S550 (WED-317)
- Sandro, Stefano Di, S369 (SAT-009)
- San, Emily Van, S581 (THU-249)
- Saner, Chetan, S554 (WED-327)
- Sanfilippo, Frank, S483 (FRI-250),
S487 (FRI-263)
- Sang, Hyunji, S477 (FRI-234)
- Sangiovanni, Angelo, S42 (OS-061),
S396 (SAT-481-YI), S397 (SAT-482),
S401 (SAT-493-YI), S700 (FRI-171)
- Sangiovanni, Letizia, S493 (FRI-281)
- Sangiovanni, Vincenzo, S215 (FRI-078-YI)
- Sangro, Bruno, S3 (GS-005), S287 (FRI-538),
S348 (FRI-555), S416 (FRI-464),
S455 (THU-501), S731 (SAT-337)
- Sangro, Paloma, S730 (SAT-337)
- Sanguinetti, Maurizio, S533 (WED-261-YI)
- Sankawa, Yuri, S320 (THU-122)
- San Martin, Javier, S698 (FRI-164)
- Sanna, Celeste, S322 (THU-127-YI)
- Sanoff, Hanna, S394 (SAT-476),
S403 (SAT-498)
- Sanoubara, Feras, S258 (SAT-130)
- Sans-Corrales, Mireia, S120 (SAT-325)
- Santamaria, Diego Burgos, S717 (WED-172)
- Santamaria, Eva, S348 (FRI-555),
S355 (SAT-543)
- Santamaría-Rodríguez, Germán,
S779 (FRI-409)
- Santangeli, Ernestina, S499 (FRI-299)
- Santangelo, Fabio, S671 (WED-457-YI)
- Santantonio, Teresa, S73 (OS-120),
S793 (WED-391), S804 (WED-414)
- Santiago, Antoine, S222 (FRI-094-YI)
- Santiago, Jesús M. Gonzalez,
S318 (THU-118)
- Santibanes, Martin De, S368 (SAT-009)
- Santini, Ferruccio, S93 (LBP-032)
- Santis, Adriano De, S829 (THU-414)
- Santis, Emanuela De, S829 (THU-414)
- Santistevé, Sara Sopena, S802 (WED-411)
- Santi, Valentina, S449 (THU-481-YI)
- Santomenna, Floriana, S466 (FRI-207-YI),
S474 (FRI-226), S482 (FRI-248-YI)
- Santopaolo, Francesco, S52 (OS-080),
S452 (THU-492), S703 (TOP-142-YI),
S705 (WED-130)
- Santoro, Armando, S438 (THU-446)
- Santos, Beatriz Gómez, S64 (OS-101-YI),
S112 (FRI-343-YI), S419 (FRI-472-YI),
S562 (TOP-229-YI), S569 (THU-210)
- Santos, Carina, S834 (THU-370)
- Santos-Ferreira, Nanci, S732 (SAT-340-YI)
- Santos-Laso, Alvaro, S318 (THU-118),
S330 (THU-155)
- Santos, Maria Dolores, S826 (THU-405)
- Sanyal, Arka, S346 (FRI-547-YI)
- Sanyal, Arun J, S2 (GS-004), S4 (GS-006),
S38 (OS-054), S72 (OS-118), S72 (OS-119),
S76 (OS-125), S467 (FRI-208),
S507 (TOP-289), S533 (WED-263)
- Sanyal, Arun J., S7 (LBO-001),
S10 (LBO-005), S93 (LBP-032),
S95 (LBP-036), S242 (SAT-082),
S465 (FRI-203), S472 (FRI-222-YI),
S523 (WED-237), S606 (SAT-201),
S607 (SAT-203), S610 (SAT-212),
S617 (SAT-239)
- Sanz de Pedro, María, S398 (SAT-485)
- Sanz de Villalobos, Eduardo,
S391 (TOP-512-YI)
- Sanz-Rodríguez, Maria, S541 (WED-284-YI)
- Sapio, Luigi, S173 (TOP-072)
- Sapisochin, Gonzalo, S368 (SAT-009),
S381 (SAT-037), S381 (SAT-039),
S445 (THU-470-YI)
- Saponaro, Anna Alessia, S429 (FRI-516-YI)
- Saqr, Al-Hussein, S84 (LBP-015)
- Saracco, Giorgio Maria, S210 (FRI-056-YI),
S451 (THU-486-YI), S458 (THU-517),
S475 (FRI-230-YI), S480 (FRI-243),
S525 (WED-243-YI)
- Saracco, Margherita, S371 (SAT-015-YI),
S378 (SAT-031-YI)

Author Index

- Saraceno, Giovanni, S680 (WED-479)
 Saracino, Annalisa, S772 (FRI-392-YI)
 Saraf, Neeraj, S158 (THU-052),
 S167 (THU-078)
 Saraswat, Vivek, S454 (THU-498)
 Saraya, Anoop, S62 (OS-098-YI),
 S158 (THU-052), S161 (THU-058),
 S167 (THU-078), S546 (WED-298-YI)
 Sarba, Ruxandra, S413 (FRI-456)
 Sarin, Shiv Kumar, S6 (GS-009),
 S30 (OS-038-YI), S67 (OS-108-YI),
 S103 (TOP-349-YI), S125 (TOP-329-YI),
 S127 (THU-318), S129 (THU-321),
 S134 (THU-339), S137 (SAT-249),
 S158 (THU-052), S161 (THU-058),
 S164 (THU-068), S164 (THU-069),
 S164 (THU-070), S167 (THU-078),
 S177 (WED-057), S199 (TOP-062),
 S200 (TOP-064-YI), S208 (FRI-053),
 S219 (FRI-088), S272 (WED-518-YI),
 S273 (WED-519-YI), S274 (WED-522-YI),
 S276 (WED-527-YI), S283 (WED-549),
 S294 (SAT-155), S346 (FRI-547-YI),
 S360 (SAT-557-YI), S745 (SAT-391)
 Sarmati, Loredana, S59 (OS-094),
 S772 (FRI-392-YI)
 Sarohi, Vivek, S158 (THU-051)
 Sarrazin, Christoph, S833 (THU-366)
 Sartini, Claudio, S477 (FRI-235),
 S486 (FRI-260), S509 (WED-197)
 Sarv, Janeli, S93 (LBP-031)
 Sasaki, Ryu, S228 (FRI-113),
 S234 (FRI-128)
 Sasaki, Yoichi, S506 (TOP-288)
 Sasaki, Yutaka, S506 (TOP-288)
 Sasso, Ferdinando Carlo, S790 (FRI-441)
 Sastre, Javier, S455 (THU-501)
 Satai, Mayur, S554 (WED-327)
 Satapathy, Sanjaya, S8 (LBO-003)
 Satoh, Takeaki, S42 (OS-062)
 Sato, Shinya, S175 (TOP-096)
 Sato, Shunsuke, S490 (FRI-272)
 Sato, Taka-Aki, S513 (WED-208)
 Satsangi, Jack, S302 (SAT-179)
 Sattar, Naveed, S138 (SAT-254)
 Satthawiwat, Nantawat, S591 (THU-281)
 Sattianayagam, Prayman, S633 (THU-029)
 Sattorov, Safarhon, S682 (WED-484)
 Saueressig, Camila, S636 (THU-044)
 Sauer, Peter, S300 (SAT-174)
 Saunbury, Emma, S210 (FRI-057),
 S687 (WED-496)
 Saunthar, Ahreni, S673 (WED-464)
 Sauri, Tamara, S444 (THU-467-YI)
 Sauter, Guido, S24 (OS-027-YI)
 Savarese, Michael, S745 (SAT-390)
 Savas, Berna, S479 (FRI-238)
 Savaş, Berna, S407 (SAT-519)
 Saverio Belli, Luca, S376 (SAT-025),
 S380 (SAT-034)
 Saviano, Antonio, S17 (OS-013),
 S172 (THU-092)
 Savino, Alberto, S325 (THU-133-YI),
 S439 (THU-447)
 Savino, Flavia, S425 (FRI-494-YI),
 S430 (FRI-519-YI)
 Savopoulos, Christos, S196 (WED-121-YI),
 S229 (FRI-117)
 Savytska, Maryana, S610 (SAT-213)
 Sawangjit, Ratree, S689 (WED-502)
 Saweres, Andrew, S491 (FRI-273-YI)
 Sawhney, Rohit, S338 (THU-177-YI),
 S400 (SAT-492)
 Sawhney, Sangeeta, S95 (LBP-036)
 Saxena, Varun, S778 (FRI-407)
 Sayaf, Katia, S592 (THU-285),
 S700 (FRI-171)
 Saydullaev, Farkhod,
 S682 (WED-484)
 Sayed, Blayne, S381 (SAT-037),
 S381 (SAT-039)
 Sayed, Nilofer, S565 (THU-200-YI)
 Sayk, Friedhelm, S582 (THU-254-YI)
 Scaldaferrì, Matilde, S451 (THU-486-YI),
 S458 (THU-517)
 Scalici, Fabrizio, S671 (WED-457-YI)
 Scalici, Marilu' Benedetta, S501 (FRI-314),
 S525 (WED-243-YI)
 Scalisi, Ignazio, S557 (WED-336)
 Scaravaglio, Miki, S81 (LBP-008),
 S96 (LBP-038), S306 (THU-093),
 S310 (THU-101), S325 (THU-133-YI),
 S380 (SAT-034)
 Schaapman, Jelte, S21 (OS-020),
 S204 (FRI-043)
 Schachteli, Fabian, S180 (WED-074)
 Schaefer, Benedikt, S515 (WED-214-YI),
 S703 (TOP-141), S708 (WED-135-YI),
 S722 (WED-183-YI)
 Schaefer, Esperance, S131 (THU-330)
 Schaefer, Liliana, S198 (WED-126)
 Schafmayer, Clemens, S56 (OS-086-YI)
 Schalkwyk, Marije Van, S756 (SAT-421)
 Scharl, Michael, S56 (OS-086-YI)
 Scharnagl, Hubert, S267 (THU-540),
 S296 (SAT-161), S383 (SAT-042)
 Schattenberg, Jörn, S508 (WED-195),
 S528 (WED-249)
 Schattenberg, Jörn M., S4 (GS-006),
 S37 (OS-051), S61 (OS-096-YI),
 S70 (OS-115), S71 (OS-117),
 S72 (OS-118), S72 (OS-119), S76 (OS-124),
 S461 (FRI-194-YI), S477 (FRI-235),
 S503 (TOP-241-YI), S504 (TOP-253),
 S505 (TOP-265), S507 (TOP-300),
 S509 (WED-196), S509 (WED-197),
 S511 (WED-201), S511 (WED-202),
 S533 (WED-263)
 Schattenberg, Jörn M., S80 (LBP-006),
 S88 (LBP-024), S91 (LBP-028),
 S141 (SAT-263), S238 (SAT-069),
 S435 (FRI-533), S463 (FRI-198),
 S464 (FRI-199), S470 (FRI-218),
 S481 (FRI-247), S482 (FRI-249),
 S484 (FRI-255), S486 (FRI-260),
 S518 (WED-223), S538 (WED-275),
 S607 (SAT-203), S611 (SAT-214),
 S648 (SAT-450)
 Schaub, Johanna, S97 (LBP-039),
 S261 (TOP-564)
 Schaufert, Wendy, S538 (WED-274)
 Scheble, Veit, S52 (OS-079-YI)
 Schedlbauer, Anna, S621 (FRI-009-YI),
 S717 (WED-171)
 Scheele, Colinda, S16 (OS-012-YI)
 Scheele, Ulrik, S565 (THU-199)
 Scheidereit, Emilia, S33 (OS-043)
 Scheiner, Bernhard, S24 (OS-027-YI),
 S51 (OS-078-YI), S52 (OS-079-YI),
 S69 (OS-112-YI), S165 (THU-071),
 S166 (THU-075-YI), S243 (SAT-086-YI),
 S250 (SAT-105), S251 (SAT-111),
 S255 (SAT-122), S257 (SAT-128),
 S436 (TOP-488-YI), S443 (THU-464),
 S445 (THU-471-YI), S621 (FRI-009-YI),
 S706 (WED-131-YI), S717 (WED-171),
 S725 (WED-190)
 Schenk, Robin P., S35 (OS-049-YI)
 Schepis, Filippo, S52 (OS-080),
 S61 (OS-096-YI), S62 (OS-099-YI),
 S258 (SAT-131)
 Scherbakovsky, Stacey, S681 (WED-482)
 Scherfler, Christoph, S722 (WED-183-YI)
 Schiano, Thomas, S374 (SAT-021)
 Schiavo, Luigi, S554 (WED-326)
 Schierwagen, Robert, S47 (OS-071-YI),
 S47 (OS-072-YI), S159 (THU-055),
 S169 (THU-083), S170 (THU-087),
 S180 (WED-074), S184 (WED-083),
 S193 (WED-111), S198 (WED-126),
 S203 (FRI-039), S259 (SAT-135),
 S272 (TOP-563), S283 (WED-548),
 S391 (TOP-511)
 Schilsky, Michael, S714 (WED-164)
 Schindler, Aaron, S404 (SAT-501-YI)
 Schinkelshoek, Mink, S278 (WED-533)
 Schlauch, Karen A., S462 (FRI-195)
 Schlecht-louf, Geraldine, S130 (THU-327)
 Schlegel, Andrea, S375 (SAT-022)
 Schleicher, Eva Maria, S230 (FRI-120),
 S249 (SAT-104-YI)
 Schleinitz, Nicolas, S710 (WED-152)
 Schlienkamp, Sarah, S94 (LBP-034)
 Schlösser, Denise, S425 (FRI-492-YI)
 Schluckebier, Julia, S699 (FRI-170)
 Schluep, Thomas, S27 (OS-032),
 S696 (FRI-161), S698 (FRI-164)
 Schmauch, Benoit, S412 (FRI-454)
 Schmaus, Hagen, S735 (SAT-363)
 Schmidbauer, Victor, S719 (WED-175)
 Schmidbauer, Viktor, S250 (SAT-106)
 Schmid, Bernhard, S72 (OS-119)
 Schmid, Roland M., S35 (OS-049-YI),
 S298 (SAT-166), S440 (THU-457)
 Schmid, Stephan, S115 (TOP-346-YI)
 Schmidt, Constantin, S24 (OS-027-YI)
 Schmidt, Hartmut, S223 (FRI-100),
 S384 (SAT-046), S443 (THU-465-YI),
 S714 (WED-164), S793 (WED-391)
 Schmidtman, Irene, S52 (OS-079-YI),
 S461 (FRI-194-YI)
 Schmidt, Sabine, S65 (OS-103)

- Schmidt, Thomas Sebastian, S48 (OS-073)
 Schmiel, Marcel, S423 (FRI-486)
 Schmist-Arras, Dirk, S278 (WED-534)
 Schmit, Nora, S678 (WED-475)
 Schmittiel, Julie, S778 (FRI-407)
 Schmittgens, Stephan, S309 (THU-100)
 Schneckloth, Terry, S146 (SAT-279)
 Schnee, Matthieu, S520 (WED-227)
 Schneeweiss-Gleixner, Mathias, S165 (THU-071), S340 (THU-180)
 Schnefeld, Helle, S77 (OS-126), S137 (SAT-250), S205 (FRI-045), S466 (FRI-206-YI), S510 (WED-199), S623 (FRI-017)
 Schnefeld, Helle Lindholm, S41 (OS-059), S153 (SAT-298), S503 (TOP-241-YI)
 Schneider, Carolin V., S392 (TOP-520), S494 (FRI-284-YI), S528 (WED-247), S567 (THU-206)
 schneider, Guenther, S560 (WED-343)
 Schneider, Hannah, S204 (FRI-042), S226 (FRI-107-YI), S226 (FRI-109), S242 (SAT-080-YI), S245 (SAT-090-YI), S762 (FRI-365-YI)
 Schneider, Hans, S653 (SAT-464-YI)
 Schneider, Kai Markus, S273 (WED-521-YI), S392 (TOP-520), S431 (FRI-522), S494 (FRI-284-YI)
 Schneider, Paul, S435 (FRI-533)
 Schnuriger, Aurélie, S729 (TOP-360-YI)
 Schöchtner, Till, S243 (SAT-086-YI)
 Schoder, Maria, S156 (TOP-097-YI), S242 (SAT-080-YI), S253 (SAT-118)
 Schoen, Cheryl, S472 (FRI-222-YI)
 Schoenlein, Martin, S51 (OS-078-YI), S443 (THU-464)
 Schoenmakers, Lotte, S61 (OS-096-YI), S540 (WED-281-YI)
 Scholtens, Joyce, S546 (WED-297-YI)
 Schöning, Wenzel, S366 (TOP-003-YI)
 Schönke, Milena, S272 (WED-517), S278 (WED-533)
 Schoonjans, Kristina, S536 (WED-271)
 Schophaus, Simon, S494 (FRI-284-YI)
 Schouten, Jeoffrey, S321 (THU-123-YI), S828 (THU-412)
 Schraauwen, Rick, S730 (TOP-384-YI)
 Schrader, Christina, S703 (TOP-141), S708 (WED-135-YI)
 Schrader, Jil Alexandra, S58 (OS-092)
 Schramm, Christoph, S5 (GS-007), S97 (LBP-039), S223 (FRI-100), S265 (THU-534-YI), S278 (WED-534), S313 (THU-106-YI), S316 (THU-113), S321 (THU-125), S327 (THU-137), S335 (THU-167), S350 (SAT-531-YI), S374 (SAT-021), S384 (SAT-046), S712 (WED-158-YI), S793 (WED-391)
 Schregel, Ida, S335 (THU-167)
 Schreiber, Licita, S770 (FRI-386)
 Schreiber, Sophia, S34 (OS-045)
 Schreiber, Stefan, S582 (THU-254-YI)
 Schreiner, Andrew, S614 (SAT-226)
 Schreiner, Sven, S34 (OS-045)
 Schreuder, Tim C.M.A., S319 (THU-120-YI)
 Schroers, Barbara, S435 (FRI-533)
 Schropp, Jonas, S393 (SAT-473)
 Schubert, Kristin, S104 (TOP-352)
 Schudoma, Christian, S48 (OS-073)
 Schuehle, Svenja, S65 (OS-103)
 Schuhbaur, Jasmin, S52 (OS-079-YI)
 Schultheiß, Michael, S69 (OS-112-YI), S161 (THU-058), S187 (WED-094)
 Schulze, Gene, S812 (WED-377)
 Schulze, Kornelius, S24 (OS-027-YI), S51 (OS-078-YI), S52 (OS-079-YI), S69 (OS-112-YI), S443 (THU-464)
 Schulze-Osthoff, Klaus, S528 (WED-249)
 Schulze, Stephanie, S316 (THU-113)
 Schulze zur Wiesch, Julian, S92 (LBP-029), S730 (TOP-369), S739 (SAT-376), S813 (WED-379)
 Schulz, Martin, S169 (THU-083), S170 (THU-087), S198 (WED-126)
 Schumacher, Jonas, S162 (THU-059)
 Schumann, Georgina, S425 (FRI-492-YI)
 Schuppan, Detlef, S106 (FRI-322), S265 (THU-534-YI), S268 (THU-546), S363 (WED-021), S585 (THU-260)
 Schuster, Alexander, S461 (FRI-194-YI)
 Schuster, Catherine, S17 (OS-013), S25 (OS-029), S31 (OS-040-YI), S42 (OS-061)
 Schütte, Sarah Lisa, S202 (FRI-038-YI), S204 (FRI-042), S242 (SAT-080-YI)
 Schüttler, Christian, S665 (WED-441-YI)
 Schütz, Angelika, S818 (THU-380-YI)
 Schwabe, Christian, S86 (LBP-019), S141 (SAT-261), S806 (WED-361), S811 (WED-374)
 Schwabe, Robert F., S24 (OS-026-YI)
 Schwabl, Philipp, S165 (THU-071), S186 (WED-089-YI), S197 (WED-122-YI), S198 (WED-125), S257 (SAT-128), S267 (THU-540)
 Schwacha-Eipper, Birgit, S69 (OS-112-YI), S373 (SAT-019), S393 (SAT-473)
 Schwartz, Zachary, S789 (FRI-436)
 Schwarz, Caroline, S253 (SAT-118), S335 (THU-166), S719 (WED-175), S773 (FRI-394), S818 (THU-380-YI), S821 (THU-390)
 Schwarzfischer, Marlene, S56 (OS-086-YI)
 Schwarzkopf, Katharina Maria, S203 (FRI-039)
 Schwarzl, Jakob, S229 (FRI-115)
 Schwarz, Michael, S28 (OS-034), S156 (TOP-097-YI), S165 (THU-071), S166 (THU-075-YI), S242 (SAT-080-YI), S243 (SAT-086-YI), S250 (SAT-105), S251 (SAT-111), S253 (SAT-117), S253 (SAT-118), S255 (SAT-122), S621 (FRI-009-YI), S706 (WED-131-YI), S717 (WED-171), S719 (WED-175), S725 (WED-190), S773 (FRI-394), S814 (WED-383), S818 (THU-381)
 Schweiger, Alexander, S702 (TOP-140)
 Schweiger, Michal, S423 (FRI-486)
 Schwenke, Carsten, S320 (THU-122)
 Schwenken, Marianna, S833 (THU-366)
 Schwinge, Dorothee, S350 (SAT-531-YI)
 Sciarrone, Salvatore, S332 (THU-161)
 Sciveres, Marco, S374 (SAT-021)
 Scivetti, Paolo, S96 (LBP-038), S306 (THU-093), S634 (THU-032)
 Scott, Deborah, S8 (LBO-003)
 Scotti, Erica, S589 (THU-274)
 Scott, Jennifer, S650 (SAT-454-YI)
 Scriccia, Sara, S554 (WED-325-YI)
 Seah, Cindy, S797 (WED-398)
 Seabagh, Mylène, S432 (FRI-525)
 Sebastian, David, S568 (THU-209)
 Sebastiani, Giada, S484 (FRI-256-YI), S496 (FRI-290), S650 (SAT-455), S683 (WED-486-YI)
 Sebode, Marcial, S44 (OS-066-YI), S115 (TOP-346-YI), S265 (THU-534-YI), S316 (THU-113), S335 (THU-167), S341 (THU-182)
 Secondulfo, Carmine, S493 (FRI-281)
 Sedki, Mai, S374 (SAT-021)
 Segal, Eran, S645 (SAT-442)
 Segal, Jonathan, S92 (LBP-030)
 Segna, Daniel, S254 (SAT-121)
 Segovia-Zafra, Antonio, S107 (FRI-324)
 Ségrestin, Bérénice, S508 (WED-194), S538 (WED-278)
 Sehemy, Lamiaa Al, S491 (FRI-273-YI)
 Sehgal, Tushar, S201 (TOP-065)
 Seidita, Aurelio, S601 (TOP-193)
 Seidner, Mark, S753 (SAT-413)
 Seifert, Tanja, S358 (SAT-551)
 Seif, Martha, S270 (THU-550)
 Sejling, Anne-Sophie, S79 (LBP-003)
 Sekaran, Anuradha, S440 (THU-456)
 Seki, Ekihiro, S39 (OS-055)
 Seko, Yuya, S537 (WED-273)
 Selcanova, Svetlana Adamcova, S172 (THU-092), S379 (SAT-033), S539 (WED-279)
 Selemani, Sarah, S388 (SAT-057)
 Selicean, Sonia, S183 (WED-082)
 Selicean, Sonia Emilia, S183 (WED-081)
 Seligson, David, S403 (SAT-498)
 Sella, Federica, S56 (OS-086-YI)
 Seltmann, Jonathan, S802 (WED-411)
 Selvaggio, Carmelo, S439 (THU-447)
 Selvestrel, Davide, S699 (FRI-167-YI)
 Selvi, Marta, S154 (SAT-304), S822 (THU-395)
 Selv, Kathirvel, S666 (WED-443-YI)
 Selzner, Markus, S381 (SAT-037), S381 (SAT-039)
 Selzner, Nazia, S9 (LBO-004), S89 (LBP-026), S374 (SAT-021), S381 (SAT-037), S381 (SAT-039)
 Semela, David, S502 (FRI-315)
 Semeniuta, Daniel, S460 (TOP-309)
 Semmler, Georg, S61 (OS-096-YI), S166 (THU-075-YI), S250 (SAT-105), S250 (SAT-106), S251 (SAT-111), S255 (SAT-122), S257 (SAT-128),

Author Index

- S340 (THU-180), S621 (FRI-009-YI), S706 (WED-131-YI), S717 (WED-171), S725 (WED-190), S818 (THU-381)
- Semmo, Nasser, S44 (OS-066-YI), S341 (THU-182), S793 (WED-391)
- Sempere, Elena Diago, S700 (FRI-171)
- Semple, Scott, S81 (LBP-007)
- Semple, Sean, S88 (LBP-022)
- Sendino, Oriol, S378 (SAT-030)
- Sendra, Carmen, S170 (THU-086), S316 (THU-114)
- Sendra-Fernández, Carmen, S779 (FRI-409)
- Seng, Dorothy, S637 (THU-046)
- Sengel, Christian, S50 (OS-077)
- Senju, Takeshi, S42 (OS-062)
- Senzolo, Marco, S62 (OS-099-YI), S237 (TOP-061-YI), S258 (SAT-131)
- Seo, Hye-Young, S112 (FRI-341)
- Seok Kim, Young, S247 (SAT-098)
- Seo, Sang Hyun, S290 (FRI-545)
- Seo, Suk, S778 (FRI-407)
- Seo, Yeon Seok, S136 (THU-348), S481 (FRI-246), S596 (THU-295), S767 (FRI-379), S774 (FRI-397), S799 (WED-404)
- Sepúlveda-Crespo, Daniel, S665 (WED-442), S751 (SAT-407)
- Seraphin, Tobias Paul, S392 (SAT-469)
- Serdjebi, Cindy, S823 (THU-397-YI)
- Serenari, Matteo, S241 (SAT-078-YI), S386 (SAT-051), S390 (TOP-509-YI), S399 (SAT-490), S704 (TOP-143-YI)
- Seror, Olivier, S50 (OS-077), S68 (OS-110), S441 (THU-459-YI), S451 (THU-487-YI)
- Serra, Carla, S457 (THU-514)
- Serra, Giancarlo, S322 (THU-127-YI)
- Serra, Isabel, S471 (FRI-219-YI)
- Serra, Marina, S322 (THU-127-YI)
- Serra, Miguel, S469 (FRI-213)
- Serra, Miquel, S503 (TOP-241-YI)
- Serrano, Gemma, S398 (SAT-485)
- Serrano-Macia, Marina, S693 (FRI-153)
- Serrano-Maciá, Marina, S194 (WED-113), S417 (FRI-466-YI)
- Serrano, Maria A., S433 (FRI-526)
- Serrano-Nieto, Juliana, S694 (FRI-153)
- Serrés, Mariana, S398 (SAT-485)
- Sersté, Thomas, S777 (FRI-406)
- Serumondo, Janvier, S686 (WED-495)
- Servant, Florence, S47 (OS-071-YI)
- Serviddio, Gaetano, S470 (FRI-215-YI)
- Servin-Caamaño, Alfredo, S140 (SAT-260)
- Sessa, Anna, S373 (SAT-020), S413 (FRI-456), S720 (WED-178), S743 (SAT-386-YI)
- Seth, Saksham, S225 (FRI-106-YI)
- Setnická, Vladimír, S539 (WED-280)
- Seto, Wai-Kay, S27 (OS-032), S86 (LBP-019), S116 (SAT-314), S161 (THU-058), S208 (FRI-053), S219 (FRI-088), S424 (FRI-490-YI), S739 (SAT-375), S745 (SAT-392), S770 (FRI-388), S797 (WED-397), S810 (WED-373-YI)
- Sevak, Jayesh Kumar, S67 (OS-108-YI)
- Sevastianos, Vasilios, S208 (FRI-052), S214 (FRI-076), S798 (WED-403)
- Sewell, Charlotte, S337 (THU-173)
- Seyec, Jacques Le, S109 (FRI-333)
- Sezgin, Orhan, S723 (WED-187-YI)
- Sguazzini, Enrico, S388 (SAT-056)
- Shadaker, Shaun, S659 (WED-427), S664 (WED-439), S675 (WED-468), S677 (WED-473), S682 (WED-484), S685 (WED-492), S691 (WED-515), S825 (THU-404)
- Shafiq, Mohsin, S24 (OS-027-YI)
- Shaheen, Abdel-Aziz, S538 (WED-274), S660 (WED-431)
- Shahi, Pradeep, S615 (SAT-231)
- Shah, Jayshri, S634 (THU-033), S639 (SAT-427-YI)
- Shah, Neil, S394 (SAT-476)
- Shah, Samir, S158 (THU-052), S167 (THU-078)
- Shah, Stuti, S352 (SAT-536)
- Shah, Tahir, S423 (FRI-487), S425 (FRI-493)
- Shah, Vijay, S134 (THU-341)
- Shaik, Sameer, S454 (THU-498)
- Shalaby, Sarah, S15 (OS-010), S179 (WED-070), S240 (SAT-074), S255 (SAT-123)
- Shalimar, Shalimar, S201 (TOP-065), S202 (TOP-066-YI), S475 (FRI-231), S506 (TOP-276)
- Sha, Meng, S387 (SAT-054)
- Shamir, Raanan, S696 (FRI-160-YI)
- Shamseddine, Nisreen, S708 (WED-136)
- Shang, Changzhen, S382 (SAT-041)
- Shang, Jia, S95 (LBP-037), S803 (WED-412)
- Shang, Ke, S102 (LBP-048)
- Shang, Ying, S2 (GS-004), S38 (OS-054), S462 (FRI-196)
- Shao, Chuxiao, S526 (WED-246)
- Shao, Congxiang, S84 (LBP-014)
- Shao, Guoliang, S447 (THU-475)
- Shao, Lan, S8 (LBO-002)
- Shao, Qing, S198 (WED-124), S359 (SAT-556-YI), S527 (WED-246)
- Shao, Yu-Yun, S438 (THU-446)
- Shapiro, James, S231 (FRI-122)
- Sharma, Aarti, S67 (OS-108-YI), S176 (WED-056), S181 (WED-076), S346 (FRI-547-YI)
- Sharma, Brij, S476 (FRI-231)
- Sharma, Gaurav, S217 (FRI-082)
- Sharma, Kanchi, S188 (WED-095-YI)
- Sharma, Manoj, S167 (THU-078)
- Sharma, Mithun, S149 (SAT-290-YI), S158 (THU-052), S208 (FRI-053), S440 (THU-456), S454 (THU-498), S701 (FRI-173), S720 (WED-180)
- Sharma, Neha, S103 (TOP-349-YI), S108 (FRI-327-YI), S125 (TOP-329-YI), S127 (THU-318), S134 (THU-339), S273 (WED-519-YI), S283 (WED-549), S294 (SAT-155)
- Sharma, Nupur, S103 (TOP-349-YI), S108 (FRI-327-YI), S125 (TOP-329-YI), S127 (THU-318), S134 (THU-339), S273 (WED-519-YI), S283 (WED-549), S294 (SAT-155)
- S127 (THU-318), S134 (THU-339), S273 (WED-519-YI), S283 (WED-549), S294 (SAT-155), S754 (SAT-415)
- Sharma, Preeti, S692 (TOP-145)
- Sharma, Priyanka, S605 (SAT-199)
- Sharma, Rajni, S700 (FRI-171)
- Sharma, Rohini, S51 (OS-078-YI), S443 (THU-464), S639 (SAT-427-YI)
- Sharma, Sanchit, S62 (OS-098-YI)
- Sharma, SatyaPriya, S602 (TOP-216)
- Sharma, Shawn, S662 (WED-436), S668 (WED-450), S679 (WED-476)
- Sharma, Shilpee, S131 (THU-331-YI)
- Sharma, Shvetank, S103 (TOP-349-YI), S108 (FRI-327-YI), S129 (THU-321), S181 (WED-076), S272 (WED-518-YI), S276 (WED-527-YI), S283 (WED-549)
- Sharma, Shyam Sunder, S225 (FRI-106-YI)
- Sharma, Simran, S348 (FRI-554)
- Sharma, Suresh, S400 (SAT-492)
- Sharma, Vikram, S632 (THU-022)
- Sharvadze, Lali, S659 (WED-427), S685 (WED-492)
- Shasthry, S. Muralikrishna, S137 (SAT-249), S164 (THU-070)
- Shawcross, Debbie L., S46 (OS-070), S47 (OS-071-YI), S48 (OS-073), S159 (THU-055), S184 (WED-083), S193 (WED-111), S282 (WED-545-YI), S588 (THU-271-YI), S654 (SAT-467)
- Shaw, Daniel, S182 (WED-080)
- Shaw, Jawaid, S161 (THU-058), S218 (FRI-086)
- Shaw, Tanya, S128 (THU-320-YI)
- Shearer, Jessica, S232 (FRI-123), S397 (SAT-483-YI)
- Sheen, I-Shyan, S414 (FRI-458), S784 (FRI-426)
- Sheikh, Muhammad Y, S8 (LBO-002)
- Sheikh, Sabreena, S506 (TOP-276)
- Shekhtman, Louis, S43 (OS-063)
- Shemuelian, Zohar, S278 (WED-534)
- Shen, Chuan, S387 (SAT-054)
- Shen, Ge, S344 (THU-191)
- Sheng, Jianlong, S100 (LBP-045)
- Sheng, Jifang, S95 (LBP-037)
- Sheng, Mingwei, S354 (SAT-542)
- Shen, Jia-Qi, S488 (FRI-267)
- Shen, Jie, S526 (WED-246), S536 (WED-272), S620 (TOP-006)
- Shen, Liang, S797 (WED-398)
- Shen, Michael, S812 (WED-377)
- Shen, Mingwang, S789 (FRI-438)
- Shen, Sheng, S95 (LBP-037)
- Shen, Weishuang, S111 (FRI-338), S111 (FRI-339)
- Shen, Yefeng, S423 (FRI-486)
- Shen, Yi, S264 (THU-532)
- Sheptulina, Anna, S501 (FRI-305)
- Sherif, Mirella, S491 (FRI-273-YI)
- Sherman, David, S634 (THU-033)
- Sherwani, Alaa, S172 (THU-090)
- Sherwani, Nouf, S172 (THU-090)
- Sheshadri, Somya, S209 (FRI-053)

- She, Shaoping, S429 ([FRI-515](#))
 Sheth, Roosey, S181 ([WED-075-YI](#))
 Shetti, Dattatrya, S349 ([FRI-556](#))
 Shetty, Kirti, S9 ([LBO-004](#)), S10 ([LBO-005](#)), S89 ([LBP-026](#)), S242 ([SAT-082](#))
 Shetty, Shishir, S423 ([FRI-487](#)), S425 ([FRI-493](#))
 Shevchenko, Andrej, S65 ([OS-104](#))
 Shibolet, Oren, S98 ([LBP-040](#)), S628 ([FRI-033](#))
 Shibuya, Akira, S349 ([TOP-552](#))
 Shi, Dongyan, S105 ([FRI-319](#)), S108 ([FRI-330](#)), S117 ([SAT-318](#)), S345 ([FRI-546](#))
 Shiffman, Mitchell, S8 ([LBO-003](#)), S80 ([LBP-006](#))
 Shiha, Gamal, S158 ([THU-052](#)), S167 ([THU-078](#)), S549 ([WED-315](#)), S624 ([FRI-020](#)), S673 ([WED-463](#))
 Shi, Haibin, S447 ([THU-475](#))
 Shih, Chin-I, S490 ([FRI-271](#)), S493 ([FRI-280](#))
 Shih, Ping-Tsung, S490 ([FRI-271](#))
 Shih, Yu-Jia, S772 ([FRI-391](#))
 Shi, Juanjuan, S195 ([WED-116](#)), S590 ([THU-279](#))
 Shi, Junping, S459 ([TOP-307](#)), S525 ([WED-244](#)), S605 ([SAT-198](#))
 Shi, Luming, S401 ([SAT-495](#))
 Shimakawa, Yusuke, S656 ([TOP-460-YI](#)), S678 ([WED-475](#)), S679 ([WED-477-YI](#)), S782 ([FRI-418](#)), S787 ([FRI-431](#))
 Shima, Toshihide, S537 ([WED-273](#))
 Shimizu, Kentaro, S506 ([TOP-288](#))
 Shimizu, Mamoru, S693 ([FRI-151](#))
 Shimizu, Masahito, S828 ([THU-413](#))
 Shimizu, Mayuko, S519 ([WED-226](#))
 Shim, Jong Joon, S247 ([SAT-098](#))
 Shim, Ju Hyun, S305 ([TOP-157](#))
 Shinde, Leela, S554 ([WED-327](#))
 Shin, Hyunjae, S517 ([WED-221](#)), S601 ([TOP-204](#)), S766 ([FRI-376](#)), S774 ([FRI-397](#)), S798 ([WED-402](#))
 Shin, Jaeseung, S410 ([SAT-526](#))
 Shin, Seung Kak, S542 ([WED-287](#))
 Shirai, Kumiko, S506 ([TOP-288](#))
 Shirazi, Rachel, S770 ([FRI-386](#))
 Shi, Stella, S102 ([LBP-048](#))
 Shivalila, Chikdu, S692 ([FRI-151](#))
 Shoaie, Saeed, S46 ([OS-070](#)), S182 ([WED-078](#)), S203 ([FRI-039](#))
 Sholy, Hisham, S774 ([FRI-395](#))
 Shou, Jianyong, S102 ([LBP-048](#))
 Shpilevaia, Elizaveta, S555 ([WED-330](#)), S561 ([WED-348](#))
 Shreekumar, Devika, S19 ([OS-018](#)), S305 ([TOP-169](#))
 Shrestha, Ananta, S158 ([THU-052](#)), S167 ([THU-078](#))
 Shringarpure, Reshma, S8 ([LBO-002](#)), S612 ([SAT-220-YI](#))
 Shrivastava, Rahul, S617 ([SAT-239](#))
 Shrwani, Khalid, S172 ([THU-090](#))
 Shu, Bin, S395 ([SAT-478](#)), S442 ([THU-462](#)), S625 ([FRI-021](#))
 Shu, Jianfen, S18 ([OS-016](#)), S80 ([LBP-006](#)), S312 ([THU-105](#))
 Shukla, Aakash, S476 ([FRI-231](#))
 Shukla, Akash, S158 ([THU-052](#)), S167 ([THU-078](#)), S554 ([WED-327](#))
 Shulman, Nancy, S78 ([LBP-001](#)), S352 ([SAT-536](#)), S808 ([WED-366](#)), S811 ([WED-374](#))
 Shumbayawonda, Elizabeth, S21 ([OS-020](#)), S524 ([WED-238](#)), S535 ([WED-268](#))
 Shun, Estie Hon-Kiu, S757 ([WED-420](#))
 Shung, Dennis, S731 ([SAT-338-YI](#))
 Shu, Xinyu, S83 ([LBP-013](#))
 Shwaartz, Chaya, S381 ([SAT-037](#)), S381 ([SAT-039](#))
 Sia, Daniela, S24 ([OS-026-YI](#))
 Sicuro, Chiara, S389 ([SAT-060](#))
 Sidali, Sabrina, S50 ([OS-077](#)), S54 ([OS-084-YI](#)), S452 ([THU-492](#))
 Siddiqi, Harris, S522 ([WED-235](#)), S543 ([WED-291](#))
 Siddiqui, Mohammad, S1 ([GS-001](#)), S364 ([WED-027](#)), S544 ([WED-294](#))
 Siddiqui, Mohammad Shadab, S366 ([TOP-004](#))
 Siddle, Matthew, S588 ([THU-271-YI](#))
 Sidiropoulos, Orestis, S454 ([THU-495](#))
 Siebler, Juergen, S327 ([THU-137](#))
 Siebner, Hartwig, S555 ([WED-331-YI](#))
 Siegel, Anne, S64 ([OS-102](#))
 Sierra, Patricia, S83 ([LBP-012](#))
 Sighinolfi, Pamela, S438 ([THU-446](#))
 Sigon, Giordano, S466 ([FRI-207-YI](#)), S470 ([FRI-215-YI](#)), S495 ([FRI-286](#))
 Sigrist, Sarah, S502 ([FRI-315](#))
 Siguencia, Jessica, S835 ([THU-372-YI](#))
 Sigüenza, Rebeca, S71 ([OS-116](#)), S596 ([THU-296](#))
 Sigurdarson, Sigurdur S., S328 ([THU-151](#))
 Si, Hooi Ling, S209 ([FRI-053](#))
 Sikadi, Beaudelaire, S224 ([FRI-101-YI](#))
 Sikaroodi, Masoumeh, S434 ([FRI-530](#))
 Siksik, Jean Michel, S512 ([WED-206](#))
 Silberstein, Francesca Ceccherini, S59 ([OS-094](#)), S772 ([FRI-392-YI](#)), S798 ([WED-399-YI](#))
 Siler, Scott, S517 ([WED-219](#))
 Silva, Andres Varela, S598 ([THU-302](#)), S599 ([THU-304](#))
 Silva, Desiree, S519 ([WED-225](#))
 Silva dos Santos, Mariana, S750 ([SAT-404](#))
 Silvain, Christine, S6 ([GS-010](#)), S387 ([SAT-052](#)), S444 ([THU-466](#))
 Silva, João, S681 ([WED-481](#))
 Silva, Joel, S52 ([OS-080](#))
 Silva-Junior, Gilberto, S180 ([WED-071](#))
 Silva, Luis Felipe, S618 ([SAT-242](#))
 Silva, Mário Jorge, S681 ([WED-481](#)), S834 ([THU-370](#))
 Silva-Ruiz, María del Pilar, S316 ([THU-114](#))
 Silva, Silvia Gomes, S362 ([WED-015](#))
 Silveira, Marina, S20 ([OS-019](#))
 Silvestri, Annalisa De, S73 ([OS-120](#))
 Silvestri, Laura, S571 ([THU-218](#))
 Silvestri, Patrizia, S368 ([SAT-009](#))
 Silvey, Scott, S60 ([OS-095](#))
 Sim, Alyssa, S826 ([THU-406](#))
 Simanjuntak, Yogy, S42 ([OS-061](#))
 Simão, André, S286 ([WED-558](#)), S358 ([SAT-554-YI](#)), S536 ([WED-271](#))
 Sim, Benedix, S139 ([SAT-256](#)), S147 ([SAT-281](#)), S366 ([TOP-004](#)), S540 ([WED-282](#))
 Simbrunner, Benedikt, S85 ([LBP-016](#)), S156 ([TOP-097-YI](#)), S165 ([THU-071](#)), S166 ([THU-075-YI](#)), S186 ([WED-089-YI](#)), S197 ([WED-122-YI](#)), S198 ([WED-125](#)), S243 ([SAT-086-YI](#)), S250 ([SAT-105](#)), S250 ([SAT-106](#)), S251 ([SAT-111](#)), S253 ([SAT-118](#)), S255 ([SAT-122](#)), S257 ([SAT-128](#)), S267 ([THU-540](#)), S621 ([FRI-009-YI](#)), S717 ([WED-171](#))
 Simeone, Irene, S88 ([LBP-023](#))
 Simin, Teo, S637 ([THU-046](#))
 Simioni, Paolo, S237 ([TOP-061-YI](#))
 Sim, Kevin, S497 ([FRI-295](#))
 Simoes, Mélanie, S720 ([WED-178](#)), S784 ([FRI-425](#))
 Simone, Fabio, S252 ([SAT-113](#))
 Simone, Giorgia De, S35 ([OS-048](#))
 Simone, Loredana, S96 ([LBP-038](#)), S215 ([FRI-078-YI](#)), S306 ([THU-093](#)), S332 ([THU-161](#))
 Simone, Paolo De, S456 ([THU-502](#))
 Simonetto, Douglas, S30 ([OS-038-YI](#)), S199 ([TOP-062](#)), S200 ([TOP-064-YI](#)), S242 ([SAT-082](#))
 Simón, María, S682 ([WED-483](#))
 Simonotti, Nicolò, S438 ([TOP-506](#))
 Simonsen, Hans Erling, S795 ([WED-394](#))
 Simonsson, Christian, S530 ([WED-255-YI](#)), S532 ([WED-259](#))
 Simón-Talero, Macarena, S705 ([WED-129](#))
 Simpson, Kara, S265 ([THU-535-YI](#))
 Simpson, Kenneth J., S9 ([LBO-004](#)), S89 ([LBP-026](#))
 Sims, Karen D, S26 ([OS-031](#))
 Sims, Karen D., S809 ([WED-371](#))
 Simu, Andreea, S324 ([THU-131](#)), S446 ([THU-473](#))
 Sim, Yu Ki, S401 ([SAT-495](#))
 Sinakos, Emmanouil, S798 ([WED-403](#))
 Sinclair, Marie, S9 ([LBO-004](#)), S89 ([LBP-026](#)), S400 ([SAT-492](#)), S402 ([SAT-496](#)), S547 ([WED-299](#))
 Singal, Amit, S51 ([OS-078-YI](#)), S200 ([TOP-063](#)), S443 ([THU-464](#)), S445 ([THU-471-YI](#))
 Singal, Ashwani K., S84 ([LBP-014](#)), S643 ([SAT-438](#))
 Singanayagam, Arjuna, S352 ([SAT-535-YI](#)), S523 ([WED-236-YI](#))
 Singer, Alexander, S643 ([SAT-436](#))
 Singer, Amanda, S667 ([WED-447](#)), S769 ([FRI-383](#))
 Singer, Michael, S426 ([FRI-495](#))
 Singh, Ankita, S554 ([WED-327](#))

Author Index

- Singh, Ayaskant, S158 (THU-052), S167 (THU-078)
- Singh, Brijesh Kumar, S55 (OS-085), S502 (FRI-316)
- Singh, Harminder, S643 (SAT-436)
- Singh, Jennifer M., S807 (WED-364), S809 (WED-370)
- Singh, Kuldeep, S693 (FRI-151)
- Singh, Parul, S177 (WED-058-YI), S188 (WED-095-YI)
- Singh, Pratishtha, S545 (WED-295-YI)
- Singh, Ravinder, S294 (SAT-155)
- Singh, Rita, S283 (WED-549)
- Singh, Satender, S279 (WED-535-YI)
- Singh, Satender Pal, S164 (THU-070)
- Singh, Shashank, S239 (SAT-070)
- Singh, Shivaram Prasad, S163 (THU-067), S285 (WED-554), S475 (FRI-231), S488 (FRI-266-YI)
- Singh, Shraddha, S137 (SAT-249)
- Singh, Shreya, S158 (THU-051)
- Singh, Swati, S6 (GS-008)
- Singh, Virendra, S152 (SAT-295), S158 (THU-051), S158 (THU-052), S167 (THU-078), S217 (FRI-082)
- Siniscalchi, Antonio, S9 (LBO-004), S89 (LBP-026)
- Sinn, Dong Hyun, S402 (SAT-497), S774 (FRI-396)
- Sinner, Friedrich, S52 (OS-079-YI), S69 (OS-112-YI), S440 (THU-457)
- Sinnreich, Magdalena Filipowicz, S291 (TOP-150-YI)
- Sint Nicolaas, Jerome, S309 (THU-100)
- Sipeki, Nora, S313 (THU-106-YI)
- Siribelli, Alessia, S824 (THU-402)
- Siripon, Nipaporn, S196 (WED-120)
- Sironi, Laura, S580 (THU-245)
- Sironi, Sandro, S439 (THU-447)
- Sisó-Almirall, Antoni, S120 (SAT-325)
- Si, Tengfei, S198 (WED-124), S359 (SAT-556-YI)
- Sitko, Marek, S821 (THU-389)
- Sittner, Richard, S161 (THU-057-YI)
- Situ, Jianwen, S757 (WED-420)
- Sivell, Chris, S350 (TOP-553)
- Sjöberg, Daniel, S12 (OS-002)
- Skinazi, Florence, S640 (SAT-430)
- Skinner, Derek, S645 (SAT-440)
- Skladany, Lubomir, S379 (SAT-033), S539 (WED-279)
- Skoura, Lemonia, S196 (WED-121-YI)
- Skovgaard, Emilie, S579 (THU-243), S626 (FRI-027), S737 (SAT-370)
- Skröder, Helena, S37 (OS-052), S464 (FRI-201)
- Skrypnyk, Igor, S121 (SAT-327)
- Skrypnyk, Roman, S121 (SAT-327)
- Skurla, Viktoria, S155 (SAT-305)
- Slaets, Leen, S79 (LBP-005)
- Sleiman, Marwan, S80 (LBP-006), S339 (THU-178)
- Slinkov, Dmitri, S11 (LBO-006)
- Slits, Florence, S189 (WED-101-YI)
- Slooter, Charlotte, S18 (OS-015)
- Slovic, Nevena, S42 (OS-061)
- Smets, Francoise, S353 (SAT-537)
- Smets, Lena, S16 (OS-012-YI), S125 (TOP-328-YI)
- Šmid, Václav, S539 (WED-280)
- Smirne, Carlo, S409 (SAT-524)
- Smith, Belinda, S679 (WED-477-YI)
- Smith, Colette, S661 (WED-432), S672 (WED-462), S684 (WED-491), S688 (WED-500)
- Smith, Daniel, S466 (FRI-207-YI), S474 (FRI-226), S482 (FRI-248-YI)
- Smith, David, S564 (THU-198), S727 (TOP-357), S728 (TOP-358-YI)
- Smither, Allison R., S326 (THU-135)
- Smith, Helen T., S485 (FRI-258)
- Smith, Hollie, S630 (THU-015-YI)
- Smith, Jeff, S88 (LBP-022)
- Smith, John, S11 (LBO-006)
- Smith, Patrick, S811 (WED-374)
- Smith, Rachel, S290 (TOP-147), S310 (THU-101), S659 (WED-428-YI), S765 (FRI-374-YI)
- Smit, Marieke, S347 (FRI-549-YI), S573 (THU-224)
- Smit, Theresa, S753 (SAT-413)
- Smolinska, Agnieszka, S195 (WED-117)
- Smout, Ayla, S267 (THU-541)
- Smyk, Wiktor, S713 (WED-161-YI)
- Smythe, Jon, S101 (LBP-046)
- Snabel, Jessica, S597 (THU-297)
- Sng, Wei Kwan, S525 (WED-242)
- Snir, Tom, S268 (THU-547), S295 (SAT-158)
- Snopkova, Svatava, S756 (SAT-422)
- Soardo, Giorgio, S238 (SAT-068), S459 (TOP-301), S704 (TOP-144-YI)
- Sobala-Szczygieł, Barbara, S821 (THU-389)
- Sobenko, Natalia, S336 (THU-170-YI), S342 (THU-185)
- Sobesky, Rodolphe, S718 (WED-174)
- Sobotka, Daniel, S250 (SAT-106)
- Socha, Łukasz, S821 (THU-389)
- Socha, Piotr, S328 (THU-152-YI), S374 (SAT-021), S578 (THU-238), S712 (WED-160), S713 (WED-161-YI)
- Soehnlein, Oliver, S133 (THU-338)
- Soe, Phymar, S659 (WED-429), S686 (WED-495)
- Soffredini, Roberta, S73 (OS-120), S781 (FRI-412)
- Sogni, Philippe, S670 (WED-455), S741 (SAT-380), S760 (FRI-361)
- Sohn, BoHwa, S68 (OS-111)
- Sohn, Joo Hyun, S148 (SAT-284), S473 (FRI-223), S553 (WED-323), S654 (SAT-465)
- Sohn, Won, S223 (FRI-099), S517 (WED-221), S766 (FRI-375)
- Soin, Arvinder Singh, S9 (LBO-004), S89 (LBP-026), S375 (SAT-023)
- Sokal, Etienne, S172 (THU-092), S353 (SAT-537)
- Solà, Elsa, S30 (OS-038-YI), S160 (THU-056), S176 (WED-055), S199 (TOP-062), S200 (TOP-064-YI)
- Soldà, Caterina, S395 (SAT-477-YI), S446 (THU-472-YI)
- Solé, Cristina, S29 (OS-037), S30 (OS-038-YI), S45 (OS-068), S141 (SAT-262), S199 (TOP-062), S200 (TOP-064-YI), S233 (FRI-126), S829 (THU-418)
- Solé, Gemma, S829 (THU-418)
- Soler, Alexandre, S53 (OS-081), S255 (SAT-123), S444 (THU-467-YI)
- Soler, Helena Martí, S39 (OS-056-YI)
- Soleri, Matteo, S404 (SAT-502-YI), S406 (SAT-514), S497 (FRI-294)
- Soler, Maria Rodriguez, S365 (TOP-002)
- Soliman, Michael, S709 (WED-138)
- Soliman, Riham, S549 (WED-315), S560 (WED-342), S624 (FRI-020), S673 (WED-463), S780 (FRI-410), S820 (THU-383)
- Solini, Anna, S619 (SAT-245)
- Sollano, Jose, S158 (THU-052), S167 (THU-078)
- Solomon, Daniel, S481 (FRI-245)
- Somasundaram, Ashwin, S394 (SAT-476)
- Somers, Nicky, S311 (THU-102-YI), S442 (THU-463)
- Sommacale, Daniele, S413 (FRI-456), S453 (THU-494)
- Sommadosi, Jean-Pierre, S749 (SAT-402), S753 (SAT-411), S753 (SAT-412)
- Somvanshi, Rajesh, S666 (WED-443-YI)
- Sonavane, Amey, S219 (FRI-088)
- Sonderup, Mark, S18 (OS-016)
- Song, Baojun, S803 (WED-412)
- Song, Byeong Geun, S402 (SAT-497)
- Song, Jeong Eun, S788 (FRI-433)
- Song, Jiangao, S300 (SAT-175), S301 (SAT-177)
- Song, Jieun, S564 (THU-198)
- Song, Jinlong, S447 (THU-475)
- Song, Peng, S566 (THU-201-YI)
- Song, PeXuan, S432 (FRI-525)
- Song, Rui, S344 (THU-191), S747 (SAT-395)
- Song, Seol Hee, S286 (WED-557)
- Song, Sherlot Juan, S475 (FRI-227), S510 (WED-198)
- Song, Sungmin, S78 (LBP-002)
- Song, Xin, S430 (FRI-517), S437 (TOP-504)
- Song, Yuxuan, S769 (FRI-382)
- Son, MinKook, S501 (FRI-306)
- Sonnenberg, Jannik, S170 (THU-087)
- Sonneveld, Milan J., S380 (SAT-035), S758 (TOP-401-YI), S761 (FRI-363-YI), S763 (FRI-367), S764 (FRI-372)
- Sood, Ajit, S158 (THU-052), S167 (THU-078)
- Sood, Siddharth, S338 (THU-177-YI), S400 (SAT-492), S632 (THU-021)
- Sophie, Ayciriex, S49 (OS-074)
- Sorah, Jonathan, S394 (SAT-476)
- Sordo, David, S337 (THU-172)
- Soresi, Maurizio, S601 (TOP-193)

- Soret, Pierre-Antoine, S313 (THU-107), S326 (THU-136), S712 (WED-158-YI)
- Sorg, Allison, S11 (LBO-006)
- Soria, Alessandro, S666 (WED-446)
- Soria, Anna, S13 (OS-005-YI), S160 (THU-056), S176 (WED-055), S468 (FRI-211), S471 (FRI-219-YI), S503 (TOP-241-YI), S541 (WED-284-YI), S711 (WED-155), S721 (WED-181)
- Soria, Isabel Carmona, S559 (WED-341), S717 (WED-172)
- Soria, Leandro, S698 (FRI-166)
- Soriano, German, S29 (OS-037), S355 (SAT-543), S700 (FRI-171)
- Sorino, Joana, S123 (SAT-334)
- Soror, Noha, S51 (OS-078-YI)
- Sorrentino, Giovanni, S699 (FRI-167-YI)
- Sorz-Nechay, Thomas, S186 (WED-089-YI), S197 (WED-122-YI), S198 (WED-125)
- Sorz, Thomas, S267 (THU-540)
- Sotiropoulos, Christos, S830 (THU-419)
- Sotty, Jules, S729 (TOP-360-YI)
- Souaré, Abdoulaye, S743 (SAT-387)
- Soua, Sabrine, S270 (THU-554)
- Soubrane, Olivier, S451 (THU-487-YI)
- Soufidi, Khalida, S314 (THU-109), S319 (THU-120-YI), S327 (THU-138)
- Soulard, Valérie, S729 (TOP-360-YI)
- Soule, Benjamin, S460 (TOP-309)
- Souleiman, Roni, S350 (SAT-532-YI), S351 (SAT-533), S353 (SAT-538-YI)
- Soulier, Alexandre, S784 (FRI-425)
- Sousa, Jacquelyn, S564 (THU-198), S727 (TOP-357)
- Sousa, María Ángeles Jiménez, S741 (SAT-379)
- Sousa-Martin, Jose Manuel, S316 (THU-114)
- Soussan, Michael, S50 (OS-077), S413 (FRI-456)
- Soussan, Patrick, S729 (TOP-360-YI)
- Soustre, Tanguy, S22 (OS-022)
- Souza de Oliveira, Juliana, S619 (SAT-248)
- Souza, Matheus, S483 (FRI-254), S616 (SAT-237), S618 (SAT-244)
- Sow, Amadou-Khalilou, S369 (SAT-010)
- So, Young Ho, S532 (WED-260)
- Sozzi, Vitina, S740 (SAT-377)
- Spaan, Michelle, S763 (FRI-367)
- Spada, Marco, S698 (FRI-166)
- Spaes, Ylang, S54 (OS-084-YI)
- Spagnuolo, Vincenzo, S824 (THU-402)
- Spalinger, Francine, S98 (LBP-041)
- Spalinger, Marianne Rebecca, S56 (OS-086-YI)
- Spanier, B.W. Marcel, S317 (THU-115-YI)
- Sparchez, Zeno, S409 (SAT-525)
- Spaulding, Aaron, S146 (SAT-279)
- Spearman, C Wendy, S18 (OS-016)
- Spedtsberg, Ida Ziegler, S153 (SAT-298), S466 (FRI-206-YI), S623 (FRI-017)
- Spegman, Doug, S641 (SAT-432)
- Spencer, Janine, S519 (WED-225)
- Sperl, Jan, S703 (TOP-141), S708 (WED-135-YI)
- Spiers, Harry, S81 (LBP-008)
- Spiezia, Chiara, S554 (WED-325-YI)
- Spiezia, Luca, S612 (SAT-219)
- Spigaroli, Margherita, S364 (WED-022)
- Spinelli, Pietro, S58 (OS-090)
- Spinetti, Angiola, S666 (WED-446)
- Sposito, Carlo, S70 (OS-114), S375 (SAT-022), S438 (TOP-506)
- Spraul, Anne, S718 (WED-174)
- Sprengers, Dave, S380 (SAT-035)
- Sprengers, Dirk, S730 (SAT-337)
- Sprinkart, Alois Martin, S258 (SAT-130)
- Sprinzak, David, S697 (FRI-163-YI)
- Sprinzl, Kathrin, S100 (LBP-044)
- Squarzone, Paola, S326 (THU-136)
- Squeo, Francesco, S96 (LBP-038), S306 (THU-093)
- Sridhar, Siddharth, S757 (WED-420)
- Srinivasan, Parthi, S128 (THU-320-YI), S281 (WED-542-YI), S388 (SAT-057)
- Sriphoosanaphan, Supachaya, S188 (WED-099-YI), S196 (WED-120), S749 (SAT-403)
- Sripongpun, Pimsiri, S396 (SAT-480-YI), S410 (SAT-529), S447 (THU-475)
- Srisoonthorn, Nunthiya, S196 (WED-120)
- S, Sharath, S149 (SAT-290-YI)
- S, Sudhindran, S9 (LBO-004)
- Stadlbauer, Vanessa, S229 (FRI-115), S284 (WED-551), S383 (SAT-042)
- Staels, Bart, S171 (THU-088), S191 (WED-105), S577 (THU-234)
- Stafford, Nina, S639 (SAT-427-YI)
- Stahl, Klaus, S115 (TOP-346-YI)
- Stalder, Anna, S291 (TOP-150-YI)
- Stallmach, Andreas, S178 (WED-060-YI), S259 (SAT-135)
- Staltner, Raphaela, S132 (THU-334)
- Stamouli, Marilena, S110 (FRI-335), S178 (WED-068-YI), S185 (WED-088-YI), S192 (WED-110), S227 (FRI-112)
- Standley, Stephany, S693 (FRI-151)
- Stanford-Moore, Adam, S571 (THU-215), S585 (THU-261)
- Stankevic, Evelina, S47 (OS-072-YI)
- Stardeleva, Kalina Grivcheva, S172 (THU-092)
- Stärkel, Peter, S151 (SAT-293-YI)
- Stashek, Kristen, S411 (SAT-530)
- Stättermayer, Albert Friedrich, S243 (SAT-086-YI), S335 (THU-166), S706 (WED-131-YI), S717 (WED-171), S725 (WED-190), S773 (FRI-394)
- Stauber, Rudolf E., S69 (OS-112-YI), S383 (SAT-042)
- Staudinger, Thomas, S340 (THU-180)
- Staufer, Katharina, S171 (THU-088)
- Stebbins, Jeffrey, S300 (SAT-175)
- Stebel, Marco, S701 (FRI-172)
- Steel, Alison, S297 (SAT-165-YI)
- Steenkiste, Christophe Van, S321 (THU-123-YI), S581 (THU-249)
- Stefan, Chris, S298 (SAT-167-YI)
- Stefanetti, Renae, S297 (SAT-165-YI)
- Stefanini, Benedetta, S395 (SAT-477-YI), S446 (THU-472-YI), S449 (THU-481-YI)
- Stefanini, Bernardo, S51 (OS-078-YI), S390 (TOP-509-YI), S395 (SAT-477-YI), S445 (THU-471-YI), S446 (THU-472-YI)
- Ștefănescu, Horia, S144 (SAT-273-YI), S151 (SAT-294), S183 (WED-082), S238 (SAT-068), S409 (SAT-525), S521 (WED-232-YI), S555 (WED-332)
- Stefano, Marianonietta Di, S777 (FRI-405)
- Steger, Maximilian, S187 (WED-092)
- Steigerwald, Sophia, S32 (OS-041-YI)
- Steindl, Carina, S191 (WED-106)
- Steiniger, Hilde, S603 (SAT-195)
- Steinhauser, Toon, S259 (SAT-134), S540 (WED-281-YI)
- Stein, Lance, S8 (LBO-003), S9 (LBO-004), S89 (LBP-026), S242 (SAT-082)
- Steinmann, Eike, S58 (OS-092), S94 (LBP-034), S730 (TOP-369), S732 (SAT-341)
- Stein, Stephanie, S350 (SAT-531-YI)
- Stella, Leonardo, S452 (THU-492)
- Stella, Sonia, S227 (FRI-110), S344 (THU-190)
- Stenbäck, Joakim, S754 (SAT-414)
- Stender, Stefan, S529 (WED-250-YI)
- Stengel, Sven, S178 (WED-060-YI), S351 (SAT-534)
- Stenzinger, Albrecht, S23 (OS-025-YI)
- Stepanova, Maria, S101 (LBP-047), S465 (FRI-202), S476 (FRI-232), S496 (FRI-291), S520 (WED-230), S572 (THU-221), S643 (SAT-438), S652 (SAT-459)
- Stepanova, Tatyana, S1 (GS-002), S92 (LBP-029), S758 (TOP-400), S764 (FRI-371), S794 (WED-392), S796 (WED-395)
- Stéphanie, Chanon, S49 (OS-074)
- Stephant, Sophie, S463 (FRI-197)
- Stephens, Camilla, S45 (OS-067), S103 (TOP-350-YI)
- Steppich, Katja, S353 (SAT-538-YI)
- Sterling, Richard, S1 (GS-001)
- Stern, Christiane, S28 (OS-034), S52 (OS-080), S550 (WED-317)
- Sterneck, Martina, S115 (TOP-346-YI), S374 (SAT-021)
- Stevens, Chris, S141 (SAT-261)
- Stevens, Lianne, S94 (LBP-033)
- Stevenson, Heather, S823 (THU-396)
- Stewart, Catherine, S724 (WED-189)
- Stewart, Stephen, S450 (THU-485-YI)
- Sticova, Eva, S21 (OS-020)
- Stiess, Michael, S70 (OS-115), S311 (THU-103)
- Stigliano, Rosa, S380 (SAT-034)
- Stillhard, Roman, S502 (FRI-315)
- Stine, Jonathan, S631 (THU-016)
- Stinson, Sara, S47 (OS-072-YI), S466 (FRI-206-YI)
- Stirnemann, Guido, S703 (TOP-141), S708 (WED-135-YI)

Author Index

- Stocco, Matteo, S700 ([FRI-171](#))
 Stockdale, Alexander J, S676 ([WED-471](#))
 Stockdale, Alexander J., S760 ([TOP-417](#))
 Stöckert, Petra, S115 ([TOP-346-YI](#))
 Stockmans, Gert, S604 ([SAT-196](#))
 Stojakovic, Tatjana, S296 ([SAT-161](#))
 Stoker, Jaap, S315 ([THU-112-YI](#))
 Stokman, Geurt, S575 ([THU-231](#)), S595 ([THU-294](#))
 Stolk, Jan, S703 ([TOP-141](#)), S708 ([WED-135-YI](#)), S720 ([WED-179-YI](#)), S721 ([WED-182](#))
 Stoll, Janis M., S715 ([WED-166](#))
 Stone, John, S710 ([WED-152](#))
 Stopfer, Katharina, S621 ([FRI-009-YI](#)), S717 ([WED-171](#))
 Stopforth, Richard, S81 ([LBP-008](#))
 Storf, Holger, S170 ([THU-087](#))
 Storm, Gert, S565 ([THU-200-YI](#))
 Storni, Federico, S373 ([SAT-019](#))
 Stoycheva, Antitsa, S564 ([THU-198](#))
 Strada, Angelo, S409 ([SAT-524](#)), S627 ([FRI-028](#))
 Strandberg, Rickard, S40 ([OS-057-YI](#))
 Strasser, Michael, S773 ([FRI-394](#))
 Strasser, Simone, S8 ([LBO-003](#)), S78 ([LBP-001](#)), S380 ([SAT-036-YI](#)), S400 ([SAT-492](#)), S401 ([SAT-495](#))
 Straub, Beate, S461 ([FRI-194-YI](#))
 Stray, Kirsten, S812 ([WED-377](#))
 Strazzabosco, Mario, S695 ([FRI-155](#)), S697 ([FRI-162](#))
 Street, Karen, S633 ([THU-029](#))
 Street, Oliver, S650 ([SAT-454-YI](#))
 Streinu-Cercel, Adrian, S1 ([GS-002](#)), S764 ([FRI-371](#)), S796 ([WED-395](#))
 Streinu-Cercel, Anca, S75 ([OS-127](#))
 Stricker, Bruno, S606 ([SAT-200-YI](#))
 Strnad, Pavel, S32 ([OS-041-YI](#)), S104 ([TOP-352](#)), S134 ([THU-340-YI](#)), S356 ([SAT-545](#)), S696 ([FRI-161](#)), S698 ([FRI-164](#)), S703 ([TOP-141](#)), S708 ([WED-135-YI](#)), S709 ([WED-138](#)), S724 ([WED-188](#))
 Ströbel, Anton, S423 ([FRI-486](#))
 Ströbel, Simon, S590 ([THU-278](#))
 Strock, Paul, S640 ([SAT-430](#))
 Stroffolini, Tommaso, S817 ([THU-378](#))
 Strömberg, Lucia Gonzales, S754 ([SAT-414](#))
 Strona, Silvia, S332 ([THU-161](#))
 Stroschia, Martina, S439 ([THU-454](#))
 Struik, Dicky, S347 ([FRI-549-YI](#)), S573 ([THU-224](#))
 Stuempflen, Marlene, S719 ([WED-175](#))
 Sturm, Ekkehard, S115 ([TOP-346-YI](#))
 Stvilia, Ketevan, S691 ([WED-515](#))
 Suarez, Armando Andres Roca, S58 ([OS-091](#))
 Suárez, Francisco, S365 ([TOP-002](#))
 Suárez, Maria Unceta, S694 ([FRI-153](#))
 Subash, Gupta, S368 ([SAT-009](#))
 Subhan, Amna, S158 ([THU-052](#))
 Subhani, Mohsan, S148 ([SAT-285-YI](#))
 Subias, Silvia, S424 ([FRI-491-YI](#))
 Subic-Levrero, Miroslava, S802 ([WED-410](#))
 Subudhi, P. Debishree, S274 ([WED-522-YI](#))
 Su, Chien-Wei, S398 ([SAT-484](#)), S663 ([WED-438-YI](#))
 Suda, Goki, S506 ([TOP-288](#)), S828 ([THU-413](#))
 Suddle, Abid, S388 ([SAT-057](#)), S709 ([WED-137-YI](#))
 Sudhindran, S, S31 ([OS-039](#))
 Sudhindran, Surendran, S89 ([LBP-026](#))
 Su, Donghan, S536 ([WED-272](#))
 Suehiro, Tomoyuki, S512 ([WED-203](#)), S542 ([WED-286](#))
 Sugahara, Go, S128 ([THU-319](#)), S288 ([FRI-540](#))
 Sugimoto, Rie, S42 ([OS-062](#))
 Sugiyama, Masaya, S736 ([SAT-365](#))
 Su, Jinpeng, S699 ([FRI-170](#)), S728 ([TOP-359-YI](#))
 Sukali, Gloria, S753 ([SAT-413](#))
 Su, Kim, S265 ([THU-535-YI](#))
 Suki, Mohammed, S563 ([THU-194](#)), S779 ([FRI-408](#))
 Suk, Ki Tae, S286 ([WED-557](#)), S602 ([TOP-216](#))
 Sukowati, Caecilia, S429 ([FRI-516-YI](#)), S792 ([FRI-444](#))
 Suksawatamnuay, Sirinporn, S196 ([WED-120](#)), S221 ([FRI-093](#)), S258 ([SAT-129](#)), S749 ([SAT-403](#))
 Sulejova, Karolina, S379 ([SAT-033](#)), S539 ([WED-279](#))
 Sulek, Karolina, S47 ([OS-072-YI](#))
 Sulkowski, Mark S., S813 ([WED-379](#))
 Sulpice, Thierry, S13 ([OS-006](#)), S597 ([THU-299](#))
 Sultana, Ashrafi, S742 ([SAT-382](#))
 Sultanik, Philippe, S207 ([FRI-050-YI](#)), S211 ([FRI-059](#)), S214 ([FRI-075](#)), S218 ([FRI-087](#)), S222 ([FRI-094-YI](#)), S222 ([FRI-095](#)), S239 ([SAT-071](#)), S441 ([THU-458](#))
 Su, Man, S161 ([THU-058](#))
 Sumida, Yoshio, S512 ([WED-203](#)), S537 ([WED-273](#))
 Su, Minghua, S209 ([FRI-053](#))
 Su, Moony, S186 ([WED-090](#))
 Sun, Beicheng, S403 ([SAT-499](#))
 Sun, Chao, S220 ([FRI-091](#)), S526 ([WED-246](#))
 Sun, Dan-Qin, S488 ([FRI-267](#))
 Sundaram, Vinay, S9 ([LBO-004](#)), S89 ([LBP-026](#))
 Sundelin, Jeanna, S93 ([LBP-031](#))
 Sun, Di, S59 ([OS-093](#))
 Sun, Frank, S304 ([SAT-185](#))
 Sung, Ji Hyun, S506 ([TOP-288](#))
 Sung, Pil Soo, S264 ([THU-530](#))
 Sun, Hongze, S622 ([FRI-010](#))
 Sun, Jian, S95 ([LBP-037](#))
 Sun, Jihan, S422 ([FRI-485](#))
 Sun, Jing, S59 ([OS-093](#))
 Sun, Kai-Hui, S729 ([TOP-368](#))
 Sun, Peng, S197 ([WED-122-YI](#)), S198 ([WED-125](#)), S267 ([THU-540](#)), S589 ([THU-274](#))
 Sun, Wei, S234 ([FRI-129](#))
 Sun, Xiaofeng, S785 ([FRI-428](#))
 Sun, Xin, S762 ([FRI-366](#))
 Sun, YiDi, S59 ([OS-093](#))
 Sun, Ying, S124 ([SAT-336](#))
 Sun, Yingji, S114 ([TOP-344-YI](#))
 Sun, Yong, S269 ([THU-549](#))
 Sun, Yu, S357 ([SAT-548](#))
 Su, Pei-Yuan, S26 ([OS-031](#))
 Surabattula, Rambabu, S265 ([THU-534-YI](#)), S363 ([WED-021](#)), S585 ([THU-260](#))
 Surace, Lidia, S619 ([SAT-245](#))
 Surace, Lorenzo, S96 ([LBP-038](#)), S306 ([THU-093](#))
 Sureau, Camille, S729 ([TOP-360-YI](#))
 Sureshan, Shruti, S274 ([WED-522-YI](#)), S279 ([WED-535-YI](#))
 Surguladze, Sophia, S664 ([WED-439](#)), S675 ([WED-468](#)), S677 ([WED-473](#)), S825 ([THU-404](#))
 Suschak, John, S515 ([WED-212](#)), S517 ([WED-219](#)), S529 ([WED-251](#))
 Sussman, Norman, S8 ([LBO-003](#))
 Sutter, Olivier, S68 ([OS-110](#)), S413 ([FRI-456](#)), S441 ([THU-459-YI](#)), S451 ([THU-487-YI](#))
 Suttichaimongkol, Tanita, S3 ([GS-005](#))
 Tutti, Salvatore, S421 ([FRI-479-YI](#))
 Su, Tung-Hung, S399 ([SAT-486](#))
 Suvitaival, Tommi, S47 ([OS-072-YI](#))
 Su, Wei-Wen, S832 ([THU-365](#))
 Suykens, Janne, S631 ([THU-020-YI](#))
 Su, Zemin, S104 ([TOP-352](#))
 Suzuki, Ayako, S55 ([OS-085](#)), S502 ([FRI-316](#))
 Suzuki, Mizuki, S502 ([FRI-316](#))
 Svačinka, Radek, S756 ([SAT-422](#))
 Svanberg, Ann Karin, S12 ([OS-002](#))
 Svegiati-Baroni, Gianluca, S215 ([FRI-078-YI](#))
 Svegliati-Baroni, Gianluca, S332 ([THU-161](#)), S395 ([SAT-477-YI](#)), S446 ([THU-472-YI](#)), S544 ([WED-293](#))
 Svicher, Valentina, S28 ([OS-034](#)), S59 ([OS-094](#)), S772 ([FRI-392-YI](#)), S777 ([FRI-405](#)), S791 ([FRI-442](#)), S798 ([WED-399-YI](#))
 Swain, Mark G, S19 ([OS-018](#)), S305 ([TOP-169](#))
 Swain, Mark G., S80 ([LBP-006](#)), S538 ([WED-274](#))
 Swaminathan, Akhilesh, S822 ([THU-391-YI](#))
 Swann, Rachael, S783 ([FRI-423](#))
 Swaroop, Shekhar, S201 ([TOP-065](#))
 Świdarska, Jolanta, S713 ([WED-161-YI](#))
 Swier, Rachel, S393 ([SAT-472](#))
 Swift, Brandon, S476 ([FRI-232](#))
 Swift, Lisa, S81 ([LBP-008](#))
 Syanda, Adam, S298 ([SAT-167-YI](#))
 Syeda, Zehra, S695 ([FRI-155](#)), S697 ([FRI-162](#))
 Sylvie, Bin, S508 ([WED-194](#))
 Symons, Julian, S564 ([THU-198](#)), S727 ([TOP-357](#)), S728 ([TOP-358-YI](#))

- Syn, Nicholas, S139 ([SAT-256](#)),
S147 ([SAT-281](#)), S366 ([TOP-004](#)),
S540 ([WED-282](#)), S565 ([THU-200-YI](#))
- Sypsa, Vana, S680 ([WED-478](#))
- Syricha, Antonia, S454 ([THU-495](#))
- Syutkin, Vladimir, S1 ([GS-002](#)),
S764 ([FRI-371](#))
- Szabo, Gyongyi, S131 ([THU-330](#))
- Szantova, Maria, S539 ([WED-279](#))
- Sze, Karen Man-Fong, S419 ([FRI-473](#))
- Taanman, Jan-Willem, S188 ([WED-099-YI](#))
- Tabak, Fehmi, S100 ([LBP-044](#)),
S805 ([WED-418](#))
- Tabala, Martine, S675 ([WED-469](#))
- Tabath, Martin, S412 ([FRI-454](#))
- Tabchouri, Nicolas, S705 ([WED-129](#))
- Tabernero, David, S662 ([WED-435](#)),
S741 ([SAT-381](#)), S746 ([SAT-393](#))
- Tacher, Vania, S413 ([FRI-456](#)),
S453 ([THU-494](#))
- Tacke, Frank, S25 ([OS-028](#)), S57 ([OS-088-YI](#)),
S203 ([FRI-040](#)), S259 ([SAT-135](#)),
S288 ([FRI-541-YI](#)), S298 ([SAT-170](#)),
S353 ([SAT-539-YI](#)), S359 ([SAT-555](#)),
S366 ([TOP-003-YI](#)), S414 ([FRI-457](#)),
S470 ([FRI-218](#)), S528 ([WED-248](#)),
S566 ([THU-201-YI](#)), S594 ([THU-291-YI](#)),
S649 ([SAT-452](#)), S716 ([WED-170](#)),
S793 ([WED-391](#))
- Tada, Toshifumi, S616 ([SAT-236](#))
- Tadjo, Thierry, S683 ([WED-486-YI](#))
- Tafader, Asiya, S60 ([OS-095](#))
- Taggart, David, S11 ([LBO-006](#))
- Taha, Amr, S673 ([WED-463](#))
- Tahata, Yuki, S506 ([TOP-288](#)),
S828 ([THU-413](#))
- Taher, Randa, S628 ([FRI-033](#)),
S789 ([FRI-437](#))
- Taib, Tarita, S552 ([WED-321](#))
- Tai, Chi-Ming, S832 ([THU-365](#))
- Tai, Dean, S56 ([OS-087](#)), S76 ([OS-124](#)),
S465 ([FRI-203](#)), S467 ([FRI-208](#)),
S515 ([WED-213](#))
- Tait, Dereck, S811 ([WED-375](#))
- Taiwo, Moyinoluwa, S131 ([THU-330](#))
- Tai, Yang, S241 ([SAT-077](#)), S622 ([FRI-010](#))
- Tai, Yunling, S197 ([WED-123](#))
- Takabatake, Hiroyuki, S122 ([SAT-332-YI](#))
- Takács, István, S72 ([OS-119](#))
- Takaguchi, Koichi, S248 ([SAT-101](#)),
S519 ([WED-226](#))
- Takahashi, Hirokazu, S147 ([SAT-281](#)),
S506 ([TOP-288](#)), S537 ([WED-273](#))
- Takahashi, Kazuhiro, S42 ([OS-062](#))
- Takai, Atsushi, S118 ([SAT-319](#))
- Takami, Taro, S828 ([THU-413](#))
- Takardaki, Anna, S196 ([WED-121-YI](#))
- Takawy, Marina, S84 ([LBP-014](#))
- Takawy, Mina, S740 ([SAT-377](#))
- Takebe, Takanori, S302 ([SAT-180](#))
- Takeda, S  n, S519 ([WED-226](#))
- Takehara, Tetsuo, S506 ([TOP-288](#)),
S828 ([THU-413](#))
- Takeuchi, Mamiko, S541 ([WED-283](#))
- Takis, Panteleimon, S282 ([WED-546](#))
- Takkenberg, R. Bart, S30 ([OS-038-YI](#)),
S199 ([TOP-062](#)), S200 ([TOP-064-YI](#)),
S204 ([FRI-043](#)), S208 ([FRI-053](#)),
S213 ([FRI-074-YI](#)), S758 ([TOP-401-YI](#)),
S763 ([FRI-367](#))
- Tak, Won Young, S3 ([GS-005](#)),
S457 ([THU-516](#))
- Talafu, Tangnuer, S783 ([FRI-419](#))
- Talal, Andrew, S670 ([WED-454-YI](#)),
S680 ([WED-478](#)), S680 ([WED-479](#))
- Talarek, Ewa, S820 ([THU-387](#)),
S825 ([THU-403](#))
- Talb  ck, Mats, S40 ([OS-057-YI](#))
- Taleb, Shakila, S695 ([FRI-155](#)),
S697 ([FRI-162](#))
- Talerico, Rosa, S703 ([TOP-142-YI](#))
- Talukdar, Saswata, S564 ([THU-198](#))
- Tamai, Tsutomu, S512 ([WED-203](#))
- Tamaki, Nobuharu, S147 ([SAT-281](#)),
S478 ([FRI-237](#)), S540 ([WED-282](#)),
S626 ([FRI-026](#))
- Tamandl, Dietmar, S436 ([TOP-488-YI](#))
- Tamayo, Juan Alfredo, S627 ([FRI-029](#))
- Tamazirt, Sonia, S41 ([OS-060](#))
- Tamim, Hani, S671 ([WED-458](#))
- Tamim, Hend, S491 ([FRI-273-YI](#))
- Tamnanloo, Farzaneh, S187 ([WED-092](#))
- Tamori, Akihiko, S430 ([FRI-518](#))
- Tam, Ying, S88 ([LBP-022](#))
- Tanaka, Atsushi, S118 ([SAT-319](#)),
S308 ([THU-098](#)), S311 ([THU-102-YI](#)),
S374 ([SAT-021](#))
- Tanaka, Kazunari, S498 ([FRI-297](#)),
S757 ([WED-421](#))
- Tanaka, Masatake, S42 ([OS-062](#))
- Tanaka, Yasuhito, S248 ([SAT-101](#)),
S288 ([FRI-540](#))
- Tanaka, Yoshiya, S710 ([WED-152](#))
- Tan, Anthony, S742 ([SAT-383](#))
- Tanasie, Ioana, S221 ([FRI-092](#)),
S324 ([THU-131](#))
- Tan, Cedric, S676 ([WED-471](#)),
S746 ([SAT-394](#))
- Tan, Cheng Peow Bobby, S578 ([THU-239-YI](#))
- Tan, Daisong, S520 ([WED-230](#))
- Tan, Darren Jun Hao, S139 ([SAT-256](#)),
S366 ([TOP-004](#)), S540 ([WED-282](#))
- Tan, Dat Ho, S552 ([WED-320](#))
- Tan, De En, S565 ([THU-200-YI](#))
- Tan, Din He, S633 ([THU-027-YI](#))
- Tandoi, Francesco, S369 ([SAT-009](#))
- Tandon, Puneeta, S161 ([THU-058](#)),
S163 ([THU-060](#)), S206 ([FRI-046](#)),
S218 ([FRI-086](#))
- Taneja, Sunil, S129 ([THU-324](#)),
S152 ([SAT-295](#)), S158 ([THU-051](#)),
S158 ([THU-052](#)), S161 ([THU-058](#)),
S167 ([THU-078](#)), S217 ([FRI-082](#))
- Tan, Elise Chia-Hui, S398 ([SAT-484](#)),
S663 ([WED-438-YI](#))
- Tan, En Ying, S524 ([WED-238](#))
- Taner, Burcin, S146 ([SAT-279](#))
- Tang, Ariel, S812 ([WED-377](#))
- Tang, Guozhi, S727 ([TOP-356](#))
- Tang, Haitao, S783 ([FRI-420](#))
- Tang, Hong, S26 ([OS-030](#)), S161 ([THU-058](#)),
S494 ([FRI-285](#)), S499 ([FRI-302](#)),
S605 ([SAT-198](#)), S803 ([WED-412](#))
- Tang, Huixin, S113 ([FRI-347](#))
- Tang, Jiayin, S422 ([FRI-484](#))
- Tang, Jinglin, S747 ([SAT-395](#))
- Tangkijvanich, Pisit, S221 ([FRI-093](#)),
S258 ([SAT-129](#)), S434 ([FRI-530](#)),
S588 ([THU-273](#)), S591 ([THU-281](#)),
S689 ([WED-502](#)), S811 ([WED-375](#))
- Tang, Liming, S566 ([THU-201-YI](#))
- Tang, Myo, S400 ([SAT-492](#))
- Tang, Qianhui, S111 ([FRI-338](#)),
S111 ([FRI-339](#))
- Tang, Ruqi, S271 ([TOP-561](#))
- Tang, Shan, S694 ([FRI-154](#))
- Tanguy, Marion, S180 ([WED-071](#)),
S193 ([WED-112](#)), S524 ([WED-239](#))
- Tang, Xiaoping, S792 ([WED-390](#))
- Tang, Yijun, S526 ([WED-246](#))
- Tang, Yuanyuan, S7 ([LBO-001](#))
- Tan, Hiang Keat, S161 ([THU-058](#)),
S169 ([THU-082](#))
- Tan, Hong Chang, S525 ([WED-242](#))
- Tan, Hua, S727 ([TOP-357](#))
- Tani, Joji, S616 ([SAT-236](#))
- Tan, Joseph, S812 ([WED-377](#))
- Tan, Michelle Siying, S565 ([THU-200-YI](#))
- Tan, Natassia, S338 ([THU-177-YI](#)),
S653 ([SAT-464-YI](#))
- Tan, Ngaiap Chuan, S525 ([WED-242](#))
- Tan, Nguan Soon, S280 ([WED-539](#))
- Tan, Nicole, S81 ([LBP-009](#))
- Tan, Soek Siam, S831 ([THU-362](#))
- Tan, Soek-Siam, S158 ([THU-052](#)),
S167 ([THU-078](#))
- Tantai, Xinxing, S235 ([FRI-131](#))
- Tantisaranon, Piraya, S396 ([SAT-480-YI](#)),
S410 ([SAT-529](#))
- Tan, Tuan Zea, S432 ([FRI-525](#))
- Tanwandee, Tawesak, S642 ([SAT-435](#)),
S796 ([WED-396](#))
- Tan, Wenting, S701 ([FRI-174](#))
- Tan, Ying, S36 ([OS-050](#))
- Tan, Youwen, S525 ([WED-244](#))
- Tao, Mengyu, S120 ([SAT-323](#))
- Tapia, Graciela, S627 ([FRI-029](#))
- Tapper, Elliot, S611 ([SAT-215](#))
- Tarchi, Paola, S429 ([FRI-516-YI](#))
- Targher, Giovanni, S488 ([FRI-267](#)),
S503 ([FRI-317](#))
- Tarmamade, Mussagy, S209 ([FRI-053](#))
- Taru, Madalina-Gabriela,
S521 ([WED-232-YI](#)), S555 ([WED-332](#))
- Taru, Vlad, S165 ([THU-071](#)),
S186 ([WED-089-YI](#)), S197 ([WED-122-YI](#)),
S198 ([WED-125](#)), S267 ([THU-540](#)),
S555 ([WED-332](#))
- Tashkandi, Abdulaziz, S671 ([WED-458](#))
- Tashkent, Yasmina, S275 ([WED-526](#))
- Tatara, Eric, S43 ([OS-063](#))

Author Index

- Tataru, Daniela, S406 ([SAT-515](#))
Tateishi, Ryosuke, S393 ([SAT-470](#)),
S437 ([TOP-505](#)), S828 ([THU-413](#))
Tateno, Chise, S128 ([THU-319](#)),
S288 ([FRI-540](#)), S735 ([SAT-364](#))
Tatman, Nick, S672 ([WED-459-YI](#))
Tatoli, Mariagrazia, S522 ([WED-233-YI](#))
Tatonetti, Riccardo, S96 ([LBP-038](#)),
S306 ([THU-093](#))
Tatsumi, Tomohide, S506 ([TOP-288](#)),
S828 ([THU-413](#))
Tatsuta, Miwa, S541 ([WED-283](#))
Taubert, Richard, S19 ([OS-017](#)),
S21 ([OS-021-YI](#)), S44 ([OS-066-YI](#)),
S115 ([TOP-346-YI](#)), S341 ([THU-182](#)),
S374 ([SAT-021](#)), S440 ([THU-457](#)),
S712 ([WED-160](#))
Taub, Karen, S576 ([THU-233](#)),
S579 ([THU-242](#))
Taub, Rebecca, S71 ([OS-117](#)), S76 ([OS-124](#)),
S141 ([SAT-263](#)), S465 ([FRI-202](#)),
S505 ([TOP-265](#)), S509 ([WED-196](#)),
S611 ([SAT-214](#)), S652 ([SAT-459](#))
Taupin, Jean Luc, S378 ([SAT-029](#))
Tauwaldt, Jan, S735 ([SAT-363](#))
Tavaglione, Federica, S535 ([WED-270](#)),
S554 ([WED-325-YI](#))
Tavakoli, Mitra, S697 ([FRI-163-YI](#))
Tavelli, Alessandro, S791 ([FRI-442](#))
Tawfik, Mohamed, S709 ([WED-138](#))
Tawfiq, Rasha, S418 ([FRI-470](#)),
S570 ([THU-213](#))
Tay, Benjamin, S540 ([WED-282](#))
Taylor, Alison, S388 ([SAT-055](#))
Taylor, John, S676 ([WED-471](#)),
S759 ([TOP-417](#))
Taylor, Martin, S416 ([FRI-463-YI](#))
Taylor, Rhiannon, S23 ([OS-024](#)),
S156 ([TOP-108](#)), S373 ([SAT-018-YI](#))
Tay, Yuh Ling Amy, S797 ([WED-398](#))
Teague, Amy, S672 ([WED-462](#))
Tedesco, Dana, S771 ([FRI-390](#))
Tedesco, Greta, S206 ([FRI-047-YI](#)),
S215 ([FRI-078-YI](#))
Tedone, Fabio, S725 ([WED-191](#))
Teerasamit, Wanwarang, S796 ([WED-396](#))
Teerasarntipan, Tongluk, S208 ([FRI-053](#))
Tefas, Cristian, S555 ([WED-332](#))
Tegtmeyer, Daniel, S115 ([TOP-346-YI](#))
Te, Helen, S9 ([LBP-004](#)), S89 ([LBP-026](#))
Teh, Kevin Kim Jun, S2 ([GS-004](#))
Teixeira, Geoffrey, S31 ([OS-040-YI](#))
Tejedor, Marta, S377 ([SAT-027](#))
Tejedor-Tejada, Javier, S139 ([SAT-257](#)),
S142 ([SAT-267](#)), S329 ([THU-154-YI](#))
Telep, Laura, S667 ([WED-447](#)),
S769 ([FRI-383](#))
Tellerup, Julie, S466 ([FRI-206-YI](#))
Tellez, Francisco Félix, S219 ([FRI-088](#))
Téllez, Luis, S52 ([OS-080](#)), S61 ([OS-096-YI](#)),
S189 ([WED-100-YI](#)), S255 ([SAT-123](#)),
S705 ([WED-129](#))
Téllez, Manuel Rodríguez, S559 ([WED-341](#))
Telli, Pelin, S377 ([SAT-028](#))
Telzerow, Anja, S47 ([OS-071-YI](#))
Temel, Ryan, S565 ([THU-199](#))
Templin, Silke, S368 ([SAT-008](#))
Temprano, Alvaro, S432 ([FRI-523](#))
ten Dijke, Peter, S263 ([THU-526](#))
Teng, Gao-Jun, S527 ([WED-246](#)),
S536 ([WED-272](#)), S620 ([TOP-006](#))
Teng, Margaret, S139 ([SAT-256](#)),
S147 ([SAT-281](#)), S366 ([TOP-004](#)),
S540 ([WED-282](#))
Teng, Wei, S414 ([FRI-458](#)), S784 ([FRI-426](#))
Teng, Xiao, S461 ([TOP-310](#)),
S551 ([WED-319](#))
Tenta, Roxani, S208 ([FRI-052](#)),
S214 ([FRI-076](#))
Teo, Wei-Quan, S169 ([THU-082](#))
Teow, Wee Jug, S578 ([THU-239-YI](#))
Tepasse, Phil Robin, S115 ([TOP-346-YI](#))
Terai, Shuji, S828 ([THU-413](#))
Teraoka, Yuji, S42 ([OS-061](#))
ter Borg, Frank, S314 ([THU-109](#)),
S327 ([THU-138](#))
ter Borg, Martijn J., S314 ([THU-109](#)),
S319 ([THU-120-YI](#)), S327 ([THU-138](#))
Teresa Arias Loste, María, S469 ([FRI-213](#))
Tergast, Tammo Lambert, S202 ([FRI-038-YI](#)),
S204 ([FRI-042](#)), S226 ([FRI-107-YI](#)),
S226 ([FRI-109](#)), S242 ([SAT-080-YI](#)),
S820 ([THU-386-YI](#))
Termite, Fabrizio, S533 ([WED-261-YI](#))
Terrabuio, Debora Raquel, S343 ([THU-188](#)),
S374 ([SAT-021](#))
Terracciani, Francesca, S96 ([LBP-038](#)),
S175 ([TOP-085](#)), S306 ([THU-093](#)),
S332 ([THU-161](#)), S554 ([WED-325-YI](#)),
S754 ([SAT-418](#))
Terracciano, Luigi, S19 ([OS-017](#)),
S438 ([THU-446](#)), S580 ([THU-245](#)),
S705 ([WED-130](#))
Terracciano, Luigi Maria, S292 ([TOP-150-YI](#))
Terranova, Antonino, S601 ([TOP-193](#))
Terra, Ximena, S580 ([THU-247-YI](#))
Terreni, Natalia, S96 ([LBP-038](#)),
S306 ([THU-093](#))
Terziroli, Benedetta, S44 ([OS-066-YI](#)),
S316 ([THU-113](#)), S335 ([THU-167](#)),
S374 ([SAT-021](#))
Terziroli Beretta-Piccoli, Benedetta,
S341 ([THU-182](#))
Tesini, Giulia, S69 ([OS-112-YI](#)),
S408 ([SAT-523](#)), S447 ([THU-474-YI](#))
Tessier, Alexia, S191 ([WED-105](#))
Testoni, Barbara, S58 ([OS-091](#)),
S808 ([WED-366](#))
Testro, Adam, S372 ([SAT-017](#))
Teti, Elisabetta, S59 ([OS-094](#)),
S772 ([FRI-392-YI](#))
Teuber, Gerlinde, S833 ([THU-366](#))
Teufel, Andreas, S52 ([OS-079-YI](#)),
S334 ([THU-164-YI](#))
Tevethia, Harshvardhan, S164 ([THU-070](#))
Tey, Yi Qing, S540 ([WED-282](#))
Thabut, Dominique, S6 ([GS-010](#)),
S41 ([OS-060](#)), S54 ([OS-084-YI](#)),
S172 ([THU-092](#)), S207 ([FRI-050-YI](#)),
S211 ([FRI-059](#)), S214 ([FRI-075](#)),
S218 ([FRI-087](#)), S222 ([FRI-094-YI](#)),
S222 ([FRI-095](#)), S239 ([SAT-071](#)),
S441 ([THU-458](#)), S486 ([FRI-259](#)),
S512 ([WED-206](#))
Thacker, Leroy, S161 ([THU-058](#)),
S163 ([THU-060](#)), S206 ([FRI-046](#)),
S208 ([FRI-053](#)), S219 ([FRI-088](#))
Thaimai, Panarat, S196 ([WED-120](#)),
S221 ([FRI-093](#)), S258 ([SAT-129](#)),
S749 ([SAT-403](#))
Thakker, Pares, S544 ([WED-294](#)),
S696 ([FRI-161](#)), S698 ([FRI-164](#))
Thalhammer, Julia, S61 ([OS-096-YI](#))
Thanapirom, Kessarin, S158 ([THU-052](#)),
S161 ([THU-058](#)), S167 ([THU-078](#)),
S196 ([WED-120](#)), S221 ([FRI-093](#)),
S258 ([SAT-129](#)), S749 ([SAT-403](#))
Thangariyal, Swati, S177 ([WED-057](#))
Thapar, Manish, S715 ([WED-165](#))
Thatcher, Amy, S631 ([THU-017-YI](#))
Thebuwana, Kunchana, S633 ([THU-029](#))
Theel, Willy, S549 ([WED-306-YI](#)),
S612 ([SAT-218](#))
Theeten, Heidi, S665 ([WED-441-YI](#))
Theise, Neil, S189 ([WED-101-YI](#))
Thennati, Rajamannar, S615 ([SAT-231](#))
Theodore, Dickens, S745 ([SAT-390](#)),
S807 ([WED-364](#)), S809 ([WED-370](#))
Théophile, Gerster, S744 ([SAT-389](#)),
S747 ([SAT-396](#))
Theret, Nathalie, S64 ([OS-102](#))
Théret, Nathalie, S261 ([THU-522](#))
Therneau, Terry, S504 ([TOP-252-YI](#))
Thévenot, Thierry, S30 ([OS-038-YI](#)),
S61 ([OS-097](#)), S199 ([TOP-062](#))
Thiam, Mamadou-Gabou, S159 ([THU-053](#))
Thiaw, Pape Omar, S743 ([SAT-387](#))
Thiele, Maja, S41 ([OS-059](#)), S47 ([OS-072-YI](#)),
S77 ([OS-126](#)), S137 ([SAT-250](#)),
S139 ([SAT-255](#)), S142 ([SAT-266](#)),
S153 ([SAT-298](#)), S205 ([FRI-045](#)),
S466 ([FRI-206-YI](#)), S503 ([TOP-241-YI](#)),
S510 ([WED-199](#)), S620 ([TOP-012](#)),
S623 ([FRI-017](#))
Thielert, Marvin, S32 ([OS-041-YI](#))
Thi, Emily P., S26 ([OS-031](#)),
S809 ([WED-371](#))
Thiery, Jean Paul, S432 ([FRI-525](#))
Thietart, Sara, S180 ([WED-071](#)),
S193 ([WED-112](#))
Thimme, Robert, S23 ([OS-025-YI](#)),
S51 ([OS-078-YI](#)), S54 ([OS-083](#)),
S187 ([WED-094](#)), S351 ([SAT-533](#))
Thing, Mira, S513 ([WED-207](#)),
S529 ([WED-250-YI](#)), S555 ([WED-331-YI](#))
Thio, Hans H.K., S319 ([THU-120-YI](#))
Thiriard, Anaïs, S131 ([THU-331-YI](#))
Thirlwell, Kayleigh, S186 ([WED-090](#))
Thi, Thu Thuy Pham, S552 ([WED-320](#))
Thi, Viet Loan Dao, S58 ([OS-092](#))
Thiyagarajah, Keerthihan, S170 ([THU-087](#)),
S734 ([SAT-361](#))

- Tholstrup Bech, Katrine, S139 ([SAT-255](#)), S142 ([SAT-266](#)), S153 ([SAT-298](#))
- Thoma, Eva, S590 ([THU-278](#))
- Thomann, Stefan, S33 ([OS-043](#))
- Thomas, Carina, S693 ([FRI-151](#))
- Thomas, Célia, S261 ([THU-522](#))
- Thomas, David, S657 ([WED-422](#)), S676 ([WED-470](#))
- Thomas, Sally, S672 ([WED-459-YI](#))
- Thomas, Sherin Sarah, S164 ([THU-069](#))
- Thomas, Wayne, S250 ([SAT-107-YI](#))
- Thomeer, Maarten, S394 ([SAT-474](#))
- Thomopoulos, Konstantinos, S830 ([THU-419](#))
- Thompson, Alexander, S400 ([SAT-492](#)), S402 ([SAT-496](#))
- Thompson, Connor, S636 ([THU-045](#))
- Thompson, Fiona, S337 ([THU-173](#))
- Thompson, Jacqui, S101 ([LBP-046](#))
- Thompson, Peyton, S668 ([WED-451-YI](#)), S675 ([WED-469](#)), S752 ([SAT-409](#))
- Thompson, Richard J., S298 ([SAT-167-YI](#)), S323 ([THU-129](#)), S331 ([THU-158](#))
- Thomsen, Karen Louise, S567 ([THU-207-YI](#))
- Thomson, Brian, S12 ([OS-004](#))
- Thomson, Rachel, S629 ([THU-008](#))
- Thorburn, Douglas, S5 ([GS-007](#)), S35 ([OS-049-YI](#)), S97 ([LBP-039](#)), S156 ([TOP-108](#)), S268 ([THU-547](#)), S290 ([TOP-147](#)), S295 ([SAT-158](#)), S308 ([THU-098](#)), S315 ([THU-111](#)), S765 ([FRI-374-YI](#))
- Thorens, Bernard, S615 ([SAT-231](#))
- Thorhauge, Katrine, S32 ([OS-041-YI](#)), S41 ([OS-059](#)), S47 ([OS-072-YI](#)), S77 ([OS-126](#)), S137 ([SAT-250](#)), S139 ([SAT-255](#)), S142 ([SAT-266](#)), S153 ([SAT-298](#)), S159 ([THU-055](#)), S205 ([FRI-045](#)), S466 ([FRI-206-YI](#)), S510 ([WED-199](#)), S620 ([TOP-012](#)), S623 ([FRI-017](#)), S703 ([TOP-141](#)), S708 ([WED-135-YI](#))
- Thranian, Arash, S325 ([THU-132](#))
- Thuluvath, Paul J., S161 ([THU-058](#)), S163 ([THU-060](#)), S240 ([SAT-076](#))
- Thumann, Christine, S25 ([OS-029](#))
- Thung, Swan N., S417 ([FRI-467](#))
- Thuresson, Marcus, S334 ([THU-165](#))
- Thursz, Mark R, S14 ([OS-008-YI](#)), S181 ([WED-075-YI](#)), S580 ([THU-247-YI](#))
- Thursz, Mark R., S8 ([LBO-003](#)), S127 ([THU-317](#)), S130 ([THU-326](#)), S145 ([SAT-274](#)), S282 ([WED-546](#)), S350 ([TOP-553](#)), S470 ([FRI-215-YI](#)), S495 ([FRI-286](#)), S782 ([FRI-418](#)), S787 ([FRI-431](#))
- Thuy, Le Thi Thanh, S261 ([THU-523](#)), S430 ([FRI-518](#))
- Thys, Kim, S813 ([WED-379](#))
- Tian, Lu, S419 ([FRI-473](#))
- Tiano, Francesca, S289 ([FRI-544](#))
- Tian, Yuan, S107 ([FRI-325](#))
- Tibbitts, Jay, S141 ([SAT-261](#))
- Tiede, Anja, S204 ([FRI-042](#)), S205 ([FRI-044-YI](#)), S226 ([FRI-107-YI](#)), S226 ([FRI-109](#)), S242 ([SAT-080-YI](#)), S245 ([SAT-090-YI](#))
- Tielemans, Merel M., S309 ([THU-100](#))
- Tiendrebego, Abdoul Salam Eric, S678 ([WED-475](#))
- Tiglao, Maria, S657 ([WED-422](#)), S676 ([WED-470](#))
- Tigue, Mark, S89 ([LBP-025](#))
- Tilden, Sally, S651 ([SAT-457-YI](#))
- Tilg, Herbert, S503 ([FRI-317](#)), S515 ([WED-214-YI](#)), S722 ([WED-183-YI](#))
- Tilley, Robert, S250 ([SAT-107-YI](#))
- Tillman, Erik, S8 ([LBO-002](#)), S612 ([SAT-220-YI](#))
- Timucin, Taner, S369 ([SAT-009](#))
- Tincani, Giovanni, S370 ([SAT-013](#))
- Tincopa, Monica, S543 ([WED-291](#))
- Ting, Hui Jun, S565 ([THU-200-YI](#))
- Tiniakos, Dina, S19 ([OS-017](#)), S454 ([THU-495](#)), S641 ([SAT-431-YI](#))
- Tiniakos, Dina G., S467 ([FRI-208](#))
- Tio, Gregory, S61 ([OS-097](#))
- Tiram, Yariv, S563 ([THU-194](#)), S779 ([FRI-408](#))
- Tiribelli, Claudio, S429 ([FRI-516-YI](#)), S701 ([FRI-172](#))
- Tischendorf, Michael, S169 ([THU-083](#)), S170 ([THU-087](#))
- Tisone, Giuseppe, S369 ([SAT-009](#))
- Tiwari, Pooja, S726 ([TOP-353](#))
- Tiwari, Rajnish, S66 ([OS-106-YI](#))
- Tiwari, Vaibhav, S177 ([WED-058-YI](#)), S188 ([WED-095-YI](#))
- Tizzani, Marco, S175 ([TOP-085](#)), S210 ([FRI-056-YI](#)), S451 ([THU-486-YI](#))
- Tjerkaski, Jonathan, S617 ([SAT-238](#))
- Toapanta, David, S115 ([TOP-346-YI](#))
- Todd, Stacy, S676 ([WED-471](#)), S759 ([TOP-417](#))
- Todorovska, Beti, S172 ([THU-092](#))
- Todt, Daniel, S58 ([OS-092](#)), S94 ([LBP-034](#)), S730 ([TOP-369](#)), S732 ([SAT-341](#))
- Toffanin, Serena, S237 ([TOP-061-YI](#))
- To-Figueras, Jordi, S45 ([OS-068](#))
- Tohme, Rania, S659 ([WED-427](#)), S664 ([WED-439](#)), S675 ([WED-468](#)), S677 ([WED-473](#)), S682 ([WED-484](#)), S685 ([WED-492](#)), S691 ([WED-515](#))
- Tokat, Yaman, S9 ([LBO-004](#)), S89 ([LBP-026](#))
- Tokumoto, Yoshio, S711 ([WED-154](#)), S722 ([WED-184](#))
- Toledano, Mireille, S406 ([SAT-515](#))
- Toledo, Claudio, S30 ([OS-038-YI](#)), S83 ([LBP-012](#)), S199 ([TOP-062](#)), S200 ([TOP-064-YI](#))
- Tolenaars, Dagmar, S296 ([SAT-160](#)), S301 ([SAT-178-YI](#))
- Tolentino, Michael, S646 ([SAT-444](#))
- Tomah, Shaheen, S515 ([WED-212](#)), S517 ([WED-219](#))
- Toma, Letitia, S211 ([FRI-058](#)), S221 ([FRI-092](#)), S324 ([THU-131](#)), S410 ([SAT-528](#))
- Toma, Mihai, S446 ([THU-473](#))
- Tomanova, Petra, S104 ([TOP-352](#))
- Tomasiewicz, Krzysztof, S834 ([THU-367-YI](#))
- Tomasini, Simone, S565 ([THU-199](#))
- Tomeno, Wataru, S541 ([WED-283](#))
- Tomé, Santiago, S139 ([SAT-257](#)), S142 ([SAT-267](#)), S365 ([TOP-002](#))
- Tomita, Kengo, S537 ([WED-273](#))
- Tomlinson, Jeremy, S135 ([THU-343](#)), S578 ([THU-236-YI](#))
- Tommaso, Luca Di, S19 ([OS-017](#))
- Tomsin, Bert, S712 ([WED-158-YI](#))
- Tondon, Rashmi, S411 ([SAT-530](#))
- Tonev, Dimitar, S21 ([OS-020](#)), S91 ([LBP-028](#)), S312 ([THU-105](#)), S321 ([THU-124](#))
- Tong, Huan, S225 ([FRI-105](#)), S241 ([SAT-077](#)), S622 ([FRI-010](#))
- Tong, Xiao-Fei, S488 ([FRI-267](#))
- Tong, Xin, S744 ([SAT-388](#)), S757 ([SAT-423](#))
- Tong, Ying, S387 ([SAT-054](#))
- Toniutto, Pierluigi, S172 ([THU-092](#)), S206 ([FRI-047-YI](#)), S215 ([FRI-078-YI](#)), S367 ([SAT-007-YI](#)), S700 ([FRI-171](#)), S804 ([WED-414](#))
- Tonnini, Matteo, S73 ([OS-120](#)), S793 ([WED-391](#)), S804 ([WED-414](#))
- Tonon, Marta, S28 ([OS-035-YI](#)), S206 ([FRI-047-YI](#)), S212 ([FRI-068](#)), S224 ([FRI-101-YI](#)), S243 ([SAT-083-YI](#)), S830 ([THU-420](#))
- Topal, Halit, S125 ([TOP-328-YI](#))
- Topazian, Mark, S161 ([THU-058](#)), S208 ([FRI-053](#)), S219 ([FRI-088](#))
- Topor, Ioan, S409 ([SAT-525](#))
- Topor, Mihai, S409 ([SAT-525](#))
- Torán, Pere, S503 ([TOP-241-YI](#))
- Tordjmann, Thierry, S348 ([FRI-555](#))
- Torella, Laura, S693 ([FRI-152-YI](#))
- Tormo, Beatriz, S700 ([FRI-171](#))
- Tornai, David, S159 ([THU-055](#)), S169 ([THU-080-YI](#)), S193 ([WED-111](#)), S313 ([THU-106-YI](#))
- Tornai, Istvan, S169 ([THU-080-YI](#)), S313 ([THU-106-YI](#))
- Torner, Maria, S192 ([WED-107](#))
- Torp, Nikolaj, S41 ([OS-059](#)), S47 ([OS-072-YI](#)), S77 ([OS-126](#)), S137 ([SAT-250](#)), S139 ([SAT-255](#)), S142 ([SAT-266](#)), S153 ([SAT-298](#)), S204 ([FRI-041](#)), S205 ([FRI-045](#)), S220 ([FRI-089](#)), S466 ([FRI-206-YI](#)), S510 ([WED-199](#)), S620 ([TOP-012](#)), S623 ([FRI-017](#))
- Torrallba, Miguel, S391 ([TOP-512-YI](#)), S738 ([SAT-374-YI](#)), S768 ([FRI-381](#))
- Torra, Mercè, S711 ([WED-155](#)), S723 ([WED-186](#))
- Torras, Claudia, S233 ([FRI-126](#))
- Torras, Clàudia, S29 ([OS-037](#))

Author Index

- Torre, Aldo, S30 ([OS-038-YI](#)), S83 ([LBP-012](#)), S157 ([THU-050](#)), S161 ([THU-057-YI](#)), S161 ([THU-058](#)), S199 ([TOP-062](#)), S200 ([TOP-064-YI](#)), S208 ([FRI-053](#)), S219 ([FRI-088](#))
- Torre, Emanuel Della, S710 ([WED-152](#))
- Torre, Giulia, S59 ([OS-094](#)), S772 ([FRI-392-YI](#)), S777 ([FRI-405](#))
- Torrens-Baile, Julen, S693 ([FRI-152-YI](#))
- Torre, Pietro, S493 ([FRI-281](#)), S554 ([WED-326](#)), S556 ([WED-333](#))
- Torre, Sara Della, S289 ([FRI-543](#))
- Torres, Daniel Rodrigo, S127 ([THU-317](#)), S130 ([THU-326](#))
- Torres, Emma, S654 ([SAT-466](#))
- Torres, Felicitas, S654 ([SAT-466](#))
- Torres, Ferran, S455 ([THU-500](#))
- Torres, Gabriela, S560 ([WED-343](#))
- Torres, Mireia, S177 ([WED-059](#)), S231 ([FRI-121](#))
- Torres, Rogelio, S654 ([SAT-466](#))
- Torrijos, Paula, S398 ([SAT-485](#))
- Tortora, Annalisa, S215 ([FRI-078-YI](#))
- Tortora, Raffaella, S175 ([TOP-085](#))
- Törüner, Murat, S479 ([FRI-238](#))
- Torzilli, Guido, S401 ([SAT-494](#)), S406 ([SAT-514](#))
- Tosca, Joan, S592 ([THU-283](#))
- Tosetti, Giulia, S9 ([LBO-004](#)), S89 ([LBP-026](#)), S227 ([FRI-110](#))
- Tosi, Delfina, S428 ([FRI-514](#))
- Toso, Alberto, S25 ([OS-029](#))
- Toso, Christian, S189 ([WED-101-YI](#)), S705 ([WED-129](#))
- Tosun, Selma, S805 ([WED-418](#))
- Tóth, Marcell, S33 ([OS-043](#))
- Touati, Nathan, S80 ([LBP-006](#)), S91 ([LBP-028](#))
- Touceda-Taboada, Sonia, S690 ([WED-513](#))
- Tough, Iain, S274 ([WED-523](#))
- Touray, Alhagie, S782 ([FRI-418](#))
- Tovar-Aguilar, Adriana, S140 ([SAT-260](#))
- Tovoli, Francesco, S390 ([TOP-509-YI](#)), S395 ([SAT-477-YI](#)), S399 ([SAT-490](#)), S446 ([THU-472-YI](#)), S452 ([THU-492](#))
- Towey, Jennifer, S654 ([SAT-467](#))
- Toyoda, Hidenori, S248 ([SAT-101](#)), S506 ([TOP-288](#)), S512 ([WED-203](#)), S537 ([WED-273](#))
- Trailin, Andriy, S349 ([FRI-556](#))
- Trainel, Nicolas, S130 ([THU-327](#)), S136 ([THU-347-YI](#))
- Trampert, David, S301 ([SAT-178-YI](#))
- Trampotová, Eliška, S697 ([FRI-163-YI](#))
- Tranah, Thomas, S46 ([OS-070](#)), S282 ([WED-545-YI](#))
- Tran, Albert, S41 ([OS-060](#)), S68 ([OS-110](#))
- Tran, Cammie, S653 ([SAT-464-YI](#))
- Tran, Doan Duy Hai, S425 ([FRI-492-YI](#))
- Tran, Henri, S648 ([SAT-449](#))
- Tran, Hung, S657 ([WED-422](#)), S676 ([WED-470](#))
- Tran, Nguyen H., S52 ([OS-079-YI](#))
- Tran, Sarah Sousa, S673 ([WED-464](#))
- Trapani, Joseph, S740 ([SAT-377](#))
- Trapani, Silvia, S367 ([SAT-007-YI](#)), S389 ([SAT-058](#))
- Traub, Julia, S229 ([FRI-115](#)), S284 ([WED-551](#))
- Trauner, Franziska, S368 ([SAT-008](#))
- Trauner, Michael, S66 ([OS-106-YI](#)), S69 ([OS-112-YI](#)), S81 ([LBP-008](#)), S97 ([LBP-039](#)), S156 ([TOP-097-YI](#)), S165 ([THU-071](#)), S166 ([THU-075-YI](#)), S186 ([WED-089-YI](#)), S197 ([WED-122-YI](#)), S198 ([WED-125](#)), S242 ([SAT-080-YI](#)), S243 ([SAT-086-YI](#)), S250 ([SAT-105](#)), S250 ([SAT-106](#)), S251 ([SAT-111](#)), S253 ([SAT-117](#)), S253 ([SAT-118](#)), S255 ([SAT-122](#)), S257 ([SAT-128](#)), S267 ([THU-540](#)), S270 ([THU-550](#)), S296 ([SAT-161](#)), S335 ([THU-166](#)), S340 ([THU-180](#)), S341 ([THU-183-YI](#)), S436 ([TOP-488-YI](#)), S621 ([FRI-009-YI](#)), S703 ([TOP-141](#)), S706 ([WED-131-YI](#)), S708 ([WED-135-YI](#)), S717 ([WED-171](#)), S725 ([WED-190](#)), S773 ([FRI-394](#))
- Trautwein, Christian, S57 ([OS-088-YI](#)), S229 ([FRI-116](#)), S259 ([SAT-135](#)), S273 ([WED-521-YI](#)), S320 ([THU-122](#)), S351 ([SAT-534](#)), S356 ([SAT-545](#)), S357 ([SAT-549](#)), S392 ([TOP-520](#)), S431 ([FRI-522](#)), S494 ([FRI-284-YI](#)), S703 ([TOP-141](#)), S708 ([WED-135-YI](#))
- Trautwein, Christoph, S65 ([OS-103](#))
- Traversa, Sergio, S592 ([THU-285](#))
- Treanor, Darren, S530 ([WED-254](#))
- Trebicka, Jonel, S9 ([LBO-004](#)), S16 ([OS-011](#)), S17 ([OS-014-YI](#)), S47 ([OS-071-YI](#)), S47 ([OS-072-YI](#)), S48 ([OS-073](#)), S83 ([LBP-012](#)), S89 ([LBP-026](#)), S133 ([THU-338](#)), S157 ([THU-050](#)), S159 ([THU-053](#)), S159 ([THU-055](#)), S161 ([THU-057-YI](#)), S169 ([THU-080-YI](#)), S169 ([THU-083](#)), S170 ([THU-087](#)), S171 ([THU-088](#)), S174 ([TOP-073](#)), S174 ([TOP-084](#)), S180 ([WED-074](#)), S182 ([WED-078](#)), S184 ([WED-083](#)), S188 ([WED-098-YI](#)), S193 ([WED-111](#)), S193 ([WED-112](#)), S198 ([WED-126](#)), S203 ([FRI-039](#)), S258 ([SAT-130](#)), S259 ([SAT-135](#)), S272 ([TOP-563](#)), S283 ([WED-548](#)), S391 ([TOP-511](#)), S579 ([THU-243](#)), S734 ([SAT-361](#))
- Treeprasertsuk, Sombat, S158 ([THU-052](#)), S167 ([THU-078](#)), S221 ([FRI-093](#)), S258 ([SAT-129](#))
- Trefois, Pierre, S360 ([WED-008](#)), S473 ([FRI-224](#))
- Treiber, Sonja, S335 ([THU-166](#)), S341 ([THU-183-YI](#))
- Treit, Peter, S193 ([WED-111](#))
- Tremblay, Mélanie, S187 ([WED-092](#))
- Trépo, Eric, S133 ([THU-335](#))
- Treviño-Garcia, Carolina, S627 ([FRI-029](#))
- Trevisani, Franco, S395 ([SAT-477-YI](#)), S449 ([THU-481-YI](#))
- Triantafyllou, Evangelos, S107 ([FRI-326-YI](#)), S181 ([WED-075-YI](#)), S352 ([SAT-535-YI](#))
- Triantafyllou, Vasiliki, S670 ([WED-454-YI](#)), S680 ([WED-478](#))
- Triantos, Christos, S798 ([WED-403](#)), S830 ([THU-419](#))
- Trifylli, Eleni-Myrto, S690 ([WED-503](#))
- Trigianos, Tammy, S394 ([SAT-476](#))
- Trillaud, Hervé, S68 ([OS-110](#)), S441 ([THU-459-YI](#))
- Trinh, Andrew, S92 ([LBP-030](#))
- Trinka, Eugen, S500 ([FRI-303](#))
- Tripathi, Dinesh Mani, S66 ([OS-106-YI](#)), S67 ([OS-108-YI](#)), S176 ([WED-056](#)), S274 ([WED-522-YI](#)), S346 ([FRI-547-YI](#))
- Tripathi, Gaurav, S103 ([TOP-349-YI](#)), S108 ([FRI-327-YI](#)), S125 ([TOP-329-YI](#)), S127 ([THU-318](#)), S134 ([THU-339](#)), S164 ([THU-068](#)), S164 ([THU-069](#)), S273 ([WED-519-YI](#)), S283 ([WED-549](#)), S294 ([SAT-155](#))
- Tripathi, Madhulika, S55 ([OS-085](#)), S502 ([FRI-316](#))
- Tripathi, Rupal, S343 ([THU-187](#))
- Tripathi, Snehlata, S693 ([FRI-151](#))
- Trivedi, Hirsch, S39 ([OS-055](#)), S200 ([TOP-063](#))
- Trivedi, Palak, S308 ([THU-098](#)), S311 ([THU-102-YI](#))
- Trivedi, Palak J., S5 ([GS-007](#)), S97 ([LBP-039](#)), S98 ([LBP-040](#)), S101 ([LBP-046](#)), S290 ([TOP-147](#)), S309 ([THU-099-YI](#)), S315 ([THU-111](#)), S321 ([THU-125](#)), S332 ([THU-160](#)), S472 ([FRI-220-YI](#)), S485 ([FRI-258](#))
- Trizzino, Arianna, S370 ([SAT-013](#))
- Troch, Killian, S53 ([OS-081](#))
- Troisi, Roberto, S386 ([SAT-051](#))
- Trojak, Aleksandra, S718 ([WED-173](#))
- Trojan, Jörg, S411 ([TOP-507-YI](#))
- Troland, Debbie, S81 ([LBP-007](#))
- Trompet, Stella, S612 ([SAT-218](#))
- Troppmair, Maria Rosina, S515 ([WED-214-YI](#))
- Troshina, Yulia, S804 ([WED-414](#))
- Trovato, Francesca M, S110 ([FRI-335](#)), S181 ([WED-075-YI](#))
- Trubert, Lise, S714 ([WED-162](#))
- Trucchi, Michelangelo, S589 ([THU-274](#))
- Truebenbach, Ines, S197 ([WED-122-YI](#)), S198 ([WED-125](#)), S267 ([THU-540](#))
- Truhn, Daniel, S567 ([THU-206](#))
- Trylesinski, Aldo, S516 ([WED-215](#)), S545 ([WED-296](#))
- Trzos, Katarzyna, S265 ([THU-533](#)), S304 ([SAT-184](#))
- Tsai, Lung-Wen, S399 ([SAT-486](#))
- Tsai, Pei-Chien, S490 ([FRI-271](#)), S493 ([FRI-280](#)), S832 ([THU-365](#))
- Tsai, Wei-Lun, S490 ([FRI-271](#)), S493 ([FRI-280](#))
- Tsai, Wen-Wei, S4 ([GS-011](#)), S575 ([THU-231](#)), S600 ([THU-336](#))
- Tsai, Ying-Nan, S795 ([WED-393](#))

- Tsakmaki, Anastasia, S274 ([WED-523](#))
 Tsankof, Alexandra, S229 ([FRI-117](#))
 Tsau, Jennifer, S544 ([WED-294](#))
 Tse, Edmund, S8 ([LBO-003](#))
 Tseng, Cheng-Hao, S795 ([WED-393](#))
 Tseng, Kuo-Chih, S74 ([OS-121](#)),
 S832 ([THU-365](#))
 Tseng, Shang-Chen, S795 ([WED-393](#))
 Tseng, Steve, S92 ([LBP-029](#))
 Tsereteli, Maia, S664 ([WED-439](#)),
 S675 ([WED-468](#)), S677 ([WED-473](#)),
 S691 ([WED-515](#)), S825 ([THU-404](#))
 Tsertsvadze, Tengiz, S659 ([WED-427](#)),
 S685 ([WED-492](#))
 Tse, Yee-Kit, S510 ([WED-198](#)),
 S761 ([FRI-362-YI](#)), S770 ([FRI-387](#))
 Tshetu, Antoinette, S668 ([WED-451-YI](#))
 Tsien, Cynthia, S9 ([LBO-004](#)),
 S89 ([LBP-026](#)), S381 ([SAT-037](#)),
 S381 ([SAT-039](#))
 Tsigalou, Christina, S358 ([SAT-551](#))
 Tsintoni, Angeliki, S830 ([THU-419](#))
 Tsirogianni, Alexandra, S358 ([SAT-551](#))
 Tsitrina, Alexandra, S268 ([THU-542](#))
 Tskhomelidze, Irina, S664 ([WED-439](#)),
 S675 ([WED-468](#)), S677 ([WED-473](#))
 Tsochatzis, Emmanouil, S248 ([SAT-100](#))
 Tsochatzis, Emmanuel, S2 ([GS-004](#)),
 S23 ([OS-024](#)), S38 ([OS-054](#)),
 S503 ([TOP-241-YI](#))
 Tso, Emily, S564 ([THU-198](#))
 Tsoriev, Timur, S501 ([FRI-305](#))
 Tsou, Hio Lam Phoebe, S174 ([TOP-084](#)),
 S700 ([FRI-171](#))
 Tsounis, Efthymios, S830 ([THU-419](#))
 Tsubota, Akihito, S248 ([SAT-101](#)),
 S616 ([SAT-236](#))
 Tsuchiya, Kaoru, S626 ([FRI-026](#))
 Tsuchiyama, Yosuke, S519 ([WED-226](#))
 Tsuji, Keiji, S118 ([SAT-319](#))
 Tsuneyama, Koichi, S519 ([WED-226](#))
 Tsuruya, Kota, S118 ([SAT-319](#))
 Tsutsui, Akemi, S118 ([SAT-319](#)),
 S519 ([WED-226](#))
 Tsutsumi, Takeya, S589 ([THU-275](#))
 Tual, Christelle, S802 ([WED-410](#))
 Tuchscher, Julia, S230 ([FRI-120](#))
 Tucker, Bethany, S198 ([WED-124](#)),
 S359 ([SAT-556-YI](#))
 Tucker, Lue-Yen, S778 ([FRI-407](#))
 Tuck, Jaclyn, S608 ([SAT-207](#))
 Tudehope, Fiona, S219 ([FRI-088](#))
 Tudrujek-Zdunek, Magdalena,
 S685 ([WED-493-YI](#)), S834 ([THU-367-YI](#))
 Tuefferd, Marianne, S810 ([WED-372](#))
 Tu, Elise, S776 ([FRI-403](#))
 Tuescher, Oliver, S461 ([FRI-194-YI](#))
 Tukebana, Bienvenu, S675 ([WED-469](#))
 Tukiainen, Taru, S562 ([TOP-240-YI](#))
 Tuli, Vishal, S266 ([THU-538](#))
 Tullio, Prestileo, S557 ([WED-336](#))
 Tulo, Adele, S36 ([OS-047-YI](#))
 Tulone, Adele, S609 ([SAT-209-YI](#))
 Tumas, Natalia, S154 ([SAT-304](#))
 Tunç, Esra, S785 ([FRI-427](#))
 Tung, Daniel, S139 ([SAT-256](#)),
 S147 ([SAT-281](#)), S366 ([TOP-004](#)),
 S540 ([WED-282](#))
 Tung, Hung-Da, S74 ([OS-121](#))
 Tuo, Shuyue, S235 ([FRI-131](#))
 Tupper, Katie, S21 ([OS-020](#))
 Tura-Ceida, Olga, S15 ([OS-010](#))
 Turan, Ilker, S211 ([FRI-067](#)),
 S336 ([THU-171](#)), S805 ([WED-419](#))
 Turati, Federica, S705 ([WED-130](#))
 Turato, Cristian, S612 ([SAT-219](#))
 Turco, Celia, S369 ([SAT-010](#))
 Turco, Elena Rosselli Del, S666 ([WED-446](#))
 Turco, Laura, S521 ([WED-232-YI](#))
 Turkal, Miranda, S266 ([THU-538](#))
 Turk, Elise, S745 ([SAT-390](#))
 Turkistani, Fatema, S687 ([WED-498](#))
 Turner, Alice, S703 ([TOP-141](#)),
 S708 ([WED-135-YI](#)), S709 ([WED-138](#)),
 S724 ([WED-188](#))
 Turner, Lucy, S765 ([FRI-374-YI](#))
 Turner, Marc, S81 ([LBP-007](#))
 Turner, Scott, S261 ([TOP-564](#))
 Turnes, Juan, S827 ([THU-410](#))
 Turon, Fanny, S52 ([OS-080](#)), S53 ([OS-081](#)),
 S61 ([OS-096-YI](#)), S240 ([SAT-074](#)),
 S255 ([SAT-123](#))
 Turriziani, Ombretta, S777 ([FRI-405](#))
 Turunç, Tuba, S805 ([WED-418](#))
 Turyadi, Turyadi, S792 ([FRI-444](#))
 Tushe, Migena, S101 ([LBP-046](#))
 Tushuizen, Maarten, S18 ([OS-015](#)),
 S382 ([SAT-040](#)), S492 ([FRI-278](#)),
 S513 ([WED-209](#))
 Tu, Thomas, S689 ([WED-501](#))
 Tuttolomondo, Antonino, S557 ([WED-336](#))
 Tutusaus, Anna, S424 ([FRI-491-YI](#)),
 S425 ([FRI-494-YI](#)), S430 ([FRI-519-YI](#))
 Tuyishime, Albert, S659 ([WED-429](#)),
 S686 ([WED-495](#))
 Tyagi, Purnima, S745 ([SAT-391](#))
 Tyc, Olaf, S171 ([THU-088](#))
 Tyson, Luke D., S14 ([OS-008-YI](#))
 Tyson, Luke D., S127 ([THU-317](#)),
 S130 ([THU-326](#)), S145 ([SAT-274](#))
 Tzadok, Roie, S237 ([FRI-136](#))
 Tzfati, Yehuda, S89 ([LBP-025](#))
 Tzig, Reut, S278 ([WED-534](#))
 Ucbilek, Enver, S219 ([FRI-088](#))
 Uchida-Kobayashi, Sawako, S430 ([FRI-518](#))
 Uchida, Takuro, S735 ([SAT-364](#))
 Uchila, Raj, S655 ([SAT-471](#))
 Ucle, Verónica, S398 ([SAT-485](#))
 Udompap, Prowpanga, S504 ([TOP-252-YI](#))
 Ueda, Yoshihide, S374 ([SAT-021](#))
 Ueno, Masayuki, S118 ([SAT-319](#)),
 S122 ([SAT-332-YI](#)), S341 ([THU-182](#))
 Ueno, Takato, S541 ([WED-283](#))
 Ueno, Yoshiyuki, S828 ([THU-413](#))
 Uguen, Thomas, S383 ([SAT-043](#)),
 S444 ([THU-466](#))
 Uhlenbusch, Natalie, S712 ([WED-158-YI](#))
 Uh, Young, S136 ([THU-348](#))
 Ulahannan, Susanna V., S51 ([OS-078-YI](#))
 Ullah, Hamid, S249 ([SAT-102](#))
 Ulrich, Rainer, S730 ([TOP-369](#))
 Uluçeçen, Sezen Genç, S551 ([WED-318-YI](#)),
 S803 ([WED-413](#))
 Ulukaya, Gulay, S417 ([FRI-467](#))
 Umar, Narmeen, S19 ([OS-018](#)),
 S305 ([TOP-169](#))
 Umehara, Hisanori, S710 ([WED-152](#))
 Umemura, Takeji, S478 ([FRI-237](#))
 Unchwaniwala, Nuruddin, S812 ([WED-377](#))
 Ungethuem, Udo, S345 ([TOP-559](#))
 Unnikrishnan, G., S31 ([OS-039](#))
 Unozawa, Hidemi, S247 ([SAT-095](#))
 Untas, Aurélie, S313 ([THU-107](#))
 Uojima, Haruki, S248 ([SAT-101](#))
 Upmanyu, Ruchi, S26 ([OS-030](#))
 Upton, Janine, S753 ([SAT-413](#))
 Upton, Paul, S179 ([WED-069](#))
 Urbani, Andrea, S533 ([WED-261-YI](#))
 Urbani, Luca, S128 ([THU-320-YI](#))
 Urban, Stephan, S74 ([OS-122](#))
 Urbonas, Gediminas, S678 ([WED-474](#))
 Ure, Daren, S128 ([THU-320-YI](#))
 Uriarte, Iker, S287 ([FRI-538](#)), S348 ([FRI-555](#))
 Uschner, Frank Erhard, S47 ([OS-071-YI](#)),
 S48 ([OS-073](#)), S157 ([THU-050](#)),
 S180 ([WED-074](#)), S203 ([FRI-039](#)),
 S283 ([WED-548](#)), S391 ([TOP-511](#))
 Uson, Eva, S83 ([LBP-012](#)), S700 ([FRI-171](#))
 Uveges, Samuel, S690 ([WED-514](#))
 Uysal, Alper, S161 ([THU-058](#))
 Uysal, Serhat, S805 ([WED-418](#))
 Uzun, Sarp, S291 ([TOP-150-YI](#))
 Uzzau, Sergio, S777 ([FRI-405](#))
 Vaccaro, Marco, S503 ([FRI-317](#)),
 S609 ([SAT-209-YI](#))
 Vaes, Wouter, S94 ([LBP-033](#))
 Vaia, Paolo, S173 ([TOP-072](#))
 Vaidya, Arun, S554 ([WED-327](#))
 Vaillant, Andrew, S28 ([OS-034](#)),
 S791 ([FRI-443](#)), S814 ([WED-383](#))
 Vainilovich, Yelena, S172 ([THU-092](#))
 Vairretti, Mariapia, S589 ([THU-274](#))
 Vaishnav, Manas, S201 ([TOP-065](#))
 Vakeeswarasarma, Vitushan, S81 ([LBP-008](#))
 Vaknin, Ilan, S268 ([THU-547](#)),
 S295 ([SAT-158](#))
 Valainathan, Shantha, S54 ([OS-084-YI](#)),
 S193 ([WED-112](#)), S524 ([WED-239](#))
 Valaydon, Zina, S400 ([SAT-492](#)),
 S402 ([SAT-496](#))
 Valbuena, Mónica Barreales,
 S139 ([SAT-257](#)), S365 ([TOP-002](#))
 Valdecantos, Pilar, S293 ([SAT-152](#)),
 S568 ([THU-209](#))
 Valdivieso, Andres, S64 ([OS-101-YI](#))
 Valdivieso, Miriam, S157 ([THU-049](#))
 Valencia, Jorge, S665 ([WED-442](#))
 Valenti, David, S484 ([FRI-256-YI](#))
 Valenti, Luca, S459 ([TOP-301](#)),
 S491 ([FRI-275-YI](#)), S496 ([FRI-290](#)),

Author Index

- S544 (WED-293), S571 (THU-218),
S593 (THU-286), S704 (TOP-144-YI),
S705 (WED-130)
Valentin, Emanuel Di, S432 (FRI-525)
Valentin, Nicolas Stankovic,
S191 (WED-105)
Valentino, Alessandro, S19 (OS-017)
Valenzi, Elena, S408 (SAT-523)
Valenzuela, María, S139 (SAT-257),
S142 (SAT-267)
Valera, Ana Lucena, S700 (FRI-171)
Valera, José Miguel, S80 (LBP-006)
Valero, Sonia, S714 (WED-164)
Valiani, Vincenzo, S96 (LBP-038),
S306 (THU-093)
Valiyeva, Leyla, S820 (THU-386-YI)
Valla, Dominique, S180 (WED-071),
S524 (WED-239), S526 (WED-245)
Valle, Mireia, S154 (SAT-304)
Valles, Foix, S9 (LBO-004), S89 (LBP-026)
Valliani, Talal, S380 (SAT-036-YI)
Valls, Imma, S822 (THU-395)
Valsan, Arun, S9 (LBO-004), S31 (OS-039),
S89 (LBP-026), S158 (THU-051),
S476 (FRI-231)
Valsecchi, Maria Grazie,
S325 (THU-133-YI)
Valverde, Angela Martinez, S293 (SAT-152),
S568 (THU-209), S574 (THU-225)
van Beek, Stijn, S321 (THU-124)
van Beers, Bernard, S526 (WED-245)
van Bergeijk, Jeroen D., S314 (THU-109),
S327 (THU-138)
van Bömmel, Florian, S52 (OS-079-YI),
S334 (THU-164-YI), S404 (SAT-501-YI),
S752 (SAT-410), S788 (FRI-434),
S793 (WED-391), S802 (WED-411)
van Dam, Lisette J.H., S319 (THU-120-YI)
Vandamme, Niels, S16 (OS-012-YI),
S292 (SAT-151-YI)
Vandecaveye, Vincent, S411 (TOP-507-YI)
van de Graaf, Stan, S296 (SAT-160),
S301 (SAT-178-YI)
van Delden, Otto, S394 (SAT-474)
van de Loo, Dominik, S115 (TOP-346-YI)
van Den Amele, Jelle, S81 (LBP-008)
Vandenbossche, Joris, S79 (LBP-005)
Van den Eede, Nele, S14 (OS-009-YI)
van den Hoek, Anita M., S597 (THU-297)
van den Hout, Wilbert, S204 (FRI-043)
van der Graaff, Denise, S584 (THU-258-YI)
Vanderhoff, Aaron, S673 (WED-464)
van der Laan, Luc, S464 (FRI-200),
S730 (TOP-384-YI)
Vanderlinden, Axelle, S730 (SAT-337)
van der Maas, Gerjan J., S319 (THU-120-YI)
van der Meer, Adriaan J., S308 (THU-098),
S309 (THU-100), S311 (THU-102-YI),
S314 (THU-109), S315 (THU-112-YI),
S319 (THU-120-YI), S321 (THU-125),
S327 (THU-138), S380 (SAT-035)
van der Merwe, Schalk, S14 (OS-009-YI),
S16 (OS-012-YI), S125 (TOP-328-YI),
S172 (THU-092)
Vanderschueren, Emma, S61 (OS-096-YI),
S246 (SAT-092-YI)
van der Velde, Jeroen, S492 (FRI-278)
van der Waaij, Lauren A., S319 (THU-120-YI)
van de Sluis, Bart, S347 (FRI-549-YI),
S573 (THU-224)
van Dijk, Remco, S763 (FRI-367)
van Doorn, Diederick, S213 (FRI-074-YI),
S219 (FRI-088)
van Duijn, Cornelia, S135 (THU-343)
van Duijn, Femke, S317 (THU-115-YI)
van Duyvenvoorde, Wim, S597 (THU-297)
van Eekhout, Kirs, S213 (FRI-074-YI)
van Erkel, Arian, S204 (FRI-043)
Vangeli, Marcello, S376 (SAT-025),
S380 (SAT-034)
van Gemert-Pijnen, Lisette,
S480 (FRI-244)
Vangipurapu, Jagadish, S562 (TOP-240-YI)
van Grunsven, Leo, S262 (THU-524-YI),
S267 (THU-541)
van Haag, Felix, S392 (TOP-520)
van Hoek, Bart, S18 (OS-015),
S204 (FRI-043), S309 (THU-100),
S314 (THU-109), S319 (THU-120-YI),
S327 (THU-138), S374 (SAT-021),
S703 (TOP-141), S708 (WED-135-YI),
S720 (WED-179-YI), S721 (WED-182)
van Hooff, Maria C., S309 (THU-100),
S311 (THU-102-YI), S314 (THU-109),
S319 (THU-120-YI), S321 (THU-125),
S327 (THU-138)
Vanhooymissen, Inge, S394 (SAT-474)
Vanhove, Trudy, S141 (SAT-261)
van Hulzen, Astrid, S763 (FRI-367)
van Kemenade, J., S319 (THU-120-YI)
van Kleef, Laurens, S464 (FRI-200),
S467 (FRI-209), S503 (TOP-241-YI),
S604 (SAT-197-YI), S606 (SAT-200-YI),
S643 (SAT-437-YI), S646 (SAT-443),
S649 (SAT-453)
van Koppen, Arianne, S513 (WED-209)
Vanlemmens, Claire, S6 (GS-010)
Vanlerberghe, Benedict, S14 (OS-009-YI)
van Meer, Suzanne, S309 (THU-100),
S314 (THU-109), S317 (THU-115-YI),
S319 (THU-120-YI), S327 (THU-138)
van Munster, Kim, S317 (THU-115-YI)
Vanni, Denise, S606 (SAT-201)
Vanni, Ester, S96 (LBP-038),
S306 (THU-093), S310 (THU-101)
van Nieuwkerk, Karin, S205 (FRI-043)
van Nuijs, Alexander, S14 (OS-009-YI)
van Putten, Paul G., S314 (THU-109),
S319 (THU-120-YI), S327 (THU-138)
van Rooij, Janne, S309 (THU-100)
van Rosmalen, Marieke, S366 (TOP-003-YI)
van Royen, Martin, S730 (TOP-384-YI)
Vanrusselt, Hannah, S728 (TOP-358-YI)
van Soest, Hanneke, S314 (THU-109),
S327 (THU-138), S763 (FRI-367)
Vanstraelen, Kim, S681 (WED-482),
S836 (THU-374)
van Velsen, Lisa M., S761 (FRI-363-YI)
Van Vlierberghe, Hans, S292 (SAT-151-YI),
S311 (THU-102-YI)
van Weeghel, Michel, S296 (SAT-160)
Vanwolleghe, Thomas, S61 (OS-096-YI),
S205 (FRI-043), S259 (SAT-134),
S386 (SAT-051), S540 (WED-281-YI),
S658 (WED-426), S665 (WED-441-YI),
S731 (SAT-337), S758 (TOP-401-YI),
S777 (FRI-406), S810 (WED-372),
S813 (WED-379)
van Zyl, Nina, S646 (SAT-444),
S672 (WED-459-YI)
Vaquero, Edith, S729 (TOP-368)
Vaquero, Javier, S276 (WED-528-YI),
S432 (FRI-525), S593 (THU-287)
Vaquero, Mirian Fernández, S65 (OS-103)
Vaquero-Rey, Aida, S362 (WED-016),
S364 (WED-028)
Vaquez Rodríguez, Sergio, S142 (SAT-267)
Vardeu, Antonella, S26 (OS-031),
S811 (WED-375)
Varela, Maria, S455 (THU-500),
S455 (THU-501)
Varela-Rey, Marta, S562 (TOP-229-YI)
Vargas-Accarino, Elena, S407 (SAT-516),
S633 (THU-028), S787 (FRI-432),
S822 (THU-395)
Vargas Blasco, Víctor Manuel,
S161 (THU-057-YI)
Vargas, Hugo, S161 (THU-058),
S163 (THU-060), S206 (FRI-046),
S218 (FRI-086), S242 (SAT-082)
Vargas, Victor, S30 (OS-038-YI),
S199 (TOP-062), S200 (TOP-064-YI)
Vargeese, Chandra, S693 (FRI-151)
Varghese, Dr. Joy, S158 (THU-052),
S167 (THU-078)
Várnai, Kinga A, S676 (WED-471)
Várnai, Kinga A., S759 (TOP-417)
Varughese, Tilly, S26 (OS-031)
Vashitshta, Chitranshu, S164 (THU-070)
Vasileiadi, Sofia, S690 (WED-503),
S823 (THU-398)
Vasilieva, Larisa, S208 (FRI-052),
S214 (FRI-076), S798 (WED-403)
Vasquez, Adriana, S146 (SAT-279)
Vasseur, Jessica, S170 (THU-087)
Vasudevan, Ashwini, S66 (OS-106-YI),
S67 (OS-108-YI), S176 (WED-056),
S177 (WED-058-YI), S346 (FRI-547-YI),
S348 (FRI-554)
Vatteroni, Maria Linda, S777 (FRI-405)
Vázquez, Alberto, S691 (WED-516)
Vázquez-Carrera, Manuel, S574 (THU-225)
Vázquez, Juan Turnes, S344 (THU-189),
S690 (WED-513)
VazRomero, Ignacio, S318 (THU-118),
S330 (THU-155)
Vecchio, Fabio Maria, S533 (WED-261-YI)
Veeckmans, Geraldine, S581 (THU-249)
Veelken, Rhea, S162 (THU-059),
S404 (SAT-501-YI)
Veenendaal, Roeland, S204 (FRI-043)
Veeracht-O-larn, Titinan, S796 (WED-396)

- Vega-Cano, Kreina Sharela, S702 ([TOP-139](#))
Vega Sáenz, José Luis, S668 ([WED-449](#))
Vidal, Sanne Skovgård, S574 ([THU-227](#)),
S580 ([THU-244](#)), S581 ([THU-248](#))
Velasco, Brian, S584 ([THU-259](#))
Velasco, Jose Antonio Velarde-Ruiz,
S161 ([THU-058](#))
Velásquez García, Héctor Alexander,
S686 ([WED-495](#))
Velazquez, René Malé, S83 ([LBP-012](#)),
S219 ([FRI-088](#))
Veldhuis, Sharon Oude, S480 ([FRI-244](#))
Veldt, Bart J., S309 ([THU-100](#)),
S314 ([THU-109](#)), S319 ([THU-120-YI](#)),
S327 ([THU-138](#))
Velez, Aryana, S661 ([WED-433](#))
Velliou, Rallia, S570 ([THU-214](#))
Velmati, Suresh, S699 ([FRI-167-YI](#))
Veloz, Maria Guerra, S388 ([SAT-057](#)),
S765 ([FRI-374-YI](#)), S820 ([THU-383](#))
Vendeville, Sandrine, S728 ([TOP-358-YI](#))
Vendrell, Marina, S362 ([WED-016](#))
Venere, Rosanna, S96 ([LBP-038](#)),
S306 ([THU-093](#))
Venerito, Marino, S52 ([OS-079-YI](#)),
S69 ([OS-112-YI](#)), S440 ([THU-457](#))
Venet, Fabienne, S22 ([OS-022](#))
Veneziano, Marzia, S175 ([TOP-085](#))
Vengohechea Llorens, Jordi,
S364 ([WED-028](#))
Venishetty, Shantanu, S149 ([SAT-290-YI](#)),
S440 ([THU-456](#)), S454 ([THU-498](#)),
S701 ([FRI-173](#)), S720 ([WED-180](#))
Venkatachalapathy, Suresh Vasan,
S161 ([THU-058](#))
Venkataraman, Jayanthi, S475 ([FRI-231](#))
Venkatasamy, Aina, S25 ([OS-029](#))
Venkatesh, Sudhakar, S52 ([OS-079-YI](#))
Vennarecci, Giovanni, S369 ([SAT-009](#))
Ventosa, Carla, S822 ([THU-395](#))
Ventura Cots, Meritxell, S142 ([SAT-267](#)),
S154 ([SAT-304](#))
Ventura, Paolo, S715 ([WED-165](#))
Venugopal, Giriprasad, S285 ([WED-554](#))
Venuto, Clara De, S206 ([FRI-047-YI](#))
Venzin, Valentina, S35 ([OS-048](#))
Verbeek, Jef, S14 ([OS-009-YI](#)),
S125 ([TOP-328-YI](#)), S321 ([THU-125](#)),
S371 ([SAT-014-YI](#))
Verbinnen, Thierry, S27 ([OS-033](#)),
S100 ([LBP-044](#)), S768 ([FRI-380](#)),
S801 ([WED-409](#)), S808 ([WED-367](#))
Verboven, Peter, S732 ([SAT-341](#))
Verburgh, Benjamin, S728 ([TOP-358-YI](#))
Vercruysse, Thomas, S807 ([WED-363](#))
Verda, Damiano, S19 ([OS-017](#))
Verdeguer, Francisco, S98 ([LBP-041](#))
Verdier, Alice, S572 ([THU-220](#))
Verdonk, Robert C., S309 ([THU-100](#)),
S314 ([THU-109](#)), S319 ([THU-120-YI](#)),
S327 ([THU-138](#))
Verdugo, Ramón Morillo, S827 ([THU-410](#))
Vereyken, Liesbeth, S732 ([SAT-341](#))
Vergani, Diego, S341 ([THU-182](#))
Vergara, Mercedes, S141 ([SAT-262](#)),
S233 ([FRI-126](#)), S311 ([THU-103](#)),
S329 ([THU-154-YI](#)), S344 ([THU-189](#)),
S829 ([THU-418](#))
Vergès, Bruno, S508 ([WED-194](#)),
S538 ([WED-278](#))
Vergis, Nikhil, S14 ([OS-008-YI](#)),
S126 ([THU-315](#)), S127 ([THU-317](#)),
S130 ([THU-326](#)), S145 ([SAT-274](#))
Verheijden, Simon, S79 ([LBP-005](#)),
S768 ([FRI-380](#)), S810 ([WED-372](#)),
S813 ([WED-379](#))
Verheij, Elwin, S94 ([LBP-033](#))
Verheij, Joanne, S394 ([SAT-474](#)),
S513 ([WED-209](#))
Verhelst, Xavier, S57 ([OS-089-YI](#)),
S143 ([SAT-268](#)), S278 ([WED-531](#)),
S292 ([SAT-151-YI](#)), S308 ([THU-098](#)),
S311 ([THU-102-YI](#)), S311 ([THU-103](#)),
S321 ([THU-123-YI](#)), S420 ([FRI-475-YI](#)),
S442 ([THU-463](#)), S631 ([THU-020-YI](#)),
S700 ([FRI-171](#)), S705 ([WED-129](#))
Verheyen, Jordi, S728 ([TOP-358-YI](#))
Verhoeven, Aswin, S278 ([WED-533](#))
Verhulst, Stefaan, S262 ([THU-524-YI](#)),
S267 ([THU-541](#))
Verjano, Francisco, S141 ([SAT-262](#))
Verkade, Henkjan J., S715 ([WED-166](#))
Verlaan, Tess, S317 ([THU-115-YI](#))
Verlinden, Wim, S828 ([THU-412](#))
Verlynde, Juliette, S640 ([SAT-430](#))
Verma, Nipun, S30 ([OS-038-YI](#)),
S31 ([OS-039](#)), S84 ([LBP-014](#)),
S129 ([THU-324](#)), S152 ([SAT-295](#)),
S158 ([THU-051](#)), S158 ([THU-052](#)),
S161 ([THU-058](#)), S199 ([TOP-062](#)),
S200 ([TOP-064-YI](#)), S217 ([FRI-082](#))
Verna, Elizabeth, S161 ([THU-058](#))
Veronesi, Valentina, S680 ([WED-479](#))
Verrastro, Ornella, S516 ([WED-215](#))
Verrier, Eloi, S734 ([SAT-348-YI](#))
Verschuren, Lars, S513 ([WED-209](#))
Verslype, Chris, S246 ([SAT-092-YI](#)),
S411 ([TOP-507-YI](#))
Verspaget, Hein W, S21 ([OS-020](#)),
S204 ([FRI-043](#))
Verstegen, Monique M.A.,
S730 ([TOP-384-YI](#))
Verucchi, Gabriella, S73 ([OS-120](#)),
S793 ([WED-391](#)), S804 ([WED-414](#))
Verwer, Bart, S213 ([FRI-074-YI](#))
Verzijl, Cristy, S573 ([THU-224](#))
Vespasiani-Gentilucci, Umberto,
S96 ([LBP-038](#)), S175 ([TOP-085](#)),
S306 ([THU-093](#)), S310 ([THU-101](#)),
S554 ([WED-325-YI](#)), S666 ([WED-446](#)),
S704 ([TOP-144-YI](#)), S754 ([SAT-418](#))
Vessby, Johan, S462 ([FRI-196](#)),
S550 ([WED-316](#))
Vesterhus, Mette, S50 ([OS-076-YI](#))
Vestito, Amanda, S241 ([SAT-078-YI](#)),
S399 ([SAT-490](#)), S704 ([TOP-143-YI](#))
Veteranos, Christos, S798 ([WED-403](#))
Vetter, Marcel, S338 ([THU-176](#))
Vettori, Giovanni, S96 ([LBP-038](#)),
S306 ([THU-093](#)), S310 ([THU-101](#))
Vettor, Roberto, S612 ([SAT-219](#))
V G, Mohan Prasad, S158 ([THU-052](#))
Viallet, Jean, S413 ([FRI-455](#))
Viana, Maria, S618 ([SAT-242](#))
Vibert, Eric, S370 ([SAT-011](#)), S378 ([SAT-029](#)),
S385 ([SAT-049](#))
Vicaud, Eric, S68 ([OS-110](#))
Viceconti, Nicholas, S533 ([WED-261-YI](#))
Vicién, Gemma Garcia, S24 ([OS-026-YI](#)),
S420 ([FRI-474-YI](#))
Victor, David W.III, S621 ([FRI-008](#)),
S625 ([FRI-023](#))
Victor, Livia, S208 ([FRI-053](#))
Vitor, Victor M., S266 ([THU-539](#))
Vidal, Jordi, S177 ([WED-059](#))
Vidal, Silvia, S355 ([SAT-543](#))
Vidal-Trecan, Tiphaine, S526 ([WED-245](#))
Vidgren, Mathias, S369 ([SAT-009](#))
Viel, Philine Witkowski Durand,
S115 ([SAT-306](#))
Viel, Sophie, S130 ([THU-327](#))
Vierling, John M., S80 ([LBP-006](#))
Viganò, Mauro, S19 ([OS-017](#)),
S96 ([LBP-038](#)), S306 ([THU-093](#)),
S310 ([THU-101](#)), S332 ([THU-161](#)),
S439 ([THU-447](#)), S470 ([FRI-215-YI](#)),
S497 ([FRI-294](#)), S705 ([WED-130](#)),
S804 ([WED-414](#))
Viganò, Raffaella, S96 ([LBP-038](#)),
S306 ([THU-093](#)), S376 ([SAT-025](#)),
S380 ([SAT-034](#)), S700 ([FRI-171](#))
Vigil, Ana Peleteiro, S432 ([FRI-523](#))
Vigneron, Paul, S413 ([FRI-456](#))
Vignone, Anthony, S175 ([TOP-085](#))
Vig, Pamela, S307 ([THU-094](#)),
S323 ([THU-129](#)), S331 ([THU-158](#))
Vijan, Ancuta, S216 ([FRI-080](#))
Vijayaraghavan, Pooja, S346 ([FRI-547-YI](#))
Vijay, Esha Bharathwaj, S280 ([WED-539](#))
Vilamil, Federico, S208 ([FRI-053](#))
Vilà, Paula Cantallops, S24 ([OS-026-YI](#)),
S420 ([FRI-474-YI](#))
Vilar Gomez, Eduardo, S469 ([FRI-213](#))
Vilarnau, Nuria, S281 ([WED-543](#))
Vilgrain, Valerie, S68 ([OS-110](#))
Villa, Erica, S438 ([THU-446](#))
Villa, Federica, S451 ([THU-486-YI](#))
Villagrasa, Ares, S142 ([SAT-267](#)),
S154 ([SAT-304](#)), S336 ([THU-170-YI](#))
Villalobos, Eduardo Sanz-de,
S738 ([SAT-374-YI](#)), S768 ([FRI-381](#))
Villamil, Alejandra, S80 ([LBP-006](#)),
S91 ([LBP-027](#)), S98 ([LBP-040](#)),
S335 ([THU-167](#)), S336 ([THU-170-YI](#)),
S341 ([THU-182](#)), S342 ([THU-185](#))
Villani, Rosanna, S175 ([TOP-085](#)),
S470 ([FRI-215-YI](#)), S496 ([FRI-290](#))
Villano, Gianmarco, S612 ([SAT-219](#))
Villanueva, Augusto, S216 ([FRI-081](#)),
S411 ([TOP-507-YI](#))
Villanueva, Cándid, S85 ([LBP-016](#)),
S231 ([FRI-121](#)), S355 ([SAT-543](#))

Author Index

- Villanueva, Marina, S103 ([TOP-350-YI](#)), S107 ([FRI-324](#))
- Villar, Carmen, S139 ([SAT-257](#)), S142 ([SAT-267](#))
- Villard, Christina, S22 ([OS-023-YI](#)), S386 ([SAT-050](#))
- Villarino, Irene, S391 ([TOP-512-YI](#))
- Villarroel, Carolina, S487 ([FRI-262](#)), S674 ([WED-465](#))
- Villavicencio, Edgar, S556 ([WED-334](#)), S641 ([SAT-432](#)), S642 ([SAT-434](#)), S654 ([SAT-466](#))
- Villela-Nogueira, Cristiane, S483 ([FRI-254](#)), S619 ([SAT-248](#))
- Villeret, Francois, S22 ([OS-022](#))
- Villesen, Ida Falk, S47 ([OS-072-YI](#)), S77 ([OS-126](#)), S137 ([SAT-250](#)), S205 ([FRI-045](#)), S255 ([SAT-122](#)), S466 ([FRI-206-YI](#)), S510 ([WED-199](#)), S620 ([TOP-012](#)), S623 ([FRI-017](#))
- Villota-Rivas, Marcela, S651 ([SAT-456](#))
- Vilsbøll, Tina, S615 ([SAT-231](#))
- Vilstrup, Hendrik, S236 ([FRI-134](#))
- Vinaixa, Carmen, S9 ([LBO-004](#)), S89 ([LBP-026](#)), S531 ([WED-257](#))
- Viñas, Laura Sererols, S24 ([OS-026-YI](#)), S420 ([FRI-474-YI](#))
- Viñas, Oriol Mirallas, S702 ([TOP-139](#))
- Vincent, Catherine, S19 ([OS-018](#)), S305 ([TOP-169](#))
- Vincentis, Antonio De, S96 ([LBP-038](#)), S175 ([TOP-085](#)), S754 ([SAT-418](#))
- Viola, Maria, S16 ([OS-012-YI](#))
- Violeta, Sargsyan, S158 ([THU-052](#)), S167 ([THU-078](#))
- Violi, Paola, S368 ([SAT-009](#))
- Vioulac, Christel, S313 ([THU-107](#))
- Vipani, Aarshi, S39 ([OS-055](#))
- Viridis, Matteo, S70 ([OS-114](#))
- Viret, Anne-Claire, S313 ([THU-107](#))
- Virseda-Berdices, Ana, S741 ([SAT-379](#))
- Virtue, Susan, S380 ([SAT-036-YI](#))
- Virzì, Alessia, S734 ([SAT-348-YI](#))
- Vitale, Alessandro, S28 ([OS-034](#)), S59 ([OS-094](#)), S376 ([SAT-024-YI](#)), S389 ([SAT-058](#))
- Vitale, Luigi Maria, S213 ([FRI-070-YI](#))
- Vitalis, Zsuzsanna, S169 ([THU-080-YI](#)), S313 ([THU-106-YI](#))
- Vitek, Libor, S539 ([WED-280](#))
- Vitellius, Carole, S456 ([THU-503](#))
- Vithayathil, Mathew, S443 ([THU-464](#))
- Viti, Vittorio, S123 ([SAT-334](#))
- Vits, Lieve, S581 ([THU-249](#))
- Vivaldi, Caterina, S51 ([OS-078-YI](#)), S69 ([OS-112-YI](#)), S395 ([SAT-477-YI](#)), S446 ([THU-472-YI](#))
- Vivarelli, Marco, S369 ([SAT-009](#))
- Viveiros, André, S375 ([SAT-023](#))
- Vizcarra, Pamela, S255 ([SAT-123](#))
- Vizzutti, Francesco, S62 ([OS-099-YI](#)), S258 ([SAT-131](#))
- Vlachogiannakos, Ioannis, S217 ([FRI-083](#)), S798 ([WED-403](#)), S800 ([WED-406](#))
- Vlachos, Iakovos, S454 ([THU-495](#))
- Vlierberghe, Hans Van, S57 ([OS-089-YI](#)), S143 ([SAT-268](#)), S278 ([WED-531](#)), S321 ([THU-123-YI](#)), S420 ([FRI-475-YI](#)), S442 ([THU-463](#)), S631 ([THU-020-YI](#))
- Vloo, Charlotte De, S321 ([THU-123-YI](#))
- Vo, Alex, S753 ([SAT-411](#)), S753 ([SAT-412](#))
- Voeller, Alexis, S663 ([WED-437](#)), S667 ([WED-448](#)), S674 ([WED-466](#)), S678 ([WED-474](#))
- Vogel, Arndt, S51 ([OS-078-YI](#)), S69 ([OS-112-YI](#)), S425 ([FRI-492-YI](#)), S443 ([THU-464](#)), S445 ([THU-470-YI](#)), S445 ([THU-471-YI](#)), S447 ([THU-475](#))
- Vogel, Georg-Friedrich, S54 ([OS-083](#))
- Vogel, Rosi, S642 ([SAT-434](#))
- Voiosu, Andrei, S216 ([FRI-080](#))
- Voiosu, Theodor, S216 ([FRI-080](#))
- Voldum-Clausen, Kristoffer, S580 ([THU-244](#))
- Volkert, Ines, S57 ([OS-088-YI](#)), S273 ([WED-521-YI](#)), S431 ([FRI-522](#))
- Volmari, Annika, S74 ([OS-122](#)), S733 ([SAT-342-YI](#))
- Volpe, Letizia Bavuso, S571 ([THU-218](#))
- Volpi, Camilla, S751 ([SAT-407](#))
- Volz, Tassilo, S733 ([SAT-342-YI](#))
- von Bergen, Martin, S104 ([TOP-352](#)), S134 ([THU-340-YI](#))
- Vondran, Florian, S425 ([FRI-492-YI](#)), S730 ([TOP-369](#))
- von Felden, Johann, S24 ([OS-027-YI](#)), S51 ([OS-078-YI](#)), S52 ([OS-079-YI](#)), S69 ([OS-112-YI](#)), S443 ([THU-464](#))
- von Felten, Stefanie, S702 ([TOP-140](#))
- Vonghia, Luisa, S37 ([OS-053](#)), S61 ([OS-096-YI](#)), S259 ([SAT-134](#)), S371 ([SAT-014-YI](#)), S540 ([WED-281-YI](#)), S581 ([THU-249](#)), S584 ([THU-258-YI](#)), S730 ([SAT-337](#))
- von Laer, Dorothee, S728 ([TOP-359-YI](#))
- von Meijenfeldt, Fien, S112 ([FRI-342](#))
- Vonschallen, Philip, S98 ([LBP-041](#)), S565 ([THU-199](#))
- von Schönfels, Witigo, S582 ([THU-254-YI](#))
- von Seth, Erik, S312 ([THU-104](#))
- Vo Quang, Erwan, S784 ([FRI-425](#)), S786 ([FRI-431](#))
- Vorobioff, Julio D., S30 ([OS-038-YI](#)), S199 ([TOP-062](#)), S200 ([TOP-064-YI](#))
- Vosbeck, Jürg, S291 ([TOP-150-YI](#))
- Vos, Dyonne, S347 ([FRI-549-YI](#))
- Vos, Harmjan, S301 ([SAT-178-YI](#))
- Vos, Xander, S213 ([FRI-074-YI](#))
- Vos, Zenzi De, S420 ([FRI-475-YI](#))
- Vrij, Ton, S317 ([THU-115-YI](#))
- Vrolijk, Jan Maarten, S309 ([THU-100](#)), S314 ([THU-109](#)), S319 ([THU-120-YI](#))
- Vrtělka, Ondřej, S539 ([WED-280](#))
- Vucur, Mihael, S259 ([SAT-135](#)), S426 ([FRI-495](#))
- Vukotic, Ranka, S619 ([SAT-245](#))
- Vu, Mylisa, S689 ([WED-501](#))
- Vuppalachchi, Raj, S7 ([LBO-001](#))
- Vyawahare, Saurabh, S592 ([THU-284](#))
- Vyberg, Mogens, S421 ([FRI-478](#))
- Vydrár, David, S756 ([SAT-422](#))
- Wack, Katy, S507 ([TOP-289](#))
- Wada, Naohiro, S235 ([FRI-130](#))
- Waddah, Mohamed, S250 ([SAT-107-YI](#))
- Waddell, Scott, S66 ([OS-105-YI](#)), S695 ([FRI-158-YI](#))
- Waddilove, Elizabeth, S675 ([WED-469](#)), S746 ([SAT-394](#)), S750 ([SAT-404](#)), S752 ([SAT-409](#)), S753 ([SAT-413](#)), S756 ([SAT-421](#))
- Wadhawan, Aishani, S129 ([THU-324](#)), S152 ([SAT-295](#)), S217 ([FRI-082](#))
- Wadhwa, Nishant, S719 ([WED-176](#))
- Wadland, Elaine, S333 ([THU-162-YI](#))
- Wafula, Rose, S684 ([WED-487](#))
- Wagner, Johannes, S368 ([SAT-008](#))
- Wagner, Lea, S205 ([FRI-044-YI](#)), S245 ([SAT-090-YI](#))
- Wagner, Mathilde, S50 ([OS-077](#)), S441 ([THU-458](#))
- Wagner, Tyler E., S326 ([THU-135](#))
- Wagner, Verena, S368 ([SAT-008](#))
- Wahab, Sabrina Ab, S552 ([WED-321](#))
- Waheed, Myra, S394 ([SAT-476](#))
- Wahid, Avista, S730 ([TOP-369](#))
- Wahli, Walter, S574 ([THU-225](#))
- Waisbourd-Zinman, Orith, S696 ([FRI-160-YI](#))
- Waisman, Ari, S65 ([OS-103](#))
- Wajcman, Dana Ivancovsky, S651 ([SAT-456](#))
- Wajsenzonz, Ines, S190 ([WED-102](#))
- Wakabayashi, Shun-ichi, S478 ([FRI-237](#))
- Wakim-Fleming, Jamile, S76 ([OS-125](#))
- Waldmann, Moritz, S24 ([OS-027-YI](#)), S316 ([THU-113](#))
- Waldschmidt, Dirk-Thomas, S52 ([OS-079-YI](#))
- Walia, Dinesh, S546 ([WED-298-YI](#))
- Walia, Nirbaanot, S161 ([THU-057-YI](#)), S203 ([FRI-040](#)), S649 ([SAT-452](#))
- Walker, Alexander, S66 ([OS-105-YI](#))
- Walker, Jill, S809 ([WED-370](#))
- Walker, Maria, S56 ([OS-086-YI](#))
- Walker, Michael A., S812 ([WED-377](#))
- Walker, Tanya, S647 ([SAT-447](#))
- Wallace, David, S388 ([SAT-057](#))
- Wallace, Zachary, S710 ([WED-152](#))
- Wallays, Marie, S16 ([OS-012-YI](#)), S125 ([TOP-328-YI](#))
- Walld, Randy, S643 ([SAT-436](#))
- Wall, Emma, S750 ([SAT-404](#))
- Wallert, Maria, S600 ([THU-314](#))
- Wallin, Jeffrey, S74 ([OS-122](#)), S738 ([SAT-373](#))
- Walmsley, Martine, S332 ([THU-160](#)), S712 ([WED-158-YI](#))
- Wan, Chunhua, S590 ([THU-280](#))
- Wandji, Line Carolle Ntandja, S6 ([GS-010](#)), S156 ([TOP-108](#)), S644 ([SAT-439-YI](#))
- Wan, Eric Yuk Fai, S116 ([SAT-314](#))

- Wang, Benny, S22 ([OS-023-YI](#)), S386 ([SAT-050](#))
- Wang, Bruce, S715 ([WED-165](#))
- Wang, Chia-Chi, S832 ([THU-365](#))
- Wang, Chih-Wen, S490 ([FRI-271](#)), S493 ([FRI-280](#))
- Wang, Cong, S183 ([WED-081](#)), S183 ([WED-082](#))
- Wang, Dong, S544 ([WED-292](#)), S806 ([WED-362](#)), S813 ([WED-381](#)), S815 ([WED-386](#)), S816 ([WED-388](#))
- Wangensteen, Kirk, S396 ([SAT-479-YI](#))
- Wang, Fengmei, S526 ([WED-246](#))
- Wang, Genshu, S271 ([TOP-562](#)), S347 ([FRI-551](#)), S363 ([WED-020](#))
- Wang, Gui-Qiang, S684 ([WED-490](#)), S790 ([FRI-439](#))
- Wang, Haiyu, S210 ([FRI-055](#))
- Wang, Hong, S605 ([SAT-198](#))
- Wang, Hongyuan, S771 ([FRI-390](#)), S797 ([WED-397](#))
- Wang, Hung-Wei, S69 ([OS-112-YI](#))
- Wang, Jia-Bo, S124 ([SAT-336](#)), S135 ([THU-342](#))
- Wang, Jian, S219 ([FRI-088](#)), S628 ([FRI-035](#)), S780 ([FRI-411-YI](#))
- Wang, Jianhong, S544 ([WED-292](#))
- Wang, Jiaqi, S745 ([SAT-392](#))
- Wang, Jie, S111 ([FRI-338](#)), S111 ([FRI-339](#)), S423 ([FRI-486](#))
- Wang, Jing, S526 ([WED-246](#)), S789 ([FRI-438](#))
- Wang, Jinhai, S235 ([FRI-131](#))
- Wang, Jiong Wei, S565 ([THU-200-YI](#))
- Wang, Juan, S594 ([THU-291-YI](#))
- Wang, Jun, S395 ([SAT-479-YI](#)), S462 ([FRI-195](#))
- Wang, Junting, S99 ([LBP-043](#))
- Wang, Junyu, S582 ([THU-251-YI](#))
- Wang, Le, S100 ([LBP-045](#))
- Wang, Lei, S161 ([THU-058](#)), S236 ([FRI-135](#)), S260 ([SAT-136](#))
- Wang, Li, S655 ([SAT-468](#)), S816 ([WED-389](#))
- Wang, Lidan, S99 ([LBP-043](#))
- Wang, Lin, S748 ([SAT-398](#))
- Wang, Lingyu, S423 ([FRI-486](#))
- Wang, Liu, S527 ([WED-246](#))
- Wang, Lulu, S505 ([TOP-264](#))
- Wang, Meng, S660 ([WED-431](#))
- Wang, Miao, S86 ([LBP-019](#)), S99 ([LBP-043](#))
- Wang, Muqi, S195 ([WED-116](#))
- Wang, Qi, S228 ([FRI-114](#)), S479 ([FRI-242](#))
- Wang, Qiuhe, S447 ([THU-475](#)), S716 ([WED-167](#))
- Wang, Rui, S271 ([TOP-561](#))
- Wang, Sai, S263 ([THU-526](#)), S287 ([FRI-539](#))
- Wang, Sarah, S76 ([OS-125](#))
- Wang, Shan, S536 ([WED-272](#))
- Wang, Shanshan, S613 ([SAT-221](#))
- Wang, Shiyu, S344 ([THU-191](#)), S355 ([SAT-544](#)), S738 ([SAT-372](#)), S815 ([WED-387](#))
- Wang, Sih-Ren, S832 ([THU-365](#))
- Wang, Sikui, S605 ([SAT-198](#))
- Wang, Su, S661 ([WED-433](#))
- Wang, Tianyuan, S280 ([WED-541](#))
- Wang, Tingyan, S676 ([WED-471](#)), S756 ([SAT-421](#)), S759 ([TOP-417](#))
- Wang, Wei, S209 ([FRI-053](#))
- Wang, Weichung, S399 ([SAT-486](#))
- Wang, Wen, S86 ([LBP-019](#)), S99 ([LBP-043](#)), S551 ([WED-319](#)), S558 ([WED-338](#))
- Wang, Wenhui, S447 ([THU-475](#))
- Wang, Wenjun, S195 ([WED-116](#))
- Wang, Xian-bo, S145 ([SAT-275](#))
- Wang, Xiao, S106 ([FRI-323](#)), S354 ([SAT-542](#))
- Wang, Xiaojuan, S442 ([THU-462](#)), S625 ([FRI-021](#))
- Wang, Xiaomei, S526 ([WED-246](#))
- Wang, Xiaowen, S271 ([TOP-562](#)), S347 ([FRI-551](#)), S363 ([WED-020](#))
- Wang, Xiaoyan, S544 ([WED-292](#))
- Wang, Xiaozhong, S209 ([FRI-053](#))
- Wang, Xinrui, S161 ([THU-058](#))
- Wang, Xiuhua, S701 ([FRI-174](#))
- Wang, Xue, S109 ([FRI-332](#))
- Wang, Xue Fei, S525 ([WED-242](#))
- Wang, Yan, S119 ([SAT-321](#)), S121 ([SAT-326](#)), S413 ([FRI-455](#)), S526 ([WED-246](#))
- Wang, Yanan, S278 ([WED-533](#))
- Wang, Yanbo, S586 ([THU-262](#))
- Wang, Yang, S124 ([TOP-312](#)), S592 ([THU-284](#))
- Wang, Yijin, S561 ([TOP-228-YI](#)), S730 ([TOP-384-YI](#))
- Wang, Yikai, S195 ([WED-116](#)), S590 ([THU-279](#))
- Wang, Ying, S558 ([WED-337](#))
- Wang, Yingling, S219 ([FRI-088](#))
- Wang, Yining, S652 ([SAT-462-YI](#)), S730 ([TOP-384-YI](#))
- Wang, Yuehua, S527 ([WED-246](#))
- Wang, Yun, S39 ([OS-055](#)), S200 ([TOP-063](#))
- Wang, Yunfang, S433 ([FRI-527](#))
- Wang, Yuqin, S578 ([THU-236-YI](#))
- Wang, Yuting, S353 ([SAT-539-YI](#))
- Wang, Zhenguang, S803 ([WED-412](#))
- Wang, Zhengxin, S775 ([FRI-398](#))
- Wang, Zhengyi, S84 ([LBP-014](#)), S275 ([WED-526](#))
- Wang, Zhidong, S241 ([SAT-077](#))
- Wang, Ziqi Vincent, S534 ([WED-267](#))
- Wan, Haitao, S573 ([THU-223](#))
- Wan, Heng, S526 ([WED-246](#)), S536 ([WED-272](#)), S620 ([TOP-006](#))
- Wan-Hin Hui, Rex, S745 ([SAT-392](#))
- Wan, Hui, S753 ([SAT-412](#))
- Wani, Qasim, S567 ([THU-203](#))
- Wan, Xueshuai, S99 ([LBP-042](#))
- Wan, Zhiping, S574 ([THU-226](#))
- Ward, John, S678 ([WED-474](#)), S686 ([WED-494](#))
- Wareing, Sue, S756 ([SAT-421](#))
- Warsop, Zakary, S656 ([TOP-460-YI](#))
- Wartel, Faustine, S168 ([THU-079](#))
- Wartski, Myriam, S50 ([OS-077](#))
- Washington, Kay, S595 ([THU-293](#))
- Wassenberg, Sebastian, S560 ([WED-343](#))
- Watanabe, Makoto, S513 ([WED-208](#))
- Watanabe, Masaaki, S118 ([SAT-319](#))
- Watanabe, Takao, S711 ([WED-154](#)), S722 ([WED-184](#))
- Watanabe, Takuya, S451 ([THU-490](#))
- Watanabe, Tsunamasa, S248 ([SAT-101](#))
- Wat, Cynthia, S26 ([OS-030](#)), S788 ([FRI-434](#))
- Watkins, Timothy R., S462 ([FRI-195](#)), S505 ([TOP-264](#)), S571 ([THU-215](#)), S585 ([THU-261](#))
- Watson, Christopher, S81 ([LBP-008](#))
- Watson, Hugh, S244 ([SAT-088](#)), S657 ([WED-423](#))
- Watt, Nicole, S573 ([THU-222-YI](#))
- Watzkenboeck, Martin, S719 ([WED-175](#))
- Wauters, Joost, S157 ([THU-049](#))
- Weavil, Josh, S10 ([LBO-005](#))
- Webb, Gwilym, S81 ([LBP-008](#))
- Weber, Achim, S702 ([TOP-140](#))
- Weber, Anna-Lena, S374 ([SAT-021](#))
- Weber, Julius, S35 ([OS-049-YI](#))
- Weber, Matthias, S230 ([FRI-120](#))
- Weber, Susanne N., S713 ([WED-161-YI](#))
- Webster, George, S710 ([WED-152](#))
- Wedd, Joel, S1 ([GS-001](#))
- Wedemeyer, Heiner, S1 ([GS-002](#)), S21 ([OS-021-YI](#)), S44 ([OS-066-YI](#)), S74 ([OS-122](#)), S75 ([OS-127](#)), S92 ([LBP-029](#)), S100 ([LBP-044](#)), S115 ([TOP-346-YI](#)), S202 ([FRI-038-YI](#)), S204 ([FRI-042](#)), S205 ([FRI-044-YI](#)), S226 ([FRI-107-YI](#)), S226 ([FRI-109](#)), S245 ([SAT-090-YI](#)), S253 ([SAT-117](#)), S350 ([SAT-532-YI](#)), S353 ([SAT-538-YI](#)), S528 ([WED-249](#)), S583 ([THU-256](#)), S712 ([WED-160](#)), S730 ([TOP-369](#)), S735 ([SAT-363](#)), S750 ([SAT-406-YI](#)), S758 ([TOP-400](#)), S759 ([TOP-416-YI](#)), S762 ([FRI-365-YI](#)), S764 ([FRI-371](#)), S793 ([WED-391](#)), S794 ([WED-392](#)), S796 ([WED-395](#)), S820 ([THU-386-YI](#))
- Wee, Aileen, S467 ([FRI-208](#))
- Weersma, Rinse, S317 ([THU-115-YI](#))
- Wege, Henning, S24 ([OS-027-YI](#)), S51 ([OS-078-YI](#)), S443 ([THU-464](#))
- Wegermann, Kara, S208 ([FRI-053](#))
- Wei, Bo, S225 ([FRI-105](#)), S241 ([SAT-077](#)), S622 ([FRI-010](#))
- Weichselbaum, Laura, S133 ([THU-335](#)), S786 ([FRI-429](#))
- Weidhase, Lorenz, S162 ([THU-059](#))
- Wei, Jinfen, S526 ([WED-246](#))
- Wei, Jinxing, S382 ([SAT-041](#))
- Wei, Lai, S100 ([LBP-045](#)), S128 ([THU-320-YI](#)), S558 ([WED-337](#)), S613 ([SAT-221](#))
- Weiler-Normann, Christina, S374 ([SAT-021](#))
- Wei, Linlin, S219 ([FRI-088](#))
- Weil-Verhoeven, Delphine, S61 ([OS-097](#)), S168 ([THU-079](#)), S200 ([TOP-064-YI](#)), S369 ([SAT-010](#)), S385 ([SAT-048](#)), S423 ([FRI-485](#)), S481 ([FRI-245](#))
- Weinbaum, Sindee, S339 ([THU-178](#))
- Weinberger, Adina, S645 ([SAT-442](#))

Author Index

- Weinmann, Arndt, S52 ([OS-079-YI](#)), S334 ([THU-164-YI](#)), S440 ([THU-457](#)), S443 ([THU-464](#))
- Weinmann-Menke, Julia, S249 ([SAT-104-YI](#))
- Weisberg, Ilan, S252 ([SAT-114](#)), S487 ([FRI-262](#)), S545 ([WED-295-YI](#))
- Weis, Nina, S795 ([WED-394](#))
- Weiss, Caroline, S32 ([OS-041-YI](#))
- Weiss, Emmanuel, S116 ([SAT-315](#)), S372 ([SAT-016](#))
- Weissenborn, Karin, S205 ([FRI-044-YI](#))
- Weiss, Karl Heinz, S716 ([WED-170](#))
- Weiss, Nicolas, S207 ([FRI-050-YI](#)), S218 ([FRI-087](#)), S222 ([FRI-094-YI](#)), S222 ([FRI-095](#))
- Weiß, Rebecca, S317 ([THU-116-YI](#))
- Wei, Xi, S400 ([SAT-491](#))
- Wei, Yu-Ju, S490 ([FRI-271](#)), S493 ([FRI-280](#))
- Welman, Christopher, S483 ([FRI-250](#)), S487 ([FRI-263](#))
- Welsch, Christoph, S170 ([THU-087](#)), S203 ([FRI-039](#))
- Weltzsch, Jan Philipp, S316 ([THU-113](#))
- Wendon, Julia, S44 ([OS-065](#))
- Wen, Gao, S129 ([THU-322-YI](#))
- Weng, Honglei, S263 ([THU-526](#)), S287 ([FRI-539](#))
- Wen-Juei Jeng, Rachel, S782 ([FRI-415](#)), S784 ([FRI-426](#))
- Wennbo, Haakan, S544 ([WED-294](#))
- Wentworth, Brian, S30 ([OS-038-YI](#)), S199 ([TOP-062](#)), S200 ([TOP-064-YI](#))
- Wen, Yilei, S99 ([LBP-043](#))
- Wen, Zhang, S235 ([FRI-131](#))
- Wen, Zhilong, S120 ([SAT-323](#))
- Werge, Mikkel, S513 ([WED-207](#)), S529 ([WED-250-YI](#)), S555 ([WED-331-YI](#))
- Wernberg, Charlotte, S139 ([SAT-255](#)), S142 ([SAT-266](#)), S620 ([TOP-012](#))
- Werner, Ellen, S309 ([THU-100](#)), S314 ([THU-109](#)), S319 ([THU-120-YI](#)), S321 ([THU-125](#)), S327 ([THU-138](#))
- Werner, Jill, S187 ([WED-094](#))
- Wernevik, Linda, S93 ([LBP-031](#))
- Wernly, Bernhard, S500 ([FRI-303](#))
- Westbrook, Rachel, S9 ([LBO-004](#)), S89 ([LBP-026](#))
- West, Claire, S380 ([SAT-036-YI](#))
- West, Joe, S399 ([SAT-487-YI](#))
- Weston, Chris J., S423 ([FRI-487](#))
- Westphal, Tim, S739 ([SAT-376](#))
- Wetten, Aaron, S297 ([SAT-165-YI](#))
- Wettstein, Guillaume, S584 ([THU-258-YI](#))
- Wheater, Valerie, S724 ([WED-189](#))
- Wheeler, Darren, S314 ([THU-110](#)), S621 ([FRI-008](#)), S623 ([FRI-015](#)), S625 ([FRI-023](#)), S627 ([FRI-030](#))
- White, Christopher, S95 ([LBP-036](#))
- Więckowski, Sebastian, S713 ([WED-161-YI](#))
- Wiedemann, Gabriela M., S35 ([OS-049-YI](#))
- Wiedemann, Toska, S170 ([THU-087](#))
- Wiegand, Johannes, S716 ([WED-170](#))
- Wiegand, Steffen, S750 ([SAT-406-YI](#))
- Wiencke, Kristine, S22 ([OS-023-YI](#)), S386 ([SAT-050](#))
- Wiener, Sebastian, S443 ([THU-465-YI](#))
- Wien, Lena, S821 ([THU-390](#))
- Wiering, Leke, S366 ([TOP-003-YI](#)), S386 ([SAT-051](#))
- Wierzbicka, Aldona, S578 ([THU-238](#))
- Wiese, Małgorzata, S578 ([THU-238](#))
- Wiese, Signe, S555 ([WED-331-YI](#))
- Wiest, Reiner, S117 ([SAT-316](#))
- Wietharn, Brooke, S51 ([OS-078-YI](#)), S69 ([OS-112-YI](#)), S443 ([THU-464](#))
- Wigg, Alan, S275 ([WED-526](#))
- Wijarnpreecha, Karn, S139 ([SAT-256](#)), S146 ([SAT-278](#)), S147 ([SAT-281](#)), S478 ([FRI-236-YI](#)), S540 ([WED-282](#))
- Wilamowski, Mateusz, S265 ([THU-533](#))
- Wild, Philipp, S461 ([FRI-194-YI](#))
- Wilkinson, Alex, S423 ([FRI-487](#))
- Wilkinson, Jennifer, S297 ([SAT-165-YI](#))
- Wilkinson, Samuel, S675 ([WED-469](#)), S752 ([SAT-409](#))
- Willars, Christopher, S44 ([OS-065](#))
- Willeford, Courtney Moc, S811 ([WED-374](#))
- Willemse, José A., S321 ([THU-125](#)), S712 ([WED-158-YI](#))
- Willemssen, Nele, S213 ([FRI-071](#))
- Willems, Ruth, S237 ([TOP-061-YI](#))
- Willemssen, Francois, S394 ([SAT-474](#))
- Williams, Dominic, S289 ([FRI-542](#))
- Williams, Nicola, S523 ([WED-236-YI](#))
- Williamson, Catherine, S274 ([WED-523](#))
- Williamson, Toni, S564 ([THU-198](#))
- Will, Nico, S350 ([SAT-531-YI](#))
- Willoughby, Catherine E., S425 ([FRI-493](#))
- Willuweit, Katharina, S384 ([SAT-046](#))
- Wilmer, Alexander, S157 ([THU-049](#)), S246 ([SAT-092-YI](#))
- Wilmink, Marijn, S56 ([OS-086-YI](#))
- Wils, Hans, S813 ([WED-379](#))
- Wilson, Debbie, S658 ([WED-425](#))
- Wilson-Kanamori, John, S105 ([FRI-318-YI](#))
- Wilson, Rickesha, S76 ([OS-125](#))
- Wilson, Wendy, S647 ([SAT-447](#))
- Windisch, Marc P., S812 ([WED-377](#))
- Wing-Ki Hui, Vicki, S154 ([SAT-302](#))
- Winikajtis-Burzyńska, Agnieszka, S308 ([THU-095](#))
- Winkler, Romy, S802 ([WED-411](#))
- Win, Rosanna, S729 ([TOP-368](#))
- Winter, Benedicte De, S581 ([THU-249](#))
- Winter, Erin, S381 ([SAT-037](#))
- Wintersteller, Hannah, S351 ([SAT-533](#))
- Winther-Jensen, Matilde, S149 ([SAT-286-YI](#))
- Wirtz, Stefan, S317 ([THU-116-YI](#))
- Wirtz, Theresa Hildegard, S229 ([FRI-116](#)), S259 ([SAT-135](#))
- Wischer, Lara, S23 ([OS-025-YI](#))
- Wisskirchen, Karin, S99 ([LBP-042](#))
- Witte, Moana, S735 ([SAT-363](#)), S750 ([SAT-406-YI](#))
- Witt, Jennifer, S205 ([FRI-044-YI](#))
- Woelfle, Joachim, S356 ([SAT-546](#))
- Wohlfeiler, Michael, S799 ([WED-405](#))
- Wohlleber, Dirk, S351 ([SAT-533](#))
- Woillard, Jean-Baptiste, S387 ([SAT-052](#))
- Wolff, Lisa, S727 ([TOP-355-YI](#))
- Wolfgang, Zimmermann Henning, S356 ([SAT-545](#))
- Wolfhagen, Frank H.J., S314 ([THU-109](#)), S327 ([THU-138](#))
- Wolfisberg, Tim, S117 ([SAT-316](#))
- Wölflle, Lena, S54 ([OS-083](#))
- Wolf, Peter, S251 ([SAT-111](#))
- Wolter, Karsten, S258 ([SAT-130](#))
- Wolters, Frank, S296 ([SAT-160](#))
- Wolters, Lena, S169 ([THU-083](#))
- Woltsche, Johannes, S229 ([FRI-115](#))
- Wong, Boris, S372 ([SAT-017](#))
- Wong, Carlos King Ho, S116 ([SAT-314](#))
- Wong, Danny Ka-Ho, S424 ([FRI-490-YI](#)), S739 ([SAT-375](#)), S810 ([WED-373-YI](#))
- Wong, Darren, S547 ([WED-299](#))
- Wong, Emily, S753 ([SAT-413](#))
- Wong, Florence, S161 ([THU-058](#)), S163 ([THU-060](#)), S206 ([FRI-046](#)), S208 ([FRI-053](#)), S218 ([FRI-086](#)), S219 ([FRI-088](#)), S242 ([SAT-082](#))
- Wong, Gerard, S826 ([THU-406](#))
- Wong, Grace, S238 ([SAT-068](#)), S797 ([WED-397](#))
- Wong, Grace Lai-Hung, S2 ([GS-004](#)), S38 ([OS-054](#)), S78 ([LBP-001](#)), S84 ([LBP-014](#)), S86 ([LBP-018](#)), S95 ([LBP-037](#)), S150 ([SAT-292](#)), S154 ([SAT-302](#)), S235 ([FRI-132](#)), S475 ([FRI-227](#)), S479 ([FRI-239](#)), S510 ([WED-198](#)), S758 ([TOP-401-YI](#)), S761 ([FRI-362-YI](#)), S770 ([FRI-387](#)), S809 ([WED-371](#)), S818 ([THU-379](#)), S836 ([THU-374](#))
- Wong, Ian, S776 ([FRI-403](#))
- Wong, Ian Chi Kei, S116 ([SAT-314](#))
- Wong, Jack Chun-Ming, S419 ([FRI-473](#))
- Wong, Kwok, S406 ([SAT-515](#))
- Wong, Man Chun, S291 ([TOP-148](#))
- Wong, Narayan, S58 ([OS-090](#))
- Wong, Philip, S484 ([FRI-256-YI](#))
- Wong, Robert, S150 ([SAT-292](#)), S154 ([SAT-302](#)), S771 ([FRI-389](#)), S788 ([FRI-435](#))
- Wong, Stanley, S40 ([OS-058](#)), S824 ([THU-399-YI](#))
- Wong, Sunny Hei, S280 ([WED-539](#))
- Wong, Tiffany, S424 ([FRI-490-YI](#))
- Wong, Vincent Wai-Sun, S2 ([GS-004](#)), S38 ([OS-054](#)), S79 ([LBP-003](#)), S84 ([LBP-014](#)), S95 ([LBP-037](#)), S150 ([SAT-292](#)), S154 ([SAT-302](#)), S235 ([FRI-132](#)), S475 ([FRI-227](#)), S479 ([FRI-239](#)), S510 ([WED-198](#)), S527 ([WED-246](#)), S536 ([WED-272](#)), S643 ([SAT-438](#)), S758 ([TOP-401-YI](#)), S761 ([FRI-362-YI](#)), S770 ([FRI-387](#)), S818 ([THU-379](#))
- Wong, William WL, S688 ([WED-499](#))

- Wong, Yu Jun, S30 ([OS-038-YI](#)),
S199 ([TOP-062](#)), S200 ([TOP-064-YI](#)),
S219 ([FRI-088](#)), S536 ([WED-272](#))
- Won Jun, Dae, S152 ([SAT-296](#)),
S477 ([FRI-234](#))
- Won Lee, Sung, S147 ([SAT-281](#))
- Won, Sung-Min, S602 ([TOP-216](#))
- Wood, Callum, S547 ([WED-302-YI](#))
- Wooddell, Christine, S27 ([OS-032](#))
- Woodhoo, Ashwin, S562 ([TOP-229-YI](#))
- Woodhouse, Charlotte, S46 ([OS-070](#))
- Woods, Kerrie, S676 ([WED-471](#)),
S759 ([TOP-417](#))
- Woods, Robyn, S653 ([SAT-464-YI](#))
- Woo, Hyun Young, S457 ([THU-516](#))
- Woo, Tiffany, S578 ([THU-239-YI](#))
- Wootton, Grace, S33 ([OS-044-YI](#)),
S34 ([OS-046](#)), S354 ([SAT-540-YI](#)),
S356 ([SAT-546](#))
- Wörns, Marcus-Alexander, S230 ([FRI-120](#))
- Worobetz, Lawrence, S19 ([OS-018](#)),
S305 ([TOP-169](#))
- Wouambo, Rodrigue Kamga,
S752 ([SAT-410](#)), S802 ([WED-411](#))
- Wozniak, Hannah, S114 ([TOP-344-YI](#))
- Wranke, Anika, S750 ([SAT-406-YI](#)),
S759 ([TOP-416-YI](#)), S762 ([FRI-365-YI](#))
- Wree, Alexander, S259 ([SAT-135](#)),
S356 ([SAT-545](#)), S359 ([SAT-555](#))
- Wright, Alexander, S530 ([WED-254](#))
- Wright, Gavin, S174 ([TOP-084](#)),
S700 ([FRI-171](#))
- Wright, Jack, S185 ([WED-088-YI](#)),
S192 ([WED-110](#)), S227 ([FRI-112](#))
- Wright, Kemi, S519 ([WED-225](#))
- Wright, Mark, S127 ([THU-317](#)),
S145 ([SAT-274](#)), S633 ([THU-027-YI](#))
- Wronka, Karolina, S338 ([THU-175-YI](#))
- Wu, Chao, S459 ([TOP-307](#)), S625 ([FRI-022](#)),
S628 ([FRI-035](#)), S744 ([SAT-388](#)),
S757 ([SAT-423](#)), S780 ([FRI-411-YI](#))
- Wu, Cheng-Heng, S414 ([FRI-458](#))
- Wu, Chi-Jung, S449 ([THU-479](#))
- Wu, Dai-tze, S59 ([OS-093](#))
- Wu, Dandan, S602 ([TOP-217](#))
- Wu, Dongbo, S494 ([FRI-285](#)),
S499 ([FRI-302](#))
- Wuestefeld, Torsten, S578 ([THU-239-YI](#))
- Wu, Haifeng, S590 ([THU-280](#))
- Wu, Hao, S225 ([FRI-105](#)), S241 ([SAT-077](#)),
S622 ([FRI-010](#))
- Wu, Haoyu, S625 ([FRI-021](#))
- Wu, Jaw-Ching, S398 ([SAT-484](#)),
S663 ([WED-438-YI](#))
- Wu, Jia-Ling, S795 ([WED-393](#))
- Wu, Jianbing, S447 ([THU-475](#))
- Wu, Jinzi J., S605 ([SAT-198](#))
- Wu, Jugang, S422 ([FRI-484](#))
- Wu, Kuan-Ta, S490 ([FRI-271](#)),
S493 ([FRI-280](#))
- Wu, Leilei, S59 ([OS-093](#))
- Wulf, Severin, S353 ([SAT-538-YI](#))
- Wu, Liandong, S767 ([FRI-377](#))
- Wu, Lili, S736 ([SAT-367](#))
- Wu, Linda, S443 ([THU-464](#))
- Wu, Ling, S106 ([FRI-322](#)), S242 ([SAT-081](#)),
S268 ([THU-546](#))
- Wu, Liyang, S219 ([FRI-088](#))
- Wu, Min, S806 ([WED-361](#)),
S807 ([WED-365](#)), S812 ([WED-378](#))
- Wu, Mingfeng, S257 ([SAT-126](#))
- Wunsch, Ewa, S308 ([THU-095](#))
- Wu, Pan, S75 ([OS-127](#))
- Wurmser, Christine, S351 ([SAT-533](#))
- Wu, Shouling, S655 ([SAT-468](#))
- Wu, Shuling, S344 ([THU-191](#))
- Wu, Shusheng, S757 ([WED-420](#))
- Wu, Trevor Kwan-Hung, S770 ([FRI-388](#)),
S810 ([WED-373-YI](#))
- Wu, Tsung-Han, S414 ([FRI-458](#))
- Wu, Wan-Jung, S75 ([OS-123](#))
- Wu, Wei, S99 ([LBP-042](#)), S260 ([SAT-136](#))
- Wu, Wen-Chih, S832 ([THU-365](#))
- Wu, Xia, S300 ([SAT-175](#)), S301 ([SAT-177](#))
- Wu, Xiaofeng, S803 ([WED-412](#))
- Wu, Xiaoli, S99 ([LBP-043](#))
- Wu, Xiaoming, S527 ([WED-246](#))
- Wu, Xiaoping, S120 ([SAT-323](#)),
S161 ([THU-058](#)), S605 ([SAT-198](#))
- Wu, Yanping, S710 ([WED-152](#))
- Wu, Yi-Ling, S795 ([WED-393](#))
- Wu, Yue, S87 ([LBP-021](#))
- Wyles, David, S769 ([FRI-383](#))
- Wynne, Alex, S822 ([THU-391-YI](#))
- Wynne-Cattanach, Kieran,
S707 ([WED-134](#))
- Wyss, Lorena, S117 ([SAT-316](#))
- Xia, Bihua, S100 ([LBP-045](#))
- Xia, Caixia, S110 ([FRI-334](#))
- Xia, Dongdong, S447 ([THU-475](#)),
S716 ([WED-167](#))
- Xia, Jie, S701 ([FRI-174](#))
- Xia, Juan, S628 ([FRI-035](#))
- Xiang, Huanyu, S269 ([THU-549](#))
- Xiang, Xiaomei, S701 ([FRI-174](#))
- Xian, Yongchao, S219 ([FRI-088](#))
- Xiao, Fei, S418 ([FRI-471](#))
- Xiao, Ji, S418 ([FRI-471](#))
- Xiao, Jiangqiang, S109 ([FRI-332](#)),
S112 ([FRI-340](#)), S260 ([SAT-136](#)),
S285 ([WED-556](#))
- Xiao, Jieliang, S147 ([SAT-281](#)),
S366 ([TOP-004](#))
- Xiao, Jing, S269 ([THU-549](#))
- Xiao, Sihao, S135 ([THU-343](#))
- Xia, Qiang, S354 ([SAT-542](#)), S387 ([SAT-054](#)),
S623 ([FRI-016](#))
- Xie, Chan, S430 ([FRI-517](#)), S437 ([TOP-504](#))
- Xie, Dong-Ying, S95 ([LBP-037](#))
- Xie, Jianping, S95 ([LBP-037](#))
- Xie, Qing, S26 ([OS-030](#)), S30 ([OS-038-YI](#)),
S95 ([LBP-037](#)), S161 ([THU-058](#)),
S199 ([TOP-062](#)), S200 ([TOP-064-YI](#)),
S208 ([FRI-053](#)), S219 ([FRI-088](#)),
S605 ([SAT-198](#)), S761 ([FRI-363-YI](#))
- Xie, Wen, S228 ([FRI-114](#))
- Xie, Yandi, S769 ([FRI-382](#))
- Xie, Yao, S344 ([THU-191](#)), S355 ([SAT-544](#)),
S605 ([SAT-198](#)), S738 ([SAT-372](#)),
S815 ([WED-387](#))
- Xie, Zhe, S699 ([FRI-170](#)), S727 ([TOP-355-YI](#))
- Xin, Jiaojiao, S105 ([FRI-319](#)), S108 ([FRI-330](#)),
S117 ([SAT-318](#)), S345 ([FRI-546](#))
- Xin, Shaojie, S158 ([THU-052](#)),
S167 ([THU-078](#))
- Xin, Zheng, S208 ([FRI-053](#))
- Xiong, Feixiang, S145 ([SAT-275](#))
- Xiong, John, S58 ([OS-090](#))
- Xiong, Kai, S260 ([SAT-136](#))
- Xiong, Xi, S116 ([SAT-314](#))
- Xiong, Ye, S780 ([FRI-411-YI](#))
- Xirodimas, Dimitris, S417 ([FRI-466-YI](#))
- Xu, Bin, S208 ([FRI-053](#)), S605 ([SAT-198](#))
- Xu, Bing, S109 ([FRI-332](#)), S112 ([FRI-340](#)),
S285 ([WED-556](#))
- Xu, Chengjian, S21 ([OS-021-YI](#))
- Xu, Chongyuan, S86 ([LBP-019](#)),
S99 ([LBP-043](#))
- Xu, Cong, S87 ([LBP-020](#))
- Xu, Dongwei, S106 ([FRI-323](#)),
S354 ([SAT-542](#))
- Xue, Feng, S100 ([LBP-045](#)), S613 ([SAT-221](#))
- Xue, Hongyuan, S775 ([FRI-398](#))
- Xue, Jiaming, S566 ([THU-201-YI](#))
- Xue, Xiulan, S803 ([WED-412](#))
- Xu, Fuyuan, S418 ([FRI-471](#))
- Xu, Guang-Hua, S786 ([FRI-430](#))
- Xu, Jason, S555 ([WED-330](#)),
S561 ([WED-348](#))
- Xu, Jia, S807 ([WED-365](#))
- Xu, Jian, S447 ([THU-475](#))
- Xu, Jianfeng, S11 ([LBO-006](#))
- Xu, Jie, S422 ([FRI-484](#))
- Xu, Jing, S357 ([SAT-547](#))
- Xu, Jingwen, S510 ([WED-198](#))
- Xu, Jun, S505 ([TOP-264](#)), S571 ([THU-215](#)),
S585 ([THU-261](#))
- Xu, Junzhong, S595 ([THU-293](#))
- Xu, Ke, S716 ([WED-167](#))
- Xu, Liang, S525 ([WED-244](#)), S776 ([FRI-404](#)),
S803 ([WED-412](#))
- Xu, Ling, S107 ([FRI-325](#))
- Xu, Lizhi, S395 ([SAT-478](#))
- Xu, Mengjiao, S344 ([THU-191](#))
- Xun, Yunhao, S531 ([WED-258](#))
- Xu, Simin, S737 ([SAT-371](#)),
S750 ([SAT-405](#))
- Xu, Tao, S447 ([THU-475](#))
- Xu, Tian, S87 ([LBP-020](#))
- Xu, Wenxiong, S109 ([FRI-331](#))
- Xu, Xiaoliang, S403 ([SAT-499](#))
- Xu, Xiaoming, S459 ([TOP-307](#)),
S502 ([FRI-316](#)), S776 ([FRI-404](#))
- Xu, Xueli, S102 ([LBP-048](#))
- Xu, Yuan, S102 ([LBP-048](#))
- Xu, Zhen, S219 ([FRI-088](#))
- Xu, Zhijie, S418 ([FRI-471](#))
- Yabut, Jocelyn, S753 ([SAT-412](#))
- Yacovzada, Nancy-Sarah, S645 ([SAT-442](#))
- Yadav, Jitendra, S554 ([WED-327](#))

Author Index

- Yadav, Kavita, S129 (THU-321), S272 (WED-518-YI), S276 (WED-527-YI)
- Yadav, Manisha, S103 (TOP-349-YI), S108 (FRI-327-YI), S125 (TOP-329-YI), S127 (THU-318), S134 (THU-339), S273 (WED-519-YI), S283 (WED-549), S294 (SAT-155)
- Yadav, Rajni, S177 (WED-058-YI), S188 (WED-095-YI), S546 (WED-298-YI)
- Yaghi, Cesar, S158 (THU-052), S167 (THU-078)
- Yagi, Takahiro, S513 (WED-208)
- Yağlı, Mehmet Akif, S377 (SAT-028)
- Yaish, Dyana, S278 (WED-534)
- Yalcin, Metin, S523 (WED-236-YI)
- Yale, Kitty, S8 (LBO-002), S522 (WED-234), S535 (WED-268), S612 (SAT-220-YI)
- Yamada, Tomoharu, S393 (SAT-470), S437 (TOP-505)
- Yamada, Tomomi, S828 (THU-413)
- Yamaguchi, Kanji, S537 (WED-273)
- Yamahira, Masahiro, S512 (WED-203)
- Yamao, Mikaru, S288 (FRI-540)
- Yamasaki, Chihiro, S288 (FRI-540)
- Yamasaki, Kazumi, S542 (WED-286)
- Yamashiki, Noriyo, S118 (SAT-319)
- Yamashita, Taro, S828 (THU-413)
- Yamazhan, Tansu, S805 (WED-418)
- Yamazoe, Taiji, S695 (FRI-159)
- Yam, Judy Wai-Ping, S739 (SAT-375)
- Yanagihara, Ted, S394 (SAT-476), S403 (SAT-498)
- Yan, Dong, S826 (THU-407)
- Yang, Aruhan, S461 (TOP-310), S551 (WED-319), S558 (WED-338)
- Yang, Changqing, S362 (WED-017-YI)
- Yang, Chan Jin, S247 (SAT-098)
- Yang, Charles, S489 (FRI-268)
- Yangcharoen, Awassada, S642 (SAT-435)
- Yang, Chen, S86 (LBP-019), S99 (LBP-043)
- Yang, Cheng Yong, S86 (LBP-019), S99 (LBP-043)
- Yang, Chenlu, S655 (SAT-468)
- Yang, Chi-Chieh, S832 (THU-365)
- Yang, Danli, S790 (FRI-440)
- Yang, Dong Hoon, S602 (TOP-216)
- Yang, Hailin, S693 (FRI-151)
- Yang, Hongbo, S708 (WED-136)
- Yang, Hui, S105 (FRI-319), S149 (SAT-287), S345 (FRI-546)
- Yang, Hwai-I, S491 (FRI-274)
- Yang, Jeng-Fu, S490 (FRI-271), S493 (FRI-280)
- Yang, Ji Won, S144 (SAT-272), S822 (THU-394)
- Yang, Ju Dong, S11 (LBO-006), S39 (OS-055), S200 (TOP-063), S216 (FRI-081)
- Yang, Ke, S20 (OS-019)
- Yang, Li, S783 (FRI-419), S785 (FRI-428)
- Yang, Ling, S605 (SAT-198)
- Yang, Liqiong, S745 (SAT-392)
- Yang, Liu, S738 (SAT-372), S815 (WED-387)
- Yang, Liuqing, S395 (SAT-478)
- Yang, Ning, S365 (WED-029)
- Yango, Jaymie, S661 (WED-433)
- Yang, Qiang, S461 (TOP-310), S551 (WED-319)
- Yang, Rui, S225 (FRI-105)
- Yang, Sheng-Shun, S26 (OS-030), S26 (OS-031), S74 (OS-121), S399 (SAT-486), S832 (THU-365)
- Yang, Shizhong, S395 (SAT-478), S433 (FRI-527), S442 (THU-462), S625 (FRI-021)
- Yang, Shufa, S447 (THU-475)
- Yang, Shuo, S230 (FRI-118), S233 (FRI-127)
- Yang, Song, S95 (LBP-037), S102 (LBP-048)
- Yang, Suzhen, S109 (FRI-332)
- Yang, Tao, S106 (FRI-323), S354 (SAT-542)
- Yang, Tianyuan, S479 (FRI-242)
- Yang, Tsung-Chieh, S256 (SAT-125)
- Yang, Xiaolan, S574 (THU-226)
- Yang, Yixuan, S440 (THU-455)
- Yang, Zeyuan, S150 (SAT-292), S154 (SAT-302), S771 (FRI-389)
- Yang, Zhenggang, S767 (FRI-377)
- Yang, Zhiwei, S726 (TOP-354)
- Yang, Zhiyun, S145 (SAT-275)
- Yankouskaya, Katharina, S356 (SAT-546)
- Yan, Libo, S87 (LBP-021), S208 (FRI-053)
- Yan, Ren, S280 (WED-541)
- Yan, Xiaomin, S780 (FRI-411-YI)
- Yan, Xuebing, S605 (SAT-198)
- Yan, Yuemei, S605 (SAT-198)
- Yan, Zhiping, S240 (SAT-075-YI), S256 (SAT-124)
- Yao, Heng, S108 (FRI-330)
- Yao, Lvfang, S100 (LBP-045)
- Yao, Naijuan, S789 (FRI-438)
- Yao, Renling, S628 (FRI-035)
- Yao, Ye, S263 (THU-526)
- Yao, Yuelin, S695 (FRI-158-YI)
- Yapıcı, Hasan Basri, S329 (THU-153)
- Yapıcı, Hasan Basri, S723 (WED-187-YI)
- Yardeni, David, S28 (OS-034)
- Yaringaño, Jesus, S702 (TOP-139)
- Yasuda, Satoshi, S512 (WED-203)
- Yasui, Yutaka, S626 (FRI-026)
- Ya, Sun, S726 (TOP-353), S732 (SAT-339)
- Yasushi, Imamura, S541 (WED-283)
- Yates, Mark, S477 (FRI-235), S486 (FRI-260), S509 (WED-197)
- Yatsushashi, Hiroshi, S542 (WED-286), S828 (THU-413)
- Yattoo, Ghulam Nabi, S167 (THU-078)
- Yaw, Lai Ping, S578 (THU-239-YI)
- Yazdi, Tahmineh, S737 (SAT-371)
- Yee, Leland J., S761 (FRI-363-YI), S771 (FRI-390), S797 (WED-397), S799 (WED-405)
- Yee, Michael, S495 (FRI-286)
- Yehezkel, Adi Sheena, S278 (WED-534)
- Yehezkel, Eyal, S308 (THU-098)
- Yeh, Julian, S101 (LBP-046)
- Yeh, Matthew, S467 (FRI-208)
- Yeh, Ming-Lun, S42 (OS-061), S490 (FRI-271), S493 (FRI-280), S832 (THU-365)
- Ye, Hua, S605 (SAT-198)
- Ye, Junzhao, S84 (LBP-014)
- Yélamos, María, S751 (SAT-407)
- Ye, Lei, S1 (GS-002), S764 (FRI-371), S796 (WED-395)
- Yen, Chia-Hsun, S449 (THU-480)
- Yen, Mark, S141 (SAT-261)
- Yen, Paul, S55 (OS-085), S502 (FRI-316)
- Yenukoti, Rohit K., S326 (THU-135)
- Yeon, Jong Eun, S596 (THU-295)
- Yeo, Yee Hui, S39 (OS-055), S200 (TOP-063), S216 (FRI-081), S459 (TOP-307), S525 (WED-244), S625 (FRI-022), S776 (FRI-404)
- Yerly, Sabine, S831 (THU-362)
- Ye, Sitao, S275 (WED-524-YI)
- Yeung, Cherlie Lot-Sum, S739 (SAT-375)
- Yeung, Steven, S584 (THU-259)
- Yew, Kuo Chao, S497 (FRI-295), S826 (THU-406)
- Ye, Xiaoting, S826 (THU-407)
- Ye, Xiuling, S241 (SAT-077)
- Ye, Yong-an, S762 (FRI-366)
- Ye, Yong'an, S755 (SAT-419), S755 (SAT-420)
- Yien Kwo, Paul, S242 (SAT-082)
- Yi, Kiyoun, S457 (THU-516)
- Yildiz, Dilek, S805 (WED-418)
- Yildiz, Ilknur Esen, S805 (WED-418)
- Yiliyaer, Guzunuer, S234 (FRI-129)
- Yilmaz, Sezai, S9 (LBO-004), S89 (LBP-026)
- Yilmaz, Yusuf, S329 (THU-153), S643 (SAT-438), S723 (WED-187-YI)
- Yimam, Kidist, S98 (LBP-040)
- Yim, Hyung Joon, S596 (THU-295), S767 (FRI-379), S799 (WED-404)
- Yim, Sun Young, S68 (OS-111)
- Yin, Benny, S693 (FRI-151)
- Yin, Dedong, S219 (FRI-088)
- Yin, Guo, S298 (SAT-170)
- Yin, Guowen, S447 (THU-475)
- Yin, James Liu, S709 (WED-137-YI)
- Yin, JingYa, S479 (FRI-242)
- Yin, Jun, S504 (TOP-252-YI)
- Yin, Shengxia, S625 (FRI-022), S744 (SAT-388), S757 (SAT-423)
- Yin, Tao, S447 (THU-475)
- Yip, Terry Cheuk-Fung, S2 (GS-004), S84 (LBP-014), S150 (SAT-292), S154 (SAT-302), S235 (FRI-132), S475 (FRI-227), S479 (FRI-239), S510 (WED-198), S761 (FRI-362-YI), S818 (THU-379)
- Yi, Shana, S662 (WED-436), S668 (WED-450), S679 (WED-476)
- Yi, Wei, S344 (THU-191)
- Yildirim, Abdullah Emre, S219 (FRI-088)
- Yildiz, Fatih, S407 (SAT-518)
- Yilmaz, Volkan, S336 (THU-171), S407 (SAT-519), S479 (FRI-238)
- Ylla, Guillem, S304 (SAT-184)
- Yogaratham, Jeysen, S87 (LBP-020)
- Yokosuka, Osamu, S158 (THU-052), S167 (THU-078)

- Yoneda, Masato, S2 (GS-004), S7 (LBO-001), S38 (OS-054), S235 (FRI-130), S537 (WED-273), S541 (WED-283)
- Yonemoto, Takuya, S123 (SAT-335)
- Yoo, Jae-Sung, S264 (THU-530)
- Yoo, Jeong-Ju, S247 (SAT-098), S652 (SAT-458)
- Yoon, Eileen, S148 (SAT-284), S152 (SAT-296), S473 (FRI-223), S477 (FRI-234), S553 (WED-323), S654 (SAT-465)
- Yoon, Jung-Hwan, S3 (GS-005), S457 (THU-515), S517 (WED-221), S575 (THU-230), S601 (TOP-204), S774 (FRI-397)
- Yoon, Sang Jun, S286 (WED-557), S602 (TOP-216)
- Yoon, Yeup, S564 (THU-196)
- Yordanoff, Ryan, S693 (FRI-151)
- Yoshida, Eric, S40 (OS-058)
- Yoshida, Osamu, S711 (WED-154), S722 (WED-184)
- Yoshida, Yuichi, S512 (WED-203), S537 (WED-273)
- Yoshiji, Hitoshi, S175 (TOP-096), S828 (THU-413)
- Yoshimura, Kentaro, S519 (WED-226)
- Yoshio, Sachiyo, S695 (FRI-159)
- Yoshizumi, Tomoharu, S9 (LBO-004), S89 (LBP-026), S375 (SAT-023)
- Yosipovitch, Gil, S340 (THU-181)
- Yotebieng, Marcel, S668 (WED-451-YI), S675 (WED-469)
- Yotsuyanagi, Hiroshi, S589 (THU-275)
- You, Dongfang, S526 (WED-246)
- You, Hong, S488 (FRI-267), S605 (SAT-198)
- Younes, Ramy, S4 (GS-006), S72 (OS-119), S477 (FRI-235), S486 (FRI-260), S509 (WED-197)
- Younes, Ziad H., S11 (LBO-006), S20 (OS-019), S98 (LBP-040)
- Young Lee, Hyo, S152 (SAT-296)
- Young, Liam, S315 (THU-112-YI)
- Youngson, Neil, S178 (WED-068-YI), S192 (WED-110)
- Younossi, Issah, S101 (LBP-047)
- Younossi, Zaid, S572 (THU-221)
- Younossi, Zobair, S95 (LBP-036), S101 (LBP-047), S465 (FRI-202), S467 (FRI-208), S470 (FRI-218), S472 (FRI-221), S476 (FRI-232), S496 (FRI-291), S520 (WED-230), S572 (THU-221), S637 (TOP-445), S638 (SAT-425), S643 (SAT-438), S651 (SAT-456), S652 (SAT-459)
- Yousefi, Keyvan, S7 (GS-012)
- You, Shihyun, S745 (SAT-390)
- You, Yixian, S494 (FRI-285), S499 (FRI-302)
- You, Zhengrui, S271 (TOP-561)
- Ytting, Henriette, S5 (GS-007), S335 (THU-167)
- Yu, Amanda, S40 (OS-058), S824 (THU-399-YI)
- Yuan, Chunwang, S357 (SAT-548)
- Yuan, Haiyang, S488 (FRI-267)
- Yuan, Jia, S235 (FRI-131)
- Yuan, Taichang, S727 (TOP-356)
- Yuan, Xiao, S69 (OS-112-YI)
- Yuan, Zihang, S111 (FRI-339)
- Yu, Catherine, S632 (THU-021)
- Yucuma, Daniela, S656 (TOP-460-YI)
- Yue, Ming, S102 (LBP-048)
- Yuen, Man-Fung, S26 (OS-030), S26 (OS-031), S27 (OS-032), S78 (LBP-001), S86 (LBP-019), S116 (SAT-314), S158 (THU-052), S167 (THU-078), S424 (FRI-490-YI), S739 (SAT-375), S745 (SAT-392), S770 (FRI-388), S806 (WED-361), S807 (WED-365), S808 (WED-367), S809 (WED-371), S810 (WED-373-YI), S811 (WED-375), S812 (WED-376), S812 (WED-378)
- Yuen, Pong Chi, S510 (WED-198)
- Yue, Wei, S87 (LBP-021), S100 (LBP-045)
- Yu, Hong, S234 (FRI-129)
- Yu, Hui, S693 (FRI-151)
- Yu, Huihong, S198 (WED-124), S359 (SAT-556-YI)
- Yu, Huiying, S736 (SAT-367)
- Yu, Jiaxin, S812 (WED-377)
- Yuksel, Muhammed, S54 (OS-083), S712 (WED-160)
- Yu, Lihua, S145 (SAT-275)
- Yu, Ming-Lung, S42 (OS-061), S74 (OS-121), S490 (FRI-271), S493 (FRI-280), S643 (SAT-438), S832 (THU-365), S836 (THU-374)
- Yu, Ming-Whei, S75 (OS-123)
- Yumita, Sae, S123 (SAT-335), S247 (SAT-095)
- Yung, Diana, S161 (THU-058)
- Yung, Rossitta, S662 (WED-436), S668 (WED-450), S679 (WED-476)
- Yun, Jae Moon, S638 (SAT-424)
- Yu, Qinwei, S111 (FRI-338), S111 (FRI-339)
- Yurdaydin, Cihan, S28 (OS-034), S736 (SAT-366), S785 (FRI-427)
- Yu, Shasha, S747 (SAT-395)
- Yu, Su Jong, S457 (THU-515), S517 (WED-221), S601 (TOP-204), S767 (FRI-379), S774 (FRI-397), S799 (WED-404)
- Yu, Xian, S86 (LBP-019), S99 (LBP-043), S807 (WED-365)
- Yu, Xiaomao, S395 (SAT-478)
- Yuzon, Jennifer, S261 (TOP-564)
- Yzet, Thierry, S413 (FRI-456)
- Zabaleta, Nerea, S693 (FRI-152-YI)
- Zabinski, Joseph, S460 (TOP-309)
- Zaboli, Shiva, S738 (SAT-373)
- Zaccherini, Giacomo, S206 (FRI-047-YI), S215 (FRI-078-YI), S700 (FRI-171)
- Zacho, Jeppe, S606 (SAT-201)
- Zachou, Kalliopi, S18 (OS-015), S44 (OS-066-YI), S322 (THU-126), S325 (THU-134), S712 (WED-160), S798 (WED-403), S800 (WED-406)
- Zafar, Paul Emile, S719 (WED-177)
- Zafar, Yousaf, S249 (SAT-102)
- Zagaria, Giuseppe, S213 (FRI-070-YI)
- Zaher, Anas, S252 (SAT-114)
- Zahhaf, Amel, S122 (SAT-331)
- Zahinos, Jesús Trejo, S662 (WED-435)
- Zaksas, Viaceslav, S678 (WED-474)
- Zalcborg, John, S400 (SAT-492)
- Zalin, Amy, S406 (SAT-515)
- Zaltron, Serena, S804 (WED-414)
- Zamalloa, Ane, S46 (OS-070), S110 (FRI-335), S128 (THU-320-YI), S178 (WED-068-YI), S185 (WED-088-YI), S192 (WED-110), S281 (WED-542-YI)
- Zaman, Saif, S695 (FRI-155)
- Zambrano-Huaila, Rommel, S15 (OS-010)
- Zamora-Olaya, Javier M., S415 (FRI-462-YI)
- Zamor, Philippe, S242 (SAT-082)
- Zamparelli, Marco Sanduzzi, S424 (FRI-491-YI), S444 (THU-467-YI), S455 (THU-500)
- Zampino, Rosa, S804 (WED-414)
- Zampogna, Christopher, S338 (THU-177-YI)
- Zanaga, Paola, S237 (TOP-061-YI), S700 (FRI-171), S818 (THU-381)
- Zanatto, Laura, S24 (OS-026-YI)
- Zanchetta, Lorena, S634 (THU-032)
- Zanetta, Chiara, S123 (SAT-334)
- Zanetto, Alberto, S237 (TOP-061-YI), S818 (THU-381)
- Zang, Chaoran, S357 (SAT-548)
- Zangneh, Hooman Farhang, S49 (OS-075-YI)
- Zani, Francesca, S96 (LBP-038), S306 (THU-093)
- Zanotelli, Maria Lúcia, S9 (LBO-004)
- Zanotto, Ilaria, S592 (THU-285)
- Zanuso, Valentina, S52 (OS-079-YI), S408 (SAT-523), S438 (THU-446), S443 (THU-464), S447 (THU-474-YI)
- Zao, Xiaobin, S194 (WED-114), S755 (SAT-419), S755 (SAT-420)
- Zapata, Carina, S627 (FRI-029)
- Zapata-Pavas, Leidy Estefanía, S417 (FRI-466-YI)
- Zarader, Jean-Luc, S207 (FRI-050-YI)
- Zarantonello, Lisa, S211 (FRI-059), S214 (FRI-075), S246 (SAT-094-YI)
- Zar, Areeb, S633 (THU-029)
- Zarauza, Yolanda, S398 (SAT-485)
- Zarbock, Alexander, S169 (THU-083)
- Zarebska-Michaluk, Dorota, S685 (WED-493-YI), S821 (THU-389), S834 (THU-367-YI)
- Zarka, Valentina, S69 (OS-112-YI)
- Zarkua, Jaba, S659 (WED-427)
- Zatsepin, Timofei, S268 (THU-542)
- Zauner, Christian, S340 (THU-180)
- Zavřelová, Jiřina, S756 (SAT-422)
- Zazueta, Godolfino Miranda, S208 (FRI-053)
- Zazzi, Maurizio, S777 (FRI-405)
- Zdráhal, Zbyněk, S134 (THU-340-YI)

Author Index

- Zefelippo, Arianna, S397 ([SAT-482](#))
Zehn, Dietmar, S351 ([SAT-533](#))
Zeina, Abdel-Rauf, S628 ([FRI-033](#))
Zein, Claudia O., S18 ([OS-016](#)),
S312 ([THU-105](#)), S326 ([THU-135](#))
Zeineddine, Fadl A., S384 ([SAT-045](#))
Zeitlhofer, Marcus, S411 ([TOP-507-YI](#))
Zekry, Amany, S161 ([THU-058](#))
Zekrya, Zohal, S572 ([THU-221](#))
Zelber-Sagi, Shira, S637 ([TOP-445](#))
Zeldin, Darryl, S580 ([THU-247-YI](#))
Zelesco, Marilyn, S483 ([FRI-250](#)),
S487 ([FRI-263](#))
Zender, Lars, S426 ([FRI-495](#))
Zeng-Brouwers, Jinyang,
S198 ([WED-126](#))
Zeng, Dawu, S803 ([WED-412](#))
Zeng, Jing, S197 ([WED-123](#)),
S523 ([WED-237](#)), S573 ([THU-223](#))
Zeng, Qinghe, S566 ([THU-201-YI](#))
Zeng, Qing-Lei, S536 ([WED-272](#)),
S620 ([TOP-006](#))
Zeng, Qingmin, S494 ([FRI-285](#)),
S499 ([FRI-302](#))
Zeng, Rebecca Wenling, S147 ([SAT-281](#))
Zeng, Yong, S447 ([THU-475](#))
Zeni, Nicola, S28 ([OS-035-YI](#)),
S212 ([FRI-068](#)), S224 ([FRI-101-YI](#)),
S243 ([SAT-083-YI](#)), S700 ([FRI-171](#)),
S830 ([THU-420](#))
Zen, Yoh, S128 ([THU-320-YI](#)),
S281 ([WED-542-YI](#)), S341 ([THU-182](#)),
S388 ([SAT-057](#))
Zerdali, Esra, S805 ([WED-418](#))
Zerial, Marino, S65 ([OS-104](#))
Zeuzem, Stefan, S92 ([LBP-029](#)),
S169 ([THU-083](#)), S170 ([THU-087](#)),
S180 ([WED-074](#)), S198 ([WED-126](#)),
S203 ([FRI-039](#)), S794 ([WED-392](#)),
S820 ([THU-386-YI](#))
Zhai, Adam, S58 ([OS-090](#))
Zhai, Panpan, S792 ([WED-390](#))
Zhai, Xing-Ran, S124 ([SAT-336](#))
Zhang, Bob, S59 ([OS-093](#))
Zhang, Boxiang, S430 ([FRI-517](#)),
S437 ([TOP-504](#))
Zhang, Chenshu, S684 ([WED-487](#))
Zhang, Chi, S684 ([WED-490](#)),
S790 ([FRI-439](#))
Zhang, Chong, S803 ([WED-412](#))
Zhang, Chunqing, S447 ([THU-475](#)),
S716 ([WED-167](#))
Zhang, Dazhi, S440 ([THU-455](#))
Zhang, Fan, S372 ([SAT-017](#))
Zhang, Feng, S236 ([FRI-135](#)),
S260 ([SAT-136](#))
Zhang, Guiying, S622 ([FRI-010](#))
Zhang, Guodong, S580 ([THU-247-YI](#))
Zhang-Hagenlocher, Chengcheng,
S300 ([SAT-174](#))
Zhang, Han, S109 ([FRI-332](#))
Zhang, Hang, S76 ([OS-124](#)),
S509 ([WED-196](#))
Zhang, Haoran, S111 ([FRI-339](#))
Zhang, Hong, S99 ([LBP-043](#)),
S551 ([WED-319](#)), S602 ([TOP-217](#))
Zhang, Hongfei, S783 ([FRI-420](#))
Zhang, Hongli, S726 ([TOP-354](#))
Zhang, Hui, S447 ([THU-475](#)),
S534 ([WED-267](#))
Zhang, Huifang, S333 ([THU-163](#))
Zhang, Ingrid Wei, S161 ([THU-057-YI](#))
Zhang, Jianhua, S102 ([LBP-048](#))
Zhang, Jianjun, S387 ([SAT-054](#))
Zhang, Jianming, S100 ([LBP-045](#))
Zhang, Jianxiong, S815 ([WED-386](#))
Zhang, Jiaqi, S301 ([SAT-176](#)), S303 ([SAT-182](#))
Zhang, Jiawei, S620 ([TOP-006](#))
Zhang, Jiaxin, S755 ([SAT-419](#))
Zhang, Jiming, S748 ([SAT-399](#))
Zhang, Jing, S227 ([FRI-111](#))
Zhang, Jingwen, S614 ([SAT-226](#))
Zhang, Ke, S99 ([LBP-042](#))
Zhang, Kewei, S716 ([WED-167](#))
Zhang, Lili, S531 ([WED-258](#))
Zhang, Lingyi, S803 ([WED-412](#))
Zhang, Linhao, S241 ([SAT-077](#))
Zhang, Lu, S344 ([THU-191](#))
Zhang, Luyong, S111 ([FRI-338](#)),
S111 ([FRI-339](#))
Zhang, Meijian, S574 ([THU-225](#))
Zhang, Meng, S195 ([WED-116](#))
Zhang, Mengmeng, S119 ([SAT-321](#)),
S121 ([SAT-326](#))
Zhang, Miaoqu, S775 ([FRI-398](#))
Zhang, Min, S605 ([SAT-198](#))
Zhang, Ming, S109 ([FRI-332](#)),
S236 ([FRI-135](#)), S260 ([SAT-136](#))
Zhang, Mingjian, S813 ([WED-381](#))
Zhang, Moran, S260 ([SAT-136](#))
Zhang, Ningning, S230 ([FRI-119](#)),
S400 ([SAT-491](#)), S405 ([SAT-503](#)),
S454 ([THU-499](#))
Zhang, Ning-Ping, S209 ([FRI-053](#))
Zhang, Ningyi, S755 ([SAT-419](#)),
S755 ([SAT-420](#))
Zhang, Qian, S257 ([SAT-126](#))
Zhang, Qin, S145 ([SAT-275](#))
Zhang, Qingling, S564 ([THU-198](#)),
S728 ([TOP-358-YI](#))
Zhang, Qingyang, S419 ([FRI-473](#))
Zhang, Qiongchi, S109 ([FRI-331](#))
Zhang, Qiran, S775 ([FRI-398](#))
Zhang, QuanBao, S775 ([FRI-398](#))
Zhang, Qun, S536 ([WED-272](#))
Zhang, Rong, S526 ([WED-246](#))
Zhang, Saisai, S424 ([FRI-490-YI](#)),
S739 ([SAT-375](#)), S745 ([SAT-392](#))
Zhang, Sen, S278 ([WED-533](#))
Zhang, Shanzhong, S806 ([WED-362](#)),
S813 ([WED-381](#)), S815 ([WED-386](#)),
S816 ([WED-388](#))
Zhang, Shaoqiu, S628 ([FRI-035](#)),
S780 ([FRI-411-YI](#))
Zhang, Shuyun, S769 ([FRI-382](#))
Zhang, Su, S708 ([WED-136](#))
Zhang, Tingyu, S762 ([FRI-366](#))
Zhang, Vanilla Xin, S419 ([FRI-473](#))
Zhang, Wanqin, S219 ([FRI-088](#))
Zhang, Wen, S240 ([SAT-075-YI](#)),
S256 ([SAT-124](#)), S710 ([WED-152](#))
Zhang, Wenhong, S26 ([OS-030](#)),
S149 ([SAT-287](#)), S536 ([WED-272](#)),
S775 ([FRI-398](#))
Zhang, Wenhua, S526 ([WED-246](#)),
S783 ([FRI-420](#))
Zhang, Wenxin, S149 ([SAT-287](#))
Zhang, Wenyan, S701 ([FRI-174](#))
Zhang, Xiangying, S107 ([FRI-325](#))
Zhang, Xiaofeng, S251 ([SAT-112](#))
Zhang, Xiaojing, S769 ([FRI-382](#))
Zhang, Xiaojun, S590 ([THU-280](#))
Zhang, Xiaoqian, S149 ([SAT-287](#))
Zhang, Xiaotao, S659 ([WED-428-YI](#))
Zhang, Xin, S94 ([LBP-034](#)),
S732 ([SAT-340-YI](#)), S732 ([SAT-341](#))
Zhang, Xing, S102 ([LBP-048](#))
Zhang, Xinyuan, S646 ([SAT-446](#))
Zhang, Xuanzhe, S526 ([WED-246](#))
Zhang, Xuehong, S646 ([SAT-446](#))
Zhang, Yang, S180 ([WED-074](#))
Zhang, Yangming, S602 ([TOP-217](#))
Zhang, Yanyun, S219 ([FRI-088](#))
Zhang, Yaodi, S161 ([THU-058](#))
Zhang, Yimin, S280 ([WED-541](#))
Zhang, Ying, S803 ([WED-412](#))
Zhang, Yinghua, S357 ([SAT-548](#))
Zhang, Yiyan, S230 ([FRI-119](#)),
S405 ([SAT-503](#)), S454 ([THU-499](#))
Zhang, Yonghong, S357 ([SAT-548](#))
Zhang, Yongjin, S447 ([THU-475](#))
Zhang, Yuewei, S442 ([THU-462](#))
Zhang, Yuguo, S605 ([SAT-198](#))
Zhang, Yuting, S526 ([WED-246](#))
Zhang, Yuwei, S527 ([WED-246](#))
Zhang, Zhengang, S95 ([LBP-037](#))
Zhang, Zhipeng, S806 ([WED-362](#)),
S813 ([WED-381](#)), S815 ([WED-386](#)),
S816 ([WED-388](#))
Zhang, Zhiyi, S628 ([FRI-035](#)),
S780 ([FRI-411-YI](#))
Zhang, Ziyang, S565 ([THU-200-YI](#))
Zhang, Ziyu, S355 ([SAT-544](#)),
S815 ([WED-387](#))
Zhang, Zongkun, S625 ([FRI-021](#))
Zhao, Caiyan, S161 ([THU-058](#))
Zhao, Derrick, S197 ([WED-123](#)),
S523 ([WED-237](#))
Zhao, Di, S86 ([LBP-019](#)),
S99 ([LBP-043](#))
Zhao, Fangcheng, S119 ([SAT-321](#))
Zhao, Hong, S684 ([WED-490](#)),
S790 ([FRI-439](#))
Zhao, Hui, S447 ([THU-475](#))
Zhao, Jieling, S263 ([THU-526](#))
Zhao, Junyu, S578 ([THU-239-YI](#))
Zhao, Junzheng, S59 ([OS-093](#))
Zhao, Longgang, S646 ([SAT-446](#))
Zhao, Meng, S424 ([FRI-490-YI](#)),
S739 ([SAT-375](#))
Zhao, Qianwen, S17 ([OS-014-YI](#)),
S182 ([WED-078](#))

- Zhao, Si, S109 (FRI-332), S112 (FRI-340), S285 (WED-556)
- Zhao, Xinyan, S119 (SAT-321), S121 (SAT-326)
- Zhao, Xun, S114 (TOP-344-YI)
- Zhao, Yang, S527 (WED-246)
- Zhao, Ying, S395 (SAT-478)
- Zhao, Yue, S423 (FRI-486)
- Zhao, Zhihao, S804 (WED-415)
- Zhayvoronok, Maksym, S610 (SAT-213)
- Zheng, Guanglei, S390 (TOP-510)
- Zheng, Huanwei, S605 (SAT-198)
- Zheng, Jiarui, S230 (FRI-118), S233 (FRI-127), S521 (WED-231)
- Zheng, Jun, S358 (SAT-550)
- Zheng, Min, S110 (FRI-334), S586 (THU-262), S767 (FRI-377)
- Zheng, Ming-Hua, S2 (GS-004), S37 (OS-053), S38 (OS-054), S488 (FRI-267), S526 (WED-246), S605 (SAT-198), S652 (SAT-462-YI)
- Zheng, Rongjiong, S783 (FRI-419)
- Zheng, Shihao, S194 (WED-114)
- Zheng, Sujun, S694 (FRI-154), S769 (FRI-382)
- Zheng, Xingrong, S430 (FRI-517), S437 (TOP-504)
- Zheng, Yanbo, S447 (THU-475)
- Zheng, Yinan, S395 (SAT-479-YI)
- Zhi, Yang, S120 (SAT-324), S122 (SAT-333)
- Zhong, Bihui, S84 (LBP-014), S100 (LBP-045)
- Zhong, Jinyi, S382 (SAT-041)
- Zhong, Min, S812 (WED-377)
- Zhong, Ming, S422 (FRI-484)
- Zhong, Victor W., S620 (TOP-006)
- Zhong, Wenting, S789 (FRI-438)
- Zhou, An, S527 (WED-246)
- Zhou, Bangguo, S333 (THU-163)
- Zhou, Bin, S95 (LBP-037)
- Zhou, Changyang, S59 (OS-093)
- Zhou, Cheng, S586 (THU-262)
- Zhou, Daqiao, S762 (FRI-366)
- Zhou, Daqiong, S227 (FRI-111), S677 (WED-472)
- Zhou, Guanlun, S784 (FRI-424)
- Zhou, Huiping, S197 (WED-123), S523 (WED-237)
- Zhou, Jiahua, S464 (FRI-200), S652 (SAT-462-YI), S730 (TOP-384-YI)
- Zhou, Li, S427 (FRI-500-YI)
- Zhou, Liyang, S792 (WED-390)
- Zhou, Qian, S119 (SAT-322)
- Zhou, Shuqiong, S98 (LBP-040)
- Zhou, Taolong, S526 (WED-246)
- Zhou, Xiao-jian, S819 (THU-382)
- Zhou, Xiaqing, S195 (WED-116)
- Zhou, Xingping, S345 (FRI-546)
- Zhou, Xiqiao, S526 (WED-246)
- Zhou, Xueyu, S303 (SAT-181-YI)
- Zhou, Yi, S701 (FRI-174)
- Zhou, Yingjiang, S564 (THU-198)
- Zhou, Yuhong, S99 (LBP-042)
- Zhou, Yusen, S526 (WED-246)
- Zhou, Zheyu, S403 (SAT-499)
- Zhou, Zhihang, S427 (FRI-500-YI)
- Zhou, Ziyi, S138 (SAT-254)
- Zhuang, Xiaodong, S42 (OS-061)
- Zhu, Chong, S36 (OS-050)
- Zhu, Chuanwu, S100 (LBP-045), S209 (FRI-053), S605 (SAT-198), S625 (FRI-022), S628 (FRI-035), S780 (FRI-411-YI)
- Zhu, Fengge, S745 (SAT-392)
- Zhuge, Yuzheng, S109 (FRI-332), S112 (FRI-340), S236 (FRI-135), S260 (SAT-136), S285 (WED-556)
- Zhu, Haoxiang, S748 (SAT-399)
- Zhu, Li, S625 (FRI-022), S628 (FRI-035), S780 (FRI-411-YI)
- Zhu, Qing, S36 (OS-050), S87 (LBP-021)
- Zhu, Siheng, S826 (THU-407)
- Zhu, Wenfeng, S271 (TOP-562), S347 (FRI-551), S363 (WED-020)
- Zhu, Wentao, S120 (SAT-323)
- Zhu, Wenwen, S454 (THU-499)
- Zhu, Xiaoli, S447 (THU-475)
- Zhu, Xiaoxue, S461 (TOP-310), S551 (WED-319), S558 (WED-338)
- Zhu, Xiaoying, S442 (THU-462)
- Zhu, Xu, S447 (THU-475)
- Zhu, Xue-jin, S135 (THU-342)
- Zhu, Yan, S701 (FRI-174)
- Zhu, Yanan, S401 (SAT-495)
- Zhu, Yanhong, S812 (WED-377)
- Zhu, Yixuan, S459 (TOP-307)
- Zhu, Yong-Fen, S526 (WED-246)
- Zhu, Yun, S119 (SAT-321), S124 (SAT-336)
- Zieglmayr, Sebastian, S213 (FRI-071)
- Ziegler, Nicole, S104 (TOP-352)
- Zieniewicz, Krzysztof, S369 (SAT-009)
- Zigmond, Ehud, S5 (GS-007), S166 (THU-076-YI), S308 (THU-098), S335 (THU-167)
- Zignego, Anna Linda, S674 (WED-467-YI)
- Žigutytė, Laura, S427 (FRI-499-YI)
- Žilincanová, Daniela, S379 (SAT-033), S539 (WED-279)
- Zilio, Gianluca, S28 (OS-035-YI), S157 (THU-050)
- Zimbardo, Angelo, S252 (SAT-113)
- Zimmermann, Tim, S363 (WED-021)
- Zimpel, Carolin, S24 (OS-027-YI)
- Zink, Joseph, S35 (OS-049-YI)
- Zinner, Carl, S291 (TOP-150-YI)
- Zinober, Kerstin, S186 (WED-089-YI), S197 (WED-122-YI), S198 (WED-125), S267 (THU-540), S436 (TOP-488-YI)
- Ziol, Marianne, S41 (OS-060), S441 (THU-459-YI), S444 (THU-466), S451 (THU-487-YI), S456 (THU-503)
- Zipprich, Alexander, S178 (WED-060-YI), S244 (SAT-087-YI), S263 (THU-527)
- Zisimopoulos, Konstantinos, S830 (THU-419)
- Zitelli, Patricia Momoyo, S9 (LBO-004), S83 (LBP-012), S89 (LBP-026), S219 (FRI-088), S619 (SAT-248)
- Žižalová, Kateřina, S539 (WED-280)
- Zlámál, Filip, S756 (SAT-422)
- Zocco, Maria Assunta, S533 (WED-261-YI)
- Zolfino, Teresa, S96 (LBP-038), S306 (THU-093), S322 (THU-127-YI)
- Zoller, Heinz, S515 (WED-214-YI), S703 (TOP-141), S708 (WED-135-YI), S722 (WED-183-YI), S773 (FRI-394)
- Zollner, Andreas, S54 (OS-083)
- Zöllner, Caroline, S793 (WED-391)
- Zompo, Fabio Del, S25 (OS-029)
- Zoncapé, Mirko, S474 (FRI-226), S492 (FRI-279-YI)
- Zonouzi, Aysan Poursadegh, S65 (OS-103)
- Zoodma, Martijn, S21 (OS-021-YI)
- Zope, Dimple, S350 (TOP-553)
- Zorza, Marta, S439 (THU-454)
- Žotkiewicz, Magdalena, S3 (GS-005)
- Zou, Guizhou, S605 (SAT-198)
- Zou, Heng, S91 (LBP-027)
- Zoulim, Fabien, S1 (GS-002), S22 (OS-022), S41 (OS-060), S58 (OS-091), S73 (OS-120), S737 (SAT-371), S764 (FRI-371), S793 (WED-391), S796 (WED-395), S802 (WED-410), S808 (WED-366)
- Zoulim, Guillaume, S423 (FRI-485)
- Zou, Zhengsheng, S119 (SAT-321), S124 (SAT-336)
- Zubiaga, Ana, S112 (FRI-343-YI), S419 (FRI-472-YI), S562 (TOP-229-YI), S569 (THU-210)
- Zucchini, Nicola, S19 (OS-017), S299 (SAT-171)
- Zucker, Jean-Daniel, S585 (THU-260)
- Zuckerman, Eli, S548 (WED-304), S774 (FRI-395), S834 (THU-371)
- Zuckerman, Inbal, S548 (WED-304)
- Zuckerman, Seth, S245 (SAT-089)
- Zucman-Rossi, Jessica, S349 (TOP-552), S415 (FRI-459)
- Zu, Hongmei, S786 (FRI-430)
- Zuin, Massimo, S725 (WED-191)
- Zuluaga, Juan Ignacio Marin, S9 (LBO-004), S89 (LBP-026)
- Zuluaga, Juan Ignacio Marín, S83 (LBP-012)
- Zuluaga, Paola, S154 (SAT-303), S190 (WED-104)
- Zuo, Mengxuan, S390 (TOP-510)
- Zurera, Coral, S190 (WED-104)
- Zvick, Joel, S98 (LBP-041)
- Zwaan, Mik, S278 (WED-533)
- Zwiebel, Maximilian, S193 (WED-111)
- Zwittink, Romy, S47 (OS-071-YI)
- Zydowicz-Machtel, Paulina, S66 (OS-107-YI)
- Zyklus, Romanas, S238 (SAT-068)

Disclosures: no commercial relationships

The following abstract submitters have indicated that they have no relationships with commercial entities that might be perceived as having a connection with their presentation:

Aaldijk Alexandra	Avellon Calvo Ana	Canivet Clémence M.
Aamann Luise	Avila Matías A.	Cantalops Vilà Paula
Ab Wahab Sabrina	Avolio Alfonso	Cantiga Cristiane
Abdelmalak Jonathan	Bablon Pierre	Capinha Francisco
Abdelrahman Basma	Babu Rosmy	Cappelli Simone
Abeysekera Kushala	Baek Yang-Hyun	Carbonell Michael
Abow-Mohamed Ikram	Balcar Lorenz	Carloni Vinicio
Abu Baker Fadi	Ballester María Pilar	Carmichael Elizabeth
Abutidze Akaki	Barajas Jorge	Carrier Paul
Aceituno Laia	Barbosa Markus Gregorio	Casirati Elia
Acevedo Haro Juan	Basheer Maamoun	Castelnuovo Gabriele
Acharya Pragyana	Bauer David	Castillo Elisa
Adali Gupse	Baumann Anja	Castoldi Mirco
Adamcova Selcanova Svetlana	Baven-Pronk Martine	Catanzaro Elisa
Adrien Bocquillon	Baweja Sukriti	Cavalletto Luisa
Ahmad Basil	Becchetti Chiara	Caviglia Gian Paolo
Ahmadizar Fariba	Bellec Claire	Cazier Helene
Ahn Jin Hee	Ben Mehrez Cyrine	Cazzaniga Giorgio
Ai Yingjie	Benedicto Ana	Celik Ferya
Aierkenjiang Malipati	Benzoubir Nassima	Cespiati Annalisa
Akarca Ulus	Beretta Laura	Chang Jason Pik Eu
Akiyama Matthew	Bernasconi Monica	Chen Rusi
Alblas Gabrielle	Bertazzoni Arianna	Chin Simone
Alenzi Maram	Bevz Tetiana	Chinellato Monica
Alfano Vincenzo	Beyene Nateneal	Cho Eun Ju
Ali Nida	Bhadoria Pooja	Choe Hun Jee
Alisi Anna	Bhattacharya Debashruti	Chon Hye Yeon
Alkhamash Maram	Bhoori Sherrie	Choudhary Nishu
Alkhoury Naim	Bihari Chhagan	Choudhury Ashok Kumar
Allen Sophie	Biriuchenko Iryna	Chuaypen Natthaya
Almeida Mathieu	Biswas Sagnik	Cives-Losada Candela
Alonso-Peña Marta	Bittencourt Paulo	Claudia Kunst
Alqahtani Saleh A.	Bittermann Therese	Clayton-Chubb Daniel
Al-Shakhshir Sarah	Björnsson Einar S.	Coelho Meine Gilmara
Alshiwanna Basheer	Blarasin Benedetta	Colecchia Luigi
Amer Johnny	Boeira Paula	Contreras Bryan J.
Andersen Mette lehmman	Bougueon Matthieu	Cordie Ahmed
Angel Dylan	Bourke Michèle	Corless Lynsey
Angelakis Athanasios	Bozon-Rivière Pauline	Corrigall Douglas
Anirvan Prajna	Bozso Boglarka	Cossiga Valentina
Anton Aina	Bozward Amber	Cox Leah
Apodaka-Biguri Maider	Brandt Annette	Crouchet Emilie
Arai Taeang	Breder Sigurd	Cruz-Ferro Elena
Arcari Ivan	Brevini Teresa	Cuadros Marta
Archer Ann	Broekhoven Annelotte	Dabbah Shoham
Ariño Silvia	Bruns Tony	Dagdeviren Sezin
Armandi Angelo	Bryce Kathleen	Dall'Alba Valesca
Armstrong Paul	Brynjulfson Lisa R. V.	Dang Shuang suo
Arora Umang	Buchanan Ryan	D'Anna Stefano
Arteta Beatriz	Calero Pérez Silvia	Das Avisnata
Arvaniti Pinelopi	Calleri Alberto	Dashdorj Arghun
Ashfaq-Khan Muhammad	Calvo Sánchez Henar	Daza Jimmy
Asteljoki Juho	Campos-Murguía Alejandro	de Boer Ynto
Attia Yasmeen	Candotti Daniel	De Broucker Chloé

de la Viña Daniela	Fürst Stefan	Hwang Jeong Ah
De Maria Nicola	Furumaya Alicia	Hydes Theresa
De Rosa Laura	Fuster-Martínez Isabel	Iborra Ignacio
De Santis Emanuela	Gabdulkhakova Adelya	Ignat Mina
De Vincentis Antonio	Gabrys Philipp	Iliescu Laura
De Vos Zenzi	Gad Shaimaa	Ingiliz Patrick
DeFelice Nicholas	Gadour Eyad	Ismail Mona
Deibel Ansgar	Gairola Abhishek	İstemihan Zülal
Del Barrio Azaceta María	Gallego-Durán Rocío	Izquierdo-Sánchez Laura
Della Corte Cristina	Gallo Paolo	Jammu Anish
Delo Joseph	Galun Eithan	Janik Maciej
Delphin Marion	Gananandan Kohilan	Jara Lorena
Deltenre Pierre	Garcia Garcia Federico	Jayanti Sri
Desbois-Mouthon Christèle	García-Gavilán María Carmen	Jegodzinski Lina
Desdouets Chantal	Garg Pratibha	Jenab Mazda
Deshpande Aditi	Gart Eveline	Jeong Jae Yoon
Determann Madita	Gazda Jakub	Jeschke Matthias
Di Girolamo Julia	Geiger Niklas	Jhahharia Ashok
Di Marco Lorenza	Getia Vladimer	Jia Tingting
Di Tommaso Luca	Ghinolfi Davide	jiang xiaoyu
Dias Marlon	Giannitrapani Lydia	Jiménez-Aguilar Juan Manuel
Dias dos Santos Diego	Giannousi Eirini	Jiménez-Franco Andrea
Diaz Juan Manuel	Giguet Baptiste	John Katharina
Dileo Eleonora	Girish Vishnu	Jördens Markus S.
Ding Rui	Giuffrè Mauro	Joung Hyunhae
Diniz Mariana	Giuli Lucia	Juanola Adria
Dinjar Kujundžić Petra	Gjini Kamela	JUN Dae Won
Dobrzniecka Anna	Gömer André	Junot Christophe
Dolce Arianna	Gómez Santos Beatriz	Jurado-Aguilar Javier
Dragan Alexandru Victor	Gomez-Jauregui Paul	Kado Akira
Du Yu	Gonçalves Araujo Joana	Kaewdech Apichat
Düll Miriam M.	Gorrell Mark	Kaji Kosuke
Dunn Winston	Graf Christiana	Kalka Iris
Duran Osman Firat	Grisetti Luca	Kao Yu-Ting
Durban Jonathan	Grossar Lorenz	Kaps Leonard
Duseja Ajay Kumar	Grzelka Malgorzata	Karbannek Henrik
Easaw Sue	Guariglia Marta	Karichashvili Lika
Ekelik Merve	Guerra Pietro	Karim Gres
El Hage Chehade Nabil	Guida Alice	Karoney Mercy
El-domiaty Nada	Guinart-Cuadra Albert	Kaur Parminder
Elkrief Laure	Gulbiani Lasha	Ke Bibo
Endo Kei	Gupta Abhishak	Keller Marisa Isabell
Erurun Hasan	H Bhat Sadam	Kelsch Lara
Evangelista Andreia	Hakeem Andrew	Kerbert Annarein
Faisal Nabiha	Hall Samantha	Keskin Onur
Fang Jing	Haller Rosa	khajuria Rahul
Felber Marco	Hamody Yara	Khanam Arshi
Feng Hao	Han Guorong	Khatua Chitta Ranjan
Fernández Javier	Harris James	Kheloufi Lyès
Fernandez Alvarez Paula	Hartl Lukas	Khoperia Anna
Fernandez-Barrena Maite G.	Har-Zahav Adi	Kimmann Markus
Fernandez-Gordón Sánchez Flor M.	Hashiguchi Taishi	Kirchner Theresa
Fiancette Rémi	Hatten Hannes	Kitto Laura
Finkel Jemima	Hermán-Sánchez Natalia	Koizumi Yohei
Finnberg-Kim Amanda	Hernández-Èvole Helena	Kong Defu
Firat Hatice Gülgün	Herrero Alba	Kornfehl Andrea
Flatley Sarah	Higuera-de-la-Tijera Fatima	Kostadinova Radina
Flores Joan Ericka	Hikita Hayato	Kotlinowski Jerzy
Foglia Beatrice	Hirooka Masashi	Kounis Ilias
Fonte Stefano	Hjorth Maria	Koutny Florian
Forlano Roberta	Ho Chun-Ting	Kovynev Artemiy
Forrest Ewan H.	Horst Ludwig J.	Krawczyk Marcin
Francoz Claire	Hountondji Lina	Kronsten Victoria
Franzè Maria Stella	Hoyle Henry	Kulkarni Anand
Freyer Erich	Hsieh Meng Lun	Kumar Pavitra
Frissen Mick	Hu Michael	Labenz Christian
Fu Xiao	Huang Yanfang	Laevens Benjamin
Fukushima Masanori	Hur Moon Haeng	Lallement Justine

Disclosures

Lalloyer Fanny	Menétrey Caroline	Petrosyan Armen
Lamarque Catherine	Meng Yao	Petryna Vitalii
Lange Naomi	Merens Vincent	Pham Thi Thu Thuy
Langer Mona-May	Meszaros Magdalena	Piermatteo Lorenzo
Lapitz Ainhoa	Meunier Lucy	Pingoy Kate
Lara-Romero Carmen	Meyer-Herbon Pamela	Piper Hanley Karen
Lasa-Elosegi Irune	Michel Maurice	Pivtorak Kateryna
Latournerie Marianne	Miglianti Michela	Placed-Gallego Cristina
Leal-Lassalle Hector	Millian Daniel	Pohl Julian
Lebossé Fanny	Minciuna Iulia	Pollicino Teresa
L'écuyer Sydnée	Mittal Ashi	Poo Jorge
Leith Damien	Moeckli Beat	Protopapas Adonis
Lekakis Vasileios	Mohamed Islam	Puchas Philip
Lepour Maxence	Mol Bregje	Pugliese Nicola
Leproux Apolline	Moles Anna	Purssell Huw
Leung Kristel	Montagnese Sara	Quach Susanna
L'Hermite Sébastien	Montague Sarah	Quelhas Patricia
Liang Xujing	Montano-Loza Aldo J	Rababoc Razvan
liew ian yang	Mor Orna	Radchenko Anastasiia
Liguori Antonio	Mücke Marcus	Ramachandran Veena
Lin Huapeng	Mukherji Atish	Ramanathan Raghu
Lindqvist Catarina	Murad Mohamad	Ramos Ballesteros Luz
Ling Sophia	Nabidzhonov Aziz	Rana Randeep
Link Frederik	Nabilou Puria	Rando-Segura Ariadna
Lo Gora	Nagao Chikako	Rashu Elias
Lombardi Rosa	Nagy Laura	Ravaioli Federico
Lombardo Antonino	Najafian Nilofar	Reinartz Groba Sara
Long Shann	Nalbant Bahar	Reißing Johanna
Loosen Sven H.	Nam Heechul	Reverter Enric
López-Vicario Cristina	Nassiri-Toosi Mohssen	Richardson Naomi
Lu Fengmin	Nautiyal Nidhi	Ring Julian
Ludwigs Lina	Nenu Iuliana	Robertson Tayla
Lumley Sheila	Niaz Qamar	Roccarina Davide
Lupberger Joachim	Niazi Shehzad	Rodrigues Inês
Lynch Erica Nicola	Nieva-Zuluaga Ane	Rohr-Udilova Nataliya
Lynn Soe Einsie	Nogami Asako	Rojas Ángela
Ma Cheng	Nováková Barbora	Román-Calleja Berenice M.
MacCarthy Hannah	Nuriyev Kanan	Román-Sagüillo Sara
Maccioni Luca	Øgaard Jonas	Romeo Mario
Magnes Marzena	Olivas Ignasi	Romero Gema
Maharshi Sudhir	Olivas Alberch Pol	Romero-Grimaldo Berta
Maheshwari Deepanshu	Onghena Louis	Romero-Gutiérrez Marta
Maimaitinijati Yusufukadier	Onoiu Alina-Iuliana	Ronca Vincenzo
Maiwall Rakhi	Osna Natalia	Rooney Michael
Makuza Jean Damascene	Ostrovskaya Anna	Roongrawee Thitaporn
Mallela Venkata Ramana	Ouchi Mayu	Rossotti Roberto
Manco Rita	Oude Veldhuis Sharon	Rossvoll Lasse
Mandea Matei	Ozari Gulnar Muge	Röttele Felix
Mann Jake	Pais Raluca	Ruiz de Gauna Mikel
Männistö Ville	Pallozzi Maria	Rydell Gustaf
Mantovani Stefania	Palma Carolina	Saidi Alina
Manuli Chiara	Pan Xingfei	Saitta Carlo
Marek George	Pandey Sushmita	Salié Henrike
Maria Arjun	Pantziros Spyridon	Salpini Romina
Markaide Enara	Panzer Marlene	Saltini Dario
Marrone Aldo	Paolini Erika	Sanchez Cristina
Marti-Aguado David	Papadopoulos Nikolaos	Sánchez Aránzazu
Martín-Escolano Rubén	Parisse Simona	Sanchez-Serrano Jose
Martinez Isabella	Parlati Lucia	Santomenna Floriana
Martínez-Arenas Laura	Pascale Alina	Santos-Ferreira Nanci
Martinez-Gili Laura	Patseas Dimitrios	Saracco Margherita
Masarone Mario	Paule Lorena	Sartini Claudio
Matsui Takeshi	Payancé Audrey	Sato Shunsuke
Maya Douglas	Pedica Federica	Saunthar Ahreni
Mbelle Mzamo	Pei Xiong	Saxena Varun
Mehta Gautam	Pelusi Serena	Sayed Nilofer
Méndez Isabel	Pennisi Grazia	Schleicher Eva Maria
Méndez-Sánchez Nahum	Pérez Diaz del Campo Nuria	Schlösser Denise

Schophaus Simon
 Schramm Christoph
 Schuehle Svenja
 Schulz Martin
 Schumacher Jonas
 Scivetti Paolo
 Segovia-Zafra Antonio
 Selvestrel Davide
 Semmler Georg
 Sendra Carmen
 Seng Dorothy
 Sepúlveda-Crespo Daniel
 Seraphin Tobias Paul
 Sererols Viñas Laura
 Seror Olivier
 Sessa Anna
 Seto Wai-Kay
 Sha Meng
 Sharma Shvetank
 She Shaoping
 Shi Juanjuan
 Shin Seung Kak
 Si Tengfei
 SIDALI Sabrina
 Silva Mário Jorge
 Silvestri Laura
 Simão André
 Simoes Eugenio Mélanie
 Siribelli Alessia
 Skrypnyk Igor
 Smets Lena
 Smith Hollie
 Smyk Wiktor
 Snorrason Bjarki Leó
 Sohn Won
 Somers Nicky
 Song Sherlot Juan
 Sonnenberg Jannik
 Souleiman Roni
 Souza Matheus
 Sposito Carlo
 Stamouli Marilena
 Stefanini Bernardo
 Strandberg Rickard
 Subhani Mohsan
 Sugiyama Masaya
 Suk Ki Tae
 Surabattula Rambabu
 Suykens Janne
 Talafu Tangnuer
 Talarek Ewa
 Tanaka Kazunari

Tangkijvanich Pisit
 Tao Mengyu
 Tashkent Yasmina
 Tejedor Marta
 Teng Margaret
 Terracciani Francesca
 Terziroli Beretta-Piccoli Benedetta
 Thanapirom Kessarín
 Thatcher Amy
 Thiyagarajah Keerthihan
 Thomas Célia
 Tincopa Monica
 Tiwari Vaibhav
 Tjerkaski Jonathan
 Tong Huan
 Torre Pietro
 Tovoli Francesco
 Trampert David
 Tran Henri
 Triantos Christos
 Tripathi Madhulika
 Troppmair Maria Rosina
 Trzos Katarzyna
 Tsereteli Maia
 Tsertsvadze Tengiz
 Tuck Jaclyn
 Tyagi Purnima
 Tyson Luke D.
 Tzadok Roie
 Ueno Masayuki
 Unozawa Hidemi
 Uzun Sarp
 Vaidya Arun
 Valainathan Shantha
 Valdecantos Pilar
 Valsan Arun
 van Doorn Diederick
 Van Melkebeke Lukas
 Vanlerberghe Benedict
 Vaquero-Rey Aida
 Vargas-Accarino Elena
 Vasudevan Ashwini
 Veelken Rhea
 Veerachit-O-Iarn Titinan
 Velliou Rallia
 Veloso Alves Pereira Isabel
 Venzin Valentina
 Verhulst Stefaan
 Viana Maria
 Viganò Raffaella
 Villagrasa Ares
 Villanueva Marina

Vitale Alessandro
 Vitellius Carole
 Vo Quang Erwan
 Voeller Alexis
 Volkert Ines
 von Meijenfeldt Fien
 von Seth Erik
 Vu Mylisa
 Waddell Scott
 Wadhawan Aishani
 Wakabayashi Shun-ichi
 Walia Nirbaanjot
 Walker Alexander
 Wan Zhiping
 Warsop Zakary
 Wei Xi
 Wetten Aaron
 Wiering Leke
 Will Nico
 Wintersteller Hannah
 Wolters Frank
 Won Sung-Min
 Woo Hyun Young
 Wronka Karolina
 Xiang Huanyu
 Xiong Feixiang
 Xue Feng
 Yadav Rajni
 Yagüe Parada Álvaro
 Yamazhan Tansu
 Yang Ju Dong
 Yangcharoen Awassada
 Yankouskaya Katharina
 Yao Naijuan
 Yoo Jae-Sung
 Yu Ming-Whei
 Yun Jae Moon
 Zachou Kalliopi
 Zafar Yousaf
 Zanetto Alberto
 Zapata-Pavas Leidy Estefanía
 Zeineddine Fadl A.
 Zerial Marino
 Zhai Xing-Ran
 Zhi Yang
 Zhou Li
 Zoncapè Mirko
 Zuckerman Eli
 Zuluaga Paola
 Zydowicz-Machtel Paulina

Disclosures: commercial relationships

The following abstract submitters have indicated that they have relationships with commercial entities that might be perceived as having a connection with their presentation:

Abbas Nadir
 Abdelgani Siham
 Aboona Majd
 Abramov Frida
 Ajaz Saima
 Ajith Ananya
 Akbary Kutbuddin
 Alard Berenice
 Alexopoulou Alexandra
 Al-Hasani Aya
 Aliane Verena
 Alimenti Eleonora
 Alitti Clémentine
 Alkhouri Naim
 Allaire Manon
 Allweiss Lena
 Alonso Cristina
 Alpert Lauren
 Altadill Ariadna
 Altmann Philipp
 Aminian Ali
 Anderson Sarah
 Angelini Giulia
 Anglero-Rodriguez Yessenia
 Apostolov Ross
 Armisen Javier
 Aseem Sayed
 Asselah Tarik
 Atkinson Stephen
 Ayada Ibrahim
 Ayonrinde Oyekoya
 Baffy Gyorgy
 Bailey Elizabeth
 Bajaj Jasmohan
 Balaseviciute Ugne
 Balkhed Wile
 Balsano Rita
 Bao Yujie
 Bardou-Jacquet Edouard
 Baron Aureole
 Barrett Jeffrey
 Bech Katrine Tholstrup
 Begum Shazia
 Benichou Bernard
 Bennett Kris
 Berberova Magda
 Bernal William
 Bernatik Sophia
 Bernstein David
 Bhuyan Muhammad Abedur Rahman
 Biermer Michael
 Bindra Jas
 Bobowski-Gerard Marie

Bogdanos Dimitrios
 Bonitz Katharina
 Boros Carina
 Bosch Anna
 Boudes Pol
 Boursier Jerome
 Brennan Paul
 Briand Francois
 Brol Maximilian Joseph
 Brosnan-Cashman Jacqueline
 Brunet Laurence
 Bruno Benjamin
 Brzdek Michał
 Buell Chelsea
 Bumbu Andreea Livia
 Burghart Lukas
 Burke Laura
 Burkhead Stephanie
 Burnside Jessica
 Buttler Laura
 Cabello Calleja Josune
 Cable Edward
 Camelo Castillo Anny
 Campana Lara
 Cançado Guilherme
 Canillas Lidia
 Cao Yuzhe
 Cappuyens Sarah
 Caraceni Paolo
 Carbone Marco
 Cardenas Andres
 Cardoso Joana
 Cardoso Delgado Teresa
 Carey Ivana
 Carvalho-Gomes Ângela
 Castera Laurent
 Cathcart Andrea
 Caussy Cyrielle
 Celsa Ciro
 Chazouillères Olivier
 Cheng Guofeng
 Choi Yun-Jung
 Chotiprasidhi Perapa
 Chotkoe Shivani
 Chu Audrey
 CHUNG Sung Won
 Cimbora Daniel
 Cinque Felice
 Clusmann Jan
 Coessens Marie
 Colapietro Francesca
 Colca Jerry
 Cole Alexander

Conway Brian
 Cooper Katherine
 Cooreman Michael
 Corpechot Christophe
 Cortese Maria Francesca
 Creamer John
 Cristoferi Laura
 Currie Sue
 Czarnecki Judith
 Da Ben L.
 Dahari Harel
 Dai Zhe
 Dajti Elton
 Daniels Samuel
 D'Antiga Lorenzo
 De Benedittis Carla
 De Creus An
 de Lédinghen Victor
 De Martin Sara
 De Monte Sara
 De Simone Paolo
 Debing Yannick
 Debroff Jake
 Del Zompo Fabio
 Dennis Andrea
 Derdak Zoltan
 Deschler Sebastian
 Dhanda Ashwin
 Di Martino Vincent
 Diamond Charlie
 Diaz-Gonzalez Alvaro
 Dobrowolska Krystyna
 Dominik Nina
 Downs Louise
 Dubourg Julie
 Duva Vita
 Edwards Lindsey
 Egge Julius
 Eggermont Fabienne
 Ehmer Ursula
 Elias Kathleen
 El-Sayed Manal
 Engel Bastian
 Erickson Mary
 Faulkes Rosemary
 Feigh Michael
 Felli Eric
 Fernandes Wendy
 Ferrandino Giuseppe
 Ferret Miñana Ainhoa
 Fiorotto Romina
 Flanagan Stuart
 Fleshman Kelly

Flisiak Robert
 Fortea Jose
 Fortuny Marta
 Fraser David A.
 Fromme Malin
 Frontino Anna Maria
 Fuchs Claudia
 Furquim d'Almeida Arno
 Gaia Silvia
 Gairing Simon Johannes
 Gambino Carmine
 Gantzel Rasmus
 Gao Lu
 Garcia David
 Garitta Elena
 Gato-Zambrano Sheila
 Geisler Lukas
 Ger Flutter
 Gerussi Alessio
 Gestels Naomi
 Gosset Andréa
 Gagnani Laura
 Grassi Alberto
 Gratacós-Ginès Jordi
 Greenman Raanan
 Griffin Laura
 Groen Roos
 Grottenthaler Julia M.
 Gruevska Aleksandra
 Gu Wenyi
 Guillot Adrien
 Guo Yifei
 Haghnjad Vincent
 Hai Hoang
 Hajarizadeh Behzad
 Halimani Noreen
 Halliday Anna
 Hansen Johanne Kragh
 Harrison Emily
 Hartsfield Cynthia L.
 Hashim Ahmed
 Hateley Charlotte
 Hauskov Sara
 Hegmar Hannes
 Heldens Anneleen
 Hernández Candido
 Hernández Conde Marta
 Hetland Liv Eline
 Heyerick Lander
 Hilliard Valerie
 Hirode Grishma
 Hockings Paul
 Hofer Benedikt
 Holmberg Marte
 Hong Jin
 Hortelano Carlos M.
 Howarth Rachel
 Hsu Heather
 HUI Vicki Wing-Ki
 Hupa-Breier Katharina Luise
 Husa jr Petr
 Hussain Nasir
 Iker Robin
 Im Gene
 Israelsen Mads
 Ivancovsky Wajcman Dana
 Izai Ryo
 Jachs Mathias

Jack Kathryn
 Jackson Edward
 Jácome-Blásquez Francisco
 Jain Harsh
 Jang Suk-Chan
 Janjua Naveed
 Jarman Georgeina L
 Jeng Rachel Wen-Juei
 Jensen Morten Daniel
 Jeschke Matthias
 Jessa Fatema
 Jiménez-Masip Alba
 Johansen Stine
 Joshi Shilpy
 Kabelitz Martin
 Kamara Elaine
 Kamlin C. Omar
 Kang Wonseok
 Kappe Naomi
 Karbannek Henrik
 Karl Anna
 Kasper Jonathan
 Kawata Kazuhito
 Kazma Rémi
 Keating Shelley
 Kendall Timothy
 Khan Shahid
 Kharbanda Kusum
 Kilany Mai
 Kilpatrick Alastair M.
 Kim Chong
 Kimura Takeshi
 King Thomas
 Kleter Bernhard
 Klöhn Mara
 Knapp Maximilian
 Kobylak Nazarii
 Kohlhepp Marlene
 Koller Tomas
 Komori Atsumasa
 Kosinska Anna D.
 Kranidioti Hariklia
 Kupcinskis Limas
 Labyed Yassin
 Lages Martins Pedro
 Lai Mason
 Lampertico Pietro
 Langenbacher Diane
 Lani Lorenzo
 Lanthier Nicolas
 Lautenbach Jennifer
 Lawitz Eric
 Lazarus Jeffrey V.
 Le Bert Nina
 Lee Jae Seung
 Lefere Sander
 Lemmens Tibo
 Lens Sabela
 Leonel Thais
 Leppkes Moritz
 Lewinska Monika
 Lewis Rhea
 Li Zhihao
 Lightstone Adi
 Lim Young-Suk
 Lindholm Schnefeld Helle
 Lindström Lina
 Lindvig Katrine

Liu Yang
 Liu Yin James
 Livingston Christine
 Llop Herrera Elba
 Llorca Anne
 Locus Tatjana
 Loomba Rohit
 López-Sáez Berta
 Louvet Alexandre
 Lovatt Jessica
 Luong Xuan
 Lyngbeck Jensen Ellen
 Macek Jilkova Zuzana
 Macias Rocio
 Mageras Anna
 Maggs Daniel
 Magyar Christian
 Mahadevan Sangeetha
 Mahmud Nadim
 Mak Lung Yi Loey
 Maldonado Adriana
 Manfredi Giulia Francesca
 Mangla Kamal Kant
 Manhas Savrina
 Marcellin Fabienne
 Mari Montserrat
 Mariño Zoe
 Marlin Taylor
 Marra Fiona
 Masood Ramsha
 Mauro Ezequiel
 Mayorca Guiliani Alejandro
 McClure Tess
 McCoullough Laura
 Medical Costello
 Melehani Jason H.
 Mendez Marinela
 Mendlowitz Andrew
 Mercier Renee-Claude
 Middelburg Tim
 Mikkelsen Anne Catrine Dagaard
 Miller Hamish
 Minami Tatsuya
 Miralpeix Anna
 Mitchell Alice
 Moga Lucile
 Mohamed Almuthana
 Møller Thomas
 Molzen Line
 Monian Prashant
 Moon Andrew
 Morgan Camille
 Morris Heather
 Morrison Martine C.
 Moruzzi Noah
 Motta Rodrigo
 Mouliade Charlotte
 Mountain Victoria
 Munteanu Mona
 Murillo Perez Carla Fiorella
 Nadal Ruth
 Nahon Pierre
 Nair Radhika
 Nanji Zehrah
 Nault Jean Charles
 Nehme Zeina
 Nguyen Duyen
 Nicolàs Olivé Aina

Disclosures

Nieves Wildaliz
Nikolaou Nikolaos
Ningarhari Massih
Nishimoto-Ashfield Akiko
Nøhr-Meldgaard Jacob
Novak Kristine
Nowak Magdalena
Nunag Dominic
O' Farrell Marie
O'Connor Ian P.
O'Dwyer Samantha
Ogawa Eiichi
Oldenburger Anouk
Oltmanns Carlos
Olveira Antonio
Oscarsson Jan
Owen Christina
Paik Woo Hyun
Palom Adriana
Panella Riccardo
Paoletti Martina
Papalamprakopoulou Zoi
Papatheodoridis George
Park Min Kyung
Parmar Deven
Parthasarathy Gopanandan
Patmore Lesley A.
Paul Katherine
Pauwels Frederik
Pavlidis Charalampos
Peiseler Moritz
Pekarska Katrina
Peleman Cédric
Peng Weng Chuan
Perez-Campuzano Valeria
Perez-Guasch Martina
Petitjean Mathieu
Pfefferkorn Maria
Pfister Dominik
PharmaGenesis Oxford
Phillips Alexandra
Piano Salvatore
Pinto Elisa
Pocurull Anna
Pomej Katharina
Pons Monica
Poynard Thierry
Protopapa Francesca
Pulaski Hanna
Puri Puneet
Pustjens Jesse
Putignano Antonella
Qiu Ke
Quaranta Maria Giovanna
Qurashi Maria
Radu Pompilia
Rajagopalan Krithika
Ramos Hilario
Rastovic Una
Ratziu Vlad
Razavi-Shearer Devin
Regnault Hélène
Remih Katharina
Ren Yayun
Rhee Hyungjin
Riva Antonio
Robaeys Wouter
Roca Suarez Armando Andres

Rodgers Helen
Rodrigo-Torres Daniel
Rodríguez-Perálvarez Manuel
Rohbeck Elisabeth
Rojo Carla
Romano Antonietta
Romero-Vico Judit
Rosado Eugenio
Rosato Valerio
Rosenberger Florian
Rosenthal Jolan
Rowe Ian
Rubinsztain Joseph
Rudler Marika
Ruiz-Cobo Juan Carlos
S. Sharath
Saeidinejad Mohammad Mahdi
Saito Takeshi
Salimzadeh Loghman
Sanchez Cristina
Sandmann Lisa
Sanyal Arun J.
Schachteli Fabian
Schaub Johanna
Scheiner Bernhard
Schneeweiss-Gleixner Mathias
Schrader Christina
Schreiber Sophia
Schreiner Andrew
Schütte Sarah Lisa
Schwarz Michael
Schwenken Marianna
Scoble Patrick
Scott Kylie
Segna Daniel
Seo Hye-Young
Serdjebi Cindy
Serfert Yvonne
Sewell Charlotte
Shaheen Abdel-Aziz
Shang Ying
Shenvi Swapna
Sheptulina Anna
Sherratt Helen
Shetty Shishir
Shih Chin-I
Shimizu Mayuko
Shulman Nancy
Shumbayawonda Elizabeth
Siddle Matthew
Siguencia Jessica
Sim Yu Ki
Simbrunner Benedikt
Sims Karen D.
Singh Jennifer M.
Skovgaard Emilie
Skröder Helena
Snir Tom
Socha Piotr
Soliman Riham
Sorensen Henrik
Soret Pierre-Antoine
Soria Anna
Sorzi-Nechay Thomas
Sridhar Siddharth
Sriphoosanaphan Supachaya
Standen Mary
Stauber Rudolf E.

Stiess Michael
Su Tung-Hung
Suess Greg
Sun Jian
Sussman Norman
Suzuki Ayako
Swearingen Kjersti
Taggart David
Tahata Yuki
Talal Andrew
Tamaki Nobuharu
Tan Cedric
Tantai Xinxing
Taru Vlad
Tavaglione Federica
Tedone Fabio
Telep Laura
Tesini Giulia
Theel Willy
Thennati Rajamannar
Thévenot Thierry
Thomann Stefan
Thompson Connor
Thuy Le Thi Thanh
Tibbitts Jay
Tillman Erik
Tizzani Marco
Torella Laura
Tornai David
Torp Nikolaj
Torrás Clàudia
Tranah Thomas
Tsai Wen-Wei
Tuli Vishal
Ursic Bedoya José
Vaillant Andrew
Van Espen Lore
van Hooff Maria C.
van Kleef Laurens
Van Renne Nicolaas
van Velsen Lisa M.
Vanderschueren Emma
Vengohechea Llorens Jordi
Verbinnen Thierry
Vergara Mercedes
Verheijden Simon
Verma Nipun
Villard Christina
Villavicencio Edgar
Vithayathil Mathew
Voldum-Clausen Kristoffer
Volmari Annika
Vyawahare Saurabh
Wang Ying
Watson Hugh
Weiss Nicolas
Weltzsch Jan Philipp
Werner Ellen
Wheeler Darren
Witte Moana
Wong Vincent Wai-Sun
Wood Callum
Wu Xia
Wunsch Ewa
Wynne Alex
Wynne-Cattanach Kieran
Xie Zhe
Xu Cindy

Yamada Tomoharu
Yamazoe Taiji
Yeh Julian
Yip Terry Cheuk-Fung
Younossi Zobair

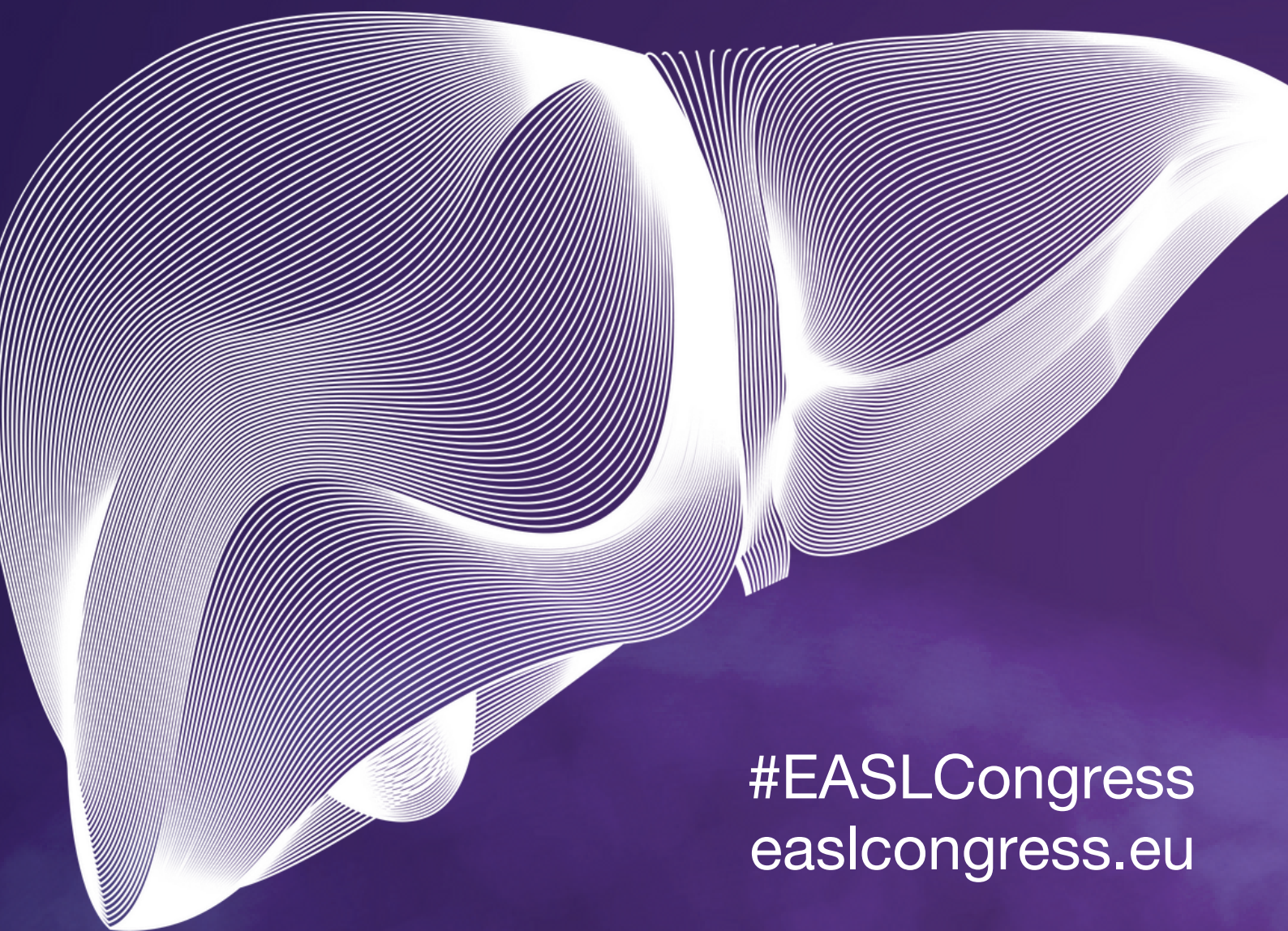
Yousefi Keyvan
Zaccherini Giacomo
Zaher Anas
Zhang Jianhua
Zhao Meng

Zheng Sujun
Zhu Qing
Žigutytė Laura

Reviewers list

We express our deepest appreciation to the following people, who have given us generous and invaluable help as abstract reviewers for the EASL Congress 2024.

Abdelmalek Manal	Goossens Nicolas	Postic Catherine
Adams Leon	Gottwein Judith	Procopet Bogdan
Affo Silvia	Gougelet Angelique	Protopopescu Camelia
Agarwal Kosh	Govaere Olivier	Rautou Pierre-Emmanuel
Aghemo Alessio	Hallsworth Kate	Reesink Hendrik W.
Andersen Jesper	Hansen Bettina	Reeves Helene
Andrade Raul Jesús	Herkel Johannes	Reid Leila
Anty Rodolphe	Hernandez-Gea Virginia	Rescigno Maria
Aspichueta Patricia	Hoare Matthew	Reverter Enric
Bañares Rafael	Hutchinson Sharon J.	Rigamonti Cristina
Bansal Ruchi	Iannacone Matteo	Rinella Mary
Baptista Pedro M.	Idilman Ramazan	Riveiro-Barciela Mar
Barfod O'Connell Malene	Iserte Gemma	Rodrigues Robim M.
Bataller Ramon	Jack Kathryn	Rodríguez-Peralvarez Manuel L.
Baumert Thomas	Jalan Rajiv	Rombouts Krista
Beckman Sonja	Kołodziejczyk Aleksandra	Ronca Vincenzo
Ben-Ari Ziv	Kondili Loretta	Rowe Ian
Bengsch Bertram	Krag Aleksander	Russo Francesco Paolo
Bosma Piter	Kwanten Wilhelmus	Rydell Gustaf E.P.
Böttler Tobias	L. Irving William	Saborowski Anna
Braconi Chiara	Lemaigre Frédéric P.	Sandman Lisa
Bureau Christophe	Licata Anna	Schaefer Denise
Buti Maria	Lleo Ana	Schattenberg Jörn
Caraceni Paolo	Longhi Maria Serena	Schnabl Bernd
Carbone Marco	Lotersztajn Sophie	Scott Charlotte
Castera Laurent	Lucifora Julie	Senzolo Marco
Castro Rui	Lupberger Joachim	Shawcross Debbie
Cazzagon Nora	Lupsor Monica	Shlomai Amir
China Louise	Luukkonen Panu	Simao Andre
Coilly Audrey	Macias Rocio	Sonneveld Milan
Coppola Nicola	Magnusson Maria	Szabo Gyongyi
Crespo Gonzalo	Mariño Zoe	Tacke Frank
Cubero Javier	Marra Fabio	Thabut Dominique
Culver Emma	Martinez-Chantar María Luz	Thiele Maja
Dalekos George	McLin Valerie	Trepo Eric
Darwish Murad Sarwa	Moreno Christophe	Trifan Anca
De knegt Robert	Morgan Marsha	Tripathi Dhiraj
Degasperi Elisabetta	Nault Jean-Charles	Trovato Francesca Maria
Degertekin Bülent	Negro Francesco	Tsochatzis Emmanuel
Desdouets Chantal	Newsome Philip	Turco Laura
Edeline Julien	Pais Raluca	Valenti Luca
Edwards Lindsey	Pallett Laura	van Bommel Florian
Elsharkawy Ahmed	Papp Maria	van Bommel Florian
Esser Hannah	Parker Richard	Verhelst Xavier
Fabrellas Nuria	Pericas Juan M.	Verma Sumita
Fisicaro Paola	Perrillo Robert P.	Verslype Chris
Folseraas Trine	Pinzani Massimo	Vinken Mathieu
Frances Ruben	Piscaglia Fabio	Westbrook Rachel
Francque Sven	Pischke Sven	Wong Vincent
Fraquelli Mirella	Pol Stanislas	Yasuko Iwakiri
Ganne Carrie Nathalie	Pollicino Teresa	Zelber-Sagi Shira
Garcia Pagan Juan Carlos	Pose Elisa	



#EASLCongress
easlcongress.eu